

SYMPOSIUM BI01

Materials Research by the LGBTQIA+ Community and a Vision for Inclusivity
April 23 - April 24, 2024

Symposium Organizers

Andrew Cairns, Imperial College London
Brett Helms, Lawrence Berkeley National Lab
Amanda Morris, Virginia Polytechnic Institute
Julia Ortony, University of California, San Diego

* Invited Paper
+ JMR Distinguished Invited Speaker
^ MRS Communications Early Career Distinguished Presenter

SESSION BI01.01: Materials Research by the LGBTQIA+ Community and a Vision for Inclusivity I
Session Chairs: Melissa Davis and Jerry Yang
Tuesday Morning, April 23, 2024
Room 326, Level 3, Summit

10:30 AM *BI01.01.01

Materials Discovery One Standard Deviation from The Mean: Finding Avalanches in Nanoparticles [Bruce E. Cohen](#); Lawrence Berkeley National Laboratory, United States

The first applications of luminescent nanocrystals to bioimaging were semiconductor quantum dots with optoelectronic properties that largely mirrored those of organics and proteins, but with substantially increased stability and brightness that have enabled single molecule and other challenging imaging applications. Building on this success, newer nanocrystals have been engineered with optical properties unlike anything found in traditional probes, including perfect photostability,¹ anti-Stokes emission a billion-fold more efficient than 2-photon excitation,² and most recently, photon avalanches hosted within nanostructures.³ Avalanches are steeply nonlinear events in which outsized responses arise from a series of minute inputs. With light, photon avalanching (PA) had been observed only in bulk materials and aggregates, often at cryogenic temperatures, preventing its application to bioimaging. In two recent studies,^{3,4} we describe the engineering and imaging of avalanching nanoparticles (ANPs), which are ~25-nm Tm³⁺-doped NaYF₄ upconverting nanoparticles that efficiently convert near infrared excitation to higher energy emission. Avalanches are steeply nonlinear events in which outsized responses arise from a series of minute inputs and, with light, photon avalanching had been observed only in bulk materials, often at cryogenic temperatures. The extreme nonlinearity of ANP emission enables sub-70 nm spatial resolution using only simple scanning confocal microscopy and before any computational analysis. Two-way NIR photoswitching of ANPs enables full optical control of photodarkening and photobrightening, and we find indefinite photoswitching of individual nanoparticles in ambient or aqueous conditions without measurable photodegradation. This enables unlimited photon collection for calculation of sub-Ångstrom localization accuracies, and we can distinguish individual ANPs within tightly packed clusters. For application of ANPs to live-cell imaging, we have developed synthetic chemistry-free methods for conjugating engineered antibodies to NP-surface SpyCatcher proteins,⁵ which bind and spontaneously form covalent isopeptide bonds with cognate SpyTag peptides. This enables controlled and irreversible attachment of antibodies to nanoparticle surfaces, for specific targeting of cell-surface receptors in quantitative live-cell study of their distribution, trafficking, and physiology.

1. Wu, S. *et al.* Non-blinking and photostable upconverted luminescence from single lanthanide-doped nanocrystals. *Proc. Natl. Acad. Sci. U. S. A.* **106**, 10917–10921 (2009).
2. Tian, B. *et al.* Low irradiance multiphoton imaging with alloyed lanthanide nanocrystals. *Nat. Commun.* **9**, 3082 (2018).
3. Lee, C. *et al.* Giant nonlinear optical responses from photon-avalanching nanoparticles. *Nature* **589**, 230–235 (2021).
4. Lee, C. *et al.* Indefinite and bidirectional near-infrared nanocrystal photoswitching. *Nature* **618**, 951–958 (2023).
5. Pedroso, C. C. S. *et al.* Immunotargeting of nanocrystals by SpyCatcher conjugation of engineered antibodies. *ACS Nano* **15**, 18374–18384 (2021).

11:00 AM BI01.01.02

Design of Iron Oxide Nanocatalysts for The Magnetic Induction-Assisted Degradation of Emergent Contaminants [Alvaro Gallo Cordova](#), Belen Corrales-Perez, Jesus G. Ovejero and M. Puerto Morales; Instituto de Ciencia de Materiales de Madrid, Spain

The application of nanomaterials in environmental remediation is of utmost importance in addressing the pressing ecological challenges of our time. Nanomaterials offer unique advantages, such as their high surface area and reactivity, which make them exceptionally effective in adsorbing, degrading, and immobilizing various pollutants in air, water, and soil. Within these nanomaterials, iron oxide nanoparticles (IONPs) stand out as great alternatives due to their low price, biodegradability and magnetic properties. Specifically, IONPs when subjected to alternating magnetic fields (AMF), generate localized heat through their physical motion or rotation of their magnetic moments [1]. This controlled heating can be harnessed to accelerate the degradation of various pollutants, including emerging contaminants (*e.g.* microplastics, antibiotics, cosmetics, etc.). Furthermore, the ability to manipulate the nanoparticles' movement through the application of external magnetic fields enables reduced operational costs for separation processes, while minimizing ecological disruption.

In this study, we developed a catalytic system via the polyol process, designed specifically for the magnetic induction-assisted degradation of organic matter. The resulting nanocatalyst (NC) displayed a multi-core structure measuring 40 nm, comprising small magnetic cores of 12 nm each [2]. These magnetic cores exhibited a well-ordered crystalline aggregation, which contributed to a collective magnetic behavior, enhancing magnetic induction heating and facilitating efficient separation due to the substantial magnetic moment per particle. To assess the industrial applicability of this approach, we

successfully scaled up the production of NCs to a gram-level with remarkable reproducibility in terms of both structure and magnetic properties. The scaled NCs were used for the magnetic induction-assisted degradation of microplastics (MPs). For this purpose, polyethylene MPs were extracted from a commercial facial scrub and we investigated a combined treatment approach for their degradation. Initially, we subjected the MPs to a hydrolysis process at 150 °C, breaking them down into monomers. Subsequently, we conducted a Fenton-like reaction, employing the as-prepared NCs in the presence of hydrogen peroxide, to degrade the hydrolyzed molecules via highly oxidative species. To assess the efficacy of this process, we monitored the changes in the Total Organic Carbon (TOC) content of the supernatant before and after each stage, which provided insights into the MPs' degradation. Notably, we observed that the mineralization of TOC was temperature-dependent, increasing from 20 to 65% at room temperature (RT) and 90 °C. This yield saw a further boost when employing IONPs as a heat source under the influence of an alternating magnetic field, likely attributable to the creation of hot spots on the surface at temperatures exceeding 80 °C.

In general, the use of magnetic nanoparticles in environmental remediation processes brings the advantages of magnetic induction heating, which can significantly reduce energy consumption and enhance the overall catalytic efficiency. As we continue to tackle the challenges of diminishing contamination and advancing sustainable energy solutions, magnetic nanoparticles represent a compelling avenue for achieving environmental remediation, making them a promising technology with the potential to reshape our approach to mitigate climate change.

Acknowledgements

This research was funded by the Spanish Ministry of Science and Innovation (AEI/FEDER, UE), project reference: TED2021-130191B-C43, PID2020-113480RB-I00 and EU project 101007629-NESTOR-H2020-MSCARISE-2020.

References

- [1] J.G. Ovejero, et al. *Nanoletters*. 21, 17 (2021) 7213–7220
- [2] Gallo-Cordova, et al. *J. Colloid. Inter. Sci.* 608, (2022) 1585-1597

11:15 AM BI01.01.03

The Future of Industrial Decarbonization and Nanotechnology through Atomic Layer Processing [David S. Bergsman](#); University of Washington, United States

Recent years have seen a surge of interest in the development of scalable tools for nanomaterials synthesis. Many emerging technologies, like solar cells, batteries, catalysts, and membranes, rely on atomically-precise materials design to operate effectively. Tools for creating these materials with increased scalability and decreased costs are thus required to enable the widespread adoption of these technologies. One suite of tools, known collectively as atomic layer processing (ALP), is particularly interesting for nanomaterials synthesis, due to its ability to create ultrathin films with sub-nanometer thickness and compositional control. ALP has also been used in the semiconductor industry over several decades, making it easy to deploy in other manufacturing processes. Commercial solar panels and battery electrodes have already started to incorporate ALP-deposited films as passivation layers. However, as demand for nanotechnology increases, there is a continued need to expand the library of materials that can be made with these tools and to accelerate the pace with which these materials are deployed.

In this presentation, in addition to highlighting my journey navigating the academic job search as a gay scientist, I will highlight how my research group at the University of Washington is expanding the applicability of ALP to create new technologies in sustainability. First, the use of vapor phase infiltration (VPI) to modify polymers will be discussed, highlighting our work to make polymer membranes conductive and to upgrade their chemical and thermal stability. Next, I will describe how molecular layer deposition (MLD) can be used to create hybrid organic-inorganic thin films, exploring our work to make atomically precise catalysts for improved electrochemical stability and activity. Last, I will describe how high-throughput materials testing is needed for rapid materials deployment, exploring our group's work to construct a high-throughput deposition system and to collect data on processing conditions into a database for additional analysis. Through these projects, our group expects to greatly expand the library of materials accessible to ALP and improve the speed with which these new materials can be translated into commercial technologies.

11:30 AM *BI01.01.04

Materials Science Challenges in Ocean-Based Carbon Removal Solutions [Kristin M. Poduska](#); Memorial University, Canada

There is a critical knowledge gap in understanding the kinetics and mechanisms of mineral formation and degradation in the context of potential technologies that are targeted for carbon capture, utilization, and storage [1]. Both crystallization and dissolution of carbonate minerals figure prominently in many such climate-change-mitigation strategies that aim for carbon dioxide removal. For example, different approaches to ocean-based alkalinity enhancement involve processes that depend on mineral surface and interfacial chemistry in order to increase water pH with concomitant atmospheric carbon removal. In this context, I will describe my team's work related to tracking changes in carbonate mineral phases, including surfaces and bulk structures, due to dissolution and recrystallization processes. In doing so, I will emphasize the urgent need for collaborations between researchers who do foundational materials science with those involved in developing monitoring, reporting, and verification protocols for potential carbon dioxide removal strategies.

- [1] Basic Energy Sciences Roundtable, Foundational Science for Carbon Dioxide Removal Technologies, US Department of Energy (2022) DOI: 10.2172/1868525

SESSION BI01.02: Materials Research by the LGBTQIA+ Community and a Vision for Inclusivity II

Session Chairs: David Bergsman and William Livernois

Wednesday Morning, April 24, 2024

Room 326, Level 3, Summit

8:30 AM BI01.02.01

Interrogating the Effects of Neutron Activation on Noble Metal Nanoparticles [Simon Scheel](#), Liane M. Moreau and Debashree Roy; Washington State University, United States

Gold nanoparticles are widely explored for applications in energy and medicine. One potential application of gold nanoparticles is the use of Au-198 nanoparticles as effective agents in prostate cancer therapy. One challenge to the synthesis of such nanoparticles is the high radioactivity and short half-life of beta-emitting Au-198 as a radiotherapeutic isotope. One solution towards generating Au-198-containing nanoparticles would be to use in-situ neutron activation of Au-197 nanoparticles. This would reduce the need to handle active material and open up options for the wide library of Au nanoparticle morphologies and ligand chemistries that have been developed. Unfortunately, to date, there is not a comprehensive understanding of how Au nanoparticles would behave in the high temperature high neutron-flux environment of a nuclear reactor. In our studies, we are looking at Au nanoparticle structure pre-

and post-irradiation within a nuclear reactor. We are using both morphology and local-structure techniques to evaluate the change in chemistry that occurs upon irradiation. In particular, SAXS and TEM will be used to analyze nanoparticle size and shape changes and XAFS and gamma spectroscopy will be used to characterize composition and local structure changes upon irradiation and beta decay of Au-198 into Hg-198.

As an LGBTQ-identifying researcher, I am deeply committed to fostering an inclusive and diverse environment within the STEM research community. It is crucial to acknowledge that embracing a broad spectrum of identities not only enriches the fabric of our scientific endeavors but also serves as a cornerstone for dismantling the challenges faced by LGBTQ+ scholars and other marginalized groups within this field. In the past, my identity has often left me feeling alienated and unwelcome in academic spaces. In primary and high school, I had to hide who I am and who I like. The schools were filled with bigotry towards the LGBTQ+ community, which left me not knowing if I was "normal" in comparison to others. This along with my parents being unsupportive of who I am made it hard for me to be excited about academia and STEM even though it's a passion of mine. In college, I have had to actively search for spaces that are explicitly LGBTQ+ friendly, which has allowed me to discover more about myself due to being able to be the true me in these situations. Luckily, in the Moreau group, I have found a scholarly space that is exceedingly accepting and inclusive of all identities. Inclusivity is more than a mere act of acceptance; it is the active cultivation of an environment where everyone can engage in their scholarly pursuits without fear of prejudice or discrimination. When the research community honors and respects the identities and experiences of all its members, it not only amplifies creativity and innovation but also empowers individuals to bring their authentic selves to their work. This authenticity, in turn, drives excellence and propels scientific progress.

8:45 AM *BI01.02.02

Modeling Small Polaron-Induced Ultrafast Ferroelectric Relaxation in BiFeO₃ [Xiaosong Li](#)¹ and Wei Xiong²; ¹University of Washington, United States; ²University of California, San Diego, United States

In this report, we employed a combination of ultrafast spectroscopic techniques and high-level calculations to uncover the complex interplay between electronic and lattice degrees of freedom in a class of strongly correlated materials. Our observations revealed a transient reduction in the electronic dipole upon optical excitation, which then recovers on 0.5 and 10 ps timescales. Time-dependent density functional theory calculations show that both ligand-to-metal charge transfer and local excitation transitions can be excited. The transient EUV dynamics captured both ultrafast free charge carrier relaxation to excitons and polaron formation. Multireference configuration interaction calculations suggest that only polaron formation is associated with the 0.5 ps electronic dipole relaxation, while the faster electronic relaxation does not contribute to changes in ferroelectric properties. Our results decode the multi-degrees of freedom associated with this ultrafast ferroelectric modulation and pinpoint the critical motion—a local polaron formation—essential for rapid ferroelectric recovery. These findings offer crucial insights into the specific lattice distortions capable of modulating the properties or phase transitions of strongly correlated materials.

9:15 AM BI01.02.03

Elimination of Tg-Confinement Effects and a Recently Revealed, Technologically Important Interfacial Phenomenon in Styrene-Based Random Copolymers Containing 2-Ethyl Hexyl Acrylate [John M. Torkelson](#); Northwestern University, United States

For two decades, i.e. slightly more than half of my professorial career, my research group has been interested in nanoscale confinement effects and the important roles of polymer interfaces, including the polymer-air interface or free surface, polymer-substrate interface, and polymer-polymer interface, on polymer dynamics. Much of this work has concerned confinement effects on the glass transition temperature (T_g) and physical aging. With ultrathin polystyrene (PS) films, the free surface plays a significant role in perturbing polymer chain dynamics, with T_g decreasing significantly with decreasing thickness below ~100 nm. Past studies by my research group have shown that changes to the PS chain architecture, from linear PS coils to cyclic PS chains with no chain ends, dense PS brushes, or PS bottlebrushes can eliminate the T_g-confinement effect in PS films as thin as ~15 nm. However, such unusual polymer architectures are unlikely to be mass produced or adopted at large scale because of complex syntheses and purification steps. Recently, we have demonstrated that such T_g-confinement effects can be eliminated in simple styrene (S)-based random copolymers containing very low levels (2 mol%, 6 mol%) of 2-ethyl hexyl acrylate (EHA). Related results are obtained with ultrathin films of 4-methyl styrene/EHA random copolymers. The special nature of the EHA comonomer is made evident by the fact that the elimination of the T_g-confinement effect is not generalizable to n-alkyl acrylate comonomers, e.g., n-butyl acrylate and n-octyl acrylate. A study of the T_g-confinement effect in 98/2 mol% and 94/6 mol% S/EHA copolymers on both piranha-treated and dichlorosilane-treated silicon wafers indicates that hydrogen bonding plays no significant role in eliminating the effect. Instead, we find a strong correlation between T_g-confinement and fragility-confinement effects, indicating that the presence of the very low levels of EHA comonomer can substantially reduce fragility in bulk copolymer, which is correlated with packing efficiency of polymer chain segments. Our results indicate that the presence of as little as 2-6 mol% EHA comonomer can fundamentally alter chain packing efficiency and the effect of a free surface on the cooperativity of polymer segmental mobility. We hypothesize that the EHA units can interdigitate due to van der Waals interactions, thereby reducing bulk fragility and the fragility-confinement effect. Capitalizing on this, we will also discuss a very recently discovered interfacial behavior of EHA-containing copolymers that is of significant technological and commercial importance. Finally, a brief comment will be made on the long-standing diversity within the materials community.

9:30 AM *BI01.02.04

Intersecting Polymer Chemistry with Sustainability in Lignin-Derivable Macromolecular Systems [Ty Christoff-Tempesta](#) and Thomas Epps; University of Delaware, United States

The valorization of lignin-derivable (LD) small molecules to polymeric materials offers a promising avenue to reduce dependences on petrochemical feedstocks in material design. However, challenges in achieving semicrystallinity and material circularity of chain-growth, LD macromolecules have limited the practical application of lignin-based polymers. Here, we describe strategies to address these targets through considerations in LD monomer design. First, we demonstrate the development of LD vinyl monomers that can undergo living polymerizations to yield stereoregular, semicrystalline macromolecules. Tailored monomer design enabled polymerization under mild synthesis conditions and gave rise to desirable crystallinities and thermal properties in the resulting macromolecules. Then, we detail the development of advanced recycling methods to thermally deconstruct high-glass-transition temperature (> 100 °C) LD polymethacrylates to their constituent monomers in high yields and purities. Understandings of the thermodynamics and kinetics underlying depolymerization enabled bulk chemical recycling of monomers that were then upcycled to value-added polymers. The discoveries described herein offer pathways to broaden the application potential of LD macromolecules and design circular LD polymeric materials.

10:00 AM BREAK

10:30 AM *BI01.02.05

Superconducting Thin-Films for Quantum Devices with Off-Line Quality Assessment [Clara M. Barker](#), Finn Squires and Susannah C. Speller; University of Oxford, United Kingdom

Quantum computers are capable of high-speed calculations, far superior to modern supercomputers. The data of each strand of the calculation does not

need to be stored permanently, but challenges include maintaining the integrity of the data (coherence) for long enough for calculations to be performed with a low error rate. To increase coherence times to useful values for multi-qubit systems, research has focussed on the design of resonators and qubits, often overlooking the design of the materials used [1]. Smart materials selection and control of the chemistry and microstructure to optimise the Q-factor of the resonators (ratio of stored energy to input energy) and increase coherence times can help make superconductor-based quantum computers more viable. Most materials used in quantum circuitry are selected for ease and reliability of deposition of multi-layered JJ structures with reasonable superconducting properties. However, it is known that other materials may have better properties if they could be optimised. For example, control of deposition flux can affect the surface roughness of a material, a parameter that can increase surface resistance and reduce the Q-factor of a quantum resonator. The structure and chemistry of the material can also impact superconducting properties. For example, changes in crystal structure, degree of crystallinity, crystallographic texture and chemical composition can affect the critical temperature of the superconductor of the film. A systematic study of carefully controlled deposition properties, linking film growth and superconducting properties, would be invaluable for assessing alternative materials for quantum resonators.

In this presentation, the results of a thorough, systematic study of the growth of superconducting materials of merit for use in quantum circuits will be reported. This study links growth parameters, material properties and superconducting performance. Initially, metal thin films- specifically niobium and molybdenum - have been deposited using magnetron sputtering, with the aim of fully understanding the deposition window before moving on to more complex materials, such as alloys and nitrides. The thin films have been analysed using SEM, XRD, XPS and AFM to determine microstructural and crystallographic properties. Electrical transport measurements have been performed to determine room temperature resistivity, transition temperature and transition width, critical field and critical current. We also aim to present preliminary low temperature microwave measurements on resonator devices. Conditions for the growth of high-quality superconducting films will be identified and this presentation will explore any links between deposition properties and material properties, to assess whether high quality room temperature and low temperature properties can be used to predict ultra-low temperature performance of materials for quantum devices.

1. Oliver, W.D. and P.B. Welander, *Materials in superconducting quantum bits*. MRS Bulletin, 2013. **38**(10): p. 816-825.

11:00 AM BI01.02.06

Modification of Perovskite Solar Cell Architecture to Increase Thermal and Mechanical Resilience [Melissa Davis](#), Kelly Schutt, Duong Nguyen-Minh, Kaitlyn VanSant, Axel F. Palmstrom and Joseph Luther; National Renewable Energy Laboratory, United States

On the cusp of commercialization and market breakthrough, perovskite solar cells have emerged as a competitor to silicon technology. Their efficiency rivals commercial products and the decreased energy for production and overall cost give perovskite solar cells an edge. However, parts of this technology still require improvement, in particular addressing their thermal and mechanical instability. These instabilities can give rise to device degradation. Comprehensive knowledge of these degradation mechanisms is required to address and solve these downfalls. In this research, we present the results of a myriad of tests, including water contact angle, kelvin probe, and double cantilever pull apart tests, designed to address these issues. As a result of the connection between instability and decreased performance, we have correspondingly altered the device architecture of standard p-i-n perovskite solar cells to improve performance. More specifically, thermal stability of devices was studied with the use of water contact angle and kelvin probe tests. Modified hole transport layers, or HTLs, were developed to ease delamination seen during tests due to thermal stress. The mechanical stability of devices was tested with double cantilever beam tests to determine mechanical weak layers. Additional modifications were added to the electron transport layers, or ETLs, to address the mechanical instability. With the adoption of these modifications within the HTL and ETL layers, this research introduces perovskite solar cells with improved thermal and mechanical resilience. These improvements will aid in this technology's path to commercialization.

11:15 AM BI01.02.07

Effects of Sulfonation Degree on Compatibility and Separation Performance of Polybenzimidazole (PBI)-Sulfonated Polyphenylenesulfone (sPPSU) Blend Membranes [Siyum S. Beshahwored](#); National Taiwan University of Science and Technology, Taiwan

Industrial liquid waste is preferred to be recycled to sustain the ecosystem. Therefore, the development of polymer-blend nanofiltration membranes with good chemical resistance and molecular compatibility is crucial. In this presentation, the molecular compatibility between polybenzimidazole (PBI) and sulfonated polyphenylsulfone (sPPSU) and their blend membranes for herbicide removal in water reuse and for drug separation in organic solvent nanofiltration (OSN) has been investigated as a function of sulfonation degree in sPPSU. Flat sheet membranes cast from PBI-sPPSU blends with a mass ratio of 1:1 were prepared. At ambient temperature, portions of them were cross-linked using trimesoyl chloride (TMC). The blend made of PBI and 12.7 mol% sPPSU showed high compatibility based on the calculated enthalpy of mixing (ΔH_m), measured dope viscosity, phase diagram, and single T_g . The TMC-modified membrane cast from this composition also exhibited higher chemical resistance, mechanical stability, narrower pore size and pore size distribution, a macrovoid-free structure, and better separation performance. All fabricated membranes were evaluated using feeds containing tetracycline (MW = 444 Da) as a model drug in ethanol and pendimethalin (MW = 281.3 Da) as a model herbicide in water. The cross-linked PBI-12.7 mol% sPPSU (12.7C) membrane exhibited rejections of >96% against low-molecular-weight pendimethalin from water and tetracycline from ethanol. It also has the capability to separate mixed solutes, even with small molecular weights. This study illustrates the effectiveness of highly compatible polymer blends with the aid of one-step cross-linking modifications for nanofiltration.

Keywords: Degree of sulfonation; Polymer blend compatibility; Single-step crosslinking; Drugs; Pesticides; Liquid nanofiltration

11:30 AM BI01.02.08

Teaching Density Functional Theory to Students of Art Conservation [Joseph W. Bennett](#); University of Maryland Baltimore County, United States

As an assistant professor that identifies as LBGTQIA+ and is employed at a minority serving institution, I am well aware of the multitude of issues surrounding diversity, equity, inclusion at the university level. My chosen field in STEM is computational materials chemistry and an issue that plagues this field is diversity in students, specifically their identities and backgrounds. This is why I've spent 3 summers as an instructor for the Baltimore SCIART program, teaching computational methods to students interested in art conservation science. While many of the students in the program identify as LBGTQIA+, the majority of students that have learned to compute surface interactions are women. Funded by the Andrew W. Mellon Foundation, the Baltimore SCIART Consortium offers a 10-week summer research experience for undergraduate students at the interface between science and art and has been developed for students from Baltimore area academic institutions with a diverse background and strong interest in art conservation science and engineering. The development of density functional methods as a nondestructive probe to study works of art is still in its infancy and here, I will discuss aspects of our inclusive teaching pedagogy and our recent successes both computing surface interactions of objects important to cultural heritage and student outcomes.

This searchable program is up-to-date as of April 15th, 2024.

SESSION BI01.03: Materials Research by the LGBTQIA+ Community and a Vision for Inclusivity III
Session Chairs: Ty Christoff-Tempesta and Alvaro Gallo Cordova
Wednesday Afternoon, April 24, 2024
Room 326, Level 3, Summit

1:30 PM BI01.03.01

A Tale from The Queer Resistance: Activism from with(in) Materials Science Jerry A. Yang and Eric Pop; Stanford University, United States

Broader sociopolitical movements toward inclusivity have brought attention to LGBTQIA+ issues in materials science, including the marginalization of LGBTQIA+ materials scientist professionals and students in the field. Previous work on LGBTQ+ students in engineering disciplines highlights the continued struggles for non-straight, non-cisgender people in STEM [1].

In this talk, I [JAY] present my current research in both materials science and engineering education while narrating my interdisciplinary journey straddling two vastly different fields of study. As a cisgender, gay, Asian-American man, my dual existence within both the materials science and engineering education research disciplines has given me unique insights into the nature of science and has substantially informed how I conceptualize equity and inclusivity in materials science.

My materials science work in two-dimensional (2D) semiconductors has shaped a large portion of my professional life. In my graduate studies at Stanford University, I currently study strain engineering 2D materials. With Prof. Eric Pop, my advisor, we have electrically and optically characterized the strain response of monolayer tungsten disulfide and molybdenum disulfide, demonstrating a ~2x improvement in electronic mobility for tungsten disulfide under ~0.3% biaxial tensile strain [2]. While my materials science work continues to satisfy me intellectually, my experimental work has often felt sterile compared to the complexities of my queer experience.

Engineering education research provides systems of thinking that enables me to deconstruct my experiences as an “outsider within” materials science [3]. In a recent study, I explored the experiences of LGBTQ+ undergraduate engineering students with a departmental survey ($n = 854$ students) and focus groups ($n = 10$). While the LGBTQ+ students in my study experienced tokenization, misgendering, and social ostracism, they found ways to actively combat these experiences and create their own supportive communities within engineering [4], [5]. With this work, I began to formulate my own understanding of inclusivity in materials science and leverage my position to advocate for queer issues. I continue my engineering education work alongside my materials science work through projects on queerness, race, and privilege in engineering education.

Before entering academia, I thought that my existences as a materials scientist, engineering education researcher, and resident gay were distinct, destined to never intersect. However, I have discovered that science is fundamentally a social endeavor, rife with the complexities of human social interaction. While using cleanroom tools may not directly summon my queerness, how I interact with my colleagues, how I present my work to my group, and how I communicate my work to the scientific community call for me to craft a professional image of myself – one that, for me, is fused with my gay identity.

I contribute my work and my story to argue for two key elements in a vision for inclusivity in materials science: first, to look beyond quantitative metrics for “diversity” and uplift the work that marginalized people are doing to resist systemic inequities, and second, to spark conversations with (queer) social justice scholars outside of materials science, who can provide valuable insight into the equity challenges facing the discipline. Inclusivity rests on recognizing both the existing climate and the agency that queer people hold in materials science and centering marginalized voices in materials science policy. I acknowledge support from the National Science Foundation Graduate Research Fellowship for this work.

[1] K. J. Cross *et al.*, *Queering STEM Culture in Higher Education* (2022).

[2] J. A. Yang, E. Pop *et al.*, arXiv:2309.10939 (2023).

[3] P. H. Collins, *Soc. Probl.*, **33**, s14 (1986).

[4] J. A. Yang *et al.*, *IEEE Trans. Educ.*, **64**, 345 (2021).

[5] J. A. Yang *et al.*, *J. Women Minor. Sci. Eng.*, **27**, 1 (2021).

1:45 PM BI01.03.02

Materials Science in The Anthropocene: Learning from Queer Advocacy William Livernois; University of Washington, United States

The Anthropocene [1], an epoch defined by human-driven planetary changes, beckons the materials science community to reconsider its role in shaping the world. [2] Although materials science offers potential sustainable solutions, the messages from both the scientific and activist communities are clear: the scale and timeline of a green transition must address the urgency of the climate crisis and the disproportionate impacts to frontline communities. [3] The queer community’s history of activism provides a blueprint of ways for materials scientists to engage in envisioning alternative futures, and the willingness to engage in transformative change. This talk will draw parallels between the messages of moral urgency from groups like Act Up during the AIDS crisis and messages of moral urgency from climate justice groups today. The theory of change of these groups will also be discussed, with the presenter drawing from personal experience as a queer scientist engaging in activism.

References:

[1] Lewis, Simon L., and Mark A. Maslin. "Defining the anthropocene." *Nature* 519.7542 (2015): 171-180.

[2] Gardner, Charlie J., and Claire FR Wordley. "Scientists must act on our own warnings to humanity." *Nature Ecology & Evolution* 3.9 (2019): 1271-1272.

[3] McCauley, Darren, and Raphael Heffron. "Just transition: Integrating climate, energy and environmental justice." *Energy policy* 119 (2018): 1-7.

2:00 PM *BI01.03.03

The "Materiality" of Sexual Orientation and Gender Identity to Materials Science: Exploring LGBTQ Participation in the Sciences Bryce E. Hughes; Montana State University, United States

In the realm of scientific pursuit, the prevailing notion often asserts that one's sexual orientation and gender identity are irrelevant—that the quality of scientific contributions is solely determined by an individual's skills and abilities. However, LGBTQ individuals exhibit a disproportionately higher attrition rate from the sciences when compared to their heterosexual and cisgender counterparts.

In this presentation, I will summarize my research on LGBTQ participation within undergraduate STEM (Science, Technology, Engineering, and Mathematics) majors. My research delves into various facets of this phenomenon, shedding light on how LGBTQ undergraduates find a sense of belonging within the heteronormative landscape of STEM disciplines. Additionally, my research investigates the influence of LGBTQ students' social networks on

This searchable program is up-to-date as of April 15th, 2024.

their commitment to pursuing STEM majors as well as how identifying as LGBTQ shapes students' perceptions of future prospects within STEM careers. Collectively, these findings emphatically affirm that LGBTQ identities do, indeed, matter within the sphere of scientific endeavors. Moreover, this research underscores how the intricate interplay between different forms of privilege and oppression continues to structure participation in STEM fields in ways that impede the overarching goals of broadening participation in STEM. My talk will then conclude with concrete recommendations and take-aways to improve the climate within materials science as well as STEM broadly.

2:30 PM BREAK

3:30 PM BI01.03.04

Designing Novel Materials for Energy Applications by Leading an Open-Minded and Diverse Research Group [Edgardo Saucedo](#); Universitat Politècnica de Catalunya, Spain

The design of novel materials for energy applications, is a fascinating field that combines in equal parts knowledge in materials science, imagination, risk, and open mind to accept and adapt non-conventional ideas. In the first part of this work, a complete novel family of van der Waals materials based on pnictogen chalcogenides ((Sb,Bi)(S,Se)(Br,I)) will be presented, as an example of out-of-the-box compounds that in principle, does not fulfil the requisites to be excellent semiconductors for energy applications, but that in real are being revealed as very promising compounds. The most relevant non-standard properties of these materials will be presented for the first time, showing that non-conventional ideas can be widely accepted with the right approach. The versatility and adaptability of this family of materials will be described, as an example of how the diversity in materials science is very relevant for progressing in this field.

In the second part of this work, the development of these new family of materials will be compared, as an example, with my career in the materials science world, where being different has been always an extra motivation. I will explain how to be part of the LGBTQIA+ community has impacting in my research career from the very beginning, starting with my PhD, my postdoctoral experience abroad, and my consolidation as independent researcher, giving me an open mind character that I have also applied in my day-to-day work through the development of new materials. Currently, I'm leading a group of 20 very diverse scientists in Barcelona, working in the development of materials and devices for energy applications, from where I'm always very committed and proactive with the visibility of the LGBTQIA+ community, and where I have created a very safe space for the diversity. I will explain how I manage my visibility as LGBTQIA+ community member, considering that I have coordinated several big European Projects with consortiums including the most relevant academic institutions, and I'm granted with a European Research Council (ERC) Consolidator Grant, which has help me to consolidate my position as Group Leader. I will also explain my interaction with my students, my colleagues in my Institution, and with collaborators worldwide, and how I apply my commitment with the diversity and visibility of the LGBTQIA+ community in my life, helping me to progress as researcher, but more important, as human being.

3:45 PM ROUNDTABLE DISCUSSION

SYMPOSIUM BI02

Broadening Participation in Materials Research and STEM
April 22 - May 9, 2024

Symposium Organizers

Chartanay Bonner, The Joint School of Nanoscience and Nanoengineering
Lisa Neshyba, University of Washington, Chemistry Department
Kristen Rahilly, Oregon State University
Michael Scheibner, University of California, Merced

* Invited Paper

+ JMR Distinguished Invited Speaker

^ MRS Communications Early Career Distinguished Presenter

SESSION BI02.01: Broadening Participation in Materials Research and STEM I
Session Chairs: Chartanay Bonner, Lisa Neshyba, Kristen Rahilly and Michael Scheibner
Thursday Morning, April 25, 2024
Room 326, Level 3, Summit

8:15 AM *BI02.01.01

Best Practices for Engaging HBCUs: Increasing URM Engagement in Materials Research [Michael L. Curry](#)¹ and Michael Schwartz²; ¹North Carolina Agricultural and Technical State University, United States; ²University of Wisconsin–Madison, United States

Only 7.7% of Chemists and 4.4% of Engineers in the US are Black, even though greater workforce diversity drives innovation and contributes to America's economic power. This warrants the exploration of new partnerships and approaches to maintain our competitiveness in the marketplace. Since its inception, Historically Black Colleges and Universities (HBCUs) have contributed to the nation's scientific and technological dominance by producing exceptional talent and cutting-edge research. HBCUs have an unparalleled impact on the education and professional development of underrepresented minorities in

chemistry, engineering, and related fields. While African Americans comprise 9% of the STEM workforce, HBCUs produce more than 24% of Black STEM undergraduates & 30% of Black science/engineering doctorates. Hence, finding new and innovative ways to tap into the human potential of the nation's 101 Historically Black Colleges and Universities for mining and investment purposes is critical. In this discussion, we will explore best practices for partnering with HBCUs as a promising approach to increase broad participation in the Materials Research community.

8:45 AM BI02.01.02

When The University and City Hall Join Forces: The STEAM BSM_UPC Project [Luis Carlos Pardo Soto](#)¹, [Artur Paz](#)¹ and [Alba Feria](#)²; ¹Universitat Politècnica de Catalunya, Spain; ²Barcelona de Serveis Municipals, Spain

Barcelona's iconic landmarks, including the Olympic Stadium, Gaudi's Park Güell, the Zoo, and the amusement park Tibidabo, serve as the backdrop for a series of STEAM activities that bring together 6,500 students from across the Barcelona metropolitan area every year. This ambitious project is made possible by the collaboration between the academic expertise of a public university like the Polytechnic University of Catalonia and the public enterprise B:SM, which oversees from Barcelona's parking system to the Zoo or the amusement park. During these events, students aged 10 to 18 engage in a range of experiments and scientific shows tailored to the unique characteristics of each location.

For example, at the Zoo, students explore life and the materials that constitute it, such as DNA and the energy-giving substances essential for life. At the Olympic Stadium, chemistry concepts are taught through an interactive show, and physics is demonstrated through a blend of a contemporary dance quartet and a scientist. In the amusement park, mobile phone sensors are utilized to investigate the movements and forces behind the rides. At the world-renowned Park Güell, we investigate how Gaudi used materials inspired by nature.

However, the project doesn't end with students. Every year, we organize training courses for teachers and public shows designed for a broader audience. These shows feature unique presentations, such as one conducted by a physicist and a violinist or a jazz band exploring the connection between music and mathematics.

Overall, this highly successful project is the result of researchers stepping out of their labs and engaging with a broad audience, and the willingness of the town hall to organize and support such impactful scientific activities.

9:00 AM BI02.01.03

Utilizing Cross-Program Collaboration to Sustain & Enhance STEM Outreach Portfolios [Mark Licurse](#), [Ashley Wallace](#) and [Eric A. Stach](#); University of Pennsylvania, United States

Effective management and growth of STEM outreach programs remains an ongoing challenge for many organizations and institutions. While the goals of broadening participation are clear and commonly shared, there is little established guidance on how to build and sustain a successful portfolio of programs. Newly funded initiatives, especially, face pressure to quickly establish programs to compete with more experienced organizations and centers but can often overwhelm limited staff. We have recently implemented an innovative model that engages participants as active contributors to improving and sustaining our portfolio of outreach programs. Rather than treating each program in isolation, this approach specifically utilizes the diverse experiences and skill sets of program participants to enhance the activities and objectives of other programs within the same portfolio. In doing so, we believe this allows for a more robust set of programs to be created and supported. We highlight how this model was implemented for three of our core programs: a summer research experience for undergraduates, a research experience for high school teachers, and a summer camp for high school students focused on materials science and engineering. The integration and exchange across programs provides benefits and extends beyond just the sharing of resources. It fosters an inclusive community in which participants' contributions matter beyond just their own experience. While tested on materials research education and outreach programs, we believe this approach of utilizing participants' strengths to enhance a portfolio of programs could be applied to STEM outreach broadly across disciplines. Crucially, the model can be integrated into existing outreach efforts, leading to continuous improvement and increased impact over time.

9:15 AM BI02.01.04

The Emergence of Transdisciplinary Material Science in Diverse Applications: Towards The Development of Frameworks for Inclusive and Diverse Perspectives of Material Science Research and Education [David Ryman](#)¹, [Saqib Ahmed](#)^{2,3} and [Sankha Banerjee](#)^{1,3}; ¹California State University, Fresno, United States; ²Buffalo State College, United States; ³University of California, Davis, United States

The field of material science is undergoing a transformative shift towards transdisciplinary approaches, demonstrating its relevance in a variety of applications. This shift is paving the way for the creation of comprehensive frameworks that foster inclusivity and diverse perspectives in material science research and education. By embracing a transdisciplinary perspective, material science is adapting to the complex and interconnected challenges of our time, promoting innovation and sustainability in a broader range of applications. This abstract provides an overview of the evolving landscape of material science, highlighting the importance of inclusive and diverse frameworks to advance the field and meet the evolving demands of modern society. The following work focuses on the transdisciplinary aspects of material science research and education in the areas spanning materials fabrication and their application in water treatment, biomedical devices, environmental impact, and economic assessment. It delves into the intersections of material science with these critical fields, emphasizing the need for a holistic understanding of materials' roles in addressing contemporary challenges. By examining materials science through the lenses of water treatment, biomedical devices, environmental sustainability, and economic evaluation, this work contributes to a more inclusive and diversified approach, fostering a more profound comprehension of the pivotal role materials play in our interconnected world. Moreover, this work extends its examination to the implementation of these approaches within the semiconductor industry. It sheds light on how these methodologies are being employed to enhance research, development, and education within this industry, ensuring the widespread dissemination of innovations and their potential to drive advancements in material science. By exploring the intersections of material science, using machine learning-based approaches, and diversity-related issues within the context of the semiconductor sector, this research contributes to a more inclusive, sustainable, and technologically advanced future.

9:30 AM BI02.01.05

How can TA Meetings Effectively Prepare TA Instruction? [Eugenia S. Vasileiadou](#); Northwestern University, United States

A General Chemistry course consists of multiple components, amongst these are recitation and office hour sections. These sections are centered on enhancing students' conceptual understanding and honing their problem-solving skills. Even without the current realization of online teaching, these objectives require a skillful synthesis of technical and pedagogical planning. The goal of this project was to examine how teaching assistant (TA) meetings can effectively prepare TA instruction in General Chemistry discussion sections with inclusive practices, considering an online teaching environment. Firstly, the challenging areas of virtual TA instruction were probed. Subsequently, five quarterly objectives for the TA meetings were determined related to the pedagogical and learning needs TAs' reported. Accordingly, biweekly presentations serving the quarterly objectives were developed, containing pedagogical strategies and resources to aid TAs' preparation for effective and inclusive instruction. Following the biweekly presentations, TAs' completed

a reflection journal based on a survey format, where overall 4 journal entries were requested. The TA reflection journal inquired if TAs accomplished the learning objectives of the biweekly presentation, as well as it included space for TAs to generate prompts and questions for the next presentation. Importantly, the TA reflection journal incorporated demographic information of TAs, where no corresponding demographics of graduate students had been collected in our Chemistry department prior. Altogether, utilizing the collaborative and informative nature of the TA meetings to the highest extent, serves as a vehicle for the pedagogical development of TAs to make effective instructional decisions that result in enhancing student learning.

9:45 AM BREAK

10:15 AM ROUNDTABLE DISCUSSION

10:45 AM *BI02.01.06

Overcoming Technology Barriers and Incorporating Culturally Responsive Outreach in Materials Research [Kyle Johnson](#)^{1,2} and Ngozi Ezeokeke¹; ¹AVELA - A Vision for Engineering Literacy & Access, United States; ²University of Washington, United States

In 2020, 11% of undergraduate students in the University of Washington's Materials Science and Engineering (MSE) department were from underrepresented minority (URM) backgrounds, with only 8% of graduate students in the department identifying as URM. In contrast, the URM population in Washington State was 21% in 2017, and 34% nationwide. High barriers of entry to the field of materials research limits who is learning about and gets involved in the field. For primary and secondary school students, these barriers include limited access to the expensive technologies required to perform materials research such as load frames, high magnification microscopes, and autoclaves. Not only is it difficult to have K-14 students engage with application or research-based material science lessons in primary or secondary school, but inequitable access to technology for Black and Latine communities are compounded by persistent economic challenges, social injustices, and human rights issues. We present sociotechnical access inequalities for Black and Latine urban communities, and our findings show that many students are hesitant to engage with already available technologies due to a lack of enticing support systems. We analyze the AVELA (A Vision for Engineering Literacy & Access) nonprofit's holistic student-led STEM engagement model leveraging near-peer mentorship, experiential learning, mentor embodied community representation, and culturally responsive lessons. Through 24 semi-structured interviews with college AVELA members, an analysis of 171 survey responses from AVELA's secondary school class participants, and an autoethnographic analysis we evaluate the model's impact on decreasing sociotechnical access inequalities. Using data from AVELA's 4 years of operation, where more than 200 university student instructors have taught to 2,500+ secondary school students in 110+ classrooms, we identify access barriers and provide principled recommendations for designing STEM education programs with a focus on materials science lessons and activities.

11:15 AM BI02.01.07

Experimenta con PREM: Outcomes and Best Practices from a Two-Decade Materials Research Summer Program for Underrepresented High School Students [Idalia Ramos](#)¹, Jose O. Sotero Esteva¹, Vibha Bansal², Francisco Bezares³, Ezio Fasoli¹, Mark Licurse⁴, Rolando Oyola¹, Nicholas Pinto¹, Juan Santana², Eric A. Stach⁴ and Ashley Wallace⁴; ¹University of Puerto Rico at Humacao, United States; ²University of Puerto Rico at Cayey, United States; ³University of Puerto Rico at Mayaguez, United States; ⁴University of Pennsylvania, United States

A long-standing partnership between the University of Puerto Rico (UPR) and the University of Pennsylvania (PENN) *Laboratory for Research on the Structure of Matter* aims at diversifying the materials research community by identifying and guiding students through a pathway from high school (and K-8) to STEM undergraduate programs, and then onto graduate school. The program is supported by the National Science Foundation *Partnerships for Research and Education in Materials* (PREM) program. The UPR-PENN PREM program targets women and students from disadvantaged backgrounds, such as low-income families, first-generation college students, and those living in geographically isolated areas in Puerto Rico, where the student population is approximately 99% Hispanic.

The *Experimenta con PREM* (ECP) summer program for high school (HS) students is a highlight of the UPR-PENN PREM. Since 2005, this two-week research experience has attracted talented students to materials research. The program started at the Humacao campus of UPR and extended to the Cayey campus in 2016. To date, approximately 400 students (68% women), from 34 towns and 59 schools in Puerto Rico have taken part in ECP. All of them graduated from high school, with 78% pursuing STEM fields.

ECP aims to foster scientific literacy and inquiry skills among students and inspire them to pursue research-oriented careers. The experience is expected to be like what they would face in a Research Experience for Undergraduates (REU), from the application process to presenting their findings. The program introduces materials science as a field that welcomes diverse interests and skills, such as materials characterization, devices, soft matter, crystals, and experimental and theoretical-computational methods. Nine UPR faculty mentors create laboratory experiences that are closely aligned with their own PREM research and that incorporate, within the time constraints, the relevant aspects of conducting research such as literature review, data collection and analysis, report, and final oral presentation. In the laboratories, HS students work in groups of up to 4 members with constant guidance from the faculty researcher and undergraduate PREM students.

Before the research experiences, the students participate in a series of workshops that help them develop soft skills that are essential for scientific research, such as diversity awareness, public communication, and laboratory safety. Additional training includes hands-on workshops on scientific writing, programming, and spreadsheet skills. The PENN partners actively contribute to the learning experience. Graduate students, post-docs and faculty members from PENN give talks, workshops and interact with the students on various topics related to materials science.

This presentation will cover the goals, components, and achievements of ECP, along with the challenges and lessons learned. We will discuss some of the best practices that emerged from our experience and how they can inform future initiatives in science education.

11:30 AM BI02.01.08

AfterSchool Academy and Teachers Camp for a Diverse Undergraduate Population [Andre Schleife](#) and Cecilia Leal; University of Illinois at Urbana-Champaign, United States

It is our goal to broaden participation in materials research starting from the undergraduate level and we particularly focus on increasing our number of students from all underrepresented groups. We find it challenging to accomplish this goal through traditional recruitment practices, including social media, email, and mail-based approaches. Our hypothesis is that we do not effectively reach our target population or reach them too late when they either have decided against college or for a different major. To mitigate this, we started pursuing a two-pronged approach reaching out to (i) high-school students directly through a newly established AfterSchool Academy and to (ii) high-school teachers by organizing a teacher's camp every summer, together with the ASM Materials Education Foundation. If successful, we envision to advertise materials research to a population of students that is still considering their college career and a population of high-school teachers that can inform students about materials research much earlier and more efficiently and deeply than mail or online campaigns. Our early success indicators are that participating students and teachers were very excited and engaged in the experimental activities and we envision to turn this into better, more diverse undergraduate enrollment over the next years. In this presentation details about both activities and their implementation from scratch will be discussed.

This searchable program is up-to-date as of April 15th, 2024.

SESSION BI02.02: Broadening Participation in Materials Research and STEM II
Session Chairs: Chartanay Bonner, Lisa Neshyba, Kristen Rahilly and Michael Scheibner
Thursday Afternoon, April 25, 2024
Room 326, Level 3, Summit

1:30 PM BI02.02.01

Materials Science and Engineering Program Needs: Students! Thomas Stoebe; University of Washington, United States

Materials Science and Engineering is a multidisciplinary field that works between the physical and biological sciences, engineering and medicine. Engineering students sometimes have difficulty determining the difference between the many opportunities in MSE and the more well defined opportunities in other engineering areas. In particular, entering undergraduate students who see themselves focused on industrial jobs often choose other engineering departments over MSE because of perceived potential future jobs.

Materials engineering, which applies the principles of materials science to practical systems, devices and processes, is an area that Materials Science can be used to attract interest among students. This has been shown based on enhanced interest in both applied experiments and demonstrations used in high school classrooms, and in special programs and camp projects in many locales. These programs include

1. Technology education workshops for teachers
2. Science and technology curriculum development based on material science and engineering, and
3. After school activities such as designing and building a guitar

The National Resource Center for Materials Technology Education (MatEdU) has collected and developed resources that provided means for materials concepts to impact areas as diverse as electronics education and advanced manufacturing, energy and critical materials utilization. Such areas can be used to inform students of their prospects in MSE. These opportunities will be developed in this presentation. General reference www.materialseducation.org.

1:45 PM BI02.02.02

Design and Delivery of Low-Cost Science Laboratory Kits for Primary- and Secondary-Level Classrooms in Eastern Africa Jill Wenderott¹, Joyce Elisadiki², Julie Fornaciari³, Danielle Butts⁴, Cecilia China⁵, Gloriana Monko² and Sossina M. Haile⁶; ¹Drexel University, United States; ²University of Dodoma, Tanzania, United Republic of; ³University of California, Berkeley, United States; ⁴University of California, Los Angeles, United States; ⁵Nelson Mandela African Institution of Science and Technology, Tanzania, United Republic of; ⁶Northwestern University, United States

Only about 30% of women students in higher education globally select science, technology, engineering, and mathematics (STEM)-related subjects, with particularly low enrollment in engineering, manufacturing, and construction (8%) and in natural science, mathematics, and statistics (5%).¹ Improving this representation is a multi-faceted challenge. Women Supporting Women in the Sciences (WS2) has been focused on spurring K-12 girls' interests in STEM and promoting women scientists as mentors to younger students. With the support of a 2020 American Physical Society (APS) Innovation Fund,² WS2 spearheaded the Lab Kit Initiative during which low-cost materials science and physics laboratory kits for K-12 students were designed and distributed to schools in eastern Africa. During the design phase, seven international teams composed of 59 volunteers (over 70% women) created 3 lab kits for primary level students and 4 lab kits for secondary level students on the topics of food science, electrostatics, light and color, and energy transfer. A key feature of the lab kits is the use of easy-to-source supplies to ensure low-cost and wide accessibility. Working with eleven partners in Ethiopia, Kenya, Rwanda, Tanzania, and Uganda, WS2 provided lab kits that engaged over 5100 students at over 40 school sites in hands-on science learning, with 62% being girls. This talk will discuss the outcomes of the Lab Kit initiative which concluded in early 2023 and future endeavors in which WS2 has been involved that are broadening the reach of our lab kits.

Women Supporting Women in the Sciences (WS2)³ is an international organization unifying and supporting graduate and professional-level women and allies in STEM.

1. Cracking the code: girls' and women's education in science, technology, engineering and mathematics (STEM) - UNESCO Digital Library. at <<https://unesdoc.unesco.org/ark:/48223/pf0000253479>>
2. APS Innovation Fund. at <<http://www.aps.org/programs/innovation/fund/index.cfm>>
3. Sciences, W. S. W. in the. Women Supporting Women in the Sciences. *Women Support. Women Sci.* at <<https://ws2global.org/>>

2:00 PM BI02.02.03

More Inclusive Q&A Sessions Will Lead to Better Science Christopher Rom; National Renewable Energy Laboratory, United States

Traditional question and answer (Q&A) sessions are a sub-optimal use of conference time because they do not engage the full audience. Since 2017, several studies in a range of academic disciplines have identified that women are under-represented among question-askers after scientific talks. Insufficiently inclusive Q&As leave thought-provoking questions un-asked, meaning our communities miss out on ideas worth hearing. Throughout my PhD and into my postdoc, I have collected data on question asking behavior at the conference talks I attended (ceramics, materials, and solid-state chemistry, broadly speaking), revealing that this disparity is present in our community too. Fortunately, prior research shows that merely discussing this trend can help balance Q&A sessions. In this presentation, I will summarize existing research on gender equity in Q&A sessions, present my own data relevant to the MRS community, and describe preliminary results from possible alternative Q&A formats. This work will spark conversations around how to structure our scientific talks to better foster learning and collaboration, boosting our ability to conduct cutting edge science.

2:15 PM BI02.02.04

Computational Course-Based Undergraduate Research Experience (CURE) for Condensed Matter Physics David A. Strubbe¹ and Enrique Guerrero^{1,2}; ¹University of California, Merced, United States; ²California State Polytechnic University, Humboldt, United States

Course-based Undergraduate Research Experiences (CUREs) are a way of bringing the excitement of research into the classroom and potentially reaching more students and reaching them earlier in their studies than would happen with the typical summer research experience or senior thesis project. Key aspects of a CURE are: students learn and use research methods, give input into the project, generate new research data, and analyze it to draw conclusions that are not known beforehand. I will show a paradigm for a computational CURE in an undergraduate/graduate condensed matter physics class at the University of California, Merced. It is based on computational studies with density functional theory, provided by a convenient GUI tool on nanoHUB (https://nanohub.org/tools/ucb_compmano) that we co-developed which requires minimal computational skills. After preparatory exercises, students calculated structures, energies, and Raman spectra of different structures and compositions of a monolayer alloy $\text{MoS}_{2-x}\text{Se}_{2(1-x)}$. They followed a defined protocol to contribute to a novel class dataset which they analyzed, and also calculated an additional property of their choice in consultation with the instructor. Studies show that CUREs improve learning, foster a sense of belonging in the field, increase retention of students in science (including going on to do summer research), and are especially beneficial for minoritized/underrepresented students such as at a Hispanic Serving Institution like UC

Merced.

2:30 PM BREAK

3:00 PM BI02.02.05

Designing Inclusive Research Experiences for Undergraduates [Rajan Kumar](#); Northwestern University, United States

Research Experiences for Undergraduates (REU) programs are a key driver for broadening participation in materials research. Every year, over 100 REU sites offer essential opportunities for students to gain hands-on exposure to materials research and develop technical skills that extend beyond the classroom. Furthermore, several of these programs aim to increase access to materials research for underrepresented students in order to help diversify academia and other research disciplines. But with increasing participation, how do we tailor REU programs to benefit students from all backgrounds? And how can we provide research opportunities that actually promote continued interest in STEM careers? In order for REU programs to have an ever greater impact, we need to focus on designing inclusive research experiences that support all students and foster a sense of belonging in materials science and engineering.

In this talk, I will introduce a template for designing inclusive undergraduate research experiences as demonstrated through the Stanford Materials Science and Engineering REU Program. Overall, our goal is to help undergraduates self-identify as materials scientists and engineers in order to encourage broader participation in STEM careers. Several important components of the REU Program will be described to identify best practices that promote positive outcomes in undergraduate research experiences, regardless of student background or preparation level. These components include program recruitment and selection, research project design, mentorship training, student programming, and program evaluation. Specific efforts related to research and communication skill development, career guidance, and community-based mentorship will also be discussed along with key outcomes from these initiatives.

3:15 PM *BI02.02.06

Empowering Diversity: Inclusive Strategies in STEM Education [Debora Monego](#)^{1,2}; ¹Heidelberg Institute for Theoretical Studies, Germany; ²Heidelberg University, Germany

In Materials Science and other STEM fields, the inclusion of diverse perspectives is more than just an added advantage, it is a necessity. Drawing from my experiences as a first-generation Latina teaching science at Columbia University, my talk will focus on fostering strategies for inclusive teaching, enhancing a sense of belonging, and empowering students to take agency in their STEM education. Practical tactics for curriculum design will be highlighted, along with discussions on challenges faced by students from underrepresented backgrounds. The goal is to craft a more inclusive environment that resonates with every student's unique journey in STEM.

3:45 PM ROUNDTABLE DISCUSSION

SESSION BI02.03: Poster Session: Broadening Participation in Materials Research and STEM

Session Chairs: Chartanay Bonner, Lisa Neshyba, Kristen Rahilly and Michael Scheibner

Thursday Afternoon, April 25, 2024

Flex Hall C, Level 2, Summit

5:00 PM BI02.03.01

Integrating Art in Materials Science Education: An Interdisciplinary STEAM Course on Metal Craft for Engineering Students [In-Suk Choi](#) and [Bog-Ki Min](#); Seoul National University, Korea (the Republic of)

We introduced an innovative interdisciplinary STEAM course for undergraduates in collaboration with the College of Fine Arts, titled "Metal Craft for Engineering Students." Designed for freshmen, this course enables students to create their own metal crafts under the guidance of Fine Arts professors. Although most participants were new to hands-on activities, they engaged in metal craftwork such as casting, hammering, and polishing, all while utilizing CAD/CAM programs for design. In conjunction with the practical craftwork, introductory lectures on physical metallurgy topics like hardening, annealing, and dislocation were delivered, contextualizing the applied theories. This hands-on approach allowed students to directly observe material thermodynamic and deformation phenomena. By melding fabrication techniques with scientific principles, the course offers a comprehensive understanding of materials science. Feedback has shown high student satisfaction, underscoring our belief that the course not only broadens perspectives but also ignites an interest in multidisciplinary research. Notably, it fills a critical void for materials science students who typically lack hands-on fabrication experience due to a curriculum predominantly focused on analysis, characterization, and theoretical modeling.

5:00 PM BI02.03.02

Broadening the Participation in Materials Research by Creating Science Identity using Near Peer Mentoring [Mary Sajini Devadas](#), [Jim Coombs](#) and [Ellen Hondrogiannis](#); Towson University, United States

Science/STEM identity" is the sense of who students are, what they believe they are capable of, and what they want to accomplish with respect to science by interacting with others in the field. This requires intervention to help the "socializers" (i.e., STEM faculty and UGs) better understand the value and purpose of science literacy themselves so as to encourage students to appreciate science, be aware of possible career options in science, and enjoy learning and doing science. The project involves building "science identity" via the active involvement of Towson University's (TU) undergraduate student researchers (UG) in 1) engagement in research with the high school (HS) recruits through the apprenticeship model, 2) outreach activities in local high schools. This results in science identity among undergraduate and high school students as they assist in workshops and internships (where they carry out authentic research) involving synthesis and characterization of nanoparticles. Through surveys collected, we show that we have built science identity and broadened the participation in student participants and in the near-peer mentors. The retention of students in STEM using this method will be discussed.

5:00 PM BI02.03.03

Bridging the Gap: A Case Study to Broadening Participation in Materials Research through Community Outreach and Education [Edgar Mejia](#)¹, [Tiara Torres-Flores](#)¹, [Zina Medina](#)², [Zhang Zhang](#)¹ and [Nancy R. Sottos](#)¹; ¹UIUC, United States; ²University of Puerto Rico at Mayagüez, United States

In the pursuit of broadening participation (BP) in Materials Research (MR) and STEM, conventional methods have often been insufficient in creating a lasting impact. This poster presents an innovative, multifaceted outreach program targeting K-5 Spanish-speaking students. The program, titled "El Verdadero Valor del Plástico (The True Value of Plastic)," serves as a case study for sustainable and effective MR outreach.

In alignment with the symposium's goals, our initiative explores the intersectionality of MR and BP by:

- Designing workshops and demonstrations centered on plastic recycling.
- Evaluating the needs of underrepresented communities to bridge gaps in scientific exposure and representation.
- Customizing workshop materials to suit diverse audiences.
- Scaling the initiative by training additional facilitators to conduct similar workshops.

Our pedagogical approach combines hypothesis-driven lessons with interactive instruction and collaborative learning, all reinforced by scientific curiosity and family engagement. Drawing inspiration and collaborating with the "Cena y Ciencias" bilingual elementary program, we offered hands-on experiences, such as transforming plastic milk jugs into coasters.

The program successfully engaged the local Spanish-speaking community, increasing awareness of the plastic waste crisis. To gauge the comprehension levels of both children and their parents, we administered a questionnaire before and after the workshop was presented. Our initiative stands as a blueprint for the effective blend of MR and BP agendas, tackling the unequal distribution of opportunities for women and other minority groups. By disseminating our best practices, we aim to contribute to the symposium's overarching objective of fostering a collaborative network committed to broadening participation in the materials science field.

5:00 PM BI02.03.04

Elementary Arts Lab: Building a Community of Scientists, Artists and Educators to Impact Local Elementary Education Elizabeth K. Allan-Cole¹, Emma Antonio^{1,1}, Katarina Lott¹, Thomas P. Chaney¹, Lacey Roberts¹, Andrew J. Levin¹, Mary Powell² and Michael Toney¹; ¹University of Colorado Boulder, United States; ²Boulder Valley School District, United States

Elementary Arts Lab is a group of artists, scientists and educators who are passionate about cultivating enthusiasm and curiosity for how we explore and interact with the world around us. We work with K-12 schools to develop and deliver curriculum that integrates movement, art and music with the physical sciences. We aim to educate and inspire children and ourselves while challenging the stereotypes of scientists and artists. Our approach uses the concept of integrated learning, or the process of making connections between multiple concepts and topics and using experience-based learning [1]. Integrated learning plays on the idea that when you experience something you are more likely to internalize the concepts you were aiming to learn [1]. Our primary aim is to create a long-term network between educators, scientists, and artists and through this network create arts-based science resources for elementary school teachers and their students.

We began our journey in 2020 at the height of the pandemic, working virtually with University Hill Elementary School in Boulder. We started with eight CU Boulder graduate students, a post-doc, and two elementary school educators, an art and music teacher, in our first phase. Together, we built science lessons for third graders that we communicated through art, dance, and music. Our initial endeavor demonstrated that students were learning and starting to internalize the science concepts we were communicating [2]. Our first expansion included building off the fourth-grade curriculum in the Boulder Valley School District (BVSD) and implementing our work at a larger scale by making lesson plans that were available to all BVSD school teachers [2]. We also worked with a class at Heather Wood Elementary School during this time and doubled our CU Boulder student involvement as well as started to incorporate undergraduate students in both science and arts. Our current phase implements continuing education for current Denver Public Schools (DPS) elementary school teachers. We work directly with DPS teachers throughout a full school year in multidisciplinary diverse teams to build integrated learning lesson plans based on class curriculum. By supporting this approach and maintaining a long-term relationship with these teachers we can indirectly impact all the students that they teach throughout their career. We have worked with more than 10 DPS teachers and have now brought in more than 50 CU Boulder graduate and undergraduate students in arts, science, and education working as a network to impact more than 350 elementary school students to date in Colorado.

Beyond our direct impact, we also aim to combat the image of a scientist or engineer for these students. We aim to bring together a diverse community and show students on classroom visits that they, too, can become scientists.

Reference:

- [1] Leslie U. Bradbury (2014) Linking Science and Language Arts: A Review of the Literature Which Compares Integrated Versus Non-integrated Approaches, *Journal of Science Teacher Education*, 25:4, 465-488, DOI: 10.1007/s10972-013-9368-6
- [2] Elementary Arts Lab Website, <https://www.colorado.edu/project/elementaryartslab/>

5:00 PM BI02.03.05

Multimodal Core-Shell Nanocomposites for Biomedical Applications Munirah Ghariani^{1,2,3}, Caroline O'Sullivan¹ and Yurii K. Gun'ko^{1,2,3}; ¹Trinity College Dublin, Ireland; ²Advanced Materials and Bioengineering Research (AMBER), Ireland; ³Science Foundation Ireland (SFI), Ireland

Multimodal nanomaterials are an important class of materials in the rapidly developing field of nanoscience. These nanomaterials have deserved a lot of attention due to their wide variety of applications including targeted cell drug delivery, biomedical imaging and cell labelling.¹ The main aim of this project was to develop new magnetic metal carbonate core-shell structures for potential biomedical applications. Calcium carbonate (CaCO₃) and magnetite (Fe₃O₄) were chosen as the functional materials for this research, thus combining the modalities of biocompatibility and magnetisation.^{2,3} Magnetic nanoparticles (NPs) have been prepared by a precipitation approach using both Fe²⁺ and Fe³⁺ salts as iron precursors in the presence of poly(sodium styrene sulfonate) (PSS). These stabilised NPs exhibited high monodispersity and stability making them ideal for further functionalization. For the very first time, the PSS-Fe₃O₄ NPs were encapsulated into CaCO₃ shell by a novel dry ice carbonation method resulting in distinctive morphological structures.

The new composites were loaded with a specific cationic dye as a model to investigate their potential drug uptake and release processes. The testing was monitored using UV-Vis spectroscopy.

This research opens up a route to new multimodal nanomaterials with unique properties making them of great interest.

Bibliography

1. S. D. Anderson, V. V. Gwenin and C. D. Gwenin, *Nanoscale Res. Lett.*, DOI:10.1186/s11671-019-3019-6.
2. H. Bahrom, A. A. Goncharenko, L. I. Fatkhutdinova, O. O. Peltek, A. R. Muslimov, O. Y. Koval, I. E. Eliseev, A. Manchev, D. Gorin, I. I. Shishkin, R. E. Noskov, A. S. Timin, P. Ginzburg and M. V. Zyuzin, *ACS Sustain. Chem. Eng.*, 2019, 7, 19142–19156.

3. A. G. Niculescu, C. Chircov and A. M. Grumezescu, *Methods*, 2022, **199**, 16–27.

5:00 PM BI02.03.06

Enhanced Immobilization of EDTA on Graphene Oxide Sponge by Siloxane Bridge for Multi-Pollutants Removal in Wastewater Yi-Ting Lai^{1,1}, Chen-Jie Liao¹, Dhanaprabhu Pattappan¹, Da-Wei Huang¹, Yu-Chin Liao¹, Yu-Hsuan Huang¹, Shu-Jun Lu¹, Po-Chun Hsu² and Ching-Lung Chen¹; ¹Ming Chi University of Technology, Taiwan; ²The University of Chicago, United States

This work developed an ethylenediaminetetraacetic acid (EDTA)-modified graphene oxide (GO) sponge to remove multi-pollutants in wastewater. During the grafting of the silicon-based EDTA (EDTA-Si) on the GO sponge, the abundant functional groups on the GO surface can interact with silane groups to form silane-bridging by removing water molecules. Thus, the silanol molecules can anchor EDTA-Si on the surface of GO, leading to stable adhesion toward the GO sponge. This proposed EDTA-Si/GO sponge can not only adsorb and chelate various heavy metals in wastewater but also degrade organic dyes by producing super radicals. This work provides a facile and eco-friendly strategy to remove heavy metals and organic pollutants in wastewater to achieve the availability and sustainable management of water with industrial applicability.

5:00 PM BI02.03.09

The Effects of Substrate Growth on VS₂ by Chemical Vapor Deposition Clara L. Jackson¹, Kedar Johnson², Elycia Wright¹, Selena Coye¹, Indika Matara Kankanamge¹ and Michael Williams¹; ¹Clark Atlanta University, United States; ²Morehouse College, United States

Vanadium disulfide (VS₂) has grown popular for its potential applications in energy storage and renewable energy due to its thin layered structure, metallic conductivity, and ability to form highly crystalline structures. Our research focuses on investigating the impact of vanadium disulfide growth on various substrates, such as sapphire, silicon oxide on silicon (SiO₂/Si), and gallium oxide (Ga₂O₃), using the chemical vapor deposition (CVD) technique. Furthermore, the research aims to identify the optimal growth parameters, including growth temperature, and carrier gas flow rate for each substrate to achieve a large coverage film. To achieve this, we use the carrier gases (Ar, Ar + H₂) while implementing the growth temperatures of VS₂ during the sample growth. We will measure the resulting materials using spectroscopic probes like photoluminescence, Raman, Fourier transform infrared (FTIR), and confocal laser optical microscopy to examine the surface morphology, structural quality, absorption, and reflection of materials.

5:00 PM BI02.03.10

Comparison of Seeding Promoters in Growth of Tungsten Disulfide by Chemical Vapor Disposition. Kedar Johnson^{1,2}, Clara L. Jackson², Elycia Wright², Selena Coye², Indika Matara Kankanamge² and Michael Williams²; ¹Morehouse College, United States; ²Clark Atlanta University, United States

Seeding promoters have been utilized to facilitate the growth of transition metal dichalcogenides via chemical vapor deposition (CVD). The choice of seeding promoter can significantly impact the resulting film's properties, including its crystallization, growth area, phase, and composition. Our study will investigate the effects of different seeding promoters on tungsten disulfide (WS₂) growth on sapphire, which is known to be challenging to control in terms of layer area, quality, and thickness. The seeding promoters we will be using in our study are sodium chloride (NaCl), zinc oxide/zinc sulfate (ZnO/ZnSO₄), and sodium sulfate (NaSO₄). We will analyze the effect of each seeding promoter on the properties of WS₂ to determine their correlation and identify the best promoter for future growth. To analyze the properties of WS₂ films, we will use confocal laser microscopy, photoluminescence spectroscopy (PL), Raman spectroscopy, Fourier transform infrared microscopy (FTIR), and x-ray photoemission spectroscopy (XPS). Our focus will be on studying these films' photoluminescence, absorption, layer thickness, impurity, optical phonon modes, and bandgap.

5:00 PM BI02.03.11

RAFT Iniferter Photopolymerization of PNIPAM based Block Copolymers Fabian Rodriguez; The University of Texas Rio Grande Valley, United States

Poly(N-isopropyl acrylamide) (PNIPAM) has been studied for various biomedical applications such as drug delivery, wound dressings, and, specifically, sensing via hydrogels due to a characteristic phase transition around 32°C. Previous work focused on the fabrication and characterization of PNIPAM based microfibers. The fibers were subsequently processed into a fibrous hydrogel to be used as biosensor. The fibrous structure was maintained as it functions as an avenue to improve the sensitivity of the biosensor by increasing the surface area. Current work focused on improving the viscoelastic behaviors of the hydrogel through the synthesis of block copolymers (BCPs) containing PNIPAM. These BCPs were synthesized using photo reversible addition-fragmentation chain transfer (RAFT). While RAFT is a commonly used controlled polymerization technique, photoinitiated RAFT can yield polymers with ultra-high molecular weights and can be performed under mild conditions. Therefore, photoinitiated RAFT is promising for synthesizing polymers ideal for ultra-thin fibers and hydrogels due to enhanced viscoelastic and mechanical properties. Alongside PNIPAM, the highly hydrophilic poly(N,N-dimethyl acrylamide) (PDMA) is a promising candidate as a stabilizing block since it improves the mechanical properties of hydrogels. A compact UV setup was implemented using a commercially available nail curing device, while also varying the distance between the reaction/light bulbs, and the light intensity through the number of said bulbs. The methodology was optimized using common lab equipment to enable widespread implementation. The physical setup was kept intentionally simple with the intent to allow small undergraduate institutions and even high schools to perform polymer synthesis, while maintaining a level of scientific refinement via the use of photo-iniferter RAFT. This project offers an avenue to broaden participation for young students and researchers to engage with and contribute to materials research by validating the potential of using commercially available equipment.

SESSION BI02.04: Test Session II
Monday Morning, April 22, 2024
BI02

SESSION BI02/MT01/QT01/QT04: Joint Virtual Session
Session Chairs: Liangzi Deng, Elif Ertekin, Toshinori Ozaki, Kristen Rahilly and Ajay Ram Srimath Kandada
Thursday Morning, May 9, 2024
BI02-virtual

10:30 AM ^BI02/MT01/QT01/QT04.01

Photoinduced Modulation of an Excitonic Resonance Coupled to Coherent Optical Phonons and The Role of Dynamical Screening in a Layered Semiconductor Selene Mor^{1,2}, Valentina Gosetti^{1,2}, Alejandro Molina-Sanchez³, Davide Sangalli⁴, Simona Achilli⁴ and Stefania Pagliara^{1,2}; ¹Università Cattolica del Sacro Cuore, Italy; ²Interdisciplinary Laboratories for Advanced Materials Physics (I-Lamp), Italy; ³University of Valencia, Spain; ⁴Università degli Studi di Milano, Italy

The ultrafast light-matter interactions in semiconductor materials are intensively studied due to their technological relevance in the field of, e.g., photovoltaics or data processing. The elementary photoexcitation of a semiconductor is the formation of an electron-hole pair, called exciton, as a result of the weak screening of the Coulomb interaction between the electron and the hole. The coupling of excitons with other excitations like, e.g., lattice vibrations (phonons) plays a pivotal role on the nonequilibrium optical properties of semiconductors, eventually governing their optoelectronic functionalities. However, how exciton-phonon coupling manifests in the time and energy domains has raised an active debate between experiment and theory in the last years [1]. Moreover, the effect of dynamical screening, i.e. of transient changes in the screening by the photoexcited quasi-free carriers, on the coupling of excitons to phonons has remained elusive. These open questions represent a forefront fundamental research challenge in semiconductor optics and an essential step toward the development of novel protocols for optoelectronic applications.

Layered semiconductors formed by van-der-Waals stacked atomic planes offer a great quantum materials platform for the study of coupled dynamics with accessible and technologically relevant energy and time scales. The quantum space confinement of mobile carriers reduces the dielectric screening, stabilizing the excitons and favoring their coupling to lattice vibrations [2].

In our work, by means of ultrafast broadband optical spectroscopy combined with ab-initio calculations of the layered semiconductor bismuth triiodide (BiI₃), we set the spectral fingerprints for the optical detection of exciton-phonon coupling in van-der-Waals layered semiconductors [2]. Our joint experimental and theoretical effort allows us to unravel the impact of exciton-phonon coupling by microscopically relating a photoinduced coherent energy modulation of the excitonic resonance to coherent optical phonons. This further enables us to track the extent of the photoinduced atomic displacement in real space with unprecedented subpicometer resolution. These findings eventually solve the debate between experiment and theory on the spectral evidences of exciton-phonon coupling, and establish the role of exciton-phonon coupling on the ultrafast exciton dynamics.

Further, we address the effect of dynamical screening on the exciton-phonon coupling in BiI₃ [3]. To this goal, we investigate the ultrafast broadband optical spectroscopy under excitation condition either resonant or off-resonance with the excitonic resonance in order to either exclude or enable the excitation of a population of quasi-free carriers. We find evidences that that the dynamical screening breaks the coupling of excitons to coherent optical phonons, thereby hindering the photoinduced modulation of the excitonic resonance.

Finally, these complementary works move a step forward in the detection of many-body couplings in layered materials by ultrafast optical spectroscopy, paving the way to optical control of an excitonic resonance on the picosecond timescale.

[1] F. Paleari, Phys. Rev. Lett. 122, 187401 (2019); C. Trovatiello, ACS Nano 14, 5700 (2020); D. Li, Nat. Comm. 12, 954 (2021); H.-Y. Chen, Phys. Rev. Lett. 125, 107401 (2020); J. Fu, Advanced Materials 33, 2006233 (2021)

[2] A. Chernikov, et al, Phys. Rev. Lett., 113, 076802 (2014); C. Jin, Nature Nanotechnology, 13, (2018); S. Dal Conte, Trends in Chemistry, 2, 1 (2020)

[3] S. Mor, et al, Phys. Rev Research, 3, 043175 (2021)

[4] S. Mor, et al., in prep.

10:45 AM BI02/MT01/QT01/QT04.03

Temperature-Dependent Phonons and Photoluminescence of WS₂ Monolayer to Bulk grown by CVD. Selena Coye¹, Kedar Johnson², Indika Matara Kankanamge¹ and Michael Williams¹; ¹Clark Atlanta University, United States; ²Morehouse College, United States

WS₂ is a layered material with unique band gap properties, making it highly promising for developing advanced electronics and optical devices. While bulk WS₂ has an indirect band gap in the near-infrared, monolayer WS₂ has a direct band gap in the visible spectrum. The optical and bandgap characteristics of WS₂ can be temperature dependent. Understanding the temperature-dependent phonon properties of materials is crucial for managing heat in electronic devices, as they impact thermal properties and scattering effects. In addition, self-heating can alter the vibrational properties of WS₂ layers, and the way electrons and phonons interact. Further, understanding the temperature-dependent A and B excitonic peaks is significant in device applications. Temperature-dependent photoluminescence and Raman spectroscopy can be utilized to identify these materials' different optical transitions and phonon properties. In this study, we will present a systematic analysis of temperature-dependent bandgap, optical transitions (including A and B exciton), electron-phonon coupling, and strain effect of WS₂ grown by chemical vapor deposition. The layers will be analyzed using photoluminescence and Raman spectroscopy techniques.

10:50 AM BI02/MT01/QT01/QT04.04

Quantum Machine Learning for The Synthesis of Photocathodes by Epitaxial Growth Salil Bavdekar, Jason B. Gibson and Richard Hennig; University of Florida, United States

We present a high-throughput, material-agnostic strategy to study promising new photocathode materials for their epitaxial growth. Cs₃Sb films grown on 3C-SiC(100) substrates with molecular beam epitaxy (MBE) display lattice parameters intermediate to fully epitaxial layers and bulk structures, indicating partial relaxation at a thickness of only 38 Å. The surface phase diagrams and structures for monolayer thin films of epitaxial Cs-Sb photocathodes on SiC substrates have been predicted using a genetic algorithm (GA) coupled with density functional theory (DFT) calculations. This information helped identify the experimental growth conditions for uniform and stoichiometric films and possible surface reconstructions. However, the computational cost of DFT calculations limits the study to a single monolayer, and the nucleation and growth of these films cannot be studied with this method.

Hence, we employ machine learning accelerated GA simulations to predict complex surface structures with larger in-place unit cells and increasing film thickness to model the transition from monolayer to bulk. Following this, the growth of Cs-Sb layers on (100) and (001) 3C-SiC substrates is studied with exascale molecular dynamics (MD) simulations. Our atomistic modeling aims to elucidate the structural transition from potentially epitaxial monolayers to bulk structures and identify structures, nucleation mechanisms, and film growth processes on (100) and (001) 3C-SiC substrates. The GA and MD simulations are powered by machine-learned ultra-fast force fields (UF³) trained on the data from the previous GA/DFT studies, greatly reducing the computational cost. The resulting structures obtained from the simulations are compared with experimental XRD and RHEED patterns, and the structural energies provide the basis for a thin-film phase diagram.

While the work here is presented for Cs-Sb films on a SiC substrate, the framework can be applied to any material system to create similar phase diagrams. These phase diagrams, along with kinetic information gleaned from the molecular-dynamics simulations, can help identify optimal experimental processing conditions during MBE growth and guide the selection of other materials systems.

11:05 AM BI02/MT01/QT01/QT04.05

Data-Driven Discovery of Dynamics from Time-Resolved Coherent Scattering Nina Andrejevic, Tao Zhou, Qingteng Zhang, Suresh Narayanan,

Mathew Cherukara and Maria K. Chan; Argonne National Laboratory, United States

Coherent X-ray scattering (CXS) techniques, including X-ray photon correlation spectroscopy (XPCS), play a critical role in the investigation of mesoscale phenomena evolving at time scales spanning several orders of magnitude. However, obtaining accurate theoretical descriptions of complex dynamics is often limited by one or more factors – the ability to visualize dynamics in real space, computational cost of high-fidelity simulations, and accuracy of approximate models. Here, we aim to bridge the gap between theory and experiments by extracting mechanistic models of dynamics directly from CXS data. To do so, we develop a data-driven framework which employs neural differential equations to parameterize unknown real-space dynamics and a computational scattering forward model to relate real-space predictions to reciprocal-space observations. This framework is shown to recover dynamics of several computational model systems, including domain synchronization, particle clustering, and source fluctuation, under various simulated conditions of measurement resolution and noise. We further demonstrate the practical application of this approach in the context of two proof-of-concept experiments. Our framework represents a general and versatile platform to discover dynamics from time-resolved CXS measurements without solving the phase reconstruction problem for a complete time series of diffraction patterns.

11:20 AM BI02/MT01/QT01/QT04.06

Pressure-Dependent Thermodynamics of Cubic Lu-H-N Solid Solutions by First-Principles Calculations and Graph Neural Networks [Pinwen Guan](#), Matthew Witman, Catalin Spataru, Vitalie Stavila and Peter A. Sharma; Sandia National Laboratories, United States

Metal hydrides are an important class of materials with high scientific significance, finding applications in various fields such as hydrogen storage, batteries, gas sensors, nuclear reactions and high-temperature superconductivity. Pressure, among others, is an important variable to control their properties. Previous computational studies of metal hydrides under high pressures usually treat them as stoichiometric compounds, without lattice disorder considered. However, when pressure becomes more moderate, lattice disorder gets more significant, as shown in the recent claimed room-temperature superconductor at near-ambient pressures, N-doped Lu hydrides, where three constituents (hydrogen, nitrogen and vacancy) have disordered occupancies in the tetrahedral and octahedral interstitial sites in the fcc Lu lattice. To consider lattice disorder dependent on pressure, in addition to other variables including temperature and composition, first-principles calculations are computationally demanding. In this work, a model of the cubic Lu-H-N solid solutions is developed by combining first-principles calculations and lattice graph neural networks to learn pressure-dependent thermodynamic quantities in the configurational space, and composition-pressure-temperature phase diagrams are derived to describe the relationship between the synthesis conditions and the resulted phase equilibria. This work can improve the thermodynamic understanding of the Lu-H-N system and help rational synthesis of N-doped Lu hydrides, as well as demonstrate an efficient approach to model pressure-dependent thermodynamics of multi-component solid solutions.

SYMPOSIUM SB01

Bioresponsive Nanotheranostics

April 23 - May 9, 2024

Symposium Organizers

Weibo Cai, University of Wisconsin--Madison

Bella Manshian, KU Leuven

Dalong Ni, Shanghai Jiao Tong University.

Ruirui Qiao, The University of Queensland

Symposium Support

Bronze

EXODUS BIO

JINAN NANOMEDICINE (HONG KONG) CO., LIMITED

Journal of Nanobiotechnology

KeAi-Bioactive Materials

POP Biotechnologies

Portrai Inc.

Promega Corporation

RAYSOLUTION Healthcare Co., Ltd

Shandong Madic Technology Co., Ltd.

United Well Technologies (China) Limited

* Invited Paper

+ JMR Distinguished Invited Speaker

^ MRS Communications Early Career Distinguished Presenter

SESSION BI02/SB01/SB03/SB05: Joint Virtual Session

Session Chairs: Dimitra Georgiadou, Philipp Gutruf and Kristen Rahilly

Thursday Morning, May 9, 2024

SB01-virtual

8:00 AM *BI02/SB01/SB03/SB05.01

Biodegradable Luminescent Porous Silicon Nanoparticles in Cancer Diagnosis and Therapy [Liubov A. Osminkina](#)^{1,2}; ¹Lomonosov Moscow State University, Russian Federation; ²Institute of Biological Instrumentation, Russian Academy of Sciences, Russian Federation

The development of new intelligent drug delivery systems to overcome unwanted side effects and maximize the therapeutic effectiveness of chemotherapy for cancer diseases is one of the main tasks of modern medicine. Active research is being conducted to explore various nanosized drug carriers (nanocarriers) for these purposes.

The use of porous silicon nanoparticles as the basis for nanocarriers is due to the unique properties of these solid-state nanomaterials, such as high biocompatibility [1] and complete biodegradability into non-toxic silicic acid [2]. The porous structure of the nanoparticles, with porosity values reaching up to 80% of their volume, provides a high drug-loading capacity for efficient drug delivery [3]. The simplicity of surface modification methods for the nanoparticles enables specific targeted delivery of various hydrophobic and hydrophilic drugs, radiopharmaceuticals, proteins, peptides, RNA, etc. into cells.

The presence of efficient luminescence in porous silicon nanoparticles allows their utilization as contrast agents for bioimaging of cells and tissues [5]. The properties of porous silicon nanoparticles, acting as photosensitizers [6], sensitizers of high-frequency electromagnetic fields [7] and therapeutic ultrasound [8], provide them with therapeutic functions and the potential for stimuli-triggered drug release from the nanopores of nanocarriers.

The research is supported by Russian Science Foundation Grant No. 24-45-20009.

References:

1. Low S.P., Voelcker N. H. "Biocompatibility of porous silicon." Handbook of porous silicon. Springer, 2014. 381-393.
2. Qurrat. S. "Biodegradability of porous silicon." Handbook of Porous Silicon (2014): 395-401.
3. Maximchik, Polina V., et al. "Biodegradable porous silicon nanocontainers as an effective drug carrier for regulation of the tumor cell death pathways." ACS Biomaterials Science & Engineering 5.11 (2019): 6063-6071.
4. Tieu T., et al. "Advances in porous silicon-based nanomaterials for diagnostic and therapeutic applications." Advanced therapeutics 2.1 (2019): 1800095.
5. Tolstik E., et al. "Linear and non-linear optical imaging of cancer cells with silicon nanoparticles." International journal of molecular sciences 17.9 (2016): 1536.
6. Timoshenko V. Yu, et al. "Silicon nanocrystals as photosensitizers of active oxygen for biomedical applications." Jetp Letters 83 (2006): 423-426.
7. Tamarov K.P., et al. "Radio frequency radiation-induced hyperthermia using Si nanoparticle-based sensitizers for mild cancer therapy." Scientific reports 4.1 (2014): 1-7.
8. Osminkina L.A., et al. "Porous silicon nanoparticles as efficient sensitizers for sonodynamic therapy of cancer." Microporous and Mesoporous Materials 210 (2015): 169-175.

8:30 AM BI02/SB01/SB03/SB05.02

Ultrasound-Guided STING Activation by Nucleotide Nanocomplex-Decorated Microbubbles for Cancer Immunotherapy Sina Khorsandi¹, Xuefeng Li², Yifan Wang², Kristin Huntoon², Adam Woodward¹, Nazia Hafeez¹, Katherlyne Nguyen¹, Connor Endsley¹, Julien Santelli¹, Wen Jiang² and [Jacques Lux](#)¹; ¹University of Texas Southwestern Medical Center, United States; ²MD Anderson Cancer Center, United States

The recent success of immunotherapy for treatment-refractory metastatic melanoma, lung cancer and renal cell carcinoma has provided a new hope that immunotherapy can be generalized to a broader range of cancers. However, many cancers do not respond to immune checkpoint inhibitors, which has limited their use to a subset of patients. There is now greater recognition that to generate optimal antitumor immunity requires activation of both innate and adaptive immune systems in patients. Innate immune cells, including macrophages and dendritic cells (DCs), possess phagocytic and antigen presenting capabilities that enable the initial immune recognition of tumor cells and serve as a link between the innate and adaptive immune systems through antigen cross-presentation and subsequent priming of T cells. In order for these professional antigen-presenting cells (APCs) to perform these immune functions, several cellular processes must be activated, including the innate immune sensor cyclic GMP-AMP synthase-stimulator of interferon genes (cGAS-STING). Agents that target the innate immune regulators, such as STING agonists are now being investigated as potential therapeutics for a wide range of human cancers. However, because STING is a cytosolic innate immune sensor, the intracellular delivery of agonists such as the negatively charged 2'3'-cyclic-GMP-AMP (cGAMP) is very challenging. Equally important, non-specific global STING activation can cause systemic inflammatory responses and toxicity. Systemic administration of STING agonists leads to dose-dependent T cell death that facilitates tumor immune evasion, further hindering the translation of STING agonists into the clinic.

To address this technical challenge and meet the clinical need, we developed a technology termed MUSIC (Microbubble-assisted Ultrasound-guided Immunotherapy of Cancer) that utilizes gas-filled microbubbles (MBs) conjugated with APC-targeting antibodies, and cationic polymers to efficiently load cGAMP via formation of nanocomplexes on the MB surface.

Our preliminary results show that, upon exposure to US, MUSIC produces robust STING activation and type I interferon responses in APCs and more efficiently primes antigen-specific CD4⁺ and CD8⁺ T cells *in vitro*. These immune stimulatory effects of MUSIC directly translated into antitumor responses *in vivo*, where we showed that the MUSIC was able to generate antitumor effects against syngeneic orthotopic primary (EO771) and metastatic (4T1) murine breast cancer models. Both models showed dramatic antitumor responses following local treatment of the primary tumor. Specifically, 6 out of 10 EO771 tumor-bearing animals were tumor-free after 50 days while 4T1 tumor-bearing mice exhibited a significant decrease of the systemic disease burden including lung metastases. We also confirmed the establishment of systemic immune memory following MUSIC treatments as mice rejected tumor cells upon re-challenge. MUSIC was also evaluated in two syngeneic murine melanoma models (B16-F10 and D4M) with 100% of D4M-tumor bearing animals and 50% of B16-tumor-bearing animals achieving complete remission when treated with a combination of MUSIC and immune checkpoints inhibitors.

MUSIC showed efficient antitumor immune responses in localized and metastatic murine breast cancer models as well as in two melanoma models leading to the establishment of immune memory (*i.e., in situ* vaccination). This nanocomplex-conjugated microbubble platform enables more efficient loading and release of cGAMP and provides a new drug delivery vehicle for further functional modifications including for loading drug or gene delivery for cancer treatment and/or vaccines.

8:45 AM *BI02/SB01/SB03/SB05.03

Neuromorphic Thin-Film-Devices for Process-In-Sensor Applications [Sung Kyu Park](#); Chung-Ang University, Korea (the Republic of)

These days, the development of sensory systems for observing the surrounding environment information is drawing a lot of attention in various fields such as self-driving, security, robotics, and internet of things (IoT). In order to efficiently convert and recognize an external stimulus into an electrical signal, the

high-performance sensory system is required. However, conventional sensor devices have been difficult to maintain and pre-process the transformed information due to their rapid recovery properties. In this regard, the human-like neuromorphic sensory systems that can efficiently recognize external information by sensing and memorizing the incoming stimulus signals is emerging. Nevertheless, to interpret incoming information, many electronic systems often need more complementary components, such as various filters or logically connected circuit structure. Such architectural complexity can limit the development of high-density and high-resolution system.

In this talk, neuromorphic sensory systems based on thin-film-devices such as amorphous indium-gallium-zinc-oxide (*a*-IGZO) and CNT thin-film-transistors (TFTs)/circuits are demonstrated by constructing hybrid heterojunction structure with various nanostructured materials as a sensing material. Specifically, through utilizing a quantum dot, nano-scaled materials, and metal chalcogenide layers integrated with *a*-IGZO TFTs exhibits evidently enhanced environmental detection ability with neuromorphic memory function. Furthermore, we will discuss a promising strategy for the facile artificial sensory systems such as neuromorphic olfactory, self-defensive, and auto controllable visual system that have low power and small size which are significant factors in neuromorphic applications.

9:15 AM BI02/SB01/SB03/SB05.04

Biomolecular Neuristors from Voltage-Activated Lipid Membranes [Michelle Makhoul-Mansour](#) and Stephen A. Sarles; The University of Tennessee, United States

Spiking neural networks (SNNs) show promise as energy-efficient and fast computing devices for adaptive spatiotemporal data processing and classification, which is critical for applications requiring efficient acquisition, and processing of time-dependent data. Taking inspiration from their biological counterparts, the artificial neuristors in SNN hardware systems have been typically designed to generate dynamic voltage spikes -i.e., *action potentials*- when a cumulative stream of received electrical inputs crosses a critical threshold. However, unlike biological neurons, action potential generation in man-made systems is achieved using complex circuitry of many solid-state devices that are often non biocompatible. Examples of artificial neurons, and *neuristor* circuits, include those based on threshold-switching memristors^[1] and organic electrochemical transistors^[2].

We recently demonstrated the use of voltage-activated lipid membranes as artificial synapses for neuromorphic computing. Advantages of this approach include the available diversity of functional biomolecules, the low voltage and power requirements, and the potential for greater biocompatibility and scalability. To-date, we have demonstrated that voltage-activated biomembranes can exhibit tunable memory resistance^[3], memory capacitance^[4], and various forms of activity-dependent plasticity that provide specific computational advantage^[5].

Herein, we study the behaviors of biomolecular neuristors consisting of voltage-activated lipid membranes exposed to alamethicin (ALM), protamine and histidine peptides. Remarkably, two distinct types of action potentials—fast (~10 ms) and slow (~1s)—have been observed, with their characteristic speeds and spike shapes differing based on the composition of the device and the direction and amplitude of the applied current. We have conducted experiments at varying compositions and concentrations of species to identify the molecular mechanisms for spike generation and develop mathematical models able to capture these behaviors.

While earlier approaches depended on complex multi-device circuitry, a biomolecular neuristor achieves this within a single stimuli-responsive biomembrane. This simplifies the fabrication process by reducing complexity, material volume, and cost, all while maintaining its adaptability to various input types. Leveraging the characteristics of synthetic biomembranes, this work can help unlock the potential for creating compact, energy-efficient, and biocompatible neuristors, thus driving progress in the realm of neural interface technology and spiking neural networks (SNNs).

[1] M. D. Pickett, G. Medeiros-Ribeiro, R. S. Williams, *Nature Materials* 2013, 12, 114.

[2] T. Sarkar, K. Lieberth, A. Pavlou, T. Frank, V. Mailaender, I. McCulloch, P. W. M. Blom, F. Torricelli, P. Gkoupidenis, *Nature Electronics* 2022, 5, 774.

[3] J. S. Najem, G. J. Taylor, R. J. Weiss, M. S. Hasan, G. Rose, C. D. Schuman, A. Belianinov, C. P. Collier, S. A. Sarles, *ACS Nano* 2018, 12, 4702.

[4] J. S. Najem, M. S. Hasan, R. S. Williams, R. J. Weiss, G. S. Rose, G. J. Taylor, S. A. Sarles, C. P. Collier, *Nature communications* 2019, 10, 1.

9:30 AM BI02/SB01/SB03/SB05.05

Single-Pulse Control of 'Trans-Memristor' Artificial Synapses [Sander Smink](#), Renée Meijer, Lennart Cool and Hans Hilgenkamp; University of Twente, Netherlands

As field-effect transistors (FETs) form the backbone of contemporary digital electronics, artificial synapses form the backbone of various realizations of analog electronics. Inspired by the operation of the brain, these elements determine the degree to which other circuit elements are coupled to each other, the synaptic weight. This weight can be programmed at will or evolved using a training algorithm, typically as a non-volatile response to pulsed input. Among other characteristics, the ideal artificial synapse has an as large as possible number of deterministically programmable states; as low as possible energy costs and delay times for both programming/training and processing; robustness against repeated cycling and stable over time; and scalability to nanoscale dimensions.

Here, we investigate the long-foreseen application of FETs as artificial synapses [1], of which a proof-of-concept was recently demonstrated by various groups [2]. A pulse-controlled switching element – in the simplest realization, a second FET – is used to place charges on the gate electrode of a FET. The channel conductivity responds to the number of charges in a well-defined, analog manner, which allows defining a synaptic weight deterministically. Like digital electronics, both programming and readout can in principle be extremely fast (picosecond timescales) and scaling is straightforward.

We present experimental results on the temporal response of the so-realized 'trans-memristors' to the application of a few voltage pulses, and discuss the dependence of this response on pulse width (~10 – 10⁴ ns), frequency (~1 – 10⁶ Hz), and charging voltage (~ ±2V). We observe that charging obeys simple resistor-capacitor behavior, which allows us to control the associated characteristic time by introducing lump circuit elements such as a series resistor. The FETs under study are micrometer-sized Au-LaAlO₃-SrTiO₃ transistors [3], which have the advantages of a single-crystalline dielectric – boosting endurance – and a low room-temperature mobility of ~1 cm²/Vs – lowering the conductance *G* to ~1 μS and thus readout power *P* ~ *U*²*G*.

Our experimental results reveal various transient effects, which we identify to be related to characteristic RC times and the FET transit time. Some transients affect the final state of the synapse and must therefore be related to the charging behavior of the gate; other transients do not and must therefore be related to the response of the channel to this charging. These results establish experimental methods to study the dynamics of field-effect artificial synapses – and FETs themselves – in detail, which are key to developing design principles that will reveal the true potential of field-effect artificial synapses as building blocks for neuromorphic hardware.

References

[1] C.A. Mead, *Proceedings of the IEEE* 78, 1629 (1990)

- [2] J. Liu *et al.* Proceedings IEDM 2021; H. Baba *et al.*, Proceedings IEDM 2021; S. Park *et al.*, Adv. Electronic Materials **9**, 2200554 (2023)
[3] B. Förg *et al.* Appl. Phys. Lett. **100**, 053506 (2012); P. D. Erkeres, *et al.*, Appl. Phys. Lett. **103**, 201603 (2013)

9:45 AM BI02/SB01/SB03/SB05.06

Economical and Convenient Fabrication of Antifouling Hydrogels for Implantable Medical Devices Hasani G. Jayasinghe and Arunachalam Muthaiyan; The University of New Mexico - Gallup, United States

Hydrogels garnered special attention as a biomaterial because these soft materials can mimic the natural environment of human tissues and are compatible with the human body. Poly(2-hydroxyethyl methacrylate)-based [poly(HEMA)-based] hydrogels have been used for biomedical applications such as soft contact lenses for decades. Despite the versatile applications of poly(HEMA)-based hydrogels attributed to their excellent biological, chemical, and mechanical properties, they show poor cell attachment. The low cell attachment on this soft material is beneficial for fabricating antifouling materials. Thus, poly(HEMA)-based hydrogels have potential applications in the medical field to prevent the growth of biofilms on medical implants and devices that stay in the human body for prolonged times. When a device remains in the human body for a long time, bacteria attach to the substrate and grow into clusters of cells known as biofilms. Biofilms are thick cell masses and resistant to antibiotics, so treating biofilms-related infections is challenging. Consequently, the biofilms grown on an implant may cause detrimental issues to the patient or damage the medical device. Therefore, searching for materials that can prevent biofilms has a vital importance. This study investigates the fabrication of a HEMA-based hydrogel with antifouling properties. Surface charge and functional groups are the key factors controlling bacterial attachment to a substrate. Therefore, we synthesize copolymers by blending HEMA with monomers such as 2-(Dimethylamino)ethyl methacrylate (DMAEMA). We prepare the polymers by changing the composition of the monomers in the reaction mixture to optimize the chemical composition of the polymer. The polymer with the optimum chemical composition should restrict the attachment of bacteria while maintaining the desired chemical and mechanical properties. The crosslinked network structure of a hydrogel determines its mechanical properties and supports the mechanical integrity of the polymer. Crosslinks also allow the polymer to absorb water excessively, making high water retention a unique feature of a hydrogel. However, the number of crosslinks in the polymer regulates its water retention capacity. Therefore, we vary the number of crosslinks by changing the amount of crosslinking agent in the reaction mixture to obtain the polymer with desirable mechanical and water retention properties. Furthermore, we investigate the effect of surface charge on controlling the bacterial attachment by introducing ionic groups to vary the surface charge. Additionally, we look into the conditions that make the synthesis process more controllable. In this study, we use a thermal initiator to initiate the polymerization reaction. Since the thermal initiation does not require sophisticated instruments, our technique makes the synthesis process convenient, simple, and economical.

10:00 AM BI02/SB01/SB03/SB05.07

Biomaterials Research Mentoring for High School Students Andrew Ulaszek, John Peponis and Yawen Li; Lawrence Technological University, United States

As a primarily undergraduate institution (PUI), Lawrence Technological University (LTU) provides ample opportunities for students to participate in research. Over 50% of the undergraduates in the Biomedical Engineering (BME) Department have conducted at least one research project before they graduate. The most active research in the BME Department is on biomaterials, with strong student interest and faculty support. Over the past five years, many high school students are also involved in semester-long biomaterials research with the BME faculty, staff and students. One group of high school students are from the Bloomfield Hills High School (BHHS) Biomedical Pathway Program (BPP), the first and only Center for Advanced Professional Studies (CAPS) program in Michigan and a nationally recognized innovative high school program that partners with industry and post-secondary institutions to provide authentic immersive learning experience for students. BPP students spend two class periods each week in their junior and senior years to develop biomedical related knowledge and skills in an immersive project-based environment. In the first year, students take classes that provide formative skills in biomedical engineering with limited classroom exposure to research and career pathways. During the second year, they are placed in host organizations that fit their career interests. Built on partnership between the BPP program and the BME Department, BME students with ongoing research projects can choose to mentor and train BPP students in the second year. Students from other high schools participate in research in the BME department either through their school internship/externship programs or over the summer. Since Fall 2019, 19 high school students have conducted research with BME faculty, staff and students. 16 of these 19 students worked on biomaterials related projects, ranging from decellularized spinach leaves, metal 3D printing, to skin tissue engineering, and bioprinted wound dressing mesh. We have developed a process to effectively mentor high school students on biomedical research. This includes targeted orientation and training of BME mentors and high school mentees, clear definition of the research scope and objectives, regular progress check and oversight of the faculty and staff, and periodic evaluation of the student learning. We report in this talk our high school research mentoring process, example projects, experience gained and lessons learned in our continuing effort to involved high school students in biomaterials research to produce high quality project outcomes with enhanced learning for all students involved.

SESSION SB01.01: Bioresponsive Nanotheranostics I
Session Chairs: Jessica Hsu and Bella Manshian
Tuesday Morning, April 23, 2024
Room 428, Level 4, Summit

10:30 AM *SB01.01.01

Engineering Biofunctional Metal-Phenolic Materials via Supramolecular Assembly Frank Caruso; University of Melbourne, Australia

The development of rapid and versatile coating strategies for interface and materials engineering is of widespread interest. This presentation will focus on our studies on the formation of a versatile class of metal-organic materials, metal-phenolic networks (MPNs), which can be formed on various substrates by coordinating polyphenols and metal ions through self-assembly. This robust and modular assembly strategy is substrate independent (covering organic, inorganic, and biological substrates) and has been used for the preparation of various materials, including thin films, particles, superstructures and macroscopic assemblies. It will be shown that a range of polyphenols and a library of metal ions are suitable for forming MPNs and that by altering the type of metal ions, different functions can be incorporated in the MPN materials, ranging from fluorescence to MRI and catalytic capabilities. Furthermore, the use of polypeptides and proteins to form engineered films and particles for a range of biological applications will be highlighted. The ease and scalability of the assembly process, combined with the tuneable properties of MPNs, provide a new avenue for functional interface engineering and make MPNs potential candidates for biomedical, environmental, and advanced materials applications.

11:00 AM SB01.01.02

DNA Origami Directed Virus Capsid Polymorphism Iris Seitz and [Mauri Kostianen](#); Aalto University, Finland

Most known viruses protect their genome by encapsulating it inside a protein capsid. Viral capsids can adopt various geometries, most iconically characterized by icosahedral or helical symmetries. The assembly process of native capsids is highly cooperative and governed by the protein geometry, protein-protein as well as protein-nucleic acid interactions. Importantly, the high control over the size and shape of virus capsids would have advantages in the development of new vaccines and delivery systems. However, tools to direct the assembly process in a programmable manner are exceedingly elusive or strictly limited to specific structures. Here, we introduce a modular approach by demonstrating DNA origami directed polymorphism of single protein subunit capsids. We achieve control over the capsid shape, size, and topology by employing user-defined DNA origami nanostructures as binding and assembly platforms for the capsid proteins. Binding assays and single-particle cryo-electron microscopy reconstruction show that the DNA origami nanoshapes are efficiently encapsulated within the capsid. Further, we observe that helical arrangement of hexameric capsomers is the preferred mode of packing, while a negative curvature of the origami structure is not well tolerated. The capsid proteins assemble on DNA origami in single- or double-layer configurations depending on the applied stoichiometry. In addition, the obtained viral capsid coatings are able to efficiently shield the encapsulated DNA origami from nuclease degradation. Our approach is, moreover, not limited to a single type of virus capsomers and can also be applied to RNA-DNA origami structures. We have for example demonstrated folded mRNA structures and identified key folding strategies to enable protein translation, without a separate origami unfolding step. Therefore, these findings may in addition find direct implementations in next-generation cargo protection and targeting strategies.

I. Seitz et al. *Nature Nanotechnology*, 2023, in press. (<https://doi.org/10.1038/s41565-023-01443-x>)

11:15 AM SB01.01.03

Protein Cages as Responsive Tools for Nanomedicine [Jeroen Cornelissen](#); University of Twente, Netherlands

Different types of protein cages are nowadays studied in the fields of nano- and materials science, because of their well-defined size and structure in the nanometer regime. Compared to more traditional polymer-based nanoparticles, these – often – virus-based materials are extremely uniform, and the position of functional groups is precisely defined. Encapsulins are protein cages found in bacteria that have interesting properties with respect to (thermal) stability and cargo loading. In the past we and others have studied the application of encapsulins, but so far, their preparation, durability and functionalization are restricted to fundamental studies.¹

Recently, we reported the design of encapsulins from two different origins (e.g., *T. maritima* and *B. linens*) with functional loops on its surface.² This allows for future site specific genetic or chemical modification. We, furthermore, optimized the cages' production and showed that, under the selected conditions, these are stable over time periods of at least a year. Both the genetic and chemical manipulation of the encapsulin based protein cages allows for the introduction of functional compounds, such as fluorescent proteins for recognition of enzymes for therapeutic applications. Exciting new developments are the introduction of moieties that respond to an external trigger, where promising results are obtained with - amongst others - light responsiveness.

The research presented in the contribution, therefore, paves the way for further design, engineering and production of encapsulins, for instance for drug delivery, vaccine development or other theranostic applications.

11:30 AM *SB01.01.04

Continuous Growth of Monodisperse Water-Dispersible Iron Oxide Nanoparticles for Potential Biomedical Applications Jing Qu¹, Joanna Wang², Jianghong Rao² and [Yongfeng Zhao](#)¹; ¹Jackson State University, United States; ²Stanford University, United States

A direct synthesis of highly water-dispersible magnetic nanoparticles has been of great interest for biomedicine, but systematic control over size has not been achieved. Here, we have developed a general method to synthesize monodisperse water-dispersible iron oxide nanoparticles with nanometer-scale size increments, ranging from 4 nm to 15 nm, in a single reaction. Precise size control was achieved by continuous growth in an amphiphilic solvent, diethylene glycol (DEG), where growth step was separated from nucleation step by sequential addition of reactant. There was only one reactant used in the synthesis, and no additional capping agents and reducing agents were required. This approach suggests the “living growth” character of the synthesis of iron oxide nanoparticles in an amphiphilic solvent. The synthetic method demonstrates high reproducibility. The as-prepared iron oxide nanoparticles are highly water dispersible without the need for any surface modification. Furthermore, the synthesized 9 nm iron oxide nanoparticles exhibit extremely high transversal and longitudinal relaxivities, as reported in the literature for sub-10 nm spherical nanoparticles. Additionally, the iron oxide nanoparticles were studied for magnetic particles imaging (MPI). The performance of MPI increases with the increase of nanoparticles size. This study will not only shed light on the continuous growth phenomenon of iron oxide nanoparticles in amphiphilic solvent but also stimulate the synthesis and application of iron oxide nanoparticles.

SESSION SB01.02: Bioresponsive Nanotheranostics II

Session Chairs: Ruirui Qiao and Hao Song

Tuesday Afternoon, April 23, 2024

Room 428, Level 4, Summit

1:30 PM *SB01.02.01

Understanding Nanomaterial Behavior in a Physiological Environment Promotes their Translational Exploration Tianjiao Chu, Christy Maksoudian, Irati Perez Gilabert, Mukaddes Izci, Bella Manshian and [Stefaan Soenen](#); KU Leuven, Belgium

The interest in the biomedical use of nanomaterials has been quite strong for several years, yet despite the excellent preclinical proof of concept data, the clinical translation of nanomedicines has remained somewhat low. One potential issue in this regard are the uncertainties related to the biodistribution and bio-effects that nanomaterials will have upon systemic administration. In the present contribution, we aim to provide an overview of some recent examples on how developments in imaging and analysis can help to overcome some of the hurdles currently associated with biomedical research involving nanomaterials.

This presentation itself will focus primarily on the role that non-invasive (optical) imaging can play in better determining the true therapeutic efficacy or potential toxicity of nanomaterials. Recent data will be discussed on the detailed characterization of tumor heterogeneity and how nanomaterials delivery to solid tumors can be improved through manipulating tumor physiology. These gained insights also led to recent advances in nanomaterial effects at the

tumor site, where we specifically look at the combined effects of nanomaterial chemistry and tumor parameters on the degree of metastases and how this can influence the choice of nanomaterials to be used. We also explore the use of engineered nanomaterials to promote anti-tumor immunity and lastly, demonstrate the ability to investigate the use of pDNA-loaded nanomaterials for therapeutic use. Together with examples of novel imaging modalities and the need for fully quantitative data, we hope that this presentation will help any interested scientists in uncovering the full potential that nanomedicines have to offer.

2:00 PM SB01.02.02

Core-Shell Semiconducting Polymer Nanoparticles for Detection and Photothermal Ablation of Breast Cancer [Nicole Levi](#) and Santu Sarkar; Wake Forest University School of Medicine, United States

Triple negative breast cancer (TNBC) is one of the deadliest among other subtypes of breast cancers due to its absence of standard biomarker expressions, and the aggressive nature of TNBC leads to low patient survival. Current treatment strategies include surgery, chemotherapy, and radiation therapy, although photothermal therapy is an evolving treatment strategy. It has recently been shown that breast cancer can harbor intracellular bacteria, which may impact therapeutic responses. Here we present the use of semiconducting theranostic polymer nanoparticles composed of a photothermal poly[4,4-bis(2-ethylhexyl)-cyclopenta[2,1-b:3,4-b']-dithiophene-2,6-diyl-alt-2,1,3-benzoselenadiazole-4,7-diyl] (PCPDTBSe) core with a fluorescent poly[(9,9-dihexylfluorene)-co-2,1,3-benzothiadiazole-co-4,7-di(thiophen-2-yl)-2,1,3-benzothiadiazole (PFBTDBT10) shell for detection and treatment of TNBC cells harboring *Staphylococcus aureus* bacteria. These dual polymer core-shell nanoparticles (CSNPs) had absorption maxima at 450 nm and 740 nm corresponding to PCPDTBSe and DBT10 respectively. The quantum yield was 9.64%. The core diameter was 83 nm and the CSNPs were 125 nm, both with negative zeta potential. Exposure of TNBC cells (MDA MB 231) to the CSNPs for 24 h resulted in a 50% reduction in viability, whereas non-tumorigenic breast epithelial cells (MCF 10A) were not impacted at 250 µg/ml in the absence of infrared light. Exposure to 800 nm resulted in a temperature change of 15°C at 250 µg/ml of CSNPs exposed to 3W of 800 nm light for 60 s. This led to a 75% reduction in uninfected MCF 10A cells, but only a 60% reduction when this cell line was infected. Uninfected MDA MB 231 cells subjected to 250 µg/ml of CSNPs and 800 nm (3W for 60 s) had a 40% reduction in viability, and the infected cells had a 70% reduction. Differences in cell response to PTT whether the cells were infected or not indicates that infected TNBC cells may be preferentially more sensitive to CSNP-induced PTT. The CSNPs could be imaged within the cells, setting the stage for using this CSNPs for detection of breast cancer and precision photothermal ablation.

2:15 PM SB01.02.03

Remote Stimuli-Responsive Nanomaterials for Regenerative and Cancer Therapy [Heemin Kang](#), Yuri Kim, Hyunsik Hong, Nayeon Kang, Sungkyu Lee and Sunhong Min; Korea University, Korea (the Republic of)

Cells constantly interact with native nanostructured extracellular matrix at the molecular level. Nanomaterials responsive to tissue-penetrative remote stimuli can be designed to present bioactive ligands or deliver functional molecules as a nanomedicine to regulate or elucidate dynamic nanoscale cell-material interactions. In this talk, I will demonstrate the design of dynamic nanomaterials that can be remotely and spatiotemporally controlled via various remote stimuli, such as magnetic field, light, self-assembling molecules, or their combinations.

In particular, I will show that magnetic field can control the motion of magnetic nanomaterials, such as reversibly controlling RGD ligand nano-coupling, nano-blocking, nano-stretching, and nano-interconnectivity with graph theory-based analysis, which can regulate the focal adhesion-mediated mechanotransduction and resultant differentiation of stem cells. Near-infrared light can activate photonic nanomaterials to trigger photoisomerization, thereby mediating the swelling of liganded supramolecular self-assembly, which can be reversibly deswelled by visible light. Such photonic control enables *in vivo* stability imaging and spatiotemporally controlled molecular delivery to regulate the adhesion-dependent pro-inflammatory vs. pro-regenerative polarization of macrophages. Furthermore, molecules and ions can reversibly induce *in situ* self-assembly of biofunctional nanomaterials.

I will also introduce a couple of representative examples of recent cancer therapies and diagnostic imaging controllable by remote stimuli, such as magnetic field, light, and ultrasound, which utilize mechanical force, 1-D nanomaterials, *in situ* self-assembly, ferroptosis, and others. These strategies can present benefits for safe personalized precision therapies while minimizing drug resistance and side effects.

2:30 PM *SB01.02.04

Recent Progress on Phototherapy [Juyoung Yoon](#); Ewha Womans University, Korea (the Republic of)

Switchable phototheranostic nanomaterials are of particular interest for specific biosensing, high-quality imaging, and targeted therapy in the field of precision nanomedicine. Here, we develop a “one-for-all” nanomaterial (NanoPcTBs) that self-assembles from flexible and versatile phthalocyanine building blocks. Fluorescence and reactive oxygen species (ROS) generation could be triggered depending on a targeted, protein-induced, partial disassembly mechanism, which creates opportunities for low-background fluorescence imaging and activatable photodynamic therapy (PDT). On the other hand, the *in vivo* specific binding between albumin and PcS, arising from the disassembly of injected NanoPcS, was recently confirmed using an inducible transgenic mouse system. In a recent investigation, we devised a novel molecular design approach to create heavy-atom-free photosensitizers for thionaphthalimides and BODIPYs. The thionaphthalimides display dramatically enhanced quantum yields for photosensitized singlet oxygen formation. Photodynamic antibacterial therapy is also regarded as an innovative and promising antibacterial approach due to its minor side effects and lack of drug resistance. Recently, we suggested that reactive differences may pave a general way to design selective photodynamic agents for ablating Gram-positive bacteria-infected diseases.

3:00 PM BREAK

3:30 PM SB01.02.06

Advanced Tissue Engineering Scaffolds Incorporated with Gold Nanoparticle-Based Theranostics for Postoperative Cancer Patients Lin Guo, Qilong Zhao, Li-wu Zheng and [Min Wang](#); The University of Hong Kong, Hong Kong

Cancer causes millions of human deaths each year and surgery has been the most commonly used method for treating many types of cancers. After surgical removal of the tumor, new tissues need to be formed at the resection site for restoring body functions. Scaffold-based tissue engineering has emerged as a viable approach for regenerating tissues in the body. Another major issue for many cancer patients, such as suffers of gastrointestinal (GI) tract cancer, is the high cancer recurrence rate. Therefore, new strategies should be investigated to detect and treat recurrent cancer for patients after their initial cancer treatment. In nanomedicine, nanodevices that provide both diagnostic and therapeutic functions (the so-called “theranostics”) appear to be highly promising for the early detection and effective treatment of cancers. In the current study, a new concurrent electrospinning and co-axial electrospray technology was developed for fabricating advanced tissue engineering scaffolds incorporated with gold nanoparticle (AuNP)-based theranostics for treating cancer patients. Model scaffolds designed for GI tract cancer patients were made using this technology. It was shown that a controlled release of AuNP-based theranostics

could be achieved for the advanced scaffolds. The study using NIH/3T3 mouse fibroblasts indicated good biocompatibility of released theranostics. HeLa cells, which have a high-level of folate receptor (FR) expression, and MCF-7 cells, which have a low-level FR expression and thus could provide a negative control in the current study, were employed for investigating the designed functions of the theranostics. *In vitro* investigations showed that the theranostics released from scaffolds could provide both diagnostic and therapeutic functions, including strongly amplified Raman signals via the surface enhanced Raman scattering (SERS) effect, active targeting, cellular imaging and photothermal therapy for HeLa cells. Our other studies also showed the potential of these advanced scaffold for GI tract tissue regeneration. Altogether, these novel scaffolds are highly promising for offering the treatment for postoperative cancer patients.

3:45 PM *SB01.02.07

Structural Immunotherapy: Spherical Nucleic Acid (SNA) Immunotherapy for HPV-Associated Head and Neck Cancer Chad A. Mirkin^{1,2} and Sergej Kudruk^{1,2}; ¹Northwestern University, United States; ²International Institute for Nanotechnology, United States

Squamous cell cancer of the head and neck (SCCHN), ranked 6th in global cancer mortality, is witnessing a transformative shift in its causation due to the escalating prevalence of human papillomavirus (HPV). Current HPV-SCCHN treatment options include surgery, chemotherapy, and radiation. Immunotherapy for HPV-SCCHN has so far been limited to commercially available immune checkpoint inhibitors targeting PD-1 or PDL-1 as a synergistic treatment to chemotherapy. However, even with these options, on average 50% of patients with SCCHN will experience a recurrence/metastasis which has a poor prognosis and a median overall survival <1 year. Therefore, there is a critical need for the development of new and improved treatment options for HPV-SCCHN. To that end, HPV oncoproteins E6 and E7 have emerged as promising targets for vaccine-based therapies. Here we employ chemically tunable spherical nucleic acid (SNA) nanostructures, consisting of a nanoparticle core densely functionalized with DNA, that incorporate selected HPV-SCCHN-specific antigens in a controlled orientation. Indeed, the three-dimensional presentation and overall structural design of SNAs enables effective entry into cells and perturbations to structural and compositional parameters can be altered to achieve a desired therapeutic outcome. Thus, SNAs for immunotherapy allows one to explore the implications of structural presentation of vaccine components in generating epitope-specific T cells. In this study, SNA-based therapeutic cancer vaccines are designed to efficiently deliver adjuvants and tumor-specific antigens, thus activating both innate and adaptive immune systems. We evaluated multiple HPV-16 antigens, with the goal of maximizing immune responses in tumor-burdened humanized murine models and patient-derived tumor spheroid samples. To identify the most potent antigen-SNA formulation, generation of antigen-specific CD8+ T-cells, cytokine production, and HPV cancer-specific cell killing are evaluated. Overall, this work highlights how the structure of SNAs is critical to designing effective therapeutics while providing insights into the molecular interactions between the immune system and cancer cells.

4:15 PM SB01.02.08

Spatiotemporally Delivery of Multiple Growth Factors from Electrospun Scaffolds through Photothermal Effect to Manipulate Skin Wound Regeneration Xindan Zhang and Jiajia Xue; Beijing University of Chemical Technology, China

Due to the increasing incidence of full-thickness skin injuries caused by mechanical trauma, burns, as well as conditions like diabetes and malignant tumors, the repair of skin wounds has become a major medical challenge in the field of wound healing. During the process of skin wound repair, different types of growth factors play specific roles at various stages, collectively promoting wound healing. In this study, we fabricated a nanofiber scaffold with surface topographical features using electrospinning. Furthermore, the scaffold was functionalized to provide the required microenvironment for skin wound repair by incorporating growth factors. To enable the spatiotemporal controlled release of these growth factors, we combined photothermal therapy with phase change materials and introduced a photomask strategy. Specifically, a three-layered sandwich-like photothermal scaffold was prepared by in conjunction with coaxial electrospinning, using polycaprolactone as the base material. The scaffold consisted of an inner layer of radially aligned nanofibers, an outer layer of random nanofibers, and an intermediate layer containing growth factors and photothermal agents in the form of phase change microspheres. By utilizing near-infrared light irradiation and the photomask strategy, the spatiotemporal controlled release of the growth factors was achieved. The multi-layered structure of the scaffold was confirmed by surface morphology analysis, and the modified surface was found to promote cell adhesion according to water contact angle measurements. Photothermal experiments and studies on growth factor release demonstrated that the scaffold could achieve spatiotemporal controlled release while maintaining photothermal stability, and the released growth factors retained their pro-angiogenic activities. *In vitro* experiments showed that the scaffold not only promoted cell proliferation but also facilitated cell migration through the combination of its topographical surface and the spatiotemporal controlled release of growth factors. Finally, an animal full-thickness skin wound model was employed to evaluate the wound healing effectiveness of the scaffold, revealing the regulatory patterns and effects of growth factors *in vivo* under programmable photothermal stimulation. In conclusion, the nanofiber scaffold with photothermal-triggered controlled release of growth factors effectively integrates the topographical structure of the nanofibers with the controllable release of growth factors. It provides a novel approach for the design of skin wound repair scaffolds and their combination with photothermal therapy to promote skin wound healing. This research holds significant potential in the fields of tissue regeneration and controlled release.

SESSION SB01.03: Poster Session: Bioresponsive Nanotheranostics

Session Chairs: Jessica Hsu and Ruirui Qiao

Tuesday Afternoon, April 23, 2024

Flex Hall C, Level 2, Summit

5:00 PM SB01.03.01

Programming Injectable DNA Hydrogels Yields Tumor Microenvironment-Activatable Chemo-Immunotherapy Yu Fan^{1,2}; ¹DWI-Leibniz Institute for Interactive Materials, Germany; ²RWTH Aachen University, Germany

Injectable hydrogels have been investigated extensively to incorporate with drugs for tumor treatment because those materials can simultaneously deliver multiple drugs to the target sites with rational ratios and minimal invasion, and elevate their tumor accumulation, blood stability, and half-lives. Importantly, the local treatment of hydrogel-encapsulated drugs showed superior tumor growth inhibition compared to the local or systemic delivery of non-encapsulated chemotherapeutics and immunomodulators. However, since current studies regarding injectable chemo-immunotherapeutic hydrogels are mainly based on the intratumoral gelation of soluble precursors, sol-gel transformation may be impeded by the complex physiological environment, resulting in the reduced cross-linking degree, abrupt drug leakage, and unpredictable pharmacokinetics. Besides, conventional polymers lack molecular, structural, and functional programmability, which results in significant challenges in tailoring the biofunctionalities of hydrogel scaffolds for intimately interacting with tumor tissue.

Here, we describe an unprecedented injectable DNA hydrogel in which the repeats of cytosine-phosphate-guanine oligodeoxynucleotide (CpG ODN) and adenosine triphosphate (ATP) aptamer are encoded on the ultralong DNA building blocks by RCA-mediated DNA polymerization. By sequentially

incorporating DNA hydrogel with immune checkpoint inhibitor anti-programmed cell death protein ligand 1 (aPDL1) and chemotherapeutic agent doxorubicin (DOX), a chemo-immunotherapeutic DNA hydrogel adjuvant (aPDL1/DOX@DNA Gel) is formed. Due to its super-soft property, this DNA hydrogel encoded with ATP aptamers can be readily injected into tumor tissues in which the overexpressed ATP binds to the corresponding aptamer. This results in the conformational change of aptamer and volume expansion of the gelmatrix to stimulate the distinct release kinetics of co-encapsulated therapeutics. DOX is first released to induce immunogenic cell death that intimately works together with the polymerized CpG ODN in gel scaffold for effectively recruiting and activating dendritic cells. While, the polymerized CpG ODN displayed very high tumor retention with a significant reduction of the systemic circulation, which is attributed to the restricted in vivo motility and metabolism of the polymerized CpG ODN, thereby reducing the adverse effects of CpG ODN while enhancing its tumor immunomodulatory efficacy. Furthermore, aPDL1 antibody was subsequently released from DNA hydrogel to block the immune inhibitory checkpoint molecules PD-L1 on the tumor cell surface, thus reversing the tumor microenvironment immunosuppression through potentiating T-cell mediated immune responses. The programmed aPDL1/DOX@DNA Gel demonstrated potent suppression of tumor growth and lung metastasis via the induced strong systemic immune response and immune memory effect. This work thus contributes to the first proof-of-concept demonstration of a programmable super-soft DNA hydrogel system that perfectly matching the sequence programmability to the synergistic therapeutic modalities based on chemotherapeutic toxicity, in situ vaccination, and immune checkpoint blockade. With the high programmability of design principle, we believe that our approach can be combined with DNA-protein conjugation chemistry, DNA nanotechnology, and microfluidic technique to develop a library of biomaterial systems in new biomedical applications beyond chemo-immunotherapy of tumors.

5:00 PM SB01.03.02

Nano Herbals for Effective Wound Healing [Aarti Shastri](#)¹, Arti Swami¹, Swarupa Hatolkar² and Sachin Bhusari³; ¹MIT World Peace University, India; ²Mrbiologist LLP, India; ³ICT Aurangabad, India

Background: The demand for Pharmacognostic-based compounds with diverse pharmaceutical activities has been escalating to combat challenges like drug resistance, emerging diseases, and the toxicity of currently used chemical compounds. The plant kingdom offers a plethora of bioactive compounds with unprecedented potential to address these difficulties, leading to a surge in novel solutions within the pharmaceutical industry. Ayurvedic formulations of Tobacco (*Nicotiana tabacum*) have emerged as a promising approach due to their established use in herbal medicine with multiple medicinal benefits.

Methods: This study aimed to explore the wound healing potential of the tobacco plant. Tobacco leaves were processed to create a traditional ayurvedic formulation, including Mashi formulations known as Anterdhum Padhati Mashi, Bahirdhum Padhati Mashi, and Muffle Furnace Mashi, following traditional ayurvedic practices. Additionally, aqueous, and alcoholic extracts of tobacco leaves were prepared. The wound healing efficacy of these formulations was assessed using an Excision model in mice.

Results: Comparative analysis revealed that the Bahirdhum Padhati Mashi with methanolic discharge exhibited significantly higher wound healing ability compared to a reference drug formulation.

Conclusion: In conclusion, the Bahirdhum Padhati Mashi derived from tobacco demonstrates promising wound healing potential and could serve as an effective wound healing agent. The findings from this experimental study support the exploration of ayurvedic formulations as potential candidates for addressing wound healing complications. Further investigations and

clinical trials are warranted to ascertain their safety, efficacy, and potential application in wound management.

Keywords: Nano particle, *Nicotiana tabacum*, wound healing, Anterdhum Padhati, Nano formulation, herbal nano formulation

5:00 PM SB01.03.03

Magneto-Responsive Textile modified by (Nano)Materials [Arkadiusz Jozefczak](#)¹, Rafal Bielas¹, Bassam M. Jameel¹, Ivo Safarik² and Peter Kopcansky³; ¹Adam Mickiewicz University, Poland; ²Czech Academy of Sciences, Czechia; ³Slovak Academy of Sciences, Slovakia

Textiles are materials made by interlocking bundles of yarns or threads. The inherent flexibility of the textile materials opens the possibilities for their functionalization. The space between the single fibers and their surface can carry additives of different functionalities, such as magnetic nanoparticles and drug molecules. Magneto-responsive textiles have emerged lately as an important carrier in various applications, including those in biomedical fields such as drug delivery, tissue engineering, and regenerative medicine. We designed and characterized simple woven and non-woven textile materials with magnetic properties that can become potential candidates for a smart magnetic platform for hyperthermia treatments [1]. When heat was induced by magneto-responsive textiles under the influence of a high-frequency alternating magnetic field, the temperature increase in tissue-mimicking phantoms depended on several factors, such as the type of basic textile material, the type of materials used for textile surface modification (magnetic fluids, magnetic Pickering emulsion), and the number of layers covering the phantom. The values of temperature elevation, achieved with the use of magnetic textiles, are sufficient for potential application in magnetic hyperthermia therapies and as heating patches or bandages. Controlled release of substances and/or nano-sized objects from the textiles triggered by high-intensity ultrasound is also possible. This paves the way for the potential use of the proposed textile materials in the theranostics paradigm.

This work was supported by project no. 2019/35/O/ST3/00503 (PRELUDIUM BIS) of the Polish National Science Centre, and project no. APVV-22-0060 of the Slovak Research and Development Agency.

[1] A. Józefczak, K. Kaczmarek, R. Bielas, J. Procházková, I. Safarik, Magneto-Responsive Textiles for Non-Invasive Heating, International Journal of Molecular Sciences 24(14) (2023) 11744.

5:00 PM SB01.03.04

In Vivo Brain Tumor Response to Magnetothermal Effect of The Optimized Magnetic Particle Imaging (MPI) Contrast Agents [Maryam Golshahi](#) and Hamed Arami; Arizona State University, United States

Magnetic Particle Imaging (MPI) has been recently developed for image-guided magnetothermal treatment of tumors in animal models. These therapies are designed based on rapid magnetization and de-magnetization of superparamagnetic nanoparticles in the presence of AC magnetic fields. This technique offers localized treatment of deep tissue and inoperable tumors due to the high tissue penetration rate of the electromagnetic fields. Also, unlike

chemotherapy approaches, which generally lead to whole-body biodistribution of the drugs, this method enables localized treatment of the tumors with minimal side-effect on other organs when intratumoral administration routes are used. Owing to their safety and tunable physicochemical properties, iron oxide nanoparticles are the optimal types of contrast agents for MPI. We have shown that since the magnetic properties of these nanoparticles are size-dependent, they play a key role in tuning the amount of heat and contrast they can generate in tumors in response to MPI magnetization. Here, we will discuss our most recent results for effective MPI imaging and magnetothermal treatment of GBM (the most deadly type of brain tumor) in mouse models. We will demonstrate the effectiveness of this technique for treatment of three types of intracranially implanted GBMs with different levels of invasiveness and growth patterns. Our survival and histological results indicated that GBM response to this treatment depends on GBM cell type, anatomical growth pattern of the tumors, and permeability of the nanoparticles within tissues. These results were used to further optimize our technique (i.e., improving the magnetization system and adjusting the nanoparticles' properties, such as core and hydrodynamic sizes and surface charges) for more effective magnetothermal treatment of different GBM models.

5:00 PM SB01.03.05

Highly Efficient Photothermal Therapy of Tumors Using Easily Prepared Nanoparticles [Songyi Lee](#); Pukyong National University, Korea (the Republic of)

The simple molecular design of small molecule-based photothermal nano-agents with high photothermal conversion efficiencies (η) remains a highly challenging obstacle in the development of new anti-tumor drugs. Although several efficient small agents have been reported, they tend to contain bulky alkyl chains and/or aromatic rings, which were introduced to enhance the photothermal effect, but result in complicated preparation procedures. Herein, we report the preparation of nano-agents from commercial reagents using a one-step organic reaction with facile purification and a subsequent simple self-assembly process in water under a flow of air overnight. The obtained nano-agents exhibited high photothermal conversion efficiencies (η) of up to 92.5%. This photothermal effect originated mainly from twisted C=N bond-induced non-radiative decay with completely inhibited radiative decay and the intersystem crossing process. In addition, the photothermal effect was enhanced by synergistic twisted intramolecular charge transfer, strong donor-acceptor interactions, various intramolecular vibrations, and the presence of rotators. The obtained nano-agents efficiently inhibited tumor growth after 10 d of photothermal therapy, and they exhibited a good biocompatibility in a mouse tumor model. This simple approach can conveniently facilitate the further development and testing of such systems.

5:00 PM SB01.03.06

Design of One-For-All Near-Infrared Aggregation-Induced Emission Nanoaggregates for Boosting Theranostic Efficacy [Huilin Xie](#) and Ben Zhong Tang; The Hong Kong University of Science and Technology, Hong Kong

Fluorescence-guided phototherapy with integrated diagnostic and therapeutic functions has great potential in the field of precision medicine, as they fully utilize light for energy conversion or transduction, and have the advantages of multifunctionality, low cost, and convenient. From a diagnostic perspective, near-infrared fluorescence imaging (FLI) has lower interference from autofluorescence, improved imaging depth, and higher sensitivity compared to conventional imaging in the visible light region. On the other hand, photothermal therapy (PTT) and photodynamic therapy (PDT) have received great research attention due to their non-invasive, controllable, and low drug resistance characteristics. PTT uses non-radiative transitions of excited molecular states to convert light energy into heat for therapy, while PDT involves energy transfer processes of excited state molecules, producing highly reactive oxygen species, inducing cell damage and apoptosis. Combining PTT and PDT with fluorescence localization of lesions could lead to better diagnostic and therapeutic effects. However, the competitive energy relaxation pathways of molecules are difficult to regulate, and the fluorescence of many planar organic molecules is quenched upon aggregation, making it difficult to achieve efficient FLI, PTT, and PDT simultaneously. Aggregate science offers more opportunities to solve this problem, as the energy dissipation pathways of aggregates are more diverse, providing more possibilities for constructing "one-for-all" phototheranostic agents and realizing their multifunctionality. Based on this, this study reports a multifunctional diagnostic and therapeutic platform with near-infrared emission, high fluorescence quantum yield, reactive oxygen species generation efficiency, and photothermal conversion efficiency. *In vivo* studies show that the use of aggregation-induced emission (AIE) nanoaggregates in this platform can make mouse tumors show bright fluorescence, while exhibiting good photodynamic and photothermal therapy effects, ultimately completely eliminating the tumors. This study is of great significance for the rational design and synthesis of multifunctional near-infrared nanoaggregates with high energy dissipation utilization efficiency for precise diagnosis and effective treatment of tumors.

5:00 PM SB01.03.07

Design and Optimization of an Electro spraying System for Bioactive Compound Nanoencapsulation for Nasal Vaccines [Sebastián León-Carvajal](#)¹, [Esteban Avendaño-Soto](#)^{2,2}, [Sebastián Zuñiga-Salazar](#)¹ and [Ricardo Starbird-Perez](#)¹; ¹Costa Rica Technological Institute, Costa Rica; ²University of Costa Rica, Costa Rica

Controlled drug release systems are innovative techniques that offer advantages over traditional methods. They enable precise localization of bioactive payloads in specific regions and provide control over drug concentration within therapeutic ranges for extended periods. One example of a controlled drug release systems are nasal vaccines, where a bioactive compound (core) is encapsulated within a biopolymer matrix (shell) in the form of micro and nanoparticles. The size and morphology of the obtained particles facilitates the controlled diffusion of the bioactive payload, and the release of the bioactive compound occurs when ambient conditions favor shell dissolution or core diffusion to the medium. Several techniques are employed to synthesize encapsulated nanoparticles, including nano-spraydrying, electrostatic-spraydrying, and electro spraying. Electro spraying is particularly interesting for the development of drug release systems because it allows the synthesis of nanoparticles without the use of high temperatures, that could potentially damage the payload. In contrast, electro spraying achieves this by applying a high electric field to electrostatically atomize and deposit generated particles onto a collecting plate for recovery. In this research, we have developed an electro spraying device that is capable of synthesizing nanoparticles based on biocompatible biopolymers, such as zein, polyvinyl alcohol (PVA), and chitosan, as well as optimized the electro spraying parameters in order to obtain homogeneous particle distribution and morphology. These systems are capable of encapsulating bioactive materials for controlled release in nasal vaccines. The implementation of this technology has the potential to enhance the biological response and, consequently, the overall effectiveness of treatments.

5:00 PM SB01.03.08

Development and Evaluation of Brimonidine Tartrate Nanoparticulate Ocular Insert [Shruti Kadam](#)¹, [Dipti Dhurat](#)¹, [Hrishikesh Khude](#)¹, [Amol Tagalpalwar](#)¹, [Akshay M. Baheti](#)¹, [Shrikant Joshi](#)² and [Anil Pawar](#)³; ¹School of Health Sciences and Technology, Dr. Vishwanath Karad MIT World Peace University, India; ²Maliba Pharmacy College, Uka Tarsadia University, India; ³Dr. Vishwanath Karad MIT World Peace University, India

Glaucoma is the second leading cause of vision loss in the world after cataracts. It is estimated that the number of people with glaucoma will be nearly 79.6 million worldwide by 2023. This alarmingly high number of anticipated patients requires urgent improvement in the current therapeutic approaches adopted for the treatment of this disease. At present, Antiglaucoma agent brimonidine tartrate is commercially available in the form of eye drops and marketed under the name of Alphagan® (0.2%) or Alphagan® P (0.1% and 0.15%). For effective management of intraocular pressure, it needs to be administered 1 to 3 drops every 6 h. The drawbacks associated with the available eye drops are short pre-corneal retention time along with poor patient compliance. The present was conducted to formulate, optimize and evaluate a brimonidine tartrate nanoparticulate ocular insert to improve patient compliance.

Nanoparticulate ocular inserts were prepared in two steps initially ionic gelation for nanoparticles and solvent casting method for the ocular insert. Release studies showed that the prepared insert releases brimonidine tartrate by zero-order kinetic up to 8 h. The inserts were evaluated for several parameters like drug-excipient interaction, thermal studies, the thickness of the insert, swelling index, and moisture studies. Furthermore, the in-vivo evaluation showed that the ocular insert has good therapeutic activity and fewer side effects as compared to other marketed formulations.

5:00 PM SB01.03.09

Confirmation of The Effect of Gold Nanoparticles on Macrophages by PEG and Analysis of Gene Expression Profiles on The Cellular Response of Macrophages Young-Hwa Kim and Kyung Hyun Min; Jeonbuk National University, Korea (the Republic of)

Purpose: Recently, understanding the relationship between immune cells and nanoparticles has played an important role in its biomedical applications. However, biological responses by nanoparticles are not clear. We investigated the effects of cellular and immune responses related to gene expression and *in vivo* behavior in murine macrophages by the gold nanoparticles (AuNPs).

Materials and Methods: To evaluate the effects of cellular responses of the hydrophilic reagent, PEG (polyethylene glycol), murine macrophage cell lines (RAW264.7) were treated with unmodified 50 nm-sized AuNPs and PEGylated 50 nm-sized AuNPs. Cytotoxicity test was performed using CCK-8 assay for 72 hrs. Morphology and intracellular localization of the AuNPs were observed by transmission electron microscopy (TEM). To analyze the modified gene expressions, total RNA was extracted from AuNPs-treated cells and whole-genome cDNA microarray analysis was performed. The uptake and clearance of ¹²⁵I-unmodified AuNPs and ¹²⁵I-PEGylated AuNPs were evaluated by serial SPECT/CT studies from 0 hr to 4 hrs after i.v injection of 11.1 MBq ¹²⁵I-AuNPs in nude mice.

Results: In Dynamic Light Scattering (DLS) analysis, the hydrodynamic size of unmodified AuNPs and PEGylated AuNPs was 49.8 ± 7.4 nm, 65.4 ± 9.2 nm, respectively. The viability of RAW264.7 cells were observed in more than 80% with 0.02 ~ 0.2 mg/mL AuNPs treatments. TEM images showed that unmodified AuNPs and PEGylated AuNPs were trapped in vesicles inside the cytoplasm of RAW264.7 cells with aggregation and separation, respectively. In the microarray analysis, significant effects were observed on gene regulations involved with immune response, oxidative stress and cell death between the unmodified AuNPs and the PEGylated AuNPs. In *in vivo* imaging, unmodified AuNPs-treated mice were observed in the liver and the spleen up to 4 hrs, however, PEGylated AuNPs were well circulated in the whole blood up to 4 hrs.

Conclusion: In this study, we investigated to understand the interaction between immune cells and gold nanoparticles, and to respond the biological mechanisms. This information would help to develop various kinds of nanoparticles with improved safety and efficacy.

5:00 PM SB01.03.10

Continuous Metal-Organic Framework Thin Films for High-Resolution X-Ray Imaging Jianxin Wang and Omar F Mohammed; King Abdullah University of Science and Technology, Saudi Arabia

In the realm of scintillator material science, the significance of scintillator screens lies in their ability to enhance imaging resolution and X-ray sensitivity. 1,2 These two factors are of utmost importance for achieving accurate medical diagnoses and treatments, improving safety inspections, and enabling comprehensive examinations of industrial equipment. 3 Presently, the dominant methods employed for creating scintillator screens primarily involve high-temperature sintering, crystal growth, and polymer doping techniques. However, these methods come with stringent synthesis requirements and grapple with challenges related to achieving uniform and extensive growth across large surfaces while minimizing light scattering. 4 The in-situ electrochemical synthesis of continuous metal-organic framework (MOF) thin films offer a solution that increases material density, reduces light dispersion, and ensures long-lasting durability. The tightly interconnected and precisely oriented growth structure of continuous MOF thin films results in a significant reduction in light scattering. 5 Consequently, the inherent characteristic of diminished light dispersion holds great promise for enhancing spatial imaging resolution in X-ray scintillators.

Herein, we present a versatile approach rooted in in-situ electrochemical-directed assembly, dedicated to crafting MOF thin films tailored for exceptional X-ray imaging capabilities. Through this electrochemical process, a series of coherent MOF thin films have been successfully synthesized, employing interconnected lanthanide metals and terephthalic acid linkers. This specific MOF thin film emerges as a standout contender, enabling high-resolution X-ray imaging while retaining X-ray sensitivity. This achievement is attributed to its superior material density, reduced light scattering, and simplified manufacturing procedure. Notably, this particular MOF thin film surpasses the majority of documented organic and traditional inorganic scintillators, achieving an X-ray imaging resolution exceeding 32 line pairs per millimeter (lp/mm). This research has the potential to elevate MOFs as highly efficient scintillators for X-ray imaging, opening up exciting opportunities in the fields of radiology and security screening applications.

References

1. Yi, L., Hou, B., Zhao, H., Tan, H. Q. & Liu, X. A double-tapered fibre array for pixel-dense gamma-ray imaging. *Nat. Photon.* 17, 494-500 (2023).
2. Wang, J.-X. et al. Heavy-atom engineering of thermally activated delayed fluorophores for high-performance X-ray imaging scintillators. *Nat. Photon.* 16, 869-875 (2022).
3. Chen, Q. et al. All-inorganic perovskite nanocrystal scintillators. *Nature.* 561, 88-93 (2018).
4. Han, K. et al. Seed-crystal-induced cold sintering toward metal halide transparent ceramic scintillators. *Adv. Mater.* 34, e2110420 (2022).
5. Zhou, S. et al. Asymmetric pore windows in MOF membranes for natural gas valorization. *Nature.* 606, 706-712 (2022).

5:00 PM SB01.03.11

Bacterial Cellulose based Modulated Drug Carriers for Transdermal Skin Patches with Diclofenac Sodium and Simvastatin: Role of Differently Soluble Drugs, Drug-Matrix Interaction and Matrix Morphology Peddapannagari Kalyani and Mudrika Khandelwal; Indian Institute of Technology, Hyderabad, India

Bacterial cellulose (BC) is a type of nanofibrous, highly crystalline cellulose that is being used as a drug carrier for two differently soluble drugs of Diclofenac sodium and Simvastatin as a model drug for likely water soluble and water insoluble drugs. One of the benefits of using BC is that it is hydrophilic and highly swellable, which means that it offers a burst release of water-soluble drugs and a limited release of hydrophobic drugs. We have modified the matrix of BC using in-situ techniques to modulate its morphological and structural properties. To achieve this, we used biopolymers of Agar and Chitosan as a modifying agent during culture, which affects density and microstructure. Chitosan also imparts additional functional groups that can modulate interaction with drugs. These polymer-modulated BCs were further modulated by varying drying conditions such as freeze drying and air drying to obtain bacterial cellulose-based modulated drug carriers as transdermal skin patches. To understand the characteristics of these drug carriers for skin

patches, conducted a range of characterization studies using SEM, FT-IR, XRD, BET analysis, water swelling and uptake studies, and drug release studies. Mathematical modeling was also fitted by use of Zero order, First order, Higuchi and Korsmayer peppas model fitting to understand the release mechanism and the factors that govern the release. The results showed that the simple modulated BC (M-BC) can release them through a swelling and diffusion-controlled first order quasi-fickian mechanism, irrespective of the drug load. The modulated Agar-BC (A-MBC) releases both drugs through swelling and Erosion driven non fickian first order diffusion kinetics. But the release in A-MBC was sustained for 3 days in water insoluble drug due to its Curley oriented denser fiber assembly making some time to release of ensnare drug molecules. On the other hand, for Chitosan-modulated BC (C-MBC), the release is greatly sustained over 14 days for water-insoluble drug (Simvastatin) through swelling, polymer relaxation and erosion following zero order- case II release through drug-matrix interaction. It seems that non-fickian release mechanism was taken place in the M-BC and A-MBC skin patches with the irrespective of the drug used. The Drug release mechanism in the C-MBC skin patch was changes from non-fickian first order diffusion kinetics for likely water-soluble drug to case II transport with zero order diffusion kinetics for water insoluble drug. This research implies the various transdermal skin patches applications like immediate potential application to sustain chronic disease management such as Vaccines, Acne, hypertension, hormonal management, thyroid treatment, cardiovascular disease, central nervous diseases, cigarette cessation, motion sickness, arthritis, diabetics, hyperlipidemia etc.

5:00 PM SB01.03.12

Brimonidine Nanoparticulate Ocular Inserts for Glaucoma Shruti Kadam¹, Dipti Dhurat¹, Hrishikesh Khude¹, Amol Tagalpalwar¹, Akshay M. Baheti¹, Shrikant Joshi² and [Anil Pawar¹](#); ¹Dr. Vishwanath Karad MIT World Peace University, India; ²Maliba Pharmacy College, Uka Tarsadia University, India

Ocular drug delivery is challenging due to the unique anatomical and physiological barriers of the eye that limit drug absorption. Conventional eye drops often have low bioavailability and short residence time on the ocular surface, requiring frequent dosing that leads to poor patient compliance. Antiglaucoma agent brimonidine is commercially available in the form of eye drops that need to be administered 1 to 3 drops every 6 h. We developed and evaluated a brimonidine tartrate nanoparticulate ocular insert to improve patient compliance. Nanoparticulate ocular inserts were prepared in two steps involving ionic gelation for the synthesis of nanoparticles and solvent casting method for the fabrication of ocular insert. The inserts were evaluated for several parameters including in-vitro release profile and in-vivo efficacy in rabbits. An in-vitro study showed the release of brimonidine from the ocular inserts by zero-order kinetic up to 8 h. The in-vivo study further validated the efficacy of these inserts in decreasing intraocular pressure. It is concluded that the brimonidine nanoparticulate ocular inserts can serve as a potential treatment option for glaucoma patients.

5:00 PM SB01.03.13

Poloxamer-Based Thin Film Ocussert for Long-Term Sustained Delivery of Dorzolamide Aishwarya V. Patil¹, Shrikant Joshi², Akshay M. Baheti¹, Amol Tagalpalwar¹ and [Anil Pawar¹](#); ¹Dr. Vishwanath Karad MIT World Peace University, India; ²Maliba Pharmacy College, Uka Tarsadia University, India

Ocular drug delivery is challenging due to the unique anatomical and physiological barriers of the eye that limit drug absorption. Conventional eye drops often have low bioavailability and short residence time on the ocular surface, requiring frequent dosing that leads to poor patient compliance. Ocular inserts or Ocussert offer a promising solution to these issues by providing controlled drug release and sustained therapeutic effects. We developed ocular inserts of dorzolamide using polymers namely polyvinyl alcohol and propylene glycol and poloxamer 407 P. The formulated dorzolamide ocular inserts were studied for in-vitro drug-release profile, ex-vivo transcorneal permeation and in-vivo efficacy in rabbits. An in-vitro study showed sustained release of dorzolamide from the ocular inserts for seven hours. Ex-vivo transcorneal permeability study demonstrated gradual transcorneal permeation of dorzolamide indicating extended-release characteristics. The in-vivo study further validated the efficacy of these inserts in decreasing intraocular pressure. It is concluded that the dorzolamide ocular inserts exhibit a controlled release profile and can serve as a potential treatment option for glaucoma patients.

5:00 PM SB01.03.14

Advanced Breast Cancer Therapy: Thermosensitive Hybrid Hydrogel (PLGA-PEG-PLGA) with Metallic Nanoparticles Enhancing Withaferin-A Release [Mythili Srinivasan](#); School of Health Sciences and Technology, Dr. Vishwanath Karad MIT-World Peace University, India

Background: Drug-delivering copolymers respond to temperature through sol-to-gel transitions. Lower transitions involve micellar growth, while upper transitions bring about micellar structure breakage. The fine-tuned PLGA-PEG-PLGA hydrogel, embedding silver or zinc nanoparticles, achieved a prolonged release of Withaferin-A.

Aim: This study sought to develop a hybrid hydrogel with in situ gel-forming for sustained release, utilizing the PLGA-PEG-PLGA copolymer and incorporating silver and zinc nanoparticles entrapped with Withaferin-A to address breast cancer.

Materials and Methods: PLGA (75:25) to PEG copolymer (3:1 ratio) formulated as *in situ* gel-forming hybrid hydrogel. Characterization involved ¹H NMR, dynamic light scattering, and rheology. Silver and zinc nanoparticles were green synthesized using *Camillia sinensis* extract, and the characteristics of the prepared nanoparticles were analyzed through FTIR, Zeta potential, XRD, TEM, and FE-SEM. Subsequent to the drug entrapment into a hybrid hydrogel, *in vitro* drug release studies were conducted using a trans-diffusion cell apparatus. In vitro cell line studies using MCF-7 and MDA-MB-231 were conducted.

Results: Silver and zinc nanoparticles exhibited a particle size of 255 nm and 128.5 nm, respectively, with zeta potentials of -17.5 mV and -12.9 mV. XRD analysis confirmed 2-theta (deg) values of 56.20 and 56.64 for silver and zinc nanoparticles, respectively. FE-SEM and TEM reports displayed spherical-shaped silver nanoparticles and cylindrical-shaped zinc nanoparticles. Hydrogels demonstrated controlled release of Withaferin-A over 39 to 43 days based on polymer concentration. Effective internalization and antiproliferative impact in MCF-7 and MDA-MB-231 breast malignancy cell lines with negligible hemolytic effects. Zinc Nps induce selective cytotoxicity and apoptosis. Silver NPs exhibited dose-dependent cytotoxicity, inducing cell death and cell cycle hindrance in breast carcinoma cells.

Conclusion: The temperature-responsive PLGA-PEG-PLGA copolymer-based hybrid hydrogel, developed by incorporating silver and zinc nanoparticles, facilitated the sustained and controlled release of Withaferin-A. The formulation exhibits potential for efficient drug delivery in breast cancer therapy, with promising physicochemical properties and drug release kinetics.

5:00 PM SB01.03.15

Advancing Glioblastoma Treatment: Aptamer-Mediated, Long-Circulating, Cationic, PEGylated Hybrid Liposomes with Bavachalcone [Ashwini Y. Chandane](#); Abhinav Education Society's, College of Pharmacy, India

Background: Glioblastoma, a formidable brain tumor, poses a significant therapeutic challenge. Current treatments face limitations due to the infiltrative nature and resistance of glioblastoma cells.

Aim: To explore the brain-targeting efficacy of cationic, long-circulating, targeting PEGylated liposomes incorporating transferrin, folate vitamins, and cationic albumin as aptamers (hybrid-liposomes). These liposomes are entrapped with poly (lactic-co-glycolic acid) (PLGA) nanoparticles containing the anticancer ligand Bavachalcone (BCN), with the goal of advancing therapeutic strategies for glioblastoma.

Materials and Methods: PLGA nanoparticles were formulated to encapsulate Bavachalcone. Characterization involved TEM, FE-SEM, FT-IR, XRD, particle size, and zeta potential analysis, confirming successful formulation. Liposomes were prepared via the ethanol-injection method and characterized using a particle size analyzer, zeta potential, TEM, and CSM. In silico studies encompassed network pharmacology, docking, and simulation for efficacy assessment. In vitro cell line studies utilized U87MG, LN-229, and T98G to evaluate cytotoxic effects.

Results: In silico studies unveiled the potential inhibitory effects of BCN on glioblastoma growth. Prepared NPs exhibited a particle size of 187 ± 0.5 nm, zeta potential of -33 mV, and drug entrapment efficiency of $89.33 \pm 0.5\%$. Liposomes displayed a favorable particle size of 175.5 ± 0.29 nm with a positive surface charge of 8.72 ± 0.53 mV. Encapsulation efficacy was measured at $77.8 \pm 0.61\%$ for BCN. In vitro drug release studies demonstrated significantly higher cumulative release rates of BCN over 82 h. Hybrid liposomes exhibited superior cytotoxicity and accelerated apoptosis in glioblastoma cell lines (U87MG, LN-229, and T98G) through MTT assays. Cellular uptake studies confirmed enhanced internalization in glioblastoma cells. Cell viability assays demonstrated improved cytotoxic effects on glioblastoma cells.

Conclusion: Bavachalcone exhibited promise against glioblastoma, supported by in silico and in vitro studies. Hybrid liposomes offer an innovative approach for enhanced drug delivery, addressing BBB challenges. This approach sheds light on the potential of natural compounds and nanotechnology for enhanced glioblastoma treatment.

5:00 PM SB01.03.16

Chitosan Modified Hydrophobic Bacterial Cellulose as Skin Patches: Role of Simvastatin as a Model Drug in The Novel Drug Delivery Applications Peddapannagari Kalyani and Mudrika Khandelwal; Indian Institute of Technology Hyderabad, India

Bacterial cellulose (BC) is nanofibrous with ultra-fine network, and hydrophilic in nature is being used as a drug carrier for immediate drug release applications. One of the benefits of using BC is that it offers a burst release of water-soluble drugs and limited to release of hydrophobic drugs for longer period. In our research, we modified BC with chitosan solution and without solution under ultrasonication by means of ex-situ modification and air dried. We achieved a water contact angle greater than 95, obtained hydrophobic modified BC as skin patches with the dimensions of 2*2 cm (about 0.79 in). To understand the characteristics of hydrophobic BC based skin patches, we conducted characterization studies by using FT-IR, DSC, BET, SEM, contact angle, swelling studies. Drug release studies were conducted by using Simvastatin as model drug for hydrophobic drug for two different concentrations. To know the drug release kinetics and mechanism of drug release, applied the various mathematical model fitting by applying Zero order, First order, Higuchi model, Korsmeyer Peppas model. The results showed that simple processed airdried BC is able to release the maximum amount of hydrophobic drug over 15 days (about 2 weeks) but chitosan modified BC has taken 40 days (about 1 and a half months) to get release maximum amount of drug. In this research, we achieved the sustain release of hydrophobic drug through effortless processes of ultrasonication and drying, but we further extend the release of hydrophobic drug by using hydrophobic modified BC. The goodness of fitting changes from first order to zero order and mechanism of drug release also changes from quasi-fickian to non-fickian for unmodified BC and hydrophobic BC respectively. Hence, we taken Simvastatin as a model drug for hydrophobic drug and maintains the drug profile over 40 days. Also, one can understand that hydrophobic modification to the BC matrix could find advantages over solubility issues of hydrophobic drugs, entrapment into the matrix, good skin permeation, good mechanical properties, long durability etc. However, BC has the emerging drug matrix for skin patches but achieving hydrophobicity with good barrier properties led to challenging outbreak for sustained release transdermal drug carrier especially long-term skin patches. The obtained chitosan modified BC skin patches most useful in the monthly basis hormonal pills for birth control and thyroid management due to missing dose may hamper the regular activity of specific glands and also maintains constant therapeutic dose over period of time. Hence, most of the marketed drugs are in the form of hydrophobic in nature, the hydrophobic BC matrix could explore the novel drug delivery applications of sustained release novel drug delivery for hormonal management, thyroid treatment, cardiovascular disease, central nervous diseases, cigarette cessation, motion sickness, arthritis, diabetics, hyperlipidemia etc.

5:00 PM SB01.03.17

Thermosusceptible Nitric-Oxide- Releasing Nitrofoam Antitumor Immune Responses with Tumor Collagen Diminution and Deep Tissue Delivery using NIR Laser- Assisted Photodynamic Therapy In-Kyu Park¹ and Yong-Kyu Lee²; ¹Chonnam National University, Korea (the Republic of); ²Korea National University of Transportation, Korea (the Republic of)

Combined cancer immunotherapy has demonstrated promising potential with an amplified antitumor response and immunosuppressive tumor microenvironment (TME) modulation. However, one of the main issues that cause treatment failure is the poor diffusion and insufficient penetration of therapeutic and immunomodulatory agents in solid tumors. Herein, a cancer treatment approach that combines photothermal therapy (PTT) and nitric oxide (NO) gas therapy for tumor extracellular matrix (ECM) degradation, along with NLG919, an indoleamine 2,3-dioxygenase (IDO) inhibitor that reduces tryptophan catabolism to kynurenine, and DMXAA, a stimulator of interferon gene (STING) agonist that stimulates antigen cross-presentation, is proposed to overcome this issue. Upon NIR (808 nm) laser irradiation, NO-GEL achieved the desired thermal ablation by releasing sufficient tumor antigens through immunogenic cell death (ICD). NO delivery triggered local diffusion of excess NO gas for effectively degrading tumor collagen in the ECM, homogeneously delivered NLG919 throughout the tumor tissue, inhibited IDO expression that was upregulated by PTT, and reduced the immune suppressive activities. The sustained release of DMXAA prolonged dendritic cell maturation and CD8⁺ T cell activation against the tumor. In summary, NO-GEL therapeutics offer a significant tumor regression with PTT and STING agonist combination that stimulates a durable antitumor immune response. Additional upregulation of IDO inhibition during PTT supplements the immunotherapy by reducing the T cell apoptosis and immune suppressive cell infiltration to TME. NO-GEL with the STING agonist and IDO inhibitor is an effective therapeutic combination to counter possible limitations during solid tumor immunotherapy.

5:00 PM SB01.03.18

Sodium Chloride Nanoparticles as Radiosensitizers Xinning Lai; University of Georgia, United States

Previous studies have demonstrated that SCNPs can enter cells through endocytosis and disrupt osmotic balance by releasing sodium and chloride ions. This process leads to cancer cell death. It's speculated that the SCNPs might affect the levels of other ions in the cells and have a significant impact on the redox balance. The research suggests that combining SCNPs with radiation therapy could enhance the effectiveness of the treatment. Radiation therapy works by ionizing molecules, especially water, to produce radicals that damage biomolecules like DNA. SCNPs might enhance this effect by promoting the production of reactive oxygen species (ROS).

In particular, we are interested in exploring SCNPs as a radiosensitizer for head and neck squamous cell carcinoma (HNSCC). HNSCC, a significant and increasingly common malignancy, often requires treatment through surgery or radiotherapy. However, these treatments have limitations, including toxicity and a high risk of recurrence. Combining chemotherapy with radiotherapy increases efficacy but also the risk of systemic toxicities. SCNPs are considered as a potential new treatment modality that could improve efficacy without adding toxicity.

In this study, we synthesized and characterized folate-conjugated sodium chloride nanoparticles (SCNPs@folate) and explored their potential as radiation sensitizers in HNSCC. Our results showed that the nanoparticles exhibited proficient cellular uptake and increased intracellular levels of sodium and chloride. Interestingly, the increase in sodium levels also causes calcium influx through the NCX, triggering an increase in ROS. We found that the ROS-

promoting effect works in tandem with IR, leading to GSH depletion, resulting in DNA and lipid damage, and ultimately cell death. Our in vitro results showed that there is a synergistic effect between SCNPs@folate and IR. In vivo studies showed that intratumorally injection of SCNPs@folate combined with irradiation resulted in a significant improvement in tumor growth inhibition compared to IR alone and a higher percentage of tumor-free mice. Taken together, our studies suggest a great potential of SCNPs@folate as a radiosensitizer in HNSCC.

SESSION SB01.04: Bioresponsive Nanotheranostics III

Session Chairs: Ruirui Qiao and Hao Song

Wednesday Morning, April 24, 2024

Room 428, Level 4, Summit

8:15 AM SB01.04.01

Multi-Pronged Approach for Targeting Oral Biofilms Keuna Jeon, Nesha Andoy and Ruby Sullan; University of Toronto, Canada

The oral microbiome is a complex system consisting of numerous bacterial species that plays host to both beneficial and harmful organisms. Among the pathogenic species in the oral cavity is *Streptococcus mutans* (*S. mutans*), the primary agent responsible for dental caries. Different antimicrobial-based strategies have been developed to tackle this problem, but the rise of antibiotic resistance among microorganisms necessitated the development of new and effective therapeutics. One such solution is the *de novo* antimicrobial peptide (AMP), GH12, which has showed potency against cariogenic bacteria. GH12 has a high content of α -helical structures that facilitate pore formation on bacterial membranes. Quorum sensing molecules such as competence stimulating peptides (CSP) have been identified as communicator molecules in bacterial species that are used to monitor not only their own but other species in their surroundings. Recently, polyserotonin (PSe) has emerged as a photothermally active nanomaterial that shows promise towards biomedical applications. In this work, I made a cocktail combining all three of the aforementioned components—AMP for bacterial killing, CSP for targeting, and PSe for localized heating—to develop a multi-pronged approach aimed to increase antibiofilm efficacy. My findings indicate that the presence of both peptides, membrane damaging and competence stimulating, in conjunction with the photothermally active PSe, effectively inhibited the growth of *S. mutans* in both planktonic and biofilm states. Overall, these results reinforced that the strategic use of multi-pronged therapeutic approaches could reduce cariogenic bacteria within the oral microbiome.

8:30 AM *SB01.04.02

Developing MRI-Based Therapeutic and Diagnostic Tools: From Cancer to Chemical Weapons Gemma-Louise Davies; University of Birmingham, United Kingdom

Magnetic resonance imaging (MRI) is a powerful non-invasive technique which becomes considerably more potent when contrast agents (CAs) are introduced. Molecular contrast agents based on Gd-chelates (e.g. Dotarem®) are regularly used in the clinic, however these usually lack specificity for selective disease or biomarker diagnostics, and can also suffer from poor signal-to-noise and blood circulation half-life, which can limit their clinical utility. Carefully designed contrast agents, and contrast agents based on nanomaterials have the potential to overcome these issues. In this talk, I will introduce our approaches to the careful design and development of MRI contrast agents tuned for different applications. I will describe nanostructured composites capable of reporting on drug release in a unique non-invasive way, of use for the pharmacokinetic mapping of drug release towards personalised medicine. I will also discuss recent advances in the diagnosis of chemical weapon poisoning using molecular contrast agents.

9:00 AM SB01.04.03

Precision in Colorimetric Sweat Sensing through Machine Learning Lijun Zhou, Minqin Zhang and Mohammad H. Malakooti; University of Washington, United States

Sweat contains diverse biochemicals that can serve as a source for detecting biomarkers, particularly in individuals with chronic conditions like diabetes. Non-invasive sweat sensors have gained popularity in various applications, promoting personalized healthcare and daily convenience. Different methods, including electrochemical, fluorescence, and colorimetric approaches, have been employed for real-time sweat analysis. Among these methods, colorimetric sensors stand out for their accuracy, stability, and portability in addition to their scalability in production processes. However, the main challenge in colorimetric sweat sensing currently lies in two areas: the need for improved sensor accuracy and the precise detection of color changes resulting from sweat exposure.

In this presentation, we will showcase the development of our sensors, offering real-time, stable, and rapid monitoring of glucose concentration and pH value without causing discomfort. The detection process takes approximately five minutes. Most notably, we address the challenge of detecting subtle color changes, which are virtually imperceptible to the naked eye, by leveraging artificial intelligence. We will discuss how the utilization of a breathable, bio-compatible, acid-base-balanced cotton substrate is the key to achieving higher color differences. In a series of experiments, we cover the fabrication and testing of two generations of pH sensors and two types of glucose sensors. We will then demonstrate the application of machine learning to our sensors and how it significantly enhances prediction accuracy. Three machine learning algorithms, namely Linear Discriminant Analysis (LDA), Support Vector Machine (SVM), and Convolutional Neural Network (CNN) are applied, demonstrating stable and excellent prediction accuracy of 90% for the test results. Finally, we will showcase the practical application of our combined pH and glucose sensors within a single substrate. This work contributes to the advancement of sensor preparation techniques and underscores the critical role of accurate machine-learning algorithms in the successful utilization of sweat sensors across various domains.

9:15 AM SB01.04.04

Collectively Interacting Colloidal Magnetic Nanoparticles with Strong AC Field Response for Remote Imaging and Thermometry Adam Biacchi, Thinh Bui, Frank Abel, Eduardo Correa, Samuel Oberdick, Curt Richter, Cindi Dennis, Solomon Woods and Angela R. Hight Walker; National Institute of Standards and Technology, United States

Colloidal magnetic nanoparticles (MNPs) are an important class of nanomaterials being investigated for use in a host of therapeutic and diagnostic modalities such as medical imaging, remote sensing, drug delivery, and hyperthermia.¹ These applications exploit the very soft ferrimagnetic magnetic behavior found in certain materials, often ferrites, when they are confined to tens of nanometers in diameter or less. Such nanomagnets can produce a strong collective response to applied alternating current (AC) magnetic fields, while simultaneously remaining dispersed in liquid media.

Recently, remote magnetic imaging of temperature has been identified as an exciting potential diagnostic application of colloidal MNPs. This thermometry measurement employs dispersed particles to construct a 3D visual representation of temperature throughout a volume. The technique, which is a variation

on the magnetic particle imaging (MPI) modality, is based on the temperature-dependent response of MNPs to an applied AC magnetic field. Additionally, when applying high-frequency magnetic fields, these MNPs can also generate localized heating, thus allowing them to function as nanotheranostics. However, significant challenges remain in the development of this technology, including a need to finely engineer MNPs to increase both their magnetic thermosensitivity and magnitude of AC response.

Here, we report on our development of MNPs, both as liquid dispersions and solid assemblies, specifically designed with a robust response to applied AC magnetic fields for imaging, thermometry, and temperature control. A series of colloidal nanocrystals based on ferrites were synthesized *via* highly tailorable and commercializable solution chemistry routes.² Careful selection of the synthetic reagents and precursor thermal decomposition kinetics allow for control of the resultant MNP composition (Fe, Co, Zn, V ratios) and size (5-80 nm). These MNPs were then investigated using solid- and liquid-phase AC and DC field magnetometry measurements. A home-built arbitrary-wave magnetic particle spectrometer was employed to perform relaxometry and measure magnetic AC susceptibility, allowing for a rigorous analysis of the temperature- and frequency-dependent AC response from 1 Hz to 30 MHz. The results were cross-correlated with detailed structural characterization including X-ray diffraction, light scattering, optical spectroscopy, and high-resolution electron microscopy to develop a set of structure-property relationships.

Finally, we tune these parameters to optimize spatial imaging of MNP magnetic response and a robust thermosensitive AC magnetic signal using magnetic particle imaging and thermometry instrumentation specifically developed for these applications.³ We find particle size and compositional doping act as levers to optimize the AC response through the manipulation of interparticle and intraparticle magnetic spin interactions. Using these guidelines, we find the set of structural parameters that produce the most robust thermosensitive magnetic response and conduct imaging experiments whereby spatial reconstructions of colloidal MNP magnetic response are generated. The key to this improved performance, in both liquid and solid media, is the field-induced linear alignment of strongly interacting MNPs, resulting in a substantially augmented magnetic anisotropy. Collectively, these studies illuminate the complex behavior of MNPs under AC driving fields, reveal extensive correlations between nanoscale structure and magnetic response, and provide guidelines for the design of MNPs used in magnetic imaging, thermal sensing, and therapeutic applications.

[1] Shasha and Krishnan *Adv. Mater.*, 33, 1904131 (2021)

[2] Biacchi *et al. Int. J. Magn. Part. Imaging*, 6, 2 Suppl 1 (2020); Biacchi *et al. Chem. Mater.*, 34, 2907-2918 (2022)

[3] Bui *et al. J. Appl. Phys.*, 128, 224901 (2020); Bui *et al. Appl. Phys. Lett.*, 120, 012407 (2022)

9:30 AM *SB01.04.05

Dynamic Nano-Assemblies for Biological Sensing, Imaging and Therapy Dai S. Ling; Shanghai Jiao Tong University, China

Inspired by the living systems that constantly undergo dynamic processes to maintain metabolic homeostasis, the Dynamic Nano-Assemblies have been developed to tackle complicated diseased environment for various biomedical applications. The materials composing the nanoparticles produce fascinating and diverse functionalities. The controllable assembly mediated by a multitude of different ligands would lead to the flexible modulation of nanomaterials' fate *in vivo*, endowing the nanoplatform with targeted delivery and accumulation to disease lesions. The clever combination of different functional components via the ligands directed co-assemblies would lead to the development of multifunctional nano-biomedical platforms for ion selective imaging, targeted delivery, fast diagnosis, biological regulation and efficient therapy. Furthermore, the ingenious control over the assembly/disassembly process based on small-sized functional nanoparticles could achieve both *in vivo* targeted delivery and stimuli-responsive disassembly for efficient disease therapy and bioelimination. Overall, dynamic nano-assemblies based biomaterials and drug delivery systems can achieve the improved diagnostic accuracy and therapeutic efficacy in many diseases including cancer, infection and neurodegenerative diseases.

10:00 AM BREAK

10:30 AM *SB01.04.06

Curcumin Derived Nanoscale Coordination Polymers for Modulating Stress Response in Plants Xin Zhang¹, Kangkang Feng², Yiyang Cong², Binqing Tao¹ and Hao Hong²; ¹Jiangsu Academy of Agriculture Sciences, China; ²Nanjing University, China

Aim/Introduction:

Different stressing factors (e.g. drought, viral infection, insects, etc.) can impose significant survival threats to plants, especially in agricultural scenarios. Strategies to alleviate these stress burdens are able to improve plant physiology and adapt them to more "unfriendly" environment. Nanotechnology is a rising star to ameliorate plant stress situation. The goal of this study is to develop a curcumin-metal coordination nanoplatform with intrinsic protecting capacity against various stressing factors in chosen plants (*Arabidopsis thaliana* and wheat selected as the patients), and it can simultaneously deliver therapeutic cargos to further improve plants survival against various stressing factors.

Materials and Methods:

Curcumin (Cur) was reacted with manganese acetate or zinc acetate by a solvothermal method to form porous nanostructures. X-ray diffraction analysis revealed the crystal structures from both Cur-Mn and Cur-Zn. The morphology, stability, and other physical properties from Cur-Mn and Cur-Zn were also evaluated. The biocompatibility of Cur-Mn/Cur-Zn was tested in *Arabidopsis thaliana* and wheat cells and plants. Subsequently, the biological impacts of Cur-Mn/Cur-Zn along with their distribution profiles in these plants were measured post the spray of a suspension of 50 µg/mL. The cargo accommodating and releasing capacity was tested for fludioxonil, a broad-spectrum bacteria and fungi killing molecule. Finally, the molecular mechanisms of Cur-Mn/Cur-Zn for stress resistance in these two plants were also explored.

Results:

Cur-Mn and Cur-Zn had a size range of 60-90 nm (measured by TEM) with good dispersity and production yields. In their structures, curcumin was coordinated with manganese/zinc to form framework structures. Cur-Mn and Cur-Zn could be internalized into *Arabidopsis thaliana* and wheat cells with no noticeable toxicity. Once applied in the plant leaves, these materials could be absorbed quickly and transported via vessels inside plant stem, and reached the roots and other plant parts in a timely manner. Pure Cur-Mn and Cur-Zn could add the drought resistance capacity to these plants, and the molecular mechanisms were clarified by RNA-seq techniques. Moreover, Cur-Zn could accommodate more than 40% w/w of fludioxonil, and protect it from UV degradation. Once applied in the field of wheat, fludioxonil@Cur-Zn could protect wheat plants from fusarium blight in a more persistent manner.

Conclusion:

As a natural compound from the plant, curcumin can coordinate with different metals to form nanosized materials, and our findings revealed that this "from plant, to plant" strategy could be an efficient tool to protect plants from multiple critical stress factors, broadly applicable in plant rescue.

11:00 AM SB01.04.07

Understanding Structure and Stability for The Development of Novel Artificial Oxygen Carriers [Martin A. Schroer](#)¹, Jan-Eric Sydow², Fabian Nocke², Ozan Karaman² and Katja B. Ferenz^{2,1}; ¹University of Duisburg-Essen, Germany; ²University Hospital Essen / University of Duisburg-Essen, Germany

Red blood cell concentrates (RBC) are an indispensable tool in various clinical scenarios; however, the available quantity is already highly limited, which will become an even more severe problem in the future. To overcome these peculiarities and limitations of RBCs, we developed albumin-derived perfluorocarbon-based artificial oxygen carriers (A-AOCs), that are comprised of a perfluorodecalin (PFD) nano-emulsion core and an albumin shell, and have already successfully supplied oxygen in extra-corporally perfused hearts and various animal models [1].

The structure and stability of A-AOCs is sensitive to changes of the carrier solution, so we need to learn more about the structure and structural changes on the nanoscale. Conventional characterization techniques lack the spatial resolution (e.g. light scattering) or need dried and consequently non-physiological samples (e.g. SEM, TEM), and thus yield limited information on A-AOC structure in solution. We therefore use X-ray scattering techniques to study A-AOCs, which do not have such limitations and allow also to study dense, opaque suspensions.

In this contribution, we present recent results of X-ray scattering measurements on A-AOCs covering a wide, clinical-relevant concentration and temperature range. We investigate A-AOCs from different synthesis approaches, using ultra-sound [2] and microfluidizing techniques, which reveal different sizes and stabilities. Based on these findings, it is now possible to optimize the synthesis parameters, in order to yield stable A-AOCs of desired size and dispersity.

This study demonstrates the huge potential of X-ray scattering for the study of pharmaceutical and medical-relevant samples [3], with direct implications for the development of new formulations.

References:

[1] J. Jägers, A. Wrobeln, K. B. Ferenz, *Pflugers. Arch.* **473**, 139 (2021).

[2] A. Wrobeln, J. Laudien, C. Gross-Heitfeld, J. Linders, C. Mayer, B. Wilde, T. Knoll, D. Naglav, M. Kirsch, K. B. Ferenz, *Eur. J. Pharm. Biopharm.* **115**, 52 (2017).

[3] S. S. Nogueira, A. Schlegel, K. Maxeiner, B. Weber, M. Barz, M. A. Schroer, C. E. Blanchet, D. I. Svergun, S. Ramishetti, D. Peer, P. Langguth, U. Sahin, H. Haas, *ACS Appl. Nano Mater.* **3**, 1063 (2020).

11:15 AM SB01.04.08

Versatile Application of Nanoscale Metal-Organic Frameworks for Intratumoral Delivery [Eunseo Choi](#) and Conroy Sun; Oregon State University, United States

Recent preclinical and clinical studies have highlighted the improved outcomes of combination radiotherapy and immunotherapy. Concurrently, the development of high atomic number (high-Z) metallic nanoparticles as radiation dose enhancers has been explored to widen the therapeutic window of radiotherapy and potentially enhance immune activation. Due to their high X-ray attenuation and high density, metal-based nanoparticles also have the potential to serve as imaging agents. Exploiting high-Z metal nanoparticles would provide clinical advantages for image-guided radiotherapy for targeted cancer treatment.

Despite the numerous advances in the field of drug delivery, there are still unmet needs that could lead to the development of a therapeutic molecule delivery carrier. In this study, we seek intratumoral delivery of metal-organic frameworks to induce a robust stimulation of anticancer immunity for a systemic and long-lasting therapeutic benefit. By utilizing hafnium and iron-based metal-organic frameworks, we target immune cells with other targeted cancer therapies for synergistic advantages. We employ this nanomaterial as a pharmaceutical carrier system for the delivery of a wide range of materials, from small molecules to macromolecules. Radiotherapy-induced local tissue damage and inflammation have the potential to generate tumor antigen and release danger-associated molecular patterns. Nanoscale metal-organic frameworks are a versatile platform for combination radiotherapy. In addition to serving as drug carriers, our high-Z metal-organic frameworks are attractive nanomaterials that serve as contrast agents in biomedical imaging. We conducted phantom studies *in vitro* and *in vivo*, using microCT for the real-time monitoring, which will facilitate advanced analysis of tumor cells and their responses to therapy. Intratumoral immunotherapy provides the capacity to manipulate the tumor microenvironment by targeting cells within the tumor microenvironment, making it an attractive therapeutic approach.

11:30 AM *SB01.04.09

Understanding Biological Processes Using Responsive Polymers and Bio-Orthogonal Chemistries [Kristofer J. Thurecht](#), Nicholas Fletcher, Gayathri Ediriweera and Craig Bell; The University of Queensland, Australia

The evolution of therapeutic systems for cancer therapy has offered the opportunity to treat more complex and refractory disease. However, there still remains key challenges around quantitatively determining the tissue specific drug release profile of therapies. It is crucial, then, for materials to be precisely engineered to allow direct assessment of their behaviour in biological systems, as well as provide feedback on biological responses. Central to this thinking is the development of theranostics, which are materials that are able to provide both spatial and temporal information about therapeutic delivery and efficacy.

Our research explores a number of avenues related to materials engineering that can provide unique insights into therapeutic efficacy of nanomedicines, where biological cues can be utilised to give realtime feedback of drug effects. Alternatively, exogenous stimuli can also be applied resulting in material changes to the delivery system. Such stimuli can be administered as applied radiation (often in the form of visible/near infrared radiation), or through chemical stimuli that take advantage of the bio-orthogonality of defined covalent reactions. Bio-orthogonal reactions that take advantage of pre-targeting, allow diagnostic and therapeutic probes to be administered with greater site-specificity to diseased tissue.

In this presentation, I will present our work exploring novel approaches to utilise the pre-targeting strategy and bio-orthogonal reactions to improve therapeutic delivery to tumours while provided realtime readout of therapeutic activity. By exploiting the multivalency and multimodality of polymeric nanomaterials, the true advantages of theranostics can be realised in nanomaterial systems.

Wednesday Afternoon, April 24, 2024
Room 428, Level 4, Summit

1:45 PM *SB01.05.01

Biomaterials to Boost Cancer Immunotherapy Zhuang Liu; Soochow University, China

Cancer immunotherapy has attracted tremendous attention in recent years. In our recent studies, by employing rationally designed biomaterials as well as nanoscale delivery systems, we are able to enhance cancer immunotherapy via developing novel nano-vaccines, modulating tumor microenvironment, and achieving combinational immunotherapy, as evidenced by various animal model experiments. In this presentation, I would introduce our latest efforts in this exciting research direction. In particular, we have tried to combine various types of local tumor treatment methods with immunotherapy using biomaterials as the bridge. Stimulated by the tumor antigens released after local tumor ablation, the triggered immunological responses in combination with immune checkpoint blockade (ICB) therapy could result in effective inhibition of tumor cells remaining in the body, promising for treatment of cancer metastasis. A strong immune-memory effect could also be observed after such treatment. Beyond that, we are also working on biomaterials that are capable of modulating tumor microenvironment for enhanced immunotherapy. A start-up company has been founded based on the technologies from our laboratory. Several pipelines are now being tested in clinical trials.

2:15 PM SB01.05.02

Lactate Oxidase Nanocapsules Boost T Cell Immunity and Efficacy of Cancer Immunotherapy Zheng Cao^{1,1}, Duo Xu¹, Wenting Chen¹, Yunfeng Lu^{2,1} and Jing Wen^{1,1}; ¹University of California, Los Angeles, United States; ²Beijing University of Chemical Technology, China

Cancer immunotherapy has reshaped the landscape of cancer treatment, but its effectiveness in solid tumors is limited by the overproduction of lactate by cancer cells. Extensive trials are being conducted to reduce lactate concentrations through inhibiting lactate dehydrogenase. However, such inhibitors often disrupt the metabolism of healthy cells and cause non-specific toxicity. In contrast to those strategies, we target lactate itself with an enzyme, lactate oxidase, which effectively reduces lactate concentrations and releases hydrogen peroxide, an immunostimulatory molecule, in the tumor microenvironment. However, recombinant lactate oxidase from microorganisms possesses short circulating half-life, low enzyme activity, and potential immunogenicity. To circumvent this limitation, we report herein a nano-encapsulating strategy to encapsulate lactate oxidase molecules within a thin polymer shell through in-situ polymerization, affording the synthesis of nanocapsules. The nanocapsules stabilize lactate oxidase and prevent it from proteolysis and denature, minimize the immunogenicity, prolong the circulating half-life, enabling their use as a potent therapeutic for cancer immunotherapy. Lactate oxidase nanocapsules can promote the proliferation and activation of effector T cells and suppress tumor-resident regulatory T cells *in vitro*. As further demonstrated in a murine melanoma model and a humanized mouse model of triple-negative breast cancer, nanocapsules avert tumor immunosuppression and enhance anti-tumor T cell immunity by upregulating gene expression for T cell recruitment and activation, as confirmed by single-cell RNA sequencing. Such multifunctional lactate oxidase nanocapsules lead to improved efficacy of immunotherapies for solid tumors.

2:30 PM BREAK

3:30 PM *SB01.05.03

Electrospun Nanofibers for Tissue Repair and Regeneration Jiajia Xue; Beijing University of Chemical Technology, China

Electrospun nanofibers have been widely applied for tissue repair and regeneration because of their advantages of mimicking the structure and composition of extracellular matrix to a certain extent. We have developed a series of scaffolds based on electrospun nanofibers to promote the repair and regeneration of peripheral nerve, bone, and skin. To improve the repair efficacy of peripheral nerve injury, we have constructed a nerve guidance conduit based on electrospun nanofibers in a bionic design to simulate the microenvironment required for nerve repair. Nerve growth factor and indocyanine green were loaded in phase change material particles and then deposited between two layers of electrospun nanofiber membranes to obtain a photothermal responsive scaffold. Upon the irradiation of a near-infrared laser, nerve growth factor was triggered to be released from the scaffold, promoting the axon extension. In addition, we deposited a density gradient of bioactive nanoparticles on the surface of uniaxially aligned fibers to guide the axon extension and accelerate cell migration along the direction of increasing the density of the nanoparticles. We further constructed degradable hydrogels in the lumen and regulated the degradation rate of the hydrogel to be increased from the proximal to distal position, allowing for the long-term delivery of growth factor loaded in the hydrogel and promoting the regeneration of sciatic nerve in rat. Additionally, we conducted large animal experiments in sheep to explore the effects of multi-channel nanofibrous nerve conduit on sheep nerve injury repair. For the repair of skin wounds, according to the demand of various growth factors in each stage of repair period, we constructed a multi-layered nanofibrous scaffold with a radially aligned nanofibrous inner surface. The scaffold effectively integrated multiple induced signals such as topography, bioactive factors and photothermal response to achieve spatiotemporally controlled delivery and accelerated wound healing. Combined with photothermal effects, we constructed a multifunctional bone repair scaffold to recruit stem cells and induce their osteogenic differentiation to improve the repair of bone defects. We also developed gradient self-assembled activated fiber scaffolds to induce osteogenic differentiation of stem cells. In summary, electrospun nanofibers can be applied to construct multifunctional tissue repair materials to promote tissue injury repair and regeneration.

4:00 PM SB01.05.04

Effects of Sequential Ultrasound Irradiation in The KHz and MHz Bands on Transdermal Administration of Biopolymeric Drugs Kengo Matsubara and Yuta Kurashina; Tokyo University of Agriculture and Technology, Japan

Introduction

Biopolymeric drugs are expected to have high efficacy and minimal side effects due to their specificity. Meanwhile, a minimally invasive method of administering these drugs is difficult to establish. As one of the attracting methods, sonophoresis is a method of drug-administering by disrupting the stratum corneum layer through the collapse of cavitation bubbles and drug infusion by the microjets induced by the bubbles (N. Deagicevic, *et al.*, *Springer* 2017). However, the amount of drugs administered by conventional techniques is limited, since the randomness of the microjets generated from cavitation bubbles makes stable drug infusion difficult. This is because the position of the bubble nucleus for the generation of cavitation bubbles is unstable and not directional.

Here, we propose an ultrasound irradiation method with multiband to achieve efficient transdermal administration of biopolymeric drugs. Especially, the synergistic effect of cavitation induced by low-frequency and acoustic streaming induced by high-frequency on drug administration is demonstrated by sequentially irradiating in the kHz and MHz bands with fluorescence-modified ovalbumin (OVA, for nano-sized drug model).

Materials and methods

Transdermal administration experiments with fluorescence-modified OVA to porcine skin irradiated by ultrasound (US) were carried out on the effectiveness of acoustic streaming by sequential irradiation in the kHz and MHz bands. Here, the irradiation distance of the acoustic streaming on the drug

dosage was evaluated. Ultrasound irradiation was experimented under the following four conditions. As a conventional method (i), US in the kHz band was applied for 10 min (control). (ii)-(iv) As the method proposed, US in the kHz band and MHz band was sequentially applied for 5 min., respectively. The MHz band was irradiated at a distance of (ii) 1 mm, (iii) 2 mm, and (iv) 3 mm. After irradiation of multiband US, the skin from each condition was lysed, and the fluorescence intensity of cyanine 5 modified OVA was measured by a spectrofluorometer to evaluate the dose of the nano-drug model quantitatively.

Results and discussion

In order to investigate the effect of acoustic streaming on the proposed method, the ultrasonic irradiation device was constructed using two types of transducers. A Langevin transducer with a resonance frequency of 45.9 kHz was used for kHz band irradiation (X. Xie, *et. al.*, *J Drug Deliv Sci Technol* 2022), and a piezoelectric device with a resonance frequency of 1.97 MHz was utilized for MHz band irradiation. The velocity of acoustic streaming is expressed as a function that depends on the distance from the irradiation source (J. Friend *et. al.*, *Lab Chip* 2019). The results obtained from the function suggest that under the conditions of this study, the flow velocity rises with increasing irradiation distance in the MHz band. This calculated outcome shows that the drug dosage increases in the range of 1 mm to 3 mm. The results of fluorescence intensity measurements for each condition suggested that the highest drug dose was obtained when the US in the MHz band was irradiated at an irradiation distance of 3 mm after irradiation of the US in the kHz band. Furthermore, as with the theoretical value, the drug dose significantly rose with increasing irradiation distance (i) vs (iv): * $p < 0.05$, (ii) vs (iv): ** $p < 0.01$, Student's *t*-test). These results suggest that sequential irradiation of the kHz and MHz bands is more effective than conventional irradiation of only the kHz band. Therefore, the acoustic streaming induced by the MHz band contributes to the improvement of drug dosage for sonophoresis. The development of the multiband US administration method enables us to propose minimally invasive biomacromolecule drug administration as an alternative to injection. Therefore, this method is expected to contribute to the development of research on biopolymeric drug materials.

4:15 PM SB01.05.05

Magnetic Liquid Marbles as Thermo-Responsive Materials under Alternating Magnetic Fields Rafal Bielas¹, Tomasz Kubiak¹, Matus Molcan², Ivo Safarik³ and Arkadiusz Jozefczak¹; ¹Faculty of Physics, Adam Mickiewicz University in Poznan, Poland; ²Institute of Experimental Physics, Slovak Academy of Sciences, Slovakia; ³Biology Centre, ISB, Czech Academy of Sciences, Czechia

Responsive materials are essential in modern scientific and industrial fields. Within this context, the potential to control these materials using external stimuli, such as magnetic fields, is of great interest. Magnetic liquid marbles—airborne droplets surrounded by particles—are emerging as suitable candidates for such purposes. For example, their ability to open and close on-demand using static magnetic fields makes them ideal for specialized tasks, such as testing fragile entrapped species [1].

When exposed to alternating magnetic fields, the internal temperature of liquid marbles rises, a phenomenon attributed to magnetic energy dissipation due to magnetic relaxation and hysteresis processes. Elevated temperature can be employed for functions like amplifying DNA contained within the particle shell of these marbles [2]. Building on this, we propose utilizing magnetic heating to modulate thermo-responsive liquid marbles.

In our experiments, we prepared liquid marbles with a ferrofluid, which included agar powder and either maghemite nanoparticles or magnetosomes (nanoparticles from magnetotactic bacteria). The droplets were coated with either polymer or bio-particles and then exposed to an alternating magnetic field with a kHz frequency. The resulting temperature increase inside the liquid marbles initiated varied reactions depending on their particle coating. With polymer particles, a combination of partial particle fusion and enhanced evaporation led to the creation of rigid magnetic shell residuals, which could be seen as precursors to a new generation of liquid marbles [3]. On the other hand, for non-thermo-responsive particle coatings, such as *lycopodium* shell, the liquid core underwent partial disintegration driven by reversal process of gelation. The diverse structures observed after the magnetic heating procedure may provide new way for developing materials suitable for applications like smart lotions or creating new types of capsules for theranostic procedures.

The work was supported by Polish National Science Center through the project no. 2019/35/N/ST5/00402.

References:

- [1] Zhao, Yan, et al. "Magnetic Liquid Marbles: Toward "Lab in a Droplet"." *Advanced Functional Materials* 25.3 (2015): 437-444.
- [2] Li, Hualin, et al. "Magnetothermal Miniature Reactors Based on Fe₃O₄ Nanocube-Coated Liquid Marbles." *Advanced Healthcare Materials* 10.6 (2021): 2001658.
- [3] Bielas, Rafal, et al. "Tunable Particle Shells of Thermo-Responsive Liquid Marbles under Alternating Magnetic Field." *Journal of Molecular Liquid* 391 (2023): 123283.

4:30 PM SB01.05.06

Radiation-Activated Ferroptosis with Liposome Nanoparticles Encapsulating 7-Dehydrocholesterol Enhancing Antitumor Immune Responses Jianwen Li, Zhizi Feng, Xinning Lai, Wei Yang, Shuyue Zhan and Jin Xie; University of Georgia, United States

In this project, we explore an approach that triggers ferroptosis and enhances antitumor immune responses by external radiation. The key component of this technology is 7-dehydrocholesterol (7DHC), a natural biosynthetic precursor of cholesterol. This zoosterol can react with radiation-induced reactive oxygen species (ROS), initiating a radical chain reaction between 7DHC and polyunsaturated fatty acids (PUFAs) in cell membranes. We show that this interaction leads to direct lipid peroxidation, culminating in cell death *via* ferroptosis. In terms of delivery, we show that 7DHC, similar to cholesterol, can be incorporated into the lipid layer of liposomes. To improve targeting, we incorporated NTS_{mut}, a ligand for NTSR1 that is overexpressed in multiple malignancies, into liposomal nanoparticles. Our tests show that these NTS_{mut}-incorporated and 7DHC-loaded liposomal nanoparticles are minimally toxic, but significantly enhance the efficacy of radiation by activating ferroptosis in cancer cells. As a highly immunogenic cell death (ICD) pathway, ferroptosis induced by our treatment further triggers the increased secretion of danger-associated molecular patterns (DAMPs) and elevated surface exposure of "eat-me" signals such as ATP, IFN- β and calreticulin. These patterns are then sensed by antigen-presenting cells such as dendritic cells (DCs), in turn boosting T cell driven adaptive immunity. Such a strategy of controlled activation of ferroptosis offers a favorable therapeutic index and opens avenues for clinical application.

4:45 PM SB01.05.07

Advancing Targeted Drug Delivery via Optimization of Drug-Loaded Polymeric Nanoparticles and Red Blood Cell-Mediated Approaches Hermon P. Girmatsion^{1,2,2}, Vincent Lenders^{1,2,2}, Bella Manshian^{1,2,2} and Guy Van den Mooter^{1,2}; ¹KU Leuven University, Belgium; ²KU Leuven, Belgium

Bronchopulmonary Dysplasia (BPD) represents a complex pathophysiological challenge in neonatal care, predominantly affecting preterm infants. Current interventions, such as mechanical ventilation and supplemental oxygen, often yield suboptimal outcomes, necessitating the exploration of novel therapeutic modalities. The administration of Dexamethasone (DEX), while effective in reducing mechanical ventilation dependency, is hindered by its severe long-term neurodevelopmental impacts and crystalline structure leading to poor solubility.

In response, our study pioneers an advanced drug delivery system involving the encapsulation of DEX within poly(lactic-co-glycolic acid) (PLGA) nanoparticles (NPs), subsequently coupled to red blood cells (RBCs). This approach aims to produce a polymer-matrix-stabilized amorphous form of DEX, ensuring sustained and localized pulmonary release. By leveraging these DEX-loaded NPs (DEX-NPs) in combination with RBCs, we aim to optimize drug circulation time, biodistribution, and targeted lung delivery, thereby attenuating systemic adverse effects of DEX.

We employed the nanoprecipitation method to synthesize drug-free and DEX-loaded NPs, thoroughly characterizing their size, polydispersity index, zeta potential, encapsulation efficiency, and DEX stabilization capability. Our results demonstrate that these polymeric NPs effectively encapsulate and stabilize DEX up to 3 mg, with higher amounts leading to crystallinity. Solvent, polymer, and drug compatibility studies indicated that PLGA stabilizes about 15% of its weight in DEX (~3 mg) with acetone or acetone: DMSO as solvents. Notably, acetone and DMSO blend markedly improved encapsulation efficiency and drug stability in PLGA nanoparticles.

In addition to these findings, we successfully coupled various types of NPs to mouse RBCs, examining the efficiency of this coupling and the biocompatibility of the resultant constructs. This element of our research was critical in assessing the feasibility and safety of the NP-RBC conjugates for *in vivo* applications. Our *in vitro* toxicity assessments across various cell lines revealed that while plain NPs exhibited limited toxicity, DEX-NPs showed higher cytotoxicity at concentrations above 0.05 mg/mL. *In vivo* studies on term-born neonate CD-1 mouse pups highlighted the superior lung targeting of NP-hitchhiked RBCs compared to free NPs.

This study emphasizes the potential of DEX-PLGA NP-RBC conjugates in revolutionizing BPD treatment. Our findings not only advocate for the targeted pulmonary delivery of therapeutics but also set a foundation for subsequent investigations into the efficacy and safety of this novel approach in the context of neonatal lung diseases.

SESSION SB01.06: Bioresponsive Nanotheranostics V

Session Chairs: Jessica Hsu and Bella Manshian

Thursday Morning, April 25, 2024

Room 428, Level 4, Summit

8:30 AM *SB01.06.01

Biomimetic Nanoparticles for Drug Delivery [Chunxia Zhao](#); The University of Adelaide, Australia

Nanotechnology holds great promise for cancer diagnosis and treatment. A wide range of nanoparticles have been developed ranging from polymer particles to lipids, proteins and other synthetic compounds for cancer drug delivery. However, only a handful cancer nanomedicines have been approved by the FDA (such as Doxil, and Abraxane). This demonstrates the huge gap between laboratory research and clinical translation of cancer nanomedicines, mainly due to several key barriers: (1) challenges in large-scale production of nanomedicine with good reproducibility and well-controlled properties; (2) incomplete understanding of the interactions between nanoparticles and biological systems; (3) targeted delivery. To address these fundamental issues, my group has been focusing on the development of platform technologies for producing nanoparticle libraries with reproducible and systematically varied properties (liposomes, polymer nanoparticles and nanocapsules) with high drug loading. We also developed different strategies for improving targeted delivery. Particularly, we developed a bioinspired nanotechnology integrating naturally derived cell membranes for enhanced biointerfacing capabilities and nanoparticles for incorporation of various payloads for targeted delivery, which provides a revolutionising strategy for fabricating nanoscale artificial cells. We have also developed biomimicking chips (Tumor-on-a-Chip, Tumor-Vasculature-on-a-Chip) to fundamentally understand nanoparticle extravasation and their tumor accumulation.

9:00 AM SB01.06.02

Soybean Oil-Derived Lipids for Efficient mRNA Delivery [Jessica Hsu](#), Zhongmin Tang and Weibo Cai; University of Wisconsin-Madison, United States

Lipids have been extensively utilized as a delivery platform for mRNA. Lipids consist of an N element-based head group with hydrophobic tails of varying composition and different length. Currently, most lipid materials are either positively charged or ionizable in nature, which allows for the formation of nanoparticles through electrostatic interactions with negatively charged mRNA. This not only serves to safeguard mRNA from enzymatic degradation but also facilitates endosomal escape, thereby ensuring mRNA expression and functions. In addition to core lipids, the delivery platform comprises helper lipids, cholesterol, and PEG lipids. Varying compositions, surface modifications, charges, and pKa values can impact mRNA expression and allow organ-specific targeting for disease treatment. Hence, continued investigation of novel lipid materials and formulations will further advance our understanding and techniques in optimizing mRNA delivery.

The ideal synthesis of lipids involves adhering to key principles, such as operating under solvent-free conditions, employing a straightforward reaction process, and eliminating the need for purification steps. These criteria aim to enhance product purity and streamline production, thereby increasing the likelihood for clinical translation. Current lipid synthesis methods involve Michael addition, epoxide ring-opening, reductive amination, and thiol-ene reactions. Furthermore, an effective lipid should encapsulate a high mRNA payload for improved expression *in vivo* and exhibit favorable biosafety without significant adverse effects. Notably, a common soybean oil derivative, rich in epoxy groups, can readily undergo ring-opening reactions with amino-containing compounds. Since soybean oil is FDA-approved and has excellent biocompatibility, it may give rise to a new class of synthetic lipid materials with the potential for mRNA delivery applications.

In our system, epoxidized soybean oil and amino-containing compounds with varying carbon chain lengths, structures, and numbers of N were the sole reactants. Lipids were synthesized via epoxide ring-opening reactions and subsequently purified through heating and rotary evaporation, all without the use of solvents. We found that the majority of lipids derived from soybean oil showed high mRNA loading capacity, thereby enhancing mRNA expression both *in vitro* and *in vivo*, all the while demonstrating excellent biosafety. In our *in vivo* studies of Luc mRNA delivery, we observed that certain lipids could enhance mRNA expression in the spleen, while others could achieve high expression in the lungs or liver. This highlights the potential utility of these lipids for precise and tunable organ targeting in the treatment of relevant diseases. In addition, soybean oil-derived lipids displayed exceptional performance in delivering Cre mRNA for gene editing. Encouraged by these results, we anticipate that soybean oil-derived lipid materials can assume a more prominent role in the realm of mRNA delivery for a diverse range of bioapplications. The synthesis of novel lipids utilizing FDA-approved substances remains a promising domain yet to be fully explored.

9:15 AM SB01.06.03

Nature-Inspired Nanoparticles for Therapeutics and Vaccine Delivery Hao Song^{1,2}; ¹The University of Queensland, Australia; ²Massachusetts Institute of Technology, United States

Recent advances in nanotechnology have greatly boosted the development of novel delivery systems for therapeutic and vaccine applications, in particular highlighting the great success of lipid nanoparticle-based mRNA vaccines fast responding to the COVID-19 outbreak. To lead a successful nanomedicine technology, the key lies in the rational design and fabrication of safe and efficient nano-carriers, while the delivery performance could be maximized by custom-designed nanoparticles considering the unique bio-interface configurations towards both cargo biomolecules and cell/tissue surfaces. Mimicking the spiky morphology of pollen and virus, which allowed enhanced interactions at bio-interfaces, here, we showcase our recent progress in the development of spiky nanoparticle-based smart therapeutics.^[1-4] Through a simple sol-gel synthesis approach, colloidal nanoparticles with an intrinsic spiky surface are fabricated and characterized by the advanced microscopy techniques of electron tomography.^[5] We demonstrated the precise control over the delicate nanotopography of spiky nanoparticles, engineering the surface chemistry,^[6] hollow interior,^[7] and asymmetry of the particles.^[8] We explored the interactions of these nature-inspired unique spiky nano-features towards both biomolecules and cells, gaining new understandings of the bio-nano-interfaces. Our findings underpinned the development of 1) a bacterial-adhesive antimicrobial nano-agent,^[1, 9-11] featuring an antibiotic-free approach to address the drug-resistance issue of infections; 2) a nano-burr hooking the rope-like DNA/mRNA molecules for efficient intracellular delivery,^[12] which allowed sufficient enzymatic protection of gene molecules and enabled of upregulated translation^[2]; 3) a pathogen mimetic adjuvant that boosts the vaccine delivery performance,^[3] including our most recent study in developing DNA and subunit (RBD) spiky nano-vaccines for SARS-Cov-2. From bench to market, this spiky nanoparticle-based delivery platform is on the translation collaborated with industrial partners toward novel nanomedicine. Our journey from fundamental research to the launching of 'NUVEC®' will also be shared in this talk.

- [1] H. Song, Y. A. Nor, M. H. Yu, Y. N. Yang, J. Zhang, H. W. Zhang, C. Xu, N. Mitter, C. Z. Yu*. *J Am Chem Soc* **2016**, 138, 6455.
- [2] H. Song, M. H. Yu, Y. Lu, Z. Y. Gu, Y. N. Yang, M. Zhang, J. Y. Fu, C. Z. Yu*. *J Am Chem Soc* **2017**, 139, 18247.
- [3] H. Song, Y. Yang, *J. Tang, Z. Gu, M. Zhang, C. Yu*. *Adv Therapeutics* **2020**, 3, 1900154.
- [4] D. Cheng, J. Zhang, J. Fu, H. Song*, C. Yu*. *Sci Adv* **2023**, 9, eadi7502
- [5] H. Song, Y. Yang, J. Geng, Z. Gu, J. Zou, *C. Yu*. *Adv Mater* **2019**, 38, 1801564.
- [6] J. Geng, H. Song*, F. Gao, Y. Kong, J. Fu, J. Luo, Y. Yang, *C. Yu. *J Mater Chem B* **2020**, 8, 4593.
- [7] E. Hines, D. Cheng, W. Wu, M. Yu, C. Xu, H. Song*, C. Yu*. *J Mater Sci* **2021**, 56: 5830.
- [8] X. Lin, W. Wu, J. Fu, Y. Yang, B. Guo, C. Yu, *H. Song*, *ACS Appl Mater Interfaces* **2021**, 13: 50695.
- [9] B. Li, Y. Liao, X. Su, S. Chen, X. Wang, B. Shen, H. Song*, P. Yue*. *J Nanobiotech* **2023**, 21: 325.
- [10] M. Zhang, J. Feng, Y. Zhong, J. Luo, Y. Zhao, Y. Yang, Y. Song, X. Lin, Y. Yang, *H. Song*, C. Yu. *Chem Eng J* **2022**, 440: 125837.
- [11] Y. Wang, Y. Yang, Y. Shi, H. Song*, C. Yu* *Adv Mater* **2020**, 32: 1904106.
- [12] B. Sun, W. Wu, E. Narasipura, Y. Ma, O. Fenton, *H. Song*, *Adv Drug Del Rev* **2023**, 200: 115042.

9:30 AM *SB01.06.04

Hydrogen Medicine and Nanomedicines Qianjun He; Shanghai Jiao Tong University, China

Hydrogen molecule has broad-spectrum anti-oxidation and anti-inflammation effects, and has exhibited clear therapeutic functions against many inflammation-related diseases and relatively high biosafety. Therefore, hydrogen therapy is an emerging and promising therapeutic strategy. But hydrogen medicine is currently facing three major issues, including (1) what is the fundamental principle of hydrogen therapy; (2) how to detect hydrogen molecules in vivo; (3) how to deliver hydrogen molecules to the focus in vivo. Aiming to these three issues, our research group has obtained a cascade of important research achievements in principle exploration, tool development, and materials application, mainly including (1) the discovery of the biological target of hydrogen molecule and the disclosure of the fundamental principle of its anti-inflammation, anti-cancer and anti-senescence functions; (2) the development of the first bioprobe of hydrogen molecule and the verification of the high biological barriers-crossing capability of hydrogen molecule; (3) the development of a series of novel biomedical materials for hydrogen delivery to enhance the efficiency of hydrogen delivery and their applications for the treatment of many major diseases. This lecture will deliver our recent research advances in these aspects.^[1-10]

Keywords: Hydrogen medicine, targeted delivery, nanomedicine, molecular imaging, nanocatalytic medicine

Reference

- Zhaokui Jin, Penghe Zhao, Wanjun Gong, Wenjiang Ding, Qianjun He, Fe-porphyrin: a redox-related biosensor of hydrogen molecule, *Nano Res.* 2023, 16, 2020.
- Shengqiang Chen, Yuanman Yu, Songqing Xie, Danna Liang, Wei Shi, Sizhen Chen, Guanglin Li, Wei Tang, Changsheng Liu, Qianjun He, Local H₂ release remodels senescence microenvironment for improved repair of injured bone, *Nat. Commun.* 2023, accepted in press.
- Qingqing Xu, Shengqiang Chen, Lingdong Jiang, Chao Xia, Lingting Zeng, Xiaoqing Cai, Zhaokui Jin, Shucun Qin, Wenjiang Ding, Qianjun He, Sonocatalytic hydrogen/hole-combined therapy for anti-biofilm and infected diabetic wound healing, *Natl. Sci. Rev.* 2023, 10, nwa063.
- Shengqiang Chen, Yanxia Zhu, Qingqing Xu, Qi Jiang, Danyang Chen, Ting Chen, Xishen Xu, Zhaokui Jin, Qianjun He, Photocatalytic glucose depletion and hydrogen generation for diabetic wound healing, *Nat. Commun.* 2022, 13, 5684.
- Bin Zhao, Lingting Zeng, Danyang Chen, Songqing Xie, Zhaokui Jin, Guanglin Li, Wei Tang, Qianjun He, NIR-photocatalytic regulation of arthritic synovial microenvironment, *Sci. Adv.* 2022, 8, eabq0959.
- Wanjun Gong, Lingdong Jiang, Yanxia Zhu, Mengna Jiang, Danyang Chen, Zhaokui Jin, Shucun Qin, Zhiqiang Yu, Qianjun He, An activity-based ratiometric fluorescent probe for in vivo real-time imaging of hydrogen molecules, *Angew. Chem. Int. Ed.* 2022, 61, e202114594.
- Yansen Xu, Mingjian Fan, Wenjuan Yang, Yonghao Xiao, Lingting Zeng, Xiao Wu, Qinghua Xu, Chenliang Su, Qianjun He, Homogenous carbon/potassium-incorporation strategy for synthesizing red polymeric carbon nitride capable of near-infrared-photocatalytic H₂ production, *Adv. Mater.* 2021, 33, 2101455.
- Bin Zhao, Yingshuai Wang, Xianxian Yao, Danyang Chen, Mingjian Fan, Zhaokui Jin, Qianjun He, Photocatalysis-mediated drug-free sustainable cancer therapy using nanocatalyst, *Nat. Commun.* 2021, 12, 1345.
- Yingshuai Wang, Tian Yang, Qianjun He, Strategies for engineering advanced nanomedicines for gas therapy of cancer, *Natl. Sci. Rev.* 2020, 7, 1485–1512.
- Penghe Zhao, Zhaokui Jin, Qian Chen, Tian Yang, Danyang Chen, Jin Meng, Xifeng Lu, Zhen Gu, Qianjun He, Local generation of hydrogen for enhanced photothermal therapy, *Nat. Commun.* 2018, 9, 4241.

10:00 AM BREAK

10:30 AM *SB01.06.05

Nanozymes and Polymers for Nitric Oxide Delivery from Prodrugs Rona Chandrawati; University of New South Wales, Australia

Nitric oxide (NO) is a potent biological molecule that contributes to a wide spectrum of physiological systems, including the cardiovascular, immune, and central nervous systems. However, NO therapeutic delivery technology remains severely limited due to the physiological properties of NO: 1) NO has a short half-life in human tissues (seconds); 2) NO can only diffuse over short distances (~100 μm), thus limiting its action to only areas near the source of delivery; and 3) NO can exert protective or deleterious effects depending on its concentration. Current strategies for NO delivery focus on encapsulation of NO donors into pre-fabricated scaffolds or an enzyme-prodrug therapy approach. The former is limited by the finite pool of NO donors available, while the latter is challenged by the inherent low stability of natural enzymes. Enzyme mimics are attractive substitutes for their natural counterparts in diverse biomedical applications because they have excellent stability against biological degradation compared with natural enzymes. In this work, we present nanoparticles and polymers that can catalytically decompose natural (endogenous) and synthetic (exogenous) S-nitrosothiols NO donors to generate NO at physiological conditions. With this approach, we envision that sustained NO delivery could be achieved by relying on life-long pools of endogenous NO donors, and when needed, on-demand NO delivery at the desired levels of NO could be realized by externally administered exogenous NO prodrugs. By tuning the concentrations of particles/polymers and NO prodrugs, physiologically relevant NO levels were generated. These materials preserved their catalytic property to generate NO for at least 6 months. The nanoparticles and polymers were immobilized in biomaterials and on surfaces, and we demonstrated the therapeutic activity of NO to inhibit cancer cell proliferation and disperse bacterial biofilms.

11:00 AM SB01.06.06

Ultrasound-Induced Cascade Amplification in Mechanoluminescent Nanotransducer for Sono-Optogenetic Deep Brain Stimulation [Huiliang Wang](#); The University of Texas at Austin, United States

Remote and minimally invasive neuromodulation is a promising approach in the advent of clinical applications. Ultrasound-triggered mechanoluminescent technology offers a promising approach for achieving remote brain modulation. However, its application has thus far been limited to shallow brain depths due to challenges related to low sonochemical reaction efficiency and restricted photon yields. Here we report a self-amplifying mechanoluminescent nanotransducer based on cascade reactions in liposomes to achieve efficient light emission upon ultrasound stimulation. As a result, blue light was generated under ultrasound stimulation with subsecond response latency. Leveraging the high energy transfer efficiency of focused ultrasound in brain tissue and the high sensitivity to ultrasound of these mechanoluminescent nanotransducers, we are able to show efficient photon delivery and activation of ChR2 expressing neurons in both the superficial motor cortex and deep ventral tegmental area (VTA). Our novel liposome nanotransducers enable minimally invasive deep brain stimulation for behavioral control in animals via a flexible, mechanoluminescent sono-optogenetic system.

11:15 AM SB01.06.07

Development of *In-Situ* Gel Containing Brinzolamide loaded Nano Structured Lipid Carrier and Its Evaluation Dipti Dhurat, Anil Pawar, Shrikant Joshi, Amol Tagalallewar and [Akshay M. Baheti](#); School of Health Sciences and Technology Dr Vishwanath Karad MIT World Peace University Pune, India

Ocular drug delivery system is most challenging and complicated to deliver drugs at the target site with its therapeutic dose. Intraocular bioavailability is only 5 to 10 % of total eye drop administered. In past few decades, researchers have attracted to nanotechnology based drug delivery system in which lipid based Nanostructured lipid carriers (NLC) appear as effective ophthalmic drug delivery system, which have, higher drug loading, stability and biocompatibility as compare to other lipid carried due to use of physiologically biodegradable lipid. The Nanostructure carrier provides more retention time, better permeation, targeted delivery, improve bioavailability, Non-toxic. Now a days, the conventional eye drops replace by Polymeric eye drop i.e. *in-situ gel*, they are liquid in nature after instillation it undergoes gelation to form viscoelastic gels triggered by stimulation such as temperature, pH and ion activation. Consequently, gel formed increases residence time, extended drug release, enhances bioavailability, reduce dosing frequency and patient compliance. The aim of this work to develop and evaluate *in-situ* gel containing Brinzolamide loaded Nano structured lipid carrier to increase its retention time, Bioavailability, Corneal permeation, reduce dose and dosing frequency.

The saturation solubility study was used to select liquid lipid. The solubility of Brinzolamide was determined in several solid lipids such as Bees wax, Stearic acid, Gelucire50/13, Palmitic acid, Glycerol mono stearate (GMS), Precirol ATO, Compritol ATO 888, cetyl palmitate. Compatibility between selected lipids was examine by preparing mixture of solid lipid and liquid lipid in a ratios of 9:1, 8:2, 7:3, 6:4, 5:5, 4:6, 3:7, 2:8 and 1:9. Only one single phase Mixtures were selected for further study. High speed homogenization method was used to prepare Brinzolamide loaded NLCs. A three-factor, three-level Box-Behnken design experimental design (BBD) was applied for evaluation of critical experimental conditions to maximize experimental efficiency and minimize experiments to optimize The particle size and particle dispersity index (PDI) of the NLCs was determined using the dynamic light scattering (DLS) at a fixed angle of 90 degree at 25 degree C using Nanophox, Sympatech, Germany. The ZP of BRZ-NLC was determined by using zeta sizer (Delsa Nano C, USA) to check electrostatic mobility and stability of formulation. The entrapment efficiency (% EE) of BEZ in NLC formulation was determined The physical state of BRZ-loaded nanostructured lipid carriers demonstrated by DSC characterization technique. BRZ-loaded NLC *in situ* gel was prepared by the cold method. The drug content was determined by HPLC. In vitro release of BRZ-loaded NLC *in situ* gel was studied on Franz diffusion cell. Transcorneal permeation studies were carried out on freshly excised goat cornea. HET CAM (Hen's egg chorioallantoic membrane) study is an alternative to the Draize *in-vivo* rabbit eye test for the recognition of ocular irritations. Therapeutic activity study was conducted with albino rabbits (1.5–2 kg) under the permission of Institutional Animal Ethics Committee (IAEC).

From solubility data Gelucire 50/13 and Oleic acid were selected as the solid and liquid lipid for NLC preparation. Amongst various ratios of solid and liquid lipid 9:1, 8:2, 7:3, 6:4, and 5:5 no phase separation and homogenous mixture was observed for 8:2 ratio, this were selected as lipids mixture. The SEM analysis reveals that spherical and smooth surface of NLC with uniform distribution of particles. BRZ content in formulated *in situ* gel was determined and found to be in range of 99.34-98.58%. BRZ-NLC shows rapid release of drug (68.33%) within 4 h and within 7 h it completely releases (94.33%) drug. This initial rapid release of drug due to the untrapped drug which release from NLC) Whereas, BRZ-NLC *in situ* have extended and slow release of drug (96.44%) up to 15 h.

11:30 AM *SB01.06.08

A Hitchhiker's and Backpacker's Guide to Drug Delivery [Samir Mitragotri](#)^{1,2}; ¹Harvard University, United States; ²Wyss Institute, United States

Nanoparticle-based drug delivery systems are widely explored to improve the biological outcome of chemo and immunotherapy. However, poor vascular circulation, limited targeting and the inability to negotiate many biological barriers are key hurdles in their clinical translation. Biology has provided many examples of successful “carriers” in the form of cells, which routinely overcome the hurdles faced by synthetic nanoparticle systems. We are exploring hitchhiking and backpacking approaches which involve combining synthetic particles with cells to drastically alter the *in vivo* fate of the particles as well as the cells. I will provide an overview of the principles and examples of hitchhiking and backpacking approaches for drug and cell therapy.

SESSION SB01.07: On-Demand Presentation
Tuesday Morning, May 7, 2024
SB01-virtual

10:30 AM *SB01.02.05

Ultrathin Nanosheets for Catalytic Cancer Therapy Sophia Gu; University of New South Wales, Australia

Nanotechnology has emerged as a promising approach for precision treatment of cancers. Two-dimensional nanoparticle-based therapeutic agents have been developed for safe and efficient treatment of cancers.¹ In this talk, I will present our recent work on development of nanosheets for catalytic cancer therapy. We have developed a sustainable method to synthesize ultrathin layered double hydroxide nanosheets via a polymer-assisted bottom-up approach,² and demonstrated high catalytic activity to disproportionate hydrogen peroxide in tumors and in-situ generated hydroxyl radicals efficiently to kill tumor cells.³ Without any drug loading, the nanosheet exhibited highly selective and specific anti-tumor effect. The hydroxyl radical generation-induced anti-tumor effect was further enhanced by cascade catalytic reactions triggered by photocatalysis.⁴ We also showed that the nanosheet generated oxygen bubbles and promoted the long-distance and directional movement toward the tumour microenvironment, thus achieving targeted delivery of therapeutic nanomedicine without traditional surface ligand modification.⁵

References

1. Cao, Z.; Li, B.; Sun, L.; Li, L.; Xu, Z.P.; Gu, Z. *Small Methods* 2019, 1900343.
2. Zhang, H.; Zhang, L.; Cao, Z.; Cheong, S.; Boyer, C.; Wang, Z.; Yun, S.L.Y.; Amal, R.; Gu, Z. *Small* 2022, e2200299.
3. Cao, Z.; Zhang, L.; Liang, K.; Cheong, S.; Boyer, C.; Gooding, J.J.; Chen, Y.; Gu, Z. *Adv. Sci.* 2018, 1801155.
4. Guo, Z.; Xie, W... Boyer, C.; Zhao, L.; Gu, Z. *Chem. Eng. J.* 2022, 137310.
5. Zhang, H; Cao, Z; Zhang, Q; Xu, J; Yun, SLJ; Liang, K; Gu, Z. *Small* 2020, 16, e2002732

SYMPOSIUM CH01

Characterizing Dynamic Processes of Materials Synthesis and Processing via In Situ Techniques
April 23 - May 7, 2024

Symposium Organizers

Liang Jin, Bioland Laboratory
Dongsheng Li, Pacific Northwest National Laboratory
Jan Ringnald, FEI Company
Wenhui Wang, National University of Singapore

Symposium Support

Bronze
Gatan

* Invited Paper

+ JMR Distinguished Invited Speaker

^ MRS Communications Early Career Distinguished Presenter

SESSION CH01.01: Crystal Growth I
Session Chairs: James De Yoreo and Dongsheng Li
Tuesday Morning, April 23, 2024
Room 442, Level 4, Summit

10:30 AM *CH01.01.01

An *In Situ* look at Interfacial Structure and Dynamics during Nucleation and Self-Assembly James J. De Yoreo^{1,2}; ¹Pacific Northwest National Laboratory, United States; ²University of Washington, United States

Interfaces play a critical role in nucleation and growth from solutions by altering the distribution of water and ions from that of the bulk, introducing an interfacial free energy that largely determines the free energy barrier to nucleation, and creating an entropic repulsion that acts as a volume exclusion force to drive colloidal assembly. The origin and characteristic length scales of these phenomena are inherently atomic-to-molecular but are manifest in ensemble dynamics and outcomes. Moreover, processes like nucleation and self-assembly arise from fluctuations, making the events that must be probed transient in nature. Consequently, in situ imaging techniques that can capture structure and its evolution, particularly at high speed and atomic-to-nm resolution, are required to build a quantitative picture of such processes. Here I use examples from and *in situ* TEM, high-speed AFM, and fast force mapping studies of interfacial structure, nucleation, and particle assembly to elucidate the mechanisms by which interfaces direct these processes, leading to unique pathways, materials, and morphologies. The results reveal the importance of surface charge, chemical gradients, and solvent organization near interfaces in determining how ordered materials emerge from the solution.

11:00 AM CH01.01.02

***In Situ* Characterization of Calcium Carbonate Crystallization on Nano-Textured Surfaces** Tobias Armstrong¹, Julian Schmid¹, Janne-Petteri Niemelä², Ivo Utke² and Thomas Schutzius^{1,3}; ¹ETH Zurich, Switzerland; ²Empa - Swiss Federal Laboratories for Materials Science and Technology, Switzerland; ³UC Berkeley, United States

Natural and technological interfaces influence the crystal nucleation and growth of calcium carbonate, including the crystallization pathways, the thermodynamic/kinetic barriers, and the crystal orientation. Predictions show that the heterogeneous nucleation rate on functionalized surfaces of the calcium carbonate polymorph calcite are 20 orders of magnitude higher compared to homogeneous nucleation. Hence, the crystallization pathway can be redirected from complex free energy landscapes towards the classical nucleation theory, allowing to compare different functionalized surface. This is exemplified by higher nucleation rates of calcite for carboxyl groups on surfaces than for thiol groups on surfaces under the same conditions. While smooth functionalized surfaces have been studied, the effect of nano-textured surfaces on calcium carbonate crystallization is unknown. Based on research for other phase change materials, it can be either: promoting or inhibiting. If calcium carbonate crystallization is promoted or inhibited by nano-textured surfaces is relevant to the understanding of calcium carbonate crystallization and facilitates rationally designed interfaces.

Here we show the effect of nano-textured functionalized surfaces on calcium carbonate crystallization. We fabricated and quantified a rationally designed nano-textured surfaces using blockcopolymer lithography, ensuring a significant amount of surface curvature features in an order of magnitude to the critical nucleus size for calcite. The fabricated nano-textured surfaces are functionalized with carboxyl groups and compared to smooth functionalized surfaces to isolate the effect of the nano-texture onto the crystallization. The investigation of the crystallization at different supersaturation conditions provides a holistic understanding of the effect on the thermodynamic as well as the kinetic barrier. *In situ* optical transmission microscopy coupled with digital holographic microscopy characterize the nucleation and single-crystal growth rates in a microfluidic cell with controlled calcium carbonate supersaturation through mixing. The analysis of the acquired microscopy images is using trained instance segmentation algorithms for accurate crystal detection.

This work shows that nano-textured surfaces promote the calcium carbonate nucleation by more than one order of magnitude compared to a smooth surface at the same supersaturation. This difference can be described by the classical nucleation theory, explaining an increasing kinetic barrier of nucleation and a decreasing thermodynamic barrier. For the tested supersaturations and nano-textures, the decreasing thermodynamic barrier outperforms the increasing kinetic barrier. While the increasing kinetic barrier is affected by a decreased monomer collision probability in the confined volumes of the nano-texture pits, the thermodynamic barrier is lowered by surface curvatures in the pits within an order of magnitude to the critical nucleus size. Besides higher nucleation rates, calcium carbonate crystallization on nano-textured surfaces shows lower induction times, higher site densities, and lower single-crystal volume growth rates. We expect that this work will provide guidance for the design of interfaces, which are needed to advance technologies relying on the understanding of the crystallization behavior of calcium carbonate and other inorganic minerals.

This project has received funding from the European Research Council (ERC), Starting Grant, under the European Union's Horizon 2020 research and innovation programme (Grant agreement No. 853257).

11:15 AM CH01.01.03

Autonomous Flow Synthesis of On-Demand Hybrid Perovskite Quantum Dots based on a Closed-Loop Feedback Control System Hoang Khang Bui and Tae Seok Seo; Kyung Hee University, Korea (the Republic of)

Nanostructured hybrid organic-inorganic lead halide perovskites quantum dots (QDs) have gained enormous attention and hold the potential to surpass traditional semiconductor nanocrystals as versatile photonic sources for displays, lighting, light-emitting diodes (LED) as well as light harvesters for photodetector devices, and solar cell. Moreover, due to the unique quantum-size effects, their optical bandgap and emission wavelength can be finely tailored by the ease of compositional control between halide ratio and adjusting the stoichiometry leading to the production of visible electromagnetic spectrum QDs. Currently, conventional flask-based synthetic platforms encounter a range of challenges from unwanted batch-to-bath variations such as precursor stability, temperature fluctuations, macro-environment kinetics.

A promising alternative is the use of continuous flow technology for the auto-production of perovskite QDs. The flow reactive chemistry in microfluidics has demonstrated rapid heat and mass transfer to speed up the chemical reaction time, precise control of the reagent volume, and reaction kinetics to produce uniform nanomaterials. Microfluidic synthesis can be integrated with an in-situ detection module so that the synthetic nanomaterials could be analyzed in real-time, which is inaccessible to the traditional flask-based methods. Moreover, all steps of microfluidic synthesis and product characterization can be software-controlled, thus ensuring time- and labor-effective QDs synthesis with high reproducibility.

One of the strategies for accelerating the identification of the most effective reaction conditions relies on automation. Automating synthesis enables quicker and more accurate procedures, including reagent loading, mixing, heating, and in-process product characterization. Furthermore, implementing an electronic feedback control module allows for the automatic optimization of reaction conditions, helping to generate the target nanomaterials with low cost and high speed. Developing a convenient and novel intelligent algorithm capable of data acquisition and analysis for resetting the reaction conditions could accelerate the transition from a manual synthetic batch process in an ordinary laboratory to a fully automatic continuous synthetic platform.

In the current work, we report an autonomous platform for self-control synthesis of desired perovskites QDs, which utilizes familiar yet efficient Proportional-Integral-Derivative (PID) algorithm. The PID controller have been used in industrial control applications for a long time since it minimizes overshoot in steady state response and lesser settling time. The PID controller has three tuning parameters: the controller gain (P term), the integral time constant (I term), and the derivative time constant (D term). The Internal Model Control methodology is a model based PID tuning techniques that has gained significant attention since it only requires one tuning parameter, namely the closed loop time constant. In conjunction with microfluidic synthesis, the PID drives an optimization in precursors regulations to rapidly return accurate specifying reaction conditions which leads to precise on-demand optical properties. To demonstrate the feasibility and efficiency of our proposed method, we have synthesized MAPbBr₃-x perovskite QDs with controlled fluorescence emission spectra in various P, I, D parameters to apparently indicate the effect of controlling to the outputs. The self-driving PID-based QDs synthesis strategy is a trade-off between target reaching time and stability, which are showcased clearly in this studies. Finally, we successfully produced two representative candidates for red-shift QDs at 650 nm and blue-shift QDs at 550 nm. This study further guides the production in large scale with simple, adaptable PID algorithm for not only lab bench synthesis but also industrial manufacturing.

11:30 AM CH01.01.04

Epitaxial Si on Epitaxial-Gd₂O₃/Si(111) Virtual Substrate Using Low-Cost RF Sputtering for Silicon on Insulator (SOI) Application Shubham Patil¹, Adityanarayan Pandey¹, Swagata Bhunia¹, Sandip Lashkare², Apurba Laha¹, Veeresh Deshpande¹ and Udayan Ganguly¹; ¹Indian Institute of Technology Bombay, India; ²Indian Institute of Technology Gandhinagar, India

There is an ever-growing need for 5G communication technology and the Internet of Things to achieve better-performing systems in speed and power consumption. Research has shown SOI technology to be very promising among different technologies (it offers low voltage and high-frequency operation capability) [1]. However, the costly smart-cut method for manufacturing SOI wafers is a challenge. Alternatively, the notion of using epitaxial rare earth (RE) oxides onto Si followed by epi-Si growth is a potential alternative to enable cheaper and high-volume manufacturing (HVM) of SOI wafers. Gd₂O₃ oxide is the most promising among all rare oxides due to its large bandgap, sufficient band offsets, stable oxidation state, and low lattice mismatch with Si(111). In this context, our group patented a methodology to produce semiconductors on an insulator substrate using an HVM-friendly RF magnetron

sputter system [2,3].

In the work, we demonstrate epitaxial-Si on epitaxial-Gd₂O₃/Si(111) substrate by RF magnetron sputtering for SOI application. The fabricated heterostructure is characterized through XPS, HRXRD, cross-sectional HRTEM, and EDS analyses, providing compelling evidence for the formation of the epi-Si(111) layer on the epi-Gd₂O₃ surface.

The cap-Gd₂O₃/Top-Si/BOX-Gd₂O₃ (capping layer (cap)/channel (Top-Si)/Buried-oxide (BOX)) stack is deposited on Si(111) substrate using RF sputtering. The box layer is deposited at 750 °C with 20 W RF power (~0.12nm/min) for 100 min, followed by intrinsic-Si deposition (~0.3 nm/min) at 100 °C temperature. The Gd₂O₃ capping layer is deposited at a higher temperature (750 °C) to crystallize the channel layer. The heterostructure is subsequently annealed at 850 °C to study the impact of rapid thermal annealing. The heterostructure thickness is 12 nm/15 nm/16 nm, confirmed using HRTEM. The capping layer is etched using an H₂SO₄: DI water wet etch, O₂ plasma ashing, followed by BHF etch. The conformal etching is verified by analyzing the XPS spectra. The absence of a Gadolinium (Gd3d and Gd4d) signature and a strong Si2p peak of bulk-Si confirms that the capping layer is properly etched. Next, HRXRD is employed to determine the structural nature of the BOX-Gd₂O₃.

The full range Φ measurements at fixed $X = 70.5^\circ$ and $2\theta = 28.44^\circ$ show two sets of peaks 120° apart correspond to the Si(-111) and c-Gd₂O₃(-222) planes.

This observation indicates a 3-fold symmetrical nature of the peaks, establishing that the (222) planes of Gd₂O₃ are grown epitaxially onto the Si(111) substrate. The Si peaks are found to be rotated by 60° relative to Gd₂O₃, suggesting the presence of an A/B twinning relationship between Si and Gd₂O₃.

The epitaxial quality of the BOX is further validated using a skew-symmetric ω -2 θ scan.

The HRTEM analysis demonstrates three key findings: (a) the formation of an atomically sharp interface at the BOX-Gd₂O₃/Si(111) interface, (b) the epitaxial nature of the BOX-Gd₂O₃ and Top-Si layers, and (c) confirmation of the A/B/A stacking arrangement of Top-Si/BOX-Gd₂O₃/Si(111). The EDS analysis further confirms the formation of a flat and homogenous interface without significant Si(Gd) out-diffusion.

In conclusion, we have developed a low-cost, high-volume, manufacturable state-of-the-art epitaxial Si-Gd₂O₃ on Si (111) substrate (SOXI) by RF sputtering. The epitaxial nature of the heterostructure is confirmed through HRXRD and HRTEM analyses. In the near future, a SOXI MOSFET demonstration should be done.

References:

[1] J. Hartmann *et al.*, IEEE CSICS, 2014. [2] Amita *et al.*, DRC, 2018. [3] Amita *et al.*, TSF, 2021

11:45 AM CH01.01.05

Iodine-Passivation Facilitates On-Surface Synthesis of Robust Regular Conjugated Two-Dimensional Organogold Networks on Au(111) [Arash Badami Behjat](#)^{1,2}, [Gianluca Galeotti](#)^{1,2} and [Markus Lackinger](#)^{1,2}; ¹Technical University of Munich, Germany; ²Deutsches Museum, Germany

Dehalogenative Ullmann-type couplings are recognized as the basis for on-surface synthesis, producing extended covalent nanostructures on metal surfaces.[1] While one-dimensional (1D) structures are typically derived from ditopic precursor molecules, two-dimensional (2D) networks like polymers can be synthesized from precursors with more than two halogen substituents. In this study, we present evidence for the debrominative coupling of a tetrabromine-substituted thiophene-rich monomer on an iodine-passivated Au (111) surface, affording well-ordered 2D organogold networks.

Previous studies have investigated the on-surface polymerization of the 2,5,9,12-tetrabromoanthra[1,2-b:4,3-b':5,6-b'':8,7-b''']tetrathiophene (TBATT) precursor on both silver (Ag) and copper (Cu) surfaces. [2, 3] These studies revealed a notable challenge arising from kinetic competition between binding motifs during the irreversible phase. As a result, the resulting networks tended to be predominantly irregular, with only small areas exhibiting regular patterns. To advance the fundamental understanding, we study the debrominative coupling of TBATT directly on pristine Au(111). When the sample is annealed at temperatures between 200 °C and 220 °C, debromination is activated, resulting in predominantly irregular networks. Interestingly, the measured intermolecular distances agree with the DFT calculated values of organometallic carbon-Au-carbon bonds instead of direct carbon-carbon bonds. Subsequently, TBATT was deposited on iodine passivated Au(111) (I-Au(111)), where we observed intact molecules either forming organized supramolecular structures or existing as dispersed single entities. Subjecting these samples to annealing temperatures of 200 °C to 220 °C induced a significant structural transformation, shifting from densely packed to a porous grid-like network.

The remarkable stability of the TBATT-derived organogold networks as evidenced by high temperature annealing, is attributed to the π -conjugation. This motivated further investigation of the network's electronic properties. The calculated electronic band structure revealed a surprisingly narrow band gap of 0.71 eV, together with dispersive bands. To confirm these DFT calculations experimentally, Scanning-Tunneling-Spectroscopy (STS) experiments were performed. The differential conductance dI/dV versus voltage V spectra indicate an electronic band gap of the order of 1.0 eV.

In conclusion, our study has demonstrated the feasibility of using I-Au(111) surfaces as effective substrates for the on-surface synthesis of covalent 2D networks through debrominative couplings. In particular, when using the TBATT precursor on I-Au(111), we achieved highly regular organogold networks, in contrast to the poor structural order observed when synthesized on pristine Au(111).

Although the domains are still relatively small, they contain a sufficient number of repeat units to allow the anthra-tetrathiophene network to develop an electronic band structure. This convergence is partly due to the 2D topology, which allows a faster evolution of electronic properties compared to 1D structures, mainly because more intermolecular bonds are formed per monomer. The influence of the iodine monolayer on the formation of highly regular organogold networks is twofold: On the one hand, iodine induces reversibility of the robust carbon-Au-carbon bonds, facilitating dynamic error correction, as confirmed by experiments where the organogold networks disintegrated when annealed in an iodine atmosphere. On the other hand, the presence of the iodine monolayer does not impose spatial constraints but instead supports the formation of exceptionally regular networks.

SESSION CH01.02: Crystal Growth II
Session Chairs: Jungwon Park and Jan Ringnald
Tuesday Afternoon, April 23, 2024
Room 442, Level 4, Summit

1:30 PM *CH01.02.01

Multi-Phasic Growth Mechanism of Colloidal Nanoparticles by Statistical Liquid Phase TEM [Jungwon Park](#); Seoul National University, Korea (the Republic of)

Nanoparticle nucleation and growth have long been of great interest in science and industry. Despite impressive advances in nanotechnology, the thermodynamic origin of nanocluster nucleation is still a mystery, and there is no quantitative understanding of nanoparticle growth dynamics. It is because of the complexity that intrinsically exists in nanoparticle growth pathways. A comprehensive understanding of the growth mechanism requires experimental investigation of nanoparticle growth from two different aspects: individual growth trajectories and kinetics in ensemble average. To address this issue, we monitor hundreds of individual trajectories of growing nanoparticles using liquid-phase transmission-electron-microscopy. Statistical analysis of ensemble growth trajectories reveals that the growth of nanoparticles can be classified into multiple distinct types and stages. We present a

microscopic model and statistical mechanical theory that provide unified, quantitative understanding of the time-dependent mean, variance, and distribution of nanoparticle size at all stages of the nanoparticle growth processes observed. We find that strongly-nonextensive free energy originating from a nanoparticle's edge interaction, motion, and conformational degeneracy, which has received little attention so far, plays an essential role in the nanocluster nucleation and non-classical growth dynamics.

2:00 PM CH01.02.02

Emergence of a Novel BCT Phase in Eutectic High Entropy Alloys during Laser Powder Bed Fusion Bingbing Zhao¹, Qingsong Shu¹, Ming Chen² and Lanting Zhang¹; ¹Shanghai Jiao Tong University, China; ²Northwestern University, United States

High entropy alloys, composed of a minimum of four principal elements, exhibit exceptional combinations of strength and ductility, along with impressive corrosion resistance and microstructural adaptability. Recent strides in eutectic high-entropy alloys (EHEAs), a subset within this category, reveal multi-phase structures and uniform microstructures in their as-cast state. Traditional metallurgical processing of EHEAs leads to limited improvements in strength and ductility due to the formation of a coarse lamellar structure. Additive manufacturing, particularly laser powder bed fusion (L-PBF), enables the construction of intricate three-dimensional structures by incrementally adding thin layers, overcoming geometric constraints. However, the phase transition process of EHEAs from liquid to as-deposited state is constrained, particularly during the rapid heating and cooling inherent in the L-PBF process. This can induce metastable phases under these non-equilibrium conditions, significantly affecting the properties of the printed EHEA. The implementation of an operando X-ray diffraction device at a synchrotron beamline, harnessing the high brilliance and swift detectors available, serves as the vital bridge to numerical methods. Our pre-alloyed powder, with a nominal composition of Ni₃₀Co₃₀Fe₁₁Cr₁₁Al₁₈, exhibits a lamellar structure consisting of B2 and FCC phases as predicted by thermodynamic phase equilibrium calculations. During the L-PBF process, a novel BCT phase emerges during solidification. Operando X-ray diffraction, employed during L-PBF, provides a real-time measurement of phase transitions and structural evolution in EHEA. This study not only establishes the relationship between processing and phase constitution but also illuminates how kinetics influence morphology and property control.

2:15 PM CH01.02.03

Understanding Graphene Inception and Growing by Investigating Early-Stage Particle Formation Ornel Padilla¹, Kyle J. Daun², Hartmut Wiggers¹ and Christof Schulz¹; ¹IVG, Institute for Energy and Materials Processes – Reactive Fluids, and CENIDE, Center for Nanointegration Duisburg Essen, University of Duisburg-Essen, Germany; ²University of Waterloo, Canada

Microwave-assisted plasma synthesis is a promising pathway for large-scale production of few-layer graphene flakes. One of the challenges associated to the advancement of this process, is to develop a better understanding of the stages of inception and growth of graphene, as well as of the connection between the synthesis conditions, the reaction conditions in the gas phase, and the quality of the material obtained.

In a microwave-assisted plasma reactor, the carbon-bearing precursor enters the plasma region and gets decomposed into smaller reactive fragments, such as C, H, H₂, C₂, C₂H₂, and CO. These reactive fragments then leave the plasma region, where they form nuclei that rapidly grow into graphene¹. The literature suggests connections between the type of structure formed and the temperature gradient, residence time, and carbon concentration in the nucleation and growing zones². Further, the use of low precursor content is common to prevent or reduce soot formation.

In this work, ethanol and ethylene are used as precursor to study graphene formation. The first one is a common precursor used in the literature, and the second one is a known key intermediate species during graphene formation. Key species formed during precursor decomposition which later become building blocks for graphene formation downstream have been analyzed in situ and through exhaust gas sampling.

Optical emission spectrometry (OES) has been performed at different heights above the nozzle of the reactor, and light collection with a plano-convex lens was used to provide good spatial resolution. Following the approach described in Ref. ³, several wavelength regions of key species light emission were selected, and for each wavelength region the measurement conditions were fixed for proper comparison of signals at different heights above the nozzle (HAN). Spectra corresponding to C and C₂ appeared at higher HAN. When increasing HAN, light emission corresponding to CH first increases and then decreases in intensity for both precursors. Emission from the H_β Balmer, important for determination the electron density, could be well distinguished from background radiation. With ethylene as precursor, C, CH, C₂, and H emissions were stronger than with ethanol. Analysis of collected material by TEM show characteristic folded layers of graphene. With ethylene as precursor graphene and soot were formed in parallel, while ethanol led to the formation of graphene only. FTIR, light scattering, and thermophoretic sampling from the post-plasma region will provide further information about particle nucleation and growth.

References

1. Dato, A. Graphene synthesized in atmospheric plasmas - A review. *J. Mater. Res.* 34, 214–230 (2019).
2. N. Bundaleska, D. Tsyganov, A. Dias, E. Felizardo, J. Henriques, F.M. Dias, M. Abrashev, J. Kissovski, A. Tatarova Microwave plasma enabled synthesis of free-standing carbon nanostructures at atmospheric pressure conditions. *Phys. Chem. Chem. Phys.* 20, 13810–13824 (2018).
3. P. Fortugno, S. Musikhin, X. Shi, H. Wang, H. Wiggers and C. Schulz, Synthesis of freestanding few-layer graphene in microwave plasma: The role of oxygen. *Carbon* 186, 560–573 (2022).

2:30 PM CH01.02.04

In Situ Observation of (Trans-) Formation of Oxide Nanoparticles during Chemical Vapor Synthesis Shradha R. Joshi, Martin A. Schroer, Maximilian Stepponat and Markus Winterer; Universität Duisburg-Essen, Germany

Characteristics of nanoparticles (NPs) such as microstructure and morphology determine their physicochemical properties and thereby their application potential. Particle characteristics and correlated properties may be optimized by tuning relevant process parameters [1].

Chemical vapor synthesis (CVS) is a dynamic gas phase synthesis to generate NPs where the formation and transformation of NPs is mainly governed by the time-temperature $T(t)$ profile in the reactor [2]. Usually, the synthesized NPs are collected and characterized ex situ to determine various characteristics. This often leads to the loss of information due to artifacts during particle collection, oxidation, hydration, surface reactions or ageing of NPs. Ex situ methods also limit insight into intermediate species. Reliable information about the dynamic processes in CVS and related particle characteristics is only accessible via in situ observation.

Here, we present results on CVS of tin oxide (SnO₂) and iron oxide (FeO_x) NPs investigated in situ using high energy X-rays at synchrotron beamlines [3]. The key challenge in these experiments is the low number density of the particles generated in the gas phase process which is about three orders of magnitude smaller than in corresponding bulk systems [4]. However, due to high intensity X-ray sources at contemporary synchrotron radiation facilities and modern X-ray detectors it is nevertheless possible to obtain scattering and spectroscopy data.

A novel mobile CVS reactor is designed for these experiments which enables control of process parameters, especially the time-temperature $T(t)$ profile and oxygen partial pressure $p(O_2)$ to produce oxide NPs. In situ small and wide-angle X-ray scattering (SAXS and WAXS) are used to study microstructure, morphology, phase composition and crystal structure. X-ray absorption spectroscopy (XAS) is performed to study electronic and local structure.

[1] M. Winterer, *Chemical Engineering Science*, 186, 2018, 135-141

[2] M. Winterer, *Nanocrystalline Ceramics: Synthesis and Structure*, Berlin: Springer 2002

[3] M. A. Schroer, A. Levish, Y. Yildizlar, M. Stepponat, M. Winterer, *Review of Scientific Instruments*, 93, 2022, 113706

[4] A. Levish and M. Winterer, *In situ cell for x-ray absorption spectroscopy of low volatility compound vapors*, *Review of Scientific Instruments*, 91, 2020, 063101

Acknowledgements: This research is conducted at PETRA III at DESY, Hamburg, Germany under the proposal numbers: I-20211391 at beamline P64 for EXAFS, I-20211320 and I-20220812 at beamline P62 for SAXS/WAXS and I-20220890 at beamline P21 for XRD. We gratefully acknowledge the German Research foundation (DFG) for funding through research unit FOR 2284 'Model-based scalable gas-phase synthesis of complex nanoparticles' (WI-981/14, INST 20876/395-1 FUGG).

2:45 PM BREAK

3:15 PM *CH01.02.06

Synthesizing Well-Defined Pre-Catalysts for Multi-Modal Studies of Electrocatalysts under Reaction Conditions See Wee Chee; Fritz Haber Institute of the Max Planck Society, Germany

Chemical conversion through renewable energy-powered electrocatalysis is a crucial technology in our green energy strategy. However, we still lack the fundamental understanding of working catalytic structures under reaction conditions needed to enable the rational design of optimal catalysts for such applications. Even though *operando* studies can be used to investigate catalysts during reaction, no single *operando* technique provides complete information about an electrocatalyst under reaction conditions because the relevant catalytic processes span several orders of magnitude in length and time scales. Hence, multiple techniques are usually needed for such studies. Ensuring that we are looking at catalysts under self-consistent reaction conditions in the different tools is not easy. The starting point towards addressing this challenge is the ability to make the samples in a controllable and reproducible manner. In this talk, I will discuss my group's work using different methods to synthesize model pre-catalysts with well-controlled characteristics for *operando* microscopy studies. Using such transferable synthesis protocols, we further bridge the gap between various techniques with targeted measurements that correlate the structure and the properties of catalysts during reaction.

3:45 PM CH01.02.07

In-Situ Synchrotron Light Studies of Cobalt Ferrite and Cobalt(II) Oxide Synthesis via The Polyol Method: Uncovering Intermediate Phases through In-Situ XRD and SAXS Monitoring Miran Baricic^{1,2}, Roxana Mirshahi², Youssef Snoussi¹, Jasper Plaisier³, Lara Gigli³, Alessandro Mariani³, Barbara Sartori³, Sophie Nowak¹, Paolo Centomo⁴, Davide Peddis⁵, Souad Ammar¹ and Carlo Meneghini²; ¹Université Paris Cité, France; ²Università degli Studi di Roma TRE, Italy; ³Elettra Sincrotrone Trieste SCpA, Area Science Park, Italy; ⁴Università degli Studi di Padova, Italy; ⁵Università degli Studi di Genova, Italy

The synthesis of cobalt ferrite (CFO) and cobalt (II) oxide (CO) nanoparticles (NP-CFO, NP-CO) through the polyol method has garnered considerable interest due to their promising applicative potential in fields such as catalysis, electronics, biomedical engineering, and magnetic materials science. Detailed knowledge of the processes taking place during synthesis is crucial information for the precise adjustment of synthesis parameters. We have used synchrotron radiation X-ray diffraction (SR-XRD) and small-angle X-ray scattering (SR-SAXS) at the Elettra synchrotron radiation facility, to monitor in situ the formation of NP-CFO and NP-CO during polyol synthesis. The analysis of time-resolved XRD and SAXS patterns provides insight into the evolving crystallographic structure and morphological changes during synthesis.

Our findings reveal curious and original insights into the evolution of the reactant during the synthesis, such as the presence of intermediates (e.g., layered hydroxide salts, LHS) and the appearance of sub-nanometre-sized precursor phases likely acting as pre-nucleation clusters of NP-CFO/CO phases. The in-situ monitoring allowed us to capture the dynamic evolution of these intermediates, providing valuable information on their formation pathways and growth kinetics, which significantly affect the nucleation and growth processes of the cobalt-based nanoparticles. The unambiguous identification of these intermediates sheds light on the intricate mechanisms governing the process and represents a crucial step towards optimising the polyol synthesis and improving the purity and crystallinity of the final products.

The understanding of the synthesis dynamics and mechanistic insights gained from this in-situ study advance tailored synthesis strategies for producing high-quality NP-CFO and NP-CO materials. This also provides relevant details for better interpretation of the magnetic properties of antiferromagnetic materials such as CO, which is critical to avoid ambiguities given its relatively low magnetic signal.

4:00 PM CH01.02.08

Multiscale Insights into Amalgamation Synthesis of Intermetallic Nanocrystals via In Situ X-Ray Scattering Florian Schenk¹, Christian Prehal² and Maksym Yarema¹; ¹ETH Zurich, Switzerland; ²University of Salzburg, Austria

Bimetallic nanocrystals are a family of materials with over > 20 000 potential members with a multitude of applications in catalysis, energy conversion and storage, plasmonics and magnetism.^[1] Recently, a general synthetic approach for colloidal intermetallics via amalgamation was presented,^[2] unlocking up to 1 000 potential new intermetallic nanocrystals. Combining pre-synthesized metal seeds with a liquid metal, the intermetallic compound is formed via fast diffusion dynamics. This overcomes challenges of combining two dissimilar metals at the nanoscale, such as contrasting oxidation potentials or epitaxial constraints. With accurate and predictive control over the size and composition, this synthesis provides access to a wide range of tailor-made intermetallic nanocrystals. Further optimization and expansion of the amalgamation synthesis, however, requires understanding of the process on the atomic as well as on the particle scale.

Here, we turn to in situ small- and wide-angle X-ray scattering as an ideal tool for observing size and size dispersion, as well as crystallinity and phase-dynamics in colloidal systems.^[3-6] We track multiscale reaction dynamics of colloidal intermetallics (Au-, Ag- and Pd-based alloys) in real time using a tailor-made reactor and reveal unprecedented reaction mechanisms in the formation of intermetallics. Furthermore, we also provide a toolbox for in situ studies of nearly every nanocrystal synthesis since the combination of reactor and in situ scattering can be applied to highly air- and moisture-sensitive protocols at temperatures up to 330 °C and down to millisecond timescales.

[1] K. D. Gilroy, A. Ruditskiy, H. C. Peng, D. Qin, Y. Xia, *Chem. Rev.* **2016**, *116*, 10414.

[2] J. Clarysse, A. Moser, O. Yarema, V. Wood, M. Yarema, *Sci. Adv.* **2021**, *7*.

[3] X. Chen, J. Wang, R. Pan, S. Roth, S. Förster, *J. Phys. Chem. C* **2021**, *125*, 1087.

[4] M. P. Campos, J. De Roo, M. W. Greenberg, B. M. McMurtry, M. P. Hendricks, E. Bennett, N. Saenz, M. Y. Sfeir, B. Abécassis, S. K. Ghose, J. S. Owen, *Chem. Sci.* **2022**, *13*, 4555.

[5] Q. A. Akkerman, T. P. T. Nguyen, S. C. Boehme, F. Montanarella, D. N. Dirin, P. Wechsler, F. Beiglböck, G. Rainò, R. Erni, C. Katan, J. Even, M. V. Kovalenko, *Science* **2022**, *377*, 1406.

[6] M. Strach, V. Mantella, J. R. Pankhurst, P. Iyengar, A. Louidice, S. Das, C. Corminboeuf, W. Van Beek, R. Buonsanti, *J. Am. Chem. Soc.* **2019**, *141*, 16312.

4:15 PM CH01.02.09

Controlled Synthesis of Self-Reduced CoO Decorated Co₃O₄ Yi-Wen Lin, Sin-Pei Wang, Yen-Ling Wang, Karan Giri, Chun-Hua Chen, Chia-Yin Cheng, Shang-Jung Wu, Wen-Chieh Hsieh and Hung-Shuo Chang; National Yang Ming Chiao Tung University, Taiwan

Nitrogen dioxide (NO₂) is a common toxic gas in automobile and locomotive emissions, industrial combustion, and power generation. Long-term exposure to nitrogen dioxide will not only cause photochemical smog and acid rain to pollute water, soil, and air but cause harm to human health, such as respiratory distress, heart failure, and pulmonary edema. Precise detection and emission control of nitrogen dioxide are thus critical.

In this study, Co₃O₄ nano-assemblies with different morphologies, including sphere, pillow-shape, and star-shape, were successfully produced via the polyol method at different reaction temperatures. The appropriate operating temperature of these three nano-assemblies for having the highest gas responses were then evaluated under 1000 ppm NO₂, and were then found to be 130 °C. The observed highest response approaching 207% was found for the pillow-shaped nano-assembly. The spherical Co₃O₄ nano-assembly was selected for the subsequent self-reduction study due to its relatively regular morphology among these three nano-assemblies. The spherical Co₃O₄ nano-assembly was then reduced in a mixture of 95% nitrogen and 5% hydrogen with various controlled temperatures and time for having a nanocomposite comprising coexisted multiple cobalt oxides. The Rietveld, x-ray photoelectron spectroscopy (XPS), and energy-dispersive x-ray spectroscopy (EDX) were mainly performed to identify the phase fraction and chemical composition. It was found that after reduction at 250 °C for 120 minutes, a heterogeneous nanocomposite comprising CoO (Co²⁺) (43 wt%) and Co₃O₄ (Co²⁺/Co³⁺) (57 wt%) can be successfully obtained. The XPS analysis confirmed that the amount of the surface adsorbed oxygen (O_c) and the oxygen vacancy (O_v) associated with O₂-ions in oxygen-deficient regions within the matrix of Co₃O₄ increase with the increase of Co²⁺ ions newly formed via the reduction procedure from Co₃O₄ to CoO, which is considered to be beneficial for improving gas sensing performance. The sensing response at 400 ppm NO₂ at 130 °C increases from 61% of the unreduced Co₃O₄ nano-assembly to 91% of the self-reduced CoO / Co₃O₄ one. Compared with CH₄, C₂H₆, C₃H₈, C₂H₅OH, and CO, the self-reduced CoO / Co₃O₄ nano-assembly exhibits excellent selectivity to NO₂. The response of NO₂ is four times higher than that of other gases. Based on the dynamic recovery test, the self-reduced CoO / Co₃O₄ nano-assembly shows a reproducible response.

Keywords: gas sensor, nitrogen dioxide sensing, Co₃O₄, reduction, selectivity, nano-assembly.

4:30 PM CH01.02.10

Characterizations of Force-Induced Mineralization Processes for Self-Adaptive Materials Sung Hoon Kang; Johns Hopkins University, United States

Adaptability is one of the hallmarks of living systems that provide resilience to survive and flourish in a dynamically changing environment. I will present self-adaptive materials that can change their mechanical properties depending on loading conditions by the coupling between stress and material synthesis. Nature produces outstanding materials for structural applications, such as bone and wood, that can adapt to their surrounding environment. For instance, bone regulates mineral quantity proportional to the amount of stress. It becomes stronger in locations subjected to higher mechanical loads. This capability leads to the formation of mechanically efficient structures for optimal biomechanical and energy-efficient performance. However, it has been challenging for synthetic materials to change and adapt their structures and properties to address the changing loading condition. To address the challenge, we are inspired by the findings that bones are formed by mineralizing ions from blood onto collagen matrices.

I will present our characterization results of a material system that triggers proportional mineral deposition from electrolytes on piezoelectric matrices upon mechanical loadings so that it can self-adapt to mechanical loadings. For example, the mineralization rate could be modulated by controlling the loading condition, and a 30-180% increase in the modulus of the material was observed upon cyclic loadings whose range and rate of the property change could be modulated by varying the loading condition. Moreover, the material system showed improved fatigue resistance from its damage mitigation mechanism with one order of magnitude slower crack propagation speed. Based on our characterization data, we developed a model to elucidate the underlying mechanism.

Our findings can contribute to new strategies for making resilient and sustainable materials for dynamically changing mechanical environments, with potential applications including healthcare, infrastructure, and vehicle.

SESSION CH01.03: Crystal Growth III
Session Chairs: Xiaoqing Pan and Haimei Zheng
Wednesday Morning, April 24, 2024
Room 442, Level 4, Summit

8:30 AM CH01.03.01

Dissolution Enables Dolomite Crystal Growth near Ambient Conditions Joonsoo Kim¹, Yuki Kimura², Brian Puchala¹, Tomoya Yamazaki², Udo Becker¹ and Wenhao Sun¹; ¹University of Michigan–Ann Arbor, United States; ²Hokkaido University, Japan

Crystals grow under supersaturated solutions. A mysterious counterexample is dolomite CaMg(CO₃)₂, an abundant sedimentary mineral that apparently cannot grow at ambient conditions, not even under highly supersaturated solutions. Using atomistic simulations, we show that dolomite initially precipitates a cation-disordered surface, where high surface strains inhibit further crystal growth. However, mild undersaturation will preferentially dissolve these disordered regions, enabling increased order upon reprecipitation. Our simulations predict that frequent cycling of a solution between supersaturated and undersaturated can accelerate dolomite growth by up to seven orders of magnitude. We validate our theory with in situ liquid cell TEM—directly observing bulk dolomite growth under supersaturation cycles. This mechanism explains why modern dolomite is primarily found in natural environments with pH or salinity fluctuations. More generally, it reveals that the growth and ripening of defect-free crystals can be facilitated by deliberate periods of mild dissolution.

8:45 AM CH01.03.02

Unveiling Multiple Transient States in Cerium Oxalate Crystallization and their Impact on Nucleation Rates Jade Raimbault¹, Maxime Durelle², David Carriere¹, Corinne Chevillard¹, Frederic Gobeaux¹, Mark Levenstein¹, Fabienne Testard¹, Florent Mallogi¹, Ovidiu Ersen³ and Dris Ihiwakrim³; ¹CEA de Saclay, France; ²University of Leeds, United Kingdom; ³Institut de Physique et Chimie des Matériaux de Strasbourg, France

Crystallization from solution can occur through a “nonclassical” route where amorphous or liquid transient species are formed prior to final crystals^[1]. These intermediates, often ignored in theoretical modeling, can however have a significant impact on crystallization mechanisms and therefore on

nucleation rates. Most industrial processes still rely on single step Classical Nucleation Theory (CNT) and then overlook cases where these routes are followed.

Cerium oxalate, a well-known surrogate for plutonium oxalate in nuclear waste recycling, shows evidence of a transient amorphous structure prior to crystallization^[2]. However, we revealed that not one, but two non-crystalline transient species are involved: amorphous nanoparticles and dense liquid droplets. Formed in less than a minute, they may also coexist depending on the chemical conditions^[3]. It challenges not only their characterization but also their theoretical description, making the validation of a nucleation model even more delicate.

We used in situ X-ray scattering at synchrotron and liquid cell TEM to characterize cerium oxalate precipitation down to the millisecond reaction times and the nanometer scale. In addition to their identification, we confirmed the amorphous and liquid nature of these intermediates. Their impact on experimental nucleation rates was also assessed and revealed a drastic increase when liquid droplets are formed, far from the values expected by a single step model. Finally, we determined the different phase transition mechanisms involved depending on the nature of the transient structure, which gives us a hint on compatible nucleation theories.

References :

- [1] Yoreo, J. J. D. *et al.* Crystallization by particle attachment in synthetic, biogenic, and geologic environments. *Science* 349, aaa6760 (2015)
- [2] Rodriguez-Ruiz, I. *et al.* Ultra-fast precipitation of transient amorphous cerium oxalate in concentrated nitric acid media. *CrystEngComm*, 20, 3302-3307 (2018)
- [3] Durelle, M. *et al.* Coexistence of Transient Liquid Droplets and Amorphous Solid Particles in Nonclassical Crystallization of Cerium Oxalate. *J. Phys. Chem. Lett.* 13, 8502–8508 (2022)

9:00 AM CH01.03.03

Formation of Highly Branched Nanocubes through Multi-Stage Oriented Attachment of Pt Nanoparticles Yuna Bae, James J. De Yoreo and Dongsheng Li; Pacific Northwest National Laboratory, United States

Crystals grow through various pathways, such as monomer-by-monomer addition and attachment processes among ions, amorphous or crystalline particles, and clusters. Oriented attachment is a common path for crystal growth. The process of particle attachment is determined by the interplay between particles, i.e. interparticle forces, including vdW attraction, hydration repulsion, steric hindrance, and electrostatic interactions, which depend on the liquid-solid interfacial structures at particle surfaces. Herein, we investigate the formation process of branched Pt nanocubes via oriented aggregation of nanoparticles using a combination of cryo TEM, liquid-phase TEM, and simulations. Initially, primary nanoparticles of 2 to 3 nm in size are generated and then agglomerated to form a cluster. This cluster will further grow through nanoparticle and cluster aggregation. The nanoparticles within the cluster are spatially separated at early stage and continuously rearrange their alignment via oriented attachments, leading to clusters with core/shell structures. The inner particles in the cluster begin to attach on the (100) plane forming the cube-shaped core. At later growth stage, nanoparticles attach along the (111) plane, forming branched rods on top of the cube as the shell. The core/shell structure finally evolves into a branched cubic mesocrystal through the gradual ordering. Low pH and high chloride ions can induce changes in the surface structure and charge between clusters and nanoparticles, leading to the nanoparticles preferentially attaching along (100) at the early stage and (111) at the later stage. Simulations based on molecular dynamics and density functional theory will be also performed to examine the influence of HCl and formates on Pt (100) and (111) surfaces, elucidating their relationship with (100) and (111) attachments at different chloride ions.

9:15 AM CH01.03.04

Inline Spectroscopic Investigation of Metal Patch Growth on Spherical Nanoparticles in Continuous Flow Julia S. Seifert, Andreas Voelkl and Robin N. Klupp Taylor; Institute of Particle Technology, Germany

Plasmon resonant nanoparticles have been extensively investigated over the last decades due to their promise in a wide range of applications (e.g. theranostics, pigments, sensors, photocatalysts). As the tunability of the resonant frequency of isotropic plasmonic nanoparticles (NPs) is limited, anisotropic particles can be used to expand the available property space. One example of anisotropic plasmonic NPs are patchy particles, where noble metal patches with controlled size and morphology are deposited onto a dielectric core particle. We have demonstrated these particles to have a wide optical tunability and scalable production in a continuous flow process. However, there is still a lack of predictive models for patch formation, hindering further process optimization. To obtain the kinetic parameters for such models, in situ characterization of the growing patches is required. Addressing this, the present contribution will give details of a purpose-built inline spectroscopic setup and the results obtained with it.

Inline measurements to understand the continuous flow growth of various types of nanoparticles have been reported in the literature. In the case of noble metal nanoparticles, a change in size and morphology can be detected via a change in the optical spectrum. Consequently, inline extinction spectroscopy offers an easily accessible tool to follow the particles' structural evolution in time.

To investigate the patch growth under well-mixed conditions, we use a continuous inline spectroscopy setup which consists of a polyamide T-mixer connected to a rectangular borosilicate glass tube. The latter is mounted on a linear stage on an optical pegboard. Via an automated protocol, the glass tube is moved through a fixed measurement position of a fiber spectrometer. Thus, each position along the glass tube corresponds to a specific reaction time. An adjustable spacer tube can be used to obtain data at later residence times.

Using measurements at different reaction conditions, we collect kinetic data for model development. To validate our measurements, we utilize a quenching approach which freezes the metal patches at various growth stages and thus enables them to be investigated via ex situ characterization techniques.

Correlating in situ and ex situ data, we show that a kinetic model for the formation of patchy particles valid for a wide range of reaction conditions can be established, paving the way for further process optimization and automation.

9:30 AM BREAK

10:00 AM *CH01.03.05

In Situ Liquid Phase TEM of Chemical Reactions and Materials Transformations Haimei Zheng; Lawrence Berkeley National Laboratory, United States

The recent development of liquid phase transmission electron microscopy (TEM) have enabled break-throughs in characterizing various chemical reactions and materials transformations. It has unveiled many materials transformation dynamics, and the structure and bonding evolution in situ/in operando with high spatial resolution. Since the electron beam for imaging can also induce perturbation to the chemical processes, it has been a concern that the observed phenomena in a liquid cell may deviate from the real-world processes. Strategies have been developed to overcome the electron-beam induced issues, and to connect the observation with the real-world chemical reactions. Here, I will discuss various strategies in using liquid cell TEM to study nucleation, growth, and self-assembly in solution, where electron beam is often used to initiate the reactions. Due to the complexity of the liquid cell TEM experiments, strategies are often employed simultaneously, for example, low dose imaging, advanced electron microscopy techniques, carefully designed

control experiments, multimodal characterization, and so on. The multidisciplinary research has opened many new opportunities by merging different expertise and approaches together stimulating innovations and fostering novel discoveries.

10:30 AM CH01.03.06

Early-Stage Nucleation Behavior of GaAs Nanowires on Si Substrate based on *In-Situ* TEM [Chen Wei](#)^{1,2}, Jean-Christophe Harmand² and Federico Panciera²; ¹Université Paris-Saclay, France; ²Centre National de la Recherche Scientifique, France

To take advantage of the unique physical properties of nanowires (NWs), it is crucial to accurately control their geometry, crystal structure, and doping level. This goal will ultimately be achieved by a deeper understanding of the growth mechanisms.

Meanwhile, the initial stages of the growth process are the least understood and have been investigated almost exclusively by ex-situ techniques. Here, we present real-time observations of the nucleation and growth of self-catalyzed GaAs nanowires using a transmission electron microscope (TEM) equipped with molecular-beam-epitaxy (MBE) sources. Custom-made floating substrates, in the form of electron-transparent <111>-oriented Si membranes, were fabricated using MEMS (Micro-electromechanical Systems) technology. A combination of finite-element simulations and Raman spectroscopy was used to accurately calibrate the sample temperature and optimize its design. The results were in good agreement and further verified by the dimension and distribution of pre-deposited Ga droplets.

Nanowires were grown directly on the membrane inside the microscope via a vapor-liquid-solid mechanism as a practical MBE configuration and the process was monitored *in situ* and in real-time with high spatial and temporal resolution. On the base of our direct observations, the main steps of this dynamic process, from Ga droplet deposition to crystal nucleation at the interface as well as the vertical growth of nanowires will be discussed.

10:45 AM CH01.03.07

Multiscale Mechanisms of Twisted Carbon Nanotube Yarns Probed *In Situ* by Soft X-Rays during Tensile Loading [Philip M. Jean-Remy](#)¹, Daniel Malone¹, Alec Schwart¹, Cheng Wang², Adam Golder¹, Eric Meshot³ and Xavier Lepro Chavez¹; ¹Lawrence Livermore National Laboratory, United States; ²Lawrence Berkeley National Laboratory, United States; ³Atomic Machines, United States

Resonant soft x-ray scattering (R-SoXS) can help realize the promise of data driven research in hierarchical materials whose structure spans multiple length-scales, such as carbon nanotube (CNT) assemblies. Our prior work demonstrated the wealth of high-resolution and statistical data R-SoXS provides about chemical and structural morphologies across different length scales in CNT materials [1]. CNTs are known as the strongest 1D material due to their covalent sp² carbon bonds, hexagonal lattice, and cylindrical shape. However, piecing together CNTs into assemblies has proven to be so far a failed strategy to achieve the same elite performance metrics as individual CNTs. This highlights a critical deficiency in understanding the effects that the processing of individual nanostructures has on the performance of their derived macroscale assemblies, thereby hindering the development of a process-structure-performance map for these materials.

In this work, we propose a new method to decouple the distribution orientation of nanoscale tortuosity and the macroscale twist of CNT dry-spun yarns under applied loads via *in-situ* R-SoXS probing at high energy (1200 eV) and low energy (280 eV), respectively. With this decoupling enabled by *in-situ* R-SoXS, we gain new insights on the deformation mechanisms of these yarns which have been structurally reinforced with a novel vapor-phase polymer that is subsequently self-crosslinking [2]. Further, we examine how both the distribution orientation of the nanoscale tortuosity of CNT bundles and the macroscale twist of the yarns evolve as a function of applied load for different processing conditions, including yarns with plasma-enhanced surface reactivity prior to the polymer reinforcement. Better understanding of the multiscale structural behavior of CNT yarns as a function of processing will allow advances for the manufacture at large scale of products based on ultra-strong, flexible, conductive fibers for aerospace, defense, communications, wearables, and biomedical industries.

1. Meshot, E. R., Zwissler, D. W., Bui, N., Kuykendall, T. R., Wang, C., Hexemer, A., Wu, K. J. J., & Fornasiero, F. (2017). Quantifying the hierarchical order in self-aligned carbon nanotubes from atomic to micrometer scale. *ACS nano*, 11(6), 5405-5416.

2. Lepro, X., Aracne-Ruddle, C., Malone, D., Hamza, H., Schaible, E., Buchsbaum, S. F., Calonico-Soto, A., Bigelow, J., Meshot, E., Baxamusa, S., & Stadermann, M. (2022). Liquid-free covalent reinforcement of carbon nanotube dry-spun yarns and free-standing sheets. *Carbon*, 187, 415-424.

Prepared by LLNL under Contract DE-AC52-07NA27344 and LDRD 20-ERD-023.

11:00 AM CH01.03.08

Synthesizing New Ternary Nitrides with Guidance from *In Situ* X-Ray Diffraction [Christopher Rom](#)¹, Shaun O'Donnell^{1,2}, Kayla Huang^{1,3}, Rebecca Smaha¹ and Andriy Zakutayev¹; ¹National Renewable Energy Laboratory, United States; ²Colorado State University, United States; ³University of Illinois at Urbana-Champaign, United States

Ternary nitrides are an important class of functional solids, most famous for underpinning high-efficiency light emitting diodes. These materials are composed of nitrogen along with two other elements (e.g., In₃Ga_{1-x}N for those light emitting diodes). However, making these materials is challenging, in part owing to the low reactivity of elemental nitrogen gas (N₂), and the propensity for nitrogen-containing solids to decompose at elevated temperatures (releasing N₂). Metathesis reactions (also known as ion exchange reactions) can help us overcome these challenges and keep nitrogen in the solid state to synthesize new ternary nitrides. For example, we have recently discovered that starting from lithium-containing precursors (e.g., Li₆WN₄), we can conduct metathesis reactions with ZnX₂ salts (X = F, Cl, Br) to synthesize new Zn ternary nitrides (e.g., Zn₃WN₄). This presentation will focus on our recent work studying these kinds of metathesis reactions using *in situ* X-ray diffraction, with an eye towards generalizing this synthesis approach to accelerate materials discovery.

11:15 AM CH01.03.09

Formation of Quasi-2D Perovskites using *In Situ* Multimodal Spin Coater with Grazing Incidence X-Ray Scattering [Aidan Coffey](#)^{1,2} and Chenhui Zhu¹; ¹Lawrence Berkeley National Lab, United States; ²University of Houston, United States

Hybrid perovskites are a class of ideal absorbing materials for solar cells that suffer from moisture and temperature instability. Single junction PVs using the hybrid perovskites MAPbI₃ and FAPbI₃ (MA= H₃CNH₂, FA= NH₂CHNH₂) have achieved a certified power conversion efficiency (PCE) over 25%, which is very close to the premier silicon PVs. To combat the instability of hybrid perovskites, 2D perovskites that feature large organic ligands that replace MA⁺ or FA⁺ in the 3D structure. Introducing electronically insulating moieties into perovskites makes crystal orientation critical to device efficiency. Nucleation and crystallization mechanisms for large organic ligands remains unknown and can be investigated thoroughly by *in situ* GIWAXS/SAXS and are vital to the development of stable perovskite solar cells.

The exploration of incorporating ligands into 2D perovskites allows another tunability parameter to control the mechanical and optoelectronic properties of perovskite materials. While incorporating organic ligands improves moisture stability, it also introduces electronically inactive components, making crystal orientation critical to photovoltaic power conversion efficiency. There have been several efforts to vertically align 2D perovskites by changing thermodynamic procedure conditions, precursor concentration, and precursor type. While there have been efforts to characterize the crystallization dynamics with the 3D perovskites (e.g. MAPbI₃), the dynamics of 2D crystallization are not well understood. To study the formation of quasi-2D films, we have fabricated a custom-made in situ multimodal spin coater system with an integrated heating stage that can be programmed with spinning and heating recipes and coupled with synchrotron-based grazing-incidence WAXS and SAXS (GI-WAXS/GI-SAXS).

Studying the crystallization of quasi-2D perovskite films using synchrotron radiation allows for reduced exposure times, ensuring high time-resolution data that is paired with in situ photoluminescence to understand how the choice of ligand affects film crystallization kinetics, crystallinity, and orientation – all of which are crucial to increasing efficiency. Using the new stage, we have studied the formation of various bithiophene-based (2T) organic ligands at a variety of n-numbers (3, 5, and 10) and compared them to the well-established butylammonium (BA) ligand. In addition, the new stage allows us to control the temperature of the substrate, allowing for the elucidation of how thermal effects can be used to leverage the formation kinetics, thus paving the way for more stable, high efficiency perovskite solar cell materials.

11:30 AM CH01.03.10

Distinguishing Classical from Non-Classical Nanoparticle Growth Mechanisms by *In-Situ* X-Ray Diffraction [Stephan Foerster](#), Manuel Wilke, Sascha Ehlert and Martin Dulle; Forschungszentrum Jülich, Germany

Hot-injection and heat-up synthesis routes are very commonly used for the controlled synthesis of nanoparticles with narrow size distribution and high crystallinity. These synthesis routes can proceed via classical or different non-classical nucleation and growth pathways, the latter often involving pre-nucleation clusters or oriented attachment. For synthetic control is important to have knowledge about the reaction pathways. To obtain fundamental insights into the nanoparticle nucleation and growth kinetics for these reactions is particularly demanding, because these synthesis routes typically involve heating to temperatures above 200°C which is challenging for many in-situ experimental techniques.

We designed glass flask reactors to perform *in situ* X-ray diffraction (SAXS/WAXS) experiments to investigate the nucleation and growth kinetics of noble metal, semiconductor and oxidic nanoparticles during heat-up synthesis up to 340°C. The analysis of the growth curves for varying heating rates, precursor/ligand ratios and plateau temperatures shows that the kinetics proceeds *via* non-classical reaction paths involving the formation of amorphous pre-nucleation clusters, nucleation, oriented attachment and final growth by monomer consumption. [1,2] Although these pathways are more complicated compared to classical nucleation and growth, one can identify kinetic phases of induction, nucleation and growth that are typically transected during the synthesis.

For a quantitative analysis of the growth curves we extended classical nucleation and growth theory to account for amorphous transient or precursor states and particle aggregation e.g. by oriented attachment during the nucleation and growth phases. We find that this non-classical model is able to quantitatively describe all experimental growth curves. The model provides fundamental insights into the underlying kinetic processes especially in the nucleation and growth phases with the occurrence of a transient amorphous state, the nucleation of crystalline primary particles, particle growth and particle aggregation, all proceeding on overlapping time scales.

The described *in situ* X-ray scattering experiments together with the extension of the classical nucleation and growth model quantitatively describe the two most important mechanisms of non-classical nucleation and growth routes, *i.e.* the formation of intermediate or transient species, and the particle aggregation processes.

[1] V. Leffler, S. Ehlert, B. Förster, M. Dulle, S. Förster, *ACS Nano* 2021, 15, 840-856

[2] V. Fokina, M. Wilke, M. Dulle, S. Ehlert, S. Förster, *J Phys Chem C* 2022, 126, 50

SESSION CH01.04: Crystal Growth IV
Session Chairs: Qian Chen and Wenhui Wang
Wednesday Afternoon, April 24, 2024
Room 442, Level 4, Summit

1:30 PM CH01.04.01

3D Structure of DNA-Protein 2D Lattice by Cryo-Electron Tomography [Jianfang Liu](#); Lawrence Berkeley National Laboratory, United States

Programmable and self-assembled two-dimensional (2D) protein lattices hold tremendous potential in the realms of biological crystalline devices and nanoscale catalysis, signifying a pivotal advancement from the fundamental building blocks towards intricate three-dimensional (3D) crystal structures. However, the creation of high-order lattices remains challenging, partly due to the lack of a tool to precisely analyze the 3D structure of each building block within short-range-ordered crystals without averaging. In this study, we leveraged advances in cryogenic electron tomography (cryo-ET) and the individual-particle electron tomography (IPET) technique to determine the 3D structure of each individual building block within short-range-ordered 2D protein-DNA origami lattices. The building block features a DNA origami octahedral cage, composed of 12 DNA helical bundles, and encapsulates ferritin molecules. Our quantitative analysis of the variations of conformations and orientational of these distinctive and asymmetric building blocks showed that ferritin loading exerted a negligible influence on the lattice unit-cell parameters. However, the flexibility of the blocks themselves and their connectors significantly affected lattice fluctuations. These findings were further validated by molecular dynamics (MD) simulations and juxtaposed with small-angle scattering (SAXS) data. This research offers an innovative approach to troubleshooting high-order crystallization by evaluating the crystal structure through the lens of the 3D structure of each unit cell.

1:45 PM CH01.04.02

Direct Observation of Key Aluminum Hydroxide Oligomers for Gibbsite Crystallization in Bayer Liquor by ToF-SIMS [Juejing Liu](#)^{1,2}, Carolyn Pearce¹, Xiaofeng Guo², Kevin Rosso¹, Zihua Zhu¹ and Xin Zhang¹; ¹Pacific Northwest National Laboratory, United States; ²Washington State University, United States

The Bayer process, discovered over a century ago, is still not fully understood with regards to the mechanism of crystallization of γ -aluminum hydroxide (γ -Al(OH)₃, gibbsite) from the Bayer liquor. In order to gain a better understanding of this process, we utilized liquid ToF-SIMS to directly observe the

evolution of Al oligomers in a sodium aluminate solution simulating Bayer liquor. Our results were then validated through in-situ Raman, SAM-NMR, and DFT simulation. By comparing the change in the relative concentration of Al oligomers with +1 and -1 charge in environments favoring the crystallization of gibbsite and solid sodium aluminate, we were able to identify three major Al oligomer candidates: iso-tetramers, iso-pentamers, and cyclic hexamers. Our in-situ Raman results demonstrated that the relative concentration of iso-tetramers and iso-pentamers saturated when crystallized gibbsite appeared, while cyclic hexamers saturated before the appearance of gibbsite. Liquid SAM-NMR and DFT simulation provided evidence that the Al oligomers were inherent in the solution, rather than fragments from bigger molecules or crystals. We believe that the iso-pentamers and iso-tetramers exhibit a higher contribution than cyclic hexamers in terms of the crystallization of gibbsite. Our study expands knowledge of gibbsite crystallization in Bayer liquor, which is crucial for optimizing Al metal production and cleaning up liquid radioactive waste at the Hanford site.

2:00 PM CH01.04.03

N Content and Stoichiometry Impact on Crystallization Kinetics of Ge-Rich GeSbTe Alloys Oumaima Daoudi¹, Yann Mazel¹, Maxime Dupraz², Hervé Roussel³, Mélanie Dartois¹, Magali Tessaire¹, Névine Rochat¹, Nicolas Bernier¹, Frédéric Fillot¹, Van-hoan Le¹, Hubert Renevier³, Emmanuel Nolot¹ and Gabriele Navarro¹; ¹University Grenoble Alpes, CEA, Leti, France; ²University Grenoble Alpes, CNRS, France; ³University Grenoble Alpes, CNRS, Grenoble-INP, LMGP, France

Phase-Change Memory (PCM) is a mature technology based on chalcogenide alloys, which has proven its suitability for next generation of non-volatile memory, in particular targeting embedded applications [1]. This result was achieved thanks to the intrinsic features of PCM in terms of scalability, fast programming and high endurance. Enrichment of GeSbTe (GST) alloys by Ge (GGST) and the introduction of light elements demonstrated to be a successful solution to enhance the data retention in PCM. This opens the possibility for this technology to target automotive applications, featuring strict specifications in terms of stability in high temperature environment [2-4]. The optimized combination of N introduction and increased Ge content delayed phase separation and crystallization processes of Ge and GST phases. This delay can be attributed to the reduced mobility of Ge atoms caused by the formation of Ge-N bonds [4, 5].

In this work, we performed *in situ* X-ray diffraction to assess how N and stoichiometry influence GGST materials during thermal annealing. Thus, the need for a beam with high energy and rapid measurements were necessary for following the amorphous-to-crystalline transition effectively.

These experiments took place at BM2-D2AM Beamline of the ESRF in November 2022. A monochromatic beam with energy of 10.9 keV and a 2D detector were used to record the scattered intensity. The result patterns were subsequently corrected and integrated to derive 1D diffraction patterns for analyses and interpretation. The diffraction peaks were fitted with Lorentzian function to extract different parameters (area, height and full width at half maximum) giving information about the crystallization evolution. In the present work, we performed annealing with different heating ramp ups for recovering activation energy by using Kissinger law [6], and then quantifying the impact of N in the different compositions.

These measurements allowed us to observe the following phenomena:

N increases the energy barrier for the crystallization of Ge cubic phase in all the GGST systems studied, while a limited impact is observed on the crystallization kinetic of the GST phase;

- The growth rate of the Ge phase is confirmed to be really high but likely limited at the interface of GeSbTe grains (i.e. where the heterogeneous nucleation of Ge takes place), i.e. the Ge grains size reaches very fast a plateau, and starts to slowly increase again only at temperatures higher than 450 °C;
- The GST phase shows a linear evolution (with respect to Ge phase), with dependent growth rate on the initial stoichiometry of the deposited alloy.
- The evolution of the parameters extracted from our measurements (i.e. crystallization temperatures, crystals sizes etc.) will be presented comparing different GGST compositions. These results will be supported with *ex situ* Raman and IR spectroscopies as well as TEM-EDX analyses.

These results bear new insights for a better understanding of the crystallization process in Ge-rich GST and the impact of N introduction in such alloys.
Haut du formulaire

[1] P. Cappelletti, et al., JAP 53, 193002 (2020).

[2] P. Zuliani, et al. IEEE TED 60, 4020-4026 (2013).

[3] I. Yang et al., H. J. Electrochem. Soc. 157, H483 (2010).

[4] L. Prazakova et al., JAP 128, 215102 (2020).

[5] G. Navarro et al., (IMW), (2016).

[6] R. L. Blaine et al., (Thermochimica Acta), (2012).

2:15 PM CH01.04.04

In Situ Near Edge X-Ray Absorption Fine Structures Spectroscopy for The Characterization of Depolymerization Rate during Polymer Recycling Zhengxing Peng, Mutian Hua, Rishabh D. Guha, Kristin A. Persson, Brett A. Helms and Cheng Wang; Lawrence Berkeley National Laboratory, United States

The circular polydiketoenamine (PDK) elastomers cover a broad range of thermo-mechanical properties to meet various application demands, and they can be fully deconstructed back to monomers through acid mediated hydrolysis. It is found that the deconstruction rates can be controlled by tuning the anions in the acidic media, i.e., the deconstruction rate is accelerated when switching from a hydrogen sulfate anion to a bromide anion. To quantitatively quantify the deconstruction rate, we developed an in-situ NEXAFS method combining with time dependent density function theory (TD-DFT) predictions to investigate the deconstruction of the PDK elastomers, which produced chemo-specific spectrums that are subsequently interpreted with specific assignment to functional groups. Briefly, we sealed a PDK403 thin film with a layer of acid in a sandwiched SiNx membrane windows as the in-situ liquid cell for the collection of NEXAFS spectrum. With careful manipulation of X-ray flux to avoid radiation damage, we consistently observed an increasing peak at 289.4 eV and a decreasing peak at 286.6 eV over time, indicating the progression of chemical transformation. With accurate peak assignment from DFT calculations, the increases at 289.4 eV is ascribed to the release of solvated T-403. The progressively increase in the peak intensity works for the quantification of depolymerization rate of PDK403. This is the first time to in situ characterize the deconstruction of crosslinked polymers as a solid that do not dissolve in a solvent environment. This methodology opens up the possibility to characterize the chemical transformations in various crosslinked vitrimers and elastomers.

2:30 PM BREAK

3:30 PM CH01.04.05

A Hard X-Ray Laboratory XES and XAFS Spectrometer Implementing Asymmetric Bragg Diffractions for High-Resolution Operando Measurements of Ni₂P Nanoparticle Electrocatalysts Anthony J. Gironda, Ricardo Rivera-Maldonado, Jared Abramson, Dawson Dean-Hill, Gerald Seidler and Brandi M. Cossairt; University of Washington, United States

X-ray spectroscopy techniques typically reserved for synchrotrons, namely x-ray absorption fine structure (XAFS) and x-ray emission spectroscopy (XES), have been undergoing a renaissance in the laboratory over the past decade. Advancements in detector technologies and Bragg optic manufacture has enabled high resolution (~1 eV) XAFS and XES spectrometers to be built in the lab. Spherically bent crystal analyzers (SBCAs) are the dominant high-

resolution hard x-ray optic both in the ongoing rebirth of laboratory-based and in synchrotron hard x-ray photon-in/photon-out methods. In almost all cases, SBCAs are implemented in a 'symmetric' configuration on the Rowland circle, wherein the diffracting crystal plane is nominally coincident with the analyzer wafer surface. The laboratory spectrometer described is a powerful characterization tool capable of *in situ* and *operando* measurements across many disciplines while implementing asymmetric Rowland geometries with many benefits.

This work details the following. First, the construction and operation of a laboratory spectrometer specialized in operating with asymmetric Rowland geometries, wherein the diffracting crystal plane is not coincident with the optical surface of the analyzer. Results indicate several benefits of such an instrument, demonstrating increased energy resolution compared to the symmetric counterpart and a massively extended energy range of a single SBCA, enabling a technique we refer to as '*hkl* hopping'. Second, the design and implementation of a low-absorption electrolytic cell optimized for transmission XAFS measurements. This cell enables *operando* x-ray measurements of catalytic materials in the laboratory due to a clear line of sight to the sample window and very thin low-Z materials to minimize unwanted x-ray absorption outside the sample. Third, the use of such a cell and the laboratory spectrometer for *operando* measurements of a Ni₂P nanoparticle electrocatalyst. Ni₂P is an earth-abundant material proposed for use as an electrocatalyst for hydrogen evolution, nitrate reduction, CO₂ reduction, and alcohol oxidation. However, Ni₂P is susceptible to oxidation. Several studies on the material and operating cell were conducted with the laboratory spectrometer, measuring the XAFS of the Ni K-edge to monitor changes in oxidation state with respect to changes in pH, air exposure, and applied potential as the cell operates and is measured simultaneously. Measured in the laboratory, synchrotron quality data of nanoparticle stability and assessment of cell performance is made possible, and through a sweeping series of experiments controlling pHs and applied potentials, a pseudo-Pourbaix diagram of nanoparticle Ni₂P can be constructed.

3:45 PM CH01.04.06

Ultrasound and Rheological Study of Oil-In-Oil Magnetic Pickering Emulsions [Bassam M. Jameel](#), Rafal Bielas and Arkadiusz Józefczak; Faculty of Physics, Adam Mickiewicz University in Poznan, Poland

Magnetic Pickering emulsion is a type of heterogeneous system consisting of stabilized immiscible liquid droplets stabilized with insoluble solid particles, such as magnetic nanoparticles. The control of the formation process and stability of such a three-phase system material is important from the application point of view. Moreover, due to its possible biocompatibility and high cargo-loading capacity, magnetic Pickering emulsions hold significant promise in biomedical and pharmaceutical applications, including therapeutic delivery and bioseparation.

This research primarily focused on characterizing magnetic Pickering emulsion stabilized using various volume concentrations of magnetic nanoparticles and with two distinct formation processes involving ultrasound homogenization and electric field. Ultrasound scattering theory, based on a so-called core-shell model, was employed to analyze ultrasound propagation through such a magnetic three-phase system. Additionally, rheological properties were measured to examine changes in the internal structure when subjected to a static magnetic field. The Herschel-Bulkley model was applied to determine the yield stress based on magnetorheology measurements. Optical microscopy was employed to verify optical changes in the system resulting from different formation processes.

The ultrasound spectroscopy results demonstrated variations in attenuation associated with different magnetic shell thicknesses, core radii, and concentrations. Fitting experimental data to the core-shell model revealed the relationship between volume concentrations and both core and shell sizes. Higher particle concentrations were found to result in a greater number of particles at the droplet interface [1], directly affecting the radius of magnetic Pickering droplets, aligning with the findings of another study [2]. Furthermore, higher volume ratios of magnetic nanoparticles exhibited a more pronounced magnetoviscous effect. Additionally, the formation process involving an electric field yielded higher dynamic yield stress [3]. This work was supported by project no. 2019/35/O/ST3/00503 (PRELUDIUM BIS) of the Polish National Science Centre.

Reference

- [1] Jameel, B., Bielas, R. and Józefczak, A., 2023. Ultrasound measurements of particle shells in magnetic Pickering emulsions. *Measurement*, 220, p.113409.
- [2] Rozynek, Z., Bielas, R. and Józefczak, A., 2018. Efficient formation of oil-in-oil Pickering emulsions with narrow size distributions by using electric fields. *Soft Matter*, 14(24), pp.5140-5149.
- [3] Jameel, B., Paulovičová, K., Tóthová, J., Rajnák, M., Molčan, M., Bielas, R. and Józefczak, A., Magnetorheological characterization of oil-in-oil magnetic Pickering emulsions. *Journal of Magnetism and Magnetic Materials*, submitted 2023.

4:00 PM CH01.04.07

SiO₂ Particles prepared from PDMS Foam/Sponge with Potential use as a Viscosity Enhancer [Yogendra Yadawa](#) and Amit Ranjan; Rajiv Gandhi Institute of Petroleum Technology, India

In this work we report a simple technique to produce SiO₂ particles with completely different morphologies, starting from the commercially available PDMS (Sylgard 184, Dow Chemicals). The process consists of first preparing a PDMS sponge by taking a solution of PDMS and cross-linkers in THF with suitable concentration and subjecting it to heating. The cross-linking reaction simultaneously occurring with the bubble formation due to boiling of the THF results in the formation of sponge-like PDMS. Subsequently, the sponge pieces are kept under two different thermal environment conditions which yield SiO₂ with entirely different morphologies in the resulting material. In the first case when the sponge is subject to slow heating to 550 °C and slow cooling, a very soft powder of SiO₂ nanoparticles is obtained. In the second case, fast heating and fast cooling of the same sponge wrapped inside an aluminum foil yields a brittle solid. The formation of amorphous SiO₂ in both the cases is confirmed from XRD and FT-IR. The SEM imaging of the soft powder shows particles of nearly spherical shape with size ranging from 100 nm to 500 nm whereas the brittle solid when crushed and ground, shows much larger particles with planar faces. The BET surface area was found to be 4.36 m²/g for the soft powders which increased considerably to 192 m²/g for the brittle solid.

We further studied the rheological alterations due to soft powder samples. A mixture of PDMS-THF solution with 1.25 wt% soft and brittle SiO₂ particles enhances the viscosity nearly 1.5 and 2 times respectively at low shear rate (1 s⁻¹). This mixture was found to homogeneously incorporate water up to a certain extent (nearly 30 wt%) beyond which the mixture was found to phase separate. The viscosity of the PDMS-THF-particle mixture with 30 wt% DI water was found to further increase by a factor of nearly 10 for soft and 20 for brittle SiO₂ particles as compared to the mixture without any water. Our formulation which is completely based on a commercially available product, will be explored towards enhancing the rheological properties of the mixture PDMS-THF-particle solutions.

Keywords: SiO₂ nanoparticles, polydimethylsiloxane (PDMS), THF, zero shear viscosity.

4:15 PM CH01.04.08

In Situ X-Ray Imaging of Droplet Drying with Dense Particle Suspensions: Exploring the Mechanism of Coffee Ring Formation [Yuanyuan Liu](#), [Wajira Mirihanage](#) and [Brian Derby](#); University of Manchester, United Kingdom

Droplet deposition and drying is a key process in many manufacturing processes including: the spray deposition of paints and coatings, inkjet printing, and the manufacture of large area electronics. During the drying of droplets that contain small particles in suspension, it is well known that, under certain

experimental conditions, the dried residue does not form a uniform deposit related to the shape of the initial liquid drop but instead a migration of particles to the pinned contact line of the drop leads to a characteristic ring deposit or *coffee stain*. In dilute particle suspensions this phenomenon is believed to be initiated by contact line pinning during evaporation, which leads to a radial outward fluid flow along the base of the drop increasing the local particle concentration at the contact line because evaporation removes the solvent. The precise conditions that trigger the formation of a coffee ring are still a topic of investigation but are believed to be associated with the mechanisms that lead to contact line pinning before the receding contact angle is reached during drying.

There has been considerable experimental study of the drop drying process and in situ imaging of dilute particular suspensions using optical microscopy and individual particle tracking experiments has prove valuable for studying the dynamics of the coffee ring and fluid flow during droplet drying. However, many of the real-world applications of droplet-based manufacture use dense particulate suspensions as the fluid or ink and, although it is known that such dense suspensions can form a coffee ring, study of droplet drying in these cases has been limited to observing the change in drop shape.

Here, we present an *in situ* study of the drying of dense suspensions of sub-micron ZrO₂ particles in aqueous suspension using a synchrotron X-Ray source to track changes in drop volume and shape during drying at 20, 45 and 60 °C on glass, silicon and Kapton substrates that show different contact angles of 24°, 36° and 73° respectively. We show that if the drop retains radial symmetry during the drying process, the signal intensity across the drop image can be transformed to determine the local density of the suspension and from this a semi-quantitative measure of the particle concentration in the liquid as a function of vertical and radial position in the drop. Hence, we can track the relative densification of the particle suspension as a function of position during the drying of the drop.

Coffee rings are found to form more easily on the lower contact angle surfaces and at higher drying temperatures where evaporation is more rapid. Our results show that the density profile across drying drop is significantly different between drops that show uniform drying and those where a coffee ring forms. In the absence of a coffee ring, densification commences across the surface of the drop in a uniform manner and there is evidence for a possible surface crust during drying. However, under the conditions that lead to a coffee ring, initial densification is also more intense at the upper surface but is now much stronger towards the contact line. It is unclear whether the surface crust formation suppresses coffee ring formation or is a consequence of its absence.

4:30 PM CH01.04.09

Continuous EELS Spectrum Imaging of Nano-Droplet Crystallization Heterogeneity [Benjamin Miller](#), Liam Spillane and Cory Czarnik; Gatan, Inc., United States

Electron energy loss spectroscopy (EELS) is a powerful technique for characterizing nanomaterials. A number of materials properties can be extracted from the information-rich spectra. One application is nano-thermometry, where the local temperature of individual metal nanoparticles can be measured by a precise determination of the plasmon peak position. As thermal expansion increases a particle's volume, the density of electrons decreases, and the energy loss of the plasmon peak shifts to lower energies. This same approach can be used to detect melting and crystallization, which result in much larger changes in the electron density. Continuous acquisition of EELS data enables precise determination of the melting and crystallization temperatures. Using the new in-situ EELS spectrum imaging features of the Continuum GIF, a continuous series of drift-corrected spectrum images can be acquired over an ensemble of particles, and the melting and crystallization behavior monitored.

In this work, we show how a series of EELS spectrum images can be acquired and processed along with the temperature data from a MEMS-based heating holder. With modern fast detectors and spectrometers, spectrum images with thousands of spectra can be acquired in less than a second, making continuous in-situ spectrum imaging feasible. The holder temperature data is automatically synchronized and correlated with EELS spectrum image data. We also show how the entire series of in-situ EELS spectrum images can be rapidly fit using the built-in NLLS tools in DigitalMicrograph, yielding series of synchronized fit maps. After summing over a single nanoparticle, plots of the peak position over time can be generated, and even plotted against the nominal temperature from the holder in scatterplots.

This new in-situ EELS spectrum imaging capability has been applied to a Sn nanoparticle sample which was oscillated above and below its melting temperature. Watching the maps of plasmon position over time reveals that while all the Sn particles crystallize during most cycles, and most particles crystallized during every observed cycle, some particles occasionally did not crystallize even though surrounding particles did. This heterogeneous and stochastic behavior at the nanoscale can only be observed with high spatial and temporal resolution. In-situ electron microscopy, and specifically in-situ EELS spectrum imaging is an excellent technique for exploring these dynamics.

4:45 PM CH01.04.10

Solid Nanoparticles and Liquid Droplets on The Path to Crystallization in Solution: Some Fundamental Questions on Nucleation Addressed with Synchrotron X-Ray Scattering Methods. [David Carriere](#); CEA, France

Crystallization from solution often involves transient, non-crystalline states like reactant-rich liquid droplets and amorphous particles [1]. This state of affairs not only challenges the chemical engineering models used to rationalize laboratory- and industrial-scale processes, but also motivates deep experimental tests of the multistep nucleation theory proposed as an alternative to the well-known classical nucleation theory of Becker and Doering [2]. However, testing both engineering and physical models requires challenging quantification of the structures and phases (sizes, volume fractions, crystallinity, compositions), down to the millisecond reaction times and sub-nanometer characteristic lengths.

Here, I will illustrate how coupling synchrotron X-ray methods and electron microscopy can tackle challenging scientific questions in the crystallization of oxide nanoparticles, vanadates and rare-earth oxalates through: 1) providing evidence of transient structures, and sometimes multiple transient structures, together with growing crystals [3–6] 2) assessing the impact of these transient phases on the final product, in particular when it consists of nanometer-sized aggregates of nanocrystals [5] 3) providing evidence of an evolution in the chemical composition of the transient phases [6] and 4) assessing the impact of the transient phases on chemical engineering models [7].

References

1. Yoreo, J. J. D. *et al.* Crystallization by particle attachment in synthetic, biogenic, and geologic environments. *Science* 349, aaa6760 (2015).
2. Vekilov, P. G. Nonclassical Nucleation. in *ACS Symposium Series* (ed. Zhang, X.) vol. 1358 19–46 (2020).
3. Fleury, B. *et al.* Amorphous to Crystal Conversion as a Mechanism Governing the Structure of Luminescent YVO₄:Eu Nanoparticles. *ACS Nano* 8, 2602–2608 (2014).
4. Baumgartner, J. *et al.* Self-Confined Nucleation of Iron Oxide Nanoparticles in a Nanostructured Amorphous Precursor. *Nano Lett.* 20, 5001–5007 (2020).
5. Freitas, A. P. *et al.* Crystallization within Intermediate Amorphous Phases Determines the Polycrystallinity of Nanoparticles from Coprecipitation. *Nano Lett.* 22, 29–35 (2021).
6. Durelle, M. *et al.* Coexistence of Transient Liquid Droplets and Amorphous Solid Particles in Nonclassical Crystallization of Cerium Oxalate. *J. Phys. Chem. Lett.* 13, 8502–8508 (2022).

7. Durelle, M. *et al.* Measurement of Nucleation Rates during Nonclassical Nucleation of Cerium Oxalate: Comparison of Incubation-Quenching and In Situ X-ray Scattering *Crystal Growth & Design* (2023)

SESSION CH01.05: Poster session I
Session Chairs: Liang Jin and Dongsheng Li
Wednesday Afternoon, April 24, 2024
Flex Hall C, Level 2, Summit

5:00 PM CH01.05.01

Atomic Scale Imaging of Defects in Solution Grown Tin Disulfide Naveen Goyal, Rajeev Kumar Rai and N. Ravishankar; Indian Institute of Science, India

Tin disulfide (SnS₂), a layered material, has gained substantial attention in recent years due to its applications in various fields, including broadband photodetection spanning from UV to NIR regions, selective room-temperature gas-sensing of NO₂, serving as an anode material in sodium-ion batteries, and application in supercapacitors.¹ These applications arise as a result of a synergistic interplay between SnS₂'s inherent properties and the precise engineering of defects, such as vacancies, dislocations, and grain boundaries.² Along with these, other defects such as ripplations are also present exclusively in layered materials.³ The control of such new defects and their influence on the properties and applications of layered materials is currently a wide subject of study.

In this study, we utilized the solution chemistry method to synthesize nanocrystals of SnS₂. The phase purity of these nanocrystals was confirmed through powder X-ray diffraction, and their uniform nanosheet morphology was evident from SEM images. We have conducted a comprehensive analysis of defects using advanced microscopic techniques, specifically using aberration-corrected scanning transmission electron microscope. By directly imaging the layers of SnS₂ along [100] zone axis, we identified the presence of various defects at the core of nanocrystal, including line and screw dislocations, voids and warping of layers. While dislocations and voids are well-documented in various materials, the ripplations appears to be a unique characteristic of van der Waals materials like SnS₂. These defects are believed to result from local variations in supersaturation during the nucleation and growth of the crystal. This type of investigation is expected to yield valuable insights for tailoring the properties of layered materials.

References:

1. Eom, T. H. *et al.* Substantially improved room temperature NO₂ sensing in 2-dimensional SnS₂ nanoflowers enabled by visible light illumination. *J. Mater. Chem. A* **9**, 11168–11178 (2021).
2. Liang, Q., Zhang, Q., Zhao, X., Liu, M. & Wee, A. T. S. Defect Engineering of Two-Dimensional Transition-Metal Dichalcogenides: Applications, Challenges, and Opportunities. *ACS Nano* **15**, 2165–2181 (2021).
3. Gruber, J. *et al.* Evidence for Bulk Ripplations in Layered Solids. *Sci. Rep.* **6**, (2016).

5:00 PM CH01.05.02

Frequency-Guided Photoreactions: A Case Study on 1,3-Dimethoxybenzene Trifluoromethylation Katsuyuki Morii^{1,2} and Mayaka Maeno²; ¹Nippon Shokubai Co Ltd, Japan; ²Osaka University, Japan

We propose a new method for controlling photochemical reactions using the frequency of the light as a parameter. The 21st century is called the century of light, and photoreaction are being actively researched. Furthermore, research is active in fields that try to apply light, such as beauty, medicine and plant cultivation. Recently, in several fields, it has been reported that time-controlled light, that is, pulsed light, has an effect beyond expectations. Therefore, in order to clarify its origin, we investigated the relationship between optical parameters of pulsed light and results with photoreactions. In this study, we conducted a pulsed-light-induced trifluoromethylation reaction under simple reaction conditions wherein we combined 1,3-dimethoxybenzene, anthraquinone, and CF₃SO₂Na without any other additives, oxidants, or reductants, and exposed the mixture to both conventional and pulsed light. The photoreaction was carried out at a temperature of 15 degree C for 20 hours. All conditions were the same except for frequency modulation, and photoreactions were performed using (a) continuous light and (b) pulsed light at 10⁵Hz and duty 0.1. Comparing entry (a) and (b), entry (a) achieves the same yield as entry (b), even though it uses only 10% of the light exposure. In addition, the amount of bis-trifluoromethylated products were decreased by half compared to entry (a). We considered it important that this result was achieved using only frequency modulation. Compared to conventional light, pulsed light yielded higher efficiency and regioselectivity, while also suppressing undesired reactions. Even more interestingly, it was found that both reaction yield and chemoselectivity varied with the frequency of the pulsed light in the range from 1.4 × 10⁻⁵ Hz to 10⁵ Hz. Notably, the total irradiation time was kept constant at 7200 s.

Our findings suggest that pulsed light offers a promising avenue for controlling photochemical reactions, and beyond traditional parameters like reagents, solution concentration, and temperature, the method of light irradiation emerges as a critical factor in photochemical processes. Furthermore, the reaction characteristics within the frequency modulation of more than 10 orders of magnitude are thought to indicate the behavior of some intermediates, substrates, and catalysts on various time scales, and it is expected that this method will be useful for evaluating the dynamics of photoreactions.

We demonstrated, for the first time, a pulsed-light-induced trifluoromethylation reaction conducted under simple reaction conditions, wherein the frequency of the pulsed source was used as an adjustable control parameter. We found that pulsed-light irradiation improved the yield and regioselectivity of the reaction. This showed that varying the parameters of the light source could be an important factor in controlling the reaction. The effect of frequency, which corresponds to the ON/OFF time ratio of the pulsed light, may be related to the lifetime of the active species and the concentration of the photocatalyst or reaction intermediates. Elucidation of the full mechanism behind the frequency-controlled photochemical reactions is expected to establish new methods for reaction control and will contribute toward the development of new reactions.

5:00 PM CH01.05.03

Synthesizing Nanomaterials with Optimal Properties using Closed Loop Optimization Brenden Pelkie, Abdul Moez and Lilo D. Pozzo; University of Washington, United States

Many nanomaterial synthesis procedures require the selection of several experimental parameters to control the properties of the material that is produced. While this can provide detailed control over material properties, navigating this high dimensional parameter space to select values that enable desired outcomes can be an intractable process. While the applications of laboratory automation makes the systematic testing of parameter combinations more accessible, complete combinatorial explorations can still be inefficient or impossible for large systems. Closed loop optimization methods like Bayesian optimization provide a method to autonomously select experimental parameter values to test, on-the-fly during an ongoing experiment. These approaches use machine learning methods to select parameters that are likely to improve a material's performance, as defined by a researcher-defined metric.

This searchable program is up-to-date as of April 15th, 2024.

Implementation of fully closed loop experiments requires capabilities for automated sample synthesis, characterization, and data processing. We are developing infrastructure to enable closed loop optimization for nanoparticle systems. To enable automated synthesis, we have developed an open-hardware robotic motion platform to enable flexible lab automation for advanced synthetic capabilities and automated flow synthesis tools for nanoparticle synthesis. Online characterization is enabled by an autosampler and automated data processing workflow for lab-scale x-ray scattering. These capabilities are applied to gain morphological control of various nanoparticle synthesis processes.

5:00 PM CH01.05.04

A Parametric Study Regarding The Influence of Fabrication Methods on The Explosive Characteristics of Porous Silicon [Nathan Heavner](#), Max Krauss, Greer Miller and Jeff Jessing; Fort Lewis College, United States

Over the past decade, extensive research has explored the reactive properties of porous silicon (PSi) when combined with chemical oxidizers. PSi detonations, capable of precise and reproducible thrust, have the potential to be utilized for advanced micro-thruster applications. By adjusting fabrication and oxidation parameters, it is possible to enhance the reactivity of chemically oxidized PSi. Changing these parameters can also provide valuable insights into the energetic yield of PSi, thus allowing optimization of propulsion characteristics. This parametric study focuses on performing the electrochemical anodization of bulk silicon (Si), using a 3:1 ratio of 49% hydrofluoric acid to ethanol (HF:EtOH) with varying current densities and anodization times to fabricate PSi. A 3.2Mol sodium perchlorate methanol solution is then applied to the PSi substrate as an oxidizer. The samples are subsequently dried using one of three methods: atmospheric drying, vacuum drying and drying in a nitrogen box. Variable drying times for each method are also reviewed. Finally, a bomb calorimeter is employed to analyze the combustive properties of the PSi samples. The results of this analysis are used to identify the optimal fabrication parameters for achieving maximum energy yield from a PSi detonation.

5:00 PM CH01.05.05

The Operando SAXS Characterization of The Binary Mixing of F127/L121 Pluronic Biomedical Hydrogels in The Self-Assembly Tz-Feng Lin and [Wei-Chieh Wang](#); Feng Chia University, Taiwan

Pluronic biomedical hydrogels (PBHs) was proposed to study the structural changes in the self-assembly of binary mixing copolymers. PBHs are served as a microenvironment and a as a targeted drug delivery system offering many attractive benefits such as intrinsic biocompatibility and controllable prolonged drug delivery. Small angle X-ray scattering (SAXS) was used to discover the self-assembled structures of the PBHs in real time with respect to the temperature variations. According to the SAXS results, structural changes of the micelle and the lamellar affected the mixing behavior of hydrophilic segments and hydrophobic segments. Thus, the transformation between the flat lamellar amphiphilic boundary and the hydrophobic core was studied. Results show that the diffusion of the amphiphilic segments in the PBHs will affect a lot across the interface between the hydrophilic corona and the hydrophobic core. Evidence are observed for the self-assembly of PBHs at the temperatures from 25 to 45 °C simultaneously.

5:00 PM CH01.05.06

Real-Time Etch End Point Detection for Silicon Biomembranes in Lung-On-A-Chip Applications [Leif Gislason](#), Sahra G. Genc, Sally Thompson and Jeff Jessing; Fort Lewis College, United States

Wet-etched thinned silicon membranes are common in the microelectromechanical system (MEMS) industry, with accuracy in dimensions, specifically thickness, being a crucial aspect to the functionality of these devices. Our research focuses on producing biomembranes for lung-on-a-chip applications. The current fabrication process of these membranes uses a heated aqueous solution of potassium hydroxide (KOH) to thin double-side polished, (100), p-type silicon wafers to sub-5 μm . Previously, our work has relied on a procedure that involves removing the membrane midway from the KOH bath, measuring with a micrometer, calculating an etch rate, and then finishing the etch based on this etch rate. This damages the silicon and ultimately compromises the quality of the resultant membrane. We propose an optical-based method to determine in real-time the thickness of the membrane as it is being etched with KOH. The setup of this experiment involves a custom fabricated enclosure for the thinned sample with apertures on both sides, with one having a light source and the other, a photodetector. Various light sources and detection wavelengths are used to investigate the optimization of light transmission through the thinning membrane so that a correlation of transmission to membrane thickness can be determined. Using scanning electron microscopy for accurate thickness determination we present a model that provides correlation with light transmission through the membrane. Our ultimate goal is to be able to determine the thickness in real-time during an etch, which will entail significant research considering it must pass through multiple media, including two glass beakers, water, and an aqueous solution of KOH and water which introduces multiple scattering events.

SESSION CH01.06: Crystal Assembly and Transformation
Session Chairs: Miaofang Chi and Dongsheng Li
Thursday Morning, April 25, 2024
Room 442, Level 4, Summit

10:30 AM *CH01.06.01

In and Out-Of-Equilibrium Assembly Dynamics of Nanoparticles [Qian Chen](#); University of Illinois at Urbana-Champaign, United States

In this talk, I will discuss our recent efforts on utilizing liquid-phase TEM imaging and associated machine-learning or computational simulation methods to understand the fundamental colloidal forces in both equilibrium and out-of-equilibrium assemblies of nanoparticles. Anisotropic gold nanoparticles are our model systems, with intriguing plasmonic properties and directional interactions. We study their nucleation pathway and growth habits in real-time in solution at the nanometer resolution, where colloidal interactions balance with mass transport to ultimately determine the size, shape and surface morphology of assembled superlattice. We study the phononic relaxation of the superlattices, where complex colloidal interactions act effectively as nanoscale springs to determine the collective structural reconfiguration. Going beyond equilibrium dynamics, we also study the external field driven assembly of nanoparticles, where hydrodynamic effects drive the nanoparticles into active "swarms" with rapidly-changing patterns. We will show new structural control and new functional relevance in these particulate systems, when we consider both the colloidal interactions and all the other factors such as diffusivity, many-body effects, and ionic flows.

11:00 AM CH01.06.02

Multiphase Silk Assembly for Two-Dimensional Bio-Crystal Film [Chenyang Shi](#) and James J. De Yoreo; Pacific Northwest National Laboratory, United States

Early insights into native silk fibroin (SF) architecture suggested that its unique structures and properties are determined by its multiscale assembly and the evolution of its secondary structure. Yet the pathways of assembly and the relationship to that evolution are poorly understood. Here we investigate SF self-assembly using in situ AFM and liquid phase infrared nanospectroscopy (nano-FTIR) and molecular dynamics. To do so, we assemble the silk at the interface between water and highly ordered pyrolytic graphite (HOPG). We find that SF grows heteroepitaxially on HOPG into highly ordered, monolayer-thick 2D nanocrystals consisting of 1D lamellae that exhibit β -sheet secondary structure and lie along the armchair direction of HOPG. Molecular dynamics simulations show that the armchair orientation is indeed energetically favored, as is polar packing to form a bilayer. As the SF concentration increases, SF assembles into multi-layers via two pathways that can occur concomitantly. One is a non-classical pathway by which a disordered metastable film forms on top of the lamellae of the first monolayer and gradually converts into the lamellar structure. The second is a classical layer-by-layer pathway by which new lamellae grow homoepitaxially on the underlying 2D lamellae nanocrystals without any evidence of an intermediate state. Applying synchrotron based tip-enhanced nano-IR to SF assembly for the first time, we demonstrate that the β -sheet conformation is adopted from largely unstructured SF in solution as the lamellae advance along the classical pathway or during the process of film transformation along the non-classical pathway. These new findings fill in the missing pieces of the puzzle showing how SF structure evolves at the liquid-solid interface and provides inspiration for the design of heterogeneous 2D SF bio-crystal film.

11:15 AM CH01.06.03

Microfluidics for Programmable Self-Assembly of Gold Nanorods Pandillapally Rama; Indian Institute of Technology Hyderabad, India

Self-assembly of nanomaterials is an effective tool for developing functional assemblies and nano devices that can be used for a multitude of electrical, biomedical, and mechanical applications to name a few. We focus on the self-assembly of anisotropic gold nanomaterials, gold nanorods (GNR) in our work, since gold nanorods possess unique optical properties that can be tailored based on their aspect ratios. The side-to-side, end-to-end and self-assembly of GNRs have been a topic of intense research due to both the challenges involved in achieving such assemblies and their application in surface enhanced Raman spectra (SERS) signal enhancements. Several studies show the assembly of GNR using solvents (Ethylene diamine tetra acetic acid (EDTA), tetra hydrofuran (THF), dimethyl formamide (DMF)), pH, temperature, surfactants, co-polymers and other conditions. However, a systematic analysis and thereby understanding of the mechanism of assembly/dis-assembly and the resultant influence of several contributing parameters is a limitation in these studies. The lack of reproducibility and kinetic control over the reaction make such analysis challenging in the methods used in the studies. In the current work, we use droplet microfluidics to analyze the solvent based (EDTA) self-assembly of GNR. The GNR are encased in a 'micro-vessel' droplet within which reaction with EDTA happens is automated and proceeds reproducibly and controllably. We vary the concentrations of EDTA, change the drop size and also the ratio of aqueous to continuous flows and look at the shift in the resonance spectral wavelength of the clusters hence formed. The spectral shifts in these studies show the individual interaction of GNR with EDTA with respect to the aspect ratio of the GNR, size and shape of the individual particles. The study also shows the effect of mixing, leading to different results in each scenario. We performed a systematic analysis of the interaction and are currently working on programming and optimizing a general assembly strategy for GNR.

11:30 AM CH01.06.04

Unraveling Self-Assembly with Liquid Resonant Soft X-Ray Scattering for *In Situ* Measurement of Mesoscale Structure with Chemical Specificity Peter Beaucage, Lucas Flagg and Dean M. DeLongchamp; National Institute of Standards and Technology, United States

Resonant soft x-ray scattering (RSoXS) is a new characterization technique that offers insights into mesoscale structure with chemical specificity and the ability to probe molecular orientation. It does this by performing conventional small-angle x-ray scattering at a series of low photon energies (285 eV at the carbon K-alpha edge) as in x-ray spectroscopy. RSoXS was originally developed around and has been applied to great effect in morphological characterization thin films of organic semiconductors. Recently, our team has developed the first quantitative fitting engine for RSoXS data using GPU-accelerated forward simulation of real-space morphologies and applied this software to measure the orientation distribution in polymer-grafted nanoparticles, reverse osmosis water membranes, and several other families of industrial materials.

The promise of RSoXS as a label-free alternative to SANS has not been fully realized, however, largely due to great difficulties in the study of liquid samples, or indeed practically any sample without significant structure factor contributions. This limitation arises because of the very feature that makes RSoXS unique: at the low photon energies used for organic molecules, a typical absorption length is about 500 nm. RSoXS measurements are, therefore, overwhelmingly conducted on thin films and typically on highly concentrated samples due to the extremely small probe volume. The design of the NIST RSoXS beamline at the National Synchrotron Light Source-II addresses this issue by incorporating a TEM port holder in the chamber; the sample thicknesses required for electron beam transparency are similar to those required for soft x-rays. We have procured a commercial TEM liquid cell capable of encapsulating a 500 nm film of flowing liquid between two thin silicon nitride membranes.

This talk will discuss the commissioning of the cell, our first RSoXS measurements of dilute biomolecules in solution, and our recent efforts to combine solution RSoXS with solution SANS measurements to obtain a greater-than-sum-of-the-parts characterization of self-assembly processes and mechanisms in bioformulations. We will discuss the future extension of the liquid RSoXS technique to the *in situ* study of electrochemically active thin films in the hydrated state, and how measurements of pure form factor scattering enabled by the liquid sample environment and combined SANS-RSoXS experiments will enable quantitative understanding of the localization of additives during complex self-assembly processes.

SESSION CH01.07: Crystal Assembly and Transformation II

Session Chair: Wenhui Wang

Thursday Afternoon, April 25, 2024

Room 442, Level 4, Summit

1:30 PM *CH01.07.01

Filming Photoinduced Ultrafast Phase Transformation of Vanadium Dioxide at The Single Nanoparticle Level Oh-Hoon Kwon; Ulsan National Institute of Science and Technology, Korea (the Republic of)

Visualizing structural rearrangements at the atomic/molecular level is essential in understanding the functions of matter. Once isolated, a molecule's intermediate and transitional structures during a chemical reaction may be routinely determined via ultrafast spectroscopy with femtosecond temporal precision. When the structural degrees of freedom increase, e.g., condensed matter comprising countless atoms or organized molecular units, local nanoscale structural defects become prevalent, and thus, the physical processes of each singularity do not proceed as those in bulk and even diverge. If controlled, these structural defects may yield functional benefits and be exploited to overcome the current technological challenges ranging from catalysis to quantum computing. Because the ensemble natures of spectroscopic measurements do not reveal the characteristic transition of each nanoscopic structure, simultaneous spatiotemporal imaging is required to resolve complex processes, hierarchically spanning small-amplitude, ultrafast atomic

displacements to collective structural rearrangements at expanded spatiotemporal scales. As an energy filter in transmission electron microscopy has improved the precision of structural determination by filtering out inelastic imaging electrons, introducing the energy filter to ultrafast electron microscopy (UEM) can advance the time resolution to the domain of atomic motion. Imaging transient structures with femtosecond temporal precision was made possible by gating imaging electrons of narrow energy distribution from dense chirped photoelectron packets, thus typically posing picosecond duration. Presented are the concept and proof-of-principle demonstration of the energy-filtered UEM achieving the temporal resolution limited by the briefness of an optical excitation pulse, i.e., 500 fs in this study, filming ultrafast insulator-to-metal phase transition of vanadium dioxide (VO_2), a representative strongly correlated system. In this study, the heterogeneous phase transformations of VO_2 nanoparticles were revealed and attributed to the emergence of a transient, low-symmetry metallic phase caused by different local strains. Our approach leads the access of electron microscopy to the timescale of elementary nuclear motions, visualizing the onset of structural dynamics of matter at nanoscales.

2:00 PM CH01.07.02

Characterization of Structural Transformations in Flash Annealed HZO Thin Films via Dynamic and Static Synchrotron Grazing Incidence X-Ray Scattering [Cristian Ruano Arens](#)¹, Valene Tjong², Balreen Saini¹, Jonathan Hartanto¹, Fei Huang¹, Chanyoung Yoo^{2,1} and Paul C. McIntyre^{1,2}; ¹Stanford University, United States; ²SLAC National Accelerator Laboratory, United States

In order to extend computational power beyond the era of conventional area scaling of semiconductor circuits, back-end-of-line (BEOL) integration is a promising pathway towards 3D integration of non-volatile memory with logic, to increase integration density and reduce latency and energy consumption associated with data transfer. With improved properties over perovskite-structure ferroelectrics, $\text{HfO}_2\text{-ZrO}_2$ (HZO) alloys are promising candidates for future nonvolatile memories because of their CMOS compatibility, sub-nanosecond switching speed, and scalability of ferroelectric properties to the nanoscale. However, synthesis of ferroelectric HZO typically requires rapid high temperature heating to form the ferroelectric phase. Flash lamp annealing (FLA) is a viable method for thermal processing of BEOL components in which sub-ms pulses of light potentially allow localization of steep temperature rises to the top layers of the device stack, and protect underlying interconnect and front-end-of-line (FEOL) structures while crystallizing higher level materials. However, the short time scales and non-equilibrium nature of the annealing technique complicates determining thermal gradients and has led groups to rely on model predictions, measurement of the underside temperature of the substrate, or comparison between the performance of devices processed using rapid thermal anneal (RTA) or FLA to estimate the temperature rise of the surface layers. Because of the strict thermal budget imposed on BEOL processing, it is vital to determine the time-temperature profile associated with non-equilibrium FLA processing.

Our work uses static and time-resolved synchrotron glancing incidence X-ray diffraction (GIXRD) for in-situ, quantitative temperature metrology to understand the temperature rise during FLA processing of $\text{TiN}/\text{HZO}/\text{TiN}$ metal-ferroelectric-metal (MFM) capacitors. Time-resolved GIXRD was performed during FLA processing to observe, in real-time, the emergence of the ferroelectric orthorhombic phase, thermal expansion of the crystal lattice, and changes in diffraction intensity due to the Debye-Waller effect under various annealing conditions. Static GIXRD was subsequently performed to carefully monitor the changes in lattice parameter and diffraction intensity at discrete elevated temperatures. After careful calibration, we were able to compare the changes in both of these parameters and quantitatively determine the temperature rise associated with various FLA conditions.

Using a sequential learning Gaussian Process, we have explored the process manifold to fabricate MFM capacitors with good remnant polarization ($P_r \sim 20 \mu\text{C}/\text{cm}^2$) and low coercive fields ($E_c \sim 1.2 \text{ MV}/\text{cm}$) while being cognizant of the thermal budget necessary to achieve devices of this performance. Thus, careful calibration has enabled exploration of the FLA processing space in effort to yield optimal ferroelectric device performance within the strict thermal budget set by BEOL processing requirements. This study has advanced in-situ temperature metrology to explore temperature transients and FLA processing effects in BEOL device stacks.

2:15 PM CH01.07.03

Investigating The Dynamics of Photo-Reversible Polymer Hydrogels using *In Situ* Shear Rheology Michael C. Burroughs, Eleanor L. Quirk, Brendan M. Wirtz, Tracy Schloemer, Dan Congreve and [Danielle J. Mai](#); Stanford University, United States

Polymeric materials are often designed to be permanent, such that single-use convenience supersedes considerations of recyclability. For hydrogels, this approach has resulted in materials comprising many components such as polymer precursors, crosslinking agents, and photoinitiators; such complex formulations preclude the chemical recovery of the original constituents. To simplify the formulation of and encode recyclability into hydrogel materials, we report photo-reversible, network-forming polymers that are crosslinked and un-crosslinked using different wavelengths of light. Light-driven un-crosslinking has potential as a low-cost, low-energy, on-demand recycling technology. Photo-reversible polymer hydrogels comprise multi-arm star polyethylene glycol with terminal anthracene groups (PEG-anthracene). PEG-anthracene undergoes photo-crosslinking upon irradiation with ultraviolet light (UV, 365 nm) and un-crosslinking upon irradiation with deeper UV light (265 nm). The photo-reversibility of PEG-anthracene with 3, 4, 6, or 8 arms (5 kg/mol per arm) was compared using UV-vis absorbance spectroscopy and *in situ* dynamic rheology. Upon 365 nm UV exposure, PEG-anthracene solutions exhibited rapid gel formation indicated by crossovers from liquid-like to solid-like behavior during *in situ* small-amplitude oscillatory shear rheology. During photo-crosslinking, more arms generally led to the quicker formation of stiffer materials. In contrast, polymers with fewer arms underwent un-crosslinking more readily, indicated by changes from solid-like to liquid-like rheological responses. PEG-anthracene with fewer arms demonstrated liquid-like “recycling windows” that allow for facile polymer solution handling prior to re-crosslinking. These findings demonstrate opportunities for on-demand recycling of photo-reversible polymers, as well as polymer structure-dependent tradeoffs between crosslinking and reversibility. Further understanding of the interplay between polymer structure, material composition, and dynamic processing will advance the use of these materials in optoelectronics, biotechnology, and sustainable additive manufacturing.

2:30 PM CH01.07.05

Synthesis of $\text{V}_2\text{O}_5\text{-Co}_3\text{O}_4$ Nanoassembled Spheres for Gas Sensing Applications Chia-Yin Cheng, Yi-Chen Chen, Chun-Hua Chen, Wen-Chieh Hsieh, Shang-Jung Wu, Yi-Wen Lin, Hung-Shuo Chang, Karan Giri and Yan-Lin Wang; National Yang Ming Chiao Tung University, Taiwan

Under the development of high industrialization, the excess of greenhouse gases has caused a global climate crisis, and thermal power generation is one of the primary sources of greenhouse gas emissions. With the rising awareness of energy conservation and carbon reduction in major industrial countries in recent years, the energy transition has become an important issue. At present, hydrogen energy is a potential sustainable energy source. The most significant advantage of using hydrogen (H_2) fuel to generate electricity is that it significantly reduces carbon dioxide emissions. However, the combustion of H_2 will still form nitrogen dioxide (NO_2), and exposure to NO_2 will cause damage to the human respiratory tract, lungs, and kidney functions. To reduce the risk of hydrogen leakage, explosion, and nitrogen dioxide harm to the human body, developing highly-sensitive gas sensing materials for detecting hydrogen and nitrogen dioxide has become an essential goal with great forward-looking and industrial application potential.

In this study, vanadium pentoxide (V_2O_5) and cobalt tetroxide (Co_3O_4) nanoassemblies with different morphologies were respectively successfully synthesized by the polyol method at different reaction temperatures. The synthesized V_2O_5 nanoassemblies can exhibit high-performance H_2 sensing properties at room temperature without catalyst modification. The Co_3O_4 nanoassemblies showed the highest response to NO_2 at an operating temperature of 130 °C. In addition, in the later stage of Co_3O_4 synthesis, vanadium acetylacetonate $\text{V}(\text{acac})_3$ was introduced to form $\text{Co}_3\text{O}_4\text{-V}_2\text{O}_5$ nano-mixed particles. Finally, a novel heterogeneous core-shell nanoassembly structure comprised a Co_3O_4 core and $\text{Co}_3\text{O}_4\text{-V}_2\text{O}_5$ mixed nanoparticle shell. When V_2O_5 , an n-type oxide, is assembled with Co_3O_4 , a p-type oxide, the formed p-n junction will result in a depletion region. The electrical charge increases when the

target gases are adsorbed and desorbed, improving the sensing sensitivity. The specific surface area of the V₂O₅-modified Co₃O₄ nano-assembled spheres is 3.2 times that of the Co₃O₄ nano-assembled spheres. At 130 °C, the sensitivity to 400 ppm NO₂ increased from 247 % to 421 %. The gas-sensing responses of the synthesized nano-assemblies are all reproducible through cyclic measurements. Compared with CH₄, C₂H₆, C₃H₈, CO, NO gases, V₂O₅ and V₂O₅ modified Co₃O₄ nanoassemblies showed excellent selectivity for H₂ and NO₂, respectively.

2:45 PM BREAK

3:15 PM CH01.07.06

Thermodynamics and Kinetics of The Crystallization of Phase Change Materials from *In Situ* Microscopy and Nanocalorimetry Isak McGieson¹, Tamara D. Koledin¹, Jim Ciston², Feng Yi³, David A. LaVan³ and Melissa K. Santala¹; ¹Oregon State University, United States; ²Lawrence Berkeley National Laboratory, United States; ³National Institute of Standards and Technology, United States

The thermodynamics and kinetics of crystallization are key to understanding the stability of glass-forming materials, including poor glass formers such as phase change materials (PCMs). PCMs are semi-conducting alloys with distinct optical and electrical properties in the amorphous and crystalline phases that make them useful for memory applications. In memory devices, amorphous bits are crystallized in nanoseconds by either laser or Joule heating, but the amorphous phase must also be stable against crystallization for long-term data retention. Crystal growth rates relevant to memory devices span orders of magnitude and fundamental questions regarding PCM crystallization mechanisms remain open, partly due to the difficulty in measuring crystallization kinetics in certain temperature regimes.

The crystal growth rate, u , has been directly measured from the glass transition, T_g , to the melting temperature for good glass formers owing to their low u . In contrast, u in PCMs can exceed 10 m/s. Thus, it is challenging to measure u directly with microscopic methods, because the small grain sizes demand high spatial resolution and the grains impinge rapidly. This has led to the use of indirect methods to study PCM crystallization such as differential scanning calorimetry (DSC). In this work nanocalorimetry with high-frame-rate transmission electron microscopy (TEM) imaging was used to investigate the thermodynamics and kinetics of the crystallization of Ag₃In₄Sb₇₆Te₁₇ and GeTe above T_g . The PCMs were deposited on individually-calibrated nanocalorimeters designed to be operated in a TEM. Direct electron detectors capture the crystal growth in the milliseconds before impingement enabling direct measurement of u . The enthalpies of crystallization are calculated from nanocalorimetry measurements. Classical models for nucleation and growth are fit against these data and models that predict the growth rate solely from DSC data are compared to the direct growth rate measurements.

3:30 PM CH01.07.07

Controlled Stepwise Wet Etching of Polycrystalline Mo Nanowires Khakimjon Saidov¹, Ivan Erofeev¹, Zainul Aabdin², Antoine Pacco³, Harold Philipsen³, Antony W. Hartanto¹, Yifan Chen¹, Hongwei Yan¹, Weng W. Tjiu², Frank Holsteyns³ and Utkur Mirsaidov¹; ¹National University of Singapore, Singapore; ²Institute of Materials Research and Engineering (IMRE), Agency for Science, Technology and Research (A*STAR), Singapore; ³IMEC, Belgium

With the persistent downscaling of integrated circuits, molybdenum (Mo) is currently considered a potential replacement for copper (Cu) as a material for metal interconnects. However, fabricating metal nanostructures with critical dimensions of the order of 10 nm and below is challenging. This is because the very high density of grain boundaries (GBs) results in highly non-uniform surface profiles during direct wet etching. Here, utilizing in-situ liquid phase transmission electron microscopy (LP-TEM), we track the etching of polycrystalline Mo nanowires (NWs) with a hydrogen peroxide solution in real-time [1]. Moreover, wet etching of Mo with conventional aqueous solutions is problematic, as products of Mo oxidation have different solubility in water, which leads to increased surface roughness. Next, we show a process for achieving a stable and uniform soluble surface layer of Mo oxide by wet oxidation with H₂O₂ dissolved in IPA at -20 °C. The oxide layer is then selectively dissolved, and by repeating the oxidation and dissolution multiple times, we demonstrate a uniform etch profile with a fine control over the metal recess. Ultimately, this presents a method of precise and uniform wet etching for Mo and other metals needed to fabricate complex nanostructures that are critical in developing next-generation electronic devices.

[1] K. Saidov, I. Erofeev, Z. Aabdin, A. Pacco, H. Philipsen, A. W. Hartanto, Y. Chen, H. Yan, W. W. Tjiu, F. Holsteyns, U. Mirsaidov, Controlled Stepwise Wet Etching of Polycrystalline Mo Nanowires. *Adv. Funct. Mater.* 2023, 2310838.

3:45 PM CH01.07.08

Force Spectroscopy and Quantitative Imaging of Hard and Soft Materials Vasileios Koutsos; Univ of Edinburgh, United Kingdom

New modes of atomic force microscopy (AFM) such as Quantitative Imaging (QI) use force spectroscopy at a high rate with direct force control and allow the high-resolution topography imaging of material surfaces while collecting simultaneously high-resolution images of adhesion, stiffness, and moduli. We applied the force spectroscopy and in particular, QI mode in different systems showing its potential to reveal unprecedented information on local material properties. We mapped the local (surface) elastic modulus of engineering polymer blends and we compared it to the bulk modulus derived from macroscopic tensile testing. The results show a remarkable agreement. We also studied the interactions of natural rubber latex films with carbon black particles (attached to the AFM tip) in aqueous solutions of ultrapure water and ultrapure water with 0.7% Ammonia. We show that in the basic 0.7% ammonia ultra-pure water solution, hydrogen ions are drawn from the surfaces leading to significantly larger negative surface charges, and therefore resulting in repulsion between the carbon black and natural rubber latex films upon the tip approach. Furthermore, we have used the superior control of the applied forces (which can be very low at the range <10 pN) of the QI mode to image and interrogate mechanically biomedical phospholipid-based microbubbles. The results demonstrate the controlled collapse of the microbubbles revealing their mechanical properties and internal structure.

4:00 PM CH01.07.09

Revealing The Kinetic Phase Behavior of Block Copolymer Complexes Using *In Situ* Solvent Vapor Isotherms Boyce Chang; Iowa State University, United States

Controlling the self-assembled morphologies in block copolymers heavily depends on their molecular architecture and processing conditions. Solvent vapor annealing is a versatile processive pathway to obtain highly periodic self-assemblies from high chi (χ) block copolymers (BCP) and supramolecular BCP complexes. Despite the importance of navigating the energy landscape, controlled SVA has not been investigated in BCP complexes, partly due to its intricate multicomponent nature. We introduce in situ measurements of characteristic absorption-desorption solvent vapor isotherms as an effective way to understand swelling and morphological evolution of BCP complexes. Using the sorption isotherms, we identify the glass transition points, polymer-solvent interaction parameters, and bulk modulus. These parameters indicate that complexation completely screens the polymer interchain interactions. Furthermore, we establish that the sorption isotherm of the homopolymer blocks serves to deconvolute the intricacy of BCP complexes. We applied our findings by developing annealing pathways for grain coarsening while preventing macroscopic film dewetting under SVA. Here, grain coarsening obeyed a power law, and the growth exponent revealed a kinetic transition point for rapid self-assembly. Overall, SVA-based sorption isotherms emerge as a critical method for understanding and developing annealing pathways for BCP complexes.

4:15 PM CH01.07.10

Mechanism Underlying Alloy Formation and Phase Segregation in Colloidal Synthesis of Multielement Nanoparticles [Azadeh Amiri](#)¹, Vitaliy Yurkiv², Abhijit Phakatkar¹ and Reza Shahbazian-Yassar¹; ¹University of Illinois Chicago, United States; ²The University of Arizona, United States

Understanding the nucleation and growth of colloidal multielement alloys remains pivotal in determining the resulting entropy-stabilized or chemically segregated nanoparticles' size, shape, and properties. Nevertheless, comprehending the complex mechanisms guiding the formation of these alloy nanoparticles or high phase segregation is incomplete. This is due to the involvement of multiple elements with distinct properties and the challenging limitations of materials characterization methods. In this study, we employed in-situ liquid cell transmission electron microscopy (TEM) technique to record the real-time colloidal synthesis of multielement nanoparticles from a precursor solution containing mixed metal salts.

The observations revealed two distinct pathways for nanoparticle formation and growth resulting in two separate sets of particles occurring within a multi-metal salt solution comprising Au, Pt, Ir, Cu, and Ni elements. Primary particles formed were 10-30 nm Au-Cu bimetallic alloy nanoparticles, while secondary particles were 1-4 nm Pt-Cu-Ir-Ni multielement alloy nanoparticles. Au-Cu bimetallic alloy nanoparticles were initially nucleated in solution, rapidly growing up to 5-10 nm. DFT calculations suggested a spontaneous reduction of Au and Cu ions on the nanoparticles' surfaces, facilitating their swift enlargement dominantly through autocatalytic surface growth. Coalescence events then merged them into larger particles, ultimately reaching sizes of 10-30 nm. In contrast, Pt-Cu-Ir-Ni multielement nanoparticles nucleated more slowly and exhibited a non-classical nucleation pathway. Starting with intermediate atomic clusters, they evolved into crystalline nanoparticles upon surpassing 2 nm. However, the surface growth of these multielement alloys through autocatalytic reduction was notably sluggish, resulting in minimal size increase for the detected small clusters or nanoparticles.

Furthermore, the surfaces of these nanoparticles were likely covered with adsorbed charged ion complexes, leading to agglomerated nanoparticles with amorphous interfaces. This hindered further growth by coalescence, as electrostatic interactions on charged surfaces limited direct nanoparticle surface-to-surface contact. Slow interatomic diffusion associated with the multielement structure might have contributed to hindering intraparticle ripening, merging, and recrystallization. The findings suggest that metal ion characteristics, particularly reduction rates and valence numbers, significantly impact particle composition during early formation stages. Differences in nanoparticle composition and surface properties, validated by DFT simulations, collectively influenced unique growth behaviors in each nanoparticle set.

This study provides valuable insights into the mechanisms underlying multielement nanoparticle formation and growth. Additionally, it illuminates the factors responsible for chemical phase segregation and emphasizes the effects of composition, surface energies, and element miscibility on the final size and structure of nanoparticles.

SESSION CH01.08: Poster Session II

Session Chairs: Liang Jin, Dongsheng Li, Jan Ringnalda and Wenhui Wang
Thursday Afternoon, April 25, 2024
Flex Hall C, Level 2, Summit

5:00 PM CH01.08.01

Evaluation of Oxidation Processes in Ti₃C₂T_x MXene using *In Situ* Electrochemical Raman Spectroscopy [Kateryna Shevchuk](#), Ruocun Wang and Yury Gogotsi; Drexel University, United States

MXenes, a large family of two-dimensional materials, have attracted a lot of interest due to their large chemistry space and diverse chemical, electrical, mechanical, and optical properties. MXenes follow the general formula $M_{n+1}X_nT_x$ ($n = 1, 2, 3, \text{ or } 4$) with M representing an early transition metal, X - carbon and/or nitrogen, and T - surface terminations (=O, -OH, and -F). In particular, MXenes' metallic conductivities and redox-active surfaces make them attractive for electrochemical energy storage. Recently, we demonstrated that partial oxidation of Ti₃C₂T_x MXene by cycling the material at 1.2 V vs. Ag wire led to enhanced pseudocapacitance in water-in-salt electrolytes. However, there is a fine line between partial oxidation of Ti₃C₂T_x MXene and complete oxidation that leads to the formation of titania and carbon. The extent of oxidation is difficult to measure with conventional X-ray and electron-based techniques. This work focuses on using in situ electrochemical Raman spectroscopy to analyze the oxidation processes in Ti₃C₂T_x MXenes at the high anodic potential. Raman spectroscopy has proven to be a powerful technique for detecting the natural oxidation of Ti₃C₂T_x MXenes. The ability to perform Raman spectroscopy in situ during electrochemical reactions will allow us to expand our knowledge of MXene electrochemistry and its partial oxidation. The findings will help achieve higher energy density in MXene-based energy storage devices.

5:00 PM CH01.08.02

Microstructure, Texture and Tensile Properties of The 50% Hot-Rolled and Subsequent Heat Treated Ti6Al4V-5Cu Alloy [Solomon K. Yeshanew](#); Dire Dawa University, Institute of Technology, School of Mechanical and Industrial Engineering, Ethiopia

In order to investigate the influence of 50% hot-rolling on the microstructure, textural evolution, and tensile properties in Ti6Al4V-5Cu alloy, an electron backscattered diffraction (EBSD) was used. To obtain a reduced textural influence behavior on the alloy, dual heat treatment schedule was specially designed. The results show that hot-rolling at high temperature significantly promote the transformation of phases to a fully α -phase structure and lamellar microstructure with different grains structure starting from elongated to coarsened appearance was produced. Hot-rolling deformation contributed for increasing the alloy texture intensity, whereas the heat treatment is important for weakening textural intensity, however, the coarsening of grains are prominent. Deformation and heat treatment temperature, therefore, an important factor affecting the texture and grain size. Using tensile testing experiment by considering 0.02 strain offset method, the yield strength of the alloy were estimated. During tensile testing process, studying strength of a material is the primary concern. Material strength could be measured in terms of either the stress essential to cause noticeable plastic deformation or the maximum stress that material can withstand. The tensile testing also provides information on the material's ductility behavior to measure how much the alloy can be deformed before fractured. Using specimen sectioned in rolling direction (90°), the true stress-strain curve revealed that the strength at which the alloy has significant plastic deformation under 0.02 offset yield strength method. The alloy revealed 35 MPa yield strength at 800 °C and its area reduction reached 168.5%, and elongation reached up to 83%.

5:00 PM CH01.08.03

Effect of Phase Composition in TiAlSiN Hard Coatings on The Behavior of Microstructure and Mechanical Properties [Bum Soon Park](#)^{1,2}, Min-Hyeok Yang^{1,2}, Jeong-Han Lee¹ and Hyun-Kuk Park¹; ¹Korea Institute of Industrial Technology, Korea (the Republic of); ²Chonnam National University, Korea (the Republic of)

The aim of this study is to investigate the structural evolution and mechanical properties of TiAlSiN coating when processed by the arc ion plating method.

The nominal compositions of the ternary alloys were designed to be $\text{Ti}_{50}\text{Al}_{45}\text{Si}_5$, $\text{Ti}_{45}\text{Al}_{45}\text{Si}_{10}$, and $\text{Ti}_{40}\text{Al}_{45}\text{Si}_{15}$ (wt.%) and mechanically alloyed by planetary ball milling to form a hard coating. The powders were densely compacted during a rapid sintering process into a ternary system coating. The evolution of the structural phase from a powder to a compact material is dominated considerably by phase states such as a solid solution or intermetallic compounds. The relationship between the physical and chemical properties during the coating process is considered to be the dominant factor controlling the orientation and morphology of that zone. The TiAlSiN coating layer was found to have hardness above 45 GPa and an adhesion above 100 N. In other words, understanding the evolution and structure of TiAlSiN helped us to produce a material with excellent properties that can be used as a hard coating. Specifically, these properties were induced by a grain refinement of the nano-crystallite structure that corresponds to an increase in the silicon nitride contents.

5:00 PM CH01.08.04

Effect of Particle Shape on Microstructure and Thermal Conductivity of Al/Graphite Materials by Spark Plasma Sintering Bum Soon Park^{1,2}, Min-Hyeok Yang^{1,2}, Yu-Gyun Park^{1,2} and Hyun-Kuk Park¹; ¹Korea Institute of Industrial Technology, Korea (the Republic of); ²Chonnam National University, Korea (the Republic of)

The Al particle shapes which are spherical, irregular and flake shape were mixed with flake type graphite. The Al-50 vol.% Gr. powders, mixed by shaking mixer, were sintered under the following process conditions; sintering temperature of 550°C, sintering pressure of 60 MPa and duration of 2 minutes at the temperature of 550°C. The relative density of the sintered body reached its highest value of 99% when the shape of the Al particles was irregular. On the other hand, the lowest value was 92% when Al particle were flake-shaped. Pores were formed due to the wettability at the Al and Gr interface, which varied with the shape of the Al powder, thereby affecting the relative density. The hardness of the Al-Gr sintered body were investigated by vickers hardness analysis depending on the Al particle type. The results showed that the hardness value increased as the relative density became higher. The propagation of micro-cracks was further extended by the pores, which are assumed to have influenced the hardness. Moreover, the results of thermal conductivity as a function of the particle type, the most important indicator of this study, demonstrated the importance of porosity and the orientation of graphite.

5:00 PM CH01.08.05

In-Situ Synchrotron Imaging of Dendrite Growth During Rapid Solidification of Ni-Base Alloys Won Sang Shin, Jun-Pyo Park and Yoon-jun Kim; Inha University, Korea (the Republic of)

An *in-situ* observation of metallic solidification using a conventional optical microscopy has been limited due to high solidification temperatures and opacity of solid metal. Hence, this study was initiated from developing an *in-situ* imaging technique using a white X-ray source generated from the synchrotron beam line operated by the Pohang Accelerator Laboratory, Pohang, Korea. Since high X-ray energies affect the scintillator, the generated synchrotron X-rays were suppressed from 15 keV to 40 keV through a Si attenuator with a sensor size of 3 mm. Then, the penetrated X-ray signals were converted to visible light by a scintillator to observe dendrite formation behaviors using an optical microscope and to record the *in-situ* optical images. The recorded images were post processed to remove noise and to make video which provides entire formation and growth behaviors of dendritic structure. Ni-base alloys were prepared by the vacuum induction melting method and machined into coupons with a dimension of 10 x 10 x 0.25 (thickness) mm. To load and hold each coupon in the furnace, two boron nitride (BN) covers wrap around a coupon like a sandwich. The sapphire glasses in the middle of the two BN covers are exposed to allow X-rays to pass through each coupon. Temperature and vacuum inside furnace were set at 1600 °C and 10^{-3} torr, respectively. Solidification commenced right after sample coupon was fully melted. Cooling rates were controlled by setting current on carbon heaters, -0.2, -0.5, and -0.8 A/min, respectively. Dendritic structure such as tip radius, arm spacing, and mushy zone under different solidification variables such as thickness of specimen and cooling rates were measured directly from *in-situ* optical images. The microstructural properties were further analyzed by optical and electron microscopies, and atom probe tomography to correlate the dendrite growth behavior, microstructure, and material properties.

5:00 PM CH01.08.06

Fabrication and Quantitative Performance Analysis of a High-Throughput CNT-DNA-Based Biosensor Bo Liu; Arizona State University, United States

The quest for highly efficient probes in the precise detection of single biomarkers has emerged as a compelling research field crucial for biological and biochemical studies. Over recent decades, this pursuit has been seen in not only small chemical probe molecules but also biomacromolecules such as enzymes, antibodies, and nucleic acids in the construction of biosensor platforms, enabling highly specific and efficient biomarker detection. Despite significant progress, there remains a pressing need to enhance biosensor performance, particularly for high-throughput clinical applications.

Among the tools contributing to single nucleotide detection, DNA-based biosensors stand out for their versatility. Their notable attributes, including good stability, high specificity, and excellent biocompatibility, make them valuable in both *in vitro* and *in vivo* applications. Here, we present a new DNA-modified CNT LoC sensor for small nucleic acid detection. Together with the probing platform, our novel biosensor platform excels in measuring the electrical signals of DNA with single-molecule precision while also enabling prolonged high-throughput measurements and the efficient screening of valuable data.

We anticipate that this platform will prove beneficial to individuals interested not only in biosensor technology but also in the broader realm of single-molecular detection.

SESSION CH01.09: Electrochemical Reactions

Session Chairs: Liang Jin and Wenhui Wang

Friday Morning, April 26, 2024

Room 442, Level 4, Summit

8:30 AM *CH01.09.01

In Situ Liquid Cell Electron Microscopy for Characterization of Dynamic Processes Shu Fen Tan; Nanyang Technological University, Singapore

Many important reactions take place in liquids, but these processes are particularly difficult to study. Liquid cell electron microscopy provides opportunities for visualizing processes in liquids with good spatial and temporal resolution. The combination of imaging and electrochemical quantification have proved especially useful in studies of crystal growth, corrosion processes and battery materials. However, it has been a significant challenge to

improve the quality and quantification of liquid cell data due to the limitation in liquid cell equipment, control of local conditions and understanding of beam effects. In this seminar, I will discuss how I use *in situ* liquid phase electron microscopy to uncover the mechanisms of chemical transformation of catalytic nanoparticles under realistic reaction conditions. I will also talk about my recent work where I (1) developed a temperature-controlled electrochemical liquid cell for understanding the detailed mechanisms by which typical catalysts change their structures under electrochemical control in liquid electrolytes; and (2) incorporated 2D materials into the electrochemical liquid cell design to improve its achievable spatial resolution and electrochemical stability. My work lays the foundation for visualizing the nanoelectrochemical structure-function relationship in the electrochemical processes, which will open new opportunities for investigating a range of problems in energy storage and electrocatalysis.

9:00 AM CH01.09.02

From Bulk-To-Nano: Advances Towards Optimization of Electrochemical Studies for Liquid-Phase Transmission Electron Microscopy Madeline Dukes, Tim Eldred, Yaofeng Guo and Katherine Marusak; Protochips, Inc., United States

Liquid-phase transmission electron microscopy (LPTEM) has advanced considerably, evolving from rudimentary static cells [1] to advanced commercial systems capable of performing a variety of functions from temperature control to electrochemistry [2]. A core limitation of any TEM study is the assumption that the limited spatial area and sampling size inherent to TEM specimen preparation accurately represents the bulk state of the material [3]. This limitation is felt even more strongly for in-situ TEM studies, where the researcher must not only contend with determining if the sample itself is representative of its bulk state, but if that sample's environment and its operando behavior remain consistent with its bulk processes and mechanisms.

Here we describe recent advancements in hardware, MEMs chip designs, and software with the end goal of improving the accuracy of replicating bulk scale results in-situ. First, integration of an external, standard reference electrode (SRE) via a "metal bridge" enables integration of conventional Ag/AgCl reference electrodes. Employing an SRE eliminates the shifting potentials introduced by on-chip pseudo-reference electrodes, such as platinum, without introducing a significant ohmic drop [4], and enables more accurate comparisons between bulk and in-situ results.

Second, it is well understood that the narrow gap between chips necessary to maintain thin enough liquid layers for good resolution in LPTEM experiments, introduces a myriad of potential artifacts due to confinement, including incomplete mixing, slow exchange of liquids and ion depletion [5]. Recently, we developed a new E-chip configuration designed to balance both thin liquid layer required for optimal resolution and a deeper flow channel to improve liquid flow characteristics. This design utilizes a 10 micron channel etched into the silicon substrate of the E-chip. The viewing region, containing the amorphous silicon nitride membrane, is isolated within the center of the E-chip on an island type structure, such that the deep flow channel surrounds it like a moat and does not interfere with the gap between the top and bottom membranes. This significantly reduces the distance over which the liquid must diffuse to reach the narrow gap between the viewing windows from >1 mm to a few tens of microns, significantly improving liquid exchange within the critical region [6].

Finally, comprehensive analysis of the electron dose during in-situ studies is necessary to disentangle beam-induced changes and behavior from a samples' inherent chemical or electrochemical behavior. We utilize a state-of-the-art machine vision software, AXON Dose, to calibrate and accurately track electron dose exposure throughout an experiment to create a record of both the electron flux, and the samples' cumulative dose exposure, on a pixel-by-pixel basis [7]. Taken in concert, these new features bring us closer to achieving the goal of accurately replicating, measuring, and observing bulk electrochemical processes at the nanoscale.

References:

1. de Jonge, N.; Ross, F. M. *Nature Nanotech* **2011**, *6* (11), 695–704.
2. Yoshida, K. et al., *Microscopy* **2023**, dfad044.
3. D. B. Williams and C. B. Carter, "Transmission Electron Microscopy: A Textbook for Materials Science," 2nd Edition, Springer, New York, 2009, pp. 3-22
4. Choudhary, S. et al., *J. Electrochem. Soc.* **2022**, *169* (111505).
5. Merkens, S. et al., *Ultramicroscopy* **2023**, *245*, 113654.
6. Merkens, S. et al., Towards sub-second Solution Exchange Dynamics in Liquid-Phase TEM Flow Reactors, 01 August 2023, PREPRINT (Version 1) available at Research Square [<https://doi.org/10.21203/rs.3.rs-3208774/v1>]
7. Dukes, M. D. et al., *JoVE* **2023**, No. 196, 65446

9:15 AM CH01.09.03

In-Situ/Operando Electrochemical Investigation of Reduced Graphene Oxide in Aqueous Solution Maria del Pilar Bernicola Garcia¹, Jose A. Garrido^{1,2} and Elena del Corro¹; ¹Catalan Institute of Nanoscience and Nanotechnology, (ICN2), CSIC and BIST, Spain; ²ICREA, Spain

The development of new carbon nano-porous materials with increased capacitance, high conductivity and electrochemical stability is of high interest for a variety of applications. It is reported an anomalous increase of the specific capacitance in nano-porous materials with a pore size below of 1 nm¹. However, the fundamental understanding of the mechanisms that involve these phenomena is still under study. Reduced graphene oxide (rGO) has gained significant attention due to its remarkable physicochemical properties such a high structural stability, large specific surface area, low cost, and availability. In the case of healthcare applications, highly porous rGO films have been widely studied because of their biocompatibility and biochemical sensing capabilities². A proper understanding of electrokinetic phenomena such as potential-controlled ionic diffusion within the nano-porous and reduction of functional groups during electrochemical operation is necessary to improve the ultimate performance of rGO-based electrodes. Also, for these applications, it is key to investigate the chemical and structural changes happening in the rGO electrodes during their electrochemical operation.

In this work, we combine different *in-situ/operando* spectroscopic techniques to understand the dynamics and irreversible/reversible chemical and structural changes within rGO-nanoporous electrodes. The high electrochemical performance of the nanoporous rGO films can be explained by different phenomena such as ionic diffusion, ionic adsorption/desorption processes, protonation mechanisms and chemical and structural changes like those induced by defects or vacancies. The electrochemical performance of the rGO-nanoporous material, in terms of specific capacitance, potential windows and impedance, is studied by cyclic voltammetry (CV) and electrochemical impedance spectroscopy (EIS). To have a deeper understanding of the fundamental phenomena that boost the electrochemical performance, we focus on the structural and chemical changes induced by the electrode-electrolyte interaction in

the nano-porous electrode. To study the structural changes that take place due to the electrode-electrolyte interaction, we have developed different custom-made electrochemical cells to couple to spectroscopic techniques like X-ray diffraction (XRD) and Raman spectroscopy. *In-situ* XRD measurements experiments give information about the impact on the rGO structure of the electrochemical operation, such irreversible/reversible changes on the interlayer distance induced by the applied potential. Operando Raman spectroscopy is used to study the structural properties of such defects, disorder and reduction degree induced by the applied potential. In this study we are able to evaluate the nature of the defects generated during electrochemical operation that impacts on the electrochemical performance³. Combined with analysis of CV coupled with electrochemical quartz crystal microbalance (EQCM), our results provide detailed information about ionic adsorption and charge transfer processes at the electrode-electrolyte. This work aims at expanding the current understanding of the properties of rGO-based nanoporous electrodes for their use as electrode material in healthcare applications.

This work has received funding from the *Project PID2020-113663RB-I00 (Neuro2Dtec) funded by MCIN/AEI/10.13039/501100011033 (Neuro2Dtec)*

1. Chmiola, J. *et al.* Anomalous Increase in Carbon Capacitance at Pore Sizes Less Than 1 Nanometer. *Science* **313**, 1760–1763 (2006).
2. Apollo, N. V. *et al.* Soft, Flexible Freestanding Neural Stimulation and Recording Electrodes Fabricated from Reduced Graphene Oxide. *Adv Funct Materials* **25**, 3551–3559 (2015).
3. Eckmann, A. *et al.* Probing the Nature of Defects in Graphene by Raman Spectroscopy. *Nano Lett.* **12**, 3925–3930 (2012).

9:30 AM BREAK

10:00 AM CH01.09.04

Corrosion Propensity of Polyester-Chromium Nitrate Coated Al7xxx Alloy in Humid Environment Joseph B. Agboola, Chiamaka M. Uzuegbu and Olatunde I. Sekunowo; University Of Lagos, Nigeria

Aircraft propeller blades are exposed to various weather and climatic conditions, such as humidity, cold, high temperatures, and wind, which over time weaken the aluminium 7xxx that they are made of due to corrosion. The present work aims to evaluate chromium nitrate's effect on corrosion resistance of Polyester-Chromium Nitrate composite coated Al7xxx alloy in a humid environment. Polyester (PE) was synthesized by condensation polymerising symmetrical 1,3,4-oxadiazole and pimelic acid using sodium lauryl sulfate as a surfactant. Polyester-chromium nitrate composite was prepared by ultrasonication method. The prepared composite was applied on the surface of Al7xxx through the dipping method and cured at room temperature for 24 hours. Scanning electron microscopy (SEM/EDS) and X-ray Diffractometry (XRD) were carried out to compare the surface structure and the morphology of the coating. The results of the electrochemical measurement showed that the 60/40% composite-coated sample exhibited better corrosion resistance compared with the uncoated and pure polyester-coated samples. Polyester chromium nitrate coated samples had a longer controlled sacrificial anodic protection on Al7xxx substrate, a lower corrosion current density (i_{corr}) and a higher corrosion potential (e_{corr}).

10:15 AM CH01.09.05

Solid-State Reaction Heterogeneity during Calcination of Lithium-Ion Battery Cathode Sugeun Jo¹, Sungjae Seo¹, Subin Choi¹, Yijin Liu², Il Sohn³, Keeyoung Jung³ and Jongwoo Lim¹; ¹Seoul National University, Korea (the Republic of); ²SLAC National Accelerator Laboratory, United States; ³Yonsei University, Korea (the Republic of); ⁴Research Institute of Industrial Science & Technology, Korea (the Republic of)

Li-ion batteries, nickel-rich cathodes, synthesis during calcination, phase transitions with solid-state reaction, spatial distribution of local chemical compositions within the particles. During solid-state calcination, with increasing temperature, materials undergo complex phase transitions with heterogeneous solid-state reactions and mass transport. Precise control of the calcination chemistry is therefore crucial for synthesizing state-of-the-art Ni-rich layered oxides (LiNi_{1-x-y}CoxMnyO₂, NRNCM) as cathode materials for lithium-ion batteries. Although the battery performance depends on the chemical heterogeneity during NRNCM calcination, it has not yet been elucidated. Herein, through synchrotron-based in-situ structural analyses, gas analysis, X-ray microscopy, mass spectrometry microscopy, we provide a reaction map for Ni-rich layered oxides (LiNi_{1-x-y}CoxMnyO₂, NRNCM) cathodes during their calcination, which includes dehydration of the precursors, the insertion of ambient oxygen, and the insertion of solid-state Li₂O₂ after Li₂CO₃ thermal decomposition. The temperature-dependent reaction kinetics, the diffusivity of solid-state lithium sources, and the ambient oxygen determine the favorable aerobic decomposition of particle shell maintaining layered structure while the anaerobic decomposition of the particle core to lithium-blocking Ni-O rocksalt. Additionally, we found that the variations in the reducing power of the transition metals (i.e., Ni, Co, and Mn) determine the local structures at the nanoscale. The investigation of the reaction mechanism via imaging analysis provides valuable information for tuning the calcination chemistry and developing high-energy/power density lithium-ion batteries.

10:30 AM CH01.09.06

Revealing CaH₂-Driven Metal Oxide Reduction Kinetics with *In-Situ* Transport Measurements Jiayue Wang^{1,2}, Yijun Yu^{1,2}, Yi Cui^{2,1} and Harold Y. Hwang^{1,2}; ¹Stanford University, United States; ²SLAC National Accelerator Laboratory, United States

Metal hydrides, such as CaH₂, have recently emerged as highly promising reducing agents for facilitating the low-temperature reduction of metal oxides. One unique advantage of hydride reduction is its capability to synthesize metastable materials that are inaccessible through conventional high-temperature reactions. Notably, researchers have harnessed hydride reduction techniques to create unusual NiO₄ square-planar coordination in nickelates to host superconductivity [1]. Beyond the realm of novel materials discovery, metal hydrides also hold substantial potential in applied engineering. For instance, previous studies have shown that CaH₂ can lower the temperature required for gas-phase H₂ reduction of iron oxide, which can benefit clean hydrogen-based ironmaking [2]. Given these promising features, there is a compelling motivation to delve deeper into the mechanics of the hydride reduction process.

In this study, we investigate the CaH₂-induced reduction kinetics of metal oxides using epitaxial α -Fe₂O₃ thin films as a model system. To elucidate the intrinsic reducing capability of CaH₂, we seal the iron oxide thin-film samples along with CaH₂ in an evacuated quartz tube and analyze the reduction behavior of iron oxide within this closed system. In particular, we have developed an experimental platform that enables real-time monitoring of the CaH₂ reduction process through transport measurements. Using this setup, we have successfully quantified the phase transformation kinetics from iron oxide to metallic iron by continuously tracking the evolution of electrical resistivity in the thin-film sample. Our results demonstrate that CaH₂ alone can effectively reduce α -Fe₂O₃ into metallic iron within a one-hour reduction treatment at 400 °C, whereas 5% H₂/Ar (99.999% purity) failed to reduce the sample at identical conditions. These findings can advance our fundamental understanding of the hydride reduction process, opening new avenues to harness this phenomenon for the exploration of emergent materials properties and the development of environmentally friendly engineering applications.

[1] D. Li *et al.*, *Nature* **572**, 624 (2019).

[2] T. Tsuchida *et al.*, *Journal of Solid State Chemistry* **302**, 122441 (2023).

10:45 AM CH01.09.07

The Scanning Transmission Electron Microscope as a Platform for Atomic Scale Synthesis Ondrej Dyck, Andrew R. Lupini, Christopher T. Nelson, Mina Yoon and Stephen Jesse; Oak Ridge National Laboratory, United States

The scanning transmission electron microscope (STEM), a workhorse instrument in materials characterization, can not only be used to observe dynamic processes with atomic resolution, but also *drive and control synthesis with atomic precision*. Through custom control of the electron beam position that actively feeds back on image, spectroscopy, and other data streams, it's possible to use focused beam energy to precisely initiate and interrupt desired transformations. This can be used for generating point defects, drilling and milling materials, changing phase, modifying bond coordination, and positioning dopants. Furthermore, control over the local environment through custom MEMS devices for heating and biasing, *in situ* evaporators, and laser irradiation, provides means to dose the sample with thermal energy, optical excitation, and reactant or dopant materials to provide the proper conditions for reactions and transformations to occur. Finally, to close the loop, the STEM can then be used in its more traditional characterization modes to image transformation processes as they occur and assess if new functional properties emerge. Presented here are recent results highlighting advancements towards such a "synthescope"[1] including new insights gained by studying the generation and temperature dependent diffusion of beam-generated single vacancies in suspended 2D materials [4,5], strategies to restrict vacancy diffusion so they can serve as sites for dopant insertion, demonstration of patterning of arrays of dopants [3], and the delivery of dopant atoms to the sample, *in situ* [2]. Development of this combination of experimental methods provides a window into the dynamic synthesis processes at fundamental length scales and a path towards fabricating materials and devices with atomically precise components for potential quantum information science applications.

This work was supported by the U.S. Department of Energy, Office of Science, Basic Energy Sciences, Materials Sciences and Engineering Division, and was performed at the Center for Nanophase Materials Sciences (CNMS), a U.S. Department of Energy, Office of Science User Facility.

1. Dyck, O., Lupini, A. R., Jesse, S. "The Synthescope: A Vision for Combining Synthesis with Atomic Fabrication". *Advanced Materials* (2023, 2023 Aug) <https://doi.org/10.1002/adma.202301560>
2. Dyck, O., Lupini, A. R., Jesse, S. "A Platform for Atomic Fabrication and In Situ Synthesis in a Scanning Transmission Electron Microscope". *Small Methods* (2023, Jul) <https://doi.org/10.1002/smt.202300401>
3. Dyck, O., Yeom, S., Lupini, A. R., Swett, J. L., Hensley, D., Yoon, M., Jesse, S. "Top-Down Fabrication of Atomic Patterns in Twisted Bilayer Graphene". *Advanced Materials* (2023, Jun) <https://doi.org/10.1002/adma.202302906>
4. Boebinger, M. G., Brea, C., Ding, L. P., Misra, S., Olunloyo, O., Yu, Y. L., Xiao, K., Lupini, A. R., Ding, F., Hu, G. X., Ganesh, P., Jesse, S., Unocic, R. R. "The Atomic Drill Bit: Precision Controlled Atomic Fabrication of 2D Materials". *Advanced Materials* **35** (2023, Apr) <https://doi.org/10.1002/adma.202210116>
5. Dyck, O., Yeom, S., Dillender, S., Lupini, A. R., Yoon, M., Jesse, S. "The role of temperature on defect diffusion and nanoscale patterning in graphene". *Carbon* **201**, 212-221 (2023, Jan) <https://doi.org/10.1016/j.carbon.2022.09.006>

11:00 AM *CH01.09.08

Fabrication Processes of Next-Gen Integrated Circuits through The Lens of In Situ Transmission Electron Microscopy Utkur Mirsaidov; National University of Singapore, Singapore

Understanding the nanoscale details of chemical and physical processes used in semiconductor manufacturing is critical for scaling and improving the performance of future integrated circuits. Here, I will review the major challenges associated with device scaling and describe how *in situ* TEM can help in the development of these processes. I will describe how direct imaging of such processes can speed up the implementation of new materials and device architectures to further enable the miniaturization of transistor footprints and improve their performance. Specifically, I will focus on etching and annealing processes used in the fabrication of both transistors and interconnects that link billions of these transistors together and to a power supply. Our studies highlight the importance of direct nanoscale dynamic visualization of chemical and physical processes for advancing the fabrication processes of integrated circuits.

SESSION CH01.10: Characterization of Catalytic Materials

Session Chairs: Miaofang Chi and Dongsheng Li

Friday Afternoon, April 26, 2024

Room 442, Level 4, Summit

1:30 PM *CH01.10.01

Unraveling Sintering Mechanisms of Precious Metal Catalysts in Diverse Gas Environments Miaofang Chi; Oak Ridge National Laboratory, United States

Heterogeneous precious metal catalysts offer the highest selectivity and activity in chemical production and combustion by-product reduction reactions. However, their efficiency is hindered by sintering, particularly in high-temperature oxidizing environments such as automotive emissions control. To address this issue, we investigate the sintering mechanisms of platinum on alumina support in various exhaust gas environments at different temperatures using *in situ* environmental scanning transmission electron microscopy (STEM). We observe that the presence of both oxygen and water vapor significantly accelerates sintering, while water vapor alone has minimal impact. Our study unveils transient nanoparticle shape instability, indicating rapid particle migration, in an oxygen and water vapor environment, contrasting with stability in a vacuum. This underscores the complex interactions between platinum, the alumina substrate, and gases, providing essential insights for the design of improved catalysts for industrial applications.

2:00 PM CH01.10.02

Effects of Crystal Lattice Deformation on Catalytic Activities Dongsheng Li; Pacific Northwest National Laboratory, United States

Deformations of hierarchical structures at the atomic scale, especially long-range ones, can significantly enhance their functional behavior, such as catalytic activity. Metastable states or grain boundaries during the synthesis and processing of nanomaterials can introduce and control deformations (strains) in crystal lattices. We design the deformations in the crystal lattice to enhance the catalytic functionality of catalysts, such as TiO₂ and platinum-group-based metals, by controlling their synthesis processes of phase transformation and particle aggregation. For example, TiO₂ polymorphs have distinct properties that have been widely employed in various applications. It is well known that these polymorphs can transform into more stable phases, such as from TiO₂-B to anatase. Here, based on results from semi-*in-situ* transmission electron microscopy, X-ray atomic pair distribution function, and density functional

theory, we will investigate the effects of lattice deformation in crystals on the catalytic activities and their controlling factors. We seek to control deformations in supporting materials and their effect on catalytic materials to uniquely tailor functionalities. These findings suggest that lattice deformations can be designed to advance new functions.

2:15 PM CH01.10.03

Strong Metal-Support Interaction makes Durable Catalysts [Ji Yang](#), David Prendergast and Ji Su; Lawrence Berkeley National Laboratory, United States

Liquid organic hydrogen carrier (LOHC) technology is a promising method for hydrogen storage and transportation by using a reversible hydrogenation–dehydrogenation cycle between aromatic compounds and naphthene, such as toluene and methylcyclohexane (MCH). A key issue in this technology is to improve the lifetime of the catalyst for MCH dehydrogenation. Here, we developed a TiO₂-supported Pt catalyst (Pt@TiO₂) by engineering a unique strong metal-support interaction (SMSI). For the first time, the monometallic Pt@TiO₂ catalyst delivers durable MCH dehydrogenation at 350 °C, without any deactivation observed within 500 h. MCH conversion of 94% and toluene selectivity of ~100% are achieved. Detailed electron microscopic and spectroscopic studies, supported by theoretical calculations, reveal that the excellent MCH dehydrogenation performance over Pt@TiO₂ is attributed to in-situ generated TiO_x-Pt^{δ+} interface induced by optimal SMSI, which immobilizes Pt nanoparticle (NP) onto TiO₂ surface and modulates electronic properties of Pt NP. MCH can be thus efficiently dehydrogenated and toluene is easily desorbed on the Pt NP surface. Our results expand the concept of classical SMSI and provide new insights into the rational design of durable supported metal catalysts based on unconventional SMSI.

2:30 PM BREAK

3:00 PM CH01.10.04

Analysis of Defects in Electrocatalysts using Variable Temperature Raman Spectroscopic Analysis of Phase Transition Mechanisms [Rodney Smith](#); University of Waterloo, Canada

Defects within solid state materials can dramatically alter material properties, but direct analysis of such defects is particularly challenging. Such analysis is impeded by the low concentrations of defects relative to bulk sites, potential co-existence of multiple defect types in any given material, possibility of dynamic changes during catalysis, and fundamental limitations inherent in every characterization technique. We analyze distortions and defects in solids through indirect analysis, where changes in structural data for series of samples are monitored as a function of some perturbation. This talk will demonstrate how we have applied variable temperature Raman spectroscopy under controlled environments to analyze phase transitions in solid state materials commonly employed as (photo)electrocatalysts, with particular interest in how defects affect features such as the presence of phase transitions and the temperature at which they occur. Discussion will be focused on the analysis of protons trapped within hematite, a commonly employed photoelectrocatalyst for the oxygen evolution reaction, and the formation of disordered carbonate-containing overlayers on a family of perovskite electrocatalysts.

3:15 PM CH01.10.05

In Situ Environmental TEM Observation of Cu/Cu₂O Interface-Modulated Methanol Reaction Dynamics [Meng Li](#)^{1,2}, Matt Curnan³, Hao Chi¹, Stephen House^{1,4}, Jimmy G. McEver¹, Dmitri N. Zakharov², Wissam Saidi^{1,5}, Goetz Vesper¹ and Judith C. Yang^{1,2}; ¹University of Pittsburgh, United States; ²Brookhaven National Laboratory, United States; ³Pohang University of Science and Technology (POSTECH), Korea (the Republic of); ⁴Sandia National Laboratories, United States; ⁵National Energy Technology Laboratory, United States

Cu-based catalysts are the most widely used commercial catalysts in methanol chemistry due to their cost-effectiveness and high reactivity with methanol. Recent studies on Cu catalyst oxidation states indicate that during the Partial Oxidation of Methanol (POM), Cu catalysts are partially oxidized, producing reactivity and selectivity changes in pertinent reactions. These changes dynamically form metal/metal-oxide (M/MO) interfaces featuring short-lived and high-energy sites, which likely contribute to measured reactivity increases near phase boundaries. However, previous studies on these reaction mechanisms have primarily focused on pure Cu or Cu₂O surfaces, rather than investigating impacts on M/MO interfaces.

In this work, using *in situ* environmental transmission electron microscopy (ETEM) with machine-learning enhanced advanced data analysis and correlated DFT simulations, we investigated the influence of Cu₂O/Cu interfacial structures on methanol reduction dynamics. The atomic-resolution reaction dynamics are observed using *in situ* ETEM under 1 Pa methanol vapor at 300 C on heteroepitaxial Cu₂O/Cu model catalysts. Our observations reveal two-stage reduction dynamics modulated by the structures of Cu||Cu₂O junctions: when the Cu||Cu₂O interface at a junction is oriented along (100), an anisotropic layer-by-layer reduction occurs at the side facets of the Cu₂O island, followed by a Cu₂O-to-Cu interfacial transformation along (100). When the Cu||Cu₂O interface is oriented along (110), isotropic reduction at both top and side facets of Cu₂O islands is observed. Using machine-learning enhanced advanced data analysis, atomic-level size evolution kinetics are extracted. Stochastic trend analysis on island size kinetics suggests two distinct kinetic stages caused by different reaction mechanisms. Using correlated density functional theory (DFT) simulations of MeOH dissociative adsorption, we found that MeOH adsorption energetics favor defect sites at Cu||Cu₂O(100) junctions, as opposed to fully coordinated sites on Cu₂O(110) surface steps or near Cu||Cu₂O(110) junctions. As the Cu||Cu₂O interface changes during the anisotropic-to-isotropic stage transition, active sites correspondingly relocate from Cu||Cu₂O(100) junctions to Cu₂O(110) surface steps. Our results emphasize the importance of M/MO interfacial dynamics during catalytic reactions, and provide new insights towards catalyst design and interface engineering.

Acknowledgements:

The authors acknowledge funding from National Science Foundation (NSF) grants DMR-1410055, CBET-1264637, DMR-1508417, DMR-1410335, and DMREF CHE-1534630, and support from Hitachi High-Tech. Technical support from the Nanoscale Fabrication and Characterization Facility in the Petersen Institute of Nano Science and Engineering at the University of Pittsburgh is appreciated. This research used the Electron Microscopy facility of the Center for Functional Nanomaterials (CFN), which is a U.S. Department of Energy Office of Science User Facility, at Brookhaven National Laboratory under Contract No. DESC0012704. J. McEver was supported in part by the U.S. Department of Energy, Office of Science, Office of Workforce Development for Teachers and Scientists (WDTS) under the Science Undergraduate Laboratory Internships Program (SULI).

8:00 AM CH01/CH03.01

The Effect Local Residual Stress States on The Internal Pore Growth in Laser-Welded Ti6Al4V [Wei Sun](#) and Xingrui Jiang; Xi'an Jiaotong-Liverpool University, China

The micron scale local residual stress states in laser-welded Ti6Al4V were characterized with focused ion beam ring-core milling coupled with digital image correlation (FIB-DIC), and its effect on the growth of welding porosity under external loading was investigated by *in-situ* tension under X-ray computerized tomography (CT). The internal pores were found to preferentially distribute along the fusion zone boundary and the weld centerline. FIB-DIC and X-ray diffraction indicated high-level tension in the vicinity of the fusion zone, balanced by the long-range compression in the base metal. Comparison with stress-free counterparts showed the residual stress significantly preponed the growth of the pores, whose aspect ratio and volume exhibited observable increments at low applied stresses. On the contrary, the pores without residual tension remained nearly undeformed until the yield point, and the relative tensile strain across the fusion zone showed a similar trend. The results demonstrated that the response of internal welding defects towards external load strongly correlates to the local residual stress states, and highlights the importance of precise measurements of the residual stress states in characteristic regions for applicational titanium laser welds.

8:05 AM CH01/CH03.02

***In-Situ* Study of Deformation Mechanisms in a Bi-Layered Bronze/Steel Sheet** [Xingrui Jiang](#)¹, Wei Sun¹, Li Rengeng², Min Chen¹ and Guohua Fan²; ¹Xi'an Jiaotong-Liverpool University, China; ²Nanjing Tech University, China

Enhancing ductility is a crucial concern within metal matrix composites. Cu-Pb bronze alloy is a commonly utilized copper-based bearing alloy, and it demands superior mechanical properties and service safety. While copper and lead exhibit excellent ductility, Cu-Pb bronze alloys experience a substantial reduction in ductility due to plastic deformation being concentrated within the low-strength Pb phase. To address this issue, we employed the solid-liquid continuous casting (SLC) method to overlay the Cu-Pb alloy onto a mild steel substrate, significantly enhancing overall ductility. We conducted an *in-situ* tensile test using a scanning electron microscope (SEM) in conjunction with Digital Image Correlation (DIC) and Electron Back-scattered Diffraction (EBSD) to elucidate the underlying mechanisms. Localized strain is distributed uniformly in the steel layer but concentrated in the Pb phase within the bronze layer. However, this localization is effectively mitigated by the layered structure, as evidenced by the high compressive strain observed in the affected zone at the bronze/steel interface. Larger misorientation angles near the copper grain boundaries indicate that the deformation of copper grains is influenced by the localized strain within the lead phase. The layered structure effectively reduces strain concentration throughout the material and accommodates the deformation incompatibility inherent in Cu-Pb bronze alloys.

8:20 AM *CH01/CH03.03

***In-Situ* TEM Study of Microstructure Evolution in Ferroelectric/ferroelastic Materials under Stress** Yifeng Ren, Jiayi Li, Zhentao Pang, Jie Wu, Shaojie Fu, Meiyu Wang and [Yu Deng](#); Nanjing University, China

In ferroelastic-ferroelectrics (FMs), stress-induced microstructure such as phase and domain can effectively enhance properties significantly. We prepared free-standing single-crystal BaTiO₃ sub-micrometer pillar as a model system to investigate microstructural evolutions in FMs under high stress loading. We directly observed and quantitatively analyzed *in situ* in a transmission electron microscope with 4D-STEM the microstructural evolutions in the pillar under various strain loading (different intensity, direction, and rate). We found that dozens of slow compression cycles (strain rate of 10⁻²/s, at 520 MPa) can induce multiple-nanodomain and multiple-phase coexistence in BaTiO₃. After unloading, the pinned boundaries and domain walls by mobile point defects can stabilize these microstructures, including metastable ones, therefore improve both functional and mechanical performance of FMs. The "brittle" FMs can in fact withstand GPa level stress without fracture, resulting in large strain (higher than 5% in BaTiO₃) under the specially designed loading ways. Our work elucidates the complex multiscale (from micrometer to unit cell scale) evolution of phase, domain microstructures and their interactions in FMs, as well as the corresponding improvement in properties under the large strain loading. Based on this, we propose a novel method for domain engineering in FMs.

8:50 AM *CH01/CH03.04

Polymers Behaviour under Ionizing Radiations: *In-Situ* Characterization of Macromolecular Defects and Outgassing [Yvette Ngono](#), Emmanuel Balanzat and Jean-Marc Ramillon; CIMAP, France

Polymers are made of long chains of repeating units linked *via* covalent bonds. Those chains are organized in function of the chemical structure of their repeating units; leading to different levels of organization. Due to these organization levels, polymers have different transition and relaxation temperatures and are more often than not semi-crystalline. Crystallites are embedded in amorphous phases and radicals created under ionizing radiations, that are the reactive species in polymers, can be trapped therein and react long after irradiation either with the oxygen or with humidity from the air.

Polymer are subjected to gas permeation and diffusion. Therefore, any analysis performed off-line, after irradiation is susceptible to represent not the state of the sample freshly irradiated but its state after subsequent post-irradiation evolution.

In order to make sure to actually study the effect of radiations, we have, at CIMAP, developed set-ups enabling to studying polymers under various temperatures and atmospheres and under different ionizing radiations be them ion or electron beams. Polymers are submitted to radiolysis and studying radiation-induced gas-emission is of great interest in assessing their ageing mechanisms, as gaseous products are the parallel of defects created in the polymer chains.

I will present not only experimental set-ups for online study of polymers but also beams available at GANIL for these studies and some results on polymers of interest.

9:20 AM CH01/CH03.05

Raman Spectroscopy: A Versatile Tool for The Studies on The Back-End of The Nuclear Fuel Cycle [Laura J. Bonales](#), Jone M. Elorrieta Baigorri, Abel Milena Pérez, Iván Sánchez García, Nieves Rodríguez Villagra and Hitos Galán Montano; CIEMAT, Spain

In recent years, Raman spectroscopy has proven to be a highly versatile characterization technique for nuclear materials research. This sensitive technique possesses, among others, two relevant features that comply with the safety conditions required when handling nuclear materials: its flexibility allows for remote, *in situ* and *ex situ* analysis, and its relative ease of use implies small sample quantities and limited effort for sample preparation. In this work, we demonstrate the usefulness of taking into consideration Raman spectroscopy for research studies on the back-end of the nuclear fuel cycle. In particular, we show some of the valuable results that can be obtained when applying this technique to: 1) the advanced characterization of nuclear fuels, 2) the evaluation of the spent nuclear fuel behavior under different storage conditions, and 3) the development and monitoring of hydrometallurgical separation processes.

9:35 AM *CH01/CH03.06

Variable-Temperature Electron Spectromicroscopy Techniques for Investigating Metal/Insulator Transitions in V2O3 Systems Laura Bocher¹, Ibrahim Koita¹, Tizei Luiz H. G.¹, Jean-Denis Blazit¹, Xiaoyan Li¹, Benoît Corraze², Julien Tranchant², Marcel Tencé¹, Laurent Cario², Etienne Janod² and Odile Stephan¹; ¹Université Paris-Saclay, France; ²Université de Nantes, France

Taming abrupt resistive transitions in functional oxides is a promising approach for developing advanced information processing and storage systems. V₂O₃ is considered a prototypical system of metal-to-insulator transitions (MITs) where they can be activated under external stimuli such as temperature (T), pressure, or chemical doping^[1] but hardly technologically feasible. Recent demonstrations from electric pulses yield MIT in (V_{1-x}Cr_x)₂O₃ systems with real potential capabilities for non-volatile memories and neuromorphic applications^[2]. Hence, understanding the V₂O₃ electronic phase separation and its local mechanisms governing the insulator/metallic (I/M) domain dynamics across the IMTs remains of interest. However, all these electronic transitions rely on their relationship between structural and electronic degrees of freedom. For instance, when cooled below 160 K, V₂O₃ presents a symmetry breaking, associated with a large volume change (+1.4%) and an MIT yielding a resistivity change of 7 orders of magnitude. This T-activated MIT has been extensively studied at the macroscopic scale^[1] and remains still a perfect arena to probe *in situ* the V₂O₃ structural and electronic evolutions at a very local scale. Recently, the microscopic electronic coexistence of I/M domains has been mapped in (V_{1-x}Cr_x)₂O₃ by *in situ* scanning photoemission spectroscopy^[3], PEEM^[4] and nano-IR^[5] with 25nm spatial resolution at best. In addition, combined micro-XRD and nano-IR experiments have highlighted competitive mechanisms between structural and electronic contributions during this MIT^[6]. These latest investigations also demonstrate the cautions and possible experimental limitations when it comes to accurately mapping the dynamics of mechanisms within regions of interest of a few tens of nm by combining different instruments, hence the need to perform structural and electronic experiments within the same instrument.

Advanced monochromated electron spectromicroscopy emerged this last decade as real game-changers for nanomaterials characterization. Here we performed *in situ* monochromated STEM/EELS experiments on the NION CHROMATEM 200 MC with variable-T options under cryo-conditions thanks to a double-tilt HennyZ cryo-holder using MEMS to vary continuously the temperature conditions across the IMTs. For each probed temperature, we associated mapping of relevant spectroscopic electronic excitations (from IR to soft X-ray) with an ultra-high EELS resolution at the nm scale and the local structural features (symmetry and lattice parameters) determined by 4D STEM nano- and microdiffraction. During low-T thermal cycling through the resistive transition, EELS spectra acquired in the low-loss regime present a characteristic signature at 1.1eV only in the metallic phase. Upon cooling, the abrupt MIT was monitored while the coexistence of I/M nanodomains was evidenced upon heating over a few degrees yielding the propagation of the electronic I/M domain wall. 4DSTEM nanodiffraction experiments reveal the local distribution of monoclinic/rhombohedral phases coexisting in the insulating domains. The observation of the low-T insulating hexagonal phase suggests an analogous paramagnetic insulating (PI) phase of large volume, as confirmed by the jumps in lattice parameters observed at the transition. These PI-like phases emerge also at the I/M domain wall, as a precursor of the metallic phase.

[1] D. B. McWhan et al. *Phys. Rev. B* **2** (1970); [2] E. Janod et al. *Adv. Funct. Mater.* **25** (2015); [3] S. Lupi, et al., *Nat. Commun.*, **1** (2010); [4] A. Ronchi et al., *Phys. Rev. B* **100** (2019); [5] McLeod et al. *Nature Physics* **13** (2017); [6] Kalcheim, Y. et al. *Phys. Rev. Lett.* **122**, (2019); [7] The authors acknowledge funding from the EDPIF, the National Agency for Research under the JCJC program IMPULSE and the program of future investment TEMPOS-CHROMATEM, and the European Union's Horizon 2020 research and innovation program under grant agreement No 823717 (ESTEEM3).

SYMPOSIUM CH02

Utilizing Advanced In Situ/Operando Transmission Electron Microscopy and Spectroscopy for the Investigation of Functional, Energy and Quantum Materials
April 23 - April 26, 2024

Symposium Organizers

Qianqian Li, Shanghai University
Leopoldo Molina-Luna, Darmstadt University of Technology
Yaobin Xu, Pacific Northwest National Laboratory
Di Zhang, Los Alamos National Laboratory

Symposium Support

Bronze
DENSsolutions

* Invited Paper
+ JMR Distinguished Invited Speaker
^ MRS Communications Early Career Distinguished Presenter

SESSION CH02.01: Exploration of Complex Oxide Heterostructures and Microelectronics Devices via *In-Situ* Electron Microscopy I
Session Chairs: Leopoldo Molina-Luna and Di Zhang
Tuesday Morning, April 23, 2024
Room 440, Level 4, Summit

10:30 AM *CH02.01.01

Advanced In Situ (S)TEM for Grain Boundary Phenomena in Oxides [Yuichi Ikuhara](#)^{1,2,3}; ¹The University of Tokyo, Japan; ²Japan Fine Ceramics Center, Japan; ³Tohoku University, Japan

Oxides have been widely used for structural applications because of their superior mechanical properties. It has been known that the behavior of GB properties is strongly dependent on the GB characters such as misorientation angle between two adjacent crystals and GB plane, however, such effect has not been clarified yet. In addition, this effect is much influenced by the dopant segregation at GBs in oxides. In this study, in order to clarify the GB atomic structures in oxides such as Al_2O_3 , ZrO_2 , SrTiO_3 , their bicrystals including various types of GBs with and without dopants were systematically fabricated. Then, the atomic structures and chemistry in thus fabricated GBs were characterized by aberration corrected STEM (scanning transmission electron microscopy), atom-resolved EDS and EELS, and the relationship between GB characters, segregated dopants and the properties for such ceramics will be discussed.

GB dynamics such as fracture and migration also play an important role in considering the sintering behavior and the properties. However, it has been still unclear as to how the GB fractures and migration proceeds at atomic scale. In this study, GB fracture and deformation are dynamically observed by TEM in-situ straining experiments using nano-indentation and newly developed MEMS straining holder. It was found that GB fracture occurs along the special crystal plane and dislocations are emitted from the crack front. Recently, we have proposed that GB migration behavior in ceramics can be precisely controlled by the aid of the high-energy electron beam irradiation. This electron beam technique was applied to directly visualize the atomistic GB migration. It was revealed that the GB migration is processed by a cooperative shuffling of atoms in GB ledges along specific routes. As a result, the GB passed through several different GB structures with low formation energies during GB migration.

References

- [1] S. Kondo, T. Mitsuma, N. Shibata, Y. Ikuhara, *Sci. Adv.*, 2[11], e1501926 (2016).
- [2] S. Kondo, A. Ishihara, E. Tochigi, N. Shibata, and Y. Ikuhara, *Nature Commun.*, 10, 2112 (2019).
- [3] J. Wei, B. Feng, R. Ishikawa, T. Yokoi, K. Matsunaga, N. Shibata and Y. Ikuhara, *Nat. Mater.* 20, 951 (2021).
- [4] J. Wei, B. Feng, E. Tochigi, N. Shibata and Y. Ikuhara, *Nat. Commun.*, 13, 1455 (2022).
- [5] S. Kobayashi, A. Kuwabara, C. A.J. Fisher, Y. Ukyo and Y. Ikuhara, *Nat. Commun.*, 9, 2863 (2018).

11:00 AM *CH02.01.02

Atomic Mapping of Polar Topologies in Oxide Superlattices [Yinlian Zhu](#)¹, Yunlong Tang² and Yujia Wang²; ¹Songshan Lake Materials Laboratory, China; ²Institute of Metal Research, Chinese Academy of Sciences, China

Since the discovery of full flux-closure domains in $\text{PbTiO}_3/\text{SrTiO}_3$ multilayers grown on GdScO_3 substrates[1], various polar topological domain structures such as vortices, skyrmions, merons and polar waves etc. were subsequently discovered in the ferroelectric films and superlattices. These polar topological structures are nanoscale objects and have potential applications in high-density non-volatile memory devices. The topological protection makes them very stable under small external stimuli and the cross-talk can be effectively avoided. Besides the industrial potential, they also possess rich emerging physical properties, such as negative capacitance, enhanced conductivity, electrocaloric effect, and so on. We choose and introduce some recent observations of polar topologies in ferroelectric films. It is pointed out that the $\text{PbTiO}_3/\text{SrTiO}_3$ system is becoming hot in modulating polar topologies these days. Both misfit strains and insulating layers play important roles in tuning the topologies. We expect more investigations to be carried out for unveiling the mask of complex structures in oxide films, multilayers and superlattices with perovskite structure.

References

- [1] Y. L. Tang, Y.L. Zhu et al., *Science* 348(2015)547-551.
- [2] The financial support from the National Natural Science Foundation of China with No. 51971223 is acknowledged.

11:30 AM CH02.01.03

Cryogenic-Monochromated STEM-EELS Analysis of Symmetry Breaking and Local Ferroelectricity in SrTiO_3 Based-Heterostructures [Aravind Raji](#)^{1,2}, Guillaume Krieger³, Xiaoyan Li¹, Yves Auaud¹, Daniele Preziosi³, Manuel Bibes⁴, Jean-Pascal Rueff^{2,5} and Alexandre Gloter¹; ¹Laboratoire de Physique des Solides Orsay, France; ²Synchrotron SOLEIL, France; ³IPCMS UMR 7504, CNRS, Universit  de Strasbourg, France; ⁴Unit  Mixte de Physique CNRS, Thales, Universit  Paris-Saclay, France; ⁵LCPMR, Sorbonne Universit , CNRS, France

The growth of oxide-based electronics is in a good pace, and the apt material knowledge obtained by advanced characterization techniques leverages the complexity in designing devices with intriguing properties. Knowledge of the atomic level arrangements in a material system enables us to make atomic level manipulations, thereby tweaking the electronics. This is made possible by one of the most advanced characterization techniques such as the Scanning Transmission Electron Microscopy (STEM). In this, in addition to obtaining a high-resolution image with good atomic phase contrast, one can have spectroscopic information representative of their electronic states through electron energy loss spectroscopy (EELS). Combining this with controllable external stimuli (Temperature, Photons, etc.) one can study a vast range of electronic and structural states in a chosen material. Some prototypical examples include temperature dependent metal-to-insulator transitions [1], photoinduced superconducting transitions [2], etc. Here we will be focusing on SrTiO_3 (STO) based heterostructures exhibiting incipient ferroelectricity as a result of broken symmetry near the interface [3]. Some examples are the Al/STO [4], and Ca -doped STO [5], and even $\text{NdNiO}_3/\text{STO}$ system that have a metal to insulator transition range spanning 150-200K [6]. Understanding the electronic origins of it is of paramount importance, and so is studying its variation with external stimuli. STO is an intriguing system that undergoes a cubic to tetragonal antiferrodistortive phase transition below 105K, and undergoes another transition to become a quantum paraelectric below 37K [7,8]. The influence of these transitions on the interface properties are of significant interest, and a spectro-microscopic study spanning the range of these transitions is much appreciated. In this regard, we carry out RT and cryogenic (~110K) STEM-EELS measurements in a monochromated Nion CHROMATEM microscope equipped with a hybrid pixel direct electron detector Medipix3 [9]. Our experiments in an $\text{NdNiO}_3/\text{STO}$ demonstrated significant fine structure variations at the $\text{Ti-L}_{2,3}$ edge, on going from RT to ~110K. It has been previously reported that the cubic to tetragonal antiferrodistortive transition in STO occurs inhomogeneously, that the surface unit cells begin this transition at around ~150K, which possibly spans to the whole STO by ~105K [10]. Hence, the fine structure variations we see at around ~110K near the interface could be representative of this transition, thereby altering the interface properties. Characterizing such variations is enabled by high-energy resolution monochromated EELS, in combination with a cryogenic system. The resolution significantly overpasses previous studies reported in this direction, where, in addition a real space mapping of the fine structure variation couldn't be done [11, 12]. An investigation in this direction paves the way to better understanding the interesting phenomena such as superconductivity and ferromagnetism that emerges at these interfaces.

- [1] Preziosi, Daniele, et al. *Nano letters* 18.4 (2018): 2226-2232.
- [2] Yang, Zhen, et al. *Small* (2023): 2304146.
- [3] Haeni, J. H., et al. *Nature* 430.7001 (2004): 758-761.
- [4] R del, Tobias Chris, et al. *Advanced Materials* 28.10 (2016): 1976-1980.
- [5] Br hin, Julien, et al. *Physical Review Materials* 4.4 (2020): 041002.
- [6] Palina, Natalia, et al. *Nanoscale* 9.18 (2017): 6094-6102.
- [7] Cowley, R. A. *Physical Review* 134.4A (1964): A981.
- [8] M ller, K. Alex, and H. Burkard. *Physical Review B* 19.7 (1979): 3593.
- [9] Tenc , Marcel, et al. *Microscopy and Microanalysis* 26.S2 (2020): 1940-1942.
- [10] Salman, Z., et al. *Physical Review B* 83.22 (2011): 224112.
- [11] Haruta, Mitsutaka, et al. *Applied Physics Letters* 119.23 (2021).
- [12] Rui, Xue, and Robert

F. Klie. Applied Physics Letters 114.23 (2019).

11:45 AM CH02.01.04

Unraveling Metal-To-Metal Hydride Phase Transformation using *In-Situ* S/TEM Techniques Gopi Krishnan¹, Lars Bannenberg², Herman Schreuders² and Joerg Jinschek¹; ¹Technical University of Denmark, Denmark; ²Delft University of Technology, Netherlands

In our relentless pursuit of solutions to advance the decarbonization of our society and economy, hydrogen stands out for its exceptional qualities as a zero-emission fuel, energy storage medium, and chemical feedstock. Nevertheless, the challenge of compact hydrogen storage remains a daunting one in both science and technology. Safe storage of hydrogen, particularly in solid forms such as metal hydrides, offers numerous compelling benefits.

However, further improving its storage properties requires a comprehensive understanding of nucleation and growth of metal-to-metal hydride phase transformation at the atomic scale. In this context, real-time visualization of the various steps of the transformation process is essential for a precise and quantitative understanding. For instance, for interpreting the hydrogen sorption property of materials, it is crucial to reveal the effect of stress/strain, the role of defects, and intermediate phase evolution during metal-to-metal hydride phase transformation.

In this study, we use MgTi thin films as a model system to study metal-to-metal hydride phase transformation using in-situ Scanning/Transmission Electron microscopy (S/TEM). The phase transition from hexagonal to face-centered cubic in Mg to MgTiH_x is tracked through crystal structure changes observed by electron diffraction (ED) and in bulk plasmon resonance detected by electron energy loss spectroscopy (EELS). We also apply in-situ 4D STEM to investigate local structural displacements and strain developed during the process. Moreover, integrated differential phase contrast (iDPC) imaging aids in pinpointing hydrogen atom positions within the lattice. By combining these methods, we gain insights into the hydrogenation process and its effects on hydrogen storage properties.

SESSION CH02.02: Exploration of Complex Oxide Heterostructures and Microelectronics Devices via *In-Situ* Electron Microscopy II

Session Chairs: Leopoldo Molina-Luna and Di Zhang

Tuesday Afternoon, April 23, 2024

Room 440, Level 4, Summit

2:00 PM *CH02.02.01

In-situ Cryogenic and Biasing STEM and EELS for Quantum Materials Shelly Michele Conroy; Imperial College London, United Kingdom

Understanding how the emergent phases of quantum materials form and behave during operation at the atomic scale is crucial to future quantum technology design. Cryogenic Scanning Transmission Electron Microscopy (STEM) and Electron Energy Loss Spectroscopy (EELS) have emerged as powerful tools, enabling scientists to explore quantum materials under extreme conditions of ultra-low temperatures, vacuum conditions and applied stimulus such as bias. This cutting-edge combination of techniques integrates the high-resolution imaging and diffraction capabilities of STEM with cryogenic technology and the analytical capabilities of EELS, allowing for the investigation of materials at these low temperature exotic emergent phases, while simultaneously probing their electronic structure.

In this presentation firstly the multiple ferroic phases below room temperature of Fe₁Boracite are investigated using a cryogenic STEM holder with temperature control. We investigate the change in strain, polarisation and domain configuration via 4D-STEM during temperature cycling and thus changing ferroic phases. By switching from 4D-STEM to EELS we can also collect changes in band gap and crystal field splitting. The dynamics of the domain wall topologies within these materials were investigated using in-situ biasing at these various temperatures and phases.

Secondly, this presentation will detail how cryogenic vacuum transfer STEM can be used to probe the superconducting phase of a doped Fe(Se,Te) system. Here we show the emergence of nanoscale superconducting puddles by complementary low temperature conducting atomic force microscopy. We could pick out these region using focused ion beam and with a vacuum transfer system we can do all sample preparation and analysis under vacuum and cryogenic conditions. We reveal the clear changes in physical structure and band gap between the superconducting and high temperature phase using controlled in-situ heating from liquid nitrogen to room temperature.

2:30 PM CH02.02.03

In-Operando Optical Tracking of Vacancy Induced Phase Change in Few-nm Thick Ferroelectric HZO Atif Jan and Giuliana Di Martino; University of Cambridge, United Kingdom

Ferroelectric random-access memories (FeRAM) switching is achieved by ferroelectric switching of dipoles. FeRAMs offer low-energy and faster switching as compared to conventional memory circuitry. They excel in power consumption and low-voltage operation when stacked against current-driven contenders. Unfortunately, FeRAMs have been restricted to niche markets due to their limited CMOS compatibility and severe scaling issues of the complex ferroelectric perovskite systems. However, the discovery of ferroelectricity in binary oxides gave an impetus for developing a universal memory concept, which may lead to a significant breakthrough in the development of memory devices. Binary oxides generally do not suffer from a "dead layer effect", which makes non-binary oxides, such as perovskites, ineffective for thin film technology. Moreover, high coercive fields inside binary oxides give them considerable resilience toward internal depolarization of the ferroelectricity, crucial to achieving scalability and overcoming the widespread reliability disadvantages of FE material. The underlying reasons for the stable ferroelectricity and distinct switching of FE domains inside binary oxides at an atomic level are poorly understood. Moreover, non-idealities seen upon continuous electronic switching cycles like wake-up and fatigue introduce uncertainties in device performance and endurance. In this work, we present the first proof of the underlying reasons for these non-idealities with cycle-to-cycle tracking of morphology changes in few-nm thick binary oxide ferroelectric ultra-thin films.

This work presents the first proof of the underlying reasons for these non-idealities with cycle-to-cycle tracking morphology changes in few-nm thick binary oxide ferroelectric ultra-thin films. With our Nanoparticle-on-Mirror (NPoM) geometry, we capture for the first time both migration of <1% oxygen ions and material phase change in just 5nm-thick binary oxide ferroelectric films when under continuous electronic switching and therefore track in real-time and in-operando the nanoscale kinetics of wake-up and fatigue in ferroelectric ultrathin memories. We use in-situ electrical and optical characterizations like darkfield scattering, photoluminescence and Raman spectroscopy to understand the nano-kinetics of the atomic level switching. The tracking of vacancy migration and phase change with the above-mentioned techniques combined with density functional theory (DFT) and finite-difference time-domain (FDTD) simulations provide the first insights into the morphological changes in ultra-thin binary oxide films [1].

[1]: A. Jan, T. Rembert, S. Taper, J. Symonowicz, N. Strkalj, T. Moon, Y. S. Lee, H. Bae, H. J. Lee, D.-H. Choe, J. Heo, J. MacManus-Driscoll, B. Monserrat, G. Di Martino, Advanced Functional Materials 2023, 33, 2214970.

2:45 PM CH02.02.04

Unveiling Texture Transfer in Dielectric Thin Films via *In Situ* Electron Microscopy Robert Winkler¹, Alexander Zintler², Oscar Recalde¹, D spina Nasioiu¹, Lambert Alff¹ and Leopoldo Molina-Luna¹; ¹TU Darmstadt, Germany; ²University of Antwerp, Belgium

Transition metal oxide (TMO) dielectric layers are pivotal for applications like field-effect transistors, supercapacitors, and emerging memories such as resistive random access memory (RRAM) [1]. Careful selection of the thin film layer materials and growth techniques in an RRAM device is essential to engineering the desired microstructure via texture transfer to improve performance and reliability [2], [3].

Usually, texture transfer is achieved via epitaxial growth at elevated temperatures, which, in the case of RRAM, might be more challenging to integrate in current complementary metal oxide semiconductor (CMOS) back-end-of-line (BEOL) processes. Therefore, a question arises if texture transfer is also possible when annealing amorphous HfO₂ thin films grown via reactive molecular beam epitaxy (RMBE) on highly textured (111) thin films. Here, we have employed in situ electron microscopy to precisely determine the minimum required temperature and the origin of grain growth.

Crystallization of amorphous HfO₂ starts at 180 °C, non-adjacent to an interface. The developing grains, as shown by automated crystal orientation mapping (ACOM) in ASTAR of the 4D-STEM data set, are nanocrystalline or amorphous until reaching an adjacent textured layer. The resulting (11-1+010) monoclinic phase of the annealed HfO₂ thin films indicates that texture transfer is possible, which is also represented in the improvement of the RRAM device's performance.

To summarize, the presented findings in our study are not only relevant in the field of dielectric thin films by connecting microstructural changes to device fabrication and performance but are generally useful when tracking the origins of grain growth with nanometer precision by analyzing 4D STEM via automated crystal orientation mapping (ACOM).

References:

- [1] R. Dittmann, S. Menzel, and R. Waser, 'Nanoionic memristive phenomena in metal oxides: the valence change mechanism', *Advances in Physics*, vol. 70, no. 2, pp. 155–349, Apr. 2021, doi: 10.1080/00018732.2022.2084006.
- [2] R. Winkler *et al.*, 'Controlling the Formation of Conductive Pathways in Memristive Devices', *Advanced Science*, vol. 9, no. 33, p. 2201806, 2022, doi: 10.1002/adv.202201806.
- [3] S. U. Sharath *et al.*, 'Control of Switching Modes and Conductance Quantization in Oxygen Engineered HfO_x based Memristive Devices', *Adv. Funct. Mater.*, Jul. 2017, doi: 10.1002/adfm.201700432.

3:00 PM BREAK

3:30 PM *CH02.02.05

Design interface and domain structure in doped BaTiO₃ systems for enhanced relaxor ferroelectric behavior and energy storage Aiping Chen¹, Di Zhang¹, Nicholas Cucciniello^{1,2}, Alessandro Mazza¹, Quanxi Jia², Michael Zachman³, Rod McCabe¹ and James M. LeBeau⁴; ¹Los Alamos National Laboratory, United States; ²University at Buffalo, The State University of New York, United States; ³Oak Ridge National Laboratory, United States; ⁴Massachusetts Institute of Technology, United States

Dielectric materials, holding charges as capacitors, are vital energy storage components of electronics and power systems. Dielectric capacitors distinguish themselves in features of ultrafast charging/discharging rates, high voltage endurance, and good reliability. Enhancing the relatively low energy densities of dielectric capacitors is essential for their applications in pulsed power equipment. Relaxor ferroelectrics are promising candidates for applications in energy storage. Therefore, considerable effort has been devoted to enhancing the energy storage via composition optimization, defect engineering, and architectural design.

In this talk, I will discuss the strategies of designing interface and domain structure in doped BaTiO₃ to achieve relaxor ferroelectrics. In the first part, I will discuss the design of (Ba_{0.7}Ca_{0.3})TiO₃ (BCT) and Ba(Ti_{0.8}Zr_{0.2})O₃ (BZT) superlattices via a high-throughput combinatorial approach. Well-controlled compositional gradient, superlattice geometry and domain size are explored by scanning transmission electron microscopy (STEM). Ferroelectric and dielectric properties identified the "optimal property point" achieved near the morphotropic phase boundary. Our results have found that relaxor-like ferroelectric behavior enhances and the leakage slightly increases with reducing the superlattice periodicity (or with more interfaces). In the second part of the talk, I will discuss strategies to further optimize domain structures and suppress the leakage current in BZT-BCT films via a machine learning approach. Sn has been identified as an ideal dopant to maintain the rhombohedral/tetragonal phase boundary, reduce leakage current and reduce the domain size below 10 nm for BZT-BCT systems and greatly enhanced relaxor ferroelectric behavior has been achieved. The large polarization and the delayed polarization saturation lead to greatly enhanced energy density of 80 J/cm³ and transfer efficiency of 85% over a wide temperature range. Such a data-driven design recipe for a slush-like polar state is generally applicable to quickly optimize functionalities of ferroelectric materials.

4:00 PM CH02.02.06

Defect Induced Memristive Switching in Off-Stoichiometric SrTiO₃ and CaTiO₃ studied by *In Situ* Transmission Electron Microscopy Changming Liu¹, Wahib Aggoune², Mohamed Abdeldayem¹, Alexander Meledin³, Houari Amari¹, Izaz-Ali Shah¹, Thilo Remmele¹, Tobias Schulz¹, Andreas Fiedler¹, Jutta Schwarzkopf¹, Matthias Scheffler² and Martin Albrecht¹; ¹Leibniz Institut fuer Kristallzuechtung, Germany; ²Humboldt-Universit t zu Berlin, Germany; ³Thermo Fisher Scientific, Netherlands

In the quest for neuromorphic computing systems that emulate the intricacies of the human brain, the transition of digital memory to an analog state is paramount. A central scientific question revolves around directing materials to incorporate synaptic plasticity. Among the most promising and technologically advanced strategies for achieving this are resistive random access memory (ReRAM) devices. Traditional ReRAMs operate through the stochastic formation and breakage of conductive filaments within an insulator storage medium, making control challenging. This paper presents a novel approach to memristive devices, focusing on single crystalline SrTiO₃ and CaTiO₃ thin films. By deliberately introducing an A cation deficiency of up to about 16% through metal organic vapor phase epitaxy (MOVPE), we have successfully realized resistive switching without the need for filament formation, achieving on/off ratios as high as 10³. Our investigation integrates various techniques, including electrical measurements, transmission electron microscopy (TEM), and in-situ X-ray studies at a synchrotron, to provide insights into the underlying mechanisms.

Our results suggest that the resistive switching phenomenon in off-stoichiometric films can be attributed to trap-assisted tunneling through Ti antisite defects, which induce a switchable polarization. Crucial parameters such as on/off ratio and retention time depend on the extent of off-stoichiometry. This study presents a comprehensive TEM analysis of these materials, including high-resolution scanning transmission electron microscopy (S-TEM), electron energy loss spectroscopy (EELS), and dynamic in-situ TEM measurements with electrical bias and heating. Our results show that approximately 50% of the V_A sites are occupied by Ti and that these antisite defects are responsible for inducing ferroelectric polarization. Differential phase contrast measurements reveal the polarization of these domains. Preliminary in-situ TEM experiments confirm the resistive switching behavior observed in ex-situ electrical measurements. Furthermore, our in-situ studies suggest that these polar defects combine under bias to form nanopolar domains that are statistically distributed throughout the film. This is visually confirmed by contrast inversion in dark-field images using forbidden reflections, consistent with macroscopic observations in synchrotron experiments. We attribute this contrast inversion to the alignment of off-centered polar defects induced by the applied electric field. Reducing the voltage to 0 V results in a stable state, albeit with the polarization erased, returning the local film to a high-

resistance state. These preliminary in-situ I-V measurements confirm our recent findings that resistive switching in Sr-deficient SrTiO₃ thin films occurs at significantly lower voltages than those required for filament formation, offering promising prospects for future neuromorphic computing applications.

4:15 PM CH02.02.07

Advanced Phase Plate Fabrication and Thin Film Characterization for TEM Imaging of Biological Samples Marcus F. Hufe¹, Mads S. Larsen¹, Stephan S. Keller¹, Marco Beleggia^{2,1} and Paul J. Kempen¹; ¹Technical University of Denmark, Denmark; ²University of Modena and Reggio Emilia, Italy

Phase plates (PPs) for transmission electron microscopy (TEM) have been a research field since 2001 [1] and are of continuing interest to enhance contrast and increase resolution when imaging biological samples [2]. The most promising PPs for soft-matter imaging are thin-film-based [3]. These include Volta-, Zernike-, and Hilbert-type PPs. Thin-film PPs are generally fabricated by hand using sputtering tools in a single-device process [4]. These PPs suffer from several limitations that plague their widespread implementation. These challenges include contamination, ease of installation and use, lack of reproducibility, and lack of full understanding and control of the induced phase shift. In this work we are using cleanroom processes to fabricate PPs that are reproducible with known parameters. In this manner we can both know and control the induced phase shift. We present the fabrication of both Zernike-type phase plate devices (ZPPs), with an ideal phase shift of $\Delta\phi = \pi/2$, and Hilbert-type PP devices (HPPs), for which $\Delta\phi = \pi$.

In order to achieve this, it is necessary to know the accurate mean inner potential (MIP) of the materials involved. For our work, the most promising thin film materials are silicon nitride and amorphous carbon. MIP values for these materials in the literature vary widely, making it difficult to fabricate a device with the ideal phase shift. The phase shift is related to the mean inner potential V_0 and the film thickness t (via an electron constant C_E) in the following way [5]: $\Delta\phi = C_E V_0 t$. We use ellipsometry and AFM techniques to determine and verify the thicknesses of the thin films. We use electron holography (EH) [6] to measure the phase shift of our devices. Using the thickness and phase shift values we can then accurately determine the MIP of our thin films. We can further use this to optimize our devices for optimal phase shift.

In addition to our material characterization, we installed the PPs in the back-focal plane of a *TF Tecnai TEM* using the existing objective aperture mechanism. We will demonstrate the functionality of our phase plate devices via contrast enhancement, using both a test sample made from thin carbon structures on a standard carbon-film TEM grid, and biological samples at cryogenic temperatures.

REFERENCES

- [1] R. Danev, K. Nagayama, Transmission electron microscopy with Zernike phase plate, 2001, Ultramicroscopy 88: 243
- [2] M. Obermair et al., Analyzing contrast in cryo-transmission electron microscopy: Comparison of electrostatic Zach phase plates and hole-free phase plates, 2020, Ultramicroscopy 218: 113086
- [3] R. M. Glaeser, Methods for imaging weak-phase objects in electron microscopy, 2013, Rev. Sci. Instrum. 84: 111101
- [4] R. Danev et al., Practical factors affecting the performance of a thin-film phase plate for transmission electron microscopy, 2009, Ultramicroscopy 109: 312
- [5] M. Malac et al., Phase plates in the transmission electron microscope: operating principles and applications, 2021, Microscopy Vol. 70, No. 1: 75
- [6] M. N. Yesibolati et al., Mean Inner Potential of Liquid Water, 2020, Phys. Rev. Lett. 124: 065502

4:30 PM *CH02.02.08

In-Situ STEM Studies of Ferroelectric Domains in Free-Standing Thin Films Tamsin I. O'Reilly¹, Kristina Holsgrove¹, Xinqiao Zhang², John J. Scott¹, Iaro Gaponenko³, Praveen Kumar^{1,4}, Patrycja Paruch³, Joshua Agar² and Miryam Arredondo¹; ¹Queen's University Belfast, United Kingdom; ²Drexel University, United States; ³University of Geneva, Switzerland; ⁴School of Mines, United States

Ferroelectrics are polar materials known for their spontaneous polarization, which can be reversibly switched by applying an external field. As these materials are cooled below their Curie temperature (T_C), the resulting domain structure and switching dynamics are driven by boundary their conditions, aiming to minimize electrostatic and elastic energy in the system.

A particularly interesting aspect of ferroelectrics is the effect that surface chemical species have on the screening mechanism, and its resulting domain structure, and vice versa, how domains affect the surface chemistry. The latter could be exploited to tailor surface reactivity for electrochemical, catalytical,[1-6] and other energy harvesting applications.[2, 7-9]

This study focuses on investigating the thermally induced behavior of ferroelectric-ferroelastic domains in free-standing thin films under different chemical environments using in-situ scanning transmission electron microscopy (STEM) techniques. The similarities and differences between these environments are discussed, along with the associated challenges.

To the best of our knowledge, this is the first time in-situ heating under controlled gas environments has been employed to study ferroelectric-ferroelastic domains. Our findings provide valuable insights into the intricate relationship between important ferroelectric characteristics such as (T_C , domain size, etc) and the chemical environment. Furthermore, this work highlights the application of in-situ gas as a powerful technique for dynamically exploring the effects of other external variables such as pressure on polar materials.

- [1] Y. Yun, E. I. Altman, *Journal of the American Chemical Society* **2007**, 129, 15684.
- [2] A. Kakekhani, S. Ismail-Beigi, *Journal of Materials Chemistry A* **2016**, 4, 5235.
- [3] T. L. Wan, L. Ge, Y. Pan, Q. Yuan, L. Liu, S. Sarina, L. Kou, *Nanoscale* **2021**, 13, 7096.
- [4] A. Kakekhani, S. Ismail-Beigi, *Physical Chemistry Chemical Physics* **2016**, 18, 19676.
- [5] Y. Li, J. Li, W. Yang, X. Wang, *Nanoscale Horizons* **2020**, 5, 1174.
- [6] A. Kakekhani, S. Ismail-Beigi, E. I. Altman, *Surface Science* **2016**, 650, 302.
- [7] H. Li, C. R. Bowen, Y. Yang, *Advanced Functional Materials* **2021**, 31, 2100905.
- [8] M. Xie, S. Dunn, E. L. Boulbar, C. R. Bowen, *International Journal of Hydrogen Energy* **2017**, 42, 23437.
- [9] S. Kim, N. T. Nguyen, C. W. Bark, *Applied Sciences* **2018**, 8, 1526.

Wednesday Morning, April 24, 2024
Room 440, Level 4, Summit

8:30 AM *CH02.03.01

High-Resolution Scalar/Vector-Field Electron Tomography Unveiling 3D Topological Spin Textures Xiuzhen Yu¹, Nobuto Nakanishi^{1,2}, Yi-Ling Chiew¹, Naoya Kanazawa³, Kosuke Karube¹, Yasujiro Taguchi¹ and Yoshinori Tokura^{1,3}; ¹RIKEN, Japan; ²Thermo Fisher Scientific, Japan; ³The University of Tokyo, Japan

The emergence of 2D topological spin textures, such as magnetic skyrmions in helimagnets, has garnered significant attention in the field of condensed matter physics and spintronics^{1,2}. However, our understanding of nontrivial 3D spin textures remains limited, primarily due to the absence of a high-resolution 3D magnetic imaging technique, especially at lower temperatures below room temperature (RT). While some progress has been made in imaging magnetic twisted structures in 3D through nanotomography³, challenges persist in accurately mapping 3D vector fields and achieving the necessary spatial resolution. These obstacles hinder our ability to comprehensively map 3D exotic spin textures in magnets with topological precision over a broad temperature range. The objective of this study is to develop a high-resolution scalar/vector-field electron tomography microscopy technique that covers a wide temperature range from 95 K to RT, enabling real-space observations of various 3D topological spin textures.

In this study, I will introduce scalar/vector-field electron tomography using 3D integrated differential-phase-contrast microscopy and discuss its applications. Specifically, I will show vortex pairs on the surface of elliptical skyrmions in an antiskyrmion-hosting magnet at RT and the formation of 'football'-like skyrmions and their heavy deformations around sample surfaces with varying temperatures in a helimagnet FeGe. This groundbreaking 3D magnetic imaging technique reveals hybrid topological spin textures, including surface spin textures such as vortices and monopoles, providing valuable insights into the topological aspects of various spin textures emerging in topological materials.

*This work was supported by Grants-In-Aid for Scientific Research (Grant No. 19H00660, 23H05431) from the Japan Society for the Promotion of Science and the Japan Science and Technology Agency CREST program (Grant No. JPMJCR1874, JPMJCR20T1).

References

- [1] Y. Tokura, and N. Kanazawa, *Chem. Rev.* 121, 2857 (2021).
- [2] N. Nagaosa, and Y. Tokura, *Nat. Nanotechnol.* 8, 899 (2013).
- [3] C. Donnelly, *et al. Nature* 547, 328 (2017); D. Wolf, *et al. Nat. Nano.* 17, 250 (2022).

9:00 AM CH02.03.02

Investigating the Resistive Switching Mechanisms of Oxide and Nitride-Based Memristor Devices via *In Situ* STEM and EELS Di Zhang¹, Rohan Dhall², Matt Schneider¹, Chengyu Song², Sundar Kunwar¹, Nicholas Cucciniello¹, Hongyi Dou³, Jim Ciston², John Watt¹, Winson Kuo¹, Michael T. Pettes¹, Haiyan Wang³, Rod McCabe¹ and Aiping Chen¹; ¹Los Alamos National Laboratory, United States; ²Lawrence Berkeley National Laboratory, United States; ³Purdue University, United States

The resistive-switching (RS) phenomenon observed in a variety of transitional metal oxides is of great research interest since it opens enormous opportunities for the next-generation electronic devices such as nonvolatile memory and neuromorphic computing units, etc. However, the RS mechanisms for many oxide- and nitride- based memristor devices are still unclear. In this project, we use *in situ* transmission electron microscopy (TEM) and Electron Energy Loss Spectroscopy (EELS) to investigate the RS mechanisms of different types of memristor devices. The high resolution STEM images captured during the *in situ* biasing experiment revealed the potential phase transition processes and polarized cations displacements, and the core EELS spectra confirmed the cations valence states change and the oxygen stoichiometry modulation during the RS processes. This study has shined great light on clarifying the RS mechanisms of different types memristor devices, which can be applied to the development of next-generation nanoelectronic devices towards advanced memory and neuromorphic computing units etc.

9:15 AM CH02.03.03

Breaking Barriers in Oxide Nanoelectronics: Advancements in *In Situ* TEM Studies Oscar Recalde¹, Tianshu Jiang¹, Robert Winkler¹, Alexander Zintler¹, Esmaeil Adabifiroozjahi¹, Yevheniy Pivak², Hector H. Perez-Garza² and Leopoldo Molina-Luna¹; ¹TU Darmstadt, Germany; ²DENSsolutions, Netherlands

In today's microelectronic industry, oxide nanoelectronics are at its core. To gain insights into the dynamic processes within these nano electronic devices at the nano and sub-nanometer scale, *in situ/operando* transmission electron microscopy (TEM) has become a vital research avenue. Recent advancements in the integration of microelectromechanical systems (MEMS) within electron microscopes have made it possible to apply various stimuli to samples directly inside the microscope, including electrical biasing.

However, achieving reliable sample preparation for these experiments using focused ion beam (FIB) techniques has been an intricate challenge. Conventional FIB methods have often led to the inadvertent creation of short circuits along the MEMS platforms and TEM devices during sample attachment and electrical contacting. This has obscured the true performance of these devices.

In this study, our innovative FIB sample preparation protocol overcomes these challenges, allowing for the dependable operation of two-terminal oxide devices within the TEM. We have investigated structural changes in materials like SrTiO₃-based memristors, Nb-doped lead zirconate titanate (PNZT) piezoelectric, and BaSrTiO₃ ferroelectric, directly correlating these observations with the simultaneous acquisition of current-voltage (I-V) curves. This has facilitated meaningful comparisons with their macroscopic counterparts.

Furthermore, our investigations encompass multi-stimuli experiments, introducing gas nano cells into the equation. Interestingly, we have observed the impact of device oxidation induced by electron beam irradiation that alters the electrical response of a SrTiO_{3-x} and BaSrTiO_{3-x} (BST) tunable dielectric device when subjected to an oxygen-rich environment.

Moreover, a suppression of leakage current in TEM lamella devices exposed to Ar/O₂ plasma cleaning has also been investigated. Additionally, the effects of electron beam irradiation on the electrical properties of oxide devices, employing them as a tool for checking sample connectivity through STEM (SE)EBIC techniques, have also been explored. These findings collectively contribute to a more comprehensive understanding of oxide nanoelectronics and their behavior at micro and sub-nanometer scales.

In conclusion, our innovative FIB-based sample preparation technique not only enables the study of nano electronic devices under various stimuli conditions within a TEM environment but also facilitates the direct correlation of electrical properties with structural changes. Moreover, we have introduced the use of gas nano cells for multi-stimuli experiments, further enhancing our ability to probe sample connectivity and uncover microstructural factors influencing current-driven mechanisms.

9:30 AM *CH02.03.04

Quantum Monochromated Electron Microscopy: Combining High Spatial and Spectral Resolution to Observe Emergent Electronic and Vibrational Properties in Nanoscaled Quantum Materials [Jordan A. Hachte](#)¹, Eric R. Hoglund¹, Harrison Walker², De Liang Bao², Geemin Kim³, Mahmut Sami Kavrik⁴, Matt Law³ and Sokrates Pantelides²; ¹Oak Ridge National Laboratory, United States; ²Vanderbilt University, United States; ³University of California, Irvine, United States; ⁴Lawrence Berkeley National Laboratory, United States

Over the last 5-10 years, the scanning transmission electron microscope (STEM) has been turned to quantum materials more and more due to the ability to correlate the subtle structural signatures of quantum phase transitions with atomistic imaging and compositional analysis. Over this same time period, monochromation for electron energy-loss spectroscopy (EELS) in the STEM has also seen a resurgence. With typical energy resolutions improving by two orders of magnitude to enable a whole host of new experiments at the high spatial resolution of the STEM. The combination of the two is truly a new opportunity for quantum materials, as it allows the ability to probe the novel quasiparticles and shallow electronic structure that mediate emergent phenomena directly at the length scales over which they occur.

In this talk, I will discuss the application of monochromated STEM-EELS to quantum nanostructured superlattices. In SrTiO₃-CaTiO₃ (STO-CTO) superlattices, where the superlattice is in the growth direction with alternating layers of STO and CTO at different unit-cell thicknesses. In this system, the period of the superlattice dominates the macroscopic properties of the material through changing the number of interfaces between the STO and CTO. However, in short period superlattices, an emergent phonon response causes the interface-density-dependency to reverse and as the material takes a new property based off of the interface octahedral tilts. I will also discuss PbSe quantum dot superlattices, where the superlattice concerns lateral, self-assembled, epitaxially-connected quantum dots that form a network analog to a cubic crystal structure. Here the electronic states delocalize across the epitaxially connected QDs to create emergent electronic structure not present in the individual quantum dots. In both cases the combination of spatial and spectral information reveal emergent spectroscopic responses in the nanostructured superlattice.

10:00 AM BREAK

10:30 AM *CH02.03.05

Investigating The Structure of Spin Qubits Using Electron Ptychography [James M. LeBeau](#); Massachusetts Institute of Technology, United States

Divacancy and vacancy-transition metal (v-TM) complexes in silicon carbide (SiC) can form the basis for optically addressable single photon emitters. The convergence of SiC's technological maturity and the compatibility of these qubits with traditional semiconductors has thus sparked considerable interest in these defects. For example, recent quantum coherence measurements of v-TM complex spin states in SiC have underscored the potential of this platform in quantum computing applications. To validate theoretical frameworks and glean insights pertinent to emitter synthesis and stability, atomic resolution electron microscopy offers direct access to their structure and interactions within their local environment.

This presentation will explore the direct observation of individual defects in a SiC film using scanning transmission electron microscopy (STEM) imaging and multislice electron ptychography. We will show how the capabilities afforded by multislice electron ptychography enable us to characterize these defects at a localized level and in 3D without the need for tomography or through-focus methods. Moreover, we will show that conventional methods, such as high-angle annular dark field STEM, can be severely limited for this type of study due to noise and are frequently obscured by surface contamination, damage, and roughness. We will demonstrate that ptychographic reconstructions can directly quantify single defects and defect complexes on a slice-by-slice basis, imparting direct 3D information. This will be explored using simulated ptychographic datasets encompassing an array of defects in various positional configurations. Finally, we will discuss the limitations of capturing three-dimensional structures and the ability to capture small displacements arising from substitution and the formation of v-TM complexes.

11:00 AM *CH02.03.06

Towards *In-Situ* Electromagnetic Field Imaging in Materials by Scanning Transmission Electron Microscopy [Naoya Shibata](#); The University of Tokyo, Japan

Differential phase contrast scanning transmission electron microscopy (DPC STEM) is a powerful technique for directly characterizing local electromagnetic field distribution inside materials and devices. In combination with tilt-scan averaging system [1,2] for suppressing diffraction contrasts, DPC STEM can be applicable to local electromagnetic field imaging even in the vicinity of crystalline defects such as heterointerfaces and grain boundaries [3,4]. The next step is to apply this technique for materials under various external conditions from low temperatures to high temperatures, electromagnetic biasing, mechanical loading and so on. In this talk, some recent developments and applications along this direction will be discussed.

[1] Y. Kohno et al., *Microscopy*, 71, 111-116 (2022).

[2] S. Toyama et al., *Ultramicroscopy*, 238, 113538 (2022).

[3] S. Toyama et al., *Nature Nanotech.*, 18, 521-528 (2023).

[4] S. Toyama et al., *submitted*.

[5] This work is supported by JST ERATO grant number JPMJER2202 and the JSPS KAKENHI (grant number 20H05659).

11:30 AM *CH02.03.07

Revealing Strain Engineering and Polar Structures for Oxides [Yunlong Tang](#); Institute of Metal Research, Chinese Academy of Sciences, China

The ability to fabricate high-quality oxide films has created a vast playground to explore emergent phenomena and exotic phases which arise from the interplay of spin, charge, orbital, and lattice degrees of freedom. Several recent progresses on the finding of new types of polar topologies in ferroelectric films will be introduced, including the observation of a periodic array of flux-closure quadrants in strained ferroelectric PbTiO₃ films [1], the observation of room-temperature polar vortices and skyrmion lattice in PbTiO₃ related superlattices [2]. Moreover, we have proposed a practical way to prepare REScO₃ ultrathin films by a combination of precision pulsed laser deposition (PLD) and controlled post-annealing, which shows the same strain engineering effects on preparing ferroelectric polar topologies [3]. In addition, strain engineering also indicates an intermediate ferroelectric-like phase during the antiferroelectric to ferroelectric transformation within the PBZrO₃ films, as revealed by atomic scale scanning transmission electron microscopy [4]. These new results indicating that designing oxide films on the atomic scale may facilitate the formation of new phase components, topologies and exploration of novel physical properties of oxide films for future electronic nano-devices.

[1] Y. L. Tang, Y. L. Zhu, X. L. Ma, *et al.*, Observation of a periodic array of flux-closure quadrants in strained ferroelectric PbTiO₃ films. *Science* 348, 547-551 (2015).

[2] S. Das, Y. L. Tang, Z. Hong, M. A. P. Gonçalves, *et al.*, Observation of room-temperature polar skyrmions. *Nature* 568, 368-372 (2019).

[3] S. J. Chen, Y. L. Tang, *et al.*, Strain engineering of ferroelectric topologies prepared on conventional SrTiO₃ substrates buffered with REScO₃ layers.

Acta Materialia 243, 118530 (2023).

[4] R. J. Jiang, *et al.*, Atomic Insight into the Successive Antiferroelectric–Ferroelectric Phase Transition in Antiferroelectric Oxides. *Nano Lett.* 23, 11522 (2023).

SESSION CH02.04: Exploration of Catalysts and 2D materials Dynamics via *In-Situ*/Cryogenic Electron Microscopy

Session Chairs: Yaobin Xu and Di Zhang

Wednesday Afternoon, April 24, 2024

Room 440, Level 4, Summit

1:30 PM *CH02.04.01

Atomic Resolution Scanning Transmission Electron Microscope Imaging of The *In Situ* Synthesis of Nanoparticle Catalysts Sarah J. Haigh¹, Yichi Wang¹, Nick Clark¹, Matthew Lindley¹, Thomas Slater² and Roman Gorbachev¹; ¹University of Manchester, United Kingdom; ²Cardiff University, United Kingdom

The shape and size of metallic nanoparticle catalysts have been shown to control the activity and selectivity for many chemical reactions. Most industrial catalysts are produced by wet impregnation and calcination, due to the scalable nature of this synthesis technique. However, a greater control of the composition, size and shape of the resulting nanoparticles is highly desirable. Understanding the interactions of metal ions with the surfaces in the wet impregnation solution, as well as better understanding of the drying behavior in hydrogen at elevated temperature would be highly desirable to support the production of the improved industrial catalysts needed to address the current energy emergency.

Our group have been developing in situ 2D heterostructure cells for atomic resolution transmission electron microscopy (TEM) imaging and analysis, using a combination of graphene, hexagonal boron nitride and MoS₂ layers to trap liquid and gas pockets and enable new functionality such as liquid-liquid mixing [1]. We have used these 2D heterostructure liquid cells to investigate the dynamic processes that occur at a solid-liquid interfaces as metal ions from solution interact with a solid support at atomic resolution.[2] For example to demonstrate the use of liquid phase imaging to probe the preferred resting sites for platinum atoms on molybdenum disulfide.[2]

We have also used in situ gas cell TEM to investigate how the morphology is determined by the wet impregnation synthesis parameters, as well as how the starting structure and composition determines the evolution of industrial supported nanoparticle catalysts during activation heat treatment.[3]

In situ TEM studies are often limited to 2D imaging, especially for highly active nanoparticle systems like PtNi, where the particle composition and morphology can be used tune the performance for the oxygen reduction reaction.[4] We have shown that the single particle reconstruction method, which is widely used in cryogenic TEM imaging of proteins, is a valuable means to probe the three dimensional structural evolution of inorganic nanoparticles.[5] This approach averages over particles present in the image with different orientation to build up a tomographic reconstruction at much lower radiation dose than is required for conventional tilt series tomography.[5] We have shown that this opens up the single particle reconstruction technique to allow 3D visualization at different time points during in a synthesis process or catalytic reaction.[6] This approach could be brought to the atomic scale through harnessing the improved imaging performance achievable with new in situ cell designs.

[1] Kelly *et al.*, *Advanced Materials* (2021) 33, 2100668;

[2] Clark *et al.*, *Nature* (2022) 609, 942;

[3] Prestat *et al.* *ChemPhysChem* (2017), 18, 2151 and unpublished work

[4] Leteba *et al.* *Nano Lett.*(2021), 21, 9, 3989–3996

[5] Wang *et al.* *Nano Lett.* (2019), 19, 2, 732–738

[6] Wang *et al.* *Small* (2023) in press

2:00 PM CH02.04.02

Advanced Transmission Electron Microscopy Application in Non-Noble Catalyst Materials for CO₂ Hydrogenation Qianqian Li; Shanghai University, China

Transmission electron microscopy (TEM) now has become one of the most influential techniques in nanoscience and nanoengineering characterization fields, which can be used to study the structure, component or valence at sub-angstrom scale. We involved the advanced Cs-corrected S/TEM to reveal the microstructural evolution of the non-noble catalyst for carbon dioxide hydrogenation. Firstly, we designed a porous Co@C catalysts derived from a novel layered metal-organic framework (MOF) with tunable pore sizes for CO₂ hydrogenation. Pointing out the dependence of the durability on the pore size. Secondly, we find the partial loss of catalytic activity of non-noble CoFe alloy catalysts, as exposed to oxygen, can be attributed to the migration of Co element from the core region of CoFe alloy to the surface. The adsorption energy of H for CoFe₂O₄ shell is stronger than Fe₃O₄ shell, so it is harder to fully desorb for H in the follow reaction process. Lastly, we revealed the non-noble catalyst structure stability optimization strategies and mechanisms in long-term reaction process for CO₂ hydrogenation. The studies above provide a new viewpoint to design high-performance catalyst and modify their structures.

2:15 PM CH02.04.03

Potential Synergism Between Sub-Nanometer Pd-Clusters and Adjacent NiO_x Domains Underneath for High-Performance CO₂ Methanation: An Ambient Pressure X-Ray Photoelectron Spectroscopy Study Amisha Beniwal and Tsan-Yao Chen; National Tsing Hua University, Taiwan

Carbon dioxide (CO₂) methanation serves as a critical process not only for the reduction of excessive CO₂ emissions but also for addressing the challenges linked to the storage and transportation of low-grade energy sources. Nevertheless, the presence of the competitive reverse water gas shift (RWGS) reaction significantly impedes the efficient production of methane (CH₄). To this end, a bimetallic nanocatalyst (NC) comprising sub-nanometer Pd clusters on Ni-oxide support (henceforth denoted as Pd@NiO_x) has been successfully synthesized through a sequential control of metal ion adsorption followed by wet chemical reduction. As prepared material achieved an impressive CH₄ production yield of about 1900 μmol/g at an operating temperature of 300°C. This remarkable performance represents a more than 10-fold improvement compared to bare Pd nanoparticles. The results of in-situ ambient pressure X-ray photoelectron spectroscopy (APXPS) unveil that the exceptional catalytic activity of Pd@NiO_x NC originates from the potential collaboration between surface-anchored sub-nanometer Pd clusters and adjacent NiO_x domains at the heterogeneous interface, where the CO₂ activation takes place. On the other hand, the NiO_x domains promote the H₂ splitting. More importantly, to the best of our knowledge, the Pd@NiO_x NC with its unique structure exhibit the highest CH₄ production yield among existing catalysts with identical loading, composition, and geometric configurations. This achievement underscores the significance of this innovative bimetallic nanocatalyst in the field of catalysis.

2:30 PM BREAK

3:30 PM *CH02.04.04

Unveiling Phase Transitions in 2D Layered Materials via Atomic-Scale Cryogenic STEM Miaofang Chi, Haoyang Ni and Hsin-Yun Chao; Oak Ridge National Laboratory, United States

Quantum materials exhibit unique phenomena and functionalities beyond classical physics. The use of 2D sheets, heterogeneous interfaces, and moiré structures has emerged as a promising method to induce exotic quantum effects. However, studying these materials using cryogenic scanning transmission electron microscopy (STEM) has been limited by stage instability. Achieving stable atomic-scale imaging at cryogenic temperatures, particularly in techniques like atomic-scale 4D-STEM imaging and monochromated electron energy loss spectroscopy (EELS), is expected to provide valuable information for probing key parameters in quantum materials. Recent improvements in stage designs and machine learning-assisted acquisition and analysis algorithms offer opportunities for related research. In this presentation, I'll discuss our on-going research using cryogenic STEM and EELS to study lattice-spin-charge coupling in 2D van der Waals materials for spintronics applications, with a specific focus on our findings regarding layer-dependent atomic structural transitions and magnetic behavior alterations for spintronics applications. Additionally, we'll cover local temperature calibration methods for cryogenic STEM and the application of machine learning for data acquisition and analysis in achieving multi-dimensional STEM mappings at cryogenic temperatures, including atomic-resolution 4D-STEM imaging and spectroscopy.

4:00 PM *CH02.04.05

In Situ Cryo 4D STEM of CDW Phase Transitions in Layered Materials Judy Cha, James Hart and Saif Siddique; Cornell University, United States

Many quantum materials possess complex electronic phase diagrams where correlated electronic phases, such as superconductivity, magnetic ordering, and charge density waves (CDWs), exist near each other. The proximity of these phases suggests that phase transitions must be understood to establish the microscopic origin for these correlated phases and to use them for applications. These phase transitions have mostly been studied using ensemble-average techniques, lacking real space information of nucleation and growth of these often-competing electronic phases. Nevertheless, such real-space information is essential for applications of quantum materials, which will be at the nanoscale where reduced dimensionality, confinement, local heterogeneities, interfaces, and defects will greatly modify the phase transitions.

In this talk, I will discuss our group's efforts on combining cryogenic scanning transmission electron microscopy (cryo STEM) and *in situ* cryo 4D STEM with *in situ* transport measurements to study the phase transition of TaS₂ in real-space with nanometer resolution as it undergoes a transition from the commensurate CDW (insulating phase) to the nearly commensurate CDW (metallic phase). We directly visualize the nucleation and growth of the NC-CDW phase out of the C-CDW phase and correlate this to the changing transport data. We establish that the phase transition starts at extended defects present in TaS₂. We also examine the pulse-induced CDW phase transition in TaS₂ and reveal the role of defects and the transition mechanism. Our findings are extended to CDWs in rare-earth tri-tellurides (RTe₃) and other layered materials.

4:30 PM CH02.04.06

STEM Imaging of AC Electric Field Driven Non-Centrosymmetric Atomic Displacements in The 2D TMD WSe₂ Christopher T. Nelson¹, Ondrej Dyck¹, Mina Yoon¹, Jawahar Almutlaq², Dirk Englund² and Stephen Jesse¹; ¹Oak Ridge National Laboratory, United States; ²Massachusetts Institute of Technology, United States

Simultaneous characterization by (S)TEM and application of electrical bias is a powerful platform to study the real-space dynamic electronic couplings at nanoscales: the length scale of interest for many electronic, quantum, and electrochemical materials and processes. Minimum acquisition times across all STEM modes favor *in situ* electrical bias experiments that are quasi-static for a good signal/noise. Exploring dynamic responses at faster time scales necessitates multi-cycle summation to overcome the shot-noise limits for a coherent source. In this work we utilize this approach to characterize moderate frequency (25kHz) AC electric-field induced response on the atomic structure of a 2D semiconductor WSe₂.

As tunable 2D direct-gap semiconductors, WSe₂ and similar Transition Metal Dichalcogenides show promise for applications in nano- and optoelectronics. Their potential lies in part with a wide library of 2D materials, TMD and otherwise, and a correspondingly large design-space for heterogeneous multi-layer engineering. Here we applied an in-plane electric field across a free-standing monolayer WSe₂ by biasing across a gap in an overlaid graphene layer. Rolling series short-dwell HAADF images were collected with a custom scan coil controller¹ while an AC 25kHz sinusoidal bias was applied. Atomic structure fluctuations vs applied voltage were determined from a workflow of phase-detection -> averaging -> binning -> atom position finding using a machine-learning model *AtomAI*². Collective atomic motion was removed, observed to be ~0.5 Å/V, owing to beam deflection by long range stray-fields. We observe a small but robust centrosymmetry breaking counter-motion between the W and Se atoms. This displacement has a total delta of ~0.5pm/V up to 4 volts (maximum applied) and can be attributed to field-induced electrical polarization. Notably, this effect was only observed for datasets collected within the electrode gap and not within the graphene electrode itself. The nominal field concentration within the former and absent in the latter strongly supports this is direct real-space observation of local field induced dynamics, specifically a fixed-frequency optical-phonon type dielectric response.

[1] Sang, X. et al. *Dynamic scan control in STEM: spiral scans*. Adv. Struct. Chem. Imag. 2, 6 (2016).

[2] Ziatdinov, M., et al. *AtomAI: A Deep Learning Framework for Analysis of Image and Spectroscopy Data in (Scanning) Transmission Electron Microscopy and Beyond*. arXiv:2105.07485 (2021)

[3] This work was supported by the U.S Department of Energy, Office of Science, Basic Energy Sciences, Materials Sciences and Engineering Division

4:45 PM CH02.04.07

Endotaxial Polytype Engineering: Enhancement of Incommensurate Charge Density Waves in TaS₂ Suk Hyun Sung^{1,2}, Pat Kezer², Nishkarsh Agarwal², Yin Min Goh¹, Noah Schnitzer³, Ismail El Baggari¹, Kai Sun², Lena Kourkoutis³, John T. Heron² and Robert Hovden²; ¹Harvard University, United States; ²University of Michigan, United States; ³Cornell University, United States

Charge density waves (CDWs) are an emergent periodic modulation of the electron density that spans a crystal with strong electron-lattice coupling. CDW phases spontaneously break crystal symmetry, facilitate metal-insulator transitions, and compete with superconductivity [1–4]. At elevated temperatures, many materials exhibit a CDW incommensurate (IC-) with the high symmetry parent phase [5–8]. Unfortunately, the IC-CDWs are inherently weak and disordered. In TaS₂, a popular layered CDW material, long-range order has not been demonstrated for the IC-CDW [9–11]. Using new methods of endotaxial polytype engineering [12] we show it is possible to restore long-range order of the IC-CDW phase. Through this process, 2D CDW layers are encapsulated within metallic polytypes to enhance charge order. Furthermore, with restored IC-CDWs we can better understand the nature of disorder in these systems. We show that the IC-CDWs in 1T-TaS₂ are hexatically disordered and undergo a continuous melting as temperature is increased. The hexatic CDW phase retains six-fold orientational order while translation order quickly decays from proliferation of defects with temperature.

Here we use endotaxial engineering to enhance CDWs—even at elevated temperatures. The polytype heterostructures consist of monolayers of octahedrally coordinated charge ordered TaS₂ embedded within matrices of metallic prismatic TaS₂. These endotaxial heterostructures have been shown to raise the critical temperature of the long-range ordered commensurate (C-) CDW phase by 150 K [12].

Surprisingly, long-range order of the IC-CDW phase is significantly enhanced in the polytype heterostructures [13]; in-situ selected area electron diffraction (SAED) of the heterostructures shows sharper and brighter superlattice peaks than the IC-CDW phase in pristine 1T-TaS₂. This enhancement of long-range CDW order is accompanied by a marked increase in the in-plane resistivity of the IC phase. The increased intensity is surprising given the number of charge ordered TaS₂ layers is decreasing.

The signature of IC-CDWs in TaS₂ is the presence of azimuthally diffused superlattice peaks decorating bright Bragg peaks in SAEDs. These azimuthally blurred superlattice peaks strongly resemble the structure factor of hexatic phases found in two-dimensional (2D) systems. 2D crystals can melt continuously through intermediate orientationally ordered hexatic phase [14–17]. Similarly, in pristine 1T-TaS₂, the IC-CDW phase is in a hexatic glassy state due to intrinsic disorder. By restoring crystallinity of the IC-CDW, we observe the full hexatic melting process: heating further melts the ordered IC-CDW phase with continuous azimuthal broadening and weakening of superlattice peaks as expected for hexatic phases.

In summary, we demonstrate that polytype engineering can stabilize fragile long-range order in IC-CDW even at high temperatures. The ordered IC-CDW phase melts continuously with hexatic characteristics.

References:

- [1] JA Wilson, FJ Di Salvo, S Mahajan *Adv. Phys.* **24** (1975) p.117.
- [2] R Ang et al., *Nat. Commun.* **6** (2015) 60981.
- [3] E Navarro-Moratalla et al., *Nat. Commun.* **7** (2016) 11043.
- [4] L Li et al., *npj Quantum Mater.* **2** (2017) 11.
- [5] J Chang et al., *Nat. Phys.* **8** (2012) p.871.
- [6] L Nie, G Tarjus, and SA Kivelson, *Proc. Natl. Acad. Sci.* **111** (2014) p.7980.
- [7] I El Baggari et al., *Proc. Natl. Acad. Sci.* **115** (2018) p.1445.
- [8] M Frachet et al., *npj Quant. Mater.* **7** (2022) p.115.
- [9] ND Mermin and H Wagner, *Phys. Rev. Lett.* **17** (1966) p.1133.
- [10] PC Hohenberg, *Phys. Rev.* **158** (1967) p. 383.
- [11] Y Imry and S-K Ma, *Phys. Rev. Lett.* **35** (1975) p.1399.
- [12] SH. Sung et al., *Nat. Commun.* **13** (2022) p.413.
- [13] SH. Sung et al., *Arxiv* 2307.04587 (2023)
- [14] JM Kosterlitz and DJ Thouless, *J. Phys. C: Solid State Phys.* **5** (1972) p.L124
- [15] BI Halperin and DR Nelson, *Phys. Rev. Lett.* **2** (1978) p.121
- [16] DR Nelson and BI Halperin, *Phys. Rev. B* **19** (1979) p.2457
- [17] AP Young, *Phys. Rev.* **19** (1979) p. 1855

SESSION CH02.05: Poster Session: Utilizing Advanced *In Situ/Operando* Transmission Electron Microscopy and Spectroscopy for the Investigation of Functional, Energy and Quantum Materials
Session Chairs: Leopoldo Molina-Luna and Di Zhang
Wednesday Afternoon, April 24, 2024
Flex Hall C, Level 2, Summit

5:00 PM CH02.05.01

***In-Situ* TEM Full Temperature Range Cooling, Heating and Electrical Biasing Sample Holder** Calvin A. Parkin, Norman Salmon and Daan Hein Alsem; Hummingbird Scientific, United States

Cryogenic cooling of specimens during scanning/transmission electron microscopy (S/TEM) has enabled the characterization of various quantum interfaces and phase interactions in strongly correlated systems. Investigation of such quantum properties at the fundamental level has historically been challenging due to inadequate spatial and temporal resolution of characterization techniques as well as inadequate sample stability. Quantum materials must be studied at cryogenic temperatures because many of the relevant properties in these quantum materials only manifest at such low temperatures.

Cryogenic S/TEM sample holders have not only enabled the study of quantum topological insulators in two-dimensional (2D) materials but also atomic resolution observation of battery interfaces, which is traditionally difficult to achieve because they are sensitive to air and prone to electron beam damage at room temperature. However, lack of biasing capability has limited the study of electrical responses in these materials systems. With increasing demand for batteries that function at high temperatures and material phase information across a wide range of temperatures from cryogenic to high temperature, expanded versatility will be required of temperature-controlled in-situ electrical biasing systems.

Here, we present a novel in-situ electrical biasing S/TEM holder that simultaneously allows electrical stimulus and high-resolution imaging of a sample in-situ across the full temperature range, from cryogenic up to high temperatures. The holder is exceptionally stable, with drift speeds across the entire temperature range comparable to standard holders at room temperature. Battery processes were demonstrated in a single nanowire system using this holder at near-liquid nitrogen temperature (<170°C) up to room temperature. Electrical biasing was performed on a nanowire sample bridging the electrodes on the biasing chip. A constant current experiment at cold temperatures on the nanowire showed a voltage drop as the reaction proceeds with the growth of a dendrite layer plated on the nanowire's surface. With the new heating capability, such experiments are extended to >1000°C using heating on the same chip that electrically biases the sample to achieve these higher temperatures. This enables studying the temperature dependence of chemical and microstructural evolution under electrical bias. Far below room temperature where on-chip temperature measurements become increasingly inaccurate, precise temperature control is maintained using a conventional resistance heater and miniature thermocouple at the sample in the TEM holder tip. At intermediately cold temperatures, the on-chip heating/temperature sensing can be combined with tip heating and temperature measurement for precisely controlled rapid heating experiments. For quantum nanomaterials, this enables their synthesis and processing to be studied across a range of different temperatures in the

low temperature regime, and their quantum response to electrical biasing to be measured at cryogenic temperatures. Batteries may now be electrochemically cycled at elevated temperature and then returned to cryogenic temperature for imaging, without the need to change holders. The cryo-biasing TEM holder with heating will empower scientists to nimbly investigate structure-property relationships in materials, specifically electronic properties, across the full temperature range. This versatile tool will accelerate the development of the next generation of electronic, quantum, and energy storage materials devices.

5:00 PM CH02.05.02

A Surface Science Investigation of Hydrocarbons Adsorption to a Ru/Al₂O₃ Catalyst Erin E. Dunphy; University of Colorado Boulder, United States

Hydrogenolysis is an extremely effective method for plastic upcycling. Specifically, Ru-based catalysts supported on metal oxides have shown high reactivity for polyethylene upcycling. Polyethylene hydrogenolysis is an extremely structure-sensitive reaction, where product distribution depends on the size of the adsorbing alkyl chain and the hydrogen availability at the metal oxide support interface. However, surface science studies are required to characterize the structural impact of these dependencies directly.

To study the arrangement of hydrocarbons to the catalyst support, we utilize X-Ray Reflectivity (XRR) and Molecular Dynamics (MD) simulations, and to study the local chemical environment changes of the Ru active site, we utilize Extended X-Ray Adsorption Fine Edge Structure (EXAFS). By utilizing hydrocarbons of various lengths (methane, hexane, dodecane, triacontane, and low-density polyethylene), we will understand preferential adsorption arrangements for undesirable and desirable product species.

We theorize that as hydrocarbon chain length increases, the polymer will adsorb to the support with increased structural order, resulting in increased adsorption potential to the Ru active site. MD simulations of n-dodecane at various temperatures indicate that the preferential adsorption of species parallel to an alumina interface changes, and the application of the distorted crystal model confirms the viability of XRR as an experimental technique, as seen in the attached image. EXAFS and XRD data are currently being processed and will yield information about the local relaxation of Ru nanoparticles and the alumina support during species adsorption.

This work aims to understand the structure and arrangement of hydrocarbons to the active metal site and the support, thus allowing for fundamental concepts to be unified and expanded upon. We anticipate our results to inspire future surface science studies to explore how different polymers adsorb to the catalyst surface—ultimately allowing for the creation of catalysts capable of mixed-polymer hydrogenolysis and reduction of energy requirements for polymer upcycling.

5:00 PM CH02.05.03

Luminescence Polarization of Rare Earth Microcrystals under High Pressure Haoran Zhao; Peking University, China

In recent years, the polarization properties of rare earth luminescent materials have attracted extensive attention. The fine spectral splittings generated by the crystal field effect has fingerprint-like polarization characteristics^[1], but its influence factors needs to be studied. High pressure is an important protocol to adjust the structure and properties of materials, which can change the unit cell parameters and local symmetry of rare earth luminescent materials, and further affect the crystal field parameters, emission wavelength and intensity^[2]. However, the effect of high pressure on the polarization of rare earth emissions has not been studied. Hexagonal phased NaREF₄, which has an anisotropic crystallographic structure, is a decent host material for emission polarization. We studied the emission polarization of NaREF₄ microcrystals under high pressure. Through adjusting the symmetry of crystal structure by high pressure, the influence of crystal structure symmetry on rare earth emission polarization was investigated, meanwhile, the correlation between the direction of emission polarization and the axis of crystal symmetry was analyzed^[3]. Taking the 700.4 nm emission as an example, its polarization degree decreased with the increased pressure, while the polarization direction rotated by 90°. These findings benefit to the in-depth understanding of the mechanism of rare earth emission polarization and are informative for the design of new rare earth polarized luminescent materials.

[Bibliography]

[1] Lyu, Z. Y.; Dong, H.; Yang, X. F.; Sun, L. D.; and Yan, C. H. *J. Phys. Chem. Lett.* 2021, 12: 11288–11294.

[2] Mei, S.; Guo, Y.; Lin, X. H.; Dong, H.; Sun, L. D.; Li, K.; and Yan, C. H. *J. Phys. Chem. Lett.* 2020, 11: 3515–3520.

[3] Zhao, H. R.; Dong, H.; Tang, X. Y.; Zhang, J. W.; Lyu, Z. Y.; Yang, X. F.; Sun, L. D.; Li, K. and Yan, C. H. to be submitted.

SESSION CH02.06: Investigation of Energy Storage Materials via Advanced *In Situ*/Cryogenic Electron Microscopy I

Session Chairs: Qianqian Li and Yaobin Xu

Thursday Morning, April 25, 2024

Room 440, Level 4, Summit

8:15 AM CH02.06.01

Electrochemical Lithium Intercalation & Exfoliation in 2D TMDs and its *In-Situ* Studies Zhiyuan Zeng; City University of Hong Kong, Hong Kong

We developed a lithium ion battery intercalation & exfoliation method with detailed experimental procedures for the mass production of 11 two dimensional TMDs and inorganic nanosheets, such as MoS₂, WS₂, TiS₂, TaS₂, ZrS₂, graphene, h-BN, NbSe₂, WSe₂, Sb₂Se₃ and Bi₂Te₃, among them 3 TMDs achieved mono- or double layer yield > 90%. This method involves the electrochemical intercalation of lithium ions into layered inorganic materials and a mild sonication process. The Li insertion can be monitored and finely controlled in the battery testing system, so that the galvanostatic discharge process is stopped at a proper Li content to avoid decomposition of the intercalated compounds. The intercalation strategy can also be used to tune 2D TMDs' physical and chemical properties for various applications. For example, we developed a one-step covalent functionalization method on MoS₂ nanosheets for membrane fabrication, which exhibited excellent water desalination performance. For lithium intercalation mechanism, the state-of-the-art *In-Situ* Liquid Phase TEM is an ideal technique for identifying the phase changes during intercalation process. With self-designed electrochemical liquid cell utilized, we can directly capture the dynamic electrochemical lithiation and delithiation of electrode in a commercial LiPF₆/EC/DEC electrolyte, such as LiF nanocrystal formation, lithium metal dendritic growth, electrolyte decomposition, and solid-electrolyte interface (SEI) formation. Combining with other *in-situ* techniques, such as *in-situ* XAS, XRD and Raman, etc, the underlying lithium intercalation mechanism in TMDs were further investigated, which render us a comprehensive understanding of the intrinsic correlation between the intercalation process and TMDs.

References:

[1] R. Yang, L. Mei, et al., H. S. Shin*, D. Voiry, Z.Y. Zeng, *Nat Protoc.*, 2022, 17, 358-377.

[2] R. Yang, et al., H. S. Shin, D. Voiry, Q. Lu, J. Li*, Z. Y. Zeng*, *Nat. Synth.*, 2023, 2, 101-118.

[2] R. Yang, L. Mei, Y. Fan, Q. Zhang, H. G. Liao, J. Yang, J. Li*, Z. Y. Zeng*, *Nat. Protoc.*, 2023, 18, 555-578.

- [3] Q. Zhang, J. Ma, L. Mei, J. Liu, Z. Li*, J. Li*, Z. Y. Zeng*, *Matter*, 2022, 5, 1235-1250.
[4] H. Peng, R. Wang*, L. Mei, et al., Z. Qian*, A. B. Farimani, D. Voiry*, Z. Y. Zeng*, *Matter*, 2023, 6, 59-96.
[5] L. Mei, et al., C. Y. Tang, D. Voiry, H. Wang*, A. B. Farimani*, Z. Y. Zeng*, *Adv. Mater.*, 2022, 34, 2201416.
[6] R. Yang, Y. Fan, R. Ye, Y. Tang, X. Cao*, Z. Yin*, Z. Y. Zeng*, *Adv. Mater.* 2021, 33, 2004862.
[7] R. Yang, Y. Fan, et al., Q. Lu, Q. Wang*, J. C. Yu*, Z. Y. Zeng*, *Angew. Chem. Int. Ed.*, 2023, e202218016.
[8] B. Tian, D. Ho*, J. Qin, et al., D. Voiry, Q. Wang*, Z. Y. Zeng*, *Prog. Mater. Sci.*, 2023, 133, 101056.
[9] R. Yang, et al., Z. Y. Zeng*, Photocatalysis with atomically thin sheets, *Chem. Soc. Rev.*, 2023, 52, 7687.

8:30 AM *CH02.06.02

Seeing the Invisible: Ultrathin (UT) Membrane Chip for Fluidic-Cell Electron Microscopy Vinayak P. Dravid; Northwestern University, United States

In the recent decade, *in-situ* or *operando* S/TEM utilizing SiN_x membrane encapsulated chips to confine fluids for electron microscopy examination has become popular. A great number of prior innovators have shown this to be an effective approach for probing fluid-surface/nanostructure interactions and related phenomena or reactions. Such a “closed cell” chip based on silicon nitride (SiN_x) membranes as electron transparent encapsulation material, has many practical and technological advantages over the differential pumping environmental TEM (ETEM). Unfortunately, however, conventional fluid-cells suffer from additional and significant electron scattering from the top and the bottom membranes, which are typically 30-50nm thick to maintain integrity/stability during the operation. Thus, the total thickness of >70-80 nm of the encapsulating membranes imposes many adverse effects on the post electron optics, such as increased chromatic aberrations. This naturally results in significant degeneration of signal quality and loss of spatiotemporal resolution, diffused interference in the electron diffraction, and plasmon-dominated electron energy loss spectra (EELS). Further, to implement advanced STEM techniques such as quantitative EELS analysis to resolve electronic structure and 4D-STEM for pixel-specific acquisition, one needs to significantly reduce electron scattering, which primarily stem from the thick SiN_x windows in gas-cells. For example, the log-ratio of scattered electron over zero-loss electron () already exceeds ~1 for two-50 nm SiN_x encapsulation (without any specimen). However, low scattering “thin” membrane is risky since the mechanical robustness is compromised, resulting in potentially catastrophic failure. Thus, novel design strategies for fabrication of stable ultrathin SiN_x membrane are needed.

We have recently developed a robust, functional and scalable backing support strategy to enable the thinnest possible (<10 nm) SiN_x gas encapsulation material [2]. Inspired by the natural honeycomb geometry, our novel design provides for honeycomb backbone that can neatly anchor ultrathin (~<10 nm) SiN_x membrane with excellent stability and consistent performance. It can still withstand up to 6 *Atm* pressure with ~50 % less bulging. Unlike graphene-based encapsulations [3], stability under the electron beam is comparable to a 50 nm SiN_x membrane, which is sufficient for most high-resolution S/TEM applications on non-electron sensitive materials.

We show that our UT chip increases contrast of typical nanoparticles at 1 *atm* Ar gas by ~70 % and the accessible information limit is enhanced by >130 % compared to the conventional encapsulation. More importantly, the is reduced from nominally ~1.0 to 0.3 using a 1 *Atm* gas cell. This greatly enhances spectral visibility and significantly improved S/N for EELS excitations. Thus, spatiotemporal detection of gas species, down to ~nanometer scale, which otherwise is unachievable with integrated residual gas analyser (RGA), is being achieved.

The presentation will cover the design and implementation of UT membrane fluid-cell for *in-situ* gas-solid interactions. [4]

References: [1] K Koo, SM Ribet, C Zhang, PJM Smeets, Rd Reis, X Hu, and VP Dravid, *Nano Lett* **22** (2022), p. 4137. doi:

10.1021/acs.nanolett.2c00893; [2] VP Dravid, X Hu, and K Koo, US Provisional Patent, No. 63413097 (2022); [3] K Koo, J Park, S Ji, S Toleukhanova, and JM Yuk, *Adv Mater* **33** (2021), p. 2005468. doi: 10.1002/adma.202005468; [4] *Acknowledgement*: This work is made use of the EPIC facility of Northwestern University’s NUANCE Center, which has received support from the SHyNE Resource (NSF ECCS-2025633), the IIN, and Northwestern’s MRSEC program (NSF DMR-1720139).

Disclosure: US Provisional Patent Application (No. 63413097) regarding this work is filed on 04-Oct-2022.

9:00 AM *CH02.06.03

In Situ Study of Electrified Solid-Liquid Interfaces using Liquid Cell TEM combining with other Advanced EM Techniques Haimei Zheng; Lawrence Berkeley National Laboratory, United States

Electrified solid-liquid interfaces play a key role in various electrochemical processes relevant to electrocatalysis, batteries, and supercapacitors. The electron and mass transport at the electrified interfaces may result in structural modifications that remarkably influence the reaction pathways.

Extensive studies of the electrified solid-liquid interfaces have been on the physisorption and chemisorption of species at the interfaces. However, the microscopic details of electrified solid-liquid interfaces, especially their atomic-scale structural evolution during electrochemical reactions, remain unclear.

In situ transmission electron microscopy (TEM) allows tracking of the evolution of individual nanocatalysts during reactions. With our development of advanced high resolution electrochemical liquid cells for TEM, we monitor the atomic dynamics of electrified solid-liquid interfaces during Cu-catalyzed CO₂ electroreduction reactions. Other techniques, such as, Cryo-EM of certain reaction states by fast freezing of the same liquid cell, chemical analysis with energy dispersive x-ray spectroscopy (EDS) and electron energy loss spectroscopy (EELS)

Our systematic study unveils fascinating atomic dynamics as well as structural and chemical evolution of the electrified solid-liquid interfaces. The combination of experimental observation and theoretical calculations reveals an amorphization-mediated restructuring mechanism resulting from charge-activated surface reactions with the electrolyte. Our results hold significant implications for utilizing interphases to control catalyst surface restructuring, thus tuning the catalytic reactions.

9:30 AM CH02.06.04

Operating a Solid Oxide Fuel Cell in The Environmental Transmission Electron Microscope Mathieu Bugnet¹, Thierry Epicier^{1,2}, Cedric Frantz³, Stefan Diethelm³, Dario Montinaro⁴, Elizaveta Tyukalova⁵, Yevheniy Pivak⁶, Jan Van Herle³, Aicha Hessler-Wyser⁷, Martial Duchamp^{5,8} and Quentin Jeangros^{7,9}; ¹University Lyon, CNRS, INSA Lyon, UCBL, MATEIS, France; ²University Lyon, UCBL, IRCELYON, France; ³Group of Energy Materials (GEM), École Polytechnique Fédérale de Lausanne (EPFL), Switzerland; ⁴SolydEra S.P.A., Italy; ⁵Nanyang Technological University (NTU), Singapore; ⁶DENS solutions, Netherlands; ⁷Photovoltaics and Thin-Film Electronics Laboratory (PV-Lab), École Polytechnique Fédérale de Lausanne (EPFL), Switzerland; ⁸MajuLab, International Joint Research Unit, CNRS, Université Côte d’Azur, Sorbonne Université, National University of Singapore, Nanyang Technological University, Singapore; ⁹Centre Suisse d’Electronique et de Microtechnique (CSEM), Saint Barthélemy

Solid oxide fuel cells (SOFC) are a class of solid-state electrochemical conversion devices that produce electricity directly by oxidizing a fuel gas. They consist in an anode-cathode duet separated by a solid electrolyte, i.e., a material conducting oxygen ions. The anode is fed with hydrogen or other fuels whereas the cathode is in contact with air, meaning oxygen. Overall, a SOFC operates thanks to the combined action of two external stimuli: a gaseous environment and temperature. Owing to the recent advances in *in situ* and *operando* transmission electron microscopy (TEM), we have set up an experiment to operate a SOFC inside an environmental TEM to identify how the device microstructure determines its electrical properties. To do so, an elementary anode-electrolyte-cathode sandwich was prepared by focused ion beam (FIB) and mounted on a heating and biasing microelectromechanical

(MEMS)-based specimen holder (DENSsolutions) and inserted in an Environmental TEM (FEI Titan ETEM), as shown in Fig. 1. Standard SOFC materials were investigated: the cathode was strontium-doped lanthanum manganite (LSM) co-sintered with yttria-stabilized zirconia (YSZ), the electrolyte was YSZ, and the anode a cermet of NiO co-sintered with YSZ. NiO was first reduced to Ni, leaving pores in the structure due to the volume loss and hence enabling the penetration of the fuel to the triple phase boundaries Ni/YSZ/porosity at the anode side. For practical reasons, we used a single chamber configuration to trigger the operation the cell: the anode and cathode were exposed simultaneously to the oxidant and reducing gases. Due to a difference in the catalytic activity between the electrodes, O₂ should reduce at the cathode, while H₂ should oxidize at the anode, thus leading to a voltage difference between the two terminals.

The reduction of NiO was first performed under a forming gas N₂:H₂ in the ratio 20:1 under 15 mbar up to 750°C (N₂ was constantly used as a mixing gas for safety reasons due to the need of mixing O₂ and H₂ in the single-chamber configuration). The O₂ to H₂ ratio was then increased to trigger the operation of the cell. A small quantity of O₂ was introduced into the microscope, leading to a total pressure of about 16 mbar at 600°C. At this point, the variation of voltage between the anode and cathode was correlated to the gas composition and the anode microstructure (see Fig. 2). The latter was analyzed by means of conventional and high-resolution imaging, diffraction, and EELS (electron energy-loss spectroscopy). The system was cycled several times by decreasing and re-increasing the O₂ concentration in the gas flow, and correlations between microstructure, gas composition, and cell voltage were established, as it will be discussed at the conference. Results were further confirmed by macroscopic *ex situ* tests in an oven using the same materials [1]. The operation of a SOFC in a single chamber configuration was demonstrated using *operando* ETEM. Such *operando* experiments open numerous perspectives to investigate the root cause of failure pathways affecting SOFCs, like poisoning of active sites or coarsening of the Ni catalyst [2].

[1] Q. Jeangros, M. Bugnet, T. Epicier, C. Frantz, S. Diethelm, E. Tyukalova, G. Pivak, J. Van herle, A. Hessler-Wyser, M. Duchamp, accepted in Nature Communications (2023). Available at <https://arxiv.org/abs/2302.12514>

[2] The authors acknowledge the French microscopy network METSA for funding and the consortium Lyon-St-Etienne de microscopie for ETEM access. The FIB preparation was performed at the facilities for analysis, characterization, testing and simulations (FACTS, Nanyang Technological University). Additional support was provided by the INSTANT project (France-Singapore MERLION program 2019-2021) and the start-up grant M4081924 at Nanyang Technological University.

9:45 AM CH02.06.05

Electric-Field-Assisted Phase Switching in GaAs Nanowires Qiang Yu¹, Khalil Hassebi¹, Khakimjon Saidov², Ivan Erofeev², Charles Renard¹, Laetitia Vincent¹, Frank Glas¹, Utkur Mirsaidov² and Federico Panciera¹; ¹Université Paris-Saclay, CNRS, Centre de Nanosciences et de Nanotechnologies, France; ²Centre for Bioluminescence, Department of Biological Sciences and Physics, National University of Singapore, Singapore

The vapor-liquid-solid (VLS) method for nanowires growth was introduced by Wagner and Ellis in the 1960s¹. Since then, intensive researches focus on engineering the morphology, composition and crystal phase of nanowires due to their promising applications in nanotechnology². While III-V bulk semiconductors generally exist in only one crystal phase, in nanowires, multiple crystal phases can coexist (polytypism). On the one hand, this phenomenon can be considered as a crystal defect; on the other hand, it enables the formation of crystal phase quantum dots (CPQDs), i.e. insertion of segments of one phase within a nanowire of a different phase. Due to the band alignment of two crystal phases and confinement of nanowire size, CPQDs feature sharp and intense spectral lines, single-photon emission and sub-nanosecond exciton lifetime³. Moreover, in contrast to compositional heterojunctions, CPQDs have intrinsically abrupt interfaces and do not suffer from alloy intermixing, which hampers precise control of the electronic properties in compositional heterostructures. However, despite over 15-year of research, technological applications of CPQDs remain severely limited by the poor understanding of the phase switching mechanisms and the difficulty of controlling their formation. In this study, beyond commonly used methods of flux and temperature modulation, we solve this issue by introducing an external electric field (E-field)⁴ to instantaneously switch the crystal phase and create GaAs CPQDs with monolayer precision. This process is monitored in real-time using in-situ transmission electron microscopy (TEM). Thanks to custom-made substrates, GaAs nanowires are grown epitaxially on Si (111) by chemical vapor deposition inside TEM. The substrate is shaped as a micro capacitor which allows us to apply an E-field up to several V/nm in the direction parallel to the nanowire growth, and this strong E-field allows to achieve phase switching faster than monolayer formation. We will present high-resolution videos showing the controlled phase switching induced by the E-field in GaAs nanowires, and the formation of single and multiple CPQDs. Finally, we will discuss the E-field-induced phase switching mechanisms and propose a model to explain the experimental results based on theoretical calculations and finite element simulations.

References:

- (1) Wagner, R. S.; Ellis, W. C. Vapor-liquid-solid Mechanism of Single Crystal Growth. *Appl. Phys. Lett.* **1964**, *4* (5), 89–90. <https://doi.org/10.1063/1.1753975>.
- (2) Bouwes Bavinck, M.; Jöns, K. D.; Zielinski, M.; Patriarche, G.; Harmand, J.-C.; Akopian, N.; Zwiller, V. Photon Cascade from a Single Crystal Phase Nanowire Quantum Dot. *Nano Lett.* **2016**, *16* (2), 1081–1085. <https://doi.org/10.1021/acs.nanolett.5b04217>.
- (3) Akopian, N.; Patriarche, G.; Liu, L.; Harmand, J.-C.; Zwiller, V. Crystal Phase Quantum Dots. *Nano Lett.* **2010**, *10* (4), 1198–1201. <https://doi.org/10.1021/nl903534n>.
- (4) Panciera, F.; Norton, M. M.; Alam, S. B.; Hofmann, S.; Mølhave, K.; Ross, F. M. Controlling Nanowire Growth through Electric Field-Induced Deformation of the Catalyst Droplet. *Nat. Commun.* **2016**, *7* (1), 12271. <https://doi.org/10.1038/ncomms12271>.

10:00 AM BREAK

10:30 AM *CH02.06.06

Insight into Energy Storage Materials Science from a Reductionist Perspective Lin Gu; Tsinghua University, China

Establishing a correlation between the structure and functionality of materials has been a long-standing challenge. Materials science based on reductionism greatly depends on one's knowledge of the elements. This understanding ranges from entirely solvable atomic energy levels to fundamentally solvable energy bands of phases under specific boundary conditions, and finally, to macroscopic material properties that may have only statistical solutions. Along this clue, here the macroscopic material is split into phase, until cell, atom, and electron step by step, exploring the material properties starting from the elementary particles. We mainly focus on band structure and dispersion relation in reciprocal space, and the distribution of four fundamental degrees of freedom (lattice, charge, orbital, spin) in real space. As a powerful characterization method, spherical aberration corrected electron microscopy could acquire information about atomic-scale structure and electronic structure, which could get rid of the constraint condition of periodic potential field, single electron approximation, and adiabatic approximation theories to obtain the structure-activity relationship in solid materials. We focused on the atomic and electronic structure of energy storage materials from lattice and charge degrees of freedom. On this basis, the direct observation of electron occupied states is realized at orbital scale, which has a substantial impact on materials' performance. This report will focus on physical mechanism of functional materials to discuss the correlation between microstructure and electronic structure based on reductionism.

11:00 AM *CH02.06.07

Cryo-EM Imaging of Li Metal Polyhedra formed by Ultrafast Electrodeposition Yuzhang Li; University of California, Los Angeles, United States

Electrodeposition of lithium (Li) metal is critical for high-energy batteries¹. However, the simultaneous formation of a surface corrosion film termed the solid electrolyte interphase (SEI)² complicates the deposition process, which underpins our poor understanding of Li metal electrodeposition. Here we decouple these two intertwined processes by outpacing SEI formation at ultrafast deposition current densities³ while also avoiding mass transport limitations. By using cryogenic electron microscopy^{4,5,6,7}, we discover the intrinsic deposition morphology of metallic Li to be that of a rhombic dodecahedron, which is surprisingly independent of electrolyte chemistry or current collector substrate. In a coin cell architecture, these rhombic dodecahedra exhibit near point-contact connectivity with the current collector, which can accelerate inactive Li formation⁸. We propose a pulse-current protocol that overcomes this failure mode by leveraging Li rhombic dodecahedra as nucleation seeds, enabling the subsequent growth of dense Li that improves battery performance compared with a baseline. While Li deposition and SEI formation have always been tightly linked in past studies, our experimental approach enables new opportunities to fundamentally understand these processes decoupled from each other and bring about new insights to engineer better batteries.

11:30 AM CH02.06.08

Combining *Operando* LCTEM and Cryogenic APT to Directly Visualise and Characterise Nanoscale Liquid-Solid Interfaces [Neil Mulcahy](#), Mary Ryan and Shelly Michele Conroy; Imperial College, United Kingdom

Materials which are critical for the creation of new technologies to tackle global problems such as climate change are often highly complex, multifarious, and difficult to characterise using standardised techniques. This is particularly the case for electrochemical systems which often contain liquid-solid or liquid-liquid interfaces involving low atomic weight, and mobile elements such as hydrogen, carbon, or lithium. These elements are notoriously challenging to quantitatively characterise in their state of interest. It is essential to gain understandings of the phase, chemistry, and morphology of these systems at multiple length scales to better understand what controls their behaviour and limits their performance. This understanding at fundamental length scales is currently limited due to a lack of high-resolution characterisation techniques which are compatible with both the liquid and solid components of the interface and those which are capable of capturing a dynamic system in its exact state of interest. This lack of understanding has ultimately limited the performance and future development of many liquid-based systems using fundamental atomic-level insights. This has crucially led to understandings of various phenomena within battery research such as dendrite growth and solid-electrolyte (SEI) interface formation remaining elusive from a fundamental perspective.

Liquid microscopy techniques have shown the greatest promise in capturing dynamic nanoscale liquid-based systems in their exact state of interest through techniques such as liquid cell transmission electron microscopy (LCTEM). LCTEM is capable of capturing solution phase static and dynamic processes at high temporal and spatial resolutions, allowing for dynamic nanoscale imaging of various processes in real-time. LCTEM has been used to probe electrochemical processes using unique cell setups allowing for electrical biasing of electrodes within the cell as an electrolytic solution is flowing. While this setup does give unique nanoscale insights into these processes, key problems with respect to spatial resolution and beam-induced effects hinder the necessary sub-nanometre spatial resolution needed to resolve these complex dynamic liquid-based electrochemical systems, particularly those containing light elements. While various strategies have been employed to overcome these problems through state-of-the-art dose limitation techniques and alternative liquid cell setups involving 2D materials, the necessary resolutions have not been achieved under *operando* conditions.

The work presented here provides an alternative approach that seeks to combine dynamic liquid microscopy techniques with high-resolution cryogenic microscopy techniques. The emerging field of cryogenic microscopy for material science has been proven capable of capturing a solid-liquid interface in its state of interest through techniques such as cryogenic STEM and cryogenic atom probe tomography (APT). Cryo APT can provide 3D compositional reconstructions of frozen nanoscale volumes with sub-nanometre spatial resolutions and has a chemical sensitivity of ppm for all elements including hydrogen, lithium, and carbon. Cryogenic microscopy techniques are however only capable of offering a snapshot of a particular system when a full dynamic understanding is required. This makes dynamic liquid microscopy techniques and high-resolution cryogenic microscopy techniques extremely complementary.

This work has successfully combined *operando* LCTEM with cryogenic APT through the use of a cryogenic FIB/SEM, vacuum cryo transfer module technology (VCTM), and an inert glovebox. The combination of these distinct microscopy techniques has allowed for dynamic sub-nanometre understandings of various phenomena within nanoscale electrochemical systems such as dendrite growth as well as SEI growth and formation. This presentation will discuss the workflow needed to realise this combination and the results produced thus far.

11:45 AM CH02.06.09

Infrared Nanospectroscopy Characterization of Initial Stages of the SEI Layer Formation at The Amorphous Si/Electrolyte Interface [Andrew Dopilka](#)¹, Jonathan M. Larson^{2,1} and Robert Kostecki¹; ¹Lawrence Berkeley National Laboratory, United States; ²Baylor University, United States

The solid electrolyte interphase (SEI) layer is a crucial component in the function and lifetime of Li-ion batteries; however, the nanoscale mechanism of its growth and evolution are often elusive due to the difficulty in characterizing its structure under *in situ* conditions. Recently, our group has been utilizing nano-FTIR spectroscopy to investigate the structure and composition of battery interfaces with nanometer scale chemical resolution in a nondestructive manner. For instance, this technique was used to probe the graphene/polymer electrolyte interface *in situ*¹ as well as the liquid/graphene interface thus allowing opportunities to characterize the electrical double layer.²

The nano-FTIR technique is implemented within an atomic force microscope using a metallic coated tip. By illuminating the tip/sample interface with a broadband infrared laser, plasmonic enhancement occurs at the apex of metallic tip inducing a nanoscopic near-field interaction with the sample. This near-field interaction couples with the infrared active vibrational modes of the sample and causes a change in the amplitude and phase of the backscattered infrared light which can be detected and then separated from the far-field signal with lock-in amplification at the tapping amplitude of the probe. The result is nanoscale, broadband infrared reflection and absorption of the sample with a probing area on the order of the tip radius (~20 nm), far beyond the diffraction limit of conventional infrared microscopy.

In this presentation, we will discuss how nano-FTIR spectroscopy is used to characterize and observe the initial formation of the SEI layer at the interface between an amorphous Si surface and a carbonate electrolyte. By fabricating a 25 nm thin, free-standing amorphous Si film and encapsulating electrolyte with this thin layer, the Si can act as a window for the infrared light as well as an electrode to apply potential to the surface and induce electrolyte decomposition. Because of the nanometer scale spatial resolution and sensitivity to the electrolyte components, we observe subtle nanoscale heterogeneities in the electrolyte composition at the interface prior to the polarization of the Si electrode. After polarization of the cell to 0.5 V vs Li/Li⁺, we observe that LiPF₆ reacts to form LiF at the surface of the Si and find further inhomogeneity in the formed layer with spatial dependent measurements. Based on the technique's high chemical sensitivity, spatial resolution, and nondestructive nature, *in situ* nano-FTIR spectroscopy is anticipated to be an important tool to unravel the elusive nanoscale formation and growth mechanisms of the SEI layer.

This research was supported by the US Department of Energy (DOE)'s Vehicle Technologies Office under the Silicon Consortium Project directed by Brian Cunningham and managed by Anthony Burrell. The work at the Molecular Foundry was supported by the Office of Science, Office of Basic Energy Sciences, of the U.S. Department of Energy under Contract No. DE-AC02-05CH11231. This research used resources of the Advanced Light Source from

beamline 2.4, which is a DOE Office of Science User Facility under contract no. DE-AC02-05CH11231

References

- (1) He, X.; Larson, J. M.; Bechtel, H. A.; Kostecki, R. In Situ Infrared Nanospectroscopy of the Local Processes at the Li/Polymer Electrolyte Interface. *Nature Communications* **2022**, *13* (1), 1398.
- (2) Lu, Y. H.; Larson, J. M.; Baskin, A.; Zhao, X.; Ashby, P. D.; Prendergast, D.; Bechtel, H. A.; Kostecki, R.; Salmeron, M. Infrared Nanospectroscopy at the Graphene-Electrolyte Interface. *Nano Letters* **2019**, *19* (8), 5388–5393.

SESSION CH02.07: Investigation of Energy Storage Materials via Advanced *In Situ*/Cryogenic Electron Microscopy II

Session Chairs: Qianqian Li and Yaobin Xu

Thursday Afternoon, April 25, 2024

Room 440, Level 4, Summit

1:30 PM CH02.07.01

Microscopic View of Carbon Dioxide Adsorption in Amine-Decorated Porous Silicates for Direct Air Capture Wei-Chang David Yang, Marcus J. Carter, John R. Hoffman, Avery E. Baumann, Christopher M. Stafford and Renu Sharma; National Institute of Standards and Technology, United States

Organic-inorganic hybrid sorbents, based on mesoporous silicates and polymers, are a leading candidate for CO₂ capture under ambient pressure, which takes advantage of the high surface area of the silicates. [1]. An impregnation process allows active functional groups, such as polymer-based alkyl amines, to decorate the internal surface of mesoporous silicates and improve the adsorption-desorption kinetics at a reduced energy expense [2]. The mesopore surface was shown to interact with aqueous polyethyleneimine (PEI) to create the amine-modified sites for CO₂ adsorption [3]. However, the beam-sensitive specimen has limited electron microscopy in measuring these adsorption sites' structure and chemistry within the nanometer-sized mesopores [4]. In this work, we adopted a new approach that combines *in situ* cryogenic scanning transmission electron microscopy (STEM) and electron energy-loss spectroscopy (EELS) in an environmental transmission electron microscope (ETEM) to probe the interactions among CO₂, PEI, and mesoporous silicates.

The ETEM is equipped with a monochromated electron source to achieve an EELS energy resolution of up to 80 meV at 80 kV and a custom-built optical spectroscopy system to measure Raman shifts from a ten-micrometer-in-diameter area centered around the electron-beam location [5]. The amine-modified silicates were prepared by impregnating about 60 wt.% of PEI with a molecular weight of 800 g/mol into pristine silicates (e.g., MCM-41). A liquid-nitrogen-cooled holder was used to freeze the amine-modified sample in the ETEM and, therefore, mitigated electron beam damages as monitored with the spatially correlated Raman spectra. We used *in situ* EELS hyperspectral imaging to benchmark the mesopore surface's interaction with CO₂, either with or without PEI impregnation. For the pristine MCM-41 mesopores, we obtained carbon K-edge maps based on the distinct π^* peak at ≈ 290 eV to show physisorption in a CO₂ environment and subsequent desorption in the ETEM baseline vacuum [6]. On the other hand, the amine-modified MCM-41 was activated at 60 °C in the ETEM baseline pressure and then exposed to CO₂. After evacuating CO₂, we froze the sample *in situ* by adding liquid nitrogen to the cooling holder. The approach allowed us to analyze EELS data obtained from specimens in the frozen state, whether they had been exposed to CO₂ or not. We identified the energy loss near edge structure (ELNES) associated with the carbonyl core to $\pi^*_{C=O}$ transition (≈ 289 eV) in ammonium carbamate [7], which indicates the formation of chemisorbed species when exposed to CO₂ under a water-free condition. Another ELNES of the amide core to π^* transition (≈ 401 eV) was also detected to support the above observation. Compared to the ETEM result, the same type of PEI film on a metal substrate was examined using polarization modulation-infrared reflection adsorption spectroscopy (PM-IRRAS). The carbamate peak intensity changes in response to the adsorption and desorption processes confirmed carbamate formation in a dry CO₂ environment.

We show here that *in situ* cryogenic STEM-EELS enables the direct observation of CO₂ chemisorption and the ability to benchmark the properties and performance of PEI-decorated MCM-41 at the nanoscale. We continue pushing the frontier of understanding the dynamic structure and chemistry in a broad range of beam-sensitive materials with our new approach to elucidate the fundamental principle that leverages adsorption sites for new direct air capture technologies.

References:

- [1] S Choi, JH Drese, and CW Jones, *ChemSusChem* **2** (2009), p. 785.
- [2] WJ Son, JS Choi, and WS Ahn, *Microporous Mesoporous Mater.* **113** (2008) p. 31.
- [3] X Xu et al., *Energy Fuels* **16**, (2002) p. 1463.
- [4] J Young et al., *Energy Environ. Sci.* **14** (2021), p. 5377.
- [5] WCD Yang et al., *ACS Appl. Mater. Interfaces* **11** (2019), p. 47037.
- [6] WCD Yang et al., *Nat. Mater.* **18** (2019), p. 614.
- [7] WG Urquhart and H. Ade, *J. Phys. Chem. B* **106** (2002), p. 8531.

1:45 PM *CH02.07.02

Autonomous Characterization for Investigating Cathode Active Materials and Solid-Solid/Solid-Liquid Interphases in Energy Storage Devices Huolin Xin, Chunyang Wang, Peichao Zou and Yubin He; University of California, Irvine, United States

The characterization of complex energy materials often requires detailed structural and functional analysis across multiple length and time scales. While *in situ* and *operando* transmission electron microscopy (TEM) provide dynamic information [1], they can be lacking in resolution and sensitivity to some degree, particularly when studying cathode active materials and solid-solid or solid-liquid interfaces/interphases [2-4]. Cryogenic electron microscopy (cryoEM) has successfully filled this gap as a 'freeze-the-moment' technique, allowing for the imaging of dose-sensitive interphases in a protected environment. CryoEM is particularly well-suited for investigating solid-solid and solid-liquid interfaces in energy materials, where these interfaces play critical roles in determining material properties and performance [4]. By combining cryoEM with an autonomous characterization system, we can overcome the limitations of human operators and improve sensitivity and resolution for these interfaces. This approach has the potential to revolutionize basic energy research, enabling comprehensive investigations of complex materials at multiple length and time scales. [5]

References:

- [1] Tension-Induced Cavitation in Li Metal Stripping, C. Wang, R. Lin, Y. He, P. Zou, K. Kisslinger, Q. He, J. Li, HL Xin, *Advanced Materials*, (2022)
- [2] Characterization of the structure and chemistry of the solid-electrolyte interface by cryo-EM leads to high-performance solid-state Li-metal batteries, R. Lin, Y. He, C. Wang, P. Zou, E. Hu, X.-Q. Yang, K. Xu & H. L. Xin, *Nature Nanotechnology*, *17*, 768–776 (2022)
- [3] Resolving complex intralayer transition motifs in high-Ni-content layered cathode materials for lithium-ion batteries, C. Wang, X. Wang, R. Zhang, T. Lei, K. Kisslinger & H. L. Xin, *Nature Materials*, (2023), *22*, 235–241 (2023)

[4] Compositionally complex doping for zero-strain zero-cobalt layered cathodes, R. Zhang, C. Wang, P. Zou, R. Lin, L. Ma, L. Yin, T. Li, W. Xu, H. Jia, Q. Li, S. Sainio, K. Kisslinger, S. E. Trask, S. N. Ehrlich, Y. Yang, A. M. Kiss, M. Ge, B. J. Polzin, S. J. Lee, W. Xu, Y. Ren and H. L. Xin, *Nature*, 610, 67–73 (2022)

[5] Supported by the Department of Energy under award no. DE-SC0021204 and the startup funding of HLX.

2:15 PM *CH02.07.03

Real-Space Visualization of Frequency-Dependent Anisotropy of Atomic Vibrations Xingxu Yan¹, Paul Zeiger², Jan Ruzs² and Xiaoqing Pan^{1,3};
¹University of California, Irvine, United States; ²Uppsala University, Sweden; ³University of California, United States

Advancements in transmission electron microscopy (TEM) have revolutionized the study of interfaces and nanostructured materials. Innovations like aberration correctors, pixelated direct electron detectors, and monochromators have enabled atomic-resolution scanning transmission electron microscopy (STEM) and electron energy-loss spectroscopy (EELS), facilitating investigations into local structure, properties, and dynamic behaviors. Using a space- and angle-resolved vibrational EELS technique, we have recently observed red shifts and intensity changes in acoustic vibration modes near a single stacking fault in cubic silicon carbide, and nanoscale composition-induced red shifts in Si optical modes in SiGe quantum dots. We also developed a method for differentially mapping phonon momenta revealing the interplay between diffuse and specular reflection. In this talk, I present a novel approach, employing dark-field monochromated electron energy-loss spectroscopy for momentum-selective vibrational spectroscopy. This technique allows us to map phonon polarization vectors. When applied to centrosymmetric cubic-phase strontium titanate, we discover two types of oxygen atoms with contrasting vibrational anisotropies below and above 60 meV, based on mean-squared displacements. These transformations are supported by theoretical models, revealing the transition from oblate ellipsoids at low energies to prolate ellipsoids at high energies. These frequency-dependent thermal ellipsoids provide insights into the thermal and optical behaviors associated with acoustic and optical phonons. Our method enables the visualization of phonon eigenvectors at specific crystalline sites, opening new avenues for exploring dielectric, optical, and thermal properties with exceptional spatial resolutions.

2:45 PM BREAK

3:15 PM *CH02.07.04

In Situ Analytical Electron Microscopy and Cryogenic Electron Microscopy for Characterizing Nanoscale Materials in Electrochemical Process Minghao Zhang¹ and Y. Shirley Meng²; ¹University of California, San Diego, United States; ²The University of Chicago, United States

Lithium-ion batteries (LIBs) commercially dominate portable energy storage and have been extended to hybrid/electric vehicles by utilizing electrode materials with enhanced energy density. However, the energy density and cycling life of LIBs must extend beyond the current reach of commercial electrodes to meet the performance requirements for transportation applications. Carbon-based anodes, serving as the main negative electrodes in LIBs, have an intrinsic capacity limitation due to the intercalation mechanism. Alternative anodes are being explored, including nanosized metal sulfides and oxides which were found to possess better cycling stability and larger reversible capacities. Recently, researchers proposed to use Li metal as the anode to achieve even higher energy density. However, the dendritic growth of Li metal during cycling will result in low coulombic efficiency as well as safety issues which is detrimental for practical applications.

Further improvements and developments of electrode materials rely on a fundamental understanding of their electrochemical cycling mechanisms. On the one hand, real-time (in situ) studies with high spatial resolution are required for characterizing microstructural evolution and specific electrochemical reactions upon cycling. In situ TEM coupled with electron energy loss spectroscopy (EELS) has thus been considered as one of the most powerful techniques for monitoring electrochemical processes in electrode materials. EELS spectra interpretation is critical for chemical information analysis including oxidation state, charge transfer, bonding environment, etc. On the other hand, metal anode and solid electrolyte interphase (SEI) are chemically reactive and sensitive to electron-beam irradiation. TEM studies of batteries in their native environment can be problematic. Cryogenic electron microscopy (cryo-EM) can potentially be a powerful technique to image beam sensitive battery electrode materials.

In this work, the lithiation mechanism of nanosized metal sulfides and oxides is explored using in situ TEM. Multi-steps lithiation mechanism was revealed with discovery of a fascinating, spontaneously formed, self-assembling nanocomposite framework. This framework provides adequate room to accommodate the volume expansion during lithiation while ensuring enhanced contact among the active materials. Probing these dynamic evolution processes is not only necessary for fundamental understanding of electrochemical mechanisms, but also beneficial for designing novel materials in batteries with improved performance. This work will also cover recent advances on cryo-EM development for metal dendritic growth and SEI. The detailed structure of electrochemically deposited Li and the SEI composition at the nanoscale were revealed with minimized beam damage during imaging. Our findings not only illustrate the capabilities of cryogenic microscopy for beam (thermal)-sensitive materials but also yield crucial structural information on the Li metal deposition.

3:45 PM CH02.07.06

Probing Volumetric Effects in Suspended Binary Superlattices of Infrared Colloidal Nanocrystals using Transmission Electron Microscopy and Optical Characterization Todd H. Brintlinger, Patrick Y. Yee, Veronica R. Policht, Paul D. Cunningham, Janice E. Boercker and Sarah Brittan; U.S. Naval Research Lab, United States

By combining two types of infrared colloidal nanocrystals (NCs) into binary superlattices, a type of 'artificial solid' can be created where the NCs would be 'atoms' and NC-to-NC interactions are 'bonds.' These binary superlattices then allow for control of desired optoelectronic properties and offer the technological advantage of scalable solution-based synthesis for low-cost infrared optoelectronics. One roadblock in these engineered systems is the small size of individual ordered domains (analogous to grain size in polycrystalline materials), which prohibits detailed understanding of structure-property relationships. Expanding on our previous work [1, 2], we manipulate the surface chemistry in these artificial solids to create enlarged (>1 μm) domains of binary components comprised of infrared plasmonic Cu_{2-x}S/PbS core/shell and excitonic PbS nanocrystals. These superlattices are suspended across holes, proving both their ability to be self-supporting as well as allowing for transmission electron microscopy and optical characterization without need to account for substrate effects. However, as structured solids with a three-dimensional extent, we then face a challenge in determining volumes of superlattice domains when suspended in this fashion. Here, we determine both thickness and spatial extent of the superlattice to define the local volume in individual superlattice domains, and then compare these to correlated photoluminescence from the same domains. Combined with time-resolved photoluminescence spectroscopy, these results suggest that energy transfer occurs between the excitonic emitters and plasmonic nanocrystals.

References

- [1] S. Brittan, N. A. Mahadik, S. B. Qadri, P. Y. Yee, J. G. Tischler, and J. E. Boercker, *ACS Appl. Mater. Interfaces* **12**, 24271 (2020).
- [2] P. Y. Yee, S. Brittan, N. A. Mahadik, J. G. Tischler, R. M. Stroud, Al. L. Efron, P. C. Sercel, and J. E. Boercker, *Chem. Mater.* **33**, 6685 (2021).

4:00 PM CH02.07.07

Reversible Oxidation of Copper via Chemical Interaction with Carbon Dioxide Investigated by Ambient Pressure X-Ray Photoelectron Spectroscopy

Haoyi Li¹, Asmita Jana¹, Angel T. Garcia-Esparza¹, Dimosthenis Sokaras², Junko Yano¹ and Ethan Crumlin¹; ¹Lawrence Berkeley National Laboratory, United States; ²SLAC National Accelerator Laboratory, United States

A fundamental understanding of the chemical interactions between copper (Cu) and carbon dioxide molecules is pivotal to gain detailed insights on the initial steps of carbon dioxide conversion on Cu surfaces. Herein, ambient pressure X-ray photoelectron spectroscopy using synchrotron radiation-based tender X-rays (4 keV) was employed to study the chemical dynamics of Cu surfaces with increasing the pressure of carbon dioxide. The surface Cu of polycrystalline metal foil was oxidized to Cu(II) upon exposure to carbon dioxide, particularly beyond 10 Torr, and then reduced back when removing the carbon dioxide gas to restore high vacuum condition. A linear correlation was built up between carbon dioxide pressure and surface Cu(II) proportion. The growth and recession of the Cu(II) overlayer is attributed to the interaction of adsorbed oxygen species from the direct dissociation of adsorbed carbon dioxide with the surface metallic Cu sites and their fast transport through the Cu(II) overlayer. The observed reversible phenomenon of the Cu(II) layer evolution induced by dissociative carbon dioxide adsorption on Cu surface has been verified on other two reported carbon dioxide-reduction systems: p-GaN/Au/Cu and p-Si/TaOx/Cu. We unveil a universal and reversible oxidation of Cu towards Cu(II) at the initial step of carbon dioxide conversion, providing atomistic insights for the design and construction of highly efficient and selective Cu-based catalysts.

4:15 PM CH02.07.08

Positron Annihilation Method of Identifying Bismuth Centers in Silicon for Quantum Computing and Communications: Effects of 15 MeV Proton Irradiation Nikolay Arutyunov¹, Vadim Emtsev², Reinhard Krause-Rehberg³, Mohamed Elsayed³, Nikolay Abrosimov⁴, Gagik Oganessian² and Vitali Kozlovski⁵; ¹MLU (Halle, Germany), IKZ (Berlin), IPLT (former Institute of Electronics), Uzbekistan; ²Ioffe Physico-Technical Institute, Russian Federation; ³Department of Physics, Martin Luther University (MLU) Halle, Germany; ⁴Leibniz-Institut für Kristallzüchtung (IKZ) Berlin, Germany; ⁵St. Petersburg State Polytechnical University, Russian Federation

In search of a high-performance interface between telecom photons and matter qubits, bismuth (Bi) centers are being scrutinized in floating zone (FZ) silicon of n-type, mostly, by the resonance and optical methods. Meanwhile, data on electron and micro-structural properties of Bi centers in silicon beyond narrow zones of the resonance and optical transitions is scarce. To gain deeper insight into properties of both the spin system and open volume related to the Bi donor center, we have probed the microstructure of the Bi center by positrons registering their two-quantum annihilation with electrons. Data about microstructure of the radiation defects formed in silicon is of paramount importance for the material which must function on the low Earth orbit satellite where the most damaging factor is the irradiation by protons of MeV energies. The challenging points in identification of the radiation defects concern practically all devices on silicon platform (e. g., of such as single-photon detectors and the devices for quantum communications).

We will discuss the data obtained, mostly, for the samples irradiated with 15 MeV protons at room temperature. For characterization of the material, low-temperature Hall's measurements were carried out on the samples-satellites.

For the first time, an inhibition and a delay of emission of two annihilation quanta has been revealed at the declining temperature, when the electron density contacting positron at the Bi center increases. This paradoxical observation performed by high-resolution positron annihilation lifetime spectroscopy is suggested to be due to non-local interaction between the nuclear (J) and electron spins of atoms of the magnetic isotope ²⁹Si (J = 1/2) and of the centers of Bi (J = 9/2) [1]. Interestingly, this interaction does not manifest itself in the enriched ²⁸Si(Bi) material (i.e., in so-called ²⁸Si "semiconductor vacuum" where the residual concentration of atoms of ²⁹Si (J=1/2) isotope ambient Bi impurity center is as low as 50 ppm). We believe that the data obtained demonstrate for the first time the influence of a non-local interaction of the spin systems of Bi (J = 9/2) and ²⁹Si (J=1/2) centers in silicon on the essentially local phenomenon of emission of the two-quantum electron-positron annihilation radiation.

The Bi center acquires an open volume V_{op} as a result of interaction with the point defects created by the proton irradiation. It is argued that the thermally stable complex $[V_{op} - Bi]$ possesses D_{3d} symmetry [1]; this comes into line with the data on the electrical properties of the electron-irradiated n-FZ-Si(Bi) material [2]. The complex manifests itself as deep donor center.

The $[V_{op} - Bi]$ center is decomposing during a fast stage of isochronal annealing over the temperature range $\Delta T_{ann} = 320$ to 470 °C [1]; the estimated activation energy is equal to $E_a = 0.89 \pm 0.08$ eV and is surprisingly close to the energy ~ 0.92 eV characterizing structural stability of the center where Bi donor impurity atom is coupled with the modeled vacancy (see [1] and references therein). It is worth mentioning that the thermally stable radiation complexes related to the phosphorus (P) impurity centers in the proton-irradiated material are annealed during a somewhat broader stage, $\Delta T_{ann} = \sim 430$ to ~ 650 °C ($E_a = 1.05 \pm 0.21$ eV [3,4]).

The results available for the Bi and P centers of radiation origin in FZ silicon are compared and the conclusion is made about necessity of reconsideration of a whole conception of formation of point radiation defects in moderately doped n-type silicon subjected to irradiation with protons and electrons [5].

[1] N. Arutyunov et al., J. Phys.: Condens. Matter, **33** (2021) 245702

[2] V. Emtsev et al., J. Appl. Phys., **134** (2023) 025103

[3] N. Arutyunov et al., J. Phys.: Condens. Matter, **25** (2013) 035801

[4] N. Arutyunov et al., Journal of Physics: Conf. Ser., **618** (2015) 012013

[5] N. Arutyunov et al., Phys. Stat. Sol. (c), **14** (2017) 1700120

SESSION CH02.08: Development of Artificial Intelligence and Novel Techniques in *In-Situ* Microscopy and Spectroscopy

Session Chairs: Leopoldo Molina-Luna and Di Zhang

Friday Morning, April 26, 2024

Room 440, Level 4, Summit

8:30 AM *CH02.08.01

Towards Artificially Intelligent Microscopy of Functional Materials Steven R. Spurgeon; Pacific Northwest National Laboratory, United States

Artificial intelligence (AI) promises to reshape scientific inquiry and enable breakthrough discoveries in areas such as quantum computing, energy storage, and advanced manufacturing. While it is now possible to produce materials in almost limitless configurations, engineering of desirable functionality depends on precise control of structure and defects across scales. Complex synthesis pathways can lead to significant deviations from idealized structures,

which occur at length and time scales that are challenging to probe experimentally and theoretically. Mastery of materials is therefore predicated on the ability to acquire and act on complex, heterogeneous, and fast-evolving microscopy data streams, a task uniquely suited to emerging AI and machine learning methods. Here I will discuss my research efforts to develop a new framework for materials discovery, leveraging embedded automation, domain-grounded analytics, and predictive control for human-like reasoning. I will show how AI is transforming the present and future of materials discovery and design, allowing us to richly manipulate matter for emerging technologies.

9:00 AM *CH02.08.02

Elucidating Metal and Oxide Nanoparticle Surface Dynamics through *In Situ* TEM and Artificial Intelligence Piyush Haluai¹, Mai Tan¹, Adrià Marcos Morales², Matan Leibovich², Sreyas Mohan², Yifan Wang¹, Carlos Fernandez-Granda² and Peter A. Crozier¹; ¹Arizona State University, United States; ²New York University, United States

Nanoparticle systems often show high degrees of instability which are strongly influenced by size and ambient environment. These dynamic structural changes modify material properties such as reactivity, phase changes and catalysis. Atomic-level surface dynamics may play a significant role in defining particle structures and functionalities but characterizing nanoparticle surface structures with high spatial and temporal resolution simultaneously has proven challenging. Transmission electron microscopy (TEM) is a key tool to visualize local atomic structure of nanoparticles. Ultrafast TEM can now achieve picosecond temporal resolution but is limited to a spatial resolution of about 2 nm. Fortunately, modern detectors now provide readout rates in excess of 1000 frames per second, offering the potential to investigate atomic-level structural evolutions with time resolutions down to a millisecond. However, in most situations, the need to limit electron dose rates results in high temporal resolution movies that are dominated by shot noise, which often obscures surface structural dynamics. In order to address this challenge, we propose a fully-unsupervised AI denoising framework, which enables recovery of atomic-resolution information from such data. The unsupervised deep video denoising framework [1] improves the signal-to-noise ratio (SNR) by a factor of 30 at a spatial resolution of 1 Å and time resolution of 10 ms. For this investigation, we explore structural dynamics of metal and oxide nanoparticle particles under combinations of CO and O₂ at temperatures up to 300°C. The enhanced time resolution reveals that supposedly stable, low-energy surfaces can display highly active dynamics, triggering nanoparticle instabilities resulting in rapid structural fluctuations. The new spatiotemporal capability enabled by the proposed framework dramatically enhances our ability to explore surface dynamics and the evolution of metastable states in nanoparticles at the atomic level, offering new insights into their functionality.

References

1. Sheth, D.Y., et al. *Unsupervised deep video denoising*. in *Proceedings of the IEEE/CVF International Conference on Computer Vision*. 2021.
2. We gratefully acknowledge the support of the following NSF grants to ASU (OAC 1940263, 2104105, CBET 1604971, and DMR 184084 and 1920335) and NYU (HDR-1940097 and OAC-2103936). The authors acknowledge HPC resources available through ASU, and NYU as well as the John M. Cowley Center for High Resolution Electron Microscopy at Arizona State University.

9:30 AM CH02.08.03

***In-Situ* Observations of Non-Classical Crystal Growth of Au Nanoparticles on Hematite** Xiang Wang¹, Sichuang Xue¹, Xin Qi², Duo Song¹, Maria Sushko¹, Xin Zhang¹ and Kevin Rosso¹; ¹Pacific Northwest National Laboratory, United States; ²Dartmouth College, United States

A significant research gap exists regarding the comprehensive investigation of crystallization mechanisms and facet-dependent stability of atomically precise metal clusters on metal oxide nanoparticles. To address this gap, our study focuses on a detailed examination of the sintering process of gold (Au) on facet-controlled hematite (α -Fe₂O₃) {104} and {001} nanoparticles through in-situ TEM observation. Our findings reveal the existence of three distinct crystal growth pathways of Au on hematite nanoparticles: Ostwald ripening, particle coalescence, and disordered intermediate-phase-mediated growth, where particle coalescence plays a dominant role in the sintering process. Furthermore, analysis of Au crystal growth kinetics on different hematite facets highlights the important influence of interfacial structure on the process, where hematite {001} stabilizes Au nanoparticles and suppresses their sintering more effectively than {104} facets. First-principles density functional theory calculations and atomistic molecular dynamics simulations with enhanced sampling provide valuable support for the crystal growth pathway selection of Au nanoparticles on hematite. Our research significantly contributes to the understanding of metal crystallization on hematite surfaces and offers essential guidelines for selecting hematite supports for heterogeneous catalysts.

9:45 AM CH02.08.04

Interface Strains in 1D and 2D Si/Ge Structures for Quantum Computing Alicia Ruiz-Caridad¹, Arianna Nigro¹, Nicolas Forrer¹ and Ilaria Zardo^{1,2}; ¹Universität Basel, Switzerland; ²SNI, Switzerland

During the last decade great efforts were put in the development of materials for quantum computing for its outstanding properties such as high speed, large store capacity and low power consumption [1]. Silicon is the preferred platform for microelectronics infrastructures due to its scalability, low economic costs, harmless for the environment, established fabrication processes and easy implementation of advanced engineering techniques [2,3]. Moreover, silicon is a good quantum material due to its long coherence time of spins of localized electrons and efficient controllability [4]. Germanium is a semiconductor material compatible with silicon. Material engineering of Si-Ge in form of epitaxial planar heterostructures or nanowires lead to enhanced mobility properties for quantum purposes. Despite, strains arising from the 4% mismatch between Ge and Si lattice parameter create defects, these defects hinder mobility. With the purpose to achieve higher mobility, scattering must be minimized by diminishing strains and interface roughness. In this regard, an effective tool to evaluate strains and interface roughness is electron microscopy combined with Raman spectroscopy which allows structural and chemical characterization of samples at the nanoscale.

In this work, we growth by chemical vapor deposition (CVD) 2D and 1D structures: (i) planar heterostructure's composed with variable percentage of Si/Ge barrier's and a Ge QW; and (ii) Ge-Si core-shell nanowires for quantum computing purposes. In a first step we chemically and structurally localized the Ge and Si by energy-dispersive X-ray (EDX) spectroscopy and scanning transmission electron microscopy (STEM) techniques. Finally, we aim to study strain of the Ge QW and core-shell interfaces by means of geometric phase analysis (GPA) and μ -Raman spectroscopy. High-resolution transmission electron microscope (HR-TEM) images of the samples were performed in a Jeol JEM F200 cFEG TEM/STEM to evaluate roughness of interfaces and defects. GPA is a microscopic technique by TEM based on the signal processing of HR-TEM images and its Fourier transform. For the μ -Raman measurements were performed at 633 nm wavelength in back scattering geometry with the help of a Horiba T64000 triple spectrometer and a liquid nitrogen-cooled CCD detector. The combination of both methods permits the control, calculation and mapping of strains in different directions (rotation χ , ϵ_{xx} , ϵ_{xy} and ϵ_{yy}) at high precision. By engineering the core-shell diameter ratio in 1D structures and Si_xGe_{1-x} composition of the barriers and Ge QW thicknesses in 2D structures, we proved and measured tensile/compressive strains in the interfaces between Ge QW and SiGe barriers and between core and shell NWs making our material suitable for integration in Si platforms for quantum computing applications.

References

- [1] M. Hirvensalo, *Quantum computing*. Springer Science & Business Media, 2003.
- [2] M.F. Gonzalez-Zalba, S. de Franceschi, E. Charbon, T. Meunier, M. Vinet, A. S. Dzurak, A. S., *Nature Electronics*,4(12), 2021, 872-884.
- [3] R.Singh, M. M. Oprysko, D. Harame, *Silicon germanium: technology, modeling, and design*,2004.

[4] A. M. Tyryshkin, S. A. Lyon, T. Schenkel, J. Bokor J. Chu, W. Jantsch, F. Schäffler J.L. Truitt, S. N. Coppersmith, M.A. Eriksson, Low-dimensional Systems and Nanostructures, **2006**, 35(2), 257-263.

10:00 AM BREAK

10:30 AM *CH02.08.05

Advanced *In-Situ* Electron Microscopy for Energy and Quantum Materials Yimei Zhu; Brookhaven National Laboratory, United States

In this presentation, I will give an overview of our recent work on advanced in-situ microscopy characterization of energy and quantum materials. I will focus on the correlation of electrons, spin and lattice and their degrees of freedom as well as the critical roles of heterogeneity, interfaces, and disorder under external electric, magnetic and photonic excitations to reveal materials' response. For instance, I will show our cryogenic microscopy study of atomically resolved imaging and electron energy-loss spectroscopy to understand the interface-enhanced superconductivity and of Lorentz phase microscopy to explore the intriguing transformations among various topological chiral spin states including skyrmions under applied electromagnetic fields. Studying spin wave dynamics in nanoscale magnetic architecture under microwave excitation and Li-ion transport mechanisms of battery materials with ionic liquid in operando will also be presented.

The author would like to acknowledge the electron microscopy group at CMPMS, BNL for assistance. The work was supported by the US DOE/BES-MSED under Contract DE-SC0012704.

11:00 AM CH02.08.06

Investigation of Dislocation-Controlled Domain Nucleation and Domain-Wall Pinning in Single-Crystal BaTiO₃ by Multi-Stimuli MEMS-Based *In Situ* TEM Tianshu Jiang¹, Fangping Zhuo¹, Oscar Recalde¹, Yevheniy Pivak² and Leopoldo Molina-Luna¹; ¹TU Darmstadt, Germany; ²DENSolutions, Netherlands

Engineering domain walls at the nanoscale to influence macroscopic functional properties presents significant potential in electromechanics and electronics. This potential is particularly apparent in introducing topological defects into functional materials, highlighting the broad possibilities in this area. However, our comprehensive understanding of defect-mediated domain nucleation and domain wall mobility remains limited.

In this work, we achieved well-aligned dislocations with {100}<100> slip systems oriented in the [001] out-of-plane direction in single-crystal BaTiO₃. This was accomplished through high-temperature uniaxial compression on a notched sample. Utilizing MEMS-based *in situ* heating and cryo scanning/transmission electron microscopy (S/TEM), we were able to observe the dislocation-mediated domain nucleation and dynamic interactions between domain walls and these topological defects. These observations spanned a wide temperature range, from -175 °C to 200 °C, covering all phases of BaTiO₃ from rhombohedral to cubic, offering high-resolution insights into the electro-mechanical interactions within this ferroelectric material. Furthermore, we explore the direct manipulation of the domain wall motion using *in situ* biasing TEM. Under various stimuli, we observed the pinning of ferroelastic domain walls by these imprinted dislocations, attributed to the stress fields from the dislocations.

Our findings not only deepen the understanding of domain wall engineering in ferroelectric materials but also introduce a novel approach suitable for both advanced nanoelectronics and bulk applications across various temperatures.

11:15 AM CH02.08.07

Facilitating *In Situ* 4D STEM with Advances in Software for Ultrafast Direct Detectors Barnaby D. Levin, Aziz Aitouchen and Benjamin Bammes; Direct Electron LP, United States

Four-dimensional scanning transmission electron microscopy (4D STEM) involves imaging a diffracted electron beam with a pixelated detector at each probe position of a STEM scan. The resulting information-rich datasets allow multiple types of analyses of a specimen, including high-resolution structural visualization, and mapping of crystal grain structure, molecular orientation, strain, electric and magnetic fields, and more [1]. Typically, 4D STEM involves recording large (several Gigabyte to several Terabyte) 4D datasets to disk to be analyzed with post-acquisition software such as LiberTEM [2], py4DSTEM [3], or custom written code. Post-acquisition analysis enables a range of complex data analysis techniques to be applied to the data, but the efficiency of 4D STEM experiments can be severely impacted by the substantial time needed to go from data acquisition to data visualization.

Lack of real-time visualization poses challenges for both manual data acquisition, and for the development of automated 4D STEM workflows. However, with ultrafast direct detectors, such as the Celeritas XS camera, able to acquire data at rates approaching 5 Gigabytes per second, developing real-time 4D STEM analysis software involves its own significant challenges. These challenges are compounded when considering *in situ* 4D STEM, (sometimes referred to as 5D STEM), where the goal is not only to record one large 4D dataset, but multiple large 4D datasets over a period of time so that dynamic processes such as changes in strain, crystal structure, or electric fields in a specimen can be observed [4].

Here, we present a new 4D STEM software platform that aims to address these challenges by leveraging GPU processing for real-time virtual STEM image generation during repeated 4D STEM acquisition. The software is compatible with Direct Electron's Celeritas XS, Celeritas, DE-16, DirectView2 and DE-64 cameras, as well as the DE-FreeScan scan generator, and allows the user to stream a series of full 4D STEM datasets to disk, even whilst simultaneously generating a live-view of up to four different types of virtual STEM image. In addition to viewing virtual images and camera frames in the software's native interface, the system can be controlled via an API, allowing for integration into 3rd-party software, as well as custom software for microscope automation.

Further developments are ongoing to augment this software platform with additional features with the goal of making 4D STEM and *in situ* 4D STEM more accessible techniques for electron microscopists to perform.

References:

- [1] Ophus C. (2019). *Microscopy and Microanalysis*, **25**, 563-582.
- [2] Clausen A. et al. (2020). *Journal of Open Source Software*, **5**, 2006.
- [3] Savitzky B. et al. (2021) *Microscopy and Microanalysis*, **27**, 712-743.
- [4] Huang, S. & Voyles, P. (2023) *Microscopy and Microanalysis*, **29**, S1, 272-273.

11:30 AM CH02.08.08

Recent Developments of High Energy Resolution X-Ray Spectroscopic Methods for Energy Materials at NSLS-II Denis Leshchey and Eli Stavitski; Brookhaven National Laboratory, United States

X-ray absorption spectroscopy (XAS), first used to be applied in the field of energy materials, such as catalysts, over 50 years ago, has evolved into an indispensable tool in the arsenal of characterization techniques. XAS is element-specific method which compatible with a variety of sample environments, enabling in situ and operando experiments. An extension of XAS spectroscopy, high energy resolution (HR) X-ray spectroscopy, a collection of techniques which resolves the energy of the fluorescence photons with high accuracy, opened new opportunities in the field [1]. Among these methods is a high-energy resolution fluorescence detection (HERFD) XAS allows to overcome the limitations of traditional XAS by selectively detecting fluorescence photon within narrow energy band. Another is Valence-to-Core X-ray Emission Spectroscopy (VtC XES) which probes electronic states in the valence band, making is a far more sensitive to subtle electronic changes than the traditional Extended X-ray Absorption Fine Structure (EXAFS). In this contribution we review recent innovations at the National Synchrotron Light Source II (NSLS-II) which enable applications of HR XAS to energy-relevant systems as well as several examples to demonstrate the advantages of these techniques.

SESSION CH02.09: New Applications in *In-Situ* Microscopy and Spectroscopy
Session Chairs: Qianqian Li, Qianqian Li, Leopoldo Molina-Luna, Yaobin Xu and Di Zhang
Friday Afternoon, April 26, 2024
Room 440, Level 4, Summit

2:00 PM CH02.09.01

Novel Environmental TEM Holder for *In Situ* Research of Nano-Electronic Devices and Energy Materials [Yevheniy Pivak](#)¹, [Oscar Recalde](#)², [Hector H. Perez-Garza](#)¹ and [Leopoldo Molina-Luna](#)²; ¹Denssolutions, Netherlands; ²TU Darmstadt, Germany

The rapid development of in situ transmission electron microscopy (TEM) has become possible due to advancements of the functionalized microelectromechanical systems (MEMS)-based sample carriers. Nowadays, there exists a great variety of MEMS chips that enable the application of an individual stimulus like thermal, electric, gas, liquid, force, etc. or, usually, a combination of two stimuli. Specifically, multi thermal and electric stimuli have been extensively used to study electronic and energy materials and devices like ferroelectrics, magnetic materials, solid state batteries, thermoelectric, memristors, solar cells and many more.

The study of structure and electrical properties of nano-electronic materials and devices is mainly performed in vacuum. This, however, doesn't represent real-life working conditions as the presence of oxygen might lead to different behaviour and properties of materials. An environmental TEM can be used to perform an in situ heating and biasing experiments in an atmosphere, but the gas pressure is limited to roughly 20 mbar which still possess a challenge. In this work we present the development of a new multi-stimuli environmental TEM sample holder. The holder allows the application of thermal and electrical stimuli in ambient environmental conditions. This is achieved through a newly designed dual chip environmental cell with an increased number of contacts. Additional electrodes on the chip are used to prepare a FIB lamella and to characterize the electrical performance of the sample either in 2- or 4-contact mode. Using a newly developed FIB sample preparation procedure, it is possible to prepare contamination-free samples on gas, heating and biasing chips with no electrical short circuits and minimized leakage currents. This development represents a significant step forward towards the realization of real operational conditions inside the TEM offering the potential to further explore and deeper understand of the real properties of nano-electronic devices and energy related materials.

2:15 PM CH02.09.02

Investigation of Amorphous Silicon Nanoparticles dispersed in Silicon Nitride Passivation Layer for Semiconductor Industry [Filippo Sabatini](#)^{1,2}; ¹Politecnico di Milano, Italy; ²ST Microelectronics, Italy

During the formation process of a typical integrated circuit (IC), a passivation layer is deposited to protect the internal semiconductor device after the metallization steps. These passivation layers are typically formed by oxide or nitride layers, most of the time deposited by plasma enhanced chemical vapor deposition (PECVD). As part of my PhD research, in collaboration between Politecnico di Milano and ST Microelectronics, I had to perform extensive characterization of different types of silicon nitride (SiN) in order to optimize its adhesion with an epoxy resin deposited on top of it. During these analysis, I detected the presence of amorphous silicon clusters dispersed within the nitride matrix through the presence of strong photoluminescence (PL) effects observed by Raman spectroscopy characterizations. Photoluminescence effects generally originate from the presence of defects or inhomogeneities of such size as to generate energy quantization. In both cases, electrons in the material, excited by the Raman laser beam, occupy energy levels intermediate to the energy gap and subsequently decay emitting photons that result in the formation of very intense bands in the Raman spectrum, called photoluminescence bands. This phenomenon was most pronounced in SiN samples with higher silicon overstoichiometry, which was intentional by company recipe and confirmed by XRD analysis. The silicon overstoichiometry thus led to spontaneous segregation of amorphous silicon into nanoparticles dispersed in the silicon nitride matrix and this phenomenon is almost nonexistent in samples with stoichiometries closer to equilibrium (%At Si/N equal to 0.75). To corroborate the assumptions made from the photoluminescence phenomenon, it was possible to directly observe the nanoparticles by TEM microscopy in some of the characterized samples.

The presence of these nanoparticles is not only interesting from an academic point of view, but could also have an interesting application aspect: one of the major criticalities of passivation layers is their high fragility, and the presence of inhomogeneous agglomerates could lead to an increase in the toughness of the material due to *crack deflection* phenomena, which have been studied for years in the field of composite materials. This effect occurs when the crack sliding is delayed by the presence of areas with a different thermal expansion index from that of the matrix: at the interface between these areas occurs the formation of compressive or tensile stress fields which attract or repel the crack tip, forcing it to deflect its path and thus increasing the energy required to slide (hence the toughness of the material). The phenomenon of *crack deflection* is generally observed in composite materials in which the inhomogeneity has a significant size, comparable to or larger than that of the crack tip. In the case of "Silicon Rich" silicon nitride (the sample with high silicon overstoichiometry), the nanoparticles observed are too small in size to make an effective contribution to the toughness of the material, and for this reason my project has now focused on finding deposition methods that can lead to the formation of larger amorphous silicon agglomerates.

Obtaining a material suitable for the role of a passivation layer that at the same time exhibits high toughness would be a great step forward in the semiconductor manufacturing industry and could solve several crack failure issues that usually form large blocking point in the development of new devices.

2:30 PM CH02.09.03

Bypassing The Energy Gap Law in Organic Semiconductors [Pratyush Ghosh](#), Richard Friend and Akshay Rao; University of Cambridge, United Kingdom

Strong nonradiative recombination mediated through exciton-phonon coupling has been a major limitation for efficient emission in organic semiconductors. This effect is far more pronounced for low energy-gap materials as predicted by the energy-gap law. High-frequency quantum modes (skeletal C-C, C=C stretching vibrations) are the major channels of non-radiative recombination.

In recent years, spin-radical doublet emitters have emerged as the highest efficiency deep red/nir OLEDs. We are exploring the vibrational coupling of the photoexcited states of these materials by tracking vibrational coherences generated by impulsive photo-excitation with an ultrashort laser pulse. This experiment is known to be impulsive vibrational spectroscopy (IVS) and our method shows the application of this technique to probe exciton-phonon coupling in semiconductors. For the CT-type doublet emitters and certain TADF, we find the absence of any coupling to high-frequency vibrational modes, which is conventionally considered unavoidable in organics. This is potential to provide a real clue behind the high photoluminescence yield of these materials. We also revealed that the extent of the high-frequency vibrational coupling is related to the nature of the delocalization of the electronic state.

With a joint contribution of IVS supported with first-principle calculations, our work suggests a molecular-level design principle of next-generation organic semiconductors with limited non-radiative loss.

2:45 PM CH02.09.04

AFM-SEM Correlative Microscopy Imaging for TEM Grid Mounted Samples Stefano Spagna¹, Kerim Arat¹, Will Neils¹, Christian H. Schwalb², Hajo Ferichs², Sebastian Seibert², Lukas Stuhn² and Marion Wolff²; ¹Quantum Design Inc., United States; ²Quantum Design Microscopy GmbH, Germany

Microscopists utilizing Transmission Electron Microscopy (TEM) and TEM based Energy Electron Loss Spectroscopy (EELS) in their studies, frequently require the characterization of physical parameters such as heights and cross-sectional shapes of the examined sample¹. Because of the typical sub-five nanometer thickness of membranes in TEM grids, Atomic Force Microscopy (AFM) measurements of grid mounted samples are presently challenging and time consuming. In this paper, we present the first truly integrated AFM and Scanning Electron Microscope (SEM) correlative workstation², which allows imaging of samples directly on a TEM grid, utilizing these two techniques. The highly integrated and easy-to-use AFM-SEM microscopy workstation opens unprecedented measurement capabilities at the nanoscale in challenging geometries. AFM-SEM imaging of TEM grid mounted samples simplifies measurement workflows to yield a higher rate of data output. In addition to topography measurement, the platform allows easy expansion of capabilities, such as elemental analysis via Energy Dispersive X-ray Spectroscopy (EDS). The rich set of AFM modes (Contact, Tapping, Off-resonance, Conductive, Magnetic, and Electrostatic) allows the extraction of various physical properties from the sample.

1 V. Reiseckr et al., "Spectral Tuning of Plasmonic Activity in 3D Nanostructures via Highly-Precision Nano-Printing", Adv. Funct. Mater. 2023, 2310110.

2 A. Alipour et al. "A highly integrated AFM-SEM Correlative Analysis Platform," Microscopy today, Vol. 31, Issue 6, Nov. 2023, 23-27.

SYMPOSIUM CH03

In Situ Characterization Methods for Nuclear Materials Applications

April 23 - April 26, 2024

Symposium Organizers

Aurelie Gentils, Universite Paris-Saclay

Mercedes Hernandez Mayoral, CIEMAT

Djamel Kaoumi, North Carolina State University

Ryan Schoell, Sandia National Laboratories

* Invited Paper

+ JMR Distinguished Invited Speaker

^ MRS Communications Early Career Distinguished Presenter

SESSION CH03.01: Equipment and *In Situ* Platforms for Characterization of Nuclear Materials I

Session Chairs: Aurelie Gentils, Mercedes Hernandez Mayoral and Djamel Kaoumi

Tuesday Morning, April 23, 2024

Room 441, Level 4, Summit

10:30 AM *CH03.01.01

***In Situ* Characterization Possibilities at The Mosaic Platform - JANNuS-Orsay Present and Future** Stephanie Jublot-Leclerc, Frederico Garrido and Aurelie Gentils; Universite Paris-Saclay, CNRS/IN2P3, IJCLab, France

Mosaic is the new name of the platform involving the ion accelerators and the tools of chemical and structural characterization of materials located at IJCLab [1]. This includes the JANNuS-Orsay experimental hall, which is in particular known from the community of nuclear materials for the diversity of ion beams that can be produced, as well as the possibilities of *in situ* characterization of the microstructural evolution of ion implanted or irradiated materials. *In situ* Transmission Electron Microscopy (TEM) with one or two ion beams can be performed in a large range of temperatures for studies at the nanometric scale. The damage induced in a single crystal can also be studied through *in situ* Rutherford Backscattered Spectrometry in Channelling

geometry (RBS-C) experiments thanks to the coupling of two ion accelerators. The possibilities, and some limitations, of these two *in situ* characterization methods currently available at Mosaic will be developed through a few examples of experiments performed on materials of interest for nuclear applications. The Mosaic platform is also in the process of completing its range of *in situ* tools for the characterization of irradiated materials with the acquisition of an X-ray diffractometer that will be modified for *in situ* measurements, and that will be available at the beginning of 2026. Examples of future possible experiments will be given along with the characteristics of this X-ray diffractometer.

The MOSAIC technical staff, in particular C. Bachelet, C. Baumier, P. Benoit-Lamaitrie, J. Bourçois, L. Delbecq, S. Hervé, C. Oriol, F. Pallier, and S. Picard, are gratefully acknowledged for their unfailing assistance during *in situ* experiments.

[1] <https://mosaic.ijclab.in2p3.fr>

11:00 AM *CH03.01.02

Developing a Comprehensive *In-Situ* Irradiation Testing Facility at Tennessee Ion Beam Materials Laboratory [Khalid Hattar](#) and Miguel Crespillo; University of Tennessee, United States

Validating and refining simulation of reactor materials evolution for either next generation fission or fusion energy systems, as well as models to extend the lifetime of current reactor fleet would benefit from controlled experiments in coupled extreme environments. This presentation will highlight the expansion of Tennessee Ion Beam Materials Laboratory (TIBML) from a world-class Ion Beam Analysis (IBA) facility based on a 3 MV Tandem Accelerator to a diverse facility designed to understand materials and device evolution in coupled extreme environments. To expand the irradiation environment, the facility will be adding a 300 keV NEC implanter, 20 kV and 5 kV Nonsequitur ion sources, a 30 kV Kimball Physics electron gun, and a Nd:YAG laser from Quantum-Ray with output energies up to 1 J at 1064 nm. The facility is already capable of performing ion irradiation and implantation experiments at temperatures ranging from 30 to 1473 K. In addition, the TIBML facility is developing capabilities to perform in-situ irradiation during photoluminescence, cathodoluminescence, ion beam induced luminescence, Raman, acoustic emission, IBA, nanomechanical testing, and Scanning Transmission Electron Microscopy (STEM). The latter will be done utilizing a highly modified JEOL 2100+ that was installed in October of 2023. The high tilt polepiece, additional electron beam condenser lens, and LaB₆ filament were selected to optimize the characterization of radiation damage. In addition, the STEM was coupled with Nanomegas Automated Crystallographic Orientation Mapping (ACOM) and Theia scientific edge computing systems for machine learning to characterize the impact of radiation damage on phase, orientation, and grain boundary evolution, as well as the size distribution of internal matrix radiation damage, respectively. This presentation will highlight the current status of the TIBML facility development and the initial results of the coupled environment. Finally, this presentation will discuss the potential future opportunities to explore increasingly complex coupled environments in a controlled manner.

11:30 AM CH03.01.03

Deployment and In-Reactor Testing of an Instrument for Real-Time Monitoring Thermal Conductivity Evolution of Nuclear Fuels [Zilong Hua](#)¹, Caleb Picklesimer¹, Austin Fleming¹, David Hurley¹, Weiyeu Zhou², Michael P. Short² and David Carpenter²; ¹Idaho National Laboratory, United States; ²Massachusetts Institute of Technology, United States

Thermal conductivity of nuclear fuels directly ties to the reactor safety and efficiency. Because of the microstructure defects generated and evolved in the extreme reactor environment, thermal conductivity of nuclear fuels reduces significantly during the reactor operation. Currently the experimental efforts on understanding such effects are primarily from the post-irradiation-examination (PIE) testing. However, an important type of phonon scatters, point defects, anneal at high temperature after the reactor shutdown and before PIE can be performed. In order to fill this technical gap, we developed an instrument that can perform real-time thermal conductivity measurements in reactor. Here we presented the latest testing results of this instrument in Massachusetts Institute of Technology Research Reactor (MITR). The final objective is to provide the routine measurement capability of thermal conductivity of nuclear fuels and materials in reactor. It will make better understandings of the scattering mechanisms between defects and thermal carriers possible, and help predict the fuel performances in reactor.

SESSION CH03.02: Equipment and *In Situ* Platforms for Characterization of Nuclear Materials II

Session Chairs: Aurelie Gentils, Mercedes Hernandez Mayoral and Djamel Kaoumi

Tuesday Afternoon, April 23, 2024

Room 441, Level 4, Summit

1:30 PM *CH03.02.01

An *In-Situ* Platform for Studying Metal Films under Simultaneous Extreme Conditions in The SEM [Benjamin K. Derby](#)¹, Eric Lang², Trevor Clark², Ryan Schoell², Jon Baldwin¹, Darrick Williams¹, Michael McBride¹, Khalid Hattar² and Nan Li¹; ¹Los Alamos National Laboratory, United States; ²Sandia National Laboratories, United States

We report on a novel technique for the in-situ characterization of a sample exposed to ion irradiation in a corrosive medium. A sample chamber has been built that can expose a metal film to a corrosive liquid environment and placed into the environmental scanning electron microscope (SEM) in line with the ion beam accelerator located at the Center for Integrated Nanotechnologies' (CINT) Ion Beam Laboratory (IBL) at Sandia National Laboratory. In this work, we expose an epitaxial Fe thin film grown on MgO to 6 MeV Fe ions while the sample surface is exposed to pure H₂O, 0.1M NaCl, and 0.1M B₄Na₂O₇ solutions. SEM imaging and post-mortem XEDS captured the complex oxide development on the surface over time. This experiment elucidates how the ion beam affected the complex oxide growth in the corrosive media, and how the surface oxide impacts further corrosion processes. This understanding will directly inform the development of new materials required for future nuclear energy sources.

2:00 PM CH03.02.02

Towards Measuring Hydrogen Dynamics in Yttrium Hydride Moderators [James Torres](#)^{1,2}, Alexander Long², Dale T. Carver², Sven C. Vogel², Aditya Shivprasad², Tyler Smith², Caitlin Kohnert², Erik Luther² and Holly Trelue²; ¹Oak Ridge National Laboratory, United States; ²Los Alamos National Laboratory, United States

A compact, nuclear microreactor that utilizes low-enriched uranium fuel is a promising solution to meet US demands in remote and decentralized energy grids. Yttrium hydride (YH) is the candidate moderator material for the microreactor design, chosen based on its superior retention of hydrogen at high temperatures. Hydrogen diffusion properties in YH are highly sought after for computer model validation and reactor prototyping. To meet design

objectives, the so-called compact dual-zone furnace was developed at the Los Alamos Neutron Science Center (LANSCE) with the goal of characterizing hydrogen diffusion in YH samples as a function of applied temperature gradients. Herein, we share our recent progress in technique and hardware developments and include initial results from recent concentration- and temperature-gradient measurements at LANSCE.[i]
[i] LA-UR-22-22241

2:15 PM *CH03.02.03

Characterization of The Solid Electrolyte Interphase with Cryogenic Ion and Electron Microscopy Hyeongjun Koh, Eric Detsi and [Eric A. Stach](#); University of Pennsylvania, United States

Characterizing the nanoscale structure and chemistry of energy storage materials is critical due to their significant impact on battery performance. However, conventional sample preparation methods required for high-resolution imaging often fundamentally alter reactive battery components. In this work, the authors employ cryogenic focused ion beam milling (FIB) in a plasma-focused ion beam/scanning electron microscope system to prepare sensitive lithium metal specimens, allowing them to assess potential ion beam damage. Cryogenic transmission electron microscopy reveals that while the lithium itself is not damaged during cryo-FIB milling, lithium oxide shells form around the sample in the instrument chamber, evidenced by diffraction data from thin lamellae prepared at two different thicknesses. Cryogenic electron energy loss spectroscopy further confirms the oxidation of lithium during sample preparation. Consulting the Ellingham diagram indicates that lithium can react with trace oxygen gas in the FIB/SEM chamber at cryogenic temperatures; notably, liquid oxygen exposure does not contribute to lithium oxidation here. This approach allowed the examination of Li metal batteries with vitrified liquid electrolytes and facilitated the discovery of an elusive solid-electrolyte interphase (SEI) component, lithium fluoride. This has not been observed when using conventional sample preparation techniques involving rinsing. Furthermore, diffraction data reveals the presence of short-range order at different regions in the SEI structures, presumably influencing and controlling lithium metal growth. Overall, these results highlight the valuable role cryogenic lift-out and cryogenic scanning transmission electron microscopy can play in enabling nano- to atomic-scale characterization of energy storage devices containing reactive materials or solid-liquid interfaces.

2:45 PM BREAK

SESSION CH03.03: *In Situ* Irradiation and TEM Characterization I
Session Chairs: Aurelie Gentils, Mercedes Hernandez Mayoral and Djamel Kaoumi
Tuesday Afternoon, April 23, 2024
Room 441, Level 4, Summit

3:15 PM *CH03.03.01

Contribution of Raman Spectroscopy to The Understanding of Defect Formation Mechanisms [Gaelle Gutierrez](#), Arthur Georgesco, Claire Onofri-Marroncle and Dominique Gosset; CEA, France

Ion accelerators have been used for decades to study radiation damage in nuclear materials, simulating their behavior in reactors. The diversity of irradiation conditions (ions, energy, fluence, temperature, etc.) is a major advantage of ion beams. This allows for systematic studies aimed at better understanding defect formation mechanisms and the resulting microstructural evolution. Additionally, the very short irradiation times and the handling of non-radioactive samples significantly reduce the cost and duration of experiments compared to reactor irradiations. The coupling of multiple ion beams, the use of heated/cooled sample holders, and the implementation of in situ characterization open the way for real-time observation of microstructure evolution under various extreme radiation conditions. Among these techniques, Raman spectroscopy provides a quick and non-destructive means to monitor vibrational mode evolution. Under irradiation, structural bands evolve, indicating the level of stress and the local structural disorder. Some bands may also appear, providing information about the level of damage and the type of defects formed.

The JANNuS Saclay platform is equipped with a Raman spectrometer installed in the triple-beam irradiation chamber [1]. This allows for in situ monitoring of vibrational modes when atomic displacements and/or ionizations and electronic excitations are generated within the structure. Studies have thus highlighted the use of Raman spectroscopy in characterizing amorphization mechanisms or phase changes occurring under irradiation [2-4]. In non-amorphizable systems, in situ measurements provide insights into damage kinetics related to the formation of point defects [5].

This paper will focus on several examples illustrating the use of ion beams coupled with Raman analyses to investigate the radiation resistance of current and future nuclear ceramic materials.

[1] S. Miro et al., J. Raman Spectrosc. 481 (2015) 45.

[2] C. Cizak et al., JNM 485 (2017) 392.

[3] A. Debelle et al., JAP 132 (2022) 085905.

[4] D. Gosset et al., JNM 476 (2016) 198.

[5] G. Gutierrez et al., J. Eur. Cer. Soc 42 (2022) 6633.

3:45 PM CH03.03.02

Uncovering Grain Boundary Metastability as a Response to Radiation in FCC and BCC Single Phase Compositionally Complex Alloys [Anne Barnett](#), Emily Hopkins, Mitra L. Taheri and Michael Falk; Johns Hopkins University, United States

Compositionally complex alloys (CCAs) are promising for the future materials of extreme radiation environments, but nuances in unique defect formation and evolution properties have yet to be thoroughly understood. In comparison to their dilute and pure counterparts, both fcc and bcc complex alloys retain local chemical order which increases the radiation tolerance due to a convoluted matrix defect bias. This bias profoundly influences grain boundary (GB) metastability under irradiation conditions, resulting in an increase in radiation tolerance with alloy complexity. A combined molecular dynamics and experimental in-situ study is preformed to demonstrate GB metastability during point defect bombardment, highlighting the fundamental differences between fcc and bcc alloys, in addition to environments with and without local chemical order.

4:00 PM CH03.03.03

Clarifying Phase Instabilities Induced by Irradiation in a FCC-Based FeNiCrMn HEA through *In-Situ* Irradiation [Antoine Dartois](#)¹, Maylise Natar¹, Brigitte Décamps², Anna Fraczkiewicz³ and Estelle Meslin¹; ¹Université Paris-Saclay, CEA, France; ²Université Paris-Saclay, France; ³MINES St-Etienne, France

Recent studies have highlighted the promising behavior of High Entropy Alloys (HEAs) under irradiation, exhibiting improved swelling resistance [1] and

reduced radiation-induced segregation (RIS) [2]. For evident safety concern, they need to maintain high single-phase stability to ensure stable mechanical properties under operating conditions.

In this context, our study focuses on the quaternary Fe₃₇Ni₃₄Cr₁₆Mn₁₃. Before irradiation, this high-purity alloy, annealed at 1473 K for 4 hours, is a single FCC phase. However, after heavy-ion irradiation within the JANNuS Saclay facility at 823 K up to 2 dpa, phase instability was detected by means of CTEM (Conventional transmission electron microscopy) and STEM/EDX (Scanning TEM/Energy dispersive X-rays) within a double-corrected Jeol Neo-ARM TEM.

It is well known that irradiation generates point defects – vacancies and self-interstitials – that subsequently agglomerate into dislocation loops, voids or precipitates [3]. Besides, net fluxes of point defects toward sinks lead to RIS potentially leading to radiation-induced precipitation (RIP) [4].

In the current study, phase instability is characterized by the precipitation of nanometer-sized Cr-Mn enriched precipitates. These intragranular precipitates have a spherical shape with an approximate diameter of 10 nm. Their crystallographic structure needs to be examined thoroughly. Considering previous analyses on similar alloys [5], a BCC phase could be expected. The matter balance between self-interstitial atoms (SIAs) and vacancies respectively stored into dislocation loops and precipitates tends to confirm the less dense BCC structure of the precipitates. We hence may expect these precipitates to result from a RIP mechanism explained by the elimination of irradiation-generated vacancies accommodating the volume mismatch between less dense precipitates and the matrix [3].

This phase instability is also correlated with a microstructural evolution. Indeed, both faulted and perfect dislocation loops are formed. According to atom probe tomography (APT) and STEM/EDX analysis, RIS occurs at these radiation-induced defects. Indeed, a strong Ni enrichment and Fe, Mn and Cr depletions, have been detected. An inverse Kirkendall model of atomic fluxes, mediated by vacancies and fitted on tracer diffusion coefficients of the well-known FeCoCrMnNi Cantor alloy, corroborates the identified RIS trend. We highlight a reduced Cr depletion, compared to conventional austenitic steels [6], potentially reducing the irradiation-assisted stress corrosion cracking (IASCC) phenomena.

In order to elucidate the precipitation mechanisms, microstructures exposed to several radiation doses have been compared. First, samples have been irradiated from 0.2 dpa to 2 dpa. Secondly, an analysis of the microstructure at increasing thicknesses has enabled us to compare various stages of irradiation progress. Indeed, point defects elimination on surfaces is stronger in thinner areas, where effective damage is therefore reduced, whereas this phenomenon is negligible in thicker areas, experiencing a stronger effective damage. On-zone axis STEM imaging shows the formation of a dislocation network, resulting from the interaction of perfect loops as well as a decrease of the density of both Frank loops and precipitates with increasing depth.

To further investigate the precipitation mechanisms, in-situ irradiations are essential. These will be conducted inside a TEM in November 2023 within the JANNuS-Orsay facilities, to track both the microstructural evolution as well as the precipitation using electron diffraction spots signal produced by the formation of Cr-Mn precipitates.

References

- [1] Jin, et al., Scripta Mat (2016)
- [2] Lu, et al., Acta Mat (2017)
- [3] Nastar, et al., Com Mat (2021)
- [4] Belkacemi, et al., Acta Mat (2021)
- [5] Parkin, et al., JNM (2022)
- [6] Kumar, et al., Acta Mat. (2016)

4:15 PM CH03.03.04

Effect of Al Addition to The Multi-Principal Elemental CrFeMnNi Alloy System in Terms of The Resulting Microstructure and Radiation Resistance Saikumaran Ayyappan^{1,1}, Kara Krogh^{1,1}, Geoffrey Beausoleil² and Djamel Kaoumi^{1,1}; ¹North Carolina State University, United States; ²Idaho National Laboratory, United States

In recent times, High-Entropy Alloys (HEAs) or Multi Principal Elemental Alloys (MPEAs) have been attracting much attention as new structural materials for nuclear reactor in-core applications due to their structural stability and excellent mechanical properties. However, their microstructural behaviour under irradiation still requires special attention. Particularly, the impact of specific chemical elements on the irradiation response of the alloys still needs to be evidenced and is at the core of this NSF funded project. The current work compares the radiation behaviour of CrFeMnNi, Al_{0.3}CrFeMnNi and Al_{0.8}CrFeMnNi alloys. The alloys, which were prepared through Plasma Spark Sintering (SPS), were irradiated in-situ in a Transmission Electron Microscope (TEM) using 1 MeV Kr⁺ ions up to 10 dpa at room temperature (RT) and at 300 °C. Since the starting microstructure depends not only on the composition but also on the way of processing, thorough pre-irradiation characterization of all the three alloys was carried out using X-Ray Diffraction (XRD) and TEM which showed the formation of (BCC+FCC) phases in major proportion. Addition of Al resulted in an increase in the proportion of BCC phase along with the formation of NiAl based ordered phase. At RT, with increased irradiation dose, the phases with more uniformly distributed elemental composition showed the dynamic formation and annihilation of irradiation induced defects. However, the Cr-segregated phase in the (Al_{0.3}CrFeMnNi) alloy showed amorphization behaviour with increasing irradiation dose. At RT, the alloys did not show the formation of voids or Radiation induced Segregation (RIS). However, at 300 °C, the alloys showed the formation of voids at doses around ~5 dpa. Also, Ni segregation at the void/matrix interfaces has been observed in the Al_{0.3}CrFeMnNi alloy at 300 °C. Overall, the void formation was observed to depend on the local chemistry and temperature of irradiation. Additionally, irradiation at 300 °C also resulted in Radiation Induced Precipitation (RIP) in these alloys, the existence of which were confirmed through extensive post-irradiation TEM diffraction analysis, which showed low intensity crystalline spots and streaks around the major diffraction spots. The Cr-rich phase in Al_{0.3}CrFeMnNi alloy showed the formation of nano-crystalline features. The Ni-rich phase showed the formation and Nano-structuring of irradiation-induced defects. The in-situ TEM experiments allowed to clearly evidence how variations in local chemistry and microstructural features in these MPEAs affect the local response to irradiation (at the nm/micron level).

8:45 AM *CH03.04.01

Dislocation Loop Evolution in Ni-Based fcc Model Alloys by *In-Situ* Self-Ion Irradiation at High Temperatures [Marie Loyer-Prost](#)¹, Kan Ma^{1,2}, Brigitte Décamps³, Liangzhao Huang¹, Maylise Nastar¹, M.A. Belghoul¹, Anna Fraczkiewicz⁴, Robin Schäublin⁵, Philippe Vermaut^{6,7} and Frédéric Prima⁷; ¹Université Paris-Saclay, CEA, France; ²University of Birmingham, United Kingdom; ³CNRS, Université Paris-Saclay, France; ⁴Ecole Nationale Supérieure des Mines de Saint Etienne, France; ⁵ETH Zürich, Switzerland; ⁶Sorbonne Université, France; ⁷ChimieParisTech, PSL Research University, CNRS, France

Austenitic Stainless Steels (ASSs) are foreseen as cladding material for next generation reactors even though their swelling under irradiation will limit the fuel burnup. Solute elements, such as titanium and carbon, efficiently reduce this swelling but the mechanism is still ambiguous.

Here we focus on the effect of a progressive addition of titanium on the microstructure evolution of nickel at small irradiation dose and on the loop interaction during irradiation. Nickel is considered as a model alloy for ASSs (same crystallographic structure). Pure Ni and nickel alloyed with various percentages of titanium (x ranging from 0.4% to 1.2% by mass), are *in-situ* irradiated at 450°C and 510°C within a Transmission Electron Microscope using the JANNuS-Orsay facility.

The *in-situ* microstructural evolution and dislocation loop characteristics are finely analyzed in function of specimen composition and doses. We reveal a strong impact of micro-alloying on microstructure: loop nature, growth rate, formation thickness, density, Burgers vector and mobility. A direct correlation of Frank loop morphology and nature is observed. Finally, a temperature-dependent critical Ti content for Frank loop nature is highlighted and discussed.

9:15 AM CH03.04.02

Investigation of Grain Growth in Nanocrystalline Oxide Thin Films during Irradiation and Heating using *In-Situ* TEM [Dmitrii Kretov](#)¹, Tiffany Kaspar², Benjamin K. Derby³ and Djamel Kaoumi¹; ¹North Carolina State University, United States; ²Pacific Northwest National Laboratory, United States; ³Los Alamos National Laboratory, United States

Grain growth, which occurs at elevated temperatures and under irradiation is manifested by an increase in the average grain size, a decrease in the number of grains, and a decrease in grain boundary total area. Nanocrystalline metals having very small sizes and high GB densities are of interest to the nuclear materials community not only for their improved mechanical properties but also for their radiation resistance, since grain boundaries are effective sinks for radiation-induced defects, ultimately impacting the radiation tolerance of nanocrystalline materials against net defect accumulation. However, even if nanocrystalline metals present increased radiation tolerance at the nanoscale, irradiation-induced grain growth is responsible for grain enlargement and annihilation of these benefits. While the literature shows several studies on this particular topic of grain growth in nanocrystalline metals, very little focus was put on grain growth in nanocrystalline oxides, especially under irradiation. The scarce available literature focuses on fuel oxides. In this work, grain growth kinetics was studied in Fe₂O₃, Fe₃O₄, Cr₂O₃ which are oxides commonly forming on components in nuclear reactor such as the ones made of steel. Thin films with nanocrystalline grain size were grown by Pulse Laser Deposition or Sputtering Deposition and subject to thermal annealing *in situ* in a Transmission Electron Microscope to follow the grain-growth. Samples were also irradiated *in situ* in the TEM at temperatures from 50 K to 773 K using 1 MeV Kr²⁺ ions to 10 dpa to study grain-growth under irradiation. Grain size was measured as a function of time for the thermal grain growth and in terms of irradiation dose (i.e. dpa) for the irradiated samples. The kinetics of grain growth was then discussed in the light of the literature and how it compares to the thermal spike model developed for metals.

9:30 AM CH03.04.03

Unveiling The Microstructural Evolution in Irradiated Zirconium Alloys Through *In-Situ* Transmission Electron Microscopy [Zhongwen Yao](#); Queen's University, Canada

Understanding the impact of irradiation on the microstructure of zirconium alloys is critical for ensuring the safety and reliability of nuclear reactors. In this presentation, we applied *in-situ* transmission electron microscopy (TEM) as a powerful tool to unravel the dynamic evolution of zirconium alloy microstructures during irradiation or after irradiation.

Through real-time TEM/STEM imaging, we explore the intricate processes taking place within zirconium alloys, such as Excel alloy, Zr-2.5Nb and Zircaloy as they are subjected to ion irradiation. We observe and analyze the complicated changes in microstructure, including a-type and c-type dislocation formation, defect accumulation, and phase transformations. These microstructural changes have a direct bearing on the material's mechanical properties and dimensional stability, making this research crucial for the nuclear industry.

This presentation highlights the invaluable contribution of *in-situ* TEM techniques in providing real-time, atomic-scale observations of zirconium alloy behavior during irradiation, paving the way for enhanced material design and reactor safety.

9:45 AM BREAK

SESSION CH03.05: *In Situ* Irradiation Characterization Methods
Session Chairs: Aurelie Gentils, Mercedes Hernandez Mayoral and Djamel Kaoumi
Wednesday Afternoon, April 24, 2024
Room 441, Level 4, Summit

1:45 PM *CH03.05.01

Real Time Monitoring of Defect Evolution and Relaxation by *In-Situ* Positron Annihilation Spectroscopy [Farida Selim](#)¹, Adric Jones², Thaighang Chung², Matthew Chancey³, Riley Ferguson³, Peter Hosemann⁴, Yongqiang Wang³ and Blas P. Uberuaga³; ¹Arizona State University, United States; ²Bowling Green State University, United States; ³Los Alamos National Laboratory, United States; ⁴UC Berkeley, United States

In-situ measurements during irradiation are critical to monitor material response to irradiation in real time; several *in-situ* techniques with remarkable capabilities have been developed to address that and examine material structure, properties, and performance under extreme radiation environments. *In-situ* TEM has been particularly powerful in monitoring the microstructural changes and growth of cavities in real time during irradiation. However, revealing the mechanisms governing early formation of defects and their evolution in extreme environments require measuring defects on all length scale from atomic- to meso-scale. Positron annihilation spectroscopy (PAS) is uniquely sensitive to atomic scale defects revealing their density and structure even in the very early stages of damage and has been shown to be an effective tool to probe vacancies and stresses in nuclear and structural materials [1,2].

Here we report the first *in-situ* PAS (iPAS) measurements during high energy ion irradiation. The measurements reveal that vacancies are formed and their number increases during collision cascades without change in structure or clustering. However, vacancies are shown to coarsen, and their structure substantially change during relaxation after ceasing irradiation. The trend is shown to dominate in the low irradiation regime and the defect density

increases linearly with irradiation time up to 0.1 dpa. In higher regime above 1 dpa, vacancies are formed and coarsen during collision cascades. Further, iPAS during annealing reveals the various recovery stages of induced radiation and the defect type involved in each stage. Lastly, I will discuss how iPAS may shed the light on the mechanism behind some interesting phenomena such as radiation induced vacancy injection in multi-phase materials that we recently observed in Fe / Fe₂O₃ bilayers.

This work was funded as part of FUTURE (Fundamental Understanding of Transport Under Reactor Extremes), an Energy Frontier Research Center funded by the U.S. Department of Energy, Office of Science, Basic Energy Sciences.

[1] Selim, F. A. "Positron annihilation spectroscopy of defects in nuclear and irradiated materials-a review." *Materials Characterization* 174 (2021): 110952.

[2] Selim, F. A., D. P. Wells, J. F. Harmon, J. Kwofie, G. Erikson, and T. Roney. "New positron annihilation spectroscopy techniques for thick materials." *Radiation Physics and Chemistry* 68, no. 3-4 (2003): 427-430.

2:15 PM CH03.05.02

***In situ* Performance of Non-Volatile Memory under Mixed Radiation Environment** [Chaitanya Sharma](#) and Juan Nino; University of Florida, United States

Nonvolatile memory technologies have paved the way for in-memory computing, eliminating the constant need to move data between storage and processing units. This reduces the von Neumann bottleneck and can significantly boost a system's effective floating operations per second (FLOPs). However, their performance evolution under irradiation from cosmic rays, solar storms, neutrons, and other secondary sources has not been extensively studied. To explore device degradation, we developed a testing apparatus at the University of Florida training reactor (UFTR) to perform *in situ* electronic measurements under varying gamma and neutron radiation profiles. The 6" diameter cylindrical setup fits inside one of the reactor beam ports and includes a Peltier thermal controller coupled to a 4-terminal electrical microprobe with variable radiation shielding. To delineate different radiation beam environments, specifically gamma rays, thermal, epithermal, and fast neutrons, shielding materials such as borated polyethylene, standard polyethylene, and lead are used. Here, we demonstrate the platform's effectiveness by examining self-directed channel (SDC) memristors, ferroelectric capacitors (FeCAPs), and resistive random-access memory (ReRAM) devices both in volatile and non-volatile configurations (i.e., 1T-1R and 1R). The experiments were conducted within the temperature range of -30° C to 120° C across a range of reactor power levels from 1W to 10kW with a total flux of 2.035 x 10⁸ particles/cm² at 100kW. We will further discuss radiation effects pertinent to various memory architectures, elaborating on device failure induced under radiation and total ionizing dose.

2:30 PM BREAK

3:30 PM *CH03.05.04

Beam-On Effects during Irradiation of Nuclear Materials [Michael P. Short](#); Massachusetts Institute of Technology, United States

In situ characterization methods for nuclear materials performance hold enormous promise for faster discovery of nuclear materials science, radiation effects, and down-selection of optimal alloys for nuclear power applications. Advancements in combining traditional irradiations and post-irradiation examination with new, rapid analysis tools promises, and will be shown in this talk, to hasten data throughput by up to 1000x compared to purely traditional methods. Particular emphasis on building robust inference models, whereby properties of ultimate interest are tightly correlated to those which are more readily measured by *in situ* techniques, will be made via illustrative examples of nuclear materials discovery, down-selection, and optimization. We specifically focus on utilizing *in situ* ion irradiation transient grating spectroscopy (I3TGS) for prediction of high-temperature superconductor performance during irradiation, rapidly exploring new ternary alloy compositions for fusion structural and functional materials, and sorting materials by their resistance to major degradation modes such as void swelling. Finally, we will present a call to collaboration and requests for input from the community, on how to best build robust and easy-to-use TGS systems to help others establish similar *in situ* capabilities of their own.

SESSION CH03.06: *In Situ* Electrochemical Methods

Session Chairs: Aurelie Gentils, Mercedes Hernandez Mayoral and Djamel Kaoumi

Thursday Morning, April 25, 2024

Room 441, Level 4, Summit

8:30 AM *CH03.06.01

Understanding Oxidation Mechanism using *In Situ* Analytical Transmission Electron Microscopy [Eric Prestat](#)¹, [Giacomo Bertali](#)², [Duc Nguyen-Manh](#)¹, [Joven Lim](#)¹, [Anicha Reuban](#)³, [Andrey Litnovsky](#)³ and [Grace Burke](#)⁴; ¹UK Atomic Energy Authority, United Kingdom; ²University of Manchester, United Kingdom; ³Forschungszentrum Juelich, Germany; ⁴Idaho National Laboratory, United States

Environment-sensitive behaviour of materials encompasses a broad range of degradation phenomena in metals and alloys. The interaction of metallic materials with the environment is of fundamental importance in understanding a material's performance in "real world" applications. Of particular significance is the effect of liquid and/or gaseous environments on the material of interest. The ability to visualize the localised changes associated with oxidation in gaseous environments and dissolution reactions in liquids coupled with qualitative STEM-XED spectrum imaging and analysis is now providing unprecedented opportunities for real-time observations that can lead to improved mechanistic understanding of nanoscale oxidation, and localised dissolution/corrosion.

In this presentation, we will discuss the application of *in situ* gas microscopy to understand the oxidation behaviour of metallic materials using open cell and closed cell system. For the closed system, two 30 nm thick SiN electron transparent membranes are used to contain up to 1 bar atmospheric pressure from the vacuum of the TEM columns. We have applied the Protochips *in situ* platforms to examine gaseous environmental interactions in structural alloys such as Ni-base alloys (Alloy 600) and tungsten. The Protochips Atmosphere system interfaced with an FEI Titan G2 200 kV S/TEM equipped with X-FEG and Super X (4 SDDs) or a JEOL NeoARM 200kV wide gap pole piece cold FEG and Dual-EDS system has been successfully used in a variety of gaseous environments. Open cell experiments were performed on a Hitachi H-9500 TEM operating at 300 kV and fitted with an add-on gas injection system for windowless environmental conditions up to -0.1 Pa at the sample.

Critical to any *in situ* experiment is the preparation of representative electron-transparent samples, so as to provide a valid link with bulk behaviour. Electron-transparent specimens were prepared using the hybrid method [1]. These specimens can then be attached to an Atmosphere heating chip with Pt. A series of examples will be discussed that are related to the detailed study of bulk material behaviour including localised oxidation reactions pertinent to stress corrosion cracking in Ni-base alloys as well as the study of oxidation of tungsten alloys. The successful experiments using the gas reaction cell

system in a variety of H₂-containing environments at elevated temperatures can be further refined to assess variables such as H₂ and O₂ partial pressures, and can also be used to assess localised reactions in 1 bar gas over a range of temperatures of interest and thus provide insight at the nanoscale about diffusion-induced grain boundary migration, internal oxidation, and the role of carbides in preferential oxidation. Similarly, S/TEM imaging and Electron energy loss spectroscopy (EELS) was used for ex situ and in situ study of the oxidation of self-passivating tungsten alloys using. Mapping the elemental distribution of W, Cr, Y at the nanoscale shows that Cr-rich grains undergoes Cr/W phase separation exhibiting characteristics of spinodal decomposition, which is in good agreement with first-principles modelling predictions. Similar Cr/W phase separation was observed at grain boundaries. The in situ (S/TEM) oxidation shows that the Cr-rich grain exhibiting Cr/W phase separation are oxidized first and formed a dense Cr oxide, providing a stable oxide layer. Additionally, in the vicinity of the yttria precipitates present at grain boundaries or grain triple junctions the oxide growth is reduced in the initial stage of oxidation. Inhomogeneity in the layer oxidation could lead to localised failure of the oxide layer, such as delamination of the protective oxide layer.

9:00 AM *CH03.06.02

***In Situ* Sample Thickness Monitoring in Simultaneous Irradiation-Corrosion Experiments** Franziska Schmidt^{1,2}, Matthew Chancey¹, Hyosim Kim¹ and Yongqiang Wang¹; ¹Los Alamos National Laboratory, United States; ²University of California, Berkeley, United States

Irradiation-corrosion experiments have recently become a popular approach to studying the simultaneous effects of both extremes on materials. Each individual experiment requires extensive preparation and yields one sample exposed to one set of conditions (temperature, damage rate, etc.) that can then be analyzed ex situ. In this talk, we will discuss the potential for the in situ monitoring of long-term (hours to tens of hours) irradiation-corrosion experiments with ion beam analysis techniques, such as particle-induced x-ray emission spectroscopy (PIXE) and Rutherford backscatter spectroscopy (RBS). Both can be used to provide information about changes in the average sample thickness while under irradiation, which is tied to corrosion kinetics. We will lay out different options for the interpretation of PIXE data based on signal from the sample alone or a mixture of sample and corrosive medium signals. The different approaches allow the use of these techniques for different combinations of samples and corrosive media, such as water, heavy liquid metals, or molten salts. As an example, we will show recent experimental data for pure Fe under proton-irradiation simultaneously corroded by lead-bismuth eutectic (LBE), a Gen-IV nuclear reactor coolant. The Fe-LBE system provides the unique opportunity to compare the accuracy of the two data interpretation options for PIXE with each other as well as with RBS, all of which provide in situ insight into Fe corrosion under irradiation not attainable from ex situ observations.

9:30 AM *CH03.06.03

Electrochemical Impedance Spectroscopic Study of Oxide Scales on 316L Stainless Steel in Molten FLiNaK Salt Jie Qiu; Xi'an Jiaotong University, China

Molten fluoride salts have been proposed to be excellent candidates as primary reactor coolant and liquid fuel in a Molten Salt Reactor (MSR) due to their advantages of high thermal conductivities, low viscosities, high boiling points and high specific heats, etc. However, the corrosion of structural materials in molten fluoride salts at high temperature is a great challenge that prevents the successful fruition of MSR. In most corrosive environments, materials derive their corrosion resistance by the formation of a protective oxide scales and/or passive films. However, these oxide films are chemically unstable in high temperature molten fluoride salts and cannot provide protection of materials from corrosion. An understanding of in-situ dissolution rate and corrosion mechanism of oxide film in fluoride salt is significantly important for the development of MSR.

In this work, coupons of 316L stainless steel (SS) were pre-oxidized in hot air and then immersed in molten FLiNaK salt at 700 °C for electrochemical experiments. The impedance of oxide films on 316L SS as a function of exposure time were investigated using in-situ electrochemical impedance spectroscopy (EIS). The oxide resistance and capacitance under different exposure time were compared. The results show that the resistance of the oxide film decreases with increasing the exposure time, due to the dissolution of the Fe and Cr elements into the molten FLiNaK salt. After experiments, the structures of the oxide film were characterized and compared.

10:00 AM BREAK

10:30 AM CH03.06.04

Understanding Transient Kinetics under Irradiation with *In Situ* EIS Franziska Schmidt, Cortney Kreller, Yongqiang Wang, James Valdez and Blas P. Uberuaga; Los Alamos National Laboratory, United States

Particle irradiation introduces a large amount of energy into a material, creating a multitude of metastable defect structures. These defects are then responsible for the microstructural evolution of the material, which often comes down to a balance of kinetic processes that determine whether the material will recover or whether larger-scale defect aggregates such as voids and loops will form. Critically, the defects most responsible for this evolution – the fastest moving defects – disappear quickly once the radiation source is removed. Thus, post-mortem examination can only provide indirect evidence of their presence and is unable to characterize neither the nature nor properties of these defects.

To better understand the transient behavior associated with fast moving radiation-induced defects, we have developed an in situ electrochemical impedance spectroscopy system that allows us to measure the conductivity of the material as it is being irradiated. This provides unprecedented insight into the kinetic nature of defects, both as the material approaches a steady-state defect concentration under irradiation and as it recovers once the irradiation source is removed.

We demonstrate this new capability on complex oxides. For example, in yttrium-stabilized zirconia, we find that there is an enhancement of the conductivity of the material during irradiation, leading to an effectively lower activation energy for conduction as the material is being irradiated. However, once the radiation source is turned off, the conductivity quickly recovers to the pre-irradiated value, emphasizing the critical need for in situ diagnostics to probe the properties of these transient defects.

10:45 AM CH03.06.05

Highlighting the Influence of Radiolysis at The Interface between 316L Stainless Steel using *In Situ* Electrochemical Techniques Nicolas Berend^{1,2,3}, Nathalie Moncoffre^{1,3}, Sabrina Marcelin^{4,3,2}, Alexis Eynard^{1,3}, Thierry Dupasquier^{1,3}, Dominique Baux^{5,3} and Bernard Normand^{4,3,2}; ¹Institute of Physics of The Two Infinities of Lyon, France; ²Université Claude Bernard Lyon 1, France; ³CNRS, France; ⁴INSA Lyon/MATEIS, France; ⁵CEMHTI, France

The study of water radiolysis at the solid/solution interface is an experimental challenge. Here, we present two original and complementary setups: the PATRICIA cell (Passivation - Tribology - Irradiation) and the RADEAU cell.

The PATRICIA configuration allows to study the tribocorrosion of a stainless steel under extreme conditions (proton irradiation, submission to radiolysis product). For instance, a proton beam can irradiate the interface formed by the contact between a liquid and a passivable material (such as 316L stainless steel). An alumina pin can induce friction on the sample's surface. Electrochemical techniques enable the *in situ* characterization of the evolution of the

RedOx potentials of the solution, as well as the evolution of the passive film present on the steel surface. Through the PATRICIA cell, we demonstrated that, regardless of the beam's energy, the corrosion potential remains unchanged. This indicates that it is the highly reactive, short-lived radiolysis products that determine the corrosion potential, rather than just long-lived radiolysis products like H₂O₂. During irradiation, the evolution of resistivity profiles within the thickness of the passive film, obtained from electrochemical impedance spectroscopy measurements, shows that the inner Cr₂O₃ layer of the passive film becomes thinner, leading to a reduction in the corrosion resistance of 316L stainless steel. This evolution could be attributed to the radiolysis of water molecules bound within the passive film.

In the RADEAU configuration, a thin layer of water is irradiated in front of a passivable material. The system's evolution is also monitored through *in situ* electrochemical techniques. In this geometry, only the water or the system {water + interface} can be irradiated, which allows for the discrimination of the passive layer's role in the corrosion process of 316L stainless steel.

These two complementary setups enable the *in situ* study of the interface's role in the mechanisms of steel corrosion.

11:00 AM CH03.06.06

Microstructure and Phase Characterization of Carbonation Accelerated Concretes Proposed for Deep Geologic Repositories using Simultaneous Synchrotron X-Ray Computed Microtomography (XCT) and Spatially Resolved Energy Dispersive X-Ray Diffraction (EDX-XRD) Yeu Chen, Anthony J. Girona, Jared Abramson and Gerald Seidler; University of Washington, United States

Long-term storage and eventual disposal of spent nuclear fuel (SNF) is a challenging materials problem, with deep geologic repositories (DGR) widely considered the best solution. The general design of DGRs is widely agreed upon, requiring an engineered barrier system (EBS) and disposal site-specific local geology to contain SNF on geologic timescales of 100,000 – 1M years, but specific details are less certain. An understanding of the stability of the materials used in the EBS in geologic conditions is crucial in a once-through nuclear cycle, such as in the United States, where SNF disposal needs are greatest. Cement and cementitious barriers are a key component in EBS systems and serve as a barrier between steel casques that contain the SNF and the local geologic environment its embedded in, creating separation of the waste from the biosphere by trapping radionuclides that escape the primary containment particularly in the first 10,000 years of storage. There are two key issues in this field of study. First, projecting the stability of cementitious materials over geologic timescales by developing an accelerated aging model that is reliable. Second, characterization techniques of corrosion mechanism in concrete, particularly specific to DGR conditions such as high pressure, high temperature, temperature cycling, radiolysis, chloride ion attack, entrapped gasses (methane, carbon dioxide), and interfacial corrosion between the steel casque and cementitious barrier. This work details a preliminary approach addressing both concerns, an accelerated aging protocol of cements in carbonating conditions and simultaneous synchrotron methods to nondestructively characterize carbonation effects on cement phase and microstructure.

To develop aging techniques, representative cement cylinders were aged in 100% CO₂ atmosphere at room and elevated temperatures for varying durations of time. The pore structure and carbonation front progression were studied using x-ray computed microtomography (XCT) finding a clear delineation between the carbonated and uncarbonated regions. Additionally, spatially resolved energy dispersive x-ray diffraction (EDX-XRD) was used to identify phase changes to the cement's alkaline portlandite buffer, a key component of the cement's barrier capabilities to radionuclides, as it was depleted with the dissolution of CO₂ into the cement's pore solution during the carbonation process. These phase changes showed clear signatures in the EDX-XRD and corroborated the carbonation depth found from the XCT. Both XCT and EDX-XRD were measured at Sector 7-BM at the Advanced Photon Source. The kinetics and near-field chemistry of concrete and cementitious materials has many unanswered questions as it's difficult to model and quantitatively measure, especially under conditions expected in DGRs. This work has shown the ability to study concrete subjected to DGR conditions and measure one of the key aspects in its usefulness as a ESB material.

SESSION CH03.07: *In Situ* Annealing Related Techniques

Session Chairs: Aurelie Gentils, Mercedes Hernandez Mayoral and Djamel Kaoumi

Thursday Afternoon, April 25, 2024

Room 441, Level 4, Summit

1:30 PM *CH03.07.01

Recrystallization Behavior of Laser Powder Bed Fused 316L Stainless Steel by *In-Situ* Annealing Yanling Ge¹, Zaiqing Que¹, Witold Chrominski², Maciej Zielinski², Kimmo Kaunisto¹ and Iwona Jozwik²; ¹VTT Technical Research Centre of Finland, Finland; ²National Center for Nuclear Research, Poland

Laser powder bed fusion (LPBF) addition manufactured (AM) 316L stainless steel (SS) shows superior mechanical and corrosion properties due to its heterogeneous microstructure. The recrystallization behavior of LPBF stainless steel is a key knowledge for application of AM material in nuclear sector. The two unique microstructure features of AM 316L, dislocation cellular structure and nanoscale oxide inclusions, are important controlling factors on recrystallization behavior and annealing structure. The recovery and recrystallization of LPBF 316L SS are analyzed with differential scanning calorimetry (DSC). The evolution of microstructure is studied with in-situ x-ray diffraction (XRD) and in-situ electron backscattered diffraction (EBSD) in scanning electron microscopy (SEM). The detailed dislocation network evolution and nanosized oxides interaction with grain boundaries during annealing are studied with in-situ transmission electron microscopy (TEM).

2:00 PM CH03.07.02

Heterogeneous Grain Boundary Corrosion in Ni-Cr Alloy Exposed to Molten Fluorinated Eutectic Salts under Applied Potential Sean Mills^{1,2}, Ho L. Chan³, Nathan Bieberdorf¹, Minsung Hong¹, Elena Romanovskaia³, Chaitanya Peddetti¹, Laurent Capolungo⁴, Mark Asta¹, John Scully³, Peter Hosemann¹ and Andrew M. Minor^{1,2}; ¹University of California, Berkeley, United States; ²Lawrence Berkeley National Laboratory, United States; ³University of Virginia, United States; ⁴Los Alamos National Laboratory, United States

Structural materials used in nuclear reactor environments are exposed to coupled extremes such as irradiation, high temperature, and corrosion which act synergistically to degrade their performance. Integral features of these processes are that defects produced under irradiation directly limit or accelerate the corrosion rates. Moreover, in molten-salt reactor environments, previous experimental work has shown that Cr dealloying is strongly coupled to the microstructure evolution of these alloys. Connecting corrosion attack with alloy microstructure such as grain boundaries and accumulating point defects is imperative to understanding underlying mechanisms. However, it is challenging to predict how varied alloying elements, salt species, and nanoscale point defects interact with one another to lead to the failure of materials, as the multiscale nature of these reactions is hidden. Until recently, the capabilities to directly measure vacancies, interstitials and black spot damage have been limited to bulk techniques such as positron annihilation spectroscopy or x-ray diffraction measurement of lattice parameters. The recent developments in 4D-STEM with high-speed direct electron detectors and atomic resolution

STEM provide an opportunity for potentially mapping point defect distributions at the nanoscale and their associated strains, both of which have far-reaching implications for detailed analysis of complex irradiation / corrosion damage.

Active corrosion mechanisms are investigated in a model Ni₈₀Cr₂₀ metal alloy exposed to molten LiF-NaF-KF eutectic (FLiNaK) at 600C. When a critical applied potential of 2.1V is reached, this enables both Cr and Ni dissolution and the formation of salt-filled corrosion channels at grain boundaries. For post-corrosion characterization, we implement microscale techniques such as energy dispersive spectroscopy (EDS) and electron backscatter diffraction (EBSD) to uncover variations in morphology and composition that are tied to non-uniform corrosion damage. This grain boundary corrosion mechanism is connected to a pure Ni de-alloyed region that forms within the salt-filled cavity. These findings are supported by phase-field modeling that describes an infiltrating salt-filled corrosion channel between two grains where Ni dissolves preferentially and re-forms on the opposing grain. This is attributed to the redox potential that is modified by the interfacial energies between grains. Building off the conditions that promote grain boundary corrosion and de-alloying, we conduct an in-situ experiment to track local changes in structure, morphology, and transport of species within a pre-fabricated salt-filled corrosion channel. The sample is annealed in the TEM at elevated temperatures (350–900C via MEMS heating + biasing holder) to simulate typical molten salt reactor operating conditions. Further, we perform simultaneous EDX-STEM and 4D-STEM to correlate changes in structure and composition that result from surface diffusion or by bulk lattice diffusion in response to non-uniform corrosion.

This extensive study aims to fundamentally improve the understanding of complex corrosion processes and provide a new pathway for engineering materials designed in future nuclear energy systems. The project is part of FUTURE Energy Frontiers Research Center (EFRC), which aims to study how the coupled extremes of irradiation and corrosion work in concert to modify the evolution of materials by coupling experiments and modeling that target fundamental mechanisms.

2:15 PM CH03.07.03

Complementing *In Situ* Microscopy with Multimodal Synchrotron Experiments in the Characterization of Radiation Damage Jason R. Trelewicz, Cormac Killeen, Yang Zhang, Spencer Thomas and David J. Sprouster; Stony Brook University, United States

The formation of gaseous defects during irradiation due to, e.g., transmutation or ion implantation, involves a transition from defect clustering to the nucleation of bubbles and its biasing to various microstructural sinks such as grain boundaries. In situ microscopy techniques are limited in their ability to resolve the behavior of sub-nanometer helium clusters during the incubation stages of bubble formation while common X-ray techniques such as X-ray diffraction (XRD) provide information specifically pertaining to changes in the lattice parameter in the presence of such defect clusters. In this study, a region of reciprocal space accessible via wide angle X-ray scattering (WAXS) is identified that allows for the direct probing of sub-nanometer helium clusters irresolvable through transmission electron microscopy (TEM) and small angle X-ray scattering (SAXS) and only indirectly quantified by an XRD lattice parameter analysis. Using WAXS in a multimodal characterization campaign with TEM informed SAXS analysis and XRD of irradiated tungsten, our experiments build a more complete picture of the transition from helium defect clustering to the nucleation of bubbles and their subsequent biasing to grain boundaries. Specifically, nanoscale cavity formation is shown to accompany clustering with increasing fluence but with cavities homogeneously distributed between the grain matrix and boundary regions of the microstructure. An increase in temperature shifted the cavity population to a bimodal distribution containing small nanometer intragranular cavities and larger cavities biased to the grain boundaries, which was accompanied by a decrease in the sub-nanometer helium cluster population. Leveraging the defect distributions as a function of fluence and temperature, the mechanisms underpinning these transitions are discussed using insights from molecular dynamics simulations. Results demonstrate the utility of our multimodal approach in probing the incubation stages of cavity formation and its subsequent transition to biased cavity populations, thereby helping to close the analysis gap between nanoscale in situ TEM imaging and atomic-scale XRD measurements.

2:30 PM *CH03.07.04

Bi-Directionally Tuning the Thermal Resistance of Materials and Interfaces with Irradiation-Induced Defects Patrick E. Hopkins; University of Virginia, United States

Materials in radiative environments (e.g., nuclear reactors, spacecraft, research instruments, among others) are subject to unique forms of damage. The microstructural damage results in a change in electron and phonon scattering rates in materials, which typically leads to a reduction in thermal conductivity. For example, in a study focused on silicon wafers irradiated with an array of ions (C²⁺, N²⁺, Al²⁺, Si²⁺, P²⁺, or Ge²⁺), we demonstrate that an increase in ion dose results in a significant reduction in thermal conductivity (up to an order of magnitude reduction) of the silicon within damaged region [1]. These reductions in thermal properties are general predicted based on the displacements-per-atom (dpa). While dpa and resulting defects lead to reductions in thermal conductivity in crystalline materials, we observe the opposite trend in thermal conductivity of amorphous materials and thermal boundary conductance across interfaces. For example, we demonstrate the ability to increase the thermal conductivity of amorphous solids through ion irradiation, in turn, altering the bonding network configuration. We report on the thermal conductivity of hydrogenated amorphous carbon implanted with C⁺ ions, in which the films' thermal conductivities reveal significant enhancement after ion irradiation, up to a factor of 3, depending upon the preirradiation composition [2]. Films with higher initial hydrogen content provide the greatest increase, which is complemented by an increased stiffening and densification from the irradiation process. This enhancement in vibrational transport is unique when contrasted to crystalline materials, for which ion implantation is known to produce structural degradation and significantly reduced thermal conductivities. At solid/solid interfaces, we also observe this ion irradiation-induced increase in thermal conductance. We experimentally demonstrate this increase in thermal boundary conductance (TBC) by ion irradiating Gallium Nitride to produce near interface point defects. GaN is bombarded with varying doses of C⁺, N⁺, and Ga³⁺ ions, with a maximum target near-interface defect density of 2%. We show an increase in the measured Al/GaN TBC. Our results show an increased level of scattering within the defected material, which assists in the thermalization between interfacial and bulk vibrational modes and decreases TBR. This is in contrast to conventional formalisms, where scattering across the interface is said to dominate thermal transport.

1. E. A. Scott, K. Hattar, E. J. Lang, K. Aryana, J. T. Gaskins, and P. E. Hopkins. Reductions in the thermal conductivity of irradiated silicon governed by displacement damage. *Physical Review B*, 104:134306, 2021.

2. E. A. Scott, S. W. King, N. N. Jarenwattananon, W. A. Lanford, H. Li, J. Rhodes, and P. E. Hopkins. Thermal conductivity enhancement in ion-irradiated hydrogenated amorphous carbon films. *Nano Letters*, 21(9):3935–3940, 2021.

3:00 PM BREAK

Thursday Afternoon, April 25, 2024
Room 441, Level 4, Summit

3:30 PM *CH03.08.01

Investigating Dislocation Loop Nucleation and Growth under Stress by *In-Situ* TEM in Al Daphné Da Fonseca¹, Thomas Jourdan¹, Fabien Onimus¹ and Frederic Mompou²; ¹CEA, France; ²CEMES-CNRS, France

Irradiation creep that occurs both under stress and irradiation flux, even at moderate temperature, has a profound impact on mechanical properties in structural materials. For instance, it leads to deleterious permanent deformation in austenitic steel vessel internals in pressurized water nuclear reactors. Although this phenomena has been documented in the 70's and 80's, experimental and theoretical investigations proposed have never found consensus so far. It was proposed that irradiation would contribute to dislocation climb but the role of anisotropic growth of irradiation loops was the subject of debates and contradictory results. From early microstructural observations, showing a bias in the development of Frank loops in austenitic steels, two models have emerged. They postulate that the applied stress biases either loop nucleation or their growth which lead to different loop populations density and size. Experimental results, provided by post-mortem TEM observations at high doses, were not able to discriminate clearly between the two models, while in-situ observations carried out in high voltage microscopes reported opposite trends.

To gain knowledge in these phenomena, we studied loop nucleation and growth during in-situ TEM experiments under stress and irradiation at low doses. To that purpose, we take advantage of the low energy displacement threshold of aluminum, to both irradiate and observe samples at the same time, in-situ in a conventional transmission electron microscope.

We show that close to the elastic limit, almost only interstitial Frank loops are formed in the {111} planes normal to the tensile direction. Deep learning and tracking approaches were used to follow the kinetics and distribution of loops during these experiments. They reveal that loop growth is in average linear with time, i.e. with electron fluence, but with numerous cases of stagnation or accelerated growth. More importantly, we demonstrate that the anisotropy of loop population is determined at early stage, probably at the nucleation, and that the growth kinetic only plays a minor role in the development of the observed loop population. These findings echo simulations performed both at atomic scale for the nucleation processes (molecular dynamics Frenkel-pair accumulation), and at mesoscale (Object Kinetic Monte-Carlo) for elastic-diffusion mechanisms of loop growth.

4:00 PM CH03.08.02

Investigating Localized Deformation in Irradiated Stainless Steels through TEM *In Situ* Straining Experiments Silvia Guerra¹, Marta Navas¹, Jia-Chao Chen², Shavkat Akhmadaliev³ and Mercedes Hernandez Mayoral¹; ¹Centre for Energy, Environmental and Technological Research, Spain; ²Paul Scherrer Institute, Switzerland; ³Helmholtz-Zentrum Dresden-Rossendorf, Germany

This research focuses on comprehending the processes occurring in austenitic stainless steels during the initial stages of deformation that can lead to localized deformation, and the impact of irradiation in the deformation modes of the material. To achieve these goals, the methodology employed in this study deals with performing in-situ straining experiments at the interior of a Transmission Electron Microscope (TEM). These experiments offer direct insights into the microstructural processes that occur in real time during sample deformation. This includes the observation of phenomena like nucleation and movement of dislocations, the interaction between dislocations and defects as well as early stages of defect-free channel formation.

These in situ straining experiments were conducted as interrupted tests, and the resulting microstructure was characterized by means of SEM/EBSD and TEM before and after each in-situ experiment in order to observe the evolution of the deformation in each sample and compare them.

The material under study is the AISI-316L, because due to its high corrosion resistance and good mechanical properties, it is a recurrent material in the construction of internal components of nuclear power plants. Two irradiation conditions have been studied, (1) with helium ions and (2) with iron ions, and each of them along with the non-implanted material, have been characterized.

A systematic study of the irradiated and deformed microstructures has been carried out with the aim to identify, describe, and classify features generated after interrupted testing and assess the influence of the irradiation conditions studied. Results will be presented and discussed.

4:15 PM CH03.08.03

Recent Innovation in Scanning Electron Microscope (SEM) *In-Situ* Extreme Micromechanical Tests in Nuclear Environments Nicholas Randall; Alemnis AG, Switzerland

Nanomechanical tests are already being used to investigate material properties at very small scales. Such testing of nuclear materials may be used to evaluate samples so small that radiation levels fall below critical thresholds, or may be used to simulate failure in the microstructure. Such measurements have moved beyond the basic measurement of hardness and elastic modulus to encompass a host of different mechanical properties such as strain rate sensitivity, stress relaxation, creep, and fracture toughness by taking advantage of focused ion beam milled geometries. New developments, such as high cycle fatigue, are extending the range of properties which can be studied at the micro and nanoscale. However, such techniques are challenging due to low oscillation frequencies, long duration of tests and large thermal drift when attempted with standard indentation instruments. Novel piezo-based nanoindentation methods are now allowing access to extremely high strain rates ($>10^4 \text{ s}^{-1}$) and high oscillation frequencies (up to 10 kHz).

Until only recently, high strain rate testing of materials at strain rates from $\sim 100/\text{s}$ – $10000/\text{s}$ has only been possible using macroscale techniques, such as split Hopkinson bar, Kolsky bars and plate impact testers. At the microscale, strain rates have typically been limited to $\sim 0.1/\text{s}$ or less, owing to limitations in instrumentation, insufficient data acquisition rates and elastic wave propagation conflicts during testing.

This talk will focus on the most recent developments in instrumentation for in-situ extreme mechanics testing at the micro and nanoscales, with specific focus on a testing platform capable of strain rate testing over the range $0.0001/\text{s}$ up to $10^7/000/\text{s}$ (8 orders of magnitude) with simultaneous high speed actuation and sensing capabilities, with nanometer and microneutron resolution respectively.

The additional challenge of performing extreme mechanics in nuclear environments and over the temperature range -150 to $1000 \text{ }^\circ\text{C}$ will be discussed together with the associated technological and protocol advances required. The inherent advantages of using small volumes of sample material, e.g., small ion beam milled pillars, will be discussed together with the associated instrumentation, technique development, data analysis methodology and experimental protocols. Some examples of test data will be presented where a wide range of strain rate has been combined with variable temperature in order to investigate rate effects as a function of temperature.

Specific focus will be given to test setup modifications required for testing of radioactive materials. Long term exposure trial data will be presented which confirms the applicability of the nanoindentation apparatus for quantitative measurements. Data will also be presented on a new stress-strain nanoindentation measurement technique which allows the localized mapping of yield point across a surface, in addition to hardness, elastic modulus and other mechanical properties (Ref. 1)

Finally, future research directions in this sub-field of micromechanics will be discussed.

References

1. R. Pero, N. Randall, D. Frey, R. N. Widmer, T. Darby, L. Aucott, C. Hardie, S. Pak, P. Maquet, A. Bushby, Stress-strain curve mapping by nanoindentation – a technique to qualify diffusion-bonded window assemblies for ITER, *Fusion Engineering and Design* 196 (2023) 113977 <https://doi.org/10.1016/j.fusengdes.2023.113977>

SESSION CH03.09: Computational and Simulation Tools Helping in the Interpretation and Management of *In Situ* Characterization Data

Session Chairs: Aurelie Gentils, Mercedes Hernandez Mayoral and Djamel Kaoumi

Friday Morning, April 26, 2024

Room 441, Level 4, Summit

8:30 AM *CH03.09.01

Advancements in Real-Time Quantification for *In-Situ* Materials in Extreme Environments Kevin G. Field^{1,2}, Hangyu Li¹, Kai Sun¹, Robert Renfrow¹, Matthew Lynch¹, Ryan Jacobs³, Aidan Pilny², Benjamin Eftink⁴, Dane Morgan³ and Chris Field²; ¹University of Michigan, United States; ²Theia Scientific, LLC, United States; ³University of Wisconsin–Madison, United States; ⁴Los Alamos National Laboratory, United States

In this talk, we discuss our recent developments on integrating automated detection of defects¹⁻⁵, stereomicroscopy^{6,7}, edge-computing⁸, and *in situ* ion irradiations to form a high-throughput, limited-bias workflow for studies on materials in extreme environments. Materials in extreme environments has been identified as a key research challenge for the materials community⁹, where radiation at elevated temperature, as well as stress, is one facet of the materials in extreme environments paradigm. Experiments on radiation-temperature effects is highly complex and dynamical, where defects are nucleated and can move in 1D and 3D with changes in their size, morphology, character, and can be annihilated. We discuss the application of machine learning to form a backbone for a high-fidelity, rapid quantification architecture that can perform 2D-projection and 3D visualization of defects and analysis of these complex dynamical events per frame and in near real-time fashion. We show that performance of deep learning methods, such as Mask R-CNN and You Only Look Once (YOLO), demonstrate performance levels that are at or exceed human performance with inference times below 100 ms. We see that such high-level model performance persists even when trained using physics-based synthetic datasets. We explore the application of deep learning coupled to tracking algorithms, such as DeepSORT, ByteTrack and BoT-SORT, to track hundreds of defects during extreme exposures, including during in-situ transmission electron microscopy (TEM) ion irradiations of several FeCrAl alloy variants on edge and near-edge computing devices. Then, we will show how object detection and tracking can be coupled with 2-tilt stereomicroscopy via the Obtain3D code package⁷ to form 3D reconstructions allowing for detailed 3D analysis such as pair distribution evolution of defects and 1D/3D diffusion of slow-moving defects under irradiation. The capabilities of this algorithm ensemble for high fidelity quantification are realized through a platform that couples a modern web application (webapp) hosted on edge or near-edge computing devices that is seamlessly coupled with a state-of-the-art *in situ* TEM ion irradiation facility. This platform enables real-time application of the algorithm ensemble and corresponding graphical displays and overlays from the *in situ* video feed during irradiation providing for *in operando* microscopy. The edge-device with a hosted webapp platform, termed TheiascopeTM, has been demonstrated for *in situ* TEM ion irradiations. It will be shown the platform is system agnostic (both in hardware and experiment) allowing for immediate feedback of materials evolution when exposed to extreme environments in other imaging systems such as scanning electron microscopy. We will conclude the discussion with recent innovations and thinking on extending the overall presented framework and advances to automated microscopy experimentation through integration with microscopy vendor software APIs.

1. Li, W., Field, K. G. & Morgan, D. *NPJ Comput Mater* **4**, 36 (2018).

2. Jacobs, R. *et al. Scientific Reports* **2023** *13*:1 **13**, 1–13 (2023).

3. Shen, M. *et al. Comput Mater Sci* **197**, 110560 (2021).

4. Jacobs, R. *et al. Cell Rep Phys Sci* (2022).

5. Shen, M. *et al. Comput Mater Sci* **199**, 110576 (2021).

6. Field, K. G., Eftink, B. P., Saleh, T. A. & Maloy, S. A. <https://doi.org/10.2172/1439930> (2018).

7. Eftink, B. P. & Maloy, S. A. obtain3D. <https://www.osti.gov/servlets/purl/1371737> (2017).

8. Field, K. G. *et al. Microscopy and Microanalysis* **27**, 2136–2137 (2021).

9. Wadsworth, J. *et al. Basic Research Needs for Materials Under Extreme Environments, June 11-13, 2007*. (2008) doi:10.2172/935440.

9:00 AM *CH03.09.02

Bubble Stability and Mobility in Nickel under *In Situ* Ion Irradiation Wei-Ying Chen, Logan Ward and Zhi-Gang Mei; Argonne National Laboratory, United States

Materials within nuclear reactors undergo irradiation that results in adverse microstructural changes, including the formation of point defects, defect clusters, voids, dislocation loops, segregation, and precipitation. The Intermediate voltage electron microscope (IVEM)-Tandem Facility at Argonne National Laboratory is a user facility for *in situ* TEM study of the radiation effects on material microstructures. It interfaces a 500 kV ion accelerator and a 20 kV helium ion source to a 300 kV Hitachi H-9000NAR TEM, allowing real-time microscopy under dual-beam ion irradiation damage/implantation with well-controlled conditions including specimen orientation, temperature, ion type, ion energy, dose, dose rate, applied strain. *In situ* TEM has unique capability to capture videos, offering quantitative insights into the dynamic process that cannot be obtained with *ex situ* experiments. Our previous study in IVEM observed voids growing or shrinking in nickel at various temperatures from 525°C to 650°C under 1 MeV krypton ion irradiation with a flux of 6.3×10^{11} ions-cm⁻²-s⁻¹. Initially, 6 samples underwent irradiation at 600°C to achieve a damage level of 0.5 dpa, which resulted in the formation of voids with an average size of about 15 nm within the TEM foil. Subsequently, the temperature was individually adjusted to 525°C, 550°C, 575°C, 600°C, 625°C, and 650°C. Following this temperature adjustment, irradiation continued for an additional 1 dpa. The stability of the voids at these new temperatures was monitored through *in situ* videos in regions where the foil thickness was approximately 100 nm. A total of about 5000 frames of videos were recorded. We applied deep learning-based semantic segmentation model (IoU score = 0.8135) to automatically analyze the videos and showed that voids shrank at low temperatures and grew at high temperatures under irradiation, where the transition occurred at 575°C (~0.5 TM). This presentation will focus on the behavior of small Kr-containing bubbles, which had a size smaller than 10 nm. Unlike larger, immobile voids, these small bubbles are mobile under irradiation. Notably, the bubbles were often found tagging along with the irradiation-induced dislocations loops. The movement of those bubbles was confined to the path where dislocation loops expanded or shrank. For bubbles not associated with dislocations, on the other hand, their movements appeared to be random. Besides, while large voids tended to grow steadily at temperatures above 575°C, the bubbles were unstable, switching between growth and shrinkage. The behavior of individual bubbles may be affected by its own unique surroundings such as nearby voids, bubbles, dislocations, and concentration of point defects. Understanding how these individual bubbles exhibited heterogeneous behavior and added up contributing to the resultant macroscopic property requires tracking capability.

We developed a tracking algorithm using Trackpy, and showed that, in average, void stability increases with void size, while void mobility decreases with void size. Nonetheless, there is significant variability in growth or mobility across voids of the same size and for the same void at different times. Besides, the analysis allows us to identify the threshold size at which bubbles transition from instability to steady growth. The temperature dependence on the bubble stability and mobility will also be discussed.

9:30 AM CH03.09.03

Kinetics Governed by Elastic Bias in *In-Situ* Electron Irradiated Aluminium: A Coupled Experimental and Modeling Study Camille Jacquelin, Thomas Jourdan, Maylise Nastar, Chu Chun Fu and Estelle Meslin; CEA Saclay, France

In this study, we investigate the direct in-situ formation of nanometer-scale radiation damage, including voids and loops, using a High-Resolution Transmission Electron Microscope (HRTEM). We observe a size-dependent effect on the shape of cavities induced by electron irradiation, with non-truncated and cross shapes appearing at sizes below 2 nm, while larger sizes exhibit truncated shapes, consistent with DFT based-equilibrium shapes. This effect is explained by our multi-scale modelling, considering the effects of finite size and network discretization on void shapes. The observed dispersion in cavity shape during their growth and shrinkage is primarily influenced by magic numbers, determined by geometry and network frustration. Additionally, not only the voids but also loops were followed in-situ. Loops grow until they eliminate at the surface, while voids go through periodic growth and shrinkage. We demonstrate that the evolution of both objects is linked and governed by elastic bias. The unexpected void shrinkage is attributed to the change of the main sink for the elimination of interstitials. Void growth occurs when the main sinks for interstitials are the strongly biased dislocation loops, generating a stronger vacancy flux towards voids. Conversely, cavity shrinkage occurs when the loops are absent, and the main sinks for interstitials are the foil surface, generating a stronger interstitials flux towards voids.

We reproduce accurately this phenomenon through Object-Kinetic Monte Carlo (OKMC) modelling.

9:45 AM CH03.09.04

Automated Defect Detection in Electron Microscopy of Radiation Damage in Metals Dane Morgan¹, Ryan Jacobs¹, Ajay Annamareddy¹, Matthew Lynch² and Kevin G. Field²; ¹University of Wisconsin–Madison, United States; ²University of Michigan–Ann Arbor, United States

In this talk, we discuss our recent work on automating detection of defects in electron microscopy images of irradiated metals relevant for advancing the capabilities of in situ defect characterization of nuclear materials [1–5]. Radiation response of materials is a critical design constraint for future nuclear fission and fusion materials. Electron microscopy is widely used to explore defects in crystal structures, but human tracking of defects can be time-consuming, error prone, unreliable, and is not scalable to large numbers of images or real-time analysis. In this work, we discuss application of machine learning approaches to find the location and geometry of different defects in irradiated alloys, such as dislocation loops, black dot interstitial clusters, and cavities. We explore multiple deep learning methods and generally find performance approaching or equivalent that of human accuracy. We explore multiple avenues of assessment, including canonical classification metrics like precision and recall of specific defect identification ($F1 \approx 0.8$), accuracy of microstructurally-relevant defect properties (e.g., average defect areal density and size distribution ($\approx 10\%$ fractional errors), and accuracy of macroscopic engineering properties such as hardening (10-20 MPa errors, or about 10% of total hardening) and swelling ($\approx 0.3\%$ swelling errors). These results suggest that specific images can have significant errors, but averaging over many images yields quite good results. We explore convergence of the results with number of training samples, finding that certain defect types are significantly less well detected, likely due both to their having reduced sampling and greater variability, as well as labeling and model limitations for small size features. Finally, we discuss recent efforts using synthetic data to improve object detection model training and reduce the need for a large corpus of labeled experimental data. We explore both deep learning approaches of image generation (namely variational autoencoders) to create synthetic dislocation loop images and physics-based electron dynamics simulations to create synthetic cavities. We generally find that the use of synthetic data is a practical path toward generating new training data essentially instantaneously, leading to improvements in object detection model performance.

1. Shen, M.; Li, G.; Wu, D.; Yaguchi, Y.; Haley, J. C.; Field, K. G.; Morgan, D.; Ridge, O.; Ridge, O. A Deep Learning Based Automatic Defect Analysis Framework for In-Situ TEM Ion Irradiations. *Comput Mater Sci* 2021, 197 (November 2020), 110560. <https://doi.org/10.1016/j.commatsci.2021.110560>.
2. Jacobs, R.; Shen, M.; Liu, Y.; Hao, W.; Li, X.; He, R.; Greaves, J. R. C.; Wang, D.; Xie, Z.; Huang, Z.; Wang, C.; Field, K. G.; Morgan, D. Performance and Limitations of Deep Learning Semantic Segmentation of Multiple Defects in Transmission Electron Micrographs. *Cell Rep Phys Sci* 2022, 100876. <https://doi.org/10.1016/j.xcrp.2022.100876>.
3. Field, K. G.; Jacobs, R.; Shen, M.; Lynch, M.; Patki, P.; Field, C.; Morgan, D. Development and Deployment of Automated Machine Learning Detection in Electron Microscopy Experiments. *Microscopy and Microanalysis* 2021, 27 (S1), 2136–2137. <https://doi.org/10.1017/s1431927621007704>.
4. Jacobs, R.; Patki, P.; Lynch, M. J.; Chen, S.; Morgan, D.; Field, K. G. Materials Swelling Revealed through Automated Semantic Segmentation of Cavities in Electron Microscopy Images. *Sci Rep* 2023, 13 (1). <https://doi.org/10.1038/s41598-023-32454-2>.
5. Jacobs, R. Deep Learning Object Detection in Materials Science : Current State and Future Directions. *Comput Mater Sci* 2022, 211 (May), 111527. <https://doi.org/10.1016/j.commatsci.2022.111527>.

10:00 AM BREAK

10:30 AM *CH03.09.05

A Comprehensive Study on The Kinetics of Defect Formation and Interaction Coupling *In-Situ* TEM with Deep Neural Networks Kory D. Burns¹, Caitlin Kohnert² and Khalid Hattar³; ¹University of Virginia, United States; ²Los Alamos National Laboratory, United States; ³The University of Tennessee, Knoxville, United States

Simulating reactor conditions inside a transmission electron microscope (TEM) gives insight into the rate of defect formation and survivability of materials in the environments in which they were designed to perform. Efforts to fully encapsulate dynamic processes occurring in a material have been challenging, owing to the large volume of information collected from an individual experiment and multiple interactions occurring simultaneously. Hereby, deep neural networks emerge as a suitable method to extract complicated information from input images and output useful analytics that help understand the physics of a reaction. This talk discusses strategies for handling a range of datasets from *in situ* TEM experiments that span different material systems, imaging conditions, and irradiation conditions to predict the stability of materials. Emphasis will be placed on developing end-to-end process flows equipped with generating synthetic data to learn feature representations of images, pattern recognition to highlight hidden trends in the data, and overall implications for the advancement of nuclear materials characterization.

11:00 AM CH03.09.06

Investigation of Extended Defect Evolution in UO₂ and ThO₂ during Ion Irradiation and Post-Irradiation Annealing Marat Khafizov¹, Joshua Ferrigno¹, Mutaz Alshannaq¹, Md Minaruzzaman¹, Kaustubh Bawane², Miaomiao Jin³, Yongfeng Zhang⁴, Boopathy Kombaiiah², Lingfeng He⁵ and David Hurley²; ¹The Ohio State University, United States; ²Idaho National Laboratory, United States; ³The Pennsylvania State University, United States;

⁴University of Wisconsin–Madison, United States; ⁵North Carolina State University, United States

A rate theory model is applied to analyze the kinetics of extended defect evolution revealed by in-situ transmission electron microscopy characterization during ion irradiation and post-irradiation annealing of uranium dioxide (UO₂) and thorium dioxide (ThO₂). The objective is to investigate mechanisms governing dislocation loop growth, unfauling of Frank loops, and extended defect coarsening. In-situ characterization of krypton ion irradiated ThO₂ reveals that loop growth is limited by the mobility of cation interstitial and loop nucleation is influenced by the mobility of both cation and anion interstitials. Similar conclusion has been obtained from ex-situ characterization of proton irradiated ThO₂. Additionally, we determined that during in-situ experiments utilizing TEM lamellae it is important to include surface as a sink for both extended and point defects. Observed extended defect coarsening under in-situ annealing is best described by coalescence mechanism resulting from migration of extended defects. This detailed understanding of extended defect evolution allows to improve assessment of physical properties important for nuclear fuel performance analysis. The established procedure also allows to infer point defect concentration, which are more impactful in determining several physical properties, such as thermal conductivity and atomic diffusion.

SYMPOSIUM CH04

Characterization of Materials Dynamics
April 23 - May 7, 2024

Symposium Organizers

Yuzi Liu, Argonne National Laboratory
Michelle Mejía, Dow Chemical Co
Yang Yang, Brookhaven National Laboratory
Xingchen Ye, Indiana University

* Invited Paper

+ JMR Distinguished Invited Speaker

^ MRS Communications Early Career Distinguished Presenter

SESSION CH04.01: Understanding Material Dynamics in Multimodalities
Session Chairs: Yuzi Liu and Xingchen Ye
Tuesday Morning, April 23, 2024
Room 443, Level 4, Summit

10:30 AM *CH04.01.01

Operando, Multimodal Characterization of Bimetallic Catalysts with Electrons and X-Rays Alexandre Foucher^{1,2}, Nicholas Marcella^{2,3}, Jennifer Lee^{4,5}, Daniel Rosen⁴, Ryan Tappero³, Christopher B. Murray⁴, Anatoly Frenkel^{2,3} and Eric A. Stach⁴; ¹Massachusetts Institute of Technology, United States; ²Stony Brook University, The State University of New York, United States; ³Brookhaven National Laboratory, United States; ⁴University of Pennsylvania, United States; ⁵University of California, Merced, United States

Alloyed nanoparticles are of increasing interest in many applications, most notably as heterogeneous catalysts. Alloying allows the tuning of composition and structure to increase functionality, most specifically reactivity and selectivity. However, harsh, reactive environments can induce changes in the structure and composition of these materials in unexpected ways, which can inhibit their performance. These materials also present a significant characterization challenge: they are tiny (from single atoms to particles of 10 nm) and can also be heterogeneous in size, composition, and structure.

I will describe how we have developed a new approach to characterize catalysts using so-called 'operando' methods to take measurements. At the same time, the materials are 'in a working condition': i.e., in a reactive environment performing their function. We use a microreactor system compatible with imaging, diffraction, and spectroscopy, using electron, photon, and x-ray probes. The presentation will describe how this multimodal approach can provide unique insights into the dynamic changes in these complex systems as they function.

There will be two specific applications. In the first portion, I will show how we can exploit an innovative colloidal synthesis method to produce highly monodisperse Cu-Pt alloy nanoparticles with a Pt-rich shell and Cu-rich core; the intermetallic CuPt phase formed after annealing shows enhanced and stable catalytic activity for CO oxidation compared to pure Pt nanoparticles or the fresh Cu-Pt particles with a Pt-shell. This synthesis route allows control over Cu-Pt nanostructures, demonstrating Cu-Pt alloys' promising catalytic properties. In the second portion, I will show how Ni-Cu alloy nanoparticles undergo compositional and morphological changes during redox cycles that simulate catalytic reactions; specifically, while Cu segregates in the fresh catalyst, oxidation at 400°C leads to restructuring into hollow particles with heterogeneous Ni-Cu composition, explaining the deactivation observed for conversion of biomass-derived 5-hydroxymethylfurfural over NiCu₃C.

11:00 AM CH04.01.02

Advancing Multimodal Characterization at The Nanoscale with The Tescan Tensor Analytical 4D-STEM Robert Stroud; Tescan USA, United States

Nanoscale imaging is important, but in materials characterization information about crystalline structure, as revealed by the diffraction pattern, and the

ability to relate that information to a particular location in the image, is equally valuable. The power of 4D analytical STEM lies in its ability to acquire complete image, crystallographic and compositional information across the field of view with nanometer-scale spatial resolution. Scientists and engineers who need this kind of information work in a variety of disciplines, including materials science, semiconductor manufacturing, pharmaceutical research, product development, and many more. Across these disciplines, practitioners were aware of the potential benefits of S/TEM but have historically been turned off by the perceived operational difficulty of the instrumentation. They want practical results, and the less time, effort, and money required to get the result, the better.

TESCAN TENSOR addresses these needs by automating almost every microscope function. This unprecedented automation is only possible because it has been integrated into the microscope design at every level from the ground up. The designers' singular focus on completely automated 4D-STEM operation has delivered a microscope without peer in that application.

The methodology behind TESCAN's Analytical 4D-STEM microscope will be explained as the solution of choice for a range of nanoscale applications. Examples including results from nickel-based superalloy indentation studies, complex semiconductors, and battery anodes will be presented.

Nickel superalloys. An investigation into the crystallographic grain reorientation caused by Vickers indentation induced plastic deformation, studied by precession-assisted 4D-STEM with automated crystal orientation analysis will be presented, including high resolution mapping of the resulting indentation induced crystallographic orientation gradient.

4D-STEM phase and orientation analysis of lithium-ion battery anode materials. Precession-assisted 4D-STEM was used to produce maps of $\text{LiTi}_2(\text{PO}_4)_3$, TiO_2 and LiTiOPO_4 phases present in spindle-like battery anode particles. 4D-STEM phase analysis will be presented showing that TiO_2 nanoparticles form a network at the $\text{LiTi}_2(\text{PO}_4)_3$ sub-particle boundaries, which may provide a more effective diffusion pathway for lithium ions at higher cycling rates.

Multimodal phase and orientation analysis of complex semiconductor devices. For semiconductor manufacturers, it is desired to have comprehensive analytical capabilities, with the ability to measure chemical and structural properties, complementary to specimen morphology, down to the sub-nanometer scale. This is generally addressed using Energy Dispersive X-Ray (EDX) mapping, defect analysis through diffraction measurements, crystal orientation and phase mapping, and critical dimension imaging. These capabilities are important as the electrical performance of devices depends strongly on the type and distribution of crystalline phases in individual layers.

The TESCAN TENSOR analytical 4D-STEM provides a unique workflow interface to facilitate efficient chemical and structural analysis using EDX mapping, and precession-assisted phase and orientation mapping. The alignment and workflow automation enables effortless, automated switching between measurements optimized for STEM imaging, EDX analysis, or analytical 4D-STEM.

With a result-centric design, TESCAN TENSOR's quality, throughput, and robustness of 4D-STEM acquisition, analysis, and processing has been optimized with state-of-the-art technologies, such as Precession Electron Diffraction (PED), 4D-STEM computing and visualization, electrostatic beam blanking, and ultra-high vacuum at the specimen area. Additionally, TESCAN TENSOR features real-time, automated data analysis and processing, which empowers an unprecedented level of system accessibility, utilization, and productivity.

11:15 AM *CH04.01.03

Understanding Particle-Mediated Growth Pathways by using Advanced Transmission Electron Microscopy and X-Ray Scattering Techniques Xin Zhang¹, Xiaoxu Li¹, Yining Wang¹, Jianbin Zhou¹, Sebastian T. Mergelsberg¹, Tuan Ho², Lili Liu¹, Honghu Zhang³, Ruipeng Li³, Mark Bowden¹, Ping P. Chen¹, Maria Sushko¹, Carolyn Pearce¹, James J. De Yoreo¹ and Kevin Rosso¹; ¹Pacific Northwest National Laboratory, United States; ²Sandia National Laboratories, United States; ³Brookhaven National Laboratory, United States

Particle aggregation involves the phenomenon of oriented attachment (OA), where crystalline particles join together by attaching to specific crystal faces with lattice matching, is a prevalent mechanism in crystal growth and has been extensively utilized in the development of hierarchically structured crystalline materials, which has been applied to catalysis, energy storage, environmental conservation, biological medicine, etc. Using a combination of advanced transmission electron microscopy (TEM) and small-angle X-ray scattering/wide-angle X-ray scattering (WAXS) techniques and computational methods, we are investigating these phenomena for several metal oxide systems and their relationship to interfacial structure in vacuum and water vapor. Here we discuss three cases. In the first, we use high-resolution TEM and scanning TEM (STEM) to explore the aggregation behaviors of hematite nanocrystals with different exposed facets including {001}, {012}, {104} and {116}. The experimental data indicates that hematite nanoparticles aggregation-based crystallization is orientation dependent (along the [001] direction), not relies on exposed facet. We then compare the results to the predictions of density functional theory (DFT) to relate the behavior to surface interactions. In the second case, we report the formation of gibbsite mesocrystals in pure water. By evaporating the suspension of monodisperse gibbsite nanoplates with a diameter of around 100 nm, plate-like mesocrystals with a diameter of up to a hundred micrometers were formed. The single crystal XRD pattern and SAXS/WAXS of the mesocrystals matched that of bulk gibbsite crystal along the specific zone axis, indicating well-aligned particles in the monocrystals. Further analysis through scanning electron microscopy (SEM) and TEM revealed a hexagonal columnar superstructure. Moreover, the *in situ* liquid phase TEM was conducted and observed the OA of a few gibbsite nanoplates in pure water, and the result matched well with *ex situ* characterizations. The MD simulation was used to investigate the energy-structure relationship for the sliding motion of two co-planar gibbsite nanoplatelets along the (010) direction. The results indicated that to obtain the first perfectly aligned configuration, sliding in the (010) direction exhibits a smaller energy barrier than sliding in the (100) direction (0.89 vs. 2.49 kcal/mol). In the third case, the measurement of anisotropic forces between rutile TiO_2 (001) nanocrystals as a function of their azimuthal orientation and surface hydration extent using a combined environmental TEM-atomic force microscopy (AFM) technique. At tens of nanometers of separation, the attractive forces are weak and show no dependence on azimuthal alignment nor surface hydration. At separations of approximately one hydration layer, attractive forces are strongly dependent on azimuthal alignment and systematically decrease as intervening water density increases. Measured forces closely agree with predictions from Lifshitz theory and show that dispersion forces are capable of generating a torque between particles to align them.

SESSION CH04.02: Advanced Characterization of Energy Materials

Session Chairs: Tianyi Li and Xianghui Xiao

Tuesday Afternoon, April 23, 2024

Room 443, Level 4, Summit

1:30 PM *CH04.02.01

Origin of Structural Degradation in Lithium Layered Oxide Cathode Luxi Li¹, Tongchao Liu¹, Ian Robinson^{2,3}, Ross Harder¹ and Wonsuk Cha¹; ¹Argonne National Laboratory, United States; ²Brookhaven National Laboratory, United States; ³University College London, United Kingdom

Li and Mn-rich (LMR) layered oxide cathode materials can substantially increase battery energy density by facilitating both cation and anion redox energy. However, the cathode material suffers from continuous voltage decay over the charge/discharge cycles and results in capacity loss. Coherent X-ray Diffraction (CXD) techniques are invaluable for investigating the morphology, structural and strain information in crystalline specimens under in-situ and operando conditions [1-2]. In this presentation, $\text{Li}_{1.2}\text{Ni}_{0.13}\text{Mn}_{0.54}\text{Co}_{0.15}\text{O}_2$ is used as a benchmark to explore the origin of structural degradation in LMR

cathode materials [3]. In-situ CXD techniques are used to visualize the strain accumulation in the charging process that leads to an abrupt oxygen loss to release the lattice strain. In the meanwhile, a new phase with a trace quantity is observed from the microbeam diffraction that supports the hypothesis of oxygen loss. These results highlight the significance of lattice strain in the voltage decay mechanism and will inspire a wave of efforts that seek novel solutions for eliminating this issue.

[1] Ian Robinson & Ross Harder, *Nat. Mater.* 8, 291–298 (2009)

[2] Luxi Li, Yingying Xie, Evan Maxey, & Ross Harder J. *Synchrotron Rad.* 26, 220-229 (2019).

[3] Tongchao Liu, Luxi Li, et al. *Nature* 606. 305-312 (2022).

2:00 PM *CH04.02.02

X-Ray Nano-Scale Spectroscopic Imaging on Battery Research – A Case Study [Xianghui Xiao](#)¹, Dong Hou², Feng Lin³ and Zhengrui Xu³;

¹Brookhaven National Laboratory, United States; ²University of Louisiana at Lafayette, United States; ³Virginia Tech, United States

Chemical reaction heterogeneity is ubiquitous at both interparticle and intraparticle scales during battery cycling. Spectroscopic imaging provides position-dependent chemical state information that is directly related to the chemical reaction heterogeneity in the samples. Transmission X-ray Microscope has been widely used in battery research as a spectroscopic imaging modality. Simultaneously, it also provides morphological structure information. In this paper, we will present a case study of the characterizations of two types of high-Ni NMC cathode materials that have different primary particle arrangement patterns. They show distinct performances at room temperature. Nonetheless, the thermal stabilities of these two types of materials are inverse compared to their electrochemical performances. The chemical state distributions and morphological structures at the single particle level show consistent evolution behaviors as the observations with neutron diffraction. The results help to reveal the fundamental mechanisms that cause the differences. The case demonstrates the capability of TXM as a spectroscopic imaging tool and its applications in battery research.

2:30 PM CH04.02.03

Boosting the CO₂ Uptake of MgO-Based Sorbents using Na₂CO₃ as Nucleation Seeds: Mechanistic Insights via *In Situ* Synchrotron XRD [Annelies](#)

[Landuyt](#)¹, Ilia Kochetov², Maximilian Krödel¹, Wendy L. Queen², Paula Abdala¹ and Christoph R. Müller¹; ¹ETH Zürich, Switzerland; ²EPFL, Switzerland

CO₂ capture, utilization and storage (CCUS) is a key technology to reach net zero CO₂ emissions and mitigate global warming. Therefore, there is an urgent need to develop functional materials that can capture and release CO₂ under industrially relevant conditions. Solid oxide materials such as MgO are earth-abundant and constitute a promising family of materials for CO₂ capture.¹ MgO-based CO₂ sorbents are characterized by favorable carbonation thermodynamics and high gravimetric CO₂ uptake capacities but display limited CO₂ uptake due to slow carbonation kinetics. The first step that partially resolves the slow kinetics involves the addition of alkali metal nitrates, which are molten under operation conditions.² Here, we show a second sorbent engineering step that effectively resolves the limited CO₂ uptake kinetics of MgO-sorbents, by co-promoting MgO with NaNO₃ and Na₂CO₃, resulting in fast CO₂ uptake rates. We demonstrate the mechanism behind this promotion via in-situ synchrotron XRD measurements (1 s resolution), revealing that Na₂CO₃ rapidly (within seconds) transforms into Na₂Mg(CO₃)₂, which acts as a nucleation seed for MgCO₃ growth. Na₂Mg(CO₃)₂ seeds facilitate MgCO₃ nucleation, which has been identified as the rate-determining step, resulting in increased CO₂ uptake kinetics (from minutes to seconds). Lastly, using electron-microscopy techniques, we visualize the nucleation of MgCO₃ directly onto the Na₂Mg(CO₃)₂ seeds. Taken together, we show that the co-promotion of MgO with Na₂CO₃ and NaNO₃ is a facile, inexpensive and highly promising strategy for improving MgO-based CO₂ capture sorbents.

[1] Dunstan, M. T. *et al. Chem Rev* 2021, 121 (20), 12681–12745.

[2] Landuyt, A. *et al. JACS Au* 2022, 2 (12), 2731-2741.

2:45 PM CH04.02.04

Depth-Profiling Spectroscopic Investigation of The Activation Mechanism of LiMn₂O₄: Micro-SORS Method Wang-Hyo Kim¹, [So Yeon Yoon](#)¹,

Myeong-Hee Lee¹, Byung-Man Kim² and Tae-Hyuk Kwon¹; ¹Ulsan National Institute of Science and Technology, Korea (the Republic of); ²University of Cambridge, United Kingdom

Lithium manganese oxide (LiMn₂O₄, LMO) stands out as a promising material for lithium-ion batteries due to its high thermal stability, low cost, abundance, and environmental compatibility. However, the dynamics of LMO's behavior in electrode is still unknown. In this study, we explore LMO as a storage electrode in photo-rechargeable batteries (PRB) using non-invasive depth profiling techniques, specifically micro-spatially offset Raman spectroscopy (micro-SORS). We delve into the Raman profiles of LMO layers, examining their variations based on depth after galvanostatic charging and discharging cycles of PRB. During these cycles, the oxidation state of manganese species shifts from Mn³⁺ to Mn^{3.5+}, accompanied by a phase transition from cubic to tetragonal. This transition results in increased capacity. To unravel this mechanism, we analyze depth-dependent Raman profiles corresponding to the phase transition throughout charging and discharging cycles. To validate our micro-SORS findings, we employ X-ray absorption fine structure (XAFS) and X-ray absorption near edge structure (XANES) techniques, confirming both oxidation states and phases. The XAFS and XANES data reveal the accumulation of an irreversible charged state (Li₂Mn₂O₄, L₂MO) over repeated charging-discharging cycles. By integrating micro-SORS analysis with this information, we pinpoint the specific site of accumulation in the electrode, elucidating the capacity increment mechanism through tracking this accumulation. While Raman analysis is common in battery research, this study marks the pioneering use of non-destructive, depth-dependent analysis using micro-SORS. This innovative approach not only provides valuable insights into battery degradation but also offers a revolutionary perspective, capturing macroscopic changes with microscopic precision.

3:00 PM BREAK

3:30 PM *CH04.02.05

Developing Automation and *In-Situ* Capabilities for X-Ray Scattering towards Autonomous Lab-At-Beamline [Ruipeng Li](#); Brookhaven National Laboratory, United States

X-ray scattering is a unique tool for revealing material structures, spanning from the atomic level to hundreds of nanometers. Its broad probe range and flexibility make it invaluable for in-situ and operando studies across various materials research fields. The development of the in-situ capabilities, coupled with technological advances in light sources and detectors, have increased our ability to explore complex material processing, resulting in vast amounts of data in more intricate parameter spaces.

In this presentation, I will discuss recent developments in in-situ capabilities at the Complex Materials Scattering (CMS) beamline of NSLS II, as well as our journey toward automation and autonomous exploration of materials. I will also outline our strategy to integrate automation, advanced data analysis, in-situ capabilities, and other characterizations to develop the beamline into an autonomous lab-at-beamline.

4:00 PM *CH04.02.06

Advancing Research with Combined Synchrotron Techniques at 7-BM NSLS II Lu Ma; Brookhaven National Laboratory, United States

At the 7-BM, NSLS II, we've developed combined synchrotron techniques for materials characterization, particularly X-ray absorption spectroscopy (XAS)/X-ray diffraction (XRD) and XAS/ Diffuse Reflectance Infrared Fourier Transform Spectroscopy (DRIFTS). These combined approaches yield numerous advantages including comprehensive analysis, real-time monitoring, and the maximization of data yield during valuable beamtime. Notably, their integration often reveals unexpected material properties and bridges gaps across varied research areas.

The combination of XRD and XAS offers an all-encompassing perspective on material structure/properties. XRD examines phase identification, crystal structure, and other microstructural properties, while XAS studies the electronic configurations, oxidation states, and the intricacies of local coordination. With XAS elucidating details of the catalyst structure and DRIFTS offering a snapshot of surface interactions and molecular dynamics, this combination proves to be a powerful tool for gaining a comprehensive view of catalytic reactions.

Leveraging these integrated techniques at the 7-BM NSLS II, we not only enhance our understanding of material properties but also set the stage for future innovations in diverse research fields.

4:30 PM CH04.02.07

Designing The Next Generation Silicon/Graphite Anodes for Lithium-Ion Batteries: From The Nanoscale to The Macroscale Benjamen Reed, Sofia Marchesini, Carmen Lopez, Andrew Wain, Rudra Samajdar, Ken Mingard, Vivian Tong, Helen Jones, Daniel O'Connor, Giannis Chatzopoulos and Andrew Pollard; National Physical Laboratory, United Kingdom

Reaching net-zero emissions and transitioning to widespread electrification of vehicles have emerged as key challenges for ensuring a sustainable future. Central to these goals is the critical role played by energy storage systems, which are pivotal in enabling the efficient utilisation and distribution of renewable energy. The advancement of energy storage technologies, particularly in the realm of lithium-ion batteries, holds the key to mitigating the challenges posed by intermittent renewable energy sources. Moreover, electrification of the transportation sector, primarily through electric vehicles, is fundamental to reducing greenhouse gas emissions.

The operating range for electric vehicles is determined by the energy density of the battery, which in the case of anode materials is directly correlated to their lithium storage capacity. While traditional graphite anodes have a theoretical capacity of 360 mAh/g, silicon has a much larger theoretical capacity (3600 mAh/g) and silicon-based lithium-ion batteries have therefore emerged as a promising technology.

However, silicon anodes suffer from large volume expansion (up to 300 %) during cycling, which cause a drop in capacity. Recent industrial advances allowed to engineer silicon/graphite composite materials with limited volume expansion and increased capacity. However, while these materials showed improved electrochemical performance, little is understood on the physicochemical mechanisms underpinning these improvements. The successful advancement of this technology necessitates a thorough understanding of intricate phenomena such as particle cracking, volume changes on various length scales (from pouch cell level down to individual particles), and the formation of solid electrolyte interphase (SEI) layers.

Herein, we employed a suite of complementary physical and chemical characterisation techniques using both post-mortem and operando methods, across a range of length scales, from pouch cells down to individual particles observed at the nanoscale. Collaboration with an industrial supplier of these anodes and cells allowed the elucidation of the material degradation phenomena and the correlation to their electrochemical cycling performance.

This work highlights the significance of integrating multiple characterisation methods to unravel the underlying degradation mechanisms in silicon-based anodes, paving the way for the design and engineering of efficient silicon and graphite anodes, thus propelling the evolution of lithium-ion battery technology.

4:45 PM CH04.02.08

Evaluations of Reaction Heterogeneities in Battery Electrodes upon Fast Charging using Operando Focused Beam X-Ray Diffraction Tianyi Li¹, Donal Finegan² and Kamila Wiaderek¹; ¹Argonne National Laboratory, United States; ²National Renewable Energy Laboratory, United States

Recently, the use of thick electrodes in lithium-ion batteries has drawn extensive attention as it effectively promotes cell-level energy density by reducing the fraction of inactive components such as separators and current collectors. However, the spatially non-uniform reaction can easily arise within a thick electrode design due to the sluggish electrolyte transport. Understanding the heterogeneous reaction and preventing it is happening are therefore critical as it may result in inferior rate performance, fast capacity degradation, and even safety hazards. This study aims to experimentally evaluate the reaction heterogeneities in thick electrodes by employing operando focused beam X-ray diffraction (XRD). We will compare the traditional graphite anode with laser ablated sample in full cells upon 6C fast charging, therefore, quantitatively assessing the degree of reaction along the depth direction in electrodes under operational conditions. A detailed comparison between the experiments and simulations will help us better understand the origin of reaction heterogeneities in electrodes and guide the design of battery materials and structures in the future.

SESSION CH04.03: Poster Session I
Session Chairs: Yang Yang and Xingchen Ye
Tuesday Afternoon, April 23, 2024
Flex Hall C, Level 2, Summit

5:00 PM CH04.03.01

Grand Canonical Monte Carlo Simulation with MOF-303 and Metal-Coated MOF-303 Jeogno An and Kunok Chang; Kyung Hee University, Korea (the Republic of)

Managing Xe/Kr radioactive novel gas generated from spent nuclear fuel is critical for both environmental and human radiation protection. While numerous experimental methods applied to find effective adsorbent, the computational simulation can help minimize experimental costs and help pre-screening effective materials. The Grand Canonical Monte Carlo(GCMC) Simulations are used to explore selective adsorptions at Metal-Organic Frameworks(MOFs). This study aims to use GCMC to select MOFs that have a large capture capacity and selective adsorption of gaseous radionuclides emitted from spent nuclear fuel such as Xe/Kr. Among the MOFs, MOF-303 shows improvement it's total uptakes and selectivity when it doped with metal such as Cu. Through GCMC calculations, the effect of Cu doping on the gas adsorption of MOF-303 was evaluated, and the effects on the capture capacity and selectivity changes were quantitatively analysed.

5:00 PM CH04.03.02

Excited-State Dynamic in Thiophene/Phenylene Co-Oligomer Nanocrystals [Andi M. Panre](#), Hitoshi Mizuno, Tomomi Jinjyo and Hiroyuki Katsuki; Nara Institute of Science and Technology, Japan

Thiophene/phenylene co-oligomer (TPCO) nanocrystals (NCs) hold strong promise for nano-environment photoluminescence probes, qubits, and quantum light source. Their optical properties show considerable versatility and flexibility depending on the size of the nanocrystals. This adaptability enhances light emission efficiency, making them a promising choice for improving organic light-emitting diodes (OLED) technology, especially as active layers. To extend the potential applications of these nanocrystals, it is essential to investigate how the size of nanocrystals is related with the excited state relaxation and photoluminescence (PL) dynamics. For example, we expect the excited state lifetime for smaller NCs should be affected by the enhanced spatial overlap of electron and hole states. In the present study, we observe the transient absorption spectrum in NCs of 5,5'-bis(4'-cyanobiphenyl-4-yl)-2,2'-bithiophene (BP2T-CN). BP2T-CN NCs with an average size of 75 nm were prepared by the reprecipitation method, which show strong yellow emission centered around 555 nm. The size-dependent steady-state optical properties were elucidated through the measurement of absorption and PL spectra. In comparison to vapor-deposited films, the BP2T-CN NCs water dispersion displayed shifts in the 0-1 and 0-2 absorption bands, attributed to lattice softening (surface effect) and quantum effects. Additionally, PL lifetime measurements yielded a decay time of 1.33 ns at an excitation wavelength of 400 nm. The transient absorption signal in the yellow-emitting BP2T-CN NCs is characterized by three exponential decays with 0.65 ps, 2.3 ps, and 75 ps components. These time constants shed light on relaxation processes, including electron trapping, intra-band relaxation, and non-radiative decay. Photoinduced absorption bands (PA, $\Delta T/T < 0$) appeared at 670-700 nm from the lowest excited state. Our findings will give a clue on the photophysical processes within these co-oligomer NCs, providing valuable insights for potential applications in optoelectronic devices and photonics, especially in OLED development.

5:00 PM CH04.03.03

Role of Aluminium in STE Engineering in Cs₂AgInCl₆:Al³⁺ Double Perovskite Nanocrystals [Rachna](#) . and Sameer Sapra; Indian Institute of Technology, India

Significant research efforts have been directed towards modification of STEs in lead-free halide double perovskite Cs₂AgInCl₆ to improve its suitability for white light applications. However, limited attention has been given to exploring the fundamental photophysical phenomenon of this material. Herein, we have demonstrated that the precise introduction of Al³⁺ can effectively adjust the material's bandgap, leading to red shifted excitation energy and enhanced STE emission. Additionally, cryogenic PL measurements discovered an inhomogeneous nature of STE emission due to the presence of defect states and is subject to thermal quenching. The increased Hyang Rhys factor show better electron phonon coupling and high density of STE states post Al³⁺ doping. Ultrafast transient absorption spectroscopy elucidated the trapping of charge carriers and provided insights into the effects of Al³⁺ doping on the formation self-trapped states. Overall, this study offers a comprehensive understanding of the origins of self-trapping in Cs₂AgInCl₆ and emphasizes the potential of compositional engineering to mitigate self-trapping in this material.

5:00 PM CH04.03.04

Microscopic Behaviour of Hydrogen and hHydrides in Atom Probe Tomography of Zirconium [Aïssatou Diagne](#) and [Lorenzo Rigutti](#); University of Rouen Normandie, France

The understanding of Zirconium (Zr) and Hydrogen (H) interactions is a topic of interest in the field of materials science. Zr is known to have a strong affinity with hydrogen, which can lead to the formation of hydrides that can affect the mechanical properties (embrittlement, cracking, etc) of the material [1]. Our studies are carried out on pure Zr analysed by laser-assisted atom probe tomography. This is complex, because the hydrogen detected during the analysis could come from the analysis chamber (parasitic hydrogen) or from the material (hydrogen contained in the material). Our results show the formation of hydrogen species H⁺, H₂⁺, H₃⁺ and hydrides ZrH_x²⁺. The evolution of the relative abundances of H⁺, H₂⁺, H₃⁺ depends on the surface field estimated from the Zr³⁺/Zr²⁺ ratios, as seen in previous studies on other materials[2]. This is not the case for the hydrides which overlap with the Zr isotopic species. In this contribution we will discuss the quantification of hydrogen and zirconium hydrides and their dependence on the field.

[1] J. Bair, M. Asle Zaeem, et M. Tonks, « A review on hydride precipitation in zirconium alloys », *J. Nucl. Mater.*, vol. 466, p. 12, nov. 2015, doi: 10.1016/j.jnucmat.2015.07.014.

[2] L. Rigutti *et al.*, « Surface Microscopy of Atomic and Molecular Hydrogen from Field-Evaporating Semiconductors », *J. Phys. Chem. C*, vol. 125, n° 31, p. 17078, août 2021, doi: 10.1021/acs.jpcc.1c04778.

5:00 PM CH04.03.05

Atomic Spatiotemporal Characterization of Light-Emitting 2D Materials by Cathodoluminescence and Femtosecond Photoluminescence Spectroscopies [Ruofei Zheng](#)¹, [Ariel Petruk](#)¹, [Kostyantyn Pichugin](#)¹, [Mike Fleischauer](#)², [Darren Homeniuk](#)², [Tyler Lott](#)¹, [Mark Salomons](#)² and [Germán Sciaini](#)¹; ¹University of Waterloo, Canada; ²National Research Council of Canada, Canada

The emerging realm of two-dimensional (2D) materials has introduced remarkable advancements in the fields of optoelectronics and photonics. To harness the full potential of these materials, a comprehensive understanding of their light-emitting characteristics at atomic spatiotemporal scales is indispensable. Cathodoluminescence (CL) integrated within a scanning electron microscope (CL-SEM) or scanning transmission electron microscope (CL-STEM) is capable of conferring material properties with sub-nanometer spatial and spectral resolutions, surpassing the limitations of traditional photoluminescence (PL) techniques imposed by the Abbe diffraction limit. Furthermore, time-resolved photoluminescence (TrPL) spectroscopy enables the characterization of ultrafast electron-hole recombination dynamics through the up-conversion technique, employing ultrashort excitation and gating laser pulses. In this context, our specifically designed sample holder and spectrometer, integrated with the high-resolution Hitachi S5500 SEM and equipped with sample loading chips featuring ultrathin windows, are aimed to develop an atomic-resolution hyperspectral CL-SEM/STEM imaging system. Additionally, in conjunction with our homemade ultrafast TrPL setup, the ultimate goal is to investigate the electronic and optical characteristics of 2D materials at the atomic scale, encompassing both spatial and temporal dimensions.

5:00 PM CH04.03.06

Photoluminescence of Up-Conversion Nanoparticles with High Spatial Resolution [Eugeniy Ermilov](#), Christian Oelsner, Volker Buschmann, Matthias Patting and Rainer Erdmann; PicoQuant GmbH, Germany

Up-conversion nanoparticles (UCNPs) are highly attractive for avoiding autofluorescence in application cases in biosensing and imaging. Characterizing the photophysical properties of such nanoparticles is essential to enhance the efficiency of preparation methods as well as their electronic and optical properties. Up-conversion is a strongly power dependent energy-transfer process which is based on excitation in the NIR and photon emission in visible range. The commonly used steady-state methods (i.e. excitation and emission spectroscopy) provide valuable insights into the photophysical of samples. However, such results give only a partial view of a sample's behavior after photoexcitation. A further piece of the puzzle is often revealed by performing

time-resolved luminescence spectroscopy. Combination of spectral and lifetime information of a sample's luminescence allows for a deeper insight into photophysical processes occurring after light absorption. This can be further enhanced by including spatial information. Time-resolved photoluminescence (TRPL) imaging is a powerful technique for characterizing and inferring structural-to-photophysical relationships in up-conversion materials. Additionally, the kind of imaging method and the power applied to the sample are further parameters which are important for understanding TRPL imaging results. Gathering such information and knowing the chosen parameters are important steps toward the optimization of structure as well as preparation process of UCNPs, resulting in increased performance of such materials.

We will demonstrate here the performance of a spectrometer-microscope assembly for characterization and analysis of UCNPs in terms of lifetime, spectral, and spatial resolution, which provides more information in combination than can be obtained using only lifetime or only steady-state experiments.

5:00 PM CH04.03.07

Multi-Modal Synchrotron X-Ray Techniques for Visualizing 3D Brittle Fracture [Sara F. Gorske](#)¹, Mythreyi Ramesh², Jun-Sang Park³, Peter Kenesei³, Hemant Sharma³, Jonathan Almer³, Peter Voorhees² and Katherine Faber¹; ¹California Institute of Technology, United States; ²Northwestern University, United States; ³Argonne National Laboratory, United States

Fracture is difficult to assess in real time. Even when crack propagation can be measured as it is occurring, usually only a 2-dimensional state can be quantified. Assessing 3-dimensional (3D) fracture has traditionally relied on post mortem analysis, but this does not capture the full intricacies of a growing crack front, such as a nonconstant velocity and shape. For brittle fracture, where very little plastic deformation occurs between the accumulation of stress concentration at a crack tip and its extension, these difficulties are compounded. Furthermore, a material's microstructure has a major effect on crack propagation, including its direction, speed, tortuosity, and even whether it arrests at points as a result of unequal stress distribution. Because of these complications, predicting crack paths, speeds, and shapes is a thorny problem which needs more in-situ data from 3D cracks occurring in real materials. Utilizing multi-modal x-ray characterization techniques available at a synchrotron source is a promising method for visualizing a crack's growth and directly relating it to the microstructure and micromechanical state of the studied material.

Our suite of multi-modal characterization techniques include far-field high-energy diffraction microscopy (FF-HEDM), near-field high-energy diffraction microscopy (NF-HEDM), and micro-computed tomography (u-CT). FF-HEDM provides per-grain elastic strain tensors, while NF-HEDM provides a high-quality shape and location for each grain. u-CT identifies the location of a crack in a material. Combining this information allows us to relate the grain structure and mechanical state found by the HEDM techniques with the crack location.

In this work, the material studied was aluminum oxynitride (AlON), a cubic ceramic with randomly oriented anisotropic grains on the order of 100 μm . The Rotational and Axial Motion System (RAMS) [1] at the 1-ID beamline of the Advanced Photon Source at Argonne National Laboratory was used to carefully grow the crack and conduct these experiments. The sample being investigated was machined into the double-cleavage drilled compression (DCDC) geometry with parallelepiped dimensions of 18 mm x 1.4 mm x 1.4 mm and a hole diameter of 0.42 mm. The application of a uniaxial compressive load caused a crack to pop in to a length on the order of 100 μm , and the crack was grown to over 1 mm by the application of further compressive load.

Every grain in the material had unique stress and strain tensors at each load that were not identical to the applied stress. Crack propagation characteristics such as its speed and path (intragranular or intergranular) were influenced as the crack interacted with these grains and complex micromechanical stress states. Because of the DCDC geometry, the crack could be grown a short distance, and then the loading could be paused along with the crack extension, creating a near in-situ state for analysis. By taking u-CT and HEDM scans in this load-controlled state, the relative extension of the crack with the increase in loading could be monitored, while also providing information on what features and grains in the microstructure caused the crack to slow down, arrest its propagation, or divert its direction of extension. We have found that certain grain orientations and accompanying stress tensors acted as barriers to crack extension and forced the crack either to change directions or to pause and accumulate enough stress concentration energy to advance. These findings can be used to inform computational methods and predictive models for future studies of brittle fracture.

[1] Shade, P. A., Blank, B., Schuren, J. C., Turner, T. J., Kenesei, P., Goetze, K., Suter, R. M., Bernier, J. v., Li, S. F., Lind, J., Lienert, U., & Almer, J. (2015). A rotational and axial motion system load frame insert for in situ high energy x-ray studies. *Review of Scientific Instruments*, 86(9), 93902. <https://doi.org/10.1063/1.4927855>

5:00 PM CH04.03.08

Thermal Stability of Calcium Carbonate and its Relationship with The Crystalline Growth of The Mineralized Phases Present in Chicken Eggshells [Nerith R. Elejalde-Cadena](#) and Lauro Bucio-Galindo; National Autonomous University of Mexico, Mexico

Biom mineralization processes in nature are associated with a structural control carried out by biomolecules (DNAs, proteins, and polysaccharides). There are two biom mineralization processes, which are usually used by living organisms in terms of producing biom minerals: (1) organic matrix-mediated biom mineralization, known to be a highly regulated and homogeneous process; (2) biologically induced biom mineralization, where mineralization deposits occur indefinitely and heterogeneously. However, little structural information is known about the macromolecules that constitute and act in the living organisms in these processes, since the level of structural organization of biom minerals is often hierarchical in different structural orders to produce a final structure with a unique morphology with properties that until now have not been reproduced by man. Among the processes mediated by a membrane, like in diatoms, of which the importance of biological entities is appreciated, there is a rigid and porous cell wall called a frustule composed of amorphous silica. It also appears in bones comprised mainly of calcium phosphate, and in eggshells whose percentage of calcium carbonate can vary depending on the species.

However, there is a lack of a universal model that will allow us to obtain information about these two biom mineralization processes. Therefore, this poster presentation will be focused on using the mineral phase and the membranes of the eggshells from chickens that are with a controlled diet (industrial sale) and those that are free (organic) as a model to differentiate the calcification, ensuring its permeability to stabilize the amorphous mineral part. By the thermal stability analysis, we will be able to obtain information on the process of formation of the eggshells as well as on the change that occurs in the membrane during the formation of crystals. The topographical analysis was performed via X-ray diffraction (XRD) and scanning electronic microscopy (SEM). The investigation has an important impact in the fields of biological and materials sciences, which would provide an effective understanding of the biom mineralization processes. Additionally, this research will also allow us to know how to mimic them since most of the studies carried out are focused on immunohistochemical studies on the formation of the chicken eggshell.

5:00 PM CH04.03.09

Monitoring Ultrafast Structural Phenomena in 2D Materials by Femtosecond Electron Diffraction [Christian Viernes](#), Sam Netzke, Kostyantyn Pichugin and Germán Sciaini; University of Waterloo, Canada

The structure of a material is a large factor determining its properties. An emerging field of research and development is in 2D materials which can exhibit

very different physical properties compared to their bulk counterparts. Transition metal dichalcogenides are of particular interest owing to their band structure tunability, such as a transformation from an indirect to direct band gap when thinned down to a monolayer and band gap shifts by vertically stacking TMDCs into a heterostructure, giving these crystals a wide range of potential applications in electronics. Additionally, TMDCs are able to crystallize into several different structures. Combined with the use of ultrafast lasers, it is possible to drive structural phase transitions allowing control and switching between desirable properties. However, in order to take advantage of these characteristics, a better understanding of the photoinduced structural dynamics is required.

In our presentation, we introduce an ultracompact 100-kV femtosecond electron diffraction (FED) setup. This instrument has been designed to produce ultrashort electron bursts, approximately 200-fs in duration, containing 10000 electrons. Ultrafast structural dynamics in solids often unfold within hundreds of femtoseconds to tens of picoseconds, necessitating cutting-edge techniques like femtosecond electron diffraction. This pump-probe method is sensitive to structural alterations. Here, an ultrafast laser splits into two beams: the pump and probe. The laser pump pulse initiates the changes whereas a time-delayed electron probe bunch monitors, stroboscopically, the sample's structure. We will show some recent FED results obtained in a model TMDC system.

5:00 PM CH04.03.10

Structural Evolution and Phase Transition of Geopolymers in Extreme Environmental Conditions: *In-Situ* SAXS/WAXS Study at High Temperatures under Uniaxial Tension S A K V Miyurudarshi Piyathilake¹, Ivan Kuzmenko², Luckshitha Suriyasena Liyanage^{3,4} and Christopher Bareither¹; ¹Colorado State University, United States; ²Argonne National Laboratory, United States; ³National Institute of Standards and Technology, United States; ⁴University of Colorado Boulder, United States

Polyethylene based geomembrane (PE GMB) waste containment infrastructures are used as barrier systems to mitigate contaminant release to protect the environment. In the field, PE GMBs are exposed to extreme environmental conditions such as harsh mining solutions, high stress and elevated temperatures that could compromise durability and performance due to geochemical reactions, microstructural phase transitions and crystallinity changes. Therefore, it is essential to investigate real-time, high temperature structural evolution of PE GMBs in the field.

In this study we performed in-situ SAXS/WAXS experiments to evaluate the impact of temperature and stress on chemically and mechanically treated PE GMBs using synchrotron radiation at Argonne National Laboratory. Initially, they were exposed to bauxite mining process solution (pH=12.3) for 10 months and 2 GPa normal stress to simulate real-world environmental conditions. Subsequently, in-situ SAXS/WAXS data was collected every 10 seconds while applying tensile stress (strain rate of 83 um/sec) at 25°C and 65°C. Tensile stress-strain traces were obtained simultaneously.

SAXS/WAXS data provide valuable insights into micro and atomic level changes as well as the microscopic phase transitions of PE GMBs. As we stretch samples at 25°C, initial isotropic 2D SAXS pattern (that corresponds to spherulitic structure of lamellae with initial long period of 20.9 nm) gradually becomes anisotropic and decreases in q-peak intensity indicating extension of the long period due to orientation of crystals along stretch direction. The intensity of the q-peak shows a significant drop at 23% of tensile strain for the untreated reference sample. However, this structural transformation occurs at 46% of strain for the treated specimens, indicating a delay compared to the untreated ones. This suggests increased material rigidity/stiffness after treatments. The formation of cross-linking due to polymer oxidation in harsh chemical environments and strain crystallization under 2 GPa stress contribute to the higher stiffness of the treated specimens. XPS and FTIR analysis confirm the formation of free radicals and oxidative byproducts (alcohols, ketones, carbonyl compounds) in the treated specimens. The tensile strength data further support these conclusions by demonstrating increased stiffness in the treated specimens. In addition, as the stress is applied, WAXS crystalline peaks from (110) and (200) planes show a reduction in crystallinity for treated and untreated specimens at 99% and 30% tensile strains respectively. These results again indicate chemically treated specimens have become stiffer and lost their original elasticity post exposure.

At 65°C, a new crystalline peak emerges with a long period of 15.7 nm representing the formation of shish-kebab superstructure consisting of long central fiber core (shish) and lamellae crystals (kebab) periodically growing along the shish under hot-stretching. This recrystallization transition occurs sooner in treated specimens which once again confirms mechanical property alteration of treated specimen under extreme environmental conditions.

Yield strength values obtained from stress-strain traces are also consistent with the increase of material rigidity after treatments. The initial yield strength of treated samples at both 25°C (11.5 MPa) and 65°C (6.4 MPa) are higher than those of untreated samples at 25°C (10.6 MPa) and 65°C (5.6 MPa). We propose in-situ SAXS/WAXS technique to study the dynamic structural evolution and phase transition phenomena in polymer based geomaterials under high temperatures, stresses, and harsh chemical environments to build robust waste containment systems to protect the environment.

5:00 PM CH04.03.11

Effect of Phase Transition caused by Different Treatment Process on Mechanical Properties of Powder Metallurgy Titanium Alloys Jie Wu; Institute of Metal Research, Chinese Academy of Sciences, China

The microstructural evolution and mechanical properties of powder metallurgy Ti-22Al-24Nb-0.5Mo prepared by combination of hot isostatic pressing, ring rolling, and heat treatment were investigated. Ring rolled and solution treatment in the ($\alpha_2 + B2 + O$) region led to the refinement of grain size and long lath O phase and α_2 phase mostly located at the grain boundaries. Aging treatment in the (B2 + O) region caused the occurrence of peritectoid reaction $B2 + \alpha_2 \rightarrow O$ owing to the segregation of the Nb element and refined the acicular O phase. The mechanical properties of PM alloys varied with the size and volume fraction of O phase and α_2 phase. The long lath O phases improve the elongation and acicular O precipitates are benefit to the elevation of alloy strength.

5:00 PM CH04.03.12

Microstructural Investigation of Work Hardening Behavior of Lightweight Steel using *In-Situ* Straining TEM Sung-Dae Kim; Pukyong National University, Korea (the Republic of)

We conducted microstructural investigations on the effect of κ -carbide precipitates on the strain hardening behavior of aged Fe-Mn-Al-C alloys. The precipitate-strengthened Fe-Mn-Al-C alloys exhibited a superior strength-ductility properties which are enabled by the strain hardening rate recovery. To understand the relation between the precipitates and strain hardening recovery, dislocation gliding alloys during plastic deformation was analyzed through in situ tensile transmission electron microscopy (TEM). The in situ TEM results confirmed the particle shearing mechanism leads to planar dislocation glide. During deformation of the overaged alloy, some gliding dislocations were strongly blocked by the large κ -carbide precipitates and were prone to cross-slip, leading to the activation of multiple slip systems. The abrupt decline in the dislocation mean free path by the activation of multiple slip leads the rapid saturation of the strain hardening recovery. It is concluded that the planar dislocation glide and sequential activation of slip systems are key to induce strain hardening recovery in polycrystalline metals. In the present study, we conducted the in-situ straining TEM experiments with a precipitation hardened (PH) Fe-Mn-Al-C alloy. By observing the dislocations/precipitates interaction in real-time, clear understandings of the hardening mechanism

could be extracted.

5:00 PM CH04.03.13

A Micro Mechanical and Chemical Analysis of a New Vitrified Rock Material for use in Environmental Sustainability Eve Meltzer and Herbert Einstein; Massachusetts Institute of Technology, United States

Extraction of the energy available via geothermal heat in the Earth could provide substantial contributions to U.S. energy needs long-term. However, there are major technical and economic limitations with the current technology available for Enhanced Geothermal Systems (EGS). I work on a new technology in the field of EGS that uses a millimeter (MM) wave gyrotron, which allows for more efficient ultra-deep drilling. The gyrotron heats rock to temperatures ranging from 1500 to 3000°C, transforming the rock into its liquid state. Upon cooling, the new material solidifies around the circumference of a well bore hole, creating a vitrified lining.

I have conducted an in-depth micro-mechanical and chemical analysis of the vitrified material from the melting and re-solidifying of basalt. Basalt is an igneous rock that forms from the solidification of molten lava and primarily consists of minerals such as plagioclase, feldspar, pyroxenes, and olivine. And thus, when heated, the elements within these minerals go through transformation processes; this includes the formation of iron oxides as well as the possible reduction of iron. To do my study I used a combination of experimental methods including Scanning Electron Microscopy (SEM), Energy Dispersive X-ray Spectroscopy (EDS), optical imagery, micro- and nano-indentation, and Raman spectrometry. These experiments allow me to quantify the micro- and nano-scale properties. The presence of mineral phase changes and elemental differences in the basalt pre- and post-melting are evident and thus understanding these differences can give insight into the future use of this material in the field of EGS, sustainable mineral extraction, and beyond.

5:00 PM CH04.03.15

Quenching Effects on Topological Defects in Magnetoelectric CuO Nanoparticles Nimish P. Nazirkar, Xiaowen Shi and Edwin Fohntung; Rensselaer Polytechnic Institute, India

CuO stands out among the few identified binary multiferroic materials, boasting a transition temperature of about 230 K — a value notably higher than other materials. In CuO, electric polarization emerges due to spontaneous magnetic order. Even a minimal application of magnetic fields can induce a transition from the paraelectric to a ferroelectric phase, observed at 213 K [1]. Interestingly, topological defects in such materials exhibit remarkably different properties at the nanoscale compared to their bulk counterparts [2]. Bragg coherent diffractive imaging has proven to be a reliable method for the three-dimensional characterization of nanoscale ferroelectrics [3,4]. By integrating magnetic quenching with Bragg Coherent Diffractive Imaging on CuO nanoparticles, we successfully investigated the nanocrystal's structural alterations and how they relate to the material's ferroelectric landscape. References:

- [1] Wang, Z., Qureshi, N., Yasin, S. et al. Magnetoelectric effect and phase transitions in CuO in external magnetic fields. *Nat Commun* 7, 10295 (2016). <https://doi.org/10.1038/ncomms10295>
- [2] X. Shi, N. P. Nazirkar, R. Kashikar, et al. Enhanced piezoelectric response at nanoscale vortex structures in ferroelectrics arXiv preprint arXiv:2305.13096 (2023).
- [3] Karpov, D., Liu, Z., Rolo, T. et al. *Nat Commun* 8, 280 (2017). <https://doi.org/10.1038/s41467-017-00318-9>
- [4] D. Karpov, Z. Liu, A. Kumar, B. Kiefer, R. Harder, T. Lookman, and E. Fohntung, *Phys. Rev. B* 100, 054432 – Published 22 August 2019

Acknowledgments

We acknowledge support from the US Department of Energy (DOE), Office of Science, under grant No. DE-SC0023148. E.F. also acknowledges support from the US Department of Defense, Air Force Office of Scientific Research (AFOSR), under award No. FA9550-23-1-0325 (Program Manager: Dr. Ali Sayir) for work on probing topological vortices and piezoelectric enhancements. This research used resources of the Advanced Photon Source (APS), a U.S. Department of Energy (DOE) Office of Science User Facility, operated for the DOE Office of Science by Argonne National Laboratory (ANL) under contract No. DE-AC02-06CH11357.

SESSION CH04.04: Dynamics Study by X-ray
Session Chairs: Tao Sun and Tao Zhou
Wednesday Morning, April 24, 2024
Room 443, Level 4, Summit

8:00 AM CH04.04.01

Modulation Excitation Coupled with X-Ray Absorption Spectroscopy for Probing The Restructuring Dynamics of Surface Species in Bimetallic Nanocatalysts Prahlad Kumar Routh and Anatoly Frenkel; Stony Brook University, United States

Rational catalyst design guided by a combined theoretical-computational-experimental approach has recently allowed the development of a “dynamic catalyst” using dilute alloy components. These bimetallic nanocatalysts possess dual functionality with a minority metal as the active element and a majority element as a less reactive environment to impart selectivity. Furthermore, the composition and pretreatment of these nanocatalysts can be used to selectively tune the active species on surface. Such dynamic restructuring of surfaces creates a complex behavior of these dynamic catalysts, under operando conditions in response to the changes in reactive environment. A notable challenge is the detailed understanding of the structure and evolving composition of catalytic species on nanoparticle surfaces during reactions. In-situ X-ray absorption spectroscopy (XAS) is a potential tool to elucidate this, but its efficacy is hampered by the dilute and varied nature of active sites. However, the dilute nature of the active sites, heterogeneity associated with nanoparticles as well as active sites, and the ensemble nature of XAS itself, presents significant challenges in sensitivity to active species.

In this work, we addressed these challenges by enhancing XAS sensitivity with a modulation excitation approach, focusing on 30% Pd-Au supported bimetallic nanocatalysts. We applied a modulation excitation approach to the X-ray absorption spectroscopy (ME-XAS) by inducing structural changes in the 30% Pd-Au supported bimetallic nanocatalysts (ca. 6 nm in diameter) via the gas (H₂ and O₂) concentration modulation and resolved the structure and kinetics of different surface species with 1s time resolution. We demonstrated that ME-XAS dramatically improves the sensitivity towards surface species in bimetallic alloys – the active species in dynamic catalysts. We isolated the minor contributions (3-7 at. %) of different surface species, such as Pd-Au ensembles and Pd oxides, from the total XAS data and discovered that they respond dynamically to the periodic modulation conditions. During the oxygen pulse, the formation of surface PdO_x species dominates over the bulk-to-surface segregation of Pd. During the hydrogen pulse, Pd dissolution within the Au

host drives the oxide decomposition. Such direct experimental measurement of the active species in various catalytic systems has been a challenge, given the heterogeneity associated with these active sites and the absence of a technique which can selectively measure the active species and its dynamic evolution as the reaction conditions progress. This work provides an experimental pathway to not only study the dynamic nature of active species but also enables designing non-equilibrium states of dynamic catalysts. The methodology and findings presented herein can be applied to a broad class of multicomponent nanoalloys and processes involving the active minority species, for which the ensemble-average spectroscopy data are dominated by spectators.

8:15 AM CH04.04.02

***In-Situ/Operando* Bragg Coherent X-Ray Diffraction Imaging for Visualization of Nanoscale Structural Evolution** [Wonsuk Cha](#); Argonne National Laboratory, United States

In the last two decades, Bragg Coherent X-ray Diffraction Imaging (BCDI) has become a powerful non-destructive 3D characterization tool for features in nanoscale [1]. Because of unique sensitivity to lattice, BCDI has been employed on various nano-scaled materials such as metal, metal oxide, and mineral, to reveal 3D map of lattice distortion and strain distribution. Adding in-situ and operando approaches to BCDI enables to address scientific questions on physics, chemistry, and materials science in recent years.

In this talk, I will introduce current state-of-art of BCDI and recent experimental results on in-situ and operando BCDI. Annealing effect on gold grains on thin films [2], relaxation of strain inside quantum materials such as nanodiamond and silicon carbide [3, 4]. Strain and defect in battery materials [5] and in catalysts [6] will be discussed. In addition, some estimates of BCDI in the near future will be discussed.

[1] M. A. Pfeifer, et al., Nature 442, 63 (2006).

[2] A. Yau, et al., Science 356, 739 (2017).

[3] S. O. Hruszkewycz, et al., APL Mater. 5, 026105 (2017).

[4] S. O. Hruszkewycz, et al., Phys. Rev. Mater. 2, 086001 (2018).

[5] A. Singer, et al., Nat. Energy 3, 641 (2018).

[6] D. Kim, et al., Nature Communications, 9, 3422 (2018).

8:30 AM *CH04.04.03

Nanoscale Imaging of Structure and Dynamics through Time-Resolved Hard X-Ray Diffraction Microscopy Martin V. Holt and [Tao Zhou](#); Argonne National Laboratory, United States

The unique imaging power of nano-focused synchrotron hard x-rays can be harnessed to provide non-destructive methods for 3D visualization of crystallographic phase and strain in solid-state materials. This gives access to understanding extremely subtle lattice perturbations ($<10^{-4}$ dc/c) near optically active defects or interfaces within fabricated heterostructures that can be located potentially microns away from surfaces without sectioning the sample. The use of time-resolved coherent synchrotron illumination synchronized to external stimuli can further augment this approach to understand excitation-driven energy flow and dynamic structure-function relationships across broad classes of classical and quantum materials for energy. Current work and future directions enabled by the near-term completion of diffraction limited storage rings such as the Advanced Photon Source Upgrade (APS-U) and correlative data synthesis with quantitative electron microscopy methods will be explored in the context of recent results

9:00 AM *CH04.04.04

Coherent Acoustic Wave Propagation in Two-Dimensional Metal Halide Perovskites [Peijun Guo](#); Yale University, United States

I will discuss our recent efforts on the development of spatiotemporal optical imaging techniques to examine coherent strain waves in quasi-two-dimensional (2D) metal halide perovskites (MHPs). Specifically, I will describe our experiments performed on a variety of 2D MHPs with different number of octahedral layers, where the experiments employ hyperspectrally-resolved pump and probe pulses and cover a unique nanosecond-to-microsecond time range. The effects of the choices on the halides and the organic cations will be discussed as well. If time permits, I will also discuss our results on the self-trapped excitons in double perovskites examined by optical-pump x-ray diffraction experiments.

9:30 AM CH04.04.05

Full-Field Strain Measurements in Homogeneous Solids: High-Resolution Speckle-Free Flux Enhanced Tomography [Zifan Wang](#); University of Cambridge, United Kingdom

X-ray computed tomography (XCT) is a reliable tool for measuring internal flaws and microstructural features in engineering materials. As an extension to XCT, Digital Volume Correlation (DVC) methodology enables tracking 3D deformations based on local grayscale contrast. Nevertheless, its applicability and spatial resolution have been limited by the need for tracer particles or inherent microstructural features that are properly distributed in the material. To address these limitations, we developed a Flux Enhanced Tomography for Correlation (FETC) technique that leverages inherent inhomogeneities in engineering materials (polymers to metals) to track 3D material point displacements without relying on artificial speckles or inclusions. Combined with a Eulerian/Lagrangian transformation in a DVC methodology, FETC allows us to measure all nine components of the deformation gradient within specimens undergoing extreme deformations at microscale resolution. FETC expands the capabilities of laboratory-based XCT and provides large datasets for data-driven constitutive modelling approaches.

9:45 AM BREAK

10:15 AM *CH04.04.06

Keyhole Dynamics in Laser Powder Bed Fusion Additive Manufacturing [Tao Sun](#); Northwestern University, United States

Laser powder bed fusion (LPBF) is the most extensively used metal additive manufacturing technology due to its unique capabilities in building parts with high geometric complexity and fine features. During the LPBF process, sparks (i.e., spattered particles) can be observed following the laser scanning path, indicating the presence of high-velocity vapor arising from the melt pool. Indeed, strong metal vaporization occurs in LPBF, resulting in recoil pressure that creates a depression in the melt pool, often referred to as a keyhole. The keyhole is an important dynamic structural feature in LPBF as it influences energy coupling, metal melting mode, and defect generation. Without a keyhole, the laser is absorbed by the metal surface only once, with significant amount of energy being reflected away. In contrast, with the presence of a deep keyhole, multiple laser absorption events occur, significantly increasing laser absorption efficiency. The laser melting mode can shift from conduction to transition, stable keyhole, and then unstable keyhole as the energy input increases. When the conduction mode is applied, lack-of-fusion voids may be generated during the build. An unstable keyhole condition also leads to porosity.

Keyhole porosity is a major defect that hinders the widespread adoption of laser-based metal additive manufacturing technologies. With simultaneous high-speed synchrotron X-ray imaging and thermal imaging, coupled with multi-physics simulations, we discovered two types of keyhole oscillation in laser powder bed fusion of Ti-6Al-4V. Amplifying this understanding with machine learning, we developed an approach for detecting the stochastic keyhole porosity generation events with sub-millisecond temporal resolution and near-perfect prediction rate. The highly accurate data labeling enabled by *operando* X-ray imaging allowed us to demonstrate a facile and practical way to adopt our approach in commercial systems.

10:45 AM CH04.04.07

Gas Pore Formation in Powder Bed Fusion [Kaitlin Lyszak](#), Erin B. Curry, Lauren A. Gorman, Donal Sheets, Lukas Lasig and Jason Hancock; University of Connecticut, United States

Additive manufacturing (AM) of metal materials based on powder bed fusion technology is widely used now in many industries. A known limitation of this type of manufacturing is the formation of gas pores in bulk material arising from stochastic events related to molten metal fluid instabilities of a vapor depression. Here we present a combined X-ray imaging and infrared pyrometry study of pore formation in repeated adjacent tracks, and quantify the correlations of pore positions and sizes for a common material (Aluminum 6061) of interest in AM as a function of its laser processing conditions. We find in both cases that an existing pore in one track often catalyzes the formation of another pore in a consecutive track at the distance of closest approach. In a raster scan strategy commonly used to construct bulk material, this phenomenon has the result of forming perforations, or lines of pores transverse to the scanning direction in a rastered patch. If controlled, this effect can be eliminated to improve the yield strength of the build, or exploited to create programmable failures for specific purposes.

Distribution A. Approved for public release: distribution unlimited. (AFRL-2023-5001) Date Approved 10-10-2023.

11:00 AM CH04.04.08

Thermal Dynamics of $\text{Na}_{0.67}\text{Ni}_{0.33}\text{Mn}_{0.67}\text{O}_2$ Cathode Materials for Sodium Ion Batteries studied by *In Situ* Analysis [Dewen Hou](#)¹, Eric Gabriel¹, Tianyi Li², Yuzi Liu² and Claire Xiong¹; ¹Boise State University, United States; ²Argonne National Laboratory, United States

Layered $\text{Na}_{0.67}\text{Ni}_{0.33}\text{Mn}_{0.67}\text{O}_2$ is an attractive cathode material for sodium ion batteries. The thermal stability of cathode materials is crucial to their practical applications. In this work, we investigate structural and morphological evolution in layered P2-type $\text{Na}_{0.67}\text{Ni}_{0.33}\text{Mn}_{0.67}\text{O}_2$ cathode materials during annealing via *in situ* synchrotron X-ray diffraction and transmission electron microscopy. Insights are obtained from two complementary *in situ* characterizations at different length scales in terms of the thermal stability of P2- $\text{Na}_{0.67}\text{Ni}_{0.33}\text{Mn}_{0.67}\text{O}_2$ cathode materials. The results indicate that the hexagonal P2 phase remains unchanged during the heat-treatment process, and thermally driven expansion/contraction of the lattice parameters exhibits an anisotropic change in the *a* and *c* directions. In addition, interfaces/grain boundaries play an important role in the structural stability, which leads to the distinct morphological evolution between the polycrystalline and single-crystal particles.

11:15 AM CH04.04.09

***Operando* XAS-XRD Reveals Structural Dynamics in CoPt Nanoparticles under Dry Reforming of Methane Conditions** [David Niedbalka](#), Marcel Janak, Diana Piankova, Paula Abdala and Christoph R. Müller; ETH Zurich, Switzerland

Gaining insight into how the geometric and electronic structure of (mono)metallic nanoparticles is modified through the addition of a second metal (bimetallic nanoparticles) and how such structural changes affect in turn their catalytic properties¹ is crucial for the rational advancement of catalysts. Further, as the structure of a catalyst is often dynamic² *ex-situ* characterization methods may be insufficient to describe the active phases of a catalyst. Therefore, *operando* studies are key to correlate a catalyst's structure to its performance while relying at the same time on well-defined model systems.

The dry reforming of methane (DRM) is a reaction that converts CH_4 and CO_2 into a synthesis gas at 600-1000 °C and is typically catalyzed by transition metals such as Ni, Co, or Pt. However, such monometallic catalysts often suffer from deactivation due to particle growth, carbon deposition, and/or oxidation.

In this study, we investigate SiO_2 -supported, bimetallic CoPt nanoparticles and their monometallic counterparts (CoPt/ SiO_2 , Co/ SiO_2 , and Pt/ SiO_2) for the DRM. Prior to the catalytic DRM tests, all catalysts were activated *in-situ* in a H_2/N_2 mixture (1-2 h). The bimetallic CoPt/ SiO_2 catalyst shows superior activity and stability under DRM conditions (800 °C and 1 bar, $\text{CH}_4:\text{CO}_2$ ratio = 1, space velocity = 30,000 $\text{ml g}^{-1} \text{h}^{-1}$) in comparison to its monometallic counterparts. Specifically, while Pt/ SiO_2 showed the lowest CH_4 conversion (10%), Co/ SiO_2 underwent deactivation, resulting in a decrease in CH_4 conversion from 30% to 15% within 120 min. Conversely, CoPt/ SiO_2 showed a stable performance of 35% CH_4 conversion over 6 h.

To elucidate the structure of the active phase in CoPt/ SiO_2 under DRM conditions, and to probe structural dynamics, we conducted *operando* experiments using combined synchrotron X-ray absorption spectroscopy (XAS) and X-ray diffraction (XRD). Co K-edge and Pt L₃-edge XAS analysis shows that in CoPt/ SiO_2 during *in-situ* H_2 activation Co and Pt become both fully reduced to their metallic states. We further observe differences in the Co K-edge and Pt L₃-edge XAS features of CoPt/ SiO_2 when compared to Co/ SiO_2 or Pt/ SiO_2 , possibly due to a charge transfer between the metals, orbital hybridization in the CoPt alloy and/or a change in the local structure of Pt and Co.³ Rietveld analysis of the acquired XRD data after *in-situ* activation at 800 °C indicates the formation of two types of CoPt alloys: an ordered (intermetallic) CoPt (52%) and a random CoPt alloy (48%). Interestingly, upon switching to DRM conditions (800 °C, $\text{CH}_4:\text{CO}_2$ ratio = 1) XRD analysis revealed an instantaneous transformation of the intermetallic phase into a random alloy. This phase transition was also evidenced in the Pt L₃-edge XAS data but did not change the electronic structure/oxidation state of Co (i.e., Co K-edge remained invariant prior to and during DRM). In contrast, under DRM conditions, Co/ SiO_2 underwent a partial oxidation showcasing the stabilization of the metallic state of Co through its alloying with Pt. This stabilization, combined with changes in the electronic/local structure and site isolation that very likely suppresses coking on Pt, contribute to the superior activity of CoPt/ SiO_2 compared to Co/ SiO_2 and Pt/ SiO_2 .

We also observe a phase transition from a random to intermetallic alloy during the cooling down to room temperature of the reacted catalyst, underscoring the significance of *operando* characterization in capturing dynamic changes and identifying the catalytically active phase.

(1) Nakaya, Y.; Furukawa, S. *Chem. Rev.* **2023**, *123* (9), 5859-5947.

(2) Chavez, S.; Werghi, B.; Sanroman Gutierrez, K. M.; Chen, R.; Lall, S.; Cargnello, M. *J. Phys. Chem. B* **2023**, *127* (5), 2127-2146.

(3) Lee, Y. S.; Rhee, J. Y.; Whang, C. N.; Lee, Y. P. *Phys. Rev. B* **2003**, *68* (23), 235111.

11:30 AM CH04.04.10

Revealing The Mechanisms of Ultrafast Transient Liquid Assisted Growth of REBCO-Type Superconducting Thin Films by Synchrotron Radiation *In-Situ* X-Ray Diffraction [Elzbieta Pach](#)^{1,2}, Lavinia Saltarelli¹, Diana G. Franco¹, Carla Torres¹, Daniel Sánchez³, Jordi Farjas³, Eduardo Solano⁴, Cristian Mocuta², Xavier Obradors Berenguer¹ and Teresa Puig¹; ¹ICMAB-CSIC, Spain; ²Soleil Synchrotron, France; ³GRMT, University of

Girona, Spain; ⁴ALBA Synchrotron, Spain

The novel ultrafast Transient Liquid Assisted Growth (TLAG) method [1-3] is an outstanding opportunity to fabricate low-cost, high throughput epitaxial superconducting $\text{YBa}_2\text{Cu}_3\text{O}_7$ (YBCO) films using scalable methods. However, the fast kinetics of this non-equilibrium process require in-situ techniques to understand its growth mechanism and determine key process parameters. A specialized instrumentation was developed to allow investigating the dynamics of TLAG process based on in-situ monitoring of the precursors reaction, intermediate phases evolution and final products of the YBCO growth by in-situ XRD at synchrotron radiation sources at acquisition times from 2 - 100 ms/frame. This set-up allows to control the key parameters of growth of the YBCO by TLAG, this includes the temperature, partial oxygen pressure, total pressure and the heating rate, as well as to perform very fast changes in total and partial oxygen pressures. Additionally, Mass Spectrometry measures the gaseous products of the reaction. Furthermore, the resistance is measured in-situ throughout all the growth process providing valuable information on the growth rate of the superconducting phase. The installation is placed in a movable rack that allows its use in different synchrotron facilities and all the equipment is time synchronized. All of the acquired data during the combined experiments is advancing our understanding of the non-equilibrium growth mechanism and pinpoints the direction to the optimal conditions for ultrafast epitaxial growth of YBCO reaching up to 1000 nm/s.

The novel ultrafast Transient Liquid Assisted Growth (TLAG) method [1-3] is an outstanding opportunity to fabricate low-cost, high throughput epitaxial superconducting $\text{YBa}_2\text{Cu}_3\text{O}_7$ (YBCO) films using scalable methods. However, the fast kinetics of this non-equilibrium process require in-situ techniques to understand its growth mechanism and determine key process parameters. A specialized instrumentation was developed to allow investigating the dynamics of TLAG process based on in-situ monitoring of the precursors reaction, intermediate phases evolution and final products of the YBCO growth by in-situ XRD at synchrotron radiation sources at acquisition times from 2 - 100 ms/frame. This set-up allows to control the key parameters of growth of the YBCO by TLAG, this includes the temperature, partial oxygen pressure, total pressure and the heating rate, as well as to perform very fast changes in total and partial oxygen pressures. Additionally, Mass Spectrometry measures the gaseous products of the reaction. Furthermore, the resistance is measured in-situ throughout all the growth process providing valuable information on the growth rate of the superconducting phase. The installation is placed in a movable rack that allows its use in different synchrotron facilities and all the equipment is time synchronized. All of the acquired data during the combined experiments is advancing our understanding of the non-equilibrium growth mechanism and pinpoints the direction to the optimal conditions for ultrafast epitaxial growth of YBCO reaching up to 1000 nm/s.

SESSION CH04.05: Self-assembly
Session Chairs: Yuzi Liu and Michelle Mejía
Wednesday Afternoon, April 24, 2024
Room 443, Level 4, Summit

1:30 PM *CH04.05.01

Peering into the Self- and Directed-Assembly of Nanoparticles [Hongyou Fan](#); Sandia National Laboratories, United States

Self-assembly of synthetic nanoparticles enables the positioning of nanoparticles into one to three dimensional ordered arrays, facilitating integration of nanoparticle lattices into nanophotonic and nanoelectronic architectures. The functional properties of these particle materials are expected to be highly sensitive to structural factors such as coordination number, degree of long-range order, or interparticle separation distance, requiring the development of robust self- and directed-assembly pathways for precise control of structural parameters to improve optical and electronic properties of functional nanoparticles. In this presentation, I will review our past efforts in development of self-assembled nanoparticles thin film arrays and in-situ structural evolution at ambient condition. I will then extend my presentation to our recent progress in development of a new Stress-Induced Fabrication method in which we applied high pressure or stress to nanoparticle arrays to induce structural phase transition and to consolidate new nanomaterials with precisely controlled structures and tunable properties. By manipulating nanoparticle coupling through external pressure, a reversible change in their assemblies and properties can be achieved and demonstrated. In addition, over a certain threshold, the external pressure will force these nanoparticles into contact, thereby allowing the formation and consolidation of one- to three-dimensional nanostructures. Through stress induced nanoparticle assembly, materials engineering and synthesis become remarkably flexible without relying on traditional crystallization process where atoms/ions are locked in a specific crystal structure. Therefore, morphology or architecture can be readily tuned to produce desirable properties for practical applications.

Sandia National Laboratories is a multimission laboratory managed and operated by National Technology and Engineering Solutions of Sandia, LLC., a wholly owned subsidiary of Honeywell International, Inc., for the U.S. Department of Energy's National Nuclear Security Administration under contract DE-NA0003525.

2:00 PM CH04.05.02

Design of Open Systems using Aqueous Polymer Solutions causing Meniscus Splitting Phenomena [Reina Hagiwara](#) and Kosuke Okeyoshi; Japan Advanced Institute of Science and Technology, Japan

Self-organization is a process commonly observed in soft matter and in spontaneous phenomena of life. Extracting and reproducing in vitro the physicochemical conditions is an important step beyond designing "life-like" materials having smart responses to environmental change. The behavior of polymeric solutions is known as viscous fingering. We have reported "meniscus splitting"^[1], in which the pattern formed on a substrate is developed into a millimeter-scale spatiotemporal structure. This is a non-equilibrium phenomenon in the controlled evaporation of polymer solution that splits the air-water interface into multiple regions. Drying an aqueous polymer dispersion from one interface in a limited space causes the polymer to precipitate at a specific position, driven by capillary forces. Also, the deposited polymer membrane has an oriented structure and becomes a functional material such as a humidity actuator^[2]. However, the specific spatiotemporal changes at the interface observed in the meniscus-splitting phenomenon have been only shown using some biopolymers, and the regulatory factors toward the universalization are unclear.

In this study, we demonstrate that meniscus splitting can happen with chemical species independence, and it is a universal phenomenon, through the experiment. Polyacrylic acid (PAAc), polyacrylamide (PAAm), and polyvinyl alcohol (PVA) were used as synthetic vinyl polymers for the demonstration. The effect of different molecular weights on the interfacial behavior was pronounced, indicating that molecular weights with appropriate viscosity are necessary for membrane formation. PAAc and PAAm exhibited a splitting pattern like that of the polysaccharides reported previously. On the other hand, PVA did not form vertical membranes, but rather horizontal ones. This difference is thought to be due to the retentivity of water, and PVA's propensity to form intra- and intermolecular hydrogen bonds. When the relative humidity was adjusted, vertical membrane was also formed for PVA as well as for the other chemical species. Furthermore, we attempted a mathematical analysis of the spatiotemporal changes in the specific interfacial shape observed during the drying process. To understand the transformation of the interface the characteristic interface curves were fitted by a hyperbolic curve or an elliptic curve. Through the fitting evaluation, it was suggested that the interface curves transformed from a hyperbolic curve to an elliptic curve during the

splitting.

Reference: [1] K. Okeyoshi, et al, *Sci. Rep.* **2017**, 7, 5615; *Polymer J.* **2020**, 52, 1185. [2] K. Budpud, et al., *Small*, **2020**, 16, 2001993.

SESSION CH04.06: Surface and Chemistry
 Session Chairs: Luxi Li and Yang Yang
 Wednesday Afternoon, April 24, 2024
 Room 443, Level 4, Summit

3:30 PM CH04.06.01

Electronic Characterization of 9A-GNR on H:Si(100) using a Scanning Tunneling Microscope Abigail Berg¹, Mamun Sarker², Anshual Saxena³, Narayana R. Aluru³, Alexander Simitiskii² and Joseph Lyding¹; ¹University of Illinois at Urbana-Champaign, United States; ²University of Nebraska–Lincoln, United States; ³The University of Texas at Austin, United States

We present the electronic characterization of a new solution-synthesized type graphene nanoribbon (GNR). The GNR was synthesized with two different precursors to form coves along the length of an N=9 armchair GNR. The GNR also contains two different functional end groups, -NO₂ and -NH₂, with each synthesized to attach to the two different precursors. Atomically precise graphene nanoribbons with functional end groups have the potential for further modification and integration into complex electronic structures. We use the dry-contact transfer (DCT) method to exfoliate the GNRs onto hydrogen passivated Si(100) in a room temperature ultra-high vacuum (UHV) scanning tunneling microscope (STM). The bandgap and density of states are probed using scanning tunneling spectroscopy (STS) and current imaging tunneling spectroscopy (CITS). We find that GNRs tend to cluster in groups and form weak bonds at the functionalized ends. We also find evidence of missing phenyl groups during synthesis which form extra-large coves in the final structure of the GNR. Simulation data indicates that the DFT bandgap is 1.4 eV and an increased density of states over the NO₂ end group. Experimentally we see that one end of the GNR appears to be metallic using STS, which we attribute to the NO₂ end group. The bandgap appears to have a lateral dependence from 1.7 eV to 2.3 eV along the GNR which will be explored in more detail. Finally, we present the effects of using nanolithography to depassivate the H:Si(100) below the GNR.

3:45 PM CH04.06.03

Effects of Anions on Phase Transformation and Crystallization of Aluminum Hydroxide Ping P. Chen, Suyun Wang, Trent R. Graham, Duo Song, Xiaodong Zhao, Zheming Wang, Carolyn Pearce, Kevin Rosso and Xin Zhang; Pacific Northwest National Laboratory, United States

Gibbsite (α -Al(OH)₃) is naturally abundant and plays a vital role as a raw material in various industrial applications. Furthermore, it constitutes a significant portion of the solid components in caustic nuclear waste at the Hanford Site (WA, USA). While extensive research has been conducted to understand gibbsite's behavior in processes such as crystallization, dissolution, phase transformation, solution chemistry, and irradiation-induced changes, the effects of co-existing high concentrations of salts on gibbsite's nucleation and growth remain a less-explored area. In this study, we investigated gibbsite crystallization from the solutions containing six sodium-based salts, specifically sodium salts of fluoride, chlorine, bromide, nitrate, phosphate, and sulfate. Our findings illuminate the diverse ways in which different anions can influence the crystal phase, structure, morphology, and growth rate of gibbsite as determined with various advanced techniques, including X-ray diffraction (XRD), Fourier-transform infrared spectroscopy (FTIR), Raman, nuclear magnetic resonance (NMR), scanning electron microscopy (SEM), and scanning/transmission electron microscopy (S/TEM). These results were further substantiated through the calculation of molecular cluster energies using density functional theory. In summary, our exploration of gibbsite crystallization in complex, multicomponent electrolytes simulates the compositional complexity encountered in nuclear waste, shedding light on the intricate interplay between gibbsite and co-existing salts.

4:00 PM CH04.06.04

Temperature-Dependent Structural and Elastic Properties of Cubic and Hexagonal Sc_xAl_{1-x}N Saskia Mihalic¹, Lucia Ciprian¹, Christopher Lüttich², Elisa Wade¹, Armin Dadgar², Björn Christian¹, André Strittmatter² and Oliver Ambacher¹; ¹University of Freiburg, Germany; ²Otto von Guericke Universität Magdeburg, Germany

The novel wide-bandgap semiconductor, Scandium Aluminum Nitride (Sc_xAl_{1-x}N) significantly enhances its piezoelectric properties compared to Aluminum Nitride (AlN). This unique increase in piezoelectric coefficient $d_{33}(x)$ makes Sc_xAl_{1-x}N a highly favorable material for numerous applications, including improved piezo-acoustic devices, which can be utilized as high-frequency filters [1]. The optimization of the devices is impeded by the trade-off between piezoelectric response and the stiffness of the crystal. To address this, a detailed investigation of the anisotropic elastic, piezoelectric, and thermodynamic properties is necessary. However, the ternary alloy Sc_xAl_{1-x}N undergoes a solid-solid phase transition from hexagonal wurtzite (wz) to cubic rock salt (rs) structure as the Sc content x increases, which differs from other ternary nitrides [2]. The coefficient $d_{33}(x)$ of wz-Sc_xAl_{1-x}N exhibits the highest values and the elastic properties undergo significant changes when the Sc content is proximate to this transition. The specific Sc:Al ratio, pressure and temperature conditions and seed layer selection (either AlN(0001) or ScN(111)) that induce this B4-B1 transition have yet been explored and will be discussed in this work. Accordingly, this study will discuss these conditions as they provide valuable insights to improve the efficiency of devices that rely on maximum piezoelectric responses. The physical properties of resonators are dependent on the operating temperature (T). The structural changes can be described utilizing lattice parameters $c(x, T)$ and $a(x, T)$, internal parameter $u(x, T)$, and elastic tensor $C_{ij}(x, T)$. In order to determine temperature-dependent structural properties of pulsed magnetron co-sputtered thin films, in-situ X-ray diffractometry measurements ranging from 300 K to 1000 K were conducted to determine the lattice parameters $c(x, T)$ and $a(x, T)$ for hexagonal and cubic Sc_xAl_{1-x}N(0001)/Si(111) thin films, respectively. The Debye model was utilized to determine the coefficients of linear thermal expansion α_a and α_c for wz-Sc_xAl_{1-x}N along the $\langle 1000 \rangle$ and $[0001]$ directions and α_a for rs-Sc_xAl_{1-x}N along the 100 directions. For the first time, the linear thermal expansion coefficient was experimentally determined for wz-Sc_xAl_{1-x}N ($0.0 < x < 0.5$) and rs-Sc_xAl_{1-x}N ($0.5 < x < 1.0$). This temperature-dependent structural information was used to compute additional structural specifications such as bond lengths and bond angles for random alloys of wz-Sc_xAl_{1-x}N and rs-Sc_xAl_{1-x}N. Scanning electron microscopy (SEM) was utilized to observe the effects of heating on surface morphology. To understand the elastic properties of wz- and rs-Sc_xAl_{1-x}N fully, various anisotropic elastic properties including shear modulus G and Young's modulus E were calculated for multiple crystallographic planes, by employing simulated tensor quantities at ambient conditions. For the first time, the in-plane epitaxial relation between rs-Sc_xAl_{1-x}N(111) and Si(111) was determined, which is rs-Sc_xAl_{1-x}N[110] || Si[100]. Further thermodynamic properties such as specific heat, heat conductivity and Debye temperature were calculated. This newfound knowledge of temperature- and direction-dependent structural and elastic properties offers the potential for improved efficiency of piezo-acoustic devices.

References

[1] N. M. Feil, E. Mayer, A. Nair, B. Christian, A. Ding, C. Sun, S. Mihalic, M. Kessel, A. Zukauskaitė, and O. Ambacher, *J. Appl. Phys.* **130**, 164501

(2021); doi: 10.1063/5.0055028.

[2] O. Ambacher, S. Mihalic, E. Wade, M. Yassine, A. Yassine, N. Feil, and B. Christian, *J. Appl. Phys.* **132**, 175101 (2022); doi: 10.1063/5.0120141.

4:15 PM CH04.06.05

Tailored Aluminum Surfaces for Adhesive Bonding – Joint Properties and Moisture induced Damage Mechanisms Jonathan Freund¹, Miriam Löbbecke¹, Frank Förste², Michael Wiedenbeck³, Ioanna Mantouvalou⁴ and Jan Haubrich¹; ¹German Aerospace Center (DLR), Germany; ²TU Berlin, Germany; ³Helmholtz-Zentrum Potsdam, Germany; ⁴Helmholtz-Zentrum Berlin, Germany

For the energy efficiency of future vehicles and aircraft, weight reductions through the use of alternative materials and joining techniques will be essential. Structural adhesive bonding is one technique to join dissimilar materials, eliminating the need for additional fasteners like bolts or rivets while enabling a uniform stress distribution across the bonded materials.

However, the fundamental understanding of the relationships between the physical and chemical surface properties of the interfaces and the resulting joint properties is needed. One major concern is joint weakening due to exposure to moisture, which has blocked the widespread uptake of adhesive bonding technologies in safety relevant applications [1]. Despite such aging process being difficult to detect non-destructively, further research into the mechanisms that cause such weakening is necessary if long-term durable adhesive joints are to be achieved.

Pulsed laser surface pretreatment of metal surfaces prior to adhesive bonding can significantly increase the mechanical strength and the long-term durability of metal-polymer joints. This benefit is often attributed to cleaning effects while also generating structures with suitable roughness on the metal surface that allow a better mechanical interlocking with the polymer matrix [2]. However, an enlarged, roughened metal oxide surface will also offer more surface area for chemical bonding with the polymer adhesive. The reasons for the improved aging properties provided by such laser surface pretreatment remains a matter of investigation, and here atomic-scale diffusion can play a role. Since the joint interface is buried and since the hydrogen and the oxygen atoms from water molecules cannot be distinguished easily from those native to the surface oxide film and polymer, it is difficult to study the diffusion in the joints.

Our study uses on a new approach for investigating the role of diffusion in modifying laser-pretreated adhesive joints. Scanning electron microscopy (SEM) can characterize the laser-modification of such surfaces down to the nanometer scale. We combined this information with observed diffusion rates determined by micro-x-ray fluorescence spectroscopy (μ -XRF) and secondary ion mass spectrometry (SIMS), which used elemental and ¹⁸O tracers, respectively. The preliminary results from our tracer studies indicate that significant diffusion in the polymer-metal interface and within the bulk polymer occurs. We also used single-lap shear tests of both unaged and hydrothermally aged specimens both with and without laser-pretreatment to link surface features and diffusion lengths with the mechanical strength of the specimens. This brought new insights concerning the mechanisms responsible for the loss of mechanical joint performance due to moisture and the role of interface features in suppressing this problem.

References

[1] R. A., Pethrick; Design and ageing of adhesives for structural adhesive bonding – A review *Journal of Materials, Design and Applications*, **2015**, 229 (5), 349-379.

[2] J. Min, H. Wang; Application of laser ablating in adhesive bonding of metallic materials: A review *Optics and Laser Technology*, **2020**, 128, 1-23.

4:30 PM CH04.06.06

Atom Probe Tomography for Dynamic Characterization of Materials Surface Phenomena Lorenzo Rigutti¹, Aïssatou Diagne¹, Samba Ndiaye¹, Christian Bacchi¹, Benjamin Klaes¹, Noelle Gogneau², Mariaconcetta Canino³ and François Vurpillot¹; ¹University of Rouen Normandie, France; ²C2N, France; ³IMM CNR, Italy

Atom Probe Tomography (APT) is a microscopy and micro-analysis technique based on field ion evaporation. Its standard application to materials science yields a *static picture* of a system, providing a set of 3D reconstructed positions of ions chemically identified through their mass/charge ratio. However, field ion evaporation is a complex *dynamic process*, driven by the system chemistry and by environmental parameters such as temperature, electric field, intensity and wavelength of laser pulses [1]. The correlated evaporation of spatially neighboring atoms, the formation and evaporation of molecular ions either through surface dynamics or through the interaction of residual gas molecules and the surface, the dissociation of molecular ions are examples of processes that occur and carry specific traces in APT datasets. This information is typically neglected in APT analysis, but may give important insight about surface chemistry under high field (with or without laser illumination), which makes of APT a technique for *dynamic studies* of material surfaces. In this contribution several examples of a dynamic use of APT will be reported: (i) the formation of molecular ions in silicon carbide, with its consequences on spatial and compositional accuracy of APT reconstructions[2], (ii) the microscopic assessment of single reactions involving molecular hydrogen adsorbed at the surface of III-N materials [3] and (iii) the field-dependent formation of hydride molecules in III-N materials.

The perspective extension of these dynamic APT approaches to other materials and surface chemical reactions will finally be discussed.

[1] M. K. Miller et R. G. Forbes, « Introduction to the Physics of Field Ion Emitters », in *Atom-Probe Tomography*, Springer, Boston, MA, 2014, p. 51. doi: 10.1007/978-1-4899-7430-3_2.

[2] S. Ndiaye, C. Bacchi, B. Klaes, M. Canino, F. Vurpillot, et L. Rigutti, « Surface Dynamics of Field Evaporation in Silicon Carbide », *J. Phys. Chem. C*, vol. 127, n° 11, p. 5467, mars 2023, doi: 10.1021/acs.jpcc.2c08908.

[3] L. Rigutti *et al.*, « Surface Microscopy of Atomic and Molecular Hydrogen from Field-Evaporating Semiconductors », *J. Phys. Chem. C*, vol. 125, n° 31, p. 17078, août 2021, doi: 10.1021/acs.jpcc.1c04778.

SESSION CH04.07: Advanced Electron Microscopy
Session Chairs: Qian Chen, Yuzi Liu and Judith Yang
Thursday Morning, April 25, 2024
Room 443, Level 4, Summit

8:00 AM *CH04.07.01

4D-STEM Imaging of The Evolution and Performance Relevance of Microstructures in Cathode Nanoparticles Qian Chen, University of Illinois at Urbana-Champaign, United States

In this talk, I will discuss our recent efforts on utilizing four-dimensional scanning transmission electron microscopy (4D-STEM) to image the microstructures in cathode nanoparticles in rechargeable multivalent-ion batteries. We use metal oxide nanoparticles, either single-crystalline or defect-laden ones, as the cathodes, which undergo electrochemically driven phase transformation during charge and discharge cycles. The phase transformation

induces the emergence of complex microstructures in the nanoparticles, such as phase orientation domains, domain boundaries, and defects such as stacking faults and dislocations. These microstructures ultimately change the energy barriers associated with ion diffusivity, the capacity, and cyclability of the battery systems. Our work demonstrates the prospect of “microstructure” engineering in energy storage materials, where spatiotemporal heterogeneity from the atomic to the nanoscale can impact macroscopic performances.

8:30 AM *CH04.07.02

Probing Grain Boundary Dynamics in Polycrystalline Materials by *In-Situ* TEM Yuan Tian, Yutong Bi and Xiaoqing Pan; University of California, Irvine, United States

Understanding grain boundary (GB) dynamics in polycrystalline materials is crucial for predicting their macroscopic properties, such as mechanical strength, ductility, and conductivity. The migration and interaction of GBs are key factors affecting the thermal and mechanical stability of these materials. In situ transmission electron microscopy (TEM) plays an important role in investigating GB dynamics at the atomic scale. However, the lack of statistics for atomic scale study presents challenges in uncovering the predominance of multiple mechanisms in certain dynamic processes. This study employs cutting-edge four-dimensional transmission electron microscopy (4D-STEM) techniques for *in situ* experiments to shed light on the mechanisms of grain boundary migration at the microstructural and statistical level.

In the first part of the study, an *in situ* 4D-STEM experiment was conducted on a Pt polycrystal thin film sample at an elevated temperature. The datasets were cyclically collected in the same region of the sample after predetermined annealing times. Crystallographic orientation information was derived from the 4D-STEM datasets through cross-correlation between the experimental and simulated diffraction patterns of the Pt sample. By utilizing grain segmentation and inter-frame association, the evolution of grain orientation and GB dynamics was traced. The observations revealed ubiquitous grain rotation and GB migration during the annealing process, as well as a strong correlation between GB migration and grain rotation. Subsequently, atomic-resolution high-angle annular dark-field scanning transmission electron microscopy (HAADF-STEM) observations of grain boundary migration were conducted on the Pt sample. These observations at the atomic scale demonstrated that GB migration occurs through disconnection propagation, leading to the induction of local shear strain. This shear strain accumulates near the GB and needs to be released before further migration can occur. The findings from this observation indicate that grain rotation and annealing twin formation serve as effective pathways for releasing the strain generated by shear-coupled GB migration. This comprehensive study provides valuable insights into the complex mechanisms governing grain boundary migration in polycrystalline materials, contributing to our understanding of their macroscopic properties and potential applications in material science and engineering.

9:00 AM CH04.07.03

Imaging Mobility of Charge Order Topology via Charge Density Wave Interferometry Suk Hyun Sung^{1,2}, Noah Schnitzer³, Ismail El Baggari¹, Lena Kourkoutis³ and Robert Hovden²; ¹Harvard University, United States; ²University of Michigan, United States; ³Cornell University, United States

Charge density waves (CDWs) are emergent correlated electron behavior that span crystals with strong electron-lattice coupling and are associated with exciting phenomena such as metal-insulator transitions and superconductivity. Often described as a superlattice crystal of electrons, CDWs can also accommodate defects such as dislocations and elastic deformations. CDW defects are of a particular interest as they are believed to dominate conductance [1] and mediate phase transitions of the charge lattice itself [2–4]. Topological defects in a CDW are even expected to locally host superconductivity [5]. Therefore, understanding the formation, destruction, and mechanics of CDW defects is paramount to harnessing the full potential of charge ordered materials.

TaS₂ is prototypical layered CDW system that hosts multiple CDW phases tuned by temperature, thickness and polytype [6–8]. Octahedrally coordinated 1T-TaS₂ at room temperature hosts a nearly-commensurate (NC-) CDW lacking long-range order, and a long-range ordered commensurate (C-) CDW below 200 K. While the nature of order in NC-CDW phase remains unclear, it is generally accepted that NC-CDW incorporates discommensurations (i.e., slips in the CDW phase) [3, 4]. Real space measurement of the nanoscale structure of the NC-CDW is complicated by out-of-plane incoherence of the CDW; features are washed out in atomic resolution measurements. Here we use CDW moiré engineering to magnify and image the structure of CDW dislocations in the NC-CDW phase of TaS₂.

We generate a CDW moiré by synthesizing an endotaxial polytype heterostructure [9] that stabilizes both NC- and C-CDW phase layers embedded in a metallic prismatic matrix. Here the long-range ordered C-CDW serves as a grating with which the NC-CDW interferes. The resulting moiré interference pattern resolves a topological defect present in the NC-CDW. This pattern effectively encodes and magnifies the phase information in the NC- and C-CDW phases, taking advantage of the fact that NC- and C-CDWs diffract electrons with only slightly different momentum. By collecting scanned nanobeam diffraction patterns (i.e., 4D scanning transmission electron microscopy (STEM)) with the convergence angle and camera length tuned such that both C and NC reflections are incident on a single pixel of an electron microscope pixel array detector (EMPAD), moiré interference patterns are speedily acquired in parallel at every point in reciprocal space that the superlattice peaks nearly coincide.

In summary, we image CDW defects by employing 4D-STEM on polytype heterostructures of TaS₂. The interference from C and NC-CDW forms a moiré pattern that encodes the phase disorder of the NC phase, allowing defects to be imaged despite the out of plane incoherence inherent to the system. This work suggests a new experimental framework that can shed light on difficult-to-study CDW mechanics.

[1] AW Tsen et al., *Proc. Natl. Acad. Sci.* **112** (2015) p.15054.

[2] WL McMillan, *Phys. Rev. B* **12** (1975) p. 1187.

[3] WL McMillan, *Phys. Rev. B* **14** (1976) p. 1496.

[4] K Nakanish and H. Shiba, *J. Phys. Soc. Jpn.* **43** (1977) p.1839.

[5] B Leridon et al., *New J. Phys.* **22** (2020) 073075.

[6] JA Wilson, FJ Di Salvo, S Mahajan *Adv. Phys.* **24** (1975) p.117.

[7] Y Yu et al., *Nat. Nanotech.* **10** (2015) 270.

[8] E Martino et al., *npj 2D Mater. App.* **4** (2020) 7.

[9] SH. Sung et al., *Nat. Commun.* **13** (2022) p.413.

9:15 AM CH04.07.04

Nanoscale Evaluation of SiO₂ Density by Stretching Vibrations Measurement using STEM-EELS Takanori Asano, Manabu Tezura, Masumi Saitoh and Hiroki Tanaka; Kioxia Corporation, Japan

SiO₂ is one of the most important dielectric materials used as gate insulators and interlayer films in nanoelectronic devices. Although the density of SiO₂ has been evaluated by the Si-O-Si stretching vibration peak using IR (infrared spectroscopy) [1] so far, there is no established technique to evaluate the density distribution in the nanoscale area. In this work, we develop a technique for nanoscale evaluation of SiO₂ using STEM (scanning transmission electron microscopy) – EELS (electron energy loss spectroscopy). While there are a number of reports on vibrational spectra measured by STEM-EELS

[2,3], a method for density evaluation using EELS has not been established yet. We found differences in the stretching vibration peaks reflecting the density between SiO₂ with different atomic structures: α -quartz (2.648 g/cm³) and silica glass (2.2 g/cm³). The dependence of the stretching peak on the thickness of the STEM specimen was investigated in detail by experiment and spectral calculation using a dielectric model.

IR spectra showed that the FWHM (full width at half maximum) of the stretching peak was larger for silica glass than for α -quartz. This corresponds to lower density in the silica glass as a result of greater variation in the Si-O-Si bond angle [3]. We also measured vibrational EELS spectra using STEM with a nanometer resolution and a high energy resolution of 16 meV (FWHM of the zero-loss peak). The FWHM of the stretching peak for silica glass was observed to be 5 meV larger than that for α -quartz, which is consistent with the IR results. On the other hand, simulations based on the Kröger formula [4] showed the experimental stretching peaks reflect both surface scattering and bulk scattering. This simulation suggests the specimen thickness is a key factor when comparing the different samples, because the contribution of surface scattering strongly depends on the specimen thickness. Thus, to establish our evaluation method by STEM-EELS, we investigated in detail the dependence of the stretching peaks on specimen thickness in the range of 30 nm to 100 nm. By comparing the FWHM of the samples with the same specimen thickness, we confirmed that there is a significant difference of more than 4 meV in the stretching peaks between silica glass and α -quartz for all the thicknesses.

We prepared α -quartz locally amorphized by electron irradiation for a longer duration (~50,000 times longer) than the vibrational EELS measurements, and investigated its density using the established evaluation method. As a result, the amorphized α -quartz was found to be denser than silica glass and to have the same density as α -quartz. This suggests that the atomic number of α -quartz is maintained during the amorphization under the low electron current (~10 pA) irradiation, which does not cause significant atomic desorption. These results indicate that vibrational EELS using STEM is a promising technique for local density analysis of SiO₂.

- [1] N. Yasuda *et al.*, Appl. Surf. Sci. 117 (1997) 216.
- [2] R.F.Egerton *et al.*, Microsc. Microanal. 26 (2020) 1117.
- [3] K. Venkatraman *et al.*, Microscopy 67 (2018) i14.
- [4] G. Lucovsky *et al.*, J. Vac. Sci. Technol. B 5 (1987) 530.

9:30 AM BREAK

10:00 AM *CH04.07.05

Dynamic Atomic-Scale Fundamental Mechanisms of the Initial Stages of Cu Oxidation Revealed by Environmental Transmission Electron Microscopy Judith C. Yang^{1,2}, Meng Li^{2,1}, Matt Curnan³, Linna Qiao⁴, Dmitri N. Zakharov¹, Guangwen Zhou⁴ and Wissam Saidi^{3,2}; ¹Brookhaven National Laboratory, United States; ²University of Pittsburgh, United States; ³Pohang University of Science and Technology, Korea (the Republic of); ⁴Binghamton University, The State University of New York, United States; ⁵NETL, United States

Surface oxidation is an important process for corrosion, which costs a few percent of the U.S. Gross Domestic Product (GDP) each year. Much is known about oxygen interaction with metal surfaces and the macroscopic growth of thermodynamically stable oxides. At present, however, the transient stages of oxidation - from nucleation of the metal oxide to formation of the thermodynamically stable oxide - represent a scientifically challenging and technologically important terra incognita. These issues can only be understood through a detailed study of the relevant microscopic processes at the nanoscale in situ. We have previously demonstrated via in situ transmission electron microscopy (TEM) that the formation of epitaxial Cu₂O islands during the transient oxidation of Cu(100), (110), and (111) films bear a striking resemblance to heteroepitaxy, where the initial stages of growth are dominated by oxygen surface diffusion and strain impacts the evolution of the oxide morphologies. To deepen our understanding of the atomic-scale dynamic processes of Cu₂O island formation on Cu during oxidation in situ, we are presently using correlated in situ high-resolution environmental TEM (ETEM) and atomistic theoretical simulations. As an example of this approach, preferential monolayer-by-monolayer growth along Cu₂O(110) planes was noted instead of along Cu₂O(100) planes. Correlated Density Functional Theory (DFT) simulations on the surface and diffusion energies during Cu₂O growth on various Cu₂O surface orientations and terminations were carried out. Our DFT results show that monolayer formation of Cu₂O along Cu₂O(110) was both thermodynamically and kinetically preferred over that of Cu₂O(100) during Cu₂O growth, which explains the observed phenomenon. These results shed new light on the epitaxial oxide growth mechanism and provide a deeper understanding of the dynamic processes involved in initial oxidation, which will ultimately help to precisely predict, design, and control nanostructured oxide growth for either corrosion-protection or creating nano-oxides for their functional properties. Furthermore, advancing hardware and software for enhancing in situ experiments will be discussed. We gratefully acknowledge support from the National Science Foundation (NSF), including NSF-CMMI 1905647, NSF-DMR 1410055, 1508417, 1410335. This research used the electron microscopy resources of the Center for Functional Nanomaterials (CFN), which is a U.S. Department of Energy Office of Science User Facility, at Brookhaven National Laboratory under Contract No. DE-SC0012704.

10:30 AM *CH04.07.06

Enabling sustainable chemical manufacturing with atomically-optimized photocatalysts Jennifer A. Dionne; Stanford University, United States

Chemical manufacturing is critical for industries spanning construction, plastics, pharmaceuticals, food, and fertilizers, yet remains among the most energy-demanding practices. Optical excitation of plasmons offers a route to more sustainable chemical synthesis. Plasmons create nanoscopic regions of high electromagnetic field intensity that can modify electronic and molecular energy levels, enable access to excited-state dynamics, and open new reaction pathways that are impossible to achieve under typical conditions. Further, plasmons can be efficiently excited with sunlight or solar-driven LEDs, for sustainable chemical transformations.

Here, we present our research advancing plasmon photocatalysis from the atomic to the reactor scale (see Figure 1). First, we describe advances in in-situ atomic-scale catalyst characterization, using environmental optically-coupled transmission electron microscopy. With both light and reactive gases introduced into the column of an electron microscope, we can monitor chemical transformations under various illumination conditions, gaseous environments, and at controlled temperatures, correlating three-dimensional atomic-scale catalyst structure with photo-chemical reactivity. Then, we describe how these atomic-scale insights enable optimized reactor-scale performance. As model systems, we consider three reactions: 1) acetylene hydrogenation with Ag-Pd catalysts; 2) CO₂ reduction with Au-Pd catalysts; and 3) nitrogen fixation with AuRu catalysts. Here, Au/Ag acts as a strong plasmonic light absorber while Pd/Ru serves as the catalyst. We find that plasmons modify the rate of distinct reaction steps differently and that reaction nucleation occurs at electromagnetic hot-spots - even when those hot-spots do not occur in the preferred nucleation site. Plasmons also open new reaction pathways that are not observed without illumination, enabling both high-efficiency and selective catalysis with tuned bimetallic catalyst composition. Our results provide a roadmap for how atomically-architected photocatalysts can precisely control molecular interactions for high-efficiency and product-selective chemistry.

11:00 AM CH04.07.07

Structural Studies of 2D Perovskites for Catalyst Support Applications by Environmental Transmission Electron Microscopy Dmitri N. Zakharov;

Brookhaven National Laboratory, United States

Two-dimensional perovskites materials gained traction for applications in various optoelectronic and sensor devices. Another potential application for this class of the material is a catalyst support, as epitaxial relationships between catalyst and support can be utilized to gain control over catalyst active sites in catalyst activity studies. Nanosheets of $\text{Sr}_2\text{Nb}_3\text{O}_{10}$ (SNO) with thicknesses down to 1.8 nm were synthesized by liquid exfoliation technique. Palladium film of a nominal thickness of 1.0 nm was deposited by electron beam evaporation to form Pd particles supported on SNO, which was picked up as a model system. Structural characterization was done in the column of C_s -corrected environmental FEI Titan scanning transmission electron microscope (ETEM). Bright field (BF) and dark field (DF) imaging revealed nanosheets of sizes of few squared micrometers. SNO flakes show contrast revealing strain and deviation from the exact [001] zone axis across the nanosheet. A perfect orientation down to the [001] zone axis was limited to a few hundred square nanometers. DF images of the SNO flakes acquired in several two-beam conditions show contrast from grain boundaries of misoriented grains. Planar defects (PD) running at an angle to the imaging plane reveal alternating contrast. Some areas show defected structure on HREM images, which also reveals itself by additional diffraction spots on the FFT in comparison with the perfect perovskites structure. In addition to vacuum environment, deposited films were also studied in the presence of Hydrogen in environmental regime of the same Titan (S)TEM. The sample was heated to 900C in the presence of 80mTorr Hydrogen. Nanoparticles supported on SNO exhibit faceted nature compared to those supported on amorphous SiN support, which potentially opens a way to controllable studies of catalyst's active sites. This research used the Electron Microscopy facility of the Center for Functional Nanomaterials (CFN), which is a U.S. Department of Energy Office of Science User Facility, at Brookhaven National Laboratory under Contract No. DESC0012704.

11:15 AM CH04.07.08

Real-Time Observation of GaN Nanowire Growth by *In-Situ* TEM Nessrine Benaziz^{1,2}, Chen Wei^{1,2}, Frank Glas^{1,2}, Noelle Gogneau^{1,2}, Charles Renard^{1,2}, Laetitia Vincent^{1,2}, Laurent Travers^{1,2}, Pavel Bulkin³ and Federico Panciera^{1,2}; ¹CNRS, France; ²Université Paris-Saclay, France; ³École Polytechnique, France

Gallium nitride (GaN) is widely used in photonic devices such as blue and white light emitting diodes and lasers. However, its large lattice mismatch with commonly used substrates such as Si (111) imposes the growth of thick and complex buffer layers to reduce the defect density. GaN nanowires (NWs) however, having a small footprint on the substrate, can easily accommodate the lattice mismatch and allow monolithic integration of high quality GaN on Si (111). Thus, GaN NWs on Si structures have been a source of great attention due to its fundamental properties and technological uses. GaN NWs can be grown with and without catalyst, but the uncatalyzed growth is preferred since it eliminates any risk of contamination. This growth mode often results in NWs having different polarities and in some cases in the simultaneous presence of both polarities on a single NW. The growth mechanism of uncatalyzed GaN NWs, in particular in the presence of multiple polarities, is not fully understood.

To shed some light on the growth of these nanostructures, we carried out in-situ transmission electron microscopy (in-situ TEM) experiments. A special TEM-compatible Si substrate with heating capability was fabricated using MEMS technology. This substrate presents a vertical (111) surface on which nanowires can be grown epitaxially and oriented perpendicular to the electron beam. The growth of GaN NWs was carried out inside the TEM by plasma-assisted MOCVD using TMGa and N_2 as precursor gases at a temperature around 850 °C. Pure wurtzite phase GaN NWs were grown epitaxially on the Si (111) substrate. The majority of NWs showed a central Ga-polar domain completely surrounded by an N-polar domain. We will present atomic resolution videos displaying the monolayer-by-monolayer growth of these NWs using both a cross-sectional and an inclined view. This second configuration reveals the nucleation site of each monolayer on the top facets (Ga-polar and N-polar) and the propagation mechanism of the monolayer. Finally, we will discuss the impact of grow conditions on the top surface morphology and the overall NW aspect ratio and present a model to rationalize our observations.

SESSION CH04.08: Ultrafast Dynamics
Session Chairs: Yuzi Liu and Michelle Mejía
Thursday Afternoon, April 25, 2024
Room 443, Level 4, Summit

1:30 PM *CH04.08.01

Ultrafast Dynamics in Materials Haihua Liu, Thomas Gage and Ilke Arslan; Argonne National Laboratory, United States

Ultrafast transmission electron microscopy (UEM) methods have become a new frontier in materials science due to the ability to follow dynamics on time scales down to hundreds of femtoseconds with nanometer spatial resolution. Imaging on ultrafast time scales reveals nonequilibrium metastable states of matter, phonon transport pathways in materials, and plasmon dynamics. This presentation will overview some of these ultrafast methods, and provide examples of how they have been used to enable new understanding of materials.

Work performed at the Center for Nanoscale Materials, a U.S. Department of Energy Office of Science User Facility, was supported by the U.S. DOE, Office of Basic Energy Sciences, under Contract No. DE-AC02-06CH11357.

2:00 PM *CH04.08.02

MeV Electron Time-Resolved Total Scattering for Material Dynamics Xijie Wang; SLAC National Accelerator Laboratory, United States

The MeV electrons produced by the photocathode RF gun made it feasible for MeV ultrafast electron scattering [1-2]. MeV ultrafast electron scattering became a new frontier in ultrafast science due to its capability of following dynamics on femtoseconds scale with the high spatial resolution and sensitivity [3-4]. Furthermore, MeV electrons experience less multiple-scattering, and possess "real" flat Ewald-sphere; MeV ultrafast electron diffraction (MeV-UED) is an ideal tool to explore both structure and dynamics using total scattering technique. Total scattering has been explored by X-ray and Neutron scattering communities to study energy materials, the time-resolved total scattering enabled by MeV-UED make it feasible to image structure dynamics and energy transfer in 2-D heterostructure [3] and revealing the intricate relation between dynamics and function of 2-D perovskite [4].

I will discuss many advantages of MeV electron for total scattering. MeV electron total scattering not only produces stronger diffraction signal and sensitive to the structure change, but also has less background and no geometric correction. Furthermore, we have experimentally demonstrated that MeV electron total scattering is capable of probing both electronic and nuclear structure dynamic [5]. MeV-UED enabled the first ultrafast operando [6] and in-situ [7] experiments.

1. X.J. Wang et al, Phys. Rev. E , 54, No.4, R3121 -3124 (1996).

2. X.J. Wang et al, Proceedings of the 2003 Particle Accelerator Conference, 2003, pp. 420-422 Vol.1, doi: 10.1109/PAC.2003.1288940.
3. J. Sood, et al, "Bidirectional phonon emission in two-dimensional heterostructures triggered by ultrafast charge transfer", Nat. Nanotechnol. 18, 29–35 (2023).
4. H. Zhang et al., "Ultrafast relaxation of lattice distortion in two-dimensional perovskites", Nature Physics **volume 19**, pages 545–550 (2023).
5. J. Yang et al, "Simultaneous observation of nuclear and electronic dynamics by ultrafast electron diffraction", Science 368, 885 (2020).
6. A. Sood et al, "Universal phase dynamics in VO₂ switches revealed by ultrafast operando diffraction", Science **373**, 352 (2021).
7. P. K. Muscher et al, "Highly Efficient Uniaxial In-Plane Stretching of a 2D Material via Ion Insertion", Adv. Mater. **33**, 2101875 (2021).

2:30 PM CH04.08.03

Capturing Laser Induced Dynamics of Materials via Ultrafast Transmission Electron Microscopy [Volkan Ortolan](#); University of Connecticut, United States

Recent developments in instrumentation have made it a very exciting time to perform both fundamental and applied research in the electron microscope. In-situ microscopy is moving forward at a rapid pace with the development of gas/liquid stages that permit reaction processes to be imaged and analyzed at atomic resolution. Moreover, the development of nanosecond and faster photoemission electron sources offers the chance to move the high spatial resolution world of electron microscopy into the ultrafast world of materials dynamics. Conventional in-situ TEM coupled with ultrafast TEM can be utilized to gain a fundamental understanding of dynamic processes occurring in materials. The combination of these capabilities allow for vast improvements of in-situ TEM studies limited by video rate in that many processes span multiple time and length scales. Ultrafast in-situ electron microscopy promises to answer challenging questions in the fields ranging from materials science and chemistry to nanoscience and biology. In this presentation, examples of ultrafast electron microscopy studies will be presented for selected systems. Short lived transient processes involved in dynamic processes in materials will be discussed to obtain new insights. Additionally, the potential of novel in-situ stages for various data acquisition schemes to push the envelope of ultrafast electron microscopy for the investigation of materials will be discussed.

2:45 PM CH04.08.04

High-Speed Imaging Techniques for Imaging High-Jitter Dielectric Breakdown [Noah Hoppis](#)¹, [Kathryn Sturge](#)¹, [Jonathan E. Barney](#)², [Brian L. Beaudoin](#)¹, [Ariana Bussio](#)¹, [Ashley E. Hammell](#)¹, [Samuel Henderson](#)², [James Krutzler](#)¹, [Joseph P. Lichthardt](#)¹, [Alexander H. Mueller](#)², [Karl Smith](#)², [Bryce Tappan](#)² and [Timothy W. Koeth](#)^{1,2}; ¹University of Maryland, United States; ²Los Alamos National Laboratory, United States

Imaging mechanically induced dielectric breakdown, which unfolds on ultra-short timescales, poses a formidable challenge. A significant hurdle in this endeavor is breakdown initiation jitter, where even a tenth of a microsecond of timing deviation can frustrate imaging efforts. Our initial attempt to use a gigahertz frame rate camera to record dielectric breakdown initiated by an exploding bridge wire detonator was hindered by pronounced initiation jitter.

To surmount this obstacle, we developed an innovative optical image delay line apparatus to mitigate the effects of breakdown jitter on imaging timing. In this presentation, we delve into the design and performance of this optical delay line apparatus, showcasing its transformative impact. The integration of the optical delay line increased image capture success rate from 25% to 94%. Moreover, it facilitated superior temporal resolution. Beyond its applicability in the realm of dielectric breakdown, this technique holds promise for imaging other high-jitter, ultra-fast phenomena

3:00 PM BREAK

3:30 PM *CH04.08.05

Imaging Quantum Coherence using Electron Wavepackets [Ido Kaminer](#)¹ and [Giovanni Maria Vanacore](#)²; ¹Technion, Israel; ²The University of Milano-Bicocca, Italy

Until recently, work in quantum optics focused on light interacting with *bound-electron* systems such as atoms, quantum dots, and nonlinear optical crystals. In contrast, *free-electron* systems enable fundamentally different physical phenomena, as their energy distribution is continuous and not discrete, allowing for tunable transitions and selection rules. Free electrons also enable unique capabilities in microscopy and spectroscopy that are otherwise inaccessible.

Recent theoretical and experimental breakthroughs involving quantum interactions of free electrons spawned an exciting new field: *free-electron quantum optics*. We developed a platform for exploring coherent free-electron interactions at the nanoscale, and used it to demonstrate the first coherent interaction of a free electron with quantum statistics of photons.

These capabilities open new paths toward using free electrons as carriers of quantum information. Concepts of quantum optics with free electrons also promote new modalities in electron microscopy. We recently demonstrated the first instance of coherent amplification in electron microscopy. Specifically, we present an algorithm-based microscopy approach that uses light-induced electron modulation to demonstrate the coherent amplification effect in electron imaging of optical near-fields. We provide a simultaneous time-, space-, and phase-resolved measurement in a microdrum made from a hexagonal boron nitride membrane, visualizing the sub-cycle dynamics of 2D polariton wavepackets therein. Our experiments show a 20-fold coherent amplification of the near-field signal compared to conventional electron near-field imaging, resolving peak field amplitudes of few kV/m.

Our vision is to develop a microscope that can image coherence, going beyond conventional imaging of matter to also *image the quantum state of matter* and probe quantum correlations between individual quantum systems.

-N. Rivera and I. Kaminer, Light-matter interactions with photonic quasiparticles, Nature Reviews Physics 2, 538–561 (2020) (Review)

-K. Wang, R. Dahan, M. Shencis, Y. Kauffmann, A. Ben-Hayun, O. Reinhardt, S. Tsesses, I. Kaminer, Coherent Interaction between Free Electrons and Cavity Photons, Nature 582, 50 (2020)

-R. Ruimy†, A. Gorchach†, C. Mechel, N. Rivera, and I. Kaminer, Towards atomic-resolution quantum measurements with coherently-shaped free electrons, Phys. Rev. Lett. 126, 233403 (2021)

-O. Reinhardt†, C. Mechel†, M. H. Lynch, and I. Kaminer, Free-Electron Qubits, Annalen der Physik 533, 2000254 (2021)

-Y. Kurman†, R. Dahan†, H. Herzig Shenfux, K. Wang, M. Yannai, Y. Adiv, O. Reinhardt, L. H. G. Tizei, S. Y. Woo, J. Li, J. H. Edgar, M. Kociak, F. H. L. Koppens, and I. Kaminer, Spatiotemporal imaging of 2D polariton wavepacket dynamics using free electrons, Science 372, 1181 (2021)

-R. Dahan†, A. Gorchach†, U. Haeusler†, A. Karnieli†, O. Eyal, P. Yousefi, M. Segev, A. Arie, G. Eisenstein, P. Hommelhoff, and I. Kaminer, Imprinting the quantum statistics of photons on free electrons, Science 373, 6561 (2021)

-A. Karnieli†, S. Tsesses†, R. Yu†, N. Rivera, Z. Zhao, A. Arie, S. Fan, and I. Kaminer, Quantum sensing of strongly coupled light-matter systems using free electrons, Science Advances 9, add2349 (2023)

-R. Dahan†, G. Baranes†, A. Gorchach, R. Ruimy, N. Rivera, and I. Kaminer, Creation of Optical Cat and GKP States Using Shaped Free Electrons, to

appear in PRX (2022); arXiv:2206.08828

-T. Bucher et al., Coherently amplified ultrafast imaging in a free-electron interferometer, arXiv:2305.04877

4:00 PM *CH04.08.06

New Approaches of Ultrafast Electron Microscopy for Quantum Materials Yimei Zhu; Brookhaven National Laboratory, United States

In this presentation, several of our research examples are selected to highlight the characterization of materials dynamics in strongly correlated systems. I will focus on ultrafast phenomena and charge-lattice and spin-lattice correlations. For instance, I will show: 1) a new two-color scheme based on near-field electron microscopy (PINEM), one for temporal gating, the other for pumping to achieve nm-fs spatiotemporal resolution to visualize ultrafast dielectric response and insulator-to-metal transition in nanowires [1]; 2) quantitative diffraction and diffuse scattering analysis to capture the photoinduced ultrafast atom dimerization and rotation dynamic pathways [2] and the evolution of optical and acoustic phonon population in charge-density-wave materials [3] using MeV-UED; and 3) study electromagnetic wave propagation in interdigitated comb device that is widely used as an antenna or sensor in mobile platforms [4] and observe spin wave dynamics under microwave excitation using the GHz electron pulser we developed at BNL. The ability to probe materials dynamic responses under RF excitations has promising applications for qubit devices and quantum information science.

Work at BNL was supported by the DOE-BES-MSED under the grant DE-SC0012704.

References:

1. X. Fu, et al., "Nanoscale-femtosecond dielectric response of Mott insulators captured by two-color near-field UEM", Nat. Comm., 11:5770 (2020).
2. J. Li, et al., "Direct detection of V-V atom dimerization and rotation dynamic pathways upon ultrafast photoexcitation in VO₂", PRX 12, 021032 (2022).
3. Y. Cheng et al., "Ultrafast formation of topological defects in a 2D charge density wave", Nat. Phys., in press (2023) (arXiv:2211.05748).
4. X. Fu, et al., "Laser-free ultrafast electron microscopy of electromagnetic wave dynamics", Sci. Adv., 6 eabc3456 (2020).

4:30 PM CH04.08.07

Interfacial Charge Dynamics in Si-Ge Heterojunctions imaged by Scanning Ultrafast Electron Microscopy Basamat Shaheen; University of California, Santa Barbara, United States

With the growing demand for efficient energy systems and electric devices, semiconductor heterostructures have garnered increasing attention due to their distinctive interfaces and synergistic effects. Understanding their fundamental nature is crucial for further developments. Surface and interfacial properties play the key role in heterostructures where the chemical composition and charge distribution change due to different sets of bonds, band structures, majority carrier concentrations, and Fermi levels. Combining the time resolution of femtosecond lasers and the spatial resolution of electron microscopes, scanning ultrafast electron microscopy (SUEM) has a unique capability to visualize charge dynamics at surfaces and interfaces. In this study, we utilize SUEM to image photocarrier dynamics in Si-Ge heterojunctions fabricated through direct wafer bonding. The charge dynamics are selectively examined across the interface and compared to the individual materials. The photo-induced SUEM contrast, corresponding to the local change in secondary electron emission, shifts from bright to dark on the Si side as it approaches the interface. On the Ge side, the contrast remains dark at the interface and beyond. Additionally, it is observed that the dispersion of the dark contrast on the Si side is wider than that on the Ge side at the interface. These findings are elucidated with insights from other surface techniques such as X-ray photoelectron spectroscopy and Kelvin probe microscopy, as well as Finite-Difference Time-Domain (FDTD) simulations of the built-in electric field across the interface.

4:45 PM CH04.08.08

Uncovering Microscopic Interactions in Skyrmion Hosts via Lattice Dynamics Andi M. Barbour¹, Myung-Geun Han¹, Fernando Camino¹, Chuhang Liu¹, Mario Cuoco², Yimei Zhu¹ and Claudio Mazzoli¹; ¹Brookhaven National Laboratory, United States; ²Consiglio Nazionale delle Ricerche, Italy

NLSL-II's Coherent Soft X-ray (CSX) beamline has world leading coherent soft x-ray flux and, as such, can provide insight to materials traditionally studied with either neutrons or electron microscopy (EM). In other words, bulk versus near-surface, respectively. The highly tunable CSX beamline can close this gap since "bulk-like" and EM specific free-standing films are readily investigated using soft x-ray resonant elastic scattering (REXS). Capitalizing on this capability, we turn to study interacting skyrmions. Most skyrmion hosting materials are conducting metal alloys (the B20 metals), and these materials do exhibit interesting skyrmion lattice dynamics. However, Cu₂OSeO₃ (CSO) offers an interesting comparison since it is a vastly different material, being an insulator and exhibiting magnetoelectric coupling – which are attractive properties for devices. We will present new findings associated with skyrmion lattice (SkL) dynamics in CSO. Recently reported rotational dynamics of the SkL are currently thought to be induced by either thermal gradients [1] or magnetic field gradients [2]. By combining coherent X-rays and REXS, we can interrogate the structure and dynamics of rotating and non-rotating SkL points in a highly controlled manner. In collaboration with LTEM researchers, we are able to expand our findings with complementary LTEM experiments.

1. Mochizuki et. al, Nature Materials 13, 241, 2014.
2. Zhang et. al, Nature Communications 9, 2115, 2018.

SESSION CH04.09: Poster Session II

Session Chairs: Yuzi Liu, Michelle Mejía, Yang Yang and Xingchen Ye
Thursday Afternoon, April 25, 2024
Flex Hall C, Level 2, Summit

5:00 PM CH04.09.01

Preliminary Study on The Microstructure Evolution and Deformation Behavior of Ti6Al4V-5Cu Alloy at Low Forming Temperatures Solomon K. Yeshanew; Dire Dawa University, Institute of Technology, School of Mechanical and Industrial Engineering, Ethiopia

The cold workability behavior of the Ti6Al4V-5Cu alloy was investigated using a hot compression experiment in the temperature range of 450 – 650 °C and strain rates interval of 10⁻⁴ – 10⁻¹ s⁻¹ with strains of 0.4 and 0.6. Deformation mechanisms and microstructural evolution of the alloy are characterized by means of the Gleeble 3800 compression test, establishing constitutive relationship that relates the microstructure of the deformed specimen with process variables (Temperature, strain rate, and strain). Unpleasant product features identified using a scanning electron microscope and an electron backscattered diffraction study, such as edge cracking defects caused by high strain conditions at low deformation temperatures (< 450 °C) and faster strain rates. Grain

boundary splitting occurs at the α/α phase interface. The splitting occurred because of the formation of weak structures due to the presence of aluminum as a major phase constituent element, indicating that pseudo-super plasticity behavior existed via the sliding of α/α phase grains. The β -phase was found in relatively dense concentrations at the grain boundary teared region of the α/α phase interface, which helped to prevent the cracked edges along the grain boundaries from widening and propagating further. On the single α -phase region, the alloy activation energy (Q) monitored to be 29.58 kJ/mol. The alloy strain rate sensitivity (m) and power dissipation efficiency (η) were also calculated as 0.45 and 22.22%, respectively. Together with the microstructure evolution, true strain-stress curve, and generated processing map, Ti6Al4V-5Cu alloy were found with low metallurgical transformation ability during forming below 650 °C (< 2.58T m).

5:00 PM CH04.09.02

Identifying Degradation Mechanism in Cathode Materials for Lithium Ion Batteries with Precession Electron Diffraction Hyungcheoul Shim¹, Young-Woon Byeon², Seungmin Hyun¹ and Jae-Pyoung Ahn²; ¹Korea Institute of Machinery and Materials, Korea (the Republic of); ²Korea Institute of Science and Technology, Korea (the Republic of)

Due to the explosive growth of the electric vehicle market, recently, attention to lithium ion batteries (LiBs) is increased. The specialty of automotive applications is promoting the development of long-life batteries based on material reliability. Developing a reliable LiB begins with understanding the mechanism of degradation of the material. In other words, based on the degradation mechanism of the material analyzed from accurate and various angles, we can propose a design method of robust material that is one step further.

In this study, we tried to analyze the cause of the deterioration of cycling characteristics for Li(Ni_{1/3}Co_{1/3}Mn_{1/3})O₂, which is mainly used as a cathode material for LiBs, by precession electron diffraction (PED). In other words, we wanted to know the causes of degradation in the whole system by analyzing the material properties at a single crystal in nanoscale. For the analysis of extremely small ranges of materials, we analyzed the degradation mechanism of the material in the sub-10nm range using Precession Electron Diffraction (PED) techniques.

The PED method can reduce the dynamic diffraction phenomenon according to the thickness of the TEM sample, so that the diffraction intensity can be quantified within a very small range. By using the PED technique based on nano-sized electron beams, we were able to map the structural change of Li(Ni_{1/3}Co_{1/3}Mn_{1/3})O₂ material in a single crystalline unit over a long period of electrochemical cycles.

It is known that the main cause of the decrease in LiB's capacity over the electrochemical cycles is the formation of an electrochemically irreversible rock salt phase inside the cathode material. However, the PED analysis showed that we could identify the existence of new metastable phase that had not discovered before. In other words, accelerated testing results revealed new unstable phases due to cation migration and found that the presence and distribution of these phases had a decisive effect on LiB's electrochemical degradation. In addition, the quantitative relationship between the strain and phase transition also could be derived. Therefore, based on these results, we expect that PED based on nano-sized electron beams can add new perspectives to the analysis of the degradation mechanism of materials for LiBs.

5:00 PM CH04.09.03

Unveiling The Distribution and Dynamic Behavior of Multi-Valent Chromium Ions in Li(Sc_{1-x}In_x)O₂:Cr Phosphors via In-Depth X-Ray Characterization Yi-Ting Tsai and Mu Huai Fang; Research Center for Applied Sciences, Academia Sinica (RCAS), Taiwan

Cr³⁺-doped inorganic compounds have played an important role in the development of near-infrared optical materials. However, the presence and distribution of multi-valent Cr ions remains unclear. In this study, we examined a series of Li(Sc_{1-x}In_x)O₂ phosphors doped with Cr³⁺ using X-ray techniques from National Synchrotron Radiation Research Center. Through high-resolution synchrotron X-ray diffraction, we identified two closely related phases within Li(Sc_{1-x}In_x)O₂. Raman spectra also confirmed distinctive scattering patterns for the two end-members of the compositional range, consistent with our XRD results. Further investigation using Cr K-edge X-ray absorption near edge structure and extended X-ray absorption fine structure techniques revealed the prevalence of Cr⁶⁺ ions in the initial samples. However, a significant shift occurred towards Cr³⁺ dominance upon water washing. We also used X-ray fluorescence and X-ray excited optical luminescence methods to analyze the source and spatial distribution of Cr³⁺ and Cr⁶⁺ ions in both as-prepared and washed samples. Our analysis indicated that Cr⁶⁺ ions aggregate within the material, while Cr³⁺ ions exhibit a more uniform dispersion. By utilizing photoluminescence, decay curve, and lineshape analyses, we were able to understand the electron-lattice interactions responsible for the optical properties. Our study explains the multi-valent, low-concentration ion distribution in solid-state materials and provides valuable insights into precise methodologies for discerning subtle alterations in crystal structures, contributing to the development of tailored optical materials.

5:00 PM CH04.09.05

Unraveling The Interfacial Behavior of Double Functionalized Silica Nanoparticles at Oil-Water Interfaces: Insights from Atomic Force Microscopy, In Operando Ultrasmall and Small-Angle and X-Ray and Interfacial Rheology Measurements Ahmed W. Alsmacii¹, Sohaib Mohammed¹, Bashayer Aldakkan¹, Nikolaos Chalmpes¹, Antonios Kouloumpis¹, Georgia Potsi¹, Greeshma Gadikota¹, Mazen Kanj² and Emmanuel P. Giannelis¹; ¹Cornell University, United States; ²King Fahd University of Petroleum and Minerals, Saudi Arabia

Tuning interfacial interactions of emulsions is of utmost importance in addressing hydrocarbon contamination of water resources and facilitating sustainable synthesis and processing of organics across different industries, such as energy recovery, pharmaceuticals, and the food industry. In this comprehensive study, we investigated the assembly of colloidal stable silica nanoparticles (NPs) at the oil-water interface, employing a novel double functionalization strategy. The NPs were functionalized with a blend of two silanes, one based on a quaternary ammonium group and the other combining primary and secondary amine groups, thereby endowing them with a positive charge. By modulating the charges on both the NP's surface groups and the oil phase, either by pH adjustments or the addition of electrolytes, we controlled the assembly and behavior of the emulsion. The careful combination of tunable charge and specifically chosen silane coupling agents provided the NPs with outstanding colloidal stability, which is significant for practical applications.

To evaluate the colloidal stability of the NPs, we conducted accelerated Space-Time Extinction Profiles (STEP[®]) measurements in brine solutions up to 60,000 ppm containing monovalent and divalent electrolytes and temperatures up to 60 °C. Remarkably, even under these harsh conditions, the NPs displayed exceptional stability. Assembly of the NPs at the oil-water interface can be controlled by controlling the pH or in the presence of electrolytes. Specifically, at pH 9 or in high salt concentrations, the interfacial tension (IFT) was substantially reduced from 35 mN/m to 5 mN/m and 2 mN/m, respectively.

To gain further insights into the interfacial properties of the emulsion, we used Ultrasmall/Small-angle X-ray scattering measurements, which unequivocally confirmed the presence of nanoparticles at the interface. Moreover, we found a correlation between the time-dependent scattering profiles and the dynamics of the growth of the interfacial film. To explore the nanomechanical characteristics of the interface, Atomic Force Microscopy (AFM) was employed. Notably, in the presence of the NPs at pH 9, the stiffness of the interface was substantially lower compared to acidic and neutral conditions, in brine or at pH 9 the assembly leads to jamming, reminiscent of an elastic membrane characterized by high dilatational and storage moduli. Leveraging the jamming phenomenon, we demonstrated the efficacy of our approach in herding oil droplets, thereby showcasing its potential for oil spill remediation. Additionally, our method facilitated the production of highly moldable and printable oil-in-water emulsions, presenting novel opportunities for various applications in the fields of environmental remediation, catalysis, drug delivery, food technology, and oil recovery.

5:00 PM CH04.09.06

Investigating The Effect of Blend Composition on The Burning Rate of PTT-PP and PTT- LLDPE Blends and Mechanism Thereof Shrikant Deo¹, Kavita Pande², Swamini Chopra³ and Dilip Peshwe¹; ¹Visvesvaraya National Institute of Technology, Nagpur, India; ²GHR Labs and Research Centre, India; ³MIT, Aurangabad, India

The present manuscript focuses on assessing the fire retardant performance of PTT polymer blended with varying proportions of PP and LLDPE, separately. This work explores the impact of varying the blend composition on the burning rate as per ASTM standard D635 for two series of blends; PTT-PP and PTT-LLDPE. The thermal degradation behavior is studied using Fourier transform infrared spectroscopy (FTIR) and the structure of the blends observed by Scanning electron microscope (SEM). The blend composition plays a vital role on the burning rate, and therefore the fire retardancy, of PPT polymer after blending. For PTT-LLDPE blends, the increase in the addition of LLDPE lowers the burning rate till 20 wt.% LLDPE. A further addition increases the burning rate of the blends due to the fact that pure LLDPE burns faster than pure PTT. In case of PTT-PP blends, the burning rate of pure PP is lower than that of pure PTT by ~22%, while the PTT-PP blends exhibit a burning rate closer to that of pure PTT. Though the PTT-PP blends may not exhibit excellent fire retardancy behavior like PTT-LLDPE blends, the addition of 15 wt.% PP can be cost effective than pure PTT, all the while exhibiting similar burning rate characteristics. Thus, this study infers that blending of PTT-LLDPE not only enhances the fire retardancy behavior of PTT by ~46%, but is also a cost effective alternative to using pure PTT. The FTIR analysis provides insight into the chemical changes occurring during the thermal degradation of the blends, thereby supporting to understand the fire-resistant mechanism of the blends.

5:00 PM CH04.09.07

Effects of Topological Parameters on Thermal Properties of Single-Walled Carbon Nanotubes by Molecular Dynamics Simulation Lida Najmi and Zhong Hu; South Dakota State University, United States

Due to their enhanced properties, carbon nanotubes (CNTs) are increasingly used in various industrial sectors. Specifically, the thermal conductivity of these materials is affected by heat transfer mechanisms across multiple scales, leading to a complex relationship between the effective response and the microscopic characteristics of the material. Due to their high thermal conductivity, CNTs have applications in various fields including electronics, materials science, and thermal management. They are incorporated into composites, films, and other materials to enhance their thermal performance. In this topic, the thermal properties of single-walled carbon nanotubes (SWNTs) are investigated using molecular dynamics (MD) simulation. The effects of the chirality, diameter, and length of SWNTs on the thermal properties were studied using the reverse non-equilibrium molecular dynamics (RNEMD) method and the carbon-carbon based Tersoff interatomic potential based on the Large-scaled Atomic/Molecular Massively Parallel Simulator (LAMMPS). The SWNTs studied have tube lengths of 5, 10, 15 and 20 nm, respectively. The thermal conductivity follows a L^B law. The exponent B is insensitive to the chiral angle of the CNT; B at room temperature is about 0.89 and 0.69 for zigzag and armchair CNTs, respectively. Although thermal conductivity increases with increasing the chiral angle, and armchair SWNTs have higher thermal conductivity than zigzag CNTs, the effect of chirality on the thermal conductivity for longer CNTs decreases. Therefore, for longer length SWNTs, the thermal conductivity of the zigzag is greater than that of the armchair ones. Through research on SWNTs of different diameters, it was found that at the same chiral angle, the thermal conductivity of SWNTs decreases with the increase in diameter, while SWNTs with greater chiral angles exhibit higher thermal conductivity than those of the same diameter. The thermal conductivity follows a D^{-B} trend, and the exponent B is insensitive to the chiral angle of the CNTs; the B of zigzag and armchair CNTs at room temperature are about 0.43 and 0.26, respectively. In addition, the thermal resistance at the CNT's interfaces was studied as a function of the nanotube spacing, overlap, and length. The simulation results were compared with the experiments and simulation results from the literature which are in agreement. The presented approach can be applied to study the properties of other advanced materials.

5:00 PM CH04.09.08

In-Situ Electron Channeling Contrast Imaging of Local Deformation Behavior of Lath Martensite in Low-Carbon-Steel Shuang Gong and Junya Inoue; University of Tokyo, Japan

This study reveals the dislocation dynamics that control the local deformation behavior of lath martensite in low-carbon steel using a combination of in-situ tensile Electron Channeling Contrast Imaging (ECCI) and X-ray based Convolutional Multiple Whole Profile (CMWP) fitting methods.

Lath martensite, characterized by distinct anisotropy in its local deformation behavior, poses challenges for its ductility in engineering applications. Unveiling the local dislocation dynamics driving this behavior is crucial for material optimization. Recent studies using X-ray and neutron diffraction line profiles have successfully employed the CMWP fitting method to probe the macroscopic evolution of dislocations in this material. Building on the foundation of this innovative approach, this study presents an integrative use of advanced X-ray analysis and in-situ tensile ECCI, which allows for microscopic direct observation of dislocation motion dynamics, directly linking them with the macroscopic evolutions.

By capturing X-ray diffraction patterns before and after a specific elongation threshold, and applying CMWP fitting, the study accurately determines the dislocation density, character, and arrangement within the lath. The analysis meticulously tracks the behavior of dislocations, identifying intra-lath crystallographic slip and boundary sliding as the two primary deformation processes. The onset of dislocation movement signifies the commencement of microscopic yielding. As the stress applied to the material increases, a transition to macroscopic yielding is observed, characterized by the ability of dislocations to navigate through and overcome densely packed dislocation walls within the laths. Near the lath boundaries, the pile-up of dislocations from out-of-lath-plane slip systems contrasts with the ongoing movement of those in-lath-plane, which are mainly responsible for plastic deformation. Further, this study successfully captures the boundary sliding phenomenon and clarifies the critical resolved shear stress (CRSS) required for this process to become the dominant form of plastic deformation following work hardening. The swift movement of the dislocation network close to the boundaries is particularly emphasized, as it plays an important role in mediating boundary sliding.

In summary, the correlation between the dislocation structure evolution observed through in-situ tensile ECCI and the evaluation made by CMWP fitting elucidate the intricate mechanism of plastic deformation in low-carbon steel lath martensite, with profound implications for enhancing the ductility of the material for industrial applications.

5:00 PM CH04.09.09

Disentangling Thermal from Electronic Contributions in The Spectral Response of Photo-Excited Perovskite Materials Lijie Wang^{1,2}, Razan O. Nughays¹, Omar F Mohammed¹ and Majed Chergui²; ¹KAUST, Saudi Arabia; ²EPFL, Switzerland

Disentangling electronic and thermal effects in photo-excited perovskite materials is crucial for photovoltaic and optoelectronic applications, but remains a challenge due to their intertwined nature in both the time and energy domains. In this study, we employed temperature-dependent variable-angle spectroscopic ellipsometry, density functional theory calculations, and broadband transient absorption spectroscopy spanning from the visible to mid-to-deep-Ultraviolet (UV) ranges on MAPbBr₃ thin films. The use of deep-UV detection opens a new spectral window that enables the exploration of high-

energy excitations at various symmetry points within the Brillouin zone, facilitating the understanding of the ultrafast responses of the UV bands and the underlying mechanisms governing them. Our investigation reveals that the photo-induced spectral features remarkably resemble those generated by pure lattice heating, and we disentangle the relative thermal and electronic contributions and their evolutions at different delay times using combinations of decay-associated spectra and temperature-induced differential absorption. The results demonstrate that the photo-induced transients possess a significant thermal origin and cannot be attributed solely to electronic effects. Following photo-excitation, as carriers (electrons and holes) transfer their energy to lattice, the thermal contribution increases from ~15% at 1 ps to ~55% at 500 ps, and subsequently decreases to ~35-50% at 1 ns. These findings elucidate the intricate energy exchange between charge carriers and lattice in photo-excited perovskite materials, and provide insights into the limited utilization efficiency of photo-generated charge carriers.

5:00 PM CH04.09.10

Highly Porous Structure Improves Molecular Dynamics of Cobalt-Based Composite Nanomaterials for Hybrid Supercapacitors [Ziwei Gan](#), Xiaohu Ren, Yongxiu Sun, Mengxuan Sun and Zhijie Li; University of Electronic Science and Technology of China, United States

Cobalt-based nanomaterials are a highly promising class of energy storage materials with high theoretical capacity and excellent long-term service life, such as metal doping and structural porousness of these cobalt-based nanocomposites, have been regarded as effective methods to further increase their active sites and improve their conductivity and performance. However, synthesizing cathode materials with high specific capacity and energy density through simplistic methods remains an immense obstacle. In this study, Mn doped cobalt-based hydroxide/sulfide nanocomposites with large pore volume as well as specific surface area were successfully synthesized. The Co(OH)₂/CoS electrode doped with Mn has better charge storage capacity (capacity increase from 586.5C g⁻¹ to 1030.8C g⁻¹ at 0.5 A g⁻¹), excellent rate performance (with a capacity retention of 75.8 % at 10 A g⁻¹). Additionally, a hybrid supercapacitor (HSC) was constructed utilizing Mn-Co(OH)₂/CoS and activated carbon (AC). HSC exhibited excellent charge storage capacity (166.3 F g⁻¹ at 0.5 A g⁻¹) and remained at 164.1 % of its original value after 30,000 cycles of testing with high current density. In addition, at a power density of 410.0 W kg⁻¹, the assembled HSC device demonstrates a significant energy density of 62.1 Wh kg⁻¹, revealing that porous Mn-Co(OH)₂/CoS electrode materials showed excellent energy storage properties.

5:00 PM CH04.09.11

Non-Newtonian Dynamics in Water-In-Salt Electrolytes [Marie-Louise Saboungi](#)¹, David Price², Andrei Dukhin³, Tsuyoshi Yamaguchi⁴ and Dongzhou Zhang⁵; ¹IMPMC -Sorbonne Université, France; ²CEMHTI, France; ³Dispersion Technology Inc, United States; ⁴Nagoya University, Japan; ⁵University of Chicago, United States

Water-in-salt electrolytes have attracted considerable interest in the past decade for advanced lithium-ion batteries, possessing important advantages over the non-aqueous electrolytes currently in use. A battery with a LiTFSI-water electrolyte was demonstrated in which an operating window of 3 V is made possible by a solid-electrolyte interface. Viscosity is an important property for such electrolytes, because high viscosity is normally associated with low ionic conductivity. Here, we investigate shear and longitudinal viscosities using shear stress and compressional longitudinal stress measurements as functions of frequency and concentration. We find that both viscosities are frequency-dependent and exhibit almost identical frequency and concentration dependences in the high-concentration region. A comparison to quasielastic neutron scattering experiments suggests that both are governed by structural relaxation of the TFSI- network. Thus, LiTFSI-water electrolytes appear to be an unusual case of a non-Newtonian fluid, where shear and longitudinal viscosities are determined by the same relaxation mechanism.

5:00 PM CH04.09.12

Evaluation of Anti-Icing/De-Icing Performance of PU Topcoat with CNT Addition in Aircraft Applications [Lee Donghyeon](#), Yang Seong Baek and Kwon Dong-Jun; Gyeongsang National University, Korea (the Republic of)

Icing on aircraft can lead to increased weight, reduced lift, and pose a risk of accidents. Methods for removing aircraft icing include the use of deicing solutions like glycol or employing techniques such as heating and vibration. However, these methods have limitations in terms of applicable areas, energy consumption, duration constraints, and low efficiency. To prevent ice formation on the aircraft itself, anti-icing methods are employed. Anti-icing methods involve surface etching on metal surfaces or the application of hydrophobic polymer coatings. Commonly used polymers for this purpose are polytetrafluoroethylene (PTFE) and polyurethane due to their ability to cure at room temperature and compatibility with base materials like epoxy. To enhance hydrophobic effects, research is exploring the addition of hydrophobic nanoparticles to create nanostructured surfaces. Nanoparticles, acting as binders, form the topcoat in the coating layer. However, nano surfaces face challenges related to durability and sustainability. In this study, a nanostructured surface was achieved by incorporating hydrophobic nanoparticles, specifically carbon nanotubes (CNT), into the polymeric topcoat. Polyurethane was utilized as the topcoat, and CNT dispersed in a solvent such as xylene was sprayed after coating. To address durability issues associated with previously researched nano surfaces, CNT was dispersed in the binder to enhance the strength of the topcoat and increase the adhesion between the binder and the exposed CNT on the surface. Additionally, the conductivity of CNT dispersed in the topcoat contributed to higher thermal conductivity compared to coating CNT only on the surface. To expose hydrophobic CNT on the surface, some hardening of the topcoat surface was induced before coating with xylene. This allowed for the manifestation of the hydrophobic effect from the carbon surface of CNT and also contributed to surface morphology effects induced by CNT. The addition of CNT increased the contact angle with water from 74.3 degrees to 121.2 degrees, resulting in a significant delay in icing effects, approximately a 260% increase. Moreover, a decrease in adhesion time and strength of ice on the surface was observed. When a current of 3V was applied, a temperature increase of about 54 degrees was noted, effectively causing the ice to melt and slide off. Ongoing research involves investigating the impact of surface roughness changes on aircraft wings or similar structures when applied as an actual model. The study aims to understand the influence of surface variations on aircraft wings and related components. This work was partly supported by Korea carbon Industry Promotion Agency grant funded by the Ministry of Trade, Industry and Energy (RS-2023-0026563). This research was supported by the National Research Foundation of Korea(NRF) funded by the Ministry of Science and ICT (RS-2023-00211944). This work was supported by Policy R&D program funded by Korea Ceramic Engineering & Technology, Republic of Korea(No. KPP23006-0-01).

5:00 PM CH04.09.13

Advanced Characterization Approaches for Anisotropic Metal Patchy Particles [Julia S. Seifert](#)¹, Andreas Voelkl¹, Dominik Drobek², Nabi E. Traoré¹, Paola Cardenas Lopez¹, Mingjian Wu², Benjamin Apeleo-Zubiri², Johannes Walter¹ and Robin N. Klupp Taylor¹; ¹Institute of Particle Technology, Germany; ²Institute of Micro- and Nanostructure Research & Center for Nanoanalysis and Electron Microscopy, Germany

Plasmon resonant nanoparticles have garnered significant interest in recent decades due to their potential as sensing or marker particles in various applications. Particularly, anisotropic plasmonic particles offer the advantage of highly tunable optical properties within a particle system. However, the increased number of shape parameters compared to isotropic particles, challenges for thorough particle characterization. Precise descriptions of particle shape and product yield are, nevertheless, indispensable for product optimization, which requires, for example, particle growth models. Therefore, in this contribution we present a variety of characterization methods used to extract information from our anisotropic particle system, obtaining the desired parameters on different levels.

We have developed several continuous flow processes for synthesizing gold and silver patchy particles whereby dielectric core particles are coated with thin islands of metal. The size, shape and morphology of the patches determine the optical resonance position which can be tuned over the visible and near-infrared spectral range. The synthesis is performed in a seed-mediated two-step process. Understanding the influence of seed particles on the growth of patches with different dimensions and morphologies is crucial. To this end, we will show how newly developed 4D-STEM analysis can resolve individual crystal grains' orientations and probe the influence of seed particles on the crystal growth directions in the patch.

On the whole patch scale, coating dimensions and morphology must be thoroughly characterized to obtain quantitative size parameters. These are essential for optical simulations and the development of patch growth models. STEM analysis and electron tomography are indispensable for revealing the patch structures where SEM imaging fails due to resolution limitations. Here we will show how these techniques can be applied to quenched samples, in which the growth has been "frozen" during patch formation, thus providing insight into the growth process. Additionally, patch shape degradation after synthesis, observed as changes in the optical spectra, can only be resolved through TEM imaging. Here, 3D data obtained from electron tomography can further be used as direct input for optical simulations to compare the obtained results with experimental spectra.

At the overall particle level, it is important to note that not every particle is coated with a patch. Determining the so-called patch yield is crucial for optimizing process efficiency. In this regard, we demonstrate the use of different methods to identify the patch yield of the product. Firstly, single particle scattering and extinction, a novel technique derived from flow cytometry, can distinguish between bare and gold-coated polystyrene particles due to their different optical responses. Secondly, analytical ultracentrifugation, as an ensemble measurement, is used to determine product yield based on differences in particle density and sedimentation velocity.

The diverse characterization methods we demonstrate for patchy particles enhance our understanding of their complex properties and synthesis. These methodologies, adaptable to other anisotropic systems, are expected to be pivotal for future advancements in plasmonic nanoparticle applications.

5:00 PM CH04.09.14

Self-Healing Polymer Composites with Enhanced Strength for Use in Protective Textiles Evan A. Griffiths, Blaine M. Barrington, Jessica M. Andriolo, Scott Coguill, Brahmananda Pramanik, Richard LaDouceur and Jack L. Skinner; Montana Technological University, United States

Self-healing materials have the potential to increase the lifetime of products exponentially through both non-reversible healing and reversible healing processes. For instance, non-reversible healing has been demonstrated with the use of micro-spheres filled with healing-compounds used to mitigate micro-crack propagation in materials like concrete or asphalt. Upon use, however, micro-sphere rupture is irreversible. Reversible self-healing traditionally takes the form of polymeric or rubber materials designed to exhibit both covalent and ionic bonds within the same material. Reversible self-healing materials not only repair other products but can have extended lifetimes themselves. However, reversible self-healing materials are often mechanically weak when compared to non-reversible self-healing materials, thereby, limiting applications. In this work we report mechanical results of aramid nanofiber (ANF) reinforcement of polycaprolactone (PCL). These results and future testing will then be applied to self-healing polymer materials to observe the mechanical reinforcement factors.

To fabricate the aramid nanofibers, macroscale fibers were broken down through hydrolysis in a dimethyl sulfoxide and potassium hydroxide solution. Fibers were then reformed through the addition of water and filtered to remove larger fibers. Following filtration, the remaining fibers were suspended in PCL that had been pre-dissolved in trifluoroethanol. The ANF/PCL suspension was sonicated for dispersion of the nanofibers within the polymer matrix. For this study, the samples examined were: 1) PCL melted and impregnated with ANFs before solidifying, 2) PCL that was solvent-dissolved before ANFs were blended into the liquid polymer and then let dry to evaporate solvent, 3) and solvent-dissolved PCL/ANF composites (1 and 2 wt%) that were embedded with ANFs before solvent was evaporated from the samples. Mechanical testing for this study included compressive, tensile and split-Hopkinson pressure bar (SHPB). Results of this testing demonstrated an increase of compressive yield strength by 22 %, an increase in tensile Young's modulus by 28 %, and a decrease in ultimate strength by 32 %. SHPB testing also revealed an increase in dynamic resistance when absorbing impacts at speeds ranging from 10 to 22 m/s where impact duration lasted as much as 23 % longer. Further testing will be performed to characterize shear performance of the samples as well as the Charpy impact energy absorption. Transmission electron microscopy and energy dispersive spectroscopy will be used to correlate embedded fiber morphologies and distributions with mechanical properties.

The primary objective of this work is to provide self-healing textiles with enhanced strength for soldiers in the field to maintain protection following damage of protective gear or uniforms. Following determination of a preferable aramid concentration in a reinforced polymer matrix, the polymer will be electrospun into fibrous textiles for further mechanical testing, to monitor properties following impact and self-repair, and determine sustainability.

SESSION CH04.10: Emerging Characterization and Modeling
Session Chairs: Tianyi Li, Michelle Mejia and Yang Yang
Friday Morning, April 26, 2024
Room 443, Level 4, Summit

8:00 AM CH04.10.01

Hydrogen Exchange and Diffusion Kinetics at Elevated Temperatures in Proton-Conducting Solid Oxide Materials Mudasir A. Yattoo¹, Sakuda Yuichi², Kataro Fujii², Masatomo Yashima² and Stephen Skinner¹; ¹Imperial College London, United Kingdom; ²Tokyo Institute of Technology, Japan

Storage of purified hydrogen is one of the central challenges in addressing climate change and reducing our reliance on fossil fuels for energy conversion and storage, and therefore there is a global surge in research and development concerning hydrogen purification and storage. In this regard, we are studying proton conduction in solid oxide materials at elevated temperatures for applications in hydrogen separation and compression membranes. Hydrogen compression is the most recommended method to store hydrogen for automotive applications as it allows an increase in the hydrogen volumetric energy density.

Traditionally the protonic conductivity in these materials is measured by indirect methods. For example, conductivity measurements in mixed gas

atmospheres, comparing for example dry N₂ with humidified N₂, thereby allowing the contribution of protons to be evaluated. In this study, we for the first time report the evaluation of protonic conductivity in BaZr_{1-x}Ce_xY_{0.2}O_{3-δ}, BaZr_{0.1}Ce_{0.7}Y_{0.2-x}Yb_xO_{3-δ}, Ba₇Nb₄MoO₂₀ and Ba₇Nb₄MoO_{20.1} by direct measurements afforded by the Isotope Exchange Depth Profiling technique with deuterium labelling. We also report the kinetics of H/D transport through the bulk materials and across metal-ceramic interfaces with a particular interest in the behaviour of the interface between the key Pd/Pd alloy catalyst component and the hydrogen-transporting oxide ceramic material. The transport and interface behaviour information will be of significance in designing hydrogen separation and compression membranes.

8:15 AM CH04.10.02

Novel Electrical Tree Type Observed using Gigahertz Frame Rate Camera to Image Dielectric Breakdown in Space-Charged Polymer [Kathryn Sturge](#)¹, Noah Hoppis¹, Ariana Bussio¹, Jonathan E. Barney², Brian L. Beaudoin¹, Cameron Brown², Bruce Carlsten², Carolyn Chun¹, Nicholas Dallmann², Jack Fitzgibbon¹, Ashley E. Hammell¹, Samuel Henderson², Miriam Hiebert¹, James Krutzler¹, Joseph P. Lichthardt², Mark Marr-Lyon², Nathan Moody², Alexander H. Mueller², Patrick O'Shea¹, Ryan Schneider¹, Karl Smith², Bryce Tappan², Clayton Tiemann², David Walter² and Timothy W. Koeth¹;
¹University of Maryland, College Park, United States; ²Los Alamos National Laboratory, United States

We have successfully imaged dielectric breakdown occurring in electron irradiated space-charged polymethyl methacrylate (PMMA) blocks at a nanosecond time resolution. These images, which are the first of their kind, reveal two distinct dielectric breakdown treeing effects, one of which is absent from the present literature on dielectric breakdown. This new mode of electrical tree formed during dielectric breakdown of a space-charged polymer demonstrates unique behavior from its better-documented and widely known “branch-type” channels, including structural and formation dynamics differences. Due to its threadlike, smooth appearance, this new type of electrical tree has been coined “vine-type,” in contrast to its “branch-type” counterpart. Both vine-type and branch-type electrical trees were imaged as they formed in the electron irradiated samples, allowing for close study of the channel formation dynamics. The speeds at which the channels form for both types were directly measured from these images and found to exceed 10⁷ m/s and 10⁶ m/s for vine-type and branch-type, respectively—speeds approaching 4% the speed of light in the material. These speeds are faster than previously predicted by models and imply the channel growth is the fastest physical phenomenon in a solid material. Further, the propagation of the electrical tree formation was imaged and three regimes of breakdown channel formation were identified and characterized for the two modes of electrical trees, solving a decades-long mystery on the plasma channel formation process in space-charge dielectric breakdown.

8:30 AM CH04.10.03

Hygromechanical Behavior of Cellulose-Based Materials [Caterina Czibula](#)¹, Ulrich Him¹ and Kristie J. Koski²; ¹Graz University of Technology, Austria; ²University of California, Davis, United States

Cellulose is the most abundant biopolymer on Earth and, as most biological materials, has a hierarchical, anisotropic structure. Its mechanical properties are strongly influenced by environmental conditions such as temperature and moisture content. Especially the influence of humidity is very difficult to investigate. In most cases, water behaves like a plasticizer and leads to lower mechanical properties, swelling of the material and shows an apparent effect on the viscoelastic behavior of the material. This has strong implications for the technical use of cellulose-based materials. The production of paper is a classic example with the material going through different process steps, which have an influence on the chemical and physical properties, and at the same time also cause different hydration states in the material. When the product is finished and put into use, the effects of moisture changes trigger undesirable effects and have an impact on service life.

Here, Brillouin Light Scattering Spectroscopy (BLS) is applied as a non-contact, optical method based on inelastic scattering of laser light by acoustic phonons in the sample material to study the mechanical properties. By using BLS, the mechanical behavior in the GHz frequency regime is investigated with a high time resolution during wetting and drying of cellulose-based materials. In this talk, first results of such experiments will be presented.

8:45 AM CH04.10.04

Interpreting Spectroscopic Data in Halide Perovskites using Bayesian Inference [Tobias Rudolph](#)¹, Chris Dreessen^{1,2} and Thomas Kirchartz^{1,3}; ¹IEK5-Photovoltaik, Germany; ²Instituto de Ciencia Molecular, ICMol, Spain; ³Faculty of Engineering and CENIDE, Germany

The characterization of recombination processes is a crucial step in the development of solar cells. TRPL is a traditional characterization method for observing recombination mechanisms, frequently used for instance in the field of lead-halide perovskites for photovoltaic and optoelectronic applications. However, especially in the fairly intrinsic lead-halide perovskites, the interpretation of data is complicated because many processes, such as different recombination mechanisms and charge transport, occur at similar time scales. While it is reasonably straightforward to solve the forward problem of simulating TRPL transients for a given set of material parameters, the inverse problem of inferring the material parameters from measured transients is difficult. Fitting analytical models typically leads to an oversimplified model while fitting numerical simulations is very time consuming.

In this study, we propose a novel approach that combines Bayesian inference with surrogate models to increase computational speed. Using our approach, we obtained results from a typical TRPL dataset in less than an hour on an ordinary desktop PC. Instead of using the drift-diffusion simulations during fitting, we used ~10⁶ simulations to train a convolutional neural network which works as a surrogate model. Reading out the surrogate model for a certain material parameter combination is approximately as fast as the evaluation of an analytical equation but allows the inclusion of significantly more complexity in the choice of model. Given the speed of comparing the output of the surrogate model with the experimental data, it becomes feasible to evaluate the physically plausible parameter space by slow methods such as grid search. This approach allows us to obtain a profound understanding of parameter correlations and can estimate fitting errors.

Conventional methods used to experimentally determine TRPL transients such as TCSPC suffer from a limited dynamic range. However, the recombination parameters only become visible in data that covers several orders (>4) of magnitude in PL intensity and time. Thus, we used a gated CCD setup to measure TRPL over a wide dynamic range of up to eight orders of magnitude. This provides insights into the recombination processes that would be difficult to obtain otherwise. A noteworthy result in the context of lead-halide perovskite thin films is the predominance of recombination via shallow defects and the apparent complete absence of deep defect recombination in the data that we observe over a wide range of compositions. We can infer important parameters, such as trap depths, trap density, and capture cross-sections from the TRPL data. Our method offers rapid and comprehensive insights into the parameters governing the recombination process in solar cells.

9:00 AM CH04.10.05

High Operation Stability of Solution-Processed Ultrathin ([John Jinwook Kim](#)¹, Haibin Su² and Wallace C. Choy¹); ¹The University of Hong Kong, Hong Kong; ²The Hong Kong University of Science and Technology, Hong Kong

Ultrathin flexible transparent electrodes (*μ*FTEs) are an indispensable component in emerging flexible electronics due to a high level of compatibility and comfortability while there is an ever-increasing demand for low-cost solution-process-based high-throughput production for *μ*FTEs. Owing to the successful advances of solution-processed nanomaterials [1], *μ*FTE composites from transparent metal-oxide-semiconductors (TMOS) and silver nanowires (*A*_gNWs) have been extensively reported. However, there is still a big gap in achieving simultaneous multi-loading operations (i.e., folding cycles with <1.5 mm radius of curvature, current bias with >300 mA cm⁻², and humid environments at 85 % of relative humidity (RH)), which is highly required as one of

the practically rigorous environments.

The fundamental bottleneck is to achieve high-quality interfaces simultaneously by performing tri-system integration in $A_gNW_{-}TMOSNP$ hybrid μ FTEs. The tri-system includes three different interfaces $A_gNW_{-}A_gNW$, $TMOSNP_{-}TMOSNP$, and $A_gNW_{-}TMOSNP$. All interfaces play key roles in the long operational stability against the simultaneous multi-loading operations. Although excellent works have been reported in the individual systems of $A_gNW_{-}A_gNW$ networks [2] and TMOS-TMOS nanocrystal films [3], importantly, the quality of $A_gNW_{-}TMOSNP$ heterogeneous interfaces needs substantially improving due to the mismatched interaction between A_gNW and $TMOSNP$. As a consequence, there are primary need to realize the tri-system integration for achieving the mechanical, electrical, and chemical stability in the solution-processed $A_gNW_{-}TMOSNP$ composites for better μ FTEs.

In this study, we develop a simple one-step *in situ* solution processed method (*i*SPM) to fabricate the solution-processed tri-system-integrated μ FTEs (greatly thin less than 1 μ m) composed of A_gNW s and $ZnONPs$ at room temperature. The *i*SPM is developed for both (i) removing the capping agents from A_gNW s and (ii) facilitating $ZnONPs$ with flexible geometric shapes through the course of the coalescence process. The provided condition from both (i) and (ii) enables the $ZnONPs$ to be capable of in situ nano-adhesion into the cleaned surface of A_gNW s via flexible geometric shapes. Fundamentally, we show the in-situ atomic passivating mechanism of A_gNW by the liquid-like spreading dynamics of solid-state $ZnONP$ being wetted on the A_gNW surface. The nanonet μ FTEs with *tri-system integration* via *i*SPM show very good mechanical-electrical-thermal-moisture stability of the current density fluctuations less than 5 % against simultaneous multi-loading fatigue tests (10,000 cyclic mechanical folding with approximately 0.5 mm of FR, continuous electrical bias of 8.4 MA cm⁻², and 85 % RH condition). The superior electrical/optical properties (<10 Ω sq.⁻¹ of sheet resistance and >88 % of diffused transmittance in the region of wavelengths 400-1000 nm) and smooth surface topography (within ~1 nm of RMS and ~5 nm of PtV roughness) have been achieved within all the *i*SPM-treated $A_gNW_{-}ZnONP$ nanonet μ FTEs. Consequently, our finding unveils the complex interfacial dynamics associated with the heterogeneous interface system between A_gNW s and $ZnONPs$ and holds great promise in understanding the in-situ nano-adhesion process and increasing the design flexibility of promising solution-processed μ FTEs.

Reference

1. Huang, Z., Ouyang, D., Shih, C., Yang, B. and Choy, W. C. H. Solution-Processed Ternary Oxides as Carrier Transport/Injection Layers in Optoelectronics. *Adv. Energy Mater.* **10**, 1900903 (2020).
2. Park, J. H. *et al.* Flash-Induced Self-Limited Plasmonic Welding of Silver Nanowire Network for Transparent Flexible Energy Harvester. *Adv. Mater.* **29**, 1603473 (2016).
3. Chen, Z. *et al.* A Transparent Electrode Based on Solution-Processed ZnO for Organic Optoelectronic Devices. *Nat. Commun.* **13**, 4387 (2022).

9:15 AM CH04.10.06

Structure and Dynamics of Water Ice Ih [Tianran Chen](#) and David A. Tennant; The University of Tennessee, Knoxville, United States

Water ice Ih is a non-periodic system with proton disorder due to the large number of possible configurations of hydrogen atoms that follow the ice rule. Understanding the structure and dynamics of water ice Ih is important for various scientific and technological applications. In this work, we measured the static and dynamic structure factors of a single crystal ice Ih at different temperatures using elastic and inelastic neutron scattering techniques. We showed that our static structure factors could be well explained by the Fourier transform of the simulated spatial configurations of water ice.

We derived the formula to calculate the dynamic structure factor of non-periodic systems. We showed the limitations of classical first-principle phonon calculations when dealing with non-periodic systems. We presented a novel method to calculate the dynamics of water ice Ih. We constructed the force constant matrices using a mathematical model based on the local symmetry guaranteed by the ice rule. The model parameters were first fitted to first-principle phonon results and then fine-tuned to fit the neutron scattering data. Our results showed the detailed short-range interactions of water ice Ih with high accuracy and corrected the underestimated hydrogen interactions using classical first-principle phonon calculations. Our results provided new insights into the lattice dynamics and thermal properties of water ice Ih and offered potential applications for understanding other non-periodic systems with local symmetry.

9:30 AM BREAK

10:00 AM CH04.10.07

Energy Storage using Order-Disorder Phase Transitions in Plastic Crystals Ares Sanuy, Gustavo Madrigal, Carlos Escorihuela, Claudio Cazorla and Luis Carlos Pardo Soto; Universitat Politècnica de Catalunya, Spain

Energy storage materials based on order-disorder phase transitions are a promising strategy for harnessing solar energy in a simple and efficient manner. Thermal energy is stored by inducing a phase transition between an ordered solid phase, where molecules are ordered both translationally and orientationally, and a plastic phase where molecules are allowed to rotate in a more or less free way. Two materials that can be used for this purpose are Neopentyl Glycol (NPG) and methylammonium-lead-iodide (MAPI), the latter having an organic molecule inserted into an inorganic framework, in contrast to the former. From a theoretical perspective, the strategy of harnessing energy through order-disorder transitions requires a deep understanding of the nature of disorder in the plastic phases. This understanding is crucial for analyzing existing materials and developing new ones based on the same principle. In this work, we present Molecular Dynamics simulations aimed at establishing a unified microscopic description that rationalizes the experiments conducted so far. Additionally, the study proposes a standardized protocol for investigating order-disorder phase transitions.

10:15 AM CH04.10.08

Unraveling The Catalytic Effect of Hydrogen Adsorption on Pt Nanoparticle Shape-Change [Cameron J. Owen](#)¹, Nicholas Marcella², Yu Xie¹, Jonathan Vandermause¹, Anatoly Frenkel^{3,4}, Ralph Nuzzo² and Boris Kozinsky^{1,5}; ¹Harvard University, United States; ²University of Illinois at Urbana-Champaign, United States; ³Stony Brook University, The State University of New York, United States; ⁴Brookhaven National Laboratory, United States; ⁵Robert Bosch LLC, United States

The activity of metal catalysts depends sensitively on dynamic structural changes that occur during operating conditions. The mechanistic understanding underlying such transformations in small Pt nanoparticles (NPs) of ~1-5 nm in diameter, commonly used in hydrogenation reactions, is currently far from complete. In this study, we investigate the structural evolution of Pt NPs in the presence of hydrogen using long time-scale reactive molecular dynamics (MD) simulations paired with experimental X-ray absorption spectroscopy. From these comparisons, we obtain atomic-level mechanistic insights into 'order-disorder' structural transformations exhibited by highly dispersed Pt NP catalysts upon exposure to hydrogen. We report the emergence of previously unknown candidate structures in the 1 nm Pt NP size range, where exposure to hydrogen leads to the appearance of a 'quasi-icosahedral' intermediate symmetry, followed by the formation of 'rosettes' on the NP surface. Hydrogen adsorption is found to catalyze these shape transitions by lowering their temperatures and increasing the apparent rates at which these candidate structures appear, revealing the mutually catalytic and dynamic nature of interaction between nanoparticle and adsorbate. This study offers a new pathway for deciphering the reversible evolution of catalyst structure resulting from the chemisorption of reactive species, enabling the determination of active sites and improved interpretation of experimental results with atomic resolution.

This searchable program is up-to-date as of April 15th, 2024.

10:30 AM CH04.10.09

Temperature-Dependent Mechanical Properties of Organic Semiconductors [Kehinde Fagbohunbe](#), Connor Callaway and Chad Risko; University of Kentucky, United States

Rationalizing the deformation of molecular and polymer-based organic semiconductors (OSC) under mechanical stress across a range of operating temperatures is critical both to the development of OSC for flexible devices and to a more general understanding of the degradation of OSC performance. Here, we develop and deploy atomistic molecular dynamics simulations to determine stress-strain relationships of molecular (i.e., non-fullerene and fullerene acceptors) and polymer (i.e., P3HT)-based OSC of interest for organic solar cells. A key goal of this work is to clarify how changes in chemical structure of the OSC building blocks, packing configurations, polymer chain entanglement, and both local and long-range material order (e.g., torsional disorder, crystallinity, etc.) influence properties such as the elastic modulus. By making connections with other (thermo)mechanical and optoelectronic works in the literature, the results discussed here seek to provide insights into upper and lower temperature limits for OSC during device operation and overall material stability.

10:45 AM CH04.10.10

Real Time Sensing of One Dimensional Nanostring Vibrations [Michael C. Skripalsh](#), Arnab Manna, Laurel E. Anderson and Arthur Barnard; University of Washington, Seattle, United States

Micromechanical resonators host localized vibrations which make them useful tools for sensing and exploring the physics of small-scale systems. Devices such as silicon nitride cantilevers or suspended carbon nanotubes can be used as sensing devices through measurements of how their resonant frequencies change due to local perturbations. The small size of these resonators enables extremely precise resolution of masses and forces. While reducing the size of mechanical resonators conceptually improves sensitivity, when a resonator is shrunk down to the molecular scale, a much more complex regime emerges. Polymers, for instance, are known to be highly entropic: coupling to their environment causes large thermal fluctuations among their many flexural modes. The dynamics of such systems are well understood in highly damped environments such as biopolymers inside a living cell. However, in underdamped environments the dynamics are largely unexplored.

In this study, single molecules of DNA are suspended between SU-8 nanopillars with superhydrophobic surfaces that clamp the DNA nanostrings to both ends. The vibrations are measured by using a scannable photonic crystal cavity coupled to a tapered optical fiber. When the cavity is positioned close to the DNA, the near field coupling between the cavity and resonator allows for real-time measurement of the flexural dynamics of the nanostring via optical readout. These measurements are conducted at room temperature and can be used to further study the complex behavior of the nanostring's flexural modes such as thermalization, nonlinear coupling, and chaotic behavior. Looking forward, resonators made from DNA can be programmed to have arbitrary structures to tune their phononic character for added functionality and to probe the physics of nanostrings.

SESSION CH04.11: On-Demand Presentation
Tuesday Morning, May 7, 2024
CH04-virtual

10:30 AM CH04.09.04

Morphology-Driven Magnetic Property Manipulation in Binary Particle Mixtures for Microscale Magnetic Control. [Khalil ur Rehman](#)^{1,2}, Mario Hofmann¹ and Ya-Ping Hsieh^{2,2}; ¹National Taiwan University, Taiwan; ²Academia Sinica, Taiwan

Magnetic microactuators and microrobots have the potential to revolutionize remote manipulation and swarm-based collaboration. Unfortunately, conventional approaches to controlling individual magnetic systems cannot be shrunk to the microscale due to fundamental challenges in the generation and modification of magnetic fields. We here demonstrate the manipulation of magnetic properties in binary particle mixtures through morphology control. A combination of ferromagnetic and non-magnetic particles demonstrates the emergence of ordering and magnetic anisotropy under conditions that induce mechanical jamming in the assembly. A combined theoretical and experimental investigation confirms the importance of arresting forces from neighboring particles as the origin of this behavior. Utilizing this insight, a novel actuator, termed "Magnet with Mechanical Tunability (MagMeT)" was developed that transduces mechanical deformation in magneto/ elastomer particle mixtures into magnetic torque. Our results open up a route toward actively controlling magnetic microrobots for future remote operating applications.

SYMPOSIUM EL01

Surfaces and Interfaces in Electronics and Photonics
April 23 - May 7, 2024

Symposium Organizers

Silvia Armini, IMEC

Santanu Bag, AsterTech

Mandakini Kanungo, Corning Incorporated

Gilad Zorn, General Electric Aerospace

* Invited Paper
+ JMR Distinguished Invited Speaker
^ MRS Communications Early Career Distinguished Presenter

SESSION EL01.01: Area Selective Deposition and Etching I
Session Chairs: Silvia Armini, Santanu Bag, Stacey Bent, Mandakini Kanungo and Gilad Zorn
Tuesday Morning, April 23, 2024
Room 348, Level 3, Summit

10:30 AM *EL01.01.01

Controlling Interfaces toward Area Selective Atomic Layer Deposition [Stacey F. Bent](#); Stanford University, United States

With the growing demands on nanostructure fabrication for advanced electronics, atomic layer deposition (ALD) continues to gain attention as an important method to achieve pattern features at the sub-10 nm length scale. Based on sequential, self-limiting vapor-surface reactions, ALD offers exceptional conformality, thickness control at the Angstrom level, and tunable film composition. Due to the chemical specificity of ALD reactions, several molecular-level system parameters can strongly impact the ALD nucleation and growth rate, including the specific substrate interface as well as the type of ALD precursor. As a result, the substrate interface and precursor selection can be tuned to intentionally control nucleation rates in ALD, which in turn provides a means to achieve selectivity on spatially patterned substrates. The resulting process of area selective atomic layer deposition (AS-ALD) has attracted significant attention in recent years. In this talk, we will provide examples of tuning surface chemistry to achieve AS-ALD. The development of inhibitory layers such as self-assembled monolayers (SAMs) and small molecule inhibitors (SMIs) to alter the native surface reactivity will be described. Some new SMIs include aryl or alkyl thiol, amine, nitro, and sulfonic acid compounds. The inhibition strategies demonstrate good selectivity in the deposition of thin films on a variety of substrate materials, and selectivity in AS-ALD can be further enhanced by choice of ALD precursor. Finally, we will describe the development of carbon-free inhibitor layers for AS-ALD.

11:00 AM EL01.01.02

Investigation of The Optical Constants of Absorbing Atomic Layer Deposition (ALD)-Grown TiO₂ Thin Films [Nimarta Chowdhary](#) and Theodosia Gougousi; UMBC, United States

Titanium dioxide, TiO₂, has been investigated extensively due to its unique and tailorable optical properties, including high refractive index, high dielectric constant, and high photocatalytic activity. The optical properties of thin films can be affected by the deposition process, composition, thickness, conductivity, and density. While TiO₂ is typically regarded as a wide band-gap semiconductor, with applications limited to the UV light range, TiO₂-based modified materials show promising results for applications with harvesting renewable solar energy. Applications of these sorts, however, require TiO₂-based materials to exhibit absorption in the visible light range. This can be achieved with band gap and optical property engineering.

For Atomic layer deposition (ALD), the process temperature is known to affect the film composition and, consequently, optical properties. We have used ALD to deposit 20-130 nm TiO₂ thin films from tetrakis(dimethyl amino) titanium (TDMAT, Ti[N(CH₃)₂]₄) and deionized (DI) H₂O at process temperatures ranging from 200 to 350°C. For films of the same thickness, the actual coloration is dependent on the deposition conditions. Control TiO₂ samples have been produced by a physical vapor deposition method (PVD) at room temperature from a TiO₂ target. X-ray photoelectron spectroscopy (XPS) analysis shows that ALD-grown TiO₂ films incorporate Ti-N/Ti-O-N metallic bonds while the PVD-produced films are purer, as expected. As the ALD process temperature increases, so is the measured at. % of Ti-O-N/Ti-N metallic bonding ranging from ~1 at. % at 250°C to ~4.5 at. % at 350°C.

Ultraviolet-visible spectroscopy (UV-VIS) confirms that the ALD-grown thin films are partially absorbing in the visible range with their absorbance dependent on the process temperature. Similar measurements have shown that PVD-grown films are transparent, as expected. The optical properties of the films have been investigated using spectroscopic ellipsometry (SE) at 380-900 nm. For these partially absorbing ALD films, conventional single-angle SE approaches fail to provide the requisite number of linearly independent equations to allow for the determination of the optical constants, n and k, and film thickness d. We have developed a modified ALD approach that produces samples on quartz substrates that are suitable to be used with a combination of single-angle ellipsometry (SE) data and intensity-based transmission (T) measurements to determine these parameters (n, k d) and their spectral dependence simultaneously.

When compared to pure PVD TiO₂ films, the partially absorbing ALD TiO₂ films exhibit a reduced n (ϵ_1) and increased k (ϵ_2), [TG5] which is consistent with the presence of TiO_xN_y bonding in the film. At 633 nm, n and k for PVD TiO₂ films are ~2.4 and 0, respectively, which is consistent with the literature. For the ALD films, the optical constants are found to depend on the ALD process temperature; values for n range from ~1.7 - 2.3, and k ranges from ~0.2 - 1.2 at 633 nm.

When the as-deposited ALD-grown TiO₂ thin films are annealed at 900°C in an argon environment, the thin film coloration changes, indicating a structural and compositional change. XPS analysis shows that the metallic bonding detectable in the as-deposited films has been removed and the films are fully oxidized TiO₂. We demonstrate that the ALD process temperature, as well as post-deposition thermal treatment for the films, are both avenues for controlling the band gap and tailoring the optical constants of TiO₂ films for a wide variety of applications.

11:15 AM *EL01.01.03

A Public-Private-Academic Partnership: The Microelectronics Commons [Alison Smith](#); NSWC Crane, United States

Public-private-academic partnerships have the potential to drive innovation by leveraging the collective expertise and resources of government agencies, industry, and academic institutions to solve complex challenges. The Microelectronics Commons (Commons) is a key national initiative that is executed with oversight from the Office of the Under Secretary of Defense for Research and Engineering's (OUSD(R&E)'s) Principal Director for Microelectronics. This effort benefits both the Department of Defense (DoD) and the United States in spurring development of a domestic microelectronics manufacturing industry by forging critical partnerships with commercial industry, academic, and government partners. The Commons supports laboratory to fabrication (lab-to-fab) testing and prototyping hubs to create a network focused on maturing emerging microelectronics technologies, strengthening microelectronics education and training, and developing a pipeline of talent to bolster local semiconductor economies and contribute to the growth of a domestic semiconductor workforce. In particular, the Commons will address the need for processes, materials, devices, and architectures to be developed and transitioned from research labs to small-volume prototyping in a fab or foundry.

11:45 AM EL01.01.04

CHIPS and Science Act: Opportunities for Materials Science Community [Santanu Bag](#); Huntington Ingalls Industries, United States

With the passage of the CHIPS and Science Act of 2022, a flurry of activity is expected to kick-off in the semiconducting research, development, and manufacturing field. Numerous programs and funding opportunities have been announced to tackle different challenges in the semiconducting value chain. The CHIPS funding will benefit not only U.S. chip manufacturers, but also tool vendors, U.S. universities, defense contractors, community colleges, K-12 STEM educational programs, and regional hubs. Materials science community plays an important part in the semiconducting industry and could be benefited from this opportunity as well. In this talk, an overview of all these opportunities will be discussed.

SESSION EL01.02: Surfaces and Interfaces I

Session Chairs: Santanu Bag, Tse Nga Ng and Angel Yanguas-Gil

Tuesday Afternoon, April 23, 2024

Room 348, Level 3, Summit

1:30 PM *EL01.02.05

Scaling and Scale Up Effects during Area Selective Deposition using Self-Assembled Monolayers and Small Molecule Inhibitors [Angel Yanguas-Gil](#); Argonne National Laboratory, United States

Area selective deposition (ASD) is a promising bottom-up patterning approach that has attracted significant interest in microelectronics. Area selective deposition methods can be roughly divided into two classes: intrinsically selective processes, which take advantage of preferential reactivity of precursors, and processes based on surface passivation. While growth selectivity is often used as a benchmark to quantify the performance of an ASD process, the scalability of ASD both in terms of pattern size (scaling) and substrate size (in terms of area and aspect ratio) is comparatively less understood.

In this presentation, I will focus on two case studies that explore the scalability of different area selective deposition approaches: the first example explores the impact of pattern size on the stability and density of defects of self-assembled monolayers (SAMs). SAMs exhibit a range of dynamic behaviors that can greatly affect their effectiveness blocking precursors: these include order/disorder transitions, non-negligible surface mobility, or the presence of so-called gauche defects. Using simple dynamic models, we have explored how pattern size affect the stability of SAMs, and how, depending on chain-chain and surface interactions, size effects can lead to substantial changes on the areal density and distributions of defects in SAMs.

In the second example, I focus on how heterogeneous processes during small molecule area selective deposition can affect the scale up of area selective deposition to large scale (i.e. wafer size) and high surface area (i.e. high aspect ratio) substrates. A key aspect of area selective deposition processes using small molecule inhibitors is the need of effectively remove them from the substrate after each ALD cycle. Through a combination of in-situ characterization techniques, kinetic models, and transport models both within features and at the reactor scale, we have explored the impact that surface kinetics has on the elimination of inhibitor molecules. Our results show that reversibility in the inhibition process can greatly increase the purge times required to effectively remove inhibitors from large area substrates, creating inhomogeneities in film thickness even when processes are fully self-limited.

These two examples exemplify the tight coupling between the fundamental aspects of area selective deposition processes and their behavior under conditions relevant for semiconductor manufacturing.

2:00 PM EL01.02.02

Synthesis and Guided Self-Assembly of Mixed-Metal Oxide Arrays from Undercooled Liquid Metal [Julia J. Chang](#), Andrew Martin, Alana Pauls, Dhanush Jamadgni and Martin M. Thuo; North Carolina State University, United States

In the Information Age, inexorable progression of big data demands rapid upgradation of modern electronics. Internet of Things (IoT), for example, requires numerous “communicable” electronics and powerful central processing units to build a “smart” world, where every physical object is digitally connected. With vast amount of high-performance electronics in-need, advancement of nanofabrication technologies become pivotal. Contradiction between better performance and lower cost, however, has long been unreconciled for electronic fabrication, and Moore’s law is an exemplary case of facing such challenge. While Moore’s law has inspired disparate advances in Complementary Metal Oxide Semiconductor (CMOS) devices (>20 doubling in transistors per chip every year), the scaling approach that drives these advances is predicted to stall after ~27 doubling events. This scaling approach faces a triple challenge in: i) continued miniaturization with concomitant need for more tools, characterization, metrology, among others, transitioning Moore’s law into ‘more’ law. ii) a looming fabrication challenge as we approach the sub nanometer-length (atomic) scale per component, and iii) global demand for more computation presents an energy and supply challenge unless new, rapid, energy efficient fabrication methods are realized. New paradigm(s) in multiscale manufacturing of microelectronics is therefore needed, among which interface-based (43 more doublings) and/or self-assembled organic (>100 doublings) post-CMOS devices pertains great potential. This calls for a significant shift in microelectronic fabrication with an emphasis to the introduction of new chemistries, composition and functionality while maintaining energy efficiency and low-cost through a device lifecycle. Liquid metal particles bear great potential to reduce energy and capital cost in functional array fabrication since they can act as a controlled reservoir for metal ions. Exploiting partial miscibility of organometallic adducts in aqueous media, steady-state kinetics *ad-infinitum* living polymerization was demonstrated using liquid metal particles as an infinitely large metal ion reservoir – the so-called HetMet reaction. This reaction led to synthesis of high aspect ratio self-assembled beams that were then translated to graphitic-carbon coated metal oxides with tunable band gaps. Herein, we extend this work by coupling the HetMet reaction with confinement from nanograting templates to separate the metal particles from the self-assembling adducts. Using molds bearing channels with desired dimensions and periodicity enables deposition of desired arrays, and exploiting fluidic dynamics of this process allows us to control both the nucleation point and the rate of ion transport to the growing seed. Driven by capillary action and solution evaporation, large-area, high-quality organometallic nanowire arrays were fabricated by D-Met, of which an in-air heat-treatment conveniently transformed the organic wires into mixed-metal oxide without compromising wire continuity or array periodicity. Besides planar patterns, fabrication of multi-layer nanostructures such as 2-layer arrays were also achieved, which is promising for design and fabrication of 3D electronics. With the high structural precision of D-Met fabricated wire arrays, we demonstrate unique electrical and optical properties including diode behavior and guided wave resonance.

2:15 PM EL01.02.03

Delafossite-Coated Cotton Fabrics and Their Potential Applications in The Textile Industry for Photocatalytic Self-Cleaning, UV-Blocking and Antimicrobial Activity [Shahria Ahmed](#), Sachin Chopra, Swati Mohan and Jasim Uddin; The University of Texas Rio Grande Valley, United States

Delafossite materials demonstrate multifunctional applications due to their excellent catalytic properties, which vary depending on their morphology, particle size, and synthetic method. Herein, a few novel applications of the delafossites are reported, which can be implemented in commercial, medical, and domestic settings. In present work we are presenting two different delafossite CuGaO₂ and CuFeO₂ nanoparticles and its composite with cotton fiber. Multifunctional cotton fabric is prepared by depositing a uniform coating layer of CuGaO₂ and CuFeO₂, exhibits excellent photocatalytic self-cleaning, UV blocking, and antimicrobial activity. CuGaO₂ and CuFeO₂ nanoparticles concentration of 1mM and 2mM were deposited over cotton fabric using citric acid as a binder by a simple sonication method. Surface analysis, bindings, stability, stain resistance, and UV blocking characteristics of the functionalized cotton fabric are performed by SEM, EDX, XRD, FTIR, and UV-vis spectroscopy. Both CuGaO₂-cotton and CuFeO₂-cotton exhibit excellent photocatalytic activity, which is evident from the UV-Vis spectroscopic analysis after mixing with methylene blue dye and subsequent exposure to simulated solar light. 2 mM CuGaO₂-cotton fabric has the highest rate of stain extinction compared to others. In addition, CuGaO₂-cotton and CuFeO₂-cotton block most of the harmful UV radiation, 95–97.5% (approx.) in the case of CuGaO₂ and 90% (approx.) in the case of CuFeO₂. The modified cotton fabrics present good antimicrobial activity against gram-positive and gram-negative bacteria, which is confirmed by antimicrobial tests with *Staphylococcus aureus* and *E. coli* bacteria. The newly fabricated cotton-delafossite composite, with all its promising applications, can be viewed as a valuable, sustainable contribution of materials science to humanity.

2:30 PM BREAK

3:00 PM EL01.02.04

Impact of The Wafer-Scale Fabrication on The Performance of Graphene-Based Flexible Microelectronics and New Strategies for Improvement
Elena del Corro¹, Marta Delga-Fernandez¹, Aina Galceran¹, Anton Guimera², Xavi Illa² and Jose A. Garrido^{1,3}; ¹ICN2, Spain; ²IMB-CNM, Spain; ³ICREA, Spain

Graphene possesses unique mechanical and electronic properties that make it a crucial material in the biomedical field. Specifically, graphene-based electronic devices have been developed and are in continuous improvement for biomedical recording, stimulating and sensing purposes^{1,2}. Despite the demonstrated capabilities of graphene-based solution-gated field-effect transistors (SGFETs) in this field, their wafer-scale fabrication process introduces uncontrolled residual charges on the graphene surface, which has an impact on the final functionality of the devices in the form of undesired doping and thus a deterioration of the general electrical performance.

In this work, we present a detailed study of the effect of residues presence at each step of photolithography in the wafer-scale fabrication process of graphene microtechnology. By means of Raman spectroscopy and spectro-electrochemistry we monitor the doping state of graphene during fabrication processes. As function of pH and the ionic strength of the electrolyte in contact with graphene, we register the frequency of the graphene's G phonon that can be directly related with the Fermi energy and doping state of graphene³.

Our study reveals that certain steps in the fabrication process leave a major amount of residues on the graphene surface that leads to inhomogeneities at cm scale in terms of device performance. With this information in hand, we propose a new fabrication strategy including the deposition of a sacrificial copper layer on graphene to protect it against induced contamination during the whole photolithography process. We analyze the impact of this additional layer on the quality of graphene material, after deposition and final etching procedures. Finalized graphene devices and electrically characterized and compared with standard technology.

REFERENCES

1. Masvidal-Codina, E., Illa, X., Dasilva, M., et al (2019) High-resolution mapping of infraslow cortical brain activity enabled by graphene microtransistors, *Nature Mater*
2. Bonaccini Calia, A., Masvidal-Codina, E., Smith, et al (2022). Full-bandwidth electrophysiology of seizures and epileptiform activity enabled by flexible graphene microtransistor depth neural probes. *Nature nanotechnology*
3. J. Yan et al., (2007) Electric Field Effect Tuning of Electron-Phonon Coupling in Graphene, *Phys. Rev. Lett*

3:15 PM *EL01.02.01

Reinforced Interfaces to Realize Multifunctional Supercapacitors Tse Nga Ng; University of California, San Diego, United States

Today's electrochemical storage devices are restricted in capacity, a key challenge that limits the operational time of wireless devices. To increase the energy storage capacity, multifunctional structures such as structural supercapacitors combine load-bearing and energy-storage functions into the same device, resulting in weight savings and safety improvements. To achieve an efficient structural supercapacitor, we developed strategies based on interfacial engineering to improve both the electrodes and electrolytes.

The structural electrodes were reinforced by coating carbon-fiber weaves with a uniquely stable conjugated redox polymer and reduced graphene oxide that raised pseudocapacitive capacitance and tensile strength. The solid polymer electrolyte was tuned to a gradient configuration, where it facilitated high ionic conductivity at the electrode-electrolyte interfaces and transitioned to a composition with high mechanical strength in the bulk for load support. The gradient design enabled the multilayer structural supercapacitors to reach state-of-the-art performance matching the level of monofunctional supercapacitors (Science Advances 2023, 9, eadh0069)

Lastly, as a feasibility study, we fabricated a structural supercapacitor to serve as the weight-bearing hull of a model boat. The boat was integrated with a solar panel for charging up the supercapacitor hull, which in turn powered up the boat motor to cruise across a pool. This demonstration showed the potential of structural supercapacitors to facilitate mass savings and increase the capacity for energy harvesting and storage in future electric systems.

3:45 PM EL01.02.06

Enhancing The Hole Conductivity of an Undoped Silicon Channel by Defect Engineering of Surrounding SiO₂ Dielectric Soundarya Nagarajan¹, Daniel Hiller², Ingmar Ratschinski², Dirk König³, Thomas Mikolajick^{1,4} and Jens Trommer¹; ¹NaMLab gGmbH, Germany; ²TU Bergakademie Freiberg, Germany; ³Australian National University, Australia; ⁴TU Dresden, Germany

The road to miniaturization in semiconductor microelectronic technology has led to an ongoing demand for identification of suitable approaches for device performance enhancements and raised requirements of new materials and device structures [1].

Here, we report the electronic device performance improvement opportunity of silicon nanostructures without direct channel doping by adding Al acceptor states into a thin SiO₂ layer surrounding the silicon [2]. This novel concept is analogous to modulation doping in III-V semiconductors. The manifestation of the dielectric by incorporation of trivalent Al impurities gives the possibility for electrons from silicon to tunnel to the acceptor states in SiO₂ yielding

silicon with holes as majority carriers. Our method removes the disadvantages of impurity doping, namely a required thermal ionization, inelastic impurity scattering, problematic dopant activation vs. out-diffusion and statistical fluctuations of dopant density [3-4]. The SiO₂ doping also facilitates interface passivation by discharging the dangling bond defects at Si/SiO₂ interface [5]. To this end, the doping approach is demonstrated on silicon channels fabricated on a silicon-on-insulator (SOI) substrate with nickel silicide contacts. The same layers sequence is extended to a transfer length measurement (TLM) structure.

It was experimentally observed that the energetic state of Al-acceptors in SiO₂ formed by atomic layer deposition of Al₂O₃ on thin thermally grown SiO₂ induces a corresponding shift in the Fermi level of silicon towards the valence band. A variation in the density of hole carriers in the silicon channel is regulated by the variation of number of ALD Al₂O₃ cycles [6] which governs both the silicon resistivity and the specific contact resistivity. The effect of addition of a monolayer of ALD Al₂O₃ is reflected in the reduction of silicon resistivity to a value as low as 0.04-0.06 Ω•cm and a contact resistivity as low as 3.5E-7 Ω•cm² [7].

A single segment of the fabricated TLM structure can also perform equivalently as a transistor with the body contact operated as a back gate. The performance of the transistor is improved by an enhanced hole carrier transport with an I_{ON}/I_{OFF} ratio of up to 10⁶ at a drain voltage of -1V. The NiSi source/drain contacts placed directly within the SOI region also undergoes a transition from Schottky to low-resistance contact as an effect of the barrier height reduction [8]. The drawbacks of conventional impurity doped devices such as dopant scattering, fluctuating device performance due to dopant diffusion, and even requirements of lightly or heavily doped source/drain regions can be circumvented by the new method. The aforesaid impurity free doping of the channel would be ideal for a high performance, high mobility device and enables new advancements encompassing areas of low-temperature physics and quantum technology.

[1] Wong, H, and Iwai, H, *Physics World* 18.9 (2005): 40.

[2] König, D, et al., *Scientific Reports* 7.1 (2017): 46703.

[3] Norris, D. J., et al., *Science* 319.5871, 1776 (2008).

[4] Nagarajan, S, et al., *Solid-State Electronics* 208 (2023): 108739.

[5] Hiller, D, et al., *J. App. Phys.* 125.1 (2019): 015301.

[6] Ratschinski, I, et al., *physica status solidi (a)* (2023): 2300068.

[7] Nagarajan, S, et al., *Advanced Materials Interfaces*, Oct 2023 (Accepted).

[8] Nagarajan, S, et al., *Device Research Conference. IEEE*, 2023.

4:00 PM EL01.02.07

Multiplexing Reactor for the High-Throughput Screening of Molecular Layer Deposition Processes [David S. Bergsman](#), Yuri Choe and Duncan Reece; University of Washington, United States

Continued progress in information and communication technologies requires sustained innovations in memory and storage devices' architecture and production processes. For example, scaling technology to sub-5nm using extreme ultraviolet (EUV) sources necessitates new processes for making hybrid organic-inorganic thin film photoresist materials that are highly adsorbing of EUV. One potential approach for making these films is through molecular layer deposition (MLD), the organic analog of atomic layer deposition. However, the discovery of desirable MLD materials is slowed by the large number of combinations of inorganic and organic reactants available.

Here, we present an approach for rapidly screening new materials deposited by MLD using a custom-built, high-throughput, multiplexing MLD-style reactor. In such a system, multiple reaction chambers are connected to shared reactants and pumping lines, allowing for the elimination of redundant reactor components and reducing capital costs compared to an equivalent number of independent systems. By carefully controlling pressure gradients in the system and valve operation, different MLD processes can be performed simultaneously in separate reaction chambers, allowing for many materials to be produced at the same time. These materials can then be screened for their properties of interest. To demonstrate this approach, a multiplexing reactor of this design was constructed with six independent reactor systems, two shared reactant manifold lines, and one shared pumping line. Using the well-studied trimethylaluminum (TMA) and water reaction into alumina, depositions in this system are shown to be reproducible, comparable to depositions shown in the literature, and without cross-contamination between chambers. In demonstration of the capabilities of this system, a TMA/water growth curve is developed using a combination of depositions in all systems, along with a measurement of the ALD temperature window using simultaneous depositions in all six chambers at different temperatures. Finally, the ability to simultaneously deposit multiple films is demonstrated using diethylzinc and one of six different organic diols. Using such a system can enable the faster screening of processes for potential materials, like photoresists, which will be needed for many electronic and photonic materials.

SESSION EL01.03: Poster Session I: Surfaces and Interfaces I

Session Chairs: Silvia Armini, Santanu Bag, Mandakini Kanungo and Gilad Zorn

Tuesday Afternoon, April 23, 2024

Flex Hall C, Level 2, Summit

5:00 PM EL01.03.01

Understanding the Degradation Mechanism of Spiro-OMeTAD during the Long-Term Operation of Perovskite Solar Cells and Mitigating it via ALD. [Mayank Kedia](#)^{1,2}, Chittaranjan Das^{1,2} and Michael Saliba^{1,2}; ¹University of Stuttgart, Germany; ²Forschungszentrum Jülich GmbH, Germany

Metal halide perovskites (MHPs) have emerged as promising photovoltaic (PV) materials with a power conversion efficiency (PCE) of 26% on the laboratory scale. Despite achieving high performance in less than a decade, device degradation under operating conditions is outcompeted in the PV market by silicon and CdTe technologies. To overcome this challenge, interface passivation with organic molecules and composition engineering are commonly explored to improve the device stability. While most studies have focused on the intrinsic stability of the perovskite active layer, there is a lack of understanding of the degradation of other charge-extraction layers and electrodes, and its effect on the final device performance upon aging.

In this work, triple-cation-based PSCs with a planar n-i-p architecture and a champion PCE of 20.1% were aged under maximum power point tracking (MPPT) for 1000 min under 1 sun illumination without any encapsulation in an ambient atmosphere. After aging, we performed soft Ar atom cluster sputtering XPS depth profiling to study the ionic motion/interactions between the perovskite active layer and the overlying charge extraction layer. In addition to iodine migration from the perovskite to the Spiro-OMeTAD/electrode interface, we observed a shift in the binding energies (BE) of the constituent species present in Spiro-OMeTAD with p-dopants lithium bistrifluoromethanesulfonimide (LiTFSI) and 4-tertbutylpyridine (tBP).

When looking specifically at the core level spectra of S 2p centered at 169.3 eV are present uniformly from the Spiro/electrode interface to the Spiro/perovskite interface in the fresh PSC. Upon aging, the S 2s exhibit a lower binding energy 168.3 eV attributing to the reduction of sulfur present in the Spiro layer. Notably, the F 1s spectrum also showed an extra peak at 685.5 eV for the aged sample from 689.0 eV for the fresh sample. Additionally, the F/S ratio changed after MPPT aging, leading to a final change in the charge extraction properties of the Spiro-OMeTAD layer, leading to the final device degradation. We observed that this chemical redistribution created pinholes in the films, leading to easier penetration of H₂O and O₂, and perovskite instability. Applying near-ambient pressure XPS (NAP-XPS) on the perovskite film with and without the Spiro-OMeTAD layer at 1 mbar of H₂O at 50 °C, 100 °C, and 150 °C showed the formation of metallic lead (Pb⁰) and iodine due to the degradation of Spiro-OMeTAD, accelerating the decomposition of the perovskite. Interestingly, our XRD results confirm that the interaction between the degraded Spiro-OMeTAD and perovskite leads to the amorphization of perovskite, which is different from what is commonly observed for PbI₂. The cross-sectional SEM image of the aged PSCs highlights the Spiro/perovskite interface as the breaking point under constant illumination.

Finally, to mitigate the instability caused by the degradation of Spiro-OMeTAD, robust passivation of ALD-deposited AlOx of <1 nm has proven to be an effective strategy for the long-term stability of PSCs. We examined the conformity of this sub-nanometer layer via HRTEM and observed the complete coverage of a rough perovskite layer (RMS ± 20 nm) by AlOx, which is difficult to obtain by the chemical deposition of organic passivation layers. In-situ electron diffraction also showed that the grown ALD layer was amorphous and acted not only as a surface passivation layer for perovskite but also as a barrier layer to prevent the degradation of perovskite as a result of the decomposition of Spiro-OMeTAD.

Overall, our work provides chemical and mechanical insights into the degradation of the overlying layer on perovskite by combining macroscopic, microscopic, and spectroscopic studies. We also decoupled the role of ALD as a passivation layer for perovskite intrinsic stability and as a nanoencapsulant layer for mitigating the phase transition to amorphous phases upon Spiro-OMeTAD degradation.

5:00 PM EL01.03.02

High Performance Organic and Inorganic Metal Halide Perovskite Phototransistors Jamal Aziz, Alexander Löwen, Zhuang Miao, Naveen Kolluru and Daniel Neumaier; University of Wuppertal, Germany

Perovskite has emerged as the promising material for optoelectronic applications, especially solar cells, owing to its high absorption coefficients. However, the research on perovskite based electrical devices raised serious concerns based on their operational instabilities and their ionic nature. This effect leads to perovskite-based field effect transistors (FETs) with low carrier mobility, high hysteresis, and high operating voltages due to long channel lengths. Here we have reported phototransistors based on MAPbI₃ and CsPbBr₃ perovskite with silicon back gate. Firstly, we reported bottom gate / top contact (BGTC) perovskite transistors with long channel lengths (170 μm) but however they exhibit poor electrical and light dependent response. In contrast, the bottom gate / bottom contact (BGBC) perovskite transistors with short channel lengths (6 μm) exhibit optimal performance. Ambipolar transport characteristic was observed at room temperature. The hole mobility presents light dependence whereas electron mobility is nearly the same under light for both organic and inorganic metal halide transistor. The photoresponsivity of 60 mA/W and detectivity of 10¹¹ Jones was observed for CsPbBr₃ phototransistors under light. The hysteresis effect of both organic and inorganic metal halide transistor was studied by changing the voltage bias and the monochromatic light intensity. The hysteresis effect in both perovskite transistors is attributed to the charge trapping process. Overall, this work paves the way for perovskite based flexible, wearable and disposable electrical devices with optimal performance.

KEYWORDS: MAPbI₃ perovskite; CsPbBr₃ perovskite; Phototransistor; Hysteresis; Responsivity

5:00 PM EL01.03.04

Improvement in Switching Characteristics and Bias Stability of Solution-Processed Zinc–Tin Oxide Thin Film Transistors via Simple Low-Pressure Thermal Annealing Treatment Junhao Feng, Sang-Hwa Jeon and Jin-Hyuk Bae; Kyungpook National University, Korea (the Republic of)

In this study, we used a low-pressure thermal annealing (LPTA) treatment to improve the switching characteristics and bias stability of zinc–tin oxide (ZTO) thin film transistors (TFTs). For this, we first fabricated the TFT and then applied LPTA treatment at temperatures of 80°C and 140°C. The LPTA treatment reduced the number of defects in the bulk and interface of the ZTO TFTs. In addition, the changes in the water contact angle on the ZTO TFT surface indicated that the LPTA treatment reduced the surface defects. Hydrophobicity suppressed the off-current and instability under negative bias stress because of the limited absorption of moisture on the oxide surface. Moreover, the ratio of metal–oxygen bonds increased, while the ratio of oxygen–hydrogen bonds decreased. The reduced action of hydrogen as a shallow donor induced improvements in the on/off ratio (from 5.5 × 10² to 1.1 × 10⁷) and subthreshold swing (8.63 to V dec⁻¹ and 0.73 V dec⁻¹), producing ZTO TFTs with excellent switching characteristics. In addition, device-to-device uniformity was significantly improved because of the reduced defects in the LPTA-treated ZTO TFTs.

5:00 PM EL01.03.05

Tunable Dielectric Properties of CVD-Processed Polymer via Click Chemistry Seongcheol Jang¹, Gunoh Lee², Kyung Jin Lee² and Hyun-Suk Kim¹; ¹Dongguk University, Korea (the Republic of); ²Chungnam National University, Korea (the Republic of)

Recently, the increasing demand for high-end displays has led to the development of flexible displays using non-traditional flexible substrates rather than traditional rigid substrate. Currently, thin-film transistors (TFTs) for flexible devices mainly use inorganic dielectrics such as SiO₂ and Al₂O₃. These inorganic gate dielectrics have critical issues to apply in flexible devices because of their high temperature process, high-cost production, and limited flexibility. Therefore, the mass production yield inevitably decreases, leading to increase in price of devices. From this point of view, polymer dielectrics have attracted considerable attention as a gate insulator for flexible transistors because of their mechanical nature. Even if polymer gate dielectrics are suitable for future flexible electronics, properties such as dielectric constant, and leakage current, are not suitable for cutting-edge devices. Also, fabrication process for polymers is usually consist of solution process, which has poor step coverage, side effect like coffee-ring effect and pinholes.

poly(p-xylylene) (PPx, commercialized name is parylene) is well known passivation materials for various electronics, which can be fabricated by chemical vapor deposition system that can give pinhole-free conformal film. Conventional parylene family, such as parylene-C, -D, -N, and -AF4 shows low dielectric constant of ~ 3, which is does not meet requirements for future advanced electronic. However, physical, dielectric, and electrical properties of parylene family can be tuned by adjusting functional groups. We reported custom synthesized parylene-ethynyl that shows higher dielectric constant, smoother surface and similar leakage current compared to conventional parylene. This approach is quite intricate as it necessitates design from the monomer.

In this work, click chemistry was employed to further tuning the properties of custom-synthesized parylene-ethynyl for dielectric layer for TFTs. IGZO oxide semiconductors were used as the active layer to demonstrate high-performance hybrid TFTs. Unlike most polymers fabricated through solution processes, parylene's fabrication method relies on the Gorham method CVD system. This system provides a thin, conformal, and pinhole-free film, resulting in a compatible interface with oxide materials. Additionally, the deposition temperature is around room temperature, and no additional high-temperature annealing is required, making it suitable for plastic substrates with low glass transition temperatures, ideal for flexible or stretchable applications. Four types of click reactions were conducted on parylene-ethynyl, and it was confirmed that all of them exhibited click reactions. After click reaction, parylene-ethynyl demonstrated an improved dielectric constant exceeding 4 without compromising film quality. Successful fabrication of IGZO TFTs combined with parylene-ethynyl showcased reliable switching properties, indicating that the combination of parylene-ethynyl with click reaction and

IGZO posed no issues at interfaces. The click reaction is anticipated to facilitate easy adjustments to the characteristics of the polymer gate dielectric. Moreover, it opens up the possibility of manufacturing a functional device utilizing the clicked part.

5:00 PM EL01.03.06

One Pot Preparation of Spherical Magnesium Silicate by W/O/W Emulsion Precipitation Method [Jung Kyeongmun](#)¹, Youngyong Kim² and Kyounghoon Lee¹; ¹Gyeongsang National University, Korea (the Republic of); ²Denve, Korea (the Republic of)

We report on the synthetic method of spherical magnesium silicate particles with a high specific surface area via a cost-effective water-in-oil-in-water (W/O/W) emulsification process. Notably, all samples of magnesium silicates prepared by this process exhibited specific surface areas ranging from 486.41 m²/g to 662.23 m²/g. In particular, the EM_2.81 sample showed approximately 1.5 times higher surface area than commercially used Magnesol XL. The high surface area originated from a high fraction of micropores. SEM analysis revealed distinct sections in the samples, indicating the optimal concentration of water glass for spherical shape maintenance. Additionally, most of the emulsion-treated EM samples displayed spherical morphology around 20 microns and demonstrated characteristics of excellent dispersion without aggregation in water. These results suggest that the W/O/W single-pot emulsification process is an effective method for producing magnesium silicate particles with high specific surface area and spherical morphology.

5:00 PM EL01.03.07

Antireflective Properties of Plasma-Polymerized Biomimetic Surfaces [Luigi P. Verdoni](#); Edmund Optics Research and Development, United States

Biomimetic surfaces inspired by Moth's eyes are characterized by the subwavelength structures that cover the eye's surface. These nanostructures, possessing tapered geometries of variable height and shape, present as a gradient refractive index and offer antireflective (AR) properties over a high angle of incidence (AOI). A facile technique utilizing inductively coupled reactive ion etching (ICP-RIE) was devised to endow the optical surface with randomly patterned subwavelength nanostructures. In this two step nanostructuring process, an etch mask and recipe were implemented to deliver AR behavior at desired wavelengths, followed by a plasma polymer deposition of a thin fluorocarbon film with a low surface energy. The resultant subwavelength antireflective surface can be tuned from the ultraviolet to infrared wavelengths and has been shown to possess utility in both antiwetting and high laser damage threshold applications.

5:00 PM EL01.03.08

Exploring Dopant Dynamics in Crystalline Germanium through Microwave Annealing (MWA) and High-Pressure Annealing (HPA): A Study on Diffusion, Activation and Recrystallization [TaiChen Kuo](#)¹ and WenHsi Lee²; ¹Chung Yuan Christian University, Taiwan; ²National Cheng Kung University, Taiwan

This study delves into the nuanced activation behavior of phosphorus and boron dopants in crystalline germanium substrates through meticulous investigation of high-pressure annealing (HPA) and microwave annealing (MWA) techniques. Phosphorus implantation at 10 keV, with a dose of 5×10^{15} atoms/cm², showcased intriguing profiles revealing a concentration peak exceeding the maximum equilibrium solubility in germanium. The subsequent HPA at 500 °C for 60 s resulted in a stable profile with a junction depth of 44.1 nm, contrasting the diffusion broadening observed at higher HPA temperatures. MWA at 3P to 5P demonstrated diffusion patterns akin to HPA at 500 °C. Sheet resistance comparisons between HPA and MWA unveiled the stability of sheet resistance in MWA, even at increased power levels (5P, 3000W, approximately 700°C), though not reaching the low resistance achieved with low-temperature HPA. Hall measurements after HPA at 500 °C revealed a decrease in sheet resistance to 0.63 Ω/square and an increase in N-carrier concentration to 5.76×10^{19} P/cm³, despite subsequent decreases in carrier concentration and mobility after 500 °C, possibly attributed to deactivation induced by high-temperature annealing. The study also explores the activation of boron, demonstrating significant enhancement through solid-phase epitaxial regrowth (SPER) with minimal diffusion, particularly notable despite the low solid solubility. The investigation involves dopant diffusion analysis using SIMS, highlighting the importance of maintaining a high dopant concentration at the surface for low contact resistivity. Sheet resistances measured by a four-point probe post-HPA and MWA underscore the effectiveness of higher temperatures in HPA for achieving high B activation through SPER. Comparative analyses and TEM images further elucidate the recovery of amorphous layers in both phosphorus and boron doping scenarios, emphasizing the advantageous SPER behavior facilitated by high-pressure annealing. In summary, this study provides comprehensive insights into the activation dynamics of phosphorus and boron in germanium substrates, emphasizing the nuanced interplay between annealing techniques and dopant behavior for advanced semiconductor device fabrication.

5:00 PM EL01.03.09

Controlled Bipolar Doping of One-Dimensional Van der Waals Nb₂Pd₃Se₈ [Bom Lee](#) and Jae-Young Choi; Sungkyunkwan University, Korea (the Republic of)

2D layered materials such as graphene, transition metal dichalcogenides (TMDCs), h-BN, and black phosphorus have been extensively studied in a wide range of applications due to their fascinating structural, physical, and chemical properties. However, as the width of the 2D semi-infinite plane becomes narrow to meet the stringent dimensional requirements of the transistor, the dangling bond density at the edge of 2D vdW increases, resulting in degradation of electronic performance. To solve such scale-down problems, research has been conducted in recent years on one-dimensional (1D) vdW materials with a further reduced dimension from a 2D structure. 1D vdW materials, where single molecular chains with strong covalent bonds are assembled by a weak vdW force, are free of broken or dangling bonds on the chain surface, even when separated by a diameter of less than 1 nm. On the basis of these structural features, various 1D vdW material-based applications have been demonstrated, such as molecular connectors, transistors, and sensors. In recent years, ternary 1D transition metal chalcogenides containing a noble metal such as Pd or Pt have gained attention as promising semiconducting materials for electronic and optoelectronic devices. For example, Nb₂Pd₃Se₈, successfully synthesized by Keszler et al. Nevertheless, research into the stable tuning of electrical properties, which is a prerequisite for basic electronic materials, is still in its infancy stage for 1D vdW materials.

In this study, we introduce a new ternary transition metal chalcogenide, Nb₂Pd₃Se₈, which was successfully synthesized via chemical vapor transport (CVT) method using iodine as a transport agent. Furthermore, we first demonstrated the chemical doping of Nb₂Pd₃Se₈, which is a representative n-type 1D vdW material, through chemically doping AuCl₃ and β-nicotinamide adenine dinucleotide (NADH) as p-type and n-type dopants, respectively. The concentration of holes and electrons controlled by varying the immersion time in the doping solution were effectively confirmed by spectroscopic and transport studies. In addition, we demonstrated an axial p-n junction on Nb₂Pd₃Se₈ that exhibits near-perfect rectifying behavior using a selective doping method. We believe that this work can promote research based on 1D vdW semiconductors for future electronic applications.

5:00 PM EL01.03.10

Improving Indoor Efficiency of Inverted Cs_{0.18}FA_{0.82}Pb(I_{0.8}Br_{0.2})₃ Solar Cells via Surface Defect Passivation [Chih-Ping Chen](#); Ming Chi University of Technology, Taiwan

The escalating energy consumption associated with the 'Internet of Things' (IoT)—involving the integration of sensors, telecommunications, remote

actuators, and smart devices—has created a growing need for consistent and sustainable energy sources. Self-powered integrated IoT devices, utilizing energy harvested from indoor photovoltaics (iPVs), have garnered significant attention. The crucial role of effectively suppressing trap-assisted recombination through the passivation of interfacial defects in perovskite has been demonstrated for sustaining high iPV performance under low light intensities. In this study, we introduced a p-i-n perovskite solar cell (PSC) that incorporates a hole-selective layer (2PACz) and employs a hybrid electron transport layer (ETL) composed of an A–D–A molecule (DTPTCY) and PCBM for the device. We constructed the PSC with the structure of ITO/NiO_x/2PACz/perovskite/PCBM(with/without DTPTCY)/BCP/Ag, and used phenethylammonium iodide to further passivate interfacial defects. Various characterization techniques, including atomic-force microscopy images, X-ray diffraction patterns, X-ray photoelectron spectroscopy, photoluminescence (PL) spectra, time-resolved PL curves, and Kelvin probe force microscopy (KPFM) were performed. We controlled the blend ratio and fabrication temperature to improve miscibility, resulting in the optimized performance. GIWAXS and AFM were employed to determine the blend morphology; KPFM and UPS were used to identify the change in energy level alignment; SCLC and TPC analysis were utilized to evaluate the change in electronic transport. Within the PCBM:DTPTCY-ETL, a fibril-like structure is formed, significantly enhancing electron mobility and effectively suppressing bimolecular recombination. This leads to a reduction in defects and lower trap density within the perovskite layer. The optimized blended ETL-based Cs_{0.18}FA_{0.82}Pb(I_{0.8}Br_{0.2})₃ PSC demonstrated outstanding performance, achieving a power conversion efficiency of 39.9% under 3000K LED illumination (1000 lux). These experimental results suggest a promising approach utilizing A–D–A molecule-based interface modification to enhance iPV performance.

5:00 PM EL01.03.11

Direct Characterization of Single-Molecule Reaction via Tip Enhanced Raman Spectrum [Ruihao Li](#); Arizona State University, United States

Characterizing chemical reactions at a single-molecule scale enables a deep understanding of the mechanism of complex chemical reactions and thus establishes new material science frameworks. Previous works explore the real-time current changes of reactants and its products to figure out the steps of the reaction process. However, it is hard to identify the paths of some reactions accurately because the current signal does not have fingerprint information of the reactants. Tip-enhanced Raman spectroscopy (TERS) can accurately characterize chemical reactions due to its ability to characterize chemical bond fingerprint information at single-molecule scale precision. By combining Raman spectroscopy with single-molecule Break Junction technology, we can control single-molecule reactions through electric fields and simultaneously observe the Raman shifts of its corresponding chemical bonds.

5:00 PM EL01.03.12

High-Performance and Stability of CsPbBr₃/WSe₂ Hybrid Photodetectors Functionalized via Quaternary Ammonium Ligand Exchange [Jae-Hyeon Ahn](#) and Jong-Soo Lee; Daegu Gyeongbuk Institute of Science and Technology, Korea (the Republic of)

The 2-Dimensional (2D) and 0-dimensional (0D) hybrid photodetector, with its high sensitivity and wavelength tunability, is reported as a promising candidate nanostructure for optoelectronic devices. The utilization of hybrid lead halide perovskite quantum dots (PQDs) in optoelectronic devices has grown due to their remarkable absorption characteristics and elevated photoluminescence quantum yield in research. Nevertheless, the stability of PQDs continues to pose a significant constraint on the overall performance of these devices. Here, it is reported that the properties and stability of the hybrid photodetectors are enhanced by surface passivation with ligand exchange using the quaternary ammonium ligand (didodecyltrimethylammonium bromide, DDAB). The average lifetime of carriers in CsPbBr₃ PQDs is extended when treated with DDAB, showing an increase of 6.68–14.88 ns compared to untreated CsPbBr₃ PQDs. Furthermore, it is verified that the resistance to damage of water is only reduced by 25.8% at PL intensity, and this stability is maintained for over 16 hours. In this study, we demonstrate the hybrid WSe₂/DDAB-capped PQDs with enhanced responsivity of $1.4 \times 10^3 \text{ A W}^{-1}$ and detectivity of 3.1×10^{13} Jones under $40.0 \mu\text{W cm}^{-2}$ of a 405 nm laser. The hybrid WSe₂/DDAB-capped PQDs exhibited a stable time-dependent responsivity, indicating a 4.5% decrease ($225.7\text{--}215.4 \text{ A W}^{-1}$) for the hybrid WSe₂/DDAB PQDs device, while the hybrid WSe₂/pristine PQDs device showed a 36% decrease ($48.3\text{--}30.9 \text{ A W}^{-1}$). The results of this work highlight the importance of the surface passivation dependence of the optical properties and stability of PQDs with 2D-0D hybrid optoelectronic devices. Our work demonstrates an effective approach to improve the photodetector performance of 2D-0D hybrid photodetector based on PQDs, which can be extended to various PQDs and TMDC semiconductors.

5:00 PM EL01.03.13

Micro-Heater Integrated Nanotube Array Gas Sensor for Parts-Per-Trillion Level Gas Detection and Single Sensor-Based Gas Discrimination [Wenyang Tang](#), Zhesi CHEN and Zhiyong Fan; The Hong Kong University of Science and Technology, Hong Kong

Ensuring chemical safety and safeguarding human health require real-time monitoring and discrimination of trace gases using appropriate gas sensors. Typically, this task involves expensive, bulky, and power-intensive devices such as optical and electrochemical gas sensors. Achieving this objective with a single, miniature, low-power semiconductor gas sensor is challenging due to selectivity issues. In this study, we demonstrated a novel gas sensor called micro-heater integrated nanotube array gas sensor (MINA sensor), which can operate in dual modes. The sensor can detect multiple gases at parts-per-trillion (ppt) level under the continuous heating (CH) mode and distinguish multiple gases under the pulse heating (PH) mode. We constructed the MINA sensor on the nano-porous anodic aluminum oxide (AAO) templates with a top-bottom electrode structure, which significantly increases the sensor's surface area for molecular access. To create the sensing material layer, we used atomic layer deposition to deposit an ultrathin and conformal SnO₂ thin film and decorated it with Pd nanoparticles. When operating under the CH mode, the MINA sensor could detect hydrogen, acetone, toluene and formaldehyde with measured LODs as low as 100 ppt, 100 ppt, 100 ppt, 4 ppb, with the corresponding theoretical LODs as 6.96 ppt, 11.88 ppt, 16.52 ppt, 70.06 ppt, respectively. Under PH mode, the MINA sensor provided varying transient responses to different gases due to the variations of gas diffusion and surface reaction activation energy of the gases. By analyzing the conductance amplitude and slope features of a single pulse, different concentrations of hydrogen, acetone, toluene, and formaldehyde can be distinguished. Furthermore, the PH mode saved 66.7% energy compared to the traditional CH mode. The remarkable capabilities of the MINA sensor make it highly appealing for various applications, including distributed low-power sensor networks and battery-powered mobile sensing systems for chemical safety, environmental monitoring, and healthcare.

5:00 PM EL01.03.14

Flexible Embedded Metal Meshes by Sputter-Free Crack Lithography for Transparent Electrodes and Electromagnetic Interference Shielding [Mohammad Mehdi Zarei](#), Mingxuan Li and Paul Leu; University of Pittsburgh, United States

Radio frequency (RF) electromagnetic radiation has revolutionized communication networks. As we become more reliant on electronic devices and systems, there is a pressing need for the development of effective EMI shielding materials. These shielding materials protect electronic components from radiation damage and block undesirable signals. Metal networks, such as metal meshes and metal nanowires, have been the subject of much research for transparent conducting electrodes with high transparency and low sheet resistance. In this abstract, we provide a novel approach in the field of crack lithography focusing on the creation of flexible embedded metal meshes. Our novel method involves the use of a self-forming crack template as a mask.

Instead of relying on traditional lithography methods that require complex and expensive equipment to create masks for etching, this approach simplifies the mask creation step through the natural formation of cracks. Our facile fabrication method involves transferring the crack patterns to a PET substrate

using RIE. The process also eliminates the need of the sputtering process, traditionally employed in crack lithography for producing conductive meshes. After removing the crack template, we fill the embedded cracks with a highly conductive Ag ink and cure the ink. Our flexible embedded Ag meshes achieve 91.3% visible transmission and sheet resistance (R_s) of 0.54, which corresponds to a figure of merit of 7500. For transparent EMI shielding, the samples exhibit an SE of 42 dB with 91.3% visible transmission

5:00 PM EL01.03.15

Superhydrophobic Surfaces and Surface Modification via Vapour Deposition Techniques Julie J. Kalmoni, Claire Carmalt and Christopher Blackman; University College London (UCL), United Kingdom

Superhydrophobicity, a common property within the field of protective coatings, was first observed in Lotus leaves where water droplets roll off the surface, taking dirt particles with them, rather than wet it.^{1,2}

To replicate this process on a synthetic scale, both micro-/nano-scale roughness and a low surface energy reagent are required.^{3,4} The latter employs the use of toxic fluorinated polymers (which also contributes to the robustness and high transparencies of the films) and requires high depositional temperatures.^{5,6} Superhydrophobic materials have potential applications in oil-water separation and photovoltaics. However the widespread application of superhydrophobic coatings has been hindered due to their typically poor durability or robustness.⁷

A relatively unexplored technique combines the use of aerosol-assisted chemical vapour deposition (AACVD) to deposit superhydrophobic polymer films along with the resultant surface modification via AACVD of metal oxides (e.g. TiO₂ and CeO₂). AACVD is a scalable technique as it involves spraying a precursor on a heated substrate. Superhydrophobic coatings are known for their self-cleaning properties but depositing thin layers of metal oxides on top has allowed us to fabricate superhydrophobic metal oxide films, enhancing the photocatalytic properties of the superhydrophobic layer and the self-cleaning properties of the TiO₂ film.

Another surface modification technique is atomic layer deposition (ALD). ALD, a branch of chemical vapour deposition (CVD), is a technique used to deposit atomic layers of complex and layered thin films. By operating at such a scale, thickness control, conformality of the films, low temperature depositions and even the ability to scale-up are possible.⁸

This research seeks to fabricate a superhydrophobic photocatalytic self-cleaning coating, first by producing a superhydrophobic film from simple and non-toxic compounds via AACVD. This depositional technique also provides the highly textured morphology required. Thin films with a rough morphology, formed through island growth of aggregates have been produced, displaying static water contact angles > 160°, transparencies > 40% and maintained superhydrophobicity after 300 tape peel cycles.⁹ Thereafter, the surfaces' properties are modified via the AACVD of TiO₂. Thus far, the deposited films are hydrophobic/superhydrophobic, exhibit photocatalytic activity and tolerate pencil hardness' of up to "6H".

This novel route could be used to produce 'easy-to-clean' coatings for slip-resistant flooring as well as coatings on solar cells.

References

- 1 W. Barthlott and C. Neinhuis, *Planta*, 1997, **202**, 1–8.
- 2 J. Jeevahan, M. Chandrasekaran, G. Britto Joseph, R. B. Durairaj and G. Mageshwaran, *J. Coatings Technol. Res.*, 2018, **15**, 231–250.
- 3 J. Huo, C. I. De Leon Reyes, J. J. Kalmoni, S. Park, G. B. Hwang, S. Sathasivam and C. J. Carmalt, *ACS Appl. Nano Mater.*, 2023, **6**, 16383–16391.
- 4 X. J. Guo, C. H. Xue, S. Sathasivam, K. Page, G. He, J. Guo, P. Promdet, F. L. Heale, C. J. Carmalt and I. P. Parkin, *J. Mater. Chem. A*, 2019, **7**, 17604–17612.
- 5 J. Y. Huang, S. H. Li, M. Z. Ge, L. N. Wang, T. L. Xing, G. Q. Chen, X. F. Liu, S. S. Al-Deyab, K. Q. Zhang, T. Chen and Y. K. Lai, *J. Mater. Chem. A*, 2015, **3**, 2825–2832.
- 6 V. H. Dalvi and P. J. Rossky, *Proc. Natl. Acad. Sci. U. S. A.*, 2010, **107**, 13603–13607.
- 7 F. Chen, Y. Wang, Y. Tian, D. Zhang, J. Song, C. R. Crick, C. J. Carmalt, I. P. Parkin and Y. Lu, *Chem. Soc. Rev.*, 2022, **51**, 8476–8583.
- 8 R. W. Johnson, A. Hultqvist and S. F. Bent, *Mater. Today*, 2014, **17**, 236–246.
- 9 J. J. Kalmoni, F. L. Heale, C. S. Blackman, I. P. Parkin and C. J. Carmalt, *Langmuir*, 2023, **39**, 7731–7740.

5:00 PM EL01.03.16

Novel Metal/2D Insulator/Metal Junctions for Rectenna Switches Evelyn Li^{1,2}, Parameswari Raju¹ and Erhai Zhao¹; ¹George Mason University, United States; ²Thomas Jefferson High School of Science and Technology, United States

The solar cell market is dominated by Silicon-based (single- or poly-crystalline) photovoltaic cells which directly convert sunlight into electricity. For example, the most commercially available Si polycrystalline solar cells have a conversion efficiency of 14–19%. In the past decades, major research efforts have been spent on improving the conversion efficiency by using multiple-junction cells and new materials, such as organic semiconductor and perovskite materials. However, sunlight is a form of electromagnetic waves with ultra-high frequency and short wavelength, in comparison to the radio frequencies which can be collected by antenna. Although the sunlight can be collected by antenna, a fast switch to rectify the sunlight signal is needed. If successful, such a rectenna solar cell can reach very high energy conversion efficiency (85% - 90%) at very low cost. The conventional radio receivers use semiconductor PN-junction-like diodes which are not able to rectify frequencies beyond tera Hertz. Metal/insulator/metal (MIM) diodes have been proposed as the switch as the electrons are tunneling across the MIM junctions at high speed. The tunneling time is defined as τ , reaching femtosecond [1], where d , m , U , e and V are barrier thickness, electron mass, barrier height, electron charge and bias across the junction. However, the conventional MIM diodes use bulk materials as the insulators which cannot be very thin and contain high-density of surface dangling bonds and defects. In this work, we applied density function theory (DFT) method to design and study MIM junctions by using two-dimensional (2D) insulators, such as mono-, bi- and tri-layer TiO₂, Ta₂O₅ and SnO₂. The 2D insulators can be obtained by oxidizing the corresponding 2D metal-sulfur materials. [2] Such 2D insulators have the smallest thickness and smoothest surface, perfect for tunneling barrier. The selection of metal electrode has a significant impact on the electrical characteristics. We found that the Au/monolayer TiO₂/Al junction exhibits the best performance in current rectifying. The tunneling time was studied by the extracted potential profile from DFT calculation, indicating the thickness and bias are the key factors. The effect of strain on the junctions was also studied. No significant effect was observed for up to $\pm 0.6\%$ of strain. In addition, the DFT-simulated current-voltage characteristics and tunneling time were modeled and fed into a rectenna circuit in Pspice. The circuit simulation showed excellent power output in the optical frequencies. Together, we will present a comprehensive study on MIM junctions using 2D insulators and their performance in rectenna circuits.

References

- [1] Fevrier, P., Gabelli, J. (2018) Tunneling time probed by quantum shot noise. *Nature Comm.* 9, 4940.
- [2] Cui, Q., Sakhdari, M., Chamlagain, B., Chuang, H., Liu, Y., Cheng, M., Zhou, Z., Chen, P. (2016) Ultrathin and Atomically Flat Transition-Metal Oxide: Promising Building Blocks for Metal–Insulator Electronics. *ACS Appl. Mater. Interfaces* 8, 34552–34558

5:00 PM EL01.03.17

Wide Working Range Mechanochromic Sensor based on Multiple Photonic Crystals and Angle Compensators Hoang Minh Nguyen^{1,2}, Kwanoh Kim², Do-Hyun Kang², Yeong-Eun Yoo^{2,1} and Jae Sung Yoon^{2,1}; ¹University of Science and Technology, Korea (the Republic of); ²Korea Institute of Machinery & Materials, Korea (the Republic of)

Flexible and wearable sensors have gained tremendous interest due to increasing demands in diverse applications such as prosthetics, personal healthcare, and e-skin. However, they are mostly based on electronic signals, restricting their potential in visualized mechanical measuring. Herein, inspired by the structural colors of natural species, we developed a novel mechanochromic sensor with a wide working range and angle compensators. Employing the colloidal lithography technique, multiple nanostructures were fabricated on a single stretchable substrate. Thus, broadening the detection range to 150% without sacrificing high sensitivity. We also introduced a novel approach using angle compensators to circumvent the issue of angle-dependent colors. By comparing the colors of rigid and stretchable photonic crystals, the users can facilely estimate the strain regardless of the incident and viewing angles. The fabrication principle in this study is based on a reusable mold, which is cost-effective for large-scale production. Thus, we believe this study will have a broad impact on the development of smart mechanochromic devices for visually measuring the deformation of materials.

5:00 PM EL01.03.18

Structural Assessment of (Sub-)Monolayer Coatings in Device Processing at High Spatial Resolving Power by TOF-SIMS Tandem MS Imaging Jacob Schmidt and Greg Fisher; Physical Electronics, United States

Surface characterization plays a pivotal role in the manufacturing process of next-generation electronic and heterogeneous devices. Characterizing the interfaces between different surfaces is especially challenging, primarily due to a lack of background information and the absence of reference spectra. This poses a significant challenge in supporting the analytical observations of emerging properties at these interfaces. Two case studies are presented here where there was little prior knowledge of the observed properties, but detailed answers were desired. In the first case, a carbon residue was observed by Auger electron spectroscopy (AES) imaging of etched e⁻ beam-patterned structures, but the source of the carbon was indeterminate. In the second case, a bi-functionalized monolayer film was ostensibly loaded with catalytically active metals to form the metal-organic ligands, but previous methods to characterize the film fell short in verifying the structure of the metal-organic ligands.

In this report, a general time-of-flight secondary ion mass spectrometry (TOF-SIMS) imaging method for unknown identification and structure elucidation is demonstrated. This method makes use of a TOF-TOF spectrometer designed for simultaneous TOF-SIMS (MS¹) imaging and tandem MS (MS²) imaging [1-4]. Ions for TOF-SIMS tandem MS imaging were produced by a Bi₃⁺ primary ion nanoprobe whereby MS¹ and MS² spectral data were generated from the same pixel in one duty cycle at a resolving power of 300 nm. Ion fluences were within the static limit (i.e. < 10¹³ Bi₃⁺/cm²) for nondestructive analysis, even where multiple analyses were conducted at the same position of the sample. Tandem MS peak attributions were made to a calculated mass accuracy ($\Delta m/z$) of ≈ 1 ppm which provides confidence in the accuracy of the molecular identifications.

In the first example, TOF-SIMS tandem MS imaging was applied to characterize the carbon-containing residues of the lithography-patterned and etched structures. Several sets of peaks were observed at $m/z > 150$ in the MS¹ spectra. It was established and verified by tandem MS imaging that the carbon observed by AES imaging on the patterned sidewalls arose from two fatty acid (FA) contaminants; specifically, the [M-H]⁻ ions of FA(12:0) and FA(16:0) were identified. Further, a $\approx 2:1$ ratio of FA(12:0) to FA(16:0) was calculated. The high m/z peaks, detected only on the Cu-plated surfaces, were attributed to metal-organic complexes of Cu with the fatty acids. In the positive ion polarity, FACu₂⁺ and FA₂Cu₃⁺ ions were identified; in the negative ion polarity, FA⁻ and FA₂Cu⁻ ions were identified. In each case, a natural Cu isotope composition was confirmed.

In the second example, TOF-SIMS tandem MS imaging was also employed to confirm the presence and elucidate the structure of metal-organic ligands of Au, Pd or Pt atoms attached to bipyridine or triphenylphosphine within patterned monolayer films. Metal atom loading was achieved after monolayer immobilization [5]. The pattern areas were readily observed based on the atomic metal ion signatures. There were a number of MS¹ precursor ions potentially related to the metal-organic ligands based on the m/z values within the anticipated range for the target structures. The 2D distribution and structure of complexed bipyridine and triphenylphosphine ligands, together with observing the natural isotope distribution of the metals, was achieved by tandem MS imaging [6].

References

- [1] G.L. Fisher, et al, Anal. Chem. 88 (2016) 6433-6440.
- [2] G.L. Fisher, et al, Microscop. Microanal. 23 (2017) 843-848.
- [3] C.E. Chini, et al, Biointerphases 13 (2018) 03B409.
- [4] T. Fu, et al, Nature Sci. Rep. (2018) accepted 06 December 2018.
- [5] R. Müller, et al, Chemistry (2018) DOI: 10.1002/chem.201803966.
- [6] R. Müller and A. Welle at Karlsruhe Institute of Technology (KIT) and C. Barner-Kowollik at Queensland University of Technology (QUB) are acknowledged for providing the samples for analysis.

5:00 PM EL01.03.19

Towards a Universal Biosensing Platform based on Graphene/Pyrene Surfaces for Neurotransmitters Marta Delga-Fernandez¹, Aina Galceran¹, Jose Caicedo-Roque¹, Xavi Illa², Jose A. Garrido^{1,3} and Elena del Corro¹; ¹Catalan Institute of Nanoscience and Nanotechnology, Spain; ²IMB-CNM, Spain; ³ICREA, Spain

The development of new therapeutic treatments and diagnosis of neural-related illnesses is linked to research in the electronic devices field. Devices as neural implants allow the recording of electrical signals to better understand the central and peripheral nervous systems^{1,2} and, therefore, advance in the diagnosis and treatment of these diseases. One of the main issues of current implants, mostly based on silicon technology (and thus, rigid) is that they are invasive. The use of graphene-based transistors may overcome this drawback, taking advantage of graphene's mechanical and electronic properties, and also opening the possibility to include chemical recording capabilities to the implant. Here, we develop a versatile graphene/pyrenebutyric acid (PyBA) platform for the detection of neurotransmitters, or other analytes of interest, while recording electrical neural activity.

To build this platform, we perform physical evaporation of PyBA, a molecule capable to interact with the p system of graphene thanks to its aromatic nature, and to covalently interact, due to its carboxylic group, with an aptamer of interest through the formation of a peptide bond. We optimize the PyBA evaporation conditions, which are those leading to the formation of a PyBA monolayer on the surface of graphene. This optimization and further detailed characterization of the pyrenebutyric layer is key for ensuring an understanding of the future sensor functionality. The viability of the system is studied with electrical characterizations of the transistors fabricated including the PyBA layer on graphene. Then, the binding of an aptamer that recognizes a specific neurotransmitter – thrombin in our particular case- is explored and used as a prove of the utility of the platform presented. Thrombin is detected by electrical characterization of the functionalized graphene transistors, while morphological characterization of the samples is performed by Atomic force microscopy (AFM) and Raman spectroscopy.

The thrombin biosensing results reveal changes in the electrical properties of graphene corresponding to each concentration tested, and the detection range achieved is correspondent to the one achieved by reported approaches based on in-liquid functionalization³ – more difficult to control-. This demonstrates the ability of the system to recognize the analyte of interest through binding to its specific aptamer. This graphene/PyBA universal biosensing platform is in the pipeline for the development of a new generation of multifunctional graphene-based neural implants.

REFERENCES

1. Masvidal-Codina, E., Illa, X., Dasilva, M., et al (2019) High-resolution mapping of infraslow cortical brain activity enabled by graphene microtransistors, *Nature Mater.*
2. Garcia-Cortadella, R., Schwesig, G., Jeschke, C., et al (2021) Graphene active sensor arrays for long-term and wireless mapping of wide frequency band epicortical brain activity, *Nat Commun.*
3. Hinnemo, M., Zhau, J., Ahlberg, P., et al (2017) On Monolayer Formation of Pyrenebutyric Acid on Graphene, *Langmuir.*

5:00 PM EL01.03.20

Cation Bonding on Functional Groups for Greatly Enhanced Dipole Moments and Excellent SERS Sensing as a Universal Approach [Ruey-Chi Wang](#) and Hsiu-Cheng Chen; National University of Kaohsiung, Taiwan

The recently developed dipole-based surface-enhanced Raman scattering (SERS) technique has ushered in a new era of opportunities for crafting cutting-edge sensing platforms, boasting a host of advantages, including the ability to identify molecules, reduced costs, and heightened sensitivity. While significant efforts have been dedicated to augmenting the molecular dipole density on the surface to enhance sensing sensitivity, the constrained dipole moments have limited further advancement and application possibilities. In the work, we present a universal method known as cation bonding to enhance the dipole moments of oxygen-containing functional groups (OFGs) with the goal of achieving high-sensitivity trace sensing through Surface-Enhanced Raman Scattering (SERS).

Utilizing Cu²⁺ as a representative model, we have demonstrated substantial enhancements in dipole moments through density functional theory-based calculations, which have been further validated through SERS measurements. These enhancements have been compared with typical OFGs and SERS platforms based on graphene oxide (GO). The analysis results from Transmission Electron Microscopy (TEM) show no formation of copper particles, while Energy Dispersive X-ray Spectroscopy (EDS) clearly indicates the presence of copper signals, which indicates the formation of copper ions on the surface and rule out common electromagnetic mechanisms. A comprehensive analysis of the electronic structures of analytes and SERS substrates has been conducted to exclude conventional chemical mechanisms. The results obtained from Infrared Spectroscopy (IR), X-ray Photoelectron Spectroscopy (XPS), and Electrostatic Force Microscopy (EFM) confirm the formation of C-O-Cu bonds and the reversal of dipole moments through copper bonding. The Cu-OFG SERS platforms thus prepared not only exhibit remarkable sensitivity in detecting Rhodamine6G (at concentrations as low as 10⁻¹⁰ M) but also prove their utility in detecting trace amounts of nitrate (at 10⁻¹⁰ M), a harmful contaminant in drinking water, and thiabendazole (at 0.01 ppm), a parasiticide used in fruit preservation. This cation bonding strategy is highly versatile, applicable to various cations, and opens the door to creating exceptional SERS platforms for a wide array of sensing applications.

5:00 PM EL01.03.21

Enhanced Hole-Injective Materials Incorporating a Series of Heteroatoms for Efficient Perovskite and Organic Solar Cells [Youngwan Lee](#) and BongSoo Kim; Ulsan National Institute of Science and Technology, Korea (the Republic of)

Inverted structure perovskite solar cells (PSCs) are focused by many researchers in both academic and industrial photovoltaic fields. Inverted p-i-n PSCs contain multiple advantages over conventional n-i-p structure PSCs including easier fabrication processing, hysteresis-free behavior, and compatibility for tandem application. However, the maximum power conversion efficiency (PCE) of inverted PSCs still lags behind that of conventional PSCs due to the limited number of well-matched charge-injection layers that can be energetically probable at the interfaces of inverted PSCs. In this work, we introduce excellent hole-injection materials for inverted PSCs. Newly synthesized hole-injection materials form a self-assembled monolayer (SAM) on a metal-oxide electrode, anchored by a phosphoric acid group, while a series of tricyclic aromatic rings containing O, S, or Se, respectively, as core heteroatom (denoted as Br-2EPO, Br-2EPT, and Br-2EPSe), directly contact with perovskite active layer. All of the SAMs on metal-oxide electrodes are energetically well-aligned with the perovskite photoactive layer at the interface. Notably, the Se-containing SAM exhibits the strongest interaction energy between the SAM and perovskite absorber, as investigated by density functional theory (DFT). The strong interaction energy at interfaces results in reduced interfacial defect density and an extended charge carrier lifetime. For device applications, PSCs introducing the Br-2EPSe SAM achieved a PCE of 22.73% between the series of SAM-based PSCs. Moreover, all of the SAMs were employed in organic solar cells (OSCs) and demonstrated good compatibility as a hole injection layer. The Br-2EPSe SAM-based OSCs demonstrated the highest PCE of 17.9% among the series of SAM-based OSCs, with enhanced short-circuit current density and fill factor.

5:00 PM EL01.03.22

Spectroscopy on The SnO₂ Buffer Layer between TCO Current Collector and Fe₂O₃ Photoelectrode [Artur Braun](#)¹, Yelin Hu^{1,2}, Florent Boudoire¹, Songhak Yoon¹, Matthew T. Mayer² and Michael Grätzel²; ¹Empa, Switzerland; ²EPFL, Switzerland

The tin oxide buffer layer between the transparent conducting oxide current collector and the hematite photoelectrode causes considerable water oxidation enhancement of that electrode. The water oxidation onset potential is lowered by 180 mV. The lifetime of photogenerated charge carriers is increased by a factor of 10. For the investigation of structure and function of the buffer layer, we designed a wedge-shaped multilayer film assembly. Oxygen 1s X-ray photoemission spectra suggest a decrease of oxygen vacancy concentration near the interface of α -Fe₂O₃ and FTO-SnO₂, when the SnO₂ buffer layer is introduced. This SnO₂ buffer layer increases the crystallinity of the hematite layer. The oxygen 1s near-edge X-ray absorption fine structure shows that the buffer layer increases the Fe 3d-O 2p hybridization and affects the quasi-Fermi level of electrons in α -Fe₂O₃. There is some indication that the α -Fe₂O₃ layer contains an adverse hole state in the valence band which disappears when the α -Fe₂O₃ layer is grown on the SnO₂ layer. This layer induces improved orbital overlap with subsequent improved charge transfer between the absorber α -Fe₂O₃ and the current collector FTO. Our experiments indicate that performance enhancement by this buffer layer is of electronic structure origin.

5:00 PM EL01.03.23

Electrically Tuneable Silicon-Based Photomodulator for THz Applications [Xavier Romain](#)¹, Peter R. Wilshaw², Rayko I. Stantchev^{3,1}, Tina Miao¹, Tim Niewelt¹, Shona McNab², Sophie L. Pain¹, Nicholas Grant¹, Ruy S. Bonilla², Emma Pickwell-MacPherson¹ and John D. Murphy¹; ¹University of Warwick, United Kingdom; ²University of Oxford, United Kingdom; ³National Sun Yat-sen University, Taiwan

Silicon is a well-established semiconductor which is extensively used in a wide variety of applications; it is the basic component for photovoltaic solar cells and is a widespread substrate in many photonic devices. More recently, silicon has found new use in the ever-growing research area of terahertz (THz) waves. For example, silicon can serve as a THz photomodulator i.e., when the silicon is illuminated by an above bandgap optical source which renders the

silicon opaque to the THz radiation. The opacity level (modulation depth) and the switching speed between the transparent and opaque states of silicon (modulation speed) are determined by the lifetime of the photoexcited charge carriers in the silicon wafer. For some applications (such as in THz single-pixel imaging) the effective lifetime of silicon is a critical parameter, which must be carefully considered to reach the best trade-off possible between the modulation depth and the modulation speed. However, neither bare silicon (too low) nor routinely surface passivated silicon (too high) yields effective lifetimes that are best suited for such THz applications. Hence we suggest a novel device configuration featuring controlled carrier lifetime modulation of Si-based THz modulators via voltage application across a transparent gate electrode.

In this work, we report the fabrication, characterisation, and implementation in a THz imaging setup of such a photomodulator. We deposited hafnium oxide via atomic layer deposition as the passivation layer on both side of a high-resistivity silicon substrate. The hafnium oxide provides a sufficient electrical insulation and an adequate surface passivation level yielding lifetimes in the hundreds of microseconds. We then coated the hafnium oxide layers with poly(3,4-ethylenedioxythiophene) polystyrene sulfonate (PEDOT:PSS) as the conductive layer for the electrical gating. The choice of PEDOT:PSS is particularly relevant for THz photomodulation as it is transparent to both the THz and the visible light. We performed an injection-dependent lifetime characterisation of the photomodulator using standard photoconductance decay (PCD) measurements while a bias voltage in a -10V to +10V range was applied between the PEDOT:PSS top layer and the silicon layer. We observed results for the effective lifetime as a function of the applied bias voltage that are consistent with similar devices previously reported in literature. We also confirmed the applied voltage homogeneity across the whole photomodulator surface by repeating a similar experiment using a photoluminescence imaging technique.

We implemented the electrically tuneable photomodulator in a THz time domain spectroscopy setup (THz-TDS) capable of single-pixel imaging. Similar to the PCD measurements, we first characterised the photomodulator effective lifetime by monitoring the THz radiation decay for a range of photoexcitation intensities and applied bias voltages. The lifetime curves extracted from this THz-TDS photomodulation configuration showed comparable trends with the lifetime curves produced by PCD. To demonstrate the potential of this electrically tuneable THz photomodulator, we performed single-pixel imaging where the photoexcitation source is now spatially structured so that the photomodulator acts as a THz spatial light modulator. We showed that tuning only the bias voltage, which controls the photomodulator effective lifetime, can massively impact the THz imaging. With such silicon-based THz photomodulator, the effective lifetime is not a constraining fixed factor but rather an additional degree of freedom for THz photomodulation.

5:00 PM EL01.03.24

Toward Solution-Processed UV Photodetectors via Atomically Thin Fluorine-Functionalized Graphene Coupled with Consecutive Carbon Quantum Dots

Po-Hsuan Hsiao, Kuan-Han Lin, Tsung-Yen Wu and [Chia-Yun Chen](#); National Cheng Kung University, Taiwan

Heterostructures stand for the artificial structures composed of two or more different solid-state materials. When the dimensionality of materials scales down to nanoscale, the interfaces associated with constitute materials play the dominant role on their materials chemistry, materials physics and even being decisive for the correlated device performances. In this presentation, the photophysical dynamics of fluorine-functionalized graphene (FF-Gra) coupled with carbon quantum dot film (CQDF) is manifested. By probing the involved electronic structures and optical transitions, bound-carrier population and dynamic phenomena is revealed, which exhibit as main features of for the modulation of photophysical origin. All these features implicate the outstanding UV-responsive flexible photodetectors with sound optical transparency, attesting external quantum efficiency (EQE) of $1.68 \times 10^9\%$, photoresponsivity of 4.66×10^6 A/W and detectivity of 2.92×10^{18} Jones based on such nonintuitive quantum-confined hybrid materials. The present photodetector design, along with the mechanism validation was anticipated to be potential for the development of next-generation optoelectronic devices with desired properties.

5:00 PM EL01.03.25

Revealing Gas Sensing Mechanism of PtO₂ Originated from The Structural Equivalence with SnO₂ [Seongsu Choi](#)¹, Yeon Sik Jung¹ and Hyeuk Jin Han²; ¹Korea Advanced Institute of Science and Technology, Korea (the Republic of); ²Sungshin Women's University, Korea (the Republic of)

Conventional gas sensing with Pt relies on the spillover effect, where Pt nanoparticles split gas molecules and disperse onto n-type semiconductors such as ZnO, WO₃, and SnO₂. In the presence of PtO, the p-type semiconductor nature of PtO creates an electron depletion region at the heterojunction with n-type semiconductors, which in turn affects the gas sensor resistance and thus provides information about the surrounding gas composition. The gas sensing mechanism of another oxidation state, PtO₂, has conventionally been considered a p-type semiconductor, similar to PtO until now. However, this traditional interpretation does not explain the increased selectivity and sensitivity observed with PtO₂ compared to both PtO and Pt. There is also a lack of research comparing the gas sensing properties based on the different oxidation states of Pt.

In this study, we suggest a novel gas sensing mechanism of PtO₂ when combined with SnO₂, originating from the structural equivalency between PtO₂ and SnO₂. Previously, it has been demonstrated that at elevated temperatures and under high O₂ partial pressure conditions, Pt in PtO₂ can replace Sn in SnO₂ lattice due to their identical rutile structure and oxidation state (4⁺) as well as their similar ionic radii. Additionally, PtO₂, known for its strong oxidizing properties, creates oxygen vacancies in a reducing gas atmosphere. These vacancies then become active sites for the adsorption of target gases, significantly enhancing gas sensor performance. To verify the sole influence of the oxidation state of Pt, we designed 3D-aligned Pt decorated SnO₂ nanowires using Thermally-assisted nanotransfer printing(T-nTP). This method improved mass transport, ensured consistent network connections, and increased the surface area, enabling specific focus on the differences originating from the oxidation state of Pt. Via annealing in an air furnace, the oxidation states of Pt were selectively altered while keeping the other conditions, such as the structure of the gas sensor and the state of the supporting material, SnO₂. Specifically, annealing the gas sensor at 900°C results in approximately 99% conversion of Pt into PtO₂. We observed that PtO₂ decoration on SnO₂ exhibited superior sensitivity and selectivity for hydrogen sulfide (H₂S) compared to Pt decoration. PtO₂ showed approximately 60 times greater sensitivity compared to the sample annealed at a lower temperature, achieving response ratios (R_{air} / R_{gas}) exceeding 50 at a concentration of 1 ppm. Overall, this study presents a newly discovered gas sensing mechanism with PtO₂ and demonstrates significantly improved sensitivity and selectivity, particularly in detecting H₂S. Moreover, the gas sensors synthesized via T-nTP offer the potential for comparative analysis of gas sensing properties across different oxidation states of other noble metals.

5:00 PM EL01.03.26

Nanoscale Morphology, Defect Identification and Electronic Spectroscopy of Thin Molybdenum Carbide (α -Mo₂C) Crystals under Ambient Conditions [Gokay Adabasi](#)¹, Saima A. Sumaiya¹, Ilker Demiroglu², Elif Okay³, Omer R. Caylan³, Goknur Cambaz Buke³, Cem Sevik⁴ and Mehmet Z. Baykara¹; ¹University of California, Merced, United States; ²Eskisehir Technical University, Turkey; ³TOBB University of Economics and Technology, Turkey; ⁴University of Antwerp, Belgium

The emerging materials family of thin transition metal carbides (TMCs) have garnered significant recent attention due to their distinctive features such as high thermal and chemical resistance, good electrical and thermal conductivity, high hardness, and potential for energy storage as well as electromagnetic shielding. The application potential of thin TMCs will strongly depend on atomic-scale structural and physical-chemical properties. On the other hand, the necessity of high vacuum and low temperatures for atomic-resolution experiments has led to a debate regarding the relevance of such characterization approaches for real-life applications.

Here, we present a nanometer- and atomic-scale characterization study of thin crystals of molybdenum carbide (α -Mo₂C) grown through chemical vapor deposition (CVD). The experiments are performed via conductive atomic force microscopy (C-AFM), under ambient conditions. It is found that the crystal surfaces are partially covered by graphene. Moreover, atomic-resolution imaging, combined with density functional theory (DFT), allows the identification of various defects found on the crystal surfaces. Finally, current vs. voltage spectroscopy performed on the defects provides information about their local influence on surface electronics.

5:00 PM EL01.03.28

Mimicking Positive Aging using Atomic Layer Deposition of Alumina in Quantum Dot Light-Emitting Diodes Haoyue Wan¹, Euidae Jung¹, Pan Xia¹, Benjamin Rehl¹, Ruiqi Zhang², Yanjiang Liu¹, Yakun Wang¹, Sjoerd Hoogland¹, Vladimir Bulovic² and Edward H. Sargent¹; ¹University of Toronto, Canada; ²Massachusetts Institute of Technology, United States

Quantum dot light-emitting diodes (QD-LEDs) frequently exhibit a unique characteristic known as positive aging, where their efficiency improves over time. In this study, we delve into the underlying causes of this behavior. Our findings suggest that the densification of the ZnMgO electron transport layer plays a pivotal role in this process. As the device undergoes shelf-aging, ZnMgO nanoparticles coalesce, leading to a reduction in leakage current and a decrease in surface vacancies within the ZnMgO layer. To expedite the device's performance without waiting for the positive aging effect, we introduced an Al₂O₃ layer via atomic layer deposition between the ZnMgO and the electrode. This modification resulted in red InP QD-LEDs showcasing a remarkable 1.3-fold boost in efficiency and a tenfold enhancement in stability, underscoring the potential of the Al₂O₃ layer in optimizing QD-LED performance.

5:00 PM EL01.03.29

Curvature-Induced Instability in Crystallization of Chiral Liquid Crystals Sepideh Norouzi¹, Jeremy R. Money¹, Jose A. Martinez-Gonzalez² and Monirosadat Sadati¹; ¹The University of South Carolina, United States; ²Universidad Autónoma de San Luis Potosí, Mexico

Crystallization in curved entities such as viral capsids, Radiolaria, and ice-freezing is ubiquitous in nature, wherein the spatial coordination of constituent materials adjusts to adequately accommodate within curvature, resulting in exotic collective properties. Herein, we investigated the nucleation and growth of blue phase (BPs) soft crystals within curved topological confinement. BPs represent 3D periodic cubic crystals while they have fluidity. They have the potential to assemble into two crystalline symmetries: BPI with a body-centered cubic structure and BPII with a simple cubic structure. These cubic crystal lattices are a few hundred nanometers and show selective Bragg's reflection with rapid sub-millisecond response times, which makes them attractive for sensing and photonic applications. They, however, exist in a very narrow temperature range and generate polycrystalline structures when confined in flat films, preventing their widespread use in most practical applications. Moreover, the growing interest in the integration of these ordered materials into miniaturized, flexible devices brings about the need to understand the effect of geometrical confinement and curved boundaries on the structure of BPs and their stability and photonic responses.

To understand how the interplay of curvature, confinement, and surface anchoring impacts the structural stability and optical response of BPs, we have confined BPs within core-shell and microdroplets with precise size and shell thicknesses. Our observations in shells indicate that increased curvature and strong spatial confinement destabilize BPI promoting its transition into configuration and optical characteristics resembling BPII. Although BPs in shells appeared polycrystalline, the inherent 3D symmetrical curvature in microdroplets facilitated the formation of monodomain crystals, eliminating the need for any specific surface treatments. Moreover, using photo-polymerization technique to stabilize defects in droplets led to an expanded thermal stability range for BPs. Yet, the phase transition temperature in these microdroplets was found to be strongly size-dependent. We have delved into the underlying principles of these molecular arrangements through both experimental and theoretical simulations. These findings can pave the way for designing optically active microstructures, addressing BP-related challenges, offering potential for cutting-edge photonic and sensing applications especially in flexible and wearable devices.

5:00 PM EL01.03.30

Local Defect-Engineering in Monolayer MoS₂ through Sulfur Vacancies Controlling with Dip-Pen Nanolithography Jinho Lee, Jeong-Sik S. Jo, Do Wan K. Kim and Jae-Won Jang; Dongguk University, Korea (the Republic of)

Molybdenum disulfide (MoS₂) is a promising layered semiconductor material that can overcome the limitations of conventional silicon-based devices. MoS₂ has a unique characteristic in which the band gap changes depending on the thickness; Monolayer MoS₂ has a direct band gap of about 1.8 eV, while multilayer MoS₂ has an indirect band gap of about 1.3 eV. Therefore, MoS₂ has potential applications in various fields such as optoelectronics, sensors, and catalysis. However, the electrical and optical properties of monolayer MoS₂ are sensitive to defects on its surface. Sulfur vacancies are the most prevalent defects in MoS₂ and they work as electron donors and trap sites. Thus, they create mid-gap states influencing the band structure and the Fermi level of monolayer MoS₂. The charge state and the local environment of the sulfur vacancies can either improve or deteriorate the electrical conductivity, the photoluminescence intensity, and the catalytic activity of monolayer MoS₂. Thus, it is crucial to control the sulfur vacancies in monolayer MoS₂ to optimize its electrical characteristics and device performance. In this study, we propose a method for local defect engineering in monolayer MoS₂. The proposed method controls sulfur vacancies through dip-pen nanolithography (DPN), a tip-based lithography technique that enables direct deposition of molecules or ions onto specific regions of the substrate surface.

5:00 PM EL01.03.31

Understanding Surfaces and Interfaces in Nanocomposites of Silicone and Barium Titanate through Experiments and Modeling Avery Pritchard¹, Vanessa Bartling¹, Heather Fuentes¹, Katrina Nelson¹, Jessica Santosa¹, Albert Dato¹, Todd Monson² and Renee Van Ginhoven³; ¹Harvey Mudd College, United States; ²Sandia National Laboratories, United States; ³Air Force Research Laboratory, United States

Computational and experimental studies into particle surfaces and particle-matrix interfaces in nanocomposites of silicone and barium titanate (BTO) nanoparticles will be the focus of this presentation. BTO is a ferroelectric perovskite that is used in electronic devices and energy storage systems because of its high dielectric constant (up to 7,000). Research has shown that the dielectric constant of BTO drastically increases to 15,000 at a BTO particle diameter of 70 nm, which is an intriguing but highly contested result. Dielectric constants of BTO nanoparticles have been determined by fabricating, characterizing, and modeling surface-functionalized BTO powders incorporated into polymer matrices. These studies have indicated that BTO particle size does impact the dielectric constant of the perovskite. However, more sophisticated modeling and advanced characterization techniques are needed to better understand the nature and complexity of interfaces formed between polymers and BTO, as well as investigate the relationships between interfacial properties, nanocomposite properties, and nanoparticle properties.

Here we present experimental and theoretical research into the preparation, transmission electron microscope (TEM) characterization, and simulation of elastomer-matrix nanocomposites containing BTO nanoparticles with diameters ranging from 50 nm to 500 nm. Methods of functionalizing the surfaces of BTO nanoparticles, preparing nanocomposites of BTO and silicone, and determining the dielectric properties of BTO-silicone nanocomposites will be shown. TEM images of BTO nanoparticles in silicone will provide insight into interface formation and be related to (1) nanocomposite properties, (2)

COMSOL models of the nanocomposites, and (3) density functional theory simulations of the interactions of water with BTO surfaces. The results from this project will advance our understanding of surfaces and interfaces in BTO-polymer nanocomposites, elucidate the particle size dependence of the BTO dielectric constant, and demonstrate an avenue toward manufacturing flexible elastomer-perovskite nanocomposites for wearable electronic devices and energy storage applications.

SNL is managed and operated by NTESS under DOE NNSA contract DE-NA0003525. This study was also supported by the National Science Foundation under Grant No. 1943599.

SESSION EL01.04: Area Selective Deposition and Etching II
Session Chairs: Silvia Armini, Santanu Bag, Erwin Kessels and Adrie Mackus
Wednesday Morning, April 24, 2024
Room 348, Level 3, Summit

8:30 AM *EL01.04.01

Plasma Processes for Isotropic and Anisotropic Atomic Layer Etching Adrie Mackus; Eindhoven University of Technology, Netherlands

The development of nanoelectronics towards increasingly complex 3D nanostructured devices requires novel combinations of anisotropic and isotropic etching. Atomic layer etching (ALE) will play an important role in the fabrication of such nanodevices because of its Ångstrom-level control and ability to uniformly etch on complex structures. Previously reported ALE processes can be classified in two main categories: plasma processes for anisotropic etching and thermal chemistries for isotropic etching.

In this contribution, results for both isotropic and anisotropic ALE will be discussed, focusing on the unique opportunities provided by plasmas. The relatively unexplored category of using plasmas for isotropic ALE allows for processing at lower temperatures and higher etch rates, as will be demonstrated for processes involving fluorination with a SF₆ plasma. Recent work also focuses on isotropic ALE based on etching by diketone dosing (e.g., hexafluoroacetylacetone) and plasma cleaning steps. Infrared spectroscopy and simulation studies revealed that the mechanism of etching with diketones involves a competition between etching and inhibition reactions.

9:00 AM EL01.04.02

Atomic Layer Deposition of WO_x-Doped In₂O₃ for High-Performance BEOL-Compatible Transistors Chanyoung Yoo^{1,2}, Balreen Saini², Jonathan Hartanto², Cristian Ruano Arens², John D. Baniecki¹, Wilman Tsai², Baylor B. Triplett² and Paul C. McIntyre^{1,2}; ¹SLAC National Accelerator Laboratory, United States; ²Stanford University, United States

Metal oxide semiconductors incorporating In₂O₃ have received significant attention as they possess high electron mobility, can be synthesized at back-end-of-line (BEOL) compatible temperatures, and exhibit excellent transistor characteristics at nanoscale dimensions. Doping In₂O₃ with several mole % tungsten oxide to form "IWO" has been reported to improve the threshold voltage stability of these semiconductor channel materials. However, currently reported film deposition for IWO is limited to sputtering, which does not allow the growth of conformal films with precise thickness and stoichiometry control on topographically complex BEOL surfaces. This limitation becomes critical when utilizing these films as channel materials in gate-all-around structures. A shift toward deposition methods that support 3D structures is necessary to address the increasing demand for high on-current.

Consequently, we use the 3D-compatible atomic layer deposition (ALD) method to deposit IWO by adjusting the cycle ratios for In and W precursors and the oxidant co-reactant, enabling precise control over the doped film composition. In addition to facilitating highly conformal film growth, ALD-grown IWO may exhibit different point defect populations and a broader process window for amorphous structure because of the lack of bombardment by energetic species that are present during sputtering. We demonstrate deposition of IWO (1~4 mol% WO_x) films using ALD and fabricate both bottom- and top-gated thin film transistors with a 3-nm thick IWO channel in a BEOL-compatible process with a maximum temperature of less than 250°C. A transistor with 2 mol% WO_x-doped IWO exhibits exceptional performance characteristics, including a subthreshold slope of 65 mV/decade, a high I_{D,sat} of 70 (W=12 μm, L=1.5 μm) at V_{DS}=1.0 V and V_{GS}=2.0 V, and remarkable stability under bias stress. The transistor showed negligible hysteresis and maintained a stable threshold voltage (V_{th}) under negative and positive bias stress conditions (ΔV_{th} = -0.06 V and +0.1 V, respectively, at an electric field of 4.2 MV/cm for 1000 seconds). This V_{th} stability under bias stress highlights the reliability of ALD-grown IWO for ferroelectric field-effect transistors and its potential to enable high-performance monolithic 3D integrated devices.

Furthermore, we explored the evolution of long-range order within the IWO films through synchrotron X-ray diffraction. We found that doping In₂O₃ with several mole % of tungsten oxide has a strong anti-correlation with both the ordering and the presence of oxygen vacancies, which are themselves strongly correlated with V_{th}. This work offers an understanding of the impact of W doping and provides insight into the reliability of In₂O₃-based oxide transistors.

9:15 AM EL01.04.03

Understanding The Formation and Evolution of Surface Oxidation Layers in Nb Thin Films Jeffrey Dhas^{1,2}, Zihua Zhu¹, Peter V. Sushko¹, Mingzhao Liu³, Ekta Bhatia⁴, Jakub Nalaskowski⁴, Sandra Schujman⁴, Corbet Johnson⁴, Tom Murray⁴, Satyavolu Papa Rao⁴ and Yingge Du¹; ¹Pacific Northwest National Laboratory, United States; ²Oregon State University, United States; ³Brookhaven National Laboratory, United States; ⁴NY Creates, United States

Surface oxides formed on metal films have a significant impact on the decoherence and stability of superconducting qubits. Niobium (Nb) exhibits a complex native oxide layer, approximately 10 nm thick, believed to harbor structural and chemical defects contributing to coherence loss in Nb-based devices. In this study, Time-of-Flight Secondary Ion Mass Spectrometry (ToF-SIMS) was used to assess the influence of different treatments on the surface oxidation layers of Nb thin films. We employed ToF-SIMS for high-resolution chemical mapping and depth profiling, combined with ex situ ¹⁸O₂ annealing experiments. This allowed us to characterize and evaluate the surface oxidation layers of Nb thin films resulting from chemical mechanical polishing (CMP) and accelerated neutral atom beam (ANAB) treatments, comparing them to native oxides formed through air exposure. By combining ToF-SIMS results with XPS and TEM studies, we revealed the differences in oxidation layer thickness and composition, including Nb₂O₅, Nb₂O₃, and NbO, on the surface. Moreover, we demonstrated that ANAB-generated oxidation layers exhibit enhanced resistance to further oxidation when compared to native oxides. This finding suggests a promising strategy for mitigating surface oxidation and improving the performance of devices based on superconducting metals.

9:30 AM BREAK

10:00 AM *EL01.04.04

Passivation of Si, Ge and SiGe Surfaces by ALD Nanolayers Erwin Kessels; Eindhoven University of Technology, Netherlands

For many (opto)electronic devices, it is vital to reduce the recombination of charge carriers at the semiconductor surfaces and interfaces. This is becoming more and more challenging due to the ongoing diversification in semiconductor materials to be used in the devices but also due to the increasing surface-to-volume ratio of the (nano)structures employed in electronics and photonics. Surface passivation can be achieved by employing ultrathin films of semiconductor or dielectric materials which often serve other functionalities in the devices too. The underlying mechanism of the surface passivation can be the reduction of surface defect states (i.e., so-called chemical passivation) and/or band bending due to so-called field-effect passivation effect (e.g., due to fixed charges in the film).

In this contribution the surface passivation by some innovative nanolayer approaches prepared by atomic layer deposition (ALD) will be presented. The focus will be on Si and Ge surfaces and also include hexagonal SiGe alloy nanowires which are of interest for nanolayers due to their direct-bandgap [1]. The nanolayers include materials such as Al₂O₃, PO_x and (doped) ZnO as well as stacks thereof [2,3,4,5]. Special attention will be given to the underlying mechanism of the surface passivation achieved as well as its relation to the properties of the nanolayers employed.

- [1] E. M. T. Fadaly, A. Dijkstra, J.R. Suckert, D. Ziss, M. A. J. van Tilburg, C. Mao, Y. Ren, V.T. van Lange, K. Korzun, S. Kölling, M. A. Verheijen, D. Busse, C. Rödl, J. Furthmüller, F. Bechstedt, J. Stangl, J.J. Finley, S. Botti, J. E. M. Haverkort, E. P. A. M. Bakkers, *Nature* 580, 205 (2020).
- [2] W. J. H. Berghuis, J. Melskens, B. Macco, R. J. Theeuwes, L. E. Black, M. A. Verheijen, W. M. M. Kessels, *J. Appl. Phys.* 130, 135303 (2021).
- [3] R. J. Theeuwes, W.J.H. Berghuis, B. Macco, W. M. M. Kessels, *Appl. Phys. Lett.* 123, 091604 (2023).
- [4] W. J. H. Berghuis, M. A. J. van Tilburg, W. H. J. Peeters, V. T. van Lange, E. M. T. Fadaly, E. C. M. Renirie, R. J. Theeuwes, M. A. Verheijen, B. Macco, E. P. A. M. Bakkers, J. E. M. Haverkort, W. M. M. Kessels, to be published.
- [5] B. Macco, M.L. van de Poll, B.W.H. van de Loo, T.M.P. Broekema, S.B. Basuvalingam, C.A.A. van Helvoirt, W.J.H. Berghuis, R.J. Theeuwes, N. Phung, and W.M.M. Kessels, *Sol. Energy Mater. Solar Cells*, 245, 111689 (2022).

10:30 AM EL01.04.05

Substrate Characteristics and Their Impact on Ruthenium Metal Growth via Atomic Layer Deposition (ALD) [Amnon Rothman](#) and Stacey F. Bent; Stanford University, United States

Noble metal thin films have attracted significant interest owing to their distinctive properties and structures, which make them ideal for applications in microelectronics, catalysis, energy, and photovoltaics. While several parameters influence the properties of these metals for such applications, the deposition process remains a critical factor. Atomic Layer Deposition (ALD) stands out as a prevalent deposition technique due to its surface-sensitive nature. The ALD process is characterized by its self-limiting surface reactions, promoting a layer-by-layer growth mechanism and allowing for precise control over film thickness and conformality. However, challenges arise in achieving continuous, pinhole-free noble metal ALD layers on oxide surfaces, often resulting in low film quality. These challenges can be traced back to the lack of adequate nucleation sites and the poor wettability of the low-surface energy substrates. We have studied the impact of substrate surface functionalization using organometallic molecules, such as trimethylaluminum (TMA) and diethylzinc (DEZ), on the nucleation and growth of Ru layers. Our results reveal an enhancement in both nucleation density and the average diameter of the Ru nanoparticles deposited, and we attribute these improvements to an increase in both nucleation sites and elevated surface diffusivity. The latter effect is speculated to result from a reduction in the substrate's surface free energy.

We also examine the influence of substrate surface characteristics, including surface termination and crystallinity, on the nucleation and growth of Ru metal via ALD. We utilize a range of substrates, including Si with native oxide, HF-etched Si, quartz, amorphous Al₂O₃, and sapphire, for the Ru metal deposition process. Surface properties such as water contact angle and surface free energy of the examined substrates are measured. The morphologies of the resulting Ru thin films are studied using scanning electron microscopy (SEM), atomic force microscopy (AFM), and grazing incidence small angle x-ray scattering (GISAXS). These analytical results are integrated with an experimental model to elucidate the differences in growth mechanisms observed across substrates. The deposited Ru coverage as well as the Ru island density and average diameter are correlated to the surface free energy of the substrate. The findings underscore the importance of substrate choice in the ALD process and broaden our understanding of Ru metal growth. This research serves as an important step in optimizing the ALD process for various applications by tailoring substrate selection.

10:45 AM *EL01.04.06

Energy Enhanced Atomic Layer Deposition (EEALD) [John F. Conley](#); Oregon State University, United States

Atomic layer deposition (ALD) is based on alternating purge-separated self-limiting surface chemical reactions in which films are deposited in a layer-by-layer fashion. Inherent advantages of ALD include atomic scale controlled growth of high quality highly conformal thin films at relatively low temperatures. A low thermal budget is often critical for BEOL processing, 3D integration, avoiding unwanted diffusion, and maintaining stable effective work functions and threshold voltages in metal/insulator/metal (MIM) and metal/oxide/semiconductor (MOS) devices and well as for deposition on glass or flexible substrates for large area electronics. While advantageous for some applications, the low deposition temperatures common in ALD can lead to incorporation of excess -OH groups or other residual impurities from unreacted ligands and result in poor stoichiometry, which may in turn lead to sub-optimal physical, optical, and electrical properties.

A number of approaches have been used to reduce impurities, increase density, improve stoichiometry and morphology, and achieve the desired properties of ALD films. One obvious approach is to increase deposition temperature. However this may move a process into the CVD regime, negating many of the benefits of ALD. The most common approach to improving film quality is post-deposition annealing (PDA) at elevated temperatures. The PDA temperatures that are typically required, however, can exceed the maximum temperature limitations of the substrate or previously formed electronics.

To maintain low thermal budget while maximizing film properties, performing annealing *during*, rather than after, ALD can be beneficial. An alternate approach to help drive reactions and reduce impurity / ligand incorporation is to add extra energy as part of each (or every few) ALD cycles or supercycles. Methods to date include in-situ rapid thermal (MTA, DADA, etc.) annealing, flash lamp annealing, plasma exposure, UV exposure, etc. I collectively refer to all of these as energy enhanced ALD (EE-ALD) [1-16]. (Note that these are distinct from plasma enhanced ALD (PEALD), see [17] for excellent review.) Documented benefits of the various forms of EE-ALD include higher GPC, denser films, lower temperature, improved dielectric constant and refractive index, lower leakage, lower residual impurities. A potential downside of energy enhancement is the additional time these steps add to the ALD super-cycle, particularly the cool down time when in-situ annealing is incorporated.

In this invited talk, I will describe, compare, and contrast the various EE-ALD techniques, focusing on mechanisms (thermal vs. chemical), placement in ALD supercycle, benefits, and drawbacks. I will also discuss the challenges to be addressed in finding the ideal EE-ALD technique. Finally, I will introduce an entirely new method of EE-ALD, microwave enhanced ALD (ME-ALD).

[1] J.F. Conley, Jr., Y. Ono, D.J. Tweet, *Appl. Phys. Lett.* **84**, 1913 (2004).

[2] J.F. Conley, Jr., D.J. Tweet, Y. Ono, and G. Stecker, in *High-k Insulators and Ferroelectrics for Advanced Microelectronic Devices*, MRS Proc. Vol. **811**, 5 (2004).

- [3] J.F. Conley, Jr., et al., in *Physics and Technology of High-k Gate Dielectrics II*, ECS Proc. Vol. 2003-22, 11 pgs.
- [4] K.H. Holden, S.M. Witsel, P.C. Lemaire, and J.F. Conley, Jr. *J. Vac. Sci. Technol. A*, 40, 040401 (2022).
- [5] T. Henke *et al.*, ECS JSSST 4, 277 (2015).
- [6] R.D. Clark *et al.*, ECS Trans. 41, 79 (2011).
- [7] V. Miikkulainen *et al.*, ECS Trans. 80, 49 (2017).
- [8] P.R. Chalker *et al.*, ECS Trans. 69, 139 (2015).
- [9] J.-C. Kwak *et al.*, ASS 230, 249 (2004).
- [10] S.K. Kim *et al.*, ESSL 14, H146 (2011).
- [11] S.Y. No *et al.*, J. ECS 153, F87 (2006).
- [12] T.L. Shih *et al.*, Sci. Rep. 7, 39717 (2017).
- [13] Österlund *et al.* JVSTA 39, 032403 (2021).
- [14] S.T. Ueda *et al.*, Appl. Surf. Sci. 554, 149656 (2021).
- [15] C.-Y. Wang *et al.*, ACS AEM 5, 2487 (2023).
- [16] M.J.M.J Becher *et al.*, Adv. Eng. Mater. 2300677 (2023).
- [17] H.B. Profijt, *et al.*, JVSTA 29, 050801 (2011).

11:15 AM EL01.04.07

High Precision Capillary Printing of Polymer Patterns for The Area-Selective ALD of Transparent Conducting Oxide [Vincent Jousseau](#)¹, Marc Pascual², Achille Guitton², Tony Jullien¹, Luana Golanski¹ and Chloe Guerin¹; ¹CEA, LETI, France; ²Hummink, France

Thin films of transparent conducting oxides (TCO) are used as electrodes for optoelectronic devices and microdisplays. However, these oxides are often difficult to pattern with standard lithography and etching processes especially in the case of ZnO, which is very sensitive to water. This problem becomes very limiting when it is necessary to reduce the characteristic dimensions of the devices (typically for structures below 5 nm). An alternative approach is the area selective deposition (ASD) of these oxides. More precisely, one way consists in using polymeric film that can act as ALD inhibiting layer and prevent deposition in certain areas.

In this work, polymeric thin films were printed by an innovative direct nanoprining technique [1]. This high precision capillary printing (HPCAP) method is directly derived from AFM technologies, replacing scanning probes by nano capillaries. These “nanopens” are filled up with a solution containing the material to deposit and can draw complex geometries at the surface of the substrate with resolution between 50 nm and tens of μm and positioning precision as low as 20 nm.

Different patterns with poly(methyl methacrylate), poly(vinyl pyrrolidone) or an epoxy-based resist (SU-8) were printed on a silicon substrate. Then, TCO films were deposited on the patterned polymers by low-temperature ALD. The film growth and material structure were analyzed using several characterization techniques including ellipsometry, atomic force microscopy, scanning electron microscopy and energy-dispersive X-ray spectroscopy.

Our results show that it is possible to produce regular micrometric polymer patterns using this HPCAP printing technique. Furthermore, this approach combines with ALD can effectively allow to localize the growth of an oxide such as ZnO. An exclusion zone around the polymer in which ZnO is not deposited is also observed depending of the polymer used. Finally, in the favorable configurations, the polymer can be selectively removed without impacting the ZnO layer. Thus, an array of pixels with 10 nm width has been successfully produced.

In conclusion, a solution combining the direct nanoprining of a polymer pattern followed by the ALD of a transparent conducting oxide appears to be a promising path toward the realization of a matrix of pixels sub-10 nm.

- [1] M. Pascual, N. Bigan, A. MBarki, R. Mental, I. Allegro, U. Lemmer, SPIE Opto 2023, 124330E

11:30 AM *EL01.04.08

Atomic Layer Etching of Metals for Microelectronics [Robert L. Opila](#) and Omar Melton; University of Delaware, United States

As microelectronics evolves more and more metals are being used. Deposition techniques like atomic layer deposition (ALD) are not always available. As a result, precise, selective etching methods are becoming more and more important. For example, magnetoresistive random-access-memory (MRAM) is a leading option for non-volatile digital data storage and depends upon precise stacking of a variety of magnetic metals. Atomic layer etching (ALE), as a time reversed ALD method, has potential for accurately etching nearly all materials, particularly those that cannot be deposited with precision. Herein, we demonstrate the etching of some transition metals used in MRAM applications, Co, Fe, and CoFeB where the tunneling barrier (MgO) acts as an etch stop. The etch is conducted using a thermal approach (versus plasma), where the film is etched by sequential dosing with two different chemical moieties, chlorine and acetylacetone (acac). Thus, optimizing kinetic factors to overcome thermodynamic limitations, thereby developing a controlled etch driving towards one atomic layer at a time. Similar techniques demonstrate that Cu is etched under comparatively mild conditions, whereas Pt requires more aggressive temperatures and pressures to facilitate the etch. Etching of candidates for lowest level metallizations will also be discussed.

SESSION EL01.05: Surfaces and Interfaces II
Session Chairs: Santanu Bag, Mandakini Kanungo and Gilad Zorn
Wednesday Afternoon, April 24, 2024
Room 348, Level 3, Summit

1:30 PM *EL01.05.01

Advancing Measurement Science for Microelectronics: CHIPS R&D Metrology Program [Marla Dowell](#); National Institute of Standards and Technology, United States

The CHIPS and Science Act of 2022 called for NIST to “carry out a microelectronics research program to enable advances and breakthroughs...that will accelerate the underlying R&D for metrology of next-generation microelectronics and ensure the competitiveness and leadership of the United States...”, NIST is leveraging its measurement science expertise, standards development contributions, and stakeholder engagement practices to address the highest priority metrology challenges identified across industry, academia, and government agencies. The program expands upon NIST’s strong track record of supporting the semiconductor technology and manufacturing ecosystem by developing, advancing, and deploying measurement technologies that are

accurate, precise, and fit-for-purpose.

Under the CHIPS and Science Act of 2022, NIST is expanding its support of the microelectronics technology and manufacturing ecosystem by developing, advancing, and deploying measurement technologies that are accurate, precise, and fit-for-purpose.

2:00 PM EL01.05.02

Probing the Interfacial Energetics in Organic Semiconductor Blends Anirudh Sharma, Jules Bertrandie, Jianhua Han, Julien F. Gorenflot, Frédéric Laquai and Derya Baran; King Abdullah University of Science & Technology, Saudi Arabia

In the realm of shrinking new-generation electronic and photonic devices, the role of functional thin-film interfaces is pivotal for optimizing device design. For example, the energetics of materials play a critical role in charge transfer at the interface between functional materials with dissimilar properties, as in the case of organic photovoltaics (OPVs).^[1] Yet, a clear correlation between material energetics at the donor (*D*) - acceptor (*A*) interface and key device parameters is missing. This is primarily because of a lack of criteria for choosing the most suitable method to determine the ionization energy (*IE*) and electron affinity (*EA*) of organic semiconductors that could precisely predict the energy level alignment at the *D/A* interfaces. Consequently, the development of state-of-the-art donor and non-fullerene acceptor materials has led to contradictory claims about the role of energetic offsets at the *D-A* interface. This makes it difficult to establish design rules for the development of future materials.

In this work, we systematically investigate the frontier molecular orbital energies of organic semiconductors and their molecularly mixed blends, as well as the impact of different solvents and molecular orientation on the resultant energies, via different probing techniques; in particular, low-energy inverse photoelectron spectroscopy (*LE-IPES*), which is a relatively novel and non-destructive technique that enables the direct determination of *EA* of organic semiconductors with high precision. By characterizing and fabricating thin films and devices based on over a dozen different *D/A* blends, we demonstrate the significant differences that have been an ongoing debate in the field for energetic losses and device performances.^[2]

We show that the *IE* and *EA* values measured using ultraviolet photoelectron spectroscopy (*UPS*) and *LE-IPES* are the most relevant in understanding the charge generation mechanism in OPVs. We further demonstrate how the energy levels of organic semiconductors evolve when blended with energetically dissimilar materials,^[3] and the impact of morphology and phase segregation on the resultant energetics. Probing a range of small molecule - small molecule and polymer: small molecule *D/A* blends, we show that the photovoltaic gap E_{pv} ($IE_{donor} - EA_{acceptor}$) measured from neat materials can be insufficient in some cases, for establishing material-property relationships in solar cells. By controlling the *D/A* ratio in molecular blend films, we probe the changes induced in E_{pv} of *D/A* blends as a result of intermixing, intermolecular, and electrostatic interactions between the *D/A* materials. We rationalize these findings to the resultant photovoltaic parameters and voltage losses in OPVs.

Lastly, from OPVs based on six different *D-A* blends having systematically varying *IE*-offsets (ΔIE), we convincingly demonstrate that ΔIE plays a crucial role in charge generation. In contrast to earlier works, we show that a vanishing ΔIE is detrimental to device performance.

Overall, these findings establish a solid base for reliably evaluating material energetics and interfacial properties toward interpreting property-performance relationships in solution-processed OPVs.

[1] S. Karuthedath, J. Gorenflot, Y. Firdaus, N. Chaturvedi, C. S. P. De Castro, G. T. Harrison, J. I. Khan, A. Markina, A. H. Balawi, T. A. D. Peña, W. Liu, R.-Z. Liang, A. Sharma, S. H. K. Paleti, W. Zhang, Y. Lin, E. Alarousu, D. H. Anjum, P. M. Beaujuge, S. De Wolf, I. McCulloch, T. D. Anthopoulos, D. Baran, D. Andrienko, F. Laquai, *Nature Materials* **2021**, 20, 378.

[2] J. Bertrandie, J. Han, C. De Castro, E. Yengel, J. Gorenflot, T. Anthopoulos, F. Laquai, A. Sharma, D. Baran, *Advanced Materials* **2022**, 2202575.

[3] X.e. Li, Q. Zhang, J. Yu, Y. Xu, R. Zhang, C. Wang, H. Zhang, S. Fabiano, X. Liu, J. Hou, F. Gao, M. Fahlman, *Nature Communications*, 2022, 13, 2046.

2:15 PM EL01.05.03

Interface Engineering with Aromatic Diammonium Acetates for Amplifying Hole Extraction in Tin Perovskite Solar Cells Donghoon Song, Yuanze Xu and Qiuming Yu; Cornell University, United States

Perovskite solar cells have emerged as one of the most promising photovoltaic technologies because of their high efficiency, solution processability, and mechanical flexibility, which enables ubiquitous energy harvesting. From device perspective, interfaces play critical roles in charge transport and collection, which turns to be particularly important for tin-based perovskite solar cells. Tin perovskite solar cells (TPSCs) stand at the forefront as toxicity-lean technology, featuring compelling properties such as the large light absorption coefficient, small exciton binding energy, ideal bandgap, slow hot-carrier cooling, and high charge carrier mobility. Especially, tin perovskites are adjustable to a bandgap of ~1.34 eV being optimal for single-junction solar cells according to the Shockley-Queisser limit. Beyond merely a toxicity issue, such superb properties drive TPSCs to an efficiency of power conversion (PCE) close to 15%. To close a gap with that (~26%) of lead counterparts, more attentions have been attracted to tailor tin perovskites to mitigate fast crystallization and Sn(II) oxidation, and to modify their interfaces to attain efficient and stable charge collection. Currently, the inverted p-i-n planar architecture is adopted widely for TPSCs because charge transport is more efficient due to the nature of p-type tin perovskites. Poly(3,4-ethylenedioxythiophene) polystyrene sulfonate (PEDOT:PSS) has been used as hole transport layer (HTL) due to the high-performance and reproducibility in an inverted planar architecture. PEDOT:PSS benefits from the demanding properties for TPSCs including a suitable work function (WF: ~5.0–5.2 eV), decent conductivity, and dopant-free merits. However, ambient annealed PEDOT:PSS thin films are terminated with a thin layer of PSS, which has acidity and is unfavorable for hole collection. We tackle this challenge via interface engineering. Specifically, we treated the surface of PEDOT:PSS using aromatic diammonium acetate salts dissolved in a highly volatile but interactive solvent, which not only modifies PEDOT:PSS itself but also its interface with tin perovskite. The salts are embedded into PEDOT:PSS to bridge and ameliorate its interface with tin perovskite and hence to amplify its hole extraction characteristics. Consequently, we attain a high device efficiency as 12.1% and impressive stability without encapsulation for ~2800 h. The materials and methodologies of our development are extendable to other perovskites- and PEDOT:PSS-based bio, energy, and electronic applications. Moreover, they can expand on surface and interface engineering to gain broader scopes, thereby lying a critical bridging stone on paths to diverse applications.

2:30 PM BREAK

3:30 PM EL01.05.04

Evaluation of Bulk and Rear Interface Passivation of Thin Film Photovoltaics by Surface Photovoltage Spectroscopy Nathan D. Rock¹, Michael Scarpulla¹, Adam Phillips², Ebin Bastola², Ed Sartor³, Andrea Mathew³ and Matthew Reese³; ¹University of Utah, United States; ²The University of Toledo, United States; ³National Renewable Energy Laboratory, United States

Thin film photovoltaics have the potential to dramatically reduce cost and carbon footprint of photovoltaic manufacture. However, current solutions like GaAs are cost prohibitive except for special applications, while more affordable CdTe, SbSe and perovskite devices lag behind silicon in efficiency. To identify and resolve these deficiencies, a fuller understanding of the role of interface and bulk passivation, diffusion length, surface recombination velocity, and band structure is necessary.

We present surface photovoltage (SPV) spectroscopy data on multiple CdTe and SbSe photovoltaic devices, comparing the effects of bulk and surface passivation strategies. The effects of doping, wet etchants, CdCl₂ annealing, and surface reconstruction are presented and the results interpreted by advanced modeling which fully describes the device under test.

Traditional methods for interpreting SPV such as the Goodman method, are only valid when diffusion length and absorption depth are both significantly less than the thickness of the sample - a situation which is not applicable to modern devices. In contrast we present analytical and computational modeling which accounts for a full device - including multiple junctions. Analytical models are used to explore the effects of a variety of parameters on SPV in the depletion region, quasi-neutral region and space charge region (SCR). The results are then validated by full device modeling in SCAPS-1D software. The effects of bulk diffusion length, doping, and recombination in each region is explored.

Finally, the understanding of how these effects combine in the final SPV signal allows for SPV to become diagnostic in evaluating the efficacy of new passivation strategies.

3:45 PM EL01.05.05

Non-Equivalent Atomic Vibrations at Interfaces in a Nitride Superlattice Eric R. Hoglund^{1,2}, Harrison Walker³, Kamal Hussain⁴, De Liang Bao³, Haoyang Ni⁵, Jefferey Baxter¹, Asif I. Khan⁴, Sokrates Pantelides^{3,5}, Patrick E. Hopkins² and Jordan A. Hachtel¹; ¹Oak Ridge National Laboratory, United States; ²University of Virginia, United States; ³Vanderbilt University, United States; ⁴University of South Carolina, United States; ⁵University of Illinois at Urbana-Champaign, United States

The structural and chemical discontinuities at interfaces in III-V material heterostructures are what lead to their emergent electronic properties. However, the spectrum of vibrations in the materials often have large mismatch and large interface thermal resistances can limit device performances. The unique structure and chemistry at interfaces in these materials do not only lead to unique electronic properties, but also unique atomic vibrations. In the case of heterostructures made from AlN-(Al_{0.65}Ga_{0.35})N -AlN, the nonequivalence of the two interfaces has long been recognized in that they host different two-dimensional carrier gasses.¹ The nonequivalence of the corresponding atomic vibrations, however, has not been investigated so far due to a lack of experimental techniques with both high spatial and high spectral resolution. Herein we experimentally demonstrate the nonequivalence of AlN-(Al_{0.65}Ga_{0.35})N and (Al_{0.65}Ga_{0.35})N-AlN interface vibrations using monochromated electron energy-loss spectroscopy in the scanning transmission electron microscope (STEM-EELS)²⁻⁴ and density-functional-theory (DFT). We demonstrate that angle-resolved STEM-EELS possesses mixed real- and reciprocal-space selectivity of the vibrational response, which enables direct mapping of the nonequivalent interface phonons between materials with different stacking order. The physical origin of the localized and nonequivalent interface behavior is then unraveled through the perspective of DFT. The results have implications on the vibrational properties of heterostructures where interfaces states increase thermal conductivity.^{3,5}

References

1. Ambacher, O. *et al.* Two-dimensional electron gases induced by spontaneous and piezoelectric polarization charges in N- and Ga-face AlGaIn/GaN heterostructures. *Journal of Applied Physics* **85**, 3222–3233 (1999).
2. Hoglund, E. R. *et al.* Emergent interface vibrational structure of oxide superlattices. *Nature* **601**, 556–561 (2022).
3. Cheng, Z. *et al.* Experimental observation of localized interfacial phonon modes. *Nat. Commun.* **12**, 6901–10 (2021).
4. Wu, M. *et al.* Effects of Localized Interface Phonons on Heat Conductivity in Ingredient Heterogeneous Solids. *Chinese Phys. Lett.* **40**, 036801 (2023).
5. Ravichandran, J. *et al.* Crossover from incoherent to coherent phonon scattering in epitaxial oxide superlattices. *Nat. Mater.* **13**, 168–172 (2014).

4:00 PM EL01.05.06

Improved Photovoltaic Performance through Ionically Regulated Space Charge Zones in α -FAPbI₃ Perovskite Solar Cells Jihyun Kim¹, Ji-Sang Park², Gee Yeong Kim³ and William Jo^{1,1}; ¹Ewha Womans University, Korea (the Republic of); ²Sungkyunkwan University, Korea (the Republic of); ³Korea Institute of Science and Technology, Korea (the Republic of)

The alpha-phase formamidinium lead triiodide (α -FAPbI₃) is considered the most promising photoactive layer material due to its narrow bandgap and superior thermal stability for perovskite solar cells (PSCs). However, interfacial lattice defects created on SnO₂ electron transport layer (ETL) due to its oxygen vacancies (V_O) and hydroxide ions (OH⁻) during the fabrication of α -FAPbI₃ thin films limit power conversion efficiency (PCE) and increase material degradation rates. Herein, the applied interfacial engineering and the regulation of space charge distribution at the FAPbI₃/SnO₂ interface are discussed, both of which are of paramount significance for solar cells. The interfaces were modified using pre-extracted NH₄⁺ ions [1], which exhibited a low migration barrier energy of 0.21 eV, as determined from density functional theory (DFT) simulations. Due to the low migration barrier energy of NH₄⁺, the FAPbI₃ perovskite top surface is p-doped, effectively aligning with hole transport layer interfaces. The redistribution of space charge zones at the FAPbI₃/SnO₂ interface is accomplished through the regulation of V_O and OH⁻, combined with the application of octyl-ammonium iodide (OAI) perovskite top passivation materials. To substantiate the impact of space charge redistribution on the photovoltaic characteristics at the FAPbI₃/SnO₂ interface, parallel conductance measurements were carried out. These measurements entailed the manipulation of FAPbI₃ thin film thickness under both dark and illuminated conditions, with the outcomes assessed through D.C and A.C polarization measurements. These results demonstrate that the regulation of space charge zones effectively enhances the modification of bifacial interfaces, leading to improved crystallinity and charge carrier extraction. Ultimately, this approach results in increased PCE up to 24.38% and enhanced operational stability for 1600 hours of PSCs.

[1] J. H. Kim, J. H. Park, Y. H. Kim, and W. Jo, "Improvement of Open-Circuit Voltage Deficit via Pre-treated NH₄⁺ Ion Modification of Interface between SnO₂ and Perovskite Solar cells", *Small*, 2204173 (2022)

SESSION EL01.06: Poster Session II: Surfaces and Interfaces II
Session Chairs: Silvia Armini, Santanu Bag, Mandakini Kanungo and Gilad Zorn
Wednesday Afternoon, April 24, 2024
Flex Hall C, Level 2, Summit

5:00 PM EL01.06.01

Operando Electrically Pumped Spectroscopy Analysis of Exciton Dynamics and Parasitic Excitons in Blue Phosphorescent Organic Light-Emitting Diodes Changmin Lee¹, Hyun Jae Lee², Tae Wook Kim², Insung Ha¹, P. Justin Jesuraj¹, Chul Hoon Kim² and Seung Yoon Ryu¹; ¹Dongguk University, Korea (the Republic of); ²Korea University, Korea (the Republic of)

Understanding exciton dynamics and optimizing device physics in phosphorescent organic light-emitting diodes (Ph-OLEDs) is essential for achieving highly efficient devices with optimal color purity. In this study, we conducted a comprehensive exploration of radiative transitions, including electromer and exciplex, within blue Ph-OLEDs using operando electrically pumped spectroscopy (EPS). EPS served as a versatile tool to simultaneously secure time-resolved electroluminescence and photoluminescence of the electronic device. Our findings revealed that Ph-OLEDs with thin emission layers (EMLs) in the range of 3–5 nm predominantly exhibited primary electromer emissions and minor interface exciplex emissions, resulting in decreased device efficiency. Conversely, thicker EMLs (30–40 nm) promoted exciplex generation at the hole transport layer/EML interface, impacting color purity due to charge balance and redshift (RZ) shift considerations. The operando EPS study detailed the origin of these parasitic excitons in device emissions, elucidating their role in reducing efficiency and color purity. These findings were substantiated through impedance analysis. Optimal efficiency and color purity were achieved with an EML thickness of 20 nm, demonstrating the absence of parasitic excitons as evidenced by EPS. The study investigates the exciton dynamics and presence of parasitic excitons in a typical blue Ph-OLED, providing valuable insights into fundamental mechanisms governing the behavior of molecular excited states. In summary, the operando EPS analysis of blue Ph-OLEDs contributes to understanding exciton dynamics and the generation of parasitic excitons. Logical modifications to the EML thickness (3–40 nm) revealed insights into RZ shifts, TAPC electromer emissions, and exciplex generation. The operando EPS approach presents a promising avenue for uncovering the origin of interface parasitic excitons, facilitating the realization of highly efficient next-generation optoelectronics.

5:00 PM EL01.06.02

Acoustic Nonreciprocity in Compact Acoustic Circulators Generated by Laser Driven Fluid Jiaxin Yang¹, Arup Neogi¹, Yuqi Jin² and Zhiming Wang¹; ¹University of Electronic Science and Technology of China, China; ²University of North Texas, United States

A circular resonant cavity was designed, using liquid as the medium and driven by laser to move and rotate the fluid. We can control the fluid motion speed by adjusting the laser power. When acoustic signals travel with or against the flow, up to 25dB of acoustic nonreciprocity is observed and faster medium flow implies greater nonreciprocity

1. Background

Acoustic isolation and nonreciprocal sound transmission are highly desirable in many practical scenarios but reciprocal transmission is not always desirable—for example, when one wants to isolate or protect a region of space allowing wave transmission in one direction yet blocking it in the opposite one. But when the fluid rotates in a circular resonant cavity, the sound travels with or against the flow exhibits significant differences. However, how to make the medium move as quickly as possible without generating noise is a problem. To solve this problem, we have introduced optical flow control technology. When a laser is irradiated on an aqueous solution mixed with gold nanoparticles, a substrate implanted with metal ions, and a metal material, the metal particles will generate ultrasonic waves due to the photoacoustic effect to drive the water flow. We designed a circular cavity to convert this linear motion into rotational motion to cause acoustic nonreciprocity.

2. Method

Design a circular resonant cavity:

The average circumference is an integer multiple of the wavelength of a 100KHz sound wave.

A window for laser incidence.

Two windows A & B for transmitting or receiving acoustic signals

Manufacturing cavity (3D printing technology).

Without laser irradiation, the water inside the cavity remains stationary:

Window A emits ultrasonic signals, while window B receives ultrasonic signals to obtain signal Static1-2.

Window B emits ultrasonic signals, and window A receives ultrasonic signals to obtain signal Static2-1.

With laser irradiation, maintaining a stable flow rate of water in the cavity:

Window A emits ultrasonic signals, while window B receives ultrasonic signals to obtain signal Flow1-2.

Window B emits ultrasonic signals, and window A receives ultrasonic signals to obtain signal Flow2-1.

Compare signal Static1-2, Static2-1, Flow1-2 and Flow2-1, and analyze the acoustic nonanisotropy.

3. Result

According to the experimental requirements, a circular cavity is designed with window Laser used for laser driven fluid motion, and windows A and B used for connecting the ultrasonic transducers. The simulation results show that the maximum nonreciprocity occurs at 101KHz, with an isolation degree of about 25dB; The experimental results show that the maximum nonreciprocity occurs at 70.5KHz, with an isolation degree of about 17dB.

4. Conclusion

1. In the experiment, the rotation of the fluid in the laser driven annular cavity was achieved, and by changing the laser power, the speed of motion from 0mm/s to 40mm/s can be controlled.

2. The higher the flow rate of the fluid in the cavity, the greater the acoustic reciprocity. By controlling the flow rate, approximately 0-25dB of acoustic isolation can be controlled.

3. This technology can be used to design and manufacture acoustic diodes and transistors.

5:00 PM EL01.06.03

Nanoscale Synergetic Effects on Ag-Hyperbolic Metamaterial Substrate for Photoinduced Enhanced Raman Spectroscopy with Ultra-Sensitivity and Reusability Muhammad Shafi¹ and Ahmed Elbanna²; ¹Southern University of Science and Technology, China; ²Nanyang Technological University, Singapore

Multilayer hyperbolic metamaterials (HMM) based SERS substrates have received special consideration owing to the support of different propagating modes such as surface plasmonic polaritons (SPP) and bulk plasmon polaritons (BPP). However, due to its weak electric field enhancement, the SPP resonance has hardly originated in the periodic stack of metal and dielectric layers. The current study introduces an innovative 3D plasmonic structure comprising silver nanoparticles (AgNPs) and HMM (4 periods of Au/TiO₂) to enable highly sensitive and reliable photo-induced-enhanced Raman spectroscopy (PIERS). The use of this hybrid substrate results in an approximate 50-fold enhancement compared to standard surface-enhanced Raman spectroscopy, marking the most substantial PIERS enhancement achieved to date. Moreover, beyond the enhanced Raman signal, the hybrid substrate offers heightened detection sensitivity, possibly owing to its capability for activation with remarkably low UV irradiation and extended relaxation times (prolonged measurement durations). Our research indicates that the localized surface plasmon resonance (LSPR) of silver nanoparticles stimulates SPP, resulting in the creation of intense hot spot zones within the nanogap areas atop the HMM structure. Furthermore, the hybrid substrate showcases exceptional photocatalytic degradation of analytes, enabling its reuse for up to 15 cycles without any decline in PIERS activity. The suggested SERS structure demonstrates the capability for precise thiram quantitative detection, achieving sensitivity limits as low as 10⁻⁷ M. This potential holds considerable promise in meeting fundamental requirements for environmental conservation and ensuring food safety.

5:00 PM EL01.06.04

Enhancing Perovskites Cell Performance through Alkali Metal Modification of TiO₂: Exploring Electronic Nature and Interface Properties Chittaranjan Das^{1,2}, Mayank Kedia^{1,2}, Rajarshi Roy¹ and Michael Saliba^{1,2}; ¹University of Stuttgart, Germany; ²Forschungszentrum Jülich GmbH, Germany

Metal halide perovskite solar cells (PSC) have achieved a remarkable efficiency above 26%, which is comparable to the conventional Si photovoltaics. In the evolution of PSC technology from dye-sensitized solar cells, TiO₂ played a pivotal role in achieving remarkable power conversion efficiency. TiO₂, as a charge extracting layer, efficiently extracts photo-generated electrons and acts as a barrier for holes. Being widely used as a blocking layer, the TiO₂ suffers from many fundamental challenges like surface defects, which work as trap states, low electron mobility, and high catalytic activity, collectively contributing to hysteresis and instability in perovskite solar cells. Therefore, to improve the electron transporting properties of TiO₂, various surface modification and doping strategies have been tried. Among various approaches, the alkali metal doping of TiO₂ has proven to be beneficial to achieving overall improvement of the PSCs' performance.

Our research explores how adding lithium (Li), sodium (Na), and potassium (K) to mesoporous TiO₂ affects its electronic properties. We also investigate the chemical interaction between the perovskite layer and TiO₂, as well as the doped TiO₂ with alkali metals. We use soft (XPS) and hard X-ray photoelectron spectroscopy (HAXPES), along with resonance photoemission spectroscopy and X-ray absorption spectroscopy (XAS). Ultimately, we evaluate how alkali metal doping influences the efficiency and stability of the device.

XPS and HAXPES analyses reveal that upon introducing Li, Na, and K to TiO₂, surface Ti⁴⁺ undergoes reduction to Ti³⁺, while bulk Ti⁴⁺ states remain unchanged. The reduction is more pronounced with Li, decreasing from Na to K. This implies Li acts as a dopant, whereas Na and K modify the TiO₂ surface. XAS studies support this conclusion, showing changes in the TiO₂ layers. Resonance photoemission spectroscopy indicates that Li induces more defect states that result from Ti⁴⁺ reduction. Upon perovskite deposition, these defect states diminish, indicating electron transfer from perovskite to TiO₂, oxidizing it. The reduction of defect states is highest in Li-doped TiO₂. Additionally, Ti2p peak shifts to lower binding energy, indicating upward band bending at the TiO₂/perovskite interface. This band bending is consistent across all TiO₂ types and their perovskite interfaces studied here. Notably, the TiO₂/perovskite interface with Na and K modifications exhibits a higher presence of Pb0 states, suggesting a defective interface. The Li doped TiO₂ based PSCs have higher power conversion efficiency compared to the others. The enhanced power conversion efficiency observed in Li-doped TiO₂-based PSCs can be attributed to the improved conductivity resulting from lithium incorporation. This augmentation facilitates the efficient transportation of photo-generated electrons. However, for sustained and stable PSC performance, Na and K-modified TiO₂ devices exhibit superior characteristics.

The spectroscopic investigation, in conjunction with device performance, shows that there is a favorable upward band bending from TiO₂ to the perovskite, and the defects of TiO₂ are passivated by the perovskite itself. Among used alkalis modifiers, the Li dopes the TiO₂ to increase the electron conductivity and with fewer interface defects, amounting to superior power conversion efficiency. On the other hand, Na and K act as modifiers for the TiO₂ layer, contributing to a more stable device performance. This stability can be attributed to their relatively larger ionic radii compared to Li.

5:00 PM EL01.06.05

Surface Engineering Studies on CsPbBr₃ Perovskites Quantum Dots for Optoelectronic Applications [Sinyoung Cho](#)¹, Jigeon Kim^{2,3}, Soon Moon Jeong¹, Min Jae Ko², younghoon kim³ and Jong-Soo Lee¹; ¹Daegu Gyeongbuk Institute of Science and Technology, Korea (the Republic of); ²Hanyang University, Korea (the Republic of); ³Kookmin University, Korea (the Republic of)

Lead halide perovskite quantum dots have been considered as the most promising materials for next-generation optoelectronics because of their high light absorption, narrow emission, and excellent photophysical and optoelectronic properties. Organic ligands with long hydrocarbon chains used as ligands in quantum dot synthesis should be exchanged to short organic/inorganic ligands for improving the charge transporting in optoelectronic device applications. However, previous research related to surface ligand exchange for solar cell application have been largely focused on iodide-based CsPbI₃ perovskite quantum dots so far. For various solar cell applications such as tandem solar cell and Building-integrated photovoltaics (BIPVs), ligand exchange studies on bromide- and chloride-based perovskite quantum dots should be performed. Herein, we demonstrate that surface ligand exchange studies of green-emitting CsPbBr₃ perovskite quantum dots, utilizing several materials such as NaOAc. Improved charge transporting property within CsPbBr₃ perovskite quantum dot thin films contribute to the electroluminescent solar cell applications with high open-circuit voltage of 1.6 V and power conversion efficiency of 3.9 %. Also, quantum dot light-emitting diodes with synthesized CsPbBr₃ perovskite quantum dots was fabricated via interfacial engineering, showing 6.5% of EQE and 22.5 cd/A of current efficiency.

5:00 PM EL01.06.06

Towards Improved Device Performance: A Study on Defects and Interfaces in MHP Devices using Electron Spin Resonance Spectroscopy [Jose A. Delgado](#)^{1,2}, Ross Kerner², Joseph Luther² and Joseph Berry^{1,2}; ¹The University of Colorado Boulder, United States; ²National Renewable Energy Laboratory, United States

Electron spin resonance (ESR) spectroscopy has been identified as a powerful method for nondestructively probing intrinsic defects and interfaces in metal halide perovskite (MHP) devices. Key challenges in MHP devices stem from defects originating from synthesis, interface reactions, lattice strain, energy level mismatches, and other interfacial issues. Furthermore, intrinsic perovskite defects, which tend to propagate post-device deployment [1–3], have substantial implications on device stability. Traditional approaches, like photoemission, often fall short in accurately characterizing these defects due to their constraints at near-surface regions. To circumvent these limitations, nondestructive methods with an acceptable probing depth and sensitivity are needed. In our study, UV and visible light sources were applied to MHP samples to analyze degradation dynamics. We acquired both ex situ and in situ EPR spectra from MHP single crystals, precursor powders, and perovskites interfaced with transport materials. The results provide valuable insights into defect origins and degradation pathways, further emphasizing the importance of a comprehensive understanding to improve MHP-based device longevity and performance.

5:00 PM EL01.06.07

Linear Stark Shift of Two-Dimensional Ga via AC Electric Double Layer Gating [Nader Sawtarie](#)¹, Jonathon Schrecengost², Krishnan Ananthanarayanan², Nithil Manimaran³, Ke Xu³, Joshua Robinson², Noel C. Giebink⁴ and Susan Fullerton¹; ¹University of Pittsburgh, United States; ²The Pennsylvania State University, United States; ³Rochester Institute of Technology, United States; ⁴University of Michigan–Ann Arbor, United States

2D polar metals (PMets) synthesized via confinement heteroepitaxy (CHet) consist of 1-3 atomic layers of metal intercalated between a SiC substrate and graphene that are theorized to have an out-of-plane permanent electric dipole moment resulting from the non-centrosymmetric interface between each layer. 2D PMets, such as bilayer Ga, exhibit unique optical absorption attributed to a quantum-confined interband transition (~1.9 eV). In this work, 2D Ga optoelectronic devices were gated using electric-double-layer (EDL) side gating with polyethylene oxide (PEO):CsClO₄. The EDL gating technique induces large (i.e., ~MV/cm) electric fields, and in this case, AC EDL gating (5 Hz) is successfully demonstrated to enable the use of a lock-in amplifier to measure small changes in reflectivity. COMSOL modeling confirms an RMS field strength of 1.36 V/nm, which agrees with the ~5% RMS channel current modulation that is detected. These high fields induce a measurable electroreflectivity ($\Delta R/R \sim 10^{-4}$) resulting from a ~1.5 meV linear Stark shift. The Stark shift resembles the first derivative lineshape of the reflectivity, corresponding to 0.05 Debye change in the permanent dipole moment. These results validate the theoretical model by providing the first direct experimental evidence for the presence of a permanent ground state dipole moment in 2D PMets, as well as demonstrate a powerful new technique to safely deploy large time varying electric fields to 2D materials in the form of AC EDL-gating.

5:00 PM EL01.06.08

Interfacing Durable Materials to Enable Structural Electronics [Georgia Kaufman](#)¹, Mychal Taylor¹, David Boese¹, Emily Huntley¹, Samuel Leguizamón¹, Michael Gallegos¹, Leah Appelhans¹, Randy Schunk¹ and Bryan Kaehr^{1,2}; ¹Sandia National Laboratories, United States; ²Center for Integrated Nanotechnologies, United States

In-mold structural electronics (IMSE) is a manufacturing approach to integrate devices into any architectural form factor, providing design freedom and device simplification while delivering advantageous size, weight and power. IMSE typically links integrated circuits and discretized by screen-printing nanoparticle-based inks onto flat, thermoplastic substrates that are molded into 3D forms—material sets/processes with widely variable interfaces that are woefully suited for demanding environmental applications. Our project seeks to demonstrate the application of more robust and reliable materials, compatible in extreme environments, such as metal foils for circuit patterning and moldable thermosets. We have explored patterning of copper foils onto b-staged and dual cure epoxies that are subsequently formed into test coupons to study interface delamination, encapsulation and environmental stability. Additionally, we have adapted the chemistry of frontal ring-opening metathesis polymerization (FROMP) of dicyclopentadiene (DCPD), a rugged thermoset material, to be compatible with IMSE. Foil patterned pre-forms are vacuum molded into devices such as 3D RF circuits, battery interconnects, and capacitive touch panels that are subsequently locked into shape at ambient temperature using FROMP. This represents a breakthrough for IMSE technologies, enabling 3D device integration into challenging environmental architectures.

5:00 PM EL01.06.09

Thermal Stability of Metastable GeSn Nanowires [Anis Attiaoui](#)^{1,2}, John Lentz¹, Jarod Meyer¹, Kunal Mukherjee¹ and Paul C. McIntyre^{1,2}; ¹Stanford University, United States; ²SLAC National Accelerator Laboratory, United States

The (Si)GeSn semiconductor material system is highly desired as a potential candidate for optical interconnects and monolithic photonic integration on Si. The demonstrated fundamental direct band gap of this complementary metal-oxide-semiconductor (CMOS) compatible semiconductor has sparked great interest due to its unique properties. Unfortunately, the low solid solubility of gray-Sn (α -Sn) in Ge (1 at.%) and the large lattice mismatch between α -Sn and Ge of approximately 14%, make it difficult to maintain its thermal stability. In fact, rapid thermal annealing (RTA) at temperatures above 400 °C leads to Sn segregation and island formation for $\text{Ge}_{0.9}\text{Sn}_{0.1}$ [1]. Moreover, the low temperature growth of GeSn (<350 °C) can promote the formation of many point defects (mostly divacancies) and act as p -type background impurities [2]. An often-observed background p -type doping of $\sim 10^{16}$ - 10^{18}cm^{-3} leads to strong electric field leakage in devices due to high parallel conductance. Consequently, it is highly desirable to enhance the thermal stability of this material. Herein, we present a method to counteract annealing-induced surface segregation of Ge core/GeSn shell nanowires grown by previously reported methods [3]. Surface passivation significantly improves the thermal stability of GeSn alloys through the atomic layer deposition (ALD) of a very thin Al_2O_3 oxide layer (< 5 nm). Next, annealing the ALD-coated NWs at different temperatures (300°C, 350°C, 400°C, 450°C, and 520°C), above the growth condition of the NWs ($\sim 275^\circ\text{C}$) was systematically investigated. First, structural characterization (X-ray diffraction and scanning electron microscopy (SEM)) demonstrated the unchanged strain state and morphology after annealing (9 ± 1 at. % Sn composition). Second, low-temperature (80K) infrared photoluminescence spectroscopy was undertaken on the annealed NWs to better quantify the recombination mechanisms after annealing. Interestingly, two key findings were observed: an average of 5-fold increase in the PL integrated intensity after annealing, and a blueshift of the band-to-band optical transition. This blueshift suggests that deep level traps are not a potential mechanism for such bandgap shift, as a bandgap contraction would be expected in that case. Understanding the mechanism behind such a blueshift is still an ongoing work. However, a plausible hypothesis can be linked to the nature of the short-range ordering in these materials, as it has been shown theoretically to be the case [4]. Third, single NW devices were fabricated to measure the resistivity variation before and after annealing. The resistivity increases from $0.28\pm 0.02 \Omega\text{-cm}$ for an as-grown NW to $0.42 \pm 0.08 \Omega\text{-cm}$, when annealed at 450°C. The resistivity increase suggests a modest decrease in the p -type carrier density of the NW. The effect of annealing on the structural and optoelectronic properties of the GeSn NW are explored in this work. Further results on the optical bandgap and resistivity changes will be reported.

References:

- [1] R. Chen, et al., *Journal of Crystal Growth* 365, 29 (2013)
- [2] S. Gupta et al., *Applied Physics Letters*, 113, 022102 (2018)
- [3] A Meng, et al., *Materials Today* 40, 101 (2020).
- [4] X. Jin et al., *Communications Materials*, 3, 66 (2022)

5:00 PM EL01.06.11

Magnetic Assembly of Vertical Nanogaps for Highly Sensitive Electrical Biosensors. [Hoang Minh Nguyen](#)^{1,2}, Jae Sung Yoon^{2,1}, Do-Hyun Kang², Yeong-Eun Yoo^{2,1} and Kwanoh Kim²; ¹University of Science & Technology, Korea (the Republic of); ²Korea Institute of Machinery & Materials, Korea (the Republic of)

Nanogap biosensors have emerged as potential tools for the detection and analysis of minuscule quantities of biomolecules, offering unparalleled sensitivity, a low limit of detection (LOD), and enhanced output signals. However, their potential is often limited by the intricate and labor-intensive processes required to precisely engineer the tiny gap between electrodes. In this work, we present an innovative fabrication method to obtain vertical nanogap platforms for electrical biosensing. Leveraging magnetic attraction, we facilitate the construction of 40 nm gaps by assembling antibody-tagged nanowires onto a nanodisk positioned between a pair of microelectrodes. An electrically conductive bridge is established when gold nanoparticles, conjugated with targeted antigen, are captured within the gaps. This results in a substantial amplification in the output current across the electrodes. Our platforms demonstrate an LOD of 18 pM with a linear dynamic detection range up to 150 pM. This approach offers a versatile biosensing platform with potential integration into a myriad of applications, from lab-on-chip systems to biomedicine and point-of-care diagnostics.

5:00 PM EL01.06.12

Adsorption Kinetic Approximation of a Mixed Alkylamido-Cyclopentadienyl Hafnium Precursor in HfO₂ Atomic Layer Deposition [Nhat-Minh Phung](#)^{1,2}, Min-Seong Kong¹, Si-Young Bae¹, Soonil Lee² and Seong-Min Jeong¹; ¹Korea Institute of Ceramic Engineering and Technology, Korea (the Republic of); ²Changwon National University, Korea (the Republic of)

In this study, the growth kinetics of HfO₂ via the atomic layer deposition (ALD) using a mixed alkylamido-cyclopentadienyl hafnium precursor are proposed based on experimental data. The hydroxyl concentration on the targeted surface, which is sensitive to the surface condition prior to the ALD, governs the saturated growth per cycle (GPC) values. Moreover, we found that the bulkiness of remaining ligands on adsorbed species hinders the adsorption of CpHf(N(CH₃)₂)₃ (Cp-Hf) molecules.

Considering this phenomena, we proposed a kinetic model by calculating the energetic terms to quantify the “steric hindrance effect” of the first elementary surface reaction of precursor Cp-Hf. The targeted Si substrates were hydroxylated at several levels to evaluate the reliance of saturated GPC and steric hindrance effect on the nature of the surface. According to the experimental ALD process, the film growth was found to be influenced by the steric hindrance factor, especially at the temperature range from 150 °C to 250 °C, but the hindrance effect decreases with increasing temperature and disappears at 300 °C. The effective activation energy of the adsorption of Cp-Hf molecules on Si substrates was estimated to be 0.2 eV. Although our present model is limited to the ALD of HfO₂, we foresee that the kinetic model could potentially assist the study of metal oxide ALD which utilizes a wide range of

precursors.

5:00 PM EL01.06.13

Forming Solid Films Containing Potassium Ferricyanide for Achieving Vibrational Strong Coupling [Roba Rashed](#)^{1,2}, Rena Klipper^{1,2} and Yaakov Tischler^{1,2}; ¹Bar Ilan, Israel; ²BINA, Israel

The phenomenon of vibrational strong coupling (VSC) presents an opportunity to exert control and to manipulate the characteristics of materials and light-matter interactions at the quantum level. Within this domain, the interaction between light and matter becomes exceedingly amplified relative to dephasing processes, rendering the light and matter sub-systems inseparable. Consequently, a novel hybrid light-matter system forms, exhibiting properties that are distinct from those of the constituent sub-systems. It has been demonstrated that VSC possesses the capability to alter the reactivity of a molecule or a catalyst for a chemical reaction and to make new sources of IR light. We choose to work with Potassium ferricyanide $K_3Fe(CN)_6$ because it is a material with a very narrow absorption spectrum even at room temperature. Ferricyanide is a strong oxidizing agent, it is a very important reference material for electrochemistry, which is very well characterized and studied, and it has even been used for VSC [S. R. Casey and J. R. Sparks, *The Journal of Physical Chemistry C* (2016) 120 (49), 28138-28143.]. Until this point in time, all of the research reports on VSC using ferricyanide and the molecules that resemble it such as Tungsten hexacarbonyl $W(CO)_6$ have been performed in solution and not in solid form. This can be a problem for some applications, namely in liquid it can be more difficult to tune the cavity resonance and to apply voltage on the solution for generating IR light emission. Here, we succeeded to form solid films containing ferricyanide where the molecules are doped into a PVA matrix that we deposit via spin coating. Initially, we tried to prepare "neat films" of potassium ferricyanide from different solvents such as water, DMSO, and methanol, using a variety of deposition techniques such as spin-coating, drop-casting, and even using UV-light, but these methods resulted in rough films, strange absorption peaks or wider absorption bands. We then tried to dope ferricyanide into various polymer matrices with different solvents, such as PMMA. In the end, we observed that the combination of ferricyanide in PVA, all dissolved in water, yielded smooth thin films, of controllable thickness ranging from 1.5 to 3.7 microns, depending on concentration in solution and spin-speed. We also observed a pronounced absorption peak at 2100 cm^{-1} and a narrow absorption spectrum of 6 cm^{-1} . Using these thin films, we can achieve VSC in high-Q DBR-based microcavities, by growing a "bottom" DBR composed of 2.5 pairs of Ge and ZnS layers, then spin-coating a thin film of ferricyanide doped into a PVA-matrix, and completing the microcavity with a top DBR.

5:00 PM EL01.06.14

Thermal Transport and Mechanical Stress Mapping of a Compression Bonded GaN/Diamond Interface for Vertical Power Devices [William Delmas](#), Amun Jarzembki, Matthew Bahr, Anthony McDonald, Wyatt Hodges, Ping Lu, Julia Deitz, Zachary T. Piontkowski and Luke Yates; Sandia National Lab, United States

In the last 20 years Gallium Nitride (GaN) electronics have outstripped conventional silicon devices in both efficiency and breakdown voltages. This enhanced performance of GaN devices comes at the cost of increased operating temperatures, kindling a need to develop more robust thermal management schema for such technologies. One such design proposes taking advantage of passive heat diffusion by bonding the GaN device to a high thermally conductive substrate, such as diamond. This would allow the heat generated in the GaN to flow into the diamond, reducing operating temperatures. To test this design, GaN and diamond die were bonded under 2 kN of force via an Ar activated intermetallic bonding layer of Ti/Au. The total bonding area of GaN/diamond stacks was quantified through confocal scanning acoustic microscopy (C-SAM), revealing both bonded and unbonded areas. These areas were confirmed to be bonded/unbonded using a combination of Focused Ion Beam milling and Transmission Electron Microscopy, with the unbonded regions being identified as a delamination at the Ti/diamond layer. Raman microscopy revealed a uniform compressive stress of <80 MPa in the well bonded areas in addition to, stress oscillations where the sample transitions from being bonded to unbonded, corresponding to a net stress differential of up to $\Delta 100$ MPa. The thermal properties of the GaN/diamond stack were measured through spatially resolved frequency-domain thermoreflectance (FDTR), with the bonded area boasting a thermal boundary conductance (TBC) of > 100 MW/m^2K . FDTR also revealed the presence of micron-scale unbonded regions that showed up as fully bonded under C-SAM. Furthermore, Co-Local Raman/FDTR mapping was demonstrated for the first time with the mapping of a micron-scale unbonded region, showing that stress differentials border the low TBC region. Overall, our work demonstrates a new method for thermal management in vertical type GaN devices that maintains low intrinsic stresses while boosting thermal boundary conductances. As the delaminations seen in these samples are on the order of a possible device (200 microns), more needs to be done to mitigate their formation during initial device fabrication and to spot them post fabrication with more sensitive techniques than C-SAM, such as FDTR.

Acknowledgements: Sandia National Laboratories is a multi-mission laboratory managed and operated by the National Technology & Engineering Solutions of Sandia, LLC, a wholly owned subsidiary of Honeywell International Inc., for the U.S. Department of Energy's National Nuclear Security Administration under contract No. DE-NA0003525. SAND2023-11173A

5:00 PM EL01.06.15

Spectroscopic Analysis of Polymer and Transition Metal Dichalcogenide Interface for Photodetection Applications [Christine McGinn](#)¹, Daniel M. Harrington^{1,2}, Edwin J. Heilweil¹ and Christina Hacker¹; ¹National Institute of Standards and Technology, United States; ²Tufts University, United States

Two-dimensional transition-metal dichalcogenides (2D TMDs) have been extensively studied for photodetection applications due to their strong optoelectronic behavior in the visible range and tunable band gap. [1] However, the optoelectronic properties of 2D TMDs can deteriorate due to surface defects and exposure to air and water. [2] Researchers have used a variety of materials to combat this degradation and passivate the surface, but polymers are ideal for passivating 2D TMDs for photodetection applications as many are transparent in the visible range. [3] Researchers have used polymers to perform significant modulation of the optoelectronic properties of hybrid devices via doping, passivation, dielectric screening, and capacitive effects. [4] These schemes illustrate that polymers can contribute multiple mechanisms to the polymer/2D TMD interface. In this work, the 2D TMD and polymer interface is assessed spectroscopically for three common polymers to evaluate the efficacy of each polymer in passivating the MoS_2 surface for photodetection applications. Evaluating this interface with spectroscopic methods, especially with ultrafast and dynamic pump probe measurements, mimics the physics occurring during photodetection operation and thus provides a clearer understanding of the fundamental physics at play.

For this study, a representative group of three commonly available polymers were chosen to understand the relative passivation effects: parylene N (Pa-N), polymethyl methacrylate (PMMA), and polyvinylidene difluoride-trifluoroethylene (PVDF-TrFE). Pa-N is an extremely inert polymer used frequently in organic electronics as a dielectric and biomedical devices as a chemical barrier. [5] PMMA is an electron beam photoresist frequently used to encapsulate 2D TMD devices for passivation. [6] PVDF-TrFE is an electroactive polymer that has been shown to be piezoelectric, pyroelectric, and ferroelectric, and as a result, is widely applied for flexible sensors. [7] PMMA and PVDF-TrFE have functional groups containing oxygen and fluorine that would be expected to better fix sulfur vacancies or provide doping than Pa-N.

Spectroscopic measurements including Raman spectroscopy, photoluminescence spectroscopy, and time-resolved terahertz spectroscopy (TRTS) were performed on these samples to observe the effect of polymer passivation on a MoS_2 monolayer. The photoluminescence measurements were done with a hyperspectral microscope to facilitate greater averaging of the photoluminescence response across the sample surface. The results of the Raman and photoluminescence spectroscopy show an n-doping effect on the MoS_2 spectra after coating with Pa-N and PMMA through a downshift in the Raman

peaks and a redshift in the photoluminescence peak. In the TRTS measurements, the peak of the response was higher for all polymer samples, which suggests more charge is generated in polymer passivated samples upon excitation either from doping or successful passivation. For PVDF-TrFE, the lifetime of the carriers was longer than any other sample. These results indicate that unpoled PVDF-TrFE best passivates the surface of the MoS₂ of the polymers tested. Further work is being done to understand the exact mechanism by which it passivates the surface, but it is suspected that the fluorine present in the PVDF-TrFE contributes electrons that help to fill the sulfur vacancies. This effect could be used successfully in photodetection to help improve the detectivity.

[1] H. S. Nalwa, *RSC Adv.*, vol. 10, no. 51, pp. 30529–30602, 2020. [2] W. Park et al., *Nanotechnology*, vol. 24, no. 9, pp. 095202, 2013. [3] J. Ma et al. *Appl. Phys. Lett.*, vol. 113, no. 1, 2018. [4] K. Cho et al., *ACS Nano*, vol. 13, no. 9, pp. 9713–9734, 2019. [5] S. Gholizadeh et al., *Scientific Reports*, vol. 13, no. 1, pp. 4262, 2023. [6] U. Ali et al., *Polymer Reviews*, vol. 55, no. 4, pp. 678–705, 2015. [7] B. Stadlober et al., *Chem. Soc. Rev.*, vol. 48, no. 6, pp. 1787–1825, 2019.

5:00 PM EL01.06.16

Improving Hazardous Gas Detection Behavior with Palladium Decorated SnO₂ Nanobelts Networks Cleber A. Amorim^{1,2}, Estacio P. Araújo³, Murilo P. Paiva², Lucas A. Moisés⁴, Kate C. Blanco⁵ and Adenilson J. Chiquito⁴; ¹Universidade Estadual Paulista, Brazil; ²University of São Paulo State–UNESP, Brazil; ³Bmo University of Technology, Czechia; ⁴Universidade Federal de São Carlos, Brazil; ⁵Universidade de São Paulo, Brazil

Transparent Conductive Oxides (TCOs) have been widely used as sensors for various hazardous gases. Among the most studied TCOs is SnO₂, due to tin being an abundant material in nature, and therefore being accessible for moldable-like nanobelts [1]. Sensors based on SnO₂ nanobelts are generally quantified according to the interaction of the atmosphere with its surface, changing its conductance [2]. The present study reports on the fabrication of a nanobelt-based SnO₂ gas sensor, in which electrical contacts to nanobelts are self-assembled, and thus the sensors do not need any expensive and complicated fabrication processes. The nanobelts were grown using the vapor–solid–liquid (VLS) growth mechanism with gold as the catalytic site [3]. The electrical contacts were defined using testing probes; thus, the device is considered ready after the growth process. The sensorial characteristics of the devices were tested for the detection of CO and CO₂ gases at temperatures from 25 to 75 °C, with and without palladium nanoparticle deposition in a wide concentration range of 40–1360 ppm. The results showed an improvement in the relative response, response time, and recovery, both with increasing temperature and with surface decoration using Pd nanoparticles. These features make this class of sensors important candidates for CO and CO₂ detection for human health.

Acknowledgments: This research was funded by FAPESP, grant number 2019/18963-6, CNPq 305656/2018-0 and 304090/2022-0. The authors are grateful for institutional support from the Department of Bi-osystems Engineering at São Paulo State University (UNESP), the Department of Physics at the Federal University of São Carlos (UFSCar), and the postgraduate program in Electrical Engineering (PPGEE/UNEPS).

Reference:

[1] E.P. de Araújo, C.A. Amorim, A.N. Arantes, A.J., *Appl. Phys. A*, 128, 1–8, 2022.
[2] T. Zhai, X. Fang, M. Liao, X. Xu, H. Zeng, B. Yoshio, D. Golberg, 6504–6529, 2009.
[3] C.A. Amorim, K.C. Blanco, I.M. Costa, E.

5:00 PM EL01.06.17

Tunable Ordering of 2D Tin on Silicon Caitlin V. McCowan and Shashank Misra; Sandia National Laboratories, United States

The optical and electronic properties of binary alloys can depend on atomic scale, site-to-site correlations. This is clearly illustrated in group IV alloys of tin, silicon, and germanium, where a direct bandgap is theoretically predicted in the random alloy, but an indirect bandgap is experimentally observed and thought to result from short range order (SRO). The balance between the deposition rates, temperature, and templating by the substrate influences the atomic-scale organization within thin films in intertwined ways, which is doubly challenging due to the atomic-scale characterization required for visualization. Here, we combine the ability to deposit materials with sub-monolayer coverage, apply heat in a separate controlled step, and *in situ* atomic-scale imaging of each discrete step with scanning tunneling microscopy (STM), to visualize the growth of Sn:Si.

The fundamental goal of our work is to systematically characterize SRO, to better understand its impact of electronic properties of a material. Existing STM work on Sn monolayers deposited on Si and Ge, in both 100 and 111 orientations, has shown the nucleation of different long-range surface reconstructions. How this influences growth is an open question, as Sn also surface segregates at moderate growth temperatures. By analyzing growth in discrete steps, comprised of Sn deposition, annealing, followed by Si deposition, and further annealing, using STM *in situ*, the dynamic nature of the thin film growth at the substrate interface can be better understood. This talk will focus on analyzing the STM data of different growth and heating combinations to reveal the forces driving ordering and surface segregation. This step-by-step mode of growth enables the creation of metastable configurations that manipulate the degree of order itself, which, in the future, can help in better understanding the relationship of order to optical and electronic properties.

SNL is managed and operated by NTESS under DOE NNSA contract DE-NA0003525

5:00 PM EL01.06.18

Fabrication of Gold Nanohole by Scanning Probe Lithography using a Sacrificial Layer and Its Applications Jeong-Sik S. Jo, Jinho Lee and Jae-Won Jang; Dongguk University, Korea (the Republic of)

Fabrication of a highly controlled gold nanohole (Au NH) is demonstrated through the use of a sacrificial layer (a tip-crash buffer layer) during scanning probe lithography. As the sacrificial layer, a poly(methyl methacrylate) layer is applied on an Au film to reduce scratches during nano-indentation by scanning probe lithography. Due to the relatively small scratches on the Au film, sub-50 nm Au NH and 15 nm gap between the Au NHs are obtained and the size of the Au NHs can be more precisely controlled compared to the Au NHs fabrication without the use of the sacrificial layer. Additionally, a multi-tip probe array was employed to showcase the mass production potential of the Au NH array. To demonstrate the applications of the Au NH array, MoS₂ hole array and conical-shaped silicon nanostructures are fabricated by using the Au NH array as a dry etching mask and a catalyst of metal-assisted chemical etching, respectively. Moreover, the Au nanoparticles trapped in Au NH shows a strong electric field by coupling between electromagnetic waves focused by the Au NH and enhanced by the Au NPs; the enhancement factor of surface-enhanced Raman scattering of 1.5×10^8 is obtained.

5:00 PM EL01.06.19

Novel Rapid Reprecipitation with Passivation Engineering for Fast Responsive and Durable Perovskite Photodetectors Byung-Gi Kim, Woongsik Jang, Ji Yun Chun, Jin Young Kim, Jihyun Lim, Zhao Yang, Suyeon Kim, Junmin Lee and Dong Hwan Wang; Chung-Ang University, Korea (the Republic of)

To develop the perovskite formation process, it becomes necessary to explore the fabricating principles underlying the photosensitive layers. To this end, various aromatic solvents with different functional groups (such as methylbenzene and chlorobenzene (CB)) are selected and analyzed during perovskite crystallization [1]. This demonstrates the excellent detectivity and fast response speed of the perovskite photodetector treated with CB, owing to its enhanced interfacial affinity with ETL and improved charge dynamic behavior. Thus, this showcases the optimization of morphological affinity and the realization of a fast and highly sensitive photodetector via selective use of anti-solvents. Meanwhile, the strategy of a highly sensitive photodetector fabrication is introduced via the relaxation effect of perovskite intermolecular exchangers [2]. Chloronaphthalene (CN) is utilized to fabricate high-quality photosensitive layers in a perovskite nucleation environment due to the unique properties of CN, such as its high boiling point and bulky naphthalene ring. Steric hindrance is thereby induced in the perovskite adduct step, delaying intermolecular interactions and creating a stable perovskite nucleation environment which promotes grain growth. Accordingly, higher crystallinity and larger grains are found in CN treated thin films. Based on this, photodetector performance is greatly improved due to the development of long grain boundary lengths as grain size increases. This is because the increase in shunt resistance and ohmic shunt within the device are suppressed, leading to improved charge transfer and recombination properties. This demonstrates improved device stability, with photodetector parameters observed for approximately 1000 hours. An advanced method for controlling the adduct phase of perovskite via 1,8-octanedithiol additive (1,8-ODT) engineering is presented [3]. In this process, 1,8-ODT is utilized as an anti-solvent additive, forming a coordination bond with Pb^{2+} ions and facilitating rapid perovskite phase conversion. The optimized photodetector exhibits low dark current density, as well as high responsivity and detectivity at 680 nm. Based on this, stability test reveals that the performance remains at approximately 90% even after approximately 260 hours. The properties of stable and recoverable perovskite photodetectors are introduced via moisture trap engineering [4]. Perovskite decomposition mechanism by moisture and the effect of moisture trap introduction are specifically proposed. The degree of hydration and perovskite photodetector characteristics are compared via solubility changes based on each H_2O content. As a result, stable photodetector driving characteristics are reproducibly observed despite moisture content when moisture trap engineering is introduced. Finally, we propose a highly sensitive photodetection strategy via passivation engineering, specifically silica nanocrystal encapsulation [5]. We designed quantum dots (QD@APDEMS) based on silane barriers with hydrophobic ligands. These quantum dots exhibit excellent dispersibility and durability, facilitating an effective film formation. This approach is applicable to bulk perovskite photosensitive layers. As a result, the introduction of QD@APDEMS leads to an improvement in charge dynamics, attributed to perovskite grain expansion and the formation of films with fewer defects. This effect can be attributed to grain boundary passivation via QD@APDEMS. Furthermore, the deep HOMO level of QD@APDEMS effectively suppresses hole charge carrier injection and shunt leakage.

- [1] Kim, B. G., et al. (2022). *Int. J. Energy Res.*, 46(7), 9748-9760.
- [2] Chun, J. Y., Kim, B. G., et al. (2022). *Appl. Surf. Sci.*, 591, 153207.
- [3] Kim, B. G., et al. (2023) *J. Alloys Compd (Special Issue)*, 172299.
- [4] Kim, B. G et al. (2022). *J. Ind. Eng. Chem.*, 116, 331-338.
- [5] Chun, J. Y., Kim, B. G., et al. (2023). *Carbon Energy*, e350.

5:00 PM EL01.06.20

Anchoring Hydroxyl Groups on Tin Oxide Nanowires Cleber A. Amorim^{1,2}, Estacio P. Araújo³, Ariano d. Rodrigues⁴ and Adenilson J. Chiquito⁴;

¹University of São Paulo State–UNESP, Brazil; ²Universidade Estadual Paulista, Brazil; ³Brno University of Technology, Czechia; ⁴Universidade Federal de São Carlos, Brazil

The nanowire functionalization process often takes place due to the need to have functional groups that enable or facilitate the chemical bonding between the inorganic material and the one intended for functionalization. In this study, we report two methods for anchoring hydroxyl groups: *i*) through nanowire growth using the vapor-solid (VS) approach, followed by treatment at various pH levels with sodium hydroxide (NaOH), and *ii*) nanowires grown using the vapor-liquid-solid (VLS) method in the presence of water vapor. Structural characterization was conducted through various techniques, including X-ray diffraction, scanning electron microscopy, UV-visible spectroscopy, Raman, and FTIR spectroscopy. Consequently, we observed the presence of OH groups on the material's surface that induced a variation in the material's bandgap when grown in the presence of water vapor. Furthermore, X-ray diffraction analysis revealed no significant alterations in the SnO_2 structure.

5:00 PM EL01.06.21

Analysis of Buried Interfaces for Device Technology by Soft and Hard X-Ray Photoelectron Spectroscopy Jennifer Mann; Physical Electronics, United States

X-ray photoelectron spectroscopy (XPS) has long been favored for its precision and reliability in discerning nanometer-thick overcoats on silicon surfaces. However, a challenge arises when using surface sensitive soft X-ray sources, as the areas of interest are often concealed beneath metal electrodes or oxide layers. While higher energy X-ray beams have enabled the detection of photoelectron signals from deeper layers, most of this analysis has been conducted at synchrotron radiation facilities. Recent advancements in lab-based hard X-ray photoelectron spectrometers (HAXPES), such as the PHI *Genesis*, have opened new accessible avenues for the routine examination of subsurface layers of technologically significant devices.

Angle-resolved or angle-dependent XPS and HAXPES (ADXPS/ADHAXPES) represent a potent, non-destructive method for providing a quantitative chemical composition depth profile for thin film structures, with thicknesses falling within the XPS or HAXPES sampling depth. This depth typically ranges from under 5-10 nanometers for an Al K alpha soft X-ray source to approximately 15-30 nanometers for a Cr K alpha hard X-ray source. Using *StrataPHI* analysis software, non-destructive XPS/HAXPES depth profiles can be reconstructed from angle-dependent photoelectron spectra. In the latest development of this software package (*StrataPHI 2.0*), spectra from both hard and soft X-ray sources can be combined. If the layer identity, order, and approximate thicknesses, are known, *StrataPHI* will recommend the X-ray source and transition to use for angle resolved measurements, reducing the overall data acquisition time.

This poster will highlight current cutting-edge and potential future directions for the integration of HAXPES and XPS in the investigation of semiconductors and nanoelectronics. It will underscore the advantages of utilizing hard X-ray sources in combination with a high-throughput, fully automated spectrometer located in a laboratory setting. These advantages encompass the ability to investigate concealed interfaces, such as electronic layers positioned beneath surface capping layers, and compositional studies within the bulk of materials and interfaces beyond the limited probing depth of soft X-rays.

5:00 PM EL01.06.22

Bismuth Surfactant Enhancement of Low-Temperature MBE-Grown GaSb Thin Films Pan Menasuta, John H. McElearney and Thomas E. Vandervelde; Tufts University, United States

Homoeptitaxial growth of GaSb is crucial for applications in mid-IR optoelectronics, such as thermal imaging, optical communication, LEDs, and thermophotovoltaic cells. At cold growth temperatures, the surface of GaSb degrades and can result in surface defects and device performance degradation. Yet, lower growth temperatures are favorable for reasons ranging from compatibility with other layers that require low-temperature growth to lowered bulk

mobility to prevent defects. Recently, we have demonstrated that bismuth surfactancy can lead to a smoother surface morphology of low-temperature-grown GaSb films. In this work, we examine the effects of bismuth surfactant at varying fluxes on the film quality of GaSb(100) grown at a cold temperature of 290 degree Celcius using molecular beam epitaxy (MBE).

A series of 200nm thick GaSb is grown via MBE in a Veeco GENxplor system in otherwise identical growth conditions except for the variation of the bismuth surfactancy flux used during growth. All films are grown at the stoichiometric point at ~0.4 monolayer (ML) per second. Bi:V flux as measured by the beam flux monitor (BFM) is varied from 0, no bismuth, to 0.2, where we have found an observable (1%) Bi incorporation. The effects of bismuth surfactant on the GaSb surface are characterized by atomic force microscopy (AFM). Raman spectroscopy is used to characterize and compare the film quality. Scanning electron microscopy (SEM) and energy dispersive X-ray spectroscopy (EDS) are used to analyze film surface and surface composition. High-resolution X-ray diffraction (HRXRD) was performed to confirm the bismuth incorporation into the films.

We concluded in our previous findings that bismuth substantially increases the two-dimensional Erlich-Schwöbel (ES) potential barrier of atomic terraces, inducing an upward adatom flux that contributes to surface smoothing. This work examines the effects of such bismuth surfactancy over a wide range of bismuth fluxes from none to some incorporation to understand how bismuth surfactancy can enhance the surface morphology and film structure of low-temperature grown GaSb. Furthermore, this research can potentially improve the growth of other homoepitaxial III-V semiconductor systems under non-ideal conditions and will contribute to the understanding of the bismuth surfactancy effects in dilute GaSbBi alloys.

5:00 PM EL01.06.23

Resolving and Engineering the Surface Chemistry of Superconducting Quantum Circuits [Mingzhao Liu](#); Brookhaven National Laboratory, United States

Superconducting qubits have emerged as one of the leading hardware platforms for realizing a quantum processor. Consequently, researchers have made significant effort to understand the loss channels that limit the coherence times of qubits made with superconducting materials. A major source of loss has been attributed to two level systems (TLS) that are present at the material interfaces in superconducting qubits. Recently, it has been shown that by substituting the superconductor niobium with tantalum, coherence times of superconducting qubits can be improved significantly. In this talk, we will discuss our studies on resolving the surface/interfacial chemical profiles at the metal-air and metal-substrate interfaces of superconducting tantalum films, to identify possible sources of TLS losses. The talk will cover the study of surface oxidation of tantalum using a combination of Hard X-ray Photoelectron Spectroscopy (HAXPES) and scanning transmission electron microscopy - electron energy loss spectroscopy (STEM-EELS), from which we can quantitatively determine the oxidation profile and atomic motifs across the ~3 nm-thick native oxide layer. We will also discuss the study of interfacial diffusion at the metal/substrate interface by synchrotron X-ray reflectivity. In the end, we will discuss a few surface and bulk engineering techniques that are used to achieve more perfect interfaces for less contribution to TLS loss.

5:00 PM EL01.06.24

Pd-Decorated SnO₂/CuO Composite Nanofiber Heterostructure as a Low ppm H₂S Gas Sensor [Shaik Ruksana](#); Indian Institute of Technology Hyderabad, India

Hydrogen sulphide (H₂S) sensing is crucial in various industrial and environmental contexts, including chemical processing, safety applications, and environmental monitoring. In this research, we introduce a hydrogen sulphide sensing structure composed of Pd-doped SnO₂/CuO composite nanofibers. The core innovation in our approach lies in the synergistic combination of electrospinning and DC sputtering techniques. Electrospinning offers nanofibers with a high surface area, tunable morphology, and enhanced gas diffusion, which significantly boosts the sensitivity of gas sensors. The XRD peaks depict the high crystalline nanofibers show rutile and monoclinic structures of SnO₂ and CuO present in the nanofibers. The surface roughness explained in FESEM analysis is the key feature for gas sensing as the diameter of the fibre reduced from 552 nm to 385 nm. The bare SnO₂/CuO nanofibers exhibited a response (Ra/Rg) of 6.95 when exposed to 50 ppm of H₂S gas at 200 °C. Pd sputtering acts as a catalyst that plays a dual role in enhancing sensitivity. Firstly, it catalytically splits hydrogen sulphide (H₂S) into SH and H radicals on its surface. This process liberates electrons, resulting in an abundance of charge carriers and significantly improving the sensor's response to H₂S. Secondly, Pd has the remarkable ability to split oxygen (O) molecules on its surface without the need for external energy. This process creates additional active sites on the sensor's surface, further enhancing its capacity to interact with gas molecules and leading to improved gas sensing performance. The presence of Pd (sputtered for 9 s) catalyses the metallization of SnO₂/CuO heterojunctions, leading to an increase in 8.5 response to 50 ppm of H₂S gas at 200 °C. This dual approach, combining the benefits of electrospinning and Pd sputtering, results in the exceptional sensitivity observed in our nanofibers. The unique properties of Pd-doped SnO₂/CuO nanofibers, such as their extraordinary sensitivity even for 0.5 ppm (response of 2.6) and selectivity for H₂S gas, make them valuable tools for various applications where the precise detection of hydrogen sulphide is paramount.

5:00 PM EL01.06.25

Enhanced Optoelectronic Properties of Green Perovskite Light-Emitting Diodes by Amino Acid-Doped PEDOT:PSS [Joonseok Kim](#), Min-Gi Jeon, Artavazd Kirakosyan, Subin Yun and Jihoon Choi; Chungnam National University, Korea (the Republic of)

Halide perovskites are promising materials for light-emitting diodes (LEDs) applications owing to their excellent optoelectronic properties such as long carrier diffusion length, high quantum yield, and facile bandgap tunability. Additionally, poly(3,4-ethylenedioxythiophene):polystyrene sulfonate (PEDOT:PSS) is commonly used as hole transport layer (HTL) in perovskite electronic devices owing to its high hole mobility, solution processability, and optical transparency. However, PEDOT:PSS can potentially degrade the adjacent layers owing to its acidic nature arising from a sulfonic acid group. Furthermore, the electrical conductivity and light emission characteristic of upper perovskite layer decrease due to phase transition from the crystalline phase to an undesired hydrated phase and decomposition of perovskite caused by the moisture absorbed by PSS chains from environment. Therefore, the acidic and hygroscopic properties of PEDOT:PSS reduce the operational stability and lifetime of perovskite LEDs (PeLEDs). Herein, we report the pH neutralization of PEDOT:PSS by adding basic amino acids, which are arginine, lysine, and asparagine. The addition of amino acids can not only modulate the pH of PEDOT:PSS, but also provide nucleation sites to perovskite crystals, and passivate the defects at the interface of PEDOT:PSS and perovskite. Thus, the addition of amino acids results in enhanced stability and photoluminescence quantum yield of the perovskite nanocrystalline layer. When the amino acid-doped PEDOT:PSS is adopted as HTL layer in PeLEDs, the external quantum efficiency (EQE) of green-emitting PeLEDs ($\lambda=518$ nm) is improved from 8.99 to 11.96 % without a shift of electroluminescence spectrum. These results demonstrate that the aforementioned disadvantages of PEDOT:PSS can be overcome, expanding the scope of application of PEDOT:PSS as HTL.

5:00 PM EL01.06.26

Enhanced NIR Photoresponse in Nanostructured Sb₂Se₃ Film on Micro-Pyramidal Silicon Substrate [Yogesh Singh](#)^{1,2}, Avriti Srivastava^{1,2}, Sanjay K. Srivastava^{1,2} and Vidya Nand Singh^{1,2}; ¹Academy of Scientific and Innovative Research, India; ²CSIR- National Physical Laboratory, India

The increasing demand for high responsiveness in imaging technology and optical communication has driven the development of photodetectors with

enhanced performance. Plasmonic sensor technologies have shown promise, but they often suffer from low optical absorption and inefficient charge carrier transport. Addressing these challenges, we present a novel approach utilizing Sb_2Se_3 , a light-sensitive material with a high absorption coefficient, in the design of a near-infrared (NIR) photodetector.

We have developed an efficient, scalable, and cost-effective NIR photodetector by depositing a nanostructured Sb_2Se_3 film onto a p-type micro-pyramidal silicon substrate, fabricated through a wet chemical etching process. Pump-probe spectroscopy was employed to investigate the impact of annealing on Sb_2Se_3 films, shedding light on their suitability for advanced photodetector applications. We excited both annealed and unannealed samples near the band gap at 650 nm (1.9 eV) with an average power of 1mW, probing the near-infrared (NIR) region spanning 800-1400 nm. The recorded kinetics at various probe wavelengths which provides crucial insights into the behavior of these materials.

The transient absorption kinetics were captured over an extended time window ranging from 0 to 6 nanoseconds. The entire spectrum is blue-shifted, a phenomenon attributed to lattice heating induced by the femtosecond laser—a well-known effect termed the Burstein-Moss shift. A negative band, centered around 850 nm, represents photoluminescence (PL) emission spectra with a longer duration due to defects within the band structure, as evidenced by a time constant (τ_4) exceeding 5 nanoseconds, accounting for nearly half of the carrier concentration. Notably, a broad photo-induced absorption (PIA) region spanning 910-1150 nm is observed, characterized by rapid decay within 1 or 2 picoseconds. The fastest time constant (τ_1) of approximately 1 picosecond is attributed to the thermal relaxation of carriers within the conduction band and the associated surface states, while a subsequent time constant (τ_2) of around 25 picoseconds adds further depth to our understanding. This study underscores the importance of annealing in optimizing the properties of Sb_2Se_3 films and contributes valuable insights into the dynamics of carrier relaxation and the role of defects in these materials. These findings are instrumental in advancing the development of high-performance photodetectors and related technologies. Our findings reveal that at the optimized thickness of the Sb_2Se_3 layer, the micro-pyramidal silicon substrate significantly enhances responsivity, achieving nearly double the performance compared to Sb_2Se_3 deposited on flat silicon or glass/ Sb_2Se_3 samples at a wavelength of 1064 nm (power density = 15 mW/cm²). Notably, the micro-pyramidal silicon-based device operates at zero bias voltage, paving the way for self-bias devices.

We report the highest specific detectivity of 2.25×10^{15} Jones at a power density of 15 mW/cm² and a bias voltage of 0.5 V. This superior performance is attributed to the field enhancement provided by the Kretschmann configuration of the silicon pyramids, creating "hot spots" at the Si/ Sb_2Se_3 junction. With a remarkable responsivity of 47.8 AW⁻¹, our design demonstrates its suitability for scalable and cost-effective plasmonic-based NIR photodetectors, addressing the need for high responsiveness in advanced imaging and optical communication applications.

5:00 PM EL01.06.27

Dark Current Suppression based on Theoretical and Experimental Investigation of Barrier Energy between Transparent Anode and Photosensitive Layer via Material Design in Organic Photodetector Woongsik Jang and Dong Hwan Wang; Chung-Ang University, Korea (the Republic of)

Organic semiconductor-based photodetectors (OPDs) have attracted a variety of attention as a substitute for photodetectors with conventional inorganic materials for image sensors with high sensitivity. The organic semiconductor has tunable optical, electrical and mechanical properties by designing their structure. OPDs are evaluated by both dark current and photocurrent. However, research to investigate the causes of dark currents has been insufficient.

Herein, we introduce non-fullerene acceptors which have opened new avenues with regard to improve the figure of merits of OPDs including wide absorption and fast response. [1] To investigate the effect of electron acceptors on dark current, OPDs are fabricated according to the types of acceptors in photosensitive layers, because anodic charge injection to acceptors has a major role of dark current under an applied reverse bias, which influences the performance of organic photodetectors. [2] The origin of dark current generated in an organic photodetector is observed through the modeling between current and voltage. To elucidate the dominant mechanism, the barrier energies in anodic contact are set from 0.6 to 1.0 eV using photosensitive layers composed of different acceptors. The current density–barrier energy characteristics measured under reverse bias strongly suggests the main source of dark current. The linear relationship observed in the current density–voltage characteristics also confirm tunnelling effects rather than thermionic emission. Consequently, the non-fullerene acceptor-based OPDs show a high detectivity and a faster response time, because of the excellent dark current suppression of the carrier injection and the low trap density of non-fullerene acceptor. Eh-IDTBR (ethylhexyl-rhodanine-benzothiadiazole-coupled indacenodithiophene) has been employed in OPDs and the results have been compared with fullerene derivatives (PC₇₁BM), in combination with electron donor PBDTTT-EFT material. eh-IDTBR based OPDs has shown excellent detectivity in comparison to PC₇₁BM based OPDs due to suppressed injected carriers and trap density. Furthermore, morphological and electrical changes depending on thermal and electrical stress have been investigated in the two different acceptor systems.

Carbon nanotubes (CNTs) have attracted huge attention owing to their outstanding flexibility, transparency, and conductivity, so that CNTs can replace an indium-tin oxide (ITO) for efficient curved and flexible photodetectors. Especially, CNTs-based electrode with high chemical resistance is the excellent candidate for organic photodetectors (OPDs), because the devices have been fabricated through solution process. In addition, The OPDs require dense nanotubes arrays to form top layers suitably to enhance the performance. The CNT electrode with high transmittance reduces dark current below pA level and exhibits the higher detectivity than that of ITO-based devices owing to its deep work function related with the high electron injection barrier energy.

[3] The flexible OPDs fabricated utilizing the CNT electrode stably operate after 500-bending tests. By investigating the charge injection mechanism according to barrier energy between transparent anode and photosensitive layer in organic photodetector, This work can help devise an effective strategy to suppress dark current for effective organic photodetector device implementation with increase of process yield and reduction of unit prices.

[1] Jang et al., Adv. Funct. Mater., 2020, 30, 2001402

[2] Jang et al., Adv. Funct. Mater., 2023, 33, 2209615

[3] Jang et al., Nano Today, 2021, 37, 101081

SESSION EL01.07: Virtual Session

Session Chairs: Silvia Armini and Catherine Dubourdieu

Tuesday Morning, May 7, 2024

EL01-virtual

8:00 AM EL01.07.01

Printable Self-Powered Electrochemical Oxygen Sensor Tianyi Liu, Vijaya Kayastha, Chandler Murray, Brock Morris, David Taggart and Jiadeng Zhu; Brewer Science, United States

Oxygen sensors have a wide range of applications, from monitoring respiration and oceanography to food and pharmaceutical industries. These sensors measure the oxygen concentration in a gas or liquid, typically air or exhaust gases, and play a crucial role in improving efficiency, reducing emissions, and ensuring safety and environmental compliance. Screen printing is a widely adopted method for producing energy storage devices, especially in printed electronics. It creates patterns of conductive materials, such as electrodes and current collectors, on various substrates. In this work, an electrochemical

sensor was fabricated using printing technology for O₂ detection at room temperature. This design consists of zinc metal as an anode and carbon-based material as a cathode. The oxygen concentration can be observed in terms of electrical signals. A complete product development process has been demonstrated, including material screening, hardware design, and sensor tests. The resultant sensor exhibits a fast response (T₉₀ ~2.7 s) and high sensitivity. Furthermore, the sensor fabrication is an environmentally friendly process with minimized consumption of toxic materials, such as Pd, and release of pollutants.

8:15 AM EL01.07.02

Efficiency Enhancement of Bifacial Sb₂Se₃ Photovoltaic Devices with Cu₂O Back Buffer: A Modeling Study Sanghyun Lee; University of Kentucky, United States

Thin-film solar cells based on an Antimony Selenide (Sb₂Se₃) absorber layer have been emerging as third-generation photovoltaic devices with promising properties. A Sb₂Se₃ absorber has 1.1 eV bandgap, a high absorption coefficient at visible light (>10⁵ cm⁻¹), good carrier mobility (<15 cm²/Vs), long carrier lifetime (<67 ns), and simple binary compound with high vapor pressure and low melting point (550 °C).

Due to the versatility of Sb₂Se₃ thin-films, Sb₂Se₃ has been studied by varying compositions and concentrations of incorporated elements for various applications. In particular, Ge-incorporated Sb₂Se₃ thin-films (hereafter, Ge-Sb₂Se₃) have been reported as a good polycrystalline absorber candidate with Ge concentration <15 %.

To further improve the efficiency of polycrystalline Sb₂Se₃ devices, both front and rear-side illumination could be captured by utilizing the bifacial device configuration of Sb₂Se₃ devices. However, developing bifacial devices has stagnated in thin-film photovoltaic technologies due to the short carrier lifetime (<100 ns) as compared to polysilicon counterparts. For instance, the record efficiency of rear-side illumination is reported as 9.2 % for CIGS, 8.0 % for CdTe, and 9.0 % for Kesterite solar cells, respectively. Designing a bifacial photovoltaic structure has been studied by several research groups and recently, a few studies of thin-film devices with a thin absorber (<2 μm) such as CIGS, CdTe, and Kesterite have been reported. By carefully selecting a transparent back buffer layer coupled with a transparent conducting back contact, a bifacial device configuration needs to be optimized in thickness and doping concentration to maximize a bifaciality factor, which is the ratio of rear-to-front efficiency to the same irradiation.

In this contribution, we have theoretically studied bifacial Ge-Sb₂Se₃ devices after fabricating Ge-Sb₂Se₃ absorber thin-films, followed by characterizing the optical properties. The optical properties of a Ge-Sb₂Se₃ absorber layer were used as input parameters for modeling and numerical simulation of the bifacial device configuration. For our analytical simulation, we have used in-house MATLAB modeling suites that have been developed in our group. We have proposed new bifacial devices to improve the overall device performance and optimized developed device models with various parameters. With a Cu₂O back buffer layer, the best efficiency of front-side illumination is 19.7 %, Voc (744.4 mV), Jsc (40.14 mA/cm²), and FF (66.1 %). For the rear-side illumination, the performance is 13.0 %, Voc (724.5 mV), Jsc (31.6 mA/cm²), and FF (56.7 %). Consequently, the bifaciality factor is 66 %.

8:30 AM *EL01.07.03

Hf_{0.5}Zr_{0.5}O₂/Al₂O₃ Bilayer Ferroelectric Tunnel Junctions: Investigations of The Chemistry of Interfaces and Films by HAXPES Wassim Hamouda¹, Ines Haeusler², Muhammad Hamid Raza¹, Keerthana S. Nair^{1,3}, Adnan Hammud⁴, Christoph Koch², Veeresh Deshpande¹, Christophe Schluter⁵ and Catherine Dubourdieu^{1,3}; ¹Helmholtz-Zentrum Berlin, Germany; ²Humboldt-Universität zu Berlin, Germany; ³Freie Universität Berlin, Germany; ⁴Fritz-Haber Institute of The Max-Planck Society, Germany; ⁵DESY, Germany

The discovery of ferroelectricity in hafnium dioxide-based ferroelectrics has revived the research on ferroelectric devices. In particular, the Hf_{0.5}Zr_{0.5}O₂ (HZO) solid solution compound provides an opportunity for back-end-of-line integrable devices due to its low crystallization temperature (< 450°C). Among the different ferroelectric-based devices, ferroelectric tunnel junction (FTJ) memories are well suited for emerging neuromorphic applications due to their low power consumption, non-volatile nature, and potential to achieve multiple resistance states through domain partial switching of domains. As the conventional metal-ferroelectric-metal FTJ stack requires an ultra-thin ferroelectric layer (1-3 nm), it is quite challenging to fabricate with a polycrystalline Hf_{0.5}Zr_{0.5}O₂ (HZO) layer. With a bilayer stack architecture based on HZO/Al₂O₃, a thicker HZO can be used (10 nm) and can still provide a high ON current as the tunneling occurs through the thin dielectric layer (~3 nm) [1]. The performance of such devices rely on the ability to stabilize a large switchable ferroelectric polarization in HZO, which is interfaced - on one side - with a dielectric and not a metal. The remanent polarization and the overall device performance also depends strongly on the nature of the bottom and top electrodes, on the presence of interfacial layers (whether intentional or not), and on the oxygen vacancies' content and distribution.

In this study, we discuss the role of processing conditions on the ferroelectric polarization and device performance of TiN / 10 nm HZO / 3 nm Al₂O₃ / W FTJs. The HZO is crystallized at 400[endif]->C for full CMOS back-end of-line compatibility. As observed in the electrical characterization, the annealing conditions of the ultrathin Al₂O₃ tunneling barrier plays a key role in the ability to stabilize and switch the polarization in the HZO layer. Hard X-ray photoelectron spectroscopy (HAXPES) was used to probe the bonds and chemistry of the different buried interfaces and layers in the stack and to quantify the oxygen vacancy content. Measurements at different synchrotron beam angles were performed to probe various depths of the HZO layer. The top Al₂O₃/W layers were investigated by combining laboratory XPS with low energy Argon ion sputtering. Complementary information was gained from scanning transmission electron microscopy (STEM) and electron energy loss spectroscopy (EELS). A strong difference in the oxygen vacancy profiles in HZO is found depending on the stack fabrication conditions. The dependence of the remnant polarization with the voltage pulse width points to the major role of charge traps in minimizing the depolarizing field. We will discuss the influence of the processing conditions on providing the needed traps for screening charges, which is essential in stabilizing the ferroelectric polarization in bilayer HZO-based FTJs.

[1] V. Deshpande *et al.*, Solid State Electronics 186, 108054 (2021).

9:00 AM EL01.07.04

Current-Voltage Versus Time: How Metallic Coatings affect Conductive Atomic Force Microscopy Interpretation on Resistive-Switching Metal Halide Perovskites Holland Hysmith¹, Neus Domingo Marimon², Sabine M. Neumayer², Stephen Jesse² and Mahshid Ahmadi¹; ¹University of Tennessee Knoxville, United States; ²Oak Ridge National Laboratory, United States

Metal halide perovskites (MHPs) are commonly studied for their solar cell applications yet are a potentially effective switching medium in memristors. A memristor by design can remember its state after external excitation is removed. This function is helpful in reducing the von Neumann bottleneck in computing by creating more powerful and compact environments for the modern world. However, MHPs are limited by their lack of commercial scaling and puzzling material phenomena that are not easily understood by scientists. To address this, using techniques like atomic force microscopy (AFM) to study MHP thin film mechanisms can help understand, quantify, and optimize MHP efficiency.

When using AFM techniques like conductive AFM (c-AFM), valuable information such as photocurrent, dark current and I-V hysteresis can be uncovered in MHP films. Although, when measuring surface morphology with an AFM tip, many factors have been reported to influence the perception of its findings: surface charges, artifacts, charge injection, wearing of the tip, etc. The AFM tip metal coating can also create undesirable and unpredictable interactions with the sample surface, especially for volatile organics such as perovskites. Therefore, we measured how cyclic voltammetry changes over time as a function of AFM metallic tip coatings on resistive-switching FACsPbI₃ thin films. This approach of c-AFM coupled with heterodyne kelvin probe

This searchable program is up-to-date as of April 15th, 2024.

force microscopy (KPFM) and time-of-flight secondary ionization mass spectrometry (ToF-SIMS) reveals the local electrical, potential, and chemical changes in the film.

Common AFM metallic coatings for c-AFM applications like platinum, diamond, and iridium were used in this study. I-V maps showed changes in the Schottky barrier with each respective tip coating and alterations to resistive switching qualities over time. Disruptions during scanning shows the potential for dragging surface charges (e.g. I_2^-) and affecting the magnitude of current measured. KPFM was measured after c-AFM to demonstrate changes in local potential among different applied sample voltages and tip coatings. Lastly, ToF-SIMS revealed multi-dimensional chemistry at the film scanning sites. The use of tools such as AFM is vital for improving the future of MHP memristors, but understanding the limitations from data interpretation and application is important for comprehending what is found.

9:05 AM EL01.03.03

Enhanced Sub-Band Gap Photosensitivity by an Asymmetric Source-Drain Electrode Low Operating Voltage Oxide Transistor [Utkarsh Pandey](#); Indian Institute of Technology (BHU), Varanasi, India

Electrical characteristics of a thin film transistor (TFT) can be tuned by using an asymmetric work function source-drain (S-D) electrode. However, to realize the effect of this asymmetric S-D electrode, a low operating voltage TFT is required. On the other hand, sub-bandgap photosensitivity of a photodetector required a suitable material interface engineering. In this work, an asymmetric S-D electrode has been used to enhance the photosensitivity of a solution processed low voltage driven metal oxide TFT. An ion-conducting LiInSnO_4 thin film has been used as the gate dielectric of this TFT that limits the operating-voltage of this TFT within 2 V whereas ZnO has been used as the channel semiconductor. This asymmetric S-D electrode of TFT allows a selective carrier (electron or hole) injection and collection from the channel. As a consequence, the On/Off ratio and photosensitivity of the device improve significantly. The On/Off ratio of asymmetric TFT is 10^2 times greater than symmetric TFT. More interestingly, the subthreshold swing (SS) of this asymmetric S-D electrode TFT (210 mV/decade), was reduced more than four times than that of the symmetric electrode (975 mV/decade) device. The $\text{LiInSnO}_4/\text{ZnO}$ interfaces states which has been identified in the UV-Vis absorption of $\text{LiInSnO}_4/\text{ZnO}$ thin film is capable to generate sub-band gap photocurrent in the devices. As a consequence, this ZnO based phototransistor can detect light efficiently ranging from 400 to 800 nm. Overall, photosensitivity of this asymmetric S-D electrode TFT has been enhanced by ~ 405 and ~ 377 times under red and blue illumination respectively with respect to the symmetric S-D electrode TFT whereas the detectivity of the device increases by ~ 10 and ~ 4 times

SYMPOSIUM EL02

Towards Atomically Precise Colloidal Materials for Conventional and Quantum Optoelectronics
April 23 - May 7, 2024

Symposium Organizers

Yunping Huang, CU Boulder
Hao Nguyen, University of Washington
Nayon Park, University of Washington
Claudia Pereyra, University of Pennsylvania

* Invited Paper
+ JMR Distinguished Invited Speaker
^ MRS Communications Early Career Distinguished Presenter

SESSION EL02.01: Breakthroughs in Colloidal Quantum Dots for Photonics
Session Chairs: Hao Nguyen and Nayon Park
Tuesday Morning, April 23, 2024
Room 347, Level 3, Summit

10:30 AM *EL02.01.01

Precision Colloidal Synthesis: How Far Can it take us in Realizing Advanced Quantum Light Sources? Jennifer Hollingsworth and [Eric Bowes](#); Los Alamos National Laboratory, United States

Core/shell heterostructuring of semiconductor quantum dots (QDs) provides a convenient platform for exploring the limits of synthetic control over quantum optical properties. Even "simple" control of component composition and feature size in a nano-heterostructure affords opportunities for band-structure engineering, which leads to altered photoluminescence properties, including emission color, lifetime, photostability, etc. More interestingly, however, colloidal synthesis provides possibilities for nearly-atomically precise manipulation of the core/shell interface. This can include alloying, introduction of defects or dopants, and selective facet growth. Here, I will describe several examples of how advanced colloidal synthesis can be used to finely tune nanoscale heterostructure to realize novel properties: dual-color emission, charged-state versus excitonic emission, and resistance to photobleaching by either dimming or catastrophic failure. First, we show that adventitious or intentional introduction of hole traps at the InP/CdSe QD interface, as well as arm length and arm diameter tuning in CdSe/CdS core/arm tetrapods, can provide conditions for realizing two-color excitonic or multi-excitonic emission, respectively, both potentially characterized by suppressed blinking. Second, we assign for the first time the synthesis-structure-function correlations for non-blinking CdSe/CdS core/shell QDs to define the limits of "on-demand" single-photon production under thermal or high-photon-flux

stress. The new insights show, e.g., the relationships between shell defects and charged-state emission and between interfacial alloying and photobleaching resistance, each precisely controlled by synthesis conditions. Taken together, the different nano-heterostructure systems reveal the opportunity for achieving designed quantum optical properties through synthesis, while the remaining limitations expose where alternative strategies might be needed to realize, e.g., transform-limited, ultrafast single-photon emitters.

11:00 AM *EL02.01.02

Soft-Electronic Quantum Dot Light-Emitting Diodes [Taeghwan Hyeon](#)^{1,2} and [Dae-Hyeong Kim](#)^{1,2}; ¹Seoul National University, Korea (the Republic of); ²Institute for Basic Science, Korea (the Republic of)

We demonstrated a wearable red-green-blue (RGB) colloidal quantum dot light-emitting diode (QD LED) array with high resolution using a novel intaglio transfer printing technique (*Nature Commun.* **2015**, 6, 7149). We also reported transparent QD LEDs with extremely high luminance and transmittance (*Adv. Mater.* **2018**, 30, 1703279). We reported a novel device design and fabrication method using metal-based etch-stop layers and a laser-assisted patterning for 3D foldable QD LEDs (*Nature Electronics* **2021**, 4, 671). Shape-tunable multiplexed phototransistor array was fabricated using an intrinsically stretchable and color-sensitive semiconducting nanocomposite consists of size-tuned quantum dots, blended in a semiconducting polymer within an elastomeric matrix (*Nature Nanotech.* **2022**, 17, 849). We report novel material and device strategies for the intrinsically-stretchable quantum dot light-emitting diode (*is*-QLED) (*Nature Photon.* In revision). We reported on the design and synthesis of highly stable, photoluminescent, and catalytically active suprastructures of (CdSe)₁₃ nanoclusters (*Nature Mater.* **2021**, 20, 650).

11:30 AM *EL02.01.03

Engineered Colloidal Quantum Dots as Universal Optical Gain Media for Solution- and Solid-State Lasers and Laser Diodes [Victor I. Klimov](#); Los Alamos National Laboratory, United States

Colloidal quantum dots (QDs) are attractive materials for applications in laser technologies. In addition to being compatible with inexpensive and easily scalable chemical techniques, they offer multiple advantages derived from a zero-dimensional (0D) character of their electronic states. These include a size-tunable emission wavelength, low optical-gain thresholds, and high temperature stability of lasing characteristics.

So far, all validated reports on colloidal QD lasing employed optically excited close-packed solid-state QD films. Two classes of QD lasers that are yet to be realized are liquid-state optically pumped devices and electrically pumped solid-state lasers (laser diodes). In both cases, a principal obstacle is very fast Auger recombination of optical-gain active multicarrier state. One consequence of fast Auger decay is the existence of a minimal (critical) QD concentration required for lasing. Due to solubility limits, this concentration is difficult to attain with liquid-state samples. Therefore, up to now, QD lasing devices have employed high-density solid-state films. Fast Auger delay also creates a serious problem when one tries to realize lasing with electrical pumping. In particular, it mandates the use of prohibitively high current densities for maintaining QDs in the inverted multicarrier state.

Here we describe how we overcome the challenge of fast Auger recombination using meticulously engineered hetero-QDs. To impede Auger decay, we modify an optical gain state so as to reduce the number of available Auger pathways. Further, we employ compositional grading of the QD interior to smoothen carrier confinement potentials and whereby suppress the strength of individual Auger transitions. As a result, our engineered QDs exhibit long optical gain lifetimes (nanosecond time scales) while still maintaining strong 3D quantum confinement. We use our novel QDs to demonstrate new types of lasing devices including prototype laser diodes and widely tunable dye-like liquid-state lasers.

SESSION EL02.02: Magic-Sized Clusters and Atomically Precise Structures
Session Chairs: Grant Dixon and Hao Nguyen
Tuesday Afternoon, April 23, 2024
Room 347, Level 3, Summit

1:30 PM *EL02.02.01

Prenucleation Clusters of Colloidal Semiconductor CdTe Quantum Dots [Kui Yu](#); Sichuan University, China

The synthesis of colloidal semiconductor quantum dots (QDs) keeps developing during the past 40 years, with limited attention paid to the evolution of prenucleation clusters. With CdTe as a model system from a non-injection-based approach, we show that prenucleation clusters form and isomerize prior to the nucleation and growth of QDs. We propose that the prenucleation clusters evolve via chemical self-assembly of Cd and Te precursors. The prenucleation clusters are relatively optically transparent, which are covalent inorganic polymers. They can transform to absorbing magic-size clusters (MSCs). Thus they are called precursor compounds (PCs) of MSCs. We placed prenucleation-stage samples obtained at 25, 45, or 80 °C into a mixture of cyclohexane (CH) and octylamine (OTA) at room temperature. We observed the presence of MSC-371, MSC-417, or MSC-448 which displayed optical absorption peaking at 371, 417, or 448 nm, respectively. Based on our experimental data, we thus hypothesize that in the reaction PC-371 forms at 25 °C, and isomerizes to PC-417 at 45 °C and to PC-448 at 80 °C. These PCs and MSCs form a group of (quasi) isomers. Our findings suggest that a multi-step non-classical model shall be taken into account to understand the nucleation and growth of colloidal QDs, instead of the one-step classical LaMer model. Furthermore, the PC-assisted transformation is the underlying cause for the step-wise spectral shift for MSCs instead of a continuous pattern.

2:00 PM EL02.02.02

The Isomer Chemistry of Magic-Sized Clusters [Youngjae Ryu](#); Pohang University of Science and Technology, Korea (the Republic of)

Magic Sized Clusters (MSCs) are small sized inorganic nanoparticles which are less 2 nm in size with a thermodynamically stable structure. Their highly surface-dependent properties facilitate the existence of various types of isomers. Particularly, isomers which exhibit dissymmetric circular dichroism signals, also known as optical isomers, are of great importance. Chiral MSCs with large circular dichroism signals will be discussed as compared to other chiral semiconductor nanocrystals. To investigate the chiroptical origins of our chiral MSCs, characterizations including XRD and Raman were conducted to explore ligand geometry and structural properties. By surface characterizations including FT-IR and TGA, we have found that particular mode of surface ligand binding is critical for the chirality. Low crystal symmetry of MSCs is thought to induce the large transition dipole moment of MSC, which in turn yields high chiroptical activity. In contrast, similar sized QDs showed silent chirality presumably due to the high crystal symmetry and the consequent low transition dipole moment. Propagation of chirality using chiral MSCs as the building block will be also addressed. We believe that unique characteristics of MSCs may open a new avenue in designing and synthesizing unprecedented chiroptical materials.

2:15 PM EL02.02.04

Atomically Precise Indium Arsenide Magic-Sized Cluster [Mahmin Choi](#)¹, Jibin Shin¹, Doeun Shim², Joongoo Kang² and Sohee Jeong^{1,1};
¹Sungkyunkwan University, Korea (the Republic of); ²DGIST, Korea (the Republic of)

In the domain of atomically precise nanoscale science, clusters serve as intermediate assemblies of atoms or molecules, stabilized with organic ligands. These formations, distinctly larger than a single atom yet considerably smaller than bulk materials, exhibit physicochemical properties divergent from established material systems. The elucidation of their structure is paramount because these clusters provide an ideal platform to clarify the intricate relationship between structure and physicochemical properties. Recently, magic-size clusters (MSCs) were discovered; these are atomically precise semiconductor clusters, and their structures have been unveiled. To clarify the relationship between the structure and physicochemical properties, the synthetic method, isolation, and characterization techniques must be refined. The Indium arsenide (InAs) quantum dot has emerged as a promising material for various infrared applications. During the synthesis of the InAs quantum dot, the presence of InAs MSC, as indicated by distinctive absorption peaks, was investigated. However, the isolation and characterization of InAs MSC have not been reported until now.

Herein, we synthesized and isolated atomically precise InAs MSCs to scrutinize their structure. With the optimal synthetic temperature, the InAs MSC revealed two distinct optical transitions. To gain a theoretical understanding, we modeled the InAs MSC using density functional theory (DFT) calculations, identifying a structure with notable stability. This model displayed two optical transitions, from HOMO to LUMO, consistent with the optical transitions we observed. The X-ray diffraction spectrum also aligned with the simulation results. For a deeper atomic-level understanding, we employed X-ray absorption spectroscopy and characterized the cluster using X-ray absorption fine structure (XAFS) techniques. By comparing with an InAs quantum dot, which is larger than the InAs MSC, we noted increases in the In-As peaks and decreases in the In-O peaks, attributable to size-dependent surface-to-volume ratios. Furthermore, spectral intensity offered insights into coordination numbers. Our fitting analysis of the XAFS spectrum enabled precise estimations of coordination numbers for various bonds. Notably, the coordination number for the In-As bond in MSC agreed with our computational predictions. Collectively, these results not only validate our theoretical model but also deepen our understanding of the structural and optical properties of InAs MSCs.

2:30 PM EL02.02.05

Structure and Reactivity of Atomically-Precise III-V Nanoclusters [Soren Sandeno](#)¹, Kyle Schnitzenbaumer², Sebastian Krajewski¹, Ryan Beck¹, Dylan Ladd³, Kelsey Levine³, Damara G. Dayton³, Michael Toney³, Werner Kaminsky¹, Xiaosong Li¹ and Brandi M. Cossairt¹; ¹University of Washington, United States; ²Transylvania University, United States; ³University of Colorado Boulder, United States

Advances in the synthesis of III-V quantum dots, including InP and InAs, have led to their development for current- and next-generation solid-state lighting, wide color gamut displays, and infrared optoelectronics. The most widely adopted synthesis of these III-V quantum dots involves indium carboxylates and E(SiMe₃)₃ (E = P, As) and is understood to proceed through the formation of metastable, atomically-precise intermediates that are often referred to as clusters. In this work, we report that the surface chemistry of In₃₇P₂₀(O₂CR)₅₁ can be leveraged to modify the core structure and control the reactivity of the clusters. Bulkier surface ligands hinder P(SiMe₃)₃ diffusion and allow for the stabilization and isolation of In₂₆P₁₃(O₂CR)₃₉, which has been characterized by single-crystal X-ray diffraction. When employing As(SiMe₃)₃ in an identical synthesis, no cluster forms and instead the inclusion of an L-type phosphine ligand is required to isolate an atomically-precise material. The surface and core of the InAs cluster are characterized, revealing important contrasts with InP with implications for understanding the landscape of accessible binary semiconductor clusters.

2:45 PM BREAK

3:15 PM *EL02.02.06

Exploring The Chemical Paths to Doped II-VI Magic Size Clusters [Kevin Kittilstved](#), Hyunggu Kim and Jillian Denhardt; University of Massachusetts Amherst, United States

The introduction of targeted, substitutional chemical dopants in a semiconductor lattice is a useful strategy to impart new functionality and in some instances emergent phenomena when synthesized at the nanometer lengthscale. One major challenge in the quantum dot field has been overcoming the thermodynamic penalty associated with introducing an impurity ion into the critical nucleus, which typically leads to an undoped core and dopants only doped in the shell or surface of the nanocrystal. The role of metastable magic size clusters in the synthesis of various quantum-confined nanostructures including doped nanostructures has received much attention in the past decade. In this talk, we will explore the common routes to prepare (doped) magic-size nanoclusters and introduce an alternate method that employs (doped) molecular clusters as single-source precursors.

3:45 PM *EL02.02.07

Doped InP Magic-Sized Clusters [Sungjee D. Kim](#); POSTECH, Korea (the Republic of)

Magic-sized clusters (MSCs) can be isolated as intermediates in quantum dot (QD) synthesis, and they provide pivotal clues in understanding QD growth mechanisms. Two families are introduced that have chlorine or zinc incorporated InP MSCs. In each family line, different MSCs could be either directly synthesized or could be converted from one to another. As the conversion proceeded, evolution from uni-molecule-like to QD-like characters was observed. Early stage MSCs showed active interstate conversions in the excited states, which is characteristics of small molecules. Later stage MSCs exhibited narrow photoinduced absorptions at lower-energy region like QDs. The crystal structure also gradually evolved from polytwistane to more zinc-blende. Other halide doped InP MSCs and Ga doped MSCs will be also discussed. MSCs show many interesting properties such as isomerization induced by adsorption of small molecules. Reversible and dramatic isomerization of MSCs will be introduced. Chiral properties of MSCs will be also discussed.

4:15 PM *EL02.02.08

Steering Doping Polarity from Synthesis Onset: Using II-V Clusters in InAs Colloidal Nanocrystals for Infrared Optoelectronics [Sohee Jeong](#); Sungkyunkwan University, Korea (the Republic of)

In the realm of nanocrystal-centric optoelectronic devices, control over the carrier type control is essential, however, integrating foreign atoms into semiconductor nanocrystal lattices remains challenging. A recent standout in this semiconductor lattice domain, Indium Arsenide (InAs) colloidal nanocrystals, has been in great attention due to their promising prospects, especially in near to short-wavelength infrared optoelectronics. In this presentation, we introduce a novel methodology where doping polarity in InAs nanocrystals is innately steered from the synthesis onset. By harnessing the capabilities of II-V clusters as reaction precursors, we offer a pathway that not only addresses existing challenges but also achieves versatile control over doping polarity with the right parameter adjustments. Our exploration underscores the robust realization of p-type doping in InAs nanocrystals, indicating their integration in state-of-the-art printed electronic architectures.

SESSION EL02.03: Synthesis of Nanocrystals and Discovery of Novel Nanomaterials
Session Chairs: Grant Dixon and Nayon Park
Wednesday Morning, April 24, 2024
Room 347, Level 3, Summit

8:15 AM *EL02.03.01

Synthesis, Interconversion and Photophysical Properties of CdSe Magic-Sized Cluster Polymorphs towards Atomically Precise Emitters Hunter Ripberger¹, Kyle Schnitzenbaumer², Lily K. Nguyen¹, Dylan Ladd³, Kelsey Levine³, Damara G. Dayton³, Michael Toney³ and Brandi M. Cossairt¹;

¹University of Washington, United States; ²Transylvania University, United States; ³University of Colorado Boulder, United States

Cutting-edge applications of quantum dots (QDs) as next generation emitters require a precise understanding of their synthesis and structure, since atom-scale differences between individual nanoparticles can result in particle-to-particle variation in their optoelectronic properties. A strategy to synthesize atomically precise QD ensembles utilizes magic-sized clusters (MSCs), which are kinetically stable, atomically defined intermediates along the QD reaction potential energy surface. The synthesis of cadmium selenide MSCs is well precedented, and recent work has established two different structural motifs: a cation-rich, “zincblende-like” tetrahedron and a “wurtzite-like,” quasi-spherical cluster with a stoichiometric inorganic core. However, the wide range of protocols used to access these species has made the direct comparison of their structure, surface chemistry, and optoelectronic properties difficult. Additionally, the physical and chemical relationship between these MSC polymorphs has yet to be established. Here, we demonstrate that both cation-rich and stoichiometric CdSe MSCs can be synthesized from identical reagents and can be interconverted through the addition of either excess cadmium or selenium precursor. The structural and compositional differences between these two polymorphs can be contrasted using a combination of ¹H-NMR spectroscopy, x-ray diffraction, pair distribution function (PDF) analysis, inductively coupled plasma optical emission spectroscopy, and UV-vis transient absorption spectroscopy. The subsequent polymorph interconversion reactions are monitored by UV-vis absorption spectroscopy, with evidence for an altered cluster atomic structure observed by powder x-ray diffraction and PDF analysis. This work helps simplify the complex picture of the CdSe nanocrystal landscape and provides a method to explore structure-property relationships in colloidal semiconductors through atomically precise synthesis. Furthermore, an understanding of polymorph structure allows us to tune the optoelectronic properties of the MSC using surface chemistry, with emission energy and quantum yield affected by the identity of the ligands.

8:45 AM *EL02.03.02

The Dream of The Perfect Nanocrystal David J. Norris; ETH Zürich, Switzerland

Quantum dots are nanometer-sized crystallites of semiconductor that have a roughly spherical shape. Due to extensive research, quantum dots are now commercially used as a robust fluorescent material in displays and lighting. However, even with our best procedures, state-of-the-art samples still contain particles with a distribution in size and shape. Because this causes variations in their optical properties, their performance for applications is reduced. This leads to a fundamental question: can we achieve a sample of semiconductor nanocrystals in which all the particles are exactly the same? In this talk we will discuss this possibility by examining two classes of nanomaterials. First, we will consider thin rectangular particles known as semiconductor nanoplatelets. Amazingly, nanoplatelet samples can be synthesized in which all crystallites have the same atomic-scale thickness (e.g., 4 monolayers). This uniformity in one dimension suggests that routes to monodisperse samples might exist. After describing the underlying growth mechanism for nanoplatelets, we will then move to a much older nanomaterial—magic-sized clusters (MSCs). Such species are believed to be molecular-scale arrangements (i.e., clusters) of semiconductor atoms with a specific (“magic”) structure with enhanced stability compared to particles slightly smaller or larger. Their existence implies that MSC samples can in principle be the same size and shape. Unfortunately, despite three decades of research, the formation mechanism of MSCs remains unclear, especially considering recent experiments that track the evolution of MSCs to sizes well beyond the “cluster” regime. Again, we will discuss the underlying growth mechanism and its implications for nanocrystal synthesis. Finally, we will present an outlook if perfect nanomaterials can be obtained.

9:15 AM EL02.03.03

Sizing Up The Electronic Structure of Atomically Precise Semiconductor Nanoparticles Eimear Madden and Martijn Zwijnenburg; University College London, United Kingdom

Empirically the effect of reducing the characteristic size of semiconductor materials on their optical and by extension electronic properties is well known. Similarly, the fact that this change with size can at least be qualitatively understood in terms of spatially constraining the excited-electron and hole pair to a volume smaller than what it would occupy in the bulk. However, when reducing the size of a semiconductor material more changes than just simply the characteristic size. The role of the surface and the nature of its termination become more important, the dielectric screening changes often reduce as more field lines travel around rather than through the semiconductor, as well as the (electronic) structure can become different to that of the bulk. This is especially true for atomically precise nanoparticles,¹ which typically are on the smaller side of the size spectrum.

To properly understand the effect of reducing the size of semiconductor materials and predict the properties of atomically precise nanoparticles of such materials one needs to perform electronic structure calculations on true nanoparticles. Such calculations should ideally consider the possible surface chemistry of the nanostructures and not assume that any of their properties, other than perhaps their internal structure, is the same as the bulk. Luckily such calculations have become tractable now, both using time-dependent density functional theory (TD-DFT) and the many-body perturbation theory combination of GW and solving the Bethe-Salpeter Equation (GW-BSE).²⁻⁴

In our contribution we will compare and contrast the results of calculations on ligand-capped cadmium sulfide nanoparticles, perhaps the archetypical atomically precise semiconductor nanoparticles, and their hydrogen terminated silicon counterparts, the c. elegans of computational nanoparticle research. Both ligand-capped binary semiconductor nanoparticles and hydrogen terminated silicon nanocrystals are interesting from an application point of view,^{5,6} but also are derived from bulk materials that are both structurally similar but electronically different. We will discuss not only how the optical and electronic properties differ between the two classes of particles and how they change with particle size but also how these changes are linked to the particles’ surface chemistry and changes in the dielectric screening and the fundamental electronic structure of the particles with particle size. An example of the latter being the onset of band-like behaviour.

1. Z. Hens and J. De Roo, *Journal of the American Chemical Society*, 2020, **142**, 15627–15637.
2. D. Rocca, M. Vörös, A. Gali and G. Galli, *Journal of Chemical Theory and Computation*, 2014, **10**, 3290–3298.
3. M. A. Zwijnenburg, *Physical Chemistry Chemical Physics*, 2021, **23**, 21579–21590.
4. M. A. Zwijnenburg, *Physical Chemistry Chemical Physics*, 2022, **24**, 21954–21965.
5. M. A. Cotta, *ACS Applied Nano Materials*, 2020, **3**, 4920–4924.
6. B. F. McVey and R. D. Tilley, *Accounts of Chemical Research*, 2014, **47**, 3045–3051.

9:30 AM EL02.03.04

Indium Coordination as a Handle for Controlling Indium Phosphide Quantum Dot and Nanowire Nucleation and Growth [Helen Larson](#) and Brandi M. Cossairt; University of Washington, United States

Indium phosphide (InP) is a less toxic semiconductor with exciting nanoscale applications in LED displays, bioimaging, and single-nanowire transistors and optoelectronics. However, colloidal InP synthesis lacks mechanisms for precursor reactivity-based size control, and standard synthesis methods rely on hazardous precursors that require high energetic input. To address these challenges, we have taken inspiration from natural biomineralization to expand control over nucleation and growth, focusing on modulating the indium coordination environment. We examined the effect of a strongly chelating anion on the nucleation and growth of InP QDs synthesized using aminophosphine chemistry. Increasing the equivalents of metal-chelating aminopolycarboxylic acid EDTA ($[\text{CH}_2\text{N}(\text{CH}_2\text{CO}_2\text{H})_2]_2$) (0–0.75 equivalents per indium) was found to decrease the final diameter of InP QDs from 4.5 to 2.3 nm by lowering the initial InP growth rate. This size trend was rationalized by invoking a continuous nucleation model in which the suppressed initial growth rates are attributed to a competitive decrease in reactivity caused by indium EDTA complexation and a lower effective concentration. In opposition to strong indium chelation by EDTA, the weak indium-binding ligands trifluoroacetate and trifluoromethanesulfonate allow the aminophosphine-based InP chemistry to access nanowires through a solution-liquid-solid mechanism. Slow phosphorus reactivity is identified by ^{31}P NMR spectroscopy which, along with the weak indium-ligand interactions and the overall reducing environment, are proposed to allow access to the indium metal necessary for nanowire growth. Transmission Electron Microscopy identifies unusual nanoribbon morphologies of zinc-blende InP. Altogether, we identify that controlling indium coordination provides a versatile handle and access to new chemistries for the nucleation and growth of InP nanocrystals.

9:45 AM BREAK

10:15 AM *EL02.03.05

Solution Synthesis Empowers Control in Inorganic Thermoelectric Materials [Maria Ibáñez](#), Tobias Kleinhanns, Mariano Calcabrini, Christine Fiedler, Sharona Horta and Daniel Balazs; ISTA, Austria

Thermoelectricity is the process of directly converting heat into electricity and vice versa, offering an environmentally sustainable means to generate electricity from wasted heat. To enhance the efficiency of this conversion, it's essential to precisely control various structural aspects beyond just the crystal structure. These aspects include defects, grain size, orientation, and interfaces. Conventional solid-state methods have limitations in achieving such precise control.

In recent years, solution-based techniques have garnered significant interest as a cost-effective and easily scalable approach for manufacturing high-performance thermoelectric materials. In this method, a powdered material is first prepared in a solution and then subjected to purification and thermal processing to produce the desired dense polycrystalline material. Unlike traditional methods, solution-based syntheses offer an exceptional level of control over various particle properties, including size, shape, crystal structure, composition, and surface chemistry. This precise control over the properties of the powder creates distinct opportunities for crafting thermoelectric materials with precisely tailored microstructural characteristics.

Throughout our research, we will illustrate various instances where exercising control over distinct nanoparticle characteristics, such as surface attributes or stoichiometry, directly influences specific properties of the dense material, thereby enabling us to fine-tune its performance optimally. Our focus will be particularly directed towards Ag_2Se , a thermoelectric material of great significance, especially in applications near room temperature.

10:45 AM EL02.03.06

HF-Free Synthesis of Colloidal A_2BF_6 Nanocrystals [Eden A. Tzanetopoulos](#), Julie Schwartz and Daniel R. Gamelin; University of Washington, United States

Fluoride-based lattices are widely studied due to their low toxicity, high photostability, and optical transparency. These properties, along with their generally low phonon energies compared to oxides, make fluoride lattices attractive hosts for luminescent impurities. In particular, A_2BF_6 ($\text{A} = \text{Na}, \text{K}, \text{Cs}, \text{NH}_4$; $\text{B} = \text{Si}, \text{Ti}, \text{Zr}, \text{Ge}$) compounds doped with Mn^{4+} in the B^{4+} site are leading candidates for narrow-line red emitters in display and lighting technologies.¹ Solution-processability of these materials would enable additive manufacturing of next-generation classical and quantum photonic structures or devices, but fluoride lattices containing tetravalent cations are essentially entirely unexplored as colloidal nanomaterials, in large part because of the current reliance upon concentrated hydrofluoric acid (HF) in nearly all doped A_2BF_6 syntheses. This talk will describe results from a versatile new synthesis² developed to eliminate the handling of HF entirely. Colloidal nanocrystals of several A_2BF_6 lattices ($(\text{NH}_4)_2\text{ZrF}_6$, Cs_2ZrF_6 , $(\text{N}[\text{CH}_3]_4)_2\text{ZrF}_6$, K_2SiF_6) have now been prepared for the first time. *In-situ* A-site cation exchange has also been demonstrated in these materials, allowing the post-synthetic conversion of, e.g., $(\text{NH}_4)_2\text{ZrF}_6$ nanocrystals into Cs_2ZrF_6 nanocrystals. Under some conditions, a nanoscale Kirkendall effect occurs that yields hollow A_2BF_6 nanostructures. Recent results showing nanocrystal size and shape control will also be discussed. These results highlight the versatility of this bottom-up synthesis for preparing a wide variety of previously inaccessible colloidal fluoride nanostructures.

References

1. "Narrow-Band Phosphors for Next Generation MiniLED and MicroLED Displays." Murphy; Camardello; Dohert; Liu; Smigelski; Setlur *SID*, **2021**, 52(S1), 902-905.
2. "HF-Free Synthesis of Colloidal Cs_2ZrF_6 and $(\text{NH}_4)_2\text{ZrF}_6$ Nanocrystals." Tzanetopoulos, E.; Schwartz, J.; Gamelin, D. R. *Chem. Commun.*, **2023**, 59, 5451-5454.

11:00 AM EL02.03.07

Colloidal Synthesis of P-Type Zn_3As_2 Nanocrystals [Seongchan Kim](#), Jaeyoung Seo, Namyoun Gwak, Seungki Shin and Nuri Oh; Hanyang University, Korea (the Republic of)

Zinc pnictides (Zn_3Pn_2 , where Pn represents P, As, or Sb) are compound II–V semiconductors composed of earth-abundant elements belonging to the II and V groups of the periodic table. These materials exhibit exceptional properties, such as high carrier mobility, low effective mass of charge carriers, anisotropic charge transport characteristics, and narrow band gaps. Notably, Zn_3As_2 , which has a band gap of approximately 1.0 eV, has significant potential for optoelectronic applications across a wide range of wavelengths. Given the substantial advantages and opportunities associated with intrinsically p-type nanomaterials, particularly considering the abundance of well-established inorganic n-type nanomaterials, Zn_3As_2 is a highly promising material owing to its inherent p-type characteristics and appropriate bandgap.

Colloidal synthesis of nanocrystals (NCs) from compound semiconductors offers precise control over their size, resulting in a wide range of tunable electrical and optical properties. These colloidal NCs, such as Zn_3As_2 NCs, exhibit characteristics that make them highly suitable for low-cost large-area processing, opening up diverse applications in fields such as solar energy harvesting and photodetection spanning the visible to infrared regions. However,

despite the outstanding properties of colloidal Zn₃As₂ nanocrystals, research in this area is lacking because of the absence of suitable precursors, the occurrence of surface oxidation, and the intricacy of the crystal structures. Zn precursors such as diethylzinc, or As precursors such as tris(trimethylsilyl)arsane exhibit high reactivity but yield Zn₃As₂ NCs that are too small. Also, previously reported Zn₃As₂ NCs have exhibited low crystallinity, which was primarily attributed to the difficulty in achieving precise stoichiometry during their formation. In this study, a novel and facile solution-based synthetic approach is presented for obtaining highly crystalline p-type Zn₃As₂ nanocrystals with accurate stoichiometry. By carefully controlling the feed ratio and reaction temperature, colloidal Zn₃As₂ nanocrystals are successfully obtained. Moreover, the mechanism underlying the conversion of As precursors in the initial phases of Zn₃As₂ synthesis is elucidated. Furthermore, these nanocrystals have been employed as active layers in field-effect transistors that exhibit inherent p-type characteristics with native surface ligands. To enhance the charge transport properties, a dual passivation strategy is introduced via phase-transfer ligand exchange, leading to enhanced hole mobilities as high as 0.089 cm² V⁻¹ s⁻¹. This study not only contributes to the advancement of nanocrystal synthesis, but also opens up new possibilities for previously underexplored p-type nanocrystal research.

11:15 AM *EL02.03.08

The Chemistry of Tin Halide Perovskite Nanocrystals [Loredana Protesescu](#); University of Groningen, Netherlands

Metal halides perovskites with nanoscale geometries have revolutionized the field of solution-processed photovoltaics and light-emitting devices due to their strong absorption and exceptional photoluminescence properties combined with a remarkable tolerance to structural defects. However, the further development of these materials to practical commercialization is hindered by their toxic components like lead and their inherent structural lability. Moreover, we still have little understanding of their crystallographic structures, chemical and physical interactions, and surface chemistry at a fundamental level.

The chemical design of metal halide perovskites proved to be the key to addressing those issues. In this work, I will discuss the physical and chemical parameters which can help us to achieve a stable, tunable and monodisperse CsSnX₃ perovskite nanocrystals with defined optical features. Pertaining to the formation energies of nanostructures, the interplay of the 2D Ruddlesden-Popper (L₂C_{n-1}Sn_nX_{3n+1}) phases with 3D CsSnX₃ nanocrystals is apparent with respect to ligand combinations (ammonium, carboxylate, phosphinate), precursor ratios and temperature when SnX₂ salt is used as a precursor. X-ray diffraction and scattering studies conjoined with optical spectroscopy and electron microscopy helps us in acquiring the useful insights into directing the chemistry of Sn-halide perovskites at nanoscale. This research work showcases the insistent necessity for the development of mechanistic understanding to design efficient synthetic routes to achieve high-quality tin-halide perovskite nanocrystals.

11:45 AM EL02.03.09

Tin Chalcogenide Colloidal Quantum Dots for Infrared Photodetection [Barbara Y. Martin](#), Jianying Ouyang, Neil Graddage, Jianping Lu, Nathan Yee, Tyler Davidson-Hall, Jianfu Ding, Tao Ye and Patrick Malenfant; National Research Council Canada, Canada

Printable, flexible and low-cost photodetectors with sensitivity in the near-infrared (NIR, 700-2500nm) window are in high demand. Much research on infrared active colloidal quantum dots (CQDs) have been conducted based on lead or mercury chalcogenides. However, environment-friendly alternatives with tunable sensitivity in the NIR and high performance should be investigated to better protect our environment. We have developed silver chalcogenide CQDs and demonstrated their application in NIR photodetection, including Ag₂Se and Ag₂Te QDs with detection up to 1.2 μm and 1.4 μm^{1,2}. To further push the sensitivity to longer wavelength, we have been developing tin telluride (SnTe) CQDs. SnTe QDs possess good optical properties in the range of 1.5-2.5 μm. So far, only a few studies were reported; the reaction mechanism is poorly understood, the synthesis is challenging and the products are prone to oxidation.

Our SnTe CQDs were synthesized with tin precursors that are less toxic, less expensive and less susceptible to oxidation than that commonly used (Bis(bis(trimethylsilyl)amino tin(II))₃). The reaction was optimized by tuning different parameters (ligands, temperature, tin precursor, etc.) to reduce the oxidation and obtain monodispersed CQDs. We were able to obtain CQDs of 12 nm with an optical sensitivity up to 2.5 μm and good stability (weeks) under air. Additionally, SnTe CQDs can be coated to obtain more stable CQDs under air. The absorbance wavelength can also be tuned with this doping from 1.2 μm to 2.5 μm with a good control by changing the reaction time.

Our developed SnTe CQDs can offer a low-toxicity route for low-cost solution-processable fabrication of high-performance infrared photodetectors with sensitivity up to 2.5 μm.

1. *ACS Appl. Nano Mater.* **2021**, 4, 13587–13601
2. *ACS Appl. Nano Mater.* **2020**, 3, 12209–12217
3. *J. Am. Chem. Soc.* **2022**, 144, 6251–6260

SESSION EL02.04: Scalability in Synthesis, Characterization and Integration of Colloidal Nanocrystals
Session Chairs: Emily Miura and Nayon Park
Wednesday Afternoon, April 24, 2024
Room 347, Level 3, Summit

1:30 PM *EL02.04.01

Sustainable, Additive, Scalable Nanomanufacturing of Quantum Materials at The Attoscale [John D. MacKenzie](#)^{1,1,2}; ¹University of Washington, United States; ²Washington Clean Energy Testbeds, United States

Conventional semiconductor processing has made immense progress in the 70 years since its introduction, pushing progress in performance, critical dimension and functionality per unit cost forward at an unparalleled rate. Even though the roadmap to single nanometer devices is still being set, it is highly likely that this field will continue to innovate given the need for increasing information processing, storage and transfer in virtual reality, artificial intelligence and the integration of electronics with virtually every aspect of our lives. At the same time, there are global concerns about climate and sustainability and, here, the future for conventional manufacturing is less certain. Whether applied to optoelectronics, microelectronics or emerging areas such as optical quantum devices, conventional approaches are dominated by cycles of subtractive and high waste lithographic processing and energy intensive and increasingly complex sets of materials that run counter to a goal of sustainable, lower carbon footprint and lower environmental impact. We

will show here that advances in solution-processable materials and corresponding additive manufacturing approaches can provide alternative, and even more capable processing routes not feasible with conventional processing.

An overview of additive nanomanufacturing will be presented along with progress towards applying electrohydrodynamic (EHD) printing as a fully additive pathway towards quantum optical devices and integrated photonics. Although nanoscale 3D printing via processes like two photon stereolithography can produce submicron structures, this is largely limited to passive materials that require subsequent subtractive processing to render functional elements. Techniques like pressure driven inkjet printing, such as piezoelectric or thermal evaporation actuated printing common to consumer inkjet systems, can digitally deposit functional materials from nanoparticle and reactive precursor inks. These types of printing have also been scaled industrially in applications such as flat panel displays. The surface energy and decreasing inertia bottlenecks for ink droplets of decreasing size and increasing surface/volume ratio leads to size and positioning accuracy limits of around 10 microns. Unfortunately, this is two or more orders of magnitude too large for applications at the leading edge of micro- and opto-electronics. Leveraging the flexibility and dynamic range inherent to electric fields, EHD printing has been shown to overcome the droplet size limitations of mechanical jetting to deterministically position functional material inks additively with zero moving part actuation.

It will be shown here that direct printing of functional materials and precursors using EHD can be pushed to deterministic positioning of quantum dots and nanocrystal precursors at the nanoscale. This includes our ability to additively pattern high index dielectrics for optical metasurfaces and shelled luminescence II-IV QDs at resolutions <100 nm from attoliter scale droplets. Our work on heterointegration of perovskite nanocrystals and QDs with photonic cavities, including selective deposition of quantum dots on free-standing close-spaced cavity pairs that demonstrate optical cross coupling will also be outlined. This demonstrates an exceptional example of heterointegration on optical structures at ambient pressures and temperatures that cannot be readily achieved by any conventional approach (e.g. semiconductor epitaxy, lithography or stochastic coating demonstrations). We will conclude with results of additive single QD deposition for devices such as single photon emission sources via dilute QD ink deposition, and formation of nanocrystals from in-situ attoliter scale reactions in printed reagent ink droplets. This will show that the resolution of techniques such as electron beam lithography can be surpassed in an additive, wasteless, sustainable scalable nanomanufacturing process.

2:00 PM EL02.04.02

Nondestructive High-Resolution Direct Optical Lithography of Colloidal Emissive Nanocrystals [Himchan Cho](#); Korea Advanced Institute of Science and Technology, Korea (the Republic of)

High-resolution precision patterning is a crucial requirement in the fabrication of immersive near-eye displays that incorporate high-color-purity emissive nanocrystals such as colloidal quantum dots and perovskite nanocrystals as color filters or electroluminescence (EL) emission layers in the form of an RGB matrix.¹⁾ Direct optical lithography, which involves a photochemical reaction of photosensitive ligands or additives, offers a new platform for patterning colloidal nanocrystals, providing high pattern uniformity with a simple procedure.²⁾ However, a significant decrease in photoluminescence (PL) quantum yield during the patterning process has been a major challenge. To address this challenge, we have developed direct, scalable, and nondestructive methods for high-resolution patterning of colloidal emissive nanocrystals without sacrificing their luminescent properties. With photochemically activated reactions, leading to *in situ* exchange³⁻⁴⁾ or crosslinking⁵⁾ of long-chain organic ligands, we have demonstrated uniform PL and EL patterns of red, green, and blue quantum dots and perovskite nanocrystals with feature sizes as small as sub-1 μm , while preserving their structural, electronic, and emissive properties. The underlying patterning mechanisms were identified by investigating the photochemical transformations of surface ligands and additives at each step of the process. Our approach provides a promising solution for patterning of colloidal emissive nanocrystals, which can be implemented in next-generation augmented reality displays and other optoelectronics applications.

References

- 1) *Advanced Materials Technologies* 2022, 2201070
- 2) *Accounts of Chemical Research* 2023, 56, 17, 2286
- 3) *Advanced Materials* 2020, 32, 2003805
- 4) *ACS Energy Letters* 2023, DOI: 10.1021/acsenerylett.3c01019
- 5) *Science Advances* 2023, 9, eadi6950

2:15 PM EL02.04.05

Data-Driven Exploration of Silver Nanoplate Formation in Multidimensional Chemical Design Spaces [Huat Thart Chiang](#), Kiran Vaddi and Lilo D. Pozzo; University of Washington, United States

Artificial Intelligence (AI) driven closed systems, which are usually composed of an AI agent to plan experiments, robots to perform experiments, and a high throughput characterization method to evaluate experiments have recently shown to be successful in optimizing structural properties of colloidal nanoparticles. However, a limitation of these kinds of systems is that they have only been demonstrated in constrained design spaces which is where the targeted structure has a high probability of being formed. In addition, while many samples are being synthesized and characterized, minimal amounts of information on the relationship between experimental design parameters and the structure of the nanoparticles is obtained from the experiment. To solve these problems, we introduce a novel AI driven closed system and test it with a model system of silver nanoparticle synthesis with the objective of synthesizing nanoplates. Our method first searches the design space for silver nanoplates based on UV-Vis spectroscopy curves, which are autonomously classified into "plates" or "not plates" using a distance metric. This information is then used to train a gaussian process classifier which then iteratively suggests experimental parameters for a new batch of samples that are likely to be nanoplates. After the chemical design space is constrained to contain mostly nanoplates, we then use small angle x-ray scattering characterization to obtain size/shape parameters. This information is used to train a gaussian process regressor, from which we can extract design rules such as the effect of the composition of the reagents on the obtained size/shape parameters.

2:30 PM BREAK

3:30 PM *EL02.04.04

Precision Synthesis and Accelerated Optimization of Colloidal Quantum Dots with Self-Driving Fluidic Labs [Milad Abolhasani](#); North Carolina State University, United States

Despite the intriguing physicochemical properties and widespread applications of colloidal quantum dots (QDs) in energy and chemical technologies, their discovery and synthesis optimization are still based on Edisonian techniques. Existing QD discovery and development strategies using batch reactors with irreproducible and uncontrollable heat/mass transport rates very often fail to comprehensively explore the vast synthesis and processing space of QDs. These limitations necessitate the development and implementation of new strategies to accelerate the pace of QD discovery and development. Recent advances in reaction miniaturization, automated experimentation, and data science provide an exciting opportunity to reshape the discovery, development, and manufacturing of QDs. In this talk, I will present a *Self-Driving Fluidic Lab* (SDFL) for accelerated discovery, optimization, and manufacturing of colloidal QDs with multi-step chemistries, through the integration of flow chemistry, online characterization, and machine learning (ML).¹⁻⁵ I will discuss how modularization of different synthesis and processing stages in tandem with a constantly evolving ML-assisted QD synthesis modeling and decision-

making under uncertainty can enable resource-efficient navigation through high dimensional experimental design spaces. Example applications of SDFs for the autonomous precision synthesis of metal halide perovskite, II–VI, and III–V QDs will be presented to illustrate the potential of autonomous labs in reducing QD development timeframe from >10 years to a few months. Finally, I will present the unique reconfigurability aspect of SDFs to close the scale gap in nanomanufacturing research through on-demand switching from reaction exploration/exploitation to smart nanomanufacturing mode.

References.

- [1] Abolhasani, M.; Kumacheva, E. The rise of self-driving labs in chemical and materials sciences. *Nature Synthesis*, 2, 483–492, 2023
- [2] Volk, A. A.; Epps, R. W.; Yonemoto, D. T.; Masters, B. S.; Castellano, F. N.; Reyes, K. G.; Abolhasani, M. AlphaFlow: autonomous discovery and optimization of multi-step chemistry using a self-driven fluidic lab guided by reinforcement learning. *Nature Communications*, 14 (1), 1403, 2023.
- [3] Volk, A. A.; Abolhasani, M. Autonomous flow reactors for discovery and invention. *Trends in Chemistry*, 3 (7), 519-522, 2021.
- [4] Delgado-Licona, F.; Abolhasani, M. Research Acceleration in Self-Driving Labs: Technological Roadmap toward Accelerated Materials and Molecular Discovery. *Advanced Intelligent Systems*, Advance Article, 2200331, 2023. <https://doi.org/10.1002/aisy.202200331>
- [5] Epps, R. W.; Bowen, M. S.; Volk, A. A.; Abdel-Latif, K.; Han, S.; Reyes, K. G.; Amassian, A.; Abolhasani, M. Artificial Chemist: An Autonomous Quantum Dot Synthesis Bot. *Advanced Materials*, 32 (30), 2001626, 2020.

4:00 PM *EL02.04.06

Autonomous Synthesis and Characterization Platforms for Parameter Space Mapping for Quantum Dots Paul Kenis and Jeff Xu; University of Illinois, United States

Controlling composition, structure, and thus properties of nanomaterials continues to be of importance to numerous fields, with potential and realized applications for colloidal nanomaterials ranging from quantum dots for displays and bioimaging, to metal nanoparticles for (electro-) catalytic conversions. The vastness of synthesis parameter space, in combination with limited understanding of the nucleation and growth mechanisms for many nanomaterials still hampers progress in identifying nanomaterials with desired properties for existing and newly envisioned purposes. Furthermore, the identification of optimal synthesis recipes for these nanostructures remains a major hurdle. To no surprise, many research efforts have been devoted to these challenges over the past 20+ years.

This presentation will focus on our efforts to develop and apply a number of enabling capabilities achieved through reactor engineering, focusing on the synthesis and characterization of quantum dots. We have demonstrated how the use of *automated flow reactors* not only helps in run-to-run reproducibility but also in uncovering mechanistic information. Examples include reactors with dedicated nucleation, growth, and shell formation zones, and investigation that revealed mechanistic insight of how water concentration affects QD synthesis outcome. In subsequent work, we employed an autonomous flow reactor system to map synthesis parameter space of specific QD systems, a project that relied on fast, fully automated in-situ characterization using UV-vis in combination with multi-step machine learning workflows. The utility of flow reactors, however, is limited when considering chemistries with longer reaction times. Hence, more recently we developed a fully *automated batch reactor* for parameter space mapping of QD synthesis via hot injection, the most frequently used method in both QD research and in QD production at scale. This batch platform is being augmented with purification capabilities, to address some of the challenges of in-line, in-situ characterization of raw reaction mixtures, and to enable using advanced optical and structural characterization methods to provide insight into the actual structure of the QD materials.

In summary, we developed an integrated approach for the rapid synthesis, purification, and characterization of QDs to determine structural properties, with ongoing work focusing on structural mapping of QD synthesis.

4:30 PM EL02.04.07

Continuous Flow Synthesis of Lead Sulfide Quantum Dots for NIR/SWIR LED Applications Pierre Machut^{1,2}, Anna Karina Antonini¹, Céline Rivaux¹, Gabriel Mugny² and Peter Reiss¹; ¹CEA, France; ²STMICROELECTRONICS, France

The development of new industrial applications in fields such as cell phones and automobiles depend on the ability to produce low-cost LEDs emitting in the NIR/SWIR range. A method for synthesizing large quantities of PbS/CdS core/shell quantum dots, known for their high photoluminescence, would enable this development.

Since the first synthesis of PbS quantum dots (QDs) using the hot-injection method in 2003,^[1] many efforts have been employed to develop monodisperse PbS quantum dots. Nowadays, the use of bis(trimethylsilyl) sulfide (TMS₂S) as sulfur precursor still remains very attractive due to the narrow size distribution giving rise to precise absorption/emission features in the NIR/SWIR region. However, scaling up this synthesis remains a challenge due to the difficulty of handling and the high toxicity of the H₂S gas released during synthesis using this sulfur precursor.

Various sulfur precursors have been utilized to prepare PbS QDs, including elemental sulfur^[2] and substituted thioureas^[3]. The latter show a great potential as the reaction rate can be adjusted over several orders of magnitude by altering their substituents, which gives access to precisely controlled particle sizes in a wide range. Moreover, there are approximately 10⁴ different thioureas that can be synthesized in simple reactions using commercially available chemicals.

To enhance the reproducibility of the syntheses and scale them up to larger quantities, continuous flow synthesis is an appealing alternative to widely used batch synthesis. Among other advantages, the strongly enhanced heat and mass transfer in small tubular reactors combined with controlled pressure can be cited. On the other hand, flow synthesis comes with several restrictions, which require in most cases an adaptation of the synthesis protocol. In particular, both the lead and sulfur precursors should be perfectly soluble at room temperature to avoid clogging, and the injected volumes should be balanced to keep consistent flow rates.

In this study, we developed new synthesis conditions affording monodisperse PbS QDs via flow synthesis exhibiting identical optical properties as with classic batch synthesis, with excitonic peak to valley ratios >3. Moreover, the excitonic peak position could be adjusted with the residence (=reaction) time, in contrast to batch reactions.

The flow synthesis of highly luminescent PbS/CdS core/shell QDs was also achieved using ex-situ prepared cadmium oleate via the cation exchange method.

Summarizing, the developed flow process gives access to grams of high-quality of PbS/CdS core/shell QDs in a couple of hours and in a highly reproducible manner, at wavelengths of particular interest for NIR QLEDs.

[1] M. a. Hines et G. d. Scholes, *Advanced Materials*, vol. 15, n° 21, p. 18441849, 2003.

[2] L. Cademartiri, J. Bertolotti, R. Sapienza, et D. S. Wiersma, *The Journal of Physical Chemistry B*, vol. 110, n° 2, Art. n° 2, 2006.

[3] J. S. Owen, M. P. Campos, G. T. Cleveland, I. J.-L. Plante, et M. P. Hendricks, *Science*, vol. 348, n° 6240, p. 12261230, 2015.

SESSION EL02.05: Poster Session I: Towards Atomically Precise Colloidal Materials for Conventional and Quantum Optoelectronics I
Session Chairs: Brandi Cossairt, Hao Nguyen and Nayon Park
Wednesday Afternoon, April 24, 2024
Flex Hall C, Level 2, Summit

5:00 PM EL02.05.01

Resonant Tunneling Transistor based on Single PbS Quantum Dot Retno D. Wulandari^{1,2,3}, Yin Dongbao², Ricky D. Septianto⁴, Yoshihiro Iwasa^{1,5}, Yutaka Majima² and Satria Bisri^{1,3}; ¹RIKEN, Japan; ²Tokyo Institute of Technology, Japan; ³Tokyo University of Agriculture and Technology, Japan; ⁴RIKEN CEMS, Tokyo Institute of Technology, Japan; ⁵The University of Tokyo, Japan

The growing need for high-performance computing continues to drive circuit and device technologies to improve in terms of speed and power. Device dimension scaling will be the most effective strategy for meeting circuit performance requirements and reducing power consumption. Colloidal semiconductor quantum dots (QDs) are highly suitable to support device miniaturization by solution processability and as platforms for quantum information science¹. The consideration of quantum mechanical effects is crucial in designing nanometer-scale electronic devices (i.e., transistors) that involve single QD. On the other hand, challenges related to the fabrication of such devices require radical solutions. Therefore, developing a bottom-up approach to enable the fabrication of high-quality single QD transistors based on the colloidal process that can easily be contacted electrically is an essential strategy that must be explored.

Here we demonstrate a resonant tunneling transistor (RTT) based on single lead sulfide (PbS) QD as a Coulomb island anchored by ligand molecules that are attached to the Au nanogap electrodes. We are utilizing two different alkane dithiol ligands which have different ligand chain length². We specifically use PbS due to its well-established synthesis process and large electron Bohr radius, thus providing stronger and more stable quantum confinement at the given QD diameters and the well-defined formation of the discrete energy levels³. We develop nanogap electrodes by combining both electron beam lithography and electroless gold plating (ELGP)⁴ to create a robust platform for the single QD device. The robust heterostructure ELGP nanogap electrode provides the capability to apply large voltage bias to the single PbS QD transistor across the two Au electrodes (the source and the drain) without breaking the device, which leads to an excellent yield. It enables us to tune the chemical potential of the PbS QD in and out of resonance with the given band energy. Consequently, we can clearly observe multiple regions of negative differential resistance (NDRs) in the current-voltage (I-V) characteristics of PbS QD devices. In addition, these NDRs can be additionally tuned by the application of a gate electric field. NDR is among the key features that can be used in modern electronic and logic circuits, which are expected to play essential roles in quantum and neuromorphic electronics⁵. This demonstration of single PbS-QD-based RTTs paves the way for the future development of solution-processable quantum electronic devices.

References:

- [1] R. D. Septianto, et al., *Nature Comm.*, **2023**, 14, 2670.
- [2] R. D. Septianto, et al., *NPG Asia Materials*, **2020**, 12, 33.
- [3] L. Liu, et al., *Nanoscale*, **2021**, 13, 14001-14007.
- [4] V. M. Serdio, et al., *Nanoscale*, **2012**, 4, 7161.
- [5] Y. Y. Choi, et al., *Appl. Phys. Express*, **2019**, 12, 125007.

5:00 PM EL02.05.02

Multi-Facet Passivated AgBiS₂ Colloidal Quantum Dot for Efficient Lead-Free Optoelectronic Dongeon Kim¹, Gaeun Cho^{1,2}, Yun Hoo Kim³, Ji Hyun Kwon¹, YeonWoo Oh¹, Minjung Yang¹, Seungin Jee¹, In Suh Lee¹, Min-Jae Si¹, Yujin Jung⁴, Ho Yeon Yang¹, Changjo Kim⁵, Han Seul Kim⁶ and Se-Woong Baek¹; ¹Korea University, Korea (the Republic of); ²Korea Institute of Science and Technology Information, Korea (the Republic of); ³Korea Institute of Science and Technology, Korea (the Republic of); ⁴National University of Singapore, Singapore; ⁵Los Alamos National Laboratory, United States; ⁶Chungbuk National University, Korea (the Republic of)

Silver bismuth sulfide (AgBiS₂) colloidal quantum dots (CQD) are promising lead-free light absorbing materials for CQD optoelectronic due to their low cost, earth-abundant element, and high absorption coefficients. However, AgBiS₂ CQD photovoltaics are hampered by low open-circuit voltage (V_{oc}) due to the complication of passivating charge neutral (100) surface of AgBiS₂. Here, we propose a ligand combination for solution ligand exchange to passivate the (100) facet of the AgBiS₂ with improved ink stability. We demonstrated that incorporating alkali metal ions can enhance the ink stability of solution ligand exchanged CQD ink and surface ligand coverage ratio. We revealed the synergetic passivating mechanism of cation ligands on AgBiS₂ CQD surface through density functional theory. This multi-facet passivated AgBiS₂ CQD solid possessed low trap density and Urbach tail. Consequently, fabricated multi-facet passivated AgBiS₂ optoelectronics showed power conversion efficiency (PCE) of 8.1 %, detectivity of over 10¹¹ around 400-930 nm, and response time of 400 ns. Which is the highest PCE and fastest response time among published solution ligand-exchanged AgBiS₂ optoelectronics showing promise for lead-free optoelectronics.

5:00 PM EL02.05.03

Colloidal InSb Quantum Dot Ink Enables III-V Group Bulk-Heterojunction Shortwave Infrared (SWIR) Photodetector Seungin Jee, Min-Jae Si, Dongeon Kim and Se-Woong Baek; Korea University, Korea (the Republic of)

Infrared (IR) optoelectronics have become important owing to their various applications, such as recognition, autonomous driving, and quantum communications. Specifically, IR detection in the shortwave IR (SWIR) spectrum (i.e., 1550 nm) is significantly important for eye safety and long-range communications. To date, the II-VI and IV-VI (e.g., HgTe, PbSe, and PbS) groups of CQDs have been widely applied to SWIR optoelectronic devices, but the use of toxic elements such as Pb and Hg limits their commercial viability. Group III-V colloidal quantum dots (CQDs) (e.g., InAs, InSb) have recently attracted significant interest as SWIR materials due to their narrow bulk bandgap and lack of toxic elements such as Pb and Hg. Herein, we synthesized of InSb CQD using the modified continuous injection method approach. This approach enables for facile tuning of bandgap at a SWIR wavelength of up to 0.9 eV with diffusion growth via monomer flux. In addition, the surface of the InSb CQD was effectively passivated and a stable CQD ink was obtained through solution-phase ligand exchange using halides and thiolates. Finally, we demonstrated a bulk heterojunction (BHJ) structure using n-type and p-type III-V CQDs. The BHJ CQD solids exhibited broad absorption up to 1600 nm and a 6-fold higher responsivity compared to the pristine InSb CQD device due to efficient charge transport.

5:00 PM EL02.05.04

Precise Doping Control of InAs Quantum Dots Using II-V Clusters Seongmin Park, Eunji Jang, Mahnmin Choi and Sohee Jeong; Sungkyunkwan University, Korea (the Republic of)

Colloidal InAs quantum dots (QDs) have tunable band gaps across the near-infrared (NIR) and short-wave infrared (SWIR) spectra, making them attractive

candidates for IR optoelectronic applications such as IR photodetectors, bio-imaging, and telecommunications. Previous studies on InAs QDs for application in optoelectronic devices have extended the size of QDs and achieved narrow size distribution based on synthetic pathways and growth mechanisms discovered through various precursors and synthesis methods. Subsequently, manipulating the electrical properties of InAs QDs through doping control has emerged as an important aspect. In particular, converting the carrier type from n-type to p-type plays a crucial role in expanding application fields. Recently, post-treatment method has been proposed that utilizes heterogeneous elements such as Zn²⁺ or Cd²⁺ precursors to lead to substitutional doping with In atoms. However, when diethylzinc or Zn-oleate was used as a p-dopant precursor, it was reported that Zn-doped p-type InAs QDs could be obtained only by highly reactive diethylzinc. Understanding the doping mechanism is essential to modulate the electrical properties of InAs QDs through doping control. Although many results of altering the carrier type have been reported, there has not yet been a clear discussion on the doping mechanism of QDs.

In this study, to understand the doping mechanism, we developed the II-V cluster as a p dopant precursor that can precisely control doping and synthesized InAs QDs with uniform size. In particular, by continuously supplying Zn-As clusters, the carrier type of the InAs QDs was gradually switched from n-type to ambipolar and eventually to p-type. This demonstrates that Zn-As clusters are effective precursors for finely controlling the carrier type. EXAFS analysis was performed to confirm the bonding between Zn and As in the InAs QD lattice, and Zn-As bonding was found only in InAs QDs showing p-type characteristics. This indicates that Zn-As clusters can be incorporated into InAs QDs by alternative doping of In with Zn under appropriate supply. To demonstrate the versatility of the II-V cluster-mediated synthesis system, Cd-doped p-type InAs QDs were also successfully synthesized using Cd-As clusters. As a result, our study provides valuable insights into the doping mechanism of InAs QDs by establishing systematic doping control conditions using II-V clusters for the first time.

5:00 PM EL02.05.05

Direct Photocatalytic Patterning of Colloidal Perovskite Nanocrystals [Seongkyu Maeng](#), Sun Jae Park, Jaehwan Lee, Hyungdoh Lee, Jonghui Choi, Jeung Ku Kang and Himchan Cho; Korea Advanced Institute of Science and Technology (KAIST), Korea (the Republic of)

Abstract:

Perovskite nanocrystals (PeNCs) are emerging materials with significant potential for various optoelectronic applications, especially in LED technologies. For their integration into AR/VR displays, precise patterning technologies are crucial [1]. However, current techniques face challenges in fabricating high-resolution PeNC patterns while preserving their unique emissive properties, due to the inherent instability of these materials. To address this challenge, we develop a direct photocatalytic patterning that can completely preserve the optical characteristics of perovskite nanocrystals (PeNCs). Solubility change of PeNCs is achieved mainly by a photoinduced thiol-ene click reaction between surface ligands and a dual-role reagent, pentaerythritol tetrakis(3-mercaptopropionate) (PTMP), where the thiol-ene reaction is enabled at a low light intensity dose (~ 30 mJ cm⁻²) by the strong photocatalytic activity of PeNCs. The photochemical reaction mechanism was investigated using various analyses at each patterning step. The PTMP also acts as a defect passivation agent for the PeNCs and even enhances their photoluminescence quantum yield (by ~5%) and photostability. Multicolor patterns of cesium lead halide (CsPbX₃) PeNCs were fabricated with high resolution (<1 μm). Our method is widely applicable to other classes of nanomaterials including colloidal cadmium selenide-based and indium phosphide-based quantum dots and light-emitting polymers; this generality provides a nondestructive and simple way to pattern various functional materials and devices [2].

References

- [1] Park et al., *Advanced Materials Technologies* **2022**, 2201070
- [2] Maeng et al., *Science Advances* **2023**, 9, eadi6950

5:00 PM EL02.05.06

Doped CeO₂ as a Probe of Active Site Speciation for Organophosphate Degradation [Emily Miura](#)¹, Ashley Oregon¹, James J. De Yoreo², Chun-Long Chen² and Brandi M. Cossairt¹; ¹University of Washington, United States; ²Pacific Northwest National Laboratory, United States

Organophosphate degradation is an important reaction for decomposing environmentally harmful compounds and recovering phosphate ions in biological molecules. CeO₂ nanocrystals have been well-studied for dephosphorylation via hydrolysis due to their stable Ce³⁺ and Ce⁴⁺ oxidation states. However, there is ambiguity regarding which defect properties of the CeO₂ surface (Ce³⁺/Ce⁴⁺ oxidation state, oxygen vacancies, faceting, and dopants) are responsible for efficient hydrolysis. Trivalent (M³⁺) dopants have been used as a tool to control the defects, such as the concentration of Ce³⁺ and oxygen vacancies, and hence the hydrolytic activity of CeO₂. Herein, we used trivalent transition metals and rare earth metals (M = Y³⁺, Cr³⁺, In³⁺, and Gd³⁺) to tune the active sites on the CeO₂ nanocrystal surface and observed the impacts of the respective metal dopant on the cerium oxide active sites for organophosphate hydrolysis. We synthesized M-doped CeO₂ via hydrothermal synthesis to yield colloiddally dispersed nanoparticles that we annealed to prime the nanocrystal surface for catalysis. We characterized their properties by powder X-ray Diffraction (PXRD), X-ray photoelectron spectroscopy (XPS), and Raman spectroscopy. Finally, we evaluated the catalytic ability using organophosphate dimethyl-*p*-nitrophenol phosphate (DMNP) and UV-visible absorption spectroscopy to monitor the degradation to *p*-nitrophenol over time. While we observed successful doping of CeO₂ by all of the dopants, their characteristics have revealed that M³⁺ dopants can both positively and negatively impact CeO₂ in our system. We propose that the CeO₂ is extremely sensitive to dopants that cause excessive lattice strain, Ce³⁺ ions, and oxygen vacancy defects. Thus, CeO₂ requires a delicate balance where the active sites are an ensemble of defects in ideal concentration and orientation on the nanocrystal surface to reach high catalytic efficiency.

References:

- (1) Tan, Z.; Wu, T.-S.; Soo, Y.-L.; Peng, Y.-K. Unravelling the True Active Site for CeO₂-Catalyzed Dephosphorylation. *Applied Catalysis B: Environmental* **2020**, *264*, 118508. <https://doi.org/10.1016/j.apcatb.2019.118508>.
- (2) Manto, M. J.; Xie, P.; Wang, C. Catalytic Dephosphorylation Using Ceria Nanocrystals. *ACS Catal.* **2017**, *7* (3), 1931–1938. <https://doi.org/10.1021/acscatal.6b03472>.
- (3) Wang, Y.; Wang, F.; Song, Q.; Xin, Q.; Xu, S.; Xu, J. Heterogeneous Ceria Catalyst with Water-Tolerant Lewis Acidic Sites for One-Pot Synthesis of 1,3-Diols via Prins Condensation and Hydrolysis Reactions. *J. Am. Chem. Soc.* **2013**, *135* (4), 1506–1515. <https://doi.org/10.1021/ja310498c>.
- (4) Vernekar, A. A.; Das, T.; Mugesh, G. Vacancy-Engineered Nanoceria: Enzyme Mimetic Hotspots for the Degradation of Nerve Agents. *Angewandte Chemie International Edition* **2016**, *55* (4), 1412–1416. <https://doi.org/10.1002/anie.201510355>.
- (5) Zhang, Z.; Wang, Y.; Lu, J.; Zhang, J.; Li, M.; Liu, X.; Wang, F. Pr-Doped CeO₂ Catalyst in the Prins Condensation–Hydrolysis Reaction: Are All of the Defect Sites Catalytically Active? *ACS Catal.* **2018**, *8* (4), 2635–2644. <https://doi.org/10.1021/acscatal.7b04500>.

5:00 PM EL02.05.07

Compositionally Engineered Ternary PbS_xSe_{1-x} Quantum Dots Active in Short-Wavelength Infrared Region [Seohee Park](#)^{1,2}, Yongwoo Jeon^{1,2}, Sung Nam Lim¹, Shin Ae Song¹, Kiyoung Kim¹, Sohee Jeong² and Ju Young Woo¹; ¹Korea Institute of Industrial Technology, Korea (the Republic of); ²Sungkyunkwan University, Korea (the Republic of)

Lead chalcogenide Quantum Dots (QDs) possess versatile attributes, primarily due to their large exciton Bohr radius and extensive infrared radiation

absorption capabilities. Among them, PbS and PbSe QDs have been integrated into various optoelectronic devices, such as solar cells and photodetectors, showcasing superior performance. Notably, their excellent absorption properties in the SWIR region underscore their potential in LiDAR systems. Although PbSe QDs display superior mobility characteristics compared to PbS,[1] they have a lower chemical yield. Furthermore, lead chalcogenide QDs exhibit size-dependent air-stability,[2] with PbSe showing significantly compromised air-stability, especially in the SWIR region. Pb_xSe_{1-x} QDs might provide an alternative solution to overcome these critical shortcomings.

Long Hu et al. highlighted enhanced mobility in FETs and better PCE in solar cells through the simple admixture of PbSe with PbS.[3] Wanli Ma et al. described Pb_xSe_{1-x} QDs that exhibited improved J_{sc} compared to PbS and enhanced V_{oc} relative to PbSe.[4] Despite the potential of Pb_xSe_{1-x} QDs in photovoltaic applications, a deeper investigate into their air-stability and other material properties remains essential. Additionally, studies to date have not conclusively explored properties concerning compositional shifts, primarily because inevitable wavelength alterations occur with changes in the anion ratio.

We successfully synthesized Pb_xSe_{1-x} QDs active in the SWIR region through a simple synthesis method by injecting a mixture of anion precursors. The QDs, synthesized uniformly, were compositionally engineered to absorb within a consistent wavelength range. Compared to the chemical yield observed in PbSe QDs, there was a marked enhancement for our Pb_xSe_{1-x} QDs with the yield being approximately three times greater. Under ambient conditions, the blue shift phenomenon resulting from oxidation is reduced and surface analysis provided evidence that the formation of Se oxide (either SeO₂ or SeO₃²⁻) was notably diminished. The mobility in FETs was improved compared to that of PbS QDs and Pb_xSe_{1-x} QDs ink was produced for the first time through a ligand exchange from long chain to short. Moreover, Pb_xSe_{1-x} in the NIR region demonstrated solar cell efficiencies exceeding 10%, the highest on record. These findings emphasize the promising future of Pb_xSe_{1-x} QDs in infrared optoelectronic applications.

References

1. Lin, Q.; Yun, H. J.; Liu, W.; Song, H. J.; Makarov, N. S.; Isaenko, O.; Nakotte, T.; Chen, G.; Luo, H.; Klimov, V. I.; Pietryga, J. M. Phase-Transfer Ligand Exchange of Lead Chalcogenide Quantum Dots for Direct Deposition of Thick, Highly Conductive Films. *J. Am. Chem. Soc.* **2017**, 139, 6644.
2. Choi, H.; Ko, J. H.; Kim, Y. H.; Jeong, S. Steric-Hindrance-Driven Shape Transition in PbS Quantum Dots: Understanding Size-Dependent Stability. *J. Am. Chem. Soc.* **2013**, 135, 5278.
3. Hu, L.; Huang, S.; Patterson, R.; Halpert, J. E. Enhanced mobility in PbS quantum dot films via PbSe quantum dot mixing for optoelectronic applications. *J. Mater. Chem. C* **2019**, 7, 4497.
4. Ma, W.; Luther, J. M.; Zheng, H.; Wu, Y.; Alivisatos, P. Photovoltaic Devices Employing Ternary Pb_xSe_{1-x} Nanocrystals. *Nano Lett.* **2009**, 9, 1699.

5:00 PM EL02.05.09

π -SnS Colloidal Quantum Dots for Field-Effect Transistors Thanyarat Phuthaphongloet^{1,2,3}, Ricky Dwi Septianto¹, Retno Miranti¹, Nobuhiro Matsushita², Yoshihiro Iwasa¹ and Satria Bisri¹; ¹RIKEN CEMS, Japan; ²Tokyo Institute of Technology, Japan; ³Tokyo University of Agriculture and Technology, Japan

Significant progress in QD optoelectronic devices and energy devices has been made mainly by Pb-based, Hg-based, and Cd-based binary compounds, or the involvement of rare noble metal alloys. While some have reached commercial markets, their high degree of toxicity is the primary concern for practical applications. We recently developed a rapid one-pot method to synthesize a novel phase of tin monosulfide quantum dots (QDs), π -SnS¹. This cubic QD phase exhibits a larger band gap bandgap (1.53–1.69 eV) than the other SnS phase (the orthorhombic α -SnS), and more thermodynamically stable. This method yields QD radii below 10 nm, allowing us to explore the quantum confinement effect, which can be utilized for high-performance photodetector devices. Despite these prospects, obtaining the scalable synthesis of this SnS QD phase with good monodispersity is still challenging. On the other hand, the electronic transport properties of this material have never been investigated, which will directly impact the design of its practical uses for electronic or optoelectronic device applications.

Here we report a controllable synthesis of monodispersed π -SnS QDs and demonstrate the field-effect transistors of colloidal π -SnS QD assemblies. We can synthesize the SnS QDs with diameters ranging from 5 nm to 8 nm and better air stability through synthesis protocol optimizations than the previously reported method. Furthermore, by performing the integration of synthesis and optical absorption measurement, we could fine-tune the synthesis methods so that we can obtain the synthesis condition boundary to obtain either π -SnS QDs or α -SnS. Synthesis temperature is found to become the critical factor that can lead to different end results. The π -SnS phase was generated at a specific injection temperature range.

We are able to fabricate field-effect transistors of the π -SnS by adapting the methods of performing ligand exchange in the solid-state phase during the layer-by-layer deposition of the QD monolayers.^[2,3] The oxide-gated π -SnS QD FETs exhibit p-type characteristics with charge carrier mobility values comparable to the early development of many other metal chalcogenides QDs. This investigation will provide insights into the factors influencing the formation of different phases of SnS QDs. Furthermore, the first success of demonstrating transistor operation of π -SnS QD assemblies presents new opportunities to investigate their charge carrier transport for developing environmentally friendly QD electronics.

Refs.: [1] R. Miranti, R.D. Septianto et al. *J. Phys. Chem. C*, 126, 11 5323 (2022) [2] R.D. Septianto, L. Liu et al. *NPG Asia Mater*, 12, 33 (2020). [3] R.D. Septianto, R. Miranti et al. *Nat. Commun.* 14, 2670 (2023).

5:00 PM EL02.05.10

Chemically and Electronically Active Metal Ions on InAs Quantum Dots for Infrared Detectors Jaeyoung Seo, Seongchan Kim, Namyoung Gwak, Seungki Shin and Nuri Oh; Hanyang University, Korea (the Republic of)

Indium arsenide (InAs), one of the III-V compound semiconductors, has a relatively small carrier effective mass, direct bandgap, and small exciton binding energy, which are attractive properties for state-of-the-art electronic and optoelectronic applications. Due to the quantum confinement effect, the nano-sized crystals of InAs can possess additional benefits, including tunable optical bandgap ranging from near-infrared (NIR) to short-wave infrared (SWIR) and versatile solution processability. Given these advantages, the IR-responsive InAs quantum dots (QDs) can be integrated as a thin solid form into various IR photosensors, enabling to apply machine vision, imaging sensors, and telecommunications. For high performance of QD-based photodetectors, it is important to obtain highly monodisperse InAs QDs and control the surface defects that can enhance the charge transport properties in QD films.

The synthesis of InAs QDs is not, however, as simple as the ionic compound semiconductor nanocrystals, because of their strong covalent bonding nature and the lack of group 15 precursors. Previous researches using continuous injection and seeded growth methods have been focused on reactivity control of highly reactive silylated or germlyated arsenic precursors, which have difficulty handling to some extent due to toxicity and pyrophoric properties of the precursors. Meanwhile, co-reduction methods with commercially available arsenic precursors are another facile approach for InAs QD synthesis. The simple heat-up process along with reducing zinc and arsenic precursors together simultaneously, may be suited for large-scale production, but it normally requires a subsequent size selection process because of a broad size distribution. Additionally, as the nanoscale III-V semiconductors suffer from the oxidative defects, the surface of InAs QDs is also prone to oxidation. It is required to eliminate the oxidative defects so that the QDs are electronically connected for efficient charge extraction without charge trapping.

In this work, we propose the synthesis approach to improve monodispersity of InAs QDs based on the co-reduction method. We introduce zinc halide

precursors as a form of coordination complex into the indium and arsenic reaction mixtures. During the synthesis, the zinc ions are chemically passivating the surface of InAs QDs, allowing to induce size-focusing as well as to remove surface defects. The surface oxide-free InAs QDs are stable enough as a colloidal form even with weakly bound ligands to facilitate the follow-up process. When InAs QDs are integrated into the infrared photodiode as an IR absorber, the surface zinc ions can electronically modulate the energy levels and carrier concentrations. The IR photodiodes with InAs:Zn QD layers exhibit higher IR sensitivity and faster response than the bare InAs QDs. We anticipate that the unique synthesis approach for InAs QDs with electronically active zinc ions should inspire QD research into a new direction for NIR and SWIR applications.

5:00 PM EL02.05.11

Interface Stoichiometry Control of InP Heterostructure Quantum Dots for Efficient Light-Emitting Diodes Seungki Shin, Nuri Oh and Jina Na; Hanyang University, Korea (the Republic of)

Colloidal quantum dots (QDs) have garnered extensive attention in optoelectronic applications due to excellent optical and electrical properties. A significant characteristic of colloidal QDs is the size-dependent optical properties. The band gap can be tuned by adjusting the particle size, enabling QDs to cover the entire visible light spectrum and near-infrared region which allows the QDs as a light-emitting diodes (LEDs), bio-imaging, photodetector, and solid-state lighting. The unique size-dependent characteristic of QDs is originate from quantum confinement effect which is observed when the QDs have smaller diameter than exciton Bohr radius. For example, the exciton Bohr radius of InP is 15 nm and 5.3 nm for CdSe. The size limitation of QDs compels the sophisticated synthesis of the emissive core materials on a nanometer scale. However, there is a rise in the surface-to-volume ratio when the size of the particles diminishes, leading to a significant increase in surface imperfections.

Indeed, the InP core exhibits photoluminescence quantum yields (PLQYs) under 1 % due to the surface defects. Forming a core/shell heterostructure in nanocrystals helps the core materials emit photons effectively. Epitaxially grown shells passivate the surface defects, such as dangling bonds, and provide the better confinement of electron/hole wavefunctions with type I band alignment. This strategy allows the InP-based QDs, which have heavy metal-free composition, to achieve near-unity PLQY. For a shell material, group II-VI materials such as ZnSe and ZnS are widely employed because they possess the wide energy band gap and low lattice mismatch with InP core. However, there is a fundamental interface misfit between the III-V composition of the InP core and the II-V composition of the shell materials. The heterogeneity between the III-V core and II-VI shell could impede radiative recombination or charge carrier transport.

In this study, we investigate the effects of interface stoichiometry in InP-based core/shell structure QDs on optical and electrical properties. We control the chemical composition at interface of InP core/shell QDs to improve the charge carrier injection efficiency in QD-based LEDs (QD-LEDs) by in-situ selenium treatment. This strategy allows the excess indium and zinc ions to be anchored on the surface during the InP core synthesis, resulting in the formation of In/Zn thin alloy layer. The surface stoichiometry of the in-situ Se-treated InP core can be tuned by controlling the feed ratio of indium and zinc precursor. The change of binding energy of selenium depending on the In/Zn feed ratio in X-ray photoelectron spectroscopy (XPS) analysis confirmed the formation of In/Zn alloy layer. Photoluminescence (PL) analysis showed that the InP core with In/Zn alloy layer exhibit higher PLQYs than InP core with Zn-rich interface even after thick shell growth. Ultraviolet photoelectron spectroscopy (UPS) analysis revealed that the in-situ Se treatment modifies the energy band alignment, leading to an enhanced charge carrier balance in QD-LEDs. As a result, the QD-LEDs based on the Se-treated InP QDs show peak current efficiency as 31.5 cd/A and a maximum luminance of 26370 cd/m² for green emission.

5:00 PM EL02.05.12

Luminescence and Covalency in Yb³⁺-Doped CrX₃ (X = Cl, Br, I) Van der Waals Compounds Thom Snoeren, Kimo Pressler, Kelly M. Walsh and Daniel R. Gamelin; University of Washington, United States

The layered 2D van der Waals ferromagnets CrX₃ (X = Cl, Br, I) are some of the most promising and well-studied materials for spintronics and related quantum systems. Despite potential applications in quantum sensing and as single-photon sources, investigations on the optical properties of CrX₃, characterized by broad *d-d* photoluminescence (PL), are severely lacking. The incorporation of carefully designed atomic defects such as lanthanides opens up a pathway to modulate the overall electronic and magneto-optical properties. Here we report preparation, structural characterization, and spectroscopic studies of all three CrX₃ compounds doped with the optical impurity Yb³⁺. 4 K PL measurements show efficient sensitization of Yb³⁺ luminescence upon photoexcitation into lattice absorption bands for all three compounds, converting their nondescript broadband *d-d* PL into sharp *f-f* emission. The PL of CrCl₃:Yb³⁺ and CrBr₃:Yb³⁺ occur at energies typical for [YbX₆]³⁻ with these halides, with PL decay times of 0.5 – 1.0 ms at 4 K, but CrI₃:Yb³⁺ displays anomalously low-energy Yb³⁺ emission and an unusually short PL decay time at 4 K. Data analysis and angular overlap model (AOM) calculations show that Yb³⁺ in CrI₃:Yb³⁺ has a lower spin-orbit splitting energy than reported for any other Yb³⁺ in any other compound. We attribute these observations to exceptionally high covalency of the Yb³⁺ *f* orbitals in CrI₃:Yb³⁺ stemming primarily from the shallow valence-shell ionization potentials of the iodide anions. These results provide rare fundamental insights into the electronic structure and luminescence of the remarkably underexplored [YbI₆]³⁻ motif.

5:00 PM EL02.05.13

Thermally-Induced Isomerization of Prenucleation Clusters during the Prenucleation Stage of CdTe Quantum Dots Zhe Wang and Kui Yu; Sichuan University, China

The evolution of prenucleation clusters in the prenucleation stage of colloidal semiconductor quantum dots (QDs) has remained unexplored. With CdTe as a model system, we show that substances form and isomerize prior to the nucleation and growth of QDs. Called precursor compounds (PCs), the prenucleation clusters are relatively optically transparent and can transform to absorbing magic-size clusters (MSCs). When a prenucleation-stage sample at 25, 45, or 80 °C is dispersed in a mixture of cyclohexane (CH) and octylamine (OTA) at room temperature, either MSC-371, MSC-417, or MSC-448 evolves with absorption peaking at 371, 417, or 448 nm, respectively. We propose that PC-371 forms at 25 °C, and isomerizes to PC-417 at 45 °C and to PC-448 at 80 °C. The PCs and MSCs are quasi isomers. Relatively large and small amounts of OTA favor PC-371 and PC-448 in dispersion, respectively. The present findings suggest the existence of PC-to-PC isomerization in the QD prenucleation stage.

5:00 PM EL02.05.14

Ligand Boosting of CsPbBr₃ Nanoplatelets for Highly Stable Efficiency Blue LED Subin Yun, Artavazd Kirakosyan, Min-Gi Jeon, Joonseok Kim and Jihoon Choi; Chungnam National University, Korea (the Republic of)

Perovskite light-emitting diodes (PeLEDs) with an external quantum efficiency (EQE) exceeding 20% have been achieved in both green and red emissions. On the other hand, the efficiency of blue perovskite materials has lagged far behind, with EQEs of 12.3% emitting the sky blue (wavelength at 475–490 nm) and 8.8% emitting the blue (wavelength at 460–475 nm). Several strategies have been proposed for the synthesis of blue-emitting perovskite nanocrystals such as (i) mixed halide perovskites and (ii) low-dimensional nanoplatelets (NPLs). Whereas the mixed halide perovskites show a variable energy bandgap, they have critical drawbacks such as a deep trap state in the bandgap owing to the formation of Cl⁻ vacancies and phase segregation arising from ion migration. In CsPbBr₃ NPLs, the emission wavelength can be controlled depending on the number of [PbBr₆]⁴⁻ layers. However, the high density

of surface defects in 2D perovskite nanocrystals results in a low photoluminescence quantum yield (PLQY), which imposes challenging issues. Here, we demonstrate that the PLQYs of CsPbBr₃ NPLs could be significantly enhanced by adopting inorganic ligands, which can effectively passivate the surface defects. To boost the PL and PLQY of NPLs, several organic/inorganic ligands (such as PbBr₂, C₆H₁₂BrN, and N₂H₃Br (HZBr)) are used. The PLQY of CsPbBr₃ NPLs is significantly enhanced from 34% to 90% when HZBr is used as the ligand can be effectively coordinated at the surface defects of the CsPbBr₃ NPLs. In addition, we conducted the cryogenic PL spectroscopic measurement. Interestingly, in the HZBr-treated sample, the activation energy for carrier trapping is increased from ~180 to 290 meV indicating that the surface vacancies and the associated defect states are well passivated. Furthermore, the exciton-longitudinal optical (LO) phonon coupling coefficient and LO phonon energy are reduced from ~280 to 100 meV and from ~30 to 20 meV, respectively. It suggests that the contribution of exciton-LO coupling to the broadening of PL became weaker.

SESSION EL02.06: Surface Chemistry, Electronic and Optical Properties of Semiconducting Nanocrystals I
Session Chairs: Hao Nguyen and Nayon Park
Thursday Morning, April 25, 2024
Room 347, Level 3, Summit

8:30 AM EL02.06.01

Chemical Modification of CdSe Nanomaterials through Carborane Ligand Exchange [Eugenia S. Vasileiadou](#), Victoria Rubio, Elijah Cook, Tasnim Ahmed, Alexander Spokoiny and Justin Caram, University of California, Los Angeles, United States

Inorganic nanocrystals capped with surfactant-like organic ligands exhibit a broad range of properties that emerge from the combination of the individual inorganic-organic components. By expanding towards functional organic ligands that are bounded on the nanocrystal surface, the charge-transport and biocompatibility of nanocrystals are enhanced, thus achieving greater chemical control of nanomaterials for targeted applications. Herein, we functionalize CdSe nanocrystals through binding with electron-donating carborane ligands (C₂B₁₀H₁₂). The synthetic preparation for CdSe quantum dots (QDs) and CdSe nanoplatelets is developed where variable concentration ligand exchange of the CdSe nanomaterials with the carborane ligands leads to changes in the photoluminescence (PL) intensity. Post-synthetic ligand exchange of the native oleate capping ligands for carborane results in a red-shift of the optical band gap of the studied CdSe QDs, while their colloidal stability is maintained based on TEM imaging. Fourier-transform infrared (FTIR) analysis demonstrates the successful incorporation of the carborane ligands onto the CdSe surfaces with the characteristic B-H resonances at 2600 cm⁻¹ and 1250-600 cm⁻¹ in the spectrum. Furthermore, we explore tuning the surface dipole of the CdSe core from a non-functional oleate ligand to functional carborane dipole, where the carborane dipole enables long-range ordering and higher control on the electronic properties of the resultant CdSe core/carborane shell. Altogether, this work illustrates the unique aspects of functional surface carborane ligands in controlling the optoelectronic and dipole properties of CdSe nanocrystals, which could advance their potential applications in solid-state device and bioimaging applications.

8:45 AM *EL02.06.02

Structural Transformations of Group III-V and II-VI Magic-Sized Clusters Driven by Atomic-Bond Exchanges [Joongoo Kang](#); Daegu Gyeongbuk Institute of Science and Technology, Korea (the Republic of)

Multistep nucleation and growth of quantum dots (QDs) involves the utilization of kinetically persistent, small inorganic clusters, specifically magic-sized clusters (MSCs), as intermediates. Therefore, understanding and control of the reactivity (or stability) of MSCs is essential to such non-classical QD synthesis. In this talk, using *ab initio* molecular dynamics (AIMD) simulations, we reveal the destabilization process of a carboxylate-ligated In₃₇P₂₀ MSC, induced by a surface ligand network modification beyond a critical limit.¹ At elevated temperatures, the release of three In(O₂CR)₃ subunits triggers the sudden loss of stability in the remaining In₃₄P₂₀ core, leading to structural transformations through In-P bond breaking and rearrangement. This isomerization manifests as an In-P bond exchange between a pair of In atoms, resulting in a “rupture” on the cluster surface. The structural disruption in the InP cluster causes noticeable changes in the simulated UV-vis absorption spectra and XRD patterns, which agree well with experimental findings² on MSC destabilization induced by reactions with primary amines at low temperatures. Our analysis elucidates that the MSC instability is driven by the intricate interactions between the surface ligand network and the inorganic core of the group III-V MSC. Finally, we discuss the fundamental differences in the isomerization of the InP MSC and a related CdS cluster of similar size,^{3,4} highlighting the distinct nature of surface ligand networks in the group III-V and II-VI cluster systems.

1. D. Shim and J. Kang, *Chem. Mater.* **2023**, *35*, 700–708.
2. D. C. Gary, A. Petrone, X. Li, and B. M. Cossairt, *Chem. Commun.* **2017**, *53*, 161–164.
3. C. B. Williamson et al., *Science* **2019**, *363*, 731–735.
4. D. Shim, J. Lee, and J. Kang, *Chem. Mater.* **2022**, *34*, 9527–9535.

9:15 AM *EL02.06.03

The Surface Chemistry of Colloidal Semiconductor Quantum Dots [Ivan Infante](#); BCMaterials - Basque Center of Materials, Spain

Despite significant progress in recent years in understanding the chemical reactions occurring on the surfaces of II-VI, III-V, and lead halide perovskite quantum dots (QDs), there are still fundamental questions that remain unanswered regarding the nature of QD surfaces, QD-ligand interactions, and the formation of trap states. Addressing these aspects is crucial for enhancing the optoelectronic efficiency of QDs.

In this study, we present a pioneering multiscale modeling approach that combines Density Functional Theory and Molecular Dynamics simulations. Our approach encompasses QDs ranging from small to real-sized QDs passivated with oleate ligands and immersed in organic solvents. Through this methodology, we gain invaluable insights into the surface characteristics and the binding energies of ligands under different experimental conditions. This methodology not only provides a deeper understanding of the intricate behavior of colloidal semiconductor nanocrystals but also paves the way for future advancements in their diverse applications.

9:45 AM EL02.06.04

Engineering The Surface Chemistry of Colloidal InP Quantum Dots for Charge Transport [Tianshuo Zhao](#)^{1,2}, Qinghua Zhao², Jaeyoung Lee², Shengsong Yang², Han Wang², Ming-Yuan Chuang², Yulian He³, Sarah M. Thompson², Guannan Liu^{2,3}, Nuri Oh², Christopher B. Murray² and Cherie R. Kagan²; ¹The University of Hong Kong, Hong Kong; ²University of Pennsylvania, United States; ³Yale University, United States

Colloidal InP quantum dots (QDs) have emerged as potential candidates for constructing nontoxic QD-based optoelectronic devices. However, charge

transport in InP QD thin-film assemblies has been limitedly explored. Herein, we report the synthesis of ~8 nm edge length (~6.5 nm in height), tetrahedral InP QDs and study charge transport in thin films using the platform of the field-effect transistor (FET). We design a hybrid ligand-exchange strategy that combines solution-based exchange with S²⁻ and solid-state exchange with N³⁻ to enhance interdot coupling and control the n-doping of InP QD films. Further modifying the QD surface with thin, thermally evaporated Se overlayers yields FETs with an average electron mobility of 0.45 cm² V⁻¹ s⁻¹, ~10 times that of previously reported devices, and a higher on-off current ratio of 10³-10⁴. Analytical measurements suggest lower trap-state densities and longer carrier lifetimes in the Se-modified InP QD films, giving rise to a four-time longer carrier diffusion length.

10:00 AM BREAK

10:30 AM *EL02.06.05

Photogenerated Spin states in Quantum Dot – Molecule Conjugates Jacob Olshansky; Amherst College, United States

The inherent spin polarization in photogenerated spin-correlated radical pairs makes them promising candidates for quantum computing and quantum sensing applications. Notably, these states are spin-polarized (non-Boltzmann populated) at moderate temperatures, and can therefore be initialized in well-defined quantum states. This feature allows them to be probed and manipulated using microwave pulses within standard electron paramagnetic resonance spectrometers equipped with pulsed lasers. Quantum dot – molecule conjugates offer a tunable platform for hosting these spin-correlated radical pairs. We have therefore designed a series of quantum dot – molecular systems that can produce photogenerated spin-polarized states. The molecules are chosen for their ability to undergo efficient charge separation, and the nanoparticle materials, ZnO quantum dots, are chosen for their promising spin properties. Transient and steady state optical spectroscopy performed on ZnO quantum dot–molecular conjugates shows that reversible photogenerated charge separation is occurring. Transient and pulsed electron paramagnetic resonance experiments are then performed on the photogenerated radical pair, which demonstrate that (1) the radical pair is polarized at moderate temperatures and well modeled by existing theories, (2) the spin states can be accessed and manipulated with microwave pulses, and (3) the spin system can be tuned with quantum dot size and molecular linker length. This work opens the door to a new class of promising qubit materials that can be photogenerated in polarized states and hosted by highly tailorable inorganic nanoparticles.

11:00 AM EL02.06.06

Erbium Spin Defects in Colloidal Ceria Nanocrystals with Near Microsecond Spin Coherence Joeson Wong^{1,2,1}, Arashdeep Thind³, Jasleen Bindra², Jiefei Zhang^{2,2}, Gregory Grant^{2,1}, Christina Wicker¹, Yuxuan Zhang¹, Jens Niklas², Oleg Poluektov², Robert F. Klie³, F. Joseph P. Heremans^{2,1,2}, David Awschalom^{1,2,2} and Paul Alivisatos^{1,1,1}; ¹The University of Chicago, United States; ²Argonne National Laboratory, United States; ³University of Illinois at Chicago, United States

We experimentally demonstrate spin coherence times approaching a microsecond in erbium doped ceria nanocrystals with an ensemble average level of a single erbium per nanocrystal. To achieve these spin coherence times, ceria was chosen as a host material with a low natural abundance of nuclear spins. As a result, we observe population lifetimes that approach a millisecond, suggesting substantial improvements to the spin coherence should be possible. We postulate that the spin coherence is limited by the nuclear spin bath of hydrogen atoms from the oleic acid ligands on the surface of the nanocrystal. Quantum beats are observed which correspond to the Larmor frequency of hydrogen, which further suggests the erbium ions are sensitive to the nearby hydrogen nuclei. Scanning transmission electron microscopy measurements combined with electron energy loss spectroscopy further show that Ce³⁺ and O vacancies are prevalent on the surface of the nanocrystal, likely playing a role in the observed spin coherence and lifetime. Nonetheless, the spin coherence already demonstrated suggests that spin defects in nanocrystals are a promising materials platform for quantum information processing.

11:15 AM *EL02.06.08

Colloidal Atomic Layer Deposition enables Synthesis of Nano-Heterostructures with Atomic Layer Precision Dmitri V. Talapin; University of Chicago, United States

In contrast to molecular systems, which are defined with atomic precision, nanomaterials generally show some heterogeneity in size, shape, and composition. The sample inhomogeneity translates into a distribution of energy levels, band gaps, work functions, and other characteristics. The lack of atomistic control during nanomaterial synthesis also limits our ability to perform “total-synthesis” of sophisticated nano-heterostructures with precisely arranged multiple components and fine-tuned properties. We discuss a general synthetic strategy which largely circumvents these limitations of traditional colloidal synthesis. Colloidal Atomic Layer Deposition (c-ALD) allows significant reduction of inhomogeneity for nanomaterials without compromising their structural perfection. We report a novel realization of c-ALD step sequence which significantly improves synthetic control and quality of synthesized nanomaterials. In traditional gas-phase ALD, the substrate and gaseous reactants act as the stationary and mobile phases, respectively. Such distinction facilitates removal of unreacted precursors by pulsing inert gas after each half-reaction. For c-ALD, we inverted the stationary and mobile phases – reactants form the stationary phase while the substrate is moved in and out of the reactor as the mobile phase. This approach brings c-ALD closer to traditional ALD and is expected to make it a similarly powerful and versatile technique. Our improved c-ALD enables synthesis of epitaxial nano-heterostructures of unprecedented complexity, ultimately enabling bandgap and strain engineering in colloidal nanomaterials synthesized with close-to-atomistic accuracy. Improved synthetic control elucidates the effects of quantum confinement and strain on the properties of semiconductor nanostructures.

11:45 AM EL02.06.09

Illuminating the Impact of Solvent and Particle Properties on Optical Manipulation of Colloidal Nanomaterials Brandon Reynolds and Matthew Crane; Colorado School of Mines, United States

The precise control over the placement of colloidal nanomaterials has led to enticing emergent phenomena including transport through superlattices, strong coupling with optical cavities for quantum applications, and hybridization when different colloidal materials are interfaced. These applications and many more require precise spatial placement of nanoparticles as well as precise control over orientation. As an example, defects in wide-band gap nanomaterials or spins in semiconductor nanomaterials offer promising solutions for quantum technologies that are inaccessible to bulk materials, if the colloidal materials can be precisely positioned in an optical cavity. This requires a tool that acts on a single colloid in three dimensions, controls the angle of the colloid, and is applicable to a variety of particles and a variety of solvents. Optical manipulation methods such as optical trapping provide a unique platform that addresses these criteria, by trapping a particle in three dimensions and allowing for orientation control through polarization. However, we have limited understanding of how optical manipulation may change in the environments necessary for colloidal nanomaterials – *i.e.* organic solvents, ligands, or high refractive index materials. Here, we investigate the impact of particle composition, geometry, and size as well as solvent identity on optical trapping forces using a combination of experiments and multiphysics simulations. We investigate the impact of key variables such as viscosity and refractive index on optical trapping strength. Combining these results, we identify key relationships between solvent and colloidal nanomaterials to manipulate and orient nanomaterials and suggest guidelines to further improve optical manipulation.

SESSION EL02.07: Surface Chemistry, Electronic and Optical Properties of Semiconducting Nanocrystals II
Session Chairs: Emily Miura and Hao Nguyen
Thursday Afternoon, April 25, 2024
Room 347, Level 3, Summit

1:30 PM *EL02.07.01

Dopants and Defects in Colloidal Nanocrystals [Daniel R. Gamelin](#); University of Washington, United States

Colloidal inorganic nanocrystals offer new opportunities for studying, cultivating, and exploiting electronic and optical effects at the nanoscale. New forms of magnetic materials at the nanoscale can reveal new behaviors relevant to high-density spintronics, spin-photonics, or related technologies, and new emissive nanostructures can open opportunities for additive manufacturing of conventional or quantum optoelectronics. This talk will describe the synthesis and physical properties of colloidal semiconductor and insulator nanostructures integrating dopants and defects as a route to controlling photonic functionality. The talk will describe the synthetic development, optical, and electronic-structural properties of these materials.

2:00 PM *EL02.07.02

Hot Electrons and Coherent Photons from Strongly Quantum-Confined Lead Halide Perovskite Nanocrystals and Their Assemblies [Dong Hee Son](#); Texas A&M University, United States

Imposing strong quantum confinement in lead halide perovskite nanocrystals enhances the electronic interactions between charge carriers and dopants within each nanocrystal and promotes the delocalization of the exciton wavefunction in the closely packed assemblies of these nanocrystals. We investigated: (i) the generation of hot electrons via exciton-to-hot electron upconversion in strongly quantum-confined cesium lead bromide (CsPbBr₃) nanocrystals doped with Mn²⁺ and (ii) the coherent photon emission from the superlattices of CsPbBr₃ quantum dots, where strong quantum confinement plays a significant role. The enhanced exciton-dopant interaction in the more strongly confined CsPbBr₃ nanocrystals proved beneficial for hot electron upconversion and allowed for the utilization of the long-lived dark exciton in such processes at low temperatures. The closely-packed QD superlattice of the strongly confined CsPbBr₃ quantum dots, which are 4 nm in size, exhibited superfluorescence from excitons delocalized across many quantum dots, rather than from an ensemble of electronically non-coupled quantum dots, especially as the temperature decreased. Positioning the superlattice within the micro-ring resonance cavity further amplified the coherent emission from the interconnected quantum dots.

2:30 PM EL02.07.03

Assessing Photoinduced Carrier and Heat Transfer in Tin-Doped Indium Oxide Nanocrystals Sara Russo, Lauren Cisneros and [Matthew Crane](#); Colorado School of Mines, United States

Degenerately doped semiconductor nanocrystals exhibit tunable localized surface plasmon resonances with strong optical absorption cross sections and band gaps. Upon excitation, these materials produce non-equilibrium carrier distributions that rapidly relax, presenting a brief window for utilization. These features mark plasmonic nanocrystals as promising candidates for new applications that require efficient light absorption and highly directed energy and carrier utilization, such as photodetectors, photovoltaics, and photocatalysts, if we can understand and engineer efficient transport mechanisms. Here, we investigate hot carrier and heat transfer from prototypical tin-doped indium oxide (ITO) nanocrystals to adsorbates as a model system for harvesting and utilizing light in plasmonic semiconductor nanocrystals. Using transient absorption spectroscopy, we track carrier and energy transfer from ITO nanocrystals to adsorbates and evaluate the impact of aliovalent dopant concentration, wavelength, and energy level alignment. We find that these variables strongly impact carrier transfer to adsorbates. Utilizing local temperature reporters, we simultaneously quantify heat transfer from ITO nanocrystals into their environment. Combining these results, we suggest general design rules to optimize carrier energy transfer from plasmonic semiconductors.

2:45 PM BREAK

3:15 PM *EL02.07.04

Anion Exchange in Discretely Grown Semiconductor Nanomaterials Yalei Deng, Xinke Kong, Lin Ru and [Yuanyuan Wang](#); Nanjing University, China

Ion exchange is emerging as a powerful post-synthetic strategy to engineer unprecedentedly high-quality nanomaterials by tuning chemical composition, crystal phase, doping, and morphology. Several heterostructured nanocrystals have been prepared through cation exchange (CE) reactions. However, in contrast to CE, the study of anion exchange (AE) processes is still in its infancy. Since the larger size and slower migration rate of anions, the exchange process usually requires high reaction temperatures, which leads to the reconstruction of the original frameworks, thus causing structural changes or collapse. Here, we used magic size clusters (MSCs) and nanoplatelets (NPLs), two discretely grown nanomaterials, as model systems to study the AE. We showed that two different AE pathways exist in the transition of MSCs, which are determined by the MSCs' compositions and structures. In addition, we achieved AE in two-dimensional nanocrystals, by which either type I or type II NPLs can be obtained without the Kirkendall effect. The heterostructured NPLs show improved optical properties. For example, the quantum efficiency of CdSe-CdS NPLs at 462 nm can be increased from 13.63% to 63.68%.

3:45 PM EL02.07.05

High Mobility and Low Trap Density in 3D PbS Quantum Dots Superlattices by PbI₂ Passivation [Jacopo Pinna](#)¹, [Elisa Pili](#)¹, [Razieh Mehrabi Koushki](#)¹, [Dnyaneshwar S. Gavhane](#)¹, [Francesco Carlà](#)², [Bart J. Kooi](#)¹, [Giuseppe Portale](#)¹ and [Maria Antonietta Loi](#)¹; ¹University of Groningen, Netherlands; ²Diamond Light Source, United Kingdom

Lead chalcogenide colloidal quantum dots (CQDs) are one of the most promising materials to revolutionize the field of optoelectronics. This is due to their unique optical properties, namely the bandgap tunability in a wide wavelength range (800 – 3000 nm). Even if the past two decades of research resulted in significant development of this technology, these materials still show moderate mobility and high trap densities, which are a limitation for their applications. Most of the problems stem from the disordered nature of the deposited films and poor control over the ligand exchange (LE). It is predicted that ordered assemblies of CQDs, the so-called superlattices (SLs), should display mobilities up to four orders of magnitude higher than the disordered counterparts. Recently, we demonstrated mobilities above 270 cm²/Vs in 3D SL of PbSe CQDs¹¹, when surface traps are filled using an ionic-gel gate. Nevertheless, using PbSe CQDs is undesirable for applications due to its tendency to oxidise very easily. On the other hand, PbS shows much higher stability even in air when proper passivation strategies are adopted. While there are several reports in the literature on PbS-based superlattices, the focus has been on structural characterisation and often transport properties are not measured. A recent report on 2D square SL with PbS CQDs demonstrated electron mobilities of 15 cm²/Vs with ionic liquid gating.

Here we demonstrate for the first time highly ordered 3D SLs of electronically coupled PbS CQDs and an effective trap passivation with iodide-based

ligands. To be suitable for photodetection, we grow films up to 220 nm of thickness with outstanding coherent ordering, both in-plane and along the thickness, as proved by electron microscopy and advanced x-ray scattering techniques. To achieve electronic coupling, we perform LE with ethylenediamine which, despite the noticeable thickness, removes the oleic acid ligand. We finally test the transport properties with an ionic-gel gated field-effect transistor and observe n-type transport, high conductance, and modulation. The measured electron mobilities achieve a maximum of 220 cm²/Vs, which is one order of magnitude above the state-of-the-art for PbS SLs with comparable gating, proving how the 3D structures outperform the 2D ones thanks to the better ordering. Finally, a passivation treatment with PbI₂ is shown to reduce the surface trap density as demonstrated by a significant reduction of the subthreshold swing. The combination of strong absorption in the short-wavelength infrared range and the record charge mobilities make these metamaterials an excellent candidate for fast-response photodetector in a wavelength range where traditional semiconductors perform poorly despite the high cost. We also demonstrate how surface trap passivation will be a key element to control in order to implement these 3D SLs in optoelectronic devices.

[1] J. Pinna, R. M. Koushki, D. S. Gavhane, M. Ahmadi, S. Mutalik, M. Zohaib, L. Protesescu, B. J. Kooi, G. Portale, M. A. Loi, *Advanced Materials* **2023**, *35*, 2207364.

4:00 PM EL02.07.06

Optical and Electrical Investigations to Unveil Charge Storage and Transport Mechanisms in ITO Nanocrystals. [Anjana P. Muraleedharan](#)^{1,2}, Nicolo Petrini¹, Sidharth Kuriyil¹, Luca Rebecchi¹, Priyadarshi Ranjan¹, Mukesh Kumar Thakur¹, Andrea Rubino¹, Nicola Curreli¹ and Ilka Kriegel¹; ¹Italian Institute of Technology, Italy; ²University of Genova, Italy

Transparent conducting oxide (TCO) zero-dimensional (0D) nanocrystals (NCs) such as Indium-Tin-Oxide (ITO) are of special importance for optoelectrical devices because of their unique features of optical transparency in the visible region and controllable electrical conductivity. In order to fully realize the potential of these materials to integrate them into useful devices, greater understanding of the charge transport in nanocrystal thin films along with a deep insight into the charge storage mechanism in solution is necessary¹. Doped metal oxide nanocrystals (MO NCs) are potential candidates for accumulating multiple electrons through the light induced doping process termed 'Photodoping'. It has been demonstrated recently that metal oxide (MO) nanocrystals can act as nanocapacitors when coupled with a suitable system acting as hole or electron acceptor, storing the charges that are generated upon illumination with photon energy above the MO bandgap². ITO NCs with different In₂O₃ (IO) shell thicknesses are charged using a UV LED in a controlled and inert atmosphere, simultaneously monitoring the changes in the absorption spectra over time with time resolution of few seconds. In this way we extract information on the dynamics of the light-driven charging process of a set of ITO/In₂O₃ core/shell (ITO/IO) NCs with "artificial" depletion regions.³ In addition, we leverage a metal-insulator-metal device configuration to probe the electronic transport in Tin doped Indium Oxide nanocrystals (ITO nanocrystals) to understand the electrical effects of photodoping.⁴ The electronic conduction in ITO NC thin film is studied in dark and light (UV) conditions in order to understand light-induced charge generation. ITO, being a wide bandgap material with high native doping levels, manifest electronic conduction that resembles semiconductor behaviour.

References:

- (1) Ghini, M.; Curreli, N.; Camellini, A.; Wang, M.; Asaithambi, A.; Kriegel, I. Photodoping of Metal Oxide Nanocrystals for Multi-Charge Accumulation and Light-Driven Energy Storage. *Nanoscale* **2021**, *13* (19), 8773–8783. <https://doi.org/10.1039/D0NR09163D>.
- (2) Kriegel, I.; Ghini, M.; Bellani, S.; Zhang, K.; Jansons, A. W.; Crockett, B. M.; Koskela, K. M.; Barnard, E. S.; Penzo, E.; Hutchison, J. E.; Robinson, J. A.; Manna, L.; Borys, N. J.; Schuck, P. J. Light-Driven Permanent Charge Separation across a Hybrid Zero-Dimensional/Two-Dimensional Interface. *J. Phys. Chem. C* **2020**, *124* (14), 8000–8007. <https://doi.org/10.1021/acs.jpcc.0c01147>.
- (3) Ghini, M.; Curreli, N.; Lodi, M. B.; Petrini, N.; Wang, M.; Prato, M.; Fanti, A.; Manna, L.; Kriegel, I. Control of Electronic Band Profiles through Depletion Layer Engineering in Core-Shell Nanocrystals. *Nat. Commun.* **2022**, *13* (1), 537. <https://doi.org/10.1038/s41467-022-28140-y>.
- (4) Müller, K.-H.; Wei, G.; Raguse, B.; Myers, J. Three-Dimensional Percolation Effect on Electrical Conductivity in Films of Metal Nanoparticles Linked by Organic Molecules. *Phys. Rev. B* **2003**, *68* (15), 155407. <https://doi.org/10.1103/PhysRevB.68.155407>.

4:15 PM EL02.07.07

The Role of Colloidal Er-Doped SiO₂ Thin-Film Interfaced with Czochralski Silicon on Enhanced Bandgap Emission for Optoelectronic Applications [Sufian Abedrabbo](#)¹, Anthony T. Fiory² and Nugehalli M. Ravindra³; ¹Khalifa University, United Arab Emirates; ²Integron Solutions LLC, United States; ³New Jersey Institute of Technology, United States

Colloidal silica bulk glass and coatings have been studied extensively for many years. In this work we report a new optoelectronic phenomenon introduced by interfacing Er-doped sol-gel silica on Czochralski silicon (Cz-Si). The discovery is noteworthy on two aspects: (i) strong enhancement of bandgap emission, and (ii) modeling the observed luminescence spectra reveals strong dominance of correlated electron-hole (e-h) radiative recombination. Colloidal interfacial reactions with Cz-Si surface are known to introduce random interfacial strain fields that favors the radiative recombination interactions. The modeling of the room-temperature photoluminescence spectra exhibit attenuates a strong attenuation of the shorter tail of the emission spectra; thus, amplifying the excitonic e-h. The presentation will also include a comparative study of the bandgap emission of thermally oxidized Cz-Si with the colloidal prepared spin-coated silica on Cz-Si to highlight the discovery.

SESSION EL02.08: Poster Session II: Towards Atomically Precise Colloidal Materials for Conventional and Quantum Optoelectronics II
Session Chairs: Brandi Cossairt, Hao Nguyen and Gillian Shen
Thursday Afternoon, April 25, 2024
Flex Hall C, Level 2, Summit

5:00 PM EL02.08.01

Surface-Mediated Photomultiplication based on Colloidal InAs Quantum Dots enabled by Dual-Ligand Passivation [Min-Jae Si](#)¹, Seungin Jee¹, Minjung Yang¹, Dongeon Kim¹, Yongnam Ahn¹, Seungjin Lee² and Se-Woong Baek¹; ¹Korea University, Korea (the Republic of); ²Korea Institute of Energy Technology, Korea (the Republic of)

For next-generation infrared (IR) detection in various applications, such as virtual reality, recognition, and quantum communication, solution-processed low bandgap semiconductors are essential for both absorption and emission of IR light. Colloidal quantum dots (CQDs) of the III-V group are of particular interest as non-toxic, band-gap-tunable materials that are suitable for IR absorbers; however, their device performance is still inferior to that of Pb-based devices. Here, we present a universal surface passivation method for InAs CQDs enabled by intermediate phase transfer (IPT). IPT is a preliminary process that exchanges native ligands with aromatic ligands on the CQD surface, yielding a highly stable CQD ink and resultant uniform film. We fabricated CQD near-infrared (NIR) photodetectors fabricated by IPT process. The precise control of surface ligands enabled by IPT allows tuning of trap state densities and surface-mediated photomultiplication, resulting in significant gain control up to ~ 10 with fast rise/fall response time ($\sim 12/36$ ns). The optimal CQD photodiodes yield one of the highest FOM's among all previously reported solution-processed nontoxic semiconductors, including organic, perovskite, and CQD, in the NIR wavelength range considering EQE versus response time (or -3 dB bandwidth).

5:00 PM EL02.08.02

Exploiting Cation Exchange to Synthesize Well-Defined Three-Component CuInS₂ Nanocrystals Ji Tianmeng; Peking University, China

Cation exchange has emerged as a compelling strategy for crafting nanocrystals with intriguing compositions and structures, overcoming limitations inherent in direct-synthesis approaches. However, well-defined synthesis of multi-component nanocrystals with a single phase by finely tuning cation exchange kinetics remains challenging. Multi-component nanocrystals, such as CuInS₂ and CuInSe₂, have attracted significant interest owing to their diverse applications in optics, electronics, and catalysis. Utilizing Cu_{2-x}S nanocrystals as the host precursors and In³⁺ as the exchange cation, we successfully synthesized monodisperse CuInS₂ nanocrystals with tunable size, morphology, and near-infrared luminescence properties. An in-depth exploration into the impact of size variations and Cu vacancies of host nanocrystals on cation exchange kinetics was conducted. Larger-size Cu_{2-x}S nanocrystals exhibit reduced vacancy density, leading to a slower rate of cation exchange and facilitating the formation of heterostructures during the cation exchange process. Comparative analysis with directly synthesized CuInS₂ nanocrystals highlighted the controllability achieved through cation exchange. This work provides valuable insights for synthesizing multi-component nanocrystals with attractive properties.

5:00 PM EL02.08.03

Synergistic Passivation of AgBiS₂ Ternary Colloidal Quantum Dots: A Strategy for Enhancing Stability and Performance Investigated with First Principles Calculations Gaeun Cho^{1,2}, Dongeon Kim¹, Han Seul Kim³ and Se-Woong Baek¹; ¹Korea University, Korea (the Republic of); ²Korea Institute of Science and Technology Information, Korea (the Republic of); ³Chungbuk National University, Korea (the Republic of)

Solution-processed semiconductors, including perovskites, colloidal quantum dots (CQDs), and conjugated polymers, have gained significant attention for their potential applications in energy conversion and optoelectronics. Such semiconductors are characterized by their printability, low cost, and large form factors. CQDs, in particular, exhibit unique physical properties, such as quantum confinement effects, which allow for tuning of optical bandgaps across the visible to infrared spectrum. The lead-chalcogenide (PbS) CQDs have the ability to tune the bandgap to the infrared (~ 1800 nm) range. This unique feature allows for the realization of low bandgap solar cells when used as back cells in multi-junction structures. The best outcomes were achieved by introducing heavy metals, such as lead (Pb), into CQD compounds. However, due to the toxicity of these metals, the commercialization of related devices was limited.

AgBiS₂, which is a ternary compound, has attracted significant attention owing to its high absorption coefficients, tunable bandgap, and environmental stability. Various strategies have been proposed to enhance the device performance of thin-film AgBiS₂ CQD solar cells, resulting in a promising current density even under ultrathin conditions. Despite these efforts, AgBiS₂ CQD solar cells demonstrate a relatively low power conversion efficiency (PCE) compared to lead-based CQD solar cells. The main drawback of solution-processed AgBiS₂ is attributed to the use of long-chain hydrocarbon ligands during the synthesis process, which impedes charge transport in practical applications. Consequently, the exchange of surface ligands emerges as a promising strategy to overcome this limitation. Nevertheless, the theoretical understanding of the surface properties of AgBiS₂ CQDs is still lacking, which can potentially influence the exchange kinetics in the synthesis process.

In this presentation, an effective passivation of AgBiS₂ CQD surface is proposed by designing a synergistic passivation strategy with [AgI₂], [AgBr₂], and Na⁺ based on density functional theory (DFT) calculations. Utilizing (111) and (100) facets which are expected to be the primary components of CQDs, single-ligand passivation calculations on each surface demonstrated that individual cations do not effectively adhere to the (111) surface. On the other hand, the simulation revealed that the synergistic ligand approach was shown to be complementary to selective surface passivation. It was found that the initial covering of the metal halide anion reconfigures the surface, leading to subsequent cation passivation. Moreover, it was also demonstrated that the synergistic exchange can easily passivate both (111) and (100), providing a uniform passivate strategy for multiple facets. Furthermore, the experiments have demonstrated the feasibility of the theoretically suggested synergistic passivation and the improvement in performance. In particular, XPS measurements indicated that stable AgBiS₂ CQD ink were realized through synergistic passivation mechanism as suggested by the simulation. Finally, the solar cell that was fabricated based on our CQD ink achieved a power conversion efficiency (PCE) of 8.14%, which is 11% higher than the previous best report.

In conclusion, our synergistic uniform passivation strategy successfully mitigates the issue of selective surface passivation of a single ligand. By uniformly passivating the CQD surface, our strategy provides a route to significantly enhance the stability and suppress the trap states. Based on this high-quality CQD solids, we also experimentally demonstrated that ink stability, short response time, and PCE of AgBiS₂ CQD-based optoelectronic devices were significantly improved. Additionally, we anticipate that such a synergistic ligand strategy will serve as a universal approach for the development of high-performance CQD-based optoelectronic devices.

5:00 PM EL02.08.04

Toward Semiconductor Lasering Cooling Using CsPbBr₃ Nanocrystals Yang Ding, Zhuoming Zhang, Jeffrey W. Peng and Masaru Kuno; University of Notre Dame, United States

Lasering an emissive material could induce refrigeration. This counter-intuitive phenomenon requires near-unity emission quantum yields (QYs) as well as efficient single-photon anti-Stokes photoluminescence (SP-ASPL) process. CsPbBr₃ nanocrystal (NC) emerge as a promising candidate due to the readily attainable near-unity QYs and high SP-ASPL up-conversion efficiency. Herein, we developed a repeatable synthetic approach that consistently yields NCs with near-unity QYs. Subsequent systematic nuclear magnetic resonance studies unveil a close-packing surface as origin of the near-unity QYs. Additionally, the synthesized NCs also manifest a near-unity SP-ASPL up-conversion efficiency, displaying non-Arrhenius behavior. This could be rationalized by our developed polaron model. Our studies of QY and ASPL performance in CsPbBr₃ NCs lays the foundation for advancing laser cooling in this material.

5:00 PM EL02.08.05

Additive Manufacturing of Nanostructures Enabled by Ligand-Salt Stabilized Polar Nanocrystal Inks Rayne T. Anderson, Stephen L. Gibbs, Daniel R. Gamelin and John D. MacKenzie; University of Washington, United States

Solution-processable semiconductor nanocrystal (NC) materials can enable the sustainable manufacturing of NC-enabled devices such as QD displays, nanophotonics, and optical quantum devices using techniques such as inkjet printing and large-area coating. A current limitation for deposition and nanoscale resolution solution-based additive manufacturing of NCs is a common requirement for nonpolar solvent systems to sufficiently stabilize NC suspensions for effective use as NC inks. In conventional printing, such as piezoelectric or liquid vaporization-based inkjet printing, non-polar inks are ejected from micromachined inkjet nozzles. In these techniques, stable printing of minimum drop volumes on the picoliter scale and printed feature dimensions down to ~10 microns are enabled in part by the low surface energy of the apolar inks. Due to the small zeta potential that the NCs have in solution; the practicality of these inks, however, is often hindered by the concentration limits of NCs in the solvent. To move towards emerging nanoscale additive nanomanufacturing with functional materials such as single NC quantum dot (QD) heterointegration or high resolution QD microdisplay fabrication. QD inks will require finite ink polarizability to enable true nanoscale deterministic positioning and attoliter scale deposition volumes. Here, we have utilized a nitrosonium tetrafluoroborate salt to ligand exchange shelled CdSe/CdS NCs to a polar solvent, N,N Dimethylformamide (DMF), that allows for high printability at low concentrations (M-10) to additively manufacture nanoscale structures. CdSe NCs in polar DMF were utilized in electrohydrodynamic ink jet (EHDIJ) printing to additively manufacture nanostructures with <100 nm dimensions with high reproducibility. The nanoparticles were stabilized in the polar solvent through tetrafluoroborate ions via ligand exchange with nitrosonium tetrafluoroborate salt. Although the photoluminescent properties of the CdSe NCs were significantly degraded after ligand exchange, shelled CdSe/CdS NCs retained their high PL quantum yields and resulted in exceptionally stable NC/DMF suspension inks for EHDIJ at attoliter and sub-100nm feature sizes. These polar NC inks also allow for high printability at lower NC concentrations of NCs than typical non-polar inks such as octane/hexadecane mixtures. This work supports polar NC inks as a pathway towards additive manufacturing of integrated single NC quantum devices leveraging electrohydrodynamics to extract droplets 104 times smaller in volume than in conventional inkjet printing using simpler, zero moving part inkjet heads where droplet size is decoupled from the mechanical orifice size.. Electrohydrodynamic inkjet printing is a promising additive manufacturing method for fabricating nanostructures for electromagnetic enhancements and optical devices. Currently, subtractive electron beam lithography is a widely used method for generating nanoscale features. However, the requirement for conductive substrates, high cost, and high fabrication time limits the adoption of this method for research environments. We demonstrate here that sub 100nm additive nanomanufacturing of functional materials and single quantum dot printing of dilute polar NC inks is now possible.

5:00 PM EL02.08.06

Kinetically Controlled Synthesis of Quasi-Square CsPbI₃ Nanoplatelets with Excellent Stability [Mengyun Chen](#) and Feng Gao; Linköping University, Sweden

Nanoplatelets (NPLs) share excellent luminescent properties with their symmetric quantum dots counterparts, and entail special characters benefiting from the shape, like the thickness-dependent bandgap and anisotropic luminescence. However, perovskite NPLs, especially those based on iodide, suffer from poor spectral and phase stability. Here, we report stable CsPbI₃ NPLs obtained by accelerating the crystallization process in ambient-condition synthesis. By this kinetic control, we tune the rectangular NPLs into quasi-square NPLs, where enlarged width endows the NPLs with a lower surface-area-to-volume ratio (S/V ratio), leading to lower surficial energy and thus improved endurance against NPL fusion (cause for spectral shift or phase transformation). The accelerated crystallization, denoting the fast nucleation and short period of growth in this report, is enabled by preparing a precursor with complete transformation of PbI₂ into intermediates (PbI₃⁻), through an additional iodide supplier (e.g., zinc iodide). The excellent color stability of our materials remains in the light-emitting diodes under various bias stress.

5:00 PM EL02.08.07

Highly Stable Blue QLEDs through Energy Level Control with Air-Stable ZnSeTe/ZnSe/ZnS Quantum Dot [Seongwoo Cho](#)^{1,2}, Sung Nam Lim¹, Shin Ae Song¹, Kiyoung Kim¹, Sohee Jeong² and Ju Young Woo¹; ¹Korea Institute of Industrial Technology, Korea (the Republic of); ²Sungkyunkwan University, Korea (the Republic of)

Next-generation high-performance displays will be made using quantum dots (QDs) with adjustable band gaps, their superior optical properties, and ease of processing in solutions. Achieving long operational lifetimes and near-theoretical-maximum external quantum efficiency (EQE) has been realized in red and green InP-based quantum dot light-emitting diodes (QLEDs) [1,2]; however, an alternative solution is necessary to cover the blue region, such as employing a ternary ZnSeTe alloy structure with a band gap around 460 nm to replace cadmium-free blue-emission quantum dots. While semiconductor quantum dots made of ZnSeTe have recently shown extremely high photoluminescence quantum yield (PL QY) and EQE, the well-known methods of highly toxic hydrofluoric acid (HF) in their synthesis have hindered their commercialization.[3] Additionally, the PL QY in ZnSe/ZnSe/ZnS quantum dots rapidly decreases under ambient conditions despite having double shells due to rapid oxidation. Furthermore, QLEDs made with these QDs have high driving voltage and short operational lifetime, which are difficult to use in practical applications. We have developed a non-toxic synthetic method that completely eliminates the need for toxic HF in the synthesis of ZnSeTe/ZnSe/ZnS heterostructure quantum dots suitable for QLED applications. Instead of using HF, we introduced excessive metal halides, resulting in significantly improved PL QY. Importantly, we have demonstrated highly stable ZnSeTe/ZnSe/ZnS quantum dots in both the solution and the solid state through a straightforward ligand exchange process, which enhances surface binding via thiolate functional groups. In QLED devices, we investigated how the Te ratio and the size of ZnSeTe QDs affect the EQE and stability. In addition, to alleviate hole transport layer (HTL) degradation, which has an adverse effect on stability in the inverted structure, the band alignment between EML and HTL was adjusted through ligand exchange in the EML. ZnSeTe QDs, stable in both material and device, make it possible to achieve complete electroluminescent QLEDs.

References

- [1] Won, Y.-H.; Cho, O.; Kim, T.; Chung, D.-Y.; Kim, T.; Chung, H.; Jang, H.; Lee, J.; Kim, D.; Jang, E. Highly Efficient and Stable InP/ZnSe/ZnS Quantum Dot Light-Emitting Diodes. *Nature* 2019, 575 (7784), 634–638.
- [2] Moon, H.; Lee, W.; Kim, J.; Lee, D.; Cha, S.; Shin, S.; Chae, H. Composition-Tailored ZnMgO Nanoparticles for Electron Transport Layers of Highly Efficient and Bright InP-Based Quantum Dot Light Emitting Diodes. *Chem. Commun.* 2019, 55 (88), 13299–13302.
- [3] T. Kim, K. H. Kim, S. M. Choi, H. Jang, H. K. Seo, H. Lee, D. Y. Chung & E. Jang, Efficient and stable blue quantum dot light-emitting diode, *Nature* 2020, 586(7829), 385-389.

5:00 PM EL02.08.08

Superatom Clusters of Bi-Icosahedral Gold: An Optical and Electrochemical Study [Mary Sajini Devadas](#), Benjamin Raufman, Catherine Connolly, Zara Freeland and Zaid Qureshi; Towson University, United States

Gold nanostructures have been the focus of research over the past two decades because of their potential as excellent two-photon absorbers, which make them good sensors and imaging agents. This is due, in part, to their size-specific properties. Of particular interest are a class of gold nanostructures called superatoms, or magic numbered clusters, that exhibit quantum confinement effects. These structures are also referred to as nanomolecules (AuNCs). They have small enough optical band gaps to absorb in the near infrared I (near IR) region (700-900 nm) which is beneficial for biological applications. One of the most investigated superatom clusters is Au₂₅L₁₈ (L = alkyl or aryl thiols) in the icosahedron geometry. Its properties have been characterized both

experimentally and theoretically. Au₂₅L₁₈, where L = hexanethiol exhibits luminescence efficiencies of $\sim 2.5 \times 10^{-4}$ in the nearIR region with cross-sections of 2700 GM at 1290 nm which can be useful for two-photon imaging with IR light. Doping the AuNC metal core with foreign atoms is considered a powerful method for transforming Au₂₅L₁₈ into stable clusters with different electronic structures resulting in increased luminescence. In addition, this can induce magnetism which is important for magnetic imaging, and computing applications. The electronic states of these clusters can further be manipulated by adding ligands containing a chromophore or possessing redox capability. While these effects are documented, the mechanisms involved remain controversial and little work has been done with respect to its bi-counterpart. The results of this study will offer more insight to better designed AuNCs with bi-icosahedral geometrical structures that are doped (Pt, Ag, Cd, Hg) for use as novel nonlinear optical materials (NLO). The electrochemical band gap and brightness factors will also be presented.

5:00 PM EL02.08.09

Magic-Sized InP Clusters as Platforms for Core-Only Emitters with Narrow Linewidths [Grant Dixon](#) and Brandi M. Cossairt; University of Washington, United States

Colloidal quantum dots (QDs) excel at converting light or electricity into bright, tunable, color-pure luminescence, a property that promises a future of display technology that can reproduce the range of spectral hues discernable to humans. While several materials are disqualified due to hazardous substance restrictions, indium phosphide (InP) is energetically qualified and not RoHS restricted. Imparting synthetic control over the resultant photophysical properties of InP is an outstanding challenge, however. Our efforts have focused on developing the synthesis of atomically precise InP magic-sized clusters that show unique and distinct photophysical behavior from their larger QD counterparts. Importantly, these clusters demonstrate exceptionally narrow emission linewidths and long-term ambient stability, making them a promising platform for emissive materials. This is achieved by exchanging carboxylic acid ligands for phosphonic acids, employing reaction additives, and exploring post-synthetic atomistic surface modifications. Despite exhibiting exceptionally narrow ensemble linewidths, the as-synthesized clusters suffer from low photoluminescence quantum yield. Low brightness is remedied by including phosphine oxides in the synthesis, which affords highly monodisperse InP nuclei demonstrating improved photoluminescence intensity and lifetimes. Ongoing and future efforts are focused on exploring the formation, physical structure, and the role of ligands and extraneous additives on modulating the surface chemistry and resultant photophysical behavior of phosphonic acid-capped InP magic-sized clusters.

5:00 PM EL02.08.10

Scalable Nanomanufacturing of Quantum Dot Heterointegrated Nanophotonic Cavities [Gregory G. Guymon](#)¹, Theodore A. Cohen¹, David Sharp¹, Purbita Purkayastha², Stephen L. Gibbs¹, Shaun M. Gallagher¹, Arnab Manna¹, Eden A. Tzanetopoulos¹, David S. Ginger¹, Edo Waks², Daniel R. Gamelin¹, Arka Majumdar¹ and John D. MacKenzie^{1,1}; ¹University of Washington, United States; ²University of Maryland, United States

Nanophotonic structures are a foundation for the emerging field of light-based quantum networks and devices. These nanoscale structures act through their ability to couple with and manipulate photons. Colloidal quantum dots (QDs) are uniquely suited to complement this range of devices due to their solution-processability, broad tuneability, and near-unity photoluminescence quantum yields, in some cases. Here we have used electrohydrodynamic inkjet (EHDIJ) printing as a highly precise and scalable nanomanufacturing method for digital deposition of attoliter-scale QD droplets to bridge the heterointegration gap between QDs and nanophotonics. EHDIJ printing is an electrophoretic additive manufacturing process that uses applied electric fields to overcome surface energy barriers to selectively deposit charged droplets and deterministically position functional materials, including QDs, down to nanoscale resolutions.

For monolithic substrate-coupled SiN nanophotonic cavities, we have shown that CsPbBr₃ QDs can be deterministically patterned over large arrays and with sub-micrometer precision using EHDIJ printing. Additionally, we collected the first high-resolution STEM images of EHDIJ printed structures, showing that the original QD structure is preserved post-printing. Furthermore, we found that QDs within these printed structures can self-assemble into superlattice domains and that ~ 200 nm diameter printed features containing ≤ 200 QDs can be produced with this technique.

Building on this capability, EHDIJ printing has been expanded to encompass heterointegration of structures that are challenging or impossible to create by conventional subtractive semiconductor processing. An example of this is the coupling of QD emitters to substrate-decoupled nanoscale resonant structures. We have demonstrated the first successful application of EHDIJ printing for the integration of colloidal CdSe/CdS QDs with suspended nanophotonic cavities, achieving selective single-cavity deposition for cavity pairs as close as 100 nm apart. PL characterization of the as-printed cavities confirmed EHDIJ printing's ability to manufacture QD-cavity and inter-cavity coupled devices, at nanoscale spacings. This broadens the horizon for new hybrid integrated device architectures that were previously considered impossible from a materials integration standpoint.

To demonstrate this broad applicability, we have also begun to apply strategies learned from these previous demonstrations onto bullseye cavity structures. These consist of semi-complete suspended concentric rings of alternating dielectrics, SiN and air. Bullseye cavities offer increased Purcell enhancement and the unique ability to direct emission from photon sources into the far field. Using EHDIJ printing, we are integrating CsPbBr₃ QDs into 500 nm diameter cavity-centered targets, while tuning the colloidal solution's concentration and chemistry to minimize the number of QDs integrated into the devices towards single QD and single photon systems.

We believe these results will motivate the development of future suspended heterointegrated devices that utilize EHDIJ printing as a sustainable, additive, and scalable method for quantum photonics nanomanufacturing.

5:00 PM EL02.08.11

Bright Colloidal Deep-Blue-Emissive Europium Halide Nanocrystals [Jaeyeong Ha](#), Seongbeom Yeon, Hyungdo Lee, Jaehwan Lee and Himchan Cho; Korea Advanced Institute of Science and Technology (KAIST), Korea (the Republic of)

Halide perovskite nanocrystals (PNCs) are gaining significant attention as light-emitting materials due to their high color purity and facile color tuning, coupled with the ease of solution-based processing. However, a significant limitation for industrialization lies in the toxic nature of Pb-based perovskites. Additionally, the photoluminescence quantum yield (PLQY) and stability of blue-emitting PNCs have lagged behind compared to the red and green counterparts.

To address these challenges, europium (Eu)-based nanocrystals, which emit deep-blue light, have been proposed as a key eco-friendly alternative. However, the inherent properties of Eu precursors: (i) low solubility and (ii) strong organic coordination, present significant obstacles for colloidal synthesis of Eu-based nanocrystals. So far, reported colloidal Eu-based PNCs have not achieved a high PLQY exceeding 6%. In this study, we present a systematic synthetic strategy of colloidal Eu-based nanocrystals with high PLQYs. We controlled the chemical interaction between the precursors and ligands, along with modulation of reaction temperature and duration. These controlled reactions led to successful synthesis of deep-blue-emitting Eu²⁺-doped CsBr, Cs₄EuBr₆/CsBr and CsEuBr₃ nanocrystals. Notably, the synthesized colloidal CsEuBr₃ nanocrystals exhibited a high PLQY of $\sim 40\%$ and a narrow spectral linewidth. Furthermore, we investigated the chemical reactions between the precursors and ligands in-depth, suggesting the synthetic mechanisms of the colloidal Eu-based nanocrystals. This study introduces great potential of Eu-based nanocrystals for solution-

processable non-toxic blue light emitters exhibiting both high PLQY and high color purity.

5:00 PM EL02.08.12

Characterization of Photogenerated Spin Qubit Pairs in Various Dye Derivative - ZnO QD Conjugates Autumn Y. Lee and Jacob Olshansky; Amherst College, United States

Previously, we have shown that upon photoexcitation of a dye molecule - quantum dot conjugated system a charge separated state can be induced. This charge separated state possess two formerly spin-paired electrons that reside in spatially separated sites, nominally labeled as spin-correlated radical pairs (SCRPs). SCRPs, also referred to as spin qubit pairs (SQPs), have unique properties which are applicable to quantum information science. These systems can act as quantum bits, qubits, operating at moderate temperatures with well-defined quantum states. In this work, we aim to expand our understanding regarding the effect that distance between dye and quantum dot (QD) has on the presence and lifetime of SQPs. We examine this causal relationship by utilizing various linker lengths, allowing us to examine a range of distances between the QD and the dye. The specific system we have chosen to study involves various carboxylate dye molecules, perylene and BPEA derivatives, and ZnO QDs. We first study their chemical interactions using absorption isotherms and then measure the photophysics of these conjugates using both steady-state and time-resolved photoluminescence spectroscopy. Swift photoinduced electron transfer from the dye derivatives to the ZnO QD is observed, and a long-lived (> 7 ns) charge separated state is generated. This charge separated state is then analyzed using laser induced time-resolved electron paramagnetic resonance spectroscopy to fully characterize the spin dynamics of the photogenerated SQPs.

5:00 PM EL02.08.13

Nonthermal Plasma Synthesis of Water-Dispersible and Photoluminescent Silicon Quantum Dots for Bioimaging with Near Infrared Emission Yeonjoo Lee¹, Mihee Kim², James H. Werner², Jinkyong Yoo² and Uwe R. Kortshagen¹; ¹University of Minnesota, United States; ²Los Alamos National Laboratory, United States

Silicon quantum dots (Si QDs) are considered as attractive probes for bioimaging applications because of their earth-abundance, and size-tunable optical properties, nontoxicity, biocompatibility and biodegradability. In this study, one-step synthesis of water-dispersible and red-emitting Si QDs is investigated using nonthermal plasma. Nonthermal plasma is popular to produce Si QDs with superior size and shape uniformities, high purity and crystallinity which are important to obtain decent and well-controlled optical properties. The one-step synthesis method is a simplified approach to produce surface-passivated Si QDs by combining QD synthesis and surface passivation processes. Therefore, it does not require additional treatments involving high temperatures and toxic chemicals; it can save energy as well as time and reduce hazardous chemicals. We prepared water-dispersible and red-emitting Si QDs using the one-step synthesis method for the first time. Si QDs were synthesized using silane as a precursor, and their surfaces were passivated by acrylic acid. In order to improve water dispersibility, oxygen gas or water vapor was added into the passivation stage. We estimated Si QDs' size from X-ray diffraction (XRD) patterns, and the estimated diameter was 4 nm. The XRD patterns also showed the Si QDs are crystalline. The hydrodynamics diameters of QDs were measured by dynamic laser diffraction to investigate water-dispersibility. 10 to 11 nm of hydrodynamic diameters meant Si QDs can disperse well enough to be used as bioimaging probes; for instance, QDs smaller than 20 nm can cross the blood-brain barrier. The Si QDs excited by ultraviolet light (400 nm) emitted red light (peak position at ~ 830 nm) with 30% of photoluminescence quantum yield. Since skin, fat, tissue, and blood are relatively transparent in the red-to-NIR range, red-emitting Si QDs can offer deeper tissue penetration resulting in improved bioimaging quality. We conducted bioimaging using 3T3 cells cultured with the Si QDs and demonstrated the Si QDs existed inside the cells emitting red light. This result showed that our water-dispersible Si QDs enables bioimaging in NIR range. Thus, this study shows that the one-step Si QD preparation method is an energy- and time-saving as well as less hazardous route for fabricating water-dispersible and photoluminescent Si QDs which are promising materials as probes for bioimaging applications as well as diagnostic tools.

5:00 PM EL02.08.14

Synthesis and Characterization of Single-Grain Epitaxially-Fused PbSe Quantum Dot Superlattices Alex Abelson^{1,2}, Caroline Qian² and Matt Law²; ¹Lawrence Livermore National Laboratory, United States; ²University of California, Irvine, United States

Epitaxially-fused superlattices of colloidal quantum dots (QD epi-SLs) may exhibit electronic minibands and high-mobility charge transport, but electrical measurements of epi-SLs have been limited to large-area, polycrystalline samples in which superlattice grain boundaries and intragrain defects suppress/obscure miniband effects. In this talk, I will first discuss the synthesis of large-grained PbSe QD SLs, including detailed analysis of their chemical and physical structure. Next, I will discuss the mechanism by which a ligand-capped PbSe QD SL is converted into an epi-SL. Finally, I will present systematic measurements of charge transport in individual, highly-ordered PbSe QD epi-SL grains. One technical challenge in making these devices is the inherent mismatch in using traditional microfabrication techniques to make single-grained devices of air-sensitive materials. Here, we demonstrate the air-free fabrication of microscale field-effect transistors (μ -FETs) with channels consisting of single PbSe QD epi-SL grains (~ 1 - 10 μ m grain sizes) and analyze charge transport phenomena in these samples. The devices exhibit *p*-channel or ambipolar transport with a hole mobility as high as 3.5 $\text{cm}^2 \text{V}^{-1} \text{s}^{-1}$ at 290 K and 6.5 $\text{cm}^2 \text{V}^{-1} \text{s}^{-1}$ at 170–220 K, one order of magnitude larger than that of previous QD solids. Device hysteresis at higher temperatures makes the true mobility-temperature curve uncertain and evidence for miniband transport inconclusive.

SESSION EL02.09: Classical and Quantum Light Sources and Other Devices from Colloidal Quantum Dots I

Session Chairs: Hao Nguyen and Gillian Shen

Friday Morning, April 26, 2024

Room 347, Level 3, Summit

8:45 AM EL02.09.01

Colloidal Quantum Dots-Based Shortwave Infrared Photodetector: From Materials to Devices Se-Woong Baek; Korea University, Korea (the Republic of)

The detection of infrared (IR) light is crucial for realizing various future applications, including recognition, bio-imaging, spectroscopy, and object inspection. In particular, utilizing photons beyond the silicon absorption band-edge (i.e., 1550 nm) becomes important to demonstrate long-range communications and quantum technologies. Colloidal quantum dots (CQDs), semiconducting nanocrystals, are promising alternative materials due to their quantum-confined bandgap tunability across visible to shortwave-infrared (SWIR) wavelengths. However, CQD-based IR optoelectronics currently face two challenges: the use of toxic elements such as Pb, Cd, and Hg, and lower performance compared to epitaxial semiconductors.

This talk showcases how to build IR devices using non-toxic CQD materials, including III-V, I-VI, and beyond. Various short-ligand passivation strategies

enable stable CQD ink, thereby rendering high-quality conductive solids. We reveal that the extent of ligand passivation yields a surface-mediated photomultiplication effect, boosting the responsivity of devices. Furthermore, we have demonstrated an efficient avalanche breakdown in the CQD multiplication layer, achieving a fast response time below the nanosecond level with a notable gain of up to $\sim 10^4$. This represents a record gain x bandwidth product among all prior solution-processed IR photodetectors operated at 1550 nm.

9:00 AM EL02.09.02

Atomistically Tailored Surface states of Indium Phosphide Quantum Dots for Shell-Less Light-Emitter Namyoung Gwak, Seungki Shin, Seongchan Kim, Jaeyoung Seo and Nuri Oh; Hanyang University, Korea (the Republic of)

The surface complexity of III-V compound QDs has been progressively elucidated through surface etching and passivation using various surface ligands. Regardless of the synthetic routes, the surfaces of highly covalent InP QDs are prone to the formation of oxidative species due to their high oxygen affinity. These surface traps act as local energy minima that hinder or delay electron-hole recombination, consequently reducing luminous efficiency. Ideally, if the surface oxides of InP QDs can be effectively removed and the exposed DBs can be passivated with additional ligands, InP cores without a pristine shell could potentially exhibit sufficient luminescent efficiency.

As part of this research endeavor, the utilization of Lewis acidic Z-type ligands for partially coupling surface atoms has shed light on the significance of surface stoichiometry and undercoordinated surface sites in the luminescence of QDs. Z-type ligand passivation has proven effective in treating the surfaces of various InP QDs, yielding consistent outcomes irrespective of their types. Recently proposed combinational ligand passivation strategies offer safer chemical routes than HF and have shown high photoluminescence quantum yield (PLQY) for InP cores without any shells, achieving 85% PLQY with the combination of $ZnCl_2$ and InF_3 , and 60% PLQY with the combination of $ZnCl_2$ -TOP and Zn-oleate. These approaches address the challenge of eliminating the remaining undercoordination despite the effective passivation of a significant number of surface DBs using Z-type ligands. Additionally, the introduction of gallium ions in a post-synthetic process of InP QDs has provided further insights into tackling surface complexity. While the enhancement of InP core luminescence has been reported through GaP shell formation, Ga cation exchange, In-Ga alloying, and additional coordination at the InP/ZnSe interface, the specific role of Ga-based ligands in altering the surface chemical state remains unclear. Overall, achieving defect-free and DB-free InP QD surfaces without shell formation while maintaining excellent luminescent properties for applications like electroluminescent (EL) devices remains an unexplored possibility. Although matching factors such as surface coordination of cations and anions and charge neutralization hold promise for eliminating surface defects in compound semiconductor QDs, further research is needed to realize the full potential of defect-free InP QDs with pristine surfaces.

To address this challenge, our novel approach focuses on controlling InP QD surface stoichiometry and coordination without the conventional growth of a complete shell. Through atomic-level modification involving proportional surface passivation using gallium chloride and zinc carboxyl groups, we successfully reduce the density of surface defect states, resulting in remarkably stable luminescence with near-unity PLQY (up to 95%). Theoretical models have offered guiding principles for identifying the chemical composition and quantity of surface traps, which can be verified through spectroscopic analysis. Remarkably, our core-only InP QDs, even without a shell, demonstrate sufficient electroluminescence in conventional LED architectures for the first time. Our findings provide valuable insights into the role of surface chemistry in controlling luminescence and present a novel strategy for developing bright and stable QDs without the necessity of a complete shell.

9:15 AM EL02.09.03

Towards Non-Blinking Strongly Confined Perovskite Quantum Dots Yitong Dong, Chenjia Mi and Matthew Atteberry; The University of Oklahoma, United States

Quantum information science has shown its capabilities to enable secure quantum communications. Single photon emitters (SPEs) emit photons one at a time and are fundamental elements of such transformative technologies. Quantum dots (QDs), an atom-like solid-state light source, can emit photons with high efficiency and thus become promising SPE materials. Colloidal cesium lead halide ($CsPbX_3$, X=Br, I) perovskite QDs are ideal for next-generation SPEs because of their high room-temperature luminescence efficiency and low-cost, scalable syntheses. Unfortunately, individual perovskite QDs show insufficient photostability and severe photoluminescence (PL) intensity fluctuations. These fluctuations, also called blinking, can lead to spectral shifts, change the fluorescence dynamics, and reduce the structural stability of perovskite QDs. This has greatly limited the spectroscopic studies for SPE developments. Unlike conventional CdSe QDs, due to the highly ionic crystal structure of perovskites, there is not yet an approach to produce a homogeneous Type-I core-shell structure for perovskite QDs that can efficiently suppress blinking.

One challenge of studying the ionic perovskite QDs is their relatively low ligand binding affinities. When preparing individual perovskite QD samples, QD colloids often need to be diluted, and the ligand can detach from the QD, introducing defects. As a result, individual perovskite QDs often show rapid PL intensity fluctuations accompanied by photodegradation. Many significant advances have been made to search for ligands that bind strongly with the surface of perovskite QDs, such as zwitter ionic and didodecyltrimethylammonium bromide ligands. However, perovskite QDs, especially for strongly size confined QDs, are still experiencing severe PL blinking with large PL "OFF" occurrences.

Here we discovered a method that can significantly suppress PL blinking and improve photostability of strongly confined $CsPbBr_3$ Perovskite QDs. $CsPbBr_3$ QDs with tunable sizes from ~ 3.5 nm to 7 nm are synthesized using the thermodynamic-equilibrium-controlled method and annealed at elevated temperatures to form a bromide rich surface. Diluted QD colloids are then used as antisolvent and nucleation centers to form a polycrystalline thin film consisting of phenethylammonium bromide (PEABr) salts. The bromide rich surface will be epitaxially anchored onto the PEABr matrix and therefore be passivated. Individual strongly confined $CsPbBr_3$ QDs embedded in the PEABr show nearly non-blinking behavior under both pulsed and cw laser excitations (non-resonant) at room temperature. Power-law analysis of the blinking traces of these perovskite QDs show very different "ON" and "OFF" powers (0.85 and 1.9). These QDs remain photostable for more than one hour under laser excitations and show very high single photon purities ($> 95\%$). Additionally, $CsPbBr_3$ QDs with sizes from 3.5 nm to 7 nm can all be passivated and stabilized using our method and show nearly non-blinking behaviors. We anticipate that these QDs will result in more accurate and detailed studies of exciton dynamics and structural-optical property relationships in strongly confined perovskite QDs.

9:30 AM EL02.09.04

Feasibility of Quantum Dot Superradiance Serguei Goupalov¹ and Mikhail O. Nestoklon²; ¹Jackson State University, United States; ²TU Dortmund, Germany

Superradiance is the collective spontaneous emission of a system of many radiative dipoles [1]. Recently, behaviors characteristic for superradiance have been reported for arrays of closely packed self-assembled colloidal lead halide perovskite quantum dots (QDs) [2,3]. The main obstacle which hinders formation of a superradiant state is the inhomogeneous broadening of the optical transitions implying variances of the resonant frequencies from one emitter to another. At first glance, in order to form a superradiant state, variances of the resonant frequencies for participating emitters should be within the radiative linewidth, which for exciton transitions in lead halide perovskite QDs is on the order of few micro-eV. However, along with the long-range interaction through the transverse electro-magnetic field, exciton radiative dipoles are subjects of short-range dipole-dipole interaction. We show that this

interaction allows one to relax the strict resonant conditions for formation of the superradiant state. Yet, we demonstrate that the dipole-dipole interaction between excitons in lead halide perovskite QDs is at least two orders of magnitude weaker than reported in literature [3] and, for closely packed QDs, amounts few tenths of a meV. We further show that retardation effect inhibits superradiance and limits the number of emitters participating in the superradiant state. This number also depends on the configuration and dimensionality of the array.

- [1] R.H. Dicke, Phys. Rev. 93, 99 (1954).
- [2] G. Raimo et al., Nature 563, 671 (2018).
- [3] D.D. Blach et al., Nano Lett. 22, 7811 (2022).

9:45 AM BREAK

10:15 AM *EL02.09.05

Programmable Quantum Nanophotonics [Arka Majumdar](#); University of Washington, Seattle, United States

Analog quantum simulators rely on programmable quantum devices to emulate Hamiltonians describing various physical phenomenon. Photonic coupled cavity arrays are a promising platform for realizing such devices. Using a silicon photonic coupled cavity array made up of high quality-factor resonators and equipped with specially designed thermo-optic island heaters for independent control of cavities, we demonstrate a programmable device implementing tight-binding Hamiltonians with access to the full eigen-energy spectrum. We report a reduction in the thermal crosstalk between neighboring sites of the cavity array compared to traditional heaters, and then present a control scheme to program the cavity array to a given tight-binding Hamiltonian. Finally, I will talk about use of colloidal materials to provide strong nonlinearity in this platform.

10:45 AM *EL02.09.06

Luminescence of Colloidal Quantum Dots in The Mid-Infrared and Beyond, and Implications for Detectors and Emitters [Philippe Guyot-Sionnest](#); University of Chicago, United States

This talk will discuss the challenges and motivations to create bright colloidal quantum dots in the mid-infrared and beyond. At all infrared wavelengths, colloidal quantum dots show enormously superior luminescence compared to organic dyes, by many orders of magnitude in the short-wave infrared. However, this talk will show that the luminescence of colloidal quantum dots is still very poor in the mid-infrared and beyond. The possible reasons will then be described, as well as some tentatives to improve the situation. Then the applications of quantum dots to detectors and emitters, in the mid-infrared and beyond, will be presented, emphasizing the connection to the challenge of luminescence.

11:15 AM EL02.09.07

Single PbS Colloidal Quantum Dot Transistors [Kenji Shibata](#)¹, Masaki Yoshida¹, Kazuhiko Hirakawa^{2,2}, Tomohiro Otsuka^{3,3,3}, Satria Bisri^{4,5} and Yoshihiro Iwasa^{4,2}; ¹Tohoku Institute of Technology, Japan; ²University of Tokyo, Japan; ³Tohoku University, Japan; ⁴RIKEN Center for Emergent Matter Science, Japan; ⁵Tokyo University of Agriculture and Technology, Japan

Colloidal quantum dots (CQDs) are small semiconductor crystals with a diameter of several nanometers [1]. CQDs exhibit excellent light emission/absorption characteristics, and their optical bandgaps are widely tunable by adjusting their size. CQDs can be treated by liquid processes, and their functionality can be controlled by selecting suitable ligands [2]. These properties make CQDs attractive candidates for use as transport channels in single-electron transistors (SETs) operating at high temperatures. However, there have been only a few evaluations of carrier transport through single CQDs in transistor geometries because of the technical difficulties in electrically accessing single CQDs prepared by bottom-up methods.

In this work, we report the first demonstration of single-CQD transistors based on commercially available high-quality PbS CQDs with oleic acid as a ligand. We made electrical contact to a single CQD using nano-gap metal electrodes and measured single-electron tunneling through the CQDs. The transport characteristics measured at 4 K strongly depend on the quantum dot size; a few-electron regime is observed in small PbS CQDs, while a many-electron regime is observed in large CQDs. From the orbital-dependent electron charging energy and conductance, we demonstrate that the tunneling barrier in this system is formed not only by the capping material but also by the intrinsic gap between the electron wavefunction in the CQDs and electrodes. Analysis of the excited states observed in the Coulomb stability diagram indicates that the confinement potential of electrons in CQDs is strongly affected by the external electric field induced by gate and source-drain voltages, suggesting the tunability of the effective confinement size of electrons and the bandgap in CQDs by the external electric field. Moreover, spin-correlated coherent carrier transport (the Kondo effect) has been observed for the first time in the CQD system; this indicates strong coupling between the electrodes and the CQDs despite the use of long-chain insulating oleic acid ligand. These results provide nanoscopic insight into carrier transport through CQDs at the single quantum dot level, which is essential for developing CQD applications in optoelectronic devices, such as solar cells and photodetectors.

Furthermore, the large charging energy in small CQDs enables SET operation at high temperature. While there is a tendency for the noise to increase at higher temperatures, we obtained diamond-like Coulomb stability diagrams even at room temperature, confirming that the devices operate as SETs at room temperature [3]. This is the first demonstration of room-temperature SET operation in semiconductor nanocrystal systems. Considering that PbS CQDs are excellent emitters and absorbers of light, our device is a platform for room-temperature SETs with good optical properties, increasing the functionality and versatility of single-electron devices. This will bring about innovation in quantum information technology.

- [1] Y. Yin and A. Alivisatos, Nature 437, 664-670 (2005).
- [2] F. de Arquer, D. Talapin, V. Klimov, Y. Arakawa, M. Bayer, and E. Sargent, Science 373, eaaz8541 (2021).
- [3] K. Shibata, M. Yoshida, K. Hirakawa, T. Otsuka, S. Z. Bisri, and Y. Iwasa, Nature Communications, in press (2023).

This work was partly carried out at the Fundamental Technology Center and the Laboratory for Nanoelectronics and Spintronics, Research Institute of Electrical Communication, Tohoku University. This work was partly supported by the Cooperative Research Projects of RIEC, JKA and its promotion funds from KEIRIN RACE, and Grants-in-Aid from the JSPS (JP20H05660, JP21K04815, and JP21K04820).

11:30 AM EL02.09.09

Mid-Infrared Cascade Intraband Electroluminescence with HgSe/CdSe Core/Shell Colloidal Quantum Dots [Xingyu Shen](#), Ananth Kamath and Philippe Guyot-Sionnest; University of Chicago, United States

Efficient infrared light sources are needed for applications like gas sensing, environmental monitoring, and spectroscopy. In the visible, electroluminescence from colloidal quantum dots is highly efficient, wavelength-tunable, and cost-effective, which inspires using the same approach in the infrared. Despite the promising performances of colloidal quantum dots light-emitting diodes in the near-infrared, mid-infrared devices show quantum

efficiencies of about 0.1% due to the much weaker emission. Moreover, these devices exclusively relied on the interband transition, restricting the possible materials.

Here, we show electroluminescence at 5 microns using the intraband transition between $1S_e$ and $1P_e$ states within the conduction band of core/shell $HgSe/CdSe$ colloidal quantum dots. With a three-monolayer $CdSe$ shell thickness, the electroluminescence efficiency is about 50-fold larger than in a device that uses the interband transition of similar-sized core-only mid-infrared $HgTe$ colloidal quantum dots. The device showed an EQE of 4.5% at $2 A/cm^2$ while the power efficiency was 0.05%. The quantum efficiency approaches that of commercial epitaxial cascade quantum well light-emitting diodes. The high emission efficiency and the electrical characteristics support a similar cascade process where the electrons, driven by the bias across the device, repeatedly tunnel into $1P_e$ and relax to $1S_e$ as they hop from quantum dot to quantum dot.

The efficiency of the device could be further enhanced through the improvement of the colloidal quantum dots synthesis and film processing. Moreover, similar intraband transitions exist in many other materials, and the cascade mid-infrared electroluminescence design could then be extended to lower toxicity systems.

11:45 AM EL02.09.10

Acceleration of Near-IR Emission through Efficient Surface Passivation and Doping of Cd_3P_2 Quantum Dots Logan Smith¹, Kathryn E. Harbison¹, Nickie Tiwari¹, Benjamin T. Diroll² and Igor Fedin¹; ¹The University of Alabama, United States; ²Argonne National Laboratory, United States

Fast near-IR (NIR) emitters are highly valuable in telecommunications and biological imaging. Colloidal synthesis is a potent method that produces a few NIR-emitting materials, but they suffer from long photoluminescence (PL) times. These long PL times are intrinsic in some NIR materials (PbS , $PbSe$) but are attributed to emission from bright trapped carrier states in others. We develop the colloidal chemistry of an overlooked II-V semiconductor cadmium phosphide (Cd_3P_2) — an alternative promising near-IR material that offers a high bandgap tunability. It is a unique material that bridges III-V and II-VI semiconductors and combines the best of both worlds: near-IR emission with solution processability. We show that as-synthesized Cd_3P_2 QDs possess substantial trap emission with radiative times $>10^1$ ns. With the help of intelligent surface passivation through shell growth or Lewis coordination, or through cationic doping, we manage to accelerate the NIR emission from Cd_3P_2 QDs by decreasing the amount of trap emission. This finding brings us one step closer to the application of colloiddally synthesized QDs as quantum emitters.

SESSION EL02.10: Classical and Quantum Light Sources and Other Devices from Colloidal Quantum Dots II

Session Chairs: Hao Nguyen and Gillian Shen

Friday Afternoon, April 26, 2024

Room 347, Level 3, Summit

1:30 PM EL02.10.01

Toward Ultrathin and Intrinsically Stretchable Optoelectronic Devices Moon Kee Choi; Ulsan National Institute of Science and Technology, Korea (the Republic of)

In recent years, deformable electronic devices have garnered significant attention for their potential in various applications, ranging from flexible displays to wearable technology. However, their mechanical rigidity and relatively large size often preclude seamless integration into flexible, curved, or dynamic environments. We explore the capabilities of ultrathin and intrinsically stretchable optoelectronic devices, such as light-emitting diodes (LEDs) and photodetectors, enabled by the synergistic incorporation of advanced nanomaterials like quantum dots and perovskites, along with cutting-edge printing techniques. The ultrathin architecture facilitates the deployment of high-definition, energy-efficient perovskite LEDs as skin-attachable electronic tattoos, as well as the use of heavy-metal-free photodetectors in wearable photoplethysmogram (PPG) sensors. Moreover, the intrinsic stretchability of displays represents a significant milestone in the design and realization of next-generation soft optoelectronic systems that can adapt to a diverse range of form factors.

1:45 PM EL02.10.02

Exploring Optoelectronic Properties of Heterostructures of Thin Films and Magic-Sized Clusters of Metal Halide Perovskites Asmitha Mekala¹, Jorge Arteaga¹, Heng Zhang², Jin Zhang² and Sayantani Ghosh¹; ¹University of California, Merced, United States; ²University of California, Santa Cruz, United States

The broad spectrum of potential applications presented by metal halide perovskites (MHPs), coupled with their straightforward manufacturing procedures, has captured considerable interest in recent years. Considerable effort has been invested in enhancing the charge transport and extraction efficiencies of MHP thin films for applications in photovoltaics and in refining the film surface quality for usage in sensing. One approach is leveraging heterostructure engineering of MHPs, and prior studies have demonstrated improved photoluminescence (PL) and emission tunability via the adaptation of this method. In our previous work, we have documented how heterostructures comprising thin films of $CH_3NH_3PbI_3$ (methylammonium lead iodide, or MAPI) and metal halide perovskite quantum dots (PQDs) result in improved stability, defect passivation, increased charge carrier lifetimes, and increased charge extraction efficiency in the MAPI films. This work focuses on charge and energy transfer in heterostructures of MAPI thin films and perovskite magic-sized clusters (PMSCs). Magic-sized clusters refer to small, well-defined stable clusters of atoms or molecules that have unique physical and optoelectronic properties, and our PMSCs are 1 – 3 nm in diameter, smaller than the typical PQDs of equivalent composition. Owing to this higher surface-to-volume ratio, PMSCs have greater potential of higher charge and energy transfer efficiencies and higher PL quantum yield. Furthermore, one of the causes affecting the quality of the MHPs films are point defects at the film surface and at grain boundaries. These defects are in the sub-nanometer spatial scale, which could be addressed better by adding the PMSCs to the MHPs film rather than PQDs.

We have conducted a comparative study of heterostructures comprising MAPI films with colloiddally synthesized PMSCs and PQDs. The deposition was carried out two ways: the first, by spin coating $MAPbBr_3$ (methylammonium lead bromide) MSCs or $MAPbBr_3$ PQDs on annealed MAPI films; the second, by adding the PMSCs or PQDs to the precursor of MAPI and annealing them together. Scanning electron microscopy and X-ray diffraction were employed to get insights into the morphological and structural characteristics of the films with PMSCs and PQDs. Confocal microscopy, PL spectroscopy and time-resolved PL measurements while varying sample temperature and excitation wavelengths were utilized to understand the energy and charge transfer mechanisms between the coated MAPI films and the PMSCs or PQDs.

2:00 PM EL02.10.03

Multimodal Strategies for Novel Material Discovery and Enhanced Halide Perovskite Emitters Alexander S. Urban¹, Nina A. Henke¹, Carola

Lampe¹, Kilian Frank¹, Stefan Martin¹, Ioannis Kouroudis², Milan Harth², Patrick Ganswindt¹, Markus Döblinger¹, Alessio Gagliardi² and Bert Nickel¹; ¹LMU Munich, Germany; ²Technical University Munich, Germany

To meet the current and future global energy demands, we must implement a dual strategy of increased renewable energy conversion and reduced energy consumption. This will require us to substantially optimize current materials or discover and develop entirely new ones, for example, for solar cells and light-emitting diodes. A material with vast potential for these applications is nanocrystalline halide perovskite. However, one of the difficulties in improving perovskites is that the fabrication can be too fast to investigate with conventional approaches, and optimizing the resulting NCs can be an extremely tedious task. In this talk, I will discuss our new multimodal approaches to determine the structure and synthesis dynamics of highly confined 1D and 2D halide perovskite nanocrystals, tailor them to specific applications, and enhance their efficiency and stability.[1,2] I will also highlight our approach to incorporate a machine-learning process to optimize syntheses with minimal data demand. Importantly, many of these novel approaches can readily be applied to other systems, greatly benefitting material discovery and development.

[1] C. Lampe, ... , A. Gagliardi, A. S. Urban *Adv. Mater.* **35**, 2208772 (2023)

[2] S. Martin, ... , A. S. Urban *Adv. Opt. Mater.* **early view**, 2301009 (2023)

2:15 PM *EL02.10.04

Metal Halide Perovskite Nanocrystals for Advanced Display Technologies Tae-Woo Lee; Seoul National University, Korea (the Republic of)

Metal halide perovskites (MHPs) have gained recognition as potential candidates for next-generation display technologies, given their high color purity, cost-effectiveness, and facile processing attributes. While several techniques have been pursued to magnify their luminescence performance and stability, they have not yet eclipsed the benchmarks set by conventional organic or inorganic quantum dot-based LEDs. In this talk, we will delve into the unique advantages and strategies involved in MHPs for display technologies using meticulously designed nanomaterials. First would be a comprehensive material strategy aimed at inhibiting defect generation in atomically precise colloidal perovskite nanocrystals (PNCs), thereby elevating their luminescent efficiency. By incorporating guanidinium (GA⁺) cations into formamidinium lead bromide (FAPbBr₃) PNCs, we could achieve a significant surge in luminous efficiency coupled with decreased amount of defect sites. [1] In addition, the incorporation of the bromine-incorporating molecule, 1,3,5-tris(bromomethyl)-2,4,6-triethylbenzene (TBTB), effectively addressed the halide vacancies. In terms of scalable manufacturing, we have pioneered a modified bar-coating process capable of producing large devices on par with the efficiencies of spin-coated counterparts at small device size. [2] In-situ type of core/shell PNC synthesis methodology on substrate will also be discussed, which facilitated the realization of perovskite LEDs with high efficiency, brightness, and stability at the same time. [3] By fragmenting large 3D crystals into nanoscale counterparts and surrounding them using covalently-bonded compact acidic organic ligands, we achieved outstanding charge confinement without compromising charge mobility. Collectively, these advancements underscore the potential of MHPs as the vanguard of self-emissive display materials.

1. Y.-H. Kim et al., *Nat. Photon.*, **15**, 148–155 (2021)

2. Y.-H. Kim et al., *Nat. Nanotechnol.*, **17**, 590–597 (2022)

3. J. S. Kim et al., *Nature*, **611**, 688–694 (2022)

2:45 PM BREAK

3:15 PM EL02.10.05

The Role of Inorganic Ruddlesden-Popper Planar Faults in CsPbBr₃ Perovskite Nanocrystals and Their Performance in LEDs Mariia V. Goriacheva¹, Alec Pickett², Payal Bhattacharya³, Suchismita Guha⁴ and Yangchuan Xing⁴; ¹University of North Dakota, United States; ²Intel Corporation, United States; ³MKS Instruments, United States; ⁴University of Missouri–Columbia, United States

Ruddlesden-Popper (RP) planar faults composed of organic layers were shown to significantly enhance stability and overall opto-electronic performance of lead-halide perovskite nanocrystals (PNCs). The observed phenomena have been mainly attributed to the moisture-repellant and electronically insulating nature of long carbon chains allowing them to shield perovskite domains from moisture while confining excitons. Similar performance enhancement is seen in PNCs with all-inorganic RP layers – insulating in nature, yet highly soluble in water. Here we attempt to define the role of CsBr RP-faults in CsPbBr₃ nanocrystals by performing a comparative analysis of nanocrystals with and without RP layers. The nanocrystals are studied as stand-alone colloids and thin films as well as emissive layers in light-emitting diodes. We find that CsPbBr₃ PNCs with RP faults possess both higher exciton binding energies and longer exciton lifetimes. The former is ascribed to a quantum confinement effect in the PNCs induced by electronically insulating CsBr layers. The latter is attributed to a plausible spatial electron–hole separation across the RP faults. A striking difference is seen in the up-conversion photoluminescence response from CsPbBr₃ PNCs with and without RPs. For the first time, all-inorganic CsPbBr₃ PNCs with RP faults are tested in light-emitting devices and demonstrated to significantly outperform non-RP CsPbBr₃ PNCs.

3:30 PM *EL02.10.06

Priming InP-Based Quantum Dots for On-Chip LED Color Conversion Zeger Hens and Pieter Schiettecatte; Ghent University, Belgium

InP-based quantum dots have emerged as an alternative for CdSe-based materials for luminescent color conversion in the visible. At the same time, color-conversion approaches are shifting from remote phosphor on-chip configurations, which implies exposure to higher light intensity and increased operation temperature. In this contribution, we discuss recent progress in the synthesis of InP-based core/shell quantum dots, reaching near unity photoluminescence quantum yield across the visible spectrum and the formation of monochromatic LEDs by means of on-chip color conversion through InP-based quantum dots. In addition, we address in detail the properties of the core/shell interface and the termination of the quantum dot outer surface that made this result possible and discuss different mechanisms of failure - leading to a deterioration of the color conversion efficiency - from an atomistic perspective.

4:00 PM EL02.10.07

Understanding Electrical Excitation Dynamics in Quantum-Dot Light-Emitting Diodes: From Steady-State to Temporal Behaviors Yunzhou Deng¹ and Yizheng Jin²; ¹University of Cambridge, United Kingdom; ²Zhejiang University, China

Light-emitting diodes based on colloidal quantum dots (QDs) promise a new generation of color-pure, cost-effective, and flexible light sources. Despite of the tremendous advances in the synthesis of QDs, the electroluminescent (EL) properties of QDs generally lag behind their photoluminescent (PL) properties. These EL-PL gaps originate from the essential difference in the charge dynamics of electrical excitation with respect to optical excitation. Here, we report our recent advances in understanding the electrical-excitation dynamics of QDs in active quantum-dot light-emitting diodes (QLEDs) in both steady-state operations, long-term evolutions, and transient EL dynamics under pulsed excitations.

First, we unraveled how the dynamic charge balance can be achieved in the steady-state operation of red, green, and blue QLEDs, leading to high-performance devices with near-limiting efficiencies [1,2]. Key to this is the sequential charge injection at single-nanocrystal level and effective blocking of

electron leakage at the polymer/QD interface. Then, we address an anomalous efficiency-elevation phenomenon induced by operational degradation. Comprehensive in-situ characterizations reveal that this is caused by the ligand migration between the electron-transport layer and the cathode, which in turn improves the charge balance in long-term operation. Finally, we report the excitation-memory effects in the transient EL dynamics of QLEDs modulated by deep-level trap states. By utilizing this unique process, we demonstrate 100 MHz modulation and data transmission based on micro-QLEDs.

[1] Deng, Y., et al., Deciphering exciton-generation processes in quantum-dot electroluminescence. *Nat. Commun.* 2020 11.

[2] Deng, Y., et al. Solution-processed green and blue quantum-dot light-emitting diodes with eliminated charge leakage. *Nat. Photon.* 2022 16.

SESSION EL02.11: Virtual Session: Towards Atomically Precise Colloidal Materials for Conventional and Quantum Optoelectronics
Session Chairs: Emily Miura and Hao Nguyen
Tuesday Morning, May 7, 2024
EL02-virtual

8:00 AM *EL02.11.01

Photo-Crosslinkable Ligands for High-Density Patterning of Perovskite Nanocrystals Zhi Kuang Tan; National University of Singapore, Singapore

The patterning of luminescent quantum dots and nanocrystals into micron-sized pixels is required for applications in electronic color displays. In the recently-developed QD-OLED technology (Quantum Dot Organic Light-Emitting Diode), semiconducting quantum dots are deposited onto blue OLED display pixels by inkjet printing methods to enhance the color quality of the displays. However, inkjet printing is prone to alignment and clogging issues, which impacts the manufacturing yield of these devices. In this talk, I will discuss the development of new crosslinkable ligands that would allow high-density patterning of perovskite nanocrystals or quantum dots by photolithography techniques. Our new ligands attach to the nanocrystals via an entropy-driven ligand exchange process. The resulting nanocrystals could be deposited onto substrates and be patterned by a photo-initiated polymerization process, similar to well-established photolithography protocols that are used in the semiconductor industry.

8:30 AM *EL02.11.02

A Path Toward Making Mid-Wave Infrared Sensing a Ubiquitous Technology Dong Kyun Ko, Mohammad Mostafa Al Mahfuz, Junsung Park and Rakina Islam; New Jersey Institute of Technology, United States

Reducing the size, weight, power consumption, and cost of infrared detectors can make the use of infrared sensing ubiquitous. In the technologically important spectral region of mid-wavelength infrared (MWIR = 3 - 5 μm), commercially available detectors suffer from the high cost associated with epitaxial growth and hybridization as well as the stringent requirement for cryogenic cooling, limiting their use to defense and space applications. The colloidal quantum dot is one of the potential materials candidate to overcome these limitations due to the availability of low-cost synthesis and wafer-scale device fabrication via solution processing. Infrared sensors based on colloidal quantum dots have been studied for decades, and harnessing the interband transition in these quantum-confined nanostructures has been the mainstream theme in optoelectronic research. More unique photophysical properties can be harnessed by utilizing the transitions within the conduction levels or valence levels, known as intraband (intersubband) transitions. In this presentation, we discuss the progress, challenges, and opportunities of MWIR sensors fabricated from Ag_2Se intraband colloidal quantum dots, a heavy metal-free colloidal nanomaterial that has merits for wide-scale adoption in consumer and industrial sectors.

9:00 AM EL02.11.03

Doubling Photoluminescence of Red-Emitting Quantum Dots by Direct Transfer from Hexane into Water Without Adding Extra Reagents Tohid Baradaran Kayyal and Marie-Christine Daniel; University of Maryland, Baltimore County, United States

The demand for converting hydrophobic nanoparticles (NPs) into water-soluble NPs, specifically red-emitting quantum dots (QDs) synthesized in organic solvents, has led to extensive research. However, the current methods for transferring these NPs face challenges related to their efficiency and a decrease in their photoluminescence quantum yield (PLQY). In this study, a remarkably facile and efficient technique was utilized to transfer oleic acid (OA)-coated CdSe/CdS core-shell QDs into water without the need for additional chemicals or agents. This process results in an unexpected increase of over 100% in PLQY upon transfer into basic water (pH 8). The transfer method is highly reproducible and can be extended to other oleic acid-based particles like magnetic NPs. The process is a straightforward method using ultrasonic assistance completed within only 4 hours at room temperature, involving the rearrangement of OA ligands at the QD surface, leading to the formation of a 'mixed' monolayer. This innovative configuration exposes approximately half of the carboxylic acid moieties to the QD surface and directs the remaining towards the aqueous medium. Density-functional-theory (DFT) calculations corroborate this rearrangement, indicating its favorable energetic state in aqueous media. The behavior of the transferred QDs was investigated and compared to that of the original QDs in hexane through absorption spectroscopy, fluorescence spectroscopy, and transmission electron microscopy. Regarding DFT calculations, Quantum ESPRESSO was utilized and CdS surfaces were generated to mimic core-shell quantum dot surfaces. This discovery can open promising avenues for employing NPs especially conventional QDs synthesized in organic solvents for applications in aqueous media. The ease of transferring QDs into a water environment will also facilitate a variety of assembly methods that rely on aqueous surface chemistry, and applications in the field of biomedical imaging.

9:15 AM EL02.11.04

Unravelling Nanocrystal Surface Structures with Relativistic DFT Calculations of Cadmium and Selenium Solid-State NMR Spectra of CdSe Nanocrystal Surfaces Rana Biswas^{1,2}, Yunhua Chen^{1,2}, Javier Vela^{2,1} and Aaron Rossini^{2,1}; ¹Iowa State University, United States; ²Ames Laboratory, United States

Semiconductor nanocrystals (NCs) offer novel tunable electronic and optical properties that depend on their size, shape and surface passivation. Semiconductor NCs exhibit multiple exciton generation and are appealing for next-generation solar cells. Surface ligands and surface sites on NCs control their nucleation, growth, colloidal stability, chemical reactivity and optical/electronic properties. However direct experimental probes of the molecular structure of NC surfaces are lacking. Solid-state nuclear magnetic resonance (SSNMR) is a powerful tool to determine the structure of NC surfaces and sites on the surface where ligands can bind.

Using CdSe as a prototypical example, SSNMR spectra have been measured to probe the structure of these nanocrystals and develop detailed models of their surface structures. DFT-optimized cluster models that represent probable molecular structures of carboxylate coordinated surface sites have been proposed. However, to the best of our knowledge, ¹¹³Cd and ⁷⁷Se chemical shifts have not been calculated for these surface models. We performed relativistic DFT calculations of cadmium and selenium magnetic shielding tensors on model compounds with previously measured solid-state NMR

spectra, with (i) the 4-component Dirac-Kohn-Sham (DKS) Hamiltonian, and (ii) the scalar and (iii) spin-orbit levels within the ZORA Hamiltonian. Molecular clusters with Cd and Se sites in varying bonding environments were used to model CdSe (100) and CdSe (111) surfaces capped with carboxylic acid ligands. Our calculations identify the observed ^{113}Cd isotropic chemical shifts $\delta(\text{iso})$ of -465 ppm, -318 ppm and -146 ppm arising from CdSeO_3 , CdSe_2O_2 , and CdSe_3O surface groups respectively, with very good agreement with experimental measurements. The ^{113}Cd chemical shifts linearly decrease with the number of O-neighbors. The calculated spans ($\delta_{11} - \delta_{33}$) encompass the experimental values for CdSe_3O and CdSe_2O_2 clusters but are slightly larger than the measured value for CdSeO_3 clusters. Relativistic DFT calculations predicted a one-bond ^{113}Cd - ^{77}Se scalar coupling of 258 Hz, in good agreement with the experimental values of 250 Hz. With a dense coverage of carboxylic acid ligands, the CdSe (100) surface shows a distribution of Cd-Se bond lengths and J-couplings. Relativistic DFT simulations aid in interpretation of NMR spectra of CdSe nanocrystals and related nanomaterials, and offer new insights into the complex structures at nanocrystal surfaces.

Supported by the U.S. Department of Energy (DOE), Office of Science, Basic Energy Sciences, Materials Science and Engineering Division. The research was performed at Ames Laboratory, which is operated for the U.S. DOE by Iowa State University under contract DE-AC02-07CH11358. We acknowledge the use of computational resources at the National Energy Research Scientific Supercomputing Center (NERSC) which is supported by the Office of Science of the U.S. DOE under contract no. DE-AC02-05CH11231.

9:30 AM EL02.11.05

Optimising Spectral Quality of Ternary Copper Dichalcogenide Core-Shell Nanoparticle Luminescent Down-Shifting Films in Controlled Environments Stefan C. Ghany and Richard A. Taylor; The University of the West Indies, St. Augustine Campus, Trinidad and Tobago

The development of luminescent down-shifting films (LDS) for spectral adaptation in controlled environment agriculture systems (CEAs) towards improved crop yields has been of tremendous focus in recent years. Due to their tunable nature, they can better utilise the sun's energy for effective light transmittance, down-shift emission into photosynthetically active radiation (PAR), while also reducing unwanted wavelengths which contribute to the generation of excessive heat within the CEAs; detrimental to crops grown in hot climates.

Copper-based dichalcogenide quantum dots (QDs) are regarded as environmentally benign materials that display desirable optical properties resulting in their use in LDS films in CEAs. In this project, a facile hot-injection colloidal synthetic protocol is employed. Highly luminescent copper indium sulphide (CIS) nanoparticles synthesised between $180 - 240$ °C and excited at 525 nm emit between 619 – 639 nm (orange – red light) of varying luminescent intensities, FWHM between 79 – 90 nm, and peaking at 230 °C after 25 minutes of growth. Particle size is largest at 10 nm under the 240 °C protocol, with triangular morphology and high crystallinity due to their sharp edges and clearly defined uniform inter-particle distances indicative of effective binding of 1-dodecanethiol and oleic acid surfactants.

Energy dispersive spectroscopic (EDS) analysis reveals that at lower synthetic temperatures between $180 - 200$ °C an off-stoichiometric copper-deficient particle with respect to indium ($\text{Cu}_{0.59}\text{In}_{0.94}\text{S}_{2.46}$ at 180 °C), produces negligible to low orange – red luminescence with direct bandgaps between 2.31 – 2.13 eV respectively after 30 minutes of growth. At higher synthetic temperatures between $220 - 240$ °C, however, the EDS data indicate a copper-rich particle with respect to indium ($\text{Cu}_{1.26}\text{In}_{0.65}\text{S}_{2.09}$) with the highest red luminescent intensity at 230 °C. Direct bandgaps decreased from 2.06 to 2.03 eV after 30 minutes of growth. Further characterization using X-ray photoelectron spectroscopy, Raman spectroscopy and time-resolved photoluminescence spectroscopy implicate several defects such as copper vacancies and interstitials influencing the remarkable luminescent properties of CIS.

Additionally, surface shelling the CIS core particles with zinc sulphide (ZnS) further tunes their optical properties for effective spectral adaptation by not only increasing the luminescent intensity through surface passivation and decreasing surface defects, but by blue-shifting its emission by cation-exchange mechanisms at the core's surface with CIS emission from 634 nm (FWHM 79 nm) at 220 °C, to 620 nm (FWHM 72 nm) CIS/ZnS shell growth at 210 °C for 30 minutes.

The highly luminescent nanoparticles will be embedded into transparent polymers of either poly(lauryl methacrylate-co-ethylene glycol dimethacrylate) (P(LMA-co-EDGM)) or poly(ethylene-vinyl acetate) (P(EVA)) to form LDS films of effective thickness to effect the desired optical properties which can enhance crop yield. The nanocomposite LDS films will be used as a prototype solar window element to evaluate the effectiveness of the QDs to spectrally adapt the solar spectrum to improve certain crop yields under controlled conditions in CEAs.

9:35 AM EL02.11.06

Green" Cu@ZnInSe/ZnSeS Core/Composition Gradient Shell Quantum Dots for Boosted Photoelectrochemical Hydrogen Production Kokilavani Shanmugasundaram¹, Lei Jin¹, Gurpreet S. Selopal² and Federico Rosei¹; ¹Institut National de la Recherche Scientifique, Canada; ²Dalhousie University, Canada

Colloidal quantum dots (QDs) are considered building blocks for solar energy devices due to their promising optoelectronic properties, such as size/shape/composition-dependent absorption and emission spectrum and high absorption coefficient. However, well-performing QDs in solar energy conversion technologies (i.e. photovoltaics or clean fuel production) are typically containing toxic heavy metals (e.g., Cd and Pb), which restricts their commercial applications. In this context, eco-friendly Cu-doped ZnInSe QDs emerged as a promising alternative due to their unique merits, including the long lifetime of charge carriers and suitable band structure for charge injection. Nonetheless, the sensitivity of the plain Cu:ZnInSe QDs may induce surface defects that act as charge recombination centers, leading to a severe deterioration of the photoelectrochemical (PEC) performance. The growth of suitable shell material is a promising approach for effective suppression of surface related defects/traps states and obtain a tailored optical response of QDs. Here, we report the synthesis of Cu:ZnInSe/ZnSeS core/composition gradient shell with tuneable shell thickness to understand the influence on optoelectronic properties, consequently PEC performance for hydrogen production. An optimized thick composition gradient shell obtained with low Se/S ratio ($n = 2$ and $r = 0.05$) showed broader absorption toward longer wavelength and high PL quantum yield. Resulting PEC device based on the Cu@ZnInSe/ZnSeS core/shell QDs with $n = 2$ and $r = 0.05$ exhibited an excellent saturated photocurrent density of 11.7 mA/cm^2 (at 1 V vs RHE) under one sun illumination (AM 1.5 G, 100 mW/cm^2), which is 96% higher than the achieved value of bare Cu@ZnInSe QDs. The investigation and its findings will be presented in detail, exploring how controlled composition gradient shell thickness influences surface passivation and carrier dynamics. In addition, the significance of composition gradient shell layer to achieve enhanced device performance will be discussed, highlighting its great potential for future eco-friendly core/shell QD-based solar energy technologies.

SYMPOSIUM EL03

Next-Generation Interconnects (Materials, Processes and Integration)—Toward Sustainable Microelectronics
April 23 - April 25, 2024

Symposium Organizers

Serena Iacovo, imec
Vincent Jousseume, CEA, LETI
Sean King, Intel Corp
Eiichi Kondoh, University of Yamanashi

Symposium Support

Silver
Tokyo Electron Limited

Bronze
Air Liquide
CEA- Leti

* Invited Paper

+ JMR Distinguished Invited Speaker

^ MRS Communications Early Career Distinguished Presenter

SESSION EL03.01: Metallization I
Session Chairs: Sean King and Eiichi Kondoh
Tuesday Morning, April 23, 2024
Room 346, Level 3, Summit

10:30 AM *EL03.01.01

Binary and Ternary Intermetallics for Advanced Interconnect Metallization Jean-Philippe Soulié¹, Nancy Heylen¹, Kiroubanand Sankaran¹, Jeroen E. Scheerder¹, Claudia Fleischmann^{1,2}, Johan Swerts¹, Zsolt Tokei¹ and Christoph Adelman¹; ¹IMEC, Belgium; ²KU Leuven, Belgium

In the recent past, alternatives to Cu metallization have elicited much interest for advanced interconnect applications due to increasing intrinsic limitations of line resistance and reliability at line widths below 20 nm [1,2]. Elemental metals with short mean free path (MFP) such as Co, Mo [3] or Ru [4] were first proposed to replace Cu and to improve line resistance and reliability. The effort has been recently extended to include binary and ternary compounds [5, 6].

Amongst binary compound metals, only certain ordered intermetallics show low bulk resistivities with values that are potentially of interest for interconnect applications. The study of binary metals for interconnect applications has therefore focused completely on intermetallic ordered compounds. *Ab initio* screening (by assessment of the $\rho_0 \times \lambda$ figure of merit together with calculations of the cohesive energy [7]) indicated that especially binary aluminides show promise for alternative metallization. The most promising materials include NiAl, CuAl, CuAl₂, RuAl and ScAl₃. Thin films of these aluminide intermetallics were then studied experimentally to assess their properties and their potential for interconnect metallization. Low thin film resistivities have been obtained for NiAl, CuAl, CuAl₂ and ScAl₃ [8, 9]. Despite different crystal structures and constituents, binary aluminide intermetallics share common properties and challenges such as crystalline order, point defects, composition control, composition uniformity, secondary phase formation, agglomeration, (interface) reactivity, or non-stoichiometric surface oxidation. These common challenges will be discussed in detail, highlighted by multiple experimental examples. We show by atom probe tomography that stoichiometric NiAl films are prone to local compositional variations on nm scales, which are difficult to detect with other techniques. For thicknesses below ~15nm, the thin film resistivity strongly increased, and the effect of annealing was reduced. Resistivity modelling found that the resistivity of thin NiAl films below ~ 15 nm was dominated by grain boundary scattering due to small grain sizes, with little impact of surface scattering. To mitigate this issue, the grain size for a given film thickness was increased by back thinning of thicker films (with larger grains) using ion beam etching (IBE) or chemical mechanical polishing (CMP). The resistivity of NiAl could be further optimized at small thicknesses by combining the back thinning experiments with epitaxial deposition: a resistivity as low as 11.5 $\mu\Omega\text{cm}$ at 7.7 nm for epitaxial NiAl on Ge (100) has been demonstrated [10], which outperforms PVD Ru and Cu at comparable thicknesses and thermal budget. We discuss prospects of such approaches for integration.

Finally, we discuss ternary compounds as replacement for Cu in advanced metallization schemes. We will discuss potential classes of materials (e.g. MAX materials) and their prospects. We introduce a materials complexity index for alternative metals to reflect the complexity of the material control. The index can also be used to develop mitigation activities to reduce complexity.

References

- [1] D. Gall, J. Appl. Phys., 127 (2020) 050901
- [2] C. Adelman *et al.*, IEEE IITC (2014) 173
- [3] V. Founta *et al.*, Materialia, 24 (2022) 101511
- [4] L.G. Wen *et al.*, IEEE IITC (2016) 34
- [5] L. Chen *et al.*, Appl. Phys. Lett., 113 (2018) 183503
- [6] K. Sankaran *et al.*, Phys. Rev. Materials, 5 (2021) 056002
- [7] S. Dutta *et al.*, J. Appl. Phys., 122 (2017) 025107
- [8] L. Chen *et al.*, Appl. Phys. Lett., 113 (2018) 183503
- [9] J-Ph. Soulié *et al.*, IEEE IITC (2021) 1
- [10] J-Ph. Soulié *et al.*, IEEE IITC (2023) 1

11:00 AM EL03.01.02

Formation of Surface Sulfide Layer on Liners for Reducing Interface Scattering of Ruthenium Interconnect [Yu-Lin Chen](#), Kai-Yuan Hsiao, Dun-Jie Jhan, Ming-Yen Lu, Pei Yun Keng and Shou-Yi Chang; National Tsing Hua University, Taiwan

Ruthenium with a low bulk resistivity, a high melting point and a short mean free path of electron is of great potential to replace copper as the next-generation metallization for low-resistance interconnects. However, the drastic resistivity scaling with the continual decrease of linewidth due to the scattering of electrons at the interfaces with dielectrics or liners needs to be minimized. Much specular scattering is expected when a layer of two-dimensional materials such as disulfides is applied to the interface, retaining the original electron density of state of the metals. Hence in this study, three types of liner materials (tantalum-titanium alloy, nitride and oxide) were deposited on silicon substrates by physical vapor deposition. Instead of complicated transfer process, sulfurization was applied onto the surface of the liner layers in a tube furnace at different temperatures, simply by using sulfur vapor or hydrogen sulfide gas, to form an ultrathin sulfide layer. Thin ruthenium films with different thickness were then deposited on the sulfurized liners for investigating the influence of the sulfide layer on interface scattering. The microstructure, chemical composition and bonding configuration of the sulfurized surface were characterized, and the resistivity scaling of the ruthenium films was examined with implementation of the Fuchs-Sondheimer and Mayadas-Shatzkes models. Experimental results indicate that, with the sulfur vapor and particularly the hydrogen sulfide gas at an appropriate temperature, an ultrathin sulfide layer of only a few nanometers thick was successfully formed on the top surface of the liners and changed the binding states from a metallic, nitride or oxide state to a sulfide state with altered binding energy. Microscopic observations revealed a crystalline structure of tantalum-titanium binary sulfide being formed, similar to the structure of two-dimensional sulfide materials. With the surface sulfide layer on the liners, the interface diffuse scattering was effectively reduced to elevate the permeability of electrons from 0.2 to 0.9, and the resistivity scaling was accordingly lessened for at least 40% at a ruthenium film thickness of below 10 nm, without a significant loss of interfacial adhesion strength.

11:15 AM EL03.01.03

In Depth Study of In-Plane Thermal Conductivity of Thin Diluted AlCu Alloy Films as Metallic Interconnects [Sara Makarem](#)¹, Daniel Hirt¹, Giovanni Steves² and Patrick E. Hopkins¹; ¹The University of Virginia, United States; ²Sandia National Laboratories, United States

Understanding the thermal conductivity trends in metallic thin films has attracted tremendous interest over the past decades due to their wide applications as interconnects in integrated circuits of electronic devices. As the dimension of the metallic interconnects has decreased comparable to the electron mean free path, size effects on the thermal transport process becomes of high importance. Reduction in size also leads to a reduction in thermal conductivity of the thin metallic films. Such a reduction will then worsen the heat transfer in the circuits and, in most cases, lead to the burnout of the circuit following by the device failure. Upon reduction in size, thermal and electrical conductivity of these interconnects are governed by emerging phenomena that challenge our understanding of the thermal and electrical conductivity of bulk materials. Matthiessen's rule combines all the non-ideal effects together through a summation rule to calculate the electronic mobility and thermal conductivity of systems subject to multiple scattering sources. Therefore, it can be readily applied to estimate the relative magnitude of different scattering mechanisms. Matthiessen's rule has been widely used to predict the phonon thermal conductivity of dielectric solids and the electrical conductivity or electronic thermal conductivity of metallic materials.

In this work we address the limitations of Matthiessen's rule in estimating thermal conductivity of Al_{99.5}Cu_{0.5} (AlCu) films at nanometer length scales and as a result of alloying. We employ ultrafast laser spectroscopic techniques such as time-domain thermoreflectance (TDTR) to directly measure the in-plane thermal conductivity of AlCu films ranging from 24 to 175 nm. We investigate the in-plane thermal conductivity trend with film thickness down to thicknesses comparable to the electron mean free path of Al which is ~19 nm. In principle, one can attribute deviations from Matthiessen's rule to three causes: (a) changes in the band structure and the phonon spectrum due to alloying (b) additional temperature-dependent scattering processes associated with solute atoms, in particular phonon-assisted impurity scattering processes, where electrons and phonons are scattered by solute atoms, and (c) the "two-band" effect where two or more groups of electrons and phonons with different relaxation times contributing to the conductivities. In addition to the experimental thermal conductivity measurements and in order to gain a better understanding of the role of electron-phonon scattering in total thermal conductivity, we measure scattering rate with IR-VASE, an spectroscopic ellipsometry technique. All the provided characterization techniques enable us to validate the contributing share of the electron-electron, electron-phonon, or electron-system boundaries scattering in total thermal conductivity of these films.

SNL is managed and operated by NTESS under DOE NNSA contract DE-NA0003525.

11:30 AM EL03.01.04

Quasi-2D Materials for Ultra-Low Resistance Electrical Interconnects [Bilal Azhar](#), Tobias Schwaigert, Qi Song, Cameron Gorsak, Yacob Melman, Darrell G. Schlom and Hari Nair; Cornell University, United States

The dramatic increase in the resistivity of interconnect lines with decreasing dimensions presents a significant bottleneck for further downscaling of integrated circuits.¹ This is because current interconnects use 3-dimensional metals which experience increased interface electron scattering as the interconnect dimensions approach their electron mean free path. A possible solution is to use metals with much lower electron mean free paths such as: W, Mo, and Ru. Metallic delafossite oxides are an alternative solution because of their inherent advantages over traditional metals such as, ultra-low room temperature resistivity, potential mitigation of interface/surface scattering due to their 2D Fermi surface, potentially decreased likelihood of electromigration, and potentially better compatibility with low-K oxide dielectrics. Metallic delafossite can prove to be a disruptive new material for ultra-scaled electrical interconnects.

Delafossites are layered oxides with the formula ABO₂ where A is a metal cation that forms 2D sheets separated by the BO₂ transition-metal oxide octahedra. In this study we focus on metallic delafossites PtCoO₂ and PdCoO₂ because of their ultra-low room temperature resistivity of 2.1 μΩ.cm and 2.6 μΩ.cm, respectively, which is comparable to the current semiconductor industry standard interconnect metal, Cu.² The metallic delafossite structure has an anisotropic nature with resistivity along the c-axis a factor of 1000 higher than resistivity within the Pt/Pd sheet. Due to the layered crystal structure, the Fermi surface of the metallic delafossites is cylindrical as for a 2D metal. This quasi-2D crystal structure can potentially mitigate interface and surface scattering since the electron Fermi velocity does not have components perpendicular to the Pd/Pt sheets. This can potentially overcome the resistivity penalty encountered by conventional 3D metals in ultrathin films (< 20 nm). Additionally, the unique Fermi surface topology allows for an electron-phonon coupling constant that is a factor of 3 lower than copper.³

In this study we investigate the structural and electrical properties of MBE-grown PdCoO₂ delafossite films. High-resolution X-Ray diffraction (HRXRD) confirms that the films are phase-pure. XRD phi scans, however, reveal in-plane twinning in these films, and the lateral size of the rotational twin domains are ~17 nm based on skew-symmetric rocking curves. We measured the resistivity of the films using a van der Pauw geometry and modelled the resistivity scaling with film thickness using Fuchs-Sondheimer (FS) and Mayadas-Shatzkes (MS) model. The upshot is that a 50 nm thick PdCoO₂ film has a resistivity of 5 μΩ.cm. Based on our resistivity fitting we find that the twin boundaries have a very low electron reflection coefficient of ~5%. This is extremely encouraging since atomic layer deposition (ALD) which is a back-end-of-the-line (BEOL) compatible synthesis technique will likely yield highly twinned delafossite thin films.

¹ D. Gall, J. Appl. Phys. **127**, 050901 (2020).

² V. Sunko, P.H. McGuinness, C.S. Chang, E. Zhakina, S. Khim, C.E. Dreyer, M. Konczykowski, M. König, D.A. Muller, and A.P. Mackenzie, Phys. Rev. X **10**, 021018 (2020).

³ C.W. Hicks, A.S. Gibbs, A.P. Mackenzie, H. Takatsu, Y. Maeno, and E.A. Yelland, Phys. Rev. Lett. **109**, 116401 (2012).

11:45 AM EL03.01.05

Ballistic Thermal Transport in TiN/TiC Multilayers due to Interfacial Elastic Modulus Enhancement Md. Rafiqul Islam¹, Elie Azoff-Slifstein², Sean King³, Daniel Gall² and Patrick Hopkins¹; ¹University of Virginia, United States; ²Rensselaer Polytechnic Institute, United States; ³Intel Corporation, United States

The scale of microelectronics is gradually reducing towards dimensions comparable with the electron mean free path. Since there is a need to dissipate ever increasing amounts of waste heat in microelectronic applications the increased device and interface density is highly undesirable. Thus, the approach of engineering materials with high densities of interfaces to achieve desirable thermal conductivity solids requires a fundamental understanding. In this work, we report on the thermal conductivity of a series of crystalline multilayers composed of alternating layers of titanium nitride and titanium carbide with varying interface densities. We deposit titanium nitride and titanium carbide superlattice films on MgO(001) by reactive magnetron sputtering in an ultra-high vacuum chamber. The alternating nitride carbide layers are formed using reactive mixtures of Ar/N and Ar/CH₄, respectively. The 1 μm thick samples are deposited at 1100 °C with alternating layer thicknesses between 1.5 and 15 nm. We directly measure the thermal conductivity of these films via the time-domain thermoreflectance technique. We find that the thermal conductivity increases with an increasing interface density indicating that the heat carriers are scattering less in the interfaces of the multilayers. This finding contradicts the traditional theory and conventional understanding. The role of interfacial nonidealities and disorder on thermal transport across interfaces is traditionally assumed to add resistance to heat transfer. The increase in thermal conductivity could be related to their increase in their elastic modulus which was measured by picosecond acoustic and nanoindentation techniques. The increase in interface density leads to a monotonically increasing elastic moduli imply a high quality of interface formation which usually results in a higher thermal conductivity. Our results demonstrate a path toward engineering thermal conductivity, thus providing a novel approach to dissipate the ever-increasing amounts of waste heat in microelectronic devices and alleviate the concern for the continuation of Moore's law.

SESSION EL03.02: Metallization II

Session Chairs: Silvia Armini and Eiichi Kondoh

Tuesday Afternoon, April 23, 2024

Room 346, Level 3, Summit

1:30 PM *EL03.02.01

Interconnect Technology for Superconducting Devices and its Interface Properties Masahisa Fujino¹, Yuuki Araga¹, Hiroshi Nakagawa¹, Katsuya Kikuchi¹ and Noboru Miyata²; ¹National Institute of Advanced Industrial Science and Technology, Japan; ²Comprehensive Research Organization for Science and Society (CROSS), Japan

Superconducting devices, such as superconducting tunnel junction (STJ), qubits, etc. can be manufactured by the current Si-based semiconductor manufacturing processes. However, circuits should be superconducting material such as Nb ($T_c=9.29$ K), Pb ($T_c=7.2$ K), In ($T_c=3.4$ K), etc.

In current technology, these devices are arranged in monolithic structures and processes, and each device should wire to control and read signal lines in the same plane. When a large number of devices and/or high-density devices are integrated, these wires would be too constrained, and several problems would be actualized, such as wiring for devices located at the chip center, crosstalk among wiring, and so on.

3D integration of qubits with interposer chips by flip-chip bonding is the proof-of-concept of large-scale qubit integration. The 3D integration approaches for qubit-based devices are the same as conventional electronic devices, including the through silicon via (TSV) process for interposers and micro bump flip-chip bonding.

3D integration for STJ would acquire the high density of sensing top electrodes for detecting x-rays from far away.

Also, the signal integrity for qubits is much better than having qubits at short distances from the control circuitry by 3D integration.

However, they use superconducting metals instead of copper and other non-superconducting materials. Most flip-chip microbump bonding processes require thermal compression bonding (TCB) at over 170 °C. Superconducting elements are easily degraded by heat.

Consequently, we apply TCB around 100 °C using In-Pb alloy.

Surface activated bonding (SAB) was also applied for room temperature bonding of Nb-Nb as superconducting metal.

Both bonding processes succeeded in confirming the superconducting interconnect.

Additionally, we discuss the superconducting interface of direct bonded Nb-Nb by T_c , and also the interfacial structure measured by polarized neutron reflectometry (PNR). The results show clear spin asymmetry in the superconducting state, as splitting is observed in the fringes of the parallel neutron (neutron spins parallel to the external magnetic field 0.1 T) reflection R^+ and the antiparallel (neutron spins antiparallel to it) reflection R^- , where the latter has become larger. This well-known effect is related to the flux penetration in the superconducting state. Therefore, unique information about the superconducting state of the buried thin film can be measured by using the polarized neutron beam. For this project, the major advantage of PNR will be to characterize the superconducting state at the deeply buried Nb interfaces sandwiched between the two substrate wafers, which would be infeasible using alternate techniques.

2:00 PM EL03.02.02

A Meta-Analysis of Non-Copper Nanowire Resistivities Sean King; Intel Corp, United States

Innovations in back-end-of-line (BEOL) interconnects over the past several decades have been driven primarily by both Moore's law mandated dimensional scaling of Cu wiring and permittivity scaling of low dielectric constant (i.e. low- k) interlayer dielectrics (ILDs) to mitigate increased resistance-capacitance (RC) delays. However, due to the demand for continued dimensional scaling, the industry now faces an exponential rise in interconnect metal line resistance created by both increased Cu resistivity size effects and limitations in thickness scaling for the Cu diffusion barrier materials needed for yield and reliability considerations. This has created an intense interest for identifying new conductors that exhibit reduced resistivity size effects and / or that require no or reduced thickness diffusion barriers. To support the identification of potential copper replacement conductors, we share a benchmarking Meta-analysis of nanowire resistivities publicly reported in the scientific literature for numerous metals including those currently under active consideration (i.e. Cobalt, Tungsten, Ruthenium, and Molybdenum) as well as up and coming metals (Iridium, Rhodium) and other potentially

overlooked metals. We will conclude by examining the supply chain challenges that may ultimately play a role in the selection of future copper replacement conductors and discuss research needed to address these challenges.

2:15 PM EL03.02.03

Highly Textured (100)-Oriented and (111)-Oriented, Cobalt Mono Silicide Nanoribbons: Material Growth and Device Fabrication Guy M. Cohen, Peter Kerns, Leonidas Ocola, Nathan Marchack, John Bruley, Franco Stellari, David Rath, Christian Lavoie and Ching-Tzu Chen; IBM T.J. Watson Research Center, United States

Topological conductors with protected surface conduction states are candidates for scaling beyond copper interconnects. The topological semimetal CoSi is used here to study the properties of this class of materials because of the well-separated surface and bulk bands in its band structure. Highly textured CoSi nanoribbons were fabricated by sputtering Co on a hot Si (111) oriented facet. The as-grown CoSi nanoribbons showed a (100) surface orientation. A further annealing resulted in rearranging the CoSi surface orientation to (111). Devices for electrical testing of the nanoribbons were fabricated by patterning (100)-oriented silicon-on-insulator (SOI) into bars, then using TMAH etching for forming (111) sidewall facets on both edges of the SOI bars. A diluted HF (DHF) clean was used to strip the native oxide and H-passivate the Si (111) facets prior to cobalt deposition. The unreacted cobalt in the field region was selectively etched leaving isolated nanoribbons on the Si (111) facets. The nanoribbons were encapsulated by a dielectric and tungsten contacts to the nanoribbons completed the device fabrication. Initial electrical characteristics of nanoribbons with a width down to 20 nm and thickness of ~3 nm were measured.

2:30 PM *EL03.02.04

Size Effects on The Electron and Phonon Scattering and Thermal Conductivity of Thin Metal Films and Multilayers for Metal Interconnects: Looking Beyond Copper Patrick E. Hopkins; University of Virginia, United States

The progressive reduction in the characteristic length scales of logic technology nodes in very-large-scale integration (VLSI) has led to the need to find replacements for copper being used as interconnects. Both the thermochemical and thermomechanical stability of Cu at these length scales, along with the strong reduction in both electrical and thermal conductivity due to length scales reducing to those less than its electronic mean free path has led to underperformance, which in part can be ascribed to deleterious heating effects. While Ru and W interconnects are currently being evaluated, a range of additional metals and metallic systems (alloys, eutectics and multilayers) are also of note due to their potential mechanical and thermal properties that are superior to Cu at the < 100 nm length scale. In this presentation, I will discuss our recent efforts in measurements of thermal conductivity and electron-phonon scattering rates of thin metal films for interest as next-generation metal interconnects, including Ru, W, Ir, Pt, Mo, Co and Ta. First, I will discuss the use of steady state thermoreflectance (SSTR) as a measurement platform to measure the in-plane thermal conductivity (k) of thin metal films. This measurement of in-plane allows for direct comparison to k derived from electrical resistivity measurements and application of the Wiedemann-Franz (WF) Law. We find that in most cases, the application of the WF law with the low temperature value of the Lorenz number does not sufficiently predict the total thermal conductivity. To understand the mechanisms that drive the thermal transport of these metal films, we use both infrared pump-probe measurements (< ps) and infrared variable angle spectroscopic ellipsometry (IR-VASE) to measure the electron scattering rates, demonstrating the relatively thickness independent scattering processes in these films, providing strong promise in the scaling of these metals to technology node length scales. Finally, I will talk about classes of multilayer metal/metal and metal nitride/metal carbides in which interfaces do not scatter electrons and phonons strongly enough to impact the thermal resistance, thus introducing a series of "interface transparent" metal multilayers that do not exhibit traditional size effects in their thermal conductivity. I will conclude by commenting on new thermal metrologies that can provide truly nanoscale thermal resistance measurements and the elucidation of new mechanisms of interfacial thermal transport.

3:00 PM BREAK

SESSION EL03.03: Etching and Bonding for Interconnects and 3D Integration
Session Chairs: Silvia Armini and Eiichi Kondoh
Tuesday Afternoon, April 23, 2024
Room 346, Level 3, Summit

3:30 PM *EL03.03.01

Pixel Pitch Hybrid Bonding and Three Layer Stacking Technology for BSI Image Sensor Kazumasa Tanida, Shigeru Suzuki, Toshiki Seo, Yasunori Morinaga, Hayato Korogi, Michinari Tetani, Masakazu Hamada, Ryuji Eto, Takeshi Yamashita, Yasuhiro Kato, Naoaki Sato, Tadami Shimizu, Tetsuro Hanawa, Hiroko Kubo, Fumitaka Ito, Yoshihiro Noguchi, Masayuki Nakamura, Ryuji Mizukoshi, Masahiko Takeuchi, Masakatsu Suzuki, Naoto Niisoe, Isao Miyanaga, Atsushi Ikeda and Susumu Matsumoto; Tower Partners Semiconductor Co., Ltd., Japan

Abstract

We have developed a pixel pitch (1.35 μm) hybrid wafer bonding technology and successfully demonstrated three layer stacked backside illuminated (BSI) image sensor fabrication with full hybrid Cu-Cu direct bonding process. We found that plasma activation condition on the bonding wafer surface is a key factor of Cu-Cu contact yield improvement for smaller size Cu contacts. Optimized pixel pitch hybrid bonding shows good electrical and reliability performances. For three layer stacking, we developed through Si via (TSV) process. The second hybrid bonding process was adapted on the first hybrid bonded wafers and it shows good electrical performances. This three layer stack technology with pixel pitch hybrid bonding is promising for many different applications.

1. INTRODUCTION

Nowadays, hybrid wafer bonding with Cu-Cu connection is a major production technology of two layer stacked backside illuminated (BSI) image sensor applied for several applications [1]. In addition, three layer stacked BSI image sensor with through Si via (TSV) connection has been introduced to high performance cameras [2]. Furthermore, three layer stacked BSI with pixel pitch Cu-Cu connection will be required in order to realize much higher performance and multi functionality image sensors. In this paper, we developed key technologies for three layer stacking. One is pixel pitch hybrid wafer bonding with minute Cu-Cu connection, the other is three layer stacking process including TSV for middle layer and the 2nd hybrid wafer bonding. Finally, three layer stacking process was demonstrated by adapting these technologies.

2. PIXEL PITCH HYBRID BONDING

Cu-Cu contact with conventional hybrid wafer bonding conditions was studied utilizing the test element group (TEG) structure of Cu-Cu connection. The Cu-Cu contact pitch is 4.00 to 1.35 μm, and Cu electrode size is 1.25 to 0.42 μm square. As the results, Cu-Cu contact yield decreased as the contact pitch and pad size became smaller. The failure was Cu-Cu open mode with small gap between upper and lower Cu electrode. Cu-N compound layer on Cu

electrode surface was identified after plasma surface activation by wafer bonder. It indicates that Cu-N compound layer was formed because Nitrogen was dosed into Cu surface during plasma activation. We considered that the Cu-N compound layer formed on both upper and lower minute Cu electrode was not broken by compressive stress of Cu thermal expansion during post annealing. Therefore, the Cu-N layer acted as a barrier, and Cu-Cu metal bonding between minute electrodes was not achieved.

N/Cu ratio of Cu electrode surface was decreased with lowering N dose of plasma condition and 1.35 μm pitch Cu-Cu contact yield (438k chains TEG) was improved. The Qual test of 1.91 μm pitch Cu-Cu contact (0.60 μm sq.) namely, electro migration (EM), stress migration (SM), temperature cycling (TMCL) and I-V, were passed.

3. THREE LAYER STACKING DEMONSTRATION

Three layer stacking was demonstrated following flow; The middle layer is bonded to the top layer by the 1st hybrid bonding with 1.91 μm pitch Cu-Cu connection. After the middle layer Si thinning, the Cu-TSV and the backside BEOL are formed. Then the 2nd hybrid bonding is done in order to bond the backside of the middle layer to the bottom layer with Cu-Cu connection. Finally, top layer Si is thinned and Al-TSV through top layer Si is formed. The stack chain TEG (10 chain circuit through Al-TSV, the 1st hybrid pixel pitch Cu-Cu, Cu-TSV, back BEOL and the 2nd hybrid Cu-Cu) shows the small resistance distribution. As the results, good electrical path of three layer stacking was established.

REFERENCES

[1] Y. Kagawa et al., "Novel Stacked CMOS Image Sensor with Advanced Cu2Cu Hybrid Bonding," Proc. of IEEE Int. Electron Devices Meeting (IEDM), 2016, pp.208-211.

[2] Y. Kagawa et al., "3D Stacking Technologies for Advanced CMOS Image Sensors," Proc. of IEEE Int. Interconnect Technology Conf. (IITC), 2021, WS-4.

4:00 PM *EL03.03.03

Direct Metal Etch of Ruthenium: Enabling Sub 20nm Pitch Interconnects Gayle Murdoch, Giulio Marti, Stefan Decoster, Souvik Kundu, Anshul Gupta, Ankit Pokhrel, Seongho Park and Zsolt Tokei; IMEC, Belgium

The realisation of Moore's law, which predicts that the number of transistors in an integrated circuit will double every 2 years, has been achieved by countless innovations in the semiconductor industry over the last 60 years. As device dimensions shrink the innovation in transistor design often grabs the headlines but of course this must be supported by innovation in the interconnect technology as the minimum metal line pitch shrinkage follows that of the gate.

Around 25 years ago the semiconductor industry made the radical transition from subtractive aluminium patterning to copper damascene, which required significantly different materials and fabrication techniques. This transition was necessary to increase the processing speed of the microchips; as the resistivity of Cu is 40% lower than Al, the RC delay is reduced, which is the performance indicator in BEOL.

In the present day, we are approaching the end of Cu damascene scaling and thus there is the requirement for another disruptive technology change to keep the RC delay at acceptable levels. Below 2nm node it is predicted that the minimum metal pitch will be < 20nm, at which point Cu damascene is not an option; even if it were possible to fill 10nm lines with Cu, the need for a metal barrier means the resistance would become too high. Therefore, we must look for an alternative interconnect material. One strong candidate is Ru, which has the convenience of having low resistivity and can be used without a barrier, giving an immediate resistance benefit for line dimensions below 12nm. Another advantage is that it can be patterned subtractively, giving access to higher aspect ratio lines than can be achieved with damascene integration schemes.

In this talk we will discuss how the subtractive patterning of Ru can realise the semi-damascene scheme which is proposed by imec as the alternative to Cu damascene at advanced logic nodes.

4:30 PM EL03.03.04

Thickness-Dependent Optical Properties of Metallic Thin Films and Their Correlation with Thermal Conductivity Saman Zare¹, Md. Rafiqul Islam¹, Sean King², Christopher Jezewski², Colin Landon², Rinus Lee³, Kandabara Tapily³, Colin Carver² and Patrick E. Hopkins¹; ¹University of Virginia, United States; ²Intel Corporation, United States; ³TEL Technology Center, United States

The semiconductor industry stands as a cornerstone of modern technology, and its relentless pursuit of miniaturization, efficiency, and performance hinges upon the precise control and understanding of materials used in electronic devices. Within this context, the study of thin films of metals takes on paramount significance. These films play a pivotal role in various semiconductor applications, as they are utilized not only as fundamental components in electronic devices but also as essential elements in the thermal management of these devices. As electronic components become increasingly compact and powerful, the efficient dissipation of heat generated during operation has become a critical challenge. Understanding the optical and thermal properties of thin metal films is instrumental in addressing these challenges, as it offers valuable insights into their potential as heat-dissipating materials and their influence on the performance and reliability of semiconductor devices.

In this study, we perform precise spectroscopic ellipsometry measurements on thin films of several metals that are of unique importance for electronic devices, including copper, iridium, ruthenium, and tungsten. Using these measurements, we determine the optical properties of these metallic thin films across a broad spectral range throughout the infrared and UV-Vis region. Through meticulous analysis involving the Drude free-electron model, we quantify variations in relaxation times and plasma energies in relation to film thickness. Furthermore, our investigation extends to exploring the intriguing interplay between size-dependent relaxation times, as derived from the Drude model, and the thermal conductivity of these metallic thin films, as measured using a thermoreflectance-based thermal conductance and ultrafast pump-probe technique. Our findings are instrumental in enhancing our understanding of these materials' behavior, with potential implications for the development of advanced electronic components.

SESSION EL03.04: Memory
Session Chairs: Sean King and Pierre Noé
Wednesday Morning, April 24, 2024
Room 346, Level 3, Summit

8:45 AM *EL03.04.01

Back End of The Line Embedded Non Volatile Memories for Microcontrollers: Constraints and Opportunities Simon Jeannot; STMicroelectronics, France

Back end of the Line embedded Non Volatile Memories for Microcontrollers: constraints and opportunities.

S. Jeannot, J. Sandrini, E. Petroni #, O. Weber, A. Conte +, A. Redaelli #, L. Laurin #, R. Ranica, F. Arnaud, J. Devin *, C. Boccaccio.

STMicroelectronics Crolles France, #Agrate-Brianza Italy, *Rousset France, + Catania Italy. Email: simon.jeannot@st.com

Embedded non-volatile memories (eNVMs) are an essential component of modern microelectronics technologies, providing a reliable and cost-effective solution for storing critical data and program code in a wide range of applications. Microcontrollers, in particular, have shown a regular increase of their market, surpassing 20 Billions dollar by year with two digits growth in the last period. They benefit from the persuasion of microelectronics intelligent products in modern life, from the automotive and industrial sector, smartcards, to the communication grid and global interconnection growing needs. From a technological point of view, Mature Floating Gates technologies are progressively replaced by new back end of the line solutions, more compliant with High K / metal technology and density increase constraints. Spin Torque Transfer Magnetic Random Access Memories (STT MRAM), Oxide Based resistive Memories (OXRAM) as well as Phase change Memories (PCM) have been introduced in the last years and are nowadays qualified in production on different nodes by majors players. Different physics and architecture involved might lead to different memory characteristics and products best suited for each technology.

Developing memories for embedded microcontrollers requires to sustain very aggressive mission profiles for memory reliability, and its introduction in the Back end of integrated circuits adds up important technology limitations. In this presentation the author will describe the constraint of eNVM for microcontrollers, both from the application and the integration side. A comparison of the different BEOL memories technologies will be done in regard to device level performance and architecture, reliability mission profiles, memory point architecture versus integration, and technology cost. A special emphasis will be applied on ePCM technology, with description of device, process flow and materials optimization involved to fulfill aggressive product requirement with competitive solutions. Lastly, emerging memory solutions for storage memories as well as working memories in "In Memory Computing" approach will be discussed, highlighting the main challenges for each competitor (FeRAM, FeFET, OTS, RERAM).

9:15 AM EL03.04.02

Experimental Characterization and 1D KMC-Based Simulation of the Reliability of 28nm BEOL Integrated VCM ReRAM Nils Kopperberg¹,

Stefan Wiefels², Karl Hofmann³, Jan Otterstedt³, Dirk Wouters¹, Rainer Waser^{1,2} and Stephan Menzel²; ¹RWTH Aachen, Germany; ²Forschungszentrum Jülich GmbH, Germany; ³Infineon Technologies AG, Germany

Valence change memory (VCM) cells are promising candidates for non-volatile memory applications and neuromorphic computing [1]. Typically, they consist of a simple metal-insulator-metal (MIM) structure, where the insulating oxide layer can be manipulated by an externally applied voltage. Thereby, oxygen vacancies can be incorporated and redistributed in a way that the resistance of the oxide layer can be switched between a high resistive state (HRS) and a low resistive state (LRS). These states can be read out non-destructively and switched very fast. Furthermore, the cells show a great scalability, CMOS (complementary metal-oxide-semiconductor) compatibility and low power consumption [2,3].

Despite their excellent characteristics, a few questions and challenges concerning the key parameter reliability are still open. During the experimental characterization of the generally great endurance of 2Mbit VCM cells, we found a rare failure mechanism in a few ppm of the cells after about 500k cycles, where the cells could not be switched back into the HRS (RESET) [4]. The investigated cells are integrated back-end-of-line (BEOL) in a 1-transistor-1-resistor (1T1R) configuration in a 28nm CMOS technology.

Based on the JART VCM 1.0 model of La Torre [5], we developed a 1D KMC simulation model to physically explain the observed failure mechanism. We show that the interplay of the transistor and the VCM cell plays an important role. In rare cases of a combination of a high resistive transistor and a very low resistive cell, the voltage dropping over the cell is not sufficient to originate the RESET. Additionally, we experimentally investigate the RESET kinetics and their dependence on the used transistor. Here again, we can explain our findings with the help of the developed 1D KMC simulation model. In conclusion, we want to point out the importance of the interplay of transistor and resistor and its understanding for the improvement of the reliability.

[1] R. Waser, R. Dittmann, G. Staikov and K. Szot, *Adv. Mater.*, 21: 2632-2663, 2009.

[2] Y. Chen, *IEEE Trans. Electron Devices*, vol. 67, no. 4, pp. 1420-1433, 2020.

[3] M. von Witzleben, T. Hennen, A. Kindsmüller, S. Menzel, R. Waser and U. Böttger, *J. Appl. Phys.*, 127 (20): 204501, 2020.

[4] N. Kopperberg, S. Wiefels, K. Hofmann, J. Otterstedt, D. J. Wouters, R. Waser and S. Menzel, *IEEE Access*, vol. 10, pp. 122696-122705, 2022.

[5] C. La Torre, A. F. Zurhelle, T. Breuer, R. Waser and S. Menzel, *IEEE Trans. Electron Devices*, vol. 66, no. 3, pp. 1268-1275, 2019.

9:30 AM EL03.04.04

Colloidal Syntheses of Novel Sb₂S₃ and Bi₂S₃ Cubic Phases for Phase Change Memory Applications Zach Wylie¹, Soohyung Lee¹, Vyvyan Dao¹, Jade Paranhos-Lopes², Nicolas M. Gaillard² and Vincent C. Holmberg¹; ¹University of Washington, United States; ²University of Hawai'i, United States

Phase change memory (PCM) is a developing technology that is set to position itself as the bridge between fast, volatile, dynamic random-access memory (DRAM) and slow, non-volatile, NAND flash storage which have become the workhorses of device architecture. To store non-volatile information, PCM typically utilizes the difference in resistance between the amorphous and metastable cubic phases of pseudo-binary GeTe-Sb₂Te₃ which undergoes a fast and reversible phase transformation. This phase change, which can occur in nanoseconds in thin films, allows for access times that can be a full order of magnitude faster than NAND flash. Despite seeming stoichiometrically imbalanced, the metastable cubic phase in Sb₂Te₃ and its alloys do not fall immediately into the more stable layered orthorhombic phase due to stabilization from a high concentration of cation site specific defects (>30%) which decreases the antibonding characteristics around the Fermi level. These defects are also responsible for the unique disorder-induced localization of states which accounts for a majority of the phase's resistance. A noteworthy computational study by Xu et al. has predicted several other metal chalcogenides that could theoretically share a similar metastable cubic phase.¹ Here, we present a direct, scalable, colloidal synthesis route for two of these previously undiscovered defect rich cubic phases for Sb₂S₃ and Bi₂S₃ nanocrystals. Solution syntheses such as these will prove invaluable for studying these and other metastable phases for use in PCM technology that would be otherwise inaccessible by other synthetic routes.

(1) Xu, Y.; Wang, X.; Zhang, W.; Schäfer, L.; Reindl, J.; vom Bruch, F.; Zhou, Y.; Evang, V.; Wang, J.; Deringer, V. L.; Ma, E.; Wuttig, M.; Mазzarello, R. Materials Screening for Disorder Controlled Chalcogenide Crystals for Phase Change Memory Applications. *Adv. Mater.* **2021**, *33* (9), 2006221.

9:45 AM BREAK

Wednesday Morning, April 24, 2024
Room 346, Level 3, Summit

10:15 AM *EL03.05.01

Boron in The Back-End: Advances in Boron-Based Solids for Interconnect Applications [Michelle M. Paquette](#); University of Missouri-Kansas City, United States

Playing a less glamorous yet critically important role, the interconnect system requires relentless innovation to support more complex and higher-density device architectures. To meet future demands, we require a constant supply of novel and better materials, material fabrication methods, and material combinations. Known for their robust mechanical, chemical, thermal, and electrical properties, boron-based solids are a compelling alternative to silicon-based solids for a range of interconnect material needs, to include low-dielectric-constant (low-k) dielectrics, etch stops, diffusion barriers, hard masks, spacers, capping layers, and other patterning-assist layers. This talk will cover advances in boron-based solids, including BC and BN, for state-of-the-art interconnect applications, touching on fundamental materials science, layer-by-layer deposition techniques, and functional and patterning applications.

10:45 AM *EL03.05.02

Porous Thin Films for Advanced Dielectrics using Molecular and Atomic Layer Deposition [Nick C. Strandwitz](#); Lehigh University, United States

Atomic and molecular layer deposition (ALD, MLD) techniques boast precise control of film thickness, conformal growth, and a wide range of material compositions. Generally, ALD and MLD thin films are non-porous, yet introduction of porosity would enable a wide range of uses ranging from catalysis to low-k dielectrics for electronics. Here, we have examined the purposeful inclusion of organic molecules including bifunctional and monofunctional alcohols during the MLD/ALD process and their subsequent removal using thermal and/or UV treatment to induce porosity. We examined the evolution of various physical and electrical properties with thermal treatment as well as the composition of these films. We found that the density and dielectric constant of these materials are smaller than the parent dense ALD oxides. This strategy is thus promising for tailor made dielectrics based on sequential self-limiting surface reactions characteristic of the ALD and MLD processes. This development parallels other methods for forming porous inorganic oxides such as terpinene inclusion in silicon-based dielectrics or block copolymer templating of inorganic solids.

11:15 AM EL03.05.03

Surface Converted Interconnected Tetrapodal Zinc Oxide for Selective Sensing Application [Barnika Chakraborty](#)^{1,2}, [Ajay Padunnappattu](#)¹, [Jürgen Carstensen](#)¹, [Rainer Adelung](#)¹, [Norbert Stock](#)¹ and [Leonard Siebert](#)¹; ¹Kiel University, Germany; ²Katholieke University, Belgium

Gas sensors, a longstanding presence in the market, have yet to reach their full potential. They lack the necessary precision for specific gas measurements. For instance, while one gas may lead to cancer and another gas might be linked to tuberculosis, a conventional metal oxide gas sensor detects both indiscriminately, failing to identify the exact gas or its concentration. This leaves ordinary consumers unable to discern the particular gas or disease they may be exposed to, even after investing in a gas sensor. Thus, achieving selectivity is paramount for gas and Volatile Organic Compound (VOC) sensors. This is where porous chemical frameworks like Metal Organic Frameworks (MOFs) or zeolites enter the scene. These materials possess defined pore sizes and selective diffusivity, allowing them to filter some gases while obstructing others, contingent on the size of the gases and the pores in MOFs/zeolites. The challenge, however, lies in their predominantly insulating nature, posing an obstacle in creating chemiresistive sensors. Therefore, for effective sensor response detection, we have opted for the well-established conducting n-type semiconductor zinc oxide.

Zinc Oxide (ZnO) is renowned for its diverse morphology, adaptable properties, and versatile applications across various fields including sensing, battery technology, catalysis, and filtration. Among the established morphologies, the tetrapodal form (t-ZnO) synthesized through flame transport synthesis is of particular interest due to its single-crystalline structure and adjustable oxygen vacancies. A versatile method of applying different metal hydroxides/oxides to coat t-ZnO in an organized manner, creating a core@shell structure of t-ZnO@M(OH)_x (where M represents metals like Cu, Co, Al, Fe, Ni, Ti, etc.) derived from a suitable metal precursor is also studied. Subsequently, we interconnect the arms of the tetrapods using a photochemical process. This development of interconnections is particularly intriguing from a sensor application perspective, as it forms stable bridge-like structures between morphologies, even those that may not conduct electricity, such as MOFs or zeolites.

The surface of t-ZnO@M(OH)_x can undergo conversions to adopt alternative structures based on the same metal framework. For example, a Cu(OH)₂ shell can give rise to a Cu-based MOF like HKUST-1, a Co(OH)₂ layer can yield a Co-based MOF like ZIF-67 and Al(OH)₃ can either convert to Al-based MOFs or serve as a source for zeolite. Likewise, t-ZnO can be readily surface converted to a Zn-based MOF, such as ZIF-8. This technique facilitates the solvothermal growth of MOFs based on any metal framework utilizing ZnO as the sensing material, all while preserving the morphology, thus enhancing selectivity towards various gases or VOCs. The interconnects grown can be precisely tailored with respect to the desired material growth, growth areas, thickness, and proximity of the self-organized flakes achieved. The ultimate objective is to create selective, sustainable, lightweight, and portable indoor gas sensors for VOCs.

In this talk, I represent how interconnected porous chemical frameworks like tetrapodal ZnO or corresponding MOFs and zeolites show promising selective filtration based on pore sizes by applying these structures to zinc oxide, a versatile semiconductor to enhance sensor selectivity, ultimately aiming to create indoor gas sensors with the capacity to detect VOCs.

Keywords: Photochemical Interconnects, Volatile Organic Compounds(VOCs), Metal-Organic Framework(MOFs), selectivity, Zinc Oxide(ZnO), Metal Coating, Indoor gas sensors, Bridge-like tunable interconnects.

11:30 AM *EL03.05.04

Interplay of electrical and mechanical behaviors in dielectrics [Fabien Volpi](#), [Morgan Rusinowicz](#), [Chaymaa Boujrouf](#), [Muriel Braccini](#), [Guillaume Parry](#) and [Marc Verdier](#); Université Grenoble-Alpes, France

Dielectric films are widely integrated into advanced devices for both their functional and mechanical properties. In terms of functional properties, dielectrics are essentially expected to prevent electrical leakages, sustain large electric fields, limit capacitive coupling... In terms of mechanical properties, dielectrics contribute to the stiffness of device architecture but, like all ceramics, they are also preferential loci for crack nucleation/propagation. Consequently, understanding the interplay between the mechanical and electrical behaviors of dielectric films is essential to predict the lifetime of functional devices.

Nanoindentation is a powerful technique to probe the mechanical behavior of small-scale systems. When combined to electrical measurements, electrical-nanoindentation can be used to assess this mechanical-electrical interplay.

In the first part of this presentation, we will show how a mechanical stress can modify the electrical conduction mechanism in an ultra-low-k dielectric

(nanoporous SiOCH film deposited on a silicon substrate). Experimentally, electrical leakage was monitored in-situ during nanoindentation with a Berkovich indenter. These experiments reveal a counterintuitive electrical conduction drop under high mechanical stresses. This phenomenon is reproduced numerically (by FEM analysis) by correcting the Poole-Frenkel conduction law with a strain-dependent factor, and described analytically in terms of space-charge build-up induced by the trapping of holes at the mechanically-generated defects. A threshold strain is identified as the keystone linking this strain-dependent conduction to the current line distribution within the dielectric.

In the second part, we show how an electrical stress can degrade the mechanical properties of dielectrics. Experiments were carried out on a wide panel of dielectric systems: high- k and low- k dielectrics, thin and thick films, with or without bottom electrodes... Thanks to the fine in-situ coupling of mechanical and electrical monitoring, a mechanical collapse of the film is observed after the application of an electrical stress. Various origins of this collapse were first ruled-out (electrostatic force, local heating...), before it was finally demonstrated that the injection of electrical charges drives this mechanical collapse. Numerical modelling (FEM analysis) is used to discuss which film property is actually modified: stiffness or hardness. This phenomenon appears to be universal, since it is observed on all kinds of dielectric systems assessed in this study.

SESSION EL03.06: Advanced Characterization

Session Chairs: Silvia Armini and Sean King

Wednesday Afternoon, April 24, 2024

Room 346, Level 3, Summit

1:30 PM *EL03.06.01

Pathfinding in Optical Critical Dimension Metrology George A. Antonelli; Onto Innovation, Inc., United States

Semiconductor manufacturing has long relied upon optical methods for non-destructive high volume critical dimensional metrology. Optical reflectometers, ellipsometers, and interferometers from the deep ultraviolet to near infrared are essential engines of discovery. The underlying architecture and operating principles of many modern optical metrology tools are directly related to their progenitor instruments. Increased complexity and continued scaling of logic and memory devices offer new metrology challenges and force the continued evolution of these tools and the introduction of new architectures. High aspect ratio and buried structures are two general areas of concern for future devices which optical metrology must address. High aspect ratio structures >100:1 have become an integral part of many semiconductor devices in a variety of applications. Conventional optical critical dimension metrology tools can address a subset of this need but fall short in some use cases. One potential solution lies in the extension of these techniques into the mid-infrared range.

The shift to a three-dimensional paradigm for transistor and interconnect geometries has led to an increase in the use of conformal and gap filling techniques to address reentrant features. Both random and systematic void formation are common defect modes in these processes. In some process flows, an opaque metal layer disrupts the conventional lithographic layer alignment requiring a different approach. Photoacoustic methods can be applied to address both issues. It is also possible to use photoacoustics to perform sub-optical resolution dimensional metrology of buried features.

In this talk, we shall briefly discuss optical methods capable of addressing these challenges. The physical principles of the proposed approaches and hardware implementation will be reviewed. Several examples drawn from memory and logic process flows will be shared.

2:00 PM *EL03.06.02

Characterizing Highly-Confined Heat Flow, Elastic, and Structural Properties of Nanostructured Semiconductors and Dielectrics using Ultraviolet Light Sources Joshua Knobloch, Brendan McBennett, Albert Beardo, Emma Nelson, Travis Frazer, Jorge N. Hernandez-Charpak, Begoña Abad Mayor, Henry C. Kapteyn and Margaret Murnane; STROBE, JILA, University of Colorado Boulder, United States

Next-generation nanoelectronic, energy, and quantum devices rely on the discovery, integration, and optimization of novel complex and nanostructured materials. As the critical dimensions of these devices shrink below 10-nm, the complex 3D geometries and physical properties—including, mechanical, thermal, and surface/interface quality—of new materials govern device efficiency and performance. However, as the complexity increases and scale decreases, conventional models fail to accurately predict the functional properties, and traditional metrology tools cannot probe the relevant behaviors on their intrinsic length- and time-scales. By harnessing tabletop sources of coherent extreme ultraviolet (EUV) light¹, novel metrology tools can characterize the elastic, thermal, and structural properties of ultrathin dielectric films and nanostructured semiconductors.

Optimized ultrathin low- k interlayer dielectric films are critical materials to improve the speed and efficiency of nanoelectronic devices. However, precise characterization of films with thickness $\ll 100$ nm is challenging for traditional methods. Using a tabletop dynamic EUV scatterometry technique, we nondestructively extract the full elastic properties of single- and bilayer a-SiC:H and a-SiOC:H ultrathin films with thicknesses down to <5 nm—revealing surprising results^{2,3}. By simultaneously extracting both Young's modulus and Poisson's ratio in a series of hydrogenated ultrathin films, we observe an unforeseen trend in the compressibility: in the presence of strong hydrogenation which reduces the bond coordination past a critical threshold, the films undergo a transition from brittle to ductile². Additionally, we find that not only doping but also surfaces/interfaces can drastically alter the mechanical properties of ultrathin films. In very thin bilayers (<5 nm) with low-hydrogen doping, surface effects induce a substantial increase in compliance—by almost an order-of-magnitude—compared with identical thicker films, an effect not observed in highly-doped systems³.

Using our dynamic EUV scatterometry technique, we also nondestructively characterize the elastic properties, thickness, porosity, and thermal behavior of thin silicon metalattice layers^{4,6}—artificial 3D solids that are periodic on the sub-100 nm length scale. By monitoring the dispersion of hypersonic surface acoustic waves, we extract the Young's modulus and thickness of silica-filled and empty-pore silicon metalattice films with 14 – 35 nm periods, agreeing well with nanoindentation and electron microscope images^{4,5}. Moreover, we nondestructively probe the porosity and interconnectivity in an empty-pore re-infiltrated metalattice and validate with electron tomography⁵. Using these characterized properties, we can subsequently analyze the exotic thermal behaviors of these nanostructured silicon materials. By tracking the cooling of laser-excited metallic nanostructures, we observe a diffusive-like heat transport behavior with an apparent thermal conductivity two-orders-of-magnitude below bulk silicon⁶, which is not predicted by traditional analytical models. To describe this behavior, we derive an analytical expression for the apparent thermal conductivity based on an analogy to rarefied gas flow in porous media⁶. We find that the physics can be separated into two components: a geometry-dependent permeability and a geometry-independent viscous component which scales universally with porosity. This analytical expression describes not only transport in silicon metalattices but also nanomeshes, nanowire networks, and porous nanowires.

¹Science **280**, 1412 (1998). ²Nano Lett. **17**, 2178 (2017). ³Phys. Rev. Mater. **4**, 073603 (2020). ⁴Nano Lett. **20**, 3306 (2020). ⁵ACS AMI **14**, 41316 (2022).

⁶Nano Lett. **23**, 2129 (2023).

2:30 PM BREAK

SESSION EL03.07: Conductors for Flexible Electronics

Session Chairs: Serena Iacovo and Fabien Volpi

Wednesday Afternoon, April 24, 2024

Room 346, Level 3, Summit

3:30 PM *EL03.07.01

Electrical and Reliability Characteristics of Low-K SiCOH Dielectrics with Metal Integration Seonhee Jang, Rajib Chowdhury and Thomas Poche; University of Louisiana at Lafayette, United States

In modern microelectronic devices, copper (Cu) and low dielectric constant (low-k) dielectric materials have been used in the back-end-of-line (BEOL) interconnects. However, the migration and diffusion of Cu into the low-k films become challenging during the integration of Cu/low-k interconnects, causing degradation of electrical performance and reliability. A metal barrier is introduced between Cu and low-k dielectrics to prevent Cu diffusion. With further scaling of technology node, the resistance of Cu metal lines significantly increases because of Cu surface and grain boundary scattering and additional metal barrier. To decrease the line resistance, the thickness of the metal barrier should be reduced. To reduce the surface and grain boundary scattering effect, different metals with low resistance can be employed. Potential candidates to replace Cu can be determined by lower product value of bulk resistivity and electron mean free path than that of Cu. Based on this criteria, cobalt (Co) and molybdenum (Mo) were selected. In this study, the integration of Co or Mo with the low-k materials was conducted and electrical and reliability characteristics were investigated. Low-k SiCOH thin films were fabricated on p-type Si (100) wafer by plasma-enhanced chemical vapor deposition (PECVD) of tetrakis(trimethylsilyloxy)silane precursor at ambient temperature. To investigate electrical and reliability characteristics of low-k SiCOH dielectrics with metal integration, metal-insulator-silicon (MIS) structures were fabricated. Four different metals Al, Cu, Co, and Mo were deposited on the low-k SiCOH films using a sputtering deposition or electron beam evaporation methods. Thickness of each metal was approximately 120-130 nm. The fabricated MIS capacitors were then annealed in N₂ atmospheres at 400 °C for 1 h. The electrical characteristics of the MIS structures were measured from capacitance-voltage (C-V) and current-voltage (I-V) curves using a semiconductor parameter analyzer. The C-V curves of Al-gate, Cu-gate, Co-gate, and Mo-gate MIS capacitors were compared before and after thermal stress. The typical C-V curves were obtained with accumulation, transition, and depletion regions from the negative to positive bias application. Depending on the type of metal-gate, the accumulation capacitance was different, suggesting that the deposition of metal gate may affect the capacitance of the underlying low-k film. The thermal annealing reduced the accumulation capacitance of the MIS capacitors. An increase in the k-value suggests that the low-k thin film was damaged by plasma during metal sputtering deposition. After annealing, the k-values were reduced, indicating that plasma-induced damage to the film could be recovered by annealing process. The shift in the C-V curve was the evidence of the diffusion of metal ions into the low-k film by annealing process. An increased leakage current after annealing demonstrates that the diffusion of metal ions occurred in the low-k film. The elemental composition including Si, O, and C was investigated by X-ray photoelectron spectroscopy (XPS). Metal diffusion into the low-k film at the interface between the low-k film and each metal after annealing affected C-V and I-V characteristics. Effects of different metals on the electrical properties and reliability of the low-k SiCOH films under thermal stress were compared in this study.

4:00 PM EL03.07.02

Stretchable High-Resolution Multifunctional Displays Jisu Yoo, Gwang Heon Lee and Moon Kee Choi; Ulsan National Institute of Science & Technology, Korea (the Republic of)

Internet of things (IoT) technology urged the development of displays, which serve as fundamental human-machine interfaces by visualizing information for the user, in order to accommodate the expanding demand of electronic systems in daily life. For this reason, multifunctional displays, instantly representing non-visible stimulation as optical information, have been actively investigated to conduct diverse remarkable electronic applications. Sound generating displays, which have only lately been highlighted, are designed as single device without additional circuitry elements, while concurrently satisfying high degrees of deformation for wearable and/or attachable device applications.

Alternative current electroluminescent (ACEL) devices are one of the promising candidates as deformable optoelectronics owing to their simple device construction, facile fabrication, mechanical robustness, stable emission, and exceptional deformability. Among them, thin-film type ACEL devices are constructed with two electrodes sandwiching emissive layer that comprises phosphors and dielectric matrix. Under AC bias, thin-film ACEL device can be operated as both EL device and dielectric actuator speaker, originated from their structural similarity, making them optimal candidates as stretchable multifunctional displays. For practical application, patterning techniques also need to be applied to ACEL device. However, existed patterning methods of ACEL device were constrained to low-resolution EL operation (pattern size > 2 mm) and reduced brightness below the industrial standard (> 100 cd/m²). Hence, it is necessary to develop effective way to achieve high-resolution multicolor patterning of devices.

Herein, we report a stretchable high-resolution multifunctional display that can work both as an input and output device. Silver nanowires (AgNWs) and conductive polymer (PEDOT:PSS) embedded in thermoplastic polyurethane (TPU) are used as stretchable electrodes, and high dielectric constant particles (BaTiO₃)-inorganic electroluminescent phosphors (ZnS:Cu)-polydimethylsiloxane (PDMS) composite is adopted as emissive layer. Through surface engineering of both stamp and the top of emissive layer, transfer printing technique for emissive layer was developed. This technique facilitates the high-resolution and multicolor patterning of emissive layer for stretchable multifunctional displays that can be stably operated under dynamic and static deformation. Owing to clear and high-resolution patterning ability, we suggested the multifunctional displays that can work both as input and output device.

4:15 PM EL03.07.03

Optimization of Reliable and Reproducible Growth of Carbon Nanotube Forests and Microstructures based on The Machine Learning-Assisted Control of Catalyst Nanoparticle Morphology Kwangjun Kim, Yongtae Kim, Minwook Kim, Rahul S. Ingole and Jong G. Ok; Seoul National University of Science and Technology, Korea (the Republic of)

Recently, the realm of carbon nanotube (CNT) applications has been expanding in accordance with the rapid growth of cutting-edge industries including secondary batteries, semiconductors, sensors, and so on. For instance, CNTs are actively used in a powder or solution form as a conductive agent for both the anodes and cathodes of secondary batteries, which, however, typically entails various physical and chemical post-treatment processes. Utilizing the CNT forests and lithographically patterned CNT microstructures in their as-grown forms may obviate the labor for harvesting (off the substrate) and subsequent post-treatment (e.g., solution preparation) and may provide more functional frameworks with controlled 3D morphology, density, and aspect ratio. This can be achieved by optimizing the morphology of catalyst nanoparticles that are converted from the thin-film catalyst layer during the annealing step of the chemical vapor deposition (CVD)-based CNT growth process. Each catalyst nanoparticle offers a growth site of each CNT, suggesting that the catalyst nanoparticle's size and density control the diameter, density, and degree of alignment of the resultant CNT forests – and thus their physical,

chemical, and electrical properties. Here we propose a machine learning-based thermal and fluid interaction analysis for the control of catalyst nanoparticle morphology during the CVD process through thermal energy-driven Ostwald ripening and subsurface diffusion. We use the thermal fluid-structure interaction (TFSI) method to analyze the heat transfer characteristics of the catalyst layer system (Fe/Al₂O₃/SiO₂). We pay more attention to the micropatterned catalyst system which exhibits considerably different heat transfer characteristics depending on the micropattern geometry as compared to the non-patterned thin-film catalyst system. Additionally, we conduct machine learning to optimize the CVD parameters for reliable growth of CNT forests on micropatterned catalyst systems with various geometries. This optimization is based solely on preprocessed SEM images of the catalyst nanoparticles. The morphological data (density, diameter, and roundness) of catalyst nanoparticles are learned, and the global optimum values for CVD parameters - temperature and time during the annealing step, as two factors dominating catalyst nanoparticulation - are proposed. The experimental growth results are presented as a validation. We demonstrate that such a reliable and reproducible CNT growth - either to a forest or microstructure - realized by taking the global optimum values can be utilized in several cutting-edge applications including neural signal recording (using 3D CNT microelectrode arrays) and stretchable strain sensors (using one-directionally aligned CNT thin films engineered from microscale CNT blade patterns).

Acknowledgment

This work was supported by the National Research Foundation of Korea (NRF) grants (No. 2021M3H4A3A02099204, and 2022M3C1A3081178 (Ministry of Science and ICT) and No. 2022R111A2073224 (Ministry of Education)) funded by the Korean Government.

4:30 PM EL03.07.04

PEDOT:PSS-Based Nanofibrous Electrodes for Flexible Transparent Electronics Xenofon Karagiorgis^{1,2}, Dhayalan Shakthivel², Gaurav Khandelwal², Rebecca E. Ginesi¹, Peter Skabara¹ and Ravinder Dahiya³; ¹Joseph Black, United Kingdom; ²James Watt, United Kingdom; ³Northeastern University, United Kingdom

The demand for flexible and transparent electronics requires electrodes capable of concurrently maintaining high conductivity, flexibility, and optical transparency. Conventional metal electrodes, such as indium tin oxide (ITO), are inadequate for this purpose due to their inherent brittleness and the scarcity of indium. Furthermore, when subjected to bending conditions, ITO on flexible substrates is prone to delamination and cracking. These challenges have urged researchers to explore alternative Transparent Conductive Electrode (TCE) materials exhibiting properties similar to ITO. These targeted characteristics include (1) high conductivity and transparency, (2) exceptional flexibility and stability under various mechanical deformations (4) large area processability, (4) cost-effective, (5) room temperature (RT) processing, and (6) readily available: i.e., abundant supply.

Our work addresses these challenges by introducing a single-step electrospinning process with post-treatment to create highly conductive, flexible, and transparent PEDOT:PSS-based fibers suitable for interconnects and electrodes. These fibrous electrodes exhibit a sheet resistance of 7 Ω/sq and electrical conductivity of 354 S/cm, which is comparable to traditional rigid and metal electrodes, such as copper, silver, and ITO (0.1 to 10 Ω/sq) all while maintaining exceptional optical transparency of 77 % at 550 nm wavelength and excellent flexibility. The previous research has explored PEDOT:PSS and PEDOT:PSS/Ag nanowires fibers with sheet resistance in the range of 600 kΩ/sq and electrical conductivity in the range of 10⁻¹²-10¹ S/cm which is very low and has no potential to replace the conventional electrodes. The electrospun nanofibers were also deposited onto different substrates with varying levels of roughness and subjected to cyclic bending tests. The fibers on the poly(caprolactone) (PCL) substrate performed best under 1000 bending cycles with a slight change in sheet resistance from 7 Ω/sq to 8 Ω/sq, while on cotton fabric and Kapton film, a slight increment was observed.

The nanofibers were demonstrated as interconnects in a simple circuit for powering a light-emitting diode (LED). Even after 1000 bending cycles, the fibers were still able to turn on the LED at the same applied voltage of 2V, despite the slight changes in their sheet resistance. The potential of electrospun nanofibers for replacing metal electrodes was evaluated by fabricating a triboelectric nanogenerator (TENG). The TENG employing the metallic electrode achieved an output voltage of 73.9 V and an output current of 6.7 μA. When the copper electrode on one side was replaced with the nanofibers, the electrical performance of the TENG showed a notable improvement, reaching 77.9 V and 7.1 μA. This work stands out due to the significantly lower sheet resistance and stability under bending cycles which is attributed to the organic-inorganic interactions of our nanofibers, positioning them as ideal for applications including touch interfaces, OLEDs, interactive displays, energy storage, and harvesting, etc.

SESSION EL03.08: Poster Session I
Session Chairs: Serena Iacovo and Eiichi Kondoh
Wednesday Afternoon, April 24, 2024
Flex Hall C, Level 2, Summit

5:00 PM EL03.08.01

IoT-Enabled Pd-Anchored CuO/SnO₂ Hybrid Thin Films via RF Sputtering for H₂S Gas Sensing Amit Kumar; Indian Institute of Technology Jodhpur, India

The advancement of various fields, including Industry 4.0, Big Data, and Machine-to-Machine technologies, is significantly influenced by the integration of the Internet of Things (IoT) and Machine Learning (ML). These technologies play a crucial role in continuously collecting and analyzing information related to parameters such as temperature, speed, pressure, health data, environmental conditions, and consumption. The development of high-performance toxic gas sensing devices is essential for public safety, environmental control, industrial operations, and other applications, contributing to improved living standards. In this context, a novel fabrication method has been devised for H₂S gas sensor prototypes. These sensors utilize noble metal-functionalized metal oxide semiconductor (MOS) chemiresistors. The fabrication process involves the growth of CuO/SnO₂ hybrid nanostructures sensing thin film on SiO₂/Si substrates using the RF sputtering method. Subsequently, Pd nanoparticles, known for their excellent gas-sensing catalyst properties, are functionalized onto the CuO/SnO₂ hybrid films using DC sputtering, with varying sputtering times of 3, 6, 9, and 12 seconds. The resulting nanostone morphology enhances gas absorption, enabling the capture of more target molecules. Notably, a 9-second Pd sputtering time significantly improves H₂S sensing compared to other gases. The CuO/SnO₂ film with Pd exhibits the highest response, registering a 74.7% response to 50 ppm H₂S and detecting concentrations as low as 0.5 ppm. These promising results are achieved at the optimal working temperature of 150 °C. Following the optimization of parameters, the technology is transferred to the development of a sensor module with IoT integration. The prototype sensor seamlessly connects to a NODEMCU-ESP8266 Wi-Fi module, establishing a link with a smartphone through a mobile hotspot. This integration enhances the real-time monitoring and data transmission capabilities of the sensor, contributing to efficient and connected systems for diverse applications.

5:00 PM EL03.08.02

Improvement of Bending Failure in DRAM Capacitors through The Utilization of EUV Patterning Seungjin Kim; Sungkyunkwan University, Korea

(the Republic of)

As the size of the dynamic random access memory (DRAM) continues to shrink, the difficulty of patterning has become increasingly challenging. Among them, the capacitor pattern, an essential element for data storage, possesses the structure with the highest aspect ratio in DRAM. Consequently, difficulties in securing yield arise due to the chronic defects such as bending and pattern collapse of the pillar-type capacitor node, impeding the overall manufacturing process. Bending of the capacitor node, generating bridges in the bottom electrodes, serves as a disruptive factor that hinders the normal operation of the memory. The bending of the capacitor occurs due to stress induced by bottom electrode oxidation during the deposition of the dielectric layer after the deposition of the bottom electrode. To prevent this, a supporter structure is being introduced. The supporter is composed of a nitride layer and is patterned for the deposition of the dielectric layer on the bottom electrode. The impact on capacitor bending varies depending on the patterning of this supporter. In this research, the improvement in capacitor bending was confirmed through the application of all cell open (ACO) supporter patterning using extreme ultraviolet (EUV). Through this, we suggest the ultimate patterning fabrication process for DRAM capacitors to overcome the scaling limits of DRAM, opening up the inevitable possibility of the EUV era, ensuring the realization of sub-10nm patterns with high guarantee.

5:00 PM EL03.08.03

In-Situ Multi-Chip Integration of Ultra-Thin-Silicon Interposer via Transfer Printing [Uhyeon Kim](#), Seungbeom Kim, Junhyung Kim, Sangyeop Lee, Agha A. Jan and Seok Kim; Pohang University of Science and Technology, Korea (the Republic of)

2.5D heterogeneous integration packaging based on interposer technology has emerged as a key technology driving 'Beyond Moore' advancements in semiconductor miniaturization. However, conventional carrier wafer techniques and flip-chip processes pose limitations when handling extremely thin components (<30µm) that can be easily distorted. In this study, an innovative In-Situ bonding process was developed using shape memory polymer (SMP) stamp-based transfer printing technology to reliably transfer ultra-thin silicon interposers at high speeds within 3 minutes. The ultra-thin silicon interposer was designed with transferable ink using transfer printing and thermal processing techniques. By predefining copper TSVs (Through-Silicon Vias) and Cu-Sn solder bumps on an SOI (Silicon On Insulator) wafer to a specific thickness, and separating the Box Layer, an independent ultra-thin interposer of 15µm thickness was manufactured. This interposer was precisely and securely transferred to the receiver substrate using an SMP (Shape Memory Polymer) stamp, designed to transfer through thermo-mechanical property. Subsequently, a low-temperature bonding method (~230°C) suitable for Cu-Sn fusion conditions was employed, successfully achieving rapid coupling for the fragile components' multi-layer integration. The bonded interposer exhibited distinct characteristics such as FIB (Focused Ion Beam) and IV curve. This ultra-thin integration technology holds promise for the utilization of brittle ultra-thin DRAM integration, specifically in applications like HBM (High Bandwidth Memory).

5:00 PM EL03.08.05

Economical Flexible Electronics Incorporating All-Solution-Processed Transistors on Paper [Chengmin Zhang](#)¹, Do Hoon Lee² and Byung Yang Lee¹; ¹Korea University, Korea (the Republic of); ²Hokkaido University, Japan

Paper electronics is receiving great interest because it is one of the best candidates for next-generation devices with many useful features such as low cost, disposability, and flexibility. However, the rough and porous surface of standard paper accelerates the spreading of liquid ink, limiting the manufacture of solution-processed paper electronics. Here, we use extremely rough and absorptive paper substrate without any treatment with an overall average RMS roughness much higher than that of general-purpose paper. The AgNW network acting as a gate electrode was formed on the paper surface by absorbing the AgNW solution (1 wt% in DI water) into the filter paper using a home-made screen printer screen printed gate electrode with low sheet resistance (9±5 Ω/sq) and low root mean square (RMS) roughness of 130±10 nm was obtained after drying for 30 min under ambient air without heating treatment. Then, the PVDF-HFP (Poly(vinylidene fluoride-co-hexafluoropropylene)) solution (20 wt% dissolved in DMF (N, N-Dimethylmethanamide)) is injected onto the surface by screen printing. In the vacuum state at a pressure of 0.002 atm for 5 min, a certain amount of PVDF-HFP solution is filtered in the AgNWs network layer and most of the solution is absorbed. As a result, a dielectric layer of less than 10 µm is cured thinly on the surface of the AgNW-assembled paper. The solution-processed flexible FETs on paper exhibit electrical performance with charge carrier mobility of 0.053 cm² V⁻¹ s⁻¹, and a current on/off ratio of 7×10². We report the development of zinc oxide nanowire (ZnO NW) field-effect transistors (FETs) on paper with facile, low-cost, and large-area manufacturing. By utilizing simple equipment such as a vacuum filter and a homemade pulling system, we could produce outstanding FETs that are desirable for cheap flexible electronic applications.

5:00 PM EL03.08.06

Electrochemical Deposition of Polyetherimide (PEI) Thin Films from Aqueous Emulsions for Structured Substrates: Towards Advanced Integrated Capacitors in Power Electronics Alexandre Seurot, Antoine Hoang, Vincent Jousseau and [Paul-Henri Haumesser](#); CEA LETI, France

In the pursuit of miniaturized high-power electronic devices, the demand for robust high-power capacitors capable of withstanding electric fields in the range of several hundred volts across micrometric dielectric layers has emerged. To miniaturize these capacitors, one possibility is to create 3D structures in a silicon wafer to maximize capacitance density by expanding the dielectric surface area. However, this approach encounters difficulties when trying to combine it with conventional inorganic dielectrics (such as SiO₂), due to the mechanical stress induced by thick films. Among suitable dielectric materials to build such devices, polyetherimide (PEI) is highly promising due to its exceptional chemical resistance and thermal stability up to 170°C. The conventional technique of spin-coating for polymer thin film deposition, however, falls short in achieving conformal deposits on 3D-structured substrates with large developed surface area. To address this limitation, we explore an electrochemical deposition process for PEI, employing an aqueous emulsion of organic droplets containing the polymer as the electrolyte.[1]

In this study, we grafted N-methylpiperazine onto the imide groups of raw PEI polymeric chains within a solvent mixture. The grafting reaction is confirmed to be quantitative through FTIR and NMR measurements. The addition of an aqueous lactic acid solution, followed by ultrasonic mixing, led to the formation of emulsions encompassing modified PEI organic droplets. These droplets exhibited an approximate diameter of 40 nm, as observed through Cryo-TEM, and zeta potentials exceeding 50 mV. These emulsions were diluted by a factor of 10 with the addition of deionized water, and were stable for at least several weeks.

Deposition experiments were conducted within a 3-electrode electrochemical cell, under mild conditions (room temperature, pH ranging from 3 to 4), utilizing Cu metal surfaces. A pulsed DC waveform with an amplitude below 2 V/SCE was employed to mitigate hydrogen evolution. Within a timeframe of 600 seconds, a PEI coating with a thickness of a few micrometers was successfully obtained.

Remarkably, our results demonstrate comparable film thickness to existing literature [1], despite using an emulsion with 20 times dilution and voltages 40 times lower. Our comprehensive investigation into the influence of deposition factors on coverage and uniformity has revealed the significant impact of hydrodynamic conditions and the pivotal role played by the pulse/tension combination in achieving distinct morphology and thickness. SEM inspection showcased a uniform film at the center with iridescence.

Following deposition, the film was thermally cured under vacuum conditions to eliminate solvents and restore the imide groups of PEI.[1] FTIR analyses confirmed excellent agreement between IR spectra of the cured and pristine polymers, as well as the elimination of amide (I and II) peaks.

This work establishes the feasibility of electrochemically depositing insulating polymeric films under mild conditions, enabled by the formation of stable emulsions containing charged polymeric droplets. This innovative electrodeposition process holds immense promise for coating substrates with complex

3D structures, contrasting with conventional dielectric deposition techniques. Importantly, this original methodology presents a potential avenue for fabricating integrated capacitors on silicon wafers, paving the way for the next generation of power electronics devices.

[1] H. QARIOUH *et al.* Polym Int. 1999, Vol. 48, p. 1183-1192

5:00 PM EL03.08.07

Investigating TDDB Reliability in Next-Generation Packaging Technology: Nano-Twinned Cu RDL Yoongu Lee, Hongik Kim, Gaeun Song, Young-Chang Joo and In-Suk Choi, Seoul National University, Korea (the Republic of)

Due to the performance improvement and miniaturization of semiconductor devices, the size of input/output (I/O) has decreased while their number has rapidly increased, surpassing the capacity of conventional printed circuit board (PCB) substrates. To address this issue, recent advanced packaging technology for 2.5D integration has applied a redistribution layer (RDL), which enables a larger number and smaller size of I/O, significantly improving signal process performance. However, as RDL becomes increasingly fine-pitched, the interlayer dielectric spacing between RDLs decreases rapidly, resulting in an increased effective electric field and raising concerns about potential dielectric breakdown. Notably, since the dielectric in RDL is organic dielectric polyimide (PI) instead of the SiO₂-based inorganic dielectric used in the conventional backend-of-line (BEOL), it is expected to be more vulnerable to time-dependent dielectric breakdown (TDDB). Therefore, this presentation will showcase the TDDB assessment of fine-pitch RDL interconnect for different RDL linewidth/space (L/S) and RDL line patterns. In particular, we compare the TDDB of interconnect with random microstructures to that with nanotwinned Cu interconnect, which is known to possess superior strength, ductility, thermal conductivity, and electromigration (EM) resistance due to its microstructure that incorporates a few nanometers thick twin boundaries within grains. Interestingly, we observed a clear difference in TDDB results between random Cu interconnect and nanotwinned microstructure. We will also discuss the cause of the difference in TDDB reliability according to the microstructure, based on the analysis of the leakage current conduction mechanism through voltage-ramping dielectric breakdown (VRDB) tests at various temperatures.

Keywords: 2.5D/3D integrated circuit (IC) integration, redistribution layer(RDL), Time-dependent dielectric breakdown (TDDB), Nano-twinned Cu

5:00 PM EL03.08.08

Sustainable Printing Processes for Chip Scale Interconnect and RF Structures on Flexible Substrates Henry Lei^{1,2} and John D. MacKenzie¹; ¹University of Washington, United States; ²NoiseFigure Research, United States

This work demonstrates the use of multiple types of sustainable high resolution additive manufacturing processes such as EHDJ (electrohydrodynamic inkjet) and piezoelectric inkjet to create chip scale interconnect and RF structures on both rigid and flexible substrates. Different types of metal based nanoparticle inks such as silver and gold are printed using a variety of methods such as direct write or drop on demand to create the desired conductive pattern. The techniques described are additive and in direct contrast to both semiconductor and PCB (printed circuit board) based metal patterning processes where metal is subtractively removed. These additive manufacturing methods may be completed in atmospheric conditions thus saving energy as vacuum is not required, unlike ebeam evaporation or other metal deposition methods in semiconductor manufacturing, nor do they require toxic chemicals, such as ferric chloride, a common copper etchant used in the fabrication of PCBs. Trace widths and spacings that range from 80 microns down to 40 microns on both rigid and flexible substrates were achieved, demonstrating these techniques' viability to create structures for chip level fan out. These techniques' capability to manufacture structures that operate at RF frequencies is shown via both a single antenna and an 1x3 antenna array that operate at the 3.6 GHz 5G n48 band. The functional antenna modules demonstrate the feasibility of these additive processes in manufacturing and prototyping for the current generation telecommunication protocols.

5:00 PM EL03.08.09

Gecko-Inspired Adhesive Conductive Film for Flexible Electronics Auriane Despax-Ferres¹, Pascal Tiquet¹, Jean-Charles Souriau², Julia De Girolamo¹ and Vincent Jousseume²; ¹University Grenoble Alpes, CEA, Liten, France; ²University Grenoble Alpes, CEA, LETI, France

A large number of flexible electronic applications are envisioned among them, wearable electronics and bio-electronics applications. One of the main challenges in this field is to integrate semiconductor devices on unconventional substrates subject to mechanical stress (bending and stretching). Interconnect technologies must be implemented at low pressure and low temperature to avoid damaging the substrate. They must also be able to withstand slight deformation, like a medical patch in contact with the skin. Currently, the solutions for interconnecting electronic components with their active face facing on substrates are mainly based on metallic soldering. These solutions are not ideal for flexible substrates as the soldering is rigid and irreversible. The used of a thin stretchable anisotropic conductive adhesive that can be used as a conductive film between the silicon device and the substrate could solve these issues.

In this work, we have developed gecko-inspired adhesive based on an arrays of microscale pillars made of polydimethylsiloxane (PDMS), a biocompatible and low-cost polymer. The pillars have mushroom-shaped tips known that are known as the most efficient form of contact. First, mushroom-shaped molds with varying geometries were fabricated in a silicon-on-insulator wafers (SOI) with typically a 2 µm-thick buried oxide layer and a thick Si top layer ranging from 15 to 25 µm. The mushroom molds were realized by standard photolithography and etching process and the surface of the molds was then covered with a hydrophobic thin film using a vapor phase process. Then, gecko-inspired films were performed using a solution of PDMS poured into the molds and spread out by spin-coating. The spin-coating parameters were adjusted to obtain films with a backing layer thickness of approximately 190 µm. Finally, the gecko-inspired films were cured at 100°C and peeled from the SOI molds. This method allow to produce microstructured films with very few defects. To make these films locally conductive, composites based on high aspect ratio multi-walls carbon nanotubes (1 wt%, mean aspect ratio of ~830) and PDMS were used. The localization of the conductive composite was performed by screen-printing. CNT-PDMS composite was deposited through a stencil composed of holes of 300 µm diameter directly on the SOI molds. After screen-printing, the CNT-PDMS was thermally cured and pristine PDMS was deposited by spin coating, cured and demolded.

The adhesion performances of the different mushroom-shaped microstructured films were characterized by compression and pull-off tests on glass and on silicon. For both surfaces, adhesion forces higher than 6 N.cm⁻² can be obtained depending on the geometry. However, the shape of the mushrooms needs to be carefully designed, as some configurations (particularly when aspect ratios are too high) are not leading to high adhesion forces. Preliminary results show also that a slight degradation of the adhesion (by a factor ~3) is observed with conductive mushrooms. This results could be related to the difference of elastic modulus induced by the presence of CNT fillers in the composite and by a difference of the surface state of the films. The electrical conductivity obtained for microstructured films is evaluated at 10⁻² S.m⁻¹ which is lower than the bulk conductivity of the composite (by one order of magnitude). The surface state of the conductive film may also be at the origin of this result, inducing a high contact resistance.

5:00 PM EL03.08.10

Advancing Precision in Transfer Systems with Shape Memory Polymers Han Jun Park, Minsu Kim, Dokyung Kyeong, Ga-in Lee and Moon Kyu Kwak; Kyungpook National University, Korea (the Republic of)

Shape memory polymers (SMPs) belong to a unique category of smart materials capable of retaining a "permanent shape" via the shape memory effect and

transitioning into a "temporary shape" under the influence of specific stimuli like heat, electricity, light, or a magnetic field. In the case of thermally triggered SMPs, they typically exist in a rigid state with a fixed permanent shape initially. However, when exposed to temperatures above their glass transition temperature (T_g), their elastic modulus decreases, enabling temporary deformation in response to an external force. Upon cooling, the elastic modulus of SMPs returns to its initial value, effectively preserving the deformed state as the temporary shape even after the removal of the external force. A defining trait of SMPs is their ability to regain their original shape and mechanical properties when subjected to thermal stimulation after adopting a temporary shape. One of the most promising applications involves utilizing the shape memory effect of SMPs in transfer systems for achieving high-precision pickup and release of delicate substrates.

Transfer system is a pivotal process in the manufacturing of displays and semiconductors, demanding the ability to transfer objects with varying surface profiles. As the demand for thinner and larger substrates continues to rise, the necessity for efficient transfer systems becomes more critical. Achieving high efficiency in pick-and-place systems necessitates both strong adhesion forces for pickup and weak adhesion forces for placement. Recent efforts have focused on dry adhesives that rely on van der Waals interactions for achieving the required adhesion switching. Dry adhesives are appealing due to their cost-effectiveness, mechanical robustness, and they are increasingly finding applications in the pick-and-place industry. Nonetheless, challenges persist in achieving stable detachment during the adhesion switching process. Several research studies have explored various strategies for designing such systems using SMPs, which include double-layer structures, surface microstructures, and dry adhesives. However, the manufacturing process of SMP-based adhesives remains time-consuming, largely due to the need for multiple material combinations and lengthy thermosetting times.

In this study, we present the design and development of a novel SMP dry adhesive that achieves highly reversible heat-actuated adhesion switching systems using Norland Optical Adhesive 63 (NOA 63). Notably, NOA 63 offers the flexibility to program the T_g based on curing conditions, facilitating the rapid and straightforward manufacture of SMP-based adhesives through UV irradiation. UV curing induces a transition in NOA 63 from a rubbery to a glassy state, reducing polymer chain mobility and diffusion. Subsequent temperature increases prompt the polymer chains to revert to the rubbery state, resuming residual reactions and elevating the material's T_g . The fabricated SMP dry adhesive exhibits outstanding adhesion performance to substrates with varying surface topographies, thanks to its ability to transition to the rubbery state above the T_g . Additionally, introducing a micro-lens pattern on the SMP dry adhesive's surface enhances both adhesion and detachment. The shape memory effect of the SMP dry adhesive facilitates the recovery of the micro-lens pattern's shape, simplifying substrate detachment. By altering the curing conditions of NOA 63, different T_g values can be programmed, resulting in varying adhesive performances at different temperatures. Furthermore, the SMP dry adhesive demonstrates remarkable mechanical durability even after repeated adhesion cycle tests. To assess its practicality, a pick-and-place experiment employing a Peltier element was conducted, confirming the feasibility of continuous fabrication through the convenient UV curing process of NOA 63 in a roll-to-roll system.

5:00 PM EL03.08.11

Vacuum- and etch-free mechanical fabrication of metal wire microtrenches interconnected by ZnO nanowires for flexible bending-sensitive optoelectronic sensors Minwook Kim, Kwangjun Kim, Rahul S. Ingole, Yongtae Kim and Jong G. Ok; Seoul National University of Science and Technology, Korea (the Republic of)

In recent years, there has been expanding interest in developing optoelectronic transducers using micro- and nanoscale materials and structures in compact, lightweight, and flexible forms. Specifically, optoelectronic micro- and nanoarchitectures composed of micropatterned electrodes connected by semiconductor nanowires (NWs) such as ZnO NWs (ZNWs) have gained considerable attention due to their good sensitivity to incident light. However, traditional methods for fabricating micropatterned electrodes often involve difficult and time-consuming processes such as vacuum deposition, optical lithography, and etching, often preventing scalability and widespread application. Additionally, synthesizing ZNWs, usually dependent on high-temperature seed sintering or chemical vapor deposition, can interrupt their practical use on flexible substrates. One tactful approach to overcoming these challenges is to create a micropatterned electrode via mechanically machining microtrenches and filling the metal wires therein, and then growing ZNWs selectively on the trench-embedded metal wires via a metal-mediated low-temperature hydrothermal process. Working on this novel strategy, we develop a vacuum- and etch-free method for the fabrication of metal-wire-embedded microtrenches interconnected by ZNWs. Our method involves the continuous mechanical inscribing of linear microtrench patterns (microgratings) on a substrate, followed by the doctor-blade-assisted embedding of solution-processable metal wires within those trenches. We then undertake the low-temperature metal-mediated hydrothermal growth of ZNWs selectively onto the metal wires, finalizing the ZNW-interconnected micrograting electrode structure. The entire process can be carried out at a low temperature without resorting to vacuum, lithography, and/or etching steps, thereby enabling the use of flexible polymer substrates of scalable sizes. The resulting flexible device can function as a bending-sensitive optoelectronic sensor with high sensitivity, as the number of ZNWs interconnecting the trench-embedded micrograting electrodes changes upon mechanical bending.

Acknowledgment

This work was supported by the National Research Foundation of Korea (NRF) grants (No. 2021M3H4A3A02099204, and 2022M3C1A3081178 (Ministry of Science and ICT) and No. 2022R111A2073224 (Ministry of Education)) funded by the Korean Government.

References

1. D. K. Oh*, W. Lee*, H. Chae, H. Chun, M. Lee, D. H. Kim, J. Kim, J. Choi, S. Hwang, M. Park, G. Yeon, S. Jung, J. Rho, and J. G. Ok (*equal contributions), Burr- and etch-free direct machining of shape-controlled micro- and nanopatterns on polyimide films by continuous nanoinscribing for durable flexible devices, *Microelectronic Engineering* 257, 111740 (Mar 2022).
2. W. Lee*, H. Chae*, D. K. Oh*, M. Lee, H. Chun, G. Yeon, J. Park, J. Kim, H. Youn, J. Rho, and J. G. Ok (*equal contributions), Solution-processable electrode-material embedding in dynamically inscribed nanopatterns (SPEEDIN) for continuous fabrication of durable flexible devices, *Microsystems & Nanoengineering* 7 74 (Sep 2021).
3. K. Yoo*, W. Lee*, K. Kang, I. Kim, D. Kang, D. K. Oh, M. C. Kim, H. Choi, K. Kim, M. Kim, J. D. Kim, I. Park, and J. G. Ok (*equal contributions), Low-temperature large-area fabrication of ZnO nanowires on flexible plastic substrates by solution-processable metal-seeded hydrothermal growth, *Nano Convergence* 7, 24 (Jul 2020).

SESSION EL03.09: ASD and Printing
Session Chairs: Silvia Armini and Eiichi Kondoh
Thursday Morning, April 25, 2024
Room 346, Level 3, Summit

8:15 AM *EL03.09.01

Novel Patterning Solutions For Scaling Interconnects Beyond 2030 Gurpreet Singh; Components Research - Intel Corp, United States

In addition to improved transistors, interconnects, and advanced packaging, scaling is a major factor in the improvement of semiconductor product performance. Scaling improves product performance by enabling lower capacitance and lower power systems, by enabling more functionality per logic block through use of additional transistors and by enabling either more cores or memory capacity per chip. Scaling is enabled by innovations in patterning, power delivery and transistor architecture. Stacked transistor architecture is expected to follow gate-all-around architecture for continued improvement in performance and density. Such an architecture could reduce the cell size by approximately 50% due to cell height reduction. However, to efficiently route an aggressively scaled cell with stacked transistors, the metal and interconnect pitch must be scaled to levels that are difficult to achieve with conventional patterning techniques. Variation control is the key challenge to pitch scaling as the edge placement margin of error is small and the large number of features required for modern circuits implies stochastic sampling in the greater than 7 sigma regime. Solutions are needed to address each component of variation, such as line roughness and size variation, via size variation, line-end pullback and overlay. One example of a powerful complementary lithography technique with superior variability control is directed self-assembly (DSA). DSA offers a fundamental advantage over conventional lithography since the line and space CDs are chemically encoded into each molecule with unprecedented accuracy. We will report on recent progress made for a process flow based on DSA that rectifies complex, multi-pitch and multi-CD EUV patterns with low integrated defects, robust electrical yield, and compatibility with standard design rules.

8:45 AM *EL03.09.02

Selective Processes to Enable Scaling: Progress, Challenges and Opportunities [Dina H. Triyoso](#), Robert Clark, Kandabara Tapily, Nathan Antonovich, Lior Huli, Ainhua Romo-Negreira, Ryota Yonezawa, Cory Wajda and Gert Leusink; TEL, United States

Selective deposition has been used in microelectronics industry for many years. These processes are mostly done at high temperature. As scaling continues, device architecture has evolved from planar to FinFET, gate all around and vertically-stacked-Complementary Field Effect Transistors (CFETs). With the stacking of devices, it is desirable to enable low temperature selective processes. In this paper we discuss three examples of selective processes which are used to help extend scaling: (1) Dielectric on Metal (DoM) to enable advanced interconnect, (2) Dielectric on Dielectric (DoD) to enable Fully Self-Aligned Via (FSAV), and (3) Combining selective deposition and etch to extend EUV scalability. These three processes are well established and not too far from high volume manufacturing (HVM). Beyond these processes, challenges in selective deposition on similar surfaces and high aspect ratio structures will be discussed.

9:15 AM EL03.09.03

Mechanisms of Area Selective- Atomic Layer Deposition and Their Impact on Feature Sizes [Katherine T. Young](#)¹, [Andy Hsiao](#)¹ and [Chris Yang](#)²; ¹Georgia Tech Research Institute, United States; ²Georgia Institute of Technology, United States

As devices have continued to scale down in size, fabrication of smaller features using novel methods has become a necessity. Strict requirements of location and alignment are often necessary and difficult to achieve with prior techniques, which has led to studies of area selective deposition. Area selective deposition, such as area selective-atomic layer deposition (AS-ALD), can be achieved by manipulating deposition preferences for different materials. A material is deposited selectively at certain locations based on the interaction of the precursors with different surfaces, so etching is not usually necessary and sometimes lithography is not necessary. AS-ALD can take advantage of the preferential deposition of the ALD precursors onto different types of materials like oxides or metals, etc. In fact, these techniques can sometimes be the only option for patterning different materials if the geometry of the surface or substrate cannot be patterned with lithography. Also, some SAM or polymer masks that have very low deposition can be patterned onto a surface so that AS-ALD can be used to pattern a single material (since the mask is later removed). This technique is especially useful for patterning materials or substrates that may be sensitive to etching. However, the selectivity between two different materials under certain deposition parameters limits the use of some materials and ALD precursors. Thus, a deeper understanding on the mechanism of area selective deposition is necessary to understand limitations on feature sizes.

This study describes the mechanisms for area selective- atomic layer deposition of common oxide materials (e.g., TiO₂ and HfO₂) on PMMA and Si and the effects of these deposition mechanisms on feature sizes. PMMA was patterned onto Si using electron beam lithography with feature sizes ranging from 5 μm down to 60 nm. ALD of TiO₂ and HfO₂ were studied to understand the selectivity of the deposition on Si vs PMMA and how that selectivity affected feature size dimensions and film thickness. The mechanisms of deposition were studied by characterizing the extent of ALD deposition before and after PMMA removal. TiO₂ was not detected on the surface of the PMMA, but after PMMA removal there was a very small amount of deposition in the location that had been coated by PMMA. It was determined that the ALD precursors are likely able to diffuse into the PMMA and still deposit at the interface between the Si and PMMA, even if it is only a trace amount. Thus, ALD of TiO₂ is highly selective for Si in comparison to PMMA; however, the effects of the PMMA side walls inhibit deposition so that the dimensions of the TiO₂ feature is smaller than the PMMA pattern. This side wall inhibition significantly affects possible feature sizes using TiO₂ and PMMA patterns. In contrast, HfO₂ is less selective than TiO₂ and demonstrates a mechanism combining selective deposition and lift-off. This lower selectivity limits possible HfO₂ thicknesses before there is blanket coverage, but it also exhibits less side wall inhibition. Significantly smaller feature sizes were obtained with HfO₂ compared to TiO₂ in these ALD conditions. Though the ALD parameters could be optimized further, these results suggest that the deposition mechanism itself, whether it is a truly area selective deposition or a combination of area selectivity and liftoff will always affect possible feature sizes.

9:30 AM EL03.09.04

Fabrication of High-Density, High-Resolution Interconnects via Acoustic Field Assisted Aerosol Jet Printing [Roxanne Kate Balaney](#) and [Tyler Ray](#); University of Hawaii, United States

The additive manufacture of production-grade flexible, large-area electronics is of intense interest to rapidly design, prototype, and fabricate electronics without reliance upon traditional electronics fabrication pathways. Such additive processes enable the direct integration of electronics on arbitrary, non-planar surfaces, expanding the potential form factors and application spaces. Of particular interest is Aerosol Jet Printing (AJP) owing to the capacity to fabricate high-resolution printed interconnects with design geometries not possible via other additive manufacturing technologies. AJP is a process by which the controlled deposition of an aerosolized, liquid ink enables the conformal printing of electronic traces. However, several key challenges, such as overspray and process drift, which restrict broad deployment of AJP and limits the feature resolution of printed interconnects. To address these challenges, we report a new type of AJP print process to control and architect aerosolized ink. Termed acoustic focusing aerosol jet printing (AF-AJP), we utilize acoustic forces (AF) to control the width of printed material by focusing the jetted material to a narrower region than what would be possible with a physical orifice alone. As the acoustic focusing effect is dependent on the ink droplet size, the utilization of acoustic focusing provides a means to “refine” the jet (especially if not material-rich) such that the deposited material has a smaller line width and exhibits a reduction in the typically observed particle overspray. We report a typical 30% reduction in trace width, sharp reduction in overspray, and an overall enhancement in print quality via this novel printing technique. We also demonstrate the utilization of AF-AJP to enable the printing of high-resolution traces with electronic materials such as graphene and MXene Ti₃C₂T_x, in order to fabricate highly conductive traces with conformal and 3D geometries.

9:45 AM EL03.09.05

A Novel Approach for High Precision Printing of Micro-Bumps Marc Pascual, Achille Guitton, Amin M'barki and Anthony Fiorini; Hummink, France

High aspect ratio micro-bumps play a critical role in flip chip applications, facilitating enhanced pixel density and reduced pixel-to-pixel coupling noise. The necessity for micro-bumps with a diameter of less than 5 μm , featuring these high aspect ratios, underscores the limitation of conventional technologies. This study discussed how HPCAP (High Precision Capillary Printing) Technology, allows the one-step fabrication of such micro-bumps. HPCAP capitalizes on capillary forces and resonance as intrinsic drivers, preventing the requirement for external energy sources. Inspired by Atomic Force Microscopy (AFM), this technique achieves remarkable precision, with up to 5 nm accuracy along the Z-axis and 20 nm along the XY axes. This level of precision ensures impeccable control over the dimensions and shapes of the micro-bumps enabling exceptional versatility in design, dimensions, and choice of materials.

10:00 AM BREAK

SESSION EL03.10: New Materials
Session Chairs: Vincent Jousseume and Sean King
Thursday Morning, April 25, 2024
Room 346, Level 3, Summit

10:30 AM EL03.10.01

Etching Characteristics of The B and N Co-Doped Amorphous Carbon Films through Nitrogen Concentration Control for Use as Hardmasks
Hongik Kim¹, Ung-Gi Kim¹, Deokgi Hong¹, Young-Chang Joo¹, Seungwu Han¹ and So-Yeon Lee²; ¹Seoul National University, Korea (the Republic of); ²Kumoh National Institute of Technology, Korea (the Republic of)

The challenge to overcome the limits of semiconductor chip shrinkage continues. Shorter-wavelength light sources, such as extreme ultraviolet (EUV), are being utilized to maximize resolution. The use of shorter-wavelength light sources leads to a decrease in the depth of focus (DOF), and consequently, a proportional reduction in the thickness of the photoresist (PR) layer. This limitation in PR layer thickness may lead to a failure in fulfilling its intended role as a mask in the etching process following lithography, risking complete loss or compromise during etching and potentially causing a deterioration in pattern quality. To address the previously mentioned issues, a sacrificial layer called the hard mask is applied between the component to be patterned and the PR. Amorphous carbon is the material that can most effectively meet various characteristics required for use as a sacrificial layer. Various approaches have been attempted to enhance etch selectivity and improve pattern quality in the etching process by altering the properties of this material. While there have been numerous studies analyzing the characteristics by doping different elements into the amorphous carbon layer, the focus has predominantly been on research related to individual elements.

We aimed to investigate how characteristics change from the perspective of etch resistance when boron & nitrogen co-doping is applied, rather than when individual dopants are applied separately. B & N co-doped amorphous carbon (a-BCN) hardmask were obtained by adjusting the nitrogen content in an amorphous carbon film supplied with sufficient boron, using the DC sputter process. The composition of the hardmask film was analyzed through XPS analysis. Subsequently, films deposited under various conditions were evaluated for their relationship with dry etching performance. In particular, we analyzed the relationship between the etching gas and the a-BCN hardmask structure in the ternary system from both physical and chemical reaction perspectives. We figured out that increased nitrogen in the film alters its density and structure, impacting physical etching processes. Additionally, DFT calculations show that higher nitrogen content increases the probability of chemical etching reactions with fluorine. The details of the physical and chemical reaction mechanisms of etching in a-BCN will be discussed in detail. Based on the implementation results of the ternary system in the hardmask, we would like to discuss the changes in etching characteristics from both physical and chemical perspectives.

10:45 AM EL03.10.02

Metal-Organic Framework Crystal Growth in Microgravity Phillip Irace, Ryan D. Reeves and Michael Roberts; International Space Station National Laboratory, United States

Crystals grown in microgravity have been shown to be larger in size, to be more uniform in size and morphology, and to contain fewer structural defects relative to Earth-grown crystals. This is due to the homogenous, diffusion-controlled growth in microgravity that results from the lack of gravity-induced convection and sedimentation. Metal-organic frameworks (MOFs) are a unique class of materials that consist of a central metal ion coordinated to organic ligands that extend to form two- or three-dimensional structures. MOFs have promising applications in electrocatalysts, photovoltaics, thermoelectrics, and electrical energy storage materials due to their tunable chemical, electrical, and mechanical properties. Persistent microgravity provides an ideal environment to study the growth of larger, higher-quality MOF crystals that will lead to more sustainable microelectronics.

The International Space Station (ISS) National Laboratory offers a unique platform in persistent microgravity that enables the elimination of gravity-driven forces to elucidate the fundamental mechanisms of growth, morphology, and defect generation in MOF crystals. An improved understanding of the fundamental mechanisms of MOF crystal formation will lead to the growth of higher-quality MOF crystals both in space and on Earth. Several organic and inorganic crystals have been grown onboard the ISS, including proteins, semiconductors, and graphene aerogels.

In this work, we will introduce the underlying physical phenomena of crystal growth in microgravity. We will present information on current ISS National Lab-sponsored research projects that are growing HKUST-1 3D MOF crystals, and hexaaminotriphenylene (HITP) and hexaaminobenzene (HIB) linker-based 2D MOF crystals. We will also discuss translational lessons learned from microgravity experiments that inform and direct terrestrial research and manufacturing. Finally, we will present opportunities for future microgravity experiments and access to ISS facilities through the ISS National Lab.

11:00 AM EL03.10.03

Highly Conductive 2D Covalent–Organic Framework Films Rui Wang, Hang Lyu and Yoonseob Kim; The Hong Kong University of Science and Technology, Hong Kong

Covalent–organic frameworks (COFs) have been widely used in electronics, catalysis, sensing, adsorption, and water purifications for their high crystallinity, porosity, and tunable functionality. However, the practical applications have been limited due to low intrinsic conductivity. Recent studies show that conjugated 2D COFs have the potential to achieve high conductivity and that the rational design of linkers and metal-containing macrocycles and synthesis optimization is important.^[1] Regarding this, our report will demonstrate a bottom-up synthesis of copper-coordinated-fluorinated-phthalocyanine (CuPc) and 2,3,6,7-tetrahydroxy-9,10-anthraquinone-based COF (CuPc-AQ-COF) films, achieving high conductivity levels.^[2] These films demonstrate an electrical conductivity of $1.53 \times 10^3 \text{ S m}^{-1}$ and a Hall mobility of $6.02 \times 10^2 \text{ cm}^2 \text{ V}^{-1} \text{ s}^{-1}$ at room temperature, rivaling that of metals. This remarkable performance is attributed to the molecular design that incorporates both 18 π electron metal-containing CuPc and a quinone-based linker, and the

significantly improved crystallinity of the films prepared via the vapor-assisted method, which all facilitate charge transport within the COFs. Density functional theory analysis further proves the intralayer donor-acceptor system and further reveals that this system has the smallest band gap between the LUMOs of CuPc center and quinone linkages compared to other published similar COFs structures.^{[3][4]} We also fabricated a field-effect transistor (FET) device with COF films exhibiting bipolar behavior, a low threshold voltage, and a high I_{on}/I_{off} . The results demonstrate the potential of the films in electronic applications. Our findings provide valuable insights into the design and fabrication of high-performance COF films. These stable, porous, and crystalline organic networks with metallic conductivity can realize advanced electronic devices, catalysis, and energy storage systems.

Reference:

- [1] Y. Yuan, K.-T. Bang, R. Wang, Y. Kim*, *Adv. Mater.* 2023, 35, 2210952.
- [2] R. Wang, H. Lyu, G. S. H. Poon Ho, H. Chen, Y. Yuan, K.-T. Bang, Y. Kim*, *Small* 2023, 2306634.
- [3] Z. Meng, R. M. Stolz, K. A. Mirica*, *J. Am. Chem. Soc.* 2019, 141, 11929.
- [4] C. Yang, K. Jiang, Q. Zheng, X. Li, H. Mao, W. Zhong, C. Chen, B. Sun, H. Zheng, X. Zhuang, J. A. Reimer, Y. Liu, J. Zhang*, *J. Am. Chem. Soc.* 2021, 143, 17701.

11:15 AM EL03.10.04

Advancements in Stretchable Displays: Exploring Serpentine Electrode Integration for Next-Generation Technologies Seungkyu Lee; Korea Advanced Institute of Science and Technology, Korea (the Republic of)

Conventional display research primarily focused on enhancing the performance of components such as pixels, luminance of light-emitting components like LCDs or OLEDs. However, the display market has been expanding towards changes in the substrate, including foldable and rollable displays. The next-generation display research is pivoting towards stretchable displays capable of adapting to various sizes and adhering to the skin (On-skin). Yet, current developments in foldable, rollable, and flexible displays react only to specific directional changes, rendering them susceptible to damage. Future electronic devices are envisioned to adhere to the skin, transition seamlessly to vehicles, and be pocket-friendly like smartphones, simultaneously changing both shape and size.

To adhere to the skin, these displays need high stretchability in all directions while maintaining their structural integrity even when twisted or bent without any defects. Previous research on stretchable displays had weaknesses such as low stretchability (below 10%) or vulnerability to repetitive motions limited to two directions (biaxial direction). Ensuring the device operates normally without faults when the substrate expands is crucial, involving components like the light-emitting diode array, electrodes, TFT, and capacitors.

The research goal is to develop a next-generation preform display platform capable of stretching, bending, twisting, and folding. This platform aims to consider various stresses occurring along all axes and requires both material-based and structural approaches to ensure stability. To create the next-generation preform display, the research is approached from three aspects, as depicted in Figure 4.

The envisioned platform seeks to effectively eliminate diverse stresses occurring in all directions while adhering well to the skin. It aims to possess significantly higher elongation properties than existing displays, ensuring high durability against twisting and folding. This advancement is anticipated to pioneer the future stretchable display market.

11:30 AM EL03.10.05

Enhancing Reliability of Stretchable Electronic Interconnect through Selective Deposition of Crosslinked PDMS Deepesh Patidar and Vijay K. Pal; Indian Institute of Technology Jammu, India

Recent research explores a novel approach to improve the mechanical reliability of stretchable interconnects, crucial components in stretchable electronics. This study introduces an innovative design approach for a stretchable electronics substrate, aiming to achieve equilibrium among factors that could induce stretch-related issues, including plastic strain, out-of-plane deformation, and interfacial delamination.

The reduction in crosslinking at the center layer of the stretchable substrate contributes to an increase in shear strain, leading to interconnect failure through interfacial delamination during stretching. Numerical analysis validates that reducing crosslinking at the center layer of the stretchable substrate contributes to minimizing equivalent plastic strain in the interconnect during stretching. Employing a PDMS 10:1 stretchable substrate to encapsulate the horseshoe interconnect results in a 32% higher plastic stress compared to PDMS 10:30. However, this also leads to an increase in maximum out-of-plane deformation from 58.12 μm to 108.43 μm and in-plane maximum shear strain from 56.4% to 77.7% at interfacial delamination locations.

In an effort to mitigate these challenges, we propose an approach involving selective crosslinking deposition on the center layer of the interconnect. This selective deposition is strategically performed at positions corresponding to delamination-prone locations, where high crosslinking PDMS is applied. In this simulation, three models were considered: A&B (10:1 & 10:1, 10:1 & 20:1, and 10:1 & 30:1). Here, B signifies the deposition of PDMS at the geometric branch, while A represents the center layer other than the geometric branch. The configuration A&B is positioned between layers of 10:1 PDMS, creating a sandwich structure. The numerical models were subjected to up to 40% elongation displacement at one end surface, considering three distinct models as explained earlier. While stretching the substrate in one direction, a lateral contraction continuously occurs due to Poisson's effect, a phenomenon analysed specifically for the 10:1&10:1 stretchable substrate.

Locally, the internal part of the interconnect is under tension, while the outer component is under compression. To further analyze the deformation effects induced by plastic strain on the interconnect, a simulation was conducted. The maximum equivalent plastic strain in the interconnect at the geometric crest concerning the strain. Notably, the maximum equivalent plastic strain for the 10:1&10:1 substrate is approximately 16.2% and 26% smaller than that for the 10:1&20:1, 10:1&30:1 substrate, respectively.

The results revealed interfacial delamination between substrates and the interconnect interface at various locations after a 40% stretch, potentially impacting stretchability. Delamination during stretching is initiated by several factors, with the failure of stretchable substrates due to in-plane shear strain being a crucial factor, as demonstrated in the literature as a significant cause of stretchable interconnect failure through delamination. In-plane shear strain counters are presented for all substrates to correlate failure locations through interfacial delamination using simulation results.

The likelihood of failure through interfacial delamination further increases due to a mismatch between the interconnect and substrate shear strain during stretching. Additionally, the maximum in-plane shear strain values for all three cases are 0.56, 0.58, and 0.65 for 10:1&10:1, 10:1&20:1, and 10:1&30:1, respectively.

By focusing on the delamination location, where in-plane shear strain is a critical factor, the high crosslinking material serves to reinforce the interconnect and substrate interface. This reinforcement helps in maintaining the structural integrity of the stretchable interconnect, ultimately reducing the forces that lead to in-plane shear strain and subsequent delamination.

SYMPOSIUM EL04

Wide and Ultra-Wide Bandgap Materials, Devices and Applications
April 22 - May 7, 2024

Symposium Organizers

Hideki Hirayama, RIKEN
Robert Kaplar, Sandia National Laboratories
Sriram Krishnamoorthy, University of California, Santa Barbara
Matteo Meneghini, University of Padova

Symposium Support

Silver

Taiyo Nippon Sanso

* Invited Paper

+ JMR Distinguished Invited Speaker

^ MRS Communications Early Career Distinguished Presenter

SESSION EL04.01: Breaking News – Diamond and Oxides

Session Chairs: Robert Kaplar and Sriram Krishnamoorthy

Monday Afternoon, April 22, 2024

Room 345, Level 3, Summit

1:30 PM EL04.01.01

High-Quality Diamond for Scientific Applications: Synthesis, Characterization and Promising Developments John Ciraldo; WD Advanced Materials, United States

Availability and production capabilities in diamond are rapidly expanding. To enable next-generation diamond-based solutions, particularly in the quantum and semiconductor realms, WD Advanced Materials (“WDAM”), in cooperation with key industry collaborators, has developed new processes for the synthesis of large-scale single-crystal diamond wafers for electronic applications. Through this talk, led by Chief Technology Officer John Ciraldo, WDAM will share an overview of recent product development breakthroughs supporting these emerging technologies, including R&D results, output from the D2 SCALE under DARPA’s LADDIS initiative, and the latest on a new U.S.-based consortium, created to supply synchrotron-grade diamond to the national market through the DOE ARDAP program. WDAM will share third-party characterization data demonstrating exceptional material quality characteristics coupled with large substrate sizes, including anonymized comparisons to other commercially available products. In furtherance of the team’s form factor expansion efforts, WDAM will also present 13mm+ wafers with full x-ray mapping, highlighting narrow rocking curves of about 30 arcseconds, ultra-high doping concentrations, and evidence of strong electronic transport properties. The discussion will conclude with a summary of new material science process and technology solutions developed at WDAM, including defect mitigation; selective patterning and deposition; heterostacks (e.g. PN/PIN junctions); and continued scale in both material size and quality.

1:45 PM EL04.01.02

Tabletop Deep Ultraviolet Transient Grating Measurements of Diamond and Silicon at Record Sub-300nm Length Scales Brendan McBennett, Emma Nelson, Theodore Culman, Albert Beardo, Henry C. Kapteyn, Margaret Murnane and Joshua Knobloch; University of Colorado and NIST, United States

Transient grating (TG) experiments provide unique insight into microscopic electron and phonon transport dynamics by interfering two laser beams on a sample surface. This results in periodic charge and phonon excitations, and is a non-contact approach – without the need to coat or pattern the sample. Visible TG experiments have observed the onset of non-diffusive heat conduction in semiconductors such as silicon [1] – however, they are limited to opaque materials and length scales set by the visible diffraction limit (>500nm). Recent extreme ultraviolet (EUV) TG implementations can probe transport at much shorter length scales but face practical limitations in manipulating the EUV light. To date, a large free electron laser facility with limited access was required to generate sufficient pump fluence [2]. Here we present a tabletop deep ultraviolet (DUV) TG beamline, which utilizes the 6.3eV / 196nm fourth harmonic of a Ti:Sapphire amplifier to achieve record tabletop excitation periodicities <300nm for the first time. The high DUV photon energy enables the investigation of wide-bandgap materials at high carrier densities, including diamond and boron nitride. Most importantly, the short DUV wavelength accesses transport on length scales that are below the visible diffraction limit, while the <300fs DUV pulse duration is critical for resolving very fast nanoscale electron and phonon dynamics. We first investigate in-plane electron diffusion in diamond, bridging the micron- and nanoscale measurements in Refs. [2] and [3] and show that comparisons between differing pump wavelengths may provide insight into the physical mechanisms modifying the electron diffusion coefficient at high carrier concentrations. We also extend the non-diffusive phonon transport measurements in silicon thin films presented in Ref. [1] to length scales almost an order of magnitude shorter, and compare to the predictions of state-of-the-art hydrodynamic and ballistic phonon transport models. This novel DUV-TG beamline provides a non-contact, tabletop route to rapidly investigate nanoscale carrier dynamics and addresses challenges associated with interfaces, defects and doping in a greatly expanded range of materials.

[1] Johnson et al., *Phys. Rev. Lett.* **10**, 025901 (2013)

[2] Maznev et al., *Appl. Phys. Lett.* **5**, eaaw5805 (2019)

[3] Malinauskas et al., *Phys. Status Solidi A* **207**, 2058-2063 (2010)

2:00 PM EL04.01.04

Materials Science and Device Technology Development for Interface-Engineered Super High-K Dielectric Nanolaminate-Based Oxides / Crystalline Diamond for New Generation High Power Electronics Orlando Auciello^{1,2}; ¹The University of Texas at Dallas, United States; ²Original

Biomedical Implants, United States

This abstract focus on describing the fundamental and applied materials science and engineering being performed to develop a new generation of transformational high-power electronics based on the integration of novel multifunctional nanolaminate-oxides thin films, with super high-dielectric constant, and single crystal diamond. Specific R&D to be discussed include:

Materials Science performed to develop transformational $\text{TiO}_x/\text{Al}_2\text{O}_3$ nanolaminates, exhibiting giant dielectric constant (up to $k=1000$), low leakage current (10^{-8} - 10^{-9} A/cm², and low losses

($\tan \delta = 0.04$), induced by a nanoscale thick Al_2O_3 layer at the top electrode/nanolaminate interface. The information to be presented will include discussion of the physics responsible for the giant dielectric constant, underlined by the Maxwell-Wagner relaxation mechanism, whereby the dielectric constant is controlled by oxygen vacancies at the nanolaminate interfaces.

Materials science and device design performed to integrate the high-K dielectric nanolaminates on single crystal diamond to fabricate the first integrated $\text{TiO}_x/\text{Al}_2\text{O}_3$ nanolaminates / single crystal diamond MOSFET devices.

Development of the lithography/RIE process to fabricate diamond-based micro / nano-electronic devices with integrated high-K dielectric $\text{TiO}_x/\text{Al}_2\text{O}_3$ nano-laminates/single crystal H-diamond surface terminated substrate, and measurement of electrical performance of first unoptimized MOSFET devices, which showed very good promising results.

The presentation will include a discussion of materials science issues that need to be addressed to optimize the performance of future $\text{TiO}_x/\text{Al}_2\text{O}_3$ nanolaminates/single crystal diamond-based micro/ nano-electronic devices, and investigate new $\text{HfO}_2/\text{TiO}_x$ nanolaminates, involving the key HfO_2 used in gates of current commercial Si-based micro/nano-electronic devices.

2:15 PM EL04.01.05

From Design to Device: Challenges and Opportunities in Computational Discovery of p-Type Transparent Conductors Rachel Woods-Robinson^{1,2}, Monica Morales-Masis³, Geoffroy Hautier⁴ and Andrea Crovetto⁵; ¹University of Washington, United States; ²National Renewable Energy Laboratory, United States; ³University of Twente, Netherlands; ⁴Dartmouth College, United States; ⁵Technical University of Denmark, Denmark

A high-performance p-type transparent conductor (TC) with a wide band gap does not yet exist, but could lead to advances in a wide range of optoelectronic applications and enable new architectures for next-generation photovoltaic (PV) devices. High-throughput computational material screenings have been a promising approach to filter databases and identify new p-type TC candidates, and some of these predictions have been experimentally validated. However, most of these predicted candidates do not have experimentally-achieved properties on par with n-type TCs used in solar cells, and therefore have not yet been used in commercial devices. Thus, there is still a significant divide between transforming predictions into results that are actually achievable in the lab, and an even greater lag in scaling predicted materials into functional devices.

In this work, we introduce a holistic “device-to-design” materials discovery framework through which to identify and contextualize various disconnects in scaling p-type TC predictions into PV devices, and we apply this framework to highlight some of the most pernicious disconnects. One set of disconnects emerges from assumptions and uncertainties in computational assessment and screening. Other disconnects stem from transforming predicted candidates into thin films in the lab: due to challenges including synthesizability, phase purity, dopability, and unwanted absorption, so far no predicted p-type TC grown in the lab performs on par with n-type TCOs. A third key set of disconnect arises from transforming predictions into scalable optoelectronic devices: challenges emerge such as making sufficient contact to the device, tuning band alignments, and growing interfaces free of defects, and other barriers.

We also discuss specific barriers related to scalability and sustainability. Although the ultimate goal of scaling PV is to mitigate climate change, input and outputs from production and deployment may cause unintentional consequences such damage to ecosystems and human health, and there is an ethical responsibility to minimize harm as we scale new materials such as TCs. Historically, life cycle assessments are conducted after technologies reach commercial scale, which can lead to “technology lock-in” that makes it challenging to replace harmful materials. To avoid “locking-in” technologies with detrimental environmental effects, we encourage materials scientists to integrate life cycle thinking throughout the design process, drawing inspiration from recent methodologies like emerging materials risk analysis and anticipatory life cycle assessment.

Lastly, we propose recommendations for materials designers to address these disconnects while designing commercially-relevant wide band gap materials. We offer guidance on how the research community can overcome such disconnects to bring our predictions into fruition in p-TCs and beyond.

2:30 PM BREAK

3:00 PM EL04.01.06

High Etch Selectivity for Dry Etching (Zn,Sn)O Thin Films to SiO₂ for Fabricating The Thin Film Transistor and 3-Dimensional Dynamic Random Access Memory Han Chul Lee^{1,2}, Jae Won Ham¹, Jinheon Choi¹, Seoyoung Jang¹ and Cheol Seong Hwang¹; ¹Seoul National University, Korea (the Republic of); ²SK Hynix, Korea (the Republic of)

Current 2D dynamic random access memory (DRAM) faces the scaling down limitation, so developing 3D DRAM is necessary to improve the integration density without relying solely on lateral device scaling. The semiconductor industry studied polycrystalline silicon as a channel material for 3D DRAM, similar to that used in 3D NAND flash memory. However, adopting polycrystalline silicon poses a critical problem due to its grain boundary effect, leading to degraded cell-to-cell uniformity. Therefore, amorphous oxide semiconductors are suggested as a potential candidate for the 3D DRAM channel materials. Amorphous zinc tin oxide (a-ZTO, Zn:Sn ratio ~ 50:50) can be a suitable channel material for 3D DRAM due to its promising electrical characteristics, such as high electron mobility, low off-current, and wide band gap. Also, it can be readily deposited by the atomic layer deposition (ALD) process, which is inevitable for 3D DRAM integration.

In fabricating 3D DRAM, etching a-ZTO film is required, but it must have a high selectivity to a sublayer, such as a gate insulator (i.e., SiO₂). Also, in 3D DRAM integration, the a-ZTO film is deposited by an ALD along the vertical channel structure, and the a-ZTO film deposited on the top portion of the pattern should be removed using the dry etching process while minimizing the damaging effect on the underlying structures. In the fabrication of a peripheral transistor, a-ZTO film out of the active region should be etched entirely while minimizing damage to the underlying thin gate insulator. The wet etching of ZTO thin films using hydrochloric acid can be used for specific cases. However, its isotropic and selective-grain boundary etching properties can pose several integration issues. Therefore, a stable dry etching process with high etch selectivity is needed. This study reports a stable dry etching process with high etch selectivity of ALD a-ZTO thin films with SiO₂ using the CH₄/N₂/Ar (30/15/31 sccm) plasma. The achieved etch selectivity was as high as 20:1.

This study also verified the possible issues in the electrical characteristics when the above recipe with high selectivity is adapted to fabricate the a-ZTO thin film transistor (a-ZTO-TFT) having TiN source and drain, 100nm-thick thermal SiO₂ gate insulator, and p⁺⁺ Si gate. For the stable operation of the TFT, a-ZTO film other than the channel region must be etched entirely away while minimizing the etching of the underlying SiO₂ layer. It is usual to over-etch the a-ZTO channel layer for this purpose. In this study, the ZTO channel etching was attempted by adopting BCl₃/N₂/Ar (15/5/30 sccm) gases, a previously reported method, and using CH₄/N₂/Ar (30/31/15 sccm) gases, a newly developed method. The over-etch was performed from 20% to 100% at intervals of

20% for each gas condition. Compared to the results of 5 over-etch conditions of applying $\text{BCl}_3/\text{N}_2/\text{Ar}$ gases, less variation of on-current ($1.27 \times 10^{-4} \text{ A} \rightarrow 4.76 \times 10^{-5} \text{ A}$ at 20.1V of gate voltage), better average subthreshold swing ($0.224 \text{ V/dec} \rightarrow 0.182 \text{ V/dec}$), and less variation of threshold voltage ($1.00 \text{ V} \rightarrow 0.70 \text{ V}$) were obtained from the 5 over-etch conditions with the $\text{CH}_4/\text{N}_2/\text{Ar}$ gases. This improvement was attributed to the improved etching selectivity of the latter compared with the former method. The presentation will report more detailed fabrication steps and electrical characteristics of the α -ZTO-TFT for their use in 3D DRAM.

3:15 PM EL04.01.07

Effect of High- k Oxide Materials on Amorphous Indium Gallium Zinc Oxide (α -IGZO) Channel in Top Gate Field Effect Transistors Reem Alshabani¹, Oliver Durnan¹, Huaqian Guo¹, Moshe Eizenberg² and Ioannis Kymissis¹; ¹Columbia University, United States; ²Technion–Israel Institute of Technology, Israel

The gate dielectric material plays a significant role in high-speed transistor operation and low power consumption in field-effect transistors (FETs). A small conduction band offset energy and a large interface trap density are common problems with high- k dielectrics with high permittivity. For that, in this work, the integration of high- k dielectrics with PECVD dielectrics has been reported to show improvements in electrical performance. Here, we integrated a high- k dielectric with (~10 nm) amorphous indium gallium zinc oxide (α -IGZO) FET with different gate dielectrics PECVD (SiO_2 and Si_3N_4). In addition, using a high- k dielectric can help overcome the problem of plasma contamination and diffusion, which can impact the device's threshold voltage and power consumption. For that, we use two of the most promising high- k dielectrics (HfO_2 and Al_2O_3). Our results showed that α -IGZO with optimized $\text{HfO}_2/\text{SiO}_2$ dielectrics has a superior electrical performance with high-field effect mobility ($50 \text{ cm}^2 \text{ V}^{-1}\text{s}^{-1}$) and an on-current of 10^{-6} A , and the value of the off-current was 10^{-13} A under 0.1 V_{DS} without any dielectric leakage. These results support the idea that increasing the gate capacitance density will improve the electrical performance and material conductivity. Integrating HfO_2 with SiO_2 improves the interface quality between the gate dielectric/channel and reduces the charge trap density and gate leakage. In contrast, there is a degradation in the electrical performance of α -IGZO FETs with $\text{Al}_2\text{O}_3/\text{SiO}_2$, related to the oxygen diffusion where more oxygen atoms diffuse from Al_2O_3 to the α -IGZO layer.

SESSION EL04.02: Vertical GaN Electron Devices
Session Chairs: Sriram Krishnamoorthy and Jingyu Lin
Tuesday Morning, April 23, 2024
Room 345, Level 3, Summit

10:30 AM *EL04.02.01

GaN Homoepitaxial Growth and Substrate-Dependent Effects for Vertical Power Devices Jennifer Hite^{1,2}; ¹U.S. Naval Research Laboratory, United States; ²University of Florida, United States

Vertical GaN power switch technology is expected to be utilized in next-generation medium to high voltage power converters due to the low ON-resistance and high breakdown voltage enabled by the improved critical electric field and mobility compared to Si and SiC-based devices. As large area substrates have become available by hydride vapor phase epitaxy (HVPE) and ammonothermal growth, the properties of nitrides are no longer dominated by defects introduced by heteroepitaxial growth, allowing recent realization of several fundamental vertical power devices, including diodes with edge termination, trench MOSFETs, and CAVETs. However, additional materials challenges are coming to the forefront that need to be understood and surmounted in order to allow vertical GaN power devices to achieve their full potential, notably the realization of repeatable thick drift layers with low background doping. To enable this, a deeper understanding of substrate preparation and the effects of the substrate and growth initiation on the characteristics of the epitaxial layers is required for MOCVD growth of homoepitaxial films. We investigate these effects on epi morphology, uniformity, and impurity incorporation by growing simultaneously on wafers from different vendors. The goal of this work is to detect and identify defects in GaN substrates with a series of quick, non-destructive, inexpensive techniques with capabilities of mapping whole wafers.

We have characterized multiple substrates from various suppliers and the homoepitaxy grown on those substrates. All the substrates had nominally similar as-received specifications (resistivity, thickness, off-cut angle, bow, surface finish). The substrates were evaluated with a variety of techniques including Raman spectroscopy, photoluminescence, white light interferometry, and Nomarski imaging, enabling to detection of different concentrations of grain boundaries, sample impurities, point defects, v-shaped pits, polishing defects, crystal stress damage, and non-uniform insulating and conductive regions. The substrates can be characterized in two different categories: those with uniform characteristics, including carrier concentration, and those without. Comparing these results to those from homoepitaxial growth on the same wafers, the effects are both subtle and overt. Macroscopic surface morphology, which has shown a direct correlation to leakage current, copies and exaggerates that of the underlying substrate. Photoluminescence of the homoepitaxial surface along with Raman spectroscopy show that non-uniformities in the substrate carrier concentration can continue into the epitaxy. Following optical characterization, vertical Schottky diodes were fabricated to evaluate device performance. While most of the films showed the ability to withstand high electric fields, those with more uniform properties in the substrate also showed more uniform electrical properties. These results show that the bulk substrates enable the path to high voltage vertical devices, but also show the significant influence that substrates can play in device performance.

11:00 AM EL04.02.02

Comparison between Sapphire and GaN Substrates for 1.2kV Rated Vertical GaN Devices Enrico Brusaterra, Eldad Bahat Treidel, Frank Brunner, Alexander Külberg, Mihaela Wolf and Oliver Hilt; Ferdinand-Braun-Institut (FBH), Germany

Vertical GaN based power switching devices, diodes and transistors, are particularly desirable due to their reduced die size in comparison to lateral heterostructures-based devices. This results in a reduction of specific on-state resistance, $R_{\text{DS(on)}} \times A$, by one order of magnitude down to 1.0 mW cm^2 . Also, vertical device concept allows for aggressive device scaling, in respect to gate periphery length per area, and enables high current densities per unit area. The targeted blocking capability of 1.2kV demands the growth of drift layers thicker than $10 \mu\text{m}$ with low residual background doping. However, the drift region conductivity, in particular for thick n -GaN drift layers, may be limited by low mobility, low carrier density, back ground compensating doping, high defect density and built-in potential barriers, having a direct impact on the device electrical performance. Previously, we provided an optimization procedure for designing the drift layer properties for a specific voltage rating, and it showed how for 1.2kV and higher it's necessary to increase the drift layer thickness above $5 \mu\text{m}$. However, growing thick GaN layers is especially challenging for foreign substrates where the lattice mismatch and thermal coefficient differences generate a series of undesirable effects, such as increase of threading dislocations density, increased leakage current, increased stiffness and fragility and increase in wafer bow. While GaN substrates may provide a better solution for the material quality point of view, costs and substrate quality may differ substantially between differently grown wafers. In this presentation we will talk about the issues of growing thick ($>5 \mu\text{m}$) GaN drift layer on Sapphire substrates for vertical high power GaN devices, how to manage the high wafer bow that makes these wafers un-processable on commercial equipment designed for flat Silicon wafers and we will compare the processed devices between sapphire and three differently grown GaN

substrates (Ammonothermal-GaN from vendor 1, “Wafer A”, and HVPE-GaN from vendor 2, “Wafer B”, and vendor 3, “Wafer C”). All processed devices showed >1.2kV breakdown voltage with different ON-state resistivity, Power-Figure-of-Merit and chip cost. *pn* diodes on Ammonothermal-GaN, “Wafer A”, show 1630V breakdown, on “wafer B” and “wafer C” 1485V and 1480V are shown respectively, all three showed avalanche breakdowns. While on sapphire, “Wafer D”, they show 1350V nondestructive breakdown due to high leakage current. The experiment starts with 4” sapphire substrate and 3×2” GaN substrates. A total of 14μm thick GaN epitaxial layers are grown on each wafer, epitaxy consists of a 2.2μm intentionally doped GaN buffer layer, a 2.4μm n⁻-GaN:Si ($N_D = 3.0 \times 10^{18} \text{cm}^{-3}$) lower highly conductive layer and a 10μm n-GaN:Si drift layer with a nominal Si concentration of $N_D = 7.5 \times 10^{15} \text{cm}^{-3}$. The effective doping has been measured by CV on diodes and changes based on the substrate material. A 500nm GaN:Mg $1 \times 10^{19} \text{cm}^{-3}$ layer with additional 30nm GaN:Mg $2 \times 10^{19} \text{cm}^{-3}$ contact layer are regrown and in-situ activated in a separate MOVPE reactor. The initial wafer bow after epitaxy grown on sapphire is ~300μm (Radius ~4m) and it would not be processable. Laser patterning is carried out in order to reduce the wafer bow by selectively introducing damage in the substrate close to the bottom interface. The patterning was realized by focusing a laser beam in the sapphire close to its back surface using a laser scriber (WSS4000), which uses a Talisker Ultra Laser from Coherent for internal layer modification. This means that the laser will be focused inside the material and, at this position, the crystal will be modified. The wavelength we use is 532nm. Used repetition rate is 40kHz at a feed speed of 400mm/s and a continuous laser power of 160mW at the point of use. Overall device performances and characteristics will be shown in the presentation, along with benchmarking and comparison of the different substrates.

11:15 AM *EL04.02.03

High-Performance Junction Diodes in GaN using Mg Implantation and Heterogeneous Heterojunctions Spyridon Pavlidis¹, Ramón Collazo¹, Zlatko Stitar^{1,2} and Fred A. Kish¹; ¹North Carolina State University, United States; ²Adroit Materials, Inc., United States

The enhanced critical electric field of wide bandgap GaN render it an attractive technology for power switching and power amplification devices. Recent improvements in epitaxy and substrate quality have made it possible to focus on the development of advanced devices with complex doping schemes and junctions. This talk will tackle two important cases: (1) vertical GaN Junction Barrier Schottky (JBS) diodes realized with Mg implantation and ultra-high pressure annealing (UHPA), as well as (2) PN junctions using III-V/GaN heterogeneous heterojunctions formed via a novel technique known as Crystal Heterogeneous Integration (CHI). In each case, it will be demonstrated that junctions with near-unity ideality factors can be achieved via careful control of the material interfaces. These results underline the promise of GaN for high performance devices, and pave the way for further innovation in device geometries.

11:45 AM EL04.02.04

pn GaN Regrowth Vertical Diodes Displaying Ten Orders of Magnitude Memory Window Stephen J. Moxim¹, Ory Maimon^{2,1}, Behrang Hamadani¹, Wei-Chang David Yang¹, Andrew J. Winchester¹, Emily G. Bittle¹, Qiliang Li^{2,1}, Albert V. Davydov¹, Travis J. Anderson³, Jennifer Hite³, Jason P. Campbell¹, Sujitra Pookpanratana¹ and Jason T. Ryan¹; ¹NIST, United States; ²George Mason University, United States; ³U.S. Naval Research Laboratory, United States

The large bandgap of GaN enable advancements in power electronics. *pn* GaN vertical diodes offer improved efficiency, size, and performance over traditional Si-based power devices making them essential components for next generation power electronic systems. *pn* GaN diode fabrication typically requires regrowth of the p-GaN layer, which is known to introduce Si impurities at the *pn* GaN interface.¹⁻³ While this does impact the performance of power devices,^{2, 4, 5} the presence of impurities at the regrowth interface has also been shown to display memristor behavior.⁶ Memristor-like behavior in GaN and other nitride device structures has also been reported.^{7,9} It is appealing to develop GaN-based memory technologies which could be integrated with GaN high electron mobility transistors. Here, we find that regrown *pn* vertical diodes display an exceptionally large memory-like hysteresis loop exceeding a previous report.⁶

The *pn* diodes were fabricated on dot-core GaN substrates. For the regrowth diode, a 5 μm unintentionally-doped drift layer (*n* between 8E15 and 2E16 cm⁻³) was first deposited, followed by ex-situ 400 nm p-layer ($N_A \approx 4 \text{E}17 \text{cm}^{-3}$). For the in-situ grown diode or “control,” a 8 μm drift layer ($n \approx 1.7 \text{E}16 \text{cm}^{-3}$) was first deposited, and subsequently followed by 400 nm p-layer ($N_A \approx 4 \text{E}17 \text{cm}^{-3}$). Metallization were identical on both sets of devices with Pd/Pt/Au on the p-GaN and Ti/Al/Ni/Au on the GaN substrate.

The regrowth *pn* diode displayed memory or hysteresis effect at forward bias with 10 orders of magnitude larger on-state current (I_{ON}) than the off-state current (I_{OFF}), while the “control” *pn* GaN vertical diodes with an *in-situ* grown interface, display no such hysteresis effect. We find that the memory endurance and retention characteristics are robust, with no appreciable degradation in I_{ON}/I_{OFF} ratio after 60k set-reset cycles. To evaluate these devices for potential use as a high temperature memory element, the presence of a reduced switching window was confirmed at temperatures up to 275 °C. To investigate the electronic differences of these two diode structures, electroluminescence (EL) measurements before and after endurance cycling were performed. While the control sample is clearly dominated almost entirely by a single spectral peak at about 3.25 eV (likely a conduction band to Mg acceptor transition), the memory-like devices have three additional strong spectral peaks whose relative contributions evolve with cycling. These three extra peaks are located at 3.1 eV (V_N to Mg acceptor), 2.9 eV (blue luminescence, BL), and 2.3 eV (yellow luminescence, YL). With increasing cycles, the 3.1 eV peak increases in relative contribution while the BL and YL features decrease. We speculate that the BL and YL defects are not critical to the memory effect. TCAD simulations of both the memory and control devices were performed, and the simulated IV characteristics of the control devices agreed with the measured electrical data. The structure of the memory devices for TCAD modelling is currently in development with transmission electron microscopy analysis to identify the regrowth *pn* GaN interface. We plan to propose a model on the origin of the memristor-like behavior in ex-situ formed *pn* GaN diodes.

1. K. Fu, et al., Applied Physics Letters **113** (23) (2018).
2. K. Fu, et al., Applied Physics Letters **118** (22) (2021).
3. M. Noshin, et al., Semiconductor Science and Technology **37** (7), 075018 (2022).
4. G. W. Pickrell, et al., Journal of Applied Physics **126** (14) (2019).
5. K. Fu, et al., IEEE Journal of the Electron Devices Society **8**, 74-83 (2020).
6. K. Fu, et al., IEEE Electron Device Letters **40** (3), 375-378 (2019).
7. J. L. Gomes, et al, physica status solidi (b) **256** (5), 1800387 (2019).
8. T. Chen, et al, IEEE Electron Device Letters **43** (5), 697-700 (2022).
9. H. Sánchez-Martín, et al, Applied Physics Letters **123** (10) (2023).

1:30 PM *EL04.03.01

Status of h-BN semi-bulk crystals [Jingyu Lin](#) and Hongxing Jiang; Texas Tech University, United States

III-nitride wide bandgap semiconductors have revolutionized the lighting industry and are poised to make a huge impact in power electronics. In the III-nitride family, the crystal growth and use of hexagonal BN (h-BN) as an ultrawide bandgap semiconductor (UWBG) are much less developed. The development of crystal growth technologies for producing semi-bulk crystals in large wafer sizes with high crystalline quality and low defect density is a prerequisite for utilizing h-BN as an UWBG electronic material. In addition to optoelectronic and electronic device applications, h-BN has another unique application for high efficiency solid-state neutron detectors because of an unusually large interaction cross-section between B-10 isotope and thermal neutrons, which however, also require the development of thick semi-bulk crystals.

In this talk, we provide a brief overview and recent progress toward the development of h-BN semi-bulk crystals by hydride vapor phase epitaxy (HVPE) and metal organic chemical vapor deposition (MOCVD). Benchmarking the crystalline and optical qualities of h-BN semi-bulk crystals with respect to the state-of-the-art millimeter-sized bulk crystal flakes grown by the high pressure/high temperature (HP/HT) and the metal flux solution methods together with photoluminescence (PL) emission and photocurrent excitation spectroscopy measurements identified that reducing the density of impurities and defects such as oxygen impurities and boron vacancies remains the most critical task for h-BN semi-bulk crystal growth. The performance of neutron detectors fabricated from semi-bulk h-BN wafers and the attainment of h-BN thermal neutron detectors with a record efficiency of 60% will also be presented. The development of high efficiency h-BN neutron detector technology serves as a stepstone for further advancing the crystal growth technology to produce electronic grade h-BN semi-bulk wafers.

2:00 PM EL04.03.03

Plasma-assisted physical vapor deposition of polycrystalline hexagonal boron nitride films [Minsuk Seo](#)¹, Leonardus Bimo Bayu Aji¹, Yan-Kai Tzeng², Sang Cheol Kim², Tian Li¹, Yilong Zhou¹, Liwen Wan¹, C.E. Kim¹, Tae Wook Heo¹, Bo Wang¹, Luis A. Zepeda-Ruiz¹, Steven Chu² and Sergei O. Kucheyev¹; ¹Lawrence Livermore National Laboratory, United States; ²Stanford University, United States

Two-dimensional hexagonal boron nitride (2D-hBN), also known as white graphene, is an electrically insulating wide-band-gap material with several emerging applications. However, most of the previous systematic work has focused deposition of cubic BN films, while the synthesis of wafer-scale hBN films with desired properties remains a challenge. Here, we present results of our ongoing systematic study of polycrystalline hBN films with thicknesses in a range of 100-6000 nm deposited by variants of reactive magnetron sputtering with a radiofrequency (RF) driven discharge. We describe how the plasma discharge characteristics and, hence, resultant major film properties can be controlled by the magnetron source design, the confining magnetic field, and process parameters such as the working gas pressure (controlling landing neutral atom ballistics and energetics), substrate temperature (adatom mobility), and substrate bias (bombarding ion energy). Even without epitaxy, with substrates held close to room temperature, hBN films are polycrystalline, characterized by a FWHM of the major E_{2g} Raman vibrational mode (1370 cm⁻¹) in the range of 40 – 100 cm⁻¹, depending on deposition conditions. The FWHM reduces to ~30 cm⁻¹ when a higher deposition temperature of 600-800 °C is used. Interestingly, all as-grown films are polycrystalline (turbostratic, with asymmetrically stacked layers) rather than amorphous even for room temperature and high deposition pressure of 50 mTorr characterized by low landing atom energetics. These film growth and characterization experiments are guided by results of in-situ plasma diagnostics, which greatly aids deposition process development.

This work was performed under the auspices of the U.S. DOE by LLNL under Contract DE-AC52-07NA27344.

2:15 PM EL04.03.04

Defect conversion in h-BN using electron beam irradiation for blue emission [Yue Xu](#)¹, Edward K. Naland¹, Zackaria Mahfoud², Chengyuan Yang¹, Andrew Bettiol¹, Michel Bosman^{1,2} and Silvija Gradecak¹; ¹National University of Singapore, Singapore; ²Agency for Science, Technology and Research(A*STAR), Singapore

Hexagonal boron nitride (h-BN) is a layered van der Waals material with a bandgap of 6 eV. Thanks to its ultra-wide bandgap, h-BN can host a series of solid-state color centers, covering a range of wavelengths from UV to the visible region. h-BN emitters have attracted particular attention, not only for their high stability and strong luminescence at room temperature, but also due to their anti-bunching behavior, a characteristic of quantum emitters. In this work, we report the controlled generation of 437 nm quantum emitters (referred to as “blue emitters”) in h-BN *via* electron beam irradiation. We demonstrate that irradiation of h-BN using 3–10 keV electron beams in a scanning electron microscope (SEM) produces the blue emitters in a spatially precise manner, as measured using photoluminescence (PL). We establish the correlation between the incident electron dose and PL intensity, indicating that the negative charge trapped in h-BN facilitates the 437 nm emission.

To explore the structural origin of the h-BN blue emitters, we introduce point defects to h-BN using a helium ion microscope (HIM) before electron beam irradiation and show that the blue emitter PL intensity increased in the defect-engineered area. Furthermore, using a scanning transmission electron microscope (STEM) coupled with cathodoluminescence (CL), we observe the real-time activation and saturation of the blue emitter in pristine h-BN. The resulting emission is stable for >1000 s, making it a promising candidate for photonic device integration. We achieved controlled production of electron beam-induced blue emitters in h-BN by tuning the electron dose and native defect density, which advances our understanding of their structural origin as the conversion of native defects in the h-BN lattice. These h-BN blue emitters with enhanced spectral stability can serve as a building block for future photonic devices.

2:30 PM EL04.03.05

Stochastic computing using stochastic memristors from solution-processed hBN [Lekai Song](#), Pengyu Liu, Jingfang Pei, Yang Liu, Songwei Liu, Yingyi Wen and Guohua Hu; Chinese University of Hong Kong, Hong Kong

As the device scaling slows down, it is getting challenging for conventional binary computing competent for the rapidly progressing big data and artificial intelligence technologies. Efficient computing paradigms call for material and device innovations. Stochastic computing with probabilistic bits is an emerging computing solution. Here, we demonstrate stochastic logic gates using stochastic volatile filamentary memristors from solution-processed insulating two-dimensional hexagonal boron nitride (hBN), and perform complex logic functions utilizing the stochastic logic gates for stochastic computing.

We start with hBN ink formulation. Briefly, an ink in isopropylalcohol/2-butanol is prepared by liquid-phase exfoliation of hBN, and is finely tuned in the composition to suit the versatile printing techniques, such as inkjet printing, spin coating, and slot-die. Silver electrodes, patterned by photolithography, are deposited to sandwich the printed hBN to develop Ag/hBN/Ag memristors. Due to the stable insulating property of hBN, the formation and disruption of the silver ion filaments in the hBN switching medium can lead to stochastic yet stable ultrafast switching and memory effect in such a metal/insulator/metal structure. As such, the memristors exhibit stochastic volatile threshold switching with a threshold voltage of ~1 V, an on/off ratio of >10⁵, a switching

speed of <300 ns, and an endurance of >10⁵ cycles. The memristors can be switched stochastically with a high speed between the ON (1) and OFF (0) states when applied with ultrafast voltage pulses. We show that the proportion of the ON states from a typical memristor device within a sampling period represents a statistical probability when a pulse train is applied. Notably, the pulse voltage can well modulate the probability, and the voltage-probability relation follows a sigmoid function. This enables the memristors to perform logic computations on the probability. To demonstrate this, the memristors are first connected to comparators as stochastic random number generators, and then connected to standard logic gates as stochastic logic gates for complex, stochastic logic operations for stochastic computing. Specifically, we hardware implement stochastic logic functions of AND, OR, XOR, and MUX gates, and construct a convolutional operator to perform edge detection of images.

Stochastic computing with probabilistic bits offers a fundamentally different computing paradigm by physically performing the computation with probabilities, potentially leading to substantial reductions in the area, power, and latency in the computing hardware. Besides, the scalable solution-processed approach allows low-cost, high-speed wafer-scale memristor array fabrication. This holds a promising prospect for the development of stochastic computing particularly at the edges with limited computational resources.

2:45 PM BREAK

SESSION EL04.04: WBG Growth and Devices
Session Chairs: Jennifer Hite and Sriram Krishnamoorthy
Tuesday Afternoon, April 23, 2024
Room 345, Level 3, Summit

3:15 PM EL04.04.01

Probing Polytype Selection during Metal-Mediated Epitaxy of GaN Quantum Dots and Nanowires [Abby Liu](#)¹, [Zhucong Xi](#)¹, [Meng Li](#)^{2,3}, [Dmitri N. Zakharov](#)³, [Fernando Camino](#)³, [Judith C. Yang](#)^{3,2}, [Liang Qi](#)¹ and [Rachel Goldman](#)¹; ¹University of Michigan, United States; ²University of Pittsburgh, United States; ³Brookhaven National Laboratory, United States

Semiconductor polytype heterostructures, which consist of chemically homogeneous structures formed via an abrupt change in crystal structure, offer opportunities for performance exceeding those of composition-based semiconductor heterostructures. Of particular interest are heterostructures formed via an abrupt change in atomic plane stacking sequence, such as the transition from the wurtzite (WZ) polytype to the zincblende (ZB) polytype. At a fixed chemistry WZ/ZB heterojunction, the lattice mismatch and thermal expansion coefficient mismatch are typically < 0.1%, leading to a negligible interfacial defect concentration. Meanwhile, the WZ/ZB band offset and polarization discontinuity are expected to lead to the confinement of a two-dimensional electron gas (2DEG) at the interface, without the need for impurity doping and/or alloying. Such heterostructures would be promising for high power electronics and single photon emitters.

It has been hypothesized that metastable nanowire (NW) polytype selection is governed by surface/interface energies, surface diffusivities, and/or droplet angles that determine ABC vs. AB stacking of atomic planes, resulting in ZB or WZ polytypes. For ZB-polytype-preferring materials, such as III-As and III-P, ZB vs. WZ polytype selection has been described by empirical “contact angle” models, enabling the design and fabrication of NW polytype superlattices. However, for GaN, a WZ-polytype preferring material, the “contact angle” models for NW polytype selection, using literature values for WZ and ZB GaN surface energies, predict ZB polytype formation, across contact angles, even though WZ GaN NWs are most frequently reported in the literature.

We recently discovered a Ga-mediated molecular-beam epitaxy (MBE) process to nucleate ZB and WZ GaN NWs on Si(001) [1]. Key to this process is a Ga pre-deposition step, in which Ga droplet arrays are formed prior to NW growth. For the ZB NW ensembles, reflection-high energy electron diffraction and x-ray diffraction suggest overall ZB-to-WZ transformations at thickness ~20 nm. High-angle annular dark-field STEM reveals WZ NWs with close-packed (0001) planes oriented along the Si [001] surface normal, i.e. [0001]-oriented WZ NWs. On the other hand, ZB NWs with the close-packed (111) planes oriented ~37° from the Si [001] surface normal, i.e. [001]-oriented ZB NWs. Interestingly, the NW axis orientation remains fixed as it transforms to the WZ polytype. We hypothesize that Si incorporation into Ga droplets influences the polytype selecting during NW growth. Preliminary energy dispersive spectroscopy (EDS) data reveals higher Si concentration within ZB NW in comparison to that within WZ GaN NWs. Correspondingly, density functional theory (DFT) calculations show that ~8 at% Si in the Ga sublattice makes ZB GaN thermodynamically more stable than WZ GaN. Thus, Si appears to be a ZB polytype stabilizer for GaN. Direct observations of GaN nucleation in an in-situ environmental TEM (ETEM) will also be presented.

This work was supported by the U.S. Department of Energy, Office of Science, Basic Energy Sciences under Award # DE-SC0023222. This research used the Electron Microscopy facility of the Center for Functional Nanomaterials, which is a U.S. Department of Energy Office of Science User Facility, at Brookhaven National Laboratory under Contract No. DE-SC0012704.

[1] Lu, H., S. Moniri, C. Reese, S. Jeon, A. Katcher, T. Hill, H. Deng, and R.S. Goldman. 2021. “Influence of gallium surface saturation on GaN nanowire polytype selection during molecular-beam epitaxy.” *Appl. Phys. Lett.* 119:031601.

3:30 PM EL04.04.02

Nitride Nanostructure Nanopatterning with Sequential Infiltration Synthesis for Optoelectronic Advancements [Sudarshana Patra](#); Illinois State University, United States

The research and development of nanomaterials for several applications have made great strides in recent years. With their unique properties on the nanometer scale, nanopatterning of inorganic materials is an emerging field with a wide range of applications such as electronics, optics, photonics, energy, and biomedical engineering. Optoelectronic devices, such as photodetectors, solar cells, and light-emitting diodes (LEDs), are crucial in converting light into electricity and vice versa. Group III nitride (III-N) materials have attracted considerable attention in this field due to their wide energy bandgap and exceptional stability. The nitride family includes significant members such as Gallium Nitride (GaN), Aluminum Nitride (AlN), Boron Nitride (BN), Indium Nitride (InN), as well as compound nitrides like InGaN and AlGaN. Among these materials, AlN and GaN are particularly noteworthy due to their exceptionally wide bandgaps, enabling emissions across the ultraviolet (UV) and visible spectrum. Planar structures of these nitrides have been widely used for blue LED applications; however, nanostructures of these materials have received significant attention recently due to factors such as the prospect of growth on low-cost dissimilar substrates, improved light extraction properties of vertical nanostructures, and better carrier confinement, *etc.* It is challenging to grow nitride materials in general due to their high-temperature requirements and lattice mismatch with conventional substrates, such as silicon (Si). Currently, nitride materials require expensive multistep processes to grow nanostructures, including chemical vapor deposition (CVD) and

sputtering, which are used to make patterns in conjunction with nanolithography. Sequential Infiltration Synthesis (SIS), an inorganic materials infiltration method, has shown potential for nanopatterning inorganic materials used in the microelectronics and optoelectronics industry. In our group, we developed nanopatterns of AlN by SIS technique that can produce scalable, well-ordered, and relatively easy integration of the patterned nanomaterials and investigate their growth mechanism and optical properties. We have used polystyrene-*b*-polymethylmethacrylate (PS-*b*-PMMA) self-assembled nanostructures as a guiding pattern and SIS as a deposition method for the AlN nanopattern. We have characterized the patterns by scanning electron microscope, x-ray photoelectron microscope, and Fourier transform infrared (FTIR) spectroscopy. This research of nanopatterning nitride materials with SIS would open new avenues for emerging nitride-based optoelectronic and other devices for large-scale growth, with any substrate, and in a cost-effective way.

3:45 PM EL04.04.03

III Nitride based Heavy Metal Ion Sensors for Smart Water Quality Monitoring [Nipun Sharma](#), Ankur Gupta and Mahesh Kumar; Indian Institute of Technology, Jodhpur, India

The group III nitride semiconductor devices like AlGaIn/GaN high electron mobility transistors (HEMT) have become the most emerging candidates in the last two and half decades. The 2DEG forms at the AlGaIn/GaN heterointerface without applying an external electric field, which makes AlGaIn/GaN HEMTs normally ON devices. There are surface states on the AlGaIn/GaN High Electron Mobility Transistor due to the availability of dangling bonds at the surface. These surface states have a significant impact on the 2DEG. By using this phenomenon, the AlGaIn/GaN HEMT are utilized for the detection of toxic heavy metal ions in water. The quick and easy monitoring of heavy metals in drinking water is utmost important due to their harmful effects on human health.

AlGaIn/GaN HEMTs with functionalized gate areas were fabricated for sensitive and selective detection of heavy metal ions such lead, and mercury. In order to study the presence of Pb²⁺ metal ions in water, the fabricated GaN HEMT sensor's gate region was functionalized using graphitic carbon nitride (g-C₃N₄) nanosheets. The limit of detection (LoD) of the g-C₃N₄ functionalized sensor, obtained a sensitivity of about 0.46 μA/ppb and 0.32 ppb as lowest limit which is substantially lower than the permissible limit as set by W.H.O. In another work on Pb²⁺ ion detection, the fabrication of AlGaIn/GaN HEMT was carried out for the detection of toxic lead ions in the water by functionalization of the Au-gated region by the 2,5-dimercapto-1,3,4-thiadiazole (DMTD). The sensor reaches the lower detection limit of 0.018 ppb. It exhibits a rapid response time of ~ 4 seconds and high sensitivity of 0.607 μA/ppb. Moreover, a study for the selectivity analysis is performed, and it is found that the sensor is highly selective towards Pb²⁺ ions. In another interesting work, we developed a sensor for highly sensitive, selective, and rapid determination of the trace amount of Hg²⁺ ions using molybdenum disulfide (MoS₂) functionalized AlGaIn/GaN HEMT. The sensor showed an excellent sensitivity of 0.64 μA/ppb and an ultra-low-level detection limit of 0.01152 ppb or 11.52 ppt (parts per trillion) with a rapid response time of 1.8 s. Moreover, the sensor exhibits the linear range of detection from 0.1 ppb to 100 ppb and highly selective behavior towards Hg²⁺ ions. To further enhance the sensitivity, we have successfully demonstrated the detection of Hg²⁺ ions using MoS₂ functionalized AlGaIn/GaN HEMT under UV illumination which showed an extremely high sensitivity of 548.07 μA/ppb with a lower detection limit of 6.15 ppt. In our another work, we observed that the fabricated sensor after functionalization with Ag-MoS₂ ensured faster electron transfer kinetics and showed out remarkable sensitivity of 1.6 mA/ppb and limit of detection (LoD) of upto 20 ppt. Along with the detection on real time water samples from lake water, a proof of concept by enabling it with IoT interface was also demonstrated. Hence, the development and performance of the AlGaIn/GaN HEMT based ion sensors suggest that these sensors have a huge potential for other heavy metal ion sensing applications

4:00 PM EL04.04.04

Metallization Scheme for 800 °C Silicon Carbide Microsystems [Robert Okojic](#); NASA Glenn Research Ctr, United States

We have developed and validated a high temperature metallization scheme that can sustain silicon carbide (SiC) microsystem operation at 800 °C in the absence of protective packaging. The metallization system consisted of the ohmic contact, diffusion barrier, and interconnect layers made up of three primary and conventional metallizations of Ti, TaSi₂, and Pt. The ohmic contact to the SiC layer is comprised of sequentially deposited Ti (100 nm)/TaSi₂ (300 nm) that provides low contact resistance, followed by the diffusion barrier layer of Ti (100 nm)/Pt (300 nm) to prevent the native oxygen and excessive upper layer platinum migrations to the underlying SiC layer. The interconnecting layer is comprised of Ti (20 nm)/TaSi₂ (20 nm)/Pt (300 nm)/Ti (20 nm)/TaSi₂ (20 nm), which also functions as a diffusion barrier against oxygen from the atmosphere. The bond pad contact layer is Ti (100 nm)/Pt (300 nm)/Au (500 nm). The metallization was implemented on the n-type epilayer of batch fabricated 4H-SiC pressure sensors to demonstrate functionality in a real device. The metallization system on the sensor was analyzed with Auger Electron Spectroscopy (AES), Focus Ion Beam (FIB) Field Emission Scanning Electron Microscopy (FE-SEM), and X-ray Photoelectron Spectroscopy (XPS) at various sections and stages during different steps of the fabrication. Further analyses were performed after fabrication at high temperature up to 800 °C in air. Electrical measurement was also performed on the bare die under a worst-case condition of no package protection of the sensor at high temperature in air.

The FIB-FESEM cross section after soaking the bare die at 800 °C in air revealed non-smooth interfaces between the layers of the oxide and metallization. The metallization on the oxide layers followed the undulating surfaces of the oxide layers, resulting in likely local discontinuities. However, these presumed discontinuities did not affect the electrical conduction path from the ohmic contact, through the interconnect, and to the bond pad. The observed rough surfaces of the oxide were believed to have occurred during the series of reactive ion etching steps of the oxide via for the ohmic contact, the interconnect, and the bond pad. Overall, the elemental analyses showed a well-preserved metallization, with only native oxygen observed in expected places. Electrically, the SiC sensors that were packaged and tested confirmed the effectiveness of the metallization scheme to support reliable operation at 800 °C. Further improvement to realize a smooth surface morphology was subsequently implemented. The complete details of this work will be presented at the meeting.

4:15 PM EL04.04.05

Dopant-selective photoelectrochemical etching of 4H-SiC for wafer-scalable SiCOI integrated photonics [Jason Lipton](#), John vajo, Adam Sorensen, Brett Yurash, Biqin Huang, Sam Whiteley, Xiwei Bai, Tong Wang, Sam Rubin, Adrian Portales, Shanying Cui and Jason Graetz; HRL Laboratories, United States

Usable quantum networks with long distance baselines requires quantum repeaters with integrated quantum memories. 4H-SiC hosts a variety of optically addressable defects, can yield low-loss photonics while being compatible with CMOS fabrication processes, and has a highly mature wafer-scale supply chain. However >3", total thickness variation (TTV) of SiC thin film during the SiC-on-insulator (SiCOI) fabrication impedes scalable fabrication of integrated photonic devices with acceptable propagation loss and efficient coupling of optical elements. While the high chemical stability of SiC makes traditional wet processes ineffective, we have demonstrated dopant-selective photoelectrochemical (PEC) etching of SiC epitaxial layers using n-type SiC as a sacrificial layer with a p-type etch stop. We apply the concept of selective PEC to a realistic SiC-on-insulator (SiCOI) stack for highly effective TTV reduction. We show that by using selective PEC etching to etch a sacrificial n-type layer and stop selectively on an intrinsic photonic layer, we are able to reduce the TTV of the SiC by over an order of magnitude. We show that the reduced TTV results in a dramatically improved yield and propagation loss of waveguides compared to the standard polishing process. The results presented here represent a step forward in realization of scalable 4H-SiC integrated photonic devices toward long-distance quantum networking.

4:30 PM EL04.04.06

Dielectric and Phase Engineering of Van der Waals Sb2O3 Films via PLD [Jing Yu](#)¹, Ruyi Jinq Ong¹, Atta Ur Rehman¹, Chris Tang¹, Wei Han² and Francis Chi-Chung Ling¹; ¹The University of Hong Kong, Hong Kong; ²Hubei University, China

Van der Waals dielectrics are broadly utilized to retain the intrinsic properties of two-dimensional (2D) electronic devices. As a 2D inorganic molecular crystal, Sb2O3 have attracted many research interests as a promising high κ gate dielectric with low-cost and CMOS compatibility. However, fabricating 2D Sb2O3 film with controllable dielectric constant and crystal phase is challenging. Here, we designed an oxygen-assisted PLD method for the phase-selective growth of α - and β - Sb2O3 thin films with super-high κ (>100) and good homogeneity by PLD. This is realized by tuning the oxygen gas pressure in the growth products to obtain two phases Sb2O3. This phase-controlled bottom-up synthesis offers a simple and efficient way for manipulating the relevant device structures and provides a general approach for producing other multi-phase materials with unique properties and allows us to characterize their intrinsic optical and electrical properties. Using dielectric and electrical measurements, we show that α phases exhibit good dielectric performance. Our Sb2O3 dielectric film not only show higher κ than other conventional dielectrics in terms of compatibility to CMOS processes, but also keeps their comparative advantages in the fabrication of high-performance electronic devices over conventional dielectrics. Our approach of fabricating Sb2O3 dielectrics using PLD may open promising opportunities to promote such unprecedented 2D devices to industry applications.

SESSION EL04.05: UWBG Nitrides

Session Chairs: Elaheh Ahmadi and Sriram Krishnamoorthy

Wednesday Morning, April 24, 2024

Room 345, Level 3, Summit

8:45 AM *EL04.05.01

Addressing Challenges in AlGaIn-Channel High Electron Mobility Transistors [Brianna A. Klein](#)¹, A. A. Allerman¹, Andrew Armstrong¹, Mary Rosprim¹, Yinxuan Zhu², Chandan Joishi², Chris Chae², Jinwoo Hwang² and Siddharth Rajan²; ¹Sandia National Laboratories, United States; ²The Ohio State University, United States

Next-generation semiconductor switches and integrated circuits require higher power density, greater customizability, and improved radiation hardness than what is commercially available today. Nitride-based Ultrawide-Bandgap (UWBG) semiconductors, namely AlGaIn (aluminum gallium nitride) are well-suited to meet these performance demands. Higher bandgaps result in exponentially higher critical electric fields, thus enabling power electronics with larger breakdown voltage and output power than devices made from conventional semiconductors (e.g., Si, GaN). In elevated temperatures, large bandgaps reduce noise and leakage from intrinsic carrier effects and thermionic emission. However, AlGaIn faces challenges in realizing low-resistance Ohmic contacts and reduced mobility due to alloy scattering.

This talk will discuss efforts at Sandia to address these challenges, as well as highlight key device results.

Significant improvements of Ohmic contacts on aluminum rich HEMTs (channel compositions of Al_{0.7}Ga_{0.3}N) have resulted in reduced specific contact resistance values, with latest developments reaching the 10⁻⁶ Ωcm^2 range. The power transistor developments have targeted increases in current and standoff voltage, while processes to realize p-AlGaIn based enhancement mode (normally off) gates have been developed.

SNL is managed and operated by NTESS under DOE NNSA contract DE-NA0003525. Research was sponsored by the Army Research Office and was accomplished under Cooperative Agreement Number W911NF-22-2-0163. The views and conclusions contained in this document are those of the authors and should not be interpreted as representing the official policies, either expressed or implied, of the Army Research Office or the U.S. Government. The U.S. Government is authorized to reproduce and distribute reprints for Government purposes notwithstanding any copyright notation herein.

9:15 AM +EL04.05.02

First Principles Modeling of High Field Transport in Ultra-Wide Bandgap Materials [Jonah Shoemaker](#), [Reza Vatan](#), [Tathagata Biswas](#), [Arunima K. Singh](#), [Marco Saraniti](#) and [Stephen M. Goodnick](#); Arizona State University, United States

Ultra-wide band gap (UWBG) materials offer the potential for greatly improved power electronic device performance due to their predicted higher breakdown fields limited by avalanche breakdown, as well as their favorable transport characteristics such as high mobility and drift velocity, which reduce on-resistance and allow for high frequency operation in power conversion applications. Experimental data on the high field transport properties of UWBG materials such as the impact ionization coefficients are relatively limited, with considerable variability. Hence, to understand the limits of performance of these materials, we report on first principles theoretical calculations of the high field transport properties of UWBG materials using a combination of ab initio calculations of the electronic and phononic structure coupled with particle based full-band Cellular Monte Carlo (CMC) high field transport simulation.

The electronic structure is computed using the GW method based on the BerkeleyGW code, which accurately predicts the bandgaps and excited states of UWBG materials. The phonon dispersion is calculated from DFPT (density functional perturbation theory) using Quantum Espresso. The full wave-vector dependent deformation potentials are computed using the GW eigenvectors as input to the EPW (electron-phonon using Wannier) code, to calculate the electron-phonon scattering rate from first principles. The calculated electronic structure, phonon dispersion, and anisotropic electron-phonon deformation potentials are then input to the CMC code. The CMC code has been developed in-house for a number of years, and simulates the dynamics of an ensemble of charge carriers using scattering rates tabulated in a large look-up table, which allows computationally efficient simulation of non-equilibrium carrier dynamics across the entire Brillouin zone. Besides electron-phonon and defect scattering, we calculate the band-to-band impact ionization scattering rate directly from the GW electronic structure, using a screened Coulomb interaction based on the full band frequency-dependent Lindhard dielectric function. Based on these scattering mechanisms as input, transport quantities such as the velocity-field characteristics and impact ionization coefficients as a function of field are calculated from full band Cellular Monte Carlo (CMC) simulation.

We have applied this framework initially to diamond in comparison to available high field transport data. One important observation is that while the critical field depends strongly on the material bandgap, the relative magnitude of the deformation potential plays an important role as well. Lower values of the deformation potential lead to more energetic electron and hole populations which favor impact ionization, hence reducing the breakdown field. We compare different approximations of the deformation potential in relation to the simulated impact ionization coefficients and their impact on breakdown. The impact of other scattering processes due to defects such as ionized impurities on the high field properties are also under investigation. We also are currently investigating other UWBG materials, specifically BN and AlN, and will report on their high field properties as well.

9:45 AM EL04.05.03

Rapid Prediction of Phonon Density of States by Graph Neural Network and High-Throughput Screening of Candidate Substrates for Wide Bandgap Electronic Cooling Ming Hu, University of South Carolina, United States

Machine learning has demonstrated superior performance in predicting vast materials properties. However, predicting a continuous material property such as phonon density of states (DOS) is more challenging for machine learning due to the inherent issues of data smoothing and sensitivity to peak positions. In this work, phonon DOS of ~5,000 inorganic cubic structures with 63 unique elements from the Open Quantum Materials Database are calculated by high precision density functional theory (DFT). With these training data, we build an equivariant graph neural network (GNN) for total phonon DOS of crystalline materials that utilizes site positions with their atomic masses as input features. The computational cost of training the GNN model is several orders of magnitude cheaper than full DFT calculations. More interestingly, the trained GNN model can predict partial DOS of the constituent atomic species even if such data were not included in the training, which demonstrates GNN's capability in predicting the species contributions (node-level) of partial DOS from the total DOS predictions without additional computational cost. We then deploy the trained GNN model to predict phonon DOS of >40,000 non-zero bandgap materials to search for thermally conductive substrates for cooling a few representative high electron mobility transistors (HEMT) in terms of high interfacial thermal conductance (ITC). Our results show that high vibrational similarity or phonon DOS overlap is not the only requirement to obtain high ITC. Instead, the average group velocity of heat source and heat sink for the acoustic branches in the phonon DOS overlap region is equally important in determining ITC. Moreover, we highlight that the lattice thermal conductivity of substrates does not always play a significant positive role in determining ITC when cooling HEMT devices. However, higher lattice thermal conductivity substrates indeed cause higher magnitudes of heat flux transporting at the interface. This work demonstrates the power of GNN models and paves the way for high-throughput screening of novel crystalline materials with desirable high ITC for phonon-mediated thermal management of wide bandgap electronics.

10:00 AM BREAK

10:30 AM *EL04.05.04

Addressing the challenges of n-type doping in AlN films grown on N-polar AlN substrate Irfan Khan¹ and Elaheh Ahmadi²; ¹University of Michigan--Ann Arbor, United States; ²University of California, Los Angeles, United States

Ultra-wide bandgap AlN has gained significant attention for high power and extreme environment applications due to its high breakdown field, high thermal conductivity and high temperature stability. However, achieving a controllable and uniform n-type doping as well as ohmic contacts with low resistance remain significant challenges for AlN based electronic and optoelectronic devices. Our work is focused on addressing these challenges on Nitrogen-polar (N-polar) AlN.

In this talk, I will present our recent results on Si-doped AlN films and polarization doping in graded N-polar AlN->AlGaIn films.

11:00 AM EL04.05.05

Adsorption controlled homoepitaxial growth of c-plane sapphire by thermal laser epitaxy Felix V. Hensling¹, Lena N. Majer¹, Sander Smink¹, Jochen Mannhart¹ and Wolfgang Braun^{1,2}; ¹Max Planck Institute, Germany; ²epiray GmbH, Germany

Its low cost, superior properties over silicon, high quality wafer availability, and the possible integration with silicon have established sapphire as widely used substrate material.[1] The ultra-wide bandgap and attractive dielectric constant of sapphire equally promise to reach regimes of semiconductor electronics and photonics thought to be impossible.[2] A cornerstone for further advancing the use of sapphire is the growth of high quality homoepitaxial sapphire films. However, epitaxial films of c-plane oriented sapphire, one of the most common cuts of sapphire, have so far been out of reach due to the preferred formation of the Al₂O₃ γ-phase.[3] Epitaxial films grown on other cuts of sapphire usually suffer from a bandgap reduction.[2,4] In the presentation, I will demonstrate that the extensive parameter space available in TLE solves those problems.[5] The CO₂-laser driven substrate heating system allows to heat sapphire substrates to their melting point. The high accessible and precisely controllable temperatures enable a smooth sapphire substrate preparation – the first step for successful homoepitaxy.[6] I further present how the crystal quality and surface smoothness of homoepitaxial sapphire increase with increasing substrate temperature in case the growth is performed in the adsorption-controlled mode. Even at high temperatures growth rates > 1 μm/h are realized. At a growth temperature of 1600 °C, the films were found to be practically undistinguishable from the underlying substrate regarding their crystallinity and optical properties, even exceeding the substrate's purity.

References

- [1] M.S. Akselrod, F.J. Bruni, "Modern trends in crystal growth and new applications of sapphire," *J. Cryst. Growth*, 360, pp. 134-145, 2012.
- [2] R. Jinno *et al.*, "Crystal orientation dictated epitaxy of ultrawide-bandgap 5.4- to 8.6-eV α-(AlGa)₂O₃ on m-plane sapphire", *Sci. Adv.*, 7, eabd5891, 2021.
- [3] H. Okumura, "Sn and Si doping of α-Al₂O₃ (10-10) layers grown by plasma-assisted molecular beam epitaxy", *JJAP*, 61, 125505, 2022.
- [4] Z. Chen *et al.* "Epitaxial growth of (Al_xGa_{1-x})₂O₃ thin films on sapphire substrates by plasma assisted pulsed laser deposition." *AIP Advances* 11, 2021.
- [5] W. Braun and J. Mannhart, "Film deposition by thermal laser evaporation," *AIP Advances*, 9, 085310, 2019.
- [6] W. Braun *et al.*, "In situ thermal preparation of oxide surfaces", *APL Mater.*, 8, 071112, 2020.

11:15 AM EL04.05.06

Metastable Shallow Donors and Origin of n-type Doping in AlN and AlGaIn Yujie Liu, Sieun Chae and Emmanouil Kioupakis; University of Michigan, United States

The n-type doping of AlN and Al-rich AlGaIn alloys through the incorporation of group-IV donors is constrained by the formation of compensating DX centers. Within the DX configuration, the bond connecting the donor atom to its adjacent N atom is disrupted, consequently causing the N atom to undergo a buckling distortion in the reverse direction. This results in the creation of a deep defect level within the band gap that is capable of trapping two electrons. Nevertheless, recent experimental works [1-4] have observed shallow donor formation and high conductivity and in Si- or Ge-implanted AlN. However, the nature of these shallow donors and the mechanism of doping remain unclear. Here, we apply predictive atomistic calculations to understand the formation of shallow donors and compensating defects in n-type AlN. We first identify that the high conductivity of Si- and Ge-implanted AlN arises from Al interstitials introduced by the ion damage. At the same time, the substitutional implanted Si and Ge ions form complexes with Al vacancies, which maintain the group-IV donors in the shallow configuration and prevent compensation. The presence of these complexes has been identified experimentally through their characteristic peaks in photoluminescence. Moreover, although the DX-center geometry is the most stable configuration of Si and Ge dopants for Fermi levels close to the conduction band, Fermi levels near the middle of the gap cause donors to adopt the shallow-donor geometry, in which Al atoms are substituted by the dopants without bond severance or strong bond distortions. This indicates that Fermi-level engineering during the material growth or

processing can stabilize donors in the shallow geometry and prevent the formation of DX centers. Furthermore, once equilibrium is re-established in n-type AlN and the Fermi level shifts closer to the conduction band, the disruption of the Si-N bond is inhibited by an energy barrier of ~1 eV, preventing the conversion of the metastable shallow Si donors into DX centers over a sufficiently long time. Our results explain the mechanisms for the efficient n-type doping of AlN and Al-rich AlGa_xN, and identify Fermi-level engineering strategies to further increase the doping efficiency and improve the conductivity.

References:

- [1] B. Neuschl et al. *Physica Status Solidi B*, 249(3): 511–515, 2012.
- [2] M. Hayden Breckenridge et al. *Applied Physics Letters*, 116(17), 2020.
- [3] R. Vermeersch et al. *Applied Physics Letters*, 119(26), 2021.
- [4] P. Bagheri et al. *Applied Physics Letters*, 122(14), 2023.

11:30 AM EL04.05.07

Comparative Study of Low-Frequency Noise in Diodes Made of Ultra-Wide Band Semiconductors Subhajit Ghosh¹, Dinusha Herath Mudiyansele², Fariborz Kargar¹, Yuji Zhao³, Houqiang Fu², Stephen M. Goodnick², Robert J. Nemanich² and Alexander A. Balandin¹; ¹University of California, Los Angeles, United States; ²Arizona State University, United States; ³Rice University, United States

In recent years, ultra-wide bandgap (UWBG) semiconductors have attracted increasing attention owing to the ever-increasing industry demand for high-power density electronics. Materials such as diamond, AlGa_xN, BN, and β -Ga₂O₃ emerged as viable alternatives to the well-established wide-bandgap technologies such as GaN and SiC. Low-frequency electronic noise produced by a device is an important metric. From one side, the level of low-frequency noise should be reduced for device applications in communications or sensors. On the other side, low-frequency noise can provide valuable information about the material quality and device reliability. The low-frequency noise includes the 1/f, flicker noise, and generation-recombination (G-R) noise with a Lorentzian-type spectrum (f is the frequency). Both 1/f and G-R noise are associated with material defects acting as trapping centers for the charge carriers. The latter can be used to understand the charge carrier dynamics and defects in materials. To some degree, the noise level can be used as a metric to assess the maturity of the material and device technology. We have conducted detailed noise studies in GaN vertical PIN diodes [1], high-current diamond diodes [2], β -(Al_xGa_{1-x})₂O₃ Schottky barrier diodes [3], and NiO_x/ β -Ga₂O₃ p - n heterojunction diodes [4]. At the presentation, we will compare the overall noise level in different UWBG technologies and comment on the effects of the material quality and device design. We will also describe the most interesting features observed in the noise spectra for some of the devices. Specifically, it was found that the noise of the diamond diodes is dominated by the 1/f and G-R noise. The G-R bulges are characteristic of diamond diodes with lower turn-on voltages. The characteristic trap time constants, extracted from the noise data, show a uniquely strong dependence on current. Interestingly, the performance of the diamond diodes improves with the increasing temperature. The noise spectral density of the β -(Al_xGa_{1-x})₂O₃ diodes, at room temperature, reveals 1/f dependence, with superimposed Lorentzian bulges at the intermediate current regimes. At the intermediate current level, the Lorentzian component belongs to the random telegraph signal (RTS) noise. The RTS noise was attributed to the defects near the Schottky barrier affecting the local electric field and the potential barrier, which correspondingly impacts the electric current.

This work was supported by ULTRA, an Energy Frontier Research Center (EFRC) funded by the U.S. Department of Energy, Office of Science, Basic Energy Sciences under Award # DE-SC0021230.

- [1] S. Ghosh, K. Fu, F. Kargar, S. Romyantsev, Y. Zhao, and A. A. Balandin, "Low-frequency noise characteristics of GaN vertical PIN diodes—Effects of design, current, and temperature", *Appl. Phys. Lett.*, 119, 243505 (2021).
- [2] S. Ghosh, H. Surdi, F. Kargar, F. Koeck, S. Romyantsev, S. Goodnick, R. J. Nemanich, and A. A. Balandin, "Excess noise in high-current diamond diodes", *Appl. Phys. Lett.*, 120, 062103 (2022).
- [3] S. Ghosh, D. H. Mudiyansele, S. Romyantsev, Y. Zhao, H. Fu, S. Goodnick, R. Nemanich, and A. A. Balandin, "Low-frequency noise in β -(Al_xGa_{1-x})₂O₃ Schottky barrier diodes", *Appl. Phys. Lett.*, 122, 212109, 2023.
- [4] S. Ghosh, D. H. Mudiyansele, F. Kargar, Y. Zhao, H. Fu, and A. A. Balandin, "Temperature dependent low-frequency noise characteristics of NiO_x/ β -Ga₂O₃ p - n heterojunction diodes", arXiv:2307.15659.

11:45 AM EL04.05.08

Novel deposition of amorphous aluminum oxide thin film using a direct liquid injection chemical vapor deposition (DLI-CVD) system Jiseon Kim^{1,2}, Wei-Fan Hsu², Simon Mellaerts², Claudio Bellani², Alberto Binetti², Koen Schouteden², Jean-pierre Locquet², Jin Won Seo² and Caroline Sunyong S. Lee¹; ¹Hanyang University, Korea (the Republic of); ²KU Leuven, Belgium

Aluminum oxide (Al₂O₃) stands out as a representative ceramic material thanks to its wide applicability, e.g., in electronic and optical devices, sensors, wear-resistant coatings, and catalyst support. Especially, amorphous aluminum oxide films hold great promise due to their flexibility, uniformity, and high dielectric properties compared to crystalline counterparts. Various deposition methods, such as sputtering, chemical vapor deposition (CVD), and sol-gel method have been used so far.

This study introduces a noble direct liquid injection CVD (DLI-CVD) technique to fabricate amorphous Al₂O₃ thin films. DLI-CVD, unlike conventional CVD process, offers various advantages: It can avoid the unnecessary decomposition of precursors prior to deposition, by making us of a vaporization chamber (Vapbox). The liquid precursor is injected into the Vapbox and transported to the deposition chamber through the nitrogen carrier gas. Simultaneously, oxygen gas is injected into the chamber for enabling the oxide film deposition. The precursor mixture is directly injected as vapor into the deposition chamber. The decomposition occurs on the surface of the substrate, where the deposition reaction is initiated. As the precursor molecules are decomposed directly on the surface, unwanted by-products can be prevented. Furthermore, strong chemical bonds between precursor molecules and organic solvent break in advance, while minimizing the required heat energy.

In this study, Al₂O₃ thin films were deposited by varying parameters such as the substrate temperature, the deposition time, and the ratio between nitrogen and oxygen gas flow. Aluminum acetylacetonate (Al(acac)₃) was selected as the aluminum precursor due to its stability, non-toxicity, and non-flammability, compared to alternatives like trimethylaluminum and aluminum chloride. X-ray reflectivity (XRR) analysis confirmed that the film thickness scaled with the substrate temperature and deposition time. Atomic force microscopy (AFM), x-ray photoelectron spectroscopy (XPS) and Fourier transform infrared spectroscopy (FT-IR) analysis elucidated the roughness, uniformity, and composition of Al₂O₃ films. Cross-sectional transmission electron microscopy (TEM) provided insights into the film morphology and growth mechanism. This work demonstrates the applicability of the novel DLI-CVD technique and enhances our understanding of this innovative thin film process.

SESSION EL04.06: Power Devices
Session Chairs: Sriram Krishnamoorthy and Baishakhi Mazumder
Wednesday Afternoon, April 24, 2024
Room 345, Level 3, Summit

1:30 PM ^EL04.06.01

Multidimensional Power Devices in WBG and UWBG Semiconductors Yuhao Zhang; Virginia Tech, United States

Power electronics technologies provide electrical energy conversion using semiconductor devices and passive components. The global power device market reaches US\$40 billion and is rapidly expanding, driven by applications like electric vehicles, data centers, consumer electronics, electric grids, and renewable energy processing.

Power device advances are driven by materials and device architectures. In addition to using wide-bandgap (WBG) or ultrawide-bandgap (UWBG) materials, multidimensional architectures – such as superjunction, multi-channel, and multi-gate – can also improve device performance, regardless of the underlying material technology. These structures enable electrostatics engineering in additional dimensions and bring the benefits of geometrical scaling into power devices.

This talk presents our efforts in developing multidimensional power devices in WBG material GaN and UWBG material Ga₂O₃, the performance of which have exceeded the 1-D power device limit of the respective material. Particular focus will be placed on GaN power FinFETs, GaN multi-channel lateral devices, as well as the vertical GaN and Ga₂O₃ superjunction devices. These devices hold great potential for advancing the speed, efficiency, and form factor of power electronics systems, and some of them are currently being commercialized. The theoretical limits, figure of merits, and scaling laws of these multidimensional power devices will also be discussed for WBG and UWBG materials. Finally, these devices provide an exciting platform to study the fundamental material properties and carrier transports in homogenous or heterogenous, charge-balanced junctions under sub-micron second fast switching conditions.

2:00 PM EL04.06.02

Design Optimization of Ultra-Wide Bandgap Power Diodes: A Co-Design Approach to Understanding the Impact of UWBG Semiconductor Materials Properties on Power Device Performance Jonah Shoemaker^{1,2}, Robert J. Kaplar², Stephen M. Goodnick¹, Reza Vatan¹, Jack Flicker², Andrew Binder² and Srabanti Chowdhury³; ¹Arizona State University, United States; ²Sandia National Laboratories, United States; ³Stanford University, United States

Ultra-Wide Bandgap (UWBG) semiconductors constitute the fourth generation of semiconductor science and technology, and as such are at the forefront of semiconductor research today. This class of materials is roughly defined as those semiconductors having a bandgap greater than that of GaN (3.4 eV). The unipolar figure of merit (UFOM) of [endif]--> is a useful metric for comparing between semiconductor materials for power device application, but (The incorporation of UWBG devices into systems is not determined on a UFOM b UFOM basis. It i, but is instead driven by the system-level benefits derived by incorporation of a device at given operational parameters (e.g. switching frequency, hold-off voltage, current-carrying ability). The various UWBG materials are at different levels stages of development for devices such as PiIn vs Schottky diodes, so a direct comparison with state-of-the-art wide bandgap materials based on device I-V curves is misleading.

In order to determine the system-level operational regimes for which various combinations of UWBG materials and diode architecture are preferred over more developed WBG devices, we have developed the optimization tool first reported in [1]. This optimizer takes various system operational parameters as input (reverse operating bias, forward current density, system frequency, etc.) and optimizes the width of the device drift region and the doping level to minimize system power dissipation. Effects particular to UWBG materials, such as incomplete ionization due to deep dopant energy depth, space-charge limited current, and doping- and device thickness-dependent breakdown fields, have been incorporated into the optimizer to more accurately model the performance of UWBG materials.

For a given device type and material, a mobility model is used to determine carrier mobilities at a given temperature, doping level, and electric field. For some materials, this mobility model is computed from various scattering contributions, while for the rest of the materials empirical models available in the literature are used instead. The operational parameters of the diode in the system are also defined. These are the reverse operating bias, forward current density, switching frequency, duty cycle, and device operational temperature. The critical fields are tabulated for various values of doping concentration and device thickness using the method described in section IIB. The optimization program then minimizes power dissipation in the system by altering device drift region thickness and doping concentration subject to the constraints described in [1]. By iterating across all available system operating parameters, it is possible to develop a map in system operating space and determine which devices/materials produce the lowest power loss for any given system operational point based on materials properties.

The resulting preferred device color-maps show a strong dependence on many of the material parameters used as input, including impact ionization coefficients, dopant activation energies, and carrier mobilities. We compare preferred device color-maps across a range of temperatures and forward current densities to show the effects of UWBG-specific effects incomplete ionization and space-charge limited conduction. Then we vary the material parameter inputs to show the sensitivity of the final color-maps on each material input. While these color-maps are always being updated with newly published results on UWBG materials, these sensitivity analyses can nonetheless give researchers a more educated insight on which materials show the greatest promise in any given region of operating space.

1. Flicker, J. and R. Kaplar, *Design Optimization of GaN Vertical Power Diodes and Comparison to Si and SiC*, in *2017 IEEE 5th Workshop on Wide Bandgap Power Devices and Applications (WiPDA)*. 2017, IEEE. p. 31-38.

2:15 PM EL04.06.03

Lateral p-GaN/AlGaN/GaN Hybrid Anode Diodes (HADs) with Hydrogen Plasma Guard Line Termination Dawei Wang, Dinusha Herath Mudiyansele, Ziyi He, Bingcheng Da and Houqiang Fu; Arizona State University, United States

Wide bandgap material GaN is promising in high-efficiency power conversion systems. To realize GaN power integrated circuits (ICs), peripheral logic circuits based on GaN are necessary, such as controllers, drivers, and protection circuits. Using the p-GaN/AlGaN/GaN high electron mobility transistors (HEMTs) platform, all these components can be integrated on a single chip, dramatically reducing parasitic effects, such as gate ringing and false turn-on of power transistors. Recently, Lateral AlGaN/GaN hybrid anode diodes (HADs) have been demonstrated on the commercial p-GaN/AlGaN/GaN platform, attracting significant attention due to the advantages of low on-resistance and low reverse leakage. It has a hybrid Schottky/ohmic anode composed of electrically connected ohmic contact and Schottky gate. The anode voltage can directly cut off the 2DEG channel at reverse bias, thus improving the reverse performance. Etching-free low-damage hydrogen plasma-treated HADs have also been demonstrated for lower turn-on voltage and lower on-resistance. However, the electric field crowding effect at the edge of the anode still exists in the previous reports.

In this work, we perform the design and fabrication of p-GaN/AlGaIn/GaN Hybrid Anode Diodes (HADs) with Hydrogen Plasma Guard Line Termination for better electric field management. The high electric field at reverse bias would extend to the whole anode-to-cathode area. The device epilayers were grown by metal-organic chemical vapor deposition (MOCVD) on a sapphire substrate, consisting of a thick GaN buffer layer, a 300 nm UID-GaN layer, a 1 nm AlN space layer, a 20 nm Al_{0.2}Ga_{0.8}N layer and a 90 nm p-GaN layer with an acceptor Mg concentration of 3×10^{19} cm⁻³. The substrate was annealed at 800 °C for 30 minutes to break the Mg-H bond and activate the p-GaN layer. The metal stack Ti/Al/Ni/Au was deposited as cathode, followed by post-annealing at 850 °C for 30s. The p-GaN layer under the cathode was etched before metal deposition for better ohmic contact. Then, several hydrogen plasma-treated patterned arrays termination, i.e., guard lines termination, were fabricated to eliminate high electric field crowding at the edge of the anode. The photoresist-based patterns were developed as the mask on the p-GaN layer. The pattern of the guard lines is different from the traditional guard ring termination for vertical GaN devices. The guard line was formed by a series of discontinuous trapezoid-like shapes for partially depleting the 2DEG channel so that the p-GaN would not cut off the 2DEG current along the whole device. The trapezoid shapes were designed for optimized electric field management. In addition, stripe edge termination structures were also introduced at the edge of the anode. Hydrogen plasma treatment was applied to the surface for 5 minutes. The photoresist was then removed using Micro Remover PG at 120 °C. The post-annealing at 400 °C was applied for hydrogen diffusion. Finally, the gate metal Ni was deposited via magnetron sputtering, followed by Au deposition using e-beam deposition. The electrical testing indicated that hydrogen plasma treatment could fully passivate the p-GaN current. The forward current and on-resistance are comparable with the previous reports. The breakdown voltage increased in the devices that have the hydrogen plasma guard line termination structure, and the on-resistance only has a slight increase. The device breakdown voltage was several-kV-class with an anode-to-cathode length (L_{AC}) from 25 to 75 μ m. The device is still under optimization for higher breakdown voltage. These results can provide critical references for the future development of high breakdown voltage lateral p-GaN/AlGaIn/GaN devices.

2:30 PM BREAK

SESSION EL04.07: WBG and UWBG Material Characterization

Session Chairs: Sriram Krishnamoorthy and Yuhao Zhang

Wednesday Afternoon, April 24, 2024

Room 345, Level 3, Summit

3:30 PM *EL04.07.01

The Application of The Photonic Atom Probe to The Study of Wide Bandgap Semiconductors Lorenzo Rigutti¹, Abraham Diaz Damian¹, Jonathan Houard¹, Enrico Di Russo², Georges Beainy¹, Pradip Dalapati¹, Angela Vella¹, François Vurpillot¹, Jean-Michel Chauveau³, Maxime Hugues⁴, Grzegorz Muziol⁵ and Henryk Turski⁵; ¹University of Rouen Normandie, France; ²University Of Padova, Italy; ³University of Versailles St Quentin, France; ⁴CRHEA, France; ⁵Unipress, Poland

The Photonic Atom Probe (PAP) allows for the measurement of Photoluminescence (PL) of a sample tip while it is being analyzed by Laser-Assisted Atom Probe. The femtosecond Laser pulse required for the La-APT measurement also serves to excite the free charge carriers, whose recombination provide the PL signal. As a consequence, it becomes possible to correlate the optical signature of the different parts of a complex structure with the 3D distribution of the contained chemical species [1].

We present an application of the PAP on III-nitride p-i-n junctions, namely a thick (> 1 μ m thickness) multi-layer structure containing InGaIn quantum wells and a buried tunnel junction [2]. Plasma-assisted molecular beam epitaxy-grown structures, which were used in the study, are characterized by diverse doping concentrations in both p- and n-type regions. The PL spectra can be correlated with the 3D chemical information from APT [3]. The PL signals exhibit indeed a donor-acceptor pair (DAP) emission, whose spectral features can be related to the 3D distribution of the Mg dopants and of the InGaIn heterostructures. These results open interesting perspectives for studies of light-emitting defects at the nanoscale.

Besides the interest of this instrument as a microscope [3], the particular conditions in which the optical signatures of localized light emitters are collected open intriguing possibilities for the study of field ion emission under high field and under laser illumination [4]. As an example, the PL spectral shift allows measuring the stress induced by the application of a strong electric field at the tip apex and its propagation through the tip. This has been evidenced both through the study of the stress-induced splitting of the zero-phonon line of the NV⁰ center in diamond [5] and of the quantum well (QW) emission in a ZnO/(Mg,Zn)O system [6], allowing measuring stress levels ranging from 9 GPa to ~1 GPa.

References

- [1] J. Houard *et al.*, *Review of Scientific Instruments*, vol. 91, no. 8, p. 083704, Aug. 2020, doi: 10.1063/5.0012359.
- [2] H. Turski *et al.*, *ECS J. Solid State Sci. Technol.*, vol. 9, no. 1, p. 015018, Dec. 2019, doi: 10.1149/2.0412001JSS.
- [3] E. Di Russo *et al.*, *Nano Lett.*, vol. 20, no. 12, pp. 8733–8738, Dec. 2020, doi: 10.1021/acs.nanolett.0c03584.
- [4] E. Di Russo and L. Rigutti, *MRS Bulletin*, vol. 47, no. 7, pp. 727–735, Jul. 2022, doi: 10.1557/s43577-022-00367-6.
- [5] L. Rigutti *et al.*, *Nano Lett.*, vol. 17, no. 12, pp. 7401–7409, Dec. 2017, doi: 10.1021/acs.nanolett.7b03222.
- [6] P. Dalapati *et al.*, *Phys. Rev. Applied*, vol. 15, no. 2, p. 024014, Feb. 2021, doi: 10.1103/PhysRevApplied.15.024014.

4:00 PM EL04.07.02

Unraveling the Atomic Mechanism of the Disorder- Order Phase transition from γ -Ga₂O₃ to β -Ga₂O₃ by in situ Transmission Electron Microscopy Martin Albrecht¹, Charlotte Wouters¹, Musbah Nofal¹, Piero Mazzolini², Jijun Zhang¹, Thilo Remmele¹, Albert Kwasniewski¹ and Oliver Bierwagen²; ¹Leibniz Institut fuer Kristallzuechtung, Germany; ²Paul-Drude-Institut fuer Festkörperelektronik, Germany

Monoclinic Ga₂O₃ (β -Ga₂O₃) is a semiconductor with a bandgap of 4.7 eV and an estimated breakdown field strength of 8 MVcm⁻¹. It has attracted considerable interest as a promising material for electronic applications such as solar blind UV photodetectors, and high power devices. In addition to the thermodynamically stable monoclinic β -phase, Ga₂O₃ can be stabilized under ambient conditions in a number of metastable structures (α -Ga₂O₃, γ -Ga₂O₃, κ -Ga₂O₃ and δ -Ga₂O₃) in which Ga cations exist in both tetrahedral (GaO₄) and octahedral (GaO₆) coordination. The polymorphic transition between β -Ga₂O₃ and γ -Ga₂O₃ has recently attracted particular attention and has become the focus of intense research efforts. These research activities were triggered by the experimental observation that after implantation of Si or Ge, used to selectively n-dope β -Ga₂O₃, a phase transition from β -Ga₂O₃ to γ -Ga₂O₃ was observed. [1,2,3] Recovery of β -Ga₂O₃ was observed after annealing. [1,2] It was also observed that β -Ga₂O₃ is extremely radiation tolerant. Since none of the other crystalline phases were observed to form, the question of a hidden structural relationship between γ -Ga₂O₃ and β -Ga₂O₃ was raised. In this paper we study the reverse direction, i.e. the disorder-order phase transition from amorphous Ga₂O₃ to γ -Ga₂O₃ and then to β -Ga₂O₃ by *in situ* transmission electron microscopy. The *in situ* studies are complemented by *ex situ* annealing experiments, the results of which are analyzed by X-ray diffraction and high resolution (scanning) transmission electron microscopy. Amorphous Ga₂O₃ deposited at 100°C by molecular beam epitaxy crystallizes

at 470°C in the γ phase, which undergoes a phase transition to the β phase above 500°C. Between 500° and 900°C we find a mixture of γ -Ga₂O₃ and the β -Ga₂O₃ coexisting. Above 950°C we find only β -Ga₂O₃. Taking into account the crystallographic symmetry relations, we construct a common lattice of both structures containing a common fcc-type sublattice occupied by oxygen atoms, the cation sites of β -Ga₂O₃ common to both phases, and partially occupied cation sites in the γ -phase corresponding to interstitial sites in the β -phase. We assign the atomic displacements within this lattice that transform γ -Ga₂O₃ (the defective spinel structure with partially occupied cation sites) into perfectly ordered β -Ga₂O₃. By its nature, this is a reconstructive disorder-order phase transition in which atoms exchange positions to the nearest neighbor sites. Few of the exchange processes we derive from crystallographic symmetry relations match those derived by Huang et al. [2,3] from analysis of atomically resolved scanning transmission electron microscopy (STEM) images of implanted β -Ga₂O₃. Our results explain, why disordering of the lattice, e.g. by implantation, causes the formation of γ -Ga₂O₃ and not any of the other phases. This would require a martensitic transition, i.e. shearing of the oxygen sublattice and not simply displacement of cations. It also explains, why annealing causes the reverse phase transition and results in a perfect β -Ga₂O₃ lattice as described by Huang et al. [2]

[1] A. Azarov, et al., Nature Communications 14, 4855 (2023)

[2] L. Huang, et al. APL Mater. 11, 061113 (2023).

[3] L. Huang et al., Appl. Phys. Lett. 122, 251602 (2023).

4:15 PM *EL04.07.03

Probing The Atomic-Scale Chemistry and Doping Defect Interactions in UWBG Semiconductors Baishakhi Mazumder; University at Buffalo, The State University of New York, United States

Ultra-wide bandgap (UWBG) semiconductors are revolutionizing high-power electronics, promising unprecedented control over conductivity and transport properties. To unleash their full potential, we must navigate the intricate interplay between material chemistry, electrical properties, and defects. Direct experimental insights into the structural and chemical components that govern electrical transport are essential, forging a connection between theory and practical application. Among UWBG semiconductors, Ga₂O₃ and its alloys shine as promising candidates for high-power electronics. Yet, their success hinges on the microstructures and nanoscale chemistry of active layers. Achieving tailored electrical properties and defect mitigation necessitates an intricate understanding of the interplay between structure and chemistry. Atom Probe Tomography (APT) is an advanced instrument that offers three-dimensional chemical imaging of individual atoms. When combined with machine learning, APT generates comprehensive datasets that shed light on material systems, offering insights into dopant solubility, dopant diffusion, impurities, vacancies, and defect complexes. These insights deepen our understanding of their impact on electrical transport, surpassing the limitations of conventional techniques.

In this work, we undertake an atomic-scale investigation of doped Ga₂O₃ and its associated alloys. This presentation underscores the critical significance of APT in elucidating the intricate structural and chemical characteristics of Ga₂O₃-based UWBG semiconductors, thereby advancing their design and development for power electronics applications. Our inquiry delves into the intricacies of doping, exerting influence on both the alpha and beta phases, while also addressing the challenges presented by defects. The knowledge gained from this analysis has the potential to reshape the synthesis of UWBG semiconductor materials, offering a new dawn for high-power electronics technology. Join us on this quest as we delve into the heart of UWBG semiconductors, where science meets innovation.

SESSION EL04.08: Poster Session

Session Chairs: Robert Kaplar and Sriram Krishnamoorthy

Wednesday Afternoon, April 24, 2024

Flex Hall C, Level 2, Summit

5:00 PM EL04.08.01

Band Gap Behavior and Order/Disorder in Sn_{1-x}Ge_xO₂ Alloys for Deep UV Transparent Conducting Oxides Sabine Hachmioune^{1,2}, Alexander Squires³, Michael B. Sullivan² and David O. Scanlon³; ¹UCL, United Kingdom; ²Agency for Science, Technology and Research, Singapore; ³University of Birmingham, United Kingdom

Transparent conducting oxides (TCOs) with deep ultraviolet (DUV) transparency have a wide range of applications, including optoelectronics, sensors, and optical coatings. However, achieving high optical transmittance in the DUV range (< 300 nm) remains challenging due to the empirical trade-off in conductivity with increasing band gap, and conventional TCOs having optical band gaps too small for DUV transparency. To address this, recent studies have shown that the addition of germanium (Ge) to rutile-SnO₂ can increase the band gap from 3.79 eV to 4.09 eV (at x = 0.7), making it a promising candidate for DUV-TCO applications.¹

In this work, we employ a comprehensive modelling approach combining hybrid-Density Functional Theory (DFT) calculations, Cluster Expansion and Monte Carlo simulations to investigate the band gap behaviour of Sn_{1-x}Ge_xO₂ alloys (0 ≤ x ≤ 1). Our methodology allows us to determine the ground state atomic structure and calculate the band structure for each composition. Additionally, we analyse the extent and impact of cation disorder in the alloyed systems.

Understanding the order/disorder behaviour in these alloyed systems is crucial as it directly influences the band gaps, electronic properties, and optical characteristics of the material. Furthermore, we explore the effect of dopants on disorder, building upon previous research that suggests the incorporation of Ta⁵⁺ impurities can enhance conductivity.¹

By elucidating the order/disorder relationships, their impact on the properties of Sn_{1-x}Ge_xO₂ alloys and the interaction of bulk disorder with impurity doping, this study provides valuable insights for the design and optimization of DUV-TCO materials.

1 Y. Nagashima, M. Fukumoto, M. Tsuchii, Y. Sugisawa, D. Sekiba, T. Hasegawa and Y. Hirose, *Chem. Mater.*, 2022, **34**, 10842–10848.

5:00 PM EL04.08.02

Self-Aligned Fabrication of Sub-50 nm Top Gate Coplanar ITO/IGZO Thin-Film Transistors without Nanoscale Patterning Jiyounghun Bang, Yeonghun Lee, Yeonsu Lee, Minjin Kwon, Hyoungbeen Ju, Hyeonjeong Sun, Sangduk Kim, Seungmin Choi, Youngsoo Noh, Hyowon Kim, Eunsuk Choi and Seung-Beck Lee; Hanyang University, Korea (the Republic of)

Amorphous oxide semiconductor (AOS) thin-film transistors (TFTs) are attracting interest due to their wide bandgap, low leakage, and capacity for low-temperature processing and have been effectively commercialized particularly in display backplane applications. One significant approach to improving the TFT's performance involves reducing the channel length to sub-micron levels. However, to fabricate nanoscale TFTs for large-scale display applications, traditional nanoscale pattern definition methods may not be applied and require the development of methods that would produce nanoscale patterns without nanolithography. We introduce a high-throughput nanoscale patterning method for fabricating top gate coplanar oxide semiconductor TFTs. Our method involves the angled thermal evaporation of an aluminum etch mask layer, taking advantage of shadowing effects induced by SiO₂ stepped spacers. First, the active channel layer, an ITO/IGZO bilayer, was sputter deposited. Then a 50 nm Mo contact metal layer was sputter deposited. Normally at this stage, a nanogap in the Mo would be introduced by nanolithography followed by reactive ion etching (RIE). However, our method defines a nanogap in the etch mask by Al angled deposition. A layer of SiO₂ is deposited on the Mo layer and an optical lithography step is used to mark the position of the SiO₂ step that will be formed by RIE down to the Mo surface. When Al is thermally evaporated at an angle on the SiO₂ step, the shadowing effect will introduce a nanogap between the Al on top of the SiO₂ step and on top of the Mo layer. Using the discontinuous Al layer as the hard mask, sub 100 nm gap in the Mo layer can be inserted by RIE, thereby forming a nanogap between the source/drain contacts. After the Al layer is removed chemically, the Al₂O₃ gate insulator and Mo top gate layers were self-aligned to the nanogap position by ALD and sputtering, respectively. By controlling the Al deposition angle and the SiO₂ step height, the nanogap width was controlled between 40 nm ~ 100 nm. Utilizing this technique, we successfully fabricated a top gate coplanar ITO/IGZO TFT with a gate length of 50 nm. Measurements showed that at a drain-source voltage of 40 mV, the device exhibited an on current of 1.3×10^{-6} A/ μm at a gate voltage of 20 V. And the off-current levels were below 10^{-14} A/cm² with a threshold voltage of -2.1 V, and a sub-threshold swing of 301 mV. The results demonstrate that this technique has the potential for broad application in large-scale nanoscale metal oxide TFT fabrication.

5:00 PM EL04.08.04

Investigating The Oxygen Defects of Nano-Heterojunction for Toxic Gas by Using Synchrotron and Raman Spectroscopy [Lin Yuru](#)¹, Chun-Yen Lai², Cheng-En Lee³, Wen-Wei Wu² and Ping-Hung Yeh³; ¹Tamkang University, Taiwan; ²National Yang Ming Chiao Tung University, Taiwan; ³Department of Physics, Tamkang University, Taiwan

In this study, a multifunctional wearable sensor with high-precision of toxic gas, nitric oxide, and multiple wavelength light detection abilities was fabricated by defect-rich nano-heterojunction SnO₂-TiO₂ nanofibers. Choosing nitric oxide as the measured gas is motivated by its potential for assessing airway inflammation by measuring its concentration in exhaled breath. While Fractional Exhaled Nitric Oxide (FENO) exists for this purpose, challenging measurement techniques and methods have hindered its clinical applicability. According to the research, the nano-heterojunction device produced in this experiment exhibits a sensitivity to low concentrations of nitric oxide that is up to seven times higher. Therefore, the ultimate goal of this experiment is to utilize the prepared nano-heterojunction device for asthma sensing.

The properties of dynamic internal charge transport and recombination process can be precisely controlled through the sol-gel drop casting method, which forms numerous oxygen defect structures at the nano-heterojunction gate between SnO₂ nanofibers and TiO₂ nanoparticles, allowing the tuning of the band gap within the range of 3.6 to 3.27 eV. The reason of band gap reducing might be a significant number of oxygen defect structures are formed at the nano-heterojunction gate, acting as generation-recombination centers to precisely trap or release free carriers. This process converts various photon energies (ranging from 365 to 520 nm) into different photocurrent levels.

To investigate the relationship between the adsorption and desorption of oxygen defect structures, the in-situ Raman spectroscopy and electrical measurement systems can be used for toxic gases detection. Furthermore, the conductivity and sensitivity of the wearable sensor for monitoring toxic gas can be enhanced through the defect-rich toxic gas molecular adhesion layer on the surface of nanofibers. The electronic structure and functionality of each oxygen defect structures, including out-of-plane oxygen defects, bridge oxygen defects, and in-plane oxygen defects, were studied using synchrotron analysis to investigate the electron transfer between the oxygen defect energy state and the conduction bands. Based on the results, the in-plane oxygen defects will be decreased, if the nano-heterojunction increases. The electrical results indicate that defects-rich SnO₂-TiO₂ nano-heterojunction nanofiber devices could be highly sensitive to toxic gases and serve as light sensing devices in our daily lives. Moreover, they are expected to be used in asthma detection in the future.

5:00 PM EL04.08.05

Addressing the orientation of defect-related crystal domains by Atom Probe Tomography in III-N heterostructures [Lorenzo Rigutti](#)¹, Jesus Cañas², Névine Rochat³, Adeline Grenier³, Audrey Jannaud³, Zineb Saghi³, Jean-Luc Rouvière², Edith Bellet-Amalric², Catherine Bougerol⁴ and Eva Monroy²; ¹University of Rouen Normandie, France; ²CEA IRIG, France; ³CEA LETI, France; ⁴CNRS Institut Néel, France

Atom Probe Tomography (APT) may be applied as a tool for the assessment of the crystallographic orientation of microstructural features. In the present study, such features are related to defects formed during the growth of AlGaIn/AlN quantum dot superlattices. These defects are the origin of the low-energy component of a bimodal luminescence emission in the 230-300 nm spectral range [1]. The defects are cone-shaped, starting at the AlN buffer/superlattice interface and propagating vertically, associated to a dislocation that produces strong shear strain and favors the formation of 30° faceted pits. They also may be responsible for local formation of misoriented domains. We show that the effective surface field intensity maps obtained through the statistics of the charge states n of the field-emitted Al ^{$n+$} ions can be used as a means to locate the direction of the [0001] crystal pole with respect to the needle axis. This provides a way to track changes of crystal orientations by several degrees and to correlate them with the morphological and chemical features of the sample. The results indicate that such misorientations can occur, but not systematically.

[1] Cañas et al., under review. <https://arxiv.org/abs/2310.04201>

5:00 PM EL04.08.06

Plasma Assisted Remediation of SiC Surfaces [Michael A. Mathews](#)^{1,2}, Andrew R. Graves^{1,3}, David R. Boris², Scott G. Walton² and Charter D. Stinespring¹; ¹West Virginia University, United States; ²U.S. Naval Research Laboratory, United States; ³The Pennsylvania State University, United States

Due to advances in chemical mechanical polishing (CMP), SiC surface quality has improved remarkably over the years. Despite this progress, there is extensive literature reporting the limitations of the CMP process. Wafers purported to have CMP surfaces can range from high-quality, optically perfect surfaces, exhibiting well-defined step and terrace structure to low-quality surfaces with highly scratched regions. Thus, methods are required to remediate these surfaces if they are to be used effectively as substrates for device fabrication. The novel surface remediation approach explored in this presentation utilizes a three-step scalable method referred to here as plasma assisted remediation. In this process, a CF₄-based inductively coupled plasma with reactive ion etch was used to remove material to a depth which was unaffected by surface and sub-surface polishing damage. This produced a planarized but carbon-rich fluorinated surface. This surface was exposed to a rapid thermal oxidation in air to oxidize and volatilize the excess carbon and fluorinated species. The resulting surface oxide was stripped using a dilute hydrofluoric acid in water solution. This process reproducibly yielded planarized, stoichiometric surfaces with low levels of carbon and oxygen contamination for both 4H- and 6H-SiC(0001) surfaces. This presentation describes x-ray photoelectron spectroscopy and atomic force microscopy studies used to characterize each step of the process and provide an understanding of the process mechanism. In addition, experimental studies under ion-rich and radical-dominant plasma conditions are reported which provide greater insight into the underlying chemistry and physics of the process.

5:00 PM EL04.08.07

Precision Gas Sensing: Tuning The Defect Energy Level of SnO₂ Nanofiber Devices by Surface Defect Engineering Cheng-En Lee¹, Lin Yuru¹, Chun-Yen Lai², Wen-Wei Wu² and Ping-Hung Yeh¹; ¹Tamkang University, Taiwan; ²National Yang Ming Chiao Tung University, Taiwan

In the last decade, surface defect engineering in metal oxide semiconductor materials is gaining more attention since it provides controllability and opens up possibilities for commercial use in various fields like gas sensors, photocatalysis, nanoparticle filters and so much more. In this work, the enhancement of gas detection ability of SnO₂ nanofiber devices (NFDs) can be achieved by using electrospinning and surface defect engineering. Increasing surface area can provide more reaction centers for gas molecules, so as to boost the detection ability of SnO₂ NFDs by colloidal film deposition. With colloidal film deposition, the sensitivity of NO gas (less than 50 ppb) detection can be increased more than three times. Furthermore, specific gas molecules can be detected by tuning the surface defect energy through nano-heterojunction integration. This is due to the variation in absorption energy among different gases. To investigate the density of states and to control the energy levels of defects, the X-ray absorption near edge structure (XANES) spectrum and Raman spectrum were used to measure SnO₂ NFDs. Based on the XANES results, the out of plane and in plane oxygen defects can be varied significantly by surface engineering. In summary, through surface defect engineering techniques, we have acquired the capability to fully control the characterization and distribution of surface defects in SnO₂ NFDs. Combining with the nanoscale advantage, we can realize low-concentration gas sensing with high precision.

5:00 PM EL04.08.08

Field-Effect Mobility Enhancement of a-InGaZnO Thin Film Transistors through Metal Capping Layer Oxidation Induced Carrier Boosting Hyeonjeong Sun, Jiyoung Bang, Hyoungbeen Ju, Seungmin Choi, Youngsoo Noh, Hyowon Kim and Seung-Beck Lee; Hanyang University, Korea (the Republic of)

Amorphous oxide semiconductor (AOS), such as amorphous In-Ga-Zn-O (a-IGZO), has gained attention as channel materials for thin-film transistors (TFTs) based on attractive benefits, including low-temperature thin-film processing, low leakage current characteristics, and excellent optical properties due to its wide band gap. However, with relatively low carrier mobility in the range of 10-40 cm²/Vs, improving the mobility becomes one of the most important research concerns of AOS TFTs. Various methods to enhance the mobility of AOS have been suggested thus far, including changes in the composition of metal cation and proportion ratio of IGZO to form strong s-orbital overlap to enhance percolation conduction. Recently, there has been active research focused on enhancing the conduction of the channel by adopting a capping layer on AOS TFT channel surfaces. Performance-enhancing strategies were reported using oxidation of Ca/Al capping layers and low-temperature crystallization of various AOS using Mo, Ti and Al. Several papers have reported on using Ti and Ta capping layers for AOS TFTs to enhance the crystallinity of the channel through low-temperature thermal annealing. Our focus was on increasing the oxygen vacancies within the IGZO channel, thereby improving its conductivity and therefore its field-effect mobility μ FE. The XPS results confirmed that Ta capping with PDA at 200 °C increased the oxygen vacancy of the IGZO film from 21% to 31% by breaking M-O bonds in IGZO and allowing oxygen diffusion to the Ta layer, which in turn acts as a carrier source. Based on the observed carrier boosting effects, the characteristics of Ta capped a-IGZO TFTs were investigated with increasing Ta coverage area. We observed that with 90% channel coverage (Ta capping) demonstrated a remarkable 875% enhancement in μ FE, increasing from 16 cm²/Vs to 140 cm²/Vs, while maintaining near-zero threshold voltage and low off-state leakage current. One problem with increasing the carrier concentration throughout the length is a severe negative shift in the threshold voltage V_{th}. The extremely high carrier concentration raises the Fermi level near the contact high enough to make the TFT operate in the depletion mode, or not turn off with nominal negative gate voltages. However, if a part of the back channel is left uncapped, the uncapped IGZO region would create a homojunction and act as a potential barrier, effectively maintaining the off-state current, while the capped IGZO region acts as a carrier-boosted region, facilitating higher channel conduction. We formed this IGZO homojunction and allowed the TFT to operate in the enhancement mode with a positive V_{th} and prevented an increase in the off-state current. As the carrier-boosted region becomes wider, the total carrier concentration increases, leading to an increase in on-current and μ FE. The results reported in this paper provide a simple method to achieve high-performance metal oxide semiconductor devices, which are expected to be applicable to various next-generation device applications.

5:00 PM EL04.08.09

GaN Nanowire Wrap-Gate Transistor: Barrier Height, Ideality Factor and Inhomogeneities at The AlGaIn/GaN Interface Yeojin Choi, Reddy S. Mallem, Yuna Lee and Sungjin An; Kumoh National Institute of Technology, Korea (the Republic of)

For the creation of next-generation nanoscale devices, it is crucial to comprehend the barrier height, ideality factor, and function of inhomogeneities at the metal/semiconductor interfaces in nanowires. Here, we study the GaN nanowire wrap-gate transistors (WGTs) drain current (I_{ds})–gate voltage (V_{gs}) characteristics over a range of gate potentials over the broad temperature range of 130–310 K. When the temperature is lowered, an unusual decrease in the experimental barrier height and an increase in the ideality factor are observed. Notably, assuming a double Gaussian distribution of barrier heights at 310–190 K (distribution 1) and 190–130 K (distribution 2), the variations in barrier height and ideality factor are attributed to the spatial barrier inhomogeneities at the AlGaIn/GaN interface in the GaN nanowire WGTs. The standard deviation for distribution 2 is lower than that of distribution 1, which suggests that distribution 2 reflects more homogeneity at the AlGaIn/GaN interface in the transistor's source/drain regions than distribution 1.

5:00 PM EL04.08.10

Li-Doped NiO/Un-Doped NiO/ β -Ga₂O₃-Based p-i-n Diode for Power Device Application Jiyoung Min¹, Madani Labeled¹, Hyungseok Kim², Kyungwoo Choi³, Teakjib Choi¹ and You Seung Rim¹; ¹Sejong University, Korea (the Republic of); ²Korea Institute of Science and Technology, Korea (the Republic of); ³Sungkyunkwan University, Korea (the Republic of)

Recently, beta gallium oxide (β -Ga₂O₃, 4.7–4.9eV), which has a wide band gap than SiC and GaN, has been attracting attentions in the field of power electronic applications [1]. The Baliga's figure of merit(B-FOM) of Ga₂O₃ is about 3000, which is 4 times that of GaN and 10 times that of SiC, and is expected to achieving high breakdown voltage at low on-resistance in the power device [2]. However, despite these high numbers, the actual reported performance of the power unit is much lower than expected. This is because it is difficult to implement p-type Ga₂O₃, which can be used as PN junction termination to improve breakdown voltage value [3]. For further improvement of devices which require lower on-resistance(R_{on}) and higher breakdown voltage, it is important to form a junction termination structure such as a guard ring and a merged structure using a p-type material even to reduce the maximum electric field of a wide bandgap materials. However, the development of p-type β -Ga₂O₃ remains insufficient, only the theoretical studies and few experimental results reported. Because a very low mobility of self-trap holes and a deep acceptor level are expected, p-type β -Ga₂O₃ may intrinsically not be practical for power device applications. As a strategy to compensate for this is to construct p-n heterojunctions by integrating n-type Ga₂O₃ with other p-type semiconductors if the interface quality is controlled in an appropriate manner [4]. In this study, a diode to form a p-n heterojunction with optimized β -Ga₂O₃ was fabricated using NiO, a material with p-type conductivity [5]. Among p-type oxide families, the wide-bandgap NiO material has promising potentials in the applications of various optoelectronic and power devices due to its high visible spectral transparency and p-type conductivity stemming from nickel vacancies or monovalent impurities [6]. It was confirmed that the p-type NiO was inserted between the β -Ga₂O₃ and the Ni Schottky junction to ensure the p-n characteristics and thus the

depletion layer expanded. In addition, the conductivity control of nickel oxide was attempted by lithium doping and oxygen concentration regulation. As a result, lithium-doped nickel oxide exhibited improved ohmic contact properties with Ni due to the thin film's low specific resistance characteristics compared to undoped nickel oxide, which induced the diode's low on-resistance. Therefore, using these current characteristics, NiO was stacked in two layers to design a heterojunction diode with a Li-NiO/NiO/ β -Ga₂O₃ structure and a device that achieves a high breakdown voltage of -1678 V while maintaining a low on-resistance of 7.1 m Ω cm²

Acknowledgments This work was supported by Korea Institute for Advancement of Technology (KIAT) grant funded by the Ministry of Trade, Industry & Energy (MOTIE, Korea) (P0012451, The Competency Development Program for Industry Specialist), the Technology Innovation Program - (20016102, Development of 1.2kV Gallium oxide power semiconductor devices technology and RS-2022-00144027, Development of 1.2kV-class low-loss gallium oxide transistor) funded by MOTIE, and Hyundai Motor Group.

References [1] M. Higashiwaki and G. H. Jessen, Appl. Phys. Lett. 112, 060401 (2018) [2] S. J. Pearton, F. Ren, M. Tadjer, and J. Kim, J. Appl. Phys. 124, 220901 (2018) [3] N. Allen, M. Xiao, X. D. Yan, IEEE Electron Device Lett. 40, 1399 (2019) [4] Y. Kokubun, S. Kubo, and S. Nakagomi, Appl. Phys. Express 9, 091101 (2016) [5] H. H. Gong, Appl. Phys. Lett. 117, 022104 (2020) [6] M. Tyagi, M. Tomar, V. Gupta, IEEE Electron Device Lett. 34, 81 (2013)

5:00 PM EL04.08.11

Cone-shaped defects on AlGa_N quantum dots for electron-beam pumped UV-emitters Jesus Cañas¹, Névine Rochat², Adeline Grenier², Audrey Jannaud², Zineb Saghi², Jean-Luc Rouvière¹, Edith Bellet-Amalric¹, Anjali Harikumar¹, Catherine Bougerol³, Lorenzo Rigutti⁴ and Eva Monroy¹; ¹CEA IRIG, France; ²CEA LETI, France; ³CNRS Institut Néel, France; ⁴University of Rouen Normandie, France

One alternative to the challenges posed by AlGa_N LEDs is the use of electron-beam pumped lamps based on AlGa_N quantum dot (QD) superlattices (SLs). This approach offers the advantage of circumventing the challenging p-type doping and contacts of AlGa_N, while providing a large active region. Previous reports from our group demonstrated UVC-emitting AlGa_N QD-SLs grown by plasma-assisted molecular beam epitaxy with internal quantum efficiency in the range of 50% [1]. However, the samples still exhibit spatial inhomogeneities and relatively wide (between ~10 and ~20 nm) emission lines, sometimes with multi-peak structure. In this contribution, we delve into the origin of bimodal emission in AlGa_N/AlN QD superlattices in the 230-300 nm spectral range. The secondary emission at longer wavelengths is linked to the presence of cone-shaped defects originating at the AlN buffer/superlattice interface and propagating vertically. These defects are associated with a dislocation that produces strong shear strain, which favors the formation of 30° faceted pits. The cone-like structures present Ga enrichment at the boundary facets and larger QDs within the defect. The bimodality is attributed to the differing QD size/composition within the defects and at the defect boundaries, which is confirmed by the correlation of microscopy results and Schrödinger-Poisson calculations [2].

[1] J. Cañas et al., under review. arXiv:2305.15825 **2023**. <https://doi.org/10.48550/arXiv.2305.15825>

[2] J. Cañas et al., under review. arXiv:2310.04201 **2023**. <https://doi.org/10.48550/arXiv.2310.04201>

5:00 PM EL04.08.12

The self-compensation process and its dependence on Ga and In donor doping in ZnO nanocrystal films Georgiy Polupan, Brahim Ei Filali and Tetyana v. Torchyńska; Instituto Politecnico Nacional, Mexico

Zinc oxide has important optical, electrical, and microstructural characteristics, important for optoelectronic applications as transparent conduction oxide (TCO) in solar cells, gas sensors, flat screens and touch panel displays, light emitting diodes, or in thermal mirrors. The conductivity of pure ZnO films is not high enough to be used as TCO windows. The important donors for ZnO film technology are the Al, Ga, In elements. However, in doped ZnO films the electron density is limited by the self-compensating effect, connected with the generation of acceptor defects to counteract of high donor doping. The nature of acceptor defects and the factors that favor the initiation of the self-compensating process remain to be studied.

The reason for the self-compensating effect can be related to the significant level of elastic stresses in doped ZnO films with high donor concentrations. It is assumed that using co-doping by Ga and In atoms with lower (Ga) and higher (In) ionic radii compared to Zn ions is expected to reduce stresses in the films and allow changing the onset of the self-compensating effect at higher donor contents. In the work presented, the variation of the optical, structural and electrical parameters of ZnO nanocrystal (NC) films doped with Ga and In atoms has been investigated. ZnO films were grown by ultrasonic spray pyrolysis with a permanent In contents of 1.0 at% or 2.0 at% and Ga contents varied in the range of 0.5 to 3.5 at%. ZnO films have been studied using scanning electron microscopy (SEM), energy dispersive X ray spectroscopy (EDS), X ray diffraction (XRD), photoluminescence (PL) and X-ray photo electronic spectroscopy (XPS).

Non-monotonic changes in the morphology of the films were revealed that correlate with non-monotonic changes of the ZnO film parameters with the variation of Ga contents. It was shown that high donor doping is accompanied by the appearance of a new near band edge (NBE) emission band, related to carrier recombination in donor-acceptor pairs (DAPs), which is a "fingerprint" of a start of the self-compensating process. The compressive stresses arising due to single In doping prevent effective oxidation in the film crystallization. The elastic stresses were calculated in ZnO films with the wurtzite crystal lattice and preferential (002) orientation. Changes in the crystal lattice parameters are detected and the stress values in the films are estimated. Doping with Ga up to 1.5-2.0 at% makes it possible to compensate the compressive stresses in the films related to In atom doping that is favored to the ZnO oxidation and dissolution of the donors at thermal annealing. The minimum electrical resistivity in ZnO:In:Ga films about 6.0x10⁻⁴ Ω cm is detected. The nature of defects generated in the self-compensating process is discussed.

5:00 PM EL04.08.13

Steady-state and transient electron transport in the two-dimensional electron gas associated with boron nitride-based heterojunctions Alireza Azimi¹, Mohammadreza Azimi¹, Michael S. Shur², Walid A. Hadi³ and Stephen K. O'Leary¹; ¹University of British Columbia, Canada; ²Rensselaer Polytechnic Institute, United States; ³Florida State University Panama City, United States

Cubic boron nitride is the latest III-V nitride-based semiconductor to draw the attention of the electronic materials community. Noting that state-of-the-art electron devices are often achieved through the use of heterojunctions, we explore possible boron nitride-based heterojunction configurations. Noticing that in the locality of a heterojunction a two-dimensional electron gas typically forms, we examine how the presence of such a gas influences the performance of boron nitride heterojunction-based devices. An electron gas can both enhance the low field mobility and influence the electron drift velocity for higher applied electric field strengths. Using a self-consistent Schrödinger-Poisson equation solver, we determine the distribution of electrons within such a two-dimensional electron gas. A comparison will then be made with results acquired using the analytical approach of Ambacher *et al.* [1]; while Ambacher *et al.* [1] applied their analysis to the case of gallium nitride-based heterojunctions, the same concepts apply here. The impact of this two-dimensional electron gas on the steady-state and transient electron transport that occurs within this material will then be critically examined. The device implications will be explored.

[1] O. Ambacher, B. Foutz, J. Smart, J. R. Shealy, N. G. Weimann, K. Chu, M. Murphy, A. J. Sierakowski, W. J. Schaff, L. F. Eastman, R. Dimitrov, A.

Mitchell, and M. Stutzmann, *J. Appl. Phys.* **87**, 334 (2000).

5:00 PM EL04.08.14

The impact of threading dislocation lines on cubic boron nitride's low-field electron mobility John Chilleri¹, Alireza Azimi², Mohammadreza Azimi², Michael S. Shur³ and Stephen K. O'Leary²; ¹New Mexico Institute of Mining and Technology, United States; ²University of British Columbia, Canada; ³Rensselaer Polytechnic Institute, United States

Threading dislocation lines are present within boron nitride's cubic phase. Within the framework of a relaxation-time approximation based low-field electron drift mobility formalism, we incorporate the treatment of threading dislocation line related scattering into this analytical framework. How the presence of threading dislocation lines influences the low-field electron transport of this material will be examined. Threading dislocation lines are found to make a significant contribution to cubic boron nitride's low-field electron transport response. The device implications of these results are then examined. A new approach to characterizing the importance of the various scattering processes is introduced as a corollary to this analysis.

5:00 PM EL04.08.15

Microwave-plasma-assisted chemical vapor deposition of BN as gate dielectric for AlGaIn/GaN metal-insulator-semiconductor high electron mobility transistors Ziyi He¹, Dawei Wang¹, Dinusha Herath Mudiyansele¹, Bingcheng Da¹, Yuji Zhao² and Houqiang Fu¹; ¹Arizona State University, United States; ²Rice University, United States

AlGaIn/GaN high electron mobility transistors (HEMTs) are considered as next-generation devices for high power and high frequency applications due to the existence of a high mobility polarization-induced two-dimensional electron gas (2DEG) at the AlGaIn/GaN interface. Nevertheless, the performance of conventional Schottky-gate HEMTs has been limited by the high leakage current. As a result, metal-insulator-semiconductor high electron mobility transistors (MISHEMTs) with gate dielectrics serve an effective solution to suppress the leakage current of conventional Schottky-gate HEMTs with the improvement of device performance. Boron nitride (BN), with an ultra-wide bandgap of ~5.2 eV, dielectric constant of 3.8, high breakdown electric fields of 12 MV/cm, high chemical stability, and excellent thermal conductivity, is promising for high-power and high-temperature electronics.

The AlGaIn/GaN HEMT structure was grown by metalorganic chemical deposition (MOCVD) on Si substrates. The Al, Ga, and N sources are trimethylaluminum (TMAI), trimethylgallium (TMGa), and ammonia (NH₃), respectively. SiH₄ was used as an n-type dopant and H₂ was the carrier gas. The structure consists of a 2.5 nm GaN cap layer, followed by a 20 nm Al_{0.25}Ga_{0.75}N barrier layer, a 1 nm AlN interlayer, a 200 nm n-GaN layer, and a 2.7 μm unintentionally doped GaN buffer layer. A ~7 nm BN thin film layer was deposited as a gate dielectric on AlGaIn/GaN HEMTs. The boron nitride film deposition was performed by microwave-plasma-assisted chemical vapor deposition using ammonia borane as the precursor. The growth temperature was 400 °C and the pressure was around 1 Torr. The MISHEMT devices are with gate width (W_G) = 100 μm, gate length (L_G) = 5 μm, gate-to-source distance (L_{GS}) = 4 μm, and gate-to-drain distance (L_{GD}) = 4 μm. The conventional Schottky-barrier-gate HEMTs were also fabricated with the same dimensions for reference. The XPS and UPS confirmed the existence of the BN film and the band alignment of BN/GaN. The transfer characteristics of BN MISHEMTs and HEMT when V_{DS} = 1 V. The MISHEMTs showed a threshold voltage of -5.9 V with a slight reduction of the maximum transconductance (g_{mmax} = 42 mS/mm) as compared with those for the HEMT (V_T = -3.2 V and g_{mmax} = 58 mS/mm, which are attributed to the insertion of BN thin film and the interface charge introduced. The MISHEMT devices exhibit a subthreshold swing of 363.8 mV/dec and a much higher I_{on}/I_{off} ratio (on the order of 10⁸) than the HEMT. The effective interface state density D_{it} can be estimated by the subthreshold swing equation to be over 1 × 10¹³ cm⁻² × eV⁻¹. The gate leakage-gate voltage (I_G-V_G) curve for the HEMT and BN MISHEMT were measured as shown, while the drain voltage and source voltage are set as 0 V. A very low gate leakage current of ~10⁻⁷ mA/mm at reverse bias was observed for MISHEMT, which is 3 orders of magnitude lower than the HEMT. The temperature dispersion from 25 °C to 205 °C of the leakage current is also analyzed. These results can serve as important references for future studies on BN-based gate dielectrics for GaN power devices.

5:00 PM EL04.08.16

Development of Ga₂O₃-based bipolar heterostructures for application of high-power electrical devices Kwangeun Kim; Korea Aerospace University, Korea (the Republic of)

Objective

The objective of this work is to develop Ga₂O₃-based bipolar heterostructures for application of high-power electrical devices. The npn Si/Si/Ga₂O₃ heterostructure was constructed through the membrane transfer method, in which the p- and n-Si membranes were sequentially transferred on the n-Ga₂O₃ substrate to form the Ga₂O₃-collector bipolar junction transistors with high-power density.

Results and discussion

β-Ga₂O₃ is a representative wide bandgap material for high-power electrical applications with the large bandgap energy and high breakdown field. The npn Si/Si/β-Ga₂O₃ heterostructures were achieved by the junction-bonding method and the electrical characteristics of back-to-back diodes were demonstrated for the development of bipolar transistors. The junction-bonded n-Si/p-Si and p-Si/n-Ga₂O₃ diodes exhibited the rectifying properties with the ideality factors under 1.4. The Ga₂O₃-collector bipolar transistors were manufactured with different thickness of p-Si base layers to improve the bipolar operation properties with high power density, gain, and cut-off frequency. The results on the formation of npn high-power heterostructures with wide bandgap materials can be applicable to the development of high-power heterojunction bipolar transistors and insulated-gate bipolar transistors.

Experimental

Sn-doped Ga₂O₃ single crystal substrate with a doping concentration of 1.7 × 10¹⁸ cm⁻³ was grown by metal-organic vapor phase epitaxy. The surface roughness of as-grown β-Ga₂O₃ was around 1 nm. The single crystal Si membranes were obtained from the top layers of highly-doped silicon-on-insulator wafers. The removal of sacrificial layer was carried out by dipping the wafers into HF solution, then the undercut Si membranes were picked up using elastomeric stamp and laminated onto the Ga₂O₃ substrate, leading to the formation of npn bipolar structures. The device fabrication was performed through semiconductor cleanroom process and the electrical characteristics were measured using semiconductor parameter analyzer.

5:00 PM EL04.08.17

On the Possibility of p-Type Doping in BaSnO₃ Joe Willis¹, Kieran B. Spooner² and David O. Scanlon²; ¹University College London, United Kingdom; ²University of Birmingham, United Kingdom

The discovery of a p-type transparent conductor would revolutionise optoelectronic devices by enabling fully transparent p-n junctions. Of particular interest are fully transparent homojunctions, which would greatly simplify the manufacturing process and potentially aid device performance. Recent work¹ has produced transparent p-n junctions from BaSnO₃, but the p-type behaviour of the compound has thus far been overlooked in the literature.

Here we seek to understand the defect and transport behaviour of p-type BaSnO₃ using hybrid density functional theory (DFT).² Group 1 metals Li, Na and K and group 13 metals Al, Ga and In are assessed as extrinsic p-type dopants on the Ba and Sn sites, respectively. We find that K and In are the most promising dopants, reaching concentrations of up to 4.7 × 10¹⁶ cm⁻³ and 1.6 × 10¹⁹ cm⁻³ respectively. Both, however, are compensated by low energy O vacancies, limiting the hole carrier concentrations to 5.2 × 10¹⁴ cm⁻³ and 9.8 × 10¹⁵ cm⁻³ respectively. Such high defect concentrations also severely limit the

electronic transport, with room temperature mobilities of $5.96 \text{ cm}^2 \text{ V}^{-1} \text{ s}^{-1}$ and $1.27 \text{ cm}^2 \text{ V}^{-1} \text{ s}^{-1}$ respectively. While this does not reach the levels seen in n-type transparent conductors, it does guide the way towards the higher doping concentrations than have so far been achieved experimentally.

[1] Kim, H. M. *et al.*, *APL Mater.*, 2016, **4**, 056105.

[2] Willis, J. *et al.*, *Appl. Phys. Lett.*, 2023, *accepted*.

5:00 PM EL04.08.18

Fabrication of broadband UV MSM photodetector using reactive sputtered nickel oxide film Swati Suman¹, Anupama Behera¹, Ashok Allamula², Satyesh Kumar Yadav² and Parasuraman Swaminathan^{1,3}; ¹Indian Institute of Technology Madras, India; ²Indian Institute of Technology, India; ³Indian Institute of Technology Bombay, India

Efficient ultraviolet (UV) photodetectors are of significant interest due to their wide area of applications, such as bio-sensing, communications, and military applications¹⁻³. In this work, a metal oxide semiconductor sandwiched between metal electrodes (MSM structure) was developed as a broadband UV photodetector. The MSM photodetectors has garnered lot of interest because of its simple fabrication design, large active area, low dark current facilitating fast response. The metal oxide used was *p*-type nickel oxide (NiO) deposited by DC magnetron sputtering technique on top of indium tin oxide (ITO). Reactive sputtering from a pure nickel target was used to deposit NiO and the effect of oxygen concentration on the morphological and optoelectronic properties of the NiO was investigated.

ITO is capable of providing good electrical conductivity and charge transporting behaviour which supports low leakage current⁴. It is a n-type degenerate semiconductor which is widely used for transparent conducting films. Among different metal oxides, NiO is a promising *p*-type semiconductor with wide band gap value (3.2 to 3.8 eV, depending on stoichiometry)⁵. In this study, we explore the fabrication and characterization of a UV photodetector using ITO and NiO heterojunction. The device performance will be optimized by varying oxygen concentration during deposition of NiO. The variation of oxygen will be done by keeping argon concentration constant. The DC magnetron sputtered NiO thin film, acts as the photosensitive layer. Silver electrodes were used as contacts for the two layers. Material characterization has been done using different techniques like XRD, SEM, UV-vis spectroscopy, Raman spectroscopy and photoluminescence spectroscopy while electrical characterization has been performed using I-V source meter and four probe. The fabricated device demonstrates good change in light to dark current at low applied biased voltage.

In conclusion, the development of UV photodetectors using DC magnetron sputtered *p*-type NiO thin films represents an encouraging route in the realm of optoelectronics. The tunability of NiO film properties at the interface with the ITO substrate provide further leverage for advancements in photon sensing.

1. Razeghi, M.; Rogalski, Journal of Applied Physics. Semiconductor ultraviolet detectors. **1996**, *79* (10), 7433-7473.

2. Yu A Goldberg, Semicond. Sci. Technol. Semiconductor near-ultraviolet photoelectronics. **1999**, *14* (7), R41.

3. Ohta, H.; Hosono, H. J. M. T., Materials Today. Transparent oxide optoelectronics. **2004**, *7* (6), 42-51.

4. Kim, H.; Lee, G.-N.; Kim, Journal of Nanomaterials. Hybrid structures of ITO-nanowire-embedded ITO film for the enhanced Si photodetectors. **2018**, *34*(12), 2625-2629.

5. Hakim, A.; Hossain, J.; Khan, K. J. R. E., Renewable Energy. Temperature effect on the electrical properties of undoped NiO thin films. **2009**, *34* (12), 2625-2629.

5:00 PM EL04.08.19

High breakdown voltage, low specific on-resistance GaN on GaN PiN diodes with low contact resistance on p-type GaN for high power applications Donghan Kim^{1,2}, Hyung-seok Lee², Hongsik Park¹, Sung-Beum Bae², Dong-young Kim² and Zin-Sig Kim²; ¹Kyungpook National University, Korea (the Republic of); ²Electronics and Telecommunications Research Institute, Korea (the Republic of)

In the last few years, wide band gap(WBG) semiconductors such as SiC, Ga₂O₃ and GaN have received considerable attention for the next-generation power electronics and RF devices. Especially GaN is promising material candidates for high power and high current applications due to its superior material properties like wide bandgap(~3.4 eV), high critical electric field(~3.5 MV/cm), high electron saturation velocities and low switching losses. For power applications, GaN-based transistors such as GaN-on-Si HEMTs have been widely used commercially since 2009. However, for mid- and high-range power applications(>~1.2 kV), it is difficult to handle power electronics with GaN-on-Si HEMTs. To handle high voltage for efficient high power applications, the chip size of GaN HEMT increases significantly, resulting in difficulty of current extraction and poor reliability. Moreover, the difficulty of growing thicker high quality GaN or AlGaN layers on a Si substrate leads to a vertical buffer breakdown which also limits the operating voltage of HEMTs below a few kV. Therefore, in this point of view, GaN-based vertical power device such as PiN diode, vertical MOSFET, CAVET attracted increasing attention due to its high breakdown voltage(>~1.2 kV) by increasing drift region thickness, while remaining the device footprint. Additionally, uniform electric field and current distribution give a superior thermal performance and increasing reliability compared to lateral GaN HEMTs. For these GaN-based vertical power devices, which include highly doped p-type GaN, the formation of ohmic contact on p-type GaN with low specific contact resistance(ρ_c) is essential in order to minimize the device specific on-resistance($R_{on,sp}$) and power losses. However, formation of ohmic contact with low specific contact resistance on p-type GaN is still challenging due to p-type GaN's wide bandgap(~6.6 eV) which leads to a high schottky barrier height at the interface of metal/p-type GaN interface. Moreover, because of the high ionization energy of the dopants(150 ~ 200 meV in the case of Mg in GaN), the activation ratio for acceptors in p-type GaN is typically below to 5%, resulting in low net hole concentrations and hole mobility.

Here, we report the formation of ohmic contact on p-type GaN with low specific contact resistance using a tri-layer Pd/Ni/Au thin films. Our work shows that specific contact resistance can be significantly reduced using Pd/Ni/Au tri-layer with suitable rapid thermal process. The role of process parameters such as temperature, time and annealing ambient were carefully studied to obtain ohmic contact on p-type GaN. We demonstrate low-specific contact resistance of Pd/Ni/Au on p-type GaN can be reached to the lowest value of $1 \times 10^{-5} \Omega \times \text{cm}^2$ by annealed at 600 °C in air condition(N₂ + O₂) for 5 min. The mechanisms of ohmic contact formation on p-type GaN were analyzed by microstructural analysis with X-ray photoelectron spectroscopy(XPS), transmission electron microscopy(TEM), and secondary ion mass spectrometry(SIMS). Additionally, We fabricated GaN-on-GaN PiN diode with Pd-based tri-layer thin films(Pd/Ni/Au) for anode in diode. This GaN-on-GaN PiN diode with Pd-based ohmic contacts on p-type GaN diode shows 30 times higher forward current compared with Ni/Au based ohmic contacts while achieving low specific on-resistance with high breakdown voltage. Therefore, low specific on-resistance($R_{on,sp}$) of 0.5 m $\Omega \times \text{cm}^2$ and breakdown voltage of 1.9 kV, corresponding to Baliga's figure of merit(BFOM) of 7.22 GW/cm², are demonstrated experimentally. Our research indicates that the formation of ohmic contact with low contact resistance on p-type GaN in vertical GaN power diode leads to high value of Baliga's figure of merit device which is suitable for next-generation high power applications

5:00 PM EL04.08.20

Optimization of growth rate and morphology of a SiC wafer by physical vapor transport method in the aids of finite element numerical simulation TsungYu Huang and Xiao Kai Lin; ming chi university of technology, Taiwan

The rapid advancement of compound semiconductors in recent years has generated considerable interest in silicon carbide, and it has steadily gained attention in the market due to its wide bandgap, high power capabilities, exceptional thermal conductivity, and a remarkable electron saturation velocity. The growing adoption of silicon carbide as the primary material for field-effect transistors by major companies has further bolstered its popularity. In terms

of silicon carbide wafer fabrication, the predominant method utilized is the physical vapor transport (PVT) process.

In the PVT process, high-purity silicon carbide powder is placed in a graphite crucible within a crystal growth furnace. The furnace employs induction coils to heat the silicon carbide powder, raising its temperature to over 2000 °C for sublimation. A single crystal seed is strategically positioned above the powder to ensure the growth of single-crystal silicon carbide. However, the PVT method faces limitations, notably the inability to monitor internal conditions during the crystal growth process. This is due to the requirement of maintaining high temperatures and a vacuum environment. As the demand for larger wafer sizes continues to rise, the internal thermal distribution within the crystal growth furnace becomes uneven. This non-uniformity results in variations in wafer curvature between the center and edges, making subsequent processing challenging.

To address these issues, our objective is to employ the finite element method to construct a comprehensive model of the crystal growth furnace. This model includes various components such as a water-cooled copper heating coil, a stainless-steel furnace cover, an argon gas atmosphere zone, a graphite lining, a graphite crucible, quartz supports, and the crystal seed. In our simulation, we couple multiple physical processes, including electromagnetic induction, heat conduction, convection, fluid distribution, mass transfer, crystal growth thermodynamics, dislocation density growth, and feedback systems to replicate the intricate crystal growth process. Our goal is to optimize the internal thermal distribution within the furnace by exploring alterations to the crucible structure and the morphology of the source materials. The primary aim is to achieve radial uniformity in the thermal field, which will result in even heating of the center and edges of wafers, effectively reducing curvature discrepancies. Furthermore, we seek to attain larger axial temperature gradients to enhance the crystal growth rate significantly.

5:00 PM EL04.08.21

Synthesis and Characterization of Single Photon Emitters from Chemically Exfoliated Hexagonal Boron Nitride Nanosheets [Edgar Dimitrov](#), George Bepete, Gothamie Ratnayake, Sahin Ozdemir and Mauricio Terrones; The Pennsylvania State University, United States

Single-photon emitters are an essential component in the emerging applications of quantum communication, quantum computing, and integrated quantum photonics. Hexagonal boron nitride (hBN) is of particular interest as a material with a wide bandgap, which allows it to host a wide range of visible to UV emitters and retain stability at room temperature. These emitters arise from spatially isolated defects which introduce mid-gap states which can be excited to act as emitting color centers. In this work, we investigate the properties of single photon emitters in hBN nanosheets, which have been generated by using commercially available hBN powders and intercalating them with molten potassium. Following alkali metal intercalation, hBN was chemically exfoliated in solution and then drop casted onto any substrate. This process introduces a variety of defects embedded in the hBN, in particular, an excess of nitrogen vacancies which has been shown by X-ray photoelectron spectroscopy (XPS). We have found that this system can host bright single photon emitters which are active at room temperature and are stable for months in atmosphere without bleaching or blinking. Through a Hanbury-Brown Twiss Interferometer we have characterized multiple emitters in the range of 570-650 nm with values $g_2(0) < 0.15$ without background subtraction, indicating high quality emitters. These findings help to provide insights into the importance of defects in hBN that are responsible for single photon emission, thus opening the possibility for tailoring these defects through chemical functionalization.

SESSION EL04.09: Gallium Oxide I

Session Chairs: Sriram Krishnamoorthy and Joel Varley

Thursday Morning, April 25, 2024

Room 345, Level 3, Summit

8:15 AM EL04.09.01

Investigation of Temperature-dependent Hysteresis and Interface Trap Density in E-Beam Evaporated NiO_x/β-Ga₂O₃ p-n Diodes [Bingcheng Da](#), Dinusha Herath Mudiyansele, Dawei Wang, Ziyi He and Houqiang Fu; Arizona State University, United States

β-Ga₂O₃, an ultra-wide bandgap (UWBG) material with a bandgap of 4.9 eV and a high breakdown field of ~8 MV/cm, holds promise for power, optical, and RF electronics. However, due to the absence of p-type Ga₂O₃, most demonstrated devices have been unipolar. This limitation is attributed to the lack of shallow acceptors and the presence of holes trapped in localized polarons. To address this, p-NiO_x has been utilized to create p-n heterojunctions with β-Ga₂O₃, resulting in devices such as p-n diodes and junction barrier Schottky (JBS) diodes. While these devices exhibit desirable properties, they also exhibit charge trapping, hysteresis in forward and reverse bias, and induced interface states at the heterojunction. This study aims to comprehensively investigate the temperature-dependent hysteresis and interface trap density in NiO_x/β-Ga₂O₃ p-n diodes on (-201) Ga₂O₃ crystal orientations.

The edge-defined film-fed grown β-Ga₂O₃ substrates were sourced from Novel Crystal Technology, Inc. (Japan) and had a n-type doping concentration of [Sn] = 5 × 10¹⁸ cm⁻³, with uniform thickness and polished front sides. Prior to device fabrication, substrate cleaning involved sequential treatments with acetone, isopropyl alcohol (IPA), and deionized (DI) water. Subsequently, electron beam (E-beam) evaporation was used to deposit Ti/Au (20/130 nm) back contacts, followed by rapid thermal annealing at 500 °C in an N₂ environment. Photolithography was employed to define circular areas of 300 μm in diameter for NiO_x and anode material deposition (Ni/Au, 20/130 nm). Layers of NiO_x (200 nm) were deposited using e-beam evaporation, and a liftoff process was executed to isolate individual devices. Post-fabrication, devices underwent annealing at 350 °C in an N₂ atmosphere for 1 minute to improve performance by reducing the number of interface states at the NiO_x/β-Ga₂O₃ heterojunction.

Preliminary findings indicate hysteresis during forward and reverse bias, but none in C-V measurements. With increasing temperature, forward bias hysteresis decreases, while reverse bias hysteresis remains constant. The experiment covers a voltage range of +3 V to -10 V. Concurrently, capacitance-frequency measurements were conducted to evaluate trap density, which varied between 5 × 10¹¹ and 2 × 10¹¹ eV⁻¹cm⁻² as the temperature ranged from room temperature to 395 K. These results suggest that temperature-dependent interface trap states contribute to the observed hysteresis in the devices. Future investigations will extend to NiO_x/β-Ga₂O₃ devices on (010) crystal orientation. Previous studies have indicated distinct electronic properties between (-201) and (010) devices due to crystal anisotropy. This study will provide valuable insights into transport properties of NiO_x/β-Ga₂O₃ p-n diodes and pave the path for device optimization by reducing interface trap states.

8:30 AM *EL04.09.02

What Is In Store for Gallium Oxide Power Devices in the Next Decade? [Man Hoi Wong](#); Hong Kong University of Science and Technology, Hong Kong

Ultrawide-bandgap semiconductors have attracted increasing interests to expand the application space for next-generation power electronics. These research efforts have been driven in large part by a need for new medium/high-voltage power devices that meet stringent requirements for system size and cost in emerging areas such as electrified transportation, motor-drive systems, and renewable energy integration with the grid. Materials with shallow hydrogenic dopants show the best projected performance for power switching. Realizing high material purity with low background compensation will enable low doping concentrations to fully exploit the intrinsic material properties. Due to the availability of shallow donors and low background impurity

compensation enabling rapid device prototyping, beta-phase gallium oxide (β -Ga₂O₃) has emerged as a relevant contender for power devices and has repeatedly pushed the boundaries of high-field performance. In addition, β -Ga₂O₃ is the only (ultra)wide-bandgap material that has a melt-grown native substrate, indicating a path to a commercially viable and cost-competitive technology.

As one of the most widely studied ultrawide-bandgap semiconductors today, β -Ga₂O₃ has attracted international attention across disciplines. Thanks to the success of high-purity homoepitaxial growths on bulk substrates, a broad portfolio of β -Ga₂O₃ devices has demonstrated favorable attributes to be the next frontier technology in power conversion, integrated high-voltage RF, and high-temperature electronics. Various strategies of field management, including edge termination techniques and multi-dimensional device architectures, have been devised to effectively harness the high critical electric field afforded by β -Ga₂O₃. Heterojunctions with β -(Al_xGa_{1-x})₂O₃ and *p*-type oxides (notably NiO) have created an abundance of new design possibilities. Additionally, reports of high-performance packaging, device robustness, and converter applications all consolidate the promise of β -Ga₂O₃ for power electronics. While β -Ga₂O₃ devices are noted for their high-temperature resilience, heat dissipation to limit the junction temperature and improve the component reliability will be critical for maximizing their performance and long-term reliability.

After the first report of a single-crystal β -Ga₂O₃ power device by Higashiwaki and co-workers in 2012, β -Ga₂O₃ has showcased technical and programmatic momentum not seen in decades since the rise of SiC and GaN research. Following a survey of the landmarks in β -Ga₂O₃ research including device engineering, process innovations, and theoretical understandings of relevant physics, I will reflect on the demonstrated benefits as well as unrealized potentials of the emerging β -Ga₂O₃ technology, then conclude with my projections of the future directions and opportunities for β -Ga₂O₃ in the coming decade.

9:00 AM EL04.09.03

MBE Growth and Properties of Monoclinic (Al_xGa_{1-x-y}In_y)₂O₃ Alloys Stephen T. Schaefer, Kingsley Egbo, Glenn Teeter, Syed Hasan, Andriy Zakutayev and Marshall B. Tellekamp; National Renewable Energy Laboratory, United States

Gallium oxide (Ga₂O₃) is an emerging ultra-wide bandgap semiconductor material that has attracted attention for its potential to outperform existing SiC and GaN based devices operating at high breakdown voltages and high temperature. The thermodynamically stable phase at room temperature and pressure is the monoclinic β -phase with symmetry *C2/m*. β -Ga₂O₃ has a direct bandgap energy of 4.76 eV and critical field as high as 8 MV/cm. Isovalent alloying of In and Al in β -Ga₂O₃ provides the ability to engineer bandgap energy and strain of the material, however the monoclinic structure is not the ground state for Al₂O₃ or In₂O₃. First-principles calculations indicate a range of bandgap energies from 7.2-7.5 eV for monoclinic θ -Al₂O₃ to 2.7 eV for monoclinic In₂O₃. The corresponding lattice mismatch to β -Ga₂O₃ ranges from about 4% for θ -Al₂O₃ to 10% for monoclinic In₂O₃. In principle the quaternary (Al_xGa_{1-x-y}In_y)₂O₃ can span this bandgap energy and strain range, providing device designers with additional degrees of freedom to tune band offsets and electronic properties.

However, efforts to synthesize isovalent alloys are complicated by their tendency to phase separate. Strain balanced alloys of (Al_xGa_{1-x})₂O₃ and (In_xGa_{1-x})₂O₃ may be able to overcome the tendency for phase separation and stabilize the monoclinic crystal, however literature reports of the quaternary (Al_xGa_{1-x-y}In_y)₂O₃ are limited to <1% unintentional indium incorporation in In-catalyzed (Al_xGa_{1-x})₂O₃.¹ The primary limitation to quaternary formation is the limited incorporation of indium at elevated growth temperatures. This limited incorporation is due to both the volatility of indium oxide and Al and Ga cation exchange reactions which replace indium in In₂O₃.²

We report on the first successful synthesis of phase pure monoclinic (Al_xGa_{1-x-y}In_y)₂O₃ by molecular beam epitaxy. Plasma-assisted molecular beam epitaxy (MBE) is used to grow (Al_xGa_{1-x-y}In_y)₂O₃ on (110) oriented Fe doped β -Ga₂O₃ substrates at 750 °C and Ga and In beam equivalent pressures (BEP) of 5×10⁻⁸ and 2×10⁻⁷ torr, respectively. The Al BEP varies from 1×10⁻⁹ to 1.5×10⁻⁸ torr. X-ray diffraction measurements of the (020) plane indicate a strained film consistent with the structural incorporation of both Al and In, and this incorporation is chemically corroborated by x-ray fluorescence (XRF) and X-ray photoemission spectroscopy (XPS). Wide-angle ω -2 θ survey scans confirm the absence of additional XRD peaks, indicating the films are monoclinic with no phase separation. Spectroscopic ellipsometry measurements show a monotonic shift in the extinction coefficient edge from approximately 4.7 to 5.2 eV with increasing Al BEP. Additional structural, chemical, optical, and electrical characterization measurements including Rutherford back-scattering spectrometry, scanning tunneling microscopy will be presented, concluding with an outlook on the applicability of these quaternary films to gallium oxide device design.

[1] P. Vogt, A. Mauze, F. Wu, B. Bonaf, and J. S. Speck, "Metal-oxide catalyzed epitaxy (MOCATAXY): the example of the O plasma-assisted molecular beam epitaxy of β -(Al_xGa_{1-x})₂O₃/ β -Ga₂O₃ heterostructures", *Appl. Phys. Express* **11**, 115503 (2018).

[2] P. Vogt, O. Brandt, H. Riechert, J. Lähnemann, and O. Bierwagen, "Metal-Exchange Catalysis in the Growth of Sesquioxides: Towards Heterostructures of Transparent Oxide Semiconductors", *Phys. Rev. Lett.* **119**, 196001 (2017).

9:15 AM *EL04.09.04

Dielectric Integration and interface defect engineering for β -Ga₂O₃ MOS devices Ahmad E. Islam¹, Ashok Dheenan², Weisong Wang³, Kevin Leedy¹, Kyle Liddy¹, Daniel Dryden¹, Guru Subramanyam⁴, Aaron Arehart², Siddharth Rajan², Kelson Chabak¹ and Andrew Green¹; ¹Air Force Research Laboratory, United States; ²The Ohio State University, United States; ³Wright State University, United States; ⁴University of Dayton, United States

Dielectric integration is always challenging for any semiconductor material when used in a metal-oxide-semiconductor (MOS) configuration. SiO₂ offers the best oxide interface on Si, mainly because the SiO₂/Si interface was carefully engineered by the pioneering works of Atalla et al. Interfacial defect engineering is currently being investigated for wide-bandgap semiconductor such as SiC. Such defect engineering solutions are, however, missing for other oxide/semiconductor interfaces involving wide or ultra-wide bandgap semiconducting materials.

The newest semiconductor β -Ga₂O₃ can be grown from melt, has a high critical electric field, a low switching loss that can be obtained at a high breakdown voltage, and an efficient high frequency performance. β -Ga₂O₃ has therefore already demonstrated promises for power switching applications with drive current > 100A and high temperature electronics with operating temperature *T* > 500 °C. The dielectric/semiconductor interface of β -Ga₂O₃ however has large interface defect density (N_{IT}) mainly due to the deposition of dielectrics after many process steps in a device fabrication process. A dielectric-early process flow is preferred for reducing N_{IT}; to enable this process, dielectrics will have to withstand all the remaining semiconductor process steps, some of which (such as dopant activation anneal) involves >900 °C process temperature. Such high *T* processes induce poly-crystallization (resulting in electrical and mass transport through the grain boundaries) in most dielectrics formed using atomic layer deposition (ALD) – a deposition process that is routinely used for all semiconductor device processes.

Till 2020, most of the MOS devices made on β -Ga₂O₃ substrates exhibited N_{IT} > 10¹² cm⁻² and, therefore, devices exhibited large hysteresis and frequency dispersion during the capacitance-voltage (C-V) and current-voltage (I-V) characteristics. Using conventional crystalline semiconductor wisdom, crystallization of dielectrics via high *T* annealing were considered for defect reduction (and hence hysteresis and dispersion reduction); this however had limited success as the resultant poly-crystalline suffered from grain boundary conduction and materials diffusion. Therefore, dielectrics with low N_{IT} and

good thermal stability still remained elusive for establishing electronic-grade semiconductor process flow for β -Ga₂O₃ devices.

In this work, we will highlight the general challenge for integrating dielectrics on β -Ga₂O₃, address the associated requirements for obtaining high-quality dielectric with low N_{IT} , and in particular discuss the integration of Al₂O₃ and SiO₂ dielectrics on (010) β -Ga₂O₃ substrates. We will discuss the role of surface roughness, surface cleanliness (using piranha treatment), surface defective layer removal (using buffered HF), and post-deposition annealing on interface defect density. We will also compare the thermal stability and interface quality of SiO₂ and Al₂O₃ dielectrics formed on β -Ga₂O₃. We will explain how interfacial crystallization of monolayer Al₂O₃ (during a low temp ALD deposition at 250 °C) enabled formation of high-quality interfaces at the Al₂O₃/ β -Ga₂O₃ interface – therefore, showed the lowest interface defect density. This is mainly because the crystal structures of γ -Al₂O₃ and β -Ga₂O₃ resembles each other and hence promotes the formation of monolayer γ -Al₂O₃ at the Al₂O₃/ β -Ga₂O₃ interface even at 250 °C deposition temperature. All these considerations have enabled us to envision pathways towards electronic-grade integration of dielectrics on β -Ga₂O₃ substrates needed to attain high breakdown voltage in power electronics applications and also to attain low frequency dispersion and high operating frequency in radio frequency applications.

9:45 AM BREAK

10:15 AM +EL04.09.05

Defects and doping in (Al,Ga)N and β -(Al,Ga)₂O₃ alloys Filip Tuomisto; University of Helsinki, Finland

Si is the n-type dopant of choice for GaN and β -Ga₂O₃. However, in (Al,Ga)N and β -(Al,Ga)₂O₃ alloys, when the Al content is increased, the the n-type conductivity produced by the added Si impurities is efficiently compensated. The critical Al fractions are about 70% for the (Al,Ga)N alloys and as low as 30% for the β -(Al,Ga)₂O₃ alloys. AlN and Al₂O₃ are well known to be poorly n-type dopable even with Si, but the detailed compensation mechanisms in the alloys are not necessarily the same as in the compounds.

Positron annihilation spectroscopy is a useful method for studying neutral and negatively charged vacancy-type defects, as well as negatively charged defects with no open volume such as acceptor impurities [1]. I will discuss the most recent results obtained in Si-doped (Al,Ga)N and β -(Al,Ga)₂O₃ alloys in the light of the compensation phenomena caused by cation vacancies, carbon impurities and Si DX center formation. The local environment of the Si dopants appears to have a strong impact on the doping efficiency.

[1] F. Tuomisto and I. Makkonen, Rev. Mod. Phys. 85, 1583 (2013).

10:45 AM *EL04.09.06

First-principles calculations on point defects and doping in (Al,Ga)₂O₃ ultrawide-band gap semiconductors Joel B. Varley; Lawrence Livermore National Laboratory, United States

Semiconductor devices utilizing ever-wider band gap materials have the promise of more compact and efficient energy conversion that can help accelerate the transformation to an energy infrastructure based primarily on renewable resources. Gallium oxide and related alloys are rapidly developing as promising material platforms for next-generation power electronics owing to their large, tunable band gaps, controllable electrical conductivity, and commercially-available single-crystal substrates that can be grown via a number of industrially-scalable processes. Analogous to the AlGaN system, the incorporation of Al into Ga₂O₃ to form (Al_xGa_{1-x})₂O₃ (AGO) alloys can lead to a significant increase of the band gap, but spanning a much larger range of ~4.8 eV-8.6 eV. AGO also exhibits the possibility of different crystal structures and lattice constants, leading to a number of possible epitaxial relationships beyond the wurtzite AlGaN system. Despite this promise, a number of questions remain as to the effectiveness of donor doping and how to overcome the possibility of compensation in the limit high Al-contents, similar to that in AlGaN. Here we assess n-type doping of Ga₂O₃ and consider the prospects of doping in the larger-gap Al-containing alloys using first-principles modelling approaches based on hybrid functional calculations. We consider a number of conventional dopants such as Si, Ge and Sn, as well as lesser-explored transition-metal donor dopants that have been identified as effective alternatives. We additionally consider the role of native cation vacancies, which are known to be potentially problematic sources of compensation. Our results identify composition regimes in AGO alloys that may be most effectively targeted for increased band gaps and effective donor doping, with composition regimes specific to particular dopant species. These results provide guidance for doping in Ga₂O₃ and related alloys incorporated into heterostructure devices. This work was performed under the auspices of the U.S. Department of Energy by Lawrence Livermore National Laboratory under Contract DE-AC52-07NA27344 and supported by the LLNL Laboratory Directed Research and Development funding under project number 22-SI-003 and the Critical Materials Institute, an Energy Innovation Hub funded by the U.S. DOE, Office of Energy Efficiency and Renewable Energy, Advanced Materials and Manufacturing Office.

11:15 AM EL04.09.07

Quantitative Modelling of Defect Concentrations in β -Ga₂O₃ for Equilibrium, Full Quenching, and Generalized Quenching Scenarios Khandakar Aaditta Arnab¹, Isaac Maxfield¹, Chenyung Lee², Elif Ertekin², Joel B. Varley³, Ymir K. Frodason⁴ and Michael Scarpulla¹; ¹University of Utah, United States; ²University of Illinois at Urbana-Champaign, United States; ³Lawrence Livermore National Laboratory, United States; ⁴Centre for materials Science and Nanotechnology Physics, Norway

β -gallium oxide (β -Ga₂O₃) is of intense current interest because of its ultra-wide bandgap, high critical field, and availability of melt-grown substrates. Point defects and complexes determine the properties of bulk crystals as well as epitaxial layers, thus, predictive models of defect concentrations under various impurity and processing scenarios are of very high value. First-principle calculations of defect energetics have provided critical insights into the defect system in β -Ga₂O₃, but translating computed enthalpies into defect concentrations corresponding to real-world crystal growth requires additional steps. Material processing in terms of growth or annealing typically controls the sample's thermochemical trajectory in terms of temperatures and partial pressures, while computational papers frequently present results holding chemical potentials constant.

Here we report quantitative modelling of equilibrium defect concentrations in Ga₂O₃, considering especially the temperature dependence of the bandgap and temperature-dependent chemical potentials from the Ga-O binary system's known thermochemistry. Additionally, we compute results for realistic sample types such as Fe- or Sn-doped wafers accounting for the fixed concentrations of these impurities as opposed to their fixed chemical potentials. Results are presented for various background n-type doping and for equilibrium and quenching, corresponding respectively to 0 or infinite cooling rates. We find significant departures from prior simpler predictions, especially in the case of the bandgap temperature dependence which tends to suppress V_{Ga} . We compare our predicted results to experimental cases such as annealing in O₂ or Ga₂O vapors.

Finally, to give semi-quantitative insight into defect concentrations expected in finite-sized samples subjected to finite cooling rates without full-fledged defect reaction-diffusion simulations, we introduce the concept of generalized quenching as a 3rd type of computation. At the heart of generalized quenching is the insight that, because of their different diffusion constants, different types of defects located at different distances from free surfaces will be "frozen-in" at different temperatures. By combining the correct series of equilibrium and quenching calculations, it is possible to predict defect concentrations present in real-world samples e.g. as a function of radius within a boule or for thin films of different thicknesses. We compare these results to the known phenomena from bulk crystal growth, indicating differences in carrier density between the center and periphery of CZ-grown boules.

11:30 AM *EL04.09.08

Lateral and Vertical β -Ga₂O₃ Transistors for Next-Generation Power Applications Kornelius Tetzner, Zbigniew Galazka, Andreas Popp, Joachim Würfl and Oliver Hilt; Ferdinand-Braun-Institut, Germany

The semiconductor β -Ga₂O₃, distinguished by its ultra-wide bandgap of approximately 4.8 eV, has gained substantial attention in recent years within the context of advancing the next generation of power electronic devices. The assessed high breakdown strength of 8 MV/cm and the resultant elevated Baliga's figure of merit exceeding 3,000 signify the potential for developing significantly more compact and, consequently, efficient power converters employing this material when compared to well-established SiC and GaN technologies. Notably, lateral β -Ga₂O₃ metal-oxide-semiconductor field-effect transistor (MOSFET) devices have exhibited remarkable performances. These transistors currently manifest an average breakdown strength of up to 5.5 MV/cm and showcase record-breaking breakdown voltages reaching 10 kV. Furthermore, the power figure of merit demonstrates a continual ascent, nearly surpassing a value of 1 GW/cm², attributed to ongoing enhancements in material quality and device optimizations.

This presentation aims to provide an overview on the current status of the process development for lateral and vertical β -Ga₂O₃ power transistor devices for high-voltage switching applications, with a specific focus on outcomes achieved at FBH and IKZ. For both scenarios, diverse approaches to bulk crystal growth, epitaxial layer structures, and device designs, tailored to attain the targeted performance parameters, will be deliberated, particularly in terms of breakdown voltage and channel current density. In this regard, we demonstrate the fabrication of lateral (100) β -Ga₂O₃ MOSFET devices with breakdown voltages up to 1.8 kV featuring a power figure of merit up to 155 MW/cm². Large periphery devices with a total gate width of 10 mm verify fast switching at 400 V with a turn-on switching speed up to 78 V/ns. In addition, the incorporation of p-type SnO highlights the considerable potential for realizing high-performance heterojunction SnO/Ga₂O₃ field-effect transistors.

Furthermore, we present vertical (100) β -Ga₂O₃ FinFET devices exhibiting enhancement-mode characteristics and a breakdown strength of 2.7 MV/cm. A comprehensive device simulation encompassing the entire FinFET structure using Silvaco Atlas identifies electric field peaks outside the active area within the SiN_x passivation layers and Al₂O₃ gate oxide, potentially serving as primary contributors to breakdown phenomena. As a culmination of these advancements, specific challenges, both in material and device domains, are identified, necessitating prospective resolutions to overcome prevailing breakdown limitations.

SESSION EL04.10: Gallium Oxide II

Session Chairs: Ahmad Islam and Sriram Krishnamoorthy

Thursday Afternoon, April 25, 2024

Room 345, Level 3, Summit

1:30 PM *EL04.10.01

Photoluminescence Mapping of Defects in β -Ga₂O₃ Matthew D. McCluskey^{1,2}, Jesse Huso², Cassandra Remple¹, John McCloy¹, Steve Rebollo³, Sriram Krishnamoorthy³ and James Speck³; ¹Washington State University, United States; ²Klar Scientific, United States; ³University of California, Santa Barbara, United States

Monoclinic gallium oxide (β -Ga₂O₃) is an ultrawide bandgap semiconductor with potential applications in power electronics. Photoluminescence (PL) spectroscopy is an important method to characterize dopants and defects in this material. Common features in the PL spectrum include the intrinsic UV band, blue and green bands that involve donor-acceptor pairs, and red emission due to Cr³⁺ impurities. PL mapping with excitation wavelengths ranging from 266 to 532 nm reveals the spatial distribution of these features with micron resolution. In Czochralski-grown β -Ga₂O₃, the Cr³⁺ emission intensity shows striations that are attributed due to inhomogeneities during growth. In addition to defects in the bulk, PL microscopy has revealed several specific defects on the surface. Some of these localized centers are very bright UV emitters. Homoepitaxial layers show defects that are observed via the shifts in the PL band, likely due to the strain field around a dislocation core. Damage due to high-intensity laser pulses results in significant changes in the intensity and energy of the UV band. *In situ* PL spectroscopy performed with a pulsed 266 nm laser shows characteristic emission peaks attributed to Ga atoms ablated from the surface.

2:00 PM EL04.10.02

Microscopic-scale Defect Identification in β -Ga₂O₃ Epitaxy Min-Yeong Kim^{1,2,3}, Andrew J. Winchester¹, Ory Maimon^{2,1}, Sang-Mo Koo³, Qiliang Li^{2,1} and Sujitra Pookpanratana¹; ¹NIST, United States; ²George Mason University, United States; ³Kwangwoon University, Korea (the Republic of)

β -gallium oxide (β -Ga₂O₃) is a promising ultrawide bandgap semiconductor for next generation high power electronics that can surpass the performance of silicon, silicon carbide, and gallium nitride. In addition, the facile growth of crystalline β -Ga₂O₃ has significantly contributed to the rapid development of β -Ga₂O₃ power devices. However, device performance issues remain, where crystalline and thin-film defects contribute to this limiting factor. Crystalline defects in technologically mature materials have been identified and classified,^{1,2} since it is economically beneficial to isolate failure mechanisms at the source rather than relying on backend testing after device fabrication. The various defects could be categorized into killer or non-killer defects, where killer defects can hinder the operation of high-performance devices by trapping charge carriers or causing increased leakage current. The defects in Ga₂O₃ are largely unclassified, therefore identifying defects that cause electrical device degradation must be solved for widespread adoption of β -Ga₂O₃.

In this work, photoemission electron microscopy (PEEM) is used to visualize micrometer-scale defects and determine their electronic impact. PEEM is based on the photoelectric effect and is a non-destructive analysis method where light is used to excite and eject electrons from the sample surface and these electrons are analyzed. We investigated the defects on commercially-available epitaxially-grown β -Ga₂O₃ on (010) β -Ga₂O₃ substrates. The epitaxy was formed by hydride vapor phase epitaxy (HVPE) with a target doping of 1 10¹⁸ cm⁻³ on the (010) semi-insulating β -Ga₂O₃ wafer. We identified two types of elongated structures on the β -Ga₂O₃ epi-layer that appear in multiple locations on the sample surface and are oriented in a parallel direction. One of these features resembles the "carrot" defect observed in SiC epitaxy.³ The carrot defect appears topographically as a bump with a density of 5 x 10⁴ cm⁻², and shows a difference in the electronic properties (either in work function and/or gap states) compared to the non-defect surroundings. The second defect, or line defect, appears as depression with a higher density of 2 x 10⁵ cm⁻² and shows no change in electronic properties compared to non-defect surroundings. The local electrical influence of these defects are investigated with tunneling atomic force microscopy (TUNA), and both defects display reduced current compared to the non-defect surroundings. Ongoing work to identify the structural origin these defects through transmission electron microscopy will be presented. Together, we will present a discussion on the nature of these distinct features and their implication on device performance.

References

1. H. Das, S. Sunkari and H. Naas, ECS Transactions **80** (7), 239 (2017).

2. P.-C. Chen, W.-C. Miao, T. Ahmed, Y.-Y. Pan, C.-L. Lin, S.-C. Chen, H.-C. Kuo, B.-Y. Tsui and D.-H. Lien, Nanoscale Research Letters **17** (1), 30 (2022).

3. M. Benamara, X. Zhang, M. Skowronski, P. Ruterana, G. Nouet, J. J. Sumakeris, M. J. Paisley and M. J. O'Loughlin, *Applied Physics Letters* **86** (2) (2005).

2:15 PM *EL04.10.03

Heterogeneous Integration with Wide and Ultrawide Bandgap Semiconductors [Mark Goorsky](#)¹, Michael Liao^{1,2}, Kenny Huynh¹ and Kaicheng Pan¹;

¹University of California, Los Angeles, United States; ²U.S. Naval Research Laboratory, United States

Combining optimal properties of different semiconductors is an especially important consideration for wide bandgap materials due to limitations in thermal conductivities, dopant activation, and compatible crystal structures. Through focus on wafer bonding techniques, we present several cases of materials combinations to achieve an improved / novel performance. First, substrate engineering describes the formation of a template layer of a wide bandgap semiconductor on a substrate with favorable lattice parameter, thermal conductivity, and / or thermal expansion coefficient. Examples include b-Ga₂O₃ and GaN template layers and demonstrate the use of bonding and exfoliation techniques to achieve the desired structures. Second, the role of different bonding practices – and the formation of novel bonding pairs – including bonding with single crystal diamond demonstrates that benefits of certain techniques compared to others. Next, interfaces can be formed without the use of foreign bonding layers. Bonding of AlN with GaN, for example, highlights the importance of substrate perfection, chemical-mechanical polishing, and surface chemistry for achieving direct bonded interfaces free of other species. Finally, the use of designed interface layers can lead to interfaces with improved thermal transport across an interface. Examples of phonon bridging layers will be described. These examples illustrate pathways to achieve the potential of ultrawide bandgap semiconductors.

2:45 PM EL04.10.04

Direct growth of wafer-scale self-separated GaN on reusable two-dimensional material substrate [Chang Hsun Huang](#)¹, Chia-Yi Wu² and Yi-Chia Chou¹; ¹National Taiwan University, Taiwan; ²National Yang Ming Chiao Tung University, Taiwan

Gallium nitride (GaN) is extensively employed in light-emitting diodes, lasers, and high-power electronic devices due to its wide direct band gap and chemical stability.¹ Given the difficulty of obtaining high-quality GaN substrates, most current GaN-based devices are heteroepitaxially grown on foreign substrates, such as sapphire, Si, and silicon carbide.² However, the conventional growth of GaN films on these substrates generates a high defect density and considerable biaxial strain, attributed to the large lattice and thermal mismatch between the GaN films and their substrates. Thus, the lack of GaN native substrates is the main obstacle for the extending development of GaN-based devices. Although several conventional methods exist for obtaining free-standing GaN, such as laser lift-off, void-assisted separation, and chemical etching of the intermediate layer between GaN and the original substrate, the process of removing the substrate from a thick GaN film is complicated, expensive, and time-consuming. Furthermore, the original substrate can be damaged or contaminated during this process.³

Recently, the van der Waals epitaxial growth of III-V films on two-dimensional (2D) materials has been proposed to effectively mitigate the lattice mismatch effect caused by the weak bonds between III-V films and 2D materials.⁴ Fluorophlogopite mica is a thermally stable material with a flexible atomic flat surface and low commercial cost, making it an ideal 2D material substrate. However, the dangling bond-free surface of 2D materials suppresses the nucleation of the III-V film, limiting the growth of large-area single crystals. Although some studies have proposed graphene as an intermediate layer in bridging techniques for growing and lifting off III-V films,⁵ the integration of GaN growth with mica for self-separation is a relatively unexplored area. In this research, we successfully grew a 2-inch thick GaN film with high uniformity on a fluorophlogopite mica substrate via hydride vapor phase epitaxy. The 2-inch thick GaN film easily self-separated from the mica substrate during rapid cooling. After the film growth process, the residual GaN on the mica substrate was effectively eliminated through deionized water, owing to the hydrophilic characteristic of mica and the weak bonding between GaN and mica. Moreover, we demonstrated the capability of reusing the mica substrates by repeatedly growing self-separated GaN films on the same substrate. Additionally, to verify that the thick GaN film was of device quality, we demonstrated a fully functional ultraviolet light-emitting diode with a wavelength of 378 nm. In summary, our proposed approach may facilitate the epitaxy of large-area single-crystalline GaN on 2D materials, offering a new substrate option in the self-separation technology of III-V materials.

References

1. W. Han et al. Synthesis of gallium nitride nanorods through a carbon nanotube-confined reaction. *Science*, 1997, 277, 1287-1289.
2. S. J. Pearton et al. GaN: Processing, defects, and devices. *Journal of Applied Physics*, 1999, 86, 1-78.
3. H. Kum et al. Epitaxial growth and layer-transfer techniques for heterogeneous integration of materials for electronic and photonic devices. *Nature Electronics*, 2019, 2, 439-450.
4. J. Yu et al. Van der Waals epitaxy of III-nitride semiconductors based on 2D materials for flexible applications. *Advanced Materials* 2020, 32, 1903407.
5. H. Kim et al. Graphene nanopattern as a universal epitaxy platform for single-crystal membrane production and defect reduction. *Nature Nanotechnology*, 2022, 17, 1054-1059.

3:00 PM BREAK

SESSION EL04.11: UWBG Optoelectronics
Session Chairs: Sriram Krishnamoorthy and Matthew McCluskey
Thursday Afternoon, April 25, 2024
Room 345, Level 3, Summit

3:30 PM *EL04.11.01

Fabrication of Vertical AlGaIn-based UV-B Semiconductor Lasers [Motoaki Iwaya](#)¹, Sho Iwayama¹, Tetsuya Takeuchi¹, Satoshi Kamiyama¹ and Hideto Miyake²; ¹Meijo University, Japan; ²Mie University, Japan

In recent years, the performance of AlGaIn-based ultraviolet semiconductor light-emitting devices has been rapidly improving; in LEDs, high-performance devices with external quantum efficiencies approaching 10% are being realized in the wide wavelength range from UV-A to UV-C. On the other hand, similarly in semiconductor lasers, device operation at room temperature has been realized in the wide wavelength range from UV-A to UV-C. The most important challenge for achieving even higher performance in the future is to increase optical output power. To increase the optical output of light-emitting devices, it is necessary to improve the external quantum efficiency of the device itself and to increase the operating current. To increase the operating current, it is essential to increase the device size, which requires the realization of vertical devices in which the current flows perpendicularly to the p-n junction. However, most of the current AlGaIn-based ultraviolet light-emitting devices use insulating sapphire or AlN as a substrate to obtain high-quality crystals, resulting in lateral devices in which the current flows horizontally in the n-type layer. Especially in semiconductor lasers, there are no reported

cases of vertical devices in UV-B and UV-C. In this report, we present the results of successful room-temperature operation of vertical AlGaIn-based UV-B laser diodes by using a laser lift-off method and a substrate exfoliation technique with heated and pressurized water. We also would like to discuss the device characteristics and other related topics.

4:00 PM EL04.11.02

Origin of strong Auger-Meitner recombination in AlGaIn deep-ultraviolet emitters [Nick Pant](#)^{1,2}, Kyle Bushick¹, Woncheol Lee¹, Chris G. Van de Walle³ and Emmanouil Kioupakis¹; ¹University of Michigan, United States; ²The University of Texas at Austin, United States; ³University of California, Santa Barbara, United States

The quantum efficiency of AlGaIn-based deep-ultraviolet (DUV) light-emitting diodes lags severely behind its visible-light counterparts. Continued advancements in the synthesis and doping of AlGaIn alloys are expected to reduce extrinsic losses, however the intrinsic energy-loss mechanisms in AlGaIn are less well understood. Auger-Meitner recombination (AMR) is a non-radiative process involving the scattering of three carriers via the Coulomb interaction that causes the quantum efficiency of light emitters to decrease (droop) at high operating powers. The importance of this non-radiative-loss mechanism in AlGaIn remains unclear, because its ultra-wide band gap makes it exceedingly difficult to simultaneously satisfy energy and crystal-momentum conservation for the direct AMR process. In this work, we develop and apply first-principles calculations based on density-functional theory to obtain mechanistic insights into the radiative and AMR processes in bulk AlGaIn alloys and AlGaIn quantum wells. We find that the additional momentum provided by electron-phonon coupling and alloy disorder lead to indirect AMR coefficients C in AlGaIn that are as large as in InGaIn ($C \sim 10^{-31} \text{ cm}^6/\text{s}$), which is known to suffer from severe efficiency droop. Moreover, we find that quantum confinement introduces a new scattering channel that significantly exacerbates AMR in AlGaIn quantum wells, leading to an enhancement of the C/B ratio (where the B coefficient quantifies the radiative recombination) by an order of magnitude relative to the bulk. We propose experimentally feasible approaches for removing disorder and minimizing quantum confinement to mitigate efficiency droop in AlGaIn DUV emitters.

4:15 PM *EL04.11.03

Surface-Emitting Lasers in The Ultraviolet Spectrum [Åsa Haglund](#)¹, Estrella Torres¹, Lars Persson¹, Giulia Cardinali², Sarina Graupeter², Dogukan Apaydin¹, Hjalmar Andersson¹, Lukas Uhlig³, Filip Hjort¹, Nelson Rebelo¹, Massimo Grigoletto², Michael Bergmann¹, Johannes Enslin², Nando Prokop², Martin Guttman², Luca Sulmoni², Neysha Lobo Ploch⁴, Munise Cobert², Tim Kolbe⁴, Ryan Page¹, Andreas Liudi Mulyo¹, Ulrich Theodor Schwarz², Philippe Tassin¹, Joachim Ciers¹, Tim Wernicke² and Michael Kneissl^{2,4}; ¹Chalmers University of Technology, Sweden; ²Technische Universität Berlin, Germany; ³Chemnitz University of Technology, Germany; ⁴Ferdinand-Braun-Institut, Germany

The recent demonstrations of edge-emitting lasers in the UVB (280 – 320 nm) operating under pulsed conditions, and in the UVC (< 280 nm) operating continuous-wave mode very well for the development of more complex laser structures in the ultraviolet (UV), such as vertical-cavity surface-emitting lasers (VCSELs) and photonic crystal surface emitting lasers (PCSELs). Recently, optically pumped versions of both of these surface-emitting lasers, emitting in the UVB and UVC, have been realized; there are, however, significant challenges precluding electrical injection. Here, we will summarize the state of the art for these UV surface-emitting lasers and outline the remaining challenges for realizing electrically injected devices.

For VCSELs, we will go in depth into our concept for achieving high reflectivity mirrors with accurate cavity lengths based on substrate removal by selective electrochemical etching. In addition to paving the way to demonstrations of both UVB and UVC VCSELs, this technology has yielded a large reduction in the lasing threshold by allowing us access to both sides of the cavity for post-growth detuning setting. It has also facilitated lasers with an inherently temperature-stable lasing wavelength by enabling the integration of materials with negative thermo-optic coefficients. Moving towards electrically driven UV VCSELs, one major challenge is applying the electrochemical etch technique to heavily doped device structures, since the doping-selective etch process can unintentionally damage doped device layers. Here, we will discuss several important steps towards overcoming this challenge, specifically, the successful substrate removal for thin-film UVB light-emitting diodes (LEDs) and resonant cavity LEDs employing tunnel junctions, without any parasitic etching of device layers. With these results in hand, the only remaining building block to electrically driven UV VCSELs is the development of an aperture scheme for horizontal current confinement.

For PCSELs, we will show single-mode devices that lase in the UVB and in the UVC under optical pumping, despite the challenging surface morphology and the inherently low refractive index of AlGaIn. A narrow beam divergence below 1° has been achieved by tailoring PCSEL parameters, such as the hole filling factor. The development of electrically injected PCSELs will benefit from the great progress that has been made for electrically injected edge-emitting lasers, since their epitaxial structures are similar. However, since PCSELs have an electrical injection path that is in the same direction as the outcoupled light they face similar challenges as VCSELs, such as achieving good lateral current spreading without the use of metals that can block the vertical emission.

The question now is, will we first see electrically driven UV PCSELs or VCSELs?

4:45 PM EL04.11.04

Fabrication of Broadband UV MSM Photodetector Using Reactive Sputtered Nickel Oxide Film [Swati Suman](#); Indian Institute of Technology Madras, India

Efficient ultraviolet (UV) photodetectors are of significant interest due to their wide area of applications, such as bio-sensing, communications, and military applications¹⁻³. In this work, a metal oxide semiconductor sandwiched between metal electrodes (MSM structure) was developed as a broadband UV photodetector. The MSM photodetectors has garnered lot of interest because of its simple fabrication design, large active area, low dark current facilitating fast response. The metal oxide used was p-type nickel oxide (NiO) deposited by DC magnetron sputtering technique on top of indium tin oxide (ITO). Reactive sputtering from a pure nickel target was used to deposit NiO and the effect of oxygen concentration on the morphological and optoelectronic properties of the NiO was investigated. ITO is capable of providing good electrical conductivity and charge transporting behaviour which supports low leakage current⁴. It is a n-type degenerate semiconductor which is widely used for transparent conducting films. Among different metal oxides, NiO is a promising p-type semiconductor with wide band gap value (3.2 to 3.8 eV, depending on stoichiometry)⁵. In this study, we explore the fabrication and characterization of a UV photodetector using ITO and NiO heterojunction. The device performance will be optimized by varying oxygen concentration during deposition of NiO. The variation of oxygen will be done by keeping argon concentration constant. The DC magnetron sputtered NiO thin film, acts as the photosensitive layer. Silver electrodes were used as contacts for the two layers. Material characterization has been done using different techniques like XRD, SEM, UV-vis spectroscopy, Raman spectroscopy and photoluminescence spectroscopy while electrical characterization has been performed using I-V source meter and four probe. The fabricated device demonstrates good change in light to dark current at low applied biased voltage. In conclusion, the development of UV photodetectors using DC magnetron sputtered p-type NiO thin films represents an encouraging route in the realm of optoelectronics. The tunability of NiO film properties at the interface with the ITO substrate provide further leverage for advancements in photon sensing.

Technol. Semiconductor near-ultraviolet photoelectronics. 1999, 14 (7), R41. 3. Ohta, H.; Hosono, H. J. M. T., Materials Today. Transparent oxide optoelectronics. 2004, 7 (6), 42-51. 4. Kim, H.; Lee, G.-N.; Kim, Journal of Nanomaterials. Hybrid structures of ITO-nanowire embedded ITO film for the enhanced Si photodetectors. 2018, 34(12), 2625-2629. 5. Hakim, A.; Hossain, J.; Khan, K. J. R. E., Renewable Energy. Temperature effect on the electrical properties of undoped NiO thin films. 2009, 34 (12), 2625-2629

SESSION EL04.12: Diamond
Session Chairs: Robert Kaplar and Sriram Krishnamoorthy
Friday Morning, April 26, 2024
Room 345, Level 3, Summit

9:30 AM EL04.12.01

Diamond: A versatile ultra-wide bandgap electronic material for many applications Subhajit Chatterjee, Bellarmine Francis, Ramasubramanian Kannan, Nikhil C and M S Ramachandra Rao; IIT Madras, India

Diamond, an exceptional ultra-wide bandgap material, has drawn a lot of attention due to its potential in quantum devices, power electronics, high-frequency devices, mechanical applications, and thermal management. Diamond's bandgap energy of 5.5 eV allows for the creation of powerful power devices like field-effect transistors and high-voltage diodes. Diamond lattice is amenable to doping and boron doped diamond makes it a potential granular superconductor for quantum devices. Nitrogen doped diamond offers potential applications in quantum computing and magnetometry. Diamond's exceptional thermal conductivity is crucial in heat dissipation and lessens the need for complex and large cooling systems – using diamond coatings. Diamond's ultra-wide bandgap helps RF devices to operate more efficiently and for longer periods of time by reducing power losses, improving breakdown voltages, and heat dissipation.

To fully realize the promise of diamond in power electronics and high-frequency applications, our group is focussed on material engineering and device design. This entails the creation of cutting-edge growing processes and doping innovations to customize the attributes of diamonds to specific needs. In conclusion, the domains of power electronics and high-frequency devices are about to undergo a revolution, thanks to diamond. With far-reaching developments for multiple industries, the utility of diamond heralds new advance and sustainable technologies. Work carried out on various aspects of diamond, in our centres, will be presented.

9:45 AM EL04.12.03

Approaches for phosphorus incorporation on (100) oriented diamond surfaces Franz A. Koeck and Robert J. Nemanich; Arizona State University, United States

Diamond based electronics, in particular for high power, high frequency and harsh ambients are evolving more rapidly in part due to the availability of high-quality substrates with increasing size. A more economical device fabrication can be achieved for larger wafers and with a (100) oriented surface. However, prominent device demonstrations for p-i-n diodes and bi-polar junction transistors utilized (111) substrates as sufficiently high phosphorus incorporation for the n-type layer is more readily achieved. We present an approach for phosphorus doping of (100) oriented surfaces that utilizes in-situ monitoring of the gas chemistry via residual gas analysis (RGA) during a pulsed deposition technique. An ASTeX style, plasma enhanced chemical vapor deposition (PECVD) system was equipped with an RGA system to monitor and control in real-time the gas chemistry during growth. Results established that the concentration of PH radicals during plasma growth was related to the incorporated phosphorus concentration. Doped diamond growth was performed on CVD type IIa (100) diamond substrates with a surface finish of 5nm Ra. Process gases included hydrogen, methane and a 200ppm trimethylphosphine (TMP) in hydrogen gas mixture. The pulsed deposition technique included growth steps separated by cooling steps where the growth process was interrupted. With optimized conditions a phosphorus concentration approaching 10^{19}cm^{-3} was measured by secondary ion mass spectroscopy (SIMS) with an abrupt doping gradient. The doping results will be described in terms of the surface chemistry and the pulsed growth technique. Improvements in phosphorus doping will be discussed in terms of miscut, growth mode (step-bunching), surface finish and surface pre-treatment processes. This research was supported by the NSF through grant DMR-2003567 and the U.S. Department of Energy, Office of Science, Basic Energy Sciences through ULTRA, an Energy Frontier Research Center under Award #DE-SC0021230.

10:00 AM BREAK

SESSION EL04.13: Emerging WBG and UWBG Materials I
Session Chairs: Robert Kaplar and Sriram Krishnamoorthy
Friday Morning, April 26, 2024
Room 345, Level 3, Summit

10:30 AM EL04.13.01

Electronic and Optical Properties of Antiferromagnetic MnF₂ Andre Schleife¹, Kisung Kang² and Yi-Ting Lee¹; ¹University of Illinois at Urbana-Champaign, United States; ²Fritz Haber Institute, Germany

In recent decades, MnF₂ has received considerable interest due to its simple antiferromagnetic structure and its promising applications in spintronic devices. While the magnetic properties of MnF₂ have been extensively characterized experimentally, theoretical approaches have failed to accurately predict its electronic structure. This is evident in the discrepancy between the values predicted by electronic-structure theory, which is less than 7.3 eV, and the measured values of more than 9.9 eV based on reflectance and absorption spectra. Furthermore, no prior computational studies have predicted its optical properties to enlighten this question. We employed DFT with the HSE06 hybrid exchange-correlation functional and applied many-body perturbation theory via GW calculations to compute the electronic structure. Subsequently, we approximated this data using a PBE+U approach and a band-dependent scissor shift to achieve a converged **k**-point sampling for Bethe-Salpeter calculations of the excitonic optical spectrum. Surprisingly, we find excellent agreement with peak positions and amplitudes of the experimental spectrum across a wide range of photon energies up to 17 eV only after assuming an additional scissor shift of 2.4 eV. To explain additional shift, we analyze the effect of the lattice parameter, the magnetic structure, and different GW methods.

10:45 AM EL04.13.02

Static and time-dependent optical properties of CuI [Andre Schleife](#) and Brian Robinson; University of Illinois at Urbana-Champaign, United States

We aim to use first-principles electronic-structure theory to explain the static and time-dependent optical properties of the wide-band gap semiconductor CuI, which is a promising candidate for a transparent conducting material. In particular, we aim to clarify the importance of the spin-orbit interaction for the appearance of an above-gap spectral feature that is reported in multiple experiments. Measurements of the linear optical properties that have been reported in the literature agree in attributing that peak in the spectrum to a spin-orbit split-off valence-band state. However, the significant oscillator strength of the peak might raise doubts about its origin due to the spin-orbit interaction. We use a combination of density-functional and many-body perturbation theory to simulate the electronic structure and optical properties including excitonic effects. Our simulations do not reproduce the experimentally reported peak structure and we show that the optical dipole transitions from the corresponding spin-orbit split-off electronic state do not show a polarization dependence. We interpret this as an indication that more direct experimental evidence is needed to support the spin-orbit origin of any feature in this spectral range. We also solve the Boltzmann transport equation to account for electron-phonon scattering as a relaxation mechanism in pump-probe experiments and implement the resulting time-dependent occupation numbers as constraint in simulations of the spectrum. Our predicted pump-probe spectra for this material show that increasing the intensity of the excitation only significantly changes the magnitude of the spectrum values, while increasing the excitation energy leads to changes in the presence of peaks, peak location, and peak width.

11:00 AM EL04.13.03

Computational Prediction of an n-type Transparent Conducting Oxide F-doped Sb₂O₅ [Ke Li](#)^{1,1}, Joe Willis^{1,1}, Seán R. Kavanagh^{2,1} and David O. Scanlon³; ¹University College London, United Kingdom; ²Imperial College London, United Kingdom; ³University of Birmingham, United Kingdom

Transparent conducting oxides possess a unique combination of optical transparency and electrical conductivity, making them indispensable in optoelectronic applications. ¹ However, the heavy dependence on a small number of established transparent conducting oxides (In₂O₃, SnO₂, ZnO and Ga₂O₃) places limitations on the number and types of devices they can support. Additionally, the high cost due to the scarcity of rare elements raises concerns about their long-term sustainability and large-scale production. ² Discovering more wide band gap oxides that can be doped to display metallic-like conductivity is therefore necessary.

In this work, we use the PBE0 hybrid functional to investigate the defect chemistry of the binary Sb(V) system, Sb₂O₅. ³ We observe a large optical band gap over 3.6 eV, enabling transparency. The calculated Sb₂O₅ electronic structure shows a dispersive conduction band minimum with low electron effective masses, revealing its n-type properties. Our defect analysis reveals that Sb₂O₅ does not display metallic-like conductivity when nominally undoped, however, F-doped Sb₂O₅ displays degenerate n-type transparent conducting behaviour. Our band alignment calculations demonstrate that Sb₂O₅ has a larger electron affinity than the established transparent conductors, which can facilitate electron extraction for organic solar cells applications. The findings of this under-explored Sb(V) binary system prove the feasibility and potential for Sb(V)-based materials to be promising transparent conducting oxides.

- (1) Jackson, A. J.; Parrett, B.; *et al.* *ACS Energy Lett.* **2022**, 3807–3816.
- (2) Mineral Commodity Summaries 2023. **2023**.
- (3) Adamo, C.; Barone, V. *The Journal of Chemical Physics* **1999**, 110 (13), 6158–6170.

11:15 AM EL04.13.04

Thermal Conversion of Ultrathin Nickel Hydroxide for Wide Bandgap 2D Nickel Oxides [Lu Ping](#), Nickolas Russo and Xi Ling; Boston University, United States

Wide bandgap (WBG) semiconductors in two-dimensional (2D) form have demonstrated great potential in 2D electronics, optoelectronics, and power industries.^{1–3} However, as an essential group of WBG semiconductors, 2D transition metal oxides (TMOs) remain largely understudied in terms of physical properties and applications in 2D electronic devices due to the lack of sufficiently large 2D crystals. Various 2D TMOs nanosheets have been produced,^{4–6} but the nanometer scale crystals are not desirable enough for 2D electronics study, which usually require larger lateral domains (>10 μm) for device design.^{7,8} And some common TMOs (e.g., Ni₃O₄) still lack of systematical study and knowledge to be designable for application studies. Therefore, we are inspired and driven to expand the 2D TMOs family from developing a universal synthesis pathway with desirably large lateral domains that will serve 2D electronics study well. Here, we present the WBG 2D nickel oxide (NiO) thermally converted from 2D nickel hydroxide (Ni(OH)₂) with largest ever reported lateral domain size (>20 μm). A facile and scalable synthesis approach is employed firstly to produce 2D Ni(OH)₂ flakes, which are subsequently transformed into NiO through a simple and controlled thermal conversion process. The morphology and structure variation is investigated and the chemical reaction during the thermal conversion under different temperature zones are established. Optical bandgap of the thermally converted 2D NiO (E_g > 3.7 eV) is higher than that of 2D α-Ni(OH)₂ (E_g > 2.5 eV), showing even better potential to serve as gate dielectric layers. The oxidation process is further studied by X-ray absorption spectroscopy (XAS) and X-ray emission spectroscopy (XES), to provide more insights and understandings on the electronic structure and bandgap of 2D NiO. We believe our investigation on 2D NiO will project and inspire more profound studies on other 2D WBG semiconductors.

Reference

1. Fujita, S. Wide-bandgap semiconductor materials: For their full bloom. *Jpn. J. Appl. Phys.* **54**, (2015).
2. Varley, J. B., Shen, B. & Higashiwaki, M. Wide bandgap semiconductor materials and devices. *J. Appl. Phys.* **131**, 1633–1636 (2022).
3. Neudeck, P. G., Okojie, R. S. & Chen, L. Y. High-temperature electronics - A role for wide bandgap semiconductors? *Proc. IEEE* **90**, 1065–1076 (2002).
4. Kalantar-Zadeh, K. *et al.* Synthesis of nanometre-thick MoO₃ sheets. *Nanoscale* **2**, 429–433 (2010).
5. Boland, J. B. *et al.* Liquid phase exfoliation of MoO₂ nanosheets for lithium ion battery applications. *Nanoscale Adv.* **1**, 1560–1570 (2019).
6. Rui, X. *et al.* Ultrathin V₂O₅ nanosheet cathodes: Realizing ultrafast reversible lithium storage. *Nanoscale* **5**, 556–560 (2013).
7. Gao, H. *et al.* Phase-Controllable Synthesis of Ultrathin Molybdenum Nitride Crystals Via Atomic Substitution of MoS₂. *Chem. Mater.* **34**, 351–357 (2022).
8. Cao, J. *et al.* Realization of 2D crystalline metal nitrides via selective atomic substitution. *Sci. Adv.* **6**, 1–9 (2020).

11:30 AM EL04.13.05

Control of ZnO defects for quantum information applications Shirin Riahi¹, Abbas Nakhband¹, [David Lister](#)¹, Manu Hegde¹, Xingyi Wang², Kai-Mei Fu² and Simon P. Watkins¹; ¹Simon Fraser University, Canada; ²University of Washington, United States

ZnO is a promising candidate for the manipulation of quantum information (QI) in a direct bandgap semiconductor. Among compound semiconductors, ZnO has very low spin orbit coupling which results in much longer spin-lattice relaxation times than GaAs, InP etc.[1] In nanostructured form, ZnO has

low surface recombination rates compared with GaAs and other compound semiconductors, meaning that it is a very strong emitter of light even for sub-optical nanowire dimensions. Donor bound exciton (D⁰X) defects such as simple substitutional group III elements are promising candidates for QI applications and can be coupled to their donor final state spins by very sharp line excitonic transitions. In addition, the exciton Bohr radius of ZnO is considerably smaller than GaAs, and InP making it less likely for donors within a NW to experience quantum confinement effects or surface fields. D⁰X centers in nanowires grown by metalorganic vapor phase epitaxy (MOVPE) achieve optical linewidths comparable to the best quality bulk material. Recently coherent optical trapping of excitons was observed in In-donors in Zn NWs grown by MOVPE. [2]

In this work, we discuss methods of achieving very low densities of such defects in ZnO in bulk and NW form. First, we show how the concentration of Ga donors can be controlled down to the 10¹⁵ cm⁻³ range by MOVPE using triethylgallium as a dopant. We use a simple model of exciton pair interactions to estimate these numbers. A second example is the so-called I₁₀ defect which is known from radioisotope studies to contain Sn on Zn site.[3] We consider 2 types of samples: (1) bulk Sn-doped ZnO grown by CVD and (2) ZnO bulk substrates implanted with Sn ions. From an application point of view, Sn implantation is a preferred method for generating these defects. We show that I₁₀ emission can be reversibly generated and destroyed by heat treatments. After annealing in a nitrogen environment at 900°C, the intensity of I₁₀ in the CVD samples can be reduced by several orders of magnitude. After such a heat treatment, by annealing under Li, the I₁₀ emission can be completely restored. This strongly suggests that I₁₀ is a complex consisting of a Sn double donor complexed with a Li acceptor. Density functional calculations are consistent with this model. This defect provides a promising avenue of study for addressing single donor spins for QI since the concentration can be carefully controlled by means of low temperature diffusion or annealing under inert gas. A set of Li-related lines D⁰X lines is also observed in addition to I₁₀.

A final issue related to the use of NWs for QI involves a broad emission band, SX, commonly seen in high purity samples in the 3.364 eV energy range. This band is attributed to excitons bound to surface states, and results in a strong background as sample purity increases and NW radius decreases. This may impact the ability to detect and control small numbers of donor spins for QI applications. We present the results of photoluminescence excitation (PLE) measurements indicating that the SX band is associated with localized surface states, with varying binding energies, rather some kind of band bending mechanism as previously proposed. The effect of surface treatments on this emission band are also discussed in this paper.

[1] Xiayu Linpeng, Maria L.K. Viitaniemi, Aswin Vishnuradhan, Y. Kozuka, Cameron Johnson, M. Kawasaki, and Kai-Mei C. Fu, Phys. Rev. Applied, 10, 064061 (2018).

[2] M. L. K. Viitaniemi, C. Zimmermann, V. Niaouris, S. H. D'Ambrosia, X. Wang, E. Senthil Kumar, F. Mohammadbeigi, S. P. Watkins, and Kai-Mei C. Fu, Nano Lett. 22, 2134 (2022).

[3] J. Cullen, D. Byrne, K. Johnston, E. McGlynn, and M. O. Henry, Appl. Phys. Lett. 102, 192110 (2013)

SESSION EL04.14: Emerging WBG and UWBG Materials II
Session Chairs: Robert Kaplar and Sriram Krishnamoorthy
Friday Afternoon, April 26, 2024
Room 345, Level 3, Summit

1:45 PM EL04.14.01

Transparent Conductive Titanium and Fluorine Co-doped Zinc Oxide Films Deposited via Aerosol Assisted Chemical Vapour Deposition Iqra Ramzan; University College London, United Kingdom

Aerosol-assisted chemical vapor deposition (AACVD) was applied to deposit highly transparent and conductive titanium or fluorine-doped and titanium-fluorine co-doped thin films on a glass substrate at 450°C. All films were characterized by X-ray photoelectron spectroscopy (XPS), X-ray diffraction (XRD), UV-Vis spectroscopy, scanning electron microscopy (SEM), and four-point probe. The films were 350-400 nm thick, crystalline, and highly transparent (80-87%). The co-doped film consists of 0.70 at.% titanium and 1 at.% fluorine, displaying a charge carrier mobility and charge carrier concentration of 8.4 cm² V⁻¹ s⁻¹, 3.97 x 10²⁰ cm⁻³, respectively. A band gap of 3.6 eV was observed for the co-doped film. Compared to the undoped and singly doped films, the co-doped film displayed a notably higher structure morphology suitable for transparent conducting oxide applications. The highly transparent and conductive titanium-fluorine co-doped films have been deposited for the first time.

2:00 PM EL04.14.02

Two excitation pathways of Pr³⁺ ion emission in HfO₂:Si:Pr films depending on crystalline phase transformations in annealing Tetyana v. Torchynska¹, Manuel Garcia Andrade¹, Georgiy Polupan¹, Larysa Khomenkova^{2,3} and Fabris Gourbilleau^{6,4}; ¹Instituto Politecnico Nacional, Mexico; ²V. Lashkaryov Institute of Semiconductor Physics at NASU, Ukraine; ³National University "Kyiv-Mohyla Academy, Ukraine; ⁴CIMAP, UMR CNRS/CEA/ENSICAEN/UNICAEN, France

HfO₂ based materials offer high refractive index and high transparency in UV-NIR spectral ranges that are promising for photonic applications. For this purpose, the stabilization of HfO₂ structure is required to minimize the optical losses in the HfO₂ based optical materials. It is known that stabilization of tetragonal/cubic structure can be achieved via HfO₂ doping with trivalent atoms, such as rare-earth (RE) elements. In this case, electrical neutrality is achieved via formation of oxygen vacancies, i.e. one vacancy for two dopant atoms. At the same time, the interaction between different ions, the RE ion excitation mechanism and their redistribution upon high temperature annealing were not well addressed.

In this report the impact of annealing on the emission and transformation of the crystalline phases in Si rich HfO₂:Pr films was investigated by analyzing the morphology, chemical composition, structure, and light emitting characteristics. The films were grown on Si substrates by radio frequency magnetron sputtering in argon plasma and annealed at T_A=1000 or 1100°C for t_A=15-60 min in inert atmosphere. The transformation of film properties was studied by means of SEM, EDS, XRD, XPS, and photoluminescence (PL) techniques.

Heat treatment at 1000°C for 30 min stimulates phase transformation together with the appearance of a tetragonal HfO₂ phase and Si quantum dot (QDs). For HfO₂ films doped with Pr ions, the stabilization of the tetragonal HfO₂ phase in annealed films was observed contrary to the monoclinic structure of pure HfO₂ films. The main reason responsible for this structural phenomenon is the formation of oxygen vacancies (V_O). The formation of Si QDs and oxygen vacancies is accompanied by the appearance of emission of rare earth (RE) ions Pr³⁺ related to the transitions in the 4f energy levels. The shape of RE-related PL spectra followed the structural transformation. Narrow RE-related PL peaks were detected in the samples annealed for 30-60 min that confirms the location of RE ions in the tetragonal phase with a high crystal field.

Annealing for 60 min stimulates the complete oxidation of the Si QDs with the formation of the tetragonal SiO₂ phase along with partial destruction of a tetragonal HfO₂ phase. This last process is accompanied by the significant increase of the intensity of Pr³⁺ ion emission. Two forms of luminescence excitation in 4f energy levels of Pr³⁺ ions are discussed, related to energy transfer to Pr³⁺ ions, first from Si QDs and then from host V_O defects in HfO₂. These changes in the excitation pathways of Pr³⁺ ion emissions are stimulated by the transformations of the crystalline phases in the thermal treatment together with the generation of host HfO₂ defects. Hafnia-based materials doped with RE elements are interesting for telecommunication technology and

applications in waveguides and optoelectronic devices.

2:15 PM EL04.14.03

UV-Selective Transparent PV Devices with Wide Bandgap ZnO_{1-x}S_x Mixed Crystal Absorbers Deposited by Atomic Layer Deposition for Seamless PV Building Integration Gustavo A Alvarez¹, Alex J. Lopez-Garcia¹, Victoria Rotaru¹, Maxim Guc¹, Jose M. Asensi López², Victor Izquierdo-Roca¹ and Alejandro Perez-Rodriguez^{1,2}; ¹Institut de Recerca en Energia de Catalunya, Spain; ²Universitat de Barcelona, Spain

One of the great limitations of integrating PV technologies on window or ceramic façades is the high light absorption of existing technologies that give these devices an opaque appearance, and other issues as weight. Therefore, when applied on glass, ceramic, or polymeric substrates they completely modify their aesthetic properties, making them practically inapplicable to the vast majority of urban buildings where aesthetic value is of fundamental importance.^[1] This is a challenge since one of the most important aspects of non-intrusive integration of PV technologies is achieving a good balance between the efficiency of the cell and the degree of transparency. In this aspect, results have shown that wide-bandgap (WBG) materials based on oxides such as ZnO or ZnO_{1-x}S_x, present reasonably good photovoltaic properties while maintaining a high degree of transparency.^[2-4] Particularly, ZnO_{1-x}S_x has been proposed as an ideal UV absorber thanks to a composition-tunable bandgap that can shift from 3.2 eV down to 2.7 eV at intermediate relative sulfur content, matching the UV spectral onset for the AM1.5G spectrum.^[5,6]

In this work, transparent PV cells based on ZnO_{1-x}S_x with a relative sulfur content of x=0.7 and the architecture SLG/FTO/MoO₃(HTL)/ZnO_{0.3}S_{0.7}/ZnO/AZO(ETL)/AZO have been fabricated and characterized. Preliminary results present the first evidence of PV effect using a fully ALD-deposited ZnO_{1-x}S_x absorber and other WBG oxide materials as carrier selective contacts. These results show a notable V_{oc} of 401 mV but a low J_{sc}, limiting the PV effect. The Average Photopic Transmittance (APT) of the device has a value of 73%, showing indeed excellent transparency and color-neutrality thanks to the use of materials with bandgaps higher than 3eV. Optical, structural and electrical characterization of the absorber and devices will be presented (Spectrophotometry, Photothermal Deflection Spectroscopy, SEM, Raman, J-V characteristics under illumination). Ongoing work based on optoelectronic characterization will determine the UV detection capabilities of this structure measuring intensity dependent J-V characteristics under UV light under no bias as well as at the maximum-power-point, which are the prominent values at which a PV device will ideally operate. By such the TPV device based on this WBG material can be multifunctional and serve as a UV detector under PV operation. Also, to increase J_{sc} and thus PCE different compositions and selective contacts are being actively studied.

This research is relevant for the advancement of thin film technologies and in particular Transparent PV technologies. The proposed architecture has the potential to revolutionize photovoltaic technology by enabling on-site generation while minimizing visual impact. It is noteworthy that ZnO_{1-x}S_x is a material composed of earth-abundant raw elements, compatible with scalable fabrication processes and can be synthesized at relatively low temperatures, which potentially allows minimizing the carbon footprint, the economic costs and energy expenditure associated with the manufacture of devices.

This work has received funding from MCIN/AEI/10.13039/501100011033 under grant numbers PID2022-138434OB-C51 and TED2021-129758B-C32 and by the NextGenerationEU/PRTR.

[1] C. J. Traverse, R. Pandey, M. C. Barr, R. R. Lunt, *Nat. Energy* **2017**, 2, 849.

[2] R. Karsthof, P. Räcke, H. Von Wenckstern, M. Grundmann, *Phys. status solidi* **2016**, 213, 30.

[3] M. Patel, H. S. Kim, J. Kim, J. H. Yun, S. J. Kim, E. H. Choi, H. H. Park, *Sol. Energy Mater. Sol. Cells* **2017**, 170, 246.

[4] R. Karsthof, H. von Wenckstern, M. Grundmann, *J. Vac. Sci. Technol. B, Nanotechnol. Microelectron. Mater. Process. Meas. Phenom.* **2016**, 34, 04J107.

[5] G. Baldissera, C. Persson, *J. Appl. Phys.* **2016**, 119, DOI 10.1063/1.4940700.

[6] A. J. Lopez-Garcia, A. Bauer, R. Fonoll Rubio, D. Payno, Z. Jehl Li-Kao, S. Kazim, D. Hariskos, V. Izquierdo-Roca, E. Saucedo, A. Pérez-Rodríguez, *Sol. RRL* **2020**, 4, 2070112.

2:30 PM BREAK

SESSION EL04.15: Breaking News – Nitrides and Other UWBGs

Session Chairs: Robert Kaplar and Sriram Krishnamoorthy

Friday Afternoon, April 26, 2024

Room 345, Level 3, Summit

3:00 PM EL04.15.01

Boron Nitride Nanotube, Its Chemistry and Application in Sensors and Transistors Jingwen Guan¹, Shiva Ashoori², Huimin Ding¹, Ping Lu¹, Eyal Roseshter³, Liliana Gaburici¹, Ravi Prakash², Stephen Mihailov¹ and Christopher T. Kingston¹; ¹Security & Disruptive Technologies Research Centre, National Research Council Canada, Canada; ²Department of Electronics Engineering, Carleton University, Canada; ³Department of Physics, Carleton University, Canada

Boron nitride nanotube (BNNT) is another emerging mankind one dimensional nanomaterial discovered at the same time frame around the years of 1990 as its counterpart carbon nanotube (CNT), but it has been much delayed in its synthesis for a large scale, its chemistry and application due to its differences in production and material characteristics from CNT. BNNT possesses a compelling set of intrinsic properties similar to CNT, such as one-dimensional tubular structures, light weight, high mechanical strength, and high thermal conductivity. But unlike CNT, BNNT is an electrical insulator with a wide bandgap about 5.5 eV, and has a hetero-atomic network of B and N in turn instead of homo-atomic of C network structure, therefore, BNNT has additional characteristics such as transparency in visible light, high thermal stability and high oxidation resistance over 900 °C in air. These properties make them high potential in many applications such as high-temperature and extreme environments, transparent armor materials, and radiation shielding protections. Especially, the polarity of B-N bonds in the BNNT network offers unique surface chemistry that can be taken in full advantages for sensing applications, for instance, due to interfacial compatibility and reactivity to its environment. We will present the use of HABS-BNNT materials produced at the National Research Council Canada (NRC) through thermal induction plasma process and the development of the surface chemistry by in-situ B-N bond cleavage with liquid bromine treatment in aqueous solution, leading to OH and amino (NH₂) dual surface functionalities at the same steps. Such functionalized BNNTs are highly soluble in aqueous and polar organic solvents by themselves without adding any surface agent. Our report will include up to today's results that such functionalized BNNTs as a sensing material for the active coating layers on optical fiber devices as well as a dielectric material for the applications in capacitors and in organic thin film transistors (OTFTs) for improving their performance and shelf life. An indicative outlook will be briefly discussed in the further development of BNNT-integrated transistors.

3:15 PM EL04.15.02

Study on Dynamic Wetting Characteristics of Al₃C-SiC System under Micro-Stretching [Yi Lv](#)^{1,2}; ¹Hubei University of Arts and Science, China; ²Hubei Longzhong Laboratory, China

Aluminum-based silicon carbide (AlSiC) is an aluminum-based silicon carbide particle reinforced composite material, which fully combines the different advantages of silicon carbide ceramics and metal aluminum, with high thermal conductivity, thermal expansion coefficient matched with the chip, low density, light weight, and high hardness and high bending strength and other advantages, is widely used in aviation, aerospace, high-speed iron and microwave and other important fields. It is the preferred material to solve the packaging thermal management problems of microelectronics, power devices and optoelectronic devices. However, in the process of preparing AlSiC composites, the wettability between silicon carbide reinforced particles and aluminum solution is often poor, and it is difficult to achieve uniform distribution of SiC particles.

Many studies showed that the wettability between the ceramic reinforcement phase and the matrix was mainly affected by three factors: temperature, Si atom concentration and SiC surface structure. However, these results were mostly obtained by experimental methods, and some experimental conditions such as droplet shape, ambient temperature and pressure were difficult to accurately control, which made these results not reproducible to a certain extent. In addition, these factors have not been used to explain the dynamic mechanism of Al droplet wetting SiC surface from the microscopic perspective. Therefore, in this study, a molecular dynamics model was established, the dynamic stretching of the 3C-SiC substrate was introduced to simulate the microvibration state of the substrate surface. First, a 3C-SiC substrate with all Si atoms and C atoms on the upper surface was established, and then some atoms were removed from the surface of Si-terminated substrate to form rectangular and wedge grooves, and then some C atoms were added to the grooves. As a result, six Al/SiC systems were constructed, including a Si-terminated system (Si), C-terminated system (C), rectangular groove system (RG), rectangular groove system embedded with atoms (RGEA), wedge groove system (WG), and wedge groove system embedded with atoms (WGEA). The size of the substrate was $87.59 \times 87.59 \times 6.57 \text{ nm}^3$, and the Al droplet size was 10.95 nm^3 . In this study, Newtonian mechanics principle was applied to solve the motion of Al atomic and molecular system on SiC surface at 1100 K. The hybrid potential functions, including Tersoff, EAM and 12-6 LJ, were used to calculate the interaction between Al, Si and C atoms respectively. The time step was 1 fs, and the system simulation times were 10^5 . In order to simulate the microvibration state and prevent atoms from squeezing or displacing each other during substrate stretching, the SiC substrate was stretched along the x-axis at a deformation rate of 10^{-3} per 100 steps, resulting in a substrate deformed only 1 nm along the x-axis in a calculated period of 10^3 fs. Then, the wettability of Al droplet on the surface of 3C-SiC was studied, including the variation trend of the wetting angle, self-diffusion coefficient and interaction energy with the simulation process.

The wetting angles of the six systems after stretching were greatly reduced, and the wettability of the substrate was improved, especially in the C-terminated system and the RGEA system. Although the interaction energy decreased and the self-diffusion coefficient increased in the WGEA system after stretching, the wetting angle of the substrate did not decrease much as expected, and even some of the wetting angles were greater than 90° , and the wettability of the substrate had not been significantly improved. This study has important application value for the preparation of a more uniform and reliable AlSiC substrate by pressure-free osmosis method.

3:30 PM EL04.15.03

Understanding the Role of Defects at Diamond/c-BN Interface: A First-Principles Study [Shikha Saini](#)¹, Kevin J. Tibbetts², Mark Polking² and Bilge Yildiz¹; ¹Massachusetts Institute of Technology, United States; ²Lincoln Laboratory, Massachusetts Institute of Technology, United States

In the realms of high-power and radio frequency electronics, diamond and cubic boron nitride (c-BN) stand out for their wide bandgaps, high thermal conductivities, high breakdown fields, and high mobilities. We have recently developed a protocol for preparing high-quality heteroepitaxial c-BN films on diamond substrates for next-generation power and RF field effect transistors (FETs). However, the development of practical electronic devices based on these heterojunctions remains challenging due to a limited understanding of the electronic structure and intrinsic interfacial defects at the diamond/c-BN interface and their impacts on dopant activation and free carrier density. Here, we present results of a first-principles study of diamond/c-BN epitaxial heterostructures. We first explore the electronic structures of different interface types, including both B and N-terminated (100) and (111) interfaces as well as the non-polar (110) interface. We analyze the band alignments for these low-index interfaces and calculate formation energies of potential substitutional, vacancy, and interstitial defects at these interfaces. Further, we analyze the stabilities of potential complexes of both multiple intrinsic defects and intrinsic defects combined with extrinsic dopants, such as Si, Mg, S, and Be, to assess the feasibility of achieving high carrier densities of both p- and n-type at the diamond/c-BN interface. We finally combine these results to determine ideal interface types, dopants, and growth conditions conducive to the formation of high-density two-dimensional electron and hole gases useful for RF FET devices. For instance, we show that B_C and C_N defects at the (110) interface induce p-type doping and lead to the formation of a two-dimensional hole gas (2DHG) in the diamond substrate. The intrinsic electron-deficient nature of these defects and the type-II band alignment are key factors in forming a 2DHG at the interface. However, we have observed that these B_C and C_N defects can be compensated by external dopants such as O and F, which are commonly introduced unintentionally in c-BN epitaxial growth processes. This leads to more stable configurations under B-rich conditions, viz. $B_C O_C$, $B_C O_N$, $C_N F_N$, and $C_N O_N$. Moreover, our calculated results for the diamond/cBN(100) interface show that interface states cross the Fermi level for both C-B and C-N interfacial bonds, indicating strong p-type (type-II band alignment) and n-type (type-I band alignment) doping, respectively. Therefore, high carrier densities on the diamond surface can be achieved through proper interface engineering with c-BN. Our comprehensive analysis reveals new insights into the structure and properties of diamond/c-BN heterointerfaces and provides a detailed roadmap for engineering next-generation power and RF FETs based on diamond/c-BN heterojunctions.

3:45 PM EL04.15.04

Revolutionizing Wafer Reusability: Innovative Porosification Techniques for Multiple Layer Transfers in Indium Phosphide [Erfan T. Osman](#), Jürgen Carstensen, Catarina Schmidt and Rainer Adelung; Christian-Albrechts-Universität zu Kiel, Germany

In pursuit of sustainable and cost-effective semiconductor manufacturing, we present ground-breaking porosification techniques tailored for multiple layer transfers in Indium Phosphide (InP) wafers, with the ultimate goal of achieving complete wafer reusability.

Indium phosphide (InP) layers have wide range applications in various optoelectronic devices, such as solar cells, light-emitting diodes (LEDs), and high-speed transistors. In most of these applications, only a layer thickness in the order of $10 \mu\text{m}$ is typically needed. The main materials and device processing standard in industry for such layers are epitaxial growth techniques (MBE, MOCVD, etc), ion cut (Smart Cut®) and chemical mechanical polishing (CMP) after a wafer bonding process. Smart Cut® and CMP both require complex and expensive preparation steps to achieve surfaces suitable for bonding. Epitaxy (heteroepitaxy) on the other hand has a difficulty in producing layers with high crystalline quality especially when there is a high lattice mismatch.

An attractive material processing alternative to these techniques is the use of electrochemical methods to grow pores with tuneable properties (pore morphologies, depths, and diameters) into the InP wafer. Such pore tunability means that at a certain desired pore depth, pore diameters can be enlarged to create a continuous cavity that can then be detached as one intact layer from the parent wafer. The parent wafer can then be recycled completely in subsequent runs. This technique provides a fast, inexpensive and simple way to transfer porous InP layers particularly in optoelectronic applications where porosity in the InP layer is an added benefit. Additionally, hetero-integration with such layers is similar to the unetched InP wafers since the entire wafer surface can be transferred.

With the aid of a special etching profile invented by us, different types of pores can be grown into InP wafers, characterised as crysto-, curro- or mixed-pores using advanced characterisation techniques. It is crucial to have precise control of these pore growth kinetics in order to achieve a high device yield

and to ensure reproducibility. This presents a challenge since electrochemical systems are complex systems containing many variables such as global and local doping differences, temperature fluctuations, heat generation and release, concentration fluctuations, surface conditions, back side contacts, etc. In these cases, quantitative approaches to estimate pore growth dynamics in semiconductor materials can be the key to producing well defined porous layers. This quantitative description of the growth kinetics is presented. The power of such a quantitative approach is that AI-driven models can be trained on this data that can then forecast pore growth dynamics in semiconductor materials, facilitating the tunability of porosity for specific applications and enhancing the reproducibility of porous layers.

Keywords: Indium Phosphide (InP), Hetero-integration, Doping Concentration, Advanced Characterisation Techniques, Materials Processing, Device Processing, Porous Structures

4:00 PM EL04.15.05

Vertical β -(Al_xGa_{1-x})₂O₃ Schottky Barrier Diodes with a BN Interlayer [Bingcheng Da](#)¹, [Dinusha Herath Mudiyansele](#)¹, [Dawei Wang](#)¹, [Abhijit Biswas](#)², [Pulickel Ajayan](#)², [Yuji Zhao](#)² and [Houqiang Fu](#)¹; ¹Arizona State University, United States; ²Rice University, United States

Ultrawide bandgap (UWBG) semiconductors have attracted significant attention due to their potential applications in power electronics, optoelectronics, and RF electronics. Among these materials, β -Ga₂O₃ stands out as a promising candidate for UWBG semiconductors owing to its notable properties such as a high breakdown field of 8 MV/cm and a wide bandgap ranging from 4.6 to 4.9 eV. Additionally, it exhibits a high Baliga's figure of merit (BFOM) in comparison to GaN and SiC. Moreover, the availability of large native substrates makes β -Ga₂O₃ highly promising for cost-effective high-voltage power electronics. By alloying β -Ga₂O₃ with Al₂O₃, (Al_xGa_{1-x})₂O₃ is produced with a tunable bandgap (e.g., 4.8-6.2 eV for $x = 0$ to 0.71). This alloy is expected to possess a higher BFOM than β -Ga₂O₃, making it more suitable for power electronic applications. Recent research has shown optoelectronic and power devices utilizing β -(Al_xGa_{1-x})₂O₃, yet most of these power devices operate laterally, which often underperforms compared to their theoretical limits. In contrast, vertical architectures dominate in commercial Si and SiC power devices, particularly in high-voltage and high-power applications. Vertical architectures offer advantages such as increased current and voltage handling capability, superior avalanche capability, absence of surface-related issues, enhanced heat dissipation, and reduced chip area.

Various methods have been proposed to enhance the reverse leakage current performance of Schottky barrier diodes (SBDs), including field plates, guard rings, and junction termination extensions. Additionally, metal-insulator-semiconductor (MIS) diodes have emerged as an appealing alternative to improve reverse performance. Introducing an ultrathin dielectric layer can effectively suppress reverse leakage current and mitigate electrical field effects at Schottky contact edges. Boron nitride (BN) is a promising candidate for MIS diodes due to its UWBG of 6 eV, high breakdown electric field of 12 MV/cm, high stability, and flat surface.

This study successfully demonstrated β -(Al_xGa_{1-x})₂O₃ metal-insulator-semiconductor (MIS) vertical diodes with a ~10 nm BN interlayer. β -(Al_xGa_{1-x})₂O₃ epilayer with an Al composition of 21% and a nominal Si doping of 2×10^{17} cm⁻³, grown by molecular beam epitaxy. BN interlayer was directly deposited on the β -(Al_xGa_{1-x})₂O₃ epilayer using pulsed laser deposition. Pt/Ti/Au was utilized on the BN layer as the top Schottky contact, while Ti/Au served as the bottom Ohmic contact. Forward and reverse I-V measurements were conducted, revealing excellent rectification with a high on/off ratio of ~10⁹. Remarkably, the insertion of the thin BN layer led to a nearly two-order decrease in reverse leakage current compared to traditional vertical β -(Al_xGa_{1-x})₂O₃ SBDs, with the turn-on voltage increasing from 1.5 to 2 V. This approach presents a promising solution to address reverse leakage current issues in β -(Al_xGa_{1-x})₂O₃-based vertical devices, paving the way for next-generation high-power electronics.

4:15 PM EL04.15.06

Developing High-Voltage AlN Schottky Barrier Diodes on AlN Substrates for Power Electronic Device Applications [Dinusha Herath Mudiyansele](#), [Dawei Wang](#), [Bingcheng Da](#), [Ziyi He](#) and [Houqiang Fu](#); Arizona State University, United States

Aluminum Nitride (AlN) is an ultrawide bandgap (UWBG) semiconductor material with a bandgap of 6.1 eV and a high critical field of 12-15 MV/cm, gaining increasing attention as a material suitable for power electronic devices. AlN, in terms of Baliga's Figure of Merit (BFOM), shows the potential to surpass other wide bandgap semiconductors like GaN, SiC, and Ga₂O₃. Despite the potential, devices based on AlN are still in the early phases of development. They encounter several challenges, including the need for high-quality epitaxial growth, establishing proper Ohmic and Schottky contacts, managing high costs, and dealing with a scarcity of conductive substrates. Recently, we have demonstrated 3 kV AlN Schottky Barrier Diodes (SBDs) with the assistance of AlN bulk substrates. Nevertheless, persistent challenges arise from the resistive nature and defects in the material, resulting in a limited understanding of the current transport mechanisms in both forward and reverse bias conditions. Additionally, under high reverse bias, the devices demonstrate elevated leakage currents, necessitating reduction for practical applications in power electronics.

In this research, AlN epilayers were grown using metal-organic chemical vapor deposition (MOCVD) with trimethylaluminum (TMAI) and ammonia (NH₃) as the Al and N sources, and SiH₄ as the *n*-type dopant Si precursor. The device structure comprised of a 1- μ m-thick resistive UID AlN underlayer, a 200 nm Si-doped *n*-AlN layer, and a 2 nm UID GaN capping layer to prevent the oxidation of underlying AlN epilayers. Subsequently, lateral SBDs were fabricated through conventional photolithography, with varying distances between the anode and cathode ($d = 5, 10, 25, \text{ and } 50 \mu\text{m}$). The device configuration included Ti/Al/Ni/Au as Ohmic contacts, and Pt/Au for the Schottky contact, with the Ohmic contacts annealed at 950 °C for 30 s in an N₂ atmosphere. Previous observations revealed that for, $d > 50 \mu\text{m}$, the devices did not exhibit breakdown up to 3 kV, necessitating control for managing the devices' breakdown and critical electrical field. Testing was conducted using a Keithly 4200 Semiconductor parameter analyzer equipped with a controllable thermal chuck, and high voltage measurements were performed using a Keysight B1505A Power device analyzer. The devices exhibited rectification ratios ranging from 10⁶ to 10⁷ as the distance changed from 50 to 5 μm . Temperature-dependent measurements indicated an increasing on/off ratio from 10⁷ to 10⁹ as the temperature varies from 293 to 623 K. Similarly, reverse leakage current testing at -40 V showed an increase from 10⁻¹² to 10⁻¹⁰ A. Breakdown testing indicated breakdown voltages of 0.62, 1.2, 2.6, and < 3 kV for devices with $d = 5, 10, 25, \text{ and } 50 \mu\text{m}$, respectively. These breakdown voltages correspond to an average electric field range of 1.1-1.2 MV/cm. While these electric fields are not high compared to other wideband gap semiconductor technologies, they represent a high value compared to the reported AlN devices without any edge termination or passivation. To enhance device breakdown, SiO₂ passivation will be implemented and tested. Additionally, field-plated structures will be explored to mitigate electric field crowding, particularly at the anode edge, and sustain high breakdown voltages. The potential for further performance enhancement through surface passivation by BN will also be investigated. This research serves as a valuable reference for the development of multi-class AlN high-voltage and high-power devices.

8:00 AM *EL04.16.01

Status and Progress of Vertical GaN-on-Silicon Devices Youssef Hamdaoui, Idriss Abid, Katir Ziouche and [Farid Medjdoub](#); IEMN-CNRS, France

Lateral GaN-on-silicon power transistors are now qualified up to 650 V voltage operation. On the other hand, the development of cost-effective GaN-based vertical devices grown on large diameter silicon substrate combines the advantages of potentially higher voltage operation with avalanche mechanism, high current, high threshold voltage together with a smaller footprint, unreachable with lateral transistors. In addition, vertical architectures rely on current conduction through a drift layer with a uniformly distributed electric field that should prevent the issue of surface charge trapping effects. Nevertheless, this technology is still at an early stage and both material and device fabrication need to be optimized. In this talk, I will discuss the status and rapid progress of fully vertical GaN-on-Silicon devices. In particular, material and processing optimization results in state-of-the-art combination of breakdown voltage (BV) and on-state resistance (Ron) with the first demonstration of avalanche capability.

8:30 AM *EL04.16.02

Recent advances in GaN microwave HEMTs: buffer-free stack and thermal management strategies [Digbijoy N. Nath](#); Indian Institute of Science, India

AlGaN/GaN microwave HEMTs are a mature technology and fast penetrating the market for 5G/wireless communication and military/strategic applications. However, challenges still remain in terms of improving the management of heat which is generated in such devices. Diamond heat sink has been extensively studied for this although commercial RF HEMTs still use Cu-heat sink. In this talk, we shall show our recent results on developing a cooling manifold using microfluidic channels whereby laser is used to etch the channels. The superiority of this approach against usual DRIE-etch based approach will be discussed along with experimental results. Our ongoing work on multi-finger X-band HEMTs with such liquid-cooling approach will be presented.

In the next part, we shall discuss our recent results on buffer-free GaN HEMTs with respect to C- and X-band performance, The study on passivation, gate dielectric and development of multi-finger HEMTs on such platforms will be presented along with load pull data.

9:00 AM EL04.16.03

Surface morphology and electrical resistivity in Ga-doped ZnO thin films: a grayscale fractal study [Chenlei Jing](#); Ankaing University, China

The Ga-doped ZnO (GZO) thin films with different sputtering pressures were prepared on glass substrates by RF-magnetron sputtering at room temperature. The surface morphologies and resistivity were examined by atomic force microscopy (AFM) and a Van der Pauw Method. The fractal geometry of films was further analyzed by the grayscale fractal study. The root-mean-square (RMS) roughness shows a decreasing trend with sputtering pressure while the fractal dimension and resistivity do not change synchronously as the pressure changes. The results show that resistivity is closely affected by the morphology like cluster height, cluster size, and the distance between adjacent clusters, and the cluster change could be obtained by the fractal spectra given by the grayscale study. What's more, resistivity is significantly related to cluster height.

9:05 AM EL04.16.04

Ballistic Quantum Transport in Terahertz Indium Gallium Nitride C-Plane and A-plane High Electron Mobility Transistors [Choudhury J. Prahara](#)^{1,2}; ¹Silicon Institute of Technology, India; ²Band Photonics Materials, United States

This paper presents numerical calculations of ballistic quantum transport in c-plane and a-plane indium gallium nitride high electron mobility transistors (HEMTs). We calculate quantum mechanical transit times across the channel region of the HEMT and take into account spontaneous and piezoelectric polarization in these materials. Unity gain frequencies of 2.8 terahertz are achievable using nanoscale device dimensions. Ballistic gate lengths of 10.8nm-15nm are obtained from quantum transport calculations. A-plane transistors are able to achieve normally-off HEMT operation due to elimination of spontaneous and piezoelectric polarization effects. A-plane transistors also offer higher immunity to gate-drain leakage and to stress-related barrier reliability issues. We explicitly take into account the effect of longitudinal optical (LO) phonon scattering rates on the ballistic device dimensions. Our calculations show that plasmon collective oscillations do not substantially affect the device dimensions in terahertz and near-terahertz regimes for typical device parameters in this material system. We also explicitly study the effect of indium percentage in the indium gallium nitride channel on device characteristics like unity gain frequencies and current densities.

9:20 AM EL04.16.05

Measuring the Static and Dynamic Disorder in β -Ga₂O₃ Using Optical Transmission [Ariful Islam](#), Nathan Rock and Michael Scarpulla; The University of Utah, United States

Gallium oxide (Ga₂O₃) has an extremely wide bandgap, predicted high breakdown field, and can be produced from melt crystal growth techniques making it attractive for next-generation high-power electronics. It is well-known that the optical transitions in monoclinic β -Ga₂O₃ are anisotropic; the threshold energies for carrier generation using linearly polarized light depend on crystallographic direction. Using transmission optical spectroscopy, which probes subtly differently than e.g., ellipsometry, we have investigated the optical transitions of Fe doped [100] β -Ga₂O₃ as function of elevated temperature, and have documented the dramatic bandgap narrowing with temperature, which was recently explained using density functional theory [1]. In addition, we have done the optical transmission of Sn doped [010], [001], [-201] at room temperature and liquid nitrogen temperature.

We elucidate the differences between ellipsometric and transmission measurements and demonstrate that transmission measurements in the literature have determined erroneous values for the bandgap because of very strong Urbach tails. We report on the anisotropy and doping dependencies of the disorder-induced tails in the optical absorption coefficient for β -Ga₂O₃ and separate the tails into static and dynamic disorder induced by phonons. Given the low symmetry of β -Ga₂O₃ and its strong electron-phonon coupling, we observed that the Urbach energy increases at elevated temperature due to the contribution of static and dynamic disorder and exhibit significant anisotropy. However, at liquid nitrogen temperature (77K), the Urbach energy for Fe-doped crystals decreases as the dynamic disorder is suppressed but increases at elevated temperatures. We also show that in the case of room temperature and liquid nitrogen temperature for Sn doped crystal. We analyze the dynamic and static components within the model of Cody et al., [2] and find that the static disorder is actually dominant. We discuss the possible microscopic origins in terms of point and extended defects; interestingly at low absorption coefficients even imperfect surface polishing may contribute. We combine the temperature dependences of the Urbach tails from our measurements with those of the optical transitions from ellipsometry [3], [4] to extract the mean square displacement-deformation potential product for Ga₂O₃ along different crystal directions. These parameters play roles in optical transitions and carrier scattering and are thus critical to measure. We elucidate open questions and opportunities especially for further theory and calculation to predict the implications on multiple properties of wider interest than the Urbach tails per-se.

9:35 AM EL04.16.06

Improving Optoelectrical Properties of Ga₂O₃ Photodetector by Reduced Graphene Oxide (rGO) Decoration for Deep UV Photodetection [Malti](#)

Kumari¹, Basanta Roui^{1,2}, S.B. Krupanidhi¹ and Karuna K. Nanda^{1,3}; ¹Indian Institute of Science, India; ²Central Research Laboratory, Bharat Electronics, India; ³Institute of Physics, India

Deep ultraviolet (200-280 nm) photodetectors have received much attention in the fields of biology, industry, military, etc. The promising optical and electrical properties of wide bandgap, n-type gallium oxide (Ga_2O_3) make it quite suitable for deep UV photodetection. Our work shows that decorating reduced graphene oxide (rGO) can further enhance the photoresponse of the Ga_2O_3 photodetector (PD). rGO - a 2D material has received a lot of interest recently because of its distinctive qualities. In this work, we fabricated rGO/ Ga_2O_3 heterostructure for deep UV photodetection where Ga_2O_3 thin film was deposited on c-plane sapphire substrate using Pulsed laser deposition, and rGO was synthesised by modified hummers method followed by thermal reduction, which was then drop casted on Ga_2O_3 film. The photoresponse of the rGO/ Ga_2O_3 PD illuminated under 250 nm light was found to be substantially higher than the Ga_2O_3 PD, indicating an improvement of photoelectric properties for the UV photodetector based on Ga_2O_3 thin film. The dark current was found to be lower for rGO/ Ga_2O_3 PD, and the illumination-to-dark current ratio ($I_{\text{illumination}}/I_{\text{dark}}$) was increased to 78.31 from 7.30 for Ga_2O_3 PD at a voltage of 5 bias and power density of 12.83 mW/cm². Thus, it can be concluded from the results that rGO/ Ga_2O_3 PDs have great promise for photodetection applications.

9:50 AM EL04.16.07

The disorder and strain transformation of $\beta\text{-Ga}_2\text{O}_3\text{:Si,N}$ after implantation to heated substrate Iraida N. Demchenko¹, Yevgen Syryanyy^{1,2}, Asiyeh Shokri¹, Yevgen Melikhov³ and Maryna Chernyshova¹; ¹Institute of Plasma Physics and Laser Microfusion, Poland; ²Warsaw University of Technology, Faculty of Electronics and Information Technology, Poland; ³Institute of Fundamental Technological Research Polish Academy of Sciences, Poland

Ga_2O_3 can become a powerful substitute for GaN in the power electronics industry in devices, such as MOSFETs and others [1-2]. Together with ion implantation, which is a versatile fabrication technique widely adopted in the mass production of commercial semiconductors, the fabrication of all-ion-implanted vertical gallium oxide transistor could greatly enhance the prospects for Ga_2O_3 -based power electronics. For the realization of such systems, ion implantation can be used for channel/contact region doping and device isolation if necessary [3]. The important limitation of implantation is the buildup of lattice disorder due to the ballistic character of this process. Consequently, there is strong motivation to study the defects formation and their transformations. The ion implantation effects in compound crystals, e.g. GaN and ZnO, have been extensively studied in the last decade [4]. In the case of Ga_2O_3 however, the mechanism of defect buildup is completely unknown. The main problem comes from the fact that the accumulation of defects and their transformations in ion implanted compound crystals is a complicated multistep process resulting in the formation of a mixture of different types of defects. It is important to identify the location of implanted ions in the bulk and thin film crystal lattice, their surroundings, interaction with the host matrix and with structural and native point defects. In addition, an important consideration for the viability of ion implantation in Ga_2O_3 is the rate of diffusion of the different impurities.

In this work, we study the effect of inserting Si/N atoms into $\beta\text{-Ga}_2\text{O}_3$ utilizing ion implantation to a heated substrate. This process of material formation offers an interesting and complex field of study, with plenty of intrinsic defects, as well as their formation into defect complexes with the implanted ion. Such complexity requires the use of a variety of complementary analytical methods in order to perform a quantitative analysis. Here, we report the results of many analytical techniques, such as Rutherford Backscattering Spectrometry, Particle Induce X-ray Emission, High-resolution X-Ray Diffraction, Raman spectroscopy, Transmission Electron Microscopy, as well as synchrotron radiation-based technique as X-Ray Absorption Near Edge Structure supported by Density Functional Theory. All of this allows us to create a novel approach to study Ga_2O_3 implanted by Si/N ions.

Acknowledgements: The work was partially supported by the Interdisciplinary Centre for Mathematical and Computational Modelling at University of Warsaw, Poland, grant ID 3557. These studies were financially supported from the project UMO-2020/39/B/ST5/03580 founded by the National Science Centre in Poland.

- [1] S.J. Pearton et al., Appl. Phys. Rev. 5 (2018) 011301.
- [2] M. Higashiwaki et al., Appl. Phys. Lett. 112 (2018) 060401.
- [3] M.H. Wong et al., IEEE Electron Device Letters 40 (2019).
- [4] A. Turos et al., Acta Materialia 134, (2017) 249.

10:05 AM EL04.16.08

Controlling The Alloy Fluctuations in AlGa_N Materials Grown by Plasma-Assisted Molecular Beam Epitaxy: Effect on Ultraviolet Light Emitting Diodes Pushan Guha Roy¹, Sayantani Sen^{1,2} and Anirban Bhattacharya¹; ¹University of Calcutta, India; ²Sister Nivedita University, India

Molecular beam epitaxy (MBE) has been extensively used for the growth of III-Nitride materials and devices as this technique has the scope of accessing a much wider range of operating parameter-space than competing technologies. These can be exploited to address the problems in the UV-LEDs, such as low internal quantum efficiency, poor p-type doping etc. This work focuses on the effect of group III/V flux ratio variation on the AlGa_N alloy properties, and consequently on the characteristics of UV emitters. Furthermore, in-situ monitoring of this parameter which is essential for accurate and reproducible growth process has been addressed.

AlGa_N alloys were grown using a VEECO GEN930 plasma-assisted molecular beam epitaxy (PA-MBE) system. The growth was monitored in real-time based on the temporal evolution of RHEED patterns and a custom designed image capture and analysis system. An algorithm was developed for the direct monitoring of excess metallic film on the growth surface using the RHEED pattern, which was found to be the critical parameter. A series of otherwise identical samples were grown under various group III/V flux ratios ranging from excess group III to near-stoichiometric, and UV-LEDs were fabricated.

For series A devices (covering the high group III flux range), a single electroluminescence peak was observed, which was red-shifted from 323 nm under III/V>1 conditions to 348 nm under III/V>>1 growth, while the intensity of the peak increased by nearly 30 times. Furthermore, the droop, that is the reduction of peak intensity with increased injection currents reduced significantly for the samples grown under III/V>>1 conditions.

These results can be attributed to the presence of in-plane compositional inhomogeneities in the active region material. For growth under excess group III conditions, a thin metallic film of Ga always remains on top of the growth surface. The Al atoms are incorporated in this film, and subsequent reaction with plasma nitrogen results in the formation of AlGa_N. As the metallic film consists of an inhomogeneous mixture of Al and Ga, the resulting AlGa_N film possesses nano-scale fluctuations in the composition. Under conditions of III/V>>1, deep level fluctuations are formed within the AlGa_N alloy, that give rise to single red-shifted peaks. These fluctuations are spatially dense, inhibiting the carriers from travelling to non-radiative recombination sites and thus reducing the probability of current droop in the devices.

For series B devices (covering the near-stoichiometric growth regime), however, clear dual-wavelength behavior was observed with two peaks at around 330 nm (P1) and 345 nm (P2). Interestingly, switching between these two peaks was observed when the duty cycle of the excitation was varied from 10% to dc values, without any change in the other excitation parameters. In this series, other devices grown under slightly different deposition conditions indicated a switching between 310 nm and 350 nm.

Under conditions of near-stoichiometry, there is nearly no metallic film on the growth surface. As liquid Ga also acts as a surfactant, the absence of it leads to limited surface adatom mobility, specifically of Al compared to Ga, which eventually result in short range fluctuations in the AlGaIn films. These give rise to two peaks of distinctly different wavelengths in the devices of series B. The wavelength-switching phenomenon is due to the difference in thermal dissociation of excitons in fluctuations of different energy depths which was confirmed by carrying out temperature dependent electroluminescence measurements.

We conclude that the emission parameters are influenced by change in growth conditions, specifically the group III/V flux ratio, generating not only single-peak LEDs that displayed significantly reduced droop but also switchable dual wavelength LEDs.

10:20 AM EL04.16.09

Effect of Copper Doping on Zinc Oxide and the Potential for Nanowire Devices [Sazzad Hussain](#) and Larry R. Carley; Carnegie Mellon University, United States

While silicon continues to dominate the semiconductor landscape, other materials have shown significant promise in conventional field-effect transistor (FET) devices as well as in optoelectronics and flexible electronics regime, zinc oxide (ZnO) being one of them. The doping of ZnO to generate carriers and consequently, designing devices of interest are active areas of research with several materials touted as possible dopants. In particular, much effort has gone into finding a reliable acceptor doping scheme as it has proven to be complicated to develop p-doped ZnO preventing the widespread use of it in certain applications. The goal of this study is to find the effects of copper (Cu) substitutional doping on ZnO using quantum mechanical computational models namely density functional theory (DFT) in conjunction with semi-empirical tight-binding extended Hückel method and non-equilibrium Green's function (NEGF). DFT is used for material property determination whereas the semi-empirical model is used for device simulations which provides some key advantages over DFT in the context of this study including a reasonable simulation time for a system with a large number of atoms as is the case with most electronic devices.

Analyses of how selectively supplanting zinc (Zn) with copper (Cu) impacts the electronic properties of the resultant structure and if the alterations can be leveraged to construct nanowire FET devices are performed. The density of states and carrier concentration calculations reveal that Cu doping of ZnO leads to p-type characteristics in the semiconductor. A massive increase in hole concentration to the order of 10^{18} cm^{-3} takes place after the addition of copper. The resultant structure is then used to build junctionless nanowire metal-oxide-semiconductor field-effect transistors (MOSFETs). The choice of the junctionless variant of the MOSFET is driven by its robust performance in the short-channel domain and fabrication simplicity. The nanoscale device exhibits excellent figures of merit including an on-current (I_{on}) of more than $500 \mu\text{A}/\mu\text{m}$ and an on-current to off-current ratio ($I_{\text{on}}/I_{\text{off}}$) of greater than 5×10^6 for certain configurations. In addition, several parameters like source/drain underlap length and work function of the gate material among others are varied, and guidelines are presented on optimization concerning $I_{\text{on}}/I_{\text{off}}$, I_{on} , and subthreshold swing (SS). The effects of different dielectric materials on the device performance are also studied. It is found that the use of high- κ dielectrics like hafnium oxide (HfO_2) can significantly improve the performance of the device. Furthermore, the merits and challenges of the modeling approach are discussed.

10:35 AM EL04.16.10

Comparative Studies on the Structural, Electrical and Optical Properties of Single-Doped (Al) and Co-Doped (Al/B, Al/In, Al/Gd) ZnO Films deposited by Sol-Gel [Angel R. Torres Duarte](#), Humberto Arizpe-Chavez, Temistocles Mendivil-Reynoso and Roberto Mora-Monroy; Universidad de Sonora, Mexico

We investigated the effects of various doping concentrations on the structural, electrical, and optical properties of ZnO films single-doped with Aluminium and co-doped with Al/In, Al/B, and Al/Gd. The purpose of this study is to explore the role of Aluminium as a dopant in the lattice of ZnO. The films were deposited on glass substrates by dip coating in sol-gel solutions. The doping concentration levels were 4, 8, and 12 %. Zinc acetate dihydrated with a constant molar concentration of 0.5 M was used as a precursor. Absolute Ethanol and Diethanolamine were used as solvent and stabilizing agents respectively co-doping was prepared in an equimolar manner. The films annealed at 500°C , were characterized by X-ray diffraction (XRD), UV-Vis-NIR spectroscopy, Atomic Force Microscopy (AFM), Scanning Electron Microscopy (SEM), and X-ray photoelectron spectroscopy (XPS). Resistivity was measured with the four-point probe method. The results revealed the formation of a nanostructured hexagonal (wurtzite) ZnO structure with no preferred orientation. The crystallite sizes decrease with the increase of dopant levels, in a general trend. Small variations in the calculated lattice parameters were attributed to the differences in the ionic radii of Zn^{2+} and the dopants. Resistivity results were related with oxygen vacancies and interstitial oxygen defects present in the high-doped samples. A red shift of the band gaps was discussed in terms of the doping levels and the Bursten-Moss effect. Also, the role of traps in the evolution of the optical band gap, was determined by the curves of $\text{Ln}(\text{Absorbance})$ and $\text{Ln}(\text{Absorption coefficient})$ as a function of the photon energy.

10:40 AM *EL04.16.11

Impact of Interface Chemistry and Crystalline Defects on The Reliability of 4H-SiC MOSFETs [Patrick Fiorenza](#); CNR-IMM, Italy

The growing silicon carbide (4H-SiC) device demand in applications with high reliability constrains (i.e. automotive etc) imposes the scientific community to acquire a deeper comprehension of the physical phenomena affecting the device integrity under prolonged stress, with a particular focus on the impact of the crystalline defects in the semiconductor epitaxial layer. However, threshold voltage (V_{th}) instability phenomena and poor field effect channel mobility (μ_{FE}) are still observed in 4H-SiC MOSFETs, and can be only partially mitigated by post-oxidation (POA) or post-oxide deposition annealing (PDA) processes.

In this context, in this invited talk, some reliability concerns affecting the performances of 4H-SiC MOSFETs are discussed. In particular, the following aspects will be addressed: the SiO_2/SiC interface chemistry and the impact of the device fabrication processes on the MOSFET threshold voltage (V_{th}) stability, and the impact of the semiconductor crystalline defect on the device lifetime.

4H-SiC MOSFETs were characterized by means of current voltage ($I_{\text{D}}-V_{\text{G}}$) transfer characteristics and capacitance-voltage (C-V) measurements. Furthermore, on selected failed devices, Scanning Transmission Electron Microscopy (STEM) analyses combined to electron energy loss spectroscopy (EELS), and electrical Scanning Probe Microscopy (SPM) analyses have been used to elucidate the physical mechanisms affecting their reliability. An important aspect is related the breakdown of 4H-SiC MOSFETs correlated to the presence of different crystalline defects in the 4H-SiC epitaxial layer. Of particular interest are the wafer level characterization of both the failed devices at $t=0\text{s}$, and of the devices showing an anomalous Fowler-Nordheim (FN) gate bias conduction. In fact, it is possible to correlate devices failing under high temperature gate bias (HTGB) stress with the presence of an anomalous FN behavior and the presence of a surface bump on the semiconductor. Moreover, the role of the threading dislocation (TD) in high temperature reverse bias (HTRB) failures was demonstrated employing high-resolution SPM techniques. These nanoscale methods elucidated the physical mechanism of the dielectric breakdown, revealing an increase of the minority carrier concentration close the insulator/semiconductor interface. Furthermore, a method to monitor the V_{th} variation from single point drain current (I_{D}) measurement using a single gate bias (V_{read}) value is presented. This method allowed to probe the interface states close to the 4H-SiC conduction and valence band edges and the amount of trapped charge at the interface close to 4H-SiC band

edges (N_{it}) an inside the near interface oxide region (NIOTs).

These finding demonstrated that the threshold voltage instability of 4H-SiC MOSFETs, associated to different trapping mechanisms, is directly related to the SiO₂/SiC interface chemistry and can be mitigated by an accurate control of the nitridation conditions of deposited oxides.

- [1] P Fiorenza, F. Giannazzo, S. Cascino, M. Saggio, F. Roccaforte. Appl. Phys. Lett. 117, 103502 (2020)
- [2] P. Fiorenza, C. Bongiorno, F. Giannazzo, M. S. Alessandrino, A. Messina, M. Saggio, F. Roccaforte; Appl. Surf. Sci. 557 149752 (2021)
- [3] P. Fiorenza, M S Alessandrino, B Carbone, C Di Martino, A Russo, M Saggio, C Venuto, E Zanetti, F Giannazzo, F Roccaforte Nanotechnology 31 (2020) 125203
- [4] P. Fiorenza, S. Adamo, M. S. Alessandrino, C. Bottari, B. Carbone, C. Di Martino, A. Russo, M. Saggio, C. Venuto, E. Vitanza, E. Zanetti, F. Giannazzo, F. Roccaforte, IEEE IRPS (2021)
- [5] P. Fiorenza, M. Zignale, M. Camalleri, L. Scalia, E. Zanetti, M. Saggio, F. Giannazzo, F. Roccaforte Mater. Sci. Semicon. Proc.169 (2024) 107866

SESSION EL04.17: On-Demand Presentation
Tuesday Morning, May 7, 2024
EL04-virtual

10:30 AM EL04.08.03

First Principle Calculation of Resistive Switching in ZnO [Satyasiban Dash](#) and Prahallad Padhan; Indian Institute of Technology, Madras, India

The resistance of the metal oxides under external bias has been observed to show brain-like synapses. Switching of resistance forms the base criterion for realizing stable neuromorphic electronic devices. Resistive switching involves the alternative change of resistance with the applied external bias. With a suitable metal-metal oxide-metal configuration, it is possible to create Resistive-Random Access Memories (ReRAMs). Unlike conventional RAMs, the RERAMs are characterized by faster switching time, low power consumption and enhanced stability. Under the condition of ON state, i.e., low resistance state, a conductive filament formed in the oxide layer due to segregation of oxygen vacancy or metal ions. In the case of the OFF state, this filament gets ruptured, leading to a high resistive state. Several metal oxides, like TiO₂, HfO₂, SrTiO₃, ZnO, etc., have shown this behaviour. The physical nature, electrical properties, and morphology of conductive filament formation have been studied through various in-situ and ex-situ techniques like transport measurement, transmission electron microscopy, x-ray photoelectron spectroscopy, and atomic force microscopy. However, the nature of electron distribution and subsequent contribution from other orbital remains tricky. In this regard, we have explored the resistive switching phenomena of ZnO on the basis of charge injection and charge removal using density functional theory. In the case of ZnO, the oxygen vacancy migration and subsequent charge transfer occur through the conductive filament. Oxygen vacancies can exist in three different states, V_{O}^{\bullet} , $V_{O}^{\bullet\bullet}$ and with two, one and zero electron, respectively. The band structure clearly shows that these oxygen vacancies act as a deep donor. The appeared near the VBM and was found to be stable at higher energy than V_{O}^{\bullet} and $V_{O}^{\bullet\bullet}$. When an electron from V_{O}^{\bullet} is removed, it forms $V_{O}^{\bullet\bullet}$ state, a metastable paramagnetic and unstable state, but upon removing the other electron, the state is very stable. The formation energy of both and is less comparable to state thus, oxygen vacancy acts as a negative U-centre point defect. For the state, the four Zn nearest neighbours are displaced inward by 12 % of the equilibrium Zn-O bond length, whereas for the V_{O}^{\bullet} and $V_{O}^{\bullet\bullet}$ states, the displacements are outward by 2 % and 23 %, respectively. In order to mimic the conductive filament, vacancies are created along [010] direction, and rupture is replicated by replacing a vacancy with oxygen. Electron localisation and band decomposed charge density calculations have confirmed the observation of conductive filament. A better understanding of the nature of resistive switching will help in the development of ReRAMs and neuromorphic electronic devices.

SYMPOSIUM EL05

Two-Dimensional (2D) Materials and Heterostructures—Large-Scale Growth and Device Integration
April 23 - May 7, 2024

Symposium Organizers

Silvija Gradecak, National University of Singapore
Lain-Jong Li, The University of Hong Kong
Iuliana Radu, TSMC Taiwan
John Sudijono, Applied Materials, Inc.

Symposium Support

Gold
Applied Materials

* Invited Paper

+ JMR Distinguished Invited Speaker

^ MRS Communications Early Career Distinguished Presenter

SESSION EL05.01: Transistors I
Session Chairs: Silvija Gradecak and John Sudijono

Tuesday Morning, April 23, 2024
Room 344, Level 3, Summit

10:30 AM DISCUSSION TIME - INTRODUCTION

10:45 AM *EL05.01.01

Will 2D Materials Play a Role in The Semiconductor Industry? [Eric Pop](#); Stanford University, United States

This talk will present my (biased) perspective on whether two-dimensional (2D) materials could play a role in the semiconductor industry. It is important to recognize that 2D materials are good for applications where their ultrathin nature gives them distinct advantages, such as flexible electronics [1] or light-weight solar cells [2]. They may not be good where conventional materials work sufficiently well, like transistors thicker than a few nanometers. I will focus on 2D materials for 3D heterogeneous integration of electronics, which has major advantages for energy-efficient computing [3]. Here, 2D materials could be monolayer transistors with ultralow leakage [4] (due to larger band gaps than silicon), used to access high-density memory [5]. Recent results from our group [6,7] and others [8] have shown monolayer transistors with good performance, which cannot be achieved with sub-nanometer thin conventional semiconductors, and the 2D performance could be further boosted by strain [9]. I will also describe some unconventional applications, using 2D materials as thermal insulators [10], heat spreaders [11], and thermal transistors [12]. These could enable control of heat in “thermal circuits” analogous with electrical circuits. Combined, these studies reveal fundamental limits and some key applications of 2D materials, which take advantage of their unique properties. **Refs:** [1] A. Daus et al., *Nat. Elec.* 4, 495 (2021). [2] K. Nassiri Nazif, et al., *Nat. Comm.* 12, 7034 (2021). [3] M. Aly et al., *Computer* 48, 24 (2015). [4] C. Bailey et al., *EMC* (2019). [5] A. Khan et al. *Science* 373, 1243 (2021). [6] C. English et al., *IEDM*, Dec 2016. [7] C. McClellan et al. *ACS Nano* 15, 1587 (2021). [8] S. Das et al., *Nat. Elec.* 4, 786 (2021). [9] I. Datye et al., *Nano Lett.* 22, 8052 (2022). [10] S. Vaziri et al., *Science Adv.* 5, eaax1325 (2019). [11] C. Koroglu & E. Pop, *IEEE Elec. Dev. Lett.* 44, 496 (2023). [12] M. Chen et al., *2D Mater.* 8, 035055 (2021).

11:15 AM EL05.01.02

Advancements in 2D Semiconductor CMOS: Length Scaling, Gate Dielectric, Doping Engineering and Machine Learning Co-Optimization [Hao-Yu Lan](#)¹, Yi Wan², Chih-Pin Lin^{1,3}, Chin-Cheng Chiang¹, Tuo-Hung Hou³, Lain-Jong Li², Joerg Appenzeller¹ and Zhihong Chen¹; ¹Birck Nanotechnology Center, Purdue University, United States; ²The University of Hong Kong, Hong Kong; ³National Yang Ming Chiao Tung University, Taiwan

This research presents recent advancements in 2D Transition Metal Dichalcogenides (TMD) Ribbon Field-Effect Transistors (RibbonFETs) as potential successors to Silicon RibbonFETs. These advancements include the scalable fabrication of ultra-narrow TMD nanoribbons, as narrow as 30 nm, leading to an impressive on-current I_{ON} of approximately 700 $\mu\text{A}/\mu\text{m}$ at $V_{DS}=1\text{ V}$. The improved electrostatics and heat distribution contribute to a significant 40% enhancement in both on-state and off-state performance. In terms of dielectric interface engineering for monolayer MoS_2 (1L- MoS_2) FETs, the integration of a high- κ TaO_x interfacial layer reduces active interface trap states and acts as an effective doping layer. This results in a superior I_{ON} of 861 $\mu\text{A}/\mu\text{m}$ at $V_{DS}=1.5\text{ V}$ and reduced contact resistance (R_C) of 230 $\Omega\ \mu\text{m}$. Dual-gate (DG) FETs achieve subthreshold swing (SS) values of approximately 70 mV/dec. Despite its small bandgap, hexagonal boron nitride (hBN) serves as a passivation and crystalline interfacial layer, improving device reliability and achieving an ideal SS of 62 mV/dec. The study also addresses reliability concerns of 1L- MoS_2 FETs on thin high- κ HfO_2 , indicating that optimized ALD processes can ensure notable stability. Furthermore, the study introduces a novel nitric oxide (NO) doping approach for monolayer tungsten diselenide (1L- WSe_2) transistors, addressing issues with high-resistive metal contact and threshold voltage. This molecular doping technique enables unipolar p-type transport and reduces Schottky barrier, resulting in a record-low R_C of 875 $\Omega\ \mu\text{m}$, the highest transconductance (g_m) of 400 $\mu\text{S}/\mu\text{m}$, and the lowest SS of 90 mV/dec. Additionally, a hybrid p-doping strategy combining tungsten oxide (WO_x) charge transfer with NO molecular doping achieves record-high I_{ON} and g_m while maintaining intrinsic channel properties. To improve the performance of 2D transistors, we propose a design and process co-optimization framework using Machine Learning (ML), similar to conventional Design of Experiments (DOE) for process optimization. Overall, these findings highlight significant progress in 2D semiconductor CMOS transistors, with a focus on length scaling, gate dielectrics, innovative p-doping techniques, and Machine Learning Co-Optimization.

11:30 AM EL05.01.03

Monolayer WSe_2 Nanoribbon Transistors with WO_x Passivated Edges [Sihan Chen](#), Yue Zhang, William P. King, Arend M. van der Zande and Rashid Bashir; University of Illinois at Urbana-Champaign, United States

Two-dimensional (2D) semiconductors like transition metal dichalcogenides (TMDs) such as MoS_2 and WSe_2 , have demonstrated record-high electron and hole mobility values with sub-nm body thicknesses,^{1,2} showing great promise to sustain the transistor scaling trend beyond silicon complementary metal-oxide-semiconductor (CMOS) technologies. Since front-end silicon transistors are moving to a gate-all-around nanoribbon architecture, TMDs will adopt a similar stacked nanoribbon geometry to be competitive.³ However, as the channel width approaches sub-100 nm, the effects of edge states of the nanoribbon channel become pronounced, limiting the carrier mobility of TMD nanoribbons.⁴ The edge states must be passivated to fabricate high-performance, ultra-scaled TMD transistors.⁵

This work demonstrates a facile edge passivation method that significantly reduces edge disorders and enhances the electrical performance of p-type monolayer WSe_2 nanoribbon field-effect transistors (FETs). We achieved this by fabricating monolayer WSe_2 nanoribbon transistors with WO_x passivated edges. The process involved using nanolithography to deposit polymer masks on prefabricated microribbon transistors, followed by a controlled remote O_2 plasma treatment. To avoid device-to-device variation, we sequentially fabricated and measured two types of nanoribbons on the same devices – passivated-edge nanoribbons and open-edge nanoribbons, with a width ranging from 50 nm to 70 nm. Open-edge nanoribbons are the nanoribbons with dangling bonds at the edges, whereas passivated-edge nanoribbons are the nanoribbons with edge atoms covalently bonded to WO_x . Compared to the open-edge nanoribbon FETs, the passivated-edge nanoribbon FETs increased the maximum current by 7–120 times, improved field-effect mobility by 6–24 times and decreased subthreshold swing by an average of $38\pm 9\%$. Hole doping induced by edge-bound WO_x was $\sim 1\times 10^{12}\text{ cm}^{-2}$. The enhanced electrical performance in passivated-edge nanoribbon FETs primarily results from reduced disorders by eliminating dangling bonds, rather than the doping effect from WO_x at the edges. Here we report, for the first time, a working p-type transistor from TMD monolayers with a channel width smaller than 100 nm. Owing to its simplicity and robustness, this edge passivation method holds the potential to become a turnkey manufacturing solution for large-scale integration of high-performance, ultra-scaled WSe_2 p-FETs into commercial silicon foundries.

References:

- (1) Liu, S.; Liu, Y.; Holtzman, L.; Li, B.; Holbrook, M.; Pack, J.; Taniguchi, T.; Watanabe, K.; Dean, C. R.; Pasupathy, A. N.; et al. Two-Step Flux Synthesis of Ultrapure Transition-Metal Dichalcogenides. *ACS Nano* **2023**, 23, 59.
- (2) Wang, Y.; Kim, J. C.; Wu, R. J.; Martinez, J.; Song, X.; Yang, J.; Zhao, F.; Mkhoyan, A.; Jeong, H. Y.; Chhowalla, M. Van Der Waals Contacts between Three-Dimensional Metals and Two-Dimensional Semiconductors. *Nature* **2019**, 568 (7750), 70–74.
- (3) O'Brien, K. P.; Naylor, C. H.; Dorow, C.; Maxey, K.; Penumatcha, A. V.; Vyatskikh, A.; Zhong, T.; Kitamura, A.; Lee, S.; Rogan, C.; et al. Process

Integration and Future Outlook of 2D Transistors. *Nat. Commun.* **2023**, *14* (1), 1–5.

(4) Chowdhury, T.; Sadler, E. C.; Kempa, T. J. Progress and Prospects in Transition-Metal Dichalcogenide Research beyond 2D. *Chem. Rev.* **2020**, *120* (22), 12563–12591.

(5) Das, S.; Sebastian, A.; Pop, E.; McClellan, C. J.; Franklin, A. D.; Grasser, T.; Knobloch, T.; Illarionov, Y.; Penumatcha, A. V.; Appenzeller, J.; et al. Transistors Based on Two-Dimensional Materials for Future Integrated Circuits. *Nat. Electron.* **2021**, *4* (11), 786–799.

11:45 AM EL05.01.04

Enhancing Carrier Mobility with Process Induced Strain in Monolayer MoS₂ Transistors [Kevin Zhao](#), Yue Zhang and Arend M. van der Zande; University of Illinois at Urbana-Champaign, United States

Two-dimensional materials are a promising candidate for future non-silicon electronics based in the "More Moore" development path, owing to their ability to circumvent many fundamental challenges hindering the continued scaling of current silicon-based technologies. Using atomically-thin channels strongly suppresses undesirable short channel effects such as drain-induced barrier-lowering and body punchthrough. However, there are important knowledge gaps in how thin film deposition materials and processes impact 2D materials properties, leading to enormous variability in reported device performance metrics. Understanding these interactions has practical implications on improving not just the reliability but also enhancing the performance of 2D transistors. Analogously, one of the many commercially implemented performance enhancement techniques in CMOS is the deposition of high stress capping layers, which increase the carrier mobilities of NMOS and PMOS transistors. The key question is how thin film deposition will impact doping and strain in 2D materials, and how to unravel their relative effects. Here, we systematically quantify the effects of thin film processed induced strain on the carrier mobility of monolayer MoS₂ transistors. To achieve this, we encapsulate the monolayer MoS₂ transistors under a HfO₂ barrier layer via atomic layer deposition before using E-beam evaporation to sequentially deposit MgO films on the same set of devices, while measuring the Raman spectra and transport between each deposition. The evaporated MgO film has a built-in internal compressive stress, which applies a tensile strain to the underlying transistor channel. This approach both maximizes data consistency by removing sample-to-sample variation.

We use vector decomposition on the Raman peak shifts in the channel to unravel the relative strain and doping induced by the film deposition. We found a systematic shift in the strain as a function of MgO thickness reaching a value of 0.45% at 150 nm. The initial deposition of MgO created a doping shift of $3 \times 10^{12}/\text{cm}^2$. The addition of the HfO₂ barrier suppressed further doping fluctuations to under $1 \times 10^{12}/\text{cm}^2$. Raman mapping confirmed the uniformity of channel strain for up to 150 nm of MgO, at which point we observe slip induced nonuniformities in the strain distribution. We measured the transfer and output characteristics of the MoS₂ transistor as a function of film thickness. Under 0.45% tensile strain, the MoS₂ transistors exhibit a electron mobility enhancement of 40%, a saturation current enhancement of 45%, and a -15 V shift in the threshold voltage. This yields the rate of mobility enhancement of n-type MoS₂ to be 90% per percent of biaxial strain.

We are now extending this experiment to p-type transition metal dichalcogenide transistors as well as compressive strains, to fully realize strain-enhanced two-dimensional CMOS logic. We are applying the Transfer Length Method to systematically isolate the relative impact of contact resistances versus channel conductivity on transistor performance. These results form a critical foundation for the design and characterization of commercialized high-speed two-dimensional integrated electronics, using existing thin-film deposition technologies in industry.

SESSION EL05.02: Transistors II
Session Chairs: Hippolyte Astier and Lain-Jong Li
Tuesday Afternoon, April 23, 2024
Room 344, Level 3, Summit

1:30 PM *EL05.02.01

Heterogeneous and Monolithic 3D Integration of 2D Materials-Based Devices for Future Computing Jinfeng Leong, Baoshan Tang, Maheswari Sivan, Jianan Li, Evgeny Zamburg and [Aaron Thean](#); National University of Singapore, Singapore

The inherent limitation of silicon-based complementary metal oxide semiconductors (CMOS) has placed constraints on the continuous performance enhancement of integrated circuits through dimension scaling. Monolithic three-dimensional (M3D) integration, which involves the stacking of devices on top of conventional silicon chips, offers promising avenues for enhancing system performance [1]. Integration of silicon-based CMOS transistors above the metal interconnect layers for massive M3D circuits compromises the devices and interconnect wires due to the high process thermal budget, necessitating exploration for low-thermal budget solutions beyond silicon. This presentation outlines our recent research efforts to explore high throughput, solution-processable 2DM compatible with semiconductor CMOS chip process technology capable of low-thermal budget heterogeneous integration. Specifically, we showed that analog memories formed from a composite stack of liquid-exfoliated MoS₂ flakes can attain superior resistive memory switching performance relative to both single-layer 2DM-based and oxide-based devices [3]. These solution-processed MoS₂ analog memories can be formed under low-thermal budgets and have been demonstrated on a wafer-level for the realization of M3D in-memory computing. Moreover, these MoS₂ analog memories can also be heterogeneously integrated with photonic neural networks to address the challenges of implementing non-linear activation functions in photonic neurons [4]. To tackle the limitations of materials and device engineering, we will also discuss system architecture-device-materials co-design strategies [4,5] to enhance overall on-chip computational functionality.

Reference:

- [1] A Thean, et al. 2022 IEDM, 12.2.1-12.2.4;
- [2] B Tang, et al. *Nat. Commun.* 2022, 13 (1), 3037;
- [3] Z Xu, et al. *Light Sci. Appl.* 2022, 11 (1), 288
- [4] M Sivan, et al. *Nat. Commun.* 2019, 10(1), 5201;
- [5] J F Leong, et al. *Advanced Func. Mat.* 2023, 2302949

2:00 PM *EL05.02.02

Semiconductor Industry Progress on 2D TMD Transistors and Challenges Ahead [Kevin P. OBrien](#); Intel - Components Research, United States

The key question is, can any material replace Silicon transistors and why would you. Both the academic and industrial communities have proposed two-dimensional (2D) transition metal dichalcogenide (TMD) semiconductors as a future option to beat silicon transistors at sub-10nm physical gate lengths. In this talk, we highlight what TMD transistors need to meet in terms of performance and architecture. In addition, we share the recent progress in the fabrication of complementary metal-oxide-semiconductor (CMOS) devices based on stacked 2D TMD nanoribbons. We will specifically highlight issues

that need to be resolved by the 2D community in five crucial research areas: contacts, channel growth, gate oxide, variability, and doping. While 2D TMD transistors have great potential, more research is needed to understand the physical interactions of 2D materials at the atomic scale.

References

O'Brien, K.P., Naylor, C.H., Dorow, C. *et al.* Process integration and future outlook of 2D transistors. *Nat Commun* **14**, 6400 (2023).

<https://doi.org/10.1038/s41467-023-41779-5>

K. P. O'Brien *et al.*, "Advancing 2D Monolayer CMOS Through Contact, Channel and Interface Engineering," *2021 IEEE International Electron Devices Meeting (IEDM)*, San Francisco, CA, USA, 2021, pp. 7.1.1-7.1.4, doi: 10.1109/IEDM19574.2021.9720651.

2:30 PM EL05.02.03

Short Top-Gate Length in 2D p-FETs achieved via Van der Waals Integration Min Sup Choi¹, Tien Dat Ngo², Tuyen Huynh² and Won Jong Yoo²;

¹Chungnam National University, Korea (the Republic of); ²Sungkyunkwan University, Korea (the Republic of)

The lack of high-performance p-type field effect transistors (p-FETs) is impeding the potential of 2D materials in upcoming CMOS technology. One potential solution to this challenge is the use of a top-gate (TG) structure with a p-doped spacer area.[1-3] However, designing and processing the device to create gate stacks presents significant obstacles in realizing ideal p-FETs and PMOS inverters. In this research, we propose a novel method for achieving high-performance lateral p⁺-p-p⁺ junction WSe₂ FETs with controlled TG length. Our approach involves the integration of self-aligned TG stacks through van der Waals (vdW) integration, followed by oxygen plasma doping in the contact spacer regions. Unlike traditional techniques, we demonstrate effective electrostatic control of 2D p-FETs by implementing the TG stacks. The use of self-aligned TG as a doping mask yields a high on-off current ratio of >10⁷, a small subthreshold swing (SS) of 98 mV dec⁻¹, and a nearly zero threshold voltage (V_{th}) in WSe₂ p-FETs. Scaling down the TG length to 300 nm results in a high on-state current of approximately 100 μA μm⁻¹, preserving on/off ratio of 10⁴. Additionally, we validate the effectiveness of our method by demonstrating a PMOS inverter with a remarkably low power consumption of ~4.5 nW.

2:45 PM BREAK

SESSION EL05.03: Transistors and Characterization

Session Chairs: Kevin O'Brien and Aaron Thean

Tuesday Afternoon, April 23, 2024

Room 344, Level 3, Summit

3:15 PM EL05.03.01

Atomic Force Microscopy for Routine, Fast and Reliable Defect Quantification in 2D Materials Kaikui Xu¹, Madisen Holbrook², Yucheng Yang¹, Luke N. Holtzman², Kristyna Yang¹, Abhay Pasupathy², Katayun Barmak², James Hone² and Matthew R. Rosenberger¹; ¹University of Notre Dame, United States; ²Columbia University, United States

Routine defect characterization is a critical capability for understanding defect-property correlations and optimizing growth of two-dimensional (2D) materials. High throughput optical methods for defect characterization, such as Raman spectroscopy, are useful for graphene, but are insufficiently sensitive to defects in some other 2D materials, such as transition metal dichalcogenides (TMDs), particularly for defect densities of about 10¹² cm⁻² or less. Typical methods for directly detecting defects at the atomic scale, such as scanning transmission electron microscopy (STEM) and scanning tunneling microscopy (STM), are effective, but they are slow and often require arduous sample preparation. There is a need for 2D material defect characterization techniques that are routine, fast, and reliable. Here, we demonstrate two atomic force microscopy (AFM)-based techniques for locating and quantifying atomic-scale defects in 2D materials. First, we show that conductive AFM can locate and differentiate the same defects as STM by comparing conductive AFM and STM on the same region of a TMD crystal¹. Our work establishes conductive AFM as a higher-throughput alternative to STM for defect quantification. Second, we show that lateral force microscopy (LFM) can locate atomic-scale defects through a direct comparison of LFM with conductive AFM on a TMD crystal². Importantly, we show that LFM can also identify atomic-scale defects in insulators, such as hexagonal boron nitride, because LFM is a purely mechanical technique. The AFM-based methods presented here enable routine defect characterization, which will facilitate rapid investigations of defect-property relationships and speed up the development of new growth processes.

(1) Xu, K.; Holbrook, M.; Holtzman, L. N.; Pasupathy, A. N.; Barmak, K.; Hone, J. C.; Rosenberger, M. R. Validating the Use of Conductive Atomic Force Microscopy for Defect Quantification in 2D Materials. *ACS Nano* 2023, 17 (24), 24743–24752. <https://doi.org/10.1021/acsnano.3c05056>.

(2) Yang, Y.; Xu, K.; Holtzman, L. N.; Yang, K.; Watanabe, K.; Taniguchi, T.; Hone, J. C.; Barmak, K.; Rosenberger, M. R. Atomic Defect Quantification by Lateral Force Microscopy. *Under Review*.

3:30 PM EL05.03.02

Overcoming Negative nFET V_{TH} in Ultra-Thin ITO-IGZO Hetero-Oxide Channel FET by Defect-Compensation to Achieve Record Mobility Sonu Devi, Chen Chun-Kuei, Manohar Lal, Evgeny Zamburg and Aaron Thean; National University of Singapore, Singapore

In this work, we have successfully demonstrated, low-thermal budget amorphous oxide-based field effect transistor (FETs) with a record ON-current (I_{D, Max}) of 790 μA/μm at V_{DS}=1V. This device shows an enhancement-mode operation (V_{TH}>0), sub-threshold slope (S.S.) <90 mV/dec., and DIBL ~20mV/V at an ultra-scaled channel length (L_{CH}) of 50 nm. The FETs have been fabricated at low-temperature (<350°C) combining sputter deposition (channel layer) and atomic layer deposition (gate insulator HfO₂), making this fabrication approach compatible with low-thermal budget Cu interconnects for back-end-of-line (BEOL). In pure ITO channel, ON-current increases with channel thickness but the V_{TH} become progressively negative and the SS is degraded. However, in hetero-junction channel, the performance of our FET is comparable to emerging two-dimensional materials and superior to that of existing metal oxides. The high performance is enabled by interfacial channel defect self-compensation in an optimized InSnOx-InGaZnOx (ITO-IGZO) hetero-junction channel. Moreover, this approach overcame the fundamental issue of negative V_{TH} seen in n-type oxide FETs due to donor-type channel oxygen vacancy (Vo) and the limited tunability of gate metal work function. Through our ITO-IGZO channel and defect self-compensation approach, our transistor effective mobility (μ_{eff}) is boosted to 110 cm²/Vs which is independent of the channel thickness (T_{CH}) when the T_{CH} is scaled down to 4 nm. This unique T_{CH}-independent mobility behaviour is not observed for IGZO or ITO mono-channel FETs. With such enhancement, our ITO-IGZO FETs exhibit the best-in-class mobility among oxide-based FETs, and are competitive to unstrained Silicon thin film and SOI FETs, while being compatible with sub-400 °C BEOL processes.

3:45 PM EL05.03.03

Er₂O₃ Top Gate MoS₂ FET with EOT Lower than 1 nm [Shuhong Li](#), Tomonori Nishimura, Kaito Kanahashi and Kosuke Nagashio; University of Tokyo, Japan

Two-dimensional (2D) molybdenum disulfide (MoS₂) has emerged as a promising channel material for the next generation of electronics, offering a solution to the scaling limitations of silicon due to its atomic thinness and the maintained mobility the layered structure brings. To achieve effective gate control of MoS₂-based field-effect transistors (FETs) while meeting scaling requirements, the integration of high dielectric (high-k) oxides onto the MoS₂ surface is essential. However, the absence of dangling bonds at the MoS₂ surface significantly hinders conventional atomic layer deposition (ALD) method for high-k oxides, which relies on an active surface as a nucleation site. Alternative techniques, like van der Waals integration, are considered as ideal for minimizing interface traps between the insulator and the MoS₂ channel. Nonetheless, both the choice of materials and the integration mechanisms are requiring further investigation from the viewpoint of real application. The judicious selection of materials and suitable integration methods is, therefore, of paramount importance for the prospective application of MoS₂ FETs in the future.

While the thermal evaporation method is widely employed for thin film fabrication, the thermal evaporation of high-k materials faces a significant challenge due to their exceptionally high melting points, often exceeding 2000°C. This makes it nearly impossible to attain the desired partial pressure for deposition. Instead, the evaporation of a metal, followed by subsequent oxidation to form high-k oxides, offers a potential solution. Herein, erbium (Er), with its oxidation product Er₂O₃, was selected as the high-k material based on a well-designed differential partial pressure system, allowing for the separated evaporation and oxidation by meticulously controlling the vapor pressure of the Er source and the partial pressure of the oxygen supply. As the result, extremely low deposition rate of approximately 0.16 Å/s was achieved. This low deposition rate is expected to have minimal impact on the intrinsic properties of the MoS₂ surface. Furthermore, the thickness of the deposited Er₂O₃ can be precisely controlled by adjusting the deposition time, offering the possibility of reducing the equivalent oxide thickness (EOT).

In this study, a dual-gated MoS₂ FET with a 3.5 nm Er₂O₃ stack was fabricated using the differential partial pressure deposition system. The top gate capacitance was evaluated through I-V characteristics, utilizing a sweep of both top gate voltage and back gate voltage. The results revealed negligible threshold shifts and on/off switching within a 1 V range, confirming a high top-gate capacitance with $k \sim 13$, resulting in an EOT of 0.94 nm. Low-temperature photoluminescence (LT-PL) and Raman characterizations indicated a lack of defect-bound exciton response, as well as no significant Raman peak shift or broadening, suggesting that the high-k deposition is non-destructive.

Moreover, the stability of Er₂O₃ and the electrical reliability of the Er₂O₃/MoS₂ gate stack were investigated over an extended period, up to 100 days. Although the reduction of the dielectric constant was observed for the Er₂O₃/MoS₂ stack, the Er₂O₃/SiO₂ stack exhibited no reduction in dielectric constant over the same duration, suggesting that stability concerns were attributed to the MoS₂ surface rather than the high-k Er₂O₃. On the contrary, the interface properties, as exemplified by the subthreshold swings (S.S.), were improved over time, which may be attributed to the relaxation of strain introduced during the high-k deposition process. These findings regarding the degradation of bulk property (k) and the enhancement of S.S. over time highlight that improving the initial interface quality between high-k materials and 2D materials will lead to enhanced bulk properties.

4:00 PM EL05.03.04

A High- κ Wide-Gap Layered Dielectric for Two-Dimensional Van der Waals Heterostructures [Aljoscha Söll](#)¹, Edoardo Lopriore^{2,2}, Asmund Ottesen^{2,2}, Jan Luxa¹, Gabriele Pasquale^{2,2}, Jiri Sturala¹, František Hájek³, Vítězslav Jary³, David Sedmidubský¹, Kseniia Mosina¹, Andras Kis^{2,2} and Zdenek Sofer¹; ¹University of Chemistry and Technology, Prague, Czechia; ²École Polytechnique Fédérale de Lausanne, Switzerland; ³Institute of Physics of the Czech Academy of Sciences, v.v.i., Czechia

Van der Waals heterostructures of two-dimensional materials have opened up new frontiers in condensed matter physics, unlocking unexplored possibilities in electronic and photonic device applications. However, the investigation of wide-gap high- κ layered dielectrics for devices based on van der Waals structures has been relatively limited. In this work, we demonstrate an easily reproducible synthesis method for the rare earth oxyhalide LaOBr, and we exfoliate it as a 2D layered material with a measured static out-of-plane dielectric constant of 9 and a wide bandgap of 5.3 eV. Furthermore, our research demonstrates that LaOBr can be used as a high- κ dielectric in van der Waals field-effect transistors with high performance and low interface defect concentrations. Additionally, it proves to be an attractive choice for electrical gating in excitonic devices based on 2D materials. Our work demonstrates the versatile realization and functionality of 2D systems with wide-gap and high- κ van der Waals dielectric environments.

4:15 PM EL05.03.05

Effects of High- κ Dielectric Encapsulation and Carrier Density on Raman Scattering in Synthetic Monolayer WS₂ [Jerry A. Yang](#), Lauren Hoang, Tara Pena, Zhepeng Zhang, Andrew J. Mannix and Eric Pop; Stanford University, United States

Two-dimensional (2D) semiconductors have gained significant interest due to their atomically thin structure, theoretically pristine van der Waals interfaces, good carrier mobility, and potential utility for future opto-electronics. Among 2D semiconductors, tungsten disulfide, WS₂ is particularly interesting, as it can exhibit electronic ambipolarity at monolayer and bilayer thicknesses [1].

Raman spectroscopy is a fast, non-destructive characterization technique that enables rapid, large-area analysis of 2D semiconductors. Previous work has utilized Raman spectroscopy to quantify the strain and carrier density in monolayer MoS₂ [2], as well as evaluate the damage induced in MoS₂ from metal deposition [3]. However, these characterization techniques have not been experimentally examined in WS₂, which features different Raman signatures from MoS₂.

Here, we investigate the effects of dielectric environment and carrier density on the Raman spectrum of WS₂. We start with three samples of monolayer WS₂ grown by chemical vapor deposition, one on SiO₂/Si and the others on sapphire. We then transfer the two sapphire samples onto 125- μ m thick polyethylene naphthalate (PEN) containing a patterned high- κ /metal-gate stack as described in [4]. We encapsulate the as-grown SiO₂/Si sample and one PEN sample with a 1.5 nm Al seed layer + 10 nm Al₂O₃ [4], then the final PEN sample with 1 nm Si seed layer + 10 nm Al₂O₃ [5].

We find that, of the primary peaks in the WS₂ Raman spectrum, the 2LA(M) peak at ~ 350 cm⁻¹ is the most sensitive to encapsulation. The as-grown, unencapsulated WS₂ on SiO₂ sample exhibited a 2LA(M) peak position $\sim 3.2 \pm 0.3$ cm⁻¹ higher than the transferred, unencapsulated WS₂ on Al₂O₃ back-gate sample. After encapsulation with the Al+Al₂O₃ layer, the 2LA(M) peak in the SiO₂ sample redshifts by an additional $\sim 1.0 \pm 0.4$ cm⁻¹ while that of the Al₂O₃ sample redshifts by $\sim 4.5 \pm 0.5$ cm⁻¹. We also find a 2 \times stronger red-shift for the 2LA(M) peak in the Si seed sample ($\sim 8.1 \pm 0.8$ cm⁻¹) than in the Al seed encapsulation sample. This indicates that the 2LA(M) peak may be useful as an optical marker for interfacial quality. In comparison, the first-order E' and A' peaks shift by less than 1.5 ± 0.5 cm⁻¹ across all samples.

We also perform *in situ* Raman measurements as a function of carrier density in the same back-gated WS₂ structure. We find that the 2LA(M) peak redshifts by 0.44 ± 0.06 cm⁻¹/V and the A' peak red-shifts by 0.24 ± 0.03 cm⁻¹/V, while the E' peak does not shift substantially. With a ~ 350 nF/cm² Al₂O₃ gate oxide capacitance, these shift rates correlate to $\sim 0.19 \pm 0.01$ cm⁻¹ per 10^{12} cm⁻² carriers for the 2LA(M) peak and $\sim 0.1 \pm 0.05$ cm⁻¹ per 10^{12} cm⁻² carriers for the A' peak. This study is the first measurement of the carrier density-dependent Raman spectra of WS₂ without ionic liquid gating, which

provides a better benchmark relative to the intrinsic carrier density of WS₂ compared with previous work [6].

Our results advance Raman spectroscopy for 2D materials in two ways: first, they extend previous studies on spectroscopic carrier density measurements to near-intrinsic carrier densities, and second, they showcase the utility of Raman spectroscopy for characterizing interactions between 2D materials and high-k dielectrics for industry-relevant integration. This work was supported in part by a NSF Graduate Fellowship (J.A.Y.), by the Stanford SystemX Alliance, and by the SRC-SUPREME Center.

- [1] G. Lee *et al.*, *ACS Appl. Mater. Interfaces*, **12**, 23127 (2020).
- [2] A. Michail *et al.*, *2D Mater.*, **8**, 015023 (2020).
- [3] K. Schauble, E. Pop *et al.*, *ACS Nano*, **14**, 14798 (2020).
- [4] J. A. Yang, E. Pop *et al.*, arXiv:2309.10939 (2023).
- [5] H. Zhang *et al.*, *Chem. Mater.*, **29**, 6772 (2017).
- [6] T. Sohier *et al.*, *Phys. Rev. X*, **9**, 031019 (2019).

4:30 PM EL05.03.06

Enhancing Single Photon Emission (SPE) Purity via Design of Van der Waals Heterostructures Hsun Jen J. Chuang¹, Christopher E. Stevens², Matthew R. Rosenberger³, Sungjoon Lee^{4,1}, Kathleen M. McCreary¹, Joshua R. Hendrickson² and Berend Jonker¹; ¹Naval Research Laboratory, United States; ²AFRL, United States; ³University of Notre Dame, United States; ⁴ASEE, United States

Single photon emitters (SPEs), or quantum emitters, are key components in a wide range of nascent quantum-based technologies. A solid-state host offers many advantages for realization of a functional system, but creation and placement of SPEs are difficult to control. We describe here a novel paradigm for encoding strain into 2D materials to create and deterministically place SPEs in arbitrary locations with nanometer-scale precision [1]. We demonstrate the direct writing of SPEs in monolayer WSe₂ using an atomic force microscope nano-indentation process. This quantum calligraphy allows deterministic placement and real time design of arbitrary patterns of SPEs for facile coupling with photonic waveguides, cavities and plasmonic structures. Because monolayer WSe₂ is a direct gap semiconductor, SPE emission at a given wavelength is often intermixed with classical light resulting from conventional excitonic recombination, reducing the purity of the quantum emission as quantified by the second order autocorrelation function $g^{(2)}(t=0)$. We show that this undesirable classical emission, arising primarily from defect bound excitonic processes, can be significantly suppressed by electrostatic gating [2] or incorporating the WSe₂ layer in a simple van der Waals heterostructure [3]. Suppression of this classical emission allows a more accurate assessment of the quantum emission character, and results in values of $g^{(2)}$ as low as 0.07 at low temperature. In addition, the SPE intensity at a given wavelength can be strongly modulated by changing the polarity of the gate bias, a feature of technological importance for practical applications. Initial results for SPEs in hBN will also be summarized, time permitting.

- [1] M.R. Rosenberger *et al.*, *ACS Nano* **13**, 904 (2019). <https://doi.org/10.1021/acsnano.8b08730>
- [2] C.E Stevens *et al.*, *ACS Nano* **16**, 20956 (2022). <https://doi.org/10.1021/acsnano.2c08553>
- [3] H.-J. Chuang *et al.*, under review (2023).

*Work done in collaboration with Matthew R. Rosenberger (Notre Dame), Hsun-Jen Chuang, Sungjoon Lee and Kathleen M. McCreary (Naval Research Laboratory), and Christopher Stevens and Joshua R. Hendrickson (Air Force Research Laboratory, Wright-Patterson AFB).

† This work was supported by core programs at NRL.

SESSION EL05.04: Poster Session I
Session Chairs: Lain-Jong Li and John Sudijono
Tuesday Afternoon, April 23, 2024
Flex Hall C, Level 2, Summit

5:00 PM EL05.04.02

Room-Temperature Direct Growth of Transition Metal Dichalcogenide Films via Remote Plasma-Assisted Chemical Vapor Deposition Jina Lee¹, Seok Joon Yun² and Ki Kang Kim¹; ¹Sungkyunkwan University, Korea (the Republic of); ²University of Ulsan, Korea (the Republic of)

Transition metal dichalcogenides (TMDs) have gained significant attention in recent years for their unique electronic and optical properties, making them promising candidates for various applications in electronic and optoelectronic devices. This study presents a novel approach for the room-temperature growth of TMDs materials utilizing a plasma-assisted chemical vapor deposition (plasma-assisted CVD) method. The conventional methods for TMDs synthesis often require high temperatures, limiting their compatibility with certain substrates and device integration processes. The proposed plasma-assisted CVD method aims to overcome these challenges by enabling the growth of high-quality TMDs films at room temperature.

The plasma-assisted approach leverages the advantages of reactive species generated in the plasma, promoting enhanced precursor reactivity and efficient material deposition at lower temperatures. The study investigates the influence of key process parameters, such as precursor gas composition, plasma power, and substrate conditions, on the growth kinetics, crystal quality, and morphology of the TMDs films. Characterization techniques, including scanning electron microscopy (SEM), transmission electron microscopy (TEM) and Raman spectroscopy, are employed to analyze the structural and morphological properties of the synthesized TMDs materials.

The findings highlight the feasibility and efficacy of the room-temperature growth of TMDs using the proposed plasma-assisted CVD method, paving the way for the development of flexible and scalable fabrication processes for TMDs-based devices. The ability to grow TMDs films at lower temperatures expands their compatibility with a broader range of substrates, offering new opportunities for integration into advanced electronic and optoelectronic applications. This research contributes to the ongoing efforts to advance the synthesis techniques of TMDs materials and unlock their full potential for next-generation electronic technologies.

5:00 PM EL05.04.03

Au Nanoparticle Floating-Gate Memristor Array for Low-Power Neuromorphic System Hongwoon Yun and Woojong Yu; Sungkyunkwan University, Korea (the Republic of)

The von Neumann architecture, which physically separates the CPU and memory devices, has been dominant for a long time. However, it has limitation in computational speed due to bottlenecks and waste a large amount of energy. To address the energy and speed issue, we made a neuromorphic system based on an Au nanoparticle floating gate memristor (AuNP-FGM).

Our memristor, utilizing graphene as floating gate, MoS₂ as channel, have been recognized for its excellent performance [1,2]. Also, it has been recognized as one of the most promising candidates for neuromorphic system [3]. In this study, by forming nanoparticles between floating gate and tunneling oxide, a two-terminal memristor which operates in the $\pm 3V$ region is fabricated. Additionally, we made a neuromorphic array, calculated the energy used for learning simulation.

Using the change of the Fermi energy level (E_F) of graphene, (AuNp-FGM) exhibits memory characteristic. The device exhibits high on/off ratio over than 10^6 , retention more than 9 hours and robust endurance more than 80,000 times. AuNp-FGM also showed low cycle to cycle variability of $C_v = 3.6\%$ ($n = 90$, $C_v =$, standard deviation, $=$ mean value). Furthermore, it showed excellent linearity, indicating applicability to neuromorphic systems. For 100 level potentiation (+4V, 0.5s), non-linearity factor ranges from 0.1 to 0.6. For 100 level depression (-3V, 0.2s), it ranges from 2.3 to 4.6 ($n = 15$). A similar trend was shown even when the number of input pulses was changed (50, 100, 200, 300, 400 inputs).

Based on AuNp-FGM, we fabricated a neuromorphic array consisting of 2 neurons and 32 synapses. Three types of data (horizontal, vertical, diagonal) were used in 40 learning simulation. The total energy consumed was 70uJ, which confirmed to be a 97% energy reduction compared to the previous experiment [3].

References

- [1] [1] Vu, Q., Shin, Y., Kim, Y. *et al. Nat. Commun.* **7**, 12725 (2016).
- [2] Q. A. Vu, H. Kim, V. L. Nguyen, U. Y. Won, S. Adhikari, K. Kim, Y. H. Lee, W. J. Yu, *Adv. Mater.* 2017, 29, 1703363.
- [3] Won, U.Y., An Vu, Q., Park, S.B. *et al. Nat. Commun.* **14**, 3070 (2023).

5:00 PM EL05.04.04

Multi-Neuron Connection Using Multi-Terminal Floating-Gate Memristor for Unsupervised Learning Mihyang Park and Woojong Yu; Sungkyunkwan University, Korea (the Republic of)

Heterosynaptic plasticity in synapses has been successfully demonstrated by multi-terminal memristor and memtransistor (MT-MEMs)^{1,2}. However, these MT-MEMs lack the capability to mimic the membrane potential of neurons in multiple neuronal connections. In this study, we demonstrate a multi-terminal floating-gate memristor (MT-FGMEM) to emulate multi-neuron connections. The variable Fermi level (E_F) in graphene allows the charging and discharging of MT-FGMEM using multiple horizontally spaced electrodes. The MT-FGMEM exhibits a high on/off ratio over 10^5 with a retention time of 1000 seconds, approximately 10,000 times higher than other MT-MEMs. The linear relationship between current (I_D) and floating gate potential (V_{FG}) in the triode region of the MT-FGMEM allows for accurate spike integration at the neuron membrane. The MT-FGMEM fully mimics the temporal and spatial summation of multi-neuron connections, based on the leaky-integrate-and-fire (LIF) functionality. Our artificial neuron consumes significantly less energy, approximately 100,000 times lower (150 pJ), compared to conventional neurons based on silicon integrated circuits (11.7 μ J). By integrating neurons and synapses using MT-FGMEMs, we successfully emulate spiking neurosynaptic training and classification of directional lines in the visual area one (V1), based on the LIF functionality of neurons and the spike-timing-dependent plasticity (STDP) of synapses. We achieved a learning accuracy of 83.08% on the unlabeled MNIST handwritten dataset in unsupervised learning based on our artificial neurons and synapses.

5:00 PM EL05.04.05

Self-Powered Asymmetric-Geometry 2D Diodes for Sensing Volatile Organic Compounds Mirette Fawzy, Amirhossein Hasani, Thushani De Silva, Michael M. adachi and Karen L. Kavanagh; Simon Fraser University, Canada

Volatile Organic Compounds (VOCs) when present in human bodily fluids such as breath, sweat, urine, tears, saliva, and blood, may be regarded as potential indicators for various health conditions and diseases. Thus, the ability to monitor and detect these VOCs can be used as a screening tool to detect diseases in the early stage when treatment options are more effective. In this work, we report the development of photovoltaic, self-powered VOC sensors based on asymmetric-geometry 2D transition-metal, dichalcogenide (TMD) diodes.

Our sensors employ mechanically-exfoliated, multilayer, TMD flakes (In₂Se₃, MoS₂, MoSe₂, and WSe₂) as the sensing channel. We exploit the geometric asymmetry of the exfoliated crystals, forming two TMD-metal contacts, of different cross-sectional lengths and areas, but with the same contact metal. This induces a diode, current-voltage characteristic with a large rectification ratio (10^5) presumably due to the 2D nature of the built-in electric field. We have used a similar diode structure for sensing biomolecules (eg. cytokines)[1].

In this work, the sensor diode is either externally biased or self-powered via a photovoltaic response, such that under UV illumination. For example, a MoS₂ device demonstrated an open-circuit voltage (V_{oc}) of 450 mV and a short-circuit current density (J_{sc}) of -1.58 mA/cm². Operating under zero applied bias, the same sensor exposed to various VOCs (acetone, ethanol, 2-propanol, butanone, hexane, and water), demonstrated sensitivities comparable to other self-powered VOC sensors (20 - 200 ppm)[2]. The mechanism is via adsorbate charge effects on the magnitude of the surface depletion and diode rectification. A current signal compared to background (responsivity) of > 60 with a response time (typically 10 sec) were measured. These self-powered portable sensors based on a simple 2D diode fabrication, is a promising candidate for a highly sensitive, and low-power, gas monitoring system.

[1] Thushani de Silva, Mirette Fawzy, et al., "Ultrasensitive rapid cytokine sensors based on asymmetric geometry two-dimensional MoS₂ diodes", **Nature Communications** (2022) 13:7593; DOI: 10.1038/s41467-022-35278-2

[2] Hoffmann, Martin WG, et al. "Solar diode sensor: Sensing mechanism and applications." **Nano Energy** 2, (2013) 514-522.

5:00 PM EL05.04.06

Synthesis of Te and Sb Doped Black Phosphorus Single Crystals, Oxidation-Resistance and Room-Temperature Gas Sensing Applications Chih-Ying Huang, Yi-Rong Wang, Ying-Hao Bai, Yi-Syuan Chen, Sin-Pei Wang, Yong-Wei Bai, Yi-Chen Chen, Yu-Jie Shih, Wen-Chieh Hsieh, Yi-Wen Lin, Chia-Yin Cheng, Shang-Jung Wu, Hung-Shuo Chang and Chun-Hua Chen; National Yang Ming Chiao Tung University, Taiwan

Black phosphorus (BP) is another highly potential semiconducting two-dimensional (2D) material after graphene and transition metal dichalcogenides (TMDCs). Its optoelectronic properties depend on the number of layers and the in-plane directions of the BP 2D structure. The optoelectronic properties range from monolayer Phosphorene to bulk BP can just link those of graphene and TMDCs, enabling 2D materials to cover a wide range of optoelectronic properties. Besides, coupled with its unique armchair wrinkled crystal structure, BP has irreplaceable advantages and can be widely used in sensing, optics, electronics, thermoelectrics, and other fields. However, since each phosphorus atom in the BP structure has a lone electron pair, it is easy to spontaneously degrade in the atmospheric environment, which significantly limits its practical application in various fields. So far, many studies have shown that the environmental stability of BP or the performance of BP components can be effectively improved by surface coating, nanostructure modification, or element doping. However, different protection strategies are often accompanied by changes in the essential characteristics of BP, and the causal relationship is still, up to now, not fully clear yet.

In this study, BP crystals were prepared by chemical vapor transport (CVT), and tellurium and antimony were respectively doped in the synthesis process to potentially change the energy band structure of BP and improve its environmental stability. The obtained BP crystals were further exfoliated by

ultrasonic liquid phase exfoliation (LPE). A series of BP nanosheets, tellurium-doped BP nanosheets, and antimony-doped BP nanosheets were prepared in the organic solvent N-methylpyrrolidone (NMP) with a 900-watt ultrasonic wave. Then, BP nanosheets with a specific size distribution are screened by centrifugal rotation speed. Then, various techniques were applied to analyze the degradation degree of these three types of BP nanosheets exposed to a specific atmospheric environment (relative humidity: 75%~90%, temperature: 23~30°C). Finally, these three types of BP nanosheets were respectively placed on the interdigitated substrate for gas sensing. It was found that the highest conversion rate of pure BP, tellurium-doped BP, and antimony-doped BP crystals can reach ~98%. According to x-ray diffraction (XRD), x-ray photoelectron spectroscopy (XPS), Raman spectroscopy, optical microscopy (OM), atomic force probe microscopy (AFM), and transmission electron microscopy (TEM) analysis, it was confirmed that the doping of tellurium or antimony is an effective strategy to improve the environmental stability of BP nanosheets. Finally, the gas sensing results show that among eleven kinds of gases (CH₄, C₂H₆, C₃H₈, NO₂, NO, NH₃, C₂H₅OH, CO, acetone, HCOH, H₂), all the prepared BP nanosheets, tellurium or antimony doped BP nanosheets exhibited highly selective responses to NO₂ and NO at room temperature. In addition, doping of tellurium and antimony could also reduce the response/recovery time to NO₂ and NO.

Keywords: black phosphorus, phosphorene, dope, anti-degradation, gas sensor

5:00 PM EL05.04.07

Novel Technique to Fabricate Thick CNT based Buckypaper for EMI Shielding Applications [Syed M. Sajid](#); Khalifa University, United Arab Emirates

Carbon nanotube thin films are very important for many applications such as radar absorbing materials (RAM), electromagnetic interference shielding (EMI), supercapacitors and lithium-ion battery (LIB). The thickness of individual buckypaper sheet, produced by the film casting technique, often falls within the range of 40-100 μm. This work presents the efforts made in producing exceptionally thick buckypapers by enhancing the film casting technique, with the aim of achieving a thickness exceeding 400 μm. The mechanical and electrical properties of the thick buckypaper is studied. The measurement of EMI Shielding Efficiency (EMI SE) was conducted to determine the corresponding parameters of electromagnetic wave absorption. The thick buckypaper fabricated using the modified SETC process demonstrates considerable potential, displaying improved or equivalent properties. The buckypaper with a thickness of 400 μm had commendable mechanical properties, namely a tensile strength of 70.10 N. Additionally, it demonstrated significant electromagnetic interference (EMI) shielding properties, with an EMI shielding effectiveness (SE) of 86.70 dB.

5:00 PM EL05.04.08

Structural and Physical Properties of Two Distinct Two-Dimensional Lead Halides with Intercalated Cu(II): A Comparative Study [Kanika Parashar](#)¹, [Zheng Zhang](#)², [Volodymyr Buturlim](#)³, [Krzysztof Gofryk](#)³ and [Bayram Saparov](#)¹; ¹University of Oklahoma, United States; ²Tulane University, United States; ³Idaho National Laboratory, United States

Transition metal cations intercalated between the two-dimensional (2D) layers of metal halides is a new and distinct category of the metal halides family. In this work we focus the synthesis and property characterizations of two layered hybrid lead halides: (1) a new compound [Cu(O₂C-CH₂-NH₂)₂]Pb₂Br₄ and (2) the reported [Cu(O₂C-(CH₂)₃-NH₂)₂]PbBr₄. These compounds have a 2D layered structure with the intercalated Cu²⁺ metals between the layers, achieved by combining metal halides with zwitterionic amino acids. The incorporation of metal organic cluster consisting of zwitterions and transition metal cation as an interlayer result in improvement of electronic charge transport properties between the layers. Physical properties like magnetization measurements and thermal conductivity have also been studied for both compounds. To gain more insights into their structural and chemical diversity, we explored the solution chemistry for the synthesis of the titled compounds. The fingerprints of formed metal-halide complexes in solution were confirmed by UV-Vis spectroscopy and small-angle X-ray scattering (SAXS) experimental techniques combined with density functional theory (DFT) calculations. Moreover compound (1) showed anisotropic charge transport properties with a good and different semiconductor resistivity measured along the a-axis and along the bc plane, respectively. The fabricated prototype detector showed response to soft low-energy X-rays at 8 keV with a detector sensitivity of 1462.7 uCGy⁻¹cm⁻², indicating its potential application for ionizing radiation detection.

5:00 PM EL05.04.09

Van der Waals Interface Engineering for Enhancement of Semiconductor Device Performance [Su-yeon Cho](#), [Do Hyeon Lee](#) and [Jun Hong Park](#); Gyeongsang National University, Korea (the Republic of)

Since the performance of semiconductor devices is highly dependent on charge injection between the metal electrode and the semiconductor channel, it is important to reduce defect density through interfacial engineering at the metal-semiconductor interface. Typically, as metal is directly deposited on the semiconductor surface to form the contact electrode, metal atoms can diffuse into the semiconductor lattice and degrade the charge injection performance. In this study, we propose a method to insert a WSe₂ layer to reduce the defect density at the metal/semiconductor interface. The WSe₂ layer inserted at the metal/semiconductor interface acts as a diffusion barrier to prevent the diffusion of metal atoms into the semiconductor lattice, thereby suppressing structural defects. The metal/WSe₂/Si diode is fabricated by transferring a WSe₂ layer thermally grown on a SiO₂ substrate to a p-type Si substrate by a wet transfer method and then depositing metal electrodes (Ni, Ag, Ti, Cr/Au) onto the WSe₂/Si substrate using an E-Beam evaporator. The C-V (Capacitance-Voltage) characteristics of the diodes confirm that the insertion of the WSe₂ layer induces a low interfacial defect density (D_{it}). Furthermore, the I-V (Current-Voltage) characterization of the diodes shows that the WSe₂ layer not only provides a diffusion barrier but also reduces the leakage current and improves the stability, thereby improving the overall diode performance. In conclusion, the interfacial control method with WSe₂ layer insertion proposed in this work provides a strategy to overcome the challenges of 2D material-based Si semiconductor technology aimed at improving performance and reliability.

5:00 PM EL05.04.10

Monolayer MoS₂ with Controllable and Localized Micro-Scale Domains of Strain enabled by Spatially Varying Nanotopography [Boran Kumral](#), [Peter Serles](#), [Akshat Rastogi](#), [Pedro G. Demingos](#), [Akhil Nair](#), [Nima Barri](#), [Cristina Amon](#), [Chandra Veer Singh](#) and [Tobin Filleter](#); University of Toronto, Canada

The remarkable strain limit of two-dimensional (2D) materials as a result of strong in-plane covalent or ionic bonding provides a straightforward means to tune electronic states by modulating the interatomic distances through mechanical strain^{1,2}. The high strain sensitivity along with low bending modulus of 2D materials make them promising candidates for eagerly sought-after gradient bandgap materials in which the bandgap spatially varies within the same material³⁻⁵. These materials would enable absorption and conversion of a broad light spectrum for use in photovoltaics, photocatalysis, and photodetectors⁶⁻⁸. Meanwhile, two-photon lithography (2PL) is newly capable of lateral resolutions below 200 nm to rapidly fabricate complex three-dimensional structures^{9,10}. Here, we use 2PL fabricated non-Euclidian nanotopography comprised of periodic undulations with spatially varying height as a patterned substrate for monolayer molybdenum disulfide (MoS₂). The monolayer conformed to the nanotopography locally strains the monolayer with both spatial and magnitudinal control. The conformity of the monolayer is characterized using scanning electron microscopy and atomic force microscopy, and the localized domains of strain in the conformed monolayer are characterized using Raman and photoluminescence spectroscopy. This study serves as a starting point for deterministic straining of 2D materials and development of 2D materials-based broad-spectrum sensing.

References

1. Sahalianov, I. Y., Radchenko, T. M., Tatarenko, V. A., Cuniberti, G. & Prylutsky, Y. I. Straintronics in graphene: Extra large electronic band gap induced by tensile and shear strains. *J Appl Phys* **126**, (2019).
2. Miao, F., Liang, S. J. & Cheng, B. Straintronics with van der Waals materials. *NPJ Quantum Mater* **6**, 2–5 (2021).
3. Kuykendall, T., Ulrich, P., Aloni, S. & Yang, P. Complete composition tunability of InGaN nanowires using a combinatorial approach. *Nature Materials* **2007** *6:12* **6**, 951–956 (2007).
4. Kim, C.-J. *et al.* On-Nanowire Band-Graded Si:Ge Photodetectors. *Advanced Materials* **23**, 1025–1029 (2011).
5. Xiao, Y. *et al.* Band structure engineering and defect control of Ta3N5 for efficient photoelectrochemical water oxidation. *Nature Catalysis* **2020** *3:11* **3**, 932–940 (2020).
6. Konstantatos, G. & Sargent, E. H. Nanostructured materials for photon detection. *Nature Nanotechnology* **2010** *5:6* **5**, 391–400 (2010).
7. Yan, J., Song, X., Chen, Y. & Zhang, Y. Gradient band gap perovskite films with multiple photoluminescence peaks. *Opt Mater (Amst)* **99**, 109513 (2020).
8. Feng, J., Qian, X., Huang, C. W. & Li, J. Strain-engineered artificial atom as a broad-spectrum solar energy funnel. *Nat Photonics* **6**, 866–872 (2012).
9. Photonic Professional GT2 from Nanoscribe, GMBH. *Nanoscribe GmbH & Co. KG* <https://www.nanoscribe.com/en/solutions/photonic-professional-gt2> (2021).
10. Vyatskikh, A. *et al.* Additive manufacturing of 3D nano-architected metals. *Nature Communications* **2018** *9:1* **9**, 1–8 (2018).

5:00 PM EL05.04.11

Semiempirical Pseudopotential Method for Low-Dimensional Materials Raj K. Paudel^{1,2}, Chung Yuan Ren³ and Yia-Chung Chang^{1,2}; ¹Academia Sinica, Taiwan; ²National Cheng-Kung University, Taiwan; ³National Kaohsiung Normal University, Taiwan

In recent years, there has been a significant focus on developing precise and efficient approaches to expedite Density Functional Theory (DFT) calculations for large unit cells. Among these techniques, the Semiempirical Pseudopotential Method (SEPM) [1] has emerged as a valuable tool for accurately determining band structures, especially in the realm of low-dimensional materials. SEPM operates by utilizing atomic pseudopotentials, which are derived from DFT calculations. Significantly, SEPM calculations offer a unique advantage compared to DFT as they eliminate the requirement for iterative self-consistent solutions in solving the Schrödinger equation, leading to a substantial reduction in computational complexity. The incorporation of both non-local and local Semiempirical Pseudopotentials in our current approach yields band structures and wavefunctions with enhanced precision compared to traditional empirical methods [2]. When applied to graphene, our model's computed band structure closely aligns with that obtained via DFT calculations [3]. Impressively, our method demands only a fraction of the time required in comparison to the CG iterative solver with self-consistent charge density from DFT. Additionally, we utilized the SEPM technique for armchair graphene nanoribbons (aGNR), achieving results that closely align with those obtained through DFT, but with significantly reduced computational time. Furthermore, we extended the application of our SEPM approach to monolayer TMDCs, adjusting the parameters to align with pertinent values obtained from DFT computations. This enables us to faithfully replicate the band structure, opening avenues for investigating the optoelectronic properties of TMDCs and exploring their potential applications in nanodevices consisting of TMDC nanostructures or related moiré structures.

References

- [1] Paudel, R.K.; Ren, C.-Y.; Chang, Y.-C. Semi-Empirical Pseudopotential Method for Graphene and Graphene Nanoribbons. *Nanomaterials* **2023**, *13*, 2066
- [2] Chelikowsky, J.R.; Cohen, M.L. Nonlocal pseudopotential calculations for the electronic structure of eleven diamond and zinc-blende semiconductors. *Phys Rev B*. **1976**, *14*, 556.
- [3] Ren C.Y.; Hsue, C.S.; Chang Y.C. A Mixed Basis Density Functional Approach for Low-Dimensional Systems with B-splines. *Computer Physics Communication*. **2015**, *188*, 94-102

5:00 PM EL05.04.12

Berry Curvature Dipole Induced Giant Mid-Infrared Second-Harmonic Generation in 2D Weyl Semiconductor Qundong Fu¹, Xin Cong², Xiaodong Xu³, Song Zhu¹ and Zheng Liu¹; ¹Nanyang Technological University, Singapore; ²University of South Florida, United States; ³Harbin Institute of Technology, China

Due to its inversion-broken triple helix structure and the nature of Weyl semiconductor, two-dimensional Tellurene (2D Te) is promising to possess a strong nonlinear optical response in the infrared region, which is rarely reported in 2D materials. We demonstrated a giant nonlinear infrared response induced by large Berry curvature dipole (BCD) in the Weyl semiconductor 2D Te. Ultrahigh SHG response was acquired from 2D Te with a large second-order nonlinear optical susceptibility ($\chi^{(2)}$), which is up to 23.3 times higher than that of monolayer MoS₂ in the range of 700-1500 nm. Notably, distinct from other 2D nonlinear semiconductors, $\chi^{(2)}$ of 2D Te increases extraordinarily with increasing wavelength and reaches up to 5.58 nm/V at ~2300 nm, which is the best infrared performance. Large $\chi^{(2)}$ of 2D Te also enables the high-intensity sum-frequency generation with an ultralow continuous-wave (CW) pump power. Theoretical calculations reveal that the exceptional performance is attributed to the presence of large BCD located at the Weyl points of 2D Te. These results unravel a new linkage between Weyl semiconductor and strong optical nonlinear responses, rendering 2D Te a competitive candidate for highly efficient nonlinear 2D semiconductors in the infrared region.

5:00 PM EL05.04.13

Growth and Characterization of 2D-MoS₂ for NO₂ Gas Application Using Chemical Vapor Deposition Method Ashok Kumar and Mahesh Kumar; Indian Institute of Technology Jodhpur, India

Gas sensors that have a low power consumption and can be easily connected into a large-scale sensor network are a necessity for the Internet of Things for environmental monitoring. The high operating temperature of semiconductor gas sensors limits their applications considering their numerous advantages which include excellent sensitivity and cost-effective. In recent years, the research curiosity in two-dimensional (2D) materials, especially molybdenum disulfide (MoS₂) has showed much more intensive attention in gas sensor due to tunable band gap, abundant edge sites and high ratio of surface to volume. Herein, the synthesis of MoS₂ nanoflower was conducted within a tube furnace using a novel three-step chemical vapour deposition (CVD) technique. This process involved the sequential deposition and sulfuration of MoO₃. The MoS₂ nanoflower were confirmed by scanning electron microscopy, Raman spectroscopy, and X-ray diffraction. The resistive gas sensors based on as-prepared bilayer MoS₂ nanoflower showed a p-type character and achieved a superior response of 16% to 100 ppm NO₂ gas, excellent reproducibility, fast response, and complete recovery at room temperature. This sensing property of the resistive gas sensor based on as-prepared MoS₂ films by the three-step CVD method represents an advance in the development of large-scale MoS₂ synthesis and gas sensor fabrication.

5:00 PM EL05.04.14

Design of Electronic Structure and Transport in S-Doped Few-Layer Graphene Armin Sahinovic^{1,1}, Paolo Fortugno^{1,1}, Nicholas Wilson^{2,2}, Hartmut Wiggers^{1,1} and Rossitza Pentcheva^{1,1}; ¹Universität Duisburg-Essen, Germany; ²University of Waterloo, Canada

Compared to a single sheet of graphene, few-layer graphene (FLG) shows additional degrees of freedom dependent on the number of layers and interlayer interactions, leading to a unique combination of surface and bulk-like states [1]. While the properties N- and S-doped monolayer graphene have been addressed previously [2,3], the interplay between defects, doping and the layered structure of FLG are largely unknown.

Based on density functional theory calculations we explore the effect of sulfur doping and vacancies on FLG. The formation energies and electronic structure of different defect types are assessed as a function of concentration and distribution. Direct incorporation of S into the lattice is associated with a high formation energy, which can be reduced by the creation of additional vacancies to bond the sulfur dopants. The most energetically favorable defect configuration is a hypervalent S bonding state in the single vacancy system. While this defect opens a small gap of 0.151 eV in the monolayer system, the multilayer system maintains a Dirac point with linear dispersion. Intriguingly, doped monolayer double vacancies promote weak ferromagnetism not present in the multilayer counterpart. We find a strong layer dependence of the doping allowing for a design of the electronic structure. The surface layers are most prone to doping, giving rise to complex buckling, resulting in a modified band structure and a band gap opening at certain doping concentrations not found for doping in the inner layers. Moreover, doping just below the surface layer allows to preserve the linear dispersion of the Dirac cone in the surface layer.

Initial experimental work on the synthesis of S-doped few-layer graphene (FLG) in a microwave plasma reactor confirms the incorporation of sulfur into the graphene structure and shows that electronic conductivity can be increased by up to 50% compared to undoped FLG. This is consistent with the transport properties, obtained via the BoltZtrap2 code [4], revealing that S doping systematically enhances the conductivity in single-layer and few-layer graphene. Charge-transfer from the doped to the surrounding pristine layers leads to indirect doping, additionally enhancing the transport in FLG compared to the monolayer case. In contrast, when FLG is doped in the surface layers the charge transfer is impeded by the buckling and local charge accommodation, thus a smaller increase of conductivity is found. In this work we show that tailoring the incorporation of S into FLG enables one to modify selectively the electronic structure in view of energy conversion and storage applications e.g. as a battery material, or in catalysis (oxygen reduction).

We acknowledge gratefully funding by the Deutsche Forschungsgemeinschaft (DFG, German Research Foundation) - IRTG 2803 - 461605777 and support of the Natural Sciences and Engineering Council of Canada (NSERC), [CREATE 565360]. Computing time was granted by the Center for Computational Sciences and Simulation of the University of Duisburg-Essen (DFG Grants No.-INST 20876/209-1 FUGG and No.-INST 20876/243-1 FUGG).

[1] F. Mak *et al.*, Proc. Natl. Acad. Sci. 107, 14999 (2010)

[2] S. Fiori *et al.*, Carbon 171, 704 (2021)

[3] J.H Lee *et al.*, Nanomaterials, 9, 268 (2019)

[4] G. K.H. Madsen *et al.*, Comput. Phys. Commun., 231, 140 (2018)

5:00 PM EL05.04.15

Direct Growth on Dielectric Substrates: Area-Selective Growth of Mono- and Bi-Layer Transition Metal Dichalcogenides WS₂ Lin-Yun Huang¹, Shih-Chu Lin¹, Ming-Chun Hsu², Ching-Hao Hsu², Yu-Tung Lin², Po-Sen Mao¹, Chih-I Wu², Wen-Hao Chang¹, Lain-Jong Li³ and Kung-Hwa Wei¹;

¹National Yang Ming Chiao Tung University, Taiwan; ²National Taiwan University, Taiwan; ³The University of Hong Kong, Hong Kong

Two-dimensional Transition metal dichalcogenides (TMDs) show great potential to surpass the latest technology node of electronic device scaling and are therefore a focus of research. Bilayer (BL) TMDs have attracted increasing attention in recent years due to their potential to outperform monolayer (ML) TMDs, which are hampered by limited carrier mobility and high contact resistance. Uniform BL TMDs have been demonstrated through the use of excess precursor, additional promoter or substrate pre-treatment methods. These methods, however, introduce random distribution or require additional transfer processes, making them impractical for large scale manufacturing. Here, we present an approach¹ that can grow area-selected uniform monolayer or bilayer WS₂ directly on dielectric substrates. This approach involves first controlling the oxidation degree of the pre-deposited tungsten metal pad, and then converting the tungsten oxide to mono- or bi-layer WS₂, respectively, thereby tuning the number of layers. Simultaneously, WS₂ would grow only around the tungsten metal pad, suggesting area selectivity. The direct-growth method provides cleaner WS₂ interfaces and thus results in improved quality and performances. The optical microscopy and Atomic Force Microscopy images show the capability of controlling the number of WS₂ layers. Furthermore, the Raman and photoluminescence spectra present the uniformity and high optical quality of the fabricated WS₂ bilayer. The Transmission Electron Microscopy (TEM) and Scanning TEM images further displays the AA stacking order of the as-grown bilayer WSe₂, which is desired to result in higher mobility. These ML and BL WS₂ were utilized in field-effect transistors, demonstrating the validity of this approach as a foundation for further device applications.

Reference

(1) Huang, L.-Y.; Li, M.-Y.; Liew, S.-L.; Lin, S.-C.; Chou, A.-S.; Hsu, M.-C.; Hsu, C.-H.; Lin, Y.-T.; Mao, P.-S.; Hou, D.-H.; et al. Area-Selective Growth of Two-Dimensional Mono- And Bilayer WS₂ for Field Effect Transistors. *ACS Materials Letters* **2023**, 5 (6), 1760-1766. DOI: 10.1021/acsmaterialslett.3c00094.

5:00 PM EL05.04.16

Synthesis of Stabilized Black Phosphorus for Gas Sensing Application Shang-Jung Wu, Chun-Hua Chen, Cheng-Ju Yang, Yi-Wen Lin, Chia-Yin Cheng, Hung-Shuo Chang, Wen-Chieh Hsieh, Yen-Ling Wang and Karan Giri; National Chiao Tung University, Taiwan

Black phosphorus (BP) is a two-dimensional material with a unique armchair-folded structure that imparts distinct electrical and optical properties in different directions, making it highly sought after in recent years. Additionally, its layered structure provides superior electron mobility, and BP exhibits tunable band structures, allowing it to excel in various applications, essentially bridging the gap between graphene and transition metal dichalcogenides (TMDCs). However, there are still significant challenges to realizing widespread applications of BP. Each phosphorus atom in the BP structure possesses lone electron pairs, making it highly susceptible to spontaneous degradation in ambient conditions, severely limiting its practical utility in various fields. Furthermore, the techniques for preparing and modifying BP are continuously evolving, making it crucial to address these issues effectively.

Keywords: black phosphorus, two-dimensional material, CVT, doping, gas sensor.

5:00 PM EL05.04.17

Direct Growth of Graphene on Dielectric Materials by Low Temperature Plasma-Enhanced CVD Umut Kaya, Hehe Zhang, Leon Lörcher, Carmen Nordhoff, Wolfgang Mertin and Gerd Bacher; University of Duisburg-Essen, Germany

Graphene offers outstanding electronic and optical properties, such as high electrical conductivity and high transparency in the UV-VIS spectral range. The most developed method for growing high quality graphene is chemical vapor deposition (CVD) on copper (Cu) substrates, where Cu has a catalytic effect on the growth. Practical applications, however, require a subsequent transfer of the graphene onto target substrates like, e.g., dielectric materials. This transfer process induces defects and contaminations, which in turn leads to reduced performance of the intended applications [1]. Thus, a direct growth on dielectric substrates, such as sapphire and (Al,Ga)N is preferable, enabling, e.g., the use of graphene as a transparent electrode for (Al,Ga)N-LEDs [2], 2D-photodetectors [3] or biosensors [4] without any complex transfer process.

We developed a low temperature plasma-enhanced CVD (PECVD) process for depositing graphene on dielectric substrates in a transfer-free approach. The PECVD process was conducted in an industrially relevant 4-inch system with methane (CH₄) as the precursor. For growing graphene on (Al,Ga)N, the conventionally used hydrogen (H₂) carrier gas was replaced by nitrogen (N₂) for preventing surface decomposition of the (Al,Ga)N [2]. Under optimized conditions, i.e., a gas mixture of CH₄/N₂, a plasma power of 40 W, a growth time of 60 min and a growth temperature of 670 °C, graphene layers with Raman intensity ratios I_D/I_G ≈ 1.6 and I_{2D}/I_G ≈ 1.4, respectively, have been realized. The sheet resistance could be reduced to < 5 kΩ/sq and the transmittance of the optimized graphene film was ≥ 90% in the UV-VIS spectral range. For graphene growth on sapphire with different crystal orientations (c-plane, ca-plane, a-plane and r-plane), no distinct dependence of the graphene quality on the crystal orientation is found, in contrast to findings for thermal CVD as reported in literature [5]. Under optimized conditions, the I_D/I_G ratio was as low as 0.7 and a sheet resistance down to 1.65 kΩ/sq could be achieved. Apparently, the PECVD process seems to provide a flexible approach for depositing graphene on dielectric substrates, where the balance between sheet resistance and optical transmittance can be willingly adjusted by the growth parameters.

[1] Wang et al., *Adv.Mater.*2016, **28**, 4956–4975

[2] Mischke et al., *2D Mater.* **7** (2020) 035019

[3] Munoz et al., *npj 2D Materials and Applications* **7**, 57 (2023)

[4] Xu et al. *Applied Surface Science* **427**, 1114–1119 (2018)

[5] Ueda et al., *Appl. Phys. Lett.* **115** (2019) 013103

5:00 PM EL05.04.19

Tunable Semiconductivity in Nitrogen-Doped Graphene Nanosheets for High Surface-Area Optoelectronics Daniel Ranke, Yingqiao Wang and Tzahi Cohen-Karni; Carnegie Mellon University, United States

Semiconducting graphene has been identified for high potential electronic and optical applications since its discovery. Previously, substitutional atomic doping of graphene, particularly nitrogen, has shown to induce semiconducting behavior. However, variability in final dopant defect states, particularly from bottom-up synthesis, results in limited control over band structure and has thus formed a firm ceiling on the application of such structures. Here we report a plasma-enhanced chemical vapor deposition approach for the synthesis of switchable p and n-type nitrogen doped vertically oriented graphene nanosheets and applications towards enhanced carrier extraction in optoelectronics. Tuning between in-situ and ex-situ nitrogen doping has shown fine control over pyridinic/graphitic nitrogen dopant ratio, in turn shifting band structures towards more electron or hole-dominated carrier transport. In conjunction with the vertical orientation and density of nanosheets, these nanostructures allowed for the development of optically active p-i-n and n-i-p heterostructures with charge storage capacity and active surface area many times greater than what is possible with traditional planar architectures. With such structures, we show a route towards developing stable, high-surface area, efficient carrier extractors for optoelectronics. Technologies that are critically limited by active surface area, such as photovoltaic electrochemical cells and optical bioelectronic stimulators, show enhanced potential for co-application with these semiconducting graphene nanostructures and pave a clear road forward toward future hybrid-nanomaterial development.

5:00 PM EL05.04.20

Molecular Dynamics Simulation of ZrS₂ Oxidation Liqu Yang, Rajiv Kalia, Aiichiro Nakano and Priya Vashishta; University of Southern California, United States

Among transition metal dichalcogenides (TMDCs) family, ZrS₂ is an important semiconductor and shows superior chemical catalytic properties and electrical properties especially with its 1T phase. ZrS₂ has been reported to be easily oxidized under native environment. Here, we perform large-scale reactive molecular dynamics simulations with optimized reactive force field to study the ZrS₂ oxidation. We present the initial oxidation events locally taking place on the ZrS₂ surface, which results in surface defects that promote further oxidation. The final product of the thermal oxidation is also investigated. This work provides an atomic-level understanding for describing and controlling the oxidation of ZrS₂ as well as for synthesis of oxide and oxysulfide products.

Acknowledgement:

Research supported by the U.S. Department of Energy, Office of Basic Energy Sciences, Division of Materials Sciences and Engineering, Neutron Scattering and Instrumentation Sciences program under Award DE-SC0023146.

SESSION EL05.05: Growth I
Session Chairs: Stephanie Law and Joan Redwing
Wednesday Morning, April 24, 2024
Room 344, Level 3, Summit

8:00 AM *EL05.05.01

Non Epitaxial Growth of Single-Crystalline TMDs on Amorphous below 400 C Jeehwan Kim; Massachusetts Institute of Technology, United States

The integration of electronics in three dimensions has gained significance in modern electronics due to limitations in scaling nanoscale devices. Vertical chip stacking reduces RC delays, leading to lower power consumption and more efficient data exchange in system-on-chip designs. Despite huge technical challenges, through-silicon-via (TSV) has been an only viable solution. A more concise and effective approach for connecting electronic devices is wafer-free monolithic 3D (M3D) integration. However, the scarcity of methods for locating single-crystalline thin film device layers at low temperatures has limited experimental demonstrations of M3D with single-crystalline devices. We now present our pioneering demonstration of single-crystal growth of TMD channel materials at 350°C on an amorphous layer-coated silicon wafer. This breakthrough allows seamless integration of single-crystalline n-type MOS devices on top of amorphous insulation layers of underlying single-crystalline p-type MOS chips. Our work establishes a foundation for advancing Moore's law. Furthermore, successfully growing single-crystalline devices on finished circuitry holds the promise of true wafer-free vertical monolithic

integration of electronics and photonics in the future.

8:30 AM EL05.05.02

Ferrecrystals: Non-Epitaxial Multilayer Growth of 2D Materials by Atomic Layer Deposition Jun Yang¹, Dongho Shin¹, Sebastian Lehmann¹, Tobias Ritschel², Jochen Geck² and Kornelius Nielsch^{1,3,4}; ¹IFW Dresden, Germany; ²Institute of Solid State Physics, TUD, Germany; ³Institute of Applied Physics, TUD, Germany; ⁴Institute of Materials Science, TUD, Germany

Atomic layer deposition is a very versatile technology for the deposition of thin films with precise thickness control on large areas, non-planar surfaces and 3D objects. The chemical reaction is surface limited, well defined and works in most cases at low temperatures (RT to 150 °C). For a number of classical van der Waals 2D materials, there have been reports on ALD of transition metal dichalcogenide (TMDC) of MoS₂, SnS₂, WS₂ and WSe₂, which also included the electronic characterization as a field effect transistor (FET).

In this work, we have fabricated by atomic layer deposition (ALD) multilayers of layered materials based on topological insulators and van der Waals materials, called *ferrecrystals*. These ferrecrystals can be tailored to exhibit unusual properties such as high electrical conductivity or low thermal conductivity or magnetic properties. A detailed ferrecrystal study was performed on ferrecrystals of Sb₂Te₃ and SbO_x, which has been grown at the same temperature as single layers of Sb₂Te₃. Without post-annealing, the electrical and thermoelectric characterisation of the highly ordered samples have been performed with the ZT-chip setup. In general, the carrier mobility is very high >150 Vs²/cm² and is even improved when the thickness of the Sb₂Te₃ layers is reduced and the number of SbO_x layers (typically 2 nm thickness) is increased. Detailed XRD investigations have been performed and an enhanced crystalline order is observed in the ferrecrystal system compared to individual layers of Sb₂Te₃. We have grown ferrecrystals based on Sb₂Te₃ and Sb₂Se₃ with tetrahedral and orthorhombic crystal structure, respectively. The p-type hole carrier concentration of Sb₂Te₃ films can be enhanced through the sublayer doping of Sb₂Se₃. The highest carrier concentration achieved was 2.5×10¹⁹ cm⁻² when the thickness ratio of Sb₂Te₃ to Sb₂Se₃ was (4 nm:2 nm). Further reduction of the Sb₂Te₃ thickness resulted in a high Seebeck coefficient of 172 μV/K at room temperature.

Reference: Jun Yang, Samik Mukherjee, Sebastian Lehmann, Fabian Krahl, Xiaoyu Wang, Pavel Potapov, Axel Lubk, Tobias Ritschel, Jochen Geck, Kornelius Nielsch, "Low-Temperature ALD of SbO_x/Sb₂Te₃ Multilayers with Boosted Thermoelectric Performance", Small 20, 2306350 (2024) <https://doi.org/10.1002/sml.202306350>

8:45 AM EL05.05.03

Plasma-Based Integrated System for Synthesis, Etching and Machine Learning of 2D TMDC Hyeong-U Kim¹, Muyeong Kim¹, Seongho Kim², Minji Kang¹ and Min Sup Choi²; ¹Korea Institute of Machinery and Materials (KIMM), Korea (the Republic of); ²Chungnam National University, Korea (the Republic of)

The research presented in this work represents a culmination of over a decade of dedicated efforts toward the development and implementation of a plasma-based integrated system for the synthesis, etching, and machine learning of two-dimensional (2D) transition metal dichalcogenides (TMDC). Our journey began in 2013 with a groundbreaking achievement: the successful synthesis of semiconducting MoS₂ at 300 °C using an inductively coupled plasma (ICP)-plasma enhanced chemical vapor deposition (PECVD) technique (PLASMART, Republic of Korea) on a 4-inch substrate. This milestone was the first step towards realizing the immense potential of 2D TMDC materials in various applications.

Building on this initial success, we continued to advance our capabilities. In 2015, we lowered the synthesis temperature to 150 °C, enabling direct deposition on polyimide substrates. This development not only expanded the range of possible applications but also demonstrated our commitment to environmentally sustainable processes. In 2020, we achieved another significant milestone by successfully synthesizing 2D WS₂, a member of the same TMDC group, in the metallic 1T phase using PECVD.

The year 2021 marked a breakthrough as we overcame previous limitations in heterostructure fabrication by creating a MoS₂-WS₂ heterostructure using H₂S + Ar plasma on a 4-inch hetero-metallic (Mo-W) layer. This achievement unlocked the potential for novel electronic and optoelectronic devices based on these heterostructures. Various forms of TMDC, all consisting of 4-5 layers, were systematically obtained, laying the foundation for further exploration. By 2023, we had established precise etching conditions at the atomic layer level using ICP-reactive ion etching (RIE) with a carefully designed three-gas mixture (Ar+O₂+CF₄) and optimized RIE utilization. This enabled us to tailor the properties of 2D TMDC materials with unprecedented precision. Furthermore, we employed density functional theory (DFT) calculations and optical emission spectroscopy (OES) diagnostic results to gain deeper insights into the plasma reaction mechanisms, shedding light on the underlying physical processes.

In a remarkable culmination of our efforts, we harnessed the power of machine learning (ML) to predict process outcomes in 2023, revolutionizing the way we approach material synthesis and etching. This achievement represents a significant leap forward in terms of efficiency and precision, with implications spanning various industries and research domains.

In summary, our research journey has led to the development of a comprehensive and versatile plasma-based integrated system for 2D TMDC materials. Over the course of a decade, we have pushed the boundaries of what is possible in material synthesis, etching, and process optimization, ultimately contributing to the advancement of science and technology.

9:00 AM EL05.05.04

Atomic Layer Deposition of WS₂ on Low-k Dielectric Substrates for Back-End-Of-Line Integration Muhammed Juvaid Mangattuchali¹, Hao Tan¹, Hippolyte P. Astier¹, Chandan Das², John L. Sudijono² and Silvija Gradecak¹; ¹NUS Singapore, Singapore; ²Applied Materials, Inc., Singapore

The progressive miniaturization of silicon integrated circuits necessitates the exploration of alternative materials for both the front-end-of-line (FEOL, transistors) and back-end-of-line (BEOL, interconnects) circuitry. Currently, the efficacy of traditional liners and barriers (e.g., Ta/TaN) requires an approximate thickness of 30-40 Å. In forthcoming sub-5 nm nodes, these components will occupy a significant portion of the interconnect cross-section, leading to a substantial increase in the resistivity of Cu interconnects. Conversely, the reduction in thickness of liner and barrier layers would result in a decrease in Cu blocking efficiency. Two-dimensional (2D) transition metal dichalcogenides (TMDs) were recently demonstrated as promising candidates for bifunctional ultra-thin liner and diffusion barrier materials in the sub-nanometer-scales. However, the majority of 2D TMDs are synthesized *via* chemical vapor deposition processes at elevated temperatures (>800°C). This makes it difficult to use them in BEOL integration, where the temperature limit is 450°C. While plasma-assisted growth offers the potential to mitigate the high-temperature requirement, it also implies poor conformality in deposition, and the emergence of plasma-induced defects in the TMDs as limitations.

Here, we present a thermal atomic layer deposition (ALD) approach that does not require plasma assistance to grow crystalline WS₂ at temperatures below 400°C, on dielectric materials, including low- k and SiO₂ substrates. This growth approach does not alter the stoichiometry of the low- k material and retains its k value, making it a suitable method for BEOL integration. The process results in layer-controlled, conformal (>95%) wafer-scale growth of WS₂ on 200 mm dielectric substrates. Furthermore, the single-layer WS₂ helps reduce Cu resistivity >70% compared to the reference low- k and SiO₂/Si substrates. Thermal and electrical stress tests on the monolayer WS₂ film reveal a high blocking efficiency against both types of stress. This low- k - compatible ALD-grown monolayer WS₂ not only addresses the downscaling challenge but also serves as an efficient bifunctional (liner and barrier) layer grown using a directly industry-compatible process.

9:15 AM EL05.05.05

Fabricating Freestanding Ultrathin Materials by Atomic Layer Deposition [Karen Ehrhardt](#), Jessica M. Coleman and Scott C. Warren; University of North Carolina at Chapel Hill, United States

Ultrathin materials have risen to an increasingly important role in recent years, both due to the nano-scaling of existing technologies and the advancement of new applications that utilize the distinct properties of ultrathin structures compared to bulk materials. Because these properties strongly depend on thickness and uniformity, vapor-based synthesis is popular. In particular, atomic layer deposition (ALD) is a popular strategy to fabricate precisely controlled ultrathin materials because of self-limiting growth and high conformality. However, to fully realize the potential of ultrathin materials from ALD, there exists a need for freestanding structures, which would allow the exploration of applications such as membranes or photolithographic pellicles. Despite the prominence of ALD, no general method of fabricating freestanding ultrathin materials with cm-scale dimension currently exists. This gap exists due to the nature of ALD, in which precursor molecules chemisorb strongly to and are difficult to remove from the substrate surface. To address the challenge of prepared freestanding ALD materials, we report a strategy of growing materials on a tailored single-crystal NaCl surface. Although NaCl is typically a poor substrate for ALD, the insertion of hydroxyl functional groups across the surface results in a heterogeneous surface that forms both bonding and nonbonding interactions with ALD materials. Once deposited, the material is easily removed under mild conditions and transferred to an arbitrary substrate. This approach yields ALD materials that have cm-scale sizes and are low in defects in cracks and pinholes. The strategy provides access to a diverse range of freestanding ultrathin compositions, creating opportunities to investigate structure-property relationships that are distinct from those in bulk material counterparts.

9:30 AM EL05.05.06

Lithographically Defined Synthesis of Transition Metal Dichalcogenides [Aidar Kemelbay](#), Ricardo Ruiz, Archana Raja, Adam Schwartzberg, Shaul Aloni and Tevye Kuykendall; Lawrence Berkeley National Lab, United States

Transition metal dichalcogenides (TMDs) possess unique and highly tunable optoelectronic properties, but their large-scale fabrication and integration is still challenging. To address this problem, we developed a "lateral conversion" technique, which enables the synthesis of TMDs with predefined thickness and shape at specific locations on a wafer. The lateral conversion of metals, metal oxides, and nitrides into metal dichalcogenides resulted in few-layer TMDs covered with a capping layer. This layer protects the delicate TMD interfaces during subsequent fabrication steps from contamination, as well as improves their air stability. We demonstrated that lateral conversion can be used to synthesize various sulfides, selenides and tellurides, as well as alloys, lateral and vertical heterostructures. The patterned TMDs can be easily transferred from growth to device substrates or directly integrated into silicon-based CMOS platforms.

9:45 AM EL05.05.07

Substrate Van der Waals Force Effect on The Stability of Violet Phosphorous [Sarabpreet Singh](#)¹, Mahdi Ghafariasl¹, Hsin-Yu Ko², Sampath Gamage¹, Robert DiStasio Jr², Michael Snure³ and Yohannes Abate¹; ¹University of Georgia, United States; ²Cornell University, United States; ³Air Force Research Laboratory, United States

The weak van der Waals (vdWs) forces between monolayers has been a unique distinguishing feature of exfoliable materials since the first isolation of graphene. However, the vdWs interaction of exfoliable materials with the substrate and how this interface force influences the interaction of vdWs materials with the surroundings have yet to be well understood. Here, we experimentally and theoretically unravel the role of vdWs forces between the recently rediscovered wide band gap p-type vdW semiconductor violet phosphorus (VP), with various substrates (including, SiO₂, mica, Si, Au) and quantify how VP stability in air and its interaction with its surroundings is influenced by the interface force. Using a combination of infrared nanoimaging and theoretical modelling we find three main factors that influence how VP interacts with its surroundings: the vdWs force at the interface, the hydrophobicity of the substrate, and substrate surface roughness. We found that VP can maintain its stability for a prolonged period if it is exfoliated on SiO₂ substrate, followed by mica and Au substrates, and is least stable when placed on a Si substrate. Our results could guide in the selection of substrates when vdW materials are prepared and more generally highlight the key role of interface force effects that could significantly alter physical properties of vdWs materials. Our findings can assist in the choice of substrates to exfoliate vdWs materials and emphasize the crucial impact that interface forces can have on altering the physical properties of exfoliable materials.

10:00 AM BREAK

10:30 AM *EL05.05.08

Wafer-Scale Epitaxy of 2D Transition Metal Dichalcogenides on Sapphire – An Enabling Technology for Large Area Devices [Joan M. Redwing](#); The Pennsylvania State University, United States

Monolayer and few-layer semiconducting transition metal dichalcogenides (TMDs), exemplified by materials like MoS₂ and WSe₂ have garnered increasing interest for next generation gate-all-around nanosheet devices and heterogeneous integration with silicon CMOS technology. The interest in TMDs arises from their ultra-thin body nature, however, realization of high-performance devices requires advances in TMD synthesis to provide wafer-scale films that can be readily integrated into devices via either direct growth or layer transfer methods. Our work has focused on the development of metalorganic chemical vapor deposition (MOCVD) as a manufacturing-compatible approach for wafer-scale semiconducting TMDs. The TMDs are grown epitaxially on c-plane sapphire by MOCVD at elevated temperatures (>800 °C) to obtain high crystal quality. Pre-annealing the sapphire surface in H₂S or H₂Se modifies the nucleation behavior of the TMDs on sapphire which is attributed to passivation of dangling bonds on the sapphire surface. Passivation of step terraces can drive nucleation to occur preferentially at step edges on sapphire leading to unidirectional domains and a significant reduction in mirror twin defects. In situ spectroscopic ellipsometry is demonstrated to be an effective real time monitor of TMD growth even at the sub-monolayer level which can be exploited to track surface coverage as a function of time under varying growth conditions. The ability to precisely control and modulate precursor flux during growth is used to synthesize in-plane heterostructures that enable localized exciton confinement and emission. Applications for wafer-scale TMD monolayers in nanoelectronics, sensing and photonics will be discussed.

11:00 AM EL05.05.09

Selective Area Epitaxy Growth of 2D Materials by Molecular Beam Epitaxy [Yongchen Liu](#)¹, [Mingyu Yu](#)¹ and [Stephanie Law](#)²; ¹University of Delaware, United States; ²The Pennsylvania State University, United States

Two-dimensional (2D) materials have exploded in popularity due to their wide range of properties and the fact that they can be stacked into devices. The vast majority of devices made from 2D materials use exfoliated flakes, which works well for creating prototypes and to understand basic physics, but exfoliation is difficult to scale up. For traditional materials, devices are fabricated using wafer-scale films and subtractive manufacturing processes. Unfortunately, wafer-scale films of 2D materials grown by physical vapor deposition or chemical vapor deposition techniques often have a high density of

grain boundaries and twin defects, which lead to unwanted conducting channels in electronic devices, non-radiative recombination pathways in optical devices, and decoherence in quantum devices. In addition, etching often damages the edges of the 2D material, further degrading device performance. One way to solve this problem is to take a new approach to the wafer-scale manufacturing of 2D material devices. Instead of growing a wafer-scale film and using subtractive techniques to fabricate devices, we use selective area epitaxy (SAE), an additive technique, to build devices from the bottom up. In SAE, a mask is patterned on the substrate before growth with precisely placed holes through to the substrate. The growth conditions are selected such that the film only nucleates and grows within the openings in the mask, thus defining the location, size, and shape of the film. By choosing the growth conditions correctly, we can ensure that only a single grain of 2D material grows in each opening, eliminating issues with grain boundaries and film coalescence. Multiple materials can be stacked together using SAE to create functional device stacks. If contacts to the stack are needed, they can be made as edge contacts before epitaxy and/or as top contacts post-growth. Using SAE, we can synthesize quantum-confined 2D materials without the need for etching, thus preserving the intrinsic properties of the material. Overall, SAE has the potential to transform growth of 2D materials for devices by enabling the synthesis of 2D materials free of grain boundaries with precise locations and sizes. In this talk, I will discuss our recent results on SAE of 2D materials using molecular beam epitaxy (MBE). MBE is an ultra-high vacuum physical vapor deposition technique, in which high-purity elemental source materials are thermally evaporated. The atoms impinge upon the substrate and react to form the film. In the past decade, MBE has been used to grow a wide range of 2D materials and heterostructures and due to its high purity, is a good choice for SAE. To begin, we explored SAE of the topological insulator Bi₂Se₃ on GaAs substrates using Al₂O₃ masks deposited by electron beam evaporation and atomic layer deposition. We find that we can obtain SAE in a narrow but reproducible growth window. We also find differences in SAE growth windows for electron beam deposited Al₂O₃ compared to atomic layer deposited Al₂O₃, likely due to the difference in smoothness and the number and density of dangling bonds. I will further show results for SAE of Ga₂Se₂ on GaAs and for Bi₂Se₃ on Si. Overall, SAE is a promising technique for the growth of high-quality 2D material devices.

11:15 AM EL05.05.10

Scalable Synthesis of Molecular-Intercalated Bulk Monolayer MoS₂ with Tailored Electron Doping Boxuan Zhou, Jingyuan Zhou and Xiangfeng Duan; University of California Los Angeles, United States

Molybdenum disulfide (MoS₂) is an extensively studied two-dimensional layered semiconductor with interesting electronic and optical properties. Monolayer MoS₂ features strong light-matter interactions due to its direct bandgap, whereas multilayer MoS₂ is an indirect bandgap semiconductor and optically inactive. The molecular intercalation of MoS₂ with organic cations offers a strategy to decouple the interlayer interaction, producing a bulk monolayer material, but is usually accompanied by a heavy electron doping effect that can diminish the intrinsic semiconductor properties or induce a phase transition. Herein, we report a chemical-dedoping strategy to tailor electron density in molecular-intercalated MoS₂, therefore retaining monolayer properties. By introducing a poly(vinylpyrrolidone)-bromine complex during the electrochemical intercalation process, we show bulk monolayer MoS₂ thin film can be produced with decoupled interlayer interaction and reduced electron concentration. The resulting thin films display strong excitonic emission, 20- and > 400 times stronger than the exfoliated monolayer and multilayer material respectively, as well as high valley polarization and enhanced photo-electric response. Our study opens a scalable path to large-area bulk monolayer MoS₂ thin films with monolayer-like optical properties and greatly increased optical cross-section, presenting an attractive material platform for both fundamental photophysics studies and scalable optoelectronic applications.

11:30 AM EL05.05.11

Wafer Scale Lateral Heterojunctions of MoS₂ and WS₂ for Photocurrent Applications Sivasakthya Mohan¹, Yuqian Gu^{1,2}, Martha Serna¹, Jia Yu¹, Shanmukh Kutagulla¹, Keji Lai¹, Kenneth Liechti¹ and Deji Akinwande¹; ¹The University of Texas at Austin, United States; ²Intel Corporation, United States

Despite the widespread research in studying the synthesis and properties of two-dimensional (2D) materials for electronic devices, there are still some intrinsic challenges such as zero bandgap (for e.g., graphene), low carrier mobilities (e.g., Transition Metal Dichalcogenides or TMDs) which prevent their successful transition to real-world applications. 2D heterostructures present new prospects for advanced materials design for specific optoelectronic and transport applications. By combining the unique properties of different 2D materials, heterostructures can be tailored suitably to possess distinct functionalities. While the fabrication of vertical heterostructures is more common through exfoliation and transfer methods, contaminations and stacking orientations between the layers often restrict their device performance¹. To this end, efforts have been made in the synthesis of lateral heterostructures where the different domains are covalently bonded and can enhance device performance.

In this work, we synthesized wafer-scale lateral heterostructures of MoS₂ and WS₂ on sapphire, through e-beam lithographic patterning followed by one-step, low-temperature sulfurization² of the thin metal films of molybdenum and tungsten. The quality and number of layers of the sulfurized heterostructures have been evaluated using optical microscopy, large-area Raman maps, and cross-section TEM. The seamless transition between the 2D TMDs at the interface has been further evaluated using high-resolution characterization techniques such as XPS, ToFSIMS, and atomic force microscopy. A scanning microwave impedance microscope (MIM) was employed to obtain the spatial conductivity resolution of the heterojunctions. Enhanced photocurrent measurements obtained on the fabricated devices pointed to potential applications in photo-sensing devices.

REFERENCES

1. Chakraborty, S. K., Kundu, B., Nayak, B., Dash, S. P., & Sahoo, P. K. (2022). Challenges and opportunities in 2D heterostructures for electronic and optoelectronic devices. *Iscience*, 25(3), 103942.
2. Gu, Yuqian, et al. "Sulfurization Engineering of One - Step Low - Temperature MoS₂ and WS₂ Thin Films for Memristor Device Applications." *Advanced Electronic Materials* 8.2 (2022): 2100515.

11:45 AM EL05.05.12

Resolution Limits and Their Effect on Structure and Morphology of Lithographically Defined TMD Synthesized by Lateral Conversion Shaul Aloni, Marco D'Allesandro, Ricardo Ruiz, Aidar Kamelbay and Tevye Kuykendall; Lawrence Berkeley National Laboratory, United States

Recently, we developed a wafer-scalable method to synthesize lithographically patterned transition metal dichalcogenides (TMDs), using a process that we call "lateral conversion." Briefly, this method relies on the diffusion of chalcogen precursors to convert metal-oxide thin-films via interlayer diffusion, which proceeds from the exposed film edges at lithographically defined locations. In this work, we explore the resolution limits of our method and its effect on its structure and properties. The synthesis approach initially relied on photolithography to fabricate structures with micron-scale resolution. In this work, we show that this method is suitable to achieve lithographically defined sub-20nm features achievable using a block copolymer lithography. We were able to develop simple transfer techniques to lift the patterned structure and transfer it to a substrate of choice such as a silicon wafer or electron transparent substrate for TEM analysis. This allowed us to study the effect of synthetic parameters on the morphology and structure of the TMD and improve the quality of the TMD films.

SESSION EL05.06: Memory Devices I
Session Chairs: Shaul Aloni and Sonu Devi
Wednesday Afternoon, April 24, 2024
Room 344, Level 3, Summit

1:45 PM EL05.06.01

Integration 3D Micro and Nano Structures with 2D Materials via Self-Assembly Approach [Zihao Lin](#)¹, Shehua C. Thorl, Chunhui Dai¹, Sodam Choi², Chiwon Ahn² and Jeong-Hyun Cho¹; ¹University of Minnesota, Twin Cities, United States; ²KAIST, Korea (the Republic of)

Two-dimensional (2D) materials have been widely researched for the past decades. Despite this, there is recently a large interest in bringing 2D materials to 3D micro/nano architectures as the later one offers many new functionalities in space dimension compared with the 2D plane, such as robotics, electronic skins, molecular sieves, and sensors. In this work, 2D materials are integrated on 3D micro and nano structures via self-assembly technique. This approach can be witnessed with several advantages. First, it is well compatible with traditional two-dimensional (2D) lithographic processes. Second, complex 3D structures which are usually challenging to achieve by traditional top-down techniques can be easily fabricated by this bottom-up method. Third, it is a manual-free and wire-free process. Moreover, it can be well applicable by patterning different kinds of materials on it with different dimensions and subsequently self-assembled together with stimulus-based active layers to realize 3D architectures, which offers great flexibility and strong functionality. Here, two fabrication processes that meet the previously mentioned benefits are introduced. They facilitate the incorporation of 2D materials, including Graphene, Graphene Oxide, and MXenes, onto a wide range of 3D micro and nanostructures. First, electron beam induced in-situ monitored self-assembly technique. 2D materials together with other active nano layers can be firstly patterned on the planar surface and then subsequently curved up to 3D nano structures stimulated by focused electron beam induced stress deformation. This technique offers nanometer resolution control of the 3D object, and the desired 3D shape can be meticulously crafted. Second, 3D self-assembly process uses stress gradient in negative photoresist (SU-8). The stress gradient in the SU-8 enables the formation of 3D graphene-based polyhedral structures. The graphene and SU-8 layers are patterned, then transitioned into 3D structures when the stress gradient, instigated by an UV-energy source, is alleviated. Simulation is performed to demonstrate the strong 3D volumetric light confinement in 3D graphene nano structures and high optical chirality in 3D graphene microstructures. The developed fabrication technique can further be used to construct 2D materials-based fluidic channels, actuators, micro/nano machines and 3D passive elements.

2:00 PM EL05.06.02

Charge Trap Engineering and Synaptic Behavior of Transition Metal Dichalcogenides Transistor, via Molecular Dynamics [MiJi Kwon](#), Yeonjin Je, Chang hwan Oh and Jun Hong Park; School of Materials Science & Engineering, Gyeongsang National University, Korea (the Republic of)

The electrical performance of semiconductor devices has a significant dependence on the surface states of the semiconductors because the channel between source and drain regions for charge carrier transports is mostly formed near the surface with applying gate bias. Therefore, it is critical to engineering the surface chemistry of the semiconductor material. Coupling an intrinsically atomically thin body with a finite bandgap, layered transition metal dichalcogenides (TMDCs) have been employed as semiconducting channel platforms with a large ON/OFF ratio and near theoretical subthreshold swing. Here, reconfigurable synapse behaviors of TMDC via molecular adsorption of chemically and the receptive layer are demonstrated with three terminal TMDC synapse devices.

Molecular adsorption on the MoSe₂ surface is induced with dipping in (NH₄)₂S(aq) diluted in H₂O with 25%, while the solution temperature is held at 50 degrees celsius. H₂S or HS molecules can be adsorbed on the MoSe₂ surface during this chemical treatment and act as trapping centers for transported carriers. The adsorbed molecules can be desorbed from MoSe₂ surfaces with wash with isopropanol.

To mimic the biological synapse, the electrical synapse response of MoSe₂ transistors is modulated by a pulse generator wherein excitatory modes; thereby synapse plasticity is controlled by spike-like gate bias as a presynaptic input. After applying pulse gate bias with 50 ms pulse duration, for bare MoSe₂ devices, there is no synapse response, including changes in conductance, consistent with the absence of the plasticity. However, after chemical treatment, molecular adsorption increases conductance upon pre-synapse inputs consistent with a significant increase from 5.9 S to 68.6 S (a postsynaptic conductance), consistent with the manifest of plasticity. The observed plasticity can disappear with the desorption of molecules from the surface of synapse devices.

To emulate the visual sensory behavior of humans, the artificial synaptic plasticity of synaptic devices has been explored by applying light pulse. As light stimulation with pulse modulation, the channel's conductance near-linearly increases as the number of light pulses increases, consistent with optical potentiation. Afterward, electric depression of molecularly functionalized synapse can be observed with the linear decrease of conductance. In addition, although it is crucial to fabricate the receptive layer in which a particular molecule reacts selectively, TMDC materials are absence of dangling bonds and surface state, resulting in degradation of selectivity. Therefore the TiOPc monolayers on the TMDC surface is deposit as the artificial receptive layer to induce the selective electric signal upon molecular absorption.

Consequently, since the present report demonstrates the reconfigurable plasticity of TMDCs synapse devices with the optically sensory response, it can be a milestone to develop a brain-inspired computing system that integrates sensory function upon chemical and optical stimulation

2:15 PM EL05.06.03

Exciton and Trion Emission in Wafer-Scale MoS₂ Layers – The Role of Bilayer Islands [Henrik Myja](#), Tilmär Kümmell and Gerd Bacher; University Duisburg-Essen, Germany

2D materials, especially the group of semiconducting transition metal dichalcogenides (TMDCs), have emerged as highly promising for electronic and optoelectronic devices over the past decades [1][2]. For industrially relevant applications, wafer-scale growth of high quality TMDCs is essential. Until today, the control of defects, crystallinity and grain size in wafer-scale synthesis via metal organic chemical vapor deposition (MOCVD) is still challenging. E.g., in molybdenum disulfide (MoS₂) or related sulfur based TMDCs, sulfur vacancies are known to lead to a background n-doping, thus affecting device performance significantly. While there are various approaches for post-growth treatments of defective TMDCs (e.g. super-acid treatment or partial oxidization), little is known about controlling sulfur vacancies and thus background doping in the growth process.

In this contribution we use confocal photoluminescence (PL) measurements with < 500 nm spatial resolution to monitor the local charge carrier distribution in MOCVD grown MoS₂ via the ratio of neutral exciton and trion emission. A 2" c-plane sapphire substrate with 1° off-axis cut is used as the growth substrate in MOCVD. The wafer-scale growth results in MoS₂ monolayers with crystal grain sizes above 50 μm as extracted from grain boundary visualization in transmission electron microscopy (TEM), and a ~15 % coverage with bilayer domains of ~500 nm in size. Despite the large grain sizes, the average PL quantum yield of the MoS₂ monolayer sample is only about 10⁻³ %. This is attributed to the high point defect density of (4.1±1.6)*10¹³ cm⁻² as determined by atomically resolved scanning tunneling microscopy (STM) [3] and the impact of interfacial defects and substrate-induced doping, respectively [4]. Surprisingly, our spatially resolved PL mappings indicate an unusual behavior for monolayer and bilayer regions on the sample. The PL obtained from monolayers is dominated by trion emission, indicating a strong influence of n-type background doping. In contrast, the PL on bilayer domains mainly shows neutral exciton emission, combined with reduced line width and a significantly enhanced intensity. This on one hand confirms literature reports on preferred nonradiative recombination via trions [5], and on the other hand hints to a suppression of background doping and thus defect

formation in bilayer areas. The latter might be highly relevant for achieving less defective TMDCs via MOCVD growth. Low temperature micro-PL mapping is used to investigate the defect structure of the samples in more detail and to verify this interpretation.

Acknowledgement:

The authors greatly acknowledge the MoS₂ growth and sample supply by imec Leuven, Belgium.

References:

- [1] Lemme, M.C., Akinwande, D., Huyghebaert, C. et al. 2D materials for future heterogeneous electronics. *Nature Communications* 13, 1392 (2022)
- [2] Andrzejewski, D., Myja, H., Heuken, M., et al. Scalable Large-Area p-i-n Light-Emitting Diodes Based on WS₂ Monolayers Grown via MOCVD. *ACS Photonics* 6, 1832 (2019)
- [3] Rybalchenko, Y., Minj, A., Medina, H., et al. Scanning tunneling microscopy for imaging and quantification of defects in as-deposited MoS₂ monolayers on sapphire substrates. *Solid-State Electronics* 209, 108781 (2023)
- [4] Yu, Y., Yu, Y., Xu, C. et al. Engineering Substrate Interactions for High Luminescence Efficiency of Transition-Metal Dichalcogenide Monolayers. *Advanced Functional Materials* 26, 4733 (2016)
- [5] Lien, D.-H., Uddin, S.Z., Yeh, M., et al. Electrical suppression of all nonradiative recombination pathways in monolayer semiconductors. *Science* 364, 468 (2019)

2:30 PM BREAK

SESSION EL05.07: Sensors
Session Chairs: Chandan Das and Oliver Fenwick
Wednesday Afternoon, April 24, 2024
Room 344, Level 3, Summit

3:30 PM EL05.07.03

Programmable Graphene e-Nose Sensor Arrays for Fast, Sensitive and Label-Free Identification of Chemical Vapors [Haolin Li](#), Anjali D. Sivakumar, Chandrakalavathi Thota, Ruchi Sharma, Xiaoheng Huang, Xudong Fan and Zhaohui Zhong; University of Michigan–Ann Arbor, United States

Conventional electrical chemical vapor sensors are mostly based on charge transfer mechanisms and have struggled with the trade-off between sensitivity and response time. To address this challenge, our groups previously demonstrated a new type of fast, sensitive, and broad-spectrum electronic vapor sensor by exploiting the fringing field capacitance effect in graphene transistors. The typically trivial fringing field capacitance change due to analyte absorption is greatly amplified by both the graphene transistor and a micro-flow channel covering the surface of graphene. In this work, we demonstrate programmable graphene e-nose sensor arrays toward true label-free sensing and identification of chemical vapors. Individual graphene sensors within the 1D sensor array (up to 1 x 9) are optimized to offer sensitive (down to picogram) and fast (sub-second) detection toward a variety of analytes. More importantly, its responsivity toward different analytes can be programmed by electrostatic gating on the graphene transistor. By combining with advanced data analysis tools, the graphene e-nose array has the potential to offer label-free chemical vapor sensing without the need to individually functionalize each sensor as in traditional e-nose devices. We will also discuss the integration of the graphene e-nose sensor array with a micro-gas chromatography chip and a smartphone-sized custom PCB board for electronic control and readout and Bluetooth data communication. The graphene e-nose sensor arrays offer a sensing platform for real-time rapid on-site monitoring of complex gas mixtures including polar, nonpolar, organic, and inorganic molecules. Furthermore, the result should pave the way for fast, sensitive, and true label-free chemical vapor sensing and identification using nanoelectronic sensors.

3:45 PM EL05.07.04

Single Crystalline and Polycrystalline 2D-Layered BiOI for Ionising Radiation Detection [Kavya Reddy Dudipala](#) and Robert L. Hoye; University of Oxford, United Kingdom

Emergence of graphene and transition metal dichalcogenides (TMDs) has escalated interest in novel 2D materials and van der Waals (vdW) solids for their applications across various scientific and engineering disciplines owing to their exceptional electrical, optical, thermal, and physical properties. In the field of medical imaging, radiological diagnostic tests like mammography/CT scan, require detection of low doses of ionizing radiation such as X-rays and γ -rays to limit radiation damage imposed on patients. Low dose radiation detection requires absorber materials with high linear attenuation co-efficient, high resistivity and large drift mobility-lifetime products.^[1] In this work, we explore 2D-layered BiOI for radiation detection, where we firstly study its photophysical properties like photoexcited charge-carrier lattice coupling dynamics and its implications for efficient detector performance. Then we demonstrate X-ray detectors based on BiOI single crystals with high sensitivities reaching $1.1 \times 10^3 \mu\text{CGy}_{\text{air}}^{-1}\text{cm}^{-2}$ and lowest dose rate directly measured upto $22 \text{ nGy}_{\text{air}}\text{s}^{-1}$.^[2] We develop scalable polycrystalline synthesis and device fabrication routes that are better suited for commercialization, through uniaxial pressing of BiOI powders/single crystals into wafers of desired thickness and through chemical vapor deposition of BiOI thick films. The results presented here highlight the potential of novel high-Z 2D materials for radiation detection applications.

1. Dudipala, K. R., Le, T. H., Nie, W., & Hoye, R. L. Z. (2023). Halide Perovskites and their Derivatives for Efficient, High-Resolution Direct Radiation Detection: Design Strategies and Applications. *Advanced Materials*, 2304523.
2. Jagt, R. A., Bravic, I., Eyre, L., Galkowski, K., Borowiec, J., Dudipala, K. R., Baranowski, M., Dyksik, M., Van De Goor, T. W. J., Kreouzis, T., Xiao, M., Bevan, A., Plochocka, P., Stranks, S. D., Deschler, F., Monserrat, B., Macmanus-Driscoll, J. L., Hoye, R. L. Z. (2023). Layered BiOI single crystals capable of detecting low dose rates of X-rays. *Nature Communications*, 14(1), 2452.

4:00 PM EL05.07.05

Highly Integrated Graphene-Based Chemical Sensing Platform for Structural Monitoring Applications [Christian E. Lopez Angeles](#) and Tomas Palacios; Massachusetts Institute of Technology, United States

Two-dimensional materials, such as graphene, hold promise for sensing applications. Graphene's remarkable surface-to-volume ratio, when employed as a transducer, enables the sensor channel to be readily modulated in response to chemical changes in proximity to its surface, effectively converting chemical signals into the electrical domain. However, their utilization has been constrained due to variations in device-to-device performance arising from synthesis and fabrication processes.

To address this challenge, we employ Graphene Field Effect Transistors (GFETs) in developing a robust and multiplexed chemical sensing array comprising tens of sensing units. This array is coupled with custom-designed high-speed readout electronics for structural monitoring applications. For example, in harsh environmental conditions, structures constructed from reinforced concrete may experience degradation due to corrosion, a chemical process initiated by carbonation and significant fluctuations in temperature and humidity. Under normal conditions, concrete maintains a pH level within the alkaline range of 13 to 14. However, when subjected to carbonation, its pH decreases to values between 8 and 9.

Our platform excels in real-time pH monitoring. By conducting I-V sweep measurements in the sensor channel, we have established a correlation between [H⁺] concentration and the gate-source voltage (V_{gs}) at graphene's Dirac point with an accuracy of roughly 98%. This system and correlation allows for the prompt detection of any deviations induced by corrosion within a concrete environment.

SESSION EL05.08: Poster Session II
Session Chairs: Silvija Gradecak and Iuliana Radu
Wednesday Afternoon, April 24, 2024
Flex Hall C, Level 2, Summit

5:00 PM EL05.08.01

Synthesis of 2D PtSe₂ Nanolayers on Glass Substrates and Their Integration in Device Applications Vera G. Marinova¹, Nikolay Minev¹ and Dimitro Dimitrov^{1,2}; ¹IOMT-BAS, Bulgaria; ²ISSP-BAS, Bulgaria

We report the synthesis details of 2D PtSe₂ layers on soda lime (glass) substrates by selenization of pre-deposited Pt films using thermally assisted conversion (TAC) method at 430°C and atmospheric pressure. PtSe₂ layers with different thicknesses were prepared by varying the Pt deposition time (Pt 3s, Pt 8s and Pt 10s), afterwards estimated by ellipsometric measurements to correspond to 7nm, 9 nm and 12nm, respectively. The X-Ray diffraction patterns showed the diffraction peaks characteristic with improving crystallinity when increasing the Pt deposition time. The Raman spectra revealed typical PtSe₂ modes, while a decrease of Se/Pt ratio and a transition from *p*-doped to *n*-doped PtSe₂ for longer Pt deposition times was found by X-ray photoelectron spectroscopy analysis. Formation of reactive oxygen species (ROS), mainly hydroxyl radicals (OH) on the PtSe₂ surface under light irradiation was demonstrated by EPR analysis.

PtSe₂ coatings demonstrate antibacterial activity against *Escherichia coli* in dark and under light irradiation owing to their 2D layered morphology, crystalline structure and optical properties. The antibacterial activity was tested applying ISO standard procedure: (i) in dark, the antibacterial activity increased with the increase of Pt deposition time and the viability of the bacteria was reduced to 30% (Pt 3s) and 15% (Pt 10s) after treatment for 6 h. The effect was attributed to the increasing film thickness, roughness and surface coverage which facilitate the mechanical destruction of the bacteria cell; (ii) under light irradiation, the activity of PtSe₂ (Pt 3s) was similar to that in dark showing low sensitivity to light. On the contrary, the PtSe₂ (Pt 8s) and (Pt 10s) appeared very effective under light, with the bacteria viability after 6 h being only 7.3% and 1.2%, respectively. The observed photo-induced antibacterial activity is related to the synergy of several parameters, i.e. high crystallinity, semiconductor behavior and chemical composition. In addition, integration of PtSe₂ as transparent, conductive layers in Polymer Dispersed Liquid Crystal (PDLC) structures operating as near infrared light shutters is demonstrated. The proposed simple and inexpensive synthesis approach opens new directions towards PtSe₂ potential technological applications, including ITO-free optoelectronics.

Acknowledgement: We acknowledge the support of the European Union's Horizon 2020 FET-PROACTIVE project TOCHA under grant agreement 824140 and Bulgarian Science Fund under the project numbers FNI KP-06-DO 02/2 and KP-06-DO 02/3 in the frames of M-ERA program project "Functional 2D materials and heterostructures for hybrid spintronic-memristive devices".

5:00 PM EL05.08.02

Telecom Quantum Emitters in Van der Waals Materials Huan Zhao^{1,2} and Han Htoon²; ¹Los Alamos National Laboratory, United States; ²Oak Ridge National Laboratory, United States

In the poster, I present the site-controlled creation of near-infrared (NIR) NIR single-photon emitters in 2D transition metal dichalcogenide (TMDC) monolayers, multilayers, and heterobilayers. The emission of non-classical light is induced through the deterministic implantation of localized strain using a scalable, nanopillar-based, strain engineering technique. The excitons trapped by the strain-induced potential wells produce bright, narrow-bandwidth photoluminescence (PL) with emission wavelength ranging from 900 nm to 1.6 μm. Our Hanbury Brown and Twiss (HBT) experiment yielded near-complete photon antibunching, unambiguously proving the quantum nature of the emitters. The high-purity single-photon emission can be maintained at liquid nitrogen temperature without a significant decrease in the emission intensity. No photon bleaching, blinking, or spectrum diffusion was observed in the time domain, suggesting the quantum emitters are photon stable. These newly discovered 2D quantum emitters extend the emission range of 2D SPEs to the NIR regime and offer new opportunities for the development of next-generation fiber-based quantum communication and quantum information applications.

5:00 PM EL05.08.05

Heterojunctions of 2D Materials for Molecular Electronics Bhartendu Papnai^{1,2} and Mario Hofmann³; ¹Academia Sinica, Taiwan; ²National Tsing Hua University, Taiwan; ³National Taiwan University, Taiwan

Molecular electronics offer an appealing alternative for future electronic devices, providing advanced functionalities that surpass the current scaling limits of silicon-based electronics. Our work demonstrates that two-dimensional (2D) materials such as graphene that come into contact with the molecular layer contribute to the formation of highly efficient devices. The fabrication of the molecular layer with Langmuir-Blodgett film was utilized to show the tunneling effect of the molecular transistor. The sharp decrease in current with increasing voltage shows a negative differential resistance effect with a high on-off ratio.

Furthermore, our research extends to the examination of thermal and thermoelectric properties within molecular junctions by incorporating molecular monolayers into a thin film configuration. Specifically, our objective is to enhance the performance of thermoelectric devices by integrating graphene-Langmuir Blodgett (LB) films. Our research also delves into Langmuir Blodgett films featuring 2D material heterojunctions, especially in the context of adaptability to diverse light sources, which is a critical aspect of our research.

5:00 PM EL05.08.06

Hydrogenated Borophene-Graphene Broadband Photodetectors for Ultrahigh Photoresponsivity Digvijay S. Tomar and Surojit Chattopadhyay; National Yang Ming Chiao Tung University, Taiwan

2D nanomaterials like graphene, hexagonal boron nitride (h-BN), black phosphorous (BP), and transition metal dichalcogenides (TMDs) have gained significant attention in the past two decades due to their distinct thermal, electrical, optical, and magnetic properties compared to their bulk counterparts[1]. In contrast, borophene, a unique 2D nanomaterial composed entirely of boron atoms, stands out for its advantages in optoelectronic device applications. These include high electrical conductivity, optical transparency in the visible spectrum, strong light-matter interaction, notable mechanical properties (high tensile strength and flexibility), the potential for superconductivity, and good chemical stability, making it suitable for harsh environments[2]. Here, we synthesized hydrogenated borophene through the thermal decomposition of NaBH_4 in the presence of H_2 . Subsequently, we fabricated a 2-terminal coplanar Borophene/Graphene/ SiO_2 /Si broadband (405-1064 nm) photodetector (PD) with high photoresponsivity (R). The Borophene/Graphene/ SiO_2 /Si PD exhibits an outstanding $R \sim 3.65 \times 10^3 \text{ A/W}$ under 405 nm laser illumination (@ 1V bias, 0.05 mW/cm²). This performance surpasses previously reported values for Borophene-based PDs, which ranged from 0.48 to 9.13 A/W [3-5]. Our PD shows short response, and recovery times of 82, and 83 ms under 633 nm laser illumination compared to previous reports in the range of 110 to 660 ms [3-5]. Our results may stir interest in Borophene for nanophotonics, and optoelectronics devices.

References

- [1] G. Wang et al., "Two dimensional materials based photodetectors," *Infrared Physics & Technology*, vol. 88, pp. 149-173, 2018/01/01/ 2018, doi: <https://doi.org/10.1016/j.infrared.2017.11.009>.
- [2] Z. Xie et al., "Two-Dimensional Borophene: Properties, Fabrication, and Promising Applications," *Research*, vol. 2020, doi: 10.34133/2020/2624617.
- [3] Y. Liu, G. Tai, C. Hou, Z. Wu, and X. Liang, "Chemical Vapor Deposition Growth of Few-Layer β 12-Borophane on Copper Foils toward Broadband Photodetection," *ACS Applied Materials & Interfaces*, vol. 15, no. 11, pp. 14566-14574, 2023/03/22 2023, doi: 10.1021/acsmi.2c23234.
- [4] Z. Wu et al., "van der Waals Epitaxial Growth of Borophene on a Mica Substrate toward a High-Performance Photodetector," *ACS Applied Materials & Interfaces*, vol. 13, no. 27, pp. 31808-31815, 2021/07/14 2021, doi: 10.1021/acsmi.1c03146.
- [5] Z. Wu et al., "Epitaxial growth of borophene on graphene surface towards efficient and broadband photodetector," *Nano Research*, 2023/09/27 2023, doi: 10.1007/s12274-023-6109-9.

5:00 PM EL05.08.07

Enhancing Gas Sensing Performance with 2D Material-Integrated Sub-Wavelength Grating Micro-Ring Resonator: Improved Sensitivity and Selective Detection Boxin Zhang, Yadendra Singh and Harish Subbaraman; Oregon State University, United States

Silicon photonics devices are widely utilized in optical gas sensing owing to their compact size and compatibility with CMOS technology. However, their limited sensitivity hampers their versatility. In this study, we introduce a highly sensitive gas sensor incorporating a 2D material gas-absorbing layer and a sub-wavelength grating (SWG) micro-ring resonator. Leveraging the large surface-volume ratio of the 2D material layer, it efficiently absorbs gas molecules and induces substantial refractive index changes during sensing. Finite-Difference Time-Domain (FDTD) simulation results will be showcased which demonstrate enhancement in both bulk sensitivity and surface sensitivity upon incorporating the 2D material layer. Moreover, the SWG design enables a larger evanescent field-analyte interaction region, resulting in an elevated quality factor for the proposed sensor. Furthermore, by coating the micro-ring resonators with different 2D materials, we envision highly selective sensor architectures.

5:00 PM EL05.08.08

Large-Scale Growth of Non-Centrosymmetric MoSe_2 by Chemical Vapor Deposition and Their Enhanced Nonlinear Optical Response Joohyeon Ahn¹, Seongju Ha², Jungseok Choi¹, Dong-Il Yeom^{1,†} and Youngdong Yoo¹; ¹Ajou University, Korea (the Republic of); ²Korea Research Institute of Standards and Science (KRISS), Korea (the Republic of)

Transition metal dichalcogenides (TMDCs) have various novel electronic and optical properties depending on their structure. Monolayer TMDCs have been used for advanced 2D electronics and 2D optoelectronics due to their exceptional physical and chemical properties. Spiral TMDCs grown through the formation of screw dislocations have been extensively utilized for nonlinear optics due to their non-centrosymmetric structure. However, large-scale growth of TMDCs remains challenging. Here, we report the large-scale growth of monolayer MoSe_2 and spiral MoSe_2 using a flux-controlled chemical vapor deposition method. With a low flux, monolayer MoSe_2 is synthesized, whereas thick spiral MoSe_2 is obtained with a high flux. With a medium flux condition, both monolayer and spiral MoSe_2 are synthesized. We utilized various analysis techniques such as optical microscopy (OM), atomic force microscopy (AFM), and Raman and photoluminescence (PL) spectroscopy for characterization of synthesized non-centrosymmetric MoSe_2 . Additionally, nonlinear optical (NLO) signal measurements of monolayer MoSe_2 and spiral MoSe_2 show the enhancement of NLO signals originating from both non-centrosymmetric structure and the excitonic resonance effects. Monolayer MoSe_2 and spiral MoSe_2 synthesized using this method are expected to be used as advanced optical materials for electronics, optoelectronics, and nonlinear optics.

5:00 PM EL05.08.09

Controllable Growth of Large Area P-Type MoS_2 with Transition Metal Doping using Confined Space CVD Muhammad Suleman, Minwook Kim and Seo Yongho; Sejong University, Korea (the Republic of)

2D molybdenum Disulfide has been used extensively as a semiconductor in recent years. Typically, MoS_2 demonstrates an N-Type Behavior as there are sulfur vacancies that are present in the material. However, the large-scale synthesis of P-Type MoS_2 and other 2D materials can still be challenging. Various methods can be used for doping the pristine MoS_2 to provide P-Type behavior and one of these methods is substitutional doping. Group VB Transition metals like Niobium (Nb), Vanadium (V) and Tantalum (Ta) can be used to achieve substitutional doping into the MoS_2 crystal lattice. In this work we have achieved P-Type behavior in CVD grown MoS_2 through a similar method. Moreover, the existence of doping atoms was confirmed by using XPS (X-ray photoelectron spectroscopy), EDX (Energy dispersive X-ray) and TEM (Transmission Electron Microscopy). The fabricated back gate FETs also confirm the behavior as a P-Type material. This proposed method for the synthesis of P-Type MoS_2 can have a lot of potential applications ranging from photodiodes, photodetectors, optoelectronics, field effect transistors, synaptic transistors, advanced materials heterostructures and energy harvesting.

5:00 PM EL05.08.10

Integrated TEM Membrane Platforms for Lateral Conversion TMD Synthesis Tevye Kuykendall, Aidar Kemelbay, Misael Campos, Alexander Herman and Shaul Aloni; Lawrence Berkeley National Lab, United States

Two dimensional transition metal dichalcogenides (TMDs) are a promising family of materials for a wide range of applications. However, their integration into traditional fabrication pipelines remains challenging. Our research has been working to develop a lithographically patterned, wafer-scalable fabrication process that we call "lateral conversion synthesis." We have demonstrated this on a host of TMDs, including W, Mo, Pt, sulfides, selenides, and tellurides,

alloys and heterostructures. We will present an overview of these results, as well as a process to directly synthesize TMDs on electron transparent membranes for performing transmission electron microscopy. We demonstrate that by using these membranes, we can resolve and optimize the crystalline microstructure, domains and lattice structures of the TMDs grown through lateral conversion.

5:00 PM EL05.08.11

Chemical Vapor Transport Growth of Selenene and its Heterostructures with TMDs [Renjith N.](#), Bhargav Rajbongshi and Manikoth Shaijumon; IISER Thiruvananthapuram, India

2-dimensional (2D) materials have attracted a lot of scientific attention recently beyond graphene, due to their distinct physicochemical features. Elemental 2D crystals have emerged as promising materials for advanced electronics and optoelectronics applications.^[1] In particular, group-VI elemental 2D semiconductors, including selenene and tellurene, have attracted significant attention for their simple composition and excellent properties, such as higher carrier mobility, better environmental stability, and high photoconductivity, which triggered intense activities on their fundamental and application-oriented research.^[2] 2D heterostructures based on various 2D layered materials with distinct properties have been demonstrated to exhibit novel physicochemical properties for their potential application in electronics, optoelectronics, and catalysis, owing to their tunable band alignment and sharp interfaces.^[3] Forming new structures by stacking transition metal dichalcogenide (TMD) layers has been explored by several groups; however, the mechanical transfer method is time-consuming and suffers from having reasonable control on the layer stacking. Single-step and two-step chemical vapor deposition (CVD) growth of lateral and vertical TMD heterostructures have been considered to be a promising approach to realize the potential applications of these heterostructures.^[4] Achieving controllable growth of high-quality, ultra-thin flakes of elemental 2D materials remains a challenge. Herein, we demonstrate a seed-assisted chemical vapor transport (CVT) growth of ultra-thin triangular flakes of highly crystalline trigonal selenium (t-Se) oriented in (0001) direction, with lateral size >30 μm .^[5,6] To study their promising photo-electrocatalytic properties and further realize the device applications, we employed a single-step CVT approach to grow selenene/WSe₂ heterostructures. Vertical heterostructures of bi-layer selenene and monolayer WSe₂ domains obtained via the CVT method are characterized by optical microscopy, transmission electron microscopy (TEM), X-ray photoelectron spectroscopy (XPS), and Raman spectroscopy. The Se/WSe₂ heterostructure exhibit improvements in the HER activity as evidenced by the overpotential which is dramatically decreased from 163 mV to 121 mV for a current density of 10 mA cm⁻² and the Tafel slope also reduces from 109 mV dec⁻¹ to 75 mV dec⁻¹ upon shining the light. The method could be extended to synthesize different 2D elemental and TMD heterostructures.

5:00 PM EL05.08.12

Direct-Growth-Enabled Monolithic Integration of Monolayer MoS₂ Vertical Field-Effect Transistors Huimin Lee¹, [Seonguk Yang](#)¹, Kihan Kim², Saeyoung Oh¹, Huyoung Jeong¹, Byungchul Jang² and Joonki Suh¹; ¹Ulsan National Institute of Science and Technology, Korea (the Republic of); ²Kyungpook National University, Korea (the Republic of)

The ultimate hyper-scaling regime for two-dimensional (2D) semiconductors requires device innovations beyond conventional planar structures, and so it is in the urgent need for developing a tailored integration solution. Recently, 2D-layered semiconductors have shown great potential as channel materials for various electronic devices due to their atomically thin structure, dangling-bond-free characteristic, and well-controlled electrostatics that can overcome intrinsic limitations as seen in sub-5-nm-body-scaling-node of silicon (Si). Nevertheless, the relevant 2D semiconductor integration has been often limited to low-fidelity transfer approaches, obviously not friendly for non-planar device structures. Here, we demonstrate vertical MoS₂ transistor and non-volatile memory with sequential growth level integrated 2D semiconductors in a 3D architecture enabling simple processes at scalable array scale with precisely fined vertical channel thicknesses down to ~ 6.5 Åm for high density. Such monolayer MoS₂-based vertical field-effect transistor (FET) shows excellent switching and leakage current characteristics with an on/off ratio of $\sim 10^8$ and a SS_{min} of ~ 77 mV dec⁻¹. Technology computer-aided design (TCAD) simulations were successfully performed to verify that the vertical MoS₂ channels aligned along the vertical sidewalls showing the capabilities of modulating the vertical transport properties via additional side control gates. Furthermore, high crystalline 2D MoS₂ was applied as a channel material for a vertical charge trap flash (CTF) memory showing excellent on/off ratio as well as reliable retention characteristics and endurance performance. This work promotes the monolithic production of vertical 2D MoS₂, which can break through the lateral integration limits, and presents a new platform as a next-generation V-NAND channel material with atomically thin conformality and high crystallinity that can be scaled up to ~ 10 μm , corresponding to V-NAND 300-layers scale.

5:00 PM EL05.08.13

Complementary 2D Tunnel FETs with Extremely Asymmetric Dual-Barrier Heterostructures [Hanbin Cho](#), Seonguk Yang, Donggyu Park and Joonki Suh; UNIST, Korea (the Republic of)

Conventional metal oxide semiconductor field-effect transistor (MOSFET) technology currently suffers from the scaling of supply voltage owing to the required power per computed bit of information tightly bound to the subthreshold swing (SS) of 60 mV/dec at room temperature. Tunneling field-effect transistor (TFET) is a promising building block for low-power and steep-slope switching applications in that the lower limit of MOSFET SS, inherently caused by thermionic emission, can be overcome by utilizing band-to-band tunneling. In this presentation, we propose the TFETs using band-offset engineering via 2D van der Waals (vdW) hetero- and multi-junctions. Indeed, 2D materials are ideally suited since they are free from non-ideal tunneling tendencies originating from lattice mismatch as seen in bulk hetero-junctions and their atom-thick body is under the complete electrostatic control. In the fabricated 2D heterostructured TFETs, SnSe₂ and SnSe not only function as the electron and hole reservoirs but provide a highly asymmetric band offset alignment to the intrinsic channel where MoS₂ and WSe₂ are employed for nTFET and pTFET, respectively. The van der Waals coupled TFETs show the promising device characteristics of low-power switching operations in terms of SS and off-current compared to MOSFETs using the same kinds of channels. In addition, complementary 2D TFETs, implemented in both n-type and p-type, expand the breadth of logic configurations. We expect to be able to leverage this naturally biased 2D material platform to implement effective low-power circuits.

5:00 PM EL05.08.14

Synthesis and Atomic-Scale Investigation of Phosphorus-Doped Graphene on Copper [Oscar Chavez](#), Jerome Brown, Owen Hudak and Li Gao; California State University, Northridge, United States

Phosphorus doped graphene has potential applications in supercapacitors, lithium ion batteries, fuel cells, and sensors. A phosphorus-containing sole precursor has been used for the synthesis of phosphorus-doped graphene on the Cu(111) surface. The surface morphology, electronic structure of phosphorus dopants, and doping-induced variation of local work function of graphene have been studied on the atomic scale by using scanning tunneling microscopy, dI/dV spectroscopy and dZ/dV spectroscopy. Bias-dependent atomic-resolution STM images of the predominant type of phosphorus dopants have been obtained. dI/dV spectra show the effect of phosphorus doping on the electronic structure of the graphene surface. dZ/dV spectra show that the local work function decreases at the phosphorus dopant site, leading to a downward energy shift of field emission resonances. X-ray photoelectron spectroscopy measurements are also performed to characterize the overall phosphorus doping properties on the sample surface. This work provides atomic-scale experimental insights into the phosphorus dopants in graphene for the first time.

5:00 PM EL05.08.15

Synthesis, Structure and Magnetic Properties of a New Spin-1 Honeycomb Lattice KNiAsO₄ with a Zig-Zag Magnetic Structure [Duminda Sanjeeva](#); University of Missouri–Columbia, United States

Identifying and characterizing new honeycomb magnetic systems are the key ingredients to explore new candidate materials for the Kitaev model as the model realizes the exact quantum spin liquids ground state. Recently the Kitaev model with higher spins ($S = 1$) systems have been proposed as candidate materials to host the quantum spin liquid state. Honeycomb compound, KNiAsO₄, is one such magnetic system and here, we present a comprehensive series of magnetic and neutron scattering measurements and evaluate the potential for Kitaev physics via the experimental determination of the spin-Hamiltonian. Bulk magnetic measurements of KNiAsO₄ reveal an antiferromagnetic transition at ~ 19 K which is generally robust to applied magnetic fields. Neutron diffraction measurements show magnetic order with a $k = (3/2, 0, 0)$ ordering vector which results in the well-known “zigzag” magnetic structure thought to be adjacent to the spin-liquid ground state. Inelastic neutron scattering experiments show a well defined gapped spin-wave spectrum with no evidence of the continuum expected for fractionalized excitations. Modeling of the spin waves shows that the extended Kitaev spin-Hamiltonians is generally necessary to model the spectra and reproduce the observed magnetic order. Overall, our results demonstrate that the KNiAsO₄ is a promising candidate to study Kitaev physics associate with spin-1 honeycomb system.

5:00 PM EL05.08.17

Photoelectric Properties of Funnel Devices Based on Asymmetrically Strained Two-Dimensional Materials [Kyung-Hwa Yoo](#); Yonsei University, Korea (the Republic of)

Strain applied to transition metal dichalcogenides (TMDs) decreases their energy bandgap. When local strains are present, a band structure resembling a funnel is created, guiding excitons toward the most strained region. In this study, we present a device with a funnel-like structure based on WS₂ and MoS₂, achieved through asymmetric strains. These strains were induced by transferring TMD flakes onto a fork-shaped SU-8 microstructure. The Raman and photoluminescence spectra peaks were observed to shift based on the morphology of the SU-8 microstructure, confirming the application of asymmetric strains on the TMDs. To examine the potential conversion of funneled excitons into electrical currents, we fabricated various devices by depositing electrodes, both symmetric and asymmetric, onto the strained TMDs. Scanning photocurrent mapping (SPCM) images exhibited a fork-shaped pattern, suggesting the likely conversion of funneled excitons into electrical currents. Specifically, funnel devices with asymmetric Au and Al electrodes demonstrated an enhancement of short-circuit current (I_{sc}) in WS₂ due to the applied strains. On the other hand, I_{sc} in MoS₂ was suppressed as the increasing strain lowered the Schottky barrier, unlike WS₂ where the Schottky barrier was not affected by the strain. These findings underscore the potential of utilizing asymmetrically strained TMDs for implementing funnel devices, and emphasize the TMD-specific impact of strains on the Schottky barrier.

5:00 PM EL05.08.18

Lithography-Free Patterned Growth of Few-Layer MoS₂ Assisted by Electron Irradiation [Haobo Li](#), Edward K. Naland and Silvija Gradecak; National University of Singapore, Singapore

Two-dimensional (2D) transition metal dichalcogenides (TMDs) have emerged as promising candidates for applications such as gas sensors, photodetectors, and channel materials in field-effect transistors, thanks to their tunable band structures, reduced leakage current, and high carrier mobility. The patterning of 2D-TMDs is critical in device fabrication, traditionally requiring a complex lithography process. We demonstrate an approach to depositing MoS₂ flakes on SiO₂/Si substrates with a predefined pattern shape, utilizing localized electron irradiation on the surface of SiO₂/Si wafers. Within the regions exposed to low-dose electron irradiation, we successfully achieve area-selective growth of MoS₂ during chemical vapor deposition (CVD) process with selectivity of >0.7 . In contrast, negative selectivity with suppressed growth is achieved in heavily irradiated areas of the substrate.

We have investigated the modification of surface potential on SiO₂/Si substrates due to localized electron irradiation using Kelvin probe force microscopy (KPFM) and demonstrated that selective growth takes advantage of the local surface potential difference. The variation of the surface potential is predictable by an analytical model. Raman spectroscopy analysis reveals the adsorption of carbon species due to irradiation, acting as a blocking layer that inhibits MoS₂ growth and contributes to the observed negative selectivity. We will discuss the role of CVD parameters (e.g., precursor flux), surface potential, adsorption of carbon species, and surface topography change observed by atomic force microscopy (AFM) in achieving the desired selectivity in CVD growth of MoS₂. Our findings pave the way for a controllable lithography-free patterned synthesis of 2D-TMD materials, eliminating the need for complex lithography processes and minimizing contamination. This study presents a promising approach to achieving a bottom-up fabrication process for the next-generation TMD-based device fabrication and its further scaling.

5:00 PM EL05.08.19

Formation of Silicon/Graphene Heterostructures through Co-Gas-Phase Synthesis [Muhammad Ali](#)^{1,2}, Hartmut Wiggers¹ and Michael Pope²; ¹University of Duisburg-Essen, Germany; ²University of Waterloo, Canada

The introduction of 2D materials as an active or enabling component is of significant interest in the field of electrochemical energy storage because it provides properties such as mechanical stability, large surface area and at the same time low material requirements. Furthermore, graphene-like 2D structures show strong electrical conductivity and electrochemical stability. While each individual 2D material has unique advantages, the deliberate assembly of heterostructures made up of different flakes in configurations such as 2D/2D or particle-flake (0D/2D) emerges as an important advancement. Such finely built heterostructures not only improve functioning but also have potential to push the performance of energy storage devices to levels that were not previously possible. A simple, competitive and scalable strategy to produce heterostructures by combining 0D nanoparticles and 2D graphene in the gas phase is reported in this research work. Gas-phase synthesis of graphene is known for more than a decade which is now further developed to give production rates of few hundred mg/h of few-layer graphene (FLG). By combining two independent gas phase reactors, this few-layer graphene is controllably mixed with other functional materials in the gas phase to obtain heterostructures without the use of structure directing agents. The reactor system was involving a microwave plasma and a hot wall reactor. Silicon nanoparticles were synthesized in the hot wall reactor, meanwhile graphene was produced in the MW plasma reactor. Both reactors were connected in such a way that the nanoparticles and graphene get in contact with each other directly in the gas phase after their inception. In this way the self-assembled heterostructures of graphene and nanoparticles are produced with the production rate reaching almost 800 mg/h. The materials were characterized with TEM, Raman spectroscopy, XPS and XRD to investigate the morphology, composition and structure. TEM images indicate silicon is present as almost spherical nanoparticles that form small aggregates. These particles are interconnected by graphene. EDX mapping shows silicon nanoparticles having graphene surrounding them. It is present between the aggregates of nanoparticles as well as connecting them to each other. Raman as well as XRD spectra confirmed the presence of silicon and graphene in heterostructures with extraordinary purity. The presence of silicon in crystalline as well as amorphous form was also confirmed from Raman spectra. It will be shown that the successful formation of 0D/2D silicon/graphene heterostructures used as anode material for lithium-ion batteries has illustrated some significant improvements. Compared to pure silicon, their combination results in excellent long-term stability of the anode while also increasing its Coulombic efficiency. Thus, the formation of these heterostructures in the gas phase offers the possibility to exploit the potential of silicon to significantly increase the anode storage capacity.

5:00 PM EL05.08.20

Wafer-Scale Synthesis of MoS₂ Atomic Layers with Different Mo Precursor Solutions and Application to Thin-Film Transistors [Woon-Seop Choi](#); Hoseo University, Korea (the Republic of)

Recently, transition-metal dichalcogenides (TMDs) have attracted much attention as new materials for electronics devices, electrocatalysts, photocatalysts, sensors, batteries, and bio-applications. Most TMDs are two-dimensional (2D) materials with a single layer. Bonds between each layer are made up of Van der Waals bonds, while intra-layer atoms bind together as covalent bonds.

Chemical vapor deposition (CVD) with sulfur gas is the most popular method for synthesizing large-scale 2D materials with high quality. Various MoS₂ can be obtained from this method using various precursors with different properties, process temperatures, and substrate materials. Solution process methods show advantages for preparing films with large size, high throughput, low cost, thickness control, and an environmentally friendly process. Even though there is sulfur in the precursors of the solution-process synthesis methods, supplementing the sulfur that is lost in the high-temperature CVD process is unavoidable.

In this study, two precursors of ammonium tetrathiomolybdate and ammonium molybdate were used in different solvent formulations to make MoS₂ crystalline by using simple thermal annealing and bottom-up thermolysis methods. These methods were relatively easy to handle, safe, and environmentally friendly processes. Importantly, these MoS₂ atomic layers were completed without additional sulfurization using CVD, but just with a single step of annealing because of sulfur-rich formulations.

The 2D atomic layers were controlled to 2 to 7 layers with precursor concentrations with both formulations, which were confirmed by STEM-FIB. Thin-film transistors (TFTs) were prepared from the solution-processed MoS₂ on Al₂O₃ and SiO₂ dielectric with thermal evaporated Al source and drain electrodes. The results show improved mobilities of 9 to 48 cm² V⁻¹s⁻¹ and reasonable on-off ratios of around 1.0×10⁵ with solid output saturations. These new methodologies can be applied to multifarious devices and have the potential for scalability in 2D MoS₂ materials.

5:00 PM EL05.08.21

Efficient Room Temperature Gas Detection Using a with Au-MoS₂ Hybrid Gas Sensor [Saurabh Rawat](#), Shivani Dangwal, Charu Dwivedi and Himani Sharma; Doon University, India

The pressing need for effective gas sensing devices is evident, given the critical role they play in environmental monitoring, industrial safety, and health diagnostics. Addressing this demand, we synthesized triangular domains of molybdenum disulfide (MoS₂) using the Chemical Vapor Deposition (CVD) method. To elevate their gas sensing potential, these MoS₂ domains were decorated with gold (Au) nanoparticles via thermal evaporation. Additionally, for sensing applications, an electrode pattern was meticulously fabricated over the MoS₂ triangular domains using thermal evaporation. The thorough characterization involved techniques like Scanning Electron Microscopy (SEM), X-ray Photoelectron Spectroscopy (XPS), Ultraviolet Photoelectron Spectroscopy (UPS), and Kelvin Probe Force Microscopy (KPFM) to determine their surface potential and electronic properties. A significant finding was that the enhanced gas sensing response observed in the Au-decorated MoS₂, which was 4.5 times greater than its undecorated counterpart, was attributed to the formation of a Schottky barrier. Capitalizing on this insight, we designed and fabricated a real-time gas sensing device, marking a transformative leap in gas detection technology.

5:00 PM EL05.08.22

A Scalable Electrochemical Intercalation of Transition Metal Dichalcogenide Powders [Nicholas Wilson](#)¹, Manila Valappil¹, Mira Mackintosh¹, Teri Siu¹, Jochen Koniczny², Michael Pope¹, Neil Graddage³ and Franziska E. Muckel²; ¹University of Waterloo, Canada; ²Universität Duisburg-Essen, Germany; ³National Research Council, Canada

Electrochemical exfoliation of transition metal dichalcogenides (TMD) is a popular method for creating large-sized and well-exfoliated sheets. Cathodic exfoliation using tetraheptylammonium bromide is a promising method for optoelectronics applications due to its ability to retain the semiconducting 2H polymorph. However, this method has several challenges. Expensive single crystals are used, which limits the amount of material generated. Additionally, the crystals expand significantly, causing sporadic and uncontrolled electrical contact to the crystal throughout intercalation. This limits the achievable degree of intercalation of the crystal.

To address these issues, we describe the construction of an electrochemical cell that can be scaled to an arbitrary size and used to intercalate TMD powders. This cell constrains material, applies a homogeneous electrical contact, and enables controlled intercalation using a reference electrode. The intercalated materials can then be easily exfoliated and dispersed by ultrasonication. We also demonstrate that the exfoliated sheets can be assembled into continuous films and coated onto arbitrary flat substrates over large areas using a modified Langmuir-Blodgett method. We use this approach to study the films as photodetectors.

Our work provides a scalable solution for intercalating TMD powders and creating well-exfoliated sheets that can be used in optoelectronics applications.

5:00 PM EL05.08.23

Fabrication of Nanostructured Molybdenum Disulfide (MoS₂) Thin Film-Based Electronic Devices Kevin Qian, Ibraheem Giwa, Fabian Sanchez, Elton Mawire, Sherwood Dong, Eric Smith, Qunying Yuan and [Zhigang Xiao](#); Alabama A&M University, United States

In this study, we report the fabrication of molybdenum disulfide (MoS₂) thin films-based electronic devices. Nanostructured molybdenum disulfide (MoS₂) thin films are grown as the active semiconducting channel material for the fabrication of MoS₂-based field-effect transistors using plasma-enhanced atomic layer deposition (ALD). MoS₂-based electronic devices such as MoS₂ field-effect transistors, inverters, and ring-oscillators are fabricated with the ALD-grown MoS₂ film using the clean room-based micro- and nano-fabrication techniques. Hydrogen sulfide (H₂S) gas is used as the S source in the growth of molybdenum disulfide (MoS₂) while molybdenum (V) chloride (MoCl₅) powder is used as the Mo source. The MoS₂ film will be analyzed by the high-resolution tunnel electron micrograph (HRTEM), scanning electron micrograph (SEM), X-ray photoelectron spectroscopy (XPS) analysis and Raman spectrum analysis. The fabricated MoS₂ device wafer will be annealed at high-temperatures (800 – 900 °C), and the electrical property of the MoS₂-based electronic devices will be measured before and after the high-temperature annealing and will be compared. The characterization results of the nanostructured molybdenum disulfide (MoS₂) thin films and the measurement results on the fabricated MoS₂-based electronic devices will be reported in the 2024 MRS Spring Meeting.

Acknowledgements: The research is supported by National Science Foundation under Grant No. ECCS-2100748.

5:00 PM EL05.08.24

High Performance GQD/Graphene Heterostructure Field Effect Phototransistor with Efficient Photoinduced Effects [Muhammad Shehzad Sultan](#)¹, Ernesto Espada Nazario¹, Bianca S Umpierre Ramos¹, Daniela D Negron Negron¹, Amanda M. Gracia Mercado¹, Wojciech Jadwisieniczak², Brad Weiner¹ and Gerardo Morell¹; ¹University of Puerto Rico - Río Piedras, United States; ²Ohio University, United States

Graphene and highly luminescent graphene quantum dots (GQDs) have been widely used in optoelectronic devices as a photoactive material. Graphene Quantum Dots (GQDs) have been widely used for various optoelectronic devices as a photoactive material due to their high absorption coefficient and tunable bandgap. However, the low mobility of GQD films results in poor charge collection and device performance. By combining GQDs with graphene into hybrid GQDs/Graphene field effect transistors, photocarriers from GQDs are transferred to graphene, improving charge collection and transport, drastically increasing the photoresponsivity. In this study, we report the preparation of a GQDs/Graphene heterostructure in order to investigate the effect of GQDs on photoactive response of graphene. Using UV-vis absorption and photoluminescence (PL) spectra, the optical properties of graphene and the GQDs/Graphene heterostructure were measured and compared. Moreover, to investigate their electronic and charge transfer properties, we fabricated field-effect phototransistors (FEPT) on pristine graphene and GQDs/Graphene heterostructure thin films and investigated their photoactive electrical properties. Under illumination, both pristine and GQDs/Graphene FEPT showed an increase in current and carrier mobility. The increased current and carrier mobility of GQDs/Graphene FEPT is due to the presence of a large number of photoexcited charge carriers. The current and carrier mobility in the GQDs/Graphene heterostructure FEPT were also lower than those in the pristine graphene FEPT. This is explained by GQDs' n-type doping effect on graphene, which reduces the accumulation of holes in the active p-channel near the insulating layer and causes charge to be transferred from the GQDs to the graphene. As a result, we discovered a charge transfer effect in the GQDs/Graphene heterostructure, which could be used in optoelectronic devices.

SESSION EL05.09: Memory Devices II
Session Chairs: Hippolyte Astier and Kalisch Holger
Thursday Morning, April 25, 2024
Room 344, Level 3, Summit

8:30 AM *EL05.09.01

Neuromorphic Circuits and Devices Based on MoS₂ Andras Kis; Ecole Polytechnique Federale de Lausanne, Switzerland

Machine learning and signal processing on the edge are poised to influence our everyday lives with devices that will learn and infer from data generated by smart sensors and other devices for the Internet of Things. The next leap towards ubiquitous electronics requires increased energy-efficiency of processors for specialized data-driven applications. I will present here how we realised an in-memory processor fabricated using a two-dimensional materials platform can potentially outperform its silicon counterparts in both standard and non-traditional Von Neumann architectures for artificial neural networks. The circuits are based on a flash memory array with a two-dimensional channel using wafer-scale MoS₂. Simulations and experiments show that the device can be scaled down to sub- μm channel length without any significant impact on its memory performance. I will then present our latest work with large-scale integrated vector-matrix multiplier circuits with over 1000 memories based on MoS₂.

9:00 AM *EL05.09.02

Compute-in-Memory Hardware based on 2D Materials for Convolution Neural Networks Kah-Wee Ang; National University of Singapore, Singapore

The exponential growth of data storage and computation requirement has imposed severe power consumption challenges for digital computers built on traditional von Neumann architecture. New computing systems using the compute-in-memory (CIM) concept could offer a potential solution to overcome the inherent energy consumption and latency issues. In particular, CIM based on analog memristors is promising to enable a low latency and energy-efficient approach for performing data-intensive tasks such as image processing by means of neural network training. Here, we demonstrate memristive crossbar arrays (CBA) using transition metal dichalcogenides for implementing convolution neural network (CNN) hardware. The memristor achieves a small switching voltage, low switching energy, and improved variability in addition to the ability to emulate synaptic weight plasticity. The CBA successfully implements both neuromorphic and matrix-heavy workloads in neural networks, including artificial-synapse-based ANN, multiply-and-accumulate (MAC) operations, and convolutional image processing with high recognition accuracy. Moreover, the column-by-column MAC operation manifests a highly parallelized computing ability, opening a route to enable hardware acceleration of machine learning algorithms for emerging artificial intelligence applications.

9:30 AM EL05.09.03

Transfer-Free Wafer-Scale Graphene Electronics on Sapphire Oliver Fenwick¹, Zhichao Weng¹, Sebastian Dixon², Lok Yi Lee², Colin Humphreys^{1,2}, Ivor Guiney², William Gillin¹, Robert Wallis², Bryan Wingfield², Paul Evans², Piotr Baginski², Jaspreet Kainth², Andrey Nikolaenko² and Joanna Baginska²; ¹Queen Mary University of London, United Kingdom; ²Paragraf Ltd., United Kingdom

The realisation of commercial graphene solid-state electronics devices has been held back by challenges of processing high-quality monolayer graphene at scale. In this work, we used wafer-scale graphene as the electrode in selected electronic devices, notably OLEDs and memristors. The graphene was grown by Paragraf Ltd using their proprietary growth process to produce high quality, monolayer graphene grown directly onto 50 mm sapphire wafers in batches of up to 37 wafers in metal-organic chemical vapour deposition (MOCVD) reactors. All processes in device production are compatible with semiconductor production lines, and we find graphene to be remarkably robust to these processes.

Graphene memristors in non-volatile memory or neuromorphic computing applications could offer high integration density as well as robustness against common memristor degradation mechanisms. The latter includes oxygen vacancy diffusion into the electrode and unwanted metal ion diffusion from the electrodes, both of which are prevented by the in-plane covalent bonding of graphene. Wafers containing 2520 memristors of different sizes with graphene electrodes were fabricated. The as-fabricated graphene memristors showed a high *ON/OFF* ratio of $10^7 \sim 10^8$ when under a bias pulsing rate of 0.5Hz – 1Hz, robust endurance (switching remained stable after >2700 cycles), stability (no device degradation after 1.8 hrs of switching at 26Hz – 46Hz) and low voltage operation (low $V_{set} \sim 1.6\text{V}$ and $V_{reset} \sim 1.55\text{V}$).

Graphene is considered as a promising material for replacing ITO, which has long term supply issues due to its limited elemental abundance, but for this to become possible. The as-grown graphene was patterned using photolithography and its conductivity was enhanced by doping with nitric acid prior to deposition of the OLED stack. The electrical and optical performances of the as-fabricated graphene-based OLEDs were identical to control devices with conventional ITO anodes [1].

[1] Weng Z. et al. **Wafer-Scale Graphene Anodes Replace Indium Tin Oxide in Organic Light-Emitting Diodes**. *Advanced Optical Materials*, 2101675 (2021). DOI: 10.1002/adom.202101675

9:45 AM EL05.09.04

Ultrathin Sb₂Te₃/Ge₄Sb₆Te₇ Superlattices for Low-Power and High-Speed Phase Change Memory Xiangjin Wu¹, Asir Intisar Khan¹, Huairuo Zhang^{2,3}, Heshan Yu^{4,5}, Albert Davydov², Ichiro Takeuchi⁴, H.S. Philip Wong¹ and Eric Pop¹; ¹Stanford University, United States; ²National Institute of Standards and Technology, United States; ³Theiss Research, Inc., United States; ⁴University of Maryland, United States; ⁵Tianjin University, China

The demand for robust and low-power nonvolatile memory is on the rise due to the rapid growth of big-data, high-performance computing, and data-centric artificial intelligence applications. Phase-change memory (PCM) based on chalcogenides has the potential to bridge the performance gap between existing storage solutions like flash and dynamic random-access memory. Traditional PCM materials suffer from issues such as high switching power and resistance drift over time [1,2]. Superlattices (SLs) made of nanometer-thin phase change materials arranged in alternating layers can overcome some of these challenges by lowering switching current and resistance drift [3,4]. However, the operation speed of these SL-PCM devices has remained slow, ~ hundreds of ns [4].

Here, we present nanoscale PCM devices (~ 40 nm bottom electrode diameter) based on Sb₂Te₃/GST467 superlattices. Unlike traditional PCM materials, GST467 contains coherent SbTe nanoclusters within the Ge-Sb-Te matrix, enhancing crystallization and lowering the melting temperature. These nanoclusters act as precursors for crystallization, boosting the switching speed of GST467. By incorporating GST467 into our superlattice PCM devices, we achieved remarkable results, including a record-low switching power density of approximately 5 MW/cm², an ultra-low switching voltage of around 0.7 V, sub-1.5 pJ switching energy, rapid switching speed of about 40 ns, low resistance drift with 8 distinct resistance states, and high endurance of ~ 2 × 10⁸ cycles.

The performance of our devices is attributed to strong heat confinement within the superlattice interfaces and their nanoscale dimensions. Additionally, the unique microstructural properties of GST467, coupled with its higher crystallization temperature, contribute to faster switching speeds and improved stability, surpassing some of the fundamental trade-offs observed in conventional PCM. Importantly, this study combines bottom-up natural interfaces in the nanocomposite with top-down superlattice interfaces in the same memory material, resulting in superior device performance.

1. H.-S. P. Wong et al., Proc. IEEE 98, 2201–2227 (2010).
2. M. Boniardi et al., IEEE Trans. Electron Devices 57, 2690–2696 (2010).
3. K. Ding et al., Science 366, 210 (2019)
4. A.I. Khan, E. Pop et al., IEEE EDL 43, 204-207 (2022)

10:00 AM BREAK

SESSION EL05.10: CMOS

Session Chairs: Kah-Wee Ang and Andras Kis
Thursday Morning, April 25, 2024
Room 344, Level 3, Summit

10:30 AM EL05.10.01

Growth of Semiconducting Graphene Nanoribbons and Single-Crystal Graphene on Germanium Robert M. Jacobberger; University of Wisconsin-Madison, United States

The chemical vapor deposition of graphene on germanium (Ge) and germanium-on-silicon (Ge-on-Si) substrates provides a scalable, industry-compatible route for integrating graphene-based devices on traditional semiconductor platforms. Here, we will discuss our work on the wafer-scale synthesis of aligned semiconducting graphene nanoribbon arrays and single-crystal semi-metallic graphene films on Ge wafers.

First, we have discovered how to drive graphene crystal growth kinetics into a highly anisotropic regime, enabling the synthesis of graphene nanoribbons with tunable sub-5-nm widths, nearly atomically defined armchair edges, atomic thickness, and unidirectional alignment on Ge(001) and vicinal Ge(001).^{1,2,3,4} This precise control over the nanoribbon width and edges transforms graphene into a semiconductor with technologically useful bandgap > 0.5 eV. The nanoribbons also exhibit high performance in field-effect transistors in terms of their on-state conductance (~10³ μS μm⁻¹) and on/off current ratio (~10⁴). Initiating the nanoribbon growth from nanoscale seeds significantly reduces ribbon-to-ribbon width polydispersity and provides control over the nanoribbon placement. Such semiconducting nanoribbon arrays with narrow widths and well-defined edges promise to meet the demands of speed, energy efficiency, density, and functionality required for next-generation semiconductor electronics and promise to meet the performance metrics set by the International Roadmap for Devices and Systems for the foreseeable future.

Second, we have elucidated the factors controlling the crystallinity of graphene grown on Ge(110) using advanced dark-field low-energy electron microscopy (DF-LEEM) and micro-low-energy electron diffraction (μ-LEED). This insight is utilized to produce large-area graphene films with minimal rotational misalignment—a major step toward realizing state-of-the-art technologies harnessing the exceptional properties of graphene lacking defective grain boundaries. We have discovered a new phenomenon in which misoriented graphene domains nucleate from the edges of unidirectionally aligned graphene islands when the islands grow over Ge surface steps, increasing polycrystallinity throughout growth. Extensive synthesis studies provide strategies for suppressing this secondary nucleation of misoriented domains to achieve graphene films in which the predominant epitaxial orientation has high coverage > 99% and low rotational spread < 0.6°. These results clarify the varying crystallinity and irreproducibility of graphene grown on Ge(110) reported in the literature, demonstrate the importance of using techniques with high spatial and angular resolution when determining if 2D materials are single crystals, and provide a route towards the large-area synthesis of single-crystal graphene on commercially available and technologically useful substrates.

- [1] R. M. Jacobberger, et al. *Nat. Commun.* **6**, 8006 (2015).
- [2] R. M. Jacobberger, et al. *ACS Nano* **11**, 8924-8929 (2017).
- [3] R. M. Jacobberger, et al. *Nanoscale* **11**, 4864-4875 (2019).
- [4] A. J. Way, et al. *Nat. Commun.* **13**, 2992 (2022).

10:45 AM EL05.10.02

A Method for Extracting 2D Semiconductor Mobility in Transistors with Gate-Voltage-Dependent Contact Resistance Robert K. Bennett¹, Lauren Hoang¹, Connor Cremers¹, Andrew J. Mannix^{1,2} and Eric Pop^{1,1}; ¹Stanford University, United States; ²Stanford Institute for Materials and Energy Sciences, United States

Emerging two-dimensional (2D) semiconductors are frequently characterized in terms of their electron and hole mobilities, which quantitatively describe the speed at which these carriers move through a material under an applied electric field. These mobilities are commonly extracted by fabricating and measuring field-effect transistors (FETs) and applying one of several techniques to estimate the 2D semiconductor's electron or hole mobility. Back-gated FETs are often used for these extractions because they can be fabricated in fewer steps and in higher yields compared to top- or dual-gated geometries. However, back-gated FETs experience *contact gating*: the electric field from the gate electrode acts on the transistor's source and drain, causing the contact resistance to decrease as the magnitude of the gate voltage increases [1–5].

Although contact gating increases the drive current that a 2D FET can achieve by minimizing contact resistance in the on-state [1, 3, 6], contact gating also modifies the shape of a transistor's transfer characteristics (i.e., I_D vs. V_{GS} characteristics, where I_D is the drain current and V_{GS} is the gate-to-source voltage). Consequently, conventional mobility extraction techniques can overestimate the mobilities of emerging semiconductors in back-gated FETs by up to an order of magnitude [2–4]. Thus, it was suggested that mobility in back-gated FETs should be estimated only at high $|V_{GS}|$ ($\gg |V_T|$, the threshold voltage) to ensure that the channel resistance, rather than contact gating, dominates the FET transfer characteristics [2, 4]. Alternatively, mobility can be accurately extracted from FETs with more complicated geometries and fabrication procedures that allow for the effects of contact gating to be eliminated (such as FETs that incorporate additional terminals to probe the channel [7]). Although these approaches may be viable in some situations, the former method can be unsuitable for transistors that experience early dielectric breakdown, whereas the latter approach can introduce additional experimental complexity during fabrication.

In this work, we propose a method of extracting a semiconductor's carrier mobility that is compatible with back-gated FETs but that does not require the FET to operate in a channel-dominated regime. This method is inspired by the conventional transfer length method (TLM) approach but makes use of a transistor's I_D vs. V_{DS} characteristics (where V_{DS} is the drain-to-source voltage), rather than its I_D vs. V_{GS} characteristics, allowing us to properly account for contact gating in back-gated FETs without having to use complicated geometries to directly probe the channel.

We validate this proposed method using current-voltage characteristics simulated by technology computer-aided design (TCAD). We find that this proposed method offers accurate mobility extraction (< 10% error) in regimes where conventional methods (including the linear extrapolation method, Y-function method, and TLM approach) overestimate mobility by > 50%. Furthermore, we demonstrate that this proposed method is robust to random variation in material quality, and we experimentally validate this method by demonstrating that experimentally-measured current-voltage characteristics of back-gated monolayer tungsten disulfide (WS_2) FETs fit the method well. Overall, we anticipate that the method we propose in this work will allow for the mobilities of emerging semiconductors to be more quickly and easily extracted without requiring sophisticated transistor geometries or complicated fabrication procedures.

References:

- [1] Z. Cheng *et al.*, *Nat. Electronics*, **5**, 416 – 423 (2022)
- [2] E. Bittle *et al.*, *Nat. Comm.*, **7**, 10908 (2016)
- [3] J. Nasr *et al.*, *Adv. Mater.*, **31**, 1806020 (2018)
- [4] I. McCulloch *et al.*, *Science*, **352**, 1521 – 1522 (2016)
- [5] W. Liu *et al.*, *ACS Nano*, **9**, 7904 – 7912 (2015)
- [6] G. Arutchelvan *et al.*, *Nanoscale*, **9**, 10869 – 10879 (2017)
- [7] C. Pang *et al.*, *Small*, **17**, 2100940 (2021)

11:00 AM EL05.10.03

Interconnect Technologies in The Ultrathin Limit: Performance of Standard and 2D Barriers and Liners in The Nanometer Thickness Regime Hippolyte P. Astier¹, Muhammed Juvaid Mangattuchali¹, Hao Tan¹, Jing Yang Chung¹, Chandan Das², John L. Sudijono² and Silvija Gradecak¹; ¹National University of Singapore, Singapore; ²Applied Materials Singapore Technology PTE LTD, Singapore

Copper wires in the back-end-of-line (BEOL) interconnects typically require two layers surrounding them: a diffusion barrier preventing Cu from diffusing into the dielectrics, and a liner, ensuring cohesive Cu wires and smooth interfaces. The current industry standards for barrier and liner applications include TaN and Ta, respectively, which then form a bilayer with a typical thickness of ~4 nm. However, with the advent of the 3-nm technology nodes, interconnect half-pitches have reached the scales of 10 nm. Consequently, the barrier/liner bilayer would represent a significant fraction of the wire cross-section and increase the wire resistance and cause significant RC delays. The polycrystalline nature of the conventional TaN/Ta bilayer films prevents formation of a continuous and effective film in the ultrathin regime. Moreover, their performance as a function of the film thickness is poorly understood, especially in ultrathin films.

In recent years, this expected limitation of conventional barriers and liners has motivated intense efforts to replace them with 2D materials, as these can be continuous yet atomically thin. However, no approach reported thus far fulfills the requirements for BEOL integration, namely low temperature (<450 °C), uniform and scalable growth, thickness control and film conformality to the substrate. We have recently developed a novel approach to growing layered films of WS_2 that fulfills all of these requirements. Our WS_2 films function as bifunctional liners and Cu diffusion barriers. We demonstrate these functionalities through electrical measurements that assess Cu film conductivity in the thin film limit, where we see a significant improvement of several orders of magnitude in Cu conductivity for Cu films of 10 nm. Their performance as diffusion barriers was assessed through time-dependent breakdown measurements, where we see the projected device lifetime increases by one order of magnitude through the utilization of single layers of WS_2 . To benchmark the performance of this new class of 2D barrier/liner layers, we compare the level of performance as a function of the film thickness both in 2D layered WS_2 films and in polycrystalline TaN films, in regimes from 4-nm thicknesses down to the ultrathin ~1 nm limit. This approach provides an ability to identify and study the thickness regime in which 2D-layer films are expected to outperform the standard TaN layers. We will also discuss measurements and modelling approaches toward evaluation of temperature-dependent diffusion barrier properties for standardized barrier evaluation in the ultrathin film limit.

11:15 AM EL05.10.04

Impact of Substrates on Graphene Sensors Masahiro Ishigami¹, Jyoti Katoch² and Michael Lodge³; ¹University of Central Florida, United States; ²Carnegie Mellon University, United States; ³Truventic LLC, United States

We have measured desorption of atomic hydrogen from graphene devices on hexagonal boron nitride and compared to our results from graphene devices on silicon oxide using transport measurements in ultra high vacuum environment. We found that atomic hydrogen desorbed at much narrower range of

temperatures on hexagonal boron nitride, indicating that chemical interaction was more uniform on hexagonal boron nitride. Our results indicated that hBN could significantly reduce the variability in interaction energies of chemical species on graphene and, as a result, it could be a better substrate for graphene-based chemical sensors.

11:30 AM *EL05.10.05

MOCVD and Device Technology of 2D-TMDC Layers and Heterostructures [Holger Kalisch](#)¹, Songyao Tang¹, Yibing Wang¹, Yingfang Ding¹, Hleb Fiadziushkin¹, Amir Ghiami¹, Michael Heuken^{1,2} and Andrei Vescan¹; ¹RWTH Aachen University, Germany; ²AIXTRON SE, Germany

Two-dimensional transition metal dichalcogenides (2D-TMDC) are attractive materials for various applications such as integration in next-generation highly scaled CMOS technology, neuromorphic computing, (opto)electronic devices and advanced sensors. However, for a successful industrial implementation, reproducible and scalable fabrication processes are required. This includes 2D material synthesis, device processing, and finally circuit integration. Regarding material deposition, MOCVD (metal-organic chemical vapor deposition) is established as a technologically mature method with excellent homogeneity, reproducibility and yield in high-volume fabrication of compound semiconductors on large wafer diameters. Developing MOCVD of 2D-TMDC requires dedicated reactor technology, in-situ monitoring techniques and elaborate deposition processes. Especially for the latter, an in-depth understanding of nucleation and growth mechanisms is a prerequisite. Another advantage of MOCVD is the option to successively deposit 2D-2D heterostructures in a continuous process, avoiding interface contaminations related to mechanical heterostructure stacking.

In many implementation scenarios, 2D integration requires a transfer of 2D films or film stacks from their growth substrates to target wafers. With respect to the atomic thickness and the “surface-only” characteristics of 2D layers, transfer and processing steps demand an even more careful consideration than known for classical bulk semiconductor structures. This especially relates to processing chemicals and all substances coming into contact with the 2D layers.

In this presentation, results of MOCVD process development of 2D materials from the (Mo,W)(S,Se)₂ family will be shown. The focus will be on growth kinetics and layer morphology. The different stages of growth starting with film nucleation, continued to lateral growth as well as finally layer coalescence and cool-down stabilization will be discussed. Critical aspects and the interplay between initial nucleation density, monolayer growth time/chalcogen precursor consumption and parasitic bilayer formation before coalescence of the first monolayer will be highlighted. Migration enhancement by reducing metal precursor supply towards coalescence is one approach to suppress premature bilayer formation, especially for W-containing materials. Limits of the parameter window set by the metal adatom migration length and parasitic carbon deposition will be addressed. Using this approach, 2D-2D heterostructures will be presented and compared to counterparts realized by mechanical stacking of monolayers.

Material characterization relies on spectroscopic in-situ reflectance measurements, SEM (scanning electron microscopy), AFM (atomic force microscopy), Raman, photoluminescence (PL) and X-ray photoemission spectroscopy (XPS). Additionally, to especially access e. g. field-effect transistor performance metrics, electrical devices have to be fabricated. In this talk, selected results from transistors and memristors processed on our layers will be presented. This topic includes details on wet and dry transfer of 2D TMDC layers onto target substrates, lithography processing, etching, metallization and device characteristics. Furthermore, first correlations between characteristics of the MOCVD processes and device metrics will be presented.

Finally, an outlook will be given including strategies to improve layer properties (e. g. by additives promoting metal adatom migration), processing steps and finally device performance.

SESSION EL05.11: Growth II

Session Chairs: Chandan Das, Robert Jacobberger, Michael Pope and Hyeon Suk Shin

Thursday Afternoon, April 25, 2024

Room 344, Level 3, Summit

1:30 PM *EL05.11.01

Wafer-Scale, Thickness-Controlled Growth of Hexagonal Boron Nitride [Hyeon Suk Shin](#); Ulsan National Institute of Science and Technology, Korea (the Republic of)

Since hexagonal boron nitride (hBN) shows unique optical properties in the deep-UV region, mechanical robustness, thermal stability, and chemical inertness, hBN thin films have gained significant attention for various applications, including nanoelectronics, photonics, single photon emission, anti-corrosion, and membranes. Thus, wafer-scale, thickness-controlled growth of hBN films is crucial to enable their industrial-scale applications. To date, considerable efforts have been made to develop continuous hBN thin films with high crystallinity, from those with large grains to single-crystal ones, and to realize thickness control of hBN films by chemical vapor deposition (CVD). However, the growth of wafer-scale high crystalline hBN films with precise thickness control has not been reported yet. The hBN growth is significantly affected by substrate, in particular the type of metals, because the intrinsic solubilities of boron and nitrogen depend on the type of metal. In this talk, state-of-the-art strategies adopted for growing wafer-scale, thickness-controlled hBN are summarized, followed by the proposed mechanisms of hBN growth on catalytic substrates. In addition, how to grow wafer-scale, thickness-controlled growth of hBN on dielectric, sapphire substrate is demonstrated.

2:00 PM EL05.11.02

Manipulating 2D Materials at The Air-Water Interface: Towards Printing on Water [Michael A. Pope](#); University of Waterloo, Canada

Conventional printing or casting approaches involving colloidal dispersions of 2D materials cannot typically yield films or prints less than 0.1 to 1 micron in thickness. On the other hand, the Langmuir-Blodgett approach can create single molecule thick films since the dispersed material is transferred or printed onto water and even after solvent evaporation, the dispersed phase or pigment remains mobile on the liquid water substrate. This mobility allows the floating material to be compressed by the moveable barriers of a Langmuir-Blodgett trough. However, this mechanical approach limits coatings to small areas (~cm²) and is not amenable to roll-to-roll, high throughput processing. In this talk, I will summarize various works from my group that aim to understand how to use this interfacial mobility to adapt the Langmuir-Blodgett approach to one capable of printing and patterning continuously and over large areas. As an example, we explore the performance of such films comprised of electrochemically exfoliated transition metal dichalcogenides as transistors and photodetectors.

2:15 PM EL05.11.03

Characterization of Hybrid Edge Results in Narrowed Bandgap of Bottom-Up Liquid-Phase Synthesis of Bent N=6/8 Armchair Graphene Nanoribbons Using Scanning Tunneling Microscopy and Scanning Tunneling Spectroscopy [Hanfei Wang](#)¹, Gang Li^{2,3}, Michael J. Loes³, Anshual Saxena⁴, Jiangliang Yin², Mamun Sarker³ and Shinyoung Choi²; ¹University of Illinois at Urbana-Champaign, United States; ²The University of Chicago, United States; ³University of Nebraska–Lincoln, United States; ⁴The University of Texas at Austin, United States

Scalable fabrication of graphene nanoribbons with narrow band gaps has been a nontrivial challenge. A unique approach has been developed to access narrow band gaps by using hybrid edge structures. Bottom-up liquid-phase synthesis of bent N=6/8 armchair graphene nanoribbons (AGNRs) has been achieved in high efficiency through copolymerization between an ortho-terphenyl monomer and a naphthalene-based monomer, followed by Scholl oxidation. Through scanning tunneling microscopy (STM) characterization, an unexpected 1,2-aryl migration has been discovered, which is responsible for introducing 60 degrees kinked structures to the GNR backbones. Topographical STM scans consistently show asymmetric internal structures in agreement with the bent GNR structure resulted from unexpected competition between the aryl 1,2-migration on the naphthalene unit and the direct cyclodehydrogenation during Scholl oxidation. Through model study, we postulate that such 1,2-migration may not occur that frequently during liquid-phase synthesis due to the more rigid C-C bonds in a polymer backbone. Such defects of turns should only take place occasionally, and the AGNRs should maintain close electronic properties to the proposed straight ribbons. The STM topography shows, except for a few straight ribbons, most ribbons contain one or two kinks in their backbone. Scanning tunneling spectroscopy (STS) was employed to fully characterize the electronic structure of this GNR. A STS bandgap of 1.7 eV is found across straight and bent AGNRs deposited on hydrogen passivated silicon surface. The STS experimental result of AGNR bandgap is well in the range of 1 eV of the optical band gap and 2.2 eV of the calculated GW band gap. Application of bent N=6/8 AGNRs in efficient gas sensing shows its potential in broad applications of other innovative uses.

2:30 PM EL05.11.04

Inductive Heating a Versatile Process for Large Scale Single-Crystal Cu(111) and Graphene Synthesis : Experiments and Thermochemical Modeling Samir Farhat^{1,2}, Wafa Alimi^{1,2}, Ivaylo Hinkov^{1,2} and Mourad Cherif^{1,2}; ¹Université Sorbonne Paris Nord, France; ²Laboratoire des Sciences des Procédés et des Matériaux LSPM CNRS, France

Inductive heating (IH) is proposed as a new concept to bring together centimeter-scale single crystal Cu(111) metal catalyst preparation and graphene growth in a combined process. Commercial polycrystalline metal catalyst is first heated by radio frequency (RF) magnetic fields. A nearly uniform magnetic field induced by Helmholtz-like coils penetrates the copper foil generating eddy currents. While the frequency of the current is being rapidly varied, the substrate temperature increases from room temperature to ~1030 °C in ~1 minute. Unlike Roll to Roll (R2R) methods where the copper is continuously passed in a hot furnace region [1], in our approach, the induction coils are moved at a constant speed generating a controlled thermal gradient. The rate of heating and cooling of the metal are hence much faster and gradient surface energy is better modulated. In addition, machine performance and maintenance costs could be reduced due to technological high-speed sealing and thermal constraints in the R2R process. In addition, for scale-up purposes, large oven are necessary to heat the metal foils. This becomes less energy efficient as system size is increased. In contrast, inductive heating only allows the heating of the thin metal films without heating the surrounding gas [2]. In our system, an edge of the Cu sheet was tapered into a tip shape, which ensured the nucleation of a single Cu(111) grain at the tip. The sliding of the coils across the copper foil caused the movement of the grain boundaries between the single crystal and polycrystalline regions and the grain of single crystal Cu(111) reached the width of the copper sheet as confirmed by XRD and EBSD. Consequently, graphene was synthesized using the same inductive heating reactor. From the optical microscopy image, all the hexagonal graphene domains are oriented in the same direction and the Raman spectrum shows the total absence of defects. We take the advantage of such system in order to better understand the mechanisms responsible for graphene growth in a chemical environment represented by a ternary C–H–Ar system. We specifically developed a thermochemical model with gas chemistry and surface reactions through Cu(111) site fraction and surface molar concentrations. The graphene growth rate is obtained by compiling the effects of gas and surface reactions *via* CHEMKIN software. The influence of the total pressure, substrate temperature and H₂, CH₄, Ar contents are obtained from the model and compared to the experiments. There was good agreement between experimental and the modeling results, providing an insight into optimizing CVD graphene growth.

References

- [1] Xu X, Zhang Z, Qiu L, et al. Ultrafast growth of single-crystal graphene assisted by a continuous oxygen supply. *Nat Nanotechnol* 2016;11:930–5.
- [2] E. Dhaouadi, W. Alimi, M. Konstantakopoulou, I. Hinkov, M. Abderrabba, S. Farhat, Graphene synthesis by electromagnetic induction heating of oxygen-rich copper foils, *Diamond and Related Materials*, Volume 132, 2023, 109659,

2:45 PM BREAK

3:15 PM EL05.11.05

Thin-Film Nanocalorimetry Study of The Melting Transitions in 2D Phase-Change Superlattices Jie Zhao¹, Asir Intisar Khan², Mikhail Efremov³, Zichao Ye¹, Xiangjin Wu², H.S. Philip Wong², Eric Pop^{2,2} and Leslie H. Allen¹; ¹University of Illinois at Urbana-Champaign, United States; ²Stanford University, United States; ³University of Wisconsin—Madison, United States

Today's nanoelectronics are reaching the limits of energy and latency for numerous data-intensive applications, including the Internet of Things (IoT) and artificial intelligence (AI). Improving the energy efficiency and speed of data storage remains at the core of tackling this grand challenge. Phase-change memory (PCM) is a storage technology combining the high speed of dynamic random-access memory and the non-volatility of flash memory. By simply stacking ~2 nm Sb₂Te₃ and Ge₂Sb₂Te₅ together, superlattice (SL) phase change memory devices demonstrated an 8 times reduction in power consumption, compared to conventional PCM devices [1]. The unexpected device-level success lies in the unique thermodynamic properties of such two-dimensional (2D) heterostructures, which, unfortunately, are inaccessible to conventional characterization methods with limited sensitivity and speed. Thus, the underlying science responsible for success has remained a mystery.

Nanocalorimetry (NanoDSC) [2, 3] is an advanced characterization method with monolayer sensitivity (~1 Å) and fast scanning rate (10⁶ K/s). This unique tool allows us to investigate the transitions of 2D heterostructure in its natural form of thin-film stacks as in SL-based PCM devices. In our recent work (2023 Nano Letters [4]), we applied NanoDSC to 65 nm Sb₂Te₃/Ge₂Sb₂Te₅ superlattices. An unexpected low-T metastable melting transition is uncovered along with an 8 times reduction in the enthalpy compared to its bulk counterparts. Such a transition provides a thermodynamic insight into the low-current switching of the superlattice PCM and advances the understanding of novel 2D heterostructures. The findings revealed here using the Nanocalorimetry technique will also inspire and enable a systematic material search for new 2D heterostructures for future energy-efficient nanoelectronics.

- [1] Khan, A. I. et al. Unveiling the effect of superlattice interfaces and intermixing on phase change memory performance. *Nano Letters* 22, 6285-6291 (2022).
- [2] Lai, S., Guo, J., Petrova, V., Ramanath, G. & Allen, L. Size-dependent melting properties of small tin particles: nanocalorimetric measurements. *Physical review letters* 77, 99 (1996).
- [3] Efremov, M. Y., Olson, E. A., Zhang, M., Zhang, Z. & Allen, L. H. Glass transition in ultrathin polymer films: calorimetric study. *Physical Review Letters* 91, 085703 (2003).
- [4] Zhao, Jie, et al. "Probing the Melting Transitions in Phase-Change Superlattices via Thin Film Nanocalorimetry." *Nano Letters* 23.10 (2023): 4587-

4594.

3:30 PM EL05.11.06

Optimizing Au-Assisted Exfoliation of Layered Materials with (3-Aminopropyl)triethoxysilane (APTES) for Large-Area Monolayers Nicolo Petri^{1,2}, Ermes Peci², Nicola Curreli^{3,1}, Francesco Bisio^{4,2}, Ilka Kriegel¹ and Anjana P. Muraleedharan^{5,6}; ¹Istituto Italiano di Tecnologia, Italy; ²Università degli studi di Genova, Italy; ³Empa-Swiss Federal Laboratories for Materials Science and Technology, Switzerland; ⁴CNR, Italy; ⁵Instituto Italiano di Tecnologia, Italy; ⁶Università Degli Studi di Genova, Italy

Two-dimensional (2D) materials have gained significant scientific interest owing to their exceptional properties and potential applications. Recently, Metal-assisted exfoliation technique has emerged as a valuable method for obtaining large and high-quality 2D monolayers. However, the process efficiency can be hampered by poor adhesion between the metal foil and the substrate. In this study, we address this issue by investigating surface functionalization of the target substrate using (3-Aminopropyl)triethoxysilane (APTES). The introduction of APTES significantly enhances adhesion between monolayers and hydrophilic substrates, overcoming delamination issues associated with the Au-exfoliation method. We perform a comprehensive comparison between APTES-functionalized Au-exfoliated flakes and those obtained through conventional scotch tape exfoliation, evaluating process yield and monolayer quality. Characterization techniques, including ellipsometry, AFM, XPS, Raman spectroscopy, and photoluminescence spectroscopy, confirm the method's effectiveness and superior outcomes in terms of yield and crystal quality. Additionally, we successfully apply this method to obtain high-quality monolayers of other materials, such as BiTeI, which we were able to characterize in terms of SHG, as theoretically predicted. Additionally, we recently refined a Metal-assisted modified exfoliation protocol, allowing for the transfer of the exfoliated flakes onto various flat substrates. This demonstrates the feasibility of achieving extensive exfoliation on rigid substrates (Si, SiO₂, ITO, Al₂O₃) as well as flexible substrates (PET, Kapton).

3:45 PM EL05.11.07

Methodology: Bayesian for Identifying Defects in Two-Dimensional Materials in a Scalable Way. Jun Wang, Na Young Kim and Kyle J. Daun; University of Waterloo, Canada

Two-dimensional transition metal dichalcogenides (TMDCs), including molybdenum disulfide (MoS₂), have many potential applications in electronic and optoelectronic devices, such as light-emitting diodes, photodetectors, and field effect transistors. However, the existence of defects such as sulfur vacancies, impurity atoms, and anti-sites impacts the optoelectronic properties of these materials. Accordingly, there is an urgent need for diagnostics that can identify defects in order to assess the functional performance of TMDC devices for scaling-up production.

In this regard, Raman spectroscopy is a promising approach for quantifying the defect concentration over industrially relevant quantities of monolayer MoS₂ efficiently. In order to obtain quantitative estimates, a measurement model is needed to connect a spectral feature (e.g., Raman shift) to the vacancy concentration, which may be derived numerically using density functional theory (DFT) or experimentally by comparing the Raman shift to the vacancy concentrations measured through other methods. More precisely, a Gaussian distribution curve representing sulfur vacancy concentration probability can be generated according to the Raman peak shift observed in the measurement spectra. In both cases, the measurement model will be subject to uncertainties due to experimental artifacts or aspects of the physical system that are excluded from the DFT simulation. Additional factors, including the number of layers, defect concentration, and doping, may also influence these spectra. Accordingly, there is a need to quantify how these parameters the uncertainty of vacancy concentration estimates, and, ideally, reduce them by incorporating complementary prior information.

Here, we propose a novel methodology that combines Raman data and Bayesian inference to identify the probability of a given concentration of sulfur vacancies which may be applied to various scales of research and production. In this methodology, a prior probability for defect concentration is calculated from the probability distribution of thermodynamic stable defect concentration data sets, which are generated in real cases. The prior probability of defect concentration is then updated with a likelihood derived from a Raman spectrum measured on a MoS₂ monolayer, leading to a posterior probability density function that comprehensively summarizes the uncertainty in the inferred sulfur vacancy.

4:00 PM EL05.11.08

Rapid Detection of Defects in Monolayer 2D Semiconductors by Polarized Raman Spectroscopy Crystal A. Nattoo, Tara Pena, Koosha N. Nazif, Amalya C. Johnson, Fang Liu and Eric Pop; Stanford University, United States

An outstanding challenge in integrating two-dimensional (2D) transition metal dichalcogenides (TMDs) into future optoelectronics is optimizing high-quality and large-scale growths of these atomically thin materials. Several methods exist for wafer- and chip-scale growths of 2D-TMDs, such as chemical vapor deposition (CVD) and atomic layer deposition (ALD). Still, we see a large degree of variability from growth to growth due to intrinsic and extrinsic factors like defects and humidity [1]. Optimizing the rapid characterization methods used to discern material quality before fabrication is essential to improve the yield of devices produced during research and development, saving time and money.

Raman spectroscopy is a non-destructive and standard characterization technique, to examine various material features such as thickness [2], doping [3], strain [4], and disorder [5, 6]. However, the effect of doping and disorder on the Raman signatures still remains to be examined in some TMD systems (e.g., WSe₂). In this work, we propose using cross-polarized Raman spectra [7] to isolate the in-plane E' mode from the out-of-plane A₁' mode with a 532 nm laser to properly examine defect-induced Raman features in two monolayer TMD materials of broad interest. Based on the phonon dispersion curves, we focus on MoS₂ and WSe₂, because they have the most suitable optical phonon energy and dispersion for this method.

The isolation of the E' mode by cross-polarization is especially effective in the case of WSe₂, which shows a strong degeneracy of the E' and A₁' modes around 250 cm⁻¹, making analysis a unique challenge. Due to the nature of defects interrupting the vibration of atoms in-plane, the transverse and longitudinal modes are the most sensitive to changes in defect density. For this reason, we study the amplitude changes of the in-plane E' mode in relation to the second order M point phonon modes that appear with increasing disorder.

After the data are collected, the spectra are fit with a Gaussian and Lorentzian spectral blend to extract the peak height, position, and full width at half-maximum (FWHM). The ratio between the left shoulder second-order phonon modes and the first-order E' mode is used as a figure of merit to estimate the expected defect density and the majority carrier mobility in the 2D material. Our approach can estimate defect densities down to the order of 10¹¹ cm⁻² using TMD samples procured by different synthesis methods. To compare the method's validity, the same samples are also characterized by conductive atomic force microscopy (c-AFM) and electrical measurements of mobility.

This rapid, non-destructive Raman characterization method can be integrated into commercial growth systems to accelerate TMD research and development for practical applications. Future work is also planned to expand these efforts to other TMDs. The work was supported by an NSF Graduate Fellowship (C.A.N.), an NSF Ascend Fellowship (T.P.), by the SRC SUPREME Center and the Stanford SystemX Alliance.

- [1] K. K. H. Smithe *et al.*, *ACS Nano*, **11**, 8456 (2017).
- [2] Y. Zhao *et al.*, *Nano Lett.*, **13**, 1007 (2013).
- [3] A. Michail *et al.*, *Appl. Phys. Lett.*, **108**, 173102 (2016).
- [4] I. M. Datye *et al.*, *Nano Lett.*, **22**, 8052 (2022).
- [5] W. Shi *et al.*, *Chin. Phys. Lett.*, **33**, 057801 (2016).
- [6] W. Shi *et al.*, *2D Mater.*, **3**, 025016 (2016).
- [7] J. Kim *et al.*, *J. Phys.: Condens. Matter*, **32**, 343001 (2020).

SESSION EL05.12: Optoelectronics
Session Chairs: Sean Li and Muhammed Juvaed Mangattuchali
Friday Morning, April 26, 2024
Room 344, Level 3, Summit

8:45 AM *EL05.12.01

Towards Large-Area Black Phosphorous Midwave-IR Optoelectronics [Ali Javey](#)^{1,2}; ¹University of California, Berkeley, United States; ²Lawrence Berkeley National Laboratory, United States

High-efficiency mid-wavelength infrared (mid-IR, 3–5 μm) optoelectronics, including light emitting diodes (LEDs) and photodetectors, are of high demand for emerging applications in spectroscopy, imaging, and gas sensing. Black phosphorus (bP) has emerged as a unique optoelectronic material for mid-IR applications with performances surpassing those of conventional III-V and II-VI semiconductors of similar bandgap. In this talk, I will present recent advancements on understanding and controlling the radiative and non-radiative recombination rates as a function of bP thickness. We observe higher photoluminescence quantum yields in bP as compared to conventional III-V and II-VI semiconductors of similar bandgaps due to the smaller Auger recombination rate. As a result, bP mid-IR LEDs with external quantum efficiency of $>4\%$ are reported, outperforming the state-of-the-art in this wavelength range. Furthermore, device encapsulation and packaging technologies are explored with extrapolated half lifetime of $\sim 15,000$ hours based on accelerated lifetime measurements. Finally, I will present strategies for large-area device fabrication and processing.

9:15 AM EL05.12.02

Photo-Gating through Unidirectional Charge Carrier Funneling in 2D TMDC / 2D Perovskite Heterostructure-Photodetectors Leon Spee¹, Julius Konietzka¹, Annika Grundmann², Martin A. Schroer¹, Markus Winterer¹, Holger Kalisch², Michael Heuken^{2,3}, Andrei Vescan², Gerd Bacher¹ and [Franziska E. Muckel](#)¹; ¹University Duisburg-Essen, Germany; ²RWTH Aachen University, Germany; ³AIXTRON SE, Germany

Two-dimensional (2D) van der Waals (vdW) semiconductors, such as transition-metal dichalcogenides (TMDCs), have garnered increasing attention as promising materials for photosensing applications. Their appeal lies in their high oscillator strength, significant electronic mobility, and remarkable mechanical flexibility, promising novel application scenarios for optical sensing in healthcare, optical communication or different lifestyle applications. However, due to their intrinsically limited light absorption, high responsivities and sensitivities are hard to achieve. To enhance photodetectivity, TMDCs are frequently integrated into functional heterostructures with other vdW semiconductors like 2D Ruddlesden-Popper Perovskites to introduce a gain mechanism. However, the processes of energy and charge carrier transfer between TMDCs and 2D Ruddlesden-Popper materials remain subjects of debate, making it challenging to elucidate the fundamental mechanism of device operation.

In this study, we present lateral heterostructure photodetectors composed of MOCVD-grown molybdenum disulfide (MoS_2) and solution processed butylammonium lead iodide (BA_2PbI_4) that exhibit significantly enhanced responsivities, reduced dark current, and increased detectivity when compared to devices using MoS_2 or BA_2PbI_4 alone. We provide compelling evidence that this improvement is linked to a gain mechanism facilitated by photo-gating within the MoS_2 channel. This photo-gating results from a unidirectional transfer of holes from MoS_2 to BA_2PbI_4 and the blocking of electrons by butylammonium ions. Our devices exhibit responsivities up to 10 A/W , which corresponds to a gain of 145. This research sheds light on the intriguing performance of heterostructure photodetectors based on 2D materials and their potential for practical device integration.

9:30 AM EL05.12.03

Graphene-Enhanced UVC-LEDs [Wolfgang Mertin](#), Johanna Meier, Hehe Zhang, Umut Kaya and Gerd Bacher; University of Duisburg-Essen, Germany

In anticipation of their promising applications in the deep-ultraviolet (UVC) spectral range, e.g., for disinfection, AlGaIn-based UVC-Light Emitting Diodes (UVC-LEDs) have experienced a lot of attention over the last decade. However, these LEDs still have lower performance regarding Wall Plug Efficiency (WPE) and External Quantum Efficiency (EQE) than blue emitting LEDs [1,2]. One reason is the low electrical conductivity of the p-AlGaIn cladding layer, which limits both, current injection in flip-chip geometry, and lateral current spreading for devices in standard geometry.

Graphene combines high electrical conductivity and high optical transparency in the UVC spectral range and has thus the potential to act as low absorbent contact layer in UVC-LEDs. Here we report on a transfer-free low-temperature approach for integrating graphene directly into AlGaIn-based UVC-LEDs at temperatures far below 1000°C . We demonstrate functional UVC-LEDs in standard as well as in flip-chip geometry.

Based on our previous work [3,4] we used a plasma-enhanced CVD graphene process to directly grow graphene on the p-AlGaIn layer of a UVC-LED at 670°C . The graphene has an optical transparency above 90% in the UVC region and an electrical sheet resistance of about $5 \text{ k}\Omega/\text{sq}$. Using the directly grown graphene as a transparent contact layer, we were able to improve the EQE of UVC-LEDs emitting at 275 nm in standard as well as in flip-chip geometry to over 5%. With these proof-of-principle experiments, we have paved the way to a large-scale integration-friendly process of graphene-enhanced UVC-LEDs.

- [1] M. Kneissl *et al.*, *Nature Photonics* **13**, 233 (2019)
- [2] S. Liang and W. Sun, *Adv. Mater. Technol.* **7** (2022) 2101502
- [3] H. Zhang *et al.*, *Materials*, **15**(6), 2203 (2022)
- [4] J. Mischke *et al.*, *2D Materials* **7**, 035019 (2020)

9:45 AM EL05.12.04

Bridging Macroscopic and Microscopic Nonlinear Optics with Layered Semiconductors [Chiara Trovatiello](#)¹, Xinyi Xu¹, Fabian Mooshammer¹, D.

Basov¹, Giulio Nicola Felice Cerullo² and P. James Schuck¹; ¹Columbia University, United States; ²Politecnico di Milano, Italy

Nonlinear frequency conversion provides essential tools for light generation, photon entanglement, and manipulation. Conventional nonlinear optical crystals display moderate second-order nonlinear susceptibilities and perform well in benchtop setups with discrete optical components. However, such crystals do not easily lend themselves to miniaturization and on-chip integration. Transition metal dichalcogenides (TMDs) possess 10-100x stronger nonlinear susceptibilities and, thanks to their deeply sub-wavelength thickness, offer a unique platform for on-chip nonlinear frequency conversion and light amplification. Recently, such giant nonlinearity has been exploited to demonstrate nonlinear light amplification at the ultimate thickness limit[1]; however, optical gain was still limited by the sub-nm propagation length.

The nonlinear conversion efficiency could be scaled by increasing the propagation length through the active medium. This is attainable by increasing the number of layers in the TMD sample. However, the nonlinear optical properties of semiconducting TMDs critically depend on their crystallographic symmetry. 2H-TMDs are naturally centrosymmetric, giving an opposite dipole orientation among consecutive layers. This results in a vanishing nonlinear susceptibility ($\chi^{(2)} = 0$) for crystals with even number of layers and precludes efficient conversion in multilayers. In contrast, 3R-TMDs naturally combine broken inversion symmetry ($\chi^{(2)} \neq 0$) and aligned layering, representing ideal candidates to boost the nonlinear optical gain with minimal footprint.

The nonlinear optical response of 3R-MoS₂ has been explored in some recent pioneering studies[2,3], so far focusing on thinner crystals, reporting the quadratic enhancement with the layer number at the 2D limit, and showing a maximum SHG enhancement of ≈ 100 occurring at specific thickness windows. Pushing towards general application, however, requires higher nonlinear enhancements and thus larger layer number, which in turn leads to more intricate interferences and interactions within the crystal.

Here we measure SHG from multilayer 3R-MoS₂ crystals with variable thickness. We report the first measurement of the coherence length of 3R-MoS₂ at telecom wavelengths. Our model is able to capture the role of phase-matching, as well as the intrinsic interference effects. At the coherence length (~ 530 nm) we achieve record nonlinear optical enhancement from a van der Waals material, i.e., $>10^4$ stronger than a monolayer, revealing the intrinsic single-pass upper limits of the material[4]. Considering that the reported conversion efficiency of monolayer MoS₂ at FW = 1560 nm is $\sim 10^{-10}$, the overall conversion efficiency of MoS₂ at the coherence length thickness will be $\sim 10^{-6}$. Further enhancement can then be achieved by regularly engineering larger crystals or waveguides with a periodicity on this length scale, or by exploiting birefringence.

Our results highlight the potential of 3R-stacked TMDs for integrated photonics, providing critical parameters for designing highly efficient on-chip nonlinear optical devices. By virtue of the exceptional nonlinear properties and the possibility of integration and phase matching in waveguide geometries, we foresee ultra-compact devices with extremely high nonlinear conversion efficiency – even exceeding multi-pass state-of-the-art photonic resonators of aluminum nitride – opening new frontiers for engineering on-chip integrated nonlinear optical devices including photonic resonators and optical quantum circuits.

[1] [Trovatello, C.](#) et al. Nat. Photonics, 15, 6-10 (2021).

[2] Shi, J. et al., Adv. Mater. 29, 1701486 (2017).

[3] Zhao, M. et al., Light: Sci. Appl. 5, e16131 (2016).

[4] Xu, X., [Trovatello, C.](#) et al., Nature Photonics, 16, 698-706 (2022).

10:00 AM BREAK

SESSION EL05.13 Optoelectronics and Magnetism I

Session Chairs: Ali Javey and Iuliana Radu

Friday Morning, April 26, 2024

Room 344, Level 3, Summit

10:30 AM *EL05.13.01

New Form of High-k Dielectrics for 2D Field-Effect Transistors [Sean Li](#)¹, Junjie Shi¹, Ji Zhang¹ and Jing-Kai Huang²; ¹University of New South Wales, Australia; ²City University of Hong Kong, Hong Kong

The integration of ultrathin insulators stands as a pivotal factor for the advancement of 2D Field-Effect Transistors (FETs) in cutting-edge technology. Presently, 2D semiconductor devices are yet to realize their complete theoretical potential, primarily due to the unavailability of suitable insulators. These insulators must strike a balance between maintaining minimal leakage currents and enabling a high gate capacitance to achieve superior gate coupling at sub-1nm Equivalent Oxide Thickness (EOT) scales. Furthermore, they must establish well-defined interfaces with the channel, exhibit minimal defect densities, and possess exceptional dielectric stability. This study showcases the power of dielectric engineering in elevating the performance of 2D FETs, offering viable avenues to develop 2D FETs characterized by remarkably low leakage currents, shorter channel lengths, and outstanding power efficiency.

11:00 AM EL05.13.02

Spatial Tuning of Light-Matter Interaction via Strain-Gradient Induced Polarization in Freestanding Wrinkled 2D Materials [Chullhee Cho](#)^{1,2}, SungWoo Nam³, Zhichao Zhang², Jin Myung Kim³, MD Farhadul Haque⁴ and Peter Snapp¹; ¹NASA Goddard Space Flight Center, United States; ²University of Illinois at Urbana-Champaign, United States; ³University of California Irvine, United States; ⁴Intel Corporation, United States

Strain engineering is an attractive strategy to design and modulate material properties, via lattice deformation, to improve modern micro and nanoelectronics device performance. To date, due to the challenge of deforming freestanding two-dimensional (2D) materials without fracture, controlled deformation of 2D materials has been demonstrated almost exclusively on substrate-supported structures, where the 2D materials are in contact with an underlying deformable substrate. However, interfacial effects arising from these supporting materials may suppress or alter the unique behavior of deformed 2D materials. To address interfacial effects, we report, for the first time, the formation of a micrometer-scale freestanding wrinkled structure of 2D materials without any encapsulation layers where we observed the enhanced light-matter interactions with a spatial modulation. Freestanding wrinkled monolayer WSe₂ exhibited about a 330% enhancement relative to supported wrinkled WSe₂ quantified through photo induced force microscopy. Spatial modulation and enhancement of light interaction in the freestanding wrinkled structures are attributed to the enhanced strain-gradient effect (i.e., out-of-plane polarization) enabled by removing the constraining support and proximate dielectrics. Our findings offer an additional degree of freedom to modulate the out-of-plane polarization and enhance the out-of-plane light-matter interaction in 2D materials.

11:15 AM EL05.13.03

Simultaneous Strain and Gate Tunability of Moiré Heterostructure Devices Jordan Fonseca¹, John Cenker^{1,2}, Mai Nguyen¹, Chaowei Hu¹, Wang Xi¹, George Rickey¹, Takashi Taniguchi³, Kenji Watanabe³, Jiun-Haw Chu¹ and Xiaodong Xu¹; ¹University of Washington, United States; ²Columbia University, United States; ³National Institute for Materials Science, Japan

Moiré heterostructures of 2D materials have served as a platform for studying and engineering a wide variety of correlated phenomena and many body physics. The atomic thickness of two-dimensional materials and the large effective lattice constant of moiré superlattices make electrostatic gating a particularly effective way to tune carrier density and thereby explore a rich phase diagram of correlated effects. Independently, two dimensional materials exhibit unusually high elasticity and can sustain significant uniaxial strain before yielding. Uniaxial strain breaks rotational symmetry and changes interatomic spacing, altering many material properties in the process. An outstanding challenge, however, is simultaneously and independently tuning uniaxial strain and electrostatic gating in-situ at cryogenic temperatures. In this talk, I will discuss our work to leverage novel approaches for efficient strain transfer to the moiré heterostructure in gateable van der Waals devices. I will show how the ability to traverse the strain-gating phase space for a high-quality transition metal dichalcogenide moiré heterostructure enables exploration of novel features in the photoluminescence spectra and discuss their origin in the underlying optoelectronic properties of this rich material system.

11:30 AM EL05.13.04

Electronic Properties of Quasi-1D Materials, TiS₃ and In₄Se₃ Alexander Sinitskij; University of Nebraska -Lincoln, United States

Two-dimensional (2D) layered materials have received much interest in recent years due to their ease of miniaturization by exfoliation techniques and very diverse physical properties. Quasi-one-dimensional (quasi-1D) materials, while seeing considerably less interest, can express many of the same desirable properties as conventional layered materials, with an added dimension of anisotropy. A representative example of quasi-1D materials is titanium trisulfide (TiS₃), a layered n-type semiconductor composed of chains of trigonal sulfur prisms with Ti⁴⁺ centers. Because of its moderate bandgap of about 1 eV, which is comparable to that of silicon, and theoretically predicted electron mobilities of up to 10,000 cm² V⁻¹ s⁻¹, TiS₃ is a promising material for electronic applications.

We demonstrate the ease of mechanical exfoliation of bulk TiS₃ crystals accompanied with theoretical calculations and show that these materials exfoliate into few-atomic-layer nanoribbons with very smooth edges. Their characterization by Raman spectroscopy shows a reliable, internally standardized shift of a few cm⁻¹ from monolayer to bulk demonstrating tunability typical of conventional layered materials. The TiS₃ field-effect transistors showed an n-type electronic transport with characteristics comparable to those of MoS₂, a popular 2D semiconductor. Their room-temperature mobilities of about 30 cm² V⁻¹ s⁻¹ were two orders of magnitude smaller than predicted theoretically, which we quantitatively explain by polar-optical phonon scattering in TiS₃. We demonstrate that TiS₃ is compatible with the conventional atomic layer deposition procedure for Al₂O₃, and the encapsulation of TiS₃ with alumina resulted in the mobility increase up to 43 cm² V⁻¹ s⁻¹. The quasi-1D TiS₃ chains exhibit an anisotropic photocurrent response to polarized light as well as a gate-tunable metal-insulator transition (MIT) and an access to the charge density wave (CDW) physics.

Many of the conclusions drawn for TiS₃ can be extended to other quasi-1D materials, such as In₄Se₃. In₄Se₃ has a different crystal structure, but it also features covalently bonded quasi-1D chains as its basic building blocks. We successfully exfoliated bulk In₄Se₃ crystals into few-nm-thick flakes with visible signatures of quasi-1D chains, similar to the exfoliated TiS₃ flakes. The In₄Se₃ flakes exfoliated on Si/SiO₂ have anisotropic electronic properties and exhibit field-effect electron mobilities of about 50 cm² V⁻¹ s⁻¹ at room temperature, as well as a polarization dependent photoresponse on a timescale of less than 30 ms. These two examples, TiS₃ and In₄Se₃, demonstrate the promise of quasi-1D materials for emerging electronic applications.

11:45 AM EL05.13.05

Investigating Magnetic Ordering in Naturally Occurring and Artificially Modified Iron-Rich Phyllosilicates Muhammad Z. Khan¹, Oleg E. Peil², Nico Klingner³, Gregor Hlawacek³, Sebastian Wintz⁴, Christian Teichert¹, Ulrich Kentsch³, Markus Weigand⁴, Daniel Knez⁵, Johann G. Raith⁶, Andreas Ney⁷ and Aleksandar Matković¹; ¹Chair of Physics, Department Physics, Mechanics and Electrical Engineering, Montanuniversität Leoben, Austria; ²Group of Computational Materials Design, Materials Center Leoben Forschung GmbH, Austria; ³Institute of Ion Beam Physics and Materials Research, Helmholtz-Zentrum Dresden Rossendorf, Germany; ⁴Department of Spin and Topology in Quantum Materials, Helmholtz-Zentrum Berlin, Germany; ⁵Institute of Electron Microscopy and Nanoanalysis, Graz Centre for Electron Microscopy, Graz University of Technology, Austria; ⁶Chair of Resource Mineralogy, Montanuniversität Leoben, Austria; ⁷Institute of Semiconductor and Solid State Physics, Johannes Kepler University, Austria

The modulation of intrinsic 2D ferromagnetism has gained significant attention and shown a great potential for spintronics. Although many two-dimensional (2D) van der Waals materials have been reported to exhibit intrinsic magnetism, there are still challenges when it comes to ambient stability, which is a crucial barrier for their integration into device applications. We propose to overcome this by exploiting naturally occurring iron-rich phyllosilicates. Phyllosilicates offer a unique opportunity to explore complex air-stable layered systems with high concentration of magnetic ions. These naturally occurring layered materials are inherently magnetic and are wide band gap insulators (i.e. 5-6 eV). These minerals integrate local moment bearing ions of iron via magnesium/aluminium substitution in their octahedral sites. Natural capping by silicate/aluminate tetrahedral groups enables air stability of monolayers.^[1] Their structure and iron oxidation states are determined via Raman and X-ray spectroscopies. Superconducting quantum interference device magnetometry measurements are performed to examine the long-range magnetic ordering. In-field magnetic force microscopy in the presence of externally applied out-of-plane magnetic field on exfoliated flakes confirms that the paramagnetic response at room temperature persists down to monolayers. We demonstrate correlations between the iron concentration, layer structure, iron oxidation states, and their magnetic response, indicating a path to design materials with higher critical temperatures via oxidation state engineering.^[2]

Furthermore, we also demonstrate a scalable approach to control and tune the concentration of magnetic species via ion implantation into pure phyllosilicate crystals. Controlling the amount of implanted magnetic ions, choosing the dopant species or even alloying in the phyllosilicate matrix will open the pathways to engineer the 2D magnetic insulators with high critical ordering temperature.

References:

- 1 - Matković, Aleksandar, et al. "Iron-rich talc as air-stable platform for magnetic two-dimensional materials." *npj 2D Materials and Applications* 5.1 (2021): 94.
- 2 - Khan, Muhammad Zubair, et al. "Probing Magnetic Ordering in Air Stable Iron-Rich Van der Waals Minerals." *Adv. Phys. Res.* (2023).

1:30 PM EL05.14.01

Tailoring The Rashba-Induced Spin-To-Charge Conversion in 2D Transition Metal Dichalcogenides Interfaced with Oxide Ferroelectrics Oliver Pauli^{1,2}, Khasan Abdukayumov², Sylvain Massabeau¹, Céline Vergnaud², Luis M. Vicente-Arche¹, Alain Marty², Lucia Iglesias¹, Matthieu Jamet² and Manuel Bibes¹; ¹Unité Mixte de Physique, CNRS/Thales, France; ²Commissariat à l'énergie atomique et aux énergies alternatives, France

The direct and inverse Rashba-Edelstein effect in condensed matter is a viable source of charge-to-spin interconversion, towards the realisation of next-generation spintronic devices. One promising way of creating Rashba spin-orbit coupling (SOC) in an otherwise centrosymmetric material system is to interface it with a ferroelectric crystal, breaking inversion symmetry with the local electric field at the interface.

Two-dimensional (2D) crystals have emerged as a new class of materials that can exhibit a large range of quantum phenomena such as superconductivity, 2D magnetism, and non-trivial topological phases [1], [2]. Of these quantum phenomena, the Rashba effect has gained popularity recently as a result of its applicability to create charge-to-spin interconversion for next-generation spintronic devices. Highly stable PtSe₂ is one such 2D material which has a centrosymmetric crystal unit cell and a band-structure that evolves drastically as a function of the number of monolayers deposited, evolving from a high band-gap semiconductor to a semi-metal [3]. Interfacing a 2D material with a ferroelectric (FE) crystal applies a strong local electric field at the interface which breaks the inversion symmetry and triggers the interfacial Rashba effect in the 2D layer. Importantly, the sign of the Rashba spin-orbit coupling depends on the direction of the FE polarisation, such that the spin texture chirality should reverse upon a change in direction of the FE polarisation [4]. This forms the basis of the functionality of a low-power FerroElectric Spin-Orbit (FESO) device.

In this work, we grow 2D materials such as PtSe₂ using molecular beam epitaxy and use a wet transfer process to interface them with a variety of ferroelectric surfaces such as LiNbO₃ substrates and BiFeO₃ thin films. The spin-to-charge conversion characteristics are then examined using a variety of experimental techniques and compared between samples with different ferroelectric polarisation directions and assessed in the context of a spin-to-charge conversion FESO device.

[1] A. K. Geim and I. V. Grigorieva, 'Van der Waals heterostructures', *Nature*, vol. 499, no. 7459, pp. 419–425, Jul. 2013, doi: 10.1038/nature12385.

[2] F. Giustino et al., 'The 2021 quantum materials roadmap', *J. Phys. Mater.*, vol. 3, no. 4, p. 042006, Jan. 2021, doi: 10.1088/2515-7639/abb74e.

[3] L. Zhang et al., 'Precise Layer-Dependent Electronic Structure of MBE-Grown PtSe₂', *Advanced Electronic Materials*, vol. 7, no. 11, p. 2100559, 2021, doi: 10.1002/aelm.202100559.

[4] S. Picozzi, 'Ferroelectric Rashba semiconductors as a novel class of multifunctional materials', *Frontiers in Physics*, vol. 2, 2014, Accessed: Mar. 10, 2023. [Online]. Available: <https://www.frontiersin.org/articles/10.3389/fphy.2014.00010>

1:45 PM EL05.14.02

Charge Carrier Balance in Scalable TMDC-Based Light Emitting Devices Tobiloba G. Fabunmi¹, Henrik Myja¹, Annika Grundmann², Kalisch Holger², Andrei Vescan², Michael Heuken³, Tilmar Kümmell¹ and Gerd Bacher¹; ¹University of Duisburg-Essen, Germany; ²RWTH Aachen University, Germany; ³AIXTRON SE, Germany

2-dimensional transition metal dichalcogenides (TMDCs) such as WS₂ are ultrathin materials with huge oscillator strength, strong in-plane bonds, and in the case of monolayers a direct bandgap. These outstanding properties have stimulated the development of various concepts for light emitting devices [1], often based on micrometer-sized flakes. Recently, a scalable device architecture has been suggested, where wafer-scale TMDCs grown by metal-organic chemical vapor deposition (MOCVD) have been embedded between electron and hole supporting layers to form a vertical p-i-n architecture [2-4]. However, the luminance of TMDC-based LEDs in cw operation at room temperature is still limited to 50 cd/m² for microscale LEDs based on mechanically exfoliated WS₂ [5] and to about 1 cd/m² for scalable, 6 mm² large devices [2], respectively. One key requirement for optimizing the luminance is a balanced electron and hole injection into the active TMDC layer. In this work, we address the electron-hole balance in scalable WS₂-based LEDs by systematically varying the architecture of electron injection layers (EIL). We fabricated three different LED archetypes: type 1 includes a ZnO EIL, type 2 contains Mg-doped ZnO as an EIL, and type 3 is a reference device without an EIL. At 5V forward bias, we observed a reduction of the current density by a factor of 10 in type 2 devices as compared to type 1. Simultaneously, the EQE was found to increase by an order of magnitude in the type 2 device compared to type 1, and a luminance of up to 3 cd/m² was obtained for type 2 devices. We attribute this to an improved electron-hole balance in type 2 devices, caused by a reduced efficiency of electron injection. Our interpretation is supported by device simulations using NextNano, which emphasizes the impact of a balanced electron and hole injection for efficient LEDs based on scalable 2D TMDCs.

References:

[1] Jiang Pu et al. *Adv. Mater.* 30, 1707627 (2018)

[2] D. Andrzejewski et al., *ACS Photonics*. 6, 1832-1839 (2019)

[3] D. Andrzejewski et al., *Adv. Opt. Mat.* 8, 2000694 (2020)

[4] H. Myja et al., *Nanotechnology* 34, 285201 (2023)

[5] D. Andrzejewski et al., *Nanoscale*, 11, 8372–8379 (2019)

2:00 PM EL05.14.04

A General Modular Assembly Approach to a Library of Hybrid Superlattices Jingyuan Zhou; University of California, Los Angeles, United States

Hybrid superlattices consisting of two-dimensional atomic crystals (2DACs) and self-assembled molecular layers allow to synergistically combine rich physical properties in solid-state 2DACs with designable molecular functionalities. Such hybrid superlattices are generally prepared by a direct chemical or electrochemical intercalation approach, and are often limited to a specific class of 2DACs or molecular systems as dictated by the relative chemical reactivity and electrochemical stability of the constituent building blocks. Self-assembly offers an alternative strategy for efficiently organizing multiple building units into ordered superstructures. In this work, we report a systematic and quantitative study of the underlying governing principle for electrostatic assembly strategy in the context of 2D-molecular hybrid superlattices, and explore it for constructing a broad library of hybrid superlattices with widely variable compositions and tunable structural configurations. By using exfoliated MoS₂ as a model system, we show a series of amines, amino acids, coordination complexes, and polymers can be assembled with MoS₂ monolayers, forming alternatively ordered hybrid superlattices. Our systematic studies reveal that electrostatic assembly process is highly analogous to classical co-precipitation of ionic solids and fundamentally governed by the charge balance and equilibrium between electrostatic repulsion and van der Waals (vdW) interaction, following Schulze-Hardy rule at Debye-Hückel approximation based on Derjaguin-Landau-Verwey-Overbeek (DLVO) colloidal theory. Based on the charge balance rule, the layer number of inclusive molecules in the resulting hybrid superlattices can be precisely tuned. Furthermore, we show this assembly strategy is highly general and can be extended to diverse 2DACs, such as TiS₂, TaS₂, WS₂, MoSe₂, SnSe, In₂Se₃, Bi₂Se₃ and Mxenes such as Ti₃C₂T_x. The formation of hybrid superlattices with

functional ions or molecules opens a new dimension to tailor and tame the fundamental physical properties of the 2DACs and enables artificial materials with exotic functions. For example, the formation of TaS₂/amine superlattice notably elevates the superconducting transition temperature (T_c). The introduction of chiral amino acids into MoS₂ interlayers effectively incorporates molecular chirality into solid-state superlattices, and the formation of MoS₂/Co(en)₃Cl₃ superlattice induces ferromagnetic properties not available in either constituent. Together, our study defines a general modular approach for the rational assembly of hybrid superlattices and artificial solids with designable structural motifs and widely tunable physical properties.

2:15 PM EL05.14.05

Towards 300 mm 2D Materials Integration: Focus on Performance, Repeatability and Fab Compatibility [Salim El Kazzi](#), Sergej Pasko, Jan Mischke, Simonas Krotkus, Emre Yengel, Apostolia Manasi and Alexander Henning; Aixtron, Germany

To reach the silicon IC-industry, 2D materials need to pass the strict requirements of the semiconductor foundries and manufacturers. At the current stage of 2D materials research, it is critical for the community to develop work on the wafer-scale integration, yield, and reproducibility instead of selecting the best-performing 'champion' device produced on smaller scale. From a growth perspective, layer uniformity and repeatability are critical factors that need to be proven for any materials system considered in the CMOS technology.

Here, we report on the scaling up of 2D materials synthesis to 300 mm substrates. We focus on the different 2D integration schemes, which rely on the growth of 2D materials on amorphous or epitaxial substrates at different temperatures. We then highlight the importance of wafer scale uniformity and run-to-run repeatability for which we try to define for the community the metrology standard of 2D wafer-scale synthesis. Finally, we will address two other key aspects related to cross-contamination and tool cleaning that are being solved to facilitate the entry of these materials into the Si-industry

2:30 PM BREAK

3:00 PM EL05.14.06

Towards CMOS-Integrated Graphene Hall Sensor Arrays with Individually Tunable Elements for High Sensitivity and Enhanced Uniformity [Vasant Iyer](#), Nishal Shah, Jaeung Ko, A.T.C. Johnson, David Issadore and Firooz Aflatouni; University of Pennsylvania, United States

Graphene Hall-effect sensors exhibit high performance comparable to state-of-the-art devices made from III-V semiconductors, with the added advantage of CMOS-compatible fabrication. These properties make graphene Hall sensors (GHSs) an attractive choice for implementing high-density magnetic sensing arrays for imaging and biosensing applications. [1] The size and effectiveness of GHS arrays are presently limited by a) low uniformity across the array arising from variable doping and fabrication mismatch, and b) the increasing need for co-integrated GHS control and readout electronics as the array size is upscaled. In this work we present and validate strategies to address both challenges, achieving progress towards large-scale GHS arrays.

We first studied the effectiveness of per-device tuning to improve response uniformity between graphene Hall elements. The conventional technique of varying the substrate voltage to tune all devices simultaneously has been shown to improve uniformity, at the expense of overall sensitivity. [2] We hypothesized that individual GHS tuning would greatly relax the tradeoff. An array of 16 GHSs was fabricated on a silicon chip, with an insulated backgate terminal underneath the active region of each sensor (10 mm x 10 mm). 10 nm HfO₂ was chosen as the insulation dielectric to enhance tuning efficacy. A CMOS-compatible voltage range of 5 V was sufficient to access all relevant regions of device operation, including the Dirac point and the maximum sensitivities in the electron and hole regimes. Characterization of multiple devices on the same chip showed non-uniformity in the optimal operating point of each GHS, arising from variations in doping across the chip. Individual backgate tuning was then used to align the responses of the sensors. The post-tuning results confirmed our hypothesis, as individual tuning improved the Hall sensitivity coefficient of variation (CV) by up to 95% compared to the scenario where all sensors shared the same backgate, with a small degradation to sensitivity (9.5%). The best-performing GHS array in our study achieved an average response of 1.17 k Ω /T with a CV of 3.4%.

We then developed techniques to monolithically integrate a GHS array within the back-end-of-line (BEOL) layers of a custom CMOS chip (designed in a 180nm foundry process) for scalable sensor control and readout. Two key challenges in graphene-CMOS BEOL integration are a) surface roughness on the uppermost layers of the chip leading to graphene tears b) surface oxidation on BEOL metals leading to non-ohmic device contacts. [3-4] To circumvent these issues, the entire sensing region of the 1.6mm x 1.2mm chip was covered with a top-metal fill in the design, with a foundry layer added to remove passivation over the top-metal fill. Sensor terminals were defined by instantiating tungsten vias between the top fill and the underlying metal layer. During post-processing, the top-metal fill was removed using a wet etch, leaving behind a planarized surface with exposed oxide-free sensor terminals. After insulating the backgate terminal, CVD-grown graphene was transferred onto the CMOS chip surface and patterned into Hall crosses at the predefined sensing sites. SEM, AFM, and Raman analysis were used to confirm successful patterning of high-quality monolayer graphene. Electrical measurements of 32 sites within the sensing surface were performed through on-chip multiplexing and indicated high yield (75%) with a measured sensitivity of 480 Ω /T. Ongoing measurements using on-chip circuitry for backgate tuning and lock-in detection of the Hall signal will also be discussed.

References:

- [1] Collomb et al., *J. Phys. Cond.Matt.* (2021)
- [2] Chen et al., *Carbon* (2015)
- [3] Dai et al., *ACS Nano* (2020)
- [4] Mortazavi Zanjani et al., *npj 2DM* (2017)

3:15 PM EL05.14.07

Ultrathin Quasi-2D Amorphous Carbon Dielectric prepared from Solution Precursor for Nanoelectronics [Fufei An](#)¹, Congjun Wang², Viet Hung Pham², Albina Borisevich³, Jiangchao Qian¹, Kaijun Yin¹, Saran Pidaparthi¹, Brian Robinson¹, Ang-Sheng Chou⁴, Junseok Lee², Jennifer Weidman², Sittichai Natesakhawat², Han Wang⁴, Andre Schleife¹, Jian-Min Zuo¹, Christopher Matranga² and Qing Cao¹; ¹UIUC, United States; ²U.S. Department of Energy National Energy Technology Laboratory, United States; ³Oak Ridge National Laboratory, United States; ⁴Taiwan Semiconductor Manufacturing Company, Taiwan

Integrating crystalline 2D semiconductors and semimetals channels with 3D bulk amorphous metal oxides generally leads to poor interfaces with high concentrations of traps and scattering centers. Low-dimensional amorphous dielectrics could be ideal for 2D-material-based nanoelectronics with their intrinsic ultrathinness and capability to maintain a smooth and homogenous 2D surface. Here we report the wafer-scale synthesis of ultrathin quasi-2D amorphous carbon with thickness down to 1–2 atomic layers from solution-processable carbon-dot precursors directly on non-catalytic substrates. The prepared one layer of coalesced carbon dots is an atomically thin, mechanically strong amorphous film predominantly composed of sp² carbon with low surface dangling bond density, and their few-layer assemblies are robust nanodielectrics with low leakage current density and high breakdown field strength.

The thickness of the prepared ultrathin quasi-2D amorphous carbon film was characterized precisely based on high-resolution cross-sectional STEM images, giving a thickness of 0.41 ± 0.04 nm. After each deposition-coalescing cycle, the thickness of the film increased precisely by 0.4 nm, which is comparable to the interlayer spacing of graphite, as measured by both AFM and TEM.

With carbon-dot precursors covalently crosslinked together, the prepared ultrathin quasi-2D amorphous carbon film is mechanically robust enough to be transferred to other substrates as a complete and continuous membrane. The transferred quasi-2D amorphous carbon was firstly suspended as freestanding nanomembranes on TEM grid for imaging. The uniform contrast throughout in the low-magnification ADF-STEM image confirms that the film is macroscopically homogenous, and the SAED patterns show a characteristic diffuse halo, which verifies its amorphous nature.

Their mechanical properties were characterized by AFM nanoindentation performed on atomically thin nanomembranes suspended over 1.2 μm wide and 3 μm deep circular holes, giving an extracted high Young's modulus of 400 ± 100 GPa, which is comparable to that of crystalline graphene and h-BN, further verifies the homogeneity and continuity of the ultrathin quasi-2D amorphous carbon prepared from the assembly and coalescence of carbon dots with strong lateral connections, which are very likely of covalent nature.

The achieved macroscopic uniformity, atomic-level thickness control, and processability allow our quasi-2D amorphous carbon films as dielectric in nanoelectronics devices, where their unique structure and properties were exploited to enable improved device performances. When utilized as gate dielectrics in graphene and 2D metal chalcogenides transistors, compared to amorphous bulk metal oxides, the ultrathin amorphous carbon films with predominant sp^2 carbon content can form clean interfaces with graphene and 2D metal chalcogenides, which leads to enhanced carrier transport mobility and minimum hysteresis. Compared to polycrystalline 2D h-BN, they have better processability and their amorphous atomic structures lead to drastically lower leakage current density ($<10^{-4}$ A/cm² with thickness down to three atomic layers of 1.6 nm) with higher dielectric strength (breakdown field above 20 MV/cm) for substantially reduced power consumption and improved device reliability.

The atomic-level thickness and the presence of large-size carbon rings inside the atomic structure of quasi-2D amorphous carbon also make its multilayered assemblies attractive for insulating ion-transport media in memristors. Their intrinsic ultrathinness and distinctive atomic structures composed of heterogeneous carbon rings offer predefined filament formation pathways across atomically thin films, leading to drastically enhanced switching uniformity, reduced energy consumption (<20 fJ per operation), and faster operating speed (<20 ns) as the switching media for electrochemical memristor, without sacrificing endurance and retention.

3:30 PM EL05.14.08

Large Area Van der Waals MoS₂-WS₂ Heterostructures for Visible-Light Photocatalysis and Energy Conversion [Giorgio Zambito](#)¹, [Matteo Gardella](#)¹, [Giulio Ferrando](#)¹, [Francesco Bisio](#)², [Maria Caterina Giordano](#)¹ and [Francesco Buatier de Mongeot](#)¹; ¹University of Genoa, Italy; ²CNR-SPIN, Italy

Two-dimensional Transition Metal Dichalcogenides semiconductors (2D-TMDs) have recently collected a strong scientific and technological interest over a broad community due to their peculiar optoelectronic response within a broadband spectrum, and to their tunable bandgap that enables promising optoelectronic and photonic functionalities. Additionally, the superior optical absorption coefficients in the Visible spectrum, enhanced by about two orders of magnitude with respect to conventional bulk semiconductors, qualify TMDs as optimal candidates for photodetection and photoconversion applications [1].

Owing to their atomically smooth surfaces and fully saturated in-plane chemical bonds, an opportunity to further engineer the optoelectronic response of a 2D device is offered by the combination of two different TMDs layers to form a van der Waals heterostructure, in which new optoelectronic properties arise from the band structure coupling of the junction [2].

Here, we demonstrate homogeneous growth of large area 2D-TMDs films by means of a physical deposition process based on Ion Beam Sputtering, followed by high temperature recrystallization in a sulfur enriched atmosphere [3,4]. The fabrication process has been subsequently optimized for the sequential synthesis of vertically stacked large area MoS₂-WS₂ van der Waals heterostructures supported on a large area graphene layer which acts as a transparent conductive window [5]. Vertical stacking of MoS₂-WS₂ heterostructure ensures a type-II staggered band alignment which in turn allows to split excitons across the junction, thus increasing the lifetime of the photogenerated carriers compared to the individual TMD components. Charge separation can be exploited both for energy conversion, since recombination rate is reduced, and for photocatalytic applications, since the separated charges on the surface can boost specific reactions. This is reflected in the superior photodissociation rate of molecular dye probes in solution near the heterostructure sample, and in the photovoltage and photocurrent measured upon illumination of the large area device.

These results show that TMDs van der Waals heterostructures represent optimal building blocks for the fabrication of self-powered photodetectors, by exploiting the charge separation of the photogenerated carriers at the 2D interface without any external bias.

[1] M. Bhatnagar et al., ACS Appl. Mater. Interfaces 2021, 13, 13508–13516

[2] D. Jariwala et al., ACS Photonics 2017, 4, 12, 2962–2970

[3] M.C. Giordano et al., Adv. Mater. Interfaces 2022, 2201408

[4] M. Gardella et al., "Maskless synthesis of van der Waals heterostructure arrays engineered for light harvesting on large-area templates", under submission

[5] M. Gardella et al., "Large area van der Waals MoS₂-WS₂ heterostructures for visible-light energy conversion", submitted at npj 2D materials and applications

3:45 PM DISCUSSION TIME - AWARDS AND CONCLUDING REMARKS

SESSION EL05.15: Virtual Session: MOCVD and Device Technology of 2D —TMDC Layers and Heterostructures

Session Chairs: Hippolyte Astier and Silvija Gradecak

Tuesday Morning, May 7, 2024

EL05-virtual

8:00 AM *EL05.15.01

Memristive Circuits based on Two-Dimensional Layered Hexagonal Boron Nitride for Radiofrequency Applications [Mario Lanza](#); King Abdullah University of Science and Technology, Saudi Arabia

Radiofrequency (RF) switches are essential components in modern communication devices, as they enable fast data transmission by driving or blocking electromagnetic signals of high frequencies (typically few/tens of gigahertz). The constant demand for higher data transmission rates requires RF switches capable of operating at higher frequencies, which represents a big challenge for commercial device technologies like field effect transistors and phase-change memristors (which are limited to ~60 GHz). In this talk I will present the fabrication of memristive RF switches, based on multilayer hexagonal

boron nitride (h-BN), capable of operating reliably at frequencies up to 260 GHz. We build the first 2D-materials-based series-shunt device configuration and readily achieve outstanding insertion loss of 0.9 dB and isolation of 35 dB at 120 GHz. We accomplish consistent ambipolar switching with low resistances down to $9.3 \pm 3.7 \Omega$ by introducing a low resistance tuning protocol, and achieve high endurance up to 2000 cycles (more than 60 times higher than previous reports on 2D-materials-based RF switches). These achievements represent a significant advancement towards next generation RF switches, as well as to the deployment of 2D materials in the semiconductors industry.

8:30 AM EL05.15.02

Lytotropic Liquid Crystal Phases as Temples for Selective Interfacial Reactions to Asymmetric Functionalization of 2D Nanomaterials at Large Scale Wei Wang; Aramco Americas: Aramco Research Center-Boston, United States

Anisotropic nanomaterials composed of two halves with different structure, chemistry, or polarity, known as Janus nanomaterials, have distinct properties when compared to symmetrically functionalized analogues. These materials have gained significant attention in many applications such as electronic thin films, drug delivery, sensors, optics, oil/water separation membranes, photoactivated micromotors, photocatalysts, and interfacial modification. Two dimensional (2D) Janus nanosheets are especially intriguing considering their interfacial properties as well as their ability to assemble into higher order and hybrid structures. In this research, we describe an approach to asymmetric functionalization of 2D nanosheets at large-scale through selective interfacial reactions using liquid crystal phases as templates. Several liquid crystal systems composed of surfactants, water and organic solvents were studied by birefringence imaging, cryo-TEM, small-angle X-ray scattering (SAXS) and small angle neutron scattering (SANS) to optimize the microstructures and stability for using as “nanoreactor” templates, and the surfactants included cationic, anionic, non-ionic and zwitterionic types. In comparison to interfacial reaction in a conventional biphasic system, the efficiency of interfacial reaction within the liquid crystal temples can tremendously increase by more than million times (in $>10^6$ order), enabling to scale up the synthesis of 2D Janus nanomaterials at industrial scale economically. Several samples of synthesized 2D Janus nanomaterials with different properties for different application have been demonstrated.

8:35 AM *EL05.15.03

Controlled Growth and Integration of 2D Semiconductors for High-Performance Electronics Minsu Seol, Junyoung Kwon, Minseok Yoo, Changhyun Kim, Huije Ryu, Eun-Kyu Lee and Kyung-Eun Byun; SAIT, Samsung Electronics, Korea (the Republic of)

2D semiconductors have received much interest as next-generation channel materials. The ultrathin nature of 2D semiconductors affords notable advantages, including enhanced electrostatic gate control and continued transistor scaling, which are pivotal for advancing electronic devices. In this talk, I am going to present our recent progress related with growth, characterization, and integration of 2D semiconductors. We have successfully grown up to 8-inch wafer-scale MoS₂ films on amorphous substrates through Metal-Organic Chemical Vapor Deposition (MOCVD). Furthermore, we have achieved the growth of single-crystalline MoS₂ on selected areas. To assess film quality, we have employed non-destructive characterization methods. Through optimized integration processes, we have demonstrated the effective fabrication of field-effect transistors (FETs) on 8-inch wafers, resulting in exceptional uniformity in electrical performance, with a success rate exceeding 90%. Statistical analyses of high-performance 2D FETs, with variations in channel length, will be presented to provide insights into their performance characteristics. Additionally, this talk explores the persisting challenges associated with materials growth and device fabrication in this field, paving the way for future advancements in 2D-semiconductor-based electronics.

9:05 AM *EL05.15.04

X-Ray Photoelectron Spectroscopy Study of 2D MoS₂/Oxide Dielectric Interface Manish Chhowalla; University of Cambridge, United Kingdom

The interface between two-dimensional transition metal dichalcogenide (2D TMDs) semiconductors and dielectric has not been as widely studied as the metal/2D TMD junction. The dielectric for 2D TMD devices must be thermodynamically and mechanically stable as well as being chemically inert. The band offset between the conduction and valence bands of the dielectric and 2D semiconductor should be at least 1eV. The 2D TMD/dielectric interface should be clean and free of defects. In this presentation, we present detailed synchrotron XOS study of 2D TMD and oxide interface. Specifically, we have studied the band offsets between MoS₂ and SiO₂, HfO₂, and ZrO₂ using XPS. We find that the dielectrics strongly dope the 2D MoS₂ with significant shift ($>1\text{eV}$) in the Fermi level. Our results provide insight into suitability of different dielectrics for 2D MoS₂ FETs.

9:35 AM EL05.15.05

Sensitivity Enhancement of CO₂ Sensors at Room Temperature based on CZO Nanorods Heterostructure Baktiyar Soltabayev¹, Yessimzhan Rajymbekov², Aidarbek Nuftolla², Amanzhol Turlybekuly¹, Gani Yergaliuly¹ and Almagul Mentbayeva²; ¹PI National Laboratory Astana, Kazakhstan; ²Nazarbayev University, Kazakhstan

Cobalt-doped ZnO (CZO) thin films were deposited on glass substrates at room temperature by RF magnetron sputtering of a single target prepared with ZnO and Co₃O₄ powders. Changes in crystallinity, morphology, optical properties, and chemical composition of the CZO thin films were investigated by varying sputtering power of 45 W, 60 W, and 75 W. All samples presented a hexagonal wurtzite-type structure with a preferential c-axis at the (002) plane along with a distinct change in strain values through X-ray diffraction patterns. Scanning electron and atomic force microscopy revealed a uniform and dense deposition of nanorod CZO samples with high surface roughness (RMS). Hall mobility and carrier concentration increased with the introduction of Co²⁺ ions into the ZnO matrix as seen from the Hall effect study. The gradual increase of applied power on the target source heavily affects the morphology of the CZO thin film, which is reflected in CO₂ sensing performance. The best gas response to CO₂ was recorded for CZO-60 W with a response of 1.45 for 500 ppm of CO₂. The distinguishing feature of the CZO sensor is its ability to effectively and rapidly detect CO₂ target gas at 27 °C.

9:40 AM EL05.15.06

Investigation of Graphene Oxide Using Transmission Electron Microscope: A Study of The Reduction Process Douglas S. Silva, Gustavo A. Viana, Jose M. Silva, Luiz C. Kretly, Tárcio A. Barros and Francisco C. Marques; State University of Campinas, Brazil

Several techniques have been used in the production of graphene, such as direct physical exfoliation of graphite and epitaxial growth of SiC surfaces [1, 2,3]. Regardless of the production process adopted, the resulting GO films are insulators with physical and chemical characteristics very different from those of pure graphene. Due to this, the implementation of processes capable of efficiently removing the presence of oxygen-containing functional groups is important to promote the properties of GO towards those of pure graphene. These processes are called “reduction” and the resulting sample “reduced GO” (rGO). Here we report a study of the reduction process using the transmission electron microscopy (TEM) technique. Variations in the electron energy loss spectroscopy (EELS) signal were also explored. It was observed that plasmon peaks, referring to sp² carbon bonds in crystalline structures, are more evident in the rGO sample compared to GO sample. The fine structure at the K edge of carbon shows difference in shape. The difference in the width, convolution and definition of the peaks can be directly linked to the density of states above the Fermi level. This fact indicates that the oxygen eliminated in the effusion spectra, which causes large variations in the electrical resistivity of the films, does not come from adsorbed water but from other sources, such as oxygen-containing functional groups, such as epoxy, carbonyl and carboxyl.

Acknowledgements:

BYD Energy Brazil, FAPESP and CNPq.

References:

- [1] K.S. Novoselov, A.K. Geim, S. V Morozov, D. Jiang, Y. Zhang, S. V Dubonos, I. V Grigorieva, A.A. Firsov, Science 306 (2004) 666–669.
- [2] C. Virojanadara, M. Syväjärvi, R. Yakimova, L.I. Johansson, A.A. Zakharov, T. Balasubramanian, Phys. Rev. B 78 (2008) 1–6.
- [3] M. Sprinkle, M. Ruan, Y. Hu, J. Hankinson, M. Rubio-Roy, B. Zhang, X. Wu, C. Berger, W.A. de Heer, Nat. Nanotechnol. 5 (2010) 727–31.

9:45 AM EL05.15.07

Use of Laser-Induced Graphene and Functionalized Magnetite Particles as Anchors in Electrochemical CA 15-3 Detection Devices Gabriela L. Araujo Bernal¹, Ramón Gomez-Aguilar² and Hugo Martinez-Gutierrez³; ¹Escuela Nacional de Ciencias Biológicas-IPN, Mexico; ²Unidad Profesional Interdisciplinaria en Ingeniería y Tecnologías Avanzadas-IPN, Mexico; ³Centro de Nanociencias y Micro Nanotecnologías-IPN, Mexico

Iron oxide particles have been used in in vitro diagnostics and theragnosis for nearly 40 years. Magnetite nanoparticles (MNPs) have become popular as supports for immobilizing biomacromolecules due to their magnetic properties, low toxicity, chemically modifiable surface, and high biomolecule loading capacity which promote constant ionic interaction. Coating magnetic nanoparticles with functional materials, such as silicon oxide (SiO₂), has been shown to improve their stability and enable the addition of various functional groups to their surface without altering their properties. The SiO₂ layer provides a chemically inert surface for the core nanomaterials in biological systems.

An ISFET, or Ion-Sensitive Field-Effect Transistor, is a type of field-effect transistor that measures ion concentration in a solution. It can be used as an immunobiosensor when combined with techniques like antibody or antigen immobilization to detect specific biomolecules such as proteins or antigens. The concentration of target biomolecules in a sample is recorded by measuring the variation of the electrical potential at the gate of the ISFET. The changes in potential are analyzed to establish a correlation between the potential change and the presence and concentration of specific biomolecules. The CA 15-3 cancer-associated antigen has been found in the serum of over 70% of patients with advanced breast carcinoma and in a small percentage of patients with non-breast malignancies. Detecting circulating levels of the CA 15-3 antigen may aid in distinguishing breast carcinoma from other dysplasias.

The upper limit of normal (ULN) for circulating CA 15-3 was set at 40 U/mL, as this threshold most adequately distinguished healthy subjects and patients with metastatic breast cancer. The levels of the antigen CA 15-3 in the serum of 500 patients with non-breast cancer, whose age ranged from 2 to 84 years were studied.

Among metallic particles, functional sable core-shell nanoparticles are promising candidates for electrochemical sensors as they can immobilize various materials of biological significance with proper chemical groups. Even if they show magnetic properties, they enable effective separation through external magnetic field induction. Magnetite, Fe₃O₄, is a prevalent iron oxide that can be converted into particles. They can be dispersed in proper solvents and have the potential to create atomic layers for example oxide surfaces (e.g., silicon or aluminum) with a suitable contact area, which can subsequently be functionalized by joining various bioactive molecules that hold high potential for use in various in vitro and in vivo applications. It is crucial to keep control over the synthesis conditions and surface functionalization of particles to achieve particles with specific dimensions, colloidal stability, and biological properties. Typically, the immobilization of peptides or proteins onto particle surfaces are conducted through the activation of 1-(3-dimethylaminopropyl)-3-ethylcarbodiimide-N-hydroxysuccinimide hydrochloride (EDC-NHS).

This work proposes immobilizing the CA 15-3 ELISA kit antibody using functionalized nanoparticles with a magnetite core and silicon oxide shell (F-NPs) with amine groups that diffuse through an immobilization platform (PI) of LIG. Stable groups are created on the functionalized particles to immobilize proteins. A reactive surface is generated by inserting various concentrations of glucose, which gives rise to an immune neutralization reaction (antigen-antibody) producing ionized species. These species are detected through an ISFET that was built on a flexible substrate and subjected to electrical potentials whose are measured between the drain, source, and gate contacts characterizing them by IV saturation curves. This process obtains a proportional relationship between the decay of the current on the device and the added glucose concentration.

9:50 AM EL05.15.08

Investigating The Influence of Multivalent Transition Metal Dopants and Capping Ligands on The Lateral Growth of Photo-Optical Cu₂MoS₄ 2D Nanostructures Using a Colloidal Method Sarika V. Chandoo and Richard A. Taylor; University of the West Indies, Trinidad and Tobago

2D transition metal dichalcogenides (TMDs) is a class of emerging materials due to their unique and unconventional properties which allows them to have a cohort of applications such as for photovoltaics and photoelectrochemical conversion. Of these, ternary TMDs are underexplored and herein, for the first-time metal-doped layered tetragonal copper molybdenum sulfide (CMS) nanostructures using a facile, economically feasible and inexpensive colloidal hot injection method were grown at relatively low temperatures of 100 and 140°C and short time of 1 hour. The morphology, structure, and optical properties of the nanostructures were analyzed by powder X-ray diffraction, high resolution transmission electron microscopy with energy dispersive X-ray analysis, X-ray photoelectron spectroscopy, Raman spectroscopy, UV-VIS absorption, steady-state and time-resolved and photoluminescence spectroscopy. We demonstrate that colloidal conditions involving fractions of oleic acid in combination with the main capping ligand oleylamine enable lateral growth of highly crystalline 2D CMS nanostructures as hexagonal shaped nanosheets and layered nanorods of approximate dimensions 17 nm and 69 nm respectively. In particular, metal doped nanostructures exhibit a correlation of metal ion fraction and particle morphology implicating impurity ions in lateral growth of high energy facets into larger domain 2D nanostructures. Overall, the data shows a correlation of structure, morphology, and stoichiometry on the optical properties such as the influence of point defects such as sulphur vacancies and dopant (Zn²⁺, Ni²⁺, Mn²⁺) substitutions and interstitials. Collectively, this study provides an avenue for the synthesis of ternary TMD 2D nanostructures primarily with shorter growth time and lower growth temperature and offer the opportunity to simply tailor the reaction conditions to afford materials with tunable properties for photovoltaic applications. Additional elements of the work entail examination of the dynamics of the growth of the 2D nanostructures using *in situ* X-ray characterization such as pair distribution function, small and wide-angle x-ray scattering and x-ray absorption spectroscopy to determine the influence of precursors, capping ligands and growth conditions on preferred edge facets. Such insights will be useful towards pinpointing specific growth factors for more targeted growth of these types of 2D nanostructures.

9:55 AM EL05.15.09

Longevity and Effectiveness of 2D-MoS₂ in Two-Terminal Devices: A Systematic Investigation Shkir Bin Mujib, Sonjoy Dey, Gurpreet Singh and Paul Owiredu; Kansas State University, United States

Two-dimensional (2D) transition metal dichalcogenides (TMDs) are strong candidates for continued scaling of transistors to improve the current Si-based technology and facilitate next-generation nanoelectronic devices such as sensors and field-effect transistors (FETs) due to their band structures and properties. Although countless published studies report the electrical properties of TMDs, many are not attentive to the testing environment or the samples' age, which we have found significantly impacts results. Herein, we utilize 2D TMDs fabricated via different top-down and bottom-up approaches, fabricate two electrode devices, and systematically investigate their longevity and effectiveness. We characterized and compared devices using IV measurements in ambient and inert conditions and found the stability of three months for the device kept at later conditions. As expected, the observed atmospheric and

aging effects have a more pronounced effect on thinner flakes. This work illustrates the importance of understanding the electrical testing environment and the impact of atmospheric aging on TMD materials.

SYMPOSIUM EL06

Complex Oxide Epitaxial Thin Films—From Synthesis to Microelectronics
April 23 - May 7, 2024

Symposium Organizers

Aiping Chen, Los Alamos National Laboratory
Woo Seok Choi, Sungkyunkwan University
Marta Gibert, Technische Universität Wien
Megan Holtz, Colorado School of Mines

Symposium Support

Silver

Korea Vacuum Tech, Ltd.

Bronze

Center for Integrated Nanotechnologies, Los Alamos National Laboratory
Radiant Technologies, Inc.

* Invited Paper

+ JMR Distinguished Invited Speaker

^ MRS Communications Early Career Distinguished Presenter

SESSION EL03/EL06/MT01: Joint Virtual Session
Session Chairs: Aiping Chen, Rodrigo Freitas and Eiichi Kondoh
Tuesday Morning, May 7, 2024
EL06-virtual

8:00 AM EL03/EL06/MT01.01

Exploring The Application of Hybrid DFTB-Molecular Mechanics Approach to Computing Optical Properties [Ruicheng Li](#), Gekko Budiutama, Keisuke Kameda, Sergei Manzhos and Manabu Ihara; Tokyo Institute of Technology, Japan

The Density Functional based Tight Binding (DFTB) method has seen a rise in adoption for materials modeling, as it permits electronic structure-level modeling of large molecules, interfaces, nanostructures, etc. with much smaller computational cost and similar accuracy when compared to Density Functional Theory (DFT) methods. The cost reduction in DFTB compared to DFT is achieved by the pre-parameterization of the elements of the Hamiltonian matrix as well as the repulsion potential between all pairs of atoms. However, parameterization for new systems with accuracies competitive with DFT in specific applications requires specialized manpower and large computational resources. This prevents the application of the DFTB method to systems for which it was not parameterized.

In our previous work (*J. Chem. Theory Comput.*, 19, 5189-5198 (2023)), a DFTB-molecular mechanics (DFTB-MM) approach was introduced to expand the applicability of DFTB by modeling the interactions of the missing Slater-Koster parameters with an interatomic interaction potential fitted with machine learning. We have shown that when interactions between the atoms do not critically affect key mechanisms of interaction, we can obtain structures and partial densities of states with a similar accuracy to full DFTB. This in principle allows the use of DFTB in systems where not all pairs of atoms have been parameterized.

Here, we further explore the capability of the DFTB-MM method to the calculation of optical properties with Time-Dependent (TD-) DFTB for the modeling of systems whose optical properties are of interest. TD-DFTB permits calculations that include a large number of excitations, which is required for systems with high densities of states, and would not be feasible with TD-DFT. In particular, we investigate interfacial charge transfer in systems such as TCNQ (tetracyanoquinodimethane) on TiO₂, whose spectra are sensitive to the computational approach. We show that key spectral features, in particular transitions that involve the interfacial charge transfer band, are similar in full DFTB and DFTB-MM, indicating that DFTB-MM is a viable approach also for optical properties.

8:15 AM *EL03/EL06/MT01.02

Braiding Lateral Morphotropic Grain Boundary in Homogeneous Oxides [Erjia Guo](#); Institute of Physics, Chinese Academy of Sciences, China

Interfaces formed by correlated oxides offer a critical avenue for discovering emergent phenomena and quantum states. However, the fabrication of oxide interfaces with variable crystallographic orientations and strain states integrated along a film plane is extremely challenge by conventional layer-by-layer stacking or self-assembling. In this talk, we will discuss the creation of morphotropic grain boundaries (GBs) in laterally interconnected cobaltite [1] and manganite [2] homostructures. Single-crystalline substrates and suspended ultrathin freestanding membranes provide independent templates for coherent epitaxy and constraint on the growth orientation, resulting in seamless and atomically sharp GBs. Electronic states and magnetic behavior in hybrid

structures are laterally modulated and isolated by GBs, enabling artificially engineered functionalities in the planar matrix. Using this method, we are able to create magnetic nanoislands with minimum size of ~35 nm in diameter, suggesting the highest possible areal density could reach upto ~ 400 Gbit/in² [3]. Our work offers a simple and scalable method for fabricating unprecedented innovative interfaces through controlled synthesis routes as well as provides a platform for exploring potential applications in neuromorphics, solid state batteries, and catalysis.

[1] S. R. Chen, et al., *Adv. Mater.* 35, 2206961 (2023).

[2] Y. Wang, et al., *Nano Res.* 16, 7829–7836 (2023).

[3] S. R. Chen, et al., *Adv. Funct. Mater.* 33, 2302936 (2023).

8:45 AM EL03/EL06/MT01.03

MoS₂/VO₂ Based Heterostructure Device for Highly Responsive Infrared Photodetection Malti Kumari¹, Basanta Rou^{1,2}, S.B. Krupanidhi¹ and Karuna K. Nanda^{1,3}; ¹Indian Institute of Science, India; ²Central Research Laboratory, Bharat Electronics, India; ³Institute of Physics, India

Vanadium oxide (VO₂) has aroused researchers' curiosity among the transition Metal Oxides (ZnO, TiO₂, Ga₂O₃, V₂O₅, SnO₂, CuO) because of its unique semiconductor-to-metal phase transition (SMT). VO₂ is an n-type semiconductor having room temperature bandgap of 0.5-0.7 eV. It undergoes a structural transformation from semiconductor monoclinic phase (low temperature) to metallic rutile phase (high temperature) at transition temperature T_c ~ 340 K exhibiting ultra-fast, fully reversible, first-order phase transition accompanied by a notable change in electronic and optical properties. Transition Metal Dichalcogenides (TMDs) have also been considerably explored due to their distinctive electronic and mechanical properties. Nowadays, TMDs (such as MoS₂, MoSe₂, SnS₂, In₂S₃, etc) are proving to be extremely promising materials because of having tunable bandgaps depending on the number of layers of the material, high carrier mobilities, and strong exciton effects. Attributed to the outstanding properties of 2D layered materials and transition Metal Oxides, these materials are well known to give ultrafast, self-biased, and broadband photodetection. In this work, we deposited VO₂ film on SiO₂ substrates by using Pulsed Laser Deposition (PLD). MoS₂ film was deposited on VO₂ film using PLD form MoS₂/VO₂ heterostructure. For MoS₂/VO₂/SiO₂ device, the responsivity was found to be 0.83A/W as compared to 4.42×10⁻⁴ A/W for VO₂/SiO₂ device at 595.83 mW/cm² power density using 1550 nm laser. Clearly, the MoS₂/VO₂/SiO₂ device shows higher photodetection and hence gives better performance than VO₂/SiO₂ device.

9:00 AM EL03/EL06/MT01.04

Epitaxial Strain Engineering of Monoclinic Bismuth Vanadate: A Path to Tailoring Optoelectronic and Photoelectrochemical Properties Erwin N. Fernandez^{1,2}, Daniel Grave³, Fatwa F. Abdi⁴ and Roel Van de Krol^{1,2}; ¹Helmholtz-Zentrum Berlin, Germany; ²Technische Universität Berlin, Germany; ³Ben-Gurion University of the Negev, Israel; ⁴City University of Hong Kong, China

Epitaxial strain engineering is a powerful tool to perturb the electronic structure of metal oxide photoabsorbers and to potentially improve its performance [1]. Little is known, however, as to the effects of epitaxial strain on monoclinic bismuth vanadate (m-BiVO₄), a transition metal oxide relevant to solar-to-fuels application. In this work, we contribute to the understanding on how epitaxial strain alters the BiVO₄ monoclinic lattice and the optoelectronic and photoelectrochemical properties of m-BiVO₄. We also reveal how the hydrostatic and deviatoric components of the strain tensor correlates with these properties. Epitaxial films of m-BiVO₄ deposited directly on yttrium-stabilized zirconia (YSZ) experiences volume-preserving deviatoric strains that modulate its Tauc bandgaps and polaronic photoluminescence emission [2]. Hydrostatic strains, on the other hand, seem to be more important for epitaxial BiVO₄ films deposited on more device-relevant indium tin oxide (ITO)/YSZ. For these fully epitaxial BiVO₄/ITO/YSZ films, compressive hydrostatic strains narrow the Tauc bandgaps and enhances the internal quantum efficiencies [3]. Epitaxial strain can thus be exploited to modulate the optoelectronic and PEC properties of BiVO₄.

[1] B. Yildiz, "Stretching" the energy landscape of oxides—Effects on electrocatalysis and diffusion, *MRS Bulletin*, 39 (2014) 147.

[2] E.N. Fernandez, D.A. Grave, R. van de Krol, F.F. Abdi, Strain-Induced Distortions Modulate the Optoelectronic Properties of Epitaxial BiVO₄ Films, *Advanced Energy Materials*, 13 (2023) 2301075.

[3] E.N. Fernandez, D.A. Grave, F.F. Abdi, R. van de Krol, *in preparation*.

9:15 AM EL03/EL06/MT01.05

Sub-1nm Wireless Local Interconnect and Photonic Millimeter Wave ULSI with the Optoelectronic Microwave CMOS Technology - Will The Cutoff Frequency and Clock Speed Races Resume? James Pan; American Enterprise and License Company, United States

Traditionally, CMOS is not considered a microwave nor light emitting device. Similar to laser or LED, and microwave devices, Photonic Millimeter Wave CMOS transistors are both light as well as microwave emitting devices. Ultra-low-resistance tunnel lasers, tunnel and avalanche millimeter wave diodes (in the drain region), avalanche photon sensors (in the well and channel regions) and MOSFET are fabricated as one integral transistor. When the MOSFET is on, all other devices are on. When the MOSFET is off, all other devices are also turned off. Potentially, CMOS may outperform these discrete lasers and microwave diodes for better quantum efficiency, reliability, and thermal stability.

Ever since AMD releases the 64-bits Athlon processor in around 2005-2006, the clock speed race for ASIC and processors has been almost stopped. Improvements of performance rely on parallel processing, multiple cores, or 3-dimensional packages. The limitation of clock speed is partially due to the RC and other delays, and electronic design and architecture, while silicon CMOS cutoff frequency may reach as high as 300GHz. With the laser millimeter wave CMOS technology, optical microwave computing may resume the races to extremely high clock speeds, with amplified bandwidth and wireless micro ULSI.

In modern societies, wireless tools, such as computers, printers, and cell phones, are replacing almost all the wired electronic tools. For RF ASICs and ULSI, typically there are many layers of backend metals, and wired local interconnects. Many of these metal wires can be eliminated by wireless designs, using new models simulated with the Photonic Microwave CMOS. The very large number (billions or even a trillion) and multiple layers of metal wires seen in ASICs and ULSI significantly retard the cutoff frequency, signal or clock speeds.

Using microwave photonic CMOS, transistor cutoff frequencies can be extended to beyond 300GHz and well into the Terahertz range. In this report, we will discuss the following:

Process integration and circuit design implementing microwave photonic CMOS to reduce the number of metal wires.

Powered optical waveguides that substantially increase the CMOS output current and speed.

Microwave computing and ASIC - using the polarized, filtered, and multiplexed technologies.

Micro-antenna designs and microwave filters for photonic microwave computing.

SRAM designs - how to design an ultra-fast microwave photonic SRAM for sub-1nm wireless processors.

CMOS VCSEL (Vertical Cavity Surface Emitting Laser) and Millimeter Wave CMOS - how to achieve 3D wireless and optical designs.

How to design logic gates with nonlinear optical materials and optical filters / polarizers.

How wireless microwave photonic CMOS and optical computing may resume the cutoff frequency and clock speed races for terahertz operations, by

replacing many of the metal wires with central micro antennas and microwave filters / polarizers.

We will also illustrate how to design wireless ASICs using negative-resistance tunnel and avalanche microwave CMOS (IMPATT, BARITT). Transferred electronic effects and photon-accelerated avalanche microwave generation significantly improve the CMOS speed and ASIC cutoff frequencies.

SESSION EL06.01: Epitaxial Growth—Strain, Defects and Interfaces I
Session Chairs: Aiping Chen and Megan Holtz
Tuesday Morning, April 23, 2024
Room 343, Level 3, Summit

10:30 AM *EL06.01.01

Synthesis of Electronic-Grade Quantum Heterostructures Chang-Beom Eom; University of Wisconsin--Madison, United States

Modern quantum materials are inherently sensitive to point defects, and require a new synthesis route to produce epitaxial oxide thin films and interfaces clean enough to probe fundamental quantum phenomena. The recent discovery of robust superconductivity at KTaO_3 (111) and KTaO_3 (110) heterointerfaces on KATaO_3 bulk single crystals offers new insights into the role of incipient ferroelectricity and strong spin-orbit coupling. Electronic grade epitaxial thin film platforms will facilitate investigation and control of the interfacial superconductivity and understanding the fundamental mechanisms of the superconductivity in KTaO_3 . The major challenge of research on KTaO_3 system is that it is difficult to grow high-quality KTaO_3 epitaxial thin films due to potassium volatility. Recently, we have developed the hybrid PLD method for electronic grade KTaO_3 thin film growth, which successfully achieves this by taking advantage of the unique capabilities of PLD to instantly evaporate Ta_2O_5 in a controlled manner and evaporation of K_2O to maintain sufficient overpressure of volatile species. We successfully synthesized heteroepitaxial KTaO_3 thin films on 111-oriented KTaO_3 bulk single crystal substrates with a SmScO_3 template by hybrid PLD, followed by a LaAlO_3 overlayer. Electrical transport data show a superconducting transition temperature of $\sim 1.35\text{K}$. We anticipate that the ability to synthesize high-quality epitaxial complex oxides such as KTaO_3 that contain volatile elements will provide a new platform for exploring new physics and technological applications arising from unique characteristics such as large spin-orbit coupling.

This work has been done in collaboration with Jieun Kim, Jungwoo Lee, Muqing Yu, Neil Campbell, Shun-Li Shang, Jinsol Seo, Zhipeng Wang, Sangho Oh, Zi-Kui Liu, Mark S. Rzchowski, Jeremy Levy.

11:00 AM EL06.01.02

Unconventional Quantum Oscillations in EuO/ KTaO_3 Heterointerface Km Rubi¹, Dumen Manish², Suvankar Chakraverty², Mun Chan¹ and Neil Harrison¹; ¹Los Alamos National Laboratory, United States; ²Institute of Nano Science and Technology, India

The coexistence of electric-field controlled superconductivity and spin-orbit interaction in two-dimensional electron gas (2DEG) based on complex oxides (e.g., SrTiO_3 and KTaO_3) hold great promise for advancement in spintronics and quantum computing. However, a comprehensive understanding of the electronic bands that give rise to the multifunctional character of these 2DEGs remains elusive. To address this, we recently investigated quantum oscillations in the magnetoresistance of a KTaO_3 -2DEG in high magnetic fields (60 T).

KTaO_3 is a 5d transition metal oxide, exhibiting a lighter effective mass of electrons and a stronger spin-orbit interaction at its conducting surface/interface than its counterpart SrTiO_3 [1-2]. A high-mobility spin-polarized 2DEG with the superconducting feature is discovered at the EuO/ KTaO_3 interface [3]. In this talk, I will present novel insights into the electronic states of the EuO/ KTaO_3 interface investigated through Shubnikov-de Haas (SdH) oscillations. Remarkably, we observed a progressive increase in cyclotron mass and oscillation frequency with the magnetic field, indicating the presence of non-trivial electronic bands [4]. Besides providing experimental evidence for topological-like electronic states in KTaO_3 -2DEG, these results shed light on the recent predictions of topological states in the 2DEG based on similar perovskite transition metal oxides.

References

- [1] K. Rubi *et al.*, npj Quantum Materials **5**, 1 (2020), King, P. D. C. *et al.* Phys. Rev. Lett. **108**, 117602 (2012).
- [2] K. Rubi *et al.*, Phys. Rev. Research **3**, 033234 (2021).
- [3] H. Zhang *et al.*, Phys. Rev. Lett. **121**, 116803 (2018), Liu *et al.*, Science **371**, 716 (2021).
- [4] K. Rubi *et al.*, arXiv:2307.04854 (2023).

Acknowledgement: We acknowledge support from the National High Magnetic Field Laboratory, supported by the National Science Foundation through NSF/DMR-1644779 and the State of Florida, and the US Department of Energy "Science of 100 Tesla" BES program.

11:15 AM EL06.01.03

High-Mobility Two-Dimensional Electron Gases based on Strain Engineered Ferroelectric SrTiO_3 Thin Films Ruchi Tomar¹, Tatiana Kuznetsova², Srijani Mallik¹, Luis M. Vicente-Arche¹, Fernando Gallego¹, Maximilien Cazayous³, Roman Engel-Herbert^{2,4} and Manuel Bibes¹; ¹Unité Mixte de Physique, CNRS, Thales, Université Paris-Saclay, France; ²Pennsylvania State University, United States; ³Laboratoire Matériaux et Phénomènes Quantiques, Université de Paris, France; ⁴Paul Drude Institute for Solid State Electronics, Leibniz Institute within Forschungsverbund Berlin eV, Germany

Two-dimensional electron gases (2DEGs) based on the quantum paraelectric SrTiO_3 display fascinating properties such as large electron mobilities, superconductivity and efficient spin-charge interconversion owing to their Rashba spin-orbit coupling.¹⁻³ However, such 2DEGs have almost exclusively been generated in SrTiO_3 single crystals, with the few attempts to replace crystals by heteroepitaxial SrTiO_3 thin films leading to low carrier mobilities. This is limiting the potential to integrate SrTiO_3 2DEGs in future devices as well as the possibility to introduce additional functionalities specific to SrTiO_3 thin films, such as strain-induced ferroelectricity. Here, we use oxide molecular beam epitaxy to grow high quality strain-engineered SrTiO_3 films that are ferroelectric up to 170 K. We then generate a 2DEG by sputtering a thin Al layer and demonstrate an increase in both the low and room temperature mobilities by up to factor of four compared to earlier literature. Furthermore, through Raman spectroscopy and magneto-transport measurements, we show that the ferroelectric character is retained after 2DEG formation. These results thus qualify our samples as ferroelectric 2DEGs up to temperatures well above previous results based on Ca- SrTiO_3 substrates ($\sim 30\text{K}$)⁴, opening the way towards ferroelectric 2DEGs operating at room temperature.

References :

1. M. Bibes, J. E. Villegas, and A. Barthelemy, Adv. Phys. **60**, 5 (2011).
2. H. Y. Hwang, Y. Iwasa, M. Kawasaki, B. Keimer, N. Nagaosa, and Y. Tokura, Nat. Mater. **11**, 103 (2012).
3. S. Varotto, A. Johansson, B. Göbel, L. M. Vicente-Arche¹, S. Mallik, J. Bréhin, R. Salazar, F. Bertran, P. Le Fèvre, N. Bergeal, J. Rault, I. Mertig & M.

Bibes, Nat. Commun., 13, 6165 (2022).

4. C. W. Rischau, X. Lin, C. P. Grams, D. Finck, S.Harms, J. Engelmayr, T. Lorenz, Y. Gallais, B. Fauqué, J. Hemberger, and K. Behnia, Nat Phys, 13, 643 (2017).

11:30 AM *EL06.01.04

Multifunctional Oxide-2DEGS for Spin-Charge Interconversion Agnès Barthelemy; Unité Mixte de Physique CNRS/Thales, France

Spin-charge interconversion in systems with spin-orbit coupling offers a new path for the generation and detection of spin currents of great potential for application in spintronics. The Rashba-type spin-orbit coupling linked to the spatial inversion symmetry breaking appearing in the two-dimensional electron gases (2DEG) formed at the interface between LaAlO₃ and SrTiO₃ [1] or by deposition of Al, Ta or Y on SrTiO₃ [2, 3], Ca:SrTiO₃ [4] or KTaO₃ [5] allows for very efficient spin to charge interconversion [1, 2, 6]. Recently, possibilities to further enlarge or control the functionalities of oxide-2DEGs have emerged. One approach relies on making the 2DEG ferroelectric by exploiting the large electric-field- or Ca-doping-induced ferroelectric character in STO, while the other is by inducing spin polarization in the 2DEG by depositing a magnetic layer on top of the 2DEG. Combining both strategies, multiferroic 2DEGs have been realized, opening an avenue for ferroelectrically controllable chiral spin textures in 2DEGs and providing a new playground for non-volatile spin-orbitronics and non-reciprocal physics. We will review our efforts to obtain such multifunctional 2DEGs [7, 8, 9, 10].

[1] E. Lesne et al., Nat. Mat. 15, 1261 (2016)

[2] D. C. Vaz et al., Nat. Mat. 18, 1187 (2019)

[3] L. M. Vincente Arche et al., Phys. Rev. Mat. 5, 064005 (2021)

[4] J. Bréhin et al., Phys. Rev. Mat. 4, 041002(R) 2020

[5] L. M. Vincente Arche et al. ; Adv. Mater. 33, 2102102 (2021)

[6] D.C. Vaz et al, Phys. Rev. Mater. 7, 071001 (2020)

[7] P. Noël et al.; Nature 580, 483 (2020)

[8] J. Bréhin et al.; Phys. Rev. Mater. 4, 041002 (2020)

[9] J. Bréhin et al.; Nat. Phys. 19, 823 (2023)

[10] G. Lazrak et al.; ArXiv. 2310.03348 (2023)

SESSION EL06.02: Epitaxial Growth—Strain, Defects and Interfaces II

Session Chairs: Ho Nyung Lee and Km Rubi

Tuesday Afternoon, April 23, 2024

Room 343, Level 3, Summit

1:30 PM EL06.02.01

The Influence of a Polar-Nonpolar Interfaces on Surface Segregation and Interface Termination: The Case of LaInO₃/BaSnO₃ Martina Zupancic¹, Wahib Aggoune², Alexandre Gloter³, Franz-Philipp Schmidt⁴, Georg Hoffmann⁵, Daniel Pfützenreuter¹, Anna Regoutz⁶, Zbigniew Galazka¹, Houari Amari¹, Oliver Bierwagen⁵, Jutta Schwarzkopf¹, Thomas Lunkenbein⁴, Kookrin Char⁷, Claudia Draxl² and Martin Albrecht¹; ¹Leibniz Institut fuer Kristallzuechtung, Germany; ²Humboldt-Universität zu Berlin, Germany; ³Université Paris-Saclay, France; ⁴Fritz-Haber-Institut, Germany; ⁵Paul Drude-Institut für Festkörperelektronik, Germany; ⁶University College London, United Kingdom; ⁷Seoul National University, Korea (the Democratic People's Republic of)

Interfacial polar discontinuities are a unique way to manipulate charge states at interfaces and to create novel two-dimensional electron states. One recent example for this phenomenon is the interface between AlN and GaN, where a discontinuity in the spontaneous polarization leads to the formation of two-dimensional electron (2DEG) or hole gas (2DHG). The polar-nonpolar interface between ABO₃ perovskite oxides offers new degrees of freedom to tune the interface states by the accessibility of mixed valence states. The accepted model explaining the formation of a 2DEG is based on the concept of charge transfer between the layers terminating the polar-nonpolar interface. To realize a 2DEG or a 2DHG control of the interface is a prerequisite. When growing the heterostructures, it is a commonly assumed that the surface termination of the non-polar layer controls the interface properties. In this contribution we provide experimental evidence demonstrating that the compensation of the polar discontinuity can drive surface segregation and consequently, control the interface termination.

We study the interface formation between the cubic wide band gap semiconductor BaSnO₃, and orthorhombic LaInO₃, by combining analytical scanning transmission electron microscopy (S)TEM, photoelectron spectroscopy and density functional theory (DFT) calculations. The samples were grown by plasma-assisted molecular beam epitaxy on DyScO₃ substrates at 835°C using a mixture of Sn and SnO₂ as a SnO source. While TEM experiments of BaSnO₃ bulk crystals and DFT agree that BaO is the most stable surface termination of BaSnO₃ over wide range of chemical potentials, we find that the interface between BaSnO₃ and LaInO₃ is terminated by SnO₂. This is consistent with the presence of a 2DEG, but also with our DFT calculations, which show this interface to be the most energetically favorable. STEM and PES show the presence of BaO on the surface of thin LaInO₃ films indicating Ba surface segregation. Based on our DFT calculations we find that the driving force for Ba segregation is the compensation of the polar discontinuity at the interface. This compensation is an effect of the gradual reduction of the octahedral tilt from the orthorhombic LaInO₃ to the cubic BaSnO₃ and the polar and non-polar distortions at the interface. In the case of the n-type SnO₂ interface, this leads to an expansion of the out-of-plane lattice spacing at the interface, which most efficiently compensates for the discontinuity. At the p-type BaO terminated interface it leads to non-polar distortions in the BaSnO₃, while polar distortions remain mainly in the LaInO₃, which compensate the polar discontinuity less efficiently. This shows that in perovskites in addition to surface energy and strain, the response of the system to compensate for the polar discontinuity must be considered as an additional driving force for segregation that can control the interface termination.

1:45 PM EL06.02.02

Orbital Engineering in Trigonal CrVO₃ Superlattices Simon Mellaerts¹, Wei-Fan Hsu¹, Claudio Bellani¹, Adolfo del Campo^{2,3}, Jesús López-Sánchez^{2,3}, Mariela Menghini⁴, Michel Houssa^{1,5}, Jin Won Seo¹ and Jean-pierre Locquet¹; ¹KU Leuven, Belgium; ²Instituto de Cerámica y Vidrio – Consejo Superior de Investigaciones Científicas, Spain; ³Instituto de Ciencia de Materiales de Madrid, Spain; ⁴IMDEA Materials Institute, Spain; ⁵IMEC, Belgium

Complex oxides form a fertile ground for a rich variety of functional phenomena that can be controlled upon doping, strain, interfacial charge transfer, confinement, and many others. Tuning these parameters often involves complex architectures such as heterostructures, superlattices or nanocomposites, with the ultimate aim to bring these quantum phenomena towards device applications. Moreover, many of the explored complex oxides are perovskites ABO₃ hosting the common high-temperature cubic structure, while materials with trigonal and hexagonal symmetry have remained largely unexplored.

In this work, we study corundum CrVO_3 ($\text{V}_2\text{O}_3/\text{Cr}_2\text{O}_3$) superlattices with symmetric periodicities ranging from 1 to 14 monolayers (ML) grown by oxide molecular beam epitaxy (MBE). By means of transport and optical spectroscopy, it is shown how the strong electron correlations in V_2O_3 are suppressed by quantum confinement. While infrared and Raman spectroscopy prove that this is accompanied by the absence of the monoclinic ground state at low temperature. By combining density functional theory (DFT) and Raman spectroscopy, it is shown that this dimensional crossover can be largely explained by a change in the orbital states dictating the phase diagram of V_2O_3 .

In a second part, we focus on the 1ML limit of superlattices, which can be considered as a new ordered ilmenite structure (R-3) and is predicted to be a ferromagnetic insulator by DFT methods. Furthermore, the capability to grow these corundum materials in a monolayer fashion unlocks a complete new set of ABO_3 materials with a trigonal symmetry (R3, R-3, R3c) where both A and B are transition metals. Finally, we also propose a way to grow these materials in the polar ordered (R3c) structure where the existence of two magnetic sublattices promises new high-temperature multiferroicity, motivating the search for novel ordered trigonal materials.

2:00 PM *EL06.02.03

Hot Complex Oxides--Turning up The Heat for Adsorption Control [Darrell G. Schlom](#)^{1,2,1}; ¹Cornell University, United States; ²Leibniz-Institut für Kristallzüchtung, Germany

It has long been known that molecular-beam epitaxy works best for materials that can be grown in an adsorption-controlled regime where thermodynamics automatically provides composition control. This is where MBE started—for GaAs and other compound semiconductors—and underlies its success for producing semiconductor films with the highest purity and mobility. The same holds for the growth of thin films of complex oxides by MBE, but the issue has been that it has not been possible to grow that many oxides in such a regime. In this talk I will describe how high substrate temperature opens the door to this desired growth regime for the growth of complex oxide thin films. Using a powerful CO_2 -laser capable of heating to substrate temperatures of 2000 °C, we have grown an increasing number of complex oxides in an adsorption-controlled regime by MBE. In this talk I will show multiple examples, but concentrate on the growth and characterization of (Ba,Sr)TiO₃ films grown by MBE at substrate temperatures in the 1200-1500 °C range.

2:30 PM EL06.02.04

Molecular-Beam Epitaxy of SrMoO₃ Films with Record Low Electrical Resistivity [Anna S. Park](#), Vivek Anil, Matthew Barone, Brendan D. Faeth, Tobias Schwaigert, Kyle Shen and Darrell G. Schlom; Cornell University, United States

Molecular-beam epitaxy of SrMoO₃ films with record low electrical resistivity

[Anna S. Park](#)^{1,2,*}, Vivek Anil^{3,*}, Matthew R. Barone^{1,2}, Brendan D. Faeth², Tobias Schwaigert^{1,2}, Kyle M. Shen^{3,4}, Darrell G. Schlom^{1,2,4,5}

¹Department of Materials Science and Engineering, Cornell University, Ithaca, New York 14853, USA

²Platform for the Accelerated Realization, Analysis, and Discovery of Interface Materials (PARADIM), Cornell University, Ithaca, New York 14853

³Department of Physics, Laboratory of Atomic and Solid State Physics, Cornell University, Ithaca, New York 14853, USA

⁴Kavli Institute at Cornell for Nanoscale Science, Ithaca, New York 14853, USA

⁵Leibniz-Institut für Kristallzüchtung, Max-Born-Str. 2, 12489 Berlin, Germany

*authors contributed equally

SrMoO₃ is the most conducting perovskite oxide (~5.1 at room temperature)^[1] about 40 times more conductive than SrRuO₃. This makes it an attractive material as a bottom electrode for perovskite heterostructures, particularly for the high-K dielectric Ba_xSr_{1-x}TiO₃^[2] Unfortunately, the synthesis of molybdates by traditional MBE is difficult due to the low vapor pressure of molybdenum.^[3] In contrast to elemental molybdenum, its oxide MoO₃ has a very high vapor pressure, which makes it a suitable candidate for a variant of MBE where a molecular beam of a metal oxide rather than its elemental counterpart is used.^[4] One challenge of using MoO₃ as a source, however, is its tendency to reduce to non-volatile MoO₂ in an ultrahigh vacuum environment. This challenge was recently circumvented by injecting a steady flow of oxygen directly into the crucible, enabling the growth of SrMoO₃ films using the stable flux of MoO₃ molecules emanating from a MoO₃ source in conjunction with the flux of strontium atoms emanating from a strontium source, both of which were contained within MBE effusion cells.^[5] The properties of oxide conductors often depend strongly on composition, where off stoichiometry can increase the room-temperature resistivity and dramatically decrease the residual resistivity ratio. This disorder is presumably responsible for the lowest room-temperature resistivity values obtained to date for SrMoO₃ films grown by conventional MBE and pulsed-laser deposition being 24 and , respectively,^[2,5] which is a factor of 5 higher than the best SrMnO₃ single crystals.^[1] Here we report the growth of SrMoO₃ in an adsorption-controlled regime where thermodynamics automatically controls film composition. To achieve this adsorption-controlled regime, substrate temperatures above 1100 °C are needed, which are unattainable in conventional oxide MBE systems. At the PARADIM thin film facility, we can reach substrate temperatures up to 2000 °C with a CO₂-laser substrate heater, allowing us to capitalize on the volatility of SrO at ~1100 °C. The resulting phase-pure epitaxial SrMoO₃ thin films are characterized by narrow rocking curves, room-temperature resistivities under and residual resistivity ratios higher than the best SrMoO₃ single crystal.^[1] We additionally map the band structure of these high-quality SrMoO₃ films with angle-resolved photoemission spectroscopy.

[1] I. Nagai, *et al. Appl. Phys. Lett.* **87**, 024105 (2005).

[2] H. Takatsu, *et al., J. Cryst. Growth* **543**, 125685 (2020).

[3] P. Saig, *et al., APL Mater.* **7**, 051107 (2019).

[4] K. Atkinson, *et al., APL Mater.* **8**, 081110 (2020).

[5] T. Kuznetsova, *et al., J. Vac. Sci. Technol. A* **41** (2023).

[6] A. Radetinac, *et al., Appl. Phys. Lett.* **105**, 114108 (2014)

2:45 PM EL06.02.05

Growth of Superconducting Sr₂RuO₄ Thin Films via Thermal Laser Epitaxy [Brendan D. Faeth](#)^{1,2}, Varun Harbola², Felix V. Hensling², Lena N. Majer², Y. Eren Suyolcu², Yu-Mi Wu², Hans Boschker³, Peter A. van Aken², Wolfgang Braun^{2,3} and Jochen Mannhart²; ¹Cornell University, United States; ²Max Planck Institute for Solid State Research, Germany; ³Epiray Gmbh, Germany

Thermal laser epitaxy (TLE) is a novel technique for thin film deposition which employs continuous wave lasers to simultaneously heat both the substrate and elemental sources. This laser heating approach allows for evaporation or sublimation of nearly all elements from the periodic table, ultrahigh substrate temperatures exceeding 2000 C, and broad compatibility with process gases at a wide range of pressures from UHV up to 1 Torr, among other benefits. As a result, TLE dramatically expands the parameter space available for thin film synthesis compared to existing epitaxy techniques. However, to date it has proven experimentally challenging to achieve simultaneous control of multiple laser based elemental sources with the flux stability and systematic fidelity necessary for the growth of ternary or multinary systems of interest such as complex oxides.

In order to establish the capabilities of TLE for the growth of such complex materials, we demonstrate here the successful epitaxial synthesis of several Ruddlesden–Popper phases of the Sr–Ru–O ternary oxide system via TLE. Near instant thermalization of both source elements and substrates from laser heating allows the process of thermodynamic phase control to be achieved rapidly during film deposition without the need for physical shuttering of sources. Additionally, we find that the “n=1” phase Sr₂RuO₄ can be reliably synthesized at substrate temperatures in excess of 1200 C and in a background environment of pure molecular oxygen, within an adsorption-controlled growth window that is inaccessible to conventional MBE approaches. We show that Sr₂RuO₄ films grown under these conditions demonstrate extremely high structural, electronic, and chemical quality, as evidenced by the appearance of superconductivity at relatively high critical temperatures. In particular, the higher growth temperatures and elemental source fluxes afforded by laser heating allow us to achieve phase pure 214 without higher-N intergrowths typically observed in MBE-grown films, and growth rates more than 10 times faster than MBE. A detailed accounting of the experimental approach, growth thermodynamics and film characterization will be discussed.

This work not only demonstrates the feasibility of TLE for the synthesis of high-quality complex oxide thin films, but also suggests new routes to achieving thin film growth in other materials systems that remain as-yet inaccessible to conventional epitaxy techniques.

3:00 PM BREAK

3:30 PM EL06.02.06

Fe Substitution Suppresses Oxygen Vacancy Formation and Stabilizes High-Valence Ni in Epitaxial La_{0.5}Sr_{0.5}Ni_{1-x}Fe_xO_{3.6} Thin Films Le Wang¹, Bethany Matthews¹, Xu He², Mark Bowden¹ and Yingge Du¹; ¹Pacific Northwest National Laboratory, United States; ²Université de Liège, Belgium

Recent discovery of superconductivity in Nd_{0.8}Sr_{0.2}NiO₂ has inspired further exploration of nickelates to gain insights into the origins of high-temperature superconductivity. However, the synthesis of Sr- or Ca-doped nickelate thin films is challenging due to the instability of high-valence Ni and the competition between perovskite and Ruddlesden–Popper (RP) phases. Our recent study revealed that Sr doping in LaNiO₃ thin films significantly reduces the Ni valence from Ni³⁺ to Ni²⁺ and results in the formation of numerous RP phases as the Sr doping level increases from 0% to 100%. Furthermore, DFT simulations on the La_{1-y}Sr_yNiO_{3.6} perovskite structures indicated a substantial decrease in the oxygen vacancy formation energy from 2.96 to 1.85 eV as y varies from 0 to 0.5. In our current work, we synthesized a series of epitaxial La_{0.5}Sr_{0.5}Ni_{1-x}Fe_xO_{3.6} (LSNFO) thin films on LSAT(001) substrates using oxide MBE. We found that partial Fe substitution for Ni in La_{0.5}Sr_{0.5}NiO_{3.6} significantly enhances the structure quality and stabilizes the perovskite structure. Ni L-edge XAS results reveal an increase in the Ni valence of LSNFO films, approaching Ni³⁺ as x increases from 0 to 0.5. At x = 0.75, the Ni valence is even higher than Ni³⁺. This is in contrast to the LaNi_{1-x}Fe_xO₃ (LNFO) system (without Sr), where the average Ni valence decreases with increasing Fe content due to charge transfer from Fe to Ni. STEM measurements confirm that the x = 0.75 sample remains in the perovskite phase but exhibits lots of RP faults and defects. On the other hand, Fe L-edge XAS results indicate that films of all Fe content show a nominally higher Fe oxidation state than a LaFeO₃ (Fe³⁺) reference. In-plane transport measurements demonstrate that the resistivity increases with Fe content in the LNFO system, but decreases initially in the LSNFO system, reaching the lowest value at x = 0.375, before rising again with x greater than 0.375. The metal-insulator transition in the LSNFO system strongly depends on Fe content, increasing with x, similar to the LNFO system. Further theoretical investigations are necessary to elucidate the influence of Fe doping on the electronic structure of the LSNFO system. In summary, these findings provide valuable insights into the design of perovskite structures featuring high-valence Ni and Fe, crucial for developing effective electrocatalysts for water splitting, as well as the creation of advanced electronic devices for solid oxide fuel cells.

3:45 PM EL06.02.07

Metal-Insulator Transition and Novel Ground States in Epitaxially Strained SmBaMn₂O₆ Thin Films Yorick Birkholzer¹, Anna S. Park^{1,1}, Noah Schnitzer¹, Evan Krysko¹, Jacob Steele¹, Hebatalla Elnaggar², Jelle Ruiters³, Koen Draijer⁴, Masoud Lazemi⁴, Qijun Che⁴, Shigeki Yamada⁵, Taka-hisa Arima⁶, Frank de Groot⁴, David Muller^{1,1,1} and Darrell G. Schlom^{1,1,7}; ¹Cornell University, United States; ²Sorbonne Université, France; ³University of Twente, Netherlands; ⁴University of Utrecht, Netherlands; ⁵Yokohama City University, Japan; ⁶University of Tokyo, Japan; ⁷Leibniz-Institut für Kristallzüchtung, Germany

For the realization of the next generation of fast, energy-efficient nanoelectronics, there is a great need for new materials whose electrical and optical conductivities can be sensitively tuned between high (on) and low (off) states by altering a thermodynamic control parameter such as strain or temperature. Unfortunately, most materials are either metallic or insulating and their conductivities cannot be changed substantially. Materials exhibiting a metal-insulator transition (MIT) above room temperature are quite rare, limiting their applicability in devices.

One noteworthy example of such a material is the A-site layer-ordered double perovskite SmBaMn₂O₆. While its synthesis in bulk form was reported by Yamada *et al.* [1], the successful growth of SmBaMn₂O₆ thin films remained elusive for over a decade. Here, we demonstrate the growth of untwinned epitaxial thin films of phase-pure SmBaMn₂O₆ on various single-crystalline oxide substrates using molecular-beam epitaxy (MBE), exploring a wide range of tensile to compressive biaxial strains. The latter has been predicted to host a different ground state based on first-principles calculations by Nowadnick *et al.* [2].

To stabilize the A-site layer-ordered double perovskite phase, we employ a two-step approach as originally described by Millange *et al.* for LaBaMn₂O₆ bulk crystals [3]. The key elements are, first, a high-temperature synthesis step of a brownmillerite-like, oxygen-deficient precursor, and second, a topotactic oxidation at low temperature. Notably, the former requires temperatures higher than 1100 °C that are unattainable in conventional oxide MBE systems. In this study, we utilize a recently installed, high-power CO₂-laser-based substrate heater at the PARADIM user facility at Cornell University, which allows growth temperatures up to 2000 °C.

Ongoing efforts entail the comprehensive investigation of the structural and spectroscopic properties of epitaxial SmBaMn₂O₆ thin films as a function of temperature and strain. To this end, we are employing an ensemble of X-ray, optical, and electrical transport techniques, alongside scanning transmission electron microscopy and electron energy-loss spectroscopy. Our aim is to elucidate potential hidden ground states and coupled structural, magnetic, and electronic phase transitions in this MIT compound.

References:

- [1] Yamada, Maeda, Arima, “Successive Electronic Transitions and Anisotropic Properties in a Double-Perovskite SmBaMn₂O₆ Single Crystal”, *J. Phys. Soc. Jpn.* **2012**, 81, 113711
- [2] Nowadnick, He, Fennie, “Coupled structural distortions, domains, and control of phase competition in polar SmBaMn₂O₆”, *Phys. Rev. B* **2019**, 100, 195129
- [3] Millange, Caignaert, Domengès, Raveau, Suard, “Order-Disorder Phenomena in New LaBaMn₂O_{6-x} CMR Perovskites. Crystal and Magnetic Structure”, *Chem. Mater* **1998**, 10, 1974-1983

4:00 PM *EL06.02.08

Structure and Properties of Low Dimensional Epitaxial Oxides; Interfaces and Superlattices [Gertjan Koster](#)^{1,2}; ¹University of Twente, Netherlands; ²MESA+ Institute for Nanotechnology, Netherlands

In complex oxide materials the occurrence of ferroelectric, ferromagnetic or other properties are for the most part determined by the detailed (oxygen) coordination of metal cations. More specifically, in the case of perovskite-type materials ABO_3 , where A and B are metal cations, by the BO_6 octahedral orientations and rotations. At interfaces in epitaxial oxide hetero structures, for example magnetic junctions or capacitive structures, this oxygen sub-lattice is found to be different from its bulk counterpart.

I will briefly introduce the status of the often-used technique to fabricate epitaxial layers, 'atomically controlled PLD', as well as give a few examples of oxygen sub-lattice and interface engineering achieved by controlled thin film parameters such as, composition, digital thickness variation, polar discontinuous interfaces or the insertion of oxide buffer layers that influence the perovskite-type BO_6 sub-lattice or related structures. I will further elaborate on the effects of such thin film parameters on the structure and properties of various model systems that have been subsequently studied by in situ characterization techniques, high resolution scanning transmission electron microscopy. More practically, often-encountered problems due to dead-layer effects and interfacial issues when integrating oxides with technical platforms such as Si or GaN, will be discussed.

SESSION EL06.03: Poster Session

Session Chairs: Aiping Chen, Woo Seok Choi and Megan Holtz

Tuesday Afternoon, April 23, 2024

Flex Hall C, Level 2, Summit

5:00 PM EL06.03.01

Lithium Incorporation in (111)NiO Epitaxial Layers Grown by Pulsed Laser Deposition Technique [Bhabani P. Sahu](#), Santosh K. Yadav, Simran Arora and Subhabrata Dhar; India Institute of Technology Bombay, India

Wide bandgap oxides such as ZnO , Ga_2O_3 and In_2O_3 have tremendous potential in UV-optoelectronics, yet the unintentional generation of certain donor type of defects in the film during growth make it challenging to achieve stable p-type doping in these materials. Nickel oxide (NiO) is a wide bandgap semiconductor of bandgap ranging from 3.6 - 4 eV. It is one of the few oxide semiconductors that exhibits stable p-type conductivity and antiferromagnetic properties with Neel temperature of 525K. The material also has high chemical and thermal stability. All these characteristics have made NiO a potential candidate for wide range of device applications such as exchange bias systems, field effect transistors, transparent hole conducting films, spintronics, UV-photodetectors and UV-LEDs. It has to be noted that stoichiometric NiO is an insulator, and p-type conduction in the film can be ascribed to the presence of nickel vacancies. However, controllable p-type doping with native defects is difficult to accomplish due to the formation of other unintentional compensating defects in the film. Intentional doping with monovalent atoms such as lithium will be interesting to explore. Keeping in mind that epitaxial films will give better device performance, there are efforts to grow epitaxial layers of NiO on different substrates such as c-sapphire, MgO and yttria-stabilised zirconia. In fact, the growth of NiO films with high epitaxial qualities have been reported by various techniques such as pulsed laser deposition (PLD), mist chemical vapour deposition, RF magnetron sputtering and molecular beam epitaxy.

Here, we study the incorporation of Li in (111) NiO epitaxial layers grown by PLD technique on c-sapphire substrates as a function of growth conditions. The structural, morphological, electrical and optical properties of the films have been systematically investigated. It has been found that the crystalline quality of these films deteriorates as the growth temperature is lowered. Surface morphology of the films, studied by atomic force microscopy (AFM) and field emission gun secondary electron microscopy (FEGSEM) shows smooth and continuous nature of the films with surface roughness lying between 0.4 - 1.4 nm. It has been found that the conductivity of the layers increases as the growth temperature is decreased. The enhancement of conductivity has been ascribed to the increase in density of nickel vacancy with the reduction of temperature. The investigation further suggests that there is a miscibility limit of Li in NiO. Li-clusters are detected in the films beyond a critical concentration of lithium. Further, it has been found that lithium inclusion results in hydrostatic tensile strain in the NiO lattice leading to the reduction of the bandgap. The study also shows that Li incorporation, which has also been verified by secondary ion mass spectroscopy (SIMS) and x-ray photoelectron spectroscopy (XPS), improves the electrical conductivity of the layers.

5:00 PM EL06.03.02

Potentiometric Detection of Serum Creatinine Utilizing Lead Dioxide and Carbon Nanotubes in a Single-Enzyme Reaction [Sung Min Jeon](#), Dayeong Choi, Han Been Lee and Gi Hun Seong; Hanyang University, Korea (the Republic of)

Creatinine (CRE) serves as the end product of creatine, responsible for energy release in skeletal muscle. The baseline concentration of serum creatinine (Scr) typically ranges from 45 μM to 90 μM in females and 60 μM to 110 μM in males. Elevated Scr levels are commonly utilized in diagnosing acute kidney injury. Ongoing research focuses on developing reliable techniques for estimating Scr due to its critical role as a biomarker of significance. The Jaffe reaction, a colorimetric method utilizing picric acid, has traditionally been employed for clinical analysis of creatinine (CRE). However, this method presents several drawbacks, including the need for pH adjustment, interference issues, and, notably, the toxicity and explosiveness of picric acid. A prominent trend in CRE detection involves electrochemical enzyme sensors, offering enhanced sensitivity and selectivity. The inclusion of creatinine deiminase (CD) in the enzymatic approach addresses the aforementioned challenges, thereby improving sensor performance and selectivity. In this enzymatic method, CD reacts with CRE to produce NH_3 , subsequently converted to NH_4^+ and OH^- in an aqueous solution. The NH_4^+ ion selective sensor and pH sensor then measure the concentration of CRE.

Single-walled carbon nanotubes (SWCNTs) are widely acknowledged for their outstanding electrical properties, characterized by high carrier mobility and current-carrying capacity, coupled with impressive chemical, thermal, and mechanical attributes. Surface modification techniques can be applied to introduce diverse functional groups on the SWCNT surface, enhancing their suitability for various applications. The incorporation of metal oxide deposits can impart electrical, electrochemical, and biocompatible properties, making them valuable in sensor manufacturing. Among the diverse applications, electrochemical pH sensors stand out, and metal oxide modification presents several advantages. These include notable sensitivity, rapid response times, prolonged operational lifespan, minimal interference with other ions, cost-effectiveness, ease of maintenance, and adaptability for miniaturization in flexible systems. While various metal oxide pH sensors such as IrO_2 , RuO_2 , TiO_2 , WO_3 , and SnO_2 have been reported in recent years, their production often involves intricate and high-temperature processes. Lead dioxide (PbO_2) emerges as a noteworthy choice for pH sensors due to its excellent electrochemical properties and straightforward fabrication method. However, PbO_2 -based pH sensors may exhibit deficiencies in oxygen or an excess of lead within the PbO_2 , potentially impacting electrochemical reactions.

In this investigation, we produced a thin film of lead dioxide deposited on carbon nanotubes (PbO_2/CNT) and developed a PbO_2/CNT ion-selective electrode ($\text{PbO}_2/\text{CNT}/\text{ISE}$). These sensors served as highly sensitive potentiometric biosensors for CRE, capitalizing on the one-step selective conversion of creatinine by creatinine deiminase. We conducted the detection of OH^- and NH_4^+ in an aqueous solution, generated through an enzymatic reaction, utilizing PbO_2/CNT as a pH sensor and $\text{PbO}_2/\text{CNT}/\text{ISE}$ as an NH_4^+ selective electrode. The obtained results reveal a remarkable sensitivity of -75.56 mV

$\log[\text{CRE}]^{-1}$ and 64.62 mV $\log[\text{CRE}]^{-1}$, with a calculated limit of detection of 0.06 μM and 0.13 μM , respectively, within the range of 10 to 400 μM . A selectivity test demonstrated robust discrimination against interfering materials in human serum, and the repeatability and long-term stability of our sensors were confirmed, indicating their high-level stability. Furthermore, recovery tests for CRE concentrations (10, 25, 50, 70 μM) in spiked human serum yielded results of 104%, 98%, 103%, and 96% for PbO_2/CNT , and 104%, 92%, 110%, and 97% for $\text{PbO}_2/\text{CNT}/\text{ISE}$. These findings underscore the reliability and reproducibility of our sensors in detecting CRE for clinical applications.

5:00 PM EL06.03.03

High Performance of Ferroelectric Synaptic Device in $\text{Hf}_{0.7}\text{Zr}_{0.3}\text{O}_2$ (HZO)/ $\text{La}_{0.7}\text{Sr}_{0.3}\text{MnO}_3$ (LSMO)/ SrTiO_3 (STO) Heterostructure by Optimizing Defect-Mediated Ferroelectric Switching Dynamics Hojin Lee¹, Joonbong Lee¹, Hyungseok Kim², Kyungwho Choi³, You Seung Rim¹ and [Taekjib Choi](#)¹; ¹Sejong University, Korea (the Republic of); ²Korea Institute of Science and Technology, Korea (the Republic of); ³Sungkyunkwan University, Korea (the Republic of)

High-performance artificial synaptic devices with linear synaptic weight and high precision are in high demand for hardware neural network (HNN) implementation. HF-based ferroelectric memristor has robust stable non-volatile analog resistive switching driven by its gradual polarization reversal. However, the high linearity and precision of the synaptic weight update are required to improve the accuracy of the neuromorphic chip application. Here, we demonstrate the high performance of ferroelectric synaptic device in $\text{Hf}_{0.7}\text{Zr}_{0.3}\text{O}_2$ (HZO)/ $\text{La}_{0.7}\text{Sr}_{0.3}\text{MnO}_3$ (LSMO)/ SrTiO_3 (STO) heterostructure, showing the high linearity ($\alpha=0.5$), effective multiple conductance states (> 40), and low cycle-to-cycle variation (2.06%). The synaptic characteristics of the device are dominantly attributed to the inhomogeneous domain nucleation, ultimately affecting the precision and linear weight update achievable in continuous polarization switching. As an artificial synapse, experimental results with electrical pulse modulation closely mimic the neuro-inspired signal process dependent on spike timing and spike rate. These results supposed that oxygen vacancy engineering in ferroelectric synaptic devices is a powerful approach to improving effective precision and overcoming the limitations nonlinear synaptic behavior for the implementation of HNN. In addition, when applied to a hardware neural network with a crossbar array (20X20), the recognition accuracy of MNIST handwriting data was recorded as 94.8%.

Acknowledgments This work was supported by the National Research Foundation of Korea (NRF) grant funded by the Korea government(MSIT) (NRF; Grant Mo. NRF-2021R1A2C2010781).

5:00 PM EL06.03.04

High-Resolution Uncooled Detector of Thermal Radiation with Resistivity Engineering [Yuhang Cai](#) and Junqiao Wu; University of California, Berkeley, United States

Uncooled infrared bolometers have become the technology of choice for applications such as thermography, firefighting, and night vision. These microbolometers detect thermal radiation from an object based on the Stefan–Boltzmann law with a thermal sensitivity, named as noise-equivalent differential temperature (NEDT). Existing methods to advance NEDT of the uncooled detectors are focused on the engineering side, with the efforts approaching the end of the roadmap. In this work, we take a distinct approach on the material side and improve the key parameter, known as temperature coefficient of resistance, by 3 times over a wide temperature range. The abrupt change of resistance comes from the metal-insulator transition of vanadium dioxide while the broad working temperature range is realized by creating a gradient-doped tungsten-doped vanadium dioxide where the tungsten fraction is judiciously graded across a thickness comparable to real products.

5:00 PM EL06.03.05

Effects of Temperature on Ruthenium Oxide Thin Films Using Pulsed Laser Deposition [Tyffani Royal](#); North Carolina Agricultural and Technical State University, United States

Within this report, experiments were conducted to determine what effects temperature has on thin film composition, crystalline orientation, and roughness. Ruthenium Oxide (RuO_2) thin films were grown using pulsed laser deposition on substrates at different temperatures (100C, 200C, 300C). The properties of the thin films were observed using X-Ray diffraction, scanning electron microscopy, and atomic force microscopy measurements. It has been observed that the increase in temperature causes an increase in density, and roughness. The RuO_2 thin films made at 500C are able to form on a substrate with strong crystalline orientation. This information can become vital in how thin films are made for their intended purpose.

5:00 PM EL06.03.06

Pulsed Laser Deposition and Characterization of Titanium Nitride and Oxynitride Thin Films for Alternative Energy Applications [Brooke Smith](#)¹, Jacob Som^{1,2} and Dhananjay Kumar¹; ¹North Carolina A&T, United States; ²Cornell University, United States

TiN_xO_y (TiNO) thin films have been grown using a pulsed laser deposition process with a wide range of x and y realized by varying the oxygen pressure. X-ray diffraction, scanning electron microscopy, and atomic force microscopy measurements have been carried out to evaluate the phase purity and microstructures of TiNO films. The electrocatalytic activities of these films were performed in KOH solution for oxygen evolution reaction. It has been observed that the electrocatalytic activities of these films depend on the growth conditions. Films grown under low oxygen partial pressure (5 mTorr) showed an overpotential of 340 mV to achieve a current density of 10 mA/cm², whereas the TiNO film grown under high oxygen partial pressure of 25 mTorr displayed the lowest overpotential of 290 mV at the same current density. This range of overpotential observed in this study is among the lowest values reported for any oxynitride systems.

5:00 PM EL06.03.07

Quantifying Oxygen Diffusion Rates at The Nanoscale in Epitaxial SrTiO_3 Films [Keon Sahebkar](#), Nathan Arndt, Sihang Hui, Brooke Lastinger, Morgan Congdon and Ryan Need; University of Florida, United States

Oxygen ion migration is an increasingly viable route to control electronic and magnetic phase transitions in nanoscale oxide thin films and harness those phase transitions for next-generation, energy-efficient electronics [1]. Nanoscale oxygen migration is central to the operation of promising emerging information technologies like resistive random-access memory and magnetoelectric memory [2,3]. Heterostructure design elements like strain, interface symmetry, and layer stacking can all control the ion diffusion rates and energy barriers that underpin the operation of these devices. However, due to the difficulty of measuring small concentrations of oxygen ions (~1 at%) moving nanoscale distances, we do not have a framework for how these heterostructure design elements can be tuned to improve and optimize device functionality. This project aims to address this by developing a methodology to quantitatively determine oxygen diffusion rates and migration energy barriers in nanoscale thin films using reflectometry techniques.

Nanoscale “oxide diffusion couples” are fabricated from epitaxially grown SrTiO_3 (STO) and a sputtered metal cap, then annealed in vacuum to drive oxygen from the epitaxial oxide layer into the metal. X-ray reflectometry (XRR) scans are taken before and after vacuum annealing and used to establish an oxygen concentration depth profile from changes to the interface roughness between the STO and metal layers. These concentration profiles are then fit to

known diffusion couple solutions to Fick's Second Law and used to calculate an oxygen diffusion coefficient for each annealing study [4]. This poster will further explain our proposed methodology and preliminary results.

References

- [1] F. Gunkel, et al., *Appl. Phys. Lett.* 116 (2020) 120505
- [2] F. Zahoor, et al., *Nanoscale Res. Lett.* 15 (2020) 90
- [3] M. Nichterwitz, et al., *APL Mater.* 9 (2021) 030903
- [4] S. Brennan, et al. *Metall. Mater. Trans. A*, 43 (2012) 4043

5:00 PM EL06.03.08

Topochemical Synthesis and Optical Properties of Epitaxially Strained SrCo(O,F)_{3-x} Thin Films Tessa D. Tucker, Zongmin Yang, David Bugallo and Steven J. May; Drexel University, United States

Transition metal oxides (TMOs) are attractive in materials science for their structural versatility and property tunability. This tunability can be further expanded by incorporating a second anion, such as F or N, to alter the metal-anion bond ionicity or the metal charge density. In this work, we report on vapor-based fluorination of epitaxial SrCoO_{2.5} films. The films are grown by oxygen-assisted molecular beam epitaxy (MBE) under conditions that result in the brownmillerite structure. Topochemical fluorination was conducted on the as-grown films at 200°C using a quartz tube furnace under Ar gas flow with poly(vinylidene fluoride) (PVDF) as the fluorine source. Fluorination reactions were performed on SrCoO_{2.5} films synthesized on STO, LAO, LSAT and GSO substrates to understand the impact of substrate-induced strain on fluorine incorporation. Fluorine incorporation was confirmed via depth-dependent elemental analysis performed with X-ray photoelectron spectroscopy (XPS). Fluorine incorporation results in an expansion of the *c*-axis parameter as determined by X-ray diffraction. Optical absorption spectra, obtained through spectroscopic ellipsometry, reveals a blue-shift of the low-energy absorption edge by 0.1 - 0.3 eV depending on the substrate. This result is attributed to a widening of the band gap due to the increased ionicity of the Co-anion bonds.

This work was supported by the National Science Foundation under grant CMMI-2001888.

5:00 PM ^EL06.03.09

High-Throughput Combinatorial Approach to The Synthesis of a Lead-Free Relaxor Ferroelectrics System Di Zhang¹, Katherine Harmon², Michael Zachman³, Ping Lu⁴, Doyun Kim⁵, Qing Tu⁵ and Aiping Chen¹; ¹Los Alamos National Laboratory, United States; ²Argonne National Laboratory, United States; ³Oak Ridge National Laboratory, United States; ⁴Sandia National Laboratories, United States; ⁵Texas A&M University, United States

Developing novel lead-free nontoxic ferroelectric materials is crucial for the next-generation microelectronic technologies in regard to clean energy and environmental sustainability. However, materials discovery and properties optimization have usually been a frustratingly slow process due to the limited throughput in traditional synthesis methods. In this work, using a high-throughput combinatorial synthesis approach, we fabricated lead-free ferroelectric superlattices and solid solutions of (Ba_{0.7}Ca_{0.3})TiO₃ (BCT) and Ba(Zr_{0.2}Ti_{0.8})O₃ (BZT) phases with compositional gradients. The high-resolution X-ray diffraction and scanning transmission electron microscopy (STEM) revealed the good film quality and well-controlled compositional gradient throughout the samples. Ferroelectric and dielectric properties identified the "optimal property point" achieved at the morphotropic phase boundary (MPB) with the composition of BZT-52BCT. The displacement vector maps revealed the tunable ferroelectric domain sizes by varying the single layer thickness of the {BCT/BZT}_n superlattices. This high-throughput synthesis approach can be applied to many other materials systems to expedite novel materials discovery and property investigations.

5:00 PM EL06.03.10

Tailoring Dielectric Permittivity in Gd_xCe_{1-x}O_{2-δ} Films by Ionic Defects Alessandro Palliotto, Nini Pryds and Daesung Park; Danmarks Tekniske Universitet, Denmark

Fluorite-based crystalline materials have the general chemical formula AX₂ (A = Ca, Hf, Zn, Zr, Ce, while X = F, O) and find wide application in fuel cells, electroceramics, oxygen sensors and exhaust reduction systems. Despite their rather simple and prototypical crystallographic structure, "fluorites" remain the subject of much academic research and unexpected scientific discoveries [1], such as ferroelectricity in HfO₂-based thin films or large electromechanical coupling in polycrystalline Gd-doped CeO_{2-x} (CGO) ceramics/films [2]. Moreover, a recent discovery has demonstrated the potential to induce significant piezoelectric effects in nominally centrosymmetric CGO by breaking symmetry through the control of ionic defects, specifically oxygen vacancies (V_O) [2]. It was found that the motion and redistribution of defects induced by an electric field results in notable changes in the dielectric permittivity of the system, which are closely associated with the magnitude of the electromechanical effects [3]. Hence, controlling the dynamic V_O in the CGO and similar oxides is key for achieving significant permittivity and electromechanical effects. In this work, we effectively tuned the V_O contents in epitaxial CGO(001) films grown on Nb-doped SrTiO₃(001) single crystal using pulsed laser deposition. Our findings show that the control of V_O contents in the epitaxial films is highly limited, regardless of the oxygen environment (oxygen partial pressure, P_O), during high-temperature growth (e.g., T = 700 °C). In contrast, an effective control of V_O contents in the epitaxial films was achieved by utilising a two-step growth technique. Subsequently, we noted a strong variation in the V_O content in the engineered CGO films and the emergence of significant apparent dielectric permittivity, thus enabling the generation of substantial electromechanical coupling and piezoelectric effect.

Reference

- [1] U. Schroeder, et al., *Nat. Rev. Mater.*, 7(8), 653–669 (2022).
- [2] D.-S. Park, et al., *Science*, 375, 653–657 (2022).
- [3] D. Damjanovic, *Rep. Prog. Phys.*, 61(9), 1267–1324 (1998).

5:00 PM EL06.03.11

Enhancement of Alkaline Hydrogen Evolution in BaRuO₃ Thin Film via Surface Self-Reconstruction Do Hyun Kim, Jegon Lee and Woo Seok Choi; Sungkyunkwan University, Korea (the Republic of)

Hydrogen production through water splitting presents a promising avenue for carbon-free energy generation. Transition metal oxides (TMOs) are pivotal electrocatalysts known for their remarkable activity and tunability. Among TMOs, perovskite Ruthenates stand out due to their significant electrocatalytic potential in driving the hydrogen evolution reaction (HER). However, the precise influence of the surface chemistry of Ruthenates in alkaline solutions on their catalytic performance in HER remains a subject of ongoing exploration.

In this investigation, we concentrate on the dynamic chemical and structural transformations occurring on the surface of cubic perovskite BaRuO₃ (3C BRO) during the HER cycle and their direct impact on HER activity. To facilitate our analysis, we utilized epitaxial thin films, meticulously crafting atomically precise crystalline surfaces. This approach allowed us to elucidate the fundamental role of the surface in catalytic activity.

Remarkably, the HER activity of the 3C BRO epitaxial thin film experiences a substantial boost through cycling in an alkaline environment. Specifically, after the initial cycle, the HER overpotential decreased from 210 to 60 mV, reflecting an impressive ~70% improvement. With continued cycling, the initially high HER activity gradually wanes, ultimately reaching a saturation overpotential similar to that of RuO₂ catalysts after approximately 50 cycles. Examination via X-ray photoelectron spectroscopy reveals that the highly active state of 3C BRO retains a similar bulk stoichiometry to the pristine 3C BRO within the thin film region. However, a noticeable reduction in the Ba/Ru ratio (~0.75) becomes apparent on the surface. Complementary observations using scanning transmission electron microscopy indicate the expansion of the Ba-deficient region across the entire film as the heightened activity diminishes. Our interpretation suggests that the initial significant activation arises from the presence of a highly active local Ba-deficient surface stabilized on the pure 3C BRO film. Subsequently, as the overall 3C BRO film loses Ba, the catalytic activity gradually diminishes. These findings offer fundamental insights into the underlying mechanisms governing the formation of a highly active catalytic surface and its stabilization strategy."

5:00 PM EL06.03.12

Enhancing High-Speed Artificial Neuron Functionality via Vanadium Oxide Resistive Switching on Perovskite Substrates Nicholas Cucciniello^{1,2}, Sundar Kunwar², Alessandro Mazza², Pinku Roy², Di Zhang², Aiping Chen² and Quanxi Jia¹; ¹University at Buffalo, United States; ²Los Alamos National Laboratory, United States

This study confronts the urgent challenge of rising energy consumption in the realm of information technology and the constraints imposed on conventional computing by issues like the Memory wall, Heat wall, and Moore's law. In response to this, there is a growing demand for a novel, energy-efficient computing paradigm inspired by the human brain, known as neuromorphic computing. These neuromorphic systems are composed of artificial synapses and neurons, with the intention of replicating the brain's nonlinear operations and its capacity for in-memory computing. Although progress has been made in creating memristive devices to mimic adaptable synaptic weights, the development of artificial neuron devices is still in its nascent stages. The use of vanadium oxide-based resistive switching is particularly promising due to its unique attributes, such as reversible phase transitions and impressive electrical conductivity, positioning it as a candidate for the development of energy-efficient, brain-inspired computing systems. This research centers on the exploration of VO_x thin films grown on La_{0.7}Sr_{0.3}MnO₃-buffered (111) perovskite substrates, with the aim of achieving low-energy consumption, a crucial advancement in the field of neuromorphic computing.

5:00 PM EL06.03.13

Characterizing Ferroelectric a/b Domain Fluctuations in BaTiO₃ through Coherent X-Ray Scattering Pooja Rao, Roopali Kukreja and Nanna Zhou Hagström; University of California, Davis, United States

Ferroelectrics are a class of functional materials which exhibit spontaneous and switchable polarization. To minimize electrostatic and elastic strain energy, ferroelectrics tend to form nanodomains of different polarization directions. Due to the stability of polarization with temperature, ferroelectrics can be considered for applications such as non-volatile memory and neuromorphic computing. However, in order to directly tune ferroelectrics for these purposes, it is important to understand fluctuation characteristics of their domains. Using x-ray photon correlation spectroscopy, we quantify timescales and length scales of fluctuations in heterogeneities of BaTiO₃. For a thin film of BaTiO₃ at nearly zero strain, the Landau-Ginzburg-Devonshire theory predicts a domain transition near 55°C from in-plane (a/b) domains to alternating in-plane and out-of-plane (a/c) domains. We focus on the diffuse scattering peaks from the a/b domain walls near the BTO (103) peak for a temperature range between 35°C to 70°C. We observed that the domains tend to remain stable at temperatures above and below the transition. However, as the transition temperature is approached, the fluctuation dynamics speed up in order to reorganize as new domains. This shows us interesting behavior of ferroelectric domains which have not been investigated yet in BaTiO₃.

5:00 PM EL06.03.14

Escalated Phase Separation Driven Enhanced Magnetoresistance in Manganite/Iridate Epitaxial Heterostructures Pinku Roy¹, Aiping Chen¹ and Quanxi Jia²; ¹Los Alamos National Laboratory, United States; ²University at Buffalo, The State University of New York, United States

Phase separation in manganites leads to unique magnetic and electronic properties. 50% Ca-doped LaMnO₃ (LCMO), at the boundary of ferromagnetic (FM) and antiferromagnetic (AFM) states in La_{1-x}Ca_xMnO₃ (0 ≤ x ≤ 1), is an ideal system to study phase separation behavior. Here, we have investigated the effect of a 5d-metal perovskite SrIrO₃ (SIO) on the phase separation, magnetic, and magnetoresistance (MR) properties of LCMO. The MR, and colossal magnetoresistance (CMR), observed in LCMO/SIO bilayers were two orders and an order of magnitude (in %) larger, respectively than that in the single-layer film. We found the coexistence of FM and AFM/CO phases was responsible for the CMR and MR enhancement in the LCMO/SIO bilayer, pointing towards the importance of the phase separation and competition of both the individual materials in enhancing their magnetic and electronic properties.

5:00 PM EL06.03.15

Functional Tin-Based Nanostructures Engineering Poting Liu^{1,2}, Anna Makarova³, Katharina Freiberg², Stephanie Lippmann², Dave Grinter⁴, Sergey Turishchev⁵ and Vladimir Sivakov¹; ¹Leibniz Institute of Photonic Technology, Germany; ²Friedrich-Schiller-University Jena, Germany; ³Free University Berlin, Germany; ⁴Diamond Light Source, United Kingdom; ⁵Voronezh State University, Russian Federation

Tin (Sn) –based nanostructures have attracted very much attention because of their superior physical and chemical properties such as high electron mobility and wide bandgap [1]. Herein, a metal organic chemical vapor deposition (MOCVD) technique is reported for the growth of unique Sn/SnO_{2-x} nanostructures with phases control by varying deposition conditions and using nanostructured/planar initial Si surfaces. Herein, we are going to discuss possible nano-engineering using nanostructured and planar silicon surfaces to create functional nanostructures with new physical and chemical properties and their characterization using large-scale synchrotron radiation based techniques. Theoretical calculations, extensive surface and bulk characterization techniques such as electron microscopy, XRD, and synchrotron radiation based XPS and NEXAFS techniques were applied to study the formation mechanisms of the unique tin-based nanostructures. An intensive oxygen exchange reaction between the planar silicon surface and a thin layer of tin (IV) oxide during the MOCVD process is observed at a tiny temperature window of 725-735 °C resulting a unique Sn:SiO₂ composite formation with the nature-similar shape of "volcanos" and "craters". The growth mechanism of the "volcano-like" nanostructures is related to the efficient oxygen retraction between the tin(IV) oxide and the silicon surface, leading to the formation of thermodynamically unstable Sn(II) oxide, which immediately disproportionates to metallic tin and SnO₂ phases localized in the SiO₂ matrix. The observed phenomenon of thin film growth at the nanoscale has similar principles to the formation of volcanos in nature, which reflects the unique relationship between the laws of nature in the nanometer and macroscale world. From another side, when the silicon nanowires (SiNWs) are used as deposition matrix, it is found a phase of Sn(0), Sn(II) and Sn(IV) distribution effect along SiNWs with controllability by varying the SiNWs matrix [2,3]. According to the detailed destructive/non-destructive surface characterization results, the significant thermal conductivity difference between bulk Si and SiNWs is responsible for a temperature gradient along SiNWs during MOCVD process and result in the reduction of Sn from precursor byproducts. These discoveries give us a new way to realize the phase-selective deposition of Sn-based functional materials and expected to adjust its functional properties in different scenarios such as photocatalyst, Li(Na) –based batteries and energy conversion and storage.

- [1] P. Liu and V. Sivakov, *Nanomaterials* 13(17), 2391 (2023).
[2] P. Liu et al., *Small* 19, 2206318 (2023).
[3] S. Turishchev et al., *Small* 19, 2206322 (2023).

SESSION EL06.04: Epitaxial Growth—Magnetism and Transport
Session Chairs: Woo Seok Choi and Le Wang
Wednesday Morning, April 24, 2024
Room 343, Level 3, Summit

8:45 AM *EL06.04.01

Richness of Spiral Magnetic States in Strontium Ferrite Thin Films [Jennifer Fowlie](#); Stanford University, United States

Perovskite strontium ferrite, SrFeO₃, hosts a variety of spiral magnetic phases at low temperature including multi-q states of different proper screw and/or cycloid ordering^[1]. Among them is a phase believed to support topologically-protected magnetic structures and may explain an observed finite-field anomaly in Hall effect^[2].

SrFeO₃ is a fascinating material because, unusually, these effects exist despite the centrosymmetry of the crystal structure. Instead of a Dzyaloshinskii-Moriya interaction, the helimagnetism has been suggested to arise due to an interplay of electronic interactions^[3].

We have optimized the growth and stability of epitaxial thin films of SrFeO₃ grown by pulsed laser deposition. Then, using resonant soft x-ray scattering, we study how these complex magnetic orderings depend on the biaxial strain state, which potentially influences the electronic structure.

- [1] Ishiwata, S. *et al.* Versatile helimagnetic phases under magnetic fields in cubic perovskite SrFeO₃, *Phys. Rev. B* **84**, 1–5 (2011).
[2] Ishiwata, S. *et al.* Emergent topological spin structures in the centrosymmetric cubic perovskite SrFeO₃, *Phys. Rev. B* **101**, 134406 (2020).
[3] Mostovoy, M. Helicoidal ordering in iron perovskites, *Phys. Rev. Lett.* **94**, 137205 (2005).

9:15 AM EL06.04.02

Properties of Barium Bismuthate Layers on Si: Molecular Beam Epitaxy Study [Islam Ahmed](#)^{1,2}, Maxim Korytov¹, Olivier Richard¹, Patrick Carolan¹, Stefanie Sergeant¹, Thomas Nuyyten¹, Thierry Conard¹, Stefan De Gendt^{1,2} and Clement Merckling^{1,2}; ¹IMEC, Belgium; ²KU Leuven, Belgium

With slowing down of Moore's law, related to scaling of integrated circuits, alternative technologies such as quantum computing require research efforts for pushing the limits of new generation of electronics. A promising approach to realize fault-tolerant quantum computations is to build qubits that are intrinsically protected against quantum errors thanks to the topological nature of the used materials. Such computations are realized when Majorana fermions are detected and manipulated. Topological superconductors are the perfect solid state material system for hosting Majorana bound states. Equivalently, an interface between a superconducting and a topological insulating layer is also expected to host such states, based on the proximity effect. Barium bismuthate (BBO) is a relevant material system because when hole-doped with potassium, it is a superconductor with a critical temperature of 29.8 K. In addition, with the spin-orbit coupling of bismuth considered, fluorine-doped BBO is predicted to be a topological insulator according to density functional theory (DFT) studies.

The work presented is related to material development and characterization of the parent compound utilizing oxide molecular beam epitaxy (MBE) process. In our work, we integrate BaBiO_x on Si(001) substrate, using an epitaxially grown strontium titanate SrTiO₃ single-crystalline buffer layer. It is demonstrated that the epitaxy of BaBiO_x is only achieved in excess of oxygen plasma because of the volatile nature of bismuth molecules reaching the substrate. Due to the high vacuum environment in the oxide chamber of the MBE machine that can reach below 10⁻⁸ torr as base pressure, ordered oxygen vacancies are created within the perovskite layers, forming a mixture of brownmillerite and perovskite phases. The mixed phase is demonstrated based on transmission electron microscopy (TEM) images. A method, in function of oxide MBE process parameters, to retrieve fully perovskite phase (with no ordered oxygen vacancies) is presented.

Due to the breathing distortion within its lattice, barium bismuthate is a Peierls insulator with an optical band gap of 1.96 eV. Optical conductivity is measured using spectroscopic ellipsometry, showing a peak centred around 2 eV. The Raman response of BBO observed at 570 cm⁻¹ is attributed to the breathing distortion of BiO₆ octahedra, which is in resonance with a laser wavelength of 633 nm. In our studies, thickness dependence of the presence of the breathing distortion is studied. In the upcoming study, a light will be shed on the band structure of fluorine-doped by measuring it using angle-resolved photoemission spectroscopy (ARPES) to detect the existence of topological states.

9:30 AM EL06.04.03

Effect of Stoichiometry on The Atomic Microstructure of Thin Film BaTiO₃ [Ashley Cavanagh](#), Larissa Little, Charles M. Brooks, Julia Mundy and Robert Westervelt; Harvard University, United States

Synthesis and characterization of thin film barium titanate is of great interest due to its promise for use in electro-optic modulators [1]. These devices require a thin film with a high electro-optic coefficient that can operate at low voltages and integrate into photonic circuits, so barium titanate's strong nonlinearity makes it an attractive candidate material. Barium titanate's ferroelectricity means that it is also of interest for applications in nonvolatile ferroelectric memories. For use in photonic devices, we must understand how variations in film stoichiometry affect the electro-optic properties, local atomic structure, and ferroelectric structure of thin film barium titanate. We use molecular beam epitaxy (MBE) to grow high quality thin films of barium titanate with a high degree of stoichiometry control. In this talk, we use high-resolution scanning transmission electron microscopy (STEM) to compare the atomic microstructure of barium titanate films of varying stoichiometries grown on strontium titanate. High-resolution electron microscopy imaging allows us to evaluate atomic-level variations in crystal structure, local defects, and electrical polarization in thin films of barium titanate. By understanding the effect of stoichiometry on these variations, we can understand the degree of stoichiometry control needed to grow barium titanate thin films that are of sufficient quality for electro-optic device applications.

* Supported in part by the NSF STC for Integrated Quantum Materials DMR-1231319, and the NSF Nanotechnology Nanotechnology Coordinated Infrastructure ECCS-1541959.

- [1] D. Zhu et al., *Integrated Photonics on Thin-Film Lithium Niobate*, *Adv. Opt. Photon.* 13, 242 (2021).

9:45 AM EL06.04.04

Tunable Electromagnetic Properties of Epitaxial Mo(d²)-Doped SrRu(d⁴)O₃ Thin Films [Rahma D. Prasetyawati](#)¹, Taehee Lee¹, Sungkyun Park²,

Tuson Park¹ and Woo Seok Choi¹; ¹Sungkyunkwan University, Korea (the Republic of); ²Pusan National University, Korea (the Republic of)

4d transition metal oxides (TMOs) offer various intriguing physical behaviors resulting from the strong interplay among charge, spin, lattice, and orbital degrees of freedom. Their electronic structure is influenced not only by the on-site Coulomb interaction (U) and spin-orbit coupling (SOC) but also by Hund's coupling (J_H). There have been several studies conducted to construct the correlated electronic phase diagram by varying the degree of those interaction parameters. One of the renowned 4d TMOs is the ferromagnetic SrRuO₃ (SRO) with 4d⁴ configuration having abundant electronic states including non-Fermi liquid and Weyl semimetal states. The intrinsic SOC coupled with its ferromagnetism is important for the emergence of the Dzyaloshinskii – Moriya interaction beneficial for the observation of exotic quantum phenomena, such as the skyrmion formation and resultant topological Hall effect [1, 2]. On the other hand, SrMoO₃ (SMO) with 4d² configuration is the other reported metallic 4d TMO influenced by Hund's coupling. However, its electronic transport mechanism is less understood compared to SRO despite its extremely small room- T resistivity with Fermi-liquid behavior [3]. Different from SRO, SMO is reported to have T -independent magnetic susceptibility exhibiting Pauli paramagnetic behavior. Previously, several attempts have been made to dope SRO thin films with 3d and 5d TM ions through Ru-site chemical substitution which results in the suppression of the ferromagnetism and emergence of metal-insulator transition in the electronic transport. In this study, we investigated the effect of Mo(4d²)-doping on SRO thin films by manipulating the degree of electronic and magnetic correlations through chemical substitution. We grew the epitaxially stabilized SrRu_{1-x}Mo_xO₃ (SRMO, $x = 0 - 0.5$) thin films using pulsed laser epitaxy by alternately ablating two targets, SRO and SMO. The Mo concentration was selectively controlled by adjusting the laser pulse numbers according to the deposition rate of each target on (001) SrTiO₃ substrates. The high quality of the resulting SRMO thin films has been confirmed by using x-ray diffraction accompanied by a systematic lattice compression per the increase in the Mo concentration. The modification of the complex 4d⁴ electronic structure by the 4d²-doping is apparent in the hybridization between Ru 4d and O 2p orbitals, inducing systematic changes in the electric and magnetic properties of SRMO epitaxial thin film. Our results present further insights into understanding the systematic changes in the electromagnetic properties of epitaxial SRMO thin films useful for spintronic device applications.

References:

- [1] Meng, Keng-Yuan *et al.*, *Nano Lett.* 2019, 19, 5, 3169–3175.
- [2] Wang, C. A. *et al.*, *Adv. Electron. Mater.* 2020, 6, 2000184.
- [3] Prasetiyawati, R. D. *et al.*, *Curr. Appl. Phys.* 2023, 53, 110.

10:00 AM BREAK

10:30 AM *EL06.04.05

Giant Topological Hall Effect and Tunable Chiral Symmetry in a Localized Asymmetric Oxide Heterostructure Xiaofang Zhai; ShanghaiTech University, China

Topological Hall effect (THE) provides the electrical detection of topologically protected chiral spin structures such as skyrmions and has attracted intensive attentions due to the potential application in future information technology. Here we found the asymmetric ruthenate/titanate heterostructure exhibiting a giant THE resistivity in striking contrast to zero anomalous Hall effect (AHE) because of localization and the quantum interference induced real space Berry phase. We further present a new technique – magnetic-field angle dependent resistance (MAR) measurement – capable to reveal emergent chiral symmetries from different chiral spin textures. Our findings reveal the localization regime to be a new playground for exploring exotic chiral spin phenomena, and demonstrate the MAR as a new technique providing evidence of real space spin chirality.

11:00 AM *EL06.04.06

Correlated Topological Oxide Heterostructures for Energy-Efficient Quantum Microelectronics Ho Nyung Lee; Oak Ridge National Laboratory, United States

Complex oxides are known to possess the full spectrum of fascinating properties, including magnetism, colossal magnetoresistance, superconductivity, ferroelectricity, ionic conductivity, and more. The breadth of remarkable properties is the consequence of strong coupling among charge, spin, orbital, and lattice degrees of freedom. Spurred by recent advances in the synthesis of such artificial materials at the atomic scale, the physics of oxide heterostructures containing atomically smooth layers of such correlated electron materials with abrupt interfaces is a rapidly growing area. We have established a growth technique to control complex oxides at the level of unit cell thickness by pulsed laser deposition. The atomic-scale growth control enables to assemble materials from atoms to functional systems in a programmable manner, yielding many intriguing physical properties that cannot be found in bulk counterparts. In this talk, examples of complex oxide thin films and heterostructures grown by advanced pulsed laser deposition and their correlated and topological properties will be presented, highlighting the importance of precision synthesis for heterostructuring, interfacing, and straining. The main topics include (1) oxide Dirac semimetals with extreme high mobility that exhibit fractional occupation of the Landau level and (2) corrected metal Pd-based delafossites as an extreme metal that may revolutionize interconnects in the next generation of microelectronics by their excellent electronic conductivity combined with Mottness.

*This work was supported by the U.S. Department of Energy, Office of Science, Basic Energy Sciences, Materials Sciences and Engineering Division.

11:30 AM *EL06.04.07

Model-Based Artificial Quantum Materials Realized in Oxide Heterostructures and Superlattices Jian Liu; University of Tennessee, United States

The complex interplay between the quantum degrees of freedom in oxides is known to cause intriguing emergent states. While the underlying physics is usually captured by model Hamiltonian, most of the known models, such as the Hubbard Hamiltonian, are difficult to resolve theoretical. This challenge calls for toy-model-based design and synthesis of novel structures for complex oxide materials synthesis. In this talk, I will discuss our recent work on experimental realization of artificial iridate superlattices that simulate the correlation-topology interplay with engineered complex hopping. While the electronic correlation stabilizes an antiferromagnetic Mott insulating ground state, their intermediate coupling strength allows significant longitudinal spin fluctuations, which allow the SU(2) symmetry-preserving and breaking components of the complex hopping to manifest as anomalous magnetoresistance and anomalous Hall effect, respectively. The latter also leads to an exceptionally large Ising anisotropy which is captured as a giant magnon gap and is an imprint of electronic topology. I will also discuss another example in pyrochlore heterostructures which simulate the spin-ice fluctuation-mediated charge transport.

This searchable program is up-to-date as of April 15th, 2024.

Wednesday Afternoon, April 24, 2024
Room 343, Level 3, Summit

1:30 PM *EL06.05.01

Phonon Decoupling in Double Perovskite Oxides Yeongrok Jin and Jaekwang Lee; Pusan National University, Korea (the Republic of)

In general, a slight displacement of an atom from its equilibrium position affects the forces on the rest of the atoms simultaneously. That's why the phonon has been considered a collective excitation in the periodic arrangement of atoms in solids. Here, using first-principles density functional theory calculations, we first demonstrate that, contrary to typical collective phonons, oxygen-octahedral and oxygen-tetrahedral phonons can be fully decoupled across the entire phonon spectrum, especially in double perovskite oxides. This decoupled oxygen tetrahedral phonon would be strongly localized and can greatly induce band flattening along a specific crystal orientation, enabling unusual site-selective control of the unit cell width domain wall.

2:00 PM *EL06.05.02

Understanding Electron and Crystal Structure Roles in Electronic Transitions of Complex Oxides: Insights Across Scales and Machine-Learning Aided Discovery of Novel Materials Alexandru Georgescu; Indiana University, Bloomington, United States

In this talk, I will discuss three main areas in the study of correlated electron materials:

- 1) Differentiating the influence of crystal structure and valence electrons in symmetry-breaking phase transitions, resolving a longstanding question in the field.
- 2) Using layered material structures as a lens to study electronic transitions at the nanoscale, backed by practical thin-film examples.
- 3) Harnessing machine learning throughout the quantum materials discovery process, from identification to synthesis.

I'll wrap up by highlighting how these advances impact the discovery and application of new quantum materials and may lead to novel applications.

2:30 PM BREAK

SESSION EL06.06: Epitaxial Growth—Microstructure and Functionalities
Session Chairs: Megan Holtz and Dongsheng Li
Wednesday Afternoon, April 24, 2024
Room 343, Level 3, Summit

3:30 PM *EL06.06.01

Quantifying 3D Chemical and Structural Order/Disorder in Thin Film Complex Oxides with Multislice Electron Ptychography James M. LeBeau; Massachusetts Institute of Technology, United States

Determining chemical and structural order/disorder within functional oxides is often key to understanding the properties of these materials, for example, relaxor ferroelectrics. Conventional techniques such as X-ray, neutron, or electron diffraction are often used to study these features via diffuse scattering, but only offer insights into the global and average local structure of a sizable material volume. While recent advances in phase contrast imaging techniques in scanning transmission electron microscopy (STEM), such as iDPC, have helped to reveal connections between local polar and chemical order, these approaches are constrained by the ability to capture only a 2D projection of the structure within a thin TEM sample. Consequently, the origins of the exceptional piezoelectric properties of these materials continue to be a subject of debate.

In this presentation, I will explore how multislice electron ptychography can be leveraged to provide nanoscale structural, chemical, and polar variations in functional oxides in 3D. First, I will present the analysis of the reconstructed phase from the thin film paraelectric Pb₂MgWO₆. I will highlight how the approach provides access to the three-dimensional structure and chemistry of inclined anti-phase boundaries in this material. The comprehensive characterization offers deeper insights into their impact on local polarization, namely stabilizing antiferroelectric distortions at the boundaries. Second, I will discuss our study of the prototypical relaxor ferroelectric Pb(Mg_{1/3}Nb_{2/3})O₃-PbTiO₃ (PMN-PT) using ptychography, where structural distortions of the cation and anion sublattices across slices are used to measure polar order in 3D. The results will be compared against conventional HAADF and iDPC imaging from the same region to provide an understanding of the sampling volume of those techniques. Finally, I will discuss how multislice ptychography offers to play a pivotal role in unraveling the intricate relationships between defects, structure, and the influence of intrinsic and extrinsic factors on the behavior exhibited by functional oxides.

4:00 PM EL06.06.02

Unravelling The Effect of Nitrogen Doping on The Structure of LaFeO₃ Epitaxial Thin Films Krishna Prasad Koirala¹, Shan Lin², Le Wang¹, Minju Choi¹, Erjia Guo², Peter V. Sushko¹, Scott A. Chambers¹, Chongmin N. Wang¹ and Yinge Du¹; ¹Pacific Northwest National Laboratory, United States; ²Institute of Physics, Chinese Academy of Sciences, China

Heteroatom doping has proven to be an effective approach for fine-tuning the electronic and magnetic properties, as well as enhancing the electrocatalytic performance in ABO₃-type perovskite oxides. Beyond the conventional cation doping at A or B-sites, partial replacement of oxygen anions in perovskite oxides by other elements, such as nitrogen (N), sulfur (S), and fluorine (F), has also been explored to modify their structure and properties. In this study, we aim to advance our understanding of how N doping in LaFeO₃ films, influences their composition and structure, subsequently affecting their electronic and electrochemical properties. High-quality N-doped LaFeO₃ (LFON) epitaxial thin films with different doping levels were grown on (001)-oriented Nb:SrTiO₃ substrates using nitrogen-plasma-assisted pulsed laser deposition. Our X-ray diffraction and scanning transmission electron microscopy (STEM) measurements revealed that while the films are coherently strained in plane, with no observed dislocations at the interface, there is a notable, up to 4% lattice expansion in the out-of-plane direction. By employing an integrated differential phase contrast (iDPC) imaging technique in STEM, we examined orthorhombic relaxation in both undoped and doped samples. We found no significant differences in octahedral tilting between them, while the doped LFON sample exhibited a higher prevalence of two orthogonal in-plane rotated structural domains. Moreover, atomically resolved electron energy loss spectroscopy (EELS) indicated that the Fe valence remains as Fe³⁺ after N doping, suggesting that the generation of oxygen vacancies serves as a compensatory mechanism for the charge difference between nitride and oxide ions. However, DFT calculations indicated that oxygen vacancies and substitutional N had little impact on the out-of-plane lattice parameter. Further experimental and theoretical investigations are necessary to uncover the underlying cause of the 4% lattice expansion in the out-of-plane direction. In summary, these findings provide a crucial guide for understanding how N

doping affects the structure and properties of complex oxides, essential for designing novel electrocatalysts for water splitting.

4:15 PM EL06.06.03

Nearly Epitaxial ZrO₂-Co Vertically Aligned Nanocomposites Thin Film with Tunable Magnetic and Optical Anisotropy [Yizhi Zhang](#)¹, Jiawei Song¹, Ping Lu², Julia Deitz², Di Zhang³, Hongyi Dou¹, Jianan Shen¹, Zedong Hu¹, Xinghang Zhang¹ and Haiyan Wang¹; ¹Purdue University, United States; ²Sandia National Laboratories, United States; ³Los Alamos National Laboratory, United States

Metamaterials have gained great research interest recently owing to their potential for property tunability, multifunctionality, and property coupling. As a new group of hybrid metamaterials, vertically aligned nanocomposite (VAN)-based thin films exhibit significant anisotropic physical properties and a broad range of property tailorability, such as optical anisotropy, magnetic anisotropy, and hyperbolic dispersion. In this work, self-assembled ZrO₂-Co hybrid thin films, with high epitaxial quality and ultra-fine vertically aligned metallic Co nanopillars (with an average diameter of ~ 2 nm) embedded in a ZrO₂ matrix, were successfully fabricated using a pulsed laser deposition (PLD) method. The Co pillar planar density can be effectively tuned, without changing the pillar size, by varying the Co concentration in the target, which results in tunable optical properties and magnetic properties. Specifically, a high saturation magnetization of 100 emu*cm⁻³, strong out-of-plane magnetic anisotropy and tailorable magnetization properties were achieved. Coupled with hyperbolic optical dispersion from 950 nm to 1500 nm in wavelength, plasmonic Co metal nanopillars, and the unique dielectric ZrO₂ matrix, this new nanoscale hybrid metamaterial shows great potential for future integrated optical and magnetic device designs.

4:30 PM *EL06.06.04

Epitaxial Memristors: Preparing for The New Generation Devices [Beatriz Noheda](#); University of Groningen, Netherlands

The search for devices that can emulate the behavior of neurons and synapses, in order to be used in brain-inspired, in-memory or on-edge computing, is extending among different research fields with an increasing number of materials scientists involved in the quest. However, the number of materials that have been considered as the key elements for these devices is restricted to the few that are compatible with CMOS integration. The need to process at low temperatures often produces polycrystalline or amorphous materials, limiting the control of the materials properties. Luckily, the emergent efforts towards epitaxial growth of complex oxides by ALD at low temperatures[1] allows us to dream of a future of epitaxial oxide microelectronics for which we want to be prepared. In this talk, we will show an example of epitaxial material that show interesting neuromorphic features, namely, self-oscillating behavior and generation of voltage spikes in epitaxial TbMnO₃, a material that does not undergo a meta-insulator transition, and can be used as a compact neuristor[2].

1. H. H. Sonstebly et al. *Nature. Comm.* 11, 2872 (2020)
- 2- M. Salverda et al. *J. Phys. D: Appl. Phys.* 55 335305 (2022)

SESSION EL06.07: Oxide Membranes
Session Chairs: Woo Seok Choi, Junwoo Son and Hua Zhou
Thursday Morning, April 25, 2024
Room 343, Level 3, Summit

8:45 AM +EL06.07.01

Exploring Opportunities and Challenges in Free-Standing Epitaxial Oxide Nanomembranes [Bharat Jalan](#); University of Minnesota, United States

With a rapidly growing family of vdW materials, the role of dielectric and metals have become more important than ever. In this talk, I will present challenges associated with the synthesis of atomically-precise three-dimensional (3D) perovskite nanomembranes followed by our group's effort to address them. Using hybrid molecular beam epitaxy that employs a metal-organic precursor, titanium isopropoxide (TTIP), to supply both Ti and oxygen (without the need for additional oxygen), epitaxial SrTiO₃ (STO) films were grown directly on a graphene layer transferred on to bulk STO substrate. Films were then successfully exfoliated and transferred onto other substrates. Using Raman spectroscopy and high-resolution X-ray diffraction, we show that the transferred STO membrane is single-crystalline and can be integrated with other vdW materials. I will also present sacrificial layer route to create oxide membranes resulting in room temperature dielectric constant of ~ 300. Finally, I will present several opportunities for materials physics and devices engineering using 3D nanomembranes.

9:15 AM EL06.07.02

Periodic Wrinkles in Freestanding Complex Oxide Membranes [Minyong Han](#), Tiffany C. Wang and Harold Y. Hwang; Stanford University, United States

A stiff film bonded to an elastic substrate shows a universal tendency to form periodic wrinkles upon application of compressive force [1]. This design principle has been employed to produce wafer-scale wrinkles in polycrystalline metal films on polydimethylsiloxane (PDMS) for applications in *e.g.* optical gratings or strain sensors [2]. When a single crystalline film is processed similarly in a non-planar morphology, a spatially graded strain state with continuously varying lattice constant can be realized. In the regime of extreme bending, the strain gradient therein is known to generate significant modifications in mechanical and electromagnetic properties of the material [3,4]. The recent development of water-soluble oxide buffer layer enables viable lift-off of complex oxide membranes to be transferred onto an arbitrary elastic substrate [5]. In this study, we adopt this technique to prepare single crystalline oxide membranes on PDMS and fabricate a variety of periodic wrinkles in a fully programmable fashion using compression amplitude and membrane thickness as control parameters. Under large compressive force, the degree of bending extends to the limit where the membrane thickness is a few percent in size compared to the radius of curvature of wrinkles. In addition, we introduce our unique sample packaging methods to characterize electrical properties of wrinkled membranes while maximally preserving the overall sample geometry and the associated strain state.

References:

- [1] Z. Y. Huang *et al.*, *J. Mech. Phys. Solids* 53, 2101 (2005)
- [2] T. Ma *et al.*, *Opt. Express* 21, 11994 (2013)
- [3] G. Dong *et al.*, *Science* 366, 475 (2019)
- [4] V. Harbola *et al.*, *Nano Lett.* 21, 2470 (2021)
- [5] D. Lu *et al.*, *Nat. Mater.* 15, 1255 (2016)

9:30 AM EL06.07.03

Maintaining The Structural Integrity of Wet-Transferred Graphene to Achieve Successful Exfoliation of BTO in Heterostructures Grown through Pulsed Laser Deposition (PLD) [Asrafal Haque](#), Suman K. Mandal, Shubham K. Parate and Srinivasan Raghavan; Indian Institute of Science, India

The epitaxial growth of functional oxides on graphene-coated substrates presents a promising avenue for producing self-standing epitaxial nanomembranes, thereby facilitating advanced scientific investigations, applications, and sustainable substrate reutilization. However, the conventional use of aggressive oxidizing conditions in the growth of epitaxial oxides can jeopardize the integrity of the graphene layer. This study introduces a systematic approach to safeguard graphene during the epitaxial growth of BaTiO₃ (BTO) on SrTiO₃ (STO) substrates coated with graphene. Our method involves an initial BTO growth phase using a laser source with a controlled aperture, thereby adjusting the growth rate to minimize damage to the underlying graphene layer. Additionally, a precisely regulated chemical vapor deposition (CVD) process is employed to grow graphene with larger grain sizes, thereby enhancing the crystalline quality of the remotely epitaxially grown BTO film. Gradual strain relaxation is observed in the resulting BTO films upon the incorporation of multiple graphene layers. The use of bilayer graphene facilitates the easy exfoliation and transfer of the BTO film to various substrates, including Si. These findings pave the way for the heterogeneous integration of different functional oxides, holding significant implications for the commercialization of perovskite oxides in flexible electronics.

9:45 AM BREAK

10:15 AM *EL06.07.04

Ferroelectric Vortex State in Twisted BaTiO₃ Membranes [Jacobo Santamaria](#); Universidad Complutense de Madrid, Spain

The wealth of complex polar topologies recently found in nanoscale ferroelectrics result from a delicate balance between the materials' intrinsic tendency to develop a homogeneous polarization and the electric and mechanical boundary conditions imposed upon them. Recently, new methods have been developed, for the realization of freestanding perovskite films, the so called oxide membranes. Membranes can be manipulated and deterministically placed on any substrate thus bypassing the limitations of conventional epitaxy. Moreover, freestanding layers can be piled up to form twisted homo bilayers. In this talk I will show that the stacking of freestanding ferroelectric perovskite layers with controlled twist angles opens an unprecedented opportunity to tailor topological polar landscapes in a way determined by the lateral strain modulation associated to the twisting. Interestingly, we find that a peculiar pattern of polarization vortices and antivortices emerges from the flexoelectric coupling of polarization to strain gradients. This finding opens exciting opportunities to create two-dimensional high density vortex crystals that would allow us to explore novel physical effects and functionalities.

Work in collaboration with

G. Sánchez-Santolino^{1,2}, V. Rouco¹, S. Puebla³, H. Aramberri⁴, V. Zamora¹, M. Cabero⁵, F. A. Cuellar¹, C. Munuera^{2,3}, F. Mompean^{2,3}, M. Garcia-Hernandez^{2,3}, A. Castellanos-Gomez^{2,3}, J. Íñiguez^{4,6}, C. Leon^{1,2}, J. Santamaria^{1,2}.

1 GFMC. Dept. Física de Materiales. Facultad de Física. Universidad Complutense. 28040 Madrid

2 Unidad Asociada UCM/CSIC, "Laboratorio de Heteroestructuras con aplicación en spintrónica"

3 Instituto de Ciencia de Materiales de Madrid ICMM-CSIC 28049 Cantoblanco. Spain

4 Materials Research and Technology Department, Luxembourg Institute of Science and Technology (LIST), Avenue des Hauts-Fourneaux 5, L-4362 Esch/Alzette, Luxembourg.

5 ICTS Centro Nacional de Microscopia Electrónica "Luis Brú" Universidad Complutense. 28040 Madrid

6 Department of Physics and Materials Science, University of Luxembourg, 41 Rue du Brill,

L-4422 Belvaux, Luxembourg

10:45 AM +EL06.07.05

Freestanding Oxides: Paving The Way for Advanced Functional Materials [Nini Pryds](#); Technical University Denmark, Denmark

Combining different materials into heterostructures stands as a foundational pillar in modern materials science. Notable instances include the advent of 2D materials and the development of van der Waals heterostructures. This presentation talks about new ways to make very thin oxide films that are almost 2D stack and twist them. These new methods open up many exciting possibilities for using these oxide materials in novel functionalities. I will in my talk focus on how these oxides freestanding membranes work and interact at their interfaces and surfaces. This research highlights the transformative potential of these materials in reshaping our understanding and approach to modern science and materials technology.

11:15 AM EL06.07.06

Transfer of Epitaxial Strained Multiferroic Thin Films on Millimeter Scale Using Rigid Substrate Epoxy Method [James P. Barnard](#)¹, Jianan Shen¹, Benson Tsai¹, Max R. Chhabra¹, Jiho Noh^{2,3}, Hyunseung Jung^{2,3}, Aleem Siddiqui², Raktim Sarma^{2,3}, Chloe Doiron^{2,3} and Haiyan Wang^{1,1}; ¹Purdue University, United States; ²Sandia National Laboratories, United States; ³Center for Integrated Nanotechnologies, United States

Multiferroic oxide thin films have diverse applications in the fields of integrated photonics, acoustic sensors, and memory devices. These devices are typically fabricated on substrates such as fused silica, lithium niobate, and silicon. However, these substrates can pose significant challenges for epitaxial growth due to their lattice structures. Pulsed Laser Deposition (PLD), a well-known technique for epitaxial thin film growth, is heavily limited by substrate selection due to its lattice parameter matching requirements, usually leading to growths being performed on SrTiO₃ (STO) or LaAlO₃ (LAO) substrates. However, a novel approach to enabling other substrates has attracted attention in recent years: film transfer. In this method, the insertion of a water-soluble layer of Sr₃Al₂O₆ (SAO) allows for epitaxial film growth while also enabling liftoff through dissolution of this sacrificial layer. The film of interest can be supported during release and transfer by attaching flexible polymer layers such as polypropylene carbonate (PPC) or poly(dimethylsiloxane) (PDMS) before dissolving the sacrificial layer. After adhering the film to the new substrate, the polymer layers can be removed. However, challenges associated with epitaxial strain have not yet been solved. Namely, when a highly strained film is released from the growth substrate, the substrate clamping effect is lost, allowing the film to wrinkle or curl to relax the strain. These deformations of the surface lead to cracks in the final transferred film, limiting the area of continuous film that can be successfully transferred. In this work, we report a new process where the rigid target substrate is adhered to the film, in this case the multiferroic Bi₃Fe₂Mn₂O₈ (BFMO) material, using epoxy prior to releasing the film from the growth substrate. This creates a "sandwich" with the BFMO film between the original substrate and new substrate. The sacrificial layer is then dissolved, leaving the film attached to the new substrate. Since the film is not allowed to flex at any time during the process, the strain cannot be relaxed to cause surface deformation, resulting in large crack-free areas of transferred film—on the scale of several millimeters rather than several hundred microns as achieved by the polymer transfer method with strained films. Finally, we will demonstrate that the transfer process preserves crystal quality and therefore the multiferroic properties of the film.

11:30 AM *EL06.07.07

Single-Crystalline Rutile Oxide Nanomembranes: Versatile Platform to Overcome Lattice Mismatch [Junwoo Son](#); Seoul National University, Korea (the Republic of)

The demand for high-performance electronics and photonics calls for the integration of heteroepitaxial oxide films with perfect crystallinity to fully exploit emerging phenomena (e.g., metal-insulator transition, high-electron mobility) from the ionic crystals. However, the requirement of the lattice matching between epilayer and dissimilar substrates drastically limits high-quality epitaxial growth, which in turn degrades the unique properties from functional oxides; this fundamental obstacle of the heteroepitaxy prevents the unrestricted integration of the single-crystalline oxide films onto any desired substrates. To overcome this fundamental limitation, here, I present our research group efforts to demonstrate the heterogeneous integration of single-crystalline rutile oxide nanomembranes with steep phase transition onto arbitrary substrates. First, we discover new combination of sacrificial layer and mild etchant by exploiting selective oxidation and transformation to layered structure, which could be exfoliated and dispersed in the solution to release millimeter-scale TiO₂ nanomembrane with any deterioration of crystal quality. Interestingly, nearly perfect single-crystallinity of transferred TiO₂ nanomembrane as a template for epitaxy permits the heterogeneous integration of single-crystal VO₂ films on silicon; indeed surprising sharp transition and the highest modulation of resistivity ratio ever reported was remarkably achieved even in the ultrathin VO₂ films on silicon, which is not achievable via direct growth [1]. Moreover, I will also present our epitaxial oxide nanomembrane as a versatile platform for steep phase transition even above critical thickness for lattice mismatch using the concept of pseudo-compliant substrates and emerging devices using single-crystalline oxide heterostructure (e.g., VO₂/PMN-PT heterostructure) [2]. Our finding will create new paradigm for the unrestricted application of emerging phenomena in oxide heterostructures on mainstream microelectronics.

This work was performed in collaboration with Dr. Dong Kyu Lee, Dr. Yunkyu Park, Sung Won Lee, Hyeji Sim, Dr. Younghak Kim, Dr. Gi-Yeop Kim and Prof. Si-Young Choi.

[1] D. K. Lee *et al.*, *Nature Commun.* **12**, 5019 (2021)

[2] D. K. Lee *et al.*, (unpublished)

SESSION EL06.08: Oxide Electronics—Ionic Motion and Ferroic

Session Chairs: Aiping Chen and Gertjan Koster

Thursday Afternoon, April 25, 2024

Room 343, Level 3, Summit

1:30 PM *EL06.08.01

Nanoscale Control of The Ionic Evolution within Complex Oxides Pu Yu; Tsinghua University, China

Over the last decades, ionic evolution emerges as a powerful tuning knob to manipulate the material functionalities of complex oxides. In this talk, we will present a few new strategies to explore ionic evolution at the nanoscale, including the scanning probe tip-induced ionic evolution and electron beam illumination induced chemical reduction. For the tip-induced hydrogen evolution, the Pt-coated scanning probe serves as an efficient hydrogen catalyst, leading to a hydrogen spillover across the nano junction between the probe and sample surface. Furthermore, the application of positively-biased voltage through the junction drives protons into the sample, while negative voltage extracts protons out, giving rise to reversible proton evolution. Due to the associated electron filling, this method can then offer an exciting opportunity to harvest advanced functions such as insulator-metal transition through the tip-induced proton evolution. Furthermore, through the electron-beam illumination with a commercial scanning electron microscope, we also demonstrated locally controlled oxygen vacancy migration in the model system of VO₂, and achieved a nano-scale structural transformation into V₂O₃. In this approach, the electron beam induces both surface oxygen desorption through radiolytic process and positively charged background through secondary electrons, which contribute cooperatively to facilitate the vacancy migration from the surface toward the sample bulk, leading to nanoscale chemical reduction through oxygen vacancy formation. We envision that these two approaches can be readily applied for other material systems, providing a promising strategy to manipulate and design novel functionalities in various materials.

2:00 PM *EL06.08.02

Solid-State Electrochemical Thermal Transistor based on Oxygen Sponge SrCoO_x (2 ≤ x ≤ 3) Hiroimichi Ohta; Hokkaido University, Japan

Thermal transistors are devices that can electrically switch “heat flow” on and off, like a semiconductor transistor that switches “electric current” on and off. We can reuse waste heat exhausted to the environment using devices composed of thermal transistors such as thermal shutters and thermal displays^[1]. Although several thermal transistors have been demonstrated thus far, the use of liquid electrolytes (or ionic liquids or ion gels) may limit the application from the viewpoint of reliability or liquid leakage^[2-4]. Very recently, we demonstrated a solid-state thermal transistor that can electrochemically control the heat flow with an on-to-off ratio of the thermal conductivity (κ) of ~4 without using any liquid^[5]. The thermal transistor is composed of a multilayer film composed of an upper electrode (Pt), strontium cobaltite (SrCoO_x), solid electrolyte (YSZ), and bottom electrode (Pt). An electrochemical redox treatment at 280 °C in air repeatedly modulates the crystal structure and κ of the SrCoO_x layer. The fully oxidized perovskite-structured SrCoO₃ layer shows a high κ ~3.8 W m⁻¹ K⁻¹, whereas the fully reduced defect perovskite-structured SrCoO₂ layer shows a low κ ~0.95 W m⁻¹ K⁻¹. We believe that all-solid-state electrochemical thermal transistors have the potential to become next-generation devices for future thermal management technology, and we are currently working on improving their characteristics^[6, 7].

References

- [1] T. Swoboda *et al.*, *Adv. Electron. Mater.* **7**, 2000625 (2021).
- [2] J. Cho *et al.*, *Nat. Commun.* **5**, 4035 (2014).
- [3] A. Sood *et al.*, *Nat. Commun.* **9**, 4510 (2018).
- [4] Q. Y. Lu *et al.*, *Nat. Mater.* **19**, 655 (2020).
- [5] Q. Yang, H. Ohta *et al.*, *Adv. Funct. Mater.* **33**, 2214939 (2023).
- [6] Z. Bian, H. Ohta *et al.*, *ACS Appl. Mater. Interfaces* **15**, 23512 (2023).
- [7] M. Yoshimura, H. Ohta *et al.*, *ACS Appl. Electron. Mater.* **5**, 4233 (2023).

2:30 PM EL06.08.03

Effect of Strain on The Proton Conduction in Multi-Oriented BaZr_{0.9}Y_{0.1}O_{3-δ} Thin Film Artur Braun¹, Muhammad S. Saleem¹ and Qianli Chen²; ¹Empa, Switzerland; ²Shanghai Jiao Tong University Joint Institute, China

For proton-conducting ceramic fuel cells, BaZr_{0.9}Y_{0.1}O_{3-δ} (BZY10) is an attractive material due to its high proton conductivity and stability. The

physical and chemical fundamentals of proton conduction in sintered pellets and thin films and their heterostructures have been explored in several studies. The search for the effect of crystallographic orientation, grains, and grain boundaries on proton transport is yet an ongoing quest. We present a study [1] on the proton conduction in a self-assembled multi-oriented BZY10 thin film grown on top of a (110) NdGaO₃ substrate. The multiple orientations are composed of different lattices, which provide a platform to study the lattice-dependent conductivity through different orientations in the vicinity of grain boundary between them and the substrate. The crystalline stacking of each orientation is determined by X-ray diffraction analysis and scanning transmission electron microscopy. The transport measurements are carried out under different gas atmospheres. The highest conductivity is 3 mS/cm at 400 °C and found under a wet H₂ environment along with an increased lattice parameter of 4.208 Å, while under O₂ and even reducing Ar atmosphere, the film shows lower conductivity and smaller lattice parameter. Our findings not only demonstrate the role of crystal lattice for conduction properties but also illustrate the importance of self-assembled strategies to achieve high proton conduction in BZY10 thin films.

[1] M. S. Saleem, Q. Chen, N. A. Shepelin, S. Dolabella, M. D. Rossell, X. Zhang, C. X. Kronawitter, F. La Mattina, A. Braun, The Role of Strain in Proton Conduction in Multi-Oriented BaZr_{0.9}Y_{0.1}O_{3-δ} Thin Film, *ACS Appl. Mater. Interfaces* 2022, 14, 50, 55915–55924, <https://doi.org/10.1021/acsmi.2c12657>

2:45 PM EL06.08.04

Polar Vortices at mmWave Frequencies Florian Bergmann^{1,2}, Peter Meisenheimer³, Bryan Bosworth¹, Nick Jungwirth¹, Ramamoorthy Ramesh⁴ and Nate Orloff¹; ¹National Institute of Standards and Technology, United States; ²University of Colorado Boulder, United States; ³University of California, Berkeley, United States; ⁴Rice University, United States

PbTiO₃-SrTiO₃ superlattice films form Polar Vortices under the right lattice periodicity conditions. Experiments at kHz and THz frequencies have already shown emergent properties of these superlattice films like negative permittivity and collective lattice dynamics. However, data in the GHz range are sparse. Measurements in this frequency range are both interesting for the fundamental understanding of Polar Vortices and for potential electronic applications of the films. Here, we report on broadband measurements from 70 kHz to 110 GHz using Coplanar Waveguide devices. We extract the permittivity of a PbTiO₃-SrTiO₃ superlattice film on a DyScO₃ substrate and compare the results to those from co-fabricated PbTiO₃ and SrTiO₃ films. For all samples, we characterize the complex in-plane permittivity in two perpendicular orientations and as a function of bias voltage. Based on our results, we discuss the potential of Polar Vortex films for mmWave applications.

3:00 PM BREAK

3:30 PM EL06.08.05

Multimodal X-Ray Studies of Remote Epitaxy of Functional Oxides and Enhanced Functionalities on Graphene Hua Zhou, Xi Yan, Hui Cao, Yan Li, Hawoong Hong, Liliana Stan, Nathan Gusinger and Dillon D. Fong; Argonne National Laboratory, United States

Future technologies are likely to exploit flexible heterostructures exhibiting multifunctional properties constructed from multiple materials. One technique for the synthesis of such systems relies on remote epitaxy, which is a novel synthesis technique that allows for the fabrication of thin, freestanding single crystals and nanomembranes. It relies on a sacrificial layer (e.g. graphene) between a thin film and a single-crystalline substrate: during film deposition, the electronic interactions across the graphene are strong enough to enable epitaxial growth but weak enough to allow mechanical release of the film. Others have demonstrated methods for the fabrication of freestanding structures, but the procedures are often materials-specific in terms of the interlayer permitting epitaxial growth. The remote epitaxy technique can be used to create single crystal heterostructures comprised of stacked epitaxial films, their properties optimized by minimizing incompatibilities between the different materials. Details regarding nucleation and growth via remote epitaxy remain unknown, however, due to the many difficulties in studying synthesis in the growth environment with atomic-scale resolution. This necessitates *in situ* studies sensitive to the atomic-level structure conducted in the growth environment. *In situ* measurements are particularly important for the synthesis of complex oxides such as perovskite oxides, where small changes to the degree of oxygen incorporation can impact the properties of the film/interface as well as degrade the graphene interlayer.

Here, in this talk, we will firstly demonstrate an *in situ* synchrotron X-ray investigation of perovskite oxide (e.g. SrTiO₃ and LaNiO₃) thin film growth by molecular beam epitaxy onto graphene few layer coated SrTiO₃ (001) substrates. X-ray phase retrieval methods were used to reconstruct the electron density profiles from X-ray crystal truncation rods measured under different growth conditions. Our *in situ* observations combined with post-growth spectroscopy provide a number of key insights regarding graphene in the synthesis environment and the resulting effects on the complex oxide/graphene heterostructure. Furthermore, we show that the graphene buffer layer could also enhance the physical properties of a functional oxide thin film grown by the remote epitaxy. We will present the study conducted on epitaxial VO₂ thin films to assess to the effect of remote epitaxy on the metal-insulator transition (MIT). The epitaxial VO₂ heterostructures were synthesized on both bare Al₂O₃ (0001) substrates and Al₂O₃ substrates coated with a bilayer graphene. While both systems exhibit the MIT, the film grown by remote epitaxy on graphene demonstrates improved transport properties. Electrical transport measurements show that the on/off ratio is enhanced by a factor of ~7.5 and the MIT switching temperature window is narrower for VO₂ thin films grown on graphene. By characterizing the heterostructures with a suite of X-ray structural, chemical, and spectroscopic tools, we find that the graphene interlayer inhibits oxygen vacancy diffusion from Al₂O₃ (0001) during the VO₂ growth, resulting in improved electrical behaviors at the MIT.

3:45 PM EL06.08.06

Scanning Oscillator Piezoresponse Microscopy: New Tools to Explore Domain Wall Dynamics Neus Domingo Marimon, Shivarajan Raghuraman, Kyle Kelley and Stephen Jesse; Oak Ridge National Laboratory, United States

Dynamics of ferroelectric domain walls associated to domain wall switching are known to depend on bulk structure, being very sensitive to defects, chemical and structural pinning sites, as well as environmental conditions, modifying the electronic boundary conditions associated with screening dynamics. However, domain walls also show a sub-coercive field dynamics as a reversible motion, with vibrational states that strongly couple to local structure and composition of the domain wall. In this presentation, we will show a novel microscopy mode based on a multifrequency approach which allows us to quantify domain wall oscillations under applied sub-coercive electric field, while simultaneously disentangle electrostatic from net electromechanical signals, which can introduce severe distortions on the net piezoelectric response around neutral domain walls. This technique allows quick visualization of domain wall displacement, their velocities and dependence on pre-existing domain configurations and defects. When applied to lead titanate, this technique shows significant oscillations of the 180° domain walls between the antiparallel c+/c- domains. Further, the displacement and velocities distinctly depend on existing a-c domain structures and relative orientations of domains. This technique can be readily applied to other heterostructures under a wide range of stimuli such as light, heat, force and bias.

4:00 PM *EL06.08.07

Unprecedented Electromechanical Response in Antiferroelectric Thin Films Lane W. Martin; Rice University, United States

Antiferroelectrics, long considered the somewhat less exciting cousin of ferroelectrics, are having their moment. These materials, which possess antipolar order (*i.e.*, antiparallel alignment of polarization at zero field), can be switched to polar (parallel) order by an external electric field thus producing a reversible antiferroelectric-to-ferroelectric phase transition and a characteristic double polarization-electric-field hysteresis loop. Such a unique field-induced antipolar-to-polar transition endows antiferroelectrics with properties that are of great interest for a range of applications including nonlinear dielectrics, capacitive-energy storage, electrothermal-energy conversion, and electromechanical actuation. While these materials have been known for many decades, they remain relatively less well studied and understood as compared to their ferroelectric relatives. To better understand the nature of such phase transitions in antiferroelectrics and to finely engineer the polarization properties for targeted applications requires that one can fabricate high-quality versions of antiferroelectric materials. In this spirit, recent years have seen a growth in efforts to study these materials, particularly as thin films. Epitaxial films offer researchers the opportunity to finely control and manipulate the structure, orientation, strain, and much more. In turn, we are offered unprecedented insights into the nature and evolution of these complex and, at times, poorly understood physical phenomena.

Here, we apply the lessons of thin-film epitaxy to the study of antiferroelectrics. This talk will provide an overview of our recent efforts to synthesize, control, and study antiferroelectric perovskite oxides. Our attention will focus on classic, prototypical antiferroelectric materials such as PbZrO_3 and PbHfO_3 and solid solutions and multilayers derived from these parent materials. In turn, we will demonstrate how epitaxy, strain, and buffer layers can allow us to finely control the orientation of the resulting orthorhombic films and, in turn, how this orientation control affects the manifestation of properties. In particular, we will explore how antiferroelectrics offer a pathway to overcome traditional limitations in the achievement of large electromechanical responses in thin-film materials. We will explore an unconventional coupling of the field-induced antiferroelectric-to-ferroelectric phase transition and the substrate constraints in these materials. A detiling of the oxygen octahedra and lattice-volume expansion in all dimensions are observed commensurate with the phase transition, such that the in-plane clamping further enhances the out-of-plane expansion. In turn, an abnormal thickness scaling is realized wherein an ultrahigh electromechanical strain (1.7%) is produced from a model antiferroelectric PbZrO_3 film of just 100 nm thick. The exceptional performance and novel mechanism provide a promising pathway to develop high-performance micro-/nano-electromechanical systems. Ultimately, antiferroelectrics represent a relatively understudied realm of ferroic materials, ripe for the application of thin-film epitaxy to accelerate our understanding and use of these interesting materials.

4:30 PM *EL06.08.08

Voltage-Gated Hybrid Ferroelectric-Superconductive Quantum Devices Maria Badarne¹, Mohammad Suleiman¹, Martin Sarott², Morgan Trassin² and Yachin Ivry¹; ¹Technion, Israel; ²ETH Zürich, Switzerland

The increasing demand for data storage and manipulation urges technological developments outside the silicon arena. Superconductors are promising for enabling low-power and quantum computing that addresses the data-consumption growth. A prominent advantage of these materials is the lack of dc electric resistance, which in turn allows zero-energy loss while transmitting electric currents. Nevertheless, following Ohm's law, the lack of resistance makes voltage biasing impossible. Thus, as opposed to voltage-gated semiconducting transistors, superconducting devices are operated with magnetic fields and RF signals, imposing large device footprint and hence hindering device miniaturization and high-density scaling. Here, we used a ferroelectric-superconducting bilayer to demonstrate voltage-gated superconducting quantum devices. Films, wires and superconducting quantum interference devices (SQUIDs) were fabricated and characterized. The ferroelectric polarization was used to produce controllable surface charge at the bilayer interface, which in turn induced changes in the quantum properties, including 54% change in the device switching current. Thus, non-volatile voltage-tunable memory hybrid quantum devices were introduced.

SESSION EL06.09: Oxide Electronics—Devices and Computing

Session Chairs: Aiping Chen and Sundar Kunwar

Friday Morning, April 26, 2024

Room 343, Level 3, Summit

8:30 AM EL06.09.01

Dynamic Processes of Oxygen Ion Exchange in Strontium Cobaltite Bilayer Thin Films Driven by Oxidation and Reduction Jill Wenderott^{1,2}, Eric M. Dufresne¹, Yan Li¹, Hui Cao¹, Qingteng Zhang¹, Narayanachari Kondapalli³, D. Bruce Buchholz³, Supratik Guha^{4,1} and Dillon D. Fong¹; ¹Argonne National Laboratory, United States; ²Drexel University, United States; ³Northwestern University, United States; ⁴The University of Chicago, United States

Transition metal oxides (TMOs) possess variable oxygen stoichiometry which can be the cause of distinct changes to physical and electronic properties. As an example, the well-studied TMO strontium cobaltite (SrCoO_x), has two structurally and electrically distinct phases – the insulating orthorhombic brownmillerite ($\text{SrCoO}_{2.5}$ – BM-SCO) and conducting cubic perovskite ($\text{SrCoO}_{3-\delta}$ – PV-SCO) – that reversibly transition via a topotactic pathway with the insertion or removal of oxygen. In the thin film form, this topotactic transition occurs while preserving high quality epitaxial films, making this material system of interest for ionotronic devices. Here, BM-SCO/PV-SCO (001) (15 nm/15 nm) heterostructures on strontium titanate (STO) (001) and the exchange of oxygen ions across this bilayer are investigated in order to understand changes to the interface under oxidizing and reducing conditions.[1] X-ray diffraction (XRD) and X-ray photon correlation spectroscopy (XPCS) studies reveal strongly asymmetric behavior with slower dynamics appearing during reducing versus oxidizing conditions and similar dynamics in the $\text{SrCoO}_{2.5}$ layer as compared to those near the heterointerface. Our results demonstrate a stable and reversible heterointerface, showcasing SrCoO_x as a model system for study of ionotronic behavior.

*Work supported by the Department of Energy, Office of Science, Basic Energy Sciences under contract no. DE-AC02-06CH11357.

[1] Wenderott, et al. Adv. Mater. Interfaces 2023, 10, 2300127.

8:45 AM EL06.09.02

What We Have Learned So Far from Phase-Field Modeling of Epitaxial Thin Films of Orthorhombic $\text{K}_x\text{Na}_{1-x}\text{NbO}_3$ Bo Wang^{1,2}, Mengjun Zhou³, Ce-Wen Nan⁴ and Long-Qing Chen²; ¹Lawrence Livermore National Laboratory, United States; ²The Pennsylvania State University, United States; ³Wuhan University of Technology, China; ⁴Tsinghua University, China

Epitaxial ferroelectric thin films often exhibit unique polymorphic phases, domain structures, and physical properties dissimilar from their bulk counterparts due to the modification of mechanical and electrical boundary conditions. While extensive knowledge has been acquired for epitaxial thin films of bulk tetragonal (such as BaTiO_3 and PbTiO_3) and rhombohedral ferroelectric materials (such as BiFeO_3), much less is known for the thin films of bulk orthorhombic ferroelectrics such as $\text{K}_x\text{Na}_{1-x}\text{NbO}_3$. In this talk, I will review our recent progress in the development and employment of thermodynamic theory and phase-field modeling for understanding the phase stability and transformation, domain and domain wall structures, and

dielectric and piezoelectric properties of KNN thin films. I will highlight the computational establishment of anisotropic misfit strain-temperature phase diagrams, theoretical prediction and experimental validation of the formation condition and configuration of two types of superdomains, and the strong domain size-dependent piezoelectricity. I will also outlook potential topics unique for the epitaxial thin films of the orthorhombic ferroelectrics. Part of this work was performed under the auspices of the U.S. Department of Energy by Lawrence Livermore National Laboratory under Contract DE-AC52-07NA27344.

9:00 AM *EL06.09.03

Rare Earth Nickelates for Neuromorphic Computing Applications Olivia Schneble^{1,2}, Christopher Muzzillo¹, Mirzo Mirzokarimov¹, Michelle Smeaton¹, Jeremy D. Zimmerman² and Marshall B. Telekamp¹; ¹National Renewable Energy Laboratory, United States; ²Colorado School of Mines, United States

As global information consumption continues to grow, the energy required to support computations is consuming a significant portion of the global energy supply. Data centers alone will consume 4.5% of all energy by 2025,¹ with computing demands doubling every 3–4 years.² Neuromorphic computing promises an energy-efficient solution based on the naturally efficient mechanisms that drive human thought and memory; it was recently calculated to outperform other technologies, including quantum computing, by at least 10,000x in terms of energy per solution.³ Spiking neural networks (SNNs) are extremely efficient, encoding information based on the time between voltage spikes defined by multiple *local* inputs. The dynamic nature of the spiking processes can be simulated in conventional semiconductors at the cost of energy efficiency,^{4,5} however a more attractive solution utilizes materials that natively produce such dynamic behavior.

Materials with an insulator-metal transition (IMT) are ideal for accessing nonlinear transport properties that could be useful in SNNs. In addition, IMTs can be highly sensitive to structure, defects, and environmental factors. Coupling fundamental mechanisms to stimuli such as electric field, electrochemical gating, and optical stimuli is an attractive way of encoding adaptive behavior that is a function of multiple input variables. Recently, IMT materials such as VO₂ and NbO₂ have been used to replicate the Hodgkin-Huxley action potential in pull-up/pull-down neuristor circuitry.^{6–8} The IMT of NbO₂ is at 1080 K, too high for energy-efficient use, while the IMT of VO₂ is at 330 K (with doping up to 370 K)⁹, meaning active cooling is required for operation with silicon CMOS, which typically operate around 400 K. Meanwhile, RNOs have a tunable IMT from 100–600 K, with known sensitivity to many inputs.¹⁰ Therefore, it is attractive to improve our understanding of RNO synthesis, control the IMT, and leverage it for neuromorphic computing applications. In this invited talk, I will overview our efforts to controllably synthesize RNO compounds (R = Gd, Eu, Sm, Nd, La) and leverage them for neuromorphic computing applications. I will first discuss synthesis of high-quality heteroepitaxial nickelate layers and bilayer stacks by RF magnetron sputtering, including successful stabilization of EuNiO₃ by RF sputtering which we have not seen reported elsewhere. I will also focus on the connection between uncontrollable synthetic parameters such as target aging and resulting film properties. In addition to RF sputtering, I will discuss synthesis of heteroepitaxial layers and bilayer stacks by pulsed laser deposition (PLD) while connecting deposition parameters to measured properties. In particular, I will present EuNiO₃/LaNiO₃ bilayers with a residual resistivity ratio ~ 7 orders of magnitude.

Finally, I will conclude with a discussion of our efforts to fabricate devices using nickelate bilayers, including a discussion of challenges and possible approaches to creating vertical devices for scalability. I will discuss our recent results of electrically-driven IMTs in NdNiO₃ and NdNiO₃/LaNiO₃ bilayers which show strong negative differential resistance (NDR) – the key electrical characteristic leveraged in neuristor circuits.

1. Liu et al. *Global Energy Interconnection* **3**, 272–282 (2020).
2. Masanet et al. *Nat Electron* **3**, 409–418 (2020).
4. Merolla et al. *Science* **345**, 668–673 (2014).
5. Merolla et al. *2011 IEEE Custom Integrated Circuits Conference (CICC)* 1–4 (2011).
6. Lin et al. *Nat Electron* **3**, 225–232 (2020).
7. Pickett et al. *Nature Materials* **12**, 114–117 (2013).
8. Kumar et al. *Nature* **585**, 518–523 (2020).
9. Schofield et al. *Chemical Communications* **58**, 6586–6589 (2022).
10. Catalano et al. *Rep. Prog. Phys.* **81**, 046501 (2018).

9:30 AM BREAK

10:00 AM ^EL06.09.04

Emerging Self-Assembled Oxide–Metal Nanocomposite Thin Films with Coupled Multifunctionalities Di Zhang¹, Shikhar Misra², Jijie Huang², Bruce Zhang², Matias Kalaswad², Robynne Paldi², Bethany Rutherford², Xuejing Wang², Jiawei Song², Aiping Chen¹ and Haiyan Wang²; ¹Los Alamos National Laboratory, United States; ²Purdue University, United States

Beyond oxide-oxide functional nanocomposite films which have been widely explored in the past two decades of this century, oxide-metal nanocomposites films have attracted increasing interests in recent years owing to their wide range of functionalities, such as metamaterials with plasmonic and hyperbolic optical properties, and ferroelectric, ferromagnetic and multiferroic behaviors. In this talk, I will focus on introducing the recently explored oxide-metal vertically aligned nanocomposite (VAN) thin films showing exotic optical, electrical, and magnetic properties coupling effect. Detailed transmission electron microscopy (TEM) and X-ray diffraction (XRD) characterization work revealed the film epitaxy and crystallographic lattice matching relation at metal/oxide interfaces. The anisotropic film morphology results in the corresponding anisotropic physical properties such as plasmonic hyperbolic dispersion and magnetism anisotropy. In situ TEM heating experiment clarified the excellent thermal stability of the oxide-metal nanocomposite thin film. The unique physical properties and coupled functionalities of the VAN films enable them to have great potential in nanoelectronic and nanophotonic devices applications.

10:30 AM EL06.09.05

Stochastic Oscillations of LaCoO₃ Memristor for True Random Number Generator Kyung Seok Woo^{1,2}, Timothy D. Brown¹, Alan Zhang¹, Elliot J. Fuller¹, R. Stanley Williams^{1,2} and Suhas Kumar¹; ¹Sandia National Laboratories, United States; ²Texas A&M University, United States

In the era of Internet of Things, information security has become significantly important. Hardware-based true random number generator (TRNG) is a crucial component of security that relies on unpredictability, and the physical stochasticity of memristors has been implemented for TRNG. Here we demonstrate LaCoO₃ memristor capable of generating random numbers using its stochastic self-oscillations. We utilized Scanning Transmission X-ray Microscopy to confirm a low to high electron-spin-state transition in the Co³⁺ ion during the insulator-metal-transition (IMT). Our LaCoO₃-based TRNG requires only one flip-flop to produce binary bits and generates the highest bit generation speed among reported volatile-memristor-based TRNGs. It successfully passed the NIST randomness test without any post-processing. Unlike Mott-transition-based memristors, such as VO₂ and NbO₂ devices, which have abrupt temperature-driven IMT, the spin-state transition of LaCoO₃ undergoes the IMT with a gradual temperature increase, leading to high endurance. This work demonstrates the advancement of memristor-based hardware security, providing a major step toward a simple, fast, and stable system.

10:45 AM EL06.09.06

Reconfigurable Cascaded Thermal Neuristors for Novel Computing Erbin Qiu, Yuan-Hang Zhang, Massimiliano Di Ventra and Ivan Schuller; University of California, San Diego, United States

In our work, we explore a novel class of spiking oscillators termed "thermal neuristors". These neuristors function and communicate exclusively through thermal processes, utilizing the insulator-to-metal transition in vanadium dioxide. We showcase a diverse range of reconfigurable electrical behaviors that closely resemble those of biological neurons, including phenomena like the all-or-nothing law, type-II neuronal rate coding law, spike-in and DC out effect, spike-in and spike-out effect, and stochastic leaky integrate-and-firing law. Remarkably, inhibitory capabilities are achieved using just a single oxide device, and the transmission of cascaded information occurs solely through thermal interactions without any intricate circuits. This research serves as the groundwork for scalable and energy-efficient thermal neural networks, advancing the field of brain-inspired computing.

11:00 AM EL06.09.07

Harnessing The Competing Roles of Charge to Design Ferroelectric-Gated Mott Transistors Yifei Hao¹, Xuegang Chen¹, Le Zhang¹, Myung-Geun Han², Wei Wang², Yue-Wen Fang³, Hanghui Chen³, Yimei Zhu² and Xia Hong¹; ¹University of Nebraska - Lincoln, United States; ²Brookhaven National Laboratory, United States; ³New York University Shanghai, China

The device concept of ferroelectric-gated Mott field effect transistors (FETs) has been intensively studied for the past three decades as a promising building block for developing energy-efficient nanoelectronics that can transcend the scaling limits of conventional semiconductor technology. The nearly metallic density of carriers within the Mott channel, however, imposes a major bottleneck for achieving substantial field effect modulation via a solid-state gate. In this study, we report a record high room temperature resistance switching in a rare earth nickelate ($RNiO_3$) channel controlled by a ferroelectric $PbZr_{0.2}Ti_{0.8}O_3$ (PZT) gate. We have systematically studied the ferroelectric field effect in $RNiO_3$ ($R = Sm, Nd, La$) to identify the optimal channel materials for constructing nonvolatile Mott transistors. For single-layer $RNiO_3$ channels, the resistance switching ratio $\Delta R/R_{on}$ peaks near the electrical dead layer thickness and then decreases abruptly due to strong depolarization in PZT. Switching the polarization of PZT induces a metal-insulator transition in the 4 uc single-layer $LaNiO_3$ channel. At 300 K, the highest $\Delta R/R_{on}$ of 1,619% is observed in 2 unit cell (uc) $LaNiO_3$ channels as it possesses the smallest electrical dead layer thickness. Devices with $RNiO_3/La_{0.67}Sr_{0.33}MnO_3$ (LSMO) composite channels exhibit up to three orders of magnitude higher $\Delta R/R_{on}$ compared with the single layer channel FETs with the same channel thickness. A record high $\Delta R/R_{on}$ of 38,540% is observed in the 2.5 uc $LaNiO_3/2$ uc LSMO bilayer channel at 300 K. Such an enhancement has been attributed to the interfacial charge transfer between $RNiO_3$ and LSMO, which reduces the net carrier density in $RNiO_3$ without compromising the screening of depolarization field in PZT. First principles calculations reveal about 0.1 electron/Mn transfer from interfacial Mn to Ni layers (or hole transfer from Ni to Mn). Both the magnitude and length scale of the charge transfer have been confirmed by atomically resolved EELS mapping. We have also studied the retention and cycling behaviors of the PZT/ $LaNiO_3$ /LSMO FETs, which reveal superior device performance compared with those of single-layer Mott channels and FeFETs exploiting polycrystalline PZT gates. Our study addresses one of the critical material challenges that limit the application potential of epitaxial ferroelectric-gated Mott transistors.

This work was primarily supported by National Science Foundation (NSF) Grant No. DMR-1710461 and EPSCoR RII Track-1: Emergent Quantum Materials and Technologies (EQUATE), Award No. OIA-2044049, and Semiconductor Research Corporation (SRC) under GRC Task Number 2831.001

11:15 AM EL06.09.08

Piezo-Strain-Controlled Phase Transition in Single-Crystalline Mott Switches for Threshold-Manipulated Leaky-Integrate-And-Fire Neurons Dong Kyu Lee, Sungwon Lee, Yunkyu Park, Si-Young Choi and Junwoo Son; Pohang University of Science and Technology, Korea (the Republic of)

Correlated oxides with strong correlations between the charge, spin, lattice, and orbital degrees of freedom present a wide array of emergent properties, such as metal-insulator transition, ferroelectricity, and superconductivity. These exotic functionalities give an opportunity to overcome the limitations of electronic devices; thus heteroepitaxial growth have been employed to synthesize these functional ionic crystals. However, unrestricted integration of emergent functionality from single-crystal oxide films is inhibited owing to the limited platforms to grow epitaxial films. Therefore, unrestricted integration of single-crystal oxide films has been of great interest to exploit emerging phenomena in artificial heterostructure. Here, we demonstrate a new strategy to integrate single-crystal (002) VO_2 thin films on highly lattice-mismatched (002) PMN-PT converse piezoelectric substrate ($\epsilon_a > 10\%$) by utilizing freestanding oxide nanomembrane (NM) as epitaxial template [1]. By selective dissolution of VO_2 sacrificial layers from TiO_2/VO_2 heterostructure grown on TiO_2 substrate by H_2O_2 solution, millimeter-size TiO_2 single-crystalline layers are integrated on PMN-PT substrate. After subsequent epitaxial growth of VO_2 films on the transferred TiO_2 NM, we create single-crystalline VO_2 /PMN-PT heterostructures with excellent sharpness of metal-insulator transition ($\Delta\rho/\rho > 10^3$) even in ultrathin (<10 nm) VO_2 films. Moreover, piezoelectric-mediated reversible strain modulation of single-crystalline VO_2 films showed unprecedented modulation of T_{MI} (5.2 K) and isothermal resistance of VO_2 ($\Delta R/R (E_g) = 20\%$ at 300 K) via effective strain transfer, which is not possible using directly grown VO_2 /PMN-PT heterostructure. Owing to the steep phase transition near the phase boundary and effective strain transfer, small changes in the lattice parameters can cause the strain induced abrupt phase transition in our VO_2 films on TiO_2 NM/PMN-PT substrate ($\Delta R/R (E_g) \approx 18000\%$ at 315K). The massive and reversible strain modulation of VO_2 epitaxial films by the VO_2 /PMN-PT heterostructure offers a new type of artificial neurons with a real-time-tuned threshold values. Our strategy to utilize freestanding oxide NMs as epitaxial template for realizing single-crystalline artificial heterojunction will provide an unique opportunity to investigate unprecedented exotic functionality for novel interfacial physics and next-generation devices.

References

[1] D. K. Lee et al., *Nat. Commun.* **12** (2019) 5019

<script src="chrome-extension://hhojmcodeegachlhfgfdhailpfhgkijnm/web_accessible_resources/index.js"></script>

11:30 AM ^EL06.09.09

Resistive Switching Oxide Nanocomposite Thin Films for Sustainable Artificial Intelligence Markus Hellenbrand¹, Ming Xiao¹, Babak Bakhtir¹, Hongyi Dou², Megan Hill¹, Nives Strkalj¹, Adnan Mehonic³, Quanxi Jia⁴, Haiyan Wang² and Judith MacManus-Driscoll¹; ¹University of Cambridge, United Kingdom; ²Purdue University, United States; ³University College London, United Kingdom; ⁴University at Buffalo, The State University of New York, United States

Artificial intelligence (AI) applications are increasingly affecting many areas of our lives. However, they are mostly being implemented in the conventional von Neumann computing architecture, which suffers from the memory bottleneck, i.e., a bottleneck in shuttling data between the memory and processing parts of the von Neumann architecture. This leads to immense power consumption due to AI applications, because with billions of parameters, they are very memory-heavy. New approaches to AI computing are thus necessary to enable a sustainable future.

One of the most promising approaches are resistive switching (RS) materials, where information is stored as the resistance state of a memory cell, rather than as charge on a capacitor as in conventional computer memory. RS materials hold promise to realise hardware neuromorphic networks, for example in the form of crossbar arrays, which make it possible to combine memory and processing into in-memory computing and thus circumvent the memory bottleneck. We developed oxide nanocomposite thin films which are based on a self-assembled phase separation on the nanoscale, and which demonstrate highly uniform and stable multi-level resistive switching. They are deposited at industry-friendly temperatures of ≤ 400 °C and demonstrate great promise in all standard figures of merit for resistive switching. In different materials systems, we achieve $\geq 10\,000$ switching cycles across a large number of devices, stable retention of up to ≥ 300 days, up to ≥ 500 resistance states, spike-timing-dependent plasticity, and fast switching down to 20 ns. These data will be presented together with compositional and structural analyses of the underlying films and the corresponding RS mechanisms.

SESSION EL06.10: Oxide Electronics—Synthesis and Characterization
Session Chairs: Nicholas Cucciniello, Megan Holtz and Yachin Ivry
Friday Afternoon, April 26, 2024
Room 343, Level 3, Summit

1:30 PM *EL06.10.01

Structural and Optical Properties of Compositionally Disordered Perovskite Metal Oxide Films Zachary Corey^{1,2}, Ping Lu³, Guanran Zhang⁴, Yogesh Sharma², Bethany Rutherford⁵, Samyak Dhole¹, Pinku Roy^{1,2}, Zhehui Wang², Yiqian Wu⁴, Haiyan Wang⁵, Aiping Chen² and Quanxi Jia¹; ¹University at Buffalo, United States; ²Los Alamos National Laboratory, United States; ³Sandia National Laboratories, United States; ⁴Alfred University, United States; ⁵Purdue University, United States

Perovskite metal oxides offer a wide range of functionalities owing to their rich compositional diversity. Experimental results have shown that much-enhanced physical properties could be achieved by forming multicomponent or high-entropy perovskite oxides. In this talk, we discuss our efforts in the design and synthesis of compositionally disordered epitaxial perovskite metal oxide films with multiple A-site cations. Using rare-earth aluminum perovskite oxide with an equiatomic ratio $(\text{La}_{0.2}\text{Lu}_{0.2}\text{Y}_{0.2}\text{Gd}_{0.2}\text{Ce}_{0.2})\text{AlO}_3$ as the model system, we show that a high entropy oxide system with equiatomic A-site cations allows for the achievement of desired optical luminescence observed in mixtures and/or doping of RE aluminates while maintaining a highly crystalline single-phase. The high crystallinity of these materials paves the way for exciting new research of high precision scintillating applications.

2:00 PM EL06.10.02

Vector Substrates: How to Grow Epitaxially Impossible Heterostructures Yu-Jung Wu¹, Varun Harbola¹, Felix Hensling¹, Hongguang Wang^{1,2}, Peter A. van Aken^{1,2} and Jochen Mannhart¹; ¹Max Planck Institute for Solid State Research, Germany; ²Stuttgart Center for Electron Microscopy, Germany

Substrates play a crucial role in thin film deposition, but they do not always align with the specific requirements of a particular experiment or application. For instance, they might be expensive or unavailable with a desired crystal lattice structure. To address this, we introduce the novel concept of "vector substrates." In this approach, the template layer for growing thin films is both chemically and structurally independent from the main substrate. Vector substrates are fabricated by transferring a membrane, which serves as the template layer and is grown on a reusable parent substrate, onto a carrier substrate. The template and carrier layers can be independently chosen and optimized, which reduces material costs and offers more flexibility. We validate the feasibility of this technology by presenting sets of vector substrates for high-quality epitaxial film growth and by demonstrating a clean interface between the transferred membrane and the carrier substrate. The vector substrate concept is in its early stages of development but holds significant promise to supplement conventional substrates and drives future advancements in substrate technology and the deposition of films and heterostructures.

2:15 PM EL06.10.03

Heterogeneous Nucleation of YBCO Film Deposited by MOD: Experimental Verification of a Thermodynamic and Kinetic Model Valentina Pinto¹, Michele De Angelis^{2,1}, Achille Angrisani Armenio¹, Andrea Augieri¹, Giuseppe Celentano¹, Andrea Masi¹, Silvia Orlanducci², Alessandro Rufoloni¹ and Massimo Tomellini²; ¹ENEA, Italy; ²Tor Vergata University, Italy

The deposition of superconducting $\text{YBa}_2\text{Cu}_3\text{O}_{7-\delta}$ (YBCO) thin film can be performed through physical and chemical methods, being the latter ones really advantageous in terms of cost-effectiveness, versatility, and simplicity. Therefore, within the last decade, the use of chemical solution deposition method, in particular the metal organic decomposition (MOD) approach, for producing epitaxial YBCO films has played an increasing role in the development of scalable processes.

In recent years, the need for a quantitative model for the YBCO heterogeneous nucleation emerged in order to better control the parameters affecting the formation of epitaxial film deposited by fluorine based MOD process. In fact, despite the great number of articles on YBCO deposition, the nucleation has been scarcely studied in the literature and only at qualitative level. However, it is a crucial step because the best superconducting properties are exhibited by YBCO film with the *c*-axis orientation. Recently, a thermodynamic and kinetic study on the heterogenous nucleation of YBCO film has been proposed in [1]. The model focused on fluorine based MOD deposition on SrTiO_3 (STO) single crystal and was developed on the basis of the classical nucleation theory providing an estimate of *c*-axis grain fraction as a function of water partial pressure and temperature. This latter calculation could constitute a useful tool to *a priori* define the proper experimental conditions for depositing highly epitaxial *c*-axis film when low crystallization temperatures may be necessary.

In the present work, the experimental verification of the model is proposed. The deposition of YBCO films on STO single crystal has been performed at different crystallization temperatures and water partial pressure values. The prepared samples have been fully characterized through the analysis of microstructure, morphology, and superconducting properties. The *c*-axis fraction has been derived by x-ray diffraction analysis and the experimental data have been described by the theoretical curves calculated from the model.

The deposition on a different substrate, namely LaAlO_3 (LAO), has been also carried out to study the effect of the substrate on YBCO nucleation kinetics. In fact, the expression for the free energy barriers includes the work of adhesion of the YBCO/substrate interface. The preliminary results obtained for YBCO/LAO samples evidenced the critical importance of this quantity and its technological implications.

In general, the present study shows that a deeper comprehension of the nucleation mechanism can lead to the improvement not only of the YBCO superconducting properties, but also of the process robustness and reproducibility.

[1] V. Pinto, G. Celentano, and M. Tomellini, *Supercond. Sci. Technol.*, vol. 33, no. 11, p. 115006, Nov. 2020, doi: 10.1088/1361-6668/abb201.

2:30 PM EL06.10.04

Bridging Thin Films Growth and Advanced Electron Microscopy to Uncover Structure-Property Correlations in Oxide Electronics Robert Winkler¹, Alexander Zintler², Oscar Recalde¹, D spina Nasiou¹, Lambert Alff¹ and Leopoldo Molina-Luna¹; ¹TU Darmstadt, Germany; ²University of

Antwerp, Belgium

Reactive Molecular Beam Epitaxy (RMBE), among other Physical Vapor Deposition (PVD) techniques, can precisely fabricate high-quality semiconductor heterostructures necessary for complex oxide electronics [1]. Their composition and crystallinity can be engineered through careful selection of growth parameters [2], [3], however are subject to the underlying layer. Here, miscut, composition and lattice mismatch impact texture transfer and thus the resulting microstructure [4].

Typically, RMBE is used to grow epitaxial thin films, yet textured thin films with defects might be more promising in oxide electronics applications like superconductors or emerging memories like resistive random access memory (RRAM). In our study, we investigated the texture relationship of TiN grown on c-cut sapphire by combining ion channeling contrast imaging (ICCI) with pole figure mapping. In addition, textured HfO₂ has been in situ grown on optimized TiN layers to investigate the impact of extended defects on RRAM performance by using atom probe tomography (APT) and operando electron microscopy. Our results indicate that a certain miscut of c-cut sapphire promotes distinct types of extended defects, which, as confirmed by elemental composition investigations using APT, are essential for RRAM operations.

Combining synthesis, macroscopic and microscopic investigation, and device characterization can bridge the information gaps required to further oxide electronics.

References:

- [1] *Beam Technologies for Integrated Processing*. Washington, D.C.: National Academies Press, 1992. doi: 10.17226/2006.
- [2] R. Winkler *et al.*, 'Controlling the Formation of Conductive Pathways in Memristive Devices', *Advanced Science*, vol. n/a, no. n/a, p. 2201806, doi: 10.1002/advs.202201806.
- [3] S. U. Sharath *et al.*, 'Control of Switching Modes and Conductance Quantization in Oxygen Engineered HfOx based Memristive Devices', *Advanced Functional Materials*, vol. 27, no. 32, p. 1700432, 2017, doi: 10.1002/adfm.201700432.
- [4] A. Zintler *et al.*, 'Enhanced Conductivity and Microstructure in Highly Textured TiN_{1-x}/c-Al₂O₃ Thin Films', *ACS Omega*, vol. 7, no. 2, pp. 2041–2048, Jan. 2022, doi: 10.1021/acsomega.1c05505.

2:45 PM EL06.10.05

Phase Change Material VO₂/Iridium/Yttria-Stabilized Zirconia Heterostructures on Silicon Christina Bestebe and Helmut Karl; University of Augsburg, Germany

External parameters like temperature, strain and electric fields can be employed to control the metal-insulator phase transition (MIT) of the strongly electron-correlated material vanadium dioxide (VO₂). This MIT is accompanied by an enormous decrease in electrical resistivity and optical transmittance in the infrared spectral region and especially the telecom window. VO₂ is thus a very promising material for hybrid optoelectronic integrated circuits [1,2]. In order to use its properties for introducing new functionality in integrated circuits based on silicon, high quality thin VO₂ films on dielectric and metallic layers are of importance.

In this work, we demonstrate epitaxial growth of VO₂ on yttria-stabilized zirconia (YSZ) and a layer stack of iridium/YSZ epitaxially grown on (001)-silicon, where the iridium layer forms a backside metallization that is used as a capacitor plate and areal contact to the VO₂ layer on top. The heterostructures were fabricated in the following way: at first, a dielectric and electrically insulating YSZ template-layer was grown epitaxially on a (001)-silicon substrate [3], followed by the growth of the VO₂ thin film, both deposited by pulsed laser deposition. Similarly, the VO₂/Iridium/YSZ heterostructure was grown, except that the iridium layer was grown ex-situ by e-beam evaporation [4,5]. The iridium layer provides a highly electrically conducting electrode allowing building capacitor structures with VO₂ to control the MIT by electric fields and to build vertical electronic switching devices for very fast sensing applications and current control.

The YSZ template-layer inhibits silicide formation by blocking diffusion of the cations to the YSZ/Si interface. Pole figures, reciprocal space maps and temperature dependent μ -Raman spectroscopy measurements reveal (010)-oriented VO₂ layers with 30° in-plane rotated crystallites and high symmetry grain boundaries on both the (001) iridium/YSZ double layer and YSZ template-layer.

Based on these multilayers metal/VO₂/iridium capacitor structures on silicon were fabricated and the effect of an electric field on the MIT were studied by μ -Raman spectroscopy and spectral reflectivity measurements.

- [1] Jostmeier Th., et al., Optically imprinted reconfigurable photonic elements in a VO₂ nanocomposite. *Applied Physics Letters* 105, (2014).
- [2] John J., et al., Multipolar resonances with designer tunability using VO₂ phase-change materials. *Physical Review Applied* 13, 044053 (2020).
- [3] Karl H., Hartmann J. and Stritzker B., Inplane lattice-constant relaxation during laser-ablation of YBCO and yttria-stabilized zirconia. *Thin Solid Films* 241, 84–87 (1994).
- [4] Fischer, et al., Preparation of 4-Inch Ir/YSZ/Si(001) substrates for the large-area deposition of single-crystal diamond. *Diamond and Related Materials* 17, 1035–1038 (2008).
- [5] Kraus T., et al., Yttria-stabilized zirconia buffered silicon to optimize in-plane electrical conductivity of [Ca₂CoO₃]_{0.62}[CoO₂] thin films. *Appl. Phys. Lett.* 104, 183104 (2014).

3:00 PM BREAK

3:30 PM EL06.10.06

Emergent Electronic and Structural Landscapes in a Novel Valence Ordered Thin-Film Nickelate prepared by Topochemical Reduction Aravind Raji^{1,2}, Zhengang Dong^{3,4}, Victor Porée², Alaska Subedi⁵, Guillaume Krieger⁶, Xiaoyan Li¹, Bernat Mundet^{7,8}, Lucia Varbaro⁷, Claribel Domínguez⁷, Marios Hadjimichael⁷, Bohan Feng^{3,4}, Daniele Preziosi⁶, Alessandro Nicolaou², Jean-Pascal Rueff^{2,9}, Danfeng Li^{3,4} and Alexandre Gloter¹; ¹Laboratoire de Physique des Solides Orsay, France; ²Synchrotron SOLEIL, France; ³City University of Hong Kong, Hong Kong; ⁴City University of Hong Kong Shenzhen Research Institute, China; ⁵Ecole Polytechnique, France; ⁶IPCMS UMR, CNRS, Université de Strasbourg, France; ⁷University of Geneva, Switzerland; ⁸Ecole Polytechnique Fédérale de Lausanne (EPFL), Switzerland; ⁹LCPMR, Sorbonne Université, CNRS, France

The on-demand design of transition-metal oxides (TMO) with emerging properties is imparted by the multivalent nature of the transition-metal ions and the accessible complexity of lattice structures [1, 2]. One can access a wide range of electronic landscapes by varying the structure and constituent elements in TMO. The oxygen dynamics in the system determines the resulting structure, and thereby their electronics. The metal hydride based topochemical reduction is one of the oxygen (de-) intercalation methods and it has been employed to synthesize otherwise difficult systems such as the infinite-layer nickelates (IL-nickelates), which was found to be superconducting upon doping [3].

In this path, from topochemical reduction of a perovskite SmNiO₃ thin-film, we obtain a novel valence-ordered and tri-component coordinated nickelate phase [4]. This new phase, with the chemical formula of Sm₉Ni₉O₂₂ (SmNiO_{2.44}) is formed by intricate planes of {303}_{pc} (subscript pc refers to pseudocubic) apical oxygen vacancies (Vo) from the parent perovskite as revealed by four-dimensional scanning transmission electron microscopy (4D-STEM). Transport measurements indicated this phase to be highly insulating, over the measured temperature range (30K - 400K). A coherent analysis between ab-initio simulations and Synchrotron based X-ray spectroscopy techniques that evidenced a strong orbital polarization elucidated that this nickelate hosts multi-valent Ni sites that are in NiO₅ pyramidal, NiO₄ square-planar, and NiO₆ octahedral coordinations. The resonant inelastic x-ray

scattering (RIXS) measurements at the O-K edge also revealed this system to be having a strong carrier localization, marked by the disappearance of a ligand-hole configuration at low temperature. The periodicity of these polyhedral ordering, that can also be interpreted as valence ordering, follows the periodicity of the apical Vo ordering. The NiO₄ square-planar sites forms at the intersection of the families of {303}_{pc} apical Vo planes, indicating a route to the infinite-layer phase.

Apart from these, this phase being an intermediate between the perovskite ABO₃ and infinite-layer ABO₂, it could have been present as a defect in many IL-nickelate samples, and caused complexity in identifying their pristine properties. The ongoing debate on the (1/3, 0, 1/3) r.l.u. Charge ordering reported in IL-nickelates is one such prototypical example [5- 10]. Our STEM-EELS analysis found quasi-2D nanodomains of (303)_{pc} apical Vo ordering in a charge ordered IL-nickelate, and its absence in a sample without charge ordering [8]. Later on, another group also reported similar Vo ordering combining with resonant x-ray scattering that directly corroborated our idea [9]. It is evident from the measurements in those thin-films and with that of Sm₉Ni₉O₂₂ that the nano-domains of (303)_{pc} ordering there was in fact the presence of nano-domains of Sm₉Ni₉O₂₂ phase as a defect. This directly questions the intrinsic nature of (1/3, 0, 1/3) r.l.u. Charge ordering reported in IL-nickelates.

This new nickelate compound provides another example of previously inaccessible materials enabled by topotactic transformations and presents a unique platform where mixed Ni valence can give rise to exotic phenomena.

[1] Dagotto, E. *Science* 309, 257–262 (2005). [2] Ahn, C. et al. *Nature materials* 20, 1462–1468 (2021). [3] Li, D. et al. *Nature* 572, 624–627 (2019). [4] **Raji, Aravind**, et al. arXiv preprint arXiv:2308.02855 (2023) (Under revision, ACS Nano). [5] Tam, Charles C., et al. *Nature Materials* 21.10 (2022): 1116–1120. [6] Rossi, Matteo, et al. *Nature Physics* 18.8 (2022): 869–873. [7] Krieger, G., et al. *Physical Review Letters* 129.2 (2022): 027002. [8] **Raji, Aravind**, et al. *Small*, 2304872. (2023). [9] Parzyck, C. et al. arXiv preprint arXiv:2307.06486 (2023). [10] Pellicciari, Jonathan, et al. arXiv preprint arXiv:2306.15086 (2023).

3:45 PM EL06.10.07

Evidence for Phase Transitions in CoFe₂O₄ and NiCo₂O₄ Thin Films in Temperature Dependent X-Ray Photoelectron Spectroscopy Arjun Subedi, Detian Yang, Xiaoshan Xu and Peter Dowben; University of Nebraska–Lincoln, United States

The temperature dependent X-ray photoelectron spectroscopy (XPS) of the CoFe₂O₄ thin film showed that core level binding energies decreased with increasing temperature. The large binding energy shifts of the Co 2p_{3/2} and Fe 2p_{3/2} core levels of CoFe₂O₄ thin film, observed at room temperature, are due to large photovoltaic surface charging. The large binding energy shifts of the Co 2p_{3/2} and Fe 2p_{3/2} core levels, in the X-ray photoelectron spectroscopy of CoFe₂O₄ thin film, decreased with increasing temperature. However, above 455 K, during annealing of the sample, shifts in the core level binding energies ceased to decrease. This shows that the prepared CoFe₂O₄ thin film can be dielectric at room temperature but more metallic at elevated temperatures. The dielectric nature of the film was restored only when the film was annealed in sufficient oxygen, indicating that the oxygen vacancies play a role in the transition of the film from dielectric (or insulating) to conducting. In contrast, similar studies on NiCo₂O₄ thin film showed that annealing of NiCo₂O₄ thin film, which was observed to be conducting, could make NiCo₂O₄ thin film insulating, and the original more metallic character of the NiCo₂O₄ thin film could be restored only when the sample was annealed in sufficient oxygen. A model that governs the core level binding energy changes, as a function of temperature, is proposed. Furthermore, restoration of the original properties or phases of the thin films after undergoing a metal-to-insulator transition illustrates routes to regulate the surface metal-to-insulator transition, especially in the case of insulating NiCo₂O₄ thin film which can undergo reversible metal-to-insulator transition with temperature. This work provides a better fundamental understanding of defect mediated surface phases for thin film oxides and opens avenues for defect assisted and/or temperature dependent future beyond CMOS devices.

4:00 PM EL06.10.08

XANES Analysis of Mn-Alloyed TiO₂ Coatings Grown by Atomic Layer Deposition: Probing The Crystallization Behavior Devan Solanki¹, Deyu Lu² and Shu Hu¹; ¹Yale University, United States; ²Brookhaven National Laboratory, United States

TiO₂ is a nontoxic, wide bandgap semiconductor with many excellent physical properties such as high chemical stability in acids and bases and good optical transparency to visible light, making it an excellent candidate for photoelectrocatalysis. Atomic Layer Deposition (ALD) enables synthesis of conformal coatings on various substrates by its layer-by-layer, surface-growth mechanism. However, controlling the crystal structure, which can modulate properties such as the band gap and band edge positions, remains a challenge as TiO₂ is often amorphous as deposited but can be annealed into multiple polymorphs such as anatase, rutile, and brookite. Despite progress in understanding the reaction mechanisms and intermediates associated with the deposition of binary materials via ALD, there are still many questions surrounding the structure-processing relationship of ternary materials. For example, the role that dopants or alloying agents play in determining key properties such as oxidation state and crystal structure remain open questions.

Methods:

The X-Ray Absorption Spectroscopy (XAS) and X-ray Absorption Near Edge Structure (XANES) measurements were conducted at the Inner Shell Spectroscopy beamline of the National Synchrotron Light Source II (NSLS-II) at Brookhaven National Lab. The data was collected at room temperature with the energy calibrated using a Ti foil. The Athena software package was used to calibrate the energy and normalize the data using the recommended parameters. XAS was collected in fluorescence mode with $\mu(E) = If/I0$ where I_f is the fluorescence intensity and I_0 the incident intensity. Each spectrum is flattened so that the overall spectrum has an asymptotic behavior approaching 1.

Results:

The primary pre-edge feature in the TiO₂ sample, centered at 4968 eV is due to the oxygen vacancies and resultant undercoordinated Ti. The absorption maximum of that pre-edge feature is unchanged after the incorporation of Mn. However, there is a narrowing of the peak in TiMnOx samples relative to the TiO₂ and an enhancement of the shoulder peak that appears at 4972 eV. The separation between the apex of the first and second pre-edge feature corresponds to the crystal field splitting energy of the Ti 3d states. This indicates that the incorporation of Mn, while not having an effect in the oxidation state of the Ti, does perturb the local steric coordination environment. Quantitative analysis of this feature was not possible due to the background variation between the different samples and the low absolute intensity of the peak. Analysis of the Mn K-edge reveals that the oxidation state of Mn in the as-grown TiMnOx is independent of Mn concentration. One explanation for this fractional oxidation state could be the incorporation of Mn into multiple different sites. The pre-edge feature is comparable to experimental and computational Mn3O4 spectra. The position of the white line can be explained either by the electrostatic model or as continuum resonances. In the electrostatic model, as the oxidation state increases, the electrons are more tightly bound to the nucleus, requiring higher energy to be excited. The continuum model considers both the excited atom and the surrounding ones, and as the absorber-scatterer distance gets shorter, the energy of the continuum state increases with $1/r^2$. As higher oxidation states result in shorter bond lengths, the energy increases as oxidation state increases. In addition, the intensity of the white line intensity is proportional to the filling of 3d orbitals. As the 3d orbitals get more occupied, the intensity of the white line goes down due to the reduction in possible population states. As the position of the white line remains constant between the as grown TiMnOx samples, the increase in sharpness of the K-edge in the 16:1 sample relative to the 2:1 sample could be explained by the combination of a slightly increased oxidation state and longer Mn-O bond.

4:15 PM EL06.10.09

Accelerating Metal Nanoparticle Exsolution by Exploiting Tolerance Factor of Perovskite Stannate Yujeong Lee, Daseob Yoon, Yeon-seo Nam, Sangbae Yu, Chaesung Lim, Hyeji Sim, Yunkyu Park, Jeong Woo Han, Si-Young Choi and Junwoo Son; Pohang University of Science and Technology, Korea (the Republic of)

Perovskite oxide (ABO_3) with catalytically active metal nanoparticles (NPs) has the potential as a promising application such as solid oxide fuel cell operated at high temperature, electrochemical reaction, energy conversion, photocatalysis and syngas conversion. In particular, *in-situ* exsolution is emerging method that metal NPs are segregated from an oxide matrix to a surface under a reducing atmosphere for enhancing the interfacial adhesion between metal NPs and the perovskite support with high electrical conductivity [1, 2].

In this presentation, we demonstrate a novel method to control a density of Ni metal NPs on surface of A-site deficient perovskite stannate matrix ($A_{0.9}Sn_{0.9}Ni_{0.1}O_{3-\delta}$, A = Ca, Sr, Ba) by manipulating distortion of SnO_6 octahedron by diffusion kinetics of Ni metal during exsolution process. Remarkably, the density of Ni NPs increases from 47 particles μm^{-2} ($Ba_{0.9}Sn_{0.9}Ni_{0.1}O_{3-\delta}$) to 304 particles μm^{-2} ($Ca_{0.9}Sn_{0.9}Ni_{0.1}O_{3-\delta}$) by decreasing the Goldschmidt tolerance factor of perovskite stannate epitaxial films. Quantitative analysis using ambient pressure X-ray photoemission spectroscopy (APXPS) during *in-situ* exsolution process experimentally confirmed that Ni diffusion is enhanced with decreasing the tolerance factor of perovskite stannates. Experimental characterization combined with theoretical calculation shows that Goldschmidt tolerance factor of perovskite stannate promote the Ni diffusion kinetics from the oxide matrix to surface by manipulating the A-O bonding strength. Motivated by the high density of Ni NPs on perovskite stannate support, *in-situ* CO oxidation was also performed using APXPS to identify the effect of the catalytic activity of perovskite stannate support with exsolved Ni NPs. This new strategy on the manipulation of tolerance factor for promoting exsolved metal diffusion kinetics can be exploited to enhance the density of populated metal nanoparticles for emerging catalytic applications.

References

- [1] Neagu, D., Tsekouras, G., Miller, D. et al. *Nature Chem* **5**, 916–923 (2013)
- [2] Yu, S., Yoon, D., Lee, Y. et al., *Nano Lett.* **5**, 3538 (2020)

SYMPOSIUM EL07

Emerging Ferroic Materials—Synthesis, Properties and Applications
April 23 - May 8, 2024

Symposium Organizers

John Heron, University of Michigan
Morgan Trassin, ETH Zurich
Ruijuan Xu, North Carolina State University
Di Yi, Tsinghua University

Symposium Support

Gold
ADNANOTEK CORP.

Bronze

Arrayed Materials (China) Co., Ltd.
NBM Design, Inc.

* Invited Paper

+ JMR Distinguished Invited Speaker

^ MRS Communications Early Career Distinguished Presenter

SESSION EL07.01: Ferroelectrics I
Session Chairs: Ruijuan Xu and Pu Yu
Tuesday Morning, April 23, 2024
Room 342, Level 3, Summit

10:30 AM *EL07.01.01

Emergent Dipolar Textures and Properties in All-Ferroelectric Superlattices Lane W. Martin; Rice University, United States

Emergent topological dipolar textures including vortices, dipolar waves, skyrmions, merons, hopfions, and more have generated considerable interest in the ferroelectrics and wider condensed-matter physics communities. The delicate balance of electric, elastic, and gradient energies of ferroelectrics can be tailored in low-dimensional forms and nanostructures to manipulate the order parameters. Exotic functional properties (*e.g.*, coexistence of phases, chirality, negative capacitance, and emergent ultrafast dynamical responses) make them interesting candidates for devices. Ferroelectric-dielectric superlattices such as $(PbTiO_3)_m/(SrTiO_3)_n$ have been widely studied as a model system in part due to the high depolarizing field boundary condition provided by the $SrTiO_3$ layer. Such layers, however, limit the incorporation of such heterostructures into devices that could use the electronic characteristics of these polar topologies.

Looking to expand upon this rich design space, we ask a simple question: can similar emergent dipolar textures be produced in all-ferroelectric (and other) heterostructures while providing additional tunability based on the susceptibilities of the constituent layers? Here, we demonstrate the formation of polar

vortices in all-ferroelectric $\text{Pb}_{1-x}\text{Sr}_x\text{TiO}_3/\text{PbTiO}_3/\text{Pb}_{1-x}\text{Sr}_x\text{TiO}_3$ trilayer and $(\text{Pb}_{1-x}\text{Sr}_x\text{TiO}_3)_n/(\text{PbTiO}_3)_n$ superlattice structures wherein $0.5 < x < 1$ grown on DyScO_3 (110) substrates. Unlike their counterparts with SrTiO_3 , the $\text{Pb}_{1-x}\text{Sr}_x\text{TiO}_3$ layers exhibit robust, in-plane ferroelectric polarization and domain structures, but still provide the appropriate boundary condition for the formation of polar vortices in the PbTiO_3 layers. We describe the manifestation of complex polar order in these structures that combines traditional ferroelectric order with emergent dipolar textures. Reciprocal space mapping studies reveal that the strontium content in the $\text{Pb}_{1-x}\text{Sr}_x\text{TiO}_3$ provides a fine control knob over the vortex periodicity; as supported by molecular-dynamics simulations. Furthermore, while recent studies on in-plane ferroelectric switching of polar vortices showed classical bistable switching, here, the in-plane polarization component of the vortices in the PbTiO_3 layers and the ferroelectric domains in the $\text{Pb}_{1-x}\text{Sr}_x\text{TiO}_3$ layers exhibit strong elastic and dipolar coupling, leading to a coercivity enhancement of the trilayer stack upon decreasing the strontium content of the $\text{Pb}_{1-x}\text{Sr}_x\text{TiO}_3$. Phase-field simulations further explain the polarization arrangement in the trilayer and the system's subsequent collective switching pathway of the two order parameters. Formation of such in-plane domains in the $\text{Pb}_{1-x}\text{Sr}_x\text{TiO}_3$ leads to the formation of a labyrinthine vortex arrangement, unlike the highly unidirectional vortices observed in $(\text{PbTiO}_3)_n/(\text{SrTiO}_3)_n$ superlattices. Further, we have explored the coupling between different emergent dipolar heterostructures of the from $\text{Pb}_{1-x}\text{Sr}_x\text{TiO}_3/\text{PbTiO}_3/\text{Pb}_{1-x}\text{Sr}_x\text{TiO}_3/\text{SrTiO}_3/\text{PbTiO}_3/\text{SrTiO}_3$. Therein, the thickness of the SrTiO_3 layer separating the two vortex structures controls the strength of the elastic and electric fields that extend between layers, affecting the sequence in which each trilayer would switch and the number of switching events. The result is an ability to produce low-field multi-state, four-step switching with robust retention and fatigue performance. Finally, in $(\text{Pb}_{1-x}\text{Sr}_x\text{TiO}_3)_n/(\text{PbTiO}_3)_n$ superlattices we have explored the dielectric tunability and out-of-plane switching and find improved tunability as a function of the chemistry of the $\text{Pb}_{1-x}\text{Sr}_x\text{TiO}_3$ layer, antiferroelectric-like switching due to an unraveling of the vortex phase upon application of the electric-field, and strong back switching on releasing the same leading to improvements in the low-field energy storage as compared to $(\text{PbTiO}_3)_n/(\text{SrTiO}_3)_n$.

11:00 AM EL07.01.04

Novel Hexagonal Ferroelectric LuGaO₃ Jesse Schimpf¹, Megha Acharya¹ and Lane W. Martin^{2,1}; ¹University of California, Berkeley, United States; ²Rice University, United States

The presence of simultaneous ferroelectric and magnetic order in hexagonal LuFeO_3 has made it a promising candidate for next-generation microelectronics. At the same time, the metastable nature of this phase makes it an interesting case study for the synthesis of novel epitaxial materials. Its utility, however, is limited by its low polarization ($<10 \mu\text{C}/\text{cm}^2$) and often poor film quality. Recent first principles predictions have identified a new hexagonal ferroelectric, LuGaO_3 , which is isostructural to LuFeO_3 but is predicted to be thermodynamically stable and exhibit a higher polarization than LuFeO_3 . While nonmagnetic, the enhanced polarization in LuGaO_3 could make it a more suitable ferroelectric, and alloying it with LuFeO_3 may serve to enhance the magnetic character while retaining more robust ferroelectricity. Overall, understanding the synthesis of newly predicted materials provides an important opportunity to verify and correct computational models, making them more reliable for future materials predictions.

Here, we demonstrate the synthesis of epitaxial, hexagonal LuGaO_3 via pulsed-laser deposition, which has not yet been reported. Extensive X-ray diffraction-based structural studies verify the hexagonal nature of this phase, while piezoresponse force microscopy studies show indications of stable, ferroelectric switching. While first principles calculations predict this phase to be thermodynamically stable (energy above hull = 0), the bulk material separates into Lu_2O_3 and $\text{Lu}_3\text{Ga}_5\text{O}_{12}$ phases. Film synthesis is even more complex and highly sensitive to growth conditions and epitaxial constraints. While (111)-oriented yttria-stabilized zirconia is the preferred substrate for hexagonal ferroelectrics like LuGaO_3 , it is also closely lattice matched with Lu_2O_3 , which forms epitaxially with surprisingly high quality under a wide range of conditions, with excess gallium being segregated to large precipitates on the surface of the film. Energy dispersive X-ray spectroscopy shows a large gallium deficiency (as much as 30% off from the target stoichiometry) in these phase-separated films, likely reducing the stability of the perovskite phase. Depositing the films at room temperature and subsequently annealing them circumvents the gallium loss enough to stabilize the hexagonal phase in extremely thin ($\sim 5 \text{ nm}$) films, while depositing in abnormally high oxygen partial pressures (1 Torr or more) has the same effect for thicker films, enabling more extensive structural and dielectric characterization which confirms the presence of a hexagonal, ferroelectric phase. We further examine the structure and dielectric properties as a function of synthesis conditions as the material transforms from predominately nonpolar Lu_2O_3 to ferroelectric hexagonal LuGaO_3 . We then compare this to LuFeO_3 , which does not exhibit the same phase separation and largely maintains the hexagonal phase regardless of the synthesis conditions. Finally, we examine the influence of alloying and multilayering of both materials to understand their stability and produce a more robust multiferroic. Interestingly, providing a thin (as little as 1-2 nm) buffer layer of LuFeO_3 is enough to stabilize hexagonal LuGaO_3 where it would otherwise phase separate on a bare substrate, further demonstrating the importance of epitaxy in phase selection. Extending this to a multilayer or solid solution has a similar effect. While such mixtures maintain robust ferroelectricity, a small degree of phase separation still persists and will likely require further tuning of the gallium chemistry to fully correct. Nevertheless, this work represents an important step toward finding a more robust hexagonal perovskite multiferroic and offers valuable insight on metastable materials synthesis.

11:15 AM EL07.01.05

Van der Waals Growth of Ferroelectric GeTe Thin Films by Industrial Magnetron Sputtering for Large-Scale Integration Pierre Noé¹, Nicolas Bernier¹, Damien Térébenec¹, Jules LaGrave¹, Alexandre Oysel-Mestre¹, Jean-Baptiste Dory¹, Théo Frottier², Salvatore Teresi², Jean-Philippe Attane², Laurent Vila² and Françoise Hippert³; ¹Univ. Grenoble Alpes, CEA, LETI, France; ²Univ. Grenoble Alpes, CNRS, CEA, SPINTEC, France; ³Univ. Grenoble Alpes, CNRS, Grenoble INP, LMGP, France

Chalcogenide materials have attracted a lot of attention over the years due to their wide range of applications. Among them, some compounds such as Ge-Sb-Te based alloys exhibit a unique portfolio of properties, which has led to their wide use for non-volatile phase-change memory applications [1,2]. In addition to memory applications, the GeTe phase-change alloy is also very promising for RF switches [3], for thermoelectrics [4,5], and offers numerous opportunities for optical applications[6] and photonics[7] as well as for the emerging field of spinorbitronics [8]. GeTe has also been the subject of numerous studies, due to the ferroelectric character of the stable rhombohedral α phase and the existence of a reversible structural transformation (around 430°C) between the rhombohedral α phase and the cubic paraelectric cubic β phase. The rhombohedral α -GeTe phase can be described as a deformed rocksalt structure that has undergone shearing along a cube diagonal ([111] or equivalent direction), with a relative displacement of the Ge and Te atoms along this direction, which is responsible for the ferroelectric properties. In the α -GeTe phase a Ge atom is surrounded by six Te atoms forming a distorted octahedron with three short and three long Ge-Te bonds. This splitting is interpreted as resulting from a Peierls distortion. These properties have sparked interest in GeTe as a ferroelectric Rashba semiconductor, combining semiconductivity, strong spin-orbit coupling and non-volatility. In addition, GeTe has recently attracted renewed interest with the demonstration of non-volatile ferroelectric control of spin-charge conversion in epitaxial germanium telluride films deposited by molecular beam epitaxy [8]. The sign of the charge current can be controlled by the orientation of the ferroelectric polarization, which can be switched by an electric gate despite the high intrinsic carrier density of GeTe. In this context, the successful deposition of high-quality epitaxial ferroelectric GeTe films using a large-scale industrial deposition process could open up a new field of applications based on the non-volatile electrical control of spin currents in semiconducting GeTe. In this presentation, I will show that the van der Waals growth of high structural quality ferroelectric GeTe thin films using industrial magnetron sputtering could be achieved, demonstrating that this material could be monolithically integrated on silicon for devices beyond CMOS such as reconfigurable spin-based and in-memory computing devices.

Key words: chalcogenide, GeTe, phase-change material, van der Waals epitaxy, ferroelectric

REFERENCES

1. P. Noé, et al., *Semicond. Sci. Technol.* **33**, 013002, (2018).
2. P. Noé and F. Hippert, "Structure and Properties of Chalcogenide Materials for PCM", in *Phase Change Memory: Device Physics, Reliability and Applications*, A. Redaelli, Éd. Cham: Springer International Publishing, 2018, p. 125–179.
3. R. M. Young, et al., 2018 IEEE/MTT-S International Microwave Symposium – IMS, pp. 832–835 (2018).
4. J. Li, et al., *J. Am. Chem. Soc.* **140**, 16190–16197 (2018).
5. Q. Tian, et al., *Nanoscale* **13**, 18032–18043 (2021).
6. P. Martinez, et al., *Adv. Mater.* **32**, 2003032 (2020).
7. J. Wang, et al., *IEEE Access* **8**, 121211 (2020).
8. S. Varotto, et al., *Nat. Electron.* **4**, 740–747 (2021).

SESSION EL07.02: Ferroelectrics II
Session Chairs: Yen-Lin Huang and Ruijuan Xu
Tuesday Afternoon, April 23, 2024
Room 342, Level 3, Summit

1:30 PM *EL07.02.01

Coexistence of Ferro- and Antiferroelectric Behavior Dennis Meier; Norwegian University of Science and Technology, Norway

Ferroelectric domain walls are a rich source of emergent electronic properties and unusual polar order. For example, recent studies showed that the polarization configuration of ferroelectric walls can go well beyond the conventional Ising-type structure, exhibiting Néel-, Bloch-, and vortex-like polar patterns.

In my talk, I will present novel types of anti-polar domain walls and discuss their structure and unusual physical properties. In the first part of my talk, I will show that charged domain walls arise in $K_3[\text{Nb}_3\text{O}_6(\text{BO}_3)_2]$. The domain wall bound charges arise from a finite canted moment associated with the material's antiferroelectric-like order, leading to distinct local piezoelectric and electrostatic responses. In the second part, I will talk about the emergence of anti-polar order at domain walls in $\text{Pb}_5\text{Ge}_3\text{O}_{11}$. The domain walls are highly mobile and exhibit an energetically costly antiparallel ordering of dipoles along the longitudinal direction, which we attribute to the hyperferroelectric nature of the system. The results provide new insight into the complex polar textures of domain walls, expanding previous studies towards anti-ferro phenomena.

2:00 PM *EL07.02.02

Dynamic Mechanical Writing of Ferroelectric Bubbles Chan-Ho Yang; KAIST, Korea (the Republic of)

Topological ferroelectric structures offering novel functionalities due to peculiar distributions of polarization and charge with long retention have been increasingly explored in a variety of dielectric systems, such as superlattices, strained films, and nanoscale islands. The polar structures, protected by topological constraints such as boundary conditions, appear as metastable states due to the interplay between strain, depolarization and gradient energies, but their precise control is still challenging. In this study, we demonstrate the observation of skyrmion-like centre-type polar bubble domains in supertetragonal BiFeO_3 thin films. These polar textures are mechanically generated by dynamic elastic force of vibrational tapping using scanning probe microscope tips. The formation of bubble domains is accompanied by emergence of strain-driven morphotropic phase boundaries wherein two competing structural phases coexist. The bubble domains can be accurately written, mechanically or electrically erased, and remain stable for longer than ~500 days. Vibrational tapping can bidirectionally switch out-of-plane polarization by exerting strong tapping force onto the elastically soft surface driven by the morphotropic phase transition, which may be attributed to non-linear flexoelectric effects in the large strain-gradient regime beyond the conventional flexoelectrical concept. Our study presents insights into dynamic mechanical switching of polarization and provides a unique pathway into topological polar structures for next-generation energy-efficient electronic applications.

2:30 PM EL07.02.03

Real-Time Imaging of Nonequilibrium Domain Evolution into a Multiferroic Phase Jan Gerrit Horstmann¹, Yannik Zemp¹, Ehsan Hassanpour Yesaghi¹, Thomas Lottemoser¹, Mads Weber² and Manfred Fiebig¹; ¹ETH Zurich, Switzerland; ²Le Mans Université, France

The properties and functionalities of multiferroic materials are governed by the microscopic domain structures of coexisting ferroic orders and their mutual coupling. Active control over multiferroic domains via external stimuli is desirable, with prominent examples in magnetoelectric inversion or transfer of domain patterns. These approaches typically harness electric or magnetic fields to affect the thermodynamically stable domain configuration within a multiferroic phase. Optical or thermal quenches through phase transitions can be used to transfer structural features between distinct phases, creating novel and potentially functional domain structures unattainable in thermal equilibrium. The impact of such transitions on multiferroic domain patterns and their dynamic evolution, however, remains a largely open subject.

In this work, we combine real-time Faraday imaging at kHz frame rates with fast optical excitations to investigate the evolution of domains across spin-reorientation transitions and into the multiferroic phase of $\text{Dy}_{0.7}\text{Tb}_{0.3}\text{FeO}_3$. We find that optically-induced thermal quenches of the system can be harnessed to imprint the characteristic bubble domain pattern of the weak ferromagnetic order at elevated temperatures onto the low-temperature multiferroic phase. We identify the quenching rate across the different spin reorientation transitions as the decisive parameter governing the domain memory and the formation of metastable domain states forbidden under equilibrium conditions. Our results highlight the potential of optical stimuli for the switching and control of multiferroic domain structures, enabling the creation of new functional states via nonequilibrium pathways.

2:45 PM EL07.02.04

Mapping Polar Distortions with Nanobeam Electron Diffraction Using A Cepstral Approach Megan E. Holtz; Colorado School of Mines, United States

Understanding local polar ordering is key to understanding ferroelectricity in thin film systems, especially for systems with small domains or significant disorder. Scanning nanobeam electron diffraction (NBED) combined with new high speed, pixelated scanning transmission electron microscopy (STEM) detectors make it possible to measure a diffraction pattern (k_x, k_y) at every scan position (x, y) . This opens doors to investigate lattice parameters, local

fields, polarization directions, and charge densities with relatively low beam dose over large fields of view. However, quantitatively extracting both the magnitude and direction of polarization vectors is still challenging. Here we use a cepstral approach, similar to a 2D pair-correlation function, to measure these local polar displacements that drive ferroelectricity. In this presentation, we will discuss the application and limits of this technique and map polar distortions across a thin film of PbTiO₃ and in relaxor ferroelectrics.

3:00 PM BREAK

3:30 PM EL07.02.05

Nanoscale Design of Polarization Using Lattice Chemistry Engineering in Layered Ferroelectrics Ipek Efe¹, Alexander Vogel², Elzbieta Gradauskaite¹, William S. Huxter^{1,1}, Christian Degen^{1,1}, Marta D. Rossell², Manfred Fiebig¹ and Morgan Trassin¹; ¹ETH Zürich, Switzerland; ²Empa–Swiss Federal Laboratories for Materials Science and Technology, Switzerland

Nanoscale electrostatic control of oxide interfaces enables physical phenomena and exotic functionalities beyond the realm of the bulk material, including superconductivity, multiferroicity, and topological properties promising for future nonvolatile memory applications. Here, by exploiting spontaneously forming charged interfaces in layered materials, we control the electrostatic boundary conditions in ferroelectric oxide heterostructures. We directly access the polarization dynamics of the layered ferroelectric model system Aurivillius Bi₃FeTi₃O₁₅ (BFTO) films during growth using in-situ optical second harmonic generation (ISHG). We identify the characteristic Aurivillius antipolar ordering of the dipoles along the growth direction, which leads to an oscillating intensity of the ISHG signal during the layer-by-layer deposition. In combination with reflection high-energy electron diffraction monitoring, we show how the polarization orientation of the films consistently changes from out-of-plane during the growth of perovskite blocks, to fully in-plane upon the completion of the unit cell with the fluorite-like (Bi₂O₂)²⁺ planes. Finally, we incorporate various functional perovskite units into the Aurivillius layered-crystal structure using the direct access to structure-dependent polarization dynamics during growth. Our work thus expands the limits of engineering the properties of layered oxide films to the sub-unit-cell-scale for the development of energy-efficient oxide electronics.

3:45 PM EL07.02.06

A Strain-Enabled Novel Multiferroic State in Barium Hexaferrite through Suppression of Quantum Paraelectricity Zhiren He^{1,2} and Guru Khalsa¹; ¹University of North Texas, United States; ²Cornell University, United States

Barium hexaferrite (BaFe₁₂O₁₉) is predicted to harbor a novel multiferroic phase within which frustrated antiferroelectricity and ferrimagnetism coexist. However, experimental studies have shown that in bulk barium hexaferrite, quantum fluctuations instead lead to a quantum paraelectric ground state at low temperature [1-2]. Strain is a popular method for tuning functional properties in epitaxial thin films and has previously been used to coax ferroelectric dipole order, for example in SrTiO₃ [3]. Similarly, recent theoretical exploration has suggested that strain may enhance antiferroelectricity in barium hexaferrite [4]. In this theoretical work, we combine first-principles calculations with quantum Monte Carlo simulations to explore the temperature- and strain-dependent properties of barium hexaferrite. We find good agreement between our model and available bulk experimental data. In the investigation of strained barium hexaferrite, we find that a modest compressive strain of approximately 1% enables the transition to a frustrated antiferroelectric phase with a critical temperature of greater than 10 K. Our results suggest that further investment in epitaxy and development of compressive substrates for hexaferrites may provide a promising route towards room temperature multiferroics.

[1] Shen et al. *Phys. Rev. B* **90**, 180404(R) (2014)

[2] Zhang et al. *Phys. Rev. B* **101**, 104102 (2020)

[3] Haeni et al. *Nature* **430** 758–761 (2004)

[4] Wang et al. *Phys. Rev. X* **4**, 011035 (2014)

4:00 PM EL07.02.07

Relaxor-Like Ferroelectric Behavior in Epitaxial NaNbO₃ Films for Capacitive Energy Storage Kevin J. Crust^{1,2}, Aarushi Khandelwal^{2,1}, Ruijuan Xu³ and Harold Y. Hwang^{2,1}; ¹Stanford University, United States; ²SLAC National Accelerator Laboratory, United States; ³North Carolina State University, United States

Electrostatic energy storage based on dielectric capacitors has garnered significant interest due to its fast charge-discharge speeds and high power density relative to electrochemical energy storage, but applications have been limited due to large leakage currents, relatively low energy storage density, and the presence of lead in materials^[1,2]. NaNbO₃ is a lead-free alternative which has received much research attention in the last decade but work has primarily focused on its bulk form, with NaNbO₃-based systems displaying both antiferroelectric and relaxor ferroelectric behaviors at room temperature with promising energy storage properties^[2,3]. Using pulsed laser deposition and selective etching, we have synthesized metal-insulator-metal heterostructures of La_{0.7}Sr_{0.3}MnO₃ and NaNbO₃ with high crystalline quality and coherent epitaxial strain across a range of thicknesses. Both strain and thickness have previously been noted to greatly affect the properties of NaNbO₃ due to the close proximity of its antiferroelectric and ferroelectric ground states^[4,5]. Through careful optimization of the growth conditions, we achieve minimal leakage current even under large external electric fields and can observe relaxor-like ferroelectric behavior in both our thinnest samples (below 50 nm of NaNbO₃) and our thickest samples (above 150 nm). This allows us to achieve improvements in both recoverable energy-storage density W_{rec} and energy efficiency η compared to previous NaNbO₃ thin films^[6,7]. This work demonstrates the potential of NaNbO₃ for dielectric energy storage and the advantages of epitaxial, single-crystal films for electrical characterization.

[1] H. Pan et al., *Science* **374**, 100-104 (2021).

[2] M.-H. Zhang et al., *Nat. Comm.* **14**, 1525 (2023).

[3] N. Luo et al., *Nat. Comm.* **14**, 1776 (2023).

[4] T. Schneider et al., *ACS Omega* **8**, 23587-23595 (2023).

[5] R. Xu et al., *Adv. Mater.* **35**, 2210562 (2023).

[6] T. Shiraiishi et al., *J. Appl. Phys.* **128**, 044102 (2020).

[7] H. Dong et al., *Ceram. Inter.* **48**, 16215-16220 (2022).

4:15 PM EL07.02.08

In Situ X-Ray Nano-Imaging of Heterogeneous Structural Response in a Relaxor Ferroelectric Aileen Luo^{1,2}, Tony Chiang³, Tao Zhou², Ziming Shao¹, Yifei Sun¹, Benjamin Gregory¹, Martin V. Holt², John T. Heron³ and Andrej Singer¹; ¹Cornell University, United States; ²Argonne National Laboratory, United States; ³University of Michigan–Ann Arbor, United States

Magnetolectric multiferroics transduce electrical and magnetic energy, which is critical for the development of new materials for sensors, motors, and computation devices. Composite heterostructures of a magnetostrictor coupled to a piezoelectric, such as the promising epitaxial FeGa on 0.7[PbMg_{1/3}Nb_{2/3}O₃] - 0.3[PbTiO₃] (PMN-PT), enable electric field control of magnetic polarization, while offering additional device utility compared to

rare single-phase multiferroics. Such systems have been studied at the micron scale, but nanoscale strain distribution changes during switching are not well characterized. We use in situ hard x-ray nanodiffraction to simultaneously measure real and reciprocal space of devices under applied DC electric field, which allows us to attribute strain and lattice rotation information at the nanoscale. By applying non-linear least squares modeling of the phase coexistence across the morphotropic phase boundary in this multiferroic heteroepitaxial system, we correlate the local strain behavior in the direction of the applied field and along the domain polarization axes. We analyze the phase distribution as a function of electrical bias and demonstrate the potential for real-time analysis in advanced microelectronics characterization.

4:30 PM EL07.02.09

Understanding Fatigue and Wake-Up in Ultra-Thin Ferroelectric $\text{Hf}_{0.5}\text{Zr}_{0.5}\text{O}_2$ Capacitors Using Cryogenic Measurements Balreen Saini¹, Chanyoung Yoo², John D. Baniecki², Wilman Tsai¹ and Paul C. McIntyre^{1,2}; ¹Stanford University, United States; ²SLAC National Accelerator Laboratory, United States

The need for logic and memory devices that are smaller, faster, and more energy-efficient is constantly growing. This has intensified the demand for innovative materials capable of scaling down and aligning with current CMOS processes. A next generation memory solution is non-volatile memories that are energy efficient and can enable new computing architectures. For high performance computing systems such as quantum computing, cryogenic embedded memories are essential that would have an added benefit of eliminating thermally induced performance degradation mechanisms. One material that shows promise for nonvolatile memory applications is HfO_2 -based ferroelectric materials and research in this area has surged due to potential memory applications such as 1T1C ferroelectric random-access memory (FeRAM) and ferroelectric field-effect transistors (FeFET).

The HfO_2 -based ferroelectric materials exhibit an increase (wake-up) or decrease (fatigue) of the remnant polarization with switching cycles which causes major reliability issues in device applications. Mechanisms such as field-induced phase evolution, domain depinning and defect redistribution with field cycling are reported to cause the observed polarization evolution with field cycling. The thermally activated nature of the above-mentioned mechanisms may produce a significant change in polarization endurance when the measurement temperature is varied. In our present work, we explore the effect of measurement temperature on the functional properties of ferroelectric $\text{Hf}_{0.5}\text{Zr}_{0.5}\text{O}_2$ (HZO) capacitors to further the understanding of mechanisms responsible for the observed endurance characteristics. Measurements are performed in a cryogenic probe station, which has the capability to reach extremely low temperatures as low as 10 Kelvin.

HZO capacitors of varying thickness (ranging from 4 nm to 10 nm) and with both Mo and TiN electrodes are examined. The HZO films have different crystalline phase fractions in the as-deposited (pristine) state. For HZO capacitors that exhibit electrical characteristics expected of films with majority ferroelectric orthorhombic phase (O-phase) in the pristine state, a decrease in remnant polarization and an increase in coercive voltage are observed as the measurement temperature is decreased from room temperature to 10 K. The polarization reduction is recovered by increasing the temperature back to room temperature, suggesting a strong effect of thermally activated domain wall motion at low temperatures. No fatigue during voltage cycling to switch the polarization is observed at low temperatures. On the other hand, pristine HZO capacitors with pinched polarization hysteresis (P-V) loops at room temperature and that, therefore, are expected to have majority non-ferroelectric tetragonal phase (T-phase), show negligible loop pinching and a large increase in switchable remanent polarization at cryogenic temperatures. This suggests that modulating the phase fraction in HZO films can change the temperature dependence of polarization switching and field cycling endurance. The rate of wake-up for these samples is reduced at low temperatures. Synchrotron X-ray diffraction measurements are performed to further understand the temperature dependence of functional properties of HZO capacitors and their relation to crystalline phase fraction.

4:45 PM EL07.02.10

Non-Zero Remnant Polarization of Anti-Ferroelectric $\text{Hf}_{0.1}\text{Zr}_{0.9}\text{O}_2$ revealed by First Order Reversal Curves (FORC) for Non-Volatile Memory Min-Hung Lee¹ and Z.-X. Li²; ¹National Taiwan University, Taiwan; ²National Taiwan Normal University, Taiwan

The data retention is one major issue of requirements for non-volatile memory (NVM) application, i.e. non-zero remnant polarization (P_r) of Ferroelectric random-access-memory (FeRAM) application at standby (bias-free) [1][2]. Recently, antiferroelectric HfZrO_2 (AFE-HZO) under built-in bias of fixed charge (Q_f) and/or interface dipole by Al_2O_3 interlayer leads applicable P_r [3][4]. Furthermore, AFE-HZO exhibits intrinsic capability of high-speed response and long endurance [5]. However, the validation of bilayer of AFE and dielectric (DE) is lack for further discussion. In this work, the technique of First-Order Reversal Curve (FORC) [6][7] will be employed to reveal the built-in bias based coercive field (E_c) distribution for AFE/DE.

The FORC diagram can determine the distribution of the E_c by multiple P-E loops measurement. The FORC distribution function $\rho(E_r, E)$ shows the concentration of E_c , and the procedure can be achieved as following. The initial field of the waveform is the saturation field (E_{sat}), sweeping from the E_{sat} to the reversal field (E_r) and then back to the E_{sat} . Then the step is repeated and E_r range is from E_{sat} reversing gradually to $-E_{\text{sat}}$. The metal/ferroelectric/metal (MFM), metal/antiferroelectric/metal (MAFM) and metal/antiferroelectric/insulator/metal (MAFIM) were prepared for FORC analysis. The MFM shows typical FE-behavior and $2P_r > 60$ mC/cm². For MAFM, the $2P_r$ almost zero due to polarization compensation at 0 MV/cm. For MAFIM, the "FE-like" characteristic is presented due to built-in bias. The origins of the built-in bias with Al_2O_3 are unbalance of surface energy for interface dipole and insufficient bonding for positive or negative fixed charge [8][9]. The single E_c distribution of MFM by FORC diagram indicates the typical FE behavior and it concentrates at ~ 1.2 MV/cm. For MAFM, there are two E_c distributions at ~ 0.5 MV/cm and 2.5 MV/cm, and this is attributed to the multi-peak of E_c for AFE. For MAFIM, the single E_c distribution is occurred at ~ 1.5 -2 MV/cm. The FORC methodology is employed to validate the built-in bias existence and non-zero P_r for AFE/DE system.

The authors are grateful for the funding support by Ministry of Science and Technology (NSTC) 112-2218-E-A49-013-MBK, 112-2221-E-002-252-MY3, 111-2221-E-002-203-MY3, and process supported by TSRI & NFC, Taiwan.

References:

- [1]. D. Takashima, "Overview of FeRAMs: Trends and perspectives," 2011 11th Annual Non-Volatile Memory Technology Symposium Proceeding, Shanghai, China, 2011, pp. 1-6.
- [2]. J. Hur et al., "A Technology Path for Scaling Embedded FeRAM to 28nm with 2T1C Structure," 2021 IEEE International Memory Workshop (IMW), Dresden, Germany, 2021, pp. 1-4.
- [3]. K.-Y. Hsiang et al., "Bilayer-based Antiferroelectric HfZrO_2 Tunneling Junction with High Tunneling Electroresistance and Multilevel Nonvolatile Memory," IEEE Electron Device Letters, vol. 42, no. 10, pp. 1464-1467, 2021.
- [4]. C.-Y. Liao et al., "Experimental Insights of Reverse Switching Charge for Antiferroelectric $\text{Hf}_{0.1}\text{Zr}_{0.9}\text{O}_2$," IEEE Electron Device Letters, vol. 43, no. 9, pp. 1559-1562, 2022.
- [5]. M. Pešić et al., "Comparative Study of Reliability of Ferroelectric and Anti-Ferroelectric Memories," IEEE Transactions on Device and Materials Reliability, vol. 18, no. 2, pp. 154-162, 2018.
- [6]. Tony Schenk et al., "Complex Internal Bias Fields in Ferroelectric Hafnium Oxide," ACS Appl. Mater. Interfaces 2015, 7, 20224–20233.
- [7]. Laurentiu Stoleriu et al., "Analysis of switching properties of porous ferroelectric ceramics by means of first-order reversal curve diagrams," Phys. Rev. B 74, 174107, 2006.
- [8] D. K. Simon et al., "On the Control of the Fixed Charge Densities in Al_2O_3 - Based Silicon Surface Passivation Schemes," ACS Appl. Mater. Interfaces, vol. 7, no. 51, pp. 28215–28222, 2015.

[9] K. Kitaa, and A. Toriumi, "Origin of electric dipoles formed at high-k/SiO₂ interface," Appl. Phys. Lett., 94, 132902, 2009.

SESSION EL07.03: Poster Session I

Session Chairs: John Heron, Morgan Trassin, Ruijuan Xu and Di Yi
Tuesday Afternoon, April 23, 2024
Flex Hall C, Level 2, Summit

5:00 PM EL07.03.02

Combining Superlattices with Co-Doping -- Toward BEoL Compatible Ferroelectric Materials with Improved Reliability at Bias and Temperature Stress David Lehninger, Ayse Sünbül, Shruthi Subramanian, Konrad Seidel and Maximilian Lederer; Fraunhofer IPMS, Germany

Interest in the concept of ferroelectric memory has been revived by the discovery of ferroelectricity in thin doped hafnium oxide films. Zirconium doped hafnium oxide (HZO) crystallizes at low temperatures (400°C and below), which makes it a compelling material for back-end of line (BEoL) implementation. Metal-ferroelectric-metal (MFM) capacitors are essential building blocks for realizing BEoL-compliant ferroelectric memory concepts. Placed in BEoL, these devices can be connected to the gate or drain contact of a standard logic device to achieve a one-transistor-one-capacitor (1T1C) ferroelectric field-effect transistor (FeMFET) or a 1T1C FeRAM, respectively. [1]

Since the discovery ferroelectricity in hafnium oxide, scientists have been working to improve key properties of these materials, including remanent polarization, endurance, retention, imprint, and wake-up. Common methods of improvement include exploring different dopants, dopant concentrations, film thicknesses, and stacking options such as interface/electrode materials and superlattices [2].

Despite significant advancements, some reliability challenges persist, such as operation under high bias and temperature stress (BTS). Especially the automotive industry's strict demands for resilience and reliability under challenging BTS conditions exacerbate the issue. Currently, the Automotive Electronic Council's quality requirements for Integrated Circuits (AEC-Q100) serve as the minimum standard for car manufacturers. Fulfilling the Grade 0 specifications, which demand stable performance within the temperature range of -40°C to 150°C, presents a major challenge for ferroelectrics with a fluorite structure.

Recently, two methods have been reported that significantly improve the stability under BTS: (1) using ferroelectric [HfO₂/ZrO₂] superlattices with relatively thick sublayer thicknesses [3], and (2) co-doping, which introduces a small amount of an additional dopant [4]. Herein, we utilize both techniques to achieve optimal reliability properties. Analytical and electrical methods were used to characterize co-doped [HfO₂/ZrO₂] superlattices with various stacking options. To gain a deeper understanding of the structural properties, X-ray diffraction (XRD) and time-of-flight secondary-ion mass spectrometry (ToF-SIMS) were conducted. Additionally, polarization versus electric field characteristics were measured to explore the electrical properties under various BTS conditions. Finally, endurance and retention characteristics under BTS conditions will be utilized to evaluate compatibility with the requirements specified by the automotive industry.

- [1] D. Lehninger et al., 2021 IEEE IITC, Kyoto, Japan, 2021, pp. 1-4.
[2] F. Ali et al., Adv. Funct. Mater. 2022, 32, 2201737
[3] D. Lehninger et al., 2023 IEEE IMW, Monterey, USA, 2023, pp. 1-4.
[4] A. Sünbül et al., Adv. Funct. Mater. 2023, submitted.

5:00 PM EL07.03.03

Tuning the Structure, Bringing The Phase Transition Temperature and Ferroelectricity Near Room Temperature in Na₂Nb_{4-x}Ta_xO₁₁ (x = 0,1,2,3 and 4) Bulk Material for Nanogenerator Applications Udhayakumar S¹, Sumit Khatua², Patro L.N² and Kamala Bharathi Karuppanan¹; ¹SRM Institute of Science and Technology, India; ²Department of Physics, SRM University AP, India

In recent times, development in health monitoring devices technology is rapidly increasing to monitor the blood pressure, body electrolyte, body temperature and breath rate due to the viral fevers especially after Covid-19. Almost all the devices are larger in size, mechanically rigid and they have longer response time. Flexible, wearable and self-powered devices such as Piezoelectric Nanogenerators (PNGs) and Triboelectric Nanogenerators (TNGs) are welcomed for the health monitoring applications [1-2]. To develop materials for low cost piezoelectric nanogenerator device applications, we made an attempt to develop a series of lead-free piezoelectric material Na₂Nb_{4-x}Ta_xO₁₁ (x= 0 to 4) and explore their structural, ferroelectric, dielectric, electronic and piezoelectric properties. Na₂Nb₄O₁₁ is one of the ferroelectric materials which is not explored much due to its high phase transition temperature nearly 393 K which is paraelectric to ferroelectric transition [3]. In order to bring down the transition temperature to room temperature (RT), we have prepared a series of Na₂Nb_{4-x}Ta_xO₁₁ (x= 0 to 4) material using solid state reaction method and explored their structural, electrical, piezoelectric and electronic properties. X-ray diffraction (XRD) and Raman spectra analysis confirms the formation of Na₂Nb₄O₁₁ material in monoclinic structure with space group of C2/c. With increasing Ta concentration, the monoclinic system changes into rhombohedral system with the space group of R-3c. The boundary between monoclinic and rhombohedral change lies in between x= 0 to 0.5. HRSEM images show that particles are spherical in shape in micron size and decreases with increasing Ta concentration. From the real part of the dielectric constant vs temperature measurements, the phase transition for pure sample is observed at 373 K and decreases to 328 K for x= 1 sample. The bandgap value of Na₂Nb_{4-x}Ta_xO₁₁ (x= 0 to 4) sample is seen to increase from 3.69 eV to 4.45 eV with increasing Ta concentration. The piezoelectric measurements show excellent piezo-response for the pure and Ta doped samples, which can be utilized for fabricating the nanogenerator devices. Nanogenerator devices of 1 x 2 cm are fabricated by mixing the Na₂Nb₄O₁₁ (x= 0 to 4) with PVDF and the piezo-response is measured using oscilloscope. Induced voltage is seen to be in the order of 500 mV to 1 V, which can be very much applicable for the health monitoring devices.

5:00 PM EL07.03.04

HoFeO₃-BaTiO₃ Nanofiber Heterostructure: Impressive Nanogenerator Performance Smita Chaturvedi^{1,2,1}, Priyank Shyam³, Supriya Sahoo¹, Mihir Iyer¹, Shivshankar Jokare¹, Avinash S. Kumbhar¹, Boomishankar Ramamoorthy⁴ and Satishchandra Ogale²; ¹Savitribai Phule Pune University, India; ²IISER Pune, India; ³Aarhus University, Denmark; ⁴IISER, India

HoFeO₃-BaTiO₃ (HFO-BTO) nanofiber multiferroic heterostructure showcase fascinating properties due to the coexistence of ferroelectric and ferromagnetic ordering. The nanofiber heterostructure is synthesized by combining the ferromagnetic component HoFeO₃, and the ferroelectric component BaTiO₃ via the electrospinning technique. The heterostructure exhibits phase fraction 3:7 of orthorhombic (Pbnm) HFO: tetragonal (P4mm) BTO. The

heterostructure indicates the possibility of tunable magnetic and ferroelectric properties by tuning the phase fraction. Inclusion of HFO-BTO heterostructure into PDMS renders impressive nanogenerator performance. This trait in the heterostructure indicates that three main factors namely structure, morphology, and composition play crucial role in tuning the properties of the compound: (i) Structure: orthorhombic and tetragonal mixed phase contributes to the distortion of TiO₆ octahedra in heterostructure: in-plane O–Ti–O angle sharply decreases as Ti atom shifts from inversion centre, giving rise to greater ferroelectric polarization. The increase in average Fe–O–Fe angle in heterostructure is 141° as compared to uncoupled HFO (139°), affects the Fe–O–Fe exchange coupling (ii) Morphology: the nanofiber heterostructure has (a) the interface induces strain field due to interface of BTO and HFO, and (b) the surface- induced strain field intrinsically present in nano-systems due to large aspect ratio (iii) Composition: The ferroelectric BTO and ferromagnetic HFO parent compounds are stabilised in heterostructure and exhibit enhanced magnetic and ferroelectric properties as compared to the individual parent compounds. Under the influence of electric as well as mechanical field, the response of HFO-BTO heterostructure based nanogenerator is superior in terms of polarization, output voltage, current density and power density.

5:00 PM EL07.03.05

Distortion of Inversion Symmetry in Biaxial Van der Waals Layered Oxide Leading to Negative Capacitance (NC) Effect and Intrinsic Ferroelectricity [Rahul Mitra](#)^{1,2,3}, [Unnikrishnan Manju](#)^{2,3} and [Yongxiang Li](#)¹; ¹RMIT, Australia; ²CSIR-IMMT, India; ³AcSIR, India

Piezoelectric materials find applications in a diverse array of devices, such as sensors, resonators, motors, actuators, high-resolution ultrasound devices, and microscopic filters for cellular communications. The synthesis of single-phase α -MoO₃ (MO) with a biaxial van der Waals (vdW) gap revealed orthorhombic *Pmcn* symmetry featuring a layered ABAB sequence with mirrored A and B layers. Applying a force magnitude of 0.5 N unveiled a force-driven dielectric constant of 12.5 in MO, showcasing distinctive dielectric saturation behavior. Ferroelectric investigations, conducted with a 10 kV/cm external electric field, demonstrated an efficiency peak of 46%, while the Berlincourt technique yielded a piezoelectric modulus (d_{33}) of 30 pC/N. Negative capacitance (NC) effects, correlated with inductive reactance and ferroelectric-induced emf per Lenz's law, were observed. Combining these characteristics, a piezoelectric energy harvester (PEH) was engineered, achieving a peak voltage of 4 V under repeated finger tapping. When subjected to a resistive load of 100 M Ω , the PEH exhibited a power density of $7.32 \times 10^{-1} \mu\text{W}/\text{cm}^2$. These findings position α -MoO₃ as an exceptional piezoelectric candidate in the realms of sensing and energy harvesting, contributing to the advancement of the Internet of Things (IoT) and Industry 4.0.

SESSION EL07.04: Magnetolectrics
Session Chairs: Ipek Efe and Di Yi
Wednesday Morning, April 24, 2024
Room 342, Level 3, Summit

8:30 AM *EL07.04.01

Sensing The Antiferromagnetic State of Multiferroics Using Spin Hall Measurements [Ramamoorthy Ramesh](#); Rice University, United States

Over the past decade the oxide community has been exploring the science of ferroic materials as crystals and in thin film form by creating epitaxial heterostructures and nanostructures. Among the large number of materials systems, there exists a small set of materials which exhibit multiple order parameters; these are known as multiferroics, particularly, the coexistence of ferroelectricity and some form of ordered magnetism (typically antiferromagnetism). The scientific community has been able to demonstrate electric field control of both antiferromagnetism and ferromagnetism at room temperature. There are some very intriguing new developments in SOT based manipulation of magnets. Particularly, the role of epitaxy and electronically perfect interfaces has been shown to significantly impact the spin-to-charge conversion (or vice versa). Current work is focused on ultralow energy (1 attoJoule/operation) electric field manipulation of magnetism with both voltage and current, as the backbone for the next generation of ultralow power electronics. We are exploring many pathways to get to this goal. In this talk, I will describe our progress to date on this exciting possibility.

9:00 AM *EL07.04.02

Polar Magnetic Metals by Design [Pu Yu](#); Tsinghua University, China

Polar metal with a combination of conflicting polarization and metallicity attracts great research interests recently with promising functionalities. Numerous searches have been carried out particularly in complex oxides with many exciting discoveries. Inspired by the promising magnetoelectric coupling in multiferroic systems with coupled polarity and magnetism, it is of fundamental interest to introduce magnetism (remove time-reversal symmetry) into polar metals to access exotic phases that might emerge through the coupled magnetic and polar orders. The difficulty in realizing a polar magnetic metal lies in circumventing the mutually exclusive requirements of polarity and metallicity, and at the same time incorporating suitable electron correlation effects to form magnetism. In this talk, I will present our recent effort to design and explore novel complex oxides with the breaking of both spatial-inversion and time-reversal symmetries, while maintaining robust metallicity. We further demonstrate that the strong coupling between the polarity and magnetism of these metallic system produces a collection of exotic properties, including the intrinsic magnetochiral anisotropy with exotic magnetic field-free nonreciprocal electrical resistivity, and an emergent Hall effect. We envision that these materials and their derivatives will serve as a model family to probe the rich spectrum of emergent states in complex oxides.

9:30 AM *EL07.04.03

Engineering Multiferroic Garnet-Perovskite and Spinel-Perovskite Nanocomposites [Caroline A. Ross](#); Massachusetts Institute of Technology, United States

Nanocomposite oxide thin films consist of two phases that grow epitaxially on a substrate. Of particular interest are multiferroic nanocomposites consisting of pillars of a ferrimagnetic spinel such as CoFe₂O₄ (CFO) within a matrix of a ferroelectric perovskite such as BiFeO₃ (BFO) grown on a perovskite substrate. BFO/CFO nanocomposites exhibit magnetoelectric coupling mediated by strain transfer at the vertical interfaces. We first discuss how patterning of substrates enables control of the locations and geometry of the self-assembled pillars. In particular, we describe the fabrication, microstructure and ferroic properties of 'sideways multilayers' consisting of parallel fins of CFO and BFO grown on (111) and (110)-oriented substrates patterned using a focussed ion beam process, including the magnetic and ferroelectric domain structure. We then demonstrate nanocomposites made from perovskites and garnets. Iron garnets (IGs) are ferrimagnetic insulators of composition R₃Fe₅O₁₂, where R is Y, Bi or a rare earth. They exhibit a range of useful magnetic properties including spin orbit torque switching, relativistic domain wall velocities of km/s, spin wave-driven domain wall motion, and magneto-optical activity. The garnet structure is incompatible with a perovskite substrate, and deposition of garnet compositions onto perovskite substrates leads to the formation of Fe-rich orthoferrites RFeO₃. Instead, we use a garnet substrate patterned with a thin seed layer of a perovskite or nanosheets of perovskite-structured Ca₂Nb₃O₁₀. Growth of garnet on these heterogeneous substrates produces IG over the bare garnet substrate and Fe-rich orthoferrite over the

perovskite seed, with vertical garnet/perovskite interfaces, where both phases have the same composition. The ferroic properties of these structurally-modulated films will be described, as well as their utility in magneto-optical and magnonic devices.

10:00 AM BREAK

10:30 AM EL07.04.04

Towards a Potential Room-Temperature Ferrimagnetic Ferroelectric [Yilin Li](#)¹, Mario Brützm², Hari Krishnan K. P.¹, Sankalpa Hazra³, Zhiren He⁴, Ramamoorthy Ramesh⁵, Natarajan Ravi⁶, Robert J. Cava⁷, Craig Fennie¹, Venkatraman Gopalan⁸, David A. Muller¹, Christo Gugushev² and Darrell G. Schlom¹; ¹Cornell University, United States; ²Leibniz-Institut für Kristallzüchtung, Germany; ³Pennsylvania State University, United States; ⁴University of North Texas, United States; ⁵Rice University, United States; ⁶Spelman College, United States; ⁷Princeton University, United States; ⁸The Pennsylvania State University, United States

Multiferroics with coupled magnetic and electric orders, although rare, hold potential for low-energy-consumption materials for logic and memory capable of electric-field control of magnetism. Barium hexaferrite (BaFe₁₂O₁₉), the most common refrigerator magnet, is predicted to gain electric polarization order at room temperature in addition to its robust ferrimagnetism under in-plane, biaxial, compressive strain [1]. The recent realization of single-crystal substrates of Sr_{1.03}Ga_{10.81}Mg_{0.58}Zr_{0.58}O₁₉ (SGMZ) [2], an insulator that is isostructural to BaFe₁₂O₁₉, enables straining BaFe₁₂O₁₉ as SGMZ has a ~1.1% smaller in-plane lattice constant. In addition to strain, to induce the ferroelectric state, an epitaxial bottom electrode is needed to control the electric state for this hexaferrite multiferroic candidate. SrCo₂Ru₄O₁₁ is a metallic ferromagnetic oxide [3], belongs to the same hexaferrite family as BaFe₁₂O₁₉, and has small (~0.3%) in-plane lattice mismatch to the SGMZ substrate. Consequently, a coherent SrCo₂Ru₄O₁₁ epitaxial thin film on the SGMZ substrate would be ideal for straining BaFe₁₂O₁₉ and serving as the bottom electrode of a metal-insulator-metal structure to test for ferroelectricity in this predicted strain-induced multiferroic.

Here we show that a 1.1% in-plane biaxial compressive strain from SGMZ substrates can be imposed on up to 27.5 nm thick BaFe₁₂O₁₉ films. The full width at half maximum (FWHM) of the X-ray diffraction rocking curve of the 0020 peak in ω ranges from 0.006° to 0.009°, the smallest ever reported. Scanning transmission electron microscopy (STEM) multislice ptychography results on a commensurately strained film clearly show local electric polarization arising from the off-center displacement of Fe³⁺ ions in the trigonal bipyramid sites, locally breaking the mirror-plane symmetry perpendicular to the c-axis of BaFe₁₂O₁₉. Second harmonic generation (SHG) proves the symmetry breaking on a larger scale from 6/*mmm* (bulk paraelectric BaFe₁₂O₁₉) to 6*mm* (fully strained BaFe₁₂O₁₉). Commensurately strained BaFe₁₂O₁₉ containing 95% enriched Fe⁵⁷ has been synthesized. Mössbauer measurement will be made on this sample to quantify the splitting between the two sites of the iron cations in the trigonal bipyramid sites.

Films of SrCo₂Ru₄O₁₁ were grown by MBE on (0001) SGMZ substrates in an adsorption-controlled regime. With matching substrates and adsorption-controlled growth, we have grown epitaxial, fully strained SrCo₂Ru₄O₁₁ thin films with even lower resistivity than SrCo₂Ru₄O₁₁ single crystals [3]. Our next step is to grow a commensurately strained metal-insulator-metal BaFe₁₂O₁₉/SrCo₂Ru₄O₁₁/SGMZ stack to test for ferroelectricity.

[1] Wang, P. S., Xiang, H.J. *Physical Review X* **4**, 011035 (2014).

[2] Gugushev, C. et al. *Crystal Growth & Design* **22** (4), 2557-2568 (2022).

[3] Shlyk, L. et al. *Adv. Mater.* **20**, 1315-1320 (2008).

10:45 AM EL07.04.05

Manipulation of Isolated Spins in Ferroelectric Oxides from First Principles [Elizabeth Nowadnick](#)¹, Bradford Barker¹, Nabaraj Pokhrel¹, Md Kamal Hossain¹, Katherine Inzani^{2,3} and Sinead M. Griffin³; ¹University of California, Merced, United States; ²The University of Nottingham, United Kingdom; ³Lawrence Berkeley National Laboratory, United States

Electric field control of single spins can probe the fundamental atomic-scale limits of multiferroic behavior. One possible platform to explore this scenario is to form isolated spin centers in ferroelectric materials via inclusion of dilute concentrations of magnetic dopants. The preferred orientation of a spin is connected to its local crystallographic environment via the spin-orbit interaction, and is described by the magnetocrystalline anisotropy energy (MCAE). In a ferroelectric material, the local crystallographic environment can be modified by structural changes that occur during polarization switching under applied electric fields, which provides a path towards electric field control of the MCAE and a magnetic dopant's spin directionality. Although the diverse properties and functionalities of ferroic complex oxides have been the subject of extensive research over the past decades, they have so far received little attention as potential platforms for electric field-based single spin processing, which is of central interest to several modern technological applications. In this work, we combine group theoretic analysis with density functional theory calculations to explore two examples of tuning the spin orientation of isolated magnetic dopant atoms in ferroelectric oxide hosts. We first consider an isolated Fe³⁺ dopant in the tetragonal, orthorhombic, and rhombohedral phases of the prototypical ferroelectric oxide BaTiO₃. We investigate how the MCAE and preferred Fe³⁺ spin orientation evolves as the material traverses these structural phases of different crystalline symmetries, linking these changes to evolution in the electronic structure. Second, we explore an isolated Fe³⁺ dopant in the low-dimensional Aurivillius ferroelectric Bi₂WO₆, tracking how the MCAE and the preferred spin orientation evolve throughout ferroelectric switching. We find that the Fe³⁺ spin aligns along a spin-easy axis in Bi₂WO₆ and that a 90° switch of the polarization direction leads to a 112° reorientation of this spin-easy axis. This work advances our understanding of electric field control of single spins, which has potential implications in the fields of spintronics and quantum computing.

11:00 AM *EL07.04.07

Designed Magnetic Texture for Spin Transport in a Multiferroic Oxide [Peter Meisenheimer](#)¹, Maya Ramesh², Sajid Husain^{3,1}, Isaac Harris^{1,3}, Shiyu Zhou⁴, Lucas M. Caretta⁴, Darrell G. Schlom², Paul Stevenson⁵, Zhi Yao³ and Ramamoorthy Ramesh⁶; ¹University of California, Berkeley, United States; ²Cornell University, United States; ³Lawrence Berkeley National Laboratory, United States; ⁴Brown University, United States; ⁵Northeastern University, United States; ⁶Rice University, United States

Antiferromagnetic-based spintronics are growing in popularity for potential applications in next-generation computational technologies due to their speeds and robustness to external fields. A key challenge in this area, however, is the control of antiferromagnetic order on the nanometer scales applicable to solid-state technologies. Bismuth ferrite (BiFeO₃) is a multiferroic material that exhibits both ferroelectric and antiferromagnetic properties at room temperature, making it a unique candidate in the development of electrically controllable magnetic devices. In BiFeO₃, the magnetic moments are arranged into a long-range spin cycloid, resulting in a unique set of magnetic properties that are intimately tied to the ferroelectric order. To date, however, understanding of this coupling between magnetism and ferroelectricity has generally relied on average, mesoscale measurements to infer the magnetic structure and behavior.

Using high-resolution nitrogen vacancy (NV) diamond-based scanning probe magnetometry, we show that this spin cycloid can be deterministically controlled with an electric field. The underlying energy landscape of the spin texture is shaped by both the ferroelectric degree of freedom and strain-

induced anisotropy, where electric fields drive magnetoelectric switching in predictable ways that can be engineered. Through precise control of the crystal structure using thin film techniques, the magnetic structure of BiFeO₃ can be tuned to control magnon transport in the material, opening the door for efficient, electrically controllable magnonic devices.

11:30 AM EL07.04.08

From Magnetostrictive Composites to Precision Magnetoelectric Field Sensing Lukas Zimoch, Stefan Schroeder, Eric Elzenheimer, Soeren Kaps, Thomas Strunskus, Franz Faupel, Michael Hoeft, Gerhard Schmidt and Rainer Adelung; University of Kiel, Germany

The demand for magnetic field sensors is rapidly increasing due to various factors, including the requirements for navigation, orientation, and motion tracking systems, as well as their growing utilization in the automotive sector and notably in biomedical applications. There are two magnetoelectric (ME) sensors discussed in this context. The first employs a magnetostrictive polymer composite (MPC) as its magnetosensitive material, which consists of ferromagnetic particles embedded within a soft polymer matrix. This capacitive sensor, featuring an electret [1], is specifically well suited for biomedical applications due to its low resonance frequency, typically around 100 Hz. To evaluate the sensor's performance, three measurements were conducted. Subsequently, a DC magnetic bias field measurement was carried out to identify the optimal operating point. In the final measurement, the sensor operated at its resonance frequency with the optimal bias field. In each measurement, the amplitude of the resonance frequency was systematically reduced to determine the minimum field the sensor can reliably detect. The resonance frequency is in the range of 50-150 Hz, largely influenced by the MPC's geometry. The sensor requires a bias field of several mT. Furthermore, these measurements confirmed that no remagnetization occurs within the sensor during the bias sweep. Even without optimization, the sensor displayed linear behavior across four orders of magnitude. The magnetic characterization of the sensor revealed that it fundamentally operates as intended, with its magnetic properties remaining stable when exposed to magnetic fields. The sensor could provide valuable insights into the common challenge faced by all magnetic field sensors, which is noise. The mechanical characteristics of the sensor are derived from the polymer matrix, while the magnetic properties are predominantly determined by the particles. Both components can be independently adjusted or altered, allowing an investigation of the individual noise components. To understand all the mechanics of the sensor a second simplified approach was adopted.

The second sensor is the most elementary version of the first sensor, where only two macroscopic ferromagnets are used emulating two particles in the composite, to understand the underlying mechanisms of the MPC. One of these magnets is mounted to a silicon cantilever, while the other remains fixed beneath it. The magnets oppose each other. When an external magnetic field is applied, superposition takes place, and the cantilever starts to oscillate. On the top part of the cantilever a piezoelectric AlN thinfilm is placed between two electrode layers. The mechanical stress of the oscillation is transduced into an electrical voltage and generates a signal proportional to the applied magnetic field. In this composition magnetic noise amplitude densities as low as 47 pT/√Hz have been measured [2]. It is possible to measure within the earth's magnetic field without sacrificing any performance. The sensor shows a sensitivity of 2170 V/T and doubles as an energy harvester. Without any optimization it was possible to generate 1.31 μW/cm²Oe² with a magnetic AC field of 20 μT in resonance.

[1] Schröder, S., Strunskus, T., Rehders, S. *et al.* Tunable polytetrafluoroethylene electret films with extraordinary charge stability synthesized by initiated chemical vapor deposition for organic electronics applications. *Sci Rep* 9, 2237 (2019). <https://doi.org/10.1038/s41598-018-38390-w>

[2] L. Zimoch *et al.*, Self-powered elementary hybrid magnetoelectric sensor, *Nano Energy*, 2023. <https://doi.org/10.1016/j.nanoen.2023.108720>

The authors acknowledge financial support by the Deutsche Forschungsgemeinschaft (DFG, German Research Foundation) – Project-ID 286471992 – SFB 1261

11:45 AM EL07.04.09

Impressive Nanogenerator Application Using Nanoscale LuFeO₃: Role of Structure and Morphology Smita Chaturvedi^{1,2}, Priyank Shyam³, Sachin Kumar Singh⁴, Avinash S. Kumbhar¹, Gopalan Srinivasan⁵ and Satishchandra Ogale^{2,6}; ¹Savitribai Phule Pune University, India; ²IISER Pune, India; ³Aarhus University, Denmark; ⁴Delhi University, India; ⁵Oakland University, United States; ⁶TCG CREST, India

In the domain of multiferroicity, Lutetium orthoferrite (LuFeO₃) represents a potentially interesting material owing to the fact that it exhibits orthorhombic (o) and hexagonal (h) structures, which significantly differ in terms of lattice symmetry and the symmetry of the surroundings of the individual cations. This difference in structural symmetry contributes to unusual changes in physical properties. In o-LFO canting of Fe moments towards c direction gives rise to weak ferromagnetism below Néel Temperature (620 K), while, ferroelectricity is unexpected due to symmetry of lattice. On the other hand, weak ferromagnetism is not allowed in h-LFO unless the moments are along the 'a' axis. Present work is intended to realize the co-existence of o-LFO and h-LFO to achieve ferroelectricity and ferromagnetism simultaneously in a single nanostructure of two different morphologies i.e. nanoparticles and nanofibers. In multiferroic LuFeO₃ the hexagonal (-h) phase is an intermediate metastable phase encountered during the amorphous to orthorhombic (-o) transformation and is ferroelectric in nature. So far h-phase has only been stabilized in a substrate-supported layered ultrathin film form. Herein we show that the surface-induced strain field intrinsically present in nano-systems can self-stabilize this phase and the hexagonal to orthorhombic phase constitution ratio depends on the shape of the nanomaterial. Thus, nanofibers (nanoparticles) strain-stabilize the o : h ratio of about 23 : 77 (75 : 25). The inclusion of nano-LuFeO₃ into PDMS renders impressive nanogenerator performance, consistent with the ferroelectric phase content. This trait in the biphasic LuFeO₃ is attributed to: (i) Structure: Orthorhombic and hexagonal mixed phase: wherein the lattice dynamics change with temperature (both in case of nanoparticles and nanofibers), (ii) Morphology: (nanoparticles and nanofibers): wherein the dynamics of interparticle interactions would differ for nanoparticles and nanofibers.

1:30 PM *EL07.05.01

Strain Manipulation of Ferroelectricity and Flexoelectricity in Freestanding Membranes [Harold Y. Hwang](#)^{1,2}; ¹Stanford University, United States; ²SLAC National Accelerator Laboratory, United States

The ability to create and manipulate materials in two-dimensional (2D) form has repeatedly had transformative impact on science and technology. We have developed a general method to create freestanding complex oxide membranes and heterostructures using epitaxial water-soluble buffer layers, with millimeter-scale lateral dimensions and nanometer-scale thickness. This facilitates many new opportunities; here we will focus on the use of membrane dimensions, tensile strain, and strain gradients to control the ferroelectric and flexoelectric response of oxide membranes.

2:00 PM *EL07.05.02

Synthesis and Properties of Single Domain BiFeO₃ Thin Films and Free-Standing Membranes Chang-Beom Eom and [Pratap Pal](#); University of Wisconsin--Madison, United States

BiFeO₃ (BFO) is positioned for success as a magnetoelectric material system, but its optimum usage in faster and more energy-efficient magneto-logic devices require advances. Most importantly, a ferroelastic and antiferromagnetic monodomain state with single-step deterministic switching is desirable for reliable low-power magnetoelectric devices with reproducibility and scaling using BiFeO₃. This would allow deterministic and robust control of both the internal magnetoelectric coupling in BiFeO₃ and the exchange coupling of its antiferromagnetic order to a ferromagnetic overlayer.

We have fabricated epitaxial (001) and (111) BFO thin films with both ferroelectric and antiferromagnetic monodomain states. Additionally, we have fabricated freestanding membranes of ferroelastic and ferroelectric monodomain BiFeO₃ using an Sr₂CaAl₂O₆ (SCAO) sacrificial layer. The membranes exhibit deterministic switching over a hundred thousand electric field cycles with lower voltage and faster switching dynamics than their thin-film counterpart. This progress is promising toward energy-efficient magnetoelectric memory devices. We will discuss additional multiferroic applications of these BFO membranes.

This work has been done in collaboration with J. L. Schad, K. J. Lee, Y. Yao, A. M. Vibhakar, R. D. Johnson, P. G. Radaelli M.S. Rzchowski and C.B. Eom.

CBE acknowledges support for this research through the Gordon and Betty Moore Foundation's EPiQS Initiative, Grant GBMF9065 and a Vannevar Bush Faculty Fellowship (ONR N00014-20-1-2844). Magnetic and transport measurement at the University of Wisconsin--Madison was supported by the US Department of Energy (DOE), Office of Science, Office of Basic Energy Sciences (BES), under award number DE-FG02-06ER46327.

2:30 PM BREAK

3:30 PM *EL07.05.04

Anomalous Hall Effect and Topological Hall Effect in NiCo₂O₄ Thin Films and Free-Standing Membranes [Xia Hong](#); University of Nebraska-Lincoln, United States

The inverse spinel ferrimagnetic NiCo₂O₄ possesses high Curie temperature and high spin polarization, making it a promising material candidate for spintronic applications. The magnetic state of NiCo₂O₄ films depends sensitively on the strain and disorder effects, which can lead to unconventional spin transport. In this talk, I will discuss our recent studies of the magnetotransport anomalies in epitaxial NiCo₂O₄ thin films and free-standing NiCo₂O₄ membranes, including linear magnetoresistance, anomalous Hall effect (AHE), and topological Hall effect (THE). NiCo₂O₄ films deposited on (001) MgAl₂O₄ substrates exhibit strong perpendicular magnetic anisotropy down to 1.2 nm (1.5 unit cell) thickness, while the (110) films possess in-plane magnetic anisotropy. Films with high crystallinity show quasi-linear magnetoresistance in magnetic fields up to 17 T with weak temperature dependence. The AHE exhibits a nonmonotonic temperature dependence and sign reversal driven by both temperature and film thickness, revealing the intricate interplay between the impurity spin scattering, band intrinsic Berry curvature, and correlation effect. THE has been observed in (110) NiCo₂O₄ films and (001) NiCo₂O₄ membranes at low temperatures. The former has been correlated with magnetic bubble domain formation, as revealed via magnetic force microscopy, suggesting the emergence of bimeron spin textures. The latter can be sensitively tuned by magnetic field cooling. Our study provides effective material strategies for designing spin transport in NiCo₂O₄ via strain and disorder, paving the path for its technological implementation. This work was primarily supported by NSF through Grant No. DMR-1710461 and EPSCoR EQUATE Award No. OIA-2044049.

4:00 PM *EL07.05.05

Atomic Scale imaging of Topotactic Phase Transitions in Freestanding Strontium Cobaltite Membranes [Seung Sae Hong](#)¹, Hudson Shih¹, Rohan Dhall² and Yayoi Takamura¹; ¹University of California, Davis, United States; ²Lawrence Berkeley National Laboratory, United States

Topotactic phase transitions (TPTs) are structural phase changes that involve the significant loss or gain of oxygen atoms while preserving the crystalline framework of the lattice. In perovskite oxides, TPTs have recently emerged as innovative pathways for designing complex oxide materials. These transitions induce dramatic alterations in metal oxidation states and atomic coordination, enabling a wide range of electromagnetic ground states, from magnetic ordering to unconventional superconductivity. Moreover, the reversible nature of TPTs holds promising implications for practical applications such as neuromorphic computing devices, garnering significant attention in both fundamental physics and device applications.

Despite the growing research interest in TPTs in recent years, the microscopic details of these transitions, encompassing both structural changes and ionic transport, remain largely unexplored. This is partly due to the constraints imposed by the thin film heterostructure geometry, which limits our ability to directly visualize the transition through conventional means. In this report, we present recent advancements in freestanding oxide membranes that enable the local nature of TPTs to be visualized using electron microscopy. As a model system to comprehend the local structure of TPTs, we examined strontium cobaltite (SrCoO_{3.8}), which can transition between a ferromagnetic metal (perovskite) and an antiferromagnetic insulator (brownillerite). Transmission electron microscopy studies of SrCoO_{3.8} membranes unveiled the formation of anisotropic domains in the midst of the transition. Furthermore, atomic-scale images revealed the intricate nature of strains and crystallographic symmetries that dictate the domain patterns. Freestanding oxide membranes offer an ideal platform for in-situ and in-operando studies of TPTs, providing insights into the predictable design of switching phenomena in oxide materials.

4:30 PM EL07.05.06

Intrinsic Properties of Ferroic Materials Independent of Substrate Effects [Varun Harbola](#), Yu-Jung Wu, Felix Hensling, Hongguang Wang, Peter A. van Aken and Jochen Mannhart; Max Planck Institute for Solid State Research, Germany

Substrates are essential in thin-film deposition, yet they do not always meet the specific requirements of a given experiment or application and, in some cases, may even hinder in intrinsic measurements of epitaxial thin films. For example, SrTiO₃, one of the most widely used substrates, goes through an

antiferrodistortive transition at 105 K which can lead to substrate artefacts extrinsic to the thin film properties grown atop the substrate. However, the bulk of the substrate in its single crystal form is not required to support epitaxy, as only the top few unit cells near the surface define the epitaxial template for thin film growth. We introduce the novel concept of "vector substrates" where the template layer for epitaxy can be chosen independently of the bulk of the substrate. Thus, by choosing the right combination of a bulk carrier substrate and the template layer, we can reduce, if not eliminate artefacts resulting from the behaviour of the bulk substrate. The fabrication of vector substrates leverages thin-film membrane technology by growing a template layer on a parent substrate and then transferring it onto a carrier substrate, thereby generating the vector substrate. By comparing the magnetism of $\text{La}_{0.67}\text{Sr}_{0.33}\text{MnO}_3$ grown on a conventional SrTiO_3 substrate and a SrTiO_3 -on-sapphire vector substrate, we show that we can indeed eliminate the extrinsic antiferrodistortive artefact on a vector substrate. Therefore, the concept of vector substrates can provide a platform to measure ferroic thin films and the characteristics independent of substrate effects.

References:

V. Harbola et al., Vector Substrates: Idea, Design, and Realization, *Adv. Func. Mater.* (In press) Article DOI: 10.1002/adfm.202306289 (2023).

SESSION EL07.06: Poster Session II
Session Chairs: John Heron, Morgan Trassin, Ruijuan Xu and Di Yi
Wednesday Afternoon, April 24, 2024
Flex Hall C, Level 2, Summit

5:00 PM EL07.06.01

Fabrication of Hybrid Particles with Dual-Functionality for EMI Shielding and Heat Dissipation Yeonju Park, HyeRyeong Oh, Hyeongkeun Kim and MyongJae Yoo; Korea Electronics Technology Institute, Korea (the Republic of)

Semiconductor packaging technology and industry are developing toward higher performance, higher integration, thinner thickness, and miniaturization. Consequently, there is a problem in that the amount of heat generated from the device increases and electromagnetic interference (EMI) occurs inside the PIM semiconductor. Therefore, packaging requires both high heat dissipation and EMI shielding performance. In this study, an insulating and heat dissipating thin film was deposited on the surface of the magnetic particles. The deposited thin film composition was analyzed through elemental analysis. The insulating properties of the fabricated particle were measured and it was confirmed that the resistance increased. Heat dissipation properties and EMI shielding properties of the fabricated particles were measured by manufacturing composite film. Our results achieved 13% increased thermal conductivity properties compared to films manufactured using pristine particles. EMI shielding characteristics were measured in the Ka band (26.5-30 GHz), and reflection and absorption performance were calculated and analyzed.

5:00 PM EL07.06.02

Magnetic Entropy Changes in Rare-Earth Tetraborides (RB₄, R = Dy, Ho, and Tm) Beongki Cho¹ and Songhee Han²; ¹GIST, Korea (the Republic of); ²Mokpo National Maritime University, Korea (the Republic of)

The RB₄ (R = Gd, Tb, Dy, Ho, and Tm) compound presents an intriguing system with simultaneous magnetic ordering and geometrical frustration, leading to a strong interaction within the material. The interaction manifests in consecutive magnetic transitions at temperatures $T = T_{N1}$ and T_{N2} (where $T_{N1} > T_{N2}$) and results in a highly anisotropic magnetic configuration when in an ordered state. In this study, we systematically investigate the anisotropic entropy change (ΔS_{AN}) of single crystals of RB₄ (R = Dy, Ho, and Tm). Our findings reveal distinct behavior: the negative entropy change above T_{N1} follows conventional field-dependence, while a positive entropy change below T_{N1} follows anomalous field-dependence. Notably, ErB₄ ($T_{N1} = 15.5$ K) and TmB₄ ($T_{N1} = 11.7$ K) demonstrate $|\Delta S_{AN}|$ values of ≈ 11.6 J/(K kg) and 10.2 J/(K kg), respectively, at $T > T_{N1}$ and for $H = 50$ kOe, accompanied by relative cooling power (RCP) values of ≈ 237.1 J/kg and 225.9 J/kg. Interestingly, DyB₄ ($T_{N1} = 20.5$ K) exhibits a significant $|\Delta S_{AN}|$ value of 18.8 J/(K kg) near $T = T_{N2}$ ($= 13.0$ K) and an RCP value of ≈ 208.39 J/kg for $H = 50$ kOe. These $|\Delta S_{AN}|$ and RCP values demonstrate the potential of these compounds for applications in refrigeration using rotational magnetocaloric effect (RMCE). Additionally, HoB₄, ErB₄ and TmB₄ exhibit also promising behavior for RMCE even at temperatures of $T < T_{N1}$ and particularly during low-field cooling ($H < 50$ kOe). This work highlights the suitability of RB₄ compounds as effective materials for RMCE cooling, covering a broad temperature range above and below the antiferromagnetic Néel temperature. Specifically, the anisotropic entropy change observed in DyB₄ near $T = T_{N2}$ holds considerable potential for RMCE applications, such as hydrogen liquefaction due to its occurrence which a limited temperature range, accompanied by large $|\Delta S_{AN}|$ and RCP values.

5:00 PM EL07.06.03

Tuning of Orientation and Magnetic Properties of Ferromagnetic Aerogels produced through a Magnetic-Field Assisted Synthesis Rosemary L. Calabro^{1,2}, Alexander D. Ciampa¹, Edward Tang¹, Kennedy V. Munz¹, Olivia S. Raykhman¹, Malina O. Hatton¹, Zachary T. Bone¹, Felita W. Zhang¹, Kelsey M. Healy¹, Peter H. Chapman¹, Stephen F. Bartolucci², Joshua A. Maurer² and John Burpo¹; ¹United States Military Academy, United States; ²U.S. Army DEVCOM Armaments Center, United States

Ferromagnetic aerogels possess many desirable properties such as low densities, high porosities and surface areas, and interesting magnetic properties which allow opportunities in a wide range of applications including sensing, energy storage, switches, theranostics, catalysis, and many others. In a majority of these applications, the aerogels consist of some type of host material such as silica or a polymer that is doped with a ferromagnetic nanomaterial. However, ferromagnetic aerogels that consist only of the magnetic material without a host are highly desirable because they allow higher magnetizations per unit mass, better exposed surfaces, and simpler structures. We have prepared magnetic nanowire aerogels using a magnetic-field assisted synthesis which allows formation of magnetic nanowire aerogels in a fast, simple, and scalable manner. In a typical synthesis, a metal salt such as iron or cobalt chloride was placed inside a magnetic field, and sodium borohydride was added dropwise as a reducing agent. This resulted in rapid formation of gels that could then be supercritically dried into aerogels or conformed into thin films depending on the desired application. The applied magnetic field strength was varied from 0 mT to 150 mT and had impact on the nanowire aspect ratios and orientation, the magnetization and coercivities of the aerogels, the mechanical properties, and the observed surface areas and porosities. Typically, low applied field strengths showed low ordering and small aspect ratios while higher applied fields increased the orientation and aspect ratios of the nanowires. Bimetallic iron-nickel aerogels were also prepared and the influence of the metal counterion was studied. The counterion not only impacted the rate of the reaction, but also the shape of the nanostructures within the formed aerogels. The iron-to-nickel ratio also influenced the nanowire length and magnetic properties. The magnetic field assisted synthesis strategy allowed rapid formation of template free ferromagnetic aerogels and can be expanded to achieve a wide range of bimetallic materials.

5:00 PM EL07.06.04

Engineering Reliability and Crystallographic Orientation by Al Doping of Ferroelectric Hafnium-Zirconium Oxide Ayse Sünbül¹, David Lehninger¹, Konrad Seidel¹, Lukas Eng² and Maximilian Lederer¹; ¹Fraunhofer IPMS, Germany; ²Institute of Applied Physics, Technical University Dresden, Germany

Due to its scalability and CMOS compatibility, ferroelectric hafnium oxide (HfO₂) has attracted attention since its discovery in 2011 [1, 2]. Many elements can be used as dopant [3, 4] to stabilize the ferroelectric (FE) orthorhombic phase of HfO₂. Especially Zr doping of HfO₂ (HZO) has some advantages for back-end-of-line (BEoL) integration, due to its low crystallization temperature [5].

FE materials can be used in memories such as ferroelectric field-effect transistors (FeFETs) that are non-volatile and applicable in low-power systems. Good endurance and retention, high remanent polarization, and high-temperature resilience are required for embedded FE memories and the automotive industry requires high-temperature operation (up to 150 °C specifications given by the Automotive Electronics Council) which is not fulfilled by current HZO devices.

Al can be co-doped into HZO (HZAO) to overcome the reliability challenges of HZO such as high-temperature, high-bias operation, endurance, and imprint limitations [6]. In this study, different Al concentrations (up to 3 at. % Al) were doped into HZO and various crystallization annealing conditions (400 °C, 650 °C, and 800 °C) were investigated.

Increasing Al concentration and increasing annealing temperature in HZAO resulted in more antiferroelectric-like behavior. Additionally, endurance at high temperatures (up to 150 °C) and high-bias conditions (up to 5 MV/cm applied electric fields) were drastically improved in HZAO compared to HZO. A correlation between crystallographic phases and electrical results (coercive field E_c and remanent polarization P_r) was made. The ratio of (111)/(002) diffraction peak intensities increases with lower Al concentrations. Increase in P_r and E_c is observed with increasing ratio of (111)/(002) diffraction peak intensities. Consequently, this work will discuss the tuning of electrical properties (such as P_r, E_c, and endurance) depending on application requirements by controlling anneal conditions and Al doping concentration. It will investigate the impacts of Al concentration and anneal conditions on reliability aspects such as enhanced endurance, reduced leakage and high temperature resilience.

[1] T. S. Böske, J. Müller, D. Bräuhäus, U. Schröder, U. Böttger. Appl. Phys. Lett. 2011; 99 (10): 102903.

[2] T. S. Böske, "Ferroelektrische Speicherzelle, Herstellungsverfahren und integrierte Schaltung mit der ferroelektrischen Speicherzelle." DE102008024519B4.

[3] T. S. Böske, et al., Appl. Phys. Lett. 2011; 99 (11): 112904.

[4] S. Mueller, et al. ECS J. Solid State Sci. Technol. 2012, 1, N123.

[5] D. Lehninger, et al., Phys. Status Solidi A, 2020, 217: 1900840.

[6] A. Sünbül, et al., Adv. Funct. Mater. 2023, Under Review.

5:00 PM EL07.06.05

Deep UV Photo Emission Electron Microscopy to Spatially Probe Work Function in Oxygen Vacancy Reduced Hf_xZr_(1-x)O₂ Fernando J. Vega Amaya¹, Alex M. Boehm², Andrew R. Kim², Samantha Jaszewski², Jon F. Ihlefeld³, Taisuke Ohta² and Thomas Beechem¹; ¹Purdue University, United States; ²Sandia National Laboratories, United States; ³University of Virginia, United States

Oxygen vacancies are known to both stabilize the ferroelectric orthorhombic phase of Hf_xZr_(1-x)O₂ (HZO) and promote leakage pathways limiting endurance of devices based on this material. For this reason, the energy states of oxygen vacancies were investigated using photoemission electron microscopy (PEEM) as their concentration was varied via laser exposure. Following a controlled oxygen vacancy (V_O) reduction via incremental and areal laser dosing on HZO, 213nm deep-ultraviolet (DUV) photoemission electron microscopy (PEEM) was used to spatially probe the resulting modification in work function. Work function was found to increase monotonically with the laser-induced reduction in oxygen vacancy concentration culminating in a total increase near 70 meV. The change implies a Fermi-level shift toward the valence band as the total available charge states are reduced as oxygen vacancies are removed. A reduction in charge states is also supported by the observed reduction in photo emission yield after laser dosing. Beyond the quantitative change, the smooth monotonic change in work-function and photoemission yield suggest the presence of a "defect band" that forms in HZO due to the presence of vacancies rather than a single discrete state.

5:00 PM EL07.06.06

La_{1-x}Sr_xCoO₃ Perovskite: Antimicrobial Properties and PVDF Based Piezoelectric Nanogenerator Through Self-Induced Polling and Sensory Application S M Anayet Ullah Shohag, Luke Franco, Adhira Tippur, Ahmed Touhami, Swati Mohan and Jasim Uddin; The University of Texas Rio Grande Valley, United States

Global demand of sustainable and efficient energy sources continues to rise of research of novel materials and their application in energy harvesting. Sr²⁺ doped Lanthanum Cobaltite (La_{1-x}Sr_xCoO₃) perovskite stands out as a promising candidate due to its unique properties and versatility as piezoelectric material as well as in antimicrobial properties. Piezoelectric Nanogenerators (PENGs), which can produce electrical energy from mechanical energy via ferroelectric effect, are one of the ambient sources of green energy. PENGs have gathered a huge attention due to cost-effectiveness, mechanical stability, and easy installation process. In this work, synthesized⁺ doped Lanthanum Cobaltite (La_{1-x}Sr_xCoO₃) perovskite, a ferroelectric material, was synthesized by sol-gel- molten-salt process and then characterized by X-ray diffraction, and scanning electron microscopy ensures the uniform morphology of nanoparticles. Further poly (vinylidene difluoride) (PVDF), N,N-dimethylformamide and acetone solution were used to make a flexible composite film using La_{1-x}Sr_xCoO₃ nanoparticles by spin coating, self-induced polling process and curing. Fourier transform infrared spectroscopy (FTIR) investigation ensures that self-induced polling process was effective to identify the structural β phase. PVDF/ La_{1-x}Sr_xCoO₃ composite film is then placed in between two copper sheets to fabricate the piezoelectric nanogenerator. The 7.5wt% PENG demonstrates the open-circuit voltage of 2.5V. The peak-to-peak voltage and peak to peak current values were also reported for all different weights, frequencies, and doping range. Finally, the PENG was used as a smart weight sensor and motion sensor to operate low-power electronic devices. Beside this we also observed antimicrobial properties of La_{1-x}Sr_xCoO₃ nanoparticles by the Kirby Bauer testing method, our synthesized La_{1-x}Sr_xCoO₃ nanoparticles showed much better activity against *Escherichia coli* and two other Bacillus species as well. This work explores La_{1-x}Sr_xCoO₃ nanoparticles potential as antimicrobial properties and piezoelectric nanogenerator for mechanical energy harvesting, contributing to greener and more sustainable energy solutions.

8:15 AM *EL07.07.02

Wake-up, Retention and Fatigue in Wurtzite Ferroelectric Films Susan E. Trolier-McKinstry; The Pennsylvania State University, United States

Ferroelectric wurtzite films typically show large polarizations of 70 – 140 $\mu\text{C}/\text{cm}^2$, coupled with coercive fields of 2 – 6 MV/cm. These films are appealing for non-volatile memory elements in ferroelectric random access memories, ferroelectric tunnel junctions, and ferroelectric diodes. It has been found that $\text{Al}_{0.93}\text{B}_{0.07}\text{N}$ and $\text{Zn}_{1-x}\text{Mg}_x\text{O}$ thin films often undergo a wakeup process associated with development of mobile interfaces on bipolar cycling. The number of cycles required for wakeup is a strong function of the switching frequency and field, with more cycles required for wakeup as the excitation frequency increases. The activation energies for wake-up typically exceed those for the activation energy for the coercive field of a fully woken-up sample. Both types of films showed excellent retention of the stored polarization state. For example, in opposite state (OS) measurements even after 3.6×10^6 sec (1000 hr.) at 200°C, the OS signal margin still exceeded 200 $\mu\text{C}/\text{cm}^2$ in $\text{Al}_{0.93}\text{B}_{0.07}\text{N}$. The predicted OS retention is 82% after 10 years baking at 200°C. $\text{Zn}_{1-x}\text{Mg}_x\text{O}$ is even more robust in opposite state retention. A key challenge is to increase the cycle lifetime by prevention of premature dielectric breakdown events.

8:45 AM EL07.07.01

Multilayered Thin Film Ferroelectric Wurtzites Robert J. Spurling¹, Chloe Skidmore¹, John Hayden¹, Josh Nordlander¹, Joseph Casamento^{1,2}, Kyle Kelley³ and Jon-Paul Maria¹; ¹The Pennsylvania State University, United States; ²Massachusetts Institute of Technology, United States; ³Oak Ridge National Laboratory, United States

We report on observations of ferroelectric switching in multilayered sputtered thin films based on wurtzite $\text{Zn}_{1-x}\text{Mg}_x\text{O}$ and $\text{Al}_{1-x}\text{B}_x\text{N}$. Ferroelectric switching is achieved in thin film stacks containing ferroelectric and polar non-ferroelectric layers. Total polarizations indicate switching is achieved across the entire film stacks, suggesting propagation of ferroelectric domains across interfaces between layers. We investigate switching pathways and wake-up behavior in these films as characterized through an array of structural and property measurement techniques. We also discuss synthesis controls in $\text{Zn}_{1-x}\text{Mg}_x\text{O}$ sputtered thin films, with an emphasis on connections between structure and electrical properties. We focus on the effect of oxygen chemical potential and temperature on film microstructure and resistivity.

9:00 AM EL07.07.03

Developing Phase Field Models for The Physical Vapor Deposition of Ferro Doped AlN John Wellington-Johnson¹, Roxanne Ware¹, Remi Dingreville² and Lauren M. Gerten¹; ¹Georgia Institute of Technology, United States; ²Center for Integrated Nanotechnologies, United States

While unique functionalities, such as ferroelectricity and ferromagnetism, have been observed in transition metal doped AlN thin films, the addition of these dopants can negatively impact the films crystalline quality. Avoiding phase segregation, surface faceting, or crystallite misorientation are critical to ensure that the full ferroic potential of these materials can be reached. Further insight into the microstructural evolution of AlN in the presence of transition metal dopants is necessary to understand the impact of these dopants on film growth and ferroelectricity.

In this work, phase field models are developed for physical vapor deposition, microstructural development, and ferroelectric response of transition metal doped AlN thin films. These models are then compared to doped AlN thin films grown by pulsed laser deposition (PLD) and sputtering. Doped AlN thin films were deposited onto platinumized silicon substrates via ultra-high-vacuum PLD, RF or DC sputtering. The substrate growth temperatures ranged from 200 °C to 800 °C with an incident laser energy from 100 to 300 mJ and a laser repetition rate of 10 Hz for PLD growth. Increasing the growth temperature decreases the full width, half maximum of the predominant (002) X-ray diffraction peaks, indicating an increase in orientation which is corroborated by the model. Atomic force microscopy and scanning electron microscopy show the evolution of the surface morphology and microstructure with changing processing conditions. Increased surface faceting is observed with increased dopant concentration and segregation as determined by X-ray photoelectron spectroscopy (XPS). There is also a clear correlation between the deposition conditions and the ferroelectric response, with increased electrical breakdown for DC sputtered films compared to RF sputtering and pulsed laser deposition. Overall, these results illustrate that the ferroelectric properties highly sensitive to the growth conditions and resulting microstructure.

9:15 AM EL07.07.04

Impact of Electrodes and Interfaces in Ferroelectric Switching of Sub-100nm $\text{Al}_{1-x}\text{Sc}_x\text{N}$ Vamshi Kiran Gogi¹, Christopher Chae², Jinwoo Hwang² and Rashmi Jha¹; ¹University of Cincinnati, United States; ²The Ohio State University, United States

Ferroelectric materials have garnered huge research interest in the last 50+ years as these materials possess a variety of interactions between electrical, mechanical, and thermal properties that can enable multiple functionalities. The reports of ferroelectric behavior in Aluminum Scandium Nitride ($\text{Al}_{1-x}\text{Sc}_x\text{N}$) has widened the potential use of ferroelectric functionality in microelectronics beyond HfO_x based ferroelectrics. Particularly, Ferroelectric Field Effect Transistor (FeFET) is a compelling application of these materials that can enable novel logic and memory devices. However, most studies have reported Ferroelectricity in thick AlScN films and more work is needed to understand their behaviour in sub-100 nanometer thickness regime. Additionally, role of electrodes and interfacial layers when AlScN is integrated in FeFETs is not well-known. This work reports the role of electrodes in Ferroelectric Switching of sub -100 nm $\text{Al}_{1-x}\text{Sc}_x\text{N}$ ($x \approx 22\%$) films. Sub-100nm $\text{Al}_{0.78}\text{Sc}_{0.22}\text{N}$ has been deposited via reactive co-sputtering and impact of electrodes such as W, Ti/Ru and Sc has been studied in metal-insulator-metal and metal-insulator-p-Si configurations. We demonstrate the effects of rapid thermal annealing and its impact on polarization in these thin films. Notably, RTA can alter the film properties and modify interfaces. On Silicon substrates, we also report the role of oxynitride formation aided defect structures in ferroelectric switching of these III-V nitrides. True Ferroelectric switching has also been investigated through PUND (Positive Up and Negative Down) analysis accounting for leakage current induced effects on these AlScN thin films grown on different metals. The film microstructures have been investigated using TEM and EDX analysis that has been correlated with electrical test data on polarization. We believe this work is important for tailoring AlScN materials and interfaces to achieve the desired FeFETs performance.

9:30 AM EL07.07.05

Synthesis of New Nitride Material Manganese Cobalt Nitride by RF Co-Sputtering Sita Dugu¹, Rebecca Smaha¹, Shaun O'Donnell², Andrew Treglia², Stephen Lany¹ and Sage Bauers¹; ¹National Renewable Energy Laboratory, United States; ²Colorado State University, United States

Transition metal (TM) nitrides have historically been used as cutting tools due to their outstanding properties such as high hardness and strength, excellent thermal conductivity, and unique electrochemical properties. In 2019, Sun *et al.* [1] constructed a stability map of inorganic ternary metal nitrides using high-throughput computational methods based on a data-mined structure prediction algorithm. While this work predicted hundreds of new ternary nitrides, only one new chemical space was predicted to contain a previously unknown compound comprising nitrogen and two TMs: MnCoN_2 . In this study, a series of Mn-Co-N thin films are synthesized by RF magnetron sputtering and characterized for structural and magnetic properties.

Combinatorial Mn-Co-N thin films are deposited using reactive co-sputtering at different temperatures ranging from 25 – 450°C and various process pressures. The phase of the as-grown material is checked by X-ray diffraction. Survey density function theory total energy calculations are performed in

parallel on six prototype structures based on zincblende or rocksalt lattices. Comparing the calculated structures with experimental diffraction patterns, the synthesized films better match the rocksalt-derived structures, which also exhibit lower formation energy than the zincblende candidates. However, only the primary diffraction peaks are seen, suggesting a large amount of cation anti-site disorder. Manganese and cobalt concentrations are measured by X-ray fluorescence and nitrogen concentration by Rutherford backscattering spectrometry, confirming nearly 1:1:2 concentrations of Mn:Co:N with some reduced N due to O impurities. Scanning electron microscopy and energy dispersive x-ray spectroscopy are also performed, which illustrated the presence of all elements at their respective energy levels. Magnetic properties for MnCoN₂ films have been studied by SQUID magnetometry, which demonstrates that the film possesses a weak moment of remanent magnetization 0.01 emu/gm and coercive field of 0.5 T. The study of moment vs temperature shows a transition temperature at ~10 K and overall antiferromagnetic correlations. To better understand the origin of the magnetic moment in the compound and its correlation with structure and stoichiometry (both anion and cation), we perform X-ray Absorption Spectroscopy (both near edge and extended fine structure). Our experimental confirmation of this new TM_1-TM_2-N ternary nitride motivates renewed effort in new materials prediction and discovery in similar ternary spaces, which we are actively pursuing. For example, in our ongoing computational search, several more TM_1-TM_2-N have been predicted as new stable nitrides.

1. Sun, W. *et al*, A map of the inorganic ternary metal nitrides. *Nat. Mater.* **18**, 732–739 (2019)

9:45 AM EL07.07.06

Hybrid Molecular Ferroelectrics, a Promising System with Unique and Outstanding Electromechanical Properties [Yuzhong Hu](#)^{1,2,3}, Marin Alexe², Hongjin Fan³, Junling Wang⁴ and Pooi See Lee³; ¹University of Heidelberg, Germany; ²University of Warwick, United Kingdom; ³Nanyang Technological University, Singapore; ⁴Southern University of Science and Technology, China

Organic-inorganic hybrid ferroelectrics (OIHF) is a novel member of ferroelectrics family comprised of both organic and inorganic parts as its building block. Since the year of 2014, tens of OIHF structures have been explored with striking progress made in electromechanical properties such as high ferroelastic strain output and piezoelectricity. Recently, giant d33 (1540 pC/N) and strain output (21.5%) were reported in this ferroelectric system, which are much higher (by around three times and two orders of magnitude, respectively) than those of lead zirconate titanate (PZT). These emerging outstanding properties indicates their bright future as lightweight and high-performance electromechanical materials. Different with the widely used piezoelectric enhancement methods such as morphotropic phase boundary (MPB) effect in oxide perovskite, the strain/piezoelectricity enhancement strategies for OIHF are involved with special molecular engineering. In addition, the bond engineering in OIHF show bright future for high-performance soft piezoelectrics. With our works, I will report: 1. The space-confinement structure enables giant strain output of 21.5% and d35 of 4800 pm/V in an OIHF. 2. The bond weakening strategy renders high-performance soft piezoelectrics, in which the materials show orders of magnitudes higher power output (11 W/m²) than general piezoelectric ceramics and simultaneously, excellent mechanical softness (0.8 GPa) better than PVDF (2 GPa). These results promise OIHF unique positions in ferroelectrics family, especially in actuator and in soft electronics applications.

Authors: Yuzhong Hu, Marin Alexe, Hong Jin Fan, Junling Wang, Pooi See Lee.

Some of the related works:

Yuzhong Hu *et al.*, *Nature Materials*, 20.5 (2021): 612-617

Yuzhong Hu *et al.*, *Nature Communications*, 13 (2022): 5607

10:00 AM BREAK

SESSION EL07.08: Hafnium Oxides I
Session Chairs: Amal El-Ghazaly and Varun Harbola
Thursday Morning, April 25, 2024
Room 342, Level 3, Summit

10:30 AM *EL07.08.01

First-Principles Studies of Hafnia Ferroelectrics -- In a Class of Their Own [Jorge Iniguez](#)^{1,2}; ¹Luxembourg Institute of Science and Technology, Luxembourg; ²University of Luxembourg, Luxembourg

Hafnia ferroelectrics hold great promise for the development of nano-devices that may take advantage of their permanent and switchable electric polarization. Hence, their technological interest has made them a focus of attention. But that is not all: surprisingly, these materials are proving to constitute a ferroelectric class of their own, displaying many intrinsic behaviors that seem genuinely unprecedented and certainly lay outside the "standard model" of soft-mode ferroelectricity in perovskite oxides. In this talk I will present first-principles results to discuss and explain some of those intriguing properties. In particular, I will discuss the evidence for (im)proper ferroelectricity -- and a possible soft-mode behavior -- in these compounds. I will also address the question of whether hafnia should be considered a triaxial, biaxial or uniaxial ferroelectric, explaining how the last option may be sufficient (and convenient) to account for the behavior of many woken-up samples. I will then show that, within such a uniaxial picture, it is possible to identify a centrosymmetric reference phase that yields a straightforward description of all the known low-energy polymorphs of these materials, evidencing how they are structurally connected. Finally, I will discuss the piezoelectric response of hafnia ferroelectrics, emphasizing the various unique features it presents (e.g., sign tunability). Time permitting, I will summarize other recent results of my group, e.g., on hafnia-based superlattices.

Work done in collaboration with Hugo Aramberri, Sangita Dutta, Binayak Mukherjee and Natalya S. Fedorova (Luxembourg Institute of Science and Technology). Funded by the Luxembourg National Research Fund through Grant INTER/NWO/20/15079143/TRICOLOR.

11:00 AM *EL07.08.02

Memristive Devices with Ferroelectric Materials [Beatriz Noheda](#); University of Groningen, Netherlands

The field of neuromorphic computing has recently broadened with the emergence of memristive devices as key elements that allow both processing and storage of information in the same unit. One of the materials classes that attract interest is ferroelectrics, as they offer non-volatile memory but also have been demonstrated to behave as memristive devices, allowing multiple resistance values and opening the possibility of their use as artificial synapses in hardware artificial neural networks, as well as in analogue information processing. I will present our work in this direction with different ferroelectric

materials (HfO₂, BiFeO₃ and BaTiO₃) and their different synaptic characteristics.

11:30 AM EL07.08.03

The Impact of Crystallinity on Ferroelectric Properties of Epitaxial Rhombohedral Hf_{0.5}Zr_{0.5}O₂ Films Ji Soo Kim¹, Maximilian Becker¹, Nives Strkalj^{1,2}, Megan Hill^{1,3}, Ziyi Yuan¹ and Judith MacManus-Driscoll¹; ¹University of Cambridge, United Kingdom; ²Institute of Physics, Croatia; ³Lund University, Sweden

Ferroelectric hafnium oxide is of great interest in the semiconductor industry due to its complementary metal-oxide-semiconductor compatibility and scalability. It has potential to be used as actuator, sensors, transducers, memories, etc. Out of all the dopants studied, zirconium doped hafnium oxide, Hf_{0.5}Zr_{0.5}O₂ (HZO), has been the most promising and widely investigated composition with reported remanent polarisation (P_r) of ~ 20 μC/cm² and coercive field (E_c) of ~ 1 MV/cm. However, there are limitations with ALD-grown ferroelectric HZO films in terms of wake-up effect, endurance and tuning of P_r and E_c for specific application such as ferroelectric random-access memory (FeRAM), ferroelectric field effect transistor (FeFET), negative capacitance field effect transistor (NCFET), and many more. In this work, model systems of HZO films were deposited by pulsed laser deposition (PLD) in which the epitaxial rhombohedral ferroelectric phase was stabilised. All the films show wake-up free ferroelectric behaviour with P_r > 7 μC/cm². With increase in laser fluence from 0.5 to 1.3 J/cm², E_c increased from ~ 2.7 MV/cm to ~ 3.3 MV/cm. In order to understand the origin of such change in ferroelectric properties, we separate out individual influences of O content, strain and microstructure via x-ray photoelectron spectroscopy, x-ray diffraction, and scanning tunnelling electron microscopy.

11:45 AM EL07.08.04

Polar Orthorhombic Phase Stabilization of Hf_{0.5}Zr_{0.5}O₂ by inserting Seed Layer of HfO₂ and ZrO₂ Yong chi Su and Yen-Lin Huang; National Yang Ming Chiao Tung University, Taiwan

Ferroelectric materials exhibit electrically switchable polarization states that can be utilized in non-volatile memory components such as ferroelectric random access memory (FeRAM), ferroelectric FET (FeFET), and ferroelectric tunnel junctions (FTJs). Among various ferroelectric materials, Hf_{0.5}Zr_{0.5}O₂ (HZO) has attracted significant interest owing to its potential for thickness scalability and compatibility with CMOS technology. However, hafnia-based ferroelectric materials still have some difficulties needing to be overcome. For example, hafnia-based materials have many polymorphs, including monoclinic phase, tetragonal phase, and orthorhombic phase. Among all the phases, only the orthorhombic phase with space group (Pca2₁) exhibits the ferroelectricity, yet it is a metastable phase for HZO. Therefore, how to stabilize the orthorhombic phase formation at a limited thickness regime is the central issue for a large-scale application of HZO. Another issue is that hafnia-based materials often suffer from the wake-up effect, which may result from the defect accumulation or the transformation from non-polar phase into polar phase. This issue is also related to the orthorhombic phase stabilization and the quality of thin films.

To address these drawbacks and improve the ferroelectric performance of HZO thin films this study proposes another approach by inserting an ultra-thin layer of HfO₂ or ZrO₂ serving as the polar phase stabilizer. This reduces the lattice mismatch between the bottom electrode (La_{0.7}Sr_{0.3}MnO₃) and the HZO layer. We found that by optimization of the insertion layer the pure polar phase of HZO can be realized in a larger growth window. We conducted the ferroelectric measurements by piezo force microscopy and ferroelectric tester to analyze the micro/macro ferroelectric properties. The wake-up and imprint effect can be measured by pulse switching measurement and first order reversal curves (FORCs) respectively. Also, by using a brand-new X-ray nano diffraction (XND) technique, it can differentiate the t-phase and o-phase with high energy resolution, which can help to prove the phase transformation from t-phase into o-phase after wake-up cycle.

Our results offer new insights into the stabilization of ferroelectric HZO and the development of wake-up-free hafnia-based devices, with the hope of paving the way for next-generation non-volatile memory applications.

SESSION EL07.09: Hafnium Oxides II
Session Chairs: Lauren Garten and Aileen Luo
Thursday Afternoon, April 25, 2024
Room 342, Level 3, Summit

1:30 PM *EL07.09.01

Hf_{1-x}Zr_xO₂-Based Ferroelectric Heterostructures for Non-Volatile Memories and Artificial Synaptic Devices Yuewei Yin and Xiaoguang Li; University of Science and Technology of China, China

The rapid development of information technology requires memory devices with fast speed, low power consumption, high density, etc. HfO₂-based ferroelectric thin films are promising for the advanced information memory devices, especially due to the good silicon compatibility and intrinsic advantages of ferroelectricity. Recently, we used atomic layer deposition to construct high-quality Hf_{1-x}Zr_xO₂ (HZO) ferroelectric thin film heterostructures and investigated corresponding prototype memory devices, including ferroelectric capacitors for FeRAM and ferroelectric tunnel junctions for neural network computing. The ferroelectric endurance properties of TiN/HZO/TiN capacitor were studied, and it was found that the ferroelectric fatigue severity increases first and then decreases with increasing pulse voltage or width. Accordingly, a recovery method by introducing wake-up effect was utilized to realize a weaker fatigue, a sufficient switched polarization (7–12 μC/cm²) by 100 ns voltage pulses, and especially an enhanced endurance of >1.01×10¹² (>5.0×10¹³ in expectation). On the basis of growing high-quality HZO heterostructure, ferroelectric tunnel junctions (FTJs) based on a SiO₂/HZO composite barrier and both conducting electrodes were designed and fabricated on Si substrates. The FTJ achieves the fastest write speed of 500 ps under 5 V or 10 ns speed at a low voltage of 1.5 V, low write current density ~1.3×10⁴ A/cm², and 8 discrete states. Interestingly, in the FTJ-based memristive synapse, gradually tunable nonvolatile conductance states (128 states) with high linearity were obtained, and by inputting the corresponding experimental results into an online neural network simulation, a high accuracy in recognizing fashion product images was achieved. These results indicate that silicon-compatible HfO₂-based ferroelectric heterostructures are important candidates for high-performance nonvolatile memory and artificial synaptic devices.

2:00 PM EL07.09.02

Ferroelectric Tunneling Junctions Based on Yttrium Doped Hafnium Dioxide Wei Chen Hung¹, Yen-Lin Huang¹ and Chun-Wei Huang²; ¹National Yang Ming Chiao Tung University, Taiwan; ²Feng Chia University, Taiwan

Hafnium dioxide (HfO₂)-based thin films are considered promising ferroelectric materials for modern semiconductor integration. Various methods have been explored to induce ferroelectricity in hafnium oxide-based thin films, including atomic layer deposition, chemical doping, and solid solution techniques. Among the diverse doping species, yttrium-doped hafnium dioxide (YHO) stands out as a novel candidate due to its robust ferroelectric

polarization, reliability, and scalability.

In this study, we are going to utilize the high ferroelectric polarization value of YHO, approximately $50 \mu\text{C}/\text{cm}^2$, to showcase ferroelectric polarization modulation of tunneling resistance. We also propose the device structure of ferroelectric tunneling junctions using YHO as the tunneling layer. We fabricate high quality epitaxial YHO thin films using pulsed laser deposition on single crystal SrTiO_3 (110)/(001) (STO) substrates. The crystal orientations of YHO were analyzed using X-ray diffraction, confirming the presence of the ferroelectric orthorhombic ($\text{Pca}2_1$) phase with two structure domains. Ferroelectric tests were carried out on our YHO films by a ferroelectric tester and piezoresponse force microscopy and ferroelectric tester.

Subsequent to the ferroelectric measurement, we utilized conductive atomic force microscopy and piezoresponse force microscopy to measure variations in polarization direction and tunneling resistance. Ultimately, we showcase the high-quality Pt/YHO/ $\text{La}_{0.7}\text{Sr}_{0.3}\text{MnO}_3$ devices and measure the resistance hysteresis loops. This innovative material holds significant potential for improving the performance and efficiency of ferroelectric tunnel junctions.

2:15 PM EL07.09.03

Influence of Stack Design on The Electrical Performance of HfZrO_2 Ferroelectric [Charlene Chen](#)¹, [Ray Meck](#)¹, [Jared McWilliams](#)¹, [Navnidhi Upadhyay](#)¹, [Mario Laudato](#)² and [Nguyen Vu](#)¹; ¹EMD Electronics, United States; ²Western Digital Corporation, United States

Hafnium-zirconium oxide (HZO) ferroelectrics have been attracting growing interest in different memory applications owing to their complementary metal oxide semiconductor (CMOS) compatibility and scaling capability [1]. Unlike their perovskite and wurtzite ferroelectric counterparts, HZO retains an excellent leakage and decent ferroelectric response at very low thicknesses [2]. This work highlights the role of bottom and top electrodes on the electrical performance of thin film HZO such as remnant polarization, endurance, and leakage. Crystallinity, thickness, and roughness of the electrodes are found to play critical roles in improving the film quality, reducing the thermal budget, and ultimately improving the electrical response of HZO films. Wake-up free sub 100 Å thick HZO films with back-end-of-line compatible annealing conditions exhibiting high remnant polarization ($2P_r \approx 54 \mu\text{C}/\text{cm}^2$) and low leakage ($10^{-5} \text{ A}/\text{cm}^2$ at 1 MV/cm) are achieved. The trade-off between polarization and the coercive field is also discussed for achieving the desired ferroelectric performance for different memory applications.

2:30 PM EL07.09.04

Integrated Ultrathin Ferroelectrics in Negative Capacitance Transistors towards Energy-Efficient High-Performance Computing [Nirmaan Shanker](#)¹, [Suraj Cheema](#)¹ and [Sayeef Salahuddin](#)^{1,2}; ¹University of California, Berkeley, United States; ²Lawrence Berkeley National Laboratory, United States

With the exponentially increasing demand for high-performance computing, the energy efficiency of transistors must continue to improve [1]. In particular, negative capacitance (NC) [2] in ferroelectric materials has emerged as a route to increase the gate capacitance, i.e. lower equivalent oxide thickness (EOT), of a transistor which can reduce the operating voltage and therefore power. However, integration of NC gate oxides in advanced silicon transistors requires ferroelectric stabilization in the ultrathin (sub-2 nm) regime on silicon, which is a significant materials challenge for conventional ferroelectrics. To overcome this, we stabilized ferroelectricity on silicon down to 1 nm [3-4] and 0.5 nm [5] in doped HfO_2 and undoped ZrO_2 , respectively, which are the high- κ dielectrics used in today's advanced logic and memory devices. Notably, these ultrathin ferroelectrics demonstrate signatures of ultrathin-enhanced polarization [3-5], in strong contrast to conventional perovskite oxide-based ferroelectrics.

Next, we leveraged the competing atomic-scale antiferroelectric-ferroelectric orders to design NC in 1.8-nm HfO_2 - ZrO_2 superlattices [6-8] and 1-nm ZrO_2 [9], the thicknesses used in today's advanced transistors and future node transistors, respectively. In contrast to the conventional ferroelectric-dielectric picture for NC stabilization, the microscopic origin of NC in these gate oxides is mixed antiferroelectric-ferroelectric order, which broadens the materials space for NC realization. Furthermore, this work establishes the first demonstrations of capacitance enhancement [6-9] in the technologically-relevant HfO_2 - ZrO_2 system, resulting in record-low EOT down to 5 Å [6-9]. Accordingly, when these NC gate oxides were integrated within transistors [6-9], due to the increase in gate capacitance without degradation in carrier velocity and reliability [6-7], record high ON current and transconductance was obtained at 90 nm channel lengths [8-9]. Additionally, there are early indications of industrial adoption as the 1.8-nm HfO_2 - ZrO_2 superlattice gate stack has successfully been integrated within a US Defense CMOS R&D Foundry [8] and an advanced FinFET transistor process in an industrial semiconductor foundry [10]. Overall, the materials breakthroughs in this work—ultrathin ferroelectricity and negative capacitance—in the simple CMOS-compatible HfO_2 - ZrO_2 material system provides a new route towards energy-efficient computing.

[1] S Datta *et al.* "Toward attojoule switching energy in logic transistors." *Science* 378, 733 (2022).

[2] S Salahuddin & S Datta. "Use of Negative Capacitance to Provide Voltage Amplification for Low Power Nanoscale Devices." *Nano Lett.* 8, 405–410

[3] S Cheema, D Kwon, [N Shanker](#) *et al.* "Enhanced ferroelectricity in ultrathin films grown directly on silicon." *Nature* 580, 478–482 (2020).

[4] S Cheema*, [N Shanker](#)* *et al.* "One nanometer HfO_2 -based ferroelectric tunnel junctions on silicon." *Adv. Electron. Mater.* 8, 2100499 (2022).

[5] S Cheema*, [N Shanker](#)* *et al.* "Emergent ferroelectricity in subnanometer binary oxide films on silicon." *Science* 376, 648–652 (2022).

[6] S Cheema*, [N Shanker](#)* *et al.* "Ultrathin ferroic HfO_2 - ZrO_2 superlattice gate stack for advanced transistors." *Nature* 604, 65 (2022).

[7] [N Shanker](#) *et al.* "On the PBTI Reliability of Low EOT Negative Capacitance 1.8 nm HfO_2 - ZrO_2 Superlattice Gate Stack on $L_g=90$ nm nFETs." in 2022 *IEEE Symposium on VLSI Technology and Circuits* (IEEE, 2022).

[8] [N Shanker](#) *et al.* "CMOS Demonstration of Negative Capacitance HfO_2 - ZrO_2 Superlattice Gate Stack in a Self-Aligned, Replacement Gate Process". in 2022 *International Electron Devices Meeting* (IEEE, 2022).

[9] [N Shanker](#) *et al.* "Ultralow equivalent oxide thickness via one nanometer ferroelectric negative capacitance." *In preparation*

[10] S Jo *et al.* "Negative differential capacitance in ultrathin ferroelectric hafnia." *Nature Electronics.* 6, 390 (2023).

2:45 PM BREAK

3:15 PM EL07.09.05

300-mm Wafer-Scale Deposition of Ferroelectric HfZrO_2 for High Electrical Performance with Back-End-Of-Line Compatible Conditions [Jared McWilliams](#)¹, [Charlene Chen](#)¹, [Ray Meck](#)¹, [Randall Higuchi](#)¹, [Ruben Waldman](#)² and [Nguyen Vu](#)¹; ¹EMD Electronics, United States; ²Applied Materials, Inc., United States

Atomic layer deposition (ALD) of hafnium oxide and zirconium oxide has been extensively studied to replace SiO_2 as dielectrics in complementary metal oxide semiconductor (CMOS) technology [1]. Since the discovery of ferroelectricity in Hafnia-based oxides in 2011 [2], there has been growing interest in developing an ALD process to achieve good ferroelectrics within the required thermal budget for back-end-of-line CMOS. This work will discuss the advantages of using ALD precursors with wide ALD windows for achieving high-quality ferroelectric HfZrO_2 films. The crystallinity of the as-deposited films can be tuned to reach the desired electrical performance by adjusting the substrate temperature within the ALD windows. A 300-mm wafer-scale deposition of HfZrO_2 with excellent uniformity across the wafer is demonstrated. The role of different underlying layers for the growth of HfZrO_2 is also

discussed. Different metals with a wide range of thicknesses are found to have an impact on the nucleation of the ligands at the surface, which affects the growth per cycle and the leakage of the films. We anticipate our results will broaden the understanding of the ALD process of ferroelectric hafnia-based oxides and bring the technology closer to manufacturing.

3:30 PM EL07.09.06

Characterizing Negative Capacitance in Ultrathin Ferroelectric HfO₂-ZrO₂ Towards Energy-Efficient Advanced Transistors Qinyuan Xue¹, Nirmaan Shanker¹, Suraj Cheema¹ and Sayeef Salahuddin^{1,2}; ¹University of California, Berkeley, United States; ²Lawrence Berkeley National Laboratory, United States

Negative capacitance (NC) [1] has emerged as a promising solution to overcome fundamental energy-efficiency limits in conventional electronics, in which internal ferroelectric order within the gate stack of a field-effect transistor can enable low-power operation. In particular, by swapping the conventional high- κ dielectric with a negative- κ ferroelectric gate stack, enhanced gate capacitance, i.e. lower equivalent oxide thickness (EOT), can be realized in advanced Si transistors, resulting in key performance benefits in transistors compared to established semiconductor foundry benchmarks [2-3]. We have previously stabilized NC in sub-2-nm HfO₂-ZrO₂ heterostructures [2-3], where we observe a capacitance enhancement, definitive proof of NC stabilization, over the SiO₂ interlayer [2-3] via small-signal capacitance measurements. However, the full internal polarization-electric field (P - E_{FE}) relation was not extracted for these NC gate oxides.

In this work, ultrafast pulsed I - V measurements are used to map the 'S'-shaped P - E_{FE} relation in various ultrathin (sub-2-nm) HfO₂-ZrO₂ NC gate stacks towards realizing both EOT and physical thickness scaling for power- and dimensional-scaling, respectively. The extracted P - E_{FE} relation shows a negative dP/dE_{FE} region, a clear signature of NC stabilization. Additionally, by integrating the P - E_{FE} relation, the characteristic ferroelectric double-well energy landscape was extracted and modelled with a Landau-Ginzburg-Devonshire framework. Both P - E_{FE} and energy landscapes were then used to quantify the degree of NC stabilization across the various gate stacks. Overall, this work further confirms NC stabilization in ultrathin HfO₂-ZrO₂ heterostructures via large-signal pulsed I - V measurements (as opposed to small-signal capacitance measurements) and provides a methodology to quantify the degree of NC stabilization.

[1] S Salahuddin & S Datta. "Use of Negative Capacitance to Provide Voltage Amplification for Low Power Nanoscale Devices." *Nano Lett.* 8, 405–410

[2] S Cheema *et al.* "Ultrathin ferroic HfO₂-ZrO₂ superlattice gate stack for advanced transistors." *Nature* 604, 65 (2022).

[3] N Shanker *et al.* "Ultralow equivalent oxide thickness via one nanometer ferroelectric negative capacitance." *In preparation.*

3:45 PM EL07.09.07

High Thermal Stability of Negative Capacitance HfO₂-ZrO₂ Superlattice Gate Stack Towards Improved Reliability and Work Function Engineering Yejin Hong¹, Nirmaan Shanker¹, Suraj Cheema¹ and Sayeef Salahuddin^{1,2}; ¹University of California, Berkeley, United States; ²Lawrence Berkeley National Laboratory, United States

Negative capacitance (NC) [1] gate oxides have emerged as a new route towards energy-efficient transistors as it can increase the gate capacitance, i.e. lower equivalent oxide thickness (EOT), which reduces the operating voltage and therefore power. We have previously demonstrated a 1.8 nm ferroelectric-antiferroelectric HfO₂-ZrO₂ superlattice (HZH) gate stack boasting a capacitance enhancement over the 8 Å SiO₂ IL layer via the NC effect [2]. Furthermore, once the HZH gate stack was integrated into 90 nm L_g silicon-on-insulator (SOI) nMOS transistors, gate leakage, electron mobility, and the PBTI reliability were unchanged relative to a conventional high- κ dielectric HfO₂ gate stack [2,3].

In this work, we investigate the thermal stability of the NC HZH gate stack at high temperatures. In particular, in advanced transistor processing, the gate oxide is subjected to several high temperature (>900°C) rapid thermal anneals in order to, for example, diffuse metal dopants (e.g. La) to adjust the effective work function, generate oxygen vacancies in the high- κ layer to lower effective work function, and improve device reliability [4,5]. After the NC HZH gate stack capped with TiN/amorphous silicon was subjected to high temperature rapid thermal anneals, we observe the EOT is unchanged before and after the high-temperature anneal, suggesting that the mixed ferroelectric-antiferroelectric structure is unaffected by the high temperature anneal and the interfacial SiO₂ did not increase in thickness. Additionally, a corresponding decrease in effective work function, consistent with prior work with high- κ HfO₂ [5], is observed, likely due to the generation of oxygen vacancies.

Overall, this work confirms the high-thermal stability of the NC HfO₂-ZrO₂ superlattice gate stack and that conventional high- κ work function tuning and reliability enhancement strategies are also compatible with the NC HZH superlattice gate stack. This takes a key step towards the integration of NC HZH superlattice gate stack in advanced transistors in semiconductor foundries.

[1] S Salahuddin & S Datta. "Use of Negative Capacitance to Provide Voltage Amplification for Low Power Nanoscale Devices." *Nano Lett.* 8, 405–410

[2] S Cheema *et al.* "Ultrathin ferroic HfO₂-ZrO₂ superlattice gate stack for advanced transistors." *Nature* 604, 65 (2022).

[3] N Shanker *et al.* "On the PBTI Reliability of Low EOT Negative Capacitance 1.8 nm HfO₂-ZrO₂ Superlattice Gate Stack on L_g = 90 nm nFETs." in *2022 IEEE Symposium on VLSI Technology and Circuits* (IEEE, 2022).

[4] H. Arimura *et al.* "Dipole-First Gate Stack as a Scalable and Thermal Budget Flexible Multi-Vt Solution for Nanosheet/CFET Devices." *2021 IEEE International Electron Devices Meeting* (IEDM, 2021)

[5] T Ando *et al.* "Simple Gate Metal Anneal (SIGMA) stack for FinFET Replacement Metal Gate toward 14nm and beyond." in *2014 IEEE Symposium on VLSI Technology and Circuits* (IEEE, 2014)

4:00 PM EL07.09.08

Low Temperature Characterization of Negative Capacitance HfO₂-ZrO₂ Superlattice Transistors Towards Cryo-CMOS Aditya D. Varna¹, Nirmaan Shanker¹, Suraj Cheema¹, Mohamed Mohamed² and Sayeef Salahuddin^{1,3}; ¹University of California, Berkeley, United States; ²Massachusetts Institute of Technology, United States; ³Lawrence Berkeley National Laboratory, United States

Cryogenic CMOS, where CMOS systems operate at liquid nitrogen temperatures, is an attractive option to reduce the energy consumption of computing as the operating voltage can be aggressively scaled due to lower subthreshold swing in transistors [1]. To realize this, several performance boosters are required, including increasing the gate capacitance of transistors without degradation in carrier transport. We have previously demonstrated a 1.8-nm ferroelectric-antiferroelectric HfO₂-ZrO₂ superlattice (HZH) gate stack boasting a capacitance enhancement over the 8 Å SiO₂ IL layer [2] via the NC effect [3] and have successfully integrated it into a 90 nm US Defense CMOS R&D technology [4]. Additionally, since no SiO₂ interfacial layer (IL) scavenging was performed, the carrier transport is not affected, resulting in a significant increase in on-current and intrinsic transconductance at room temperature [2, 4].

In this work, we characterize 90-nm L_g nMOS and pMOS transistors integrating the NC HZH gate stack down to 77 K. From cryogenic RF characterization, we observe that the capacitance enhancement is maintained, suggesting that the mixed ferroelectric-antiferroelectric structure is stable at 77 K. Additionally, due to enhanced injection velocity at cryogenic temperatures, we observe 35% and 25% improvement in transconductance for nMOS and pMOS devices, respectively, at 77 K. Overall, this work confirms that NC is stabilized in the HZH gate stack down to cryogenic temperatures and can be an attractive option to realize cryo-CMOS systems.

[1] S. Datta *et al.* "Toward attojoule switching energy in logic transistors." *Science* 378, 733 (2022).

[2] S Cheema *et al.* "Ultrathin ferroic HfO₂-ZrO₂ superlattice gate stack for advanced transistors." *Nature* 604, 65 (2022).

- [3] S Salahuddin & S Datta. "Use of Negative Capacitance to Provide Voltage Amplification for Low Power Nanoscale Devices." *Nano Lett.* 8, 405–410
 [4] N Shanker *et al.* "CMOS Demonstration of Negative Capacitance HfO₂-ZrO₂ Superlattice Gate Stack in a Self-Aligned, Replacement Gate Process." in *2022 International Electron Devices Meeting (IEEE, 2022).*

4:15 PM EL07.09.09

Enabling Low Coercive Voltage in Hf_{0.5}Zr_{0.5}O₂/BaTiO₃ Heterostructure via Double Ferroelectric Coupling Yen cheng Chiu and Yen-Lin Huang; National Yang Ming Chiao Tung University, Department of Materials Science and Engineering, Taiwan

In recent years, hafnium-based binary oxides, particularly Hf_{0.5}Zr_{0.5}O₂ (HZO), have garnered significant attention due to their stable ferroelectric properties at the nanoscale and compatibility with Complementary Metal-Oxide Semiconductor (CMOS) devices. However, maintaining ferroelectricity at extremely thin thicknesses is often hindered by a substantial coercive field, limiting the applicability of ferroelectric HZO in low-power applications. Typically, reducing the operating voltage compromises the stability of ferroelectric polarization. In this context, we introduce a novel approach to achieve lower operating voltage by creating a heterostructure consisting of perovskite/fluorite ferroelectric layers. When compared to fluorite ferroelectrics, perovskite ferroelectrics, such as BaTiO₃ (BTO) thin films, exhibit a significantly lower coercive field. In our study, we showcase the high-quality heterostructure of BTO/HZO, which is fabricated by pulsed laser deposition, and we characterize the ferroelectric properties through piezo force microscopy and a ferroelectric tester. By incorporating the low-voltage switchable BTO layer, we have the potential to induce critical domain nucleation in the BTO layer, leading to a lower switching voltage for the HZO layer. This innovative approach leverages the advantages of both materials to address the challenges associated with high switching voltages in HZO and the integration of perovskite ferroelectrics into the CMOS process. Our findings may pave the way for enhanced performance and efficiency in ferroelectric-based devices, such as Ferroelectric Field-Effect Transistors (Fe-FETs) and Ferroelectric Tunnel Junctions (FTJs).

4:30 PM EL07.09.10

Load Line Analysis of The Memory Window in Amorphous Indium-Gallium-Zinc Oxide-Based Ferroelectric Thin-Film Transistor Jae Hoon Lee^{1,2}, Yong Hee Lee¹, Joon-Kyu Han^{1,3} and Cheol Seong Hwang¹; ¹Seoul National University, Korea (the Republic of); ²SK Hynix Semiconductor Inc., Korea (the Republic of); ³Sogang University, Korea (the Republic of)

Ferroelectric thin-film transistors (FeTFTs) attract a great deal of interest for their potential to reduce operating voltage and enhance durability in non-volatile memories by minimizing the interfacial layer through the use of amorphous oxide semiconductors (AOS) instead of silicon (Si). Especially, FeTFTs with amorphous indium-gallium-zinc oxide (*a*-IGZO) channels offer high on-off ratios, fast operation speed, and compatibility with complementary metal-oxide-semiconductor (CMOS) technology. The Memory Window (MW) of FeTFTs holds significant importance, particularly in applications such as multilevel cell non-volatile memory and neuromorphic systems. However, there have been limited reports on the MW achievable with n-type *a*-IGZO, primarily due to the scarcity of hole carriers necessary for polarization switching.

This study investigates the attainable MW through load line analysis in FeTFTs. Load line analysis is a widely used technique that enables a comprehensive graphical representation of the intricate operation of solid-state circuits with nonlinear charge-voltage or current-voltage responses. In contrast to ferroelectric field-effect transistors (FeFETs) based on Si, which can secure an MW at the twice coercive voltage ($2V_c$) level, the inherent characteristics of FeTFTs based on AOS material result in an inevitably smaller MW due to the absence of an inversion mode.

Furthermore, the influence of various process conditions in FeTFTs is explored, including the atomic layer deposition temperature of the aluminum-doped hafnium oxide (HAO) ferroelectric layer, rapid thermal annealing temperature for crystallization of the HAO layer, and the thickness of the *a*-IGZO channel. Aluminum is selected as the impurity for hafnium oxide due to its thermal stability and compatibility with CMOS processes. The impact of these process variables on ferroelectric performance in metal-ferroelectric-semiconductor-metal capacitors and the FeTFT structures is analyzed by evaluating polarization-voltage, capacitance-voltage, and current-voltage characteristics under various conditions. In addition, load line analysis is performed at each process condition based on these characteristics. These findings can potentially guide the development of high-performance FeTFTs with optimized MW for various applications.

4:45 PM EL07.09.11

Large Electromechanical Coupling in Zr-Doped Ceria Maxim Varenik¹, Boyuan Xu², Tali Pechersky-Savich¹, Junying Li³, Ellen Wachtel¹, David Ehre¹, Prahlad Routh³, Sergey Khodorov¹, Anatoly Frenkel³, Yue Qi² and Igor Lubomirsky¹; ¹Weizmann Institute of Science, Israel; ²Brown University, United States; ³Stony Brook University, United States

We have investigated the electrostriction (ES) effect in Zr-doped ceria (Zr_xCe_{1-x}O_{2,δ}) ceramics. ES is a second order electromechanical response, *i.e.*, strain, u , is proportional to M^*E^2 , where E is the applied electric field and M is the longitudinal electrostriction strain coefficient. Large ES in ceria has generally been associated with oxygen vacancies (V_O) which provide charge compensation for aliovalent dopants or for cerium reduction (Ce³⁺). The ES induced by V_O is restricted to frequency <1 Hz and low saturation strain ($|u_{sat}| < 15$ ppm).

Doping CeO₂ with Zr results in a large ES strain coefficient, reaching $|M| = 10^{-16} \text{ m}^2/\text{V}^2$ for $x=0.1$. This effect persists to frequency ≥ 3 kHz with $|u| \geq 220$ ppm, making Zr_{0.1}Ce_{0.9}O₂ competitive with the best commercial electrostrictor (PMN-PT15), but with ~ 100 times lower dielectric permittivity and three-fold higher elastic modulus. XAS data, DFT modelling and *ab initio* molecular dynamics (AIMD) calculations demonstrate that elastic dipoles formed by Zr-doping are dynamic. In the absence of an E-field, [ZrO₈]-local bonding units remain, on average, centered with respect to the second (cation) coordination shell. Due to bond anharmonicity displacement of Zr by an E-field requires less energy than displacement of the host cations, resulting in a large dynamic elastic dipole. This polarizable elastic dipole gives rise to large electrostrictive strain and constitutes the first example of non-classical electrostrictors (NCES) relying solely on substitutional point defects.

$|M|$ of Zr-doped ceria increases exponentially with Zr content for $x=0-0.1$, suggesting that the contribution of Zr-ions to electrostrictive strain may not be simply additive. Zr-doping also increases the relative dielectric permittivity, from ~ 26 ($x=0$), to ~ 220 ($x=0.1$) and lowers the elastic modulus from 227GPa ($x=0$) to 214GPa ($x=0.1$), even though the number of chemical bonds remains unchanged. AIMD calculations report that stiffness for moving [CeO₈]-local bonding units is essentially isotropic and is 2-2.4 times higher than for [ZrO₈]. Stiffness for moving [CeO₈] first nearest neighbor to Zr, is only slightly decreased from that in the bulk. These results can provide the theoretical basis for the reduction of the Young's modulus and increase in the dielectric permittivity with Zr doping.

When the concentration of Ce³⁺ is ≥ 100 ppm in Zr_xCe_{1-x}O_{2,δ}, accompanied by the formation of oxygen vacancies (V_O) for charge compensation, ES is suppressed. In addition, by co-doping Zr_{0.1}Ce_{0.9}O₂ with 0.5mol% of aliovalent cations - Ca, Sc, Yb or La - we observed that the aliovalent dopant reduces the electrostriction strain coefficient by more than an order of magnitude and restores the values of Young's modulus and dielectric permittivity to values close to those of undoped ceria. Since all these co-dopants, irrespective of valence and ionic radius, lead to a similar result, we concluded that the species responsible for the suppression of electrostriction in Zr doped ceria must be the oxygen vacancies. This finding is supported by XAS measurements and AIMD calculations. Fourier transform of Zr K-edge EXAFS spectra reveal that, even though the molar ratio Zr_{Ce}: V_O is 40:1 in the co-doped compounds, oxygen vacancies nevertheless succeed in introducing enhanced disorder into the second coordination shell (cation) of Zr. DFT modelling predicts that a [ZrO₇- V_O] local bonding unit is stiff and asymmetrically distorts adjacent unit cells, leading to an elastic interaction length in the lattice between Zr-ions \geq two-and-a-half-unit cells, which, in the absence of oxygen vacancies, can allow limited collective motion. However, such collective motion does not lead to

a phase transition even at 123 K, implying that interaction between Zr-ions is neither sufficiently strong nor sufficiently long-range to produce freezing of the displacement, an effect that has been observed for perovskite relaxors.

SESSION EL07.10: Poster Session III
Session Chairs: Morgan Trassin, Ruijuan Xu and Di Yi
Thursday Afternoon, April 25, 2024
Flex Hall C, Level 2, Summit

5:00 PM EL07.10.01

Strain-Driven Solid–Solid Crystal Conversion in Chiral Hybrid Perovskites with Paramagnetic-To-Ferromagnetic Transition Haining Zheng and Kian Ping Loh; National University of Singapore, Singapore

Hybrid organic–inorganic perovskites (HOIPs) are promising stimuli-responsive materials (SPMs) owing to their molecular softness and tailorable structural dimensionality. The design of mechanically responsive HOIPs requires an in-depth understanding of how lattice strain induces intermolecular rearrangement that impacts physical properties. While chirality transfer from an organic cation to an inorganic lattice is known to influence chiral-optical properties, its effect on strain-induced phase conversion has not been explored. As opposed to achiral or racemic organic cations, chiral organic cations can potentially afford a new dimension in strain-responsive structural change. Herein, we demonstrate that mechanical strain induces a solid phase crystal conversion in chiral halide perovskite single crystals (*R/S*)-(FE)₂CuCl₄ (FE = (4-Fluorophenyl)ethylamine) from a 0D isolated CuCl₄ tetrahedral to 1D corner-sharing CuFCl₅ octahedral framework via the incorporation of Cu...F interaction and N–H...F hydrogen bonding. This strain-induced crystal-to-crystal conversion involves the connection of neighboring 0D CuCl₄ tetrahedra via Cu²⁺–Cl[–]–Cu²⁺ linkages as well as the incorporation of an F-terminated organic cation as one of the X atoms in BX₆ octahedra, leading to a reduced band gap and paramagnetic-to-ferromagnetic conversion. Control experiments using nonchiral or racemic perovskite analogs show the absence of such solid phase conversion. To demonstrate pressure-sensitive properties, the 0D phase is dispersed in water-soluble poly(vinyl alcohol) (PVA) polymer, which can be applied to a large-scale pressure-induced array display on fibrous Spandex substrates via a screen-printing method.

Reference:

Zheng H.; Zhang R.; Wu X.; Zhang Q.; Wu Z.; Wong P. D. W.; Chen J.; Xu Q.; Loh K. P. *J. Am. Chem. Soc.* 2023, 145, 3569–3576.

5:00 PM EL07.10.02

Filterless Visible-Range Color Sensing and Wavelength-Selective Photodetection Using Bandgap Engineered Ferroelectric Ceramics Vasili Balanov¹, Filip Temerov¹, Vladimir Pankratov², Wei Cao¹ and Yang Bai¹; ¹University of Oulu, Finland; ²University of Latvia, Latvia

Photosensors, photodetectors, or color sensors are key components for various optical and optoelectronic applications. Semiconductor-based photodetection has been a dominator which is excellent at measuring the photon intensity of incident light. However, the wavelength of the incident light to be measured must be known beforehand and it mostly depends on auxiliary methods to filter unknown wavelengths. In this work, an alternative but simple mechanism that is using a monolithic, bandgap-engineered photoferroelectric ceramic to blindly determine the wavelength and intensity of incident light at the same time is demonstrated. The photoferroelectric compound is Ba- and Ni-codoped (K,Na)NbO₃ exhibiting a direct band gap of ≈2 eV and a spontaneous polarization of ≈0.25 C/m². The band–band charge carrier transition is confirmed by multiple characterization methods of photoluminescence, photodielectric spectroscopy, and photoconductivity. The existent optoelectrical cumulative effect enabled by the simultaneous narrow bandgap and strong ferroelectricity allows to reliably distinguish the wavelengths of 405, 552, and 660 nm as well as the power density ranging from ≈0.1 to 10 W/cm², with the photoresponsivity of up to 60 μA/W.

5:00 PM EL07.10.03

First Principles Insights into Phase Transitions, Disorder and Electronic Properties of Lead-Free Ba-Based Tetragonal Tungsten Bronzes Benjamin A. Williamson, Nora S. Løndal and Tor Grande; Norwegian University of Science and Technology, Norway

Tetragonal tungsten bronzes (TTBs), with the general formula A₂A₁C₄B₁B₂O₃₀, are a family of ferroelectric materials, which, due to their broad compositional space and structural flexibility make them a suitable framework for tuneable lead-free oxide ferroelectrics.

The Ba-containing TTBs such as Ba₄Na₂Nb₁₀O₃₀ (BNN) with a T_c of ≈560°C[1] is of particular interest in high temperature applications where there is a lack of suitable materials. Previous experimental work on substituting the A-site Na cation with larger alkali metals: K and Rb, show a systematic decrease in T_c in addition to uncovering the integral role that cation disorder plays on the structural parameters of these systems.[1]

However, there is little in terms of mechanistic understandings of these compositions using first principles characterisation techniques. In this work, density functional theory (DFT) calculations using both standard and hybrid functionals are performed on BNN-based compositions: Ba₄A₂M₁₀O₃₀ (A = Na, K, Rb; M = Nb, Ta). In particular, we probe the origin of the high T_c as well as the thermodynamics of disorder. In particu

and the trends associated with the compositional engineering, as well as the thermodynamics of disorder and its effect on structural and electronic properties. The effects of this study are discussed in line with experimental work done in parallel as well as implications for the future direction of these materials.

5:00 PM EL07.10.04

Chlorine Substituted Organic Linker in Two-Dimensional Halide Double Perovskite Ferroelectric with Directional Dependence Properties Shubham A. Rajput, Sudhadevi Antharjanam and Aravind Kumar Chandiran; Indian Institute of Technology Madras, India

Ferroelectric materials have garnered significant interest due to their unique electrical and structural properties, holding immense promise for diverse electronic applications. This study introduces a novel 2D layered halide double perovskite ferroelectric material denoted as Cl_{1.14}Br_{2.86}PA₄AgInBr₈ (CPAIn). Through the strategic substitution of halogenated A-site organic linker 3-chloropropylammonium, CPAIn demonstrates exceptional non-centrosymmetric properties and remarkable ferroelectric behaviour, with a Curie temperature (T_c) of 197°C. One of the key findings of this research is CPAIn's anisotropic ferroelectric behaviour, characterized by a notably high spontaneous polarization (P_s) of 6.25 μC.cm⁻² along the perpendicular orientation to the octahedral layers. This observation underscores its potential for applications requiring precise control over polarization direction. Notably, the material exhibits differential resistivity along distinct crystallographic axes, with resistance measuring 9.71 MΩ.cm along the parallel direction

and 18.81 M Ω .cm along the perpendicular direction. This variance is attributed to the role of organic cations as insulators, modulating charge transfer dynamics within the material. As demonstrated by CPAIn, the ferroelectric characteristics present intriguing opportunities for future development and construction of advanced electronic devices. This endeavour represents a noteworthy advancement in tapping into the complete capabilities of ferroelectric materials for a diverse array of technological uses. The distinctive qualities of CPAIn outlined in this investigation render it an attractive contender for further research and pragmatic integration into cutting-edge electronic devices.

5:00 PM EL07.10.05

Synthesis and Characterization of Tellurium Doped Tin Sulfide (SnSTe) Bamidele O. Onipede¹, Hui Cai^{1,2} and Matthew E. Metcalf¹; ¹University of California, United States; ²Lawrence Berkeley National Laboratory, United States

The presence of a spontaneous electric dipole even in the absence of an applied external electric field defines ferroelectric materials. By symmetric requirements, this is possible only in non-centrosymmetric structures where non-zero net polarization is possible. Bulk 2D Tin sulfide (SnS), an exciting member of the group IV-VI semiconductor materials with ferroelectric properties exhibits centrosymmetry which can be broken by doping. In this work, we successfully synthesized tellurium doped SnS, achieving different doping concentrations via the traditional chemical vapor deposition method. The samples were characterized via Optical microscopy, Raman spectroscopy, X-Ray Photoelectron spectroscopy and Atomic Force Microscopy. By tuning the growth parameters, we have been able to determine optimal growth parameters for these doped crystals, thus precise control has been achieved. Hence, this work would open fresh opportunities for bulk ferroelectric 2D SnS with future potential use in high quality, scalable, tunable, and high-performance technological applications.

5:00 PM EL07.10.06

Zwitterion-Based Organic High-k Dielectric Materials Simranjeet Kaur¹, Renita M. D'Souza², Timothy L. Kelly², Vance E. Williams¹ and Loren G. Kaake¹; ¹Simon Fraser University, Canada; ²University of Saskatchewan, Canada

Most high-k dielectrics known are based on inorganic materials, where large polarization is due to the slight separation of positive and negative charges in response to an applied field. Organic materials on the other hand, tend to have very low dielectric constants because of the low atomic number of their constituents. However, organic materials offer many advantages including easy of processing and mechanical flexibility. Zwitterionic molecules have charged groups that can be spatially separated by tens of angstroms. However, they are underexplored as dielectric materials. We report the synthesis of a novel zwitterionic molecule which melts below 100 °C. The compound was blended with poly(methyl methacrylate) and its dielectric properties were studied. The frequency-dependent capacitance depends strongly on the amount of zwitterion in the film and on the temperature of the device. At low concentrations of zwitterion and low temperatures, the film shows small capacitance (~3 nF/cm²). Above a specific concentration and temperature, capacitance is greater than 10 μ F/cm², consistent with electrostatic double layer formation. In order to achieve this high of a capacitance value, the bulk of the film must be field-free. As such, we suggest that zwitterions exhibit strong electrostatic correlation behaviour. This interpretation is supported by grazing incidence wide angle x-ray experiments which show evidence of zwitterion crystallization only at high concentrations. This demonstrates a non-electrolyte dielectric with a very high capacitance and illustrates the importance of the nanoscale electrostatic environment on the properties of this class of materials.

5:00 PM EL07.10.07

Depolarization Field Driven Photovoltaic Effect in 2D Ferroelectric α -In₂Se₃ Shahriar Muhammad Nahid¹, SungWoo Nam² and Arend M. van der Zande¹; ¹University of Illinois Urbana Champaign, United States; ²University of California Irvine, United States

The ultimate limit of bulk photovoltaic energy conversion efficiency in ferroelectrics at the nanoscale depends on the mechanism of electron and hole separation. Understanding the underlying mechanism will enable new design principles for utilizing the bulk photovoltaic effect (BPVE) in next generation optoelectronic devices, such as self-powered photodetectors or solar cells. In contrast to conventional ferroelectrics, 2D ferroelectric α -In₂Se₃ has two advantages for BPVE based solar cells. First, the band gap is 1.3 eV, close to the ideal value for utilizing the solar spectrum, and much smaller than most wide bandgap ferroelectric oxides. Second, they naturally exist at nanoscale dimensions with stable ferroelectricity down to a monolayer. The key goals are to characterize the thickness dependent BPVE in α -In₂Se₃ and understand the dominant mechanism.

Here, we fabricate graphene- α -In₂Se₃-graphene heterostructures, where the thickness of α -In₂Se₃ varies between 18-50 nm, and characterize the transport under illumination. We use scanning photocurrent and photovoltage microscopy to map the short-circuit current density (J_{sc}) and open-circuit voltage (V_{oc}). We also measure the transport under varying intensities.

The photocurrent and photovoltage maps show that both the J_{sc} and V_{oc} prevails only in the region overlapped by the top and bottom graphene. The J_{sc} is antiparallel to polarization. All these observations confirm the BPVE in the heterostructures. The transport measurements under illumination show that the J_{sc} and efficiency decay exponentially with thickness. The direction of the photocurrent and its exponential decay with thickness confirm the depolarization field as the origin of the photovoltaic effect in α -In₂Se₃. We also find that the depolarization field is inversely proportional to thickness and reaches 158 KV/cm for 18 nm α -In₂Se₃. Moreover, the depolarization field model allows us to predict a nonmonotonic trend of photoconductivity with thickness where it is expected to peak for 6 nm thick α -In₂Se₃. The transport measurements depict that $J_{sc} \propto \text{Intensity}^\beta$ where β varies from 0.6 to 1.2 with increasing thickness. The photoresponsivity reaches 1.8 mA/W under 1 W/cm² intensity for 18 nm α -In₂Se₃. This is comparable to other 2D ferroelectrics and almost 4 to 2200 times higher than conventional bulk ones.

Our study demonstrates the relative importance of depolarization field in 2D ferroelectrics over other mechanisms, such as shift current or Schottky barrier effect, and provides design principles for optimizing the efficiency of BPVE based energy harvesting.

SESSION EL07.11: Emerging Ferroics II
Session Chairs: Seung Sae Hong and Ruijuan Xu
Friday Morning, April 26, 2024
Room 342, Level 3, Summit

8:30 AM *EL07.11.02

Ferroelectric Control of Conduction in The Pb(Zr_{0.2}Ti_{0.8})O₃/Bi₂O₂Se Heteroepitaxy Ying-Hao Chu; National Tsing Hua University, Taiwan

The search for 2D semiconductors with excellent electronic performance and stability in the ambient environment is urgent. Bi₂O₂Se, an air-stable layered oxide, has emerged as a promising new semiconductor with excellent electronic properties. Studies demonstrate that its layered nature makes it ideal for fabricating electronic devices down to a few atomic layers. The Bi₂O₂Se-based top-gated field-effect transistor device shows

excellent semiconductor device properties, including high carrier mobility ($\sim 28,900$ cm²/Vs at 1.9 K and 450 cm²/Vs at room temperature) and superior current on/off ratio with the almost ideal subthreshold swing. In addition, the moderate bandgap (~ 0.8 eV) of Bi₂O₂Se makes its device suitable for room temperature operation while requiring only a relatively low operation voltage. These fascinating properties, chemical stability in the ambient environment, and easy accessibility make Bi₂O₂Se a promising semiconductor candidate for future ultra-small, high-performance, and low-power electronic devices. Moreover, as the Bi-O layer in Bi₂O₂Se is structurally compatible with many perovskite oxides with interesting physical phenomena, it is feasible to fabricate heteroepitaxy/superlattices between Bi₂O₂Se and perovskite oxides to pursue novel emergent physical phenomena in hybrid heterostructures. The study combines an epitaxial ferroelectric Pb(Zr_{0.2}Ti_{0.8})O₃ (PZT) layer with the Bi₂O₂Se layer. The ferroelectric polarization of the PZT layer serves as a control parameter to modulate the semiconducting behaviors of the Bi₂O₂Se layer. The as-grown polarization leads to charge depletion and, consequently, low conduction. Switching the polarization direction results in charge accumulation and enhances the conduction at the Bi₂O₂Se layer. The origin of this modulation is attributed to a change in the electronic structure due to the ferroelectric polarization states, evidenced by X-ray photoelectron spectroscopy and cross-sectional scanning tunneling microscopy/spectroscopy. Control of the conduction at this new heterostructure delivers a pathway of non-volatile controlling on layered semiconductors for next-generation transistors.

9:00 AM EL07.11.01

Giant Optical Second Harmonic Generation from SnS with Ferroelectric Stacking [Redhwan A. Moqbel](#)^{1,2,3}, Ryo Nanae⁴, Satsuki Kitamura⁴, Chi-Cheng Lee⁵, Kosuke Nagashio⁴ and Kung-Hsuan Lin²; ¹National Taiwan University, Taiwan; ²Academia Sinica, Taiwan; ³Taiwan International Graduate Program, Taiwan; ⁴The University of Tokyo, Japan; ⁵Tamkang University, Taiwan

In recent years, substantial attention has been directed towards two-dimensional SnS, a member of the group IV monochalcogenides, owing to its exceptional physical properties. Theoretical predictions have emphasized the potential of SnS monolayer to display significant second harmonic generation (SHG) due to its in-plane ferroelectricity. However, the synthesis of monolayers with considerable lateral dimensions remains challenging due to the formidable inter-layer forces between SnS layers. For a large SnS bulk crystal, the layers are typically stacked with an antiferroelectric order (AB stacked), and the ferroelectric property disappears. In this work, we successfully fabricated a sizable flake (approximately 8x8 μm) consisting of a few layers of SnS with ferroelectric stacking (AC stacking), which enables optical measurement feasible. We found giant SHG from AC-SnS, surpassing that of MoS₂ monolayers by 50 times. The SHG susceptibility was experimentally estimated as 85 pm/V, which is much stronger than the value (~ 2 pm/V) of a typical nonlinear crystal such as BBO and KTP crystals. We have also investigated the angle-resolved SHG patterns and found there is good agreement between experimental and theoretical data. We further developed angle-resolved SHG microscopy as a tool for identifying single or multiple domains in SnS flakes. Orientations of polarization in different domains have been clearly obtained by this technique. From the results of cross-sectional transmission electron microscopy, we found some region that the stacking order of layers is neither AB nor AC stacking. We have also investigated the effect of stacking disorder to the angle-resolved SHG patterns.

9:15 AM EL07.11.03

Defects and Domain Walls in Soft Ferroelectric CsGeX₃ (X = Cl, Br, I) [Kristoffer Eggestad](#), Benjamin A. Williamson, Dennis Meier and Sverre M. Selbach; Norwegian University of Science and Technology, Norway

Conductive domain walls (DWs) hold promise for nanoscale, energy-efficient multi-level diodes and neuromorphic circuitry. In CsGeX₃, caesium and halogen vacancies are intrinsic point defects that can induce electrons and holes, respectively. Controlling the formation and position of vacancies can in principle give switchable local n-type or p-type conductivity at DWs and enable new concepts for DW-based circuitry. This requires a material where mobile point defects of both positive and negative charge can accumulate at DWs. CsGeX₃ is here chosen as our model system due to the possibility of having mobile caesium and halogen vacancies.

We use density functional theory (DFT) to study intrinsic point defects and DWs in CsGeX₃. Using *hybrid* DFT we investigate electronic structure and defect formation energies in bulk, showing highly mobile holes and free electrons, as well as relatively shallow defect levels. Additionally, a study on point defect mobility in bulk, reveals exceptionally mobile anion vacancies with migration barriers comparable to Li vacancies in the best solid-state electrolytes. Furthermore, we investigate possible DWs and show that parallel and head-to-tail Y-type 71-degree DWs are the most stable DWs. Moreover, the mobility of DWs, with and without point defects in their vicinity, has been studied, showing extremely mobile DWs, implying that polarisation can easily be switched. Finally, the possibility of reversible p- and n-type conductivity in DWs in CsGeX₃ and other similar materials is discussed.

9:30 AM EL07.11.04

Two-Dimensional MOF-Based High-Performance Ferroelectric Field-Effect-Transistors with an Ultralow Off-State Current [Jiangyu Li](#); Southern University of Science and Technology, China

Two-dimensional (2D) ferroelectrics open a new realm of nonvolatile memory and computing devices, while metal-organic framework (MOF) materials offer tremendous possibilities to design and optimize ferroelectric performance. Building a ferroelectric field effect transistor (FeFET) by integrating a 2D MOF ferroelectric gate with a 2D semiconducting channel provides new strategies towards ultralow power nonvolatile memory devices, yet no 2D MOF was found to be ferroelectric yet. Here we successfully develop 2D ferroelectric MOF nanosheets, {CuIIL₂}n-MOF, and confirm its ferroelectricity down to 7 nm. A large polarization of ~ 14.2 μC/cm², a small coercive field of ~ 33.3 V/μm, and excellent durability $>10^6$ cycles are found in 2D {CuIIL₂}n-MOF nanosheets. This enables us to fabricate FeFETs using 2D {CuIIL₂}n-MOF as the gate and MoS₂ as the channel, achieving an on/off ratio of 10⁷ with the ultralow low off-state current of 100 fA and tunable memory window, making it exceptional among known FeFETs and very promising for next-generation ultralow power memories and computing devices.

9:45 AM EL07.11.05

Understanding The Formation of Ferromagnetic CuCr₂Se₄ Nanocrystals [Samantha Harvey](#), Jonathan DeStefano, Jiun-Haw Chu, Daniel R. Gamelin and Brandi M. Cossairt; University of Washington, United States

Spinel (AB₂X₄) are a unique class of materials that exhibit a range of magnetic, optical, and magneto-optical properties tunable through choice of A and B site cations. While many of the oxides have been synthesized at the nanoscale, research into nanocrystalline chalcogenide spinels is lacking. Amongst these the copper chromium chalcogenides are of particular interest for their high Curie temperatures (>350 K) and large magneto-optical Kerr effects. Only a handful of reported syntheses for these materials exist, with conflicting magnetic properties (e.g. superparamagnetic vs. ferromagnetic), minimal mechanistic understanding, and no optical data. Here, we delve deeper into the synthesis of this material. Binary copper selenide forms as an intermediate followed by Cr diffusion into the lattice. Upon ramping the reaction temperature, magnetism is slow to turn on as evident by magnetic susceptibility measurements. After approximately 40 minutes at 340°C ferromagnetic ordering appears concurrently with a change in lattice parameter, crystallite size, and stoichiometry suggesting annealing and cation diffusion. Magnetic circular dichroism data of nanocrystal films is similar to magneto-optical Kerr rotation spectra of single crystals exhibiting a NIR feature that overlaps with telecommunications wavelengths.

Current and future directions involving doping, cation exchange, and spectroelectrochemistry are also discussed.

10:00 AM BREAK

SESSION EL07.12: Magnetic Heterostructures, Actuators and Sensors
Session Chairs: Seung Sae Hong and Ruijuan Xu
Friday Morning, April 26, 2024
Room 342, Level 3, Summit

10:30 AM *EL07.12.02

Increasing Magnetic Anisotropy at The Nanoscale for Micromagnetic Actuators Amal El-Ghazaly, Yulan Chen and Ludovico Cestarollo; Cornell University, United States

When scaled down to micrometer dimensions, magnetic actuators along with other micromagnetic devices strongly depend upon their nanoscale behavior. For example, magnetorheological elastomers (MREs), which are composites of a polymer matrix and a magnetic filler, will stretch, bend, and generally behave in a manner that is intrinsically linked to the properties of the magnetic filler. However, the extent by which a magnetic material can bend and deform is proportional to its elasticity and inversely proportional to the cube of its thickness. Thus, high-resolution actuation and bending of MREs at the microscale requires an MRE of thickness similarly at the microscale and a magnetic filler that is much smaller – on the order of nanometers.

In this talk, we will present a direct comparison of actuation by microparticle-filled and nanoparticle-filled elastomer thin films, illustrating that higher actuation response at small applied magnetic fields (<100 mT, typical of integrated devices) can be achieved by the nanoparticle films [1]. Therefore, MRE microactuators using magnetic nanoparticles are desirable. However, magnetic particles are known to lose their anisotropy and ferromagnetic behavior as the dimensions are reduced to the nanoscale. Thus, nanoparticle MRE actuation can be further increased with improved nanostructures having increased remanent magnetic moment.

We will show that synthesis of high saturation magnetization $\text{Fe}_{65}\text{Co}_{35}$ (230 emu/g) magnetic nanoparticles addresses this obstacle head on, bringing both anisotropy and strong ferromagnetism down to this size regime and achieving *6x higher remanent magnetization* than conventional ferrous magnetic nanoparticles (maghemite, steel, and pure Fe). Furthermore, synthesis of self-assembled Fe-Co nanochains (theoretical 1-dimensional nanostructures) doubles the nanoscale anisotropy by adding shape anisotropy to the existing magnetocrystalline anisotropy [2, 3]. Of particular importance is that these nanochain structures with aspect ratios exceeding 10:1 can be synthesized in high concentration solutions without the need for an external field, thereby simultaneously allowing yield to increase while simplifying the synthesis process.

Finally, these anisotropic 1-dimensional nanostructures, i.e. nanochains, are hypothesized to produce the maximum actuation response from the MRE microactuators when the filler concentration is optimized. We will present our experiments that show that an optimal volume concentration of nanochains in the elastomer matrix exists, at 6 vol.%, such that it minimizes the antiferromagnetic chain-to-chain interactions while maximizing remanence ($0.43M_s$). Capitalizing on these results, an optimized soft actuator was made with the nanochains and shown to provide large actuation at fields <100 mT. Multiple modes of actuation will be illustrated including, lateral bending, twisting, and vertical bending.

[1] L. Cestarollo, S. Smolenski, A. El-Ghazaly, *ACS Applied Materials & Interfaces*, 2022.

[2] Y. Chen, A. El-Ghazaly, *Small*, 2023.

[3] Y. Chen, ... A. El-Ghazaly, *Advanced Functional Materials*, 2023.

11:00 AM EL07.12.01

Amplifying Spin-Orbit Torque Efficiency via a Crystallographic Approach Chi-Yen Huang, Chao-Yao Yang and Yen-Lin Huang; National Yang Ming Chiao Tung University, Taiwan

Currently, transition-metal-oxide based spintronics have sparked a tremendous research interests thanks to their non-trivial properties in solid-state physics and soon become potential candidates to participate into the spin-orbit torque (SOT) technology in the third generation of magnetoresistive random access memory. Recent studies have highlighted the ability of epitaxially grown SrIrO_3 to generate a spin current with remarkable charge-to-spin conversion efficiency. However, a comprehensive study of crystallographic dependence of SOT effect in single crystal SrIrO_3 thin films remains lacking. To address this gap, we prepare $\text{SrIrO}_3(001)/\text{La}_{0.7}\text{Sr}_{0.3}\text{MnO}_3(001)$ epitaxial bilayers on the SrTiO_3 single crystal substrates by using pulsed laser deposition technique. The SrIrO_3 layer serves as a spin generator with orthorhombic symmetry, facilitating the study of anisotropic SOT effects, while LSMO functions as a ferromagnetic layer with in-plane magnetic isotropy for spin detection. Employing a loop-shift method on Hall bar devices with different crystallographic orientations, we observed that applying current along the [110] direction of SrIrO_3 resulted in nearly five times higher SOT efficiency compared to applying current along the [100] direction, as indicated by the peak shift (H_{eff}) relative to the sensing current amplitude. This outcome reveals a robust correlation between the crystal structure and the SOT effects, offering an ideal platform for manipulating SOT properties in TMO-based spintronic devices.

11:15 AM EL07.12.03

High Aspect Ratio Magnetostrictive Particles for Structurally Integrated Sensors and Transducers Andrew Charles^{1,2}, Andrew Rider¹, Sonya Brown² and Chun Wang²; ¹Defence Science and Technology Group, Australia; ²University of New South Wales, Australia

Magnetostriction is a property of many magnetic materials whereby they exhibit a deformation in response to a change in magnetization, which is thus applicable to various sensor, actuators and transducer applications. Terfenol-D, $\text{Tb}_x\text{Dy}_{1-x}\text{Fe}_2$ ($x \approx 0.3$), exhibits the largest known room temperature magnetostriction of >2000 ppm, followed by Galfenol, $\text{Fe}_{1-x}\text{Ga}_x$ ($x \approx 0.2$), with magnetostriction values of up to 400 ppm.

The use of these alloys in particulate form is particularly advantageous, as the combination with a supporting matrix allows the production of active devices of complex geometries with tailorable properties. Notably, the use of a non-conductive polymer matrix drastically reduces eddy current losses in produced composites, allowing for operational use at high frequencies. This has enabled the exploitation of these alloys in various strain-coupled magnetoelectric applications through use of a piezoelectric matrix. Tailoring of the polymer and magnetostrictive phases can also yield improvements in mechanical properties, which is particularly useful for structurally integrated sensor and transducer applications.

Through the use of flake-shaped particulates, shape anisotropy can be exploited to bring about enhancements in the specific strain of these magnetostrictive phase/polymer composite systems. To further these efforts, in this work we explore the production of these flake-shaped geometries using high-energy ball milling and quantify the effects this technique has on the crystal structure of polymer embedded Galfenol and Terfenol-D particulates. The work provides

useful insights into the material processing requirements to optimize the performance of these alloys in multi-functional composite applications such as structurally integrated sensors and transducers.

11:30 AM EL07.12.04

Understanding Magnetic Nanochain Interactions for Reconfigurable Soft Actuators Yulan Chen¹, Karthik Srinivasan², Marcus Choates³, Ludovico Costarollo¹ and Amal El-Ghazaly¹; ¹Cornell University, United States; ²Boise State University, United States; ³The Pennsylvania State University, United States

Reconfigurable soft actuators hold great promise for applications ranging from mobile electronics to medicine, but they require more in-depth studies to improve the extent and efficiency of their actuation. Magnetic soft actuators are attractive candidates for these applications due to the extent of their deformation in external magnetic fields and the speed of their response. However, relatively little attention has been devoted to the influence of the shape and concentration of the magnetic filler (typically in the form of microparticles or other microstructures) on the properties of the assembled actuator. Here, we study the importance of these parameters and observe their influence on the actuator's properties, ranging from its magnetic to its mechanical characteristics.

In particular, this study delves into the potential of magnetic nanochains to offer soft actuators both the benefits of magnetic responsiveness and the additional feature of reconfigurability due to their enhanced anisotropy. We synthesized iron-cobalt nanostructures including nanoparticles and self-assembled nanochains using a magnetic field-free assembly method. The nanostructures were investigated to understand their individual and collective magnetic behaviors. After synthesis, an external magnetic field was applied to align the nanostructures. Nanochains largely remained in their single-particle-wide form but organized into longer lines of chains separated by regular distances; the synthesized nanoparticles, on the other hand, formed multi-particle-wide elongated strands with the width of a few micrometers. In both cases, alignment of the nanostructures led to an augmentation of their collective magnetic properties compared to when they were randomly oriented. However, the nanochains demonstrated a more pronounced enhancement (2x increase) in magnetic remanence compared to the case of nanoparticles. To further investigate the magnetic behavior of the nanochains and their potential as a filler for soft magnetic actuators, their properties were systematically studied as a function of filler concentration, i.e., spatial density. It was discovered that there exists a threshold concentration where the interactions between nanochains transition from ferromagnetic coupling to antiferromagnetic coupling. This resulted in a trend of initially increasing and subsequently decreasing remanence and coercivity as the concentration was increased. The maximum remanent concentration for a collective magnetic nanochain system was achieved at a filler concentration of 6 vol%, which yielded an M_r/M_s ratio approaching 0.5.

Furthermore, we successfully fabricated a reconfigurable magnetic composite film by incorporating the optimal concentration of magnetic nanochains into an elastomer matrix. A soft actuator was made with two separate magnetic panels. The panels could be either encoded with the same magnetization orientation or opposite magnetization orientation to achieve various actuation modes. Subsequent reprogramming could be achieved through the application of a magnetic field to one or both panels. This actuator exhibited shape-morphing behaviors in the form of S-shaped twisting or either lateral or vertical U-shaped bending, respectively, in response to the magnetic field and could be repeatedly reprogrammed. Thus, we demonstrated the construction of reconfigurable magnetic soft actuators capable of large, efficient deformation in small actuation fields (less than 400 Oe). This research emphasizes the potential of magnetic nanochains as effective magnetic fillers and determines the optimal concentration of this magnetic filler for the development of reconfigurable, highly-elastic actuators.

SESSION EL07.13: Bulk Ferroics
Session Chairs: Kevin Crust and Aileen Luo
Friday Afternoon, April 26, 2024
Room 342, Level 3, Summit

1:30 PM EL07.13.01

Energy Storage Properties of Samarium-Doped Bismuth Sodium Titanate-Based Lead-Free Ceramics Xuyao Tang¹, Zimeng Hu¹, Vladimir Koval², Bin Yang³, Graham Smith³ and Haixue Yan¹; ¹Queen Mary University of London, United Kingdom; ²Slovak Academy of Sciences, Slovakia; ³University of Chester, United Kingdom

Due to worldwide environmental regulations, lead-free relaxors, namely $\text{Bi}_{0.5}\text{Na}_{0.5}\text{TiO}_3\text{-}6\text{BaTiO}_3$ (BNT-6BT) are being extensively studied as an alternative candidate for energy storage applications. Here, Sm was introduced at different A sites of the relaxor system; specifically, the Sm-doped BNT-6BT system was designed to replace Bi (BNT-Bi), Na (BNT-Na), and both the Bi and Na ions (BNT-BiNa) by Sm ions. It was found that the BNT-Bi sample possesses high piezoelectricity ($d_{33}=117.3 \text{ pC N}^{-1}$), whereas the BNT-Na and BNT-BiNa ceramics show exceptionally high values of the energy storage density and efficiency. To define the energy storage performance, a new concept based on determining the recoverable energy storage intensity is proposed in the present work. This allows bypassing the high applied electric fields in determining the value of the energy storage density. An ultrahigh recoverable energy storage density (4.41 J cm^{-3}), excellent energy storage efficiency (83.96%) and superhigh recoverable energy storage intensity ($19.17 \times 10^{-3} \text{ J kV}^{-1} \text{ cm}^{-2}$) were achieved in the BNT-BiNa ceramics simultaneously. Furthermore, the energy storage characteristics exhibit an excellent stability over a wide temperature range from 25 °C to 150 °C. Thus, the developed Sm-doped BNT-6BT ceramics show great potential for piezoelectric and high-power energy storage applications.

This paper has been published in Chemical Engineering Journal 473 (2023) 145363, <https://doi.org/10.1016/j.cej.2023.145363>

1:45 PM EL07.13.02

Field Sensitive $\text{Ba}_{1-x}\text{Sr}_x\text{Ti}_{0.89}\text{Hf}_{0.11}\text{O}_3$ Ceramics with Super High Dielectric Tunability Wanting Hu, Haixue Yan, Xuyao Tang, Samrawit D. Hailu and Isaac Abrahams; Queen Mary University of London, United Kingdom

Barium strontium titanate ($\text{Ba}_{1-x}\text{Sr}_x\text{TiO}_3$, BST) is a promising candidate for tunable components but the tunability of BST is relatively low and the mechanisms of tunability and the impact of electric fields on the dielectric properties of BST ceramics require more comprehensive research. Here, by introducing Hf and adjusting the content of Sr, the transition in BST ceramics turn to the diffuse phase. There are at least two distinct polar structures, which is suggested by different current peaks in current-electric field loops. The developed ceramics show super high dielectric tunability (up to 68%) which can be attributed to the different polar structures having significantly sensitive to applied electric fields. Compared to pure BST ceramics or other doped variants, the designed BST exhibit nearly twice the increase in dielectric tunability and hold great potential for widespread use in tunable devices including phase shifters, resonators, filters, voltage-controlled oscillator.

2:00 PM EL07.13.03

Facile Mechanochemical Synthesis of Lead-Free Piezoelectric Perovskite Potassium Niobate Incorporated with Tungsten [Latha Nataraj](#), Anthony Roberts, Scott Walck, Tucker Moore, Kenneth Strawhecker and Kristopher Darling; US ARL, United States

A quest for non-toxic alternatives to conventional lead-based ferroelectric and piezoelectric materials has led to avid research in complex perovskite oxides and systems characterized by morphotropic phase boundary due to the abrupt increase in the dielectric and piezoelectric constants occurring in this region. Niobate perovskites like the (K,Na)NbO₃ (KNN) family have emerged as some of the most important lead-free ferroelectric and piezoelectric materials. Engineering of facile, economical, and environmentally safe synthesis methods for such materials pose challenges to ensuring chemical homogeneity and achieving desired structures. Further, it has been demonstrated that doping positively influences properties such as morphology, texture, crystalline structure, and polarization of KNN. Here, we report solvent-free mechanochemical synthesis of single-phase lead-free piezoelectric perovskite oxide (W-KNN) of KNN incorporated with Tungsten (W), using a simple high-energy ball-milling process with shorter processing times and lower calcination temperatures than those reported in literature. The characterization of the derived powder confirms the structure, morphology, crystallinity, and chemical composition of the material synthesized. Local piezoelectricity is confirmed on the synthesized material for various application-specific device configurations. The presented method could also pave the way for a rapid, facile, and faster synthesis mechanisms at lower processing temperatures for other promising functional oxides.

2:15 PM EL07.13.05

Novel Photocaloric Effects in Archetypal Ferroelectrics for Solid-State Cooling Applications [Claudio Cazorla](#); Universitat Politècnica de Catalunya, Spain

Solid-state cooling represents an energy efficient and ecologically friendly solution to the environmental problems posed by conventional refrigeration technologies based on compression cycles of greenhouse gases [1-3]. Upon small and moderate magnetic, electric and/or mechanical field shifts, promising caloric materials experience large adiabatic temperature variations ($|\Delta T| \sim 1-10$ K) as a result of phase transformations entailing large isothermal entropy changes ($|\Delta S| \sim 10-100$ J K⁻¹kg⁻¹). Solid-state cooling relies on such caloric effects to engineer multi-step refrigeration cycles. Nevertheless, conventional magneto-, electro- and mechano-caloric effects present a series of critical drawbacks that keep hindering their practical implementation in commercial refrigeration devices. For example, operation temperature conditions should be close to zero-bias transition points, since otherwise the required driving fields grow unfeasibly too large, but these only serendipitously occur at ambient conditions. Here, we will show, based on advanced first-principles simulation methods, that macroscopic light-driven phase transitions in ferroelectrics have the potential to overcome such a materials selection limitation. In particular, we demonstrate for the archetypal ferroelectric KNbO₃ the existence of giant photocaloric effects (i.e., $|\Delta T| \sim 10$ K and $|\Delta S| \sim 100$ J K⁻¹kg⁻¹), that is, induced by light absorption, over a vast temperature span of several hundreds of Kelvin containing room temperature. Our results can be qualitatively generalized to other ferroelectrics displaying similar types of ferroelectric to paraelectric phase transitions [4].

[1] I. Takeuchi and K. Sandeman, Phys. Today 68, 48 (2015)

[2] C. Cazorla, Appl. Phys. Rev. 6, 041316 (2019)

[3] C. Menéndez-Muñiz, R. Ruruli and C. Cazorla, Phys. Chem. Chem. Phys. 25, 17450 (2023)

[4] C. Paillard, et al., Phys. Rev. Lett. 123, 087601 (2019)

2:30 PM EL07.13.06

Light-Induced Color Change and Negative Photoconductivity in Bandgap Engineered Lead Titanate Ceramics [Yang Bai](#)¹, Suhas Yadav¹, Ofir Rudich², Or Shafir² and Ilya Grinberg²; ¹University of Oulu, Finland; ²Bar-Ilan University, Israel

Motivated by the principle of above-bandgap photovoltage and thus the theoretical possibility of breaking the Shockley-Queisser limit, research interest in bandgap engineering of conventional ferroelectric materials is on the rise. Due to the reduced bandgaps and the resultant interaction between the incident photon energy and the unit cells and domains, many fundamentally interesting phenomena have been observed in ferroelectrics under visible light, including photo-excited domain switching and photoferroelectric cumulative effect. These phenomena could result in optical and optoelectrical applications far beyond the bulk photovoltaic effect. This talk will report a newly synthesized PbTiO₃-based ceramic that is modified to achieve a narrow band gap, which has been predicted via calculations by the density functional theory (DFT). This new material changes its color from maroon to brown when exposed to visible light, accompanying with negative photoconductivity. A hypothesis to explain the phenomena could be that the photo-excited electrons might reduce Ti⁴⁺ to Ti³⁺, causing the color change. Meanwhile, the leftover photo-excited holes might contradict the pristine n-type conduction and thus decreasing conductivity under illumination. This interesting phenomenon may be useful for optical or optoelectronic components requiring property change under visible light, such as photo-sensitive membrane, photosensor, and photo-resistive switch.

2:45 PM EL07.13.07

Enhanced Spontaneous Ferroelectric Polarization in Sm-Doped BaFe_{0.2}Ti_{0.8}O₃ Ceramics [Anumeet Kaur](#)^{1,2} and Arkaprava Das³; ¹Guru Nanak Dev University, India; ²Global Group of Institutes., India; ³University of Tübingen, Germany

We investigate the origin of progressive spontaneous polarization enhancement at room temperature (RT) in Ba_{1-x}Sm_xTi_{0.8}Fe_{0.2}O₃ (BTO) solid solution (x = 0, 0.10, 0.15, 0.20) with increasing Sm doping. X-ray diffraction and Raman spectroscopic results confirm A (Sm_{Ba}) and B (Fe_{Ti}) site cationic substitution and increase in the tetragonality. The cooperative off-centering phenomena promote inter-polar clustering via nucleation causing an enhancement in remnant polarization and coercive field with increasing Sm doping. Microscopic observation has indicated the presence of multivariant ferroelectric domain fringes along with more compact and larger grain distribution at the highest Sm concentration. The continuous reduction in oxygen vacancy density observed from X-ray photoelectron spectroscopy results in domain wall depinning and easier domain switching. The X-ray absorption spectra for Ti L_{3,2} shows the increase of $\langle \text{Ti}^{3+} \rangle$ with increasing Sm doping, indicating enhanced Ti 3d¹ occupancy. The increase of $\langle \text{Ti}^{3+} \rangle$ with increasing Sm doping, indicating enhanced Ti 3d¹ occupancy.

mso-ansi-language:EN-IN">$O\ 2p$ orbital hybridization. The first-principles density functional theory calculation also indicates that doping induced increment in $Ti\ 3d/Sm\ 4d$ [1] [if gte msEquation 12]$O\ 2p$ orbital hybridization which weakens the short-range repulsion between core orbitals and facilitates the ferroelectricity enhancement. Such in-depth understanding permits us to tune the controlling parameters in optimizing the ferroelectric ordering at RT with appropriately co-doped BTO-based ceramics.

SESSION EL07.14: Virtual Session
Session Chairs: John Heron and Ruijuan Xu
Wednesday Afternoon, May 8, 2024
EL07-virtual

4:00 PM *EL07.14.01

Large Magnetic Proximity Effect in Manganite Oxide Heterostructures Suryakanta Mondal, Naveen Negi and [Bhagwati Prasad](#); Indian Institute of Science Bangalore, India

The fabrication of spintronic devices necessitates the use of multi-layer structures made up of diverse magnetic materials. Such magnetic structures lead to a wide range of interface effects, prominent among which is the proximity effect. Manganite oxide thin film heterostructures are potential candidates for a comprehensive exploration of these proximity effects, primarily because manganites showcase emergent phenomena due to the dynamic interplay among charge, spin, orbital, and lattice degrees of freedom [1]. Some of their fascinating properties are colossal magnetoresistance and metal-insulator transitions. These properties arise from the intricate interactions among charge carriers, spin ordering, and lattice distortions, and they can be modulated by external stimuli like magnetic or electric fields. The physical attributes of manganites, such as $Sr_{1-x}SrxMnO_3$ (SSMO), undergo significant changes with alterations in the Sr doping percentage. Depending on the doping ratio, SSMO can exhibit ferromagnetic, antiferromagnetic, or even mixed magnetic phases [2]. The extensive variety of phenomena that can be tuned based on Sr concentration in SSMO highlights its scientific importance and makes it a compelling subject for the study of diverse properties [3, 4]. In this study, we investigated the magnetic proximity effect in SSMO bilayer and tri-layer heterostructures. Initially, we deposited a single layer of ferromagnetic metal (FMM) and an antiferromagnetic insulator (AFI) onto a $SrTiO_3$ (STO) substrate using the pulsed laser deposition (PLD) technique. Their magnetic attributes were assessed with a SQUID magnetometer, and the results were consistent with earlier reports. Subsequently, we laid down a bi-layer stack of FMM/AFI and a tri-layer configuration of AFI/FMM/AFI on the STO substrate. We observed a marked increase in magnetic moment across these structures, indicating that the magnetic proximity effect in the heterostructures was the main contributor. In conclusion, manganite heterostructures present a promising avenue for further exploration of novel electronic and magnetic phenomena at their interfaces. References: 1. Y. Tokura, Reports Prog. Phys. 69, 797 (2006). 2. Kurbakov et al., Journal of Physics: Condensed Matter. 20, 104233 (2008). 3. Bhagwati Prasad, et al., Advanced Materials 27, 3079 (2015). 4. Bhagwati Prasad and M. G. Blamire, Appl. Phys. Lett. 109, 132407 (2016).

4:30 PM EL07.14.02

Emergence of Dynamic Memory and Perturbation Effect in $Dy_{2-x}Fe_xTi_2O_7$ Pyrochlore Oxides [Pramod Yadav](#) and Pavan Nukala; Indian Institute of Science, India

Investigation of topological materials and their exotic properties, along with understanding crucial exponents, holds great interest for the advancement of next-generation devices. A particular focus lies in the study of out-of-equilibrium properties observed in $Dy_2Ti_2O_7$ spin ice, which presents unique opportunities to comprehend the intricate magnetic behavior found in disordered magnetic materials. Through our experimental analysis, we have discovered the magnetic field-induced anomalous thermomagnetic hysteresis, a phenomenon exclusively observed in temperature- and magnetic field-dependent AC susceptibility measurements. Notably, this observed memory effect exhibits a strong dependence on both thermal and non-thermal driving variables. We have identified that even a minor substitution of the Heisenberg Fe-spins within the Ising matrix, formed by Dy ions, significantly alters the memory effect. Our results clearly demonstrate that defects play a crucial role in the dynamic magnetic properties, which are particularly pronounced in the out-of-equilibrium state. This phenomenon is believed to arise from the combined influences of geometric frustration, disorder, and the cooperative nature of spin dynamics exhibited by these materials. The emergence and controllability of the memory effect with thermomagnetic variables and substitution present a promising foundation for future applications of quantum-based devices.

4:45 PM *EL07.14.03

Polar Topological Defects in Ferroelectric Nanostructures: Novel Features and Phenomena [Laurent Bellaiche](#); University of Arkansas, United States

About twenty years ago, electrical topological defects were predicted in ferroelectric nanostructures [1-3]. These fascinating objects are now forming one active and exciting research field, since they have the potential to revolutionize technologies but also yield striking phenomena (see, e.g., Refs. [4-7] and references therein).

The aim of this Talk is to reveal and explain, via the use of first-principle-based atomistic effective Hamiltonians and state-of-the-art experimental growth and characterization techniques, the emergence of novel features, all associated with polar topological states. This includes:

Their activation by THz pulses and twisted light [8-10],

Their role in creating magnetism in nominal non-magnetic systems [11],

The systematic control of their motions across thin films [10,12,13],

The unusual lattice vibrations and soft modes responsible for their condensation [14,15],

The transitions between different topological states [16-20], and

The occurrence of novel phases and phenomena, such as polar solitons in low-dimensional multiferroics [21], quantum-induced dipolar liquid states and quantum criticality [22] and electrical hopfions [23].

The authors at Arkansas thank the Vannevar Bush Faculty Fellowship (VBFF) from the Department of Defense, the MonArk NSF Quantum Foundry supported by the National Science Foundation Q-AMASE-I Program under NSF Award No. DMR-1906383, the ARO Grants No. W911NF-21-1-011 and W911NF-21-2-0162 (ETHOS), the DARPA Grant No. HR0011727183-D18AP00010 (TEE Program), and the ONR Grant N00014-21-1-2086. The research at University of New South Wales (UNSW) is supported by DARPA Grant No. HR0011727183-D18AP00010 (TEE Program), partially supported by the Australian Research Council Centre of Excellence in Future Low-Energy Electronics Technologies (project number CE170100039) and funded by the Australian Government.

References:

- [1] Ivan I. Naumov *et al.*, Nature (London) 432, 737 (2004).
- [2] I. Kornev *et al.*, Physical Review Letters 93, 196104 (2004).
- [3] H. Fu and L. Bellaiche, Physical Review Letters 91, 257601 (2003).
- [4] Vivasha Govinden *et al.*, Nature Materials 22, 553-561 (2023).
- [5] Javier Junquera, *et al.*, Reviews of Modern Physics 95, 025001 (2023).
- [6] Lu Han *et al.*, Nature 603, 7899 (2022).
- [7] Shuai Yuan *et al.*, Physical Review Letters 130, 226801 (2023).
- [8] Peng Chen *et al.*, Physical Review B 107, L060101 (2023).
- [9] Sergey Prosandeev *et al.*, Advanced Electronic Materials, 2200808 (2022).
- [10] Lingyuan Gao *et al.*, under review.
- [11] Lingyuan Gao *et al.*, Physical Review Letters, in press.
- [12] Sukriti Mantri *et al.*, under review.
- [13] Sergei Prokhorenko *et al.*, under review.
- [14] Suyas Rijal *et al.*, under review.
- [15] Maxim A. Makeev *et al.*, in preparation.
- [16] Vivasha Govinden *et al.*, Physical Review Materials 7, L011401 (2023).
- [17] Vivasha Govinden *et al.*, Physical Review Materials 5, 124205 (2021).
- [18] Y. Nahas *et al.*, Nature Communications 11, 5779 (2020).
- [19] Qi Zhang *et al.*, Advanced Functional Materials 1808573 (2019).
- [20] Qi Zhang *et al.*, Advanced Materials 29,1702375 (2017).
- [21] Vivasha Govinden *et al.*, Nature Communications 14, 4178 (2023).
- [22] W. Luo *et al.*, under review.
- [23] Suyash Rijal *et al.*, in preparation.

5:15 PM EL07.14.04

Structural, Magnetic and Magnetocaloric Study of Rare-Earth and Cobalt Co-Doped $\text{La}_{0.8}\text{RE}_{0.2}\text{Cr}_{0.5}\text{Co}_{0.5}\text{O}_3$ ($x = 0.2$; RE = Nd and Gd) Chromite Jolaiikha Sultana¹, Surendra Dhungana¹, Santosh K. Chhetri², Jin Hu² and Sanjay R. Mishra¹; ¹The University of Memphis, United States; ²University of Arkansas, Fayetteville, United States

Heavy rare earth chromite's, specifically RCrO_3 (where R represents Ho, Er, Yb, Lu, and Y), are a class of advanced multifunctional materials that demonstrate multiferroicity, which combines ferroelectricity and canted antiferromagnetism. These materials have significant promise for utilization in magnetic refrigeration applications. This work presents structural, magnetic and magnetocaloric effect (MCE) observed in polycrystalline orthochromites $\text{La}_{0.8}\text{RE}_{0.2}\text{Cr}_{0.5}\text{Co}_{0.5}\text{O}_3$ that have been doped with rare-earth and cobalt elements. The materials were synthesized by the sol-gel auto combustion method. XRD pattern reveals that all the samples crystallize in the perovskite phase with an orthorhombic structure (space group Pbnm). The lattice parameter of the powder samples was calculated from the XRD pattern refinement, which showed a decrease in lattice parameter and volume upon rare-earth substitution. This systematic change in the lattice volume is the result of the lanthanide contraction of the ionic radii of rare earth elements. Magnetic measurement shows Paramagnetic (PM) to Canted Antiferromagnetic (CAFM) transition with Néel temperature (T_N) below 300K and paramagnetic Curie-Weiss temperature (θ) undergoing shift towards lower temperature upon RE and Co co-doping. An increase of considerable magnitude in magnetization has been observed in the doped compounds because of the development of ferromagnetic properties. All the doped compounds showed an enhancement in MCE performance compared to the pristine compound. The compound $\text{LaCr}_{0.5}\text{Co}_{0.5}\text{O}_3$ exhibited a maximum change in magnetic entropy of $0.07\text{Jkg}^{-1}\text{K}^{-1}$ when subjected to an applied field of 5T. The Nd and Co co-doped $\text{La}_{0.8}\text{Nd}_{0.2}\text{Cr}_{0.5}\text{Co}_{0.5}\text{O}_3$ compound showed the highest magnetic entropy change of $6\text{Jkg}^{-1}\text{K}^{-1}$, whereas the Gd and Co co-doped $\text{La}_{0.8}\text{Gd}_{0.2}\text{Cr}_{0.5}\text{Co}_{0.5}\text{O}_3$ compound showed magnetic entropy change of $4\text{Jkg}^{-1}\text{K}^{-1}$, both under a 5T applied field. Due to the substantial rise in magnetic entropy change, these materials have potential for use in magnetic refrigeration applications at low temperatures.

5:20 PM *EL07.14.05

Tunneling in Ferroelectric Heterostructures: A Tale of Two Interfaces Nagarajan Valanoor; UNSW Sydney, Australia

The various demonstrations of robust ferroelectricity down to a few unit cells at room temperature has triggered the quantum era of ferroelectrics. Nearly two decades ago the concept of a ferroelectric tunnel junction (FTJ) was brought to the fore leading to a flurry of activity in the field of polarization control of tunneling current and related tunneling electro-resistance (TER) effects studies. In this presentation we cover two types of new ferroelectric devices based on the tunneling effect, both founded on the control of electrode/ferroelectric interface in an II oxide heterostructure.

The first part of the talk discusses our recent demonstration of a ferroelectric resonant tunneling diode (RTD), which exploits the switchable electric polarization state of the quantum-well (QW) barrier to tune the device resistance at room temperature. We show robust room-temperature ferroelectric-modulated resonant tunneling and negative differential resistance (NDR) behaviors in all-perovskite-oxide $\text{BaTiO}_3/\text{SrRuO}_3/\text{BaTiO}_3$ RTDs. The resonant current amplitude and voltage are tunable by the switchable ferroelectric polarization of the ultrathin BaTiO_3 layers with the NDR ratio modulated by ~ 3 orders of magnitude and an OFF/ON resistance ratio exceeding a factor of 20 000. An average tunnel lifetime of 0.47 fs on the resonant states is obtained, which is orders of magnitude smaller than those obtained in semiconductor QWs. This work appears in Ma *et al.*, Adv. Mater. 2022, 34, 2205359.

In the second study we explore how electronic phases at the interfaces can be deterministically harnessed to modulate the TER. We find a large tunneling electroresistance (TER) of 6 orders of magnitude when inserting a 0.5 nm-thick $\text{La}_{0.8}\text{Ca}_{0.2}\text{MnO}_3$ layer between the Pt/ BaTiO_3 interface in Pt/ $\text{BaTiO}_3/\text{Nb:SrTiO}_3$ ferroelectric tunnel junctions (FTJs), benefitting from the double interface effect. That is, both the $\text{BaTiO}_3/\text{Nb:SrTiO}_3$ and $\text{La}_{0.8}\text{Ca}_{0.2}\text{MnO}_3/\text{BTO}$ interfaces are synchronously metal or insulator phases in response to the ferroelectric polarization switching, thus amplifying the difference in resistance between the high resistance state (OFF state) and low resistance state (ON state). It is found that a thicker $\text{La}_{0.8}\text{Ca}_{0.2}\text{MnO}_3$ layer leads to the decrease of the TER. This is attributed to the decreased barrier height/width at the $\text{BaTiO}_3/\text{Nb:SrTiO}_3$ interface as revealed by analysis of the electron transport mechanism. We show it occurs by Fowler-Nordheim (FN) tunneling. Our reports provide a pathway, namely interface control of the oxide heterostructure, to achieve high-performance ferroelectric tunneling devices for future oxide electronics at the nanoscale.

The speaker would like to acknowledge the support of an Australian Research Council (ARC) Discovery Project and Australian Research Council Centre of Excellence in Future Low-Energy Electronics Technologies (Project No. CE170100039) grant.

SYMPOSIUM EL08

Plasmonics and Metasurfaces—Design, Materials and Applications
April 22 - May 7, 2024

Symposium Organizers

Yao-Wei Huang, National Yang Ming Chiao Tung University
Min Seok Jang, Korea Advanced Institute of Science and Technology
Ho Wai (Howard) Lee, University of California, Irvine
Pin Chieh Wu, National Cheng Kung University

Symposium Support

Bronze

APL Quantum

Kao Duen Technology Corporation
Nanophotonics Journal

* Invited Paper

+ JMR Distinguished Invited Speaker

^ MRS Communications Early Career Distinguished Presenter

SESSION EL08.01: Photonics Resonance Designs for Biomedical Imaging, Sensing and Spectroscopy Application

Session Chairs: Ho Wai (Howard) Lee and Pin Chieh Wu

Monday Morning, April 22, 2024

Room 340/341, Level 3, Summit

8:45 AM EL08.01.02

Integrating Surface-Enhanced Raman Spectroscopy and Electrokinetics for Bacterial Identification in Wastewater Yirui A. Zhang, Liam Herndon, Punng Padhy, Babatunde Ogunlade, Alexandria Boehm and Jennifer A. Dionne; Stanford University, United States

Antibiotic-resistant bacterial infections claim over 1.2M lives annually and are projected to be the main cause of death in 30 years [1]. Elevated pathogen levels in wastewater are one of the first indicators of disease outbreaks, making wastewater a powerful tool for surveilling the infections present in a community [2]. However, bacterial WBE presents outstanding challenges; current culturing or fluorescence-based methods [3] to identify bacteria are slow and costly, and not suitable for high-throughput screening of diverse bacterial species. Further, the complex substances in wastewater can interfere with chemical probes or cause false negative results.

In this study, we develop a generalized enrichment with Raman-machine learning spectroscopy (GERMS), employing surface-enhanced Raman spectroscopy (SERS) [4] and integrating it with electric fields and machine learning models [5], to enable rapid and amplification-free bacteria identification in filtered wastewater, even at low concentrations down to 10^4 cells/mL. To achieve this, we first synthesize gold nanorods designed to electrostatically bind with bacteria, enabling SERS measurements from the cell surfaces. We perform SERS measurements on various bacteria, including *Staphylococcus aureus*, *Staphylococcus epidermidis*, and *Escherichia coli*, across a concentration range spanning from 10^9 down to 10^4 cells/mL. Spectral clustering analysis reveals that as the concentration decreases, bacterial signals become progressively more challenging to distinguish from the background wastewater. Furthermore, we incorporate electrokinetic effects into SERS by employing gold microelectrodes to apply external electric fields and leveraging dielectrophoresis [6] to rapidly displace and enrich bacteria within minutes. Microscopy directly visualizes the enrichment of bacteria with nanorods, leading to a remarkable increase in Raman signal intensities by up to tenfold under external electric fields for bacterial concentrations from 10^6 down to 10^4 cells/mL. This enhancement has the potential to extend the detection sensitivity to environmentally-relevant concentrations. In addition, through data science approaches, we identify biologically significant "fingerprint" Raman peaks that characterize proteins, nucleic acids, and lipids on bacterial surfaces. This discovery holds promise for the rapid identification of bacterial species for wastewater-based epidemiology.

[1] Thompson, T. *Nature*. (2022)

[2] Keshaviah, et al. *The Lancet Global Health*. (2023)

[3] Jahn, et al. *Nature Microbiology*. (2022)

[4] Tadesse, et al., *Nano Lett.* (2020).

[5] Ho, et al., *Nat. Comm.* (2019).

[6] Pethig. *John Wiley & Sons* (2010).

9:00 AM EL08.01.03

Evaluating The Refractometric Sensing Performance of Plasmonic Titanium/Hafnium Nitride Nanohole Arrays Beyza N. Gunaydin^{1,1}, Meral Yuce¹ and Hasan Kurt^{2,3}; ¹Sabancı University, Turkey; ²Imperial College London, United Kingdom; ³Istanbul Medipol University, Turkey

Noble metals, such as gold and silver, have conventionally been the preferred materials for plasmonic applications owing to their elevated electrical conductivity, surface plasmon frequencies within the visible spectrum, and chemical stability. However, they are increasingly expensive to utilize, incompatible with conventional CMOS process, difficulties in large-scale manufacturing, and have low melting temperatures at the nanoscale. In this perspective, refractory group IVB metal nitrides present a remarkable ability to modulate their plasmonic behavior within the visible to near-infrared range as alternatives to noble metals. These materials can exhibit exceptional resistance to high temperatures, mechanical robustness, compatibility with CMOS

technology, chemical inertness, and outstanding compatibility with prevailing electronic platforms. Thus, these properties render group IVB metal nitrides, especially titanium nitride (TiN) and hafnium nitride (HfN), highly promising candidates for diverse plasmonic applications.

In this study, we have investigated the optical properties of TiN and HfN thin films using variable angle spectroscopic ellipsometry, focusing on the Ar:N₂ ratio to improve the metallic properties of thin films. X-ray diffraction and Raman spectroscopy have been thoroughly carried out on thin TiN and HfN films to assess the stoichiometry and structure of thin films with different gas flow rates. In addition, periodic nanohole arrays of TiN and HfN (especially HfN is a hard material, called conductive ceramic) were successfully fabricated by electron beam lithography (EBL) and induced coupled plasma reactive ion etching (ICP-RIE) to evaluate the refractometric sensing of plasmonic assays. Finally, to explore the potential of plasmonic metal nitrides as alternatives to noble metals, the refractive index sensitivities of TiN and HfN nanohole arrays were investigated using a custom micro-spectrometry setup under different mediums. The refractive index sensitivities for TiN and HfN nanohole arrays achieved 180 and 631 nm/RIU, respectively. This study provides unique insights into the behaviors of TiN and HfN nanohole arrays in refractometric sensing applications, and the full potential of refractory metal nitrides in plasmonics is yet to be realized.

9:15 AM EL08.01.04

Temporal Vs Stable Plasmonic Anticounterfeit Tags for Structural Health Monitoring Studies Maha Ibrar, Megan Knobloch, Zachery Mccurtain, David Crandall and Sara Skrabalak; Indiana University Bloomington, United States

Proliferation of counterfeit goods has resulted in exorbitant economic fallout, device reliability issues, and health and safety concerns. Hence, developing anticounterfeit platforms has become imperative for reliable and cost-effective authentication, tracking of products, and detection of potential tamper activity. Here, we report covert anticounterfeit platforms where plasmonic nanoparticles (NPs) were used to develop tags to authenticate goods. The two platforms developed are Unique images and Physical Unclonable Functions (PUFs). Fabrication of Unique images entails assembling plasmonic nanoparticles in arrays with the help of templates, whereas PUFs result from light scattering from randomly drop casted NPs. These techniques allow critical goods to be facily tagged, and the resultant pattern from either a nanoparticle assembly or individual NPs is analyzed with darkfield optical microscopy imaging. Au and Ag NPs were prioritized due to their tailorable optical responses in the visible spectrum. The sensitivity of metal nanoparticles (particularly Ag) to the environment was also leveraged as a monitor of structural health and to show evidence of tampering. Functionalized Ag NP inks were used to create tags that serve as temporal sensors where changes in color response were tracked with variable exposure times to ambient environmental conditions. These temporal sensors are authenticated with machine learning protocols that keep track of the optical changes with time.

9:30 AM EL08.01.05

Scalable Manufacturing, Transfer and Integration of Metasurfaces for Biosensing Hao Wang, Ashish Pandey, Nanzhong Deng and Haogang Cai; New York University, United States

Building upon a long-established history of plasmonic and nanophotonic biosensors, the recent advancements in metasurfaces have brought to light exciting new possibilities, such as tailor-designed high-Q resonances, spectrometer-less and imaging-based sensing. However, there is still a major challenge towards the widespread implementation of metasurface technology, for either sensing or wavefront engineering: optical metasurface manufacturing largely relies on electron beam lithography (EBL), which provide high resolution at a price of low throughput. It is difficult for EBL to offer either high-volume production or large area metasurfaces. Moreover, EBL-compatible substrates are planar and bulky, usually orders of magnitude thicker than the metasurface itself. Conventional substrates not only nullify the reduced footprint advantage of metasurfaces, but also limit their application scenarios.

To address these challenges, we demonstrate scalable manufacturing of metasurfaces using the self-assembly approach known as nanosphere lithography, which is versatile in terms of material selection, nanopattern geometry and dimension tunability. Through a process called "Marangoni convection", polystyrene (PS) latex beads float at the air-water interface and eventually self-assemble into hexagonally close-packed pattern upon addition of surfactant. Nanosphere hexagonal arrays can be formed on a wider range of substrates, and then used as masks for metal deposition or etching to create complementary geometries of nanohole and nanodisc arrays, respectively. Oxygen plasma is used to etch the PS beads for fine tuning of the feature size in the nanoscale. After removing and cleaning of the PS beads layer, the metallic nanopatterns can be directly used as plasmonic metasurfaces for biosensing, or used as etching masks for pattern transfer into the underlying dielectric materials. Recently, dielectric metasurfaces are drawing increasing attention for sensing applications due to their advantages of negligible ohmic loss and high-Q resonances, compared to the plasmonic counterparts.

Taking gold nanohole arrays as an example, the metasurface geometric parameters are tuned by the following: the period is determined by the original PS bead size, the nanohole diameter is determined by the Oxygen plasma etching, while the thickness is determined by electron beam deposition. We started with 600 nm PS beads assembly on glass coverslips, and etched the diameter to 360 nm for gold deposition of 50 nm. For the optofluidic integration, a polydimethylsiloxane (PDMS) chamber was formed in a mold, and then bonded on top of the metasurface after Oxygen plasma treatment. Microfluidic tubes were inserted to the PDMS chamber, forming inlet and outlet channels. In the medium of DI water, a transmission resonance dip was found near 700 nm wavelength using a spectroscopy setup. By changing media with different refractive indexes (RI), the bulk RI sensitivity was measured as 550 nm/RIU, with a limit of detection down to $\sim 2 \times 10^{-4}$ RIU. The sensing performance matches well with finite-difference time-domain (FDTD) simulations, and approaches that of the state-of-the-art devices manufactured by EBL. The metasurface sensor was used to detect the specific binding between protein A/G and antibody, which can be further customized for various biosensing targets.

In summary, we demonstrated the scalable manufacturing and optofluidic integration of metasurface biosensors. They provide high sensing performance comparable to EBL, while the high through and low cost make them more suitable for point-of-care testing. The scalable manufacturing and our recently developed metasurface transfer technique largely expand the selection of substrates, which will enable promising applications such as the integration of flexible/wearable devices and lab-on-fiber technology for in vivo sensing and diagnostics.

9:45 AM EL08.01.06

Terahertz Monitoring of Gas-Matter Interactions: Exploring Interatomic and Interfacial Dynamics through Palladium Nano-Film Hybrid Metasurfaces Jinwoo Lee^{1,2}, Jongsu Lee¹, Geon Lee^{1,3}, Ryu Yong-Sang² and Minah Seo^{1,2}; ¹Korea Institute of Science and Technology(KIST), Korea (the Republic of); ²Korea University, Korea (the Republic of); ³Seoul National University, Korea (the Republic of)

Terahertz (THz) technology is an attractive optical sensing platform that offers accurate approaches for the real-time investigation of intrinsic materials in non-invasive and non-contact manners. In addition, using metamaterials that have been extensively researched recently, diffraction-limit and absorption cross-section-limit can be overcome [1]. Here, we monitored molecular dynamics by gas-matter interactions including interatomic and interfacial reactions such as absorption, desorption, adsorption, and catalytic reaction. In-situ THz measurement using nano-patterned slot antennas is introduced to investigate Palladium (Pd) based interatomic and interfacial gas-matter interactions. Interatomic interaction which is atomic scale changes can be measured using our geometrically optimized nano-slot structure, which consists of a narrow gap of approximately 14 nm between a gold wall and a deposited Pd metal thin film. Furthermore, we manipulated nano-slot structures to maximize the sensitivity of THz signals in terms of water, formed by the Pd catalytic reactions, and their absorption. Our proposed experiment aims to analyze the dynamics of interatomic hydrogenation, interfacial oxygen adsorption, and water-forming reactions in a highly consistent and dependable manner, enabling real-time analysis [2].

The molecular dynamics are interpreted by THz transmittance measurement under the various gas concentrations including N₂, H₂, and O₂. The molecular

dynamics can be determined by inspecting resonance frequency shifts and transmittance changes in the transmitted resonance signals that were filtered by our nano-slot structures. The Pd hydrogenation process, the oxygen adsorptions, and the catalytic water formation reactions according to the various concentrations of H₂, O₂, and N₂ were dynamically measured by resonance frequency and transmittance response.

The atomic scale response, such as hydrogen absorption, desorption into the Pd lattice, and catalytic water formation response which is a relatively huge scale can be measured in a reliable manner using such a long wave-length light. In addition, by interpreting inclinations that are plotted on the map composed of the amount of resonance frequency and transmittance response, not only the three different dynamics can be classified, but also a complex hidden process of water-forming reactions can be tracked.

Acknowledgement: NRF (2023R1A2C2003898, CAMM-2019M3A6B3030638, 2021R1A2C2009236), KIST (2E32451)

References

- [1] Nanoscale Terahertz Monitoring on Multiphase Dynamic Assembly of Nanoparticles under Aqueous Environment, *Adv. Sci.* 8, 11, 2021
- [2] Naked-eye observation of water-forming reaction on palladium etalon: transduction of gas-matter reaction into light-matter interaction, *Photonix*, 1, 2023

Keywords: Metamaterial, Terahertz spectroscopy, Palladium film

10:00 AM BREAK

10:30 AM *EL08.01.07

Passive and Active Metasurfaces for Wireless Telemetry Sensors Hanwei Wang, Xiaodong Ye, Yulei Shen, Yun-Sheng Chen and Yang Zhao; University of Illinois Urbana-Champaign, United States

In this talk, I will discuss both the theoretical design and experimental realization of metasurfaces aimed at enhancing the efficiency and operational range of wireless charging for surgically implanted biosensors. I will delve into several design concepts of metasurfaces including auto-reconfigurability, magnetic mode forming, and Parity-Time (PT) symmetric metasurfaces, which hold the potential for achieving unity efficiency. My discussion will extend to the inverse design principles and their impact on mode optimization. Further, I will explore the practical applications of these theoretical concepts by introducing the metasurface as a wearable device designed to sustainably power a surgically implanted bio-potential sensor, encompassing electromagnetic compatibility with both in vitro and in vivo demonstrations.

11:00 AM EL08.01.08

Designing Spoof Plasmonic Metasurfaces for Microwave Frequencies and Applications in Biological Processing Zachary Nichols and Chris D. Geddes; University of Maryland, Baltimore County, United States

Plasmonic metasurfaces are a growing subclass of metamaterials which are materials whose properties are based on their structure rather than their composition and can be tuned and designed for different applications as a result. Metasurfaces are the two-dimensional analogs of three-dimensional metamaterials and plasmonic metasurfaces are those that use electron oscillations in metals, termed plasmons, to achieve their desired properties. Most applications of plasmonic materials have been limited to the visible and UV frequency ranges of light since lower frequency photons have insufficient energy to excite plasmons in metals, however "spoof plasmons" which mimic normal plasmons, have been created in the terahertz and microwave frequency ranges by utilizing subwavelength metal structures in periodic arrays. Spoof plasmonic metasurfaces (SPMs) are metasurfaces that can mimic plasmonic metasurfaces at lower frequencies by utilizing properties of spoof plasmons. In this work, we have designed several SPMs for use in the microwave frequency range using a combination of computational modeling and physical testing. SPMs were designed *in-silico* using finite-difference time-domain (FDTD) methods and then fabricated for physical testing with microwave irradiation. Once designed, these SPMs were assessed for their utility as a sample processing platform for biological samples such as microbes, nucleic acids, and proteins in a variety of laboratory assays such as genomic sequencing or diagnostic polymerase chain reaction (PCR). While many applications of metasurfaces to biological problems have been focused on sensing biological signals and imaging, this work is focused on using their properties to process biological samples via light-matter interactions and their products. Thus far this work has shown promise in applying SPMs to a new area of biological processing as well as exploring existing metasurface design principles for alternative applications.

11:15 AM EL08.01.09

In-Situ Raman/SERS Photocatalysis mediated by Coupling NaREF₄ Upconversion Nanoparticles with Plasmonic Gold Nanoparticles to Reaction Conversion of 4-Aminothiophenol to 4,4'-Dimercaptoazobenzene Gesiane Pinha Sousa¹, Anerise De Barros¹, Flavio Makoto Shimizu^{2,1}, Fernando Aparecido Sigoli¹ and Italo O. Mazali¹; ¹Universidade Estadual de Campinas, Brazil; ²Centro Nacional de Pesquisa em Energia e Materiais, Brazil

Lanthanide-doped upconversion nanoparticles (UCNPs) absorb low-energy photons, in the near-infrared region (NIR), and emit high-energy photons, in the visible or ultraviolet region (UV/Vis). This property of radiation emissions can be used to promote plasmonic photocatalytic reactions by coupling UCNPs with plasmonic nanoparticles. For this, the highly crystalline β -NaYF₄:Yb₃₊, Er³⁺@NaYF₄:Nd³⁺@NaYF₄ UCNPs capped with an amino-modified nanosized silica shell were coupled with gold nanospheres (13 ± 2 nm). The plasmonic-driven dimerization of 4-aminothiophenol (4-ATP) to 4,4'-dimercaptoazobenzene (DMAB) was carried out solely by using the UCNP visible emissions to excite the gold nanoparticle localized surface plasmon resonance band. The reaction was monitored in situ through surface-enhanced Raman spectroscopy (SERS) and optimal conditions were achieved in order to eliminate secondary influences during spectra acquisition. The SERS substrates containing either UCNPs@SiO₂-NH₂/Au or SiO₂-NH₂/Au nanoparticles were prepared by the drop-cast method in silicon substrates. In the studied reaction conditions, plasmonic photocatalytic activity was observed only in the substrates containing UCNPs and Au nanoparticles. The plasmonic-driven reaction was achieved by UCNPs excitation with a 980 nm laser (25.7 mW), aligned in a Raman spectrometer, only after 5 s of exposition. Interactive document mapping (IDMAP), which is an unsupervised pattern recognition method, was applied to analyze the numerous SERS spectra acquired during the plasmonic photocatalytic measurements. The high values found for the silhouette coefficient (0.88 for the Si₂SiO₂-NH₂/Au and 0.76 for the Si₂NYF@SiO₂-NH/Au substrate) indicate that strong discrimination among the Raman spectra was achieved. Thus, through IDMAP, it was observed that the SERS spectra obtained for the substrates containing either UCNPs@SiO₂-NH₂/Au or SiO₂-NH₂/Au corresponded to spectral features, respectively, from the DMAB product and the 4-ATP reagent, evidencing that, in the optimized reaction conditions, the dimerization occurred only through the interaction of the UCNPs with the Au nanospheres.

11:30 AM EL08.01.10

Fluorophore Induced Plasmonic Current (FIPC) for The Detection of Biological Species for The Purposes of Assay Development and Onsite Detection Dan Pierce; University of Maryland, United States

The recent COVID-19 pandemic has made it abundantly clear that there is a growing need for the capacity to have analytically precise detection of pathogens be performed as quickly as possible for the best public health outcome. Fluorophore Induced Plasmonic Current (FIPC) is a newly developed

testing modality that is based upon the principles of modern fluorescence detection, but differs in its implementation and applicability. Where a traditional fluorescence-based assay would require a laboratory environment and an expensive fluorimeter, an FIPC only requires a current detection device and an excitation source to achieve similar results. Based on the properties of FIPC wherein a fluorophore that is excited close to the surface of a plasmonically active metal nanoparticle film is able to transfer a portion of its excitation energy to the film, these proposed assays revolve around this property for the detection of various fluorescent tags and probes for the analytical detection of DNA and proteins. The goal of this presentation is to demonstrate the advances made in the assay development side of FIPC research, and to highlight its strengths and identify its shortcomings when compared to traditional fluorescence detection.

11:45 AM EL08.01.11

Low-Loss Plasmonics with Nanostructured Potassium and Sodium-Potassium Liquid Alloys [Ankun Yang](#); Oakland University, United States

Alkali metals have low optical losses in the visible to near-infrared (NIR) compared to noble metals. However, their high reactivity prohibits the exploration of their optical properties. Recently sodium (Na) has been experimentally demonstrated as a low-loss plasmonic material. Here we report on a thermo-assisted nanoscale embossing (TANE) technique for fabricating plasmonic nanostructures from pure potassium (K) and NaK liquid alloys. We show high-quality-factor resonances from K as narrow as 15 nm in the NIR, which we attribute to the high material quality and low optical loss. We further demonstrate liquid NaK plasmonics by exploiting the Na-K eutectic phase diagram. Our study expands the material library for alkali metal plasmonics and liquid plasmonics, potentially enabling a range of new material platforms for active metamaterials and photonic devices.

SESSION EL08.02: Metasurfaces, Plasmonics and Breaking News Presentations

Session Chairs: Yao-Wei Huang and Min Seok Jang

Monday Afternoon, April 22, 2024

Room 340/341, Level 3, Summit

1:45 PM *EL08.02.01

Meta-Optics for Image and Spectral Classification [Jason G. Valentine](#); Vanderbilt University, United States

Here, we demonstrate how meta-optics can be designed, and realized, to work in concert with a digital back-end for a range of tasks including image and spectral classification. In the case of image classification, the meta-optic serves to off-load computationally expensive tasks into an optical front-end, speeding computational speed while lowering energy consumption. For spectral classification, meta-optics serve as complex filters which are used in conjunction with a digital neural network to achieve a compact flow cytometer capable of classifying up to four unique fluorophores, and their combinations.

2:15 PM EL08.02.03

Printable, Emissivity-Adaptive and Albedo-Optimized Radiative Covering for Dynamic Radiative Thermal Management [Jiachen Li](#)^{1,2,1}, Kaichen Dong^{1,3}, Ruihan Guo¹, Tiancheng Zhang¹ and Junqiao Wu^{1,2,1}; ¹University of California, Berkeley, United States; ²Lawrence Berkeley National Laboratory, United States; ³Tsinghua University, China

Radiative cooling technology utilizes thermal emission to cool buildings and uses outer space as a natural heat sink. Traditional radiative cooling materials focus on static, cooling-optimized material properties to maximize the cooling power, but the constant strong cooling causes overcooling in cold climates, which increases energy budget in the HVAC system. Recently, advances in temperature-adaptive structures have been made to solve the overcooling issue. However, great challenges remain in their fabrication feasibility, and their unoptimized solar heating that may override the radiative cooling benefit. In this work, we develop a printable, emissivity-adaptive and albedo-optimized covering (PEAC) based on recyclable materials with roll-to-roll fabrication. With a metastructure embedded with the phase change material vanadium dioxide, PEAC automatically switches its sky-window emissivity from 0.25 to 0.85 when the surface temperature exceeds a preset transition temperature, whereas delivering an albedo that is optimized for maximal year-round energy saving or thermal comfort in a given climate. Numerical simulations and outdoor experiments show that PEAC outperforms radiative cool roofs in terms of annual energy saving in most climates, especially those with substantial seasonal variations. PEAC can also be applied to objects in addition to building roofs and walls, such as space objects, tents, and vehicles.

2:30 PM BREAK

3:00 PM EL08.02.04

Low-Dimensional Phonon-Polariton Materials for Higher-Order Hyperbolic Dispersion and Efficient Thermal Transport [Guanyu Lu](#)¹, Zhiliang Pan¹, Christopher R. Gubbin², Ryan A. Kowalski¹, Xun Li³, James R. McBride¹, Rinkle Juneja³, Mackey Long¹, Lucas Lindsay³, Simone De Liberato², Deyu Li¹ and Joshua D. Caldwell¹; ¹Vanderbilt University, United States; ²University of Southampton, United Kingdom; ³Oak Ridge National Laboratory, United States

Phonon polaritons are stimulated by coupling infrared photons with the polar lattice vibrations. Such quasi-particles offer low-loss, highly confined electromagnetic energy propagation at subwavelength scales. Here, we discuss the launching and manipulation of higher-order hyperbolic phonon polaritons (HPhPs) in low-dimensional materials.¹ Additionally, we discuss how non-equilibrium phonon polaritons in these materials can further enhance thermal transport as additional energy carriers.²

HPhPs in low-symmetry polar crystals offer ray-like light propagation with out-of-plane or in-plane hyperbolic wavefronts at deep-subwavelength scales. While hyperbolic dispersion in HPhPs implies multiple propagating modes at a given frequency, experimentally launching and probing the higher-order modes, especially for in-plane HPhPs, remains challenging. We report the experimental observation of higher-order in-plane HPhP modes, stimulated on the 3C-SiC nanowire (NW)/ α -MoO₃ heterostructures. This demonstrates the advantage of leveraging both the low-dimensionality and low-loss nature of polar NWs to launch higher-order HPhP modes within two-dimensional α -MoO₃ crystals.

One-dimensional polar NWs not only bridge the wavevector mismatch between free-space light and the higher-order, high-momenta HPhPs but could also significantly impact thermal transport. While optic phonons typically contribute minimally to thermal conductivity, their hybridization with photons as phonon polaritons could facilitate conductive heat transfer in nanostructures. Although some signs of progress in phonon-polariton-mediated heat conduction have been made, experimental efforts so far suggest only very limited contribution from such modes. Here, by combining nanoscale real-space

mapping of phonon polaritons within 3C-SiC NWs with direct thermal transport measurements of these NWs (coated with gold as an efficient polariton launcher), we unambiguously demonstrate phonon-polariton-mediated heat conduction, resulting in orders of magnitude enhancement compared to equilibrium predictions.

1. Lu, G.; Pan, Z.; Gubbin, C. R.; Kowalski, R. A.; De Liberato, S.; Li, D.; Caldwell, J. D., Launching and Manipulation of Higher-Order In-Plane Hyperbolic Phonon Polaritons in Low-Dimensional Heterostructures. *Adv Mater* **2023**, *35* (22), e2300301.
2. Pan, Z.; Lu, G.; Li, X.; McBride, J. R.; Juneja, R.; Long, M.; Lindsay, L.; Caldwell, J. D.; Li, D., Remarkable heat conduction mediated by non-equilibrium phonon polaritons. *Nature* **2023**, *623* (7986), 307-312.

3:15 PM EL08.02.05

An Abnormal Single Molecule Detection by Plasmonic InGaN Quantum Dots Thi Anh Nguyet Nguyen and [Kun-Yu Lai](#); National Central University, Taiwan

Detecting single molecules is a formidable challenge. Surface-enhanced Raman spectroscopy (SERS) is one of the few techniques that can achieve the goal. To verify the presence of single molecules with SERS, the bianalyte proof is the most adopted approach since it is a statistical result from thousands of spectra, rather than the conclusion based on the blinking signals at few selected spots. However, the bianalyte method relies on an undesirable nature of SERS, i.e., the hot spot (SERS-active regions) is too small (< 10 nm) to cover two or more molecules. Since it is extremely difficult to control the size of a hot spot in a scalable manner, only a very limited portion (< 1%) of the diluted molecules can yield detectable Raman signals.

In this work, we demonstrate an abnormal single-molecule signal by SERS, covering 89.6% of the scanned spots. The result was achieved by making the hot spot big enough to simultaneously boost the signals from two or more single molecules. The hot-spot expansion was accomplished by coupling the localized surface plasmons at every Au nanoparticle with electrons confined by the subsurface InGaN quantum dots (QDs). This SERS configuration allows all of the dense Au nanoparticles to become the intensity-boost centers. Thus, any single molecule adsorbed on the SERS substrate can be easily captured by the Au-QD complexes, making single-molecule detection a prevailing event, instead of a rare instance.

With the greatly expanded SERS-active region, the single molecules can deliver stable signals by staying within the “hot surface” before and after the thermal diffusion upon laser excitation. This is not achievable with the conventional hot spots, where blinking signals are often observed by the SERS detection of diluted analytes. Our approach not only changes the bianalyte principle, but also allows researchers to analyze the molecular dynamics with reliable data.

SESSION EL08.03: Thermal Emission with Nanostructure and Nonreciprocal System

Session Chairs: Ho Wai (Howard) Lee and Pin Chieh Wu

Monday Afternoon, April 22, 2024

Room 340/341, Level 3, Summit

3:30 PM *EL08.03.01

Harnessing The Infrared: Materials and Structures for Breaking Reciprocity and Control of Thermal Radiation [Harry A. Atwater](#); California Institute of Technology, United States

In this talk I will discuss materials and photonic design concepts that allow us to experimentally observe breaking of optical reciprocity for thermal radiation, as well as metastructures that allow for considerable control of the thermal emission angular distribution. Thermal emission—the process through which all objects with a finite temperature radiate electromagnetic energy—has generally been thought to obey reciprocity, where the absorbed and emitted radiation from a body are equal for a given wavelength and angular channel. This equality, formalized by Gustav Kirchhoff in 1860, is known as Kirchhoff's law of thermal radiation and has long guided designs to control the emitted radiation. There is considerable interest and numerous theoretical proposals for design of nonreciprocal absorbers that violate the Kirchhoff thermal radiation law. Until recently however, there were no experiments demonstrating this concept. I will discuss direct observation of the inequality between the spectral directional emissivity and absorptivity for an InAs photonic metastructure arising from the non-diagonal permittivity tensor of InAs at the epsilon-near-zero condition under an externally applied magnetic field. The magneto-optic response of magnetic Weyl semimetals is characterized by non-diagonal permittivity governed by the nontrivial Berry curvature that exists between recombinant Weyl nodes. I will also discuss reciprocity breaking in the magnetic Weyl semimetal $\text{Co}_3\text{Sn}_2\text{S}_2$, confirmed via observation of a net reflectance modulation that is nearly an order of magnitude higher than that of the typical transverse magneto-optical Kerr effect in ferromagnets, without the concurrent application of any external magnetic field, and discuss implications of these findings.

4:00 PM EL08.03.02

Thermal Imaging through Hot Emissive Windows [Ciril Samuel Prasad](#)¹, Henry O. Everitt² and Guru V. Naik¹; ¹Rice University, United States; ²DEVCOM Army Research Laboratory - South, United States

The challenging problem of enhancing thermal emission in some directions while suppressing it in others is exacerbated for hot windows because they must remain transparent in the same spectral window. This complex problem has prevented applications such as infrared imaging through hot windows, whose own thermal emission is strong enough to blind the camera [1]. Here, we demonstrate a solution to this long-standing challenge by replacing the hot emissive window with one coated with an asymmetrically emitting thermal metasurface. By engineering the imaginary index of refraction to produce an asymmetric spatial distribution of absorption losses in its constituent nanoscale resonators, the metasurface suppresses thermal emission towards the camera while being sufficiently transparent for thermal imaging.

We create the constituent resonators of the asymmetric loss metasurface by coupling nanoscale Si discs with distinct losses [2, 3, 4]. These silicon nanodiscs separated by SiO_2 spacer support a quasi-bound state in the continuum (q-BIC) mode. These photonic modes couple to each other under normally incident input excitation with coupling strength that can be tuned by varying the spacer thickness. We identify that, when the resonators are weakly coupled, the eigenmodes of the system are distributed asymmetrically across the resonators with a large fraction of photon energy confined in the lossless resonator and hence causes strong asymmetry in the far-field thermal radiation from the metasurface [4].

The asymmetry in energy confinement also causes the resonance dip in the transmission spectra to be narrow and as a result, enhances the overall transmission in the spectral bandwidth of the thermal camera. Thus our metasurface design, inspired by non-Hermitian optics, balances the need for good transmittance and emissivity asymmetry required to achieve thermal imaging through an emissive hot window. Our metasurface window, operating at 873 K, enhanced the thermal imaging contrast by nearly 2 times when compared to a conventional window at the same temperature. This demonstration

illustrates the power of using the imaginary index as a design parameter for nanophotonic thermal devices, thereby enabling novel functionalities for energy, imaging, and sensing applications.

Reference

1. L. Lorah, E. Rubin, *The Infrared Handbook*, WL Wolfe and GJ Zissis, eds., Office of Naval Research, Washington, DC (1978).
2. Chloe F Doiron and Gururaj V Naik. Non-hermitian selective thermal emitters using metal–semiconductor hybrid resonators. *Advanced Materials*, 31(44):1904154, 2019.
3. Frank Yang, Ciril S Prasad, Weijian Li, Rosemary Lach, Henry O Everitt, and Gururaj V Naik. Non-hermitian meta-surface with non-trivial topology. *Nanophotonics*, 11(6):1159–1165, 2022.
4. Frank Yang, Alexander Hwang, Chloe Doiron, and Gururaj V. Naik. Non-Hermitian metasurfaces for the best of plasmonics and dielectrics. *Opt. Mater. Express*, OME, 11(7):2326–2334, Jul 2021.

4:15 PM EL08.03.03

Far- and Near-Field Heat Transfer in Transdimensional Plasmonic Film Systems Svend-Age Biehs¹ and Igor Bondarev²; ¹University of Oldenburg, Germany; ²North Carolina Central University, United States

Radiative heat transfer in transdimensional plasmonic film systems is analyzed using the confinement-induced nonlocal electromagnetic response model built on the Keldysh-Rytova electron interaction potential [1]. Results are compared to the local Drude model routinely used in plasmonics. The former predicts greater Woltersdorff length in the far-field and larger film thickness at which heat transfer is dominated by surface plasmons in the near-field, than the latter. Analysis performed suggests that the theoretical treatment and experimental data interpretation for thin and ultrathin metallic film systems must incorporate the confinement-induced nonlocal effect to provide reliable results in radiative heat transfer studies. The fact that the enhanced far- and near-field radiative heat transfer occurs for much thicker films than the standard Drude model predicts is crucial for thermal management applications and in general for the development of new quantum photonics materials based on ultrathin metallic films and metasurfaces of controlled thickness. The latest experiments to confirm this fact will also be reported [2].

References:

- [1] S.-A. Biehs and I.V. Bondarev, *Adv. Optical Mater.* 11, 2202712 (2023).
- [2] H. Salihoglu, et al., *Phys. Rev. Lett.* 131, 086901 (2023).

4:30 PM *EL08.03.04

3D Meta-Optics for Sorting Light and Image Processing Andrei Faraon; California Institute of Technology, United States

35 words abstract: Structuring optical properties with a spatial resolution much smaller than the relevant wavelength of light leads to optical structures with non-intuitive optical response. I discuss our recent progress in designing and fabricating these structures.

Modern imaging systems can be enhanced in efficiency, compactness, and range of applications through introduction of multilayer nanopatterned structures for manipulation of light based on its fundamental properties. I discuss several recent implementations of this type of devices for sorting light based on wavelength, polarization and spatial modes. Then I present devices for optical image processing like edge detection with enhanced optical bandwidth. Implementations at mid infrared and shorter wavelengths is discussed.

References

- [1] Roberts, G.; Ballew, C.; Zheng, T.; Garcia, J.C.; Camayd-Muñoz, S.; Hon, P W C; Faraon, A; 3D-Patterned Inverse-Designed Mid-Infrared Metaoptics , *Nature Communications* volume 14, Article number: 2768 (2023) <https://www.nature.com/articles/s41467-023-38258-2>
- [2] Ballew, C; Roberts, G; Faraon, A; Multi-dimensional wavefront sensing using volumetric meta-optics , (2023), *Optics Express*, Vol. 31, Issue 18, pp. 658-669 (2023), [<https://doi.org/10.1364/OE.492440>],
- [3] Camayd-Muñoz, R; Ballew, C; Roberts, G; Faraon, A; Multi-functional volumetric meta-optics for color and polarization image sensors, *Optica*, Vol. 7, Issue 4, pp. 280-283 (2020), [<https://doi.org/10.1364/OPTICA.384228>],.

SESSION EL08.04: Advanced Tunable Nanophotonics and Quantum Emission Control

Session Chairs: Harry Atwater and Min Seok Jang

Tuesday Morning, April 23, 2024

Room 340/341, Level 3, Summit

10:30 AM *EL08.04.01

Path Towards Large Space Bandwidth Product Spatial Light Modulator Arka Majumdar; University of Washington, Seattle, United States

Shaping an optical wavefront with sub-wavelength spatial resolution is important for various applications with far-reaching scientific and technological impacts (e.g., in adaptive optics and imaging through turbid, disordered media) and commercial interest (e.g., LIDAR for autonomous transportation and pixelated holography). The primary enabling technology for such capability is a compact optical phase shifter, which can change the phase of the incident light by a full 360 degree with low energy and high frequency (~MHz). Existing tunable optical technologies cannot provide this functionality; mechanically tunable modulators can reach a speed of only a few kHz, while liquid-crystal based modulators operate at 100's of Hz. The pixel size of the spatial light modulator is also on the order of tens of wavelengths, which increases the energy consumption per pixel.

In this talk, I will discuss our effort to tune meta-optics using non-volatile phase-change materials. Additionally, I will talk about varifocal meta-lens using micro-mechanical actuators. Apart from physical tuning, we can also implement varifocal functionality using computational techniques. Finally, I will discuss the issues of scalability of meta-optics based spatial-light modulation, and how we can use static meta-optics to effectively scale the number of tunable pixels in a spatial light modulator.

11:00 AM EL08.04.02

Enhanced Quantum Properties of Single Photon Emitters in Hexagonal Boron Nitride Flakes Using Plasmonic Nanocavities Abdelghani Laraoui¹,

Mohammadjavad Dowran¹, Ufuk Kilic¹, Suvechhya Lamichhane¹, Adam Erickson¹, Sy-Hwang Liou¹ and Christos Argyropoulos²; ¹University of Nebraska-Lincoln, United States; ²The Pennsylvania State University, United States

Recently, single-photon emitters (SPEs) in solid-state materials have drawn a huge interest for different usages in quantum sensing and quantum nanophotonics [1]. Significant developments led to the finding of a variety of atom-like SPEs in low-dimensional and two-dimensional (2D) materials, such as hexagonal boron nitride (hBN), which exhibit favorable quantum properties at room temperature, making them highly desirable element for integrated quantum photonic circuits [2]. One major challenge of using these SPE host 2D materials in such applications is their low quantum efficiency with a fluorescence emission rate way below 0.5 Mc s^{-1} .

In this work, we use composite nanophotonic structures based on gap plasmonic modes, integrated with hBN multilayered flakes, to achieve a speedup and enhancement in the quantum interaction processes at room temperature. We first created a high density ($> 0.5 \text{ SPE}/1 \mu\text{m}^2$) of stable SPE in thin (thickness $\leq 35 \text{ nm}$) hBN flakes deposited on a Si/SiO₂ substrate by using a high-temperature (1100 °C) annealing method under O₂ flow. We then transferred the annealed hBN flakes with SPEs to epitaxial gold (Au) film (thickness $\sim 100 \text{ nm}$), grown on Si substrate, and characterized their quantum properties using a home-built confocal fluorescence microscope [3]. We demonstrated a plasmonic enhancement of SPE properties from the nanograins (size 50- 65 nm), found in the Au film, manifested by a decrease of quantum emitter lifetime by one order of magnitude and an increase of the emitter fluorescence by $\sim 392\%$ [4].

To enhance further the quantum properties of SPEs on a selected thin hBN flake we spin coated commercial silver nanocubes (SNCs) with size of 100 nm on the annealed Au/Si substrate. We optimized the spin coating parameters to increase the chance of getting the SNCs coupled spatially with the SPEs [3]. We observed plasmon nanocavity enhancement of SPE properties near the SNCs on top of the hBN flake manifested by a decrease of emitter lifetime by 100%, and a fluorescence enhancement of 200% [4]. The overall saturation counts is $> 2 \text{ Mc/s}$ for some of the SPEs in the plasmonic (metallic) Au/hBN/SNC nanocavities in comparison to $\sim 0.25 \text{ Mc/s}$ for SPEs in just hBN flakes deposited on SiO₂/Si substrates. The presented two order of magnitude enhancement of SPE quantum properties at room temperature is further investigated by using COMSOL numerical simulations. The hBN flakes are integrated into the fabricated nanophotonic cavities that are characterized by an optical frequency resonance response where light-matter interaction is particularly enhanced [4]. [1] M. Atattire et al., Nat Rev Mater 3, 38–51 (2018). [2] J. D. Caldwell, et al., Nat. Rev. Mat. 4, 552-567 (2019). [3] M. Dowran, et al., Adv. Opt. Mat. 11 (16), 2370062 (2023). [4] M. Dowran et al., under preparation.

Acknowledgement: This material is based upon work supported by the NSF/EPSCoR RII Track-1: Emergent Quantum Materials and Technologies (EQUATE), Award OIA-2044049. The research was performed in part in the Nebraska Nanoscale Facility: National Nanotechnology Coordinated Infrastructure and the Nebraska Center for Materials and Nanoscience (and/or NERCF), which are supported by NSF under Award ECCS: 2025298, and the Nebraska Research Initiative. Christos Argyropoulos acknowledges partial support from NSF Award DMR: 2224456.

11:15 AM EL08.04.03

Zero Diffraction: A Novel Approach for High-Contrast Switching of Light Patrick Goern, Andreas Henkel, Sven O. Schumacher, Christopher Knoth and Maximilian Buchmueller; University of Wuppertal, Germany

The ultrafast electro-optic Pockels effect is widely used for modulating light in terms of its intensity, phase, and polarization, because controlling these parameters is the basis of modern information and communication technology. However, other applications, including displays, scanners, or solar concentrators, also require the control of geometric parameters of light, such as its pathway in space. Until today, the efficient spatial control of light remains challenging.

The common approach for achieving spatial control involves modifying optical components. These modifications often rely on the mechanical movement of lenses, mirrors or gratings, which is much slower compared to modulations based on the Pockels effect. Recent reports propose novel approaches based on interference. [1] In these cases, the optical components remain mostly unchanged, but their interaction with light strongly depends on the light's properties like phase or momentum leading to a limited set of operation parameters.

Here, we propose a novel approach for controlling the diffraction of light at a leaky waveguide grating using the ultra-fast Pockels effect. The leaky waveguide grating is illuminated by two symmetrical incident plane waves. By tuning the relative phase between the two waves, the diffraction can be entirely suppressed, termed *zero diffraction*. [2] Therefore, this phenomenon enables to control the diffraction of light with infinite contrast. Remarkably, it not only occurs at singular spectral positions but on continuous curves in the energy–momentum space.

In analogy to our recent report, we first investigate a standalone grating and a symmetric waveguide grating under symmetric dual-plane wave incidence. Simulations using rigorous coupled wave analysis (RCWA) show that the diffraction efficiency can be controlled with an average contrast below 100. Zero diffraction cannot be found in either of these cases.

In the next step, we introduce leakiness and find zero diffraction for plane waves. We demonstrate the experimental feasibility of these theoretical findings using real laser beams instead of plane waves. For that purpose, a symmetric waveguide grating is placed between two lithium tantalate (LiTaO₃) wafers of opposite crystal direction. The high refractive index of the LiTaO₃ introduces leakiness, while the opposite crystal direction maximizes the relative phase shift when applying an electric field across the entire waveguide stack. After creating symmetrically propagating beams, we measure the optical power diffracted at the waveguide grating as a function of the applied field strength and find a maximum contrast of 1236.

This way, we also show how zero diffraction can be applied in a nonlinear waveguide in order to control trapping and detraping of light. The position where a directed laser beam is detrapped from the surface can be selected with an electric field without any mechanics. Laser displays based on zero diffraction would be more efficient than liquid crystal displays as are not based on absorption. Instead, they extract the light only where it is needed. At the same time, such laser displays could be completely transparent and promise immense possibilities in terms of color rendering due to the narrow spectrum of the laser.

[1] M. Meudt, A. Henkel, M. Buchmüller, and P. Görrn, *Optics*, **2022**

[2] A. Henkel, S.O. Schumacher, M. Meudt, C. Knoth, M. Buchmüller, and P. Görrn, *Adv. Phot. Res.*, **2023**

11:30 AM EL08.04.04

Metamaterial-Controlled Parity-Time Symmetry in Non-Hermitian Wireless Power Transfer Systems Hanwei Wang, Xiaodong Ye and Yang Zhao; University of Illinois at Urbana-Champaign, United States

Wireless power transfer (WPT) technologies contain two main categories, radiative and non-radiative. Non-radiative WPT utilizes the magnetic near-field to carry energy and is more commonly used due to its advantages of high-power volume and safety. The receiving (Rx) resonator couples with the transmitting (Tx) resonator through magnetic mutual induction. Inductive WPT systems can be described as non-Hermitian systems through coupled-mode theory. Power transfer in such systems is efficient when forming PT-symmetric states, which could be guaranteed by the physical symmetry in a strong

coupling regime. However, spontaneous symmetry breaking happens in the weak coupling regime as the increasing of the Tx-Rx separation, where the resonant states become anti-PT-symmetric.

Relay resonators can be used to increase the overall coupling and, therefore, increase the maximum Tx-Rx separation for the PT-symmetric state. The PT-symmetric states in such systems are also known as the topological edge state for magneto-inductive waves, which have been used for mid-range WPT and frequency-robust WPT. However, one drawback of the relay resonators is the potential involvement of higher order resonant states of the system; many of the states are anti-PT symmetric. To avoid these states, spatial arrangement of the relay resonators needs to be symmetric and the geometry of the Tx and Rx resonators need to be identical. Such requirements are impractical in many applications, such as free-positioning WPT.

Metamaterials, demonstrating excellent ability in manipulating electromagnetic and acoustic fields and waves, show great potential in solving this challenge. Researchers have developed metamaterials to control the PT-symmetry for above-unity transmission and reflection, nanoscale sensing, and coherent perfect absorption. However, such an approach remains challenging for WPT systems due to the lack of accurate control in the metamaterial's resonance mode. In our previous works, we have demonstrated a quasi-Hermitian metamaterial that can achieve on-demand field-shaping for magnetic resonance imaging and WPT. In this conference presentation, we will extend the theory by showing metamaterial-controlled PT-symmetry in a non-Hermitian WPT system.

We derive the states of the system and show that a PT-symmetric state can be achieved with certain metamaterial's configuration. The sizes of the Tx and Rx do not need to be identical, and their physical positions are not limited as long as operating in the strong coupling regime. We prove that the state is stable when the system operates in a strong coupling regime. We theoretically and experimentally demonstrate the transition between anti-PT-symmetric and PT-symmetric states controlled by the metamaterial's configuration. We further show that the PT-symmetric state can be achieved with different spatial arrangements of the Rx resonator. This technique largely increases physical freedom of Tx and Rx and provides a paradigm for designing many-body WPT systems.

11:45 AM EL08.04.05

Ultrafast Collapse of Molecular Polaritons to Pure Molecular Transition in Plasmonic Photoswitch-Nanoantennas Joel Kuttruff¹, Marco Romanelli², Esteban Pedrueza-Villalmanzo³, Jonas Allerbeck⁴, Jacopo Fregoni⁵, Valeria Saavedra-Becerril⁶, Joakim Andréasson⁶, Daniele Brida⁷, Alexandre Dmitriev³, Stefano Corni² and Nicolò Maccaferri^{8,7}; ¹Universität Konstanz, Germany; ²Università degli Studi di Padova, Italy; ³University of Gothenburg, Sweden; ⁴Empa-Swiss Federal Laboratories for Materials Science and Technology, Switzerland; ⁵Universidad Autónoma de Madrid, Spain; ⁶Chalmers University of Technology, Sweden; ⁷University of Luxembourg, Luxembourg; ⁸Umeå University, Sweden

Molecular polaritons are hybrid light-matter states that emerge when a molecular transition strongly interacts with photons in a resonator. At optical frequencies, this interaction unlocks a way to explore and control new chemical phenomena at the nanoscale. Achieving such control at ultrafast timescales, however, is an outstanding challenge, as it requires a deep understanding of the dynamics of the collectively coupled molecular excitation and the light modes. Here, we investigate the dynamics of collective polariton states, realized by coupling molecular photoswitches to optically anisotropic plasmonic nanoantennas. Pump-probe experiments reveal an ultrafast collapse of polaritons to pure molecular transition triggered by femtosecond-pulse excitation. Through a synergistic combination of experiments and quantum mechanical modelling, we show that the response of the system is governed by intramolecular dynamics, occurring one order of magnitude faster with respect to the uncoupled excited molecule relaxation to the ground state. Our results provide exciting foundation for the further exploration of the synthesis and characterization of strongly coupled photoswitch systems, towards a full control of ultrafast chemical processes at the nanoscale.

SESSION EL08.05: Low Dimensional Metasurfaces and Metamaterials

Session Chairs: Ho Wai (Howard) Lee and Jason Valentine

Tuesday Afternoon, April 23, 2024

Room 340/341, Level 3, Summit

1:30 PM EL08.05.01

Active Excitonic 2D Metasurfaces Using Exciton Polaritons in Monolayer TMDs Thomas Bauer and Jorik Van de Groep; University of Amsterdam, Netherlands

Monolayer transition metal dichalcogenides (TMDs) like WS₂ exhibit strong exciton resonances in the visible spectral range that govern their optical response. The excitonic light-matter interaction in these 2D quantum materials is inherently strong and highly tunable, which can be leveraged to realize mutable flat optical elements as well as novel spin-valley coupled information carriers. To unleash the full potential of exciton-enhanced wavefront shaping and active optical switching in atomically thin metasurfaces, it is essential to gain a detailed understanding of the exciton's quantum mechanical properties and its coupling to hybrid light-matter quasiparticles known as exciton polaritons.

Recently, it was shown theoretically that exciton polaritons can exist as excitations from the continuum of three-dimensional electromagnetic modes even for atomically thin layers of materials. Coupling to such 2D exciton polaritons (2DEPs) was subsequently demonstrated experimentally in a free-standing monolayer membrane via photoluminescence excitation and outcoupling through a photonic crystal. Realizing such a strongly coupled light-matter state in on-chip photonic environments promises new opportunities for tunable wavefront shaping, photonic sensing, as well as probing of fundamental quantum-mechanical properties of light scattering by excitons.

However, direct integration of coherently coupled 2DEP functionality into nanopatterned monolayers on substrates has so far remained elusive due to the stringent requirements on the dielectric environment as well as monolayer quality to support 2DEPs.

Here, we experimentally demonstrate active control of coherent coupling to 2DEPs in a monolayer of WS₂ on a quartz substrate, allowing for enhanced photonic functionality given directly by the geometry of the monolayer itself. We accomplish guiding along the monolayer by managing the refractive index contrast between the top and bottom side via a 230nm thick capping layer of PMMA. Using guided mode resonances in sub-wavelength gratings structured in mm-sized continuous WS₂ monolayers, we realize polarization-selective dynamic phase control of light scattered coherently off the hybrid light-matter state. The sub-wavelength nature of the grating together with the high quality and homogeneity of the initial monolayer leads to an electrically and/or thermally tunable phase modulation of the reflected light when exciting close to the 2DEP guided mode resonance.

Further utilization of photonic metasurface concepts allows for active amplitude switching of higher diffraction orders via binary blazed gratings, leading to

expected modulation depths exceeding 80% stemming from an atomically thin optical element. This opens a path to full active control over the complex optical response in tailored atomically thin metasurfaces via exciton resonance tuning.

1:45 PM EL08.05.02

Asymmetric Propagation of Hyperbolic Polaritons in MoO₃ and β -Ga₂O₃ Heterostructures Saurabh Dixit¹, Maximilian Obst², José Á. Cuervo³, Giulia Carini⁴, Ryan Kowalski¹, Aitana T. Martín-Luengo³, Gonzalo Alvarez Perez³, Katja Diaz-Granados Santos¹, Aditha Senarath¹, Niclas Müller⁴, J. Michael Klopff⁵, Lukas Eng², Susanne Kehr², Thomas G. Folland⁶, Pablo Alonso Gonzalez³, Alex Paarmann⁴ and Joshua D. Caldwell¹; ¹Vanderbilt University, United States; ²Technische Universität Dresden, Germany; ³University of Oviedo, Spain; ⁴Max Planck Society, Germany; ⁵Helmholtz-Zentrum Dresden-Rossendorf, Germany; ⁶The University of Iowa, United States

Opposite signs of the dielectric permittivity along different principal directions of optical materials (hyperbolic anisotropy) allow for exotic quasiparticles to be formed due to the hybridization of photons and phonons (phonon polariton) in the mid-infrared spectral region. Phonon-polaritons in such hyperbolic materials enable the confinement of electromagnetic waves at the nanoscale, which offers mechanisms to induce large enhancements of the optical response and reduce the footprint of photonic devices such as molecule sensors, polarizers, waveplates, optical modulators, IR sources and detectors, and many others. To design nanophotonic devices, it is necessary to engineer the characteristic features of phonon polaritons, like propagation direction and distances. It has been demonstrated that characteristic features of hyperbolic phonon polaritons can be engineered via the choice of crystal symmetry. Hyperbolic polaritons in crystals with varying symmetries from hexagonal, such as boron nitride (h-BN), exhibit isotropic propagation in plane, whereas reducing to orthorhombic structures like MoO₃ and V₂O₅, results in directional propagation. Monoclinic systems, such as β -Ga₂O₃ or CdWO₄, with further reduced symmetry exhibit exotic phenomena in the form of shear, whereby the polariton wavelength and direction of propagation disperse with changing frequency. This provides an additional degree of freedom to manipulate polariton propagation. By employing twisted low symmetry structures, such as twisted slabs of MoO₃, highly directional propagation with minimal divergence can be observed (canalization) at specific 'magic' angles. Yet, it remains unclear if such canalization can be observed in twisted structures of different Bravais lattices. Here, we investigate heterostructures of MoO₃ orthorhombic and Ga₂O₃ (monoclinic) to determine the role of twisting with non-degenerate polariton resonances, as well as the potential influence of shear. By investigating a series of MoO₃ slabs twisted with respect to the a-axis of β -Ga₂O₃ we observed the change in the direction of propagation along with asymmetric dispersion via a scattering-type SNOM coupled to a free-electron laser. It is determined that the high asymmetry in the propagation in the twisted structure is driven principally by the twist angle, rather than the inherent shear in the underlying β -Ga₂O₃, indicating that the propagation direction can be dictated via twist angle, making such heterostructure platforms designable for future nanophotonic devices such as sensors, chiral sources, IR imaging components, and many others.

2:00 PM EL08.05.03

Polariton Design and Modulation via Van der Waals / Doped Semiconductor Heterostructures Mingze He¹, Joseph R. Matson¹, Mingyu Yu², Angela Cleri², Sai Sunku³, Eli Janzen⁴, Stefan Mastel⁵, Thomas G. Folland⁶, James Edgar⁴, D. Basov³, Jon-Paul Maria², Stephanie Law² and Joshua D. Caldwell¹; ¹Vanderbilt University, United States; ²The Pennsylvania State University, United States; ³Columbia University, United States; ⁴Kansas State University, United States; ⁵Autocube, Germany; ⁶The University of Iowa, United States

Due to the long free-space wavelength of mid- to far-infrared (IR) light, the realization of deeply subdiffractional photon confinement via the stimulation of polaritons is critical for IR nanophotonic applications, such as miniaturized optical components, on-chip photonics, polariton waveguides, and nanolasers. Specifically, hyperbolic polaritons supported in extremely anisotropic media, i.e., those featuring permittivity tensor components with opposite signs along different optical axes, can offer significant promise for many nanophotonic applications where stronger confinement and improved control over propagation are beneficial. Applications of these properties include hyperlensing, metasurface-based optical components, quantum optics, and probes of nanoscale defects. While hyperbolicity was first demonstrated with artificial dielectric/metal stacks, it was later discovered that a list of natural materials, including hexagonal boron nitride (hBN), MoO₃, V₂O₅, support hyperbolic phonon polaritons (HPhPs). Such HPhPs in natural crystals feature exceptionally low optical losses, as the polaritons are derived from optic phonons instead of scattering from free carriers. Compared to surface polaritons, HPhPs offer further confinement of long-wavelength light to deeply subdiffractional scales. Furthermore, the evanescent field of volume propagation could interact with the local environment, e.g., substrate, allowing for tuning of wavevectors without modifying the hyperbolic media itself. Therefore, it is possible to realize polaritonic resonators and near-field polariton propagation without deleterious etching of hyperbolic materials. While it is promising to utilize the substrate-induced effect in engineering polaritonic devices, conventionally used noble metal and dielectric substrates restrict the tunability of this approach, leaving most of the wavevectors in the dispersion inaccessible. Here, we present our recent work on exploiting substrate induced HPhP tuning. We demonstrate that using doped semiconductors, e.g., InAs and CdO, can enable near-continuous tuning and access to both the maximum and minimum wavevectors (~8.3 times experimentally demonstrated). We further elucidate HPhP tuning with the plasma frequency of an InAs substrate, which features a significant wavevector discontinuity and modal order transition when the substrate permittivity crosses -1 in the Reststrahlen band. Around the transition point, the HPhP system is sensitive to perturbations, e.g., the working frequency, InAs plasma frequency and superstrate, thus it is suitable for sensing and modulation applications. Although the loss of HPhPs peaks around the transition point, where the largest tunability is observed, we highlight that the increased loss can be neglected in some proposed applications/devices. We also illustrate that the hBN/InAs platform allows for active modulation at picosecond timescales by photo-injecting carriers into the InAs substrate, demonstrating a dynamic wavevector change of ~20%. Overall, the demonstrated hBN/doped semiconductor platform offers significant improvements towards manipulating HPhPs, and enormous potential for engineered and modulated polaritonic systems for applications in on-chip photonics and planar metasurface optics.

2:15 PM *EL08.06.02

Strong Field Enhancement Based on Manipulation of Anapole State in Dielectric Metasurface Wen-Hui (Sophia) Cheng and Meng-Hsueh Tsai; National Cheng Kung University, Taiwan

Resonant metamaterials and metasurfaces cause by light-matter interaction in sub wavelength structures have been a hot research topic recently due to its potential in progressing the conventional devices. Anapole, a new hybrid mode is formed by overlapping toroidal dipole (TD) and electric dipole (ED) mode. Since the far field radiations of TD and ED are antiphase, destructive interference between them will turn this hybrid mode into a dark mode with strong near field. In addition, the electric field can be further enhanced by incorporating the slot effect, which happens to fulfill the continuity of electric displacement field at interfaces of low-refractive-index and high-refractive-index material. In this work, we propose a dielectric metasurface which can support anapole mode and introduce slot effect to manipulate field enhancement. The structure is composed of a concentric circle and ring, with a middle bar connecting them. We find the middle bar and gap are critical and give rise to the tunability. From the multipole decomposition, a combination of TD and ED with same amplitude can be corresponded to the anapole mode. It shows that the middle bar creates a path for displacement current passing through it, supporting the nonradiative mode with high quality factor. The strong near field enhancement and high Q demonstrated is believed to be useful for many applications including PL control and nonlinear effect.

Keywords: Anapole, Slot effect, Metasurface, Dielectric, Field enhancement

2:45 PM EL08.05.05

Weak Coupling of WSe₂ to Plasmonic Surface Lattice Resonance [Stanislav Tsoi](#), Marc Christophersen, Joseph A. Christodoulides, Hsun Jen J. Chuang, Paul D. Cunningham, Adam D. Dunkelberger, Kathleen M. McCreary, Nicholas Proscia and Igor Vurgaftman; U.S. Naval Research Laboratory, United States

Weak coupling of light emitters to optical cavities facilitates efficient photon extraction by directing their emission into cavity modes instead of random directions in free space. Monolayer transition metal dichalcogenides (TMDs) are 2D semiconductors with the direct band gap attractive for future nanoscale optoelectronics. The present experimental work investigates weak coupling of monolayer WSe₂ to a metasurface cavity, consisting of a lattice of plasmonic nanodisks and supporting surface lattice resonances (SLRs) propagating in its plane. The nanodisks were fabricated from aluminum and WSe₂ mechanically transferred on top of the cavity. Angle-resolved photoluminescence (PL) measurements show efficient light emission by WSe₂ into the SLRs. The most efficient emission appears to take place into spectrally narrow modes resulting from interference of two counter-propagating SLRs, a previously unreported behavior in metasurface cavities. The obtained results suggest the opportunity to control the interference modes via geometrical factors of the lattice and thus tune the strength of its coupling to emitters, including the possibility of strong coupling.

3:00 PM BREAK

SESSION EL08.06: Nanophotonics and Plasmonics
Session Chairs: Yao-Wei Huang and Arka Majumdar
Tuesday Afternoon, April 23, 2024
Room 340/341, Level 3, Summit

3:30 PM EL08.06.01

Plasmon Enhanced Light Emission in Metal Halide Perovskite Nanowires [Tintu Kuriakose](#)¹, Qingyu Wang¹, Hao Sha², Shengfu Yang² and Robert A Taylor¹; ¹University of Oxford, United Kingdom; ²University of Leicester, United Kingdom

Photonic nanowires based on semiconductor materials have potential applications in light generation, propagation, detection, and amplification at the nanoscale and play a key role in the development of integrated photonic/electronic devices. To achieve the best optical performance for these applications it is crucial to enhance the photon conversion efficiency of the nanowires. A promising way to enhance light emission from nanowires is to combine semiconductors with noble metals. The strong confinement of electromagnetic field resulting from plasmonic structures can effectively transfer surface plasmon resonance energy to semiconductors via excited electrons and thus effectively enhance the photoluminescence (PL) yield. However, the synthesis of hybrid metal-semiconductor nanowires having desirable optical properties has proven challenging due to the non-wetting between the two types of materials.

Here we report plasmon-enhanced light emission from a hybrid nanowire consisting of noble metal and semiconductor materials. The demonstration is performed in a cesium lead halide perovskite-based four-layer structure (CsPbBr₃/PMMA/Ag/Si) designed to limit plasmonic losses in the metal while exhibiting efficient surface plasmon-photon coupling at moderate power. We used solution processing to make the nanowires, which were then spin-coated onto a Si substrate coated with Ag nanoparticles. These were produced by using quantized vortices in superfluid helium, which circumvents the non-wetting between the two types of materials. We employ temperature-dependent micro-photoluminescence spectroscopy (from 4 K to 300 K), to study the optical properties of the nanowires. We excite the individual nanowires by considering several configurations with Ag nanoparticle diameters ranging from 7 to 10 nm and PMMA layer thicknesses ranging from 5 to 25 nm to better understand the optical performance. The study, conducted with 100 fs laser pulses at a repetition rate of 76 MHz and at an excitation wavelength of 400 nm reveals that a 5 nm thick PMMA layer and 7.5 nm sized Ag nanoparticles enhanced the PL intensity by approx. 40% compared to pure semiconductor structures at 4 K. In addition, we investigate the emission dynamics of carriers and excitons in the nanowires using time-resolved photoluminescence spectroscopy techniques. Observation shows enhanced carrier recombination dynamics due to plasmonic interactions with the perovskite. These results show a potential way to excite hybrid nanowires at sufficiently low photon density so that single photon excitation/emission could be possible from these structures. Moreover, this fundamental demonstration confirms a proof-of-concept for further work involving plasmon-enhanced light emission from core-shell metal/semiconductor nanowires and opens the door for realizing lead halide perovskite-based micro and nanolasers in the visible range and more broadly for developing on-chip nanophotonic devices.

3:45 PM *EL08.05.04

Functional Materials for Next Generation Photonic Chips [Volker J. Sorger](#), Nicola Peserico, Russell Schwartz, Hao Wang, Chandraman Patil and Hamed Dalir; University of Florida, United States

Emerging and functional materials are critical for next-generation optoelectronic device performance, energy efficiency, and application capabilities. In this presentation we share recent developments on efficient, fast, and compact electro-optic modulators, as well as sensitive photodetectors with high gain bandwidth products, as part of advanced integrated photonic circuits. The second part of the presentation then shows how these emerging device-level technologies enable performance gains for photonic-electronic heterogeneous integrated AI chiplets to accelerate machine learning applications such as matrix-matrix multiplications and convolution operations.

4:15 PM EL08.06.03

Disordered Meta-Doublets for Unidirectional and Synergistic Imaging in The Mid-Infrared [Romil Audhkhasi](#), Maksym Zhelyeznyakov, Anna Wirth-Singh and Arka Majumdar; University of Washington, United States

Recent advances in metamaterials have enabled the realization of complex optical functionalities within a compact form factor. The vast number of design degrees of freedom in such systems provides the ability to manipulate optical waves in the spatial and spectral domain, thereby enabling the development of photonic devices for a broad range of applications. Here, we propose an all-silicon metamaterial platform for advanced imaging applications in the mid-infrared wavelength range. Specifically, we design large aperture, all-silicon meta-optic doublets for unidirectional and synergistic imaging at a wavelength of 4 μm . The large design space afforded by metamaterials often makes it challenging to optimize such devices for a desired functionality using a conventional forward design approach. Here we develop a differentiable model that maps the structure of our meta-atoms to their optical response. Our algorithm uses this model iteratively to modify the structural parameters of our devices and optimize a figure of merit that mathematically describes the desired optical response. The phase profiles of our optimized devices possess a large degree of disorder that is tailored to realize the required imaging functionality. When illuminated by a plane wave in the forward mode, our unidirectional imager generates an intense spot on its optic axis at a predefined

focal length. In the reverse mode, the imaging performance is significantly reduced, accompanied by a dramatic reduction in light intensity on the focal plane. On the other hand, our synergistic imager is optimized to enable imaging only when the constituent meta-optics are used in conjunction with each other. We envision our devices to provide new avenues for the development of metamaterial imaging platforms for applications in defense and data security.

4:30 PM *EL08.06.04

Electrolyte-Gating for Metasurfaces and Large-Area Fabrication Vivian Ferry; University of Minnesota, United States

Alternative materials for metasurfaces enable new properties and lay the foundation for advantage applications. This talk will discuss two strategies for new, tunable metasurfaces. The first part of the talk will discuss the use of electrolyte gating to control the optical properties of materials, focusing on $\text{La}_{1-x}\text{Sr}_x\text{CoO}_{3-d}$ (LSCO) as an exemplary case. We fabricate electric double layer transistors using LSCO and an ion gel, and under application of positive gate voltage gating facilitates the formation and migration of oxygen vacancies, and a transition from a perovskite phase to an oxygen-vacancy-ordered brownmillerite phase. This is accompanied by substantial change in optical properties, as measured with spectroscopic ellipsometry. The talk will discuss how LSCO can be incorporated with metasurfaces to produce tunable optical response. The second part of the talk will discuss a new strategy for fabricating large-area metasurfaces, using roll-to-roll compatible additive manufacturing methods. This method, which uses solution-based inks to create the metasurfaces, can pattern a variety of materials, including metals, dielectrics, and semiconductor nanocrystals, and also create multilayer structures.

SESSION EL08.07: Poster Session I

Session Chairs: Yao-Wei Huang and Ho Wai (Howard) Lee

Tuesday Afternoon, April 23, 2024

Flex Hall C, Level 2, Summit

5:00 PM EL08.07.01

Polarization-Multiplexed Metalens for Far-Field Super-Resolution Imaging Yaxi Liu, Bohan Zhang, Qiushuang Lian, Shuai Wang and Yuanmu Yang; Tsinghua University, China

Recent decades have seen an increasing interest in developing super-resolution imaging methods that allow overcoming the diffraction limit. Near-field imaging methods achieve super-resolution by collecting evanescent waves with high spatial frequency components, often having subwavelength working distances or requiring the sample to be placed near a specially structured hyperlens. On the other hand, far-field super-resolution microscopy imaging with fluorescent substances often requires staining the sample. For non-invasive far-field super-resolution imaging systems based on a super-oscillatory lens, the field-of-view is limited by the unwanted sidelobes and sidebands. The throughput efficiency of the super-oscillatory lens dramatically decreases with the reduced size of the main focal spot. Here, we propose a far-field non-invasive super-resolution imaging method based on polarization-multiplexed metalens. By designing and optimizing the polarization-multiplexed, multi-channel point spread functions of the metalens, the system can obtain multi-channel optical information in a single shot. As a result, we obtain a digitally synthesized point spread function with a center hot spot with a small full width at half maximum as well as suppressed sidelobes and sidebands. Such a compact, single-shot super-resolution imaging system could enable new applications in diverse areas ranging from remote sensing to microscopy over a wide field-of-view.

5:00 PM EL08.07.02

Hotspot at Dimer, Small Aggregate and 2D Nanoassembly by Near-Field Scanning Optical Spectroscopy Mohammad Kamal Hossain; King Fahd University of Petroleum & Minerals, Saudi Arabia

Nanoassembly of noble metal nanoparticles facilitates surface plasmon confinements, and such localizations can coalesce and percolate due to a small variation in local nanogeometry. However, realizing such confinement by conventional microscopic and spectroscopic techniques has been challenging until now. We report near-field optical confinement observed by an aperture near-field scanning optical microscopy (a-NSOM). Three typical constructs of gold nanoparticles, viz., archetype dimer, nanoassembly of a few nanoparticles, and long-range two-dimensional (2D) nanoassembly, were investigated. Surface-sensitive techniques such as near-field surface-enhanced Raman scattering (SERS) and near-field surface-enhanced two-photon-induced photoluminescence (TPI-PL) have been recorded using a-NSOM. Well-correlated optometry was confirmed amongst the SERS, TPI-PL, and shear-force topographies of the abovementioned constructs tapping simultaneously at the very same spot of interest.

Distinctive aggregates and 2D nanoassemblies of gold nanoparticles (~100 nm diameter) were fabricated by the "sandwich technique", wherein the droplet on a silane-treated treated cover-slip was sandwiched by another glass slide. Monomers, dimers and nano-assemblies of various sizes were confirmed by a field-emission scanning electron microscope. The specimens were spin-coated with Raman active dyes, Rhodamine 6G. A fs-Ti: sapphire laser ($\lambda=800\text{nm}$, $<100\text{fs}$, 80MHz) and He-Ne laser ($\lambda=632.8\text{nm}$) were coupled to the a-NSOM to carry out TPI-PL and SERS measurements. Au-coated tapered optical fiber was used to carry the excitations and act as an apertured probe (aperture ~ 50–100 nm) to scan the specimen. The emitted signals were collected by an objective lens and transferred to an avalanche photodiode (for single-channel detection) and/or to a polychromator-CCD (for multichannel detection). As expected, optical signals from SERS and TPI-PL were found to be confined and localized at the interstitials of dimers, whereas coalescence and hybridization of such nearby confinements for nanoassemblies were observed. For long-range 2D nano-assembly, optical confinements were more complex and homogeneously distributed apart from the edge effect in this context. Finite-difference time-domain (FDTD) simulations were carried out to validate the results obtained in this investigation. FDTD models were designed so that the geometries and parameters closely represent the constructs under investigation and the a-NSOM setup. Such a direct observation with high spatial resolution is required to comprehend the origin of the localized electromagnetic (EM) field at the "hotspot" and the EM amplification factor in surface-sensitive optical processes.

The author acknowledges the Interdisciplinary Research Center for Sustainable Energy Systems (IRC-SES), Research Institute, King Fahd University of Petroleum and Minerals (KFUPM), Dhahran 31261, Saudi Arabia (Grant # INRE2318).

5:00 PM EL08.07.03

Arrays of Split-Ring Resonator embedded in a Free-Standing Gold Membrane for Surface-Enhanced Infrared Absorption Biosensing Platform Chieh-Chun Chang^{1,2} and Yun-Chong Chang^{1,2}; ¹Academia Sinica, Taiwan; ²National Taiwan University, Taiwan

In this study, free standing gold (Au) membranes with embedded arrays of split-ring resonator (SRR) were fabricated using modified nanospherical-lens lithography. The diameter of the polystyrene nanosphere used is 2 nm. The SRR-shaped photoresist (PR) patterns were achieved by exposing ultraviolet light at a tilt angle while rotating the sample and subsequent PR development. A thin Au layer was evaporated onto the rotating sample at an oblique angle and the evaporated Au only covered the surface area, resulting the Au membranes with embedded SRR arrays. The Au membrane was released from the

substrate by dipping into the solvent and was recovered onto a stainless-steel plate with micron-sized holes. The Au membrane suspended within the micron-sized hole is the free-standing gold Au membrane with embedded SRR arrays. Surface plasmon resonance (SPR) of the fabricated SRR is in the mid-infrared, which was confirmed by the theoretical simulation. The structural parameters of the SRR were tuned so the SPR is within the molecular infrared signature region between 400 to 4000 cm^{-1} . 4-aminothiophenol (4-ATP) molecules were applied to the Au membrane and their absorption signal around 1490 and 1600 cm^{-1} , which are correspondent to the vibrational modes of C=C bond and NH_2 scissoring, are greatly enhanced. Therefore, the proposed gold membrane with embedded SRR array can be ideal platform for surface enhanced infrared absorption spectroscopy.

5:00 PM EL08.07.04

Infrared Magnetic Hyperbolic Metamaterials [Swati Parmar](#), Yayoi Takamura and J. Sebastian Gomez-Diaz; University of California, Davis, United States

Magneto-optic (MO) materials represent a fascinating realm where the manipulation of magnetic spins is intricately entwined with the control of light propagation.^{1,2} Our research delves into harnessing the potential of established MO effects—Faraday, Voigt, and Kerr effects—to steer, sense, manipulate, and process infrared light through ferromagnetic hyperbolic metamaterials (HMTM). The core of our innovation lies in the integration of ferromagnetic oxides with gold nanorods, creating broadband HMTM that exhibit epsilon-near-zero (ENZ) properties. Additionally, we leverage infrared surface plasmons supported at the interface between the HMTM and air to amplify MO effects, forging a synergistic relationship between magnetics and plasmonics. This magneto-plasmonic synergy not only opens avenues for developing compact nonreciprocal devices but also facilitates the creation of magnetic field-sensitive hyperbolic composite materials, enabling the precise manipulation of electromagnetic waves at the nanoscale. Our objective is to contribute to technologies at the intersection of magneto-optics and plasmonics.

In our fabrication process, nanocomposite films consist of vertically aligned gold (Au) nanopillars within ferromagnetic (La,Sr)MnO₃ (LSMO) oxide matrices, achieved through pulsed laser deposition. X-ray diffraction confirms the highly epitaxial nature of the (001)-oriented ferromagnetic LSMO film along, while X-ray reflectivity attests to the uniformity of electron density and high-quality surfaces and interfaces with a film thickness of approximately 30 nm. Detailed analysis through atomic force microscopy and scanning electron microscopy reveals the formation of Au nanopillars with diameter of around 45 nm within the LSMO matrix. X-ray photoelectron spectroscopy of the Au 4f and Mn 2p core levels highlights that the electronic structure of the nanocomposite displays a correlation between Fermi energy and electrical conductivity.

Notably, Fourier transform infrared (FTIR) microscopy uncovers a highly reflective band observed between approximately 12.2 μm and 8 μm optical phonon wavelengths. Ellipsometry microscopy further demonstrates the presence of double negative materials in our engineered nanocomposite. Further, we employed scanning near-field optical microscopy nano-FTIR, providing high-resolution insights with 10 nm spatial resolution. This technique not only enables chemical analysis but also characterizes local electromagnetic fields, offering a comprehensive understanding of the intricacies within our magneto-plasmonic nanocomposite.

References:

1. Jijie Huang, Han Wang, Zhimin Qi, Ping Lu, Di Zhang, Bruce Zhang, Zihao He, and Haiyan Wang, Multifunctional Metal–Oxide Nanocomposite Thin Film with Plasmonic Au Nanopillars Embedded in Magnetic La_{0.67}Sr_{0.33}MnO₃ Matrix, *Nano Letters* 2021 21 (2), 1032-1039.
2. Leigang Li, Liuyang Sun, Juan Sebastian Gomez-Diaz, Nicki L. Hogan, Ping Lu, Fauzia Khatkhatay, Wenrui Zhang, Jie Jian, Jijie Huang, Qing Su, Meng Fan, Clement Jacob, Jin Li, Xinghang Zhang, Quanxi Jia, Matthew Sheldon, Andrea Alù, Xiaoqin Li, and Haiyan Wang, Self-Assembled Epitaxial Au–Oxide Vertically Aligned Nanocomposites for Nanoscale Metamaterials *Nano Letters* 2016 16 (6), 3936-3943.

5:00 PM EL08.07.05

Laser-Based Facile Fabrication of Plasmonic Gold Nanostructures and Their Sensory Applications [Do-Hyun Kang](#), Nguyen H. Minh, Ga-Eun Han, Jae Sung Yoon, Kwanoh Kim and Yeong-Eun Yoo; Korea Institute of Machinery and Materials, Korea (the Republic of)

Plasmonic nanostructures presenting localized surface plasmon response (LSPR) have attracted great attention in diverse sensory applications. Susceptible change of LSPR peak wavelength to the environmental stimulus, such as molecular binding, has been exploited to detect rare biomolecules at extremely low concentrations. In addition to such biomolecule sensing, the LSPR peak change to the distance variation between individual plasmonic nanostructures has been used to equipment-free colorimetric sensing of mechanical strain. Various nanolithography techniques have been employed to craft plasmonic metal nanostructures to realize the above-mentioned sensor applications; however, there is still a need for a low-cost, simple, fast, and scalable fabrication method to achieve reliable and reproducible LSPR sensors. Herein, we introduce a laser scribing-based technique for rapid formation and patterning of plasmonic gold nanostructures. In our process, a high-power laser beam melts a thin gold film on glass or quartz substrates, and subsequent dewetting of the melted gold results in nano-island structures consisting of surface-bound gold nanoparticles with an average diameter of 42 nm. We have been successfully applied the plasmonic structures to the highly-sensitive and selective immunoassay of the SARS-CoV-2 nucleocapsid protein, enabling the diagnosis of recently prevalent infectious disease, COVID-19. On the other hand, we have also developed a technique to transfer the gold nanostructures from the hard quartz substrate to the soft and flexible elastomer tape, aiming to create convenient colorimetric strain sensors capable of detecting mechanical motions of human bodies or mechanical behaviors of building structures.

5:00 PM EL08.07.07

Molecular Reporter-Immobilized Ag-Au Shell-Satellite Nanoassemblies for a SERS-Based Galactose Sensor Eun Hae Heo and [Hyejin Chang](#); Kangwon National University, Korea (the Republic of)

Galactosemia is a genetic metabolic disorder caused by a deficiency of galactose-degrading enzymes, leading to the accumulation of galactose and its metabolites in the body. The early diagnosis of galactosemia is crucial, as it can lead to death if left untreated. In this study, we present a surface-enhanced Raman spectroscopy (SERS) sensor based on a capillary tube for the convenient and sensitive detection of galactose. To enhance the SERS signal, we introduced gold nanoparticles (Au NPs) onto the surface of silver nanoshells (Ag NSs) to create an Ag-Au shell-satellite nanoassemblies on the inner wall of a capillary. We then fabricated a Ag-Au shell-satellite structured SERS sensor using 4-mercaptophenylboronic acid (4-MPBA) as a Raman reporter molecule. The galactose detection method relied on the conversion of 4-MPBA to 4-mercaptophenol (4-MPhOH) due to the production of hydrogen peroxide (H_2O_2) resulting from the oxidation of galactose by enzyme (galactose oxidase, GOx). A new SERS band was observed, which can be attributed to the H_2O_2 produced during the reaction between galactose and GOx. Additionally, we observed an increase in the band intensity ratio between 418 cm^{-1} and 390 cm^{-1} (I_{390}/I_{418}) as a function of galactose concentration. This strategy for galactose SERS detection based on a capillary tube-based SERS biosensor demonstrates its potential as an early galactosemia diagnosis platform.

5:00 PM EL08.07.08

Enhanced Room-Temperature NIR Plasmonic Photodetection and Photoelectron Spectroscopy [Eslem N. Abubakr](#)^{1,2,3}, Masaaki Oshita¹, Shiro Saito³ and Tetsuo Kan¹; ¹The University of Electro-Communications, Japan; ²Aswan University, Egypt; ³IMRA Japan Co., LTD., Japan

The development of plasmonic photodetectors, especially in the near-infrared (NIR) region, has gained significant attention due to their non-destructive nature. It is essential to provide absorption of longer wavelengths in the most accurate, reliable, and repeatable manner; however, fabricating NIR detectors can be challenging due to their inherently low energy. Prior studies have laid a solid foundation for NIR detection and spectroscopy. However, responsivity was limited to a few tens of $\mu\text{A/W}$, and spectroscopy of the longer wavelength range of NIR beyond 1400 nm is not yet clearly demonstrated. In this work, we achieved remarkable detection over a wide range of wavelengths up to 2300nm with distinguished responsivity. Our emphasis lies in the extension of the spectral range for reconstructive spectroscopy into longer NIR wavelengths, fostering enhanced understanding and application possibilities.

Gold is widely used in semiconductor manufacturing processes; however, it forms unstable contacts with Si, leading to potential device reliability issues. The introduction of an interlayer not only enhances device adhesion but also modifies charge carrier generation and transport processes. A low Schottky-barrier photodetector with a plasmonic assist that receives Near-infrared (NIR) light at room temperature was demonstrated. A comparative study of Schottky plasmonic photodetectors employing titanium (Ti) as a Schottky interlayer metal, a diffusion barrier, an adhesion promoter, and to suppress the formation of intermetallic compounds or plasmonic resonance shifts with enhanced absorption led to a tenfold increase in device responsivity compared to previous studies. The study meticulously engineered a grating structure with a pitch of 1.4 μm . Grating design is determined by extensive experimental and modeling, ensuring a wavelength-specific plasmonic photodetection and a near one-to-one correspondence between incident angles and wavelengths within the NIR region.

It exhibited an exceptional photocurrent response at room temperature and zero biasing conditions, characterized by high linearity and sensitivity. In addition, it exhibited high sensitivity to low light intensities (less than 25 μW at 1900 nm). The device exhibited the capability to demonstrate clear SPR peaks for NIR even with parallel exposure to visible light and maintained high stability with neither hysteresis nor deterioration in photocurrent measurements over a time span of 240 days so far. The sharp and selective SPR peaks facilitated expanding the spectral range for reconstructive spectroscopy to longer wavelengths. Since the degree of surface sensitivity can be controlled by collecting photoelectrons emitted at different emission angles to the surface plane by changing the incident photon energy, the reconstruction of multiple parallel incident wavelengths could be successfully demonstrated. Making it a very powerful technique for investigating the electronic and chemical structures of various nanolayers and devices for green chemistry. This research represents a significant leap in NIR photodetection and spectroscopy, with far-reaching implications across applications such as gas sensing.

Light acquisition for 1.2–2.3 μm -long NIR wavelengths became possible through a single device and applicable in gas sensing, particularly within the vibrational absorption bands of alkane groups. This research builds upon a comprehensive array of experimental results, encompassing devices with diverse geometries and multiple interlayers, including Au, Ti, Mo, and Cr. These findings provide valuable design guidelines for optimizing device structures and insights into their application for various scenarios.

5:00 PM EL08.07.09

Nano-Metamaterial Design and Fabrication, Hybridized with Various Nanostructures for Gigantic THz Electromagnetic Wave Modulation and Their Biochemical Applications [Minah Seo](#)^{1,2}, Geon Lee¹ and Jinwoo Lee^{1,2}; ¹Korea Institute of Science and Technology, Korea (the Republic of);

²Korea Univeresity, Korea (the Republic of)

Large-scaled metamaterial design and fabrication, hybridized with various nanostructures for gigantic terahertz (THz) electromagnetic wave modulation and their applications. Their potential applications as highly sensitive target molecule-specific sensors, amplifying interactions between light and materials, are particularly noteworthy [1-2]. On the one hand, the terahertz (THz) waves offer non-destructive interactions with molecular modes for the sensing purpose, and reasonable process capabilities in terms of fabrication size. Metamaterials operating at this range, with similar-sized structures (micrometer scale), can be manufactured using photolithography methods on a wafer-to-chip basis. Notably, a large-area nanoscale process was successfully developed by selectively combining different techniques based on their intended purpose. This structure takes the form of a slot-shaped antenna, with a width of hundreds of nanometers and a high aspect ratio, extending tens of micrometers in the transverse direction. To enhance sensitivity and minimize noise levels, over 1,000 antennas per sensor chip were designed and arranged in an array configuration. The design of the metamaterial was thoughtfully engineered to enable the tuning of its resonant frequency by adjusting the antenna's length. Furthermore, the additional nanostructures including nanowires, self-assembled nanoparticles, 2D materials such as MXene, graphene, and catalytic materials as well were integrated to get further functionality. This innovative feature allows excellent detection of trace amounts of biomaterials, leading to several groundbreaking research outcomes at the forefront of the field.

In conclusion, we successfully produced nanoscale THz metamaterials using various process equipment, enabling high field enhancement, thus improving sensing and imaging ability. These THz metamaterial sensing chips demonstrated the ability to detect even DNA nucleotides, COVID viruses, microplastics, and trace biochemical substances with greatly improved sensitivity compared to existing light sources [3-4]. Its unique and powerful capabilities offer significant advancements in sensing and control applications, promising to revolutionize electro-optics and open up new possibilities across various industries.

References

- [1] Y. Roh et al., Ultrastrong coupling enhancement with squeezed mode volume in terahertz nano-slots, *Nano Letters* 23, 7086 (2023)
- [2] G. Lee et al., Frontiers in Terahertz Imaging Applications beyond Absorption Cross Section- and Diffraction-Limits, *ACS Photonics* 9, 1500 (2022)
- [3] S. Lee et al., Detection and discrimination of SARS-CoV-2 spike protein-derived peptides using THz metamaterials, *Biosensors and Bioelectronics* 113981 (2022)
- [4] E. Yu et al., Nanoscale terahertz monitoring on multi-phase dynamic assembly of nanoparticles under aqueous environment, *Advanced Science* 2004826 (2021)

Acknowledgment: The National Research Foundation of Korea (NRF) (2023R1A2C2003898), and KIST Institutional Program (No. 2E32451)

Keywords: Metamaterial, Terahertz spectroscopy, nanostructures

5:00 PM EL08.07.10

Silver Nanowire Transparent Radiative Shield for Personal Heating Textiles [Genesis M. Higueros](#)^{1,2} and Po-Chun Hsu²; ¹Duke University, United States; ²The University of Chicago, United States

Heating requirements for residential and commercial dwellings result in significant financial costs and deleterious environmental effects. Personal thermal management textiles (PTMTs) regulate the wearer's body temperature by controlling the material's intrinsic optical properties. Passive heating materials suppress radiative heat losses and therefore eliminate energy usage for building heating requirements. Guided by a numerical theoretical approach, a transparent radiative shield (TRS) is designed capable of human body heat suppression and simultaneous visible light transmittance anticipated from commercial textiles. Simulations for visible transmission and mid-infrared reflectance of silver nanowire (AgNW) network are based on Mie scattering and a wire-mesh equivalent sheet impedance model, respectively. TRS achieves high infrared light reflectance (low emissivity of 35%) and visible light transparency values of 75% (400-800 nm). Fabrication of TRS is a simple, scalable process consisting of a AgNW network and thermoplastic elastomer protective layers granting notable stretching capabilities and mechanical robustness. TRS may conform to any body shape or object. The novel theoretical approach permits a scalable pathway towards low emissivity and visibly transparent textiles for personal thermal comfort.

5:00 PM EL08.07.11

Enhancing CsFAMA Perovskite Solar Cells with Plasmonic TiN Nanoparticles: Structural, Morphological and Optical Effects Oleksii Omelianovych, Liudmila Larina and Ho-Suk Choi; Chungnam National University, Korea (the Republic of)

Perovskite solar cells have undergone significant advancements in recent years, with a strong focus on optimizing perovskite crystallization and surface passivation. One promising avenue for improving the light absorption and electrical properties of perovskite layers is the incorporation of plasmonic nanoparticles. In this study, we investigate the effects of TiN nanoparticles on the structural, morphological, electrical, and optical properties of Cs_{0.05}(FAPbI₃)_{0.83}(MAPbBr₃)_{0.12} (referred to as CsFAMA) perovskite.

Prior to conducting experimental measurements, we performed optical finite-difference time-domain (FDTD) simulations to assess the anticipated impact of embedding TiN nanoparticles into CsFAMA on the optical absorbance spectra. Our simulations revealed moderate increases in absorbance within the visible range, accompanied by notable enhancements in the near-infrared region. Subsequent real UV-Vis-NIR measurements closely aligned with the simulation results, with one exception: the overall reflectance of TiN-containing perovskite films exhibited a decrease. We attribute this phenomenon to the higher crystallinity and larger size of CsFAMA grains, as confirmed through X-ray diffraction (XRD) and scanning electron microscopy (SEM), respectively.

To gain further insights into the structural and morphological changes resulting from the presence of TiN nanoparticles, we conducted an aging study on as-deposited, unannealed CsFAMA films for a duration of 3 hours, followed by XRD measurements on the aged films. Our observations and XRD results indicate that as the content of TiN nanoparticles increases, the re-dissolution of CsFAMA becomes more pronounced, suggesting a larger quantity of trapped solvents within the perovskite film. Consequently, the apparent increase in grain size can be attributed to the ability of TiN nanoparticles to adsorb trace amounts of dimethyl sulfoxide (DMSO), leading to a less rigid perovskite film that crystallizes at a slower rate, thus facilitating the growth of larger crystals. These findings are in line with TGA and DSC measurements results.

X-ray photoelectron spectroscopy (XPS) analysis revealed the absence of TiN on the perovskite surface, indicating that the TiN nanoparticles are situated either at the TiO₂/CsFAMA interface or within the CsFAMA structure. Finally, we constructed perovskite solar cells incorporating TiN nanoparticles, resulting in increased efficiency related to an improvement of all electrical properties of solar cell (Jsc, Voc and FF). Our measurements of the incident photon-to-electron conversion efficiency (IPCE) demonstrated enhanced performance arising from both the larger size of perovskite grains and electron transfer from plasmonic nanoparticles at resonance wavelengths. Larger size of grains led to reduction in the recombination, as evident from PL results. As a result the incorporation of TiN led to increase in PCE from 19.5% to 21%.

In summary, the presence of TiN nanoparticles significantly influences the structural, morphological, electrical, and optical properties of CsFAMA perovskite. The incorporation of TiN nanoparticles leads to improved absorbance, enhanced crystallinity, larger grain sizes, and increased efficiency of perovskite solar cells. These findings contribute to the ongoing efforts to advance the development of high-performance perovskite-based photovoltaic devices.

5:00 PM EL08.07.12

Photothermal Enhancement Effects of Plasmonic Nanoparticles on Diels-Alder Reactions towards The Development of Solar Light Enhanced Recyclable Epoxy Arnob Dipta Saha, Madeline Finale, Julio Cubillas, Youngmin Lee, John McCoy and Sanchari Chowdhury; New Mexico Tech, United States

Thermosets are suitable candidates for vast range of applications such as in adhesives, electronics, automotives, aerospace, and household devices due to their superior mechanical properties, high chemical resistance, and thermal stability. However, irreversible crosslinking of thermosets poses problems for their recycling. We have developed light mediated recyclable epoxy incorporating thermo-reversible covalent adaptable network (Diels-Alder (DA) reactions) into it and mixing that with refractory plasmonic titanium nitride (TiN) nanomaterials. Plasmonic TiN nanomaterials can absorb broad spectrum visible light to generate localized heat to drive Diels-Alders reactions enabling reversible polymerization and depolymerization. Nanoparticles loading and their dispersion in the polymer matrix is optimized to maximize their photothermal efficiency. It was found that these nanoparticles can absorb visible light to drive the Diels-Alder (DA) reactions efficiently to reversibly liquefy the epoxy for reprocessing. We used in situ FTIR to study the kinetics of Diels Alder reactions driven by photothermal effects and compared that with conventional heat driven reaction kinetics. One of our key findings is that the kinetics of Diels-Alder reactions are significantly different with light induced photothermal heat generation in comparison to conventional heating even though the bulk temperature of the sample is similar. This indicates the local heat generation around the nanoparticles and the interaction of reactants with nanoparticles may affect the Diels-Alder reactions differently than the bulk heating. Further studies are being done to understand the exact mechanisms behind the photothermally induced Diels-Alder reactions.

5:00 PM EL08.15.04

Far Field excitation of Polaritons in Photonic Hypercrystals of Van der Waals Materials Nihar R. Sahoo and Anshuman Kumar; Indian Institute of Technology Bombay, India

This study delves into the realm of in-plane Hyperbolic Phonon polaritons (HPhPs), intriguing quasiparticles arising from the strong interaction between photons and optical phonons in hyperbolic materials. While these hold immense promise in various domains such as sensing, thermal emission, and high-resolution imaging, their technological application has been hampered by a substantial momentum mismatch between photons and in-plane HPhPs. Previous experimental demonstrations have primarily relied on intricate and costly near-field detection schemes.

In this work, we present a pioneering approach, exemplified by α -MoO₃, showcasing the potential of constructing photonic hypercrystals. This innovative concept not only enables the far-field excitation of in-plane HPhPs but also offers the ability to fine-tune the far-field response by introducing controlled twists in the hypercrystal lattice relative to the lattice of α -MoO₃. These findings represent a significant stride forward, promising the development of practical in-plane HPhP devices while also providing access to novel fundamental physics of such materials via conventional and well-established far-field measurement techniques.

The study systematically explores biaxial van der Waals (vdW) crystals, focusing on α -MoO₃, wherein HPhPs exhibit pronounced sensitivity to the crystal's basal plane direction. The isofrequency contours in these cases take on a hyperbolic geometry, a stark departure from the circular contours observed in uniaxial vdW materials like h-BN. This biaxial hyperbolicity in vdW crystals opens up unprecedented opportunities for manipulating and tailoring infrared light waves and energy flow at the nanoscale, offering intriguing optical phenomena such as negative refraction, topological transitions, light canalization, and twist photonics.

The research confronts the longstanding challenge of momentum mismatch for far-field excitation of phonon polaritons. Previous studies have proposed patterning the vdW crystal with various materials to surmount this limitation. This work, however, introduces the concept of a photonic hypercrystal, involving periodic structural modulations in a hyperbolic material. By employing α -MoO₃ as a model system, we demonstrate the feasibility of far-field excitation of in-plane HPhPs, showcasing a new dimension of control over light-matter interactions.

In essence, this study represents a transformative advancement in the understanding and utilization of in-plane hyperbolic vdW crystals. The results not only deepen our comprehension of the intricate interplay between light and these hypercrystals but also lay the foundation for the practical realization of phonon polariton-based devices. These findings hold broad implications, extending from the realm of nanophotonics to the burgeoning field of twist photonics, opening up a new chapter in the exploration of advanced photonic technologies.

SESSION EL08.08: Nonlinear Optics and Extreme Light-Matter Interaction with Metasurfaces and Plasmonics

Session Chairs: Ho Wai (Howard) Lee and Pin Chieh Wu

Wednesday Morning, April 24, 2024

Room 340/341, Level 3, Summit

8:00 AM EL08.08.01

Moiré Photonic Crystal enabled Optical Vortex Generation through Bound States in The Continuum [Tiancheng Zhang](#)¹, Kaichen Dong^{1,2}, Jiachen Li^{1,3}, Fanhao Meng^{1,3}, Jingang Li¹, Sai Munagavalasa¹, Costas Grigoropoulos¹, Junqiao Wu^{1,3} and Jie Yao^{1,3}; ¹University of California, Berkeley, United States; ²Tsinghua Shenzhen International Graduate School, China; ³Lawrence Berkeley National Laboratory, United States

The twisted stacking of van der Waals crystals has led to the emerging moiré physics as well as intriguing chiral phenomena such as chiral phonon and photon generation. Along with the surge of research into moiré physics of two-dimensional materials, moiré patterns in photonic systems have also drawn broad attention. In this work, we identified and theoretically formulated a non-trivial twist-enabled coupling mechanism in twisted bilayer photonic crystal (TBPC), which connects the bound state in the continuum (BIC) mode to the free space through a twist-enabled “moiré channel”. Moreover, the radiation from TBPC hosts an optical vortex in the far-field radiation with both odd and even topological orders. We quantitatively analyzed the twist-enabled coupling between the BIC mode and other non-local modes in the photonic crystals, giving rise to radiation carrying orbital angular momentum. The optical vortex generation is robust against geometric disturbance, making TBPC a promising platform for stable vortex generation. Furthermore, the incorporation of TBPC and micro/nanoelectromechanical systems (MEMS/NEMS) could lead to the creation of tunable vortex beams with adjustable topological orders, beam center positions, divergence angles, etc. As a result, TBPCs not only provide a new approach to manipulating the angular momentum of photons, but may also enable novel applications for integrated optical information processing and optical tweezers. Due to the intrinsic similarities between photonic systems and condensed matter systems, this work may also guide the exploration of orbital angular momentum and spin-orbit coupling in moiré van der Waals structures. Our work broadens the field of moiré photonics and paves the way toward the practical application of moiré physics.

8:15 AM *EL08.08.02

A Materials' Screening Paradigm for Thermophotovoltaic Optical Emitters Declan S. Kopper¹, Margaret A. Duncan¹, Tao Gong¹, mariama dias², Stuart S. Ness¹, Scott J. McCormack¹, Jeremy N. Munday¹ and [Marina S. Leite](#)¹; ¹University of California, Davis, United States; ²University of Richmond, United States

Thermophotovoltaics (TPV) represent a promising route for converting heat into usable electricity via a clean energy paradigm. Yet, the material options used to date for the optical emitters substantially restrict the power conversion efficiency of this process. Here, we provide a survey of material options, based on a dual-layer emitter stack (coating + substrate) that could be scaled up. We screened the optical behavior of >2,800 material combinations with melting point >2,000 °C, comprising refractory silicides, borides, carbides, nitrides, etc. [1]. The mismatch in permittivity allowed for emission control, key for the successful employment of high performing TPV. We identified optical emitters for TPV with theoretical efficiency >50% for GaSb solar cells, while considering both optical properties and thermochemical stability. We analyzed the promising SiC/AlN option, where we found this material combination to be stable up to 1,200 °C in air and 1,500 °C in inert environments [2], using in situ high-temperature optical measurements [3]. Further, we quantitatively assessed the maximum power conversion efficiency using this emitter for TPV systems comprised of InGaAsSb, InGaAs, Ge, GaSb, and Si photovoltaics. The material screening approach implemented here could be expanded to additional high-temperature photonic devices, such as thermal regulation ones, and barrier coatings for extreme environmental conditions.

[1] M. R. S. Dias et al. *Joule* 7, 2209 (2023).

[2] M. Duncan et al. In preparation (2024).

[3] T. Gong et al. *ACS Appl. Opt. Mater* 1, 1615 (2023).

8:45 AM EL08.08.03

Unfolding The Origin of Titanium Nitride's Ultrafast Optical Nonlinearity [Silvia Rotta Loria](#)¹, Beatrice Roberta Bricchi¹, Andrea Schirato^{1,2}, Luca Mascaretti³, Andrea Li Bassi^{1,4}, Bruno Palpant⁵, Margherita Zavelani-Rossi^{1,6} and Giuseppe Della Valle^{1,6}; ¹Politecnico di Milano, Italy; ²Italian Institute of Technology, Italy; ³Palacký University Olomouc, Czechia; ⁴Center for Nano Science and Technology - IIT@PoliMi, Italy; ⁵Université Paris-Saclay, CNRS, ENS Paris-Saclay, CentraleSupélec, LuMIn, France; ⁶IFN-CNR, Italy

In the last decade, Titanium Nitride (TiN) has been brought into the spotlight as a promising alternative plasmonic material to noble metals, such as gold and silver [1]. Indeed, it boasts a refractory character, CMOS- and bio-compatibility, tunable permittivity at the synthesis stage, and epsilon-near-zero properties at optical wavelengths. On top of that, TiN shows an extremely rapid hot-electron relaxation time (< 100 fs), one order of magnitude lower than noble metals such as, e.g., gold [2]. This property is extremely appealing to exploit TiN as a novel material in devices for all-optical-modulation.

Nevertheless, in order to perform device design, the bare knowledge of the hot-carriers cooling time is not sufficient. A comprehensive model, able to predict how the broadband dielectric properties of the material are modulated, upon ultra-rapid photoexcitation, is essential.

In this work, we develop an original numerical model, able to disclose the origin of TiN's giant optical nonlinearity. Starting from a rate-equation model, we evaluate the increments in carrier and lattice temperatures following photoexcitation. Then, we manage to disentangle the interband and intraband contributions to the permittivity modulation, on a broad spectral domain, pointing out the key role of interband transitions in the first instants (< 150 fs) of TiN optical dynamics. The calculations are validated on ultrafast pump-probe spectroscopy experiments, starting from the simplest TiN structure: a 200 nm-TiN film on glass. The sample is excited with an ultrashort pump at ~ 500 nm, and probed with a broadband pulse, having a temporal resolution of ~ 100 fs [3]. The model is then implemented to study the ultrafast optical nonlinearity in TiN nanostructures. Specifically, we focus on a lattice of TiN nanodisks in air and on a colloidal solution of TiN nanospheres in water. For both systems, the comparison with ultrafast pump-probe measurements [4],[5] shows accurate results. As a further step, we aim at studying the hot-carriers induced optical nonlinearity on a even more complex structure, namely a TiN-based metasurface.

Our work provides a powerful tool: indeed, starting from the actual experimental conditions, such as the pump fluence or the nanostructure geometry, we are able to predict the ultrafast optical properties of virtually any TiN-based sample over a broad spectral range. This paves the way to the design and demonstration of new TiN-based devices for ultrafast plasmonics applications.

References:

- [1] G.V. Naik *et al.*, *Adv. Mater.*, 25, 3264 (2013).
- [2] B.T. Diroll, *et al.*, *Adv. Opt. Mater.*, 8, 2000652 (2020).
- [3] S. Rotta Loria *et al.*, *Adv. Optical Mater.*, 11, 2300333 (2023).
- [4] T. Reese *et al.*, *ACS Photonics*, 8, 1556 (2021).
- [5] S. Adhikari *et al.*, *Phys. Rev. Appl.*, 15, 024032 (2021).

9:00 AM EL08.08.04

Nonlinear Optical Colloidal Three-Dimensional Metacrystals Ye Zhang and Chad A. Mirkin; Northwestern University, United States

Atomic and molecular structure inversion symmetry breaking in naturally occurring crystals dictate their physical properties including nonlinear optical effects, piezo-/ferroelectricity, and nonreciprocal charge transport behavior. With metamaterials composed of nanoscale building blocks (*i.e.*, meta-atoms), the spatial inversion symmetry violation on planar surfaces leads to spin-controlled photonics as well as nonlinear optical metasurfaces. While low-symmetry three dimensional (3D) metacrystals can be synthesized, limitations in long-range order and control over resulting symmetries inhibits the investigation of the symmetry-property relationships in these systems. Here we present a DNA-mediated gold nanoparticle assembly approach to create 3D colloidal crystals which can be designed to deliberately access high- or low-symmetry phases. By manipulating particle shape, size, and DNA design, we effectively tune the crystal symmetries of the superlattices in a controllable manner. Access to these different symmetries and facile transitions among them enable us to explore the symmetry-dictated functionalities of these colloidal crystals. Further, we investigate how the resulting crystal symmetry relates to their nonlinear optical interactions and identify that the non-centrosymmetric crystal functions as an effective nonlinear optical metacrystal, where second harmonic generation (SHG) arises from the asymmetrical distribution of the local electric field around the close-packed plasmonic nanoparticles. Moreover, this non-centrosymmetric colloidal metacrystal represents the first 3D nonlinear optical metamaterial developed through a bottom-up approach and exhibits a high maximum SHG conversion efficiency, notably surpassing the efficiencies observed in the majority of plasmonic 2D metasurfaces by two orders of magnitude.

9:15 AM *EL08.08.05

Modeling The Nonlinear Optical Response of ENZ Films Adam Ball¹, Ray Secondo^{2,3}, Yaqub Mukhtar¹, Samprity Saha¹, Jingwei Wu¹, Dhruv Fomra^{4,1}, Jacob Khurgin⁵ and Nathaniel Kinsey¹; ¹Virginia Commonwealth University, United States; ²Azimuth Corporation, United States; ³Air Force Research Laboratory, United States; ⁴NIST, United States; ⁵Johns Hopkins University, United States

The epsilon-near-zero (ENZ) regime of optical materials represents the transition point between metallic (negative permittivity) and dielectric (positive permittivity) response, similarly characterized by strong alterations in reflection, transmission, and absorption. This intriguing region of optical response has given rise to range of unique effects in both the linear and nonlinear optics fields, including wavelength expansion, slow light, and field confinement. In particular, the ability of the ENZ regime to enhance various nonlinear optical effects has garnered significant attention in recent years. Among them, a key is the ability to modulate the refractive index of the ENZ film on the order of unity on a picosecond timescale via nonlinear optical excitation. This has given rise to a significant interest in utilizing ENZ films for a number of optical devices including saturable absorbers, nonlinear activation functions, optical switches, and more. However, key to designing these devices is understanding the nonlinearity and modeling the change in complex index (permittivity) that will be experienced for a given excitation. In this talk we will highlight our recent efforts to model the intensity dependent index of Drude-based ENZ thin films, highlighting the Nonlinear Epsilon Near Zero (NLENZ) Calculator application available online via nanohub.org. We will introduce the basic theory of the non-parabolic conduction band and how it gives rise to nonlinear response of ENZ materials. We will then provide a high level outline of the models for interband and intraband nonlinearities, culminating in the use of the NLENZ app to predict the nonlinear properties of the material, using only experimental parameters and the material band structure, which can then be extracted and used in combination with other FEM or FDTD solvers for complex device design. We expect this tutorial style talk to be of interest to researchers and materials scientists who are interested in working with ENZ materials in new devices or developing new materials with an ENZ response, and hope to support the further development and study of these unique effects by furthering the ability of the community to simulate material and device responses incorporating ENZ.

9:45 AM BREAK

10:15 AM EL08.08.06

Analysis of Near-Field Patterns generated by Propagating Polaritons Minsoo Jang, Sergey Menabde, Jacob Heiden and Min Seok Jang; Korea Advanced Institute of Science and Technology, Korea (the Republic of)

Polaritons are quasi-particles that are excited by the coupling of light and charges within a material. They are closely related to the motion of charges in matter, which gives them a deep connection to material properties. Additionally, in specific low-dimensional materials, they exhibit a high level of light-matter interaction and confinement. Polaritons hold significant value in the field of nanophotonics, and current research is underway in areas such as light absorption, thermal emission, biosensing, and beam deflection. However, directly measuring the complex propagation of polaritons remains a challenging aspect of research due to the difficulty of near-field measurements.

Scattering type scanning near-field optical microscopy (s-SNOM) enables the simultaneous measurement of the amplitude and phase of the near field by utilizing a metallic atomic force microscopy (AFM) tip as a near-field antenna and the interferometric coupling of this signal with the base signal. Typically, s-SNOM excites complex propagating polaritons through the tip and material edges and images them. In the past, Fourier transform (FT) was used on the image profile to extract real momentum, but the damping term was determined through direct fitting or by directly fitting complex momentum from the beginning. This method poses challenges in mixed signal analysis and background removal. Additionally, for edge-launched polaritons, the polariton momentum can shift depending on the edge angle, but this shift has not been considered in recent high-effective-index materials like hBN or MoO₃.

In this study, we first present a standardized method for analyzing the complex momentum of propagating polaritons. To analyze polariton momentum, we fit the FT signal of propagating polaritons with a function obtained by FT of the analysis model. We confirmed a perfect fit and also revealed the relationship between the full-width half-maximum (FWHM) of the FT signal and the damping of propagating polaritons, confirming a specific ratio of . This method using FT makes it easier to analyze comprehensive signals compared to the traditional direct fitting method and offers an advancement in analyzing the loss of polaritons based on the existing Fourier transform approach.

Secondly, we established an analytical model for tip and edge polaritons and experimentally demonstrated edge-oriented momentum shifts that occur during measuring process in edge mode. We measured polaritons on hBN transferred onto crystalline gold. Polaritons launched from the clear atomic gold

edge generate modes known as hyperbolic phonon-polaritons (HPP) and hyperbolic image polaritons (HIP) that propagate on both the glass substrate and crystalline gold. We measured the polariton by rotating gold edge at 45-degree angles and confirmed that the degree of shift matched the theoretical model. Furthermore, for HPP, it was observed that HPP exhibited a maximum momentum shift of approximately 8% even at a high effective index of 12.54.

10:30 AM *EL08.08.07

Plasmonics Platforms for Strong Coupling [Matthew T. Sheldon](#); University of California, Irvine, United States

Nanophotonic and plasmonic architectures present a compelling platform for investigating strong coupling phenomena. These nanofabricated optical structures enable precise tailoring of electromagnetic modes on sub-wavelength scales, leading to significant coupling interactions within near-field "hot spots". Recent advancements from our laboratory have showcased ultrastrong coupling to vibrational modes using innovative plasmonic cavity designs. The sub-wavelength localization of these platforms facilitates strong coupling to fewer molecules compared to traditional Fabry-Pérot (FP) cavities, potentially limiting contributions from "dark states" in polariton chemistry.

A notable feature of plasmonic-based cavities is their compatibility with established surface science techniques, such as confocal molecular Raman spectroscopy. With these tools, our recent studies have uncovered unique temperature-dependent dehydration behavior of transition metal salt films on plasmonic substrates, suggesting resonant thermal energy transfer when vibrational strong coupling is present. This discovery hints at the potential of pronounced thermal gradients within the near-field of plasmonic substrates.

Furthermore, our research delves into the design of cavities that support sub-radiant modes that exhibit higher q-factors, leading to stronger coupling interactions with molecular samples. Preliminary results indicate that these sub-radiant cavity modes with quadripolar field symmetry achieve very strong coupling with molecular samples, while offering a modification of the usual optical selection rules for bright and dark (N-1) polariton states.

11:00 AM EL08.08.08

Visualizing Chiral Plexitons at Room Temperature Using Tip-Enhanced Photoluminescence [Thomas P. Darlington](#)¹, [Kevin W. Kwock](#)¹, [Matthew Strasbourg](#)², [William Hayes](#)¹, [Nicholas Borys](#)² and [P. James Schuck](#)¹; ¹Columbia University, United States; ²Montana State University, United States

Chirality is a fundamental property of nature, arising naturally in many systems, ranging from the structure of molecules to the spiral arms of galaxies. Structural chirality leads to circular dichroism, where photons of right or left handedness experience contrasting refractive indices for a particular molecular enantiomer. This phenomenon plays a crucial role in the chemical identification of molecules in the food and drug sciences. In the field of quantum optics, chiral single photon sources have gained increased interest due to their inherent non-reciprocity¹, allowing for realization of novel optical devices such as single photon isolators and circulators². A requirement in many quantum optical applications is the realization of polariton states through strong coupling of a cavity optical field with a material dipole excitation. In this regime, substantial recent work has focused on plexitons, strongly coupled excitons with nanocavity plasmon-polaritons, due to their ultra-confined cavity volumes (<10 nm³). These small volumes allow for strong coupling to be readily achieved at elevated temperatures, with Rabi splittings of 50 – 400 meV in a wide array of excitonic systems ranging from quantum dots^{3,4}, monolayer transition metal dichalcogenides⁵, to molecular J-aggregates⁶. However, despite the explosion of the scientific efforts on the topic, chirality in plexitonic systems has yet to receive significant experimental attention.

In this presentation I will show our recent experimental efforts on imaging chiral plexitonic states formed with commercial CdSe/ZnS quantum dots with a gap-mode plasmonic cavity. Using tip-enhanced photoluminescence (TEPL), we are able to map out the nanocavity-quantum dot response, revealing a naturally asymmetric spatial profile for nanocavities formed with commercially available silver nano-optical probes and gold substrates, a common cavity geometry. Our nano-optical measurements further show positional control of the quantum dot emission energy, with an upper and lower polariton branches forming in the TEPL spectrum depending on the probe-dot separation and orientation, demonstrating the plexiton nature of the emission. Using a novel nano-optical imaging method that integrates TEPL with single photon avalanche photodiodes (SPADs) and time correlated single photon counting hardware, we map out the degree of circular polarization as a function of probe-dot position, showing polarization ratios as large as 80%, that is controllable by varying the x,y,z position of the nano-optical probe. Our results demonstrate the ability to imprint chiral behavior on quantum-emitter-based polaritons using plasmonic nanocavities, and provide important insight into development of chiral quantum optical devices.

1. Lodahl, P. et al., *Nature* **541**, 473-480 (2017).

2. Chen, D., He, R., Cai, H., Liu, X. & Gao, W., *ACS Nano*, **15**, 1912-1916 (2021).

3. Park, K.-D. et al., *Science Advances*, **5**, eaav5931 (2018).

4. Groß, H., Hamm, J. M., Tufarelli, T., Hess, O. & Hecht, B., *Science Advances* **4**, eaar4906 (2018)

5. Qin, J. et al., *Physical Review Letters* **124**, 063902 (2020).

6. Wersäll, M., Cuadra, J., Antosiewicz, T. J., Balci, S. & Shegai, T., *Nano Letters* **17**, 551-558 (2017).

11:15 AM *EL08.08.10

Perspectives of Design, Materials, Manufacturing and Applications for Optical Metasurfaces [Junsuk Rho](#); Pohang University of Science and Technology, Korea (the Republic of)

In this talk, I will represent AI-designed metasurfaces, new materials and three low-cost manufacturing: 1) nanoimprinting with high-refractive-index dielectric particle embedding resin (PER), 2) bandgap engineering of hydrogenated amorphous silicon (a-Si:H), and 3) atomic-layer coating on imprinted resin. a-Si, TiO₂, and ZrO₂ PERs are used for metasurfaces at infrared (940 nm), visible (532 nm), and ultraviolet (325 and 248 nm), respectively; measured efficiencies reach 47% (940 nm), 91% (532 nm), 72% (325 nm), and 49% (248 nm). PER metasurfaces with an inverse design provide 3D, full-color holography at visible. The bandgap of a-Si:H is engineered to suppress optical losses, realizing metasurface efficiencies of 42% (450 nm), 65% (532 nm), and 75% (635 nm). We deposit an atomic layer on resin for 12-inch metasurfaces, achieving measured efficiencies of 61% (450 nm), 78% (532 nm), and 65% (635 nm). Finally, the recent development of mass production and manufacturing of metasurfaces and nanophotonic structures, and future direction with a bigger vision will be discussed.

1:30 PM *EL08.09.01

Metasurfaces for Future Sensing, Imaging and Display Technologies [Mark L. Brongersma](#); Stanford University, United States

Metamaterials are a new, emerging class of high-performance materials that derive their unique, physical properties from the way they are structured. In this presentation, I will focus on the creation of 2-dimensional metamaterials (i.e. metasurfaces) by nanopatterning glass, semiconductor and metal films. I will argue that these metasurfaces are ideal building blocks for the next generation of optical elements and optoelectronic devices.

I will highlight how metasurface functionalities can start to impact a variety of optical sensing, imaging and display technologies. For example, I will show how one can create transparent optical sensors on glass substrates that can extract valuable information from an optical scene. I will also discuss the use of integrated metasurfaces for new imaging modalities. The proposed optical elements can be fabricated by scalable fabrication technologies, opening the door to many commercial applications.

2:00 PM EL08.09.02

Highly Collimated and Polarized Light Emitting Metasurface for AR displays [JP Berenguer](#)¹, Fenghao Xu², Qitong Li¹, Jung-Hwan Song¹ and Mark L. Brongersma¹; ¹Stanford University, United States; ²Stanford University, United States

Major technical challenges must be overcome in order for augmented reality (AR) technologies to fulfill its revolutionizing promises. Current solutions for AR displays suffer from very low efficiencies and large form factors, mostly due to the use of grating-based waveguides and polarizing optical elements. Therefore, there is a growing need for nanophotonics designs that can focus light emission at desirable in-coupling locations for maximum throughput and with a high degree of polarization to avoid the use of bulk polarizers.

Here, we present and characterize a directional and polarized light-emitting metasurface based on a generic GaN LED. We engineered arrays of Mie nanoresonators that preferentially couple to one linear polarization and make use of quasi-guided modes to achieve focused emission. We will discuss the underlying theory for optimal metasurface design and emitter placement as well as present photo and electroluminescence angle-resolved data to confirm a major enhancement in directionality, polarization, and overall efficiency as compared to a commercial LED. This work provides a feasible metasurface design tailored to improve μ -LEDs for next-generation display technologies and represents a significant advancement in the field of light emission control.

2:15 PM EL08.09.03

Compact Structured Light Generation and Depth Perception from Integration of Metasurface and PCSEL [Yao-Wei Huang](#)¹, Wen-Cheng Hsu^{1,2}, Chia-Hsun Chang¹, Yu-Heng Hong² and Hao-Chung Kuo^{1,2}; ¹National Yang Ming Chiao Tung University, Taiwan; ²Hon Hai Research Institute, Taiwan

We demonstrate a novel depth sensing system that utilizes metasurfaces and photonic crystal surface-emitting lasers (PCSELs), realizing structured light generation and facial recognition in monocular depth sensing. Our single-shot system projects approximately 45,700 infrared spots from an about $300^2 \mu\text{m}^2$ metasurface area, which is 233 times smaller than the commercial diffractive optical element (DOE) based dot projector used in the Face ID on iPhone. The system is lens-free and power consumption due to the utilization of PCSEL, reducing 5-10 times of power compared to dot projectors based on vertical-cavity surface-emitting laser (VCSEL) array. Our proposed system addresses the limitations of traditional structured light depth sensing technology, offering significant advantages in terms of size, power consumption, and potential for integration into wearable devices.

2:30 PM BREAK

SESSION EL08.10: Wave Front Control Metasurfaces—Design and Fabrication

Session Chairs: Yao-Wei Huang and Min Seok Jang

Wednesday Afternoon, April 24, 2024

Room 340/341, Level 3, Summit

3:30 PM EL08.10.01

Single-Gate Active Beam Steering Graphene Metasurface [Sangjun Han](#), Jinseok Kong and Min Seok Jang; Korea Advanced Institute of Science and Technology, Korea (the Republic of)

Optical beam steering is a next-generation technology with applications in optical communications, laser patterning, three-dimensional laser point clouds and LiDAR systems. Conventional beam steering devices based on mirrors rotated by motors have a 360° horizontal field-of-view, but suffered from its bulky size and high heat generation. MEMS-based LiDAR, which combines an actuator and a micro-scanner, and flash LiDAR, based on diffractive elements, were adopted to address those issues. However, they still suffered from low durability and significant power consumption. Metasurface-based beam steering device offers several breakthroughs, including miniaturization, reduced power consumption, reduced heat generation and higher frame rates. Active metasurface beam steering device can be implemented utilizing liquid crystals, phase change materials, or carrier injection into Transition metal dichalcogenide monolayers or conductive oxides. However, previous studies have faced challenges such as a small field-of-view within a few degrees, poor diffraction efficiency or directivity. In conventional electrically tunable beam steering devices, they generally require a complex circuit driver inside to individually control each metaatom. Those system may also involve dielectric breakdown problems between adjacent metaatom. To scale up to practical beam steering technologies in the future, it is necessary to simplify the driving mechanism and improve performance.

In this study we developed a beam steering technique using only single-gate voltage. The limitations in design freedom imposed by removing a complex circuit driver can be overcome by carefully determining the structural parameters of the metasurface. In conventional forward design, a local periodic approximation is commonly adopted to understand overall performance of metasurface in metaatom level. However, this approximation is not appropriate when there are significant interferences between neighboring metaatoms, resulting in unwanted sidelobes and poor directivity. Recently, inverse design, which determines structural parameters based on its performance, has been introduced to address these shortcomings. We used a genetic algorithm to efficiently deal with large design hyperspace and find a device structure with high directivity and field-of-view without a complex circuit configuration. The metasurface consists of a gold grating and a graphene ribbon array with different widths and gaps. The height, width, gap and operating wavelength of the metasurface were optimized as design parameters. The designed metasurface is placed on a gold back reflector and a 200 nm low-stress silicon nitride dielectric spacer.

We measured modulation in diffraction efficiency and directivity at the 0th and -1st diffraction angles by varying a gate voltage applied to the device. When the gate voltage of 10 V is applied, the directivity at the 0th diffraction angle (45°) is approximately 0.675. This value decreases as the gate voltage is gradually decreased, reaching 0.325 at a gate voltage of -70 V. Meanwhile, the diffraction efficiency reaches 16%, gradually decreases to 8.5% when the

gate voltage decreases. This confirms that the reflected wavefronts can be actively switched with a field-of-view of 68° with single-gate voltage.

3:45 PM *EL08.10.02

Design and Fabrication of Large-Scale Meta-Optic Devices Xingjie Ni; The Pennsylvania State University, United States

Metasurfaces, artificially engineered ultrathin subwavelength nanostructures with exceptional light control capabilities, have the potential to revolutionize conventional optics. However, the traditional methods for creating these metasurfaces are slow, expensive, and lack scalability. To address this, we have developed a cost-effective and scalable design and fabrication method for large-scale meta-optic devices that work in both the visible and infrared regimes. We showcase several examples, including a single-lens telescope using a wafer-scale metalens, inch-scale meta-optic correctors, and a metasurface-enabled real-time hyperspectro-polarizometry camera. Our technology facilitates versatile light control in scalable, compact, multifunctional flat optics devices with significant potential for real-world applications.

4:15 PM ^EL08.10.03

Machine Learning-Enabled Photonic Metamaterials Jonathan A. Fan; Stanford University, United States

In this talk, I will discuss advances in photonic engineering in which machine learning approaches to device implementation unlock new functional capabilities. First, I will discuss new concepts in nanostructure geometric parameterization, inspired from the computer graphics community, which enable freeform layouts to be specified in a manner that can be differentiated and maintain hard constraints. Second, I will show how deep generative networks can be used to perform population-based global optimization, producing best in class devices. Third, I will show how physics-augmented deep networks can serve as accurate surrogate electromagnetic solvers and how innovations in network architecture can enable these solvers to generalize to arbitrary sized domains and grayscale dielectric media. We anticipate that the ability for deep learning models to dramatically accelerate and even automate the simulation and design of photonic systems will push the innovation cycle in all domains of photonics research.

4:45 PM EL08.10.04

Modulating Color Response in Polymeric Photonic Crystals through Refractive Index Tuning with Gold Nanoparticles Chen Chen and Yadong Yin; University of California, Riverside, United States

Responsive photonic crystals with high brightness, straightforward fabrication, and excellent tunability are in high demand for a wide range of potential applications, including sensors, printing, and display units. In this study, we present an innovative design of highly-ordered photonic crystals with tunable color response through gold (Au) deposition using a space-confined seeded growth method.

The pivotal aspect of modulating color response is controlling the deposition of Au nanoparticles (NPs) within the hollow polymeric shells. Benefiting from the strong interaction between AuNPs and resorcinol-formaldehyde (RF) polymer, even the addition of tiny Au NPs leads to an unexpected decrease in the effective refractive index of the core-shell NPs. Compared to other plasmonic materials, Au exhibits a unique ability to significantly reduce the effective refractive index.

Leveraging the continuous decrease in refractive index during AuNPs growth, we fabricate a series of composite films displaying blue-shifted colors. The structural color can be easily modulated over a broad spectral range by simply adjusting the hollow shells, resulting in more abundant colors with rich saturation. Moreover, the blue-shift effect can be eliminated through Au removal, allowing for reversible color changes. Simple fabrication, flexible adjustment, and outstanding optical properties of our composite film make it a promising choice for the development of functional colorimetric sensors in the future.

SESSION EL08.11: Poster Session II
Session Chairs: Yao-Wei Huang and Min Seok Jang
Wednesday Afternoon, April 24, 2024
Flex Hall C, Level 2, Summit

5:00 PM EL08.11.01

Tuning Nonlinear Optical Properties of Titanium Nitride Nanocrystals Carla Berrospe-Rodríguez¹, Ariana Sabzeghabae², Guillermo Aguilar¹ and Lorenzo Mangolini²; ¹Texas A&M University, United States; ²University of California, Riverside, United States

Titanium Nitride (TiN) nanomaterials have become a research interest since their present interesting photothermal and absorption/scattering properties. This novel material has a localized surface plasmon resonance response (LSPR) in the NIR window, in addition to having a higher thermal stability-resistivity compared to the commonly used plasmonic Gold (Au) or Silver (Ag) nanoparticles. Furthermore, several studies have confirmed the biocompatibility and low cost of fabrication of TiN nanoparticles with the intention of replacing Au for biomedical applications. [1] Currently, TiN nanoparticles are studied for implant coatings, photothermal therapy and bio-sensing, among other.

The search of plasmonic nanomaterials with tunable nonlinear optical properties has become crucial for laser-based applications in integrated electronics, biomedical and imaging, to mention a few [2]. Particularly, saturable absorption and self-focusing effect, are desirable third order nonlinearities for the design of non-reciprocal light propagation optoelectronic devices, high resolution spectroscopy, thermal lenses, and optical switches. Previous studies demonstrated non-linear absorption coefficients for TiN higher than Au, under the same laser radiation conditions. [3] Furthermore, the agglomeration of these nanoparticles can be utilized to enhance scattering properties, making these colloidal solutions ideal for tunable absorption. Therefore, it is of high value to investigate non-linear optical properties of TiN nanoparticles and TiN clusters in the NIR regime for the above-mentioned applications, particularly in the biomedical field.

In this work, the optical nonlinearities of TiN as a function of nanoparticle concentration in DI water solutions were investigated. Additionally, the effect of nanoparticle clustering, fabricated by 1 μm size clusters of 50 nm TiN nanoparticles, on nonlinearities was studied. It was found that the nonlinear absorption coefficient increases linearly with concentration for both models, however clusters required higher concentrations to exhibit similar values in absorption. Similarly, the optical threshold of reverse saturable absorption for cluster solutions was higher compared to the freestanding nanoparticles due to the collective scattering phenomenon. Finally, the self-focusing effect on TiN nanoparticles was explored on the continuous regime. Kerr lens with focal length as a function of solution concentration were obtained. The refractive index changes, due to photothermal effects and diffusive heat transfer,

produced changes in the beam diameter and consequently on the laser fluence. This work provides a comprehensive study of the tunability of nonlinear properties by the parameters of concentration and agglomeration.

References.

- [1] G. V. Naik, V. M. Shalae, A. Boltasseva, Adv. Mater. 2013, 25, 3264.
- [2] Capretti, A., Wang, Y., Engheta, N., & Dal Negro, L. (2015). *Acs Photonics*, 2(11), 1584-1591.
- [3] A. N. Sabzehabae, C. Berrospe, L. Mangolini, A. Aguilar, J. Biomed. Mater. Res., Part A2021, 109, 2483

5:00 PM EL08.11.02

Leveraging Correlations between The Statistics and Spectral Properties of Random Metasurfaces for Multi-Wavelength Cryptography Romil Audhkhasi, Maksym Zhelyeznyakov, Steven Brunton and Arka Majumdar; University of Washington, United States

Randomness and disorder are abundant in nature and help in sustaining the environment around us. In particular, random optical media encountered in various varieties of insects, birds and marine organisms are naturally optimized to offer survival advantage in their respective habitats. Historically, photonics researchers have focused their attention on periodic and ordered systems, and randomness has often been viewed as undesirable. In recent years, the broad range of functionalities exhibited by random optical media have prompted researchers to explore materials with tailored disorder for various applications. As opposed to their periodic counterparts, the vast design space afforded by disordered photonic devices provides greater flexibility in achieving tailored optical responses. However, the expanded design space makes it challenging to map the structural degrees of freedom of random photonic devices to their optical properties. This necessitates the identification of a tractable set of parameters that can be used to characterize random optical media. Here, we investigate correlations between the configuration statistics of random metasurfaces and their spectral response. Our metasurfaces consist of a two-dimensional array of silicon nanopillars with random widths on a silica substrate. We explore the effect of tuning the probability distribution characterizing the nanopillar widths on the wavelength-dependent transmissivity of the random metasurface in the 400 – 800 nm wavelength range. Furthermore, we exploit the correlations between the configuration statistics of the random metasurfaces and their spectral properties to design a photonic device encoding spectrally encrypted image data in the visible wavelength range. Our findings offer new insight into the optical properties of random media and provide avenues for developing such systems for a broad range of applications.

5:00 PM EL08.11.03

Engineering The Properties of Metal Nanoparticle Arrays for Optoelectronic Applications Gavin Farmer, Chris Littler, Athanasios Syllaios and Usha Philipose; University of North Texas, United States

This work focuses on a technique for the fabrication of ordered metal nanoparticle arrays with tunable particle diameter and inter-particle distance. The nanoparticle arrays were formed by a sequential solid state de-wetting process, using evaporated gold to fill the dimples of an anodized alumina membrane. The results show a direct correlation between the particle size and interparticle distance, factors that are determined by both the geometry of the dimples in the membrane as well as the volume of the evaporated gold. An experimental threshold for the evaporated gold film was determined, such that beyond a certain limit the existing nanoparticles were unable to preserve their ordering and spacing. This technique allows for fabricating ordered nanoparticle arrays with diameters ranging from 55 nm to about 85 nm, with inter-particle spacing's ranging from 10 nm to about 40 nm. This work is significant because ordered arrays of metal nanoparticles exhibit localized surface plasmon resonance, a phenomenon that can be taken advantage of in sensing applications

5:00 PM EL08.11.04

Aqueous Synthesis of Silver Nanocubes and Their Sensing Capabilities Annabella Talbott¹, Anika Guo^{1,2}, Nigel Ng¹ and Ying Bao¹; ¹Western Washington University, United States; ²University of Oregon, United States

Metallic nanoparticles are of great interest because they have shown promise in many fields like biomedicine, imaging, and sensing because of their chemical and physical properties. A focus has been put on controlling the morphology of metallic nanoparticles since specific characteristics (size, shape, composition, and structure) can impact the nanoparticles' properties and applications. Amidst these structures, sharp tips are of interest for enhancing related applications, as they allow for "hot spots" on the nanoparticles. Specifically, silver nanocubes (AgNCs) are desirable for sensing due to the "hot spots" located at their sharp corners, as well as the heightened plasmonic properties of silver. Typically, AgNCs are synthesized through a polyol process, but other methods are being explored due to the polyol process having been found to be toxic to the environment. In this work, an aqueous method of synthesizing the AgNCs was employed, and the effects of specific components of the synthesis and their resulting impact on the AgNCs were studied. This was done using UV-Vis spectroscopy and scanning transmission electron microscopy (STEM) to characterize the size and morphology of synthesized AgNCs. The refractive index sensitivity of varied sized AgNCs has been evaluated which shows a larger cube size has higher refractive index sensitivity. Furthermore, the synthesized AgNCs also were used for sensing iodide with the assistance of copper. In the future, the sensitivity of detecting iodide using various-sized AgNCs will be studied. The sensing of iodide using coated AgNCs will also be studied.

5:00 PM EL08.11.05

Iridescent Structural Color from Ultra-Low Refractive Index Aerogel as Fabry-Perot Cavity Dielectric Jennie Paik¹, Wei-Jie Feng¹, Sean Clark² and L. Jay Guo¹; ¹University of Michigan–Ann Arbor, United States; ²University of Florida, United States

Iridescent color-shift pigments are widely used across industries, from automotive and architectural coatings to cosmetics and packaging. To achieve a vibrant, iridescent, and lasting color, thin-film interference is used to generate structural color. By tuning the refractive index, thickness, and geometry of the component films, a wide range of vivid and iridescent colors can be produced. One strategy to produce iridescent films is to layer a thin, high refractive index (RI) film atop a thicker, low refractive index dielectric, thus allowing large optical path length variation within the dielectric. Artificial structural engineering of the low-RI layer by using a dielectric aerogel can reduce the RI of the low-RI layer, thereby imparting iridescence. Commercial iridescent color-shift pigments layer materials of large refractive index differences, such as TiO₂ (RI = 2.2) and SiO₂ (RI = 1.46). However, the lowest refractive index of a naturally occurring solid dielectric is close to 1.37 (i.e. MgF₂), which is still not significantly lower than SiO₂. To address this, we developed a structure using SiO₂ aerogel as the low-RI dielectric, whose ultralow refractive index arises from artificial structural engineering towards high porosity, and demonstrated its performance in a TiO₂/SiO₂/Si system. The ultra-low refractive index of aerogel is close to that of air (n~1.06), thus the color can travel a very long trajectory on the CIE diagram upon angle variation. To our knowledge, this work is the first to employ an ultra-low RI aerogel dielectric as a resonator in a FP cavity. To achieve high reflection and angle-dependent color, we utilize silicon dioxide (SiO₂) aerogel, which is an extremely porous network of SiO₂ and has a RI close to that of air (~1.06). Using titanium dioxide (TiO₂, RI ~1.8-2) as a high RI layer, we can achieve the highly iridescent structural color capable of traveling near completely around the CIE diagram upon angle variation. **By tuning the refractive index, thickness, and geometry of the aerogel layer, we control the reflection dip's shape, therefore producing a wide range of vivid and iridescent colors.**

5:00 PM EL08.11.06

Effect of pH on The Self Assembly of Janus Particles [Maria Iftesum](#)¹, Mohan K. Dey¹, Alisha Prasad², Jin G. Lee³, Shirin Parvin⁴, Meng Lu⁴, Ram Devireddy¹, Bhuvnesh Bharti¹ and Manas R. Gartia¹; ¹Louisiana State University, United States; ²Catalent Pharma, United States; ³University of Colorado Boulder, United States; ⁴Iowa State University of Science and Technology, United States

The use of pH-adjusted self-assembly in Janus particles is a promising approach for controlling Raman scattering. These Janus particles, known for their asymmetry in composition and properties, provide distinct benefits for crafting precise nanostructures in surface-enhanced Raman scattering (SERS) applications. The study investigates using pH-controlled self-assembly of Janus particles to observe the changes in their Surface-Enhanced Raman Scattering (SERS) and Raman signals. Characterization methods such as scanning electron microscopy (SEM) and focused ion beam (FIB) technology were implemented for detailed information regarding the shape, size variation, and inner structure of Janus particles. Various analytical techniques, including TEM, EDAX, and elemental mapping, were employed to assess the assembled Janus particles by examining their elemental composition and how it is distributed. By adjusting the pH of the solution, electrostatic interactions between the Janus particles were manipulated, leading to controlled aggregation and spatial arrangement. As the pH value rises, the gap between the particles widens. At specific pH levels, self-assembly of Janus particles occurs, forming ordered nanostructures that concentrate analyte molecules. This spatial confinement caused significant changes in electromagnetic field intensity and Raman signals. Optimal pH selection enables control over interparticle spacing, plasmonic coupling, and electromagnetic field distribution, leading to remarkable modulation of Raman signals. This research also focused on analyzing electromagnetic fields, uncovering how electric and magnetic fields are distributed between Janus particles when exposed to excitation light. A decrease in Raman Intensity with the increasing number of Janus particles were observed at the Raman wavenumber. Using Finite-Domain-Time-Difference (FDTD) simulations, a decrease in electromagnetic field intensity with the number of particles were also observed, which validates our experimental finding. Analyzing the structure and optical and electromagnetic properties of Janus particles will further help us understand their behavior and potential applications. pH-tuned Janus particle self-assembly shows promise in creating sensitive and selective Raman sensing platforms. This research advances our understanding of Janus particle assembly for SERS-based sensing, with broad applications in areas like chemical analysis, bioassays, and environmental monitoring.

5:00 PM EL08.11.07

Visible Light Mediated Deposition of Pt Nanocatalyst on Refractory Plasmonic Titanium Nitride Nanoparticles [Hirithya Sharad Jeyashangaraj](#), Sanchari Chowdhury and Naomi Helsel; New Mexico Institute of Mining and Technology, United States

Plasmonic photocatalyst can efficiently absorb light to generate photoexcited electrons to drive energy extensive catalytic reactions including CO₂ reduction, water splitting and solar energy conversion. We have successfully synthesized composite plasmonic catalysts by visible-light-induced deposition of transition metal nanocatalysts such as Pt on refractory plasmonic titanium nitride (TiN) nanoparticles. Titanium nitride nanoparticles can absorb broad spectrum solar light to generate photoexcited electrons which reduce transition metal precursor salts to deposit the metal atoms on the surface. We could deposit different size of Pt nanocatalysts on titanium nitride by varying the photodeposition process conditions such as light intensities and duration of light illumination. We are studying the effect of light intensity, irradiation time and wavelength dependence of Pt precursor reduction rate to understand the reaction mechanism of Pt nanocatalysts deposition. The findings of this study can be used to develop a visible light mediated synthesis of single atom plasmonic catalysts under mild conditions, which has been a bottleneck for their widespread applications.

5:00 PM EL08.11.08

Large-Grain Thin Films of Biaxial Hyperbolic α -MoO₃ Using Alkali Metal Compound-Assisted Vapor Transport Deposition [Ryan Spangler](#)¹, Joshua D. Caldwell², Patrick E. Hopkins³ and Jon-Paul Maria¹; ¹The Pennsylvania State University, United States; ²Vanderbilt University, United States; ³University of Virginia, United States

As the application space of mid-IR technologies continues to expand, materials with new and advanced properties become of interest. α -MoO₃ is a transparent, layered semiconductor that can exhibit biaxial hyperbolicity of the dielectric function, where the optical properties can be switched from out-of-plane hyperbolic to in-plane hyperbolic by varying the mid-IR wavelength. This opens up opportunities for planar emitters, non-reciprocal plasmon waveguides, and directional collimation of energy within nanomaterials via long-lifetime hyperbolic phonon polaritons. However, research on these properties has been predominantly performed on samples of exfoliated flakes of α -MoO₃, with thin film fabrication techniques being relatively undeveloped. This is in part due to the difficulty of producing the large grains necessary for many polaritonic experiments of in-plane anisotropic crystals. Therefore, the experimental flexibility of α -MoO₃ studies has been historically limited and it is of great interest to repeatedly produce large single crystals in thin film form. In this work, a physical vapor transport technique is developed which uses alkali metal compounds to promote grains possessing lateral dimensions of hundreds of μ m to few mm. We observed that this technique overcomes the poor film texturing and morphology that is observed in α -MoO₃ grown on most substrates. Data will be presented on the film morphology and crystallinity as functions of different growth parameters including substrate composition and preparation, growth temperature, and presence of alkali metal compounds. Additionally, the applicability of this synthesis technique to the nanophotonics community will be demonstrated by characterizing the optical and hyperbolic phonon polariton properties of the synthesized films. This synthesis technique opens up new capabilities for controllable fabrication of large-area α -MoO₃ crystals for nanophotonics and polaritonics research.

SESSION EL08.12: Light Field Detection and Sensing
Session Chairs: Matthew Sheldon and Pin Chieh Wu
Thursday Morning, April 25, 2024
Room 340/341, Level 3, Summit

8:45 AM *EL08.12.01

Monocular Metasurface Camera for Multidimensional Light Field Sensing [Yuanmu Yang](#); Tsinghua University, United States

Conventional camera systems can only detect light intensity while losing important information about the target scene, including depth, polarization, and spectrum. In order to further obtain the multi-dimensional light-field information of the target object, it is often required to use bulky and expensive instruments. Metasurface is composed of an array of optical antennas that can manipulate the amplitude, phase, polarization, and spectrum of light at the subwavelength scale. By replacing conventional diffractive of refractive elements with metasurfaces in imaging systems, one may be able to build optical sensors for high-performance multidimensional light sensing with low size, weight, power, and cost. Here, I will present our group's recent effort to replace conventional camera lenses with metalenses. By leveraging the unique capability of metasurface to tailor the vectorial field of light, in combination with an advanced image retrieval algorithm, we aim to build compact camera systems that can capture multi-dimensional light field information of a target scene in a single shot under ambient illumination conditions. Specifically, I will show how we use a polarization-multiplexed metalens for imaging through turbid

water (Laser & Photonics Reviews 15, 2100097 (2021)). Recently, we further extended such a concept to build a monocular camera that can capture a 4D image, including 2D all-in-focus intensity, depth, and polarization of a target scene in a single shot (Nature Communications 14, 1035 (2023)). I would also like to present our effort to commercialize flat-optics-based passive monocular 3D cameras, which drastically differ from existing 3D imaging hardware, including LiDAR and binocular cameras. The miniaturized 3D camera module may be seamlessly integrated with smartphones, AR/VR headsets, and robots for a variety of applications, including face and gesture recognition, spatial localization and mapping, and collision avoidance.

9:15 AM EL08.12.03

Direct Measurement of Radiation Pressure Forces on Membrane Lightsails Lior Michaeli, Ramon Gao, Michael Kelzenberg, Claudio Hail, John Sader and Harry A. Atwater; California Institute of Technology, United States

We report direct measurement of radiation pressure forces exerted on a 100-nm-thick silicon nitride lightsail membrane. Our sensitive measurements rely on three key components: a noise-robust common-path interferometer with picometer resolution, rational design of the tethered lightsail for enhanced mechanical susceptibility, and an off-resonant driving scheme for quasi-static, linear dynamics. Ultrathin lightsails, propelled to relativistic speeds by laser radiation pressure, are being actively explored as a new generation of interstellar spacecraft probes, spearheaded by the Breakthrough Starshot Initiative [1,2]. Realizing laser-driven lightsails necessitates precise characterization of the optical forces on a material platform capable of exhibiting mechanical, beam-riding, and thermal stability. For a laser power density of 200 W/cm² at 514 nm, we measure displacements of ~10 pm, resulting from optical forces of ~30 fN. Contrary to optical trapping of microscopic objects, motion is induced by a collimated laser beam filling substantial part of the lightsail, mimicking the initial acceleration stage of interstellar lightsails. Furthermore, to predict the tilt-dependent dynamics of subwavelength thick lightsails, we characterize the non-intuitive trend of the optical force versus incidence angle in the range of ±20° for TE and TM polarization. Our study represents a critical milestone in realizing an experimental testbed for lightsail characterization, thus advancing the development of laser-driven spacecraft, and opening the door for manipulation of macroscopic objects through optical forces.

9:30 AM *EL08.12.04

Let's Twist Again: High-Quality-Factor Metasurfaces to Enhance Spin In Molecules and Monolayer Materials Jennifer A. Dionne; Stanford University, United States

Many inversion-asymmetric materials, including chiral molecules and certain van der Waals materials, exhibit a differential absorption of left and right circularly polarized light that is nearly five orders of magnitude less than their absorption of unpolarized light. Such weak differential absorption challenges applications such as single molecule circular dichroism spectroscopy, all-optical enantio-specific synthesis, and efficient valleytronic data encoding for quantum information. Here, I describe approaches to enhance helicity-dependent optical absorption, emission, and carrier relaxation in molecules and monolayered materials. We rely on high-quality-factor (high-Q) metasurfaces, which, when placed in the near-field of a molecular or monolayer sample, precisely control the amplitude, phase, and polarization of light. Each metasurface enables substantial and uniform-sign enhancements of both the electric and magnetic fields of light, with local photon spin fields that can be enhanced by several orders of magnitude.

First, we show how high-Q metasurfaces enable circular dichroism from a molecular monolayer. We fabricate silicon metasurfaces and functionalize them with short, ~10-mer DNA oligonucleotides. We measure their circular dichroism in a home-built table-top polarization sensitive spectrometer, and also show how this technique is sensitive to changes in the CD handedness through double-stranded to single-stranded DNA denaturing. Next, we show metasurface designs that can enable high-yield enantioselective photochemistry at visible and ultraviolet wavelengths. By overlapping the metasurface optical resonances with the chiral molecular resonance, we project a 2000-fold improvement in the yield of a photoionization reaction. Finally, we extend this platform for valleytronic applications with two-dimensional transition metal dichalcogenides (TMDCs). We integrate TMDC monolayers with high-Q metasurfaces to improve and control valley-specific absorption and emission, to realize solid-state, optically addressable spin qubits. Through the coupling to the metasurface modes, the degree of polarization of exciton and trion emission from each valley can be enhanced, even up to 190K. Combining Si-compatible photonic design with molecular and 2D materials integration, our work makes an important step toward all-optical enantioselective sensing and separation as well as on-chip quantum optical information systems approaching room-temperature operation.

10:00 AM BREAK

SESSION EL08.13: Dielectric Metasurfaces
Session Chairs: Jennifer Dionne and Ho Wai (Howard) Lee
Thursday Morning, April 25, 2024
Room 340/341, Level 3, Summit

10:30 AM *EL08.13.01

Novel Dielectric Metasurfaces for DUV Photonics Bo Ray Lee, Ting An Shu, Pei Ying Ho, Mao Feng Jiang, Yu Chieh Peng, Kuan-Heng Chen, Jia Hua Lee, Yu Chia Chung, Yu Jie Wang, Der-Hsien Lien, Tzu-En Lin, Chao-Hsin Chien, Ray Hua Horng and Ming Lun Tseng; National Yang Ming Chiao Tung University, Taiwan

Deep ultraviolet (DUV) light covers wavelengths from 200 nm to 300 nm and has diverse applications including imaging, sensing, and medical treatments. Developing efficient and robust metasurfaces is crucial for improving the relevant DUV technologies. Here, we present innovative DUV dielectric metasurfaces providing field enhancement and several unique properties. By employing the photon doping effect and including a quasi-bound state in the continuum in the design, we realize a Si metasurface capable of showing a DUV plasmonic resonance. The field enhancement and the durability of biochemistry-related solvents of the sample enable its applications for DUV sensing applications. In addition, to generate strong field enhancement, we use low-loss HfO₂ to create a dielectric metasurface. Combining HfO₂'s optical properties with novel designs results in multiple high-quality factor resonances and significant field enhancement. These results will advance the development of ultrasensitive biosensing chips within this crucial wavelength range.

11:00 AM EL08.13.02

Extremely Confined THz Phonon Polaritons in HfS₂ and HfSe₂ Ryan Kowalski¹, Gonzalo Alvarez Perez², Maximilian Obst³, Katja Diaz-Granados Santos¹, Giulia Carini⁴, Aditha Senarath¹, Saurabh Dixit¹, Niclas Müller⁴, J. Michael Klopff⁵, Thomas G. Folland⁶, Lukas Eng³, Susanne Kehr³, Pablo Alonso Gonzalez², Alex Paarmann⁴, Richard Haglund¹ and Joshua D. Caldwell¹; ¹Vanderbilt University, United States; ²University of Oviedo, Spain; ³Technische Universität Dresden, Germany; ⁴Fritz-Haber Institute, Germany; ⁵Helmholtz-Zentrum Dresden-Rossendorf, Germany; ⁶The University of Iowa, United States

Plasmonics and polaritonics have enabled the field of nanophotonics to reduce the wavelength of light to length scales far below the diffraction limit, leading to optoelectronic devices miniaturization and enhanced light-matter interactions. Traditionally, complex heterostructures were necessary to achieve the desired confinement capabilities. Coherently coupled vibrations in polar dielectrics, or phonon polaritons, are an attractive alternative to realize these goals as they use a different mechanism intrinsic to the material, to compress light. Quality phonon polaritonic materials possess a large splitting between the transverse optic (TO) and longitudinal optic (LO) phonons, which results from a strong internal electric dipole. Within the TO-LO splitting, or Reststrahlen band, the dielectric permittivity becomes negative, opening the door for phonon polaritons. Traditionally, the dominant spectral range for phonon polaritons has been the mid-infrared (mid-IR), despite a rich potential for nanophotonic materials at far-infrared (far-IR) and terahertz (THz) frequencies where molecular vibrations and rotations are observed. The transition of plasmonics and polaritonics into the far-IR and THz has been stunted due to a lack of materials that can host phonon polaritons.

Transition metal dichalcogenides (TMDs) are commonly studied in the near-infrared (near-IR) and visible wavelengths, specifically for the excitonic properties in MoS₂, MoSe₂, WS₂, and WSe₂. However, the phonon resonances of these TMDs are not strong and do not possess large TO-LO splitting, making them a poor candidate for infrared nanophotonics. Conversely, Group-IVB TMDs such as HfS₂ and HfSe₂ have exceptionally large Reststrahlen bands (> 100 cm⁻¹), a priority for phonon polaritonics. They are also two-dimensional (2D) van der Waals crystals, making them even more attractive for nanoscale optics. Furthermore, due to the crystals' anisotropy, the dielectric permittivity between the in-plane (ϵ_{xy}) and out-of-plane (ϵ_z) directions differs with respect to the incident wavelength, which separates the Reststrahlen band into two dispersion bands, elliptic ($\epsilon_{xy}^* \epsilon_z > 0$) and hyperbolic ($\epsilon_{xy}^* \epsilon_z < 0$). In the hyperbolic regions, the isofrequency contour becomes an open hyperbola with extraordinary waves that do not have a momentum (k) limit, facilitating extreme compression of the free-space wavelength ($k = 2\pi/\lambda$).

In this study, we use polarized Fourier transform infrared (FTIR) spectroscopy to extract the anisotropic IR permittivity of HfS(e)₂ and reveal the exceptional TO-LO splitting in the mid- to far-IR. Within these broad bands, we image the near-field optical signal of phonon polaritons and measure confinement of the free-space wavelength by a factor of more than 100. Finally, by varying the substrate permittivity, we demonstrate tunable control of the coupling strengths between the hyperbolic phonon polaritons and epsilon-near-zero polaritons in HfSe₂. By examining an underexplored class of materials, this work directs the search for quality nanophotonic materials, in particular those that facilitate access to far-IR/THz wavelengths, a spectral range that suffers from limited optical materials.

11:15 AM *EL08.13.03

Metasurfaces for Light Detection and Ranging [Patrice Genevet](#); Colorado School of Mines, United States

Metasurfaces are versatile optical components that can distribute optical power in desired regions of space, thus holding great potential for on-chip integration of miniaturized optoelectronic and imaging systems[1]. Using metasurfaces, we reported advanced LiDAR technology that leverages from ultrafast low FoV deflectors cascaded with large area metasurfaces to achieve large FoV (150°) and high framerate (kHz)[2]. Additionally, achieving wide-angle 3D imaging is becoming essential nowadays for autonomous robotic systems, yet most of the available solutions fail to simultaneously measure back-scattered from multiple directions. Inspired by arthropods eyes, we conceive a metasurface can overcome the limitation of curved optics, achieving panoramic vision. On-chip vertical integration of directional metalenses on the top of a planar array of detectors enables a powerful insect-inspired LiDAR vision that is capable of 3D imaging over a wide field of view[3]. The use of our disruptive LiDAR technology with advanced learning algorithms offers perspectives to improve perception and decision-making process of ADAS and robotic systems.

[1] "Crossing of the branch cut: the topological origin of a universal -phase retardation in non-Hermitian metasurfaces", R Colom, E Mikheeva, K Achouri, J Zuniga-Perez, N Bonod, O JF Martin, S Burger, and P Genevet, *Laser & Photonics Reviews* 2023, 2200976

[2] "Metasurface-enhanced Light Detection and Ranging Technology" RJ Martins, E Marinov, M. Aziz Ben Youssef, C Kyrou, M Joubert, C Colmagro, V Gâté, C Turbil, PM Coulon, D Turover, S Khadir, M Giudici, C Klitis, M Sorel and P Genevet, *Nature Communications* 13, 5724 (2022)

[3] "Bio-inspired flat optics for directional 3D Light Detection And Ranging", C Majorel, A Loucif, E Marinov, RJ Martins, A Patoux, PM Coulon, V Brandli, E Charbon, C Bruschini, and P Genevet, (submitted 2023)

11:45 AM EL08.13.04

Silicon Nanophotonics for Multi-Omic Marine Detection [Halleh Balch](#)¹, Sahil Dagli¹, Varun Dolia¹, Kai Chang¹, Greg Doucette², William Ussler³, Chris Scholin³ and Jennifer A. Dionne¹; ¹Stanford University, United States; ²NOAA/National Center for Coastal Ocean Science, United States; ³Monterey Bay Aquarium Research Institute, United States

The oceans are host to diverse marine microorganisms that are capable of cycling nearly all chemical elements and are responsible for over half of the oxygen on earth, forming a key part of our carbon cycle. Yet, studying the marine microbiome remains an outstanding challenge. Very few marine microbes have been successfully cultured under laboratory conditions and culture-independent methods like metagenomics and mass spectroscopy are incompatible with the real-time and in situ measurements necessary to study how physico-chemical drivers impact microbial nutrient cycling.

Here, we present our approach based on high quality factor silicon nanophotonics to simultaneously and rapidly measure multiple 'omic' signatures from marine ecosystems. Our metasurfaces are composed of sub-wavelength silicon nanobars on sapphire substrates. First, by introducing small biperiodic perturbations to the lateral block dimension, free space radiation can be coupled into guided mode resonances to produce high-Q resonances with Q factors exceeding 10³ in aquatic environments. We demonstrate in simulation and experiment that by varying the biperiodic perturbation from 10 nm to 50 nm, the quality factor can be modulated from 10²-10⁴ and that the local electric field can be driven to the silicon surface, increasing the overlap between the field and the binding surface by nearly four-fold. We experimentally demonstrate that by introducing tapered photonic mirrors, the resonator cavity length can be reduced by 10X while retaining Q-factors exceeding 3000, and that the long resonance lifetimes together with the increased field penetration at the binding surface results in strong spectral shifts of the resonance mode due to small perturbations to the local dielectric environment. We fabricate our metasurfaces by e-beam lithography and demonstrate that the optical responses of individual resonators can be spatially resolved as individually addressable finite 'pixels' and simultaneously read out on a 2D InGaAs CCD array in a cross-polarized reflection configuration.

Using this platform, we demonstrate quantitative and amplification-free detection of DNA and the harmful algae bloom toxin, microcystin, which poses a threat to drinking and agricultural water supplies. We selectively target nucleotides and the toxin microcystin on the same multiplexed platform using tailored surface functionalization of self-assembled monolayers (SAM) and a competitive antibody binding assay. We observe in both calculations and experiments that consecutive molecular layers generate 0.5 nm - 4 nm shifts to the resonant wavelengths as sequential layers bind to the resonator surface. Finally, I will discuss the integration of our high-Q metasurfaces with flow-through microfluidics and an autonomous robotic water sampler developed at the Monterey Bay Aquarium Research Institute (MBARI), that offers a pathway for in situ phycotoxin detection, processing, and analysis.

SESSION EL08.14: Active Control Metasurfaces and Metamaterials

Session Chairs: Ho Wai (Howard) Lee and Pin Chieh Wu

Thursday Afternoon, April 25, 2024

Room 340/341, Level 3, Summit

1:30 PM *EL08.14.01

Photonic Integrated Circuits with Inverse Design Kiyoul Yang; Harvard University, United States

In this presentation, we will discuss a gradient-based optimization of nanophotonic device design, known as photonic inverse design, along with its applications in silicon photonic data communications and quantum nonlinear photonic experiments.

2:00 PM EL08.14.02

Acoustically Modulated Gap Plasmons Skyler P. Selvin, Majid Esfandyarpour, Mohammad Taghinejad and Mark L. Brongersma; Stanford University, United States

Among all techniques used to modulate light, mechanical modulation techniques hold high promise due to their ability to alter the optical permittivity to a greater extent than any other modulation technique. However, typical mechanical techniques employing acoustic waves and the photo-elastic effect, such as Acousto-Optic Modulators (AOMs), struggle to efficiently modulate light due to the weak refractive index modulation that acoustic waves impose on optical materials. Micro-Electromechanical Systems (MEMS) can be more efficient, but are limited in speed and spatial resolution. The ideal mechanical system would thus combine the advantages of both AOMs and optical MEMS. Here, we present and characterize a Nano-Electromechanical System (NEMS) acousto-optic resonator, which comprises a gap plasmon resonator with a deformable gap filler. The plasmonic gaps confine light to nanometer-sized regions, enabling small nanometer-scale movements to significantly and efficiently modulate the optical scattering spectra. Surface acoustic waves (SAWs) are emitted and shaped under an array of these gap plasmon resonators, facilitating spatially tunable optical scattering. We show time-resolved optical spectra and demonstrate high-frequency continuous optical beam steering by sweeping the input SAW frequency. This work represents a significant advancement in the field of acousto-optic modulation, and provides a new platform to investigate soft materials at the nanometer and nanosecond scale.

2:15 PM EL08.14.03

Tunable Metal-CP-Metal Metasurface with Intrinsically Reflective IR-Electrochromic Conducting Polymer (CP) Ting-Hsuan Chen^{1,2} and Po-Chun Hsu²; ¹Duke University, United States; ²The University of Chicago, United States

Electrochromic conducting polymers (CPs) have made significant contributions on actively tunable applications from visible light to infrared (IR), including metasurfaces, plasmonics, and personal thermoregulation. By varying their charge concentration and localization, the interaction between CPs and electromagnetic waves is therefore modulated. Until recently, most CP-based IR-electrochromic studies focused on thin-films toggling between transmissive and absorptive state, due to the trade-off between electrical conductivity and ionic diffusion kinetics. Compared with the transmission modulation strategies, electrochromism based on intrinsic reflectance opens the opportunities to create substrate-agnostic devices.

In this presentation, we propose a tunable metal-CP-metal tunable metasurface by incorporating lossy metals with CP to achieve large tunability of absorption and emission in mid-to-long IR spectrum. The device utilizes the CP as the active material to modulate between reflective and absorptive states. Our study shows the active material, chemically synthesized camphor sulfonic acid doped polyaniline (PANI-CSA), can simultaneously achieve intrinsic reflectance and large mid-IR electrochromic contrast. The IR-spectroscopic ellipsometry and electrochemical characterization explains the correlation between the electrochemical kinetics and the charge localization during the modulation process. Finally, we will discuss and compare the several materials and design properties that affect the overall performance and efficiency in IR electrochromic metasurfaces.

2:30 PM ^EL08.14.04

Gap-Plasmon-Enhanced NbN Superconducting Photon Detectors at Single-Photon Level Yu-Jung Lu^{1,2}; ¹Academia Sinica, Taiwan; ²National Taiwan University, Taiwan

Single-photon detectors have been widely studied for decades because of their unique capability to resolve photon numbers, enabling many applications in quantum information technologies. Compared to other types of single-photon detectors, niobium nitride (NbN) superconducting nanowire single-photon detectors are promising candidates and are commercially available today. However, the absorption coefficient of superconducting NbN in the visible range is typically low, resulting in low quantum efficiency and low signal-to-noise ratios. In the present work, we use a novel approach to enhance the visible-light photoresponse in NbN superconducting microwire photon detectors (SMPDs) by integrating them with gap plasmon resonators (GPRs). This talk describes how we observe the plasmonic NbN SMPDs can achieve a 233-fold enhancement in the phonon-electron interaction factor (γ) compared to pristine NbN SMPDs under resonant conditions with illumination at 532 nm. The nonlinear photoresponse in the visible region is attributed to the gap-plasmon-induced heating that breaks the superconducting state to normal. In addition, an impressive detection efficiency of 98% was achieved using these plasmonic SMPDs. Our results open new opportunities for designing sensitive quantum detectors for quantum information processing, quantum optics, imaging, and sensing at visible wavelengths. The detailed mechanisms and possible applications will be discussed.

2:45 PM BREAK

3:15 PM *EL08.14.05

High-Efficiency Electrically Tunable Active Metasurfaces at Telecommunication Wavelengths Ruzan Sokhoyan, Martin Thomaschewski and Harry A. Atwater; California Institute of Technology, United States

We theoretically discuss different design pathways towards achieving high-efficiency active metasurfaces. We demonstrate electrically tunable active metasurfaces, which can dynamically manipulate the wavefront of the reflected light in the near-infrared wavelength range while exhibiting optical efficiencies > 80%. Our active reflective metasurfaces consist of a gold (Au) back reflector, followed by a silica spacer (SiO₂) on top of each we place an array of amorphous silicon (a-Si) pillars [1]. The quality factors of the designed metasurfaces can adopt values ranging from a few 100s up to 60,000. We achieve a dynamically tunable optical response by integrating an electro-optically tunable lithium niobate layer (LNO) layer into the resonant metasurface structure and introducing indium tin oxide (ITO) interconnects. By applying electrical bias, we achieve a dynamically tunable phase shift of 236° when the refractive index of the LNO layer varies between 2.212 and 2.208. The optical efficiency of the designed metasurface is > 80 % for all the considered values of the applied bias, and the Q-factor of the considered resonance is 40,000. In alternative implementations, we use ITO or tungsten disulfide (WS₂) as dynamically tunable materials and present realistic active metasurface designs adapted to the choice of the active material. Finally, we analyze the beam steering performance of the designed metasurfaces considering the cases of both two-dimensional and one-dimensional beam steering.

The designed high-efficiency metasurfaces could be useful for a number of applications such as free-space optical communications, light detection and ranging (LiDAR), and laser-based additive manufacturing.

[1] Ruzan Sokhoyan, Claudio U. Hail, Morgan Foley, Meir Y. Grajower, and Harry A. Atwater, "All-dielectric high-Q dynamically tunable transmissive metasurfaces", arXiv:2309.08031v1.

3:45 PM *EL08.14.06

Electrochemically Active Metasurfaces Po-Chun Hsu; The University of Chicago, United States

Electrochemistry is a powerful tuning knob for inducing drastic material property change. By applying an electrical bias while using counterions to maintain charge neutrality, electrochemistry can vary the carrier density or even trigger a phase transformation in an electrically addressable manner. Electrochemistry is an ideal tool in many applications where tunable range, scalability, or non-volatility is crucial. However, electrochemically active metasurfaces are still largely underexplored, probably due to the lack of a property database to perform metasurface design and optimization. More co-development is needed among fundamental materials science, metasurface design, and electrochemical device engineering. In this talk, I will present two examples of electrochemically active metasurfaces. (i) Conducting polymer near-perfect dynamic thermal emitter. We conducted infrared ellipsometry to measure the potential-dependent optical property and designed a tunable MIM near-perfect absorber for wearable variable emittance (WeaVE) devices for personal thermoregulation. (ii) Reversible metal electrodeposition for active beam steering metasurface. Because reversible electrodeposition can create and dissolve metals on demand, active metasurface can be achieved by creating and dissolving the meta-atoms or affecting the periodicity. As a proof of concept, we will demonstrate a reflection-type beam steering metasurface based on this principle and discuss the outlook and future challenges and opportunities.

4:15 PM EL08.14.07

Stop Coloring Inside The Lines- Meniscus-Guided Printing of Nanoparticle Films John R. Crockett, Kyung Sun Park, Yen-Chi Chen, Ying Diao and Qian Chen; University of Illinois at Urbana-Champaign, United States

Meniscus-guided printing has become a well-known technique for the application of polymer films. The ability to control orientation and thickness along with the ease of scaling have made it a low cost and effective process that is even used in manufacturing OLED displays. This research investigates the use of meniscus-guided printing for the simultaneous self-assembly and deposition of anisotropic gold nanorods. Through varying the speed, concentration of nanorods, energy of surface interactions, and size of substrate we have achieved deposition of several patterns with features from the millimeter to the nanoscale. This method can alleviate the necessity of costly and time-consuming templating or lithography steps, instead by controlling the confinement of the solution, and its interaction with the substrate, nanoparticle films can be templated and printed simultaneously.

SESSION EL08.15: Poster Session III

Session Chairs: Ho Wai (Howard) Lee and Pin Chieh Wu

Thursday Afternoon, April 25, 2024

Flex Hall C, Level 2, Summit

5:00 PM EL08.15.01

Realizing Full-Spectral Image Encryption in The Infrared Using an Electrically Tunable Metasurface and a Matched Detector Romil Audhkhasi¹ and Michelle Povinelli²; ¹University of Washington, United States; ²University of Southern California, United States

The ability of metasurfaces to manipulate optical waves in the spatial and spectral domain has provided new avenues for the development of compact and secure data storage platforms. Here we present an encryption system consisting of an electrically tunable metasurface and a matched detector for secure encryption of grayscale images in the 8 – 12 μm wavelength range. In the proposed scheme, the encrypted image corresponds to the spatially varying thermal intensity of the metasurface as captured by its matched detector. In contrast to previous metasurface-based encryption schemes, the current approach leverages the full spectral response of the associated photonic devices to achieve secure encryption while circumventing the need for an increased device size. Using examples of single and multi-image encryption, we show that the optical properties of either the metasurface or matched detector alone do not reveal any meaningful information about the encrypted image, thereby validating the security of the proposed scheme. The electrical tunability of the metasurface provides additional security as the image can only be retrieved by operating it at a predefined voltage level. We believe that our results provide intriguing possibilities for the development of compact and secure object tagging and anti-counterfeiting applications in the infrared.

5:00 PM EL08.15.02

Manipulating Confined Infrared Light via Polaritonic Design of Sub-Diffractive $\alpha\text{-MoO}_3$ Wedges Ethan Ray^{1,2}, Mingze He², John Buchner², Saurabh Dixit² and Joshua D. Caldwell²; ¹Georgia Institute of Technology, United States; ²Vanderbilt University, United States

The Mid-infrared (mid-IR) spectrum of light is crucial for various applications, including thermal imaging, molecular sensing, and free-space communication. However, the application of long free-space wavelengths of mid-IR light is limited in chip-scale devices due to the diffraction limit. This problem can be circumvented by using hyperbolic materials where the dielectric permittivities along the principal crystal directions exhibit opposite signs in the mid-IR spectral region. It has been well-demonstrated that hyperbolic materials (e.g. h-BN, $\alpha\text{-MoO}_3$, $\alpha\text{-V}_2\text{O}_5$) can confine high-momentum (short wavelength) electromagnetic waves in the form of hyperbolic phonon polaritons (HPhPs)- quasi-particles made from the hybridization of charged dipoles (phonons) and photons (an external light source). The propagation behavior of these HPhPs can be tuned and confined in deep sub-diffraction volumes using sub-wavelength structures, which offer distinct opportunities in the form of chip-scale nano-photonics devices for integrated optics and photonics applications.

In this work, we investigate sub-wavelength wedges of a hyperbolic material ($\alpha\text{-MoO}_3$) to demonstrate in-plane focusing of electromagnetic waves beyond the diffraction limit and a transition of polaritonic propagation in the forbidden direction of the $\alpha\text{-MoO}_3$ crystal. We design our wedges by optimizing lateral dimensions and wedge thickness using 3D numerical simulations via COMSOL Multiphysics. Numerically, we observed transitions from adiabatic compression to standing wave in polaritonic modes through changing wedge vertex angles (θ_v). For $10^\circ < \theta_v < 30^\circ$, we observe a compression factor (i.e. ratio of wavelength in standing wave region to the adiabatically compressed region in the wedge) of 2.89 (at 700 cm^{-1}) and 1.42 (at 900 cm^{-1}) that converge to 1 upon increasing vertex angle. Further, we investigate the effect of geometrical confinement at vertex angles $120^\circ < \theta_v < 150^\circ$ on propagation direction and found that a high vertex angle of wedge enables the propagation of HPhPs in the forbidden direction. After establishing these theoretical foundations, we

fabricated such wedges and characterized them with scattering-type Scanning Near-field Optical Microscopy (s-SNOM). Through s-SNOM, we found the presence of adiabatically compressed waves confined at the tip of the wedge at lower vertex angles and node formation along the forbidden propagation direction at high vertex angles. This work offers a novel tunable parameter for manipulating mid-IR light propagation in α -MoO₃ sub-wavelength structures. Further, these findings open avenues for chip-scale mid-IR nanophotonic devices and optical components with the ease of van der Waals integration for integrated optics and photonics applications.

5:00 PM EL08.15.03

New Design Principle of Chemically Tunable Bulk Hyperbolic Metamaterials Hyungseok Lee^{1,1}, Jong-Young Kim² and In Chung^{1,1}; ¹Seoul National University, Korea (the Republic of); ²Korea Institute of Ceramic Engineering and Technology, Korea (the Republic of)

Conventional hyperbolic metamaterials are fabricated to form artificial nanoscale structures that are designed to interact with light uniquely. In addition to the difficulty in theoretical prediction of the structures to induce desired properties, their structures had to be realized by technically challenging nanofabrication techniques. Herein, we present a new facile design principle to realize bulk metamaterials with a hyperbolic dispersion tunability. Using two exfoliated inherent hyperbolic materials as a building block, hexagonal boron nitride (h-BN) and graphite/graphene, we developed the facile synthesis method to obtain their heterostructured nanohybrid powders via self-assembly between two functionalized building blocks. Afterwards, the resulting powders were consolidated into dense bulk pellet using spark plasma sintering. The final bulk products comprise the alternating nanoscale layers of h-BN and graphite/graphene. Depending on the mixing ratio and thickness of the constituent building blocks their microstructures were delicately altered, consequently serving as a fine tool to control the hyperbolic responses. Remarkably, embedding a trace of rhombohedral boron nitride (r-BN) also anisotropically changes both type-I and type-II hyperbolic resonance modes and negative permittivities, thus indicating that r-BN acts as a 'dopant' in h-BN/graphite metamaterial system. For the first time, our work demonstrates the real bulk metamaterials with finely tunable hyperbolic dispersions by modulating chemical compositions. Negative permittivities are observed for the incident infrared light along both the in-plane and out-of-plane directions. Our achievement can serve a potential platform to rationally design and conveniently realize scalable bulk metamaterials without need of complicated fabrications.

5:00 PM EL08.15.05

Terahertz Time Domain Transmission Spectroscopy of Magnetic Nanoparticles for Frequency Selective Surface Application Kousik Pradhan¹, Sumit Saxena¹, Shobha Shukla¹, Siddhartha Duttgupta¹ and Sriganesh Prabhu²; ¹Indian Institute of Technology Bombay, India; ²Tata Institute of Fundamental Research, India

Terahertz time-domain spectroscopy (THz-TDS), is an effective method for characterizing materials and monitoring processes. Metals, electronics, 2D materials, and even superconductors have all been tested with this technique, which does not require physical touch to obtain accurate results. Terahertz (THz) spectroscopy has developed as a method for investigating dielectric and transient photoconductive characteristics of materials over the past few decades. Since it can measure electrical resistance without touching the sample and has a temporal precision of a few picoseconds. Due to the low energy of THz radiation and the narrow pulse width, THz-TDS technology is non-destructive when used for extracting visual data from materials (picosecond range). This paper reveals optical parameters extraction methods by using THz transmission spectroscopy technology. In summation, materials with a low absorption of terahertz radiation can benefit from the adaptability of transmission methods, while materials with a high absorption capacity can take advantage of the advantages of reflection methods. To measure the magnetic material's optical properties like refractive index and absorption coefficient, we employ a transmission-type terahertz time domain spectroscopic instrument. The observations and analysis are performed in both the time domain and frequency domain, and we examine the transmission of terahertz radiation through a polymer based magnetic nanoparticle substance at frequencies from 0.1 to 3 terahertz (THz). In the past few years, magnetic materials based on frequency selective surfaces (FSS) have become indispensable in the design of gigahertz (GHz) and terahertz (THz) millimeter-wave filters, polarizers, absorbers, EMI shielding, antenna reflectors, and radar applications. In this research, ferrite was used to produce a microstructured FSS on a quartz substrate. Frequency Domain (FD) solvers included in the CST MWS commercial software package, which is based on the Finite Integration Technique (FIT), are used to evaluate the FSS's efficiency. Here, we demonstrate a terahertz filter made from arrays of circular holes in a quartz substrate, which acts as a frequency selective surface (FSS). We shall show the properties of FSS terahertz-wave transmission using a finite difference time-domain approach. Researchers looked examined the suggested design over a range of frequencies from 0.2 THz to 3 THz. The proposed structure's complementary behaviour is also statistically analysed. We evaluate the proposed layouts by investigating their most elemental characteristics, such as their transmittance and polarisation. The response of the proposed structure to a broad variety of incidence angles is also investigated. Additionally, at the frequency selective surface of the magnetic material, polarisation insensitivity is achieved for the TE and TM stimulated mode. This research presents the detailed layout and analyses of the evaluated parameters for the proposed terahertz wave filter. The suggested terahertz wave filter's parameters are then fine-tuned. The filter we describe has the potential to be widely used in future terahertz wave systems due to its low manufacturing costs and simple design.

5:00 PM EL08.15.06

Dynamic Tuning between a Reflecting Mirror and a Transmitting Window by Nano Sphere Lithography and Electrochemistry TsungYu Huang and Cheng-Yuan Xiao; Ming Chi University of Technology, Taiwan

In the ever-evolving landscape of technology, electronic devices such as displays, solar panels, and touchscreens have become indispensable to our daily lives. These devices rely on a critical component known as transparent conductive electrodes. In the past, indium tin oxide (ITO) was the common material for these electrodes. However, ITO has certain drawbacks. Its inherent oxide nature makes it brittle and susceptible to damage, and indium is a precious metal, with high cost. To overcome these challenges, researchers have explored novel nanostructures that serve as alternatives to traditional ITO electrodes. Yet, most of these nanostructures come with a drawback, i.e., they tend to possess fixed conductivity and transmittance values after production, lacking the ability for dynamic modulation.

To address this limitation, in this work, we combine nanosphere lithography, indium tin oxide deposition, and the electrodeposition of silver to design and fabricate a dynamic tuning between a reflecting mirror and a transmitting window. To fabricate such a device, first of all, we spin-coated polystyrene nanospheres for a uniform mask. The corresponding spacing among nanospheres was further modified by reactive ion etching. Next, ITO was deposited to form a continuous hollow hole array. Then, the electroplating of silver was carried out. By controlling parameters of electrochemical reaction, we could fine tune the corresponding thickness of silver and the open of the hole array for active manipulation of transmittance of the proposed devices. The electroplating behavior of the device and the transmittance for different thickness and morphology of the device were further predicted by two simulations. The first simulation focused on the transmittance of the proposed device by tuning the periodicity and the opening of the devices and the thicknesses of both ITO and silver. The second simulation involves the electrochemistry reaction. The potential variables included material parameters of electrodes and electrolytes, applied current, electrodeposition area, and thickness to anticipate the experimental outcomes.

5:00 PM EL08.15.07

Configurational Tunable Mie, Plasmonic and Diffractive Structural Colors in a Single Design Youngji Kim^{1,2}, Joshua D. Caldwell¹ and Jerome Hyun²; ¹Vanderbilt University, United States; ²Ewha Womans University, Korea (the Republic of)

We have developed a structural color design capable of displaying Mie resonant, plasmonic, and diffractive colors within a single design, depending on the configuration of imaging setup. Previous research achieved two distinct colors arising from the same resonance mechanism by introducing anisotropy into the structural parameters of a 2D array and selectively displaying each color based on the polarization. In this study, however, we store and display multiple colors within a single design by employing a 1D metallodielectric grating composed of TiO_x nanowires sandwiched between two Ag layers. Choice of polarization allows for either an electric dipole Mie resonance or a localized surface plasmon resonance to occur independently, generating striking differences in color. Furthermore, the selection of numerical aperture (NA) can further extend the color modulation, as collected diffracted light wavelength is determined by the NA. We also demonstrate the color modes from the 1st order diffraction. All resonance mechanisms and imaging configurations depend solely on the two spatial parameters and their combination: the period and the width of the nanowire. Finally, we demonstrate four levels of encoded images produced from a single set of the gratings under different imaging setups. These findings open up new possibilities for applications, such as image encryption and data storage, and so on.

5:00 PM EL08.15.08

Coupling Surface Plasmon Polaritons to Surface Acoustic Waves Felix Kimeu, Derricka Jones, Renny Fernandez and Doyle Temple; Norfolk State University, United States

The interaction of surface acoustic waves (SAWs) with incident beams to excite surface plasmon polaritons (SPPs) represents an exciting and promising area of exploration in photonics, biotechnology, and nanoscience. This combination of acoustic and optical effects offers fresh opportunities for investigating and controlling surface-related phenomena and devices. The incorporation of SAWs and SPPs provides a unique platform with diverse applications, such as sensing, imaging, and signal processing, capitalizing on their combined strengths in propagation, high sensitivity, adjustable spectral properties, and precision. Our hypothesis suggests that through meticulous selection of the metal for the sensing area, precise control of the metal film's thickness, and accurate adjustment of the SAW frequencies, we can attain exact resonance. Using computational software, Mathcad in the design phase, we carry out simulations to determine the SAW frequencies necessary for achieving optimal coupling with incident beams of varying wavelengths. The research investigates the choice of the metal film at the sensing region and its thickness influences alterations in reflectivity at specific thicknesses of the metal film, and how these alterations affect the sensor's overall performance. The objective is to establish a robust theoretical foundation for the sensor's operation while considering the influence of different metals on its sensitivity and selectivity. The fabrication of the actual sensor prototype is outlined as a crucial aspect of future work, leveraging the insights gained from the simulations of different metals and variation of the thickness to build a functional and efficient SAW-SPP sensor. Additional future steps include calibrating and fine-tuning the sensitivity of the prototype to enhance its performance, as well as ascertaining its selectivity using different analytes.

5:00 PM EL08.15.09

Cost-Effective Wide-Angle High-Performance Mid-Wavelength Infrared Polymeric Polarizers by Sulfur-Rich Polymers Gyeongyeon Bae, Woongbi Cho and Jeong Jae Wie; Hanyang University, United States

Mid-wave infrared (MWIR) detectors have a wide range of applications in various fields, including non-invasive medical diagnosis, gas detection, and night vision. The IR polarization can significantly improve the resolution of IR images by selectively transmitting transverse magnetic fields (TM). However, state-of-the-art MWIR polarizers mainly use ceramic materials such as ZnS, ZnSe, and Ge. Although these materials offer excellent IR transmission and polarization properties, the material costs are expensive, and their crystalline structures require specialized etching equipment for processing. Toward cost-effective fabrication of MWIR 1D polarizers, we recently reported high-fidelity thermal imprinting of sulfur-rich polymer (SRP) by inverse vulcanization of elemental sulfur with diisopropylbenzene (DIB). The SRPs are mainly composed of elemental sulfur, which is a byproduct of the petroleum refining process. However, 1D polarizers lack the ability to precisely manipulate the incoming light because they cannot accurately classify incoming light from various directions. In addition, the glass transition temperature (T_g) of DIB-based SRP is close to room temperature, suffering from dimensional stability to maintain the shape of the polarizer in practical applications. In this presentation, we discuss strategy to enhance T_g of SRP for thermal nanoimprinting of 2D nanostructured polarizer. We systematically fine-tuned various thermal nanoimprinting conditions for high-fidelity imprinting of the 2D patterns. This innovative 2D nanostructured polarizer, based on SRP, presents a cost-effective solution for MWIR applications, enhancing image quality and expanding its practical utility.

Mid-wave infrared (MWIR) detectors have a wide range of applications in various fields, including non-invasive medical diagnosis, gas detection, and night vision. The IR polarization can significantly improve the resolution of IR images by selectively transmitting transverse magnetic fields (TM). However, state-of-the-art MWIR polarizers mainly use ceramic materials such as ZnS, ZnSe, and Ge. Although these materials offer excellent IR transmission and polarization properties, the material costs are expensive, and their crystalline structures require specialized etching equipment for processing. Toward cost-effective fabrication of MWIR 1D polarizers, we recently reported high-fidelity thermal imprinting of sulfur-rich polymer (SRP) by inverse vulcanization of elemental sulfur with diisopropylbenzene (DIB). The SRPs are mainly composed of elemental sulfur, which is a byproduct of the petroleum refining process. However, 1D polarizers lack the ability to precisely manipulate the incoming light because they cannot accurately classify incoming light from various directions. In addition, the glass transition temperature (T_g) of DIB-based SRP is close to room temperature, suffering from dimensional stability to maintain the shape of the polarizer in practical applications. In this presentation, we discuss strategy to enhance T_g of SRP for thermal nanoimprinting of 2D nanostructured polarizer. We systematically fine-tuned various thermal nanoimprinting conditions for high-fidelity imprinting of the 2D patterns. This innovative 2D nanostructured polarizer, based on SRP, presents a cost-effective solution for MWIR applications, enhancing image quality and expanding its practical utility.

SESSION EL08.16: Metastucture Designs and Fabrication for Light Manipulation and Sensing

Session Chairs: Ho Wai (Howard) Lee and Ruzan Sokhoyan

Friday Morning, April 26, 2024

Room 340/341, Level 3, Summit

10:30 AM EL08.16.01

Probing The Impact of Interfaces on Thin-Film Lithium Niobate Electro-Optic Device Performance Matthew Yeh¹, David R. Barton^{1,2}, Gavin Smith¹, Evelyn L. Hu¹ and Marko Loncar¹; ¹Harvard University, United States; ²Northwestern University, United States

Thin-film lithium niobate on insulator (TFLN) has emerged as a strong candidate platform for integrated classical and quantum photonics due to its large linear electro-optic (EO) effect and wafer-scale availability. Driven by breakthroughs in nanofabrication, the EO interaction strength has greatly improved over the bulk, unlocking a new class of devices such as high-bandwidth and energy-efficient modulators, ultrafast pulse generators, and microwave-to-

optical transducers. Despite rapid advances in device functionality, however, material understanding has fallen behind. In particular, it is generally recognized that the reliability of TFLN modulators is subject to unstable EO response at dc and low frequencies. This instability is especially disruptive to the advancement of large-scale photonic circuits and cryogenic applications such as quantum photonics, which require precise index reconfigurability and low-power operation. Post-processing techniques such as thermal annealing have been developed to reduce these deleterious effects, but the microscopic origins of instability remain unclear.

Here, we combine measurements of the material structure, electronic properties, and EO device performance to identify a mechanistic insight for low-frequency instability in TFLN. All devices are fabricated on 600 nm thick x-cut lithium niobate on insulator wafers, and we explore modifications to the fabrication process that affect both bulk and interface properties. First, we correlate electronic transport measurements with improvements in the EO response magnitude to show that annealing reduces charge leakage pathways in TFLN. However, SIMS measurements of the elemental composition show that simultaneously additional dielectric relaxation pathways are introduced; annealing in the presence of a cladding oxide creates an interface by which lithium can diffuse out of the TFLN.

Next, we show through XPS that the etch chemistry and acid cleans used in our thin-film processing dramatically affect the surface chemistry of TFLN. Dry etching with an Ar plasma reduces Nb and creates a damaged amorphous surface layer, whereas employing a C_3F_8 -based chemistry creates a prominent F peak stemming from the formation of LiF_x salts or fluoropolymers. The surface Li:Nb ratio can be restored both by specific chemical cleans that remove the damaged layer or thermal annealing. Surprisingly, forming metal contacts to LN surfaces that have been cleaned or annealed actually reduces the EO response magnitude and degrades the stability. Together, these measurements indicate that the metal-TFLN interface also plays a key role in determining EO device performance.

10:45 AM EL08.16.02

A Battery-Free Stretchable Strain Sensor Using Plasmon-Based Structural Color [Naoji Matsuhisa](#)^{1,2}, Riku Nakagawa^{1,2}, Keinosuke Soda², Yushi Suzuki², Hiroki Kajita² and Toshiharu Saiki²; ¹University of Tokyo, Japan; ²Keio University, Japan

Soft and stretchable sensors offer superior skin conformability, enabling the capture of high-quality biometric signals. Among these, color-based sensors can be operated without batteries and read using devices like smartphone cameras, making them easy to use. While there have been advancements in strain sensors using structural colors, such as photonic crystals [1,2], their applications are limited due to challenges in tuning device softness.

Here, we introduce a battery-free, soft, and stretchable strain sensor using structural color that combines plasmon resonance and interference effects. The device structure comprises 4 stacked layers: a high-refractive-index ($n=1.55$) polymer, a low-refractive-index ($n=1.33$) polymer, gold nanoparticles, and a black silicone substrate. Structural coloration emerges from the interference of reflected light from gold nanoparticles, where plasmon resonance takes place, with the reflected light at the interface of the top high and low-refractive-index layers. Applied strain changes the thickness of a low-refractive-index polymer layer to induce different structural colors. This color can be adjusted by modifying the thickness of the low-refractive-index polymer layer and the gold nanoparticle size. Given our structural color layer is ultra-thin, under 1 μm , its flexibility is easily adjustable with additional PDMS layers. A particular device displayed a reflection peak of 730 nm (red) at 0% strain and 665 nm (green) at 60% strain. Moreover, our sensor adapted to finger joints and exhibited a distinct color shift during finger bending.

1. Yue, Y. et al. Mechano-actuated ultrafast full-colour switching in layered photonic hydrogels. *Nat. Commun.* 5, 4659 (2014).

2. Park, T. H. et al. Block copolymer structural color strain sensor. *NPG Asia Materials* 10, 328–339 (2018).

11:00 AM EL08.16.03

Investigation of The Nanoparticle – Support Interaction Effects of Plasmonic Gold Nanoparticles Deposited on Steel and Aluminum [Rosemary L. Calabro](#)^{1,2}, John Burpo¹, Stephen F. Bartolucci² and Joshua A. Maurer²; ¹United States Military Academy, United States; ²U.S. Army DEVCOM Armaments Center, United States

Plasmonic nanoparticle (NP) based sensors have been developed to detect a wide range of analytes based on the principles of localized surface plasmon resonance (LSPR). With LSPR, the peak wavelength of absorption and scattering can shift, broaden, narrow, or be amplified or suppressed based on an interaction with the analyte of interest, allowing an optical readout. However, factors such as near-field coupling, size effects, and surface environment of the NPs can also influence the LSPR properties. Practical implementation of LSPR based sensors requires deposition of the NPs on a substrate, however most studies thus far have focused on very crystalline or pristine materials. We investigated the NP-substrate interaction effects of gold nanoparticles (AuNPs) on two industrially relevant substrates: steel and aluminum. AuNPs were drop cast on the substrates and the change in reflectivity was measured. The spectral properties were also compared to AuNPs in solution. Near field-coupling of the AuNPs was observed when the samples were transferred from water to isopropyl alcohol due to partial nanoparticle agglomeration, however this coupling effect was not observed when the particles were deposited from the isopropyl alcohol to the substrates, despite being aggregated together on the substrate. This suggests that the AuNP coupling effect to the substrate is much stronger than any NP interactions with each other. Shifts in the peak wavelengths were observed when depositing the AuNPs on the substrates, with AuNPs deposited on steel typically exhibiting a redder shift compared to AuNPs on aluminum. Variable angle measurements showed that the AuNPs absorbed strongly at low angles of incidence, with decreasing absorption as the angle increased. Other factors such as the separation of specular and diffuse reflectance, AuNP shape and size, different capping agents, and the surface roughness of the substrates were also considered. The results from this study provide valuable insight into NP – substrate interactions and will help better design LSPR based sensors for a wide range of industrial applications.

11:15 AM *EL08.16.04

Scalable Classical and Quantum Light Sources [Boubacar Kante](#); University of California, United States

The scaling of lasers and in-particular of surface emitting lasers is a multi-decade long question that has been investigated since the invention of lasers in 1958. It is an important question with numerous applications. In this talk, I will propose and discuss an intriguing solution to this question that we named the Berkeley Surface Emitting Laser (BerkSEL) and it is the world's first scale-invariant laser. In the second part of the talk, I will discuss our demonstration of the first deterministic quantum light source in silicon that emits single photons in the telecom band. The work opens unique perspectives for scalable quantum networks.

11:45 AM EL08.16.05

Light-Controlled Disorder-Engineering of Optical Metasurfaces: Aspects of Design and Applications [Maximilian Buchmueller](#), Sven O. Schumacher and Patrick Goerm; University of Wuppertal, Germany

Metasurfaces have become one of the cornerstones of modern nanotechnology. In planar optics, they enable the precise control of phase, amplitude, and polarization of light at the nanoscale, which has led to advances in numerous application fields, including sensing, nonlinear optics, and optical modulators.

However, their implementation often requires surface nanostructuring, based on complex design and fabrication methods such as electron-beam lithography or focused ion-beam milling. In addition, exploiting narrow spectral features, e.g., for sensing, is accompanied by high demands in terms of precise post-process alignments with respect to probing light, which is challenging particularly in the scope of miniaturization and device integration.

Here, we demonstrate the fabrication of optical metasurfaces exploiting the plasmon-mediated growth of silver nanoparticles (AgNPs). The particle growth is based on the reduction of silver ions in an aqueous solution. Incident light interacts with the localized surface plasmon resonances (LSPRs) of the AgNPs, and thus enables to enhance the reduction kinetics of the silver ions and support the particle growth at intensity hotspots. The changing scattering properties of the growing ensemble of particles can further influence the distribution of intensity hotspots and thus influence the growth positions of other AgNPs. The resulting metasurface shows an optical response, which is highly sensitive to changes in the electromagnetic environment.

The morphology of the resulting metasurfaces shows different features of engineered disorder, including disordered hyperuniformity. These features can be linked to the electromagnetic waves involved in the fabrication process.[1,2] By varying the illumination properties during the growth using incident waves with individual wave-front profiles, penetration depths into the solution and different frequencies, we demonstrate the vast design freedom of the presented method. It is even possible to simultaneously incorporate multiple waves into the fabrication process and thus to increase the amount of structural information stored in the metasurfaces.

As a first application scenario, we show that the metasurfaces are directly applicable as self-optimized optical sensors. The sensors are both instantaneously tailored and intrinsically aligned to the probing light source, as the fabrication and probing environment can be identical. The inherent sensitivity of the optical response to any variations of the electromagnetic environment thus enables high-performance nanoplasmonic sensing without the need for any post-process alignments. We found a sensing performance in terms of a Figure of Merit* of 968. [1]

Furthermore, we show that our method also renders it possible to harness short-range surface plasmon polaritons (SR-SPPs) in smooth ultra-thin silver films using a Kretschmann-Raether geometry. [3] Typically, it is challenging to utilize SR-SPPs in planar stack geometries, because of their high effective mode index. Nanostructuring ultra-thin metal films (around 20nm thickness), or placing metallic nanostructures in close proximity to the planar film for coupling is technologically challenging and can strongly influence the SR-SPP properties. The new possibilities given by our method promise great potential for sensing single surface binding events and high resolution imaging applications due to their strong field enhancement and localization. First promising results also suggest the possible use of other noble metals instead of silver, such as gold, for biological and medical applications.

[1] I. Shutsko, M. Buchmüller, M. Meudt, and P. Görrn, *Adv. Opt. Mat.*, **2022**

[2] I. Shutsko, M. Buchmüller, M. Meudt, and P. Görrn, *Adv. Mat. Tech.*, **2022**

[3] M. Buchmüller, I. Shutsko, S.O. Schumacher, P. Görrn, *ACS Appl. Opt. Mat.*, **2023** (accepted)

SESSION EL08.17: Nanostructure Design, Fabrication and Characterization

Session Chairs: Boubacar Kante and Ho Wai (Howard) Lee

Friday Afternoon, April 26, 2024

Room 340/341, Level 3, Summit

1:30 PM EL08.17.02

Electrically Gated Organic-Based Metadevice for THz Amplitude Modulation Federico Grandi^{1,2}, Cristiano Bortolotti^{1,3}, Francesco Modena³, Lorenzo Gatto², Matteo Butti³, Iain McCulloch⁴, Caterina Vozzi², Mario Caironi², Giorgio Ernesto Bonacchini³ and Eugenio Cinquanta²; ¹Politecnico di Milano, Italy; ²CNR-IFN, Italy; ³Istituto Italiano di Tecnologia, Italy; ⁴University of Oxford, United Kingdom

In the last years, the interest in THz technologies has increased rapidly due to their applicability across several application scenarios like telecommunication and sensing, with recent developments overarching the fields of optics and electronics [1]. Despite their scientific and technological appeal, THz waves have a major drawback coming from the absence of optoelectronic techniques and devices that can manipulate such light waves. To solve this issue, one of the most promising approaches relies on the use of metasurfaces [2], engineered composites whose optical properties can be specifically tailored to interact with THz waves. Therefore, research is now focused on trying to design reconfigurable metamaterials, also known as metadevices, able to modulate the amplitude, phase, and frequency of THz pulses, to achieve the highest modulation depth and switch speed possible [3]. Among the plethora of proposed modulation strategies based on optical, electro-mechanical, or thermal stimuli, electrically-tuned THz metadevices represent a flourishing approach that directly benefits from the development of novel and unconventional transistor configurations.

In our work, we explore for the first time the functioning and the effectiveness of an organic semiconductor-driven metadevice based on a matrix of metal Split-Ring Resonators, which can modulate the amplitude of a THz pulse passing through them [4]. This approach has already been shown to work nicely in the microwave spectral region [5] but has not yet been applied in the THz range. The modulation capabilities come from the electrically driven change of charge carrier density in the organic semiconductor, which enables the metadevice to act as an optical transistor, varying THz transmission around a specific frequency (~0.7 THz) with modulation depths of approximately 65%. These performances, which are comparable with current state-of-the-art technologies but with a way lower driving voltage (<1 V) result from the unique 3-dimensional charge modulation properties of a new class of organic mixed ion-electron conductors based on conjugated polymers with glycolated sidechains, such as the emerging p(g2T-TT) semiconductor.

Also, another key aspect of our work is to show that it is then possible to shift towards mass-scalable and cost-effective manufacturing techniques exploiting high-throughput deposition methods for both the metamaterial matrix and the organic semiconductor, on either rigid or flexible plastic substrates, without losing modulation efficiency.

In conclusion, we hope that this work will lead to the further development of metadevice technologies based on organic semiconductors, with the future aim of improving the effectiveness of this modulating technique in the THz spectral region, especially in terms of modulating speed. Moreover, this device development comes together with an ongoing study on the THz properties of this emerging class of organic semiconductors, leading to fundamental scientific insights that could also find application in other areas, such as electronics and bioelectronics.

[1] Samizadeh Nikoo, M., & Matori, E. (2011). *Nature* **614**, 451–455 (2023). <https://doi.org/10.1038/s41586-022-05595-z>

[2] Degl'Innocenti, R., Lin, H. & Navarro-Cía, M. (2022). *Nanophotonics*, 11(8), 1485-1514. <https://doi.org/10.1515/nanoph-2021-0803>

[3] Wang, L., Zhang, Y., Guo, X., Chen, T., Liang, H., Hao, X., Hou, X., Kou, W., Zhao, Y., Zhou, T., Liang, S., & Yang, Z. (2019). *Nanomaterials*, 9(7), 965. <https://doi.org/10.3390/nano9070965>

[4] Chen, H., Padilla, W. J., Zide, J. M. O., Gossard, A. C., Taylor, A. J., & Averitt, R. D. (2006). *Nature*, 444(7119), 597–600. <https://doi.org/10.1038/nature05343>

[5] Bonacchini, G. E., & Omenetto, F. G. (2021). *Nature Electronics*, 4(6), 424–428. <https://doi.org/10.1038/s41928-021-00590-0>

1:45 PM EL08.17.03

Emergent Opportunities with Magnesium for Green Photonics Peifen Lyu, Tao Gong and Marina S. Leite; University of California, Davis, United

States

Structural color generation exploiting nanophotonics or plasmonic behaviors has burgeoning applications in displays, lasers, sensors and other optical sources due to promising advantages such as durability, environmental friendliness, and compatible integration with monolithic fabrication compared to traditional pigments and dyes. While conventional metals (e.g., Au, Ag and Cu) and their alloys are the focus of current optical research, magnesium (Mg) as an earth-abundant material, with biodegradability and CMOS compatibility, has not been fully explored in photonic applications. In our present works [1, 2], we have already established a novel platform for transient color filters/superabsorbers based on Mg and other dielectric thin films with angle-insensitive response and capabilities for fast fading of single vivid hues when exposed to water. These results motivate us to now pursue the realization of sophisticated 3D nanostructures that will form the building blocks of degradable/biocompatible devices. Based on our preliminary optical simulations using Finite-Difference Time-Domain (FDTD) for selected nanostructure configurations [3], all of the structures exhibit pronounced blueshift of their scattering peak frequency with decreased sizes (i.e. due to the etching process of Mg in water). These resonance shifts beget a plethora of applications in photonic devices. For example, it can produce a smooth transition of hues in color display devices for dynamic color tuning. Besides, we perform near-field scattering measurements with Mg nanostructures *in situ* to experimentally demonstrate the transient behavior as the Mg dissolves in a controlled manner. This helps us to achieve our long-term goal of realizing Mg-based devices for next-generation CMOS-compatible and green photonic devices.

1. Gong, T., P. Lyu, and M.S. Leite, Scalable Superabsorbers and Color Filters Based on Earth-Abundant Materials. *ACS Applied Optical Materials*, 2023. 1(4): p. 825-831.
2. Lyu, P., et al., Transient Structural Colors with Magnesium-Based Reflective Filters. *Advanced Optical Materials*, 2022. 10(13): p. 2200159.
3. Farinha, T.G., et al., Selective etching properties of Mg thin films and micro/nanostructures for dynamic photonics [Invited]. *Optical Materials Express*, 2021. 11(5): p. 1555-1565.

2:00 PM BREAK

2:30 PM EL08.17.04

Solution-Processed *In-Situ* Grown Ag-TiO₂ Nano-Schottky Junction Thin Films for Hot-Electron based Photodetection and Energy Conversion
Bhola N. Pal; Indian Institute of Technology, India

It is not very easy to capture hot plasmonic electrons for photodetection or solar energy conversion. In this work, an *in situ* grown Ag-TiO₂ nano-Schottky junction thin film has been deposited by a solution process technique, that contains a highly dense silver (Ag) nanoparticle (NP) surrounded by TiO₂. This Ag-TiO₂ nano-Schottky junction has a low barrier height and a high interface area with the least interface state, which enables efficient hot-electron transfer to the conduction band of TiO₂, which is realized in the external quantum efficiency (EQE) data. This EQE data shows intense photocurrent formation in the region of plasmonic absorption of Ag NP, indicating the primary contribution of hot electrons on photocurrent production. As a consequence, a narrowband photodetector with full width at half-maximum (FWHM) of ~55 nm is fabricated by utilizing this Ag-TiO₂ nano-Schottky junction thin film. This photodetector is fabricated on a glass substrate in a photoconductor geometry that shows a peak detectivity of 3.19×10^{11} Jones at 420 nm with a response time of ~2 s. Besides, this Ag-TiO₂ thin film has been utilized as photoanode for highly enhanced electro-photocatalytic H₂ generation. Photoelectrochemical measurement of optimized Ag(NPs)-TiO₂ thin film photoanodes showed a high photocurrent generation at a density of 42 mA cm⁻² in 1 M KOH solution, which is three orders of magnitude higher than that of pure TiO₂, and stability for more than 1.5 h. An intense photocurrent generation in the region of plasmonic absorption of Ag NPs has been observed that reveals direct evidence of plasmon-induced hot electrons for solar energy conversion.

References:

1. Solution-Processed Ag-TiO₂ Nanostructure-Based Schottky Junction Thin Films for Narrowband Hot-Electron Photodetectors S Hazra, SV Singh, S Dahiya, PK Aich, B N Pal; *ACS Appl. Nano Mater.* 2023, 6, 16, 15119–15127
2. Direct Evidence of an Efficient Plasmon-Induced Hot-Electron Transfer at an *In Situ* Grown Ag/TiO₂ Interface for Highly Enhanced Solar H₂ Generation Satya Veer Singh, M. Praveen Kumar, Sengen Anantharaj, Bratindranath Mukherjee, Subrata Kundu, and Bhola N. Pal; *ACS Appl. Energy Mater.* 2020, 3, 2, 1821–1830

2:45 PM EL08.17.05

Chemical Growth of Chiral Plasmonic Metamaterials Shuai Feng, Blake Povilus, Jaewoo Park and Sui Yang; Arizona State University, United States

Controlling the polarization states of light through chiral metamaterials offers unprecedented opportunities in realizing novel functions including optical switches, modulators, wave isolation and phase shifter. The realization of metamaterials can be made from top-down and bottom up, either from lithographic methods such as EBL or self-assembly for nanoparticle coupling. However, significant challenge exists in controlling symmetry functions directly by the growth. Here we show that the direct chemical growth of chiral plasmonic metamaterials. This work provides a new metamaterials fabrication platform for symmetry control leading to the properties and applications previously deemed unfeasible.

3:00 PM EL08.17.06

Synthesis and Photocatalytic Activity of Porous Bimetallic Plasmonic Nanoparticles Formed on Solid Substrates Harshitha Rajashekhar, Navneet Kumar, John Garcia, Damini Vrushabendrakumar and Karthik Shankar; Univ of Alberta, Canada

Plasmonic catalysis aims to extract useful work from the surface plasmon resonance phenomenon in order to assist or drive a chemical reaction. Nanoparticles (NPs) composed of plasmonic metals such as Au, Ag, Cu and Al resonantly interact with light through the excitation of localized surface plasmon resonance (LSPR) modes which subsequently decay to produce highly energetic "hot carriers". There are two major technical obstacles that prevent the efficient utilization of hot carriers to drive chemical reactions. The first limitation is that plasmonic NPs are frequently synthesized as colloidal suspensions while a number of heterogeneous catalytic reactions require the catalyst to be anchored to a solid-state support. The second limitation arises due to the relative chemical inertness of noble metals, particularly gold, which prevents the adsorption of most types of reactant molecules on the surface of the plasmonic NP catalyst. As a consequence of the second limitation, plasmonic metal NPs often demonstrate low catalytic activity for many chemical reactions. In recent years, there has been growing interest in bimetallic nanostructures that combine the optical characteristics of plasmonic metals with the catalytic properties of metals such as Pt and Pd. In this work, we attempted the precise fabrication of diverse bimetallic plasmonic photocatalysts with a porous structure to overcome both the aforementioned technical problems. Porous bimetallic plasmonic nanoparticles with large surface areas possess an enhanced capacity to adsorb reactant molecules (compared to their monometallic counterparts) increasing their overall catalytic efficiency. In this work, we present a dealloying technique to fabricate porous bimetallic nanostructures on solid substrates and investigate their activity for the vapor phase transformation of CO₂ and H₂O into hydrocarbons at close to room temperature. We also analyze the photocatalytic ability of the as-fabricated porous bimetallic nanostructures in the decolorization of methylene blue (MB) dye. Scavenger studies indicate photogenerated electrons to be the active species responsible for photocatalytic activity. In both CO₂ photoreduction and dye photodegradation, bimetallic porous AuPt NPs outperform monometallic

porous Au NPs by nearly 33%. These results have important implications for more energy efficient, sustainable heterogeneous catalysis under milder conditions of temperature and pressure. This work also presents the application potential for the use of porous bimetallic plasmonic catalysts in water remediation and the generation of solar fuels.

3:15 PM EL08.17.07

Engineering Chiral Plasmonic Nanocrystals via Controllable Photoetching of Silver Nanorods with Circularly Polarized Light [Tian Qiao](#), Tsumugi Miyashita, Anne Ashworth and MingLee Tang; The University of Utah, United States

Chiral plasmonic nanostructures have shown great potential for photonics and sensing applications. Chiral molecules and micelles have been demonstrated to be effective sources of chirality, enabling the colloidal production of large-scale, homogeneous chiral plasmonic nanocrystals. Recent investigations have explored the use of circularly polarized light (CPL) as a chirality source to fabricate chiral Au/PbO₂ heterostructures or as an additional ingredient in chiral molecule-directed synthesis to enhance the optical dissymmetry of the nanocrystals further. However, the mechanism by which these chiral structures develop with CPL has remained largely unexplored. Our latest study has revealed that the wavelength of CPL is a critical factor in determining the shape of chiral Au/PbO₂ heterostructures and their resulting chiroptical properties. Here, we further demonstrate that the asymmetry of the initial plasmonic nanocrystals plays a crucial role in generating more chiral nanostructures. Specifically, we utilized silver nanorods with varying aspect ratios as the starting materials. Ag was oxidized at selective sites upon circularly polarized excitation to create chiral structures. Our results indicate that the optical activity of resulting chiral nanostructures increases with the aspect ratio of the starting nanocrystals. Besides, tuning the excitation wavelength with Ag nanorods of a larger aspect ratio can yield higher contrast of chiral morphologies due to the larger number of higher-order modes accessible in these nanocrystals. Our study underscores the importance of carefully selecting the starting material and excitation wavelength to maximize chiral plasmonic nanocrystals' shape and optical dissymmetry when using CPL as the chirality source. Besides, the non-toxic chiral Ag nanocrystals are more suitable for bio-compatible systems than chiral Au/PbO₂ nanostructures.

SESSION EL08.18: Virtual Session
Session Chairs: Yao-Wei Huang and Pin Chieh Wu
Tuesday Morning, May 7, 2024
EL08-virtual

8:00 AM *EL08.18.01

Flat Optics: Arbitrary Wavefront Control with Metasurfaces and Metalenses for High Volume Applications [Federico Capasso](#); Harvard University, United States

We will discuss metasurfaces that enable light's spin and orbital angular momentum to evolve along the propagation direction and nonlocal supercell designs that demonstrate multiple independent optical functions at arbitrary large deflection angles with high efficiency. 2D phase and polarization singularities ("structured dark") have been realized, as well as 0D singularities. I will present active metasurfaces for high-speed optical modulation at telecom wavelengths based on electrooptic polymers and Si and give the state-of-the-art of commercial metalenses including their high-volume manufacturing for consumer electronics. Finally, we will discuss our recent work on metalenses for the EUV (50 nm wavelength) based on vacuum guiding.

8:30 AM EL08.18.02

Investigation of Exciton-Plasmon Interaction in 2D Hybrid Nanostructures [Dmitry Murausky](#) and Pavel Malakhovsky; Research Institute for Physical and Chemical Problems, Belarus

Two-dimensional hybrid nanostructures composed of plasmonic and excitonic nanoparticles attract great interest in the range of applications such as solar photovoltaics, photoelectrochemical catalysis and biosensing. We developed novel 2D hybrid structures via depositing close-packed monolayers of hydrophobic Zn-CuInS₂/ZnS quantum dots (CIS QDs) atop silver nanoplates (AgNPLs) electrostatically deposited onto thin (~20 nm) optically and e-beam transparent polycationic film. To study exciton-plasmon interaction the optical properties of these hybrid structures were compared with CIS QDs films without AgNPLs. Photoluminescence quenching for samples with CIS QDs monolayer atop AgNPLs was revealed. According to the time-resolved photoluminescence measurements plasmon-excitonic interaction leads to a pronounced lifetime shortening. We analyzed polarization photoluminescence spectra of the samples to reveal the resonance energy transfer from CIS QDs to AgNPLs. We found that the ratio of p- to s-polarized emission light intensity is about 2 times less for samples with AgNPLs, due to contribution from indirectly excited AgNPLs plasmon scattering. CIS QDs demonstrate intrinsic reversible photoinduced PL quenching and we utilized variations in the quenching kinetics to reveal the FRET effect. A 30% reduction in the PL intensity of CIS QDs monolayers was observed, while CIS QDs atop AgNPLs showed no noticeable tendency to PL quenching due to competitive FRET channel. Such hybrid exciton-plasmon nanostructures are perspective for nanophotonic devices with modulating emission. This work was partially supported by BRFFR X22Turk-004 and CHEMREAGENTS 2.1.04.01 projects.

8:45 AM *EL08.18.03

Wide Field-Of-View Metasurface Optics [Juejun Hu](#); Massachusetts Institute of Technology, United States

Field-of-view (FOV) is an important performance metric of optical systems. In traditional optics, expanding the FOV necessarily involve increasing the number of optical elements at the expense of system size and complexity. Metasurfaces offer a promising solution to overcome this limitation, enabling wide-FOV systems with reduced element count while suppressing optical aberrations. In this talk, I will discuss the basic theory guiding the design of wide-FOV imaging and projection optics, and demonstrate wafer-scale, industry-standard foundry manufacturing of wide-angle metasurface optics for applications spanning imaging, sensing and display.

9:15 AM EL08.18.04

SERS Substrate Using Ag@ZnO Composite Coated on Electrospun Cellulose Acetate Fibers by Sputtering Deposition under Limited Adatom Mobility [Adrian Camacho-Berrios](#)¹ and Oscar M. Suárez²; ¹University of Puerto Rico at Ponce, Puerto Rico; ²University of Puerto Rico at Mayagüez, Puerto Rico

The present straightforward fabrication methodology of plasmonic substrates is based on Ag@ZnO nanocomposites deposited on cellulose acetate fibers. Magnetron sputtering combined with electrospinning allowed for different morphologies of ZnO and Ag at the nano and microscale. We examined the

morphology and structural properties of the substrates by electron microscopy, Raman spectroscopy, and FT-IR spectroscopy. The results show that ZnO nanocolumns on the cellulose acetate fibers and Ag nanoparticles with various sizes and shapes can form on the ZnO surface. Also, we demonstrated the potential of substrates for surface-enhanced Raman scattering (SERS) applications by using benzenethiol and rhodamine 6G as probe molecules. Our results showed that the experimental substrates exhibited good SERS performance and reproducibility. Our method is simple, versatile, and scalable and could be applied to other metal/oxide systems for plasmonic applications.

9:30 AM *EL08.18.05

Design and Applications of Chiral and Quasi-Bound-States-In-The-Continuum Metasurfaces [Stefan A. Maier](#)^{1,2}; ¹Monash University, Australia; ²Imperial College London, United Kingdom

My talk will discuss the design and applications of chiral and quasi-BIC metasurfaces for a variety of applications, from energy conversion and light harvesting to interactions with two-dimensional semiconductors. Examples include suppression of exciton-exciton annihilation and controlled enhancement and suppression of light emission, as well as strong-coupling, amongst others. A focus will lie on metasurfaces that can be generated using straightforward nanofabrication techniques with a robustness to defects.

10:00 AM *EL08.18.06

Meta-Fibers: Merging Optical Fibers and Nanophotonics Through 3D Nanoprinting [Markus Schmidt](#); Leibniz Institute of Photonic Technology, Germany

Synopsis: Here, we will demonstrate how the combination of optical fibers and nanostructures creates a new category of fiber-integrated devices – meta-fibers, achieved by leveraging 3D nanoprinting. Essential results are high-NA holographic meta-lenses for optical trapping, multifocus generation via single-point phase-engineering, achromatic metasurface-based lenses, and dielectric ring-like gratings for boosting incoupling efficiencies.

Introduction: The development of nanostructures on fiber end faces offers a promising approach for unlocking new functionalities across various fields, such as biophotonics, quantum technologies, and optical sensing. Conventional top-down fabrication methods usually fail as the fiber geometry is complementary to that of planar substrates (e.g., wafers). In this presentation, we show on several examples that 3D nanoprinting using direct laser writing circumvents this bottleneck, allowing to implement intricate nanostructures on the end face of optical fibers.

Optical trapping with single fiber: Effective light focussing is crucial for numerous applications, while optical fibers have limitations due to the divergence of the emitted light. Here, we used 3D nanoprinting to integrate ultra-high NA holographic meta-lenses onto functionalized single-mode fibers, achieving record-high NA of up to 0.9 with diffraction-limited spots. This breakthrough allowed us to optically trap microspheres and bacteria with individual single-mode fibers, overcoming a significant limitation of fiber optic.

Achromatic light focusing: An open issue in the field of telecommunication is achromatic light focusing, for which no satisfactory solution exists so far. By integrating a nano-printed metasurface-based lens onto a fiber, we have been able to achromatically and efficiently focus the output light of a SMF-28 over the entire telecommunications range. Key is the use of nanopillars of different heights, representing a unique degree-of-freedom provided by the nanoprinting process that is crucial to wavelength independent light focussing.

Boosting in-coupling efficiency: Conventional commercial fibers suffer from low NS, restricting light incoupling to small angles. We have solved this problem by integrating axial-symmetric ring-type nanogratings onto the core of SMF-28, improving the incoupling efficiency at near-grazing incidence by more than four orders of magnitude. Additionally, incoupling at preselected angles and across large angular intervals by employing an optimization procedure was additionally shown. This approach overcomes the low NA limitation of commercial fibers and can lead to advancements in the field of fiber optics.

Summary: We have demonstrated that meta-fibers represent a new category of fiber-integrated devices that offer unprecedented applications for fiber optics. With the implementation of versatile application strategies, we anticipate broader use of meta-fibers in various fields, including quantum technology, bioanalytics, and nanophotonics.

10:30 AM EL08.18.08

A Nanostructured Microarray-Based SERS Sensor Targeted at Multiplex Mycotoxins Detection in Food and Feedstuff Using Handheld Apparatus Rohit K. Singh, Narsingh R. Nirala and [Giorgi Shtenberg](#); ARO, Research Organization, Volcani Institute, Israel

Food and agricultural commodities contamination by various toxigenic molds is a seriously neglected problem, affecting ~25% of the world's crops with staggering economic losses. Regardless of decades of extensive research, mycotoxins continue to penetrate the food chain through food and feed crops and pose health risks to humans and livestock. Herein, we present a newly developed nanostructured microarray (5 by 5 sensing spots) based on silver-coated porous silicon used as a surface-enhanced Raman scattering (SERS) transducer. The unique microarray was facilitated without the need for any micro/nano-fabrication (clean-room) facilities. The inherent surface void and pore morphology (82±2% and ca. < 9 nm, respectively) were physically optimized to augment the SERS effect while achieving an enhancement factor of $> 1.03 \times 10^8$. Under optimized conditions, three common mycotoxins (aflatoxin B1, fumonisin B1 and ochratoxin A) in feed ingredients and agricultural products were simultaneously assessed using a portable Raman device (1.5 µL sample analyzed in 30 min). The optical response was inversely proportional to the metabolite concentration upon selective interaction with anti-target mycotoxin aptamers modified sensing spots. The calculated limits of detection were 0.01, 0.6 and 0.9 ng/mL (part per billion, ppb) for aflatoxin B1, fumonisin B1 and ochratoxin A, respectively, within the dynamic range of 0.1-1000 ppb. Furthermore, the selectivity, regeneration and overall shelf-life were thoroughly evaluated while depicting satisfactory performances (no interferences with interfering mycotoxins, four regeneration cycles and five weeks of stability, respectively). Finally, the practicality of the developed SERS assay was elucidated in various matrices (e.g., maize, rice and wheat), with recovery values of 95–103%. The successful validation of actual samples' analysis emphasizes the platform's reliability, robustness and suitability for practical use of multi-target analytes detection, including on-site operation.

10:45 AM EL08.18.09

Plasmonic and Plasmon-Free Nanostructured SERS Sensors Tania K. Naqvi, Prabhat K. Dwivedi and [Manish M. Kulkarni](#); IIT Kanpur, India

Surface-enhanced Raman scattering (SERS) is employed for identification and detection of several types of analytes such as environment contaminants, explosives, pathogens, and biomarkers from body fluids for preventive healthcare. SERS outperforms the number of other analytical tools especially for detection of analytes at a trace level. In recent years, with advancements in small size Raman spectroscopy tools, portable, on-field, analysis of real-world complex compounds and point-of-care SERS devices is becoming a reality. However, to this end, there is a need to develop highly sensitive, label free and reproducible SERS sensors.

We demonstrate here fabrication of some plasmonic and plasmon-free SERS sensors and detection of analytes using portable Raman setup. The SERS sensors were developed using different nano/microfabrication techniques such as electrospinning, lithography and self-assembly. We compare the performance of plasmon free SERS sensors obtained via different polymeric carbon precursors and with plasmonic sensors for detection of standard analytes and selective explosives and biomarkers.

SYMPOSIUM EN01

Application Targets for Next Generation Photovoltaics
April 23 - April 26, 2024

Symposium Organizers

Ardalan Armin, Swansea University
Christoph Brabec, FAU Erlangen-Nuremberg
Nicola Gasparini, Imperial College London
Ellen Moons, Karlstad University

* Invited Paper
+ JMR Distinguished Invited Speaker
^ MRS Communications Early Career Distinguished Presenter

SESSION EN01.01: Organic Photovoltaics
Session Chairs: Christoph Brabec and Nicola Gasparini
Tuesday Morning, April 23, 2024
Room 331, Level 3, Summit

10:30 AM *EN01.01.01

Material and Device Design for Multijunction Perovskite Solar Cells Rene A. Janssen^{1,2}; ¹Eindhoven University of Technology, Netherlands; ²Dutch Institute for Fundamental Energy Research, Netherlands

Metal halide perovskite solar cells have advanced into a viable option for future renewable energy. Record single and tandem junction all-perovskite solar cells already provide power efficiencies of over ~26% and ~29%, respectively. A next target in photovoltaic energy conversion can possibly be met by developing perovskite triple or even quadruple junction solar cells. While these hold a promise to afford higher efficiencies, they require developing stable perovskite sub cells with bandgaps in the range of 1.8 to 2.3 eV, i.e., a range that has not received much attention so far. These wide-bandgap perovskites often suffer from more pronounced voltage losses due to non-radiative bulk and interfacial charge recombination. In developing new perovskite sub cells, photocurrent spectroscopy and absolute photoluminescence spectroscopy are used in combination with bulk and interface passivation strategies to eliminate these losses. This has enabled to reduce the voltage deficit over a wide range of bandgap. Guided by optical modelling, monolithic multi-junction solar cells have been fabricated by stacking two and three different bandgap perovskite sub cells in series using recombination junctions designed to provide near-zero electrical and optical losses. Collectively, these strategies enable monolithic tandem and triple junction solar cells with a power-conversion efficiency of over 26%.

11:00 AM EN01.01.02

Towards Highly Efficient Upscaled Organic Solar Cells: Solvents, Fabrication and The Role of Charge Carrier Dynamics Eva Mazzolini^{1,2}, Richard A. Pacalaj¹, Bhushan Patil³, Yuang Fu⁴, Rahul Patidar³, Xinhui Lu⁴, Trystan Watson³, Zhe Li², James Durrant¹ and Nicola Gasparini¹; ¹Imperial College London, United Kingdom; ²Queen Mary, University of London, United Kingdom; ³Swansea University, United Kingdom; ⁴The Chinese University of Hong Kong, Hong Kong

Organic solar cells (OSC) using non-fullerene acceptors in the Y6 family have now surpassed 19% efficiency. However, these lab-scale, state-of-the-art devices are usually processed using halogenated solvents, which are not suitable for up-scale. As the solvent used during deposition of the OSC's active layer has a significant impact on its microstructure, and therefore the device performance, one of the first steps towards industrialization is to start with materials that are already soluble in greener alternatives.

Moreover, there is still a large performance gap between spin-coated, hero cells and large-scale modules. This is due, among other factors, to the difficulties in maintaining an optimal active layer morphology when switching to industrial fabrication techniques. To bridge this gap, it is paramount to study the photophysics of devices made with scalable techniques, such as blade coating and slot-die coating.

In this work, we demonstrate highly efficient organic solar cells fabricated with spin-coating, blade coating, and slot-die coating techniques, using PM6 and Y12 in *o*-xylene as electron donor and electron acceptor materials, respectively.

We then investigate the differences and similarities between these techniques with a variety of optoelectronic techniques, including transient photovoltage, charge extraction, and GIWAXS, to determine charge carrier dynamics, morphology, photovoltaic performance, and stability.

Finally, this work demonstrates the application of green-solvent processed OSCs as semi-transparent devices with over 40% visible transmittance and a

fully solution-processed stack.

11:15 AM *EN01.01.03

Singlet Exciton Decay is The Main Competing Pathway to Free Charge Generation in Organic Solar Cells with Low Energetic Offset Dieter Neher; University of Potsdam, Germany

Since the advent of low bandgap non-fullerene acceptors (NFAs), the performance of organic solar cells (OSCs) has improved significantly. In combination with donor materials with complementary absorption, such NFA-based bulk heterojunction blends show efficient conversion of photons into electrons over a broad spectral range. Therefore, an important topic of current OSC research is to reduce the voltage loss by non-radiative recombination while maintaining the short-circuit current (J_{sc}) and the fill factor (FF) at a high level. The most popular approach to optimize the open circuit voltage of NFA-based blends is to reduce the HOMO-HOMO energy offset. Unfortunately, this is generally accompanied by a significant reduction of J_{sc} and FF - the reason for this being controversially discussed in the literature.^[1-4]

Here we combine a wide range of methods, from spectroelectrochemistry to determine the blend energetics, to femtosecond transient absorption to study the early excitation dynamics, to bias-dependent photoluminescence spectroscopy in the steady state, to study the mechanisms and efficiency of free charge generation in relation to the HOMO-HOMO offset in selected Y-based blends. We find no evidence of the hybridisation of the interfacial charge transfer (CT) state with the local singlet exciton (LE), nor do we observe significant losses due to non-radiative CT recombination competing with charge separation. Instead, singlet exciton decay is identified as the main competing pathway for free charge generation in low energy offset OSCs. This interpretation is consistent with the observed strong decrease in J_{sc} when the HOMO-HOMO offset decreases from 0.32 eV to 0.17 eV. Our results show that the optimal range of the HOMO-HOMO offset for achieving optimal performance is quite narrow and lies at 0.3 eV - the exciton binding energy of Y6 aggregates.^[5]

[1] B. Sun, N. Tokmoldin, O. Alqahtani, A. Patterson, C. S. P. De Castro, D. B. Riley, M. Pranav, A. Armin, F. Laquai, B. A. Collins, D. Neher, S. Shoaee, *Adv. Energy Mater.* **2023**, 2300980, DOI 10.1002/aenm.202300980.

[2] M. Pranav, T. Hultsch, A. Musiienko, B. Sun, A. Shukla, F. Jaiser, S. Shoaee, D. Neher, *APL Mater.* **2023**, 11, DOI 10.1063/5.0151580.

[3] D. Qian, S. M. Pratik, Q. Liu, Y. Dong, R. Zhang, J. Yu, N. Gasparini, J. Wu, T. Zhang, V. Coropceanu, X. Guo, M. Zhang, J. L. Bredas, F. Gao, J. R. Durrant, *Adv. Energy Mater.* **2023**, 2301026, 1.

[4] J. S. Müller, M. Comí, F. Eisner, M. Azzouzi, D. Herrera Ruiz, J. Yan, S. S. Attar, M. Al-Hashimi, J. Nelson, *ACS Energy Lett.* **2023**, 8, 3387.

[5] S. Shoaee, H. M. Luong, J. Song, Y. Zou, T. Nguyen, D. Neher, *Adv. Mater.* **2023**, DOI 10.1002/adma.202302005.

SESSION EN01.02: Perovskite – Performances and Stability

Session Chairs: Nicola Gasparini and Rene Janssen

Tuesday Afternoon, April 23, 2024

Room 331, Level 3, Summit

1:30 PM *EN01.02.01

Printed Solar – Green Energy for Industrial, Warehouse and Commercial (IWC) Buildings Paul Dastoor, Daniel Elkington, Warwick Belcher and Nathan Cooling; University of Newcastle, Australia

Printed solar modules based on organic photovoltaic materials offer significant promise as a next-generation solar energy technology manufactured using roll-to-roll printing. A relatively mature technology, printed solar weighs less than 300 g per square metre, is less than 0.3 mm thick and can be adhered to roofing and other structures using adhesives. Moreover, detailed economic modelling has demonstrated that by focussing on low-cost materials and manufacturing techniques, printed solar is commercially compelling even at relatively low device efficiencies and lifetimes [1].

A key application target for printed solar is the Industrial, Warehouse and Commercial (IWC) building sector. The size of the sector is significant with the area of IWC roofing conservatively estimated to be more than 100 million square metres in Australia [2] and over 4 billion square metres worldwide [3]. Over 70 % of IWC roofs are manufactured to the minimum specification and these “slender” roofs are low weight bearing and incapable of supporting the weight of conventional silicon solar panels which typically weigh around 20 kg per square metre.

In this paper we outline our work in developing large area printed solar for IWC applications in Australia, encompassing material synthesis, device development, demonstration installation, economic modelling and recycling. With modelled payback times of less than 2 years for a typical IWC roof, printed solar offers significant potential for sustainable energy generation in the sector.

1. Mulligan, C.J., Bilén, C., Zhou, X., Belcher, W.J. and Dastoor, P.C., 2015. Levelised cost of electricity for organic photovoltaics. *Solar energy materials and solar cells*, 133, pp.26-31. DOI: 10.1016/j.solmat.2014.10.043

2. Seifhashemi, M., Capra, B.R., Miller, W. and Bell, J., 2018. The potential for cool roofs to improve the energy efficiency of single storey warehouse-type retail buildings in Australia: A simulation case study. *Energy and Buildings*, 158, pp.1393-1403. DOI: 10.1016/j.enbuild.2017.11.034

3. Lapis, R., Bozonnet, E., Salagnac, P. and Abadie, M.O., 2018. Optimized design of low-rise commercial buildings under various climates–Energy performance and passive cooling strategies. *Building and Environment*, 132, pp.83-95. DOI: 10.1016/j.buildenv.2018.01.029

Acknowledgements

This work was performed in part at the Materials Node (Newcastle) of the Australian National Fabrication Facility (ANFF), which is a company established under the National Collaborative Research Infrastructure Strategy to provide nano- and microfabrication facilities for Australia’s researchers.

2:00 PM EN01.02.02

Self-Promoted Vertical-Gradient Hole Transport Layers for Flexible Large-Area Perovskite Modules Wallace C. Choy; University of Hong Kong, China

While the power conversion efficiency (PCE) of single-junction perovskite solar cells (PSCs) has increased to over 26%, there are some challenges to achieving flexible large-area PSCs with good long-term stability for practical applications. In this work, we demonstrate a self-assembled gradient $Ti_3C_2T_x$ MXene incorporated PEDOT:PSS HTL for promoting flexible large-area PSCs by establishing half-caramelization-based glucose-induced MXene

redistribution. Through this process, the $\text{Ti}_3\text{C}_2\text{T}$, MXene nanosheets are spontaneously dispersed and redistributed at the top region of HTL to form the unique gradient distribution structure composed of MXene:Glucose:PEDOT:PSS (MG-PEDOT). Our results show that the MG-PEDOT HTL not only offers favorable energy level alignment and efficient charge extraction, but also improves the film quality of the perovskite layer featuring enlarged grain size, lower trap density, and longer carrier lifetime. Consequently, the power conversion efficiency (PCE) of the flexible device based on MG-PEDOT HTL is increased by 36% compared to that of pristine PEDOT:PSS HTL. Meanwhile, the flexible perovskite solar minimodule (15 cm^2 area) using MG-PEDOT HTL achieves a PCE of 17.06%. The encapsulated modules show remarkable long-term storage stability at 85degC in ambient air (~90% efficiency retention after 1200 hours) and enhanced operational lifetime (~90% efficiency retention after 200 hours) [1]. With the adoption of the flexible transparent electrodes [2] and the introduction of a new modification on the perovskite active layer, the power-per-weight of our flexible PSCs reaches about 8 W/g while the power-per-weight of PEN/ITO-based control about 1-1.5 W/g. The work contributes to the development of flexible PSCs for practical applications.

[1] R. Zhang, W.C.H. Choy, et al, Adv. Funct. Mater., 33, 2210063, 2023.

[2] J. Kim, W.C.H. Choy, et al, Adv. Energy Mater., 10, 1903919, 2020.

2:15 PM *EN01.02.03

Natural Sunlight for Stability Testing of Perovskite Solar Cells Iris Visoly-Fisher; Ben-Gurion University of the Negev, Israel

A major challenge facing the development of perovskite-based solar cells is combining high efficiency with long-term stability. Outdoor stability testing under natural sunlight provides the most relevant test of performance dynamics under operational conditions. Understanding these cells' recovery properties under natural diurnal light-dark cycling can point to methods to extend its lifetime. Sunlight intensity/ concentration -dependent studies of perovskite-based devices elucidated the effect of bias applied to the solar cells on its lifetime and degradation mechanisms. Accelerated stability studies under different sunlight concentrations were examined to determine their relevance to degradation at operational conditions.

2:45 PM EN01.02.04

Fabrication of PEDOT Thin Films using Oxidative Chemical Vapor Deposition to Enhance The Stability of Perovskite Solar Cells Meysam Heydari Gharahcheshmeh; San Diego State University, United States

The practical applications of perovskite solar cells (PSCs) have been hindered by stability issues. One key factor contributing to this limitation is the inherent acidity of the commonly used hole transport layer, poly(3,4-ethylene dioxythiophene):polystyrene sulfonate (PEDOT:PSS), which can compromise the stability of PSC devices. To address this challenge, this study explores an innovative approach that leverages oxidative chemical vapor deposition (oCVD) with antimony pentachloride (SbCl_5) as a liquid oxidant. This method is employed to fabricate stable and ultrathin, highly conformal PEDOT films, offering a promising alternative as a hole transport layer in PSCs. The oCVD-grown PEDOT-Cl thin films, produced using liquid SbCl_5 oxidant, exhibit outstanding optoelectronic properties, precise control over nanostructure, stability, and integration capabilities. These qualities make them a robust and efficient choice for use as a hole transport layer in PSCs. Incorporating oCVD PEDOT-Cl thin films as the hole transport layer in PSCs results in a remarkable PCE of 20.74%. This surpasses the PCE of 16.53% achieved by spin-coated PEDOT:PSS thin films treated with the dimethyl sulfoxide (DMSO) polar solvent. Moreover, PSCs incorporating oCVD PEDOT-Cl thin films demonstrate a notable 2.5 \times enhancement in stability compared to their PEDOT:PSS-DMSO counterparts. This technological advancement paves the way for the development of PSCs with not only high performance but also enhanced stability.

Keywords: Oxidative Chemical Vapor Deposition, PEDOT, SbCl_5 Oxidant, Perovskite Solar Cells

3:00 PM EN01.02.05

Attaining Long-Term Stability, Pure Phase and High Efficiency Beyond 23% in FAPbI_3 Perovskite Solar Cells via CsSCN Additives Ahmed Fouad Musa^{1,2} and Tzu-Chien Wei¹; ¹National Tsing Hua university, Taiwan; ²Al-Azhar University, Egypt

Perovskite solar cells (PSCs) have garnered substantial attention due to their exceptional power conversion efficiency (PCE) and cost-effective fabrication. Among the semiconductors, the cubic α -phase of formamidinium lead triiodide (FAPbI_3) has emerged as the most promising choice for creating highly efficient and stable perovskite solar cells. Maximizing the performance of this material is of paramount importance to the perovskite research community. However, thin FAPbI_3 films tend to undergo a phase transition from the photoactive black α -phase to an inactive yellow δ -phase when the temperature drops below 150°C. In this study, we explored the impact of introducing cesium thiocyanate (CsSCN) into the perovskite precursor solution. This addition facilitated the creation of a stable perovskite film with a larger grain size, even at a lower temperature of 100°C. The role of SCN^- anions proved critical in promoting the formation and stabilization of α - FAPbI_3 below its thermodynamic phase transition temperature. Notably, the inclusion of the CsSCN additive resulted in a remarkable enhancement of the power conversion efficiency (PCE) of the devices, exceeding 23%. This performance improvement can be attributed to several factors, including the formation of a stable perovskite film with larger grains, a film that is more uniform and compact, reduced defects, and improved charge transport properties. Furthermore, X-ray diffraction analysis verified that the CsSCN additive facilitated the formation of pure α -phase perovskite crystals, eliminating undesirable secondary phases. These findings underscore the effectiveness of CsSCN as an additive in achieving stable and high-performance α - FAPbI_3 perovskite solar cells with a pure phase composition.

Keywords: Perovskite solar Cells, Formamidinium lead triiodide, Cesium thiocyanate.

3:15 PM BREAK

SESSION EN01.03: Perovskite Applications

Session Chair: Paul Dastoor

Tuesday Afternoon, April 23, 2024

Room 331, Level 3, Summit

3:45 PM EN01.03.01

Perovskites in Space: Promising Results Aboard Two ISS Missions Samuel Erickson¹, William Delmas^{2,1}, Calista Lum^{3,1}, Jorge Arteaga¹, Kaitlyn VanSant⁴, Joseph Luther⁴, Timothy J. Peshek⁵, Lyndsey McMillon-Brown⁵ and Sayantani Ghosh¹; ¹University of California, Merced, United States; ²Sandia National Laboratories, United States; ³University of California, Irvine, United States; ⁴National Renewable Energy Laboratory, United States; ⁵NASA Glenn Research Center, United States

The rapid commercialization of low Earth orbit (LEO) and NASA's return to the moon will require next-generation photovoltaic materials with high specific power and defect tolerance. Perovskite solar cells (PSCs) are an excellent candidate for such missions, having demonstrated their resilience against the unique stressors of space. These include rapid temperature cycling with each orbit, high-energy particle radiation, increased ultraviolet light in the AM0 spectrum, and exposure to atomic oxygen. This work discusses the effects of LEO on metal halide perovskite (MHP) samples from two recent Materials International Space Station Experiment (MISSE) missions. MISSE-15, launched in 2021, included eight PSCs of varying architecture and absorber composition to test several prototype devices. The cells were placed in open circuit at zenith orientation (facing normal away from the Earth) outside the ISS for 6 months before returning to Earth for characterization. MISSE-16 included five encapsulated methylammonium lead iodide (MAPI) thin films with different cover glass layers to test the effects of UV radiation. Upon return, all samples were investigated with high-resolution spectroscopy and microscopy. Photoluminescent (PL) emission and recombination lifetime data from the MISSE samples were compared with control devices to quantify how the former changed under LEO conditions.

Ultimately, all MHP samples showed strong PL emission intensity and little sign of chemical degradation. MISSE-16 films were encapsulated with long pass and band pass UV filters instead of standard top glass to expose each sample to specific UV wavelengths. This test was designed to study if and how MHPs would be affected by various UV bands in combination with the space stressors previously described. All five samples exceeded expectations, returning uniform, emissive, and energetically stable. Of the eight PSCs aboard MISSE-15, only the two CsPbI₂Br cells experienced absorber failure. These cells returned nearly transparent due to CsPbI₂Br photobleaching. The remaining six PSCs, including two each of MAPI, triple cation, and formamidinium-rich triple cation cells, returned with their absorber layers intact. Unfortunately, all cells experienced degradation to their top electrodes (Al or Ag depending on PSC), resulting in no electrical response in post-flight tests. This appears to be caused by ion migration, likely iodide, between the MHP and the metal. However, all MHP films were stable and emissive in regions without contacts and only slightly altered in areas behind the damaged contacts, further confirming the resilience of MHPs. Future MISSE missions will soon launch containing PSCs with indium tin oxide and Au contacts which are known to prevent ion transfer. Overall, the high stability and PL response of MHP films and cells demonstrates their ability to withstand the harsh environment of space.

*This work was supported by NASA grant no. NNN18ZHA008CMIROG6R and NSF grant no. NSFDGE-2125510.

4:00 PM EN01.03.02

Computational Exploration of Perovskite-Inspired ABX₃ Structures for Inorganic Solar Harvesting Materials Wonzeo Jung^{1,2}, Suim Lim^{1,2}, Jiho Lee³, Changho Hong³, Yong Youn¹, Seungwu Han³, Kihwan Kim¹, Joo Hyung Park¹ and Kanghoon Yim¹; ¹Korea Institute of Energy Research, Korea (the Republic of); ²Chungnam National University, Korea (the Republic of); ³Seoul National University, Korea (the Republic of)

In the last decade, hybrid organic-inorganic perovskites (HOIPs) have shown remarkable potential in enhancing the efficiency of solar cells. However, their practical application has been hindered by issues related to instability, primarily stemming from their inherent vulnerability to humidity and heat. To overcome the instability, which may originate from their organic components, the development of fully inorganic perovskites with comparable performance could be the solution for next-generation solar-cell materials. In our research, we explore all known ABX₃ inorganic compounds obtained from structure databases in search of novel materials for solar energy harvesting. Driving inspiration from the perovskite structure, which offers several advantages in photovoltaic properties, we systematically screen and classify materials featuring the connectivity information between octahedra composing the structures. Consequently, we have successfully classified the target structures in terms of dimensionality and porosity. To predict the photovoltaic performance of those perovskite-inspired structures, we conduct high-throughput screening, taking into account critical factors such as band gaps, optical absorbance, effective masses, synthesizability, and defect tolerance. As a result, we propose several new candidate materials for fully inorganic photovoltaic absorbers. Additionally, we analyze the overall trends in photovoltaic properties across the various structural types within our classification. We anticipate that this talk will offer valuable insights for discovering and designing new inorganic solar-cell absorbers from an expanded material pool.

4:15 PM EN01.03.03

HOMO Energy Level Modulation with Fluorinated Poly(aryl)amines for Wide-Bandgap Perovskite Solar Cells Tom Macdonald; University College London, United Kingdom

Fluorination stands out as an effective strategy to narrow the energy gap between HTMs, such as Poly(aryl)amines (PTAA), and perovskite materials. We demonstrate the synthesis of six novel fluorinated PTAA derivatives and present innovative methods for introducing trifluoromethyl (CF₃) groups into PTAA structures. Our investigation, incorporating electrochemical and optical spectroscopy analyses, highlights the significant influence of both the position and quantity of fluorine atoms on PTAA's energy levels. Additionally, we demonstrate that fluorine atoms and CF₃ groups impact orbital level structures differently, advancing our understanding of PTAA's role in PSCs. Importantly, we have fabricated wide-bandgap PSCs with fill factors exceeding 80%, short-circuit current densities surpassing 17 mAcm⁻², and power conversion efficiencies exceeding 17%. Notably, this was achieved without implementing surface passivation, underscoring the potential for optimizing high-performance HTMs in PSCs.

4:30 PM EN01.03.04

Efficient Indoor Light Harvesting with High Band Gap Perovskite and Sodium-Ion Battery Tsvetelina Merdzhanova¹, Li-Chung Kin^{1,2}, Zhifan Liu¹, Hans Kungl², Sergey Shcherbachenko¹, Thomas Kirchartz¹, Rüdiger-A. Eichel², Uwe Rau^{1,3} and Oleksandr Astakhov¹; ¹Forschungszentrum Jülich GmbH, Institut für Energie- und Klimaforschung (IEK-5-Photovoltaik), Germany; ²Forschungszentrum Jülich GmbH, Institut für Energie- und Klimaforschung (IEK-9 Grundlagen der Elektrochemie), Germany; ³Jülich Aachen Research Alliance (JARA-Energy) and Faculty of Electrical Engineering and Information Technology, RWTH Aachen University, Germany

Integrating storage technologies in renewable energy systems of the future is one of the most important problems of the moment. Recent development trends in small scale consumer electronics towards implementing "Internet of Things" and smart house/smart cities concepts make it imperative to have cheap, wireless power solutions for electronics that operate all day. The combination of photovoltaic (PV) devices with rechargeable batteries represents a viable strategy for powering such low power electronic devices. With the increasing use of indoor LED (light emitting diode) lighting worldwide, the matching spectrums of LED output and the absorption spectrum of lead halide perovskite solar cells (PSC) affords an opportunity to reuse emitted light with high efficiency to feed low power electronics. Recently, lead halide perovskite cells and modules have demonstrated efficiencies under artificial lighting of more than 30 % [1] with a record of 40.1 % achieved with an extra thick absorber layer [2]. The main reason is the very close overlap of the external quantum efficiency in lead halide perovskite solar cells with the emission spectrum of an LED lamp. However, there are not many publications showing a combination of perovskite-battery devices working efficiently under low light LED illumination intensities.

The aim of the work is to demonstrate a successful and highly efficient energy harvesting and storage under a wide range of light emitting diode (LED) illumination intensities by applying lead halide perovskite solar module directly coupled to a high-rate capable next generation sodium ion battery. Direct coupling of PV and batteries require fabrication of perovskite solar module with tailored current-voltage (IV) characteristic to match battery voltage under target irradiance conditions. A 3-cell perovskite module with CH₃NH₃Pb(I_{0.8}Br_{0.2})₃ absorber layer and fullerene electron transport layer were fabricated with a conversion efficiency of 17.8 %, with a fill factor of 81.3 %, short-circuit current density of 5.91 mAcm⁻² and open-circuit voltage of 3.71 V under

AM.1.5 illumination. To test the PSC modules for indoor battery charging under LED lighting a sodium ion battery with metallic sodium anode and cathode made from sodium titanium phosphate ($\text{NaTi}_2(\text{PO}_4)_2$) coated onto sheets of carbon nano-felt (NTP@CNF) was chosen due to its high charge rate capability, low charge-discharge overpotential and distinct charge and discharge voltage plateau. LED illumination intensity was attenuated by using neutral density filters.

High efficiency indoor charging of advanced sodium ion battery based on sodium titanium phosphate ($\text{NaTi}_2(\text{PO}_4)_2$) coated onto sheets of carbon nano-felt coupled with a perovskite solar module with $\text{CH}_3\text{NH}_3\text{Pb}(\text{I}_{0.8}\text{Br}_{0.2})_3$ absorber layer under LED illumination was demonstrated. We have directly coupled both devices without any power electronics and achieved overall PV-Battery efficiency of 24.3% at 300 lx LED lighting. Under target LED illuminance of 300 lx, the perovskite solar cell shows PCE of 29.4%, and coupling factor of 0.87, and roundtrip battery efficiency of 94.9 % [3].

References

- [1] Cheng, R.; et al., *Advanced Energy Materials*. 2019, 9, 1901980. <https://doi.org/10.1002/aenm.201901980>
- [2] He, X.; et al., *Advanced Materials*. 2021, 33, 2100770. <https://doi.org/10.1002/adma.202100770>
- [3] Kin L.C.-; et al. *Cell Reports Physical Science* 2022, 3, 101123.

4:45 PM EN01.03.05

Scaling of Perovskite Solar Cells with Carbon Nanomaterials Wei Wei; Wichita State University, United States

Perovskite solar cells (PSCs) that utilize carbon materials as the electrodes provide a great opportunity to enhance the stability and performance meanwhile reduce the cost. Carbon-based electrodes have been reported to be an alternative owing to material abundance, low cost, industrially mature preparation and excellent stability. In this talk, we will first introduce our recently designed chemical reaction for hydrogenated carbon preparation. Then its application for high performance perovskite solar cells will be presented. Last, the potential of using slot-die coating for large-area PSCs will be discussed.

SESSION EN01.04: Poster Session
Session Chairs: Nicola Gasparini and Paul Meredith
Tuesday Afternoon, April 23, 2024
Flex Hall C, Level 2, Summit

5:00 PM EN01.04.01

Absorption Enhancement in Perovskite based Thin Film Solar Cells using Whispering Gallery Modes of Dielectric Spheres Ayusmin Panda; Indian Institute of Technology Madras, India

Organic and inorganic halide perovskite solar cells (PSC) are regarded as a promising candidate for next-generation photovoltaic technology owing to their low-fabrication methods and higher power conversion efficiency. PSC devices with adequate trapping of incident light, have been proposed in two different novel configurations. One with the inclusion of pristine TiO_2 microspheres and the other with CsPbI_3 coated TiO_2 microspheres, exhibiting resonating whispering gallery modes (WGM). The absorption in the CsPbI_3 active layer is enhanced due to the presence of WGM microspheres. The incoming electromagnetic wave couples with TiO_2 microsphere and forms confined resonating modes. Since, the in-coupling element is lossless, energy stored in microspheres is absorbed efficiently by the underlying active perovskite material. Thus, the devices show a higher current density in the range of **25 mA/cm²**, which is almost **50%** more than a conventional PSCs device. The performance of the designed PSCs have been tested numerically using 3D full-field finite difference time-domain (FDTD) simulation tool. Further, different designs have been discussed for deciding the appropriate position of WGM spheres w.r.t thin-film PSCs featuring back-reflector and optimized anti-reflecting coating. We have also studied the influence of multi-sized array of spheres as well as perovskite coated dielectric spheres to propose an analytical model based on temporal coupled mode theory.

5:00 PM EN01.04.02

A Breakthrough in Indoor Light Energy Recycling: Dye-Sensitized Photorechargeable Batteries So Yeon Yoon, Myeong-Hee Lee and Tae-Hyuk Kwon; Ulsan National Institute of science and Technology, Korea (the Republic of)

Global energy consumption continues to escalate daily, accompanied by the rapid depletion of fossil fuel resources. The imperative for technological and economic progress has led to increased combustion of fossil fuels, resulting in diminishing reserves, environmental pollution, and extreme weather events. In response to the urgent challenges of energy depletion and environmental pollution, the exploration and development of renewable and recycling energy sources have become paramount. Among these sources, indoor light, constituting 10% of total energy consumption and widely available, has attracted significant attention. However, despite its advantages, indoor light recycling has proven challenging due to the absence of suitable technology.

Recently, a groundbreaking solution has emerged in the form of dye-sensitized photorechargeable batteries (DSPBs), designed to harvest and store energy under indoor light conditions. DSPBs represent a seamlessly integrated system comprising a dye-sensitized solar cell (DSSC) and a Li-ion battery. Their photocharging process is balanced by the spontaneous internal thermodynamic reaction between the redox materials in dye-sensitized solar cells and the redox Li-ion storage materials. Previous studies have showcased the remarkable efficiency of DSPBs, achieving a high light-to-storage efficiency of up to 13.2%. This efficiency translates into recycling 1% of total energy consumption, equivalent to the energy consumption of ammonia synthesis. However, a challenge remains in their energy density for operating devices.

In this study, we address this limitation by incorporating redox targeting materials inspired by the redox flow battery system into DSPBs. These materials facilitate energy harvesting by regenerating the redox material in DSPBs based on the Nernst equation. Consequently, the energy densities increased approximately threefold compared to previous conditions. This innovative approach not only provides a sustainable solution for indoor light energy recycling but also holds the potential to revolutionize the way we harness and utilize energy. Our research opens new avenues for enhancing energy efficiency, marking a significant step toward a more sustainable energy future.

5:00 PM EN01.04.04

Scalable, Low-Temperature Fabrication of High-Performance Perovskite Solar Modules and Their Application to Photo-Rechargeable Batteries Young Yun Kim, Sehee Kim, Jungdon Suk and Nam Joong Jeon; Korea Research Institute of Chemical Technology, Korea (the Republic of)

A fabrication of perovskite solar cells (PSCs) by scalable processes in large-area is prerequisite for the PSCs to fully utilize the inherent advantages of perovskite such as superior charge-transport properties, high absorption coefficient, flexible and light-weight form factors. Large-area perovskite solar

modules (PSMs) can be utilized in self-powered personal mobility and electronics, smart textiles, custom-shaped building-integrated photovoltaics, and so on.

Although several demonstrations of scalable production of PSCs have been reported, successful demonstration of fully scalable production of large-area PSMs is still lacking. The major obstacles are uniform wet-film formation via scalable process in large-area, and complete phase conversion of perovskite precursor to photoactive phase. Therefore, reliable scalable production methods should be established including wet-film formation and phase conversion steps.

In addition, the direct integration of energy generation and storage devices have attracted a lot of interest recently in order to correspond to the fluctuation of power input from the Sun and increasing demand for self-powered electronics. However, inherent mismatch of voltage and current range for charging and discharge from PSCs to Li-based batteries is a major obstacle to realize the direct integration between them. Additionally, power output from PSCs under continuous light illumination, and storage capacity from charging-discharging cycles from Li-ion batteries should be retained.

In this work, we successfully demonstrate high-performance PSMs and photo-rechargeable batteries by directly integrating PSMs and Li-ion batteries in a single substrate. All the layers constituting PSMs can be fabricated via solution shearing coating, with optimized rheological and interfacial properties, at a low temperature (<160 °C). An electron transporting layer (ETL) is designed to be uniform and compact in large-area, by systematically investigating the effect of leaving group in sol-gel precursor and applying an optimal tin precursor with organic crosslinkers. As a result, high-efficiency over 24% can be achieved, retaining over 90% relative efficiency compared to initial one after over 2000 h. Complete conversion of perovskite precursor to photoactive phase in a large area can be achieved via careful selection of proper antisolvent and bathing in it.

PSMs are carefully designed to have a proper area and structure to exactly match the charging voltage-current range of high-capacity Li-ion batteries. Consequently, over 20% efficiency of PSMs and over 14% of overall charging to storage efficiency can be achieved. The photo-charging can be repeatedly conducted over 50 cycles because of stable power output and storage of integrated PSMs and Li-ion batteries.

5:00 PM EN01.04.05

Passivate Leakage Current via Active Layer and Electron Transport Layer Engineering for Enhanced Perovskite Optoelectronic Performance and Stability [Junmin Lee](#), Woongsik Jang, Byung Gi Kim and Dong Hwan Wang; Chung-Ang University, Korea (the Republic of)

ABSTRACT BODY:

Perovskite optoelectronic devices have garnered immense attention in recent years due to their exceptional efficiency, low-cost fabrication, and potential to revolutionize the field of photovoltaics. However, enhancing their stability and performance remains a critical challenge [1,2]. This study delves into the systematic investigation of perovskite optoelectronics, focusing on the pivotal role played by the active layer and electron transport layer (ETL) in determining device efficiency and stability [3]. We investigate the role of the electron transport layer (ETL) in enhancing the charge carrier transport and extraction processes. PDI-derivatives, such as PDIN, PDINO, and PDINN which are well-known and used material in organic optoelectronic devices' electron transport layer, has high electron affinity, charge transport properties, and good chemical and thermal stability etc [4]. However, it was difficult to apply it on the perovskite layer because the alcohol-based solvent was used, so we solved this and applied it to the PSC device of the NIP structure. It was confirmed that by applying PDINN on the PCBM layer, the defects of the PCBM layer were effectively passivated to reduce shunt leakage and at the same time suppress dark current. This process consequently suppresses the thermal degradation of the device and improves the stability of the device. Furthermore, we present a meticulous exploration of various active layer chemical physical process and their impact on the perovskite optoelectronic devices. Until now, it has been known that the grain size in the perovskite active layer is largely influenced by the time and temperature of the annealing process [5]. We note the relationship between the force and buoyancy acting on the active layer by the density of the washing solvent during the washing process, confirming that the lower density washing solvent receives lower buoyancy and consequently induces the formation of a larger grain size. It can be explained by the LaMer model, which represents the speed and time relationship between reaching the supersaturated state from the saturated state, confirming that the dark current is suppressed by reducing grain boundary concentration and passivate the leakage current through it [6]. This, in turn, leads to improved detection performance of the perovskite photodetector. Moreover, we have also conducted research to overcome the shortcomings of perovskite materials that are vulnerable to moisture [7]. A moisture trap capable of trapping water molecules is put into a perovskite solution to remove an infinitesimal amount of remaining moisture through over-night stirring, forming a well-oriented perovskite crystal, and preventing oxidation generated by internal moisture meeting the upper electrode when the device is driven, thereby improving device durability. In summary, our research offers valuable insights into the intricate interplay between the active layer composition, ETL properties, and the overall performance and stability of perovskite optoelectronic devices.

[1] Jang, W., Lee, J. M., Kim, B. G., Lim, J., Yang, Z., & Wang, D. H. (2023). *Crystal Growth & Design*, 23(9), 6916-6925.

[2] Kim, B. G., Jang, W., Chun, J. Y., Lee, J., & Wang, D. H. (2022). *Journal of Industrial and Engineering Chemistry*, 116, 331-338.

[3] Lee, J., Kim, B. G., & Wang, D. H. (2023). *Solar RRL*, 7(3), 2200937.

[4] Yao, J., Qiu, B., Zhang, Z. G., Xue, L., Wang, R., Zhang, C., ... & Li, Y. (2020). 11(1), 2726.

[5] Kim, H. D., Ohkita, H., Benten, H., & Ito, S. (2016). *Advanced materials*, 28(5), 917-922.

[6] Whitehead, Christopher B., Saim Ozkar, and Richard G. Finke. *Chemistry of Materials* 31.18 (2019): 7116-7132.

[7] Wang, Q., Chen, B., Liu, Y., Deng, Y., Bai, Y., Dong, Q., & Huang, J. (2017). *Energy & Environmental Science*, 10(2), 516-522.

5:00 PM EN01.04.06

Investigating The Suitability of All-Perovskite Tandem Photovoltaics for Indoor Applications [Jarla Thiesbrummel](#)^{1,2}, Etienne Beier², Lucas Holte², Jonathan Warby², Fangyuan Ye^{3,2}, Henry J. Snaith¹ and Felix Lang²; ¹University of Oxford, United Kingdom; ²University of Potsdam, Germany; ³East China University of Science and Technology, China

To enable Internet of Things (IoT) applications powered by indoor photovoltaics, it is essential to attain high open circuit voltages. This eliminates the need for step-up transformers to supply the voltage required by the different IoT applications. Although so far, only single junction perovskite solar cells have been investigated for indoor use, all-perovskite tandems could be adapted such that their bandgaps are suitable for indoor illumination, with the advantage of providing a much higher open circuit voltage than single junctions. Here, for the first time, we present an all-perovskite tandem solar cell based on bandgaps that have been specifically tailored to indoor light sources. The performance of these tandems is evaluated for two different types of indoor illumination, and at different illumination strengths. Furthermore, a sub-cell-selective investigation of both sub-cells reveals their individual performance, and provides crucial insights into the factors limiting the tandem efficiency under different illumination conditions. Finally, the general suitability of all-perovskite tandem solar cells for indoor applications is discussed.

5:00 PM EN01.04.07

Indenofluorene-Based Polymer Donor containing The Structural Structure of Pyrolopyroledione [Youngeup Jin](#)¹, Suhee song², Jin Young kim² and Rajalingam Agneeswari¹; ¹Pukyong National University, Korea (the Republic of); ²Ulsan National Institute of Science and Technology, Korea (the Republic of)

We synthesized three new polymers, namely **P1-P3**, incorporating electron-donating 6,12-dihydro-6,6,12,12-tetraoctyl-indeno[1,2-b]fluorene (IF) and

structural isomers of weak and strong electron-accepting 2,5-dioctyl-4,6-di(thiophen-2-yl)pyrrolo[3,4-c]pyrrole-1,3(2H,5H)-dione (IFPPD) or 2,5-bis(2-ethylhexyl)-3,6-di(thiophen-2-yl)pyrrolo[3,4-c]pyrrole-1,4(2H,5H)-dione (LFPPD) or both the IFPPD and LFPPD units as an effort to study the performance of IF-based polymers on non-fullerene acceptor-based organic solar cells (NFA-OSCs). Polymer **P1** exhibited absorption from 300 nm to 450 nm with an optical bandgap (E_g) of 2.39 eV but polymers **P2** and **P3** showed extended absorption up to 700 nm with an E_g of 1.75 eV. The determined highest occupied molecular orbital/lowest occupied molecular orbital (HOMO/LUMO) levels for **P1–P3** were -5.44 eV/ -3.05 eV, -5.26 eV/ -3.51 eV, and -5.39 eV/ -3.64 eV, respectively. The NFA-OSCs made by using each of **P1–P3** as an electron donor and Y6 as an electron acceptor gave a maximum power conversion efficiency (PCE) of 0.8%. We also utilized **P1–P3** as a co-adsorber and fabricated ternary NFA-OSCs using **P1–P3**:PM6:Y6 blends. It was noted that the performance of the ternary devices was lower than that of the binary devices made from PM6:Y6 blend

SESSION EN01.07: Perovskite Applications
Session Chairs: Nicola Gasparini and Tom Macdonald
Thursday Morning, April 25, 2024
Room 331, Level 3, Summit

8:45 AM *EN01.07.01

Photovoltaic Response and Mechanical Properties of Stretchable Solar Cells [Antonio Facchetti](#)^{1,2}; ¹Georgia Institute of Technology, United States; ²Northwestern University, United States

Recently, the power conversion efficiencies (PCEs) of rigid organic solar cells (OSCs) and all-polymer solar cells (all-PSCs) and have surpassed 19% and 18%, respectively, principally reflecting the introduction of (polymerized) small molecule acceptors. Here we report the synthesis of new acceptor semiconductors having fully conjugated and partially nonconjugated cores/backbones as well properly designed sidechains enabling both high efficiency ultra-high stretchability. Thus, all blend films were characterized by morphological, microstructural, and spectroscopic techniques and tensile experiments indicates that our blends can achieve ultimate strains surpassing 60%. Equally important, devices based on these blends achieve power conversion efficiencies > 16%, corroborating the molecular design of the new acceptors. Overall, these results convey important implications for developing future ductile and stretchable electronics.

9:15 AM EN01.07.02

Luminescent Solar Concentrator Greenhouses for Concurrent Energy Generation and Lettuce Production in The United States [Kristine Q. Loh](#), Nathan J. Eylands, Uwe R. Kortshagen and Vivian Ferry; University of Minnesota, United States

Agrivoltaic systems promote dual land use by strategically combining photovoltaics (PV) and agriculture. One application space is in greenhouses, where PV glazing can offset or completely meet high energy demands from greenhouse operations. However, fully opaque PVs generate electricity at the expense of light transmission, thereby eliminating crop photosynthesis. Luminescent solar concentrators (LSCs) have received growing interest in the agrivoltaics community as their higher transparency can benefit crop yield while concentrating light onto small-area PV cells. Integrating LSCs into greenhouse roofs presents a promising opportunity to provide clean energy without significantly compromising crop yield; however, the LSC design considerations that balance transmission and electricity generation need to be better understood.

This work presents a modeling framework to evaluate the tradeoff between light used for energy generation and light used for crop growth in LSC greenhouses. Our model incorporates solar resources, heat and energy, power generation, lettuce (cv. Rex) crop yield, and economic models. Using data pulled from NASA and NREL, we determine the hourly power generation and energy demands for operating LSC greenhouses in Arizona (AZ), Florida (FL), Minnesota (MN), and Pennsylvania (PA). We compare two periodic LSC roof structures: a small-area 8 x 8 cm² LSC film surrounded by 2 cm-wide PV cells (36% PV coverage) and a large-area 24 x 24 cm² film surrounded by 2 cm-wide PV cells (15% PV coverage), as well as a conventional glass greenhouse. We also study three non-toxic luminophores previously evaluated as LSC roof materials: copper indium sulfide/zinc sulfide quantum dots (CIS/ZnS), silicon quantum dots (Si), and Lumogen Red 305 molecular dye (LR305).

First, we determine the influence of the luminophore spectrum and concentration in the LSC films on lettuce growth. CIS/ZnS and Si quantum dot roofs absorb blue light, while LR305 roofs absorb green light. We find that in all cases, the quantum dot roofs lead to higher lettuce yields than the dye roofs due to the reduction in blue light fraction.

Next, we study the impact of luminophore concentration on energy generation and the potential for net zero energy (NZE) greenhouses, where the total energy demand is met by the power produced by the PV cells. In AZ and FL, all small-area LSC greenhouses are NZE as the higher PV coverage allows for more energy generation. No LR305 large-area LSC greenhouses are NZE due to reabsorption losses and a lower PV coverage. All MN and PA LSC greenhouses have an energy deficit due to the high heating demands in these cold climates. However, for small-area LSC greenhouses in PA, the PV cells could meet roughly 1/3 of the energy demand.

Lastly, we calculate the net present value (NPV) to evaluate the tradeoff between crop yield and energy generation. We find that crop yield is the most significant determinant for the NPV, with higher yields leading to more profitable greenhouses. LSC greenhouses in AZ and FL can be more profitable than conventional greenhouses. In MN and PA, small-area LSC greenhouses are less profitable than conventional glass greenhouses. Still, large-area LSC greenhouses can be more profitable in PA due to improvements in crop yield and energy offset provided by the PV cells. The profit from AZ and FL LSC greenhouses can be further improved through net metering, where surplus energy is sold back to the grid. Overall, this study furthers understanding of the balance between power generation and light transmission in LSC-based greenhouses.

9:30 AM EN01.07.03

Constructing a Cascaded Type Perovskite/Perovskite Heterostructure with Transfer Printing Technique for Efficient Solar Cells [Anjali Thakran](#)^{1,2}, Mario Hofmann¹ and Chih Wei C. Chu²; ¹National Taiwan University, Taiwan; ²Academia Sinica, Taiwan

The perovskite/perovskite heterostructures, based on mixed-halide perovskites, manifest solution-processability, low-temperature, and competent efficiency like tandem solar cells. However, the current challenges of limited fabrication routes on solution-based materials, the interaction of the top layer with the underlying layer, solvent compatibility, and unmatched band alignment can cause poor performance and long-term stability issues. Herein, we have designed and demonstrated a sequential spin and transfer printing technique to fabricate a perovskite/perovskite device architecture (p-i-n type). We integrated Br-based perovskites (1.7 eV bandgap) as a bottom layer and Sn-based perovskites (1.2 eV bandgap) as a top layer with a thin interlayer. Due to

This searchable program is up-to-date as of April 15th, 2024.

cascaded-type band alignment between the top and bottom layer, a smooth extraction and transfer of photo-carriers happened, which boosted power conversion efficiency compared to a single-junction counterpart. With further morphology investigation, we found that SEM and AFM analysis confirmed that the crafted perovskite film with a modified PDMS stamp provides a smooth surface, fewer pinholes, and better interface quality. The high crystalline nature with larger grain size, lesser grain boundaries, and defects across interfaces in heterostructure film helps to suppress recombination losses at the interfaces. The printed layer positively impacts morphology, improving the heterostructure's power conversion efficiencies (PCE). Apart from PCE, the well-distinguished top and bottom layer, as investigated with XPS analysis, greatly helps to maintain the stability of ~1000 hours. With our ongoing investigation, we are focusing on the variation of top and bottom layer composition with consideration of active bandgap of 1.7 eV/ 1.6 eV, 1.7 eV/ 1.5 eV, 1.7 eV/1.4 eV, and 1.7 eV/1.3 eV and investigate heterostructures potential to maintain stability and performance of perovskite-based solar cells. Our technique can be adopted for low-temperature processable layer printing, including HTLs, ETLs, or any interlayer, and promotes low-weight, portable, and flexible photovoltaic devices. Additionally, this strategy is advantageous for implementing traditional Si solar cells and multi-junction tandem structures.

9:45 AM BREAK

SESSION EN01.08: Prototypes and PV in the Real World
Session Chairs: Nicola Gasparini and Tom Macdonald
Thursday Morning, April 25, 2024
Room 331, Level 3, Summit

10:15 AM *EN01.08.01

Organic Photovoltaic Sails for Maritime Decarbonation and BIPV Applications [Guillaume Wantz](#); University of Bordeaux, France

After briefly presenting the recent results obtained at lab scale in particular on water-processed OPV cells with record efficiencies, this presentation will mainly focus on the use of OPV modules in specific novel applications. In the frame of the start-up company "HEOLE", OPV-based sails have been manufactured incorporating OPV modules directly into the flexible and lightweight fabrics. These sails have been tested in real life, on multiple actual sailboats sailing since May 2022. Results on the monitored solar electricity and energy yields will be discussed as a promising direction for OPV deployment. Additionally, OPV sails have been combined with green roofing for rooftop application. Green roofing is an efficient strategy to enhance thermal insulation of buildings. However, green roofing cannot be easily combined with traditional opaque crystalline silicon prohibiting the plants development. The semitransparency of OPVs enables this combination with plant growing underneath the solar modules. The experimental roof is operational since April 2023 in southern Germany. Results of monitoring will be presented and discussed.

10:45 AM *EN01.08.02

High Performance Energy Harvesting Cells for Powering Consumer Electronics and IOT Devices [Kethinni Chittibabu](#), Bates Marshall, Sammaiah Thota, Debora Martino, Chris Turkstra and Joshua Wright; Ambient Photonics Inc, United States

Dye sensitized solar cells (DSSC) are very attractive for indoor light harvesting technology due to spectral tuning of DSSC to match ambient light spectrum. Ambient Photonics Inc has developed photovoltaic cells that perform well under a variety of indoor and diffused outdoor irradiating conditions. Ambient technology enables the development of battery free devices in consumer electronics and smart sensor applications.

11:15 AM *EN01.08.03

Solid Transparent Photovoltaics for Invisible Energy Supplies on Human Interface Applications [Joondong Kim](#); Incheon National University, Korea (the Republic of)

Humans have been widely using fossil fuels due to their ease of consumption for energy production with substantial concern. United Nations reported the World Commission on Environment and Development for "Our Common Future". Sustainable development is defined as "meeting the needs of the present without compromising the ability of future generations to meet their own needs." Renewable and sustainable energy resources are among the pivotal issues of sustainability, and photovoltaic power is a powerful shifter of the energy paradigm.

Photovoltaic energy production provides a great opportunity to support global energy demand. If we can transparently produce energy, we may apply invisible power generators to residential architectures to supply energy without losing visibility. Transparent Photovoltaic (TPV) is the technology of solar cells to convert light to electric energy beyond the darkness. Different from the typically dark or opaque solar cells, TPV is transparent by passing the visible range lights due to the wide-energy bandgap of metal-oxides. And thus, human beings may not recognize the existence of TPV entities but the electric energy is generated through the invisible power generator. This kind of invisible TPV may open a new era for on-demand energy supplying system, by being applied in windows of cell phones, displays, vehicles, and buildings.

Beyond the energy issues, transparent power generation can interface to human for bioelectronics, communications and memory devices. One day, human will use the invisible energy and relevant devices without losing a vision. "There's plenty of room at the bottom (Richard Feynman)" to explore the future technologies with the energy ubiquity.

SESSION EN01.09: Tandem and Stability
Session Chairs: Joondong Kim and Guillaume Wantz
Thursday Afternoon, April 25, 2024
Room 331, Level 3, Summit

1:30 PM *EN01.09.01

Strategies for Resilient Organic Photovoltaics [Derya Baran](#); King Abdullah University of Science and Technology, Saudi Arabia

Organic solar cells (OSCs) offer a distinct set of advantages among next-generation photovoltaics, i.e. their flexibility, lightweight design, low-cost manufacturing, and semi-transparency. Substantial efforts have been invested in boosting device efficiency, and this potential is now underpinned by

impressive laboratory-scale efficiencies approaching 20%. As efficiency gradually approaches commercialization requirements, the stability of OSCs becomes increasingly paramount in academic research. Numerous factors can influence device stability, including delamination of the photo-active layer or interface triggered by oxygen and water, light-induced chemical alterations in materials, and thermally induced morphological changes. Therefore, it is imperative to comprehend the stability bottlenecks of high-efficiency systems at this stage towards real-world applications.

In this talk, I will elaborate on the stability of various non-fullerene acceptors (NFAs) and different polymer donors for OSC. We established a connection between the molecular structure of Y-series NFAs, specifically the endgroup and side-chain, and their photostability, ultimately affecting the device's lifetime. We also explored the significance of various polymer donors in determining device longevity and highlighted the side-chain-induced degradation pathway in polymer donors. We further provided theoretical tools for understanding the photostability of polymer donors. Photochemical degradation in both Y-NFAs and polymer donors, under illumination, leads to a significant increase in trap-assisted recombination, resulting in decreased device performance under outdoor conditions. We systematically compared the photostability, thermal stability, and outdoor stability of devices fabricated with state-of-the-art materials, aiming to gain a comprehensive understanding of how the photoactive layers influence long-term performance in the hot and sunny climate of Saudi Arabia. Furthermore, I will propose new strategies to simultaneously improve the photostability, thermal stability, and outdoor stability of devices for resilient organic photovoltaics. Overall, our findings offer valuable insights for the design and synthesis of photoactive materials, with the goal of achieving both high efficiency and long-term stability in OSCs for real-world applications.

2:00 PM *EN01.09.02

Combined ML, DFT and Drift-Diffusion Model for Fabrication and Optimization of DSSCs and PSCs. [Andrews Nirmala Grace](#); VIT University, India

The development of highly efficient third generation solar cells (Dye sensitized solar cells (DSSCs) and Perovskite solar cells (PSCs)) is greatly hindered by the lack of a reliable and understandable Machine Learning (ML) model. In this study, a ML model is developed by integrating machine learning and computational quantum chemistry, DFT and drift diffusion modelling. The model is accurate, robust, and capable of interpretation. Utilizing this model, virtual screening and synthetic accessibility evaluation are conducted to discover novel absorbers that are efficient and easily synthesized for use in DSSCs and PSCs. Ultimately, a rigorous selection process has identified a subset of organic dyes that exhibit both high power conversion efficiency and synthetic accessibility, from an initial pool of over 5000 possibilities. In the context of deducing plausible chemical rules for high-performance absorbers, the interpretability of the model is utilized. This utilization is anticipated to facilitate future advancements in the practical applications of DSSCs and PSCs.

2:30 PM BREAK

3:30 PM EN01.09.03

Voltage-Matched Configurations for Monolithically Series-Connected All-Perovskite Double- and Triple-Tandem Solar Modules [Yasuhiko Takeda](#), Ken-ichi Yamanaka and Naohiko Kato; Toyota Central R&D Labs Inc, Japan

We designed all-perovskite (PVK) double- and triple-tandem solar modules.¹ Monolithically series-interconnected structures were adopted, because these offer high scalability by exploiting the advantages of thin-film modules over wafer-based crystalline-silicon modules. We revealed the voltage-matched configurations and their variants improve the annually averaged conversion efficiencies outdoor with potentially higher durability and lower costs compared with those of the conventional current-matched configurations.

Although the combination of PVK top cells and crystalline-silicon bottom cells has been realized higher conversion efficiencies of double-tandem modules at present, all-PVK tandem modules have various advantages of scalability, lightweight, and suitability for mass production. Therefore, improvements in the efficiencies of all-PVK modules are extremely important. Thus, to find the suitable module configurations, we modeled the photovoltaic performance of single PVK cells with different bandgaps by reference to previous experimental data. Then, we optimized the cell widths and transparent-electrode thicknesses used for the monolithically series-interconnected modules, along with the PVK bandgaps. Finally, we evaluated the annually averaged conversion efficiencies under various meteorological conditions using a database.

The conventional current-matched two-terminal double-tandem (Double-2T) modules have an advantage of a simple structure. The current matching condition requires the use of a large-bandgap PVK top cell. However, the photovoltaic performance currently lowers with increasing bandgap. This lowers the module efficiency. By contrast, the efficiency of another conventional configuration: four-terminal double-tandem (Double-4T) modules is less sensitive to the PVK bandgaps. This allows us to use more efficient and durable PVK compositions. However, Double-4T complicates the power-conditioning system, and hence it is not suitable for practical use. The voltage-matched double-tandem (Double-VM) module consists of the parallel-connected top and bottom modules, in which plural top cells and bottom cells are connected in series, respectively, so that the voltages of the maximal-power points (V_{MPP}) of these modules are approximately the same as each other. We revealed that Double-VM combines the advantages of Double-2T and Double-4T, and mitigates their shortcomings.

The voltage-matched triple-tandem modules also offer similar advantages to those of Double-VM. However, the use of three substrates covered with transparent conductive oxide films increases the optical loss and ohmic loss, resulting in lower efficiencies than those of the triple-tandem 2T modules. To solve this issue, we proposed a new configuration of the triple-tandem series/parallel-connecting voltage-matched (Triple-SPVM) module, in which the middle-bottom module consisting of directly series-connected middle and bottom cells is connected to the top module in parallel. The use of only two substrates improves the efficiency and lowers the cost. The current mismatch between the series-connected middle and bottom cells is not a great issue, because of slight changes in the relative solar spectrum in the relevant near-infrared range. Thus, Triple-SPVM is the best suited for practical use.

An emerging application of solar modules is power supply to electrochemical reactors for CO₂ conversion to useful organic substances. Direct connection of these two devices is exactly an artificial-photosynthetic device, and stores time-varying solar energy. It is of great importance for efficient conversion of CO₂ that the device operates at V_{MPP} of the solar modules. Double-VM and Triple-SPVM are suitable for this application, because V_{MPP} of the module is tunable by changing the series-connected cell numbers in each submodule.^{2,3}

References

1. Y. Takeda, et al., submitted.
2. Y. Takeda, J. Appl. Phys. 127, 204503 (2020).
3. Y. Takeda, J. Appl. Phys. 132, 075002 (2022).

3:45 PM *EN01.09.04

Exploiting The Synergy between Perovskite and Organic Photovoltaics in Semi-Transparent Solar Cells and Modules [Aldo Di Carlo](#)^{1,2}; ¹University of Rome Tor Vergata, Italy; ²Consiglio Nazionale delle Ricerche, Italy

Metal halide perovskites, characterized by tunable bandgaps, cost-effectiveness, and excellent optoelectronic properties, find diverse applications from indoor photovoltaics to tandem integration with silicon. Notably, their tunable bandgap enables transparent photovoltaics, a transformative technology for building-integrated photovoltaics (BIPV). Photovoltaic windows represent a compelling application, where visible light transmission is crucial, allowing for effective conversion of near-infrared (NIR) and/or near-ultraviolet (NUV) light into electrical energy. This technology holds particular promise in urban settings with limited rooftop space for traditional photovoltaics. The ability to continuously adjust the bandgap of halide perovskite materials across a broad

spectrum facilitates the development of semi-transparent solar cells and modules with high visual transmittance. Through bandgap optimization, tandem configurations with NIR organic solar cells can be designed to enhance efficiency without compromising average visual transmittance (AVT). This coupling can be boosted by a specific light management optimization that allows to increase the current density and/or the AVT and consequently the light utilization efficiency (LUE) of the cell. Numerical simulations suggest that optimized tandem architectures, leveraging photonic crystals and materials, can achieve a 15% power conversion efficiency with a 50% AVT.[1] The EU CITYSOLAR consortium [2] addresses this challenge through tailored strategies, encompassing material optimization, light management, and innovative characterization approaches. This presentation highlights the consortium's progress in surpassing the state of the art, showcasing diverse fabrication techniques, from solution processes to physical deposition, for see-through photovoltaics. Beyond solar cells, module-level developments, including a low-temperature, full blade-coating method for depositing semi-transparent FAPbBr₃-based perovskite modules on 300 cm substrates [3] and innovative coupling between top perovskite module and bottom organic module [4] are discussed.

Work performed within the CITYSOLAR consortium (www.citysolar-h2020.eu)

[1] D Rossi, K Forberich, F Matteocci, M Auf der Maur, HJ Egelhaaf, Christoph J Brabec, Aldo Di Carlo "Design of Highly Efficient Semitransparent Perovskite/Organic Tandem Solar Cells" *Solar RRL* 6 (9), 2200242

[2] <https://www.citysolar-h2020.eu/>.

[3] Jessica Barichello, Diego Di Girolamo, Elisa Nonni, Barbara Paci, Amanda Generosi, Minjin Kim, Alexandra Levchenko, Stefania Cacovich, Aldo Di Carlo, Fabio Matteocci "Semi-Transparent Blade-Coated FAPbBr₃ Perovskite Solar Cells: A Scalable Low-Temperature Manufacturing Process under Ambient Condition" *Solar RRL* Volume 7, 2200739 (2022)

[4] J. Wachsmuth, A. Distler, C. Liu, T. Heumüller, Y. Liu, C. M. Aitchison, A. Hauser, M. Rossier, A. Robitaille, M-A. Llobel, P.-O. Morin, A. Thepaut, C. Arrive, I. McCulloch, Y. Zhou, J. C. Brabec, H.-J. "Fully Printed and Industrially Scalable Semitransparent Organic Photovoltaic Modules: Navigating through Material and Processing Constraints", *Solar RRL* 7, 2300602 (2023)

Acknowledgments

This research has received funding from the European Union's Horizon 2020 research and innovation programme under grant agreement No 101007084 (CITYSOLAR). We acknowledge all the research team at CITYSOLAR consortium for their support.

4:15 PM EN01.09.05

High-Performance Monolithic Perovskite/Organic Tandem Solar Cells Hin-Lap Yip: City University of Hong Kong, Hong Kong

The emergence of solution-processed organic and metal halide perovskite solar cells can transform the landscape of photovoltaic technology in delivering scalable and high-performance solar cells to provide sustainable green energy. While the power conversion efficiencies (PCEs) of both single-junction organic solar cells (OSCs) and perovskite solar cells (PSCs) are rapidly ascending to >19% and >25%, respectively, their maximum efficiency is limited to ~33% accordingly to the Shockley-Queisser model for single-junction devices. However, it is possible to significantly increase the efficiency of solar cells by constructing a tandem device that consists of multiple light absorbers with considerably different bandgaps to reduce the solar cells' overall transmission and thermalization losses.

In this talk, I will discuss our work on developing high performance monolithic perovskite/organic tandem solar cells comprising a wide bandgap perovskite (WBG) front cell and a narrow bandgap (NBG) organic rear cell connected through a recombination junction. The WBG (E_g: 1.7-1.85 eV) PSCs are chosen for the front cell due to their strong and broad absorption for visible light, smaller voltage loss, and higher photoresponse compared to their organic counterparts with approximate bandgap. While NBG (E_g: 1.1-1.25 eV) OSCs can offer better near-infrared absorption tunability and stability compared with the Sn-based NBG perovskites, making them favorable candidates for the rear cell.^[1] Moreover, the advantage of the perovskite and organic light absorbing layers being processed from orthogonal solvents imposes fewer constraints on the choice of the materials for constructing the recombination junction and provides better flexibility on the device design of tandem solar cells.

To demonstrate state-of-the-art perovskite/organic tandem cells, an integrated strategy combining materials, interface, optical, and process engineering was adopted to optimize the two subcells and the interconnect junction simultaneously.^[2-5] In addition, a comprehensive optoelectronic model is being developed to simulate the electrical and optical properties of the tandem solar cells and to provide guidelines to optimize their device performance. The successful development of perovskite/organic tandem cells will have far-reaching impacts on producing high efficiency, low cost and scalable PV cells for clean energy production.

Reference:

[1] Yip, H.-L. et al, Renewed Prospects for Organic Photovoltaics. *Chemical Reviews* 2022, 122, 95

[2] Yip, H.-L. et al, Homogeneous grain boundary passivation in wide bandgap perovskite films enables fabrication of monolithic perovskite/organic tandem solar cells with over 21% efficiency. *Advanced Functional Materials* 2022, 32, 2112126.

[3] Yip H.-L. et al, Dual Sub Cells Modification Enables High Efficiency n-i-p Type Monolithic Perovskite/Organic Tandem Solar Cells. *Advanced Functional Materials* 2023, 33, 2212599.

[4] Yip, H.-L et al, All-Inorganic Perovskite-Based Monolithic Perovskite/Organic Tandem Solar Cells with 23.21% Efficiency by Dual-Interface Engineering. *Advanced Energy Materials*, 2023, 13, 2204347.

[5] Yip, H.-L et al, Optimizing Crystallization in Wide Bandgap Mixed Halide Perovskites for High Efficiency Solar Cells. *Advanced Materials* 2023, 35, 2306568

4:30 PM EN01.09.06

Toward Long Term Organic Solar Cell Device Stability via Thermocleavable Donor and Acceptor Active Layer Haoyu Zhao¹, Jordan Shanahan², Soumya Kundu¹, Guorong Ma¹, Andrew Bates¹, Wei You² and Xiaodan Gu¹; ¹University of Southern Mississippi, United States; ²University of North Carolina at Chapel Hill, United States

The performance of organic solar cell (OSC) was surged during past decades, however, the insufficient efforts to improve stability set the barriers to realize the practical applications for OSC devices. The morphological stability of OSC bulk heterojunction layer (BHJ) is apparently affected by the molecular mobilities of donors/acceptors under operational conditions. The introduction of thermocleavable side chains provides an effective and efficient method to reduce the dynamics of conjugated polymers (CP) to improve the thermal stability as evidenced by the enhanced T_g after fully cleavage. Furthermore, the newly synthesized donor-acceptor conjugated polymers (DA CPs) with thermocleavable contents were expected to achieve both good performance and stability for long term usage. This work focused on the investigations of the morphological changes as well as phase separation behaviors for thermocleavable donor/acceptor BHJ blend film. The solar cell devices were also prepared to evaluate the performance under various conditions. Finally, our work revealed the good performance and stable morphology over long term at elevated temperatures after alkyl side chains were completely removed, which could provide a pathway to improve the stability of optoelectronic properties in future OSC devices.

SESSION EN01.10: Inorganic Photovoltaics
Session Chairs: Nicola Gasparini and Julianna Panidi
Friday Morning, April 26, 2024
Room 331, Level 3, Summit

10:30 AM *EN01.10.01

The Benefits or Circular Recycling for Terawatt Photovoltaics Ian Marius Peters and Misha Sytnyk; Helmholtz Institute Erlangen Nürnberg, Germany

Solar energy and wind power stand as the twin cornerstones of the 21st-century energy revolution. Acknowledged by the Intergovernmental Panel on Climate Change (IPCC), the installation of solar panels and wind turbines emerges as the most potent and cost-effective means to decarbonize our energy systems. To attain the ambitious goal of limiting global temperature rise to 2 degrees Celsius, we must embark on the massive deployment of tens of billions of solar panels, necessitating the mobilization of several hundred million tons of raw materials. Encouragingly, the global industry is taking formidable strides to meet this challenge, projecting annual production capacity to exceed 1 terawatt peak (TW_P) before 2030, along with rapid expansion across the globe.

Yet, as we fast-forward a few decades, a pivotal decision looms on the horizon. As these solar panels reach the end of their operational life, we find ourselves at a crossroads – we can either discard these modules in landfills or we can opt for a more sustainable and forward-thinking approach. This approach involves integrating them into a circular system, fostering their reuse, repair, and eventual recycling.

Notably, we are not bound by resource constraints; although exceptions like silver exist, alternative materials are readily available. Thus, the option of dumping solar panels would not fundamentally hinder the realization of a renewable energy system operating at 100% capacity. However, opting for circular treatment offers an array of compelling benefits, rendering dumping the less favorable choice. Circular handling invariably encompasses the recovery and restoration of the materials and components involved, ensuring that these resources maintain their utility and minimize waste. The rate at which this recovery occurs must align with the pace of production, underscoring the imperative for our circular treatment capacity to match our production capacity.

Given the staggering scale of photovoltaic production, non-circular processes will become increasingly infeasible. The photovoltaic market is poised to become a major consumer of reclaimed products, further incentivizing circular strategies. In this presentation, we will delve into the dynamics that will steer a terawatt photovoltaic market toward circular recycling. Furthermore, we will explore the potential of emerging photovoltaic technologies, which hold the promise of enabling more processes with unprecedented material recovery and reuse, cementing the path toward a sustainable and circular energy future.

11:00 AM EN01.10.02

Ultrathin a-Si:H/Oxide Transparent PV Devices Deposited onto Architectural-Compatible Glass and Ceramic Substrates Alex J. Lopez-Garcia¹, Gustavo A Alvarez¹, Eloi R. Costals², Pablo Ortega², Cristobal Voz², Joaquim Puigdollers² and Alejandro Perez-Rodriguez^{1,3}; ¹Institut de Recerca en Energia de Catalunya, Spain; ²Universitat Politècnica de Catalunya, Spain; ³Universitat de Barcelona, Spain

Transparent Photovoltaics (TPV) is an emergent branch in the toolkit of PV that promises to extend the potential applications of PV and complement the most mature strategies that are limited in terms of on-site integration and applicability, especially into architectural components.^[1] The most important feature of PV devices is power output (i.e. efficiency). However, this approach brings in another critical feature almost at the same level of importance, which is the transparency and aesthetics of the device, which have to meet certain standards that can differ depending on the specific application and/or integration. As such, it adds some degree of complexity when optimizing, as other properties become more important. For TPV to be implemented in real-world scenarios they do not need to compete with high efficiency devices, rather they must be tailored to maximize efficiency with special care on transparency and aesthetic characteristics. For cost competitiveness, existing and mature industrialized materials (earth-abundant and non-toxic) and processes are a good starting point for first implementations. Developing such devices can potentially allow for fast-developing integration in areas such as building-integrated PV (BIPV) in the form of façade windows and other glazing elements, or to be integrated ubiquitously into sensors and future IoT devices with low-power requirements, as well as in Agrivoltaics (APV). Recent work has effectively studied the use of a-Si:H/oxide structures on glass substrates for TPV, showing some limitations especially in terms of V_{oc}.^[2,3]

In this work, we present inorganic-based TPV devices relying on ultrathin a-Si:H as absorber and different oxides as carrier selective contacts and transparent electrodes. In an innovative approach, we have inserted a high dipolar moment molecule (PAMAM-G3 dendrimer) at the ETL/absorber interface. This interface modification allows working with oxide charge transport layers (CTLs) that offer high transparency while eliminating surface energy barriers that decrease the resulting V_{oc} of the device, avoiding doping strategies (i.e. a-Si:H(p), a-Si:H(n)) and reducing costs due the low-temperature deposition processes. This new solution has allowed a record Light Utilization Efficiency (LUE) of 0.85%, by improving V_{oc} from 410 (reference) to 781 mV (PAMAM G3), still not reached by state-of-the-art devices with these materials, with negligible reduction in Average Photopic Transmittance or Color Rendering Index. The basic device structure is SLG/FTO/AZO/PAMAM-G3/ZnO/a-Si:H(30nm)/MoO₃/ITO. At the present time, spectrophotometry and J-V measurements under AM1.5G illumination (from the front and back sides) as well as Spectral Response measurements have been carried out. We report also on the bifaciality aspect of the architecture, showing almost unity bifacial factor, due to the ultrathin absorber coupled to wide-bandgap CTLs that make the device optically symmetric. Additionally, reference devices without dipoles have been also deposited onto ceramic substrates successfully and will be presented, confirming the potential of this approach to be integrated in different architectural environments such as glass and ceramics.

The work presented is of high relevance for the development of the field of inorganic thin film Transparent PV technologies, especially those working on ultrathin absorbers. It might also spark interest in thin film technologies in general that rely on advanced ETL/Active layer/HTL architectures.

This work has received funding from MCIN/AEI/10.13039/501100011033 under grant numbers PID2019-109215RB-C41 and TED2021-129758B-C32 and by the NextGenerationEU/PRTR.

[1] C. J. Traverser, R. Pandey, M. C. Barr, R. R. Lunt, *Nat. Energy* **2017**, 2, 849.

[2] S. Kim, M. Patel, T. T. Nguyen, J. Yi, C. P. Wong, J. Kim, *Nano Energy* **2020**, 77, 105090.

[3] A. J. Lopez-Garcia, O. Blazquez, C. Voz, J. Puigdollers, V. Izquierdo-Roca, A. Pérez-Rodríguez, *Sol. RRL* **2022**, 6, 2100909.

11:15 AM EN01.10.03

A Phenomenological Figure of Merit for Photovoltaic Materials Andrea Crovetto; Technical University of Denmark, Denmark

I propose a figure of merit Γ_{PV} to estimate the maximum efficiency attainable by a generic non-ideal PV absorber in a planar single-junction solar cell under the non-concentrated AM1.5G spectrum. This efficiency limit complements the more idealized limits derived from fundamental physics, such as the Shockley-Queisser limit and its subsequent generalizations. Specifically, the present figure-of-merit approach yields stricter efficiency limits applicable to realistic PV absorbers with various imperfections, including finite carrier mobilities and doping densities. Γ_{PV} is a function of eight properties of the absorber that are both measurable by experiment and computable by electronic structure methods. They are: band gap, non-radiative carrier lifetime, carrier mobility, doping density, static dielectric constant, effective mass, and two parameters describing the spectral average and dispersion of the light absorption

coefficient. Γ_{PV} has high predictive power (absolute efficiency error less than $\pm 1.1\%$) and wide applicability range. The Shockley-Queisser limit and its generalizations are reproduced by Γ_{PV} . Simpler figures of merit proposed by others are also included as special cases of Γ_{PV} .

For a generic PV absorber at any stage of development, determination of its Γ_{PV} figure of merit helps understand whether imperfect PV performance is intrinsic to the material (inadequate bulk properties at the current stage of development), or if it “only” requires a different device structure, contact layers, or improved interface properties. I will show the outcome of this analysis for 25 PV absorbers with record PV efficiencies between 0% and 85% of their Shockley-Queisser limit. Using a local version of the Γ_{PV} figure of merit, a material-specific optimization strategy is laid out for any experimentally synthesized PV absorber, by specifying the bulk properties that should most urgently be improved to increase their PV efficiency.

11:30 AM EN01.10.04

Photochromic Dyes for Semi-Transparent Solar Cells and Solar Mini-Modules with Light-Adjustable Transmittance and High Colour Rendering Index Renaud Demadrille¹, Samuel Fauvel¹, Antonio J. Riquelme¹, Diego Mirani¹, Johan Liotier¹, Valid M. Mwalukuku¹ and Stéphanie Narbey²; ¹CEA, France; ²Solaronix, Switzerland

Among the emerging photovoltaic technologies, dye-sensitised solar cells (DSSCs) have recently achieved power conversion efficiencies (PCE) above 15% and have demonstrated good stability, with lifetimes exceeding 12 years in real-world conditions. These devices can be coloured and semi-transparent, making them very attractive for both building-integrated photovoltaics (BIPV) and agrivoltaics (Agri-PV). However, to integrate these cells into windows for use in buildings or greenhouses, it is often necessary to find the right compromise between transparency and efficiency.

In this talk, we will present our recent work aimed at developing new photochromic dyes specifically designed for use in photovoltaic devices.^[1] We will present the synthetic routes to these photochromic photosensitizers and detail their optoelectronic and photochromic properties. We will show that by modifying the substitution of dyes from the diphenylmethopyran family, it is possible to modulate their absorption range in the visible, to control their discoloration kinetics and to reduce the recombination processes in solar cells.^{[2][3]}

We will then show that these dyes can be used to fabricate a new generation of semi-transparent solar cells and solar modules capable of self-regulating their optical transparency and energy conversion efficiency as a function of light intensity.

Thanks to the molecular engineering of these photosensitizers and the development of novel formulations for the electrolytes, we will show that solar modules with a transmittance varying between 50 and 65% as a function of light exposure and a color rendering index above 95 can be obtained.^[4]

References :

- [1] Huault et al., *Nature Energy*, 2020, 5, 468-477.
- [2] Mwalukuku et al., *Adv. Energy Mater.*, 2023, 13, 2203651.
- [3] Riquelme et al., *ACS Appl. Energy Mater.* 2021, 4, 9, 8941–8952.
- [4] Fauvel et al., *Chem. Sci.*, 2023, 14, 8497-8506.

11:45 AM EN01.10.05

Over 18% Efficiency Kesterite Solar Cell under Indoor Illumination Conditions Yuancai Gong¹, Alex Jimenez Arguijo^{2,1}, Axel Gon Medaille¹, Outman El Khouja³, Romain Scaffidi⁴, Guy Brammertz⁴, Denis Flandre⁵, Bart Vermang⁴, Aurelian Catalin Galca³, Alejandro Perez-Rodriguez², Sergio Giraldo¹, Edgardo Saucedo¹ and Zacharie Jehl Li-Kao¹; ¹Universitat Politècnica de Catalunya, Spain; ²Institut de Recerca Energètica de Catalunya, Spain; ³National Institute of Materials Physics, Romania; ⁴IMEC, Belgium; ⁵Université Catholique de Louvain, Belgium

Indoor photovoltaic (IPV) cells have the potential to power distributed and remote sensors, actuators, and communication devices, enabling the widespread implementation of the Internet of Things (IoT). Commercial (c-Si, CIGS, CdTe) and emerging (perovskite, organic solar cells) photovoltaic technologies face several challenges for indoor applications, including cost, toxicity, stability, and/or spectral mismatch. In contrast, kesterite materials are composed of earth-abundant, non-toxic elements and exhibit excellent stability, with a wide bandgap tunability between 1.0 eV up to 2.1 eV. This technology has recently achieved certified efficiencies of 14.9% under AM1.5G for the narrow band gap (Se-rich; 1.1 eV) compound and 11.4% for wider bandgap (S-pure; 1.5 eV), demonstrating its high efficiency potential.

In this work, we present the first complete theoretical and experimental study of the behavior of kesterite solar cells under indoor illumination conditions, with different high efficiency devices. First, we will show that the most relevant and mature photovoltaic technology, that is c-Si, expectedly drops the performance in indoor conditions due to its narrow band gap. Hence, the use of wide band gap materials is required for a good performance in indoor conditions. We will show that, under indoor conditions, the wide band gap (S-pure; 1.5 eV) can achieve efficiencies above 20%.

The experimental results demonstrate the excellent optoelectronic properties under low injection conditions, showing that the efficiency of narrow bandgap (12% efficiency in AM1.5G conditions) is practically unchanged with the AM1.5G light intensity down to 0.2 suns. To further support the high potential of kesterite materials for low injection applications we studied the narrow bandgap device performance under simulated indoor conditions by red shifting the typically used indoor spectra, corresponding to the blackbody emission at 2700K, 3000K, 4000K and 5000K. These spectra can be achieved using a calibrated LED based solar simulator. As predicted from the numerical simulation results, the devices demonstrate an outstanding efficiency over 18%.

These results motivate the development of efficient kesterite solar cells with a wider bandgap, specifically tailored for IPV applications. The indoor performance of the wide bandgap kesterite material has been studied using the same experimental procedure, revealing a performance of above 12% under simulated indoor conditions, consistently with the numerical simulation. The charge carrier extraction is analysed with spectral response (External quantum efficiency, EQE) and the changes induced by indoor light are characterized by performing EQE under dark and indoor illumination conditions.

Furthermore, to prevent interface recombination and drastically improve the IPV performance two strategies will be presented: (i) Ge alloying to further widen the bandgap and minimize the spectral mismatch, and (ii) device engineering by using passivation interlayers (e.g. Al₂O₃), adjusting the thermal post deposition treatment conditions or employing other electron-selective contacts (e.g. ZnSnO).

Therefore, the pathway for achieving efficiencies over 20% for indoor kesterite solar cells will be presented. These original ideas will set the stage for affordable, bio-safe, and durable indoor solar cells. It will also provide a technical approach for the comprehensive design of other emerging PV technologies.

SESSION EN04.05/EN01.05: Joint Session I—Organic Photovoltaics – from Fundamentals to Upscaling I

Session Chairs: Mariano Campoy-Quiles and Safa Shoaee

Wednesday Morning, April 24, 2024

Room 328, Level 3, Summit

8:30 AM *EN04.05/EN01.05.01

Exploring charge pair generation in single-component macromolecular materials for photovoltaic energy conversion [Jenny Nelson](#), Flurin Eisner, Mohammed Azzouzi and Jolanda Simone Müller; Imperial College London, United Kingdom

The discovery of several new classes of electron-accepting molecule that work well as electron acceptors at molecular heterojunctions had led to a strong increase in the power-conversion efficiency in organic solar cells, from 11 to 19% in the last 5 years. The impressive performance of the new materials and the range of chemical structures has led to interest in whether alternatives to the traditional 'bulk heterojunction' architecture for an organic solar cell can be found.

One approach concerns structures where, through chemical design, electron-rich and electron-poor components of a single macromolecular material are constrained to have a particular geometry relative to each other, being electronically coupled either through space or through bond. In a second intriguing development, devices based on a single molecular material have been reported deliver relatively high charge-generation efficiency in the absence of a donor-acceptor interface. This latter example challenges the current understanding of how free charges are generated in organic semiconductors. Achieving efficient energy conversion with a single macromolecular component would be both interesting and practically useful.

In this work, we report on studies of the design, characterisation and modelling of both types of structure, including a variety of non-fullerene acceptors, and macromolecular compounds with tethered donor and acceptor type domains. By combining experimental characterisation under varying conditions (field, temperature, excitation) with molecular and device-level calculations, we endeavour to relate exciton and charge dissociation efficiency in single-component devices to molecular parameters.

9:00 AM *EN04.05/EN01.05.02

Homo- and Heteromolecular interactions and Their Relevance for Morphological and Mechanical Stability of Non-Fullerene Organic Solar Cells [Harald Ade](#); North Carolina State University, United States

Organic solar cells (OSCs) are one of the most promising cost-effective options for utilizing solar energy in high energy-per-weight or semi-transparent applications. Recently, the OSC field has been revolutionized through synthesis and processing advances, primarily through the development of numerous novel non-fullerene small molecular acceptors (NFA) with efficiencies now reaching >19% when paired with suitable donor polymers. The device stability and mechanical durability of these non-fullerene OSCs is critical and developing devices with high performance, long-term morphological stability, and mechanical robustness remains challenging. Yet, morphological and mechanical stability is a prerequisite for OSC commercialization. Here, we discuss our current understanding of the phase behavior of OSC donor:acceptor mixtures and the relation of phase behavior and the underlying hetero- and homo-molecule interactions to performance, processing needs (e.g., kinetic quenches), and morphological and mechanical stability. Characterization methods range from SIMS and DSC measurements to delineate phase diagrams and miscibility to x-ray scattering to determine critical morphology parameters and molecule packing and dynamic mechanical analysis (DMA) to assess specifically the hetero-interactions. The results presented and its ongoing evolution are intended to uncover fundamental molecular structure-function relationships that would allow predictive guidance on how desired properties can be targeted by specific chemical design. Comparative studies show that the molecular hetero-interactions between the donor and NFA are not always the geometric mean of the homo-interactions. The presentation will focus on these heterointeractions and the results underscores the limited success often encountered when Hansen Solubility Parameters and surface energies are used to estimate molecular interactions [1]. Additional insights into the molecular interactions are also provided and the relevance discussed in rubber-toughening of OSCs with a SEBS additive [2].

References.

1. "Molecular interactions that drive morphological and mechanical stabilities in organic solar cells" S Siddika, Z Peng, N Balar, X Dong, X Zhong, W You, H Ade and BT O'Connor, *Joule* **7**, 1593 (2023)
2. "Rubber-Toughened Organic Solar Cells: Miscibility–Morphology–Performance Relations" AA Shafe, HM Schrickx, K Ding, H Ade, and BT O'Connor, *ACS Energy Letters* **8**, 3720-3726 (2023)

9:30 AM EN04.05/EN01.05.03

Sustainability Considerations for High Performing Organic Solar Cells [Julianna Panidi](#); Imperial College London, United Kingdom

Organic semiconductors are an emerging class of materials with various optoelectronic applications. The high commercialisation potential of this technology is evidenced by a few companies that have already launched their products into the market or are working towards this goal. Solution-processed organic electronics have a high potential to reduce the carbon footprint of the semiconductor industry if they are developed further and increase their market share.

In my talk, I will introduce sustainable routes to manufacture solution-processed organic electronics. Particular focus will be given to organic solar cells, which recently attracted immense attention due to the development of a new family of semiconductors that allows highly efficient light harvesting in indoor and outdoor conditions. One current limitation, though, is the use of not eco-friendly solvents and materials during the device development stages. Most organic electronic devices require halogenated and non-halogenated aromatic solvents during their fabrication. For large-scale production and further commercialisation, this is a key limitation. This arises from the fact that organic semiconductors are highly soluble in this category of solvents, which are often carcinogenic or toxic to the human reproductive systems and negatively impact the environment. Here, I will show high-performing organic solar cells fabricated from biomass-based solvents. In addition, recycling considerations are required for any product entering the market. Lastly, I will demonstrate a tool that enables quick solvent screening and the link between organic solar cells' performance in an effort to replace the use of toxic ones.

Overall, this work highlights the importance of replacing harmful chemicals and materials in the organic electronics fabrication stages, resulting in faster and wider commercialisation and new market opportunities.

Panidi, J. *et al.* Biorenewable Solvents for High-Performance Organic Solar Cells. *ACS Energy Lett* **8**, 3038–3047 (2023).

9:45 AM EN04.05/EN01.05.04

Structure Control during *In Situ* Printing of Donor-Acceptor Blend Films for Organic Solar Cells [Peter Muller-Buschbaum](#); Technical University of Munich, Germany

Among the next generation solar cells, in particular organic photovoltaics are gaining impact as a promising alternative to conventional silicon-based solar cells. However, despite big achievements in terms of power conversion efficiencies in the last years, it remains an unresolved challenge to fabricate large-area organic solar cells without sacrificing efficiencies. The reason behind is that basic understanding is still very limited due to the complexity of the systems. Moreover, presently a substantial number of researchers use spin-coating for film deposition, which is not compatible with the needs of a large scale production. Thus, using up-scalable deposition methods such as printing are of immanent interest. [1] Large-area printing such as slot-die coating involves complex hydrodynamic processes and simply transferring optimized parameters from spin-coating studies has only limited success. Thus, in the present work, we use advanced scattering methods such as grazing incidence small and wide angle X-ray scattering (GISAXS and GIWAXS) in situ during

printing of donor:acceptor blends to gain fundamental understanding about the underlying film formation processes. Different examples of polymer donors and small molecule acceptors are presented and the resulting morphologies are correlated with solar cell device performance. A special emphasis is put on the shift towards more environmentally friendly solvents, [2] which will be also a pre-requisite to promote a large-scale production of organic solar cells.

[1] Adv. Energy Mater. **13**, 2203496 (2023)

[2] Adv. Mater. **32**, 2002302 (2020)

10:00 AM BREAK

10:30 AM *EN04.05/EN01.05.05

Semitransparent Organic Photovoltaics with High Average Visible Transmittance Thuc-Quyen Nguyen; University of California, Santa Barbara, United States

Organic Photovoltaics (OPVs) offer sustainable, solution-processable, and cost-effective energy harvesting solutions. While opaque devices underwent enormous progress in the past decade, it remains a challenge to meet the high transparency requirements for integrated semitransparent OPVs (ST-OPVs) for buildings, skylights, skyscrapers, or greenhouses. In this work, we investigate the charge generation-recombination dynamics in three semitransparent blend systems with varied donor concentrations to understand the performance limitations. We also study the effect of the optical expediency of Au, Ag, Al, and graphite as back electrode material on ST-OPVs and show that 'one size fits all' is not a valid approach for choosing the back electrode material. It is important to consider the active layer absorption, active layer thickness and application in selecting the back electrode material. We demonstrate that using the dilute donor approach with an appropriate back electrode can yield devices with 73 % average visible transmittance.

11:00 AM EN04.05/EN01.05.06

Exciton Delocalization Induced by Aggregation for Efficient Non-Fullerene Organic Photovoltaics Robert J. Westbrook¹, Kui Jiang², Cheng Zhong³, Jianxun Lu⁴, Francis R. Lin², Sei-Hum Jang¹, Jie Zhang⁵, Yuqing Li⁴, Zhanhua Wei⁴, David S. Ginger¹ and Alex Jen^{2,1}; ¹University of Washington, United Kingdom; ²City University of Hong Kong, Hong Kong; ³Wuhan University of Technology, China; ⁴Huaqiao University, China; ⁵Shenzhen Institute of Advanced Technology, China

Intimate π -stacking in organic semiconductors is known to form aggregates, which drive dissociation of photogenerated excitons through delocalization of exciton wavefunctions [1-3]. In particular, the onset of non-fullerene acceptors (NFAs) such as Y6 has seen a dramatic rise in discussion of exciton delocalization and its relation to (acceptor-donor) hole transfer [4-6]. Here, we explore the concept of exciton delocalization and show that such treatment is necessary to accurately describe charge separation in high performance OPV blends based on D18:Y6. Specifically, we evaluate how π -interactions in aggregates contribute to delocalization strength, revealing that the formation of delocalized excitons in strongly π -interacting materials opens a new pathway for free carrier generation. This pathway partially bypasses the formation of performance-limiting singlet and triplet charge-transfer states in OPV blends and improves the internal quantum efficiency in OPVs to realize power conversion efficiencies of >19%. We further show that the extent of delocalization can be tuned with precise structural modifications of organic donor and acceptor molecules. Ultimately, we provide an insight into overcoming the fundamental limit of OPVs associated with intrinsic material properties. Designing materials with more pronounced delocalization character should maximize the exciton dissociation efficiency and minimize the terminal back recombination, pushing OPVs forward closer to theoretical efficiency limits [7].

[1] Rao, A. *et al.* The role of spin in the kinetic control of recombination in organic photovoltaics. *Nature* **500**, 435-439 (2013)

[2] Gélinas, S. *et al.* Ultrafast Long-Range Charge Separation in Organic Semiconductor Photovoltaic Diodes. *Science* **343**, 512-516 (2014)

[3] Tamai, Y. *et al.* Ultrafast Long-Range Charge Separation in Nonfullerene Organic Solar Cells. *ACS Nano* **11**, 12473-12481 (2017)

[4] Price, M. B. *et al.* Free charge photogeneration in a single component high photovoltaic efficiency organic semiconductor. *Nat. Commun.* **13**, 2827 (2022)

[5] Zhang, G. *et al.* Delocalization of exciton and electron wavefunction in non-fullerene acceptor molecules enables efficient organic solar cells. *Nat. Commun.* **11**, 3943 (2020)

[6] Wang, R., Zhang, C., Li, Q., Zhang, Z., Wang, X., Xiao, M. Charge Separation from an Intra-Moiety Intermediate State in the High-Performance PM6:Y6 Organic Photovoltaic Blend. *J. Am. Chem. Soc.* **142**, 12751-12759 (2020)

[7] R. Westbrook, K. Jiang *et al.*, Exciton Delocalization Induced by Aggregation in Polymer Donor for Efficient Non-fullerene Organic Photovoltaics. *Under Review*

11:15 AM EN04.05/EN01.05.07

Bifacial Indoor OPVs: Investigating The Influence of Vertical Stratification on Performance Symmetry of Semi-Transparent OPVs Gulzada Beket^{1,2}, Anton Zubayer¹, Uli Wurfel³, Thomas Österberg², Jonas Bergqvist² and Feng Gao¹; ¹Linköping University, Sweden; ²Epishine AB, Sweden; ³Fraunhofer Institute for Solar Energy Systems ISE, Germany

The demand for sensors in building digitalization is growing rapidly due to the increased need for better monitoring. However, Internet-of-Things (IoT) sensors typically rely on batteries, leading to high maintenance costs and environmental concerns related to battery recycling. One of the innovative solutions is harvesting ambient light to power these sensors. Organic Photovoltaics (OPVs) offer a promising approach due to their semi-transparency and high power-per-weight ratio, making them suitable for integration with IoT devices like electronic shelf labels and asset tracking labels. The synthesis of organic semiconductor materials for OPV gives flexibility which allows to design material systems which surpass state-of-the-art inorganic PVs for indoor applications.

Recent advancements in solution-processable, flexible, and semi-transparent indoor OPVs made by roll-to-roll and lamination technologies have opened the door to large-scale industrialization of IOPVs¹, reducing manufacturing costs by eliminating vacuum processing and scarce materials. Nevertheless, semi-transparent IOPVs may exhibit performance asymmetry when illuminated from different sides (cathode/anode illumination), which is problematic for IoT sensors requiring bifacial use.

In our study, we investigate the link between performance asymmetry and vertical phase segregation in semi-transparent IOPVs featuring various photoactive layers, including fullerene and non-fullerene-based materials. Through a combination of optoelectronic characterizations and simulations, we identify that a filtering layer within the photoactive layer does not contribute to photocurrent extraction and is the source of observed cathode/anode performance asymmetry².

Our investigation delves into the vertical arrangement of the cathode and anode stack, utilizing techniques such as Neutron and X-Ray Reflectivity, Time-of-Flight Secondary Ion Mass Spectrometry, and Ellipsometry. We find that certain photoactive layers, while highly efficient for indoor use, tend to phase separate when deposited on the cathode electrode, creating a physical barrier and causing trap-assisted recombination when illuminated from the anode side. Furthermore, we found that some photoactive layers remain vertically homogeneous, regardless of the electrode used, presenting the potential for electrically symmetric semi-transparent IOPVs.

Through thorough screening, we identify a photoactive layer system that not only delivers high and air-stable indoor performance but also exhibits perfect symmetry when illuminated from either the anode or cathode side. These findings offer a comprehensive understanding of how photoactive layers affect electrical symmetry in semi-transparent IOPVs, especially for bifacial applications. Our research contributes valuable insights for designing photoactive layers to achieve air-stable, and electrically symmetric semi-transparent IOPVs for various applications in the field of IoT sensors.

References:

1. Bergqvist, J. *et al.* Asymmetric photocurrent extraction in semitransparent laminated flexible organic solar cells. *npj Flex. Electron.* **2**, (2018).
2. Rodríguez-Martínez, X. *et al.* Air Processing of Thick and Semitransparent Laminated Polymer:Non-Fullerene Acceptor Blends Introduces Asymmetric Current–Voltage Characteristics. *Adv. Funct. Mater.* 2301192 (2023).

11:30 AM *EN04.05/EN01.05.08

Photovoltaic Enabled Indoor Light Harvesting Paul Meredith; Swansea University, United Kingdom

By the mid-2020s it is predicted that billions of sensors and other IoT devices will be deployed worldwide monitoring every aspect of our environment. These devices require electrical power with batteries being the preferred choice when hard-wiring is impractical or too expensive. Other alternatives to batteries are being advanced and particularly for the indoor environment harvesting the 'free' artificial and / or externally transmitted light seems a tangible possibility.

It is becoming more appreciated that the design of an optimised and integrated PV system for indoor light harvesting is very different to conventional solar cells. Artificial lighting sources have bespoke spectral characteristics (consider warm and cool white LEDs) radically different to AM1.5G, and indoor lighting is low intensity (< 500 lux). The question thus arises – what type of PV is best suited to this emerging application? Answering this question involves thermodynamic considerations such as the optimal bandgap in the radiative limit, generation and transport losses under low photo-generated carrier concentrations, additional voltage losses due to shunt, etc. We must also consider architectural approaches such as doubly transparent contacts and cell interconnection to deliver appropriate voltages and currents.

In my talk I will expand upon these basic considerations for the specific case of organic and organohalide perovskite PV and compare and contrast with other systems including silicon and compound semiconductors. Specifically, I will discuss the optimum bandgap for typical indoor lighting sources and advance a new predictive model to assess the performance of various materials. This analysis allows for the specification of design rules for indoor light harvesting.

SESSION EN04.06/EN01.06: Joint Session II—Organic Photovoltaics – from Fundamentals to Upscaling II

Session Chairs: Paul Meredith and Dieter Neher

Wednesday Afternoon, April 24, 2024

Room 328, Level 3, Summit

1:30 PM *EN04.06/EN01.06.01

Shedding Light on The Dark Side of Triplets: Exploring Their Potential Safa Shoaee^{1,2}; ¹University of Potsdam, Germany; ²Paul Drude Institute for Solid State Electronics, Germany

The top-performing organic solar cells (OSCs) currently achieve similar peak external quantum efficiencies and fill factors as traditional photovoltaic devices. Nevertheless, they experience significantly elevated voltage losses, primarily stemming from nonradiative recombination, imposing a significant constraint on their performance. To explore the potential influence of triplet states on this phenomenon, we investigate PM6:0-IDTBR system. While we suspect that the open-circuit voltage (VOC) is constrained by the energy of the triplet state, the measured non-radiative voltage loss is surprisingly minimal. By comparing as-prepared and thermally annealed blends, we demonstrate that triplet-triplet annihilation - under operating conditions - may potentially offset the detrimental effects of triplet-induced dark losses.

2:00 PM EN04.06/EN01.06.02

Potential and Limitations of High Performance and Scalable Evaporated Organic Solar Cells Richard A. Pacalaj^{1,1}, Yifan Dong², Roderick Mackenzie³, Ivan Ramirez⁴, Mehrdad Hosseini⁴, Martin Pfeiffer⁴, Eva Bittrich⁵, Julian E. Heger⁶, Peter Muller-Buschbaum^{6,6}, Pascal Kaienburg⁷, Moritz Riede⁷, Jiaying Wu⁸ and James Durrant^{1,1,9}; ¹Imperial College London, United Kingdom; ²National Renewable Energy Laboratory, United States; ³Durham University, United Kingdom; ⁴Heliatek GmbH, Germany; ⁵Leibniz Institute of Polymer Research, Germany; ⁶Technische Universität München, Germany; ⁷University of Oxford, United Kingdom; ⁸The Hong Kong University of Science and Technology, China; ⁹University of Swansea, United Kingdom

The bulk heterojunction (BHJ) active layer of organic photovoltaics (OPV) is typically deposited either via thermal evaporation (small molecule donors, fullerene acceptors) or by solution processing (polymer donors, non-fullerene acceptors). The commercial viability of thermal evaporation has been proven for organic light emitting diodes (OLED), including the deposition of complex multilayer stacks and co-evaporated BHJs. Evaporated blends in OLEDs and OPVs have been shown to be more stable than their solution processed counterparts. Furthermore, the solvent free deposition lowers the environmental impact compared to solution processed technologies. Looking at the power conversion efficiency (PCE), Heliatek GmbH achieved an OPV record PCE of 13.2 % with an evaporated tandem cell in 2016. Since then, novel solution processable polymers and non-fullerene acceptors paved the way for performance increases beyond 19 % that could not be matched by evaporated OPVs. As a result, the academic community is today largely focussed on lab scale performance increases and reproducible upscale of solution processed OPVs, leading to a lack of studies addressing the limitations of high performance, industrially relevant evaporated OPV materials.

A key bottleneck in evaporated OPVs is the trade-off between efficient charge collection and maximising absorption by increasing the active layer thickness. This is evident from the high losses in fill factor for active layer thicknesses beyond 50 nm while solution processed cells often perform best at thicknesses >100 nm. Studies on solution processed devices showed that active layer blends with efficient collection (high mobility vs. slow non-geminate recombination) exhibit a phase separated morphology. This is often achieved through post-deposition optimisation (e.g. thermal annealing, solvent vapour annealing). Similar studies on the connection between morphology, recombination kinetics and mobility in evaporated OPVs are key to identifying ways to increase their performance through improved deposition control and molecular design.

Here, I will present a study on a state-of-the-art evaporated small molecule donor paired with C₆₀. The acceptor-donor-acceptor type small molecule was synthesized by Heliatek. Devices with different active layer morphologies were studied. A wide range of optical (photoluminescence, ultrafast spectroscopy) and optoelectronic device measurements (transient photovoltage, charge extraction) demonstrate that the low and imbalanced charge carrier mobility is a key bottleneck even in the optimised blend. An in-depth characterisation of the active layer morphology (RSoXS, GIWAXS) enables us to

identify the aspects of the morphology that should be addressed to further improve performance. I will contrast our findings about the collection efficiency with results from solution processed devices (PM6:Y6, BTR:PCBM) as well as giving an outlook for feasible performance improvements based on drift-diffusion simulations (OghmaNano).

2:15 PM EN04.06/EN01.06.03

Enhanced Solid-Liquid Phase Separation and Carrier Transfer for High-Performance Organic Solar Cells by Modulating The Mixing Gibbs Free Energy Wallace C. Choy; University of Hong Kong, China

The similar conjugated backbone of donor/acceptor material and fast film-formation kinetics have led to spinodal-decomposition-orientated phase separation that the film presents an intimately mixed morphology and random molecular orientation and thus critically hinders the carrier extraction for high-performance non-fullerene organic photovoltaics. To solve the issue, we enhance the mixing Gibbs free energy-triggered solid-liquid phase separation during the film formation process by solidifying one component and solvating the other based on a liquid additive. Following the liquid evaporation process, a favorable vertical distribution is obtained. Meanwhile, the prolonged solvation process enlarges the domain size and assists the molecules to diffuse and orient properly, enabling better exciton/charge dynamics during the power conversion processes. In detail, we alter the phase separation behavior from original liquid-liquid de-mixing to solid-liquid de-mixing during the film formation process to prolong the phase separation and assist the molecules to further orient. Finally, we achieve the donor/acceptor phase separation with the enlarged phase domains, favorable vertical distribution, and significantly ordered crystal orientation [1], which contributes to a high fill factor of >80%. The corresponding device power conversion efficiency (PCE) reaches 18.72% with a short-circuit current density (J_{sc}) of 27.30 mA/cm² and open-circuit voltage (V_{oc}) of 0.854 V. Importantly, the better light stability is also captured in the more phase-separated device. This work optimizes donor/acceptor vertical distribution and orientation by enhancing the solid-liquid phase separation via a predictable method for realizing high-performance and stable organic photovoltaics [2].

[1] X. He, W.C.H. Choy, et al, *Small Methods*, 2022, 2101475.

[2] X. He, W.C.H. Choy, et al, *Adv. Energy Mater.*, 202203697, 2023.

2:30 PM BREAK

3:30 PM *EN04.06/EN01.06.04

Efficient and Stable Organic Photovoltaics Thomas D. Anthopoulos; King Abdullah University of Science and Technology, Saudi Arabia

Organic photovoltaics (OPVs) show great potential as a complementary technology to traditional silicon-based photovoltaics due to their lightweight, flexible, and potentially low-cost properties. However, they face challenges such as poor operational stability and lower power conversion efficiency (PCE) compared to commercial solar cell technologies. In recent years, there have been significant advancements in materials and cell architectures to enhance the PCE of OPVs. This presentation will focus on practical new strategies to improve OPVs' efficiency and operational stability. Specifically, it will discuss the innovative use of charge-extracting interlayers, which help increase the efficiency of next-generation OPVs. The benefits of these interlayers include a higher open-circuit voltage, reduced recombination losses, and improved operational stability. Additionally, recent progress in utilizing molecular dopants to enhance the PCE of advanced OPVs will be presented, demonstrating their effectiveness in improving the cell's fill factor and short-circuit current density. Moreover, it will be shown that combining innovative charge-extracting interlayers with molecular dopants and advanced functional material formulations can lead to even more significant improvements in efficiency and device stability.

4:00 PM EN04.06/EN01.06.05

Origin of Temperature-Driven Morphology Changes in High-Performance Bulk Heterojunction Active Layer of Organic Solar Cell Device Haoyu Zhao, Nathaniel L. Prine, Guorong Ma, Soumya Kundu, Andrew Bates and Xiaodan Gu; University of Southern Mississippi, United States

The performance of conjugated polymer-based organic solar cell (OSC) device relies on the bulk heterojunction morphology of the electron donor and acceptor blend. The morphology including the average domain size, crystallinity, and phase purity of donor/acceptor blend determines the device performance. Although the power conversion efficiency (PCE) of OSC is above 19%, the origin of the instable performance over longer times remains poorly understood. In this work, we conducted multiple characterization techniques to explore the dynamic, temperature-dependent morphology of a state-of-the-art donor polymer (PM6) blended with a non-fullerene small-molecule acceptor (Y6). Particularly, we focused on the thermal analysis of the donor and acceptor using fast scanning calorimetry (Flash DSC) to understand the crystallization kinetics. Combined with the assistance of atomic-force microscopy paired with infrared microscopy (AFM-IR) and X-ray scattering, we concluded the origin of PCE loss can be attributed to the severe phase separation caused by acceptor diffusional crystallization. The pure Y6 showed growing crystallization as annealing temperature increased. And the isothermal crystallization growth of blend was further accelerated due to diffusions of Y6. As the blend is maintained at elevated temperatures, the formation of Y6 crystalline domains induced phase separation with donors, as evidenced by the domain purities via AFM-IR characterizations. The influences of small molecules crystallization were characterized by the performance changes for solar cell device. This study will contribute to the development of more reliable, efficient and commercially viable OSC in the future.

4:15 PM EN04.06/EN01.06.06

Radiation Hardness of Organic Solar Cells Yongxi Li^{1,2} and Stephen R. Forrest^{1,3,4}; ¹University of Michigan, United States; ²Michigan Materials Research Institute, United States; ³Departments of Physics, United States; ⁴Departments of Material Science and Engineering, United States

Over the past few decades, space exploration has opened up new frontiers in both scientific knowledge and technological innovation. These endeavors have created new opportunities for addressing global challenges. As we set our sights on the forthcoming era of space exploration, the demand for substantial power looms large. Electric propulsion, driven by solar energy, emerges as a pivotal technology to support these capabilities.

Organic photovoltaic cells (OPVs), in particular, have exhibited great promise for solar power generation in space due to their incredibly high specific power, reaching up to 40 kW/kg¹, compared, for example to the ubiquitously employed Si cells of ~ 1 kW/kg². Furthermore, OPVs have the ability to withstand tensile strains exceeding 300% when supported by elastomeric materials, making them far more flexible than their inorganic counterparts³. The continuous advancement of organic materials has enabled the power conversion efficiency (PCE) of OPVs to exceed 20%^{4,5} and intrinsic operational lifetime over 30 years⁶, making them competitive with other thin-film inorganic photovoltaic devices. The only pervasive myth associated with OPVs is that the materials are intrinsically vulnerable to degradation when exposed to high energy incident radiation.

In this work, we found that carefully selected and designed organic materials and device structure are capable of showing high radiation hardness. Previous studies have identified proton irradiation as a prominent source of radiation-induced damage to photovoltaic systems in space, generating vacancies, interstitials, or complex defects within semiconductor materials⁷. Through simulations of proton energy loss per unit depth using SRIM/TRIM, we found that proton energies exceeding 100 keV can traverse the organic active layer without inducing collisions, consequently yielding a low total vacancy count. This phenomenon is attributed to the relatively slim nature of the organic active layer within OPV cells, measuring only a hundred nanometers in thickness,

rendering them comparatively transparent to high-energy particles. To evaluate the proton tolerance of OPVs, we fabricated devices based on the two most reliable OPV configurations demonstrated by our lab. The results demonstrated that the PCE of the OPV device can be maintained even at energies as high as 1 MeV and fluences up to 10^{12} cm⁻², equivalent to 20 years of operation in low Earth orbit (LEO) missions. Remarkably, this performance surpasses that of crystalline silicon (c-Si) cells, which undergo around 40% degradation, and perovskite cells, which show nearly 10% degradation at the same fluence. This compelling evidence suggests the potential of OPVs to offer extraordinarily long operational lifespans in space environments.

References:

1. Zheng, X. *et al.* Versatile organic photovoltaics with a power density of nearly 40 W g⁻¹. *Energy Environ. Sci.* (2023) doi:10.1039/D3EE00087G.
2. Kaltenbrunner, M. *et al.* Flexible high power-per-weight perovskite solar cells with chromium oxide–metal contacts for improved stability in air. *Nat. Mater.* **14**, 1032–1039 (2015).
3. Cardinaletti, I. *et al.* Organic and perovskite solar cells for space applications. *Sol. Energy Mater. Sol. Cells* **182**, 121–127 (2018).
4. Zheng, Z. *et al.* Tandem Organic Solar Cell with 20.2% Efficiency. *Joule* **6**, 171–184 (2022).
5. Cui, Y. *et al.* Single-Junction Organic Photovoltaic Cell with 19% Efficiency. *Adv. Mater.* **33**, 2102420 (2021).
6. Li, Y. *et al.* Non-fullerene acceptor organic photovoltaics with intrinsic operational lifetimes over 30 years. *Nat. Commun.* **12**, 1–9 (2021).
7. Kirmani, A. R. *et al.* Countdown to perovskite space launch: Guidelines to performing relevant radiation-hardness experiments. *Joule* **6**, 1015–1031 (2022).

4:30 PM EN04.06/EN01.06.07

The Determination of Referenced HOMO/LUMO Levels with Pulse Radiolysis Michele Myong, Mrinalni Iyer, Yaejin Kim, John Miller and Matthew Bird; Brookhaven National Laboratory, United States

With organic photovoltaic (OPV) power conversion efficiencies nearly at 20%, and their emerging applications in photocatalysis, knowledge of the driving force for electron transfer is vital for understanding how to further optimize these materials.

Pulse radiolysis (PR) enables the rapid generation of excess, free charges in any solvent without the need for electrolyte or electrodes. Relative one-electron redox potentials of pairs of solutes can be determined through charge transfer equilibria measurements with PR. This approach offers the tantalizing possibility of determining accurate, referenced one-electron redox potentials of conjugated polymer chains in nonpolar environments, something that has been desperately needed in the field of organic electronics since its inception.

The two leading approaches for estimating HOMO and LUMO levels in these highly conjugated materials come from onset potentials obtained by CV or UPS/IPES measurements on films. Both methods give important information but, even in the best case, we expect 50-100 mV accuracy which could correspond to orders of magnitude variation in electron transfer rates. Remarkably, one of the leading OPV blends of PM6 and Y6 has been reported to have a HOMO offset of 90 meV with CV but 700 meV with UPS. The PR method may help to understand these differences. We have developed a “redox ladder” in o-xylene to serve as a measuring stick to get internally referenced redox potentials in a nonpolar media. The ladder is constructed from numerous equilibrium constants for electron or hole transfer between pairs of small molecules. The choice of o-xylene gives nonpolar redox potentials and enables both reduction and oxidation processes to be studied. Newer “green” OPV materials are designed to be soluble in o-xylene.

We have performed these measurements to determine accurate one electron redox potentials for several common conjugated polymers and small molecules including PM6, Y6, P3HT, IDTBT, PFO, PCPDTBT, F8BT with respect to the Fc/Fc⁺ couple in o-xylene. We hope this method will provide a reliable measure of the inherent redox properties of single conjugated polymer chains and we plan to expand it to include aggregated polymers to determine how inter-molecular interactions affect redox potentials.

SYMPOSIUM EN02

Cutting-Edge Materials Design Toward Advanced Energy Harvesting—From Modeling to Manufacturing
April 23 - April 26, 2024

Symposium Organizers

Jinbo Bai, CNRS ECParis
Daniel Hallinan, Florida State University
Chang Kyu Jeong, Jeonbuk National University
Andris Sutka, Riga Technical University

* Invited Paper

+ JMR Distinguished Invited Speaker

^ MRS Communications Early Career Distinguished Presenter

SESSION EN02.01: Piezoelectric Systems and Self-Powered Bioelectronics

Session Chairs: Chang Kyu Jeong and Kwi-II Park

Tuesday Morning, April 23, 2024

Room 332, Level 3, Summit

11:00 AM *EN02.01.02

Photoresponsive Piezoelectric Ceramics for Multisource Energy Harvesting and Sensing Yang Bai; University of Oulu, Finland

Among all kinetic energy harvesters, those made from piezoelectric materials are considered the most efficient when working at resonance of the electromechanical coupling process. High-performance piezoelectrics, such as piezoceramics and single crystals, are usually oxide perovskite ferroelectrics which also exhibit photovoltaic effect. This fact offers a unique opportunity to integrate light harvesters with the piezoelectric ones in a single material to achieve multi-source energy harvesting and/or sensing. Coupling multiple energy in one material promotes self-sufficiency and sustainability of energy harvesters and associated electronic systems. Strong piezoelectricity has been thought to inevitably lead to wide photonic band gaps, and vice versa, narrow band gaps eliminate piezoelectricity. This view, however, is being changed. This talk will walk through the achievements in recent years in terms of band gap engineering of piezoelectric materials with an emphasis on works carried out by the speaker's research group, including piezoelectric compositions based on the potassium niobate and lead titanate perovskite solid solutions.

11:30 AM EN02.01.03

Self-Powered Gas Sensing based on Triboelectric Effect via Metal-Organic Frameworks Alibek Kakim, Baktiyar Soltabayev, Amanzhol Turlybekuly and Gulnur Kalimuldina; Nazarbayev University, Kazakhstan

Triboelectric nanogenerators (TENG) have demonstrated potential for ambient energy harvesting and sensing applications in different fields in the last decade. In this work, we focus on unveiling the usage of TENG as a self-powered gas sensor. The conventional sensors for detecting environmental gas concentrations are powered by batteries, which limits their usage. We propose the development of a self-powered portable gas sensor based on the TENG incorporated with MOF particles with comparable accuracy to the conventional sensors. MOFs have charge-trapping properties resulting from the ionic interactions of the metallic ions. While MOFs are widely used for gas storage, their gas sensing capabilities, such as TENG, need further research. Specifically, MIL-125 and ZIF-8 MOFs have promising potential. ZIF-8 has garnered significant interest as a gas sensor due to its two distinct advantages compared to traditional zeolites. Firstly, ZIF-8 boasts larger pore dimensions (approximately 1.6 nanometers) and typically exhibits smaller crystal sizes, increasing surface area. Secondly, ZIF-8 demonstrates a notable hydrophobic characteristic. MIL-125 is a promising gas-sensing material due to its large surface area, adjustable pore size, and controllable surface properties.

11:45 AM EN02.01.04

On-Skin Breathable Triboelectric-And-Electromagnetic Liquid-Metal Nanogenerator for Extracting Biomechanical and Electromagnetic Energy and as Whole-Body Epidermal Self-Powered Sensors Ying-Chih Lai; National Chung Hsing University, Taiwan

On-skin electronics can be conformably deployed on body for health monitoring, assisted living, and human/computer interfaces. However, developing corresponding energy devices is a critical challenge. Herein, a permeable and stretchable multifunctional liquid-metal electronic skin that can generate electricity by recovering ambient electromagnetic pollution (from surrounding electrical appliances) and biomechanical energy (from body movements) is presented for epidermal energy and self-powered sensing applications. To the best of our knowledge, this is the first demonstration that a breathable on-skin device can convert ambient electromagnetic pollution into useful electricity. The device was constructed using two stretchable microfibrillar films sandwiching self-organized mesh-like and wrinkled liquid metal that affords electricity via induced electrification (± 9.3 V, ± 1.7 μ A; 60 Hz) and triboelectricity (205.6 V, ± 2.3 μ A; 4 Hz). Its applicability in powering electronic devices has been demonstrated. Moreover, it can serve as an epidermal self-powered sensor for continuously monitoring whole-body physiological signals and motions of the eyelids, face, throat, chest, and limbs, thus demonstrating its potential to remotely collect clinical and biomechanical information. Finally, it was used as an interface in diverse system-level applications. These results shed light on new directions in on-skin energy and sensing, enabling to usher electronics toward untethered and diversified applications.

Ref.

[1] Ying-Chih Lai*, et al., *Advanced Energy Materials*, 2021, 202100411. (Selected as VIP paper and front cover)

[2] Ying-Chih Lai*, et al., *Nano Energy*, 2022, 95, 107035

SESSION EN02.02: From Fundamentals to Materials for Electromechanical Coupling Devices

Session Chairs: Chang Kyu Jeong and Dong-Myeong Shin

Tuesday Afternoon, April 23, 2024

Room 332, Level 3, Summit

2:00 PM *EN02.02.02

Approaches Toward Efficient Piezoelectric based Energy Harvesting Chong Yun Kang; Korea Institute of Science and Technology, Korea (the Republic of)

Due to relatively low power generation capability and energy conversion efficiency, however, these harvesting technologies have been applied only to limited applications. In order to solve these issues, here, we address three type of piezoelectric energy harvesting. First, we design and demonstrate a piezoelectric/electromagnetic hybrid energy harvester that can generate significant amount of electricity at vibration environments. Oval-like configuration using two curved piezoelectric energy harvesters based on MFC (Macro-fiber composite) piezoelectric material induces large displacement of a permanent magnet installed at the end of the top surface which allows efficient power generation both piezoelectric and electromagnetic energy harvesters. Second, we introduce a PVDF-based piezoelectric energy harvester applicable to roads. The PVDF-based piezoelectric energy harvesters provide a competitive power output at small vertical displacements with proper module design, making the tough piezoelectric materials suitable for efficient and durable roadway energy harvesting. Finally, we demonstrate an ultra-wide bandwidth piezoelectric energy harvesters through the automatic resonance tuning. Piezoelectric energy harvesters typically exhibit sharp peak in output power around resonance frequency. We expect that the automatic resonance tunable piezoelectric energy harvester can provide the much-needed breakthrough in the deployment of mechanical energy harvesters for naturally occurring vibrations.

2:30 PM BREAK

3:00 PM *EN02.02.03

Cooperative Contact Electrification enabled by Control Over Electron and Ion Transfer Directions Xiaoting Ma, Jiaming Zhou, Eunjong Kim, Jingyi Gao and [Dong-Myeong Shin](#); University of Hong Kong, Hong Kong

Contact electrification (CE) is a phenomenon that occurs when two materials are brought into contact and exchange charges. Although recent studies show that CE between two solids including metals, semiconductors and nonionic polymers is basically due to electron transfer, the mechanism for CE involving ionic materials remains controversial. In this paper, the CE process between single-ion conducting materials (SICM) and fluorinated ethylene propylene (FEP) is systematically investigated to elaborate the electrification mechanism when ions are participating in CE. In the study, electron thermionic emission method was also used to separate the contributions of ion transfer and electron transfer in the total static charges when varying the environmental humidity. Furthermore, molecular dynamics simulations were performed to reveal the molecular interactions and dynamics of the polymer surfaces, mobile ions and water molecules at the interface. The results show that ion transfer is an important mechanism in the CE of FEP/SICM pairs and that higher humidity leads to more free ions and higher contribution of ion transfer in the total transferred charges. Our research not only provides new insights into the mechanism of contact electrification that involves ion transfer but also introduces a unique category of triboelectric materials that are single-ion conducting.

3:30 PM EN02.02.04

Sustainable and High-Performance Triboelectric Nanogenerator Based on Sulfur-Rich Polymer/MXene Composites [Woongbi Cho](#)¹, Sungsu Kim¹, Hyeonhoo Lee¹, Nara Han^{2,3}, Hyunki Kim², Minbaek Lee², Tae Hee Han¹ and Jeong Jae Wie^{1,3,4}; ¹Hanyang University, Korea (the Republic of); ²Inha University, Korea (the Republic of); ³State University of New York College of Environmental Science and Forestry, United States; ⁴The Michael M. Szwarc Polymer Research Institute, United States

Sulfur-rich polymer (SRP) is a great candidate to construct a waste-based but high-performance triboelectric nanogenerator (TENG), as elemental sulfur is a huge waste from the petroleum refining process and possesses the highest level of electron affinity (-200 kJ mol^{-1}). In our previous reports, the SRP-based TENG outperformed polytetrafluoroethylene (PTFE), one of the state-of-the-art triboelectric materials, by directly fluorinating the surface of SRP and adapting a blend system with fluoropolymer. However, these strategies raised environmental concerns about using F_2 gas and per- and poly-fluoroalkyl substances (PFAS), which are toxic to humans. Herein, we introduce the SRP/MXene composites to circumvent environmental issues and to achieve a high-performance triboelectric nanogenerator (TENG). We achieved the maximized MXene distribution in SRP with minimized MXene content by introducing the segregated structure. This well-distributed MXene enhances triboelectrification through the enhanced dielectric constant via microscopic dipole interactions at the interface between SRP and MXene. As a result, SRP/MXene-based TENG demonstrated a record high peak voltage of 331.4 V and peak current of 19.6 μA , which are 2.9 times and 19.5 times higher than those reported in previous SRP-based TENGs. The used SRP/MXene film also can be recycled by regrinding and compressing due to its dynamic bond exchanging property, and the recycled SRP/MXene film maintains its modulus and triboelectric output performance. Finally, scaled-up 4-inch SRP/MXene film-based TENG demonstrated a record high peak power density of 3.89 W m^{-2} after applying corona discharging, surpassing the reported SRP-based TENG.

3:45 PM EN02.02.05

A Volume Effect based Triboelectric Nanogenerator for Omnidirectional Wave Energy Harvesting [Jiaming Zhou](#), Xiaoting Ma, Eunjong Kim and [Dong-Myeong Shin](#); University of Hong Kong, Hong Kong

The marvel of the liquid-solid triboelectric nanogenerator (LS-TENG) has been demonstrated in its efficient energy harvesting via the contact electrification effect between liquid and solid triboelectric materials. The insufficient contact problems and wear issues frequently encountered in solid-solid TENGs are avoided through this technology. Nevertheless, the droplet-based LS-TENG has been plagued by problems of continuous falling droplets, which limits its practical application. Herein, we present an innovative droplet-based omnidirectional triboelectric nanogenerator (DB-TENG) utilizing the volume effect of droplets for efficient harvesting of ocean wave energy. With a unique concentric circular electrode pair built on an oblate plate, the DB-TENG achieves a significant improvement in output performance compared to traditional liquid-solid TENGs, with a maximum output voltage of 160V, which is 16 times higher, and a maximum current of 4000 nA, which is 40 times higher. This volume effect DB-TENG can perform reliably under extreme conditions of high humidity or high concentrations of salt, acid, or alkali solutions, making it a flexible tool for all types of working environments with enhanced reliability and reduced maintenance costs. What's more, the DB-TENG's omnidirectional capabilities make it suitable for capturing energy from various directions of ocean waves. The TENG's performance in ocean wave energy harvesting is evaluated and compared with traditional TENGs, demonstrating superior results in terms of output voltage and current. The proposed design holds significant potential for practical applications in blue energy harvesting and can inspire the development of self-sufficient ocean sensors. Overall, this study highlights the importance of volume-effect in enhancing the output performance of TENGs and presents a promising approach for efficient and sustainable ocean wave energy harvesting.

SESSION EN02.03: Mechanism and Manufacturing for Energy Harvesting

Session Chairs: Yang Bai and Andris Sutka

Wednesday Morning, April 24, 2024

Room 332, Level 3, Summit

9:00 AM *EN02.03.01

Advances in Plasma-Enabled Nanomaterial Synthesis for Enhanced Energy Harvesting Devices [Ana Borrás](#), Javier Castillo-Seoane, Xabier Garcia-Casas, Juan Delgado, Fernando Nunez-Galvez, Melania Sanchez, Lidia Contreras-Bernal, Jorge Budagosky, Vanda Godinho, Victor Lopez-Flores, Carmen Lopez-Santos, Juan Sanchez-Valencia, Angel Barranco and Javier Castillo-Seoane; CSIC, Spain

In this communication, we will present our latest advances in the development of nanostructured thin films and supported core@multishell nanomaterials for energy harvesting. The foundation of the synthetic approach centers around the utilization of a one-reactor system,^[1] where we integrate various industrially scalable vacuum and plasma deposition methods for tailored nanostructured thin film deposition and the fabrication of one-dimensional devices. The transition from conformal layers to core@multishell devices is driven by the application of single-crystalline organic nanowires as supported soft templates compatible with a wide array of substrates.^[2,3] We demonstrate the integration of materials, spanning from plasma polymers to sculptural hybrid halide perovskites and metal oxide nanotrees, onto energy harvesting devices such as solar cells, piezoelectric, pyroelectric, triboelectric, and hybrid nanogenerators. Our presentation highlights the role of micro and nanostructures and interface control in optimizing these energy-harvesting solutions.^[4-9]

[1] Castillo-Seoane, J., Borrás, A. et al. (2021) *Nanoscale* 13:13882.

- [2] Montes, L., Borrás, A. et al. (2021) Adv. Mater. Interf. 21:2100767.
[3] Borrás, A., Groening, A. et al. (2010) Langmuir 26:5763.
[4] Castillo-Seoane, J., Borrás, A., Sánchez-Valencia, J. R. et al. (2022) Adv. Mater. 34:2270137.
[5] Obrero, J., Borrás, A., Barranco, A. et al. (2022) Adv. Ener. Mater. 12:2200812.
[6] Barranco, A., Borrás, A., Sánchez-Valencia J. R. et al. (2020) Adv. Ener. Mater. 10:1901524.
[7] Filippin, A. N., Borrás, A. et al. (2019) Nano Energy 58:476-483.
[8] García-Casas, X., Borrás, A. et al. (2022) Nano Energy 91:106673.
[9] García-Casas, X., Borrás, A. et al. (2023) Nano Energy 114:108686.

9:30 AM EN02.03.02

Machine Learning Aided Exploration of Chalcogenide-Based Solid Solutions for Photovoltaic Applications Cibrán López Álvarez^{1,2}, Ivan Caño Prades^{1,2}, Jose M. Asensi López³, Zacharie Jehl Li-Kao^{1,2}, Edgardo Saucedo^{1,2} and Claudio Cazorla^{1,2}; ¹Polytechnic University of Catalonia, Spain; ²Barcelona Research Center in Multiscale Science and Engineering, Spain; ³University of Barcelona, Spain

Ternary chalcogenides, of general formula ABC (A = {Bi, Sb}, B = {S, Se}, C = {I, Br}), conform a new family of promising photovoltaic solar cell absorbers [1], with band-gaps lying between 1.5-1.9 eV and high absorption coefficients ($\sim 10^5 \text{ cm}^{-1}$).

Chalcogenide-based tandem solar cells have revolutioned the landscape of photovoltaic energy conversion in the past years as a promising alternative to single-junction silicon-based panels (e.g., tandem solar cells). Given the great stability of this novel family, solid solutions of chalcogenides [2], of general expression $\text{Bi}_x\text{Sb}_{1-x}\text{S}_y\text{Se}_{1-y}\text{I}_z\text{Br}_{1-z}$, present extraordinary possibilities in terms of device tunability and efficiency, something that has not been explored so far to the best of our knowledge.

We present a comprehensive study of the energetic stability and optoelectronic properties of chalcogenide-based solid solutions covering all possible compositions that is based on a combination of first-principles calculations and novel deep learning techniques. Experimental validation is as well obtained from the synthesis and characterization of a solid-solution in the laboratory. Finally, a realistic BiSb-BiSeI tandem device is optically simulated and optimized, showing a very competitive short-circuit current of 18.65 mA/cm².

- [1] I. Caño-Prades, A. Navarro-Güell, E. Maggi et al., SbSeI and SbSeBr micro-columnar solar cells by a novel high pressure-based synthesis process, J. Mater. Chem. A, 2023, doi: 10.1039/D3TA03179A
[2] I. Caño-Prades, P. Vidal-Fuentes, A. Gon-Medaille et al., Challenges and improvement pathways to develop quasi-1D (Sb1-xBix)2Se3-based materials for optically tuneable photovoltaic applications. Towards chalcogenide narrow-bandgap devices, Sol. Energy Mater. Sol. Cells., 2023, doi: 10.1016/j.solmat.2022.112150

9:45 AM EN02.03.03

Three-Dimensional Physical Modeling of The Wet Manufacturing Process of Solid-State Battery Electrodes Mohammed Alabdali¹, Franco M. Zanotto¹, Marc Duquesnoy¹, Anna-Katharina Hatz², Duancheng Ma², Jérémie Auvergniot², Virginie Viallet¹, Vincent Seznec¹ and Alejandro A. Franco¹; ¹LRCS - Université de Picardie Jules Verne, France; ²Umicore, Belgium

We present an innovative three-dimensional physics-based modeling workflow that addresses the issue of poor performance of Solid-State Battery (SSB) cells due to the challenging design and manufacturing of composite electrodes with appropriate ionic and electronic conductivities. While modeling approaches have been utilized in the literature to investigate the influence of stochastically-generated microstructures on their conductivities, computational simulations able to predict the influence of manufacturing parameters on the SSB electrode microstructures remain elusive [1]. We present a novel physics-based computational modeling framework able to numerically investigate the impact of wet manufacturing process parameters (e.g. formulation, drying rate, calendaring degree) on the properties of SSB tape casted composite electrodes. In analogy to our previous work on the simulation of the manufacturing process of Lithium Ion Battery electrodes [2], the Coarse-Grained Molecular Dynamics (CGMD) is adapted and used here for the simulation of the manufacturing process of SSB composite electrode cathode based on the physical interactions among individual particles representing the materials constituting the slurry and the formed electrode (i.e. NMC622, Carbon-Binder Domain and Li₆PS₅Cl) involved in the wet manufacturing process. By encompassing the entire process of wet manufacturing of SSB electrodes, from the slurry to the calendaring, the model is able to predict the correlations between manufacturing parameters and electronic and ionic conductivities of the electrodes. We show why and how this model constitutes an important tool to assist in the optimization of interfaces between the materials in the electrodes, leading to improved SSB performance and durability.

References

- [1] M. Alabdali, F. M. Zanotto, V. Viallet, V. Seznec, A. A. Franco, Curr Opin Electrochem 2022, 36, DOI 10.1016/J.COELEC.2022.101127.
[2] M. Alabdali, F. M. Zanotto, M. Duquesnoy, A.K. Hatz, D. Ma, J. Auvergniot, V. Viallet, V. Seznec, A. A. Franco, J Power Sources 2023, 580, DOI https://doi.org/10.1016/j.jpowsour.2023.233427.

10:00 AM BREAK

10:30 AM *EN02.03.04

Harvesting Motion via Polymers: From Mechanisms to Electricity Peter C. Sherrell^{1,2}, Ronald Leon², Andris Sutka³ and Amanda Ellis²; ¹RMIT University, Australia; ²The University of Melbourne, Australia; ³Riga Technical University, Latvia

For many centuries people have pondered (notably and dubiously Thales of Miletus)^[1] why some materials become electrically charged when brought into contact with other, dissimilar, materials. We now know that this charging phenomena is governed either by piezoelectricity from deformation, for non-centrosymmetric unit cells, or contact electrification (also known as triboelectricity) from interfacial friction. While piezoelectricity (and ferroelectricity) is well understood, the mechanisms of contact electrification remain a subject of debate in the literature.^[2] This debate on the driving force being electron-, ion-, or material-transfer,^[2-3] coupled to poor measurement techniques leading to conflation of piezoelectric and contact electrification,^[4-5] has limited the design of optimal polymer energy harvesters.

If we can develop improved understandings of how polymers charge from friction, we can design devices that can capture motion to harvest electricity,^[6] drive chemical reactions,^[7] or even enable wound healing.^[8]

To address this lack of understanding, we have studied how polymers generate charge at a contact interface. This has linked the polarity of generated charge directly to polymer structure via cohesive energy density,^[9] and surface topography.^[10] These relatively simple understandings have enabled the production of layer-by-layer 'laminated' assemblies from arbitrary polymers.^[11] These laminates, which function purely off contact electrification and

interfacial friction, generate internal dipole moments that mimic piezoelectric polymers – enabling exceptionally efficient vibrational energy harvesting. Finally, we demonstrate the use of recycled foamed/expanded polystyrene to fabricate such laminates, capable of harvesting over 12 μA and 200 V from just 16 N of force. Moving forwards, these laminates, as well as piezoelectric polymers,^[12] are being studied tools to drive catalytic reactions ranging from fuel production through to small molecule synthesis.

This talk aims to provide a pathway to design highly efficient electromechanically active surfaces from polymers towards catalysis and sustainable chemistry.

References:

- [1] P. Iversen, et al., *Journal of Electrostatics* **2012**, *70*, 309, 10.1016/j.elstat.2012.03.002
- [2] D. J. Lacks, et al., *Nature Reviews Chemistry* **2019**, *3*, 465, 10.1038/s41570-019-0115-1
- [3] A. Šutka, et al., *Advanced Materials Interfaces* **2023**, *n/a*, 2300323, 10.1002/admi.202300323
- [4] R. T. Leon, et al., *Nano Energy* **2023**, *110*, 108445, 10.1016/j.nanoen.2023.108445
- [5] A. Šutka, et al., *Adv. Mater.* **2020**, *32*, 2002979, 10.1002/adma.202002979
- [6] A. Šutka, et al., *ACS Applied Energy Materials* **2023**, 10.1021/acsam.3c01196
- [7] J. Zhang, et al., *Journal of the American Chemical Society* **2021**, *143*, 3019, 10.1021/jacs.0c11006
- [8] F.-C. Kao, et al., *Science and Technology of Advanced Materials* **2022**, *23*, 1, 10.1080/14686996.2021.2015249
- [9] P. C. Sherrell, et al., *ACS Applied Materials & Interfaces* **2021**, *13*, 44935, 10.1021/acsami.1c13100
- [10] O. Verners, et al., *Nano Energy* **2022**, *104*, 107914, 10.1016/j.nanoen.2022.107914
- [11] A. Linarts, et al., *Small* **2023**, *19*, 2205563, 10.1002/sml.202205563
- [12] N. A. Shepelin, et al., *Nature Communications* **2021**, *12*, 3171, 10.1038/s41467-021-23341-3

11:00 AM EN02.03.05

Innovative ITO Nanocrystals for Sustainable Thin Film Fabrication in Optoelectronics and Clean Energy Printing Using Solution Processing Techniques Ivet Maqueira Albo^{1,2}, Luca Rebecchi^{1,2}, Andrea Rubino¹ and Ilka Kriegel¹; ¹Italian Institute of Technology, Italy; ²Università degli Studi di Genova, Italy

To address the growing global energy demand while mitigating environmental concerns, innovative technologies and materials for clean and sustainable energy generation are essential. Transparent Conducting Oxides (TCO), like Indium Tin Oxide (ITO), play a pivotal role due to their exceptional transparency in the visible spectrum and metal-like electron mobility. These materials not only show great promise in the field of optoelectronics but also significantly contribute to enhancing the capabilities and sustainability of cutting-edge printing technologies. Recent efforts have been directed toward implementing transparent conductive inks, which offer the potential for solution processing and the use of flexible substrates. This work primarily focuses on the synthesis and characterization of ITO nanocrystals (NCs) and the subsequent fabrication of thin films using various solution-based deposition techniques. The synthesis of Indium Tin Oxide (ITO) nanocrystals employs a precise slow injection technique that provides meticulous control over dopant positioning within the crystal lattice. By fine-tuning the injection rate and duration, it becomes possible to precisely adjust dopant concentration and distribution, thereby ultimately affecting the thin film properties. This is related to the control of dopant segregation and activation. Characterization techniques such as spectroscopy, electron microscopy and electrical conductivity measurements can directly relate to the dopant placement in the nanocrystals. This comprehensive analysis greatly enhances the potential of TCO nanoparticles in solution-based thin film production, contributing to a more sustainable and energy-efficient future.

11:15 AM EN02.03.06

Unlocking The Pt Sintering Prevention Mechanism by Trace Amount of Atomic Layer Deposition Shyama C. Mandal^{1,2}, Gennaro Liccardo^{1,2}, Bang T. Nhan¹, Matteo Cargnello^{1,2}, Stacey F. Bent^{1,2} and Frank Abild-Pedersen²; ¹Stanford University, United States; ²SLAC National Accelerator Laboratory, United States

The catalytic performance of Pt-based metals has long been recognized for its remarkable activity. Nevertheless, the sintering of Pt during the reactions diminishes its active sites, ultimately resulting in reduced reactivity. Therefore, it is imperative to inhibit the sintering of Pt during the reactions. In this context, we have conducted atomic layer deposition (ALD) of Al_2O_3 and ZrO_2 onto Pt nanoparticles and observed the prevention of sintering. For a comprehensive understanding of this phenomenon, we focused on the theoretical investigation on Pt(111) terrace sites and Pt(211) step sites. Step sites are particularly susceptible to detachment, which can lead to Ostwald ripening, ultimately resulting in the deposition on larger nanoparticles. During our investigation, we considered various ALD species that could form during the process and calculated their binding energies on terrace and step sites. Our calculations revealed that most of the species exhibited a preference for binding to step sites, suggesting their ability to stabilize the steps. Additionally, we proposed a possible ALD mechanism and calculated the reaction free energies for each elementary steps on both the ALD recipes. These calculations indicated that the most favorable intermediate on Pt(211) step sites would be $\text{Al}_2(\text{OH})_6$ and $\text{Zr}(\text{OH})_4$ for the Al_2O_3 -based and ZrO_2 -based ALD processes, respectively. The ALD sample exhibited lower catalytic activity compared to Pt supported on Al_2O_3 during combustion of propene. However, an increase in catalytic activity has been observed after aging the ALD sample. This could be attributed to the opening of the ALD layers during aging or the diffusion of Pt through defects in the ALD layer. Notably, our calculated binding energies showed that Pt has a stronger binding within the ALD layer, suggesting the possibility of Pt diffusion through the ALD layer and its subsequent participation in the catalytic reaction. In summary, our research demonstrates that even trace amounts of ALD can effectively stabilize supported Pt catalysts, mitigating sintering-related deactivation and significantly enhancing the efficiency of the catalyst.

11:30 AM EN02.03.07

A Comparative Study of Switched-Capacitor and Inductor-Based Boost Converters for Indoor Light Energy Harvesting Tharaka Kaushalya^{1,2}, Markus Littow², Eetu Virta¹, Tarmo Ruotsalainen², Jari Juuti¹ and Yang Bai¹; ¹University of Oulu, Finland; ²Nordic Semiconductor Finland Oy, Finland

With the development of sustainable and energy-efficient smart buildings and cities, scavenging indoor light energy to power the Internet of Things (IoT) has become an increasingly attractive solution. This solution helps to extend the lifespan of devices by reducing the frequency of battery replacement whilst resulting in less battery waste. However, the energy that can be harvested from an indoor light environment is limited compared to natural, outdoor sunlight, emphasizing the importance of efficiency of the entire energy harvesting system rather than that of individual harvesters. Power management circuitry plays a crucial role here but there has not been a system-level study for different power management schemes when connected to both harvesters and batteries whilst working under real lighting conditions. In this talk, performances of both a Switched-Capacitor (SC) and an Inductor-based (IN) boost converter will be evaluated with reference to their charging efficiencies when connected to photovoltaic cells and Li-ion batteries under indoor office light. Results suggest that, although the IN converter tends to be cumbersome, it provides unbeatably high and stable battery charging efficiency across a broad range of light intensities compared to the SC converter even though the latter is specifically designed for low-power applications competing with the IN counterpart.

11:45 AM EN02.03.08

Developing Triboelectric Materials for High-Performance Generators [Andris Sutka](#)¹, [Kaspars Malnieks](#)¹, [Artis Linarts](#)¹, [Linards Lapčinskis](#)¹ and [Peter C. Sherrell](#)^{2,3}; ¹Riga Technical University, Latvia; ²RMIT University, Australia; ³The University of Melbourne, Australia

Triboelectric generators are the most promising mechanical to electrical energy converters at a small scale because they can extract energy from a huge range of mechanical sources: from motion, ambient vibrations, noise, and even from water droplets. However, their performance is limited due to low surface charge density and output power.

Herein, we will describe various approaches for increasing the triboelectric surface charge density. These will include MM ordering [1], functionalization [2], controlling interfacial strain [3], and exploiting volumetric dipoles [4,5]. We will show enhancement from controlled net surface charge polarity, intensified organo-ion transfer, and the complementary induction from triboelectric or piezoelectric dipoles in volume. We will look at the perspective of combining these approaches for providing generators with high performance up to 50 W/m².

References

- [1] Šutka et al., *Adv. Mater. Technol.* **2022**, 2200162
- [2] Germane et al., *Mater. Adv.* **2023**, 4, 875-880
- [3] Verners et al., *Nano Energy* **2022**, 104, 107914
- [4] Linarts et al., *Small* **2023**, 2205563
- [5] Šutka et al., *ACS Applied Energy Materials* **2023**, 6, 9300-9306

SESSION EN02.04: Emerging Materials for Energy Harvesting

Session Chairs: Jinbo Bai and Chang Kyu Jeong

Wednesday Afternoon, April 24, 2024

Room 332, Level 3, Summit

1:30 PM *EN02.01.01

Self-Powered Flexible Piezo-Sensor and MicroLED: Toward Commercialization [Keon Jae Lee](#); Korea Advanced Institute of Science & Technology, Korea (the Republic of)

This seminar introduces two recent progresses of self-powered flexible devices; piezo-sensors and microLED. The first part will introduce flexible inorganic piezoelectric membrane that can detect the minute vibration of membrane for self-powered acoustic sensor and blood pressure monitor. Speaker recognition has received spotlight as personalized voice-controlled interface, smart home, biometric authentication. The conventional speaker recognition was realized by a condenser type microphone, which detects sound by measuring the capacitance value between two conducting layers. The condenser type microphone, however, has critical demerits such as low sensitivity, high power consumption, low recognition rate and an unstable circuit due to the large gain amplification. Herein, we reported a machine learning-based acoustic sensor by mimicking the basilar membrane of human cochlear. Highly sensitive self-powered flexible piezoelectric acoustic sensor with a multi-resonant frequency band was employed for voice recognition. Convolutional Neural Network (CNN) were utilized for speaker recognition, resulted in a 97.5% speaker recognition rate with the 75% reduction of error rate compared to that of the reference MEMS microphone. In addition, wearable piezoelectric blood-pressure sensors (WPBPS) were developed for continuous non-invasive arterial pressure monitoring. WPBPS achieves a high normalized sensitivity (0.062 kPa⁻¹), and fast response time (23 ms). The transfer function of a linear regression model converts flexible piezoelectric sensor signals into blood pressure values. Clinical validation of WPBPS was performed on 35 subjects/175 measurements, that satisfies international standard of blood pressure measuring devices.

The second part will discuss the highly efficient flexible micro LED for displays and biomedical applications. Flexible displays can be easily affixed anywhere, such as on the surfaces of human skin, clothes, automobiles and buildings. III-V inorganic LEDs have superior characteristics, such as long-term stability, high efficiency, and strong brightness compared to OLED. However, due to the brittle property of inorganic materials, III-V LED limits its applications for flexible electronics. Here we introduce the flexible GaAs/GaN microLED using innovative micro-vacuum transfer technology. The superb properties of flexible inorganic LED enable not only full-color displays and wearable phototherapy patches like hair growth, melanogenesis inhibition and pancreas cancer. In addition, combining with optogenetic mouse models, flexible microLED stimulates the neurons of motor cortex for manipulating mouse body movements and synchronized electromyogram (EMG) signals.

2:00 PM *EN02.04.01

Piezoelectric Biomaterials and Devices for Energy Harvesting and Application in Cardiovascular Systems [Xudong Wang](#); University of Wisconsin--Madison, United States

Nanogenerator (NG) is a promising solution to biomechanical energy harvesting inside human body. So far, many technology innovations have advanced the NG technology toward a broad range of biomedical applications. Among many potential directions, cardiovascular applications possess substantial significance given the wide spread of cardiovascular diseases and high demands of cardiovascular electronic devices. In this talk, I introduce our most recent development of piezoelectric materials and composites that are particularly designed for implantable NG applications for both hearts and blood vessels. First, new ferroelectric composites are presented as a new material used in 3D printing for directly manufacturing of piezoelectric architectures with tunable piezoelectric and mechanical properties. Artificial blood vessels and stents are developed using this new technique that enable in vivo monitoring of blood pressure and early detection of blockage. Materials and devices that enables effective energy harvesting from hearts will also be introduced, showing a promising solution for long-term in vivo operation for powering cardiovascular electronics. Toward the end, other relevant challenges, such as device safety, biocompatibility, and packaging issues will also be discussed, together with additional novel application potentials for NGs for cardiovascular systems.

2:30 PM BREAK

3:30 PM *EN02.04.03

Discovering Giant Magnetoelastic Effect in Soft Systems for Bioelectronics [Jun Chen](#); University of California, Los Angeles, United States

The magnetoelastic effect, also named as Villari effect and discovered in 1865 by Italian experimental physicist Emilio Villari, is the variation of the magnetic field of a material under mechanical stress. This effect is usually observed in rigid metal and metal alloys with an externally applied magnetic

field and has been ignored in the field of soft bioelectronics for the following three reasons: the magnetization variation in the biomechanical stress range is limited; the requirement of the external magnetic field induces structural complexity and bulky structure, and there exists a gigantic mismatch of mechanical modulus up to six orders of magnitude difference between the rigid magnetoelastic materials and the soft human tissues. In 2021, we discovered the giant magnetoelastic effect in a solid soft polymer system, later in a liquid permanent fluidic magnet, which paves a fundamentally new way to build up intrinsically waterproof and biocompatible soft bioelectronics for diagnostics, therapeutics, and energy applications. Our group at UCLA is currently pioneering this research effort of harnessing giant magnetoelastic effects in soft systems for healthcare and energy.

4:00 PM EN02.04.04

High-Performance PVDF/PMMA Porous Matrix-Based Triboelectric Nanogenerators [Assem Mubarak](#), Gulnur Kalimuldina, Bayandy Sarsembayev and Zhanat Kappassov; Nazarbayev University, Kazakhstan

The increasing demand for flexible and wearable devices is driven by ongoing advancements in intelligent electronics technology, coupled with the growing importance of the Internet of Things (IoT) in biomedical applications. Modern electronics must exhibit specific characteristics, including a lightweight design, high conductivity, good dielectric permittivity, low dielectric loss, and exceptional breakdown strength. Polyvinylidene fluoride (PVDF), a polymer known for its high triboelectric charge density, is a common piezoelectric material used in nanogenerators like triboelectric nanogenerators (TENGs). However, obtaining PVDF with a high β -phase content using conventional methods, typically employed for membrane materials, poses a significant challenge due to its high resistance and the inherent difficulty in polarization.

Therefore, this research study employs a novel quenching method to prepare a PVDF/PMMA porous matrix with a predominant β -phase content of around 86%, offering a relatively simple and cost-effective approach. The fabricated TENG device exhibited an impressive output power output of approximately 750 mW per and demonstrated excellent mechanical robustness, enduring more than 30,000 cycles. This mechanical robustness is three times higher than that of previous PVDF-based TENGs. Overall, this study demonstrates the potential application of a PVDF/PMMA porous matrix TENG device, fabricated through a simple and cost-effective method, highlighting its versatility and efficiency for various practical purposes.

4:15 PM EN02.04.05

Metal-Organic Frameworks for Textile based Triboelectric Nanogenerators [Gaurav Khandelwal](#), Charchit Kumar, Satyaranjan Bairagi and Daniel Mulvihill; James Watt School of Engineering, University of Glasgow, United Kingdom

Metal-organic frameworks (MOFs) are crystalline porous materials composed of metal ion coordinated with an organic ligand. MOFs has numerous advantages including high surface area, tunable size, ease of post synthetic modifications, high porosity. Further MOFs offers specific pore size which can be advantageous for highly selective self-powered sensors based on triboelectric effect. However, majority of MOFs based TENG uses powders attached on the conductive tape by applying high pressure and blowing off the unattached particles. This widely used approach is unsuitable due to poor device reproducibility, repeatability and stability. Further, TENGs active layers designed by above method cannot be used for self-powered physical or chemical sensors. In case of physical sensors like pressure sensor, high pressure can lead to the transfer of material on the opposite contact layer. While in case of chemical sensors addition of analyte can lead to removal of material, thus making device unreliable. This work discusses the advantages and the challenges of MOFs for TENGs. Then MOFs are introduced for TENG based self-powered sensor applications with ZIF-8 based tetracycline sensor and Cu-Asp based thioacetamide sensor as examples. Finally, the talk will discuss the growth of MOFs on the textile substrates for TENGs, their triboelectric behaviour and potential for self-powered applications.

SESSION EN02.05: Poster Session I
Session Chairs: Chang Kyu Jeong and Kwi-II Park
Wednesday Afternoon, April 24, 2024
Flex Hall C, Level 2, Summit

5:00 PM EN02.05.01

Flexible and Wearable Thermo/Piezo-Electric Hybrid Energy Harvesters Cheolmin Kim, Hyeon Jun Park, Gwang Hyeon Kim, Bitna Bae, HakSu Jang and [Kwi-II Park](#); Kyungpook National University, Korea (the Republic of)

Thermoelectric and piezoelectric hybrid generators (TPHG) are attractive candidates for powering wearable body sensor networks continuously and permanently owing to their excellent access to human-generated energy. First, to achieve the enhanced piezoelectricity of flexible piezoelectric composites-based films, we have demonstrated the flexoelectric-boosted electromechanical properties of piezoelectric nanoparticles using an induced built-in strain gradient in heterogeneous core-shell nanostructure for enhancing the intrinsic piezoelectricity of pure BaTiO₃ nanoparticles. We have also demonstrated the enhanced poling efficiency in nanocomposite made of P(VDF-TrFE) and porous BaTiO₃ nanofibers. Moreover, we have developed the high-temperature workable f-PEH comprising the high T_c KNN-based ceramics and a thermally stable polyimide (PI) matrix which can be a promising candidate for developing f-PEH and self-powered sensors working in high-temperature environments. Next, to realize the flexible thermoelectric energy harvesting technology, we have fabricated the tailorable f-TEHs based on thermoelectric films and papers made by dispersing the Bi₂Te₃ particles inside polymeric and cellulose matrices, respectively. Finally, the hybrid generator was assembled through simple drop-casting and gravitational settling effect, for the first time. The film layer sedimented with the conductive thermoelectric particles simultaneously served as an electrode and a bottom substrate for piezoelectric energy harvesting. The proposed design concept for f-TPHG can aid in the development of high-performance multisource energy harvesting devices for wearable sensors.

5:00 PM EN02.05.02

Enhanced Triboelectric Performance of Surface-Modulated 2D MoS₂ via Pulsed Laser-Directed Thermolysis for Self-Powered Wearable Electronics Hee Yoon Jang¹, Chang Kyu Jeong² and [Seoung-Ki Lee](#)¹; ¹Pusan National University, Korea (the Republic of); ²Jeonbuk National University, Korea (the Republic of)

In recent times, two-dimensional (2D) transition metal dichalcogenide (TMDC) nanomaterials have emerged as leading contenders for advancing the realms of flexible, transparent, and wearable electronics. Yet, there exists a conspicuous dearth in the exploration of their inherent properties in the domain of triboelectric nanogenerators (TENGs), a foremost technology for mechanical energy harvesting. This study presents a novel, rapid, ambient, wafer-scale, and patternable methodology for the synthesis of 2D MoS₂ through pulsed laser-directed thermolysis. Our groundbreaking laser synthesis approach facilitates the imposition of internal stress on the MoS₂ crystal by modulating its morphological characteristics, resulting in a surface-modulated MoS₂ TENG device that exhibits power generation amplified by approximately 40% relative to its flat MoS₂ counterpart. Distinctly, in comparison to analogous

MoS₂-based TENG devices, our model achieves superior energy harvesting metrics (reaching peaks of ~25 V and ~1.2 μA) without the requirement of supplemental materials, even in scenarios where the opposing triboelectric surface exhibits a marginally varied triboelectric series. This augmentation in triboelectrification can be ascribed to both alterations in work function and the amplification of surface roughness. Conclusively, the directly synthesized MoS₂ patterns are adeptly employed to craft a self-sustaining flexible haptic sensor array. The methodology delineated herein aims to galvanize expansive research into the triboelectric potentials and diverse applications of 2D TMDC nanomaterials.

5:00 PM EN02.05.03

Anomalous Output Performance Enhancement of Triboelectric Nanogenerators by Manipulation of Surface Molecular Dipoles Ruey-Chi Wang and Hsiu-Cheng Chen; National University of Kaohsiung, Taiwan

Since the invention of triboelectric nanogenerators (TENGs), numerous strategies have been proposed to boost their performance by altering the triboelectric materials, typically centered on increasing work function disparities or effective contact areas. However, in this study, we introduce a novel approach that significantly enhances output performance through the manipulation of surface molecular dipoles, a departure from conventional methods. In our research, we demonstrate a significant improvement in TENG output performance by manipulating surface dipoles, achieved by bonding copper ions to the oxygen-containing functional groups on the surface of graphene oxides. This bonding causes a reversal in the orientations of surface molecular dipoles, resulting in the enhancement of TENG output. Remarkably, the variations in TENG output performance due to these surface modifications are contrary to what would be predicted based solely on differences in work functions, as determined by Kelvin probe force microscopy. This observation suggests that factors beyond work functions play a pivotal role in governing TENG performance. We propose a self-bias-enhancement model by surface dipoles and further testifies it by polling processes. This mechanism is expected to have universal applicability to other materials aimed at enhancing the performance of TENGs and self-powered devices.

5:00 PM EN02.05.04

Computational Investigation of Low-Dimensional Materials for Spacesuit Applications Simone Lang and Shiru Lin; Texas Woman's University, United States

Modern Space Suit materials maintain properties that shield astronauts from radiation, severe lunar temperature, and microparticles; while upholding lightweightness, flexibility and tensile strength on long space missions. Most spacesuit materials are made from nylon, synthetic fabrics and synthetic polymers. High density polyethylene (HDPE) is a popular polymer for space applications due to their resistance properties from secondary radiation exposure and their richness in hydrogen atoms. However, HDPE lacks tensile strength, therefore causing urgency to find a material that will absorb well and maintain excellent properties with HDPE. In this project, low-dimensional materials, including graphene, graphene oxide and boron oxide are explored for spacesuit material additives HDPE, because of their successful electrostatic, thermal and mechanical properties. Density Functional Theory (DFT) computations are used to investigate the adsorption interactions between low-dimensional materials with HDPE with the variable of angle dependence. Moreover, exploring their ability to maintain radiation resistance, thermal cycling and electrostatic properties.

5:00 PM EN02.05.05

Influence of Relaxor Piezoelectric Polymer Matrix on Piezoelectric Nanocomposites-Based Energy Harvesting Hyunseung Kim^{1,1}, Wook Jo², Seung-Hyun Kim³ and Chang Kyu Jeong^{1,1,1}; ¹Jeonbuk National University, Korea (the Republic of); ²Ulsan National Institute of Science and Technology, Korea (the Republic of); ³Brown University, United States

Piezoelectric nanocomposites consisting of a polymer matrix and ceramic fillers are candidate components of flexible, wearable, and self-powered electronic devices. The physical discrepancy between ferroelectric polymers and ceramics in a piezoelectric interface makes it difficult to assemble efficient hybrid piezoelectric nanocomposites without polarization and extraneous artifacts. Here, we describe the effect of a relaxor ferroelectric terpolymer matrix on the piezoelectric output, which can enhance the energy harvesting or sensor performance of piezoelectric composite device of nanocomposite generators with filler nanoparticles of lead zirconium titanate. The dielectric property and reduced ferroelectric hindrance of the proposed terpolymer matrix provides more poling to align the polarization of piezoelectric ceramic fillers compared with a normal ferroelectric copolymer matrix. Therefore, relaxor ferroelectric polymers can be better than normal ferroelectric polymers as the matrix of hybrid polymer-ceramic piezoelectric nanocomposite. This research provides important physical information about the interface between a polymer matrix and ceramic fillers in flexible piezoelectric nanocomposite applications.

5:00 PM EN02.05.06

Dual Contribution of Charge Loss Reduction and Charge Generation Assisted by Electronegative Double-Layered Triboelectric Nanogenerator Arun Mondal, Mohd Faraz, Mamta Dahiya and Neeraj Khare; Indian Institute of Technology Delhi, India

Converting ambient mechanical vibrations into electricity is a promising approach to providing independent power sources for smart portable electronic devices[1]. Triboelectric nanogenerator (TENG) is one of the very promising choices in the research community for harvesting mechanical energy for their easily available resources and simple fabrications. The major problem of a TENG device is the loss of generated negative surface charges of the electronegative layer before it can be captured. In the present work, we have fabricated a double-layered structure for the electronegative part to engineer the dual contribution: reduction in the surface charge loss and the improvement in the surface charge generation during contact electrification. The double-layer structure of the electronegative layer is a stacking of two different composite polymers, in which the bottom part is the NaNbO₃ nanocubes incorporated PDMS layer, and the top part is the composite of PVDF and MXene Ti₃C₂T_x flakes, which is named as 15MP/15NP (PVDF+15wt% MXene/PDMS+15wt% NaNbO₃). An enhancement of 2.5 times in open-circuit voltages (V_{OC}), 2.5 times in short-circuit currents (I_{SC}), and 2.2 times in the transferred charges (Q_{SC}) have been observed in 15MP/15NP-based TENG. It also exhibits a large 7-fold enhancement compared to the bare PVDF, where the bare PVDF-based TENG shows a power density of 19 μW/cm², whereas the 15MP/15NP-based TENG shows 134 μW/cm². The enhancement in the electrical outputs in 15MP/15NP is due to the improved surface charge retention of the electronegative layer. The KPFM study confirms that the surface potential in the 15MP/15NP has been reduced significantly compared to bare PVDF, resulting in an increased work function, which enhances the surface charge density during contact electrification and improves the electrical outputs. [2]. The incorporation of NaNbO₃ in the PDMS layer improved the dielectricity and internal polarization of the PDMS+NaNbO₃ composite, which reduced the surface charge loss that arises from the internal electric field generated between the negative surface electrons and positive induced charges on the back electrode. Additionally, the incorporation of MXene in the PVDF layer effectively improved the electronegativity of the friction layer because of their surface-terminated electronegative -F groups and microcapacitive structure[3].

References

[1] A. Mondal, M. Faraz, N. Khare, Magnetically tunable enhanced performance of CoFe₂O₄-PVDF nanocomposite film-based piezoelectric nanogenerator, Appl. Phys. Lett. 121 (2022) 103901–103906. <https://doi.org/10.1063/5.0102253>.

[2] H.H. Singh, D. Kumar, N. Khare, Tuning the performance of ferroelectric polymer-based triboelectric nanogenerator, *Appl. Phys. Lett.* 119 (2021). <https://doi.org/10.1063/5.0057640>.

[3] H.Q. Wang, J.W. Wang, X.Z. Wang, X.H. Gao, G.C. Zhuang, J.B. Yang, H. Ren, Dielectric properties and energy storage performance of PVDF-based composites with MoS₂/MXene nanofiller, *Chem. Eng. J.* 437 (2022) 135431. <https://doi.org/10.1016/j.cej.2022.135431>.

5:00 PM EN02.05.07

Hybrid Biomechanical Energy Harvesting for Wearable Microgrids Jiseok Kim and Il-Kwon Oh; Korea Advanced Institute of Science and Technology, Korea (the Republic of)

With increasing interest in battery-free electronic devices, researchers are exploring ways to convert biomechanical energy from the human body into electrical energy. However, the commercialization of energy harvesting devices poses significant challenges. Such challenges can be attributed to various factors as follows; 1) The low efficiency of energy conversion results in a lack of viable electronic components for real-world applications. Additionally, the use of biomechanical energy harvesting devices may increase metabolic energy and causes discomfort. To address these challenges, this study proposes an innovative air-pumping-based energy harvesting device that aims to enhance energy conversion efficiency while minimizing user inconvenience. The device compresses rubber bladders through repetitive ground impacts during walking. It releases compressed air to induce rotor rotation hence converting low-frequency reciprocating motion that arises from impacts into high-frequency rotary motion to increase efficiency in electricity generation with a low crest factor. Unlike conventional energy harvesting devices, which generate single-pulse and discontinuous energy harvesting signals from low-frequency movements, this approach enables continuous energy harvesting by converting rotational motion. Additionally, it can be made of lightweight materials for a simple air-pumping mechanism rather than heavy mechanical components. The rotary energy harvester employs a hybrid energy harvesting technology that utilizes both an electromagnetic and tribovoltaic generator. The latter exploits the friction at the metal-semiconductor Schottky interface to produce unidirectional direct current beyond the energy barrier. This hybrid energy harvester facilitates the continuous operation of healthcare monitoring sensors when seamlessly integrated into smart wearable systems. We conclude that this technology is ideal for ensuring uninterrupted healthcare monitoring. In conclusion, the hybrid biomechanical energy-harvesting device developed in this research presents a promising solution for enabling the continuous operation of smart wearable systems, especially healthcare monitoring sensors, by utilizing energy harvested during daily walking activities.

5:00 PM EN02.05.08

Enhanced Output Performance of Triboelectric Nanogenerator Based on Sulfur-Rich Polymer with Controlled Composition Gradient Minji Bak^{1,2}, Woongbi Cho¹, Sungsu Kim¹ and Jeong Jae Wie^{1,3,2}; ¹Hanyang University, Korea (the Republic of); ²The Michael M. Szwarc Polymer Research Institute with Composition Gradient, United States; ³State University of New York College of Environmental Science and Forestry, United States

Elemental sulfur of seven million tonnes is annually generated as a by-product from petroleum refining processes. Hence, the upcycling of elemental sulfur has gained significant attention owing to its high economic feasibility and environmental-friendliness. In previous reports, the sulfur-rich polymer (SRP) is utilized for the high-performance negatively chargeable friction layer in a triboelectric nanogenerator (TENG). Because the SRP has the highest electron affinity of -200 kJ mol^{-1} in the periodic table except for halogenic elements and precious metals like Au, Pt. In this study, we introduce a structural approach with composition gradient for improving TENG performance. A thin dielectric layer is typically favorable for high performance due to increased charge induction, but excessive thinness reduces surface charge density due to charge recombination. To prevent the recombination, a charge trapping layer (CTL) is employed for enhancement of surface charge density. Increasing sulfur content in SRP leads to a higher dielectric constant, resulting in the generation of more charge through triboelectrification. At the same time, the benzene content decreases, which reduces charge capture ability. This is because aromatic polymers have non-uniform energy levels along their polymer chain, containing numerous charge trapping sites. We optimize TENG performance by creating a monolithic film with spatially controlled elemental sulfur and benzene content through dynamic covalent bonding by the thermal processing of two films with different sulfur contents.

5:00 PM EN02.05.09

Big Data Analysis for Cell Efficiency Prediction with Multi Wafer Quality Data Sung Ho Hwang^{1,2}, Yoonmook Kang¹, Hae-seok Lee¹ and Dongchul Suh³; ¹Korea University, Korea (the Republic of); ²Research Institute for Energy Technology, Korea (the Republic of); ³Hoseo university, Korea (the Republic of)

In photovoltaic (PV) products, three key parameters, namely high power, low cost, and high energy yield, have been the primary focus of investigation within both academic and industrial contexts. From a cost reduction perspective, the wafer has traditionally been the most expensive material in module manufacturing. In 2021, crystalline wafers (mono and multi) dominated the market, holding approximately 95% of the share. Within this, multi wafers accounted for around 15%. More recently, larger wafers like M10 and M12 have been adopted in the PV industry, continuing this trend. Given this market situation, reducing the cost of wafers has become a highly effective endeavor. Wafer manufacturers have been striving to produce thinner wafers to maximize the quantity from ingots.

Simultaneously, cell manufacturers have been working on methods to identify and separate lower-quality wafers before the manufacturing process begins. These lower-quality wafers can result in cells with reduced efficiency, making them unsuitable for module production, as they fail to meet the required power specifications. This decrease in cell efficiency has imposed a significant burden on cell manufacturers, leading to losses in materials, gases, chemicals, and production. Consequently, the development of improved screening methods is a critical and necessary step for cell manufacturers.

In this study, various properties of multi wafers, such as lifetime, dark area, dark edge area, edge defect, defect, resistivity, total thickness variation (TTV), saw mark, wafer thickness, and grain defects, were monitored and evaluated alongside final data on cell efficiency, short-circuit current, and open-circuit voltage during mass production. This analysis was conducted on Passivated Emitter Rear Contact (PERC) multi cells, using several tens of thousands of wafers. The performance of all tools was also assessed to establish a connection with these wafer quality parameters.

Several parameters demonstrated a strong correlation with cell efficiency. This correlation allows for the cell efficiency prediction based on wafer quality without any additional processes. This predicted cell efficiency was compared with the mass production data, revealing a significant correlation.

As a result of this study, cell manufacturers can identify and eliminate low-quality wafers that pose a risk of resulting in low cell efficiency during mass production. This process can ultimately lead to cost reduction by saving on gas, chemicals, process time, and pastes. Consequently, this study has the potential to contribute to reducing the levelized cost of electricity (LCOE) in the PV industry.

5:00 PM EN02.05.10

Metallic Glass Thin Film Electrodes for Chemically and Mechanically Stable Interface for Flexible Electronics Jae Sang Cho¹, Woongsik Jang¹, Keum Hwan Park² and Dong Hwan Wang¹; ¹Chung-Ang University, Korea (the Republic of); ²Korea Electronics Technology Institute, Korea (the Republic of)

Metallic glasses (MGs) or amorphous alloys gained attentions for their attractive mechanical properties and chemical stabilities, which originate from the randomly oriented atomic arrangement in the MGs that results in their strong strain-resistance and chemical inertness. MGs are often characterized by the absence of grain boundaries, which are often responsible for initiating catastrophic mechanical failures and corrosion (and other chemical reactions). Recently, their applicability in thin film via physical vapor deposition method have motivated researchers to replace electrode materials to MG thin films. MG thin films exhibit varying electrical and mechanical characteristics depending on their atomic compositions, thus should be analyzed thoroughly before replacing conventional electrode materials for the electrodes. Here, we present intriguing cases of adopting MG thin films for electrodes of organic photovoltaic cells and sensors. Through detailed investigations on MG thin films, fabrication of thin film devices with enhanced stability and flexibility is achieved. In specific, amorphous metallic surface in contact with polymers circumvents oxidation reaction caused by ambient air, which prevents formation of insulating oxides and loss of electrical conductivity of the electrode itself. In addition, MG thin film exhibited high crack resilience in bendable and stretchable devices, which yielded flexible devices with high flexibility and reliability.

Reference (1) *Organic Electronics* 84 (2020): 105811.

Reference (2) *Electrochimica Acta* 446 (2023): 142053.

Reference (3) *Journal of Alloys and Compounds* 944 (2023) 169219.

5:00 PM EN02.05.11

3D Printed Ni-Mo Catalysts for High Performance HER at a High Current Density Yanran Xun and Jun Ding; National University of Singapore, Singapore

Developing efficient water splitting at high current density ($>500 \text{ mA cm}^{-2}$) is essential for its scalability. [1] Electrochemical water splitting is one of the most promising technological approaches for producing green hydrogen, and it plays a crucial role in achieving carbon neutrality. [2] In the meantime, additive manufacturing as a simple and facile method has attracted researchers' interest for the past decades, and a couple of outstanding works about using 3D printing to fabricate electrodes for water-splitting have been done. [3]–[5] Here, we reported a series of monolithic 3D-printed Ni-Mo alloy electrodes for highly efficient water splitting at high current density (1500 mA cm^{-2}) with excellent stability and bubble removal behavior, which provides a solution to scale up Ni-Mo catalysts for HER to industry use. All possible Ni-Mo metal/alloy phases were achieved by tuning the atomic composition and heat treatment procedure, and they were investigated through both experiment and simulation, and the optimal NiMo phase shows the best performance. Density functional theory (DFT) calculations elucidate that the NiMo phase has the lowest H_2O dissociation energy, which further explains the exceptional performance of NiMo. In addition, the microporosity was modulated via controlled thermal treatment, indicating that the $1100 \text{ }^\circ\text{C}$ sintered sample has excellent catalytic performance, which is attributed to the high electrochemical surface area (ECSA). Finally, the 4 different macrostructures were achieved by 3D printing, and they further improved the catalytic performance. The gyroid structure exhibits the best catalytic performance of driving 500 mA cm^{-2} at a low overpotential of 228 mV and 1500 mA cm^{-2} at 325 mV as it maximizes the efficient bubble removal from the electrode surface, which offers the great potential for high current density water splitting.

[1] Y. Luo, Z. Zhang, M. Chhowalla, and B. Liu, *Adv. Mater.*, vol. 34, no. 16, p. 2108133, (2022)

[2] X. Liu, M. Gong, S. Deng, T. Zhao, J. Zhang, and D. Wang, *J. Mater. Chem. A*, vol. 8, no. 20, pp. 10130–10149, (2020)

[3] S. Chang *et al.*, *Adv. Energy Mater.*, p. 2100968, (2021)

[4] R. A. Márquez *et al.*, *ACS Appl. Mater. Interfaces*, p. acsami.2c12579, Sep. (2022)

[5] I. Sullivan *et al.*, *ACS Appl. Mater. Interfaces*, vol. 13, no. 17, pp. 20260–20268, (2021)

5:00 PM EN02.05.12

Hydrophobic-Barrier-Assisted Formation of Vertically Layered Metal Electrodes within a Single Sheet of Paper for a Foldable Radio Frequency Energy Harvesting System In Hyeok Oh, Eiyong Park, Sinil Kim, Sungjoon Lim and Suk Tai Chang; Chung-Ang University, Korea (the Republic of)

Radio frequency energy harvesting (RFEH) systems have emerged as a critical component for powering devices and replacing traditional batteries, with paper being one of the most promising substrates for use in flexible RFEH systems. However, previous paper-based electronics with optimized porosity, surface roughness, and hydroscopicity still face limitations in terms of the development of integrated foldable RFEH systems within a single sheet of paper. Here, we present a novel integrated foldable RF energy harvesting system based on vertically separated metal electrodes within a single sheet of paper by using a combination of hydrophobic wax printing and water-based solution process. Our fabrication approach provided stable horizontal conductive patterning with high conductivity, vertical separation of electrodes, and more importantly connection through a via-hole inside a paper substrate. The via-hole processing is a key factor that dramatically expands the design freedom of the harvesting system. When the via-hole cannot be implemented, the harvester should be positioned in the same plane or use the multilayer and additional connecting line. Thus, by applying our novel fabrication process, all-in-one type foldable RF energy harvesting system can be realized by integrating RF antenna, RF to DC rectifier, and supercapacitor within only a single sheet of paper. The proposed RFEH system exhibits an RF/DC conversion efficiency of 60% and an operating voltage of 2.1 V in 100 s at a distance of 50 mm and a transmitted power of 50 mW . The integrated RFEH system also demonstrates stable foldability, with RFEH performance maintained up to a folding angle of 150° . Our single-sheet paper-based RFEH system thus has the potential for use in practical applications associated with the remote powering of wearable and Internet-of-Things devices and in paper electronics.

5:00 PM EN02.05.13

High Efficiency Triboelectric Generator by Combining Acoustic Metamaterial Absorber and Isotropic Spring TsungYu Huang and Wei-Zhi Weng; Ming Chi University of Technology, Taiwan

Due to the current energy shortage and the growing environmental awareness, researchers around the world have been dedicating significant efforts to the development of green energy solutions. One area of particular interest is the exploration of eco-friendly and semi-permanent devices for power systems. Among these, the triboelectric nanogenerator has garnered significant attention due to its ability to efficiently convert weak mechanical energy into electrical energy. This simple, high energy density, and cost-effective device make triboelectric generator a prime candidate for alternative power sources, especially in the context of sustainable energy solutions. In addition to the energy crisis, urban areas are currently grappling with severe noise pollution, which has led to an increase in irritability and negatively impacts on their overall quality of life. In response to this challenge, researchers have developed innovative acoustic metamaterials capable of absorbing incident sound waves efficiently, even at sub-wavelength thicknesses. This technological advancement offers a promising opportunity to address both the energy shortage and noise pollution simultaneously. In this study, our goal is to integrate an acoustic metamaterial absorber, isotropic springs, and nanoscale triboelectric generators to convert the original noise pollution into electrical energy that can be used to power low-power devices. The first component of our integrated system is the acoustic metamaterial absorber, which we have designed as a quasi-Helmholtz resonator. This absorber is specifically engineered to achieve perfect absorption of incident sound waves at sub-wavelength thicknesses. It operates as an efficient noise-capturing device, thereby significantly reducing noise pollution in urban areas. The second essential element of our system is the isotropic spring, which we have incorporated within the acoustic metamaterial absorber. This spring is designed to capture and store the mechanical energy generated by sound waves. To optimize the energy conversion process, we must carefully consider the characteristics of the noise we aim to

capture. General traffic noise, for instance, typically has a frequency of around 2000 Hz and a decibel level of approximately 90 dB. These values serve as crucial parameters for our design and performance assessment. In our simulation, we have set the sound pressure of the incident sound wave to 1×10^6 to represent the real-world noise pollution scenario. By accurately modeling this scenario, we can better evaluate the effectiveness of our system in capturing and converting noise into electrical energy. The heart of our innovation lies in the positioning of two different materials for triboelectric generation. We have strategically placed these materials at a location with the maximum displacement between the components of the isotropic springs and the side walls of the acoustic metamaterial absorber. This placement is critical to ensuring the efficient conversion of mechanical energy into electrical energy. In our simulation, we have found that the relative displacement between the spring and absorber is approximately 1.8 mm, which is a promising result indicating the potential for effective energy conversion. In conclusion, our innovative approach to addressing both the energy shortage and noise pollution in urban areas offers a promising solution.

Keywords: Acoustic Metamaterials, Absorber, Isotropic Spring and Nanogenerator

5:00 PM EN02.05.14

Plasma Enhanced Attachment of Graphene Dispersed Conductive Polymer to 1D Nanofibers for Sensing and Nanogeneration Elmmmer A. Vera Alvarado, Md. Abdur Rahman Bin Abdus Salam, Ali Ashraf and Karen Lozano; The University of Texas at Rio Grande Valley, United States

Nanogeneration, an emerging area where nanotechnology meets energy harvesting, has the potential to transform how we provide power to our increasingly miniaturized and portable electronic devices. The concept of nanogeneration, which involves the utilization of nanoscale materials and processes to generate electricity from surrounding sources. Nanogeneration encompasses various technologies like piezoelectric nanomaterials, thermoelectric generators, and triboelectric nanogenerators, which make it possible to transform mechanical movements, temperature variations, and even environmental vibrations into electrical power. Polyvinylidene fluoride (PVDF) is a semi-crystalline thermoplastic fluoropolymer known for its remarkable piezoelectric properties. PVDF is a commonly employed material for piezoelectric sensors, serving to measure pressure, force, acceleration, and vibration in various devices. These sensors are applied in industrial monitoring, medical equipment, and consumer electronics. In this study, the Forcespinning® (FS) method was utilized to fabricate PVDF nanofiber mats, which then were cut into small strips for nanogeneration and sensing tests. A conductive polymer ink, composed of poly(3,4-ethylenedioxythiophene) polystyrene sulfonate (PEDOT:PSS) and graphene nanoflakes, was created and diluted in a 1:1 ratio with deionized water, which was later applied using a dip-coating process on the nanofibers. These nanofibers were initially subjected to a 3-minute plasma etching process to eliminate excessive beading. The specific time was decided after several trials at different times under the plasma treatment, the samples were characterized by Scanning Electron Microscopy (SEM) and it was observed that as the treatment time increased, the finer the fibers became, decreasing the fiber diameter by approximately 500 nm from the pristine nanofibers. The plasma process was done to enhance the adhesion of 2D material particles to the nanofibers, confirmed by SEM. The microscopic images of untreated PVDF nanofibers following the 3-minute plasma treatment displayed a noticeable decrease in the number and dimensions of bead-like structures, along with a substantial reduction of 500 nm in nanofiber diameter. Additionally, the images revealed a strong adhesion between the conductive polymer ink and the nanofibers. Moreover, the coated nanofibers presented an approximate electrical conductivity of 250 kΩ, as well as an average output voltage of 50 mV for single finger pressing, comparable to the work performed by Rahman et al., where a voltage of 75mV was obtained from graphene-coated nanofibers [1]. Further tests for sensing and conductivity of these samples are to be performed, showing a promising advancement for low-powered sensors and energy harvesting.

References:

[1] Rahman, M. A., Rubaiya, F., Islam, N., Lozano, K., & Ashraf, A. (2022). Graphene-coated PVDF/pani fiber mats and their applications in sensing and nanogeneration. *ACS Applied Materials & Interfaces*, 14(33), 38162–38171. <https://doi.org/10.1021/acsami.2c09045>

5:00 PM EN02.05.15

Towards 1-Watt Capable Rotary Triboelectric Nanogenerators for Power at Sea Griffin Trayner, Calum Kenny and Jim McNally; National Renewable Energy Laboratory, United States

Increasing at-sea power generation by Triboelectric Nanogenerator (TENG) energy harvesters in the order of 1-Watt will create significant opportunities to power ocean observation buoys and distributed sensor nodes by extending mission time and increasing sensor payload [1]. Of the many possible configurations of harvesting wave energy with TENGs, we document the rationale for choosing and developing a rotary TENG that operates by the freestanding mode. The rotary TENG prototype consists of two plates, a rotor and a stator, to take advantage of the various mechanisms of converting wave action into rotational motion. We have constructed a testing apparatus that allows us to vary several key parameters of the device: distance between rotor and stator, triboelectric material, rotational speed, number of electrodes and output load impedance. Preliminary results show that when driven at a constant 500 rpm, we can achieve a power density of 0.7 W/m³. A variable speed motor drives the rotor, which can be driven using a velocity profile informed by the equivalent to the output from a wave energy converter (WEC). This profile may be generated by the hydrodynamic simulation software WEC-Sim. The optimized rotational TENG can be stacked and driven by a single shaft, increasing the energy density of the device. The output of such a TENG could be used to power devices in the ocean at a low cost and high durability.

References:

1. A. LiVecchi, "Powering the Blue Economy: Exploring Opportunities for Marine Renewable Energy in Maritime Markets," (2019).

5:00 PM EN02.05.16

Moisture Activated Zinc Ion Battery for Leak Detection Signaling Dylan D. Edmundson and Anthony Dichiaro; University of Washington, United States

Every year \$6 billion worth of potable water is lost to undetected leaks in addition to \$20 billion spent on property damage in the U.S alone [1-3]. While many leak detection systems exist that use acoustic, thermal, and video detection principles, they often suffer from low signal to noise ratios, poor sensitivity, and require technician operation [4]–[6]. To overcome these challenges researchers have begun investigating new and inventive bio-based solutions such as conductive paper resistive sensors [7], [8]. While these systems are quite effective, they are difficult to implement in residential homes due to the expense of installation and the need of continuous monitoring and power supply. To overcome these drawbacks, a fully autonomous leak detection system was envisioned, where a leak can produce power through mechanisms such as moisture enabled generators (MEGs) however, the extremely low power production of MEGs is insufficient for WIFI signaling. In this study a zinc ion battery inspired device is developed in pursuit of a fully autonomous detection system. Zinc microspheres are embedded in a carbon nanotube/cellulose composite using a scalable paper manufacturing method. Using this anode with a moisture wicking electrolyte separator and manganese oxide cathode, a water activated battery was produced capable of powering a WIFI device signaling the presence of a leak.

Sources:

[1] O. US EPA, "Fix a Leak Week," Feb. 03, 2017. <https://www.epa.gov/watersense/fix-leak-week> (accessed May 18, 2023).

[2] "Average monthly cost of water United States 2019," *Statista*. <https://www.statista.com/statistics/720418/average-monthly-cost-of-water-in-the-us/>

(accessed May 18, 2023).

[3] "Water Damage Statistics [2023]: Claim Data & Facts," *iPropertyManagement.com*. <https://ipropertymanagement.com/research/water-damage-statistics> (accessed May 28, 2023).

[4] H. Fan, S. Tariq, and T. Zayed, "Acoustic leak detection approaches for water pipelines," *Autom. Constr.*, vol. 138, p. 104226, Jun. 2022, doi: 10.1016/j.autcon.2022.104226.

[5] J. D. Butterfield, R. P. Collins, and S. B. M. Beck, "Influence of Pipe Material on the Transmission of Vibroacoustic Leak Signals in Real Complex Water Distribution Systems: Case Study," *J. Pipeline Syst. Eng. Pract.*, vol. 9, no. 3, p. 05018003, Aug. 2018, doi: 10.1061/(ASCE)PS.1949-1204.0000321.

[6] Y. A. Khulief, A. Khalifa, R. B. Mansour, and M. A. Habib, "Acoustic Detection of Leaks in Water Pipelines Using Measurements inside Pipe," *J. Pipeline Syst. Eng. Pract.*, vol. 3, no. 2, pp. 47–54, May 2012, doi: 10.1061/(ASCE)PS.1949-1204.0000089.

[7] S. Goodman, A. Song, R. Fitzpatrick, and A. Dichiaro, "Development of carbon nanotube: cellulose composites using a simple papermaking process for multifunctional sensing applications," *Proc. Spie*, vol. 10165, p. 101650N, 2017, doi: 10.1117/12.2257364.

[8] S. M. Goodman *et al.*, "Scalable manufacturing of fibrous nanocomposites for multifunctional liquid sensing," *Nano Today*, vol. 40, p. 101270, Oct. 2021, doi: 10.1016/j.nantod.2021.101270.

[9] D. Shen *et al.*, "Moisture-Enabled Electricity Generation: From Physics and Materials to Self-Powered Applications," *Adv. Mater.*, vol. 32, no. 52, p. 2003722, 2020, doi: 10.1002/adma.202003722.

SESSION EN02.06: Miscellaneous Energy Harvesting
Session Chairs: Jinbo Bai and Seoung-Ki Lee
Thursday Morning, April 25, 2024
Room 332, Level 3, Summit

8:00 AM *EN02.06.01

Paper-Based Electrokinetic Power Generator Dylan D. Edmundson and [Anthony B. Dichiaro](#); University of Washington, United States

Wearable devices integrated with microprocessors and multifunctional sensors are gaining momentum in a variety of industries over the past decade. Such advancements significantly exceed the development pace of portable power sources. Most batteries, besides posing serious sanitary and environmental concerns, are unfit for wearable devices, which require flexible, lightweight, reliable, and long-lasting systems with power densities of at least several tens W/kg. The autonomous scavenging of energy from the ambient environment offers a sustainable solution to power wearable sensors over long periods without the need to recharge. Nanogenerators (NG), such as triboelectric, piezoelectric, and thermoelectric generators, have been developed to harvest renewable energy from ambient sources that can be used to power portable electronics. Among them, moisture-enabled generators or MEGs are a class of NG that generate electricity from moisture transport mechanisms, giving them a great advantage as water is inherently present in the air everywhere in the world. MEGs are typically made up of conductive materials that form an electric double layer when contacted by water. As water molecules move through a porous material, viscous shear forces create a charge gradient causing a potential difference and inducing current. Inspired by the Earth's hydrological cycle, transpiration-driven electrokinetic power generators (TEPGs) take advantage of transpiration forces using asymmetric wetting mechanisms to increase fluid transport without the need for flowing bodies of liquid water. The present research leverages the biodegradable nature, flexibility, and light weight of lignocellulosic paper and combines them with the excellent properties of carbon nanotubes to prepare electrically-conductive capillary pumps. This innovative papertronics is cost-effective, recyclable, and can be manufactured using easily scalable papermaking processes. As-produced TEPG materials were thoroughly characterized and achieved a sustained open circuit voltage and short circuit current of 225 mV and 7 μ A, respectively, from the transport of a 10 μ L aqueous aluminum sulfate solution. The power output was improved further by using an optimized active electrode design, yielding OCV and SCC values over 1 V and 3 mA, respectively. A single device exhibited an impressive maximum power density of 50 W/kg, which when connected in series and parallel, could supply power for some common electronic systems.

8:30 AM EN02.06.02

Streamlining The Hydration of Micron-Sized Aluminum Particle Surface Towards Enhanced Power Generation [Mahmuda Ishrat Malek](#) and [Michelle L. Pantoya](#); Texas Tech University, United States

Aluminum particles possess a core-shell configuration in which an aluminum core is covered by a passive alumina (Al_2O_3) shell. This Al_2O_3 shell acts as both a heat sink and a barrier for reactions which impedes the process of harnessing the substantial chemical energy potential of Al, which stands at 31MJ/Kg. Hydrating the Al surface has the potential to replace the Al_2O_3 shell with $\text{Al}(\text{OH})_3$, a material with favorable properties for energy extraction. While nano-sized Al particle surfaces can be hydrated by controlling the pH, micron-sized particles require external heating and subsequent aging because of 90% decrease in surface energy. Applying temperature above 35C to Al-water solution can expedite the formation of AlOOH and prolonged aging can lead to excessive consumption of Al core, both of which have adverse effect on the potential energy of the sample. For small amount of Al powder (230mg) controlling the temperature at 35C for a minimum of 18 hrs, $\text{Al}(\text{OH})_3$ shell formation in place of Al_2O_3 can be achieved with 96% Al core still unconsumed. To hydrate a larger amount of powder (2gm) in a short period of time, high temperature (100C) is necessary to produce $\text{Al}(\text{OH})_3$. Heating Al powder for 25mins at this temperature can produce 5% $\text{Al}(\text{OH})_3$ with most of the Al cores (95%) unconsumed. Moving up to 30mins the powders have a trace of 3% AlOOH . TEM images of 18hrs at 35C and 25mins at 100C both have similar fuzzy surfaces. Upscaling the hydration process for micron-sized Al powder can lead to a time-saving method for larger quantities of Al and aid in producing modified shell-core properties that can be exploited for enhancing power generation techniques.

8:45 AM EN02.06.03

Performance Enhancement of Moisture-Induced Power Generators under Ambient Conditions through Flashlight-Induced Graphitization of FeCl_3 -Impregnated Cellulose Papers [Daewoong Kim](#), [Jakyung Eun](#), [Hyunsoo Han](#) and [Sangmin Jeon](#); Pohang University of Science and Technology, Korea (the Republic of)

We introduce a novel approach for the fabrication and performance enhancement of moisture-induced power generators (MPGs) utilizing flashlight-induced graphitization (FIG). FeCl_3 -impregnated cellulose papers (FCPs) were photothermally converted into graphitized cellulose papers (GCPs) with a hierarchically porous structure by flashlight irradiation under ambient conditions. During the photothermal conversion process, Fe^{3+} ions partially convert into iron oxide compounds with limited solubility, highlighting that FeCl_3 serves multiple roles such as catalyst for graphitization, moisture absorber, and charge carrier. When a bilayered cellulose paper (BCP), formed by stacking GCP on top of FCP, was exposed to moisture, a potential difference was generated between the collecting electrodes due to the concentration gradient of dissociated Fe^{3+} ions within the BCP, with higher concentration in FCP

and lower concentration in GCP. The resulting migration of Fe^{3+} ions from FCP to GCP caused electron movement along the external circuit. The BCP-based MPG exhibited continuous voltage and current outputs, with maximum values of 0.39 V for voltage and $28.6 \mu\text{A}/\text{cm}^2$ for current density at 45% relative humidity, marking a significant breakthrough in MPG performance under ambient humidity conditions.

9:00 AM EN02.06.04

Multidimensional Analysis of Moisture-Induced Power Generator Using Quartz Crystal Microbalance Hyerim Baek, Jihun Choi, Hyewon Lee and Sangmin Jeon; Pohang University of Science and Technology, Korea (the Republic of)

A novel quartz crystal microresonator was developed as a moisture-induced power generator (MPG) through constructing an interdigitated electrodes-lateral field excited (IDEs-LFE) quartz resonator. This system enabled the simultaneous measurement of both the electrical output of the MPG and the resonant frequency shift of the quartz crystal (QC) in real time. The SCP film, composed of sodium alginate, carbon nanoparticles and polyvinyl alcohol was coated onto the IDEs which were deposited on the top surface of the QC. Following the coating process, a voltage of 1 V was applied across the IDEs to construct ion concentration gradient, resulting in the generation of electricity during the adsorption of water molecules. Two symmetrical electrodes which were deposited on the bottom surface of the QC were employed to monitor the adsorption of water molecules into the SCP film by measuring the change in resonant frequency during oscillation. By conducting simultaneous measurements of the resonant frequency shift and electrical output under varying humidity conditions, parametric plots were established that correlate the electrical output with the resonant frequency shift. This dynamic interplay between resonant frequency shifts and electrical output provided insights into the impact of moisture adsorption on MPG performance.

9:15 AM EN02.06.05

Electrochemical Kinetic Energy Harvesting Mediated by Ion Solvation Switching in Two-Immiscible Liquid Electrolyte Donghoon Lee¹, You-Yeob Song², Angyin Wu¹, Jia Li³, Jeonghun Yun¹, Dong-Hwa Seo² and Seok Woo Lee^{1,3}; ¹Nanyang Technological University, Singapore; ²Korea Advanced Institute of Science and Technology, Korea (the Republic of); ³Rolls-Royce at NTU Corporate Lab, Singapore

Kinetic energy harvesting (KEH) is the process of converting mechanical energy, typically in the form of motion or vibrations, into electrical energy using specialized devices or systems.[1] KEH is of significance in the realm of renewable energy, as it enables the harnessing of otherwise wasted or underutilized kinetic energy sources, thereby contributing to the development of sustainable power generation and self-sustaining electronic devices.[2] Nonetheless, presently existing techniques, like those relying on friction and deformation, require high-frequency kinetic energy and call for materials possessing exceptional durability.[3] Also, those methods have extremely high impedance, leading to reduced current and power outputs, thus constraining their practical applications.[4]

Herein, we propose an electrochemical KEH system that employs a two-phase immiscible liquid electrolyte, specifically combining aqueous and ionic liquid components, with Prussian blue analogue (PBA) electrodes. This system is designed to capture and harness kinetic energy from gentle and low-frequency mechanical motions while reducing impedance of the system. Starting from the state of equilibrium, where both PBA electrodes are submerged in distinct phases of the immiscible electrolyte, the open-circuit potential difference between these electrodes experiences an increment. This increase in potential difference enables the conversion of kinetic energy, associated with the movement of the electrodes into their respective phases, into electrical energy. The system generated $6.4 \mu\text{W cm}^{-2}$ of peak electrical power, accompanied by 96 mV of peak voltage and $183 \mu\text{A cm}^{-2}$ of peak current density when connected to a load resistor of 300 Ω . The applied load is three orders of magnitude smaller than what is conventional KEH methods. Furthermore, the proposed method demonstrated a continuous current output of around $5 \mu\text{A cm}^{-2}$ over one hundred seconds, at the frequency of 0.005 Hz for 23 cycles without any degradation in performance. Through computational simulations, we have determined that voltage between PBA electrodes originates from the difference in solvation Gibbs free energy within each phase of the two-phase electrolyte. The elimination and subsequent reformation of solvation shells surrounding solvated cations serve as the driving force for both the generation of voltage and the flow of electrons within the system. Moreover, we have effectively demonstrated the capability of our system within a microfluidic device, thereby paving the way for diverse applications. The microfluidic kinetic energy harvester is composed of identical PBA thin-film electrodes and the two-phase electrolyte. By utilizing the conversion of kinetic energy to drive the two-phase electrolyte through the microfluidic channel, our system attained a peak power density of 200nW cm^{-2} . In conclusion, we recognized the possibility of harvesting kinetic energy from solvation Gibbs free energies in the two-phase electrolyte mediated by ion-hosting materials and furnished persuasive evidence of its viability as a power source for self-powered devices. The incorporation of our system into the microfluidic harvester endows it with advantages for powering wearable electronics and Internet of Things (IoT) applications.

Abstract original from, [Preprint] *Research Square*, DOI: 10.21203/rs.3.rs-3296359/v1

[1] *Applied Energy*. 2021, 286, 116518.

[2] *Nano Energy*. 2017, 39, 9-23.

[3] *Energy & Environmental Science*, 2022, 15, 82.

[4] *Nature*, 2020, 578, 392-396.

9:30 AM EN02.06.06

Wearable Device Monitoring Cough with Piezoelectric Energy Harvester as a Simultaneous Sensor and Battery Life Extender Yang Bai, Jaakko Palosaari, Eetu Virta and Miika Miinala; University of Oulu, Finland

Cough is the most common symptom for which individuals seek medical advice. However, wireless and autonomous tools and standards for cough monitoring are lacking, possibly due to issues of measurement reliability and device lifespan. This work utilizes the piezoelectric energy harvesting concept to sense coughing signals. Different from conventional sensing techniques, the piezoelectric harvester here converts energy of muscle movement triggered by cough into electricity which then charges a capacitor, rather than being directly read by the microcontroller. The capacitor will accumulate energy for a certain period and then the capacitor voltage will be read by the microcontroller. This simple change of data collection mechanism magnificently reduces the duty cycle of the entire electronic system whilst maintaining high accuracy of recording the history of coughs. Proven in clinical trials, the battery life of the device has been significantly extended to longer than a week compared to approximately only overnight where conventional sensing techniques are implemented, even if using the same piezoelectric harvester (sensor). The newly developed system can then be used to autonomously monitor and analyze cough data of in-/outpatients for daily, research and clinical purposes and thus to improve prediction and management of severe respiratory diseases.

9:45 AM BREAK

Thursday Morning, April 25, 2024
Room 332, Level 3, Summit

10:15 AM *EN02.07.01

Designing Solid Polymer Electrolytes for Energy Storage and Harvesting [Christopher Li](#), William R. Fullerton and Tongjie Zhang; Drexel University, United States

Solid polymer electrolytes (SPEs), with a unique combination of electrochemical and mechanical characteristics, are promising for a wide range of energy storage and harvesting applications. The molecular architecture and structure of SPEs provide a versatile platform for tailoring materials' properties to suit specific application needs. This presentation will focus on the morphology and network structure effects on ion transport, electrodeposition, and the formation of metal dendrites. We demonstrate that the tortuosity resulting from the morphology of SPEs can be employed to fine-tune ion transport and guide the growth of metal dendrites. On the other hand, mechanically modulating the internal SPE structure can provide an alternative approach to controlling dendrite growth. By tuning SPE's molecular structure and chemistry, we can adjust the electrochemical and mechanical properties for improved battery performance while elucidating how these affect the underlying transport mechanism and electrodeposition behavior.

10:45 AM *EN02.07.02

A Modular Solid-State Electrolyte Platform Based on a Charged Double Helical Polymer [Louis A. Madsen](#); Virginia Tech, United States

Our group has been developing a class of rigid solid electrolytes based on a highly charged double helical polyanion self-assembled with ion-containing fluids. We term this class of materials *molecular ionic composites* (MICs). These materials are highly thermally stable, and can reach ~ 1 GPa tensile modulus and > 1 mS/cm ionic conductivity with only 10-20% polymer content, and even with a substantial loading of cations like Li⁺ or Na⁺. Although MICs are macroscopically solid, the nanoconfined and partially ordered ions inside move only modestly slower (ca. a factor of 3) than in the neat precursor fluid. We can modulate the mechanical, transport, and chemical/thermal stability properties of MICs over wide ranges by changing the content and molecular weight of the polymer, and the chemistry of the ions and other mobile components. I will discuss the state of understanding of MICs, from the dependence of multi-scale morphology and transport on composition and liquid crystallinity, to the influence of specific molecular interactions on properties. I will discuss progress toward practical alkali-metal batteries, as well as extensions beyond our original MIC materials that include (1) segregation of highly Li-conductive nanocrystalline phases, and (2) high modulus thermo-reversible hydrogels.

11:15 AM *EN02.07.03

Coarse-Grained Molecular Dynamics Simulations of Polymer-Grafted Nanoparticle Systems [Lisa M. Hall](#); Ohio State University, United States

Grafting polymer chains to nanoparticle surfaces, creating polymer-grafted nanoparticles (PGNs), allows for nanocomposites with a uniform and controllable distribution of inorganic particles in an organic matrix. Such materials are of interest as membranes for separations and dielectric materials, among other applications. The nanoparticle size, graft length, and graft density together set the interparticle spacing, as well as the degree to which conformations of chains on nearby particles can overlap, which impacts the local and overall material properties. Specifically, at high enough graft densities, the polymer conformations are stretched (brushlike) near the surface, then approach random walk conformations further from the surface if the grafts are long enough. We use a simple, efficient coarse-grained model to study how key controllable parameters such as graft density impact the chain conformations and local and overall properties. In particular, from molecular dynamics simulations, we analyze the structure, segmental and chain dynamics, and mechanical properties for a variety of polymer-grafted nanoparticle systems, including dilute PGNs in solvent and PGN monolayer films. We find an intermediate graft density leads to a relatively precise interparticle spacing along with a significant amount of overlap of polymers on nearby nanoparticles, which provides increased toughness versus high graft density systems.

11:45 AM EN02.07.04

Developing High-Performance Piezoelectric ZnS:Mn²⁺ Nanoparticles for Enhanced Mechanoluminescence and Piezocatalysis [Zhongxiang Wang](#) and Yadong Yin; University of California, Riverside, United States

Piezoelectric materials, featured by their non-centrosymmetric structures and unique charge separation properties under mechanical stimulation, hold significant promise for applications spanning pressure sensing, optogenetics, and piezocatalysis. However, existing materials often exhibit large particle sizes, posing challenges in specific applications like optogenetics, where nanoscale dimensions are required for barrier-free circulation through blood vessels. Furthermore, reducing particle size to the nanoscale offers increased surface area and enhanced reactant adsorption, a pivotal factor in catalytic performance. Thus, developing a straightforward method to produce highly piezoelectric nanomaterials is of great significance. Herein, we introduce a novel approach for synthesizing ZnS:Mn²⁺ nanoparticles, employing the self-assembly of ZnS:Mn²⁺ quantum dots, followed by high-temperature calcination. During calcination, the ZnS:Mn²⁺ quantum dot assemblies transform into individual nanoparticles, accompanied by a phase transition from sphalerite to wurtzite structure. This sintering process is spatially confined within a silica layer, preventing nanoparticle interconnection. Subsequent etching of the silica layer using NaOH results in ZnS:Mn²⁺ nanoparticles with an average size of approximately 150 nm. These ZnS:Mn²⁺ nanoparticles exhibit exceptional piezoelectricity, featuring a piezoelectric coefficient (d_{33}) of up to 25 pm/V as measured via Piezoresponse Force Microscopy (PFM). Notably, this d_{33} value is around eight times higher than the literature-reported d_{33} value of ZnS (3.2 pm/V). It is worth mentioning that the d_{33} value exhibits variations dependent on calcination temperature and duration. Furthermore, the ZnS:Mn²⁺ nanoparticles display robust mechanoluminescence, both when dispersed in a PDMS film and an aqueous solution under focused ultrasound excitation. This mechanoluminescent emission from the nanoparticles has potential applications in controlling neural stem cell activities. Moreover, the piezoelectric ZnS:Mn²⁺ nanoparticles demonstrate excellent performances in piezocatalytic dye degradation, effectively decomposing organic dyes like rhodamine B and methylene blue. The degradation process is attributed to the generation of reactive oxygen species from the combination of charge carriers and OH[•]/O₂ in the solution, a mechanism supported by Electron Spin Resonance (ESR) measurements. The introduction of h⁺, hydroxyl radical, and superoxide radical scavengers into the reaction system significantly reduces the degradation rate, further substantiating the catalytic mechanism. Compared to undoped ZnS nanoparticles synthesized in a similar manner, ZnS:Mn²⁺ nanoparticles exhibit superior piezocatalytic performance due to defect-induced polarization. Intriguingly, both mechanoluminescence and piezocatalysis are contingent on the non-centrosymmetric wurtzite structure of ZnS and its associated defect-induced polarization, each showcasing different optimal dopant concentrations and operating under distinct ultrasound frequencies.

Thursday Afternoon, April 25, 2024
Room 332, Level 3, Summit

1:30 PM EN02.08.01

Soft-Matter Engineering for Thermoelectric Wearables with Unprecedented Power Generation [Youngshang Han](#) and Mohammad H. Malakooti; University of Washington, United States

Stretchable thermoelectric generators (S-TEGs) have recently drawn attention since they can compliantly be attached to complex surfaces to induce temperature change or harvest electricity from waste heat. Unlike conventional thermoelectric modules that are rigid and brittle, flexible thermoelectric devices commonly comprise elastic polymers with encapsulated semiconductor pellets. This stretchable device architecture also provides conformal contact with curved surfaces such as the human body. We have designed multifunctional elastomer composites to enhance the heat management and deformability of these emerging TEGs. Our approach involves dispersing liquid metal droplets within elastomers to create liquid metal elastomer composites (LMECs). LMECs with microdroplets exhibit high thermal conductivity while remaining electrically insulating, serving as thermal interface materials in the devices. Additionally, we have embedded hollow thermoplastic microspheres in the base elastomer to synthesize soft matter with low thermal conductivity, which separates the top and bottom thermal interface layers and encapsulates the semiconductor pellets. The difference between the conductivity of the two elastomer composites facilitates a larger heat flux in thermoelectric semiconductors, leading to improved device performance.

In this talk, we will begin with a brief overview of TEGs that utilize liquid metals and bismuth telluride semiconductors. Following this introduction, we will present our new findings on the design rationale of S-TEG, focusing on the improvement of energy harvesting performance at low-temperature gradients, along with enhancing mechanical resilience and stretchability. In particular, we will highlight the essential role of device structure in thermoelectric energy conversion, utilizing both numerical simulations and experimental analyses to illustrate our findings. The resulting S-TEG design is optimized for efficient thermal management, resulting in a notable power harvesting performance increase, exceeding baseline levels by more than sixfold. The electromechanical and energy harvesting characterization of this engineered S-TEG will be presented to showcase its full potential for a range of emerging applications. To conclude, we will explore the practical applications of these thermoelectric generators across various use cases.

1:45 PM EN02.08.02

Nanocomposite Ceramics Materials for Energy Harvesting and Heat Management Zouhair Hanani¹, Brigita Rozic¹, Daoud Mezzane², Mimoun El Marssi³, Anna Morozovska⁴, Serhii Ivanchenko³, Hana Uršič¹, Matjaz Spreitzer¹ and [Zdravko Kutnjak](#)¹; ¹Jozef Stefan Institute, Slovenia; ²University Cadi Ayyad, Morocco; ³University of Picardie Jules Verne, France; ⁴National Academy of Sciences of Ukraine, Ukraine

Today's quest for sustainable energy solutions through greener energy harvesting and heat-management technologies has recently developed a significant interest in new flexible and biocompatible nanocomposite ceramics with large electromechanical, triboelectric, and electrocaloric (EC) effects [1]. Therefore, an overview of experimental and theoretical investigations of the large EC, piezoelectric, and triboelectric response in flexible ceramic nanocomposites exploiting enhanced multiferroic properties of ferroelectric nanoparticles within the polymer matrix will be presented in this contribution. Specifically, the enhanced EC response in lead-free BCZT and BaTiO₃-based nanoparticles will be reviewed, including flexible polymer composites' large energy harvesting potential [2]. The impact of filler's dielectric permittivity and aspect ratio in high-k polymer and the benefits of combining 1D and 3D nanofillers on enhanced properties of flexible nanocomposites will be discussed [3]. [1] Z. Kutnjak., B. Rozic, R. Pirc., Wiley Encyclopedia of Electrical and Electronics Engineering, 1-19 (2015). [2] Z. Hanani et al., Nano Energy 81, 105661 (2021). [3] Z. Hanani et al., Nanoscale Adv. 4, 4658 (2022).

2:00 PM EN02.08.03

Soft Caloric Materials for Green Cooling Technologies Devid Cresnar¹, Matic Morgan¹, Bostjan Zalar¹, Samo Kralj², Zdravko Kutnjak¹, Gregor Skacej³ and [Brigita Rozic](#)¹; ¹Jozef Stefan Institute, Slovenia; ²FNM, University of Maribor, Slovenia; ³FMF, University of Ljubljana, Slovenia

With increased environmental awareness, the search for an environmentally friendlier heat-management device has been the topic of many scientific studies. Materials with large caloric effects, such as the electrocaloric (EC) and elastocaloric (eC) effects, have the promise of realizing new solid-state refrigeration techniques. A review of recent direct measurements of the large EC effect in liquid crystals (LCs) and large eC effect in liquid crystal elastomers (LCEs) [1, 2] will be given in this contribution, including the application aspect. In particular, in smectic LCs and mixtures of LCs with functionalized nanoparticles, the EC effect exceeds 8 K and the eC in main-chain (MC) LCEs exceeds 2K with the eC responsivity about three orders of magnitude larger than the average eC responsivity found in the best shape memory alloys. However, both soft materials can play a significant role as active cooling elements and parts of thermal diodes or regeneration material in developing new cooling devices. [1] D. Črešnar et al, J. Phys. Energy 5: 045004, 2023. [2] A. Rešetič et al, Nat Comm 7: 13140, 2016.

2:15 PM EN02.08.04

Direct Thermal-To-Pneumatic Body Heat Harvesting to Power Soft Actuators [Marquise D. Bell](#), Aman I. Eujayl, Sofia Urbina, Anoop Rajappan, Barclay J. J. Te Faye Yap, Evan Noce, Megan Enriquez and Daniel J. Preston; Rice University, United States

Wearable assistive devices have emerged as a viable aid in performing activities of daily living for people with physical disabilities, a group representing up to 27% of the U.S. adult population [1]. In particular, soft wearable assistive devices—most of which are pneumatically actuated [2]—can help those with limited mobility and dexterity caused by physical disabilities. A common limitation of these pneumatic assistive devices, however, is that they typically require a tether to an external pressure source, limiting adoption. Researchers have attempted to address this limitation by investigating methods to use the human body itself as a power source through various energy harvesting techniques, including implementation of piezoelectric, triboelectric, and thermoelectric devices [3,4]. However, these electronic energy harvesting approaches require multiple energy conversion steps for operation of pneumatic assistive devices (i.e., a mechanical or thermal input is converted first to electrical energy and then finally to pneumatic energy).

To address these energy conversion limitations, mitigate portability concerns caused by tethers to external power sources, and appeal to a larger percentage of those with physical disabilities, we developed a wearable textile-based system that bypasses the intermediate electrical conversion step by directly converting heat harvested from the body to pneumatic energy using a low-boiling-point fluid (LBPF). Our system consists of two pouches—a “warm” and “cool” pouch, thermally insulated from one another—where heat emitted from the body vaporizes a LBPF in the warm pouch to drive pneumatic actuation. After actuation, the vapor phase of the LBPF is recovered via condensation in the cool pouch, which is exposed to the lower temperature of the ambient compared to that of the body. Following eventual depletion of the LBPF in the warm pouch after a number of actuation cycles, the device can be flipped, placing the now-fluid-filled cool pouch in contact with the user to continue to vaporize the LBPF in a repeatable manner.

We characterized the system performance by modeling the transient pressure response, power output, efficiency, and life cycle of the device and compared modeling results with experiments, as well as with comparable thermal-to-electronic energy harvesting devices used in wearables in prior work. Our model uses fundamental thermodynamic and heat transfer principles to show how the frequency of operation and geometry of the device affect the overall system

performance. We also demonstrated the practicality of this system with a user applying the device to pneumatically actuate an assistive actuator for grasping. This work enables the use of body heat as a viable power source for pneumatically actuated assistive devices that can be used to enhance mobility assistance.

- [1] CDC, "Disability Impacts All of Us Infographic | CDC," Centers for Disease Control and Prevention. Accessed: Oct. 15, 2023.
[2] B. Jumeat, M. D. Bell, V. Sanchez, and D. J. Preston, "A Data-Driven Review of Soft Robotics," *Adv. Intell. Syst.*, vol. 4, no. 4, p. 2100163, 2022.
[3] Z. Zhou *et al.*, "Smart Insole for Robust Wearable Biomechanical Energy Harvesting in Harsh Environments," *ACS Nano*, vol. 14, no. 10, pp. 14126–14133, Oct. 2020.
[4] Y. Liu *et al.*, "Advanced Wearable Thermocells for Body Heat Harvesting," *Adv. Energy Mater.*, vol. 10, no. 48, p. 2002539, 2020.

SESSION EN02.09: Poster Session II
Session Chairs: Jinbo Bai and Andris Sutka
Thursday Afternoon, April 25, 2024
Flex Hall C, Level 2, Summit

5:00 PM EN02.09.01

Printed Triboelectric Nanogenerator Incorporating MXene-Enhanced PVBVA for Skin-Interactive Devices and Touch-Sensing Arrays [Ajay Pratap](#)¹, Isaac Little¹, Fereshteh Rajabi Kouchi¹, Hailey Burgoyne¹, Naqsh Mansoor¹, Tony Varghese¹, Zhangxian Deng^{1,1,2}, and David Estrada^{1,1,2}; ¹Boise State University, United States; ²Idaho National Laboratory, United States

The adoption of soft contact structure designs in triboelectric nanogenerators (TENGs) has been a favored approach to enhance their durability. However, this method often presents a significant challenge to achieving high output performance. TENGs are often limited by their reliance on specific tribo-materials, which can restrict their practicality and performance. To address these limitations, we use additive electronics manufacturing methods for TENG fabrication, which enables energy generation from various tribomaterials, including human skin [1-3]. Our innovation lies in the integration of a high-performance polymer, Poly (*vinyl butyral-co-vinyl alcohol-co-vinyl acetate*) (PVBVA), with Ti₃C₂ MXenes [4], two dimensional transition metal carbides etched from the Ti₃AlC₂ MAX phase ceramics. Inks from these materials are formulated for microdispense printing and printed onto aluminum substrates using a Hyrel extrusion printer. This combination significantly enhances the triboelectric properties of the manufactured TENG device. Our findings show that the PVBVA layer alone yields a triboelectric output of approximately 110 V. However, with the introduction of MXene at a concentration of 2.75 mg/ml, the output escalates to 150 V, and further increases to 250 V at a concentration of 5.5 mg/ml, demonstrating a substantial enhancement in performance. Beyond energy harvesting, we leveraged this TENG technology in a water energy harvesting system, effectively extracting energy from sources such as raindrops. Additionally, we developed a 2 x 2 touch sensor array utilizing this technology. This sensor array can generate charge through the triboelectric effect and dynamically map the output voltage values in response to touch, showcasing its potential for human-machine interaction and touch-sensitive interfaces.

In summary, our research introduces a groundbreaking approach to TENG fabrication by combining 3D printing technology with a PVBVA-MXene composite. This leads to TENGs with markedly improved triboelectric performance. The versatility of these TENGs not only enables efficient energy harvesting from environmental sources like rain but also holds significant promise for applications in touch-sensitive devices. This makes them a valuable asset for developing self-powered devices and interactive interfaces in fields such as healthcare and robotics.

References: [1] Sun, Y.; Li, Y.Z.; Yuan, M. Requirements, challenges, and novel ideas for wearables on power supply and energy harvesting. *Nano Energy* **2023**, *115*, 108715. [2] Wang, W.; Xu, L.; Zhang, L.; Zhang, A.; Zhang, J. Self-Powered Integrated Sensing System with In-Plane Micro-Supercapacitors for Wearable Electronics. *Small* **2023**, *2207723*. [3] An, B.W.; Shin, J.H.; Kim, S.Y.; Kim, J.; Ji, S.; Park, J.; Lee, Y.; Jang, J.; Park, Y.G.; Cho, E.; Jo, S. Smart sensor systems for wearable electronic devices. *Polymers* **2017**, *9*(8), 303. [4] Naguib, M.; Kurtoglu, M.; Presser, V.; Lu, J.; Niu, J.; Heon, M.; Hultman, L.; Gogotsi, Y.; Barsoum, M.W.; Two dimensional nanocrystals produced by exfoliation of Ti₃AlC₂. *Adv. Mater.* **2011**, *23*(37), 4248–4253.

5:00 PM EN02.09.02

Solvo-Voltaic Energy Harvesting for Distributed Electronic Systems Jihpeng Sun, Jongbin Won and [Albert T. Liu](#); University of Michigan–Ann Arbor, United States

Electricity is the central energy currency in artificial programmable systems, akin to the role ATP plays in biological systems. Next-generation off-the-grid electronic systems call for alternative modes of energy harvesting. With numerous engineering possibilities in areas like circulating medical diagnostic devices and remote sensors in previously inaccessible locations, the Achilles' heel for such an electronic system at an extremely small length-scale has by and large been the energy constraint. While there has been tremendous progress toward improving the energy and power densities for traditional energy storage devices such as microbatteries and supercapacitors, their disadvantageous volumetric scaling poses fundamental constraints on important energy metrics that limit the application space of these electricity-demanding on-board electronics. To bridge this energy gap, we explore different liquid-based energy harvesting methods more broadly known as the 'solvo-voltaic' effect, a phenomenon whereby various local energy inputs are converted into electricity within a quantum-confined nanostructure (*e.g.*, single-walled carbon nanotube, or SWCNT) by virtue of interactions with the surrounding solvent molecules. This technique stands out as a promising candidate to complement existing energy generation schemes like the photovoltaics, whose utility is diminished where visible light is not present, such as in the body.

5:00 PM EN02.09.03

Suppressing Conduction Losses of Polymer Composites Dielectrics for High-Temperature Capacitive Energy Storage [Minhao Yang](#), Yanlong Zhao and Zepeng Wang; North China Electric Power University, China

Electrostatic capacitor that capitalizes on the rapid electric field-induced polarization and depolarization effects in dielectric materials to store and release electrical energy is one of the most important passive components in modern electronic devices and electrical power systems. The energy storage performance of electrostatic capacitors is mainly determined by the dielectric inside. Compared with inorganic dielectrics, polymer dielectrics from synthetic resins exhibit stable dielectric performance over a wide range of frequencies, superior high voltage endurance, excellent flexibility and processing properties. High-temperature resistance ability of polymer dielectrics is extremely important for the harsh operating environment with high temperature requirements. Nevertheless, most polymer dielectrics are more vulnerable to high temperatures due to their low glass transition temperature (T_g). The capacitive performance of polymer dielectrics degrades rapidly at high temperatures and electric fields, which is mainly attributed to the exponential increase of conduction loss. The increased leakage current further leads to an undesirable temperature rise inside the polymer dielectrics and consequently accelerates the thermal runaway of capacitors. Therefore, inhibiting the conduction loss of polymer dielectrics is extremely important for high-temperature

capacitive performance.

The bulk-limited conduction and electrode-limited conduction are the two main mechanisms inside the polymer dielectrics. With increasing the electric field and temperature, more trapped charge carriers are thermally activated to overcome the potential barrier of traps, even though the carrier energy is lower than the maximum energy of the potential barrier, and participate in the electrical conduction. Therefore, the conduction loss inside polymer dielectrics displays an exponential growth with temperature under high electric field. Introducing more deep charge traps is beneficial to suppress the bulk-limited conduction. Incorporating a small amount of wide bandgap inorganic fillers or small organic molecules with strong electronegativity into the high-temperature resistant polymer dielectrics is an effective method to increase the density of deep traps and trap depth. These fillers can act as trap centers to immobilize the charge carriers and constrain their mobility inside polymer composites, accordingly leading to the reduction in conduction loss. As for the electrode-limited conduction loss, charge carriers from the electrode can gain sufficient energy provided by thermal activation to overcome the energy barrier at metal-dielectric interface and increase the conduction loss. increasing the barrier height at the electrode/polymer interface is helpful for the suppression of electrode-limited conduction loss. Inserting a charge-blocking layer such as highly insulated inorganic and organic layers between the electrode and polymer dielectric can significantly increase the barrier height for the charge injection from the electrode.

From this, we unify the bulk and electrode-limited conduction losses and simultaneously suppress these two types of conduction loss through the surface engineering of polymer composites dielectrics. The leakage current at high temperatures and electric fields is significantly inhibited and the breakdown strength is greatly improved compared with un-modified polymer dielectrics. Accordingly, the polymer composites dielectrics exhibit superior capacitive performance with high discharged energy density and discharge-charge efficiency at high temperatures.

5:00 PM EN02.09.04

Printed Piezoelectric Transducers for Highly Integrated Motion, Vibration and Magnetic Waves Harvesting: From Simulation-Guided Design to High-Throughput Fabrication Philipp Schöffner, Asier Alvarez Rueda, Oliver Werzner, Andreas Petritz, Jonas Groten and Barbara Stadlober; Joanneum Research Forschungsgesellschaft mbH, Austria

Many application fields for energy harvesting require compact devices featuring a high integration density that can be realized with low-cost, high-throughput fabrication methods. We present multiple types of energy harvesters (EH) based on compact printed piezoelectric transducers for energy harvesting of motions, vibrations and magnetic stray fields in home and industrial environments. The EH design is guided by FEM simulations to optimize both conversion efficiency and electrical output characteristics to meet the requirements of low-power IoT electronics. For smart wearable and healthcare applications, we have previously demonstrated a 2.5 μm thin imperceptible energy harvesting device with integrated, ultraflexible organic diodes for rectification.^[1] Most recently, we accomplished a few millimeter thin smart floor piezoelectric harvester that generates up to 6 $\mu\text{J}/\text{step}$ at only 1 mm vertical displacement.^[2] For harvesting of machine vibrations under realistic conditions, we demonstrate an energy harvesting system tuned to the main vibration frequency (50 Hz) of an electric vacuum pump. It is capable of harvesting up to 138 mJ per day, which is sufficient to power a wireless sensor node for condition monitoring of the engine.^[3] Finally, we will take a look at the simulation-driven design of weak magnetic stray field ($\sim 100 \mu\text{T}$) harvesters with in-situ tunable resonance frequency and < 1 mm displacement amplitude.

[1] Petritz, A. et al. Imperceptible energy harvesting device and biomedical sensor based on ultraflexible ferroelectric transducers and organic diodes. *Nat. Commun.* 12, 2399 (2021). <http://dx.doi.org/10.1038/s41467-021-22663-6>

[2] Rueda, A. A. et al. Optimization and realization of a space limited sens-PEH for smart floor applications. *Nano Energy* 109248 (2023). <https://doi.org/10.1016/j.nanoen.2023.109248>

[3] Rueda, A. A. et al. Low-frequency vibrational energy harvesting with fully printed multi- and single stack piezoelectric transducers. *Under review*

5:00 PM EN02.09.05

Ultra-High Durability and Performance of a Proton Composite Membrane containing long-Chain Amino Sulfonated Poly(arylene ether) and Cerium Oxide-Titanium Carbide over 1000 Hours for Hydrogen Fuel Cells Ae R. Kim, Milan B. Poudel and Iyappan Arunkumar; Jeonbuk National University, Korea (the Republic of)

As a key component of proton exchange membrane fuel cells (PEMFCs), the durability of the proton exchange membranes (PEMs) directly determines the service life of the PEMFCs. In this study, poly(arylene ether) containing amino and trifluoromethyl units (AFPAE) was synthesized by nucleophilic aromatic polycondensation followed by nucleophilic substitution to obtain butyl sulfonated poly(arylene)(SAFPAE). $\text{CeO}_2\text{-TiC}$ prepared by the hydrothermal process were incorporated into the SAFPAE matrix and the content of the $\text{CeO}_2\text{-TiC}$ was optimized. The morphological, physicochemical, and electrochemical investigation of the prepared membranes demonstrated that the random dispersion of the $\text{CeO}_2\text{-TiC}$ in the SAFPAE matrix improves the thermal and mechanical stability as well as water adsorption, ion exchange capacity and proton conductivity. Particularly, the optimized SAFPAE/ $\text{CeO}_2\text{-TiC}$ exhibited high current output and power output at 20% relative humidity and 60 °C outperforming commercial membranes. Most importantly, the SAFPAE/ $\text{CeO}_2\text{-TiC}$ composite membrane demonstrated MEA durability over 1100 h under low humidity 20% RH operating conditions and was about 4.4 times more stable than pristine SAFPAE. SAFPAE with a special structure of hydrophilic backbone containing trifluoromethyl group and long aliphatic sulfonic acid group to create nano-sized proton conduction channels whereas, TiC provides mechanical support and CeO_2 improves the durability of PEM by scavenging free radicals. Therefore, the SAFPAE/ $\text{CeO}_2\text{-TiC}$ composite membrane reported in this study is a potential candidate for high-performance and durable PEMFC, suggesting its applicability in future large-scale PEMFC.

5:00 PM EN02.09.06

Synthesis Characterization and Electrochemical Evaluation of Quaternized Poly(2,6-dimethyl-1,4-phenylene oxide)/Ionic Liquid Composite Membrane for Anion Exchange Membrane Fuel Cell Application Ramasamy Gokulapriyan, Beom Ho Kim, Hyo Bin Kwak and Dong J. Yoo; Jeonbuk National University, Korea (the Republic of)

Quaternized poly(2,6-dimethyl-1,4-phenylene oxide) (QPPO) serves as a polymer electrolyte membrane facilitating hydroxide ion conduction, whereas with limited hydroxide conductivity and certain physicochemical drawbacks. To address this, modifications are necessary to enhance its overall performance. Composite membranes of QPPO and an ionic liquid were fabricated using the solvent casting technique. The ionic liquid, which contains quaternized imidazole groups, enhances hydroxide transport pathways within the QPPO membrane. Varying weight % of the ionic liquid were incorporated into the QPPO membrane during fabrication. The role of the ionic liquid in the QPPO membrane is to increase the bound water content and develop a hydrogen bonding network with the hydroxide ion transport channels, thereby increasing the hydroxide ion conductivity. Remarkably, the optimized QIL-8% composite membrane exhibits superior hydroxide conductivity compared to the QPPO membrane, achieving 135 mS cm^{-1} at 90 °C, while the QPPO membrane reached 56 mS cm^{-1} at the same temperature. Additionally, the QPPO/ionic liquid composite membranes exhibit appreciable water uptake, swelling ratio, thermal, and mechanical properties. In single-cell tests, the QIL-8% composite membrane achieves a maximum power density of 328 mW cm^{-2} at 60 °C, under conditions of 70% humidity on the anode side, 100% humidity on the cathode side, and an H_2/O_2 flow rate of 100/200 mL min^{-1} . Overall, this study illustrates the enhancement of QPPO membrane performance through the incorporation of synthesized ionic liquids.

5:00 PM EN02.09.07

Efficient Hot Electron Transfer and Improved Lifetime of Charge Carriers at The 1P Hot State in Sb₂Se₃/CdSe p-n Heterojunction [Arshdeep K. Sohal](#)¹, Tanmay Goswami¹, K. Justice Babu¹ and Hirendra N. Ghosh²; ¹Institute of Nanoscience and Nanotechnology, India; ²National Institute for Science Education and Research, India

Utilization of hot carriers is very crucial in improving the efficiency of solar energy devices. In this work, we have fabricated Sb₂Se₃/CdSe p-n heterojunction through cation exchange process for the very first time and explored their interfacial photophysical processes with help of ultrafast transient absorption spectroscopy. In the transient study, the heterosystem was consisted with both the signature of Sb₂Se₃ and CdSe. Interestingly, the 1P excitonic bleach was found to be more prominent in the heterosystem. This is itself a testimony for hot electron migration from Sb₂Se₃ to CdSe QDs. From the comparative dynamic profiles, we found that both the 1P and 1S bleach signals are slower in the heterosystem, which again substantiates the electron migration phenomena. In fact, the hetero-system slowed down the 1P signal more efficiently than that of the 1S one. This is an incredible observation, as hot electron migration influenced the separation of charge carriers in a hot excitonic state (1P), not in the usual lowest excitonic state (1S). Enhanced charge carrier lifetime of the hot state would be helpful in the extraction of those charge carriers in a device set up. Our detailed spectroscopic investigation in this p-n heterojunction would help in the fabrication of many new heterojunctions and uplift the field of condensed matter based opto-electronic devices.

5:00 PM EN02.09.08

Machine Alignment Methods for Precision Roll-Forming of A5052 Aluminum Sheets: Achieving Smooth Finishes and Microstructure Evaluation. [Krishna S. Bhandari](#); Jeju National University, Korea (the Republic of)

The roll-forming process stands as a crucial technique in shaping metal sheets across diverse industries, ranging from jewelry and aerospace to the automobile sector. Ongoing research endeavors center on achieving precision in shaping and minimizing defects, with a particular focus on challenges like spring-back—the tendency of a metal sheet to revert to its original shape post-formation. This scientific investigation has a dedicated purpose: to enhance the alignment of roll-forming machines, thereby ensuring the production of precise and smooth profiles. The study places special emphasis on a5052 aluminum sheets, a material prevalent in various industrial applications. Delving into the specifics, the research scrutinizes the intricacies of roll-forming a5052 aluminum sheets, providing a comprehensive examination of the associated challenges and opportunities. Beyond this, the study explores the integration of cutting-edge technologies to optimize the alignment and formability of roll-forming machines. These technologies encompass laser alignment, real-time feedback sensors, CNC systems for precise control, machine learning algorithms for adaptive processes, and finite element analysis for comprehensive simulation. The overarching objective is clear: to optimize both the alignment and formability of the roll-forming process, which will be used in sensor-making technology to additive manufacturing and nanomaterials. Through this, the research aims to contribute to the advancement of manufacturing techniques, ensuring the production of high-quality and accurately shaped metal profiles and materials across various industrial applications.

5:00 PM EN02.09.10

A Skin-Wearable Triboelectric Nanogenerator for Self-Powered Motion Monitoring and Energy Harvesting [Agha A. Jan](#), Seungbeom Kim, Junhyung Kim, Sangyeop Lee, Uhyeon Kim and Seok Kim; Pohang University of Science and Technology, Korea (the Republic of)

Self-powered and wearable pressure sensors based on triboelectric nanogenerators (TENGs) have gained attention as promising candidates for tactile sensing and energy harvesting because of their design compatibility and ability to operate at low frequencies. While much research has focused on enhancing tribo-negative materials for flexible TENGs, the limited choices for tribo-positive materials have been a limiting factor. A crucial challenge in the development of wearable sensors is achieving biocompatibility without compromising broad-range sensitivity and energy-harvesting capabilities. Here we report a TENG based skin-wearable and self-powered pressure sensor by a simple fabrication using layer by layer deposition method. The flexible layered triboelectric nanogenerator (L-TENG) features a dielectric-to-dielectric configuration, with polytetrafluoroethylene (PTFE) and polymethyl methacrylate (PMMA) films serving as negative and positive triboelectric layers, respectively. These layers are sandwiched within a flexible and biocompatible polydimethylsiloxane (PDMS) matrix. A nanostructured PDMS surface obtained by oxygen plasma served as the structural backbone for the bottom indium tin oxide-copper electrode and overlying tribo-positive PMMA layer. The self-powered L-TENG sensor exhibited a broad range dual pressure sensitivity of 7.287 mV/Pa for low pressure and 0.663 mV/Pa for higher pressure ranges. Additionally, the L-TENG sensor adeptly detected physiological motions such as wrist extension and flexion, and finger bending angles while efficiently harvesting wasted energy from routine physical activities like walking and jogging. Notably, the maximum peak-to-peak voltages of 18.3 V and 57.4 V were measured during these motions. The L-TENG holds vast potential in wearable technology, spanning applications in healthcare, human-machine interfaces, and the powering of microelectronics from physical activities.

Keywords: skin-wearable, self-powered, wearable pressure sensing, triboelectric nanogenerator (TENG), energy harvesting, human motion monitoring

5:00 PM EN02.09.11

Tribovoltaic Devices based on Sliding Contact TiO₂ Films [Andris Sutka](#)¹, Kaspars Malnieks¹, Peter C. Sherrell² and Osvalds Verners¹; ¹Riga Technical University, Latvia; ²RMIT University, Australia

Tribovoltaic (TV) devices are motion-based energy harvesters with high local current densities that can be generated. Debate remains surrounding the fundamental charge generation mechanism of TV devices. Here, we study the charge generation mechanism for TV device fabricated from thin films of the world's most common oxides, TiO₂. We compare the TV performance under contact with metals of varying work functions, contact areas, and applied pressure. The resultant current density shows little correlation with the work function of the contact metal and a strong correlation with the contact area. Considering other effects at the metal–semiconductor interface, the thermoelectric coefficients showed a clear correlation with the tribovoltaic current density. We put in front the need to consider a variety of mechanisms to understand the tribovoltaic effect and design future exemplary TV devices.

SESSION EN02.10: Energy Harvesting Devices and Applications

Session Chairs: Jinbo Bai and Rusen Yang

Friday Morning, April 26, 2024

Room 332, Level 3, Summit

8:30 AM *EN02.10.01

Surface Charge Effects: An Advantage for Enhancing The Piezoelectric Conversion Efficiency in GaN NWs [Noelle Gogneau](#)¹, Pascal Chretien²,

Amaury Chevillard¹, Tanbir Kaur Sodhi^{1,2}, Szu-wei Chen¹, Laurent Couraud¹, Laurent Travers¹, Jean-Christophe Harmand¹, François Julien¹, Maria Tchernycheva¹ and Frederic Houze²; ¹Center for Nanosciences and Nanotechnologies, France; ²Group of Electrical Engineering of Paris, France

For powering micro-devices with strong dimension constraints (smaller than 1 cm² or 1 cm³), it is crucial to develop ultra-compact piezoelectric nanogenerators characterized with a high conversion efficiency per surface/volume unit. To reach this objective, we must both improve the electromechanical conversion efficiency of the active material and optimize the generator design to maximize the piezoelectric system performances in response to the environmental mechanical and vibration inputs.

1D-nanostructures have emerged as system of interest for developing ultra-compact piezoelectric generators. This interest lies in their quasi-lattice perfection and large surface-to-volume ratio, which confer to NWs larger degree of elastic deformation without mechanical deterioration and higher sensitivity to applied forces in comparison with their 2D-film counterparts and conventional bulk piezoelectric materials. In addition, sub-100 nm-wide NWs present the particularity to exhibit specific properties that can lead to a strong modulation of their characteristics. Among these “new properties”, we can cite the exaltation of the piezoelectric coefficients, the formation of nano-contact at the NW/electrode interface allowing an enhanced energy harvesting, or the modulation of the free carrier concentration due to the surface charge (SC) effects. Regarding this last property, simulations have recently established that these SC effects can be advantageous for improving the piezoelectric response of the NWs, since they can limit, in given conditions, the screening by the free carriers of the piezoelectric charges.

Since the expression of the SC effects depends on the NW dimensions and on the NW environment (in other terms of the soft matrix embedding them into nanogenerator devices), the in-depth understanding of the relationship between the SC effects and the piezoelectric conversion capacities of the NWs is now a prerequisite for further improving the device performances and thus approaching a future technological transfer.

To investigate the SC effects in sub-100 nm-wide GaN NWs, we use a systematic multi-scale analysis going from the growth of the GaN NWs by plasma-assisted Molecular beam epitaxy and their possible post-treatment for modulating their surface trap density, to the fabrication and testing of piezoelectric nanogenerators, passing through the characterization of single NWs using nano-characterization tools based on atomic force microscope equipped with electrical modules.

We experimentally highlight that the electromechanical coupling coefficient of GaN NWs is strongly affected by the expression of the SC. By finely adjusting the NW dimensions, we demonstrate that the SC effects can be advantageous for strongly improving the electromechanical conversion efficiency of GaN NWs up to 43%. We also establish that the piezoelectric response of the GaN NWs is sensitive to their direct environment. We confirm experimentally that the SC are useful for improving the piezo-conversion, and evidence that by properly engineering the GaN NWs surfaces, the piezoelectric response of the GaN NW-based nanogenerators can be enhanced. Finally, by architecting the nanogenerator design with regard to the deformation mode (direct compression or vibration) and the targeted application, we demonstrate generated power density in the $\mu\text{W-mW/cm}^3$ range in response to mechanical inputs miming the environmental ones (equivalent forces of few Newton in the 1-200 Hz frequency range).

9:00 AM EN02.10.02

Versatile Thiol-Amine Chemistry for The Synthesis of Complex Chalcogenides and Chalcogenides: New Opportunities to Develop Earth-Abundant Materials for Energy Applications Ivan Caño Prades¹, David Rovira Ferrer¹, Maykel Jiménez Guerra¹, Jonathan Turnley², Marcel Placidi¹, Joaquim Puigdollers¹, Rakesh Agrawal² and Edgardo Saucedo¹; ¹Universitat Politècnica de Catalunya, Spain; ²Purdue University, United States

Earth-abundant chalcogenides and chalcogenides are garnering substantial attention as innovative semiconductors compatible with solar energy harvesting, thermoelectric, pyroelectric applications and other optoelectronic technologies.¹ Among them, van der Waals materials possess an anisotropic crystal structure resulting from covalently-bonded ribbons along one crystallographic direction, which leads to unique electrical properties (e.g. enhanced carrier transport) when the material is correctly oriented. Among recent successes Sb₂(S,Se)₃ solar cells have achieved efficiencies above 10%², and SbSX (X=I,Br) micro-scale devices have been synthesized for the first time showing excellent optoelectronic properties³. However, although the synthesis techniques used so far have enabled significant progress, it is necessary to explore manufacturing routes that are more cost-effective, scalable and versatile in terms of composition and chemical doping.

Molecular precursor ink deposition is an excellent approach for thin film synthesis, being a low-energy, low-cost and versatile method, allowing various compositional analysis by modifying the stoichiometry of the precursor solutions, its integration into distinctive scalable deposition methods (including roll-to-roll coating), and deposition on flexible and non-planar substrates. In particular, thiol-amine solvent systems have recently demonstrated great potential to synthesize chalcogenide compounds (typically poorly soluble in polar solvents), producing promising results for Cu₂ZnSnS₄ and BaZrS₃, but there is still little information regarding van der Waals materials with low-dimensionality.^{4,5}

In this work, Sb₂Se₃, Sb₂S₃ and Sb₂(S,Se)₃ thin films have been synthesized by dissolving either the chalcogenide itself or the constituent elements into different mixtures of ethandithiol and amines/diamines, followed by spin-coating and a short hot-plate annealing at 300 C. Then, different post-deposition treatments have been explored using a tubular furnace under chalcogen atmosphere to coalesce crystallites and to selectively orient texture in the (001) direction, improving the quality of devices. Additionally, different doping strategies have been investigated to tune the conductive type and carrier concentration. For n-type doping, Sb₂Se₃ samples have been prepared incorporating NH₄Cl and SbCl₃ to the precursor solution (Cl-doping).⁶ On the other hand, p-type doping strategies have been investigated through Sn-doping and synthesis of Se-rich samples, resulting in an increase of the V_{oc} of photovoltaic devices. Structural, compositional and electronic characterization have been performed by X-ray diffraction, microscopy, X-ray and UV photoelectron spectroscopy (determination of valence band and Fermi level), Seebeck coefficient and JV measurements.

Additionally, the universality of the thiol-amine solvent for chalcogenides will be discussed, presenting its successful implementation for synthesis on other systems, including emerging chalcogenides (e.g. SbSI, SbSeI) and Ag-based anti-perovskites (Ag₃SI). The latter has a cubic structure analogous to standard perovskite (switching anions by cations and vice-versa), bandgap around 1 eV, and shows superionic behavior above room temperature. Overall, this work demonstrates the viability of thiol-amine solvents to synthesize a broad range of cutting-edge complex chalcogenide materials, allowing composition and doping control, and opening the door to explore new properties for energy harvesting applications.

1 *Chem. Rev.* **123**, 1, 327-278 (2023)

2 *Nat Energy* **5**, 587–595 (2020)

3 *J. Mater. Chem. A*, **11**, 17616-17627 (2023)

4 *Chem. Mater.* **27**, 6, 2114-2120 (2015)

5 *Chem. Mater.* **31**, 15, 5674-5682 (2019)

6 *Chem. Mater.* **32**, 6, 2621-2630 (2020)

9:15 AM *EN02.10.03

Self-Assemblies of Piezoelectric Metabolites and Their Energy Harvesting Applications Rusen Yang; Xidian University, China

Piezoelectric metabolite materials have received increasing attention in recent years owing to their inherent biological nature and efficient energy conversion capability, and piezoelectric metabolite self-assemblies are considered as promising smart materials for energy, sensor, robotics, healthcare, and many other areas. Rational material design is important to enhance their piezoelectric and biological activity. Herein, recent advancements to piezoelectric biomaterials, such as amino acids and peptide-based micro/nanostructures, are provided. Synthetic methods, morphological features, and piezoelectric performance of piezoelectric biomaterials are presented. The effect of growth direction, phase and structure of piezoelectric biomaterials on their piezoelectric activity are discussed. The applications of piezoelectric biomaterials in the field of nanogenerators are provided at the end.

9:45 AM BREAK

10:15 AM *EN02.10.04

Materials for Triboelectric Energy Harvesting: Current Situation and Some Thoughts [Alain Sylvestre](#)¹, Simon-Emmanuel Haim¹ and Armine Karami²; ¹University Grenoble Alpes, CNRS, Grenoble INP, G2Elab, Grenoble, France; ²CNRS, France

The triboelectric effect is as old as the hills, and the first reported effects of electrification date back to Thales of Millet in 600 BC. However, it was only in the 17th century that experimental evidence of triboelectricity was found, and in the next century that electrostatic generators began to appear, their benefits not being exploited until much later. Triboelectric generators for energy harvesting are a very recent development, not even 15 years old. The advent of these generators and their popularity stem from the work of Prof. Zhong Lin Wang and his team at the Georgia Institute of Technology. They develop triboelectric nanogenerators (TEENGs). Paying attention with the 'nanogenerator' term, which should not be taken to mean a nanometer-sized generator, but a generator that generally includes nanomaterials within it. More generally today, TEENG is the established term for triboelectric generators dedicated to energy harvesting, even if nanomaterials are not present. While the basic concept of triboelectricity is well established, with positive and negative charges separating when two materials rub or make contact, many questions remain. This separation of charges is not necessarily two-sided (i.e. negative charges on one material and positive charges on the other), and research has shown the co-presence of positive and negative charges on the same surface after contact. Generally, electron transfer is involved, but sometimes also ion transfer, as well as material transfer when surfaces come into contact: in some situations, it's a point of debate. Likewise, the development of nanocomposites raises another question regarding the ranking of these new materials in the classification of the triboelectric series. Some studies show that preconditioning of materials can promote or conversely reduce triboelectricity: is there a sound strategy for implementing this route? As far as the basic operating modes for developing TEENGs are concerned, there are several approaches: vertical contact-separation, sliding, free-standing, single electrode... Should one mode be favored over another in terms of expected performance if application requirements do not dictate it? How is performance in terms of energy harvested or produced truly calculated or estimated, and how can performance be easily compared between TEENGs?

Through an abundant panorama of works from the literature on TEENGs and their applications, we will attempt to shed light on some of these questions, and to highlight the advantages, difficulties and cautions to be taken in the announced promises in the actual use of these generators for energy harvesting. We will also present our research work on TEENGs through the development of a test bench dedicated to the precise characterization of these materials in sliding mode, as well as a consolidated theoretical study enabling us to evaluate performance on resistive or capacitive loads. This theoretical study also led to a proposal for optimal TEENG operation, which we then validated experimentally.

10:45 AM EN02.10.05

Sustainable Energy Harvesting by Employing Biocompatible Ferroelectric Molecular Cu(II) Complexes [Rajashi Haldar](#); Indian Institute of Technology Bombay, India

To address the escalating global energy consumption, resulting in swift depletion of non-renewable fossil fuels, it is imperative to explore alternative approaches. A smart way to tackle this problem is harnessing abundant, renewable but otherwise wasted environmental energies (vibrations, pressure, heat, solar, tidal) and converting them into useful electrical energy, with the help of the self-powered nanogenerators (SPNGs). Researchers have employed pure inorganic materials like bulk oxides (perovskites and ceramics), polymers, organic molecules, even peptides and organic-inorganic hybrid structures for this purpose. [1] Among these, the oxide systems show excellent piezo and ferroelectric as well as energy harvesting properties but they suffer from huge disadvantages like costly high temperature synthesis methods, almost zero mechanical flexibility, tunability of properties in the long-range and of course bio-incompatibility due to the presence of toxic heavy metals. In case of polymers or peptides, stabilizing the polar ferroelectric state which is required for the application purpose (for example β -state of PVDF) is an extremely daunting task. Alternatively, hybrid organic-inorganic perovskite systems offer low temperature and easy processing method, as well as great output performances but these systems also suffer from a number of problems, including the stability of reactive metal halide bonds under aerobic conditions and moisture and the presence of toxic heavy metal ions like lead (Pb). [2] By careful molecular engineering and controlled design strategy, we have overcome almost all of the above-mentioned caveats by employing bio-compatible discrete molecular complexes, which is an active area of research in the current scenario. They are light weight, mechanically flexible and easily polarizable in presence of an electric field, making them perfectly suitable to use in various energy harvesting nanogenerators. The Cu(II) metal based molecular complexes synthesized by us not only provide high values of piezoelectric co-efficients (d_{33} = 10-30 pm/V), comparable to the popular bulk materials like LiNbO₃, ZnO and polymers like PVDF, PVDF-TrFE etc., but also has appreciable spontaneous polarization values as well, leading to appreciable energy harvesting capabilities in both single-crystal and composite forms. We have shown to obtain a high value of output voltage of 8 V, power density of 0.85 μ W/cm² and an output current of 5 μ A, with a discrete molecular ferroelectric complex which is used in the form of a flexible composite film with a non-polar polymer matrix polyvinylalcohol (PVA), and . [3] Our efforts successfully afford an efficient route of energy harvesting which can be modified for futuristic applications. On the other hand, an open circuit output voltage of (7.4 V/cm²) and an appreciable pyroelectric coefficient of 29 μ C/m²K was obtained by a single-crystal based device made by us using another biocompatible molecular complex. In contrast to the single crystals of conventional bulk oxides, single crystals of the discrete molecular complexes are easier to synthesize and can be envisaged for various other applications such as anisotropic sensors, ultrasound transducers, and acoustic devices so as to avoid multidirectional mechanical and heat flux fluctuation aided artifacts. This opens up a lot of possibilities for molecular complexes in real-world applications.

References:

- [1] C. R. Bowen, H. A. Kim, P. M. Weaver and S. Dunn, *Energy Environ. Sci.*, 2014, **7**, 25–44.
- [2] T. Vijayakanth, D. J. Liptrot, E. Gazit, R. Boomishankar and C. R. Bowen, *Adv. Funct. Mater.*, 2022, **32**, 2109492
- [3] R. Haldar, A. Kumar, B. Mallick, S. Ganguly, D. Mandal and M. Shanmugam 2023, **62**, 202216680

SYMPOSIUM EN04

Beyond 20% Efficiencies with Organic Solar Cell Devices
April 23 - April 26, 2024

Symposium Organizers

Derya Baran, King Abdullah University of Science and Technology
Dieter Neher, University of Potsdam
Thuc-Quyen Nguyen, University of California, Santa Barbara
Oskar Sandberg, Åbo Akademi University

Symposium Support

Silver

Enli Technology Co., Ltd.

Bronze

1-Material, Inc.

* Invited Paper

+ JMR Distinguished Invited Speaker

^ MRS Communications Early Career Distinguished Presenter

SESSION EN04.01: Concepts and Designs of Efficient Organic Photovoltaics I

Session Chairs: Derya Baran and Ivan Kassar

Tuesday Morning, April 23, 2024

Room 328, Level 3, Summit

10:30 AM *EN04.01.01

Bilayers, Gradients and Funnel: Harvesting Excess Energy to Surpass The Shockley-Queisser Limit Constantin Tormann¹, Dorothea Scheunemann¹, Clemens Goehler¹, Tanvi Upreti² and Martijn Kemerink¹; ¹University of Heidelberg, Germany; ²Linköping University, Sweden

Compared to inorganic solar cells, the energy losses in organic photovoltaics (OPV) are still (too) large. Fortunately, a significant fraction of these losses results from a relatively slow relaxation of photogenerated charges in the disorder-broadened density of states. In previous work, we have already shown that the slowness of the mentioned thermalization leads to a 0.1-0.2 V higher open circuit voltage (Voc) in OPV devices than would be expected for instantaneous thermalization. Here, we will discuss strategies to harvest even larger parts of this excess energy, even beating the Shockley-Queisser limit for the constituent material.

Specifically, we experimentally and numerically show how inhomogeneous distributions of electron donating and accepting phases can be used to entropically drive positive and negative charge carriers towards the anode and cathode, respectively. First, we analyze simple step-like bilayer devices without any built-in voltage (Vbi) to single out the contribution of said mechanism to Voc. Next, we discuss how more suitably chosen gradient profiles can be used to improve actual devices that do have a finite Vbi. Combining these concepts, we demonstrate that in optimized, funnel-shaped morphologies the enhanced, non-equilibrium diffusivity of photogenerated charges can be rectified, allowing to surpass the Shockley-Queisser limit for the same material in absence of gradients and under near-equilibrium conditions. Finally, we use a cellular automaton model to show a realistic pathway to generate the proposed funnel-like morphologies in actual donor-acceptor blends.

11:00 AM EN04.01.04

Degradation Mechanisms in Highly Efficient Organic Solar Cells Based on Non-Fullerene Acceptors Klaus Meerholz; Univ of Cologne, Germany

During recent years, organic solar cells composed of different donor-acceptor-type polymers and non-fullerene acceptors (NFA) have approached and even exceeded the 20% hurdle. However, still questions remain regarding their long-term stability, i.e. the degradation processes involved.

Here, we present a comprehensive study on ca. 10 different NFAs and try to derive structure/property relations regarding their chemical stability / degradation mechanism, respectively. Experiments include the 1) analysis of the chemical stability of the NFAs themselves by mass spectrometry, 2) electrochemical stability tests of the radical anions ("electrons"), 3) solar cell devices based on PCE-12 and the NFAs, respectively, as prepared ones as well as aged by accelerated life-time testing, and 4) chemical analysis of the degradation products.

11:15 AM *EN04.08.02

Interface Engineering in Organic Solar Cells Huiqiong Zhou; National Center for Nanoscience and Technology, China

Solution-processed organic solar cells (OSCs) have attracted much attention due to their low cost, flexibility and high transparency. Recently, the power conversion efficiency (PCE) of OSCs is approaching 20%. However, the unsatisfied interface issues limit further improvement in PCEs and stability of OSCs, through affecting the physical processes such as exciton separation and/or charge transport/extraction/recombination in the device. Our recent study on interface engineering in OSCs has shown that the introduction of new electron transporting materials could enhance the PCE and suppress the photodegradation at the cathode interface, achieving over 10000 hours of storage and thermal stability in OSCs. An original strategy for selecting an optimal interfacial layer based on the surface energy has been proposed, to optimize the morphology of the active layers by regulating the surface energy and its microscopic distribution of the interface layer. At the end, we have constructed semi-transparent devices by utilizing optical microcavities, achieving high uniformity of device transmission and controllable adjustment of reflection color, which offers a viable design strategy for semi-transparent OSCs toward applications in next-generation smart photovoltaic windows.

This searchable program is up-to-date as of April 15th, 2024.

SESSION EN04.02: Concepts and Designs of Efficient Organic Photovoltaics II
Session Chairs: Ivan Kassal and Dieter Neher
Tuesday Afternoon, April 23, 2024
Room 328, Level 3, Summit

1:30 PM *EN04.02.01

Organic Solar Cells: Concepts towards The Single Junction Limit and Beyond [Christopher J. Brabec](#)^{1,2} and Larry Lüer¹; ¹FAU Erlangen-Nuremberg, Germany; ²Forschungszentrum Jülich GmbH, Germany

Thanks to the development of novel electron acceptor materials, power conversion efficiencies (PCE) of organic photovoltaic (OPV) devices are now approaching 20%. Further improvement of PCE is complicated by the need for a driving force to split strongly bound excitons into free charges, causing voltage losses. This presentation discusses recent approaches to find efficient OPV systems with minimal driving force, combining near unity quantum efficiency (maximum short circuit currents) with optimal energy efficiency (maximum open circuit voltages). We discuss apparently contradicting results on the amount of exciton binding in recent literature, and approaches to harmonize the findings. We then present a comprehensive view on motifs providing a driving force for charge separation, namely hybridization at the donor:acceptor interface and, polarization effects in the bulk. Apart from controlling the energies of the involved states, these motifs also control the dynamics of recombination processes, essential to avoid voltage and fill factor losses. Importantly, all motifs are shown to depend on both molecular structure and process conditions. The resulting high dimensional search space advocates for high throughput (HT) workflows. The final part of the presentation presents recent concepts for architectures allowing to bypass the single junction limit for organic photovoltaics.

2:00 PM *EN04.02.02

Critically Assessing The Potential and Challenges of Machine Learning for Designing Organic Photovoltaic Devices [Martin Seifrid](#); North Carolina State University, United States

Due to the complexity of designing organic semiconducting materials (OSCs) and devices, researchers have long used computational tools to screen candidate molecular structures and gain further insight into physical processes. Machine learning (ML) is emerging as a powerful tool for accelerating this even further. While processing conditions are known to play a significant role in determining PCE, ML has so far only been used to predict the power conversion efficiency (PCE) of organic photovoltaics (OPV) from molecular structure alone

In this talk, I will discuss how we can integrate device fabrication data into ML models, as well as best practices of ML for OPV. One of the key challenges of gathering such datasets is the difficulty of extracting data from the literature. We have created the first dataset containing both molecular structure and device processing conditions. We find sobering evidence of the low quality of such data, which is particularly important if we seek to use ML to accelerate the development of OPVs and OSCs. Many are aware of the widespread problem of the low quality of literature data, which affects numerous fields and is not discussed openly enough. The question for the future of ML and meta-analyses based on datasets derived from the literature becomes: what do we do going forward?

I will initiate a discussion with the community about what we can do to make generating large OPV and OSC datasets easier and more reliable, both in the short and long terms. In particular, I will outline a set of standards that could help make reporting and collecting data more robust.

2:30 PM EN04.02.04

Experimental and Theoretical Understanding of The Y6:Rubrene Upconverting Bilayer [Jarvist M. Frost](#) and Hanbo Yang; Imperial College London, United Kingdom

Photon upconversion via triplet-triplet annihilation (TTA) is a promising approach to overcome the detailed balance limit of single band-gap photovoltaics. However, low triplet densities in the bulk often limit TTA efficiency. Recently, Izawa et al. [1] demonstrated a new bilayer upconversion architecture comprising a non-fullerene acceptor (Y6) and rubrene. Photoexcitation of Y6 is believed to produce charge-separated states at the interface, which then recombine with normal spin statistics (avoiding the energetic cost of inter-system crossing), generating a high density of triplets in the rubrene which then fuse into higher-energy emissive singlets. Despite this promising 2021 result, details of the upconversion mechanism and dynamics in this system remain largely unexplored.

We study this system with complementary experimental and theoretical techniques.

Performing optical and electron paramagnetic resonance (EPR) spectroscopy helps us understand the nature of the photo excited states and how their population changes with time. EPR spectroscopy directly detects the spin of the photo excited species. Interpretation of this data is greatly helped by simulation of the non-adiabatic dynamics. This multi scale modelling approach starts with molecular dynamics (to get a representative interface) and then quantum chemistry (to understand and parameterise the eigenstates) and then a path-integral approach to the non adiabatic dynamics (to simulate the reduced density matrix as a function of time). The path integral approach to non adiabatic dynamics offers a principled and consistent hierarchy of simulation methods from fully quantum to semi-classical, ensuring trust in the results.

Our motivation for developing such a detailed understanding of the Izawa and Hiramoto Y6:Rubrene bilayer system is to then be able to make suggestions for synthesis for materials that have a higher upconversion efficiency and therefore can be used to engineer high efficiency photovoltaic systems. These upconversion based system would use large band-gap solar cells, making use of earth abundant chalcogenide and oxide semiconductors, and non donor-acceptor organic photovoltaics.

[1] Izawa, S., Hiramoto, M. (2021). Efficient solid-state photon upconversion enabled by triplet formation at an organic semiconductor interface. *Nature Photonics*, 15(12), 895–900. <https://doi.org/10.1038/s41566-021-00904-w>

2:45 PM DISCUSSION TIME

3:00 PM BREAK

SESSION EN04.03: Device Physics I—Models and Experiments
Session Chairs: Oskar Sandberg and Martin Seifrid
Tuesday Afternoon, April 23, 2024
Room 328, Level 3, Summit

3:30 PM *EN04.03.01

Delocalisation in Device-Scale Drift-Diffusion Models [Ivan Kassal](#); University of Sydney, Australia

In organic semiconductors, even small amounts of delocalisation can considerably enhance charge and exciton transport as well as charge separation. We recently developed delocalised kinetic Monte Carlo (dKMC), the first computational method able to describe the motion of partially delocalised charges [1] and excitons [2] in organic semiconductors on mesoscopic time and length scales, while considering the critical influence of energetic disorder, quantum-mechanical couplings, and polaron formation. dKMC has revealed new, basic physics of transport in organic semiconductors and can explain why mobilities predicted by traditional kinetic Monte Carlo are usually too low, showing that delocalisation over just a few molecules can increase mobilities by orders of magnitude [1,2]. Similarly, applying dKMC to the two-body problem of charge separation reveals a decisive enhancement of internal quantum efficiency (IQE) from a small amount of delocalisation [3,4].

In this talk, I will show that the benefits of delocalisation—first identified on the mesoscopic scale—also improve performance on the macroscopic, device scale. To do so, we have parametrised drift-diffusion models using dKMC to arrive at the first delocalisation-aware device models.

Our parametrisation relies on several new computational approaches. The first is jumping kinetic Monte Carlo (jKMC), a model that approaches the accuracy of dKMC, but with a computational cost comparable to conventional KMC [5,6]. Rates entering jKMC are simple modifications of ordinary Marcus hopping and can be used to include delocalisation effects in any existing KMC code. The low computational cost of jKMC also allows us to carry out the first calculations of all remaining parameters necessary for drift-diffusion models, which could not be computed by fully quantum techniques. These include steady-state mobilities, generation rates, and carrier recombination rates, processes that we show are also significantly affected by even modest delocalisation.

Putting all the ingredients together, our delocalised drift-diffusion code [7] can compute JV curves while faithfully capturing charge and exciton delocalisation. The results confirm the importance of delocalisation in device performance and help explain recent high-performance blends that defy explanation using classical models.

[1] Daniel Balzer, Thijs J.A.M. Smolders, David Blyth, Samantha N. Hood, and Ivan Kassal, *Chem. Sci.* **12**, 2276 (2021).

[2] Daniel Balzer and Ivan Kassal, *J. Phys. Chem. Lett.* **14**, 2155 (2023).

[3] Daniel Balzer and Ivan Kassal, *Sci. Adv.* **8**, eab19692 (2022).

[4] Daniel Balzer and Ivan Kassal, *arXiv:2308.15076* (2023).

[5] Jacob T. Willson, William Liu, Daniel Balzer, and Ivan Kassal, *J. Phys. Chem. Lett.* **14**, 3757 (2023).

[6] Jacob T. Willson, Daniel Balzer, and Ivan Kassal, *arXiv:2308.13194* (2023).

[7] Tom Grayson and Ivan Kassal, in preparation (2024).

4:00 PM EN04.03.02

Disorder-Effect on The Photophysics of Solution Processed Polymeric Photovoltaic Materials through Sequential QM/CMD Approach L. R.

Franco¹, C. Marchiori¹, D. Valverde², Yoann Olivier², Ellen Moons¹ and [Moyses Araujo](#)¹; ¹Karlstad University, Sweden; ²University of Namur, Belgium

The development of new organic photovoltaic materials based on non-fullerene acceptors (NFAs) has led to a significant increase in the power conversion efficiency of organic photovoltaics (OPV) in the last years [1]. However, the fundamental understanding of the charge photogeneration mechanism at the molecular level is still lacking, a scientific challenge whose solution could be the watershed in the discovery of novel OPV materials. To contribute to this end, we have developed a multi-scale method that combines Quantum Mechanics (QM) calculations and Classical Molecular Dynamics (CMD) simulations within the scope of a sequential QM/CMD approach [2] to assess the photophysics of organic-polymeric photovoltaic materials. Despite being a well-established method to study small and medium-sized molecules in solution, it has not yet been applied to investigate polymer films cast from solution. Our methodology starts with the simulation of film formation through solvent molecules evaporation procedure using CMD simulations. Afterwards, additional CMD simulations are carried out on the obtained film to generate uncorrelated configurations to be subsequently used on the properties' calculations. The latter is assessed through an electronic embedding scheme where a pre-defined molecular region of the generated configuration is treated at the QM level, incorporating explicit effects of the environment. The quality of the force field parameters adopted in the CMD simulations has also been carefully analyzed. For the QM calculations, density functional theory (DFT) and its time-dependent version (TD-DFT) have been employed along with the wavefunction-based method ADC(2) [3]. The latter has been widely used as reference method to assess the accuracy of TD-DFT method on the description of vertical excitation energies and excited-state potential energy surfaces. We have focused the study on the PF5-Y5 polymer [4,5], which can be seen as a model system to study covalently bound donor-acceptor interfaces. First, we have analyzed the structure of the films, focusing, for instance, on the tendency to stabilize π - π stacking conformations. Then, the dynamics and molecular environment effects on the electronic transitions have been quantified with an improved description of the optical absorption. The recently developed double-hybrid functionals [6], which include a MP2-like perturbation in the correlation part, were found to be the best theory-level within TDDFT framework to describe the singlet-triplet energy gaps in this complex donor-acceptor polymer. The comparisons with experimental results confirm the suitability of the developed s-QM/CMD approach, highlighting the importance of properly describing the disorder, dynamics and molecular environment effects in the modeling of the electronic properties of OPV materials.

References

1. A. Armin et al. *Advanced Energy Materials* **11**, 2003570 (2021).
2. K. Coutinho et al. Springer, Dordrecht, 2008. 159-189.
3. A. Tajti et al. *J. Chem. Theory Comput.* **16**, 468 (2020).
4. Q Fan et al. *Energy & Environmental Science* **13**, 5017 (2020).
5. I. Jalan et al. *Journal of Materials Chemistry C* **11**, 9316 (2023).
6. D. Mester et al. *J. Chem. Theory Comput.* **18**, 1646 (2022).

4:15 PM EN04.03.03

A Digital Twin to Overcome Long-Time Challenges in Photovoltaics Larry Lürer¹, Ian Marius Peters², Ana Suncana-Smith³, Eva Dorschky³, Björn M.

Eskofier³, Frauke Liers³, Jörg Franke³, Martin Sjarov³, Matthias Brossog³, Dirk Guldi³, Andreas Maier³ and Christoph J. Brabec^{1,2}; ¹i-MEET, Germany; ²Forschungszentrum Jülich GmbH, Germany; ³Friedrich-Alexander-Universität Erlangen-Nürnberg, Germany

The recent successes of emerging photovoltaics are largely driven by innovations in material science. However, closing the gap to commercialization still requires significant innovation to match contradicting requirements such as performance, longevity and recyclability. In this contribution, we suggest a layout of a Digital Twin for PV materials able to provide the necessary acceleration of innovation.

The rationale of the Digital Twin is to bridge the gap between first principles calculations, currently not able to predict the crucial solid state properties for emerging PV materials, and high throughput experimentation, currently not able to provide datasets of the necessary scale needed to train generative artificial intelligence (AI) models.

The crucial aspect of our layout is featurization, that is, identifying and retaining only the relevant and non-redundant information present in a dataset. This allows designing fast proxy experiments and surrogate models across all relevant scales. We will learn more from faster and simpler experiments, and the resulting massive (but cheaply acquired) dataset will allow building better approximate models for solid state structure from chemical structure, closing the gap for molecular inverse design, that is, from a set of desired properties all the way back to molecular structure.

Our proposed layout of the Digital Twin combines machine learning approaches, as performed in materials acceleration platforms (MAPs), with physical models and digital twin concepts used in engineering. This layout will allow using high-throughput (HT) experimentation in MAPs to improve the parametrization of quantum chemical and solid-state models. In turn, the improved and generalized models can be used to obtain the crucial structural parameters. HT experimentation will thus yield a detailed understanding of generally valid structure-property relationships. Most importantly, and different from black-box AI approaches, our physics-aware approach can benefit from human abstract thinking, increasing the chance for breakthrough innovation. Building a Digital Twin in PV materials is agile. We show that some of the necessary building blocks are already available, doing useful work today. Finally, we identify promising approaches for the open challenges such as fast scale-bridging surrogate models and large scale optimization under uncertainty.

4:30 PM EN04.03.04

The Photocurrent in Organic Solar Cells does not Vanish at Open-Circuit Clemens Göhler, Mónica Dyreby, Alexander Flamm and Martijn Kemerink; Institute for Molecular Systems Engineering and Advanced Materials, Universität Heidelberg, Germany

Organic solar cells (OSCs) had been around for several decades while scoring considerably worse efficiencies than their inorganic counterparts. Recently discovered materials have closed the gap considerably and optimized OSCs can now reach close to 100% conversion yield between incident photons to extracted charge carriers. Still, they suffer from losses to the open-circuit voltage and fill factor, and conventional equilibrium charge carrier dynamics fail to exactly reproduce their current-voltage-characteristic. Instead, non-thermalized charge carrier distributions—due to incomplete relaxation in a disordered density of states—provide better agreement, yet with at times uncommon ramifications: here, we will show that a non-neglectable photogenerated current under open-circuit conditions is a general feature of OSCs.

In more detail, we have investigated the internal quantum efficiency of photogenerated charges in non-fullerene acceptor OSCs in the steady state. Therefore, we have first measured their external quantum efficiency spectrum under different experimental conditions, including a constant background illumination. Utilizing a small signal light source, modulated at low frequencies, and varying the working conditions from reverse (collection) to forward (injection regime) fields, allowed us to determine how efficient photogenerated charges can be extracted at any point on the current-voltage-curve. We find that while the yield decreases towards open-circuit, it does not vanish completely and some 10-20% of the short circuit yield remains; therefore, the resulting photocurrent has to be compensated by charge injection in order to reach zero net current. In a subsequent step, we were able to reproduce these experimental findings with kinetic Monte-Carlo device simulations involving non-equilibrium dynamics with decoupled photo- and injection currents.

4:45 PM EN04.03.05

How 'Hot' are The Charges in OPV? Priya M. Viji, Constantin Tormann, Clemens Goehler, Dorothea Scheunemann and Martijn Kemerink; Universität Heidelberg, Germany

The question of whether charge transport in operational organic solar cells (OSC) occurs far-from-equilibrium or not is of significant practical and fundamental importance. While the equilibrium picture of the OSC assumes that the photogenerated charge carriers quickly lose their energy and attain lattice temperature, kinetic Monte Carlo (kMC) simulations of OSC have consistently shown that photogenerated charge carriers are extracted before reaching thermal equilibrium energy: the population thermalizes, albeit to an effective temperature that exceeds that of the lattice [1].

Probing the distribution of photogenerated charges possessing this excess energy has proven to be notoriously hard. In this work, we use Johnson thermometry to measure the temperature of the photogenerated carriers carried out by cross-correlated current noise spectroscopy. Two representative material systems, P3HT:PCBM and PM6:Y6, are tested against their inorganic counterpart, silicon. The experiments univocally prove, in stark contrast to silicon photovoltaics, that charges in operational OSC are not thermalised and are almost twice as hot as the lattice. The experimental findings are confirmed by kMC simulations. The simulations show that the energetic disorder in organic semiconductors is not only the reason for slow thermalisation but also for the high effective temperature observed in the Johnson thermometry experiments.

Our results imply that OPVs are truly far from equilibrium systems, which opens realistic prospects to mitigate the thermalisation losses and eventually beat the near-equilibrium thermodynamic limit [2]. In fact, the results presented show that even regular OPVs are Hot-Carrier Solar Cells in the sense that excess energy contributes to output power.

References

- [1] A. Melianas, M. Kemerink, A. Melianas, and M. Kemerink, *PROGRESS REPORT 1806004 (1 of 23) Photogenerated Charge Transport in Organic Electronic Materials: Experiments Confirmed by Simulations*, (2019).
- [2] T. Upreti, C. Tormann, and M. Kemerink, *Can Organic Solar Cells Beat the Near-Equilibrium Thermodynamic Limit?*, J. Phys. Chem. Lett. **13**, 6514 (2022).

SESSION EN04.04: Poster Session
Session Chair: Oskar Sandberg
Tuesday Afternoon, April 23, 2024
Flex Hall C, Level 2, Summit

5:00 PM EN04.04.01

Effects of Deposition Angle on The Thin Film Quality of Indium Tin Oxide Grown by Magnetron Sputtering [Tabitha Amollo](#)^{1,2} and Qi H. Fan¹;

¹Michigan State University, United States; ²Egerton University, Kenya

Indium tin oxide (ITO) has been widely used as a transparent electrode in various applications including solar cells, liquid crystal displays, plasma displays, smart windows, and light emitting diodes (LEDs). Many of these applications require low-temperature deposition of ITO thin film. But it remains a challenge to achieve satisfactory electrical conductivity and optical transmittance at low deposition temperatures. This work proves that the sputtering deposition angle has significant effects on the ITO film microstructure and properties. The ITO thin films are grown by a unique single beam ion source enhanced magnetron sputtering. The sputtering and ion beam directions relative to the substrate surface are varied from 30 to 90 degrees and the film structure and properties are subsequently investigated. X-ray diffraction is used to determine the film microstructure. Atomic force microscopy (AFM) and scanning electron microscopy (SEM) are used to characterize the morphology of the thin films. The thin films' electrical conductivity and carrier mobility are determined from four-point probe and Hall effect measurements, respectively. Optical transmittance spectra are obtained using UV-Vis spectroscopy. This study contributes to the advancement of thin film growth mechanisms

5:00 PM EN04.04.02

Attaining a Remarkable Efficiency of 11.57% in a Polymer Solar Cell Submodule with a 55 cm² Active Area using 1D/2A Terpolymers and Nonhalogenated Solvents [Hyeonwoo Jung](#)¹, Sung-Ho Jin², Chang Eun Song³ and Youngu Lee¹; ¹DGIST, Korea (the Republic of); ²Pusan National University, Korea (the Republic of); ³Advanced Energy Materials Research Center, Korea Research Institute of Chemical Technology, Korea (the Republic of)

Polymer solar cells (PSCs) employing a bulk heterojunction structure exhibit a significant potential as energy sources for advanced portable electronic devices due to their low weight, scalable roll-to-roll (R2R) processing, and cost-effectiveness. Recent advances in the design of high-performance photoactive materials and device structure optimization, have resulted in a remarkable increase in the power conversion efficiency (PCE) of PSCs, surpassing 19 %. Recently, the PM6 copolymer has been widely used in the photoactive layers of PSCs due to its high crystallinity, superior hole mobility, and strong pre-aggregation behavior. However, achieving high-performance PSCs based on the PM6 polymer normally requires the use of halogenated solvents such as chloroform and chlorobenzene. Unfortunately, the use of these halogenated solvents is limited in mass production because of environmental toxicity concerns. Furthermore, due to the strong temperature dependent aggregation property of the PM6 polymer, PM6-based large-area PSCs fabricated using large-scale coating methods exhibits a significant reduction in PCE. For example, PM6-based small-area (0.12 cm²) PSCs exhibits a PCE of 15.1 %. However, the PCE of PM6-based large-area (54.5 cm²) PSC submodules can be significantly reduced to 8.73 %. This decrease in performance of PM6-based large-area PSCs in nonhalogenated systems can be attributed to the oversized domains and nonuniformity in the photoactive layer, leading to an increased cell-to-module (CTM) loss. The undesirable morphology of the PM6-based photoactive layer can be controlled using a high-temperature (HT) process such as a hot solution and/or preheated substrates. However, such a complicated process is unsuitable for the production of cost effective and highly reproducible R2R PSC modules. Therefore, it is necessary to develop new p-type polymer for high-performance large-area PSC modules based on simple processes and minimize the CTM loss in nonhalogenated systems.

Terpolymers composed of three different monomers have recently attracted attention as promising p-type polymer. Terpolymers can accurately control physicochemical properties, such as frontier energy levels, light harvesting ability, pre-aggregation behavior, miscibility, and crystallinity, by introducing a third component directly into the donor-acceptor (D-A) copolymer backbone.

Herein, we synthesize a new series of 1D/2A terpolymers for developing room-temperature (RT) and nonhalogenated solvent processed high-performance PSCs submodules. The terpolymers are composed of three components: benzo[1,2-b:4,5-b']dithiophene (BDT-F), thieno[3,4-c]pyrrole-4,6(5H)-dione (TPD-TT), and benzo-[1,2-c:4,5-c']dithiophene-4,8-dione (BDD). Three PBTPtBD terpolymers (i.e. PBTPtBD-25, PBTPtBD-50, and PBTPtBD-75) are synthesized using different ratios TPD-TT to BDD composition ratios, corresponding to TPD-TT contents of 25 %, 50 %, and 75 %, respectively. The composition ratio of the TPD-TT and BDD components can be used to control the light harvesting ability, energy level, molecular ordering, and charge transport properties of the PBTPtBD polymers. A grazing incidence wide-angle X-ray scattering and contact angle analysis shows that the PBTPtBD-75:BTP-C11 blended film exhibits a predominant face-on orientation with good miscibility. The RT and nonhalogenated solvent processed PBTPtBD-75:BTP-eC11 PSC exhibit a high PCE of 15.55 %. Furthermore, PBTPtBD-75:BTP-eC11-based PSC submodules, processed with *o*-xylene under RT conditions, achieve a notable PCE of 11.57 % over a 55 cm² active area. This PCE value is among the highest reported in single-junction PSC submodules processed with nonhalogenated solvent.

5:00 PM EN04.04.03

Green Solvent Enables Record Performance in Model PCDTBT:PCBM Through Reduced Recombination [Acacia Patterson](#), Awwad N. Alotaibi, Obaid Alqahtani and Brian A. Collins; Washington State University, United States

Organic solar cells (OSCs) are promising as a printable and massively scalable solar energy source, with efficiencies approaching 20%. For OSC production, toxic, halogenated solvents are typically used, limiting processing options for efficiency gains as well as prospects for commercialization. Additionally, there are inadequate connections between the complex nanomorphology and charge dynamics that occur during device operation to fully exploit and enhance performance gains. Here, we show how a non-halogenated solvent CS₂ can not only reduce toxicity but also result in a record high efficiency (30% higher than previous records with traditional halogenated solvents) for a model system PCDTBT:PCBM. We apply time delayed collection field (TDCF) in a comprehensive charge loss analysis under device-relevant conditions to reveal significant suppression of bimolecular recombination that explains the performance difference. This ultimately enables enhanced absorption with thick active layers that are more relevant to industrial production. Furthermore, we apply advanced X-ray techniques to demonstrate that the enhanced device dynamics and performance originate from increased nanodomain purity and crystalline order due to altered interaction with the host solvent. Moving forward, this work reveals a new emphasis on green processing solvents for scaleup that may also enable new record OSC efficiencies.

5:00 PM EN04.04.04

Dimerized Small-Molecule Acceptors Enable High-Performance Organic Solar Cells with High Open-Circuit Voltage and Prolonged Life-Time [Jinwoo Lee](#)¹, Cheng Sun², Yun-Hi Kim² and Bumjoon Kim¹; ¹Korea Advanced Institute of Science and Technology, Korea (the Republic of); ²Gyeongsang National University, Korea (the Republic of)

The power conversion efficiencies (PCEs) of small molecule acceptor (SMA)-based organic solar cells (OSCs) have remarkably increased in recent years, but their thermal and long-term stability are insufficient for commercialization. In addition, the low open-circuit voltage (V_{oc}) of OSCs, compared to those of other types of solar cells (i.e., perovskite solar cells), should be addressed to further improve their PCEs. Here, we demonstrate that the dimerization of an SMA resolves the performance limitations of SMA-based OSCs, in terms of stability and V_{oc} . The dimerized SMA (DYBO) connected by a benzodithiophene (BDT) conjugated linker affords OSCs with excellent PCEs (> 18%), which outperform OSCs based on its monomer counterpart (MYBO, PCE ~ 17.1%). The electron-donating BDT linker in DYBO effectively upshifts the lowest unoccupied molecular orbital energy level and reduces the voltage loss, synergistically increasing the V_{oc} of DYBO-based OSCs. Importantly, DYBO-based OSCs exhibit excellent thermal and photo stability. For example, DYBO-based OSCs retain more than 80% of their initial PCE even after 6000 hr of thermal exposure at 100 °C, whereas the PCE of MYBO-

based OSCs sharply degrade to ~80% of their initial value in only 36 hr. The improved stability of DYBO-based OSCs is attributed to (1) the high glass transition temperature (T_g) of DYBO of 179 °C (the T_g of MYBO is 80 °C) due to its extended chain, which stabilizes the blend morphology under thermal stress, and (2) the improved miscibility of DYBO with the BDT-based polymer donor. Thus, we highlight the significance of the molecular design of dimerized SMAs in realizing OSCs with excellent PCEs and stabilities.

5:00 PM EN04.04.05

Design of Mechanically-Robust Naphthalenediimide-Based Polymer Additives for High-Performance, Intrinsically-Stretchable Organic Solar Cells Chulhee Lim¹, Sanghun Park¹, Dong Jun Kim¹, Sunjoo Kim², Taek-Soo Kim¹ and Bumjoon Kim¹; ¹Korea Advanced Institute of Science and Technology, Korea (the Republic of); ²Chung-Ang University, Korea (the Republic of)

High-molecular-weight electro-active polymer acceptor (P_A) is effective in simultaneously increasing photovoltaic performance and mechanical integrity of organic solar cells (OSCs) based on a polymer donor (P_D) and a small molecule acceptor (SMA). In this work, we develop a new naphthalene diimide (NDI)-based P_A , named P(NDI2OD-TCVT), and employ it as a P_A additive in a P_D :SMA blend to fabricate high-performance and mechanically robust OSCs. Copolymerization of NDI, bithiophene, and cyano-vinylene units ensures the n-type characteristics of the P(NDI2OD-TCVT). Noticeably, the cyano-vinylene group alleviates the crystalline nature of the NDI and bithiophene units, providing inter-domain bridges by being a tie molecule. As we vary the weight-averaged molecular weight (M_w) of the polymer, we find that the backbone structure enables a significant reduction of the critical molecular weight that ensures mechanical robustness. High crack-onset strain (COS) of 30.1% is achieved in the P(NDI2OD-TCVT) film with a relatively low M_w of 109 kg mol⁻¹, which is a stark contrast to the COS value (1.8%) of the reference P(NDI2OD-T2) film with similar M_w of 126 kg mol⁻¹. In addition, we find that incorporation of P(NDI2OD-TCVT) enhances the photovoltaic performance of the P_D :SMA-based OSCs, achieving a high power conversion efficiency (PCE) of 16.8%. Benefitted from the significantly enhanced mechanical properties of P(NDI2OD-TCVT), we also demonstrate the highly efficient and intrinsically stretchable organic solar cells (IS-OSCs). The IS-OSCs with 10 wt% of P(NDI2OD-TCVT) featured a PCE of 12.6% and retained 85% of the initial PCE after 100 cycles of stretching at 20% strain and releasing, outperforming those of P(NDI2OD-T2)-based IS-OSCs.

5:00 PM EN04.04.07

Highly Stable Organic Solar Cells with Fullerene as Interfacial Compatibilizer Guan-Lin Chen, Shih-Hao Wang, Kai-Wei Tseng, Ching-I Huang and Leeyih Wang; National Taiwan University, Taiwan

The emerging technology of organic solar cells faces challenges related to long-term durability due to the combined effects of moisture, thermal, and photo stresses. To address this issue, we introduced a novel interfacial stabilizer, fullerene, $C_{60}(OH)_x$, which substantially improved the durability of organic solar cells to cope with environmental stress. This study utilized X-ray photoelectron spectroscopy and Fourier-transform infrared spectroscopy to confirm that $C_{60}(OH)_x$ forms hydrogen bonds with both the oxygen atoms of ZnO and the fluorine atoms of Y6. As a result, the compatibility and charge transport between the electron transport layer (ETL) and the organic photoactive film were significantly improved, thereby stabilizing the interface. By incorporating the ZnO/ $C_{60}(OH)_x$ ETL, the power conversion efficiency of the ternary PM6:Y6:PC71BM solar cell was increased from 16.1% to 17.8%. More importantly, such ZnO/ $C_{60}(OH)_x$ device maintained 80% of its original performance (T_{80} lifetime) after being annealed at 65 °C for more than 6,973 hours in N_2 . The T_{80} lifetime at room temperature (25 °C) was estimated to exceed 34,635 hours. Detailed characterizations demonstrated that $C_{60}(OH)_x$ can passivate the surface with regard to defects and effectively facilitated free radical scavenging. Overall, the ZnO/ $C_{60}(OH)_x$ device retained 91% of its initial PCE after continuous light soaking with a solar simulator at one-sun intensity for over 1,200 hours in N_2 . For a relative humidity of 50% at 25 °C, the un-encapsulated ZnO/ $C_{60}(OH)_x$ device exhibited a T_{80} exceeding 1,323 hours. The successful showcasing of this new interfacial stabilizer can spur additional research and momentum towards the advancement of future photovoltaic technologies.

5:00 PM EN04.04.08

Atomic Layer Deposition of Tin Oxide Electron Transport Layer for High-Performance Organic Solar Cells with Inverted Structure Lorenzo Di Mario, David Garcia Romero, Han Wang, Eelco K. Tekelenburg, Sander Meems, Teodor Zaharia, Giuseppe Portale and Maria Antonietta Loi; University of Groningen, Netherlands

OSCs with the inverted n-i-p structure are considered more suitable for commercialization compared to those with conventional p-i-n structure, due to the superior stability of the materials used. However, the highest efficiencies (close to 20%) are currently achieved exclusively using the conventional structure. In fact, efficiencies above 17% from OSCs with the inverted structure are scarcely reported, mainly due to the low values of fill factor (FF) which characterize devices in this configuration. Electron and hole transport layers play a crucial role in determining the performance of OSCs. Therefore, a proper selection of them is essential to achieve higher efficiency in OSCs with inverted structure and to close the gap with devices with conventional structure.

Transparent conductive oxides are usually employed as electron transport layers (ETLs) in OSCs with inverted structure. Among them, zinc oxide (ZnO) is the most studied and adopted, since it provides a good band alignment with the organic semiconductors and it can be easily deposited from solution. Tin oxide (SnO_2) represents a valid alternative to ZnO as ETL, offering superior transparency to the visible light and higher electron mobility. Moreover, unlike ZnO, SnO_2 is reported to have an excellent ambient stability and to not cause any photocatalytic degradation of the organic materials [1].

A broad use of SnO_2 as ETL in OSCs is currently hindered by the difficulty in fabricating films of the material with low defect density. SnO_2 films for OSCs are often obtained from solution processing, starting from nanoparticle colloidal dispersions, with the result of a high defect density, especially on the surface. Moreover, organic ligands, used to stabilize the nanoparticle dispersions, often leave residuals in the deposited film, which can compromise the interface with the active layer. As a result, the overall performance of OSCs with SnO_2 as ETL is often poor, with in particular low values of FF [2].

In this work, highly efficient OSCs with inverted structure are demonstrated by using as ETL SnO_2 deposited by atomic layer deposition (ALD). ALD is an industrial grade technique which can be applied at the wafer level and also in a roll-to-roll configuration. ALD allows obtaining compact layers of SnO_2 with exceptional quality and low defect density. SnO_2 fabricated by ALD already attracted attention in the research field of photovoltaic, for perovskite [3] and tandem solar cells [4]. Nonetheless, its use in OSCs is scarcely reported and its potential not yet fully exploited. By using ALD to deposit the SnO_2 ETL, we fabricated OSCs with PM6:L8-BO active layer, reaching a champion efficiency of 17.26% and a record FF of 79%. The devices fabricated outperform not only solar cells using SnO_2 nanoparticles casted from solution (PCE 16.03%, FF 74%) but also those utilizing the more common ZnO (PCE 16.84%, FF 77%). Furthermore, the OSCs with ALD SnO_2 show a higher stability under illumination in comparison with those utilizing ZnO. The outstanding results achieved are demonstrated to arise from a superior quality of the interface between the ALD SnO_2 film and the active layer and, thus, from a reduced charge carrier recombination [5].

[1] Y. Jiang, et al., *Mater. Horiz.*, **2019**, 6, 1438–1443.

[2] L. Hu, et al., *J. Mater. Chem. C*, **2020**, 8, 12218–12223.

[3] L. Xiong, et al., *Adv. Funct. Mater.*, **2018**, 28, 1802757.

[4] K. O. Brinkmann, et al., *Nature*, **2022**, 604, 280–286.

[5] L. Di Mario, et al., *Adv. Mater.*, **2023**, 2301404.

5:00 PM EN04.04.09

Anisotropic Nature of Vibronic Coupling, Singlet Fission and Triplet Transport of Single Crystalline Acenes (n=4-6) Yi Rao; Department of Chemistry and Biochemistry, Utah State University, United States

The escalating global energy predicament implores for a revolutionary resolution—one that converts sunlight into electricity—holding the key to supreme conversion efficiency. We embark on the exploration of the principle of generating multiple excitons per absorbed photon, a captivating concept that possesses the potential to redefine the fundamental confines of conversion efficiency, albeit its application remains limited in photovoltaic devices. At the nucleus of this phenomenon are two principal processes: multiple exciton generation (MEG) within quantum-confined environments, and singlet fission (SF) inside molecular crystals. The process of SF, characterized by the cleavage of a single photogenerated singlet exciton into two triplet excitons, holds promise to potentially amplify photon-to-electron conversion efficiency twofold, thereby laying the groundwork to challenge the detailed balance limit of solar cell efficiency. Our discourse primarily dissects the complex nature of SF in crystalline organic semiconductors, laying special emphasis on the anisotropic behavior of SF and the diffusion of the subsequent triplet excitons in single-crystalline polyacene organic semiconductors. We initiate this journey of discovery by elucidating the principles of MEG and SF, tracing their historical genesis, and scrutinizing the anisotropy of SF and the impact of quantum decoherence within the purview of functional mode electron transfer theory. We present an overview of prominent techniques deployed in investigating anisotropic SF in organic semiconductors, including femtosecond transient absorption microscopy and imaging as well as stimulated Raman scattering microscopies, and highlight recent breakthroughs linked with the anisotropic dimensions of Davydov splitting, Herzberg-Teller effects, SF, and triplet transport operations in single-crystalline polyacenes. Through this comprehensive analysis, our objective is to interweave the fundamental principles of anisotropic SF and triplet transport with the current frontiers of scientific discovery, providing inspiration and facilitating future ventures to harness the anisotropic attributes of organic semiconductor crystals in the design of pioneering photovoltaic and photonic devices.

5:00 PM EN04.04.10

Probing Nanomorphology of Guest Component in Ternary OPVs Tanner M. Melody, Acacia Patterson and Brian A. Collins; Washington State University, United States

Recent advancements in organic photovoltaic (OPV) solar technology show that with the inclusion of a third guest component to the traditional binary devices, efficiencies can surpass 20% which are comparable or even above competing technologies. The addition of ternary components contribute to increasingly complex nanomorphologies that most characterization techniques cannot determine. Our objective is to identify these key nanostructures that maximize the ternary advantage. First, we characterize the thermodynamic mixing of donor and acceptor molecules in phase-separated equilibrium states via surface energy measurements combined with the blend demixing experiments we have previously demonstrated using spectral X-ray microscopy. We then determine the dominant paradigm ternary morphology that enhances performance using traditional GIWAXS in conjunction with chemical sensitive nanopores such as spectrally resolved RSoXS analysis and STXM directly on high performance active layers. Uncovering the morphological pathways that these ternary components provoke will allow us to inflect the fabrication process of these devices to maximize the ternary advantage for commercially viable, high-performance OPVs.

5:00 PM EN04.04.11

Solvent Effect on Doctor Blade Coating Process for Large-Area Organic Solar Cell Modules Soonil Hong¹, Byoungwook Park¹, Chandran Balamurugan², Jinho Lee³ and Sooncheol Kwon²; ¹Korea Research Institute of Chemical Technology, Korea (the Republic of); ²Dongguk University, Korea (the Republic of); ³Incheon National University, Korea (the Republic of)

Efforts to commercialize organic solar cells (OSCs) through the development of roll-to-roll compatible modules have faced challenges in optimizing printing processes to achieve laboratory-level performance in fully printable OSC architectures. In this study, we present efficient OSC modules fabricated using only printing methods. The effect of processing solvents on the morphology of key layers applied with the doctor blade coating method, including the hole transport, photoactive, and electron transport layers, was systematically evaluated with a focus on processability. The results showed that bathocuproine (BCP) processed from volatile alcohols required a delicate balance between wettability and vaporization, which contrasts with the results for spin-coated films. The fully printed OSC modules with uniform and continuous BCP layer formation achieved a remarkable power conversion efficiency of 10.8% with a total area of 10.0 cm² and a geometrical fill factor of 86.5%.

SESSION EN04.07: Device Physics II—Exciton and Charge Carrier Dynamics

Session Chairs: Tayebah Ameri and Thomas Anthopoulos

Thursday Morning, April 25, 2024

Room 328, Level 3, Summit

8:30 AM *EN04.07.01

Charge Generation in Neat Non-Fullerene Acceptor Domains Kaila Yallum and Natalie Banerji; University of Bern, Switzerland

Non-fullerene acceptors (NFAs) are exciting molecules allowing high efficiency in organic photovoltaic (OPV) blends with conjugated polymers. Interestingly, charges can also be generated by neat NFA films without additional donor. To understand the origins of exciton dissociation in neat NFAs, we have looked at the impact of aggregation, external electric field and non-linear effects. We used solvatochromism in order to gain insight on charge redistribution after excitation in isolated NFAs. We found that unaggregated NFAs feature a more dipolar excited state, revealing intramolecular charge transfer (ICT) character. This ICT character, however, is not enough to generate separated charges. Aggregation is the key to exciton dissociation in neat NFAs, which we observe with TA of solutions and films of several different NFAs. To explore the impact of an electric field on exciton dissociation in neat NFA devices, we used bias-dependent external quantum efficiency (EQE) and transient absorption (TA) spectroscopy. Electromodulated differential absorption (EDA) measurements then allowed us to observe charge transport under bias. Excitation correlation spectroscopy and fluence-dependent TA finally revealed how non-linear effects can increase the charge yield. Lastly, we comment on whether the neat domain charge generation significantly affects the photophysics of blends or not.

9:00 AM *EN04.07.02

Understanding Processes Limiting Charge Collection in Organic Solar Cells Oskar Sandberg¹ and Ardalan Armin²; ¹Abo Akademi University, Finland; ²Swansea University, United Kingdom

Organic solar cells have many advantageous properties including tailorable light absorption, low embodied energy manufacturing, structural conformality,

and low material toxicity. However, owing to their low charge carrier mobilities, the competition between extraction and recombination of photogenerated charge carriers is an important factor limiting the performance of organic solar cells. This competition is further complicated by the inevitable presence of contact-induced dark carriers in the device. In this work, we clarify the effect of contact-induced dark charge carriers on photovoltaic device performance through theoretical device simulations. We find that first-order recombination between photogenerated carriers and contact-induced dark carriers is the dominant bimolecular recombination channel limiting charge collection in state-of-the-art organic solar cells. Furthermore, analytical models for the current-voltage characteristics are established. This work provides intriguing insights into the fundamental limits set by charge transport in organic photovoltaic devices.

9:30 AM EN04.07.03

Singlet Exciton Fission Sensitization of Silicon Photovoltaics Narumi Wong¹, Collin F. Perkinson¹, Kangmin Lee¹, Aaron Li¹, Kwanyong Seo², William Tisdale¹, Mouni G. Bawendi¹ and Marc Baldo¹; ¹Massachusetts Institute of Technology, United States; ²Ulsan National Institute of Science and Technology, Korea (the Republic of)

The efficiencies of crystalline silicon solar cells, the current industry standard for photovoltaics, are approaching the Shockley-Queisser limit. One method of going beyond this limit is to sensitize the silicon (Si) by using organic molecules that can perform singlet exciton fission (SF), a carrier multiplication process that can create two triplet excitons (electron-hole pairs) from a single photon. Successful transfer of these two triplet excitons to silicon can result in increased photocurrent and improved efficiencies.

Previous work has shown coupling between Si and the archetype singlet exciton fission material tetracene in the presence of passivating interfacial layers of hafnium oxynitride through magnetic-field dependent photocurrent [1]. However, the electrical device performance did not show an enhancement from tetracene due to insufficient passivation and poor carrier extraction from the surface [1]. We have developed a new interfacial heterostructure that both provides surface passivation of defects and facilitates intermediate charge transfer states for triplet exciton transfer from tetracene to silicon. Additionally, using silicon photovoltaic device architectures with shallow junctions and high carrier extraction efficiency at the surface, we demonstrate enhancements in short circuit current from singlet exciton fission in tetracene for the first time.

[1] Einzinger, M., Wu, T., Kompalla, J.F. *et al.* Sensitization of silicon by singlet exciton fission in tetracene. *Nature* **571**, 90–94 (2019).

9:45 AM EN04.07.04

Electroabsorption Spectroscopy to Probe Charge Transfer Character in Donor/Acceptor Materials for Organic Photovoltaics Urvashi Bothra¹, Robert J. Westbrook¹, Demi Liu¹, Jian Wang¹, Mark Ziffer² and David S. Ginger¹; ¹University of Washington, United States; ²Columbia University, United States

We perform electroabsorption (EA) spectroscopy to understand charge transfer in polymer donor/acceptor blend systems comprised of three different acceptors: (i) fullerene acceptor, (ii) non-fullerene acceptor (IT-series), and (iii) non-fullerene acceptor (Y-series). We observe that the EA spectrum of polymer/fullerene blends and the blend based on 3,9-bis(2-methylene-(3-(1,1-dicyanomethylene)-6,7-difluoro-indanone))-5,5,11,11-tetrakis(4-hexylphenyl)-dithieno[2,3-d:2',3'-d']-s-indaceno[1,2-b:5,6-b']dithiophene (IT-4F) exhibit features which primarily correspond to first derivative of absorbance at the first optical transition, suggesting localized exciton formation upon photoexcitation. In contrast, the EA spectrum from the blend based on 2,2'-(2Z,2Z)-((12,13-bis(2-ethylhexyl)-3,9-diundecyl-12,13-dihydro-[1,2,5]thiadiazolo[3,4-e]thieno[2",3":4',5']thieno [2',3':4,5]pyrrolo[3,2-g]thieno[2,3':4,5]thieno[3,2-b]indole-2,10-diyl)bis(methanylylidene))bis (5,6-difluoro-3-oxo-2,3-dihydro-1H-indene-2,1-diylidene)dimalononitrile (Y6) is dominated by second derivative of absorbance spectrum, indicating formation of excited state with charge transfer (CT) characteristics upon photoexcitation. We carried out EA of neat Y6 and observed that the signal in blend originates primarily from Y6. Among the studied polymer donors and acceptors, Y6 exhibits the highest dipole moment change of 7.5 ± 2.5 Debye, consistent with a high degree of CT character, and a relatively large polarization volume of $361 \pm 70 \text{ \AA}^3$, suggesting better electron delocalization than other NFA acceptors such as IT4F. Further, we have also developed a new method to resolve CT state in the donor/acceptor blend by observing an additional feature in the EA of blend film at low energy, which is not present in the neat materials. These results provide evidence of EA spectroscopy in resolving the CT state across multiple polymer/non-fullerene acceptor blends and understanding the uniqueness of the Y6 acceptor due its large dipole moment change upon photoexcitation.

10:00 AM BREAK

10:30 AM EN04.07.05

Elucidating The Performance Impeding Role of Exciton Dissociation in Low Offset Nonfullerene Acceptor-Based Solar Cells Atul Shukla¹, Manasi Pranav¹, Bowen Sun¹, Rong Wang², Larry Lier², Christoph J. Brabec², Safa Shoaee¹ and Dieter Neher¹; ¹University of Potsdam, Germany; ²Friedrich-Alexander-Universität Erlangen-Nürnberg, Germany

The performance of organic solar cells has made large strides with power conversion efficiencies exceeding 19%, and the milestone of 20% well within sight¹. The emergence of non-fullerene acceptors (NFAs) has played a vital role in these advancements². Particularly, organic blends comprising of NFAs with polymeric donors (D) having low energetic offset between the ionization energies (ΔE_{IE}) of the two components have demonstrated excellent photovoltaic performance with superior charge generation yields in conjunction with reduced voltage losses^{3,4}. However, the process of free charge generation and the origin of performance limiting loss pathways has been a subject of debate. More specifically, the critical role of low ΔE_{IE} on the voltage losses and charge-generation efficiencies ask for a more detailed analysis. In this work, we systematically explore the role of energetic offset through methodical assessment of free charge generation process in a sample set of Y-series acceptors (Y6 and Y5) with well know polymeric donor, PM6. Herein, the PM6:Y5 material system is found to have a relatively lower energetic offset as compared to high performing system PM6:Y6. Our sample set uses the NFAs Y5 and Y6 blended with different molecular weights of the polymer donor PM6, spanning a large PCE range from 15% to 1%. This poor photovoltaic performance is further accompanied with pronounced field-dependence of free charge generation as demonstrate *via* time delayed collection field (TDCF) measurements. Using transient absorption spectroscopy (TAS), we find that the poor performing PM6:Y5 material system suffers from inefficient charge transfer at the interface, ultimately limiting the overall photovoltaic performance of Y5 based blends. We highlight the significance of driving force through field-dependent TAS measurements by demonstrating concomitant increment in free charge generation and exciton dissociation yields under the application of external electric field. These results supported with bias-dependent steady-state and transient photoluminescence studies provides a holistic view of the overall process and propounds that poor exciton dissociation is one of the main performance limiting channel in materials systems with diminishing energetic offset.

References.

1. Liu, F., Zhou, L., Liu, W., Zhou, Z., Yue, Q., Zheng, W., Sun, R., Liu, W. Y., Xu, S., Fan, H., Feng, L., Yi, Y., Zhang, W., Zhu, X., Organic Solar Cells with 18% Efficiency Enabled by an Alloy Acceptor: A Two-in-One Strategy. *Adv. Mater.* 2021, 33, 2100830
2. Armin, A., Li, W., Sandberg, O. J., Xiao, Z., Ding, L., Nelson, J., Neher, D., Vandewal, K., Shoaee, S., Wang, T., Ade, H., Heumüller, T., Brabec, C.,

- Meredith, P., A History and Perspective of Non-Fullerene Electron Acceptors for Organic Solar Cells. *Adv. Energy Mater.* 2021, 11, 2003570.
3. Bertrandie, J., Han, J., De, C. S. P., Yengel, E., Gorenflot, J., Anthopoulos, T., Laquai, F., Sharma, A., Baran, D., The Energy Level Conundrum of Organic Semiconductors in Solar Cells. *Adv. Mater.* 2022, 34, 2202575
4. Zhong, Y., Causa, M., Moore, G.J. et al. Sub-picosecond charge-transfer at near-zero driving force in polymer:non-fullerene acceptor blends and bilayers. *Nat Commun.* 2020, 11, 833.

10:45 AM EN04.07.06

Activationless Charge Transfer Governs Photocurrent Generation in Organic Photovoltaic Blends [Yifan Dong](#)¹, Deping Qian², Helen Bristow³, Tack Ho Lee⁴, Hyojung Cha⁵ and James Durrant^{1,6}; ¹Imperial College London, United Kingdom; ²Fujian Normal University, China; ³King Abdullah University of Science and Technology, Saudi Arabia; ⁴Pusan National University, Korea (the Republic of); ⁵Kyungpook National University, Korea (the Republic of); ⁶Swansea University, United Kingdom

Organic photovoltaics (OPVs) have recently shown substantive progress in device efficiency, driven in particular by advances in non-fullerene acceptor design and suppression of energy offsets between exciton (S_1) and charge-transfer (CT) states. Ultrafast charge transfer (< 200 fs) from polymer donors to fullerene acceptors has often been observed and attributed to the origin of efficient photocurrent generation in polymer:fullerene blends. While efficient charge photogeneration has also been observed in polymer:non-fullerene OPVs, several studies have reported much slower CT rates on the order of tens of ps. As suggested in Marcus theory, higher activation energy barriers could be the origin of slower CT rates. However, it remains unclear whether the suppressed S_1 -CT offset and/or the hybridisation/thermal equilibrium between S_1 and CT states would lead to higher barriers for charge generation and hinder charge transfer in such small-offset OPV blend systems. Herein, utilizing temperature-dependent transient absorption spectroscopy for a range of polymer:non-fullerene and polymer:fullerene OPV blends, we elucidate that the activation energy for charge generation is below 15 meV, implying that activationless charge generation pathway governs photocurrent generation in archetypal polymer based OPVs including the highly efficient low-offset PM6:Y6 blend. Suppression of the energy offsets in non-fullerene based OPVs does not lead to any increase in activation energy barriers for charge separation. While charge transfer is activationless, bimolecular recombination of charges proceeds with a high activation barrier of several hundreds of meV. Efficient charge photogeneration is universal among the blends studied herein and is not a limiting factor for device performance, while the geminate and/or no-geminate recombination losses appear to be the limiting factors.

11:00 AM EN04.07.07

Origin of Electric Field Dependence of Charge Generation in Organic Photovoltaics with Planar and Bulk Heterojunctions [Kyohei Nakano](#), Yumiko Kaji and Keisuke Tajima; RIKEN CEMS, Japan

Efficient, electric-field independent charge generation in the photo-electron conversion process in organic photovoltaics (OPVs) leads to high short-circuit current (J_{SC}) and fill factor (FF). However, the origin of the electric field-dependent charge generation in OPVs is still unclear. In this study, we fabricated bulk- and planar-heterojunction (BHJ and PHJ) type OPVs with the same donor (PM6) and acceptor (Y6) materials and investigated their charge generation process. The state energies of the singlet excited (S_1) and charge transfer (CT) states were experimentally quantified. In addition, the molecular orientation was determined by variable angle spectroscopic ellipsometry (VASE). The charge generation process in the BHJ is electric-field independent, while that in the PHJ is strongly electric-field dependent. The state energy offset between S_1 and CT states in the PHJ is 70 meV smaller than that in the BHJ, indicating that insufficient energy offset is one of the origins of the electric-field dependent charge generation in the PHJ. We also fabricated the PHJ with acceptors exhibiting different molecular orientations to figure out the effect of the relative molecular orientation between the acceptor and the donor domain on the charge generation process. We observed that the acceptor with face-on orientation to the donor domain showed field-dependent generation, whereas that with end-on (the direction of the end edge of the molecular long axis) orientated one had field-independent generation. The results suggest that the energy difference between S_1 and CT states and the molecular orientation in the BHJ film must be considered to realize high-performance OPV devices.

11:15 AM *EN04.07.08

Triplet Excitons in Organic Solar Cells [Alexander Gillett](#); University Of Cambridge, United Kingdom

Driven by the development of non-fullerene electron acceptor materials, the performance of organic solar cells (OSCs) has recently shown a remarkable improvement, with power conversion efficiencies nearly doubling from 11% to 19% in less than 10 years. However, the efficiency of OSCs is still lower than inorganic technologies, where efficiencies of $>20\%$ are commonplace. This is primarily due to excessive non-radiative recombination in OSCs, which reduces the open circuit voltage from the radiative limit.

In our work, we have identified recombination via low energy triplet excitons as a key factor responsible for the large non-radiative losses in OSCs. In state-of-the-art systems, such as 'PM6:Y6', up to 90% of the charge carrier recombination proceeds via triplet exciton states; this reduces the open circuit voltage by up to 60 mV. To address this issue, we propose two viable strategies. First, through the identification of systems where recombination via triplet excitons is suppressed, we demonstrate that significant hybridisation of the molecular triplet exciton and triplet charge transfer state can disfavour terminal recombination into the former. Second, we show that triplet-triplet annihilation has the potential to mitigate against triplet exciton losses by recycling up to half of these states formed back into singlet excitons, providing an opportunity for radiative recombination to occur. Therefore, our findings provide a framework to alleviate non-radiative losses via triplet excitons in OSCs, which could push efficiencies towards and beyond the 20% milestone.

11:45 AM EN04.07.09

Fluorescent Emission Enhanced Efficient Organic Photovoltaic Cells [Guodan Wei](#); Tsinghua-Berkeley Shenzhen Institute, China

Compared with non-fullerene acceptor (NFA), which has the advantages of high crystallinity and exciton diffusion coefficient, the polymer donors are limited by large Stokes shift and energy disorder, showing a lower exciton diffusion distance and higher non-radiative energy loss which limit their application in organic solar cells (OSCs). Herein, we reported a simple reverse-sensitization strategy and an organic small molecule thermally activated delayed fluorescence (TADF) material (BPhA-QAO) was designed and synthesized, which as solid additives was introduced into the widely studied PM6:BTP-4F based OSCs to enable a significant efficiency increase from 16.3% to 18.2%. The champion solar cell has efficiency close to 19.0%. Ultrafast optic and spectroscopic studies reveal that BPhA-QAO can transfer its long-lifetime singlet excitons to the polymer donor through energy transfer to ensure adequate exciton lifetime to expand its diffusion distance, and achieve better exciton dissociation efficiency. Morphological studies show that BPhA-QAO promotes the formation of more J-type aggregation for PM6, while inhibiting the stacking behavior of BTP-4F, regulating the degree of phase separation, and forming smaller domain sizes. Conductive AFM (C-AFM) shows that more thorough mixing of donor/acceptor improves the efficiency of exciton dissociation and charge transfer. This work demonstrates that the introduction of small molecule TADF materials based on the reverse-sensitization strategy is an effective strategy to achieve highly efficient organic solar cells larger than 20%.

SESSION EN04.08: Engineering Interfaces and Active Layer Properties
Session Chairs: Brian Collins and Chad Risko
Thursday Afternoon, April 25, 2024
Room 328, Level 3, Summit

1:30 PM *EN04.08.01

Aggregation Control of Organic Photovoltaic Molecules toward High Performance [Tao Wang](#); Wuhan University of Technology, China

The emergence of new organic semiconductors has driven the continuous development of organic solar cells, with the power conversion efficiency of single-junction devices having passed 19%. The strong intermolecular interactions between organic semiconductors lead to the self-assembly of them into hierarchical aggregates, which exhibits vastly different optoelectronic properties compared to those of the single molecules. Revealing and controlling the complex aggregation structure of organic semiconductors, and establishing the key relationship between structure and the power conversion process, is vitally important toward high performance organic solar cells, but remains as a grand challenge.

We have developed a number of physical and chemical approaches to tune the hierarchical aggregates of organic photovoltaic molecules: We developed the heating-induced aggregation strategy to suppress the large-size aggregation of crystalline semiconductors, realizing the conversion from large-size aggregation to small aggregation, which broadens the light absorption range and enhances exciton splitting; we developed the solution-induced aggregation strategy, realizing the conversion from random aggregation to ordered aggregation, which increases the light absorption intensity and improves charge transport; we also developed the small-molecular fibrillization strategy, realizing the conversion from short-range aggregation to long-range aggregation, which resolves the serious charge recombination issue during charge hopping and achieves a device efficiency of over 19%. The correlation between aggregates and light absorption, exciton dissociation and charge transport processes is eventually established to direct the future development of organic solar cells.

2:00 PM *EN04.01.05

Towards High-Performance Organic Solar Cells Deposited from Nanoparticle Dispersions Felix Manger, Philipp Marlow, Jonas Armleder, Karen Fischer, Holger Röhm, Christian Sprau and [Alexander Colsmann](#); Karlsruhe Institute of Technology, Germany

Record power conversion efficiencies of organic solar cells are most often achieved upon deposition from toxic solvents such as chloroform. Yet, organic solar cells can reach their full potential only if high performance is coupled with eco-friendly processing of organic semiconductors instead. Recent reports have demonstrated that organic nanoparticle dispersions are a viable route to combine sustainable production with maintaining high power conversion efficiencies. As of today, omitting surfactants for the stabilization of the dispersions appears mandatory when targeting highest solar cells performance since surfactants would remain in the solar cell and affect the formation of the delicate bulk-heterojunction. When using electrostatic stabilization instead, so far, only selected donors can be combined with selected absorbers in selected dispersion media to produce stable nanoparticle dispersions. In this work, design criteria will be discussed how to select the components of the dispersion. The role of the ionization potential of donors, the miscibility of donors and acceptors as well as the properties of the dispersion medium are elucidated. Stabilization concepts of the dispersions are compared for their process viability.

[F. Manger et al., Adv. Energy Mater. 2023, 2202820; F. Manger et al., Adv. Funct. Mater. 2022, 2202566; P. Marlow et al., Nanoscale 2022, 14, 5569-5578]

2:30 PM EN04.08.03

Ester-Functionalized Poly(thiophene vinylene) with Controlled Molecular Weights for High-Performance Intrinsically-Stretchable Organic Solar Cells [Tan Ngoc-Lan Phan](#), Jinwoo Lee and Bumjoon Kim; Korea Advanced Institute of Science and Technology, Korea (the Republic of)

Poly(thiophene vinylene)s (PTVs) are a promising type of polymer donors (PDs) for organic solar cells (OSCs) owing to their advantages of simple chemical structures and straightforward synthesis. However, the structural rigidity of PTVs results in the formation of thin films with inadequate mechanical properties for application in intrinsically stretchable (IS)-OSCs. In this work, we prepare a new ester-functionalized PTV with controlled molecular weights (MWs) (PETTCVT-X, X = L, M, and H) and demonstrate efficient and mechanically durable IS-OSCs. The crystallinity of the PTVs increases gradually with increasing MW, yielding enhanced hole mobility and suppressed charge recombination of the OSCs. Moreover, both the mechanical stretchability and electrical properties of the PTVs are improved notably with increasing MW. Consequently, rigid-OSCs featuring a PTV with the highest MW (PETTCVT-H) exhibit the highest PCE (15.3%) and crack-onset strain (COS, 8.3%) among the series, compared to lower values for the low- (PETTCVT-L, PCE = 9.7% and COS = 1.2%) and medium-MW counterparts (PETTCVT-M, PCE = 12.5% and COS = 4.3%)-based OSCs. Accordingly, the IS-OSCs utilizing PETTCVT-H present the highest initial PCE (10.1%) and stretchability (strain at PCE80% (retaining 80% of the initial PCE) = 16%). This work leverages the use of PTV for high-performance IS-OSCs.

2:45 PM EN04.08.04

Unraveling The Impact of Polymer and Solvent Additives on Aggregated Y6 Thin Films using Electroabsorption Spectroscopy [Sudhi Mahadevan](#)¹, Shanchao Ouyang¹, Liu Taili² and Sai Wing Tsang¹; ¹City University of Hong Kong, China; ²Yunnan Normal University, China

Organic photovoltaic cells (OPVs) using Y6 non-fullerene acceptors (NFA) have recently achieved record-breaking efficiencies with negligible photovoltage loss. According to GIWAXS and theoretical calculation results, Y6 exhibits unique molecular packing, significantly contributing to the overall charge transfer (CT) properties. In this report, we will demonstrate the application of electroabsorption (EA) spectroscopy to examine the impact of different aggregates on the intermolecular CT characteristics of Y6 and also the directional molecular orientation in thin films. To probe the intermolecular interactions in Y6, we fabricated and tested solid-solvation thin films by dispersing Y6 molecules in various organic polymers. We also used solvent additives such as DIO and CN to study the aggregation effect and corresponding charge transfer characteristics of Y6 in the second harmonic EA spectrum. Interestingly, the added polymers and solvent additives lead to aggregation-induced spectral shifts and broadening of both optical absorption and electroabsorption spectra. The differences in aggregated and non-interacting molecular distribution due to solvent additives in Y6 have been quantitatively evaluated using Franck-Condon analysis. From EA fitting results, it is found that along with increased dipole moment, the change in polarizability during aggregation contributes to the strong CT character, which has been overlooked in previous works. An exciton recombination model is proposed to validate the CT property by considering the spatial overlap of the electron-hole wavefunctions. These findings give insight into the impact of different polymer and solvent additives on the morphology and CT characteristics of Y6 thin films. Also, this can be an important step towards upscaling highly efficient organic photovoltaics.

3:00 PM BREAK

3:30 PM *EN04.08.05

Precise Control of Nanostructures in Organic Photovoltaics beyond Mixed Bulk Heterojunction Keisuke Tajima; RIKEN Center for Emergent Matter Science (CEMS), Japan

Current organic photovoltaics (OPVs) achieve high conversion efficiencies through donor/acceptor interpenetrated bulk heterojunction (BHJ) structures. In general, BHJ structures are created by simply mixing two materials, electron donor and acceptor, but there are challenges in building nanostructures that are optimal for charge generation and their stability. For example, prolonged heat treatment causes donor/acceptor phase separation, which reduces conversion efficiency. More precise control of the nanostructures in OPVs beyond the simple mixed BHJ is needed to improve the efficiency and robustness of the devices.

One strategy we have investigated is the use of photocrosslinkers. We have introduced singlet photocrosslinkers based on diazine (2Dz) or azide (2Bx) into BHJ to stabilize the morphology of mixed BHJ films. The photocrosslinking reactions in BHJs have significant detrimental effects on the performance of OPVs. This is in striking contrast to previous reports on organic field-effect transistors, where these singlet crosslinkers can solidify the films without affecting the charge transport properties. Based on the OPV results with the layer-by-layer deposited films and the transferred films, we found that the crosslinking reactions had greater effects on the non-fullerene acceptor than on the donor polymer. The photoluminescence measurements suggested that the crosslinkers could react with the π -conjugated backbone of the non-fullerene acceptor to form trace amounts of by-products that cause strong exciton quenching. These results indicate that the use of the "universal" singlet photocrosslinkers in OPVs requires careful selection of the organic semiconducting materials and crosslinkers. In the talk, we will also discuss other strategies recently employed in our group to control nanostructures and molecular orientations in OPVs.

4:00 PM *EN04.08.06

High-Throughput Screening of Materials for Rainbow Multi-Junction Organic Solar Cells Mariano Campoy-Quiles; ICMAB-CSIC, Spain

Single-junction organic solar cells (OSC) nowadays have reached promising power conversion efficiencies around 19%. Besides new materials, going beyond the current efficiencies could, in principle, be achieved by multi-junction devices, which promise a reduction in thermalization losses [1]. For this promise to become a reality, two items should be addressed, namely, the multi-junction geometry and the screening of materials with very different gaps. In this talk, we will present a multi-junction in-plane spectral splitting geometry that we call Rainbow solar cells [2]. In this geometry, a series of sub-cells are placed next to each other laterally, and illuminated through an optical component that splits the incoming white beam into its spectral components, thus matching local spectrum and absorption for each sub-cell. The fabricated n-terminal devices are capable of extracting the maximum power of each sub-cell without the need for current matching nor processing challenges. We demonstrate the concept for PM6:IO-4Cl and PTB7-Th:COTIC-4F blends, as high and low band-gap sub-cells, respectively. In agreement with simulations, we show an efficiency increase of around 30% of the Rainbow geometry with respect to our best single junction device [2]. Finally, we use high throughput methods based on gradients on the parameters of interest [3] to screen tens of materials exhibiting either wide band gap or narrow bandgap, and thus pushing the efficiency of the Rainbow multi-junction further up.

[1] I. M. Peters et al, *Prog. Photovolt.* 31 (2023) 1006.

[2] M. Gibert-Rocat et al, *Adv. Mater.* (2023) <https://doi.org/10.1002/adma.202212226>

[3] X. Rodríguez-Martínez et al, *Ener. Environ. Scien.* 14 (2021) 986.

4:30 PM EN04.08.07

Open Circuit Voltage Losses in Organic Planar and Bulk Heterojunction Solar Cells - The Role of Interfacial Energetics Richard A. Pacalaj¹, Yifan Dong², Tack Ho Lee³, Yang Fu⁴, Yi-Chun Chin¹, Lucy Hart¹, Ji-Seon Kim¹ and James Durrant¹; ¹Imperial College London, United Kingdom; ²National Renewable Energy Laboratory, United States; ³Pusan National University, Korea (the Republic of); ⁴The Chinese University of Hong Kong, Hong Kong

The introduction of non-fullerene acceptors (NFAs) has led to a surge in the record power conversion efficiency (PCE) of bulk heterojunction (BHJ) organic photovoltaics (OPV) now exceeding 19%.¹ These achievements were made in part due to the greater flexibility in tuning their energetic levels. Narrow bandgap NFAs enable improved absorption extending into the near-infrared region. Particularly successful candidates like Y6 and IT-4F have also been shown to exhibit long exciton diffusion length exceeding 30 nm.² At the same time, the possibility to better match the energy levels with complementary absorption donor polymers helped to decrease the energy offset related voltage losses. Despite this reduction in interfacial energy offsets, OPVs still exhibit larger voltage losses relative to their effective bandgap than other inorganic photovoltaic technologies. A better understanding of the involved voltage losses and how to further reduce them constitutes the main challenge on the quest to breach the 20% PCE threshold.

Up until now, efficient OPVs consisted of a bulk heterojunction (~ 10nm domain sizes) to enable efficient exciton separation while also allowing for thick active layers (~ 100nm) to maximise absorption. However, the large area of the donor/acceptor interface contributes to the observed voltage losses through the increased recombination rate.³ Given the high exciton diffusion length of NFAs like IT-4F and Y6, this raises the question of whether a planar heterojunction (PHJ) architecture could yield reduced voltage losses at the limited well-defined interface while also enabling high photocurrents through tuning the acceptor layer to the exciton diffusion length.

Here, we study the charge generation and voltage loss characteristics of a series of well-defined PHJs (including IT-4F/PM6 and Y6/PM6) produced by a polymer film transfer method⁴ as well as evaporated PHJs. Through optical and optoelectronic measurements, we assess the charge generation and voltage loss characteristics compared to their BHJ counterparts. A special emphasis is put on the comparison of interfacial energetics – especially the observed morphology dependent electrostatic effects due to the high quadrupole moment in high performing NFAs. Our findings have implications for the optimisation of future low voltage loss device structures as well as for the understanding of interfacial electrostatic effects in BHJs and PHJs.

1. Zhu, L. *et al.* Single-junction organic solar cells with over 19% efficiency enabled by a refined double-fibril network morphology. *Nat. Mater.* **21**, 656–663 (2022).

2. Firdaus, Y. *et al.* Long-range exciton diffusion in molecular non-fullerene acceptors. *Nat Commun* **11**, 5220 (2020).

3. Vandewal, K. *et al.* Increased Open-Circuit Voltage of Organic Solar Cells by Reduced Donor-Acceptor Interface Area. *Adv. Mater.* **26**, 3839–3843 (2014).

4. Lee, T. H. *et al.* Planar Organic Bilayer Heterojunctions Fabricated on Water with Ultrafast Donor-to-Acceptor Charge Transfer. *Solar RRL* **5**, 2100326 (2021).

4:45 PM EN04.08.08

Targeting Defects on Metal-Oxide/Organic Interfaces: Maximizing The Charge Extraction of Organic Solar Cells David Garcia Romero, Lorenzo Di Mario, Feng Yan, Carolina M. Ibarra Barreno, Suhas Mutalik, Loredana Protesescu, Petra Rudolf and Maria Antonietta Loi; University of Groningen, Netherlands

Metal-oxide transport layers have become an essential building block for fabricating thin-film solar cells. In particular, the robustness, inert nature, easy processability from solution, and high carrier mobilities offered by several both n-type, such as SnO₂ or ZnO, and p-type, like NiO_x or MoO_x, have made them promising candidates for improving performance and scaling up organic solar cells^{1,2}. Nevertheless, the inherent formation of surface traps during the

fabrication process, originating either from structural defects or from ligand residuals, can influence negatively the solar cell characteristics and device stability, and ultimately make them fail to become a standard transport layer.

Herein, we have studied independently two different systems: firstly an n-i-p structure using SnO₂ as the bottom n-type layer and, secondly, a p-i-n structure with a bottom NiO_x as the p-type layer. In both cases, commercially available well-known colloidal inks were employed.

For the first case, s-shaped J-V curves and poor device stability evidenced the suboptimal interface quality with SnO₂. We identified the presence of potassium ions as stabilizing ligands, staying on the film surface as trap sites. By removing them with a simple washing with deionized water, we remove the s-shape and improve the device efficiency from 12.82% to 16.26% and the stability to maintain up to ≈87% after 100 hours³.

In the second case, a low V_{OC} is found when NiO_x is used as the hole transport layer with the same active layer. Through the combination of multiple spectroscopic methods, we pinpoint the specific NiO_x structural surface defects that are limiting the charge extraction, and we propose a passivation strategy using carbazole-based self-assembly monolayers (SAMs). We demonstrate the passivation mechanism and we generalize it by screening out several SAMs. After all the optimization, solar cells with around 18% of power conversion efficiency are demonstrated.

[1] Fakhruddin, A., Vasilopoulou, M., Soultati, A., Haider, M.I., Briscoe, J., Fotopoulos, V., Di Girolamo, D., Davazoglou, D., Chroneos, A., Yusoff, A.R.b.M., Abate, A., Schmidt-Mende, L. and Nazeeruddin, M.K., Sol. RRL, 2021, 5: 2000555.

[2] R. Sorrentino, E. Kozma, S. Luzzati and R. Po, Energy Environ. Sci., 2021, 14, 180—223

[3] Garcia Romero, D., Di Mario, L., Yan, F., Ibarra-Barreno, C. M., Mutalik, S., Protesescu, L., Rudolf, P., Loi, M. A., Adv. Funct. Mater., 2023, 2307958.

SESSION EN04.09: Active Layer Composition and Morphology

Session Chairs: Xinhui Lu and Tao Wang

Friday Morning, April 26, 2024

Room 328, Level 3, Summit

8:30 AM *EN04.09.01

Combined Dynamics and Nanostructure Analyses for Paths that Maximize NFA Solar Cell Performance [Brian A. Collins](#); Washington State University, United States

Organic solar cells stand on the precipice of >20% efficiencies and large-scale commercialization. Unfortunately, constrictive processing options and a lack of direct connections between nanostructure, device dynamics, and performance hold back the promise of this exciting technology. I will describe our efforts in combining device-relevant loss analyses with quantitative nanostructure characterization to reveal key considerations in maximizing device performance. In particular, one barrier to scaleup is runaway crystallinity of NFA solar cells where slight fluctuations in additive concentrations compromise even lab-scale devices. We find that expanding processing toward non-halogenated additives both halt runaway crystallinity and work toward less-toxic manufacturing. However, only a detailed connection between the new morphology and device dynamics can reveal the opportunities for further improvements. Applying these processing and measurement strategies will be critical to understanding and mastering new materials breakthroughs that launch the technology toward a new solar future.

9:00 AM *EN04.09.02

Multicomponent Blend Strategy for Enhanced Performance and Longevity in Organic Photovoltaics [Tayebeh Ameri](#)^{1,2}; ¹Kiel University, Germany; ²University of Edinburgh, United Kingdom

Organic photovoltaics have made remarkable progress in recent years, achieving power conversion efficiencies of over 19% in laboratory-scale devices, marking a significant step towards their commercial viability. This advancement can be attributed to the integration of non-fullerene acceptor materials and the adoption of the multicomponent/ternary blend approach within the organic photovoltaic technology.

However, the organic photovoltaic community, focused on enhancing the power conversion efficiency, had previously overlooked the critical aspects of lifetime and stability issues for more than a decade. Recent efforts have focused on addressing these concerns, with numerous studies conducted to comprehend the degradation mechanisms and improve the overall longevity of organic photovoltaics.

This presentation will delve into the development of the ternary blend approach, which has not only elevated the power conversion efficiency but also enhanced the open circuit voltage and fill factor. We will provide insights into the working principles and the underlying mechanisms governing the open circuit voltage in ternary systems, consisting of a polymer donor, a nonfullerene acceptor, and a fullerene acceptor. Furthermore, we will explore how this approach can effectively address stability issues linked to the commonly used zinc oxide electron transport layer, thereby significantly improving the photostability of organic photovoltaics.

9:30 AM EN04.09.03

Controlling All-Polymer Solar Cell Morphology and Performance via Systematic Fluorination of Both Donor and Acceptor Polymers [Yilei Wu](#) and Zhenan Bao; Stanford University, United States

The influence of the conjugated backbone fluorination on the blend film morphology and photovoltaic characteristics of all-polymer solar cells (all-PSCs) is systematically investigated. The fluorination effect analysis of both donor and acceptor polymers is enabled by implementing a random terpolymerization strategy which produces conjugated polymers with tunable fluorine-containing monomer loading. Experimental results reveal that systematic fluorination variation greatly influences both inter-chain interactions and solubility parameters, and ultimately the degree of phase separation and morphology evolution. Specifically, increasing fluorine content for both polymers reduces blend film domain sizes and enhances donor-acceptor polymer-polymer interfacial areas, affording increased short-circuit current densities (J_{sc}). Moreover, the greater temperature-dependent aggregation (TDA) of fluorinated polymers in the solution-phase minimizes disorder and intermixed feature proliferation accompanying increasing fluorination, which would otherwise promote charge-carrier recombination, reducing cell fill factors (FF). The optimized photoactive layers exhibit well-balanced exciton dissociation and charge transport characteristics, providing solar cells with a significant power conversion efficiency (PCE) enhancement versus devices with nonoptimal fluorination content. Overall, it is shown that proper and precise tuning of both donor and acceptor polymer is critical for optimizing all-PSC performance. Modification of a single component, on the other hand, may lead to local maximum PCE. This study provides a general synthetic methodology to predictably access conjugated polymer blends with desired fluorine-content and highlights the importance of optimizing both donor and acceptor components to achieve the full potential of all-PSCs devices.

9:45 AM EN04.09.04

Structurally Pure and Reproducible Polymer Materials for High-Performance Organic Solar Cells – Insights in the Chemical Structures of PM6 and D18 Sander Smeets^{1,2}, Jochen Vanderspikken^{1,2}, Quan Liu^{1,2}, Tyler Quill³, Sam Gielen^{1,2}, Laurence Lutsen^{1,2}, Koen Vandewal^{1,2} and Wouter Maes^{1,2}; ¹Hasselt University, Belgium; ²IMEC, Belgium; ³Stanford University, United States

While (push-pull) semiconducting polymers are now displaying better device performances than ever before, their commercial uptake remains limited, in part due to challenges in terms of reproducibility. Next to consistent device fabrication, continuous material quality is of high importance to obtain optimal and reliable performance metrics. Often the assumption is made that the “drawn” chemical structure is representative of the active material used in applications such as polymer-based solar cells. It has, however, become clear that this is not always the case. In this work, we assess the structures of two top-performing organic solar cell donor polymers, PM6 and D18, both for commercial and synthesized samples.¹¹ Using matrix-assisted laser desorption/ionization time-of-flight mass spectrometry (MALDI-ToF MS) we analyze the chemical structures in detail. We also introduce an approach to limit structural defects and study the impact on device performance. Next to that, we translate the synthesis of these polymer materials to a droplet flow protocol, not only to limit batch variability but also as a means to achieve reproducible molar masses. In general, flow chemistry offers benefits such as easier scalability and enhanced safety at larger scale. Droplet-flow synthesis in particular has demonstrated excellent reproducibility, both in terms of molar mass distribution and optoelectronic properties of push-pull conjugated polymers. This allows a detailed investigation of the impact of chemical structure and molar mass on blend morphology and solar cell performance.

10:00 AM BREAK

SESSION EN04.10: Interrogation and Control of Structure and Dynamics I

Session Chair: Keisuke Tajima

Friday Morning, April 26, 2024

Room 328, Level 3, Summit

10:30 AM *EN04.10.01

Understanding The Crystalline and Amorphous Morphology of Organic Solar Cells using Grazing-Incidence X-Ray and Neutron Scattering Techniques Xinhui Lu; The Chinese University of Hong Kong, Hong Kong

Organic photovoltaic molecules or polymers typically form semicrystalline thin films. It is widely recognized that the bulk heterojunction (BHJ) morphology of organic photovoltaic thin films, which consists of both crystalline and amorphous regions, plays a crucial role in determining the performance of devices. However, understanding the intricate three-dimensional multi-length scale morphology of these thin films remains a grand challenge. In this talk, we will present our recent progress on decoding the complex BHJ morphology of OPVs and developing strategies to control the morphology to enhance device performance. In addition to employing conventional techniques like GISAXS/GIWAXS, we will introduce two innovative methods: GTSAXS, which allows for the quantification of vertical nanomorphology, and GISANS combined with deuteration, a technique used to detect amorphous phase structures. Armed with these state-of-the-art scattering techniques, we investigated the optimal active layer morphology for OPVs, aiming at understanding the impacts of amorphous and crystalline phase structures on device performance and to advance the practical applications of these devices. Furthermore, these scattering techniques can also be applied in material science, chemistry, biology and condensed matter physics studies. By modifying the wavelength of the probing beam and the experimental geometry, a variety of sample types, such as solutions, powders, surfaces and thin films, can be studied, covering wide length scales as well as versatile dynamic and kinetic behaviors.

11:00 AM EN04.04.06

Evidence for Entropy-Driven Charge Separation in Non-Fullerene Acceptor/Polymer Bulk Heterojunction Kushal Rijal¹, Neno N. Fuller¹, Fatimah H. Rudayni^{1,2} and Wai-Lun Chan¹; ¹University of Kansas, United States; ²Jazan University, Saudi Arabia

Organic photovoltaics (OPVs) based on non-fullerene acceptors (NFAs) have achieved power conversion efficiencies close to 20%. These NFA OPVs can efficiently generate free carriers at the donor/acceptor (D/A) interface despite a very small energy level offset. However, why efficient charge separation can occur with a minimal energy loss is still not clear. We will present our recent time-resolved two-photon photoemission (TR-TPPE) spectroscopy measurements on exciton dynamics in a representative NFA/polymer blend, the Y6/PM6 bulk heterojunction (BHJ). We find that charge transfer (CT) excitons are formed within a few picoseconds after the photoexcitation. Subsequently, an energy uphill process occurs in which the energy of the CT exciton is increased by 0.15 eV on the 10-100 ps timescale. We attribute this energy uphill process to the conversion of bound CT excitons to free electron-hole pairs. The observed energy uphill process is rather anomalous because excited electrons typically lose their energy to the environment when no external electric field is applied. We propose that the energy uphill charge separation process is driven by entropy. The entropy-driven charge separation would be promoted by the specific nanostructure of NFA BHJs. This work is based upon work supported by the U.S. Department of Energy, Office of Basic Energy Sciences, under Award No DE-SC0024525.

11:15 AM EN04.10.03

Study on The Network Formation Mechanism of The Photoactive Domains in Organic Photovoltaics Jinsung Kim¹, Yepin Zhao¹ and Yang Yang^{1,2}; ¹University of California, Los Angeles, United States; ²California NanoSystems Institute, University of California, Los Angeles, United States

Organic photovoltaics (OPVs) have emerged as a promising technology for clean energy generation, characterized by their cost-effectiveness, solution processability, and high transparency. In recent years, there has been a spike in power conversion efficiency from the continuous development of nonfullerene small molecule acceptors. However, despite recent performance improvements, a comprehensive mechanism analysis on the network formation of the donor and acceptor domains needs more investigation. In this study, the morphology transition mechanism of the bulk-heterojunction network was studied to identify the photoactive domain formation process. In-situ UV-vis absorption analysis showed that the donor polymers established a network framework, acting as a structural body in the system, with small molecules subsequently penetrating this structure. It was also confirmed by mapping the solidified network, visually showing clear donor and acceptor domains. Crucially, the drying environment during the deposition of donor and acceptor solutions plays a pivotal role in determining the network structure. Leveraging this insight, a novel additive material that effectively controls the drying speed of acceptor molecules was employed, resulting in improved performance of OPV devices. Lastly, the system was also applied to fabricate semitransparent OPV with over 3.5 light utilization efficiency values.

11:30 AM EN04.10.04

Identify The Physical Processes occurring in Poly-Small-Molecule Acceptor-Based All-Polymer Bulk Heterojunction Solar Cells [Shahidul Alam](#) and Frédéric Laquai; King Abdullah University of Science and Technology, Saudi Arabia

For some fundamental reasons, the performance of all-polymer solar cells is behind the state-of-the-art in small molecule non-fullerene acceptor bulk heterojunction organic solar cells. This work investigates the efficiency-limiting processes in all-polymer solar cells using blends of the common donor polymer PBDB-T and PM6 with two acceptor polymers, namely PYN-BDT and PYN-BDTF. These compounds function as macromolecular absorbers with large optical cross-sections extending to around 900 nm due to their π -extended naphthalene rings. Combining data from steady-state optical spectroscopy and time-resolved photoluminescence, transient absorption, electron spin resonance, and time-delayed collection field experiments provides not only a concise but also quantitative assessment of the losses due to limited photon absorption, geminate and non-geminate charge carrier recombination, field-dependent charge generation, and inefficient carrier extraction. Kinetic parameters obtained by pulsed laser spectroscopy are used to reproduce the experimentally-measured device IV characteristics and indicate that low fill factors originate either from non-geminate recombination competing with charge extraction or from a pronounced field dependence of charge generation, depending on the donor polymer. The methodology presented here is generic and can be used to quantify the loss processes in BHJ OSCs, including both all-polymer and small-molecule NFA systems.

11:45 AM EN04.10.05

Interface Energy Level Offset of Organic Solar Cells Measured by UPS and IPES and Its Correlation with Voc and CT Exciton Energy Gyuhyeon Lee¹, Younghwan Kim¹, Min-Jae Maeng¹, Kyu-Myung Lee¹, Jong-Am Hong¹, Kyung-Geun Lim² and [Yongsup Park¹](#); ¹Kyung Hee University, Korea (the Republic of); ²KRISS, Korea (the Republic of)

In organic light-emitting diodes (OLEDs) and heterojunction organic solar cells (OSCs), the energy offset between HOMO and LUMO, also called the transport gap (E_t) is substantially different from optical gaps due to the relatively large exciton binding energies. However, the inability to independently measure the LUMO levels makes it hard to elucidate important things like electron injection barrier at the cathode in OLEDs and the voltage loss mechanisms in Voc of OSCs.

We have recently developed highly sensitive inverse photoemission spectroscopy (IPES) instrument specifically for the LUMO level measurement of organic semiconductors. In combination with the existing ultraviolet photoemission spectroscopy (UPS) we determined all the relevant transport energy levels (HOMO, LUMO, Fermi level and vacuum level) in any organic semiconductor surface and interface. In addition, combination of the electron source for IPES and the electron energy analyzer for UPS allowed us to utilize reflection electron energy loss spectroscopy (REELS) to determine the gaps. We first demonstrate that all these measurements can be performed for an identical sample as a function of thickness. We also determine the energy levels at both C60/pentacene and C60/CuPc interfaces so that the factors affecting the voltage losses that led to observed Voc value of the model planar heterojunction organic solar cells can be evaluated.

In addition, we fabricated bilayer model organic solar cells using C60/pentacene and C60/CuPc pairs. The deposition sequence of each layer was alternated resulting in four different types of devices, namely, C60/pentacene, pentacene/C60, C60/CuPc, and CuPc/C60. We confirmed that there exists interfacial energy offset difference between C60/pentacene and pentacene/C60 devices, which is also reflected in Voc values of respective devices. This is due to the difference in molecular orientation for pentacene depending on the deposition sequence in this binary system. On the other hand, we could not observe any dependence of Voc on deposition sequence of C60 and CuPc devices nor could we measure any energy offset at the interface, where the molecular orientation is expected to be independent of deposition sequence. We further investigate the charge transfer (CT) exciton energies for all the devices by using sensitive external quantum efficiency (EQE) measurement. These combined measurements led us to identify the most important parameter in determining the Voc of these model bilayer organic solar cells.

This work was supported by Korea Basic Science Institute (National Research Facilities and Equipment Center) grant funded by the Ministry of Education (2021R1A6C101A437) and National Research Foundation of Korea (NRF) BRL program grant funded by the Korean government (MSIT) (2022R1A4A3030766).

SESSION EN04.11: Interrogation and Control of Structure and Dynamics II

Session Chair: Keisuke Tajima
Friday Afternoon, April 26, 2024
Room 328, Level 3, Summit

1:30 PM *EN04.11.01

Interrogating Structure, Dynamics, and Disorder in Organic Semiconductors [Chad Risko](#); University of Kentucky, United States

The design of π -conjugated polymers for solution-deposited organic semiconductors commonly considers the chemical modulation of (i) the π -conjugated backbone to modify the electronic and optical characteristics and (ii) the alkyl-based side chains to govern solubility. During solution deposition and solidification of the semiconductor, physical interactions among these constituents and their solution environment play an important, yet not well understood, role. Here we will discuss the development of computational models to interrogate how the chemistry of π -conjugated polymers impact polymer structure and dynamics and the resulting properties of materials derived from these building blocks. The chemical insight developed through these investigations is beginning to refine and offer new understanding essential to the development of next generation organic semiconducting active layers.

2:00 PM EN04.11.02

Overcome The Limits of Conductivity in Doped Organic Semiconductors [Eva Röck](#) and Natalie Banerji; DCBP, Switzerland

We study the conductivity of doped organic semiconductors and vary (i) the electrostatic environment with anion exchange of the dopant and (ii) the dielectric constant with oligo ethylene glycol side chains. Since organic semiconductors are commonly disordered materials such as polythiophenes, it is crucial to look at the conductivity on different length scales. The comparison between electrical four point probe and optical THz time domain spectroscopy is the experimental core of this study resulting in the conductivity over the long-range (millimeters) and short-range (nanometers) respectively.

Anion exchange from F_4TCNQ^- to PF_6^- doubles the short-range conductivity of $P(g_2T-T)$ up to 610 S/cm, which is related to an increased density of contributing charges. Similarly for $P(g_3BTTT)$ upon anion exchange the conductivity doubles to 1280 S/cm. Since PF_6^- is smaller than F_4TCNQ^- we suggest the improvement stems from a better insertion of the anion rather than an electrostatic effect. Hereby, we see an increased density of contributing

This searchable program is up-to-date as of April 15th, 2024.

charges while their mobility is limited. This is verified by fitting the short-range conductivity with the Drude-Smith model for disordered systems. Furthermore, we track the changes in absorbance in-situ during chemical doping and electrochemical doping and find a substantial relation between polaron/bipolaron ratio and the best conductivity.

Oligo ethylene glycol side chains increase the short-range conductivity by increasing the number of contributing charges and their mobility in comparison to P3HT with alkyl side chains. We find that glycolated side chains help the absolute conductivity as well as its restoration (>90%) from the short-range (nanometers) to the long-range (millimeters) transport. The improvement hereby can be assigned to (i) the higher dielectric constant as well as (ii) lower energetic disorder. Understanding the conductivity on the short- and long-range is key for designing efficient devices based on doped organic semiconductors.

SYMPOSIUM EN05

Advances in Material, Catalyst and Device Design for Scalable Solar Fuel Production
April 22 - April 24, 2024

Symposium Organizers

Demetra Achilleos, University College Dublin
Virgil Andrei, University of Cambridge
Robert Hoye, University of Oxford
Katarzyna Sokol, Massachusetts Institute of Technology

Symposium Support

Bronze

Angstrom Engineering Inc.
National Renewable Energy Laboratory

* Invited Paper

+ JMR Distinguished Invited Speaker

^ MRS Communications Early Career Distinguished Presenter

SESSION EN05.01: (Photo)electrocatalytic CO₂ Reduction
Session Chairs: Demetra Achilleos and Virgil Andrei
Monday Morning, April 22, 2024
Room 335, Level 3, Summit

8:30 AM +EN05.01.01

Photoelectrochemical CO₂ Reduction: The Spotlight on The Light Absorber [Francesca M. Toma](#)^{1,2}; ¹Helmholtz-Zentrum Hereon, Germany; ²Lawrence Berkeley National Laboratory, United States

Light-driven CO₂ reduction into chemicals is considered as a promising way to meet carbon neutral targets. Photoelectrochemical (PEC) CO₂ reduction has attracted significant attention as a prevailing way to store intermittent solar energy in fuels and chemicals as well as closing the chemical carbon cycle. Unfortunately, thermodynamically viable photocathode materials for this process favor hydrogen evolution reaction (HER), thus leading to either insufficient activity or selectivity for CO₂ reduction reaction (CO₂RR). Besides the thermodynamic requirement, the semiconductor/electrolyte interface also plays a pivotal role in defining the performance of photoelectrodes, which can directly affect light driven CO₂RR efficiency and determine the product selectivity.

Here, we show few examples of how light absorber materials can be used in integrated photoelectrochemical cells or when directly interfaced with the electrolyte for CO₂RR. Specifically, we show how one can improve the stability and performance of photoelectrodes for PEC CO₂RR in systems that use Cu₂O or halide perovskite materials. In addition, we will discuss how ZnTe can enable photo-generated charge carrier transfer, but also acted as electrocatalyst for boosting carbon product selectivity and suppressing HER. Our work demonstrates that the fundamental understanding of the processes at the photoelectrode/electrolyte interface allows the systematic improvement of photoelectrode stability of CO₂RR selectivity.

9:00 AM EN05.01.02

CO₂ Electrolysis in Aqueous Media with Almost 100% Selectivity for CO Production by Water-Soluble Cobalt Dimethyl-Bipyridine Complex [Takeshi Morikawa](#)^{1,2}, [Tomiko M. Suzuki](#)¹, [Kengo Nagatsuka](#)², [Takamasa Nonaka](#)¹, [Yuichi Yamaguchi](#)², [Naonari Sakamoto](#)¹, [Takeshi Uyama](#)¹, [Keita Sekizawa](#)¹ and [Akihiko Kudo](#)²; ¹Toyota Central R&D Labs, Japan; ²Tokyo University of Science, Japan

We developed a water-soluble Co complex with dimethyl-bipyridine ligands ([Co(dmbpy)₃]³⁺, dmbpy: 4,4'-dimethyl-2,2'-bipyridine), which electrochemically reduces CO₂ to CO with almost 100% selectivity in an aqueous medium without an organic solvent. The reaction overpotential was 270 mV, and the Co complex (hereafter, [Co-dmbpy]) facilitated carbon dioxide reduction reaction (CO₂RR) to produce carbon monoxide (CO) with an almost 100% selectivity (against competitive H₂ production) at a low potential of -0.80 V vs. NHE (pH 6.8). We discuss a possible CO formation mechanism based on static and *operando* analyses combined with DFT calculations.[1]

A cyclic voltammetry (CV) of [Co-dmbpy] (0.3 mmol L⁻¹) measured in an aqueous NaHCO₃ (0.1 mol L⁻¹) solution bubbled with CO₂ exhibited a higher

reaction current than that in Ar bubbling (adjusted to pH 6.8) within the range of -0.4 to -1.6 V (vs. NHE). The DFT calculations suggested that a ligand-decoordinated species of $[\text{Co}(\text{dmbpy})_2]^{3+}$ is formed as an active monomer catalyst by the decoordination of one dmbpy ligand, which is consistent with an observed -1.5 eV shift in *operando* X-ray absorption spectroscopy (XANES) spectra obtained under an electrical bias in the aqueous NaHCO_3 (0.1 mol L^{-1}) solution bubbled with CO_2 . Therefore, it is strongly suggested that a one-dmbpy-decoordinated species is the active catalyst, and a rate-determining step is a CO_2 coordination to the Co center of one-electron injected species $[\text{Co}(\text{dmbpy})_2]^+$.

We have also reported artificial photosynthetic systems consisting of metal complexes and two coexisting semiconductors, which produce formic acid or CO under visible light irradiation by the Z-scheme (2-step photoexcitation) mechanism like photosynthesis in plants in a particulate dispersion setup. [2-3] The use of the aqueous dispersion of particulate photocatalysts for a membrane-free and one-compartment reactor is a simple and scalable approach to producing valuable chemicals. In particular, a system containing $[\text{Co}(\text{dmbpy})_2]^{3+}$ generated CO with a product selectivity of 98% (and H_2 of 2%). The reaction accompanied O_2 production under visible light irradiation, which suggested this photocatalytic system utilized H_2O as an electron donor for the CO formation. The ability of electrochemical CO_2RR over the $[\text{Co}(\text{dmbpy})_2]$ with a nearly 100% CO selectivity contributed to the extraordinarily high CO selectivity of 98 % in the Z-scheme photocatalytic system by receiving photoexcited electrons in the conduction band of a particulate semiconductor in an aqueous media.

CO is a desirable target product made from CO_2 and H_2O because it can be converted into various hydrocarbons via Fischer–Tropsch synthesis. Gaseous CO exhibits low solubility in aqueous media, making its collection easier than liquid products such as formic acid. Therefore, photocatalytic and (photo)electrochemical CO production using H_2O is valuable.

References

- [1] T. M. Suzuki, A. Kudo, T. Morikawa, *Chem. Commun.* (2023) in press, DOI <https://doi.org/10.1039/D3CC003940D>.
- [2] T. M. Suzuki, A. Kudo, T. Morikawa, et al., *Chem. Commun.*, 54 (2018) 10199-10202.
- [3] T. M. Suzuki, A. Kudo, T. Morikawa, et al., *Appl. Catal. B.*, 316 (2022) 121600.

9:15 AM EN05.01.03

Molecule-Derived Coatings Improve The Selectivity and Durability of CO_2 Reduction on Chalcogenide Photocathodes Joel Haber¹, John M. Gregoire¹, Yungchieh Lai¹, Lan Zhou¹, Kevin Kan¹, Nicholas Watkins¹, Jonas Peters¹, Theodor Agapie¹, Christopher Muzzillo² and Andriy Zakutayev²; ¹California Institute of Technology, United States; ²National Renewable Energy Laboratory, United States

Direct solar-driven conversion of carbon dioxide to chemicals and fuels requires identification of efficient, durable, and selective photocathodes. Chalcogenide p-type semiconductors, exemplified by chalcopyrite $\text{Cu}(\text{In,Ga})\text{Se}_2$ (CIGS), have been effectively deployed as photocathodes. However, selectivity toward CO_2 reduction and durability of the commonly used CdS buffer layer remain unsolved challenges. We have demonstrated that for the wide band gap CuGa_3Se_5 chalcopyrite absorber these challenges are well addressed by an organic coating generated in situ from an $\text{N,N}'$ -(1,4-phenylene)bispyridinium ditriflate salt in the electrolyte. The molecular additive provides a 30-fold increase in selectivity toward CO_2R products compared to the unmodified system and lowers Cd corrosion at least 10-fold. This dual functionality highlights the promise of hybrid solid-state-molecular photocathodes for enabling durable and efficient solar fuel systems. This presentation will highlight the variations in product selectivity and durability observed for different combinations of coatings derived from molecular precursors in the electrolyte with photocathodes including CuGa_3Se_5 and $\text{Cu}(\text{In,Ga})\text{Se}_2$, with and without CdS buffer layers.

9:30 AM EN05.01.04

CO_2 Reduction under Realistic Ambient Conditions with Directly coupled PV-EC Device Tsvetelina Merdzhanova¹, Thérèse Cibaka¹, Oleksandr Astakhov¹, Guangxin Liu², Chuyen Pham², Marc Heggen³, Peter Strasser⁴ and Uwe Rau^{1,5}; ¹Forschungszentrum Jülich GmbH, Institute of Energy and Climate Research (IEK-5-Photovoltaik), Germany; ²Forschungszentrum Jülich GmbH, Institute of Energy and Climate Research (IEK-11-HI-ERN), Germany; ³Forschungszentrum Jülich GmbH, Ernst Ruska-Centre for Microscopy (ER-C 1), Germany; ⁴Technical University of Berlin, Institute of Chemistry, Germany; ⁵Jülich Aachen Research Alliance (JARA-Energy) and Faculty of Electrical Engineering and Information Technology, RWTH Aachen University, Germany

Long-term storage in molecules like fuels or other industrially useful chemicals is most relevant for counterbalancing natural yearly oscillations in photovoltaic power generation. We address this challenge via ‘artificial leaf’ approach – conversion of carbon dioxide (CO_2), water (H_2O) and sunlight into valuable chemical products. This approach facilitates further deployment of photovoltaics and simultaneously utilizes exhaust or atmospheric CO_2 with potential to entirely close CO_2 cycle. Conversion of CO_2 into chemical fuels such as syngas (mixture of CO and H_2 products) is demonstrated with photoelectrochemical (PEC) devices, direct electrolysis, and direct photovoltaic-driven electrolysis (PV-EC). The PV-EC approach in direct connection is attractive as a good compromise between the design flexibility and high solar to chemical efficiencies. In this work we design, and test ‘A-leaves’ with emulated PV devices reproducing IV characteristics of real PV modules in the field at most relevant irradiance/temperature combinations. The characteristic operating point were obtained using the NREL public database for SHJ module installed in Eugene USA. With our newly developed PV emulator routine any PV IV can be replicated at high accuracy and at the same PV part of the PV-EC system can be adjusted to required size matching the size of the lab scale CO_2 reduction EC cell. In our work PV module of emulated area of 51.7 cm^2 drives flow-type stack EC cell (area 8.8 cm^2) with silver/gas diffusion layer (GDL) cathode [1] and iridium oxide anode. The EC cell consists of two electrode chambers separated by a Nafion membrane (N117, thickness 0.007 inch) and a 1 mol/l KHCO_3 electrolyte saturated with CO_2 (20 $\text{cm}^3\text{min}^{-1}$) flowing in both chambers. We have chosen five most probable irradiance and temperature combinations out of variety of ambient conditions with the highest PV energy generation, i.e., the PV-EC device is optimized for the region of major PV energy generation. In our case this is 1 Sun irradiance and 45°C PV temperature. Performance, power coupling and CO and H_2 products evaluation have been investigated in the context of most relevant PV irradiance (1 – 0.2 Sun) and temperature (25 – 45 °C) obtained from real PV data. Power coupling, or power matching between the photovoltaic and electrochemical components have been quantified with ‘coupling factor’ C – coefficient indicating proximity of the working point (WP) of the PV-EC device to the maximum power point (MPP) of the PV module.

High degree of coupling, more than 0.9 and solar-to-chemical efficiency in the range from 7.5 % to 10.8 % is observed at the most relevant PV irradiance (1 – 0.2 Sun) and temperature (25 – 45 °C). Successful production of CO with by-product of H_2 in the ration of 3:1 with Faradaic efficiency (F_E) of 70 - 100% was measured via chromatographic analytics. Over the experiment, operating voltages of 2.6 - 3.1 V and current densities 9 - 44.9 mA/cm^2 were observed. Energy loss analysis of PV-EC device at 1 Sun 45 °C was performed. SHJ module converts 22.5 % of solar power into electric power and due to relatively low PV-EC coupling loss, 21.3 % of the initial sun power reaches the EC cell. At the working voltage (V_{WP}) of 3.1 V and working current density of 44.9 mA/cm^2 , EC operates at 70 % Faradaic efficiency and 13.8% overpotential loss that translates into solar-to-chemical efficiency (STC) of 7.5 % estimated by using the equation:

$$\text{STC} = \text{PVeff.} \times \text{C} \times (\text{Ecell}/V_{\text{WP}}) \times F_E$$
 where Ecell is the energy stored in product CO or H_2 in voltage.

- [1] Liu, G., et al., *Chemical Engineering Journal* 2023, 40, 141757.

9:45 AM EN05.01.05

Controlling Methanol Selectivity on Immobilized Cobalt Phthalocyanine on Carbon Nanotubes for Photoelectrochemical and Electrochemical

CO₂ Reduction Calton J. Kong^{1,2}, Thomas Chan^{2,3}, Grace Rome⁴, Darci Collins⁴, Alex King^{2,1}, Rajiv Ramanujam Prabhakar², Sarah Collins⁴, Michelle Young², Mickey Wilson⁴, Finn Babbe², Tobias Kistler², Myles Steiner⁴, Adele Tamboli⁴, Emily Warren⁴, Cliff Kubiak³, Joel W. Ager² and Annie Greenaway⁴; ¹University of California, Berkeley, United States; ²Lawrence Berkeley National Laboratory, United States; ³University of California, San Diego, United States; ⁴National Renewable Energy Laboratory, United States

Electrochemical CO₂ reduction (CO₂R) using heterogenized molecular catalysts usually yields 2-electron reduction products (CO, formate); recently, it has been reported that certain preparations of immobilized cobalt phthalocyanine (CoPc) produce methanol (MeOH), a 6-electron reduction product. Here, we demonstrate the significance of the role mass transport plays in CoPc selectivity to different CO₂R products. Specifically, a moderate linear flow velocity of 8.5 cm/min has the highest MeOH selectivity at 35%, with higher flow rates increasing CO selectivity and lower flow rates increasing HER, suggesting that CO is a free intermediate. We use a simple, physically mixed, polymer free preparation of CoPc on multiwalled carbon nanotubes (MWCNT) to achieve moderate MeOH selectivity in near-neutral aqueous conditions at -1.2 V vs RHE. An onset potential of -0.8 V vs. RHE for MeOH was observed with increasing Faradaic efficiency until it reaches a relative maximum at -1.2V vs. RHE and lowering as the reductive potential increases. The catalyst was made compatible with Au planar substrates using a poly(3,4-ethylenedioxythiophene) polystyrene sulfonate (PEDOT:PSS) adhesion layer. Using the PEDOT:PSS adhesion layer, we integrated the CoPc catalyst onto a multijunction GaInP/GaAs three terminal tandem (3TT) solar cell, that could operate two separate electrodes at different potentials. We achieved 4% FE toward MeOH on the 3TT solar cell at +0.2 V vs RHE, demonstrating that the 3TT can be used as a platform for future study of tandem photoelectrochemical systems.

SESSION EN05.02: Perovskite and Organic Semiconductors
Session Chairs: Virgil Andrei and Robert Hoyer
Monday Afternoon, April 22, 2024
Room 335, Level 3, Summit

1:30 PM *EN05.02.01

Organic Semiconducting Polymer Photocatalysis for Water and CO₂ Reduction [Iain McCulloch](#); University of Oxford, United Kingdom

Green hydrogen, produced from water using renewable energy, is expected to become a prominent renewable fuel of the future, providing clean, carbon neutral energy for a wide range of industrial applications. It can also provide complementary energy storage in combination with intermittent solar energy. However, competitive economic solar generated hydrogen production on a large scale remains challenging. One promising approach is photochemical water splitting, using light absorbing nanoparticle semiconductors that can drive redox reactions on their surface. The more light the photocatalytic nanoparticle absorbs, the more efficiently it can split water into hydrogen and oxygen. Traditionally, wide bandgap inorganic semiconductors have been used for photocatalytic applications. However, these materials almost exclusively absorb UV light which only carries a small fraction (<5%) of solar energy, limiting their efficiency. In this presentation, the development of photocatalysts fabricated from organic semiconductors, chemically tuned to absorb strongly throughout the UV-visible spectrum will be discussed. We demonstrate a larger solar to hydrogen efficiency than traditional inorganic photocatalysts with the potential to achieve solar hydrogen production at a lower levelized cost. We have developed organic semiconductor nanoparticles that contain an internal donor/acceptor heterojunction between two organic semiconductors with a type II energy level offset. The donor/acceptor heterojunction greatly improves charge generation within the nanoparticles, which in turn greatly improves their hydrogen production efficiency. We demonstrate a substantial increase in the H₂ production efficiency by tuning the nanoparticle composition. We also observe that the high efficiency of these nanoparticles originates from their ability to generate exceptionally long-lived reactive charges upon illumination, increasing their likelihood to participate in a photocatalytic reaction. In addition, we will discuss solution-processable, linear conjugated polymers of intrinsic porosity for gas phase carbon dioxide photoreduction. The polymers' photoreduction efficiency is investigated as a function of their porosity, optical properties, energy levels and photoluminescence. All polymers successfully form carbon monoxide as the main product, without the addition of metal co-catalysts. The best performing single component polymer yields a rate of 66 $\mu\text{mol h}^{-1}\text{m}^{-2}$, which we attribute to the polymer exhibiting macroporosity and the longest exciton lifetimes. The addition of copper iodide, as a source of a copper co-catalyst in the polymers shows an increase in rate, with pTA-Ph (the most active) achieving a rate of 175 $\mu\text{mol h}^{-1}\text{m}^{-2}$. The polymers are active for over 100 hours under operating conditions. This work shows the potential of processable polymers of intrinsic porosity for use in the gas phase photoreduction of carbon dioxide towards solar fuels.

2:00 PM EN05.02.02

Defect-Passivated Perovskite Photoanode coupled with Iodide Oxidation Reaction enabling Efficient Stable Unbiased Hydrogen Production [Juwon Yun](#), Young Sun Park, Hyungsoo Lee, Wooyong Jeong, Chang-Seop Jeong, Gyumin Jang, Chan Uk Lee, Jeongyoub Lee, Subin Moon, Soobin Lee and Jooho Moon; Yonsei University, Korea (the Republic of)

Defect-passivated perovskite photoanode coupled with iodide oxidation reaction enabling efficient stable unbiased hydrogen production

Juwon Yun, Young Sun Park, Hyungsoo Lee, Wooyong Jeong, Chang-Seop Jeong, Chan Uk Lee, Jeongyoub Lee, Subin Moon, Soobin Lee, Sumin Kim, Junhwan Kim, and Jooho Moon*

¹Department of Materials Science and Engineering, Yonsei University
50 Yonsei-ro Seodaemun-gu, Seoul 120-749, Korea

*E-mail address : jmoon@yonsei.ac.kr

The unassisted photoelectrochemical (PEC) hydrogen production is one of the promising candidates to replace the carbon-based energy sources. However, the previously reported photoanodes have suffered from low efficiency resulting from poor light absorption and limited charge separation capability. Lead halide perovskite has emerged as a promising breakthrough to overcome the limitations of conventional photoanode materials (such as BiVO₄, Fe₂O₃, Ta₃N₅, Sb₂S₃, and WO₃) owing to its tunable bandgaps, excellent hole mobility, and long hole-diffusion length. These superior properties enable perovskite-based photoanode to achieve remarkable high-performance parameters including a photovoltage of ~ 1.1 V and a photocurrent density of around 23 mA cm⁻². However, there are still challenges in achieving competitive hydrogen production, particularly in terms of onset potential and long-term stability. The poor onset potential can be attributed to the high thermodynamic potential (1.23 V with respect to reversible hydrogen electrode (V_{RHE})) required for the oxygen evolution reaction (OER) and the sluggish kinetics of OER involving a four-electron transfer process. Moreover, the charge accumulation due to interfacial defects and slow charge transfer reaction result in efficiency loss and photoelectrode degradation. Herein, we report a straightforward strategy to improve the onset potential and durability of perovskite photoanode. This approach involves simple defect passivation method by decorating 4-methoxyphenethylamine on electron transport layer (ETL), effectively suppressing efficiency loss and charge

accumulation at ETL/perovskite interface. Furthermore, we replace the OER with the iodide oxidation reaction (IOR) by employing an active IOR catalyst ($\text{Co}_{0.2}\text{Ni}_{3.5}\text{S}_2$) to enhance the kinetics of charge transfer reaction. The combined effects of interface engineering and the IOR catalyst are manifested by the enhanced PEC performance and stability. The perovskite photoanode reveals a $-0.2 V_{\text{RHE}}$ onset potential and improved fill factor along with a high durability for 200 h. We additionally demonstrate unbiased hydrogen production consisting of single perovskite photoanode and Pt catalyst achieving the operation current of 12 mA cm^{-2} and stable operation for 24 h.

2:15 PM EN05.02.03

A Polymer Overlayer Generates Long-Lived Charges in PM6:Y6 Bulk-Heterojunction Photoanodes with Improved Photoelectrocatalytic Performance [Tack Ho Lee](#); Pusan National University, Korea (the Republic of)

Photogenerating charges with long lifetimes to drive catalysis is challenging in organic semiconductors. Here, we investigate the role of a PM6 polymer overlayer on the photoexcited carrier dynamics in a PM6:Y6 bulk-heterojunction (BHJ) photoanode undergoing ascorbic acid oxidation. With the additional polymer layer, the hole lifetime is increased in the solid state BHJ film. When the photoanode is electrically coupled to a hydrogen-evolving platinum cathode, remarkably long-lived hole polaron states are observed on the timescale of seconds under operational conditions. We demonstrate that these long-lived holes enable the organic photoanode with the polymer overlayer to show enhanced ascorbic acid oxidation performance, reaching $\sim 7 \text{ mA cm}^{-2}$ at $1.23 V_{\text{RHE}}$ without a co-catalyst. An external quantum efficiency of 18% was observed using 850 nm excitation. We propose that the use of an organic overlayer can be an effective design strategy for generating longer charge carrier lifetimes in organic photoanodes for efficient oxidation catalysis.

2:30 PM EN05.02.04

Days-Long Stable Bias-Free Solar Hydrogen Generation by Perovskite and Organic Photoanodes [Matyas Daboczi](#), Flurin Eisner, Joel Luke, Junyi Cui, Filipp Temerov, Shi Wei Yuan, Noof Al Lawati, Jolanda Simone Müller, Ji-Seon Kim, Jenny Nelson and Salvador Eslava; Imperial College London, United Kingdom

Conversion of solar energy into hydrogen by photoelectrochemical water splitting is an emerging technology with large potential for sustainable green hydrogen generation. However, reaching the combination of high performance, stable and inexpensive photoelectrodes remains a scientific challenge. Solution-processable perovskite and organic photoactive materials have shown remarkable efficiency in solar cells, and they are extremely promising candidates for photoelectrochemical devices, but their application so far has been limited by their instability in aqueous media. In this presentation, we will show both perovskite and organic photoanodes applying NiFeOOH-functionalized self-adhesive graphite sheet, providing a simple, cost-effective approach to prevent degradation by the aqueous environment and eliminate almost all electrical losses between the photoactive layer and the water oxidation-catalyst.

The all-inorganic perovskite photoelectrodes incorporate solely Earth-abundant materials and apply a low annealing temperature carbon paste with tuned energy level CsPbBr₃ photoactive layer. Controlling the perovskite phase by a facile chemical bath method allows to achieve a pure 3D CsPbBr₃ layer with 8.1 mA cm^{-2} photocurrent density at $+1.23 V_{\text{RHE}}$ (close to the radiative efficiency limit of CsPbBr₃) with record perovskite photoanode stability: 100% of stabilized photocurrent density maintained for more than 100 h. Devices with $>1 \text{ cm}^2$ area, and low-temperature processing will also be demonstrated.¹ We will also discuss our most recent results towards reaching bias-free water splitting with these CsPbBr₃ photoanodes by applying high porosity electrospun top electrode layers.

The polymer:non-fullerene acceptor containing organic (PM6:D18:L8-BO) photoanodes achieve breakthrough photocurrent densities over 25 mA cm^{-2} at $+1.23 V_{\text{RHE}}$ and remarkable, days-long operational stability. We will discuss strategies of how the continuous operation of the organic photoanode could be extended even further. Finally, polymer:polymer photoelectrodes, as well as monolithic organic tandem photoanodes (*i.e.*, two photoactive layers integrated into one photoanode to generate high photovoltage) with exceptionally low, negative onset potential and bias-free water splitting in two-electrode setup with solar-to-hydrogen efficiency reaching 5% will also be presented.

References:

1. Daboczi, M. *et al.* Scalable All-Inorganic Halide Perovskite Photoanodes with $>100 \text{ h}$ Operational Stability Containing Earth-Abundant Materials. *Advanced Materials* 2304350 (2023) doi:10.1002/ADMA.202304350.

2:45 PM EN05.02.05

Organic Semiconductor-BiVO₄ Tandems for Solar-Driven H₂O and CO₂ Splitting [Celine W. Yeung](#)¹, Virgil Andrei^{1,1}, Tack Ho Lee^{2,3}, James Durrant² and Erwin Reisner¹; ¹University of Cambridge, United Kingdom; ²Imperial College London, United Kingdom; ³Pusan National University, Korea (the Republic of)

Photoelectrochemical (PEC) devices offer great promise for simultaneous solar light harvesting and chemical storage, converting water and CO₂ into value-added products.¹ While progress has been made to improve their solar-to-fuel conversion efficiencies, most conventional inorganic prototypes face challenges in terms of insufficient photovoltage, moisture instability, high material cost or toxicity.²⁻⁵ In this work, we introduce PEC devices based on an organic π -conjugated donor-acceptor bulk heterojunction, protected by a carbon-based encapsulant to produce green H₂ and the platform chemical CO. By rationally combining design strategies from both organic photovoltaic and PEC fields, the photocathodes achieve long-term H₂ production over 300 h, which is tenfold higher than reported systems. Further interfacing the devices with a molecular CO₂ reduction catalyst allow for tunable and selective CO production under 0.1 sun. The complementary light absorption of these photocathodes with BiVO₄ enable their assembly into a standalone artificial leaf, demonstrating unassisted concurrent CO₂ reduction and water oxidation over 96 h. This establishes a new path for organic semiconductors, as we approach the composition, function, and efficiency of natural leaves.

References:

1. Tuller, H. L. Solar to fuels conversion technologies: a perspective. *Materials for Renewable and Sustainable Energy* **6**, 3 (2017).
2. Lin, Y. *et al.* Amorphous Si Thin Film Based Photocathodes with High Photovoltage for Efficient Hydrogen Production. *Nano Letters* **13**, 5615-5618 (2013).
3. Goto, Y. *et al.* A particulate (ZnSe)_{0.85}(CuIn_{0.7}Ga_{0.3}Se₂)_{0.15} photocathode modified with CdS and ZnS for sunlight-driven overall water splitting. *Journal of Materials Chemistry A* **5**, 21242-21248 (2017).
4. Pan, L. *et al.* Boosting the performance of Cu₂O photocathodes for unassisted solar water splitting devices. *Nature Catalysis* **1**, 412-420 (2018).
5. Andrei, V. *et al.* Scalable Triple Cation Mixed Halide Perovskite-BiVO₄ Tandems for Bias-Free Water Splitting. *Advanced Energy Materials* **8** (2018).

3:00 PM BREAK

SESSION EN05.03: Oxides and Oxide Perovskites
Session Chairs: Robert Hoye and Katarzyna Sokol
Monday Afternoon, April 22, 2024
Room 335, Level 3, Summit

3:30 PM *EN05.03.01

Linking Defect Chemistry to Photo- and Electrocatalytic Performance Ludmilla Steier; University of Oxford, United Kingdom

Doping or alloying strategies are heavily employed in the design of new catalysts for photoelectrochemical, photochemical and electrochemical conversion reactions with enhanced solar energy harvesting efficiencies and/or desired surface chemistry. In the electrochemical reduction of CO₂ for example, efforts are focused on the development of electrocatalysts with high activity and selectivity towards C₂, products ideally breaking the scaling relations currently observed for metal surfaces.¹ In photoelectrochemical and photocatalytic devices research has focused on developing catalysts with light harvesting in the visible, strong surface electric fields and long charge carrier lifetimes.^{2,3} In both, electro- and photocatalytic systems, perovskite oxides have been employed heavily, offering a more versatile defect chemistry platform.

Here, I will showcase some of our studies on oxide perovskite materials employed in photo- and electrocatalysis discussing links between defect chemistry and catalytic performance. One example will be the visible light absorber (La,Sr)(Rh,Ti)O₃ employed in the Z-scheme photocatalyst sheet device from Profs. Wang and Domen which led to a record 1% solar-to-hydrogen efficiency.^{4,5} Taking inspiration from this material, we have been investigating the performance of other dopants and compositions in photo- and electrocatalytic conversion of CO₂ leading us to look very closely into the material surface compositions and the ways of reporting of catalytic activity.

1 Stephens, I. E. L. *et al.* 2022 roadmap on low temperature electrochemical CO₂ reduction. *Journal of Physics: Energy* **4**, doi:10.1088/2515-7655/ac7823 (2022).

2 Corby, S., Rao, R. R., Steier, L. & Durrant, J. R. The kinetics of metal oxide photoanodes from charge generation to catalysis. *Nature Reviews Materials* **6**, 1136-1155, doi:10.1038/s41578-021-00343-7 (2021).

3 Luo, H. *et al.* Progress and Perspectives in Photo- and Electrochemical-Oxidation of Biomass for Sustainable Chemicals and Hydrogen Production. *Advanced Energy Materials* **11**, 2101180, doi:https://doi.org/10.1002/aenm.202101180 (2021).

4 Wang, Q. *et al.* Scalable water splitting on particulate photocatalyst sheets with a solar-to-hydrogen energy conversion efficiency exceeding 1%. *Nature Materials* **15**, 611-+, doi:10.1038/nmat4589 (2016).

5 Moss, B. *et al.* Linking in situ charge accumulation to electronic structure in doped SrTiO₃ reveals design principles for hydrogen-evolving photocatalysts. *Nature Materials* **20**, 511-517, doi:10.1038/s41563-020-00868-2 (2021).

4:00 PM EN05.03.02

Ti₃C₂T_x MXene as Effective Conductive Material for Enhancing the Activity of Cu-Doped TiO₂ Nanotube Photocatalysts – Application in Photooxidation and in H₂ Production Gilles D. Berhault, Ziba Roostaei, Frédéric Dapozze and Chantal Guillard; CNRS, France

Photocatalysis is one of the most promising approach for photon energy conversion and environmental remediation. In this respect, TiO₂ is the most used semiconductor due to its high photocatalytic response. However, TiO₂ also presents a high propensity for electron-hole recombination. To solve this issue, several options were found to limit recombination: cationic doping, change of the semiconductor morphology or addition of C allotropes.

Previous studies performed in our group have shown that 1D TiO₂ nanotubes can help in enhancing the separation of electron-hole pairs resulting in higher photooxidation while doping by copper allows increasing the response under visible light. Another option is to add a conductive material which can enhance the transport of photoelectrons from TiO₂ to Cu. Previous work performed using graphene oxide showed the validity of this approach but also the instability of this material under irradiation. An alternative solution is to use the emerging class of MXene compounds which were found to exhibit very high conductivity.

The objective of this work will then be to synthesize Cu/Ti₃C₂T_x/TiO₂ systems in which the Ti₃C₂T_x MXene will be evaluated for its propensity in enhancing the transport of photoelectrons, improving in this way the separation of electron-hole pairs. Comparison will be performed between 1D TiO₂ nanotubes and a P25 reference while Cu/Ti₃C₂T_x/TiO₂ will be applied for both photooxidation (formic acid photodegradation) and for H₂ production.

Materials and Methods

Ti₃C₂T_x MXene layers were obtained by HF etching of Ti₃AlC₂ MAX precursors to remove Al. TiO₂ nanotubes were obtained under hydrothermal alkaline conditions. Two series of impregnation were performed: first, GO or MXene were impregnated onto P25 or TiO₂ nanotubes while Cu(NO₃)₂·3H₂O was then impregnated onto the resulting materials.

Results and Discussion

Systematic comparisons between P25 and nanotubes were done during the construction of various Cu/TiO₂, MXene/TiO₂ and Cu/MXene/TiO₂ configurations. Results emphasized the important role played by surface oxygen vacancies in the enhancement of the photooxidation activity. While the addition of Cu onto P25 induces the creation of new oxygen vacancies onto P25 improving its photooxidation efficiency, on TiO₂ nanotubes, copper interacts mainly through the consumption of these surface oxygen vacancies initially present on the titanium oxide surface. Beneficial effects were the observed only at low Cu loadings. Photocurrent analysis also emphasized the strong increase in conductivity resulting from the addition of Ti₃C₂T_x. This high conductivity enhancement leads to a substantial increase of the photocatalytic response in photooxidation with an activity of Cu/Ti₃C₂T_x/P25 150 % higher than for P25 and 50 % higher than for Cu/P25 while the highest activity was reached using Cu/Ti₃C₂T_x/TiO₂ nanotubes.

In H₂ production, surface oxygen vacancies play a more indirect role since their consumption through copper addition favors a higher Cu-Ti interaction and a better transfer of electrons from TiO₂ to Cu. This leads to very active Cu/TiO₂ nanotube systems for H₂ production. Surprisingly, the addition of Ti₃C₂T_x leads to an apparent lower H₂ evolution activity. H₂ chemisorption analysis reveals in fact that Ti₃C₂T_x plays the role of an excellent trap for the hydrogen produced which is then stored inside our materials revealing in this way the ability for H₂ storage of Ti₃C₂T_x MXene.

Conclusion

The utilization of Ti₃C₂T_x MXenes as conductive materials enhancing the transport of photoelectrons from a semiconductor, TiO₂ to an electron acceptor, Cu has been demonstrated in photooxidation. Results also emphasized the important role played by surface oxygen vacancies while Ti₃C₂T_x MXene was found to present quite interesting properties as H₂ storage material.

4:15 PM EN05.03.03

Ceria and Metal Ferrite Core-Shell Nanoparticle for Solar Thermochemical Fuel Production Ziyao Wu¹, Aniket S. Patankar¹, Ahmed Ghoniem¹, Xiaoyu Wu², Wonjae Choi³ and Harry Tuller¹; ¹Massachusetts Institute of Technology, United States; ²University of Waterloo, Canada; ³Ewha Womans University, Korea (the Republic of)

Two-step metal oxide-based Solar Thermochemical Hydrogen Production (STCH) is an emerging technology that directly utilizes high-temperature heat to split water and carbon dioxide, producing hydrogen and carbon monoxide, respectively. Using heat can be a more cost-effective source than electricity, particularly for high-capacity factors and continuous fuel production. However, to achieve ambitious targets like the US DOE HydrogenShot (\$1/kg-H₂), significant efficiency gains and cost reductions are essential. Optimizing the redox material is pivotal in advancing STCH fuel production.

Ceria (CeO₂) is the state-of-the-art redox material in STCH systems due to its high-temperature stability, fast reduction and water-splitting kinetics, and thermodynamic properties. Yet, its limited oxygen-carrying capacity (OCC), compared to perovskites and iron oxides, results in diminished fuel productivity and solar-to-fuel efficiency. Larger quantities of ceria are needed, leading to larger reactors and higher costs.

Metal-substituted ferrites are another STCH material class with 3-5 times higher OCC compared to ceria. However, ferrites can experience sintering and rapid deactivation at high temperatures (~1500°C), causing a marked decrease in fuel productivity after a few cycles. This sintering effect enlarges particle size, and the inherent low ion diffusivity in spinel slows water-splitting kinetics, ultimately leading to material deactivation. Doping ferrites with different cations or combining with inert supports like zirconia has proven inadequate in preventing ferrite agglomeration [1].

In our previous work, we introduced a composite STCH redox material combining magnesium ferrite (MgFe₂O₄) and ceria. We hypothesize that such a composite can combine the high OCC of ferrites with the thermal stability and high oxygen diffusivity of ceria. Our system-level thermodynamic analysis showed that a composite with 50 wt-% ferrite produces twice as much hydrogen per unit mass as ceria and increases STCH efficiency from 33% to 35.3% [2].

In this presentation, we will discuss our experimental efforts with ceria-ferrite composites. We will present the synthesis and characterization of core-shell composites, with a Mg-ferrite core and a ceria shell. Ceria was chosen as the shell material because of its low sintering, fast redox kinetics, and high oxygen diffusivity. We compare the performance of the core-shell composite with that of simple mechanical mixtures in which ferrite and ceria powders are mixed and pressed into a porous pellet. A combination of Infrared furnace experiments and thermogravimetric analysis is used to measure the OCC of composites at STCH-relevant conditions. The experiments involve thermochemical cycles by switching the temperature between reduction (1400°C-1500°C) and water/CO₂ splitting (700°C-900°C), changing the gas environment, and monitoring the real-time gas composition using an in-line mass spectrometer. We measure OCC and fuel production profiles over several consecutive STCH cycles to study the sintering or other forms of degradation composites. The ferrite content in the composite is varied to measure its impact on OCC and degradation.

Ex-situ X-ray diffraction (XRD), SEM and TEM imaging, and surface area measurements will be used to characterize the evolution of composite chemistry and morphology during STCH cycles. This work aims to demonstrate the potential of ferrite-ceria composites and core-shell structures as leading an STCH redox material, setting the stage for scaled-up studies in the future.

[1] Miller et al. *Advanced Energy Materials*, 4(2), 1300469 (2014).

[2] Patankar, PhD thesis, MIT (2023)

SESSION EN05.04: Nanostructuring
Session Chairs: Virgil Andrei and Katarzyna Sokol
Tuesday Morning, April 23, 2024
Room 335, Level 3, Summit

10:30 AM *EN05.04.01

Nanoengineering Interfaces in The Biomolecular Devices for Solar-To-Chemical Conversion Joanna Kargul; University of Warsaw, Poland

Combining the highly active and stable natural photocatalysts with various electrode materials open an avenue for the selective production of target chemicals at ambient conditions using non-toxic and cost-effective biomaterials. Here, I present the rational bottom-up design of conductive bio-organic interfaces within the biomolecular systems based on the robust photoenzyme, photosystem I (PSI) that yields the significantly enhanced solar conversion efficiency and stability. The PSI biophotocatalyst is interfaced with various cost-efficient, transparent electrode materials in the orientation controlled manner for the generation of green electricity and fuel. The performance of such devices can be greatly improved by tailoring the structure of the organic molecular wires based on pyrene-nitrilotriacetic acid, terpyridine or diazonium salt ligands coordinated with various transition metals to ensure the generation of unidirectional electron transfer and minimisation of wasteful back reactions. Incorporating plasmonic nanoparticles in the bio-organic interface improves the light-harvesting, photocatalytic activity and long-term photostability of PSI. Such rational design paves the way for the generation of viable and sustainable technologies for solar energy conversion into fuel and other carbon-neutral chemicals.

Acknowledgements: Support from the Polish National Science Centre (Solar-driven chemistry 2 SUNCOCAT grant no. 2022/04/Y/ST4/00107) and the European Horizon Europe Research and Innovation Programme (SUNER-C CSA, GA no. 101058481) is greatly acknowledged.

11:00 AM EN05.04.02

GaAs@TiO₂ Core-Shell Nanowire-Based Electrode and Co Catalyst for Enhanced Hydrogen Generation Thomas Dursap¹, Mariam Fadel², Cristina Tapia Garcia², Céline Chevalier¹, Hai-Son Nguyen¹, Emmanuel Drouard¹, Philippe Regreny¹, Solène Brottet¹, Michel Gendry¹, Alexandru Danescu¹, Matthieu Koepf², Vincent Artero², José Penuelas¹ and Matthieu Bugnet³; ¹University Lyon, CNRS, ECL, INSA Lyon, UCBL, CPE Lyon, INL, France; ²University Grenoble Alpes, CNRS, CEA, IRIG, Laboratoire de Chimie et Biologie des Métaux, France; ³University Lyon, CNRS, INSA Lyon, UCBL, MATEIS, France

Photoelectrochemical cells (PEC) are appealing devices for the production of renewable energy carriers. In this context, III-V semiconductors such as GaAs are very promising materials due to their tunable bandgaps, which can be appropriately adjusted for sunlight harvesting. Because of the high cost of these semiconductors, the nanostructuring of the photoactive layer can help to improve the device efficiency as well as drastically reduce the amount of material needed. III-V nanowire-based photoelectrodes benefit from the intrinsically high aspect ratio of nanowires, their enhanced ability to trap light as

well as their improved charge separation and collection abilities, and thus are particularly attractive for PECs. However, III-V semiconductors often suffer from corrosion in aqueous electrolytes, preventing their utilization over long periods under relevant working conditions.

In this study, the influence of the geometry of GaAs semiconductor as photocathodes for the water reduction was investigated. Photocathodes made of GaAs nanowires [1, 2] and protected with thin TiO₂ shells were prepared and studied under simulated sunlight irradiation to assess their photoelectrochemical performances in correlation with their structural degradation [3]. A strong improvement of the cell efficiency was demonstrated for the 1-dimensional NW geometry compared to its thin film counterpart, which is mainly due to a significant reduction of light reflected by the electrode. Morphological and electronic parameters, such as the aspect-ratio of the nanowires and their doping pattern were found to strongly influence the photocatalytic performances of the system. This work highlights the advantageous combination of nanowires featuring a buried radial p-n junction with Co-nanoparticles used as hydrogen evolution catalyst. The nanostructured photocathodes exhibit significant photocatalytic activities, comparable with previous noble-metal based systems tested under similar conditions (0 V vs. RHE, pH = 7). Furthermore, the stability of the NW-based photocathode over time was significantly improved with the deposition of a thin TiO₂ protective layer, leading to an increase of the Faradaic efficiency of the photocathodes by a factor 3 after 13 hours. The fabricated photocathodes display photocurrent density up to 1.15 mA/cm² at 0 V vs RHE under neutral conditions. Nevertheless, it would lead to solar-to-hydrogen performances below 1% in tandem photoelectrochemical cells. This calls for future tenfold improvement of the performances of such scalable materials to allow for a viable solar hydrogen technology. Still, such performance is at the state of the art for similar GaAs photoelectrodes, and demonstrates the potential of GaAs nanostructured semiconductor for photo-driven hydrogen production.

[1] T. Dursap *et al.*, *Nanoscale Advances* (2020).

[2] T. Dursap, *et al.*, *Nanotechnology* (2021).

[3] T. Dursap, *et al.*, *under review* (2023).

Acknowledgments

The authors acknowledge funding from the French *Agence Nationale de la Recherche* for funding (project BEEP 18-CE05-0017-01, Labex ARCANE and CBH-EUR-GS (ANR-17-EURE-0003)).

11:15 AM EN05.04.03

Single Atom Catalyst-Like Strontium Doping of Titania Nanotube Arrays for CO₂ Photoreduction Damini Vrushabdrakumar, Navneet Kumar, Harshitha Rajashekhar, Kazi M. Alam and Karthik Shankar; University of Alberta, Canada

This study focuses on the details concerning the adsorption mechanisms, surface electronic band structure and structural disorder in anodically formed TiO₂ nanotube arrays (TNTAs) due to the surface doping of strontium Sr²⁺ metal cations that end up being widely dispersed on the surface of the TNTAs. The surface doping was achieved using an electrochemical cathodic treatment in a Sr²⁺-containing aqueous electrolyte. Sr²⁺ surface dopants also modified the crystallographic texture of the nanotubes.³ X-ray diffraction patterns and Raman spectra confirmed the induced lattice strain, reduced crystallite size, and phonon confinement in the TNTAs due to Sr-doping.² The absence of segregated phases of Sr or SrO or SrTiO₃ led to the conclusion that Sr atoms were high entropy surface dopants in TiO₂, widely dispersed on the surface of the TNTAs and approaching single atom catalysts insofar as the surface distribution of dopant Sr atoms is concerned. Fourier transformed infrared (FTIR) spectra of the Sr cathodized TNTAs indicated the presence of a small population of bridging bidentate carbonate adsorbate on Sr doped TNTA surfaces exposed to CO₂.³ Sr-doping reduced the work function of TNTAs and caused appreciable downward band-bending of 0.25 eV resulting in an electron accumulation layer at the surface. We hypothesize that such an electronic band-structure makes it easier for photogenerated electrons to be transferred to surface adsorbates for CO₂ reduction. The electrochemically cathodized Sr-doped TNTAs exhibited a more than 3-fold enhancement in the rate (25 μmol g⁻¹ h⁻¹) of CO₂/CO transformation in surpassing the output of bare TNTA (7.7 μmol g⁻¹ h⁻¹), thereby impressively improving the photocatalytic performance.

References:

1. Kisslinger, R.; Askar, A. M.; Thakur, U. K.; Riddell, S.; Dahunsi, D.; Zhang, Y.; Zeng, S.; Goswami, A.; Shankar, K., Preferentially oriented TiO₂ nanotube arrays on non-native substrates and their improved performance as electron transporting layer in halide perovskite solar cells. *Nanotechnology* **2019**, *30* (20), 204003.

2. Hamedani, H. A.; Allam, N. K.; Garmestani, H.; El-Sayed, M. A., Electrochemical Fabrication of Strontium-Doped TiO₂ Nanotube Array Electrodes and Investigation of Their Photoelectrochemical Properties. *The Journal of Physical Chemistry C* **2011**, *115* (27), 13480-13486.

3. Luo, C.; Zhao, J.; Li, Y.; Zhao, W.; Zeng, Y.; Wang, C., Photocatalytic CO₂ reduction over SrTiO₃: Correlation between surface structure and activity. *Applied Surface Science* **2018**, *447*, 627-635.

11:30 AM EN05.04.04

Surface Ferroelectric Effect in Oxygen Deficient (111) Strontium Titanate Single Crystals Controls Photoelectrochemical Water Oxidation Samutr Assavachin, Chengcan Xiao, Tatiana Mamani, Davide Donadio and Frank E. Osterloh; University of California, Davis, United States

Ferroelectric materials such as BaTiO₃ have a permanent electric polarization that can be controlled with an external applied electric field. Here we demonstrate a surface ferroelectric effect in oxygen deficient (111) SrTiO_{3-x} and its application to improve photoelectrochemical water oxidation for the first time. After hydrogen-annealed (111) SrTiO_{3-x} single crystals are polarized with an electric field of 11 kV cm⁻¹ under argon flow, the anodic water oxidation photocurrent increases from 0.99 to 2.22 mA cm⁻² at 1.23 V RHE (60 mWcm⁻², UV illumination) or decreases to 0.50 mA cm⁻², for the opposite field orientation. The polarization also modifies the surface photovoltage signal of the material and its flat band potential, based on Mott-Schottky measurements. This is attributed to an electric dipole near the (111) SrTiO_{3-x} surface, which controls the potential drop across the depletion layer and charge transfer at the solid-liquid junction. Based on DFT calculations the electric polarization results from the migration of oxygen vacancies between SrTiO_{3-x} surface and sub-surface regions. The use of the surface ferroelectric effect to modify the junction and photoelectrochemical properties of a non-ferroelectric material is expected to be of interest for solar energy conversion and information technology applications.

11:45 AM EN05.04.05

Thermochemical Properties of ABO₃-Type Compounds for Solar Fuel Generation Sossina M. Haile; Northwestern University, United States

Solar-driven thermochemical production of chemical fuels using redox active oxides has emerged as an attractive means for storing solar energy for use on demand. In this process, a reactive oxide is cyclically exposed at high temperatures to an inert gas, which induces partial reduction of the oxide, and subsequently to an oxidizing gas of either H₂O or CO₂, which reoxidizes the oxide, releasing H₂ or CO. While it is widely recognized that the *capacity* for fuel production is dictated by the thermodynamic properties of the oxide, here we show that the *rate* of fuel production is also often directly given by these properties. Recognizing this behavior, we report the thermodynamic properties, specifically the enthalpy and entropy of reduction, of a range of previously unexplored ABO₃-type compounds and identify those with promising characteristics for efficient thermochemical fuel production.

SESSION EN05.05: Carbonaceous Materials for Photocatalysis
Session Chairs: Demetra Achilleos and Katarzyna Sokol
Tuesday Afternoon, April 23, 2024
Room 335, Level 3, Summit

1:45 PM *EN05.05.01

Transient Absorption Spectroscopy/Microscopy of Carbon Nitride Photocatalysts for Biomass Photoreforming Robert Godin; The University of British Columbia, Canada

Polymeric photocatalysts made of Earth-abundant elements have been extensively developed over the past decade to take advantage of their synthetic tunability.¹ Within this family, carbon nitrides (CN_x) are emerging as leading photocatalysts because of their high photocatalytic performance combined with good stability and facile synthesis.^{2,3} However, significant gaps remain in our knowledge of the photophysical properties of these organic polymeric materials. Determining the pathways and mechanism of photoinduced processes will greatly aid our efforts to engineer better CN_x photocatalysts for solar fuel production and other photocatalytic processes.

We are taking the next step to develop a full picture of the charge carrier dynamics by expanding our spectroscopic capabilities to transient absorption microscopy (TAM). Notably, our first-of-its-kind TAM system monitors the microsecond – second timescales relevant to the complex multi electron redox reactions that occur to produce solar fuels. Spatial mapping of the charge carrier dynamics on the micron scale provides novel insights into the heterogeneity in individual CN_x particles. This new tool allowed us to unearth a multiscale heterogeneity where the charge carrier dynamics differ from particle to particle and different behavior within individual particles on ~ 10 micrometer length scales can be observed. These new insights into the heterogeneity of charge carrier dynamics in CN_x particles can push the field into uncovering the optimal structure and local environment in defect-rich organic semiconductors such as CN_x. We are taking this knowledge and applying it to systems of biomass photoreforming for the simultaneous breakdown of organic matter and H₂ evolution.

(1) Wang, Y.; Vogel, A.; Sachs, M.; Sprick, R. S.; Wilbraham, L.; Moniz, S. J. A.; Godin, R.; Zwiijnenburg, M. A.; Durrant, J. R.; Cooper, A. I.; Tang, J. Current Understanding and Challenges of Solar-Driven Hydrogen Generation Using Polymeric Photocatalysts. *Nat. Energy* **2019**, *4* (9), 746–760. <https://doi.org/10.1038/s41560-019-0456-5>.

(2) Liu, C.; Liu, J.; Godin, R. ALD-Deposited NiO Approaches the Performance of Platinum as a Hydrogen Evolution Cocatalyst on Carbon Nitride. *ACS Catal.* **2023**, *13* (1), 573–586. <https://doi.org/10.1021/acscatal.2c04795>.

(3) Ohemeng, P. O.; Godin, R. Methylated Precursor Leads to Carbon Nitride (CN_x) with Improved Interfacial Interactions for Enhanced Photocatalytic Performance. *Sustainable Energy Fuels* **2023**. <https://doi.org/10.1039/D2SE01636B>.

2:15 PM EN05.05.02

On The Scarcity or Not of Carbon-Based Overall Water Splitting Photocatalysts Martijn Zwiijnenburg; University College London, United Kingdom

Since the discovery in 2010 that carbon nitride combined with suitable co-catalysts could in the presence of appropriate electron donors and acceptors drive both the reduction of protons to molecular hydrogen and the oxidation of water to molecular oxygen, carbon-based materials have received an enormous amount of interest as potential light absorbers for photocatalytic water splitting. Now probably more than 200 different carbon-based materials, mostly conjugated polymers, are known to be active for hydrogen evolution in the presence of a sacrificial donor such as triethanolamine or ascorbic acid, and platinum or palladium nanoparticles that act as co-catalyst and site of the hydrogen evolution.¹ In contrast, a much smaller number of carbon-based materials have been reported to be active for the oxygen evolution half-reaction. The number of carbon-based materials experimentally active for overall water splitting can be counted on the fingers of one or two hands.

Based on the scarcity of materials that are active for overall water splitting one could naively assume that such activity is a rare property of carbon-based materials. That carbon-based materials generally just do not have the ionisation potential / valence band maximum position to drive water oxidation. In my contribution I'll discuss the results of computational high-throughput screening of thousands of conjugated polymers which shows that this is not necessarily the case, or at least not for polymers.² Approximately, a similar fraction of the library of 3000+ conjugated polymers is predicted to be thermodynamically able to drive overall water splitting as is predicted to be active for sacrificial hydrogen evolution. Although the ability to drive overall water splitting combined with a small enough optical gap that a large part of the solar spectrum is absorbed is predicted to be relatively rare for this material class. Finally, I'll discuss why we think the real reason behind the scarcity of carbon-based overall water splitting photocatalysts is not thermodynamics but the need for well-optimised co-catalysts and why thus future work on co-catalysts and/or combining polymers into heterojunctions, like recently explored experimentally by Kosco and co-workers,³ can rescue large numbers of carbon-based photocatalysts from the proverbial scrap heap of history.

¹ Y. Wang et al. *Nat. Energy* 2020, 5, 633.

² B. Saunders et al. *Sustainable Energy Fuels*, 2022, 6, 2233.

³ J. Kosco et al. *Nat. Mater.* 2020, 19, 559.

2:30 PM EN05.05.03

Efficient Z-Scheme Configuration for Photocatalytic CO₂ Reduction through g-C₃N₄ and Cs₃Bi₂Br₉ Heterojunctions Enhanced by Reduced Graphene Oxide Yasmine Baghdadi and Salvador Eslava; Imperial College London, United Kingdom

Photocatalytic CO₂ reduction is pivotal for progressing solar fuel technologies, demanding catalysts with enhanced efficiency. Combining the optoelectronic characteristics of Cs₃Bi₂Br₉ and the versatility of g-C₃N₄, this study aims to create a synergistic platform for photocatalysis, harnessing the unique strengths of each semiconductor to enhance overall performance in applications such as solar fuel generation and photocatalytic CO₂ reduction. Building on our previous studies where the ratio of g-C₃N₄ to Cs₃Bi₂Br₉ was optimized for high CO₂ conversion to CO, this study presents a dual-modification approach to amplify the performance of g-C₃N₄ as a photocatalyst. Surface modifications, including exfoliation for increased surface area and surface oxidation for improved charge separation, were employed on g-C₃N₄. The introduction of reduced graphene oxide (rGO) at various ratios, integrated into both bulk and exfoliated g-C₃N₄, effectively mitigated charge recombination. An optimal rGO/g-C₃N₄ ratio was identified, showcasing superior efficiency.

Importantly, the study also introduces a hybrid inorganic/organic heterojunction by combining the optimized rGO/g-C₃N₄ with Cs₃Bi₂Br₉ into a Cs₃Bi₂Br₉/rGO/g-C₃N₄ Z-scheme composite. This synergistic integration resulted in a remarkable increase in photocatalytic activity, reaching 54.3 (± 2.0) μmol g⁻¹ e⁻ h⁻¹ on an electron basis for CO, H₂, and CH₄ production, surpassing pure Cs₃Bi₂Br₉ (11.2 ± 0.4 μmol g⁻¹ e⁻ h⁻¹) and bulk g-C₃N₄ (5.5 ± 0.5 μmol g⁻¹ e⁻ h⁻¹).

A comprehensive characterization shows the charge transfer mechanism within the composite to take place via the rGO, acting as a solid redox mediator, in

a Z-scheme heterojunction where Cs₃Bi₂Br₉ drives the reduction and g-C₃N₄ the oxidation, explaining its enhanced photocatalytic activity. The successful formation of this high-performance heterojunction underscores the composite's potential as an efficient photocatalyst for CO₂ reduction, promising substantial advancements in solar fuel technologies and aligning with sustainable energy goals.

¹ Cs₃Bi₂Br₉/g-C₃N₄ Direct Z-Scheme Heterojunction for Enhanced Photocatalytic Reduction of CO₂ to CO

Yasmine Baghdadi, Philipp Temerov, Junyi Cui, Matyas Daboczi, Eduardo Rattner, Michael Segundo Sena, Ioanna Itskou, and Salvador Eslava

Chemistry of Materials 2023 35 (20), 8607-8620

DOI: 10.1021/acs.chemmater.3c01635

2:45 PM EN05.05.04

Earth-Abundant Co-Catalysts to Replace Noble Metals in Photocatalysis Judith Zander and [Roland Marschall](#); University of Bayreuth, Germany

Climate change due to rising CO₂ concentrations in the atmosphere require the transformation from a fossil-fuel based energy economy towards a sustainable, emission-free one centred around renewable energy sources. Photocatalysis offers the possibility to directly obtain H₂ as a green fuel from water under irradiation of a photocatalyst with a suitable band gap for light absorption. Up to date, photocatalytic hydrogen evolution (HER) can, however, still not compete with traditional hydrogen production processes, such as steam reforming, due to low efficiencies [1]. Co-catalysts can be added to a photocatalytic system to improve the separation of excited charge carriers, provide additional active sites, lower the overpotential of a reaction, and thus increase the overall activity. Many common co-catalysts are noble-metal-based, though [2]. Therefore, the addition of a noble co-catalyst increases the material costs. This is also a common problem in electrochemistry, where platinum is used as standard material for the hydrogen evolution reaction. In recent years, sulphides and phosphides, such as MoS₂, have emerged as earth-abundant alternatives and subsequently been employed as co-catalysts in photocatalysis as well [3]. Nickel and iron based materials are especially interesting for the hydrogen evolution reaction, since both metals are common motifs in hydrogenase enzymes [4].

We herein present binary and ternary sulphides and oxides as novel, earth-abundant co-catalysts on TiO₂, with a special focus on Ni₂FeS₄. All of the presented materials can be obtained as nanoparticles in a very fast microwave-assisted solvothermal reaction at temperatures not exceeding 200 °C. The synthesis time can be decreased down to 1 min, without a significant loss of product crystallinity and no impedimental effects on the activity. The addition of the transition metal sulphides to P25 TiO₂ could significantly boost the activity for photocatalytic hydrogen evolution under 1 sun solar light irradiation, as well as under UV irradiation. A combination of control experiments, material characterisation and the realisation of astonishingly low transition metal loadings of 0.5 wt.% (< 0.3 wt.% of metals) underline the role of Ni₂FeS₄ and other sulphides as efficient co-catalysts that show promise for replacing noble metal co-catalysts.[5]

References

- [1] L. Lin, T. Hisatomi, S. Chen, T. Takata, K. Domen, Trends in Chemistry 2 (2020) 813.
- [2] J. Yang, D. Wang, H. Han, C. Li, Acc. Chem. Res. 46 (2013) 1900.
- [3] K. Chang, X. Hai, J. Ye, Adv. Energy Mater. 6 (2016) 1502555.
- [4] M. Isegawa, T. Matsumoto, S. Ogo, Dalton Trans. 51 (2022) 312.
- [5] J. Zander, R. Marschall, J. Mater. Chem. A 11 (2023) 17066.

3:00 PM BREAK

SESSION EN05.06: Value-Added Products
Session Chairs: Demetra Achilleos and Katarzyna Sokol
Tuesday Afternoon, April 23, 2024
Room 335, Level 3, Summit

3:30 PM *EN05.06.01

Turning Waste into High Value Chemicals with Electricity [Magdalena Titirici](#); Imperial College London, United Kingdom

In this talk I will present out latests advances in converting bio-based products such as glycerol, 5-hydroxymethylfurfural or PET waste into valuable chemicals including lactic acid, FDCA and glycolic acid including some fundamental mechanistic studies, upscale oportunities and life cycle assesment of such processes.

4:00 PM *EN05.06.02

Coupling Hydrogen Production and Upgrading of Chemicals in Oxide-Based Photoelectrochemical Device [Fatwa F. Abdi](#); City University of Hong Kong, Hong Kong

Green H₂ has been recognized as an important element in efforts to decarbonize our fossil fuel-dependent society. One method to produce green H₂ is solar water splitting in a photoelectrochemical (PEC) device. Solar-to-hydrogen (STH) efficiencies of up to 30% have been demonstrated but these high efficiencies could only be achieved using expensive and non-scalable photoelectrodes—the approach therefore still results in a hydrogen cost that is not competitive. One obvious approach is to develop novel photoelectrode materials that are low-cost and highly efficient. For example, earth-abundant complex metal oxides have been explored, and several promising ones have been identified. Here, our efforts in developing tin tungstate (α-SnWO₄) as a photoelectrode material will be discussed.[1-3] Alternatively, co-production of valuable chemicals can be introduced in the PEC cell to increase the competitiveness of the overall system. For example, we recently coupled a homogeneous hydrogenation reaction with PEC-generated hydrogen inside a single device.[4,5] Using the hydrogenation of itaconic acid (IA) to methyl succinic acid (MSA) as a model proof-of-concept reaction, solar-driven H₂-to-MSA conversion as high as ~50% was demonstrated using our BiVO₄-based PEC device. Although still demonstrated in the laboratory scale, life-cycle net energy assessment and technoeconomic analysis reveal that the concept indeed offers a very promising return. Finally, further implications and optimization potentials of this coupled PEC hydrogenation approach, also beyond the demonstrated hydrogenation of IA to MSA, will be discussed.

References

1. P. Schnell et al. *Adv. Energy Mater.* 11, 2021, 2003183
2. P. Schnell et al., *Chem. Mater.* 34, 2022, 1590
3. P. Schnell et al. *Solar RRL* 7, 2023, 2201104
4. X. Zhang et al. *Nat. Commun.* 14, 2023, 991

5. K. Obata et al. *Nat. Commun.* 14, 2023, 6017

4:30 PM EN05.06.03

Aqueous Z-Scheme Photocatalytic CO₂ Reduction by Dispersed Semiconductor Particles of Metal Sulfide and Oxide in Synergy with Dual-Functional Metal-Complex Tomiko M. Suzuki¹, Shunya Yoshino², Keita Sekizawa¹, Yuichi Yamaguchi², Akihiko Kudo² and Takeshi Morikawa¹; ¹Toyota Central R&D Labs., Inc., Japan; ²Tokyo University of Science, Japan

The photocatalytic carbon dioxide reduction reaction (CO₂RR), which can generate useful chemicals, is essential for realizing a carbon-neutral society and a circular economy.

To utilize visible-light energy and water as with natural photosynthesis, a 2-step photoexcitation mechanism (Z-scheme) that transfers electrons via two semiconductor photocatalysts is feasible [1]. Although an aqueous suspension of particulate photocatalysts in one-pot is an ultimately simplified and scalable approach, previous demonstrations have suffered from very low CO₂ selectivity against undesirable hydrogen production [1-3].

In this study, we demonstrate a simple activation methodology to overcome the issue by the combination of one molecule together with two semiconductor particulates in a water-filled one-pot reactor, achieving unparalleled selectivity of almost 100% of CO.

A simple mixture of two particulate semiconductors, a metal-sulfide, (CuGa)_{0.3}Zn_{1.4}S₂ as a CO₂ reduction photocatalyst (0.1 g) and a metal-oxide (BiVO₄) as a water oxidation photocatalyst (0.1 g) and a newly designed water-soluble molecular Co complex, [Co(4,4'-dimethyl-2,2'-bipyridine)₃]²⁺ ([Co-dmbpy]) were added to an aqueous solution of 10 mmol L⁻¹ NaHCO₃ (120 mL). Under CO₂ gas bubbling into the reactor and irradiation with visible light ($\lambda > 420$ nm), CO and a much smaller amount of hydrogen were continuously generated, while formate was almost undetectable. CO was generated with 98% product selectivity with respect to the total reduction products (CO, H₂, and HCOO⁻) after 56 h. The CO generation rate of this system was increased by 1–2 orders of magnitude (38 $\mu\text{mol h}^{-1}$) relative to that obtained with a previously reported visible light-driven Z-scheme photocatalytic reaction using an aqueous suspension system, and was comparable to water splitting H₂ synthesis by the Z-scheme mechanism under similar conditions.

The simultaneous evolution of O₂ was confirmed, which clarified the extraction of electrons from water molecules with irradiated BiVO₄ necessary for CO₂RR in the Z-scheme mechanism. Experimental studies and calculations suggest that the Co complex acts dual-functionally in synergy with (CuGa)_{0.3}Zn_{1.4}S₂ and BiVO₄: it behaves as an efficient ionic electron mediator, and also acts as a new active CO₂RR cocatalyst after a structural change following the acceptance of photoexcited electrons from (CuGa)_{0.3}Zn_{1.4}S₂ [4, 5]. This simple method, operating in a self-optimizing manner in solution, has great potential to help achieve sustainable, highly active artificial photosynthetic systems.

References

[1] W. Zhang, et al., *Angew. Chem. Int. Ed.*, 59 (2020) 22894-22915. [2] S. Yoshino, A. Kudo, et al., *Acc. Chem. Res.*, 55 (2022) 966-977. [3] T. M. Suzuki, A. Kudo, T. Morikawa, et al., *Chem. Commun.*, 54 (2018) 10199-10202. [4] T. M. Suzuki, A. Kudo, T. Morikawa, et al., *Appl. Catal. B.*, 316 (2022) 121600. [5] T. M. Suzuki, A. Kudo, T. Morikawa, et al., *Chem. Commun.* 59 (2023) 12318-12321.

SESSION EN05.07: Device and Interface Design

Session Chairs: Virgil Andrei and Robert Hoyer

Wednesday Morning, April 24, 2024

Room 335, Level 3, Summit

8:15 AM EN05.07.01

Flow Photoelectrochemical Devices for Converting Carbon from the Ocean Bin Liu¹, Zheng Qian^{2,1} and Shu Hu¹; ¹Yale University, United States; ²Tsinghua University, China

The capture and utilization of the dissolved inorganic carbon in seawater, i.e., 2 mM bicarbonates, offer an appealing approach to mitigate environmental concerns and advance the realization of a carbon-neutral society. Unbiased solar-driven photoelectrochemical (PEC) CO₂ reduction leads to sustainable production of chemicals and fuels. However, the development of reactors for unbiased PEC CO₂ capture and in-situ utilization in seawater has been scarcely reported, due to the lack of reactors that elegantly balance mass transfer and flow field design with PEC CO₂ reduction. We effectively achieve protons transportation and sequent in-situ conversion of freshly generated CO₂. We will describe the design and realization of 3D-printed reactors for unbiased PEC CO₂ capture and in-situ conversion in seawater, in which the locally generated CO₂ at BiVO₄ photoanodes can be brought to the neighboring Si photocathodes for CO₂ reduction reaction by optimized flow field, reducing the protons transfer distance and improving the local CO₂ concentration on the surface of Si photocathodes. With this, we achieved excellent CO₂ capture velocity and outstanding solar to fuels (STF) efficiency of 0.71%: CO selectivity was increased from 3 to 19% compared with the conventional “artificial leaf” configuration of back-to-back photoanodes and photocathodes. A flowing reactor module is demonstrated for realistic ocean operation.

8:30 AM EN05.07.02

Atomic Layer Deposition of Defect-Engineered TiO_x and TaO_x Protective Coatings for Photoelectrochemistry Tim Rieth, Oliver Bienek, Julius Kühne and Ian D. Sharp; Technische Universität München, Germany

Photoelectrochemical (PEC) energy conversion provides a viable route to chemical fuel production from solar light. Several different PEC design approaches exist, ranging from single photoelectrodes to tandem configurations of photoanodes and -cathodes to buried photovoltaic junctions. However, common to each of these designs is a central materials challenge of achieving simultaneous stability, efficiency, and scalability. Furthermore, the coupling of the semiconducting photo absorber and catalytic components demands sophisticated solid state interface engineering. In this talk, we focus on the stabilization of this semiconductor/electrolyte interface with functional conformal coatings grown by plasma-enhanced atomic layer deposition (PE-ALD). We investigate defect-engineered electron-selective titanium oxide (TiO_x) protection layers for efficient InP photocathodes and identify ALD pathways to optimize interfacial and bulk charge transport, as well as to tune the driving force for photovoltage generation [1]. Furthermore, we use PE-ALD to deposit ultra-thin tantalum oxide (TaO_x) protective coatings showing improved chemical stability compared to titanium oxide in alkaline and acidic environments. In addition to possessing excellent optical transparency, the conductivities of TaO_x layers can be tuned over several orders of magnitude by introducing electronic defects via hydrogen plasma sub-cycles during the ALD process. Spectroscopic methods including X-ray photoelectron spectroscopy (XPS), photothermal deflection spectroscopy (PDS), and spectroscopic ellipsometry (SE) are employed to characterize and understand the introduced defects and correlate the electronic properties to the PEC performance. Overall, the demonstrated route to ALD-based defect-engineering enables precise control over the properties of ultra-thin layers, facilitating not just improved corrosion protection layers but also tunable semiconductor/dielectric interfaces.

[1] Bienek, O. et al. Engineering Defects and Interfaces of Atomic Layer Deposited TiO_x Protective Coatings for Efficient III-V Semiconductor

Photocathodes. *ACS Photonics* (in press). <https://doi.org/10.1021/acsp Photonics.3c00818>

8:45 AM EN05.07.03

Directing The Path with Directional Properties: Unravelling Anisotropic Carrier Mobility, Lifetime and Surface Defects in Oxides for Solar Fuels Generation Linfeng Pan¹, Linjie Dai¹, Jingshan Luo², Anders Hagfeldt², Michael Graetzel² and Samuel D. Stranks¹; ¹University of Cambridge, United Kingdom; ²École Polytechnique Fédérale de Lausanne, Switzerland

The concept of solar fuels holds great promise for the sustainable production of fuels through the utilization of solar energy. Over the last ten years, oxide photocathodes, such as Cu₂O, have showcased performance comparable to that of photoelectrodes relying on well-established photovoltaic materials. Our work has demonstrated several record tandem solar water splitting devices based on the state-of-the-art Cu₂O photocathodes featuring a radial junction design and effective hole transport strategies. Nevertheless, a significant challenge found was the occurrence of considerable charge carrier recombination within the bulk of the photoabsorber, a common issue commonly observed in oxide semiconductors. Here, we demonstrate Cu₂O photocathodes with performance beyond the state-of-the-art by exploiting a novel conceptual understanding of carrier recombination and transport in single-crystal Cu₂O thin films with adjustable crystal orientations. The combination of the unique thin film materials platform and a series of optoelectronic characterizations, including a customized broadband femtosecond transient reflection spectroscopy, precisely quantified unprecedented anisotropic carrier mobilities, lifetimes and diffusion lengths. Notably, it was discovered that these properties exhibit significant disparities along different crystal orientations, with one orientation manifesting significantly superior properties compared to the others. To exploit the findings, polycrystalline Cu₂O photocathodes with extremely pure selected crystalline orientations and terminating facets were fabricated, delivering current density 70% more current density compared to the state-of-the-art electrodeposited devices at 0.5 V versus a reversible hydrogen electrode under simulated air mass 1.5 G illumination, and stable operation over 100 hours. Furthermore, we will share recent research outcomes that elucidate the significance of facet-dependent defects in their contributions to photoelectrochemical applications.

9:00 AM EN05.07.04

Anisotropic Conductive Adhesive for Semi-Monolithic Integration of Multi-Junction PV and PEC Devices Kai C. Outlaw-Spruell^{1,2}, Christopher Muzzillo³, Kai Zhu³ and Nicolas Gaillard^{1,2}; ¹Hawaii Natural Energy Institute, United States; ²University of Hawaii, United States; ³National Renewable Energy Laboratory, United States

Although foundational to multi-junction (MJ) photovoltaic (PV) and photoelectrochemical (PEC) device synthesis, monolithic integration presents major limitations in process compatibility. Consequently, conductive adhesive-based interconnection scheme emerged as a suitable method to overcome limitations and to integrate incompatible material classes into MJ devices without compromising the integrity of the constituent layers. As the conductive adhesive generally employ a polymer matrix, the conductivity of this composite material depends on the conductive filler material. Among which, a core-shell type silver coated PMMA (Ag-PMMA) conductive microsphere filler has gained significant interest in the PV and PEC community due to its ability to exhibit reliable out-of-plane electrical conductivity (0.1 Ω-cm²) and good optical transparency (T > 90%), as we demonstrate for an epoxy-based transparent conductive composite (TCC) consisting of low particle loading (0.1 - 5 vol%).

By implementation of the Ag-PMMA based TCC paired with a device exfoliation method, further referred to as semi-monolithic integration, independently processed substrate-grown single junction (SJ) devices were successively bonded and exfoliated onto a single host substrate to create a MJ device. As a proof-of-concept demonstration, we constructed the world's first whole-chalcopyrite triple junction MJ device comprising 1.13 eV and 1.44 eV Cu(In,Ga)Se₂ and 1.85 eV CuGa₃Se₅ sub-cells, with the TCC acting as the recombination layer between each sub-cell. The device exhibited a V_{OC} of 1.85 V and is capable of splitting water with an STH efficiency of 3% in a PV-electrolysis configuration.

Although the use of Ag-PMMA based TCC has shown to be an effective approach to prepare MJ devices, mechanical and electrical design and optimization is required to reliably appropriate the TCC as an optoelectronic device interconnect and to scale the semi-monolithic integration method. In the context of mechanical optimization, it has been shown that the degree of deformation of conductive microsphere filler is a key factor in establishing electrical connections. Up until now, the load-deformation characteristic of a single Ag-PMMA microsphere has not been measured. As such, we present in this communication a mechanical model based on measured load-deformation characteristics of a single Ag-PMMA microsphere to facilitate a spring model to better predict the deformation of multi-particle systems with respect to applied load. Furthermore, a finite element electrical model is implemented to determine the effects of sub-cell charge transport layer properties and electrical contacts on parasitic resistive losses. Hence, we demonstrate the critical factors influencing the quality of TCC as an anisotropic electrical interconnection layer, and provide a computational mechanical and electrical model to understand and mitigate parasitic resistive losses.

9:15 AM EN05.07.05

Interface Engineering and Characterization of BiVO₄ Photoanodes Boosted with 2D Interlayers and Co-Catalysts Junyi Cui and Salvador Eslava; Imperial College London, United Kingdom

Photoelectrochemical conversion of water using solar energy offers a clean solution to the world energy requirements of a sustainable future. Achieving its full potential depends on developing inexpensive photoanodes that can efficiently absorb solar light and drive the difficult oxygen evolution reaction (OER), which requires 4 electrons per molecule, and currently hampers reaching high solar to hydrogen efficiencies.

In this talk, I will first present recent developments we have achieved in my group in the preparation of inexpensive BiVO₄ photoanodes functionalized with 2D bismuthene. Partially oxidized two-dimensional (2D) bismuthene is prepared by reduction of BiCl₃ and demonstrated to be an effective, stable, functional interlayer between BiVO₄ and the archetypal NiFeOOH co-catalyst. Comprehensive (photo)electrochemical and surface photovoltage characterizations show that NiFeOOH passivates hole trap states of BiVO₄; however, it is limited in influencing electron trap states related to oxygen vacancies (V_O). Loading bismuthene on BiVO₄ photoanodes fills the V_O-related electron traps, leading to more efficient charge extraction. This is confirmed by kelvin probe measurements. Moreover, bismuthene increases adsorption sites for reaction intermediates and increases interfacial band bending boosting hole charge flux to the electrolyte. With the synergistic interaction of bismuthene and NiFeOOH on BiVO₄, this composite photoanode achieves a 5.8-fold increase in photocurrent compared to bare BiVO₄ reaching a stable 3.4 (±0.2) mA cm⁻² at a low bias of +0.8 V_{RHE} or 4.7(±0.2) mA cm⁻² at +1.23 V_{RHE}. The use of 2D bismuthene also boosts other photoanodes such as hematite, demonstrating its wide potential to boost the performance of photoelectrodes for energy conversion applications.

In a second part of my talk, I will present our study on the role of composition and interactions between BiVO₄ and core-shell structured bimetallic nickel-cobalt phosphide co-catalysts with varying metal ratios to improve their photoanodic performance. The best performance obtained from BiVO₄/Ni_{1.5}Co_{0.5}P and BiVO₄/Ni_{0.5}Co_{1.5}P photoanodes achieved a photocurrent of 3.2 (±0.14) mA cm⁻² at +1.23 V_{RHE}, a 3.5-fold increase in photocurrent compared with bare BiVO₄. Through an extensive characterization considering interfacial energetics, hole storage, and catalytic ability, we have discovered that the

enhanced photoelectrochemical performance cannot be solely attributed to the catalytic activity of the co-catalysts. Instead, it arises from a synergistic interplay involving effective band bending, catalytic activity, and capacitive ability. The contact between the core-shell metal phosphides, BiVO₄, and the electrolyte creates three pathways for hole injection into the electrolyte, all of which are notably enhanced by the presence of a second metal cation in the co-catalysts. Kinetic studies demonstrate that the BiVO₄/metal phosphide photoanodes show significantly improved interfacial charge injection due to a lower charge-transfer resistance, enhanced OER kinetics, and larger surface hole concentrations. Moreover, by analysing the distribution of relaxation times, we can distinguish the kinetics of various processes, including bulk charge carrier transport, hole injection through different pathways, and surface recombination. This analysis provides deeper insights into the carrier dynamics within these photoanode/cocatalyst systems.

To conclude, these results provide key insights into the preparation of BiVO₄ photoanodes boosted with interlayers and co-catalysts to achieve its full potential and pave the way to rationally design other complementary photoelectrodes.

Cui, J.; Daboczi, M.; Regue, M.; Chin, Y.; Pagano, K.; Zhang, J.; Isaacs, M.A.; Kerherve, G.; Mornito, A.; West, J.; Gimenez, S.; Kim, J.; Eslava, S. *Adv. Funct. Mater.* 2022, 32, 1-12

Cui, J.; Daboczi, M.; Cui, Z.; Gong, M.; Flitcroft, J.; Skelton, J.; Parker, S.C. *Eslava, S. Small* 2023, 2306757

9:30 AM *EN05.07.06

Monolithic Photoelectrochemical Tandem Devices consisting of Tunnel Oxide Passivated Contact Silicon and BiVO₄ enabling Unassisted Water Splitting Gihun Jung¹, Choongman Moon¹, Filipe Martinho², Yun Seog Lee³, Stela Canulescu² and Byungha Shin¹; ¹Korea Advanced Institute of Science and Technology, Korea (the Republic of); ²Technical University of Denmark, Denmark; ³Seoul National University, Korea (the Republic of)

A tandem photoelectrochemical (PEC) water-splitting device for solar hydrogen production consists of two light absorbers with different bandgaps. Silicon photoelectrodes have been widely investigated in PEC applications because their bandgap (1.12 eV) is suitable for the bottom cell of a tandem device. We apply a tunnel oxide passivated contact (TOPCon) on the front and back sides of a Si wafer to prepare a TOPCon Si PEC device. Photocathodes and photoanodes based on TOPCon Si exhibit remarkable versatility across a wide pH spectrum (0–14), generating photovoltages ranging from 640–650 mV under 1 sun illumination, marking the highest values achieved among crystalline Si photoelectrodes. TOPCon Si demonstrates excellent thermal stability, enduring a high processing temperature of up to 600 °C for 1 h in ambient air. These advantages of TOPCon Si provide high efficiency and great design flexibility for monolithic tandem cells. TOPCon Si is integrated with BiVO₄, a large bandgap top cell consisting of earth-abundant and non-toxic elements, in monolithic construction—a wireless PEC tandem cell. A dual-junction monolithic tandem cell consisting of NiOOH/FeOOH/BiVO₄/SnO₂/Ta:SnO₂(TTO)/TOPCon Si yields a maximum photocurrent density of 1.4 mA cm⁻² (equal to the solar-to-hydrogen conversion efficiency of 1.72%) when illuminated with air mass 1.5 G simulated solar irradiation, which is the highest value among dual-junction monolithic PEC cells except for III-V materials. Transparent and conductive TTO grown by pulsed laser deposition serves as a recombination layer to achieve effective integration. In addition, the TTO provides chemical and physical protection, allowing the surface of the TOPCon Si to exhibit 24 h of tandem cell stability under weak base electrolyte conditions. The SnO₂ hole-blocking layer inserted between TTO and BiVO₄ enhances the charge separation of BiVO₄, allowing device to achieve high efficiency. Furthermore, we present artificial leaf-type monolithic tandem cells consisting of NiFe/BiVO₄/SnO₂/TTO/TOPCon Si/Ag/Ti/Pt. Additionally, if time permits, I will also discuss our recent research involving the utilization of halide perovskite/Cu(In,Ga)Se₂ tandem devices for unassisted water splitting.

10:00 AM BREAK

SESSION EN05.08: Stability and Scalability
Session Chairs: Virgil Andrei and Robert Hoyer
Wednesday Morning, April 24, 2024
Room 335, Level 3, Summit

10:30 AM *EN05.08.01

Photo-Electrochemical Water Splitting to Generate Hydrogen Fuel: The Importance of Accurately Benchmarking Efficiency, Challenges with System Scale Up and Protective Barriers for Corrosion Mitigation Todd G. Deutsch, Myles Steiner and James L. Young; National Renewable Energy Laboratory, United States

Solar-to-hydrogen (STH) conversion efficiency a common figure of merit for evaluating and comparing research results, and it largely establishes the prospect for successfully introducing commercial solar water-splitting systems. Present measurement practices do not follow well-defined standards, and common methods consistently overestimate performance. To remedy this need we confirmed underestimated influence factors and proposed experimental strategies for improved accuracy.

Our focus was tandem (dual absorber) devices that have the prospect for greater STH efficiency, but increased complexity that requires more careful consideration of characterization practices. We performed measurements on an advanced version of the classical GaInP₂/GaAs design while considering (i) calibration and adjustment of the light source, (ii) validation of results by incident photon-to-current efficiency (IPCE), and (iii) definition and confinement of the active area of the device.

We initially measured 21.8% STH efficiency using a tungsten broadband light source, a calibrated GaInP₂ photovoltaic reference cell, and epoxy-encased photocathodes. In contrast, integrating experimental IPCE over the AM 1.5G reference solar spectrum showed that less than 10% STH conversion is possible. We performed a set of on-sun measurements that gave 16.1% STH efficiency before eliminating indirect light coupled to the sample by using a collimating tube and 13.8% STH efficiency. However, the value still significantly exceeded the current density expected according to the quantum efficiency measured via IPCE. Finally, suspecting that the illuminated area is poorly defined by epoxy, we use a compression cell for an epoxy-free area definition, resulting in 9.3% STH efficiency – a number corroborated by our IPCE results.

The second part of this talk will identify the challenges encountered while scaling the inverted metamorphic multijunction (IMM) III-V absorber areas of from ~0.15 cm² up to 16 cm² and incorporating them in a photoreactor capable of generating 3 standard liters of hydrogen in 8 hours under natural sunlight. To successfully scale photo-electrochemical water-splitting technologies from bench to demonstration size requires addressing predictable and unpredictable complications. Despite using Comsol multiphysics to model our photoreactor and identify suitable specifications for a prototype, several practical issues were uncovered during testing that led to multiple iterations of photoreactor design between the initial and final generation. Several bottlenecks that ranged from counter electrode composition and orientation to bubble removal needed redress in order to meet our performance targets. Ultimately, the demonstration-scale system was able to generate nearly twice the target volume of hydrogen in an 8-hour outdoor trial.

While III-V semiconductors have achieved high photo-electrochemical (PEC) conversion efficiencies, they are remarkably unstable during operation in a harsh electrolyte. The final part of this talk will focus on the degradation mechanism of IMM III-V cells and surface modification strategies aimed at protecting them from photocorrosion. We applied noble metal catalysts, oxide coatings by atomic layer deposition, and MoS₂ in an effort to protect the GaInP₂ surface that was in contact with acidic electrolyte. We also grew epitaxial capping layers from III-V alloys that should be more intrinsically stable than GaInP₂. The ability of the various modifications to protect the IMM's surface was evaluated by operating at each electrode at short circuit for extended periods of time. We will elaborate on the challenges of this mode of protection and new methods of protecting perovskite photo absorbers will be introduced.

11:00 AM EN05.08.02

An Artificial-Photosynthetic System Consisting of Solar-Driven Reaction and Product Isolation Processes to yield only Pure Formic Acid Yasuhiko Takeda, Shintaro Mizuno, Masahito Shiozawa, Natsumi Nojiri, Takeshi Morikawa and Naohiko Kato; Toyota Central R&D Labs Inc, Japan

We proposed a concept of an artificial-photosynthetic system to produce pure formic acid using only CO₂, water, and solar energy, generating no waste.¹ The system consists of a solar-driven reaction process and a product isolation process. We proved the concept by small-scale experiments, and constructed a practically large-sized reactor as the first step toward widespread use of artificial photosynthesis.^{2,3}

We adopted a single-compartment configuration of the solar-driven reactor without ion-exchange membranes and a near-neutral pH electrolyte of a potassium phosphate buffer aqueous solution to simplify the reactor structure. The large-sized reactor was composed of eight-stacked cathode/anode-electrode pairs of 1 m×1 m in size and powered by crystalline-silicon solar cells on the reactor housing via a DC-DC converter. The raw material of 100% CO₂ gas was dissolved in the electrolyte and supplied to the cathode-electrode surfaces uniformly with the help of well-designed flow channels. The electrochemically synthesized formic acid was dissolved in the electrolyte and ejected from the reactor. We developed a Ru-complex-based cathode catalyst and a IrO_x-based anode catalyst, and achieved a Faradaic efficiency as high as 96% for the formic-acid synthesis at an extremely low operating voltage of 1.65 V (overpotential of only 0.22 V) and a large current of 65 A, resulting in a high solar-to-chemical energy conversion efficiency of 10.5%. In addition, we tackled to improve both activity and durability of the cathode and anode electrodes,^{4,5} and to realize direct reduction of CO₂ in a flue gas to eliminate CO₂ capture processes.⁶ Further, we designed tandem solar modules suitable for direct coupling with the reactors using organic-inorganic hybrid perovskite solar cells.⁷

The next challenge was isolation of the synthesized formic acid dissolved in the aqueous electrolyte. The formic acid cannot be isolated by distillation because of its boiling point (101 °C) almost the same as that of water. Thus, we developed an isolation process on the basis of reactive extraction, including three sequential steps.¹ The first step was reactive extraction of the formic acid from the electrolyte using an extraction solution composed of an organic base (trioctylamine, TOA, boiling point 366 °C) as an extractant and an organic solvent (dichloromethane, DCM, boiling point 40 °C) as a diluent. Although formic acid is highly miscible in water, it was extracted into DCM because the formic acid formed a complex salt with TOA that is insoluble in water. The second step was removal of DCM from the mixture of the extracted formic acid, TOA, and DCM produced in the first step, by evaporation at 40 °C. Finally, the residue was heated at 160 °C for isolation of the formic acid by distillation in the third step. The large differences in the boiling points among these three chemicals secured few contaminations in the second and third steps. In addition, the composition of the electrolyte was tuned for promotion of the formation of the formic acid-TOA complex salt. Thus, we achieved an over 90% isolation yield of pure formic acid. The new electrolyte was confirmed to lower the conversion efficiency by only 10% (relative) and to secure similarly high durability compared with the original electrolyte. The great feature of the isolation process is that all the electrolyte, TOA, and DCM are reused for the next synthesis and isolation after the formic acid is isolated. Thus, we established a highly sustainable artificial-photosynthetic system that consumes no chemicals other than the raw materials of CO₂ and water, or generates no waste.

References

1. M. Shiozawa, et al., in preparation.
2. N. Kato, et al., *Joule* 5, 687 (2021).
3. N. Kato, et al., *ACS Sustain. Chem. Eng.* 9, 16031 (2021).
4. M. Shiozawa, et al., *Electrocatalysis* 13, 830 (2022).
5. N. Kato, et al., in preparation.
6. Y. Takeda, et al., *J. CO₂ Util.* 71, 102472 (2023).
7. Y. Takeda, *J. Appl. Phys.* 132, 075002 (2022).

11:15 AM EN05.08.03

Utilizing Three-Terminal IBC-Based Si Solar Cells as a Platform to Study The Durability of Photoelectrodes for Solar Fuel Production Darci Collins^{1,2}, Zebulun Schichtl¹, Nathan Nesbitt¹, Annie Greenaway¹, Valentin Mihailtchi³, Daniel Tune³ and Emily Warren¹; ¹National Renewable Energy Lab, United States; ²Colorado School of Mines, United States; ³International Solar Energy Research Center, Germany

Unassisted, photoelectrochemical (PEC) reactions, such as H₂ generation and CO₂ reduction, are limited by the durability of the immersed semiconductor and catalyst. While great strides have been made to improve stability under illumination, dark stability remains relatively unexamined and presents great challenges. Typically, semiconductors require the use of protection layers to drive the PEC reactions of interest. Cathodic protection is an established electrochemical method for preventing electrode degradation in harsh conditions. Similar protection strategies cannot be applied to traditional two-terminal (2T) semiconductor photoelectrodes because of their inability to pass reverse bias current in the dark. New, three-terminal (3T) photovoltaic (PV) architectures can remove the limitations of traditional 2T photoelectrodes by the addition of an extra electrical contact which provides an alternative low resistance path to drive electrochemical reactions, even in the dark. 3T Si interdigitated back contacted (IBC) cells have n+ and p+ doped back contacts, similar to a traditional IBC cell, with an additional conductive front n+ contact to create the third terminal. Here, we investigate how 3T Si PV can be operated as photocathodes to understand new protection methods for photocathodes in aqueous environments without protection layers. We characterize performance of the 3T electrode in a regenerative redox electrolyte, methyl viologen, to decouple catalysis from photocathode device performance. The 3T Si electrode is used as a platform to understand the applications of cathodic protection to electrodes in photoelectrochemical systems. The 3T architecture provides additional capabilities to PEC systems such as cathodic protection, the ability to drive reactions with or without illumination, and in-situ switching between different operational modes. During experiments, the 3T photoelectrode is wired in the diode mode during illumination and wired in ohmic mode in the dark, where the cathodic protection is applied. We show that bare 3T-based Si photocathodes maintain PEC activity in methyl viologen electrolyte after several hours of light/dark cycling. This work helps advance PEC use in real-world conditions where durability under variable illumination must be considered. Future work includes modeling 3T architectures and cathodic protection in fuel forming reactions and experimentally adding Pt and Cu catalysts to extend this work to systems for H₂ generation and CO₂ reduction.

Wednesday Afternoon, April 24, 2024
Room 335, Level 3, Summit

3:30 PM *EN05.09/EN11.02.01

Large Scale Solar Hydrogen and Fuels Production Systems Using Particulate Photocatalysts Kazunari Domen^{1,2}; ¹Shinshu University, Japan; ²The University of Tokyo, Japan

Sunlight-driven water splitting has been studied as a means of producing renewable solar hydrogen. Overall water splitting using particulate photocatalysts is of growing interest as a means of producing renewable hydrogen, because systems based on particulate photocatalysts can be spread over large areas using potentially inexpensive processes.¹ A solar hydrogen production system based on 100-m² arrayed photocatalytic water splitting panels and an oxyhydrogen gas separation module was recently built, and its performance and system characteristics, including safety issues, were reported.² In addition, the hydrogen produced can be used to convert carbon dioxide into chemical fuels.³ However, it is essential to radically improve the solar-to-hydrogen energy conversion efficiency (STH efficiency) of photocatalysts and to develop suitable reaction systems.⁴ In my talk, recent advances in photocatalytic materials and reaction systems for hydrogen and fuel production will be presented.

The author's group has studied various semiconductor oxides, (oxy)nitrides, and (oxy)chalcogenides as photocatalysts for water splitting.⁵ SrTiO₃ is an oxide photocatalyst that has been known to be active in overall water splitting under UV irradiation since 1980. Recently, the apparent quantum yield of overall water splitting using SrTiO₃ has been improved to more than 90% at 365 nm, corresponding to an internal quantum efficiency of nearly unity, by refining the preparation conditions of the photocatalyst and the loading conditions of the cocatalysts.⁶ This observation means that particulate photocatalysts can drive the endergonic overall water splitting reaction with almost no recombination loss as in photon-to-chemical conversion processes during photosynthesis. However, for practical solar hydrogen production, it is essential to develop photocatalysts that are active under visible light. Ta₃N₅,⁷ Y₂Ti₂O₅S₂,⁸ TaON,⁹ BaTaO₂N¹⁰, SrTaO₂N¹¹ have been shown to be active in photocatalytic overall water splitting via one-step excitation under visible light. It is also possible to combine hydrogen evolution photocatalysts (HEPs) and oxygen evolution photocatalysts (OEPs) to split water into hydrogen and oxygen via two-step excitation. Such a process is widely known as the Z-scheme. Particulate photocatalyst sheets consisting of La- and Rh-codoped SrTiO₃ as HEP and Mo-doped BiVO₄ as OEP immobilized on Au and C layers split water into hydrogen and oxygen with STH efficiencies exceeding 1.0%.^{12,13} Some (oxy)chalcogenides and (oxy)nitrides with long absorption edge wavelengths are also applicable to Z-scheme photocatalyst sheets and hold the promise of realizing greater STH efficiencies.

References:

1) Hisatomi *et al. Nat. Catal.* **2019**, *2*, 387. 2) Nishiyama *et al. Nature* **2021**, *598*, 304. 3) Yamada *et al. ACS Engineering Au* **2023**. DOI: 10.1021/acseengineeringau.3c00034. 4) Hisatomi *et al. Next Energy* **2023**, *1*, 100006. 5) Chen *et al. Nat. Rev. Mater.* **2017**, *1*, 17050. 6) Takata *et al. Nature*, **2020**, *581*, 411. 7) Wang *et al. Nat. Catal.* **2018**, *1*, 756. 8) Wang *et al. Nat. Mater.*, **2019**, *18*, 827. 9) Xiao *et al. Angew. Chem. Int. Ed.* **2022**, *134*, e202116573. 10) Li *et al. ACS Catal.* **2022**, *12*, 10179. 11) Chen *et al. J. Am. Chem. Soc.* **2023**, *145*, 3839. 12) Wang *et al. Nat. Mater.* **2016**, *15*, 611. 13) Wang *et al. J. Am. Chem. Soc.* **2017**, *139*, 1675.

4:00 PM *EN05.09/EN11.02.02

Advancing Solar Harvesting Technology with Kesterite-Inspired Absorbers and High Throughput Materials Discovery Lydia H. Wong; Nanyang Technological University, Singapore

The quest for harnessing solar energy to produce both electricity and fuel represents an enduring pursuit in the realm of renewable energy. Although conventional solar panels have found application in solar fields and rooftops, the realization of this vision necessitates the development of advanced technologies involving innovative materials and novel manufacturing processes. These advancements aim to extend the application of solar energy to diverse contexts such as windows, vehicles, and complex substrates. Despite the identification of numerous photoabsorbers with potential as solar cell materials, only a limited few have transitioned into commercial use.

This presentation will delve into the recent endeavors of our research group, focusing on kesterite-inspired absorbers [1], with a specific emphasis on the effects of doping and cation substitutions in Cu₂CdSnS₄ photoabsorbers. We will demonstrate how substitutions involving Ag and Ge impact the structure and optoelectronic characteristics of this material [unpublished findings]. Additionally, we will discuss our research in high-throughput synthesis and characterization techniques, which have led to the discovery of new dopants that enhance the charge transport properties of FeVO₄ photoanodes [2] and ternary Fe-Co-Ni oxide catalysts for the Oxygen evolution reaction [3].

References

[1] S. Lie, L.H. Wong* *et al.*, *J. Mater. Chem. A*, **2022**, *10*, 9137-9149
[2] H. Nguyen, L.H. Wong* *et al.*, *Solar RRL*, **2021**, *4* (12), 2000437
[3] M. Ahmed, L.H. Wong* *et al.*, *Small*, **2023**, *19* (2), 2204520

SESSION EN05.10: Poster Session
Session Chairs: Demetra Achilleos and Virgil Andrei
Wednesday Afternoon, April 24, 2024
Flex Hall C, Level 2, Summit

5:00 PM EN05.10.01

Simultaneous Photo Protecting and Tuning Selectivity of Cs₃Bi₂Cl₉ during Photoreduction of CO₂ to HCOOH Using Ir/IrO_x Govardhan Pandurangappa, Raghuram Chetty and Aravind Kumar Chandiran; Indian Institute of Technology Madras, India

Tuning the selectivity with the improved activity of photocatalysts during the photoreduction of CO₂ to value-added chemicals is one of the main bottlenecks in the field of artificial photosynthesis. Here we have investigated lead-free, bismuth-based Cs₃Bi₂Cl₉ perovskites as photocatalysts for the photoreduction of CO₂ in the solid-liquid phase. The main CO₂ photoreduction products include CO, CH₄ in the gas phase, and HCOOH in the liquid phase. Cs₃Bi₂Cl₉ showed high activity and good selectivity towards HCOOH, with a 553 ± 21 μmol g⁻¹ yield at the end of the 5-hour reaction. There was decreased activity of the Cs₃Bi₂Cl₉ due to the formation of the secondary phase of BiOCl. A composite photocatalyst Cs₃Bi₂Cl₉-Ir/IrO_x showed a higher selectivity towards HCOOH with a yield of 789 ± 43 μmol g⁻¹ at the end of the 5-hour reaction which was 1.5 times higher than the yield on pristine

material. This was the highest yield of HCOOH ever reported for this class of materials. The presence of Ir/IrO_x provided the reaction with much-needed hydroxyl groups for the photoreduction of CO₂. Further, Ir/IrO_x delayed the catalyst deactivation thereby retaining its activity for longer cycles by altering the photo-generated charge recombination process and prolonging their lifetimes making them available for the valuable photoreduction of CO₂. This work provides a simple yet effective strategy to tune the selectivity and improve the performance of photocatalysts for CO₂ photoreduction.

5:00 PM EN05.10.02

Solar Driven CO₂ Reduction to CO Catalyzed by Mn-Complex supported on Carbon Nanohorn in an All Earth Abundant System [Teppe Nishi](#), Shunsuke Sato, Keita Sekizawa, Tomiko M. Suzuki, Keiichiro Oh-ishi, Naoko Takahashi, Yoriko Matsuoka and Takeshi Morikawa; Toyota Central R&D Labs., Inc., Japan

CO₂ conversion technology have been developed for carbon neutral society. A lot of catalysts to convert CO₂ to chemicals have also been developed. Our group also reported CO₂ reduction catalysts. In particular, Mn-complex catalyst supported on multi-walled carbon nanotubes (MWCNTs) can catalyze CO₂ reduction reaction to CO at low overpotential (ca. 100 mV) [1]. In addition to the electrocatalytic activity, solar-driven CO₂ reduction to CO using Ni-doped β-FeOOH as an anode and Si solar cell was also reported [2]. Here, we report a carbon support effect to enhance the electrocatalytic activity [3]. We used MWCNTs, carbon nanohorns (CNHs), graphene platelets (GNPs), carbon black (CB) and carbon nanofibers (CNFs). Electrocatalytic activities Mn-complex supported on various carbon supports were measured in CO₂ saturated aqueous 0.1M K₂B₄O₇ + 0.2M K₂SO₄ solution at an applied potential of -1.0 V vs Ag/AgCl. Among the various carbon materials, CNHs were the best supports to enhance the catalytic activity toward CO₂ reduction to CO. Faraday efficiency of CO was 87%. The superior activity was speculated to the high specific surface area and hydrophobic nature. The water-drop contact angle revealed hydrophobicity of CNHs and MWCNTs. It is expected that a superior local environment for highly selective CO₂ reduction can be provided by hydrophobic supports by keeping water away from the electrode surface. In contrast, hydrophilic carbon supports resulted in the increase of Faraday efficiency of H₂. Additionally, specific surface area of CNHs (410 m²/g) was larger than other carbon supports. It is concluded that these properties resulted in the enhancement of catalytic activity of Mn-complex.

Because CNHs was revealed to enhance the catalytic activity of Mn-complex for CO₂ reduction to CO, we demonstrated solar-driven CO₂ reduction to CO using Mn-complex supported on CNH as a cathode electrode, Ni doped β-FeOOH supported on single walled carbon nanotube (SWCNT) as an anode electrode and polycrystalline Si solar cell. A solar-to-CO conversion efficiency was 3.3 %.

[1] S. Sato et al., ACS Catal., 2018, 8, 4452-4458.

[2] T. Arai, et al., Chem. Commun., 2019, 55, 237-240.

[3] T. Nishi et al., ChemNanoMat 2021, 7, 596.

5:00 PM EN05.10.03

Experimental Characterization of Three-Terminal Tandem Photoelectrode Voltages for Photoelectrochemical Applications [Grace Rome](#)^{1,2}, Myles Steiner², Emily Warren² and Annie Greenaway²; ¹Colorado School of Mines, United States; ²National Renewable Energy Laboratory, United States

Sustainably produced liquid fuels are necessary for a clean energy future, especially for energy intensive applications such as aviation where batteries are presently not sufficiently energy dense. Photoelectrochemical carbon dioxide reduction (PEC CO₂R) is a possible route to the production of sustainable fuels. However, there are an abundance of different products from CO₂R, making selective production of a single chemical difficult and requiring expensive, energy intensive product separation. One method to improve selectivity is to design cascading reactions, such as reducing CO₂ to CO and then subsequently reducing the CO to higher order (C₂₊) products.^[1] Each reaction within the CO₂R cascade occurs at a specific thermodynamic potential, requiring a specific voltage, and has a specific stoichiometry, requiring a specific electron flux or current density. The reactions of interest for a PEC CO₂R cascade would take place on a single photoelectrode, requiring first step products to move only on the order of millimeters to the second reaction site. This work aims to develop and characterize a III-V-based photoelectrode that can drive such a cascade CO₂R photoelectrochemically, using sunlight as the energy input.

A three-terminal tandem (3TT) is a type of multijunction photovoltaic device where a middle terminal is added between the two subcells that comprise the tandem, rather than having no extra terminal (as in a two-terminal tandem) or having the two subcells electrically separated (a four-terminal tandem).^[2] Connecting any two of the three contacts generates a different voltage, enabling a single device to supply the different potentials required for CO₂R cascade reactions. Current densities can be manipulated by changing the relative areas of the terminals. The GaInP/GaAs 3TT tandem used in this work has two terminals contacting the electrolyte, each of which drives one step of the CO₂R cascade; the photoelectrode is illuminated from opposite side, through a third terminal. Previous modelling work^[3] has shown that a 3TT tandem could drive a PEC CO₂R cascade and possibly improve product selectivity over simpler photoelectrodes. However, the fundamental behaviors of 3TT photoelectrodes are not yet understood in relationship to the performance of 3TT photovoltaics. This work experimentally characterizes the PEC behavior of a 3TT photoelectrode. Potential and current relationships will be characterized both dry and under electrochemical conditions to provide insight into what standard reduction potentials are possible with a GaAs/GaInP 3TT device. Dry power contour plots will be used to find the max power point, as simple current-voltage curves cannot fully define 3TT operation due to presence of the middle contact.^[4] Non-aqueous PEC measurements, using regenerative redox couples, will be performed in combination with light filtering (to select the GaInP or GaAs subcell) to learn about the operational window of each electrolyte terminal. In summary, this work aims to control a 3TT photoelectrode for PEC CO₂R as a step towards the goal of sustainable fuel production.

[1] Gurudayal, D. Perone, S. Malani, Y. Lum, S. Haussener, J. W. Ager, *ACS Appl. Energy Mater.* **2019**, 2, 4551–4559.

[2] E. L. Warren, W. E. McMahon, M. Rienäcker, K. T. VanSant, R. C. Whitehead, R. Peibst, A. C. Tamboli, *ACS Energy Lett.* **2020**, 5, 1233–1242.

[3] C. J. Kong, E. L. Warren, A. L. Greenaway, R. R. Prabhakar, A. C. Tamboli, J. W. Ager, *Sustain. Energy Fuels* **2021**, 5, 6361–6371.

[4] J. F. Geisz, W. E. McMahon, J. Buencuerpo, M. S. Young, M. Rienäcker, A. C. Tamboli, E. L. Warren, *Cell Rep. Phys. Sci.* **2021**, 2, 100677.

5:00 PM EN05.10.04

Direct Z-Scheme Heterostructure of In-Situ Planted ZnO Nanorods on g-C₃N₄ Thin Sheets Sprayed on TiO₂ Layer: A Strategy for Ternary-Photoanode Engineering towards Enhanced Photoelectrochemical Water Splitting [Ahmed E. Aboubakr](#), Mahmoud K. Hussien, Amr Sabbah, Kuei-Hsien Chen and Chen-Hsiung Hung; Academia Sinica, Taiwan

In this study, we focused on optimizing the photoanode, which is crucial for the practical applications of photoelectrochemical water splitting (PEC-WS). We describe an improved fabrication method that is efficient and scalable. This approach enhanced the separation and transfer of charge carriers for photoelectrochemical water splitting in solar-driven hydrogen production. We followed a procedure that enables the in-situ growth of ZnO nanorods on g-C₃N₄, resulting in a ZnO/g-C₃N₄ composite with an enhanced specific surface area. The as-fabricated composite exhibits interfacial Zn-N bonding interactions, as evidenced by XPS Zn 2p and N 1s spectra. This composite material demonstrated improved efficiency in charge migration and a lower charge recombination rate with a Z-scheme type charge separation, supported by data from time-resolved photoluminescence spectroscopy (TRPL) and photoelectrochemical impedance spectroscopy (PEIS), as well as from theoretical calculation. We achieved this by designing a highly efficient Z-scheme

TiO₂/g-C₃N₄/ZnO photoanode. PEC-WS measurements showed that TiO₂/g-C₃N₄/ZnO photoanode improved the produced photocurrent by about 160-, 40-, 20-, 8-, 2-, and 2-fold, relative to pristine g-C₃N₄, pristine ZnO nanorods, ZnO/g-C₃N₄ composite, pristine TiO₂, TiO₂/ZnO, and TiO₂/g-C₃N₄, respectively, versus reversible hydrogen electrode (RHE) at 1.23 V. The DFT results contributed to a deeper understanding of the mechanism of the photocatalytic process and confirmed that the as-fabricated ternary heterojunction promoted the separation/transfer efficiency of the photogenerated charge carriers, thereby promoting the activity of the photocatalytic process. This work could pave the way for the better fabrication of ternary-based photoanodes; we used an airbrushing procedure under mild heating to deposit ZnO/g-C₃N₄ on TiO₂ and obtained a photoanode with a ternary composition. This photoanode displayed efficient charge separation and transfer due to the improved interface properties. Furthermore, utilizing this strategy of spraying the as-synthesized ZnO/g-C₃N₄ photocatalyst over the TiO₂-coated FTO under moderate heating results in a homogeneous distribution of the components. To the best of our knowledge, this is the first study to use these strategies to fabricate such ternary photoanodes. So, our strategy could pave the way for synthesizing various g-C₃N₄-based ternary composites for PEC-WS. We believe this work will be of high interest because our approach is applicable to many ternary heterostructures and could be widely used as a universal strategy to increase the photocatalytic performance of various composites toward PEC-WS.

5:00 PM EN05.10.06

Designing New Metallic Catalysts by Transversing The ‘Hidden’ Compositional Terrain Qinrui Liu, Md T. Islam and Scott Broderick; University at Buffalo, United States

To discover materials with enhanced catalytic behavior, we convert the complex elemental feature space into a connected network, representing the similarities and underlying physics of catalytic alloys. A challenge in the design is due to limited number of property measurements, thereby making typical data driven modeling inaccurate and uncertain. To address this challenge, we apply a random walk approach to capture the reaction behaviors and link the kinetic and chemical behaviors of the alloys. The results lead to a more comprehensive understanding of metallic catalysts design with the most promising chemistries identified across a variety of gas reactions. Through this work, the design space is reduced and the necessary experiments are defined.

5:00 PM EN05.10.07

Enhancement of The Photoelectrochemical Performance of TiO₂ Nanotube Arrays through Sensitization with Electrochemically Deposited CdSe Nanoparticles Damini Vrushabendrakumar, Harshitha Rajashekhar, Navneet Kumar, Kazi M. Alam and Karthik Shankar; University of Alberta, Canada

This study presents an approach to enhance the photoelectrochemical water-splitting performance of highly transparent TiO₂ nanotube arrays (TTNTAs) through electrochemical deposition of CdSe nanoparticles (NPs) in aqueous electrolytes containing a mixture of CdCl₂ and SeO₂.¹ CdSe is particularly attractive as a sensitizer due to its broad visible light absorption (enabling increased photogeneration of carriers), quantum confinement effect and strong photoluminescence emission which can be spectroscopically monitored to understand the interfacial energy level configuration and electron injection efficiency (into TiO₂). While CdSe NPs formed by colloidal and/or SILAR (sequential ionic layer adsorption and reaction) routes have been extensively used to sensitize various wide band gap semiconductor nanostructures, there are far fewer reports on sensitization using electrochemically synthesized CdSe quantum dots. TTNTAs were fabricated via a facile and well-established electrochemical anodization process.² The top surfaces and lateral walls of TTNTAs were selectively decorated with CdSe NPs. A major advantage of the electrochemical deposition process is the number of process variables that can be adjusted in order to deterministically control the particle size and size distribution of the CdSe NPs decorating the TTNTAs. These process variables include the concentration & relative ratio of the Cd and Se precursors in electrolyte, the applied electrochemical potential and the duration of the electrodeposition process. The structural and optical properties of the CdSe-doped TTNTAs were systematically characterized. Sensitization of TTNTAs with CdSe NPs led to improved light absorption and charge separation efficiency.³ The photoelectrochemical activity for water splitting was evaluated, demonstrating enhanced hydrogen and oxygen evolution reactions under visible light illumination. The synergistic effects of transparent TTNTAs and CdSe nanoparticle decoration resulted in a significant improvement in the overall water-splitting performance. This work provides valuable insights into the design of efficient and partially transparent photoelectrodes for solar-driven water splitting, paving the way for sustainable hydrogen production.

References:

1. Yang, L.; Luo, S.; Liu, R.; Cai, Q.; Xiao, Y.; Liu, S.; Su, F.; Wen, L., Fabrication of CdSe nanoparticles sensitized long TiO₂ nanotube arrays for photocatalytic degradation of anthracene-9-carboxylic acid under green monochromatic light. *The Journal of Physical Chemistry C* **2010**, *114* (11), 4783-4789.
2. Kisslinger, R.; Askar, A. M.; Thakur, U. K.; Riddell, S.; Dahunsi, D.; Zhang, Y.; Zeng, S.; Goswami, A.; Shankar, K., Preferentially oriented TiO₂ nanotube arrays on non-native substrates and their improved performance as electron transporting layer in halide perovskite solar cells. *Nanotechnology* **2019**, *30* (20), 204003.
3. Seabold, J. A.; Shankar, K.; Wilke, R. H.; Paulose, M.; Varghese, O. K.; Grimes, C. A.; Choi, K.-S., Photoelectrochemical properties of heterojunction CdTe/TiO₂ electrodes constructed using highly ordered TiO₂ nanotube arrays. *Chemistry of Materials* **2008**, *20* (16), 5266-5273.

5:00 PM EN05.10.08

Supercharging Solar Fuel Production: Harnessing Sub Bandgap Energy in Mo-Doped BiVO₄ Photoanode to Enhance Photoelectrochemical Reaction via Triplet-Triplet Annihilation Upconversion Prashanth Venkatesan and Ruey-An Doong; National Tsing Hua University, Taiwan

Developing solar-based empowered technology is an important issue to realize a zero-carbon world. Among various forms of solar energy utilization, photoelectrocatalysis (PEC), which involves a direct solar to chemical energy conversion by light-matter interaction, exhibits a relatively high theoretical efficiency. PEC uses semiconductors to absorb photons to produce effective electron-hole pairs for a redox reaction. Several concepts have been proposed and demonstrated to improve the separation and utilization of the excitons. However, few attempts have been made to engineer the light to enhance the PEC efficiency by broadening the range of the solar spectrum that the semiconductor can utilize. The upconversion (UC) process induced by triplet-triplet annihilation (TTA) is an intermolecular energy transfer process by restoring the energy in triplet-state molecules to produce a high-energy singlet state to enhance the UC process. It is noted that the UC process, which uses the solar spectrum as the light source can convert the sub-bandgap photon into the absorbing range of the PEC semiconductors. Therefore, incorporating PEC with TTA-UC appears to be the most suitable process to enhance the efficiency of PEC by utilizing the abundant visible light from solar light.

In this study, the benchmark TTA-UC chromophores, 9,10-diphenylanthracene (DPA) sensitized by platinum octaethylporphyrin (PtOEP) are used. They are dissolved in oleic acid to upconvert the green light (532 nm) to blue light (400 – 480 nm) in an ambient environment. The phosphorescence of PtOEP is quenched by DPA based on the Stern-Volmer relation, indicating that the triplet energy transfer between the two chromophores is effective. The optimal concentrations of PtOEP and DPA are 20 μM and 8 mM, respectively. For ease of implementation, PtOEP/DPA containing oleic acid is emulsified and acts as soft templates during the sol-gel process of tetraethyl orthosilicate (TEOS), yielding to UC active SiO₂ nanocapsules. The TEM images suggested that a silica shell encapsulates oleic acid with a diameter of 200 – 300 nm with a thickness of 10 nm. The upconverting composite film is prepared using the SiO₂ nanocapsules. Semitransparent Mo: BiVO₄ photoanode is synthesized by spin coating technique. The incorporation of upconverting composite film with Mo:BiVO₄ photoanode shows an enhanced photocurrent density from 1.09 mAcm⁻² to 1.24 mAcm⁻², equivalent to an increase of 14%. With a 490 nm long pass filter a 45% increase at 1.23 V_{RHE} is observed corresponding to a current density increase from 0.24 mAcm⁻² to 0.35 mAcm⁻².

5:00 PM EN05.10.09

A Novel Approach to Anti-Soiling Coatings for Solar Modules by use of Lanthanide Oxide Films [Jayna K. Patel](#), Ivan Parkin and Claire Carmalt; University College London, United Kingdom

Advances in solar module utilities underpin an important approach for novel sources of renewable energy. However, soiling remains a major obstacle when considering the use of solar modules as a sustainable replacement for electricity generation. Thus, there is an evident need for self-cleaning solar utilities. We present the design, synthesis and application of inorganic rare oxide layers (Ce_2O_3 , Er_2O_3) which have been deposited by aerosol assisted chemical vapour deposition (AACVD) with intrinsic hydrophobicity. Water contact angles of up to 103° were established across the deposited thin films, inferring their self-cleaning potential.

The reduced number of examples of lanthanide oxide complexes for hydrophobic coatings using AACVD within the literature, prompted our investigation into the synthesis of volatile lanthanide β -diketonate precursors, a novel approach to self-cleaning solar modules. Notably, inorganic rare Earth oxide layers (Ce, Y, Lu, Er) have proven through various applications to be durable, UV stable, oxidant resistant and have intrinsic hydrophobicity with a water contact angle range of 110 – 125° .^{1,2} Likewise, β -diketone ligands complexes have proven to serve as effective and stable precursors. Compounds of the type $[\text{M}(\text{Y})_{3,4}]$ have been synthesised via adaption of a known synthetic route to $[\text{Ce}(\text{thd})_4]$ and $[\text{Er}(\text{thd})_3]$.^{3,4} Where; M = lanthanide metal (Ce, Er) and Y = thd (dipivaloylmethane), dbm (dibenzoylmethane).

AACVD of the synthesised complexes yielded lanthanide oxide films on fluorine tin doped (FTO) glass under a constant flow of nitrogen. Thermogravimetric analysis of these compounds indicated suitable deposition temperatures ranging from 400 – 600°C . The most hydrophobic coatings were attained by deposition of cerium oxide onto FTO at temperatures between 400 – 500°C . These rare oxide thin films were intrinsically analysed using surface analysis and characterisation techniques. Whereby X-ray photoelectron spectroscopy confirmed the presence of a mixed phase system of Ce(III) and Ce(IV) across the surface. Further analysis of the deposited thin films was conducted using SEM and XRD to determine the surface morphologies of these hydrophobic coatings.

References

1. G. Azimi, R. Dhiman, H. M. Kwon, A. T. Paxson and K. K. Varanasi, *Nature Materials*, 2013, **12**, 315-320.
2. Y. Zhao, *Materials*, 2012, **5**, 1413-1438.
3. M. Becht, T. Gerfin and K. H. Dahmen, *Chemistry of Materials*, 1993, **5**, 137-144.
4. K. J. Eisenbraun and R. E. Sievers, *Journal of the American Chemical Society*, 1965, **87**, 5254-5256.

5:00 PM EN05.10.10

Highly Efficient and Stable Dye-Sensitized Photoelectrochemical Cells via Cascade Charge Transfer [Jun-Hyeok Park](#), Ji-Wook Jang and Tae-Hyuk Kwon; Ulsan National Institute of Science and Technology, Korea (the Republic of)

Dye-sensitized photoelectrochemical cells (DSPECs) have shown promise in artificial photosynthesis for water splitting, but they face obstacles such as low photocurrents (0.01 – 2.2 mA/cm^2) and limited stabilities (0.01 – 2 h , maintaining over 90% of initial photocurrent) due to degradation/decomposition of dye-sensitized photoelectrodes, along with inefficient charge transfer processes in aqueous electrolytes forming adaptive junction. To overcome these fundamental issues, we developed a “cascade-type” dye-sensitized photoelectrode utilizing platinum-sputtered nickel foil to encapsulate both the dye-sensitized TiO_2 layer and redox mediator electrolyte. This buried junction design enables spatially controlled cascade charge transfer, highly effective photoconversion, and active water oxidation facilitated by Ni-based catalysts, all without undesirable current leakage. By conducting a comprehensive study involving three redox electrolytes and optimizing water oxidation catalysts, our best-performing photoelectrode achieves a photocurrent of 14.5 mA/cm^2 , Faradaic efficiency of approximately 98%, and photostability of 30 h under AM 1.5G illumination.

5:00 PM EN05.10.11

Effect of Protonation on The Photocatalytic CO_2 Reduction by Linear Conjugated Polymers containing Benzo[c]cinnoline Structure [Kuang-Hao Cheng](#)^{1,2}, Shih-Hsuan Lin¹, Cheng Wei Cai², Leeyih Wang², Kun-Han Lin³ and Jyh-Chien Chen¹; ¹National Taiwan University of Science and Technology, Taiwan; ²National Taiwan University, Taiwan; ³National Tsing Hua University, Taiwan

In this study, we polymerized NDI-BZC and DPP-BZC utilizing the naphthalene diimides (NDI) and diketopyrrolopyrrole (DPP) as acceptor benzo[c]cinnoline (BZC) as donor, and obtained the polymers NDI-BZC-H and DPP-BZC-H by hydrochloric acid protonation, respectively. We consider that the photocatalytic carbon dioxide redox reaction consists of two half reactions: the oxidation of water and the reduction of carbon dioxide. The oxidation of water is essential in this process. In this experiment, we use protonation to increase the hydrophilicity of the polymer. However, an excessive increase in hydrophilicity will lead to a competing reaction of hydrogen generation and CO_2 reduction. Therefore, it is crucial to precisely control the increase in hydrophilicity. We introduced BZC as a donor, which possesses an azo-functional group for protonation to precisely enhance the donor's hydrophilicity and facilitate the oxidation reaction with water. The precise enhancement of hydrophilicity proves to be beneficial for water oxidation efficiency without adversely affecting CO_2 adsorption. The success of protonation is confirmed by the signal shift of the azo-functional group and the appearance of Cl signals in the XPS analysis. Additionally, contact angle measurements demonstrate an increase in hydrophilicity, leading to a doubled efficiency of pure water system. After the addition of the sacrificial, the efficiency of DPP-BZC-H reached $235\text{ }\mu\text{mol g}^{-1}\text{ h}^{-1}$, and the efficiency of NDI-BZC-H reached $343\text{ }\mu\text{mol g}^{-1}\text{ h}^{-1}$. The results clearly emphasize the critical role of increasing hydrophilicity in CO_2 reactions, particularly when it occurs at the appropriate site. The distinctive characteristic of the azo group in BZC enables precise control over the protonation position, resulting in a significant enhancement of efficiency. These remarkable capability make BZC as a highly promising candidate in the field of CO_2 reduction.

5:00 PM EN05.10.12

Two Dimensional Janus Ga_2SX_2 (X = O, S, Se, and Te) Monolayers as Efficient Piezo- and/or Photocatalyst for Green Hydrogen Generation [Devender Takhar](#)¹, [Balaji Birajdar](#)¹ and [Ram Krishna Ghosh](#)²; ¹Jawaharlal Nehru University, India; ²IIT, India

Developing innovative and environmentally friendly hydrogen generation technologies are pivotal for transition to a carbon-neutral future. In this regard, the integration of photocatalytic and piezoelectric properties of semiconductor catalyst have proved beneficial. As polar nature of piezoelectric materials provides a drive force to photo-generated charge carriers thus enhancing their separation and reducing recombination. Additionally, piezoelectric materials generate a potential under oscillatory strain, commonly known as piezo-potential, can alone initiate the water redox reaction. Therefore, in this study we explore the potential of piezoelectric Janus Ga_2SX_2 (X=O, S, Se, Te) monolayers as efficient piezo- and/or photocatalyst, leveraging density functional theory (DFT) simulations. Our investigation encompasses a comprehensive examination of the structural, electronic, optical, mechanical and piezoelectric properties. Except Ga_2SO_2 all monolayers exhibit semiconducting behaviour, featuring indirect band gaps within the range of 1 eV to 2.7 eV . The band

edges are favourable to straddle the photocatalytic water redox reaction under the solar illumination. Moreover, the generated piezo-potential exceeds 3 V which originate from superior piezoelectric and mechanical properties demonstrating the piezo-catalytic water splitting ability. In summary, these findings open new avenues for the development of piezo- and photocatalytic technologies for clean and sustainable hydrogen production.

5:00 PM EN05.10.13

Modulation of Structural, Electronic and Electrocatalytic Properties of Pulsed Laser Ablated Ruthenium Oxide Thin Films for Oxygen and Hydrogen Evolution Reactions Ikenna C. Chris-Okoro¹, Sheilah Cheron¹, Swapnil Nalawade¹, Mengxin Liu¹, Valentin Craciun^{1,2}, Shyam Aravamudan¹, Maria D. Mihai^{2,3}, Soyoun Kim⁴, Junko Yano⁴ and Dhananjay Kumar¹; ¹North Carolina Agricultural and Technical State University, United States; ²Horia Hulubei National Institute for Physics and Nuclear Engineering, Romania; ³University Politehnica of Bucharest, Romania; ⁴Lawrence Berkeley National Laboratory, United States

This study presents a detailed optimization study of the structural, electronic, and electrocatalytic properties of ruthenium oxide thin films grown using the pulsed laser ablation (PLA) process. The study begins by growing substrate-film interdiffusion-free sub-stoichiometric (RuO_{2-x}), stoichiometric (RuO_2), and hyper-stoichiometric (RuO_{2+x}) epitaxial ruthenium oxide films with controlled orientation at relatively low deposition temperatures on single-crystal substrates with different crystal structures and surface orientations, such as (110) and (100) oriented rutile TiO_2 , (100) oriented perovskite SrTiO_3 and LaAlO_3 , and (0001) oriented hexagonal sapphire. The synthesis of the substrate-film interdiffusion-free RuO_2 films has been possible due to the axial velocity of laser-ablated neutral and ionic species as high as $\sim 10^5$ m/s (kinetic energy ~ 3 eV), which compensates for the high substrate temperatures nearly by 50 °C. The next part of the study is focused on the use of x-ray photoelectron spectroscopy (XPS) and Rutherford Backscattering Spectrometry (RBS) measurements to confirm that the oxygen content of RuO_2 films increases from $x = 0.5$ to $x = 1.0$ with an increase in oxygen growth pressure from 5 mTorr to 100 mTorr. Further characterization of the RuO_2 films was carried out using x-ray diffraction, atomic force microscopy, four-probe resistivity, spectroscopic ellipsometry, and soft x-ray absorption spectroscopy (XAS) at the O K-edge analysis before and after electrocatalytic property measurements. The study has provided insights to overcome the stability problem of RuO_2 often encountered during the electrocatalytic water oxidation and reduction process. Using the ability to synthesize RuO_2 with the same stoichiometry on substrates with different crystal structures, lattice constants, and orientations, we have developed a better understanding of the effect of surface tension and lattice-matched interfacial structures on electrocatalytic oxidation and reduction of water.

This work was supported by a DOE EFRC on the Center for Electrochemical Dynamics and Reactions on Surfaces (CEDARS) via grant # DE-SC0023415. The authors (IK, VC, and DK) also acknowledge the support of the NSF PREM via grant # DMR-2122067 PREM.

5:00 PM EN05.10.15

Enhanced Stability, Photoluminescence and Charge Transport Properties of TiO_2 -Coated CsPbBr_3 Quantum Dots for Photoelectrochemical Solar Fuel Production Paravee Vas-Ummuay and Parina Nuket; Chulalongkorn University, Thailand

All-inorganic cesium lead bromide perovskite quantum dots (CsPbBr_3 QDs) exhibit excellent optical and electrical properties such as strong light absorption, tunable band gap, long diffusion lengths, ambipolar charge transport, and high charge carrier mobility. Therefore, they have been widely used for light-energy conversion including photovoltaic (PV) and photoelectrochemical (PEC) applications. However, CsPbBr_3 QDs have suffered from instability against the environmental factors in broad applications due to the inherent perovskite properties. This work thus aimed for two purposes. The first is to enhance the stability of CsPbBr_3 QDs, and the second is to use CsPbBr_3 QDs as a light-harvesting material incorporated with TiO_2 electrode for PEC oxidation of methanol. For the first aspect, TiO_2 coating on CsPbBr_3 QDs by ex-situ and in-situ methods was performed to prevent the agglomeration of the nanocrystals and to improve the stability of CsPbBr_3 QDs without heat treatment at high temperatures. The stability test revealed that TiO_2 -coated CsPbBr_3 QDs prepared from the in-situ method exhibited a significant stability improvement against toluene, ultrasonication treatment in water, and light illumination. Furthermore, the results demonstrated the remarkable enhancement of photocurrent generation due to a suitable alignment of energy levels of TiO_2 and CsPbBr_3 and a stable structure of QDs, which plays an important factor in improving the PEC performance. Therefore, it was proved to be used as a good light-harvesting and electrode material in various photoelectrochemical applications. For the second aspect, the photocurrent generation via PEC oxidation of methanol was studied using surface-modified TiO_2 -coated fluorine-doped tin oxide (FTO) as a photoanode in combination with CsPbBr_3 QDs dispersed in an electrolyte solution. Detailed studies revealed that surface modification of the TiO_2 layer was crucial for good interfacial adhesion of CsPbBr_3 QDs, which were surrounded by hydrophobic ligands, with the TiO_2 surface. Self-assembled monolayers of octadecylphosphonic acid (ODPA) were applied on the TiO_2 surface, resulting in the change of hydrophilic nature to a superhydrophobic surface. The photoluminescence measurement of the ODP A-modified TiO_2 /FTO photoanode demonstrated a significantly higher photoluminescence intensity than that of the unmodified one, indicating that CsPbBr_3 QDs were well adsorbed on the TiO_2 surface. The photocurrent was generated via methanol oxidation by holes in CsPbBr_3 QDs. The current-voltage measurements revealed that in the presence of methanol, the current density was increased from 1.2 mA/cm^2 (without methanol) to the maximum of 1.6 mA/cm^2 under visible light irradiation, indicating that methanol was a sacrificial hole scavenger. As a consequence, the multicomponent ODP A-modified TiO_2 /FTO photoanode in combination with CsPbBr_3 QDs together with the efficient hole scavenger of methanol in the system has been shown to promote the PEC oxidation performance, which can be applied in any PEC solar fuel production.

5:00 PM EN05.10.16

Electrochemical CO_2 Reduction to Methane with Remarkably High Faradaic Efficiency in The Presence of a Proton Permeable Membrane Hanqing Pan; University of Nevada, Las Vegas, United States

The combustion of fossil fuels is a major contributor to rising levels of anthropogenic carbon dioxide (CO_2) in the atmosphere. Due to the adverse effects of climate change caused in large part by CO_2 , new technologies must be developed that contribute to a global renewable energy supply. Electrochemical reduction of CO_2 offers a viable pathway to generating value-added products and synthetic fuels to meet our future energy demands while decreasing greenhouse gas emissions. By constructing electrocatalysts capable of modulating proton transfer, we are able to tune product selectivity. Previous studies have demonstrated that two-electron products (CO and HCOOH) can be produced with high selectivity, but multiple-electron transfer products (CH_4 , CH_3OH , and C_2^+ products) typically are produced at much lower Faradaic efficiencies. In this work, we construct polymer-modified Cu electrodes that exhibit extraordinarily high CH_4 production (88% Faradaic efficiency). These electrodes afford a new strategy for increasing the selectivity of CO_2 reduction electrocatalysts, an attribute that is key in developing industrially-relevant CO_2 conversion devices. Nafion is a widely used fluoropolymer that is often mixed with electrocatalysts to facilitate proton transport. In contrast to these Nafion-catalyst composites, this work studies electrodes covered by Nafion overlayers for the CO_2 reduction reaction. By varying the thickness, substrates, and voltage, we perform a detailed study of the effect of Nafion overlayers on metal and carbon mesh electrodes for CO_2 reduction. Depending on the thickness of the Nafion membrane, CO_2 reduction occurs at either the polymer-electrolyte interface or electrode-polymer interface. A Nafion overlayer of 15 μm on a Cu electrode enables an extraordinarily high yield of CH_4 production (88% Faradaic efficiency) at a low overpotential (540 mV) via the stabilization of metal-bound CO intermediates. To the best of our knowledge, this yield is the highest for electrocatalytic CO_2 reduction to CH_4 production at room temperature reported.

5:00 PM EN05.10.17

Preparation of MOFs Coupled-LaFeO₃ Nanosheet for Electrochemical CO₂ Conversion [Iltaf Khan](#), Munzir H. Suliman and Muhammad Usman; King Fahd University of Petroleum and Minerals, Saudi Arabia

The rapid growth of modern industries has led to increased energy demand and worsened fossil fuel depletion resulting in global warming while organic pollutants pose significant threats to aquatic environments due to their stability, insolubleness, and non-biodegradability. So, scientists are investigating high-performance materials to resolve these issues. In this study, we prepared LaFeO₃ nanosheets (LFONS) employing a solvothermal method via a soft template such as polyvinylpyrrolidone (PVP). The LFONS have good performance regarding surface area and charge separation as compared to LaFeO₃ nanoparticles (LFONP). To improve the efficiency of LFONS, it was further modified with Ag and ZIF-67 and utilized for CO₂ conversion. Herein, the results confirm that Ag-doped and ZIF-67 coupled LFONS (ZIF-67/Ag-LFONS) exhibit superior performance compared to pristine LFONP. In addition, the stability tests confirm that our optimal sample is the most active and stable among various nanocomposites. Ultimately, our studies will pave the new gateway for cost-effective, eco-friendly, and electroactive nanomaterials for CO₂ conversion.

5:00 PM EN05.10.18

Unveiling the Optimal Interfacial Synergy of Plasma Modulated Trimetallic Mn-Ni-Co Phosphides: Tailoring Deposition Ratio for Complementary Water Splitting [Nageh K. Allam](#); American University in Cairo, Egypt

Designing highly active, durable, and nonprecious metal-based bifunctional electrocatalysts for overall water electrolysis is of urgent scientific importance to realize sustainable hydrogen production, which remains a grand challenge. Herein, an innovative approach is demonstrated to synthesize flower-like 3D homogenous trimetallic Mn, Ni, Co phosphide catalysts directly on nickel foam *via* electrodeposition followed by plasma phosphidation. The electrochemical activity of the catalysts with varying Mn: Ni: Co ratios is assessed to identify the optimal composition, demonstrating that the equimolar trimetallic phosphide yields an outstanding HER catalytic performance with a current density of 10 mA/cm² at an ultra-low overpotential of ~14 mV, outperforming the best-reported electrocatalysts. This is asserted by the DFT calculations, revealing a strong interaction of the metals and the P atom, resulting in enhanced water activation and optimized G_{H*} values for the HER process. Moreover, this optimal composition appreciably catalyzes the OER by exposing more intrinsic active species *in-situ* formed on the catalyst surface during the OER. Therefore, the Mn₁-Ni₁-Co₁-P-(O)/NF catalyst exhibits a decreased overpotential of ~289 mV at 10 mA/cm². More importantly, the electrocatalyst sustains perfect durability up to 48 h at a current density of 10 mA/cm² and continued 5000 cycling stability for both HER and OER. Meanwhile, the assembled MNC-P/NF||MNC-P/NF full water electrolyzer system attains an extremely low cell voltage of 1.48 V at 10 mA/cm². Significantly, the robust stability of the overall system results in remarkable current retention of ~96% after a continuous 50 h run. Therefore, this study provides a facile design and a scalable construction of superb bifunctional ternary MNC-phosphide electrocatalysts for efficient electrochemical energy production systems.

5:00 PM EN05.10.19

Atomically Dispersed Transition Metal Single Atoms for Photocatalytic CO₂ Reduction and NO Removal [Thang Q. Nguyen](#)^{1,2,3}, Amr Sabbah², Li-chyong Chen² and Kuei-Hsien Chen¹; ¹Institute of Atomic and Molecular Science, Academia Sinica, Taiwan; ²Center for Condensed Matter Sciences, National Taiwan University, Taiwan; ³National Tsing Hua University, Taiwan

The development of single-atom-supported metal oxides has inspired extensive interest in energy catalysis, offering a promising avenue for combating environmental pollution and converting greenhouse gas emissions into valuable products. Single-atom-supported metal oxide catalysts have garnered significant attention for their unique ability to bridge the gap between surface reactions and efficiency. Identifying the precise atomic-level active sites where these reactions occur is pivotal for advancing research in this domain. In this study, we presented a facile approach for synthesizing atomically-dispersed nonprecious metal-modified metal oxide catalysts. By carefully tuning the transition metal single-atom ratios, exceptional photocatalytic efficiency in the conversion of nitric oxide (NO) with an impressively low conversion of toxic nitrogen dioxide (NO₂) and enhanced photocatalytic CO₂ reduction were achieved. Insights into the mechanistic aspects of the photocatalytic NO oxidation reaction are garnered through scavenger trapping and electron paramagnetic resonance experiments employing 5,5-dimethyl-1-pyrroline N-oxide (DMPO). Furthermore, *in-situ* diffuse reflectance infrared Fourier transform spectroscopy (DRIFTS) and *in-situ* X-ray absorption spectroscopy techniques are employed to elucidate reaction intermediates and mechanisms governing the photocatalytic reduction of CO₂ into CO. This study highlights the potential of single-atom-supported metal oxides in advancing the fields of sustainable chemistry and air purification, offering a promising avenue for addressing pressing environmental challenges.

5:00 PM EN05.10.20

Chalcohalide Nanocrystals for Solar Energy Harvesting: Synthesis, Characterization and Photocatalytic Applications [Irina Gushchina](#)¹, Stefano Toso², Bo-An Chen¹, Carlo Giansante³, Masaru Kuno^{1,1} and Liberato Manna²; ¹University of Notre Dame, United States; ²Istituto Italiano di Tecnologia, Italy; ³Consiglio Nazionale delle Ricerche, Italy

Despite the pressing needs imposed by climate change, we have not yet managed to harvest the full potential of the sun as an abundant and fully renewable energy source. Scientists globally have invested significant resources to better understand how to capture this vast energy capital: the most renowned is arguably photovoltaics, but it is not the only one. Another promising route is storing the energy of the sun by forming new chemical bonds, through a process called photocatalysis.

Recently, a new group of semiconductors known as chalcohalides has come to the attention of the community as promising active materials. Many compounds of this class can be prepared with cheap, vastly abundant, and nontoxic elements, which would make them ideal candidates for large-scale applications. In this project, we aimed to synthesize metal chalcohalide nanocrystals with varying compositions, crystal structure, and morphology. We considered both phases that have been already obtained colloiddally, but whose photocatalytic potential is still to be explored (e.g., Bi₂S₃, Bi₁₂S₁₈X₂, and Pb₄S₃X₂, where X=Cl, Br, I), as well as materials known in bulk but never explored before at the nanoscale (e.g., Pb₇S₂Br₁₀, or the lead-free AgBiSCl₂ and CuBiSCl₂). We optimized the synthetic methods for each material and characterized their optoelectronic properties to identify the best candidates for photocatalytic applications. Additionally, catalytically active metal tips were grown on top of chalcohalide nanocrystals to form functionalized heterostructures with improved energy conversion efficiency. Finally, the most promising candidates were tested as active materials in a liquid-medium photocatalytic test cell, leading to new industry-viable materials for light-to-chemical energy conversion.

5:00 PM EN05.10.21

Empirical and Theoretical Investigations into the Mechanism of Wireless CO₂ Reduction over Modified g-C₃N₄ Photocatalyst [Mahmoud K. Hussien](#)¹, Amr Sabbah¹, Putikam Raghunath², Shu-Chih Haw³, Kuei-Hsien Chen⁴ and Li-chyong Chen¹; ¹National Taiwan University, Taiwan; ²National Yang Ming Chiao Tung University, Taiwan; ³National Synchrotron Radiation Research Center, Taiwan; ⁴Academia Sinica, Taiwan

The light-driven reduction of carbon dioxide holds promise for CO₂ mitigation and the conversion of CO₂ into valuable fuels and chemicals. While extensive efforts have been dedicated to elucidating the mechanistic aspects of photocatalytic CO₂RR, the majority of reported studies have primarily focused on liquid-phase reactions using metal-based photocatalysts. In this investigation, we systematically explore the water-vapor assisted CO₂RR employing a modified, metal-free g-C₃N₄-based photocatalyst without the incorporation of any cocatalyst, photosensitizer, or sacrificial reagent. Our

approach utilizes In-Situ FTIR, DFT calculations, and operando XAS to deepen our understanding of the reaction mechanism. Furthermore, this study yields significant insights into the dynamics of charge carriers and the identification of active sites, thereby advancing our comprehension of the entire photocatalytic process.

5:00 PM EN05.10.23

Facile One-Step Synthesis of Cu₂O Photocathode coated with ZnO Nanoparticles for Enhanced Photoelectrochemical Property Huang Yu Hao, Po Yu Lai and Chien-Neng Liao; National Tsing Hua University, Taiwan

Cuprous oxide (Cu₂O) is a promising photoelectrode material for photoelectrochemical (PEC) water splitting due to its suitable band structure, environmental acceptability, non-toxicity, and ease of fabrication. In this study, ZnO nanoparticles coated Cu₂O films (ZNC) were electrodeposited on fluorine-doped tin oxide (FTO) substrates using a CuSO₄ solution with varying ZnSO₄ content. The ZNC film exhibited a 35% enhancement in photocurrent density compared to the pristine Cu₂O film. Several characterization techniques were employed to uncover the impact of ZnO NPs on the PEC enhancement of the ZNC films, including x-ray photoelectron spectroscopy, electrochemical impedance spectroscopy, and photoluminescence spectroscopy. Additionally, Pd nanoparticles were introduced onto the surface of the ZNC films, and a thin trisodium citrate (TSC) layer was applied as a passivation treatment to improve the performance and stability of the ZNC photoelectrodes during PEC water splitting.

SYMPOSIUM EN03

Sustainability of Emerging Photovoltaics
April 24 - April 25, 2024

Symposium Organizers

Juan-Pablo Correa-Baena, Georgia Institute of Technology
Vida Engmann, University of Southern Denmark
Yi Hou, National University of Singapore
Ian Marius Peters, Helmholtz Institute Erlangen Nuremberg

* Invited Paper

+ JMR Distinguished Invited Speaker

^ MRS Communications Early Career Distinguished Presenter

SESSION EN03.08: Poster Session I: Sustainability of Emerging Photovoltaics

Session Chairs: Yi Hou and Ian Marius Peters

Wednesday Afternoon, April 24, 2024

Flex Hall C, Level 2, Summit

5:00 PM EN03.08.01

Improvement of Optical Properties of CZTSSe-Based Solar Cells and Photocathode Devices via Cd Doping Suyoung Jang and Jin Hyeok Kim; Chonnam National University, Korea (the Republic of)

Cu₂ZnSn(S,Se)₄ material is a material that replaces CuInGaSe₂, which is currently being researched, and is attracting attention as an eco-friendly and economical material because it does not use indium or gallium. However, various studies are being conducted to improve CZTSSe devices due to their low solar cell efficiency and low hydrogen conversion efficiency in PEC water splitting. Among them, cation doping is known to significantly contribute to improving device performance by improving the optoelectric properties of CZTSSe thin films. Cations doped into CZTSSe include various elements such as Ge, Cd, and Ag, and among these, Cd can be easily doped using the Chemical Bath Deposition method. Cd is doped into CZTSSe to control secondary phase and void formation, and when applied to a device, it improves photocurrent and improves light-hydrogen conversion efficiency. In this study, CZTSSe was doped with Cd by deposition time (9.5, 10.5, 11.5 minutes) using the CBD method to analyze its single thin film properties, and solar cells and PEC photocathodes were manufactured under the same conditions to measure device characteristics. As a result, the thin film sample doped with Cd for 11.5 minutes showed excellent photoelectric properties, solar cell efficiency was measured up to ~8%, and photocurrent was measured up to ~15 mA/cm² as a PEC photocathode.

5:00 PM EN03.08.02

Perylene Diimide Derivatives with Various Ionic Functionalities as Cathode Interlayers for ZnO-Free Inverted Non-Fullerene Organic Solar Cells Dong Hwan Son, Rahmatia Fitri Binti Nasrun, Qurrotun Ayuni Khoirun Nisa, Indah Salma Sausan, Young-Seok Lee, Ka In Kang and Joo Hyun Kim; Pukyong National University Daeyeon Campus, Korea (the Republic of)

Perylene diimide (PDIN) derivatives, possessing various ionic functionalities, have been synthesized and utilized as cathode interlayers (CIL) in inverted-type non-fullerene organic solar cells (NFOSCs). CILs including polyfluorene derivatives and PDIN are commonly employed as prospective non-fullerene CILs due to their advantageous low-energy levels. However, the main drawback of PDI derivatives is exhibiting strong aggregate, primarily due to their pronounced π - π stacking tendency, and this aggregation adversely impacts their morphology and transport characteristics. Therefore, it is necessary to modify the geometry with appropriate functional groups of PDI derivatives to adjust the planarity of PDIs and control their energy level. In this study, we

modified CILs based on PDIN derivatives for inverted NFOSCs. To our knowledge, perylene diimide featuring ammonium oxide as its terminal group (PDIN-O) was inserted between the active layer and the metal cathode, typically placed on top of the photoactive layer, in conventional OSCs. This positioning helped eliminate the need for heat treatment. To overcome the thermal issue, we modified PDIN by changing the side-chain functionality. We synthesized a series of materials based on PDIN with different terminals which are amino N-ethyl-iodo (PDIN-I), amino N-ethyl-bromo (PDIN-Br), amino N-butane sultone (PDIN-BS), and amino N-oxide (PDIN-O). In our study, we introduced various counterions into the PDIN to examine their impact on photovoltaic performance to replace the ZnO layer. Inverted-type NFOSCs were constructed with the following configuration: ITO/PDIN derivatives/PM6:Y6BO/MoO₃/Ag. The reference device (ITO/ZnO/PM6:Y6BO/MoO₃/Ag) was also prepared for comparison to investigate the photovoltaic characteristics of PDIN derivatives in NFOSCs. The power conversion efficiency (PCE) of the inverted-type device utilizing PDIN-O is 12.5%, which is lower due to its poor thermal stability, with degradation starting at around 100°C. In contrast, devices employing PDIN-I, PDIN-Br, and PDIN-BS achieved PCE values of 15.5%, 15.0%, and 15.0%, respectively. These values are nearly identical to the PCE of the device using ZnO (15.0%). The combined improvements of short circuit current (J_{sc}) and fill factor (FF) contribute significantly to the performance of the device. The highest PCE obtained is 15.5% achieved by PDIN-I as CIL which is slightly higher than the device based on ZnO. This improvement is a result of the increase in the J_{sc} of 28.2 mA/cm² from the device based on ZnO (25.9 mA/cm²). However, in terms of the FF of the device based on PDIN-I showed a slightly lower value of 68.6% than that of the device based on ZnO (70.8%). Introducing the quaternary ammonium ion and zwitterion into the PDIN backbone enhanced the performance of the devices compared to a device based on PDIN-O. Expanding the size of the counter anion led to a reduction in the effective work function of ITO. The size of the counterion affects the magnitude of the interfacial dipole and results in increasing the device performance. In addition, these CILs retained their original PCE after 30 hours of thermal and photo-aging, proving their effectiveness as an oxygen-blocking layer at the device interface. This study demonstrates the capacity to regulate CIL and thus provides insight into the fabrication of low-temperature processible ZnO-free NFOSCs.

5:00 PM EN03.08.03

Physical Structure Effect of TiO₂ Compact Layer for Enhanced Photoelectric Efficiencies Chia-Yi Huang¹ and Tz-Feng Lin²; ¹Tunghai University, Taiwan; ²Feng Chia University, Taiwan

One of the urgent challenges for sustainable energy is to hold the global warming back before 2050 in response to the global net-zero mission. An awareness of that is the green energy in demand and the use of solar energy would continue to cover the deficient of clean energy. Dye-sensitized solar cells (DSCs) would one of the promising photovoltaic technologies for renewable applications since 1990 in balancing an infrastructure cost and electricity production. This study fabricates a planar and stereo TiO₂ compact layer on a fluorine-doped tin oxide glass substrate with a Pt layer. Photolithography and physical structural design were used to build planar and stereo structures. The Pt layer gives rise to the protrusive structure of the counter electrode by sputtering and lift-off process. Then, porous semiconductor materials made of fine or coarse TiO₂ nanoparticles was coated on the planar and stereo structure. Experimental results reveal that the photoelectric efficiency of the DSCs is higher than that of a DSCs without a specific physical structure one. As a result, the protrusive Pt layer not only can increase the photoelectric efficiencies of DSCs but also serves as a facilitated electron transport channels. In addition, this result was verified by the electrochemical impedance spectra of the two DSCs. The proposed method has advantages in easy fabrication of electrode structures with respect to acceptable production cost.

5:00 PM EN03.08.04

Solar-Thermal Hybrid Concept of Energy Harvesting with Printed Perovskite and Organic Photovoltaic Cells Sarath Witanachchi¹, Derick C. DeTelle¹, Christian Coris¹, Gina Pantano¹, Brianna Pecourt¹, Hasitha Weerasinghe², Mei Gao² and Luke Sutherland²; ¹University of South Florida, United States; ²Commonwealth Scientific and Industrial Research Organization (CSIRO), Australia

In this paper we are reporting the results from an experimental project conducted in collaboration with CSIRO Australia to enhance power generation by integrating screen-printed flexible perovskite and organic cells with thermoelectric modules. While solar modules have the potential to generate significant currents based on the solar radiation intensity, achieving required voltages require a series connection of multiple devices. On the other hand, thermoelectric modules (TE) that convert heat into electricity generates high voltages, but the current is limited by the intrinsic properties of the thermoelectric materials. Under the new hybrid concept, high voltages generated by TE modules are combined with the high currents generated by PV cells. Four thermoelectric modules placed in a 150°C temperature gradient and connected in series can generate voltages over 7V. The printed perovskite cells used in the study showed a short-circuit current of 22 mA/cm² and an open circuit voltage of 4.8v. The hybrid of the PV-TE combination in a unique configuration has resulted in power outputs that are 4x higher than the PV module alone. A computational model developed for the hybrid correlate well with the experimental data. The circuit design, the IV-characteristics, and the conditions for optimum power generation in the hybrid configuration with possible waste-heat sources will be presented. The project was supported by an NSF IRES grant.

5:00 PM EN03.08.06

Assessment of Potential Environmental and Health Risks for Key Components of Solar Module Hi Gyu Moon, Jong-Su Seo and Chang-Beom Park; Korea Institute of Toxicology, Korea (the Republic of)

To address the serious challenges of climate change and global energy security, investment in renewable energy sources has increased significantly in Asia, Europe and globally. Among them, wind and solar power plants are expected to make the largest contribution to global decarbonization, ranking first and second in projected capacity by 2050. To date, the development and improvement of photovoltaic technology based on energy storage technology has received considerable attention, but the potential environmental risks are still unknown. Additionally, there is currently insufficient toxicological and environmental risk information to assess potential risks. However, several studies have reported that lead, tin, cadmium, silicon, and copper, which are the main components of damaged products, are harmful to the ecosystem and human health when discharged to landfills. Therefore, we evaluated the toxicity and human risk of the main components of solar panels, including related research trends, and then propose optimal government policies for solar cell to protect the environment and the human body.

SESSION EN03.13: Poster Session II: Sustainability of Emerging Photovoltaics
Session Chairs: Yi Hou and Ian Marius Peters
Thursday Afternoon, April 25, 2024
Flex Hall C, Level 2, Summit

5:00 PM EN03.13.01

Eco-design Strategies from R&D Level Towards a Sustainable Perovskite Tandem Technology Nouha Gazbour^{1,2}, Beatrice Drevet¹, Sjoerd Veenstra²

and Delfina Munoz¹; ¹Commissariat à l'énergie atomique et aux énergies alternatives (CEA), France; ²TNO, Partner in Solliance, Netherlands

The solar photovoltaic (PV) energy has become a fast-growing competitive sector. Innovation is a prerequisite for the survival of many PV companies. In the last years, the perovskite solar cells has gained much attention in the solar community because of the high efficiencies obtained in single and multi-junction devices and low fabrication projected cost. Due to the massive scale of the energy sector, it is essential that this new emerging PV technology progresses in a way that is consistent with the requirements of sustainable development before large scale deployment.

Sustainability is defined as an interaction between economic, social, technical and environmental criteria. Nevertheless, R&D activities are often focused on technical and economic improvements as a priority to enter the market. In addition, the limitations of current eco-design tools, as identified in the literature, hinder their adoption by R&D organizations. In fact, environmental impact assessment is relatively complex for a non-mature technology under development because its characteristics and manufacturing processes are not yet fully defined. Life Cycle Assessment (LCA) is a reliable environmental assessment tool, but it is limited to the evaluation of the investigated technology without proposing eco-design alternatives.

This study proposes a methodology to provide eco-design strategies from the earliest stages of design to develop sustainable all-perovskite tandem technology. In the research stage, the device architecture is often not defined yet. Therefore, we start with a review of the existing LCA studies on perovskite solar cells to identify the hotspots from an environmental point of view. Then, the list of the reported materials that could be used for the solar cell, including packaging materials, is defined. We analyze this list from an environmental point of view based on results obtained from the literature and legislative constraints. Finally, we propose eco-design guidelines that could reduce the cost, increase the performance, and decrease the environmental impact for the development of a sustainable perovskite tandem solar cell technology.

Based on this approach, key recommendations toward a sustainable perovskite tandem technology are :

- For the Transparent Conductive Oxide (TCO), indium-containing oxides are good candidates from a technical and economical point of view. However, indium is a critical material. Aluminum-doped zinc oxide (AZO) would be a more suitable candidate but vigilance is required on the electricity required for its production process.
- For the metal electrodes, copper should replace silver for economic and environmental criteria. However, there are few studies in the literature on its technical reliability.
- Fullerene (C₆₀) remains technically one of the best electron transport layer materials, but attention must be paid to its environmental impact and its high production cost.
- The contribution of the material of the perovskite layer to the environmental impact in the module is small. Nevertheless, some components in the layer and auxiliary materials need to be eco-designed
- Compared to glass, polymer-packaging materials do not pose a problem from economic and environmental points of view. Their choice must be based on technical criteria, primarily good barrier properties.
- In view of the circularity potential, a closed loop wet chemical recycling process is preferable over other approaches such as thermal decomposition, electrochemical refinement, or physical separation routes (e.g. adsorption/desorption).
- The challenges addressed by this recycling process are i) green solvent recycling development, ii) complex perovskite composition separation and recovery (with a focus on lead recovery and reuse), and iii) functional layer recovery.

These recommendations will help to guide technological choices from the early design process to ensure the development of sustainable perovskite tandem technology.

5:00 PM EN03.13.02

Breaking News on Highly Efficient Inorganic Tin-Lead Perovskite Solar Cells [Ting Zhang](#)¹, Feng Qian¹, Shihao Yuan¹, Zhi D. Chen² and Shibin Li¹;

¹University of Electronic Science and Technology of China, China; ²University of Kentucky, United States

To date, hybrid lead halide perovskite (LHP) solar cells have achieved great advances on a PCE from 3.8%¹ to an impressive certified value of 26.1%² within fourteen years. Despite the high efficiency of state-of-the-art lead-based perovskite solar cells is approaching the market-dominant silicon photovoltaic technology, they still face two concerns, e.g. poisonous Pb and non-ideal bandgaps for single-junction solar cells. To addressing this issue, according to Shockley-Queisser (S-Q) limit theory³, alloying tin (Sn) into B site is more effective to obtain less toxicity and preferable bandgap for a single-junction solar cell, which can yield the maximum efficiency with bandgap energies ranging from 1.2 to 1.4 eV, at which the solar spectrum utilization and the photocarrier relaxation would be optimized and balanced. Among these Pb-Sn alloyed perovskites, inorganic tin-lead perovskites are attractive candidates owing to their additional merit of inherent compositional stability.

Inorganic tin-lead perovskites have been investigated with low exciton binding energy, high charge mobility, high absorption coefficients and thermal stability. Encouraged by these outstanding properties, lead-rich CsPb_{0.9}Sn_{0.1}IBr₂ PSCs with a wide bandgap of 1.79 eV were first reported in 2017⁴, which obtained an efficiency of 11.33%; up to 2023, Zhang et al. reported a record PCE of 17.19% based on low-bandgap (1.34 eV) CsPb_{0.7}Sn_{0.3}I₃ PSCs via a post treatment method⁵. As seen from the simple development of inorganic Pb-Sn PSCs progress, the PCE still lags far behind their Pb-based analogs and Pb-Sn hybrid counterparts and the origin remains unclear. In addition to the common challenges of easy oxidation of Sn²⁺, crystallization regulation has been crucial yet less explored in low-bandgap CsPb_xSn_{1-x}I₃ PSCs. This could be ascribed to the lower enthalpy of the Cs⁺ in comparison with MA⁺ or FA⁺, which endows the crystallization kinetics quite different from their hybrid counterparts. It is thus imperative to acquire in-depth understanding of the unique crystallization dynamics of cesium tin-lead perovskites, which would provide guidance of the solidification process of cesium tin-lead perovskites and therefore high optoelectronic films and devices.

In this breaking news, for the first time, Shibin Li and colleagues reveal the B-site initiated asynchronous crystallization of inorganic tin-lead halide perovskites by comprehensive in-situ and ex-situ characterizations as well as molecular dynamics calculations⁶. Then, a novel synchronous alloying process is developed using a novel Sn-perovskite-targeted crystallization regulator. The regulator suppresses the asynchronous crystallization by enhancing the formation barrier energy of CsSnI₃, endowing a synchronous Sn and Pb alloying reaction in precursor film, achieving a homogeneous film after the annealing process. Finally, a record-high PCE of 17.55% is obtained for modified CsPb_{0.7}Sn_{0.3}I₃ solar cells, in a sharp contrast to the control device which shows a PCE of 3.6%. More importantly, B-site synchronous alloyed target devices show impressive stability with negligible degradation either at 65 °C over 3500 h for the net films or under continuous LED illumination for 700 h.

Research on Pb-Sn alloyed perovskites mostly focuses on the anti-oxidation of tin and is still at a relatively early stage, but the work of Shibin Li and colleagues provides a valuable B-site initiated synchronous crystallization approach to create highly efficient PSCs. Their proposed approach would be applicable to other high-performance and stable optoelectronic devices based on Pb-Sn alloyed perovskite.

Reference

¹ *J Am Chem Soc* **2009**, *131*(17): 6050-6051.

² National Renewable Energy Laboratory, "Photovoltaic World Records. NREL," can be found under <https://www.nrel.gov/pv/interactive-cell-efficiency.html> **2023**.

³ *Nat Energy* **2018**, *3*(10): 828-838.

⁴ *J Am Chem Soc* **2017**, *139*(40):14009-14012.

⁵ *Chem Eng J* **2024**, *479*:147554.

⁶ *Appl Phys Rev* **2023**, *10*(4).

5:00 PM EN03.13.03

Theoretical Guided Material and Interface Optimization for High Performance Perovskite/Organic Tandem Solar Cells Zonglong Zhu; City University of Hong Kong, Hong Kong

Addressing the pressing challenges of rising global energy needs and achieving carbon neutrality to protect the environment necessitates the development of a practical solution. The emergence of solution-processed organic and metal halide perovskite semiconductors, and their resultant solar cells, could potentially instigate a revolution in photovoltaic technology, enabling the delivery of scalable, high-performance solar cells for sustainable green energy production. Despite the power conversion efficiencies of both single-junction organic solar cells and perovskite solar cells rapidly reaching over 19% and 26% respectively, their maximum efficiency is confined to around 30% as per the Shockley-Queisser model for single-junction devices. However, by fabricating a multi-junction device with multiple light absorbers possessing significantly varied bandgaps, the efficiency of solar cells could potentially be augmented to over 40%.

In this talk, I will introduce high-performance monolithic perovskite/organic tandem solar cells with PCE>26%. These encompass a wide bandgap perovskite front cell and a narrow bandgap organic rear cell connected via a recombination junction. We have selected wide bandgap perovskite solar cells for the front cell due to their robust absorption for visible light, minimal voltage loss, and superior photoresponse. Meanwhile, narrow bandgap organic solar cells could potentially offer superior near-infrared absorption tunability and stability, making them ideal candidates for the rear cell of the tandem cells. To demonstrate the potential of perovskite/organic tandem solar cells, we employ an integrated strategy that combines materials, interface, optical, and process engineering.

5:00 PM EN03.13.04

Systematic Study of The Effect of A-Site Engineering on The Crystallization Kinetic of Sn-Pb Perovskite Changyong Kim, Ayoung Lee, Sangheon Lee, Sangjun Park and Donghoo Kim; Korea University, Korea (the Republic of)

Perovskites with narrow band gaps exhibit high theoretical efficiency, and there is still considerable room for improvement at the current stage. Introducing a combination of Sn and Pb into metal halide perovskites is way to obtain narrow band gap perovskites. For high-quality Sn-Pb perovskite formation requires delicate controlled crystallization rate of the perovskite precursor solution. However, due to the fast crystallization kinetics of high Lewis acidic Sn²⁺ the reaction between SnI₂ and methylammonium iodide (MAI)/ formamidineum iodide (FAI) proceeds notably quicker than that involving PbI₂. Consequently, as the Sn content increases in Sn-Pb binary perovskite films, the rapid nucleation rate by Sn²⁺ crystallization kinetics leads to smaller crystal grain sizes and a higher density of defects. This uncontrollable crystallization and reaction competition of organic ammonium with Sn and Pb make it hard to fabricate of high-quality perovskite film.

At present, the most high-performing Sn-Pb perovskite based solar cells consist of an A-site mixture of FA and MA. The doping of various inorganic cations on the A-site of perovskite has been reported as one of the advantageous candidates for controlling the crystallographic kinetics to improve the performance and stability of perovskite solar cells. However, in the binary B-site of Sn-Pb perovskite, there is a lack of systematic research on the effect of the A-site composition by reacting more complex.

In this study, we have carried out a systematic study of the effect of inorganic cations on the fast and complex crystallization process of Sn-Pb perovskites. Finally, we have demonstrated the several composition design rule of Sn-Pb perovskites to reach a photovoltaic conversion efficiency exceeding 22%.

TAG : Perovskite, Narrow band gap, Inorganic cation, A-site engineering, Composition design

5:00 PM EN03.13.05

Stable and Efficient Halide Perovskite Solar Cells by Using Guanidinium-Incorporated Quasi-2D Perovskite Layer Matthew T. Bamidele and Do Young Kim; Oklahoma State University, United States

Halide perovskite solar cells are a rising star in the photovoltaic community due to their remarkable performance and rapid progress. Solution processability of hybrid perovskite semiconductors makes these materials especially attractive for low cost and scalable manufacturing. While halide perovskite solar cells already show remarkable improvement with a power conversion efficiency above 25%, poor stability under ambient environmental conditions of heat, humidity, and light is the major issue hindering the commercialization of this technology. Layered two-dimensional (2D) perovskites have been extensively investigated for improving the stability of perovskite solar cells while sacrificing efficiency. In this study, we have explored pathways to improve the stability of perovskite solar cells while maintaining their efficiency by using a 2D perovskite layer. First, halide perovskite solar cells using quasi-2D guanidinium-based halide perovskites synthesized with lead acetate (PbAc) have higher efficiency and stability compared to perovskite solar cells with quasi-2D perovskite synthesized from traditional lead iodide (PbI). This is due to a characteristic perpendicular orientation of the quasi-2D perovskite crystal structure, which can facilitate charge extraction. The power conversion efficiency of quasi-2D perovskite solar cells using PbAc is approximately two times higher than solar cells using Pbl. Another intriguing aspect of guanidinium-based quasi-2D perovskite solar cells is a continuous improvement in efficiency that spans several weeks. This observed enhancement is attributed to age-induced recrystallization, showcasing the material's potential for prolonged stability and delay in the onset of device degradation. As a result, the quasi-2D perovskite solar cells maintained almost the same performance even after 3,000 hours. Also, we present an alternative approach that improves the performance of halide perovskite solar cells by introducing an orderly stacking of MAPbI₃ film as a 3D halide perovskite light-harvesting layer on top of a quasi-2D GA₂MA₄Pb₅I₁₆ halide perovskite layer. The power conversion efficiency of quasi-2D/3D perovskite solar cells is approximately 20% higher than that observed for 3D perovskite-based solar cells fabricated under the same conditions. The observed improvement is attributed to the superior crystallinity and excellent film quality achieved by the coherent stacking of 3D MAPbI₃ on top of quasi-2D GA₂MA₄Pb₅I₁₆ perovskites. Additionally, the improved photovoltaic performance of these quasi-2D/3D perovskite solar cells does not compromise their durability. Even after 1,900 hours of storage, the devices maintained about 98% of their initial performance.

SESSION EN06.04/EN03.04: Joint Session: Advances in Solution Processed Photovoltaics

Session Chairs: Yi Hou, Yong Feng Mei and Ian Marius Peters

Wednesday Morning, April 24, 2024

Room 333, Level 3, Summit

8:15 AM *EN06.04/EN03.04.01

Biocarbon from Algae, Cellulose and Sewage Sludge as Sustainable Composites for Energy Storage Theotime Béguerie¹, Amel Cydric Ghogia¹, Lina María Romero Millána¹, Shamala Gowri Krishnan¹, Majd El Saddik¹, Elsa Weiss¹, Claire White^{2,2}, Kuo Zeng³ and Ange Nzihou^{1,2}; ¹Université de

Toulouse, France; ²Princeton University, United States; ³Huazhong University of Science & Technology, China

This presentation will discuss the synthesis, characterization, and utilization of a novel family of biocarbon-based composites for electrochemical and heat storage. The composites are produced by the pyrolysis and carbonization of various biomass (algae, cellulose biomass, and municipal sewage sludge) inherently containing or doped with catalytic metal such as Iron and Calcium at lower temperature (<1400°C) than the standard carbonization temperature (>1800°C) or processed with molten salt (Na₂CO₃-K₂CO₃). In this process, the biocarbon is transformed from a randomly organized carbon to a graphite-like material (organized and structured carbon) showing a high graphene rate structure. The Carbon structure and composition changes in the composites have been investigated from nano to bulk scales in combining XRD, HRTEM and RAMAN. This has enabled to probe changes in biochar nanostructure and crystalline graphitic domains catalyzed by the inclusion of metal such as iron and Calcium. The encapsulation of iron particles by graphitic phase (graphene sheets) and the carbon-metal bonding during the pyrolysis and carbonization were uncovered using XPS. Key properties for energy storage applications such as the remanent magnetization, the coercive field, the specific heat, the thermal and electric conductivities, the thermal stability including the mechanical properties will be discussed. Biocarbon from algae for example, rich in nitrogen showed a high specific surface area of 2009.26 m²/g with high specific capacitance of 230.2 F/g at 0.25 A/g and a capacitance retention of 75.54% at 2 A/g. This work provides a green and promising approach to produce heteroatom-doped capacitive biocarbon with superior properties for energy storage.

8:45 AM EN06.04/EN03.04.02

Heteroepitaxial Crystal Growth of Halide Perovskite for n-i-p Structure [Yun-Kyeong Hong](#), Sanghee Yang and Hui-Seon Kim; Inha University, Korea (the Republic of)

Perovskite solar cells (PSCs) have rapidly achieved high power conversion efficiency since its first solid-state application in 2012, leading to an outstanding PCE of 26.1% in 2023. Nevertheless, the stability issue still hinders the commercialization. While the chemical composition of perovskite material has been carefully engineered to extract the best optoelectronic properties and the phase stability as well, the lattice strain has recently emerged as one of the key parameters determining the phase stability of perovskite film. Here we employ an interlayer, formamidinium tin halides (FASnCl_xBr_{2-x}), between SnO₂ (electron transport layer) and perovskite, where the heteroepitaxial crystal growth of perovskite film on the interlayer is enabled by tuning its lattice distance (*d*), ranging from 0.342 nm (FASnCl_x) from 0.365 nm (FASnBr₂), as evidenced by transmission electron microscopy. While the large difference in *d* between the interlayer and the perovskite film (>10%) negligibly affect the crystal growth, the smaller mismatch in *d* (<10%) affects the perovskite crystal growth and thus leads to a strain relaxation at the interface of perovskite film. Therefore, the resulted relaxation of tensile strain at the bottom interface of perovskite film is comparably beneficial for the phase stability of α -FAPbI₃, though 2% in-plane residual tensile strain is still remaining, which is in accordance with the monitored film stability in ambient air. Kelvin probe force microscopy is also measured to elucidate the effect of FASnCl_xBr_{2-x} interlayer on energy level alignment, where the changed band banding, coupled with defect reduction, at the interface is likely responsible for the enhanced recombination resistance and open-circuit voltage of PSCs.

9:00 AM EN06.04/EN03.04.03

New Dopant for FAPbI₃ Film in Perovskite Solar Cells [Ju-Hye Choi](#)¹, Yu-Na Kim² and Hui-Seon Kim¹; ¹Inha University, Korea (the Republic of); ²Korea Institute of Energy Research, Korea (the Republic of)

A great effort has been made on the chemical composition of perovskite film in perovskite solar cells (PSCs), where formamidinium lead iodide (FAPbI₃) recently achieved the highest power conversion efficiency (PCE) of 26.1% in 2023. One of the most important challenges is securing the phase stability of FAPbI₃, which is prone to convert from α -phase to δ -phase without additive engineering. Therefore, additive plays an important role in FAPbI₃ not only by affecting the phase stability via interaction in the grown lattice but also by controlling the crystal growth through interaction with precursors. In this study we incorporate hydroxylammonium formate (HAHCOO) in the perovskite precursors for FAPbI₃, coupled with methylammonium chloride. Fourier transform-infrared spectroscopy reveals that lone pairs in HA⁺ and HCOO⁻ effectively act as Lewis base and interact with Pb²⁺ as Lewis acid in perovskite precursors and leads to increased grain size (~1500 nm) and uniformity (1500 nm of FWHM), as evidenced in scanning electron microscope images. In the meantime, HA⁺ is assumed to substitute for FA⁺ because the ionic radius of HA⁺ (0.216 nm) ranges between methylammonium cation (MA⁺, 0.18 nm) and FA⁺ (0.22 nm), which is indirectly evidenced with a variation in binding energy from x-ray photoelectron spectroscopy measurement. On the other hand, HCOO⁻ acts as an anion vacancy passivator at grain boundaries and top surface and closely correlates with the increased surface recombination resistance of PSCs. The inclusion of new additive, HAHCOO, therefore successfully leads to PCE increase from 18.9% to 20.1% with an increased long-term stability.

9:15 AM EN06.04/EN03.04.04

A Strategy for Modifying ZnO-Free Inverted Organic Solar Cells using a Naphthalene Diimide as Cathode Interlayers [Rahmatia Fitri Binti Nasrun](#), Qurrotun Ayuni Khoirun Nisa, Dong Hwan Son, Indah Salma Sausan, Young-Seok Lee, Ka In Kang and Joo Hyun Kim; Pukyong National University, Korea (the Republic of)

Perylene diimide featuring ammonium oxide as its terminal group, often referred to as PDIN-O, is a widely recognized cathode interlayer utilized in conventional organic solar cells (OSCs). As naphthalene diimide demonstrates a lower LUMO level compared to perylene diimide, we selected it as the core to gain additional control over the LUMO level of materials. Small molecules (SMs) generate a favorable interfacial dipole through the introduction of ionic functionality at the side chain of naphthalene diimide. When employing SMs as cathode interlayers in conjunction with an active layer composed of a non-fullerene acceptor (PM6:Y6BO), the power conversion efficiency (PCE) showed an enhancement. The results revealed that the OSC using naphthalene diimide with ammonium oxide as its terminal group (NDIN-O) exhibits inadequate thermal stability, resulting in irreversible damage to the interlayer-cathode contact, thereby contributing to a low PCE of 11.1%. To overcome the disadvantage, we have introduced NDIN-Br and NDIN-I, both of which possess a higher decomposition temperature. We achieved an impressive PCE of 14.6% in the device utilizing NDIN-Br as an interlayer, which is almost the same as the PCE of the ZnO-based device (15.0%). The device incorporating NDIN-I demonstrates an enhanced PCE of 15.4%, slightly surpassing the ZnO-based device. These results suggest a viable alternative to the ZnO interlayer, which typically requires precise control of the sol-gel transition through high-temperature annealing, often reaching up to 200°C. This alternative approach could potentially reduce the manufacturing costs of OSCs.

9:30 AM *EN06.04/EN03.04.05

Organic Photovoltaic Materials: Decreasing Synthetic Complexity through Scalable “Cascade” Approaches [Dario Pasini](#)¹, Andrea Nitti¹, Riccardo Po² and Gabriele Bianchi²; ¹University of Pavia, Italy; ²Eni S.p.A., Italy

Organic electronic materials offer advantages such as flexibility, low cost, and easy processability using simple solution processing methods. They are π -extended organic compounds and polymers with suitable semiconducting properties, typically obtained through linear and multi-step synthetic approaches. Such approaches have yielded highly performing compounds and polymers through complex, multi-step synthesis, limiting their scalability for industrial applications. Sustainability and scalability of the synthetic process plays a fundamental role for definitive consecration of the organic electronic materials, and generally they depend on: (a) the number of synthetic steps; (b) the cost of the materials; (c) yields; (d) the number of steps of purification that require

column chromatography. A unique parameter (synthetic complexity, SC) have been recently proposed to rationalize the field of materials used in the Organic Photovoltaic arena (OPV).¹

In this contribution, we will report recent developments on the use of “cascade” reaction protocols to address annulations and formation of π -extended polymers for OPV. Such protocol condenses in an one-pot cascade fashion both direct (hetero)arylation (DHA) and intramolecular cross-aldol condensations.²⁻⁵ The application of such protocol has been used with success for the synthesis of thienoacene scaffolds such as naphthothiophenes (NTs), benzodithiophenes (BDTs) and anthradithiophenes (ADTs) in a single and double annulation fashion. ADT and BDT derivatives were incorporated into polymers and the properties of bulk-heterojunction solar cells will be presented.

References

- [1] R. Po, G. Bianchi, C. Carbonera, A. Pellegrino, *Macromolecules* **2015**, 48, 453–461
- [2] G. Forti, R. M. Pankow, F. Qin, Y. Cho, B. Kerwin, I. Duplessis, A. Nitti, S. Jeong, C. Yang, A. Facchetti, D. Pasini, T. J. Marks, *Chem. Eur. J.*, **2023**, 29, e202300653
- [3] G. Bianchi, C. Carbonera, L. Ciammaruchi, N. Camaioni, N. Negarville, F. Tinti, G. Forti, A. Nitti, D. Pasini, A. Facchetti, R. M. Pankow, T. J. Marks, R. Po, *Sol. RRL* **2022**, 6, 2200643.
- [4] M. Penconi, G. Bianchi, A. Nitti, A. Savoini, C. Carbonera, D. Pasini, R. Po, S. Luzzati, *Adv. Energy Sustain. Res.* **2021**, 2, 2100069.
- [5] A. Nitti, G. Forti, G. Bianchi, C. Botta, F. Tinti, M. Gazzano, N. Camaioni, R. Po, D. Pasini, *J. Mater. Chem. C* **2021**, 9, 9302-9308.

10:00 AM BREAK

SESSION EN06.05/EN03.05: Joint Session: Metal Management and Stability
Session Chairs: Yi Hou and Ian Marius Peters
Wednesday Morning, April 24, 2024
Room 333, Level 3, Summit

10:30 AM *EN06.05/EN03.05.01

Lead Sequestration and Recycling in Perovskite Solar Cells Kai Zhu; National Renewable Energy Laboratory, United States

Organic-inorganic hybrid halide perovskites have rapidly become a focal point of the photovoltaic (PV) community as a promising next-generation PV technology. The certified efficiencies of single-junction perovskite solar cells (PSCs) and perovskite-based tandem cells have reached 26.1% and 33.7%, respectively. However, all of the current state-of-the-art perovskite-based PV devices contain lead (Pb) ions. The toxic Pb could pose a potential threat to the environment and public health. To address this potential challenge for future market adoption of perovskite PV technologies, we need to develop proper Pb management strategies for both perovskite devices in operation and those at the end-of-life. In this talk, I will first provide an overview of the potential Pb toxicity issue and some common strategies to address it. Then I will present our recent studies in this research area. Specifically, I will discuss our efforts on developing on-device Pb sequestration to prevent the leakage of Pb ions from broken perovskite PV devices under severe weather conditions. I will also discuss how to make our Pb sequestration approach scalable for industrial applications. In addition, I will discuss our efforts on recycling Pb from end-of-life perovskite PV devices. Finally, I will present our perspective on making perovskite PV a sustainable technology.

11:00 AM EN06.05/EN03.05.02

Environmental Impacts of Pb Leaching from Halide Perovskites Iris Visoly-Fisher¹, Arindam Mallick¹, Mendez Lopez Rene D.² and David Cahen³; ¹Ben-Gurion University of the Negev, Israel; ²Bar Ilan University, Israel; ³Weizmann Institute of Science, Israel

A significant concern is accidental Pb leaching from PSCs and modules, due to the well-documented Pb toxicity. Review of the current knowledge shows that this threat is found to be comparable to that posed by currently used Pb-containing products, and a plethora of measures are available to mitigate the environmental impact of Pb.[1] However, Pb leaching from damaged PSCs may imply a significant environmental impact on the surrounding soil in the case of module damage. We have examined the penetration profile of Pb from aqueous solutions of dissolved Pb-perovskite into the soil, and the Pb²⁺ adsorption mechanism to soil particles. The penetration profiles in all studied soils showed high affinity for Pb adsorption to soil, hence shallow immobilization of the Pb cations in all studied soils, with negligible odds of reaching and contaminating ground water. We, therefore, suggest that Pb in PSCs and its effect on the environment are not as concerning, as they seem to be.[2]

[1] A. Mallick, I. Visoly-Fisher, *Pb in halide perovskites for photovoltaics: reasons for optimism*, *Mater. Adv.* (2021) 2, 6125 - 6135

[2] A. Mallick, R. D. Mendez Lopez, G. Arye, D. Cahen, I. Visoly-Fisher, *Soil adsorption and transport of lead in the presence of perovskite solar cell-derived organic cations*, *J. Hazardous Materials* (2023) 451, 131147.

11:15 AM EN06.05/EN03.05.03

Tautomeric Mixture Coordination Enables Efficient Lead-Free Perovskite LEDs Virginia Carnevali¹, Lorenzo Agosta¹, Nikolaos Lempesis¹, Haizhou Lu^{1,2}, Ursula Rothlisberger¹ and Michael Graetzel¹; ¹École Polytechnique Fédérale de Lausanne, Switzerland; ²Southeast University, China

Lead halide perovskite light-emitting diodes (PeLEDs) have demonstrated remarkable optoelectronic performance. However, there are potential toxicity issues with lead and removing lead from the best-performing PeLEDs—without compromising their high external quantum efficiencies—remains a challenge. Here we report a tautomeric-mixture-coordination-induced electron localization strategy to stabilize the lead-free tin perovskite TEA₂SnI₄ (TEAI is 2-thiopheneethylammonium iodide) by incorporating cyanuric acid. We demonstrate that a crucial function of the coordination is to amplify the electronic effects, even for those Sn atoms that aren't strongly bonded with cyanuric acid owing to the formation of hydrogen-bonded tautomeric dimer and trimer superstructures on the perovskite surface. This electron localization weakens adverse effects from Anderson localization and improves ordering in the crystal structure of TEA₂SnI₄. These factors result in a two-orders-of-magnitude reduction in the non-radiative recombination capture coefficient and an approximately twofold enhancement in the exciton binding energy. Our lead-free PeLED has an external quantum efficiency of up to 20.29%, representing a performance comparable to that of state-of-the-art lead-containing PeLEDs. We anticipate that these findings will provide insights into the stabilization of Sn(II) perovskites and further the development of lead-free perovskite applications.

SESSION EN06.06/EN03.06: Joint Session: Advances in Recycling and Circularity
Session Chairs: Yi Hou and Ian Marius Peters
Wednesday Afternoon, April 24, 2024
Room 333, Level 3, Summit

1:30 PM *EN06.06/EN03.06.01

Circular Economy for Photovoltaics in Service of Energy Transition Heather Mirletz, Silvana Ovaitt and Teresa Barnes; National Renewable Energy Laboratory, United States

The challenge of energy transition is immediate and immense; current projections target 75 TW of photovoltaics (PV) capacity by 2050. While any transition to renewable energy technology is preferable to the current fossil-based system, it is ideal to improve the sustainability of PV to minimize negative environmental and social impacts. Circular economy (CE) has been proposed as a method to improve the sustainability of PV, especially for emerging materials like perovskites. CE is a set of actions, principles, and systems which aim to design out waste and keep products and materials in use, to reduce environmental impacts and enable sustainable development. At the most basic level, CE is “reduce, reuse, recycle”, the R-actions, in ranked order. CE of a PV technology can be metricized in a variety of ways, such as the Material Circularity Indicator (Smith and Jones, Ellen MacArthur Foundation, 2019) or recycling rates. Unfortunately, standard CE metrics have several shortcomings for measuring renewable energy technologies in the context of deployment for energy transition (Figge 2018, Saidani 2019):

only measure mass flows

de-prioritization of the use phase in favor of mass circularity when scoring

tight focus on a single product scale

The use phase and energy flows of PV are key to energy transition, and therefore need to be quantified. Additionally, correlating product-scale to system-scale is necessary for quantifying the environmental impacts of energy transition. Life Cycle Assessment (LCA) can address some of these concerns, but also focuses on a single product scale and has trouble capturing the dynamics of system-scale energy transition, such as the interaction of module lifetime with manufacturing demands for energy transition deployment schedules.

Therefore, we developed an open-source Python-based system dynamics model to quantify the mass, energy and carbon impacts of CE R-actions for PV technologies in the energy transition; PV in the CE (PV ICE) (Ovaitt & Mirletz 2021). The tool captures supply chains from material extraction through end of life, incorporating 5 circular end of life pathways. PV ICE takes in any evolving bill of materials, module properties and deployment schedule to support researchers and decision makers with data-backed insights.

In this work, we quantify and compare proposed CE sustainable PV module designs and lifecycle management strategies, spanning currently commercialized technologies, government and industry technology targets, and several low Technology Readiness Level (TRL) emerging PV technologies, including perovskites. Our analyses capture the projected evolutions of lifetime, efficiency and material circularity of these PV technologies, as well as their material supply chains.

Our analyses emphasize the importance of examining a suite of metrics to identify priorities and tradeoffs, and inform design or lifecycle management decisions holistically. Previous analyses have demonstrated the central importance of PV module lifetime to support energy transition while minimizing impacts. High levels of material circularity (>90%) enable minimizing lifecycle wastes, can reduce virgin material demands if paired with improving efficiency, but demonstrate tradeoffs in energy return on investment.

In the fervor of new material and technology development, it is important to remember that CE is not the end goal; decarbonization and energy transition are the end goal. CE should be used in service to improve the sustainability of PV, and R-actions evaluated for their usefulness and efficacy to this end.

2:00 PM EN06.06/EN03.06.02

Novel Mechano-Chemical Approach to Achieve Rapid Delamination of Glass from Solar Panels Ankit Ankit, Jeremy K. Ang, Ying Sim and Nripan Mathews; Nanyang Technological University, Singapore

With growing global cumulative photovoltaics (PV) installation, end-of-life (EoL) PV panels are expected to grow as well, with reports predicting this number to reach 78 million tonnes by 2050. This huge amount of PV waste does not only present a looming environmental challenge but also an opportunity to recover valuable materials embedded in the panels.

Different generations of PV technologies (1st Gen - Crystalline silicon (c-Si), 2nd Gen - Thin film (CIGS, CdTe) and 3rd Gen - Emerging PV (Perovskite, Bifacial)) have presence in the market currently. Out of all of these technologies, c-Si modules have the largest market share. Irrespective of their differences, the device stack for these PV technologies follows a sandwich structure, with the active layer (comprising metals and semiconductors) layered between polymeric encapsulants and glass. These insulating layers ensure a longer lifetime for panels in the field.

However, the same device structure creates challenges to recover valuable materials efficiently. Different approaches have been developed to separate the layers of solar panels. Thermal approaches burn the polymeric layers. However, they can produce toxic gases and affect the purity of active layer materials. Mechanical approaches crush the panel and sieve into different fractions. However, that often leads to undesired cross-contamination and affects the output yield and quality. Chemical approaches can give high output yield and purity and rely on dissolution of the polymeric encapsulant to separate the layers. However, they can take a long time (up to 7 days) making it less attractive.

Herein, we report a novel mechano-chemical approach that relies on weakening of bonds between glass layer and encapsulant layer through use of a green solvent. Cleaving of glass from the solar panels is achieved through mechanical processing. This process achieves rapid delamination of glass from solar panels (<4 hours) and high purity (>98%) glass cullet, while providing access to the active layer of the panel. The process has been demonstrated for c-Si panels and can be translated to different generations of solar panels.

2:15 PM EN06.06/EN03.06.03

From Lead Bullets to Solar Cells: A Two-Step Approach to Repurpose Contaminated Lead Misha Sytnyk¹, Zhenni Wu^{1,2}, Jiyun Zhang^{1,2}, Benfang Niu^{1,2}, Jens Hauch¹, Christoph J. Brabec^{1,2} and Ian Marius Peters^{1,2}; ¹Forschungszentrum Jülich GmbH, Germany; ²Friedrich-Alexander-University Erlangen-Nuremberg (FAU), Germany

Lead perovskite solar cells have emerged as a groundbreaking technology. The unique properties of lead perovskite materials, such as their high absorption coefficient and tunable bandgap, make them ideal candidates for next-generation photovoltaic applications.

Despite their promise, perovskite solar cells pose environmental concerns, particularly in the recycling and sourcing of lead halides. Conventional methods of lead extraction and processing contribute to ecological degradation. To address these challenges, this research proposes a sustainable solution grounded in the principles of a circular economy, aiming to repurpose lead waste into valuable materials for solar cell fabrication.

The environmental challenge posed by lead waste is twofold. On the one hand, there is the potential for lead waste from the burgeoning perovskite

This searchable program is up-to-date as of April 15th, 2024.

industry. On the other, there are existing sources of lead waste, such as metal plating industry, mining industry, homes built before 1986, lead-acid batteries, that are highly contaminated and pose a long-standing environmental hazard. It's important to note that even so-called "lead-free" plumbing may contain up to 8 percent lead.

Our approach is a two-step process designed to tackle this issue head-on. The first step involves a novel electrochemical method that will be presented in detail at the conference to convert contaminated lead into lead iodide (PbI₂). As the lead waste source, we utilized XVII century lead bullet balls. The electrochemical recovery process is robust, accommodating a wide range of contaminants including the 15% Carbon, 10% Oxygen, 0.5% Silicon, 1% Bismuth, 1% Copper, and 1% Zinc we found in the bullets. Remarkably, the process achieves a Faradaic efficiency close to 1, indicating near-complete conversion of lead to PbI₂.

The second step involves further purification of the synthesized PbI₂ through single-crystal growth. This results in a 35% yield of pure PbI₂, with the remaining material being recyclable for subsequent purification loops.

The synthesized PbI₂ is not only suitable for immediate use in solar cells but has also been successfully utilized to fabricate a working solar cell.

Additionally, it offers a high yield rate of approximately 1g per hour. This yield rate is scalable by simply increasing the electrode area, making the process suitable for industrial applications.

This research has far-reaching implications. It not only addresses the immediate problem of recycling perovskite solar cells for a circular economy but also offers a viable solution to the broader issue of lead waste management. By converting contaminated lead into a valuable material for efficient perovskite solar cell fabrication, we can potentially eliminate both current and future concerns related to lead waste.

2:30 PM BREAK

SYMPOSIUM EN06

Make Energy Materials Sustainable Again

April 23 - May 9, 2024

Symposium Organizers

David Cahen, Weizmann Institute and Bar-Ilan University

Jihye Kim, Colorado School of Mines

Clara Santato, Ecole Polytechnique de Montreal

Anke Weidenkaff, Technical University of Darmstadt

* Invited Paper

+ JMR Distinguished Invited Speaker

^ MRS Communications Early Career Distinguished Presenter

SESSION EN03/EN04/EN05/EN06: Joint Virtual Session

Session Chairs: Virgil Andrei, David Cahen, Robert Hoye, Clara Santato and Anke Weidenkaff

Thursday Morning, May 9, 2024

EN06-virtual

8:00 AM *EN03/EN04/EN05/EN06.01

Scalable Routes to Functional Materials: Photocatalytic, TCO and Anti-Soiling Coatings Claire Carmalt and Mingyue Wang; University College London, United Kingdom

The search for efficient materials for sustainable infrastructure is a key challenge to address the global environmental crisis. Sunlight-activated coatings, particularly those produced from scalable technologies, are sought in the glass industry for applications in self-cleaning windows. Current research involves developing processes towards sustainable and inexpensive functional materials including photocatalysts, anti-soiling coatings, transparent conducting oxides (TCOs) and photoelectrochemical films on float glass. For example, we have been developing sustainable upscaled routes to TCO materials from precursors containing earth abundant elements (titanium, aluminium, zinc) with equivalent or better figures of merit to existing TCOs. Our method uses aerosol assisted chemical vapour deposition (AACVD) to develop large scale coatings. Compared to conventional CVD, the AACVD method uses aerosol droplets to transport precursors, with the aid of an inert carrier gases. Therefore, in AACVD volatility is no longer crucial and this allows for a wider choice of precursors being available for use and can lead to high quality films at low cost.

Recent work has also investigated a range of bismuth-based materials for a number of applications. For example, adherent coatings of phenethylammonium bismuth iodide have been deposited via AACVD. The film morphology was found to depend on the deposition conditions and substrates, resulting in different optical properties to those reported from their spin-coated counterparts. Bismuth oxyhalides, BiOX (X = Cl, Br, and I), are of interest in a range of applications including photoelectrochemical (PEC) sensing, pollutant degradation and water splitting, with particular focus as emerging materials in photocatalytic applications. We recently reported visible-light-active iodide-doped BiOBr thin films fabricated via AACVD. The impact of dopant concentration on the structural, morphological, and optical properties was studied and the photocatalytic properties of films were evaluated. An optimized material was identified as containing 2.7 atom% iodide dopant. We have also synthesised BiOI and ZnO heterojunction materials. It was found that the BiOI/ZnO structure was far less active towards PEC water oxidation, while the ZnO/BiOI heterojunction showed a significant enhancement in activity compared with its parent materials. The ZnO/BiOI heterojunction, with a 120 nm thick ZnO film, exhibited the best PEC performance through studying the

influence of the ZnO film thickness and deposition temperature.

AACVD has also been used to develop thin films of other functional materials, including processes towards sustainable and inexpensive anti-soiling coating on float glass and photocatalytic films.

References:

1. Wang, M.; Carmalt, C. J., *ACS Appl. Energy Mater.* 2022, 5, 5434.
2. Marchand, P.; Hassan, I. A.; Parkin, I. P.; Carmalt, C. J., *Dalton Trans.*, 2013, **42**, 9406.
3. Wang, M.; Sanchez-Perez, C.; Habib, F.; Blunt, M. O.; Carmalt, C. J., *Chem. - Eur. J.*, 2021, **27**, 9406.
4. Wang, M.; Quesada-Cabrera, R.; Sathasivam, S.; Blunt, M. O.; Borowiec, J.; Carmalt, C. J., ACS Applied Materials & Interfaces *Article ASAP*, DOI: 10.1021/acsami.3c11525.
5. Wang, M.; Kafizas, A.; Sathasivam, S.; Blunt, M. O.; Moss, B. Gonzalez-Carrero, S.; Carmalt, C. J., *Applied Catalysis B: Environmental*, 2023, 331, 122657.

8:30 AM EN03/EN04/EN05/EN06.02

Preparation of High-Efficiency All-Perovskite Tandem Solar Cells [Huan Bi](#)¹, Hiroshi Segawa², Saulius Grigalevicius³, Qing Shen¹ and Shuzi Hayase¹; ¹The University of Electro-Communications, Japan; ²The University of Tokyo, Japan; ³Kaunas University of Technology, Lithuania

Although the efficiency of the organic-inorganic hybrid perovskite solar cell (PSCs) has reached 26.2%, it still has not surpassed silicon-based solar cells. At the same time, poor stability also makes the competitiveness of single-layer PSCs not obvious compared with silicon solar cells. Since 2015, narrow bandgap PSCs have been widely reported due to their better light absorption. However, wide bandgap perovskites should not be neglected as they are important for fabricating tandem PSCs. Here, we demonstrate a series of monolayer molecules with different alkyl chain lengths as interfacial modifiers to modify the PTAA and perovskite layer for improving the optoelectronic properties of PSCs by improving the quality of perovskite films and increasing the transport and extraction of interfacial carriers. The target device achieves a PCE of 16.57%, which is one of the highest PCE of the WBG-PSCs. Besides, the all-perovskite tandem solar cells with the WBG-Pb-perovskite solar cells and the narrow bandgap Sn/Pb perovskite solar cells gave a high PCE of 25.24%.

Here, we fabricated the wide bandgap PSCs with or without SAM modification. We found that the champion control device with a PCE of 14.46% (a short circuit current (J_{SC}) of 17.15 mA/cm², an open-circuit voltage (V_{OC}) of 1.117 V, and a fill factor (FF) of 75.53%), while the devices based on 3,3PrPACz, 4,3BuPACz, and 6,3HePACz modification got the highest PCE of 15.49% (a J_{SC} of 17.59 mA/cm², a V_{OC} of 1.141 V and an FF of 77.20%), 16.57%, and 15.29%, respectively. According to the corresponding incident photon-to-electron conversion efficiency (IPCE) spectra of the best-performing control device and PTAA/monolayer molecules devices, with the integrated current densities of 16.99 mA/cm² for the control device, 17.34 mA/cm² for the 3,3PrPACz-modified device, in good agreement with the J - V characterization. Finally, all-perovskite tandem solar cells were fabricated further to improve the PCE of PSCs. The J - V curves of all perovskite tandem solar cells modified by 3,3PrPACz show a high PCE of 25.24% was obtained (a J_{SC} of 17.115 mA/cm², a V_{OC} of 1.814 V, and an FF of 81.3%) with forward scan and 24.50% with reverse scan (a J_{SC} of 17.161 mA/cm², a V_{OC} of 1.800 V and an FF of 79.3%), which shows the negligible hysteresis. <div id="gtx-trans" style="position: absolute; left: 485px; top: 401.594px;"> <div class="gtx-trans-icon">

8:45 AM EN03/EN04/EN05/EN06.03

Efficiency Improvement Mechanism by Light and Dark Soaking for CdSe_xTe_{1-x} Thin-Film Solar Cells through Novel In-Situ Dopant Profiling [Sanghyun Lee](#)¹ and Kent Price²; ¹University of Kentucky, United States; ²Morehead State University, United States

Cadmium Telluride (CdTe) thin-film solar cells have shown remarkable efficiency and durability in the past decade, reaching over 22.1 % in laboratory-scale tests, close to the theoretical Shockley-Queisser limit of ~30 %. Furthermore, they have also been widely deployed in commercial applications, with more than 30 GWp of modules installed worldwide. CdTe is the leading thin-film technology for cost-effective solar energy production due to its low fabrication costs, high-power conversion efficiency, reasonable long-term performance stability, and short energy-payback time. Recently, researchers have explored the use of Se to create band grading either in addition to or as a replacement for CdS. CdSe_xTe_{1-x} is a promising material with bandgap lowering below 1.4 eV, which allows the short-circuit-current (J_{sc}) to approach its theoretical limit. For a long period, CdS was regarded as a crucial component for achieving high performance. Cells made without CdS (i.e., a direct CdTe junction to the transparent conducting oxide electrode) exhibit very low open circuit voltages (V_{oc} and fill factors (FF), implying that the CdTe/oxide interfaces were of low quality. Although CdS has a benefit in that intermixing eases the lattice mismatch at the interface, this approach has a drawback: it also reduces the photocurrent by absorbing light in the 300 - 525 nm range. This means less light reaches the active layer of the solar cell, resulting in efficiency loss. Hence, recent efficiency improvement has focused on introducing Se to create band grading either in addition to or as a replacement for CdS. CdSe_xTe_{1-x} is promising, with bandgap lowering below 1.4 eV, enabling J_{sc} to be close to its theoretical limit.

In this study, we have fabricated CdSe_xTe_{1-x} devices by vapor transport technology (VTD) and investigated the detailed improvement mechanism of efficiency improvement through in-situ Cu dopant profiling under various light and dark soak conditions. Moreover, devices were stressed at elevated temperatures simultaneously under various bias conditions, both with illumination and in the dark. During light soaking, different intensities of light and wavelengths were tested to characterize devices. In addition, we modeled the result with our in-house MATLAB modeling suites, which we developed in our group to understand the efficiency improvement mechanism. Connected to the external TCAD simulators (Synopsys Sentaurus), we modeled and explained the results with different input parameters based on the dopant in-situ profiling. The results indicate that CdSe_xTe_{1-x} devices have shallow donor and acceptor energy states near the main front junction interface, and acceptor activation energy (E_a) is approximately 0.3 - 0.4 eV based on light and voltage-biased quantum efficiency at different temperatures. The Cu dopant concentration is approximately 5×10^{14} cm⁻³ under no bias conditions. However, a peak doping concentration evolves toward the front CdSe_xTe_{1-x} junction during in-situ measurements. The weak blue light (0.01 sun at 450 nm) can dramatically improve the carrier collection as compared to the same intensity of red light (660 nm). Interestingly, the stability of CdSe_xTe_{1-x} solar cells was found to be bias-dependent and device-specific during light and dark soaking. CdSe_xTe_{1-x} devices without Cu dopant demonstrated a reduction of depletion width under voltage and light-biased conditions. The depletion width of CdSe_xTe_{1-x} devices without Cu is reduced to approximately 24 % under applied voltage biases and dark soaking conditions as compared to no bias condition, while efficiency, J_{sc} , and V_{oc} decreased. Under light soaking conditions at 85 C, the increase in V_{oc} and efficiency depends on the thickness of CdSe deposition thickness.

9:00 AM EN03/EN04/EN05/EN06.04

Investigation and Application of Thin Films of Photoluminescent Pigment for Utilization of Ultraviolet Light in Solar Cells Otávio J. Oliveira, Thais Crestani, Natália F. Coutinho, Ana P. Monteiro, Tarcio A. Barros and [Francisco C. Marques](#); State University of Campinas, Brazil

Although silicon and perovskite solar cells have achieved efficiency as high as 26 %, their efficiency is still limited by several factors. One of the proposed mechanisms to circumvent these problems is to use wavelength shifters materials. Here we investigate the properties of thin film of low-cost photoluminescent pigment currently used in coatings, graphic arts, cosmetics and adhesives. The aim was to evaluate the capability of shifting the

ultraviolet light to the wavelength where silicon solar cells are more efficient (around 600 nm). Precursor solutions were prepared by dissolving the orange pigment on ethanol. Thin film deposition was performed by spin-coating technique. After each deposition, the substrates were placed on a heating plate in order to evaporate the solvent. The pigment was characterized by X-ray diffraction, AFM, UV-Vis transmittance, photoluminescence. The XRD diffractograms are compatible with the expected structure of organic pigments, they present an amorphous characteristic. Photoluminescence measurements show the PL emission covers a range of 500 – 650 nm, which are in the region of the highest efficiency of silicon solar cells. Thin films deposited by spin coating show good uniformity. UV-Vis spectra show some absorption bands related to specific structures of the pigment and/or impurities. The absorption occurs in the wavelength range from 300 to 700 nm, been more intense in the UV range. This absorption corresponds to the one associated with the conversion of the UV light in visible light. The PL emission, on the other hand, is shifted to the 550 to 700 nm range. This result shows that the film made of pigment, deposited by spin coating, works as a wavelength shifter.

9:05 AM EN03/EN04/EN05/EN06.05

Exploring Carbon Nanoflake Based Materials for Charge Transport Layers of Perovskite Solar Cells: A Combined DFT-DFTB Study Including Effects of Solid-State Packing [Ruicheng Li](#)¹, Keisuke Maeda¹, Man-Fai Ng², Keisuke Kameda¹, Sergei Manzhos¹ and Manabu Ihara¹; ¹Tokyo Institute of Technology, Japan; ²Institute of High Performance Computing, Singapore

One of the biggest difficulties in the commercialization of perovskite solar cells (PSCs) lies in their charge transport layers. Charge transport materials are needed to achieve high performance with PSCs, but hole transporting materials (HTM) and electron transporting materials (ETM) used in high-performance lab-scale PSCs are relatively high-cost. Meanwhile, high-performance HTMs typically require the use of dopants that are detrimental to cell stability, while the commonly used metal oxide ETMs suffer from low electron mobility and photo-generated oxygen vacancies, which result in photocurrent hysteresis and serious interface recombination that affects the performance of the device. Carbon-based materials, in particular carbon nanoflakes (CNF) and carbon quantum dots (CQD), have been increasingly used in charge transport layers and electrodes for PSCs. There are practically limitless possibilities of designing such materials with different sizes, shapes and functional groups, which allows modulating their properties such as band alignment and charge transport. Solid-state packing further modifies these properties. However, there is still limited insight into electronic properties of this type of materials as a function of their chemical composition, structure, and packing. Here, we study the dependence of band alignment and charge transport characteristics on chemical composition and structure of commonly accessible types of nanoflakes and functional groups and further consider the effect of their solid-state packing. We use a combination of density functional theory (DFT) and density functional-based tight binding (DFTB) to get electronic structure level of insight at scales relevant to experiments. We find that CNFs must have sizes as small as 1.3 nm to provide band alignments suitable for their use as hole transport materials with the commonly used MAPbI₃, certain functional groups are able to change the band alignment so strongly that the same carbon nanoflake might act as either hole transport material or electron transport material. We show that both the shape of the CNF and inter-flake interactions can significantly modify band alignment by more than half an eV; solid-state packing has a moderate effect on HOMO of less than half an eV, whereas the effect on LUMO can be on the order of one eV.

9:20 AM EN03/EN04/EN05/EN06.06

Design and Synthesis of Zn-Based Metal Organic Frameworks (MOF) for Adsorptive Removal of Pharmaceutical Contaminants [Anam Afaq](#) and Sarang Gumpfekar; IIT Ropar, India

Metal-organic frameworks (MOFs) are porous, crystalline, hybrid materials with high surface area, large pore volume, various topologies and tuneable functionality that make them unique. Conventionally, MOFs are synthesized using the autoclave-based hydrothermal method at relatively higher temperatures in a batch process. In this study, we synthesized Zn-based MOFs using a continuous flow reactor at a lower temperature. We compared the properties with the same MOF synthesized using a batch hydrothermal reactor. A continuous flow microreactor was fabricated for large-scale production of MOFs with homogeneous morphology. It was a circularly coiled reactor made of 316 stainless steel with a total volume of 14 ml. It offered improved heat and mass transfer which resulted in less reaction time, high space-time yield, higher reaction rate, precise control of residence times and control of MOF size and morphology. In this work, we showed that the Zn-based MOF can be synthesized in a continuous flow reactor in less time (2 hours) and at low temperatures (55°C) as compared to the batch process (48 hours and 180°C). Further, the MOF was used to remove pharmaceutical contaminants **Estradiol valerate** and **17 α -ethylestradiol** from model wastewater. Estradiol valerate and 17 α -ethylestradiol are synthetic estrogens found in contraceptive pills and are considered emerging pollutants. The batch adsorption experiments were performed at different adsorbent amounts, extraction time, temperature, pH and ionic strength for both the contaminants to optimize the adsorption process. **Langmuir model** fitted the isotherm data, and the **pseudo-second-order model** fitted the kinetic data for Estradiol valerate and 17 α -ethylestradiol adsorption. Overall, this study presents a continuous flow reactor system to synthesize MOFs at large scale with reproducible properties and its use as an adsorbent to remove pharmaceutical contaminants.

9:25 AM EN03/EN04/EN05/EN06.07

Synthesis of Green Metallic Nanoparticles by Plants: A Sustainable Approach [Krishna Yadav](#)¹ and Dharmveer Yadav^{2,2}; ¹Malaviya National Institute of Technology, India; ²Indian Institute of Technology Bombay, India

The synthesis of metallic nanoparticles has gained significant attention in the field of nanotechnology due to their unique physicochemical properties and diverse applications. However, conventional methods for nanoparticle synthesis often involve the use of hazardous chemicals and energy-intensive processes, leading to environmental concerns. Therefore, there is an increasing demand for the development of sustainable and eco-friendly approaches for nanoparticle synthesis. This eco-friendly and sustainable approach utilizes the bioactive compounds present in various parts of plants, such as leaves, stems, and roots, to facilitate the reduction and stabilization of metallic ions into nanoparticles. These compounds can effectively convert metal ions into metallic nanoparticles, eliminating the need for harsh chemicals and reducing the detrimental impact on the environment. Green metallic nanoparticles synthesized by plants exhibit unique optical, electrical, and catalytic properties, making them ideal for a wide range of applications. These include biomedical applications, such as drug delivery, imaging, and antimicrobial agents, as well as environmental remediation. Lastly, this work highlights the various challenges and future perspectives to further synthesize biogenic metal nanoparticles toward environmental and pharmaceutical advances in the coming years.

9:30 AM EN03/EN04/EN05/EN06.08

Effect of Solar Concentration on Poly (ethylene terephthalate) Degradation Using a Compound Parabolic Concentrator (CPC). [Lol-chen Alegria](#)¹ and Maria D. Baeza²; ¹Universidad Autónoma del Estado de México, Mexico; ²Centro de Investigación en Tecnología Avanzada (CIATEQ), Mexico

This study provides insights into the thermal properties and composition changes in PET after exposure to concentrated solar radiation using a Compound Parabolic Concentrator (CPC). We compare these effects to those resulting from exposure to an accelerated weathering chamber and the ambient conditions, aiming to assess the advantages and disadvantages of using solar concentrators for polyester degradation.

The observed alterations in coloration, increased fragility and deformation of the PET sheets indicate that a degradation process occurs during the CPC

exposure periods. Results obtained from Differential Scanning Calorimetry (DSC) reveal a significant increase in crystallinity fraction in the material exposed within the concentrator; whereas specimens subjected to weathering chamber and ambient conditions displayed effects related to physical aging. Furthermore, data obtained from Thermogravimetry Analysis (TGA) exhibited a reduction in thermal stability and maximum degradation temperature, with more pronounced effects observed in the specimens degraded within the CPC. Fourier Transform Infrared spectroscopy (FTIR) also displayed reduced intensity in the spectra as a result of degradation, without the presence of functional groups that indicate the formation of final products.

9:35 AM EN03/EN04/EN05/EN06.09

High-Performance Ternary Organic Solar Cells based on Peryleneimide Acceptors Yong Zhang, Ming Liu, Xianxian Ge and Daoyuan Chen; Harbin Institute of Technology, China

Organic solar cells (OSCs) have received widely attention in the recent years, the power conversion efficiencies (PCEs) of OSCs based on non-fullerene acceptors have beyond 17%. In terms of further improving the photovoltaic performance, a lot of strategies have been conducted from materials and device engineering. Among them, ternary blending is believed to be the most effective method to enhance the PCEs. In the ternary blend OSCs, it contains two or more donors and one acceptor, or two or more acceptors and one donor, which could be tune the morphologies of active layers, and enhance the Voc, Jsc and/or FF so as to obtain a higher PCE than that of binary device. In the current state-of-the-art ternary OSCs, the third component commonly is based on the fullerene, ITIC or Y-series acceptors, however, these third component (acceptor) mostly possess the weak sun-light absorption, multi-steps synthesis with high cost, the overlap on absorption with the main acceptor. Thus, the development of low cost third component (acceptor) will be a promising way to further lower the fabrication cost of OSCs, and also face a lot of challenges. Recently, based on our previous works[1,2], we have developed a quasi-two dimensional perylene diimide FPDI-2PDI, and apply it in the ternary devices of PM6:Y6. The results showed that PM6:Y6:FPDI-2PDI ternary OSCs gave a Voc of 0.848V, a Jsc of 27.47 mA/cm² and a FF of 77.2%, providing a PCE of 18%, which is much higher than the 16.63% of PCE in the binary PM6:Y6 device.[3] Further, we developed another novel three-dimensional TPA-4PDI, and the ternary OSC can obtain the PCE of 18.29% with simultaneously enhanced Voc, Jsc and FF.[4]

References:

- [1] Yin, Y. L.; Zhan, L. L.; Liu, M.; Yang, C. Q.; Guo, F. Y.; Liu, Y.; Gao, S. Y.; Zhao, L. C.; Chen, H. Z.; Zhang, Y. *Nano Energy*, 2021, 90, 106538.
- [2] Yin Y. L.; Zhang, W. X.; Zheng, Z.; Ge, Z. Y.; Liu, Y.; Guo, F. Y.; Gao, S. Y.; Zhao, L. C.; Zhang, Y. *J. Mater. Chem. C*, 2020, 8, 12516.
- [3] Liu, M.; Ge, X. X.; Jiang, X.J.; Chen, D. Y.; Guo, F. Y.; Gao, S. Y.; Peng, Q.; Zhao, L. C.; Zhang, Y. *Nano Energy*, 2023, 112, 108501.
- [4] Liu, M.; Ge, X. X.; Jiang, X.J.; Guo, F. Y.; Gao, S. Y.; Peng, Q.; Zhao, L. C.; Zhang, Y. *Adv. Funct. Mater.*, 2023, 33, 2300214.

9:50 AM EN06.09/EN03.09.05

The Genesis Device[®]: A Revolution in Large Scale Decarbonization Stuart Licht^{1,2,3}, ¹George Washington University, United States; ²Carbon Corp, Canada; ³C2CNT LLC, United States

CO₂ is a highly stable molecule. This stability had been considered an insurmountable barrier to its transformative removal from its role as a greenhouse gas. The C2CNT[®] (CO₂ To Carbon Nanomaterial Technology) process breaks through this barrier by using an energetic (high temperature), carbon rich (molten carbonate), transition metal nucleated environment, electrolytically splitting of CO₂ to graphitic carbon nanomaterials (and O₂). Built from the same fundamental graphene structure as graphite, which has a geologic lifetime, these nanocarbon products can permanently bind the transformed CO₂ to mitigate global warming. Their value arises from the properties of graphene such as high strength and conductivity, solid lubrication, electronic and catalytic activity tuned by distinctive 0D, 1D and 2D morphologies.

Control of the electrochemical conditions tuning C2CNT[®] to selectively produce 17 unusual nanocarbons is described in:

"Controlled Growth of Unusual Nanocarbon Allotropes by Molten Electrolysis of CO₂",

Liu, Licht, Wang, Licht, *Catalysts*, **12**, 125, 2022.

and

"Controlled Transition Metal Nucleated Growth of Carbon Nanotubes by Molten Electrolysis of CO₂",

Liu, Licht, Wang, Licht, *Catalysts*, **12**, 137, 2022.

The value of these nano graphitic carbons arises from the unique properties of graphene such as exceptional strength, high conductivity, solid lubrication, electronic and catalytic activity as modified by their distinctive 0D, 1D and 2D shapes. These nanocarbons are useful in a range of applications in the carbon fiber, polymer, electronic, medical, transportation, steel, cement and power sectors.

The C2CNT[®] process received the 2021 Carbon XPRIZE XFactor award for producing the most valuable product from CO₂. The process and new materials chemistry has been rapidly scaled as described in a growing body of proprietary IP, including selected US patents: US9,080,244, US9,297,082, US9,683,297, US9,758,881, US10,637,115, US10,730,751, US11,028,493, US10,982,339, US11,094,980,

and from 2022 onward patents: US11,346,013, US11,401,212, US11,402,130, US11,434,574, US11,512,398, US11,542,609, US11,613,815, US11,616,659, US11,633,691, US11,643,735, US11,680,325, US11,724,939, US11,732,368, US11,746,424, US11,767,260, US11,767,261, as well as a growing list of international patents and patents pending.

A C2CNT process[®] Genesis Device[®] CCUS demonstration using the has been built in Calgary, and a large-scale Genesis Device[®] CCUS plant, the GC3 project, is scheduled in Edmonton, producing 7,500 tonnes of carbon nanotubes transforming the CO₂ emission at the Genesee power plant.

Some of the 30 C2CNT[®] related publications are presented at:

<https://carboncorp.org/climate-change-solution>,

These publications include:

"STEP generation of energetic molecules: A solar chemical process to end anthropogenic global warming" Licht, *J. Phys. Chem. C*, **113**, 16283, 2009.

"Efficient Solar-Driven Synthesis, Carbon Capture, and Desalinization, STEP: Solar Thermal Electrochemical Production of Fuels, Metals, Bleach" Licht, *Advanced Materials*, **47**, 5592 (2011).

The discovery of the electrochemical nucleated growth of graphitic nanocarbons in:

"One-pot synthesis of carbon nanofibers from CO₂",

Ren, Li, Lau, Urbina, Licht *Nano Letters*, **15**, 6142, 2015.

"Recent Advances in Solar Thermal Electrochemical Process (STEP) for Carbon Neutral Products & High Value Nanocarbons," Ren, Yu, Peng, Lefler, Li, Licht, *Accounts of Chemical Research*, **52**, 3177 (2019).

“Amplified CO₂ greenhouse gas removal with C2CNT carbon nanotube-material composites”, Licht, Xinye, Licht, Wang, Swesi, Chan, *Materials Today Sustainability*, **6**, 100023 (2019).

and

“The green synthesis of exceptional braided, helical carbon nanotubes and nanospiral platelets made directly from CO₂,” Liu, Licht, Licht, *Materials Today Chemistry*, **22**, 100529 (2021).

SESSION EN06.01/EN03.01: Joint Session: Sustainable Materials I
Session Chairs: David Cahen, Jihye Kim, Clara Santato and Anke Weidenkaff
Tuesday Morning, April 23, 2024
Room 333, Level 3, Summit

10:30 AM *EN06.01/EN03.01.01

“Deep Materials Sustainability”: From Sourcing, to The Use Phase, to End-Of-Life Vanni Lughì; University of Trieste, Italy

For a material to be truly sustainable, all phases of the material’s life cycle should be sustainable: sourcing, manufacturing, transport, use, End-of-Life (EoL). In this contribution, I will introduce the concept of “Deep Materials Sustainability”, where all phases of the life cycle are addressed simultaneously, and will discuss some examples.

The ideal case is one where a material is synthesized through a sustainable process utilizing renewable and/or recycled material sources, it minimizes the transport phase impact (e.g. by being lightweight), it is used in applications aimed at increasing the sustainability of a system (e.g. an efficient thermal insulation for buildings), and it can be recovered and reused with minimal loss and downcycling. The metrics for measuring “sustainability” depend on the goal. For environmental sustainability, typical metrics are energy consumption, CO₂ emitted, tonnage of raw materials – all measured throughout the entire life cycle. Social sustainability is also gaining interest, and meaningful metrics are being developed in the field of critical and strategic materials. Most desirably, however, sustainability should be considered as a combination of all of the above.

I will review some examples where new materials are designed with the specific purpose of optimizing the environmental sustainability of the phases of the material’s life cycle. This underlying approach resembles that of “design for disassembly” or that of “design for recycling”. However, these approaches are focused on the design of the overall system, in order to favor the recovery of the materials and their recycling, respectively; in these approaches, the material is seen as a passive element, which is recycled simply by virtue of its intrinsic properties (good examples of this are thermoplastic materials and metals). Instead, here we shift our focus on new materials, where there is an effort of conceiving, designing and realizing them to optimize the specific properties that maximize the performance in environmental applications, while simultaneously pursuing circularity by both using sustainable material sources (e.g. renewable and/or recycled), and laying out an EoL path enabling reuse, remanufacture, or recycle.

I will discuss in more detail one example of such a material characterized by “deep sustainability”, where we co-developed a highly efficient thermal insulation foam along with its recycling process, and the foam material was a composite consisting of an alginate matrix and recycled fiber glass as the filler – i.e. a combination of renewable and recycled materials. The recycling process exploits the reversibility of the molecular assembly mechanism in the ion-assisted gelification of alginate, which is the first step in the fabrication of our material. At the end of life of the insulating foam – e.g. when the highly porous microstructure of the material starts degrading, along with the thermal insulation performance – a chelation agent is utilized to sequester the ions and disassemble the matrix, making possible the full recovery of the initial material source. Reversing chelation by changing the pH enables re-gelification and successively re-creation of the foam. The process can be repeated multiple times, and the new foam shows unaltered thermal insulation properties, as assessed via thermofluorimetry and calorimetry. SEM and micro-computed tomography are used to characterize the microstructure of the foams, and a Life-Cycle Assessment is carried out, showing a rather promising environmental footprint.

This case shows the feasibility of a sustainable material for a sustainable energy application: a foam based on a natural source, incorporating waste material, fully recyclable, and that is an effective thermal insulator – simultaneously addressing, in the spirit of circular economy, the issue of energy efficiency, of sustainable materials sourcing, and the material end-of-life.

11:00 AM EN06.01/EN03.01.02

Enhancing Thermal Insulation Performance through Entropy Stabilization in Rare-Earth Zirconate Structures Myeungwoo Ryu, Ganggyu Lee, Seungwoo Lee, Seunggun Choi, Seungcheol Myeong, Minsung Kim, Gunwoo Cha, Chanjin Park, Ungyu Paik and Taeseup Song; Hanyang University, Korea (the Republic of)

Thermal barrier coating (TBC) materials utilize ceramics with low thermal conductivity and exceptional thermal durability. The gas turbine market has recently seen a growing demand for thermally insulating materials suitable for operating temperatures exceeding 1200 °C, achieved aiming greater thermal conversion efficiency. In this study, we synthesized high-entropy A₂Zr₂O₇ zirconate ceramics by incorporating five cations of similar ionic radius into the A³⁺ cation site through a conventional solid-state reaction, and we demonstrated their superior thermophysical properties. The high-entropy oxide (HEO) ceramics exhibited consistently low thermal conductivity, ranging from room temperature to 1000 °C, mainly due to lattice distortion induced in the crystal structure. Furthermore, we introduced divalent cations to the A³⁺ cation site to increase oxygen vacancies within the structure, thereby reducing heat transfer caused by phonons. These A₂Zr₂O₇ zirconate HEOs demonstrate improved thermal barrier performance compared to yttria-stabilized zirconia (YSZ), which is a conventional TBC material. This highlights their potential application as next-generation TBC materials.

11:15 AM EN06.01/EN03.01.03

Investigation of Deposition Methods for Self-Cleaning Polymer Coatings Cesar III Reyes; University College London, United Kingdom

A self-cleaning effect can be achieved using superhydrophobic surfaces (i.e., water contact angle > 150°) through the Lotus effect, where water droplets can remove contaminants such as dust as they slide across a water-repellent surface.¹ This effect is achieved by a combination of a rough surface morphology and a low surface energy material. Surface morphology is typically determined through the deposition method, and aerosol-assisted chemical vapour deposition (AACVD) has often been used as a one-step method to attain both properties using an innately hydrophobic material (e.g., polymers).² Often, these coatings require reapplication once physically damaged; therefore, a self-healing approach was of interest. Transparent, self-healing hydrophobic coatings have been synthesised using polymeric materials such as epoxy resin (EP) and PDMS (polydimethylsiloxane, Sylgard 184) components with contact angles ca. ~105° and optical transparencies ~88% with respect to pristine glass at 91% transparency in the 400-800 nm wavelength range. Coatings were deposited using easy-to-scale methods such as spray, spin, and dip-coating and compared to other methods such as

AACVD.³ Contact Angle Hysteresis (CAH) measurements were used to determine the optimal easy-to-scale method. Samples were subject to plasma-treatment-testing, UV-exposure, and scratch testing, followed by heat treatment at 200 °C as the trigger to the self-healing process. The optimal coating (through spray-coating) was EP/PDMS in an ethyl acetate solvent without the PDMS curing agent, which displayed the most consistent self-healing character whilst still being transparent and hydrophobic. Coatings were characterised using FTIR, XPS, SEM, EDS, AFM, and UV/Vis spectroscopy. Templating materials with a desired morphology such as a diffraction grating, sandpaper, Cunanoneedles, and physically/chemically etched Al sheets was also investigated by creating PDMS templates which were applied onto polymer coatings to replicate the surface morphology. Using the templating approach, these techniques were studied to find a pathway to create self-healing superhydrophobic surfaces with supplementary characteristics either from additive nanoparticles or replicated surface morphologies.

References: 1) W. Barthlott and C. Neinhuis, *Planta*, 1997, 202, 1–8. 2) J. Huo, C. I. De Leon Reyes, J. J. Kalmoni, S. Park, G. B. Hwang, S. Sathasivam and C. J. Carmalt, *ACS Appl. Nano Mater.*, DOI:10.1021/acsanm.3c02575. 3) X.-J. Guo, C.-H. Xue, S. Sathasivam, K. Page, G. He, J. Guo, P. Promdet, F. L. Heale, C. J. Carmalt and I. P. Parkin, *J. Mater. Chem. A*, 2019, 7, 17604–17612.

11:30 AM EN06.01/EN03.01.04

Transparent Liquid-Repellent Coatings from Fluorine-Free Building Blocks with Excellent Substrate Independent Adhesion Priya Mandal, Vikaramjeet Singh and Manish Tiwari; University College London, United Kingdom

The research on liquid-repellent surfaces/interfaces has progressed rapidly in the last decade owing to their universal importance in fundamental research and practical applications. Ranging from energy and healthcare sectors to contamination prevention, (anti-)condensation, anti-icing, anti-biofouling, etc. The issue that limits the practical implementation of such materials can be broadly divided into two categories: i) the use of hazardous fluorine-based molecules due to their extremely low surface energy which are bio-persistent, and ii) low adhesion with underlying substrates which makes them susceptible to mechanical damage. Due to global warming and the increasing scarcity of resources, there is an immediate need to find ways toward more robust and sustainable developments. To this end, engineering robust and resilient surfaces with overall durability using environmentally safe chemicals can address some of these challenges.

Herein, we come up with a strategy to address these important challenges by rationally selecting polyurethane due to its excellent substrate-independent adhesion and metal-organic frameworks (MOF) which provide precision nanotextures (nanohierarchy) and impeccable intercalation characteristics. We present a water-based spray formulation of non-fluorinated amphiphobic (repellent to water and low surface tension liquids) coatings by combining commercial polyurethane and nanohierarchical MOF followed by post-functionalization with flexible alkyl silanes. The resulting surfaces are smooth, highly transparent, and exhibit excellent amphiphobicity towards a wide range of low surface tension liquids from water to alcohols and ketones. These coatings are able to sustain heating up to 200 °C and cyclic tape-peeling, are resistant to high-speed water jets (~35 m/s), and feature very low ice adhesion of ≤30 kPa which is well below the threshold of anti-icing surfaces (<100 kPa). Multi-functionality, robustness, and scalability (production and applicability, both), make this formulation a potential alternative to PFC-based hazardous coatings.

SESSION EN06.02/EN03.02: Joint Session: Thermoelectrics
Session Chairs: David Cahen, Jihye Kim, Clara Santato and Anke Weidenkaff
Tuesday Afternoon, April 23, 2024
Room 333, Level 3, Summit

1:30 PM *EN06.02/EN03.02.01

High Performance Flexible and Scalable Thermoelectric Device and its Application as a Self-Sufficient Power Supply for Wearable Electronic Devices Deepa Madan; University of Maryland, United States

Additive manufacturing has been investigated as a more time, energy, and cost-efficient method for fabricating thermoelectric generators (TEGs). Early results have been promising but are held back by the necessary inclusion of a high-temperature, long-duration curing process to produce high-performance thermoelectric (TE) films. This work investigates the synergistic effect of four factors – a small amount of chitosan binder (0.05wt%), a heterogeneous particle size distribution, the application of mechanical pressure, and thickness variation – on the performance of p-Bi_{0.5}Sb_{1.5}Te₃ (p-BST) and n-Bi₂Te_{2.7}Se_{0.3} (n-BTS) TE composite films. The combination of these four factors controls the micro and nanostructure of the films to decouple their electrical and thermal conductivity effectively. This resulted in figures of merit (ZTs) (0.89 and 0.5 for p-BST and n-BTS, respectively) comparable to other additive manufacturing methods despite eliminating the high-temperature, long-duration curing process. The process was also used to fabricate a 6-couple TEG device which could generate 357.6 μW with a power density of 5.0 mW/cm² at a temperature difference of 40 K. The device demonstrated air stability and flexibility for 1000 cycles of bending. Finally, the device was integrated with a voltage step-up converter to power a LED and charge and discharge capacitor at a temperature difference of 17 K, demonstrating its applicability as a self-sufficient power source.

2:00 PM *EN06.02/EN03.02.02

Pursuing Sustainable Thermoelectrics Wenjie Xie^{1,2}, Xingxing Xiao¹, Jinxue Ding¹, Wei Li¹ and Anke Weidenkaff^{2,1}; ¹Technical University of Darmstadt, Germany; ²Fraunhofer IWKS, Germany

Thermoelectricity offers a direct and highly efficient approach for converting heat into electricity, relying on two key factors: Carnot efficiency and the materials-dependent property, *ZT*. In the last two decades, tremendous efforts have been made to develop high *ZT* thermoelectric materials, and the bulk *ZT* has reached above 3. Energy converters for renewable or sustainable energy technologies have to be based on materials that are not a burden to the environment, do not contain critical elements and guarantee a short energy payback time. Besides improving the conversion efficiency and other performance factors, sustainability has to be considered when designing novel thermoelectric materials and devices. In this talk, we will introduce novel synthesis strategies for oxide and silicon-based thermoelectric materials. We will delve into the concept of Entropy Engineering, a method that can extend the lifetime of (oxide) thermoelectric materials. Moreover, we will showcase one example where waste Si from the solar cell industry is transformed into valuable products, specifically in the synthesis of MnSi_{1.75} alloy. This underscores the potential to convert waste into valuable resources, contributing to both sustainable energy and responsible material usage.

2:30 PM EN06.02/EN03.02.03

High-Performance CNT-Based Green Thermoelectric Composites and Device Siqi Liu¹ and Chaobin He^{1,2}; ¹National University of Singapore, Singapore; ²Institute of Materials Research and Engineering (IMRE), Singapore

Thermoelectric (TE) materials and devices which can harvest electricity in the low-temperature range from the temperature difference of human body and surroundings therefore attracts great attention. However, conventional TE devices are mainly assembled on general plastics, where materials for TE legs assembly normally are costly and scarce and environmentally damaging. Therefore, development of environmental-friendly TE materials and devices attracts huge attention in perspective of sustainability. Biodegradable composites are termed as green composites and effectively used as sustainable alternative. In this work, CNT/polycaprolactone (PCL) composites were fabricated. Beside the biodegradability, the composites showed enhanced TE properties with the existence of PCL with nearly 4 times power factor increase compared with neat CNT. This work provides a novel strategy for high-performance green TE composites for sustainable future.

2:45 PM EN06.02/EN03.02.04

Emerging Chalcogenides: A New Family of Perovskite-Inspired Sustainable Energy Materials [Ivan Caño Prades](#)¹, Cibrán López Álvarez¹, David Rovira Ferrer¹, Marcel Placidi^{1,2}, Claudio Cazorla¹, Joaquim Puigdollers¹ and Edgardo Saucedo¹; ¹Universitat Politècnica de Catalunya, Spain; ²Institut de Recerca en Energia de Catalunya, Spain

In the last ten years, lead-halide perovskites have achieved outstanding performance in photovoltaics, X-ray detectors and other optoelectronic applications. Significantly, they can be synthesized via cost-effective low-temperature methodologies, which represent an improvement in terms of sustainability compared to physical vapor processes, normally requiring high temperatures and vacuum. However, the presence of Pb and stability issues have raised the question of whether the exceptional properties present in lead-halide perovskites could be replicated in other materials. Among the different known approaches to develop perovskite-inspired materials, here we have fabricated emerging chalcogenide semiconductors with structure analogous to perovskite, and others which have different structure but similar electronic features.

Belonging to the first group, silver and copper chalcogenides - (Ag,Cu)₃SX (X=I,Br) - stand out for their crystalline structure analogous to perovskites, albeit switching cation sites by anions and vice-versa. They are constituted by earth-abundant and non-toxic components, and their bandgap in the 0.9 - 1.1 eV range indicates that they could be suitable for single-junction solar cells or tandem configurations. So far, powders and pellets have been mostly fabricated using costly and time-consuming approaches which involve high temperature and vacuum, and lack adaptability in terms of composition and doping. Alternatively, in this work we present a novel procedure to prepare (Ag,Cu)₃SX (X=I,Br) polycrystalline thin films by molecular precursor ink deposition, using thiol-amine solvent mixtures. This methodology offers advantages in terms of cost-effectiveness, versatility, scalability and sustainability, opening the door to explore new compositions, properties and applications of the ecologically benign chalcogenide anti-perovskite system. Samples have been extensively studied by X-ray diffraction, microscopy and optoelectronic characterizations.

Another approach to develop perovskite-inspired materials consists in developing materials which are electronically analogous, i.e., they have similar electronic characteristics at the band structure. In this regard, it is particularly interesting to seek materials which exhibit the same features which make lead-halide perovskites tolerant to defects. Indeed, despite having high defect densities, hybrid perovskites exhibit low non-radiative recombination rates. This phenomenon has been suggested to emerge from having bonding orbitals at the conduction band, and antibonding contributions at the valence band.¹ Therefore, it is expected that materials with similar electronic structure, such as ternary chalcogenides SbSX and BiSX (X=I,Br), can replicate the beneficial defect tolerance of perovskites. In addition, these materials are constituted by relatively earth-abundant and low toxic components, they are stable, have bandgaps in the 1.5 - 2.0 eV range, and can be synthesized at low temperatures, which makes them ideal as a viable alternative to perovskites. In this work, experimental and theoretical analyses will be presented, including the characteristics of the band structure (obtained by first-principle calculations), structural and optical properties (X-ray diffraction, spectroscopy analyses), and prototype PV devices, demonstrating their potential as a sustainable alternative for energy harvesting applications.

To sum up, this work presents two different families of emerging chalcogenide materials, constituted by relatively earth-abundant elements and manufactured by low-temperature environmentally-friendly techniques, which are inspired in different ways by the successful lead-halide perovskites (structure analogous and electronic analogous respectively), suggesting new, more sustainable ways to develop semiconductor materials for energy applications.

1 *Chem. Mater.* **29**, 11, 4667-4674 (2017)

3:00 PM BREAK

SESSION EN06.03/EN03.03: Joint Session: Sustainable Materials II
Session Chairs: David Cahen, Jihye Kim, Clara Santato and Anke Weidenkaff
Tuesday Afternoon, April 23, 2024
Room 333, Level 3, Summit

3:30 PM *EN06.03/EN03.03.01

Solution Processed Nanomaterials for Solar Technologies [Federico Rosei](#)^{1,2}; ¹University of Trieste, Italy; ²INRS, Canada

We describe wet chemistry approaches, solution based synthesis and hydrothermal processing of various nanomaterials, primarily Quantum Dots (QDs). By varying the size, shape and composition of the QDs we are able to optimize their bandgap and optoelectronic properties. The QDs are then used as building blocks to fabricate three types of solar technologies: (i) Quantum Dot Solar Cells [1,2]; (ii) Quantum Dot Photoelectrochemical cells for Hydrogen Production [3-11]; (iii) Luminescent Solar Concentrators [12-15] and in optical nanothermometers [16-18].

References

[1] *Adv. Func. Mater.* **27**, 1701468 (2017); [2] *Nano Energy* **55**, 377 (2019); [3] *Nano Energy* **31**, 441 (2017); [4] *Appl. Cat. B* **250**, 234 (2019); [5] *Appl. Cat. B* **264**, 118526 (2020); [6] *J. Mater. Chem. A* **8**, 20698 (2020); [7] *Nano Energy* **79**, 105416 (2021); [8] *Appl. Cat. B* **280**, 119402 (2021); [9] *Nano Energy* **81**, 105626 (2021); [10] *Chem. Eng. J.* **429**, 132425 (2022); [11] *Nano Energy* **100**, 107524 (2022); [12] *Adv. En. Mater.* **6**, 1501913 (2016); *Nano Energy* **37**, 214 (2017); [13] *Nano Energy* **44**, 378 (2018); [14] *Nano Energy* **50**, 756 (2018); [15] *J. Mater. Chem. A* **8**, 1787 (2020); [16] *ACS Phot.* **6**, 2479 (2019); [17] *ACS Phot.* **6**, 2421 (2019); [18] *Small* **16**, 2000804 (2020).

4:00 PM EN06.03/EN03.03.02

Fabricating Air-Stable Copper Films with Exceptional Electrical Conductivity without Sintering [Jessica Pereira](#)^{1,2}, Oleg Makarovskiy¹, David

Amabilino³ and Graham Newton¹; ¹University of Nottingham, United Kingdom; ²University of Southampton, United Kingdom; ³Consejo Superior de Investigaciones Científicas, Campus Universitario de Bellaterra, Spain

Copper is an excellent electrical conductor, nearly matching the conductivity of silver (Cu: 5.96×10^7 S/m vs Ag: 6.30×10^7 S/m), but at a fraction of the cost (Cu: \$ 0.28/oz vs Ag: \$ 21.6/oz) making it an ideal choice for cost sensitive large area applications which are in high demand. However, unlike silver, copper has a much higher susceptibility towards oxidation, a risk that is particularly acute in particulates and suspensions with high surface to volume ratio, which generates additional processing complications including the need for surface passivation and inert environments for processing as well as sintering. The use of fossil fuel based long-chain hydrocarbon ligands to passivate copper is the common approach in the field but decomposition of such ligands to fabricate functional conductive films require high sintering temperatures and controlled conditions. Moreover, with the rapid growth of the flexible and wearable electronics industry, sintering becomes increasingly less practical as most substrates used in this sector are temperature sensitive. Herein, a new approach to fabricating conductive air-stable copper films with resistivities close to that of bulk copper is demonstrated which only requires compression at room temperature, completely removing the need for any form of sintering. This approach facilitates the generation of highly conductive simple unsupported copper films as well as intricate patterns on paper and printed circuit board substrates with an aqueous, biopolymer stabilised copper ink formulation. The remarkable conductivity and oxidative stability of the copper films, coupled with the sustainability of the approach have the potential to precipitate a paradigm-shift in the use of copper inks for printable electronics.

4:15 PM EN06.03/EN03.03.03

Designing Sustainable Permanent Magnets: Alloying Additions and Magnetocrystalline Anisotropy in L1₀ FeNi Christopher D. Woodgate¹, Laura H. Lewis^{2,2} and Julie Staunton¹; ¹University of Warwick, United Kingdom; ²Northeastern University, United States

We report results from an holistic approach for modelling both atomic ordering and subsequent magnetocrystalline anisotropy energy (MAE) of magnetic materials with application to the design of novel, rare-earth-free permanent magnets. This computationally efficient technique allows for fast exploration of the materials design space and could open up a new route for materials discovery and manufacturing. Here we report recent results concerning the class of magnetic materials which chemically order into the L1₀ structure. These materials typically have large MAE values appropriate for advanced permanent magnets, with prime examples being FePt and CoPt that contain elements of high criticality. *Ab initio* theory has previously confirmed that it is the tetragonal, L1₀ order that produces the high MAE values measured in these materials [1]. There is therefore a desire to discover new L1₀ materials which are made using more-abundant elements, but which still retain desirable magnetic properties. One such candidate material is L1₀ FeNi, found in meteoritic, tetrataenite samples. This material is known to have a high uniaxial anisotropy, but a low chemical ordering temperature and sluggish kinetics make it challenging to manufacture in a laboratory setting.

Here, we consider introducing a third element into the binary Fe-Ni composition to promote ordering tendencies and enhance its predicted MAE. Systems with the general formula Fe_{50-x}Ni_{50-y}X_{x+y} (X=Pt, Co, Al) were investigated. Crucially, our modelling predicts the nature of any chemical order [2] and goes on to predict the MAE for a given system [1], using the same *ab initio* formalism for both aspects of the modelling approach. The ordering behaviour predicted on adding these dopants is rich and a variety of chemical orderings are obtained. Interestingly, we find that it is often the addition of light elements such as Al which enhance the MAE the most. We are also able to study the impact of magnetic order on predicted atomic order and show that annealing samples in an applied magnetic field may enhance chemical ordering [3].

Acknowledgements

We gratefully acknowledge the support of the UK EPSRC, Grant No. EP/W021331/1. C.D.W. is supported by a studentship within the UK EPSRC-supported Centre for Doctoral Training in Modelling of Heterogeneous Systems, Grant No. EP/S022848/1. This work was also supported in part by the U.S. Department of Energy, Office of Basic Energy Sciences under Award Number DE SC0022168 (for atomistic insight) and by the U.S. National Science Foundation under Award ID 2118164 (for advanced manufacturing aspects).

References

- [1] J. B. Staunton et al., Phys. Rev. B **74**, 144411 (2006).
- [2] C. D. Woodgate and J. B. Staunton, Phys. Rev. B **105**, 115124 (2022).
- [3] C. D. Woodgate D. Hedlund, L. H. Lewis, J. B. Staunton, Phys. Rev. Mater. **7**, 053801 (2023).

SESSION EN06.07/EN03.07: Joint Session: Photovoltaics and Supercapacitors
Session Chairs: David Cahen, Jihye Kim, Clara Santato and Anke Weidenkaff
Wednesday Afternoon, April 24, 2024
Room 333, Level 3, Summit

3:30 PM *EN06.07/EN03.07.01

Lead-Free Perovskite Derivatives Toward Eco-Friendly Indoor Photovoltaics Vincenzo Pecunia; Simon Fraser University, Canada

Indoor photovoltaics present a compelling solution for powering the ever-expanding array of Internet-of-Things (IoT) smart sensors in a sustainable manner. The emergence of halide perovskites as promising absorbers for indoor photovoltaics has ignited significant interest due to their favorable optoelectronic characteristics. Nevertheless, the deployment of indoor photovoltaic devices in close proximity to end-users raises concerns about the toxicity associated with the lead content found in mainstream halide perovskites. This has spurred the search for alternative, lead-free perovskite derivatives for efficient indoor photovoltaics without lead toxicity concerns. We first demonstrated this concept with Cs₃Sb₂I_{9-x}Cl_x, enabling indoor photovoltaic efficiencies already in the range of mainstream, commercial indoor photovoltaics. Furthermore, our investigations revealed that the spectroscopic limited maximum efficiency for this and other lead-free perovskite derivatives under indoor lighting conditions can reach approximately 60%, showcasing their immense potential through further materials and device optimization. In fact, the demonstrated photovoltaic efficiency of Cs₃Sb₂I_{9-x}Cl_x was sufficient to power printed digital gates via millimeter-scale indoor photovoltaic devices, confirming the opportunity already provided by this technology toward self-powered electronics with potentially low environmental impact. We extended our exploration to Cu-Ag-Bi-I absorbers, tailoring the microstructure and device architecture to achieve enhanced indoor photovoltaic efficiencies and ensuring reliable operation under realistic illumination levels as low as 200 lux, all while exhibiting favourable air stability. Recognizing the importance of sustainability in emerging technologies, we additionally conducted a thorough assessment of the environmental impacts of various lead-free perovskite derivatives in the context of indoor photovoltaics. Our findings identified the most promising compositions from a sustainability perspective, offering crucial guidance to the research community developing lead-free perovskite derivatives to enable eco-friendly self-powered smart sensors for a green IoT revolution.

4:00 PM EN06.07/EN03.07.02

Oxide-Halide Perovskite Composites for Simultaneous Recycling of Piezoceramics and Solar Cells Mohadeseh Tabeshfar¹, Sivagnana Sundaram Anandkrishnan¹, Mikko Nelo¹, Maliha Siddiqui², Jani Peräntie¹, Pavel Tofel³, Heli Jantunen¹, Jari Juuti¹ and Yang Bai¹; ¹University of Oulu, Finland; ²CEITEC-Central European Institute of Technology, Czechia; ³Brno University of Technology, Czechia

Global concerns regarding energy and the environment have created an urgent demand for sustainable manufacturing, usage, and disposal of electronic components. Piezoelectric and photovoltaic components are being extensively used due to the rapid development of the Internet of Things (IoT) and green energy production, which require large quantities of piezoelectric sensors/energy harvesters and solar cells as functional components and power sources. Thus, recycling these two essential types of components needs to be carefully considered. This work develops upside-down composites to recycle waste oxide perovskite-based piezoceramics and organometal halide perovskite-based solar cells. Production of the recycled and reusable materials requires only a marginal energy budget, while achieving a high level of material densification and excellent sensing capabilities. This work offers an energy- and environmentally friendly approach for recycling hazardous and high energy-consuming elements, as well as giving a second life to the functionality of waste piezoelectric and photovoltaic components.

4:15 PM EN06.07/EN03.07.03

Enhancing Fluorophore-Induced Plasmonic Current for Converting Solar Energy Lahari Saha¹ and Chris D. Geddes^{1,2}; ¹University of Maryland, Baltimore County, United States; ²Institute of Fluorescence, United States

Biological chromophores and certain model organisms present a unique opportunity in solar energy harvesting. Currently, solar energy conversion efficiency rates are in the low 20s, necessitating multiple panels to generate electricity. This is a problem since many agricultural farms are transitioning into solar farms, supporting the growing demand for electricity and further deepening existing food crisis. Therefore, the system's efficiency, stability, and longevity are crucial. Advances in plasmonic materials offer promising results due to their compatibility with fluorescent biosensors and various fluorophores, suggesting potential applications in solar energy conversion. In this presentation, we discuss a technology called fluorophore-induced plasmonic current (FIPC), where plasmonic thin films and a fluorophore solution are used to generate current. We consider a few methods to increase current produced by FIPC for example, annealing thin films and incorporating metallic colloids in the fluorophore solutions. Key takeaway on annealing thin films suggests an increase in current response within the working range and lowering signal to noise ratio, leading to a stable baseline current. Preliminary data on metallic colloids mixed with fluorophore solutions indicate an *exceptional* increase in current generation. Future work in this project will translate our present findings to biological chromophores.

4:30 PM EN06.07/EN03.07.04

Carbon-Based Photoabsorbers for Sustainable Energy Applications Demetra S. Achilleos¹, Caoimhe Maher¹, Hatice Kasap² and Erwin Reisner²; ¹University College Dublin, Ireland; ²University of Cambridge, United Kingdom

The continuous air and water pollution arising from the accelerated consumption of fossil fuels and organic pollutants, respectively, emphasize the need for society to move towards renewable "green" resources, and environmentally sustainable processes. Photocatalysis is a promising approach for mitigating simultaneously both the energy and environmental concerns.¹ However, the development of economically and environmentally sustainable photocatalytic processes creates the pressing need for new materials of low cost and toxicity, such as photoabsorbers and catalysts, which maintain substantial performances.

Carbon dots (CDs) and carbon nitride (CN_x) can efficiently serve as photoabsorbers for this purpose since they fulfil these requirements.²⁻⁶ In particular, they are hydrophilic materials of low toxicity which are chemically and photochemically robust, can be synthesized at low cost, and show optimum photocatalytic properties upon pre-designed synthesis. In this work, we describe the synthesis of CN_x and CDs from low-cost organics and/or Earth abundant waste (circular economy), the structure of which bestows the derived photoabsorbers with distinctive photocatalytic performances. These light harvesters, when combined with noble-metal free catalysts in aqueous photocatalytic systems, not only facilitate "green", solar-driven fuel synthesis but also waste/water pollutant utilization. The use of waste and aqueous pollutants, eliminates the need for additional sacrificial reagents traditionally used in great excess, which add to the overall cost of the process, and result in toxic by-products.⁷ We anticipate that this approach could be a breakthrough in the development of scalable, economically, and environmentally sustainable systems, which can efficiently serve energy and environmental applications.

References

1. Kamat, P. V.; Bisquert, J., *J. Phys. Chem. C* **2013**, *117*, 14873-14875.
2. Achilleos, D. S.; Kasap, H.; Reisner, E., *Green Chem.* **2020**, *22*, 2831-2839.
3. Achilleos, D. S.; Yang, W.; Kasap, H.; Savateev, A.; Markushyna, Y.; Durrant, J. R.; Reisner, E., *Angew. Chem. Int. Ed.* **2020**, *59*, 18184-18188.
4. Kasap, H.; Achilleos, D. S.; Huang, A.; Reisner, E., *J. Am. Chem. Soc.* **2018**, *140*, 11604-11607.
5. Kasap, H.; Godin, R.; Jeay-Bizot, C.; Achilleos, D. S.; Fang, X.; Durrant, J. R.; Reisner, E., *ACS Catalysis* **2018**, *8*, 6914-6926.
6. Ren, J.; Achilleos, D. S.; Golnak, R.; Yuzawa, H.; Xiao, J.; Nagasaka, M.; Reisner, E.; Petit, T., *J. Phys. Chem. Lett.* **2019**, *10*, 3843-3848.
7. Pellegrin, Y.; Odobel, F., *C. R. Chim.* **2017**, *20*, 283-295.

4:45 PM EN06.07/EN03.07.05

Hybridization of Magnetic Fe₃O₄ with Mn-MOFs for High Performance Supercapacitor Saumaya Kirti, Shobha Shukla and Sumit Saxena; Indian Institute of Technology Bombay, India

Encapsulating guest compounds in metal-organic frameworks (MOFs) architectures is one of the most promising paths to achieve properties beyond those of the pristine MOFs and/or guest species. Contrary to the conventional host/guest composites encapsulating guest species inside MOF cavities, core-shell architectures exhibit a better accessibility to the pores ensuring an optimal diffusion of the substrate while presenting a unique structure that prevents the aggregation and the runoff of the active guests and ensures a tight interaction between core and shell, leading to synergistic effects. Herein, the integration of Fe₃O₄ with manganese-based MOF i.e., Fe₃O₄@Mn-MOF-NH₂ with varying shell thickness and hierarchical pore structure is synthesized. As a proof of concept, the obtained Fe₃O₄@Mn-MOF-NH₂ composite is used as an active material for supercapacitor applications which showed an enhancement of ~80% with respect to pristine compounds.

Wednesday Afternoon, April 24, 2024
Flex Hall C, Level 2, Summit

5:00 PM EN06.08.01

Closed-Loop, Rapid Polymer Welding Using Radio-Frequency Heating Aniruddh Vashisth and Surabhit Gupta; University of Washington, United States

Polymer components are becoming more prevalent in load-bearing applications due to their superior strength-to-weight ratio. Thermoplastics, particularly, have gained traction in recent years due to their ability to be molded, recycled, and reused. Effective welding and joining methods are essential to facilitate the assembly of intricate thermoplastic parts; but these manufacturing processes are energy expensive and depend on the processed materials. We have developed an energy efficient closed-loop method that utilizes a recent discovery that radiofrequency (RF) fields rapidly heat up carbonaceous materials. We developed a machine capable of monitoring the material's pressure, deformation, and thermal response during the assembly process; this closed-loop system does not require human intervention to process the materials. In this work, we will show that the closed-loop machine can rapidly weld thermoplastics using RF heating at the bondline; to process these materials, we can control the pressure or displacement of the welds to ensure desired mechanical properties. Our initial experiments showed that we can successfully weld polylactic acid (PLA) coupons with graphitic RF susceptors at the bond line in less than 2 minutes, utilizing less than 50 W of RF power. The weld properties show no significant variation within a 0 to 0.3 MPa pressure range. However, an increase in out-of-plane welding displacement enhances the modulus and strength of the weld. This work introduces an energy-efficient, automated system for welding polymer composites using RF fields, showing promise for diverse manufacturing applications. The machine can be used in three control settings: hold, displacement, and pressure control. We saw excellent RF heating response of conductive carbonaceous coatings on polymers; this rapid heating was used for RF processing and bonding thermoplastics using less than 50 W of RF input powers in an automated manner.

5:00 PM EN06.08.02

Electrochemical Methods of Carbon-Negative Ironmaking for Green Steel Paul A. Kempler, Berkley Noble and Anastasiia Konovalova; University of Oregon, United States

Iron and steel are important feedstocks for energy materials and infrastructure but are produced with concomitant greenhouse gas emissions. Iron reduction, typically accomplished using coal or natural gas, can be driven electrochemically which provides a potential path to a fully electrified and carbon-neutral steelmaking process. We have developed the chlor-iron process, a low-temperature (<100 C), electrochemical cell that directly reduces solid iron oxide particles to high-purity iron metal at the cathode while co-producing sodium hydroxide and chlorine. The production of co-products consumed at the ~100 million tons per year scale provides a cost-competitive pathway for electrochemical ironmaking. Moreover, the co-produced hydroxide can be used for direct CO₂ capture and mineralization, leading to a net-negative process for ironmaking. Here, we report results on the mechanism of electrochemical direct oxide reduction, the effects of iron ore feedstocks on selectivity towards iron metal, and prototypes for a cell producing iron and chlorine at current densities > 100 mA cm⁻².

5:00 PM EN06.08.03

Reinforcing Strategy in The Fabrication of GO-Reinforced Al-Matrix Composite Using Single Pass Friction Stir Processing Soumyabrata Basak^{1,2}, Han-Gyeol Yoo³, Van Cong Phan², Sung Tae Hong², Sam Y. Anaman³ and Hoon-Hwe Cho³; ¹Korea Institute of Industrial Technology, Korea (the Republic of); ²University of Ulsan, Korea (the Republic of); ³Hanbat National University, Korea (the Republic of)

The influence of carbonaceous components (graphene oxide, GO) on the microstructure and mechanical properties of aluminum (Al) matrix composite fabricated by single-pass friction stir solid-state processing (FSP) is studied. GO powder is introduced onto the commercially pure Al plate using adhesive, eliminating typical secondary manufacturing stages. As a result, this technique becomes more cost-effective and energy-efficient than other conventional approaches. The presence of GO within the Al matrix is initially characterized using Raman spectroscopy and secondary ion mass spectrometry, followed by detailed electron microscopy studies. TEM studies show a reasonable amount of dislocation accumulation at the matrix particle interface without other chemical reactions. Due to continuous dynamic recrystallization, EBSD analysis reveals a significant grain refinement in FSPed Al (FSP-only condition without GO reinforcement) and FSP with GO conditions. The microhardness map of FSP with GO characterizes an overall improved hardness value than the FSPed Al and reveals the maximum hardness zone at the advancing side of the stir zone. The advancement of mechanical properties is primarily due to GO particles and their interaction with the Al matrix. The tensile strength and ductility are improved in the FSP with GO condition compared to the base material and FSPed Al condition.

5:00 PM EN06.08.04

Boron Nitride Nanomaterials for Gas Storage and Separation Using Mechanochemistry Srikanth Mateti and Ying Chen; Deakin University, Australia

2D h-BN, also known as white graphene, has a similar honeycomb structure to graphene, with alternating boron and nitrogen atoms consisting of strong sp² covalent in-plane bonding and weak van der Waals forces between layers. h-BN has unique properties; it is a lubricant due to its layered structure. BN is an electrical insulator (with a bandgap of approximately 5.9eV) at the same thermally conductive and also has high mechanical strength, large thermal conductivity and low dielectric constant. Hydrogen is increasingly being touted as one sustainable solution to globe clean energy problem. But one of the main challenges is the lack of a safe and cost-effective storage and transport technique. Solid-state storage technology is considered to overcome this challenge by storing enormous quantities of gases in solid materials. Currently, hydrogen storage and transport happen majorly in three ways, compressed gas and carrier gas then decompose. Due to reasons of material properties and operating costs, large amounts of gaseous hydrogen are usually not stored at pressures exceeding 100 bar in aboveground vessels and 200 bar in underground storages [1]. Currently commercially available have utilized an onboard storage pressure of 700 bar, but storage tanks capable of storing hydrogen at such pressures are expensive. To decompose ammonia to form hydrogen, transport losses are 34-36% [2]. And Liquid hydrogen storage needs an extremely low boiling point of hydrogen (-253°C at 1 bar) which is energy intensive and expensive. Thus, urgent need to find alternative and sustainable ways to store hydrogen gases. In this, we discuss possible and sustainable and safe ways of storing and transporting hydrogen in powder form. This talk will provide insights on the mechanochemical approach to store and separate various gases.

[1]. Y. Cao, J. Renewable Mater., 2021, doi: 10.32604/jrm.2021.015722

[2]. <https://www.edisongroup.com/wp-content/uploads/2021/07/Finding-the-sea-of-green230721-3.pdf>

5:00 PM EN06.08.05

A Novel Cobalt Chloride Hydrate Modified Co-MOF Derived Carbon Microspheres as Anode Materials for Lithium Ion Batteries Lei Jiang^{1,2} and Bohejin Tang²; ¹KU Leuven, Belgium; ²Shanghai University Of Engineering Science, China

In this work, the carbon-microsphere loaded with cobalt chloride hydrate (CCH@CM) was prepared via a collaborative and chlorination strategy derived from ZIF-67 precursor, which exhibits a superior electrochemical performance as a lithium-ion battery anode material. The synthesized CCH@CM obtained a high initial discharge capacity (947 mAh g⁻¹) and the capacity attenuation rate is close to zero after 200 cycles at the current density of 100 mA g⁻¹. The porous structure derived from ZIF-67 not only can provide a conductive path, which increases the transport of electrons and lithium ions, but also alleviate volume expansion. The presences of -Cl/H₂O groups provide active sites for the anchoring of Li⁺. As the first successful synthesizing the cobalt chloride hydrate (CCH) from ZIF-67, good electrochemical performance provides a promising for the large-scale application in lithium ion batteries.

5:00 PM EN06.08.06

Recycle Waste Gloves for Oxygen Evolution Reduction in Alkaline Water Electrolysis Tzu Hsuan Chiang, Ji-Min Chang and Rui En Li; National United University, Taiwan

Nitrile gloves have gained widespread use as disposable gloves in various sectors, including hospitals, scientific laboratories, manufacturing facilities, halls, and museums, thanks to their superior mechanical strength compared to vinyl gloves and other alternatives. Due to the ongoing COVID-19 pandemic, the global production of discarded gloves has soared, estimated at more than 76 million monthly. Unfortunately, dealing with and reintroducing this waste into the reuse cycle is costly and time-consuming. Regrettably, many disposable gloves eventually find their way into oceans and other water bodies, slowly deteriorating and fragmenting into microplastic particles. Marine animals swiftly ingest these microplastics, leading to blockages and permanent damage to their internal organs. Consequently, finding a practical solution to this substantial waste issue is paramount.

A study was conducted to create FeWO_x-NG electrocatalysts by recycling waste nitrile gloves through the oxygen evolution reaction (OER) in alkaline water electrolysis (AWE). While AWE is a preferred technology for green hydrogen production, its adoption has been impeded by the high cost associated with the necessary capital investment in electrolysis and renewable energy systems. Furthermore, the commonly used precious electrocatalysts contribute to AWE's elevated costs and superior gas evolution performance. The oxygen evolution reaction (OER) is the rate-limiting step in alkaline water electrolysis. It makes electrocatalyst performance in OER a crucial factor in enhancing its hydrogen evolution reduction (HER) capabilities. Leveraging recycled waste nitrile gloves, this study developed an OER electrocatalyst with Fe and W precursors (FeWO_x-NG) to reduce the electrocatalyst's cost.

The study results demonstrate that FeWO_x-NG exhibits a smaller overpotential and Tafel slope at a 10 mA/cm² current density in alkaline electrolytes compared to RuO₂. This improved performance could enhance alkaline water electrolysis efficiency and promote more efficient hydrogen evolution.

5:00 PM EN06.08.07

Exploring The Potential and Performance Constraints of Ni-Rich LiNi_{0.9}Co_{0.1}O₂ through DFT Research Temitayo O. Ikuerowo¹, Omotayo Salawu² and Olusegun Tomomewo¹; ¹University of North Dakota, United States; ²Texas A&M University, Qatar

The high-capacity but unstable LiNiO₂ (LNO) cathode material for lithium-ion batteries can be improved through partial substitution with cobalt. First-principles calculations were performed to study the impact of 10% cobalt doping on the structural, electronic, defect, and lithium diffusion properties of LiNi_{0.9}Co_{0.1}O₂ (NC91). The layered structure is retained but the band gap decreases significantly with 10% Co. Formation energies reveal oxygen vacancies and antisite defects still occur; however, Ni sites near Co are least favorable for antisite formation. The energy barrier for Li migration is substantially lower in NC91 than LNO, indicating enhanced Li mobility with 10% Co. While the Co doping improves Li transport, additional doping is likely required to sufficiently suppress cation mixing and oxygen loss. This work provides fundamental insights into the structure-property relationships resulting from low levels of cobalt doping in Ni-rich cathodes.

5:00 PM EN06.08.08

Utilizing Date Seed-Derived Hard Carbon in Lithium-Ion Batteries Operating at Low Temperatures Nurbolat Issatayev¹, Kazna Tassybay¹, Arailym Nurpeisova^{1,2,3}, Zhumabay Bakenov^{1,2,3} and Gulnur Kalimuldina¹; ¹Nazarbayev University, Kazakhstan; ²National Laboratory Astana, Kazakhstan; ³Institute of Batteries LLC, Kazakhstan

The performance of traditional Li-ion batteries deteriorates when operating at sub-zero temperatures. This is mainly due to the slow diffusion of Li-ions in the commercial graphite anode, which can retain about 12% of its capacity at -20 °C. To solve this issue, recently, many alternative anodes have been explored. However, most of the electrodes proposed to date involve complex fabrication methods, complicating their practical implementation. Therefore, we propose cost-effective anode material as porous structured nitrogen-doped hard carbon synthesized from biowaste (date seeds) with further LiF modification to achieve an artificial LiF-rich SEI layer. The prepared anode material achieved a specific 525 and 280 mAh g⁻¹ capacity after 100 cycles at 0.1 C at room and -20 °C temperatures, respectively. It could deliver 72 mAh g⁻¹ after 500 cycles, even at a high current of 2C at -20 °C. To elucidate the superior electrochemical performance of LiF-modified hard carbon, post-mortem Transmission Electron Microscope (TEM) and X-ray Photoelectron Spectroscopy (XPS) analyses and the Li-ion storage mechanism at low temperatures were studied. The former showed that the LiF-modified electrode has a uniform, thin, and LiF-rich SEI layer that alleviates the penetration and/or integration of ions into graphic layers of hard carbon. The latter illustrated the dominance of the pseudo-capacitive storage mechanism of hard carbon anode, which contributes significantly to high performance at low temperatures.

5:00 PM EN06.08.09

Synergistic Interaction between Ruthenium Catalysts and Grafted Niobium on SBA-15 for 2,5-Furandicarboxylic Acid Production using 5-Hydroxymethylfurfural Hyun Sung Kim¹ and Hangil Lee²; ¹Pukyong National University, Korea (the Republic of); ²Sookmyung Women's University, Korea (the Republic of)

This study entailed the synthesis of a novel Ru-bound catalyst decorated on Nb-grafted SBA-15. An Nb-grafted SBA-15 support with varying Si/Nb ratios was utilized as a support for Ru nanoparticles. The effect of Nb grafting on the immobilized Ru nanoparticle catalyst was systematically investigated, and its catalytic performance in the synthesis of furan dicarboxylic acid using 5-hydroxymethylfurfural (HMF) under base-free reaction conditions was evaluated. The results indicate the increased productivity of the Ru/Nb-grafted SBA-15 catalyst, with a yield exceeding 99%, representing a significant advancement in catalysis. This study also affords insights into the complex relationship between the catalytic activity and selectivity and its unique surface attributes. Moreover, acidic sites were created, and the electron density within the active sites was modulated by generating monomeric Nb oxide species on the SBA-15. Additionally, the role of high-electron-density Ru atoms in facilitating the efficient adsorption and activation of HMF, resulting in enhanced catalytic efficacy, was highlighted.

5:00 PM EN06.08.10

Material advancement for iron-based redox flow batteries for grid-scale storage Buddhinie S. Jayatilake, Anna Ivanovskaya, Alexandra Overland, Swetha Chandrasekaran and Auston Clemens; Lawrence Livermore National Laboratory, United States

Iron-based redox flow batteries are low-cost candidates for grid-scale energy storage due to their scalability and low cost. Compared to the current state-of-the-art redox flow batteries based on vanadium redox chemistry, iron shows the potential to achieve DOE's cost targets LCOS, \$0.05/kWh due to its natural abundance and eco-friendliness. Our recent studies show pathways for overcoming material challenges associated with iron-based systems. Iron deposition process limits the storage capacity and efficiency of the system. Our findings show that engineered electrolytes and 3D electrodes can minimize parasitic losses by 15%, improve the durability and enhance storage capacity by 25%.

5:00 PM EN06.08.12

Lead Halide Perovskite Pixel Arrays Fabricated by Ultrathin Reusable Metal Mask Zhao Sun¹, Zhuofei Gan¹, Jianwen Zhong¹, Liyang Chen², Zijie Jiang¹ and Wendi Li¹; ¹The University of Hong Kong, China; ²ETH Zurich, Switzerland

In recent decades, metal halide perovskites have emerged as a highly promising class of materials for optoelectronic devices, owing to their exceptional properties, which include a tunable bandgap, a significant optical absorption coefficient within the visible light, and long carrier diffusion length^[1-4]. Nonetheless, achieving high-resolution patterning of perovskite arrays presents challenges due to their inherent instability when exposed to conventional photolithography solvents. In this work, we proposed a universal approach to pattern high-resolution perovskite arrays using an ultrathin reusable metal mask. A two-step sequential approach utilizing a designed metal mask is employed to achieve the controlled fabrication of micro and nanometer-resolution perovskite arrays. Through this generic and straightforward patterning process, we successfully fabricated perovskite arrays in red, green, and blue (RGB) colors, varying in shapes and sizes, with a minimum diameter of 500 nm perovskite pixel arrays. Moreover, the patterned perovskite arrays exhibit excellent photoelectric properties, including comparable light absorption and considerable lifetime. Furthermore, we investigated a transfer method to assemble multi-color perovskite arrays, enabling the creation of full-color images that significantly contribute to the progress of screen display technologies. Additionally, we presented photodiode stack arrays with a sandwich structure for each stack, demonstrating the capability of our approach in both solution and evaporation processes, which is unprecedentedly achieved. The patterned perovskite photodiode stack arrays exhibit outstanding electronic performance, showcasing lower open circuit voltage and comparable stability under diverse levels of illumination intensity. The fabricated ultrathin and high-resolution metal mask holds significant potential in the development of micro and nanoscale photoelectronic devices such as LEDs and solar cells. This method enables the patterning of perovskite micro-arrays on versatile substrates with reusable metal mesh templates and can be further applied to other materials to facilitate the development of micro-structured optoelectronic devices.

References

- [1] W. S. Yang, J. H. Noh, N. J. Jeon, Y. C. Kim, S. Ryu, J. Seo, S. I. Seok, *Science* **2015**, 348, 1234.
- [2] W. Wu, X. Wang, X. Han, Z. Yang, G. Gao, Y. Zhang, J. Hu, Y. Tan, A. Pan, C. Pan, *Advanced Materials* **2019**, 31, 1805913.
- [3] X. Han, W. Wu, H. Chen, D. Peng, L. Qiu, P. Yan, C. Pan, *Advanced Functional Materials* **2021**, 31, 2005230.
- [4] L. N. Quan, B. P. Rand, R. H. Friend, S. G. Mhaisalkar, T.-W. Lee, E. H. Sargent, *Chemical reviews* **2019**, 119, 7444.

5:00 PM EN06.08.13

Sustainable Electroceramics in a Circular Economy Jinxue Ding^{1,2}, Anke Weidenkaff^{1,2} and Wenjie Xie^{1,2}; ¹Technical University of Darmstadt, Germany; ²Fraunhofer Research Institution for Material Recycling and Resource Strategies IWKS, Germany

Defossilisation with renewable energy converters require tailored electroceramics and an infrastructure partially based on critical materials. The renaturation and transformation to a future green circular economy has to be based on a fundamental recovery of nature with circular materials and innovations. The development of recyclable materials for energy harvesting and conversion requires sustainable large-scale production from secondary raw materials. The decision making for future resilient energy systems has to be based on environmental aspects as well as on performance criteria defined by a holistic life cycle assessment.

Here efficient synthesis methods for materials with a programmable lifetime and regenerativity will be introduced as a suitable approach. The design of circular high performance materials uses theoretical predictions and the criticality analysis of applied elements to improve the cycle life of future solar and wind energy converters.

5:00 PM EN06.08.14

Remarkable Enhancement of Thermal and Dielectric Properties of Layered Double Hydroxides and Graphene Fillers Reinforced Poly(vinyl alcohol) Nanocomposite for Energy Applications Ritu^{1,2,3}, Shadi Houshyar¹, Lijing Wang¹, Manoj Kumar Gupta^{4,3} and Manoj Kumar Patel^{2,3}; ¹RMIT University, Australia; ²CSIR-Central Scientific Instruments Organisation, India; ³Academy of Scientific and Innovative Research, India; ⁴CSIR-Advanced Materials and Processes Research Institute, India

In this work, we have synthesized the zinc-aluminum layered double hydroxide (ZnAl LDH) nanostructures using cost-effective hydrothermal technique. The ZnAl LDH and graphene-based poly(vinyl alcohol) (PVA) nanocomposites are fabricated. The crystal structure, morphology, thermal, and dielectric properties of pristine PVA and ZnAl LDH and graphene-based PVA nanocomposites films were investigated using X-ray diffraction, HR-transmission electron microscopy, thermo gravimetric analysis, and impedance analyzer. HRTEM analysis reveals the hexagonal nanoplates shape-like morphology of Zn-Al layered double hydroxides with an average thickness of 40-50nm and size of 400-600nm. High thermal stability was observed from ZnAl LDH and graphene-reinforced nanocomposite. Enhanced thermal stability of 250°C and low weight loss was observed from ZnAl LDH reinforced PVA-based nanocomposites compared to pristine PVA. Zn-Al LDH nanoplates-graphene-PVA based nanocomposites showed ultra-high dielectric constant of 794 as compared to the ZnAl LDH-PVA nanocomposites (334) and pristine PVA sample (35). Low dielectric loss of 0.27, 0.18, 0.38 was observed for pristine PVA, ZnAl-LDH-PVA and ZnAl-LDH-graphene-PVA nanocomposites. The large enhancement of the dielectric constant and thermal stability were discussed in terms of improved crystallinity, interfacial polarization and formation of nanodipoles in the matrix. This study reveals a significant role of LDH-graphene-based hybrid nanocomposites in optoelectronics, energy storage, sensors, energy conversion and thermally stable devices.

5:00 PM EN06.08.15

Exploring Hydrogen Storage Efficiency in MgH₂ Using Charred Nanomaterials: A Computational Analysis Integrating DFT and Machine Learning Approaches Fernando Soto and Joshua Lilly; Penn State University Greater Allegheny, United States

Hydrogen, as a clean energy carrier, holds significant potential for reducing CO₂ emissions and diversifying the energy mix (1-3). However, the practical implementation of solid-state hydrogen storage, particularly in hybrid energy systems (HES), faces challenges related to kinetics, stability, and safety (4). This study performs a computational exploration of magnesium hydride (MgH₂) integrated with char nanomaterials, aiming to enhance the efficiency of hydrogen storage systems. We investigate the use of charred nanomaterials as a novel approach to address the fire risk and safety concerns associated with MgH₂, as well as to improve its hydrogen desorption kinetics. We hypothesize that charred nanomaterials can act as dual-function agents, catalyzing hydrogen release while also offering protection against combustion.

To test our hypothesis, we employ Density Functional Theory (DFT)-based simulations complemented with machine learning techniques. Our study

models include various configurations of MgH₂ clusters in contact with charred carbon fragments doped with heteroatoms like Oxygen, Nitrogen, and Iron, alongside O₂ molecule environments to simulate combustion processes. These models are analyzed to understand the stability and interaction dynamics under varying conditions. Our findings reveal that charred nanomaterials significantly influence the hydrogen desorption properties of MgH₂, indicating a promising pathway towards safer and more efficient hydrogen storage. The charred structures, particularly when doped with heteroatoms, not only catalyze hydrogen release but also mitigate risks associated with MgH₂'s reactivity, offering a holistic solution to the current limitations in hydrogen storage technology.

This computational study provides crucial insights into the design of advanced materials for hydrogen storage, offering a sustainable solution to energy storage challenges in HES. It opens up avenues for further experimental validation and development of MgH₂-based hydrogen storage systems, contributing to the advancement of clean energy technologies.

References

- L. Schlapbach, A. Züttel, Hydrogen-storage materials for mobile applications, *Nature*, 414 (2001) 353-358.
M. Carmo, D.L. Fritz, J. Mergel, D. Stolten, A comprehensive review on PEM water electrolysis, *International Journal of Hydrogen Energy*, 38 (2013) 4901-4934.
Y. Cheng, R. Zheng, Z. Liu, Z. Xie, Hydrogen-based industry: a prospective transition pathway toward a low-carbon future, *National Science Review*, 10 (2023).
G. Glenk, S. Reichelstein, Economics of converting renewable power to hydrogen, *Nature Energy*, 4 (2019) 216-222.

5:00 PM EN06.08.16

Building a Rechargeable Voltaic Battery via Reversible Oxide Anion Insertion in Copper Electrodes Jose F. Florez Gomez¹, Nischal Oli¹, Songyang Chang², Shen Qiu², Swati Katiyar², Ram Katiyar¹, Gerardo Morell¹ and Xianyong Wu²; ¹University of Puerto Rico at Rico-Rio, Puerto Rico; ²University of Puerto Rico at Río Piedras, Puerto Rico

The Voltaic battery (zinc-copper battery) is the very first battery built by humanity, which plays a critical role in battery development history. However, the inevitable copper ion dissolution-crossover issue leads to its primary battery nature. The ion-exchange membranes and alkaline electrolytes represent two leading approaches to mitigate this issue; however, they incur the disadvantages of complicated battery design, high cost, and zinc anode corrosion. Herein, we build a rechargeable zinc-copper Voltaic battery from simple and cost-effective electrode/electrolyte materials, where the cathode is a nano-sized copper, and the electrolyte is a near-neutral zinc sulfate solution. Interestingly, the copper electrode experiences a synergistic cation-anion insertion reaction, where copper transforms to zinc-copper alloy (Zn_xCu) during discharge and converts to copper (I) oxide (Cu₂O) during charge. Therefore, multivalent Zn²⁺ cations and multivalent O²⁻ anions participate in the redox reaction, giving a high capacity of ~370 mAh g⁻¹. Moreover, the structural similarity between Zn_xCu, Cu, and Cu₂O endows high reaction reversibility, leading to impressive cycling of ~500 cycles. Such a concerted cation-anion insertion is rarely reported in the battery field, which offers a mechanism-based approach for developing high-capacity and long-cycling multivalent-ion batteries.

SESSION EN06.09/EN03.09: Joint Session: Decarbonization
Session Chairs: David Cahen, Jihye Kim, Clara Santato and Anke Weidenkaff
Thursday Morning, April 25, 2024
Room 333, Level 3, Summit

8:15 AM EN06.09/EN03.09.01

Fit-To-Purpose Batteries. An Ecodesign-Based Approach to Power Portable Applications Marina Navarro-Segarra¹, Carles Tortosa^{2,1}, Neus Sabate^{3,2} and Juan Pablo Esquivel^{1,4,2}; ¹BCMaterials, Spain; ²Fuelium, Spain; ³Instituto de Microelectrónica de Barcelona, IMB-CNM (CSIC), Spain; ⁴Ikerbasque, Spain

Batteries have become an essential power source, due to their capability to deliver high energy densities in a portable manner. However, a close look into conventional portable battery life cycles reveals, that they still follow an obsolete linear model. They are manufactured at specific locations causing scarce material exhaustion, transported thousands of kilometres for its use and then disposed of, sometimes before even its complete depletion. Then, during portable batteries' end-of-life, only a small percentage are recycled, typically using energy intense processes, whereas the rest ends up incinerated or in landfills, generating greenhouse gas emissions and poisoning terrestrial and marine ecosystems. Furthermore, it is forecasted that the upcoming wave of power-hungry Internet-of-Things (IoT) sensing nodes will increase exponentially the portable battery demand in the near future. Thus, aggravating the environmental impact associated with electronic devices production and the generation of waste electrical and electronic equipment (WEEE). For portable batteries to stop contributing to environmental damage, and become an example for sustainable technological development, it is crucial to change the way the batteries value chain is approached.

This work presents a rationale for ecodesign portable batteries by re-thinking their life-cycle under an environmentally conscious framework. Through careful device design and advocating for a 'fit-to-purpose' approach, the development of these batteries is paired with the application value chain, in such a manner that even the power source end-of-life is redefined according to the use-case scenario. In order to ground these ideas, several examples of these ecodesigned portable power sources will be presented.

First, a paper-based battery in a lateral flow assay format intended to power portable diagnostic devices. These liquid activated batteries can be fabricated under the same procedures used in the rapid test industry and have shown the ability to power the most relevant features needed in portable medical devices, such as sensors, displays, wireless communications or heating.

Secondly, a bio-based battery using laser induced graphene current collectors in a cardboard tape format for smart packaging. These batteries have the capability to power typical applications envisioned by the sector, such as digital displays and wireless trackers. As validated by normalized evaluation methods, these batteries are compliant with current paper and cardboard recycling processes.

Finally, different approaches of biodegradable batteries for precision agriculture will be presented. These batteries made with organic materials can power sensing devices that measure parameters in soil and the environment and then send the data by Bluetooth communication. The capability to undergo biodegradation has been assessed experimentally using normalized tests as a way to minimize energy consumption at the end-of-life.

Developed under this rationale, environmental sustainability has been placed as a core priority to guide the batteries' conception and materialization, from materials to end-of-life. Hence all materials used as electrodes, electrolytes, or structural components are abundant, non-toxic and renewable; selected to meet the specific end-of-life requirements and endow a safe and ethical manufacturability.

8:30 AM EN06.09/EN03.09.02

A Coplanar Edible Rechargeable Battery with Increased Capacity and Durability Valerio Galli^{1,2}, Valerio F Annese¹, Giulia Coco^{1,2} and Mario Caironi¹; ¹Istituto Italiano di Tecnologia, Italy; ²Politecnico di Milano, Italy

Edible electronics is an emerging research field focused on developing safe-to-ingest devices entirely made of food and food additives. Being intrinsically non-toxic and biodegradable, this technology can find applications in many scenarios, from healthcare to agrifood. Starting from common food additives like activated carbon, edible gold, ethyl cellulose, and beeswax, we developed the first edible rechargeable battery entirely made of food materials. The chemistry is based on two small redox-active molecules found in food, riboflavin, and quercetin, used as the anode and the cathode, respectively.^[1] Here we present a coplanar edible battery, characterized by an electrode configuration that eases compatibility and integration with electronic components. The battery provides an open-circuit voltage of ~0.65 V with a specific capacity of 20 $\mu\text{Ah cm}^{-2}$, a two-fold increment with respect to our first prototype, thanks to increased electrode mass loading. The beeswax encapsulation yields excellent operational stability, characterized over a two-week period and in different environmental conditions. As proof of the compatibility with traditional electronic devices, the battery was successfully used to power up resistive sensors, including thermistors and photoresistors. Multiple batteries were also employed to supply power to an Internet of Things module which can acquire humidity and temperature information and transmit data in real-time via Bluetooth. The high degree of versatility of our technology goes beyond the proposed proof-of-concept: we envision edible batteries as a promising alternative to traditional ones in low-power applications, such as agrifood sensor networks and food monitoring.

[1] Ilic, I. K., Galli, V., Lamanna, L., Cataldi, P., Pasquale, L., Annese, V. F., Athanassiou, A., & Caironi, M. (2023). An edible rechargeable battery. *Advanced Materials*, 35(20), 2211400.

8:45 AM *EN06.09/EN03.09.03

Advanced Characterization and Modeling to Understand Hydrogen Production by Solid Oxide Electrochemical Cells David S. Ginley¹, Michael J. Dzara¹, Brandon Wood², Harry W. Abernathy³, Olga A. Marina⁴, Brian Gorman⁵, Heather Slomski⁵, Mike Tucker⁶, Micah Casteel⁷, Nicholas Strange⁸ and Sarah Shulda¹; ¹National Renewable Energy Laboratory, United States; ²LLNL, United States; ³NETL, United States; ⁴Pacific Northwest National Laboratory, United States; ⁵Colorado School of Mines, United States; ⁶Lawrence Berkeley National Laboratory, United States; ⁷Idaho National Laboratory, United States; ⁸SLAC National Accelerator Laboratory, United States

Functional oxides are becoming more important in a wide variety of renewable applications, ranging from high temperature electronics, electric vehicles, and solid oxide electrolysis/fuel cells (SOEC/SOFC). They must meet a diversity of characteristics to achieve desired functionality in these harsh environments. Hydrogen is considered an enabler for the transition to sustainable and renewable society. Production of green hydrogen is a strong focus of modern research given the current global market of 170 billion dollars. Among the approaches for hydrogen generation are the use of SOECs. These utilize a stack of high temperature oxides operating in H_2 /steam. While direct electrochemical measurements are key for quantifying progress towards the DOE Hydrogen Earthshot Goal of 1\$/kg in the next decade they are insufficient to provide detailed materials science investigation of degradation pathways. We report on the development of a suite of synchrotron and conventionally based analysis tools to provide a set of detailed morphology, phase, and composition data which both provide detailed information about degradation mechanisms and provide foundational information for predictive models leading to ultimate materials improvement.

The solid oxide layers that comprise SOECs typically feature a layered structure composed of a Ni-YSZ fuel electrode/YSZ electrolyte/Gadolinium doped Ceria barrier layer and a Lanthanum Strontium Cobalt Iron Oxide oxygen electrode. The phase behavior especially at interfaces is complex starting from the deposition of materials to behavior during extensive aging. Recent analysis has confirmed a number of potential degradation mechanisms are operable including Sr, Ni, and Ag migration, interfacial phase formation and grain coarsening. We will discuss how a combination of synchrotron X-ray diffraction (XRD), nanoscale X-ray computed tomography (nano-XCT), and other X-ray spectroscopy techniques combined with electron microscopy can provide coupled insights on the nature of these mechanisms which can be incorporated into computational models which can provide predictive insights on cell/stack longevity. We also discuss how button cells can inform large area and stack behavior.

We will discuss our recent development of an in-operando system intended for the synchrotron techniques, especially XRD, to probe cell performance in real time.

Advanced characterization can couple to cell development and electrochemical testing towards achieving DOE Hydrogen Earthshot Goals.

This work is authored by the National Renewable Energy Laboratory (NREL), operated by Alliance for Sustainable Energy, LLC, for the U.S. Department of Energy (DOE) under Contract No. DE-AC36-08GO28308. David Ginley, Sarah Shulda, Robert Bell, Nick Strange, Heather Slomski and Michael Dzara are funded primarily by the EERE Hydrogen and Fuel Cell Technology Office; The views expressed in the article do not necessarily represent those of the DOE or the U.S. Government.

9:15 AM EN06.09/EN03.09.04

Artificial Chlorophyll-Inspired: Photonic Crystals-Based Photocatalyst for Carbon Dioxide Conversion as Gaseous Fuel Fang-Yu Liang¹, Po-Jung Huang² and Yen-Ping Peng¹; ¹National Sun Yat-Sen University, Taiwan; ²National Central University, Taiwan

The PCN-222(M)/IOT heterostructure is constructed (created) by combining the narrow bandgap metalloporphyrin metal-organic framework (PCN-222) with the wide bandgap inverse opal TiO_2 (IOT). PCN-222 grows in situ on the surface of the inverse opal under hydrothermal conditions, forming a tightly connected interface that enables the rapid separation and transfer of electrons and holes.

Inspired by natural photosynthesis, this research contributes to the development of artificial CO_2 photoreduction catalysts. The construction of Z-scheme heterojunctions is an effective strategy for enhancing the photocatalytic activity of semiconductor materials by isolating photogenerated electron-hole pairs. In this study, the morphologies, structures, and photoelectric characteristics of materials acquired through the synthesis of P(M:metal)/IOT heterostructures were characterized. These heterostructures were evaluated for their photocatalytic CO_2 reduction capabilities, revealing their superior performance compared to IOT and PCN-222. Under visible light illumination, the P(Fe)/IOT heterostructure achieved impressive yields of CH_4 and C_2H_4 . The enhanced photoactivity is attributed to the efficient spatial separation of photogenerated electrons and holes via a Z-scheme charge transfer mechanism. This research provides valuable insights into the design and fabrication of novel Z-scheme photocatalytic systems for environmental remediation and energy conversion. The P(M)/IOT heterostructure combines a narrow band gap metalloporphyrin metal-organic framework (PCN-222) with a wide gap inverse opal TiO_2 (IOT) via in-situ growth under hydrothermal conditions. This results in a tightly connected interface that facilitates rapid electron-hole separation and transfer. The high photocatalytic activity of P(M)/IOT is attributed to its strong visible light absorption and efficient charge separation within the heterointerface, also providing bionic chloroplast microenvironmental strategies for effective photocatalytic carbon dioxide reduction.

9:30 AM EN06.09/EN03.09.06

Highly Efficient Carbon Mineralization Using Amine-Functionalized Magnetic Nanoparticle Clusters Hyunsoo Han and Sangmin Jeon; POSTECH, Korea (the Republic of)

Carbon mineralization, which transforms carbon dioxide (CO₂) into a stable form such as calcium carbonate or magnesium carbonate, has emerged as a promising technology for long-term CO₂ storage. In this study, we developed amine-functionalized magnetic nanoparticle clusters (A-MNPs), that enhance both CO₂ capture and its subsequent mineralization, by hydrothermal method and immobilization of (3-Aminopropyl)triethoxysilane (APTES). The surface of A-MNPs was covered by the APTES monolayer with approximately 100% coverage. A-MNPs expanded the surface area of CO₂ bubbles and led to amine-CO₂ coupling, improving CO₂ uptake. Subsequently, the injection of calcium chloride into the CO₂-saturated A-MNP solution resulted in carbon mineralization (i.e. CaCO₃ formation) with improved efficiency. Additionally, the shapes of CaCO₃ could be adjusted by adding anionic surfactants to the solution. Since A-MNPs can be controlled by magnetic force, they can be recovered using a magnet and reused more than 10 times without a loss in their catalytic activity, offering an efficient and sustainable method for CO₂ storage.

9:45 AM EN06.09/EN03.09.07

N-Doped Carbon Dots Embedded in Electrospun Cellulose-Derived Nanofibers: A Novel Approach to Pseudosupercapacitors with Enhanced Faradic Activity Jesus Vazquez-Chavez, Michael W. Thielke, Carlos Mingoés and Ana Jorge Sobrido; Queen Mary University of London, United Kingdom

The sustainable energy storage landscape is rapidly evolving, with innovations driven by the necessity to meet increasing global energy demands. In this context, pseudosupercapacitors emerge as a new solution, closing the gap between batteries and supercapacitors, by achieving the high energy density of batteries with the rapid charge-discharge cycles of supercapacitors. The key to harnessing the potential of pseudosupercapacitors lies in the development of electrodes that demonstrate superior faradic activities and high-capacity retention.

Our research presents a pioneering effort in this direction, focusing on the synthesis of pseudosupercapacitor electrodes from electrospun cellulose acetate nanofibres embedded with N-doped carbon dots. Electrospinning is a widely used technique known for its adaptability in fabricating carbon fibres. With its intrinsic capability to produce fibres boasting a high surface-to-volume ratio, electrospinning not only permitted the integration of the N-doped carbon dots in the fibres, but also allowed fine control over the fibre diameter and nitrogen concentration. By manipulating electrospinning parameters, we achieved fibres ranging from 220 nm to 850 nm, presenting a trade-off between surface area and mass transport efficiencies. Cellulose acetate was chosen as carbon source and as an alternative to usually employed polyacrylonitrile (PAN), to increase the sustainability of our approach.

The carbon dots, synthesized through a microwave-assisted method using citric acid and urea, showcased a high faradic activity (here include values for faradic capacity and capacity retention after xx cycles) even after the deacetylation and carbonization as they were incorporated into the cellulose acetate matrix. Their N-doped nature contributes to enhanced electronic properties. Pyridinic N and pyrrolic N have been shown to be responsible for active redox sites for faradic activity whereas graphitic N is thought to contribute to the enhancement of conductivity of the resultant electrodes.

In conclusion, we present a multidimensional approach to a novel pseudosupercapacitor electrode fabrication. By integrating microwave-assisted synthesized n-doped carbon dots within electrospun cellulose acetate nanofibres, we not only address the technical challenges of achieving high specific capacitance, but also present an environmentally conscious blueprint. With promising preliminary results in electrochemical and analytical characterization, our research aims to expand the current design of pseudosupercapacitor and their implications for sustainable energy storage.

10:00 AM BREAK

SESSION EN06.10/EN03.10: Joint Session: Resource Recovery
Session Chairs: David Cahen, Jihye Kim, Clara Santato and Anke Weidenkaff
Thursday Morning, April 25, 2024
Room 333, Level 3, Summit

10:30 AM *EN06.10/EN03.10.01

Recovery of Lithium and Heavy Non-Ferrous Metals from Spent Lithium-Ion Batteries Valery Kaplan, Ellen Wachtel and Igor Lubomirsky; Weizmann Institute of Science, Israel

When compared with nickel-cadmium or nickel-hydride batteries, lithium-ion batteries (LIBs) provide significant advantages as a power source for electric vehicles and for small mobile devices. However, LIBs contain a variety of toxic and ecologically harmful substances, such as heavy metals, organic and inorganic compounds, thereby creating a challenge for clean end-of-life (EoL) disposal. But why throw away EoL LIBs when the grade of cobalt and lithium in the complex lithium/cobalt oxide cathodes is higher than that in pristine lithium and cobalt ores? Recycling these valuable metals efficiently and with minimal environmental impact has therefore become an effort of significant economic, health and ecological importance, as well as of reducing tense international relations. To this end, we have worked to develop a (laboratory-scale) procedure for recycling EoL laptop LIBs containing LiCoO₂, LiNiCoO₂, and/or lithium-nickel-cobalt-aluminum oxide without the necessity of using acid/bases or costly reagents and without generating hazardous liquid waste. Following removal of the non-metallic container, the battery elements undergo crushing/milling; no other component separation procedure is performed or required. One hour dilute natural gas (4 vol.% in N₂) sintering under reducing conditions (673– 1123 K), followed by ice-water leaching, is used to efficiently separate Li from the heavy metals in the form of lithium carbonate at high yield and purity; 0.5 h smelting (1773 K) of the remaining metal clinker in air with sodium tetraborate as flux, allows recovery of the heavy, non-ferrous metals (Ni, Co, Cu and their alloys) as mm-size ingots (39% Co, 32.2% Ni, 26.3% Cu). Iron compounds, remanent Li, Al and unburnt graphite are removed as slag. Neither corrosive acids nor costly reagents are required, and hazardous liquid waste is not generated.

11:00 AM EN06.10/EN03.10.02

Separating Materials for Recycling Processes Mmantsae M. Diale; University of Pretoria, South Africa

Recycling is a circular economy system that allows participants to add value to cleaning the environment. Materials have been the major role player in improving old engineering systems and producing newest technologies to reduce the carbon footprint. There is a great effort in plastic recycling where profits are made, and poverty reduced to address the UN sustainable goals for 2030. Phosphors and other identifiers have been used to identify different plastics during separation. Similarly, paper and bottles can have additives and nanostructures that will make it easy to separate such materials during recycling. We report on the work done to identify glass, paper and plastic in recycling and make it a smooth process to produce new products. In addition, we have also embarked on educating the garbage pickers to enhance profits by proper separation.

11:15 AM EN06.10/EN03.10.03

Electrochemical Separation Technologies for Resource Recovery and Recycling Seoni Kim¹ and Jin Soo Kang²; ¹Ewha Womans University, Korea (the Republic of); ²Seoul National University, Korea (the Republic of)

Global efforts toward carbon neutrality have impacted the industry and the market in various directions, and this is causing rapid changes in the production, use, and supply chain of various resources. For instance, explosive growth of the electric vehicle (EV) market induced significant increments of demands for lithium and other relevant elements. Meanwhile, it should be noted that the production of such resources from ores often result in a large amount of CO₂ emission and environmental pollutions, which endangers the sustainability of our world. Therefore, there is a wide agreement on the importance of developing clean technologies for recovering and recycling resources from various sources, which even include wastes. Herein, our recent research works on electrochemical separation technologies for efficient resource recovery and recycling will be presented. Electrode materials that have favorable crystal structures for highly selective extraction of specific elements are introduced, together with discussions on their behaviors during the operation. Based on these understandings, rationally designed resource-recovery electrodes are developed, and their performance and reliability are evaluated and demonstrated.

11:30 AM EN06.10/EN03.10.04

Selective and Sequential Precipitation for Critical Mineral Extraction from Electronic Waste Qingpu Wang¹, Elias Nakouzi¹ and Chinmayee Subban^{1,2}; ¹Pacific Northwest National Laboratory, United States; ²University of Washington, United States

The recycling of critical materials from electronic waste (e-waste) shows a great potential for urban mining. However, convective separation methods are often chemical- and energy-intensive as they mainly rely on organic ligands, ionic liquids, and ion-selective membranes and/or electrodes. The sustainable production of valuable critical elements from e-waste requires a paradigm shift away from currently used resource-intensive processes. We present a novel approach based on the coupling of ion diffusion and precipitation kinetics. Simply by placing a mixed salt solution on top of a hydrogel loaded with a precipitating agent, we obtained spatially separated precipitates along the reactor. Our proof-of-concept has been demonstrated for sequentially precipitating transition metals with modeled feedstocks representative of lithium-ion battery cathodes and rare earth elements from NdFeB permanent magnets. We expect this approach to be broadly relevant to chemical separations from complex feed streams and diverse chemistries—enabling more sustainable materials extraction and processing.

11:45 AM EN06.10/EN03.10.05

Economically Sustainable Recycling of MAPbI₃ Perovskite Solar Cells Zhenni Wu^{1,2}, Misha Sytnyk¹, Jiyun Zhang^{1,2}, Gülüsüm Babayeva², Simon Arnold², Jens Hauch^{1,2}, Christoph J. Brabec^{1,2} and Ian Marius Peters^{1,2}; ¹Forschungszentrum Jülich, Helmholtz Institute Erlangen-Nürnberg for Renewable Energies (HI ERN), Germany; ²Friedrich-Alexander-Universität Erlangen-Nürnberg, Germany

Recycling becomes ever relevant with exponentially expanding photovoltaic deployment. Yet, the recycling of commercial silicon photovoltaic modules often falls behind in preserving the quality of materials due to inadequate separation of mixed components. Conversely, the solution processing feature of nascent but propitious perovskite solar cells facilitates simplified component separation. Herein, we report a recycling approach for a planar MAPbI₃ perovskite solar cell, resulting in recycled materials that can be integrated into new cells without compromising their quality. Prior to integration into cell construction, all the collected materials underwent corresponding purification or modification treatments. The hole transport material, Spiro-OMeTAD, was purified with column chromatography. The absorber material, MAPbI₃, was crystallized using anti-solvents. And the recovered old ITO/SnO₂ was coated with fresh SnO₂ for quality rejuvenation. The resulting recycled materials, whether used individually or combined, all lead to cell efficiencies comparable to those of cells constructed with entirely virgin materials. Based on a techno-economic analysis, the developed recycling approach has demonstrated economic viability at both laboratory and industrial scales.

SESSION EN06.11/EN03.11: Joint Session: Energy Systems II
Session Chairs: David Cahen, Jihye Kim, Clara Santato and Anke Weidenkaff
Thursday Afternoon, April 25, 2024
Room 333, Level 3, Summit

1:45 PM *EN06.11/EN03.11.01

Sustainable Off-Grid Hybrid Energy Systems: The Case of The Astronomical Telescope AtLAST Sabrina Sartori; University of Oslo, Norway

Production and use of hydrogen as a green and renewable fuel are increasingly considered as a central component in the transition to a green economy. Green hydrogen, i.e. hydrogen produced by water electrolysis with electricity from renewable energy sources, could abate CO₂ emissions and replace fossil fuel usage within transport, heating, stationary applications and various industrial processes. In this talk we will present our latest work on off-grid low carbon renewable energy-based systems (RES) setups for the newly planned Atacama Large Aperture Submillimeter Telescope (AtLAST) and compare them to business-as-usual diesel power generated systems. We consider systems built near the telescope on the Chajnantor plateau at ~5000 m and systems at a Valley Site, 2500 m above sea level, near the town of San Pedro de Atacama (also off-grid).

Technologies included in the designed systems are photovoltaics, batteries, and hydrogen technology, sizing them according to the telescope's projected energy demand and reliability requirements, cost assumptions for the year 2030 and site-specific characteristics (including a particular interest on the effect of high altitudes on hydrogen-based components). We assess whether 100% RES scenarios are favorable from an environmental point of view in the categories climate change, mineral resource depletion and water use. The system boundary includes the production of components, their transport to the energy system site, and the operation and maintenance of the system.

We find that 100% RES scenarios have a lower CO₂e impact than high-renewable scenarios, however, the latter lower the mineral resource depletion and water use by about 27% compared to 100% RES scenarios. Applying hybrid energy storage systems increases the water use impact, while reducing the mineral resource depletion.

An additional aspect of interest in our study is the proposition of a socially accepted renewable energy system where we combine an energy system model with a participatory multi-criteria analysis.

Results reveal that a renewable energy system supplying the telescope could also cover 66% of the nearby community's energy needs of San Pedro de Atacama, without additional capacity. Stakeholders inputs show this as the most attractive solution by developing an energy system where all of them benefit. Replicating similar energy systems at nearby telescopes could reduce fossil fuel-based energy generation by 30GWh annually, cutting emissions by 18-24ktCO₂eq while contributing to acceptability of new infrastructures and energy justice.

Acknowledgments

This work received fundings from the European Union's Horizon 2020 research and innovation programme under grant agreement No. 951815 (AtLAST project). Acknowledgments to the team of WP5 (Environmental Sustainability) at UiO, Isabelle Viole, Guillermo Valenzuela-Venegas, Marianne Zeyringer. Special thanks to our astronomy colleagues for the cooperation in the interdisciplinary project AtLAST.

2:15 PM EN06.11/EN03.11.02

Analysis of Inception Sites of Vented Water Trees in a Laboratory Aged High Voltage XLPE Subsea Cable Sofie B. Hårberg¹, Cedric Lesaint², Sigurd Wenner³, Inger-Emma Nylund¹, Per Erik Vullum³, Sverre Hvidsten² and Mari-Ann Einarsrud¹; ¹NTNU, Norway; ²SINTEF Energy, Norway; ³SINTEF Industry, Norway

The use of lead sheaths in future subsea high voltage power cable designs will not be possible, or subject to a strict authorization processes because lead is a candidate for future inclusion by the European Chemicals Agency in the REACH Annex. "Wet design" subsea cables with no metallic barrier have been developed and are available for voltages up to 66 kV. Using the wet design also for higher voltages is very attractive to avoid the use of lead or metallic sheaths. However, in such cables, water molecules can permeate into the polymeric cable insulation system during service. As subsea high voltage cable cores have up to now been in dry service conditions, the knowledge on their performance when subjected to water is not known.

In this work, XLPE cable cores have been subjected to wet ageing following the recommendations in CIGRE TB 722. The electrical ageing was performed at 500 Hz with an equivalent electrical stress at the conductor screen of 10 kV/mm. The cable was helically spirialized into 2 mm thick samples. The vented water trees which appeared from the semi-conductive screens were made visible using a water pre-treatment supersaturating the tree channels. The water trees were located, and the inception sites were cryo-microtomed. The sites were assessed using Energy Dispersive X-Ray analysis (EDX) and Electron Energy Loss Spectroscopy (EELS) to determine the chemical composition of the section analyzed by Scanning Transmission Electron Microscopy (STEM). More than 5 vented water tree inception sites from the same cable were analyzed. The overall composition of inorganic elements was analyzed using Inductively Coupled Plasma Mass Spectrometry (ICPMS).

The cable insulation and semi-conductor sections that were analyzed by ICPMS revealed the presence of ionic species such as Na⁺ or K⁺. More localized investigation at the inception sites of the water trees was conducted by EDX and EELS analysis with respect to inorganic elements, and the results were compared to those obtained by ICPMS.

2:30 PM EN06.11/EN03.11.03

Innovative Energy Harvesting from Salinity Gradients: Asymmetric Flow-Electrode Capacitive Mixing with MnO₂-Coated Activated Carbon Insung Hwang¹, Seungcheol Myeong¹, Seunggun Choi¹, Hyungjun Lee^{1,2}, Minsung Kim¹, Han Seung Min^{1,2}, Hongjun Park¹, Bobae Lee¹, Ungyu Paik¹ and Taeseup Song^{1,1}; ¹Hanyang University, Korea (the Republic of); ²Korea Institute of Ceramic Engineering and Technology, Korea (the Republic of)

Salinity gradient power represents a promising source of renewable energy, and flow-electrode capacitive mixing (F-CapMix) offers an innovative approach to harnessing this energy potential. However, conventional F-CapMix systems encounter limitations in power density due to the restricted charge storage capacity inherent in porous carbon materials, which operate via the electrical double-layer mechanism. In this study, we introduce manganese dioxide-coated activated carbon (MO@AC) as a novel flow-electrode material for F-CapMix applications, placing specific emphasis on the introduction of an asymmetric flow-electrode system. We conduct a comprehensive assessment of the electrochemical properties of both activated carbon (AC) and MO@AC-based flow-electrodes, with particular attention to their suitability as positive and negative electrodes for symmetric and asymmetric F-CapMix configurations. Notably, it becomes evident that remarkable performance enhancements are exclusively observed in the context of the asymmetric F-CapMix system, thus underscoring the heightened efficacy of the MO@AC material within this asymmetric framework. Remarkably, employing MO@AC as the flow-electrode in the asymmetric F-CapMix configuration yields an impressive power density of 2.22 W/m² through reversible redox reactions involving Na⁺ ions. These findings not only expand the horizons of potential applications but also underscore the transferability of our strategies to various materials engaged in redox reactions with Na⁺ and Cl⁻ ions within the realm of F-CapMix systems.

2:45 PM EN06.11/EN03.11.05

Stretchable Plant-Based Redox-Diffusion Battery Aiman Rahmanudin^{1,2} and Klas Tybrandt^{1,2}; ¹Linköping University, Sweden; ²Wallenberg Wood Science Centre, Sweden

Stretchable batteries are essential for the realisation of autonomous and conformable wearable electronics that interface intimately with the human body. In existing battery designs, the predominant use of unsustainable transition metal-based active materials and non-biodegradable petroleum-based elastomers contribute to the environmental problem of e-waste and the mining of finite resources. Moreover, increasing the active material content often leads to stiffer electrodes with poor mechanical properties. Here, we developed a stretchable battery design – the redox-diffusion (RD) battery - based on soluble plant-based redox-active biomolecules infiltrated within a cellulose-based 3D porous electrode scaffold. The redox reaction is mediated by diffusion of dissolved biomolecules within the pores of the 3D scaffold. It decouples the active material loading from the mechanical structure of the electrodes to afford high mass loadings (> 40 mg cm⁻²) of the redox-active biomolecules. The electrode achieved a high capacity of 28.6 mAh/cm³ with a skin-like Young's modulus of 110 kPa and stretchability up to 200 % strain. The RD design is facilitated by the development of a stretchable ion-selective membrane separator to allow the utilisation of two separate redox couples while preventing crossovers. This enabled a full cell with stable electrochemical performance under stretching. The utilisation of plant-based materials for the battery components (electrode, separator, current collector, and encapsulation) enabled the full degradation of the cell into benign products. The work emphasises on the importance to encompass not only high battery performance but considers the human and environmental impact of the materials used and disposal of the cell at the end-of-life.

3:00 PM BREAK

SESSION EN06.12/EN03.12: Joint Session: Sustainable Materials III
Session Chairs: David Cahen, Jihye Kim, Clara Santato and Anke Weidenkaff
Thursday Afternoon, April 25, 2024
Room 333, Level 3, Summit

3:30 PM *EN06.12/EN03.12.01

Unlocking the Catalytic Potential of LiCoO₂: Innovative Exfoliation Strategies and Applications [Alp Sehirlioglu](#)¹, Kevin Pachuta¹, Benjamin Hirt¹, Huaixuan Cao², Micah Green² and Emily Pentzer²; ¹Case Western Reserve University, United States; ²Texas A&M University, United States

LiCoO₂ (LCO) stands as a prototypical cathode material within the realm of Li-ion batteries, bearing the critical elements of lithium (Li) and cobalt (Co), which are concurrently acknowledged for their potential toxicity. The foremost frontier for repurposing LCO lies in the catalytic realm, precisely aimed at decomposing environmental contaminants. Past endeavors in employing LCO for photocatalysis, electrocatalysis, and thermocatalysis have borne fruits of considerable promise. LCO not only contains a transition metal oxide but also boasts a layered structure, facilitating the processes of delithiation and intercalation. These techniques are conventionally wielded in the chemical exfoliation of layered oxide materials.

The typical process of chemical exfoliation in crafting nano-sheets from layered oxide materials comprises two primary steps: protonation and intercalation, involving the integration of bulky molecules with counter ions. While the ultimate outcome manifests in the form of nanosheets, the exfoliation process provides an array of intermediate forms and byproducts, all with promising structural and functional attributes, particularly in the context of catalytic performance.

In this presentation, we utilize three distinctive forms of LCO powder: (i) post-protonation via acid treatment, (ii) post-base treatment – marking the powders as ready for exfoliation, and (iii) nanosheets integrated into armored particles via Pickering emulsions. Our case of applications spans diverse domains, including methylene blue degradation, carbon monoxide oxidation, ammonium perchlorate decomposition, and bisphenol A (BPA) removal from water. Realizing the full potential of these applications necessitates a profound comprehension of the chemical, structural, and morphological forms that emerge during these processes.

Our exploration will be enriched by novel processing methods that expand beyond the conventional two-step procedure, rendering it possible to fabricate these products in a pH-neutral aqueous medium as opposed to the highly alkaline nanosheet solution with a pH exceeding 13, typical of traditional techniques. Furthermore, we will delve into supplementary methodologies designed to stabilize the nanosheets in various non-aqueous solvents and enhance nanosheet production yields. The precise yield is intricately governed by an interplay of parameters, encompassing acid concentration, base concentration, and base type, akin to a 'Goldilocks effect.' These processing conditions also exert a profound influence on the efficacy of the resulting powders and nanosheets as catalytic materials, with exceptionally narrow processing windows dictating extraordinary performance metrics.

The intricate interplay of parameters is also critical to the stability and uniformity of Pickering emulsions, with key variables encompassing the type and concentration of salts, the nature of the oil medium, and the specific nanosheet type employed, encompassing exfoliated LCO and graphene oxide (GO). The catalytic performance for all the examples provided is underpinned by the inherent attributes of Co as the transition metal, the presence of H⁺ within the structure, A-site vacancies, oxygen vacancies, and the stratified architecture itself.

4:00 PM EN06.12/EN03.12.02

Nanostructured Sustainable Materials for Solar Energy Conversion: Fe-Based Absorbers and Catalysts [Roland Marschall](#); University of Bayreuth, Germany

Efficient conversion and storage of solar energy are crucial steps in the establishment of a renewable and carbon neutral energy supply. Photocatalysis and photoelectrochemistry are considered promising to make use of the large amounts of sunlight that reach the surface of earth. They render the direct conversion of light into chemical energy possible, e.g. solar fuels like hydrogen or ammonia. In recent years, earth-abundant Fe-based materials like spinel ferrites have emerged as auspicious materials for these applications. They have the inherent ability to absorb a large part of the visible light spectrum with band gaps around 2 eV, while some of them being also very good electrocatalysts. My group utilizes modern synthesis techniques to prepare nanostructured Fe-based materials for the generation of solar fuels.

In recent years, we have developed fast microwave-assisted sol-gel syntheses yielding phase-pure spinel ferrite nanoparticles of e.g. MgFe₂O₄, CuFe₂O₄, NiFe₂O₄, MnFe₂O₄ and ZnFe₂O₄ at temperatures as low as 170-200 °C.[1,2] The crystallite size can be tailored in-situ or by post-synthetic heat treatment, however the materials are already (partly) crystalline as-prepared, with specific surface areas of around 200 m²/g and good colloidal stability. Some syntheses even take only several minutes. Photocatalytic and electrocatalytic experiments will be presented, as well as the conversion of some spinel oxides into (oxy)sulfides and perovskites for electrocatalytic water splitting.[3,4] Moreover, a direct microwave-assisted synthesis for nickel-iron sulphide nanosheets for electrocatalytic CO₂ reduction and photocatalytic HER will also be presented.[5,6]

Finally, the potential of using a heterojunction of iron sulphide and carbon nitride for light-induced reduction of N₂ to ammonia will be introduced.[7]

Literature:

[1] A. Bloesser et al., ACS Appl. Nano Mater. 2020, 3, 11587. [2] C. Simon et al., Chem. Eur. J. 2021, 27, 16990. [3] D. Tetzlaff et al., Faraday Discussions 2019, 215, 216. [4] D. Tetzlaff et al., Energies 2022, 15, 543. [5] C. Simon et al, ACS Appl. Energy Mater. 2021, 4, 8702. [6] J. Zander et al., J. Mater Chem. A 2023, 11, 17066 [7] J. Zander et al., Adv. Energy Mater. 2022, 12, 2202403.

4:15 PM EN06.12/EN03.12.03

Mesoporous Zn-Doped MnCo₂O₄ Nanoparticles for Asymmetric Supercapacitor Application [Prem Sagar Shukla](#)¹, Anant Agrawal², Anurag Gaur³ and Ghanshyam D. Varma¹; ¹Indian Institute of Technology Roorkee, India; ²National Institute of Technology Kurukshetra, India; ³Netaji Subhas University of Technology, India

Energy sources that are reliable as well as sustainable have become essential in the present technological world. Our dependency on fossil fuels has its limitations, is not sustainable, and has a number of consequences, including greenhouse gas emissions, water pollution, and hazardous waste. Researchers have focused on supercapacitors as next-generation energy storage devices due to their quick charge/discharge rate and outstanding cycle stability. Because of their excellent power delivery and quick charging characteristics, supercapacitors have significant advantages for high-power applications. This study aims to determine how Zn doping at the cobalt site of MnCo₂O₄ affects its electrochemical properties. In this approach, we have synthesized Zn-doped MnCo₂O₄ nanomaterial abbreviated as ZMCO for supercapacitor electrodes. The XRD and HRTEM results confirm the presence of cubic phase of ZMCO. Surface area and morphology were also studied through BET and FESEM measurements, respectively. Among all the samples, MnZn_{0.4}Co_{1.6}O₄ shows better electrochemical performance due to its larger specific surface area and mesoporous distribution of pore size. Moreover, the single electrode showed excellent cycling stability along with good coulombic efficiency. To evaluate the practical utility of the synthesized nanomaterial, an asymmetric supercapacitor (ASC) device was fabricated. The device was fabricated with the ZMCO nanomaterial as a cathode and activated carbon as an anode electrode. The device exhibited a higher power density and specific energy density. The device also shows excellent cycling stability in PVA/KOH gel electrolyte. Additionally, a single device illuminates a red LED, while connecting two devices in series illuminate red and green LED. We believe Zn doped MnCo₂O₄ provides a lot of potential for making higher-performance supercapacitor devices because of its simple synthesis process and superior electrochemical characteristics.

4:30 PM EN06.12/EN03.12.04

Forming Nanoscale Sculptured Surfaces for Advanced Electrical Bonds by Environmentally Friendly Electrochemical Etching [Jannik Rank](#), Jörg Bahr, Jürgen Carstensen and Rainer Adelung; Kiel University, Germany

With the modern advances in high performance adhesives, bonded joints are more and more competitive or are even outperforming mechanical joints and welds. Bonded joints exhibit many benefits compared to mechanical joints in respect of thickness, weight, force distribution, application and especially for dissimilar material bonding. The connection of different materials with fundamentally different properties is crucial for applications such as multi-material automotive bodies and composite materials for the aerospace sector. Thereby, the wide range of different favorable materials and the resulting different surface properties create high demands on the adhesives and often require complex surface preparation involving hazardous chemicals.

This work uses an electrochemical nanoscale sculpting process with a seawater-like electrolyte for an eco-friendly surface preparation and nearly perfect bonding on various metals such as aluminum, stainless steel and brass.

The strong adhesion is achieved by creating sub-micron undercuts that facilitate mechanical interlocking of adhesive and material. Chemical surface-to-surface interaction becomes less relevant, resulting in bonds that are limited by intrinsic fracture strength of the used adhesive. The undercuts are produced by a highly selective pulsed electrochemical etching, resulting in three-dimensional formation of chemically stable surfaces.

Additionally, brass can selectively be leached by the same process. Upon leaching, the structured surfaces are copper-rich and show extraordinarily good wettability for solder. For common tin-based solders, this work shows a contact angle near zero with several times larger spreading compared to a mechanical cleaned and roughened surface.

Since the chemical surface interaction is no longer decisive for the bonding strength, it also becomes possible to use completely new types of adhesives with superior bulk properties, that would otherwise lack the chemical properties for sufficient surface adhesion. This can not only be used to increase mechanical strength of a joint but is also promising for joining with electrically conductive adhesives as an alternative to soldering. Typical conductive adhesives consist of a conductive filler (e.g., metal particles) and an adhesive as binder, resulting in a tradeoff between bonding and conductivity properties.

This work will evaluate nano structured surfaces and their use for mechanically strong, conductive-bonded joints.

4:45 PM EN06.12/EN03.12.05

A Biodegradable and Stretchable Battery [Filippa Wentz](#)^{1,2}, Aiman Rahmanudin^{1,2} and Klas Tybrandt^{1,2}; ¹Linköping University, Sweden; ²Wallenberg Wood Science Center, Sweden

Next generation wearables will interface intimately with the human body. They will be used for health monitoring, soft robotics, and futuristic consumer electronics such as e-skin and e-textiles. For seamless integration with the human body, mechanical properties such as stretchability, softness and bendability need to be optimized. Extensive research has already been done on improving the mechanical properties of various components, such as transistors, conductors, diodes, sensors etc., to complement next-generation wearables. Batteries give autonomy to these wearables, by providing a portable power source. However, as the complexity of wearable devices increase, so would the energy demand and form factor. Capacity is often sacrificed increasing stretchability and reduction of size, since lowering the loading of active material reduces the capacity. Additionally, a growing issue is the accumulation of hazardous e-waste and mining of finite resources. Since the battery is often the most toxic and unsustainable part of electric devices, due to the use of harmful organic electrolytes and critical raw materials. Therefore, the development of batteries that are environment and human friendly is urgently needed.

Zn-ion batteries show great potential as a sustainable alternative to current Li-ion battery technology. Zn has a high theoretical capacity, is biodegradable and abundant, and can operate in safe and sustainable aqueous electrolytes. Today, most biodegradable batteries lack the mechanical properties needed (i.e. stretchability) for next-generation wearables. Only a handful biodegradable and stretchable batteries have been reported. However, their electrochemical performance is limited. The aim of this work is to address the abovementioned challenges by designing the first biodegradable and stretchable Zn-ion battery that can also deliver a high capacity.

Here, we studied the use of biomass-derived polymers in all components of the biodegradable and stretchable battery. For the active electrode, we developed a new biodegradable elastomeric binder by copolymerizing a polyester, poly(glycerol sebacate) (PGS), with a protein (gelatine). The gelatine improved the electrolyte uptake and the stretchability of the active electrode which resulted in improved capacity. A gelatine/cellulose-based composite was used in the electrolyte. It enhanced the adhesion to the electrodes which is critical for stretchability and increased the electrochemical stability by suppressing Zn dendrite and passivation layer formation. PGS was also used in the encapsulation which permitted the biodegradation of the full cell. Lastly, at the battery's end-of life the components are degraded into non-toxic products, many of which are today used in skincare or dietary supplements.

SESSION EN06.13/EN03.14: Joint Session: Breaking News

Session Chairs: David Cahen, Yi Hou, Clara Santato and Anke Weidenkaff

Friday Morning, April 26, 2024

Room 333, Level 3, Summit

8:30 AM EN06.13/EN03.14.01

Optimized Extraction of Mesoporous Nanocomposites from Spent Li-Ion Batteries and Their Use to Construct High-Performance Supercapacitor Devices with Ultra-High Stability [Nageh K. Allam](#); American University in Cairo, Egypt

Lithium-ion batteries (LIBs) are one class of the most significant energy storage devices used nowadays. However, a huge number of spent batteries bring harmful resource waste and environmental hazards as LIBs are mainly composed of heavy metals and organic electrolytes. Consequently, recycling spent LIBs has become a hot topic lately, where researchers are actively working to develop a plethora of methods to extract valuable metals and components. In this study, mesoporous Li-Ni-Mn-Co oxide nanoparticles have been successfully extracted from spent Li-ion batteries using a simple microwave/precipitation method. The as-extracted Li-Ni-Mn-Co oxides were used to construct functional supercapacitor devices. However, the as-extracted oxides showed poor stability and low conductivity. To enhance their cycling stability and conductivity, fullerene (C₇₆) is used as a carbon additive to form Li-Ni-Mn-Co oxide/C₇₆ nanocomposite materials. The morphological, structural, and compositional analyses of those composites were performed using FESEM, HRTEM, XRD, and XPS techniques. The Li-Ni-Mn-Co oxide/C₇₆ nanocomposites exhibit higher conductivity and wettability with an enhanced gravimetric capacitance of ~357 Fg⁻¹ at 1.0 Ag⁻¹. The asymmetric supercapacitor devices deliver specific energy as high as ~10 Wh/kg at a specific power of ~800 W/kg with a superior retention rate of ~115% after 20,000 cycles with ~100% Coulombic efficiency.

8:45 AM EN06.13/EN03.14.02

Unleashing Moisture Content as a Capacitance Deciding Factor for Supercapacitors derived from Wild Orchid [Abhay Deshmukh](#); Rashtrasant Tukadoji Maharaj Nagpur University, India

All carbonaceous materials manifest Electrical double layered capacitor (EDLC) type behaviour. Still, drawbacks like cost-effectiveness and availability of precursor materials provide a spotlight on "Biomass derived carbons" as electrode material for supercapacitors. Nevertheless, different types of biomasses show uniqueness in their properties and thus reveal differences in carbon materials derived from them. During carbonizing or pyrolysis of biomass, a factor called moisture is generally ignored or removed by simply drying the sample in an air oven. Here in this work, we choose leaves of a wild orchid (*Vanda Tasselleta*) which is an abundantly available species of plant from the Indian subcontinent to Indochina, to establish a relation between moisture content in biomass, rate capability and capacitance of electrode material. Interestingly out of five variations viz normal leaves without treatment, dried leaves, soaked leaves, a mixture of dried and normal leaves, and -20 °C samples, carbon derived from normal leaves shows the highest capacitance of 213.43 F/g at 0.5 A/g without any activation. But fascinatingly normal leaves without treatment show the lowest rate capability of only 35.53 % which is approximately half of the rate capability obtained for dry leaves of wild orchids exhibiting 124.78 F/g capacitance at 0.5 A/g. Moreover, our work demonstrates the dependence of pore size distribution on the amount of moisture intact in wild orchid leaves with the help of characterization techniques. Finally, a two-electrode symmetric device was fabricated showing high capacitance and capacitance retention which shows practical application of wild orchid leaves as supercapacitor electrode material.

9:00 AM EN06.13/EN03.14.03

Cost-Effective Fabrication Process in 24 Hours for Supercapacitors [Satnam S. Mattu](#); Rastrasant Tukadoji Maharaj Nagpur University, India

In the ever-expanding realm of modern science and electronics, the demand for miniaturized and flexible energy storage devices is growing to enhance people's lives with compact and adaptable electronics. Currently, the prevalent use of micro-batteries in portable devices presents a significant drawback, marked by their short life spans of only a few hundred to several thousand cycles, thus frequent replacement is required but becomes problematic in the context of implantable biochips. Not only this, connecting micro-batteries by some combination to provide high power makes it even bulkier. In stark contrast, micro-supercapacitors with an increase in a number of advantages like flexibility, remain lightweight with high power discharge. Apart from this manufacturing cost-effective micro-supercapacitors in less time is a task. Thus, this work addresses the making of micro-supercapacitors from highly porous pseudocapacitive material MOFs (metal organic framework) using LASER ablation technique. The substrate used here is a normal paper where deposition of material is exhibited using a very simple method and finally scribing it using CO₂ LASER scribing. Different designs of MSCs are also explored and finalized in-plane concentric shape which provides a wide voltage window from 0 to -0.8 V as well as from 0 to 0.8 V at high scan rates showing the highest areal capacitance of 57 μF cm⁻². Moreover, making use of gel electrolyte and showing capacitance in microns increases its feasibility for flexible devices. Finally, to show the practical application of the electrode several LEDs were blinked by stacking prepared MSC. Thus, the cost-effective method is implemented with a claim of manufacturing micro-supercapacitors in a single day.

9:15 AM EN06.13/EN03.14.04

Fabrication of Fully Sustainable Electrospun Fiber-Reinforced 3D Carbon from Waste as Scalable Electrodes in Energy Storage Materials [Michael W. Thielke](#), Luis M. Murillo Herrera, Carlos Mingoes and Ana Jorge Sobrido; Queen Mary University of London, United Kingdom

Carbon fibers for the new batteries have been of interest for a long time based on their advantageous shape that provides stability, flexibility and a high surface area, lightweight, and high electrical conductivity. Most of the current reported and commercial carbon fibers are derived from using polyacrylonitrile, a synthetic polymer obtained from crude oil. Due to the finite nature and environmental impact of sourcing and refining crude oil, it is necessary to find sustainable alternatives to ensure the filling of the demand in the future.

Fully sustainable alternatives have been reported based on the use of biopolymers. A promising candidate as precursor for carbon fibers is lignin, the main byproduct of the paper and pulp industry and the second most abundant biopolymer that is rich in aromatic carbon groups. Carbonizing lignin therefore, results in a high yield of carbon fibers. To ensure enough entanglement of the molecular chains, that allows the formation of stable fibers, the high molecular weight fraction of lignin is extracted, allowing the fabrication of pure lignin fibers without the use of additional synthetic polymers as carrier. One technique to fabricate fibers that have been of particular interest is electrospinning. Through the use of a high voltage field, the electrostatic forces draw a polymer solution to fibers in submicron diameter ranges, lower than any of the other commercially used techniques to fabricate fibers. Due to the enormous surface area to volume ratio, these fibers have been at the center of interest in various applications, including energy storage systems and (electro)catalysis. In addition to the relatively simple setup, electrospinning is the ideal technique to explore the properties of new materials in a laboratory scale. In larger scaled energy storage systems, such as flow batteries, electrospun fibers show a disadvantage due to the limited thickness of the fiber mat can reach compared to other spinning processes due to the relatively small fabrication scale and process that uses the electric field. To overcome this issue, we created a 3D structure based on lignin fibers through the lyophilization of the electrospun lignin fibers. The structure was obtained through a sonification process of the fibers in an aqueous solution of potato-based protein, another byproduct of the potato starch industry. In addition to enhancing stability in its dimensions, the soluble protein increases the mass of the resulting carbon, as well as the introduction of heteroatom doping of nitrogen and sulfur within the carbon for electrocatalytic improvement. After the lyophilization process, the combination of the lignin fibers and the potato protein form a fiber-reinforced sponge structure, an ideal precursor for fully sustainable 3D carbon structures, and adjustable in size and dimensions.

It was shown that with the ideal ratio of protein to lignin fibers, a full coverage of the fiber could be achieved, and in addition, the carbon shows an improvement in the electrochemical catalysis of V⁴⁺/V⁵⁺ redox reaction, important for the use of the redox-flow battery. In comparison to the unsustainable, commercial felts that are predominantly used in the past, the sustainable alternative 3D freeze-dried carbon shows significantly better performance in cyclic voltammetry measurements and electrochemical impedance spectroscopy (EIS), and could further improve the performance of an asymmetrical flow battery.

9:30 AM EN06.13/EN03.14.05

Long-Term Stability of Hygroscopic Hydrogels by Preventing Metal Ion-Mediated Degradation [Chad Wilson](#), Carlos D. Diaz, Lorenzo Masetti, Xiao-Yun Yan, Will Chang Liu, Shucong Li, Gang Chen and Xuanhe Zhao; Massachusetts Institute of Technology, United States

Recent developments in material chemistry highlight hygroscopic hydrogels as promising candidates for use in sorption systems, with applications ranging from atmospheric water harvesting to energy storage and thermal management. However, material lifetime remains a significant limitation to realizing cost-effective high-performance devices. In this work, we consider deployment of lithium chloride-loaded polyacrylamide (PAM + LiCl) hydrogels at elevated temperatures on a variety of potential system substrates, correlating lifetime and cyclability of the gels to device design and material choice. We show that the presence of metallic ions in the system leads directly to material degradation via radical formation in the gels. Moreover, metallic ion absence results in consistent cyclic sorption performance and a gel lifetime of over 8 months. This work demonstrates the long-term stability of PAM + LiCl hydrogels, and provides initial design guidelines for its repeatable, cost-effective implementation in future sorption systems.

9:45 AM EN06.13/EN03.14.06

Recycling Polystyrene Waste into Electromechanically Responsive Materials by Producing Multilayered Films from Bilayers with Asymmetric Triboelectric Properties [Andris Sutka](#)¹, Anna Šutka¹, Artis Linarts¹ and Peter C. Sherrell²; ¹Riga Technical University, Latvia; ²RMIT University,

Australia

Millions of tons of foamed polystyrene (FPS) are produced annually. FPS is a major environmental problem. Polystyrene is slow to biodegrade, with an estimated decomposition time of up to 500 years. FPS contains 95% of air, and thus, it has a very low extent of recycling. According to a study by the California Integrated Waste Management Board, less than 1% of FPS was recycled in 2019. At the same time, FPS fills up 25% to 30% of landfill space by volume around the world.

Here, we report the upcycling of FPS waste into electromechanically responsive triboelectric laminates (TLs). These TLs possess internal triboelectric dipoles offering an alternative to ferroelectric fluoropolymers. The piezoelectric contact-mode testing showing a FPS laminate is comparable to state-of-the-art piezoelectric fluoropolymers for overall electromechanical conversion. Piezoelectric fluoropolymers are critical electromechanically responsive materials for flexible energy harvesting and sensors. However, their production results in the release of significant amounts of toxic substances into the environment, and as such, these fluoropolymers are at risk of being banned by the European Union. Our alternative flexible electromechanically responsive materials can replace piezoelectric fluoropolymers, thus enabling rapid integration into current technology standards.

10:00 AM BREAK

10:30 AM EN06.13/EN03.14.07

Waste to Product: Green Production Processes for a Circular Economy [Anke Weidenkaff](#), Wenjie Xie and Jinxue Ding; Technical University of Darmstadt, Germany

The energy transition to defossilisation will be built on renewable energy converters which require tailored materials and a new infrastructure partially based on critical materials. This transformation to a future fossil free green circular economy will be based on sustainable materials production processes and ecologic innovations. The development of renewable materials for renewable energy converters requires sustainable large-scale production from secondary raw materials. The decision making for future resilient energy systems has to be based on environmental aspects as well as on performance criteria defined by a holistic life cycle assessment.

In this lecture an efficient recycle precursors production for materials with a programmable lifetime and regeneration will be introduced as a suitable approach. The design of circular high performance materials uses theoretical predictions and the criticality analysis of applied elements to improve the cycle life of future energy converters such as thermoelectric generators and refrigerators, batteries, electrolyzers, fuel cells, plasmalysers, hydrides and solar watersplitting cells.

10:45 AM EN06.13/EN03.14.08

Supercritical CO₂ Assisted Aerosol Synthesis of HKUST-1 Nanoparticles in a Continuous Flow Reactor [Ji Feng](#), Almond Lau and Igor Novoselov; University of Washington, United States

Metal-organic Frameworks (MOFs) are very promising materials for gas sensing, catalysis, energy storage, water purification and drug delivery due to their high porosity, tunable pore sizes, adequate chemical and thermal stability, and various structures and compositions. Downsizing MOFs to the nanoscale brings superior properties over their bulk analogs, such as high surface-to-volume ratio, rich exposed metals and ligands, short diffusion path for reactants, which all contribute to improved performances. While great efforts have been made to reduce the particle sizes by controlling the reaction kinetics or terminating the particle growth with additives, large-scale synthesis of MOF nanoparticles with simple methods remains a challenge. Here, we report supercritical CO₂ assisted synthesis of HKUST-1 nanoparticles in a continuous flow reactor. This method yields pure and thermal stable HKUST-1 nanoparticles with median sizes of 98-212 nm and BET surface area of 1613-1887 m²/g in the residence time of just 3 seconds without any additives. Supercritical CO₂ and ethanol with a mole ratio of 9:1 are used as co-solvents for the fast precipitation of HKUST-1 nucleus and crystal growth. A typical dry yield of 53.7 wt% is achieved with 0.1 M copper precursor at 75 °C and 13 MPa. Size analysis of the products obtained at different copper concentrations shows the influence of supersaturation and fluid phase behavior to the nanoparticle formation. Fractal dimension analysis indicates that the growth is caused by aggregation of primary nanocrystals, indicating a non-classical crystal growth mechanism. The use of supercritical CO₂ saves the use of organic solvents. In addition, super critical CO₂ has physical properties such as natural abundance, non-flammability, and low toxicity, making this synthesis a green and sustainable method for the scalable production of MOF nanoparticles.

11:00 AM EN06.13/EN03.14.09

Laser-Induced Graphitization of Lignocellulosic Cellulose Nanofiber Films Intended for Electronic and Energy Storage Applications [Anna Fall](#); University of Washington, United States

Graphitic carbon is a popular crystalline form of carbon commonly used in electronics and energy storage applications (Bressi et al., 2023). There is a large push to reduce the environmental impact of the production of graphite and graphene by finding environmentally and economically friendly alternative methods of production. It is possible to synthesize graphitic carbon utilizing laser irradiation on lignocellulosic cellulose nanofiber (LCNF) films to produce graphitic carbon intended for flexible electronic and energy storage devices (Lee & Jeon, 2019).

Flexibility and durability of the films were improved by adding polyvinyl alcohol (PVA) to create an LCNF and PVA nanocomposite. This study used a 10W Snapmaker CO₂ laser module to convert a film comprised of this nanocomposite into a graphitic carbon structure. LCNF was produced by alkaline peroxide pulping of wheat straw, mechanical treatment, and peracetic acid (PAA) treatment (Pascoli et al., 2023). Characterization of the prepared material includes Raman Spectroscopy, XRD, SEM, and conductivity. After testing various film compositions and laser settings, optimal conditions were discovered and are ready to be implemented for creating flexible electronic and energy storage devices.

Sources

Bressi, A. C., Dallinger, A., Steksova, Y., Greco, F. (2023). Bioderived Laser-Induced Graphene for Sensors and Supercapacitors. *ACS Applied Materials & Interfaces*, 15(30), 35788-357814. 10.1021/acsmi.3c07687.

Lee, S. & Jeon, S. (2019). Laser-Induced Graphitization of Cellulose Nanofiber Substrates under Ambient Conditions. *ACS Sustainable Chemistry & Engineering*, 7(2), 2270-2275. 10.1021/acssuschemeng.8b04955.

Pascoli, D. U., Dichiaro, A., Gustafson, R., Bura, R. (2023). A Robust Process to Produce Lignocellulosic Nanofibers from Corn Stover, Reed Canary Grass, and Industrial Hemp. *Polymers*, 15(4), 937. 10.3390/polym15040937.

11:15 AM EN06.13/EN03.14.10

Production of High-Quality Biogas Using Recycled Trimetallic Nanoparticles from Electronic Waste [Nageh K. Allam](#); American University in Cairo, Egypt

A plethora of nanoparticles (NPs) significantly enhanced the biogas production from organic waste anaerobic digestion upon their optimized addition to the reactors. In this study, trimetallic Sn-Mn-Fe.NPs, recovered from waste-printed circuit boards, were used to enhance the quality and productivity of the anaerobic digestion (AD) of cow manure as an organic substrate. This study aims to make the biogas production process more efficient and economically sustainable, taking into account the environmentally friendly nature of the AD process. The obtained nanoparticles were characterized using scanning electron microscopy (SEM), high-resolution transmission electron microscopy (HRTEM), and X-ray diffraction (XRD) techniques. Various concentrations (20, 50, and 100 mg/L) of the trimetallic Sn-Mn-Fe NPs were added to the biogas reactors, which were made of 1000-ml autoclave glass bottles to host the animal waste during the AD process. The pressure of the biogas produced was monitored daily for 45 days as retention time, and the volume of the produced biogas was calculated at a constant temperature (15 °C) and pressure (1.013 bar). Generally, NP-based reactors showed superiority in biogas production over blank reactors. Also, among the different concentrations, the best biogas-producing digester (RC2200) revealed the highest performance with a 113.6% enhancement in biogas production. In addition, it showed a significant increase of 231.2% in methane production.

11:30 AM EN06.13/EN03.14.11

Material Stability and Durability Testing Using the Extreme Space Environment in Low Earth Orbit Phillip Irace, Ryan D. Reeves and Michael Roberts; International Space Station National Laboratory, United States

The extreme environment of space provides an ideal domain for testing the stability and durability of materials for use in multiple applications both in space and on Earth. Materials exposed to the harsh space environment in low Earth orbit (LEO) are subject to atomic oxygen (AO) erosion, ultraviolet (UV) radiation, ionizing radiation, vacuum, thermal cycling, and temperature extremes. Depending on the material, each of these factors can lead to significant material degradation. For materials used in space applications, space exposure testing is critical for evaluating the performance of the material. For materials designed for Earth applications, long-term space exposure provides a mechanism for accelerated material degradation testing, where the impact of space-exposure can be correlated to degradation via Earth-based testing to identify failure modes and evaluate the lifespan of the material. The International Space Station (ISS) National Laboratory offers an ideal platform for long-term exposure to the extreme space environment in LEO, particularly because power, data, and imaging can be provided *in-situ* and samples can be returned to Earth for postflight analysis and comparison to ground samples. Some materials that have been investigated using ISS external platforms include silicon-, organic-, copper-zinc-tin-sulfide (CZTS), and perovskite-based 3D photovoltaic cells; methylammonium lead tribromide (MAPbBr₃) and methylammonium lead triiodide (MAPbI₃) perovskites; Beta Barium Metaborate (BBO) lenses; biomaterials; polymers; ceramics; and metals. In addition, several electronic, photonic, and other devices have been tested in the harsh space environment outside the ISS.

In this work, we will introduce the damage mechanisms present in the extreme space environment. We will discuss how the magnitude of each damage mechanism is affected by sample orientation: nadir (Earth-facing), zenith (space-facing/opposite of nadir), ram (direction of travel), and wake (opposite of ram). We will present case studies of materials and devices for both space- and Earth-based applications that were investigated using ISS external platforms, including the performance of 3D photovoltaic cells, perovskites, and polymers. We will also discuss translational lessons learned from space-exposure experiments that inform and direct terrestrial research and materials science. Finally, we will present opportunities for future space-exposure experiments and access to ISS facilities through the ISS National Lab.

SYMPOSIUM EN07

Thermal Transport and Energy Conversion
April 22 - May 7, 2024

Symposium Organizers

Woochul Kim, Yonsei University
Sheng Shen, Carnegie Mellon University
Sunmi Shin, National University of Singapore
Sebastian Volz, The University of Tokyo

* Invited Paper

+ JMR Distinguished Invited Speaker

^ MRS Communications Early Career Distinguished Presenter

SESSION EN07.01: Breaking News
Session Chairs: Woochul Kim and Sunmi Shin
Monday Morning, April 22, 2024
Room 344, Level 3, Summit

10:45 AM EN07.01.01

Solid-State Electrochemical Thermal Transistors with Large Thermal Conductivity Switching Width Ahrong Jeong¹, Zhiping Bian¹, Mitsuki Yoshimura¹, Bin Feng², Yuichi Ikuhara², Yusaku Magari¹ and Hiromichi Ohta¹; ¹Hokkaido University, Japan; ²The University of Tokyo, Japan

Thermal transistors that electrically switch heat flow on and off have attracted growing attention as thermotronic devices such as thermal shutters and

thermal displays. In 2023, we demonstrated the world's first solid-state electrochemical thermal transistors with SrCoO_x ($2 \leq x \leq 3$) as the active layer.^{1,3} The thermal conductivity (κ) on/off ratio was approximately 4 and κ switching width was $2.85 \text{ W m}^{-1} \text{ K}^{-1}$. Here, we demonstrate solid-state thermal transistors with a large κ switching width of $9.5 \text{ W m}^{-1} \text{ K}^{-1}$. We used CeO₂ thin films as the active layer directly deposited on the solid electrolyte YSZ substrate using the PLD method. A Pt thin film was deposited on the surface of the CeO₂ thin film and the back surface of the YSZ substrate using the sputtering method to create an all-solid-state thermal transistor. When the CeO₂ thin film was once reduced and then oxidized, the κ was approximately $2.5 \text{ W m}^{-1} \text{ K}^{-1}$ in the most reduced state, and κ increased with oxidation to $11.8 \text{ W m}^{-1} \text{ K}^{-1}$. This reduction/oxidation was repeated 5 times and the average value of κ was $2.5 \text{ W m}^{-1} \text{ K}^{-1}$ after reduction and $12 \text{ W m}^{-1} \text{ K}^{-1}$ after oxidation. The CeO₂-based solid-state electrochemical thermal transistors might have the potential for thermotronic devices such as thermal shutters and thermal displays.

[1] Q. Yang *et al.*, *Adv. Funct. Mater.* **33**, 2214939 (2023).

[2] Z. Bian *et al.*, *ACS Appl. Mater. Interfaces* **15**, 23512 (2023).

[3] M. Yoshimura *et al.*, *ACS Appl. Electron. Mater.* **5**, 4233 (2023).

11:00 AM EN07.01.02

Multi-Luminophores-Multi-Waveguide Architecture Luminescent Solar Concentrator with Record Power Conversion Efficiency of 7.8% Waad Naim^{1,1,2}, Fahad Mateen^{1,1,2}, Christopher Herrera^{1,1,2}, Aria Vahdani^{1,3}, Jesse Cantrell^{1,3}, Babak Borhan^{1,3} and Richard Lunt^{1,1,2}; ¹Michigan State University, United States; ²Molecular and Organic Excitonics Lab, United States; ³Department of Chemistry, United States

Among the different solar technologies, luminescent solar concentrators (LSCs) display a versatile solar harvesting platform due to the broad spectrum of color options, low cost, and their ability to harvest both direct and diffuse sunlight. LSCs consist of a lightguide doped or coated with luminophores that absorb sunlight and re-emit photons at a longer wavelength. The majority of emitted photons are waveguided via total internal reflection towards the edge-mounted photovoltaic (PV) cells. Indeed, the maximum theoretical efficiency of a black LSC absorbing throughout the visible spectrum is 33.7%, similar to the Shockley-Queisser limit of a single junction solar cell. This value is obtained assuming that the absorption, luminescence, and collection efficiencies are all 100%. However, based on practical considerations, this value is reduced to 23.5% for an ideal condition, and 18.0% for a general one, due to non-ideal luminescent molecules and re-absorption losses. Today, the highest reported power conversion efficiency (*PCE*) of an opaque LSC ($5 \times 5 \text{ cm}^2$, paired with four GaAs cells attached in parallel to the sides) is 7.1% based on a set of two organic luminophores with total absorption ranging from 350 nm to 600 nm. The reported External Quantum Efficiency (*EQE*) measurement highlighted that at higher wavelengths (beyond the bandgap of both used luminophores), there is still a response due to incident light that is scattered at the diffuse backside mirror. Recently, it has been agreed upon in a consensus statement that the direct illumination of the edge-mounted PV is considered a mismeasurement or an artifact, significantly leading to an overestimated short-circuit current density (J_{SC}).

Diverse classes of luminophores with various wavelength-selectivity have emerged, including organic dyes, nanoclusters, quantum dots, and rare-earth ion complexes. Combining multi-luminophores in LSC allows maximizing the light-absorbing ensuring a full-spectrum harvesting. However, the coupling between different luminophores often leads to a reduction in the efficacy of this approach. This suggests that the optimization of the architecture of the LSC is just as crucial as that of the luminophores. To demonstrate the potential of full-spectrum LSC, we present a novel LSC design based on an optimized multi-waveguide architecture with multi-luminophores. In contrast to existing designs, our methodology involves effectively harvesting through the ultra-violet (UV), visible (VIS), and near-infrared (NIR) regions of the solar spectrum, highlighting the airgap strategy to isolate the absorption/emission bands. We then select, synthesize, and optimize luminophores that target each of these spectral regimes with the highest achievable photoluminescence quantum yield (*PLQY*). Thus, our LSC design comprises of organic molecules, quantum dots, and nanoclusters, each discreetly incorporated within an independent waveguide. Among these luminophores, a newly synthesized Donor-Acceptor-Donor (DAD) organic molecule, distinguished by its near-unity *PLQY* and absorption spectrum spanning the 300 nm to 600 nm wavelength range, leads to one of the highest *PCEs* reported for a single component LSC of 5.7% (4.5% with black background). By optimizing the single components and the architecture, we demonstrate that this multi-luminophores LSCs ($50.8 \times 50.8 \text{ mm}^2$) achieve a *PCE* of 7.8% with a specular-reflective background, establishing a new benchmark for *PCE* among opaque LSC devices.

11:15 AM EN07.01.03

Active Heat Transfer Fluids: Liquid Coolants Containing Self-Propelled Microparticles for Heat Transfer Enhancement Jacob Velazquez¹, Darsh Devkar², Sajad Kargar¹, Amit K. Singh¹ and Jeffrey L. Moran¹; ¹George Mason University, United States; ²University of Virginia, United States

Liquid coolants are critical components of many modern technologies, such as hybrid electric vehicle batteries, solar receivers, and cooling systems for electronics. Sustaining the growth of these technologies while limiting their carbon footprint requires coolants that transfer heat efficiently. Since the 1990s, significant research has been conducted into the use of suspended nanoparticles to improve coolant performance. The resulting suspensions, known as *nanofluids*, typically exhibit higher thermal conductivity than the liquids alone, since the particle material is typically more thermally conductive than the liquid. However, the improvements provided by nanoparticles are fundamentally limited by the particles' inability to move on their own through the liquid, and thus agitate convective mixing that could dramatically improve performance.

In this work, we explore the use of self-propelled particles (SPPs), which are colloids that can move autonomously in liquids using energy from their local environment, to accelerate heat transfer in liquids. As they move, SPPs induce disturbance flows in the surrounding liquid, and we hypothesize that this "micro-stirring" effect can enhance the heat transport rate by an amount depending on the SPPs' size, speed, and volume fraction. We demonstrated this concept experimentally by placing an SPP suspension in contact with a heated surface; for a constant heat flux, a more effective coolant should result in a lower temperature of the heated surface. By measuring the temperatures of the heater & background fluid, as well as the heat flux, we can quantify SPP-induced increases in the convective heat transfer coefficient (HTC), a widely-recognized metric of heat transfer efficiency. We present data for the HTC of various SPP suspensions under various experimental conditions. The results will inform the prospective use of coolants containing SPPs, which we refer to as "active heat transfer fluids," in a variety of cooling applications in the energy, environmental, and biomedical sectors.

11:30 AM EN07.01.04

Intelligent Radiative Thermostat Induced by Near-Field Radiative Thermal Diode Yang Liu and Yi Zheng; Northeastern University, United States

A radiative thermostat system senses its own temperature and automatically modulates heat transfer by turning on/off the cooling to maintain its temperature near a desired set point. Taking advantage of far- and near-field radiative thermal technologies, we propose an intelligent radiative thermostat induced by the combination of passive radiative cooling and near-field radiative thermal diode for thermal regulation at room temperature. The top passive radiative cooler in thermostat system with static thermal emissivity uses the cold outer space to passively cool itself all day, which can provide the bottom structure with the sub-ambient cold source. Meanwhile, using the phase-transition material vanadium dioxide, the bottom structure forms a near-field radiative thermal diode with the top cooler, which can significantly regulate the heat transfer between two terminals of the diode and then realize a stable temperature of the bottom structure. Besides, the backside heat input of the thermostat has been taken into account according to real-world applications. Thermal performance of the proposed radiative thermostat design has been analyzed, showing that the coupling effect of static passive radiative cooling and dynamic internal heat transfer modulation can maintain an equilibrium temperature approximately locked within the phase transition region. Besides,

after considering empirical indoor-to-outdoor heat flux, rendering its thermal performance closer to that of passive solar residential building walls, the calculation result proves that the radiative thermostat system can effectively modulate the temperature and stabilize it within a controllable range. Passive radiative thermostats driven by near-field radiative thermal diode can potentially enable intelligent temperature regulation technologies, for example, to moderate diurnal temperature in regions with extreme thermal swings.

11:45 AM EN07.01.05

Thermoreflectance-Based Thermometry of Silicon Thin Films with Resonantly Enhanced Temperature Sensitivity Xinchao Wang, Changxing Shi, Qifan Zheng, Jan Maroske and Dakotah Thompson; University of Wisconsin-Madison, United States

We demonstrate a thermoreflectance-based thermometry technique with an ultimate temperature resolution of 60 μK in a 2.6 mHz bandwidth. This temperature resolution was achieved using a 532 nm-wavelength probe laser and a ~ 1 μm -thick silicon transducer film with a thermoreflectance coefficient of $-4.7 \times 10^{-3} \text{ K}^{-1}$ at room temperature. The thermoreflectance sensitivity reported here is over an order-of-magnitude greater than that of metal transducers, and is comparable to the sensitivity of traditional resistance thermometers. Supporting calculations reveal that the enhancement in sensitivity is due to optical interference in the thin film.

SESSION EN07.02: Thermal Transport Across Interfaces/Thermal Transport in Nanoscales
Session Chairs: Sheng Shen and Sebastian Volz
Tuesday Morning, April 23, 2024
Room 327, Level 3, Summit

10:45 AM *EN07.02.01

Rethinking Evaporation and Condensation Gang Chen; Massachusetts Institute of Technology, United States

Although ubiquitous in nature and industrial processes, transport processes at the interface during evaporation and condensation are still poorly understood. Experiments have shown temperature discontinuities at the interface during evaporation and condensation but the experimentally reported interface temperature jump varies by two orders of magnitude. Even the direction of such temperature jump is still being debated. In this talk, I will first discuss a thermomolecular emission for thermal evaporation, analogous to the thermionic emission mechanism. Starting from the kinetic theory, we derive interfacial mass flux and heat flux conditions, which are used to solve the coupled problem between the liquid and the vapor phase during evaporation and condensation. Our model shows that when evaporation or condensation happens, an intrinsic temperature difference develops across the interface, due to the mismatch of the enthalpy carried by vapor at the interface and the bulk region. The vapor temperature near the interface cools below the saturation temperature on the liquid surface during evaporation and heats up above the latter during condensation. However, many existing experiments have shown an opposite trend to this prediction. We explain this difference as arising from the reverse heat conduction in the vapor phase. Our model results compare favorably with experiments on both evaporation and condensation. We show that when the liquid layer is very thin, most of the applied temperature difference between the solid wall and the vapor phase happens at the liquid-vapor interface, leading to saturation of the evaporation and the condensation rates and the corresponding heat transfer rate. This result contradicts current belief that the evaporation and condensation rates are inversely proportional to the liquid film thickness. For the two parallel plate problem with evaporation on one side and condensation on the other, we will explain several paradoxical predictions including inverted temperature profile in the vapor phase.

[1] G. Chen, "On the molecular picture and interfacial temperature discontinuity during evaporation and condensation," *Int. J. Heat & Mass Transfer*, 191, 122845, 2022.

[2] G. Chen, "Interfacial cooling and heating, temperature discontinuity and inversion in evaporation and condensation," *Int. J. Heat & Mass Transfer*, <https://doi.org/10.1016/j.ijheatmasstransfer.2023.124762>.

[3] G. Chen, "On paradoxical phenomena during evaporation and condensation between two parallel plates," *J. Chem. Phys.*, 10.1063/5.0171205, 2023.

11:15 AM EN07.15.18

Evaluating The Vibrational Character of Thermal Carriers across Order–Disorder Phase Transitions Rahil Ukani¹, Qichen Song¹, Catherine Thai¹, Alexander D. Christodoulides², Yookyung Moon¹, Dehong Yu³, Caleb Stamper⁴, Jinyoung Seo¹, Jonathan A. Malen² and Jarad A. Mason¹; ¹Harvard University, United States; ²Carnegie Mellon University, United States; ³Australian Nuclear Science and Technology Organisation, Australia; ⁴University of Wollongong, Australia

Materials containing aligned alkyl chains have shown considerable promise for energy applications, including solid-state cooling through caloric effects. Understanding how heat flows through these chains—particularly during phase transitions—can enable precise manipulation of their thermal transport properties, which are critical to optimizing efficiency in practical applications. Many of these materials offer tunable interchain chemistries and thermally responsive structural dynamics, which can offer molecular-level insights—and thus control—of heat conduction mechanisms. Here, we examine thermal transport in two classes of two-dimensional (2-D) layered crystals whose alkyl chains undergo thermally induced order–disorder transitions: (1) hybrid perovskites, and (2) organic salts. Variable temperature frequency-domain thermoreflectance (FDTR) measurements of analogous 2-D perovskite and organic salt structures allow us to describe the role of chemical interactions and chain confinement in dictating thermal conductivity. Microscopy and nanomechanical characterizations similarly describe the influence of structural features and microstructure. Through quasielastic and inelastic neutron scattering, we highlight how the vibrational nature of thermal energy carriers changes as the alkyl chains in these materials transition from ordered to dynamically disordered states. These complementary techniques allow us to detail the key chemical levers that tune thermal transport in phase change materials. Our investigations reveal a comprehensive picture of the mechanisms underlying thermal conduction across phase changes of confined alkyl chains, and how interlayer chemistry regulates heat flow in complex crystals.

11:30 AM EN07.02.03

Non-Equilibrium Thermal Resistance from Phonons and Electrons Across Solid Interfaces Jinchen Han and Sangyeop Lee; University of Pittsburgh, United States

Understanding interfacial thermal resistance has focused on atomistic-scale phenomena such as carrier transmission functions across the interface. In this presentation, we discuss a phenomenon at micrometer scale for interfacial resistance: relaxation of non-equilibrium carriers through scattering. The widely used Landauer formalism assumes incident carriers have an equilibrium distribution, but the actual distribution can be highly non-equilibrium due to the interfacial scattering. The carriers with non-equilibrium distribution are relaxed by carrier scattering at micrometer scale and the Boltzmann's H-theorem

dictates entropy generation and thermal resistance during this relaxation process. To capture such process, we solve the Boltzmann transport equation with ab initio inputs. Our work shows two important facets of carrier non-equilibrium near interface and interfacial thermal resistance. First, we highlight significance of spectral heat flux mismatch for the interfacial thermal resistance. An example is a Si-SiGe alloy interface where the phonon dispersion is matched exactly but exhibits a substantial interfacial resistance. Second, we discuss the energy exchange between electrons and phonons in metal-insulator interfaces. We focus on how electron-phonon scattering influences the relaxation of thermal carriers near the interface as well as its impact on the entropy generation and non-equilibrium thermal resistance.

11:45 AM EN07.02.04

Modelling Hydrodynamic Heat Conduction Signatures in Experiments Using The Full Scattering BTE [Aleksei Sokolov](#)^{1,2}, Jamal A. Haibeh² and Samuel C. Huberman²; ¹Technical University of Berlin, Germany; ²McGill University, Canada

The early experimental studies of anomalous thermal transport include second sound observations by Jackson et al (PRL 1970) and ballistic transport observations by Northrop and Wolfe in PRL (1979). Recent experimental techniques allow gathering temperature data with high spatial and temporal resolution, one can directly observe the evolution of a transient temperature field, such as the decay of ultrafast Gaussian heating in Transition metal dichalcogenides, as demonstrated by Varghese et al. in (Rev. Sci. Instrum. 2023) or a ring heating geometry which yielded an observation of 'lattice cooling', i.e., the temperature field may locally become lower than the initial background temperature (Jeong et al. in PRL 2021). These contemporary experimental techniques drive a need for theoretical descriptions based on microscopic principles. One such approach requires solutions to the Boltzmann Transport Equation where the collision term is described by the full scattering matrix, going beyond the Relaxation Time Approximation which fails to describe the heat conduction process in the hydrodynamic phonon regime. As shown by Chiloyan et al (PRB 2021), the BTE with a full scattering matrix can be efficiently solved for an initial sinusoidal temperature profile, also known as the Transient Thermal Grating (TTG) geometry, yielding a semi-analytical solution. Building upon this result, we propose a novel numerical method. It is based on pre-sampling solutions of the BTE with a full scattering matrix for TTG initial conditions with different sinusoidal excitation wavelengths, calculated using ab initio force constants and a semi-analytical solution. This response is then used to construct the solution of the Linear Boltzmann Transport Equation for arbitrary heating geometries as a superposition of responses of different spatial spectra. This approach is used to simulate the Gaussian and ring heating geometries for a few materials, including graphene, graphite and MoS₂.

SESSION EN07.03: Radiative Heat Transfer
Session Chairs: Baowen Li and Sheng Shen
Tuesday Afternoon, April 23, 2024
Room 327, Level 3, Summit

1:45 PM *EN07.03.01

Thermal Transport and Conversion Using Photonic Nanostructures [Renkun Chen](#); University of California, San Diego, United States

Photonics can be harnessed to engineer and in certain cases enhance thermal energy transport and conversion processes due to favorable characteristics of thermal photons relative to phonons under certain conditions, such as long wavelength, long propagation length, high speed, and spectral tunability. Here we present our work on thermal transport and conversion in nanostructures over the past few years. First, we showed that the coupling between photons and traditional heat carriers such as phonons and electrons can be utilized to manipulate radiation and conduction heat transfer in polar dielectric and metallic nanostructures. In particular, we observe enhanced effective emissivity and thermal conductivity in rationally designed nanostructures of polar dielectrics and metals. Second, we developed high-temperature selective emitters based on photonic metamaterials. While selective emitters have been extensively studied previously, they are often not stable at high temperature due to the presence of nanoscale interfaces. We use novel material and structural designs to achieve high temperature stability. These selective emitters could be utilized for converting optical and electrical energy more efficiently into thermal energy within a desirable spectrum that are useful for systems such as thermophotovoltaic and infrared heating.

2:15 PM *EN07.03.02

Energy Transfer and Conversion in Nanoscale Gaps [Pranod Sangi Reddy](#); University of Michigan, United States

Understanding radiative heat transfer in nanoscale gaps and devices is of considerable interest for creating novel energy conversion devices. In this talk, I will first describe ongoing efforts in our group to experimentally elucidate nanoscale radiative heat transfer. I will present our recent experimental work where we have explored how radiative heat transfer is modified in nanoscale gaps at room temperature and cryogenic temperatures. Specifically, I will describe a variety of instrumentation including novel nanopositioning platforms and microdevices, which we have developed to accomplish these measurements. Further, I will discuss possible applications of near-field thermal radiation for energy conversion and photonic cooling. Finally, I will briefly outline how these technical advances can be leveraged for future investigations of nanoscale heat transport and near-field thermophotovoltaic energy conversion.

2:45 PM EN07.03.04

Optical Interrogation of Subsurface Nanogap Thermal Transport [Zachary T. Piontkowski](#), Amun Jarzembki, Wyatt Hodges, Anthony McDonald, Matthew Bahr, William Delmas, Ping Lu and Julia Deitz; Sandia National Laboratories, United States

Nanoscale thermal transport has received significant attention for next-generation energy conversion and thermal management applications. In particular, state-of-the-art experiments have shown for vacuum gap distances down to 10 nm that thermal transport is governed by near-field thermal radiation, and can be enhanced by orders of magnitude above the Planck black body limit. Moreover, radiative thermal transport is bridged to heat conduction by so-called acoustic phonon tunneling at contact, which can be controlled via external forces. However, to perform such complex experiments, precision measurement of heat flow and isolation from parasitic conduction are required. Here, we demonstrate the utility of hyperspectral frequency-domain

thermoreflectance (FDTR) for the interrogation of thermal transport across subsurface nanogaps, alleviating the extreme challenges faced by nanoscale thermal transport experiments.

FDTR is a pump-probe optical technique sensitive to the thermal properties of an underlying material system. Here, a periodically modulated pump beam deposits energy into the sample, where subsequent temperature oscillations are monitored by a continuous wave probe beam via the thermoreflectance effect. Measurement of the phase lag between the thermal oscillations and periodic heating enables quantification of thermal properties through parametric fitting with the heat diffusion equation. In particular, FDTR at low pump frequencies can quantify and image interfaces up to 200 μm below the surface. We demonstrate FDTR's ability to interrogate subsurface nanogaps by looking at heterogeneously integrated gallium nitride (GaN) with diamond substrates and silicon with silicon substrates. We show that FDTR can precisely quantify the thermal conductivity of air trapped in sub-200 nm gap that is 15 μm below the GaN surface. Similarly, we use hyperspectral FDTR imaging to map a mechanical standing wave in a silicon membrane supported by a silicon substrate, which spatially modulates the gap thermal conductance. Thus, FDTR eliminates the need for microfabricated precision calorimeters and thermally insulated gap supports through spatial mapping of subsurface thermal boundary conductances.

Acknowledgements: Sandia National Laboratories is a multi-mission laboratory managed and operated by the National Technology & Engineering Solutions of Sandia, LLC, a wholly owned subsidiary of Honeywell International Inc., for the U.S. Department of Energy's National Nuclear Security Administration under contract No. DE-NA0003525. SAND2023-11105A

3:00 PM BREAK

SESSION EN07.04: Thermal Measurement Techniques
Session Chairs: Renkun Chen and Pramod Sangi Reddy
Tuesday Afternoon, April 23, 2024
Room 327, Level 3, Summit

3:30 PM *EN07.04.01

TDTR-Based Thermal Conductivity Mapping – Challenges and Applications Yee Kan Koh; National University of Singapore, Singapore

Over the past two decades, time-domain thermoreflectance (TDTR) has been developed into a versatile tool to measure the thermal conductivity of thin films and substrates. Variants of TDTR have been developed, to address the specific needs. For example, beam-offset TDTR has been developed to measure the in-plane thermal conductivity of the thin films. Dual-frequency TDTR has been developed to measure the thermal resistance of buried thin films and interfaces. These various TDTR variants are paramount to advance the knowledge of heat transport in different types of nanostructures and across interfaces. One variant of TDTR that is less explored is to use TDTR for thermal conductivity mapping. In this talk, we will present our recent work to develop and apply TDTR for thermal conductivity mapping. We will share the challenges we faced, including how to ensure smooth surfaces for mapping and how to interpret the results. We will also share our recent works to apply TDTR to map the thermal conductivity of twisted bi-layer graphene and electrodes in the Li-ion batteries. For the first example, we map the thermal conductivity CVD-grown twisted bilayer graphene on single-layer graphene substrates. With the mapping, we are able to accurately measure the thermal conductivity difference between the bilayer and single layer graphene, as a function of the twisted angle between the graphene flakes. In the second example, we map the thermal conductivity of graphite and LCO electrodes of Li-ion batteries. We discuss how we interpret the mapping results, including our measurements near the boundaries of the electrode powders. Our works suggest that TDTR-based thermal conductivity mapping could be a powerful tool to study heat transport in complex composites.

4:00 PM EN07.04.02

Nanoscale Temperature Mapping for Operating Devices with Reflection Electron Elastic Energy Thermometry (REEET) Menglong Hao^{1,2}, Qiyue Zheng^{3,2,4}, Ziwen Zou¹, Xing Xiang³, Saad Sbsafiullah³, Yuhang Cai², Junqiao Wu^{2,4} and Chris Dames^{2,4}; ¹Southeast University, China; ²University of California, Berkeley, United States; ³The Hong Kong University of Science and Technology, Hong Kong; ⁴Lawrence Berkeley National Laboratory, United States

Experimental characterization of nanoscopic temperature distribution and heat transfer in devices with ever-decreasing feature size is fundamental to realizing next-generation chip-level thermal management and validating and unifying fundamental non-diffusive thermal models. However, existing scannable thermal metrologies have their limitations. For instance, scannable far-field optical methods suffer from diffraction-limited spatial resolution; scanning probe techniques are complex due to the tip-sample thermal contact and sometimes perturb the sample thermal field, despite offering nanoscale resolution; TEM-based thermometries require impractically thin, electron-transmissible samples. A flexible metrology that can directly map temperature fields with 10s of nanometer spatial resolution for practical working devices is still lacking.

In this work, we develop a novel nanoscale thermal imaging methodology built upon Reflection Electron Energy Loss Spectroscopy (REELS) in SEM. This method, termed Reflection Electron Elastic Energy Thermometry (REEET), directly measures the mean kinetic energy of thermally-vibrating atoms in materials leveraging the quasi-elastic peak of electrons in the spectrum. Our calibration experiments and first-principles-based calculation of kinetic energy confirmed the physical model for REEET based on simple individual electron-nucleus scattering constrained by conservation laws under the Born approximation. The relative temperature sensitivity of the technique is estimated as $\sim 0.09\%/K$ for light elements such as C and Si at 300-600 K, which compares favorably with other electron-beam-based thermometry.

We used REEET to demonstrate far-field temperature mapping of nanostructured graphitic thin film devices with 300-400 nm feature size, as well as a 250-nm diameter multiwalled carbon nanotube, both under Joule heating. Local hotspots with peak temperature rise of 500-800 K in these nanodevices can be visualized with a spatial resolution estimated as 30-50 nm. The temperature profiles can be well described by our analytical and finite element modeling based on modified Fourier's law using suppressed thermal conductivity of ~ 480 and $\sim 360 \text{ W m}^{-1} \text{ K}^{-1}$ for graphite and MWCNT, respectively. These results

are consistent with prior reports on such carbon materials on substrates due to the Casimir size effect and interface scattering. Additionally, the 2-kV 3-nA electron beam is found to have negligible impact on the lattice temperature rise (<0.1 K) in such devices based on our Monte Carlo simulations (CASINO) and a multi-temperature model.

4:15 PM EN07.04.03

Thermal Diffusivity Measurement of Thin Films by Fourier Transform Thermo-Reflectance Method under Front Heat – Front Detect Configuration [Takahiro Baba](#)¹, Tetsuya Baba¹ and Takao Mori^{1,2}; ¹National Institute of Materials Science (NIMS), Japan; ²University of Tsukuba, Japan

Thermo-reflectance method is one of the few methods which can measure thermal transport properties in the cross-plane direction of thin films. Thermo-reflectance method under front heat – front detect (FF) configuration, so-called time domain thermo-reflectance (TDTR), is commonly used because it can be applied to a wide variety of samples including non-metallic thin films. In FF configuration, both pump beam and probe beam are focused at the same spot on the surface of a sample and temperature response from the surface is observed. In this case, the temperature response is significantly affected by the penetration of pump beam, which depends on the absorption coefficient of the surface. In TDTR method, a metallic layer, sometimes called transducer, is generally deposited on a sample to safely observe thermo-reflectance signals. In most cases, heat diffusion time in the transducer is assumed to be infinitesimal and the layer can be regarded as heat bath with known heat capacity. To determine thermal effusivity of the sample below the transducer, the rate of temperature decrease is analyzed. This means the penetration of pump beam, which affects the initial distribution of temperature, is not considered. This approach has some ambiguity because thermal diffusion in the transducer can significantly affect the determination of the thermal effusivity of the sample. To examine this issue, we propose an analytical approach which considers the effect of penetration of pump beam. Our approach attributes to recent developments in thermo-reflectance method. The electrical delay technique has enabled the technique to observe temperature response in longer timescale than pulse interval of pump laser, which demonstrates the periodic nature of the temperature response. In our recent study, we developed an analytical approach based on Fourier analysis, which can consider the periodicity and improve the robustness and reliability of determination of thermal properties by thermo-reflectance method. Thanks to this new analytical approach, we could also develop a mathematical model which can consider the contribution from the penetration of pump beam, whereas our conventional model assumes that the energy of pump beam is entirely absorbed at the surface without penetration. We could examine how the penetration affects the temperature response and improve the robustness and reliability of determination of thermal properties by thermo-reflectance method under FF configuration. We measured some actual thin films by picosecond thermo-reflectance method under FF configuration. We are going to introduce notable developments in thermo-reflectance method and actual results obtained from these samples, and discuss the robustness and reliability of the determination.

4:30 PM EN07.04.04

Direct Measurement of Ballistic Electron Transport and Negative Thermal Diffusion during Non-equilibrium Heating of Metals Pravin Karna¹, Md Shafkat Bin Hoque², Patrick Hopkins² and [Ashutosh Giri](#)¹; ¹University of Rhode Island, United States; ²University of Virginia, United States

We experimentally show that the ballistic length of hot electrons in laser-heated gold films can exceed ~ 150 nm, which is $\sim 50\%$ greater than the previously reported value of 100 nm inferred from pump-probe experiments. We also find that the mean free path of electrons at the peak temperature following interband excitation can reach upward of ~ 45 nm, which is higher than the average value of 30 nm predicted from our parameter-free density functional perturbation theory. Our first-principles calculations of electron-phonon coupling reveal that the increase in the mean free path due to interband excitation is a consequence of drastically reduced electron-phonon coupling from lattice stiffening, thus providing the microscopic understanding of our experimental findings. We also show that the strength of electron-phonon coupling not only dictates the mean free paths, but also controls a peculiar spatial shrinking of the electronic temperature profile immediately after the electrons have thermalized with the ‘colder’ lattice.

4:45 PM EN07.04.05

Experimental Extraction of Phonon Scattering Lifetimes in MoS₂ Using Transient Grating [Nikhil Malviya](#) and Navaneetha Krishnan Ravichandran; Indian Institute of Science Bangalore, India

In crystalline semiconductors, heat is predominantly transported via the collective vibrations of lattice atoms, and the quanta of the normal modes of these lattice vibrations are called phonons. The resistance to thermal transport in a crystal is caused by the scattering of phonons among themselves, which is driven by the anharmonic crystal potential in pristine semiconductors. During these scattering events, phonons tend to attain equilibrium, and the corresponding time involved, called the phonon lifetime, is an important quantity to determine phonon-specific thermal properties, for example, the distribution of heat-carrying phonons. The transient grating (TG) is a well-established non-contact optical pump-probe technique that is often used experimentally to probe the phonon specific mean free paths, and hence the phonon lifetimes [1,2]. Here, we probe the phonon lifetimes for van der Waals materials like layered MoS₂ using the TG setup. For MoS₂, by comparing our measurements with the predictions from the complete solution of the governing equation for phonon transport, the Peierls-Boltzmann equation (PBE), from first principles, we uncover a significant contribution of momentum conserving Normal scattering as well as the higher-order scattering among four phonons to the total phonon lifetimes. We also discuss the suitability of the computationally inexpensive approximation to the PBE - Callaway model for MoS₂, motivated by its widespread success for several ultrahigh thermal conductivity materials uncovered recently [3].

In the TG technique used in this work, two short pump lasers are made to interfere and get absorbed into the sample, resulting in a spatially sinusoidal temperature grating, with a characteristic period Λ . The decay of this impulsive temperature profile is probed using another probe laser beam. By comparing the observed temperature decay with that calculated from the PBE, the effective thermal conductivity of the sample as a function of Λ can be obtained, from which phonon-specific properties, such as the phonon lifetimes, can be extracted [1,2]. Our experimental measurements highlight the significant contribution of four-phonon scattering to thermal resistance in MoS₂ around and beyond room temperature. By comparing our experimental measurements on phonon lifetimes with the first-principles predictions, we conclude that the Normal processes dominate the total scattering rates at low phonon frequencies in MoS₂, particularly around and below room temperature. Interestingly, we find that four-phonon Normal scattering rates are much stronger than the three-phonon Umklapp scattering rates, which is quite unusual compared to several other materials studied earlier [4]. The comparison of our experimental measurements with first principles predictions also reveal strong anharmonic renormalization of phonon frequencies in MoS₂, even at room temperature, thus significantly affecting its thermal conductivity. We believe that our experimental findings, with insights from predictive first principles calculations, will provide clarity on the nature of phonon-phonon interactions in layered and low-dimensional materials.

This work is supported by the Prime Minister's Research Fellowship (02-01036) and the Science and Engineering Research Board's Core Research Grant No. CRG/2020/006166 and the Mathematical Research Impact Centric Support Grant No. MTR/2022/001043.

References:

- [1] J. A. Johnson, A. A. Maznev, J. Cuffe, J. K. Eliason, A. J. Minnich, T. Kehoe, C. M. Torres, G. Chen, and K. A. Nelson, Phys. Rev. Lett. 110, 025901 (2013).
- [2] N. K. Ravichandran, H. Zhang, and A. J. Minnich, Phys. Rev. X 8, 041004 (2018).

[3] N. Malviya and N. K. Ravichandran, Phys. Rev. B 108, 155201 (2023).

[4] N. K. Ravichandran and D. Broido, Phys. Rev. X 10, 021063 (2020).

SESSION EN07.05: Poster Session I: Thermal Transport and Energy Conversion I

Session Chairs: Woochul Kim and Sunmi Shin

Tuesday Afternoon, April 23, 2024

Flex Hall C, Level 2, Summit

5:00 PM EN07.05.01

Thermal Conductance of Buried AlN Interfaces Measured by Dual-Frequency Time-Domain Thermoreflectance Yi Jiang¹, Ravikiran Lingaparthi², Casimir Chan², Alex Tian Long Seah², Kirill Shabdurasulov^{2,3}, Nethaji Dharmarasu², K Radhakrishnan^{2,3} and Yee Kan Koh¹; ¹Department of Mechanical Engineering, National University of Singapore, Singapore; ²Temasek Laboratories, Nanyang Technological University, Singapore; ³School of Electrical and Electronic Engineering, Nanyang Technological University, Singapore

Thermal management is a critical concern in microelectronic devices, especially for third-generation semiconductor devices that are based on GaN and AlN due to high power density during operations. An in-depth understanding of their thermal properties is essential for thermal management, such as interfacial thermal conductance between different layers. However, accurately measuring the thermal conductance in buried interfaces, particularly in epitaxial growth interfaces, is substantially challenging due to its low measurement sensitivity. Conventional time-domain thermoreflectance (TDTR) technique can only achieve around 40% of uncertainty, or not able to separate the thin film thermal conductivity and the buried interfacial thermal conductance. In this study, we utilize dual-frequency TDTR technique with Monte Carlo simulations to precisely quantify the thermal conductance of buried AlN interfaces with various substrates.

Firstly, we deposit AlN on common substrates, specifically, sapphire, silicon, and 4H-SiC, using molecular beam epitaxy (MBE). We carefully control the thickness of AlN to be 100 nm for the best experiment sensitivity. The quality of the AlN films is assessed by atomic force microscopy (AFM) and the picosecond acoustics technique of TDTR. Subsequently, TDTR measurements are performed at modulation frequencies of 18.9 MHz and 5.4 MHz, which leads to two different thermal penetration depths. To enhance the sensitivity of thermal conductance of AlN/substrate interfaces, we analyse the ratio of TDTR signals between 18.9 MHz and 5.4 MHz measurements. In addition, we employ Monte Carlo simulations to statistically estimate the uncertainty by considering results from both measurements and their ratio. The measurement uncertainty is reduced to approximately 1/3 of the conventional single-frequency TDTR measurements.

Our method can accurately measure the interfacial thermal conductance between AlN and different substrates with each result exhibiting an uncertainty of less than 16%. Among these substrates, the high interfacial thermal conductance of AlN/4H-SiC (~450 MW/m²K) provides a promising prospect for effective heat dissipation across the interface.

In summary, this study demonstrates a dual-frequency TDTR technique with Monte Carlo simulations that significantly enhances the precision by 3 times in interfacial thermal conductance measurements of buried interfaces with just 100 nm of AlN. This technique contributes to a guidance of interfacial thermal conductance measurements and exploring thermal management further in electronic devices.

5:00 PM EN07.05.02

Dual-Functional Wood for Thermal Management of Buildings through Radiative Cooling and Thermal Energy Storage Bernadette Magalindan¹, Lyu Zhou¹ and Shuang Cui^{1,2}; ¹The University of Texas at Dallas, United States; ²National Renewable Energy Laboratory, United States

Passive thermoregulation of buildings presents a sustainable means to alleviate the ever-growing demand for thermal comfort. Although emerging radiative cooling technologies effectively enable one-way heat rejection and achieve cooling, they alone cannot fully satisfy the thermal comfort needs that arise from all types of weather – namely, the need for warmth in cold weather. In this work, we developed a dual-functional material, composed of microencapsulated phase change materials (MPCMs) embedded in delignified wood pulp, for energy-efficient thermal management of buildings through radiative cooling and thermal energy storage (TES). In warm weather, radiative cooling assists the re-crystallization of MPCMs; in cold weather, TES serves as a valuable complement to radiative cooling by preventing excessive cooling and offering space heating. The dual-functional material exhibits 92% of solar reflection that ascribes the scattering by the wood pulp and MPCMs, whereas the intrinsic emissivity of cellulose produces a strong radiative cooling effect. Meanwhile, TES through MPCMs achieves a latent heat of 150 J/g with excellent shape stability. This material's superior thermoregulation enabled by the synergistic TES and radiative cooling properties is demonstrated by outdoor testing, showcasing the substantial energy-saving potential of this innovative approach. Additionally, fabricating the material from abundant cellulose promotes carbon sequestration and offers a promising avenue for the development of sustainable building materials for energy-efficient thermal regulation.

5:00 PM EN07.05.03

Decoupling Electronic and Thermal Transport in Spinel Oxide Ashutosh Srivastava, Madhubanti Mukherjee and Abhishek K. Singh; Indian Institute of Science, Bengaluru, India

Decoupling electronic and thermal transport properties remains the biggest challenge in finding efficient thermoelectric materials. We demonstrate an approach to decoupling the complex interdependence among electrical conductivity, Seebeck coefficient, and lattice thermal conductivity in spinel oxides. Utilizing the effects of tetrahedral and octahedral coordination on bonding characteristics, we demonstrate tuning the electronic and thermal transport properties of cobalt-based spinel oxides ACo₂O₄. Tetrahedrally coordinated cation A (Zn/Cd) controls the electronic transport, while thermal transport has been controlled by octahedrally coordinated cation B (Co). The combination of heavy bands and contribution of the tetrahedrally coordinated environment of Co near valence band maxima (VBM) and conduction band minima (CBM) results in an enhanced power factor. Additionally, the substitution of Cd for Zn on an octahedrally coordinated cation site leads to one order of magnitude reduction in the lattice thermal conductivity (κ_l). This reduction is attributed to the significant mass difference, phonon modes, phonon lifetime, and remarkably strong anharmonic scattering introduced by Cd. Simultaneously achieved high power factor and low lattice thermal conductivity resulting in an enhanced figure of merit value of 1.68 for Cd-spinel. The approach of decoupling atomic contributions utilizing various cationic sites demonstrates a potential route to enhance thermoelectric performance.

5:00 PM EN07.05.04

Temperature Dependent Electron Emission in Focused Ion Beam Microscopes Wyatt Hodges, Julia Deitz, Luis Jauregui, Daniel Perry, Joseph Boro and Jessica Duree; Sandia National Laboratories, United States

Transistors in mass produced consumer electronics have characteristic dimensions on the nanometer scale, with companies such as Intel and Samsung

continuously working to increase transistor density by fabricating smaller components. Thermal management (i.e., temperature during use) plays a key role in effective operation of these devices. However, measuring temperature of nanometer scale components presents a challenge. Optical techniques commonly used in failure analysis, such as IR thermography, are diffraction limited and cannot effectively access the nanoscale. Contact techniques such as scanning thermal microscopy offer nanoscale resolution, but parasitic losses from the scanning tip limit temperature sensitivity. Transmission electron microscopy has been used to demonstrate thermal effects with nanometer resolution but can only accommodate devices that have been thinned to ~100 nm. Scanning electron microscopy shows some promise as a noncontact technique that has topographical resolution of ~1 nm and has shown preliminarily to have temperature dependence in secondary electron counts.

Here we examine thermal effects in Focused Ion Beam (FIB) microscopes. FIB microscopes offer several advantages over using a single beam SEM instrument: (1) the ion beam does not generate backscattered electrons, improving signal to noise ratio, (2) the ion beam can mill samples, allowing measurements of subsurface features in devices without breaking vacuum, and (3) FIB tools are almost exclusively manufactured as dual beam FIB-SEMs, so electron beams are simultaneously accessible. Using the FIB-SEM we demonstrate temperature dependence in grayscale intensity in semiconductor images. We additionally show results of energy mapping at different temperatures at multiple temperatures using the through lens detector built into FIB-SEM microscopes. Comparison of temperature dependent effects in SEM and FIB images are discussed. We also examine the additional considerations of accelerating voltage, power normalization, ion implantation, and spatial resolution.

Sandia National Laboratories is a multimission laboratory managed and operated by National Technology & Engineering Solutions of Sandia, LLC, a wholly owned subsidiary of Honeywell International Inc., for the U.S. Department of Energy's National Nuclear Security Administration under contract DE-NA0003525.

5:00 PM EN07.05.05

Electromagnetic Wave-Absorbing and Heat-Managing Magnetic Composite Membrane Engineered via an Atomized Aerosol Process Jeong Seung-Jae, Mi Se Chang, Jae Won Jeong, Sangsun Yang and Young-Tae Kwon; Korea Institute of Materials Science, Korea (the Republic of)

Rapid advancements in fifth-generation (5G) telecommunications have generated a demand for enhanced connection and data transmission, which are expected to significantly affect various fields. The rise of networks operating within higher frequency bands compared to previous wireless technologies has prompted the need for the development of electromagnetic wave (EMW) absorbers to alleviate signal interference, EMW pollution, and potential health risks. Among the notable materials, soft magnetic materials with high saturation magnetization and low coercivity facilitate effective EMW absorption ranging from 2 to 18 GHz. However, the low complex permeability of commonly available soft magnetic materials shows limited EMW absorbing characteristics. Here, we present the shape-modulated FeCo-boron nitride (BN) soft magnetic particles prepared via an atomized aerosol process for EMW absorption and thermal management. Shape modulation has become a widely used method to raise the Snoek's limit of spherical particles and thus enhance the complex permeability and the ferromagnetic resonance of the material. New class of the chemical process designed in this work allows a one-step synthesis of composites with three different structures, including spheres, cubes, and hollows, without requiring any shape-controlling additives. The FeCo-BN composite membrane demonstrates enhanced complex permeability and effective impedance matching, leading to a high reflection loss value of -46.4 dB at 11.3 GHz. In addition, the incorporation of BN nanomaterials enabled the effective dissipation of heat converted from EMW energy. Overall, our research findings in shape modulation process and material designs highlight promising opportunities for the EMW absorbing and thermally managing membranes.

5:00 PM EN07.05.06

Precision Microengineering of Curved Metallic Heat Transfer Surfaces for Fouling Inhibition Liyang Chen¹, Julian Schmid¹, Tobias Armstrong¹ and Thomas Schutzius^{1,2}; ¹ETH Zurich, Switzerland; ²University of California, Berkeley, United States

Crystallization fouling, an undesirable process where scale forms on surfaces, is pervasive in nature and technology, negatively impacting the energy and water industries. Work has progressed towards realizing surfaces with intrinsic antifouling properties, however, realizing precise, defect-free topography over large areas with complex curvature remains challenging. In this work, we successfully developed a technique allowing us to impart precise surface microstructure array patterns onto metallic heat transfer surfaces with isotropic and anisotropic curvatures. The patterning on curved surfaces is realized by four steps: photoresist microstructure generation on planar substrates; structure transfer to curved metallic surfaces under heat and pressure; metal deposition by electroplating/electroless plating; photoresist removal. We conducted preliminary tests on the heat transfer performance of copper substrates with and without micropatterns in heat-exchanger-like conditions and the results show that the surface micropatterns can effectively modify the heat transfer coefficient of the metallic substrate and the structures possess good tolerance to fluidic friction. Durable curved (super)hydrophobic metallic surfaces can be realized with such stable microstructures, which are promising to mitigate fouling issues and energy loss by inhibiting the onset of nucleation and reducing the adhesion of limescale crystallites.

5:00 PM EN07.05.07

Understanding Phonon Mediated Lattice Thermal Conductivity in Magnetic Trihalides Ashutosh Srivastava¹, Heda Zhang², Chunqiang Xu², Subhendra D. Mahanti², Xianglin Ke² and Abhishek K. Singh¹; ¹Indian Institute of Science, India; ²Michigan State University, United States

The investigation of phonon-mediated behaviours in transition metal trihalide systems is becoming an area of growing interest in fundamental research. The insulation of quantum magnet trihalides in both bulk and two-dimensional (2D) layers is a valuable avenue for investigating spin liquid phenomena, spintronics, magnetism in 2D and bulk systems, and thermal transport. The investigation of thermal transport mechanisms involving phonons in the presence of spins has received limited attention thus far. The present study has investigated the harmonic and anharmonic vibrational characteristics of magnetic bulk CrCl₃ and CrI₃ by the use of density functional theory (DFT) and subsequent experimental validation. Theoretical findings underscore the significance of van der Waals and magnetic interactions in ensuring the dynamical stability of these systems. The vibrational spectra of CrCl₃ and CrI₃ exhibit notable distinctions, mostly due to the presence of a phonon band gap in CrI₃. In particular, low-energy phonons in CrI₃ are predominantly influenced by iodine contributions. The phononic vibrational spectrum of CrCl₃ exhibits an intriguing anisotropic lattice thermal conductivity (κ_l), with higher κ_l values observed in the in-plane direction compared to CrI₃. Conversely, CrI₃ demonstrates larger κ_l values in the out-of-plane direction when compared to CrCl₃. It is demonstrated that despite the higher scattering strength of phonons in CrCl₃ due to its higher phonon group velocities, the heat transfer capacity of CrCl₃ surpasses that of CrI₃. Our study offers a fundamental comprehension and valuable insights into the phononic heat conduction in magnetic bulk transition metal trihalide materials.

5:00 PM EN07.05.08

Synergistic Effect of Radiative Cooling and Thermal Energy Storage for Advanced Thermal Management Lyu Zhou, Roma Avhad and Shuang Cui; University of Texas at Dallas, United States

Recent research endeavors strive to develop sustainable thermal management methods to confront the threats posed by extreme weather events and global

energy crisis. Thermal energy storage (TES), which harnesses the latent heat of phase change materials (PCMs), is a promising technology that has been extensively explored for thermal management. However, the practical implementation of TES in buildings faces inherent limitations, including issues related to shape stability, supercooling, slow charging/discharging rates, and limited storage capacity. Here we report a shape stabilized PCM composite that overcomes these challenges by exploring the synergetic effect of TES and passive radiative cooling (PRC), which consists of polyethylene glycol (PEG) as PCM and functionalized boron nitride (fBN) particles as solar scatterers. The inclusion of fBN particles induces a Mie-scattering effect and combines with the intrinsic thermal emission of PEG, resulting in an impressive solar reflectivity of 84.5% and a thermal emissivity of 95.0%. Meanwhile, the composite also achieved a latent heat of 97.1 J/g with excellent shape stability promoted by the interaction between fBN with PEG. Compared to traditional TES, this synergetic effect of PRC and TES promises more efficient thermal regulation by (1) effectively charging PCM during nighttime, (2) maximizing daytime cooling capabilities, and (3) mitigating the impact of supercooling effect. Our modeling study showed that the proposed dual-functional composite could extend the effective TES period by over 50% within a 24-hour cycle. The field test also demonstrated a PRC effect of 3.5 °C below ambient during night, which facilitated the charging of PCMs via crystallization. All these benefits are particularly promising for developing sustainable building thermal management.

5:00 PM EN07.05.09

Temperature-Dependent Optical Properties of Monocrystalline CaF₂, BaF₂, and MgF₂ Qifan Zheng, Xinchao Wang and Dakotah Thompson; University of Wisconsin-Madison, United States

The alkaline earth metal difluorides are critical optical components for applications in non-contact temperature sensors, thermal imaging, and infrared spectroscopy due to their characteristically low refractive index and wide optical transparency spanning the ultraviolet to mid-infrared. Despite their technological importance, a systematic investigation into the temperature dependence of their optical properties is lacking. In this study, spectroscopic ellipsometry was used to obtain the refractive index of monocrystalline CaF₂, BaF₂, and MgF₂ for wavelengths between 220 nm and 1700 nm, and for temperatures between 21 °C and 368 °C. The refractive index of CaF₂ and BaF₂ was observed to decrease linearly with increasing temperature, which can be largely attributed to a reduction in the mass density due to thermal expansion. In contrast, the refractive index of MgF₂ was found to vary nonlinearly with temperature, which suggests competing effects from the material's electronic polarizability. The temperature-dependent refractive index data reported here provide a finely-resolved mapping of the thermo-optic coefficient for these three materials, which could inform the development of optical devices operating at elevated or unsteady temperatures.

5:00 PM EN07.05.10

Transient Active Cooling of Microscale Hot Spots Using Thermoelectric Devices Yihan Liu¹, Hao-Yuan Cheng², Jonathan A. Malen² and Feng Xiong¹; ¹University of Pittsburgh, United States; ²Carnegie Mellon University, United States

Thermal management of microprocessors suffers from transient local hot spot induced by circuits such as clock generator. Embedded thermoelectric devices (TEDs) are promising to remove heat from local hot spots with passive cooling by the Fourier law and active cooling by thermoelectric effect with transient electrical power supplied. In this work, we introduce an analytical model to describe the temperature response of a periodically heated hot spot, which is actively cooled by a thermoelectric cooler operating at the same frequency. The analytical result is experimentally validated with frequency domain thermal reflectance (FDTR) measurements made directly on an actively cooled Si TED where the transient local hot spot is replicated by laser. We further demonstrate a practical and energy efficient method to actively cancel the TED's surface temperature variations based on our model's analytical result. We then apply this method to cancel the transient temperature variation of $2.35 \pm 0.26\text{K}$ at 10 kHz on the Si TED's hot side surface. Our model's result and the active cooling method is promising for analysis and optimization of cooling systems for transient localized hot spots in integrated circuits.

5:00 PM EN07.05.11

Improved Durability Nanotextured Aluminum Surfaces for Jumping Droplet Thermal Rectification Trevor J. Shimokusu¹, Frank Robinson², Alia Nathani¹, Zhen Liu¹, Te Faye Yap¹, Daniel Preston¹ and Geoffrey Wehmeyer¹; ¹Rice University, United States; ²NASA Goddard Space Flight Center, United States

Jumping droplet thermal diodes (JDTDs) offer new capabilities for passive thermal rectification in thermal management of buildings, electronics, and batteries.^[1-3] However, the durability of JDTD devices is limited because the superhydrophobic (SHPB) surface degrades upon continuous exposure to condensing water vapor.^[4] In addition, most prior JDTDs documented in the literature have been constructed with copper surfaces, although aluminum surfaces are preferable for lightweight applications.^[2,3,5-8]

In this work, we quantify the durability of novel SHPB aluminum surfaces and JDTD devices. We manufacture our Al-based surfaces using scalable surface functionalization techniques based on hydrothermal nanostructuring, silanization, and a dip coat deposition of Teflon AF (amorphous fluoropolymer). We show that dip-coating Teflon AF on top of TFTS monolayer-coated nanostructured surfaces enhances surface durability compared to non-Teflon coated surfaces, thereby enabling prolonged operation and comprehensive thermal testing of the JDTD. Contact angle measurements, environmental scanning electron microscope (ESEM) images, and X-Ray photoelectron spectroscopy (XPS) measurements indicate slight changes in the surface topology and chemical composition after dip coating, confirming that the deposited coating is thin (<20 nm).

Using our SHPB surfaces, we parametrically study steady-state thermal rectification as a function of gap height, fluid fill ratio, and heating orientation of the JDTD. We identify tradeoffs between the performance and the orientation dependence of operation by controlling the gap height and charge level. At larger gap sizes and lower charge levels, we observe enhanced thermal rectification only when the JDTD is heated from the bottom, while minimal thermal rectification is measured when the JDTD is heated from the top. At moderate charge levels and smaller gap sizes, operation is sustained in both orientations, but thermal rectification is reduced. We demonstrate a maximum thermal rectification ratio of 30 plus/minus 1.

To investigate potential implementation in thermal energy storage and harvesting applications, we show that the Al JDTD enables a half-wave thermal rectifier circuit that rectifies time-periodic temperature profiles, achieving thermal circuit effectiveness values up to 30 % of the ideal-diode limit at rectification ratios near 5. When coupled with thermal capacitances, such time-periodic thermal rectification could aid cold energy storage for passive cooling of components subjected to time-periodic thermal boundary conditions. Thus, our findings showcase the functionality of Al-based surfaces for thermal rectification and could guide future work aiming to apply Al JDTDs for improved thermal management.

References

- [1] H. Zhao, Y. Wu, H. Sun, B. Lin, M. Zhong, G. Jiang, S. Wu, *Renewable Energy* **2023**, 119278.
- [2] J. B. Boreyko, C.-H. Chen, *International Journal of Heat and Mass Transfer* **2013**, 61, 409.
- [3] F. Zhou, Y. Liu, S. N. Joshi, E. M. Dede, X. Chen, J. A. Weibel, in *2017 16th IEEE Intersociety Conference on Thermal and Thermomechanical Phenomena in Electronic Systems (ITherm)*, IEEE, Orlando, FL, **2017**, pp. 521–528.
- [4] M. J. Hoque, J. Ma, K. F. Rabbi, X. Yan, B. P. Singh, N. V. Uput, W. Fu, J. Kohler, T. S. Thukral, S. Dewanjee, N. Miljkovic, *Applied Physics Letters*

2023, 123, 110501.

[5] J. B. Boreyko, Y. Zhao, C.-H. Chen, *Appl. Phys. Lett.* **2011**, 99, 234105.

[6] J.-X. Wang, P. Birbarah, D. Docimo, T. Yang, A. G. Alleyne, N. Miljkovic, *Phys. Rev. E* **2021**, 103, 023110.

[7] B. Traipattanakul, C. Y. Tso, C. Y. H. Chao, *International Journal of Heat and Mass Transfer* **2019**, 135, 294.

[8] M. Y. Wong, Y. Zhu, Y. Zeng, T. C. Ho, Y. Yang, H. Qiu, C. Y. Tso, *Advanced Engineering Materials* **2022**, 24, 2100958.

*This work was supported by a NASA Space Technology Graduate Research Opportunity (80NSSC20K1220).

5:00 PM EN07.05.12

Effect of Fluorination on The Thermal Conductivity of Graphite Fluoride (CF) Wonsik Lee, Seungbin Han and Hyejin Jang; Seoul National University, Korea (the Republic of)

For thermal management applications, there are surging demands for materials with high thermal conductivity and electrically insulating properties. Graphite fluoride (CF), one of the novel graphene-based layered materials, has emerged as a promising thermal management material owing to its similar crystal structure to that of graphite yet electrically insulating properties, i.e., electronic band gap of over 3 eV. CF is expected to show high thermal conductivity due to its structural similarity to graphite. However, the degree of which fluorination alters the thermal conductivity is largely unexplored, and even the thermal conductivity is not experimentally established. Here, we report the through- and in-plane thermal conductivity of mechanically exfoliated CF flakes for the first time by using time-domain thermoreflectance (TDTR). At room temperature, a 70-nm-thick CF flake shows $(1700 \pm 300) \text{ W m}^{-1} \text{ K}^{-1}$ for in-plane direction, which is about 90 % of that of graphite, and $(4.0 \pm 0.8) \text{ W m}^{-1} \text{ K}^{-1}$ for through-plane direction. The through-plane thermal conductivity of CF flakes shows quasi-ballistic behavior for thicknesses $< 200 \text{ nm}$, which is similarly observed in graphite but shows two times higher through-plane thermal conductivity than that of graphite. We calculate the phonon properties of monolayer graphene and graphene fluoride to reveal the intrinsic phonon transport mechanisms by solving the phonon Boltzmann transport equation (BTE). BTE estimates the thermal conductivity of graphene and graphene fluoride as $3000 \text{ W m}^{-1} \text{ K}^{-1}$ and $270 \text{ W m}^{-1} \text{ K}^{-1}$, respectively. Phonon mode thermal conductivity indicates that the fluorination opens an out-of-plane acoustic (ZA) phonon scattering channel and the ZA phonon contribution to the thermal conductivity of CF is greatly suppressed, compared to the case of graphene. To understand the discrepancy in thermal conductivity between the experimental and theoretical results, we characterize the chemical and optical properties of exfoliated CF flakes to correlate those properties with thermal conductivity results. We believe this work reveals the role of functional groups on thermal conductivity in graphene/graphite-derivative materials.

5:00 PM EN07.05.13

Development and Validation of Calcium Chloride Hexahydrate-Based Eutectic Systems Denali Ibbotson, Derian Morphew, Bryan Duong and Patrick Shamberger; Texas A&M University, United States

As the use of different renewable energies becomes more common and widespread, the need for different technologies to store that available energy to use at a later time will only grow. Therefore, in order to move towards the decarbonization of the energy grid, effective thermal energy storage systems will be integral in this process. One method that is used to increase HVAC system efficiency and to allow for more efficient load displacement is the incorporation of phase change materials (PCMs) into thermal energy storage systems. PCMs can passively store and release heat, thus allowing for a pathway in order to displace peak energy load for buildings that will better align with the available excess energy generation. However, robust and economical phase change materials that are tailorable to a specific desired energy storage temperature are needed to accomplish this task. Salt hydrates represent one class of PCMs of interest due to their high volumetric energy densities, low cost, and the ability to tailor the energy storage temperature through the design of custom salt hydrate eutectics. However, they can also experience undercooling, a nucleation-limited phenomena which results in the existence of a metastable liquid below the melting point. This phenomena can lead to undesired issues, including incongruent melting and phase segregation. Thus, eutectic mixtures of salt hydrates are often used, as they tend to melt at a single-valued temperature and are a chemically related family of PCMs that enable bespoke PCMs with specifically defined eutectic temperatures. Though, within eutectics, undercooling can still be prevalent, and thus nucleation particles can be added to the system to induce nucleation. However, the effect of nucleation particles is not well understood when the nucleating system contains multiple compounds, as the different phases present within the eutectic can affect how and where nucleation will occur.

In this study, we first explored pseudo-binary and ternary eutectic systems with the intent of identifying systems with closely spaced eutectic temperatures. Specifically, we investigated several different pseudo-binary and ternary calcium chloride hexahydrate ($\text{CaCl}_2 \cdot 6\text{H}_2\text{O}$) - based eutectic systems, with several different eutectic components such as calcium bromide hexahydrate, magnesium chloride hexahydrate, potassium chloride, ammonium chloride, and urea. Calcium chloride hexahydrate is a stoichiometric salt hydrate of interest for use in thermal energy storage systems because it is a low cost salt hydrate that melts at 29°C . However, calcium chloride hexahydrate is also prone to undercooling and phase segregation related to incongruent melting behavior. Therefore, several different calcium chloride hexahydrate-based eutectic systems were identified and evaluated, in order to develop a family of PCMs with specifically defined eutectic temperatures. We utilized calorimetric techniques to measure undercooling in small quantities of calcium chloride hexahydrate with different eutectic components, and differing weight percentages of the other component. We observed in several cases that the eutectic composition can have a reduced melting temperature by up to 10°C , which allows for a wider available range of melting temperatures. We will present several different eutectic systems and how melting and solidification in these eutectic systems can often be affected by the addition of nucleation particles, when compared to the base stoichiometric system. Additionally, we will also present the effects of the presence of multiple phases and how they can affect the nucleation behavior.

5:00 PM EN07.05.14

Impact of Cooling Rate and Thermal Mass on Supercooling in a Salt-Hydrogel Complex for Thermal Energy Storage Youngmun Lee, Daniel Hsieh, Sung Bum Kang, Paul V. Braun and Sanjiv Sinha; University of Illinois at Urbana Champaign, United States

Glauber's salt is a promising phase change material for building thermal management because of its high latent heat, acceptable melting temperature of 32.3°C for indoor air^{1,2}. Despite these advantages, the practical application of Glauber's salt in thermal energy storage systems is still challenging due to supercooling and phase segregation¹⁻³. Here, we report the impact of temperature ramp rate and thermal mass on the supercooling of Glauber's salt through the DSC and T-history experiment. The ramp rate effect was studied with a wide range of ramp rates in 1 to $10^\circ\text{C}/\text{min}$ in DSC and 1 to $4^\circ\text{C}/\text{min}$ in the T-history experiment. The thermal mass effect was investigated by comparing DSC and T-history experiment. The latent heat was also analyzed for different ramp rates and thermal mass conditions. The melting temperatures of Glauber's salt from the two techniques were identical while freezing temperatures were different because of the thermal mass effect. During freezing in the T-history experiment, the latent heat was reduced by around 75% to the latent heat in melting due to supercooling and phase segregation. To overcome this bottleneck, we developed a novel hydrogel complex that reduces the supercooling and prevents phase segregation to maintain volumetric energy density for 100 cycles. Thermodynamic analysis accounting for composition shows that a higher salt composition can further enhance the volumetric energy storage density. For example, a 10% increase in the weight percentage of salt leads to about 50% enhancement in volumetric energy storage density.

References:

1. D. R. Biswas, *Solar Energy*, **19**, 99–100 (1977).
2. S. M. Hasnain, *Energy Conversion and Management*, **39**, 1127–1138 (1998).
3. Byung Chul Shin, Sang Done Kim, P. Won-Hoon, *Energy*, **14**, 921–930 (1989).

5:00 PM EN07.05.15

Thermal Conductivity of Individual Ceramic Fillers and Their Application to Thermal Interface Materials Woo Hyun, Jee-Hoon Kim and Hyejin Jang; Seoul National University, Korea (the Republic of)

Oxide ceramic fillers, such as Al₂O₃ and MgO, have been commonly used for thermal interface materials (TIMs) due to their affordable cost and decent thermal conductivity, i.e., 30 and 48 W m⁻¹ K⁻¹ for each bulk material. In addition, hydroxide fillers, such as Al(OH)₃ and Mg(OH)₂, have recently been noticed due to their shorter processing time, lightweight nature, and excellent flame retardancy, which are beneficial compared to oxide fillers. While the thermal conductivity of ceramic fillers is one of the most important properties for the performance of TIM, the direct evaluation of the fillers has remained challenging. Thus, the thermal conductivity of bulk materials has been assumed for the fillers when designing the TIMs. In this study, we employed time-domain thermoreflectance (TDTR) to measure the thermal conductivity of individual ceramic filler particles at 300K. For Al₂O₃ and MgO, the filler size in the range of 60–120 μm is investigated, and thermal conductivity varies depending on the filler size. For example, the thermal conductivity of Al₂O₃ decreases from (30±6) to (7.0±1.2) W m⁻¹ K⁻¹ when the filler size is reduced from 120 to 70 μm. The thermal conductivity of MgO decreases from (47±7) to (23±3) W m⁻¹ K⁻¹ when the filler size decreases from 100 to 60 μm. The hydroxide fillers show much smaller and a broad range of thermal conductivity, i.e., 3.4–10 W m⁻¹ K⁻¹ for Al(OH)₃, and 0.7–3.0 W m⁻¹ K⁻¹ for Mg(OH)₂. We attribute this distribution of thermal conductivity to the layered structures and weak hydrogen bonding between layers of the hydroxide fillers. The effects of crystal structures and microstructures on the thermal conductivity will be discussed. Furthermore, to reveal the relation of the thermal conductivity of fillers to that of TIM, we prepare the TIMs using these fillers and measure their thermal conductivity using the steady-state ASTM D5470 method. We expect our work to provide a practical guideline for selection of filler types and sizes for TIMs, based on the thermal conductivity values of actual fillers measured by using TDTR.

5:00 PM EN07.05.16

Supramolecular Interactions lead to Remarkably High Thermal Conductivities in Interpenetrated Two Dimensional Porous Crystals Jaymes Dionne¹, Ashutosh Giri¹ and Patrick E. Hopkins^{2,2,2}; ¹University of Rhode Island, United States; ²University of Virginia, United States

The design of innovative porous crystals with high porosities and large surface areas has garnered a great deal of attention over the past few decades due to their potential for a variety of applications, including flexible electronics, gas storage, and catalysts, among others. However, heat dissipation poses a major challenge in porous crystals and enhancing heat dissipation is key to realizing their potential. In this work, we use systematic atomistic simulations to show that the interpenetration of two, two-dimensional frameworks possess remarkable thermal conductivities at high porosities compared with their single three-dimensional framework and interpenetrated three-dimensional framework counterparts. Typically, high thermal conductivities are associated with low porosities; however, this work provides an alternative method to retain high porosities while drastically enhancing the thermal conductivity of the porous crystal. We attribute this to lower phonon-phonon scattering and vibrational hardening from supramolecular interactions that restrict atomic vibrational amplitudes, enhancing heat conduction. We also show this for realistic systems, with a two-dimensional interpenetrated framework of COF-1 achieving an order of magnitude increase in thermal conductivity when compared to its three-dimensional counterpart, COF-300. This introduces a new regime of materials design that combines ultrahigh thermal conductivities with ultralow mass densities via the interpenetration of two-dimensional porous crystals.

5:00 PM EN07.05.17

Investigation of Grain Effect in Heat Transfer for less than - 10nm Local Areas of HfO₂ Thin Film Deposited with Atomic Layer Deposition Seunghoe Koo, Jaehee Park, Junki Jung and Kyeongtae Kim; Incheon National University, Korea (the Republic of)

Recently, the rapid development of the material science and nano-atomic technology has led to the development of device made up of dozens of atoms such as nanoparticles(0D), nanowires(1D), 2D atomic materials, ultra-thin film. In particular, the atomic layer deposition(ALD) method is attracted attention as a key technology that can produce ultra-thin films at the atomic level. In the ultra-thin film, because the size of a material becomes similar to or less than the size of the quantum mechanical wave of particle or the energy carrier's collision distance (mean free path, MFP), a novel quantum mechanical characteristics occurs. Therefore, novel heat transfer mechanisms should exist in angstrom-scale materials. We can predict that a difference or a restriction in the quantum heat transfer exist based on the crystal structure and thin-film thickness obtained from previous theoretical studies. However, the heat transfer mechanism has not been proven owing to the difficulty of the experimental approach and the lack of measurement techniques in the atomic or angstrom scale. In addition, only the totally averaged thermal conductivity is reported regarding the annealing effect of the thin film, and the relationship between grain size and heat transfer by annealing is not closely analyzed. In this study, we used scanning thermal microscopy(SThM) to investigate heat transfer differences occurring in a local area less than ~10 nm in HfO₂ thin films. The difference in averaged thermal conductivity and distribution of thermal conductivity in the local area according to the thickness of the thin film was investigated. In addition, the crystal structure was changed through annealing, and the thermal conductivity of the thin film according to grain size was investigated. The thermal transfer mechanism investigated in this work according to the crystal structure will be an important background for the development of innovative device using ALD method. It is also expected that the SThM system used in this study will be actively used for future research that can provide insight of new heat transfer mechanisms in the atomic scale.

5:00 PM EN07.05.18

Low Thermal Conductivity and High Thermoelectric Performance in Toxic-Element-Free Inverse-Perovskite Oxide Xinyi He¹, Shigeru Kimura¹, Takayoshi Katase¹, Terumasa Tadano², Satoru Matsuishi¹, Hidenori Hiramatsu¹, Hideo Hosono¹ and Toshio Kamiya¹; ¹MDX Research Center for Element Strategy, International Research Frontiers Initiative, Tokyo Institute of Technology, Japan; ²Research Center for Magnetic and Spintronic Materials, National Institute for Materials Science, Japan

Given the recently increasing energy crisis, there has been a growing focus on thermoelectric technology for converting waste heat energy into electrical power. The energy conversion efficiency (ZT) of thermoelectric materials, defined as $ZT = S^2\sigma T\kappa^{-1}$, is determined by the key factors: the Seebeck coefficient (S), the electronic conductivity (σ), and thermal conductivity (κ), which includes both electronic (κ_{ele}) and lattice (κ_{Lat}) contributions. Therefore, high ZT thermoelectric materials require large S and high σ to achieve a high power factor ($PF = S^2\sigma$), along with low κ to create a sizable temperature gradient. To date, high thermoelectric ZT values has primarily been demonstrated in heavy metal chalcogenides, but the use of toxic elements, such as Pb and Te, is not preferred for widespread practical applications of thermoelectricity. In this study, we propose inverse perovskite-type oxide Ba₃SiO as a novel class of toxic-element-free thermoelectric materials with high ZT reported so far. First, we experimentally demonstrate that undoped Ba₃SiO bulks exhibit rather high $ZT = 0.16\text{--}0.84$ at $T = 300\text{--}623$ K. In addition to these promising experimental results, we demonstrate that the maximum ZT is estimated to be 2.14 for Ba₃SiO at $T = 600$ K when optimally doped, based on the first-principles carrier and phonon transport calculations. The maximum ZT value of Ba₃SiO is notably higher than those of environmentally benign thermoelectric materials, and it is comparable to those of the high ZT

thermoelectric materials composed of heavy and toxic elements in the same temperature range.

We elucidate the origin of high ZT for Ba_3SiO and the underlying physical mechanisms through a combination of the experimental analysis and the first-principles calculations. We observed that Ba_3SiO bulks exhibit remarkably low lattice thermal conductivity (κ_{lat}) of 1.00 W/(mK) at $T = 300$ K, which is significantly lower than 8.2 W/(mK) of the normal perovskite SrTiO_3 bulk, and even lower than 1.7–2.0 W/(mK) of Bi_2Te_3 and PbTe bulks. The crystal structure of Ba_3SiO is constructed from the highly distorted O– Ba_6 octahedra framework with weak O–Ba ionic bonds, which provides low phonon group velocity and strong phonon scattering. Additionally, Ba_3SiO possesses favorable band structures for achieving a high PF, where the valence band around the Fermi level arises from the p state of the negatively charged Si anion with large ion size, and their highly dispersive bands with multiple valley degeneracy enable both high σ and high S , simultaneously, leading to the high ZT for Ba_3SiO originating from the low κ_{lat} and the high PF. These results suggest that inverse-perovskite oxides are promising and environmentally benign thermoelectric materials, offering a compelling alternative to current practical materials composed of heavy and toxic elements.

5:00 PM EN07.05.19

Binder-Free Boron Nitride Spheres Enhanced Quasi-Isotropic Thermal Conductivity of Polymer Composites Hongbo Jiang, Qiran Cai and Ying Chen; Deakin University, Australia

Heat dissipation has become increasingly crucial in modern highly integrated and miniaturised electronic devices to improve their reliability and performance. Thanks to the high thermal conductivity and electrical insulation, boron nitride nanosheets (BNNSs) are usually used as fillers to construct thermally conductive polymer composites for heat dissipation. However, limited to the low dispersibility, high aspect ratio, and anisotropic thermal conductivity of BNNSs, the resulted thermal conductive composites based on polymer matrix showed an unsatisfied thermal conductivity, especially in the out-of-plane direction, due to the "lie-down" structures of the BNNSs fillers. In this work, micro-sized, binder-free boron nitride spheres (BNSs) have been successfully synthesized using a two-step process of thermal spray drying and high-temperature sintering; and a facile and efficient method to measure the thermal conductivity of BNSs, based on the factors impacting the BNSs' thermal conductivity, including precursor, polymer binder and sintering temperature, was developed. With optimised conditions, BNSs have a high, isotropic thermal conductivity of 37.2 W/mK. Based on the high thermal conductive and binder-free BNSs, a poly(vinyl alcohol) (PVA)/BNS composite film was successfully fabricated, and the out-of-plane thermal conductivity of this composite film is significantly enhanced to 8.1 W/mK, while the in-plane thermal conductivity, up to 10.6 W/mK, is not sacrificed, indicating the quasi-isotropy in thermal conductivity. The significant thermal conductivity enhancement (~3700%) of PVA is attributed to the formation of isotropic thermally conductive networks within the polymer matrix and strong interactions between BNNSs inside BNSs. This study provides a practical route to fabricate BN-enhanced composite films with isotropic thermal conductivity and promising materials that are valuable for heat dissipation in new-era advanced electronics and related applications.

5:00 PM EN07.05.20

Thermal Interface Engineering Using Layer-By-Layer Carbon Nanotube-Polyethylenimine Functional Nanostructures between Phase Change Materials and Aluminum Heat Sinks Jiheon Kim, Jaemin Lee and Wonjoon Choi; Korea University, Korea (the Republic of)

Phase change materials (PCMs) and heat sinks (HSs) can be integrated rationally to complement the inherent constraints of both technologies. However, adding PCMs to HSs frequently causes additional thermal resistances and unstable contact interfaces during solid-liquid phase transitions. In this study, we present the utilization of layer-by-layer (LbL) assembly to enhance functional interfaces between a multiwalled carbon nanotube (MWCNT) and polyethylenimine (PEI) on the surfaces of PCMs and HSs to enhance thermal management capabilities. The MWCNT-PEI percolation networks on an aluminum HS are effectively created by the LbL approach reported in this study, which involves the direct synthesis of electrostatically attached nanocoatings using a solution-based process. The HS channels are filled with a phase change substance (n-eicosane) to complete the PCM-HS assembly. The PCM and HS interface is stabilized over repeated solid-liquid phase transitions owing to the functional interface's optimization of the porous structures and a large increase in the active surface area enabling effective thermal transport. A comparison between the developed specimens (bare and PCM-filled HSs without LbL interfaces) highlights the improved thermal performance, particularly in transient and static operating conditions. The LbL functional interfaces show lower temperatures than the PCM-HS without MWCNT-PEI bilayers under different thermal loads (30, 40, and 50 W). The set point temperatures (SPTs) are chosen to be 40°C, 50°C, and 60°C for an objective and precise comparison. The LbL-assembled MWCNT-PEI coatings considerably increase the times to reach all SPTs. Using the LbL interface improves the effectiveness by more than 10%, according to experimental assessments of real-time temperature responses under different heating power levels and the time required to reach target temperatures. Furthermore, the LbL interfaces effectively mitigate thermal shock and overload issues during intermittent thermal loads. The developed LbL interface presents a versatile and scalable approach for creating PCM-filled HSs with advanced thermal properties that surpass the capabilities of traditional heat sinks.

5:00 PM EN07.05.21

Nanostructured Anodic Aluminium Oxide (AAO) with Metal Coating Optimized for Passive Radiative Cooling Alba Díaz-Lobo¹, Marisol Martín-González¹, Angel Morales-Sabio² and Cristina V. Manzano¹; ¹Micro and Nanotechnology Institute, Spain; ²Centro de Investigaciones Energéticas, Medioambientales y Tecnológicas, Spain

Currently, one third of the total energy consumption is already used for cooling in modern countries. An alternative way to achieve thermal comfort is becoming crucial to face this trend, and a passive cooling technology is a strong candidate that should be considered. Specially, when passive thermal management is achieved by using low-cost and easy-scalable to industry materials. In this sense, this study shows the possibilities of nanostructured anodic aluminium oxide (AAO) for passive radiative cooling: first, we analyse in detail the influence of all morphological parameters and the effect of the chemical structure on the optical response as well as on the passive radiative cooling performance; second, considering the most suitable kind of AAO nanostructures for passive cooling, we characterise different metal coating on the AAO nanostructures. Hence, we found the wavelength regions where the alumina thickness, the pore diameter, the interpore distance, the porosity and the incorporated counterions show the major impact in the optical response of the AAO nanostructures. We also improve the cooling performance of these AAO nanostructures by metal coating. A maximum temperature reduction of 11.7 K is experimentally measured under direct sunlight in a summer day in Spain. The results of this work demonstrate the enormous potential of AAO nanostructures to be used in thermal management applications and to contribute to a sustainable future energy.

5:00 PM EN07.05.22

Remarkable Suppression of Thermal Transport by Inhomogeneous Strain Lin Yang¹, Deyu Li² and Peng Gao¹; ¹Peking University, China; ²Vanderbilt University, United States

There is a mantra in the realm of material mechanics, "smaller is stronger", the science of which took root in the 1950s and is vigorously developing today. As nanomaterials are mechanically much stronger, significantly higher strains can be applied to tune their physicochemical properties than is possible with traditional materials. Based on this, we can rationally engineer a spectrum of advanced functionalities ranging from transistors, solar cells and photodetectors to batteries, superconductors, and electrocatalysis. Despite extensive investigations into strain-engineered electronic properties, the intricate phonon transport mechanism subjected to inhomogeneous strain remains an issue of debate. This is especially frustrating given that precise thermal

management stands as a critical bottleneck to device efficiency and lifespan.

One prevalent method for introducing strain involves growing thin epitaxial layers on substrates with lattice mismatch, such as Si on SiGe, and research has been conducted to investigate thermal transport through various epitaxial layers. However, although low thermal conductivity (κ) values even below their alloy counterparts have been observed, the effects of strain gradient through the epitaxial layers are experimentally difficult to decouple from the interfacial phonon boundary scattering effects, which presents a daunting challenge to draw a solid conclusion on the physical origin of the ultra-low κ . Similarly, although dislocations and vacancies could scatter phonons in various functional devices, it remains a formidable challenge to isolate their effects from that of long-range strain fields introduced by these defects, which could also impede thermal transport via an increase in vibrational anharmonicity. Consequently, questions regarding the cause of the unusual and somewhat perplexing thermal behavior in these functional materials have lingered unanswered.

To date, while elastic strain engineering often relies on highly inhomogeneous stress produced by nanoscale deformation (e.g., by epitaxial layer growth, defects and vacancies, or lithography patterning), most studies of strain effects on thermal transport have centered around materials under simplified condition of uniform stress. The major challenges in experimentally quantifying the effects of inhomogeneous strain on thermal transport include applying stress exclusively without introducing confounding factors (e.g., interfaces and defects), and combining thermal measurements with atomically resolved characterization of the strain field and phonon spectra. Here, we induce inhomogeneous strain through bending individual silicon nanoribbons on a custom-fabricated microdevice, and measure its effect on thermal transport while characterizing the local strain and vibrational spectra using atomically resolved electron energy-loss spectroscopy (EELS). Our results show that a strain gradient of 0.112% per nanometer could lead to a drastic thermal conductivity (κ) reduction of 37.4%, which is over 3-fold of previously demonstrated κ modulation under uniform strain. Taking advantage of recent progress in electron energy loss spectroscopy equipped with a monochromator in an aberration corrected scanning transmission electron microscope (STEM), we directly measured the local phonon modes and correlated them with the nanometer-scale strain gradient. Results show that the bending-induced lattice strain gradient significantly alters the vibrational states and broadens the phonon spectra. Coupled with *ab initio* theoretical modeling, this broadening effect is shown to enhance phonon anharmonicity and shorten phonon lifetimes, ultimately contributing to suppressed thermal conductivity.

5:00 PM EN07.05.23

Assessing Multivariate Thermal Transport Relationships in Pump-Probe Experiments Using Sensitivity Matrix Jing Tu and Wee-Liat Ong; Zhejiang University, China

Sensitivity analysis is a powerful technique to analyze the behaviors of models and experimental data in diverse fields.¹⁻⁴ Most state-of-the-art characterization techniques rely on fitting experimental data to a theoretical multivariate model. Such a model often has multiple unknown parameters at the same time. These unknowns are either determined independently or, when impractical, are fitted together in a single set of measured data. It is well-known that such a multivariate fit can become invalid, especially when these unknowns are related.⁵ To complicate matters, such a relationship can change with a different sample configuration and measurement conditions. Unfortunately, few rigorous methods exist to evaluate the validity of such a fit or uncover the governing transport relationships under different measurement conditions.

Here, we formulate a systematic approach based on sensitivity analysis to uncover the governing physics in a complex multivariate theoretical model and assess the feasibility of performing a multivariate fit. A sensitivity matrix of the unknown variables is constructed and, later, decomposed using the singular-value decomposition (SVD) method. The resulting solution of three matrices provides insight to the fitting process. The rank of the rectangular diagonal matrix with non-negative real numbers on the diagonal reveals the number of independent fit-able variables within the tested range. Under certain conditions, the associated complex unitary matrix contains information of the thermal transport relationships in the measured system. Different pump-probe techniques for thermal characterization are used to illustrate the capability of this method. We found that the existing experience-based criteria,^{5,6} e.g., the overlapping sensitivity curves to identify related parameters or the non-overlapping and distinct sensitivity curves for multivariate suitability, are inadequate and applicable only in certain situations. Also, our method can uncover the governing heat transfer relationships through different multilayer samples and measurement conditions. This method can apply to most measurement techniques relying on multivariate theoretical models in various disciplines and can help to improve their measurement validity and throughput.

Reference:

1. Razavi, S. *et al.* The Future of Sensitivity Analysis: An essential discipline for systems modeling and policy support. *Environ. Model. Softw.* **137**, (2021).
2. Saltelli, A., Jakeman, A., Razavi, S. & Wu, Q. Sensitivity analysis: A discipline coming of age. *Environ. Model. Softw.* **146**, 105226 (2021).
3. Kala, Z. Sensitivity analysis in probabilistic structural design: A comparison of selected techniques. *Sustain.* **12**, (2020).
4. Qian, G. & Mahdi, A. Sensitivity analysis methods in the biomedical sciences. *Math. Biosci.* **323**, 108306 (2020).
5. Yang, J., Ziade, E. & Schmidt, A. J. Uncertainty analysis of thermoreflectance measurements. *Rev. Sci. Instrum.* **87**, (2016).
6. Schmidt, A. J., Cheaito, R. & Chiesa, M. A frequency-domain thermoreflectance method for the characterization of thermal properties. *Rev. Sci. Instrum.* **80**, 094901 (2009).

5:00 PM EN07.05.25

In-Situ Long Term Stability Analysis of Hygroscopic Hydrogels for Energy and Water Applications Joseph P. Mooney^{1,2}, David Keisar¹, Carlos D. Diaz¹ and Bachir El Fil¹; ¹Massachusetts Institute of Technology, United States; ²University of Limerick, Ireland

Thermal energy storage serves a pivotal role in bolstering both energy efficiency and sustainability by enabling the controlled capture and release of heat, thus mitigating energy wastage and facilitating the seamless integration of renewable energy sources. Desiccant-based thermal energy storage (TES) systems leverage moisture-absorbing materials to efficiently store and discharge heat, offering a promising avenue for sustainable and efficient energy management. Hygroscopic hydrogels, as potential desiccant materials, offer a compelling prospect due to their high energy densities and cost-effectiveness. While our understanding of the kinetics and transport mechanisms of hygroscopic hydrogels is advancing, there remains a critical knowledge gap concerning their long-term stability and performance. Furthermore, the translation of insights gained from Dynamic Vapor Sorption (DVS) cyclability analysis to a larger scale and its relevance to TES systems operating in pure vapor environments warrants comprehensive investigation. In this study, we have developed a comprehensive test facility that assesses the long-term stability of hygroscopic hydrogels and other sorbents in pure vapor at vacuum pressures. With this facility, we can control the relative vapor pressure and chamber temperature that the sorbents are exposed to, emulating relative humidity (RH) conditions. Moreover, insights into aspect ratio and thickness scaling on a device size sample can inform the limits of diffusion limits of the material.

In this study, we fabricate PAM-LiCl hygroscopic hydrogels with salt loadings of 1 gg^{-1} and 5 gg^{-1} . We subject the gels to an RH swing of 30% to 70% – allowing the hydrogels to equilibrate at each RH level. This is achieved through the thermal cycling of the gels between 30 °C and 60 °C on a 25 mm x 50 mm temperature-controlled plate while fixing the chamber vapor pressure at 3 kPa. We measure both the kinetics and load swing of these hydrogels by mounting the plate to a precision strain gauge (< 0.1 g error). This analysis demonstrates that the hydrogels maintain > 90% of their performance, after 100 thermal desorption-adsorption cycles. We also qualitatively show that no visual variation between cycles was observed in the gels. These novel insights

have significant implications for understanding the long-term stability and, importantly, for optimizing the design of hygroscopic hydrogels for broader and more efficient energy storage systems.

SESSION EN07.06: Thermal Transport in Amorphous Materials
Session Chairs: Yee Kan Koh and Jaeyun Moon
Wednesday Morning, April 24, 2024
Room 327, Level 3, Summit

8:45 AM *EN07.06.01

Phonon Transport of Disordered Materials with Nanostructures [Junichiro Shiomi](#); The University of Tokyo, Japan

Phonon engineering of crystalline materials by nanostructures has made great progress in the past decades, and the next non-trivial challenge is how to engineer phonons in disordered materials. We have studied nanostructured amorphous materials such as amorphous superlattices [1] and amorphous phononic crystals (amorphous thin films with holes) [2]. There, by applying the Allen-Feldmann theory, which divided heat carrier into propagons, diffusons, and locons, we found that not only the transport of propagons but also that of diffusons is effectively hindered by the nanostructure interfaces. To gain further direct insight, inelastic x-ray scattering was performed. Partially disordered materials are also of great interest from an academic and industrial point of view. This includes materials consisting of crystalline and amorphous portions, e.g., polycrystals with disordered interfaces. Disordered grain boundaries have been found experimentally to selectively inhibit phonon transport rather than electron transport. Furthermore, a black box model of disordered silicon grain boundaries was successfully performed, revealing that the main structural factors that determine transport are different for phonons and electrons [3]. Crystalline materials with distorted lattices, such as cellulose nanofibers, are also interesting. The thermal conductivity of cellulose nanofibers was found to be greatly enhanced by controlling the arrangement of the constituent cellulose nanofibrils and the hydrogen bonds between the fibrils [4].

[1] Y. Liao, S. Iwamoto, M. Sasaki, M. Goto, J. Shiomi, *Nano Energy* 84, 105903 (2021).

[2] N. Tambo, Y. Liao, C. Zhou, E. M. Ashley, K. Takahashi, P. F. Nealey, Y. Naito, J. Shiomi, *Science Advances* 6, eabc0075 (2022).

[3] C. Lortaraprasert, J. Shiomi, *npj Computational Materials* 8, 219 (2022).

[4] G. Wang, M. Kudo, K. Daicho, S. Harish, B. Xu, C. Shao, Y. Lee, Y. Liao, N. Matsushima, T. Kodama, F. Lundell, L. D. Sooderberg, T. Saito, J. Shiomi, *Nano Letters* 23, 1144-1151 (2023).

9:15 AM EN07.06.03

Effect of Linker Chemistry, Linker Length and Temperature on The Thermal Conductivity of Vinylogous Urethane Dynamic Network [Peng Lan](#), Seongon Jang, Christopher M. Evans and David Cahill; UIUC, United States

Covalent adaptable networks (CANs) have been heavily studied in recent years as promising candidates for recyclable polymer in applications like shape memory materials, shockwave energy-dissipative materials, and flexible electronics. However, the thermal management of polymeric materials in these devices is still an urgent issue, since polymers generally have low thermal conductivity (as 0.2 W/m K) which can lead to thermally-induced aging. Moreover, the effect of bond exchange dynamics, linker chemistry and temperature on the thermal conductivity of CANs is still unclear. In this work, a series of vinylogous urethane dynamic networks (VU- x E) were synthesized from tris(2-aminoethyl)amine and di-acetoacetates with ethylene linkers (E = ethylene) and varied linker length ($x = 2-22$ carbon atoms). Thermal conductivity was measured by frontside frequency-domain probe beam deflection (FD-PBD). In comparison to the ethylene network with benzene diboronic acid bonds, neither linker length dependence nor temperature dependence of thermal conductivity shows a monotonic trend as in the case of VU- x E network. The thermal conductivity of these VU networks at room temperature varies from 0.20 W/m K to <0.1 W/m K as the linker length increases from $x = 2$ to $x = 22$. At high temperature approaching glass transition ($T_g \sim T_g + 20$ K), a drop of thermal conductivity is observed by FD-PBD and as the temperature grows higher ($> T_g + 30$ K), the thermal conductivity retains to that of low temperature ($< T_g$). We hypothesized that this drop of thermal conductivity near T_g in FD-PBD is due to combined dynamics of monomer chain motion and bond exchange. The morphology of these VU- x E networks were also studied using WAXS for both fresh and annealed samples. Apart from amorphous halo peak at $\sim q_{II} = \sim 14 \text{ nm}^{-1}$ and broad ethylene chain stacking peak at $\sim q_{II} = \sim 4 \text{ nm}^{-1}$, no obvious crystalline peak is seen for all networks. Such a behavior is different from our previously studied ethylene network with boric acid dynamic bonds, where longer network ($x > 10$) exhibits slow crystallization (with crystallinity > 78% in WAXS) at room temperature. We attributed this difference to the fact that VU bonds have a much slower bond exchange than boric acid. Furthermore, we investigated the effect of linker chemistry on the thermal conductivity, by changing the ethylene linker to ethylene oxide (VU- x EO, $x = 6, 9, 12, 18, 36$ atoms). Similar linker length dependence of thermal conductivity is observed for these ethylene oxide VU network. But no EO chain stacking peak q_{II} is seen in WAXS spectra as the linker length increases, suggesting that the presence of oxygen atoms in EO linker will disturb the chain stacking and make the network less capable of crystallization. This work provides new design rules for thermal conductivity of dynamic polymer networks and how to control the crystallization depending on linker length, chemistry, and dynamic bond type.

9:30 AM EN07.06.04

Thermal Conductivity of 2H and 2H3R Niobium Diselenide Polymorphs [Sungjin Park](#)¹, Kyomin Kim², Kwangrae Kim¹, Jong-wook Roh³, Aloysius Soon¹, Wooyoung Lee¹ and Woochul Kim¹; ¹Yonsei University, Korea (the Republic of); ²LIG Nex1, Korea (the Republic of); ³Kyungpook National University, Korea (the Republic of)

Niobium diselenide (NbSe₂) is a two-dimensional van der Waals material whose 2H3R polymorph was discovered recently [1]. The 2H3R polymorph of NbSe₂ possesses a different stacking sequence when compared to the 2H polymorph due to the weak van der Waals bonding between the layers and therefore possesses different physical properties. Previous research has shown that difference in stacking sequence in two-dimensional materials can alter their electrical and thermal properties [1,2]. In this work the thermal conductivity of the 2H and 2H3R polymorphs of NbSe₂ was measured and compared. The in-house T-bridge method was used in the measurement of thermal conductivity [3]. The T-bridge method measures the thermal conductivity of a sample through difference in heat conduction from a suspended heater to a heatsink. NbSe₂ samples of various thicknesses were prepared for both polymorphs. Measured thermal conductivity results showed that the 2H3R polymorph shows lower thermal conductivity compared to the 2H counterpart of similar thickness. Theoretical calculation was performed to study the cause of the difference in thermal conductivity and revealed that the lower thermal conductivity of the 2H3R polymorph was induced by the greater phonon-phonon scattering of the 2H3R polymorph than that of the 2H polymorph.

[1] H. Moon, J. Kim, J. Bang, S. Hong, S. Youn, H. Shin, J.W. Roh, W. Shim, W. Lee, *Nano Energy* 78, 105197 (2020)

[2] P. Erhart, P. Hyldgaard, D. O. Lindroth, *Chemistry of Materials* 27, 551-5518 (2015)

[3] J. Kim, D. J. Seo, H. Park, H. Kim, H. J. Choi, W. Kim, *Review of Scientific Instruments* 88, 054902 (2017)

9:45 AM EN07.06.05

Modulating The Thermal Transport of MAPbI₃ Hybrid Perovskites and The Effect on its Population-/Coherence-Channel Jin Yang¹, Yuting Yu¹, Ankit Jain² and Wee-Liat Ong¹; ¹Zhejiang University, China; ²IIT Bombay, India

Hybrid halide perovskites, with their favorable carrier recombination time and ultrashort phonon mean-free paths, are potential candidates for numerous energy conversion applications like photovoltaics and thermoelectrics. The origin of the ultralow thermal conductivity in the prototypical methylammonium lead triiodide (MAPbI₃) is of intense research interest for improving and modulating its energy conversion performance.[1] So far, such an understanding remains elusive in the MAPbI₃ at above room temperatures (that exists as a cubic phase) despite numerous efforts[2] and under external modulation fields.

Using molecular dynamics and the Wigner transport equation,[3] we first report the discovery of several cubic-phase MAPbI₃ (c-MAPbI₃) local energy minimum structures.[4] These stable structures are amenable to lattice dynamics-based calculations to produce positive phonon dispersions. Our results reveal a coherence-channel-dominated thermal transport mechanism in the c-MAPbI₃ crystals. Interestingly, an inter-conversion between the population- and coherence-channel occurs when the c-MAPbI₃ changes across these energetically equivalent structures at the same temperature. Such an effect is yet to be observed in simple atomic crystals.

Next, we looked at how external pressure fields and electric fields affect the thermal transport of MAPbI₃. An external pressure increases the c-MAPbI₃ thermal conductivity of the phonon population-channel contribution, similar to trends in many crystals. However, little effect on the coherence-channel contribution is observed. This unusual trend impedes the thermal conductivity increase for this c-MAPbI₃ and imparts a trend that mirrors that of a diamond[5]. On the other hand, the electric field has little effect on c-MAPbI₃ although the polar MA cations are affected by the electric field.

Our work also shows that existing thermal transport intuitions based on the phonon gas model can be misleading in such hybrid crystals. Further, the dominance of the non-traditional coherence-channel of phonons can affect the interpretation of other phonon-mediated processes in MAPbI₃ and other hybrid perovskites.

References:

- [1] M.A. Haque, S. Kee, D.R. Villaiva, W. Ong, D. Baran, Halide Perovskites: Thermal Transport and Prospects for Thermoelectricity, *Adv. Sci.* 7 (2020) 1903389. <https://doi.org/10.1002/adv.201903389>.
- [2] T. Zhu, E. Ertekin, Mixed phononic and non-phononic transport in hybrid lead halide perovskites: Glass-crystal duality, dynamical disorder, and anharmonicity, *Energy Environ. Sci.* 12 (2019) 216–229. <https://doi.org/10.1039/c8ee02820f>.
- [3] M. Simoncelli, N. Marzari, F. Mauri, Unified theory of thermal transport in crystals and glasses, *Nat. Phys.* 15 (2019) 809–813. <https://doi.org/10.1038/s41567-019-0520-x>.
- [4] J. Yang, A. Jain, W.L. Ong, Inter-channel conversion between population-/coherence-channel dictates thermal transport in MAPbI₃ crystals, *Mater. Today Phys.* 28 (2022) 100892. <https://doi.org/10.1016/j.mtphys.2022.100892>.
- [5] J. Yang, A. Jain, L. Fan, Y.S. Ang, H. Li, W.L. Ong, Anomalous Pressure-Resilient Thermal Conductivity in Hybrid Perovskites with Strong Lattice Anharmonicity and Small Bulk Modulus, *Chem. Mater.* 35 (2023) 5185–5192. <https://doi.org/10.1021/acs.chemmater.3c00935>.

10:00 AM BREAK

SESSION EN07.07: Extreme Thermal Conductivity Materials
Session Chairs: Jonathan Malen and Junichiro Shiomi
Wednesday Morning, April 24, 2024
Room 327, Level 3, Summit

10:30 AM +EN07.07.01

Unconventional Approaches to High or Tunable Thermal Conductivity in Solids Li Shi; The University of Texas at Austin, United States

Materials with an either high or tunable thermal conductivity can find applications ranging from thermal management of microelectronics to electrification of industrial heating processes. Wide-bandgap diamond and semi-metallic graphite achieve record-high thermal conductivity values because strong covalent bonding of light carbon atoms gives rise to a large thermal conductivity contribution from phonons, the energy quanta of lattice vibrations. Such conventional criteria for a high lattice thermal conductivity have recently been upended by the establishment of a phonon band engineering approach to high-thermal conductivity semiconducting cubic boron arsenide (c-BAs) made of both light and heavy elements. This paradigm shift is not only motivating heterogeneous integration of c-BAs heat spreaders with other semiconductors for enhanced thermal and electronic performance, but also the search of other compounds with a high thermal conductivity, including semi-metallic theta-tantalum nitride (theta-TaN). Compared to this recent progress in the research of ultrahigh-thermal conductivity materials, the study of tunable solid-state thermal transport has still been largely limited to tuning of the lattice and electronic contributions through structural and magnetic phase transitions, respectively. Besides providing an update on experimental progresses and applications of high-thermal conductivity c-BA, theta-TaN, and graphitic materials, this presentation will introduce recent efforts of utilizing interlayer excitons and flat moiré electron bands to realize tunable thermal transport along and between two-dimensional heterostructures.

11:00 AM *EN07.07.02

Extreme Materials Design for Thermal Transport and Energy Conversion Yongjie Hu; University of California, Los Angeles, United States

Controlling thermal transport is critical for many applications including electronics and energy technologies. In this talk, I will highlight my group's recent efforts [1-6] in creating innovative materials and devices to push the boundaries of heat dissipation. First, I'll discuss our advancements in developing emerging semiconductors with high thermal conductivity and their integration with wide-bandgap/ultra-wide bandgap semiconductors to enhance heat dissipation in power electronics. Notably, we discovered cubic boron arsenide (BAs) and boron phosphide (BP) with a high thermal conductivity up to 1300 W/mK at room temperature, surpassing most common semiconductors and metals [1]. We've successfully integrated BAs with GaN HEMTs [2], achieving a record thermal boundary conductance and outperforming diamond/SiC cooling devices. Using self-assembly manufacturing [3], we've developed scalable and flexible high-conductivity BAs-polymer interfaces for efficient cooling in LEDs and wearables. Moreover, our fundamental study has explored BAs as a showcase platform for high-order phonon anharmonicity physics [4] and non-perturbative quantum theory [5]. Finally, I'll discuss our recent advances in solid-state thermal regulation for heat flow and phonon control [6]. References:[1] *Science* 361, 575-578 (2018). [2] *Nature Electronics* 4, 416-423 (2021). [3] *Nature Communications* 12, 1284 (2021). [4] *Nature* 612, 459-464 (2022). [5] *Phys. Rev. B* 108, L140302 (2023). [6] *Science*, to appear.

11:30 AM EN07.07.03

Origin of Extreme Thermal Properties in Amorphous Diamond [Jaeyun Moon](#) and Zhiting Tian; Cornell University, United States

Structural disorder hinders propagation of vibrational heat carriers, leading to intrinsically low thermal conductivity in amorphous solids. Recently, bulk amorphous diamond with hardness and elastic modulus exceeding those of its crystalline counterpart was synthesized and thermal conductivity of $\sim 25 \text{ Wm}^{-1}\text{K}^{-1}$ was reported at room temperature, higher than any other bulk amorphous solids and even some crystals. In this work, we explore the microscopic thermal transport mechanism in amorphous diamond through both computational and experimental techniques and discuss its implications in thermal transport in solids.

11:45 AM EN07.07.04

Proton Collective Quantum Tunneling Induces Anomalous Thermal Conductivity of Ice Under Pressure Yufeng Wang, Kuang Yu and [Bo Sun](#); Tsinghua University, China

Ice is one of the most ubiquitous substances in the universe. Understanding its thermal conduction properties is crucial for exploration of the evolution and dynamics of icy planets. Moreover, ice itself serves as an ideal model to study proton's quantum effects in the hydrogen bond networks, which has received enormous attention in physical chemistry and condensed matter physics.

It is believed that protons tunnel in the hydrogen bond network in ice and the tunneling is local compared with the wavelength of heavy phonon; as such, the quantum nature of the proton dynamics would not strongly affect the thermal conduction of ice, and the thermal conductivity as a function of pressure should increase following the classical Leibfried-Schlömann equation.

In stark contrast, we observed anomalous, nonmonotonic behavior in the thermal conductivity of H_2O and D_2O ice above 20 GPa that breaks the classical rule. Such anomaly is revealed to be caused by global collective quantum tunneling involving several tens of molecules. It is the first time that quantum tunneling in ice is observed at such a large spatial scale, opposing to all previous studies which assumed that local or synchronized tunneling within a limited size (such as six-member rings) dominates in ice.

Moreover, the tunneling dynamics in the ice VII-X phase transition region has been a long-standing challenge to understand using conventional spectroscopic methods. In this work, we provide a completely new approach that can directly probe the global dynamics of the phase transition with unambiguous experimental measurements.

SESSION EN07.08: Polaritonic Heat Transfer

Session Chairs: Yongjie Hu and Li Shi

Wednesday Afternoon, April 24, 2024

Room 327, Level 3, Summit

1:30 PM +EN07.08.01

Thermal Transport Mediated by Non-Equilibrium Surface Phonon Polaritons Zhiliang Pan¹, Guanyu Lu¹, Xun Li², Lucas Lindsay², Joshua D. Caldwell¹ and [Deyu Li](#)¹; ¹Vanderbilt University, United States; ²Oak Ridge National Laboratory, United States

Surface phonon polaritons (SPhPs), hybrid quasi-particles resulting from coupling between infrared photons and optical phonons, could play significant roles in near-field radiation. More recently, it has been predicted that SPhPs can also contribute to heat conduction along polar thin films and nanowires; however, direct and conclusive experimental evidence for SPhP-mediated heat conduction has been scarce. Here we report on significant enhancement of the thermal conductivity of 3C-SiC nanowires when the end(s) of the nanowires are coated with a thin layer of gold that can serve as efficient SPhP launchers. Through measuring the same 3C-SiC nanowires with and without gold coating at the end(s), we show that the SPhPs launched by the gold coating can remarkably enhance the thermal conductivity of the uncoated wire segment from the value of the same wire without gold coating. Interestingly, it is found that the SPhP-mediated thermal conductivity is orders of magnitude higher than the Landauer limit predicted based on the equilibrium Bose-Einstein distribution function over the entire measurement temperature range. We attribute this unexpected discovery to the partial ballistic propagation of SPhPs along the SiC nanowire with a number density well beyond the value determined by the Bose-Einstein distribution function. The understanding of non-equilibrium SPhP transport is supported by the observation that the extracted SPhP-mediated thermal conductivity is proportional to the length of the gold coating at the end(s) of the nanowire, which provides important insights into the SPhP excitation process. The highest SPhP-mediated thermal conductivity at room temperature reaches a value of 5.8 W/m-K, a few times of the phonon-mediated thermal conductivity for some technologically important thin films such as silicon oxide and nitride. This discovery of non-equilibrium SPhP-mediated heat conduction implies novel cooling strategies utilizing SPhPs as effective thermal energy carriers.

2:00 PM EN07.08.02

Guided Polariton Thermal Radiation [Sebastian Volz](#); CNRS, France

Phonons are the quasiparticles of lattice vibrations and represent the primary heat carriers in bulk dielectric materials. The thermal conductivity of dielectric membranes is thus typically driven by acoustic phonons that is usually assimilated to a gas of particles, and generally reduces with the membrane thickness due to the increasing frequency of surface scattering events. In the light of the ever-increasing miniaturization of devices with enhanced rates of operation, this reduction in the thermal conductivity causes overheating, low reliability, and reduced lifetime of electronic components. Yet, while the thermal transport via acoustic phonons might be at the limit, the heat dissipation might be enhanced via optical phonons coupled with surface electromagnetic waves.

Over the past decade, substantial research efforts have been devoted to the study of these surface waves, because the surface effects predominate over the volumetric ones in nanostructures with high surface-to-volume ratio. Some types of surface electromagnetic waves may even carry heat and thus improve the thermal performance and stability of nanoscale devices.

One type of such surface waves is the surface phonon-polaritons (SPhPs), which occurs as a hybrid of optical phonons and surface electromagnetic waves. The SPhPs are essentially evanescent waves that propagate along the surface of polar dielectric membranes.

We will first demonstrate the existence and the properties of those SPhPs in thin SiO_2 films and especially uncover that the propagation lengths of those waves reach the range of hundreds of micrometers, which is orders of magnitude longer than the typical mean free path of acoustic phonons. Theoretical models predict that such a long propagation length enables SPhPs to conduct more thermal energy than phonons when the membrane thickness is reduced below 100 nm.

We will then corroborate the significant contribution of SPhPs to heat flux in silica membranes, in a restricted temperature range and also, in a wide temperature range, in silicon nitride membranes where SPhP thermal conductivity becomes predominant at 800K. An additional confirmation was finally provided by showing the size dependence of thermal conductivity due to the ballistic contribution of SPhP.

2:15 PM EN07.08.03

Long-Range, Short-Wavelength and Ultrafast Heat Conduction driven by Three Plasmon Modes supported by Graphene Jose Ordóñez^{1,2}, Yuriy Kosevich², Masahiro Nomura^{2,1} and Sebastian Volz^{1,2}; ¹CNRS, Japan; ²The University of Tokyo, Japan

By leveraging the unique two-dimensional structure of graphene with its ability to support the propagation of surface plasmon-polaritons, we demonstrate the existence and propagation of three hybrid modes of surface plasmon polaritons supported by two graphene monolayers coating a solid film. These modes propagate long distances with short wavelengths, which are suitable features to enhance the heat conduction along the film interfaces. For a Si film with a thickness of 15 nm and a length of 5 mm at 300 K, we find a plasmon thermal conductivity of $13.6 \text{ Wm}^{-1}\text{K}^{-1}$, which represents 67% (26%) of its phonon Si (Si+graphene) counterpart. This thermal energy appears due to the coupling of plasmons propagating at speeds comparable to the speed of light in vacuum. The plasmonic heat conduction driven by two-dimensional materials thus appears as a major and unexpected mechanism for controlling temperature in solid-state systems without changing their internal structure and at rates faster than the ones of phonons and electrons.

2:30 PM BREAK

SESSION EN07.09: Thermal Transport in Crystals

Session Chairs: Deyu Li and Sunmi Shin

Wednesday Afternoon, April 24, 2024

Room 327, Level 3, Summit

3:30 PM *EN07.09.01

Engineering and Probing Phonons and Thermal Transport Begoña Abad Mayor, Chaitanya Arya, Giulio de Vito, Yashpreet Kaur, Grazia Raciti, Aswathi K. Sivan, Jose Manuel Sojo Gordillo, Saeko Tachikawa, Johannes Trautvetter and Ilaria Zardo; University of Basel, Switzerland

The recently growing research field called “Nanophononics” deals with the investigation and control of vibrations in solids at the nanoscale. Phonon engineering leads to a controlled modification of phonon dispersion, phonon interactions, and transport [1, 2]. However, engineering and probing phonons and phonon transport at the nanoscale is a non-trivial problem.

In this talk, we discuss how phononic properties and thermal transport can be engineered and measured in nanowires and the challenges and progresses in the measurement of the thermal conductivity of nanostructures and low dimensional systems. The concept of phonon engineering in nanowires is exploited in GaAs/GaP superlattice nanowires [3]. We experimentally show that a controlled design of the nanowires’ phononic properties can be decided à la carte by tuning the superlattice period [4].

We also investigated thermal rectification in semiconducting gallium arsenide nanowires with an abrupt change in diameter [5], also called telescopic nanowires. We measured rectification values ranging from 2 to 7% at a range of ambient temperatures, with rectification values increasing for larger temperature gradients. The direction of rectification and its dependence on temperature gradient is confirmed by ab-initio calculations using the acoustic mismatch model, taking into account the contribution from interfacial thermal resistance.

Finally, Raman thermometry is used to probe the temperature profile in nanostructures upon application of a thermal gradient, enabling the differentiation between different thermal transport regimes.

References

- [1] M. Maldovan, *Nature* **503**, 209 (2013).
- [2] S. Voltz, et al., *Eur. Phys. J. B* **89**, 15 (2016).
- [3] O. Arif et al., *Nanoscale* **15**(3), 1145-1153 (2023).
- [4] A. K. Sivan, et al., *ACS Applied Nano Materials* **Article ASAP**, DOI: 10.1021/acsnm.3c04245
- [5] W. Kim, A. Fontacuberta i Morral, *Nano Lett.* **18**, 49-57 (2018).

4:00 PM EN07.09.02

Narrowband Thermal Phonon Motion Under Atomic-Scale Local Resonance Conditions Albert Beardo¹, Paul Desmarchelier², Prajit Rawte¹, Chia-Nien Tsai¹, Konstantinos Termentzidis² and Mahmoud Hussein¹; ¹University of Colorado Boulder, United States; ²University of Lyon, France

Thermal energy conduction in nanostructures involves various atomic-scale phonon mechanisms with a complex interplay between wavelike and particle behavior. In nanoscale configurations where the feature sizes are smaller or on the order of the phonon mean free path, it is possible to engineer the wavelike behavior to, for example, impede heat conduction—which is favorable for thermoelectric energy conversion. While reducing the dimensionality or introducing obstacles to the heat flow in nanostructures can reduce the thermal conductivity [1], it can also limit the thermoelectric figure of merit ZT. Control of sub-phonon mean free path properties, on the other hand, offers the potential to improve ZT. One approach along this path involves the introduction of resonating substructures to a conventional material, such as silicon, to form a *nanophononic metamaterial* (NPM) [2]. These substructures create standing phonon waves that couple with the in-plane propagating phonons causing a significant modification of the dispersion relation, reduction of the phonon group velocities, creation of mode localizations, and ultimately decreasing the lattice thermal conductivity—all without affecting the electronic properties [3].

In this work, we use narrowband wave-packet excitations to investigate the impact of local resonances on the room temperature phonon transport in NPMs in the form of nanopillared membranes and compare with corresponding nanostructures that do not include local resonances. Our results provide an in-depth analysis elucidation of the underlying phonon localization effects associated with the local resonances. By controlling the wave-packet frequency, we are able to distinguish the role of the local resonances on the thermal energy propagation from other effects that also influence the total lattice thermal conductivity such as phonon-boundary scattering. These observations open exciting new possibilities for experiments to further unlock the potential of atomic-scale local resonances.

[1] D. Li, Y. Wu, P. Kim, L. Shi, P. Yang, and A. Majumdar, *Appl. Phys. Lett.* **83**, 2934-2936, (2003).

[2] B.L. Davis and M.I. Hussein, *Phys. Rev. Lett.* **112**, 055505, (2014).

[3] B.T. Spann, J.C. Weber, M.D. Brubakera, T.E. Harveya, L. Yang, H. Honarvar, C.-N. Tsai, A.C. Treglia, M. Lee, M.I. Hussein, and K.A. Bertness, *Adv. Mater.* **35**, 2209779 (2023).

4:15 PM EN07.09.03

Unrevealing The Unexpected Large Thermal Boundary Resistance induced by Inelastic Heat Carrier Trapping at GaN-Diamond Interface Bin Xu¹, Shiqian Hu², Rulei Guo¹, Fengwen Mu³ and Junichiro Shiomi¹; ¹The University of Tokyo, Japan; ²Yunnan University, China; ³Chinese Academy of Sciences, China

The rapid advancements in the wide band gap semiconductors like gallium nitride (GaN), silicon carbide (SiC), and gallium oxide (Ga₂O₃), have revolutionized various fields, including electric vehicles, mobile devices, and next-generation telecommunications. With the increase in power and the reduction in device size, the elevating heat density via self-heating makes thermal management a significant issue. One of the most promising solutions is integrating the devices with high thermal conductivity diamond substrates. However, this will introduce additional thermal boundary resistance (TBR) at the semiconductor/diamond interface and impedes heat dissipation.

In such kinds of interfaces, the substantial differences in Debye temperature between diamond and semiconductors like SiC, GaN, or Si would lead to a significant mismatch in phonon modes at the interface, where the traditional acoustic mismatch model (AMM) and diffuse mismatch model (DMM) are no longer applicable as the inelastic phonon scattering is non-negligible. Moreover, this interface is typically composed of amorphous layers when using room temperature bonding techniques, which is essential to avoid thermal damage and thermal-induced strain in the devices. The amorphous layers not only bring large TBR but also increase the complexity of the behavior of heat carriers at the interface because the heat conduction in amorphous materials differs from crystalline materials and involves different heat carriers: the delocalized heat carriers (propagons and diffusons) and localized heat carriers (locons). The mechanism of heat conduction at such an interface is still to be elucidated, posing difficulty in interfacial structure design for reducing TBR for the semiconductor-on-diamond systems.

This study investigated the thermal boundary resistance (TBR) in the GaN/diamond system, a representative case of semiconductor-on-diamond structures. We employed an innovative room-temperature surface-activated bonding (SAB) technique to control the thickness and structure of the interfacial layer precisely. As a result, a multi-layer heterogeneous interfacial layer was generated, bonding the GaN to the diamond substrate. This interface includes a SiO_x-enriched region sandwiched between two diffusive regions as characterized by transmission electron microscope (TEM) and energy dispersive X-ray spectroscopy (EDX) analysis. We then used time-domain thermoreflectance (TDTR) measurement to investigate the TBR. The increase in the total thickness of the interfacial layer leads to a nonlinear variation in TBR. More surprisingly, the increase in the thickness of the interfacial layer provides counterintuitively huge thermal resistance, far exceeding its diffusive limit. To unravel this phenomenon, we performed molecular dynamics (MD) simulations to analyze the density of state (DOS) of heat carriers and their spectral heat conduction at the interfacial, which shows the existence of the local low-frequency states in the SiO_x-enriched region and the resultant conversion of phonon frequencies through an inelastic process in this region. This discovery challenges the traditional belief that interfacial inelastic scattering consistently improves heat conduction by opening up new inelastic pathways, while the pathways were limited in our specific case instead. This phenomenon can be further intensified by increasing the thickness of either the SiO_x-enriched region or the two diffusive regions, ultimately promoting the TBR of the GaN/diamond interface. Leveraging these innovative insights into the physics of interfacial heat conduction, a record low TBR of 8.3 m²-K/GW among direct bonded GaN/diamond interface was achieved. This breakthrough has significant implications for efficient interfacial heat dissipation.

4:30 PM EN07.09.04

Thermal-Response Functions computed from First Principles with Applications to Two-Dimensional Materials Patrick K. Schelling and Antonio Martinez Margolles; University of Central Florida, United States

Thermal response, or alternately thermal susceptibility, is a useful way to describe the propagation of energy in response to an external heat pulse. The particular advantage of this approach is that there is no a priori assumption made as to whether transport is ballistic or diffusive. Here I present an approach to compute thermal response functions using input from Density-Functional Theory (DFT) calculations. Calculations are presented for two-dimensional materials at low temperatures. The results demonstrate the propagation of second sound in graphene, with insight into length and timescales where ballistic transport can be expected. Comparison is made to recent experimental results. Finally, the work is discussed in the context of phonon Boltzmann theory in the relaxation time approximation.

4:45 PM EN07.09.05

Effective Interface Engineering for Phonon Manipulation in Multi-Layered Semiconductor Systems Hong Lu; Nanjing University, China

Effective thermal management in functional devices has become more and more important as the demands on device performance keep increasing continuously [1]. Interfaces are crucial to device functionality. However, they could inevitably cause heat accumulation. So, it is essential to be able to manipulate the thermal transport through interface engineering. The semiconductor/semiconductor and metal/semiconductor interfaces are two types of important interfaces in the study of thermal transport, especially in semiconductor devices. The change of interface structure is bound to affect its transport properties. Therefore, it is expected that the regulation of phonon transport behavior can be realized through the design of unique multi-layered structures and utilization of effective interface engineering.

In this work, we have designed a series of multi-layered semiconductor structures and grown them using molecular beam epitaxy (MBE). Owing to the atomic-level control of growth, MBE offers us more freedom to realize high quality multi-layered samples with delicate structural parameters, including single monolayered superlattices. Manipulation of long-wavelength phonons is especially important for these structures as their developments continue to pursue the limit of thermal conductivity. Here, the experimental demonstration of manipulating and probing long-wavelength phonon thermal transport in Al_xGa_{1-x}As/Al_yGa_{1-y}As and InAs/AlAs superlattices will be reported. A direct experimental approach is demonstrated to probe and monitor the contribution of long-wavelength phonons to the thermal conductivity, based on the quasi-ballistic transport principle of phonons. In addition, we have observed evidence of coherent phonon transport up to 500 K. Effective interface manipulation in some artificial metal/semiconductor interfaces will be presented and discussed too. This demonstration holds the very promise to be a universal strategy for manipulating and probing phonon thermal transport in various application scenarios, including microelectronics, thermoelectrics, and optoelectronics.

[1] D. G. Cahill, P. V. Braun, G. Chen, D. R. Clarke, S. Fan, K. E. Goodson, P. Keblinski, W. P. King, G. D. Mahan, A. Majumdar, Nanoscale thermal transport II, *Appl. Phys. Rev.* **1** (2014) 011305.

Wednesday Afternoon, April 24, 2024
Flex Hall C, Level 2, Summit

5:00 PM EN07.10.01

Towards Scalegophobicity: Soft Surface Microengineering for Microfoulant Repellency [Julian Schmid](#)¹, Tobias Armstrong¹, Fabian J. Dickhardt¹, SK Rameez Iqbal¹ and Thomas Schutzius^{1,2}; ¹ETH Zurich, Switzerland; ²University of California, Berkeley, United States

Particulate and crystallization fouling, ubiquitous in nature and technology, pose significant challenges to the efficiency of water treatment, desalination, and energy conversion processes. Current solutions rely heavily on active methods like antiscalant additives or mechanical removal, necessitating a shift towards sustainable, passive strategies, such as surfaces with inherent self-cleaning or anti-fouling properties. Existing research has focused on modifying the surface energy and texture of rigid materials for anti-fouling surfaces, overlooking the potential of compliant materials with intrinsic foulant-repellent properties. The intricate interplay of substrate compliance, composition, and surface texture in an aqueous environment and their impact on microfoulant adhesion at the microscale remain largely unexplored. In this study, we employ a micro-scanning fluid dynamic gauge (μ -sFDG) setup to conduct in-situ shear removal experiments for calcium carbonate and polystyrene micro-foulants on compliant anti-fouling surfaces. Guided by adhesion and fluid mechanics theory, and through rational micro-engineering of compliant materials, our findings reveal counterintuitive results: compliant materials surpass their rigid counterparts in anti-fouling performance. This research provides promising insights for the design of compliant interfacial materials capable of achieving high anti-fouling efficacy against particulate and crystallization fouling across various industrial applications including water and energy conversion systems.

5:00 PM EN07.10.02

Thermoelectric Properties of Monolayer HfI₂, an Electride with Electrons on The Interstitial Sites [Yi-Ming Zhao](#), Chun Zhang, Sunmi Shin and Lei Shen; National University of Singapore, Singapore

Two-dimensional (2D) thermoelectric materials are particularly suitable for wearable devices due to the flexible monolayer structure, which will supply power for other carried devices.¹ However, the electrical conductivity (σ) of 2D material is usually lower compared with the bulk counterparts because of a lower electron mobility induced by a higher density of scatterings.² Recently, Zhang et al. found that two MoS₂-like structures, ZrI₂ and HfI₂ with long carrier-lattice distance (d_{c-l}) exhibit a high hole mobility up to 4000 cm²V⁻¹s⁻¹.³ We notice that the ZrI₂-type structures are electrifies with excess electrons occupying the interstitial sites increasing the d_{c-l} .⁴ Such a unique charge distribution should undergo a weaker perturbation under the displacements of atoms, then the carrier mobility and the σ will be high. The figure of merit (ZT) of ZrI₂ reaches 1.2 at 900K under hole doping,⁵ but the relation between the charge distribution and the transport properties is still not clear enough in these electrifies.

Here, we investigate the thermoelectric properties of monolayer HfI₂ using first-principles calculations by fully considering the electron-phonon interaction using EPW⁶ code. The thermoelectric properties including Seebeck coefficient (S), σ and electron thermal conductivity (κ_e) are calculated by solving the Boltzmann transport equation beyond the constant relaxation time approximation implemented with BoltzTraP2 code.⁷ The lattice thermal conductivity (κ_l) is calculated by the ShengBTE code.⁸

We found that the hole doping tends to soften the acoustic phonon modes due to the interstitial distributed charge states and low density of states (DOS) near the valence band maximum (VBM), while the electron doping decreases the phonon relaxation time obviously because of a stronger electron-phonon interaction (EPI) induced by the high DOS near conduction band minimum (CBM). The carrier relaxation time at the VBM is obviously higher than that near the CBM due to the weaker lattice perturbation. The p-type σ is also higher than the n-type one under the same concentration. But the p-type S value is lower than the n-type one due to a lower DOS near VBM. The p-type power factor (PF) is larger than the value of n-type more dominated by σ .

The κ_l of HfI₂ is only 9.1 W/m-K within three-phonon interaction at room temperature lower than that of ZrI₂ (20.3 W/m-K⁵). The phonon relaxation time contributed by the electron-phonon scattering is even smaller than that of the three-phonon scattering at low phonon frequency range. The electrons near CBM will scatter the phonons due to the strong EPI. As a result, the κ_l decrease by 1.5 W/m-K when considering the electron-phonon scattering. The final ZT value reaches 0.86 at 1200K under p-type doping.

In summary, the HfI₂ with anionic electrons near the VBM exhibit a high mobility and σ under hole doping due to the weaker lattice perturbation. Our work reveals the role of interstitial distributed anionic electrons on the electron and phonon transport in the electride system, which gives insights for the further design of high-performance thermoelectric materials.

(1) Kanahashi, K.; Pu, J.; Takenobu, T. *Adv. Energy Mater.* **2020**, *10* (11), 1902842.

(2) Cheng, L.; Zhang, C.; Liu, Y. *Phys. Rev. Lett.* **2020**, *125* (17), 177701.

(3) Zhang, C.; Wang, R.; Mishra, H.; et al. *Phys. Rev. Lett.* **2023**, *130* (8), 087001.

(4) He, J.; Chen, Y.; Wang, Z.; et al. *J. Mater. Chem. C* **2022**, *10* (19), 7674-7679.

(5) Wen, J.; Peng, J.; Zhang, B.; et al. *Nanoscale* **2023**, *15* (9), 4397-4407.

(6) Ponc e, S.; Margine, E. R.; Verdi, C.; et al. *Comput. Phys. Commun.* **2016**, *209*, 116-133.

(7) Madsen, G. K. H.; Carrete, J.; Verstraete, M. J. *Comput. Phys. Commun.* **2018**, *231*, 140-145.

(8) Li, W.; Carrete, J.; A. Katcho, N.; et al. *Comput. Phys. Commun.* **2014**, *185* (6), 1747-1758.

5:00 PM EN07.10.03

Near-Field Thermal Radiation across Solid-State Gaps Mackey Long, [Hakan Salihoglu](#) and Joshua D. Caldwell; Vanderbilt University, United States

Near-field thermal radiation has attracted great interest due to heat transfer exceeding blackbody radiation by several orders at nanoscale separation gaps. Although extensive research is devoted for understanding of physics, feasibility of near-field based thermal devices with large scales is extremely low owing to the difficulty in controlling and sustaining the corresponding separations between heat exchanging materials in macroscales. In this study, we explore near-field radiation through solid-state gaps sandwiched between heat exchanging materials with large lateral dimensions. Our theoretical design employs solid-state thin films as a separating medium. We derive a multimode, nanoscale heat transfer model by incorporating Boltzmann's equation to fluctuational electrodynamics, and compare energy transport capacity of thermal radiation and conduction across the thin film and interfaces at both sides of the film. Our systematic approach enables defining key dimensions and parameters that govern radiation and conduction heat transfer through the solid-state gap. Using quasi steady-state approximation, this study also investigates and compares heat transfer dynamics of radiation and conduction across the film and the interfaces of the film in time domain. This study will shed light on the feasibility of solid-state based near-field thermal radiation and has potential to open a new avenue for possible application of near-field enhancement using macroscale devices.

5:00 PM EN07.10.04

Inhibiting Crystallization Fouling Using Nano-Micro-Engineered Heat Transfer Surfaces [Julian Schmid](#)¹, Tobias Armstrong¹, Niklas Denz¹, Diego R. Pi eiro¹ and Thomas Schutzius^{1,2}; ¹ETH Z urich, Switzerland; ²University of California, Berkeley, United States

Fouling of heat transfer surfaces is a widespread problem in the energy conversion and water treatment industries where thermally insulating deposits lead to significant performance reduction. Crystallization fouling, an important subset of fouling, occurs when water containing retrograde soluble salts like calcium sulfate, makes contact with a heated surface leading to the nucleation and growth of a surface deposit, termed "scale". However, we currently lack detailed information on the effect of surface texture, composition, and environmental conditions on the onset of scale nucleation, growth, and adhesion which is crucial for comprehending the complexity of scaling since it is a multiphase problem that starts at the nano-micro scale. Furthermore, we lack rational strategies for passively combatting this important problem. Here we show that nano- and micro-textured superhydrophilic surfaces outperform hydrophilic, hydrophobic and superhydrophobic surfaces regarding the delay of nucleation and observable growth of forming deposits in laminar and turbulent conditions. For this purpose, a novel continuous flow experimental setup mimics a cooling section of a heat exchanger and allows to holistically investigate the onset, growth, removal of deposit with its influence on the heat transfer process. Simultaneous visual microscopic *in-situ* observation and heat transfer resistance measurements provide insight into nucleation, growth, and adhesion of nano-micro-engineered substrates. We found that the degassing of dissolved gases on the heated substrate, their affiliation to the substrate, and the subsequent evaporation of water into the new phase is important for scaling in flow conditions. We anticipate that our holistic experimental setup provides profound information on the fundamental aspects of scaling and our nano-micro-engineered surfaces contribute to the development of advanced thermal interface materials that inherently prevent and/or repel scaling to contribute to a sustainable future in energy conversion.

5:00 PM EN07.10.05

Thermal Characterization of Ultra-Thin Suspended Silicon Nitride Platforms [Hwijong Lee](#)¹, Ethan Scott^{1,2}, John N. Nogan¹, Don Bethke¹, Peter A. Sharma¹, Tzu-Ming Lu¹ and C. Thomas Harris¹; ¹Sandia National Laboratories, United States; ²University of Virginia, United States

Silicon nitride is widely used in the microfabrication of thermal sensors due to its favorable material properties. While numerous studies have leveraged thin silicon nitride membranes for highly sensitive thermal measurements, there have been limited reports concerning membranes and platforms with thicknesses well below 100 nm. Herein, we report on the development of low-stress, suspended platform devices designed to facilitate the thermal characterization of membranes spanning a thickness range from 120 nm down to less than 10 nm. Depending upon the membrane thickness, we observe a substantial reduction in the thermal conductivity from $2.4 \text{ W m}^{-1} \text{ K}^{-1}$ to $1.2 \text{ W m}^{-1} \text{ K}^{-1}$ near room temperature. These platforms in this low thickness regime can significantly enhance the performance of devices requiring thermal isolation, such as bolometers, calorimeters, and gas sensors.

*This work was performed, in part, at the Center for Integrated Nanotechnologies, a U.S. DOE, Office of Basic Energy Sciences, user facility. Sandia National Laboratories is a multitechnology laboratory managed and operated by National Technology & Engineering Solutions of Sandia, LLC, a wholly owned subsidiary of Honeywell International, Inc., for the U.S. DOE's National Nuclear Security Administration under contract DE-NA-0003525. The views expressed in the article do not necessarily represent the views of the U.S. DOE or the United States Government.

5:00 PM EN07.10.06

Super-Resolution Thermometry via Computational Correction to Overcome Diffraction Limit [Edward D. Walker](#) and Thomas Beechem; Purdue University, United States

A computational enhancement is proposed, allowing for the realization of optical thermometry at spatial resolutions beyond the diffraction limit. Since the temperature measurement is a weighted average over the beam spot, the spot needs to be much smaller than the region of interest for accurate measurements. If it is too large, averaging creates a smoothing effect, flattening the measured profile. The simple solution is to more tightly focus the beam in order to create a smaller spot size. However, there is a limit to how much a beam of a given wavelength of light can be focused, known as the diffraction limit. For a diffraction limited system, then, there is a minimum temperature profile that is resolvable. To counter this, the relationship between the true profile, flattened profile, and beam shape can be put into the form of an integral equation, whose solution is the "true" profile. This equation takes a form that is similar in structure to problems in fields such as electromagnetism, image processing, and heat conduction. By studying how those fields approach the problem, their solutions can be used to create a set of corrective methods to undo the smoothing effect. Applying these to existing Raman systems allows for accurate measurements at scales up to 5x smaller than currently possible, improving spatial resolution without changing the underlying hardware.

5:00 PM EN07.10.07

Reversible Polymerization Chemistry for Compact Thermochemical Energy Storage Systems [Mayur S. Prabhudesai](#), Meysiva Veerabagu, Paul V. Braun and Sanjiv Sinha; University of Illinois at Urbana Champaign, United States

Thermal energy storage (TES) can be an effective alternative to electrochemical batteries in applications where the end usage is primarily heat¹. Within TES, thermochemical energy storage (TCS) based on reversible chemical reactions have been demonstrated for high-temperature applications via gas-gas or solid-gas reactions based on ammonia, sulfuric acid, limestone, etc². However, the development of these inorganic systems is limited by material degradation with cycling, hysteresis losses, and complex equipment and operation. Recent studies have explored organic reactions that operate in a homogeneous phase for low to medium temperature TCS applications³. With significant advances in chemically recyclable polymers⁴, we investigate here the polymerization/depolymerization chemistry of ϵ -caprolactone/polycaprolactone as a viable candidate for TCS. This chemistry is advantageous from an applications perspective due to a simple operation as a closed system and a broad range of charge/discharge temperatures suitable for water heating (100 – 200 °C). Preliminary studies confirm high conversion in the forward direction (polymerization) and selective formation of the monomer in the reverse direction. We find the heat of reaction obtained from DSC experiments ($\sim 140 \text{ J/g}$) to be consistent with prior literature values⁵. We discuss ongoing experiments to enhance the monomer yield during depolymerization and to quantify heat of polymerization (storage capacity) using a laboratory-scale reactor. This work advances the usage of organic compounds for TES applications and could form the basis for further identification of similar chemistries.

1. Odukomaia, A. et al. Addressing energy storage needs at lower cost via on-site thermal energy storage in buildings. *Energy and Environmental Science* vol. 14 5315–5329 Preprint at <https://doi.org/10.1039/d1ee01992a> (2021).

2. Prieto, C., Cooper, P., Fernández, A. I. & Cabeza, L. F. Review of technology: Thermochemical energy storage for concentrated solar power plants. *Renewable and Sustainable Energy Reviews* vol. 60 909–929 Preprint at <https://doi.org/10.1016/j.rser.2015.12.364> (2016).

3. Spotte-Smith, E. W. C., Yu, P., Blau, S. M., Prasher, R. S. & Jain, A. Aqueous Diels–Alder reactions for thermochemical storage and heat transfer fluids identified using density functional theory. *J Comput Chem* **41**, 2137–2150 (2020).

4. Coates, G. W. & Getzler, Y. D. Y. L. Chemical recycling to monomer for an ideal, circular polymer economy. *Nature Reviews Materials* vol. 5 501–516 Preprint at <https://doi.org/10.1038/s41578-020-0190-4> (2020).

5. Lebedev, B. V et al. The thermodynamics of ϵ -caprolactone, its polymer and of ϵ -caprolactone polymerization in the 0-350 K range. *Polymer Science U.S.S.R* vol. 20.

5:00 PM EN07.10.08

A Personal Cooling Garment with Flexible Thermoelectric Devices and Heat Sinks [Ethan Sun](#)^{1,2}, Tianshi Feng² and Renkun Chen²; ¹The Bishop's

School, United States; ²University of California, San Diego, United States

Global warming is causing more intense, more frequent, and longer periods of extreme heat events, which have caused numerous diseases and, in some cases, fatalities, among patients, the elderly, and outdoor workers such as those in the agriculture and construction sectors and firefighters. A lightweight personal cooling garment could be a game-changing solution to protect at-risk population and workers. However, today's personal cooling garments are not adequate as they are often too bulky and heavy, have limited cooling duration, and have no or limited temperature controllability. Hence, there is a strong need for a personal cooling garment with effective cooling, adjustable temperature, lightweight, is flexible & wearable, consumes less power (high coefficient of performance), and has low cost. Here we present our work on a personal cooling garment with flexible thermoelectric devices and heat sinks. This work leverages our earlier concept of developing flexible thermoelectric devices using high-performance rigid thermoelectric pillars. Here, we integrated individual thermoelectric devices into a flexible garment with the hot side cooled by flexible heat sinks. The garment is optimized with a finite element model for minimal weight. The performance of the garment under various heat flux levels and environmental temperatures was characterized. The results show that the garment can deliver high-flux cooling in a hot environment with high coefficient of performance (COP > 1). The technoeconomics and potential applications of this garment are also discussed.

5:00 PM EN07.10.09

Identifying Molecular Scale Interactions of Nucleating Agents with Salt Hydrates for Thermal Energy Storage Applications [Mayur S. Prabhudesai](#), Sung Bum Kang, Youngmun Lee, Daniel Hsieh, Jay M. Taylor, Paul V. Braun and Sanjiv Sinha; University of Illinois at Urbana Champaign, United States

Latent heat based thermal energy storage is of interest as a method to mitigate and time-shift thermal load peaks and hence reduce energy demands for heating and cooling buildings. Notably, Glauber's salt (GS) presents a good choice as a phase change material (PCM) for building applications because it has a melting point near room temperature (i.e., 32.4 °C), a large heat of fusion and energy density, and is low cost (~ \$100/ton). However, there are several known limitations to using GS as a PCM, such as incongruent melting, high degree of supercooling, and formation of other hydration states, which renders GS unsuitable for practical use. Inorganic crystals acting as nucleating agents can avoid some of these issues with GS [1]. Understanding nucleation behavior through typical calorimetry experiments offers limited insight into the molecular-scale mechanisms. Here, we report isothermal titration calorimetry [2] to investigate the interactions between sodium sulfate salt and an organic nucleating agent - glycine. Our experiments provide qualitative and quantitative understanding of how glycine interacts with sodium sulfate across various temperatures. The findings offer insights into the nucleation onset temperature (24°C) and underscore the pivotal role of glycine's zwitterionic structure in facilitating nucleation. This preliminary work provides a foundation for subsequent exploration of nucleating agents that would be incorporated in different salt hydrate systems.

1. Purohit, B. K., and V. S. Sista. "Inorganic salt hydrate for thermal energy storage application: A review." *Energy Storage* 3, no. 2 (2021): e212.
2. Velázquez-Campoy, Adrián, Hiroyasu Ohtaka, Azin Nezami, Salman Muzammil, and Ernesto Freire. "Isothermal titration calorimetry." *Current protocols in cell biology* 23, no. 1 (2004): 17-8.

5:00 PM EN07.10.10

Prediction and Characterization of Barocaloric Effects in Plastic Crystals Using Molecular Dynamics [Carlos Escorihuela Sayalero](#), Luis Carlos Pardo Soto, Pol Lloveras, Josep Lluís Tamarit and Claudio Cazorla; Universitat Politècnica de Catalunya, Spain

The energetic challenges of the present times demand the renewal of the technologies that harm the global environment. Amongst them, the scientific efforts towards developing cooling technologies based on the barocaloric effect (BC) present as a promising alternative to the conventional use of greenhouse-effect gases. Materials displaying BC present typically a large entropy change across a first order solid to solid phase transition. Such large entropy difference is usually related to order-disorder phase transitions, as is the case in some plastic crystals such as [CH₃NH₃]PbI₃. There is however a lack of understanding of the atomistic mechanisms driving this effect, which is necessary in order to move towards a feasible solid-state cooling technology. In this work we revise the atomistic origin of the entropy in disordered systems, and present a novel general methodology to calculate the BC estimators by using molecular dynamics NpT simulations using any source of atomistic potential available to the user. We present as well the application of this method to the analysis of [CH₃NH₃]PbI₃ and LiCB11H12 barocaloric potential.

5:00 PM EN07.10.11

Thermal Transport in Quasi-1D Van der Waals Crystal Nanowires [Zhiliang Pan](#), Lin Yang, Qian Zhang and Deyu Li; Vanderbilt University, United States

van der Waals (vdW) crystals represent a class of interesting materials with extraordinary bonding anisotropy. The break of symmetry induces rich physics and exotic transport phenomena. So far, extensive efforts have been made to explore the thermal properties of a plethora of two-dimensional (2D) vdW crystals. However, efforts on one-dimensional (1D) vdW materials remain largely in theory except some experimental work on single-walled carbon or boron nitride nanotubes.

Here we report on systematic studies of the thermal/mechanical properties of a group of quasi-1D vdW crystal nanowires composed of covalently bonded molecular chains assembled together via weak vdW interchain interactions. In the study of Ta₂Pd₃Se₈ nanowires, the thermal conductivity increases with the wire diameter up to 110 nm despite the weak interchain interaction. Measurements of the thermal conductivity for different sample lengths suggest a partial ballistic phonon transport over 13 μm at room temperature, which is induced by the propagation of phonons along the molecular chains. One interesting property of quasi-1D vdW crystals is charge density wave (CDW) phase transition, which can alter the free electron density without introducing dopants. Taking advantage of the CDW phase transition in NbSe₃ nanowires, we have observed distinct signatures of the electron-phonon (e-ph) interactions on the lattice thermal conductivity of NbSe₃ nanowires. With the development of CDWs, the carrier concentration reduces dramatically, which suppresses the e-ph interaction strength and results in an uprise in the lattice thermal conductivity. Furthermore, a tunable e-ph interaction is achieved through modulating the electric field along the chain. Above the threshold electric field strength, the condensed free electrons due to CDW can be depinned, leading to a higher electron thermal conductivity. Counterintuitively, the total thermal conductivity upon depinning is suppressed, which is due to the lower lattice thermal conductivity as a result of the enhanced e-ph scattering. The most exotic feature is found in ultrathin NbSe₃ nanowires where the thermal conductivity increases with the wire length following a 1/3 power law up to >42.5 μm, a signature of superdiffusive transport of 1D phonons. It is shown that this superdiffusive transport is due to excitation of 1D phonons as a result of the enhanced along-chain Young's modulus when the nanowire diameter becomes smaller than 26 nm. Our results show that as the wire diameter reduces from 26 nm to 6.8 nm, the Young's modulus increases by more than 5 times, which leads to a thermal conductivity enhancement by about 25 folds. The enhanced Young's modulus allows for excitation of high frequency 1D phonons along the molecular chains, which are responsible for the superdiffusive phonon transport in ultra-thin NbSe₃ nanowires. These findings disclose interesting thermal transport phenomena in quasi-1D vdW crystal nanowires, and the unique thermal properties could find important applications in thermal engineering.

5:00 PM EN07.10.12

Anharmonic Effects in Heat Capacity of Solids [Jaeyun Moon](#); Cornell University, United States

Heat capacity is a measure of how much energy heat carriers carry; therefore, it directly impacts performance and efficiency of various energy applications such as thermal storage and heat exchangers. For dielectric solids, heat capacity is most typically described by a purely harmonic oscillator model. This coupled with how these weakly interact anharmonically determine lattice thermal conductivity in various calculation schemes. In this work, we explicitly characterize individual mode contributions to heat capacity in some simple crystals such as argon and silicon and find that in contrast to common assumptions based on harmonic oscillators, each mode is strongly anharmonic especially at high temperatures, leading to the breakdown of the equipartition theorem. We discuss implications of our findings in the context of thermal transport in solids.

5:00 PM EN07.10.13

Predicting Phonon Transport in Disordered Alloys from a Highly Accurate Machine Learning Interatomic Potential [Hsin Lin](#)¹, Hao-Jen You¹, Liang-Zi Yao¹, Yi-Ting Chiang¹, Yen-Fu Liu², Tzen Ong¹, Yueh-Ting Yao² and Tay-Rong Chang²; ¹Academia Sinica, Taiwan; ²National Cheng Kung University, Taiwan

The II₂IV family of materials, such as Mg₂Si, Mg₂Sn, Sr₂Si, and Sr₂Ge, among others, are highly regarded as promising high-performance thermoelectric materials. In our previous research, we calculated the maximum figure of merit ZT for the promising II-IV family thermoelectric compounds Sr₂Si and Sr₂Ge, yielding values of 1.15 and 1.44 at 900 K through first-principles calculations. To improve thermoelectric performance, the common practice involves alloying to reduce lattice thermal conductivity and enhance the Seebeck coefficient. Nevertheless, determining the optimal alloy ratios through first-principles calculations can be quite challenging because disordered effects require a large supercell in the computations. Here, we introduce a highly accurate machine learning interatomic potential (MLIP) for Sr₂Si_{1-x}Ge_x disordered alloys. This MLIP is created through a machine learning technique trained on first-principles density functional theory (DFT) data, and it attains accuracy levels comparable to those achieved with DFT. This approach empowers us to carry out efficient molecular dynamics simulations for entire alloy concentration $0 \leq x \leq 1$ in Sr₂Si_{1-x}Ge_x and make accurate thermal property predictions. Our work provides a solution to explore compositions that offer the most potential for high-performance thermoelectric disordered alloys while assessing the contributions of phonon modes to phonon transport.

5:00 PM EN07.10.14

Thermal Transport in 2D Materials Using Tersoff Interatomic Potentials [Adil Muhammed](#)^{1,2}, Subramanian Sankaranarayanan^{1,2}, Aditya Koneru^{1,2}, Kiran Sasikumar³ and Partha Sarathi Dutta^{1,2}; ¹University of Illinois Chicago, United States; ²Argonne National Laboratory, United States; ³Avant-Garde Materials Simulation, Germany

Understanding thermal behavior in two dimensional (2D) materials is important for advancing nanoelectronics and thermoelectric applications, as these materials can exhibit exceptionally tunable thermal conductivities. Especially, emerging 2D materials like Silicene, Arsenene, Bismuthene and Antimonene are necessary as they find applications in a wide range of electronic and thermal devices. In this work we perform molecular dynamic simulations to understand thermal transport of these 2D nanomaterials and their corresponding nanotubes using equilibrium molecular dynamics with the Green-Kubo formalism. We utilize our in-house Tersoff models optimized against different polymorphs across local and global properties. Also, we present the impact of understanding the phonon dispersion predictions made by these models on thermal conductivities. This can greatly aid in optimizing better force-fields which in turn can create accurate surrogate models for inverse design of these thermal materials.

5:00 PM EN07.10.15

Probe Beam Deflection Technique with Liquid Immersion for Rapid Measurement of Thermal Conductance [Jinchi Sun](#) and David Cahill; University of Illinois at Urbana-Champaign, United States

Time-domain thermoreflectance (TDTR) and frequency-domain thermoreflectance (FDTR) are well-established techniques for spatially resolved measurements of thermal conductivity and thermal boundary conductance. In these methods, a metal coating serves as a thermometer, generating a thermoreflectance signal. To enhance the signal-to-noise ratio, a frequency-domain probe beam deflection (FD-PBD) was developed, which utilizes the probe beam deflection caused by thermal expansion. FD-PBD is only sensitive to in-plane thermal diffusivity. To introduce sensitivity to through-plane thermal conductance, FD-PBD is adapted by immersing the Al-coated sample in a dielectric liquid. The thermometer now becomes the probe beam deflection which is due to the refractive index gradient in the liquid resulting from temperature changes. This modified approach, named as liquid immersion probe beam deflection (LI-PBD), allows us to measure the thermal conductivity of thin films, thermal boundary conductance, and the thermal conductivity of bulk materials, all without the need for prior knowledge of heat capacities. The measured values agree with reference values within 10%. Rapid mapping of thermal boundary conductance is demonstrated, with the data acquisition time per point required to achieve a noise-induced uncertainty of 1% significantly reduced to 3 milliseconds. Both spatial resolution and maximum probing depth can be adjusted by varying the radius of the focused laser beams. This technique facilitates imaging of defects buried at different depth below the surface.

5:00 PM EN07.10.16

The Role of Deposition Temperature on The In-Plane Thermal Conductivity of Aluminum Scandium Alloys [Daniel M. Hirt](#), Md. Rafiqul Islam, Md Shafkat Bin Hoque, Sara Makarem and Patrick E. Hopkins; University of Virginia, United States

The advancement of modern electronic devices has been limited by a thermal engineering problem existing at the nanoscale: how to reduce the thermal load on critical components of a device. Hillocks, which form due to differences in thermal expansion between a film and its substrate, are a significant limitation to integrated circuit fabrication. Hillocks can cause problems in integrated circuits such as dielectric cracks and interconnection shortages that result in unreliable devices. Aluminum (Al), the current choice for electrical traces in integrated devices due to its low resistivity, is particularly susceptible to hillock formation when heated. Recent advances have shown that alloying scandium with aluminum can help mitigate this issue. Furthermore, the aluminum scandium alloy (Al₃Sc) also has a higher melting point than Al thus making it a potential alternative to Al for high temperature applications. Combining these properties with its low electrical resistivity makes Al₃Sc an excellent choice for the next generation of electrical interconnects. However, a detailed study into the thermal properties of Al₃Sc alloy as well as the scattering mechanisms that contribute to its thermal conductivity is still missing in literature.

In this work we investigate the in-plane thermal conductivity and electron-phonon coupling factor of aluminum scandium alloys deposited at different temperatures with time-domain thermoreflectance (TDTR). For these experiments, we use a Al_{0.8}Sc_{0.2} (Al_{0.8}Sc_{0.2}-SiO₂-Si) structure deposited at various temperatures. Our measurements reveal that higher deposition temperatures yields higher in-plane thermal conductivity in aluminum scandium alloys. We attribute this to an increased formation of Al₃Sc crystalline regions for films that were deposited at higher temperatures. In order to investigate the role of electron-phonon scattering on the measured drop in the in-plane thermal conductivity, we performed our TDTR measurements with an infrared probe laser. By measuring the electron-phonon coupling constant at different deposition temperatures we show that the electron-phonon coupling constant remains relatively constant with deposition temperature. This suggests that a reduction in electron-boundary scattering due to increased formation of Al₃Sc is the primary reason for enhanced thermal conductivity at higher deposition temperatures. Our measurements provide insight into the role of different scattering mechanisms on the thermal conductivity of intermetallic alloys.

5:00 PM EN07.10.17

Phonon Thermal Transport in Semiconductors Studied Using a Neural Network Assisted Solution of The Peierls-Boltzmann Equation [Navaneetha Krishnan Ravichandran](#); Indian Institute of Science, India

Unusual thermal transport phenomena such as the hydrodynamic and Poiseuille phonon flow arise out of strong coupling among phonons in certain solid-state crystalline materials, and find applications in thermal cloaking and shielding of semiconductor devices and in the development of low thermal noise detectors. The linearized Peierls-Boltzmann equations (LPBE), which form a set of multi-dimensional and coupled partial differential equations, govern the coupled dynamics, transport and equilibration of phonons in these systems. Hence, solving the LPBE is a crucial step towards discovering new materials that display these unusual, yet technologically important phenomena.

However, predictive solutions of the LPBE including lowest-order interactions among three phonons and higher-order interactions among four phonons with *ab initio* inputs from density functional theory, which will serve as search tools for new materials, have been computationally intractable until recently [1, 2]. Even considering these recent advances, the computational cost due to the high dimensionality of the LPBE, large number of phonon polarization for the materials with complex crystal geometries and the need to resolve highly localized, temporally evolving interactions among phonons makes these conventional methods unsuitable for the rapid search of new materials that show exceptional hydrodynamic phonon transport.

To overcome this problem, here we develop a neural network scheme to solve the steady-state and the transient LPBE, which enables rapid convergence of the steady-state solution of the LPBE and allows for computationally efficient high temporal resolution of localized interactions among phonons under transient transport conditions, which is particularly important to search for materials with strongly hydrodynamic phonon flow. We show that, for materials with complex crystal structures beyond the cubic geometry such as bulk MoS₂, graphite, w-GaN and hBN, where hydrodynamic transport is possible at cryogenic conditions, the neural network scheme significantly outperforms the conventional iterative solution of the LPBE under both steady-state and transient conditions. Our findings highlight the computational advantages of adopting this new neural network-based first principles solver for the LPBE, which can have significant impact in the research areas of developing robust, efficient computational tools for materials discovery.

This work is supported by India's Science and Engineering Research Board through the Core Research Grant No. CRG/2020/006166 and the Mathematical Research Impact Centric Support Grant No. MTR/2022/001043. The presenter also acknowledges the Infosys Young Investigator award for support.

[1] Tianli Feng, Lucas Lindsay, and Xiulin Ruan, Phys. Rev. B 96, 161201(R), 2017.

[2] Navaneetha K. Ravichandran and David Broido, Phys. Rev. X 10, 021063, 2020.

5:00 PM EN07.10.18

Molecular Aspect Ratio Effect on Axial Thermal Transport in Solution-Spun Carbon Nanotube Fibers [Yingru Song](#)¹, Michelle D. Chaves¹, Ivan R. Siqueira¹, Ognyan Stefanov¹, Natsumi Komatsu², Junichiro Kono¹, Matteo Pasquali¹ and Geoffrey Wehmeyer¹; ¹Rice University, United States; ²University of California, Los Angeles, United States

Neat, densely packed, and highly aligned carbon nanotube fibers (CNTF) have appealing room-temperature axial thermal conductivity (κ) and thermal diffusivity (D) for applications in lightweight axial heat spreading or flexible thermal connections. Although increasing the molecular aspect ratio (i.e., ratio of nanotube length to nanotube diameter) of the constituent single-wall and few-wall carbon nanotubes (CNTs) is expected to improve and by reducing the number of interfaces along the axial direction per unit length, no prior work has quantified the molecular aspect ratio effect on thermal transport for solution-spun CNTF. Here, we perform self-heated steady-state and three-omega thermal measurements at room temperature on suspended CNTF in vacuum. The CNT molecular aspect ratios range from 960 to 5600, as quantified by rheological measurements of liquid crystalline CNT solutions. The thermal measurement results show that κ increases from 1.5 ± 0.1 to 1.5 ± 0.1 W/mK with increasing aspect ratio. The axial electrical conductivity also increases from 1.5 ± 0.1 to 1.5 ± 0.1 S/m with increasing aspect ratio, and the Wiedemann-Franz law predicts the electronic contribution to κ is for the highest sample. CNTF made with varying volume fraction of constituent high- and low- κ CNTs generally fall within typical macroscopic rule-of-mixtures bounds for κ and D . The thermal diffusivity scales with κ , leading to a sample-averaged volumetric heat capacity of 1.5 ± 0.1 . Thus, this work shows that increasing the molecular aspect ratio enhances κ and D of solution-spun CNTF, motivating further investigation into thermal transport mechanisms and applications of carbon nanotube fibers.

5:00 PM EN07.10.19

Bioengineering a Reversible Thermal Conductivity Switch in Tandem Repeat Proteins [Emma Tiernan](#)¹, John Tomko¹, Benjamin Allen², Melik Demirel³ and Patrick E. Hopkins¹; ¹University of Virginia, United States; ²Tandem Repeat Technologies, Inc, United States; ³The Pennsylvania State University, United States

The reversible regulation of heat transport within a material provides the user the ability to control its temperature as well as that of its surroundings. To achieve this nanoscale regulation, a material must be able to switch between thermally conductive and insulative states. In recent years it has been shown that thin films of certain tandem repeat proteins can achieve this thermal switch by simply hydrating and dehydrating the film. One material that is able to serve as a thermal switch is a synthetic bio-polymer whose sequence is inspired by those found in squid ring teeth (SRT). These SRT bio-polymers consist of repeating amorphous and crystalline domains which rely on hydrogen bonding and other intermolecular forces to retain their folded conformation. The addition and removal of water to these films will enhance or disrupt the intermolecular forces, thus encouraging or inhibiting the transport of heat.

In these experiments, we used time-domain thermoreflectance (TDTR) to monitor the thermal conductivity switch of SRT thin films under varying hydrating conditions. TDTR is an optical pump-probe technique for measuring thermal conductivity of microscale material systems, where a low power "probe" beam monitors the change in reflectivity of a metal transducer on the sample surface in response to a modulated heating "pump" laser. By applying an analytical solution to the heat conduction equation, we calculate thermal conductivity and other thermal properties of the material. We show that by modifying the composition of the hydrating solution, we are able to obtain a thermal conductivity switch ratio of four between ambient and hydrated states.

5:00 PM EN07.10.20

Anti-Environmental Aging Passive Daytime Radiative Cooling Paint [Jianing Song](#) and Xu Deng; University of Electronic Science and Technology of China, China

Passive daytime radiative cooling technology presents a sustainable solution for combating global warming and extreme weather, with great potential for diverse applications. The key characteristics of this cooling technology are the ability to reflect most sunlight and radiate heat through the atmospheric transparency window. However, the required high solar reflectance is easily affected by environmental aging, making the cooling ineffective. We demonstrate a facile strategy to use titanium dioxide nanoparticles, with UV resistance, forming hierarchical porous morphology via evaporation-driven assembly, which guarantees a balanced anti-soiling and high solar reflectance, rendering anti-aging cooling paint (AACP) based coatings. We challenged

the AACP coatings against simulated 3 years of natural soiling and 1 year of natural sunshine, and found that the solar reflectance only declined by 0.4% and 0.5% compared with the un-aged ones, barely affecting the cooling performance. Our AACP is scalable and can be spray coated on desired outdoor architecture and container, presenting durable SDRC, promising for real-world applications.

SESSION EN07.11: Data-driven High Throughput Computations

Session Chairs: Sheng Shen and Ilaria Zardo

Thursday Morning, April 25, 2024

Room 327, Level 3, Summit

8:30 AM *EN07.11.01

Physics-Informed Neural Networks for Solving Phonon Boltzmann Transport Equation [Tengfei Luo](#), Jiahang Zhou and Ruiyang Li; University of Notre Dame, United States

The phonon Boltzmann transport equation (pBTE) has been proven to be capable of precisely predicting heat conduction in sub-micron electronic devices. However, numerically solving pBTE is extremely computationally costly due to its high dimensionality, especially when phonon dispersion and time evolution are considered. In this study, we use physics-informed neural networks (PINNs) to solve pBTE for multiscale non-equilibrium thermal transport problems both efficiently and precisely. In particular, a PINN framework is devised to predict phonon energy distribution by minimizing the residuals of governing equations, boundary conditions, and initial conditions without the need for any labeled training data. With phonon energy distribution predicted by the PINN, temperature and heat flux can be obtained thereby. In addition, geometric parameters, such as characteristic length scale, are also considered as a part of the input to PINN, which makes our model capable of predicting heat distribution in different length scales. Furthermore, 1D to 3D heat conduction problems are studied under our PINN framework, and the results show excellent agreement with numerical and FEM solutions. Moreover, our PINN framework has proved to be far more efficient compared to existing pBTE numerical solvers. With superiorly high efficiency and accuracy, the proposed method shows great promise for practical applications, such as thermal design and thermal management of microelectronic devices. Besides pBTE, we have also extended the applicability of the PINN framework for modeling coupled electron-phonon (*e-ph*) transport. *e-ph* coupling and transport are ubiquitous in modern electronic devices. The coupled electron and phonon Boltzmann transport equations (BTEs) hold great potential for the simulation of thermal transport in metal and semiconductor systems. However, solving the BTEs is often computationally challenging due to their high dimensional complexity and wide span heat carrier properties, hindering large-scale thermal modeling at the device level. In this work, we present a PINN framework for solving the coupled electron and phonon BTEs. Instead of relying on labeled data, the proposed framework directly learns the spatiotemporal solutions (i.e., the electron and phonon distribution functions) within a parameterized space by enforcing physical laws. The efficacy of this framework is demonstrated through its ability to accurately resolve temperature profiles in low-dimensional thermal transport problems and visualize the ultrafast electron and phonon dynamics in laser heating experiments on thin metal films. The results indicate that our approach can accurately describe non-equilibrium *e-ph* energy transfer with improved efficiency, opening new avenues for the predictive design and optimization of micro- and nanostructures.

9:00 AM EN07.11.03

Screening Ultralow Thermal Conductivity from 150,000 Crystals by Sub-Trillion-Scale Atomic Data Integrated Deep Learning Approach [Ming Hu](#); University of South Carolina, United States

Existing machine learning potentials for predicting phonon properties of crystals are limited to either small amount of training data or a material-to-material basis, primarily due to the exponential scaling of model parameters with the number of atomic species or elements. This renders high-throughput infeasible when facing large-scale new materials. Unlike previous machine learning models with inherently limited training on small data and global properties, we develop Elemental Spatial Density Neural Network Force Field (Elemental-SDNFFF) with abundant atomic level environments as training data. Benefiting from this innovation, we integrate ~50 million atomic data to train a single deep neural network without increased expensive ab initio simulations. The effectiveness and precision of the Elemental-SDNFFF approach is demonstrated on a set of 150,000 inorganic crystals spanning 63 elements in the periodic table by prediction of complete phonon properties. Our algorithm achieved a competitive force root mean square error of about 40 meV/Å and a speed-up of 3 – 4 orders of magnitude in comparison to first principles. Self-improvement schemes such as active learning and data augmentation techniques are also incorporated allowing human-free refinement of the force accuracy on arbitrary combinations of chemistries. Deep insight into the ultralow lattice thermal conductivity (<1 W/mK) of predicted structures are gained by p-d orbital hybridization analysis and charting the thermal conductivity data in the bonding-antibonding map, which offers a quick approach for future screening of crystals with strong intrinsic phonon anharmonicity. Our model also quantitatively reveals the correlation between off-diagonal coherence and diagonal populations and identifies the distinct crossover from particle-like to wave-like heat conduction. Our algorithm is promising for accelerating discovery of novel phononic crystals for emerging applications, such as heat dissipation in electronics, thermoelectrics, and coherent phonons for quantum information technology.

9:15 AM EN07.11.04

Advancing Thermal Management in Buildings Globally: Machine Learning-Optimized Dynamic Window Materials [Yuan Gao](#), Jacob Jonsson, Charlie Curcija, Simon Vidanovic and Tianzhen Hong; Lawrence Berkeley National Laboratory, United States

Dynamic window materials represent a significant advancement in energy-efficient building technology, offering a promising approach to intelligent thermal management and energy conversion in architectural applications. Leading areas of interest in dynamic window research include hydrogels, passive radiative cooling materials, dynamic devices based on reversible metal electrodeposition. These cutting-edge materials are capable of dynamically altering their optical and thermal properties in response to external environmental variations, thereby efficiently managing light and heat transfer within buildings. However, dynamic window materials face significant challenges in their development and application. First and foremost, these materials are often optimized based on specific weather conditions rather than a comprehensive, global spectrum. Achieving continuous optimization on a global scale proves to be difficult due to the immense volume of calculations required. This lack of universal optimization may limit their efficiency across diverse climate zones. Furthermore, there is a noticeable gap in the presence of robust indicators to quantify the dynamic performance of these materials. This void in performance metrics poses a challenge, as without clear quantification, it becomes difficult to determine the true value of these windows, especially since their dynamic features may be superfluous in certain climatic conditions.

To address these issues, we proposed novel indicators to evaluate the necessity level of using dynamic windows in buildings for different climates. We use thermochromic (TC) materials as examples to demonstrate this concept for passive dynamic windows. Through an unprecedented global-scale analysis, we executed more than 2.8 million simulations across over two thousand global locations covering most of the Köppen climate classifications in the world. A typical commercial office space, which is adapted from Department of Energy's prototype building model, is used for EnergyPlus simulation in this study. Beyond typical office space, whole commercial and residential buildings are also used for analysis. World heatmaps of indicators for dynamic TC windows

have been obtained by artificial neural networks (ANNs) trained by data from various conditions: differing material properties, window configurations, building and environmental circumstances. The ANN inputs include geographic (latitude) and weather (solar radiation and air temperature) data that can be extracted from weather files and is publicly available as the information in a world-map format. The good linear regressions between target and prediction indicate that the performance indicators can be well predicted from the inputs through ANNs, which are optimized by a hyperparameter tuning process. The heatmaps of indicators obtained from ANNs reveal that TC windows with optimal transition temperatures lack dynamism in most of low-latitude tropical regions, functioning similarly to static windows in terms of energy savings. Seasonal dynamics of TC windows appear more important for energy saving compared with daily fluctuations. Surprisingly, optimal transition temperatures correlate more with clear-state solar transmittance than with dark-state. This insight is unprecedented in existing literature.

To assist researchers in optimizing and evaluating TC materials and windows, we provide an open-source Python tool (<https://github.com/LBNL-ETA/PyDynamicWindow>, a private repository, will be published soon) to quickly obtain a world heatmap of desired indices or optimal properties within seconds by simply inputting the fixed material properties. Besides thermochromic, other dynamic window materials will also be included in this Python tool in the future. With this powerful tool, researchers can identify climate conditions for dynamic windows and improve their materials and products for target climates.

9:30 AM BREAK

SESSION EN07.12: Modeling Phonons, Electrons and Their Interactions
Session Chair: Tengfei Luo
Thursday Morning, April 25, 2024
Room 327, Level 3, Summit

10:30 AM *EN07.12.01

Atoms to Devices: Predicting Thermal Properties of Materials in Technological Applications [Sanghamitra Neogi](#); University of Colorado Boulder, United States

Recent advances of atomistic modeling techniques have shown remarkable accuracy while predicting heat transport mechanisms in isolated nanoscale systems, such as thin films with confining surfaces, single solid-solid interfaces between materials with different degrees of crystallinity or disorder. Heat is mostly carried by phonons in semiconductors and insulators. When the system size becomes comparable to the characteristic lengths of phonons, heat conduction is affected by phonon confinement and enhancement of scattering due to boundaries, interfaces, and various defects. Phonon confinement results in localization of modes in spatial regions. The effect of scattering mechanisms on phonon transport properties could also be highly varied. The thermal transport properties of nanoscale systems that include multiple confining surfaces, interfaces, and materials with different degrees of crystallinity or disorder, is far from understood. The computational costs of atomistic approaches prohibit us to explore the complete structural parameter space of large systems, that influence phonon transport. The state-of-the-art (SoA) deeply scaled sub-10 nanometers transistors are heterogeneous structures that include nm-scale crystalline semiconductors, disordered dielectric materials and metals, within confining interfaces. The confined geometry results in a net increase of the power density within the structures. The associated self-heating accelerates the defect generation mechanisms leading to decline of performance and reliability issues. The SoA thermal models of microelectronic circuits utilize continuum level models to predict the temperature distribution in the structures, even after 40+ years of being declared outdated. The models also incorporate input from non-continuum models that are better suited to describe the physics at smaller length scales. However, the transistor-level thermal properties are often approximated from the bulk thermal properties or computed using effective models. The effective models include several parameters that need to be calibrated using measurement data. The calibrated parameters may not even accurately represent behavior in dynamic operating conditions. The heat transfer in nm-scale systems can be drastically different from their bulk counterparts. The effective models does not include these details and as a result, cannot explain thermal bottlenecks or runaways or reveal any mitigation strategies. A predictive thermal model must consider the effects of confinement to accurately predict temperatures and identify thermal bottlenecks. In the past decades, algorithmic improvements, and dramatic increase of computing power, have enabled rigorous techniques such as molecular dynamics (MD) simulations to accurately model heat transport in finite systems, with disordered components and interfaces. MD simulations implicitly include the full dynamics of anharmonic interactions and do not make any assumptions about scattering mechanisms. In this talk, I will discuss how we use atomistic modeling approaches combined with machine learning methods to predict thermal properties of sub-10-nm confined geometry field effect transistors and other complex devices.

11:00 AM EN07.12.02

Monte Carlo - Finite Element Mixed Model for Heat Transport on Electronic Devices at The 20 nm Scale [F. Xavier Alvarez](#), Jordi Tur and Albert Beardo Ricol; Universitat Autònoma de Barcelona, Spain

Simulation of the thermal evolution of actual electronic devices is a very challenging topic. Heat transport at the nanoscale does not behave as in the macroscale [1-2]. This is a problem for engineers, as they cannot predict the thermal response of their devices with accuracy.

In the last years, the Kinetic Collective Model (KCM) has been used to develop a finite element tool to describe the thermal evolution of electronic devices with great accuracy using the Guyer and Krumhansl hydrodynamic equation. The results obtained from this approach fit extraordinarily to experiment with characteristic scales up to 400 nm using only ab initio parameters [1-2], but for smaller devices, effective values for the parameters are required. In that situations, some corrections are required in order to predict the experiments.

We present the Higher Order Perturbation (HOPE) an improvement of the KCM-hydrodynamic approach [4-5]. This new method allows to obtain a full predictive finite element model for thermal transport at the 20nm scale. The model is obtained from the split of the Boltzmann Transport Equation (BTE) in two terms, a first one that describes the hydrodynamic behavior and a second one with the residual terms that describes the evolution of the perturbations of higher order. From the solution of the residual term using a Monte Carlo approach we derive a boundary correction term that modifies the hydrodynamic boundary conditions. With this correction, the applicability of our finite element tool is significantly improved. We compare the results obtained from our simulations with experimental data of devices in the 200-20 nm range.

Bibliography

[1] Beardo, A. et al. (2021) *Observation of second sound in a rapidly varying temperature field in Ge*. Science Advances, 7(27), eabg4677.

<https://doi.org/10.1126/sciadv.abg4677>

[2] Beardo, A. et al. (2021) *A General and Predictive Understanding of Thermal Transport from 1D-and 2D-Confined Nanostructures: Theory and Experiment*. ACS NANO, 15(8), 13019–13030. <https://doi.org/10.1021/acsnano.1c01946>

[3] Alajlouni, S. et al. (2021). Geometrical quasi-ballistic effects on thermal transport in nanostructured devices. NANO RESEARCH, 14(4), 945–952. <https://doi.org/10.1007/s12274-020-3129-6>

[4] Sendra, L. et al. (2021). Derivation of a hydrodynamic heat equation from the phonon Boltzmann equation for general semiconductors. Phys Rev B, 103(14). <https://doi.org/10.1103/PhysRevB.103.L140301>

[5] Sendra, L. et al. (2022). *Hydrodynamic heat transport in dielectric crystals in the collective limit and the drifting/driftless velocity conundrum*. Phys Rev B, 106(15). <https://doi.org/10.1103/PhysRevB.106.155301>

11:15 AM EN07.12.03

Study of Interfacial Thermal Resistance of Heterostructures Using Machine Learning (ML)-Molecular Dynamics [Tianli Feng](#); University of Utah, United States

Diamond, as an ultra-wide bandgap semiconductor, holds significant potential in many cutting-edge applications from electronics, nanotechnology, biosensors and quantum information processing, owing to its ultra-high thermal conductivity and mobility. The interfacial thermal conductance between diamond and metals is crucial for the thermal management of diamond-based electronic devices and determines the maximum working temperature. However, current knowledge about the metal/diamond thermal interfacial transport is still very limited. There is no reliable interatomic potential between metals and diamond. In this work, we train machine learning interatomic potentials at the interface based on density functional theory (DFT) calculations. The accuracy of the potential is validated against DFT calculations. Using the potentials, we conduct MD simulations and obtain the interfacial thermal conductance. Different surface terminations of diamond have been studied. The results from this research should have significant contribution to improved understanding of interfacial thermal properties, which is key to developing new diamond-based electronics devices.

11:30 AM EN07.12.04

Active Learning Exploration of Thermally Conductive Polymers Under Strain [Renzheng Zhang](#), Jiaxin Xu, Hanfeng Zhang and Tengfei Luo; University of Notre Dame, United States

Finding amorphous polymers with higher thermal conductivity (TC) is technologically important, as they are ubiquitous in a wide range of applications where heat transfer is crucial. While TC is generally low in amorphous polymers, it can be enhanced by subjecting them to strain since it facilitates the alignment of polymer chains. However, using the conventional Edisonian approach, the discovery of polymers that may have high TC after strain can be time-consuming and lack guarantee of success. In recent years, machine learning approaches have shown promise in the prediction of polymer properties with high accuracy and efficiency. In this work, we employ an active learning scheme to speed up the discovery of amorphous polymers with high TC under strain. Polymers under strain were simulated using molecular dynamics (MD), and their TCs were calculated using the non-equilibrium MD method. A Gaussian Process Regression (GPR) model is then trained using these data. The GPR is used to screen the PoLyInfo database, and the predicted mean TC and uncertainty are used towards an acquisition function to recommend new polymers. The TC results of these selected polymers are then labeled using MD simulations and the obtained data are incorporated into the training set, initiating a new iteration of the active learning cycle. Over a few cycles, we identified more strained polymers with significantly higher TC than the original dataset, and the results offer valuable insights into the structural characteristics that contribute to enhanced energy conduction from a physical perspective.

11:45 AM EN07.12.05

Phonon Diffraction and Interference [Konstantinos Termentzidis](#)¹, Paul Desmarchelier², Efstathios Nikidis³, Yoshiaki Nakamura⁴, Anne Tanguy² and Joseph Kioseoglou³; ¹CNRS, France; ²Université de Lyon, France; ³Aristotle University of Thessaloniki, Greece; ⁴University of Osaka, Japan

We have observed phonons diffraction and interference patterns at the atomic scale, using molecular dynamics simulations in systems containing crystalline silicon and nanometric obstacles as voids or amorphous-inclusions. The diffraction patterns caused by these nano-architected hybrid systems of the same order as the phonon wavelengths are similar to the ones predicted by a simple Fresnel- Kirchhoff integral. These findings give evidence of the wave nature of phonons, can help to a better comprehension of the interaction of phonons with nanoobjects and at long term can be useful for intelligent thermal management and phonon frequency filtering at the nanoscale.

SESSION EN07.13: Phonon Engineering
Session Chairs: Sanghamitra Neogi and Sebastian Volz
Thursday Afternoon, April 25, 2024
Room 327, Level 3, Summit

1:30 PM *EN07.13.01

Thermal Conductivity and Elastic Modulus in Two-Dimensional Hybrid Metal Halide Perovskites: From a Molecular Engineering Perspective Ankit Negi¹, Liang Yan², Cong Yang¹, Yeonju Yu³, Subhrangsu Mukherjee¹, Andrew Comstock¹, Ziqi Wang¹, Dali Sun¹, Harald Ade¹, Qing Tu³, Wei You² and [Jun Liu](#)⁴; ¹North Carolina State University, United States; ²University of North Carolina at Chapel Hill, United States; ³Texas A&M University, United States

Device-level implementation of soft materials demands a comprehensive understanding of their thermal conductivity and elastic modulus to mitigate thermo-mechanical challenges and ensure long-term stability. Thermal conductivity and elastic modulus are usually positively correlated in soft materials, such as amorphous macromolecules, which poses a challenge to discover materials that are either soft and thermally conductive or hard and thermally insulative. Here, we show an anomalous correlation of thermal conductivity and elastic modulus in two-dimensional (2D) hybrid organic-inorganic perovskites (HOIP) by engineering the molecular interaction between organic cations. When replacing the organic cation from a softer alkyl ligand to a more rigid aryl ligand, we find that elastic modulus increases but thermal conductivity decreases, which provides a route to engineer thermal conductivity and elastic modulus independently. We further conducted molecular dynamics simulation to understand the molecular interactions and this anomalous

dependence. Introducing chirality into the organic cation induces a unique molecular packing, leading to the same thermal conductivity and elastic modulus regardless of the composition for all half-chiral 2D HOIPs. This finding provides substantial leeway for further investigations in chiral 2D HOIPs to tune opto-electronic properties without affecting the thermal and mechanical stability.

2:00 PM EN07.13.02

Understanding Effects of Gas Molecules on Thermal Transport in Metal–Organic Frameworks [Yukyung Moon](#), Rahil Ukani, Qichen Song, Joy Cho and Jarad A. Mason; Harvard University, United States

Metal–organic frameworks (MOFs)—porous crystals composed of metal nodes and organic linkers—are promising materials for a wide range of applications, notably in gas storage and separations. Despite ultrahigh porosities, large internal surface areas, and highly tunable structures, realizing the full potential of MOFs has been hindered in part by their inadequate thermal properties. MOFs typically possess low thermal conductivities ($< 2 \text{ W m}^{-1} \text{ K}^{-1}$), which can dictate gas adsorption dynamics under practical loading rates. While it has been suggested that the presence of gas molecules within the pore can impact the propagation of phonons, it has been challenging to experimentally examine the effects of interactions at the pore wall. Recent studies have sought to measure the thermal conductivities of various MOFs, and molecular dynamic simulations have been employed to elucidate the factors governing their intrinsic transport properties, but the microscopic mechanisms underlying the effects of adsorbates remain underexplored. Here, we present experimental investigations of thermal transport in zeolitic imidazole framework-8 (ZIF-8) under systematically varied gas environments. We employ the frequency-domain thermoreflectance (FDTR) technique to probe thermal conductivity in single crystals of ZIF-8 with chemically diverse gas adsorbates. This approach enables us to investigate how the interaction energies between gas molecules and the pore walls influence transport pathways along the porous framework. Our FDTR measurements reveal that gases with higher adsorption capacity, such as CO_2 , result in a notable decrease in the thermal conductivity of ZIF-8 compared to adsorbates with a lower adsorption capacity such as N_2 . Additionally, variable-temperature FDTR measurements provide insight into the kinetics of gas molecules confined within the pores of ZIF-8. Our research illuminates the dynamic interplay between gas adsorption and the thermal properties of ZIF-8, offering new mechanisms to chemically modulate thermal transport in porous materials systems.

2:15 PM EN07.13.03

Anomalous Thermal Transport of Two-Dimensional Materials in Contact with Metal due to Complex Phonon Scattering [Jie Sun](#), Bin Xu, Rulei Guo and Junichiro Shiomi; Tokyo University, Japan

Heat dissipation is paramount in the realm of modern electronics, encompassing chips and wearable devices, whose typical candidates are the two-dimensional (2D) materials due to their superior intrinsic electrical, optical or phonon properties. However, these materials are seldom found in a freestanding state when integrated into devices, often integrated with crystalline semiconductors, metals, or flexible polymers. Thermal management strategies for such devices typically rely on a macroscopic perspective, which may lack precision. Employing the techniques of machine-learning-based interatomic potentials within DFT-level quality, together with the theory of phonon coherence and scattering from different orders, the heat transport of the 2D materials combined with substrates are investigated. Contrary to conventional expectations of hindered thermal transport, our findings reveal that the thermal conductivity of graphene remains invariant when placed on a substrate. This invariance is attributed to the suppression of four-phonon scattering, a consequence of symmetry-breaking effects. The more intriguing phenomenon is the observed enhancement of thermal conductivity when germanene is placed on the substrate. This outcome defies expectations and can be attributed to the competing mechanisms: increased third-order anharmonicity and decreased fourth-order anharmonicity. Besides, an increase in coherent phonon transport due to the reduced disparities in the frequencies of various phonon modes also accounts for the enhanced thermal transport. In conclusion, our study has unveiled both the invariant and enhanced heat transport in 2D materials when combined with substrates. This investigation, driven by the microscopic phonon transport theorem, offers a fresh perspective on heat dissipation in electronic devices.

2:30 PM EN07.13.04

Unlocking Rayleigh's Law Limit of Phonon Transport for Extremely Low Thermal Conductivity by Materials Informatics [Meng An](#), Wenyang Ding, Jiang Guo and Junichiro Shiomi; The University of Tokyo, Japan

Engineering materials with extremely low thermal conductivity are crucial and desirable for many applications such as thermal management of electronic devices, thermal insulation and thermoelectric conversion. Recently, two-dimensional (2D) materials with heteroatoms from multiple distinct materials blocks show excellent properties and are considered as the promising candidates for constructing integrated circuits and quantum computers. However, Rayleigh's law implies that acoustic phonons, which carry most of the heat, are insensitive to scattering by atomic-scale defects. Therefore, realizing low thermal conductivity of lateral heterostructure with complex composition and diverse arrangement remains challenging due to the high degree of freedom and complex objectives. Herein, we develop a hybrid materials informatics approach which combines the variational autoencoder and Bayesian optimization to design two-dimensional patterned graphene/h-BN lateral heterostructure with extreme low thermal conductivity. With only several hundred training data sets, new structure with extremely low thermal conductivity can be quickly determined in a compressed latent space by calculating far less than 0.0001% of the total candidate structures, which greatly decreases the design period and cost. More interestingly, the thermal conductivity of newly obtained structure is much lower than that of randomly arranged graphene/h-BN lateral heterostructure, where the extracted phonon relaxation time of newly obtained structure from phonon energy spatial density are calculated to demonstrate the validity of Rayleigh's law. Finally, the mode-resolved atomistic Green's function (AGF) method was utilized to calculate the phonon modal transmission of newly obtained structure and analyze the elastic phonon scattering behavior. This study not only can be easily extended to other thermal conduction metamaterials with higher dimensional features but would be beneficial to screening the phonon transport mechanism of two-dimensional heterostructures with multiple thresholds of thermal conductivity.

2:45 PM EN07.13.05

Tailoring Thermal Conductivity Anisotropy Using Ion Beam Modification [Marat Khafizov](#)¹, Vinay Chauhan¹, Hao Ma², Zilong Hua³, Azat Abdullaev⁴, Shadman S. Priam¹, Saqeeb Adnan¹, Erika Nosal¹, Michael Manley², Zhandos Utegulov⁴, Lingfeng He³ and David Hurley³; ¹The Ohio State University, United States; ²Oak Ridge National Laboratory, United States; ³Idaho National Laboratory, United States; ⁴Nazarbayev University, Kazakhstan; ⁵North Carolina State University, United States

We demonstrate utilization of energetic particle to introduce few nanometer-sized features in crystalline solids leading to changes in thermal transport. This integrated analysis includes ion irradiation, microstructure characterization using transmission electron microscopy, measurement of thermal conductivity tensor using spatial domain thermoreflectance, and modeling of thermal conductivity accounting for observed nanostructure. In cubic CeO_2 bombarded with 2 MeV energy protons faulted dislocation loops are formed. These loops have long range strain field resulting in significant reduction of thermal conductivity. Aligned ion tracks in Al_2O_3 generated by bombardment with 167 MeV xenon ions modify its thermal conductivity anisotropy, where thermal conductivity along direction perpendicular to ion channels exhibits larger conductivity reduction compared to direction parallel to the channels. Lastly, we show modification of conductivity anisotropy in hexagonal delta-phase U-Zr alloy, caused by formation of platelet nanoprecipitates. For the latter case, the anisotropic modification is also observed in phonon lifetimes measured using inelastic X-ray scattering.

3:00 PM BREAK

SESSION EN07.14: Thermal Transport Modulation
Session Chairs: Hyejin Jang and Jun Liu
Thursday Afternoon, April 25, 2024
Room 327, Level 3, Summit

3:30 PM *EN07.14.01

Tuning Thermal Transport and Magnetization Dynamics in Functional Materials Xiaojia Wang; University of Minnesota, Twin Cities, United States

In this talk, I will highlight the ongoing research efforts of our group focused on tailoring thermal transport and magnetization dynamics in functional materials for applications including active thermal control and energy-efficient spintronics. Our research leverages ultrafast laser-based metrology techniques, specifically the basic time-domain thermoreflectance and advanced time-resolved magneto-optical Kerr effect configurations. I will begin by discussing our work in solid-state control of thermal transport in nanoscale perovskite oxides, using lanthanum strontium cobaltite (LSCO) and strontium stannate (SSO) as model systems. We have successfully manipulated thermal transport through structural engineering. Notably, we have demonstrated continuous tuning of LSCO thermal conductivity by a factor of over five. This tuning is achieved via a room-temperature electrolyte-gate-induced non-volatile topotactic phase transformation from perovskite to brownmillerite, accompanied by a metal-insulator transition.

The second part of the talk will feature L10-FePd, a promising material candidate for energy-efficient and non-volatile spintronic devices with large areal densities. We have conducted systematic investigations into the influence of buffer-layer engineering on perpendicular magnetic anisotropy (PMA, crucial for switching speed) and Gilbert damping (related to energy consumption). Additionally, I will delve into the effects of temperature on both PMA and damping to better address the technological viability of L10-FePd for spintronic applications.

4:00 PM EN07.14.02

Reversible and High-Contrast Thermal Conductivity Switching in a Flexible Covalent Organic Framework Possessing Negative Poisson's Ratio Sandip Thakur and Ashutosh Giri; University of Rhode Island, United States

The ability to dynamically and reversibly control thermal transport in solid-state systems can redefine and propel a plethora of technologies including thermal switches, diodes, and rectifiers. Current material systems, however, do not possess the swift and large changes in thermal conductivity required for such practical applications. For instance, stimuli responsive materials, that can reversibly switch between a high thermal conductivity state to a low thermal conductivity state, are mostly limited to thermal switching ratios in the range of 1.5 to 4. Here, we demonstrate reversible thermal conductivity switching with an unprecedented 18 \times change in thermal transport in a highly flexible covalent organic framework with revolving imine bonds. The pedal motion of the imine bonds are capable of reversible transformations of the framework from an expanded (low thermal conductivity) to a contracted (high thermal conductivity) phase, which can be triggered through external stimuli such as exposure to guest adsorption and desorption or mechanical strain. We also show that the dynamic imine linkages endow the material with a negative Poisson's ratio, thus marking a regime of materials design that combines low densities with exceptional thermal and mechanical properties.

<https://doi.org/10.1039/D3MH01417G>

4:15 PM EN07.14.03

Thermal Rectification Mediated by Polaritonic Heat Conduction Sichao Li and Sunmi Shin; National University of Singapore, Singapore

The pursuit of advanced thermal management solutions for applications spanning electronics, buildings, and energy conversion/storage has intensified with the exploration of thermal rectification. While previous studies have several approaches using phase-change materials, heterostructures, or mechanical deformation, thermal rectification ratios have consistently lagged behind those observed in electrical or optical transport. This challenge originates from the diffusive nature of heat conduction mediated by classical heat carriers, e.g., phonons and electrons. Here, we leverage surface phonon polaritons (SPhPs), a coupled energy carrier arising from the interaction between optical phonons and photons, to enhance thermal rectification. Theoretical predictions suggest that these distinctive heat carriers exhibit anomalously long propagation length over 100s μm . In our study, various long and thin polar dielectric nanostructures, e.g., SiO₂ nanowalls, were designed and integrated into a suspended thermometry platform to facilitate the probe of polaritonic thermal conductance. To demonstrate the asymmetric heat transfer across forward and reverse directions, we controlled the coupling coefficient of surface-guided waves by incorporating grating structures into one side of the thermometry platform. In this presentation, we will discuss the rationale behind the design of nanostructured heat channels and thermometers, showcasing their critical role in realizing asymmetric transmittance of quasi-ballistic heat transport.

4:30 PM EN07.14.04

Thermal Transistor and Thermal Regulator Devices Utilizing Temperature-Dependent Magnetic Forces Lorenzo Castelli, Ajay Garg, Qing Zhu, Trevor J. Shimokusu, Pooja Sashital and Geoffrey Wehmeyer; Rice University, United States

Switchable and nonlinear thermal devices are enabling technologies for applications ranging from waste heat scavenging to solid-state cooling and battery thermal management. Existing high-performance passive switching devices operating near room temperature rely primarily on thermal expansion to open or close gaps between surfaces; however, many thermal expansion switches have substantial thermal hysteresis and/or require large device thicknesses. Here, we demonstrate passive thermal switching with several devices that use temperature-dependent magnetic forces to make and break mechanical contact between thermally conductive elements. Our devices rely on the reversible paramagnetic/ferromagnetic phase transition of the magnetically soft material gadolinium, which has a convenient Curie temperature near 20°C for room temperature switching. We use this magnetically-actuated mechanism to construct a thermal regulator,¹ which is a two-terminal device in which the steady-state thermal conductance can be passively tuned between an ON or OFF value by the temperature of the control thermal terminal. We also demonstrate the first reported thermal transistor,² which is a three-terminal device in which the temperature at the gate terminal controls the source-drain heat flow in a manner that leads to heat flow switching and amplification. The thermal regulator displays an average thermal switch ratio of 34 (uncertainty +30, -13) in vacuum with switching temperatures near 20°C and a 5°C thermal hysteresis. The magnetic actuation mechanism leads to relatively low thermal hysteresis and smaller thicknesses (<2 μm) as compared to the prior thermal expansion demonstrations. Similarly, the thermal transistor displays an average source-drain thermal switch ratio of 109 (uncertainty +62, -38) in vacuum with switching gate temperatures near 25°C and a 7°C thermal hysteresis. The thermal transistor displays measured heat flow amplifications near

30, meaning that a small gate heat flow can drive a larger source-drain heat flow, and has characteristic thermal time constants ranging from 4 to 17 minutes. We quantify the durability and performance of both devices over >1000 cycles and find that the regulator switch ratio decreases by a factor of four after cycling and long-duration (0.5 year) storage. We construct proof-of-concept thermal circuits to demonstrate that these nonlinear thermal devices enable thermal logic operations, passive heat flow routing, and temperature regulation capabilities. Thus, our demonstrations of passive heat switching using a magnetic thermal regulator and thermal transistor will motivate further research implementing nonlinear thermal elements for advanced thermal management.

This work was supported by an Early Career Faculty grant from NASA's Space Technology Research Grants Program (Grant #80NSSC20K0066), by a NASA Space Technology Graduate Research Opportunity (Grant # 80NSSC20K1220), and by a grant from the Welch Foundation (Grant No. C-2023).

References:

1. L. Castelli, A. Garg, Q. Zhu, P. Sashital, T. J. Shimokusu, G. Wehmeyer, A thermal regulator using passive all-magnetic actuation, *Cell Reports Physical Science*, **4**, 101556, 2023
2. L. Castelli, Q. Zhu, T. J. Shimokusu, G. Wehmeyer, A three-terminal magnetic thermal transistor, *Nature Communications*, **14**, 393, 2023

4:45 PM EN07.14.05

Asymmetric Thermal Transport and The Influence of Contact Resistance in Telescopic Nanowires Yashpreet Kaur¹, Saeko Tachikawa¹, Jose Manuel Sojo Gordillo¹, Milo swinkels¹, Matteo Camponovo¹, Anna Fontcuberta i Morral², Riccardo Rurali³ and Ilaria Zardo¹; ¹University of Basel, Switzerland; ²EPFL, Switzerland; ³ICMAB-CSIC, Spain

Heat dissipation has become a critical problem in the performance of electronic devices, thus reducing their lifespans [1]. To cope with this, researchers are using several approaches like thermoelectric generators, coolers, thermal diodes, heat guides, and more [2]. A thermal diode works as a rectifier, allowing the flow of heat preferentially in one direction. In our current research, we have studied telescopic nanowires for their thermal transport and rectification capabilities [3].

A telescopic nanowire is a quasi-one-dimensional structure with a thick and a thin part having diameters of 300 and 90 nm, respectively, with a transition region in between. The GaAs telescopic nanowires are grown by MBE technique using the VLS mechanism [4]. Thermal conductivity measurements of one-dimensional (1D) structures were conducted using thermal bridging technique [5]. Thermal rectification ratios of up to 8% were measured as a function of applied temperature bias.

Further, the temperature jump at the contacts is extracted using Raman thermometry [6] while applying different temperature biases. In numerous instances within the literature, this crucial contact contribution tends to be overlooked despite its substantial influence on the determination of thermal properties. In our case, a thermal contact resistance of $(2.71 \pm 8.43) \times 10^8 \text{K/W}$ was estimated and compared to reference homogeneous nanowires. This enables a corrected estimation of the rectification from the nanostructure. The thermal mapping along the nanowire axis was also done to extract the thermal conductance of the corresponding thick and thin parts.

These results underscore the significance of accounting for thermal contact resistance in accurately characterizing the thermal properties of nanowire-based systems. Moreover, this is the first experimental study on telescopic nanowires indicating rectification and an important contribution towards the development of thermal circuit elements.

- [1] M. Maldovan, *Nature* 503, 209 (2013)
- [2] S. Volz, *The European Physical Journal B* 89, 1 (2016)
- [3] X. Cartoixà, L. Colombo and R. Rurali, *Nano Letters* 15, 8255 (2015)
- [4] W. Kim, A. Fontcuberta i Morral, *Nano Letters* 18, 49 (2018)
- [5] L. Shi, A. Majumdar, *Journal of Heat Transfer* 125, 881 (2003)
- [6] Doerk et al., *ACS Nano*, Vol.4, 4908-4914 (2010)

SESSION EN07.15: Poster Session III: Thermal Transport and Energy Conversion III
Session Chairs: Jaeyun Moon and Sunmi Shin
Thursday Afternoon, April 25, 2024
Flex Hall C, Level 2, Summit

5:00 PM EN07.15.01

Low-Dimensional Heat Conduction in Surface Phonon Polariton Waveguide Yu Pei, Li Chen, Wonjae Jeon, Zhaowei Liu and Renkun Chen; UCSD, United States

Heat conduction in solids is governed by Fourier's law, describing a diffusion process primarily driven by phonons and electrons with short wavelengths and mean free paths. Non-Fourier heat conduction, observed in exotic systems, remains elusive in typical solids. Surface phonon polaritons (SPhP) are evanescent surface waves resulting from the collective oscillation of atoms on the surface of polar dielectric materials. They couple thermal photons and optical phonons, potentially contributing significantly to heat conduction, particularly in nanostructures with diminished volumetric heat conduction by phonons and electrons. Unlike thermal radiation, SPhP waves carry a high energy flux along the solid surface, acting as thermal waveguides. Surface phonon polaritons (SPhP) offer a promising avenue for extraordinary heat transfer due to their longer wavelength and propagation length. However, their low energy flux has hindered direct observation of SPhP-mediated heat conduction.

Here, we demonstrate direct observation of enhanced thermal conductivity mediated by SPhP in SiO₂ nanoribbon waveguides. To distinguish SPhP from phonons, the waveguide cross-section must be reduced. However, this introduces challenges related to wave leakage and inefficient coupling with thermal reservoirs. Our study addresses these challenges by designing nanoribbon waveguides of SiO₂ with controlled SPhP mode size and efficient coupling to thermal reservoirs using an absorber. We directly observe an increased thermal conductivity in these waveguides, surpassing the limit of phonon thermal conductivity by up to 34%. Moreover, we observe non-Fourier behavior in SPhP thermal conductance over 50-100 μm distances at room and high temperature, indicating the unique characteristics of polaritonic heat conduction. Our work represents the first direct observation of enhanced thermal conductivity mediated by SPhP and provides insights into the potential of manipulating heat conduction beyond traditional limits. These findings open up

new possibilities for engineering thermal transport in various applications.

5:00 PM EN07.15.02

High Thermal Conductive Liquid Crystal Elastomer Nanofibers Jingxuan Wang¹, Yue Wen¹, Duo Pan^{1,2}, Shulang Lin¹, Chinnappan Amutha¹, Qiguang He³, Chuntai Liu², Zhiwei Huang¹, Shengqiang Cai⁴, Seeram Ramakrishna¹ and Sunmi Shin¹; ¹National University of Singapore, Singapore; ²Zhengzhou University, China; ³The Chinese University of Hong Kong, Hong Kong; ⁴University of California, San Diego, United States

Liquid crystal elastomers (LCEs), consisting of polymer networks and liquid crystal mesogens, show reversible phase change induced by thermal stimuli. However, the kinetic behavior is limited by the inherently low thermal conductivity of polymers. Transforming amorphous bulk into fiber-like forms enables us to enhance the thermal conductivity by aligning polymer chains. Rigid networks of crosslinked polymer have challenged to fabricate nanofibers of it while the existence of the crosslinks in LCEs is crucial to shape reversible transformation of the elastomers. In this study, hydrodynamic alignment was employed to orient the LCE domains assisted by controlled in-situ crosslinking. A drag force was applied to a suspended individual single polymer fiber anchored to a micro-thermometry device. This process remarkably cuts down the fiber diameter to sub-microns. We observed the highly enhanced thermal conductivity of LCE nanofibers (<100 nm in diameter) which is one order of magnitude higher than that of bulk counterpart. To further elucidate the size-effect on heat transfer in LCE fibers, temperature-dependent analysis was made with various diameters of LCE fibers.

5:00 PM EN07.15.03

Nanoscale Thermal Transport in SiC: Effects of Inter-Grain Misorientation, Grain Size and Crystal Anisotropy Omid Farzadian, Yanwei Wang and Zhandos Utegulov; Nazarbayev University, Kazakhstan

Detailed understanding of the thermal transport across grain boundaries (GBs) and nano-size grains in nanocrystalline thermal functional materials is essential for optimizing their performance across variety of advanced energy applications [1,2]. This study aims at elucidating the nature of inter-grain heat transport as well as spatially-resolved thermal conductivity κ inside small grains by controlling the misorientation tilt angles θ , grain sizes D and crystal anisotropy to advance our fundamental insight into thermal transfer in nanocrystalline materials.

For a detailed atomistic treatment of interfacial heat transport across GBs in SiC bi-crystals, non-equilibrium molecular dynamics (NEMD) simulations are employed. We focus on the (hk0)[001] family of symmetrical tilt GBs, where [001] represents the tilt axis, (hk0) signifies the GB plane with tilt angle θ . The primary interest in structural analysis of GBs revolves around uncovering the atomistic configuration that represents the lowest energy state for a specific θ , commonly referred to as the ground-state structure. To discern this equilibrated state for each GB, we employ an optimization procedure involving the conjugate gradient (CG) method [2,3].

To examine the heat propagation behavior across these GBs, a temperature gradient is imposed on both ends of the SiC structure. It is anticipated that κ of nanocrystalline material will be significantly lower than that of the bulk single crystal due to the presence of thermal resistance at the GB interfaces, defined as the Kapitza resistance R . The variation of R with θ across individual GBs is studied with minimized GB energy. Observed asymmetry in R with respect to $\theta = 45$ degrees is due to two dissimilar atoms (Si and C) present in the lattice.

Moreover, we employ perturb MD [3] to compute spatially-resolved anisotropic local thermal conductivities in SiC by varying D and θ . It was explored that the intra-grain κ decreases with the reduction of D and also varies with the rise of θ in the cross-GB and along-GB directions. The κ remains relatively uniform within the grain interiors but decreases near the GB plane. It should be noted that this reduction is more dominant in larger grains than in smaller ones. This observed phenomenon is discussed in terms of the enhanced phonon scattering in the nanoscale vicinity from GBs, phonon mean free paths, interatomic interaction within a diatomic SiC crystalline lattice across the GBs connecting grains misoriented from each other at various tilt angles directly affecting inter- and intra- grain phonon mediated heat transport.

References:

- [1] J. P. Crocombette and L. Gelebart "Multiscale modeling of the thermal conductivity of polycrystalline silicon carbide" J. Appl. Phys. 106, 083520 (2009)
- [2] M. Wojdyr, S. Khalil, Y. Liu and I. Szulfarska "Energetics and structure of <0 0 1> tilt grain boundaries in SiC", Modelling Simul. Mater. Sci. Eng. 18 075009 (2010)
- [3] S. Fujii, K. Funai, T. Yokoi and M. Yoshiya "Grain-size dependence and anisotropy of nanoscale thermal transport in MgO" Appl. Phys. Lett. 119, 231604 (2021)

5:00 PM EN07.15.04

Theory of The Soret Effect in Liquids and Solids Patrick K. Schelling; University of Central Florida, United States

The Soret Effect, also known as thermodiffusion, is the flow of matter in response to externally applied heat sources. This effect is important in a number of applications including crystal growth and analysis interactions between biomolecules, and may present opportunities for guided materials synthesis using temperature gradients. While this effect has been known for some time, predictive models and microscopic understanding have been lacking. We have recently demonstrated that the Soret effect is closely connected to the response of a system to the internal stresses induced by a heat source. In particular, as a system approaches mechanical equilibrium, density gradients develop, and the difference in response to these density gradients is responsible for the observed concentration gradients. Using two-component Lennard-Jones liquids as an example, it is shown that an analysis of the dependence of the partial pressures of the two components on concentrations, namely via second derivatives of the partial pressures, the sign and magnitude of the Soret effect can be established. The results suggest how thermodiffusion in solids either of interstitials or alloys via a vacancy mechanism can be understood.

5:00 PM EN07.15.05

Wood Waste-Based Thermal Insulation Foam for Building Energy Efficiency Amanda Siciliano¹, Xinpeng Zhao¹, Dr. Jan Kosny² and Liangbing Hu¹; ¹University of Maryland, United States; ²University of Massachusetts Lowell, United States

Wood, a renewable resource with passive carbon sequestration abilities, has a history of use within construction materials because of its cheap, abundant, and sustainable nature; however, natural wood's low porosity makes it an unfit candidate for readily producible and highly efficient thermal insulation materials, leading to a high overall thermal conductivity (> 0.1 W/(mK)). Furthermore, the fabrication process of wood-based building insulation materials generally involves chemical- and time-consuming drying methods (e.g., freeze-drying, solvent exchange, overnight curing), resulting in high manufacturing costs. In this work, we illustrate the development and characterization of sustainable wood waste-based thermal insulation foam fabricated through a rapid hot-pressing technique, demonstrating significant product tunability, manufacturing scalability, and time- and cost-efficiency. This method significantly improves the manufacturability of wood-based thermal insulation materials by eliminating solvents from the fabrication process. Performance characterization of wood waste-based thermal insulation foam exhibits a density of 0.2 g/cm³, thermal conductivity of 0.03 W/(mK), and compressive

strength of ~1 MPa at 10% strain. This example of the quick development of efficient sustainable thermal insulation materials shows promise for addressing complex thermal transport challenges with applications in various sectors including electronics, manufacturing, buildings, and transportation.

5:00 PM EN07.15.06

Temperature-Vacuum Swing Desorption in Sorbent-Based Atmospheric Water Harvesting Devices: An Approach to Energy Savings Bachir El

Fill¹, Chenyang Li¹, Yang Zhong¹, Hyeongyun Cha¹, David Keisar¹, Mengjiao Wu², Pasquale Fulvio², Jamie Salinger², Jay Lin² and Krista Walton²;

¹Massachusetts Institute of Technology, United States; ²Georgia Institute of Technology, United States

To meet the increasing global demand for clean and potable water, sorbent-based atmospheric water harvesting (SAWH) is a promising solution. However, challenges remain owing to the complexity of system integration and energy-intensive nature of the regeneration process. The desorption process has long been a bottleneck, directly affecting both the energy efficiency and deployment scalability. Conventionally, the regeneration of sorbents has been dominated by two primary methods: temperature-swing desorption (TSD) and vacuum-swing desorption (VSD). In temperature-swing desorption, heat is typically applied to release the adsorbed water molecules from the sorbent making it prevalent for sorbents with high water capacity but consequently demanding high energy inputs. Conversely, vacuum-swing desorption employs pressure alterations to induce desorption, favored for its operational simplicity, but sometimes limited by its efficacy with certain sorbents. Both methods, while effective, bear significant energy costs, sometimes overshadowing the net water extraction gains and constraining the broad adoption of AWH, especially in regions with limited energy infrastructure. In this work, we delve into the application of a hybrid temperature-vacuum swing desorption (TVSD) as an approach aimed to optimizing the energy consumption in the regeneration of solid sorbents used in AWH devices.

This hybrid approach harnesses the synergistic benefits of both desorption techniques, aiming to minimize the overall energy consumption. To understand this more, we have developed thermo-fluidic models to simulate and optimize the desorption process. Additionally, we conducted experiments under various pressure ranging between 14 to 300 mbar and with desorption temperatures as low as 27°C to 80°C. Preliminary findings indicate that TVSD can achieve energy saving by ~33% when compared to conventional temperature swing desorption, for hierarchical silica impregnated with salts. Thereby rendering AWH systems more viable in energy-constrained settings.

In conclusion, TVSD offers a promising avenue for improving the energy efficiency of sorbent regeneration in AWH systems. We continue to optimize this method across various operating conditions, the integration of temperature and vacuum swings stands as a novel solution to enhance the sustainability and accessibility of atmospheric water harvesting.

5:00 PM EN07.15.07

Thermoelectric Properties of Stressed p-Doped Polycrystalline Hollow Nanotubes Jose Manuel Sojo Gordillo^{1,2}, Yashpreet Kaur¹, Saeko Tachikawa³,

Giulio de Vito¹, Alex Morata² and Ilaria Zardo¹; ¹University of Basel, Switzerland; ²Catalonia Institute for Energy Research - IREC, Spain; ³National Institute of Advanced Industrial Science and Technology - AIST, Japan

Thermoelectric generators have the potential to efficiently convert waste heat into valuable electrical power. However, conventional thermoelectric materials face limitations in terms of efficiency, scarcity, high cost, and scalability, impeding their widespread adoption. Nanoengineering techniques have emerged as a promising solution to enhance the thermoelectric properties of abundant and inexpensive materials like silicon. Nevertheless, the integration of these nanostructures on a large scale, necessary for efficient waste heat recovery, remains a significant challenge.

Recently, a novel class of nano-enhanced materials in the form of extensive, paper-like fabrics composed of nanotubes has been developed, offering a cost-effective and scalable approach to thermoelectric power generation [1]. However, the fundamental properties of the building blocks of these fabrics, namely the p-type silicon nanotubes, have not been individually investigated to date.

This study conducts electrothermal measurements using microfabricated suspended nitride membranes to characterize the thermoelectric properties of these nanotubes, including the electrical and thermal conductivity as well as the Seebeck coefficient. Furthermore, Raman thermography is employed in order to accounting for the effects of thermal contact resistance in the thermal conductivity measurement. Raman spectroscopy is also used to examine the residual mechanical stress in the nanotubes and investigate its relationship with the observed thermoelectric properties. A network model is proposed to link the macroscopic thermal properties of the fabrics with those of the nanotubes. Additionally, the study investigates the light absorption within these hollow structures. Finally, the effects of SiGe alloy on the properties of the nanotubes are compared and discussed.

By understanding the interplay between the morphology, structure, and thermoelectric properties of the nanotubes, a pathway can be established for the development of more mechanically stable and efficient fabrics, with the potential for commercializing waste heat recovery through this technology.

[1] Morata et al. "Large-area and adaptable electrospun silicon-based thermoelectric nanomaterials with high energy conversion efficiencies" *Nat. Comm.* (2018), 4759, 9(1)

5:00 PM EN07.15.08

Thermal Studies of Au–BaTiO₃ Nanoscale Hybrid Metamaterial Haomin Li¹, Benson Tsai², Fabian J. Medina¹, Qiyu Chen¹, Haiyan Wang² and Qing

Hao¹; ¹The University of Arizona, United States; ²Purdue University, United States

With embedded periodic vertical nanopillars, oxide-metal nanocomposite thin films hold significant potential for various applications, including magnetic data storage, energy storage, plasmonics, optics, sensors, multiferroics, and spintronics.¹ In these thin films, electron-phonon coupling at the metal-oxide interface plays a crucial role in restricting the in-plane thermal transport. When the corresponding interfacial resistance becomes a critical factor, these thin films become particularly intriguing when compared to extensively studied periodic nanoporous thin films. In general, such periodic structures are used for both photonics and phononics devices, where periodic nanostructures are used to manipulate the wave propagation within the structure by tuning the dispersion relation of photons and phonons. The interplay between optical photons and phonons also leads to important applications such as optomechanical waveguides and resonators.²

This study focuses on systematically measuring the in-plane thermal conductivity of Au–BaTiO₃ nanocomposite thin films with sub-100 nm feature sizes.³ The measured samples are fabricated as a metal-coated suspended bridge for 3 omega measurements⁴ to extract both the specific heat and in-plane thermal conductivity. Thermal analysis is further carried out to gain a deeper understanding of thermal transport across the metal-oxide interface and within the periodic patterns. Transmission electron microscopy studies are carried out to reveal the defects at the metal-oxide interfaces, which may largely impact the thermal transport.⁵ Our study provides important guidance for the thermal management of the related plasmonic or other devices using these composite thin films.⁶

References:

1 Misra, S. & Wang, H. Review on the growth, properties and applications of self-assembled oxide–metal vertically aligned nanocomposite thin films—current and future perspectives. *Materials Horizons* **8**, 869–884 (2021).

2 Safavi-Naeini, A. H., Van Thourhout, D., Baets, R. & Van Laer, R. Controlling phonons and photons at the wavelength scale: integrated photonics meets integrated phononics. *Optica* **6**, 213–232 (2019).

3 Zhang, D., Qi, Z., Jian, J., Huang, J., Phuah, X. L., Zhang, X. & Wang, H. Thermally Stable Au–BaTiO₃ Nanoscale Hybrid Metamaterial for High-Temperature Plasmonic Applications. *ACS Applied Nano Materials* **3**, 1431–1437 (2020).

4 Hao, Q., Xu, D., Zhao, H., Xiao, Y. & Medina, F. J. Thermal Studies of Nanoporous Si Films with Pitches on the Order of 100 nm -Comparison between Different Pore-Drilling Techniques. *Scientific Reports* **8**, 9056 (2018).

5 Giri, A., Walton, S. G., Tomko, J., Bhatt, N., Johnson, M. J., Boris, D. R., Lu, G., Caldwell, J. D., Prezhdo, O. V. & Hopkins, P. E. Ultrafast and Nanoscale Energy Transduction Mechanisms and Coupled Thermal Transport across Interfaces. *ACS Nano* **17**, 14253-14282 (2023).

6 Cunha, J., Guo, T. L., Della Valle, G., Koya, A. N., Proietti Zaccaria, R. & Alabastri, A. Controlling light, heat, and vibrations in plasmonics and phononics. *Advanced Optical Materials* **8**, 2001225 (2020).

5:00 PM EN07.15.09

Completely Passive Capture of Carbon Dioxide from Air Using Solar Energy [Jian Zeng](#)¹, Hsinhan Tsai², Ravi Prasher³, Jeffrey Long² and Sean Lubner⁴; ¹The Hong Kong University of Science and Technology (Guangzhou), China; ²University of California, Berkeley, United States; ³Lawrence Berkeley National Laboratory, United States; ⁴Boston University, United States

In addition to reducing greenhouse gas emissions, it is now imperative that we implement direct air capture (DAC) of CO₂ from the atmosphere at a scale of hundreds of giga metric tons before the year 2100 to avoid catastrophic climate change. Development of a viable DAC technology is still limited by the high cost and high energy consumption that result from a low adsorbent capture capacity, requirements for expensive, cumbersome infrastructure, and widespread societal acceptance challenges. In this work, we aim to address all three of these challenges and have designed and demonstrated a completely passive DAC device with a projected net CO₂ capture cost as low as 80 \$ t_{CO2}⁻¹, lower than the 'Carbon Negative Shot' 2030 goal (100 \$ t_{CO2}⁻¹) and potentially profitable at 100 \$ t_{CO2}⁻¹ with the 45Q carbon tax credit. Our DAC device captures CO₂ passively at night and desorbs CO₂ passively during the day. It uses solar energy as the sole energy source with minimum maintenance requirements. The modular design and passive operation of the system should enable deployment across broad geographic regions far from infrastructure centers, thereby enabling a distributed, self-powered solution to the problem of removing dilute CO₂ from the atmosphere. It further combines low-cost solar-thermal and low-risk photovoltaic technologies, facilitating installation at different scales in any corner of the world with abundant solar resources.

5:00 PM EN07.15.11

Sub-Micron Resolution Mapping of Thermal Properties in CVD and MBE-Grown MoS₂ via Nanoscale Thermoreflectance Microscopy [Briam M. Foley](#)¹, Patrick E. Hopkins^{2,1} and John T. Gaskins¹; ¹Laser Thermal Inc, United States; ²University of Virginia, United States

As with most other functional properties of 2D materials, thermal energy transport via phonons can be impacted quite dramatically through their scattering by a variety of material defects. These phonon scattering events in 2D systems arise from the plethora of defects and interfaces that arise from both the growth parameters and post-processing steps that are often required to manipulate the 2D materials functionalities. The thermal transport properties of 2D materials at and around these defect phonon scattering sites, which often have length scales and spacings on the order of a few to 10's of nanometers, are difficult to isolate and measure individually with the thermal measurement techniques available previously. For example, optical based techniques for measuring thermal properties of 2D materials (e.g., Raman, TDTR) are ultimately diffraction limited and thus restricted in-practice to areal spatial resolution on the order of single micrometers. Techniques using lasers coupled with AFM-tips (e.g., Nano-FTIR) have shown promise in achieving sub-diffraction limited areal resolution to qualitatively interrogate optically excited surfaces, but lack the opto-thermal transduction power afforded by thermoreflectance-based methods to ensure accurate measurement of local temperature and thermal wave modulation.

Here, we introduce a novel approach called Nanoscale Thermoreflectance Microscopy (NTM), capable of characterizing the thermal properties of 2D materials with ~10 nm areal spatial resolution. Thermal maps of CVD and MBE-grown molybdenum disulfide (MoS₂) are presented, quantifying the impact of the chosen growth method on material quality through direct visualization of how the thermal resistance increases near defects such as wrinkles/boundaries, adlayer nucleation sites, etc. These local increases in resistance are attributed to the impact of the defect in question on phonon transport. As a result, this new capability enables an estimation of the length scales over which various defect structures exert influence over phonon transport in these 2D materials, providing important thermal insight to guide future synthesis, processing and device-integration efforts using this important family of materials.

5:00 PM EN07.15.12

Enhancing Building Thermal Management with Thermochemical Materials-Based Thermal Energy Storage [Sumanjeet Kaur](#), Andrew Martin, Alondra Perez, Drew Lilley and Ravi Prasher; Lawrence Berkeley National Laboratory, United States

Buildings drive energy consumption worldwide, particularly in the United States. Thermal loads, which contribute significantly to CO₂ emissions, must be addressed for deeper adoption of renewable energy. On-site Thermal Energy Storage (TES) is vital for reducing peak loads and managing renewable energy intermittency. Thermochemical Materials (TCMs), which consist of reactive pairs of inorganic salts and water vapor, exhibit notable advantages as they have a higher theoretical energy density of approximately 500 kWh/m³ and exhibit minimal self-discharge since energy is stored within chemical bonds. This makes them uniquely suited as compact, stand-alone solutions for daily-seasonal energy storage within buildings. However, TCMs face challenges related to material instabilities at both the salt particle level and reactor level (packed beds of salt). These issues result in poor multi-cycle efficiency and a high levelized cost of storage.

In response to these challenges, this study offers valuable insights into strategies aimed at mitigating chemical instabilities within the salt at both the material and composite levels. Additionally, it explores pathways to enhance heat and mass transport performance at the reactor level, thereby paving the way for more efficient and cost-effective thermal energy storage solutions.

5:00 PM EN07.15.13

Unveiling High-Order Phonon Physics: High-Pressure Thermal Transport in Extreme Materials [Suixuan Li](#)¹, Zihao Qin¹, Huan Wu¹, Man Li¹, Martin Kunz², Ahmet Alatas³, Abby Kavner¹ and Yongjie Hu¹; ¹University of California, Los Angeles, United States; ²Advanced Light Source, Lawrence Berkeley National Laboratory, United States; ³Advanced Photon Source, Argonne National Laboratory, United States

High pressure provides a new dimension for exploring the transport physics and properties of materials. Over the past century, tremendous efforts have been made to study thermal transport under high pressure. However, the first-principles phonon theory for understanding thermal transport under high pressure has been rarely applied. Here, for the first time, we studied high pressure transport and identified high order anharmonic behaviors beyond the classical textbook understanding. We conducted in-situ experiments, incorporating thermal transport, vibrational spectroscopies, and synchrotron X-ray experiments. These measurements were juxtaposed with first-principles calculations, shedding light on the microscopic dynamics underlying heat transfer. Our finding uncovering high-order anharmonic behaviors beyond traditional comprehension based on classical physics. Our development enables new research platforms and provides fundamental insights into thermal transport under extreme conditions. **Reference:** S. Li, Z. Qin, H. Wu, M. Li, M. Kunz, A. Alatas, A. Kavner, Y. Hu, "Anomalous thermal transport under high pressure in boron arsenide," *Nature* **612**, 459 (2022). <https://www.nature.com/articles/s41586-022-05381-x>

5:00 PM EN07.15.14

Molecular Dynamics Study of The Heat Transport Mechanism of Cu_{2.8}Se Using Machine Learning Potential Tomu Hamakawa and Junichiro Shiomi; The University of Tokyo, Japan

Cu_{2.8}Se is a material that exhibits the high thermoelectric performance of $zT=1.5$ at 1000 K [1]. This high thermoelectric performance is due to its extremely low lattice thermal conductivity at high temperatures. For example, 0.5 W/mK at 1000 K was reported for Cu₂Se [1]. This value is comparable to that of liquid and amorphous materials. Cu_{2.8}Se superionic conduction causes such low lattice thermal conductivity. At high temperatures (>410 K), Cu ions move between the fcc-structured selenium [1,2]. Such a material with liquid-like properties for phonon transport and crystal-like properties for electrons is called "phonon-liquid electron-crystal (PLEC)". It has been explored for candidate thermoelectric materials.

The "liquid-like" nature of Cu ions in PLEC materials makes it hard to treat heat transport in a perturbative manner. Thus, it requires computationally demanding *ab initio* molecular dynamics (AIMD) simulation. On the other hand, the use of machine learning potentials in calculating thermal conductivity has been increasing in recent years [3,4]. Machine learning potentials are developed to approximate interatomic potentials using machine learning. They can reduce the computational cost to the same extent as empirical potentials while maintaining the accuracy of *ab initio* calculations. The Beheler-Parrinello type potential using Neural Networks is one of the machine learning potentials [5].

In this study, we constructed the interatomic potential of Cu_{2.8}Se based on Moment Tensor Potential [6] and calculated thermal properties by MD simulations. We tested our potential, and MD trajectories on our potential showed Cu ions' liquid-like properties. We performed the Non-equilibrium Molecular Dynamics (NEMD) method for calculating the lattice thermal conductivity, and we got the calculated thermal conductivity of 0.5 W/mK at 700 K. Moreover, we derived the relation between thermal conductivity and diffusion coefficient. From this relation, we investigated the contribution of Cu ions transport and found that the hopping transport of Cu ions is dominant in heat transport.

[1] Huili Liu, et al., *Nat. Mater.*, **11**, 422–425, 2012. [2] Hyoungchul Kim, et al., *Acta Mater.*, **86**, 247–253, 2015.

[3] R. Li, et al., *Mater. Today Phys.*, **12**, 100181, 2020. [4] Pavel Korotaev, et al., *Phys. Rev. B*, **100**, 144308, 2019.

[5] Jörg Behler, et al., *Phys. Rev. Lett.*, **98**, 146401, 2007. [6] Novikov Ivan S, et. al. *ML: Sci. & Tech.*, **2**, 025002, 2021

5:00 PM EN07.15.15

Thermal Boundary Conductance at High Temperatures Samreen Khan and Richard B. Wilson; University of California, Riverside, United States

Understanding the physics of thermal boundary conductance is essential for thermal management of semiconductor devices. Thermal boundary conductance between two materials has been shown to depend on atomic scale details like interfacial bonding, interfacial roughness, and interfacial layers. The intrinsic vibrational properties of the materials at the interface also affect thermal boundary conductance¹. Surprisingly, only a few experimental studies of thermal boundary conductance at high temperatures exist. This prevents testing of theories for how inelastic processes contribute to thermal conductance^{2,3}. Inelastic processes at the interface between dissimilar materials are expected to be most important, and more noticeable at high temperatures. In this study, we present results of time domain thermoreflectance (TDTR) measurements of the thermal boundary conductance for nitride-metal/group-IV-semiconductor interfaces between 80 and 800 K. The nitride-metals (TiN and HfN) and group-IV-semiconductors (Ge, Si, SiC, and diamond) have systematic differences in bulk vibrational properties. By comparing the conductance vs. temperature of these systems, we determine the effect of vibrational similarity on inelastic scattering processes. We show that the average probability for interfacial energy transmission increases significantly with temperature by comparing the measured conductance values to theoretical predictions for the elastic and inelastic limits of the constituent materials. In diamond systems, the transmission probability of thermal energy triples from 20% at 300 K to 60% at 900 K. Our findings fill an important gap in the literature for how interfacial conductance evolves at high temperatures, and tests burgeoning theories^{2,3} for the role of inelastic processes in interfacial thermal transport.

References

(1) Khan, S.; Angeles, F.; Wright, J.; Vishwakarma, S.; Ortiz, V. H.; Guzman, E.; Kargar, F.; Balandin, A. A.; Smith, D. J.; Jena, D.; Xing, H. G.; Wilson, R. Properties for Thermally Conductive Interfaces with Wide Band Gap Materials. *ACS Appl Mater Interfaces* **2022**, *14* (31), 36178–36188. <https://doi.org/10.1021/acsmi.2c01351>.

(2) Guo, Y.; Zhang, Z.; Bescond, M.; Xiong, S.; Nomura, M.; Volz, S. Anharmonic Phonon-Phonon Scattering at the Interface between Two Solids by Nonequilibrium Green's Function Formalism. *Phys Rev B* **2021**, *103* (17). <https://doi.org/10.1103/PhysRevB.103.174306>.

(3) Säskilähti, K.; Oksanen, J.; Tulkki, J.; Volz, S. Role of Anharmonic Phonon Scattering in the Spectrally Decomposed Thermal Conductance at Planar Interfaces. *Phys Rev B* **2014**, *90* (13), 134312. <https://doi.org/10.1103/PhysRevB.90.134312>.

5:00 PM EN07.15.16

Strong, Scalable and Anisotropic Wood Composites for High-Performance Thermal Energy Storage in Buildings Bernadette Magalindan¹, Gustavo Felicio-Perruci¹, Yudong Li², Kyle Foster², Charles Booten², Hongbing Lu² and Shuang Cui^{1,2}; ¹The University of Texas at Dallas, United States; ²National Renewable Energy Laboratory, United States

Thermoregulation in America's buildings by heating, ventilation, and air conditioning (HVAC) consumes 11% of the nation's total energy use and emits 309 million metric tons of CO₂ in a single year. One promising solution for energy-efficient thermoregulation involves thermal energy storage (TES) through phase change materials (PCMs) integrated into building envelopes. Recent endeavors have explored the encapsulation of solid-to-liquid PCMs in delignified wood; however, the resulting composite is weak due to the removal of lignin, the natural binding agent in wood. Additionally, the scalability of delignification methods is limited by the slow and inhomogeneous permeation kinetics of the chemical treatment. Here, we transform the most commonly used building construction material—wood—into a microporous, anisotropic, strong, and scalable matrix for PCM encapsulation by selectively removing hemicellulose using a chemical-free, pressurized hot water treatment that preserves lignin. Additionally, the exterior of the wood was selectively densified by controlled hot-pressing, enhancing mechanical strength while allowing high PCM loading within the microporous core of the matrix. Following PCM infiltration, the composite exhibits a mechanical strength of 50 megapascals, comparable to that of natural wood, and achieves a latent heat of 55 J/g for TES. The low-carbon fabrication of the composite in addition to the reduced HVAC-associated carbon emissions enabled by TES promotes the sustainability of the built environment.

5:00 PM EN07.15.17

Manipulation of Near-Field Radiative Heat Flow via Mid-Infrared Plasmonic Coupling Saman Zare¹, William D. Hutchins¹, Maxwell Tolchin², Angela Cleri², Mingze He³, Joshua D. Caldwell³, Jon-Paul Maria² and Patrick E. Hopkins¹; ¹University of Virginia, United States; ²The Pennsylvania State University, United States; ³Vanderbilt University, United States

With the continuous reduction in the size of electronic devices to the nanoscale, it becomes imperative to gain a deep understanding of heat transport mechanisms at these levels. In recent years, breakthroughs in nanotechnology and radiative engineering have introduced thermal radiation as a promising mechanism to tailor both the magnitude and direction of heat transfer. The use of metamaterials enhances our capability to manipulate radiative heat flow

in nanoscale systems, particularly in the context of near-field radiation, which can significantly exceed the blackbody limit by multiple orders of magnitude. Heat transport in the near field of metamaterials depends on their geometry, optical properties of the constituent materials, and interfacial properties. By fine-tuning interfaces in or underneath a metamaterial we can manipulate heat flux, and facilitate an augmented flow of radiative heat from specific spectral modes into bulk heat carriers. One proposed way to tune this flow is by capitalizing on the hybridization of resonant modes in plasmonic materials. Highly doped cadmium oxide (CdO) is poised as an exceptional candidate for that purpose as it allows for high electron mobilities while maintaining dielectric properties mechanically. Also, sub-wavelength films of CdO support epsilon-near-zero (ENZ) modes in the mid-infrared range of the spectrum. Most importantly it has been shown that carefully constructed multilayers of CdO with varying carrier densities exhibit tunable hyperbolic plasmonic dispersion properties, allowing for carrying heat across interfaces at a significantly higher rate than conduction. In this research, we conduct experimental investigations into the interactions between hyperbolic plasmon-polaritons (HPPs) within a layered hyperbolic metamaterial (HMM) and ENZ modes within a doped CdO thin film. Our approach involves employing a unique ultrafast pump-probe technique that enables the precise detection of heat transfer modes with sub-picosecond temporal resolution. This technique relies on a wavelength-tunable mid-infrared probe pulse, allowing us to directly interface with plasmonic heat carriers, thereby providing a direct assessment of polariton dynamics within nanoscale material systems. By utilizing this method, we investigate the ultrafast thermally-induced near-field coupling of HPP and ENZ modes via far-field sensing. Furthermore, we explore the impact of a MgO dielectric gap positioned between the HMM and ENZ layers on the efficiency of near-field coupling between HPP and ENZ modes, and we demonstrate the capability of tuning the near-field radiative heat transfer by introducing a dielectric spacer in an HMM/ENZ structure. Our results provide a new path for novel designs of plasmonic devices with far-reaching applications in tailored thermal emission and thermal management of microelectronics.

5:00 PM EN07.15.19

High Temperature Thermal Conductivity Measurement Using Two-Color Thermal Imaging [Hao-Yuan Cheng](#), Alexander Myers and Jonathan A. Malen; Carnegie Mellon University, United States

This research explores measuring the thermal conductivity of various materials at high temperatures (up to 4000 K). We use the two-color thermal imaging technique with a commercial color camera to measure the temperature distribution on a sample heated by the high-power laser heat source of a Directed Energy Deposition (DED) additive manufacturing machine. The technological requirement to evaluate materials for use in high temperature environments, particularly in the world of additive manufacturing and aerospace, has dramatically increased in recent years. Developing a technique capable of measuring the thermal conductivity of materials up to 4000 K will provide tremendous insights to improve the manufacturing process of different materials. Conventional methods such as the “flash” method have been improved to measure the thermal conductivity of materials up to 3000 K but this approach has challenges including the ability to reach higher temperatures. Electric pulse methods can also reach high temperatures but are applicable only to electrically conductive samples. Using the newly developed two-color thermal imaging method, we are capable of capturing the thermal conductivity of materials with high positional and temporal resolution. This study focuses on developing an apparatus to measure the temperature distribution of a material under a given heat source using the two-color imaging method, then deriving the temperature dependent thermal conductivity using least squares fitting with FEA models. We evaluate the robustness of our proposed method using materials with well-known high temperature thermal conductivity, such as Tungsten, Tungsten Carbide, and Tantalum.

5:00 PM EN07.15.20

Determination of Thermal Conductivity in Metals Under High Temperature and Pressure: A First Principles Study [Pravin Karna](#)¹, [Oleg Prezhdo](#)², [Patrick E. Hopkins](#)³ and [Ashutosh Giri](#)¹; ¹University of Rhode Island, United States; ²University of Southern California, United States; ³University of Virginia, United States

Metallic structures find applications across a wide range of challenging environments, including situations involving high temperatures and pressures like nuclear reactors, plasmonics, pressure calibrators, and interconnects. These metals exhibit distinct properties when subjected to extreme conditions, which might not be apparent under ambient conditions. We employ first principles calculations to investigate the interaction between electrons and phonons in these conditions for various metals: free-electron metal (Al), noble metals (Au, Ag, Cu), and a transition metal (W). This analysis reveals how these metals respond to extreme conditions and sheds light on their thermal and electrical characteristics in such environments. Our calculations encompass the thermal conductivity of these metals under extreme conditions, factoring in both electron-phonon and electron-electron interactions. Furthermore, by computing the spectrally resolved electron-phonon coupling parameter at high pressures, we calculate the contribution of different phonon modes in scattering with electrons. This research offers valuable insights into the processes of electron-phonon scattering under high temperatures and pressures, uncovering a new realm of electrical and thermal transport properties in metallic materials.

5:00 PM EN07.15.21

Effect of Interface Curvature at The Axial Junction in Silicon-Germanium (Si-Ge) Nanowires [Oreoluwa O. Adesina](#) and [Laura de Sousa Oliveira](#); University of Wyoming, United States

Due to a wide array of potential applications, such as thermal management, thin-film technologies, microelectronics, and semiconductor and optical devices, thermal transport in silicon-germanium (Si-Ge) materials, including nanowires, is an area of continued interest. Thermal transport in small-scale heterogeneous systems is controlled by interfacial thermal resistance but the relative contributions of different transport mechanisms (e.g., elastic and inelastic phonon scattering) remain elusive. Our work is expected to further our understanding of phonon thermal transport and the role of boundary scattering at the interfaces of low-dimensional materials. The curvature and sharpness of the interface at the heterojunctions in Si-Ge nanowires depend on their growth environment. Herein, we evaluate the effect of interfacial curvature at the axial junctions in Si-Ge nanowires. We employ the non-equilibrium molecular dynamics (NEMD) Muller-Plathe method (with the Tersoff potential) to model thermal transport in nanowires with lengths between 100 nm and 1.3 μm and varying interfacial curvatures. Boundary resistance is probed for directional transport between both Si and Ge and Ge and Si. We have observed an overall weak dependence of thermal conductivity on curvature, and that the effect of curvature on thermal transport is dependent on nanowire length. The evolution of the wave-packet kinetic energies during the course of a simulation provides a more comprehensive picture of the wave behavior of phonons across the Si-Ge interface.

5:00 PM EN07.15.22

Unlocking Enhanced Thermal Conductivity in Polymer Blends through Active Learning [Jiaxin Xu](#) and [Tengfei Luo](#); University of Notre Dame, United States

Polymers play an integral role in various applications, from everyday use to advanced technologies. In the era of machine learning (ML), polymer informatics promises to become a valuable tool for efficiently designing and developing polymeric materials. However, the focus of polymer informatics has predominantly centered on single-component polymers, leaving the vast chemical space of polymer blends relatively unexplored. This study employs a high-throughput molecular dynamics (MD) simulation approach combined with active learning (AL) to uncover polymer blends with enhanced thermal conductivity (TC) compared to the constituent single-component polymers. Initially, TC values for about 600 amorphous single-component polymers and

approximately 200 amorphous polymer blends with varying blending ratios are determined through MD simulations. The optimal representation method for polymer blends is also identified, which involves a weighted sum approach that extends existing polymer representation from single-component polymers to polymer blends. An AL framework, combining MD simulation and ML models, is employed to explore the TC of an unlabeled dataset comprising approximately 550,000 potential polymer blends. The AL framework proves highly effective in accelerating the discovery of high-performance polymer blends for thermal transport. Additionally, we delve into the relationship between TC, radius of gyration (R_g), and hydrogen bonding, highlighting the roles of inter- and intra-chain interactions in thermal transport in amorphous polymer blends. A significant positive association between TC and R_g improvement and an indirect contribution from H-bond interaction to TC enhancement are revealed through a log-linear model and odd ratio calculation based on the polymer blend dataset, emphasizing the impact of increasing R_g and H-bond interactions on enhancing polymer blend TC.

SESSION EN07.16: Thermoelectrics
Session Chairs: Masahiro Nomura, Jae Sung Son and Sebastian Volz
Friday Morning, April 26, 2024
Room 327, Level 3, Summit

8:30 AM *EN07.16.01

Si-Based Planar-Type Thermoelectric Generators over $1 \mu\text{Wcm}^{-2}\text{K}^{-2}$ Masahiro Nomura; The University of Tokyo, Japan

Thermoelectrics energy harvesting is one of the key technologies for carbon neutrality. This talk introduces recent advances in Si-based thermoelectric generators (TEGs) and we demonstrate a planar-type double-cavity Si TEG with phononic nanostructures based on a phonon-engineered design. The planar-type device was fabricated in an SOI wafer with CMOS and MEMS processes to largely integrate the device. By using phononic nanostructures and three-dimensional thermal design, we achieved over $100 \mu\text{Wcm}^{-2}$ output power density at a temperature difference of lower than 10 K. We fabricated the Si TEG in an SOI wafer with a 1.1- μm -thick n-type poly-Si device layer and a 1.5- μm -thick BOX layer. The phononic crystal (PnC) structures are an array of circular holes with a period of 300 nm and a neck size between 8 and 100 nm. It was designed to reduce the thermal conductivity of poly-Si by considering the phonon mean free path spectrum. The cap wafer is designed for efficient cooling of the device. This double-cavity thermal design leads to a high-power density of the device. We found that more than 30% of the temperature difference between the upper and bottom of the device was applied in the thermoelectric material thanks to the careful thermal design of the double cavity structure. This thermal design is an important key factor, as well as the ZT of the thermoelectric material. Our TEG showed the output power density of more than $100 \mu\text{Wcm}^{-2}$ at a lower than 10 K temperature difference between the devices (a few Kelvin in thermoelectric material). The obtained normalized performance of over $1 \mu\text{Wcm}^{-2}\text{K}^{-2}$ is, to our knowledge, the highest-performing planar-type Si thermoelectric generator reported to date.

9:00 AM *EN07.16.02

Geometric Design and 3D Printing of Thermoelectric Materials and Devices Jae Sung Son¹, Seungjun Choo¹, Jungsoo Lee², Seong Eun Yang² and Keonkuk Kim²; ¹Pohang University of Science and Technology, Korea (the Republic of); ²Ulsan National Institute of Science and Technology, Korea (the Republic of)

Heat is omnipresent in natural and artificial environments, more than 60% of which is dissipated. Thermoelectric (TE) power generation can provide a unique solution to convert this dissipated, wasted heat into useful energy, that is, electricity. The performance of thermoelectric modules, typically composed of cuboid-shaped materials, depends on both the materials' intrinsic properties and the temperature difference created. Despite significant advancements in the development of efficient materials, macroscopic thermal designs capable of accommodating larger temperature differences have been largely underexplored because of the challenges associated with processing bulk thermoelectric materials. At this moment, three-dimensional (3D) printing technology can maximize the flexibility in the design and fabrication of TE modules into more efficient structures. Herein, we present the design strategy for various thermoelectric materials for enhancing power generation performances using a combination of finite element modeling and 3D printing. The macroscopic geometries are designed and realized by the 3D printing processes, leading to significant enhancements in the temperature difference within devices and the resulting output powers. The proposed approach paves the way for designing efficient thermoelectric power generators.

9:30 AM EN07.16.03

All-Silicon Micro-Thermoelectric Generator for IoT Applications Jose Manuel Sojo Gordillo^{1,2}, Denise Estrada-Wiese³, Alex Rodriguez-Iglesias³, Marc Salleras³, Alex Morata², Albert Tarancón² and Luis Fonseca³; ¹University of Basel, Switzerland; ²Catalonia Institute for Energy Research, Spain; ³Institute of Microelectronics of Barcelona, Spain

In the next decade, a new digital revolution will be held over the expansion of the Internet of Things (IoT), involving the deployment of trillions of nodes in multiple locations. The exponential growth of these kind of wireless devices represents a major challenge in terms of their energy supply [1]. Among the available environmental sources, heat can be harvested by means of thermoelectric devices [2]. This work presents a new generation of densely packaged all-silicon microthermoelectric generators (μTEGs) with planar architecture.

Optimized p-doped silicon nanowires with 80 ± 30 nm in diameter are epitaxially integrated as dense arrays into these generators for an improved performance [3]. A procedure to reliably place a heat sink on top of the devices, boosting the fraction of external thermal gradient captured by the thermoelectrically active nanowires, is described. These improvements boost the generated voltage up to six times with respect to that of a bare μTEG , leading to output powers well within the range of IoT needs ($10\text{--}100 \mu\text{W/cm}^2$). Specifically, the μTEG on top of a heat source above 200°C and under still air convection conditions generates more than $10 \mu\text{W/cm}^2$. When exposed to the same temperatures and to an airflow of 1.3 m/s (equivalent to a light breeze) the power density increases above $80 \mu\text{W/cm}^2$.

Moreover, a long-term stability study running the device in load matching conditions for a period of 1000 h does not show degradation below 200°C . Finally, the suitability of connecting the μTEG with the current state of the art DC-DC converters is discussed, showing how eventual transients in real operation conditions could allow the device to reach the required cold start-up voltages.

Overall, the results shown here demonstrate the readiness of the presented μTEG as a valid power source for IoT applications at the microscale.

[1] E. Hittinger, P. Jaramillo, "Internet of things: Energy boon or bane?" Science 364(6438), 326–328 (2019).

[2] E. Bell, "Cooling, Heating, Generating Power, and Recovering Waste Heat with Thermoelectric Systems." Science 321(5895), 1457–1461 (2008).

[3] J.M. Sojo-Gordillo, et al., "Tuning the thermoelectric properties of boron-doped silicon nanowires integrated into a micro-harvester." Advanced

Materials Technologies 7(2101715) (2022).

9:45 AM EN07.16.04

Geometric Thermo Electricity (GTE) - Towards "Junction-Less" Unconventional Thermoelectric Devices Oleg V. Kolosov¹, Alexandros El Sachat², Charalambos Evangelis¹, Sergio Gonzalez-Munoz³, Peng Xiao⁴, Elisa Castanon⁴, Edward McCann¹, Matthew Hamer⁴, Johanna Zultak⁴, Olga Kazakova³ and Roman Gorbachev⁴; ¹Lancaster University, United Kingdom; ²NCSR "Demokritos", Greece; ³ICN2, Spain; ⁴The University of Manchester, United Kingdom; ⁵National Physical Laboratory, United Kingdom

Traditionally, thermoelectric (TE) phenomena require junctions between two dissimilar materials to either generate the current when opposing junctions are held at two differing temperatures (Seebeck effect) or to cool and heat the opposing junctions when the external current is applied (Peltier effect). The two materials must have a different thermoelectric (Seebeck) coefficient, S (defined as the voltage V per temperature difference ΔT) in order to observe either Seebeck or Peltier effect. Nevertheless, the recently discovered phenomenon of "Geometrical Thermoelectricity", GTE [1] indicated that a nanoscale constriction (of the order of 50-200 nm) in the monolayer of two-dimensional material (2DM) graphene on the insulating SiO₂/Si substrate acts as de-facto different material with the different Seebeck coefficient, changing the Seebeck coefficient solely by geometrical patterning and allowing to create TE devices out of a single material [2], avoiding the need for another material and a junction between two materials.

Here we investigate the origin of the GTE phenomenon using a well-defined structure of graphene encapsulated between hexagonal boron nitride (hBN) layers with asymmetric constrictions (flat-taper/flat-flat/taper-flat) and under different polarity of the carriers using the back-gating. By using Scanning Thermal Gate Microscopy (STGM) [3] where a heated nanoscale tip of an atomic force microscope is scanned across the material or device surface to produce a map of thermovoltage as a function of tip position, we established that the GTE modification of Seebeck coefficient does not a) depend of the symmetry of the junction nor b) on the polarity of the carriers (electrons or holes) and therefore c) is directly linked solely to the geometrical dimensions of the constriction.

Furthermore, we explored whether GTE can be used for modification of the Seebeck coefficient in the area of 2D material rather than for a single point (nanoscale constriction). We performed the FIB milling of arrays of holes of about 50 nm in diameter in a thick 50 nm layer of 2D material SnSe₂ using the varying pitch, density and ordering, showing that it is indeed possible to create multi- μ m size areas of material with a very different Seebeck coefficient. By combining STGM with scanning thermal microscopy (SThM) [4] we found that the holes modify the heat transport on the distance of less than 20 nm, whereas the modification of the Seebeck coefficient is extended to the distances larger than 500 nm, suggesting the characteristic TE modification length is linked with the charge carriers.

In summary, we conclusively linked the GTE phenomenon to the geometrical factors and demonstrated that such an effect is present in other 2D materials such as dichalcogenide SnSe₂. We also showed the one can create large areas of multilayer 2D material building de-facto a new material with different TE properties while preserving its heat transport performance, paving the way for the much broader applications of GTE effect for the nanoscale and microscale cooling, heat manipulation and TE energy generation.

References

- [1] A. Harzheim, J. Spiege, C. Evangelis, E. McCann, V. Falko, Y. W. Sheng, J. H. Warner, G. A. D. Briggs, J. A. Mol, P. Gehring, O. V. Kolosov, Nano Letters 2018, 18, 7719. <https://doi.org/10.1021/acs.nanolett.8b03406>
- [2] A. Harzheim, F. K onemann, B. Gotsmann, H. van der Zant, P. Gehring, Advanced Functional Materials 2020, 30, 2000574. <https://doi.org/https://doi.org/10.1002/adfm.202000574>
- [3] A. Harzheim, C. Evangelis, O. V. Kolosov, P. Gehring, 2D Materials 2020, 7, 041004. <https://doi.org/10.1088/2053-1583/aba333>
- [4] S. Gonzalez-Munoz, K. Agarwal, E. G. Castanon, Z. R. Kudrynskiy, Z. D. Kovalyuk, J. Spiege, O. Kazakova, A. Patan e, O. V. Kolosov, Advanced Materials Interfaces 2023, 10, 2300081. <https://doi.org/https://doi.org/10.1002/admi.202300081>

10:00 AM BREAK

10:30 AM *EN07.16.05

Unusually Large Anomalous Nernst Effects in Partially-Crystallized Ferromagnetic Metallic Glasses Hyungyu Jin and Hyun-Woo Lee; Pohang University of Science and Technology, Korea (the Republic of)

Nernst effect is a well-established thermoelectric effect where electrons traveling along the direction of a temperature gradient are deflected by the Lorentz force into the transverse direction perpendicular to both temperature gradient and applied magnetic field. As a result, a finite electric field develops along the transverse direction. In magnetic or topological materials, such transversal deflection occurs owing to different mechanisms classified into intrinsic and extrinsic origins, and the phenomenon is called the anomalous Nernst effect (ANE). Recent studies reported that a large ANE arises in materials possessing a large Berry curvature near the Fermi level. Since its origin is intrinsic electronic band topology, such a large ANE is observed in specific crystalline orientations which requires the use of single crystalline materials. Contrary to the growing research interest in discovering new materials with large Berry curvatures, much less attention has been paid to extrinsic aspects of ANE.

In this talk, we show that unusually large ANE can be obtained even in amorphous ferromagnetic metals, when the degree of disorder within the materials is properly controlled. By applying varied heat treatment conditions to initially amorphous materials, we were able to prepare samples with different crystallinity. Intriguingly, samples with partial crystallization show the largest ANEs, comparable to those of the single crystalline state-of-the-art materials. The fact that the ANEs of fully-crystallized samples are far smaller suggests a significant role of extrinsic contribution to the observed large ANEs in partially-crystallized samples. Such large extrinsic contribution is further supported by detailed analysis of anomalous Hall effect, which reveals an unprecedented scaling relation between the longitudinal resistivity and Hall resistivity. Our work sheds new light on disordered materials as promising candidates for large ANE with better mechanical robustness than their single crystalline counterparts.

Acknowledgement

This work was supported by Samsung Research Funding & Incubation Center of Samsung Electronics under Project Number SRFC-MA2002-02 and by the National Research Foundation of Korea (NRF) grants funded by the Korea government (MSIT) (NRF-2022M3C1A3091988) and by the Ministry of Education, Science and Technology (RS-2023-00252296).

11:00 AM *EN07.16.06

Advanced Energy Materials and Devices for Low-Grade Heat Harvesting and Flexible Thermal Sensing Dongyan Xu; The Chinese University of Hong Kong, Hong Kong

With the recent advance of the internet of things, wearable technology, and soft robotics, there is a great interest to develop low-cost energy harvesting devices for converting low-grade heat into electricity and flexible sensors for artificial thermal sensation. In this talk, I will share our recent research efforts in these directions through exploring three effects: (1) thermoelectric effect; (2) thermogalvanic effect; and (3) thermodiffusion effect. Specifically, we

developed flexible micro thermoelectric generators (TEGs) with high power density and light weight by integrating pulsed electroplating with microfabrication processes. Compared to traditional electron-based thermoelectric materials, redox couples and ionic thermoelectric (iTE) materials using ions as charge carriers can achieve much larger thermopowers typically on the order of mV/K. Recently, we report polarized electrolytes consisting of Γ/I_3^- redox couple, methylcellulose (MC), and KCl with ultrahigh thermopowers of -8.18 mV/K for n-type and 9.62 mV/K for p-type. Thermoresponsive MC enables polarization switching from n-type to p-type above the gelation temperature, while the giant thermopowers mainly come from the thermogalvanic effect of the Γ/I_3^- redox couple enhanced synergistically by MC and KCl. We also developed an iTE hydrogel with a thermopower of 24.17 mV/K and flexible thermal sensor arrays for human-machine interaction.

11:30 AM EN07.18.06

Thermal Characterization of GeTe PCM based Reconfigurable Devices Zexiao Wang, Xiu Liu, Hyeonggyun Kim and Sheng Shen; Carnegie Mellon University, United States

Nanophotonic devices with adjustable optical response can be achieved through phase change materials (PCMs) such as Germanium Tellurium alloy (GeTe). GeTe can be rapidly melt-quenched or annealed between amorphous and crystalline states with large contrast of electrical and optical properties, making it a good candidate in reconfigurable electromagnetic devices, optical devices, and memory devices. However, challenges exist on the thermal aspect of GeTe PCM, where the cooling rate high as 1 K/ns from the melting point of 1000 K is required for quenching process. The stringent thermal requirements possess high demands on both heating power and heat dissipation ability. Currently several different heating approaches are adopted to achieve phase change in GeTe based nanophotonic devices, including hot plate, pulsed laser, and integrated electrical heater. However, reversible switching of GeTe covering a large area remains difficult, and the device-level understanding of the thermal and electrical properties is still elusive for the GeTe reconfigurable devices.

In this work, device level thermal modelling is conducted for a representative GeTe switching heater device, which includes a Si substrate, an AlN insulation layer, an electrical heater made from tungsten, an Al₂O₃ separation layer, and the GeTe phase change material on the top. Frequency domain thermoreflectance (FDTR) method is adopted for thermal characterization, where thermal properties of a multi-layered structure can be determined through pump-probe laser heating and curve fitting to an analytical heat conduction model. The most thermally sensitive material parameters, including thermal conductivity and heat capacity of Si, AlN and GeTe layers, as well as the thermal boundary resistance between AlN and tungsten heater, are characterized through FDTR with delicately designed multi-layered samples.

Based on the thermal measurement results, an actual GeTe switching heater device is designed with 8-unit heater layout covering the phase change region of 25×12.5 μm². A finite element model is established for the heater device to predict the steady state and transient thermal responses. To validate the thermal measurement results and the finite element model, the heater device is also fabricated and experimentally tested. The steady state thermal response is measured through a thermal mapping system; the transient response is reflected through a phase change test with pulse voltage input. Both the steady state temperature profile and the amorphized GeTe region under pulse input show high agreement between simulation and experiment, proving the accuracy of the thermal measurement and the finite element model. This work extends the thermal understanding of the GeTe based reconfigurable devices, and provides a general workflow on comprehensive thermal modelling of nanofabricated heater structures.

SESSION EN07.17: Energy Conversion and Storage
Session Chairs: Hyungyu Jin and Dongyan Xu
Friday Afternoon, April 26, 2024
Room 327, Level 3, Summit

1:45 PM *EN07.17.01

Triboelectrics and Tribovoltaics for Energy Harvesting Sang-Woo Kim; Yonsei University, Korea (the Republic of)

Energy harvesting systems based on triboelectric nanomaterials are in great demand, as they can provide routes for the development of self-powered devices which are highly flexible, stretchable, mechanically durable, and can be used in a wide range of applications. Ultrasound was used to deliver mechanical energy through skin and liquids and demonstrated that a thin implantable vibrating triboelectric nanogenerator is able to effectively harvest it. Secondly the presenter is going to introduce a two-dimensional (2D) materials-based tribotronics for possible future application toward tactile sensors, robots, security, human-machine interfaces, etc. The triboelectric charging behaviors of various 2D layered materials including graphene, MoS₂, WS₂, etc were investigated in order to decide the triboelectric position of each 2D material using the concept of a triboelectric nanogenerator, which provides new insights to utilize 2D materials in triboelectric devices, allowing thin and flexible device fabrication. Finally I will introduce a novel tribovoltaic effect, which can generate DC power output through the coupling of tribo exciton and drift by built-in electric field to overcome the limitations of conventional AC power-generating triboelectric nanogenerators. It was found that DC power can be generated at dynamic perovskite/CTL heterojunctions by electrical carrier generation from triboelectrification between two layers, which is different from the electric energy generation by photon excitation in solar cells. The tribovoltaic effect enables a paradigm shift in energy harvesting by enhancing battery charging efficiency based on an innovative working mechanism.

2:15 PM EN07.17.02

Dynamically Tunable Solid-State Thermal Energy Storage Shuang Cui^{1,2} and Judith Vidal, Ph.D.²; ¹The University of Texas at Dallas, United States; ²National Renewable Energy Laboratory, United States

Thermal energy storage (TES) utilizing phase-change materials (PCMs) holds substantial promise in various applications, such as climate control in buildings and thermal management for batteries and electronics. A critical challenge in PCM-based TES applications is the limited tunability of the operating temperature, especially for the near-ambient applications, as the PCM has a fixed transition temperature as designed. or instance, within buildings, the required operating temperature can significantly fluctuate between summer and winter, and even exhibit notable diurnal variations. This results in suboptimal PCM utilization, often leading to incomplete melting or no phase transition at all. Recent efforts have aimed to enhance the tunability of thermal materials and devices, enabling dynamic changes in their properties and performance. However, most of these endeavors have primarily concentrated on modifying thermal transport properties, such as thermal conductivity, while neglecting thermodynamic characteristics, specifically the transition temperature of materials. Changing the transition temperature using external stimuli like pressure, electric fields, or magnetic fields presents a non-trivial task, as the required magnitude of the stimulus to achieve a sizable change in T_m is typically large, and the enthalpy change at T_m is only moderate for thermal storage applications. Additionally, handling the liquid phase of PCMs during phase transitions (melting) has hindered practical TES implementation. To address these challenges, this work reports a solid-state, tunable TES utilizing shape stabilized PCMs. This innovative tunable TES

achieves an impressive dynamic transition temperature tunability of up to 10°C and enables outstanding shape stability over a month without leakage during melting. Such advancements offer the potential for simplified and safer TES device and system designs. Furthermore, the tunable TES exhibits exceptional cyclability, maintaining TES capacity across more than 100 cycles, thus presenting a promising avenue for practical applications.

2:30 PM EN07.17.04

Physics-Based Prediction and Design of Absorption Properties of Moisture-Capturing Hydrogels [Carlos D. Diaz](#), Lorenzo Masetti, Miles Roper, Kezia Hector, Yang Zhong, Zhengmao Lu, Gustav Graeber, Jeffrey C. Grossman and Gang Chen; Massachusetts Institute of Technology, United States

Moisture-capturing hydrogels have emerged as promising low-cost sorbent materials for applications including thermal management, thermal energy storage, and atmospheric water harvesting. Despite extensive efforts in the synthesis of novel hydrogels, there is a major knowledge gap between the synthesis variables and the material properties, which hinders the design of properties and system-level optimization. In this work, we develop physics-based models to predict the properties of moisture-capturing hydrogels from their composition. We develop and experimentally validate thermodynamic models that accurately predict the water uptake and absorption enthalpy as a function of humidity as relevant hydrogel synthesis variables are changed. We also develop mass transport models, using a convection-limited transport description, that accurately predict experimental absorption and desorption speeds. This work represents a major step in the design of moisture-capturing hydrogels, enabling application optimization for high performance thermal management of electronics, buildings, and people, heat storage, and atmospheric water production.

2:45 PM EN07.17.05

Hydrogel-Salt Hydrate Composite for Highly Stable Heat Energy Storage with Reduced Supercooling [Sung Bum Kang](#), Youngmun Lee, Wonsik Eom, Wuchen Fu, Mayur S. Prabhudesai, Daniel Hsieh, Sameh Tawfik, Nenad Miljkovic, Sanjiv Sinha and Paul V. Braun; University of Illinois at Urbana-Champaign, United States

Phase change materials (PCM) have potential for use in thermal energy storage in buildings, medical devices, and water heat pumps. Sodium sulfate hydrate (SSD) is appealing due to its high energy storage capability and affordability. However, SSD has issues including high supercooling (> 15°C) and low thermal cyclic stability. In this study, we introduced an ionic molecular nucleating agent that decreases the supercooling temperature to under 2°C. When this SSD was combined with a hydrogel, it maintained its thermal energy storage capacity for over 100 cycles without any decline. The success is attributed to the polymer confining the SSD crystals, preventing large-scale phase separation and the nucleating agent which resulted in nucleation of many small SSD crystals at small undercoolings rather than a small number of larger crystals. As a proof-of-application, we synthesized this composite at a kg scale and demonstrated its properties in a close to real-world demonstration.

3:00 PM BREAK

SESSION EN07.18: Thermal Management and Characterization

Session Chairs: Taeyong Kim and Woochul Kim

Friday Afternoon, April 26, 2024

Room 327, Level 3, Summit

3:30 PM EN07.18.01

Ultra Low-Cost Phase Change Hydrogel for Building Thermal Regulation [Lyu Zhou](#), Zainab Faheem and Shuang Cui; University of Texas at Dallas, United States

Energy-efficient thermal management for buildings is one of the keys to our sustainable future, as the demand for thermal comfort has increased swiftly under the impact of extreme weather. Tremendous research endeavors have been reported in recent decades, striving to tackle thermal management tasks using sustainable methods such as radiative cooling, evaporative cooling, and smart window. Thermal energy storage (TES), which utilizes latent heat of phase change materials (PCMs), also received emerged interest for its ability in mitigating temperature fluctuations and sustaining thermal comfort without extra energy input. However, practical implementation of PCMs is constrained by cost, shape stability, and energy density. Here we report an inorganic PCM composite based on sodium sulfate decahydrate (SSD). In contrast to most organic PCM, SSD has an ultralow cost (1.60 \$/kWh) and high energy density (254 J/g), making it a promising PCM for building thermal management. To address the intrinsic limitations of SSD in shape stability and phase separation, we introduced another low-cost hydrogel, i.e., poly (acrylamide-co-acrylic acid), to encapsulate SSD through swelling. In particular, we optimized hydrogel composition by exploring the hydrolysis effect, and achieved a swelling ratio of 29.96 g/g in 70 wt% SSD solution. The obtained phase change hydrogel exhibited a melting latent heat of 133.32 J/g with melting temperature of 32.84 °C, while withholding excellent shape stability after 500 hundreds thermal cycles. This demonstrated thermal properties promise a cost-effective PCM for building thermal regulations.

3:45 PM EN07.18.02

Broadband Thermal Management Using Smart Cooling Films [Will Chang Liu](#); Massachusetts Institute of Technology, United States

With the escalating trend of climate change, we are under severe pressure to increase the resilience of commercial and residential buildings and vehicles. Smart lighting and thermal management of windows promise to improve indoor thermal comfort with minimum added carbon footprints. We report a passive smart cooling technology for thermal management throughout the spectrum from visible to mid-infrared regions by using a thermochromic hydrogel network integrated with an optically transparent polymer coating for radiative cooling. We have achieved excellent optical properties, including luminous transmittance of 81.8% and solar transmittance modulation of 74.8%, to intelligently minimize direct solar radiation. Notably, merging the light management of thermochromic hydrogel networks with the thermal management of daytime radiative cooling films enables us to minimize secondary radiation from hot window surfaces, contributing to overall cooling power. To the best of our knowledge, this is the first demonstration of the integration of a thermochromic smart medium and passive radiative cooling film into a single cooling apparatus in a field test. Through this integration, we achieved an indoor temperature drop of up to 5.1 °C on summer days with zero energy consumption. Additionally, our material and device designs offer advances far beyond spectrum tunability and cooling power. The mechanical flexibility and moldability of the hydrogel network promise extensive applications for our technology in buildings, vehicles, and other complex geometric shapes with intelligent cooling needs, distinguishing it from any prior liquid-based counterparts. We believe that the broad thermal management of thermo-responsive hydrogel networks and visually transparent radiative cooling coatings could usher in a new paradigm for extending the scope of space temperature control, bringing tangible benefits to real-world applications aimed at alleviating global cooling needs.

4:00 PM EN07.18.03

On-Demand Modulation of Radiative Cooling Performance with Hygroscopic Salt-Cellulose Fiber for Building Applications Huajie Tang and Dongliang Zhao; School of Energy and Environment, Southeast University, China

Radiative cooling of buildings with low carbon footprints has drawn widespread attention. However, the possible overcooling effect at night may increase building heating energy consumption in transition seasons, especially in mild climates. Herein, we developed a simple, low-cost, and high-performance hygroscopic salt-cellulose fiber to modulate diurnal radiative cooling performance. With the transition of desorption and adsorption of the cooling fiber, the sub-ambient temperature reduction can reach 2.4 °C during the day, and be limited to below 2 °C at night. The daytime cooling performance is dominated by thermal radiation when ambient relative humidity is low, and dominated by evaporation when relative humidity is high. The nighttime adsorption enthalpy is contributed by multiscale mechanisms, including the adsorption of hydrophilic functional groups, capillary condensation, as well as the deliquescence of CaCl₂ salt. The profusion of cellulose and hygroscopic salt features desirable cost-effectiveness, and the simple preparation process allows large-scale applications.

4:15 PM EN07.18.04

Cell-Level Mapping of The Thermal Conductivity of Electrode Composites in Lithium-Ion Batteries Juwei Sun and Yee Kan Koh; National University of Singapore, Singapore

In Lithium-ion batteries (LIB), the surface of the active material serves as the primary site for reactions and heat generation. Also, it is the place where the hotspots trend to emerge. Localized high temperatures within the micrometer range can trigger a series of chain reactions, leading to uncontrollable thermal runaway in batteries. Therefore, a detailed understanding of the thermal properties of LIB electrodes is of paramount importance. Previous research has used various methods, for example, laser flash and steady-state measurement, to measure the thermal properties of electrode composite or active materials. However, the previous research typically treats the thermal properties of LIB electrodes as a macroscopic characteristic, failing to provide detailed information about real electrodes. The objective of this study is to produce micrometer-scale resolution mapping for the thermal conductivities of the electrodes.

We adapted TDTR technology, which is a well-established optical pump-probe technique, to perform experiments. In TDTR, the pump laser beam heats the sample surface, and the reflected probe beam is detected to analyze the thermal response of the sample. Before conducting the experiment, we took multiple steps to ensure that the sample would yield a sufficient reflected probe signal. We utilized ion milling techniques to polish the electrode's cross-sectional surface until its Root Mean Square (RMS) roughness within a 10um x 10um area was reduced to less than 50nm. We selected graphite and lithium cobalt oxide (LCO) electrodes, both made from active material particles of approximately 20um in size for the experiment. The local measurement was first conducted under three different conditions: 1) 6um spot size laser at 18.9MHz heating frequency, 2) 3um spot size laser at 9.8MHz heating frequency, and 3) 3um spot size at 5.4MHz heating frequency. We fitted the obtained thermal response signal with a thermal model. From this, we derived an isotropic thermal conductivity for LCO, and an anisotropic thermal conductivity for graphite. Finally, we conducted scanning experiments on the electrode within a 30µm x 30µm area. Data was collected at 1 um intervals during the scan. The scanning results clearly indicate the thermal conductivity of each component, with distinct boundaries that align well with the SEM images.

Our study provides detailed thermal properties at high spatial resolution, enabling the calculation of the temperature distribution during battery operation and the prediction of hotspot emergency conditions. This study facilitates the development of thermal management strategies at the electrode level in LIBs, addressing the safety concerns at their root.

4:30 PM EN07.18.05

In Vivo Thermal Conductivity Measurement of Blood-Perfused Tissue Accounting for The Effect of Blood Flow Gimin Park¹, Boksoon Kwon², Sang-Kyu Kim² and Woochul Kim¹; ¹Yonsei University, Korea (the Republic of); ²Samsung Advanced Institute of Technology, Korea (the Republic of)

Understanding the thermal properties of human tissue is crucial for evaluating their ability to regulate temperature, assessing the effectiveness of thermotherapy techniques, designing skin-contact medical devices, and optimizing thermal comfort in different environments. Traditional measurement methods primarily conducted on nonliving materials involve modifying the material's geometry and placing the material in a vacuum environment, which is not achievable for living human beings. Moreover, the presence of blood flow and perfusion of tissue introduces advection effects described by Pennes' bioheat equation, and its influence on thermal response at the skin must be considered when measuring thermal conductivity. Previous studies have often been unable to isolate the effect of blood perfusion, resulting in the quantification of effective thermal conductivity, which exhibits a strong temperature dependence due to vasomotion's role in dissipating excess heat or conserving heat in cold conditions. In this study, we employ sinusoidal heating and transient plane source heating to subsequently measure the blood perfusion rate and thermal conductivity exclusively at the skin by controlling the thermal penetration depth. Analytical solution to the transient bioheat equation allows us to separate the influence of blood perfusion when obtaining the thermal conductivity attributed solely to conduction. Tissue temperatures ranging from 30.5°C to 35.5°C yielded tissue thermal conductivity averaged at 0.334 ± 0.035 W/m-K. This value of thermal conductivity agrees well with that of excised human epidermis (0.21 – 0.41 W/m-K) [1]. As expected, the blood perfusion rate increased with increasing tissue temperature from 0.143×10^{-3} to 3.421×10^{-3} m³/s/m³, which is typical for convective heat transfer coefficients ranging from 5 to 15 W/m²-K. By measuring the thermal conductivity of blood-perfused skin, we hope to enhance the design and performance of wearable devices, improve the efficacy of thermoregulation techniques, and advance the understanding of various skin-related disorders and conditions. The insights gained from these studies have the potential to revolutionize fields such as biomedical engineering, personalized medicine, and thermal comfort optimization, ultimately benefiting human health and well-being.

[1] Xu, F., Lu, T. J., Seffen, K. A., & Ng, E. Y. K. (2009). Mathematical modeling of skin bioheat transfer. *Applied mechanics reviews*, **62** (5).

SESSION EN07.19: Virtual Session: Thermal Transport and Energy Conversion
Session Chairs: Shuang Cui and Sunmi Shin
Tuesday Morning, May 7, 2024
EN07-virtual

8:00 AM EN07.19.01

High-Powered Superhydrophobic Pyroelectric Generator via Water Droplet Impact Jeonghoon Han¹, Seongjong Shin², Seungtae Oh³, Heejae Hwang⁴, Dukhyun Choi⁵, Choongyeop Lee³ and Youngsuk Nam²; ¹Korea Institute of Energy Research, Korea (the Republic of); ²Korea Advanced Institute of Science and Technology, Korea (the Republic of); ³Kyung Hee University, Korea (the Republic of); ⁴Korea Institute of Science and Technology, Korea

(the Republic of); ⁵Sungkyunkwan University, Korea (the Republic of)

Recent studies on water-based pyroelectric generators (PyGs), which convert thermal energy to electrical energy, have focused on different operational modes like water evaporation, water stream, and droplet sliding. However, the development of sustainable, high-powered generators and comprehensive theoretical models has been limited. In response, our research introduces a superhydrophobic (SHPo) PyG, exploiting the characteristics of lead magnesium niobate-lead titanate (PMN-PT) coated with titanium dioxide nanoparticles. We analyzed power density by considering the phase transient temperature that maximizes the pyroelectric coefficient of PMN-PT, testing various Weber numbers and droplet diameters within a moderate operating temperature range of 40°C to 80°C. Considering the dynamic characteristics of water droplet on SHPo surfaces, we suggest the peak current model that can accurately predicting the actual peak current. Also, the maximum power density of 54.5 $\mu\text{W}/\text{cm}^2$ at a droplet diameter of 3.6 mm and a PMN-PT temperature of 80°C, a noteworthy improvement over 3 times higher than previous water-based PyGs. Our results enhance the understanding of the pyroelectric effect coupled with drop impact dynamics and outlines novel strategies for designing high-performance water-based PyGs.

8:15 AM EN07.19.02

Integrating Porous Copper for Supercooling Mitigation in Gallium-Based Phase Change Material Thermal Storage Seokkan Ki¹, Seongjong Shin¹, Sumin Cho², Soosik Bang¹, Dongwhi Choi² and Youngsuk Nam¹; ¹Korea Advanced Institute of Science and Technology, Korea (the Republic of); ²Kyung Hee University, Korea (the Republic of)

Phase change materials (PCMs) undergo a transition from solid to liquid, absorbing a substantial amount of latent heat, making them suitable for systems that efficiently store and release heat as needed. Research on PCMs is actively pursued in various fields such as energy harvesting, air conditioning, and electronic device thermal management. Paraffin has been extensively utilized in PCM research primarily due to its high specific latent heat (~230 kJ/kg) and cost-effectiveness. Nevertheless, challenges arise when paraffin is applied to systems requiring rapid thermal response, such as electronic devices, due to its low thermal conductivity of approximately 0.2 W/mK.

To address these challenges, researchers have turned to gallium-based liquid metals with an appropriate specific latent heat (80 kJ/kg) and a comparatively high thermal conductivity of approximately 40 W/mK. While gallium may possess a lower specific latent heat per unit mass compared to paraffin-based PCMs, its density exceeds that of paraffin by more than six times. As a result, the specific latent heat per unit volume increases, enabling efficient heat absorption within confined volumes. Furthermore, gallium exhibits high thermal conductivity, enabling rapid system response under conditions of fluctuating thermal load. However, gallium faces a supercooling issue, where it remains in a liquid state after absorbing heat and fails to transition back to a solid state when the temperature drops below its freezing point. In this context, resolving the supercooling problem is imperative for the successful application of gallium in PCM systems.

This study suggests a gallium-porous copper composite to mitigate gallium's supercooling issue. Deoxidized gallium and porous copper were efficiently combined to create the composite material in a low-concentration hydrochloric acid environment. The porous structure increased the surface area, and the intermetallic compound CuGa₂ that formed at the interface facilitated heterogeneous nucleation, reducing the supercooling of gallium. The quantitative performance of supercooling mitigation was verified through differential scanning calorimetry and multi-cycle heating and cooling experiments.

8:30 AM EN07.19.03

Assessing Lattice Thermal Conductivity of Topological Insulator Bi₂Se₃ by Temperature-Dependent Raman Spectra Vipin K. E and Prahallad Padhan; Indian Institute Of Technology Madras, India

Topological insulators (TIs) have emerged as a fascinating material class that exhibits unique electronic properties, making them promising candidates for various technological applications. One of the promising areas where TIs hold great potential is thermoelectricity. Unlike conventional materials, TIs possess a non-trivial band gap in their bulk states but harbor conducting surface states due to the presence of robust, spin-polarized, and topologically protected electronic states. The conducting surface states of TIs, known as topological surface states (TSS), have a linear energy-momentum dispersion relationship, which can lead to high electron mobility and improved electrical conductance. This unique electronic structure offers an advantage over conventional thermoelectric materials, where achieving both high electrical conductivity and low thermal conductivity is challenging.

The pursuit of highly efficient thermoelectric (TE) materials hinges on understanding their electrical conductivity (σ), Seebeck coefficient (S), and thermal conductivity (κ_L). Among these, thermal conductivity (κ_L) plays a pivotal role and is a critical factor in TE efficiency. This study delves into the reduction of κ_L , focusing on hexagon-shaped nanocrystals cluster of Bi₂Se₃, synthesized via the hot-injection technique employing non-toxic solvents. The nanocrystals' temperature-dependent Raman spectra were analyzed to determine the average Debye temperature (θ_D) and Gruneisen parameter (γ), utilizing the bond order-length-strength correlation theory (BOLS).

At room temperature, κ_L of the Bi₂Se₃ nanocrystals was evaluated as 1.85 $\text{Wm}^{-1}\text{K}^{-1}$ using θ_D and γ obtained from BOLS theory, closer to the simulated values of 1.4 $\text{Wm}^{-1}\text{K}^{-1}$ in-plane and 0.4 $\text{Wm}^{-1}\text{K}^{-1}$ out-of-plane direction.

Our theoretical studies adopting 3 phonon process demonstrate that over 54 % of in-plane cumulative κ_L , and around 12 % of out-of-plane cumulative κ_L are contributed by the modes below 2 THz, which are dominated by the Bi atom. The ratio of in-plane cumulative κ_L to out-of-plane cumulative κ_L at 5 THz is ~ 3.58, establishing the anisotropic κ_L of Bi₂Se₃. Further our mean free path (λ) dependent κ_L studies demonstrated the cumulative κ_L in the plane is dominated by the phonons with a mean free path below $\lambda \sim 15$ nm, while along the out-of-plane directions, the phonons with an λ of ~ 5 nm have strong contributions. The Bi₂Se₃ is an anisotropic system, and the cumulative thermal conductivity as a function of the λ displays that a major contribution is arising from the shorter mean free path. This scattering is the main cause of low lattice thermal conductivity in the investigated system.

The introduction of nanostructuring-induced grain boundaries in Bi₂Se₃ obstructs long-mean-free-path phonons. Furthermore, intentional doping can also significantly reduce the phonon mean free path, effectively lowering κ_L . Anisotropic phonon scattering, facilitated by weak Van der Waals forces between quintuple layers in the out-of-plane direction, alongside acoustic-optical phonon scattering and anharmonicity, impeded efficient thermal energy transport in Bi₂Se₃, resulting in reduced κ_L .

This research demonstrates a method for determining κ_L from temperature-dependent Raman spectra and sheds light on the potential of intentional nanostructuring and doping to optimize TE materials. These findings are instrumental in advancing the understanding of materials that enhance the TE quality factor and, consequently, the figure of merit, offering a promising avenue for future research in the realm of thermoelectrics.

8:35 AM *EN07.19.04

Plasmon Thermal Conductivity of a Thin Metal Film Bong Jae Lee; KAIST, Korea (the Republic of)

The well-known classical size effect causes decreased thermal conductivity of thin films at the nanoscale, which usually results in hot-spot formation and device performance deterioration. Recent research has revealed a novel heat transfer mechanism based on the use of surface electromagnetic waves in a polar dielectric, specifically Zenneck surface modes. Surface plasmon polaritons (SPPs) are a type of surface electromagnetic wave that is associated with free electrons within metals and so functions as a heat carrier. Thermally excited SPPs have been used to manipulate the near-field thermal radiation across

a broad spectrum in lossy metals and heavily doped semiconductors. This presentation will discuss our most recent results about the surface-plasmon-enhanced in-plane thermal conductivity of a thin metal film on a glass substrate.

9:05 AM EN07.19.05

Mechanism of Transition Metal-Assisted Healing of Defective Graphene [Anbarasan Radhakrishnan](#) and Jae Hyun Park; Gyeongsang National University, Korea (the Republic of)

In graphene synthesis, the emergence of atomic vacancy defects is inevitable. These defects compromise the lattice's capacity to conduct heat, resulting in a diminished thermal transport efficiency for graphene-based devices. The introduction of adatoms to these vacancies termed the healing of defected graphene, has been identified as a method to enhance thermal conductivity. However, the details of the healing process remain unclear. This study delves into the mechanism underlying the healing of mono-vacancy (MV) defected graphene using Pt atoms, employing neural network potential (NNP)-assisted molecular dynamics (MD) simulations. In contrast to the marginal increase in thermal conductivity observed with pure Pt atoms, healing with C-Pt fragments significantly elevates the lattice thermal conductivity of defected graphene as the healing progresses. Upon full healing, the thermal conductivity of defected graphene healed by C-Pt fragments reaches 5.2 times that of the pre-healing state. During the healing process with C-Pt fragments, the fragments dissociate, allowing Pt atoms to move freely on the surface while carbon atoms remain stationary at the vacancies. Subsequently, Pt atoms gather to form a metal cluster, influencing the distribution of phonon density of states and causing a change in lattice thermal conductivity. The study also explores alternative transition metals such as Ni and Pd, with the resulting lattice thermal conductivities for C-Ni, C-Pd, and C-Pt fragment-healed graphene recorded as 382.1 W/m K, 976.9 W/m K, and 1159.7 W/m K, respectively. This variation is attributed to differences in mass and adsorption energy. The findings of this research present the effectiveness of utilizing transition metals as a promising strategy for rectifying defective graphene and controlling lattice thermal conductivity, particularly for applications in thermal management.

This work was supported by the National Research Foundation of Korea funded by the Ministry of Science and ICT under Grant (2022M1A3C2074536, Future Space Education Center) and Grant (2021R1A2C2004207).

9:10 AM EN07.19.06

Solar-Thermal Energy Harvesting to Achieve Water Desalination Taylor Moore¹, [Rana Biswas](#)^{1,2} and Meng Lu¹; ¹Iowa State University, United States; ²Ames Laboratory, United States

Harnessing solar energy to desalinate water is a critical need in many areas of the world where water supplies are scarce, or in regions affected by natural disasters. To address this problem, we developed a novel small-scale solar-thermal energy harvesting scheme to rapidly heat water to boiling, enabling distillation, water desalination, and generation of potable water.

We performed outdoor experiments demonstrating that concentrated solar power can heat water to boiling effectively and achieve desalinate water on a small scale. Using a 1.5 m dish shaped mirror to concentrate solar energy on a flask of water we achieved boiling of water within 1 hour. To accelerate the solar-thermal energy harvesting process we compare the performance of absorbing carbon-black coatings on glass flasks with uncoated flasks. We discuss the use of photonic structures that enhance thermal emission in relevant wavelength windows and describe preliminary measurements with these structures. We measured the conductivity (κ) and concentration of total dissolved solids (TDS) in the starting water solution to be 4.32 milli-S/cm and 2.2 ppt respectively and found that these decreased to 20 micro-S/cm and 10 ppm in the distillate achieved with solar-thermal energy conversion, illustrating excellent desalination. To calibrate the outdoor solar-thermal energy conversion results we performed baseline indoor water distillation experiments. We found that the decreases of conductivity and TDS are in outdoor experiments are comparable with those achieved in benchmark indoor distillation experiments. We discuss pathways for scale-up of solar-thermal energy harvesting and water desalination to larger scales. The critical thermal transport processes will be described.

The work was partially supported by Iowa State University through the ECpE FuTure Grant and the ISU Honors program.

9:15 AM *EN07.19.07

Rattling of Three-Fold Coordinated Copper in Sulfides: A Blockade for Hole Carrier Delocalization but a Driving Force for Ultralow Thermal Conductivity [Emmanuel Guilmeau](#); CRISMAT, France

Copper-rich sulfides are attracting a wide attention for energy conversion applications due to their environment compatibility, cost effectiveness and earth abundance. Herein, based on a comparative analysis of the structural and transport properties of state-of-the art Cu-rich sulfides, we highlight the role of the cationic coordination types and networks on the electrical and thermal properties. By combining experiments and theory, we show that the ultralow thermal conductivity originates mainly from the very high anisotropic thermal vibration of copper due to its threefold coordination. Density functional theory (DFT) calculations reveal that these Cu atoms are weakly bonded and, thus, give rise to low-energy, Einstein-like vibrational modes that strongly scatter the heat-carrying acoustic phonons. Importantly, we demonstrate that the three-fold coordination of copper causes a hole blockade. This phenomenon hinders the possibility to optimize the carrier concentration and electronic properties through mixed valency $\text{Cu}^+/\text{Cu}^{2+}$, differently from tetrahedrite and most other copper-rich chalcogenides, where the main interconnected Cu-S network is built of CuS_4 tetrahedra. The comparison between various copper-rich sulfides demonstrates that seeking for frameworks characterized by the coexistence of tetrahedral and threefold coordinated copper is very attractive for the discovery of efficient thermoelectric copper sulphides. Considering that lattice vibrations and carrier concentration are key factors for engineering and controlling all transport phenomena (electronic, phonon, ionic...) in copper-rich chalcogenides for various types of applications, our findings on the structure/properties relationships can serve as new guidelines for the design of functional materials for the generation of sustainable energy with wide-ranging applications.

9:45 AM EN07.19.08

Strain-Driven Anomalous Lattice Thermal Conductivity in BaPdS_2 [Xiao X. Yu](#)^{1,2}, Can Wu¹, Jia W. Hong² and Bo Xu¹; ¹Yanshan University, China; ²Beijing Institute of Technology, China

Strain engineering is one of the most promising and effective routes toward continuously turning the electronic and optical properties of materials, while thermal property is generally believed to be sensitive and positive with the mechanical compress strain. In this paper, we investigated the lattice thermal conductivity of zigzag chain-like wrinkled structure BaPdS_2 with uniaxial compress strain along c -axis based on first-principles calculations and phonon Boltzmann transport equation. Unlike the commonly belief that the lattice thermal conductivity increases (or decrease) with compress (or tensile) strain for bulk materials, it is found that the $\kappa_{\text{latr-c}}$ was nearly unchanged and $\kappa_{\text{latr-a}}$ was increased exceptionally for BaPdS_2 with strain imposed in c -axis. The unusual strain dependence thermal conductivity in c -axis was mainly attributed to the enhanced phonon phase space that neutralized the weakened anharmonicity and the enhanced group velocity. While the abnormal increased $\kappa_{\text{latr-a}}$ is attributed to the weak anharmonicity with compress strain perpendicular to a -axis, equivalent to uniform biaxial tension strain in ab plane. In addition, high thermal conductivity anisotropy was observed because of the large group velocity disparity along a - and c -axis. The finding discovers materials with unusual thermal conduction mechanism under strain along different directions, as well as provides new material platforms for potential heat-routing or heat-managing devices.

SYMPOSIUM EN08

Advancements in Thermoelectric Materials, Module Technology and Applications
April 23 - May 8, 2024

Symposium Organizers

Ernst Bauer, Vienna Univ of Technology
Jan-Willem Bos, University of St. Andrews
Marisol Martin-Gonzalez, Inst de Micro y Nanotecnologia
Alexandra Zevalkink, Michigan State University

* Invited Paper

+ JMR Distinguished Invited Speaker

^ MRS Communications Early Career Distinguished Presenter

SESSION EN02/EN08: Joint Virtual Session
Session Chairs: Jan-Willem Bos and Alexandra Zevalkink
Wednesday Morning, May 8, 2024
EN08-virtual

8:00 AM EN02/EN08.01

Enhanced Biomechanical Energy Harvesting and Gesture Monitoring: Superhydrophobic, High-Performance Hybrid Piezo-Triboelectric Nanogenerator Using Flexible Nanofibers [Sushmitha Veeralingam](#), Jun S. Choi, Tran D. Khanh, Kampara R. Kishore, Seung B. Jung and Jong W. Kim; Sungkyunkwan University, Korea (the Republic of)

The burgeoning field of nanogenerators presents ongoing challenges in elevating performance through innovative strategies and architectures. This study addresses these challenges by synergistically combining the distinct properties of piezoelectric nanogenerators (PENG) and triboelectric nanogenerators (TENG). It harnesses the bulk polarization effect inherent in PENG and the contact electrification and electrostatic induction in TENG, thereby leveraging their combined strengths. Our focus is the development of a novel hybrid piezo-triboelectric nanogenerator (HPTENG), which employs a multi-layered nanofiber architecture, showing significant promise for applications in flexible electronics and electronic skins. This work introduces composite nanofibers composed of polyvinylidene fluoride (PVDF)-MoS₂-MXene (PMMX), capitalizing on the superior piezoelectric effect of MoS₂-PVDF and the two-dimensional structure and abundant dangling bonds of MoS₂-MXenes. We synthesized MXene (Ti₃C₂) via chemical etching and MoS₂ using the hydrothermal method. The resulting TENG, employing PMMX nanofibers as the negative triboelectric layer and Nylon 6,6 nanofibers as the positive layer, exhibited an open-circuit voltage (Voc) of 25 V and short-circuit current (Isc) of 1.2 μ A. The PENG displayed a Voc of 10 V and Isc of 2.0 μ A. Notably, the HPTENG demonstrated enhanced performance with a Voc of 100 V and Isc of 6.0 μ A. This amplification can be attributed to the synergistic Piezoelectric-Triboelectric (TE-PE) effect, facilitating the conversion of random, low-frequency mechanical energy into electricity by altering the charge density in electrodes under external forces. Our study further emphasizes the necessity of augmenting the electrical performance of PENGs and TENGs to improve energy harvesting efficiency and signal-to-noise ratio. The practicality of HPTENG was validated by attaching it to various human joints, including fingers, elbows, palms, and knees, effectively monitoring real-time motion during activities like bending, running, and walking. Additionally, the need for hydrophobicity in wearable devices, to mitigate the influence of sweat, is addressed through contact angle studies of electrospun PMMX fibers, which demonstrated a significant angle of 117.5 degree, confirming their hydrophobic nature. The promising results of this study highlight the potential of HPTENG as an effective system for human gesture monitoring. The unique material composition and straightforward fabrication strategy presented here pave the way for novel solutions in the realm of advanced energy harvesting.

8:05 AM *EN02/EN08.02

Flexible Self-Charging Power Sources [Ruiyuan Liu](#); Soochow University, China

Flexible power sources are key power solutions towards wireless wearable electronics, untethered soft robotics, and medical care. However, the high power consumption of various components in modern flexible electronics with limited volume raises great challenges for their sustainable operation. A flexible self-charging system that can harvest energy from the working environment and simultaneously charge energy-storage devices to supply power is a promising strategy. Flexible self-charging devices based on solar cells, triboelectric nanogenerators (TENGs), hydrovoltaics, and other emerging energy harvesting technologies hold the advantages of high power density and lightweight. Therefore, they would meet the critical requirements of next-generation soft electronics. In this presentation, the integration of several energy harvesting and storage devices will be introduced, regarding the materials, designs and applications.

Reference:

1. K. Ni, B. Xu, Z. Wang, Q. Ren, W. Gu, B. Sun, **R. Liu***, X. Zhang*. **Advanced Materials** 2023, 35, 202305438.
2. C. Zhang[#], M. Nayeem[#], Z. Wang[#], X. Pu, C. Dagdeviren*, Z. L. Wang*, X. Zhang*, **R. Liu***. **Progress in Materials Science** 2023, 138, 101156.
3. B. Shao, Y. Song, Z. Song, Y. Wang, Y. Wang*, **R. Liu***, B. Sun*. **Advanced Energy Materials** 2023, 13, 2204091.
4. **R. Liu***, Z. L. Wang, K. Fukuda*, T. Someya*. **Nature Review Materials** 2022, 7, 870.
5. C. Zhang[#], M. Wang[#], C. Jiang, P. Zhu, B. Sun, Q. Gao*, C. Gao*, **R. Liu***. **Nano Energy** 2022, 95, 106991.

8:35 AM EN02/EN08.03

Artificial Intelligence Guided Thermoelectric Materials Design and Discovery [Guangshuai Han](#), Na Lu and Yining Feng; Purdue University, United States

Materials discovery from vast repositories of Earth's resources remains a significant impediment to revolutionary technological advancements. The labor-intensive and time-consuming nature of this process hampers the exploration of novel materials. While machine learning techniques have demonstrated their potential in expediting materials discovery, the challenge lies in obtaining effective material feature representations and achieving precise predictions of material properties. This research endeavors to establish an automated framework for material design and discovery, harnessing the power of data-driven AI models. Initially, we have developed a range of diverse material descriptors to enhance the representation and encoding of the distinctive characteristics of materials. This, in turn, leads to improved predictive performance across various molecular properties. As a baseline, we have focused on predicting thermoelectric (TE) properties of materials to demonstrate the framework's effectiveness. Remarkably, our proposed framework attains an accuracy rate exceeding 90% in forecasting TE properties. Moreover, our AI models have identified 6 promising p-type TE materials and 8 promising n-type TE materials. To validate our predictions, we have compared them with Density-functional Theory (DFT) calculations, and they align with the TE properties obtained from experimental results. By harnessing the potential of machine learning, deep learning, and data mining, this endeavor holds the potential to transform the paradigm of high-performance energy harvesting materials design, ushering in a new era of sustainable and efficient energy utilization.

8:50 AM EN02/EN08.04

Fabrication of Polyvinylidene Fluoride-Co Hexafluoropropylene (PVDF-HFP) Staple Yarns Using Discrete Electrospun Nano filaments and Evaluation of Their Mechanical and Piezoelectric Properties [Adaugo M. Enuka](#) and Vincent Z. Beachley; Rowan University, United States

Textiles fabricated from biocompatible and biodegradable polymers, such as Polyvinylidene fluoride-co hexafluoropropylene (PVDF-HFP), hold immense promise for various biomedical applications, including scaffolds and implants. Electrospinning, a well-established nanofiber fabrication technique, allows for producing nanofibers with exceptional properties at high throughput. One intriguing application of electrospinning is the creation of nano yarns spun from nanofibers. However, the conventional approach employs continuous filaments, limiting the control over filament parameters. An alternative approach involves the fabrication of yarns using discrete filaments, termed "staples," enabling precise tuning of filament parameters as fiber spinning and yarn spinning occur separately. Building upon previous work, this study introduces a high-throughput yarn-spinning device capable of producing staple yarns with repeatable and consistent parameters. By decoupling the electrospinning and yarn-spinning processes, we harness the unique properties of nanofibers and gain control over their parameters, a feat unattainable with current yarn fabrication methods. This advancement will facilitate an in-depth investigation into the impact of tunable fiber parameters on yarn mechanics. PVDF-HFP staple yarns are crafted from electrospun nanofilaments with varying parameters, such as draw ratio, density, segment length, and more, and their effects on yarn mechanical properties are explored.

Methods: Electrospinning and fiber collection are carried out using a Track electrospinning system. A potential difference is applied between the polymer tip (30% w/v PVDF-HFP in a 2:1 DMF: Acetone solution) pumping needle and the collection tracks. Continuous collection of fibers onto a roving track produces discrete filaments. These filaments are then transported to a spinning device that converts them into staple yarns. Mechanical testing and characterization adhere to ASTM D2256 standards.

Textile products created from biocompatible polymers, such as Polyvinylidene fluoride-co hexafluoropropylene (PVDF-HFP), find applications in biomedical technology. Electrospinning, a widely employed nanofabrication technique, enables the production of nanofibers with superior properties at a rapid production rate. One intriguing application of electrospinning is the creation of nano yarns spun from nanofibers. Currently, nano yarns are produced using continuous filaments.

PVDF-HFP exhibits remarkable properties, including excellent chemical resistance, high stability, low dielectric loss, a high dielectric constant, and biocompatibility. When electrospun, PVDF-HFP yields nanofibers with exceptional mechanical strength and an impressive surface area-to-volume ratio. Post-drawing of thin films enhances the β -phase content of these fibers. This copolymer boasts diverse applications, from developing susceptible sensors for measuring blood pressure and joint pressure to transforming mechanical energy from body movements into electrical energy. PVDF-HFP is also well-suited for energy harvesting systems in implantable medical devices. Furthermore, PVDF-HFP is being investigated for actuators and transducers capable of converting electrical energy into mechanical motion and finding applications in medical devices, such as microsurgical tools and drug delivery systems. The ongoing research aims to transform electrospun PVDF-HFP filaments into yarn using a specialized spinning device to assess the piezoelectric responses of the resulting yarns for various biomedical applications. This study presents a significant advancement in developing PVDF-HFP staple yarns, offering a more versatile and tunable approach for biomedical applications. Integrating electrospinning and yarn spinning at distinct stages enables precise control over yarn parameters, expanding the potential for harnessing the remarkable properties of PVDF-HFP in diverse medical devices and systems.

9:05 AM EN02/EN08.05

Macro-Scale Patterning for Hierarchically Designed Thinner Peltier Sheets [Norifusa Satoh](#)¹, Jin Kawakita¹ and Junnosuke Murakami²; ¹National Institute for Materials Science, Japan; ²Sekisui Chemical Company, Limited, Japan

Towards the Global Cooling Pledge launched on CoP28 at Dec. 5, 2023, reducing over 60% greenhouse gas emissions from the cooling sector [ref. 1], thermoelectrics (TEs) has a great potential because Peltier human cooling devices directly cool down the body temperature not the entire room temperature to save 10-times energy consumption compared to air conditioners only [ref. 2,3]. To slim the thickness and enhance the contacting body area when using the same amount of TE materials [ref. 3,4], we have been developing thinner Peltier sheets using sticky TE materials [ref. 5,6] based on a hierarchical multi-component strategy turning element composition of TE particles for high Seebeck coefficient at atomic scale [ref. 7], controlling the surface of TE particles for small interfacial electric resistance at nano scale [ref. 7], and minimizing thermal conductivity and absorbing mechanical bending stress by hybridizing organic solvent with the TE particles [ref. 6] and adopting ultra-thin high performance foam at micro-scale [ref. 3]. Instead of the benefits on flexibility and in the rate of heat transfer [ref. 3,4], however, Peltier sheets tend to ruin the cooling performance. Since thinner design requires higher current at the maximum operating point, more Joule heat is generated at the electrodes sandwiching the TE materials to reduce the temperature difference formed within the TE materials based on Peltier effect. Especially, narrow electrode patterns adopted for the TE generation modules to accumulate the thermopower based on Seebeck effect in series and drive booster circuits [ref. 5] generates Joule heat in general. Through surveying various pattern combination between sticky TE materials and electrodes at macro-scale, herein, we propose a different patterning rule than that for TE generation modules.

[ref. 1] <https://news.un.org/en/story/2023/12/1144382>

[ref. 2] Itao et al. J Jpn Soc Precis Eng 2016;82:919-924 (in Japanese).

[ref. 3] Satoh et al. MRS Adv 2023;8:781-786.

[ref. 4] Satoh et al. MRS Adv 2023;8:446-450.

[ref. 5] Satoh et al. Sci Technol Adv Mater 2018;19:517-25.

[ref. 6] Satoh et al. MRS Adv 2020;5:481-487.

[ref. 7] Satoh et al. Soft Sci 2022;2:15.

9:10 AM EN02/EN08.06

Procedure of Failure Analysis on Commercial Available Thermoelectric Modules Karl-Heinz Gresslehner¹, Martin Krenn¹, Patrizia Lerner², Lukas Gupfinger¹ and Bernhard Sonderegger¹; ¹Johannes Kepler University Linz, Austria; ²University Graz, Austria

In this work, the procedure of a failure analysis on commercial available thermoelectric modules (TE-M) is presented. Due to the research activities in recent years, TE-materials become excellent candidates for power generation devices (TEG) which can be used in the mid- and high-temperature range up to 500 °C on the hot side of the TE-M. Now, in order to bring TE-M from laboratory status to industrial applications, it is very important that the intrinsic positive properties of a TEG, such as no moving parts, easy scalability, etc. can be fully exploited through a high long-term stability / reliability.

To quantify reliability, appropriate stress tests / reliability tests must be performed and defective modules must be analyzed for their failure mode and failure cause / failure location using non destructive (NDE) and destructive evaluation (DE) techniques. Failure analysis is a complex process of collecting and analyzing data to determine the failure mode / failure mechanism and location of the failure in a TE-M (root cause failure analysis). The results of failure analysis now allow the weaknesses of the component to be identified and help to understand the mechanisms and causes of failures, making it possible to undertake corrective measures to optimize the product and guarantee its quality and reliability. In this context, a rough distinction between so-called 'soft' and 'hard' failures is helpful. A soft failure means that the TE-M is working, but is out of specification, generally resulting in an increased internal resistance due to degeneration. A hard failure means that the TE-M is completely inoperable, i. e. no current can flow due to delamination or a gap (e. g. defective soldering or broken leg).

In this work we present the applicability of the NDE methods measuring the internal resistance (for soft and hard failures), IR-thermography (for soft failures), scanning acoustic microscopy (for hard failures) and X-ray computed tomography (mainly for hard failures). After NDE, DE methods of embedding the TE-M, cutting, grinding and polishing the surface where applied, followed by the NDE analysis methods using optical microscopy, SEM and EDS to determine the location of the defect.

Acknowledgments

This work was financially supported by the voestalpine Stahl GmbH and Energie AG Oberösterreich Umwelt Service GmbH. The authors would like to thank Peltron GmbH Peltier-Technik for supplying thermoelectric modules free of charge.

9:15 AM EN02/EN08.07

Defects Engineering in Thermoelectric Copper-Based Sulfides Emmanuel Guilmeau; CRISMAT, France

Among the various possibilities offered by the periodic table, copper-rich sulfides represent a formidable source for the discovery of low cost and environmentally benign thermoelectric materials. Copper-rich sulfides form an important class where univalent copper is the dominant element, giving the possibility of creating hole carriers in the conductive "Cu-S" network for the generation of *p*-type thermoelectrics. During this presentation, recent advances in synthetic minerals and new sulphide compounds will be shown. Some peculiar structural features in connection with atomic and nanoscale order/disorder phenomena and defects engineering were carefully examined to establish rules and correlations between the crystal structures, nano-microstructures, electronic structures, vibrational and thermoelectric properties.

9:30 AM EN02/EN08.08

Effect on Thermoelectric and Mechanical Properties of Interstitial Void Filling by Cu in ZrNiSn HH Alloy Shamma Jain^{1,2}, Ajay K. Verma^{1,2,3}, Kishor K. Johari^{1,2}, Christophe Candolfi⁴, Bertrand Lenoir⁴ and Bhasker Gahtori^{1,2}; ¹CSIR-National Physical Laboratory, India; ²Academy of Scientific & Innovative Research (AcSIR), India; ³RMIT University, Australia; ⁴Institut Jean Lamour UMR 7198 CNRS - Université de Lorraine Campus ARTEM, 2 allée Andre Guinier, BP 50840, Nancy 54011, France, France

Widely explored ZrNiSn half-Heusler (HH) alloy has an interpenetrating fcc cubic crystal structure with four vacant positions in the unit cell, where the elemental substitution at these voids by off-stoichiometric composition could play an imperative role in the optimization of electronic transport by tuning the band structure and band gap, as well as it can reduce the phonon transport by interstitial point defect scattering. In the present study, off-stoichiometric compounds are synthesized opting a fast and facile route of arc melting and spark plasma sintering by surplus Cu in ZrNiSn system to fill the available voids at 4d ($\frac{3}{4}$, $\frac{3}{4}$, $\frac{3}{4}$) in the HH unit cell. Here, 0-4% Cu excess was used to easily occupy the vacant site which can improve the thermoelectric properties. The XRD results reflect that up to 2% Cu partially occupied the vacant site. The electronic transport enhances with the Cu excess by increased carrier density due to shifting of fermi level as reflected by reduced chemical potential. Further, this Cu excess of upto 2% significantly reduces the thermal conductivity due to interstitial point defect phonon scattering. The figure-of-merit *ZT* enhances ~ 45% with the peak value 0.81 at 775 K which is the result of interstitial filling of 2% Cu in ZrNiSn. The mechanical properties also improved upto 2% Cu excess, confirming interstitial filling strengthen the mechanical properties.

9:35 AM *EN02.04.02

Materials and Device Strategies for Energy Nanogenerators Pooi See Lee; Nanyang Technological University, Singapore

Tribo- and piezo-electric nanogenerators (TENG and PENG) are deemed as low-cost, and effective distributed energy conversion of mechanical energy to electricity, which allow us to harvest wasted mechanical energy from the environment or human motion. Device design and materials composition are the two important approaches in addressing the challenges in improving the output power of TENG and/or PENG. One of the device engineering involves generation of continuous direct current electricity from dynamic p-n or Schottky junctions to achieve tribovoltaic nanogenerator (TVNG). By incorporating ferroelectricity, we aim to control the interfacial energy band bending to regulate work function for enhanced current output. The materials composition used is a lead-free perovskite-based (3,3 difluorocyclobutylammonium)₂CuCl₄ ((DF-CBA)₂CuCl₄) that is coupled with Al metal to form Schottky junction TVNG.[1] The system provides excellent surface charge modulating capacity and high work function regulation via an electrical poling control. On the other hand, in harnessing mechanical bending motion through PENG, an auxetic structure on polymer substrate was fabricated with 3D printing. A synclastic effect of the auxetic structure is harnessed to achieve bending mode flexible energy harvesting of PENG will be introduced.[2] Further work progress on gas-solid interacted TENG will also be introduced.

References:

1. F. Jiang, G. Thangavel, X. Zhou, G. Adit, H. Fu, J. Lv, L. Zhan, Y. Zhang, P. S. Lee, Adv. Mater. 2023, 35(31), 2302815.
2. X. Zhou, K. Parida, J. Chen, J. Xiong, Z. Zhou, F. Jiang, Y. Xin, S. Magdassi, P. S. Lee, Adv. Energy Mater. 2023, 13(34), 2301159.

Tuesday Morning, April 23, 2024
Room 336, Level 3, Summit

10:30 AM *EN08.01.01

Electronic Transport Simulations in Thermoelectric Materials beyond The Constant Relaxation Time Approximation Neophytos Neophytou¹, Zhen Li¹ and Patrizio Graziosi²; ¹University of Warwick, United Kingdom; ²CNR, Italy

The large variety of complex electronic structure materials and their alloys offer highly promising directions for improvements in ZT originating from the power factor (PF). The electronic structure of novel materials contains rich features such as many valleys (typically included in machine learning descriptors [1]), warped features, elongated features, anisotropic bands, resonant states, topological states, and more. The transport dynamics also involve complex scattering physics. Many theoretical studies provide very useful direction in identifying and optimizing these materials, most of them, however, based on the constant relaxation time approximation, which brings an arbitrary degree of error, both qualitatively and quantitatively.

Here we describe our advanced electronic Boltzmann transport simulator, *ElecTra* [2], together with a method we developed to obtain accurate scattering rates from ab initio calculations. We demonstrate its capabilities in a series of investigations: i) regarding the importance of including all relevant scattering mechanisms in electronic transport computation [3]; ii) regarding the possibility to obtain ultra-high PF in low bandgap materials with highly asymmetric transport properties between the conduction and valence bands [4, 5]; iii) regarding the influence of the shape of the electronic structure with its elongated features and high band anisotropy on the PF, where we show that 2-3x PF variations are observed based on the band shape complexities alone; iv) regarding the possibility of reliably computing transport properties of complex band materials with low symmetry and large unit cells in realistic time scales entirely from first principles.

References

- [1] P. Graziosi, C. Kumarasinghe, N. Neophytou, *ACS Appl. Energy Mater.*, **3**, 6, 5913-5926 (2020)
- [2] P. Graziosi, Z. Li, N. Neophytou, *Computer Physics Communications*, **287**, 108670 (2023)
- [3] P. Graziosi, C. Kumarasinghe, N. Neophytou, *J. Appl. Phys.*, **126**, 155701 (2019)
- [4] P. Graziosi, N. Neophytou, *J. Phys. Chem. C*, **124**, 34, 18462 (2020)
- [5] P. Graziosi, Z. Li, N. Neophytou, *Appl. Phys. Lett.*, **120**, 072102 (2022)

Acknowledgments

This work has received funding from the European Research Council (ERC) under the European Union's Horizon 2020 research and innovation programme (grant agreement No 678763) and from the UK Research and Innovation fund (project reference EP/X02346X/1).

11:00 AM EN08.01.02

The Importance of Electronic Relaxation Times in Complex Fermi Surfaces Øven Andreas Grimenes¹, Ole Martin Løvrvik² and Kristian Berland¹; ¹Norwegian University of Life Sciences, Norway; ²SINTEF Industry, Norway

The difficult task of optimizing the thermoelectric figure of merit (zT) has often been approached by reducing lattice thermal conductivity, such as by nanostructuring or alloying. This strategy has led far, but to engineer even better materials we need to include other strategies. Another popular approach, especially in computational studies, is to engineer band structures that give more favorable electron transport properties. Generally, electron transport is characterized by the transport distribution, that is, the density of states (DOS), where each state is weighted by the square of its group velocity times the relaxation time of that state. A rapidly increasing transport distribution next to the band gap tends to give a higher zT . By aligning bands and valleys, the electronic structure can achieve a higher density of states without a reduction in group velocity. In the commonly used constant relaxation time approximation (CTRA) this band alignment will always be favorable for zT . By more accurate modeling of the scattering rates, we show that moving beyond CTRA is vital to get accurate predictions of zT . The alignment of multiple bands or valleys will generally lead to more electron scattering and lower relaxation times. This effect is especially prominent for materials with complex "extended" Fermi surfaces that result in a large scattering space for electrons.

We use first principle methods to investigate numerous complex semiconductors with unusual band structures and give extra attention to the specific case of the full-Heusler CsK2Sb. This material has an exotic Fermi surface with extended 2D-like features. We also predict a very low predicted lattice thermal conductivity with the Temperature Dependent Effective Potential (TDEP) method. This leads to a very high predicted zT under CTRA. With more accurate modeling of the electric transport properties with scattering rates modeled in AMSET the expected zT is reduced, revealing the shortcomings of the constant relaxation time approximation and the necessity to move beyond it. We also show this trend in several other materials with complex Fermi surfaces.

Finally, we present a counterexample, ZrNiSn. The three-fold degenerate conduction band minimum is not promising under CTRA. However, the simple shape of the Fermi surface and large k -space distance between its Fermi pockets results in relaxation times much longer than the 10 fs often used in CTRA. This increases the n-type zT of ZrNiSn significantly. We conclude that while complex Fermi surfaces indeed can provide very good electronic transport properties, it is essential to include estimations for scattering rates in such materials. These results can help aid the design of future thermoelectric materials with superior properties.

11:15 AM EN08.01.03

High-Throughput Thermoelectric Materials Screening by Novel Deep Convolutional Neural Network with Fused Orbital Field Matrix and Composition Descriptors Ming Hu; University of South Carolina, United States

Thermoelectric materials assist in generating or harvesting energy through converting waste heat into reusable electricity. Thermoelectric materials are also widely used in real-world applications, such as refrigerators and cooling electronics. However, most popular and known thermoelectric materials to date were proposed and found by intuition, mostly through experiments. Unfortunately, it is extremely time and resource consuming to synthesize and measure the thermoelectric properties through trial and error experiments. Here, we develop a convolutional neural network (CNN) classification model that utilizes the fused orbital field matrix (OFM) and composition descriptors to screen a large pool of materials to discover new thermoelectric candidates with power factor higher than $10 \mu\text{W}/\text{cmK}^2$. The model used a few thousand data generated by density functional theory (DFT) coupled with AMSET, a package for calculating electronic transport properties that does not assume constant relaxation time for electrons, thus ensuring more reliable electronic transport properties calculations. The classification model was also compared to traditional machine learning algorithms, such as light gradient boosting and random forest. With the classification model we screened >35,000 structures with non-zero band gap from the Open Quantum Materials Database (OQMD). We identified lots of potential high performance thermoelectric materials with $ZT > 1$ across wide temperature range for both n- and p-type doping with

different doping concentrations, including quaternary Heuslers, half-Heuslers, and more material families. Insight into the correlation between high power factor and some representative material descriptors was also gained by feature importance analysis and maximal information coefficient, which provides new simple routes for fast screening thermoelectrics from large-scale material pool in the future.

11:30 AM EN08.01.04

Composition Engineering of Thermoelectric Performance of High-Entropy Ge-Te Based Alloys by First Principles Han Meng, Masato Ohnishi and Junichiro Shiomi; The University of Tokyo, Japan

The thermoelectric effect offers a promising pathway for energy harvesting through direct converting waste heat into electricity, however, it is mainly limited by the performance of thermoelectric material evaluated by figure of merit $ZT = S^2\sigma/\kappa$, where S , σ , and κ are Seebeck coefficient, electrical conductivity, and total thermal conductivity, respectively. To pursue good thermoelectric performance, various successful strategies have been proposed to enhance electrical transport properties through the creation of ordered band structure and reduce lattice thermal conductivity by introducing disordered atomic arrangement, following the phonon-glass electron-crystal concept. However, further improvement in thermoelectric performance requires the decoupling of electrical and thermal transport properties and their simultaneous optimization.

High-entropy material, where a stabilized structure coexists with disordered atomic arrangement, hold tremendous potential for enhancing thermoelectric performance. This potential arises from the ability to maintain long-range order in atomic arrangement to support efficient electrical transport, while simultaneously introducing short-range disorder through lattice distortion, which effectively scatter phonons and lead to low thermal conductivity. The GeTe that stabilizes as a rhombohedral lattice at room temperature by distorting high-temperature cubic structure, has been demonstrated to exhibit high thermoelectric performance. Most recently, a significant improvement in ZT , reaching 2.7 at 750 K, has been achieved in high-entropy GeTe-based alloys. This accomplishment was realized in several sample with specific composition by increasing the entropy, which enhanced crystal symmetry to promote delocalization of electron distribution and concurrently localize phonons to effectively hinder the propagation of transverse phonons. However, the high-entropy concept also offers a means to create crystals with an extended chemical composition range, providing ample room for optimizing electronic properties by modulating phase composition and band structure across a wide spectrum of chemical composition.

In this study, we take a significant stride towards engineering the composition for thermoelectric performance of high-entropy GeTe-based alloys. To predict the formation energy, we employed cluster expansion to construct a machine learning model, which was trained and validated using datasets generated from first-principles calculations. Through the Monte Carlo simulation, the configurations with low formation energy were suggested by sampling the structure for various composition, incorporating silver, lead, and antimony atoms as solutes. We designed seven distinct composition-changing paths that involved the alloying of one element, two elements, and all elements, allowing the thorough investigation on the impact of alloying each individual element component as well as their collective influence on ZT . For each composition, the average ZT was calculated from five possible configurations by semi-classical Boltzmann transport theory within relaxation time approximation. The analysis of electrical transport properties through electronic band structure and charge distribution, along with the examination of thermal conductivity via phonon dispersion relations and phonon properties, unveiled the underlying mechanism responsible for the compositional dependence of ZT . This study not only demonstrates the potential for optimizing thermoelectric performance of GeTe-based alloys, but also encourages further exploration of high-entropy alloys in the future.

11:45 AM EN08.01.05

Discovery of Multi-Anion Antiperovskite $X_6\text{NFSn}_2$ ($X = \text{Ca}, \text{Sr}$) as Promising Thermoelectric Materials by Computational Screening Dan Han^{1,2,3}, Bonan Zhu², Zenghua Cai⁴, Kieran Spooner^{2,3}, Stefan S. Rudel¹, Wolfgang Schnick¹, Thomas Bein¹, David O. Scanlon^{2,3} and Hubert Ebert¹; ¹University of Munich (LMU), Germany; ²University College London, United Kingdom; ³University of Birmingham, United Kingdom; ⁴Suzhou University of Science and Technology, China

The thermoelectric performance of existing perovskites lags far behind that of state-of-the-art thermoelectric materials such as SnSe.^{[1], [2]} Despite halide perovskites showing promising thermoelectric properties, namely, high Seebeck coefficients and ultralow thermal conductivities, their thermoelectric performance is significantly restricted by low electrical conductivities. Here, we explore new multi-anion antiperovskites $X_6\text{NFSn}_2$ ($X = \text{Ca}, \text{Sr}$ and Ba) via B-site anion-mutation in antiperovskite and global structure searches, and demonstrate their phase stability by first-principles calculations. Ca_6NFSn_2 and Sr_6NFSn_2 exhibit decent Seebeck coefficients and ultralow lattice thermal conductivities ($< 1 \text{ W m}^{-1} \text{ K}^{-1}$). Notably, Ca_6NFSn_2 and Sr_6NFSn_2 show remarkably larger electrical conductivities compared to the halide perovskite CsSnI_3 . The combined superior electrical and thermal properties of Ca_6NFSn_2 and Sr_6NFSn_2 lead to high thermoelectric figure of merit $ZT \sim 1.9$ and ~ 2.3 at high temperatures. Our exploration of multi-anion antiperovskites $X_6\text{NFSn}_2$ ($X = \text{Ca}, \text{Sr}$) realizes the “phonon-glass, electron-crystal” concept within the antiperovskite structure.^[3]

[1] Zhou C, Lee Y K, Yu Y, et al. Nature materials, 2021, 20(10): 1378-1384.

[2] Lee W, Li H, Wong A B, et al. Proceedings of the National Academy of Sciences, 2017, 114(33): 8693-8697.

[3] Han D, Zhu B, Cai Z, Spooner B, Rude S, Schnick W, Bein T, Scanlon D and Ebert H, Matter., 2023, submitted.

SESSION EN08.02: Novel Materials and Half-Heusler Alloys

Session Chairs: Ran He and Paz Vaquero

Tuesday Afternoon, April 23, 2024

Room 336, Level 3, Summit

1:30 PM *EN08.02.01

Engineering Electronic Properties of Thermoelectric Semiconductors Jeff Snyder; Northwestern University, United States

Engineering Electronic Properties of Thermoelectric Semiconductors

G. Jeffrey SNYDER

Department of Materials Science and Engineering, Northwestern University

jeff.snyder@northwestern.edu

thermoelectrics.matsci.northwestern.edu

Thermoelectric semiconductors often have complex electronic properties yet they can be modeled with a simple effective mass model. Good thermoelectric materials require a high weighted mobility [1] which serves as the electronic component to the thermoelectric quality factor [2] that determines peak zT . Often complex band structures with multi-valley Fermi surfaces are associated with high weighted mobility. This complexity arises from orbital chemistry as well as structure. Band convergence combined with the physics of avoided crossings can also be used to explain the band structures and provide strategies for band engineering Half Heusler materials [6].

Many thermoelectric materials such as Bi₂Te₃ are topological insulators (TI). The correlation can be understood in that the band inversion that causes TI can lead to band warping that leads to high valley degeneracy and low transport mass. [4]

In some systems the Fermi surface pockets can be anisotropic and even non-ellipsoidal, such as the tubes of Fermi surface found in SrTiO₃ and Pb and Ge Chalcogenides [5]. Tubes or sheets of Fermi surface rather than ellipsoidal pockets leads to a density of states like 1D or 2D low dimensional materials. By engineering the orbital chemistry complex behavior and unusual properties can be devised even in 3D materials.

[1] Snyder et al. *Advanced Materials*, 32, 2001537 (2020)

[2] X. Y. Zhang et al., *Science Advances* 6, (2020)

[3] Snyder et al. *Advanced Functional Materials*, 202112772 (2022)

[4] Toriyama et al. *Cell Reports Physical Science* 4, 101392 (2023)

[5] M. K. Brod et al, *Journal of Materials Chemistry A*, 9, 12119, (2021)

[6] M. K. Brod et al, *MRS Bulletin* 47, 573–583 (2022)

2:00 PM EN08.02.02

Zn_{0.5}Ti_{0.5}NiSb – A New Aliovalent Half-Heusler Alloy with Intrinsic Low Thermal Conductivity Blair F. Kennedy¹ and Jan-Willem Bos²; ¹Heriot-Watt University, United Kingdom; ²University of St Andrews, United Kingdom

Half Heusler (HH) alloys are leading contenders for thermoelectric power generation and cooling. Traditional XYZ HH materials are characterised by large electronic power factors, $S^2\sigma$, and are limited by high lattice thermal conductivity, κ_{lat} , which limits the achievable figure of merit, zT .¹

Recently a new class of HH materials has emerged that uses mixtures of aliovalent elements. The archetypal example is the TiFe_{0.5}Ni_{0.5}Sb family, which is a mixture of 17 electron TiFeSb and 19 electron TiNiSb. Hence, an equal mixture of these ternary systems achieves the required average 18 valence electron count required for semiconducting behaviour. In comparison to regular XYZ materials, these complex compositions are characterized by low κ_{lat} and modest $S^2\sigma$, leading to zT approaching unity.² This approach is general, and can also be applied to the X and Z sites, leading to work on X'_{0.5}X''_{0.5}YZ and XYZ'_{0.5}Z''_{0.5} compositions by multiple groups.³

As part of this recent new direction of research, this contribution is focused on the aliovalent Zn_{1-x}Ti_xNiSb system, which links 17 electron ZnNiSb with 19 electron TiNiSb. The x = 0.5 composition has exactly 18 valence electrons. Samples were prepared between 0.40 ≤ x ≤ 0.65; with x < 0.4 not accessible under the used conditions, whilst Ti-rich samples can likely be prepared over the full range (to x = 1). This difference occurs because TiNiSb forms with Ti vacancies and is close to an 18-electron system, hence removing the electronic driving force for insolubility.

In terms of thermoelectric properties, the samples are characterised by very low κ_{lat} , $\kappa_{lat,340K} = 2.5 \text{ W}\cdot\text{m}^{-1}\cdot\text{K}^{-1}$, comparable for all investigated samples. The electronic response suggests a small bandgap, $E_g = 0.4 \text{ eV}$, with evidence for bipolar transport. Varying the composition away from x = 0.5 leads to a transition towards p- (x < 0.5) or n-type (x > 0.5) degenerate semiconducting behaviour. The best observed performance is $zT = 0.18$ for p-type Zn_{0.6}Ti_{0.4}NiSb and $zT = 0.33$ for n-type Zn_{0.4}Ti_{0.6}NiSb.

The origin for the low κ_{lat} in these materials is not fully resolved. Typically, mass and strain disorder are the main drivers of phonon scattering. However, for the aliovalent HH materials, atomic mass and size differences are typically small, whilst the velocity of sound is only about 10-20% reduced compared to the XYZ materials. We have used synchrotron X-ray total scattering and pair distribution function analysis to probe the local structure of Zn_{0.5}Ti_{0.5}NiSb. This confirms that there is not a large source of local lattice strain, e.g. the Ti-Ni and Zn-Ni distances are comparable. Hence, the structure does not substantially deviate from the average unit cell obtained from diffraction. This suggests that differences in bond strength (bond disorder) may play a crucial role in the low κ_{lat} in the aliovalent HH materials.

References

1. R. J. Quinn and J.-W. G. Bos, *Materials Advances*, 2021, 2, 6246-6266.

2. Z. Liu, S. Guo, Y. Wu, J. Mao, Q. Zhu, H. Zhu, Y. Pei, J. Sui, Y. Zhang and Z. Ren, *Advanced Functional Materials*, 2019, 29, 1905044.

3. P.-F. Luo, S. Dai, Y. Zhang, X. Liu, Z. Li, J. Zhang, J. Yang and J. Luo, *Journal of Materials Chemistry A*, 2023, 11, 9125-9135.

2:15 PM EN08.02.03

Thermoelectric Compounds TZnSb, T = Ti to Ni ? Peter F. Rogl¹, Raimund Podloucky¹, Gerda Rogl¹ and Ernst Bauer²; ¹Univ Wien, Austria; ²TU Wien, Austria

We present results of a combined experimental and first-principles study on compounds TZnSb (T=Ti to Ni). Physical properties i.e. electrical resistivity (4.2 - 800 K), Seebeck coefficient (300 - 800 K), specific heat (2 - 110 K), Vickers hardness and elastic moduli (RT) have been defined for the aforementioned polycrystalline single-phase materials. From X-ray single crystal and Rietveld analyses all these phases, of which TiZnSb and Cr_{1-x}ZnSb are novel representatives, were found to crystallize with the ordered MnAlGe-type (space group *P4/nmm*), whereas NiZnSb is a half Heusler phase. The thermal stability has been investigated by differential thermal analysis.

For the polycrystalline compounds TZnSb (relative densities >90%) the electrical resistivity is gradually changing from typical metallic behaviour (TiZnSb) to semiconductor-like features with resistivities decreasing with rising temperature (T=V,Cr). Specific heat curves Cp vs T and Cp/T vs T² of TiZnSb and CrZnSb conform with a simple metal behaviour revealing Sommerfeld coefficients of 6.4 (1) mJ/molK² and 12.4 (2) mJ/molK² and low-temperature Debye-temperatures of 273(5) K and 245(5) K, respectively.

Rather low Seebeck coefficients ($|S_V| < 30 \mu\text{V/K}$), power factors ($\text{pf} < 0.05 \text{ mW/mK}^2$) and an estimated thermal conductivity of $\lambda < 6 \text{ mW/(cmK)}$, yield low thermoelectric figures of merit consistent with the rather metallic behavior of the materials. It should be noted that TiZnSb and VZnSb reveal negative Seebeck values with shallow minima at about 500 K, whereas CrZnSb exhibits a positive Seebeck coefficient which gradually tends towards zero at 800 K. Indentation hardness and elastic moduli of TZnSb were extracted employing the accelerated mechanical property mapping (XPM) mode and were found to be within $5.5 \pm 1 < H_V < 6 \pm 1 \text{ GPa}$ and $E = 100 \pm 10 \text{ GPa}$ for T=Ti, V, but somewhat lower $E = 80 \pm 10 \text{ GPa}$ for CrZnSb. The Poisson ratio in all cases was $\nu = 0.24$ (taken from DFT calculations).

A detailed analysis of the structure types TZnSb adopted by the 3d transition elements clearly reveals that electropositive elements T=Ti, V, Cr, Mn, Fe crystallize with the tetragonal MnAlGe-type but with rising electronegativity T=Fe, Co, Ni incline to the cubic half-Heusler structure or to a (2a×2a×2a) superstructure of it. The case of Fe with three modifications constitutes the border range.

A variety of physical properties are derived from first principles such as structural and magnetic structural stabilities, charge transfer and atomic size,

elastic properties, electronic structure (density of states, band structure), electronic transport properties (Seebeck coefficient and resistivity) within Boltzmann's transport theory. All the results are obtained for fully relaxed structural parameters. Concerning magnetic ordering the in-plane antiferromagnetic ordering of T-magnetic moments in the tetragonal MnAlGe-type is dominant. The influence of T- vacancies for VZnSb and Cr_{1-x}ZnSb are investigated and the results emphasize the role of such vacancies.

2:30 PM EN08.02.04

Mapping The Configuration Space of Intrinsic Properties and Dopability of Half-Heusler Compounds [Angela Pak](#)¹, [Kamil Ciesielski](#)², [Eric Toberer](#)² and [Elif Ertekin](#)³; ¹University of Illinois at Urbana Champaign, United States; ²Colorado School of Mines, United States; ³University of Illinois at Urbana-Champaign, United States

In this work, we utilize computational approaches to navigate the half-Heusler phase space to identify patterns in how properties relevant to thermoelectric (TE) materials vary with chemistry. Identifying novel TE materials is a challenge due to the unique, and typically disparate, set of intrinsic properties required (thermal and electronic conductivity) together with the need to access high p-type or n-type carrier concentrations. Although half-Heuslers have long been known as candidate TE materials, the hundreds of compositions that have been experimentally realized represent a small proportion of the possible chemistries. Of these possible chemistries, we focus on the 1,126 that are expected to be semiconductors based on the "18 valence electron rule". In addition to fundamental understanding, design rules that link chemistry to indicators of TE performance such as carrier mobilities, band edge density of states, band edge degeneracy, and thermal conductivity are useful for accelerated materials discovery. Towards identifying these design rules, we evaluate candidate half-Heusler transport properties using first-principles simulations and semi-empirical models. This approach utilizes a filtering scheme that successively eliminates compounds based on their electronic structure, TE performance, stability, dopability, and transport properties. The analysis yields trends across chemical phase space. For instance, Rh and V-containing chemistries consistently have strong n-type TE performance, Ni and Sb-containing chemistries are consistently strong p-type performers, and Ta, or W-containing chemistries are good for both p and n-type performance. Furthermore, good n-type TE is found to arise from chemistries exhibiting high electronic carrier mobility as a result of low band mass, while for p-type performance a high band degeneracy at the valence band edge further enhances performance. Chemistries that exhibit good TE performance for both n and p-type were found to have comparatively low thermal conductivities relative to what is typical for half-Heuslers. This presentation will focus on the key results of the computational analysis and a comparison to experiment, the features of half-Heusler compounds that make them particularly suitable for TE applications, and ongoing work in stochastic assessment of trends using machine learning.

2:45 PM EN08.02.05

Effect of Magnetic Entropy in The Thermoelectric Properties of Fe-Doped Fe₂VAl Full-Heusler [Tarachand Tarachand](#)¹, [Naohito Tsujii](#)¹, [Takao Mori](#)^{1,2}, [Fabian Garmroudi](#)³ and [Ernst Bauer](#)³; ¹National Institute for Materials Science, Japan; ²Graduate School of Pure and Applied Sciences, University of Tsukuba, Japan; ³Institute of Solid State Physics, Technische Universität Wien, Austria

Spin entropy is involved in the transport of heat/charge carriers in magnetic materials, and can provide new opportunities to improve the conversion efficiency of thermoelectric materials over that of the conventional case [1-3]. Here, we have explored the effect of magnetic entropy on thermoelectric properties of well-characterized Fe-doped full-Heusler, Fe_{2-x}VAl_{1-x} with x = 0-0.1. These samples are prepared by arc melting, spark plasma sintering and annealing, producing high-density crystalline products. The low-temperature magneto-thermoelectric measurement shows exotic results, including a significantly high power factor near 300 K.

The itinerant weak ferromagnetic behavior of studied samples is confirmed from the magnetization. A systematic increase in magnetic transition temperature (T_c; 40 K to 223 K) and saturation magnetization (M_s; 0.13 to 0.41 μ_B/Fe) with increasing Fe doping (x = 0 to 0.1) is observed. Applying a magnetic field causes a clear suppression in the magnitude of thermopower (S) and S/T (entropy term) with a negative magnetoresistance near the T_c for all the samples, demonstrating a clear effect of spin fluctuation [2]. The spin fluctuation leads to an enhancement in S of ~34% than diffusion thermopower and hence a whopping enhancement in thermoelectric power factor of 18% for x=0.1 at the T_c. The temperature-dependent behavior of S ruled out the contribution of magnon drag. Interestingly, Fe doping can shift the T_c towards room temperature and lead to a spin fluctuations induced enhancement in the S, but, it also increases the overall carrier density and hence deteriorates the magnitude of S. Multiparabolic band model fitting reveals the formation of additional spin states with large effective mass near the Fermi level, which can be eliminated/suppressed by applying the magnetic field. Callaway model fitting of thermal conductivity reveals Fe doping increases the number of point defects, causing a significant reduction in lattice thermal conductivity. This study demonstrates the role of spin fluctuation in enhancing the thermopower/ thermoelectric performance of Fe-doped Fe₂VAl and opens a vista for the strategy's applicability for various thermoelectric materials.

References

- [1] S. Hébert, R. Daou, A. Maignan, S. Das, A. Banerjee, Y. Klein, C. Bourges, N. Tsujii, T. Mori, *Sci. Technol. Adv. Mater.*, **22**, 583-596 (2021).
- [2] N. Tsujii, A. Nishide, J. Hayakawa, T. Mori, *Sci. Adv.* **5**, eaat5935 (2019).
- [3] K. Vandaele, S. J. Watzman, B. Flebus, A. Prakash, Y. Zheng, S. R. Boona, J. P. Heremans, *Materials Today Physics*, **1**, 39-49 (2017).

Acknowledgments

This work was supported by the Japan Science and Technology Agency (JST), MIRAI program grant (JPMJMI19A1).

3:00 PM BREAK

SESSION EN08.03: Materials for Thermoelectric Modules

Session Chair: Jeff Snyder

Tuesday Afternoon, April 23, 2024

Room 336, Level 3, Summit

3:30 PM *EN08.03.01

Beyond Bismuth Telluride: Magnesium-Based Compounds Redefine Thermoelectric Excellence [Pingjun Ying](#), [Heiko Reith](#), [Kornelius Nielsch](#) and [Ran He](#); Leibniz-Institut für Festkörper- und Werkstoffforschung, Germany

Thermoelectric (TE) technology converts heat directly into electricity, and is a promising source of clean electricity. Commercial TE modules are based on Bi₂Te₃ compounds because of their unrivalled TE properties at low-grade heat-related temperatures (<550 K). However, the scarcity of elemental Te severely limits the applicability of these modules. Here, we present the performance of TE modules assembled from Te-free compounds, including p-type

MgAgSb and *n*-type Mg₃(Sb,Bi)₂, using a simple, versatile and therefore scalable processing routine. We demonstrate module-level conversion efficiencies of 3% and 8.5% for temperature differences of 75 K and 260 K, respectively, as well as maximum cooling of 72 K when used as a cooler. These proofs of principle will pave the way for robust, high-performance and sustainable solid-state power generation and cooling to replace the highly rare and toxic Bi₂Te₃.

4:00 PM *EN08.03.02

Simultaneous Enhancement of Efficiency and Output Power in GeTe/Mg₃Sb₂-Based Thermoelectric Generator Tsutomu Kanno; Panasonic Holdings Corporation, Japan

Recently, there have emerged many reports on thermoelectric generators (TEGs), claiming record-breaking efficiency values. From a viewpoint of practical applications, a problem is the trade-off between the efficiency and the output power in the presence of electrical contact resistance. Thus, high efficiency does not necessarily lead to high cost-performance (W/\$).

Here, to break the trade-off, we develop GeTe/Mg₃Sb₂-based TEGs with minimal electrical contact resistance and total thermal resistances. Our TEG allows for simultaneous boost in the efficiency and the output power (10.1% and 1.94 W/cm²), owing to excellent material performance and high input heat flow [1]. We also discuss a simple and reliable protocol to avoid errors in efficiency measurement [2].

References

[1] F. Ando, H. Tamaki, Y. Matsumura, T. Urata, T. Kawabe, R. Yamamura, Y. Kaneko, R. Funahashi, T. Kanno, Dual-boost thermoelectric power generation in a GeTe/Mg₃Sb₂-based module, *Materials Today Physics*. (2023) 101156.

[2] T. Kanno, F. Ando, Y. Matsumura, T. Urata, H. Tamaki, R. Funahashi, Avoiding errors in efficiency measurements of high-performance thermoelectric generator modules: Toward best practices for materials researchers, *Materials Today Physics*. 36 (2023) 101171.

4:30 PM EN08.03.03

Implication of Alloying The Anionic Framework in Mg₃Sb₂ for *p*-Type Zintl Thermoelectrics Nagendra S. Chauhan and Takao Mori; NIMS, Japan, Japan

Solid solutions of *n*-type Mg₃Sb₂ has garnered growing attention due to its remarkable thermoelectric potential for harnessing low grade waste heat. However, achieving high performing *p*-type conduction around room temperature has remained challenging, fundamentally due to greater degeneracy in conduction band relatively to the valence band. As a Zintl compound, β-Mg₃Sb₂ crystal structure constitutes of an anionic framework of double layer [Mg₂Sb₂]²⁻ wherein Mg²⁺ cations are located between these layers. In this work, we present the implication of (Bi, Sn, Ge, Te) alloying at the anionic framework of Mg₃Sb₂ solid solutions to favorably tune the *p*-type conduction for attaining higher power factors by band engineering. Altering the anionic framework through alloying resulted in modifying the electronic structure to enhance the valley degeneracy at the top of valence bands. Simultaneously, the prospects of enhancing phonon scattering by the distorted lattice, point defects, and nano-precipitates was examined for attaining lower lattice thermal conductivity at near room temperature. The alloyed *p*-type Mg₃(Sb,Bi,Ge,Sn,Te)₂ with its tailored properties, shows promising potential as an economical alternative to α-MgAgSb, thereby facilitating the practical realization of Mg₃Sb₂-based thermoelectric power generators for harnessing low-grade heat.

4:45 PM EN08.03.04

Highly Improved Thermoelectric Performance in Periodically Ablated BiSbTe: WSe₂ Nanostructured Films Karan Giri, Yan-Lin Wang, Ling-Chun Chao, Chuan-Wen Wang, Hung-Shuo Chang, Wen-Chieh Hsieh and Chun-Hua Chen; National Yang Ming Chiao Tung University, Taiwan

An innovative technique has been developed to combine two different layered materials, bismuth antimony telluride (BiSbTe) and tungsten diselenide (WSe₂), which are well-known for their great efficacy in waste heat recovery and extremely low thermal conductivity, respectively. To enhance the thermoelectric properties even more, WSe₂ as a secondary target is encapsulated periodically in the primary target Bi_{1.5}Sb_{0.5}Te₃ using a pulse laser deposition technique. The WSe₂ for the first time, is co-ablated with the BiSbTe at four distinct deposition temperatures, resulting in hetero-nanocomposite thin films. Various characterization techniques are employed to determine thermoelectric properties. Both x-ray diffraction (XRD) and Raman spectroscopy validate the existence of WSe₂ and Te as heterogeneous phases. The sharp XRD peaks observed indicate strong crystallinity and evidence that the crystals are grown in a highly *c*-oriented manner. The electrical transport properties are greatly improved due to the optimized hole concentration, resulting in significantly high electrical conductivity in hundreds to thousands of S cm⁻¹ for the samples grown at 573 K and 723 K, respectively. Furthermore, the room temperature and temperature-dependent Seebeck coefficient measurements exhibit highly optimized values, providing evidence of a satisfactory trade-off between the thermoelectric parameters. The overall outcome is a significant increase in the power factor which is computed up to 156 μW cm⁻¹ K⁻², demonstrating outstanding room temperature thermoelectric performance. In addition to electrical characteristics, the specimens have a low electronic thermal conductivity, *k_e*. The calculated room temperature *k_e* values are 0.10 W m⁻¹ K⁻¹ and 0.87 W m⁻¹ K⁻¹ for the samples grown at 573 K and 723 K, respectively. Additionally, a qualitative measurement of lattice thermal conductivity was conducted through Raman spectroscopy under different laser power conditions, providing enough room for the highly improved figure of merit value. The enhanced thermoelectric transport characteristics of the periodically encapsulated WSe₂ in the BiSbTe matrix place it among the best thermoelectric materials with excellent performance for thermoelectric conversion, such as solid-state refrigeration and power generation.

SESSION EN08.04: Thermal Transport and Phonon Dynamics

Session Chairs: Eleonora Isotta and Lilia Woods

Wednesday Morning, April 24, 2024

Room 336, Level 3, Summit

8:15 AM EN08.04.01

Experimental Demonstration of Inverse-Designed Nanostructures with Ultra-Low Thermal Conductivity Giuseppe Romano; Massachusetts Institute of Technology, United States

Tailoring heat transport at the nanoscales is crucial to several applications, such as thermal energy harvesting and heat management. First-principles calculations and mesoscales models, such as the Boltzmann transport equation (BTE), have provided tremendous help in understanding the effect of material composition on thermal transport. However, materials engineering in this space is mostly done with trial. In this talk, we will report numerical

optimization and experimental demonstration of nanopatterned Si membranes with ultra-low thermal conductivity. Shape optimization is performed by density-based topology optimization, a technique commonly employed for elastic materials, and the adjoint mode-resolved BTE [1]. The fabrication of the optimized structures is carried out with Focused Ion Beam, and the effective thermal conductivity is measured with the thermal transient grating technique. Manufacturing constraints, such as minimum length scales, are taken into account by adding suitable constraints to the optimization algorithm. With a patterning resolution of about 70 nm and a film thickness of 50 nm, we record a thermal conductivity as low as 1.7 W/mK. Exploiting a deep synergy between theory and experiments, our work pushes the limits of low-thermal-conductivity materials, opening up novel routes for high-efficiency thermoelectric materials.

[1]G. Romano and S.G. Johnson. *Structural and Multidisciplinary Optimization* 65, 297

8:30 AM *EN08.04.02

Simulations Guiding Phonon Thermal Conductivity Reductions [Lucas Lindsay](#); Oak Ridge National Laboratory, United States

Minimizing lattice thermal conductivity has been a goal for engineering enhanced thermoelectric figures of merit for over a decade, both intrinsically (e.g., material choices) and extrinsically (e.g., defects and nanostructuring). In the context of numerical simulations, we discuss phonon scattering details that underlie thermal resistance in bulk, nanostructured, and alloyed materials. We highlight promising routes for decreasing lattice thermal conductivity, limitations on these, and challenges faced in simulations of realistic materials. We use large-scale mass disorder models, temperature-dependent effective potentials, density functional theory, and Boltzmann and Wigner transport methodologies to understand how alloy disorder, temperature renormalization, correlations, and phonon dispersion features govern thermal transport in materials of potential interest for thermoelectric applications.

L.L. acknowledges support from the U. S. Department of Energy, Office of Science, Basic Energy Sciences, Materials Sciences and Engineering Division.

9:00 AM EN08.04.03

Thermoelectric Power Factor Enhancement in Hybrid Solid/Liquid Porous Material Systems: A Simulation Approach Pankaj Priyadarshi, Neophytos Neophytou and [Vassilios Vargiamidis](#); University of Warwick, United Kingdom

Prior experimental work has demonstrated the possibility of large improvements in the thermoelectric (TE) power factor of porous media when intercalated with electrolytes filling their pores [1]. Surprisingly, in many cases both the electrical conductivity and Seebeck coefficient were increased, offering large improvements to the power factor (PF). These improvements were attributed to charge exchange between the solid medium and the electrolyte, with strong dependence on the type of solid and the type of electrolyte used.

In this work we examine theoretically this complex system and provide directions for optimization. For this, we have developed an advanced simulator and theoretical models to accurately describe the TE behavior of a hybrid porous-solid/electrolyte system in the presence of large degree of nanostructuring. We have developed a novel Monte Carlo algorithm specifically designed for large scale thermoelectric simulations in porous nanostructured media [2]. Our code includes many features beyond the state-of-the-art in Monte Carlo simulations, which allow for drastic computational savings of at least an order of magnitude, making large scale simulations feasible. We then developed a model for the addition of the electrolyte within the pores of the solid medium, whose interaction with the solid is computed in a self-consistent manner by solving the Poisson equation. This provides the charge exchange and band variations that the solid thermoelectric material experiences. Once this is achieved, the Monte Carlo simulator provides the thermoelectric coefficients.

We show that it is possible to achieve very high power factor improvements using this solid/liquid hybrid material direction. This happens in two ways: 1) Appropriate choice of an electrolyte can cause favourable band bending in the solid material, resulting in increased carrier density and conductivity, at the levels which optimize the power factor. 2) Rather than relying on intentional doping, we enhance charge density within the material domain by the use of the electrolytes into the pores. This avoids the strong ionized impurity scattering associated with the doping typically required, since now this is achieved electrostatically.

Finally, the simulator we present goes beyond this system, and can be generally used to enable the understanding of transport in highly disordered nanostructured TE materials in a very effective and efficient way.

Acknowledgements:

This project has received funding from the European Union's Horizon 2020 research and innovation programme under grant agreement No 863222 (UncorrelaTEd).

References:

- [1] L. Marquez-Garcia, B. Beltraan-Pitarch, D. Powell, G. Min, and J. Garcia-Cannadas, *ACS Applied Energy Materials* 1, 254 (2018)
- [2] Pankaj Priyadarshi and Neophytos Neophytou, 'Computationally efficient Monte Carlo electron transport algorithm for nanostructured thermoelectric material configurations,' *Journal of Applied Physics* 133, 054301 (2023).

9:15 AM EN08.04.04

Thermal Conduction Pathways within Complex Polycrystalline Microstructures [Younggil Song](#), Nick C. Du, Dong-Xia Qu and Tae Wook Heo; Lawrence Livermore National Laboratory, United States

The effective thermal conductivity (TC) of a material is determined by various microstructural factors. Different phases in a material often have distinct thermal conductivities and their geometrical configurations dictate the thermal pathway. In addition, the thermal resistance of the crystalline surface disturbs the thermal transport, while it can be enhanced by the crystalline surface coated by a high conductive material. Due to these various and complicated factors, investigations for effective TCs within polycrystalline microstructures have been limited to the controlled microstructures under selected TC regimes. In this study, we use the numerical method to estimate effective TCs within complex multi-phase systems, which are validated using experimental measurements. For simulations, our comprehensive mesoscale model [1, 2] is used to investigate microstructure-aware effective TC variations within porous materials. The model can compute effective TC within realistic digital microstructures with diffuse interfaces using the FFT method, and the simulation results show quantitative agreement with the experiments [1]. In order to characterize the TC behaviors for porous microstructures, we carried out simulations with wide TC ranges of both the gas and the solid phases. The simulations show two different regimes for the TC variations due to (i) the porosity of a microstructure and (ii) the TC difference between the two phases. We suggest the semi-analytical model by introducing structure and intensification factors to capture the effective TC variations [2]. Additionally, we simulated the effective TCs for a ternary system (Fe, Fe₂O₃, and Air) within porous microstructures, which show reasonable agreement with experiments. Moreover, our simulation method can be extended to evaluate the effective TCs by varying additives and their topological features. We expect our combined experimental, analytical, and numerical approach can shed light on how the effective TC of a complex microstructures can be tailored, allowing for better designing materials microstructures for improved thermal conductivities under the wide range of operation conditions.

This work was performed under the auspices of the U.S. Department of Energy by Lawrence Livermore National Laboratory under Contract DE-AC52-07NA27344.

[1] D.-M. Kim et al., *Enhancement of effective thermal conductivity of rGO/Mg nanocomposite packed beds*, Intern. J. Heat Mass Transf. 192 (2022) 122891.

[2] Y. Song and T.W. Heo, *Mesoscale modeling and semi-analytical approach for the microstructure-aware effective thermal conductivity of porous polygranular materials* (Submitted, <http://dx.doi.org/10.2139/ssrn.4574964>).

9:30 AM EN08.04.05

From Rattling to Incipient Ionic Conductivity: Neutron Scattering Studies of Tetrahedrite Paz Vaqueiro¹, Sebastian Long¹, Shripama Mukherjee¹, David Voneshen² and Anthony V. Powell¹; ¹University of Reading, United Kingdom; ²ISIS Pulsed Neutron and Muon Source, Rutherford Appleton Laboratory, United Kingdom

The thermoelectric performance of tetrahedrites, which are minerals composed predominantly of environmentally-friendly and abundant copper and sulfur, is currently attracting considerable interest. Tetrahedrites, which are *p*-type materials with low lattice thermal conductivities, crystallise in a collapsed sodalite structure in which corner-sharing CuS₄ tetrahedra form cages. Each cage contains an octahedral cluster formed by six trigonal-planar copper cations.

We have exploited a range of neutron scattering techniques to investigate the origin of low thermal conductivity in tetrahedrite, Cu₁₂Sb₄S₁₃, which has been previously attributed to the rattling vibrations of the trigonal-planar copper ions and has also been linked to a phonon instability arising from a low-temperature phase transition. Analysis of neutron and synchrotron X-ray diffraction data collected on tetrahedrite shows that copper rattling is a direct consequence of a tetragonal-to-cubic phase transition at 90 K, which results in a sharp increase, by approximately 200%, of the atomic displacement parameters of the trigonal-planar copper cations. This phase transition occurs because of the orbital degeneracy of the highest occupied 3d cluster orbitals of the copper clusters found inside the sodalite cages. In the high-temperature cubic phase, the trigonal-planar copper cations form regular octahedral Cu₆⁷⁺ clusters, which are electronically degenerate. Below 90 K, tetrahedrite contains pentameric Cu₅⁷⁺ clusters. The Jahn-Teller electronic instability which leads to the formation of “molecular-like” Cu₅⁷⁺ clusters, suppresses copper rattling vibrations due to the strengthening of direct copper-copper interactions. At temperatures above 200 K, quasielastic neutron scattering (QENS) measurements on tetrahedrite, Cu₁₂Sb₄S₁₃, and copper-rich tetrahedrite, Cu₁₄Sb₄S₁₃, combined with molecular dynamics simulations, reveal that copper ion diffusion occurs. However, although the copper ions are mobile between 200 and 400 K, they are largely trapped inside the sodalite cages. Analysis of inelastic neutron scattering (INS) data reveals the presence of a low-energy optical mode at 3-4 meV, which can be attributed to the intra-cage diffusion of the trigonal-planar copper ions. This low-energy optical mode, which softens on cooling revealing strong anharmonicity, is capable of strongly scattering the heat-carrying acoustic phonons, and hence lowers the lattice thermal conductivity.

9:45 AM EN08.04.06

Thermoelectric Enhancement under Hydrodynamic Regime in Interconnected Nanowire Networks F. Xavier Alvarez, Jordi Tur and Albert Beardo Ricol; Universitat Autònoma de Barcelona, Spain

Recent advancements in the field of thermoelectric materials have highlighted the substantial benefits of employing 3D interconnected nanowire scaffolds. These scaffolds have demonstrated a significant enhancement in thermoelectric efficiency when compared to 1D nanowires and films grown under similar electrodeposition conditions. A key contributing factor to this improvement is the marked reduction in thermal conductivity (κ) observed in Bi₂Te₃ 3D nanonetworks, while concurrently preserving high electrical conductivity.

Employing a comprehensive approach, we have conducted an in-depth analysis of these structures, employing the Guyer and Krumhansl Equation through a Finite Element methodology, coupled with ab initio calculations for the transport parameters from the Kinetic Collective Model (KCM). Our findings have revealed that the laplacian (viscous) term in the Guyer and Krumhansl Equation is chiefly responsible for the observed reduction in heat flux within the interconnections. Specifically, the hydrodynamic nature of heat within these interconnected regions has led to a remarkable decrease in the thermal conductivity, as compared to that of the individual nanowires lacking such interconnections.

Through this investigation, we shed light on the critical influence of hydrodynamic effects on heat transport in intricate nanowire networks, offering valuable insights for the development of more efficient thermoelectric materials..

10:00 AM BREAK

SESSION EN08.05: Computational Guided Materials and Defect Engineering

Session Chairs: Johannes de Boer and Neophytos Neophytou

Wednesday Morning, April 24, 2024

Room 336, Level 3, Summit

10:30 AM *EN08.05.01

Adventures and Challenges in Computation-Guided Design and Discovery of Thermoelectric Materials -- from Direct Physical Modeling to Language Models Elif Ertekin; University of Illinois at Urbana-Champaign, United States

My presentation will highlight some of our recent attempts to make the computation-experiment handshake applied to the discovery and optimization of thermoelectric materials. We will describe the importance and state-of-the-art of accurate simulations of both intrinsic material properties and dopability in computation-guided search for new materials, focusing on the design space of diamond like semiconductors, ordered vacancy compounds, binary chalcogenides, and half-Heuslers. Finally, we'll discuss where computational approaches have success and what aspects are missing and should be realized to enable true computation-guided design and optimization -- focusing on strategies to optimize doping and carrier concentrations, and alloying strategies. Time-permitting, I will depart from direct physical modeling to show some of our recent work in the use of language-based representations in the search for thermoelectric materials and discuss some observations of the merits and possible shortcomings of data-based methodologies.

11:00 AM EN08.05.02

Investigating The Potential of III-V Type-I Clathrates as Thermoelectrics: A Computational Perspective [Alexander Squires](#) and David O. Scanlon; University of Birmingham, United Kingdom

The significant impact of III-V semiconductors on the electronic materials landscape is indisputable, demonstrated by their widespread use in high-profile applications such as integrated circuits, LEDs, and advanced photovoltaics. Innovations in materials discovery have ushered in the synthesis of type-I clathrate structures with a III-V host framework, exhibiting remarkable p-type mobilities [1]. Clathrate structures, consisting of nanometre-sized polyhedral cages encapsulating guest atoms or molecules, have stirred interest as prospective battery electrodes, photovoltaics, but most relevantly as thermoelectrics [2]. The highly electronically conductive framework coupled with weakly bound "rattler" guest atoms leads to fast electron transport and poor thermal transport, thus fulfilling the 'phonon-glass electron crystal' concept and paving the way for exceptional thermoelectric materials. Despite this notable potential, there exist significant discrepancies previous theoretical predictions and experimental studies of these materials' properties [1], which our research aims to resolve. In our study, we integrate atomistic simulations with data-driven methodologies to screen and characterize both existing and novel clathrates within the III-V compositional space. Employing the SMACT materials informatics tool [3], we efficiently navigate the vast compositional search space of III-V clathrates using economical heuristic tools, refining the search by evaluating the stability of the proposed clathrates using density functional theory. We further utilized spin-orbit coupling corrected hybrid density functional theory to provide a comprehensive first-principles characterization of these materials' electronic structures. Finding that this alone does not reconcile the experimental-theoretical disparities, we explore the strong influences of disorder and off-stoichiometry on their target properties. Our findings present deeper insights into this exciting class of materials, and offers a range of potential new applications.

1. Owens-Baird et al., Journal of the American Chemical Society, 2020, 142, 4, 2031–2041
2. Krishna, L., & Koh, C., Inorganic and methane clathrates: Versatility of guest–host compounds for energy harvesting. MRS Energy & Sustainability, 2, E8, 2015.
3. Davies et al., SMACT: Semiconducting Materials by Analogy and Chemical Theory. Journal of Open Source Software, 2019, 4(38), 1361

11:15 AM EN08.05.03

Advancing Thermoelectric Materials: A CALPHAD Approach to Charged Defects in Semiconductors [Adetoye H. Adekoya](#) and Jeff Snyder; Northwestern University, United States

Thermoelectric (TE) devices that offer a route for energy recovery/production often need to be optimized by doping with other elements to improve the thermoelectric figure of merit (zT) which qualifies the efficiency of the device. The solubility of these elements in the bulk system is usually in such dilute concentrations that they can best be described as 0-D defects in an otherwise essentially uniform crystal. However, these defects/dopants are essential to the efficient performance of thermoelectric devices. As a result, an accurate understanding of the solubility limits of these dopants is necessary for the manufacture of high-performing Thermoelectrics. Phase diagrams, which are lines of equilibrium or phase boundaries at specific thermodynamic conditions, can be useful for visualizing the solubility limit. To that end, the method called Computer Coupling of Phase Diagram and Thermochemistry, or alternately Calculation of Phase Diagrams (CALPHAD) is an established technique for visualizing the phase diagram of material systems. In our previous work, we showed that CALPHAD is a viable tool to both visualize the effects of the dominant defects on the shapes of the phase diagram as well as provide an estimate of the defect concentration. We further extend those principles into describing charged defects in semiconductors. The CALPHAD technique has been used extensively as a thermodynamic framework to optimize the manufacture of alloys by modeling the Processing, structure, properties, and performance relationship. By developing a formalism for describing these charged defects in a CALPHAD framework, we set the stage for a more complete integration of CALPHAD with thermoelectric materials and semiconductors in general

11:30 AM EN08.05.04

Multi-Objective Optimization of Thermoelectric (TE) Performance in Binary Chalcogenides through Computational Assessment of Extrinsic Dopants [Ferdaushi A. Bipasha](#) and Elif Ertekin; University of Illinois at Urbana-Champaign, United States

We demonstrate a computational approach to optimize the dopant profile of a thermoelectric material, accounting for the effect of the dopant on multiple interrelated indicators of performance. While most computational studies of dopants in TE materials primarily focus on optimization of carrier concentrations with the assumption that bulk/intrinsic properties of the material remain unchanged, in cases of high concentrations doping can affect other aspects of performance through modifications to carrier mobilities, thermal conductivity, and density of states. These competing effects often make it challenging to identify optimal doping concentrations. In this work, we use the example of Ga and Sb co-doping as a case study for the multi-objective optimization of n-type achievable TE performance in the group IV-VI binary chalcogenides with AB stoichiometry. Although recent reports show improved performance in n-type PbS based on co-doping with Ga and Sb, a predictive model that describes doping effects on multiple properties would reveal ultimate performance achievable and the carrier concentrations at which it occurs. We present models to assess how co-doping with Ga and Sb affect carrier mobilities, thermal conductivity, electronic density of states, and carrier concentrations in PbS and PbSe. The density of states analysis on PbS and PbSe show increased dos curvature after Ga, Sb co-doping. The defect properties show the stability of the co-doped system over a single dopant, which shows the stability of co-doped Ga-Sb defect would be stable over single point defect Ga and Sb. Our analysis reveals opportunities for multi-objective optimization of TE properties through understanding the change in effective mass, mobility, thermal conductivity, and optimized carrier concentration.

11:45 AM EN08.05.05

Micro Thermoelectric Devices: From Thermal Management to Powering the Internet of Things Heiko Reith¹, Nithin Pulumati¹, Aditya Dutt¹ and [Kornelius Nielsch](#)^{1,2,3}; ¹IFW Dresden, Germany; ²Institute of Applied Physics, TUD, Germany; ³Institute of Materials Science, TUD, Germany

Micro-thermoelectric devices (μ TEs) hold significant potential for various applications in the biomedical field, powering internet-of-things devices, and thermal management. To enable their use in such applications, robust packaging is crucial, allowing direct thermal contact between the μ TEs and the target heat sink and source. However, conventional packaging techniques designed for larger modules are unsuitable for μ TEs due to excessive thermal resistance between the capping material and the device, which hampers performance. In this study, we present the fabrication of μ TEs using optimized geometry and contact resistance, coupled with a novel packaging technique that seamlessly integrates with on-chip systems. Our fabrication process involves the creation of micro thermoelectric coolers (μ TECs) with vertically free-standing leg pairs, eliminating the need for a top plate. To meet real-world requirements, we embed these free-standing devices to form a flat surface at the top level, ensuring direct thermal contact with the heat sink. This embedding not only enhances mechanical stability but also provides chemical stability. We employ photoresist as the filling material due to its low thermal conductivity and excellent processability. By characterizing the μ TECs with and without photoresist using a thermoreflectance thermal imaging technique, we analyze the devices' cooling efficiency and the impact of the photoresist matrix on their performance. The fabrication process of the μ TEC involves a combination of photolithographic patterning and electrochemical deposition of $\text{Bi}_2(\text{Te}_{1-x}\text{Se}_x)_3$ and Te, which serve as the n-type and p-type thermoelectric materials, respectively. Through optimization of the geometry and contact resistance of the μ TECs, we achieved a maximum cooling effect of approximately 10.8 K at an applied electrical current of 235 mA. Furthermore, our reliability studies demonstrated a rapid response time of 700 μ s and over 100 million cooling cycles without device failure. We also conducted finite element analysis to investigate the impact of geometry and contact

resistance on the cooling power density and net cooling temperature, offering valuable guidelines for fabricating thermoelectric coolers with optimal performance. In the case of embedded μ TECs, the photoresist matrix acts as a thermal shortcut that results in additional thermal loss, leading to a slight reduction of the maximum cooling from 10.8 K to 9.6 K. This decrease can be attributed to thermal loss through the polymer. Nevertheless, the embedded devices exhibit a rapid cooling response time of 721 μ s and demonstrate only a slight reduction in cycling reliability, with a lifespan of 85 million cycles. These embedded, optimized, stable, and easily scalable μ TEs present exciting opportunities for widespread applications in the biomedical field, powering internet-of-things devices, and localized heat management.

References: 1. Zhang, Q., Deng, K., Wilkens, L., Nielsch, K. et al. Micro-thermoelectric devices. *Nat. Electron.* 5, 333–347 (2022). 2. Dutt, A. S., Deng, K., Li, G., Pulumati, N., Ramos, D. L., Barati, V., Garcia, J., Perez, N., Nielsch, K., Schiering, G., Reith, H., *Adv. Electronic Mater.* 8, 2101042 (2022). 3. Li, G., Garcia Fernandez, J., Lara Ramos, D.A., Nielsch, K. et al. Integrated microthermoelectric coolers with rapid response time and high device reliability. *Nat. Electron.* 1, 555–561 (2018)

SESSION EN08.06: Novel Architecture and Applications
Session Chairs: Saniya LeBlanc and Marisol Martín-González
Wednesday Afternoon, April 24, 2024
Room 336, Level 3, Summit

1:30 PM EN08.06.01

Thermoelectric-Photoelectrochemical Water Splitting under Concentrated Solar Irradiation Virgil Andrei; University of Cambridge, United Kingdom

Photoelectrochemical (PEC) systems utilize sunlight to directly convert water and carbon dioxide into useful chemicals like hydrogen, synthesis gas, or ethanol. Such devices may lower the costs of sustainable fuel production by integrating light harvesting and catalysis in one compact device.^[1] However, light absorption suffers losses from thermalization and the inability to use low-energy photons, which limits the overall solar-to-chemical conversion efficiency.^[2,3] Here, we demonstrate that PEC reactors can utilize this waste heat by integrating thermoelectric modules, which provide additional voltage under concentrated light irradiation.^[3] While most single semiconductors require external bias, we already accomplish unassisted water splitting under 2 sun irradiation by wiring a BiVO₄ photoanode to a thermoelectric element, whereas the photocurrent of a perovskite-BiVO₄ tandem system is enhanced 1.7-fold at 5 sun. This strategy is particularly suitable for photoanodes with more positive onset potentials like hematite, with thermoelectric-perovskite-Fe₂O₃ systems achieving a 29.7 \times overall photocurrent increase at 5 sun over conventional perovskite-Fe₂O₃ devices without light concentration. This thermal management approach provides a universal strategy to facilitate widespread solar fuel production, as light concentration increases output, reduces the reactor size and cost, and may enhance catalysis.^[3]

We further reveal the recent success of thermoelectric composites in other material science applications. While thermoelectric pastes consisting of conductive powders in a polymer matrix display limited power factors,^[4] their hydrophobicity proves essential for effective moisture protection of PEC devices and solar cells. Accordingly, a graphite epoxy paste encapsulant extends the lifetime of metal halide perovskite photocathodes to 4 days under operation in water,^[5] and increases the stability of a BiOI photocathode for H₂ evolution from minutes to months.^[6] This material allows the manufacturing of flexible, lightweight devices, which float on water similar to lotus leaves.^[7] Those devices are compatible with large-scale, automated fabrication processes, which present the most potential towards future real-world applications.^[8]

[1] Andrei, V.; Roh, I.; Yang, P. *Sci. Adv.* 2023, 9, eade9044.

[2] Andrei, V.; Bethke, K.; Rademann, K. *Energy Environ. Sci.* 2016, 9, 1528–1532.

[3] Pornrunroj, C.; Andrei, V.; Reisner, E. *J. Am. Chem. Soc.* 2023, 145, 13709–13714.

[4] Andrei, V.; Bethke, K.; Rademann, K. *Phys. Chem. Chem. Phys.* 2016, 18, 10700–10707.

[5] Pornrunroj, C.; Andrei, V. et al. *Adv. Funct. Mater.* 2021, 31, 2008182.

[6] Andrei, V.; Jagt, R. A. et al. *Nat. Mater.* 2022, 21, 864–868.

[7] Andrei, V.; Ucoski, G. M. et al. *Nature* 2022, 608, 518–522.

[8] Sokol, K. P.; Andrei, V. *Nat. Rev. Mater.* 2022, 7, 251–253.

1:45 PM EN08.06.02

Kirigami-Inspired Organic and Inorganic Film-Based Flexible Thermoelectric Devices with Built-In Heat Sink Chongyang Zeng and Emiliano Bilotti; Imperial College London, United Kingdom

Thermoelectric (TE) technology presents a unique opportunity to convert waste heat directly into electricity, offering a promising solution to address energy harvesting and sustainability challenges. However, conventional TE devices with π -type structures always need a heat sink to thermally link to the air during operation which remains a significant limitation for their practical applications.

Herein, we report a new configuration of a TE device that has a built-in heat sink for the first time. Furthermore, the device modified with shape-memory polymer films can be self-folded into a hexagonal structure via heating above its glass transition temperature. We demonstrate the feasibility of our design through experimental characterization and modelling. The device with built-in fins exhibits superior thermoelectric performance with both organic (carbon nanotube veils) and inorganic (bismuth telluride, Bi₂Te₃) TE materials. The maximum power output of the Bi₂Te₃-based device can reach 180 μ W, which is 4.4 times higher than that of the carbon-based device (41 μ W) when the temperature difference is 43 K and airflow is 1.5 m s⁻¹. Bi₂Te₃-based devices show better TE performance but less stability compared to carbon-based devices. Moreover, carbon-based devices can be self-folded via external temperature stimulus and keep resistance no change (95 Ω) while Bi₂Te₃-based devices cannot.

This work provides a path to optimize the thermoelectric performance of TE devices by designing rational structures. This approach has the potential to reduce the cost, mass, and volume of TE devices, making them more attractive for a wide range of applications, such as waste heat recovery, energy harvesting, and thermal management.

2:00 PM *EN08.06.03

Thermoelectric Transport with Metamaterials Lilia Woods; University of South Florida, United States

Thermoelectricity is a basic transport phenomenon encompassing thermodynamically reversible heat-to-electricity conversion. Much of the current research in this area has been focused on the electronic, phonon, and transport properties of materials as a viable route to optimize existing and engineer new compositions for better practical devices. Here I would like to explore a macroscopic perspective that helps us think differently of controlling

thermoelectricity. Using thermodynamics, circuit theory, and transformation optics an efficient approach is offered for the design of thermoelectric metamaterials with targeted functionalities. For example, thermoelectric cloaks and rotators can be achieved by enforcing preservation of the invariance of the governing and constitutive thermodynamic equations. Using basic relations for in-parallel and in-series connected components, the independent control of the coupled via Seebeck coefficient thermal and heat currents can also be achieved. Our pathways for constructing metamaterials capable of achieving such functions is especially exciting for the construction of actual devices.

2:30 PM BREAK

SESSION EN08.07: Printing Techniques
Session Chairs: Koji Miyazaki and Zhifeng Ren
Wednesday Afternoon, April 24, 2024
Room 336, Level 3, Summit

3:30 PM *EN08.07.01

Process-Structure-Property Relationships for Laser Additive Manufacturing of Thermoelectric Materials for Low and High Temperature Applications Saniya LeBlanc; The George Washington University, United States

Thermoelectric materials enable direct, solid-state conversion of heat to electricity and vice versa, so they offer functional power generation and heat pumping capabilities. Additive manufacturing offers the potential to structure thermoelectric materials and devices at multiple length scales, thus improving both intrinsic properties, overall system performance, and application integration. We report on experimental and computational investigation of process-structure-property relationships for laser powder bed fusion of thermoelectric materials including bismuth telluride (for applications near 100°C) and silicon germanium (for applications near 1000°C). Strategies for non-spherical powders were developed, and the process parameters that lead to conduction mode melting were determined. The process has been demonstrated on multiple tools, both custom setups and commercial tools. The structure of both single melt tracks and bulk parts were characterized at nano-, micro-, and meso-scales for varying process parameters such as laser power, scan speed, and powder layer thickness. Finite element modeling of laser energy deposition and heat diffusion within the powder bed resulted in simulations of spatial and temporal temperature gradients during laser processing of thermoelectric material. These simulations were compared to in situ, long wavelength infrared sensor data collected during processing experiments. The ratio of temperature gradient and solidification rate was used to predict the transition between equiaxed and columnar grains and compare the prediction to the experimentally observed grain morphology. A kinetic Monte Carlo simulation was used to simulate the formation of grain structure during solidification. Thermoelectric properties (Seebeck coefficient, electrical conductivity, and thermal conductivity) were measured on fabricated bulk samples, and structure and property characterization results indicate a link between the process-dependent nanostructure and the Seebeck coefficient, including a transition between n- and p-type behavior and graded Seebeck coefficient. These results indicate functional grading of thermoelectric properties during the additive manufacturing process may be possible. Finally, the power generation performance impact of unique device shapes (e.g., layered, hourglass, and hollow shapes) enabled by additive manufacturing was modeled for high and low temperature and heat flux boundary conditions, and selected promising shapes were fabricated. This work provides knowledge about how rapid melting and solidification of thermoelectric materials during laser additive manufacturing impacts the material structure and properties. The results show how variations in process parameters can be leveraged to enable functional grading of thermoelectric properties within the material by manipulating the material at the nano and micro-scales. The additive manufacturing technique enables fabrication of unique shapes at the mesoscale that show improvements for system-level performance of thermoelectric devices.

4:00 PM EN08.07.02

3D Ink Printing and Casting of Nb_{0.8}Ti_{0.2}FeSb and Half-Heusler Thermoelectric Couples Alexander Proschel, Duncan Zavanelli, Jeff Snyder and David C. Dunand; Northwestern University, United States

Current manufacturing processes for inexpensive, mechanically stable, high performing p-type half-Heusler Nb_{0.8}Ti_{0.2}FeSb such as ball milling and hot pressing are unsuitable for continuous processing, geometrically limited, and require subsequent slicing and assembly steps to fabricate thermoelectric couples. Additionally, current assembly of half-Heusler couples typically relies on brazing or soldering, both of which are unsustainable for long-term use. Thus, new additive manufacturing synthesis of Nb_{0.8}Ti_{0.2}FeSb and half-Heusler couples is necessary to improve utility and eliminate the costly slicing and assembly steps. This talk will present a new procedure for ink casting of bulk Nb_{0.8}Ti_{0.2}FeSb with subsequent half-Heusler couple assembly as well as direct 3D ink printing of a complete half-Heusler thermoelectric couple. This synthesis approach utilizes polymer-based inks loaded with elemental metallic precursor powders which can be co-printed or cast at ambient temperature to produce thermoelectric legs or complete half-Heusler couples.

4:15 PM EN08.07.03

Flexible, Scalable and Reliable Fully Screen-Printed Thermoelectric Generators Irene Brunetti^{1,2}, Federico Ferrari³, Nathan James Pataki⁴, Sina Abdolhosseinzadeh⁵, Lambert Jan Anton Koster³, Jakob Heier⁵, Ulrich Lemmer², Martijn Kemerink⁶ and Mario Caironi⁴; ¹InnovationLab, Germany; ²Karlsruhe Institute of Technology (KIT), Germany; ³University of Groningen, Netherlands; ⁴Istituto Italiano di Tecnologia (IIT), Italy; ⁵Swiss Federal Laboratories for Materials Science and Technology (Empa), Switzerland; ⁶Heidelberg University, Germany

Global energy demand is expected to increase by almost 50% in the next 20 years. Currently, traditional energy sources such as oil, gas, and coal have played a significant role in global energy production. However, they are also responsible for the increase in pollution and are harmful to human health. New energy sources are necessary to support this high demand, in a sustainable way. The thermal energy can be converted into electrical energy in a completely eco-friendly way thanks to thermoelectric generators (TEGs). Due to their flexibility, lightness, affordability, and natural abundance, organic thermoelectric materials are the perfect competitors for making flexible TEGs that can readily conform to complex surfaces. However, up to now, the research has primarily focused on making simple proof-of-concept devices not application-oriented, to highlight the thermoelectric performance of the organic materials. Moreover, demonstrator-devices typically show performance that is far below what one would expect based on the figures of merit of the constituent materials.

Here, we present a new fabrication method to make vertical, fully printed, large-area, flexible, monolithic TEG with a high-density of thermocouples scalable up to m², compatible with all the screen-printable inks with performance that matched the expectations based on the figures of merit of the constituent materials.

The TEGs were made screen printing five layers on top of each other on a 25 μm thick Kapton substrate, recreating the Π-shape structure, where device legs are oriented perpendicular to the heat flows. A silver bottom contact necessary for the electrical connection was screen printed, followed by an insulator layer with cavities designed to create a mask for the vertical thermocouples. Successively, the p-type layer and the silver layer were screen-printed

to fill alternatively the cavities, thereby creating the vertical thermocouples. Finally, the top silver contact was screen printed to electrically complete the circuit.

We demonstrated the scalability of the process employing as p-type the well-known and commercially available poly(3,4-ethylenedioxythiophene) polystyrene sulfonate (PEDOT:PSS) to make vertical TEGs composed of 4 and 8 thermocouples, with a surface area of 0.5 cm² and 1 cm², respectively. The devices exhibited an ideal behaviour perfectly scalable in accordance with numerical simulations. After the validation of the fabrication method, we utilized a recently reported additive-free graphene, not previously assessed for thermoelectric applications, as p-type material to make a vertical TEG composed of 8 thermocouples. The power output at a $\Delta T = 25^\circ\text{C}$ provided by the additive-free graphene device was over five times higher than that of the PEDOT:PSS TEG. Additionally, the measures were once again in accordance with numerical simulation. The additive-free graphene TEG provides a remarkable, among the organic thermoelectric TEG, power density of 15 nW/cm² at $\Delta T = 29,5^\circ\text{C}$.

Scaling this device to a 100 cm² large TEG will result in a power output of 1.5 μW , sufficient to power low-energy electronic devices such as sensors, wearables, and wireless communication systems.

The fully screen-printable large-area TEGs presented are also extremely lightweight and flexible. Specifically, the additive-free graphene TEG provides an estimated power output of 1 $\mu\text{W/g}$, and its internal device resistance remained constant even when the device was rolled into a cylinder with a bending radius of 1 cm.

Future work for this technology will involve making larger devices on thinner substrates to considerably increase the power output. Using a 5 μm substrate the power output of a 100 cm² additive-free graphene TEG will increase by an order of magnitude. Furthermore, due to the versatility and reliability of the process, it will also be possible to use inorganic materials as active inks with enhanced thermoelectric performance to further increase the power output.

4:30 PM EN08.07.04

Laser Powder Bed Fusion of Bismuth Telluride on Plastic Foil as a Simple Route for The Scalable Fabrication of Flexible and Large-Area Thermoelectric Generators Isidro Florenciano, Francisco Molina-Lopez, Yuan Tian and Heyi Xia; KU Leuven, Belgium

Thermoelectric generators (TEGs) are solid-state devices that convert waste heat into electrical energy. Conventional manufacturing methods struggle to meet the requirements of scalability and compatibility with unconventional form factors required for emerging applications such as wearables and large-area electronics. In contrast, additive manufacturing techniques offer scalability, reduced material waste, and the ability to conform to various shapes, expanding their potential applications. In particular, Laser Powder Bed Fusion has shown tremendous potential to manufacture high-performing pellets with laser-tunable nanostructure. However, the compatibility with flexible substrate and large-area patterning remains to be demonstrated.

Our work demonstrated the additive manufacturing of high-performing inorganic flexible TEGs by laser powder bed fusion directly onto flexible polyimide foil. We achieve maskless and large-area patterning of thick films of Bi₂Te₃-based materials deposited from a slurry. By reusing the unexposed powder we minimize material waste. Mechanical interlocking enables simultaneous patterning, sintering, and attachment of films to the flexible substrate, enabling the creation of a highly flexible device adaptable to different shapes.

Moreover, the material structure and chemical composition, and the associated performance, can be precisely tuned by the laser power and scanning speed. For instance the unique microstructure of the laser-printed material imparts remarkable flexibility to the typically brittle Bi₂Te₃ thick films. Samples can withstand extreme bending with a radius of curvature as small as 0.75 mm while experiencing minimal changes in performance over a 10 mm bending radius. Additionally, we can simultaneously modify the stoichiometry of the material to optimize its power factor. This innovative approach holds promise for the advancement of flexible TEGs and their diverse applications.

4:45 PM EN08.07.05

Flexible Thermoelectric Generators based on Template- Assisted Electrodeposition of Bismuth Telluride inside Commercial Filters Olga Caballero-Calero, Pablo Cerviño Solana, M. Jesús Ramirez Peral, Miguel Angel Tenaguillo Arrese and Marisol Martín-González; IMN-CNM, Spain

Miniaturized thermoelectric generators utilizing bismuth telluride (n-type) and tellurium (p-type) semiconductors have been fabricated within commercial polyester filters. Employing electrochemistry for fabrication for both the electrical contacts and the active thermoelectric material, we create an intricate network of nanostructured bismuth telluride or tellurium, which is electrically connected to the top and bottom electrodes. The control over the electrochemical process allows us to maintain the flexibility of the commercial filter in the final device. It is mandatory to be flexible in applications such as harvesters of body heat to power wearable devices, where adaptability to human skin is essential.

Electrochemical deposition is a cost-effective and scalable fabrication method, that does not use high vacuum or expensive facilities, but has the advantage of allowing conformal growth of the material when a template is used. Given that the commercial filters have hollow structures in the order of tens to hundreds of nanometers in diameter and microns in length, the obtained material will be nanostructured with those dimensions. Our work demonstrates enhanced thermoelectric performance compared to electrodeposited thin films due to the nanostructure [1]. Also, with the control of the different parameters during the electrochemical deposit (temperature, applied voltage, etc.), the stoichiometry, morphology, and crystallographic orientation can be tailored. Once the samples were grown, scanning electron microscopy images, X-Ray diffraction images, and Raman spectroscopy were used to get complete information on the material and optimize the filling of the template, the material composition (which is crucial in the case of bismuth telluride), and crystal orientation to have the best performing material for applications in the out-of-plane direction, that is, with the temperature gradient applied in the direction of the thickness of the template. Once these first parameters were optimized, and a high filling ratio of nanostructures oriented along the [110] direction with stoichiometric composition was obtained [2], the transport properties were also measured (Seebeck coefficient and electrical conductivity) to fine-tune and optimize the material.

For the final thermoelectric generator, which uses the gold electrode evaporated in one of the faces of the filter to perform template-assisted electrochemical deposition as the bottom electrode, a top electrical contact needs to be implemented. This has been made by electrochemically depositing nickel on top of the previously grown bismuth telluride or tellurium nanostructure. In this way, the electrical contact between the different nanostructures of thermoelectric material and the top electrode is granted, and a macroscopic electrode is formed on the top of the filter, which simplifies the use of the generator.

Finally, the optimization of the geometry of the thermoelectric generators was firstly studied by simulations carried out with COMSOL MULTIPHYSICS and then implemented in actual devices. For the moment, thermoelectric generators consisting of 2 or 4 pairs of legs fabricated inside the commercial filter have been implemented.

References

- [1] A Ruiz-Clavijo et al., *ACS Applied Energy Materials* **4**, 13556 (2021).
- [2] A. Ruiz-Clavijo et al. *Nanomaterials* **8** 345 (2018).

SESSION EN08.08: Poster Session I
Session Chairs: Jan-Willem Bos and Alexandra Zevalkink
Wednesday Afternoon, April 24, 2024
Flex Hall C, Level 2, Summit

5:00 PM EN08.08.01

Theoretical Investigations of Electronic, Thermodynamic and Thermoelectric Properties of Filled Skutterudites ThFe 4 P 12 and CeFe 4 P 12 Using DFT Calculations [Abdelkader Alleg](#); Laboratory for Physical Sciences, Algeria

The structural, mechanical, electrical, thermodynamic and thermoelectric properties of CeFe₄P₁₂ and ThFe₄P₁₂ employing first-principles calculations together with semi-classical Boltzmann Transport equations are investigated. It has been firmly proved that these materials fall within the category of semiconductors. The existence of band gap energies measuring 0.436 eV and 0.52 eV, respectively, supports the basis for this classification. Both materials are stable in terms of mechanics and dynamics. The Seebeck coefficient for ThFe₄P₁₂ is 827 μ V/K, while CeFe₄P₁₂ is 667 μ V/K at ambient temperature. For both materials, the highest recorded figure of merit values for both materials is 0.96 for ThFe₄P₁₂ and 0.97 for CeFe₄P₁₂ at 300 K. Therefore, the theoretical findings provide a strong justification for future experimental investigations. Keyword: Thermoelectric; Skutterudites; ThFe₄P₁₂; CeFe₄P₁₂

5:00 PM EN08.08.02

An Efficient High-Throughput Approach for Investigating Anharmonic Lattice Dynamics [Hrushikesh P. Sahasrabudhe](#)^{1,2}, [Zhuoying Zhu](#)², [Junsoo Park](#)^{2,3}, [Alex M. Ganose](#)^{2,4}, [Rees Chang](#)^{2,5}, [John W. Lawson](#)³ and [Anubhav Jain](#)²; ¹University of California, Berkeley, United States; ²Lawrence Berkeley National Laboratory, United States; ³NASA Ames Research Center, United States; ⁴Imperial College London, United Kingdom; ⁵University of Illinois at Urbana-Champaign, United States

This work introduces a high-throughput framework specifically designed for anharmonic phonon calculations. The method is based on the efficient fitting of the force constant (FC) matrix implemented in the hiPhive¹ framework and subsequent calculation of harmonic and anharmonic properties. In particular, we determined the set of optimal parameters: FC fitting methods, cutoffs, supercell size for finite displacement DFT calculations, the magnitude of atomic displacements, and the number of perturbed supercells. Our workflow can calculate phonon band structure, phonon DOS, finite temperature free energy, heat capacity, coefficient of thermal expansion (α), and lattice thermal conductivity (κ). A temperature-induced anharmonic phonon renormalization (APRN)² scheme to tackle dynamical instability is also included in the workflow, which is shown to predict the finite temperature stability of cubic GeTe³ and ZrO₂⁴ phases.

Our workflow exhibits an impressive 100 to 1000X speedup compared to conventional approaches when calculating anharmonic vibrational properties. We conduct a rigorous benchmarking process against experimental measurements, encompassing α , κ , and computationally calculated phonon DOS. The α and κ obtained from the workflow agree well with the experimentally reported values with a Pearson correlation coefficient of 0.94 and 0.99, respectively. The Pearson correlation coefficient of phonon DOS varies from 0.63 in CdSe to 0.96 in BP.

In this workflow, we integrate lattice dynamic packages like hiPhive with the Materials Project (MP)⁵ tech stack using Atomate2. We aim to use this workflow to curate a high-quality dataset of materials with finite temperature phase diagrams and anharmonic vibrational properties in a high-throughput way. This dataset will make it possible to identify novel thermoelectric materials, solid-state ionic conductors for solid-state batteries, photovoltaic absorber materials, and solar cells. It will also aid in the predictive synthesis of solid-state reactions.

1. Eriksson, F., Fransson, E. & Erhart, P. The Hiphive Package for the Extraction of High-Order Force Constants by Machine Learning. *Adv. Theory Simul.* **2**, 1800184 (2019).
2. Xia, Y. Revisiting lattice thermal transport in PbTe: The crucial role of quartic anharmonicity. *Appl. Phys. Lett.* **113**, 073901 (2018).
3. Anharmonic stabilization and lattice heat transport in rocksalt β -GeTe | Applied Physics Letters | AIP Publishing. <https://pubs.aip.org/aip/apl/article/113/19/193902/35993>.
4. Tolborg, K. & Walsh, A. Exploring the High-Temperature Stabilization of Cubic Zirconia from Anharmonic Lattice Dynamics. *Cryst. Growth Des.* **23**, 3314–3319 (2023).
5. Jain, A. *et al.* Commentary: The Materials Project: A materials genome approach to accelerating materials innovation. *APL Mater.* **1**, 011002 (2013).

5:00 PM EN08.08.03

Developments in Thermal Transport Property Measurement of Thermoelectric Thin Films and Determination of Interfacial Thermal Resistance by Thermo-Reflectance Method [Takahiro Baba](#)¹, [Tetsuya Baba](#)¹ and [Takao Mori](#)^{1,2}; ¹National Institute of Materials Science (NIMS), Japan; ²University of Tsukuba, Japan

Thermo-reflectance method, also called time domain thermo-reflectance (TD-TR) method can measure thermal transport properties in the cross-plane direction of thin films, which is important for evaluation of thermoelectric thin films. Recently the method achieved notable developments. The rise of electrical delay technique has enabled the method to observe temperature response in longer timescale than pulse interval of pump beam, which demonstrate periodic nature of thermo-reflectance signals. In our recent study, we developed an analytical approach based on Fourier analysis, which can consider the periodicity of thermo-reflectance signal into consideration and improved robustness and reliability of the determination of thermal properties. To evaluate thermal transport in thermoelectric thin films, it is also important to consider the transport across interfaces between materials, which is generally called interfacial thermal resistance. Picosecond thermo-reflectance method is suitable to measure the interfacial thermal resistance which has very short characteristic time. Thanks to our approach based on Fourier analysis, we could consider the contribution from interfacial thermal resistance between thin film and substrate by extending the mathematical model in frequency domain. We could finally achieve quantitative evaluation of interfacial thermal resistances by measuring only one sample, whereas a conventional approach to evaluate interfacial thermal resistances needs to prepare thin films with different thickness. In the conventional approach, each thin film should be sandwiched between two metallic films with the same thickness. This approach has some ambiguity because it is difficult to confirm that thin films with different thickness have the identical characteristics. We have measured actual thermoelectric thin films by picosecond thermo-reflectance method. In TDTR method, a sample is generally measured under front heat - front detect (FF) configuration, but we have utilized a thermo-reflectance method under rear heat - front detect (RF) configuration as well. The thermo-reflectance method under RF configuration, sometimes called ultrafast laser flash method, has smaller uncertainty compared to the method under FF configuration. This time we are going to introduce recent developments in thermo-reflectance method and share some notable results of thermal transport property measurements of thermoelectric thin films.

5:00 PM EN08.08.04

Controlling Defects in Epitaxial Thin Film Growth of $Mg_2Sn_{1-x}Ge_x$ by Modulating Mg Flux Rate in MBE [Kenneth M. Senados^{1,2}](#), Takashi Aizawa², Isao Ohkubo², Takahiro Baba^{1,2}, Akira Uedono¹, Takeaki Sakurai¹ and Takao Mori^{1,2}; ¹University of Tsukuba, Japan; ²National Institute for Materials Science, Japan

Defects manipulation in thermoelectrics is emerging as a key in optimizing their performance. However, because thin film processes differ from bulk synthesis methods, the manipulation of defects in thin films vary significantly from their bulk counterparts. We explore in this study how Mg flux rate modulation in molecular beam epitaxy (MBE) growth affects the defects formation of $Mg_2Sn_{1-x}Ge_x$ ($x = 0.05$ and 0.12) epitaxial films. Mg flux rates were varied in the range of Mg : Sn(Ge) = 3.9-9.1, while Sn and Ge flux rates were fixed at $1.65 \text{ atoms} \times \text{s}^{-1} \text{ nm}^{-2}$. Although the relative Mg supply rate largely exceeded 2, the obtained films consisted of Mg_2Sn phase as a main component, because the excess Mg can easily evaporate at the growth temperature of 380°C . However, the Mg flux rate can impact the film growth dynamics.

Higher Mg flux rates substantially enhance carrier mobility, Seebeck coefficient and eventually the power factor, which is linked to the reduction of vacancy-type defects detected in the positron annihilation spectroscopy measurements. Simultaneously, the films' X-ray diffraction (XRD) indicated higher crystallinity at higher Mg flux rates. Cross-sectional transmission electron micrographs of films reveal Moiré patterns. EDS measurements at the Moiré patterns for the low Mg flux rate film show Mg-poor regions, suggesting Mg vacancies (V_{Mg}). On the other hand, at the high Mg rate, the presence of Mg interstitials (I_{Mg}) is hinted within the Moiré patterns. The formation of Moiré patterns can be associated with strain relaxation, and their increased occurrence at higher Mg flux rates could be attributed to the role of Mg in altering strain distributions and controlling the defects. Structural analysis through XRD pole figures also unveiled the presence of stacking faults in the films. The total thermal conductivity measured at room temperature of the thin films tends to decrease with an increasing Mg flux rate. These findings suggest a delicate balance between improved overall crystal structure and the presence of localized structural variations that may contribute to the decrease in thermal conductivity and total improvement of the thermoelectric properties of Mg-based thin films.

5:00 PM EN08.08.05

Role of Spin-Orbit Coupling in Determining The Transport Properties of NbFe (As, Sb, Bi) Half - Heusler Compounds [Sara Shivalingam Goud¹](#), Amrita Bhattacharya¹ and Ashok Arya²; ¹Indian Institute of Technology Bombay, India; ²Bhabha Atomic Research Centre, India

Half – Heusler (HH) alloys have proven to be promising materials for thermoelectric (TE) energy conversion due to their remarkable electronic transport properties and good mechanical stability. However, relatively large lattice thermal conductivity (κ_L) limits their performance. For the past two decades, lowering κ_L in these materials without reducing their power factor ($PF = S^2\sigma$; S - Seebeck coefficient, σ - electrical conductivity) using various microstructural engineering techniques has been the primary interest of research. $RFeSb$ ($R = V, Nb, Ta$), a class of Fe – based HH compounds have emerged as high-performing p -type thermoelectric materials. Major theoretical works on these compounds are focussed on understating the band structure related transport properties under the rigid band (RB) and constant relaxation time approximations (CTR). The effect of spin-orbit coupling (SOC), which has a significant influence on the band structure due to the presence of heavy elements has not been investigated thoroughly. This study mainly focuses on investigating the role of SOC on transport properties of NbFeX ($X = As, Sb, Bi$) alloys using density functional theory (DFT) based electronic structure calculations. Electronic band structure calculations revealed that the splitting in the energy levels has increased as the element gets heavier (As Sb Bi) and the band degeneracy at the valence band maximum (VBM) which occurs at L point in the Brillouin zone for NbFeBi is broken. Due to the different magnitudes of splitting at different chemical potentials, opposing trends in transport properties (S and σ) are observed at lower and higher chemical potentials. The varying trends are mainly due to the change in the number of bands available for conduction and their topology at the extrema for different doping concentrations when SOC is included in the calculation. Lattice thermal conductivity calculations are performed to get a comprehensive insight into the thermoelectric performance of these compounds and the calculations revealed that NbFeBi has the lowest κ_L when compared to NbFeAs and NbFeSb with a phonon band gap due to the suppression of the acoustic modes as Bi is relatively heavier than As and Sb. With a large reduction in the lattice thermal conductivity and a favorable splitting of energy levels due to SOC, NbFeBi is found to best-performing p -type TE material when compared to NbFeSb and NbFeAs, with the highest figure of merit (zT) of 1.6 at 1100 K emphasizing the importance of SOC in thermoelectric transport.

5:00 PM EN08.08.06

Impact of Excess Cu on Phase Separation and Thermoelectric Properties of Arc Melted $Ti_{0.5}Zr_{0.5}NiCu_ySn$ [Blair F. Kennedy¹](#) and Jan-Willem Bos²; ¹Heriot-Watt University, United Kingdom; ²University of St Andrews, United Kingdom

Alloys based on $XNiSn$ ($X = Ti, Zr$ or Hf) are leading n-type half-Heusler thermoelectrics.¹ They have large power factors $S^2\sigma$, but are limited by an inherently high lattice thermal conductivity, κ_{lat} . Alloying Ti, Zr and Hf on the X-site in the crystal structure affords significant reductions of κ_{lat} . However, Ti and Zr/Hf mix poorly during materials synthesis, typically resulting in the presence of multiple HH phases in the final product.^{2,3} The presence of multiple HH phases has been attributed to phase segregation, and has been linked to low κ_{lat} , below values expected from alloying. In this contribution, the impact of excess Cu on the HH phase distribution of $Ti_{0.5}Zr_{0.5}NiCu_ySn$ ($y = 0.025, 0.1$) is discussed. Structural characterisation of samples treated at varying temperatures reveals minimal impact on the phase distribution for $y = 0.025$, compared to not having Cu. By contrast, samples with $y = 0.1$ show improved homogeneity and can be made single phase at high temperature. The homogeneous $y = 0.1$ sample has the lowest κ_{lat} of all samples, confirming that alloying is the dominant phonon scattering effect. A highest $zT = 0.7$ is found for multiphase $Ti_{0.5}Zr_{0.5}NiCu_{0.025}Sn$, with a lower $zT = 0.5$ observed for single phase $Ti_{0.5}Zr_{0.5}NiCu_{0.1}Sn$. This lower value is due to over-doping and a compromised $S^2\sigma$.

This work demonstrates that (1) the poor mixing of Ti and Zr/Hf in $XNiSn$ alloys is predominantly a kinetic effect and not driven by thermodynamic phase segregation. (2) That there is no evidence that multiphase behaviour leads to significant reductions of κ_{lat} in our samples.

References

1. R. J. Quinn and J.-W. G. Bos, *Materials Advances*, 2021, **2**, 6246-6266.
2. M. Schwall and B. Balke, *Materials*, 2018, **11**, 649.
3. A. Page, A. Van der Ven, P. F. P. Poudeu and C. Uher, *Journal of Materials Chemistry A*, 2016, **4**, 13949-13956.

5:00 PM EN08.08.07

Alloying-Induced Structural Transition in The Promising Thermoelectric Compound $CaAgSb$ [A K M Ashiqzaman Shawon¹](#), Weeam Guetari¹, Kamil Ciesielski², Rachel Orenstein², Jiaxing Qu³, Elif Ertekin³, Eric Toberer² and [Alexandra Zevalkink¹](#); ¹Michigan State University, United States; ²Colorado School of Mines, United States; ³University of Illinois at Urbana-Champaign, United States

AMX Zintl compounds, crystallizing in several closely related layered structures, have recently garnered attention due to their exciting thermoelectric properties. In this study, we show that the orthorhombic $CaAgSb$ can be alloyed with hexagonal $CaAgBi$ to achieve a solid solution with a structural transformation at $x \sim 0.8$. This transition can be seen as a switch from 3D to 2D covalent bonding, in which the interlayer $M-X$ bond distances expand while the in-plane $M-X$ distances contract. Measurements of the elastic moduli reveal that $CaAgSb_{1-x}Bi_x$ becomes softer with increasing Bi content, with the

exception of a step-like 10% stiffening observed at the 3D-to-2D phase transition. Thermoelectric transport measurements reveal promising Hall mobility and a peak zT of 0.47 at 620 K for intrinsic CaAgSb, which is higher than previous reports for unmodified CaAgSb. However, alloying with Bi was found to increase the hole concentration beyond the optimal value, effectively lowering the zT . Interestingly, analysis of the thermal conductivity and electrical conductivity suggests that the Bi-rich alloys are low Lorenz-number (L) materials, with estimated values of L well below the non-degenerate limit of $L = 1.5 \times 10^{-8} \text{ W}\cdot\Omega\cdot\text{K}^{-2}$, in spite of the metallic-like transport properties. A low Lorenz number decouples electrical and electronic thermal conductivity, providing greater flexibility for enhancing thermoelectric properties.

5:00 PM EN08.08.08

Thermal and Electrical Transport Properties of Novel Metal $\text{Ln}_2\text{M}_2\text{O}_5\text{Ch}_2$ Compounds for Thermoelectrics Kieran B. Spooner¹, Joe Willis², Katarina Brlec² and David O. Scanlon¹; ¹University of Birmingham, United Kingdom; ²University College London, United Kingdom

Heat loss wastes 50 % of global energy production,¹ making its reduction or utilisation essential in controlling and meeting our ever-increasing energy demand with renewable energy and reducing the effects of global heating. Thermoelectric materials, which convert heat into electricity, are the ideal candidates for this task, however the highest efficiency materials tend to contain rare or toxic elements such as Pb, limiting their potential uses. Therefore, the discovery of efficient, earth-abundant and non-toxic thermoelectrics is of great importance.

The recent analysis of $\text{Y}_2\text{Ti}_2\text{O}_5\text{S}_2$ as a thermoelectric² has revealed $\text{Ln}_2\text{M}_2\text{O}_5\text{Ch}_2$ to be a promising family for further investigation as thermoelectric materials. Here, we study $\text{Ln}_2\text{M}_2\text{O}_5\text{Ch}_2$, ($\text{Ln} = \text{Sc}, \text{Y}, \text{La}$; $\text{M} = \text{Ti}, \text{Zr}, \text{Hf}$ and $\text{Ch} = \text{S}, \text{Se}, \text{Te}$), first finding the kinetically and thermodynamically stable structures, before identifying their n-type preference via band alignment. Finally, we explicitly calculate the electronic and phononic scattering rates in order to calculate their thermoelectric performance, quantified by the dimensionless figure of merit, zT .

[1] Firth, A. et al, *Appl. Energy*, 2019, **235**, 1314

[2] Brlec, K. et al., *J. Mat. Chem. A*, 2022, **10**, 16813

5:00 PM EN08.08.09

Exploring Electronic and Thermal Conduction in Lanthanum Diselenide Christopher Savory^{1,2}; ¹University of Birmingham, United Kingdom; ²University College London, United Kingdom

Thermoelectric materials, converting heat into electricity, represent a key part of the energy generation economy, particularly when used for waste heat collection from other industrial processes. Many of the highest performing materials have issues with sustainability, in containing less abundant elements such as Te, or toxic elements such as Pb. Efforts to explore and develop new thermoelectrics are important to improve the diversity of materials – not only to drive for more sustainable compounds but also to tackle different optimal temperature ranges for specific waste heat applications.¹ LaSe_2 has seen recent investigation as a p-type transport material with intrinsic carrier concentrations beyond 10^{19} cm^{-3} ,² although with limited exploration for the microscopic origin of its favourable electronic behaviour. In this study, we examine LaSe_2 using multiple computational techniques to explain its electronic and thermal transport properties. Initially, we establish the key role of Se-Se dimerization in the structure of the compound in engineering valence band dispersion using a combination of hybrid Density Functional Theory and GW calculations.³ We move on to calculate electronic transport properties beyond the relaxation time approximation within the recently-developed AMSET code, allowing the calculation of individual scattering mechanisms, and establish the likely limits to carrier mobilities.⁴ Finally, we calculate the thermal transport properties of LaSe_2 , with comparison between the hiphive and ALAMODE packages^{5,6} to establish the suitability of LaSe_2 as a p-type thermoelectric, and the possibility for more earth abundant polychalcogenides.

1. Caballero-Calero, O.; Ares, J. R.; Martín-González, M. *Adv. Sustain. System* **2021**, *5* (11), 2100095.

2. Gao, G.; Tong, L.; Yang, L.; Sun, C.; Xu, L.; Xia, F.; Geng, F.; Xue, J.; Gong, H.; Zhu, J. *Appl. Phys. Lett.* **2021**, *118* (26), 261602.

3. Huo, L.; Savory, C., *ChemRxiv* **2023**, doi:10.26434/chemrxiv-2023-8jn8b-v3.

4. Ganose, A. M.; Park, J.; Faghaninia, A.; Woods-Robinson, R.; Persson, K. A.; Jain, A. *Nat. Commun.* **2021**, *12* (1), 2222.

5. Eriksson, F.; Fransson, E.; Erhart, P. *Adv. Theory Simul.* **2019**, *2* (5), 1800184.

6. Tadano, T.; Gohda, Y.; Tsuneyuki, S. *J. Phys. Condens. Matter* **2014**, *26* (22), 225402.

5:00 PM EN08.08.10

Ultra Low Thermal Conductivity and Enhanced Thermoelectric Properties of High Entropy Half Heusler Ankit Kumar, S.S Vishak, Prasenjit Ghosh and Surjeet Singh; Indian Institute of Science Education and Research, India

We have witnessed a dramatic reduction of lattice thermal conductivity and improved thermoelectric performance by increasing configurational entropy and tuning carriers of half Heusler (hH) systems. Lattice thermal conductivity is a major player in the thermoelectric performance. κ_L of double hH $\text{Ti}_2\text{FeNiSb}_2$ is less compared to conventional hH like TiCoSb because of Fe and Ni occupying same site. By increasing the number of component at same site, κ_L can be reduced. In this report we show an unexplored double hH $\text{Hf}_2\text{FeNiSb}_2$ and some high entropy (HE) hH alloys created by adding more components at Hf and Fe/Ni site. We have further engineered the bands to increase the band gap in order to counter bipolarity. The carriers were optimized by tuning Fe/Ni concentration in the synthesized HE $\text{TiHf}(\text{FeCoNi})_{0.667}\text{Sb}_2$. κ_L of $0.88 \text{ Wm}^{-1}\text{K}^{-1}$ was obtained for $\text{TiHf}(\text{Fe}_{0.5}\text{CoNi}_{1.5})_{0.667}\text{Sb}_2$ with maximum zT of 0.46 at 973 K. In the p-type region the maximum zT of 0.32 was obtained. This work demonstrates the effectiveness of the high entropy strategy in double hH compounds and the potential of the new concept of high entropy hH compounds as high-performance thermoelectric materials.

5:00 PM EN08.08.12

Favourable Interface Contacts for Thermoelectric Devices Ajay K. Verma^{1,2,3}, S. R. Dhakate^{2,3}, Sumeet Walia¹ and Bhasker Gahtori^{2,3}; ¹RMIT University, Australia; ²CSIR- National Physical Laboratory, India; ³Academy of Scientific & Innovative Research (AcSIR), India

A solid-state thermoelectric device directly transforms the waste heat into useful electricity. Although the practical applications of TE devices are confined owing to their low efficiency. The efficiency of TE devices depends on several parameters such as performance and compatibility of both p- and n-type thermoelectric materials, as well as compatibility of contact material. Further, a crucial aspect of enhancing thermoelectric performance lies in the engineering of contact interfaces within these devices. Various aspects of interface engineering, including contact material selection, surface passivation, and interface morphology control will be discussed here. Along with that will focus on the strategies to tailor interface properties to maximize charge carrier transport while minimizing thermal conduction, with low thermomechanical stresses. Therefore, understanding the key issue of unfavorable contact interfaces in TE devices and its possible solutions could hasten the development of several practical applications.

5:00 PM EN08.08.13

Oxide Thermoelectric Materials for Green Energy Generation Kriti Tyagi, Rohit Yadav and S. R. Dhakate; CSIR-National Physical Laboratory, India

BiCuSeO oxy-chalcogenides are considered promising thermoelectric materials due to high Seebeck coefficient values combined with intrinsically low thermal conductivity. BiCuSeO showcases properties of a semiconductor and possess low electrical conductivity values. The two essential steps that must be taken in sequence to create test materials for use in thermoelectric modules are the calcination of the mixed precursors (BiCuSeO) and subsequent consolidation into precisely dense pellets by spark plasma sintering (SPS) technique. By tracking the evolution of structural and morphological measurements, the current work optimizes the processing times for ball milling and calcination on the phase formation of polycrystalline BiCuSeO powder. The work also focuses on designing different synthesis routes and their comparison to find out the most suitable route for synthesizing pristine BiCuSeO.

5:00 PM EN08.08.14

Computational Design of SiGeSn Alloys for Thermoelectric Applications Li-Wen Lin and Szu-Chia Chien; National Central University, Taiwan

Owing to the increasing demand for sustainable energy, significant effort has been made towards the development of energy-related materials. Among various candidates, thermoelectric materials have drawn considerable attention. Si-Ge alloys have a long history as effective thermoelectric materials for waste heat recovery. More importantly, recent studies have shown that Si-Ge alloys with the Ge content of 20% possess excellent material properties as thermoelectric materials¹. By introducing Sn into Si-Ge alloys, the thermal conductivity can be reduced with a small impact on electrical conductivity, thus making SiGeSn alloys promising thermoelectric candidates. However, challenges in precise composition control and complex synthesis methods in experiments may limit their studies and applications². To this end, this work seeks to employ computational methods to help search for the optimal composition ratios of SiGeSn alloys with the aim of facilitating the development of SiGeSn thermoelectric materials.

In this work, the Alloy Theoretic Automated Toolkit (ATAT), utilizing special quasi-random structure (SQS) modeling, is employed to create random $\text{Si}_x\text{Ge}_y\text{Sn}_z$ alloys with various Si, Ge, and Sn content. The electronic structure characteristics are calculated using density functional theory (DFT) as implemented in the Vienna *Ab-initio* Simulation Package (VASP)³, whereas their thermoelectric properties are assessed by BoltzTraP2 software, which applies the Boltzmann Transport Equation (BTE) for obtaining key thermoelectric parameters such as the Seebeck coefficient, electronic conductivity, electronic thermal conductivity, and power factor⁴. Our result shows that with the composition of $\text{Si}_4\text{Ge}_1\text{Sn}_1$, the highest figure of merit of around 0.8 can be achieved. By integrating these computational tools, this work offers comprehensive insights into the intricate correlation between composition ratios and the thermoelectric properties in SiGeSn alloys. It is anticipated that the findings from this work can offer insights into the design of high-performance thermoelectric materials.

References

1. Lee, Y.; Alexander J. P.; and Hwang, G. S., *Phys. Chem. Chem. Phys.* 2016, 18, 19544-19548.
2. Wirths, S.; Buca, D.; Mantl, S., *Prog. Cryst. Growth Charact. Mater.* 2016, 62, 1-39.
3. Kresse, G.; Furthmüller, J., *Phys. Rev. B* 1996, 54, 11169.
4. Madsen, G. K. H.; Carrete, J.; Verstraete, M. J., *Comput. Phys. Commun.* 2018, 231, 140-145.

5:00 PM EN08.08.16

Drastic Lowering of Lattice Thermal Conductivity induced by Aliovalent Substitution of TiCoSb-Based Half-Heusler Compound Dipanwita Bhattacharjee¹, Nagendra S. Chauhan², Tanmoy Maiti³, Yury V. Kolen'ko⁴, Yuzuru Miyazaki⁵ and Amrita Bhattacharya¹; ¹Indian Institute of Technology Bombay, India; ²National Institute for Materials Science, Japan; ³Indian Institute of Technology Kanpur, India; ⁴International Iberian Nanotechnology Laboratory, Portugal; ⁵Tohoku University, Japan

The performance of the state-of-the-art ternary half-Heusler (HH) compounds is limited by their intrinsically high lattice thermal conductivity (κ_L). In this study, we present a stable n-type biphasic-quaternary (Ti,V)CoSb HH alloy that is equivalent to previously reported nanostructured HH alloys in terms of lattice thermal conductivity ($\kappa_L \sim 2$ W/mK) within a temperature range of 300-800 K. Aliovalent substitution of TiCoSb, resulting in an effective 18.5 valence electron count ($\text{Ti}_{0.5}\text{V}_{0.5}\text{CoSb}$), results in a significant reduction in κ_L and synergistic enhancement of the power factor with a peak zT of $0.4 (\pm 0.05)$ at 873 K. The lowering of κ_L in $\text{Ti}_{0.5}\text{V}_{0.5}\text{CoSb}$ HH alloy is attributed to an enhancement in phonon scattering driven by spinodal decomposition upon annealing. First-principles DFT calculations are performed to investigate the structure, stability, electronic structure, and transport properties of the synthesised alloy, which accredits the decrease in lattice thermal conductivity to the alloy's increased anharmonicity. The changing electronic band-structure upon substitution and an increase in carrier concentration have a good correlation with the observed electrical characteristics. Hence, new prospects for discovering biphasic-quaternary HH compositions with intrinsically lower κ for potential thermoelectric applications are supported by this study.

5:00 PM EN08.08.17

Defect Engineering in Bi_2Se_3 by Tuning Synthesis Conditions - A Combined Experimental and Theoretical Study Michael Toriyama¹, Andrei Novitskii², Illia Serhienko^{2,3}, Takao Mori^{2,3}, Jeff Snyder¹ and Prashun Gorai⁴; ¹Northwestern University, United States; ²National Institute for Materials Science, Japan; ³University of Tsukuba, Japan; ⁴Colorado School of Mines, United States

Recently, Bi_2Se_3 has emerged as a promising n-type counterpart to p-type BiCuSeO in thermoelectric (TE) devices. However, there are significant variations in the reported charge carrier concentration of Bi_2Se_3 spanning several orders of magnitude, resulting in diverging reports of TE properties. These predominantly arise from the disparate synthesis routes used, which in turn affect the defect thermodynamics in the system. In this study, we employ a combined experimental and theoretical approach to demonstrate how defect engineering controlled by synthesis conditions can be used to tailor the transport properties of n-type Bi_2Se_3 . Through first-principles calculations, we identify the dominant native defect in Bi_2Se_3 as the donor-like selenium vacancy (V_{Se}). We predict that increasing the synthesis temperature (T_{SSR}) of nominally undoped Bi_2Se_3 will lead to an increase in V_{Se} and, consequently, electron concentration. We observe a rise in carrier concentration by nearly two orders of magnitude between samples synthesized at $T_{\text{SSR}} = 773$ K and $T_{\text{SSR}} = 1173$ K. This results in the enhancement in both the quality factor and the TE performance with a remarkable zT value of 0.25 at 773 K achieved for self-doped Bi_2Se_3 . Our findings underscore a noteworthy relationship between processing conditions and the transport properties of Bi_2Se_3 rooted in defect engineering.

5:00 PM EN08.08.18

Side-Chain Engineered p or n-Type Nonaqueous Polymeric Ionic Gels for Sustainable Ionic Thermoelectrics Sungryong Kim, Seyeong Lim and Taiho Park; Pohang University of Science and Technology, Korea (the Republic of)

Although ionic hydrogels have been developed recently for innovative wearable electronics, they necessitate high humidity to diffuse ions in water and fast self-healing, which negatively impacts their performance and stability in ambient conditions (e.g., dry environments). In this study, a series of p- and n-type polymeric ionic gels (PIGs) with different ratios of ionic side chains are synthesized to allow only single-type ions to pass through them. The results

demonstrate that our repeatedly stretchable PIGs are transparent, thermally robust up to 125 °C, and self-healing. Among the series of PIGs, p- and n-type PIGs with 75% ion moieties (P75 and N75) exhibit the optimum ionic conductivity (σ_i) (4.1×10^{-4} and 2.7×10^{-4} S cm⁻¹) and ionic Seebeck coefficients (S_i) (5.84, and -4.18 mV K⁻¹) under ambient conditions (25 °C and relative humidity (RH) of 30%), resulting in ZT_i values of 1.87×10^{-3} and 1.18×10^{-3} . Moreover, the σ_i and S_i of PIGs were almost consistent under extremely low RH 10%. Accordingly, P((EMIM⁺)[SPA])_{0.75-r}-MA_{0.25} (P75) and P((APTA)[TFSI])_{0.75-r}-MA_{0.25} (N75) are used to achieve stretchable ionic thermoelectrics (iTEs) with stable operability under ambient conditions (RH of 30%), satisfying all of the requirements. The iTEs with five pairs of p/n couples exhibit a thermovoltage of up to -0.8 V.

5:00 PM *EN08.08.19

Engineering Thermoelectric Transport in Transparent Conducting Oxides Vinayak B. Kamble, Soumya Biswas, Saptak Majumder and E. Jagadeswara Reddy; Indian Institute of Science Education and Research (IISER) Thiruvananthapuram, India

A number of oxides, including ZnO, ITO, SrTiO₃ and cobalt oxides are promising candidate as environment friendly thermoelectric (TE) materials[1-3]. However, high thermal conductivity is the primary factor which hinders their application and leads to poor TE figure of merit (zT). Here we demonstrate that microstructure engineering through Al doping and reduced graphene oxide /graphite additives leads to selective enhancement in phonon scattering in ZnO thereby increasing its TE efficiency[4]. The incorporation of trace Al doping with 1.5 wt% RGO into ZnO (AGZO) has been found to show significant improvement in zT (=0.52 at 1100 K) which is an order of magnitude larger compared to that of bare undoped ZnO. Tunneling spectroscopy performed on bare as well as composite particles reveals that the band gap of ~ 3.4 eV for bare ZnO reduces effectively to ~ 0.5 eV upon RGO encapsulation, facilitating charge transport. The Al doping, defect engineering and RGO encapsulation synergistically brings about drastic reduction of thermal conductivity, through enhanced interfacial and point defect-phonon scatterings. These opposing effects on electrical and thermal conductivities leads to enhancement in the power factors as well as the zT value[5]. Our subsequent efforts with highly ITO oxides will be presented in the later half.

References

- [1] M. H. N. Assadi, J J Gutiérrez Moreno, M. Fronzi, *ACS Applied Energy Materials* **3**, 5666-5674 (2020)
- [2] J. He, Y. Liu, R. Funahashi, *Journal of Materials Research* **26**, 1762 (2011)
- [3] J. W. Fergus, *Journal of the European Ceramic Society* **32**, 525-540 (2012)
- [4] A. S. Dutt, S. Biswas, K. Dabral, K.; P. Rajasekar, V. B. Kamble, *AIP Conference Proceedings* **2297**, 020005 (2020)
- [5] S. Biswas, S. Singh, S. Singh, S. Chattopadhyay, K.K. H. De Silva, M. Yoshimura, J. Mitra, V. B. Kamble, V. B., *ACS Applied Materials & Interfaces* **13**, 23771–23786, (2021)

5:00 PM EN08.08.20

Sustainable Metal Phosphide Thermoelectrics with Promising Performance Robert Quinn¹, Rajan Biswas² and Jan-Willem Bos²; ¹Heriot-Watt University, United Kingdom; ²University of St. Andrews, United Kingdom

There is a continued need for discovery of new thermoelectric materials. Metal phosphides are an emerging class of thermoelectrics with promising figures of merit, approaching $zT = 1$ in n-types and $zT = 0.5-0.8$ in p-types.¹

Despite the low atomic mass of phosphorous, structural complexity leads to low thermal conductivities across a range of materials and the main challenge is to embed better electrical properties.¹ Phosphorous has a range of possible oxidation states, affording diverse chemical bonding and a wide range of available structures for exploration.

We have investigated a series of ternary metal phosphides and have discovered promising thermoelectric performance in MgCuP, CaCuP and CaAgP.^{2,3,4} In all cases, metal deficiency leads to degenerate p-type conduction and the figures of merit fall between $zT = 0.4-0.5$ at 660-773 K. CaCuP in particular is promising as this composition has the best electronic properties amongst all reported metal phosphides.^{2,3} Modelling shows CaCuP can reach $zT = 1$ in alloyed compositions if control of doping can be achieved. MgCuP has a lower symmetry structure and achieves a similar zT on account of a lower thermal conductivity.² CaAgP has been considered as a candidate topological nodal line semimetal. However, our work shows that CaAgP forms with high concentrations of Ag vacancies, and the stable phase CaAg_{0.9}P behaves like a regular highly doped semiconductor.⁴

This contribution will summarise our recent metal phosphide work, including phase boundary mapping and alloying in the CaCuP system and discuss some of the general conclusions from our recent review.¹

References

- [1] R.J. Quinn and J.W.G. Bos, *Journal of Materials Chemistry A* **11** 8453 (2023).
- [2] R.J. Quinn and J.W.G. Bos, *Chemical Communications* **58**, 11811 (2022).
- [3] R.J. Quinn, R. Biswas and J.W.G. Bos, *ACS Applied Electronic Materials* (2023), DOI: 10.1021/acsaelm.3c00828
- [4] R.J. Quinn and J.W.G. Bos, *Applied Physics Letters* **120**, 073903 (2022).

5:00 PM EN08.08.21

Enhanced Density of States Mass in Cu Containing XNiSn Half-Heusler Alloys – A New Route Towards High Thermoelectric Performance Robert Quinn¹, Sonia Barczak¹ and Jan-Willem Bos²; ¹Heriot-Watt University, United Kingdom; ²University of St. Andrews, United Kingdom

Half-Heusler alloys are leading contenders for application in commercial thermoelectric generators. They combine strong performance with good engineering properties and thermal stability.¹ There has been great progress in p-type half-Heusler alloys in the past decade, with $zT = 1.5$ achieved in NbFeSb and ZrCoBi. There have been fewer developments in n-type Heusler alloys with the best performance in compositions based on ZrNiSn, with peak $zT = 1.2-1.3$.

We have investigated the use of interstitial Cu in the XNiSn half-Heusler alloys. This cheap base metal is an alternative to the usual n-type dopant Sb. In addition to being an efficient n-type donor, its use leads to a suppression of thermal conductivity and a more homogeneous microstructure.²⁻⁴ Our latest work reveals an enhanced density of states effective mass, $m_{DOS}^* \sim 4.1 m_0$, for Cu-doped XNiSn half-Heusler samples rich in X = Ti. This enhancement over typical values of $3 m_0$ occurs without substantial drop in electron mobility. This enables improved power factors and peak $zT = 1$ at 773 K in TiNiSn-based samples with interstitial Cu used as a mineraliser, dopant and to suppress thermal transport.³ Bandstructure calculations show the emergence of a second band at the conduction band minimum. This brings the performance of TiNiSn-based compositions close to the leading n-types based on Sb-doped ZrNiSn and is a significant development.

This contribution will summarise our current understanding of the impact of interstitial Cu in the XNiSn Heuslers, which goes beyond carrier doping and affects underlying electronic properties and microstructure of these materials.

References

- [1] R. J. Quinn and J.W.G. Bos, *Materials Advances*, **2** 6246 (2021).
- [2] S. A. Barczak et al. *ACS Applied Materials and Interfaces* **10**, 4786 (2018)
- [3] S. A. Barczak et al. *Journal of Materials Chemistry A* **7**, 27124 (2019).
- [4] J. E. Halpin et al. *ACS Applied Electronic Materials* **4**, 4446 (2022).
- [5] R. J. Quinn et al. *Submitted* (2023).

5:00 PM EN08.08.22

Ab Initio Investigation of Thermoelectric Properties of Two-Dimensional MOFs Masoumeh Mahmoudi Gahrouei, Emmanuel Odogwu, Nikiphoros Loki Vlastos and Laura de Sousa Oliveira; University of Wyoming, United States

Recent studies have shown that metal-organic frameworks (MOFs) have potential as thermoelectric materials, and the topic has received increasing attention. The main motivation for this project is to further our knowledge of thermoelectric properties in MOFs and find which available density functional based tight-binding method can accurately predict (at least trends in) the electronic and thermoelectric properties of MOFs at a lower computational cost than standard density functional theory. In this work, the monolayer, AA, and AB-stacked $Zn_3C_6O_6$, Zn-NH-MOF and $Ni_3(HITP)_2$ MOF structures have been investigated. Our results indicate that tight-binding density functional theory, especially GFN-xTB, a less computationally expensive first principles-based approach, can be used reliably to speed up predictions of the MOFs' electronic, phonon and thermoelectric properties. Phonon dispersion calculations of the $Zn_3C_6O_6$ and Zn-NH MOFs show that AB-stacking results in the most stable structure whereas for $Ni_3(HITP)_2$ both AA and AA slipped stacking are dynamically stable. To estimate the figure of merit, for the aforementioned MOF geometries, the electrical conductivity and Seebeck coefficient are computed (with a constant carrier relaxation time) along with the lattice thermal conductivity (using third-order force constants). We report on these results, including how the thickness and doping are expected to affect the thermoelectric properties of semiconducting MOFs.

5:00 PM EN08.08.23

A Computational Investigation of Bi_2MO_4Cl ($M = Y, La$ and Bi) as Thermoelectric Materials Shipeng Bi¹ and David O. Scanlon²; ¹University College London, United Kingdom; ²University of Birmingham, United Kingdom

In the process of primary energy consumption, a large amount of waste heat is generated. Thermoelectric materials (TEs) can convert waste heat energy into electric energy, which is crucial to solving the current energy crisis and mitigating global warming. In general, the performance of TEs can be determined by the dimensionless figure of merit, ZT , that is evaluated from its electronic and thermal properties. However, it is difficult to maximise ZT due to the interaction between different parameters.

In recent years, mixed anionic oxides have shown great potential in the field of TEs.¹⁻³ Recently, the mixed anionic oxides Bi_2MO_4Cl ($M = Y, La$ and Bi) was shown to exhibit excellent stability in photocatalytic water oxidation reactions,⁴ but their thermoelectric properties have not been explored. We postulated that this quaternary structure with heavy elements will lead to a low lattice thermal conductivity, and they can be synthesised at a relatively high temperature, thus can maintain stability at high temperatures, so we performed density functional theory (DFT) calculations to study the thermoelectric performance of Bi_2MO_4Cl ($M = Y, La$ and Bi). Our results showed that Bi_2MO_4Cl ($M = Y, La$ and Bi) belongs to p-type TEs and exhibits an average ZT of about 1 at 1000 K.

References

- 1 M. Einhorn, B. A. D. Williamson and D. O. Scanlon, *J. Mater. Chem. A*, 2020, **8**, 7914-7924.
- 2 K. Brlec, K. B. Spooner, J. M. Skelton and D. O. Scanlon, *J. Mater. Chem. A*, 2022, **10**, 16813-16824.
- 3 W. Rahim, J. M. Skelton and D. O. Scanlon, *J. Mater. Chem. A*, 2021, **9**, 20417-20435.
- 4 A. Nakada, D. Kato, R. Nelson, H. Takahira, M. Yabuuchi, M. Higashi, H. Suzuki, M. Kirsanova, N. Kakudou, C. Tassel; et al., *J. Am. Chem. Soc.*, 2021, **143**, 2491-2499.

5:00 PM EN08.08.24

Thermoelectric Enhancement of Thin Si Films by means of Block Copolymer Driven Nanostructuring Alex Rodriguez-Iglesias¹, Inigo Martín-Fernández¹, Francesc Pérez-Murano¹, Joaquín Santander¹, F. Xavier Alvarez², Aitor F. Lopeandia², Luis Fonseca¹, Llibert Abad¹, Marc Salleras¹ and Marta Fernández-Regúlez¹; ¹Instituto de Microelectrónica de Barcelona (IMB-CNM, CSIC), Spain; ²Universitat Autònoma de Barcelona, Spain

Thermoelectricity explains the conversion of heat into electricity and vice versa, and a plethora of applications are available nowadays for thermoelectric systems in the fields of cooling, power generation and sensing. Traditionally, the most used thermoelectric materials have been based on chalcogenides, as the main reason that has driven the material choice has been the maximization of the thermoelectric figure of merit (ZT). This figure of merit indicates the performance capabilities of a material as a thermoelectric, and depends on its Seebeck coefficient and its electrical and thermal conductivities.

Nevertheless, these widely used materials are based on alloys of scarce, expensive, and toxic elements (Bi, Te, etc.) that are difficult to integrate within the semiconductor industry. On the contrary, silicon (Si) is a poor thermoelectric material when in its bulk form but it has been shown to improve around 100 times its thermoelectric performance when it is nanostructured in two- or one-dimensional structures, then becoming a competitive alternative [1]. This improvement is mainly justified by the effective reduction of the phononic thermal conductance in the nanostructured material.

In this contribution, we present the study of suspended Si ultra-thin films as thermoelectric material, which are much easier to integrate into semiconductor technologies. Although the enhancement in thermoelectric performance of thin films is modest when compared to one-dimensional structures, this is compensated and enhanced by introducing surface nanostructuring with the aim to reach thermoelectric figures of merit similar to the best reported values in the literature for Si structures. These structures are based on rough surface Si nanowires (NWs), whose large-scale fabrication remains unsolved as the synthesis of high density and uniform Si NW arrays with homogeneous nanoscopic surface morphology is a challenging process. Here, we present a cost-effective and scalable approach for the fabrication of the membranes by block copolymer (BCP) nanopatterning. BCP based technologies present manufacturing advantages, as it is a technology easy to scale up for high-volume manufacturing, very cost-effective and capable of achieving sub-10 nm resolution [2].

Nanostructured Si membranes are fabricated on the device layer of a Silicon on Insulator (SOI) wafer with ultrathin device layer (30 – 50 nm). A thin film BCP is self-assembled perpendicularly oriented to the Si surface. The BCP used for surface nanostructuring is polystyrene-block-poly(methylmethacrylate) (PS-b-PMMA) with cylindrical or lamellar morphology and a period between 28 and 80 nm. After self-assembly, the PMMA block is selectively removed, and PS features are transferred into the Si underneath by reactive ion etching (RIE). As a result, we obtain a nanostructured surface with a hexagonal distribution of holes when a BCP with cylindrical morphology is used as a mask, and a fingerprint-type nanostructuring when a lamellar BCP is used as a mask. The period of such structures is controlled by properly blending BCPs of different molecular weights and the depth and the shape of the walls are tuned by the RIE conditions. The final structures are doped by spin-on dopant to achieve an optimal doping concentration, 10^{19} - 10^{20} cm⁻³, for thermoelectric applications. This method has been chosen because it's a low cost, wafer scale compatible and non-destructive process, and the

characterization of the doping values obtained has been done with the 4-probe method on the thin films. We will study the effect of surface nanostructuring on the thermoelectric performance. The thermal conductivity of the membranes will be evaluated using the $3w$ Völklein approach on an appropriate test structure, in order to find the most optimal nanostructuring conditions for thermoelectricity.

[1] D. Dávila, et al. *Nano Energy* 2012, 1 (6), 812

[2] C. Pinto-Gómez et al. *Polymers* 2020, 12(10), 2432

SESSION EN08.09: Novel Materials
Session Chairs: Susan Kauzlarich and Alexandra Zevalkink
Thursday Morning, April 25, 2024
Room 336, Level 3, Summit

8:30 AM *EN08.09.01

Structure and Property Relationship in GeTe based Thermoelectric Materials Yong Yu, Wu Wang, Lin Xie and Jiaqing He; Southern University of Science and Technology, China

The performance of thermoelectric materials is mainly governed by the materials' electrical and thermal conductivity properties and a number of new materials and structures have been exploited in order to optimize the energy conversion efficiency. Especially, nanostructure engineering via dopants, precipitates or phase/twin/grain boundaries is found to be effective in increasing the conversion efficiency by reducing the thermal conductivity. However, a direct correlation of these nanostructures to the material's property is yet to be elucidated. Nowadays, with the rapid development of aberration-corrected transmission electron microscopy (TEM), the resolution of electron microscopes takes a leap forward to sub-angstrom and sub-eV, which allows a direct access to a material's structure and chemical composition at an atomic scale.

The presentation will start with a brief and realistic coverage of the emerging and maturing themes in the context of energy sources, efficiency, charge storage and distribution. It will illustrate GeTe as one example of emerging excitements in nanostructured materials and systems for thermoelectric materials. It will highlight the role of advanced and classical electron microscopy in unravelling the structure of the constituents and their intimate interplay in governing key phenomena in thermoelectric materials.

9:00 AM EN08.09.02

Defect-Driven Thermoelectric Performance in Disordered Cd-Doped AgSbTe₂ Sabrine Hachmioune^{1,2}, Chenguang Zhang³, Jose R. Gomez³, Maheswar Repaka², Kedar Hippalgaonkar^{2,3}, Michael B. Sullivan² and David O. Scanlon⁴; ¹UCL, United Kingdom; ²Agency for Science, Technology and Research, Singapore; ³Nanyang Technological University, Singapore; ⁴University of Birmingham, United Kingdom

With an increasing demand for efficient and environmentally friendly energy conversion technologies, thermoelectric materials play a pivotal role in harnessing waste heat for power generation. In this work, we focus on enhancing the thermoelectric performance of AgSbTe₂, a well-known high-performance material that has garnered significant attention for its exceptional performance in mid-temperature range applications.¹ Previous works showed the high ZT could be further improved by Cd-doping to achieve a maximum ZT of 2.6 at 573 K.² This improvement in performance was attributed to cationic ordering and tuning of the disorder in the material. This study presents a comprehensive experimental and theoretical investigation of the thermoelectric properties of cadmium-doped silver antimony telluride (Cd-doped AST).

Single-phase Cd-doped AST samples were successfully synthesised, exhibiting notably high-power factor values. Remarkably, a peak power factor of $\sim 20 \mu\text{Wcm}^{-1}\text{K}^{-2}$ was achieved, demonstrating the material's exceptional electrical conductivity. Furthermore, thermal conductivities as low as $0.5 \text{ Wm}^{-1}\text{K}^{-1}$ were observed at 330 K. This research also investigates the influence of growing under silver and tellurium poor conditions.

Employing first-principles hybrid-density functional theory (DFT) calculations, we systematically analyse the defect landscape within AgSbTe₂. By quantifying the concentration and distribution of defects, we unveil their effect on the crystal lattice structure and electronic band structure. The impact of Cd-doping on the electronic band structure was analysed to understand the underlying mechanisms responsible for the observed changes in thermoelectric performance.

By understanding the interplay between disorder-induced defects and thermoelectric performance, we aim to pave the way for the design and optimisation of advanced thermoelectric materials for efficient energy conversion applications. The combined experimental and theoretical approach offers a robust framework for the design and optimisation of thermoelectric materials contributing to the advancement of sustainable energy technologies.

1 Y. Zhang, Z. Li, S. Singh, A. Nozariasbmarz, W. Li, A. Genç, Y. Xia, L. Zheng, S. H. Lee, S. K. Karan, G. K. Goyal, N. Liu, S. M. Mohan, Z. Mao, A. Cabot, C. Wolverton, B. Poudel and S. Priya, *Adv. Mater.*, 2023, **35**, 2208994.

2 N. Cheng, R. Liu, S. Bai, X. Shi and L. Chen, *J. Appl. Phys.*, 2014, **115**, 163705.

9:15 AM EN08.09.03

Micro/Nano-Scale Structural and Thermoelectric Characterization of Magnesium Silicide-Based Composite Materials: Investigating Self-Diffusion of Constituent Elements, Band Alignment and Transport Properties Sanyukta Ghosh¹, Harshita Naithani¹, Mohamed Abdelbaky², Eleonora Isotta³, Byungki Ryu⁴, Wolfgang Martin², Gregor Oppitz¹, Eckhard Müller¹ and Johannes de Boor¹; ¹German Aerospace Center (DLR), Germany; ²University of Duisburg-Essen, Germany; ³Northwestern University, United States; ⁴Korea Electrotechnology Research Institute, Korea (the Republic of)

The ability of thermoelectric (TE) materials to produce electrical power from otherwise wasted thermal energy has propelled this field into the spotlight, with immense potential for addressing critical issues such as energy efficiency, sustainable power generation, and environmental conservation. The effectiveness of a TE generator is intricately linked to the performance of its constituent TE materials, which, in turn, is constrained within uniform bulk materials by the interplay of three fundamental TE transport properties: the Seebeck coefficient, electrical conductivity, and thermal conductivity. The precise manipulation of the electronic band alignment at the micro/nanoscale can serve to disentangle these TE properties by selectively filtering out detrimental spectral fractions of the charge carriers. Among the diverse array of TE materials, magnesium silicide-based materials are the preferred choice for this purpose due to their spontaneous formation of nanostructured composites comprising distinct phases with varying band gaps dependent on the Si:Sn ratio, driven by a miscibility gap in the solid solution series. Furthermore, these materials are emerging as compelling candidates due to their potential to serve as cost-effective and environmentally friendly components, showcasing exceptional TE properties within the mid-temperature range of

500-800 K. However, the conventional bulk property measurements often lack the sensitivity required to detect the subtle effects of charge carrier filtering, necessitating micro/nano-scale characterizations of TE properties (Seebeck coefficient and thermal conductivity) of multi-phase materials. In our research, we have integrated several locally resolved experimental techniques with electronic transport modeling. The transient Seebeck microprobe, with its micron-scale resolution, allows us to map the distribution of the Seebeck coefficient. Combining the Seebeck coefficient map and the compositional map, obtained by establishing a simple correlation between the grey value in backscattered electron (BSE) images and the chemical composition from EDX point analysis, enables a local correlation between the Seebeck coefficient and the phase composition in multiphase materials. Moreover, employing transport modeling offers insights into the local distribution of the reduced Fermi level and the alignment of valence and conduction bands, enabling the generation of a micro-scale carrier concentration map. Furthermore, utilizing Kelvin probe force microscopy with nano-scale spatial resolution can provide the value of the Fermi level position with respect to the vacuum level, enabling generation of the same carrier concentration map at the nano-scale. Our work also demonstrates the potential of selective doping, using Bi as a dopant, to precisely modify the band positions of individual phases, a prerequisite for material enhancement by energy filtering. This localized characterization technique also aids our understanding of the inter-diffusion of Mg, Si, and Sn from one phase to another, resulting in distinct changes in the thermoelectric properties of each phase. This knowledge is vital for optimizing thermoelectric properties, as it can either amplify or attenuate the effects of selective doping. Hence, this integrated approach represents a crucial step towards optimizing composite materials through effective energy filtering.

9:30 AM BREAK

10:00 AM *EN08.09.04

New Members of The $\text{Ca}_{14}\text{AlSb}_{11}$ Structure Type: Structure and Thermoelectric Properties [Susan M. Kauzlarich](#); University of California, Davis, United States

Compounds of the $\text{Ca}_{14}\text{AlSb}_{11}$ structure type show some of the highest zT s at high temperatures for p-type compounds. We have shown that preparing these phases with binary precursors of the appropriate composition provides a high-fidelity route to phase pure powders. This allows for broad exploration of this structure type and the resulting thermoelectric properties. We have initiated an investigation of the Eu- and As-containing compounds. In principle, for $\text{Eu}_{14}\text{MAS}_{11}$, the following compounds should be possible with $M = \text{Mn, Zn, Cd, Mg, Fe}$. I will present the synthesis of these phases, and the thermoelectric properties and compare them with other compounds of this structure type.

10:30 AM EN08.09.05

Cu_2SiSe_3 as a Self-Doped Thermoelectric [Adair Nicolson](#)¹ and David O. Scanlon²; ¹University College London, United Kingdom; ²University of Birmingham, United Kingdom

Thermoelectric materials can convert thermal energy into electrical energy, taking advantage of the waste heat generated during many industrial processes. Currently, some of the best performing materials are chalcogenides containing toxic elements such as PbSe and PbTe.^[1] Therefore, there is a need for research into new thermoelectric materials, which contain earth-abundant and non-toxic elements.

Kesterites, for example CuZnSnS (CZTS), have been shown to have lattice thermal conductivity lower than PbTe, and equivalent to PbSe, showing that a low lattice thermal conductivity can be achieved without the inclusion of heavy atoms by increasing the structural complexity of the material.^[2] However, generating sufficient charge carriers through doping is a challenge, due to the complex quaternary defect chemistry. Taking inspiration from the kesterites, we have computationally investigated the ternary Cu_2SiSe_3 as a potential thermoelectric, as it has been previously shown to be intrinsically p-type due to the high concentrations of copper vacancies.^[3] There is also a large dopability window to increase the concentration of charge carriers further.

In this work we use the AMSET^[4] code to calculate the electronic transport properties using the momentum relaxation time approximation and which when combined with lattice thermal conductivities calculated using Phono3py^[5], with force-constants fitted using the hiphive package^[6], enabling the calculation of the thermoelectric figure of merit, zT . A zT of 0.91 is predicted in a self-doped crystal at 800 K, increasing to > 1.5 at higher carrier concentrations.

[1] Xiang, H. et al., Adv. Sustain. Syst., 2022, 6, 2100457

[2] Skelton, J. M. et al., A. APL Materials, 2015, 3, 041102

[3] Nicolson, A. et al., J. Mater. Chem. A, 2023, 11, 14833-14839

[4] Ganose, A. M. et al., Nat. Commun., 2021, 12, 2222.

[5] Togo A., Phys. Rev. B, 2015, 91, 094306.

[6] Eriksson F., et al. Adv. Theory Simul. 2019, 2, 1800184

10:45 AM EN08.09.06

Changes in Physical Properties for HPT-Processed p-Type Skutterudite $\text{DD}_{0.7}\text{Fe}_3\text{CoSb}_{12}$ [Gerda Rogl](#)¹, Vilma Bursikova², Kunio Yubuta³ and Peter F. Rogl¹; ¹University of Vienna, Austria; ²Masaryk University, Czechia; ³Kyushu University, Japan

To build thermoelectric generators, which can directly convert heat into electricity, materials with a high figure of merit, ZT are essential. Severe plastic deformation (SPD) via high-pressure torsion (HPT) was successfully applied to produce in a fast and energy saving way bulk nanostructured skutterudites directly from powders. SPD introduces many defects into the sample and in parallel the crystallite size is significantly reduced. HPT-processed $\text{DD}_{0.7}\text{Fe}_3\text{CoSb}_{12}$ is a high-quality thermoelectric material with $1.12 < ZT < 1.35$ at 750 K. During measurement-induced heating these defects anneal partially out, and the grains grow. It was observed that while heating HPT processed material from room temperature to about 850 K, changes of the temperature-dependent physical properties, most of all the electrical resistivity, the density, and the thermal expansion occur more or less simultaneously around 600 K. For the first time we have combined *in situ* TEM observations as well as measurements of the elastic modulus and hardness in order to get a deeper insight into the microstructural behavior of a p-type skutterudite, $\text{DD}_{0.7}\text{Fe}_3\text{CoSb}_{12}$ (DD = didymium) during increasing temperature from 300 K to 823 K.

11:00 AM EN08.09.07

$\text{BaCu}_{2-x}\text{T}_x\text{P}_2$ ($T = \text{Al, Ga, In, Si, or } \{\text{Si+Zn}\}$): A New Group Semiconducting 'Golden Geese' in The ThCr_2Si_2 Family with Ultra-Low Thermal Conductivity and High Seebeck Coefficient [Arka Sarkar](#)^{1,2}, Gayatri Viswanathan^{1,2}, Stasia Harycki¹, Andrew P. Porter¹, Alexander Gundlach-Graham¹, Aaron Rossini¹ and Kirill Kovnir^{1,2}; ¹Iowa State University, United States; ²Ames Laboratory, United States

ThCr_2Si_2 -type layered materials are a large family of compounds with applications ranging from thermoelectricity to magnetism, with most of them showing metallic behavior. In this study, we synthesized a variety of new ThCr_2Si_2 -type materials with the general formula $\text{BaCu}_{2-x}\text{T}_x\text{P}_2$ ($T = \text{Al, Ga, In, Si, or } \{\text{Si+Zn}\}$), most being charge balanced semiconductors, a rarity in this family. They all crystallize in the ThCr_2Si_2 -type tetragonal $I4/mmm$ space group,

with Cu/T jointly occupying the same 4d crystallographic site. In the case of BaCuAlP₂ and BaCu_{1.33}Si_{0.67}P₂, Ba atom occupies a single crystallographic site. However, the introduction of Zn in the BaCu_{1.33}Si_{0.67}P₂ system results in the expansion of the unit cell by 4%, splitting the Ba atom along the crystallographic c-direction. Similar structural distortions are observed for BaCuGaP₂ and BaCuInP₂ as well. Such structural disorder of the Ba atoms leads to the occurrence of clathrate-like rattling behavior along the c-direction, as observed from heat capacity measurements. This in turn leads to ultra-low thermal conductivity (as low as ~0.4 W/m-K at 550 °C) at high temperatures. All BaCu_{2-x}T_xP₂ materials show semiconducting behavior, making them potential solar absorbers. The composition with the lowest Zn-content, BaCu_{1.5}Zn_{0.2}Si_{0.5}P₂, exhibits a clear semiconductor-to-metal transition upon heating above 155 K. The materials show high Seebeck coefficients, such as ~300 μV/K at 550 °C for BaCuAlP₂, making them promising candidates for thermoelectric applications. Band structure and density-of-states calculations on ordered hypothetical structures reveal clear semiconducting nature for the triel-based materials and semi-metallic nature for the Si-based ones.

11:15 AM EN08.09.08

Exploration of The Effects of Yb₁₁Sb₁₀ and Yb₁₀MnSb₉ Secondary Phases on The High Performing Zintl Thermoelectric Material Yb₁₄MnSb₁₁

Leah E. Borgsmiller and Jeff Snyder; Northwestern University, United States

The high performing Zintl thermoelectric material Yb₁₄MnSb₁₁ has been of interest to the thermoelectrics community for years. However, a major challenge with this material is that it exists in a very busy region of phase space, making it susceptible to having considerable amounts of secondary phases. In particular, the Yb₁₁Sb₁₀ phase has been repeatedly reported as a negative secondary phase, but there have been discrepancies in the literature regarding the effect of this phase as a secondary phase in 14-1-11. Since the Yb₁₁Sb₁₀ material is a poor metal, it would be expected to hinder thermoelectric performance, and yet there have been studies where large amounts of this metallic phase have relatively no effect on transport, and even one case where it seemed like the Yb₁₁Sb₁₀ phase contributed to an improvement in the thermoelectric performance. Recently, a related phase, Yb₁₀MnSb₉ has been reported and has been shown to have a high Seebeck coefficient and ultralow thermal conductivity making it a decent p-type thermoelectric material. Despite having very different properties, Yb₁₁Sb₁₀ and Yb₁₀MnSb₉ have extensive crystallographic and stoichiometric similarities, which makes distinguishing between these two phases difficult, especially if they are only present in small amounts as a secondary phases. In this work, we consider the properties of these two possible secondary phases and explore the consequences of these materials as secondary phases in the high performing Yb₁₄MnSb₁₁ material.

11:30 AM EN08.09.10

Enhanced Thermoelectric Performance in Hybrid Inorganic-Organic Conducting Polymer Systems Iris Nandhakumar¹, Pawan Kumar², Syed

Zulfiqar Hussain Shah^{2,1} and Kedar Hippalgaonkar^{2,3}; ¹University of Southampton, United Kingdom; ²IMRE, Singapore; ³NTU, Singapore

Wearable technologies such as smart watches, smart glasses or even smart pacemakers have caused a paradigm shift in consumer electronics with huge potential in areas such as healthcare, fashion and entertainment (e.g. augmented reality glasses). Currently these devices are still powered by batteries needing frequent replacement or recharging, a key challenge holding back wearable electronics. Thermoelectric generators (TEGs) can provide a potential solution as a wearable power source: they can convert heat into electricity, are safe, long-lasting and maintenance-free with zero-emissions. The Seiko Thermic watch (which generated 60 μW/cm² at DT= 5 K^[1]) and the recently released Matrix PowerWatch are just some examples of how TEG technology has already been implemented in commercial devices. Current TEGs however are plagued by low efficiencies, high manufacturing costs, and are fabricated onto rigid substrates which makes them difficult to integrate into many applications that require conformal installation. To date most thermoelectric (TE) materials under study have been inorganic chalcogenides such as Bi- or Pb-based compounds (e.g. Bi₂Te₃ and PbTe, ZT ~ 1), intermetallics (e.g. half-Heusler alloys), and clathrates and skutterudites. Interest in organic conducting polymers (OCPs) is rapidly growing due to their mechanical flexibility, low thermal conductivities, elemental abundance, low cost and toxicity as well as solution processability. The TE performance of OCPs however still lags behind that of conventional inorganic TE materials which remain the state of the art for applications near room temperature. Recently hybrid inorganic-organic TE materials composed of inorganic nanostructures and OCPs have emerged as a promising class of flexible high performance TE materials. The TE hybrid materials use the OCPs as the mechanical binder providing flexibility whilst simultaneously contributing to the thermoelectric properties of the composite. This has demonstrated PFs exceeding those of either constituent. The reason for this enhancement is still under debate, however Kumar et al. demonstrated that the enhancement in the PEDOT:PSS-Te(Cux) system was dominated by the effects of polymer morphology at the organic-inorganic interface and interfacial charge transfer and not by energy filtering as has previously been assumed. We present the results of an in-depth study on flexible tellurium nanowire-P3HT hybrid systems with significantly enhanced power factors that can be rationalised in terms of the Kang-Snyder model on charge transport.

SESSION EN08.10: Thermoelectric Modules and Thin Films

Session Chairs: Thierry Caillat and Maria Ibáñez

Thursday Afternoon, April 25, 2024

Room 336, Level 3, Summit

1:30 PM *EN08.10.01

The Role of Thermoelectric Property Variations Over Time and Temperature in The Life Performance of Radioisotope Thermoelectric Generators Thierry Caillat; Jet Propulsion Lab, United States

Radioisotope Thermoelectric Generators (RTGs) have been successfully used to power various NASA spacecrafts and rovers. The flight-proven Multi-Mission Radioisotope Thermoelectric Generator (MMRTG) uses PbTe/TAGS thermoelectric materials and is currently used on the Curiosity and Perseverance Mars rovers. The concept of a skutterudite based MMRTG was first proposed in 2013. It is based on retrofitting the flight-proven MMRTG with higher-efficiency thermoelectric couples based on skutterudite materials developed at NASA's Jet Propulsion Laboratory (JPL) while keeping the balance of the system virtually unchanged. The General-Purpose Heat Source (GPHS-RTG) uses SiGe thermoelectric materials and has been used on several NASA missions, including the Voyager spacecrafts. The degradation of the RTG power over time is controlled by several degradation mechanisms, including the changes in thermoelectric properties over time and temperature. The contribution of these changes for several RTG thermoelectric material systems is reviewed and discussed.

2:00 PM EN08.10.02

Macroscopic Thermoelectric Legs Obtained by Encapsulating Forests of Self-Supporting Silicon Nanowires Dario Narducci, Federico Giulio and Antonio Mazzacua; University of Milano Bicocca, Italy

The application of nanotechnology in the development of novel thermoelectric materials has yielded remarkable advancements in their efficiency. In many

instances, dimensional constraints have resulted in a beneficial decoupling of thermal conductivity and power factor, leading to large increases in the achievable thermoelectric figure of merit (ZT). As a major example, single-crystalline silicon ZT increases by nearly two orders of magnitude when transitioning from bulk single crystals to nanowires. However, the practical implementation of nanostructured materials in thermoelectric devices remains somewhat restricted, not only due to manufacturing complexity and associated costs but also due to the limited power that nanomaterials deliver because of the reduced heat capture section [1]. Metal-assisted chemical etching offers a potential solution to overcome such limitations, enabling the production of dense, cost-effective forests of silicon nanopillars [2]. Nevertheless, use of pillared silicon chips in thermoelectric devices necessitates the non-trivial establishment of low-resistance electrical and thermal contacts atop the Si nanopillars. Furthermore, the residual single-crystalline silicon membrane adds thermal and electrical resistances that degrade the device performances. In this regard, we will present and compare strategies for achieving high-quality contacts through electroplating [3] and by embedding pillars into appropriate electrical and thermal insulators. Additionally, nanowire embedding will be shown to be of use also to encapsulate quasi-ordered millimeter-long nanowire aggregates, named 'nanofelts', that are obtained by fully etching thick silicon chips [4]. This provides a novel path to employ Si nanostructures with enhanced ZT to make thermoelectric legs with macroscopic sizes.

[1] Heremans, J. P.; Dresselhaus, M. S.; Bell, L. E.; Morelli, D. T.; Nat. Nanotechnol. 2013, 8 (7), 471–473.

[2] Magagna, S.; Narducci, D.; Alfonso, C.; Dimaggio, E.; Pennelli, G.; Charai, A.; Nanotechnology 2020, 31 (40), 404002.

[3] Dimaggio, E.; Pennelli, G.; Nano Lett. 2016, 16 (7), 4348–4354.

[4] Giulio, F.; Puccio, L.; Magagna, S.; Perego, A.; Mazzacua, A.; Narducci, D.; ACS Appl. Electron. Mater. 2023, accepted.

2:15 PM EN08.10.03

Thermoelectric Modules and Applications: An Industrial Perspective Aniruddha Ray and Maarten den Heijer; RGS Development, Netherlands

Over the past quarter-century, NASA has maintained a cadence of missions utilizing radioisotope power systems (RPS) at a rate of approximately one mission every ten years. At present, the sole flight-qualified RPS in NASA's inventory is the Multi-Mission Radioisotope Thermoelectric Generator (MMRTG), which boasts an initial power output of around 120 watts. Additionally, NASA and the U.S. Department of Energy (DOE) jointly oversee the development of the Next Generation Radioisotope Thermoelectric Generator (NGRTG), expected to provide an initial power output ranging between 250 and 270 watts.

There is currently an unmet need for low-power generators with a projected initial power output of 15 watts. To address this gap, RGS Development and UDRI conducted a concept study to explore the feasibility of low-power RPS based on a single General Purpose Heat Source (GPHS).¹ Thorough thermoelectric calculations were performed to optimize the design of the current generation of RGS Thermagy architecture, which employs an all-silicon-germanium module. This optimization allows for efficient utilization of available heat flux via a suitable heat interface to meet the required power outputs. Furthermore, by concentrating the heat flux on a smaller hot side surface area of the thermoelectric module, a mechanically robust pellet-based next-generation Thermagy module is envisioned.

In terrestrial applications, RGS has undertaken several noteworthy projects focused on power generation through waste heat recovery in various heavy industries, including Tata Steel, Elkem, and ArcelorMittal. These experiences have underscored the need for mid-temperature Thermoelectric Generator (TEG) devices capable of handling high temperatures, reaching up to 600°C. In response to this demand, RGS is advancing the application of nanostructured SiGe materials, known for their higher average ZT values, while concurrently developing telluride-free thermoelectric modules designed to operate at temperatures up to 350°C in a recently funded EU Horizon project.²

RGS has developed significant expertise in various areas, including COMSOL simulations, thermo-mechanical engineering, interface engineering, device aging, and testing, positioning the company to offer TEG solutions for both single-stage and cascaded device architectures tailored to a range of source temperatures and heat flux densities.

¹ K. Sherick, A. Ray, P. Berneron, A. Tolson, C. Barklay, M. D. Heijer, Feasibility of a Low-Power RTG Concept Utilizing a GPHS Heat Source, Proc. of the Nuclear and Emerging Technologies for Space, May 7-11 (2023), Cleveland, Ohio, USA

² <https://www.start-heproject.com/>

2:30 PM EN08.10.04

Optimal Transient Operation in Thermoelectric Cooling and its Relation to Thermoelectric Properties Jaden Lucas, Udit Halder, Lakshmi Amulya Nimmagadda, Prashant Mehta and Sanjiv Sinha; University of Illinois at Urbana-Champaign, United States

It has been well known for many decades that there exists an optimal Peltier current to achieve the best performance in steady-state Peltier cooling. At this constant current, there is a minimum steady-state cold-end temperature that can be achieved across a thermoelectric cooler. However, in a transient operation over a short time window, the temperature drop can be improved with a transient current pulse where the minimum transient temperature depends on the shape of the current pulse [1]. Here, we apply optimal control theory to find for the first time, a temperature minimizing *transient* current pulse. We consider a thermoelectric cooler with a heat load at the cold end, and model it as a discrete control system and use gradient descent to find a cost-minimizing current [2]. The optimal current diminishes the temperature rise due to the low frequency components of the heat loads, and this performance improvement depends strongly on thermal conductivity [3]. We also consider transient cooling of a thermoelectric below the minimum steady-state temperature. We observe that an optimal current pulse holds the temperature below its steady-state value for longer than a comparable constant current pulse. This work provides new insights into the upper limit of the transient performance of thermoelectric coolers.

R. Yang, G. Chen, A. R. Kumar, G. J. Snyder, and J.-P. Fleurial, "Transient cooling of thermoelectric coolers and its applications for microdevices," *Energy Conversion and Management*, 2005.

D. P. Bertsekas, *Nonlinear programming*, 3rd ed. Belmont, Mass: Athena scientific, 2016

P. E. Gray, *The Dynamic Behavior of Thermoelectric Devices*. The MIT Press, 1960.

2:45 PM EN08.10.05

Boron-Mediated Interface Engineering for Enhancing The Thermoelectric Performance of Bi₂Te_{2.7}Se_{0.3} Films Yen-Ling Wang, Karan Giri, Chuan-Wen Yang, Ling-Chun Chao, Hung-Shuo Chang, Wen-Chieh Hsieh and Chun-Hua Chen; National Yang Ming Chiao Tung University, Taiwan

Nanostructuring has become one of the most practically proven and effective strategies in enhancing the thermoelectric figure of merit, which significantly propels thermoelectric materials to the forefront of progress in fundamental research and advanced applications. Accompanied by nanostructuring, heterogenization, which frequently shows excellent synergistic effects with nanostructures, has appeared as an appendable and feasible solution for a

further breakthrough.

Hexagonal boron nitride (h-BN), exhibiting remarkable thermal and chemical stability, is a potential candidate as the heterogeneous additive since the thermal conductivity of a single h-BN is much lower than that of graphene. In this work, to improve the thermoelectric properties of Bi₂Te_{2.7}Se_{0.3} (BTS) thin films, BTS and h-BN were co-deposited on a SiO₂/Si substrate by a dual-beam laser system. The BN addition is expected to synergistically optimize the thermoelectric properties and stability of the BTS films.

According to the x-ray diffraction, the crystal structure of the formed BTS:BN hetero-nanostructured films deposited at a temperature higher than 400 °C shows a preferred orientation of (00l), which significantly improves the carrier mobility (~105 cm²V⁻¹s⁻¹). The optimized Seebeck coefficient is -197 μVK⁻¹ and the corresponding power factor is 29 μWcm⁻¹K⁻². Raman spectroscopy was performed to analyze the thermal transporting of the formed BTS:BN films. A non-local thermal equilibrium phenomenon of Raman signal collapse at lower laser energy was found, indicating that introducing the BN additive can effectively reduce the thermal conduction of the BTS films and, thus, can effectively improve the thermoelectric performance.

3:00 PM BREAK

3:30 PM *EN08.10.06

Recent Progress on Thermoelectric Materials and Modules [Zhifeng Ren](#); University of Houston, United States

Thermoelectric modules based on thermoelectric materials can either generate cooling/heating using electrical power or electrical power from heat. Thermoelectric property improvement of materials is only the first step for thermoelectric modules for a variety of applications. How to make efficient modules is equally important as the materials improvement. The thermoelectric properties of the traditional materials are not good enough to make efficient modules to compete with the traditional coolers using compressor or steam engines. However, in the past fifteen years, we have been able to not only achieve some good progress on improving the thermoelectric properties of the traditional materials but also discover new materials with better properties and lower cost. At the same time, thermoelectric modules have also been improved for record-breaking cooling and power generation performances due to the advance in module fabrication. In this talk, I will present some of the advances in both the materials and devices.

4:00 PM EN08.10.07

A Path to Sustainable and Scalable Production of High-Performance Thermoelectric Materials [Maria Ibáñez](#)¹, Tobias Kleinmanns¹, Francesco Milillo², Mariano Calcabrini¹, Christine Fiedler¹, Sharon Horta¹ and Daniel Balazs¹; ¹ISTA, Austria; ²UNIBA, Italy

Over the past few years, there has been a significant surge in interest surrounding solution-based techniques due to their cost-effectiveness and scalability in the production of high-performance thermoelectric materials. This approach involves the synthesis of particles in a solution, followed by their purification and thermal processing to yield the desired dense polycrystalline material. In contrast to traditional methods, solution-based syntheses offer the ability to manipulate particle characteristics, including size, shape, crystal structure, composition, and surface chemistry, to an unprecedented degree. This fine-tuned control over powder properties opens up distinct opportunities for crafting thermoelectric materials with meticulously controlled microstructural attributes.

In this presentation, our primary focus will be on Ag₂Se, an important thermoelectric material for harnessing thermoelectricity at or near room temperature, an area where the selection of high-performing materials is currently limited. While Ag₂Se shows great promise, the main problems are the large discrepancy in the reported thermoelectric properties and difficulties in replicating its exceptional performance. These discrepancies often stem from the intricate control of defects within the material, such as vacancies, interstitial atoms, dislocations, grain boundaries, and precipitates.

We will show that our solution-based synthesis method enables precise defect control, especially avoiding fluctuations in stoichiometry. Additionally, we will illustrate how we can fine-tune microstructural defects, including strain, dislocations, and grain boundary density, leveraging the characteristic phase transition of Ag₂Se during the sintering process. Our results will highlight that besides stoichiometry, the microstructure is crucial for tuning Ag₂Se transport properties and how this control can be provided by our novel synthetic route. Furthermore, we will highlight the sustainability and scalability of our approach, where solvents can be recycled and energy consumption minimized, contributing to a more environmentally friendly production process.

4:15 PM EN08.10.08

Optimization of Sb₂Te₃ and Bi₂Te₃ Thermoelectric Films for Infrared Detection and Energy Harvesting [Rumana Zahir](#)¹, Robert E. Peale^{1,2}, Javier Gonzalez², Darian Smalley¹, Masahiro Ishigami¹, Akash Hari Bharath¹, Kalpathy Sundaram¹ and Edgar Nino¹; ¹University of Central Florida, United States; ²Truventic LLC, United States

We are developing antenna-coupled thermoelectric junctions for infrared detection and energy harvesting. COMSOL Multiphysics simulations identify Sb₂Te₃ and Bi₂Te₃ thermoelectric materials as ideal for the thermocouple junction at the antenna feed. Joule heating at the antenna feed from currents induced by antenna-collected radiation generates thermoelectric voltage and current for detection and energy conversion. In this work, we optimized the properties of RF sputtered telluride films for these applications. We performed a two-level full factorial optimization experiment with three factors: Argon gas pressure, substrate temperature, and RF power. Their low and high values were 7 and 8 mTorr, 175 and 225 deg C, and 15 and 25 W, respectively. The resulting eight depositions were performed using glass substrates in randomized order. A mid-point deposition at 7.5 mTorr, 200 deg C, and 20 W RF power was performed to reveal curvature in the main effects. We found for Sb₂Te₃ a maximum Seebeck coefficient of 149 μV/K, minimum resistivity 88 μΩ-m, and a maximum power factor (squared Seebeck coefficient over resistivity) of 1 μW/cm-K². Main effect plots, which are the response (power factor) averaged over two of the factors plotted vs the third, reveal that the power factor was most sensitive to changes in substrate temperature and least sensitive to variations in RF power. All main-effect plots show strong negative curvature. The mid-point response was significantly higher than those of the end points. The maximum power factor was achieved on the low-side of the midpoint. Interaction-effect plots are the response averaged over one of the factors plotted vs a second factor, for each value of the third factor. These reveal no significant interaction between gas pressure and RF power and the most significant interaction between RF power and substrate temperature. SEM images reveal a microstructure comprising ellipsoidal grains with half-micron major axis dimension. Similar results for Bi₂Te₃ will be presented. Photolithographically patterned bowtie-antenna-coupled thermocouples demonstrate successful deposition and lift-off. Response of this device to mm-wave radiation from a backward wave oscillator is consistent with COMSOL predictions.

4:30 PM EN08.10.09

Enhancing Thermoelectric Properties of Semicrystalline Conjugated Polymers through Controlled Tie Chain Incorporation [Wenjin Zhu](#) and Henning Sirringhaus; University of Cambridge, United Kingdom

Conjugated polymers are promising materials for thermoelectric applications, however, at present few effective and well understood strategies exist to further advance their thermoelectric performance. Here we report a new model system for better understanding the key factors governing their thermoelectric properties: aligned, ribbon-phase poly[2,5-bis(3-dodecylthiophen-2-yl)thieno[3,2-b]thiophene] (PBTTT) doped by ion-exchange doping. Using a range of microstructural and spectroscopic methods we study the effect of controlled incorporation of tie-chains between the crystalline domains through blending of high and low molecular weight chains. The tie chains provide efficient transport pathways between crystalline domains and lead to

significantly enhanced electrical conductivity of 4810.1 S/cm, that is not accompanied by a reduction in Seebeck coefficient nor a large increase in thermal conductivity. We demonstrate respectable power factors of $172.6 \mu\text{W m}^{-1} \text{K}^{-2}$ in this model system. Our approach is generally applicable to a wide range of semicrystalline conjugated polymers and could provide an effective pathway for further enhancing their thermoelectric properties and overcome traditional trade-offs in optimization of thermoelectric performance.

SESSION EN08.11: Poster Session II
Session Chairs: Jan-Willem Bos and Alexandra Zevalkink
Thursday Afternoon, April 25, 2024
Flex Hall C, Level 2, Summit

5:00 PM EN08.11.01

Defect Engineering of Transparent Thermoelectric Copper Iodide through Low Energy Ion Implantation Martin Markwitz^{1,2,3}, Peter P. Murmu², Ben J. Ruck^{1,3}, Takao Mori^{4,5} and John V. Kennedy^{2,3}; ¹Victoria University of Wellington, New Zealand; ²GNS Science, New Zealand; ³The MacDiarmid Institute for Advanced Materials and Nanotechnology, New Zealand; ⁴National Institute for Materials Science (NIMS), Japan; ⁵University of Tsukuba, Japan

Copper iodide (CuI) is a non-toxic earth-abundant wide bandgap semiconductor with many potential technological applications in transparent electronics. Transparent conducting p-type semiconductors CuI and CuAlO₂ have lower electrical conductivities compared to their doped n-type counterparts In₂O₃:Sn or ZnO:Al. CuI possesses the highest electrical conductivity of its class as a transparent p-type semiconductor ($\sigma \sim 10^2 \text{ Scm}^{-1}$) due to its high hole mobility ($\mu \sim 10^1 \text{ cm}^2 \text{V}^{-1} \text{s}^{-1}$) and carrier concentration ($p \sim 10^{19} \text{ cm}^{-3}$) whilst boasting a large Seebeck coefficient ($\alpha \sim 280 \mu\text{VK}^{-1}$), mainly attributed to p-type doping with copper vacancies (V_{Cu})^[1,2]. Intrinsic doping via controlling deposition conditions and extrinsic doping with chalcogens allows for control over the crystal quality and carrier concentration^[3,4,5,6,7]. Sulfur and selenium doping increases the CuI carrier concentration ($p \sim 10^{20} \text{ cm}^{-3}$)^[4,6]. Optimizing the intrinsic defect structures in undoped CuI is predicted to yield even higher electrical conductivity^[8]. Ion implantation, a well-established microfabrication technique, can be used for defect engineering via noble gas implantation, known to also improve thermoelectric properties by reducing lattice conductivity and vacancy doping^[9].

In this work, we elucidate the role of intrinsic point defects in low-energy noble gas ion implanted into ion beam sputtered CuI thin films. Ion energies 13, 27, and 70 keV were used to implant neon, argon, and xenon with fluences between 5×10^{14} ions cm^{-2} and 1.92×10^{16} ions cm^{-2} . Microstructural, compositional, and electronic characterization showed stoichiometric γ -CuI. Moderate implantation fluences ($\leq 2 \times 10^{15}$ ions cm^{-2}) led to a 100% increase in carrier concentration ($\sim 1 \times 10^{20} \text{ cm}^{-3}$) without significant loss in Seebeck coefficient ($\sim 200 \mu\text{VK}^{-1}$) or carrier mobility ($\sim 9 \text{ cm}^2 \text{V}^{-1} \text{s}^{-1}$). This led to the increase of the power factor by two-fold to $\alpha^2 \sigma \sim 540 \mu\text{Wm}^{-1} \text{K}^{-2}$. Transport of Ions in Matter (TRIM)^[10] simulations showed that the damage per atom (DPA) ranged between 1.2 and 16. Density functional theory (DFT) calculations showed that Frenkel pairs (low formation energy defect complexes) are likely produced through ion implantation. We will present detailed results discussing the relationship between point defect formation and thermoelectric performance of CuI thin films supported with Monte Carlo simulations and DFT calculations.

References:

[1] Yang, C. *et al.* (2017), Nature Communications 8(1), 16076. [2] Yang, C. *et al.* (2016), Proceedings of the National Academy of Sciences 113.46, 12929-12933. [3] Grauzinyte, M. *et al.* (2019), Physical Chemistry Chemical Physics, 21, 18839-18849. [4] Murmu, P. P. *et al.* (2022), ACS Applied Energy Materials, 3(10), 10037-10044. [5] Ahn, K. *et al.* (2022), Chemistry of Materials, 34(23), 10517-10527. [6] Storm, P. *et al.* (2021), Physica Status Solidi RRL, 15, 2100214. [7] Markwitz, M. *et al.* (2023), Surfaces and Interfaces, 41, 103190. [8] Willis, J. *et al.* (2023), Chemistry of Materials, 35(21), 8995-9006. [9] Burcea, R. *et al.* (2022), ACS Applied Energy Materials, 5(9), 11025-11033. [10] Ziegler, Z. F. *et al.* (2010), Nuclear Instruments and Methods in Physics Research Section B: Beam Interactions with Materials and Atoms, 268(11-12), 1818-1823.

5:00 PM EN08.11.02

Transparent and Flexible Graphene-Based Temperature Sensor via p-n Junction Soomook Lim¹, Hyeon-Jong Lee¹ and Ji Won Suk^{1,1,2}; ¹Sungkyunkwan University, Korea (the Republic of); ²Sungkyunkwan University Advanced Institute of NanoTechnology, Korea (the Republic of)

As the demand for wearable devices surges, there is a growing need for flexible and transparent temperature sensors capable of monitoring changes in body and surrounding environments [1]. Among many two-dimensional (2D) materials, graphene has garnered significant attention due to its exceptional electrical properties, flexibility, and transparency, rendering it suitable for a diverse range of applications, including flexible transparent electrodes, sensors, and optoelectronic devices [2]. Thermocouples, based on the thermoelectric effect, offer an alternative way for temperature monitoring in wearable devices because of their self-powering capability and high accuracy. Thermoelectric devices using a combination of p- and n-type graphene have exhibited noteworthy sensitivity to temperature [3]. Achieving p- and n-type properties in graphene typically involves controlling its electrical properties of graphene via charge transfer doping. However, ensuring the stability of n-type graphene generated by the surface doping poses a considerable challenge in the development of graphene-based thermoelectric temperature sensors [4]. In this work, a transparent, flexible graphene-based temperature sensor was developed by chemical doping of graphene and encapsulation with a thin oxide layer. Monolayer graphene was synthesized using chemical vapor deposition (CVD) on copper foil and transferred to a flexible polyethylene terephthalate (PET) film. Half of the monolayer graphene on the PET film was doped by polyethyleneimine (PEI) coating, resulting in the formation of a p-n junction for thermoelectric sensing. The fabricated graphene thermocouple showed high sensitivity suitable for daily use in wearable devices, along with high flexibility and optical transparency. To overcome the inherent air instability of the PEI coating, the sensor was encapsulated with a thin oxide layer using atomic layer deposition (ALD). Aluminum oxide (Al₂O₃) was chosen for encapsulation due to its widespread use as a stable barrier material against air. The thickness of the aluminum oxide layer was controlled to minimize any degradation in sensor performance. This study demonstrates the potential of monolayer graphene as flexible and transparent temperature sensors for wearable devices.

[1] Kim, Seungwon, *et al.*, *J. Mater. Sci. Technol.*, 172, 15-22, 2024
[2] Weiss, Nathan O., *et al.*, *Adv. Mater.*, 24, 5782-5825, 2012
[3] Hwang, Hyeon Jun, *et al.*, *Carbon*, 201, 467-472, 2023
[4] Cha, Myoung-Jun, *et al.*, *RSC Adv.*, 4, 37849-37853, 2014

5:00 PM EN08.11.03

Transverse Seebeck Effect Devices for Heat Flux Sensing in Hot Environments up to 500°C Kenneth McAfee, Peter Sunderland and Oded Rabin; University of Maryland, United States

Utilizing the Transverse Seebeck Effect (TSE), heat-flux sensing devices were designed, built and tested, demonstrating the linearity of the heat-flux-to-voltage transduction. We introduce new testing protocols that (1) demonstrate that the electrical signal results from the TSE and not from the conventional Seebeck effect, and (2) provide reliable values for the sensitivity of the sensor (i.e. calibration curves) at elevated temperatures. We introduce new materials as practical TSE transducers. Through materials selection and sensor design, the range of temperatures of operation of the heat-flux sensors has been extended up to 500 degrees Celsius, with the potential to exceed 1000 degrees Celsius upon the identification of appropriate adhesives. These heat-flux sensors fill in a technical void that is currently present in thermal systems metrology, superseding the state-of-the-art Schmidt-Boelter heat-flux sensors under extreme environments, due to their simpler and rugged construction. [Funding: US Department of Energy, Award DE-FE0031902].

5:00 PM EN08.11.04

Tuning Solvent Properties for Efficient N-Type Doping of Highly Aligned Wet-Spun CNT Fibers: Achieving High-Performance Wearable Thermoelectrics SungJun Kim, Yong Kim and Woong-Ryeol Yu; Seoul National University, Korea (the Republic of)

The highly oriented structure of wet-spun carbon nanotube (CNT) fibers makes them a promising candidate for high performance wearable thermoelectric fibers. This orientation facilitates remarkable electrical conductivity without increasing carrier concentration, which would otherwise decrease the Seebeck coefficient. However, their highly packed structure hinders the infiltration of chemical dopants, making it more challenging to prepare N-type CNT fibers through conventional wet processes like dipping, brushing, or spraying of chemical dopants. This study investigates the role of solvent properties in enabling efficient N-type doping of highly aligned CNT fibers. Wet-spun CNT fibers with varying winding rates were prepared to explore the impact of their degrees of orientation on the doping process, as highly aligned structure hinders the sufficient N-type doping. Among the various solvent properties, the Hansen solubility parameter, which represents the affinity with CNTs, has a significant influence on the N-type doping process. By optimizing solvent properties, even for the case of highly aligned CNT fiber with high electrical conductivity of ~ 1.0 MS/m, a desirable N-type Seebeck coefficient of -39 $\mu\text{V/K}$ was achieved, leading to power factor of ~ 1.5 $\text{mW/m}^2\text{K}^2$.

5:00 PM EN08.11.05

Stretchable Ag_2Se Thermoelectric Fabric without Thermal Treatment for Wearable Sensors Chaebeen Kwon and Taeyoon Lee; Yonsei University, Korea (the Republic of)

With the rapid advancements in the textile-based electronics, smart fibers have emerged as a pivotal component of functional textiles, distinguished by their remarkable responsiveness to a wide array of external stimuli. These smart fibers boast an extensive range of capabilities, including sensory functions and the capability for energy harvesting. This innovation is currently driving the emergence of novel fiber-based wearable electronics, encompassing applications such as electronic skin, health sensor, and interfaces for human-machine interaction. As the field of fiber-based wearable electronics continues to evolve, the integration of thermoelectric (TE) materials into the fibers has become a significant development. TE materials possess the unique ability to efficiently convert temperature gradients into electrical output voltage, and vice versa. This integration introduces a groundbreaking ability to harvest electrical energy from the natural heat generated by the human body. Furthermore, TE fibers enable the detection of temperature variations and changes in posture through the measurement of output voltage and resistance, respectively.

The pursuit of using inorganic TE materials for wearable applications has garnered significant attention in recent research. Among these efforts, silver selenide (Ag_2Se)-based materials have emerged as promising candidates due to their unique TE properties. Incorporating Ag_2Se into fibers has been a cautious endeavor in several studies, primarily due to the rigidity associated with inorganic TE materials. Yang et al. suggested approach to creating a three-dimensional TE generator with biaxial stretchability. By integrating inorganic Ag_2Se film strips into a knit fabric, aligned with the vertical heat flux direction, a stable temperature gradient of 5.2 $^\circ\text{C}$ was achieved when in contact with the wrist at room temperature. Research is currently underway to explore TE units in fiber form, rather than in film, to enhance their suitability for wearable electronics applications. Vinodhini et al. reported a one-step solvothermal method to integrate Ag_2Se and Ag_2S with conductive carbon fabric (CF). Ag_2Se CF and Ag_2S CF exhibited power factors of 6.7 $\mu\text{W/mK}^2$ and 24 $\mu\text{W/mK}^2$, respectively. However, during the material synthesis process, applying heat at 180 $^\circ\text{C}$ for 24 hours frequently results in the formation of rigid structures. The only research on non-thermal Ag_2Se fabric has been recently reported. Liu et al. introduced two-step impregnation method for fabricating a three-dimensional TE network. The TE network demonstrates an elongation of over 100%. The resulting network-based TE generator achieves an output power of 4 $\mu\text{W/cm}^2$. Nonetheless, the process can become complicated and time-consuming due to multiple steps. For the effective integration of Ag_2Se into wearable electronics, a simple and non-thermal approach is essential.

Herein, we have fabricated a stretchable Ag_2Se TE fabric through simple and non-thermal process. Ag_2Se nanoparticles (NPs) were densely and rapidly formed within the cotton fabric using a chemical reduction method, without the need for thermal treatment. Due to the durable NP networks, the stretchable Ag_2Se TE fabric exhibited remarkable electrical stability under repeated conditions of 20% lateral strain and 16 kPa normal pressure. Remarkably, it maintained its electrical path even under strain of 200%, surpassing thermally treated Ag_2Se TE fabric in both electrical and mechanical performance. Moreover, the TE unit exhibited a power factor of 9.80 $\mu\text{Wm}^{-1}\text{K}^{-2}$ with an electrical conductivity of 134.45 Scm^{-1} and a Seebeck coefficient of -26.98 μVK^{-1} at 370 K. To demonstrate the practical utility of our work, we developed a haptic sensing glove capable of detecting changes in strain, pressure, and temperature. This glove effectively alerted users to potential hazards related to elevated temperatures and exhibited accurate sensing capabilities for both pressure and tensile forces.

5:00 PM EN08.11.06

Stretchable Thermoelectric Fibers Using CuI Nanoparticle Networks for Multi-Sensing Wearable Electronics Sanghyeon Lee; Yonsei University, Korea (the Republic of)

Recently, the field of biomedical engineering and robotics has witnessed wearable sensor that is able to imitate functions of human skin. Wearable sensor is required the characteristics such as flexibility and stretchability with capacity that converts external stimulate including temperature, pressure, displacement, pulse, electrocardiograph (ECG) signals, tactile sensations, to electrical signals. Recently, thermoelectric materials that transform reversibly the temperature gradient into an electrical output voltage have been applied to detect changes in temperature through output voltage and current.

To applied wearable sensor, there are several strategies as followings: (1) structural innovations of inorganic thermoelectric materials, (2) materials innovations of organic thermoelectric materials. Although inorganic materials have high figure of merit (zT) and high electrical conductivity, inorganic materials are difficult to deform mechanically due to brittleness. To solve the limitation of rigidity, thermoelectric device consisted with inorganic materials designed by kirigami/origami structure. However, this structure not only has limitation of deformation but also is too complicated to integrate in wearable device. In case of organic thermoelectric materials, the thermoelectric performances are poorer than that of inorganic thermoelectric materials. To improve thermoelectric performances, organic materials are chemically doping. However, the efficiency and stability of chemical modification are always unsatisfactory.

Herein, we fabricated stretchable thermoelectric copper iodide nanoparticles (CuINPs) embedded fibers. CuINPs, which is promising and ecofriendly thermoelectric materials, are densely formed inside and outside of the polyurethane (PU) fiber using the chemical reaction methods. This method consists of two steps: (1) the fiber immersed in Cu precursor to absorbed Cu ions in the PU matrix, (2) the absorbed fiber reacted with I precursor to synthesis CuINPs. CuINPs embedded fiber achieves a power factor of 18.31 $\mu\text{Wm}^{-1}\text{K}^{-2}$ with electrical conductivity of 5.99 S/cm and Seebeck coefficient of 175.8 μVK^{-1} at room temperature. Moreover, the resistance of the fiber increased with increasing tensile strain. The Seebeck coefficient of the fiber constantly

remained with changing strain of fiber. We demonstrated a sensing system that can detect pressure and temperature changes simultaneously. This facile CuINPs embedded fibers will pave the way for applying inorganic TE materials in a stretchable form in wearable electronics.

5:00 PM EN08.11.07

Enhancing Thermoelectric Efficiency of Bi₂Te₃ Nanoribbons through *In-Situ* F₄-TCNQ and *Ex-Situ* Cr Interfacial Alloying Jun Beom Park, Rijan Karkee and Michael T. Pettes; Los Alamos National Laboratory, United States

Nanostructured Bi₂Te₃ shows promise in enhancing thermoelectric characteristics by theoretical prediction, but its practical performance often falls short of bulk Bi₂Te₃ due to defects, impurities, and surface oxidation. Addressing this, precise control of the nanostructured surface's chemical potential is crucial for achieving long-lasting, high-performance thermoelectric materials and devices. Various techniques, including oxygen plasma treatment, non-oxidizing superacid treatment, and atomic layer deposition (ALD) of Al₂O₃, have been explored to engineer the surface of Bi₂Te₃. Additionally, extrinsic doping by coating metallic or carrier-rich layer has shown promise in modulating carrier concentration and chemical potential.

In this presentation, we introduce two distinct strategies to enhance the thermoelectric performance of Bi₂Te₃ nanoribbons through the incorporation of external dopant layers: an *in-situ* F₄-TCNQ layer and an *ex-situ* Cr layer. The *in-situ* coated F₄-TCNQ layer induces a transformation of the major carrier from *n*-type to *p*-type, resulting in 6-times enhancement of the Seebeck coefficient. Moreover, the core-shell structure effectively shields the core from oxidation, demonstrating the absence of surface oxidation or loss of thermoelectric properties even after one month in ambient air. On the other hand, the surface-coated Cr layer is confirmed to induce a 70% reduction in nanoribbon resistance along with a 24% increase in the Seebeck coefficient, which resulting 2-times enhancement of thermoelectric figure of merit (*zT*). Our findings underscore a promising approach to practical application of nanostructured Bi₂Te₃, surpassing the performance of bulk material.

5:00 PM EN08.11.08

Low Thermal Conductivity and High Thermoelectric Performance in GeTe-Based Medium-Entropy Thermoelectric Material by Sb-Se Alloying Cheng-Ruei Wu and Chien-Neng Liao; National Tsing Hua University, Taiwan

Germanium telluride (GeTe) is a promising thermoelectric material with great tunability in transport properties, but the rhombohedral-cubic phase transition restricts the applications. A substantial research effort has been dedicated to electronic band modulation and thermal conductivity reduction through partial cation substitution. On the other hand, anion substitution has received much less attention due to limited miscibility. In this study, we synthesize GeTe-based medium-entropy alloys (MEAs) with notable (Se) substitution at Te sites and (Sb) at Ge sites by powder metallurgy to suppress the phase transition and achieve the cubic GeTe. The thermal conductivity of GeSbSeTe-based alloy (GSST-8) is significantly reduced due to severe lattice distortion while maintaining decent thermoelectric power factor. The GSST-8 exhibits an extremely low thermal conductivity of 0.68 W/mK and a high Seebeck coefficient (> 220 μ V/K) over a temperature range of 300 – 623 K. As a result, a high *zT* of ~0.3 at 323 K and ~1.24 at 623 K can be achieved in GSST-8. The transport properties of the pristine GSST-8 have been further improved with optimized carrier concentration and mobility through minor doping element and annealing. The influence of dopant and annealing on the band structure and thermoelectric properties of GSST-8 compounds is studied

5:00 PM EN08.11.09

Cu₂ZnSiTe₄: A Potential Thermoelectric Material with Promising Electronic Transport Himanshu Sharma¹, Bhawna Sahni², Tanusri Saha-Dasgupta³ and Aftab Alam¹; ¹Indian Institute of Technology, Mumbai, India; ²University of Warwick, United Kingdom; ³S. N. Bose National Centre for Basic Sciences, Kolkata, India

Transition metal-based quaternary chalcogenides have attracted a lot of interest for a variety of renewable energy applications, especially thermoelectrics (TE). Although this class of compounds have low symmetry and complex structure which contribute to low lattice thermal conductivity, achieving a high figure of merit (*ZT*), is still a challenge for this class of materials for use in TE applications due to low values of power factor. Here, we used first-principles calculation to study the TE properties of a novel system, Cu₂ZnSiTe₄, with promising electronic transport. The heavy chalcogen 'Te' atom, contributes to the comparatively low bandgap of 0.58 eV. This results in a promising power factor of 3.95 (n-type) and 3.06 (p-type) mWm⁻¹K⁻² at 900 K, together with a favourable electronic band topology. Additionally, 'Te' atoms are responsible for the mixing of the optical and acoustic phonon branches, which at high temperature results in low lattice thermal conductivity (about 0.7 mWm⁻¹K⁻¹). The compound yields a promising TE figure of merit (*ZT* ~2.67 (n-type) and ~2.11 (p-type) at 900 K. We predict Cu₂ZnSiTe₄ as a viable option for TE applications. We believe our study will motivate experimentalists to explore this compound for future investigation for TE applications.

5:00 PM EN08.11.10

Investigate NaGeSbO₅ as a Transparent Thermoelectric Xiaoyu Jia¹, Joe Willis¹ and David O. Scanlon^{1,2}; ¹University College London, United Kingdom; ²University of Birmingham, United Kingdom

Transparent conducting oxides (TCOs) are a unique class of oxide materials that exhibit both transparency and electronic conductivity simultaneously. Thermoelectrics (TEs) are a class of materials that can directly convert heat and electricity mutually. Their Seebeck effect allow thermoelectric devices to recover waste heat and convert it into electrical power. The discovery of high performance transparent thermoelectric materials can potentially develop novel applications such as smart windows and screens with energy harvesting, cooling, and thermal sensing functionalities.

In this project, NaGeSbO₅ was chosen due to its complex crystal structure, which typically leads to low lattice thermal conductivities. The (n-1)d¹⁰ns⁰sp⁰ electronic configuration of Ge(IV) and Sb(V) is expected to yield a dispersive conduction band minimum, similar to the known TCOs.

State-of-the-art ab initio calculations were performed using the VASP code to understand its thermoelectric capability. The initial steps involved evaluating the thermodynamic stability versus known compounds within Na-Ge-Sb-O phase space by CPLAP[1] and optimizing the geometry. Following this, we studied the band structure of NaGeSbO₅ and found its band gap is wide enough to ensure optical transparency. Subsequently, the band alignment was calculated using SURFAXE[2] to examine the doping preference. AMSET[3] code was then used to assess the charge transport properties, and an exploration of lattice dynamics was undertaken through the utilization of Phonopy[4] and hiPhive[5]. The stability at high temperature up to 1100 K has been experimentally confirmed.[6] The thermoelectric figure of merit (*ZT*) at this temperature was predicted to reach 1.09 at a specific carrier concentration, indicating the potential for setting a record in thermoelectric performance. In-depth defect engineering will be undertaken with the goal of attaining the optimal *ZT*.

1. J. Buckeridge, D. O. Scanlon, A. Walsh, C. R. A. Catlow, *Computer Physics Communications*, 2014, **185**, 330.
2. K. Brlec, D. Davies, D. O. Scanlon, *Journal of open source software*, 2021, **6**, 3171.
3. A. M. Ganose, A. J. Jackson, D. O. Scanlon, *Nat. Commun.*, 2021, **12**, 2222.
4. A. Togo, I. Tanaka, *Scripta materialia*, 2015, **108**, 1359.
5. F. Eriksson, E. Fransson, P. Erhart, *Adv. Theory Simul.*, 2019, **2**, 1800185.
6. B. V. Mill, A. V. Butashin, S. Yu. Stefanovich, *Russian Journal of Inorganic Chemistry*, 1993, **38**, 947.

5:00 PM EN08.11.11

High Thermoelectric Performance in n-Type PbSe via Embedding Coherent Endotaxial Nanostructure [Hyungseok Lee](#) and In Chung; Seoul National University, Korea (the Republic of)

PbSe has been regarded as a potential candidate for replacing state-of-the-art thermoelectric (TE) PbTe-based materials, owing to the scarcity of Te. In contrast to the progress in a p-type counterpart, effective strategies to enhance TE performance of n-type PbSe have been rare until recently. For example, band convergence to decouple Seebeck coefficients and electrical conductivity for higher power factor has not been possible because of a large energy gap between first and second conduction bands in contrast to the case of its p-type version. As a result, TE performance of n-type PbSe has been improved by reducing thermal conductivity.

In this presentation, we report a new high-performance n-type PbSe thermoelectric system embedded with a very low concentration nanoscale, semiconducting alloys. Through atomic-resolved TEM, we observed the formation of coherent interfaces between the surrounding matrix and endotaxial nanostructures. The coherent nanostructure gives additional phonon scattering mechanisms induced by mass fluctuation across the interface, remarkably suppressing a lattice thermal conductivity down to $\sim 0.32 \text{ W m}^{-1} \text{ K}^{-1}$. Concurrently, incorporating alloys effectively manipulate the electronic band structure, consequently increasing the conduction band effective mass maximum and a magnitude of Seebeck coefficient. Both effects synergistically improve the TE performance, showing a record-high TE figure of merit, ZT, of ~ 2.0 at 823 K, for all n-type PbSe and PbTe-based materials to date. This result shows that the strategy of designing coherent endotaxial nanostructures could be an effective means of controlling charge and thermal transport properties independently.

SESSION EN08.12: Topological Materials
Session Chairs: Ernst Bauer and Kornelius Nielsch
Friday Morning, April 26, 2024
Room 336, Level 3, Summit

8:30 AM *EN08.12.01

Room Temperature Minimum Thermal Conductivity in 3D Weak Topological Insulators [Jihui Yang](#); University of Washington, United States

In contrast to the conventional belief that the consideration for topological insulators (TIs) as potential thermoelectrics is due to their excellent electrical properties benefiting from the topological surface states, our work shows that the 3D weak TIs, formed by alternating stacks of quantum spin Hall layers and normal insulator (NI) layers, can also be decent thermoelectrics because of their thermal transport. We found that the 3D weak TI $\text{Bi}_{14}\text{Rh}_3\text{I}_9$ possesses the minimum thermal conductivity at room temperature, very unusual for a crystalline material. Our work revealed that the topologically "trivial" NI layers play a surprisingly critical role in hindering phonon propagation. The weak bonding in the NI layers gives rise to significantly low sound velocity, and the localized low-frequency vibrations of the NI layers cause strong acoustic-optical interactions and lattice anharmonicity. All these features are favorable for the realization of exceptionally low lattice thermal conductivity, and therefore present remarkable opportunities for developing high-performance thermoelectrics in weak TIs.

9:00 AM *EN08.12.02

Ta₂PdSe₆: A Guide Towards High Performance Thermoelectric Semimetals [Akitoshi Nakano](#) and Ichiro Terasaki; Nagoya University, Japan

Thermoelectric materials attract great interest due to their promising application to power generation and Peltier cooling devices. Semiconductor thermoelectrics has been mainstream thus far, since the existence of a bandgap makes a large thermopower (S), and tuning the carrier polarity easy by carrier doping. Semiconductor physics predicts that the carrier concentration of around 10^{19} cm^{-3} is appropriate to achieve high $S \sim 200 \mu\text{V/K}$, and high conductivity (σ) $\sim 10^3 \Omega^{-1}\text{cm}^{-1}$. Bi_2Te_3 , the most representative thermoelectric material thus far, well exemplifies the prediction and shows the best thermoelectricity around 300 K. On the other hand, semimetals, in which electrons and holes necessarily coexist, have been out of range of the searching field for the thermoelectric materials, since the compensation between electrons and holes degrades the net S . We have recently discovered that a transition-metal chalcogenide Ta_2PdSe_6 exhibits an extraordinary thermoelectric property despite its semimetal character [1][2]. Ta_2PdSe_6 crystallizes in a layered structure, each layer of which consists of quasi-one-dimensional chains formed by prismatic TaSe_6 and square-planer PdSe_4 . The thermoelectric property measured along this direction is highly exotic; an ultra-high σ above $10^6 \Omega^{-1}\text{cm}^{-1}$ is compatible with a substantial S of $40 \mu\text{V/K}$ at 20K. As a result, the Peltier conductivity $P (= S\sigma)$ is the highest among the thermoelectric materials thus far. The value of $100 \text{ Acm}^{-1}\text{K}^{-1}$ means that a 1cc sample can generate a current of 100 A when it is put across a temperature difference of 1 K. Furthermore, we have found that thermal conductivity of Ta_2PdSe_6 is relatively small ($100 \text{ Wm}^{-1}\text{K}^{-1}$) for such good electrical conductor associated with significant violation of the Wiedemann-Franz law. As a result, the thermoelectric figure of merit $z (= S^2\sigma\kappa^{-1})$ of Ta_2PdSe_6 at 13 K becomes as high as 0.04, which is comparable to the value of Bi_2Te_3 at 300 K. Roughly speaking, 60 times larger thermal conductivity is cancelled by 60 times larger power factor ($= S^2\sigma$) in Ta_2PdSe_6 as compared Bi_2Te_3 . The comparable z from distinct transport parameters strongly indicates a new design rule of high-performance thermoelectric semimetals. In the presentation, we will discuss the origin of the anomalous transport properties of Ta_2PdSe_6 from the viewpoint of the carrier dynamics.

References

- 1) A. Nakano, A. Yamakage, U. Maruoka, H. Taniguchi, Y. Yasui, and I. Terasaki, J. Phys. Energy 3, 044004 (2021)
- 2) A. Nakano, U. Maruoka, and I. Terasaki. Appl. Phys. Lett. 121, 15 (2022)

9:30 AM EN08.12.03

Are Topological Insulators Promising Thermoelectrics? [Michael Toriyama](#) and Jeff Snyder; Northwestern University, United States

Some of the best thermoelectric (TE) materials to date are also topological insulators (TIs). While many studies have investigated the effects of topologically-protected surface states on TE properties, it is still unclear how the bulk band structure of a TI can benefit the TE performance. Here, we perform high-throughput transport calculations using density functional theory (DFT) to reveal that TIs, when properly optimized, tend to outperform normal insulators as TEs. Models based on Boltzmann transport theory show that warping driven by band inversion, a key characteristic of TIs, is beneficial for TE performance because of reduced transport mass and effectively higher valley degeneracy. The model also reveals that the band inversion strength is a critical material property dictating the TE performance, where TIs with strongly inverted bands exhibit higher zT . We suggest potential avenues for tuning the band inversion strength and, as a result, enhancing the TE performance in TIs, such as alloying and strain engineering. The study marks TIs as serious candidates for TE applications owing to band inversion-driven warping.

9:45 AM EN08.12.04

Seebeck Coefficient Enhancement by Quantum Confinement Effect in Superlattice Nanocomposites [Ting Meng](#) and Yang Zhao; University of Science and Technology of China, China

Thermoelectric devices enable the bidirectional conversion between thermal and electrical energy, which has great potential in energy harvest and thermal management, etc. This work proves experimentally that the quantum confinement effect could improve the thermoelectric properties of low-dimensional film materials effectively. The quantum wells formed by embedding ErAs nanoparticles with diameter of around 2 nm in $\text{In}_{0.53}\text{Ga}_{0.47}\text{As}$ matrix lead to drastic changes in the material band structure and convert the semimetal ErAs into a semiconductive state. The size confinement increases the asymmetry in the distribution of the density of electron states near the Fermi level and thus improves the Seebeck coefficient. Here, we report that the Seebeck coefficient and power factor of $\text{In}_{0.53}\text{Ga}_{0.47}\text{As}$ films assembled with ErAs nanoparticles are increased by 2.2 times and 5 times at 516 K, respectively.

10:00 AM BREAK

SESSION EN08.13: Disordered Materials
Session Chairs: Theodora Kyratsi and Jihui Yang
Friday Morning, April 26, 2024
Room 336, Level 3, Summit

10:30 AM *EN08.13.01

Unlocking High-Performance Thermoelectrics: From Phase Engineering to Entropy-Enhanced Materials [Mercuri G. Kanatzidis](#); Northwestern University, United States

In the rapidly evolving field of thermoelectric materials, significant strides have been made to improve material properties and energy conversion efficiency. This talk will traverse multiple avenues of cutting-edge research to showcase advancements in our group in thermoelectric materials and applications. We will present our efforts on Ga-doped n-type PbTe thermoelectric materials that undergo dynamic phase conversion through Cu₂Se alloying. The addition of Cu₂Se enhances electrical transport properties while reducing lattice thermal conductivity. At elevated temperatures, the material undergoes dynamic changes in its phase compositions, achieving a promising ZT for n-type systems of ~1.63 at 823 K for intermediate-temperature applications. Transitioning to p-type lead chalcogenides, these materials exhibit superior thermoelectric performance due to valence band convergence. Improvements on n-type materials are more difficult because of the absence of easy electronic band convergence. However, introducing GaSb doping into their n-type counterparts has led to significant improvements as well. This intervention causes conduction band convergence and increases the average power factor, culminating in a high ZT of across a wide temperature range. Building on our previous results, we have also explored the fascinating realm of entropy-engineered materials, using the $\text{PbGeSnCdxCdxTe}_{3+x}$ family as a case study. The high-entropy effect from alloying not only stabilizes the material's cubic phase but also significantly improves thermoelectric properties to a maximum ZT of 1.63 at 875 K. PbS-based compounds are less well-developed but can become key players in this arena. By alloying PbS with GeS, we achieved a multi-tiered optimization of its electrical and thermal transport properties, involving Ge²⁺ substitution, the formation of a secondary phase of Pb₅Ge₅S₁₂, and enhanced electron mobility. The resultant 14% GeS-alloyed samples yield a ZT of 1.32 at 923 K, outperforming standard Sb-doped PbS by approximately 55% and setting a new benchmark for n-type PbS-based thermoelectric systems. This presentation aims to provide new insights and spark interdisciplinary discussions on optimizing thermoelectric materials for a sustainable energy future.

11:00 AM EN08.13.02

Optimized Thermoelectric Performance and Plasticity of Ductile Semiconductor $\text{Ag}_2\text{S}_{0.5}\text{Se}_{0.5}$ via Dual-Phase Engineering [Hao Wu](#); Nanjing Tech University, China

Inorganic semiconductor Ag_2S with excellent plasticity is highly desired in flexible and wearable thermoelectrics. However, the compromise between plasticity and thermoelectric performance limits the advances in Ag_2S -based thermoelectric materials and their devices. Here, a 0.5 mol.% Ag_2Te -alloyed $\text{Ag}_2\text{S}_{0.5}\text{Se}_{0.5}$ bulk material is designed, which has a competitively high near-room-temperature figure of merit of ≈ 0.43 at 323 K and an ultra-high bending strain of $\approx 32.5\%$ without cracks. Introducing Ag_2Te can optimize the carrier concentration and mobility of the $\text{Ag}_2\text{S}_{0.5}\text{Se}_{0.5}$ matrix due to its metal-like conducting features, leading to a maximum power factor of $\approx 6 \mu\text{W cm}^{-1} \text{K}^{-2}$. Simultaneously, Ag_2Te induces Ag-poor amorphous phase boundaries, serving as buffer layers to enhance the overall plasticity. Moreover, such amorphous phase boundaries combined with multiscale phonon scattering sources can significantly suppress the lattice thermal conductivity to $\approx 0.28 \text{ W m}^{-1} \text{K}^{-1}$ at 323 K, leading to a high figure of merit. This study demonstrates an innovative route to simultaneously boost the thermoelectric performance and plasticity of ductile semiconductors.

11:15 AM EN08.13.03

Zigzag Ag_2Se Nanorod Arrays with Ultrahigh Room Temperature Thermoelectric Performance and Superior Mechanical Properties [Jamal A. Khan](#) and Jitendra P. Singh; Indian Institute of Technology Delhi, India

Ag_2Se is an intriguing material for room temperature energy harvesting. Herein, we report the fabrication of zigzag Ag_2Se nanorod arrays by Glancing angle deposition technique (GLAD) followed by simple selenization in a two-zone furnace. The thermoelectric performance was investigated by varying the number of zigzag arms. The novel Ag_2Se zigzag nanorod arrays with four arms shows an excellent $zT = 1.42 \pm 0.15$ and power factor of $3202.21 \pm 105.23 \mu\text{W/m-K}^2$, respectively at 300 K. The superior thermoelectric performance of four arm zigzag Ag_2Se nanorod arrays compared to one arm Ag_2Se nanorods could be ascribed to the unique nanocolumnar architecture that not only offers a preferential path for carrier transport but also enhanced the scattering of phonons at the tilted rough boundaries and interfaces. The synergetic dependence between the tilt structure and the thermoelectric properties opens a new avenue to fabricate scalable nanostructure thin films for practical applications in next-generation thermoelectric devices.

11:30 AM EN08.13.05

High-Performance Ionic Thermoelectric Materials by Ionic Doping [Jianyong Ouyang](#); National University of Singapore, Singapore

Ionic thermoelectric materials have been attracting more and more attention mainly because of their high thermopower. Their thermopower can be tens mV/K, higher than that of electronic thermoelectric materials by 2-3 orders in magnitude. The thermopower of ionic thermoelectric materials arises from the accumulations of cations and anions at the two ends of a sample under temperature gradient. We found that ionic doping can greatly increase the difference in the mobilities of cations and anions and thus improve the thermopower. By ionic doping, we observed high thermoelectric performance on

both p-type and n-type thermoelectric materials. The ZT_i value can be higher than 6 at room temperature.

SESSION EN08.14: Local Transport Measurements
Session Chairs: Elif Ertekin and Dario Narducci
Friday Afternoon, April 26, 2024
Room 336, Level 3, Summit

1:30 PM *EN08.14.01

Understanding The Impact of Microstructure and Interdiffusion in Mg₂Si-Based Thermoelectric Materials by Integral and Locally Resolved Measurements Johannes de Boor^{1,2}, Amandine Duparchy¹, Sanyukta Ghosh¹, Aryan Sankhla¹, Harshita Naithani¹, Gregor Oppitz¹, Mohamed Abdelbaky², Wolfgang Mertin², Byungki Ryu³, Sungjin Park³, Sudong Park³ and Eckhard Müller¹; ¹German Aerospace Center, Germany; ²University of Duisburg-Essen, Germany; ³Korea Electrotechnology Research Institute, Korea (the Republic of)

Alternative thermoelectric materials that can substitute the commercially dominant bismuth telluride technology are highly desirable for heat conversion and thermal management applications. Alternative thermoelectric materials that can substitute the commercially dominant bismuth telluride technology are highly desirable for heat conversion and thermal management applications. Magnesium silicide based solid solutions Mg₂X (X = Si, Ge, Sn) are among the most promising thermoelectric (TE) materials due to very good thermoelectric properties, low cost of raw materials and environmental compatibility. We have demonstrated technological maturity with prototypes of p- and n-type Mg₂X and p-MgAgSb/n-Mg₂X, the latter reaching conversion efficiencies > 6.5% (T_c = 25 °C; T_h = 300 °C) and power densities of ~1 W/cm², comparable to commercial bismuth telluride modules.

However, stable thermoelectric properties are of utmost importance for successful large-scale application. Intrinsic defects like Mg interstitials and Mg vacancies affect the properties of Mg₂X significantly, therefore Mg diffusion is a potential concern here. Annealing experiments and in-situ measurements at high temperature show that degradation of Mg₂X is a two-step process, where in the first step loosely bound excess Mg sublimates from the surface, reducing the charge carrier concentration, and only in the second step, after the solubility limit of Mg vacancies has been reached, Mg₂X decomposes into other phases. Variation of the annealing temperature allows us to develop a kinetic model which can be used to predict material stability at different application temperatures, we also find indications that this process can be decelerated by sealing of the surfaces.

Furthermore, we find that diffusion phenomena are relevant even at room temperature, changing the thermoelectric properties on a scale of months to years if stored under laboratory atmosphere. Microstructural investigations by SEM, EDX and AFM indicate that the observed changes are related to Mg diffusion inside the material, in line with conclusions from high temperature experiments. They furthermore show that the diffusion constant is highly selective on the Si:Sn ratio of the material, with diffusion being much faster in Sn-rich material. Comparison of different microscopic mechanisms of bulk diffusion by first-principles calculations reveals that Mg transport via Mg vacancies is the most relevant mechanism. We can furthermore show that the drift kinetics of the thermoelectric properties is related to the amount of excess Mg added during synthesis and that high-performance samples with improved stability can be synthesized by omitting excess Mg.

The chemical and structural complexity of this material class allows for employing advanced material improvement strategies, in particular selective scattering of charge carriers on (self-assembling) nanostructures (“energy filtering”). This can be achieved by a locally varying electronic band structure, feasible in Mg₂Si_{1-x}Sn_x by changing the band gap via the Sn content x and energetically adjusting the band edges in grains of different compositions by selective doping. To test selective doping strategies, a local charge carrier concentration measurement is highly useful. We will show that transient microprobe measurements of the Seebeck coefficient can be used to that purpose with a local resolution down to ~5 μm. For carrier concentration determination with sub-μm resolution we employ a combination of the AFM-based Kelvin Probe Force Microscopy for work function measurements, SEM for determination of the composition, first-principles calculations for band offset predictions and modelling based on the Boltzmann transport equation. Our results reveal an inhomogeneous distribution of the dopant Bi among several observed Mg₂Si_{1-x}Sn_x phases and confirm the feasibility to tune the local carrier concentration to control the electronic band structure alignment.

2:00 PM EN08.14.02

Optimization Study of (Ta_{0.4}Nb_{0.4}Ti_{0.2})–Fe–Sb Half-Heusler Thin Films Using Combinatorial Synthesis, High-Throughput Power Factor Mapping and Thermoreflectance Thermal Property Measurements Dylan J. Kirsch¹, Joshua Martin¹, Nathan Johnson², Suchismita Sarker³, Rohit Pant⁴, Ronald Warzoha⁵, Apurva Mehta⁶ and Ichiro Takeuchi⁴; ¹National Institute of Standards and Technology, United States; ²Carl Zeiss Research Microscopy Solutions, United States; ³Cornell University, United States; ⁴University of Maryland, United States; ⁵U.S. Naval Academy, United States; ⁶SLAC National Accelerator Laboratory, United States

Half-Heusler (hH) thermoelectric (TE) intermetallic alloys are promising candidates for commercial modules, but their conversion efficiency can be limited due to high thermal conductivity. One method to improve hH alloy performance is to decrease the lattice contribution to the thermal conductivity through solid-solution alloying. Several publications reported p-type NbFeSb hH alloys can accommodate off-stoichiometry on the Fe- and Sb-sites, which could positively impact the both the electrical properties and the thermal properties, similar to the lattice thermal conductivity decrease observed via Ta-alloying. Combinatorial approaches are an ideal method to explore hH alloy properties and phase stability with the advantage of rapid sample fabrication and characterization of a wide range of compositions. This approach can provide insights into materials systems that could be missed using conventional approaches but requires unique and custom synthesis and transport property measurement instrumentation. Both continuous-spread composition gradient and homogeneous discrete co-sputtered combinatorial thin film synthesis methodologies were leveraged to produce maps of the composition-structure-property relationships as a function of Fe- and Sb-content in (Ta_{0.40}Nb_{0.40}Ti_{0.20})–Fe–Sb hH alloys for the first time. The Seebeck coefficient and electrical resistivity were measured using our custom-built high-throughput scanning probe. Thermal conductivity and heat capacity were measured on our discrete combinatorial hH thin films using a custom-built, automated Frequency Domain Thermoreflectance (FDTR) instrument. Maximum TE figure-of-merit zT values at room temperature are calculated to be ≈ 0.08 for compositions (Nb_{0.41}Ta_{0.33}Ti_{0.26})_{28.5}Fe_{40.3}Sb_{31.2} and (Nb_{0.42}Ta_{0.33}Ti_{0.25})_{35.0}Fe_{31.7}Sb_{33.3} having thermal conductivity values ≈ 2.25 ± 0.27 W m⁻¹ K⁻¹. Our custom suite of high-throughput combinatorial instruments can now measure all of the properties needed to calculate the zT of any promising and unoptimized TE material system.

2:15 PM EN08.14.03

Microscale Imaging of Thermal Conductivity Suppression at Grain Boundaries Eleonora Isotta¹, Shizhou Jiang¹, Alexandra Zevalkink², Jeff Snyder¹ and Oluwaseyi Balogun¹; ¹Northwestern University, United States; ²Michigan State University, United States

Grain boundaries have a central importance in materials science. They can critically control thermal and electrical transport, determining the performance of energy and electronic materials. In thermoelectric materials, grain boundaries can be leveraged to suppress the thermal conductivity, but can also detrimentally suppress the carrier mobility. Grain boundaries are not all equal: they are associated to several degrees of freedom, and can come in multiple

orientations, symmetries, and chemistries. Recent evidence suggests that some types of grain boundaries could be more beneficial than others for the thermoelectric performance. Despite the importance, we lack a clear understanding of how grain boundaries modify the microscale transport owing to the scarcity of local investigations. Usually the role of grain boundaries is inferred from bulk, effective measurements. However, understanding how grain boundaries impact transport locally is a crucial perspective to enable grain-boundary engineering for the next generation of high-performance thermoelectrics.

In this work, we image the thermal conductivity of individual grain boundaries via spatially-resolved frequency-domain thermoreflectance. Measurements with microscale resolution reveal a suppression in thermal conductivity at grain boundaries both in thermoelectric SnTe and multicrystalline silicon. In contrast to conventional thermal modeling, which assumes that all boundaries are perfect scatterers and lead to uniformly suppressed thermal conductivity, we observe a non-uniform suppression localized within a few microns of a boundary. Furthermore, not all grain boundaries behave the same: misorientation angle, symmetry, and morphology are found to strongly correlate with the effective thermal boundary resistance. Extracting transport properties from microscale imaging can provide comprehensive understanding of how microstructure works. This development can improve our understanding of carrier-defect interactions, advancing the engineering of materials for thermoelectrics.

2:30 PM EN08.14.04

Using Bulk Thermoelectric Measurements to Identify Grain Boundary Transitions in NbFeSb [Duncan Zavanelli](#)¹, Ruben Bueno Villoro², Ran He³ and Jeff Snyder¹; ¹Northwestern University, United States; ²Max-Planck-Institut für Eisenforschung GmbH, Germany; ³Leibniz Institute for Solid State and Materials Research Dresden, Germany

Grain boundaries have seen much recent interest for improving the performance of thermoelectrics, with their capacity to reduce thermal conductivity. Thermally activated charge carrier scattering from grain boundaries is detrimental to performance, far outweighing the benefits to thermal conductivity in many materials. If charge scattering of grain boundaries could be reduced or eliminated, then reducing grain size could be used to improve the thermal properties of many thermoelectrics. In half-Heusler materials, experimental observations have shown that compositional changes at the grain boundary from dopant segregation are correlated to a reduction in the detrimental scattering from boundaries. However, there is currently no good method to identify this behavior based on bulk thermoelectric measurements. In this presentation, we propose a method to model the behavior of grain boundaries such that transitions in grain boundary properties can be identified. This enables the identification of changes in chemistry or structure of grain boundaries prior to in depth characterization of individual grain boundaries in the material.

2:45 PM EN08.14.05

Enhanced Thermoelectric Performance in Sputtered Epitaxial Fe₂VAl Thin Films via Crystal Orientation Selection Jose María Domínguez-Vázquez, Olga Caballero-Calero, Alfonso Cebollada, [Andres Conca](#) and Marisol Martín-González; Instituto de Micro y Nanotecnología, IMN-CNM, CSIC (CEI UAM+ CSIC), Spain

Heusler intermetallic compounds present a wide variety of compositions that fulfill the requirement of avoiding toxic or scarce elements. The Fe₂VAl family of Heusler alloys shows a large potential and versatility for thermoelectric thin films with tunable properties via doping with additional elements such as Ti, Ta, Si, W, and others [1-3]. The doping allows the fabrication of p- and n-type alloys in the same family, which simplifies future thermoelectric device fabrication. While the undoped alloy Fe₂VAl is a p-type material, the introduction of W, Si, or Ta results in a n-type one. P-type alloys are obtained with Ti and Zr, both with an increase in Seebeck values compared to the undoped case. The addition of these materials can also be performed in an off-stoichiometric manner [4,5].

Sputter deposition is a well-established, inexpensive, and very versatile technique for the fabrication of a wide variety of material systems. The chemical composition can be highly controlled by the simultaneous use of several magnetrons with different elements (codeposition) to achieve the desired film content or doping concentration, which is needed to optimize the thermoelectric properties [6].

From a fundamental point of view, the possibility to explore the influence of crystal orientation on thermoelectric performance is very appealing, offering a perfect scope for experiment versus theory comparison. In this sense, physical vapor deposition techniques are excellent tools for obtaining thin films with desired orientations through the use of adequate substrates in terms of crystal symmetry and lattice match. In this contribution, we present results on Fe₂VAl thin films fabricated by magnetron dc sputtering. Two different sample series have been prepared with varying deposition temperatures (RT-950°C) and with two different substrates and, consequently, two crystalline orientations owing to the different epitaxial relations. Films grown on MgO (100) are (100)-oriented, while Al₂O₃ (11-20) substrates induce a (110) orientation. In both cases, the (111) diffraction peak Fe₂VAl corresponding to the L₂₁ fully ordered phase can be observed in asymmetric configuration diffraction measurements.

The results of the characterization of the thin films with X-Ray Diffraction and SEM imaging are shown, proving epitaxial growth for both series. The electric conductivity, Seebeck parameter, and power factor are reported. We observe a large difference in the thermoelectric performance depending on the growth orientation of the films.

With these results, we prove the large potential of sputtering to produce high-quality Fe₂VAl films ready for further desired compositional variation and tuned doping via codeposition.

References

- [1] Nishino, Y. IOP Conference Series: Materials Science and Engineering, IOP Publishing, 142001 (2011)
- [2] K. Renard, et al., Journal of Applied Physics, **115** (3), 033707 (2014).
- [3] B. Hinterleitner, et al., Nature, **576** (7785), 85-90 (2019).
- [4] B. Hinterleitner, et al., Physical Review B **102** (7), 075117 (2020).
- [5] M. Mikami, et al., Journal of Applied Physics **111** (9), 093710 (2012).
- [6] A. Conca, et al., ACS Applied Electronic Materials (2023), DOI: <https://doi.org/10.1021/acsaem.2c01772>

Acknowledgments

Financial support by the Ministerio de Ciencia e Innovación with the ThermHeus (TED2021-131746B-I00) project and the ERC Advanced Grant POWERbyU (ERC-2021-ADG-101052603) is acknowledged. We acknowledge the service from the MiNa Laboratory at IMN, and funding from CM (project S2018/NMT-4291 TEC2SPACE), MINECO (project CSIC13-4E-1794) and EU (FEDER, FSE).

3:00 PM BREAK

SESSION EN08.15: Sustainable and Flexible Modules
Session Chairs: Jan-Willem Bos and Tsutomu Kanno
Friday Afternoon, April 26, 2024
Room 336, Level 3, Summit

3:30 PM *EN08.15.01

Heat Conduction in a Printed Thermoelectric Film [Koji Miyazaki](#); Kyushu University, Japan

We have developed printed thermoelectric thin films using inorganic materials such as Bismuth Telluride. The process involved crushing the material into fine powders and mixing it with polyamic acid in an organic solvent. The resulting viscous solution was screen-printed onto a substrate and annealed in an Argon atmosphere. The heated polyamic acid transformed into polyamide at 400°C, acting as an adhesive between the thermoelectric powders. However, we found that the electrical conductivity of the resulting film was very low due to the low packing density. To address this issue, we decided to create a composite material by incorporating printable materials. We chose the lead-free halide perovskite, CsSnI₃, which displayed relatively good thermoelectric properties as a printable material. We mixed the Halide perovskite into the Bismuth Telluride solutions and printed them onto the substrate. After heating the film on a hotplate, the halide perovskite precipitated in the pores, resulting in a composite film of Bi₂Te₃/CsSnI₃. This composite film displayed improved electrical conductivity and low thermal conductivity, while the Seebeck coefficient slightly decreased. We also found that the thermal conductivities of both Bismuth telluride and Halide perovskite were low, and the high interfacial thermal resistance between them was measured to be in the order of 10⁻⁷K/(m²•W) using the differential 3omega method. This high interfacial thermal resistance explained the low thermal conductivity of the composite film, following a conventional model with interfacial thermal resistance. Ab initio calculations helped us understand the mechanisms behind the high interfacial thermal resistance. We believe that our printing process can be applied to other thermoelectric materials, allowing us to create film-shaped thermoelectric generators. Then, we applied the present printing technique to Cobalt antimonide Skutterudite. The Cobalt antimonide shows a high power factor at room temperature although thermal conductivity is also high. The effective thermal conductivity of the printed film is low, as well as keeping a relatively high power factor at room temperature. The packing density should be increased to improve the electrical conductivity of the printed Cobalt antimonide Skutterudite. This method can be applied to make thermoelectric energy harvester for room temperature use.

4:00 PM EN08.15.02

An Organic Thermoelectric Generator by Local Doping of Highly-Aligned Polymer Films [Nathan James Pataki](#)^{1,2}, [Shubhradip Guhait](#)³, [Martin Brinkmann](#)³ and [Mario Caironi](#)¹; ¹Istituto Italiano di Tecnologia, Italy; ²Politecnico di Milano, Italy; ³Centre National de la Recherche Scientifique (CNRS), France

The growing number of distributed microelectronics in the Internet of Things (IoT) requires versatile, scalable and affordable power sources. Heat-harvesting organic thermoelectric generators (TEGs) are regarded as a potential key component of the future energy landscape. Research surrounding the structure-property relationships in organic thermoelectric materials has led to extraordinary advances in the power factors of preferentially aligned polymer films [1-2], yet there has been little effort to actually leverage these advances and transfer aligned polymer films into a functional TEG. In this work, a previously reported shear-force method is used to induce in-plane orientation of regioregular poly(3-hexylthiophene) (P3HT) and poly[bis(thiophen-2-yl)thieno[3,2,b]thiophene (PBTTT) films which are then floated onto ultrathin parylene substrates. A scalable inkjet printing method along with an ink formulation of the p-type dopant tris(4-bromophenyl)ammoniumyl hexachloroantimonate, known as magic blue (MB), enabled high-precision local doping of the oriented polymer films to pattern a conductive TEG architecture. This novel fabrication method was used to scale the oriented TEGs up to 10 thermocouple pairs resulting in a maximum power output of 1.1 nW and an open circuit voltage of 6.6mV at ΔT=50K. This work represents the first example of an oriented organic TEG and demonstrates the value of local doping as a precise and scalable fabrication method for future TEGs.

[1] Viktoriia Untilova, Till Biskup, Laure Biniek, Vishnu Vijayakumar, and Martin Brinkmann
Macromolecules 2020 53 (7), 2441-2453

[2] Vijayakumar, V., Zhong, Y., Untilova, V., Bahri, M., Herrmann, L., Biniek, L., Leclerc, N., Brinkmann, M., Bringing Conducting Polymers to High Order: Toward Conductivities beyond 10⁵ S cm⁻¹ and Thermoelectric Power Factors of 2 mW m⁻¹ K⁻². Adv. Energy Mater. 2019, 9, 1900266.

4:15 PM EN08.15.03

2D/3D-Printed Bismuth Telluride-Based Flexible Thermoelectrics for Low-Scale Energy Harvesting [Francisco Molina-Lopez](#); KU Leuven, Belgium

The swift development of the Internet of Things (IoT) and wearable electronics is urgently demanding innovative power solutions. Batteries alone can barely satisfy this demand for two main reasons: Firstly, battery replacement limits the implementation of some scenarios of the IoT in which nodes might be highly distributed in difficult access locations; Secondly, batteries are often too bulky and rigid to be seamlessly integrated on thin and soft wearable electronics, or small IoT nodes. Thermoelectric generators (TEGs) refer to renewable power sources able to assist -or even replace- batteries by generating electricity from the abundant waste heat in the environment. Conveniently, it has been suggested that for low-power applications, TEs can surpass other thermal engines in terms of efficiency.[1] Furthermore, TEs are also capable of on-demand cooling and heating. However, to meet the form factor required by the IoT and wearables (namely repeated bendability/stretchability, conformability to curved surfaces, and large areas), important advancements must be made on traditional TEGs, which are rigid, and hard to scale up to large-area devices.[2]

My group is working towards the development of high-performance thermoelectric materials that can be directly 2D- or 3D-printed on flexible substrates. In particular, I will describe our progress in the formulation of bismuth telluride powder as a printable paste/ink, and the process of selective laser sintering and the direct ink writing (DIW) to form in-plane and through-plane TEGs, respectively. Printing techniques can potentially reduce the material waste and cost of TEGs. Moreover, in combination with a flexible substrate, printing enables innovative device architectures, such as large-area and flexible devices that can be easily integrated on the skin/smart textiles to power wearables using the heat emitted by the human body, as well as adapt to hot curved surfaces, like hot pipes or engines, to power IoT nodes. Because we target energy harvesting around room temperature, bismuth telluride is used as a benchmark material to showcase our processes and device architectures. However, our technology is likewise compatible with emerging polymeric materials, which will be also presented for comparison. If successful, this line of research will holistically tackle the main bottlenecks of TEGs, paving the way to their broad implementation in wearables and other low-power energy harvesting applications.

Acknowledgments

This work was supported by the European Research Council (ERC) under the European Union's Horizon 2020 research and innovation programme: Grant Agreement No. 948922 – 3DALIGN; the Research Foundation - Flanders (project number 11E2621N); and the Internal Funds KU Leuven, C1 project C14/21/078.

[1] C. B. Vining, Nat. Mater. 2009, 8, 83.

[2] F. Molina-Lopez, In 2020 IEEE Sensors, IEEE, Rotterdam, 2020, pp. 1–4.

4:30 PM EN08.15.04

Electrodeposited Silver Selenide Films: From Pourbaix Diagram to a Flexible Thermoelectric Module [Cristina V. Manzano](#), Cristina Llorente del Olmo, Olga Caballero-Calero and Marisol Martín-González; Institute of Micro and Nanotechnology, Spain

In the last few years, the exploration of new thermoelectric materials with low-toxicity, earth-abundance, and high-efficiency has become essential. Following this trend, sustainable, easily scalable, and cost-effective fabrication methods, such as electrochemical deposition, are also desirable. In this work, the Pourbaix diagram of silver–selenium–water was developed to find an adequate pH and reduction potential for the electrodeposition of stable silver selenide. Based on this diagram, a solution without the incorporation of additives was developed. Silver selenide films were electrodeposited at different reduction potentials, and after the deposition, the compositional, morphological, and structural characterizations of the silver selenide thin films were analysed. The thermoelectric properties of the electrodeposited silver selenide films were measured at room temperature. The maximum power factor was found for the films grown at 0.071 V with a value of 3421 ± 705 mW/mK² and a thermal conductivity of 0.56 ± 0.06 W/mK. Even better, when it can be done by employing a technique that is easily scalable to an industrial level and allows large areas to be obtained, such as electrodeposition. Finally, films with similar properties were deposited on a flexible Kapton substrate (see Figure 1). A unileg thermoelectric power generator was produced with maximum output powers of 14.7, 29.4, and 37 mW under temperature differences of 10, 15, and 19 K, respectively; and maximum power densities of 55.1, 110.1, and 138.6 mW/m² under temperature differences of 10, 15, and 19 K, respectively.

4:45 PM EN08.15.05

Advances in Soft and Wearable Energy Harvesters Using Stretchable Thermoelectrics [Mason Zadan](#), Dinesh K. Patel, Anthony Wertz and Carmel Majidi; Carnegie Mellon University, United States

To improve operational lifetimes of wearable electronics, energy harvesting solutions must be introduced to offset the limitations of current battery technologies. These solutions must both have energy harvesting performance metrics that can meaningfully extend the operational lifetime of wearable health monitoring systems, along with being biocompatible. Soft and deformable materials must be introduced to replace the rigid components of these systems to allow for these energy harvesters to not impede movement. Currently, various wearable energy harvesting solutions have been introduced including piezoelectric, triboelectric, dielectric elastomer, and thermoelectric generators. While these systems have been developed to be deformable and stretchable, the energy densities still must be improved to meaningfully increase power output while not sacrificing mechanical performance. Thermoelectrics, in particular, have the advantage of operating off of temperature differentials and not requiring biomechanical movement. When a temperature difference is applied across oppositely doped thermoelectric semiconductor junctions, a voltage is generated through the Seebeck effect. Conversely, when a current is driven across the semiconductor junctions, a temperature potential can be generated through the Peltier effect.

In this talk I will discuss recent work on the creation of soft and stretchable thermoelectric generators along with their introduction as a power source for wearable electronic devices. To replace rigid materials such as ceramic thermal interfaces and copper interconnects, we introduce 3D printed elastomers and eutectic gallium indium liquid metals as material replacements for the device substrate and conductive traces. Device packaging and fabrication is discussed for multiple generations of these devices. Seebeck and Peltier characterization along with electromechanical characterization is reported, highlighting performance metrics under strain. Wearable integration is also reported with on-body testing conducted to better understand the relative performance changes during wear. Separately, recent integration of these TEGs into soft robotics is discussed through their combination with liquid crystal elastomer shape memory polymers. These TEGs are introduced as both the heating and cooling element along with energy harvesting capabilities.

SYMPOSIUM EN09

Nanostructured Electrocatalysts for Energy Applications
April 23 - May 8, 2024

Symposium Organizers

Christopher Barile, University of Nevada, Reno
Nathalie Herlin-Boime, CEA Saclay
Michel Trudeau, Concordia University
Edmund Chun Ming Tse, University Hong Kong

* Invited Paper

+ JMR Distinguished Invited Speaker

^ MRS Communications Early Career Distinguished Presenter

SESSION EN09.01: Synthesis for (Electro)catalysis I
Session Chairs: Christopher Barile and Edmund Chun Ming Tse
Tuesday Morning, April 23, 2024
Room 337, Level 3, Summit

10:30 AM *EN09.01.01

Phase Engineering of Nanomaterials (PEN) [Hua Zhang](#)^{1,2}; ¹City University of Hong Kong, China; ²City University of Hong Kong Shenzhen Research Institute, China

In this talk, I will summarize the recent research on phase engineering of nanomaterials (PEN) in my group, particularly focusing on the rational design and synthesis of novel nanomaterials with unconventional phases for various promising applications. For example, by using wet-chemical methods, for the first time, we have successfully prepared novel Au nanostructures (e.g., the hexagonal-close packed (*hcp*) 2H-Au nanosheets, 4H-Au nanoribbons, and crystal-phase heterostructured 4H/*fcc* and *fcc*/2H/*fcc* heterophase Au nanorods), epitaxially grown metal nanostructures on the aforementioned unconventional Au nanostructures and 2H-Pd nanoparticles, and amorphous/crystalline heterophase Pd, PdCu, Rh and Rh alloy nanosheets. In addition, by using gas-solid reactions, metastable 1T'-phase group VI transition metal dichalcogenides (TMDs), e.g., WS₂, WSe₂, MoS₂, MoSe₂, WS₂Se_{2(1-x)} and MoS₂Se_{2(1-x)}, have been prepared. Moreover, the salt-assisted 2H-to-1T' phase transformation of TMDs have been achieved, and the phase transformation of TMDs during our developed electrochemical Li-intercalation process has been observed. Impressively, the lithiation-induced amorphization of Pd₃P₂S₈ has been achieved. Currently, my group focuses on the investigation of phase-dependent physicochemical properties and applications in catalysis, (opto-)electronic devices, clean energy, chemical and biosensors, surface enhanced Raman scattering, photothermal therapy, etc., which we believe is quite unique and very important not only in fundamental studies, but also in future practical applications. Importantly, the concepts of phase engineering of nanomaterials (PEN), crystal-phase heterostructures, and heterophase nanomaterials are proposed.

11:00 AM EN09.01.02

Atomic Layer Deposition of Noble Metal Nanoparticles for Catalytic Applications [Jan M. Macak](#)^{1,2}; ¹University of Pardubice, Czechia; ²CEITEC, Czechia

Platinum group metals such as Pt, Ru, Pd, Ir, etc., have superior performance for various catalytic applications.^[1] Due to their scarcity, efforts were being made to reduce or replace these noble metals. Atomic Layer Deposition (ALD) is one among the best technique to facilitate lowering of loading mass on a support of interest.^{[2],[3]} Furthermore, ALD is the most suitable technology that can decorate high aspect ratio and high surface area substrate architectures.^[4] Due to the governing surface energy variations between noble metals and support surfaces, the growth initiates as nanoparticles (NP) and with a further increase in ALD cycles the agglomeration among NP's dominates over the individual NP size increase, thus developing thin films of relatively higher thickness. The surface energy variations are also known to increase the nucleation delay of noble metals especially for Ru considerably. In this regard our efforts were laid to improve the functionality with pretreatments on carbonaceous supports which were shown promising to reduce the nucleation delay of ALD deposited Ru.

For electrocatalytic applications, it is important to choose the right substrates. Among available substrates, carbon papers (CP) and titania nanotube (TNT) layers are best choices considering their physio-chemical properties, availability, vast literature, and low costs incurred using these as support substrates in electrocatalysis and photocatalysis. Several surface modifications for CP's and variations on morphological aspects of TNT layers had received a great attention from applied fields due to their improved surface area, conductivity and stability.^{[5]-[8]} Uniformly decorating these CP's and TNT layers by NPs or thin films of catalysts proved to be highly efficient with no boundaries on applications.^[9]

The presentation will introduce and describe the synthesis of different noble metal NPs by ALD on various aspect ratio TNT layers and CP substrates. It will also include the corresponding physical and electrochemical characterization and encouraging results obtained in electrocatalysis.

References

Huang, Z. F. *et al. Advanced Energy Materials* vol. 7 (2017) 1700544.

Yoo, J. E. *et al. Electrochem. commun.* **86**, (2018) 6

Anitha, V. C. *et al. J. Catal.* **365**, (2018) 86.

Zazpe, R. *et al. Langmuir* **32**, (2016) 10551.

Sopha, H. *et al. Appl. Mater. Today* **9**, (2017) 104.

Macak, J. M., Zlamal, M., Krysa, J. & Schmuki, P. *Small* **3**, (2007) 300.

Liu, C., Sun, C., Gao, Y., Lan, W. & Chen, S. *ACS Omega* **6**, (2021) 19153.

Sitaramanjaneya M. Thalluri & Macak, J. M. *Small* **19** (2023) 2300974.

Dvorak, F. *et al. Appl. Mater. Today* **14**, (2019) 1.

11:15 AM *EN09.01.03

Nanomaterials for Energy: Controlling Properties through Controlled Synthesis [Sophie Cassaignon](#); Sorbonne University, France

In the realm of applied research for energy, the continuous quest to offer innovative materials with novel properties remains a perpetual challenge. These properties are often tailored to suit specific applications. To approach this challenge effectively, one must master the four fundamental characteristics of a material. The first of these, which dictates its intrinsic properties, is its composition and the crystalline phase it assumes, especially in the case of crystalline solids. The second aspect to consider is the size of the primary objects that constitute the solid. On a larger scale, texturing techniques such as creating porous materials, multi-scale architectures, and superstructures are also used. Finally, the shaping of materials into various forms like films or powders also plays a critical role in determining the material's properties within the final device.

On the side of fundamental research, it is imperative to understand the intricate relationship between a material's structure, morphology, texture, and the specific property we aim to target. The synthesis of the material should not rely on a mere "trial and error" approach; instead, it should be grounded in a profound understanding of the parameters governing reactivity.

Despite the wealth of crystalline phases associated with metals, oxides, carbides, and more, new structures are consistently being discovered, often characterized by unique properties. These structures are frequently beyond the reach of traditional high-temperature synthesis methods. Instead, they can be effectively realized through gentler and more innovative synthesis techniques, such as Sol-Gel chemistry. Operating at lower temperatures, Sol-Gel chemistry facilitates the attainment of metastable states of matter, often emphasizing kinetic control over thermodynamic control. Furthermore, certain phases exist only at extremely small particle sizes, corresponding to the nanoscale. Mastering Sol-Gel chemistry and its key parameters, typically involving concentration, temperature, or pH in the case of aqueous solutions, offers the most suitable means of structuring materials at this scale.

In the presentation, we will explore specific examples of nano-oxides like TiO₂, WO₃, Na₃V₂(PO₄)₂F₃... and their applications in the realms of energy and the environment.

11:45 AM EN09.01.04

Magnetic-Field Assisted Synthesis of Transition Metal Aerogels Allows Formation of High Surface Area Electrocatalysts [Rosemary L. Calabro](#)^{1,2}, [Garret A. Longstaff](#)¹, [Edward Tang](#)¹, [Veronika M. Xiao](#)¹, [Alexander D. Ciampa](#)¹, [Kennedy V. Munz](#)¹, [Enoch A. Nagelli](#)¹, [Stephen F. Bartolucci](#)², [Joshua A. Maurer](#)² and [John Burpo](#)¹; ¹United States Military Academy, United States; ²U.S. Army DEVCOM Armaments Center, United States

Transition metal aerogels (TMAs) have emerged as promising electrocatalysts for a variety of reactions due to their lightweight properties, conformability, porous natures, and high surface areas allowing many available sites for charge transfer and catalytic activity. The catalytic properties of the TMAs can be tuned based on the elemental composition, surface environment, and structural properties, allowing opportunities to design a wide range of TMAs that can

catalyze a variety of reactions. An ongoing challenge is that traditional methods to prepare TMAs suffer drawbacks such as aggregation, slow reactant diffusion times, a need for templates which can block catalytic active sites, and formation of a brittle final product. We have developed a magnetic-field assisted synthesis strategy to produce iron aerogels that addresses these limitations. In a typical synthesis, a ferric chloride metal salt solution was placed inside a 150 mT magnetic field. Sodium borohydride was then added as a reducing agent which resulted in immediate formation of a gel. This gel was rinsed and then either supercritically dried into an aerogel or pressed into a thin film. Scanning electron microscopy (SEM) shows that the aerogels consist of iron nanowires that are intertwined with each other, and nitrogen porosimetry confirms that they have high surface areas and porosities. The lack of templates or surfactants in synthesis allows exposed surfaces available for electrocatalysis. The iron nanowire network within the aerogel allows improved mechanical properties relative to TMAs prepared through alternate methods. The aerogels were then used as a sacrificial template for galvanic displacement with platinum which allowed dissolution of the iron and formation of high surface area platinum nanotubes. SEM shows the platinum tubes retain the nanowire network of the iron template, and electrochemical impedance spectroscopy (EIS) and cyclic voltammetry (CV) indicate high electrochemical accessible surface areas for electrocatalytic applications. This strategy was also applied to cobalt nanowire synthesis with subsequent thermal annealing to Co_3O_4 for pseudocapacitor applications, and for formation of bimetallic iron-nickel aerogels which are promising as electrocatalysts for water splitting.

SESSION EN09.02: Synthesis for (Electro)catalysis II
Session Chairs: Christopher Barile and Edmund Chun Ming Tse
Tuesday Afternoon, April 23, 2024
Room 337, Level 3, Summit

1:30 PM EN09.02.01

Ordered Metal Nanowire Networks for High Performance Catalytic Electrodes [Adam Squires](#); University of Bath, United Kingdom

We present a new method for the production of ordered 3D metal-nanowire network films using a coating of lipid inverse cubic phase as the template for electrodeposition. We have produced platinum films which show a previously unreported "single diamond" nanoarchitecture with tunable nm-scale pore and wire diameters, and lattice parameters down to below 10 nm. The nanoarchitecture gives high electrocatalytic performance and stability towards fuel cell oxidation reactions; and the production and removal of the template is facile, using mild conditions and green solvents (water, ethanol) in simple half-hour steps, representing an attractive route to high performance nanomaterials.

1:45 PM EN09.02.02

Fast and Facile Microwave Synthesis of Cubic CuFe_2O_4 Nanoparticles for Electrochemical CO_2 Reduction Judith Zander and [Roland Marschall](#); University of Bayreuth, Germany

Electrochemical CO_2 reduction is a promising strategy for the sustainable synthesis of carbon-based chemicals or fuels such as CO , or CH_4 . [1] Copper-based materials are of special interest due to their broad substrate scope. While copper itself is the first known metal catalyst able to directly yield CH_4 , CO , methanol, or C_2 products such as ethanol can also be obtained, e.g. from oxide derived catalysts. [2][3] Another interesting copper oxide is the spinel CuFe_2O_4 , due to its versatile electronic and magnetic properties. Those can be tuned *via* variations in the cation distribution between octahedral and tetrahedral sites. [4] Changes in the cation distribution, or degree of inversion, can additionally lead to a structural transformation between the cubic and tetragonal form, due to the strong Jahn-Teller effect of Cu^{2+} . Both degree of inversion and structure are strongly dependant on the synthesis conditions. [4] In this contribution we introduce a fast microwave-assisted solvothermal synthesis of cubic CuFe_2O_4 . Very short synthesis times of 1 min and low temperatures of 120 °C in ethylene-glycol/water mixtures could be realised, without a loss of phase-purity and no necessity for subsequent thermal treatment. [5] The degree of inversion was found to decrease with increasing synthesis time, whereas the particle size and crystallinity was almost independent of the synthesis conditions. The influence of the synthesis conditions – and thus material properties – on the activity in electrochemical CO_2 reduction to CO in 0.1 M KHCO_3 was investigated. The best activity was obtained for CuFe_2O_4 with an intermediate degree of inversion of approx. 0.75, together with a large crystallite size and micro-strain. Since hydrogen was produced as the only site-product, CuFe_2O_4 can be an interesting candidate for the production of syngas.

References:

- [1] Q. Lu, F. Jiao, *Nano Energy* **2016**, 29, 439
- [2] S. Nitopi, E. Bertheussen, S. B. Scott, X. Liu, A. K. Engstfeld, S. Horch, B. Seger, I. E. L. Stephens, K. Chan, C. Hahn, J. K. Nørskov, T. F. Jaramillo, I. Chorkendorff, *Chem. Rev.* **2019**, 119, 7610
- [3] D. Raciti, C. Wang, *ACS Energy Lett.* **2018**, 3, 1545
- [4] R. Zhang, Q. Yuan, R. Ma, X. Liu, C. Gao, M. Liu, C.-L. Jia, H. Wang, *RSC Adv.* **2017**, 7, 21926
- [5] J. Zander, M. Weiss, R. Marschall, *Adv. Energy Sustainability Res.* **2023**, 2200184

SESSION EN09.03: Water Splitting
Session Chairs: Christopher Barile and Edmund Chun Ming Tse
Tuesday Afternoon, April 23, 2024
Room 337, Level 3, Summit

2:00 PM *EN09.03.01

Engineering Stable Multiscale Electrocatalyst Architectures for Efficient Alkaline-Membrane Water Electrolysis [Shannon W. Boettcher](#)^{1,2};

¹University of Oregon, United States; ²University of California, Berkeley, United States

Commercialized membrane electrolyzers use acidic proton exchange membranes (PEMs). These systems offer high performance but require the use of expensive precious-metal catalysts such as IrO_2 and Pt that are nominally stable under the locally acidic conditions. Alkaline-exchange-membrane (AEM) electrolyzers in principle offer the performance of PEM electrolyzers with the ability to use earth-abundant catalysts and inexpensive bipolar plate materials. I will present our work in understanding the chemical and electrochemical processes in earth-abundant water-oxidation catalysts, including the use of integrated reference-electrode device architectures and cross-sectional materials analysis, as well as progress in building high-performance AEM

electrolyzers. Baseline electrolyzers operate at 1 A cm⁻² in pure water feed at < 1.9 V at a moderate temperature of ~70 °C using either IrO₂ or Co₃O₄ anode catalyst layers, PiperION alkaline ionomers, and stainless-steel porous transport layers. These devices, however, degrade rapidly compared to PEM electrolyzers. The voltage profile corresponding to degradation has initial fast (~10 mV/h) and steady-state slow components (~1 mV/h), which we link to chemical and structural changes in the ionomer-catalyst reactive zone. We further discover that dynamic Fe-based OER catalysts – that have world-record performance in traditional liquid alkaline electrolyzer systems – perform poorly with enhanced degradation rates in alkaline membrane electrolysis, illustrating fundamentally different chemical design principles for OER catalysts. We use these principles to create advanced catalysts with surface and bulk properties tuned for AEM electrolysis applications leading to enhanced performance. I will also highlight promising new chemical strategies to mitigate degradation using novel ionomers and passivated electrolyte-electrode-catalyst compositions and interfacial architectures.

2:30 PM EN09.03.02

Two Dimensional Materials and Their Heterostructures for Ampere-Level Direct Seawater Splitting Suraj Loomba, Muhammad Waqas Khan, Muhammad Haris and Nasir Mahmood; RMIT University, Australia

Green hydrogen has emerged as the potential replacement for fossil fuels; however, more than 20 billion m³ of water would be required to meet the future demand of 2.3 Gt of hydrogen per year, which is almost equal to the water needs of a country with a population of more than 60 million. Currently, most of the current industrial processes require purified freshwater for the electrolysis process, which is a limited resource, and utilizing freshwater to meet increasing hydrogen demands can lead to a drinking water crisis. Seawater, an almost unlimited resource, can be a potential feedstock for water electrolysis. However, the complex composition and presence of chloride anions in the seawater can interfere with the electrolysis process. Although desalination has been suggested for seawater purification, the economics of scale do not justify the set-up of the plant. Therefore, synthesizing materials that can withstand complex seawater composition and deliver enhanced performance and long-term stability in direct seawater is crucial.

In my previous work, I developed porous sheets of 2-dimensional (2D) N-NiMo₃P, which required an overpotential of only 35 mV and 346 mV to acquire 10 mA cm⁻² for hydrogen evolution reaction (HER) and oxygen evolution reaction (OER) in alkaline seawater, respectively. The presence of Ni and N resulted in enhanced electrical conductivity by assisting in the redistribution of the charge states and the metal-non-metal bond lengths while the pores catered for faster mass transport and increasing active sites. Furthermore, the presence of polyanions (phosphate, nitrate) on the surface safeguarded the catalyst against chlorine chemistry, preventing chlorine evolution reaction at the anode. As a result, the catalyst was stable for over 100 hours of continuous operation. Although the HER performance of the catalyst was exceptional, the long-term operation and anodic performance still needed to be improved to realize the commercial applications.

Learning from my previous work, I have developed a 2D heterostructure catalyst for ampere-level anodic reaction. The as-synthesized catalyst possesses the advantages of its constituent 2D materials while alleviating their disadvantages. The materials are bonded via unique bonds at the heterointerface, which helps in optimizing the surface geometries for selective reactions while also modulating the hydroxyl anions at the interface, which play a crucial role in averting the chlorine chemistry at the anode by repelling the chloride anions. As a result of the unique bonded heterointerface, the material can deliver approximately 10x better performance while also being 65% more economical than commercial IrO₂ for anodic reaction. Furthermore, the catalyst can operate stably for over 1000 h without any current losses. To further confirm the exceptional stability, the working electrode was left idle in the electrochemical system for 5 days and then tested again, where it retained more than 90% of its initial current density after 3 days of continuous operation, making it integrable with renewable power sources. Hence, the interfacial engineering method to obtain a unique bonded heterointerface can be a potential strategy to synthesize a 2D heterostructure catalyst for industrial direct seawater splitting.

2:45 PM EN09.03.03

Electrochemical Water Oxidation over Core/Shell structured Hyperfine β-FeOOH (akaganeite) Crystalline Nanorods coated with Bias-Responsive Amorphous Ni(OH)₂ Tomiko M. Suzuki, Takamasu Nonaka, Akihiko Suda, Yoriko Matsuoka, Keita Sekizawa, Yusaku F. Nishimura, Satoru Kosaka, Tepei Nishi, Shunsuke Sato, Takeo Arai and Takeshi Morikawa; Toyota Central R&D Labs, Japan

The water oxidation to extract electrons from water molecules for the oxygen evolution reaction (OER) is essential for the development of a sustainable system to synthesize valuable chemicals such as hydrogen and organic compounds from H₂O and CO₂. The catalysts consisting of earth-abundant elements are required for the system integration with minimized cost and total CO₂ emission in its lifecycle.

We have developed a 10 nm-sized highly crystalline red rust catalyst for OER composed of pure β-phase FeOOH(Cl) hyperfine nanorods (an average diameter of 3 nm and a length of 14 nm) synthesized by a facile one-pot process at room temperature and ambient pressure.[1] This one-pot process yields β-FeOOH(Cl) nanorods sizing more than 10 times smaller than those by conventional methods. The process also enables doping with Ni ions in the crystal lattice (β-FeOOH(Cl):Ni) and simultaneous surface-coating with amorphous a-Ni(OH)₂ (a Ni to Fe ratio up to 22 at.%), which forms a core/shell structure.[2] The overpotential for electrochemical OER over anodes stacked with the core/shell β-FeOOH:Ni/a-Ni(OH)₂ was 170 mV, and an OER current of 10 mA/cm² was obtained at an overpotential of 430 mV in a 0.1 M KOH solution. The high current density at low potential compared with many Fe-rich oxide and (oxy)hydroxide electrodes reported previously.

X-ray absorption fine structure analysis (XAS), Mössbauer spectroscopy, X-ray photoelectron spectroscopy (XPS), field emission scanning electron microscopy (FESEM), X-ray diffraction (XRD), and impedance spectroscopy suggested that surface coating with the a-Ni(OH)₂ lowered the OER overpotential of β-FeOOH(Cl), resulting in reduced total impedance in the electrode. Mössbauer spectroscopy suggested interaction between Fe and Ni species [2], and *operando* X-ray absorption spectroscopy (XAS) under biased conditions in the aqueous solution revealed a characteristic behavior that does not occur in Fe-Ni mixed oxide systems.[3] The nearest neighbor structure and valence of Fe³⁺ ions did not change under the OER conditions. In contrast, Ni ions showed second nearest neighbor ordering which was assignable to β-Ni(OH)₂, and a fraction of Ni²⁺ ions was partially oxidized to Ni³⁺ at the bias for OER. This is presumably the change at the interface of the β-FeOOH:Ni nanorods and the surface a-Ni(OH)₂. This Ni valence change was reversible, following the sweep of the electrical bias. These findings show an essential role of Fe-Ni interactions in the core/shell β-FeOOH:Ni/a-Ni(OH)₂, accompanied by Ni species' structural and partial valence change under the electrical bias.

Further, after treatment in an alkaline solution of the β-FeOOH:Ni/ a-Ni(OH)₂ stacked electrode operates long-term OER even in a nearly neutral pH solution. The electrode as an anode was series-connected with a Mn-complex catalyst cathode for CO₂ reduction and a Si solar cell in a one-compartment reactor to construct a system mainly consisting of earth-abundant elements.[4] Under a nearly neutral pH solution bubbled with CO₂ (pH 6.9), the system produced CO and achieved solar-to-chemical energy conversion efficiency of 6.6 % in a single electrolyte solution. A long-term OER in the nearly neutral pH solution performed after a specific treatment of β-FeOOH:Ni/ a-Ni(OH)₂ will also be presented.

References

- [1] T. M. Suzuki, T. Nonaka, A. Suda, N. Suzuki, Y. Matsuoka, T. Arai, S. Sato and T. Morikawa, *Sustain. Energy Fuels*, 1 (2017) 636-643.
- [2] T. M. Suzuki, T. Nonaka, K. Kitazumi, N. Takahashi, S. Kosaka, Y. Matsuoka, K. Sekizawa, A. Suda and T. Morikawa, *Bull. Chem. Soc. Jpn.*, 91 (2018) 778–786.
- [3] T. Morikawa, S. Gul, Y. F. Nishimura, T. M. Suzuki and J. Yano, *Chem. Commun.*, 56 (2020) 5158-5161.
- [4] T. Arai, S. Sato, K. Sekizawa, T. M. Suzuki and T. Morikawa, *Chem. Commun.*, 55 (2019) 237-240.

3:00 PM BREAK

3:30 PM *EN09.03.04

Toward Cost-Effective Ensembles of Artificial Photosynthetic Nanoreactors for Solar Water Splitting Zejie Chen¹, Sam Keene¹, Justin T. Mulvey¹, Pushp Raj Prasad¹, William Gaieck¹, Gabriel S. Phun¹, William D. Stinson², Robert S. Stinson², Luisa Barrera³, Tea Yon Kim¹, Brian T. Zutter⁴, Aliya S. Lapp⁴, Soyoung Kim⁵, Wenjie Zang¹, Mingjie Xu¹, Fikret Aydin⁶, Yaset Acevedo⁷, Jennie Huya-Kouadio⁷, Brian D. James⁷, Tuan Anh Pham⁶, Tadashi Ogitsu⁶, Akihiko Kudo⁸, Junko Yano⁵, Joseph P. Patterson¹, Xiaoping Pan¹, Alec Talin⁴, Katherine Hurst⁹, Daniel Esposito², Rohini Bala Chandran³ and Shane Ardo¹; ¹University of California Irvine, United States; ²Columbia University, United States; ³University of Michigan, United States; ⁴Sandia National Laboratories, United States; ⁵Lawrence Berkeley National Laboratory, United States; ⁶Lawrence Livermore National Laboratory, United States; ⁷Strategic Analysis, Inc., United States; ⁸Tokyo University of Science, Japan; ⁹National Renewable Energy Laboratory, United States

In 2021, the U.S. Department of Energy (DOE) announced its first Energy Earthshot on green hydrogen production, with a cost target of \$1/kg within a decade. To put this value in perspective, astonishingly, at least 80% of this cost will be needed to pay for the operating expenditures alone of future utility-scale electricity from photovoltaics. This fact motivates less-expensive means than photovoltaics to generate and collect photogenerated mobile charge carriers, and/or exceedingly low capital cost electrochemical reactors operating at exceptionally low overpotentials. This latter option represents a paradigm shift from state-of-the-art electrolyzers that currently benefit from operation at high current densities, and thus relatively high overpotentials.

Optically thin photosynthetic nanoreactors transmit significant amounts of sunlight, and therefore each operates at a low current density. When combined with the multiplicative output of having many nanoreactors in an ensemble, detailed-balance solar-to-hydrogen energy conversion efficiencies are simulated to exceed those of optically thick photoelectrochemical designs. In efforts to attain these predicted higher efficiencies, Ensembles of Photosynthetic Nanoreactors (EPN) DOE Energy Frontier Research Center (EFRC) is performing detailed studies on the properties of state-of-the-art doped SrTiO₃ and BiVO₄ photocatalyst nanoparticles.

During my talk, I will share our recent collaborative discoveries in atomic-layer-deposited ultrathin oxide coatings to impart redox selectivity and materials stability, single-photocatalyst-nanoparticle photoelectrochemical behavior and mobile charge carrier properties, and atomic-level information on dopant distributions and materials interfaces obtained from electron microscopies and X-ray spectroscopies. I will also describe a new low-cost reactor design that we are developing. Collectively, our discoveries provide new design guidelines, and motivate additional basic science research pathways, for the development of stable composite materials to serve as active components in cost-effective artificial photosynthetic devices.

4:00 PM EN09.03.05

Electrolyte-Assisted Polarization in BiFeO₃/Nickel Foam for The Enhancement of Electrocatalytic Water Splitting Heng-Jui Liu¹, Yue-Wen Fang², Feng-Shuo Li¹, Chih-Yen Chen³, Sheng-Zhu Ho⁴, Ching-Yu Chiang⁵ and Yi-Chun Chen⁴; ¹National Chung Hsing University, Taiwan; ²University of the Basque Country, Spain; ³Nation Yang Ming Chiao Tung University, Taiwan; ⁴National Cheng Kung University, Taiwan; ⁵National Synchrotron Radiation Research Center, Taiwan

Efficient and long-lasting electrocatalysts with superior performance are essential for the efficient and sustainable production of green hydrogen, ensuring high yield and minimal energy consumption. Electrocatalysts based on transition metal oxides have a significant advantage due to their abundant natural resources, adjustable physical properties, and their compatibility with various solutions. Among the various oxide catalyst materials, ferroelectrics have received attention for their semiconducting properties and switchable spontaneous polarization, particularly as promising photoelectrodes in solar water splitting. However, their potential as electrocatalysts has been largely overlooked until now. Here we present an effective electrocatalytic electrode composed of a BiFeO₃/nickel foam heterostructure. This heterostructure exhibits a lower overpotential and higher current density compared to a bare nickel foam electrode. Additionally, when in contact with an alkaline solution, the interaction between hydroxyls and the BiFeO₃ surface induces a significant area of upward self-polarization. This phenomenon reduces the adsorption energy of subsequent adsorbates and enhances the efficiency of the oxygen and hydrogen evolution reactions. Our work illustrates a unique approach, utilizing functional semiconducting materials for the development of highly efficient electrocatalytic electrodes.

4:15 PM EN09.03.06

Rational Synthesis of PbTe/Ti₃C₂T_x MXene Nanocomposite as Electrocatalyst for Overall Water Splitting Tata Sanjay K. Sharma and Won Mook Choi; University of Ulsan, Korea (the Republic of)

Constructing a pivotal electrocatalyst for electrochemical water splitting is a crucial task to which two-dimensional (2D) lead telluride PbTe is ascribed as a suitable substitution for platinum (Pt). However, due to its limited active sites, sluggish kinetics, and low electrical conductivity a cocatalyst is needed. To overcome this, we fabricated a one-step solvothermal technique in which we combined dual-phase PbTe, with titanium carbide (Ti₃C₂T_x) MXene, to attain a wide range of solar absorption and effective charge separation. Several spectroscopical analysis were performed to understand the physicochemical and optoelectronic properties of a prepared electrocatalyst. XRD-Rietveld refinement discloses PbTe as an octahedral crystal system of the Fm3m space group where Ti₃C₂T_x was successfully transformed from Ti₃Al₂C-MAX phase to MXene phase of C2/c space group with orthorhombic structure. The catalytic activities of fabricated electrocatalysts were evaluated using electrochemical HER, and OER to investigate overall water splitting. This facile integration of PbTe with Ti₃C₂T_x not only increased interlayer 2D distance it also suppressed MXene oxidation and restacking enriching catalytic stability and conductivity. Thus, the promoted electrocatalyst emerges to establish further developing prospects in developing feasible catalysts using rational atomic modeling.

4:30 PM EN09.03.07

Chemovoltaic Energy Conversion on Semiconductor Surface Mahdi Alizadeh Kouzeh Rash, Ivan Radevici, Shengyang Li and Jani Oksanen; Aalto University, Finland

The chemovoltaic effect, which involves the generation of electronic excitation through exergonic redox reactions, has emerged as a crucial phenomenon with extensive implications. This effect has been observed on metallic surfaces of Schottky junctions, offering valuable insights into the intricate dynamics of chemically active collisions and having the possibility to open new avenues for energy conversion. One particularly promising application of the chemovoltaic effect is its potential to demonstrate direct chemical energy harvesting by semiconductor solar cells.

This study explores the exciting possibilities of chemovoltaic energy conversion by semiconductors and introduces the concept of an electrolyte-free fuel cell. This novel fuel cell is based on a Gallium Arsenide (GaAs) diode, specially designed to demonstrate electrochemical fuel oxidation and oxidant reduction reactions directly on its conduction and valence bands. The overarching goal is to determine if renewable chemical energy, as well as light, can be used to produce electricity efficiently and sustainably by hybrid cells.

To test the viability of this concept, we developed a thermodynamic charge transfer model to explain the chemovoltaic effect of renewable fuels on semiconductor surfaces, and experimentally demonstrated the electricity generation. Our modelling results indicate that redox reactions occurring between a fuel and an oxidizer on the photovoltaic cell's surface can chemically excite the semiconductor. This excitation, in turn, triggers a splitting of the Fermi

level for both the conduction and valence bands, thereby enabling the direct conversion of chemical energy into electricity. This effect is experimentally observable when the GaAs surface of a specially designed photovoltaic cell is exposed to liquid or vapor-phase methanol in the presence of oxygen or hydrogen peroxide, affirming the potential of the electrolyte-free fuel cell as a new technology in energy conversion. Excitation is also observed for H₂ and O₂ gases which are in-situ generated by splitting of water in KOH (0.05 M) solution in vicinity of the device surface using a separate potentiostat setup. Our findings not only demonstrate the feasibility of chemovoltaic energy conversion with renewable fuels but also suggest a pathway towards practical implementation. A deeper comprehension of the energy conversion process and its potential requires further endeavors in system optimization, cell design enhancement, and the exploration of pertinent materials and catalysts. The chemovoltaic fuel cell offers a unique and versatile platform for capturing energy ideally from a range of renewable chemical sources, potentially providing new solutions for the growing demand for sustainable power generation.

4:45 PM EN09.03.08

Covalent S-O Bonding Enables Enhanced Photoelectrochemical Performance of Cu₂S/Fe₂O₃ Heterojunction for Water Splitting Artur Braun¹ and Jian Jun Wang²; ¹Empa, Switzerland; ²Shandong University, China

Premature charge recombination and slow kinetic for oxygen evolution reaction have widely limited the application of hematite (α -Fe₂O₃) for water splitting. We designed [1] a Cu₂S/Fe₂O₃ heterojunction and discovered that the formation of covalent S-O bonds between Cu₂S and Fe₂O₃ can improve the photoelectrochemical performance and stability for water splitting. Compared with bare Fe₂O₃, the heterostructure of Cu₂S/Fe₂O₃ permits the photoelectrode enhanced charge separation and charge transfer, and an extended range for light absorption, and decreased charge recombination rate. Additionally, due to the thermal properties of Cu₂S, the heterostructure exhibits locally a higher temperature under illumination, profitable for increasing the rate of oxygen evolution reaction. Following this slight improvement, the photocurrent density of the heterostructure is enhanced by a factor of almost 2 to around 1.2 mA/cm² at 1.23 V versus reversible hydrogen electrode. This work may provide guideline for future in the design and fabrication of highly efficient photoelectrodes for various reactions.

[1] Yan Zhang, Yuan Huang, Shi-Shi Zhu, Yuan-Yuan Liu, Xing Zhang, Jian-Jun Wang, Artur Braun, Covalent S-O Bonding Enables Enhanced Photoelectrochemical Performance of Cu₂S/Fe₂O₃ Heterojunction for Water Splitting, Small Vol. 17, Issue 30, (2021), 2170154, <https://doi.org/10.1002/sml.202170154>

SESSION EN09.04: Poster Session I

Session Chairs: Nathalie Herlin-Boime, Michel Trudeau and Edmund Chun Ming Tse
Tuesday Afternoon, April 23, 2024
Flex Hall C, Level 2, Summit

5:00 PM EN09.04.01

Proton Incorporation and Electrical Leakage in BaZrO₃ and BaCeO₃ Andrew Rowberg¹, Meng Li², Tadashi Ogitsu¹ and Joel B. Varley¹; ¹Lawrence Livermore National Laboratory, United States; ²Idaho National Laboratory, United States

BaZrO₃ (BZO) and BaCeO₃ (BCO) are among the best electrolytes for proton-conducting solid-oxide electrolysis cells (p-SOECs). Protons (H_i⁺) are introduced via hydration of oxygen vacancies (V_O²⁺) via the reaction V_O²⁺ + H₂O → 2H_i⁺. This reaction requires acceptor doping with an element such as yttrium (i.e., Y_{Zr}⁻) to introduce V_O²⁺. However, acceptor doping carries an additional consequence of increasing electrical leakage in devices, which can limit their Faradaic efficiency and performance in devices. To understand the factors leading to electrical leakage, we perform first-principles calculations based on density functional theory (DFT) with a hybrid functional. First, we study the properties of hole and electron polarons in BZO and BCO, finding that hole polarons form favorably in both materials, while electron polarons can only be stabilized in BCO and in Ce-containing alloys. In general, doped BZO and BCO will have low electron concentrations, but larger concentrations of hole polarons may be present. To reduce the resultant risk of *p*-type electrical leakage, we find it to be advantageous to avoid extreme O-rich conditions and high dopant concentrations.

In addition, high ionic conductivity in BZO and BCO relies on them having large proton concentrations. We study avenues to achieve this goal by calculating the formation energy of H_i⁺ and how the concentration of protons and other relevant defects change under different experimental conditions. Proton concentrations will be highest under wet conditions, with V_O²⁺ becoming more dominant at drier conditions. Our results identify that higher protonation levels correlate with lower concentrations of hole polarons, implying lower electrical leakage with higher hydration levels. In addition to the protonation pathway mediated by V_O²⁺, we also investigate an alternative mechanism via hydroxyl migration (OH_i⁻). However, we find this process to be less favorable than V_O-mediated hydration except at extremely wet conditions.

Additionally, we study migration mechanisms for charge carriers near other defects or impurities as a proxy for grain boundaries, which play an important role in determining device performance. Our results suggest a complex behavior can result for mobile species like H_i, where migration kinetics can be influenced by other defects that may be present (e.g. cation vacancies) and compositional variation due to alloying. Our results provide crucial insights for understanding the complex behavior of these devices *in situ*. Determining how to promote ionic conductivity at the expense of electrical leakage is critical to optimizing their performance in p-SOECs and related devices.

This work was performed under the auspices of the U.S. DOE by Lawrence Livermore National Laboratory under Contract DE-AC52-07NA27344.

5:00 PM EN09.04.02

Z-Scheme CBO@MoS₂ System for Enhanced H₂O₂ Photosynthesis with Mechanistic Insights Akshay Tikoo, Nikitha Lohia, S.S.C. Kondeti and Praveen Meduri; Indian Institute of Technology Hyderabad, India

Photocatalysts often have limited light absorption capabilities and suffer from rapid electron hole recombination[1]. This issue can potentially be addressed through suitable band edge line-up of two or more semiconductors, particularly z-scheme systems, which have superior charge separation and light harvesting properties[2]. The present study explores a z-scheme system with CBO (Copper bismuth oxide) and MoS₂ (molybdenum sulfide), which have good light harvesting abilities and efficient charge separation. CBO has a narrow bandgap, good light harvesting capability, and high negative conduction band potential[3]. However, pristine CBO has high charge recombination and unfavourable band edge line-up with the water oxidation reaction. MoS₂, a 2D material is recognized as an excellent co-catalyst for advanced oxidative processes with improved light harvesting, efficient interface charge transfer, and separation[4]. CBO@ MoS₂ is synthesized using two step hydrothermal method. The synthesized catalyst is characterized using several techniques, including XRD, Raman, PL, UV-Vis, and TEM. The catalyst has shown a significantly higher H₂O₂ production rate of 1457 μM h⁻¹ and a current density of

-1.6 mA cm⁻² at 0.2 V, both of which are an order of magnitude higher than the pure components. The improved photocatalytic activity of CBO@ MoS₂ is mainly attributed to the efficient separation of the electron-hole pairs due to staggered band alignment and the z-scheme heterojunction that retains the strong redox ability of both CBO and MoS₂. Mechanistic insight in H₂O₂ production is also provided using mott-schottky analysis, scavenger study and kinetic modelling.

References

- [1] J. Deng, Y. Ge, C. Tan, H. Wang, Q. Li, S. Zhou, K. Zhang, Degradation of ciprofloxacin using α -MnO₂ activated peroxymonosulfate process: Effect of water constituents, degradation intermediates and toxicity evaluation, *Chemical Engineering Journal*. 330 (2017) 1390–1400. <https://doi.org/10.1016/j.cej.2017.07.137>.
- [2] Y. Duan, L. Deng, Z. Shi, L. Zhu, G. Li, Assembly of graphene on Ag₃PO₄/AgI for effective degradation of carbamazepine under Visible-light irradiation: Mechanism and degradation pathways, *Chemical Engineering Journal*. 359 (2019) 1379–1390. <https://doi.org/10.1016/j.cej.2018.11.040>.
- [3] S. Pulipaka, N. Boni, G. Ummethala, P. Meduri, CuO/CuBi₂O₄ heterojunction photocathode: High stability and current densities for solar water splitting, *Journal of Catalysis*. 387 (2020) 17–27. <https://doi.org/10.1016/j.jcat.2020.04.001>.
- [4] K.F. Mak, C. Lee, J. Hone, J. Shan, T.F. Heinz, Atomically thin MoS₂: a new direct-gap semiconductor, *Phys Rev Lett*. 105 (2010) 136805. <https://doi.org/10.1103/PhysRevLett.105.136805>.

5:00 PM EN09.04.03

Oxygen Evolution Reaction at Low Overpotential Catalyzed by Nanostructured CuO derived from 2 nm-Sized Colloidal Clusters generated by Laser Ablation at The Air-Liquid Interface Teppe Nishi, Shunsuke Sato, Takeo Arai, Yusuke Akimoto, Kosuke Kitazumi, Satoru Kosaka, Naoko Takahashi, Yusaku F. Nishimura, Yoriko Matsuoka and Takeshi Morikawa; Toyota Central R&D Labs., Inc., Japan

Because oxygen evolution reaction is one of the key factors for artificial photosynthesis of chemicals or fuels from CO₂, a lot of catalysts have been developed. Here, we report CuO catalyst derived from 2 nm-sized Cu based clusters prepared by laser ablation at the air-liquid interface using a colloidal solution as a target[1]. First, colloidal solution was prepared by laser ablation of Cu powder precipitated in a flask filled with pure water. Pulsed laser light was irradiated through the bottom of the flask. After laser irradiation for 1 h, we obtained colloidal solution. Then, laser ablation at the air-liquid interface using a colloidal solution was carried out. After laser ablation at the air-liquid interface, a drastic color change from black to a transparent green was observed. Scanning transmission electron microscopy image revealed monodispersed small cluster formation (ca. 2 nm). Colloidal clusters were stably dispersed in water without any chemical reagents for a few years. To investigate the electrocatalytic activity toward oxygen evolution reaction, colloidal solution was deposited on a carbon paper substrate. After deposition, X-ray diffraction pattern revealed Cu₂(NO₃)(OH)₃ formation on carbon paper. After pre-electrolysis in Ar-purged 1.0 M aqueous Na₂CO₃ solution (pH 11.3) at an applied potential of 1.72 V vs RHE for 1h, most of Cu₂(NO₃)(OH)₃ was changed into CuO. Tafel slope of 54 mV/dec and overpotential of 540 mV was required for 10 mA/cm² in Ar-purged aqueous 1.0M Na₂CO₃ solution. In addition to 1.0 M Na₂CO₃, electrocatalytic activity in KBi buffer (pH 9.2) was also measured. Tafel slope of 88 mV/dec and overpotential of 570 mV at 1.0 mA/cm² was required. In the stability test in both electrolytes for 24h, stable current density were recorded. Scanning electron microscopy images obtained after electrolysis revealed nanostructured CuO formation. Our catalyst exhibited the lowest overpotential for OER rather than those for the previously reported CuO catalyst.

- [1] T. Nishi et al., *ACS Appl. Energy Mater.* 2020, 3 8383-8392.

5:00 PM EN09.04.04

Schiff Bases Complexes prepared from Polyethylene Terephthalate and Amine for Alkaline Water Electrolysis Tzu Hsuan Chiang and Si-Rong Xu; National United University, Taiwan

Alkaline water electrolysis is considered a viable technology for large-scale hydrogen production due to its use of non-precious metal catalysts. This process involves two half-slow-rate electrochemical reactions, the hydrogen evolution reaction (HER) and the oxygen evolution reaction (OER). In contrast to non-precious metal electrocatalysts, typically employed for acid-media reactions to enhance slow electrochemical activities, precious metals like Ir/Ru compounds for OER and Pt for HER are used. However, relying on such relatively scarce and precious catalysts is not advisable, as it significantly inflates the cost of hydrogen production and hampers future industrial scalability. Consequently, there is a pressing need to develop high-performance non-precious metal alternatives.

This study investigates metal Schiff base complexes derived from polyethylene terephthalate (PET) and various amines. PET materials have been used for packaging since the 1960s, with global consumption surpassing 24 million tons annually and continuing to rise. While PET's durability is advantageous, its downside is its slow biodegradation rate, taking up to 500 years to decompose in landfills when disposed of as waste. Unfortunately, many developing countries have low PET recycling rates.

PET is a condensation polymer synthesized from terephthalic acid (BDC) and ethylene glycol (EG). The degradation of PET was achieved through a solvent-assisted glycolysis process using EG to obtain BDC. BDC contains carbonyl groups capable of reacting with amine compounds to form Schiff bases. These metal Schiff bases are formed when Schiff base ligands' azomethine groups (–RC=N–) coordinate with metal ions. The study meticulously screened amines' chemical composition and compound ratios to identify those exhibiting optimal electrochemical properties. Furthermore, the study delves into the mechanism and effects of these Schiff bases on OER/HER.

Diverse Schiff bases were synthesized by combining terephthalic acid (TPA) with various amine compounds, including ethylenediamine (EDA), diethylenetriamine (DETA), triethylenetetramine (TETA), tetraethylenepentamine (TEPA), and pentaethylenhexamine (PTHA). In the context of alkaline water electrolysis, the two-electrode cell employing the unheated Fe_{0.5}Cu_{0.5}Mo_{0.5}-SB-TEPT @NF couple as both the anode and cathode exhibited higher levels of H₂ and O₂ production compared to the Pt/C and RuO₂ couple at 100 mA/cm².

The study expects that metal Schiff bases will demonstrate outstanding electrolysis performance in alkaline water electrolysis, offering innovative applications for PET recycling and contributing to the resolution of the waste PET problem.

5:00 PM EN09.04.05

Laser-Synthesis of Nanostructured Carbides Molybdenum Catalysts for HER/OER Reactions Guillaume Dubois¹, Fabien Grasset², Corinne Lagrost¹, Tetsuo Uchikoshō³, Franck Tessier¹, Nathalie Herlin-Boime⁴ and Suzy S. Surlbe⁴; ¹Université de Rennes, France; ²LINK, IRL3629 CNRS-Saint-Gobain-NIMS, Japan; ³NIMS, Japan; ⁴CEA, France

Platinum doped materials are very efficient for electrocatalytic reaction and H₂ production. However, platinum being a scarce and expensive element, carbides and nitrides could be an interesting alternative to make this technology economically viable. Indeed, transition metal carbides and nitrides demonstrate very interesting electrocatalytic properties, close to those of noble metals.^{1,2} In this context, molybdenum (Mo)-based electrocatalysts materials are very promising and are currently attracting a growing interest in the energy field.

We report here the synthesis of molybdenum nitrides and carbides using the laser pyrolysis method for the overall water splitting reactions (hydrogen evolution reaction HER and oxygen evolution reaction OER)³. The laser pyrolysis process is a facile, scalable, environmental synthesis of small-sized, highly specific surfaces, well dispersed, and electrochemically accessible. The resulting Mo based materials were characterized with several

complementary techniques (XRD, SBET measurement, SEM, etc.). We also demonstrate that these materials show some electrocatalytic activity for HER reaction.

References

1. Hargreaves, J. S. J. et al. *Coord. Chem. Rev.* 257, 2015-2031 (2013).
2. Wang, H. et al. *Chem. Soc. Rev.* 50, 1354-1390 (2021).
3. Caroff, T. et al. *Nanomanufacturing* 2, 112-123 (2022).

5:00 PM EN09.04.06

Sulfur-Doped Activated Carbon derived from Discarded Surgical Masks for High-Performance Supercapacitors [Hsiu-Ying Chung](#) and Zhi-Bin Huang; National Sun Yat-sen University, Taiwan

Consumption and discarded face masks are urgently driven by the spread of COVID-19 and the flu epidemic and general medical operations. To reduce the severe environmental pollution, the discarded surgical masks were recycled and subsequently prepared as high-added value supercapacitor electrode materials for energy storage. This study synthesized sulfur-doped activated carbon from the discarded face masks. Additionally, nanoscale manganese oxide was incorporated into sulfur-doped activated carbon to improve the electrochemical properties of supercapacitors. The resulting porous materials were analyzed using SEM, BET and XPS. Due to the synergistic effect of activated carbon and nanomanganese oxide, the capacitance of the hybrid electrode increased by more than 20%, and the capacitance retention rate was approximately 80% after 500 cycles.

5:00 PM EN09.04.07

Mechanistic Insight into Dual-Atom Catalysts for The Oxygen Reduction Reaction [Courtney Brea](#)¹ and Guoxiang (Emma) Hu²; ¹Queens College (City University of New York), United States; ²Georgia Institute of Technology, United States

Incorporating a second transition metal to iron-nitrogen-carbon single-atom catalysts (Fe-N-C SACs) to design dual-atom catalysts (DACs) was demonstrated to offer a promising opportunity to enhance the oxygen reduction reaction (ORR). However, it has been challenging to clearly elucidate the structure-property relationship at the atomic level. Here we apply a computational workflow integrating configuration generations, phase diagram constructions, and reaction free energy calculations to provide an insightful understanding of the active site structures and catalytic mechanisms of ORR on DACs. Using Fe-Cu as an example, we generated all possible configurations by tiling the hexagonal lattice and investigate their atomic structures under reaction conditions. We find for a wide range of the electrode potential, the Fe site is covered by an *OH intermediate while the Cu site is not covered by any intermediates. With the OH-ligated structures, we identify the configurations which possess higher catalytic activity than Fe-N-C and Pt(111). We find ORR on Fe-Cu DACs proceeds via the associative pathway, and the desorption of *OH is the rate-determining step. Further analysis reveals a linear correlation between the limiting potential and the magnetic moment on Fe. These mechanistic insights pave the way for the rational design of efficient platinum group metal-free (PGM-free) catalysts for ORR.

5:00 PM EN09.04.08

Electrochemical CO₂ Reduction over Nanoparticles derived from an Oxidized Cu-Ni Intermetallic Alloy [Tomiko M. Suzuki](#), Toshitaka Ishizaki, Satoru Kosaka, Naoko Takahashi, Noritake Isomura, Juntaro Seki, Yoriko Matsuoka, Keiichiro Oh-ishi, Ayako Oshima, Kosuke Kitazumi, Keita Sekizawa and Takeshi Morikawa; Toyota Central R&D Labs., Inc., Japan

Research and development on the electrocatalytic CO₂ reduction reaction (CO₂RR) to valuable hydrocarbons and alcohols has attracted great interest because of the potential to produce sustainable fuels. To date, copper (Cu) and Cu-based compounds are the most studied metal electrocatalysts that have demonstrated the ability to convert CO₂ and CO into large amounts of C2 and C3 molecules [1]. Furthermore, studies of Cu particle catalysts have reported that their particle size, crystalline phase, and morphology are highly correlated with C2 selectivity [2]. As one approach to control C2 selectivity on Cu catalysts, the use of Cu-based bimetallic alloys has been reported [3], especially the combination of Cu with CO-producing metal species such as Ag, Au, Zn, and Pd. On the other hand, combinations of Cu with hydrogen-producing elements such as Fe, Ni, and Pt have been reported to improve the activity and selectivity of hydrogen production compared to pure Cu electrodes, making it difficult to improve C2 and C3 activity with these combinations. In this study, we demonstrate that Ni species have a positive effect on the formation of C2 compounds in the CO₂RR of Cu-based catalysts. To avoid size-dependent selectivity of copper catalysts, Cu-Ni interatomic alloy NPs (0-83 at% Ni as Ni/(Cu + Ni)) of various compositions with diameters around 10 nm were synthesized by one-pot and two-step synthesis using copper(II) acetylacetonate and nickel(II) chloride [4]. Since these Cu-Ni NPs were easily spontaneously oxidized in air at room temperature, these partially oxidized NPs were loaded onto carbon paper supports and used as electrocatalyst. The electrochemical CO₂ reduction reaction was evaluated using a three-electrode system in a closed batch single-compartment reactor filled with 0.05 M KHCO₃ aqueous solution bubbled with CO₂. Electrolysis was performed at -1.2 V (vs. RHE) using a catalytic electrode as the working electrode, a Pt wire as the counter electrode, and an Ag/AgCl electrode as the reference electrode. The CuNi-NP was driven as a catalyst for hydrogen production in the early stages of the electrolysis, but activated into an excellent CO₂ reduction catalyst in the subsequent electrolysis. The dependence of the C2 selectivity on the Ni content was investigated using various activated Cu-Ni NPs electrodes. Activated Cu-Ni (3-32 at%-Ni) alloy nanoparticles enhance selectivity for ethylene and ethanol formation over oxide-derived Cu nanoparticles by electrochemical CO₂RR in aqueous solution. The Cu-Ni (19 at%) NPs exhibited 35% efficiency for C2 and the suppression of H₂ formation down to 9%. These results demonstrate that the addition of Ni to the Cu NPs facilitates C-C bond formation. The activated catalyst consists of metallic Cu, Cu-O, Ni, and Ni-O species, as confirmed by X-ray absorption spectroscopy measurements [5].

The present research suggests that further investigation is worthwhile to broaden the possibility of an unprecedented oxide-derived Cu-Ni and other CO₂RR catalysts.

References

- [1] Y. Hori, et al., *Chem. Lett.*, (1985) 1695-1698. [2] A. Loiudice, et al., *Angew. Chem. Int. Ed.*, 55 (2016) 5789-5792. [3] S. Nitopi, et al., *Chem. Rev.*, 119 (2019) 7610-7672. [4] R. Watanabe, T. Ishizaki, *J. Mater. Chem. C.*, 2 (2014) 3542-3548. [5] T. M. Suzuki, T. Morikawa, et al., *Chem. Commun.*, 56 (2020) 15008-15011.

5:00 PM EN09.04.09

Computational Chemistry on Investigating Copper, Nitrogen-Doped Graphene Catalyst for CO₂ Reduction Reactions [Youjin Kim](#) and Shiru Lin; Texas Woman's University, United States

With the growing use of fossil fuels, CO₂ emissions are also sharply increasing. This increase directly correlates to the recent global warming issues, affecting the environment, human survival, and development. the CO₂ reduction reaction (CO₂RR) is a potential solution to reducing CO₂ levels by converting CO₂ into fuels and raw materials. CO₂RR will not only be environmentally sustainable but will also be more economically sustainable. A CO₂ reduction reaction is a series of chemical reactions that converts CO₂ into potential products and applications. The products of CO₂RR include C1 products, such as CO, HCOOH, and CH₄, and C2+ products, including C₂H₄, ethanol. However, not all CO₂RR products are of equal importance and have similar

applications. For example, a C1 product, such as CH₄, or methane, is mainly used in natural gas and metal smelting. On the other hand, a different C1 product, CO, carbon monoxide, is used directly as fuel. Therefore, the selectivity of catalysts toward CO₂RR is crucial. Out of various catalysts, Cu stood out from the many catalysts for CO₂RR because of its appreciable CO₂RR catalytic performance. In our project, we use 4N@Cu, 4C@Cu, and 3C@Cu graphene material for CO₂RR by density functional theory (DFT) computations. In our research, we investigate different reaction pathways and products to see their reaction energies and find whether 4N@Cu, 4C@Cu, and 3C@Cu graphene are ideal catalysts for CO₂RR.

5:00 PM EN09.04.10

Deciphering The Activity of Co-, Fe- Co-Doped NiS supported on Carbon Cloth prepared via a Novel Strategy for Promoted Water Splitting
Ahmed E. Aboubakr, Amr Sabbah, Mahmoud K. Hussien, Kuei-Hsien Chen and Chen-Hsiung Hung; Academia Sinica, Taiwan

Water electrolysis via affordable and efficient electrocatalysts under industrial conditions plays a key role in large-scale green hydrogen production. Since the electrocatalysts may undergo undesired in-situ transformations under high current density, the fabrication of single-phase multi-element sulfides with desired composition is crucial and challenging for the development of sulfide catalysts. In this context, we developed a facile and scalable method to construct Fe and Co co-doped NiS supported on carbon cloth (Fe, Co-NiS-CC). A specific compound of metal sulfide was prepared that can be sprayed on the carbon cloth before being pyrolyzed, resulting in a specific phase of NiS directly attached to the substrate. The presence of dopants and the pyrolysis conditions could control the as-formed phase of NiS. The optimized electrode of Fe, Co-NiS-CC exhibits remarkable performance for industrial water splitting (6 M KOH, 70 °C), achieving a current density of 1000 mA cm⁻² at a potential of about 1.698 V. The in-situ XAS and Raman measurements and the characterization of the post-electrocatalysts along with the theoretical calculations revealed that the high performance and long-term stability were attributed to the regulation of electronic configuration and the sustained single-phase of doped sulfides, directly grown on carbon cloth. Therefore, high-performance sulfide electrocatalysts can be stabilized by multi-element doping with the formation of polysulfide species that prevent the leaching of the elements and the destruction of the real active catalysts.

5:00 PM EN09.04.11

Metal Nanoparticles Supported on Hexagonal Boron Nitride Nanosheets as an Efficient Catalysts for Oxygen Evolution Reaction Conghang Ou, George Bepete, Zhuohang Yu, David Sanchez and Mauricio Terrones; The Pennsylvania State University, United States

The oxygen evolution reaction (OER) is a crucial step in the electrochemical water-splitting process that can be used as a competitive and sustainable method for clean energy production, energy storage, and electrochemical sensing applications. However, due to the commonly sluggish kinetics of the OER steps, newer catalytic materials that can lower the reaction overpotential are pivotal to enhance the overall OER efficiency. In this work, ultrathin hexagonal boron nitride (hBN) nanosheets fabricated by a molten metal assisted intercalation method is used as the supporting structure for metal nanoparticle deposition, then employed as efficient catalyst material for OER in alkaline environments. Different metals and metal combinations including Pt, Pd, Ru, Fe, Ni, NiFe, PtAg, and PdAg are tested in these catalyst systems as dopant materials. Aligning with the goal of using non-precious metal-based catalysts as the alternative to the current benchmarks of Ir and Ru based OER catalysts, our hBN supported Fe nanoparticle sample exhibited competitive electrochemical performance and low overpotential. Additionally, annealing of the hBN supported Fe sample in Ar at 800°C showed further improvements of such catalytic activity and an increased current density. High-resolution transmission electron microscopy (HRTEM) was done to reveal the structural and crystallinity characteristics of the metallic nanoclusters and/or atomically dispersed metal atoms confined on the hBN framework. X-ray photoelectron spectroscopy (XPS) is carried out to characterize the changes of chemical valence state of the dopant metals before and after annealing to offer more insights into the OER reaction mechanism. Electrochemical cycling testing was conducted to evaluate the stability of the metal-doped hBN catalysts that could be applied to hydrogen fuel cells and/or metal-air batteries.

5:00 PM EN09.04.12

Solvent-Tailored Solvothermal Synthesis of 1T-VS₂ Nanostructured Electrode Materials for Electrochemical Energy Storage Applications Rahul S. Ingole¹, Minwook Kim¹, Kwangjun Kim¹, Yongtae Kim¹, Snehal L. Kadam² and Jong G. Ok^{1,1}; ¹Seoul National University of Science and Technology, Korea (the Republic of); ²Seoul National University, Korea (the Republic of)

This study explores the electrochemical energy storage properties of 1T-VS₂ nanostructured electrode materials synthesized via a facile solvothermal method using three different solvents: ethylene glycol, ethylenediamine, and N, N-dimethylformamide (DMF). The use of different solvents in solvothermal reactions offers several advantages, including better control over the surface morphology and size of the nanostructures, as well as the ability to synthesize nanomaterials on a variety of substrates. The solvent-mediated synthesized 1T-VS₂ nanostructured electrode materials were characterized to explore the structural and morphological properties and composition of electrode materials via different analytical methods such as X-ray diffraction (XRD), X-ray photoelectron spectroscopy (XPS), field emission scanning/transmission electron microscopy (FESEM/TEM), and Brunauer-Emmett-Teller (BET) for surface area analysis. Furthermore, the electrochemical energy storage performance of 1T-VS₂ electrode materials was investigated systematically in a 6 M KOH electrolyte. The results show the 1T-VS₂ nanostructured electrode synthesized using DMF solvent exhibits the highest specific capacitance of 753.21 F/g with 75.96% columbic efficiency at 20 mA/cm² current density compared to the others. The nanostructures also exhibited good long-term cycle stability, retaining over 87% of their initial capacitance after 1000 galvanostatic charge-discharge cycles. The enhanced specific capacitance and capacitance retention over a long cycle life justify the 1T-VS₂ nanostructures as superior electrode materials for electrochemical energy storage applications. For real-life demonstration, a symmetric prototype supercapacitor device has been fabricated using symmetric electrodes and an aqueous electrolyte. The symmetric device shows promising electrochemical energy storage properties.

Keywords:

1T-VS₂ nanostructures, solvent-mediated solvothermal, electrochemical energy storage

Acknowledgment:

This work was supported by the National Research Foundation of Korea (NRF) grants (No. 2021M3H4A3A02099204, and 2022M3C1A3081178 (Ministry of Science and ICT) and No. 2022R111A2073224 (Ministry of Education)) funded by the Korean Government.

5:00 PM EN09.04.13

Synthesized Transition Metal-Based Nanosheet Electrocatalysts for Alkaline Water Electrolyzers Seunghun Lee¹, In Tae Kim², Yoo Sei Park² and Yangdo Kim¹; ¹Pusan National University, Korea (the Republic of); ²Chungbuk National University, Korea (the Republic of)

Hydrogen is a completely carbon-free energy source with high energy density and conversion efficiency, and it has become a promising alternative to fossil fuels. The best way to produce green hydrogen without carbon emissions is through water electrolysis. Water electrolysis involves two reactions: the oxygen evolution reaction (OER) and the hydrogen evolution reaction (HER). Although HER is produce hydrogen, production efficiency is more directly associated with OER.

The two most famous water electrolysis technologies are alkaline water electrolyzers (AWEs) and proton exchange membrane water electrolyzers (PEMWEs). The recently developed AEM electrolyzer exhibit both the advantage of AWE, PEM electrolyzers mentioned above. This electrolyzer can greatly reduce the ohmic loss using solid ionomer membrane and is operated in alkaline condition, allowing the use of non-precious metals as

electrocatalysts. Although, the cost of hydrogen production can be reduced by using non-precious metal electrocatalysts, the performance of AEM water electrolyzers is still lower than that of PEM electrolyzers due to the sluggish electrocatalyst kinetics for oxygen evolution reaction (OER). To overcome this obstacle, it is strongly necessary to develop high-performance and cost-effective OER electrocatalysts.

In this study, we developed Cu(OH)₂ nanosheets onto ZIF67 for OER electrocatalyst. The obtained material, labeled as CuOH₂@ZIF67, improves its conductivity and intrinsic activity. In addition, the AEM electrolyzer equipped with CuOH₂@ZIF-100 shows better performance at high current densities than that of RuO₂ by reducing the mass transport of the AEM electrolyzer. Our approach is suitable for large-scale hydrogen production as an OER catalyst since it does not require precious metals and enables cost-effective, high-efficiency catalyst production through simple synthesis

5:00 PM EN09.04.14

Templated Multiwall Polycrystalline MoS₂ Nanotubes with Tunable S-Vacancies for High-Performance H₂ Evolution Reaction [Yang Tian](#); University of Arkansas, United States

As the demand for clean energy intensifies, hydrogen (H₂) emerges as a leading candidate for next-generation energy solutions. Currently, the catalysis for the hydrogen evolution reaction (HER) predominantly relies on noble metals like platinum, which are scarce and economically unsustainable for large-scale applications. Consequently, there's an urgent need for cost-effective, abundant, and efficient catalysts. MoS₂, a low-cost material, has been identified as a potential platinum substitute due to its ability to significantly reduce overpotential in H₂ production. While 2D MoS₂ has demonstrated promising HER results, its synthesis via chemical vapor deposition (CVD) is costly and complex, hindering large-scale production. In this study, we present a novel approach to synthesize templated multiwall polycrystalline MoS₂ nanotubes using hydrothermal methods. Comprehensive characterization using XRD, EDX, and XPS confirmed the successful coating of MoS₂ on Titanate nanofiber surfaces. By controlling sulfur vacancies on the MoS₂ surface, we can modulate the HER performance. Our optimal conditions yielded an overpotential of approximately 280 mV at 10mA cm⁻² with a MoS₂ coating ratio of 1 wt% when treated at 240°C for 5 days.

5:00 PM EN09.04.15

SUNER-C: Unlocking The Renewable Energy Future [Nathalie Herlin-Boime](#)¹, [Nathan Coutard](#)², [Bert Weckhuysen](#)² and [Frederic Chandezon](#)³; ¹CEA Saclay, France; ²U Utrecht, Netherlands; ³CEA - University Grenoble Alpes, France

How can we achieve the EU's goal of becoming the first climate-neutral continent by 20250? SUNER-C is a EU-funded Coordination and Support Action (CSA) aiming to contribute to this objective, targeting the next generation of energy carriers to replace fossil-fuels.

29 EU partners gather to work on building an ecosystem of companies, researchers, societal actors and policymakers, to accelerate the transition of technologies on solar fuels and chemicals, from the laboratory to large-scale industrial applications.

The main objectives of the project are:

Creation of an innovation ecosystem on solar fuels and chemicals

Develop a Strategic Technological Roadmap for the broad implementation in the industry and in society

Prepare a Large-Scale Research and Innovation (LRSI) initiative, ready to be launched after the CSA

Promote communication, dissemination and education of the next generation of Europeans

SUNER-C is an instrument for the SUNERGY community to develop and expand the innovation ecosystem working on the conversion and storage of renewable energy into fossil-free fuels and chemicals, both through indirect processes and direct conversion of solar to chemical and energy products.

The SUNERGY community, formed by +300 supporters, aims at developing a common vision and a technological roadmap for accelerating the scale-up of technologies, focusing on enabling a circular economy through developing closed carbon and nitrogen cycles.

5:00 PM EN09.04.16

Synthesis of MFI and BEA Type Zeolite Membrane Reactor [Abduljelil W. Sabir](#) and [Pyung Soo Lee](#); Chung Ang University, Korea (the Republic of)

Zeolite membranes was found to be an appealing material for separation and catalytic chemical reactions considering suitable pore diameter, catalytic characteristic together with their thermal and chemical stability. This study presents fabrication of MFI type and BEA type single layer and MFI/BEA bilayer membranes. First both zeolite type crystals were prepared by hydrothermal reaction in a self-pressured autoclave reactor. Primary growth was conducted by seeding the zeolite crystals on porous α -alumina support. Thereafter, secondary growth solution was made accompanied by hydrothermal treatment for secondary growth. The manipulation of synthesis time and temperature was conducted in order to achieve a continuous and defect-free membrane, while also attaining the desired optimal thickness range of 5 μ m-7 μ m. Membrane morphology and thickness was characterized via FE-SEM. Furthermore, the performance of the membranes evaluated in pervaporation-assisted catalytic esterification of alcohol and carboxylic acid.

5:00 PM EN09.04.17

Interfacial Polymerization of Covalent Organic Frameworks for The Application of Ammonia Production [Chi-Cheng Chen](#)¹, [Ming-Chung Wu](#)^{2,3} and [Tz-Feng Lin](#)¹; ¹Feng Chia University, Taiwan; ²Chang Chung University, Taiwan; ³Chang Gung University, Taiwan

Novel supramolecular structural design, covalent organic frameworks (COFs), was determined by various exact chemical structures such as benzobisthiazole, benzene-1,3,5-tricarbaldehyde, benzene-1,4-diamine, or 2,4,6-Triformylphloroglucinol etc. derivatives. The one-pot synthesis of COFs was achieved from the monomers which was dissolved in the unmixed Brønsted acid and Brønsted base under the Schiff-base reaction system. NMR, TGA, DSC, SEM, PLM, FTIR, contact angle and X-ray scattering (SAXS/WAXS) were used to detect the relationship of effective ammonia production and intermolecular exchange reaction, in order to control the processing conditions. An overall understanding of the physical mechanism of COFs nafion film would be investigated according to the influence of the structural changes on the crystallinity as well as crystal phase morphology. Therefore, our work demonstrates a practical potential for COFs as an ammonia production platform.

5:00 PM EN09.04.18

On The Interplay of Quantum Capacitance and Pseudocapacitance in rGO with Regulated C/O Ratios [Archana Sharma](#) and [Alok Shukla](#); Indian Institute of Technology Bombay, India

Supercapacitors have evolved as mature energy storage devices, utilizing graphene as electrodes to store charge electrostatically. During the process, electric double layers are formed at electrode/electrolyte interface, offering electric double layer capacitance (EDLC). Although large surface area and high conductivity of graphene are favorable for enhanced EDLC, intrinsically low quantum capacitance of graphene limits the overall performance. In recent years, reduced graphene oxide (rGO) has been increasingly gaining favor as an alternative material based on graphene owing to its cost-effective means of production. Experimental characterizations have identified abundant epoxy and hydroxyl functional groups on its basal plane, while hosting relatively fewer carbonyl and carboxyl groups at its edges. Interestingly, these oxygen-containing species on the surface of rGO serve as electrochemically active sites for enhanced pseudocapacitance in aqueous EDLCs. While rGO electrodes have demonstrated superior performance compared to graphene electrodes, the reported capacitances have shown inconsistent responses to different C/O ratio. This highlights the necessity to comprehend the impact of the degree of

reduction on the total capacitance and theoretical simulations can offer valuable insights to decouple the contributions to the total capacitance. Therefore, in this work, density functional theory (DFT) calculations have been employed for studying the capacitive behavior of rGO functionalized with epoxy and hydroxyl functional groups with different coverages on their basal planes. We have considered the cases for low-level, medium-level and high-level oxygen functionalization depending upon the C/O ratio. Under low-level oxygen functionalized graphene (LOFG), rGO with C/O ratios of 8, 6.4 and 5.33 are considered, while for medium-level oxygen functionalized graphene (MOFG) and high-level oxygen functionalized graphene (HOFG), rGO with 4.57, 4, 3.55 and 3.2, 2.9, 2.66 C/O ratios are considered, respectively. We have computed EDLC of rGO subjected to different degrees of reduction using implicit solvent model. The computation of EDLC from this method is validated by first calculating EDLC of graphene (116.52 Fg^{-1}) and compared with the experimental value ($125\text{-}135 \text{ Fg}^{-1}$). Our calculations show that dispersed coverage of rGO with more of epoxy groups offer relatively higher EDLC than that with more of hydroxyl groups. However, in both the cases, EDLC decreases monotonically for decreasing C/O ratio. Quantum capacitances (C_Q) of LOFG, MOFG and HOFG are directly related to the changes in density of states (DOS) near the Fermi level. LOFG with more epoxy groups have zero bandgap, possessing higher C_Q while MOFG & HOFG with more hydroxyl groups have lower bandgap opening, possessing higher C_Q . As bandgap gets wider, maximum C_Q is obtained at higher voltages. OH-induced enhancement in quantum capacitance (C_Q) tends to be more dramatic with positive polarity because of relatively very low band gap than possessed by graphene with more epoxy functionals. Pseudocapacitance (C_{pseudo}) too exhibits the similar pattern, depicting decreased capacitance with decreasing C/O ratio. Such a behavior is explained by studying the variation in dipole moment and work function change. Maximum total capacitance is offered by rGO at C/O ratio of 5.33, well in accordance with an experimental study. Suppression of EDLC is mitigated by the enhancement in both C_{pseudo} and C_Q for LOFG while only increased C_Q compensates for MOFG. This study motivates future investigations into control and careful optimization of the oxygen content to balance the oxygen induced influences on electrical capacitance and quantum capacitance.

5:00 PM EN09.04.19

Gas Adsorption on Nanoporous Materials for Carbon Capture Applications: A First Principles Study Thomas Sadowski^{1,2}, Cristian Sayers^{1,2}, Ericka Barnes^{1,2} and Christine Broadbridge^{1,2}; ¹Southern Connecticut State University, United States; ²CSCU Center for Nanotechnology, United States

The world's continued reliance on fossil fuels as the predominant energy source has remained almost unchanged despite significant advancements in renewable and sustainable energy technologies. This persistent dependence necessitates implementing focused initiatives to mitigate carbon dioxide emissions. Traditional carbon capture and storage technologies used in industrial applications rely on chemisorption between CO_2 and a suitable solvent; however, in recent years, physisorbent solids have emerged as an attractive alternative, offering notable energy-efficient benefits. The journey towards fully harnessing the inherent capabilities of these innovative materials is riddled with various obstacles and difficulties, as these materials can be costly to produce and evaluate, possibly limiting their discovery through traditional trial-and-error physical experimentation and observation. Hence, the utilization of computational techniques that possess the capability to forecast material properties effectively has immense value within this domain. The key figure of merit in determining the appropriateness of a specific material for carbon capture is the enthalpy of adsorption, the thermodynamic parameter characterizes the alteration in energy that occurs when a gas molecule adheres to a solid surface. In this study, the enthalpy of adsorption was calculated between the metal-organic framework (MOF) Cu-BTC and the components of ambient air (N_2 , O_2 , CO_2 , and H_2O) within the plane-wave density functional theory (DFT) formalism. Cu-BTC is commercially available and has been intensely investigated for its potential as a sorbent material for post-combustion carbon capture as well as direct air capture applications. A variety of exchange-correlation functionals and van der Waals correction schemes were considered, and the calculated enthalpies were compared with existing experimental results. The goal of this study is the establishment of a computational workflow that can be extended to less well-studied materials such as MIL-100 (Al) and biochar, thereby providing theoretical insight into future experimental studies and increasing the range of materials potentially utilized in carbon capture methods.

5:00 PM EN09.04.20

Development of Vanadium Oxide/Manganese Selenide Nanocomposite as Robust Bifunctional Electrocatalyst for Oxygen Evolution Reaction and Hydrogen Evolution Reaction Sumaira Manzoor, Safyan Akram Khan, Shahid Ali and Muhammad Mansha; Interdisciplinary Research Center for Hydrogen and Energy Storage, King Fahd University of Petroleum, Saudi Arabia

For the expansion of alternative energy structure, it is crucial to develop a bifunctional electrocatalyst for the water splitting process. In this study, we present a novel nanocomposite of Vanadium Oxide and manganese Selenide ($\text{V}_2\text{O}_5/\text{MnSe}$) directly grown on copper foam (CF) using straightforward hydrothermal method, and then characterized via different analytical characteristics. After that the fabricated nanocomposite demonstrates the exceptional electrocatalytic activity for both the hydrogen evolution process (HER) and the oxygen evolution reaction (OER) in a 1.0 M KOH solution. At a current density of 10 mAcm^{-2} , $\text{V}_2\text{O}_5/\text{MnSe}$ has exceptionally low overpotentials of 130 mV for HER and 217 mV for OER. Due to the protective properties of the V_2O_5 layers, the catalyst demonstrates exceptional stability of 50 h in alkaline environments. Furthermore, the fabricated nanocomposite $\text{V}_2\text{O}_5/\text{MnSe}$ also shows the tafel slope of 44, and 69 mV/dec for OER and HER, respectively. Hence, the increased catalyst efficacy is a result of the synergistic interaction between the V_2O_5 and MnSe. On the other hand, the presence of MnSe nanoparticles dispersed precisely and inhibit the aggregation process effectively, maximizing active site exposure. In addition, the presence of V_2O_5 shields these exposed metal particles while increasing the material's electrical conductivity. This study reveals a feasible process for the production of bifunctional electrocatalysts with superior performance and stability. These findings introduce novel concepts for advancing the field of water splitting to produce green energy, which will contribute to the ongoing development of electrocatalytic technology.

5:00 PM EN09.04.21

Electrocatalytic Properties of Pulsed Laser-Deposited Titanium Dioxide and Titanium Oxynitride Thin Films Grown on Photo-Adsorbing Single Crystal Substrates with Different Orientations Sheilah Cheron¹, Ikenna Chris-Okoro¹, Swapnil Nalawade², Soyoung Kim³, Jacob Som⁴, Dhananjay Kumar¹ and Tanja Cuk⁵; ¹North Carolina Agricultural and Technical State University, United States; ²Joint School of Nanoscience and Engineering, United States; ³Lawrence Berkeley National Laboratory, United States; ⁴Cornell University, United States; ⁵University of Colorado at Boulder, United States

The research focuses on the growth of (photo)electrocatalytic titanium dioxide (TiO_2) and Titanium oxynitride (TiON) thin films epitaxially grown on single crystal substrates at different orientations. The films are used as catalysts to examine the electrochemical reactions during water-splitting with the aim of producing hydrogen. The films were grown using pulsed laser deposition (PLD), which has many advantages, including fast response time, energetic evaporants, and congruent evaporation. These advantages were used to determine the optimal growth conditions, which, when combined with careful substrate selection, led to oxide and oxynitride films with well-defined strain and well-controlled vacancies. Furthermore, since PLD can transfer the composition of the target having elements with vapor pressures as different as 10^6 from each other, it can enable the incorporation of non-Ti cations into TiO_2 and TiON (photo)electrocatalytic films. Soft X-ray absorption spectroscopy at the Ti L-edge, O K-edge, and N K-edge was collected on the TiON samples to obtain information regarding the electronic structure. This controls afforded by pulsed laser deposition (PLD) allows us to tailor the band edges of semiconductors and to evaluate the creation and evolution of water-splitting intermediates as a function of potential and/or photo triggers. This capability is then used to examine the hydrogen evolution reaction (HER) and oxygen evolution reaction (OER) mechanisms on oxide and oxynitride catalysts.

5:00 PM EN09.04.22

4-Electron Oxygen Reduction Reaction via Transition Metal Phthalocyanines Functionalized Three-Dimensional (3D) Fuzzy Graphene Seonghan Jo¹, Lance Kavalsky², Venkat Viswanathan² and Tzahi Cohen-Karni¹; ¹Carnegie Mellon University, United States; ²University of Michigan, United States

Rechargeable metal-air batteries and proton exchange membrane fuel cells are regarded as next-generation energy devices for clean power generation. However, the sluggish rate of the oxygen reduction reaction (ORR), attributed to its complex reaction steps, and the absence of cost-effective and highly stable electrocatalysts seriously restrict energy efficiency and commercialization of these devices. Recently, we reported that nanowire templated 3D fuzzy graphene (NT-3DFG) exhibited remarkable 2-electron ORR performance due to its hierarchical structure composed of exposed single-layer graphene edges that readily functionalized by oxygen in situ under alkaline ORR conditions. Here, we synthesized a highly improved electrocatalyst for 4-electron ORR by modifying the surface of NT-3DFG by iron phthalocyanine (FePc@NT3DFG). FePc@NT3DFG exhibited notable efficiency (half-wave potential of 0.910 ± 0.001 V vs. RHE), low selectivity (3.1 ± 1.0 % H₂O₂), and improved long-term stability (96.0 ± 0.2 % current retention at 30 hours). We attribute this performance to the interaction between Fe active sites and *in-situ* functionalized oxygen groups at the edge of graphene layers, adjusting the electro-configuration of Fe as well as stabilizing the atomic structure during the reactions. Moreover, additional transition metals phthalocyanine displayed the same tendency to favorable for 4-electron ORR. This work provides an increased understanding of tuning electro-configuration from graphene edge-based substrates for 4-electron ORR and offers directions for future electrocatalyst design.

5:00 PM EN09.04.23

Facile Synthesis of Ag₂S Quantum Dots for Energy Storage and Sensing Applications. Sharath S C¹, Naveen Narasimhachar Joshi² and M. N. Kalasad¹; ¹Davangere University, India; ²Centennial Campus North Carolina State University, United States

Herein, we report the synthesis of Ag₂S Quantum dots by co-precipitation method using the silver, thiol molecules (stabilizing agent) and sulfur (S) S-complex in molarities. The synthesized Ag₂S Quantum dots were characterized by different techniques by using optical absorption, wavelength tunable photoluminescence emissions in the visible range, FTIR, PXRD, TEM, HRTEM, SAED and EDX. From XRD patterns estimated particle sizes are found of 6.50 nm with a monoclinic phase of the Ag₂S quantum dots. The morphological study was made by performing transmission electron microscopy (TEM) images to confirm a spherical shape and the average particle size estimated from the micrographs is 7 nm. The electrochemical measurements as cyclic voltammetry (CV), electrochemical impedance spectroscopy (EIS) and Galvanostatic charge/discharge (GCD) and differential pulse voltammetry (DPV) profile in a three-electrode configuration system for prepared nickel mesh electrode. Initially, the CV curves of Ag₂S QDs electrodes were performed at scan rates ranging from 20 to 100 mVs⁻¹. A consistent enhancement in current responsiveness can be observed for 1M KOH electrolyte [27]. The regression values (R²) of Ag₂S QDs (0.99807) are enhanced. These values signify a reversible and diffusion-controlled redox reaction of the electrodes. The impedance spectra demonstrated that charge transfer resistance (R_{ct}) is enhanced with a low capacitance value of Ag₂S. There is a distinctive depressed semicircle representing the charge transfer resistance in the high-frequency region, along with a slope that is associated with the Warburg impedance observed in the low-frequency range. Nyquist plot of Ag₂S electrode, after and before cycling was carried out [28]. Galvanostatic charge/discharge (GCD) exhibited supercapacitor performances with high specific capacitance at different current density (140 Fg⁻¹ at 1 Ag⁻¹) with the potential window 0-4 V and it shows a maximum specific capacity compared to other reported sulfur-based materials. The potential generated in Ag₂S electrode was observed from GCD curves of the first 20 and 200 cycles. After 200 cycles of charge discharge, the coulombic efficiency of was 96% [22,29]. The Differential Pulse Voltammetry (DPV) technique was used to sense the tartaric acid of 0.1M with a linear range of 50 to 1000mM and shows the Limit of Detection about 84.9mM, this shows an extraordinary sensing behaviour of Tartaric acid in the KOH solution with the sensitivity of the sensor about 1.51×10^{-7} A/cm², stability (25 days) and the surface coverage area is 7.23×10^{-10} mol cm⁻². This Organic acid sensor shows a high selectivity among (Oxalic acid, Citric acid, Mallic acid and Ascorbic acid)]. As a result, Ag₂S Quantum dots, synthesized through co-precipitation, show promise as high-performance supercapacitor electrode materials. They offer high capacitance and efficient charge transfer, making them a compelling alternative to toxic materials. Additionally, they exhibit remarkable sensitivity and selectivity as a tartaric acid sensor. Overall, this research underscores their versatility in energy storage and chemical sensing applications.

5:00 PM EN09.04.24

The Effective 2D Interlayer Architecture of Cu₂WS₄@N-Doped Graphene Nanocomposite for Oxygen Reduction Reaction and Rechargeable Zn-Air Battery Ranjith Balu^{1,2}, Debabrata Chanda^{1,2}, Mikiyas Mekete Meshesha^{1,2}, Seok Gwon Jang^{1,2} and Bee Lyong Yang^{1,2}; ¹Kumoh National Institute of Technology, Korea (the Republic of); ²bGHS (Green H₂ System) Co., Ltd., Korea (the Republic of)

A new research trend is exploring highly efficient and prolonged catalysts for oxygen evolution reaction (OER) and oxygen reduction reaction (ORR). Even though, it remains a considerable challenge to understand electrochemical performance enhancement in this field. Herein, we synthesized an interlayered architecture of Cu₂WS₄@NG nanocomposite and are reported as efficient cathode materials for flexible Zinc-Air batteries. Hierarchical porous interlayers create more active sites due to the unique interlayer architecture. As a result of the synergistic interaction between Cu₂WS₄@NG interfaces, the rate of charge transfer is facilitated, the number of active sites is increased, and OER/ORR kinetics is positively influenced in an alkaline environment. Theoretical studies indicate that the interlayered architecture tuning of the electronic structure of Cu₂WS₄@NG nanocomposite, which is significantly increases the electrical conductivity and catalytic activity. The prepared catalyst will be delivers an excellent half-wave potential for ORR and a low overpotential for OER. Furthermore, the quasi-solid state flexible ZACs will be fabricate and testing for commercial purpose.

Acknowledgement

This work was supported by the Technology development Program (RS-2023-00218808) funded by the Ministry of SMEs and Startups (MSS, Korea), Technology development Program (Project No.: S2960707) funded by the Ministry of SMEs and Startups (MSS, Korea). By the Basic Science Research Program through the National Research Foundation of Korea (NRF) funded by the Ministry of Education, Science, and Technology (MEST) [grant numbers: 2021R1A2C1006010]. and by the Technology development Program (RS-2023-00218808) funded by the Ministry of SMEs and Startups (MSS, Korea)

5:00 PM EN09.04.25

More than a Matrix: Tailoring Catalytic Sites in Graphitic Carbon Nitride Joel R. Pennings, Mustafa Yavuz and Michael Pope; University of Waterloo, Canada

Graphitic carbon nitride (g-C₃N₄) is a promising multifunctional 2D material, especially popular as an eco-friendly and accessible catalyst in oxygen reduction reactions (ORR), hydrogen evolution reactions (HER), and fuel cells [1]. However, the application of g-C₃N₄ is restricted by a natively high e-/h+ recombination rate, poor conductivity, and low surface area, resulting in somewhat sluggish and limited catalytic performance. Research towards ameliorating these limitations has shown that coordinating metals in the lattice gallery space and non-metal substitutional doping are incredibly effective tools for tailoring selective and high-performing catalytic materials [2]. Critically, these tools are often studied in isolation or with sub-optimally prepared g-C₃N₄, which fails to address the various challenges holistically [3-5]. Our work demonstrates strong improvements in the baseline performance of g-C₃N₄ due to pre-polymerization supramolecular assembly coupled with extensive exfoliation. We also show that this g-C₃N₄ synthesis method is highly

compatible for both metals coordinated to the nitrogen lone pairs and substitution covalently bonded dopants. These results show uniquely tailored, catalytically active sites in the material, specifically improving the ORR and HER performance. Specifically, we fabricated exfoliated g-C₃N₄ nanosheets with transition metals (Fe/Na/Co/Mg/Pd) strongly coordinated to the active sites, which had been secondarily engineered via covalently bonded interstitial dopants (P/S). These materials were subjected to ORR and HER electrochemical assessments and traditional characterization techniques to preliminarily grasp the advantages and limitations of our material preparation procedures. These material variations offer a wide range of selectivity towards catalytic systems and applications while wholistically improving the catalytic performance and preserving the stability, and sustainability of the g-C₃N₄ system.

Related group papers:

- [1] J. Pennings et al., "Femtosecond laser irradiation as a novel method for nanosheet growth and defect generation in g-C₃N₄," *Nanotechnology*, vol. 34, no. 41, p. 415603, Jul. 2023, doi: 10.1088/1361-6528/acda3e.
- [2] T. R. Aldhafeeri, M. Uceda, A. Singh, M. Ozhukil Valappil, M. W. Fowler, and M. A. Pope, "Embedded Platinum–Cobalt Nanoalloys in Biomass-Derived Laser-Induced Graphene as Stable, Air-Breathing Cathodes for Zinc–Air Batteries," *ACS Appl. Nano Mater.*, vol. 6, no. 10, pp. 8302–8314, May 2023, doi: 10.1021/acs.nano.3c00564.
- [3] G. F. Hawes, S. Rehman, Y. Rangom, and M. A. Pope, "Advanced manufacturing approaches for electrochemical energy storage devices," *International Materials Reviews*, vol. 68, no. 3, pp. 323–364, Apr. 2023, doi: 10.1080/09506608.2022.2086388.

Related sources:

- [1] J. Wen, J. Xie, X. Chen, and X. Li, "A review on g-C₃N₄-based photocatalysts," *Applied Surface Science*, vol. 391, pp. 72–123, Jan. 2017, doi: 10.1016/j.apsusc.2016.07.030.
- [2] A. K. Mrinalini Kalyani, R. Rajeev, L. Benny, A. R. Cherian, and A. Varghese, "Surface tuning of nanostructured graphitic carbon nitrides for enhanced electrocatalytic applications: a review," *Materials Today Chemistry*, vol. 30, p. 101523, Jun. 2023, doi: 10.1016/j.mtchem.2023.101523.
- [3] Q. Zuo et al., "Ultrathin Metal–Organic Framework Nanosheets with Ultrahigh Loading of Single Pt Atoms for Efficient Visible-Light-Driven Photocatalytic H₂ Evolution," *Angewandte Chemie International Edition*, vol. 58, no. 30, pp. 10198–10203, 2019, doi: 10.1002/anie.201904058.
- [4] J. Jiang et al., "Sulfur-doped g-C₃N₄/g-C₃N₄ isotype step-scheme heterojunction for photocatalytic H₂ evolution," *Journal of Materials Science & Technology*, vol. 118, pp. 15–24, Aug. 2022, doi: 10.1016/j.jmst.2021.12.018.
- [5] X. Zhu et al., "Design and Architecture of P-O Co-Doped Porous g-C₃N₄ by Supramolecular Self-Assembly for Enhanced Hydrogen Evolution," *Catalysts*, vol. 12, no. 12, Art. no. 12, Dec. 2022, doi: 10.3390/catal12121583.

5:00 PM EN09.04.26

Rational Development of Nanostructured Catalyst with Tuneable Electronic Properties towards Electrochemical Ammonia Synthesis [Ashmita Biswas](#) and Ramendra Sundar Dey; Institute of Nano Science and Technology, Mohali, India

Ammonia, once a benchmarking element in fertilizer industries has now embarked into the energy sector as a potential carrier of H₂ as a fuel. This has significance to achieve the "NET-ZERO" targets of the society, towards sustainability. It is noteworthy that, the electrochemical ammonia synthesis is capable of reserving green hydrogen that is being sought nation-wide as an alternative of the non-renewable energy sources. Ammonia in itself can act as a fuel or it can be dehydrogenated to extract the H₂ enabling a circular economy. In the current frontier of the world, this holds utmost importance as the storage, handling, transportation and shipping of this green ammonia is comparatively cheaper than liquid hydrogen and hence of potential interest. However, the demand of green ammonia production is although high but the electrochemical methods and components require rigorous optimizations to attain the desired goal.

In this realm, our group works on the development of electrocatalysts and electrode-electrolyte systems capable of overcoming the rate-limiting steps of the electrochemical ammonia synthesis by nitrogen reduction reaction (NRR) at the cost of low energy barrier. Since NRR is a complicated multi-stepped process, we have ventured that the elementary steps and the reaction kinetics heavily depend on the electronic properties of the catalyst impacting the binding strength of the intermediates on the electroactive site. The descriptors include the position of Fermi level and metal d-band center, work function, density of states, charge distribution and polarizability that not only dictate the activation of N₂ (which is very difficult otherwise) and also determine the reaction pathway. In our case-studies, it has been observed that the catalyst designing with hetero-atom doping, interface engineering as well as vacancy engineering has been proven to be efficient in provoking N₂ adsorption over proton adsorption over the active site. A better proton adsorption initiates hydrogen evolution reaction (HER) that lowers the possibility of NRR on catalyst surface with a sacrificial NH₃ yield rate and Faradaic efficiency (FE). With the differential atomic polarizability in our developed systems, we are able to deviate this HER path to adjacent atoms, while preserving the active center for NRR. This is how we tend to improve the NH₃ yield rate and FE upto the industrial scale periphery.

Finally, we have developed an electrolyzer with which we are able to control the overpotential of the NRR. Basically, the electrocatalysts are not strong enough to break the even stronger N≡N. So, a huge power input incurs sufficient energy consumption to produce the value-added ammonia, which ultimately becomes equivalent to that consumed in the Haber-Bosch process. However, with the developed electrolyzer system, we are able to manipulate the kinetics of the NRR-coupled-oxygen evolution reaction and the less overpotential enabled a better electrical to chemical energy conversion efficiency of the system, which has potential to be commercialized and scaled-up to meet the industrial scale demands of ammonia.

References:

- Proceedings of the National Academy of Science of the United States of America*, 2022, 119 (33), e2204638119,
J. Chem. Phys. 2023, 158, 201103,
Nano-Micro Letters, 2022, 14, 214,
ACS Nano, 2021, 15, 20364–20376,
Inorg. Chem. 2023, 62, 34, 14094–14102.

5:00 PM EN09.04.27

Modulating Active Sites in Metal Oxides for Deeper Insights into CO₂ Reduction [Amr Sabbah](#)¹, Thang Q. Nguyen², Kuei-Hsien Chen² and Li-chyong Chen¹; ¹National Taiwan University, Taiwan; ²Academia Sinica, Taiwan

The pursuit of CO₂ reduction through catalytic processes holds significant promise in addressing climate change. Metal oxide-based catalysts are among the most promising candidates, as they provide invaluable insights into reaction mechanisms and subsequent catalytic enhancements. This presentation delves into the intricate world of active site modulation within metal oxides especially the n-type semiconductor of the Aurivillius oxides family, a pivotal aspect for a deeper comprehension and optimization of CO₂ reduction. Through the systematic manipulation of these active sites, we uncover essential insights into the mechanisms governing CO₂ reduction and its fine-tuning. This study explores a range of modeling approaches, including the manipulation of oxygen vacancies, dopants, heterostructuring, and single atom modifications, each contributing distinct effects to tailor the catalytic properties of metal oxides and enhance their performance in CO₂ reduction. By dissecting these methodologies, our objective is to advance our comprehensive understanding of active site modulation and its pivotal role in the development of efficient and sustainable CO₂ reduction technologies.

5:00 PM EN09.04.28

Microwave-Assisted Molten Salt Synthesis of Chevrel Phase Chalcogenides [Ankita Kumari](#), Johnathan D. Rivera and Jessica C. Ortiz-Rodriguez; University of California, Davis, United States

The increase in energy demand has brought the challenge of developing efficient energy-conversion technologies. Currently, natural gas reforming is the most common method to generate hydrogen fuel, but this process is energy-consuming and also releases greenhouse gases into the atmosphere. Renewable hydrogen production has long been considered a clean energy carrier and a highly promising alternative to transition away from fossil fuels. Alternatively, electrochemical proton reduction is a sustainable and green method for producing hydrogen gas – a process that leaves virtually no carbon footprint when coupled to renewable sources of electricity. Chevrel phase (CP; $M_xMo_6S_8$; M=alkali, alkaline earth, transition, and post-transition metal), a class of molybdenum chalcogenides are especially attractive due to their tunable composition and lower coordination on their molybdenum moieties which has led to previously observed catalytic activity for oxygen evolution, hydrogen evolution, and CO₂ reduction reactions. Theoretical studies under various reaction conditions agree that proton adsorption interactions in the chevrel phase occur through the undercoordinated chalcogen-molybdenum bridging site. Hence, reducing the size of the CP particles will increase the surface-to-volume ratio exposing a more undercoordinated Mo-S bridging site for proton adsorption. Traditionally CPs were synthesized by high-temperature solid-state reactions which can take several days and require extremely high-energy input. Although some approaches have been made to reduce the preparation time of CPs, the methods either suffer from uncontrolled particle size, high level of agglomeration, presence of MoS₂ impurities, or high energy input. This work presents an efficient route to synthesize size-controlled ternary Chevrel phase chalcogenides (Cu₂Mo₆S₈) by a microwave-assisted molten salt approach. This methodology has significantly reduced the reaction times from days to minutes resulting in significant time and energy savings yielding highly crystalline, faceted morphology of CPs. The phase, morphology and surface chemistry of the resultant materials were characterized by X-diffraction (XRD), scanning electron microscopy (SEM), Energy dispersive X-ray Spectroscopy (EDX), and X-ray photoelectron spectroscopy (XPS). The electrochemical reactions were done in a three-electrode cell with Ag/AgCl as the reference electrode, graphite as the counter electrode, and catalyst ink on Toray paper as the working electrode.

5:00 PM EN09.04.29

Dispersion and Stability Mechanism of Heterogeneous Catalysts [Sang-Wook Han](#)¹, Eun-Suk Jeong¹ and In-Hui Hwang²; ¹Jeonbuk National University, Korea (the Republic of); ²Argonne National Laboratory, United States

The dispersion and stability of noble-metal catalysts on transition-metal-oxide supports are considerably important for practical applications of the catalysts. Pt nanoparticles are uniformly and highly dispersed on transition-metal oxides when hydrogen peroxide (H₂O₂) is applied before calcination at 500 °C. The influence of H₂O₂ on the dispersion and the stability of Pt nanoparticles on titania-incorporated fumed silica (Pt/Ti-FS) supports was examined using in-situ X-ray absorption fine structure (XAFS) measurements at the Pt L₃ and Ti K edges as well as density functional theory (DFT) calculations. The local structural and chemical properties around Pt and Ti atoms of Pt/Ti-FS with and without H₂O₂ treatment were monitored using *in-situ* XAFS during heating from room temperature to 500 °C. XAFS revealed that the Pt nanoparticles of H₂O₂-Pt/Ti-FS are highly stable and that the Ti atoms of H₂O₂-Pt/Ti-FS support form into a distorted-anatase TiO₂. DFT calculations showed that Pt atoms bond more stably to oxidized-TiO₂ surfaces than they do to bare- and reduced-TiO₂ surfaces. XAFS measurements and DFT calculations clarified that the presence of extra oxygen atoms due to the H₂O₂ treatment plays a critical role in the strong bonding of Pt atoms to TiO₂ surfaces.

5:00 PM EN09.04.30

Enhanced Photocatalytic Reduction of CO₂ to CO Using Cs₃Bi₂Br₉/g-C₃N₄ Direct Z-Scheme Heterojunctions [Yasmine Baghdadi](#) and Salvador Eslava; Imperial College London, United Kingdom

Lead-free halide perovskite derivative Cs₃Bi₂Br₉, has proven to possess optoelectronic characteristics suitable for photocatalytically reducing CO₂ to CO. However, further research is needed to boost the separation of charges in order to improve the overall efficiency of this photocatalyst. This study presents the synthesis of a hybrid heterojunction composed of inorganic and organic materials, combining Cs₃Bi₂Br₉ with g-C₃N₄ at various ratios. This was accomplished by growing Cs₃Bi₂Br₉ crystals on the surface of g-C₃N₄ using a straightforward antisolvent crystallization method. The resulting powders demonstrated increased photocatalytic CO₂ reduction in the gas phase with water vapor, producing 14.22 (±1.24) μmol of CO per gram per hour with a 40% Cs₃Bi₂Br₉ content, compared to 1.89 (±0.72) and 5.58 (±0.14) μmol CO g⁻¹ h⁻¹ for pure g-C₃N₄ and Cs₃Bi₂Br₉, respectively. Photoelectrochemical measurements revealed enhanced photocurrent in the composite further proving improved charge separation. Additionally, stability tests showed that the heterojunction remained structurally stable even after 15 hours of illumination. Analysis of the band structure alignment and selective metal deposition indicated the formation of a direct Z-scheme heterojunction between the two semiconductors, which led to a significant improvement in charge separation and an overall enhancement in CO₂ reduction.¹

¹ Baghdadi, Y. *et al.* Cs₃Bi₂Br₉/g-C₃N₄ Direct Z-Scheme Heterojunction for Enhanced Photocatalytic Reduction of CO₂ to CO. *Chemistry of Materials*, doi:10.1021/acs.chemmater.3c01635 (2023).

SESSION EN09.05: CO₂ Reduction
Session Chairs: Michel Trudeau and Edmund Chun Ming Tse
Wednesday Morning, April 24, 2024
Room 337, Level 3, Summit

8:30 AM EN09.05.01

Strategies for Improving The Microenvironment in Electrochemical CO₂ Reduction Using Nanostructured Catalysts [Andrew B. Wong](#); National University of Singapore, Singapore

The electrochemical CO₂ reduction reaction (CO₂RR) represents a promising approach toward the carbon-neutral generation of hydrocarbons. However, despite intense research efforts, the need remains to increase selectivity and activity for electrocatalysts for CO₂RR. In order to accomplish these goals, there has been increasing interest in optimizing the microenvironment to boost the activity and selectivity of electrocatalytic sites for CO₂ conversion. However, the functional understanding of how to tune the microenvironment is still under development.

This presentation discusses several strategies that are being pursued in my research group to illustrate design principles to optimize the microenvironment for CO₂ conversion, which include:

- (1) Nanostructured model systems to illustrate control of diffusion via engineering electrode structure at micro- and nano-length scales

(2) Nanostructured model systems to harness localization of tandem catalysts.

This talk will also share perspectives about harnessing nanoscale materials to control and enhance the microenvironment in order to enhance CO₂ conversion.

8:45 AM EN09.05.02

Transition Metal Doped Electrospun Fibers as Freestanding Electrodes for Carbon Dioxide Electroreduction [Hattie Chisnall](#), Michael W. Thielke and Ana Jorge Sobrido; Queen Mary University of London, United Kingdom

The electrochemical carbon dioxide reduction reaction (CO₂RR) is a promising route to reducing excess atmospheric CO₂ emissions and producing valuable commodity chemicals. While there are upwards of 16 products accessible via the multi-electron, multi-step reduction, each pathway is required to proceed via an initial electron transfer from CO₂ to the anion radical, CO₂*⁻. This first electron transfer step, being the most energetically demanding, proves difficult in the absence of a catalyst due to the high overpotential (-1.9V vs SHE) required to reduce the thermodynamically stable, linear CO₂ molecule. The success of CO₂RR is therefore guided by efficient electrocatalysts which circumnavigate such high activation energies and promote favourable kinetics. The design of selective electrocatalysts which offer high faradaic efficiencies, reduced overpotentials, and provide high current densities has thus inspired an extensive area of research.

Transition metals have been consistently established as highly efficient electrocatalysts within this field. Within this reach, we have investigated two promising morphologies of active site: molecular-based catalysts with well defined active sites which demonstrate high selectivity for the 2-electron reduction of CO₂ into CO and in situ formed copper nanoparticles, which facilitate CO₂ conversion into C₂+ products. The former has inspired investigation into the electrocatalytic behaviour of phthalocyanine complexes: aromatic, macrocyclic molecules consisting of four isoindole subunits with a central cavity which supports a metal atom. While distinct transition metal sites within the molecular cavity offer improved selectivity and work well to suppress the competing hydrogen evolution reaction (HER), they fail to offer pathways beyond C₁ products. Attempts to access more energy dense products have been made via controlled in situ growth of copper nanoparticles during simultaneous carbonisation of the graphitic matrix. While an intermediate binding energy to *CO is responsible for the well-known propensity of copper to facilitate electrochemical CO₂ reduction to C₂+ products, restraint of particle size and regulation of crystal facets via temperature control allow the user significant control over product selectivity and overall catalytic efficiency.

Freestanding electrocatalysts offer a significant advantage over commonly used catalytic inks as they provide a larger surface area. We have elected to synthesise freestanding nanofibrous mats via electrospinning polymer solutions followed by a carbonisation step. Polyacrylonitrile, a widely-available synthetic polymer, used as a precursor allows fabrication of conductive fibres with advantageous nitrogen doping. Likewise, electrospinning bio-mass derived lignin can introduce oxygen-functionalities with the added advantage of avoiding petrochemical-derived precursors. Heteroatom functionalities may act to both bolster performance of the overall catalyst through their inherent activity and also to anchor active sites to the surface of the support. The covalent binding of molecular catalysts via the central transition metal onto such supports has demonstrated improved charge transfer when compared to those which rely on isolated molecular catalysts or those bound through pi-pi stacking. In the case of freestanding carbon fibers with in situ deposition of copper nanoparticles, the distribution of uniformly sized catalytic particles is enabled throughout the graphitic fibres.

9:00 AM EN09.05.03

Comparison of Mono- and Multi-Layer MoS₂ within Non-Aqueous Reactive Carbon Capture and Conversion (RCC) Conditions [Kingston Robinson](#)¹, Rowan Brower¹, Jose L. Perez Gordillo^{2,1} and Jesus M. Velazquez¹; ¹University of California, Davis, United States; ²University of Puerto Rico at Humacao, United States

With a need to reduce global emissions and scale up alternative energy sources to fossil fuels, RCC integrates CO₂ capture and conversion into a singular electrochemical, thermal, or biological process as a feedstock for value added chemicals. Despite significant progress in CO₂ electrocatalyst design to improve efficiency, reproducibility, and selectivity in aqueous media, achieving the same milestones within non-aqueous media under RCC conditions remains a challenge. However, preliminary results show that single crystal molybdenum disulfide (MoS₂) exhibits high efficiency (~65%) towards CO production under non-aqueous RCC with ionic liquids. The electrocatalytic behavior of MoS₂ can be controlled by exposing edge and terrace active sites through surface defects or by modulating its structure through compositions such as thin film monolayers and multi-layer nanosheets. It is hypothesized that by decreasing MoS₂ layers, further efficiency and selectivity of CO₂ reduction products under relevant non-aqueous RCC conditions will be observed due to increased surface area of active sites. Two different synthetic pathways are detailed in this work, shear exfoliation of bulk MoS₂ to yield dispersions of nanosheets and metal organic chemical vapor deposition (MOCVD) of monolayer MoS₂ thin films. The shear exfoliation process is a combination of mechanical and liquid-phase techniques, utilizing a homogenizer along with chemical exfoliation from different surfactants. Exfoliating agents such as sodium cholate resulted in MoS₂ nanosheets with large terraces while polyvinylpyrrolidone (PVP) resulted in small nanoparticle MoS₂ sheets. Therefore, size distribution of MoS₂ sheets may be controlled with the type of exfoliating agent. Our MOCVD process utilizes Mo(CO)₆ and diethyl sulfide (DES) as metal organic precursors flown in a vapor phase with Ar and H₂ gas for deposition onto Si/SiO₂ wafers. At optimal chamber pressure and temperature as well as precursor/gas flow rates, deposition of nucleation zones, monolayers, and few layered structures occur as a function of time. Shear exfoliated nanosheets and MOCVD deposited monolayers will be tested against single crystal MoS₂ under relevant non-aqueous RCC conditions with ionic liquids.

9:15 AM EN09.05.04

Regulating Spillover Effect in Cu-Ag via Zeolite Frameworks for Efficient CO₂ Electroreduction [Dohun Kim](#)¹, Joon Y. Kim², Woosuck Kwon¹, Taemin Lee¹, Uk Sim² and Dae-Hyun Nam¹; ¹Daegu Gyeongbuk Institute of Science and Technology, Korea (the Republic of); ²Korea Institute of Energy Technology (KENTECH), Korea (the Republic of)

Electrochemical CO₂ reduction reaction (CO₂RR) has been regarded as a promising green technology for lowering atmospheric CO₂ level and producing value-added products. For multi-carbon (C₂+) chemical production, Cu-based electrocatalysts have been developed by various strategies, such as defect engineering, alloying with other metals, and morphological engineering. Among these various strategies, the spillover effect between Cu and Ag has been considered as an effective avenue for modulating CO₂RR selectivity and activities. However, previous works about spillover effect have focused on controlling the Cu/Ag ratio rather than regulating the interface reaction between Cu and Ag.

Herein, we propose a novel strategy to optimize spillover effect on the Cu surface by modulating anion species in zeolite framework-augmented gas diffusion electrode (GDE). In CO₂RR, anions such as Cl⁻, Br⁻, and I⁻ can modulate the Cu surface oxidation states and create Cu (0)-Cu (I) mixed sites which facilitate C-C coupling by modifying *CO binding. However, these anions can easily migrate to the anodic side by crossover in anion exchange membrane under high current density conditions. Thus, we augmented AgX (X = Cl, Br, and I)-incorporated zeolite A (AgX-Zeolite A) on Cu electrocatalysts to modulate spillover effect by restricting anion migration. They showed lower hydrogen production and more efficient CO₂RR compared to bare Cu electrocatalysts in 1 M KOH electrolyte conditions. Especially, AgCl-, AgBr-, and AgI-Zeolite A on Cu electrocatalysts exhibited 586.3, 495.8, and 456.4

mA/cm² as maximum partial current densities for C₂₊ products. This trend is in inverse relationship with the electronegative force of anion species. With increasing electronegative force, the Cu (I) sites become more dominant rather than Cu (0)-Cu (I) mixed sites. However, AgCl-, AgBr-, and AgI-Zeolite A on Cu electrocatalysts showed the 0.89, 1.17, and 1.14 as Faradaic efficiency (FE) ratio of ethanol (C₂H₅OH)/ethylene (C₂H₄), respectively. These results verified that anion species stabilized by zeolite framework not only accelerate C₂₊ production but also steer the CO₂RR pathway to specific products *via* spillover effect. Our work provides an insight of zeolite framework-augmented GDEs for high rate and selective C₂₊ chemical production in CO₂RR.

9:30 AM EN09.05.05

Cation Exchange Ionomer-Based Microenvironment Control of Gas Diffusion Electrode for Efficient CO₂ Electroreduction Yujin Lee¹, Daewon Bae¹, Woosuck Kwon¹, Hansol Choi², Hyungju Ahn³, Chang Hyuck Choi², Chanyeon Kim¹ and Dae-Hyun Nam¹; ¹Daegu Gyeongbuk Institute of Science & Technology (DGIST), Korea (the Republic of); ²Pohang University of Science and Technology (POSTECH), Korea (the Republic of); ³Pohang Accelerator Laboratory (PAL), Korea (the Republic of)

Electrochemical CO₂ reduction reaction (CO₂RR) where CO₂ is converted into a high-value-added compound can be a great strategy for carbon neutrality. Gas diffusion electrode (GDE) which allows the formation of triple phase boundary (TPB) of catalyst, electrolyte, and CO₂ gas has been widely applied for CO₂RR. It results in overcoming the CO₂ solubility limitation in double phase boundary (DPB) of electrolyte and catalyst, and thus increases the CO₂ availability. However, the volume of TPB where the reaction occurs is much smaller than the volume of DPB. Therefore, it is important to increase the volume of TPB for CO₂RR activity. Cation exchange ionomer enables us to control the volume of TPB. The hydrophobic chains of ionomer that play a role as gas channel and hydrophilic ionic groups that form a water matrix increase the volume of TPB in GDE-based systems. Here, we verify the effect of ionomer on CO₂RR performance in 1 M KOH electrolyte by controlling CO₂/H₂O ratio and CO₂ availability near GDE-based Cu catalyst surface. To distinguish the effect of each part of ionomer, we control the variables of ionomer; (1) Controlling the length of side chain with the application of Nafion as long side chain (LSC) ionomer and Aquivion as short side chain (SSC) ionomer, (2) Fixation of equivalent weight (EW). Compared to the maximum H₂ partial current density (J_{H2}) of 71.3 mA/cm² at bare Cu, Nafion decreases the maximum J_{H2} to 11.5 mA/cm² while Aquivion decreases it to 26.4 mA/cm². On the other hand, the maximum CO partial current density (J_{CO}) is 75.1 mA/cm² at Nafion whereas it is 24.1 mA/cm² at Aquivion. Nafion and Aquivion also improve the maximum C₂H₄ partial current density (J_{C2H4}) to 169.5 and 173.3 mA/cm², respectively. Based on the characterization of ionomers in GDE, we found that LSC ionomer can induce a higher CO₂/H₂O ratio than SSC ionomer and increase CO₂ availability near the active site. Also, we assume that it affects the CO₂RR selectivity by tuning the local OH⁻ concentration. Improved OH⁻ formation by high current density CO₂RR at ionomer-augmented catalysts affects the surface charge density that can enhance CO₂RR selectivity. Therefore, the key factor of ionomer effect on CO₂RR performance enhancement is regulation of the water concentration near the catalyst surface which impacts the CO₂ availability and ion conductivity through this water matrix. We expect that this work will suggest a more accurate understanding of the mechanism of ionomer effect on CO₂RR and strategy for optimizing the microenvironment of catalyst for efficient CO₂RR.

9:45 AM EN09.05.06

Cationic Cu Species Tracked via Operando X-Ray Microscopy during CO₂ Electrocatalysis and Their Role in Boosting C-C Coupling Activity Jongwoo Lim^{1,2}, Juwon Kim¹, Si Young Lee³, Se-Jun Kim⁴, Bonho Koo¹, Namdong Kim⁵, Matthew Markus⁶, David Shapiro⁶, Shu-Chih Haw², Daan Hein Alsem⁷, Norman Salmon⁷, Hyungjun Kim⁴ and Yun Jeong Hwang¹; ¹Seoul National University, Korea (the Republic of); ²National Synchrotron Radiation Research Center, Taiwan; ³University of Michigan–Ann Arbor, United States; ⁴Korea Advanced Institute of Science and Technology, Korea (the Republic of); ⁵Pohang Light Source, Korea (the Republic of); ⁶Advanced Light Source, United States; ⁷Hummingbird Scientific, United States

Unraveling and guiding the dynamic evolution of active species in efficient electrochemical CO₂ reduction (ECR) catalysts remains a challenge. Through observing the chemical and morphological changes of high-performance ECR catalysts in action, we pinpointed the essential intermediate species that lead to highly active surfaces and notably improved C–C coupling activity. Operando scanning transmission soft X-ray microscopy, a method that illustrates the nanoscale chemical composition distribution of Cu-based catalysts during ECR, showed that the emergence of partial Cu⁺ phases and surface Cu₂⁺ phases are key to the dynamic dissolution-redeposition mechanism and heightened C–C coupling activity, respectively. We further established that this dissolution-redeposition process is electrochemical formation Cu²⁺ phases, even at elevated cathodic potentials. Our correlative microscopy and electrochemical analysis strengthen the substantial contribution of Cu₂⁺ phases toward C-C coupling. In addition, DFT calculations corroborated that Cu₂⁺ phases amplifies C–C coupling activity.

10:00 AM BREAK

10:30 AM *EN09.05.07

Vibrational Spectroscopy at Electrified Interfaces: Electrochemical CO₂ Reduction Reaction Heng-Liang Wu^{1,2,1}; ¹National Taiwan University, Taiwan; ²National Synchrotron Radiation Research Center, Taiwan

The solid-liquid interfacial reactions play a crucial role in controlling the performance and stability of electrocatalysts¹⁻⁴. In situ vibrational spectroscopy techniques such as Raman and surface-enhanced infrared absorption spectroscopy (SEIRAS) are the powerful tools for examining the surface-adsorbed intermediates on the solid-liquid interfaces. In this talk, we report our use of in situ SEIRAS, Raman, and X-ray absorption spectroscopy to investigate the electrochemical CO₂ reduction mechanism over the Cu-based electrocatalysts. The Cu-based electrodes with different oxidation states result in the formation of various CO intermediates such as CO_{atop} and CO_{bridge}. The co-existence of CO_{atop} and CO_{bridge} corresponds to the selectivity of CO₂-to-C₂H₄ reaction. Also, the bimetallic electrocatalysts are developed for efficient CO₂-to-HCOOH and CO₂-to-CO conversion processes. We found that the surface-adsorbed COO species with different binding structures play crucial role in the reduction process. The electronic structures of Cu-based electrocatalysts are associated with the formation of surface-adsorbed intermediates and electrocatalytic properties. The formation of surface-adsorbed intermediates and reaction mechanism associated with CO₂-to-HCOOH and CO₂-to-CO reactions over the bimetallic electrocatalysts will be discussed in detail.

References

- [1] T. Cheng, H. Xiao, W. A. Goddard, *J. Am. Chem. Soc.*, 138, 13802 (2016).
- [2] T.-C. Chou, C.-C. Chang, H.-L. Yu, W.-Y. Yu, C.-L. Dong, J. Velasco-Vélez, C.-H. Chuang, L.-C. Chen, J.-F. Lee, J.-M. Chen, and H.-L. Wu, *J. Am. Chem. Soc.*, 142, 2857 (2020).
- [3] X. Mo, X. Gao, A. V. Gillado, H.-Y. Chen, Y. Chen, Z. Guo, H.-L. Wu, E. C. M. Tse, *ACS Nano*, 16 12202 (2022).
- [4] K. B. Ibrahim, T. A. Shifa, M. Bordin, E. Moretti, H.-L. Wu, A. Vomiero, *Small Methods*, 2300348 (2023).

11:00 AM EN09.05.08

Role of Reservoir and Diffusion for Electrocatalytic CO₂ Reduction to Ethylene on Cu Sydney H. Hemenway^{1,2}, Chansol Kim^{1,3}, Nitish Govindarajan⁴, Junho Park^{1,2}, Anya Zoraster^{1,2}, Calton J. Kong^{1,2}, Rajiv R. Prabhakar¹, Joel Varley⁴, Hee-Tae Jung³, Christopher Hahn⁴ and Joel W. Ager^{1,2,1}; ¹Lawrence Berkeley National Laboratory, United States; ²University of California, Berkeley, United States; ³Korea Advanced Institute of Science and Technology, Korea (the Republic of); ⁴Lawrence Livermore National Laboratory, United States

Electrochemical CO₂ reduction (EC-CO₂R) on Cu is a promising approach to produce value-added-chemicals using renewable feedstocks. The ability of Cu to produce multi-carbon products during electrochemical CO₂ reduction is conventionally understood in terms of the binding energy of the crucial CO intermediate and the existence of active sites which facilitate C-C coupling. Yet the vast differences in activity and selectivity towards single and multi-carbon products produced by various Cu preparations suggest that this picture is incomplete. In this work, we find that the effective catalytic activity towards ethylene improves with a larger fraction of **less active** sites acting as reservoirs of *CO on the Cu surface. This surprising finding can be explained by the rapid supply of *CO from reservoir to active sites which increases the effective activity of active sites. Experimental evidence is provided by real-time measurements of mass flow exiting a gas diffusion electrode cell held at a fixed potential and subjected to different precursor feeds. When the precursor feed is switched from inert Ar to CO, CO reduction to C₂₊ products begins promptly, as expected. However, when the precursor feed is switched from CO to Ar, CO reduction continues for several seconds (delay time) before transitioning to hydrogen evolution. Control experiments establish that some Cu preparations, most notably oxide-derived Cu, can maintain COR activity in the absence of the gas phase precursor due to reservoir sites on the Cu surface that bind CO but do not convert it. We introduce a microkinetic model which shows that the delay time originates from a less active *CO reservoir that exhibits fast diffusion to active sites on the surface of OD-Cu. Experiments find that delay time and *CO reservoir sizes are affected by the catalyst preparation, applied potential, and microenvironment. Notably, we associate large *CO reservoir surface coverages (maximally 86±5% at -1.52 V vs. SHE) with increased ethylene production. We also estimate that *CO can travel long distances (up to 10s of nm) prior to reaction. We propose a broader scope for EC-CO₂R catalyst design: in order to design high C₂₊ activity, in addition to active sites, the role of less active sites in controlling the *CO availability must be considered.

11:15 AM EN09.05.09

Copper Silicophosphides: New Ternary Nanocrystals as Electrocatalysts for Carbon Monoxide Reduction [Anissa Ghoridi](#)^{1,2}, [Ngoc-Huan Tran](#)^{3,1,2}, [Carlos V. Mendonça Inocêncio](#)^{1,2}, [Amandine Séné](#)^{1,2}, [Marzena Baron](#)^{1,2}, [Emile Defoy](#)^{1,2}, [Daniel Janisch](#)^{1,2}, [Fernando Igoa Saldana](#)^{1,2}, [Edouard De Rolland Dalon](#)^{1,2}, [Antoine Miche](#)^{1,2}, [Christel Gervais](#)^{1,2}, [Cristina Coelho-Diogo](#)^{1,2}, [Sandra Casale](#)^{1,2}, [Pierre-Olivier Autran](#)⁴, [Andrea Zitolo](#)⁵, [Isabelle Génois](#)^{1,2}, [Marc Fontecave](#)^{3,1,2} and [David Portehault](#)^{1,2}; ¹CNRS, France; ²Sorbonne Université, France; ³Collège de France, France; ⁴European Synchrotron Radiation Facility, France; ⁵Synchrotron SOLEIL, France

Incorporating *p*-block elements into transition metals offers a mean to fine-tune their electrocatalytic properties through localized structural distortion, charge transfer, and hybridization^[1]. Beyond simply doping, the design of compounds with specific compositions and crystal structures can significantly expand the range of accessible properties. Notably, copper phosphides and silicides have been explored for their efficiency as catalysts or pre-catalysts in electrochemical water splitting^[2] and as anodes in Li-ion batteries^[3,4]. However, the properties of ternary copper silicophosphides, which possess unique structures distinct from binary phases, have been little investigated. Currently, only three ternary copper phases are known (CuSi₂P₃, CuSi₄P₃, Cu₄SiP₈)^[5,6], and have remained at the status of scientific oddities.

To boost catalytic activity and selectivity for the generation of high-value added products containing C-C bonds in the electrocatalysis of the CO₂ reduction reaction (CO₂RR) and of the CO reduction reaction (CORR), one approach is to create single metal active sites, which can deeply modify catalytic cycles compared to metal clusters or nanoparticles^[7,8]. However, maintaining these single atom sites in an isolated state during electrocatalysis poses a significant challenge. Our strategy focuses on stabilizing these sites within crystallographic structures by seeking additional stabilization through the promotion of covalent bonding to establish a rigid crystal structure. It is also imperative to design nanostructures with a high surface-to-volume ratio, thereby amplifying catalytic activity. Copper silicophosphides present an ideal candidate for this purpose.

Here, we present the first synthesis of copper silicophosphide (CuSi₂P₃ and CuSi₄P₃) nanocrystals using molten salts as reaction media, promoting the nucleation of nanoparticles while limiting their growth^[9]. *In situ* X-ray diffraction measurements conducted at the ESRF ID11 synchrotron beamline during the synthesis reveal the crystallization mechanism from the initial metal salts to the ternary phases. Following a comprehensive characterization of the nanomaterials, including their structure, composition, and morphology (TEM, HRTEM, STEM-EDX, EDS mapping, XPS), we will delve into the promising electrocatalytic properties of CuSi₂P₃ for CORR, studied via *in situ* X-ray absorption spectroscopy at the SOLEIL SAMBA synchrotron beamline.

[1] Chen, T. et al. *J. Am. Chem. Soc.* **2019**

[2] Kong, L. et al. *RSC Adv.* **2016**

[3] Liu, Z. ; Yang, S. et al. *Angew.Chem. Int.Ed.* **2020**

[4] Zeng, X. C. et al. *Nanoscale.* **2018**

[5] Wang P. et al. *Dalton Transaction.* **2009**

[6] Kaiser, P. and Jeitschko, W. *Z. anorg. allg. Chem.* **1995**

[7] Karapinar et al. *Angew. Chem. Int. Ed.* **2019**

[8] Karapinar et al. *ChemSusChem.* **2020**

[9] Portehault, D. et al. *Chem. Soc. Rev.* **2022**

11:30 AM EN09.05.10

Bimetallic Interface Control of Cu₂O Nanocrystals for Efficient CO₂-to-C₂₊ Chemical Conversion [Seolha Lim](#), Woosuck Kwon and Dae-Hyun Nam; Daegu Gyeongbuk Institute of Science and Technology, Korea (the Republic of)

Electrochemical carbon dioxide reduction reaction (CO₂RR) is promising in the pursuit of carbon neutrality, as it converts CO₂, the primary contributor to global warming, into valuable high-end fuels and chemical feedstocks. Copper (Cu) is the only metal that has an appropriate *CO binding energy for C-C coupling. Cu-based CO₂RR electrocatalysts can produce multi-carbon (C₂₊) chemicals such as ethylene, ethanol, and acetic acid. Nonetheless, they suffer from low selectivity for producing specific products. Particularly, bimetallic systems including Cu with secondary metals such as Au and Ag for their weak *CO bonds, emerge as a promising strategy to enhance the production of C₂₊ chemicals. However, the focus of Cu-based bimetallic catalysts has primarily been optimizing the ratio of secondary metals, overlooking the significance of interface control for efficient CO₂RR.

In this study, we fabricated the facet-controlled Cu₂O nanocrystals (NCs) and studied the effect of bimetallic interface design on the CO₂RR. Cu₂O NCs includes cube with (100) facets, cuboctahedron (cubo) with (100) and (111) facets, and octahedron (octa) with (111) facets. We introduced Ag and Au as secondary metals to facet controlled Cu₂O NCs through galvanic replacement. Shape and size distributions of the secondary metal were affected by surface energy and the surface atomic diffusion rate. These factors proved to be pivotal in the fabrication of three distinct catalysts, each characterized by varying Cu-Ag, Cu-Au interfacial compositions. In general, Cu₂O cube with low-surface-energy exhibited segregation and agglomeration at the interfaces, whereas Cu₂O cubo and octa with high-surface-energy formed well-dispersed interfaces. Bare Cu₂O cube exhibited a 40% Faradaic efficiency (FE) for C₂₊ products and achieved H₂ FE of 19% at -0.73 V (vs RHE). Ag-augmented Cu₂O cube significantly improved selectivity by reaching 57% FE for C₂₊ and suppressing H₂ with a FE of 13% at -0.78 V (vs RHE). In contrast, the Au-augmented Cu₂O cube promoted H₂ with 25% FE and C₂₊ with 33% FE at -0.99 V (vs RHE), resulting in reduced performance. To gain deeper insights into the intermediate behavior of *CO, *in-situ* Raman spectroscopy was employed, highlighting

the critical importance of the metal effect in CO₂RR. Remarkably, it was observed that CO derived from Ag had a more pronounced impact on increasing *CO coverage on the Cu surface compared to that of Au. Furthermore, the relatively higher portion of high-frequency band (HFB) *CO_{atop} represents efficient C-C coupling. This study sheds light on the bimetallic interface design of Cu-based active sites for efficient C₂, chemical production in CO₂RR.

11:45 AM EN09.05.11

Atomic Layer Deposition of Cu Electrocatalysts on Gas Diffusion Electrodes for CO₂ Reduction Julia D. Lenef¹, Si Young Lee¹, Kalyn M. Fuelling¹, Kevin E. Rivera Cruz¹, Aditya Prajapati², Daniel O. Delgado Cornejo¹, Tae Cho¹, Kai Sun¹, Eugenio Alvarado¹, Timothy S. Arthur³, Charles A. Roberts³, Christopher Hahn², Charles C. McCrory¹ and Neil P. Dasgupta¹; ¹University of Michigan, United States; ²Lawrence Livermore National Laboratory, United States; ³Toyota Research Institute of North America, United States

Electrochemical recycling of carbon dioxide into value-added products is a promising strategy to mitigate climate change as the CO₂ reduction reaction (CO₂RR) can be driven using renewable electricity (i.e. wind, solar). So far, copper metal is the only known single element catalyst to form multi-carbon products, such as ethylene and ethanol, from CO₂RR. Numerous synthesis strategies have been employed to deposit copper-based catalysts including sputtering, evaporation electrodeposition, and solution processing; however, they do not enable atomically precise control of film thickness and particle size and have limited conformality on 3-D substrates such as carbon gas diffusion electrodes. To address this knowledge gap, we fabricate Cu catalysts using plasma-enhanced atomic layer deposition (PE-ALD) with varied PE-ALD cycle numbers on 3D carbon electrodes to achieve precise control of catalyst loading. A polycrystalline Cu metal layer was confirmed by grazing incidence X-ray diffraction. The catalyst surface morphology was probed by scanning electron microscopy and atomic force microscopy, highlighting the island-growth mode of the metal catalyst.

We demonstrate that Cu surfaces prepared by PE-ALD can reduce CO₂, forming value-added products such as carbon monoxide, methane, and ethylene. Parasitic hydrogen evolution was minimized to Faradaic efficiencies of ~10%, as quantified using *in situ* gas chromatography measurements. We further demonstrate a selectivity over 40% Faradaic efficiency for ethylene production, which is among the highest values reported to date in an H-cell geometry. Compared to evaporated Cu catalysts, we show significant methane suppression for the PE-ALD Cu. Finally, we demonstrated stability for up to 15 h for CO₂ reduction products with minimum loss in the ethylene production rate. In summary, we demonstrate CO₂RR using PE-ALD of Cu catalysts with high selectivity and stability, which provides a pathway to conformal deposition on 3D substrates with precise control of particle size and catalyst loading.

SESSION EN09.06: Fuel Cells—Membranes
Session Chairs: Jacques Huot and Michel Trudeau
Wednesday Afternoon, April 24, 2024
Room 337, Level 3, Summit

1:45 PM EN09.06.01

Pyrolysis of Conductive 2D Coordination Polymers for Use as Solid Acid Fuel Cell Electrode Materials James Ridenour¹, Bethany M. Hudak¹, Olga Baturina¹, Hannah Ashberry², William A. Maza¹, Brian Chaloux¹ and Albert Epshteyn¹; ¹US Naval Research Laboratory, United States; ²Former NRC Fellow - US Naval Research Laboratory, United States

The U.S. Department of Defense has shown great interest in the development of next-generation hydrogen-based energy systems that have long-term power-output, higher energy density, lower production and maintenance costs, and greater reliability [1]. In pursuit of those goals, solid acid fuel cells (SAFCs), which use solid acid electrolytic membranes (e.g. CsH₂PO₄) and operate at higher temperatures (150 – 300 C) compared to polymer electrolyte membranes (PEMs, <100 C), have shown great promise since their initial discovery two decades ago [2,3]. Yet, due to corrosive and reductive chemistries as well as the higher temperatures required, current electrode paradigms are ill-suited for direct translation from PEM fuel cells. SAFC electrodes need to be both thermally stable and chemically resistant to the corrosive environment of the solid acid electrolyte and fuel streams, porous to facilitate mass transport of fuels to the triple phase boundary, electrically conductive, and catalytic towards hydrogen oxidation or oxygen reduction. Metal-organic coordination polymers [4] are well suited for investigation as precursor compounds for SAFC electrode materials based on the requisite properties for SAFC electrodes. We have investigated several compounds as porous scaffold-like architectures suitable for pyrolysis in inert atmospheres to create metal-doped carbonized materials. These are highly electrically conductive and porous to facilitate nano-Pt catalyst impregnation and gas transport. Materials were characterized by powder X-ray diffraction and thermogravimetric analysis for bulk structure and stability and electrochemical impedance spectroscopy for electrical conductivity while pyrolysis was studied with TEM by *in situ* heating under vacuum. Pyrolysis of carbon-based coordination polymers generates carbonized materials with greater chemical stability and *in situ* TEM pyrolysis characterization was utilized to monitor thermally induced changes in the carbonized materials.

[1] Hydrogen fuel cells for Unmanned Systems, Briefing to: DOE Hydrogen and Fuel Cell Technical Advisory Committee, Washington DC https://www.hydrogen.energy.gov/pdfs/htac_mar19_06_swiderlyons.pdf (accessed October 10, 2023)

[2] S. M. Haile, C. R. I. Chisholm, K. Sasaki, D. A. Boysen, T. Uda, *Faraday Discussions*, 134, (2007) 17-39.

[3] D. A. Boysen, T. Uda, C. R. I. Chisholm, S. M. Haile, *Science*, 303, (2004) 68-70.

[4] L. S. Xie, G. Skorupskii, M. Dinca, *Chem. Rev.*, 120, 16, (2020) 8536-8580.

2:00 PM EN09.06.02

Investigation of Pt-Based Nanoparticle Degradation in Catalyst Layers through Automated Electron Tomography Lynda Amichi¹, Haoran Yu¹, Obaid Rahman¹, Amir Ziabari¹, Jose' D. Arregui-Mena¹, Laure Guetaz² and David Cullen¹; ¹Oak Ridge National Laboratory, United States; ²Commissariat à l'énergie atomique et aux énergies alternatives, France

Proton exchange membrane fuel cells (PEMFC) are promising devices for the deployment of hydrogen-powered heavy-duty vehicles, which provide higher efficiencies than internal combustion engine vehicles and similar driving ranges and fueling times. However, PEMFCs still encounter durability challenges, mainly due to catalyst degradation in the cathode. Mitigating these performance losses requires a better understanding of the degradation mechanisms under heavy-duty accelerated stress tests (ASTs) ¹. Electron tomography is a key tool for high-resolution three-dimensional analysis of Pt and PtCo nanoparticle spatial distribution to determine the rate and type of degradation as a function of position on the carbon support ².

In this work, we developed an automated electron tomography workflow performed in scanning transmission electron microscopy (STEM) mode and utilizing SerialEM ³ for data acquisition. We applied a super-voxel model-based iterative reconstruction with adaptive regularization (MBIR-ARAR) for artifact reduction ⁴ and performed segmentation of the nanoparticles and carbon using the commercial software Avizo. This workflow allowed us to

differentiate Pt-based nanoparticles located on the exterior of the carbon support from those within the pore structure, which enabled assessment of the relative stability of interior versus exterior nanoparticles.

In this study, the catalyst powder was scraped from electrodes and drop-cast on tomography TEM grids. We compared Pt and PtCo catalyst particle size distributions at the beginning of test (BOT) and end of test (EOT). The findings indicated a noticeable increase in particle size, regardless of location, and a significant portion of particles remaining within the carbon pores. Simultaneously, there is evidence of an expanding size distribution of closed pores after the AST, possibly stemming from carbon corrosion. These observed degradation mechanisms challenge the assumption that Pt dissolving primarily on the carbon support interior and re-depositing on the surface is a major contributor to ECSA decline, suggesting that factors such as carbon corrosion, dissolution of exterior nanoparticles, and/or particle coalescence also contribute to ECSA loss. This shows the importance of automating the electron tomography workflow, i.e., acquisition, reconstruction, and visualization, for increasing sampling and determining statistical parameters for the measurements. The outlook for utilizing low-dose cryo-tomography for limiting damage to the catalyst, support, and especially proton-conducting ionomer will be discussed ⁵.

References:

1. Cullen, D. A. *et al.* New roads and challenges for fuel cells in heavy-duty transportation. *Nat. Energy* **6**, 462–474 (2021).
2. Padgett, E. *et al.* Editors' Choice—Connecting Fuel Cell Catalyst Nanostructure and Accessibility Using Quantitative Cryo-STEM Tomography. *J. Electrochem. Soc.* **165**, F173 (2018).
3. Mastronarde, D. N. Automated electron microscope tomography using robust prediction of specimen movements. *J. Struct. Biol.* **152**, 36–51 (2005).
4. Ziabari, A. *et al.* Reducing Artifacts in BF and HAADF-STEM Images of Pt/C Fuel Cells using MBIR-ARAR. *Microsc. Microanal.* **29**, 1385–1387 (2023).
5. Girod, R., Lazaridis, T., Gasteiger, H. A. & Tileli, V. Three-dimensional nanoimaging of fuel cell catalyst layers. *Nat. Catal.* **6**, 383–391 (2023).

This material is based on work performed by the Million Mile Fuel Cell Truck (M2FCT) Consortium, technology manager Greg Kleen, which is supported by the U.S. Department of Energy, Office of Energy Efficiency and Renewable Energy, Hydrogen and Fuel Cell Technologies Office. Electron microscopy research was supported by the Center for Nanophase Materials Sciences (CNMS), which is a US Department of Energy, Office of Science User Facility at Oak Ridge National Laboratory.

2:15 PM EN09.06.03

Strategies Towards Low-Ir-Catalysts for PEM Electrolysis: From Support Material and Morphology to Depositing Iridium Oxide Melisande Kost¹, Markus Döblinger¹, Dina Fatthakova-Rohlfing² and Thomas Bein¹; ¹LMU Munich, Germany; ²FZJ, Germany

The transition from fossil fuel based and CO₂-intensive energy production to a future sustainable energy-based economy requires solutions for efficient energy conversion and storage for later re-electrification of green energy such as solar or wind power. One possibility is to convert energy from sustainable sources into chemical energy in the form of hydrogen by electrolysis of water. To meet this challenge, Proton Exchange Membrane (PEM) electrolysis is a powerful state-of-the-art technology that uses scarce iridium-based catalysts to promote the oxygen evolution reaction (OER). To improve the sustainability and economics of the PEM process, it is necessary to minimize the use of rare and precious iridium to reduce the overall density of iridium-based catalysts for the OER.

Here we present different strategies for the synthesis of low overall iridium OER catalysts. In addition to the choice of support material and support morphology, we also consider the coating strategy to produce highly active and durable catalysts.

The coating of corrosion-resistant high surface area metal oxide supports of various morphologies with an ultrathin layer of amorphous iridium hydroxide by a simple wet chemical synthesis at low temperature and ambient pressure or by a hydrothermal approach leads to the formation of interconnected amorphous hydrous iridium oxide particles. In a subsequent step, the amorphous phase is oxidized at elevated temperatures using an Adams fusion salt melt. This process allows for a controllable phase transformation and crystallization to form a layer of interconnected partially crystalline IrO₂ nanoparticles of ≈1.5 - 2 nm domain size on the surface of the supporting metal oxides, thus providing an electrical percolation path in the catalyst layer. The appropriate choice of support material in terms of crystal lattice parameters can modulate the crystal growth of the iridium oxide in terms of epitaxy and significantly increase the stability due to tight anchoring to the support. The final core-shell nanostructures comprise highly active iridium oxide with total Ir weight fractions as low as 7 at% on SnO₂ nanoparticles, compared to a state-of-the-art benchmark catalyst with 56 at% Ir supported on TiO₂ nanoparticles. Transmission electron microscopy (TEM) imaging was used to elucidate the impact of different core-shell designs, with a particular focus on iridium coating and crystallinity. Rotating disc electrode (RDE) measurements were also carried out to assess the electrochemical properties of each catalyst.

2:30 PM BREAK

SESSION EN09.07: Characterization and Mechanisms
Session Chairs: Nathalie Herlin-Boime and Michel Trudeau
Wednesday Afternoon, April 24, 2024
Room 337, Level 3, Summit

3:30 PM *EN09.07.01

Use of X-Ray, Synchrotron and Neutron Diffraction for The Development of Metal Hydrides Jacques Huot; UQTR, Canada

Metal hydrides are attractive solutions for hydrogen storage in a wide range of applications going from fuel cell submarine down to smart phones. In metal hydrides hydrogen is chemically bonded to other elements to form an alloy. Therefore, knowledge of the crystal structure of the metal hydride in its hydride and dehydrided state is essential. Conventional X-ray diffraction gives important information such as crystal structure, crystallite size, microstrains, etc. However, in-situ investigation of fast kinetics is basically impossible with this technique. Synchrotron radiation provides a large flux of photons that enable the recording of phase change of very fast hydrogenation/dehydrogenation kinetics. Unfortunately, X-ray diffraction is not suitable to locate the hydrogen atom in the crystal lattice. Neutron diffraction is practically the only technique that could give the localization of the hydrogen in a metal hydride. However, another synchrotron technique, the Extended X-Ray Absorption Fine Structure (EXAFS) could probe the local environment of each type of atoms.

In this talk, we will briefly discuss each of these techniques and give the advantages and inconvenience of each of them. Examples on the utilization of X-

ray, synchrotron and neutron diffraction for the development and fundamental understanding of metal hydrides will be given.

4:00 PM EN09.07.02

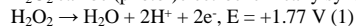
Selective Water Oxidation to H₂O₂ on TiO₂ Surfaces with Sub-Surface Redox-Active Allosteric Sites [Devan Solanki](#) and Shu Hu; Yale, United States

Hydrogen peroxide H₂O₂, is a versatile chemical with applications ranging from industrial to household use such as pulp bleaching, wastewater treatment, and sterilization. In addition to these established uses, H₂O₂ is emerging as a green energy carrier which can release 96 kJ *mol⁻¹ of energy via exothermic chemical decomposition with only water and oxygen as by-products. Currently, more than 95% of H₂O₂ produced globally originates from anthraquinone autooxidation. This process requires precious metal catalysts and expensive liquid-liquid extraction processes that are only feasible for large-scale chemical plants.

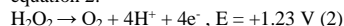
Electrochemical and photochemical syntheses are promising alternatives for distributed H₂O₂ production. H₂O₂ can be produced by 2e⁻ processes both via oxidatively, via water oxidation reaction (WOR) or reductively via oxygen reduction reaction (ORR). These approaches take advantage of abundant energy sources, i.e., renewable electrical or solar energy, and enables the storage of intermittent energy as the free energy of chemical bonds for distributed energy storage. In this work we focus on the water oxidation pathway.

Electrochemical Charge Transfer:

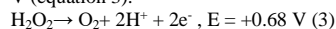
H₂O₂ can be (photo-)electrochemically synthesized via a two-electron (2e⁻) water oxidation pathway, as shown in equation 1.



However, existing catalysts often exhibit low faradaic efficiency (FE) due to the competitive four-electron (4e⁻) pathway of O₂ evolution reaction (OER) equation 2.



The thermodynamic driving force for OER is always at least +0.54 V greater than that of the 2e⁻ H₂O₂ pathway which can allow the undesired O₂ evolution pathway to overcome any kinetic barriers and dominate. In addition, the produced H₂O₂ can be over-oxidized to O₂ at an excess potential of at least +1.09 V (equation 3).



Thus, the partial oxidation of water to hydrogen peroxide presents a model system of a common challenge in catalysis where the desired product is kinetically feasible but thermodynamically unfavorable.

Conclusion:

In this work, we utilize X-ray Photoelectron Spectroscopy to quantify the presence of Mn(III) defect states within the TiO₂ band gap which are energetically aligned to peroxide generating reactive intermediates. During operation, the energy levels of CB and VB of TiO₂ are fixed, or “pinned”, at -0.05 and 3.29 VRHE, respectively, yet the empty states of the Mn defect states can precisely align with the energetics of H₂O₂ producing intermediates. Under a higher applied potential, i.e., +2.3 V, there would exist a moderate overpotential for the 2e⁻ water oxidation, but such a potential also enables the other pathways including 1e⁻ water oxidation to produce radicals, leading to an overall reduction in H₂O₂ production rates due to the reduced selectivity. Thus, this strategy of defect state tuning is best suited to low overpotentials, 90% at < 150 mV overpotentials was achieved for H₂O₂ production, accumulating 2.97 mM H₂O₂ after 8 hours. Nanoscale mixing of MnOx and TiOx resulted in a partially filled, highly conductive Mn intermediate band (IB) within the TiO₂ mid-gap to transport charge across the TiMnOx coating. This IB energetically matched that of H₂O₂-producing surface intermediates, turning a wide bandgap oxide into a selective electrocatalytic material that can operate in the dark.

4:15 PM EN09.07.03

Kinetic Mechanisms of M-N-C Electrocatalysts Saerom Yu, Zachary Levell and [Yuan Yue Liu](#); The University of Texas at Austin, United States

Single metal atoms embedded in nitrogen doped graphene (M-N-C) has attracted wide interest as electrocatalysts for various reactions. Although there have been many studies on the thermodynamic mechanisms (mostly based on computational hydrogen electrode model or its variants/derivations), the kinetic mechanisms are less understood partly due to the complexity of simulating reaction kinetics at electrochemistry interface. Using an advanced model developed recently in my group, I will show its application to elucidate the mechanisms of M-N-C for CO₂ reduction and oxygen reduction.

4:30 PM EN09.07.04

Synchrotron Radiation Characterization to Understand The Nature of Catalysts during Operation [Yan-Gu Lin](#); National Synchrotron Radiation Research Center, Taiwan

Catalysis has been tightly associated to X-ray spectroscopy from the very beginning, and this happy wedding is still holding and faithful. Catalysts studied at beamlines are quite a mirror of the needs of our society, reflecting current issues on global warming, oil shortage and economic struggles. In the recent years, the transition of dynamic atomic/electronic structure has been demonstrated to be induced by some external stimulus during catalysis, which enable one to potentially manipulate the unpaired electrons at the metal centers, thus directly influencing their dynamic structure as well as resulting nature. In this respect, the recent research trends have increasingly transferred from optimizing catalysts to making clear the real active species of the catalysts, especially understanding the underlying mechanisms behind these catalytic reactions. Abundant synchrotron-based X-ray spectroscopy methods, including in-situ/operando measurement have been developed and applied, offering nonnegligible characterization assistance to researchers in the field of catalysis, material and chemistry. Regarding the advanced in situ/operando approaches, ongoing characterization efforts employing X-ray absorption spectroscopy (XAS) particularly have successfully unveiled the potential-induced or photo-driven changes in local geometry of the active sites. In this talk, I will illustrate a part of the activities of the NSRRC beamlines through examples to show the establishment of the correlation between atomic/electronic structure and the catalytic properties. The experimental results demonstrate that the operando X-ray characterization provides the unique information for understanding the real reaction mechanism.

References

- [1] Peng, C.K.; Lin, Y.C.; Chiang, C.L.; Qian, Z.; Huang, Y.C.; Dong, C.L.; Li, J.F.; Chen, C.T.; Hu, Z.; Chen, S.Y.; [Lin, Y.G.](#); Zhang-Rice singlets state formed by two-step oxidation for triggering water oxidation under operando conditions. *Nature Communications*, 2023, 14, 529.
- [2] Lim, S.C.; Chiang, C.L.; Peng, C.K.; Wu, W.B.; Lin, Y.C.; Lin, Y.R.; Chen, C.L.; [Lin, Y.G.](#); Realizing the bifunctional electrocatalysis via local charge rearrangement of α -CrOOH-modulated Co@CoMoOx for overall water splitting. *Chemical Engineering Journal*, 2023, 452, 139715.
- [3] Li, Y.; Peng, C.K.; Hu, H.; Chen, S.Y.; Choi, J.; [Lin, Y.G.](#); Lee, J.M.; Interstitial boron-triggered electron-deficient Os aerogels for enhanced pH-universal hydrogen evolution. *Nature Communications*, 2022, 13, 1143.
- [4] Lin, Y.C.; Peng, C.K.; Lim, S.C.; Chen, C.L.; Nguyen, T.N.; Wang, T.T.; Lin, M.C.; Hsu, Y.J.; Chen, S.Y.; [Lin, Y.G.](#); Tailoring the Surface Oxygen Engineering of a Carbon-Quantum-Dot-Sensitized ZnO@H-ZnO_{1-x} Multijunction toward Efficient Charge Dynamics and Photoactivity Enhancement. *Applied Catalysis B: Environmental*, 2021, 285, 119846.

4:45 PM EN09.07.05

Revealing The Roles of Oxygen Vacancies in Single Atoms to Sub-Nanometers Scaled Metal Oxide Clusters for The Oxygen Reduction and

Hydrogen Evolution Reactions via *In-Situ* X-Ray Absorption Spectroscopy [Dinesh Bhalothia](#); National Tsing Hua University, India

Regardless of the well-explored role of oxygen vacancies in metal-oxide nanoparticles (NPs), oxygen vacancies have rarely been correlated with the dimensions of NPs. In this context, we report a systematic study to uncover the fundamental mechanisms between dimension effects and the catalytic activity of oxygen vacancies enriched cobalt-oxide (CoOx) from a single atom to sub-nanometer scale clusters. To demonstrate such a concept, we report a nanocatalyst (NC) comprising CoOx-clusters decorated Pd NPs on the Co-oxide support (denoted as CPCo). For the optimum case, a single Co atom with oxygen atoms (denoted as CPCo-1) delivers an unprecedented high mass activity (MA) of 4394 mA_{mgCo}⁻¹ at 0.85 V vs RHE and 426 mA_{mgCo}⁻¹ at 0.90 V vs RHE in alkaline oxygen reduction reaction (ORR) (0.1 M KOH), which surpasses the commercial J.M.-Pt/C (20 wt%) catalyst by 65-times. On top of that, the CPCo-1 NC exhibits remarkable durability in an accelerated durability test (ADT) with a progressively increased MA by 40 % (6,140 mA_{mgCo}⁻¹) as that of the initial condition after 20 k cycles. On the other hand, a sharp fall down in the catalytic performance is observed, when oxygen vacancies are created in CoOx species with increased dimensions. Through in-depth physical characterization, electrochemical analysis, and in-situ X-ray absorption spectroscopy (XAS), we demonstrated the conceptual framework of potential synergism between the oxygen vacancies enriched CoOx species and neighboring metallic Pd-sites. In this event, the surface-anchored CoOx species coupling with oxygen vacancies promotes the O₂ splitting, while the neighboring Pd-sites simultaneously trigger the O^{ads} relocation (i.e. OH⁻ desorption) step. In addition, the cobalt oxide support underneath assists the electron injection to surface Pd-sites.

SESSION EN09.08: Poster Session II

Session Chairs: Christopher Barile, Nathalie Herlin-Boime, Michel Trudeau and Edmund Chun Ming Tse

Wednesday Afternoon, April 24, 2024

Flex Hall C, Level 2, Summit

5:00 PM EN09.08.01

Enhancing Energy Efficiency in Bicarbonate Electrolysis through The Development of an Au-NiO-CNT Catalyst for Glycerol Oxidation [Dohee Kim](#)¹, [Hyeonuk Choi](#)¹, [Hojung Lee](#)², [Yoonyoung Kim](#)³, [Eunui An](#)¹, [Youngkook Kwon](#)² and [Jihun Oh](#)¹; ¹Korea Advanced Institute of Science and Technology, Korea (the Republic of); ²Ulsan National Institute of Science and Technology, Korea (the Republic of); ³Korea Institute of Energy Research, Korea (the Republic of)

Reducing emitted CO₂ through direct air capture is crucial to mitigate climate change. Bicarbonate electrolysis is a method that facilitates CO₂ reduction by utilizing bicarbonate generated from aqueously captured CO₂, ultimately yielding syngas or CO as a product. However, the overall energy efficiency of bicarbonate electrolysis is impeded by the high theoretical voltage associated with the oxygen evolution reaction (OER) occurring at the anode. To enhance energy efficiency and bolster the economic viability of this process, it is important to design reactions and catalysts that can simultaneously produce valuable products at the anode while reducing operating voltage.

Here, we proposed a novel cell architecture that combines biomass upgrading, glycerol oxidation (GEOR) for glycolic acid (GCA) production with bicarbonate electrolysis. GCA serves as a monomer for bio-plastics, Poly(lactic-co-glycolic acid) (PLGA), but its current production relies on fossil fuels. In this work, to achieve sustainable GCA production via GEOR, we introduced Au catalyst design that incorporates NiO support and multi-walled carbon nanotubes (MWCNTs) to enhance the selectivity of GCA production through a synergy effect. We then successfully demonstrated that the addition of 4 wt% MWCNTs on Au-NiO catalyst leads to a remarkable achievement of 36% GCA selectivity and 28% glycerol conversion at 0.9 V (V vs. RHE) and 2 h in 0.1 M glycerol and 1 M KOH for GEOR. This showed that a 4.6-fold increase in glycerol conversion and a twofold increase in GCA production compared to the conventional Au-CB catalyst. Additionally, by controlling MWCNT ratio of Au-NiO catalyst, it showed that the amount of Au-NiO catalyst required to achieve 10% glycerol conversion at 0.9 V (V vs. RHE) was reduced by 20 wt%. We conducted operando raman analysis to gain mechanistic insights. Our findings suggested that during GEOR, the NiO support undergoes a transformation into Ni(OH)₂, and introduction of MWCNTs on NiO promotes formation of Ni(OH)₂. Additionally, our electrochemical impedance spectroscopy (EIS) indicated that MWCNTs improve the electrical conductivity of NiO, which could facilitate Ni(OH)₂ formation. Therefore, we demonstrated that the reaction between adsorbed glycerol on Au and Ni-OH transformed on the NiO support, resulting in enhanced conversion of glycerol to GCA. Finally, by combining bicarbonate electrolysis, we achieved an H₂/CO ratio of about 2.34 through bicarbonate electrolysis and a GCA selectivity of 26% through GEOR at 200 mA/cm². This accomplishment confirms the successful development of an efficient system, proficiently yielding valuable compounds at both electrodes.

5:00 PM EN09.08.02

Zirconium Phosphate Layered Nanomaterials as Supports for Earth-Abundant Electrocatalysts for The Oxygen-Evolution Reaction [Jorge L. Colón](#)¹, [Yannelly A. Serrano-Rosario](#)¹, [Sebastián Muñoz-Torres](#)¹, [Daniella M. Gibson-Colón](#)¹, [Biao Liu](#)¹, [Gabiella A. García-Machado](#)¹, [Antonio Torres-López](#)², [Louise M. Defebve](#)² and [Christopher J. Pollock](#)²; ¹University of Puerto Rico at Río Piedras, United States; ²Cornell University, United States

We are studying new applications of layered zirconium phosphate (ZrP) inorganic nanomaterials [1]. The θ phase of ZrP can be directly ion-exchanged with metal complexes and catalysts, producing intercalated phases useful for artificial photosynthesis schemes for water splitting, amperometric biosensors, and drug delivery applications. Recently, we have demonstrated improved electrocatalytic activity of ZrP nanomaterials loaded with metal ions suitable for the oxygen evolution reaction of water splitting. Electrocatalysts have been incorporated as intercalated species, surface bound, on exfoliated layers, and on nanoparticles of different morphologies (hexagonal platelets, cubes, rods, and spheres). Single and bimetallic electrocatalysts based on earth-abundant materials have been studied. Reduction in overpotentials and increases in mass activity have been achieved. Mixed metal NiFe-intercalated ZrP electrocatalysts at 90% Fe metal content proved to have superior OER electrocatalytic performance (decreased overpotentials, increased mass activities, reduced Tafel slopes) compared to adsorbed counterparts. We have recently prepared CoFe electrocatalysts systems and again the intercalated bimetallic system is more active than the surface-adsorbed one. We are starting to work also with Mn electrocatalysts. We are exploring OER activities of other mixed-metal catalysts on ZrP, bifunctional catalysts, and operando synchrotron X-ray absorption spectroscopy studies to elucidate the nature of the active species. We are also exploring efficient solar H₂ production using these supports.

Reference

[1] M. V. Ramos-Garcés; J. González-Villegas; A. López-Cubero; J. L. Colón. New Applications of Zirconium Phosphate Nanomaterials. *Acc. Mater. Res.* **2021**, 2, 793-803. DOI: 10.1021/accountsmr.1c00102.

5:00 PM EN09.08.04

Superior CO₂ Electroreduction Performance on Co-Ni-Nitrogen Bimetallic Sites [Jianping Chen](#) and [Weining Wang](#); Virginia Commonwealth University, United States

The electrochemical reduction of carbon dioxide (CO₂ ECR) plays a crucial role in transitioning towards a sustainable energy and chemical industry. This process has the potential to not only address the rising CO₂ levels but also utilize it as a resource to produce valuable fuels and chemicals. Electrocatalysts are essential in CO₂ ECR, as their ability to selectively and efficiently convert CO₂ offers significant environmental and economic benefits. Our research, focusing on nanostructured electrocatalysts for energy applications, introduces an innovative nanostructured catalyst that represents a significant advancement in CO₂ ECR technology for energy generation and conversion.

Regarding CO₂ ECR, a wide range of catalysts including metals, alloys, metal oxides, functionalized carbons, and metal complexes have been studied for their effectiveness. Despite their remarkable CO₂ conversion capacity, challenges such as sub-optimal energy efficiency, varying activity levels, and undesired hydrogen evolution reactions (HER) present significant obstacles. Addressing these challenges, our study introduces a novel electrocatalyst featuring diatomic metal-nitrogen sites (Co-Ni-N-C). This catalyst is synthesized through a unique process involving ion exchange using a zeolitic imidazolate framework (ZIF) as a precursor, followed by pyrolysis. This method results in nitrogen-doped graphitic carbon, effectively anchoring the Co-Ni bimetallic active sites.

This work highlights the potential of nanostructured single-atom catalysts (SACs) and dual-active site catalysts (DASCs) in CO₂ ECR. Transition metal SACs, such as Ni-SAC on nitrogen-doped graphene, have previously shown promising results in CO₂ conversion efficiency. However, our Co-Ni-N-C catalyst takes a step forward by demonstrating a CO yield rate of 53.36 mA mg cat.⁻¹ and a CO Faradaic efficiency of 94.1% at an overpotential of -0.27 V. This performance showcases that Co-Ni-N₆ moiety plays a crucial synergistic role in promoting and sustaining these exceptional ECR activities. Spectroscopic, microscopic, and density functional theory analyses collectively reveal the synergistic role played by the Co-Ni-N₆ moiety in enhancing catalytic activity. This synergy is crucial in promoting and sustaining exceptional ECR activities. The findings not only emphasize the effectiveness of nanostructuring in electrocatalyst design but also shed light on the pathways for developing various advanced catalysts for sustainable energy conversion. Therefore, our study offers a novel perspective in the field of CO₂ ECR, opening new avenues for the development of efficient, nanostructured catalysts for energy applications.

5:00 PM EN09.08.05

High-Entropy Alloy Nanocrystals with Controlled Compositions and Surface Structures for Catalytic Applications Younan Xia; Georgia Institute of Technology, United States

We recently developed a robust method for the facet-controlled synthesis of nanocrystals with an ultrathin shell made of a nearly equimolar RuRhPdPt quaternary alloy. Our strategy involves the use of well-defined Rh cubic seeds, halide-free precursors, and a method for precisely controlling the reaction kinetics of different precursors. In the setting of dropwise addition, the precursors with different reactivities can be reduced at about the same pace for the generation of an alloy with a uniform and well-controlled composition. The core-shell nanocubes show greatly enhanced activity toward ethanol oxidation when benchmarked against Pd and Pt counterparts. Combining *in situ* and *ex situ* electron microscopy studies, we also demonstrate that the core-shell nanocubes possess good thermal and electrochemical stability in terms of both geometrical shape and elemental composition, with their cubic shape and alloy composition retained when annealing at 500 °C or after long-term electrochemical cycling. It is expected that the synthetic approach can be further extended to fabricate multi-metallic catalysts with enhanced activities toward a variety of thermal and electrochemical reactions.

5:00 PM EN09.08.06

Engineering Efficient Electrocatalysts: Non-Precious Bimetallic ZIF-Based Hybrid Nanocomposites for Oxygen Reduction Reaction Mahshid Mokhtarnejad, Erick Ribeiro, Dibyendu Mukherjee and Bamin Khomami; The University of Tennessee, United States

Synthesis of metal oxides/metal-organic frameworks (MOFs) into hybrid nanocomposites (HNCs), wherein transition metals combined with carbon (C) matrices, due to the excellent conductivity and high porosity present an attractive and cost-effective alternative for engineering electrocatalysts used for oxygen reduction reaction (ORR) in anion exchange membrane fuel cells (AEMFCs). To that end, improving the performance of these materials by adjusting their composition, structure, size, and morphology through an efficient synthesis process is of great technological importance. In this context, the Laser Ablation Synthesis in Solution in Tandem with Galvanic Replacement Reaction (LASiS-GRR) technique is employed as a fast, facile, and green approach for the synthesis, and precise control of complex hierarchical bimetallic Zeolitic Imidazolate Framework (ZIF) structures. Specifically, this novel one-pot, two-step LASiS-GRR process allows for the optimization and of the composition, structure, size, and morphology of Co-based MOFs encapsulated within Zn-based porous MOF crystals “dubbed” Co/ZIF-67@Zn/ZIF-8. The pyrolytic post-processing of these crystals leads to the development of HNCs exhibiting superior ORR electrocatalytic performance in AEMFCs. Overall, this research not only sheds light on the impact of two distinct salt precursors on particle size and morphology during LASiS but also showcases the exceptional performance and stability of post-pyrolytic (ZnO/ZIF@C) HNCs in AEMFC applications as non-precious ORR electrocatalysts when compared to state of art Pt- and platinum-group metals (PGM)-based electrocatalysts.

5:00 PM EN09.08.07

Biaxial Strained MoS₂ Nanoshells with Controllable Layers Boost Alkaline Hydrogen Evolution Tao Zhang; Nanyang Technological University, Singapore

Strain in layered transition-metal dichalcogenides (TMDs) is a type of effective approach to enhance the catalytic performance by activating their inert basal plane. However, compared with the traditional uniaxial strain, the influence of biaxial one and TMDs layer number on local electronic configuration remains unexplored. Herein, via a new *in situ* self-vulcanization strategy, we realize biaxial strained MoS₂ nanoshells in the form of single-crystalline Ni₃S₂@MoS₂ core-shell heterostructure, where the MoS₂ layer is precisely controlled between 1 to 5 layers. In particular, the electrode with bilayer MoS₂ nanoshells shows a remarkable hydrogen evolution reaction activity with a small overpotential of 78.1 mV at 10 mA cm⁻², and negligible activity degradation after durability test. Density Functional Theory calculations reveal the contribution of optimized biaxial strain together with the induced sulfur vacancies, and identify the origin of superior catalytic sites in these layer-resolved MoS₂ nanoshells. This work highlights the importance of the atomic-scale layer number and multiaxial strain in unlocking the potential of two-dimensional TMDs electrocatalysts.

5:00 PM EN09.08.08

Unleashing the Full Potential of Heterostructured Nickel-Cobalt Phosphate for Optically Active High-Performance Asymmetric Quasi-Solid-State Supercapacitor Devices Nageh K. Allam; American University in Cairo, Egypt

The rational design of hybrid systems that combine capacitor and battery merits is crucial to enable the fabrication of high-energy and power-density devices. However, the development of such systems remains a significant barrier to overcome. Herein, we report the design of a Ni-Co phosphate (Ni_{3-x}Co_x(PO₄)₂·8H₂O) nanoplatelet-based system via a facile coprecipitation method at ambient conditions. The nanoplatelets exhibit multicomponent synergy, exceptional charge storage capabilities, rich redox active sites (ameliorating the redox reaction activity), and high ionic diffusion rate/electron transfer kinetics. The designed Ni_{3-x}Co_x(PO₄)₂·8H₂O offered a respectable gravimetric specific capacity and marvelous capability rate (966 and 595 C g⁻¹ at 1 and

15 A g⁻¹) over the Ni₃(PO₄)₂·8H₂O (327.3 C g⁻¹) and Co₃(PO₄)₂·8H₂O (68 C g⁻¹) counterparts. Additionally, the nanoplatelets showed enhanced photoactive storage performance with a 9.7% increase in the recorded photocurrent density. Upon integration of Ni_{3.4}Co_x(PO₄)₂·8H₂O as a positive pole and commercial activated carbon as a negative pole, the constructed hybrid supercapacitor device with PVA@KOH quasi-gel electrolyte exhibits great energy and power densities of 77.7 Wh kg⁻¹ and 15998.54 W kg⁻¹ with remarkable cycling stability of 6000 charging/discharging cycles and prominent Coulombic efficiency of 100%. Interestingly, two assembled devices are capable of glowing a red LED bulb for nearly 180 s. This research paves the way to design and fabricate electroactive species via a facile approach for boosting the design of a plethora of supercapattery devices.

5:00 PM EN09.08.09

Optimized V-Doped Defective TiO₂/α-(Fe₂O₃)_{1-x}(Cr₂O₃)_x Heterojunctions for Photo-Assisted Supercapacitor Devices: Insights on the Materials Integrity and Dual Conversion-Storage Mechanism [Nageh K. Allam](#); American University in Cairo, Egypt

Energy conversion and storage integrated power units suffer from multiple engineering issues. Replacing two devices (solar cell and supercapacitor assembly) with one device (photo-enhanced supercapacitor- PSC) requires materials with emerged dual solar-electrochemical storage attributes. Herein, a propitious approach is developed to fabricate all visible light-enhanced semisolid flexible PCS. Nanoflakes-based p-n junction α-(Fe₂O₃)_{1-x}(Cr₂O₃)_x photocathode is synthesized directly on industrial waste stainless steel mesh (316L-SS). Alongside, three TiO₂-based electrodes are utilized as positive photoactive electrodes. Tuning the optical properties of TiO₂ is displayed via doping with mixed valence vanadium (V⁴⁺/V⁵⁺) together with thermal hydrogen annealing. This is revealed via the reduction of the bandgap energy from 2.89 to 2.15 eV, which can be ascribed to the induced oxygen vacancies. The device can sustain up to 1.6 V potential window with 91% stability after 350 successive charge/discharge cycles with the possibility of performance regeneration to its 100% retention. An illustration of the photo-storage mechanism is proposed based on the X-ray photoelectron spectroscopy, X-ray crystallography, and band position/alignment results. Quasi-reversible water splitting/formation is concluded as the main storage mechanism in the semisolid state electrolyte under illumination conditions.

5:00 PM EN09.08.10

Fe-Single-Atom Catalysts on Nitrogen-Doped Carbon Nanosheets for Electrochemical Conversion of Nitrogen to Ammonia [Nageh K. Allam](#); American University in Cairo, Egypt

Electrochemical nitrogen reduction reaction (NRR) has been established as a promising and sustainable alternative to the Haber–Bosch process, which requires intensive energy to produce ammonia. Unfortunately, NRR is constrained by the high adsorption/activation of the N₂ energy barrier and the competing hydrogen evolution reaction, resulting in low faradic efficiency. Herein, a well-dispersed iron single-atom catalyst was successfully immobilized on nitrogen-doped carbon nanosheets (Fe_{SAC}-N-C) synthesized from pre-hydrothermally derived Fe-doped carbon quantum dots with an average particle size of 2.36 nm and used for efficient electrochemical N₂ fixation at ambient conditions. The as-synthesized Fe_{SAC}-N-C catalyst records an onset potential of 0.12 V_{RHE}, exhibiting a considerable faradic efficiency of 23.7% and an NH₃ yield rate of 3.47 μg h⁻¹ cm⁻² in aqueous 0.1 M KOH electrolyte at a potential of -0.1 V_{RHE} under continuous N₂ feeding conditions. The control experiments assert that the produced NH₃ molecules only emerge from the dissolved N₂-gas, reflecting the remarkable stability of the nitrogen–carbon framework during electrolysis. The DFT calculations showed the Fe_{SAC}-N-C catalyst to demonstrate a lower energy barrier during the rate-limiting step of the NRR process, consistent with the observed high activity of the catalyst. This study highlights the exceptional potential of single-atom catalysts for electrochemical NRR and offers a comprehensive understanding of the catalytic mechanisms involved. Ultimately, this work provides a facile synthesis strategy of Fe_{SAC}-N-C nano-sheets with high atomic dispersion, creating a novel design avenue of Fe_{SAC}-N-C that can vividly have potential applicability in the large spectrum of electrocatalytic applications.

5:00 PM EN09.08.11

3D Vertical Graphene Nanofibers with High Defect Density and Nitrogen Doping for Electrocatalytic Hydrogen Evolution Reaction [TaeGyeong Lim](#)¹, [Sang Ho Shin](#)¹ and [Ji Won Suk](#)^{1,2}; ¹Sungkyunkwan University, Korea (the Republic of); ²Sungkyunkwan University Advanced Institute of NanoTechnology, Korea (the Republic of)

The production of clean hydrogen using water electrolysis is a crucial element in achieving sustainable energy production and utilization systems.[1] A key challenge in attaining sustainable hydrogen production via water electrolysis lies in the development of suitable electrocatalyst materials for the hydrogen evolution reaction (HER), aiming to replace conventional noble-metal-based electrocatalysts with earth-abundant alternatives.[2] Graphene-based materials have emerged as promising candidates for metal-free electrocatalysts due to their exceptional electrical conductivity, high specific surface area, and chemical stability.[3] The electrocatalytic performance of graphene-based materials has notably advanced with the introduction of heteroatom doping or defects.[4,5]

In this study, we synthesized three-dimensional (3D) vertical graphene nanofibers (VGNFs) with unique 3D structures, serving as metal-free electrocatalyst for HER. The freestanding 3D VGNF sheets were synthesized via facile and scalable processes employing the electrospinning method combined with thermal chemical vapor deposition. The 3D VGNFs exhibited high defect density and nitrogen doping, which are favorable traits for enhancing electrocatalytic HER. In addition, they displayed hierarchical pore structures with high specific surface area. Therefore, the 3D VGNFs demonstrated outstanding HER performance, presenting a low overpotential and robust stability when evaluated in a 0.5 M H₂SO₄ acidic solution.

[1] Huang, Huajie, et al., *Adv. Mater.*, 31, 1903415, 2019.

[2] Huang, You-guo, et al., *Int. J. Hydrog. Energy*, 41, 3786-3793, 2016.

[3] Ali, Asad, and Pei Kang Shen., *Carbon Energy*, 2, 99-121, 2020.

[4] Jiao, Yan, et al., *Nat. Energy*, 1, 1-9, 2016.

[5] Jia, Yi, et al., *Adv. Mater.*, 28, 9532-9538, 2016.

5:00 PM EN09.08.12

Impact of Surface Defects like Vacancies and Dopants on The Design of Energy-Efficient Ag Nanoparticle/Ligand-Based Catalysts for Electroreduction of CO₂ [Asmita Jana](#), [Jin Qian](#) and [Ethan Crumlin](#); Lawrence Berkeley National Laboratory, United States

Capture and subsequent conversion of CO₂ to value-added chemicals is a promising strategy to tackle the increase in CO₂ concentrations in the atmosphere. CO₂ electroreduction to CO is often the first step in such a conversion, necessitating the design of effective electrocatalysts that can not only produce CO with high selectivity but also do so energy-efficiently. The Ag-Nanoparticle/Ordered Ligand Interlayer (Ag-NOLI) catalyst produces CO at high selectivity. However, to achieve the catalytically active phase, the material needs to be biased to a large negative potential. Thus, any effort to create the catalytically active phase at lower magnitudes of negative potential can pave the way towards designing a more energy-efficient catalyst. We used density functional theory calculations to engineer the Ag surface by introducing vacancies, and Cu and Ag dopants, evaluated the relative energies of all the configurations, and computed the transition potentials needed to get to the catalytically active phase. We found that while introducing Ag vacancies and Cu dopants increase the magnitude of the transition potential, the opposite is seen with Au dopants, making Au dopants a suitable design modification.

Moreover, while Cu increases the stability of all the phases compared to Ag, Au decreases it. The source of this Cu < Ag < Au energy trend was evaluated and we found that the ligand-surface interaction was the most prominent contributor compared to other interactions in the system. Finally, we found that the trend in the ligand-surface interaction energy can be attributed partially to the intrinsic chemical interaction between the surface and ligand atoms, by investigating systems where the geometry of the topmost layer was kept fixed. Overall, this Cu < Ag < Au energy trend can be ascribed partially to the electronegativity differences with O, making it an important descriptor in the design of energy-efficient Ag-NOLI-based catalysts.

5:00 PM EN09.08.13

Thermodynamic Prediction of Gas-Solid Reactions for the Synthesis of Transition Metal Carbides Catalysts Sang-Ho Oh¹, Dohun Kim², Ji-Yong Kim¹, Geosan Kang¹, Jooyoung Jeon¹, Miyoung Kim¹, Young-Chang Joo¹ and Dae-Hyun Nam²; ¹Seoul National University, Korea (the Republic of); ²Daegu Gyeongbuk Institute of Science and Technology, Korea (the Republic of)

Transition metal carbides have garnered significant attention due to their extensively adjustable physicochemical characteristics based on their structure, phase, and polymorph, making them highly versatile in a broad spectrum of electrochemical applications owing to their unique d-band electronic structures. Nevertheless, the synthesis of metal carbides and the precise control of their phases and structures present formidable challenges. In comparison to other metal compounds like oxides, sulfides, and phosphides, metal carbides exhibit the highest Gibbs free energy of formation (ΔG°), indicating the lowest inclination for synthesis. Additionally, the formation of metal carbides requires stringent processing conditions due to the preferential oxidation of metals in the presence of atmospheric oxygen. Typically, metal carbides are generated through carburization and carbothermic reduction using methane and graphite. However, the sluggish kinetics of carbon (C)-induced reactions demand elevated temperatures, leading to undesired sintering and aggregation. Moreover, an excessive supply of C sources inevitably results in coke encapsulation and precipitation.

In this work, we describe an approach for the predictive synthesis of nanostructured Mo carbides, achieved by steering the equilibrium reactions involving oxocarbons (carbon monoxide (CO) and carbon dioxide (CO₂)) during the calcination process. Oxocarbons engage in two equilibrium reactions: the Boudouard reaction ($2CO(g) \leftrightarrow CO_2(g) + C(s)$) and the CO/CO₂ redox reaction ($2CO_2(g) \leftrightarrow 2CO(g) + O_2(g)$). This phenomenon allows for concurrent C–O reactions (selective C combustion) and Mo–C interactions (Mo carbide formation) within the nanofibers, serving as a framework for the initiation and growth of Mo carbides. This process enables precise manipulation of the phases and structures of Mo compounds. Since inducing selective redox reactions in multi-atomic systems like Mo–C–O poses significant challenges, requiring considerable trial and error in experimentally determining process variables. Hence, the specific prediction of processing parameters becomes imperative.

We successfully established processing windows for nanoscale carbide synthesis by thermodynamically forecasting oxocarbon-mediated gas-solid reactions. By computing ΔG° for Mo compound formation, we present a method for discovering specific processing windows to control the phases of diverse Mo compounds. Concurrently, the extent of selective C combustion is anticipated through pO₂ calculations to regulate the porosity of C nanofibers and diffusion behavior of Mo. By utilizing the thermodynamically predicted processing window, we not only controlled a wide range of Mo phases (MoO₂, α -MoC_{1-x}, and β -Mo₂C) but also manipulated various nanostructures (nanoparticle, spike, stain, and core-shell) by steering diffusion during the phase synthesis process in the Mo compounds/C nanofibers.

Moreover, to confirm the connections between material and properties in nanostructured Mo carbides, we examine their catalytic performance in the hydrogen evolution reaction (HER). Our results demonstrate a performance achievement, with an overpotential of 152 mV @ 10 mA cm⁻¹, accomplished through the formation of active nano-spikes of Mo₂C on C nanofibers. We expect that the predictions of element supply and spontaneous reactions will offer valuable insights to researchers involved in the synthesis and structural manipulation of diverse catalysts based on transition metal compounds.

5:00 PM EN09.08.15

Ammonia-Fueled Proton Ceramic Fuel Cells with Atomic Layer Deposited Palladium Catalysts Joon Hyung Shim; Korea University, Korea (the Republic of)

The study investigates the efficacy of protonic ceramic fuel cells (PCFCs) operating in an ammonia-fuel environment, focusing on enhancing their performance. PCFCs, known for lower operational temperatures, faced limitations in ammonia decomposition rates, which were remediated by introducing a catalyst. Specifically, treating the PCFC anode with a palladium (Pd) catalyst resulted in remarkable improvements. Compared to untreated counterparts, the treated PCFCs exhibited a substantial increase in performance, achieving a peak power density over 0.3 W/cm² at 500 °C, nearly doubling the output. The process involved depositing Pd catalysts via atomic layer deposition onto the anode surface, where a blend of nickel oxide and BaZr_{0.2}Ce_{0.6}Y_{0.1}Yb_{0.1}O_{3- δ} facilitated Pd penetration into the porous interior. This treatment significantly enhanced current collection and notably reduced polarization resistance, particularly evident at lower temperatures, ultimately bolstering overall performance. Importantly, impedance analysis confirmed the catalyst's role in augmenting the current flow and mitigating resistance, contributing to the observed improvements. Moreover, stability tests showcased the treated PCFCs' superior durability compared to untreated samples, suggesting the catalyst's role in enhancing long-term stability. These findings underscore the potential of this methodology as a promising avenue for achieving high-performance and resilient PCFCs in the context of ammonia injection environments. In summary, the study's approach of integrating a Pd catalyst into PCFCs operating under ammonia injection demonstrates substantial enhancements in performance, particularly at lower temperatures. The catalyst deposition technique enhances current collection, reduces resistance, and significantly improves durability, marking a significant stride toward realizing high-performing and stable PCFCs in ammonia-based energy systems.

5:00 PM EN09.08.16

Interplay of Oxygen and Sulphur Surface Sites in Controlling OER Kinetics on Cobalt Electrocatalyst supported on Porous 3-D Porous Hard Nanocarbons Subham Yadav and Chandramouli Subramaniam; Indian Institute of Technology Bombay, India

Hydrogen being a clean fuel has gained worldwide attention for improving its greener production pathways to meet energy demands. Electrocatalysis proven to be efficiently producing H₂ and O₂ via water splitting which has its own limiting step. Oxygen evolution reaction (OER) due to the involvement of 4e⁻ transfer in alkaline media. Transition metal oxides/oxyhydroxides are widely explored electrocatalysts for OER. Herein, we explored Cobalt sulphide nanoparticles with surface oxygen sites (Co_xS_yO^{*}) supported on nanocarbon floret (NCF) as electrocatalyst for OER. Interplay of these surface sulphur and oxygen sites in water splitting kinetics has been studied by comparing pristine and modifying the catalytic surface (by varying the ratio of oxygen and sulfur sites) via electrochemical impedance spectroscopy, linear sweep voltammetry. The lowest overpotential ~ 350 mV and charge transfer resistance (R_{ct} ~ 21 Ω @ 1.6 V vs RHE) observed with using pristine Co_xS_yO^{*}@NCF catalysts. The results indicates significance of synergetic role of oxygen and sulphur sites for efficient water splitting.

5:00 PM EN09.08.17

Plasma-Treated 1D Transition Metal Dichalcogenides for Efficient Hydrogen Evolution Reaction Alex Laikhtman¹, Arie Borenstein², Alla Zak¹ and Asmita Dutta³; ¹Holon Institute of Technology (HIT), Israel; ²Ariel University, Israel

Significant research endeavours have been dedicated to the search for highly efficient and cost-effective electrocatalysts for the Hydrogen Evolution Reaction (HER). Tungsten disulphide (WS₂) nanotubes were previously demonstrated for electrocatalysis performances owing to their unique chemical structure and physical properties. In this study, we report a new method of surface modification through cold radiofrequency (RF) plasma. The effect of

two plasmonic ions (D_2^+ and Ar^+) on WS_2 nanotubes has been investigated. The plasma-treated samples showed improved performances in HER electrocatalysis. Based on experimental results, both Ar and D_2 plasma treatments, when performed separately, show similar effects on electrocatalysis performances with improved HER overpotentials of 348 and 343 mV at $-10\text{mA}/\text{cm}^2$ compared to 567 mV of the pristine WS_2 nanotubes. On the other hand, combined treatment by Ar and then by D_2 radio frequency plasma notably decreases the overpotential to 264 mV. Hydrogen is considered a promising alternative for energy production due to its high energy density, high calorific value, and zero environmental effect of combustion products. To avoid the risk of the continuous exploitation and increased consumption of fossil fuels, the efficient and sustainable electrocatalysts for HER is required.

Among all the known HER catalysts, Pt-group metals have been utilized as the most effective electrocatalysts for HER in an acidic medium. However, the low abundance and high cost considerably limit its large-scale application. The preferred electrocatalyst material should lower the activation energy so the process consumes less energy at fast reaction kinetics of the HER.

Two-dimensional transitional metal dichalcogenides (TMDs) are an emerging class of materials with advantageous properties for a wide range of applications such as nanoelectronics, nanophotonics, sensing, etc. Due to the very distinctive characteristics such as robustness, low cost, ease of intercalation, and accessibility to structural modification, this group of compounds exhibit excellent electrochemical characteristics. WS_2 is a representative member of the TMD family. One-dimensional (1D) WS_2 nanotubes are extensively studied for their unique structural and electronic properties. Among other applications, WS_2 nanotubes demonstrated efficient catalytic performance for HER. WS_2 nanotubes feature unique physical and chemical behavior originating from the lattice strain raised by the tubular curvature. Yet, this specific class of pristine inorganic nanotubes possesses fewer active sites and thus eventually suffers from the low affinity of WS_2 nanotubes for proton adsorption. Among different methods, plasma treatment was reported to modify the surface of WS_2 nanoparticles effectively. Low-power RF plasma treatment increases the number of disordered sites at the surface layer and produces atom vacancies, thus significantly enhancing energy conversion performance. Herein, we demonstrate the surface modification of WS_2 nanotubes by plasma treatment. This plasma modified WS_2 nanotubes used as catalyst reveal improved HER performance.

To summarise, we have successfully formed plasma-treated WS_2 nanotubes, which provides a high concentration of active catalytic sites for electrocatalytic reaction. As a result, the HER catalytic activity of all the treated samples significantly improved compared to pristine WS_2 nanotubes. Plasma treatment induces material modification by creating defects and disorders of the nanotube surface. Additionally, RF plasma treatment helps the incorporation of oxides hydrophilic groups inside the system, which promotes fast electron transfer. The effective lowering of overpotential for HER activity was achieved due to the simple, scalable, cost-effective, and less time-consuming plasma treatment on of the semiconductive WS_2 nanomaterial, demonstrates efficient and stable HER electrocatalytic performance.

5:00 PM EN09.08.18

An Improved Non-Enzymatic Glucose Sensor Using a Simple Metal Ion Tuning in Nickel-Aluminum Layered Double Hydroxides [Sreejesh Moolayadukkam](#), Priyanka Datta, Dhruvajyoti Chowdhury and Ishwar K. Puri; University of Southern California, United States

Lifestyle diseases, such as Diabetic Mellitus where patients cannot process glucose effectively, are an increasing cause of human mortality. Glucose molecules in food and the human bloodstream are typically determined with relatively expensive enzyme-based sensors that are error prone due to enzyme degradation. Non-enzymatic sensors do not experience enzyme instability and offer an inexpensive alternative, but competing electrochemical reactions due to dissociation of water molecules at the electrode can lead to inaccurate measurements. Hence, new sensors must be designed with new materials that have accurate glucose adsorption and electrocatalytic performance. Layered double hydroxides (LDHs) with tunable skeletons and multiple metal ions are interesting candidates. We design and test non-enzymatic glucose sensors with nickel-aluminum LDHs, which are hydrothermally synthesized with Ni:Al ratios of 1:1, 3:1, and 4:1. X-ray diffraction (XRD) and scanning electron microscopy (SEM) morphological studies confirm the formation of pure LDH phases. The most robust glucose sensing occurs with the 3:1 metal ion ratio while the 1:1 ratio produces poorest sensing with the 4:1 ratio producing an intermediate result. Through chronoamperometry (CA), the sensor shows good sensitivity ($31.206\ \mu\text{A}\ \mu\text{M}^{-1}\ \text{cm}^{-2}$) and selectivity against common interfering species, and a response time lower than 4s. We demonstrate that sensing capabilities can be enhanced using simple engineered materials to develop high-performing non-enzymatic glucose sensors.

5:00 PM EN09.08.19

Enhancing Ammonia Production Rate from Electrochemical Nitrogen Reduction by Modifying Cu Catalyst and Three-Phase Boundary [Jeehye Kim](#)^{1,2}, Ji Hee Jang³, Mathieu Doucet¹, Hanyu Wang¹, Youn Jeong Jang³ and Jae Sung Lee²; ¹Oak Ridge National Laboratory, United States; ²Ulsan National Institute of Science and Technology, Korea (the Republic of); ³Hanyang University, Korea (the Republic of)

Ammonia (NH_3) is a critical component in fertilizer and other essential industrial chemical production, making it the second largest synthetic chemical worldwide (> 200 million tons). However, the traditional Haber-Bosch process requires massive energy input and results in the emission of a large amount of carbon dioxide [1,2].

The electrochemical nitrogen reduction reaction (eNRR) driven by renewable electricity under mild condition emerges as a sustainable method for NH_3 production to minimize carbon footprint [3,4]. We are focusing on the development of an effective eNRR system using Cu-based electrocatalysts in gas diffusion electrode (GDE) system with modification of three-phase interfaces. To overcome the low affinity of Cu for N_2 , phosphorus activation was applied to create electron-deficient Cu sites for better N_2 adsorption and activation. Additionally, we address the limited solubility of nitrogen in aqueous electrolytes by incorporating a GDE coated with polytetrafluoroethylene (PTFE). This setup optimizes the three-phase interfaces among water, gaseous N_2 , and the catalyst. Our innovative approach in a flow-type cell achieves a Faradaic efficiency of 13.15% and an ammonia production rate of $7.69\ \mu\text{g}\ \text{h}^{-1}\ \text{cm}^{-2}$ at $-0.2\ \text{V}_{\text{RHE}}$. This represents a 59.2-fold increase in NH_3 production rate compared to electrodeposited Cu electrodes, highlighting the potential of our strategies in practical systems [3].

[1] Y. Zeng, C. Priest, G. Wang, G. Wu, Restoring the Nitrogen Cycle by Electrochemical Reduction of Nitrate: Progress and Prospects, *Small Methods*, 4 (2020) 2000672.

[2] B. Yang, W. Ding, H. Zhang, S. Zhang, Recent Progress in Electrochemical Synthesis of Ammonia from Nitrogen: Strategies to Improve the Catalytic Activity and Selectivity, *Energy Environ. Sci.*, 14 (2021) 672-687.

[3] J. Kim, C.H. Lee, Y.H. Moon, M.H. Lee, E.H. Kim, S.H. Choi, Y.J. Jang, J.S. Lee, Enhancing Ammonia Production Rates from Electrochemical Nitrogen Reduction by Engineering Three-Phase Boundary with Phosphorus-Activated Cu Catalysts, *J. Energy Chem.*, 84 (2023) 394-401.

5:00 PM EN09.08.20

Non-Noble Metal Oxide (WO_3), Sulfide (MoS_2) and Carbide (MoC) for Electro and Photoelectrocatalytic Hydrogen Evolution Reactions [Jae-Jin Shim](#), Muhammed Shafi Parasseeri and Al Mahmud Abdullah; Yeungnam University, Korea (the Republic of)

Nonprecious transition metal electrocatalysts are cost-effective, possess catalytic solid performance, and are scalable for hydrogen generation via water splitting, which provides clean and sustainable energy. Developing an efficient catalyst for hydrogen evolution reaction (HER) based on metal oxide, sulfide, and carbide has been studied worldwide to replace the expensive noble metal PtC. In this work, selected oxide, sulfide, and carbide (WO_3 , MoS_2 , and MoC), together with other metal compounds, have been studied. The 2D molybdenum disulfide is a challenge because of the restacking of MoS_2 layers, which leads to insufficient access to active sites. In this study, the drawbacks of 1T MoS_2 catalyst were overcome by employing carbon nano-onion

(CNO). This CNO-MoS₂ exhibited an excellent HER performance with an overpotential of 53 mV vs. RHE and a Tafel slope of 40.8 mV dec⁻¹ for over 25 h, showing it one of the best HER catalysts next to platinum. 3D core-shell heterostructures of WO₃/Bi₂MoO₆/Co-Pi and BiVO₄/MoS₂ were also synthesized using hydrothermal synthesis/ electrodeposition and electrodeposition/plasma-enhanced atomic layer deposition (PEALD). The former hetero-photocatalyst exhibited significantly high photoelectrochemical activity, where its photocurrent efficiency was 4.6 times greater than that of the constituent WO₃. For the BiVO₄/MoS₂ photoelectrode, an optimal thickness of the MoS₂ layer was controlled by the number of PEALD cycles. The highest photocurrent (2.1 mA cm⁻²) was produced from the electrode with a 6 nm layer-thickness, 2.4 times higher than the pristine BiVO₄. Thermal pyrolysis created a carbon-encased, nitrogen-rich γ -MoC/NiC composite that contains rGO. The overpotential at 10 mA cm⁻², of γ -MoC/NiC@rGO for HER is 185 mV, whereas it is 298 mV for OER. The Tafel slopes for HER and OER are relatively modest, at 78 and 80 mV dec⁻¹, respectively. This study highlights a new, highly stable, highly performing non-noble metal catalyst for electrochemical water splitting applications.

SESSION EN09.09: Batteries and Supercapacitors
Session Chairs: Nathalie Herlin-Boime and Cédric Tard
Thursday Morning, April 25, 2024
Room 337, Level 3, Summit

8:30 AM *EN09.09.01

Organic Chemistry—A Tool for Improved Performance of Lithium Secondary Batteries [Charlotte Mallet](#); Hydro Quebec, Canada

Hydro-Québec's Center of Excellence in Transportation Electrification and Energy Storage has been a world-class innovation hub in the field of battery materials for electric vehicles as well as other energy storage applications for more than 40 years. The Center's efforts are primarily focused on advanced lithium-ion batteries and solid-state batteries. Its know-how, extensive intellectual property portfolio and cutting-edge facilities draw interest from around the world and make it an essential partner for major industry players involved in the development of next generation battery materials and technologies.

This presentation will outline our major breakthroughs leveraging our strong expertise in organic chemistry. By dint of multidisciplinary team, our work is rooted in understanding degradation phenomena of battery systems and aims to provide solutions based on the structure-property relationships of materials, which resulted in 40 patents with new concepts since 2015.

To tackle the challenges related with high voltage cathodes like LMFP or NMC, we developed new additives to protect electrolyte-cathode interface and limit degradation phenomena such as transition metal dissolutions^{1,2} or electrolyte side reactions.³ In addition, we developed new binders or co-binders to improve low temperature applications, increase C-rate performance,⁴ and polymers to eliminate different types of gas by in-situ trapping.⁵ Our works include synthesis of new kind of salts for liquid and solid lithium batteries.⁶ We also developed new organic cathode materials with high operation voltage up to 4.5V, and high specific capacity of 692 mAh/g. The cycle life was tested with polymer electrolyte system at 40°C.⁷ Finally, another major project is protection of lithium metal anode by different organic compound deposition method like spray-coating or solution casting. This protective organic layer stabilized Li metal interface providing enhanced performance with various electrolyte chemistries such as liquid, polymer, and sulfide electrolyte.⁸ The organic and polymer chemistry team of center of excellence has developed a lot of creative solutions to address a wide range of issues such as stability, efficiency, low temperature performance and low cost.

1. C. Mallet, J.-C. Daigle, S. Rochon and K. Zaghbi, Hydro-Quebec, Murata Manufacturing Co., Ltd. 2020 Patent Number: WO2020034031
2. Mater. Adv., 2021, 2, 253-260
3. C. Mallet, S. Rochon and K. Zaghbi, Hydro-Quebec, Murata Manufacturing Co., Ltd. 2020 Patent Number: WO2020069619
4. K. Zaghbi, M. Beaupre, C. Mallet, J.-C. Daigle, Y. Asakawa and S. Uesaka, Sony Corporation, Hydro-Quebec 2019, WO2019006560
5. Scientific Reports (2020, 10, 10305)
6. C. Mallet, S. Rochon, A. Lafleur-Lambert, S. Uesaka and K. Zaghbi, Hydro-Quebec, Sony Corporation 2018, WO2018176134
7. J.-C. Daigle, A. Lafleur-Lambert, S. Rochon, Y. Asakawa, C. Mallet and K. Zaghbi, Hydro-Quebec, Murata Manufacturing Co., Ltd. 2019, WO2019210411
8. C. Mallet, S. Verreault, J. Pronovost, S. Rochon, J.-C. Daigle, K. Amouzegar, et al., Hydro-Quebec, Murata Manufacturing Co., Ltd. 2020, WO2020034036

9:00 AM EN09.09.02

A Systematic Study of NiCo Layered Double Hydroxide Grown on Porous Carbon for Hybrid Supercapacitor Electrodes: Growth Method, Morphology and Composition [Geonho Kim](#), Dongjun Kim and Jiwon Kim; Yonsei University, Korea (the Republic of)

Supercapacitors have drawn an extensive attention for their high power density and excellent cycling stability to meet a rapidly growing demand for high-capacity energy storage systems. Specifically, metal (e.g., Ni, Co, Fe, Al, Mn, and its combinations) layered double hydroxides (LDHs) have been integrated to supercapacitor electrodes owing to their seamless ion transport through interlayer. LDHs are often hybridized with conductive materials to facilitate charge transport since low conductivity of LDHs hinders the supercapacitors to reach their theoretical capacitance (e.g., ~3,000 F g⁻¹ for pristine NiCo LDH). Although diverse forms of LDH hybridized carbon electrodes are designed, it has not yet been systematically studied how morphology and composition simultaneously affect the performance of supercapacitors.

Accordingly, we have systematically controlled the synthetic method/condition of growing metal LDHs on nitrogen doped porous carbons (NPCs) and studied their effects on electrical performance as hybrid electrodes of supercapacitors. In detail, various metals (i.e., Ni, Co, and NiCo) have been deposited on NPCs by both electrodeposition (i.e., 100, 300, 500, and 1000 mC) and solvothermal method. NPC was chosen as carbon electrodes since it can improve the rate performance as well as structural stability of electrodeposited LDHs owing to its higher conductivity, specific surface area, and hydrophilicity compared to other carbon-based materials with free-standing structure for electrodeposition compatibility. The supercapacitor with electrodeposited NiCo LDH@NPC electrodes exhibited higher specific capacitance than those of either Ni or Co LDH@NPC electrodes, since coexistence of metals shows a synergistic effect on storing higher energy via multiple reduction-oxidation (redox) reactions. Among NiCo LDH@NPC electrodes, the electrode with the total deposited charge of 500 mC (NiCo500 LDH@NPC) showed the highest capacitance of 3,155.52 F g⁻¹. These results might be ascribed to three main factors: (i) multiple redox reactions from Ni-Co coexistence, (ii) shortened hydroxide (OH⁻) ion diffusion length due to the uniform distribution of LDH in nanomesh structure, and (iii) facilitated OH⁻ ion accessibility into active materials owing to broader interlayer of LDH. Furthermore, an asymmetric supercapacitor (NPC||NiCo500 LDH@NPC) achieved energy density of 39.22 Wh kg⁻¹ at a power density of 913.87 W kg⁻¹ and 80.00% retention after 20,000 cycles.

9:15 AM EN09.09.03

Microwave Synthesis for Trimetallic Needle Structures coupled with N-Doped Carbon for Highly Boosted Bifunctional Oxygen Catalysts for Zn–Air Batteries [Hoyoung Jang](#), Youngsun Cha and Wonjoon Choi; Korea University, Korea (the Republic of)

Energy storage systems play a crucial role in expanding the capabilities of sustainable energy sources and addressing existing energy issues associated with environmental pollution concerns. While versatile renewable energy sources have been developed over the past decade, their large-scale implementation inherently requires the use of highly efficient yet robust energy storage solutions. Metal-air batteries have recently been attracting attention as a promising candidate for next-generation storage cells due to their high theoretical capacity and eco-friendly use of oxygen. Among various types of metal-air batteries, the Zn-air battery has notably demonstrated a high theoretical energy density of 1860 Wh/kg, while ensuring cost-effective production, safety, and environmental compatibility. The primary emphasis in the development of rechargeable Zn-air batteries has been on improving stability and energy efficiency. The challenge of achieving high energy efficiency lies in the substantial overpotential of the constituent materials, which impacts the effectiveness of both the oxygen reduction reaction (ORR) and the oxygen evolution reaction (OER). Noble metal-based electrocatalysts such as Pt/C and Ir/C exhibit remarkable electrochemical performances in ORR and OER. However, its widespread application is limited due to its high cost and stability issue.

In this work, we report a facile synthesis route of trimetallic bifunctional catalysts with N-doped carbon, with their low overpotential and high stability comparable to precious metals. The formulation of the precursor solution is conducted by precisely mixing 0.3 M iron nitrate hexahydrate ($\text{Fe}(\text{NO}_3)_3 \cdot 6\text{H}_2\text{O}$), 0.3 M nickel nitrate hexahydrate ($\text{Ni}(\text{NO}_3)_2 \cdot 6\text{H}_2\text{O}$), 0.3 M cobalt nitrate hexahydrate ($\text{Co}(\text{NO}_3)_2 \cdot 6\text{H}_2\text{O}$), 1.2 M urea ($\text{CO}(\text{NH}_2)_2$), and 0.4 M ammonium fluoride (NH_4F) in 100 ml of deionized (DI) water. The melamine foam was soaked in this solution and it was subjected to heating in an oven at 130 degrees Celsius for a duration of 5 h as an integral step in the synthesis process. Then, the catalyst is directly fabricated using microwave heating for 20 seconds at 1000 W power. Scanning electron microscopy images illustrate the morphology transition of the catalysts at each stage of the synthesis process. Optimizing the microwave heating exposure leads to the creation of uniform metal oxides, as validated through transmission electron microscopy analysis. The composition and chemical state of the elements constituting the catalyst surfaces are precisely examined using X-ray photoelectron spectroscopy and X-ray powder diffraction.

The electrochemical performance of the developed catalysts is examined using a potentiostat in a three-electrode electrochemical cell with a rotating ring disk. The optimized trimetallic (Fe-Ni-Co) catalysts exhibit a low overpotential (0.071 V), similar to that of Pt/C and Ir/C. Under the full cell test, the catalysts obtain stable performances for 300 h in repetitive charge/discharge cycles for an hour interval, and the specific capacitance reaches 769 mAh g⁻¹ at 10 mA cm⁻². We believe that this rational synthesis strategy toward a facile fabrication process will contribute to developing novel active materials with mesoporous structure and large surface area, potentially useful for diverse electrochemical energy storage systems. Furthermore, the outcome of this work will inspire novel design of high performance electrocatalysts and other energy-related hybrid materials using transition metals.

9:30 AM *EN09.09.04

Confining Highly Redox-Active Atoms in Stable Insertion-Type Anode Materials for Alkali Metal-Ion Batteries [Dominic Bresser](#); Karlsruhe Institute of Technology, Germany

The unique combination of exceptional energy and power density along with the continuous decrease in cost have made lithium-ion batteries the electrochemical energy storage technology of choice for small-scale and large-scale applications.^[1–3] However, the use of graphite as active material for the negative electrode is intrinsically limiting the possibility to rapidly charge these batteries.^[4] Herein, a new class of active materials is presented that provides comparable charge storage capacities at much faster rates. This new class of materials is based on the introduction of highly redox-active atomic centers into stable metal oxide host structures. These host structures are well preserved upon continuous lithium cation insertion and deinsertion following a solid-solution-type mechanism, while the introduction of these highly redox-active atomic centers allows for the duplication and triplication of the charge storage capacity compared to the nanoparticulate metal oxide host structures alone. Remarkably, the redox centers are reversibly reduced to the metallic state at the atomic level without affecting the surrounding crystal structure. When replacing lithium cations by sodium or potassium cations, essentially the same mechanism is observed, apart from the expected “size effect”, highlighting the exceptional versatility of this new class of battery electrode materials.

References

- [1] B. Scrosati, J. Garche, *Journal of Power Sources* **2010**, *195*, 2419.
- [2] B. Nykvist, M. Nilsson, *Nature Clim. Change* **2015**, *5*, 329.
- [3] M. Armand, P. Axmann, D. Bresser, M. Copley, K. Edström, C. Ekberg, D. Guyomard, B. Lestriez, P. Novák, M. Petranikova, W. Porcher, S. Trabesinger, M. Wohlfahrt-Mehrens, H. Zhang, *Journal of Power Sources* **2020**, *479*, 228708.
- [4] J. Asenbauer, T. Eisenmann, M. Kuenzel, A. Kazzazi, Z. Chen, D. Bresser, *Sustainable Energy Fuels* **2020**, *4*, 5363.

10:00 AM BREAK

SESSION EN09.10: HER, OER and ORR Reactions I
Session Chairs: Dominic Bresser and Edmund Chun Ming Tse
Thursday Morning, April 25, 2024
Room 337, Level 3, Summit

10:45 AM EN09.10.01

Balancing Volmer Step by Dual-Active Domains for Electrocatalytic H₂ Formation [Jinsong Zhou](#)^{1,2}; ¹City University of Hong Kong, China; ²ETH Zürich, Switzerland

The reaction kinetics of hydrogen evolution reaction (HER) is primarily determined by balancing the Volmer step in alkaline/neutral media. The bifunctional effect as a proposed strategy divides the reaction process of water dissociation and intermediates ad-/de-sorption. However, sluggish OH⁻ desorption plagues water re-adsorption, leading to the active domain's poisoning effects. In addition, some active sites may even directly act as spectators and do not participate in the reaction. The activity comparison under approximate nanostructure between bifunctional effect and single-functional-domain is not fully understood.

We adopted a facile three-step strategy to successfully grow MoS₂ on cobalt-containing nitrogen-doped carbon nanotubes (Co-NCNTs), forming obvious dual-active domains. The active domains of Co-NCNTs and MoS₂, with the tuned electronic structure at the heterointerface, trigger the bifunctional effect

to balance the Volmer step and boost the catalytic activity. The HER driven by the bifunctional effect could significantly optimize the Gibbs free energy of water dissociation and hydrogen adsorption, resulting in fast reaction kinetics and superior catalytic performance.

11:00 AM EN09.10.02

The Effect of C₆₀ Support on The Electrochemical Activity of Pd and Pt Particles [Sergey Kozlov](#), Mohammed Aliasgar and Fernando Buendia; National University of Singapore, Singapore

Engineering nanoparticle-support interactions is a powerful strategy for improving the activity and stability of heterogeneous catalysts. In this contribution, we show how such interactions can also improve the electrocatalytic performance of Pd and Pt nanoparticles. First, we demonstrate how the interactions between Pt nanoparticles and C₆₀ nanosheets lead to higher catalyst activity in alkaline hydrogen evolution reaction (HER) compared to unsupported Pt nanoparticles or Pt nanoparticles on graphene [1]. The nanoscale roughness of the C₆₀(110) support surface helps to stabilize ~2 nm large crystalline Pt particles between appropriately spaced rows of C₆₀ molecules. Our density functional (DFT) simulations reveal the strong polarization of electron density on the interface between similarly sized Pt particles and the C₆₀(110) surface due to the transfer of ~2 electrons from each particle to the support. The polarized electron density on the Pt/C₆₀ interface results in a significant variation of H binding energies, which are known to govern the HER activity of the catalyst. Curiously, our microkinetic modeling shows that such variation dramatically increases the rate of both Volmer, Heyrovsky, and Tafel steps by up to 100 times on the interface sites and decreases HER overpotential by almost 0.1 V at 10 mA/cm² under alkaline conditions, in line with experimental observations. The calculated simultaneous acceleration of both Volmer and Heyrovsky steps indicates that the introduced diversity of the active sites on the nanoparticle-support interface effectively allowed us to overcome the limitations of Sabatier activity volcano for hydrogen evolution reaction on transition metals. Moreover, the interactions between metal nanoparticles and fullerene support can also affect the phase transitions in the former. For example, we show how nanoparticle-support interactions alter the onset electrode potential for β-hydride formation in Pd nanoparticles, which notably changes their electronic structure and catalytic properties. As a result, the activities of Pd/C₆₀ catalysts in HER and CO₂ reduction reactions significantly differ from those of unsupported Pd nanoparticles.

References:

[1] Chen, Aliasgar, Buendia, Zhang, Zhao, Lian, Wen, Yang, Sun, Kozlov, Chen, Wang, *Diversity of platinum-sites at platinum/fullerene interface accelerates alkaline hydrogen evolution*, **Nat. Commun.** 2023, 14, 1711

11:15 AM EN09.10.03

Bifunctional Nickel Cobalt Phosphorus Sulfide Electrocatalyst for Simultaneous Hydrogen Evolution and 5-Hydroxymethylfurfural Oxidation Kuan-Mei Hung and Jih-Jen Wu; National Cheng Kung University, Taiwan

The replacement of the O₂ evolution reaction of electrocatalytic water splitting with a thermodynamically more favorable reaction has attracted considerable attention for simultaneous value-added feedstock formation coupled with H₂ production. The electrocatalytic oxidation of renewable biomass platform chemical 5-hydroxymethyl furfural (HMF) to 2,5-furandicarboxylic acid (FDCA), a valuable bio-monomer of polyethylene furanoate (PEF), has emerged as a promising sustainable route for biomass valorization. In this work, bifunctional nickel cobalt phosphorus sulfide nanosheet arrays (NCPS) were constructed on Ni foams as the electrodes of a two-electrode electrolytic H cell for simultaneous electrocatalytic hydrogen evolution and HMF oxidation (HMFOR) to FDCA in 0.1 M KOH. With the addition of 5 mM HMF in the electrolyte, the cell voltage required to afford the current density of 10 mA cm⁻² is less 153 mV than water electrolysis. It indicates the superior energy conversion efficiency of NCPS for electrocatalytic HER and HMFOR compared to water splitting. The amounts of H₂ and FDCA produced over NCPS in the two-electrode configuration were measured at a constant cell voltage of 2.12 V (the anode potential of 1.6 V vs. RHE) for 78 min to pass the charge of ~34.8 C. In the anodic chamber of the H cell, the HMF conversion is 95.01%, and the selectivity for forming FDCA is 89.06% with the Faradaic efficiency of FDCA is 86.83%. The generated H₂ in the cathodic chamber reaches a Faradaic efficiency of 96.07%. The XPS analyses indicate that the Ni²⁺/Ni³⁺ and Co²⁺/Co³⁺ ratios in the NCPS couples alter after the HER and HMFOR, suggesting that the Ni and Co sites play crucial roles in the electrocatalytic reactions. The influences of chemical and electronic structures on the electrocatalytic activity of NCPS will be discussed in this presentation.

11:30 AM EN09.10.04

Bimetallic Fe/Co Sites for Oxygen Reduction Reaction [Xin Li](#)^{1,2,3} and Michael K. Leung¹; ¹City University of Hong Kong, Hong Kong; ²Tsinghua University, China; ³University College London, United Kingdom

Double atom catalysts (DACs), featuring dual metal atoms dispersed on supports, provide innovative avenues for accelerating the sluggish kinetics of the oxygen reduction reaction (ORR). In this study, we have engineered a double-atom metal site consisting of iron (Fe) and cobalt (Co) anchored within a triazine-based covalent organic framework (Fe/Co-COF) with different Fe/Co ratios. This framework is derived from the assembly of 4,4'-(1,3,5-triazine-2,4,6-triyl) trianiline and ace-naphthenequinone monomers, resulting in a highly π-π conjugated structure. The COF structure incorporates two adjacent =N- groups, each featuring a lone pair that can coordinate with Fe and Co. We assessed the ORR performance in an O₂-saturated 0.1 M KOH electrolyte, where the Fe₂/Co₁-COF catalyst, with Fe at 1.27wt% and Co at 0.65wt%, exhibited a remarkable half-wave potential (E_{1/2}) of 0.95 V (vs RHE). Moreover, it displayed impressive durability, enduring 100,000 voltage cycles with only a 25 mV E_{1/2} loss. This performance outstrips that of commercial Pt/C catalysts and virtually all other reported single atom-based catalysts. The improved activity is ascribed to the higher metal loading, a synergistic catalytic mechanism, and the presence of more intricate and adaptable active sites on the Fe/Co-COF surface.

Highlights:

In the realm of electrocatalysis, single atom catalysts (SACs) have garnered significant attention, particularly those with the metal-N-C structure. However, standard EXAFS fitting struggles to differentiate metal-C/N/O coordination, raising doubts about whether N truly coordinates with metal. In our work, ex-situ vtc-XES measurements were employed, confirming the coordination of Fe-N and Co-N.

We conducted *in-situ* X-ray Absorption Near Edge Structure (XANES) measurements to uncover the real active sites and determine the changes in metal electronic and coordination structures under the conditions of the oxygen reduction reaction. Our findings unveil the presence of synergistic Fe-N and Co-N active sites in Fe₂/Co₁-COF, demonstrating a mutually beneficial effect on overall ORR performance.

11:45 AM EN09.10.05

Photocatalysis and Photosensitization Using Atomically Precise Metal Nanoclusters for Solar Energy Harvesting and Conversion [Nicola Pinna](#), Yu Wang and Ye Liu; Humboldt-Universität Berlin, Germany

Metal nanoclusters (NCs) with atomic precision are a unique family of metal nanomaterials that are readily crystallized into single crystals, representing ideal models to unravel structure-property relationship at atomic level. By tuning the number of metal atoms in the core, the composition and the protecting ligand of metal NCs, their physicochemical properties can be precisely controlled. The strong, broad light absorption ability and the long-lived excited

states make metal NCs promising candidates as photosensitizer, and might replace traditional dyes. Their discrete energy levels allow them to prevent charge recombination at the semiconductor by efficiently separate the photoinduced charge carriers. Moreover, these metal NCs themselves can act as active catalysts. In the first part of the talk, we demonstrate the differences of working principle between metal NCs and their particle counterparts in photocatalytic system. The metal NC modified TiO₂ catalyst is found to exhibit a five times higher performance than TiO₂ modified with metal nanoparticles in the photocatalytic H₂ production reaction.^[1] In the second part, we present the strategy to tune the charge transfer pathways of metal NCs sensitized semiconductors in photoelectrochemical system. While metal NCs serve as catalyst for oxidation reactions when loaded on n-type semiconductor, they serve as catalyst for reduction reactions when loaded on p-type semiconductor.^[2] In the last part, we will use Au₂₅ NC as an example to demonstrate how the protecting ligand and the composition of the metal NC influence the overall performance of a NC/semiconductor system in photocatalytic H₂ production.^[3]

[1] Wang, Y.; Liu, X.-H.; Wang, Q.; Quick, M.; Kovalenko, A. S.; Chen, Q.-Y.; Koch, N.; Pinna, N. *Angew. Chem. Int. Ed.* **2020**, *59*, 7748-7754.

[2] Wang, Y.; Liu, X.-H.; Wang, R.; Cula, B.; Chen, Z.-N.; Chen, Q.-Y.; Koch, N.; Pinna, N. *J. Am. Chem. Soc.* **2021**, *143*, 9595-9600.

[3] Liu, Y.; Wierzbicka, E.; Springer A.; Pinna N.; Wang, Y. *J. Phys. Chem. C* **2022**, *126*, 1778-1784.

SESSION EN09.11: HER, OER and ORR Reactions II
Session Chairs: Sophie Cassaignon and Sandrine Lyonnard
Thursday Afternoon, April 25, 2024
Room 337, Level 3, Summit

1:30 PM EN09.11.01

Interfacial Engineering of RuO_x on Rutile TiO₂ Supports to Boost the Acidic Oxygen Evolution Reaction Hyunseok Yoon and Dong-Wan Kim; Korea University, Korea (the Republic of)

As global concerns about crises such as climate change and fossil fuel depletion increase, the importance of hydrogen energy is being further emphasized. In particular, there is growing interest in the commercial feasibility of using polymer electrolyte membrane water electrolysis (PEMWE) for large-scale production of green hydrogen. However, there are significant obstacles to overcome, mainly related to the slow kinetics of the acidic oxygen evolution reaction (OER) that occurs at the anode. Ruthenium (Ru)-based materials (e.g. RuO₂), which are much more abundant and have relatively high OER activity, are very attractive alternatives to rare iridium (Ir)-based materials such as IrO₂, the most commercialized acidic OER catalyst. Nonetheless, Ru has a critical drawback in that it is easily over-oxidized and dissolved as a soluble species (Ru³⁺) under acidic OER operating conditions. Therefore, additional research is required to find solutions to this issue. In this study, we tried to develop a highly efficient and durable Ru-based acidic OER electrocatalyst, employing interfacial engineering. Ruthenium oxide (RuO_x) nanoparticles were coated on the surface of one-dimensional (1D) rutile TiO₂ nanofibers using a facile hydrothermal method. Introducing rutile TiO₂ as a support is advantageous in enhancing the OER stability and promoting an interfacial affinity with the catalyst due to its excellent corrosion resistance and the common crystal structure sharing with RuO_x. Notably, the size, morphology, and crystallinity of Ru species crystal grains on the TiO₂ surface changed depending on the pH conditions during the reaction process. When RuO₂ was grown in the form of a large nanosheet with high crystallinity through alkaline pretreatment (RT-NSs), it was less affected by strain effect and showed OER performance with no significant difference from general RuO₂. On the other hand, in the case of a sample composed of a small nanoparticle film on a TiO₂ support synthesized in an acidic solution (RT-NPs), the interfacial synergy with TiO₂ was maximized, showing excellent OER activity. Finally, we achieved enhanced acidic OER performance by improving stability through a low-temperature post-annealing process.

Acknowledgement:

This work is supported by the National Research Foundation of Korea (NRF) Grant funded by the Ministry of Science and ICT [NRF-2020R1A6A1A03045059].

1:45 PM EN09.11.02

Effective Catalysts Design for Selective OER in Seawater Sharafadeen Gbadamasi, Suraj Loomba, Muhammad Haris, Muhammad Waqas Khan and Nasir Mahmood; RMIT University, Australia

The oxygen evolution reaction (OER), a significant half-reaction in electrocatalytic water splitting to produce green hydrogen, has received considerable research attention. Currently, state-of-the-art water splitting technology utilises the expensive and scarce noble metal-based catalysts and freshwater, a limited resource, as it constitutes less than 1% of the world's total water. To this end, alternative feedstocks, such as seawater, need to be explored, which account for approximately 96.5% of the world's total water.

In recent years, research on developing efficient catalysts for seawater has been gaining significant attention. However, the complex nature of seawater and the presence of dissolved ions like chloride ions (Cl⁻) have made seawater splitting more challenging. The Cl⁻ ions can induce electrode corrosion and have the capacity to engage in competing reactions with the oxygen evolution reaction (OER) at the anode. This necessitates developing highly active electrocatalysts that are exclusively selective towards OER and possess long-term stability. Based on this, I have developed a two-dimensional heterostructure catalyst that achieved 2 A before 2V, was stable for over 500 h and was exclusively OER selective in natural seawater. The catalyst benefits from the synergistic effects between the component 2D materials and strong electronic interactions between them.

2:00 PM *EN09.11.03

Electrochemical Activity of Iridium Oxides for OER: Porosity, Crystallinity and Nanocages Cédric Tard¹, Silvia Duran¹, Marine Elmaalouf², Andrea Zitolo³, Benedikt Lassalle³, Cédric Boissière⁴, Marco Faustini⁴, Marion Giraud² and Jennifer Peron²; ¹Ecole Polytechnique, France; ²Université Paris-Cité, France; ³Synchrotron Soleil, France; ⁴Sorbonne Université, France

Iridium oxide is still considered the superior material for the oxygen evolution reaction (OER) in acidic environment, as it maintains both high activity and stability, making it the benchmark material for green hydrogen production.^[1] Despite the numerous studies describing the activity of IrO₂ materials for the OER, it is crucial to have a thorough understanding of its functional principles in order to optimize and rationalize its utilization. Towards this objective, we have been able to produce porous iridium-based mixed oxides using aerosol chemistry via a sol-gel process,^[2] to decouple the electronic processes from the structural transformations.^[3] Indeed, the oxidation of iridium from IrO₂ occurs upon calcination, but is not related to the crystallization of the material itself. The measurements demonstrate that short-range ordering, corresponding to sub-2nm crystal size, is controlling the activity of the materials. This is the case regardless of the initial oxidation state and composition of the calcined iridium oxides, as evidenced by XAS, XRD and XPS measurements. Regarding other types of porous materials, we have also been able to prepare hierarchical structures of IrO₂ based on Pearson's hard and soft acid-base

theory and characterize their outstanding activity toward the OER.^[4]

[1] Chatenet, M. *et al.*, *Chem. Soc. Rev.* **2022**, *51*, 4583–4762.

[2] a) Faustini, M. *et al.*, *Adv. Energy Mater.* **2019**, *9*, 1802136; b) Duran, S. *et al.*, *ChemElectroChem* **2021**, *8*, 3519–3524.

[3] Elmaalouf, M. *et al.*, *Nat. Commun.* **2021**, *12*, 3935.

[4] Elmaalouf, M. *et al.*, *Chem. Sci.* **2022**, *13*, 11807–11816.

2:30 PM BREAK

3:00 PM EN09.11.04

Investigation of Active Factors for Oxygen Reduction Reaction by Titanium Oxide Model Electrode Takahiro Saida, Miyu Mashiyama and Takahiro Maruyama; Meijo University, Japan

Polymer electrolyte fuel cells (PEFCs) are one of the low-environmental-impact power sources. However, the broad commercialization of PEFCs has been slow. One reason for this is that the electrocatalyst of PEFCs is the high manufacturing cost and low durability. Titanium oxide-based catalysts have attracted attention as the candidate for low-cost and highly durable electrocatalysts. Titanium oxide-based catalysts need to address the drawback of poor catalytic activity.

Currently, introducing the oxygen vacancies and doping the other metal atoms are known to enhance the oxygen reduction-reaction (ORR) activity on titanium oxide. Generally, the catalytic reaction progresses at the low coordination site on the surface. Introducing oxygen vacancies leads to an increase in low-coordination sites, which means increasing the activity sites. As a result, the ORR activity of titanium oxide is improved by introducing oxygen vacancies. In addition, the oxygen vacancy changes the electron structure of titanium oxide and provides electron conductivity. From the results of the DFT calculation, it was reported that the low-coordination metal site, which was formed by oxygen vacancy, and the neighborhood structural oxygen played an important role in ORR. On the other hand, the structural analysis results using the pair distribution functions (PDFs) method using X-ray showed that the active site was related to the crystal distortion site and no confirmed oxygen vacancies. One of the problems in titanium oxide-based catalysts is that the active site and reaction mechanism are still unclear. For this reason, the design of new catalysts must rely on rules of thumb. Clarifying the active control factor for ORR on titanium oxide is one of the effective approaches to the high activity close to platinum-based catalysts.

In this study, a titanium oxide model electrode formed by a mono-layer of the titanium oxide nanosheets was used to separate the effects from the low coordination site and the crystal distortion. A titanium oxide nanosheet is composed of octahedrons centered on Ti atoms. Thus, the variation of Ti valence is linearly related to the number of low-coordination sites.

The crystal distortion was evaluated by in-plane XRD and grazing-incidence XAFS measurements in synchrotron radiation facilities. In particular, the local coordination structure of the titanium-oxide model electrode was investigated from pre-peak before the adsorption edge and EXAFS region in the obtained XAFS spectrum. The Ti valence was estimated from the energy of half value at the edge jump intensity in the XAFS spectrum. The number of oxygen vacancies on a titanium-oxide model electrode was roughly controlled by the calcination temperature with hydrogen flow conditions. Electrochemical measurements were performed in a three-electrode cell with 0.1 M HClO₄ electrolyte.

The structure of the titanium-oxide model electrode was changed from the lepidocrocites structure to the anatase structure with increasing calcination temperature. The local coordinate structure was also transformed with increasing calcination temperature. At that time, the Ti valence was gradually elevated from 3.47 to 3.92. The ORR activity of the model electrode was enhanced by the calcination with hydrogen flowing until the beginning of the phase transition to the anatase structure. The distortion of the crystal structure was most significant after the phase transition. However, the ORR activity was low compared to before the phase transition. Introducing the oxygen vacancies to the titanium-oxide model electrode clearly enhanced the ORR activity and gave its structure a very slight crystal distortion. At this time, it is forecasted that the crystal distortion is more effective in ORR activity on titanium oxide rather than the number of oxygen vacancies. However, the permissible crystal distortion rate may be narrow, and the phase transition probably leads to the degradation of the ORR activity.

3:15 PM EN09.11.05

High-Performance Mo-N-C Electrocatalyst for Efficient Oxygen Reduction and Evolution Reaction Nadezda Kongi¹, Gulnara Yusibova¹ and Yevgen Karpichev²; ¹Institute of Chemistry, University of Tartu/University of Tartu, Estonia; ²Tallinn University of Technology, Estonia

Despite notable advancements in the development of catalysts for both the oxygen reduction reaction (ORR) and oxygen evolution reaction (OER), there exists a persistent demand for materials that are more efficient and cost-effective. M-N-C (metal-nitrogen-carbon) materials have emerged as promising solutions that are efficient, low-cost, and sustainable. This study presents the synthesis of Mo-N-C catalysts through a novel metal-organic framework precursor, along with comprehensive characterizations involving X-ray diffraction, transmission electron microscopy, and X-ray photoelectron spectroscopy. These catalysts, owing to their highly porous structure and a high density of active sites, demonstrate remarkable performance and stability for both ORR and OER. Our findings underscore the potential of Mo-N-C catalysts as efficient and economical alternatives to noble-metal-based catalysts for ORR/OER.

3:30 PM EN09.11.06

MOF-Based Architectures towards Higher Activity Oxygen Reduction Reaction Catalysts Albert Epshteyn, William A. Maza, Benjamin L. Greenberg, James Ridenour, Bethany M. Hudak, Olga Baturina, Boris N. Feykelson and Brian Chaloux; U.S. Naval Research Laboratory, United States

The electrocatalyst responsible for carrying out the oxygen reduction reaction (ORR) at the hydrogen fuel cell (FC) cathode has a demanding task to perform in a highly acidic environment and under a corrosive potential. Despite its cost, platinum (Pt) has become the most common catalyst proven to have high activity and durability towards ORR catalysis. There is, therefore, a need to design and develop more cost-effective catalysts that can either replace or reduce Pt content. A key challenge in the design of ORR catalysts is maximizing the conduction and utilization of electrons, protons, and oxygen to the active sites on the electrode surface. For use in intermediate temperature hydrogen fuel cells, which operate above the boiling point of water, the ability to minimize transport barriers in the electrolyte material and optimizing the way it couples to the ORR catalyst is of great importance to maximize catalytic turnover and efficiency. To that end, we have set out to develop approaches toward using metal-organic frameworks (MOFs) as templates for high-surface-area platinum structures to develop high-performance ORR catalysts. As a proof-of-concept, we have chosen the highly robust and well-known UiO series, which among other benefits has the potential for pore-size tuning that should be conducive for effective gas transport. The MOF synthesis has been optimized to target well-defined, single crystalline MOF particles with shape control and narrow size distributions and scaled to multi-gram batches. Subsequently, we have explored different approaches to deposit Pt onto these MOF nanoparticles using methodologies that include colloid-derived methods, as well as solvothermal and atomic layer deposition (ALD) approaches. In this work we compare the different Pt deposition approaches by assessing the relative ORR activities and correlate the results to X-ray photoelectron spectroscopy (XPS) and the catalyst morphology as determined by high-resolution transmission electron microscopy (HR-TEM).

3:45 PM EN09.11.07

Current Density – Voltage (i-V) Dependence of Polymer Electrolyte Electrochemical Cells (PEEC) on The Cell Components of Gas Diffusion Layers (GDLs) and Cell Sealings Miyuki Nara, [Katsushi Fujii](#), Takeharu Murakami, Takayo Ogawa and Satoshi Wada; RIKEN, RAP, Japan

Hydrogen production using water electrolysis in polymer electrolyte electrochemical cells (PEEC) is an attractive technique. The PEEC is known to be relatively strong for input energy fluctuation from a reliability point of view; thus, it is a suitable technique for fluctuating renewable energy storage. The current density characteristics as a function of PEEC voltage are critical for improving the efficiency of hydrogen production from renewable energies. Research is continuing to improve an oxygen evolution catalyst whose overvoltage is relatively high compared to that of hydrogen evolution and using a thinner polymer electrolyte membrane to reduce the series resistance. The PEEC cell structure consists of endplates, gas diffusion layers (GDLs), catalyst-coated membranes (CCM), and gas and supplied water-sealing materials. These components were not considered to improve PEEC performance. However, these structures affect electron, water, and gas electron flows. Thus, the effect of these components on the PEEC performance is discussed here. The influence of the GDL thickness and porosity was evaluated by current density-voltage (i-V) characteristics and electrochemical impedance spectroscopy (EIS). A PEEC with a thicker and higher porosity GDL improved the i-V characteristics. It was also found that the thickness of the seal has an appropriate relationship with the internal parts. The series resistance evaluated by EIS decreased with an improvement in the i-V performance. From these results, the reason for this i-V characteristic change is estimated to be changing the flow of electrons and/or the flows of the source material of water and/or of the produced gas oxygen or hydrogen.

SESSION EN09.12: Virtual Session
Session Chairs: Christopher Barile and Edmund Chun Ming Tse
Wednesday Morning, May 8, 2024
EN09-virtual

8:00 AM EN09.12.01

Modelling of Natural-Like Grain Generation of TiO₂ and its effect on Band Structures [Takuma Okamoto](#)¹, Anastassia Sorkin², Keisuke Kameda¹, Wang v. Hao², Manabu Ihara¹ and Sergei Manzhos¹; ¹Tokyo Institute of Technology, Japan; ²National University of Singapore, Singapore

TiO₂ is widely used in various electrochemical technologies including photosynthesis catalyst and optical applications such as dye sensitized solar cell, perovskite solar cells and batteries. Its polycrystal structure affects electronic properties, for example, introducing trap states into the band structure both in the bulk and at the interfaces and affects the ion and electron transport. It is difficult to understand these effects experimentally especially in bulk, therefore computational studies of effects of microstructural features are desired. These kinds of calculations have been done using models with a specific, postulated grain boundary. However, real materials have a distribution of grain boundaries. In mono-elemental materials like Fe and Si, generation of grain structures have been reported using Molecular Dynamics (MD), but for ceramics containing several kinds of atoms, it is more difficult. In this study, natural-like generation of grain boundaries is explored using MD at a million-atom scale. Different types of temperature schedules are explored, and different structures are obtained by different heat treatments. To facilitate the formation of grains, spherical seeds that are randomly located and oriented are introduced. Temperature dependence of the grain sizes of the obtained structures is investigated. Furthermore, the effects of the microstructural features on the band structure are computed using large-scale Density-Functional Tight-Binding calculations (DFTB). Differences in the electronic properties between ideal crystal and different grainy structures are compared.

8:15 AM EN09.12.02

Effects of Nanosizing of Zirconia and Bandstructure Modulation on Catalytic Activity: Insights from a Combined Density Functional Tight Binding – Order(N) Density Functional Theory Study [Kexin Chen](#)¹, William Dawson², Takahito Nakajima², Aulia S. Hutama³, Keisuke Kameda¹, Sergei Manzhos¹ and Manabu Ihara¹; ¹Tokyo Institute of Technology, Japan; ²RIKEN Center for Computational Science, Japan; ³Universitas Gadjah Mada, Indonesia

Zirconia based materials are widely utilized in the electrodes of solid oxide fuel cells and electrolysis cells. Interactions of small molecules with zirconia surfaces are of key importance in these applications. Numerous theoretical reports have focused on periodic models, while the properties of materials at the nanoparticle or cluster scales may differ markedly from their bulk counterparts. However, ab initio level understanding of gas adsorption behavior on Zirconia at this scale remains limited. We will present a comparative analysis based on first principles and semiempirical calculations of cubic ZrO₂ nanoparticles, varying in size from a few tens to a thousand atoms. This is achieved by combining density functional-based tight-binding (DFTB) and order-N DFT to balance computational cost and increase scalability. The band structure of the nanoparticles, which proves sensitive to oxygen deficiencies, exerts a significant influence on gas adsorption behavior. Notably, nanoparticles can exhibit intrinsic as well as p- and n-doped characteristics corresponding to O-rich or O-poor conditions. The n-type particles display heightened reactivity for the adsorption of CO and CO₂ gases on their surfaces with promoted electron transfer from zirconia adsorbents to the adsorbed molecules, which is useful for their catalysis, with the effect stronger due to nanosizing. Our results suggest good potential of nanosizing and bandstructure engineering in zirconia nanoparticles to achieve enhanced gas adsorption and catalytic performance, thus presenting promising utilization prospects in energy devices.

8:30 AM EN09.12.03

Chemical Vapor Deposition of Ru/RuSe₂ Catalyst for Electrolytic Hydrogen Evolution Reaction [Daba D. Megersa](#)¹, Gutema T. Gudena¹, Youngho Kim² and Hak K. Yu^{1,3}; ¹Ajou University, Korea (the Republic of); ²Korea University, Korea (the Republic of); ³Ajou University, Korea (the Republic of)

The current trend of synthesis in preparing catalysts for hydrogen evolution reaction (HER) is heavily dependent on solution processing which takes a great deal of time and is mostly not suitable to prepare supported structures. Solution processing has advantages to prepare controlled stoichiometry nano particles, while the prepared nano particles end up in another step of dispersing them into a solvent and coating onto desired substrate, which results in long process and sometimes poor adhesion of catalysts to the substrates. We believe chemical vapor deposition is less utilized in synthesis of supported catalysts for HER. In this regard the essence of this work was to provide a simple alternative synthesis route for catalysts used in HER. Therefore, this work demonstrates a one-step synthesis of highly stable Ru/RuSe₂ nanoparticles (NPs) on carbon paper using low temperature and pressure chemical vapor deposition (CVD), resulting in a heterointerface with multiple active sites for catalysis. The catalyst exhibited outstanding performance for the hydrogen evolution reaction (HER) in an alkaline solution, with low overpotentials and fast hydrogen adsorption and desorption kinetics. The Ru/RuSe₂/C nanoparticle structure has potential for large-scale production and can be used as an efficient catalyst for HER.

8:45 AM EN09.12.04

Transition Metal- Metal Carbide decorated N-Doped Carbon Framework as Efficient Dual Mott-Schottky Electrocatalysts for Water Splitting Gokul Raj, Debanjan Das, Bidushi sarkar, Shauvik Biswas and Karuna K. Nanda; Indian Institute of Science, India

Transition metal carbides (TMCs) have garnered significant attention as effective electrocatalysts for the hydrogen evolution reaction (HER), offering a highly active and stable alternative to precious metals like platinum, because of their d-band electronic structure resembling that of platinum. In this study, we address the challenge of developing a top-tier bifunctional electrocatalyst for efficient water splitting by employing a dual transition metal approach to electronically modify bimetallic carbides. Here, we have designed a composite structure through an in-situ fabrication process, featuring N-doped carbon nanotubes (CNT) and graphene, which serve as anchors for Co/MoC, Co/WC, and Co/VC. This integrated pyrolysis technique promotes synergistic interactions among these components and creates dual Mott-Schottky junctions, resulting in a bifunctional catalyst capable of catalyzing both the hydrogen evolution reaction (HER) and the oxygen evolution reaction (OER) with exceptional activity in both acidic and basic environments. Furthermore, it demonstrates excellent performance in water splitting under basic conditions, requiring a relatively low cell voltage of approximately 1.686 V to generate a current of 10 mA/cm² while maintaining good stability. This superior performance is attributed to the cooperative electron transfer between the Co and MoC moieties and the defects induced by nitrogen doping in the graphene/CNT-based conductive network, distinguishing it from other recently reported Mo-based carbide materials.

8:50 AM EN09.12.05

Dual-Function Electrochromic Smart Window based on PEDOT:PSS /Graphene and Cesium Tungsten Oxide for Transmittance Modulation and Near Infrared Shielding Lung-Hao Hu and Kai-Sheng Hsiao; National Sun Yat-Sen University, Taiwan

In this study, transparent conductive layers, which were made with the combination of few-layer graphene ink and poly(3,4-ethylenedioxythiophene) polystyrene sulfonate (PEDOT: PSS) by spin-coating method were utilized on an electrochromic device (ECD). Moreover, a dopant with excellent solar radiation shielding ability, cesium tungsten oxides, was added into the conductive layers, developing a cost-efficient electrochromic smart window with improved near infrared shielding feature. The present device was assembled with five primary layers, including two transparent conductive layers, two complementary electrochromic layers (Prussian blue as the cathode and PEDOT: PSS as the anode) and PC/LiClO₄ liquid electrolyte in the middle. The sheet resistance, electrochemical properties, optical performance, structure morphology and heat insulation ability of the devices were characterized by four-probe measurement with LCR meter, cyclic voltammetry (CV), vis-NIR spectrometer, field emission scanning electron microscopy (FE-SEM) and self-made heat insulative chamber test, respectively. The results show that the sheet resistance of the PEDOT: PSS/graphene/CsWO₃ film with the thickness of 500nm to 600nm, is 0.77Ω/sq. And the films' visible light transmittance is 80.2% at 550nm wavelength. The transmittance of colored and bleached states at 700nm wavelength was 19.7% and 52.9%, respectively, having the maximum optical contrast about 33.2%. The coloration efficiency (CE) of the device was 435.04 cm²C⁻¹. And the response time of the device switching between colored and bleached state is 1.7s and 0.7s, respectively. With the cesium tungsten oxides nanoparticles coated inside the transparent conductive layer, the transmittance of the NIR can be blocked by the ECD about 77.4% utmost, effectively isolating outdoor thermal radiation. In the insulating test with 100W Halogen lamp irradiating 10 cm from the heat insulative chamber for 1 hour, the simple coating layer of PEDOT: PSS/ graphene/ CsWO₃ film on glass substrate can achieve a lower indoor temperature difference, 4 °C compared to the normal glass window, performing good heat shielding ability with single film. In addition, the comparison of the ECD with/without CsWO₃ doping presents that the CsWO₃ doped ECD can significantly expand the indoor/outdoor temperature difference between colored and bleached states from 4.5 to 24.7°C. The outcomes indicate that the CsWO₃ doped ECD can improve the two-way heat insulative ability of the device, absorbing the heat coming from the outside and providing the heat leaking out from the inside.

9:05 AM EN09.12.06

High Catalyst Performance of 2D π-d Conjugated TM₃B₃N₃S₆ for Hydrogen Evolution Reaction Yongxiu Sun, Mengxuan Sun, Xiaohe Ren, Ziwei Gan and Zhijie Li; University of Electronic Science and Technology of China, China

Single-atom catalysts (SACs) for the hydrogen evolution reaction (HER) is an efficient electrochemical pathway to produce the green production. However, the development of HER process is hampered by the lack of high-performance electrocatalysts. In this work, we proposed a new π-d conjugated structure of the Ti₃B₃N₃S₆ monolayer as the single-atom catalysts for the HER process by using the density functional theory (DFT) calculations. The calculated results show that the Ti atom is active site of the Ti₃B₃N₃S₆ monolayer with the high catalytic activity ($\Delta G_H = -0.14$ eV) for HER. The electronic properties of the Ti₃B₃N₃S₆ monolayer were explored by the electron localization function (ELF), Bader charge analysis and the polarized density of states (PDOS) density analysis. The Ti₃B₃N₃S₆ monolayer can promote the electronic transfer during the HER process, which indicates that the Ti₃B₃N₃S₆ monolayer can be considered to investigate the catalytic activity for HER. The Gibbs free energy of H atoms adsorption on the Ti₃B₃N₃S₆ monolayer is -0.14 eV. Furthermore, the origin of high catalytic activity for the Ti₃B₃N₃S₆ monolayer was explored by the analysis the PDOS of the H adsorption on the Ti₃B₃N₃S₆ monolayer. Therefore, our work propose a new and high catalytic single-atom catalyst for the HER.

9:10 AM EN09.12.07

Development of Cs_xWO₃ Nanoparticles for Electrochemical Reduction of CO₂ to Formate Ramsha Saleem and Rana Rashad Mahmood Khan; Government College University Lahore, Pakistan

CO₂ is a greenhouse gas that mainly contributes to major environmental issues. Several strategies have been developed to alleviate the effects of the increased CO₂. Among all, converting CO₂ to valuable products is a bird-two-stone approach as it reduces the atmospheric concentration of CO₂ and gives us the fuels to replace renewable energy sources. To commercialize these processes, highly efficient catalysts are required. In recent years, bimetallic nanoparticles have gained significant attention as the second metal influences the electronic properties of the first metal and, thus catalytic efficiency. We synthesized Cs_xWO₃ nanoparticles as a novel catalyst for electrochemical reduction of CO₂ to formate by hydrothermal method and WO₃ nanoparticles to compare the results. We characterized them by UV-visible, FTIR, SEM-EDX, and XRD. The bandgap of WO₃ was decreased from 2.67 eV to 1.87 eV when Cs was incorporated over them. SEM images revealed that Cs_xWO₃ nanoparticles were rougher and more porous than WO₃ nanoparticles. The WO₃ and Cs_xWO₃ nanoparticles were employed as working electrodes in H-type cells, and CV, LSV, and CA evaluated their electrochemical performance. LSV was used to calculate the onset potential, and the onset potential for Cs_xWO₃ was found to be -0.7 V vs Ag/AgCl. The electrochemical results showed that the maximum Faradaic efficiency and partial current density of formate over WO₃ nanoparticles were 50 % and -13.5 mA/cm², respectively. The FE and partial current density were increased to 76 % and -19 mA/cm², respectively, when Cs_xWO₃ was employed as a working electrode. Moreover, Cs_xWO₃ nanoparticles were stable at -1.33 V vs Ag/AgCl for 3 h. The high FE, low overpotential, and stable electrocatalysis proved that incorporating Cs over WO₃ nanoparticles improved its efficiency, and Cs_xWO₃ nanoparticles can be used on a large scale in the future with little modifications.

9:25 AM EN09.12.08

Synthesis of Porous Bimetallic Nanocatalyst for Selective Formate Production by CO₂ Electroreduction Rana Rashad Mahmood Khan; Government College University Lahore, Pakistan

The emission of CO₂ into the air is causing a severe environmental problem because of the continuously increasing demand for fossil fuels. To fulfill these demands sustainably, the conversion of CO₂ into fuels has attracted profound research. The possible CO₂ conversion products are CO, hydrocarbons, and alcohols that are used as a chemical feedstock. Particularly, the electrocatalytic formation of formate is of great interest and have a potential for the development of an economically feasible process.

We prepared the Ag₂SnO₃ nanoparticles by a simple and cost-effective chemical reduction method. We conducted the electrochemical conversion of CO₂ to formate in aqueous electrolyte media at pH 6.8. The two-compartment cell (H type cell) was used for electrochemical measurements. The absorption maxima, the energy bandgap, surface morphology, catalytic composition, crystallinity, crystallite size, crystal facet, and electrochemical activity of the electrocatalyst were probed. The linear sweep voltammetry was used to record the polarization curve/current response. The catalyst shows porous/sponge-like morphology. The electrochemical results show higher current density (~26 mA/cm²), long term stability, product selectivity, and higher faradaic efficiency (FE) on the bimetallic electrocatalyst electrode. The highest FE for the only liquid product (formate) was 89% at -1.3 V vs. Ag/AgCl with a Tafel slope of 174 mV/decade. The faradaic efficiency was found high as compared to the monometallic (Ag, Sn) nanoparticles. The high FE and product selectivity indicates the synergistic effect between these metals.

9:40 AM EN09.12.09

Stabilization of PtRu Alloy Nanocatalysts by Encapsulation with Niobium Oxide [Annabelle M. Hadley](#)¹, Frode Seland² and Byron D. Gates¹; ¹Simon Fraser University, Canada; ²NTNU, Norway

The threat of climate change motivates us to reduce our reliance on fossil fuels and transition to renewable energy infrastructure. Direct methanol fuel cells (DMFCs), in which electrocatalysts harness electricity from the reaction of methanol and oxygen, are an attractive clean energy technology because of the high energy density and ease of transport and storage of methanol compared to hydrogen. However, there remains much to improve upon in terms of the durability, and as a consequence the economic viability, of DMFCs. This project focuses on the durability of the anodic electrocatalysts which facilitate the methanol oxidation reaction. A platinum-ruthenium alloy is the most commonly used electrocatalyst towards the methanol oxidation reaction due to its high performance. The high activity and selectivity of the platinum is additionally imparted high tolerance for poisoning byproducts of methanol oxidation [carbon monoxide (CO)] by alloying with ruthenium. Unfortunately, the ruthenium is known to dissolve from the alloy and reduce the CO tolerance of the catalysts.

This project explored encapsulating the PtRu nanoparticle catalysts with porous niobium oxide to stabilize the PtRu alloy. Niobium oxide was chosen due to its high corrosion resistance and previous studies showing its stabilization of ruthenium. PtRu alloyed nanoparticles were synthesized *via* electrodeposition on a glassy carbon electrode substrate and subsequently encapsulated by an electrophoretic deposition method adapted from Penner *et al.*¹ The morphology and composition of the catalyst and encapsulating layer were characterized by scanning and transmission electron microscopy, energy dispersive X-ray spectroscopy, X-ray photoelectron spectroscopy, Raman spectroscopy, and optical microscopy. The activity and durability of pristine and encapsulated PtRu catalysts were evaluated by cyclic voltammetry, chronoamperometry, and electrochemical impedance spectroscopy. Carbon monoxide stripping and the double layer capacitance method was used to study changes in the electrochemically active surface area before and after deposition of the niobium oxide. Access to the electrocatalyst surfaces through the encapsulating layer was maximized by the addition of surfactants and the application of different potentials during the deposition of the niobium oxide to improve its porosity. The niobium oxide was shown to improve the stability of the PtRu alloy and maintain the CO tolerance of the alloy well beyond that of the un-encapsulated catalyst. The stabilization of PtRu imparted by the encapsulation of niobium oxide herein is promising for the stabilization of alloyed nanoparticle catalysts towards a wide range of electrocatalytic applications.

1. Jha, G.; Tran, T.; Qiao, S.; Ziegler, J. M.; Ogata, A. F.; Dai, S.; Xu, M.; Thai, M. L.; Chandran, G. T.; Pan, X.; Penner, R. M. Electrophoretic Deposition of Mesoporous Niobium(V)Oxide Nanoscopic Films. *Chem. Mater.* **2018**, *30*, 6549-6558.

SYMPOSIUM EN10

Novel Approaches to Synthesize and Characterize Stable Halide Perovskites and their Devices

April 22 - April 26, 2024

Symposium Organizers

Ivan Mora-Sero, Universitat Jaume I

Michael Saliba, University of Stuttgart

Carolin Sutter-Fella, Lawrence Berkeley National Laboratory

Yuanyuan Zhou, Hong Kong University of Science and Technology

Symposium Support

Silver

Journal of Energy Chemistry

* Invited Paper

+ JMR Distinguished Invited Speaker

^ MRS Communications Early Career Distinguished Presenter

SESSION EN10.01: Characterization
Session Chairs: Erin Ratcliff and Michael Saliba
Monday Afternoon, April 22, 2024
Room 347, Level 3, Summit

1:15 PM *EN10.01.00

Novel Multifunctional Additives for Enhancing The Efficiency and Stability of Perovskite Solar Cells and Their Tandem Solar Cells with Organics Alex Jen; City University of Hong Kong, Hong Kong

Minimizing energy loss and increasing the quality of crystalline perovskite films are keys to improve the performance and long-term stability of perovskite solar cells. To address these challenges, we have developed several multifunctional, nonvolatile additives that can be used to modulate the kinetics of perovskite film growth to enable large-sized grains and coherent growth of perovskites from bottom to surface to be achieved. The improved film morphology resulted in significantly reduced non-radiative recombination, helping enhance the power conversion efficiency (PCE) of inverted (p-i-n) device to ~26% with low energy loss and good stability. In addition, these multifunctional additives can also be applied to address one of the most challenging problems involved in large bandgap perovskites and their derived devices for single junction and tandem solar cells. The commonly observed halide segregation critically limits the stability of mixed-halide perovskites under device operational conditions. There is a strong indication that halide movement/oxidation is the primary driving force behind halide de-mixing. To alleviate this problem, we have developed a series of multifunctional mediators that can suppress these factors while simultaneously passivate defects through tailored substitution. These effects enable wide-bandgap (1.81 eV) perovskite solar cells to achieve an outstanding PCE >20%, with 95% of its initial PCE retained after tracking at maximum power point for 500 h. Integrating this layer into a monolithic perovskite-organic tandem solar cell as a wide-bandgap subcell afforded a record-high PCE of 26.1% and impressive long-term operational stability.

1:45 PM EN10.01.01

Stress Relaxation in Metal Halide Perovskites and use of Controlling Film Stress to Improve Stability Nicholas Rolston¹, Muneeza Ahmad¹, Carsen Cartledge¹, Gabriel McAndrews², Antonella Giuri³, Aurora Rizzo³ and Michael D. McGehee²; ¹Arizona State University, United States; ²University of Colorado Boulder, United States; ³CNR Nanotec, Italy

Challenges to upscaling metal halide perovskites (MHPs) include mechanical film stresses which accelerate degradation, dominate at the module scale, and can lead to delamination or fracture. In this work, we demonstrate open-air blade coating of single-step coated perovskite as a scalable method to control residual film stress after processing and introduce beneficial compression in the thin film with the use of polymer additives such as gellan gum and corn starch.

Given the strong link between residual stress and degradation, we assessed the stability of perovskite films with different residual stress states. Perovskite films on silicon and glass were stress engineered using additives to either be tensile or compressive and aged under either high heat or humidity conditions (85°C vacuum or 85% relative humidity). A control MAPbI₃ film spin coated without additives was also added as a reference under 85% relative humidity. The samples were periodically removed, and the stress was remeasured in ambient conditions (22°C and 40% RH). The highly tensile samples experienced stress relaxation quickly in the humid environment due to moisture induced degradation. This effect was not observed for samples with compressive stress, which also did not experience visible degradation during the 100-hour exposure. We performed XRD measurements on these films to verify degradation and the tensile sample had PbI₂ peaks after the aging experiment, whereas the compressive sample had lower intensity PbI₂ peaks and still had MAPbI₃ in the film. This confirms that perovskites are more structurally stable when exposed to environmental conditions while in compression. Samples were reannealed to ensure that trapped moisture was not the cause of the relaxation, and there was no change observed in the stress. Therefore, residual moisture is not the explanation for stress reduction.

A similar experiment was conducted for thermal stability at 85°C under vacuum to monitor the changes in stress under thermal aging. Once again, stress relaxation was observed for the highly tensile sample with gum. The improvement in stability was visually apparent since the tensile films turned completely yellow after being aged for 100 hours while the compressive one remained largely in the black photoactive phase. The samples with additives took longer to visibly degrade, which also points towards their improved stability. The tensile stress was therefore relaxing as the film degraded due to the strained bonds likely enabled the methylammonium cation to diffuse out, whereas a compressive stress showed better stability and unchanging stress under heat, similar to the effect observed with aging in high humidity.

A thermal cycling experiment was also conducted for a tensile and compressive sample to monitor the perovskite films as the temperature changes between -40 to 85°C. The experiment ran for 200 cycles and the results supported what was observed under high heat and humidity conditions. The tensile sample relaxed by 180 MPa and turned completely yellow. However, the compressive sample was stable both in terms of its appearance and film stress. A spin coated MAPbI₃ film without additives (with tensile residual stress) was kept as the control sample. In all three aging conditions, films with residual tensile stress degraded significantly faster. The degradation also corresponded to stress relaxation in the perovskite film as the phase changed, marking the first time for which changes in stress have been directly mapped to stability. Stress relaxation has been observed in many other material systems (*i.e.*, polymers and metals) when exposed to tensile stress. Perovskites therefore act similarly, and despite their brittle nature, share in this property.

This discovery of a new mechanism underpinning MHP degradation shows that film stress can be used as a parameter to screen MHP devices and modules for quality control before deployment as a design for reliability criterion.

2:00 PM EN10.01.02

Interpreting Halide Perovskite Semiconductor Photoluminescence Kinetics Margherita Taddei¹, Sarthak Jariwala², Robert J. Westbrook¹, Shaun M. Gallagher¹, Aaron Weaver¹, Henry J. Snaith³ and David S. Ginger¹; ¹University of Washington, Italy; ²Twelve, United States; ³University of Oxford, United Kingdom

Drawing from both experimental data and simulation, we highlight best practices for fitting time-resolved photoluminescence (TRPL) decays on halide perovskite semiconductors now widely studied for applications in photovoltaics and light-emitting-diodes (LEDs). We focus on three key observations. First, at low excitation intensities, high-quality perovskites often show pseudo-first-order kinetics, consistent with classic minority carrier lifetimes. Second, non-single-exponential decays frequently observed at low excitation intensity often have significant contributions from spatial heterogeneity. We recommend fitting such decays by stretched exponentials, where the stretching factor (β) can be used to characterize the heterogeneity of the local lifetime distribution. Third, PL decay kinetics can depend on the excitation wavelength. We discuss how penetration depth, carrier diffusion, and surface recombination affect measurements, and make recommendations for choosing experimental parameters suited to the question at hand. Accounting for these factors will provide more reliable and physical interpretation of carrier recombination and better understanding of non-radiative losses in perovskite semiconductors.

2:15 PM EN10.01.03

Advancing Photovoltaic Performance and Stability of Perovskite Solar Cells Using a Solid-State Multi-Modal Electrochemical Approach Juan F. Tirado, Mriganka Singh, Michel De Keersmaecker and Erin L. Ratcliff; University of Arizona, United States

Analysis and characterization of buried interfaces in metal halide perovskite (MHP) devices has always been a major challenge in advancing device performance and stability, particularly under conditions of operation including light bias and charge transport. Recently, our group has developed a solid-state electrolyte “peel and stick” spectro-electrochemistry methodology in order to directly study the energy levels and charge extraction capabilities of the buried interface between ITO/MHP under *operando* conditions. Moreover, this tool allows including redox probes in the solid electrolyte in order to measure near-gap and mid-gap defect densities of MHP with quantification limits around $\sim 10^{14} \text{ cm}^{-3}$, which is below the space-charge limited current methodology or conventional spectroscopic techniques.

Our approach overcomes a major challenge to industrial adaptation and manufacturing at scale of printable electronics. Generally, interface modifications at charge-selective-layer/MHP bottom contacts are speculated to improve performance through correlations with indirect measurements and a demonstration of a change in power conversion efficiency. For instance, photoelectron spectroscopies can only determine the chemical environment and energetics at the MHP surface, which is widely recognized to be dependent on buried interface chemistries that cannot be probed with subsequent layer deposition. Similarly, time-resolved photoluminescence spectroscopy is restricted to measuring the net total change in carrier lifetime but lacks exact information on charge extraction/injection at the buried interface with the MHP.

In this context, herein we extend the use of our “peel and stick” electrochemistry platform to assess the effect of partial device stacks comprised to transparent conductive oxide/hole-transporting-layer (HTL)/MHP interfaces, systematically modified using ionic liquids and phosphonic acids. Our approach is exquisitely sensitive to small changes in energetics, monitored through injection barriers, and charge extraction capabilities of HTL/MHP interface in a p-i-n Perovskite Solar Cells (PSCs) configuration. Remarkably, we demonstrate the correlation between interface charge extraction “quality” and photovoltaic response of p-i-n PSCs so that our solid-state electrochemical platform may advance the device performance by probing the buried interface.

Similarly, we take advantage of this powerful tool to explore MHP stability under thermal and illumination stress conditions and to measure the effect of HTL nature by quantifying the near-gap defect densities. Ultimately, by combining this approach with complementary spectroscopies, we are able to provide new insights into the degradation processes occurring in the MHP and corresponding devices. Thus, we highlight the potential of our solid-state electrochemistry methodology to become a very useful tool for advancing the behavior and stability of MHP and PSCs, which is necessary in order to find proper materials and interface treatments to increase PSCs stability to commercial level requirements.

2:30 PM EN10.01.04

***Operando* Trapped Carrier Dynamics in Perovskite Solar Cells Observed via Infrared Optical Activation Spectroscopy** Ziming Chen; Imperial College London, United Kingdom

Metal halide perovskites show promise for cost-effective and high-efficiency photovoltaics. Recent progress in perovskite solar cells (PeSCs) has achieved a certified power conversion efficiency (PCE) of approximately 26.0%. To push PeSCs closer to the Shockley-Queisser limit and enhance their performance, reducing non-radiative recombination caused by carrier ‘traps’ is crucial under standard sunlight conditions. Understanding these trap states and trapped carrier dynamics is vital to minimise performance losses.

To overcome the limitations of conventional spectroscopic techniques like time-resolved photoluminescence and transient absorption, which lack the necessary selectivity for detecting trapped carriers, we used a novel method called infrared optical activation spectroscopy, specifically optical pump-IR push-photocurrent (PPPc), to monitor trapped carriers in real-time during PeSC operation. PPPc involves generating band-edge carriers with a visible ‘pump’ beam, followed by carrier trapping. Subsequently, trapped carriers absorb IR ‘push’ beam photons, returning them to the band states. IR-detrapped carriers contribute to additional device photocurrent, allowing us to assess trapped carrier concentration and dynamics based on the amplitude and behaviour of IR-induced photocurrent.

Here, we employed PPPc (both its time-resolved and quasi-steady-state versions) to investigate how the surface passivation process and strain of perovskite make an impact on the trapped carrier dynamics, respectively:

1) To study surface passivation effects, we fabricated $\text{FA}_{0.99}\text{Cs}_{0.01}\text{PbI}_3$ PeSCs with and without surface passivation. Our device structure was ITO/SnO₂/FA_{0.99}Cs_{0.01}PbI₃/(OAI)/Spiro-OMeTAD/Au, where n-octylammonium iodide (OAI) served as a passivator for both cation and halide vacancies at the FA_{0.99}Cs_{0.01}PbI₃ surface.

We found that bulk traps filled rapidly (within 10 ns) due to nearby photocarrier trapping, while surface trap filling was slower (tens to hundreds of ns) and involved band-edge carrier drift/diffusion to the perovskite surface. The filling of surface trap states created an interfacial charge layer that screened the internal field and slowed carrier drift/diffusion. This process was also influenced by device temperature. The surface-passivated device exhibited faster saturation of trapped carrier concentration compared to the pristine device with higher trap density. Our kinetic model estimated a ~ 50 times reduction in trap states after surface passivation. Notably, the activation energy of trap state bands (~ 280 meV) remained nearly identical in both devices, indicating that surface passivation reduced trap numbers without changing trap types.

2) To investigate the impact of strain, we fabricated two perovskite films with varying strain levels: MA_{0.95}GA_{0.05}PbI₃ with tensile strain and MA_{0.95}GA_{0.05}Pb(I_{0.95}Br_{0.05})₃ with free strain due to Br (with smaller size) compensation in the lattice.

We found that non-radiative recombination loss was suppressed in the strain-free perovskite, which resulted in better emission properties and higher device performance. Considering trap-assisted recombination is the main process accounting for the non-radiative recombination loss, again, the combination of both quasi-steady-state and time-resolved PPPc measurements revealed that strain relaxation reduced trap density, shallowed trap depth, as well as prolonged trapped carrier lifetimes. Hence, this mitigated trap-assisted recombination losses in the strain-free device. This study represents the first explicit correlation between strain engineering and its effects on overall trap-assisted recombination processes.

2:45 PM EN10.01.05

Origin of Open-Circuit Voltage Losses from Energy-Level Misalignment between Metal Halide Perovskites and Hole Transport Layers Jae Eun Lee¹, Silvia G. Motti^{1,2}, Robert D. Oliver^{1,3}, Siyu Yan¹, Henry J. Snaith¹, Michael B. Johnston¹ and Laura Herz^{1,4}; ¹University of Oxford, United Kingdom; ²University of Southampton, United Kingdom; ³The University of Sheffield, United Kingdom; ⁴Technical University of Munich, Germany

Metal halide perovskites (MHPs) show great potential in multijunction photovoltaics applications due to their tunable bandgaps through compositional mixing on the halide site. However, wide-bandgap MHPs (>1.7 eV) typically suffer from greater open-circuit voltage (V_{OC}) losses compared to their narrow-bandgap counterparts (~ 1.6 eV) owing to energy-level misalignment with charge extraction layers. Herein, we investigate the origin of such losses, focusing on the energy level misalignment between the valence band maximum and the highest occupied molecular orbital (HOMO) for a commonly employed combination of perovskite with various halide compositions and hole transport layers.[1] Our research combines time-resolved photoluminescence spectroscopy and numerical modelling to reveal the origin of V_{OC} losses, which stem from the accumulation of holes in the HOMO of hole transport layers, followed by subsequent non-radiative across-interfacial recombination via interfacial defects. By simulating an ideal choice of hole transport material to pair with a mixed-halide MHP whose 1.8-eV bandgap is optimized for tandem solar cells, we demonstrate a potential reduction in V_{OC} losses originating from energy level misalignment. Our findings underscore the pressing need for tailored charge-extraction materials with improved

energy level alignment to enhance the efficiency of solar cells based on wide-bandgap mixed halide MHPs.

[1] Lee, JE et al. Energy & Environmental Science. (2023) manuscript under review.

3:00 PM BREAK

SESSION EN10.02: Stability I
Session Chairs: Tim Kodalle and Yuanyuan Zhou
Monday Afternoon, April 22, 2024
Room 347, Level 3, Summit

3:30 PM *EN10.02.01

Advancing Perovskite Solar Cell Development and Stability Using In-Line Electrochemical Methodologies [Erin L. Ratcliff](#); University of Arizona, United States

This talk will discuss established (spectro)electrochemistry-based measurement science approaches to quantify the distribution and energetics of donor and acceptor defects in prototypical perovskite solar cell materials and partial device stacks.

We utilize a solid-state electrolyte top contact that equilibrates with the perovskite film to create “half-cells” of device-relevant material stacks and study them under solar cell-relevant electric fields. This allows us to spectroscopically assess onsets in valence and conduction bands under *operando* conditions, as well as quantify near-band edge defects using redox-active hole or electron capturing molecular probes. The combination of spectroscopy and electrochemistry characterizes the energetic distribution of donor defect states at an energy resolution of <10 meV in “stoichiometric” triple cation, mixed halide perovskite thin films (Cs_{0.05}FA_{0.79}MA_{0.16})Pb(I_{0.87}Br_{0.13})₃ or CsFAMA, under device-relevant electric fields (i.e. electrochemical biasing). Limits of detection are at the 10¹⁴ defects/cm³. Such detection limits are better than spectroscopic, electronic and photoemission protocols, with speciation (anion versus cation defects) not available in those other approaches.

The technique is exquisitely sensitive, allowing for detection of clear differences in buried perovskite/metal oxide interfaces to better understand photovoltaic performance. Ongoing efforts to characterize defects and distributions include both nickel oxide nanoparticles and sputtered nickel oxide hole-transport contacts, modified with molecular species. Advancements towards development of in-line characterization (i.e., roll-to-roll) and connections to stability will also be described and benchmarked with respect to photoluminescence and photoelectron spectroscopies.

4:00 PM EN10.02.02

Multifunctional Polymeric-Nanofiber Reinforcement of Perovskite Solar Cells for Improved Mechanical Stability without Performance Trade-Off [Adam Printz](#), [Anton Samoylov](#), [Kenneth Lang](#), [Patrick Lohr](#), [Matthew Dailey](#), [Yanan Li](#) and [Euan McLeod](#); University of Arizona, United States

Metal halide perovskites have been demonstrated to be extremely fragile materials that can fracture at low applied stresses. Previous efforts to mechanically reinforce perovskite films have focused on the extrinsic mechanical shielding such as polymer scaffolding, but these implementations demonstrated to date either have performance trade-offs or require complex manufacturing steps. I will discuss a perovskite-polymeric nanofiber composite that increases the mechanical toughness without an efficiency tradeoff. The fracture energy, G_c , of this nanocomposite is 500% higher ($2.34 \pm 1.67 \text{ J m}^{-2}$) than in pristine perovskite ($0.40 \pm 0.16 \text{ J m}^{-2}$). The nanocomposites were observed via scanning electron microscopy (SEM) and atomic force microscopy (AFM) to be homogeneous in the vertical direction, and x-ray diffraction (XRD) showed that the films were of similar quality to pristine perovskite (no lead iodide growth), but with a decrease in orientation. Furthermore, we show that there is no trade-off in device efficiency despite the integration of the insulating nanofibers, which we show is likely due to beneficial light scattering that increases current generation.

4:15 PM EN10.02.03

Increasing Halide Perovskite Scalability and Stability with Food Additives [Carsen Cartledge](#), [Muneeza Ahmad](#) and [Nicholas Rolston](#); Arizona State University, United States

In this work, we report on a polymeric additive endemic to the food industry, gellan gum, as a means of enabling scalable, open-air manufacturing of halide perovskites with improved stability characteristics under high heat and humidity conditions.

As the global demand for scalability escalates, traditional perovskite inks designed for small scale fabrication in inert environments like spin coating have been found to produce pinholed, incomplete, and shunted films when utilized in more scalable open-air processes like blade coating. Interestingly, gellan gum enables viable films through the critical transition of well-studied spin coating inks into solutions that are compatible with blade coating. By working as a non-toxic and efficient rheological modifier in combination with a pure dimethyl sulfoxide solvent system, gellan gum enables longer periods for crystallization which eliminates the formation of a patchy network of needle-shaped crystals attributed to the PbI₂ phase of perovskites in favor of larger spherulitic grains which results in smoother, more uniform films in a one-step coating method. In fact, the use of this additive reduces surface roughness of ambient blade coated films from 138nm using an unmodified ink to 35nm when gellan gum is incorporated.

Similarly, hyperspectral photoluminescence data reveals that gellan gum decreases the defect density between grains. In films with low gum concentration the intensity of the photon flux decreases when moving from the grain centers to the boundaries which could be explained by thinner coverage in those areas; however, the opposite trend is true for samples with higher gum concentration. This indicates the additive decreases the defect density through passivation and induces a corresponding reduction in non-radiative recombination centers. This reduction in defects, and therefore improvement in stability, is supported by XRD data demonstrating increased crystallinity through ordered texturing.

Additionally, open-air blade coated gellan gum samples feature an intrinsic compressive stress above 1wt% additive which contrasts with traditional tensile stress found in spin coated films. Not only does compressive stress indicate increased resistance to delamination and fracture under thermal and environmental conditions, but it is also associated with an increase in the activation energy for ion migration. For example, when aged under 85% relative humidity for 100 hours, a compressive film processed with gellan gum features very little change in compressive stress, from 50MPa to 75MPa, while a tensile sample can experience dramatic tensile relaxation from 450MPa to 200MPa. Under thermal aging at 85 degrees Celsius for 100 hours, a similar stress trend is observed, and the compressive film visually retains the black photoreactive phase while tensile samples turn completely yellow, indicative of degradation to PbI₂.

XRD data confirms that aged tensile control samples feature an increase of PbI₂ and a weakening of the perovskite peaks while aged compressive gum samples generate spectrums with markedly less prominent PbI₂ peaks and relatively unchanged perovskite peaks. Furthermore, when compared to a similar

polysaccharide biopolymer like cornstarch, gellan gum enables a reduction in additive concentration from 5wt% with an associated compressive stress of 35 MPa, to only 1wt% inducing compressive stresses of 75 MPa.

Overall, open-air blade coating of single-step gellan gum-halide perovskites reduces defect densities at grain boundaries and improves stability and manufacturability with compressive stresses that may limit ion migration leading to increased resiliency to heat, humidity, and illumination. In designing for reliability, this work mitigates some of the fundamental degradation mechanisms preventing halide perovskites from reaching service lifetimes comparable to incumbent PV technologies.

4:30 PM EN10.02.04

Ionic Self-Diffusion Approaches: Enhancing Stability and Efficiency in Perovskite Solar Cells through Ion Migration Suppression and Fermi Level Tuning [Jihyun Kim](#)¹, Ji-Sang Park², Gee Yeong Kim³ and William Jo^{1,1}; ¹Ewha Womans University, Korea (the Republic of); ²Sungkyunkwan University, Korea (the Republic of); ³Korea Institute of Science and Technology, Korea (the Republic of)

Lead halide perovskites have garnered attention as potential energy-harvesting materials for optoelectronic devices due to their remarkable photovoltaic properties. Among these, the FA cation demonstrates the most promising performance and attributes to the formamidinium lead triiodide (FAPbI₃) perovskite, which has a narrow bandgap (E_g) and great thermal stability. Despite FAPbI₃ perovskite displaying great stability as an absorber layer for perovskite solar cells, issues of device instability persist due to adsorbed Pb²⁺ or I⁻ at the oxide surface which induced the ion migration of iodine vacancies. This phenomenon generates the hysteresis loop and accelerates degradation rate in photovoltaic performance. In this study, we customized the charge-selective interfaces, revealing the induced adjustment of the Fermi level at the FAPbI₃/SnO₂ junction by ionic diffusion into the bulk. This adjustment enhances charge transport and mitigates ion migration. These findings were confirmed using computational simulations and ultraviolet photoelectron spectroscopy. To understand ion migration mechanism at the FAPbI₃/SnO₂ interface, we analyze the normalized ionic and electronic conductance as functions of film thickness through D.C polarization measurements. The space charge zone of cation and anion-treated SnO₂ (NH₄⁺-SnO₂ and Cl⁻-SnO₂) [1], [2] was found to exhibit reduced zones under induced light. Based on our findings, it is evident that interfaces modified with cationic and anionic treatments lead to a decrease in Pb²⁺ and I⁻ absorption at the oxide surface. Additionally, these modifications enhance charge transport while significantly minimizing the occurrence of interfacial defects. As a result of this approach, the power conversion efficiency (PCE) increased to 24.38%, and the operational stability of perovskite solar cells (PSCs) was extended to 1600 hours.

[1] J. H. Kim, J. H. Park, Y. H. Kim, and W. Jo, "Improvement of Open-Circuit Voltage Deficit via Pre-treated NH₄⁺ Ion Modification of Interface between SnO₂ and Perovskite Solar cells", *Small*, 2204173 (2022)

[2] J. H. Kim, Y. S. Kim, H. R. Jung, and W. Jo, "Chlorine-passivation of the ozone-treated SnO₂ thin films: occurrence of oxygen vacancies for manipulation of conducting states and bipolarities in resistive switching", *Applied Surface Science* 555, 149625 (2021)

4:45 PM EN10.02.05

A Bifunctional Organic Salt as *p*-Type Dopants of Spiro-OMeTAD for Perovskite Solar Cells with Enhanced Stability [Sung-Kwang Jung](#) and Jin-Wook Lee; Sungkyunkwan University, Korea (the Republic of)

2,2',7,7'-tetrakis(N,N-di-*p*-methoxyphenyl-amine)9,9'-spirobifluorene (spiro-OMeTAD) has been a commonly employed in hole transport layer (HTL) for normal-structured perovskite solar cells (PSCs). Lithium bis(trifluoromethane)sulfonimide (Li-TFSI) is introduced into the spiro-OMeTAD as a *p*-type dopant to improve conductivity and band alignment to facilitate hole extraction. However, the lithium salt causes undesired side effects such as enhanced hygroscopicity, migration and accumulation of Li cations, and formation of by-products, which can lead to degradation of PSC performance and stability. Herein, we propose an alternative organic salt dopant, tetramethylammonium bis(trifluoro-methane)sulfonimide (TMA-TFSI). The TMA-TFSI reacts with the top surface of formamidinium lead iodide perovskite, forming a tetramethylammonium lead iodide film acting as a surface passivation layer of underlying perovskite thin film, contributing to an enhancement of open-circuit voltage of the devices. Furthermore, TMA-TFSI enhances resistance of the HTL against harsh environmental conditions, such as humidity and high temperature, owing to suppressed ion migration and hydrophobic nature. Resultingly, the TMA-TFSI-based devices demonstrate superior stability under high temperature (~85 degrees Celsius) and maximum-power-point tracking compared to those based on Li-TFSI.

5:00 PM EN10.02.06

Reduced Recombination via Tunable Surface Fields in Perovskite Solar Cells [Dane W. DeQuilettes](#)^{1,2}, Jason J. Yoo¹, Roberto Brenes¹, Felix U. Kosasih³, Madeleine Laitz¹, Benjia Dou¹, Daniel Graham⁴, Kevin Ho⁴, Yangwei Shi⁴, Seong Sik Shin^{5,6}, Caterina Ducati³, Mounji G. Bawendi¹ and Vladimir Bulovic¹; ¹Massachusetts Institute of Technology, United Kingdom; ²Optigon Inc., United States; ³University of Cambridge, United Kingdom; ⁴University of Washington, United States; ⁵Korea Institute of Science and Technology, Korea (the Republic of); ⁶Sungkyunkwan University, Korea (the Republic of)

The ability to reduce energy loss at semiconductor surfaces through passivation or surface field engineering has become an essential step in the manufacturing of efficient photovoltaic (PV) and optoelectronic devices.¹ Similarly, surface modification of emerging halide perovskites with quasi-2D heterostructures is now ubiquitous to achieve PV power conversion efficiencies (PCEs) > 22% and has enabled single-junction PV devices to reach >26%, yet a fundamental understanding to how these treatments function is still generally lacking. This has established a bottleneck for maximizing beneficial improvements as no concrete selection and design rules currently exist. Here we uncover a new type of tunable passivation strategy and mechanism found in perovskite PV devices that were the first to reach the > 25% PCE milestone, which is enabled by surface treating a bulk perovskite layer with hexylammonium bromide (HABr). We uncover the simultaneous formation of an iodide-rich 2D layer along with a Br halide gradient achieved through partial halide exchange that extends from defective surfaces and grain boundaries into the bulk layer. We demonstrate and directly visualize the tunability of both the 2D layer thickness, halide gradient, and band structure using a unique combination of depth-sensitive nanoscale characterization techniques. We show that the optimization of this interface can extend the charge carrier lifetime to values > 30 μ s, which is the longest value reported for a direct bandgap semiconductor (GaAs, InP, CdTe) over the past 50 years. Furthermore, we show that this heterostructure is well suited for a host of optoelectronic devices where we achieve a new benchmark for perovskite/charge transport layer surface recombination velocity with values < 7 cm s⁻¹. Importantly, this work reveals an entirely new strategy and knob for optimizing and tuning recombination and charge transport at semiconductor interfaces and will likely establish new frontiers in achieving the next set of perovskite device performance records.

5:15 PM EN10.02.07

Light Makes Right: Laser Polishing for Surface Modification of Perovskite Solar Cells [Mayank Kedia](#)^{1,2} and Michael Saliba^{1,2}; ¹University of Stuttgart, Germany; ²Forschungszentrum Jülich GmbH, Germany

Interface engineering is a common strategy for passivating surface defects to attain open circuit voltages (V_{oc}) in perovskite solar cells (PSCs). Although a large volume of reports highlights the potential of chemical passivation, an additional solvent-based processing step increases the challenges of upscaling

and reliability. Moreover, as the library of chemical passivators consistently expands, there is no consensus on the result risking that each perovskite composition needs its tailor-made solution. Hence, a solvent-free, up-scalable, and one-size-fits-all approach is desirable.

In this work, we introduce the concept of polishing a perovskite thin-film surface using a nanosecond (ns) pulsed ultraviolet laser to reduce surface defects, such as dangling bonds, undesirable phases, and suboptimal stoichiometry. Careful control of laser energy and scanning speed improves the photophysical properties of the surface without compromising the thickness. A detailed and complementary analysis of the perovskite top layer and the full device using photoluminescence imaging and Kelvin Probe Force Microscopy reveal the removal of *dark spots* that act as traps for photogenerated carriers, resulting in surface homogeneity and narrowing of the band gap. Using laser polishing, a record V_{oc} of 1.21 V is achieved for planar PSCs with a triple cation composition ($E_g \sim 1.61$ eV), showing an improved perovskite/hole transport interface by mitigating surface recombination losses. We measure an efficiency boost from 18.0% to 19.3% with an improved stability of up to 1000 h. The polishing effect on the MAPbI₃ perovskite is also studied to explore the versatility of this method.

Furthermore, the same laser is employed to fabricate ultra-thin perovskite films up to ~ 50 nm achieving a V_{oc} of 1.15 V, which is one of the highest reported so far for such semi-transparent PSCs. These results open the door to a new class of surface modification without any structural damage using lasers for interface passivation and semi-transparency in well-controllable, automated, scalable, and solvent-free surface treatments.

5:30 PM EN10.02.08

Highly Efficient Perovskite Blue Light-Emitting Diodes [Jian Mao](#)^{1,2} and Samuel D. Stranks¹; ¹University of Cambridge, United Kingdom; ²Fudan University, China

Lead halide perovskite has attracted extensive attention during the past decade for applications in light-emitting diodes because of its wide emission tunability, high color purity, high quantum yield, and easy solution processibility. Despite the exciting progress of perovskite green, red, and near-infrared LEDs, fabrication of perovskite blue LEDs with high external quantum efficiency (EQE), high brightness, and high color purity remains a considerable challenge. Here, we report efficient perovskite blue LEDs with a world-record EQE of surpassing 22%, a peak luminance above 7000 cd/m², and a full width at half maximum of 15 nm. Besides, the devices exhibit a stable electroluminescence spectrum at constant elevated current injection. This performance is achieved by carefully manipulating the growth of perovskite into thin films with homogeneous isolated grains, which not only improve the light outcoupling efficiency but also enhance the spectrum stability.

5:45 PM EN10.02.09

Dual Strategies with Defect Suppression and Hole Transporting Bilayer for Inverted Perovskite Solar Cell (PCE ~24%) [Hyunjung Shin](#), Hyoungmin Park, Hyeon Jun Jeong, Yongjae In and Urasawadee Amornkitbamrung; Sungkyunkwan University, Korea (the Republic of)

A growing interest in inverted structure perovskite solar cells (i-PSCs) is underway due to their higher stability and potential applications in tandem structures. Typical organic/polymeric hole-transporting layers (HTLs) often faced limitations in improving stability due to intrinsic hygroscopic nature, acidity, intrinsic instability, and non-uniform coating. On the other hand, self-assembled monolayers (SAMs) have demonstrated better stability and higher device performance. Nevertheless, challenges persist, such as non-uniform coating and the hydrophobicity, when perovskite's layers were fabricated on the top of SAMs. Inorganic hole transport layers like NiO can offer better stability and higher performance compared to organic HTLs, but surface defect-related undesirable reactions have been reported. In this study, an ultra-thin NiO (4nm) using atomic layer deposition (ALD) was applied, forming an ALD-NiO/SAMs bi-layer HTL. The use of ALD-NiO showed superior uniformity compared to traditional sol-gel and nano-particulate films' preparation methods, ensuring uniformly formed bi-layers with SAMs. Together with bi-layer strategy, perovskite composition engineering and defect suppression were also conducted. The molecules with both electron donating cation and pseudo halide anion, pyridinium tetrafluoroborate (PyBF₄), were added into perovskite precursor solution to suppress defects in perovskite layers. The suppressed defect was analyzed with thermal admittance spectroscopy. Finally, i-PSCs based on the bi-layer of ALD-NiO/SAMs with defects suppressed perovskite layers demonstrated high power conversion efficiency of 24.0%.

SESSION EN10.03: Stability II

Session Chairs: Marina Leite and Carolin Sutter-Fella

Tuesday Morning, April 23, 2024

Room 334, Level 3, Summit

10:30 AM *EN10.03.01

Facet Engineering for Stable and Efficient Perovskite Solar Cells [Nam-Gyu Park](#); Sungkyunkwan University, Korea (the Republic of)

Since the first report on 9.7 percent efficient solid state perovskite solar cell in 2012 by our group, the record power conversion efficiency of 26.1 percent was reported in 2023. In addition, more than 33 percent was demonstrated from a tandem structure with silicone bottom cell in 2023. This underlines that commercialization of perovskite solar cells is just around the corner. However, long-term stability is still challenging. To achieve highly stable perovskite solar cells, several approaches have been proposed and tried. Among them, we report here the facet engineering approach to improve stability of perovskite solar cells. Dependence of photocurrent generation, moisture stability and passivation on perovskite facets will be discussed in detail.

11:00 AM *EN10.03.02

High-Throughput Experiments and a Machine-Learning-Driven Analysis to Characterize the Stability of Halide Perovskites [Marina S. Leite](#); University of California, Davis, United States

Machine learning (ML) is a powerful tool to accelerate the development of halide perovskite materials and devices. Because this burgeoning class of material for photovoltaics entails a colossal chemical composition space, ML is very suitable to replace the conventional trial-and-error approach used in their characterization. Thus, there has been a pressing need within the materials research community to identify ML models that can be implemented to inform the physical and chemical behavior of the perovskites. We apply ML models varying from echo state networks to statistical models to classify and predict physical properties such as hole transport layer electrical conductivity, halide perovskite photoluminescence response, the power conversion efficiency of photovoltaic devices, etc. Specifically, we use *in situ* environmental optical measurements to predict the optical behavior of Cs-FA perovskites for 50+ hours, upon materials' exposure to moisture. Here, we compare linear regression, echo state network, and seasonal auto-regressive integrated moving average with eXogenous regressor algorithms and attain accuracy of >90% for the latter. Our high-throughput measurements and ML-

supported analyses validate the potential of ML to detect and forecast hybrid perovskites' response with a variety of chemical compositions.

11:30 AM EN10.03.03

Improving Stability of Triple-Cation Perovskite Solar Cells under High-Temperature Operation [Amy E. Louks](#)^{1,2}, Robert Tirawat¹, Mengjin Yang¹, Severin N. Habisreutinger¹, Steven P. Harvey¹, Kelly Schutt¹, Kai Zhu¹, Joseph Berry^{1,3,3} and Axel F. Palmstrom¹; ¹National Renewable Energy Laboratory, United States; ²Colorado School of Mines, United States; ³University of Colorado Boulder, United States

Metal halide perovskite (MHP) photovoltaic performance required for commercial technology encompasses both efficiency and stability. Advances in both these parameters have recently been reported; however, these strategies are often difficult to directly compare due to differences in perovskite composition, device architecture, fabrication methods, and accelerated stressors applied in stability tests. Reported strategies to increase efficiency of perovskite photovoltaics include ink additives, pre- or post-treatments to the perovskite absorber, and choice of contact materials. While these methods may be effective for boosting the initial performance of MHPs, there is a distinct lack of standardized accelerated stability testing data showing the effects of these modifications on the operational stability. This work focuses on using individual and combinations of additive, post-treatment, and contact layer strategies from recent perovskite literature reports. A standardized accelerated testing protocol of light, heat (70 °C), and bias (modified ISOS-L-2) was applied throughout this study to evaluate overall performance impact across device architectures.

Initially, CsMAFA perovskites with an ink stoichiometry of Cs_{0.05}MA_{0.16}FA_{0.79}Pb(I_{0.84}Br_{0.16})₃ were investigated. Visible degradation was quickly observed across all devices tested with this composition. Time of flight secondary ion mass spectrometry (ToF-SIMS) analysis revealed lateral phase halide phase segregation under these elevated temperature test conditions, which was not induced at lower temperatures. Reduction of the bromine content on the X site to a composition of Cs_{0.05}MA_{0.16}FA_{0.79}Pb(I_{0.92}Br_{0.08})₃ mitigated this effect and provided a baseline platform for the broader study of additives, post-treatments, and alternative transport layers to determine the effect the interaction of each has on the stability of the device.

Through analysis of over 1000 devices, we identify the hole transport layer as the most significant factor toward improving performance at elevated temperature. Out of all the combinations tested, the four most stable architectures incorporated a NiOx contact. Post-treatment approaches targeting the perovskite/ETL interface showed positive effects on the initial performance of TC8Br devices but did not lead to significant stability improvements. This observation highlights that passivation approaches for perovskite solar cells should more regularly undergo accelerated aging tests that include exposure to light and heat to unambiguously establish whether the proposed passivation approach is worthwhile. Fundamentally, we observe that these p-i-n devices are stability limited by the HTL, consistent with recent trends in literature. This work therefore motivates the continued development of high-performance HTLs to realize stable and efficient perovskite solar cells.

SESSION EN10.04: Tandems and Wide Bandgaps
Session Chairs: Annalisa Bruno and Carolin Sutter-Fella
Tuesday Afternoon, April 23, 2024
Room 334, Level 3, Summit

1:45 PM *EN10.04.01

Vapor Phase Deposited Perovskite for Single Junction and Tandem Solar Cells [Henk J. Bolink](#); University of Valencia, Spain

We will report on the progress on vapor phase deposited perovskites both for single junction and for Si tandems. Using substrate configuration we optimize the incoupling of sunlight which leads to current densities very close to the detailed balance limit. Impact of deposition speed will be commented upon.

2:15 PM EN10.04.02

Reverse-Bias Resilience of Monolithic Perovskite/Silicon Tandem Solar Cells [Zhaojian Xu](#)¹, Helen Bristow², Maxime Babics², Badri Vishal², Erkan Aydin², Randi Azmi², Esma Ugur², Bumin Yildirim², Jiang Liu², Ross Kerner³, Stefaan De Wolf² and Barry P. Rand¹; ¹Princeton University, United States; ²King Abdullah University of Science and Technology, Saudi Arabia; ³National Renewable Energy Laboratory, United States

Metal halide perovskites have rapidly enabled a range of high-performance photovoltaic technologies. However, catastrophic failure under reverse voltage bias hinders their commercialization. In this work, we demonstrate that by employing a monolithic perovskite/silicon tandem structure, the perovskite subcell can be effectively protected by the silicon subcell under reverse bias, owing to the low reverse-bias diode current of the silicon subcell. As a result, the tested perovskite/silicon tandem devices show superior reverse-bias resilience compared to perovskite single-junction devices in both long-term reverse voltage biasing tests at the single-cell level and partial shading tests at the module level. These results highlight that, compared to other perovskite technologies, monolithic perovskite/silicon tandems are at a higher technology readiness level in terms of tackling the reverse-bias and partial shading challenge, which is a considerable advantage towards commercialization.

2:30 PM EN10.04.03

Rational Design of Photoelectrochemical Perovskite-BiVO₄ Tandem Devices for Stable Fuel Production [Virgil Andrei](#); University of Cambridge, United Kingdom

Metal halide perovskites have emerged as promising alternatives to commonly employed light absorbers for solar fuel synthesis, enabling unassisted photoelectrochemical (PEC) water splitting^[1,3] and CO₂ reduction to syngas.^[2,4] While the bare perovskite light absorber is rapidly degraded by moisture, recent developments in the device structure have led to substantial advances in the device stability. Here, we give an overview of the latest progress in perovskite PEC devices, introducing design principles to improve their performance and reliability. For this purpose, we will discuss the role of charge selective layers in increasing the device photocurrent and photovoltage, by fine-tuning the band alignment and enabling efficient charge separation. A further beneficial effect of hydrophobicity is revealed by comparing devices with different hole transport layers (HTLs).^[1,3] On the manufacturing side, we will provide new insights into how appropriate encapsulation techniques can extend the device lifetime to a few days under operation in aqueous media.^[1,2] To this end, we replace low melting alloys with graphite epoxy paste as a conductive, hydrophobic and low-cost encapsulant.^[3,5] The combined advantages of these approaches are demonstrated in a perovskite-BiVO₄ tandem device archiving selective unassisted CO₂ reduction to syngas.^[4] These design principles are successfully applied to an underexplored BiOI light absorber, increasing the photocathode stability towards hydrogen evolution from minutes to months.^[6] Finally, we take a glance at the next steps required for scalable solar fuels production, showcasing our latest progress in terms of device manufacturing. A suitable choice of materials can decrease the device cost tenfold and expand the device functionality, resulting in flexible, floating artificial leaves.^[7] Those materials are compatible with large-scale, automated fabrication processes, which present the most potential towards future real-

world applications.^[8,9] Such PEC systems approaching a m² size can further take advantage of the modularity of artificial leaves.^[10]

- [1] Andrei, V. et al. *Adv. Energy Mater.* 2018, 8, 1801403.
- [2] Andrei, V.; Reuillard, B.; Reiser, E. *Nat. Mater.* 2020, 19, 189–194.
- [3] Pornrunroj, C.; Andrei, V. et al. *Adv. Funct. Mater.* 2021, 31, 2008182.
- [4] Rahaman, M.; Andrei, V. et al. *Energy Environ. Sci.* 2020, 13, 3536–3543.
- [5] Andrei, V.; Bethke, K.; Rademann, K. *Phys. Chem. Chem. Phys.* 2016, 18, 10700–10707.
- [6] Andrei, V.; Jagt, R. A. et al. *Nat. Mater.* 2022, 21, 864–868.
- [7] Andrei, V.; Ucoski, G. M. et al. *Nature* 2022, 608, 518–522.
- [8] Sokol, K. P.; Andrei, V. *Nat. Rev. Mater.* 2022, 7, 251–253.
- [9] Andrei, V.; Roh, I.; Yang, P. *Sci. Adv.* 2023, 9, eade9044.
- [10] European Commission; Directorate-General for Research; Innovation. Artificial photosynthesis : fuel from the sun : EIC Horizon Prize; Publications Office of the European Union, 2022. DOI: 10.2777/682437.

2:45 PM EN10.04.04

Unveiling Non-Fullerene Routes: Strategic Design of Wide Bandgap Inverted Perovskite Solar Cells with SnO₂ Layers Sung Yong Kim¹ and Jun Hong Noh^{1,2,3}; ¹Korea University, Korea (the Republic of); ²KU-KIST Green School Graduate School of Energy and Environment, Korea University, Korea (the Republic of); ³Department of Integrative Energy Engineering Korea University, Korea (the Republic of)

Recently, metal halide perovskites have garnered attention in photovoltaic research, experiencing a substantial increase in efficiency, achieving an impressive 26.1%. Within this realm, the inverted perovskite solar cell structure is notable for avoiding stability issues associated with the transport layer, such as Spiro-MeOTAD in regular perovskite solar cells. However, to date, the majority of high-efficiency inverted structures employ fullerene derivatives like C60 and PCBM as Electron Transport Layers (ETLs), posing difficulties in commercialization due to their long-term stability and cost-related challenges. Consequently, inorganic materials like SnO₂, TiO₂, and Nb₂O₅ have emerged as potential ETL candidates, with SnO₂ being the most extensively used material in n-i-p structures due to its high electron mobility, wide bandgap, and low cost.

We report achieving a high efficiency of 18.3% at a 1.77eV bandgap, utilizing synthesized SnO₂ nanoparticles, dispersed in a non-damaging solvent, as an Electron Transport Layer (ETL) in an inverted structure. This efficiency is the highest achieved using SnO₂ in inverted structures, even without considering the bandgap. In order to mitigate defects originating from the expanded SnO₂ surface area attributed to the small particles, ethylenediamine (EDA) was employed for passivation. Notably, EDA exhibited a bifunctional role between the perovskite and SnO₂ layers. In order to validate this, observations of a reduction in defects and an enhancement in charge transportation between the perovskite/SnO₂ interfaces will be conducted, utilizing Photoluminescence (PL) and X-ray Photoelectron Spectroscopy (XPS) analytical techniques.

3:00 PM BREAK

SESSION EN10.05: Upscaling and Industrial Considerations
Session Chairs: Henk Bolink and Michael Saliba
Tuesday Afternoon, April 23, 2024
Room 334, Level 3, Summit

3:30 PM *EN10.05.01

Advances in Materials and Process for Sustainable Perovskite Solar Cells Hyun Suk Jung^{1,2}; ¹Sungkyunkwan University (SKKU), Korea (the Republic of); ²SKKU Institute of Energy Science and Technology (SIEST), Korea (the Republic of)

All solid-state solar cells based on organometal trihalide perovskite absorbers have already achieved distinguished power conversion efficiency (PCE) to 26.1% and further improvements are expected up to 27%. Now, the research on perovskite solar cells (PSCs) has been moving toward commercialization. To facilitate commercialization of these great solar cells, some technical issues such as long-term stability, large scale fabrication process, Pb-related hazardous materials, and environmentally-burdened toxic solvent-based process need to be solved.

This talk is dealing with our recent efforts to facilitate commercialization of perovskite solar cells. For examples, we introduce a recycling technology of perovskite solar cells, which covers the regeneration process of Pb contained perovskite layer as well as recycling process of Au electrodes and transparent conducting oxide glass. Also, novel strategies for recycling toxic solvents such as DFM, used in fabricating PSCs are introduced, which is critical to realize close loop recycling process of PSCs. Finally, recent studies for achieving high efficiency PSC using ecofriendly solvent are demonstrated.

4:00 PM *EN10.05.02

Vacuum Processed Perovskites for Optoelectronic Devices Annalisa Bruno; Nanyang Technological University, Singapore

Metal-halide perovskites (MHP) are one of the most promising low-cost optoelectronic materials due to their excellent optoelectronic properties and fabrication versatility. The need to transfer the existing technology into large areas by industrial-compatible high throughput methods is becoming more urgent [1].

Thermal evaporation is a promising MHP fabrication technique to bring this technology closer to reliable and extended production by relying on excellent size scalability, fine composition control, surface adaptability, and enabling precision in layer thickness and fine control on composition [2-7]. On one hand, this annealing-free deposition process guarantees a strain-free perovskite and PSCs with remarkable thermal stability and structural robustness [4]. On the other, thermal evaporation of perovskite has expanded the horizons of thin film fabrication, proving the ability to produce ultrathin perovskite films as the base of multi-quantum well (MQW) structures.

Controlling the optoelectronic features of thin films and nanostructured materials, capitalizing on the quantum confinement effects, can open up a novel pathway for investigating cutting-edge phenomena and for new optoelectronic applications.

References

1. J. Avila et al., *Joule* 2017, 2, 431; F. Kosaisih et al., *Joule* 2022, 12, 2692; Y. Vaynzof, *Adv. Energy Mat.* 2020, 10, 2003073
2. J. Li et al., *Joule* 2020, 4, 1035
3. H.A. Dewi et al., *Sust. Energy & Fuels.* 2022, 6, 2428

4. E. Erdenebileg, et al Solar RRL, 2022, 6, 2100842
5. H.A. Dewi, et al., Adv. Funct. Mater. 2021, 11, 2100557
6. J. Li et al., Adv. Funct. Mater. 2021, 11, 2103252
7. E. Erdenebileg et al., Material Today Chemistry, 2023, 30, 101575

4:30 PM EN10.05.03

Sustainable Solvent Management for Viable Perovskite Solar Cell Recycling Process [Hee Jung Kim](#)¹, Oh Yeong Gong¹, Young Ju Kim¹, Geon Woo Yoon¹, Gill Sang Han², Hyunjung Shin^{1,3} and Hyun Suk Jung^{1,3}; ¹Sungkyunkwan University, Korea (the Republic of); ²Korea Research Institute of Chemical Technology, Korea (the Republic of); ³SKKU Institute of Energy Science and Technology, Korea (the Republic of)

Sustainable recycling technologies of perovskite solar cells (PSCs) at the end of life is inevitable for commercialization, which can reduce the environmental impacts as well as re-fabrication cost. Thus, several efforts have been made to recycle toxic Pb compounds and expensive components in PSCs. However, most recycling strategies included dissolving layers such as perovskite and charge transfer layer by using organic solvents, which can cause harmful effects on environmental, health, and safety. Nevertheless, studies related to these toxic solvents used in recycling processes have not yet been considered.

Here, we introduce a novel approach that recovers and reuses toxic solvents used in the recycling process. First, detailed evaluations were conducted to assess the effects of residual substances in PSC-dissolved solvents. Then, two-step dissolution process, which selectively dissolve spiro-OMeTAD and perovskite layer by layer, was introduced to minimize the factors affecting the efficiency reduction. PSCs were immersed in chlorobenzene and N,N'-dimethylformamide (DMF) solvents in sequence, and each solvent was recovered for reuse in the re-fabrication of PSCs. Especially, the recovered DMF was filtered by nano-absorbents for removing and managing toxic Pb ions. The recovered solvents were reused as precursor solvents to re-fabricate PSCs, and the dissolved spiro-OMeTAD also reused without any loss. Our results demonstrate the feasibility of a toxic solvent recycling process for PSC re-fabrication, which achieved a power conversion efficiency of 25.02%, comparable to that of the original PSCs (25.12%), as well as recycling of the dissolved hole conducting materials.

4:45 PM EN10.05.04

Open-Air Spray Deposition with Rapid Plasma Curing for High-Throughput Manufacturing of Low-Cost Perovskite Solar Modules [Austin Flick](#), Justin P. Chen, Thomas W. Colburn, Abigail Carbone, Francisco Barrera, William Cai and Reinhold H. Dauskardt; Stanford University, United States

Successful commercialization of perovskite solar devices requires significant focus on scalable, low-cost manufacturing techniques. The solution processability of the perovskite layer yields a compelling candidate for low-cost solar energy production, though efforts to develop complementary low-cost transport layers, electrodes, and barrier layers are essential. Ultrasonic spray deposition provides a platform for high-throughput production, complemented with open-air plasma curing for rapid crystallization as previously demonstrated in rapid spray plasma processing (RSPP) of perovskite films.^[1-3] Large-area spray deposition paired with ultrafast plasma-assisted crystallization enables processing speeds up to 20 cm/s, demonstrating the highest throughput and lowest cost perovskite manufacturing method. However, remaining vacuum-dependent transport layer and electrode depositions—including sputtering and thermal evaporation—create significant bottlenecks in production with elevated module costs.

In this work, open-air spray deposition with rapid plasma and near infrared curing sources are employed throughout the entire thin-film architecture for high-throughput production of low-cost additive-free inverted p-i-n perovskite devices. Ultrasonic spray deposition with rapid plasma curing is utilized for transparent conducting oxide (TCO) front electrode and perovskite layer production, meanwhile spray deposition with near infrared curing is employed across the transport layers and rear metal electrode. Validation of individual film morphologies and optoelectronic properties demonstrate large-area defect-free films deposited at linear throughputs of 10 – 20 cm/s. TCO front electrodes with >90% visible transmittance and Haack figure of merit (T_{10}/R_{SH}) of 0.01 Ohm^{-1} are achieved with >80% fill factor compatible transport layers, enabling 20% device efficiencies and >18% module efficiencies across 25 cm^2 .

Complementary technoeconomic analysis at 100 MW production scale demonstrates >50% cost reduction employing the developed open-air manufacturing techniques compared to conventional vacuum-based manufacturing. The high-throughput techniques enable reduced dependence on equipment, facilities, and labor costs, yielding considerable economies of scale beyond 1 GW production. The open-air spray deposition platform for perovskite module production provides a pathway towards reduced levelized cost of energy for photovoltaics below \$0.02/kWhr.

[1] Hilt, F., Hovish, M.Q., Rolston, N., Bruning, K., Tassone, C.J., and Dauskardt, R.H. "Rapid Route to Efficient, Scalable, and Robust Perovskite Photovoltaics in Air." *Energy Environ. Sci.*, **2018**.

[2] Hovish, M.Q., Rolston, N., Bruning, K., Hilt, F., Tassone, C.J., and Dauskardt, R.H. "Crystallization Kinetics of Rapid Spray Plasma Processed Multiple Cation Perovskites in Open Air." *J. Mater. Chem. A*, **2020**.

[3] Rolston, N., Scheideler, W.J., Flick, A.C., Chen, J.P., Elmaraghi, H., Sleugh, A., Zhao, O., Woodhouse, M., and Dauskardt, R.H. "Rapid Open-Air Fabrication of Perovskite Solar Modules." *Joule*, **2020**.

SESSION EN10.06: Poster Session I

Session Chairs: Carolin Sutter-Fella and Yuanyuan Zhou

Tuesday Afternoon, April 23, 2024

Flex Hall C, Level 2, Summit

5:00 PM EN10.06.01

Correlating Halide Segregation with Iodide Oxidation via *In-Situ* Opto-Gravimetric Analysis [Zhaojian Xu](#) and Barry P. Rand; Princeton University, United States

Halide oxidation plays an important role in halide segregation and degradation of metal halide perovskites. However, a direct and quantitative measurement of halide oxidation in solid-state perovskite samples is still required to fully understand and evaluate the effect of halide oxidation. In this work, we employed a quartz crystal microbalance to achieve an *in-situ* opto-gravimetric measurement of solid-state perovskite films and quantify the iodine loss rate under light excitation. Combining photoluminescence, X-ray photoelectron spectroscopy, X-ray diffraction, and *in-situ* opto-gravimetric measurements on a series of mixed-halide perovskite with different halide ratios, we are able to explain the degradation mechanism of mixed-halide perovskite under prolonged light illumination (photolysis of iodine), and demonstrate an identical compositional threshold for both light-induced halide segregation and iodide oxidation. These results not only reveal the correlation between light-induced halide segregation and iodide oxidation, which experimentally proves

the photoelectrochemical origin of light-induced halide segregation, but also provide a powerful tool to quantitatively study halogen loss and degradation kinetics of metal halide perovskites.

5:00 PM EN10.06.02

Utilizing Machine Learning and Diode Physics to Optimize Photovoltaic Performance in Sequentially Processed Perovskite Solar Cells Jeongbeom Cha and Min Kim; Jeonbuk National University, Korea (the Republic of)

Organic-inorganic lead halide perovskite photovoltaics are well-known for their exceptional solution processability. However, achieving uniformly crystalline perovskite films often requires complex deposition methods. To solve this challenge of the perovskite deposition method, several studies have been performed to utilize deposition parameters such as concentrations of the annealing temperatures, precursor solution, and spin-coating speeds. Unfortunately, most of these studies have been conducted on trial-and-error approaches, which are resource-intensive and time-consuming. Nowadays, machine learning techniques have considered as powerful tools for utilizing complex experimental parameters and predicting the device performance, making more efficient analysis of parameter spaces.

In our study, we combined Shockley diode-based numerical analysis with machine learning techniques to analyze the photovoltaic characteristics of the device and utilize their photovoltaic performance by considering experimental variables. The application of the Shockley diode equation allowed us to extract photovoltaic parameters and predict power conversion efficiencies, contributing to our understanding of charge recombination and device physics. Using machine learning techniques, we trained a machine learning model using current-voltage curves that are sensitive to changes in manufacturing conditions. This enabled us to identify the optimal settings for improved device performance.

Our harmonized approach not only reveals the relationship between experimental conditions and device performance, but also simplifies the optimization process, reducing the need for extensive trial-and-error experimentation. This methodology shows great promise in advancing the development and fine-tuning for next-generation perovskite solar cells.

5:00 PM EN10.06.03

Assembly-Coating through Marangoni and Capillary Convection Manipulation of Colloidal Droplets on a Substrate for Robust Luminescence Jin Young Kim, Byung Gi Kim, Woongsik Jang and Dong Hwan Wang; Chung-Ang University, Korea (the Republic of)

Recently, lighting and display technologies require high-resolution, and research into materials that produce vivid and natural colors is required [1,2]. In particular, semiconductor material selection and layering for key energy sensing components in industrial applications is important [3]. Quantum dots (QDs) are attracting attention as next-generation functional materials, but due to the nature of colloidal particles, it is difficult to deposit them evenly and uniformly on the substrate. Therefore, discussion is still needed to understand and solve the evaporation mechanism of drying a solution containing colloidal particles on a substrate. In general, when depositing a colloidal suspension on a solid substrate, non-uniform surfaces (coffee rings, multi-ring patterns, etc.) are mainly observed due to evaporation of the solvent [4,5]. At the evaporation location, the particles are circulated by the inward and outward flow of the droplets. As a result, colloidal particles move to the tri-contact line, resulting in irregular surface deposition, and many studies have been conducted to prevent this. However, a system that uniformly coats the entire surface of the substrate with a colloidal solution has not been studied. In this study, we focused on surface uniformity and luminescence efficiency by relating Marangoni flow and capillary flow to the inclination angle of the substrate. Perovskite QDs were used as colloidal particles, and the coating method was improved by tilting the substrate by manipulating the directions of the two main flows (Marangoni and capillary). Due to this, the internal flow circulation time of the droplet was different on the flat and inclined substrates, which extended the Marangoni flow and led to a uniform surface. In addition, lubrication theory was applied to the colloid applied to the inclined surface to analyze the correlation between the inclination angle of the substrate and the Marangoni and capillary numbers. It was found that the higher the Marangoni number, the more uniform the coating, and as the angle of the substrate increases, the shaded area increases, making the surface more non-uniform [6]. At an angle of 3°, the Marangoni and capillary flows circulated almost similarly, leading to a uniform surface, which was confirmed to not lose luminescence even in a thermal evaporation environment. In addition, as a result of manufacturing a diode device and evaluating the charge transport characteristics according to the quality of the QD thin film, improved hole carrier transport and extraction characteristics were observed. These results suggest that it may help improve the deposition quality of colloidal solutions that require uniform surfaces in applications.

[1] J. Y. Kim, B. G. Kim, W. Jang, D. H. Wang, *ACS Sustainable Chem. Eng.* 2022, 10, 3, 1115-1124.

[2] J. Y. Kim, W. Jang, J. Lim, D. H. Wang, *Inorg. Chem.* 2023, 62, 29, 11665-11673.

[3] J. Y. Chun, B. G. Kim, J. Y. Kim, W. Jang, D. H. Wang, *Carbon Energy*, 2023, 5, e350.

[4] J. Zhang, Z. Zhu, Z. Yu, L. Ling, C.F. Wang, S. Chen, *Mater. Horiz.* 2019, 6, 90-96.

[5] L. Shmuylovich, A.Q. Shen, H.A. Stone, *Langmuir* 2002, 18 (9), 3441-3445.

[6] A. Gençer, C. Schütz, W. Thielemans, *Langmuir* 2017, 33 (1), 228-234.

5:00 PM EN10.06.04

Thermally Evaporated High-Performance Metal Halide Perovskite Transistors Youjin Reo¹, Huihui Zhu^{1,2}, Ao Liu^{1,2} and Yong-Young Noh¹;

¹Pohang University of Science and Technology, Korea (the Republic of); ²Northwestern University, United States

Advances in metal halide perovskites for optoelectronic devices have resurrected their potential as channel layer for transistors. Over the past several years, notable performances have been reported for solution-processed metal halide perovskite transistors through fine-tuning of material composition, crystallization and device structure.¹⁻³ However, their ionic nature allows the channel layer to be susceptible to common solvents used in lithography, which is challenging for complex circuit integration, large-area or micro-scale electronics. Here, we present thermally evaporated metal halide perovskite, caesium-tin-iodide, as a channel layer for high-performance p-channel thin-film transistor. While thermal evaporation is a mature fabrication technique, the low crystallinity of deposited thin-films, when compared with those from solution-process, was a fundamental bottleneck. The chemical reaction can take place by overcoming high energy barrier for diffusion and solid-solid interaction, unlike fast ionic reactions of the solution-process.^{4,5} By incorporating chloride-based additives that accelerate the solid-state diffusion under high thermal energy and alkali metal iodide additives that modulate the formation of nucleation sites, we achieved a highly crystalline film and high-performance thin-film transistor with field-effect hole mobilities over 30 cm²V⁻¹s⁻¹ and on/off current ratios exceeding 10¹⁰. High reproducibility and operational stability were attained in large-area wafer-scale to micro-scale devices, accentuating the highly promising and industry-ready thermally evaporated metal halide perovskite thin-film transistors.

1. H. Zhu et al. *Nat. Electron.* 6, 650-657 (2023).

2. A. Liu et al. *Nat. Electron.* 5, 78-83 (2022).

3. A. Liu et al. *Nat. Electron.* 6, 559-571 (2023).

4. D. Lin et al. *Mater. Today Adv.* 16, 100277 (2022).

5. Y. Vaynzof. *Adv. Energy Mater.* 10, 48, 2003073 (2020).

5:00 PM EN10.06.05

Down Layer Intercalation Control of Cesium Halides into MAPbI₃ Framework for High Stable Perovskite Solar Cells Yue Feng¹, Shahiduzzaman Md.², Munkhtuul Gantumur¹, Masahiro Nakano³, Makoto Karakawa^{1,2,3} and Tetsuya Taima^{1,2,3}; ¹Graduate School of Frontier Science Initiative, Kanazawa University, Japan; ²Nanomaterials Research Institute, Kanazawa University, Japan; ³Graduate School of Natural Science and Technology, Kanazawa University, Japan

Perovskite solar cells (PSCs) have attracted considerable interest of the researchers and achieved the power conversion efficiency (PCE) of 26.1%. However, low stability is still the most challenging issue for PSCs that needs to be solved. Up to date, introduction of a small amount of cesium halides (CsX) particularly CsCl, CsBr and CsI into perovskite precursor solution showed improved device performance. However, this method leads to the formation of pinholes during the spin-coating and imperfect surface coverage of the perovskite due to the limited solubility of these materials and has difficulties to control Cs⁺ concentration as well as thickness of the film. Previously, our group has successfully intercalated CsI into perovskite MAPbI₃ framework and achieved a PCE of 18.43% and remained above 80% of their initial output after 6000 h storage in open air (non-encapsulated) [1]. Precise intercalation of CsX technology has not yet studied widely. In this study, we introduced vacuum deposited CsX (CsCl, CsBr and CsI) thin layers into solution processed host perovskite MAPbI₃ film from down layer to promote precise intercalation, resulted in high-quality perovskite film for high stable PSCs. The use of CsX layer greatly altered the perovskite morphology to produce large grain sizes, as a result of the precise intercalation of the CsX molecules into the host MAPbI₃. We tested thermal stability of perovskite films and found that after heating at 85 °C on hot plate at relative humidity of 50% to 60% for more than 24 hours, Cs-containing perovskite films showed higher stability than pristine MAPbI₃ film. After that, PSCs were fabricated by using CsX intercalated perovskite films and evaluated device performance and stability. PSCs made with CsCl, CsBr, and CsI intercalation exhibited PCEs of 15.64%, 15.97% and 15.74%, respectively whereas the pristine MAPbI₃ based device showed PCE of 15.33%. Furthermore, the light-soaking of devices prepared with CsCl, CsBr and CsI intercalation remained 76.9%, 77.2% and 71.2%, respectively, of their initial efficiencies, while the pristine MAPbI₃ device showed only 4.3% of its initial efficiency after 120 minutes of light illumination (1 sun). More importantly, a similar trend with the CsCl, CsBr, and CsI-based PSCs were observed for the moisture stability for 3000 h storage at ambient with a relative humidity range of 50–60%. This CsX intercalation technology will enable a significant improvement in the device operational stability and processing reproducibility.

5:00 PM EN10.06.06

Process Optimization of Chemical Vapor Deposition of MAPbBr₃ for Optoelectronic Applications Jona Riedel¹, Franziska E. Muckel², Michael Heuken^{1,3}, Andrei Vescan¹ and Holger Kalisch¹; ¹RWTH Aachen University, Germany; ²Universität Duisburg-Essen, Germany; ³AIXTRON SE, Germany

With growing commercial interest in halide perovskite (HP) thin-film applications, the question which deposition techniques can meet the requirements of industrial scalability and reproducibility becomes increasingly important. At the current time, solution-based methods which are prominent in research are limited to small areas, low reproducibility and are not able to meet special requirements such as deposition on structured substrates. Promising alternatives are vapor-based techniques like vacuum thermal evaporation (VTE) or chemical vapor deposition (CVD) which are well established in the field of semiconductor manufacturing.

At CST (RWTH Aachen University), we have designed and built a custom showerhead-based CVD tool for the deposition of HP thin films by thermal evaporation of halide salts into a heated carrier gas stream. The usage of an inert carrier gas such as N₂ at low vacuum around 5-10 hPa allows for the simultaneous or alternating evaporation of both metal-halide as well as organo-halide salts in a single process. The latter materials are typically difficult to use in high-vacuum techniques like VTE due to their large vapor pressures and low sticking coefficients. In addition, unlike quartz furnace CVD setups found in research literature, our tool features separate sources for different precursor salts. Temperature-controlled substrates are mounted in a heated showerhead-based reactor chamber allowing for uniform deposition on areas up to 100 cm².

While different HP materials have been successfully prepared in our tool, benchmarks for both LEDs and solar cells are lagging behind those of devices based on HP films prepared by spin coating. A typical feature of our CVD films is a reduction of photoluminescence (PL) intensity compared to spin-coated reference samples by 2-3 orders of magnitude. Times-resolved PL spectroscopy indicates the presence of a fast, non-radiative recombination channel in CVD samples absent in their solution-processed counterparts, which likely impedes efficient operation of both LEDs and solar cells. By sequential deposition of PbBr₂ and MABr to form MAPbBr₃ using combinations of CVD and solution deposition, we investigated the influence of both precursors and processes. We observed that spin-coated PbBr₂ layers can be easily converted to MAPbBr₃ layers with strong PL intensity using CVD-MABr, while simultaneously grown CVD-MAPbBr₃ as well as CVD-PbBr₂ films converted by either CVD-MABr or MABr solutions share a low PL intensity. This is in accordance with literature which comprises numerous reports on the conversion of lead-halide precursor films from solution or VTE via MABr-CVD, but lacks reports on the usage of lead halide salts as separate precursors under low vacuum. Unlike reports from high-vacuum evaporation, we observe strong evidence for the dissociation of thermally evaporated PbBr₂. Notably after prolonged evaporation of PbBr₂ precursor material, metallic residues can be found in the crucible. This indicates an at least partial dissociation of PbBr₂ into elemental Pb and volatile Br₂. Due to the high vapor pressure of Br₂ the deposition conditions inside our reactor can be expected to be Br-rich. This could facilitate the formation of intrinsic defects related to excess Br, like Br interstitials, and give a reason for the low PL intensity found when evaporated PbBr₂ is part of the process. Nevertheless, we were able to increase the PL intensity of MAPbBr₃ by 1-2 orders of magnitude by thermal annealing of PbBr₂ precursor layers for up to 3 h at 200-310 °C in N₂. A similar effect can be observed by increasing the substrate temperature during PbBr₂ deposition from 100 °C to above 200 °C, supporting the assumption of a volatile species like Br poisoning our HP. The combined results show a clear path to directly avoid the suspected negative impact of PbBr₂ dissociation in CVD of HPs.

5:00 PM EN10.06.07

Structure and Properties of Novel Mixed Organics Hybrid Lead-Halide Phase (1-NA)(1-MQ)Pb₂I₆ Yang Goh, Megan Cassingham, Peter Djurovich, Mark E. Thompson and Brent Melot; University of Southern California, United States

Low dimensional hybrid organic-inorganic lead-halide structures are gaining interest due to their structural flexibility and tunability compared their parent 3-D perovskite structure. By combining the tunability of organic chromophores and the desirable optical properties of perovskites, we aim to develop a new portfolio of hybrid organic-inorganic lead-halide materials. In order to achieve a mixed organics hybrid lead-halide phase, several 1-naphthylamine isomers were used to synthesize new 1-D hybrids to screen for similar crystal structures to the known 1-D hybrid, 1-naphthylammonium lead iodide (1-NA)PbI₃. 1-methylquinolinium iodide (1-MQ)PbI₃ has a similar structure, and a mixed organics hybrid phase, (1-NA)(1-MQ)Pb₂I₆ is successfully synthesized. (1-NA)(1-MQ)Pb₂I₆ shows clear ordering of the organics, which is the first we are aware of in these systems. We will discuss the optical and dielectric properties of the end members, (1-NA)PbI₃ and (1-MQ)PbI₃, as well as the mixed organics hybrid phase, (1-NA)(1-MQ)Pb₂I₆, and how that relates to their respective structures.

5:00 PM EN10.06.08

Direct Photo-Patterning of Perovskite Nanocrystals with Siloxane Resin Showing Highly Stable Luminescence Jinmin Park¹, Sang Woo Bae¹, Junho Jang², Hyukmin Kwon¹, Byeong-Soo Bae², Young-Hoon Kim¹ and Do Hwan Kim¹; ¹Hanyang University, Korea (the Republic of); ²Korea Advanced Institute of Science and Technology, Korea (the Republic of)

Metal halide perovskite nanocrystals (PeNCs) are promising light emitting materials for color-converting light-emitting diodes (CC-LEDs) due to their

high absorption coefficient, narrow full width at half maximum (FWHM) and easily tunable bandgap. However, PeNCs face challenges, such as instability against chemicals and high humidity, as well as limited patternability without any additive, which limit their potential as color conversion layer (CCL) in CC-LEDs. Also, there are no reports regarding stable PeNCs patterns, despite the achievements of their high-resolution patterning using ligand crosslinkers.

Herein, we report highly stable PeNCs (green emitting MAPbBr₃/resin composites) patterns encapsulated in siloxane resin which is synthesized by the sol-gel reaction between methoxy groups of (3-methacryloxypropyl) trimethoxysilane (MPTS) and hydroxyl groups of diphenylsilanediol (DPSD). The synthesized siloxane resin provides physical protection to core materials by crosslinking between methacrylate functionalized siloxane resin and unsaturated hydrocarbon of organic ligands (e.g., oleic amine or oleic acid) via UV-induced free radical reactions, resulting in direct optical patterning without ligand crosslinkers.

By introducing the siloxane resin, PeNCs patterns demonstrate high photoluminescence quantum yield (PLQY) in various harsh conditions: in DI water (> 100 days), ambient conditions (> 150 days) and under 40 °C/RH 70% (> 8 hours) without additional encapsulation process, since the siloxane resin suppresses hydrolysis of PeNCs and controls permeation of H₂O molecules moderately. Moreover, direct optical patterning with siloxane resin can be applied to various inorganic light emitting materials (red emitting CdSe QDs/resin composites).

We believe that our material design, which combines MAPbBr₃ and CdSe QDs with siloxane resin, will offer a universal solution, demonstrating high levels of pattern stability in harsh conditions while enabling direct optical patterning without the need for ligand crosslinkers, simultaneously.

SESSION EN10.07: Devices
Session Chairs: Jin-Wook Lee and Michael Saliba
Wednesday Morning, April 24, 2024
Room 334, Level 3, Summit

8:00 AM *EN10.07.01

Insights into Hybrid Perovskites Ink Reactivity and Evolution to Polytypes [Silvia Colella](#)^{1,2}; ¹CNR-NANO, Italy; ²University of Bari, Italy

Metal halide perovskite (MHP) semiconductors are excellent candidates for contemporary optoelectronics innovation, particularly for photovoltaics.[1] The advantages of this class of materials derive from their hybrid nature, allowing for straightforward fabrication processes, and from their unique optoelectronic properties. A typical 3D organic-inorganic perovskite has a chemical formula of ABX₃, where A is an organic cation (such as MA [methylammonium] or FA [formamidinium]), B is a metal cation (such as Pb²⁺), and X is a halogen anion (such as I or Br).[2] However, recent advances have also explored more complex compositions embedding diverse cations/anions.[3] These materials are prepared by simple and straightforward solution processing, the material precursors dissolved in a solvent undergoes self assembly into a perovskite structure during spin-coating onto a substrate under mild thermal annealing. As the technology continues to mature, this still is a key advantage, allowing for affordable and scalable processing. Understanding perovskite ink properties is therefore a fundamental requirement towards industrialization, with special regards to their evolution over time. It has been demonstrated that even for the simplest system, the precursor solution is a complex – and dynamic – dispersion which contains not only solvated ions but also lead halide complexes, colloids and aggregates of different natures and dimensions. In these complex dispersions, multiple chemical species are present and can interact – or react – between each other or with the solvent. We have proved the existence of a reactivity between two of the perovskite components – MA and FA – in the precursors solutions, that leads to the formation of a novel condensation product, methylformamidinium (MFA). We have studied different parameters that affects such reactions kinetics, therefore modifying the ink composition over time, and proposed solutions to overcome these issues.[4] With the aim of correlating the solution chemistry with the film structural properties, through the synergic use of solution Nuclear Magnetic Resonance (NMR) spectroscopy, X-ray Diffraction and Density Functional Theory (DFT) calculations, we have recognized and explained for the first time a correlation between the aging of perovskite precursor solutions, the presence of MFA species in solution and the emergence of photoinactive hexagonal polytypes (6H and 4H) [5] Starting from the known reactivity of the chemical species present in ink solutions, we outline the directions towards which future research efforts should be directed.[6] References: [1] Jeong, J., Kim, M., Seo, J., Lu, H., Ahlawat, P., Mishra, A., Yang, Y., Hope, M.A., Eickemeyer, F.T., Kim, M., et al. (2021). Pseudo-halide anion engineering for *α*-FAPbI₃ perovskite solar cells. *Nature* 592, 381–385. [2] Snaith, H.J. (2013). Perovskites: The emergence of a new era for low-cost, high-efficiency solar cells. *Journal of Physical Chemistry Letters* 4, 3623–3630. [3] McMeekin, D.P., Sadoughi, G., Rehman, W., Eperon, G.E., Saliba, M., Hörantner, M.T., Haghighirad, A., Sakai, N., Korte, L., Rech, B., et al. (2016). A mixed-cation lead mixed-halide perovskite absorber for tandem solar cells. *Science* 351, 151–155. [4] Valenzano, V., Cesari, A., Balzano, F., Milella, A., Fracassi, F., Listorti, A., Gigli, G., Rizzo, A., Uccello-Barretta, G., and Colella, S. (2021). Methylammonium-formamidinium reactivity in aged organometal halide perovskite inks. *Cell Reports Physical Science* 2, 100432. [5] Gianluca Bravetti, Nicola Taurisano, Anna Moliterni, Jose Manuel Vicent-Luna, Davide Altamura, Federica Aiello, Nadir Vanni, Agostina Lina Capodilupo, Sonia Carallo, Giuseppe Gigli, Gloria Uccello-Barretta, Federica Balzano, Cinzia Giannini, Shuxia Tao, Silvia Colella, Aurora Rizzo (2023). Solution Aging Promotes Hexagonal Polytype Formation in Mixed Cation/Halide Perovskites, accepted. [6] Rizzo A., Listorti A., Colella S. (2022). Chemical insights into perovskite ink stability. *Chem*, 8, 1, 31–45

8:30 AM EN10.07.02

Bi-Directional Simultaneous Cation/Anion Engineering of Formate Complex for Holistic Management of Perovskite Solar Cells [Min Ju Jeong](#); Korea University, Korea (the Republic of)

Pseudo-halide anion formate (HCOO⁻) has been widely recognized as crystallization agent to control the crystal growth without inducing any changes in the band-gap. However, there is a lack of understanding regarding the effect on perovskite films depending on the chemical bonding state of formate. In this work, we demonstrated the distinguishable crystallization behavior of FAPbI₃ film by comparing the formate complexes with different bonding state. In addition, we found that the distinct passivation mechanisms depending on the cations of formate complexes, which resulted in the differences in device performance. Notably, sodium formate (NaFo) showed bi-directional behavior of cation and anion, eliciting a distinction from other formate complexes. As a result, the NaFo device showed an enhanced power conversion efficiency (PCE) of 25.6% with a high open-circuit voltage (V_{oc}) of 1.18 V, achieving 95% of the Shockley-Queisser limit at the PV band-gap of 1.53 eV. This work provides insights of the effect of crystallization by the chemical bonding state of formate as well as different passivation mechanism depending on the cations of formate complexes.

8:45 AM EN10.07.03

Electrically Induced Directional Ion Migration in Two-Dimensional Perovskite Heterostructures [Jee Yung Park](#), Yoonho Lee and Letian Dou; Purdue University, United States

Understanding ion migration in halide perovskite materials is key to enhancing both device performance and stability. The introduction of two-dimensional (2D) perovskites has improved stability, spurring increased interest in understanding ion migration in these materials. Hindered by the challenge in building

a reliable device platform, prior studies primarily focused on heat and light induced ion migration. Here, we construct a high-quality single crystal 2D perovskite heterostructure, free from grain boundaries and impurities. Using a device platform fabricated through a multi-step dry transfer process to realize near defect-free van der Waals contact, we achieve real-time visualization and imaging of directional ion migration. Notably, aside from the expected directional ion migration driven by the electric field, we discover the unique behavior of halide anions inter-diffusing against the field under strong and prolonged bias. Spatial confocal photoluminescence mapping reveals a halide migration channel that aligns with the crystal edge of high electrical conductivity, highlighting the role that electric current plays in ion migration. Finally, after a sustained mild bias, stable junction diodes exhibiting ~1000-fold forward to reverse current ratio are realized due to directional ion migration-induced asymmetry. This study unveils important fundamental insights on halide migration under electrical bias, paving the way toward high-performance electronic and optoelectronic devices.

9:00 AM EN10.07.04

***In Situ* Polymerization of Cross-Linked Perovskite–Polymer Composites for Highly Stable and Efficient Perovskite Solar Cells** He Guo and Hyun Suk Jung; Sungkyunkwan University, Korea (the Republic of)

Mixed-halide perovskites have emerged as outstanding light absorbers that enable the fabrication of efficient solar cells; however, their instability hinders the commercialization of such systems. Grain-boundary defects and lattice tensile strain are critical intrinsic-instability factors in polycrystalline perovskite films. In this study, the light-induced cross-linking of acrylamide (Am) monomers with non-crystalline perovskite films was used to fabricate highly efficient and stable perovskite solar cells. The Am monomers induced the preferred crystal orientation in the polycrystalline perovskite films, enlarged the perovskite grain size, and cross-linked the perovskite grains. Additionally, the liquidity of Am effectively released lattice strain during perovskite-film crystallization. The cross-linked interfacial layer functioned as an airtight wall that protected the perovskite film from water corrosion. Devices fabricated using the proposed strategy showed an excellent power conversion efficiency (*PCE*) of 24.45% with an open-circuit voltage (V_{OC}) of 1.199 V, which, to date, is the highest V_{OC} reported for hybrid PSCs with electron transport layers comprising TiO_2 . Large-area perovskite solar cell modules fabricated using the proposed strategy showed a *PCE* of 20.31% (with a high fill factor of 77.1%) over an active area of 33 cm², with excellent storage stability.

9:15 AM EN10.07.05

Metal-Organic Chemical Vapor Deposition of Hybrid Perovskites Alicia Bryan, Jonathan Meyers, Lorenzo Serafin and James Cahoon; University of North Carolina at Chapel Hill, United States

Hybrid perovskites (HPs) have become widely recognized in the chemistry and materials science communities as a promising candidate for the next generation of efficient optoelectronic and photovoltaic devices. Their unique hybrid organic-inorganic nature affords HPs an exciting blend of electronic and structural properties, and yields both advantages and challenges in fabrication. The vast majority of HP fabrication methods to date have focused on simple solution processing, while comparatively few vapor-phase HP deposition methods have been developed, and these broadly rely on single-source evaporation of solid HP perovskite crystals or dual-source coevaporation of precursor salts. However, these methods suffer from limited control over reactant vapor pressures and temperatures that in turn lead to limited control over final film composition and morphology. In light of this, we have developed a metal-organic chemical vapor deposition (MOCVD) method for HP fabrication to enable precise control of composition, stoichiometry, and film morphology. Using our custom-built reactor equipped with vapor precursors including methylamine, tetraethyllead, and hydrogen halide gasses, we have successfully deposited continuous thin films of phase-pure $CH_3NH_3PbI_3$ perovskites as confirmed using X-ray diffraction, UV-visible and photoluminescence spectroscopy, and scanning electron microscopy. We further probed deposition on a variety of substrates including FTO-glass, silicon oxide, and organic-functionalized materials to investigate the vital relationship between substrate identity and film nucleation and growth dynamics.

9:30 AM BREAK

SESSION EN10.08: Synthesis and Formation
Session Chairs: Monica Morales-Masis and Carolin Sutter-Fella
Wednesday Morning, April 24, 2024
Room 334, Level 3, Summit

9:45 AM *EN10.08.01

Revisiting Crystal Growth and Composition Engineering for Reproducible Fabrication of High-Performance Perovskite Solar Cells Jin-Wook Lee; Sungkyunkwan University, Korea (the Republic of)

Metal halide perovskite solar cells (PSCs) have been spotlighted as a promising next-generation photovoltaic technology. Recently, there has been a surge of efforts in the commercialization of PSCs in academia and industries worldwide with record power conversion efficiencies over 26% for both n-i-p and p-i-n structured devices. Nevertheless, their subpar operational durability, module scalability, and material toxicity are challenges often brought up as the major barriers hindering practical commercialization. The poor reproducibility of PSCs has been relatively overlooked, but negatively impacts institutional research laboratories, start-up companies, and large established corporations all alike. Reproducible fabrication of PSCs is a critical consideration for market viability and practical commercialization. In this work, I will discuss the critical functions of atmospheric humidity to regulate the crystallization and stabilization of formamidinium lead triiodide (FAPbI₃) perovskites. We demonstrate that the humidity content during processing underlies profound variations in perovskite stoichiometry, thermodynamic stability, optoelectronic quality and thus reproducibility of PSCs. In second part of the presentation, I will discuss the interplay between composition of perovskite, and performance and stability of inverted PSCs. We rationalize the difference in widely used perovskite compositions in n-i-p and p-i-n PSCs.

10:15 AM *EN10.08.02

Unlocking Versatility: Innovative Crystallization Strategies for Metal Halide Perovskites and Their Application Potentials Pablo P. Boix; Instituto de Tecnología Química (UPV-CSIC), Spain

Metal halide perovskite crystals in the macro and nano scales can leverage the huge versatility of the perovskite family. They present exceptional optoelectronic properties that make them attractive for a variety of applications. However, these structures usually depend on complex synthesis processes, where the ligands play a dominating role, or are limited by growth form factor and surface losses.

We present crystallization insights that enable less demanding synthesis processes, such as a promising sol-gel approach [1] for humidity-triggered nanoparticle crystallization or a contactless surface passivation technique for large crystals. The particularity of these systems can be adapted to specific applications such as memristive devices or downconversion films with efficiencies >95%, which also serve as a platform to characterize the fundamental

working mechanisms of these materials.

The combination of the crystallization control with additive engineering also opens new routes for lead-free perovskite photovoltaics, improving their ambient and operational stabilities.

References

[1] Noguera-Gómez et al., *Matter* 5, 1–12

Acknowledgment

The work was partially funded by MCIN/ AEI through project TED2021-131600B-C32, by Generalitat Valenciana via Pla Gent-T (grant CIDEXG/2022/34) and by the research project no. PID2020-119628RB-C31 funded by MCIN/ AEI /10.13039/501100011033.

10:45 AM EN10.08.03

Light-Induced Halide Sublimation and Diffusion in 2D Halide Perovskites Yanqi Luo¹, Shuchen Zhang², Jia-Shiang Chen¹, Xuedan Ma¹, Ke Ma², Junjing Deng¹, Yi Jiang¹, Luxi Li¹, Barry Lai¹, Si Chen¹, Sarah Wiegold¹ and Letian Dou²; ¹Argonne National Laboratory, United States; ²Purdue University, United States

To address stability challenges in two-dimensional (2D) perovskite semiconductor materials, an improved understanding of the degradation origins and pathways under external stimuli is needed. Here, we investigate the evolution of halide redistribution within various 2D halide perovskites ($n = 1$ to 3) lateral heterostructures using *in-situ synchrotron* nanoprobe X-ray fluorescence (nano-XRF) microscopy. The heterostructures comprise distinguishable iodine (I) and bromine (Br) regimes laterally. Continuous UV exposure leads to iodine sublimation in high-dimensional 2D perovskites and a visible amount of Br diffusion to the previously iodine-rich regime. In contrast, bromine is relatively more stable than iodine in $n = 2$ and 3 heterostructures, with no significant change in total Br concentration. Additionally, combining nano-XRF mapping and X-ray absorption spectroscopy, we found a reduction of dimensionality in the previously iodine-rich regime in crystals with $n > 1$ after UV exposure, indicating significant structural reconfiguration beyond ion migration. These findings provide new insights into the photo-induced ion migration and degradation mechanisms of 2D perovskite materials and shed light on future materials design.

11:00 AM EN10.08.04

3D Printing of Vertical Heterostructures of Two Dimensional Halide Perovskites Sixi Cao and Ji Tae Kim; The University of Hong Kong, Hong Kong

The integration of different materials into heterostructures allows for the manipulation of interfaces and electronic structures, playing a crucial role in various modern electronics and optoelectronics applications, such as solar cells, light-emitting diodes, lasers, self-powered photodetectors, transistors, and large-scale electronic circuits¹⁻³. Two-dimensional (2D) halide perovskites have gained significant attention due to their superior optoelectronic properties and high stability, making them promising candidates for next-generation multifunctional devices^{4,5}. The heterojunctions formed by 2D halide perovskites exhibit high tolerance to lattice mismatch and low intrinsic anionic diffusion at the interface, thanks to the presence of the organic layer in the 2D quantum well, which enhance their stability and performance in optoelectronic integrated device⁶. However, achieving controllable integration of 2D perovskites remains a challenge due to their mobile and fragile crystal lattices⁷. solution and gas-solid phase intercalation have been reported for fabricating 2D perovskite-based lateral and vertical heterostructures^{8,9}. Nevertheless, these methods suffer from limitations, including a lack of scalability and limited control over the morphology of the resulting heterostructures, which hinders large-scale production and integration of 2D perovskite nanowire heterostructures into practical devices. In this work, we propose a novel approach for fabricating freestanding layer perovskite nanowire heterostructures using a 3D printing method. This level of control ensures uniformity and reproducibility, facilitating the deterministic fabrication of arbitrary vertical heterostructures and multi-heterostructures using 2D perovskites. Our printed heterojunction nanowires showed an excellent stability with suppressed anionic diffusion at the interface. By offering greater structural degrees of freedom, our approach allows for the precise definition of the electronic structures of the heterojunctions.

Reference

1. Y. Liu *et al.*, Van der Waals heterostructures and devices. *Nature Reviews Materials* 1, (2016).
2. Y. Liu, Y. Huang, X. Duan, Van der Waals integration before and beyond two-dimensional materials. *Nature* 567, 323-333 (2019).
3. A. Castellanos-Gomez *et al.*, Van der Waals heterostructures. *Nature Reviews Methods Primers* 2, (2022).
4. K. Leng, W. Fu, Y. P. Liu, M. Chhowalla, K. P. Loh, From bulk to molecularly thin hybrid perovskites. *Nature Reviews Materials* 5, 482-500 (2020).
5. J. C. Blancon, J. Even, C. C. Stoumpos, M. G. Kanatzidis, A. D. Mohite, Semiconductor physics of organic-inorganic 2D halide perovskites. *Nat Nanotechnol* 15, 969-985 (2020).
6. Akriti *et al.*, Layer-by-layer anionic diffusion in two-dimensional halide perovskite vertical heterostructures. *Nat Nanotechnol* 16, 584-591 (2021).
7. J. Chen *et al.*, Oriented Halide Perovskite Nanostructures and Thin Films for Optoelectronics. *Chem Rev.* (2021).
8. E. Shi *et al.*, Two-dimensional halide perovskite lateral epitaxial heterostructures. *Nature* 580, 614-620 (2020).
9. D. Pan *et al.*, Deterministic fabrication of arbitrary vertical heterostructures of two-dimensional Ruddlesden-Popper halide perovskites. *Nat Nanotechnol* 16, 159-165 (2021).

11:15 AM EN10.08.05

Enhancing Crystallization Kinetics in Glass-Forming Halide Perovskites using Organic Cation Isomers Akash Singh, Yi Xie, Curtis Adams III and David B. Mitzi; Duke University, United States

The recent exploration of glass-forming hybrid metal halide perovskites (MHPs) has opened new possibilities to extend their applications beyond the well-established realm of optoelectronic research, which primarily focuses on their crystalline variants. In this regard, it is imperative to diversify the range of glass-forming MHP compositions and manipulate their crystallization kinetics through synthetic structural engineering. Herein, we conducted a comparative study involving two MHPs that possess subtly different structural characteristics, utilizing isomer organic cations while maintaining the same chemical composition. Our investigation sheds light on how these alterations in the position of functional groups profoundly influence the kinetics of both glass formation and cold crystallization. One of the MHPs, (S)(-)-1-(1-naphthyl)ethylammonium lead bromide (S(1-1)NPB), exhibits a lower melting point (T_m) of 175 °C and readily transforms into a glassy state at a critical cooling rate (CCR) of 20 °C/min. In contrast, (S)(-)-1-(2-naphthyl)ethylammonium lead bromide (S(1-2)NPB) displays a higher T_m of 193°C, and requires a CCR of 150,000°C/min, necessitating the use of ultrafast calorimetry for glass formation. The examination of the underlying crystallization kinetics, performed using iterative calorimetry and the Kissinger modeling technique, further indicates a small activation energy barrier (E_A) for crystallization in S(1-2)NPB.

We also investigate the interplay between structural and thermodynamic features that engenders distinct glass formation and crystallization behavior using a comprehensive analysis of the organic-inorganic hydrogen bonding interactions in the crystalline state and a careful examination of the enthalpy and entropy balance across the melting transition. These analyses highlight the strengthened hydrogen bonding in S(1-2)NPB and the reduced entropy of melting as the key factors contributing to the higher T_m and CCR, as well as a lower E_A , observed in comparison to S(1-1)NPB. The results presented in this

study establish a framework for evaluating the impact of structural elements on the kinetics of glass formation and crystallization, serving as a new material design strategy to diversify the family of glass-forming MHPs and extending their potential applications in areas demanding faster switching speeds such as memory, computing, metamaterials, and reconfigurable photonic devices.

11:30 AM EN10.08.06

A Templating Approach to Controlling the Growth of Co-Evaporated Halide Perovskites [Siyu Yan](#)¹, Jay Patel¹, Jae Eun Lee¹, Karim Elmestekawy¹, Sinclair R. Ratnasingham¹, Qimu Yuan¹, Laura Herz^{1,2}, Nakita K. Noel¹ and Michael B. Johnston¹; ¹University of Oxford, United Kingdom; ²Institute for Advanced Study, Technical University of Munich, Germany

Metal halide perovskite semiconductors have shown significant potential for use in photovoltaic devices. While fabrication of perovskite thin-films can be achieved through a variety of different techniques, thermal vapour deposition is particularly promising, allowing for high-throughput fabrication and large-scale production. However, the ability to control the nucleation and growth of these materials, particularly at the charge-transport layer (CTL)/perovskite interface, is critical to unlocking the full potential of vapour-deposited perovskite photovoltaics, since the surface of the substrate material exerts a substantial impact beyond the interface, leading to alterations in the morphology of the entire film. As a result, for vapor-deposited perovskites, it is crucial to choose the right CTLs to ensure uniform deposition of alkylammonium halides and appropriate crystallization of the perovskite material. This not only limits the range of available substrates, but also requires extensive experimentation to optimize the evaporation parameters for different types of substrates. This issue limits the economic feasibility of industrial applications, as the most attractive scale-up technique is to produce all device layers on the same vacuum fabrication lines. Therefore, the ability to decouple the nucleation and growth of coevaporated perovskite films from the influence of substrate materials is of the utmost importance.

We highlight our recent work [Yan et al., ACS Energy Lett. (2023)] wherein we explored the use of a templating layer to control the growth of co-evaporated perovskite films, and found that such templating reproducibly leads to highly oriented films with identical morphology, crystal structure, and optoelectronic properties, independent of the specific substrate on which the perovskite was deposited. When incorporated into solar cells, devices based on this approach showed reproducible improvements, yielding vapour-deposited FA_{0.9}CS_{0.1}PbI_{3-x}Cl_x solar cells with steady-state solar-to-electrical power conversion efficiencies over 19.8%. This report provides an effective and reproducible method for controlling the buried charge transport layer/perovskite interface in vapor-deposited perovskite solar cells, further increasing the competitiveness of this deposition technique, moving the field closer to large-scale fabrication of a wide-range of efficient perovskite optoelectronic devices.

Yan, S. et al., A Templating Approach to Controlling the Growth of Coevaporated Halide Perovskites, ACS Energy Lett. 2023, 8, 10, 4008–4015 DOI: 10.1021/acsenerylett.3c01368

11:45 AM EN10.08.07

Exploring The Relationship between The Local Structure of Lead Halide Perovskites and Their Macroscopic Properties [Milos Dubajic](#); University of Cambridge, United Kingdom

Characterised by their exceptional optoelectronic characteristics, hybrid halide perovskites have gained prominence as a viable class of materials for energy conversion applications. Their marked impact is especially noticeable in the field of solar cell technology, where they have demonstrated substantial progress in efficiency. Despite these advancements, fully decoding their unique properties continues to pose a scientific enigma. Of particular interest is the local structure of these materials, which often diverges from their average configuration, and is hypothesised to be a significant determinant of their macroscopic properties.

We employed temperature-dependent diffuse X-ray scattering on a series of perovskite single crystals, enabling us to accurately characterise the local structure in real-space across all crystallographic phases of these perovskites. By developing a simple, computationally inexpensive model that accurately mirrors the experimental diffuse scattering, we were able to gain insights into how the local structure can be modulated through the substitution of A and X-site cations.

By employing a variety of optical microscopy techniques on identical compositions, we established a direct correlation with the emergence of ferroelastic properties in these materials.

Our study thereby underscores the critical role of compositional engineering in tailoring the local structure and, by extension, the macroscopic properties of hybrid halide perovskites.

SESSION EN10.09: Detectors

Session Chairs: Pablo P. Boix and Yuanyuan Zhou

Wednesday Afternoon, April 24, 2024

Room 334, Level 3, Summit

1:45 PM EN10.09.01

Robustness and Versatility of CsPbBr₃ Perovskite Detectors in Extreme Radiation Environments [Mercuri G. Kanatzidis](#); Northwestern University, United States

The burgeoning field of radiation detection has witnessed a significant interest in semiconductors that can operate under harsh conditions and high photon fluxes. We present a comprehensive study on CsPbBr₃, a perovskite-based semiconductor, showcasing its potential as a robust and cost-effective alternative to conventional Cd_{1-x}Zn_xTe (CZT) detectors. Our research reveals that CsPbBr₃ detectors demonstrate minimal degradation even after exposure to 1 Mrad of Co-60 gamma radiation, maintaining high energy resolution and hole mobility. Many of these detectors also continue to function after a 10 Mrad dose over 3 days, indicating that device failure is more likely related to electrode-material interactions rather than intrinsic material degradation. I will also present the behavior of these detectors under extreme x-ray flux conditions. Utilizing ultrahigh flux synchrotron x-rays and advanced pump-and-probe techniques, we examine the polarization effects and discover their correlation with deep defects generated by intense radiation. Importantly, we find that the polarization can be mitigated by stronger applied electric fields and reduced carrier traps. Additionally, we employ thermally stimulated current spectroscopy to identify trap states and their impact on performance. Our findings suggest that CsPbBr₃ detectors fabricated with low defect concentrations (<1 x 10¹⁴ cm⁻³) show appreciable performance and stability. Another remarkable aspect of our research is the use of solution-

processed perovskites for hard X-ray and gamma-ray detection. These solution-grown CsPbBr₃ detectors display excellent photocurrent linearity and sensitivity, even under ultrahigh x-ray fluxes, substantiating their wide applicability in high-flux environments. Comparisons between solution-grown and melt-grown crystals reveal comparable performance in terms of defect concentration and overall detector efficacy. There is a compelling case emerging for the use of CsPbBr₃-based detectors in a variety of high-stress applications, ranging from industrial settings to space explorations while highlighting strategies for further optimizing these promising materials.

2:00 PM EN10.09.02

Multi-Energy X-Ray Imaging Technology for Security Check [Tengyue He](#) and Omar F Mohammed; KAUST, Saudi Arabia

Conventional grayscale single-energy X-ray imaging technology (SEXIT) often struggles to accomplish outstanding material-specific functions. While dual-energy X-ray imaging technology (DEXIT) partially compensates the limitation, its implementation typically demands dual detectors or twice X-ray exposures. Besides, valuable spectral photon information is abandoned by both SEXIT and DEXIT.^{1,2} Herein, we have developed an inventive multi-energy X-ray imaging technique (MEXIT) designed by multiple scintillators with a ΔE -E telescope structure. Specifically, three distinct scintillators convert and assign X-rays from different energy bins into individual visible light information in an energy sequence. Emerging scintillation materials of metal halides were employed.³ The carefully selected filters were inserted into them, enabling the combined radioluminescence (RL) to span the entire visible range (350 nm to 800 nm) devoid of any overlap. Consequently, substances with different CT numbers can be readily discriminated through their corresponding emission colors. Moreover, notable spatial imaging resolutions that exceeds 22 lp mm⁻¹ across all X-ray energy were achieved by MEXIT. The conceptual demonstration was conducted in a scenario for the inspection of various substances with complicated composition, where the ΔE -E telescopic scintillator allows effective screening of different substances based on X-ray energy bins. Different ROIs (region of interests) are available to be extracted by the original images. Our study presents a promising avenue for achieving MEXIT and extends it to trichromatic vision, introducing innovative perspectives for various scientific and practical fields. To the best of our knowledge, no prior reports exist of a similar design capable of translating X-ray energy into an ultrabroad RL spectra using three distinct scintillation materials to achieve multi-energy X-ray imaging.

1. Ran, P. *et al.* Multispectral Large-Panel X-ray Imaging Enabled by Stacked Metal Halide Scintillators. *Advanced Materials* **34**, 2205458 (2022).
2. Shao, W. *et al.* Transparent Organic and Metal Halide Tandem Scintillators for High-Resolution Dual-Energy X-ray Imaging. *ACS Energy Letters* **8**, 2505-2512 (2023).
3. Zhou, Y., Chen, J., Bakr, O. M. & Mohammed, O. F. Metal Halide Perovskites for X-ray Imaging Scintillators and Detectors. *ACS Energy Lett.* **6**, 739-768 (2021).

2:15 PM EN10.09.03

Two-Dimensional Hybrid Halide Perovskite as Highly Efficient β -Ray Scintillator by Incorporation of Aromatic Cations [Dongjun Kim](#), Seoyoung Yoon and Jiwon Kim; Yonsei University, Korea (the Republic of)

Scintillators are extensively employed in the fields of security inspection, industrial product analysis, and medical diagnosis, owing to their capability of converting high-energy ionizing radiation (e.g. α -, β -, γ -, X-, and neutron rays) into visible light. Specifically, organic scintillators – including single crystals, liquids, and plastics – are primarily utilized for detecting β -ray. However, organic single crystal scintillators, such as anthracene and naphthalene, encounter limitations associated with complexity in crystal growth and potential carcinogenicity resulting from the sublimation of substances. Liquid scintillators pose challenges in terms of manufacturing, transportation, storage, and handling due to their vulnerability to oxygen and flame. Meanwhile, plastic scintillators exhibit drawbacks owing to their low glass transition temperature of polymers and poor irradiation hardness. Consequently, organic-inorganic hybrid halide perovskites have emerged as a promising alternative scintillator for high light yield, tunable emission wavelength, and low-temperature solution processability. To enhance the scintillation efficiency of perovskites, comprehensive investigations on their structure and composition have been preceded. Specifically, two-dimensional (2D) perovskites are known to exhibit higher light yield and faster scintillation decay compared to three-dimensional (3D) perovskite owing to higher exciton binding energy. Moreover, long aliphatic molecules were introduced as organic cations of 2D perovskite to enhance the capturing efficiency of β -rays. Nevertheless, 2D perovskite incorporating aromatic molecules, which are known to facilitate the absorption and release of energy, has not yet been developed as a scintillator. Herein, we developed blue-emitting 2D hybrid halide perovskites and evaluated its scintillation properties under various types of radiation. More specifically, ammonium derivatives from organic scintillators (i.e. anthracene, naphthalene, or stilbene) were employed as cations, where aromatic rings effectively serve as centers for the absorption of radiation energy. The synthesized 2D perovskite exhibited a photoluminescence (PL) peak centered at 410 nm, along with a notably high PL quantum yield of 64.5%. Furthermore, it demonstrated highly efficient scintillation property under X-ray and β -ray (C-14, Ni-63). In this study, we proposed a new strategy to enhance scintillation efficiency by incorporating organic scintillator cations into 2D hybrid halide perovskites, thereby paving a way for applications in future nuclear radiation monitoring devices.

2:30 PM BREAK

SESSION EN10.10: Light-Emitting Diodes
Session Chairs: Henk Bolink and Michael Saliba
Wednesday Afternoon, April 24, 2024
Room 334, Level 3, Summit

3:30 PM *EN10.10.01

Perovskite Light-Emitting Diodes for Next-Generation Data Communications [Wei Zhang](#); University of Surrey, United Kingdom

Light-emitting diodes (LEDs) are ubiquitous in modern society. However, future applications of light-emitting diodes (LEDs) will not be limited to the fields of lighting and displays. As billions of Internet of Things (IoT) devices are already connected, the demand for data communication systems with low-cost and low-power consumption is dramatically increasing. It has been widely expected that LED-based links will act as key elements in the next-generation data communication systems¹. The conventional III-nitride micro-LEDs have the potential to provide a modulation bandwidth of several hundred MHz, however, their complex fabrication process and high manufacturing costs pose significant challenges for their integration into next-generation communication systems where the considerations on costs and compatibility are sometimes prioritized over speed in current communication scenarios.

Metal halide perovskites are emerging classes of semiconductors that have recently showed great potentials in the optoelectronic devices such as high-

performance photovoltaics, photodetectors and LEDs². Their widely tuneable properties such as bandgap and electronic energy levels can be tailored through synthesis and composition engineering^{3,4}. Another distinct advantage is that these emerging materials can be solution-processed and deposited on different types of substrates under ambient conditions which are attractive for low-cost high-throughput industrial-scale fabrication. These fascinating features make metal halide perovskites promising materials for LED applications. Although prior research has progressed substantially in optimizing their external quantum efficiency for the applications in lighting and displays, the modulation characteristics of perovskite LEDs remain unclear.

In this talk, I will review the challenges that exist in developing practical high-speed LEDs, and highlight the most recent advance in the development of emerging LED materials—organic semiconductors, colloidal quantum dots and metal halide perovskites—for use in optical communications. I will then introduce a holistic approach that we developed most recently for realizing fast perovskite photonic sources on silicon based on tailoring alkylammonium cations in perovskite systems⁵. Under optimal conditions, we achieved device modulation bandwidths of 42.6 MHz and data rates above 50 Mbps, with further analysis suggesting that the bandwidth may exceed gigahertz levels. Finally, I will summarize the general principles that will support the future development of perovskite light sources for next-generation data-communication architectures, which might open up new possibility of integration with micro-electronics platforms.

References

1. Aobo Ren, et al. Emerging light-emitting diodes for next-generation data communications. *Nature Electronics* 4, 559–572 (2021).
2. Wei Zhang, et al. Metal Halide Perovskites for Energy Applications. *Nature Energy* 1, 16048 (2016).
3. Xueping Liu, et al. Stabilization of photoactive phases for perovskite photovoltaics. *Nature Reviews Chemistry* 7, 462–479 (2023).
4. Dongtao Liu, et al. Strain analysis and engineering in halide perovskite photovoltaics. *Nature Materials* 20, 1337–1346 (2021).
5. Aobo Ren, et al. High-bandwidth perovskite photonic sources on silicon. *Nature Photonics* 17, 798–805 (2023)

4:00 PM *EN10.10.02

Molecular Interface Engineering and Optical Design for High-Efficiency Perovskite LEDs Hin-Lap Yip; City University of Hong Kong, Hong Kong

Metal halide perovskite light-emitting diodes (PeLEDs) have the potential to significantly impact next-generation lighting and display technology. However, their full promise has yet to be unlocked, particularly for blue and white PeLEDs. These devices face unique challenges such as maintaining stability, achieving high efficiency, and obtaining pure color emission, especially for blue light, due to the inherent material and device-related difficulties. Our research tackles these issues through a multifaceted strategy designed to optimize the performance and efficiency of PeLEDs. We commence with interfacial engineering, introducing a self-assembled monolayer (SAM) with functional hole injection properties between the NiOx and poly(9-vinylcarbazole) hole injection layers. This approach effectively mitigates common obstacles such as weak interfacial adhesion, high interfacial trap density, and mismatched energy levels. The introduction of the SAM has successfully led to blue PeLEDs with external quantum efficiencies (EQEs) exceeding 15% and green devices with EQEs of 26.0%. In addition to enhancing efficiency, the introduction of the SAM also augments the device response speed by reducing interfacial capacitance and resistance. These advancements together pave the way for the development of more efficient, brighter, and faster responding perovskite LEDs, thereby broadening their potential applications in various fields. Furthermore, we have developed an advanced device structure that optically couples a blue PeLED with a red-emitting perovskite nanocrystal layer, leading to the creation of efficient white PeLEDs. This innovative strategy utilizes near-field effects to facilitate the extraction of trapped blue photons' optical modes to the red perovskite layer, resulting in white PeLEDs achieving EQEs over 12% - a significant advancement in white PeLED performance.

4:30 PM EN10.10.03

Semitransparent OLEDs with Ultrathin Light Emitting Layer and Extraordinarily Thick Perovskite Hole Transport Layer Michele Forzatti, Sang-Hyun Chin, Daniel Tordera and Henk J. Bolink; Universitat de Valencia, Spain

Organic light-emitting diodes (OLEDs) have had a huge gain in popularity by virtue of their simple fabrication process, thin structure and for the possibility to devise transparent devices. However, the production of stable, cheap and efficient devices remains a challenge. Ultrathin nondoped emitting layers have been investigated as a way to simplify fabrication process and lower material consumption, but the consequent reduction in thickness may decrease device stability. Overcoming this issue with thicker transport layers is alluring but tough, as organics have intrinsically low charge-carrier mobilities. On the other hand, metal halide perovskites (MHPs), promising materials in many fields of optoelectronics, have also been used as charge transport materials, where their transparency in the visible region and high hole conductivity make it possible to increase the thickness of the layer to the micrometer-scale without increasing the operation voltage or reducing luminous efficiency.

In light of this, we developed a semitransparent OLED having a thick cesium lead chloride all-inorganic perovskite hole transport layer, an ultrathin (<0.1 nm) [Ir(ppy)₂acac] film as emitting layer and a semitransparent top indium-tin oxide contact deposited on top of a thin metallic layer. The resulting devices have a thickness exceeding 1 μm, a combined peak luminance of over 1000 cd m⁻², a current efficiency of 34 cd/A and a transparency in excess of 60% over the visible spectrum above 480 nm. The hole transporting CsPbCl₃ layer includes two thin (2 nm) CsCl layers at the interfaces, which have been demonstrated to be able to passivate interfacial halide vacancies, improving the photoluminescence and reducing exciton quenching in turn. The nature of the ultrathin layer was investigated by means of contact angle measurement, which confirmed that the molecules forming the LEL are not in the form of a neat layer. The metallic layer could be deposited with little damage to the underlying organic layers but despite its low thickness, essential to guarantee transparency, it still protected towards the final ITO sputtering deposition. The combination of transparent top electrode, thick perovskite HTL and ultrathin LEL, described herein for the first time, entails a reduction in material and fabrication costs and is promising towards future cheap and stable semitransparent OLEDs.

4:45 PM EN10.10.04

Overcome Charge Transfer Barrier via Electrostatically Stabilized CsPbBr₃ Nanocrystals for Efficient Perovskite Light-Emitting Diodes Min-Gi Jeon, Artavazd Kirakosyan, Kim Joonseok, Subin Yun and Jihoon Choi; Chungnam National University, Korea (the Republic of)

Electrically insulating organic ligands with long hydrocarbon chains cause bottlenecks, which hinder efficient charge injection and transportation in CsPbBr₃ nanocrystal (NC)-based light-emitting diodes (LEDs). Shorter ligand exchange with precise control of the surface ligand density through additional purification processes is a common strategy used to improve charge transport in optoelectronics. However, practical applications have been limited owing to poor structural integrity and colloidal stability associated with the low steric hindrance of short surface-capping ligands. Here, we report a post-synthesis treatment on CsPbBr₃ NCs using hydrazine monohydrobromide (N₂H₅Br; HZBr), and tetrafluoroborate derivatives (XBF₄, X=Na⁺, NO⁺, NH₄⁺, ...). Despite their short molecular structure, these inorganic ligands provide an excess amount of charged ions to the NC surface, enhancing the colloidal dispersion of the CsPbBr₃ NCs through electrostatic stabilization. Cryogenic photoluminescence spectroscopic analysis identified that the exciton-phonon coupling at the surface of CsPbBr₃ NCs is significantly reduced by the presence of short inorganic ligands, preventing the formation of both permanent and transient exciton traps. Furthermore, enhanced surface stabilization to improve the radiative recombination was accomplished by excess Br⁻ and F⁻ anions passivating Br⁻ ion vacancies at the CsPbBr₃ NC surfaces. LEDs based on the short inorganic ligands-treated CsPbBr₃ NCs showed improved

maximum current efficiency of 19.46 cd/A, and the external quantum efficiency of 6.04 % increased by a factor of 2.8. Additional electron and hole-only device measurements affirmed the enhanced hole-electron injection and transport into the CsPbBr₃ NCs.

5:00 PM *EN10.10.05

PLD of Metal Halide Perovskites: From *In-Situ* Photoluminescence During Growth to Efficient Solar Cell Devices [Monica Morales-Masis](#); University of Twente, Netherlands

The dominance of vapor phase deposition in semiconductor technology extends to various applications, such as commercial thin-film PV manufacturing. Physical vapor deposition (PVD) of thin film materials offers distinct advantages, including conformal deposition, precise thickness control, and scalability. An underexplored alternative within PVD for metal halide perovskites (MHP) is pulsed laser deposition (PLD). We have recently demonstrated that PLD facilitates single-source vapor phase growth and stoichiometry control of MHPs; and solar cell devices with PLD-perovskites exceeding 19% efficiency. Furthermore, the growth control afforded by PLD, encompassing thickness and deposition rate, allows the epitaxial formation of MAPbI₃ on lattice-matched substrates. To delve into the growth mechanisms at different PLD deposition rates for halide perovskites (e.g., high rates for solar cell applications or low rates for epitaxy), we conduct in-situ photoluminescence measurements during film growth, complemented by an in-depth ex-situ analysis using PL, XRD, MAS ss-NMR, and XPS. We discuss the role of the deposition parameters, deposition rate and PLD target composition on final film quality. The role of the substrate or contact layers on the film morphology, optoelectronic quality, and final device performance will be furthermore discussed. Combining PLD-controlled growth with insights into structural-property relationships provide important insights into the vapor-phase growth of MHPs, which can be applied in more PVD beyond PLD. All these are important steps forward in the controlled growth and future scalability of optoelectronic materials for efficient devices, both single junction and tandem solar cells.

References

[2] <https://doi.org/10.1002/admi.202000162> [3] <https://doi.org/10.1021/acs.chemmater.1c02054> [4] <https://doi.org/10.1002/adfm.202300588> [5] <https://doi.org/10.21203/rs.3.rs-3671187/v1> [6] <https://doi.org/10.21203/rs.3.rs-3730125/v1>

SESSION EN10.11: Poster Session II
Session Chairs: Henk Bolink and Michael Saliba
Wednesday Afternoon, April 24, 2024
Flex Hall C, Level 2, Summit

5:00 PM EN10.11.01

Effect of Interfacial Modification on Spray-Coated Lead-Free Cs₂AgBiBr₆ Double Perovskite Solar Cells Kun-Chin Wei¹, Hsin-Jung Wu¹ and [Chih-Liang Wang](#)²; ¹National Chung Hsing University, Taiwan; ²National Tsing Hua University, Taiwan

The Cs₂AgBiBr₆-based double perovskites have recently been reported as alternatives to hybrid lead halide perovskites due to the improved stability and nontoxicity. However, the conversion efficiency of Cs₂AgBiBr₆ solar cell remains low due to inherent film-related defects. In this regard, the lead-free Cs₂AgBiBr₆ double perovskite solar cell was firstly studied by a spray coating to systematically understand the influence of spraying time, substrate temperature, and surrounding atmosphere on the spray-coated film. The interface between the spray-coated Cs₂AgBiBr₆ film and hole transport layer or electron transport layer was further modified by the dye layer, such as N719 and Z907. The result showed that the surrounding atmosphere from the solvent vapor during the spray deposition can play a key role in the growth of the high-quality Cs₂AgBiBr₆ resulting film. In addition, the insertion of the dye layer in Cs₂AgBiBr₆ solar cells showed a positive effect on the light absorption, charge carrier recombination, carrier extraction, and energy level alignment. The SEM, XRD, and UV-vis were carried out to understand the surface morphology, crystallization, phase purity and optical property of different spray-coated Cs₂AgBiBr₆ films. The electrochemical impedance spectroscopy was performed to figure out the electrical properties and the charge recombination of Cs₂AgBiBr₆ solar cell with and without the insertion of the dye layer. More details related to the stability and performance of the Cs₂AgBiBr₆ solar cells, influenced by the spray coating process and dye layer, will be reported in the presentation.

5:00 PM EN10.11.02

Understanding Nucleation and Film Growth of Perovskite in Confined Volume Printing [Matthew Dailey](#) and Adam Printz; University of Arizona, United States

Despite the promising characteristics of metal halide perovskites for optoelectronic applications, these materials are highly unstable to environmental factors such as moisture and heat. These instabilities stem predominantly from grain boundary defects, such as halide vacancies that allow more facile ion migration. One strategy to improve the stability of perovskites is to reduce the surface area of the grain boundaries within the film by increasing the grain size. A one-step pathway to increased grain size is limiting nucleation of crystallites followed by rapid growth, resulting in films with fewer, larger crystals. Batch processes have been developed to grow monocrystalline perovskite with confined volumes; however, these processes are slow and not scalable for manufacturing. Conversely, scalable printing techniques such as slot die coating or doctor blading provide limited control over nucleation and growth of crystallites. We have developed a printing process that bridges the gap between scalability and control over crystallization that we call Restricted Area Printing by Ink Drawing (RAPID). RAPID prints films from confined volumes (between a superstrate and substrate) in a continuous process.

Film growth with RAPID can be tuned by controlling the working parameters that dictate the nucleation and growth—confinement gap, residence time, and temperature. We will show the influence of the solvent evaporation rate, distance between substrate/superstrate, and surface chemistry on both the substrate and superstrate on the nucleation and growth of perovskite thin films. Finally, we will demonstrate RAPID-printed perovskite thin films with domains greater than 20 μm and no lead iodide can be achieved in ambient conditions without the need for post processing.

5:00 PM EN10.11.03

Elevating Perovskite Solar Cells: Advances in Scalable Thin Film Deposition and Degradation Insights [Randall Headrick](#)¹, [Seid Yimer Abate](#)^{1,2}, [Pramod Baral](#)², [Gary E. Carver](#)¹ and [Richards G. Miller](#)^{2,1}; ¹University of Vermont, United States; ²Verde Technologies Inc., United States

In the rapidly evolving landscape of perovskite solar cells (PSCs), two pivotal challenges take center stage: (i) pioneering scalable thin film deposition techniques and (ii) unraveling degradation mechanisms. This presentation converges groundbreaking research encompassing scalable thin film deposition, high-efficiency solar cells, in-situ synchrotron X-ray diffraction studies, spatially resolved photoluminescence analysis, and accelerated degradation investigations under maximum power point tracking conditions.

At the heart of this presentation lies the development of scalable thin film deposition techniques, with a special emphasis on the innovative Verde Slot Coater [Ref 1]. Engineered to bring perovskite solar cells closer to commercial viability, the Verde Slot Coater represents a significant leap forward. It addresses the challenges of achieving uniform coating and effectively bridges the gap between laboratory-scale experiments and large-scale production. Most notably, this innovation has resulted in achieving over 18% power conversion efficiency (PCE) for 1.25 cm² solar cells, underlining the potential of scalable manufacturing methods within the perovskite industry.

We have also embarked on a journey towards long-term stability, guided by cutting-edge research methodologies. Specifically, we have begun studies of Formamidinium Lead Iodide (FAPbI₃) thin film devices. FAPbI₃ is slightly unstable with a Goldschmidt tolerance factor just above 1.0, making it susceptible to transforming into the undesirable hexagonal phase. Through in-situ synchrotron X-ray diffraction studies, we gain invaluable insights into the degradation processes that influence perovskite thin films over time. This research enables us to track the evolution of multiple phases over time, exploring responses to varying conditions such as temperature, light exposure, and humidity, across timescales from seconds to hours.

In the race to ensure PSCs can endure real-world challenges, accelerated degradation studies conducted under maximum power point tracking conditions provide indispensable insights. These studies simulate practical scenarios, enabling researchers to evaluate the resilience of perovskite solar cells and optimize their performance for long-term reliability. Furthermore, the use of spatially resolved photoluminescence studies (SRPL) during accelerated degradation investigations offers a microscopic understanding of degradation with a spatial resolution of 1 micron. By pinpointing specific regions of degradation and identifying potential mitigation strategies, this research substantially contributes to the long-term durability of perovskite solar cells.

The presentation will provide the latest results for each facet of the research outlined above. It encapsulates the spirit of innovation in perovskite solar cell research, emphasizing scalable manufacturing, high efficiency, and an in-depth exploration of degradation mechanisms. It invites us to closely scrutinize the path toward more robust and commercially viable perovskite solar cells.

Ref 1: Wan, J., Li, Y., Benson, J., Miller, R., Zhernenkov, M., Freychet, G. & Headrick, R. L. Dynamic processes in transient phases during self-assembly of organic semiconductor thin films. *Molecular Systems Design & Engineering* 7, 34-43, doi: <https://doi.org/10.1039/D1ME00078K> (2022).

5:00 PM EN10.11.04

Sn-Based Perovskite Solar Cells: Additive Engineering and Surface Modification to Improve Stability Ashrafur Islam and Md. Emrul Kayesh; NIMS, Japan

Perovskite solar cells (PSCs) have attracted much attention because of the fast progress of their power conversion efficiency (PCE), from 3.8% to 25.7% in the past 14 years [1]. However, the toxicity of Pb effectively hinders the large-scale commercial production of PSCs. Therefore, researchers have turned their attention to Sn-based perovskite due to their similar or even superior optoelectronic properties, such as optimum band gap, higher charge carrier mobility, and low exciton binding energy [2–3]. However, the stability of the Sn-based PSCs is low compared to Pb-based PSCs, which limits the practical use of the solar cells. One of the reasons for this low stability is the rapid crystallization, which results in inhomogeneous films with a lot of pin holes. Another reason is the easy oxidation of Sn²⁺ to Sn⁴⁺, which leads to high nonradiative recombination of carriers, low efficiency, and low stability. According to recent studies, Sn²⁺ oxidation is more dominant on the perovskite surface [2].

To enhance the quality of perovskite film, additive engineering is a well-known process for Sn-based PSCs to slow down the crystallization rate [3]. Recently, polydentate additives have shown effectiveness in modulating the growth of Sn-based perovskite films [4]. However, the stability of perovskite film is dependent on crystallinity and pin-hole-free large-grain compact films. The highly oriented crystal offers smooth charge transfer, whereas the larger grain reduces the grain boundaries, which are regarded as the recombination centers for the charges. In this work, we used a bifunctional additive in Sn precursor solution that acted as a modulator to dictate the growth of perovskite film and were able to fabricate highly crystalline and stable uniform perovskite film.

The additive-added FASnI₃ film showed large and compact grains without any pinholes. This is because the bifunctional additive had a strong interaction with SnI₂ through hydrogen bonding, which delayed the FASnI₃ crystal growth. At the same time, the bifunctional groups helped to create strong adherence between perovskite and PEODOT:PSS and dictated the growth of perovskite crystals in a preferred orientation. The XRD pattern of the modified FASnI₃ film remains unchanged for up to 3h when exposed to air, which indicates that the addition of this bifunctional additive to the precursor solution significantly enhanced the environmental stability of the FASnI₃ film.

With the addition of a bifunctional additive, the PCE jumped from 10.0% to 13.2%. It is important to state that the addition of the additive significantly improved the open circuit voltage (V_{OC}) from 0.85 V to 0.95 V as well as the short circuit current (J_{SC}) from 16.5 mA/cm² to 18.2 mA/cm². The enhancement of V_{OC} may be due to the suppression of leakage current with the addition of additives in the precursor solution, as we confirmed from our dark current measurement. This modification also reduced the charge recombination center, such as Sn⁴⁺ content in the film, as we observed from the XPS result. The PCE of the modified PSC retained its 90% initial PCE even after 100h. As a result, we achieved a certified (AIST, Japan) PCE of over 12% with superior device stability for Sn-based PSCs.

References

- NREL Best Research-Cell Efficiency Chart. [<https://www.nrel.gov/pv/cellefficiency.html>]
Zhang, J., Yu, C., Wang, L., Li, Y., Ren, Y., & Shum, K. *Scientific Reports*, 2014, 4, 1-6.
Kayesh, M. E., Matsuihi, K., Kaneko, R., Kazaoui, S., Lee, J. J., Noda, T., Islam, A. *ACS Energy Letters*, 2018, 4, 278-284.
Hu, S., Otsuka, K., Murdey, R., Nakamura, T., Truong, M. A., Yamada, T., Wakamiya, A. *Energy & Environmental Science*, 2022, 15, 2096-2107.

5:00 PM EN10.11.05

p-Type Doping of Cs₂SnI₆ Halide Perovskites Using Charge Transfer Dopants Alex Kratzer and Shubhra Bansal; Purdue University, United States

Perovskite solar cells (PSCs) have shown remarkable progress in recent years, surpassing the efficiency of conventional thin-film photovoltaic (PV) technologies such as CdTe and CIGS. The recent discoveries in organic-inorganic hybrid PSCs resulting from synergistic optimization of the perovskite absorber layer have generated remarkable development in device efficiency from 3.8% in 2009 to the present state-of-art 25.7%. Organic-inorganic halide perovskites have also shown 31.3% efficient tandem devices with Si bottom cells. Mixed-halide and mixed-cation systems have demonstrated high efficiency, improvement in stability and reduced hysteresis. The emergence of 2D perovskite passivation and 2D/3D heterojunctions, have shown promise by enhancing the long-term stability of Pb-based halide PSCs, however, addressing toxicity challenge is crucial for large scale adoption.

A2BX₆ is a defect variant of the general perovskite structure ABX₃ where half of the vacant B-cations results in corner-sharing octahedron of anions [BX₆]²⁻ and A-cation occupying the sites between the octahedron in 12-fold coordination. Alteration and substitution of B-cations and/or halogen anions (Cs₂Tel₆, Cs₂PtI₆, Cs₂PtBr₆, Cs₂TiBr₆, Cs₂AgBiBr₆, Cs₂AgBiCl₆, etc.) offer a multitude of features in these double perovskite structures with enhanced thermal and moisture stability. Cs₂SnI₆ double perovskite has emerged as a promising light absorber, with a 4+ oxidation state of tin and shorter Sn-I bond length (2.85 Å vs. 3.11 Å in CsSnI₃), making it oxidation resistant and air-stable. Cs₂SnI₆ has a direct bandgap of 1.3-1.6 eV, and the closed-packed halide

framework results in dispersed conduction and valence bands leading to low electron effective masses of 0.48m₀ for electrons and 1.32m₀ for holes. Cs₂SnI₆ exhibits electron and hole mobilities of 310 cm²V⁻¹s⁻¹ and 42 cm²V⁻¹s⁻¹, respectively, and is believed to be an ambipolar material due to formation of n-type iodide vacancies/tin interstitials or p-type cesium vacancies. Devices up to 5% PCE have been demonstrated with enhancements such as Cl, F, Rb, Ag, In doping; ZnO nanorod electron transport layer (ETL); ethylene diamine post-deposition treatments. However, state-of-art Cs₂SnI₆ devices show high bulk and interface recombination as indicated by low carrier lifetime and high dark saturation current. Power conversion efficiency of > 5% has been demonstrated for planar p-i-n Cs₂SnI₆ devices; however, to increase the device efficiency further robust methods of defect passivation and improved doping density are needed. Here we will present the results of a controlled study on charge transfer doping using molecules such as F4TCNQ for Cs₂SnI₆. When applied to MAPb_{0.5}Sn_{0.5}I₃, the electrical conductivity increased by 5 orders of magnitude, the hole density increased by 1 order of magnitude, and the passivation of charge carrier traps increased the carrier recombination lifetime. The molecular dopant F4TCNQ also fits the criteria to be an effective p-type dopant for Cs₂SnI₆, due to its lowest unoccupied molecular orbital (LUMO) value being less than the valence band maximum (VBM) value, so as to facilitate effective charge transfer for holes. Data on film processing, doping density and carrier lifetime will be presented for Cs₂SnI₆ processed by doctor blade method with and without molecular dopants. The effect of the dopants on phase stability, absorption bandgap will also be studied.

5:00 PM EN10.11.06

Optimal Interface Engineering through SAM Energy Alignment & Functionalization [Hannah K. Contreras](#)¹, Yangwei Shi¹, Fangyuan Jiang¹, Declan McCarthy², Aidan O'Brien¹, Seth R. Marder² and David S. Ginger¹; ¹University of Washington, United States; ²University of Colorado Boulder, United States

Open circuit voltage losses (V_{OC}) in the perovskite top cell remain a significant challenge for the commercialization of perovskite tandem solar cells. We show through simulations that common hole transport layers like PTAA and Me-4PACz are energetically mismatched with the perovskite active layer which lowers the quasi-Fermi level splitting and limits V_{OC} , particularly for wide bandgap compositions relevant to tandems ($E_g \geq 1.7$ eV). We identify the ideal energy offset between the hole extraction and the wide bandgap perovskite layers and modulate the anode work function to this ideal using novel halide self-assembled monolayers (SAMs) as interface modifiers. Mixing these SAMs allows for selective tunability of both wettability and work function. Using a two-step SAM-perovskite deposition, we have not found a clear correlation between improved alignment of the SAM-modified ITO-perovskite interface and improved V_{OC} in solar cell devices. However, we found that mixing the SAMs into the perovskite precursor solution using a one-step deposition method improves their solar cell performance. This suggests that interfacial chemistry, including SAM functionalization and SAM interactions with perovskite in solution, may supersede energy alignment as the primary factor currently limiting V_{OC} . Understanding their respective roles will enable the development of efficient wide gap perovskite devices for Si-tandem applications.

5:00 PM EN10.11.07

Efficient and Stable Perovskite Quantum Dot Photovoltaics enabled by Using Dopant-Free Hole Transport Materials with Rigid Segments [Seyeong Lim](#), Sungyong Kim and Taiho Park; Pohang University of Science and Technology, Korea (the Republic of)

CsPbI₃ perovskite quantum dots (PQDs) with ideal optoelectronic properties offer high thermal stability for photovoltaics. In device fabrication, a ligand exchange process is required to enhance electrical coupling within PQDs. However, this dynamic ligand exchange is imperfectly performed, resulting in surface traps and inevitable exposure of PQDs to external conditions containing H₂O or O₂. So far, most PQD photovoltaics (PQDPVs) have adopted Spiro-OMeTAD as hole transport material (HTM), which requires deliquescent dopants to enhance its hole mobility, resulting in moisture that penetrates the perovskite crystal and greatly accelerates the decomposition of PQDs. In this point of view, hydrophobic HTMs on the PQD surface are crucial for achieving high device stability. Conjugated polymeric HTMs basically have strong molecular packing for efficient charge transport, but excessive intermolecular interactions degrade film-forming properties in perovskite, which causes interfacial nonradiative recombination. In this respect, side chain engineering (e.g., extended-, polar-, and asymmetric-side chains) is developed for optimizing the morphology. Nevertheless, these strategies reduce the charge hopping efficiency. Therefore, in this study, we propose a novel D-A conjugated polymeric HTM design employing unsubstituted rigid segments and fabricate three D-A conjugated polymeric HTMs: Asy-PDTS, Asy-PSDTS, and Asy-PSeDTS. Particularly, Asy-PSeDTS with a rigid segment locally induces strong intermolecular interactions, enhancing the charge hopping efficiency while exhibiting appropriate intermolecular interaction to maintain excellent film-forming properties. Owing to this synergy, Asy-PSeDTS-based PQDPVs achieved 15.2% power conversion efficiency (PCE) and maintained 80% of the initial PCE after 40 days, which is the highest PCE and stability among dopant-free HTM-based PQDPVs so far.

5:00 PM EN10.11.08

Electrochemical Impedance Spectroscopy on Perovskite Inks to Probe Ion Pairing in Solution [Keenan W. Wyatt](#); University of Colorado Boulder, United States

Hybrid perovskite solar cells (PCS) are a disruptive technology with their rapid improvement in power conversion efficiencies over the last decade. At the laboratory scale, solution processed PCSs are studied to inform the eventual commercialization which is likely to use a slot dye coating process. Many steps in the PSC device fabrication process have been optimized, however there is still a lack of understanding of the solution chemistry and chemical species prior to the crystallization and annealing to perovskite phase. During the crystallization, solvent is expelled with the addition of anti-solvent or with a purge of nitrogen. Initially, the ratio of solvent molecules to ions is dominated by the solvent, especially in low concentration solutions. As solvent is driven off, the ratio of solvent molecules to ions begins to be dominated by ions until a solubility limit is reached and precipitate is formed then an eventual crystallization. In the interim, before any precipitation or crystallization, the solution will undergo concentration dependent regions of ion pairing which directly influence the kinetics of crystallization. Here, we use electrochemical impedance spectroscopy (EIS) to probe the ion pairing in different concentrations of perovskite inks and complement our results with pair distribution function from the total scattering of x-rays.

5:00 PM EN10.11.09

Mechanism of the Anomalous Dependence between Spin-Orbit Coupling and Dimensionality in Lead Halide Perovskites [Yeming Xian](#), Xiaoming Wang and Yanfa Yan; University of Toledo, United States

The spin-orbit coupling (SOC) effect of lead (Pb) atoms is a consequential attribute of the unique optoelectronic and defect properties of lead halide perovskites (LHPs). It has been found that the SOC effect varies significantly as the structural dimensionality changes with an anomalous dependence; i.e., while the SOC strength monotonically decreases as structural dimensionality decreases from three-dimensional (3D) to two-dimensional (2D) and then to one-dimensional (1D), the zero-dimensional (0D) SOC strength is greater than the 1D SOC strength. The underlying mechanism of such a SOC dimensionality dependence anomaly remains elusive. In this work, we show that Pb 6p energy splitting increases from 3D to 2D and to 1D LHPs due to the increased degree of distortion, leading to a reduced SOC strength. However, the degree of distortion decreases for the 1D to 0D transformation, resulting in reverse SOC enhancement. The mechanism described in this work can be employed to regulate the SOC effect in the design of perovskite materials.

5:00 PM EN10.11.10

Understanding the Structure-Property Relationship of Two-Dimensional Metal Halide Perovskites [Yumeng Song](#) and Philip Chow; The University of Hong Kong, Hong Kong

Yumeng Song, Philip C.Y. Chow*
Department of Mechanical Engineering, The University of Hong Kong,
Hong Kong SAR, China
pcyc@hku.hk

Two-dimensional (2D) metal halide perovskites have emerged as promising materials for next-generation solar cells and light-emitting diodes thanks to their outstanding optoelectronic properties, facile tunability, and superior stability over their 3D counterparts. However, the detailed structure-property relationship of 2D perovskites underlying their optoelectronic properties has remained unclear. In this project, we design and synthesize a variety of 2D perovskite single crystals, in both Ruddlesden-Popper and Dion-Jacobson phases. We then use a combination of steady-state and time-resolved optical spectroscopy methods to characterize the exciton properties and dynamics, specifically focusing on how they are affected by changes in structural properties. Our results will help us develop a fundamental understanding of 2D perovskites and enable rational material design and development.

SESSION EN10.12: Passivation and Interlayers I
Session Chairs: Virgil Andrei and Hin-Lap Yip
Thursday Morning, April 25, 2024
Room 334, Level 3, Summit

8:15 AM EN10.12.01

Mitigating Iodine Diffusion by a MoO₃-Organic Composite Hole Transport Layer for Stable Perovskite Solar Cells [Jisu Hong](#)¹, Zhaojian Xu¹, Dominique Lungwitz¹, Jonathan Scott¹, Holly Johnson¹, Yun-Hi Kim², Antoine Kahn¹ and Barry P. Rand¹; ¹Princeton University, United States; ²Gyeongsang National University, Korea (the Republic of)

Halide perovskite solar cells (PSCs) exhibit commercialization potential, but long-term stability still has to be addressed. Among various products of perovskite decomposition, iodine species are of considerable concern due to their high vapor pressure and corrosive nature. To address this, a small-molecule hole transport layer (HTL), 4,4',4''-tris[(3-methylphenyl)phenylamino]triphenylamine (m-MTDATA), is used, and *p*-doped using molybdenum trioxide (MoO₃) to prevent an alternative oxidation reaction with iodine species that are released from iodide perovskites upon degradation. The resulting m-MTDATA:MoO₃ composite HTL demonstrates high conductivity and suppressed iodine permeation. We demonstrate that m-MTDATA:MoO₃ HTLs employed in PSCs improve stability under both thermal and voltage bias stress compared to devices with a conventional doped 2,2',7,7'-tetrakis[N,N-di(4-methoxyphenyl)amino]-9,9'-spirobifluorene (spiro-OMeTAD) HTL.

8:30 AM EN10.12.02

Time-Resolved Electrostatic Force Microscopy Measures Effect of Phosphonic Acid Hole Transport Layers on Lead Halide Perovskite Carrier Dynamics on the Nanoscale [Madeleine Breshears](#), Rajiv Giridharagopal, Justin Pothoof and David S. Ginger; University of Washington, United States

Phosphonic acid hole transport layers (HTLs) demonstrate great promise in improving lead halide perovskite device performance metrics such as open circuit voltage and radiative recombination lifetime. As perovskite thin films exhibit morphological features on the scale of hundreds of nanometers, and carrier dynamic processes on the order of microseconds and below, it is important to investigate the effects of these HTLs at sub-diffraction limited lengthscales with high temporal resolution. Time-resolved electrostatic force microscopy (trEFM) is an atomic force microscopy method that measures photoinduced charging in samples under realistic intensities with sub-microsecond time resolution and nanometer-scale spatial resolution. Here, we use trEFM to investigate the effect of two phosphonic acid HTLs, MeO2PACz and Me4PACz, on carrier dynamics at grains and grain boundaries. We find that phosphonic acid HTLs promote slower dynamics as captured by trEFM, which agrees with bulk carrier lifetime measurements and provides a nanoscale view of charging dynamics. Furthermore, we observe variation in those dynamics across grain boundaries, with grain boundaries exhibiting slower charging compared to grain centers. The microsecond timescales suggest that trEFM measures fast capacitive charging, which may be convolved with carrier trapping, non-radiative recombination, and ion motion. These experiments indicate that trEFM is a powerful tool for probing dynamic processes in perovskites at the nanoscale.

8:45 AM EN10.12.03

Halide Choice is Critical for The Formation of 2D/3D Perovskites and Their Performance in Solar Cells [Raphael F. Moral](#)^{1,2}, Carlo Andrea Riccardo Perini³, Tim Kodalle¹, Ahyoung Kim¹, Finn Babbe¹, Nao Harada⁴, Philip Schulz⁵, Naomi S. Ginsberg⁶, Ruipeng Li⁷, Shaul Aloni¹, Craig Schwartz², Juan-Pablo Correa-Baena³ and Carolin M. Sutter-Fella¹; ¹Lawrence Berkeley National Laboratory, United States; ²University of Nevada, Las Vegas, United States; ³Georgia Institute of Technology, United States; ⁴L'Institut Photovoltaïque d'Île-de-France, France; ⁵Centre National de la Recherche Scientifique, France; ⁶University of California, Berkeley, United States; ⁷Brookhaven National Laboratory, United States

2D/3D perovskite solar cells (PSCs) hold great promise for photovoltaics applications.¹ The key to the development of stable and efficient devices is the synergy between the higher ambient stability of 2D phases and the outstanding electrical and optical properties of 3D halide perovskites. These materials also have high versatility in terms of composition, allowing for different material design and engineering strategies. The vast list of molecules (spacers cations) that can be used for the synthesis of the 2D phases also poses a challenge to the development of these materials.² Each of these spacer cation presents a different reactivity with the underlying 3D perovskite, encouraging trial-and-error approaches rather than a rational design of stable 2D/3D interfaces.³ For example, the choice of the halide anion, both in the spacer cation and in the 3D perovskite, greatly influences materials' photovoltaic and device properties.⁴ To provide more insights into the formation and ionic dynamics of these complex interfaces, we examined the impact of halide choice (I and Br) in 3D perovskites treated with phenylethylammonium salts (PEAI and PEABr, respectively). We evaluated the formation of layered perovskites using PEAi and PEABr salts on top of 3D perovskites with pure iodine and mixed halides, Cs_{0.17}FA_{0.83}PbI₃ and Cs_{0.17}FA_{0.83}PbI_{2.5}Br_{0.5}, respectively, before, during, and after annealing at 65 °C for 30 minutes. Through various spectroscopic techniques, we revealed that PEABr reacts less readily with the 3D film compared to PEAi to form the 2D phases. As a consequence of this lower reactivity, PEABr can diffuse through the grain boundaries as an ionic pair, and this behavior was revealed by X-ray photoelectron spectroscopy (XPS). Also, the mixed-halide 3D perovskite is less reactive than its pure-iodine counterpart. The lower reactivity of PEABr may be attributed to the higher lattice energy of ammonium bromides in comparison to ammonium iodides,⁵ and similar reasoning applies to the mixed-halide 3D perovskite. Consequently, PEAi presents higher passivation ability than PEABr, and the best device performance and reproducibility were achieved with PEAi-treated

Cs_{0.17}FA_{0.83}PbI₃. Our work provides valuable insights into the fundamental properties and formation mechanisms of 2D/3D perovskites, which is crucial for advancing these photovoltaic devices.

9:00 AM EN10.12.04

Preventing Metal Shunting in Perovskite Solar Cells during Reverse Bias [Daniel A. Morales](#) and Michael McGehee; University of Colorado Boulder, United States

Perovskite solar cells (PSCs) are emerging as promising materials for photovoltaic energy conversion due to their rapidly increasing power conversion efficiencies and cost-effective fabrication procedures. Many research efforts are currently dedicated to investigating external stressors that perovskite solar cells experience in the field – oxygen, elevated temperatures, and moisture/humidity. However, there remains a knowledge gap concerning the behavior of this technology when subjected to another real-world external stressor for solar panels – reverse bias.

PSCs typically exhibit low breakdown voltages in reverse bias (<5V), making the integration of traditional bypass diodes used in Si arrays difficult due to the increased production costs^{[1][2]}. Therefore, numerous efforts have been made to identify and address the root causes of reverse bias-induced degradation of PSCs. These breakdown mechanisms of PSCs have been directly correlated with voltage-induced ion migration and the formation of hotspots when using metal electrodes^{[2][3]}. The diffusion of metallic species in PSCs has been recorded during regular operation, but is accelerated under reverse bias conditions as elevated electric fields facilitate ion migration and initiate interactions between mobile ions and metal species at the contacts.

We have studied a wide variety of strategically chosen perovskite solar cells under reverse bias, and we observe the formation of these metallic shunts in PIN architectures with metal electrodes. We employed metals with various electrochemical reactivities (Ag, Au, Cu, & Al) and found that metal shunting is most prominent in silver metal electrodes, one of the most popular contact materials used in perovskite solar cells. Metal diffusion/shunting most-often results in catastrophic failure of the device when returned to normal operating conditions. We attribute this metal shunting behavior to the preferred oxidation state of the metals and the increased activation energy for these metal ions to diffuse through the perovskite device architecture. We show that metal shunting/diffusion in our inverted perovskites can be prevented by simply using higher oxidation-state metals (Au, Cu, & Al). We also investigate the application of interlayer additives, including barrier layers deposited via atomic layer deposition (ALD), chromium (Cr), benzotriazole (BTA), and other chelating agents commonly employed in water treatment facilities to address metal accumulation.

[1] E. J. Wolf, "Designing Modules to Prevent Reverse Bias Degradation in Perovskite Solar Cells when Partial Shading Occurs," *Solar RRL*, 2021.

[2] C. Wang, "Perovskite Solar Cells in the Shadow: Understanding the Mechanism of Reverse-Bias Behavior toward Suppressed Reverse-Bias Breakdown and Reverse-Bias Induced Degradation," *Advanced Energy Materials*, vol. 13, no. 9, 2023.

[3] A. Bowring, "Reverse Bias Behavior of Halide Perovskite Solar Cells," *Advanced Energy Materials*, vol. 8, no. 8, 2017.

9:15 AM EN10.12.05

All Inorganic Layer Perovskite Solar Cells Based on Oxide/Halide/Oxide Architecture [Soo Woong Jeon](#), Min Ju Jeong and Jun Hong Noh; Korea University, Korea (the Republic of)

Inorganic CsPbI₂Br perovskite has outstanding thermal stability and substantial potential for semi-transparent solar cells. However, Cesium-based perovskite solar cells (PSCs) exhibit phase instability due to the perovskite film's moisture penetration. Therefore, 2,2',7,7'-tetrakis(N,N-di-p-methoxyphenylamine)-9,9'-spirobifluorene (spiro-OMeTAD) which has been commonly used as hole transporting layers (HTLs) in high-performance PSCs is not suitable for CsPbI₂Br-based PSCs. Herein, we report all inorganic layer PSCs based on oxide/halide/oxide architecture for the high stability and performance of PSCs. We introduced nickel oxide (NiOx) nanoparticles overlayer on the perovskite layer as HTLs. As a result, the all-inorganic layer device shows an improved thermal stability and power conversion efficiency (PCE) of 16.67%. In addition, we fabricated the semi-transparent devices by sputtering the tin-doped indium oxide (ITO) as an electrode, which achieved an average visible transmittance higher than 20%. All inorganic layer PSCs with oxide/halide/oxide also showed superior storage stability without encapsulation under 10% relative humidity, retaining over 85% of initial PCE for 1000 h. We believe that this architecture with n-type oxide/inorganic perovskite/p-type oxide represents a cornerstone for the high stability of PSCs.

9:30 AM EN10.12.06

Irreversible Performance Degradation Driven by Lithium-Ion Migration in FAPbI₃ Perovskite Solar Cells [Seung-Gu Choi](#) and Jin-Wook Lee; Sungkyunkwan University, Korea (the Republic of)

The typical n-i-p structured perovskite solar cells (PSCs) incorporate 2,2',7,7'-Tetrakis (N, N-di-p-methoxyphenylamine)-9,9'-spirobifluorene (Spiro-OMeTAD) as a hole transporting material. The chemical doping process of the spiro-OMeTAD involves a redox reaction with bis(trifluoromethane) sulfonimide lithium salt (Li-TFSI) accompanying complex side reactions of which impact on device performance is not fully understood. Here, we investigate correlation between aging dependent device performance of widely used formamidinium lead tri-iodides (FAPbI₃) based PSCs and migration of lithium-ion (Li⁺) generated from Li-TFSI. The cross-sectional Kelvin probe force microscopy unraveled aging time dependent change in hetero-interface energetics in PSCs, which was correlated with progressive migration of Li⁺ ions generated from Li-TFSI confirmed by Time-of-flight secondary ion mass spectroscopy. Comprehensive analysis revealed that the Li⁺ migrate from spiro-OMeTAD to perovskite, SnO₂ and their carrier extraction interfaces to induce phase back conversion of α -FAPbI₃ to δ -FAPbI₃ with local microstrain, and consequent generation and migration of iodine defects and dedoping of the spiro-OMeTAD. The rapid performance drop of PSCs even aging under dark conditions was attributed to a series of these processes. Our work unraveled the hidden side effect of Li⁺ ion migration in FAPbI₃ based PSCs that can guide further work to maximize the operational stability of the PSCs.

9:45 AM EN10.12.07

Effective Addition of Cation and halides in FAPbI₃ Perovskite Solar Cells by Multiple Thermal Co-Evaporation [Ha Kyung Park](#) and William Jo; Ewha Womans University, Korea (the Republic of)

Metal halide perovskite solar cells (PSCs) have rapidly advanced as a next-generation solar cells with high efficiency over 25%. Among the various fabrication methods for the perovskite, thermal evaporation stands out as a suitable option for scaling up commercialization. However, achieving precise stoichiometry with multiple sources is challenging when using a co-evaporation method due to their varying volatility. In this study, multiple co-evaporation method was designed to fabricate the stoichiometrically mixed cation and halides PSCs using two sources. Formamidinium iodide (FAI) and lead iodide (PbI₂) were co-evaporated followed by the co-evaporation of methylammonium iodide (MAI) and PbI₂ or methylammonium bromide (MABr) and lead bromide (PbBr₂). The deposition rates and thickness of secondly co-evaporated layer were controlled to achieve stoichiometry of mixed cations and halides precursors. After that, samples were annealed to form FAPbI₃, (FA,MA)PbI₃, and (FA,MA)Pb(I,Br)₃ films. The completed PSCs were semi fully-vacuum-deposited, except for the hole transport layer. Among the samples, (FA,MA)Pb(I,Br)₃ solar cells showed the highest performance of 11.38% efficiency with improved open-circuit voltage of 25 mV and current-voltage hysteresis. Herein, band gap of MA and Br added FAPbI₃ slightly increased indicating only small amount of MAPbI₃ and MAPbBr₃ phases formed. Still, mixed cations samples showed improved absorbance compared to FA cation only sample. In conclusion, multiple co-evaporation is effective method for mixing cations and halides in PSCs.

10:00 AM BREAK

SESSION EN10.13: Strain and Single Crystals
Session Chairs: Silvia Colella and Carolin Sutter-Fella
Thursday Morning, April 25, 2024
Room 334, Level 3, Summit

10:30 AM EN10.13.01

High Mobility Anthracene-Based Perovskites: Tunable Phase Morphology via GIWAXS [Damara G. Dayton](#)¹, Pattarawadee Therdkatanyuphong¹, Junxiang Zhang¹, Yifan Dong², Keith P. White¹, Tatiana Temofeeva³, Kathryn Bairley¹, Michael Toney¹, Seth R. Marder¹ and Matthew C. Beard²;
¹University of Colorado Boulder, United States; ²National Renewable Energy Laboratory, United States; ³New Mexico Highlands University, United States

Exploiting the inherent stability of two-dimensional metal halide perovskites (2D MHPs) is a desirable approach to enable scaled production of perovskite solar cells. The addition of a light-absorbing 2D MHP passivation layer promises to address the poor stability plaguing 3D MHPS- degradation induced by ambient moisture, oxygen, and light.[1] Despite recent achievements in this area, the community lacks a consensus of thin film processing controls towards preferential orientation for high photoconductivity in 2D MHPs, nor an understanding of how 2D MHP polymorphism influences charge transport and device efficiency. In this work, an anthracene-based family of spacer cations were used to synthesize two-dimensional MHPs with record-breaking carrier mobility values in the n=1 2D MHP class of materials. The band structures of the anthracene-based family of organic cations are compatible with that of the lead-iodide octahedra, and thus offer desirable charge transport properties due to electronic coupling and wavefunction hybridization. The position and length of the alkylamine on the anthracene cation greatly influence the film's morphological response when solution processed across a binary solvent system compositional loading series. The polar aprotic solvents NMP and DMF were selected for this study due to their similar properties and common use in the perovskite community. Characteristic trends in photoconductivity and morphology are apparently correlated, unique to each cation. The photoconductivity of these anthracene-based Ruddleston-Popper 2D Lead Iodide MHPs was interrogated with time-resolved Microwave Conductivity (TRMC) and Terahertz Spectroscopy (TRTS). TRTS provides picosecond resolution of charge carrier mobility and diffusion lengths, complementary to the longer nanosecond timescales of carrier lifetimes probed by TRMC. TRMC measures the change in microwave power reflection coefficient from the sample cell relative to a control, from which the conductivity of the sample can be calculated. [2] From this work, we present record values for mobility and demonstrate correlations between alkylamine local chemistry and solvent interactions, and the photoconductivity of these films to the equilibrium polymorphic phase distribution and degree of orientation of the 2D MHP lamella parallel to the substrate. Grazing Incidence Wide Angle X-ray Scattering (GIWAXS) is an incredibly powerful technique enabling a comprehensive analysis of phase behavior- including octahedral tilting, degree of orientation, phase distribution, crystallinity, strain, static disorder and stacking faults.[3] In addition to this analysis via internally developed programs, we show GIWAXS simulations in agreement with the experimental data utilizing solved single crystal structures for two of the cations. Additionally, the crystallographic space group was determined for a particular cation which was unable to yield a single crystal. Herein, this analysis is used to propose generally applicable processing and design rules for high mobility 2D MHP passivation layers for use in MHP device applications.

10:45 AM EN10.13.02

How The Dynamics of Attachment to The Substrate Influence Stress in Metal Halide Perovskites [Gabriel McAndrews](#)^{1,2}, Boyu Guo³, Daniel Morales¹, Aram Amassian³ and Michael D. McGehee^{1,1,1}; ¹University of Colorado Boulder, United States; ²National Renewable Energy Laboratory, United States; ³North Carolina State University, United States

Metal halide perovskites, hereon referred to perovskites for simplicity, are a promising class of semiconductors eagerly researched for their use in photovoltaic and optoelectronic applications. Despite low fabrication cost and superb initial efficiencies, improvements to the operational stability of perovskites would aid extensive deployment in both terrestrial and space applications. Mechanical stress is an important, but often misunderstood factor impacting chemical and structural degradation as well as reliability during extreme temperature cycling. Tension has been linked to accelerated formation of undesirable PbI_2 which has been attributed to decreased activation energy for ion migration.^[1,2] In addition, the brittle nature of polycrystalline metal halide perovskite films leaves them susceptible to fracture and delamination.^[3] Therefore, it is crucial to accurately identify and reduce sources of tension that arise from film formation processes and in response to environmental exposure.

The formation of perovskite thin films using solution processing methods usually includes a thermal annealing step to fully convert the film from intermediate to perovskite phases. The field has primarily focused on thermal strain originating from an order of magnitude difference in coefficient of thermal expansion (CTE) between perovskite and substrates used for photovoltaic applications, such as silicon and glass.^[2] Consequently, tensile stress is predicted to develop in the perovskite layer while cooling back to room temperature due to the film's constraint to the substrate and inability to fully contract.

Here, we show that a simple application of the CTE mismatch equation inaccurately predicts residual stress in perovskite films. For example, despite similar CTEs, there is a 60 MPa stress difference between narrow bandgap "SnPb Perovskite" ($\text{Cs}_{0.25}\text{FA}_{0.75}\text{Sn}_{0.5}\text{Pb}_{0.5}\text{I}_3$) and popularized "Triple Cation Perovskite" ($\text{Cs}_{0.05}\text{MA}_{0.16}\text{FA}_{0.79}\text{Pb}_{(0.83\text{Br}_{0.17})_3}$). We probe the cause of residual stress variation in metal halide perovskite with a combination of *in situ* absorbance and substrate curvature measurements during the spin coating, anneal, and cooldown procedures. This reveals that the degree of partial attachment prior to the anneal can reduce residual tension following cooldown. Additionally, we demonstrate the dynamic nature of stress in perovskite with evidence of tensile stress relaxation which is accelerated by the presence of moisture and oxygen. In turn, we propose a new framework to understand the relationship between stress and degradation as films with tension are driven to uptake moisture and oxygen to release stress. Finally, we present a critical perspective on stress engineering strategies based on high CTE buffer or interlayers which are claimed to modify thermal stress in the perovskite.^[4] We show that these strategies are not grounded in thin-film mechanics as the stress in the perovskite in response to temperature changes is dominated by the thickest, stiffest layer, such as glass.

[1] J. Zhao, Y. Deng, H. Wei, X. Zheng, Z. Yu, Y. Shao, J. E. Shield, J. Huang, *Sci. Adv.* **2017**, 3, ea05616.

[2] N. Rolston, K. A. Bush, A. D. Printz, A. Gold-Parker, Y. Ding, M. F. Toney, M. D. McGehee, R. H. Dauskardt, *Adv. Energy Mater.* **2018**, 8, 1802139.

[3] C. Ramirez, S. K. Yadavalli, H. F. Garces, Y. Zhou, N. P. Padture, *Scr. Mater.* **2018**, 150, 36.

[4] D.-J. Xue, Y. Hou, S.-C. Liu, M. Wei, B. Chen, Z. Huang, Z. Li, B. Sun, A. H. Proppe, Y. Dong, M. I. Saidaminov, S. O. Kelley, J.-S. Hu, E. H. Sargent, *Nat. Commun.* **2020**, 11, 1514.

11:00 AM EN10.13.03

Suppressing Trap-Assisted Recombination in Perovskite Solar Cells via Strain Relaxation Beier Hu; Imperial College London, United Kingdom

Intraband trap states can be formed unavoidably during the solution-processed fabrication of perovskite solar cells (PeSCs). Their existence contributes to non-radiative recombination loss via trap-assisted recombination pathways in PeSCs, leading to insufficient power conversion as well as a higher intraband trap states can be formed unavoidably during the solution-processed fabrication of perovskite solar cells (PeSCs). Their existence contributes to non-radiative recombination loss via trap-assisted recombination pathways in PeSCs, leading to insufficient power conversion as well as a higher probability of lattice decomposition. Particularly, regarding the soft nature of perovskites, one should consider the impact of local lattice strain on the properties of trap states. However, the relationship between strain and trap-assisted recombination has not been disclosed systematically and comprehensively.

Herein, we fabricated two perovskite films with different strain levels, i.e., $\text{MA}_{0.95}\text{GA}_{0.05}\text{PbI}_3$ with tensile strain and $\text{MA}_{0.95}\text{GA}_{0.05}\text{Pb}(\text{I}_{0.95}\text{Br}_{0.05})_3$ with free strain due to the compensation of the smaller-size Br towards the expanded lattice. To access the critical factors that affect the trap-assisted recombination including the number of traps, depth of traps, and lifetime of trapped carriers, we employed the advanced visible-pump-IR-push photocurrent spectroscopy (PPPC) on devices based on the aforementioned perovskite films with and without strain. PPPC is a highly selective technique for observing localized state behaviours of PeSCs under operational conditions, to display a full scenario of the regulated trapped carrier dynamics after strain manipulation. Steady-state and time-resolved PPPC measurements evidenced that the strain relaxation was able to reduce the density of traps, shallow the depth of traps, and prolong the lifetime of trapped carriers, alleviating the trap-assisted recombination loss in the strain-free device. To the best of our knowledge, this is the first report which provides an explicit correlation between strain engineering and its impacts on the overall trap-assisted recombination processes.

11:15 AM EN10.13.04

Lattice Volume Anchoring Attenuates Natural Performance Loss in Perovskite Solar Cells during Day/Night Cycling Tiankai Zhang and Feng Gao; Linköping University, Sweden

It is commonly believed that perovskite solar cells (pero-SCs) show enhanced stability under day/night cycling due to reported self-healing effect in the dark. However, it is discovered that the operational lifetime of highly efficient FAPbI₃ pero-SCs is in fact much shorter under day/night cycling mode, being into question the widely accepted approach to estimate the pero-SCs' operational lifetime based on continuous mode testing. We reveal the key factor to be the lattice volume change during the operation, an effect which gradually relaxes under the continuous illumination mode but cycles synchronously under the cycling mode. The cycled lattice volume change results in plastic deformation and deep trap accumulation during operation, decreasing the ion migration potential and hence the lifetime under the cycling mode. To address the challenges induced by the synchronously cycled lattice volume, we introduce Ph-Se-Cl to stabilize the perovskite lattice during day/night cycling. As a result, the pero-SCs achieved the certified efficiency of 25.6% and a 10-time improved T80 lifetime under the cycling mode (ISOS-LC-2 suggested protocol) after the modification. Our results uncover the unique degradation mechanism caused by the cycling mode and highlight the necessity of lattice volume fixing to prolong the real working lifetime of pero-SCs.

11:30 AM EN10.13.05

Advancing Perovskite Single Crystal Fabrication: Enhanced Crystallinity and Reproducibility through Feedback Control of Linear Growth Rate Yuki Haruta, Antoine Pavesic Junior and Makhsud Saidaminov; University of Victoria, Canada

Lead halide perovskites have gained significant attention in recent years thanks to their excellent photon absorption capabilities and charge transport properties, raising high expectations for diverse device applications such as solar cells and X-ray detectors. However, their instability presents a major challenge that demands resolution. Notably, perovskite single crystals are known to exhibit substantially higher durability compared to polycrystalline films, with an even higher degree of crystallinity suggesting enhanced stability. Nevertheless, conventional methods for synthesizing perovskite single crystals have often been relatively straightforward, yet challenging to consistently produce high-quality single crystals. In light of this, our research focused on controlling the linear growth rate of the single crystals which has been likely overlooked in the conventional methods. Methylammonium lead tribromide (MAPbBr₃) single crystals are fabricated as a case study. Our novel approach combines in-situ imaging techniques to monitor crystal growth rates with a conventional solvent evaporation method. When the crystal growth deviates from the desired rate, our system provides feedback to adjust growth conditions accordingly. Through this approach, we successfully maintain a constant linear growth rate for over 60 hours, leading to the reproducible synthesis of single crystals with enhanced crystallinity.

The degree of crystallinity is quantified by measuring the rocking curves of the (100) plane of the obtained MAPbBr₃ single crystals. This work uncovers the critical role of controlling the linear growth rate, rather than the mass growth rate, in achieving superior crystallinity and reproducibility. MAPbBr₃ single crystals grown with a linear growth rate of less than 0.3 mm h⁻¹ exhibit narrow rocking curves, with a full width at half maximum (FWHM) of 19.0±2.7 arcsecs (n=17), while growth rates exceeding 0.3 mm h⁻¹ results in a FWHM of 27.9±10.0 arcsecs (n=15). The best crystal achieves a remarkable FWHM of 15.3 arcsecs, the narrowest reported for MAPbBr₃ single crystals, comparable to a commercial silicon wafer. Note that these excellent FWHM are achieved with centimeter-scale single crystals. This research emphasizes the pivotal importance of linear growth rate control in single crystal growth.

11:45 AM EN10.13.06

Slow Spontaneous Enhancement in Efficiencies of Single-Crystal Metal Halide Perovskite Solar Cells Vishal Yeddu¹, Parinaz Moazzezi¹, Bekir Turedi^{2,2}, Muhammad N. Lintangpradipto^{2,2}, Dongyang Zhang¹, Soumya Kundu¹, Deepak Thrithamarassery Gangadharan¹, Reuven Gordon¹, Osman M. Bakr^{2,2} and Makhsud Saidaminov^{1,1,1}; ¹University of Victoria, Canada; ²King Abdullah University of Science and Technology, Saudi Arabia

Perovskite solar cells exhibit an interesting phenomenon known as spontaneous efficiency enhancement (SEE), where their efficiencies gradually improves over a few days. Numerous mechanisms have been proposed to explain this behavior in polycrystalline perovskite solar cells. However, investigations into such phenomena have not been extended to single-crystal perovskite solar cells (SC-PSCs). In this presentation, we present our findings of a relatively slow (approximately 20 days) SEE in single crystal methylammonium lead iodide perovskite solar cells. We show that the average PCE of SC-PSCs increases by at least 50% upon storage in an inert atmosphere for two weeks.

Our studies have revealed that SEE in SC-PSCs can be attributed to the slow escape of solvent trapped by the perovskite single-crystal thin films. We have demonstrated that SEE can be significantly accelerated through a heat treatment of at 40 °C. This work provides a ground for fast-tracking the progress of single-crystal perovskite solar cells.

Reference:

1. Yeddu, V.; Moazzezi, P.; Turedi, B.; Lintangpradipto, M. N.; Zhang, D.; Kundu, S.; Thrithamarassery Gangadharan, D.; Gordon, R.; Bakr, O. M.; Saidaminov, M. I. Slow Spontaneous Efficiency Enhancement of Single-Crystal Perovskite Solar Cells Due to Trapped Solvent. *ACS Appl. Energy Mater.* **2023**, *6* (4), 2257–2264.

SESSION EN10.14: Beyond Photovoltaics
Session Chairs: Sascha Feldmann and Carolin Sutter-Fella
Thursday Afternoon, April 25, 2024
Room 334, Level 3, Summit

1:30 PM EN10.14.01

Perovskite Nanocrystals for Down Conversion Displays and AR/VR Application Tae-Woo Lee^{1,2}; ¹SN Display, Korea (the Republic of); ²Seoul National University, Korea (the Republic of)

Colloidal perovskites nanocrystals (PeNCs) have been proven to possess high color purity (FWHM ~ 20 nm), high photoluminescence quantum yield (PLQY) and low-cost solution processability, making them promising candidates for the next generation light emitters. However, poor stability and the potential toxicity issues arising from lead leakage have hindered the commercialization of PeNCs. Furthermore, light-induced halide segregation limits the spectral stability of red and blue perovskite nano crystals, restricting their spectral tunability.

Here, first of all, we have developed ultra-stable and bright PeNCs by constructing a multi-layer structure. The multi-layer structure improved aging stability under 60 °C and 90% relative humidity condition and the photostability. Furthermore, this structure successfully prevents the leakage of lead, significantly reducing the toxicity of the nanocrystal film. Secondly, we have developed polymer matrix to improve stability of PeNC film. The polymer matrix successfully prevents degradation of PeNC by external condition and halide, leading to stable PeNC down conversion films with long lifetime under 60 °C and 90% relative humidity condition and under high flux (100 mW/cm²). With efficient and stable PeNC down conversion film, we successfully demonstrated a 28-inch monitor and a 10.1-inch tablet that surpasses existing products in terms of vivid images, achieving Rec. 2020 over 95%. Our work sheds great light on the potential that PeNCs can be commercialized in the near future.

1:45 PM EN10.14.02

Trap-Free Field Effect Transistors based on Epitaxial Single-Crystal Perovskites Vladimir V. Bruevich and Vitaly Podzorov; Rutgers University Physics Department, United States

Lead-halide perovskites have emerged as important semiconducting materials suitable for a variety of optoelectronic applications. Further advances in the field will rely on establishing the basic properties of these materials. We report the first experimental realization of the *intrinsic* (not dominated by defects) charge conduction regime in metal-halide perovskite field-effect transistors (FETs). The advance has been enabled by: i) a new vapor-phase epitaxy technique that results in large-area single crystalline all-inorganic cesium lead bromide (CsPbBr₃) films with excellent structural and surface properties, including atomically-flat surface morphology, essentially free from defects and traps at the level relevant to device operation; ii) an extensive materials analysis of these films using a variety of thin film and surface probes certifying the chemical and structural quality of the material; iii) the fabrication of nearly ideal (trap-free) FETs with textbook FET characteristics superior to any reported to date. These devices have allowed the investigation of the intrinsic carrier mobility as a function of temperature via both FET and gated Hall-effect measurements. The intrinsic mobility of our CsPbBr₃ FETs was found to increase on cooling from ~ 30 cm²V⁻¹s⁻¹ at room temperature to ~ 250 cm²V⁻¹s⁻¹ at 50 K. The combination of photo-Hall, gated Hall, and FET measurements reveal the intrinsic band transport occurring in these devices, with the mobility limited only by phonon scattering. The outstanding quality of these devices is largely due to the atomically flat, single crystalline morphology of the epitaxial CsPbBr₃ films achieved over macroscopic length scales, as confirmed by comprehensive structural, morphological and surface analysis.

The epitaxial CsPbBr₃ FETs exhibit no degradation over a long-term storage in air (as tested for up to several months) or during extended electric measurements (that sometimes run for several weeks on end), with the exceptions of driving the FETs into a saturation regime or micro crack formation at low temperatures. While the encapsulation of the perovskite in parylene may have contributed to the excellent operational stability of our FETs, our as-grown uncoated perovskite films did not exhibit noticeable degradation during a prolonged storage in the regular laboratory air (ranging in duration from days to weeks).

Establishing the intrinsic (phonon-scattering limited) mobility can not only serve as a rigorous test for theoretical models of carrier transport but can also reveal the ultimate fundamental limits of mobility in these materials, as well as point to a path for future innovation to still newer and improved perovskite systems. Additionally, our findings suggest that epitaxial perovskites offer an ideal platform for fundamental studies on charge transport in this class of materials. The robust, simple, and effective method for fabricating perovskite FETs that exhibit stable and ultimately efficient intrinsic charge transport paves a way for a plethora of new perovskite-based devices, such as light emitting FETs, electrically pumped injection lasers, better radiation detectors, sensors and memories.

Reference:

Bruevich, V., Kasai, L., Rangan, S., Hijazi, H., Zhang, Z., Emge, T., Andrei, E. Y., Bartynski, R. A., Feldman, L. C., Podzorov, V., Intrinsic (Trap-Free) Transistors Based on Epitaxial Single-Crystal Perovskites. *Adv. Mater.* 2022, 34, 2205055. <https://doi.org/10.1002/adma.202205055>

2:00 PM EN10.14.03

High-Resolution Multicolor Transfer Printing of Perovskite Nanocrystals for Ultrathin Skin-Attachable Displays. Gwang Heon Lee¹, Jong Ik Kwon¹, Gyuri Park², Jae Hong Jang¹, Jiwoong Yang² and Moon Kee Choi¹; ¹Ulsan National Institute of Science and Technology, Korea (the Republic of); ²Daegu Gyeongbuk Institute of Science and Technology, Korea (the Republic of)

Over the past decade, the development of wearable displays with ultrahigh definition has garnered considerable attention in the information technology. Wearable displays exhibit mechanical deformability, allowing them to conformally attach to various objects with curvilinear surfaces. Technological advances to achieve deformable form factors enable mechanical changes such as bending, rolling, and twisting. In parallel to the advanced at form factors, high-definition red/green/blue (RGB) subpixels are crucial for visualizing diverse information on the compact screens of wearable displays. Despite the recent advancements in display technology, the development of high-definition full-color wearable light-emitting diodes (LEDs) remain an unresolved problem.

Metal halide perovskite have gained attention as promising light-emitting substances due to their narrow full-width half-maximum, high photoluminescence, and color tunability. Furthermore, the extremely thin construction of perovskite light-emitting diode (PeLEDs) (<1 μm, excluding the thickness of the substrate) make them highly promising for candidates for application to ultrathin and deformable displays. With recent advances in synthesis and device engineering, progress in this field has led to impressive external quantum efficiency (EQE) values, with red, green, and blue PeLEDs achieving 25.8%, 28.9%, and 18%, respectively. Most previous studies predominantly centered on optimizing PeLED performance via monochromatic perovskite nanocrystal (PeNC) films produced by spin-coating techniques. However, manufacturing full-color displays on the commercial scale requires the development of patterning methods to ensure the seamless integration of RGB subpixels within electroluminescent (EL) devices.

Conceptually, the RGB patterning of PeNCs have several requirements : 1) Preservation of device layer integrity and no contamination during the patterning process 2) high reproducibility and 3) high-resolution patterning capabilities, particularly at the sub-micrometer scale. Unfortunately, conventional patterning methods (e.g., photolithography and inkjet printing) of perovskite materials are unsuitable for the fabrication of highly efficient PeLEDs. Photolithography suffer from the degradation of perovskite materials by ultraviolet(UV) light , moisture and polar solvents, owing to their ionic

bonding nature. Ink jet printing is applicable to multicolor pixelation of PeNCs through additive patterning. However, the additives (i.e., polymer matrix, surfactant, and viscosity modifier) suppress the EL device performance. Dry transfer printing employing a viscoelastic stamp represents a strategic choice for producing high-definition PeNC pixels for EL devices. This method circumvents the use of wet chemicals, mitigating concerns about solvent compatibility and cross-contamination between different colored pixels. Nonetheless, this approach has seen limited application in the case of PeNCs. The low interaction energy among PeNCs can lead to internal film cracking during the transfer process

Here, we demonstrate high-resolution dry transfer printing for ultrathin wearable displays. Specifically, we employ a simple and effective double-layer transfer printing method with an additional organic layer between PeNCs and a poly(dimethylsiloxane) (PDMS) stamp. The organic layer serves to prevent internal cracks in the transferred PeNCs layer. Furthermore, the pressure applied during the transfer printing process reduces the interparticle distance in the transfer-printed PeNCs layer, enabling the highly efficient PeLEDs, which exhibit peak EQE of 15.3%, 14.8%, and 2.5% for red, green, and blue PeLEDs, respectively. Finally, we demonstrate ultrathin, skin-attachable PeLEDs based on this patterning method. The realization of high-resolution RGB patterns using double-layer transfer printing may open up unique opportunities for wearable displays with various form factors.

2:15 PM EN10.14.04

Halide Perovskites as Thermoelectric Materials Oliver Fenwick; Queen Mary University of London, United Kingdom

Halide perovskites are well known as promising candidates for photovoltaics and light-emitting diodes. Additionally, promising thermoelectric performance has been reported for a small number of halide perovskites, with this class of materials offering ultralow thermal conductivity, good Seebeck coefficients and potential advantages in processing and sustainability. However, there is not yet a good understanding of how thermoelectric performance of halide perovskites can be optimised. This talk will cover the origins of ultralow thermal conductivity and quantify both the Lorenz number and the thermal boundary resistance [3] in polycrystalline films. Extrinsic doping and self-doping will be discussed as methods to optimise the thermoelectric figure of merit zT , with values of zT reaching 0.14 in CsSnI_3 [2] The case of self-doping by Sn-oxidation in CsSnI_3 will be examined in detail and strategies to improve performance and control the rate of oxidation by modification of deposition procedures, or by using mixed halide and mixed metal stoichiometries will be presented. Thin-film vapour deposition, single crystal growth [1] and solid-state synthesis of pellets will be discussed, along with doping techniques to improve stability and conductivity.

[1] Tang, W; Zhang, J; Ratnasingham, SR; et al., **Substitutional doping of hybrid organic-inorganic perovskite crystals for thermoelectrics**, *J. Mater. Chem. A* 2020, **8**, 13594 – 13599.

[2] Liu, T; Zhao, X; Li, J; Liu, Z; Liscio, F; Milita, S; Schroeder, BC; Fenwick, O **Enhanced control of self-doping in halide perovskites for improved thermoelectric performance**, *Nature Communications*, 2019, **10**(1):5750.

[3] Liu, T; Yue, SY; Ratnasingham, SR; Degousée, T; Varsani, PR; Briscoe, J; McLachlan, MA; Hu, M; Fenwick, O **Unusual thermal boundary resistance in halide perovskites: A way to tune ultralow thermal conductivity for thermoelectrics**, *ACS Applied Materials and Interfaces*, 2019, **11** (50), 47507–47515.

2:30 PM EN10.14.05

A Molecular Clamp Approach to Layered Halide Perovskite Nanowires Wenhao Shao, Jeong Hui Kim and Letian Dou; Purdue University, United States

Layered materials can be exfoliated into atomically thin 2D sheets or further fragmented into quantum dots, forming the foundation of numerous technology breakthroughs since the discovery of graphene. However, achieving 1D nanostructures from these materials with inherent in-plane symmetry remains a demanding yet rewarding endeavor. To date, only a few material-specific top-down methods exist, such as creating 1D nanoribbons of graphene and transition metal dichalcogenides through physical or chemical etching and unzipping from carbon nanotubes. The pursuit for a simpler and more universal bottom-up approaches with superior tunability, scalability, and capabilities to create precise and complex epitaxial structures therefore continues, necessitating a fundamental redesign of the crystal growth mechanism.

Here, we addressed this demand using organic-inorganic hybrid layered perovskites as a model system. Distinct from inorganic layered materials, hybrid semiconductors allow the incorporation of tailor-designed organic spacers with directional supramolecular synthons that communicate beyond single-molecule level. In this regard, a new “molecular clamp” approach is proposed to restrict crystal growth along all crystallographic directions except for [110] and thus to regulate 1D nanowire growth. Our approach is widely applicable to synthesize a range of high-quality 2D perovskite nanowires with large aspect ratios and tunable chemical compositions. These nanowires form exceptionally well-defined and flexible cavities that exhibit versatile unusual optical properties beyond conventional perovskite nanowires including anisotropic emission polarization, low-loss waveguiding (below 3 dB/mm), and efficient low-threshold light-amplification (below 20 $\mu\text{J}/\text{cm}^2$). Our approach highlights the unique structural tunability of organic-inorganic hybrid semiconducting materials by synergizing the merits of each, which also brings unprecedented morphological control to layered materials.

2:45 PM EN10.14.06

Degradation Mechanism of Colloidal Perovskite Nanocrystals and its Stabilization Strategy Qingsen Zeng, Huanyu Zhou and Tae-Woo Lee; Seoul National University, Korea (the Republic of)

The commercialization of colloidal perovskite nanocrystals (PeNCs) has been impeded by their rapid degradation in response to environmental factors and potential toxicity concerns due to lead leakage. Furthermore, the spectral stability of red-emitting and blue-emitting PeNCs is limited by light-induced halide segregation, restricting their spectral tunability.

Herein, we present a novel approach to address these issues. We have developed a facile and versatile method based on hierarchical confinement, involving the construction of a multi-layered structure. This technique facilitates the fabrication of CsPbBr_3 PeNC films with a photoluminescence quantum yield (PLQY) exceeding 84%. Importantly, the hierarchical confinement method significantly enhances the aging stability of CsPbBr_3 PeNCs, extending their operational lifetime at 60°C and 90% relative humidity and under blue light irradiation to 3400 hours and over 6000 hours, respectively. Moreover, this hierarchical confinement strategy proves to be versatile, effectively stabilizing mixed halide perovskite lattices, thereby suppressing halide segregation in mixed halide red-emitting PeNC films (QY: 83%) and blue-emitting PeNC films (QY: 40%) for 800 hours and 500 hours, respectively.

Most importantly, the hierarchical confined structure successfully prevents the leakage of lead ions, mitigating the toxicity concerns associated with the PeNC film material. Consequently, these findings render the PeNCs biocompatible, paving the way for their utilization in wearable devices and virtual/augmented reality display applications in the future.

3:00 PM BREAK

SESSION EN10.15: Emission
Session Chairs: Jacek Jasieniak and Carolin Sutter-Fella
Thursday Afternoon, April 25, 2024
Room 334, Level 3, Summit

3:30 PM *EN10.15.01

Light Emission from Localization in Halide Perovskites – Composition, Doping, Dimensionality [Sascha Feldmann](#); Harvard University, United States

Halide perovskites are fascinating semiconductors for light-emitting applications. Compared to conventional inorganic covalent semiconductors like silicon or GaAs, perovskites are structurally soft and often more disordered. Understanding the consequences of this remains a key challenge for commercialization.

Here I will present our recent mechanistic insights from spectroscopy on the role of composition, doping and dimensionality to control light emission through localization in these materials, including the introduction of a new method of doping halide perovskites at room temperature and its impact on excitation dynamics.

4:00 PM EN10.15.02

Tailoring The Optoelectronic Properties of Tin-Based Perovskite Light-Emitting Diodes [Ece Aktas](#); University of Naples Federico II, Italy

Two-dimensional perovskite thin films have shown tremendous potential as active materials for light-emitting diode (LED) applications, thanks to their remarkable optoelectronic properties and high environmental stability compared to their three-dimensional counterparts. However, achieving precise control over their composition and morphology remains a significant challenge. To overcome these issues, a strong coordinating agent, several functionalized bulky cations, and an increasing number of precursor materials have been applied. In this study, we investigate the influence of additives on the growth and performance of 2D tin-based perovskite thin films in nonoxidative solvent. We employed advanced characterization techniques such as UV-Vis absorption spectroscopy, X-ray diffraction, scanning electron microscopy, and photoluminescence spectroscopy to understand its effect. By systematically varying the processing parameters, including the amount of additive and the deposition conditions, we gain insights into the underlying mechanisms governing the film formation and properties. As a result, the 2D tin-based perovskite LED device had a low turn-on voltage of 1.75 V, and a maximum external quantum efficiency of ~2.2% in a nonoxidative solvent. The optimized thin film compositions and processing conditions from this research will facilitate the development of good-performance tin-based perovskite LEDs with enhanced external quantum efficiency, stability, and color purity. Furthermore, this work will contribute to the advancement of additive engineering strategies for the scalable fabrication of perovskite-based LEDs, fostering their integration into next-generation solid-state lighting technologies.

4:15 PM EN10.15.03

How Pinholes in Perovskite Films Create Stealthy ETL-HTL Diodes that Slightly Reduce Efficiency and Dramatically Enhance Reverse Bias Shunting [Samuel A. Johnson](#) and Michael D. McGehee; University of Colorado, Boulder, United States

Solution processing metal halide perovskites has advantages for scaling up manufacturing, but reproducibility and reliability are complicated by physics dictating coating (e.g. surface tension and dewetting). Void defects and pinholes form via tension created by volume reduction during the drying phase. We systematically investigate the origin and impacts of 'void defects' and reveal five common defect formation mechanisms that can result in points where the intrinsic perovskite absorber is missing. At most of these sites, metal- electron transport material (ETM)-hole transport material (HTM)- metal diodes exist. We determined how much current can pass through these defect diodes by making diodes without the perovskite layer and measuring the current-voltage curve. We found that the current turned on between 0.4 and 0.8 V depending on which contact layers we used. Dark Lock-in Thermography (DLIT) of a perovskite solar cell shows localized regions begin to heat under forward bias, but only above the turn-on voltage of transport-layer diodes indicating diode-like defect response in real devices. An important consequence of this behavior is that the defect diodes do not pass current near 0 V where the shunt resistance is typically measured by taking the slope of the current-voltage curve. They do, however, pass significant current at the maximum power point and the open circuit voltage. Consequently, they have a more detrimental effect on device performance than most people realize. These defects have even more important consequences when the cells are operated in reverse bias, which can happen when a panel is partially shaded. These defects enable break down at lower voltages and shunt current, resulting in local ohmic heating, followed by the melting and propagation of burning metal shunts across the surface. This effect produces catastrophic degradation of the solar module. It is therefore critical to mitigate such defects for widespread implementation of perovskite PV. We demonstrate optical profilometry and PL-mapping as high-throughput detection methods for these defects as well as improved particle control and solution wetting as possible preventative measures. Elimination or passivation of these defects will prevent localized loss and enhance long-term reliability of perovskite solar cells, paving the way for successful commercial perovskite solar cell production.

4:30 PM EN10.15.04

Bismuth: An Infrared-Emitting, Deep-Level Trap in CsPbBr₃ [Kyle Sengdikoski](#)¹, Brendon T. Jones², Michael H. Stewart¹, Barbara A. Marcheschi¹, Todd H. Brintlinger¹, John Lyons¹ and Sarah Brittan¹; ¹U. S. Naval Research Laboratory, United States; ²Florida State University, United States

Halide perovskites have already demonstrated impressive optoelectronic performance in applications ranging from photovoltaics, to light-emitting diodes and lasers, to X-ray and gamma-ray detectors and scintillators. Understanding how extrinsic dopants behave in this class of materials is a critical next step to gaining greater control over the stability and performance of this versatile class of materials.

While Bi³⁺ was originally proposed as a potential n-type dopant in lead halide perovskites, experiments and theory clearly demonstrate that it is a deep-level trap that gives rise to broad near-infrared emission. We synthesized a series of crystals of CsPbBr₃ doped with Bi content ranging from 0.01 to 0.32 atomic percent, as quantified by inductively coupled plasma optical emission spectroscopy (ICP-OES). The absorption edge shifts redder with Bi incorporation, but density function theory (DFT) calculations show that this increased absorption comes from the electronic structure of Bi as a deep-level trap, not from a shift in the CsPbBr₃ band edge. Indeed, all doped crystals emit both narrow band-edge (2.37 eV) and broad defect-level (1.12 eV) photoluminescence at room temperature, consistent with our theoretical prediction. We also apply STEM-EDS to the most heavily doped samples to characterize the spatial uniformity of the Bi incorporation within the CsPbBr₃ crystals. Our combined results demonstrate the power of current theoretical approaches to predict defect behavior in halide perovskites, which will be invaluable in guiding the development of these materials.

4:45 PM EN10.15.05

Photoluminescence Enhancement of Perovskite Quantum Dot@Polymer Nanocomposite via Silver Epoxy Paste Treatment for Time-And Environment-Dependent Optical Encryption [Jaehyeok Ryu](#), Jiyeon Lee, Dongjun Kim and Jiwon Kim; Yonsei University, Korea (the Republic of)

In an increasingly digital and interconnected world, advanced information encryption techniques became imperative for ensuring the confidentiality,

integrity, and availability of data. The integration of perovskite quantum dots (PQDs) with polymers has garnered considerable attention in the field of optical encryption for their eminent photoluminescence (PL) property and improved stability. Herein, we have designed a time- and environment-dependent optical encryption/decryption method based on the PL enhancement of CsPbBr₃ QD/polydimethylsiloxane (PDMS) nanocomposite film using a conductive Ag epoxy paste. Ag epoxy paste treatment was conducted by a thermal treatment subsequent to applying the Ag epoxy paste on the surface of nanocomposite film, followed by the removal of cured paste with ease. The Ag⁺ ions from the Ag epoxy paste diffuse into the PDMS matrix and passivate the surface defects of CsPbBr₃ QDs, resulting in enhanced PL properties (e.g., intensity, lifetime, PL quantum yield (PLQY)) of the nanocomposite film. In order to enhance the image contrast for an optical encryption, surface defects have further been generated by ligand purification of CsPbBr₃ QDs during the synthesis of nanocomposite film. By controlling the treatment duration and external environment, Ag epoxy paste treatment was utilized as a time-dependent information encryption/decryption method via regulation of the PL intensity. Specifically, an encrypted information was initially concealed under daylight and disguised by a fake information under UV light, which was decrypted over time owing to the differences in the degradation rates of PQDs. Once the information had been confirmed by an intended receiver, the leakage of information was further avoided with a subsequent water immersion, in which the decrypted information permanently reverts to the initial fake information via PL intensity inversion between treated and untreated region. In this work, we propose novel applications of commercially available Ag epoxy paste as a method for surface defects passivation in PQDs embedded in polymer matrix and as a strategy for optical encryption/decryption, providing a high level of security with multiple encryption states and a straightforward decryption.

SESSION EN10.16: Poster Session III
Session Chairs: Michael Saliba and Carolin Sutter-Fella
Thursday Afternoon, April 25, 2024
Flex Hall C, Level 2, Summit

5:00 PM EN10.16.01

Beginner's Guide to Visual Analysis of Perovskite and Organic Solar Cell Current Density-Voltage Characteristics [Albert These](#)^{1,2}; ¹Institute Materials for Electronics and Energy Technology, Germany; ²Friedrich-Alexander-Universität Erlangen-Nürnberg, Germany

The current density-voltage characteristic (JV) is a critical tool for understanding the behaviour of solar cells. In this poster, I will present an overview of the key aspects of JV analysis and introduce a user-friendly flowchart that facilitates the swift identification of the most probable limiting process in a solar cell, based mainly on the outcomes of light-intensity-dependent JV measurements. The flowchart was developed through extensive drift-diffusion simulations and a rigorous review of the literature, with a specific focus on perovskite and organic solar cells. Moreover, the flowchart proposes supplementary experiments that can be conducted to obtain a more precise prediction of the primary performance losses. It therefore serves as an optimal starting point to analyse performance losses of solar cells.

5:00 PM EN10.16.02

Grain-Boundary Grooves in Perovskite Solar Cells Mingwei Hao¹ and [Yuan Yuan Zhou](#)²; ¹Hong Kong Baptist University, Hong Kong; ²The Hong Kong University of Science and Technology, Hong Kong

Metal halide perovskites (MHPs) have shown great potential as light absorbers in solar cells, achieving high power conversion efficiencies and approaching industrialization standards. In order to fully harness the capabilities of MHPs, it is imperative to delve deeper into the understanding of their microstructural characteristics and provide valuable insights into the properties, performance, and stability of MHPs, paving the way for advancements in material design, device engineering, and fabrication techniques. Here, we introduce a typical microstructure referred to as the grain boundary groove. We provide a detailed examination of its formation, the influence of it, and various approaches for its control. By studying this microstructural characteristic, we aim to offer a fresh perspective and contribute to the understanding of perovskite microstructures and their influences.

5:00 PM EN10.16.03

Investigation of Interface Engineering for High-Performance All-Inorganic Cs-Based Perovskite Solar Cells Gaukhar Nigmatova¹, Gulzhan Zhumadil¹, Menghua Cao², Yu Han², Zhuldyz Yelzhanova¹, Vladimir Pavlenko¹, Hryhorii Parkhomenko¹, Marat Kaikanov¹, Mannix Balanay¹, Askhat J.¹, Gang Li², Zhiwei Ren² and [Annie Ng](#)¹; ¹Nazarbayev University, Kazakhstan; ²The Hong Kong Polytechnic University, Hong Kong

The halide perovskite solar cells (PSCs) have emerged as a promising photovoltaic technology for the generation of cost-effective renewable energy. Over the past decade, a significant progress has been made in improving the power conversion efficiency (PCE) and stability of PSCs. Among the various types of PSCs, all-inorganic CsPbI₂Br PSCs have recently garnered increasing attention due to their excellent thermal stability and promising photovoltaic properties, with a bandgap size suitable for efficient light harvesting, particularly in short-wavelength portion for tandem device applications.

This work focuses on investigating interface engineering techniques to further enhance the performance of all-inorganic cesium-based PSCs in ambient and protonated irradiation condition. The first technique involves the growth of two-dimensional (2D) Ruddlesden-Popper mixed halide perovskite nanostructures on the surface of CsPbI₂Br. The deposition of Cs₂PbX₄ (where X=I and Br) requires precise processing conditions, allowing for good control of the Cs₂PbX₄ morphology. This controlled growth of 2D nanostructures improves the interface quality between the perovskite layer and the hole transport layer, thereby enhancing charge transport properties. Consequently, a significant enhancement in the PCE and device stability can be achieved. The impact of incorporating an ionic liquid (IL) in the bulk of CsPbI₂Br perovskite is also investigated. Experimental results demonstrate that the use of [EMIM+][PF6-] IL promotes the formation of highly crystalline perovskite thin films, leading to a reduction in the defect density of the perovskite material. This reduction in defects improves carrier recombination processes, resulting in enhanced PCE and stability of the devices under harsh ambient conditions.

Through systematic optimization processes of interface engineering, a PCE above 17% can be achieved, accompanied by a significant improvement in the device lifetime. To understand the underlying mechanisms of these interface engineering techniques, comprehensive experimental characterizations were conducted. These characterizations include analyzing the morphology, crystal structure, carrier transport dynamics, and recombination processes etc. The results obtained from this work provide valuable insights into the effectiveness of interface engineering strategies for all-inorganic Cs-based perovskite materials, contributing to the advancement of this type of PSCs in the community.

5:00 PM EN10.16.04

Trap Density and Energy States in Organic-Inorganic Halide Perovskite Thin Films: A Study of Thickness Variations Using Drive Level

Capacitance Profiling and Admittance Spectroscopy [JaeGwan Sin](#)¹, Jaeho Kim¹, Gisung Kim¹, Mijung Kim¹, Moonhoe Kim¹, Hyojung Kim^{1,2} and Jung Yup Yang¹; ¹Kunsan National University, Korea (the Republic of); ²The Institute of Basic Science, Korea (the Republic of)

Recently, organic-inorganic halide perovskite (OIHP) materials have gained significant prominence in various applications, especially in renewable energy and semiconductor technology, such as photovoltaic and thin film transistor (TFT) devices. Thickness of the OIHP film is an important factor in determining device characteristics. For example, an OIHP thin film thickness of approximately 30 nm must be achieved in order to achieve optimal on/off ratios and high mobility for TFT devices. Despite its critical importance, the relationship between halide perovskite film thickness and trap density has not been comprehensively explored. In this research, drive-level capacitance profiling (DLCP) and temperature derivative admittance spectroscopy (TAS) were used to investigate changes in trap energy and density depending on the thickness of the OIHP film. The DLCP and TAS methods were employed to explore the intricate relationship between OIHP film thickness and trap characteristics, providing insights into their effects on charge transfer dynamics and overall stability. From the DLCP and TAS analysis, it was observed that as the OIHP film thickness decreases, the trap density rapidly increases from $10^{15}/\text{cm}^3$ to $10^{17}/\text{cm}^3$ at the 0.35 eV trap energy level, due to the increasing influence of the interface caused by the reduction in OIHP film thickness. The defect energy level of 0.35 eV appears as an iodine interstitial defect, and we were able to improve device performances by applying an interface passivation process to remove iodine interstitial defects. We believe that this study provides a detailed analysis of the complex relationship between OIHP film thickness and trap states and can provide key research directions for OIHP-based photovoltaic and semiconductor devices and provide guidance for device optimization.

5:00 PM EN10.16.05

Damage-Free Process of Metal Electrode Using Plasma-Assisted Vapor Deposition for Halide Perovskite Devices [Gisung Kim](#)^{1,2}, Mijung Kim², [JaeGwan Sin](#)², [Hyojung Kim](#)³, [Kang-il Lee](#)¹, [Yongsup Choi](#)¹ and [Jung Yup Yang](#)^{2,3}; ¹Korea Institute of Fusion Energy, Korea (the Republic of); ²Kunsan National University, Korea (the Republic of); ³The Institute of Basic Science, Korea (the Republic of)

In response to fossil fuel depletion and global warming, research and development of new and renewable energy are recognized as crucial tasks worldwide. Solar cells, which utilize unlimited solar energy to generate electricity in an environmentally friendly manner, are at the forefront of new renewable energy technologies. Next-generation perovskite solar cells have emerged as promising candidates, owing to their cost-effectiveness and simplified low-temperature processes. The structure of a perovskite solar cell typically consists of glass/transparent electrode/electron transport layer/perovskite (light absorption layer)/hole transport layer (HTL)/metal electrode. The HTL, predominantly composed of organic materials like Spiro-OMeTAD, PTAA, and P3HT, etc. is susceptible to plasma damage when metal electrodes are formed using the commonly employed vacuum physical vapor deposition (PVD) method, limiting its utility. Although the thermal evaporation method is employed in the metallization process, it also carries the disadvantage of uneven metal particle deposition, resulting in reduced transparency and conductivity of the thin film. To overcome these challenges, this research focuses on fabricating perovskite solar cells with high-quality and damage-free metal electrode deposition on organic materials using plasma-assisted vapor deposition (PAVD). Unlike conventional methods, PAVD technology does not require heating the substrate to enhance the thin film. Instead, it converts the interior of the thermal evaporation source into a plasma state, thereby transforming the metal particles into a high-energy state. As a result, the metal particles firmly bond to the substrate without the need for additional energy, like heat. This process results in the formation of high-quality and low-resistance metal thin films. The morphology, structure, and electrical characteristics of the metal thin film formed using PAVD were compared with those obtained using the thermal evaporation method. Furthermore, the relationship between the deposition method and the device characteristics was investigated. Given the critical importance of metal electrode quality and resistance in large-area perovskite monolithic modules, this research also concentrated on their application in large-area modules. The large-area perovskite modules fabricated with the PAVD metal electrode show over a 1% improvement in efficiency compared to those using the evaporation method. In addition, improvements in long-term stability characteristics were observed. In the future, the PAVD technology is expected to be highly utilized as a damage-free electrode deposition process for electronic devices using organic thin film layers due to its high quality and low resistance.

5:00 PM EN10.16.06

Controllable Synthesis of 0D/3D Perovskite Heterostructure for High-Performance and Stable X-Ray Detection Devices [Thanh Hai Le](#); Los Alamos National Laboratory, United States

Despite the impressive optoelectronic performance, perovskite-based detectors are poorly stable under operation, failing by far the market requirements. Various technological approaches have been proposed to overcome the instability problem caused by the migration of halide ions, which, while delivering appreciable incremental improvements, are still far from a market-proof solution. Here, we demonstrate that a zero-dimensional PEA_2ZnI_4 induces more robust surface passivation on 2D perovskite single crystal and stronger n-N isotype two-dimensional/zero-dimensional heterojunctions than its lead-based counterpart. The 0D/2D forms an exceptional gradually-organized multi-dimensional interface that yields up to 30% external quantum efficiency which 8% higher than 2D perovskite device. Our device maintains 100% initial efficiency after 1000 on-off cycles and after >70 hours under continuous illumination of 178.7 $\mu\text{Gy/s}$ and an applied voltage of 10V. In addition, the unencapsulated device exhibited zero performance loss under normal measured and storage conditions (temperature: 25 °C, humidity: 20 to 60%) in 2 months. Our findings expand the material library for low-dimensional interface engineering and open an opportunity for the timely commercialization of perovskite x-ray detectors.

5:00 PM EN10.16.07

Conductivity Analysis of a Polycaprolactone/Carbon Nanotube Composite for use in Electrospun Photovoltaics and Flexible Electronics [Luke J. Suttay](#)¹, Dennis J. Moritz², John Borkowski², Jessica M. Andriolo¹ and Jack L. Skinner¹; ¹Montana Technological University, United States; ²Montana State University, United States

In recent years, conductive electrospun (ES) microfibers have gained traction for use in flexible electronics and perovskite photovoltaics. ES fibers are attractive for their large surface-area-to-volume ratio and relative strength. Conductivity in ES nanofibers has been accomplished using conductive or semiconducting polymers. Alternatively, conductivity in polymer thin films can be accomplished through addition of carbon nanotubes (CNTs) or graphene.

Previously, we formed hybrid perovskite crystals encased in ES fibers *in situ* that demonstrated improved stability in humid conditions. In other work, we used melt electrospinning to produce conductive graphene-doped polymer fibers. Additionally, we have utilized the previously established method of multiwalled CNT (MWCNT) dispersion by combined use of a hydroxy-functionalized and unfunctionalized MWCNT blend in polycaprolactone (PCL) matrix to fabricate a conductive PCL/MWCNT composite. Thin films of the composite were measured using a four-point probe and demonstrated a maximum conductivity of 0.3765 S/cm. In the present work, the hydroxy-functionalized and unfunctionalized MWCNTs will be replaced with hydroxy functionalized and unfunctionalized metallic single-wall carbon nanotubes (MSWCNTs) to achieve larger conductivity values in the composite material in preparation for electrospinning of a multi-layer solar cell structure.

Triaxial ES will be used to form the multi-layer solar cell structure described. In the design, a conductive PCL core will be coated with the previously

established perovskite-polymer composite. The exterior layer of the solar cell fiber structure will consist of a polymeric electron transport layer (ETL). In this work, each layer of the device will be characterized. Conductivity of a PCL thin-film doped with a mixture of functionalized and unfunctionalized MSWCNTs will be evaluated for conductivity via a non-destructive four-point probe method. Conductivity characterization will be used to determine the percolation threshold and preferable ratios for the MSWCNT-doped PCL composite used as the core of the functional fibers proposed. MSWCNT dispersion in the composite as a function of sonication time will be characterized through crystallinity analysis via Raman spectroscopy and electron microscopy.

Presented work will include conductivity characterization of the PCL/MSWCNT composite material and fabrication methods of a four-layer thin film photovoltaic system consisting of the conductive MSWCNT/PCL composite, a polymer-encapsulated hybrid perovskite layer, a polymeric ETL, and a transparent conductor. This work will provide the foundational preliminary data for future fabrication of an ES perovskite solar cell. The design is achieved without a hole transport layer, which has previously been established as non-consequential to perovskite solar cell performance. After adequate conductivity is achieved, the conductive ES nanofibers will be used as a central electrode in a concentric, triaxial ES photovoltaic cell.

5:00 PM EN10.16.08

Electronic Coupling in Low Dimensional Hetero-Metallic Halide Hybrids Janardan Kundu; Indian Institute of Science Education and Research, India

Low dimensional metal halide hybrids (2D, 1D, 0D) incorporating hetero-metal halide units is of fundamental importance to understanding electronic coupling between distinct excitons of the constituent metal halide units. However, synthesis of such multicomponent one phase systems is challenging. In this talk, I will highlight our current efforts on exploiting various synthetic strategies towards phase pure multi-metallic halide hybrids. I will present the photo-physical properties of such multi-metallic halide hybrids that manifest emissive properties arising due to electronic cross-talk/coupling between the multiple metal halide centers. I will discuss the relevant mechanism/pathway of the observed electronic coupling highlighting energy transfer interaction that are mediated through the structural components of the low dimensional metal halide hybrids. I will conclude my talk by emphasizing the need of robust theoretical calculations and ultra-fast spectroscopy to provide insight to the observed electronic coupling effects in low D hybrids.

5:00 PM EN10.16.09

High-Performance Photodetector and Angular-Dependent Random Lasing from Long-Chain Organic Diammonium Sandwiched 2D Hybrid Perovskite Non-Linear Optical Single Crystal Rajesh Kumar Ulaganathan¹, Pradip Kumar Roy², Raghavan Chinnambedu Murugesan³, Ambika Subramanian⁴, Chang-Yu Lin⁴, Chi-Te Liang² and Raman Sankar¹; ¹Academia Sinica, Taiwan; ²National Taiwan University, Taiwan; ³Aston University, United Kingdom; ⁴Chung Yuan Christian University, Taiwan

3D organic-inorganic metal halide perovskites are excellent materials for optoelectronic applications due to their exceptional properties, solution processability, and cost-effectiveness. However, the lack of environmental stability highly restricts them from practical applications. Herein, a stable centimeter-long 2D hybrid perovskite (N-MPDA)[PbBr₄] single crystal using divalent N1-methylpropane-1,3-diammonium (N-MPDA) cation as an organic spacer, is reported. The as-grown single crystal exhibits stable optoelectronic performance, low threshold random lasing, and multi-photon luminescence/multi-harmonic generation. A photoconductive device fabricated using (N-MPDA)[PbBr₄] single crystal exhibits an excellent photoresponsivity ($\approx 124 \text{ AW}^{-1}$ at 405 nm) that is ≈ 4 orders of magnitudes higher than that of monovalent organic spacer-assisted 2D perovskites, such as (BA)₂PbBr₄ and (PEA)₂PbBr₄, and large specific detectivity ($\approx 10^{12}$ Jones). As an optical gain media, the (N-MPDA)[PbBr₄] single crystal exhibits a low threshold random lasing ($\approx 6.5 \mu\text{J cm}^{-2}$) with angular dependent narrow linewidth ($\approx 0.1 \text{ nm}$) and high-quality factor ($Q \approx 2673$). Based on these results, the outstanding optoelectronic merits of (N-MPDA)[PbBr₄] single crystal will offer a high-performance device and act as a dynamic material to construct stable future electronics and optoelectronic-based applications.

5:00 PM EN10.16.10

Co-Deposition of Hole-Selective Contact and Absorber for Improving The Processability of Perovskite Solar Cells Xiaopeng Zheng¹ and Joseph Luther²; ¹University of Chinese Academy of Sciences, China; ²National Renewable Energy Laboratory, United States

Simplifying the manufacturing processes of renewable energy technologies is crucial to lowering the barriers to commercialization. In this context, to improve the manufacturability of perovskite solar cells (PSCs), we have developed a one-step solution-coating procedure in which the hole-selective contact and perovskite light absorber spontaneously form, resulting in efficient inverted PSCs. We observed that phosphonic or carboxylic acids, incorporated into perovskite precursor solutions, self-assemble on the indium tin oxide substrate during perovskite film processing. They form a robust self-assembled monolayer as an excellent hole-selective contact while the perovskite crystallizes. Our approach solves wettability issues and simplifies device fabrication, advancing the manufacturability of PSCs. Our PSC devices with positive-intrinsic-negative (p-i-n) geometry show a power conversion efficiency of 24.5% and retain >90% of their initial efficiency after 1200 h of operating at the maximum power point under continuous illumination. The approach shows good generality as it is compatible with different self-assembled monolayer molecular systems, perovskites, solvents and processing methods.

5:00 PM EN10.16.11

Advancing Operational Stability of Inverted Perovskite Solar Cells Utilizing Parylene-C Encapsulation Techniques Elnaz Ghahremani Rad, Abraha Tadese Gidey, Towhid H. Chowdhury and Alexander R. Uhl; The University of British Columbia, Canada

Following advancements to increase the efficiency of perovskite solar cells, the current emphasis is mainly on enhancing their operational stability. Various methods of encapsulation have been employed to safeguard perovskite solar cells from environmental factors and preserve their efficiency. Recent research studies have primarily focused on using organic/inorganic multilayers to create a more robust barrier against the degradation of perovskite solar cells. However, the commercial feasibility of employing inorganic materials might be limited due to their high-cost fabrication process and low flexibility. The encapsulation techniques using polymers stand out for their versatility in material selection and functionality, making them suitable for manufacturing flexible devices. Polymers efficiently act as encapsulants, preventing the infiltration of water and oxygen into the perovskite layer while also inhibiting the release of perovskite composition. One such polymer, parylene-C, offers cost-effective extrinsic protection against environmental harm, mainly humidity and oxygen, to uphold the performance and reliability of perovskite solar cells. In our study, we utilized a multilayer deposition of parylene-C with a high light and low water vapor transmission rate, uniformly applied across the surface of the perovskite solar cells. To assess the operational stability of these devices, we employed ISOS-D1 and D2 protocols including conditions such as ambient/ambient and 85 /ambient, pertaining to temperature/relative humidity. The obtained results underscore the durability of parylene-C coated perovskite solar cells compared to their unencapsulated counterparts.

5:00 PM EN10.16.12

Novel 3D Cubic Topology in Hybrid Lead Halides with a Symmetric Aromatic Triammonium Exhibiting Water Stability Eugenia S. Vasileiadou¹, Imra S. Tajuddin¹, Michael C. De Siena¹, Vladislav V. Klepov¹, Mikael Kepenekian², George Volonakis², Jacky Even², Lukasz Wojtas³, Ioannis Spanopoulos³, Xiuquan Zhou¹, Abishek Iyer¹, Julie L Fenton⁴, William Dichtel¹ and Mercouri G. Kanatzidis¹; ¹Northwestern University, United States;

²Univ. Rennes, France; ³University of South Florida, United States; ⁴The Pennsylvania State University, United States

The limitations of three-dimensional (3D) perovskites are related to their narrow structural tunability of the organic cations and their moisture sensitivity. Herein, we report a new family of 3D cubic hybrid metal halides (T-Et₆)₃Pb₁₁X₃₁ (X = I, Br), where T is 1,3,5-tris-(4-aminophenyl)benzene. The materials are synthesized through an *in situ* N-alkylation of T and an efficient one-step solvothermal reaction containing ethanol, initiating a tunable synthetic avenue for the acquisition of structurally complex hybrid halides with luminophores. (T-Et₆)₃Pb₁₁X₃₁ consist of an unprecedented *1a3* framework of [Pb₁₁X₃₁]⁹⁻ one-dimensional (1D) chains embedded with (T-Et₆)³⁺ cations, affording an overall 3D topology. The constituent [Pb₁₁X₃₁]⁹⁻ chains include exclusively octahedral lead halide units with clusters of face- and edge-sharing connectivity, giving rise to weak broad emission centered at ~660 nm observed at 78 K. (T-Et₆)₃Pb₁₁I₃₁ demonstrates water stability for at least 7 days. Synthesis through ambient pressure results in tunable structural variations of zero-dimensional (0D) structures rendering T₇Pb₃Br₂₇DMF and T₂Sn₃Br₁₈4H₂O.5Br₂, both of which feature blue PL emission at room temperature.

SESSION EN10.17: Modeling

Session Chairs: Dane DeQuilettes and Wei Zhang

Friday Morning, April 26, 2024

Room 334, Level 3, Summit

8:00 AM EN10.17.01

Anisotropy and Exciton Self-Trapping in the 1D Perovskite C₄N₂H₁₄PbBr₄ from First Principles Rijan Karkee and David A. Strubbe; University of California, Merced, United States

Low-dimensional organic-inorganic metal halide hybrids have remarkable optical and electronic properties and better stability against heat and moisture. We study a 1D perovskite of formula C₄N₂H₁₄PbBr₄, consisting of PbBr chains separated by organic cations. Experiments showed a large Stokes shift (0.83 eV) with broadband emission [Nat. Commun. 8, 14051 (2017)] which hints at interesting photo-physics involving self-trapped excitons. We calculate the highly anisotropic optical, bandstructure, vibrational, and transport properties of this 1D perovskite, which could be used for polarized photodetectors and LEDs. The bands are highly dispersive along Pb-Br chains and nearly flat along other directions, leading to a factor of 100 in conductivity as calculated by Boltzmann transport. We find an indirect gap and a direct gap which is just slightly higher in energy. Our GW/Bethe-Salpeter equation calculations using BerkeleyGW show strong anisotropy in absorption, especially in the lowest exciton which has a binding energy of 0.83 eV [Small Struct. 4, 2200378 (2023)]. We calculate excited-state forces based on these results and our vibrational calculations to find the coupling of excitons and phonons, from which we can predict exciton self-trapping and get insight into mechanisms of broadband emission.

8:15 AM EN10.17.02

Unravelling Rashba Effect through Spin Texture Evolution in Uni-Dimensional Confined Halide Perovskite under Compression Jagjit Kaur and Sudip Chakraborty; Harish-Chandra Research Institute, India

The pursuit of uni-dimensional hybrid halide perovskites holds significant importance in the field of spin-optoelectronics due to quantum confinement effect. Moreover, such confined systems with constituent heavy elements (Pb, Bi, etc) could be prone to Rashba effect considering relativistic spin-orbit coupling (SOC) and inversion symmetry breaking. The repercussion of Rashba splitting could be very well reflected in charge carrier recombination rate, which is significant for manifesting efficient photovoltaic devices. One way to manipulate such recombination rate is through tuning the Rashba splitting corresponding to the spin texture of such materials under the external pressure or structural compression. In this work, we have envisaged such evolution paradigm in one of the promising non-centrosymmetric hybrid halide perovskite through rigorous electronic structure calculations. The electronic and optical properties along with the Rashba splitting and spin texture are being systematically observed within the thermodynamic limit of under compression equivalent to 9.6 GPa in this promising halide perovskite. Our study successfully reveals the intriguing transition of electronic band structure from indirect to a direct bandgap phenomena under compression in addition to an interesting red shift in the optical absorption spectra. To accurately describe the spin polarization both in-plane and out-of-plane, we have explored a three-dimensional Rashba model. The in-plane spin-texture has been found to arise from the octahedral distortion along the b-direction. The fundamental interplay between structural distortions and the Rashba-splitting in the considered one-dimensional system under the influence of compression along with the evolution of spin texture could very much hold potential for the pursuit of sustainable energy.

8:30 AM EN10.17.03

Intrinsic Limits of Charge Carrier Mobilities in Halide Perovskites: From 3D to Layered Materials Bruno Cucco^{1,2}, Joshua Leveillee², Jacky Even³, Mikael Kepenekian¹, Feliciano Giustino² and George Volonakis¹; ¹Univ Rennes, ENSCR, INSA Rennes, CNRS, ISCR (Institut des Sciences Chimiques de Rennes), UMR 6226, France; ²Department of Physics, Oden Institute for Computational Engineering and Sciences, The University of Texas at Austin, United States; ³Univ Rennes, INSA Rennes, CNRS, Institut FOTON, UMR 6082, France

Over the past decade, we have witnessed the emergence of metal halide perovskites as a most formidable building block for emergent solar cells with record-breaking performances. Recently, 2D/3D materials that combine these ABX₃ (3D) metal halide perovskites with their layered (or 2D) counterparts, have enabled the fabrication of photovoltaic devices that are both stable and highly efficient. [1] Yet, it is well-known that layered perovskites exhibit poor charge carrier transport in comparison with 3D perovskites. [2] To date, the underlying mechanisms behind the reported reduced mobilities remain elusive. In this work, we employ a combination of state-of-the-art *ab initio* approaches [3] and symmetry analysis to explore the electron-phonon coupling mechanisms in layered halide perovskites. We start from the three-dimensional perovskite CsPbBr₃ and model the cases of layered *n* = 1 (Cs₂PbBr₄) and *n* = 2 (Cs₃Pb₂Br₇). We show that the diminished charge carrier mobilities in layered systems primarily originate from differences in the carrier's lifetimes. We identify the vibrational modes contributing to charge carrier scattering and associate them with polar-phonon scattering mechanisms arising from long-range Fröhlich coupling and non-polar optical deformation potential scattering processes. Furthermore, we show that the charge carrier mobilities are not only reduced by the increased polar-phonon interactions but also by an abrupt increase in the electronic density of states near the band edges. Our findings uncover the electron-phonon coupling mechanisms that intrinsically limit the charge carrier transport of layered metal halide perovskites, which is critical for their application in any optoelectronic device, such as solar cells.

JE acknowledges the support of the MERANET project Phantastic.

[1] I. Metcalf, S. Sidhik, H. Zhang, A. Agrawal, J. Persaud, J. Hou, J. Even, and A. D. Mohite. *Chem. Rev.* 123, 9565-9652, 2023.

[2] S. G. Motti, M. Kober-Czerny, M. Righetto, P. Holzhey, J. Smith, H. Kraus, H. J. Snaith, M. B. Johnston, L. M. Herz. *Adv. Funct. Mater.* 33, 2300363, 2023.

[3] H. Lee, S. Poncé, K. Bushick, S. Hajinazar, J. Lafuente-Bartolome, J. Leveillee, C. Lian, F. Macheda, H. Paudyal, W. H. Sio, M. Zacharias, X. Zhang, N. Bonini, E. Kioupakis, E. R Margine, F. Giustino. *arXiv:2302.08085*, 2023.

8:45 AM EN10.17.04

Combining First-Principles Simulations and Combinatorial Synthesis: Effects of Exciton Binding Energy Halide Perovskite-Based Optoelectronic Devices [SangMyeong Lee](#), Hee Jung Kim, Young Ju Kim, Geon Woo Yoon, Oh Yeong Gong and Hyun Suk Jung; Sungkyunkwan University, Korea (the Republic of)

Halide perovskites (HPs) have garnered significant attention in optoelectronics due to their excellent optoelectronic properties. The performance of HP optoelectronics is affected by the exciton binding energy, which represents the combined energy of electron-hole pairs. Therefore, a method that can comprehensively and rapidly explore and measure changes in exciton binding energy based on HP composition is highly valuable. In this study, we report the effects of HP optoelectronic properties depending on the HP compositions using a combination of first-principles simulations and combinatorial synthesis. The first-principles simulations confirm that an increase in the concentration of halide ions leads to an increased band gap, strengthening the Coulomb interactions. We demonstrate that an increase in the band gap corresponds to a decrease in relative permittivity when fabricating HP thin films with a halide compositional gradient using combinatorial synthesis. Furthermore, we measured the photoelectric conversion efficiency and responsivity of HP-based optoelectronics depending on exciton binding energy, including time-resolved photoluminescence. The results indicate that the dissociation of electron-hole pairs increases with a reduction in exciton binding energy, thereby improving device properties. Thus, this study suggests a high-throughput screening method that combines first-principles simulations and combinatorial synthesis to explore the effects of HP properties on optoelectronics.

SESSION EN10.18: Optical Management
Session Chairs: Raphael Moral and Michael Saliba
Friday Morning, April 26, 2024
Room 334, Level 3, Summit

9:00 AM *EN10.18.01

Towards Semi-Opaque Perovskite Solar Cells via Molecular Templates [Jacek Jasieniak](#); Monash University, Australia

Metal halide perovskite semi-transparent perovskite solar cells (ST-PSC) have drawn great interest for applications in building integrated photovoltaics (BIPV), such as solar windows. Conventionally, ST-PSC are realised by thinning the perovskite absorber layer to allow partial light transmission, while also replacing the opaque back electrode with one that is transparent. This approach has been shown to produce efficient and stable cells, with window-grade levels of transparency (>30%). However, their main drawback is the unavoidable perceived colour (typically red to yellow) due to the optical bandgap lying within the visible range, which lowers the colour-rendering index (CRI) and therefore impedes their application in BIPV. A possible path to overcome this hurdle is by patterning the solar cell in a way that selected regions are entirely transmissive, while others remain fully absorbing. Such semi-opaque configurations can support greater efficiencies and color purity levels than ST-PSC. Towards this technological evolution, here, we explore a low-cost and efficient method for patterning metal-halide perovskites via stamping of a hydrophobic template on substrates. The facile approach is demonstrated to be scalable and suitable for both flexible and rigid substrates. It further removes the need for post-processing, thus minimizing potential lithographic steps, and the burden they pose. The use of such patterned perovskite films are considered within semi-opaque solar cell configurations, highlighting the challenges and the major opportunities that such patterned films and this form of solar cell architecture present.

9:30 AM EN10.18.02

Multi-Spectral Optical Platform of Luminescent Patterns by Single-Shot Optical Lithography [Hyewon Shim](#), Geonwoong Park, Hyunsuk Yun, Sunmin Ryu, Yong-Young Noh and Cheol-Joo Kim; Pohang University of Science and Technology, Korea (the Republic of)

Integration of numerous optical materials with different band gaps forms the basis of a multispectral technology. While step-by-step integrations are the prevailing manufacturing approach, realizations of complex patterns with increasing numbers of material units by high definition and reproducibility remain challenging, preventing the wide implications of the multispectral platform. Here, we report optical lithography to spatially control the optical band gaps of semiconductor alloys by composition modulations with a single-shot expose. Luminescent patterns with intrinsic emission wavelengths, spanning the entire visible-spectral range are designed to realize functional multispectral films. With programmed correlations between spatial and spectral information, we fabricate multivariate optical filters for dispersive optics-free spectroscopy with a high spectral resolution and wavelength-selective encoding patterns for encryptions with precise spectral programming. The fabrication is at room temperature, and compatible with various device platforms for monolithic integrations.

9:45 AM EN10.18.03

Photon Management for Efficient and Stable Large-Area Perovskite Solar Cells via Luminescent Thin Films of Platinum(II) Complex [Eunhye Hwang](#)¹, Hak-Beom Kim², Dong Suk Kim¹ and Tae-Hyuk Kwon¹; ¹Ulsan National Institute of Science and Technology, Korea (the Republic of); ²Korea Institute of Energy Research, Korea (the Republic of)

As a representative photon management strategy converting high-energy photons into low-energy ones, photon downshifting in photovoltaic applications can be realized by introducing strongly luminescent materials that are properly designed to have spectral overlap with the corresponding light absorbers. Especially for perovskite solar cells (PSCs), photon downshifting has been suggested as an effective way to overcome UV-related problems such as exciton loss, thermalization, and catalytic decomposition of the photoactive layers. However, it is still challenging to achieve thin-film photon downshifting layers (PDLs) with high photoluminescence quantum yields (PLQYs) and versatility for fabrication, considering upcoming high-performance and large-area PSCs.

Herein, to enhance UV stability without any loss in photocurrent generation, a highly blue-emissive Pt(II) complex is developed for effective photon management in high-performance PSCs. Thin PDLs based on the Pt(II) complex are fabricated on glass substrates of PSCs using ultrasonic spray deposition, leading to significant improvement in PLQY and facile production of large-area PDLs. By introducing the PDLs, a maximum device performance of 22.03% is achieved for large-area PSCs with an active area of 25 cm². Owing to their long-range photon downshifting effect, in which absorbed UV photons are converted into visible emission, remarkable improvements in UV stability of PSCs are realized with the PDL coating. In terms of

efficient photon management, luminescent thin films of UV-to-visible converting Pt(II) complex suggest wide ranging applicability that can further improve the performance and stability of other optoelectronic devices.

10:00 AM BREAK

SESSION EN10.19: Lead-Free, Lead-Reduced, Perovskite-Like Materials
Session Chairs: Sascha Feldmann and Raphael Moral
Friday Morning, April 26, 2024
Room 334, Level 3, Summit

10:30 AM EN10.19.01

Material and Device Stability of Lead-Tin Perovskite Solar Cells [Florine Rombach](#) and Henry J. Snaith; University of Oxford, United Kingdom

Narrow bandgap perovskite solar cells based on mixed lead-tin perovskites tend to suffer from poor stability under operating conditions. This impedes the successful development of all-perovskite tandems. We explore the causes of this instability under extended periods of combined 65°C thermal and 1 sun illumination stressing, using a range of structural, optical, and electronic characterization techniques on lead-tin perovskite films, half-stacks and devices.

We show that the phase, absorbance, morphology and mobility of lead-tin perovskite films are stable on timescales that exceed those of device degradation, although we reveal an interesting pattern of phase segregation after stressing for much longer amounts of time. Additionally, we observe only a slight increase in background carrier density and a moderate decrease in charge carrier lifetime during the first few hundred hours of stressing. We simulate the impact of these properties on device performance using SCAPS, and argue that these changes can only partially account for the observed device degradation.

A close investigation of the EQE and J-V characteristics of devices reveals the formation of a charge extraction barrier in aged devices. We find that the impact of this barrier is hugely decreased in very fast J-V scans, suggesting that mobile ions contribute significantly to device degradation. We quantify the increasing impact of mobile ions on device performance during aging, and furthermore reveal that the extent of this impact is strongly related to the hole transport layer used in devices.

Ultimately, we identify a rapidly worsening impact of mobile ions during aging as the major cause of the observed device performance degradation. The segregation of a non-perovskite CsSnI₃ degradation phase and an increasing defect density are also expected to limit the stability of lead-tin perovskite solar cells over longer timescales. Finally, we propose solutions related to both bulk perovskite composition and device architecture to overcome these challenges.

10:45 AM EN10.19.02

Highly Efficient and Stable Thermal Evaporated Lead-Tin Perovskites [Heon Jin](#) and Henry J. Snaith; University of Oxford, United Kingdom

Multi-junction tandem solar cells, utilizing complementary bandgaps, offer the potential to surpass the detailed balance limit for single-junction perovskite solar cells (PSCs). Through the tunability of perovskite bandgaps and recent advancements in mixed lead-tin (Pb:Sn) narrow bandgap PSCs, it is now possible to create highly efficient multi-junction solar cells solely using perovskites, achieving certified PCEs of up to 26.4% in all-perovskite tandem solar cells.

However, there are two main challenges when using Pb:Sn perovskites. Firstly, methylammonium (MA) has been traditionally used in the most efficient Pb:Sn PSCs, but its thermal and chemical stability concerns prompt the search for MA-free alternatives. Second, conventional solution processing methods remain prevalent in lab-scale Pb:Sn PSCs fabrication. There were many attempts to thermal evaporate Pb:Sn as this method presents significant advantages, including high-quality thin film fabrication, precise thickness control, elimination of toxic solvents, large-scale compatibility, and reproducibility. Vacuum evaporation can also be applied to the fabrication of all-perovskite tandem solar cells without damaging underlying layers. Although vacuum deposition has proven successful in achieving high-efficiency and large-area PSCs for Pb-based perovskites, its application to Pb:Sn perovskites is less explored. Ball et al. and Igual-Munoz et al. are among the few to report Pb:Sn PSCs using vacuum evaporation.

In this work, we demonstrate that through careful control of the environment and some fine-tuning, it is possible to deposit Pb:Sn perovskite films of high quality through thermal evaporation. We compare devices made using this method to those made from similar state-of-the-art solution processed methods. Our work demonstrates that it is possible to approach the performance of solution processed devices within a workable processing window using vacuum evaporation. Our champion devices reach PCEs of 17%, surpassing previously set records of 14% for thermally coevaporated Pb:Sn devices. This was done without requiring additional passivation or bulk additive, which are used in the previous reports.

11:00 AM EN10.19.03

Local Background Hole Density Drives Non-Radiative Recombination in Tin Halide Perovskites [Robert J. Westbrook](#)¹, [Margherita Taddei](#)¹, [Rajiv Giridharagopal](#)¹, [Meihuizi Jiang](#)², [Shaun Gallagher](#)¹, [Kathryn Guye](#)^{1,3}, [Aaron Warga](#)¹, [Saif Haque](#)² and [David S. Ginger](#)^{1,3}; ¹University of Washington, United Kingdom; ²Imperial College London, United Kingdom; ³Pacific Northwest National Laboratory, United States

Tin halide perovskites, with the general formula ABX₃ [A = Formamidinium (FA), B = Sn, X = Br, I], offer a narrower bandgap (~1.3 eV) than their lead counterparts, making them suitable candidates for the light-absorbing semiconductor in single-junction photovoltaic devices. Moreover, this attribute makes tin halide perovskites integral to all-perovskite tandems, with the best-performing cells incorporating a 50-50 Sn-Pb composition in the low bandgap component. Nevertheless, record-breaking pure-Sn devices still exhibit severe losses in both open-circuit voltage (V_{OC}) and short-circuit current (J_{SC}), keeping power conversion efficiencies well below theoretical limits.

Non-radiative voltage loss is directly linked to decreases in the photoluminescence quantum yield (PLQY), and thus the prevalence of non-radiative recombination.[1] This picture is complicated in Sn perovskites given that the presence of Sn⁴⁺ impurities in the precursor solution leads to both the introduction of background hole dopants (serving to *increase* the PLQY) and non-radiative recombination centers (serving to *decrease* the PLQY). [2] We use the observation of pseudo-first order photoluminescence (PL) decay kinetics in Sn perovskite films to establish a method for characterizing the hole dopant level and non-radiative recombination rate constant with combined time-correlated single photon counting (TCSPC) and photoluminescence quantum yield (PLQY) measurements. We find that untreated FASnI₃ films exhibit large hole doping concentrations of $p_0 > 8.8 \times 10^{18} \text{ cm}^{-3}$, which is reduced to $p_0 \sim 10^{16} \text{ cm}^{-3}$ after precursor sublimation and SnF₂ treatments. While it is well known that the radiative recombination rates are increased with p_0 , we reveal that the non-radiative rate is also increased. Employing hyperspectral photoluminescence microscopy, we find that microscale p -type regions

in untreated FASnI₃ films are centers for non-radiative recombination, which are diminished in films with $p_0 \sim 10^{16} \text{ cm}^{-3}$. We find significant PL heterogeneity even in FASnI₃ films with moderate dopant levels, suggesting that new strategies to eliminate deleterious defects in FASnI₃ should be developed. [3]

[1] Y. Shi *et al.*, (3-Aminopropyl)Trimethoxysilane Surface Passivation Improves Perovskite Solar Cell Performance by Reducing Surface Recombination Velocity. *ACS Energy Lett.* **2022**, 7 (11), 4081–4088. <https://doi.org/10.1021/acsenergylett.2c01766>.

[2] D. Meggiolaro *et al.*, Tin versus Lead Redox Chemistry Modulates Charge Trapping and Self-Doping in Tin/Lead Iodide Perovskites. *Journal of Physical Chemistry Letters* **2020**, 11 (9), 3546–3556. <https://doi.org/10.1021/acs.jpclett.0c00725>.

[3] Westbrook *et al.*, Local Background Hole Density Drives Non-Radiative Recombination in Tin Halide Perovskites, *Under Review*

11:15 AM EN10.19.04

Quantifying Spatiotemporal Signal in Photothermal Heterodyne Imaging of Metal-Halide Perovskites Lauren Cisneros and [Matthew Crane](#); Colorado School of Mines, United States

Resonant pump-probe spectroscopies like photothermal heterodyne imaging have emerged as promising approaches to selectively measure the distribution of chemical species with high spatial and temporal resolution. In photothermal heterodyne imaging, a pump resonant with an electronic or vibrational transition of the species of interest heats the sample, and a higher energy probe measures differential reflectance (or transmittance) due to heating. For materials research, pump-probe photothermal spectroscopies thus offer an attractive and unique tool to evaluate the spatial distribution of “dark” species including, *e.g.* defects or molecules without significant radiative transitions. However, the conditions under which signal is optimized in thin films, including metal-halide perovskites, is not well understood, and approximations are frequently used to describe differential reflectance or transmittance signal. Here, we develop a multiphysics simulation implemented with a finite-difference method to quantify transient photothermal heating and the resulting differential reflectance signal. Using this approach, we investigate the conditions that optimize spatiotemporal resolution in alloyed methylammonium and formamidinium metal-halide perovskite thin films and evaluate these simulations experimentally. Combining these results, we identify key figures of merit to optimize spatiotemporal resolution in thin films and find that significant information about spatial distribution is buried within the temporal signal.

11:30 AM EN10.19.05

3D Lead-Organoselenide-Halide Perovskites and Their Mixed-Chalcogenide and -Halide Alloys Jiayi Li¹, Yang Wang², Santanu Saha³, Zhihengyu Chen⁴, Jason Misleh¹, Karena Chapman⁴, Jeffrey Reimer², Marina R. Filip³ and Hemamala Karunadasa¹; ¹Stanford University, United States; ²University of California, Berkeley, United States; ³University of Oxford, United Kingdom; ⁴Stony Brook University, The State University of New York, United States

Following our previous report of organosulfide-halide perovskites (RS)PbX₂ (X = Cl, Br; RS = organosulfide ligand), we present the first examples of organoselenide-halide perovskites (RSe)PbX₂ (RSe = organoselenide ligand) using organoselenide zwitterionic ligands, occupying both the X and A sites in the prototypical ABX₃ perovskite lattice. We applied X-ray diffraction/scattering measurements to study the average structures of the organochalcogenide-halide perovskites, with disordered organic components and anion sites. Considering the heteroanionic nature of these materials, we collected solid-state ⁷⁷Se and ²⁰⁷Pb NMR to probe the local coordination environments at Pb centers and anion (X/Se) distributions, complemented by theoretical simulations. The experimental results support the fully disorder distribution of organochalcogenide in (L)PbX₂. The band structures calculated by density functional theory (DFT) of (SeCYS)PbX₂ closely resemble those of (CYS)PbX₂ with chalcogenide dominating the valence band maximum (VBM). Due to the higher energy of Se 4p orbitals compared to the S 3p orbitals, (SeCYS)PbX₂ exhibit considerable bandgap (E_g) decrease, with $E_g^S = 2.07$ and 1.86 eV for X = Cl and Br, respectively. We further demonstrate different methods to alloy the halides (Cl/Br) and chalcogenides (S/Se) to obtain a continuous bandgap tuning. Overall, the expansion of this novel family of organochalcogenide-halide perovskites can provide new handles to tune the band structures of halide perovskites, and the comprehensive understanding of both average and local structures sets the foundation to further optimize the optoelectronic properties.

11:45 AM EN10.19.06

Structure and Stability of Multi-Component B-Site Mixed CsBX₃ Metal Halide Perovskites [Riley W. Hooper](#), Brian Phan, Trinanjan Dey, Cole Butler, Jonathan Veinot and Vladimir Michaelis; University of Alberta, Canada

ABX₃ [A = Cs, FA, MA; B = Pb, Sn, Ge; X = Cl, Br, I] metal halide perovskites have dominated the research landscape since the first demonstration of MAPbI₃ as an absorber layer for dye-sensitized solar cells.¹ Since then, developments in this space have realized perovskites for widespread applications in LEDs, photovoltaics, sensing, radiation detection, lasing, and more.^{2,3} The ubiquity of perovskites today is partly due to their facile synthesis via multiple routes, their tolerance to high defect concentrations, and highly tunable composition whereby properties can be defined. Of late, low-dimensional perovskite-based materials, alloys, or high entropy systems (with multiple elements at the same site) have brought renewed interest.⁴

Widespread deployment of ABX₃ perovskites has been slowed by the inclusion of the toxic heavy metal Pb, and material instability to heat and moisture. An attractive method for promoting the formation of the desired phase(s) while limiting degradation involves site-mixing. A- and X-site mixing is currently applied to materials in state-of-the-art compositions for the current best-performing prototype solar cells. Only limited examples showing mixing at the B-site have appeared and most involve Pb-Sn derivatives that only reduce Pb content in the material, without completely eliminating it. Sn-Ge mixed perovskites have received some attention, and exhibit improved stability and solar cell performance than previous Ge-based perovskites.^{5,6} A detailed understanding of the phenomena leading to such improvements using a suite of bulk spectroscopic and diffraction methods can provide insight into the mechanisms at play. Specifically, NMR spectroscopy offers atomic-level precision of the local chemical environment and has been used with much success for studying challenging and interesting perovskite materials.⁷⁻¹⁰ Together, this toolkit can provide the means for rational design of new materials for advanced solar absorbers.

Our work explores new systems of mixed B-site perovskites, starting with lead-free Sn-Ge solid solutions of the formula CsSn_xGe_{1-x}Br₃. Their optical properties and structure were explored using optical band gap measurements, XRD, SEM/EDX, and ¹³³Cs NMR spectroscopy. We then investigate the impact of halide identity on the mixed Sn-Ge system, and explore the possibility of a triple B-site mixed Pb-Sn-Ge perovskite.

References

- (1) Kojima, A.; Teshima, K.; Shirai, Y.; Miyasaka, T. *J. Am. Chem. Soc.* **2009**, 131 (17), 6050-6051. DOI: 10.1021/ja809598r.
- (2) Kim, J. Y.; Lee, J. W.; Jung, H. S.; Shin, H.; Park, N. G. *Chem. Rev.* **2020**, 120 (15), 7867-7918. DOI: 10.1021/acs.chemrev.0c00107.
- (3) Jena, A. K.; Kulkarni, A.; Miyasaka, T. *Chem. Rev.* **2019**, 119 (5), 3036-3103. DOI: 10.1021/acs.chemrev.8b00539.
- (4) Xiao, Z.; Song, Z.; Yan, Y. *Adv. Mater.* **2019**, 31 (47), e1803792. DOI: 10.1002/adma.201803792.
- (5) Xi, J.; Loi, M. A. *ACS Energy Lett.* **2021**, 6 (5), 1803-1810. DOI: 10.1021/acsenergylett.1c00289.
- (6) Ke, W.; Stoumpos, C. C.; Kanatzidis, M. G. *Adv. Mater.* **2019**, 31 (47), e1803230. DOI: 10.1002/adma.201803230.

- (7) Hooper, R. W.; Ni, C.; Tkachuk, D. G.; He, Y.; Terskikh, V. V.; Veinot, J. G. C.; Michaelis, V. K. *J. Phys. Chem. Lett.* **2022**, *13* (7), 1687-1696. DOI: 10.1021/acs.jpcllett.1c04033.
- (8) Karmakar, A.; Bhattacharya, A.; Bernard, G. M.; Mar, A.; Michaelis, V. K. *ACS Mat. Lett.* **2021**, *3* (3), 261-267. DOI: 10.1021/acsmaterialslett.0c00596.
- (9) Bernard, G. M.; Karmakar, A.; Michaelis, V. K. *Reference Module in Chemistry, Molecular Sciences and Chemical Engineering*, Elsevier, **2021**. DOI: 10.1016/B978-0-12-823144-9.00018-2
- (10) Kubicki, D. J.; Stranks, S. D.; Grey, C. P.; Emsley, L. *Nat. Rev. Chem.* **2021**, *5* (9), 624-645. DOI: 10.1038/s41570-021-00309-x.

SESSION EN10.20: Passivation and Interlayers II
Session Chairs: Tim Kodalle and Michael Saliba
Friday Afternoon, April 26, 2024
Room 334, Level 3, Summit

1:30 PM *EN10.20.01

Halide Perovskites based Indoor Photovoltaics: Role of Composition Tuning and Interfacial Layers Shaoyang Wang¹, Paul Edwards², Maged Abdelsamie³, Peter Brown¹, David Webster¹, Arvydas Ruseckas¹, Robert W. Martin², Carolin M. Sutter-Fella³, Graham Turnbull¹, Ifor Samuel¹ and Lethy Krishnan Jagadamma¹; ¹University of St Andrews, United Kingdom; ²University of Strathclyde, United Kingdom; ³Lawrence Berkeley National Laboratory, United States

With the explosive development of the Internet of Things (IoT) technology, indoor photovoltaics (IPVs) are becoming a promising candidate to sustainably power billions of wireless sensors for secured and smart buildings. Among the various photovoltaics technologies available today, halide perovskite-based IPVs are most promising for integration with IoT because of their excellent optoelectronic properties, easy and cost-effective processability using solution-based methods such as roll-to-roll printing, high specific power, and earth-abundance. The low intensity of the indoor light sources means the absence of beneficial light-induced trap filling of the perovskite photoactive layer. This demands stringent defect minimisation approaches at every functional layer to maximize the power conversion efficiency of IPVs and thereby reduce the efficiency gap (more than 20 % now) between the theoretically predicted and experimentally observed power conversion efficiency of IPVs. In this talk, I will discuss the effect of active layer composition tuning and the role of interfacial layers in maximizing efficiency and suppressing the hysteresis effects under indoor lighting. While tuning the composition of the halide perovskites we observed that the fast processing of the triple anion perovskite composition enables the retention of Chlorine and enhances the photovoltaic device performance under indoor lighting. The kinetics of chlorine incorporation/escape was investigated by in situ grazing incidence wide-angle X-ray scattering and correlated the Cl content with the photovoltaic device performance. The selection of organic vs oxide-based transport layers and the effect of light soaking and J-V hysteresis under indoor lighting will also be discussed in detail.

2:00 PM EN10.20.02

ALD-SnOx as a Top Layer and Hole Transport Layer to Improve The Thermal Stability of Lead-Free Tin Perovskite Solar Cells Takeshi Kitamura and Shuzi Hayase; The University of Electro-Communications, Japan

Lead perovskite solar cells (Pb-PSCs) have attracted significant worldwide attention due to their rapid increase in power conversion efficiency (PCE) from 3.8% to 25.8%. However, lead toxicity is a concern for their commercialization. Among lead-free alternatives, tin perovskite solar cells (Sn-PSCs) have the highest PCE (>14%) due to their narrow band gap (1.4 eV), low exciton binding energy, and high carrier mobility.

Despite the vigorous efforts to improve the efficiency of Sn-PSCs, thermal stability is still a critical issue that has not been solved. Inverse structure devices using poly(3,4-ethylenedioxythiophene) poly(styrenesulfonic acid) (PEDOT:PSS) as the hole transport layer (HTL) are commonly used for highly efficient Sn-PSCs. However, the PEDOT:PSS layer has hygroscopic and acidic properties that reduce the stability of the solar cell. Therefore, Sn-PSCs without PEDOT:PSS is an important research item in terms of stability. In addition, the diffusion of iodine ions within the tin perovskite layer reduces device stability. Therefore, preventing iodine ion diffusion is also important to improve the stability of Sn-PSCs.

Previous studies have reported that ALD-SnOx (x = 1.7-1.8) can serve as HTLs in tin-lead alloy perovskite solar cells. Furthermore, our previous study demonstrated that SnOx (x = 1.7-1.8), obtained by plasma oxidation of metallic Sn, can serve as HTLs in Sn-PVK-PV with PCEs exceeding 14%. We have also found that tin oxide nanoparticle layers, which are commonly used as electron transport layers (ETLs) in Pb-PSCs, can operate as HTLs in Sn-PSCs. These SnOx layers are partially composed of Sn²⁺ rather than Sn⁴⁺ and exhibit bipolar carrier transport. Sn-PSCs with tin oxide nanoparticle HTLs exhibit higher stability than PEDOT:PSS HTL devices. Therefore, tin oxide HTLs may be effective to enhance the stability of Sn-PSCs.

ALD-SnOx in the top layer has been reported to improve stability in Pb-PSCs by preventing the diffusion of iodine ions.

In this report, we first replaced HTL with ALD-SnOx to improve the thermal stability of Sn-PSCs. In addition, ALD-SnOx was also introduced in the top layer.

In the presentation, the mechanism of thermal stability improvement by ALD-SnOx will be discussed.

2:15 PM EN10.20.03

Synergistic Effect of Charge-Modulated Molecular Passivation in MA/Br-Free Perovskite Solar Cells Dhruba B. Khadka, Yasuhiro Shirai, Masatoshi Yanagida, Hitoshi Ota and Kenjiro Miyano; National Institute for Materials Science (NIMS), Japan

Molecular passivation represents a promising avenue for enhancing both the efficiency and operational stability of perovskite solar cells. This work reports on the effect of diammonium iodide functional molecules featuring aryl or alkyl cores onto 3D-perovskite surfaces. Our findings reveal the remarkable efficacy of piperazine dihydriodide, characterized by an alkyl core and electron-rich -NH terminal, in mitigating surface and bulk defects while modifying surface chemistry and improving carrier extraction efficiency. This results in an impressive efficiency of 23.17% (1 cm² area) with superior long-term stability. Device analysis substantiates that these robust bonding interactions reduce defect densities in the perovskite film and suppress ion migration. This report will shed light on the synergistic effect of bifunctional molecules in defect mitigation, opening avenues for design strategies centered on bonding-regulated molecular passivation to enhance solar cell performance and stability.

2:30 PM BREAK

SESSION EN10.21: Composition Analysis and Degradation
Session Chairs: Virgil Andrei and Lethy Krishnan Jagadamma
Friday Afternoon, April 26, 2024
Room 334, Level 3, Summit

3:00 PM EN10.21.01

Taming Phase Transitions in Two-Dimensional Hybrid Perovskites Connor G. Bischak; The University of Utah, United States

Metal halide perovskites often exhibit phase transitions that occur near room temperature. Typically, efforts have focused on suppressing phase transitions for optimal device stability. Yet, strategies to control these phase transitions could lead to new applications in memory storage, thermal energy storage, and switchable optoelectronic devices. We demonstrate that we can control the temperature of the order-to-disorder phase transition of two-dimensional Ruddlesden Popper perovskites through alkyl cation alloying. We also connect structural transformations to changes in photophysical properties and show that changes in photoluminescence wavelength and intensity are tied to octahedral distortions in the perovskite crystal lattice. Last, using photoluminescence imaging, we image the dynamics of the phase transition and show that the nature of these dynamics depends on the alkyl cation length.

3:15 PM EN10.21.02

The Role of Mobile Ions in The Early Performance Degradation of Perovskite Solar Cells Jarla Thiesbrummel^{1,2}, Sahil Shah², Vincent Le Corre³, Henry J. Snaith¹ and Martin Stoltterfoht^{2,4}; ¹University of Oxford, United Kingdom; ²University of Potsdam, Germany; ³Friedrich-Alexander-Universität Erlangen-Nürnberg, Germany; ⁴The Chinese University of Hong Kong, Hong Kong

In the last decade, perovskite semiconductors have triggered a revolution in solar cell research. However, there remain some critical issues concerning the stability of metal-halide perovskites, which need to be overcome to enable a large scale commercialisation of perovskite photovoltaics. While the rather poor environmental stability of these perovskites is usually attributed to their ionic nature rendering them sensitive to moisture and oxygen, the actual contribution of mobile ions to the total degradation loss under different environmental conditions is poorly understood. Here, we reveal that the initial degradation of perovskite semiconductors is largely the result of mobile ion-induced internal field screening - a phenomenon that has not been previously discussed in relation to the degradation of perovskite solar cells. The increased field screening leads to a decrease in the steady-state power conversion efficiency mainly due to a large reduction in current density, while the efficiency at high scan speeds (>1000 V/s) where the ions are immobilized is much less affected. We also show that interfacial recombination does not increase upon ageing, yet the open-circuit voltage decreases as the result of an increase in the mobile ion density upon ageing. Furthermore, similar ionic losses appear under different external stressors, in particular when there are free charges present in the absorber layer. Finally, we generalize these findings beyond triple cation solar cells by showing the same degradation mechanisms take place in perovskites with a range of different compositions, including methylammonium leadiodide ('MAPI'), formamidinium cesium leadiodide ('FACs'), and several mixed-halide perovskites with different bandgaps. This work reveals a key degradation mechanism, providing new insights into initial device degradation before chemical or extrinsic mechanical device degradation effects manifest, and it highlights the critical role mobile ions play therein. It highlights the importance of efficiently managing mobile ions and their effects to enable long term stability in perovskite-based photovoltaics and move towards commercialization.

3:30 PM EN10.21.03

Potential of Perovskite Doping Unlocked: Shaping The Future of Energy and Electronics Zuzanna Molenda¹, Dario Bassani² and Lionel Hirsch¹; ¹IMS-Bordeaux, France; ²ISM, France

Doping of metal halide perovskites (MHPs) is the next, essential step towards the implementation of perovskite semiconductor technology for electronic devices. Nonetheless, only a limited number of successful doping instances have been documented, and it is frequently mistaken for additives, grain passivation, or surface functionalization, none of which affect the semiconductor's charge carrier density. Due to the ionic character of the perovskite crystal, the introduction of heterovalent ions is accompanied by the counter ions that balance out the potential doping effect. Here we present a use of homovalent yet metastable ions, in particular Sm²⁺, to substitute Pb²⁺ in MAPbI₃ (MA = methylammonium). Sm²⁺ ions spontaneously oxidize to Sm³⁺, once incorporated into the crystal lattice and each of them releases one electron to the conduction band. The oxidation of samarium ions is confirmed by the analysis of the Sm 3d core level in the X-ray photoelectron spectrum (XPS). Residual content of the oxidized form of Sm³⁺ present in the doping solution allows to observe a slight shift of the Sm 3d peak towards higher binding energy, suggesting the environment change of the Sm³⁺ ion, once introduced inside the perovskite film. Together with the shift of the XRD pattern upon doping, this supports the hypothesis that the dopant ion is incorporated and stabilized in the crystal lattice. At the same time, the crystal structure of the doped perovskite layer is conserved and no phase separation is observed from the XRD patterns. Ultraviolet photoelectron spectroscopy (UPS) shows a shift of the Fermi level (E_F) by around 0.5 eV towards the conduction band, proving the doping to be n-type. The increase of the free electron density in the conduction band is the direct reason for the conductivity increase for the doped films by 3 orders of magnitude. Using the Mott-Schottky method, the ionized charge carrier density is estimated to be 10¹⁷ cm⁻³ for the sample showing the highest conductivity increase, which suggests the ionized dopant concentration in the doped perovskite film to be around 0.01% (Pb density in MAPbI₃ ≈ 20²¹ cm⁻³). The discrepancy between this result and the doping concentration stemming from the XPS measurement, which is calculated to be around 20%, leads to two possible explanations. Either the majority of the Sm²⁺ introduced to the perovskite polycrystalline film resides at grain boundaries and therefore does not act as a dopant or the dopant is only partially oxidized in normal conditions, exhibiting the freeze-out effect. The dopant activation energy (the energy necessary to oxidize all the Sm²⁺ ions to Sm³⁺) of around 350 meV seems to support the latter hypothesis and is in agreement with the energy between the E_F and conduction energy (E_C). The presented method allows to reach the highest to-date conductivity increase for the n-type and may become a protocol for the efficient n-type doping of MHPs. To illustrate one of its applications, we fabricated perovskite solar cells (PSC) with poly(triaryl amine) (PTAA) as a hole transporting layer (HTL) (p-side) and Sm-doped MAPbI₃ (n-side), without the electron transporting layer (ETL). Additionally, we used gold as an electron collecting electrode ($W_{Au} = 5.22$ eV). The strain-induced ohmic contact between highly doped perovskite and Au allows to minimize the series resistance at this interface and an efficient electron collection. This shows the potential of flexible electrode selection for the doped PSC. Therefore, the ETL-free n-doped PSC retains the same PCE as the reference sample (with PCBM as an ETL), in spite of the simplified architecture that decreases the fabrication cost and the number of interfaces.

3:45 PM EN10.21.04

Spatially Resolved Parameter Mapping and Degradation of Perovskite Solar Cells Akash Dasgupta and Henry J. Snaith; University of Oxford, United Kingdom

Perovskite solar cells have made significant strides towards maturity; however, two major challenges persist: stability and up-scalability. Achieving uniform deposition methods is crucial for ensuring the suitability of devices for large-scale production. Furthermore, a comprehensive understanding of degradation mechanisms is essential for mitigating these effects and improving stability. In this study, we introduce a novel approach that integrates photoluminescence imaging with drift diffusion simulations which incorporate the effects of mobile ions. By employing machine learning techniques, we

generate inferred maps of various material parameters. These maps are then tracked throughout the aging process to analyse their spatially resolved temporal evolution during degradation, enabling us to distinguish between bulk. Our findings reveal that macroscopic-scale spatial defects propagate outward, ultimately resulting in device degradation across the entire area. By distinguishing between bulk and surface degradation, our technique provides an additional dimension of insight into the heterogeneous nature of degradation in perovskite solar cells. This enables meaningful comparisons and enhanced comprehension of different treatments and processes. We expect analysis using our approach to enable the field to target sources of inhomogeneity and degradation more precisely, paving the way towards commercialisation.

4:00 PM EN10.21.05

In-Situ Spatially-Resolved Analysis of Degradation in Perovskite Solar Cells [Dana Kern](#), Jack Schall, Goutam Paul, Steve Johnston, Andrew Norman, Harvey Guthrey, Nikita S. Dutta, Chun-Sheng Jiang and Andrew Glaws; National Renewable Energy Laboratory, United States

Long-term durability of metal halide perovskite solar cells (PSCs) can be impacted by both the intrinsic nature of the as-designed device stack as well as unintentional local nonuniformities. Here, we present methods for spatially-resolved in-situ degradation analysis during perovskite stress testing. We use repeated bias/rest cycles from timescales of minutes up to 100 hours to separately assess metastability in comparison to irreversible degradation. We visualize device evolution in-situ under light or electrical bias, either in surface view using electro-optical imaging or in cross-section using kelvin probe force microscopy. We further demonstrate multi-scale investigation of defects, from rapid electro-optical screening of the full device area down to nanoscale microscopic characterization to reveal the underlying chemical or structural nature of defects. Our results inform methods to screen for defects in PSCs, as well as further development of accelerated stress testing and degradation analysis which will become essential for perovskite devices to improve their durability and enter the commercial market.

4:15 PM EN10.21.06

From Electrically Assisted Amplified Spontaneous Emission to Injection Lasing with Metal Halide Perovskites [Iakov Goldberg](#), Karim Elkhoully, Xin Zhang, Nirav Annavarapu, Sarah Hamdad, Guillaume Croes, Cedric Rolin, Jan Genoe, Weiming Qiu, Robert Gehlhaar and Paul Heremans; IMEC, Belgium

Metal halide perovskites have emerged as promising gain media for thin-film laser diodes. However, achieving electrically excited amplified spontaneous emission (ASE) and lasing in perovskite light-emitting diodes (PeLEDs) is challenged by the conflicting requirements of high conductivity and high net modal gain of the device stack. We break this trade-off by developing a transparent PeLED architecture that combines excellent current-injection properties with low optical losses [1]. The device is operated at 77 K and delivers current densities above 3 kA cm^{-2} with irradiance values above 40 W cm^{-2} , whilst displaying an ASE threshold of $9.1 \text{ } \mu\text{J cm}^{-2}$ using 2.3 ns optical laser pulses. By co-exciting the PeLED with optical pulses that are synchronized with the leading edge of an intense electrical pulse, we achieve a reduction of the ASE threshold by $1.2 \text{ } \mu\text{J cm}^{-2}$, showing that electrically injected carriers contribute to optical gain. This breakthrough addresses the first essential pre-condition for perovskite laser diodes. A perovskite gain layer with a three-dimensional morphology has been used in this work, showing that there is potential for the reduction of the amplification threshold through elaborate quantum confinement engineering.

Integration of an optical cavity, which does not compromise PeLED performance, is a critical next step in transitioning from optical amplifier structures to laser diodes. It is noteworthy that reaching injection lasing might turn out to be more accessible than cavity-free electrically stimulated ASE. Specifically, when studying standalone perovskite films deposited over distributed feedback structures, we have achieved an optically pumped lasing threshold that is a factor of ~ 2 lower than the ASE threshold of neat films [2]. Consequently, we propose an integration route where the resonators are embedded into the substrate with a planarized arrangement of alternating materials with differing refractive indices. This approach eliminates challenges associated with the thin-film deposition atop corrugated surfaces, such as increased leakage currents, strong local electric fields, and nonuniform current distribution. Finally, we show that such a planarized grating can be married with the proposed transparent PeLED architecture, where efficient mode coupling is facilitated by the use of a thin bottom transparent electrode [3]. We believe that this alternative integrating scheme will accelerate the development of thin-film perovskite injection lasers.

[1] Elkhoully, K., Goldberg, I., Zhang, X. et al. Electrically assisted amplified spontaneous emission in perovskite light-emitting diodes. *Nat. Photon.* (2024). <https://doi.org/10.1038/s41566-023-01341-7>

[2] Annavarapu, N., Goldberg, I., Hamdad, S. et al. Four-Dimensional Design Space of High-Q Second-Order Distributed Feedback Perovskite Lasers. *Advanced Optical Materials* (2024). Accepted (adom.202302496).

[3] Goldberg, I., Annavarapu, N., Leitner, S. et al. Multimode Lasing in All-Solution-Processed UV-Nanoimprinted Distributed Feedback MAPbI_3 Perovskite Waveguides. *ACS Photonics* (2023). <https://doi.org/10.1021/acsp Photonics.3c00206>.

4:30 PM EN10.21.07

Facile and Composition-Flexible Alternate Route to Perovskites [Dean G. Grier](#), Tapan K. Jena, Yuvraj Patil and Philip Boudjouk; North Dakota State University, United States

Halide perovskites have emerged as promising candidates for a variety of applications, including solar cells and light emitting diodes. In the field of photovoltaics, power conversion efficiencies have risen rapidly and competitively over the past several years, although environmental stability remains a focus of study. Herein we report a method for synthesizing a variety of phase pure perovskites through a simple solution method followed by mild thermolysis. Our group has previously successfully demonstrated synthesis of metal chalcogenide semiconductors as well as nanocomposites of polymers with metal chalcogenide semiconductor quantum dots, through the use of organometallic single source precursors. The approach allows access to compositions across the periodic table, including those from Groups 13-15, 14-16, and 12-16. Following on from this work, we turned our approach to perovskite materials. In this study, we demonstrate synthesis of the all-inorganic lead-free perovskites A_2SnX_6 , with $\text{A}=\text{Cs, Rb, K}$, and $\text{X}=\text{Cl, Br, I}$.

SYMPOSIUM EN11

Emerging Inorganic Semiconductors for Solar Energy and Fuels
April 24 - May 8, 2024

Symposium Organizers

Andrea Crovetto, Technical University of Denmark
Annie Greenaway, National Renewable Energy Laboratory
Xiaojing Hao, Univ of New South Wales
Vladan Stevanovic, Colorado School of Mines

* Invited Paper
+ JMR Distinguished Invited Speaker
^ MRS Communications Early Career Distinguished Presenter

SESSION EN10/EN11: Joint Virtual Session
Session Chairs: Tim Kodalle and Ivan Mora-Sero
Wednesday Morning, May 8, 2024
EN11-virtual

8:00 AM *EN10/EN11.01

Less Defect and Stable Perovskite Nanocrystals: Optical Property and Photoexcited Carrier Dynamics [Qing Shen](#), Yusheng Li and Hua Li; The University of Electro-Communications, Japan

Perovskite nanocrystals (PNCs) have gained significant attention for both fundamental research and applications of optoelectronic devices owing to their appealing optoelectronic properties and excellent chemical processability. For their wide range of potential applications, synthesizing PNCs with high crystal quality and stability is of crucial importance. Recently, we have succeeded in synthesis of phase stable and less defect PNCs, including APbX₃ NCs (A: FA, MA, Cs; X: I, Br, Cl), Sn-Pb alloyed NCs and Sn-based PNCs [1-7]. We have demonstrated that a high room-temperature photoluminescence quantum yield (PL QY) of close to 100% can be obtained in the Pb-based PNCs, signifying the achievement of ignorable less trapping defects in the PNCs. Ultrafast kinetic analysis with time-resolved transient absorption spectroscopy evidences the negligible electron or hole trapping pathways in our PNCs, which explains such a high quantum efficiency. In addition, photoexcited hot and cold carrier dynamics as well as charge transfer were systematically investigated [4,8,9]. Solar cells based on these high-quality PNCs exhibit power conversion efficiency of over 15%, showing great promise for practical application. In addition, through metal doping and Sn (IV) control [5-7,10], we found that Sn(IV)-induced defects and distortions could be reduced greatly in Sn and Sn-Pb PNCs. As a result, stable Sn and Sn-Pb PNCs with ultra long carrier lifetimes (> 180 ns) were realized. Our findings provide new insights into the materials design strategies for improved optoelectronic properties of Sn-containing perovskites [10].

References

1. F. Liu and Q. Shen et al., ACS Nano 11 (2017) 10373
2. F. Liu and Q. Shen et al., J. Am. Chem. Soc. (2017), 139, 16708.
3. F. Liu and Q. Shen et al., Chem. Mater. 32 (2020) 1089.
4. C. Ding and Q. Shen et al., Nano Energy 67 (2020) 104267.
5. F. Liu and Q. Shen et al., Angew. Chem. Int. Ed. 59 (2020) 8421.
6. J. Jiang, F. Liu, Q. Shen and SX. Tao, J. Mater. Chem. A 9 (2021) 12087.
7. F. Liu and Q. Shen et al., ACS Appl. Nano Mater. 4 (2021) 3958.
8. Hua Li and Q. Shen et al., Adv. Mater. 35 (2023) 2301834.
9. Yusheng Li and Q. Shen et al., arXiv preprint arXiv:2209.02202.
10. Yusheng Li and Q. Shen et al., submitted.

8:30 AM EN10/EN11.02

High Stability of Sn-Based Perovskite by Adding Reducing Agents for Perovskite Solar Cells [Teresa S. Ripolles](#); University of Valencia, Spain

Tin-based (Sn) halide perovskites have become one of the most prospective photovoltaic materials due to their optoelectronic properties, high photoconversion efficiency and relatively low toxicity.[1][2] Nevertheless, the rapid crystallization of tin-based perovskite and the easy oxidation of Sn²⁺ to Sn⁴⁺ under ambient conditions increases the interest of the scientific community.[3] To avoid these undesirable processes, we will address by two different methods, for instance, (i) organic cations engineering in Sn-based halide perovskite microcrystals, and (ii) adding reducing agents in three dimensional perovskite thin film.

On the one hand, Sn-based halide perovskite microcrystals have been synthesized by hot-injection method to control the dimensionality by changes the concentration of reactants. The physical properties suggest high photoluminescence quantum yield (PLQY) of 75% and 25% for chloride-based and bromide-based, respectively, and almost negligible for 2D Sn-based microcrystals.

On the other hand, increasing the perovskite dimensionality, we suggest adding a variety of additives that act as reducing agents with different nature in thin film. The addition of these novel materials into the FASnI₃ (FA is formamidinium) perovskite solution controlled the oxidation reaction and improved the surface morphology. An inverted perovskite solar cell was prepared and characterized. Due to the Sn⁴⁺ concentration is reduced in the Sn-based perovskite layer, the power conversion efficiency in a solar cell and the cell stability under ambient conditions are improved notably in comparison with the pure FASnI₃.

References

- [1] Malekshahi Byranvand, M., Zuo W., Imani R., Pazoki M., Saliba M. (2022) 'Tin-based halide perovskite materials: properties and applications' Chemical Science, 13, 6766. DOI: 10.1039/d2sc01914k (Accepted 23rd May 2022).
- [2] Li M., Li F., Gong J., Zhang T., Gao F., Zhang W.-H., Liu M. (2022) 'Advances in Tin(II)-Based Perovskite Solar Cells: From Material Physics to

Device Performance' Advanced Science News, 3, 2100102. DOI: 10.1002/ssr.202100102 (Published online: 5th October 2021).

[3] Abdel-Shakour M., Chowdhury T. H., Matsuishi K., Bedja I., Moritomo Y., Islam A. (2021) 'High-Efficiency Tin Halide Perovskite Solar Cells: The Chemistry of Tin (II) Compounds and Their Interaction with Lewis Base Additives during Perovskite Film Formation' Solar RRL, 5, 2000606. DOI: 10.1002/solr.202000606 (Published online: 9th December 2020).

8:45 AM EN10/EN11.03

Investigating The Influence of Multivalent Transition Metal Dopants on Copper Antimony Sulphide Thin Films for Enhanced Photovoltaic and Electrochemical Properties Kimberly A. Weston and Richard A. Taylor; The University of The West Indies, Trinidad and Tobago

Undoped non-stoichiometric semiconducting copper antimony sulphide (CAS) thin films were deposited at 500, 550 and 600 °C onto glass substrates by aerosol-assisted chemical vapour deposition (AACVD) at different flow rates and copper concentrations using metal diethyldithiocarbamate precursors. For thin films deposited at an optimal flow rate, data from powder X-ray diffraction (p-XRD), X-ray photoelectron spectroscopy (XPS), Raman spectroscopy, and scanning electron microscopy-energy dispersive X-ray spectroscopy (SEM-EDS) suggest a correlation of composition of the non-stoichiometric sulphur-deficient tetrahedrite phase (cubic structure) microcrystalline CAS (Cu₁₂Sb₄S₁₃) thin films with particle sizes ranging from 0.1 to 4 µm. For undoped thin films, visible optical absorption and cyclic voltammograms (CV) show a bandgap of ~2.1 eV is likely associated with compositional variations involving intrinsic lattice defects, including shallow electronic states such as copper interstitials (Cu_i^{•••}) and vacancies of sulphur (V_s^{••}) as deep-lying donors, and copper-antimony anti-sites (Cu_{Sb}^{••}) and antimony vacancies (V_{Sb}^{••}) as deep-lying acceptors. Additionally, upper first row transition metal divalent (M²⁺) ions such as Mn²⁺, Co²⁺, Ni²⁺ and Zn²⁺ were incorporated into tetrahedrite phase CAS (rCAS) thin films at optimal temperature, 550 °C and flow rate, 150 sccm. M²⁺ ions incorporated (M_r-rCAS) exhibit tunable composition-driven electronic structure for small M²⁺ content influencing narrower bandgaps between 1.7 and 1.9 eV. The Raman data suggest that the phase purity is affected by small fractions of the famatinite (tetragonal) phase. Additionally, rCAS and M_r-rCAS thin films were deposited on conducting substrates (ITO/FTO) and were found to be efficient as a novel catalyst for the hydrogen and oxygen evolution reactions in water splitting. Overall, the thin films display broad emission of fast dual radiative recombination, and an additional recombination pathway exhibited for M_r-rCAS associated with divalent ion-related point defects. These results show the utility of AACVD in tuning compositional and optical and electrochemical properties of undoped rCAS and M_r-rCAS thin films for possible applications in photovoltaics and electrochemical conversion.

9:00 AM EN10/EN11.04

Lead-free Perovskites: Toward an Opto-Electronics based on Abundant Elements and Low Temperature Synthesis Ilhem Elgargouri^{1,2}, Hind Kadiri¹, Akram Alhoussein¹, Rached Ben Hassen² and Gilles Lerondel¹; ¹Université de Technologie de Troyes, France; ²University of Tunis El Manar, Tunisia

The depletion of natural resources today necessitates a reevaluation of technological development, considering both material abundance and energy-efficient processes while maintaining device efficiency. This research presents a comprehensive investigation into the design and synthesis of advanced thin films materials for improved optoelectronic applications. By exploring the unique properties of lead-free perovskites oxides, we aimed at engineering materials with enhanced electrical conductivity, stability, and optical properties.

For this work, we chose two types of perovskites oxides: SrSnO₃ and LaVO₃. The reason behind this choice is the combination of abundance, non-toxicity, and low-cost production of these materials along with the tunable bandgap, the stability and durability.

In this study, we will detail the tailored synthesis process with sol-gel method using different percentages of doping. We discuss the systematic characterization of the resulting thin films through various analytical tools.

Nontoxic, relatively cheap precursors, and solvents were used without generating waste materials. The viscosities were controlled, and the resulting resins were spin-coated on Silicon and Quartz. The wet films were then annealed at 673 K to remove organic material and crystallized at 1173 K for 1h in air. Using scanning electron microscopy, the film thickness was found to be around 200nm with a highly uniform and homogeneous surface. X-ray diffraction confirmed the perovskite phase with an intense peak at 32°, and optical measurements proved the transparency of 80% in the visible range with an absorption in the UV range around 300nm.

The results reveal a clear correlation between the synthesis parameters and the optoelectronic performance of the materials, demonstrating the feasibility of optimizing these materials characteristics through precise control of the synthesis process.

The objective of this work is the realization of optoelectronic components (pn junction) based on doped perovskite oxide semiconductors (SrSnO₃: Sb@SrSnO₃: Al on ITO and LaVO₃) synthesized using an ecofriendly environmental synthesis (sol-gel process). Application as light absorbers or barrier layers in highly efficient solar cells are foreseen. Other applications are also possible (e.g., LEDs).

This work contributes to the ongoing efforts to develop sustainable and efficient materials for optoelectronic devices and underscores the pivotal role of advanced material synthesis techniques in achieving this goal.

9:05 AM *EN10/EN11.05

Computational Workflows for an Accelerated Design of Novel Materials and Interfaces Ivano Eligio Castelli; Technical University of Denmark, Denmark

The development of automated computational tools is required to accelerate the discovery of new functional materials, to speed up the transition to a sustainable future. Here, I address this topic by designing new electrodes with controlled interfaces for different applications which accelerate the transition to a sustainable future. These workflows are implemented in the framework of Density Functional Theory (DFT), using MyQueue and the Atomistic Simulation Environment (ASE). In the first part of my talk, starting from our recent work on a fully autonomous workflow, which identifies materials to be used as intercalation electrodes in batteries, based on thermodynamic and kinetic descriptors like adsorption energies and diffusion barriers,¹ I will describe a new modular approach to estimate electronic and ionic mobility in energy materials useful for a variety of applications, from batteries and fuel cells and solar energy conversion and storage. A substantial acceleration for the calculations of the kinetic properties has been obtained due to a recent implementation of the Nudged Elastic Bands (NEB) method, which takes into consideration the symmetries of the system to reduce the number of images to calculate. Moreover, we have established a surrogate model to identify the transition states, which can further reduce the computational cost to at least one order of magnitude.^{2,3} In the second part of my talk, I discuss how engineering the interface can positively impact surface properties for electrochemical water splitting: I apply strain engineering and external stimuli to switch material's polarization to decrease the reaction overpotential in oxynitride materials for the oxygen evolution reaction.^{5,6} In the last part of my talk, I will describe my vision for autonomous computational workflows, namely the creation of workflows for interface and their integration with experimental workflows.

References

- [1] F. T. Bölle, N. R. Mathiesen, A. J. Nielsen, T. Vegge, J. M. García-Lastra, and I. E. Castelli, Batteries & Supercaps 3, 488 (2020).
- [2] F. T. Bölle, A. Bhowmik, T. Vegge, J. M. García-Lastra, and I. E. Castelli, Batteries & Supercaps 4, 1516 (2021).
- [3] B. H. Sjölin, P. B. Jørgensen, A. Fedrigucci, T. Vegge, A. Bhowmik, and I. E. Castelli, Batteries & Supercaps 2023, e202300041 (2023).
- [4] Z. Lan, D. R. Småbråten, C. Xiao, T. Vegge, U. Aschauer, and I. E. Castelli, ACS Catal 11, 12692

(2021).

[5] C. Spezzati, Z. Lan, and I. E. Castelli, *Journal of Catalysis* 413, 720 (2022).

SESSION EN11.01: Phosphide PV I
Session Chairs: Andrea Crovetto and Xiaojing Hao
Wednesday Afternoon, April 24, 2024
Room 335, Level 3, Summit

1:30 PM *EN11.01.01

Experiments toward High-Performance Zintl Phosphide Solar Absorbers Sage Bauers¹, Obadiah Reid¹, David Fenning², Andriy Zakutayev¹, Jifeng Liu³, Kirill Kovnir⁴ and Geoffroy Hautier³; ¹National Renewable Energy Laboratory, United States; ²University of California, San Diego, United States; ³Dartmouth College, United States; ⁴Iowa State University of Science and Technology, United States

Most photovoltaic absorber materials development is done on materials with known or slightly modified structural prototypes; for example, kesterite, chalcopyrite, and zincblende are all derived from mutations to the diamond crystal structure. It is rare and sometimes transformative—such as in halide perovskites—when new structural classes of absorber materials are discovered. The AM_2P_2 (A = alkaline earth cation such as Ba, Ca, Sr and $M = 2+$ cation such as Zn, Cd) compounds have previously been described as semiconducting zintl phases and are structurally distinct to widely studied PV materials. However, these have attracted recent interest from theory as materials with solar-spectrum matched band gaps and tolerance to intrinsic point defects. $BaCd_2P_2$ is particularly compelling with a direct 1.45 eV band gap and mostly comprising inexpensive elements already used in solar absorber applications, thus having high-grade feedstocks already available. Here, we report on the synthesis and properties of $BaCd_2P_2$ and related AM_2P_2 materials. $BaCd_2P_2$ can be synthesized in powder form from elemental precursors using conventional solid-state reaction methods. The material forms in a $P-3m1$ crystal structure ($CaAl_2Si_2$ prototype) and is stable in open air heating up to 300 °C as well as in acids, bases, and at even higher temperatures in inert environments. $BaCd_2P_2$ powder shows strong band-to-band photoluminescence that is stable at elevated temperature and time-resolved microwave conductivity shows long photoexcited carrier lifetimes of around 30 ns, which is already longer than observed in some much more mature absorber technologies. Since the direct-gap AM_2P_2 materials will be most compelling as thin film absorbers, we also discuss several ongoing efforts to realize these compounds in thin film format.

2:00 PM *EN11.01.02

Emerging Cu-Based Phosphides as Contacts and Absorbers for Solar Energy Conversion Andrea Crovetto^{1,2,3} and Andriy Zakutayev¹; ¹National Renewable Energy Laboratory, United States; ²Technical University of Denmark, Denmark; ³Helmholtz-Zentrum Berlin, Germany

Many new contact and absorber materials have been studied in the past decade for solar energy conversion applications. For example, research into emerging chalcogenides expanded from zincblende-derived CdTe, CuInSe₂ and Cu₂ZnSnS₄ to include non-tetrahedrally bonded compounds like 1D-bonded Sb₂S₃, layered CuSbS₂ chalcostybites, or BaZrS₃ perovskites.

There are much fewer known phosphide solar materials, besides II-IV-P₂ derivatives of GaP (e.g. ZnSnP₂, ZnSiP₂) and their binary constituents (e.g. Zn₃P₂) studied as absorbers, or wide band gap bipolar dopable BP that has been considered for contact applications. Nevertheless, the reported semiconductor properties and initial device performances of phosphide materials are quite promising and deserve further research attention.

This presentation will highlight a few emerging phosphide materials based on Cu, as potential transparent contact and light absorber layers in solar energy conversion devices. The first example is experimental demonstration of high electrical conductivity and measurement optical transparency in theoretically predicted CaCuP sputtered thin film material [1]. The second example is two-step synthesis and semiconductor property measurements of CuP₂ – one of the first known phosphorus-rich semiconductors in thin film form [2].

General synthesis and characterization challenges associated with doing experiments on the phosphide class of materials will be also discussed.

[1] *Chem. Sci.* 13, 5872 (2022)

[2] *J. Am. Chem. Soc.* 144, 13334 (2022)

2:30 PM BREAK

SESSION EN11.03: Poster Session I
Session Chairs: Annie Greenaway and Vladan Stevanovic
Wednesday Afternoon, April 24, 2024
Flex Hall C, Level 2, Summit

5:00 PM EN11.03.01

Biased Photoreflectance Spectroscopy for Characterization of Band Bending in Compound Solar Cells Isshin Sumiyoshi and Yoshitaro Nose; Kyoto University, Japan

Introductions

The optimization of pn junctions is an inevitable subject to realize high performance of emerging solar cells. Junction capacitance, derived from overall capacitance of a solar cell through an equivalent circuit, widely used to evaluate band bending in a pn junction. However, in emerging solar cells, the electrical properties and band structures of layers or junctions other than the target are often unknown, thereby introducing various unknown factors into the evaluation of specific physical properties.

In this study, we present a characterization technique of pn junctions through Franz-Keldysh oscillations (FKOs). FKOs can be observed in spectra of modulation spectroscopy, such as photoreflectance (PR) and electroreflectance (ER). Analyzing the oscillation periods in spectra provides the internal electric field applied to the pn junctions, offering a means to estimate band bending. Furthermore, we propose applying a bias voltage to solar cells during

PR measurement, denoted as biased PR (B-PR) measurement. Through this method, we attempted to evaluate the interface states within pn junction.

Experimental methods

We performed PR measurements on pn junction solar cells using ZnSnP₂ (ZTP) bulk crystals and GaInP thin film as absorbing layers, representing emerging and highly efficient solar cells, respectively.

The PR and B-PR measurement was conducted at room temperature using a PR measurement system (Seishin Trading Co. Ltd). A YAG laser ($\lambda=532$ nm) was used as a pump beam and its modulation frequency was set at 711 Hz. The probe beam was a monochromatized light from Xenon lamp. In the B-PR measurement, a bias voltage ranging from -5 to +1.4 V was applied to the solar cells using a source meter (Keithly 2400) and Au probes.

Results and discussions

In the PR spectra of the ZTP solar cell measured without bias voltage and any contacts, FKOs with up to the 5th extrema were observed at photon energies higher than the bandgap of ZTP (1.64 eV). The internal electric field in ZTP layer around the pn junction was determined to be 87 ± 8 kV cm⁻¹, derived from the FKOs period following the theory proposed by Aspnes and Studna [2]. Assuming an uniform acceptor concentration of 5.5×10^{16} cm⁻³ in the ZTP layer, we estimated the charge distribution around the pn junction using the Poisson's equation. As the results, we determined the depletion layer width and the surface potential at the pn junction in ZTP side as 83 nm and +0.47 eV from the valence band maximum (VBM) of ZTP, respectively. It is here emphasized that the above results were obtained with contactless.

FKOs were observed over a bias voltage range from -5 to +1.4 V also in the B-PR spectra. Following the above-mentioned analysis, we obtained the bias voltage dependence of the surface potential. In the absence of interface states at a pn junction, the surface potential is expected to monotonically increase with rising reverse bias. This behavior is theoretically expressed through the Poisson's equation. However, the experimental results deviate from the theoretical curve, exhibiting plateau regions around bias voltage of 0 and -4 V. The applying of bias voltage to a solar cell corresponds to the control of the Fermi level. The deviation in the bias dependence of the surface potential from the theoretical curve may be attributed to the occupation (emission) of electrons at interface states. Such transitions of electrons are facilitated by approach of the Fermi level to the interface level. In the ZTP solar cells, the levels of the plateau regions were +0.45 eV and +1.3~+1.5 eV from the VBM of ZTP. In the presentation, we will discuss the consistency between the B-PR measurement and conventional capacitance measurement, using GaInP III-V solar cells together with ZTP solar cells.

References

- [1] I. Sumiyoshi and Y. Nose, J. Appl. Phys. **133**, 235702 (2023).
- [2] D.E. Aspnes and A.A. Studna, Phys. Rev. B **7**, 4605-4625 (1973).

5:00 PM EN11.03.02

Recent Progress on The Application of Spectroscopic Ellipsometry for a Multilayer Analysis of CdTe-Based Solar Cell Structures Incorporating Magnesium-Zinc Oxide Transparent Layers Mohammed Alaani¹, Prakash Koirala¹, Balaji Ramanujam¹, Ambalanath Shan¹, Adam Phillips¹, Nikolas Podraza¹, Stephen K. O'Leary² and Robert Collins¹; ¹The University of Toledo, United States; ²University of British Columbia, Canada

We present some recent progress that has been made on the application of an optical function parameterization of polycrystalline Mg_xZn_{1-x}O (MZO) thin films on the bandgap that has been used for the metrology of CdTe-based solar cell structures that incorporate MZO thin films as high resistivity transparent (HRT) layers. The acquired parametric expressions are applied to facilitate the mapping spectroscopic ellipsometry (M-SE) of device structures consisting of glass/SnO₂:F/MZO. M-SE is shown to provide maps in the MZO effective thickness and bandgap within confidence limits of ± 1 nm and ± 0.003 eV, respectively. As a second application of this parameterization, performed on an as-deposited glass/SnO₂:F/MZO/CdS/ CdTe device structure, has been made using through-the-glass spectroscopic ellipsometry (TG-SE). Such an analysis is also shown to provide the MZO effective thickness and bandgap. The outcome of the TG-SE analysis for this device structure enables simulations of the external quantum efficiency (EQE) spectrum of the resulting solar cell assuming different recombination losses within the individual layers of the structure. A comparison of these simulations with the experimental EQE spectrum reveals improved current collection from the front of the device incorporating an MZO HRT layer.

5:00 PM EN11.03.03

A Detailed Investigation on The Photothermal Properties of SnFe₂O₄ as a Photocatalyst for Wastewater Treatment Lei Liu and Chunli Liu; Hankuk University of Foreign Studies, Korea (the Republic of)

SnFe₂O₄ is a magnetic semiconductor with a spinel crystal structure. Due to its relatively narrow bandgap of less than 2.0 eV, SnFe₂O₄ holds promising potential for achieving a full spectral response to the solar radiation with enhanced energy utilization. However, research on its photothermal effects has been limited so far. In this study, we successfully synthesized narrow-bandgap SnFe₂O₄ (1.62 eV) via hydrothermal synthesis. Using Chlorotetracycline (CTC) as a model antibiotic pollutant, we investigate the photothermal properties of SnFe₂O₄ in various catalytic modes. Thermal catalytic experiments at different temperatures, photocatalytic experiments with various light wavelengths, and photothermal catalytic experiments under simulated solar light were conducted to evaluate the photoexcitation and thermal excitation properties.

Our findings reveal that SnFe₂O₄ efficiently utilizes different spectral regions of sunlight: photothermally activated under UV and visible light and mainly thermally excited under near-infrared light. Furthermore, CTC degradation experiments have shown that SnFe₂O₄ can degrade CTC effectively under real outdoor sunlight. Even under cloudy weather conditions, SnFe₂O₄ retains catalytic activity if the ambient temperature can be kept at higher than 35°C. Therefore, this narrow-bandgap catalyst possesses the remarkable capability to enhance solar energy utilization significantly. Thus, it is believed to promise the design of a full solar spectrum photocatalyst for wastewater treatment.

5:00 PM EN11.03.04

Efficient Photocatalytic Degradation of Pharmaceutical Residues with Ni-TiO₂/gC₃N₄ Heterojunction Yiting Xiao, Yang Tian and Jun Zhu; University of Arkansas, Fayetteville, United States

The proliferation of pharmaceutical residues in natural water systems has emerged as a significant environmental concern over the past decades. In response to these contaminants of emerging concern (CECs), our study introduces an innovative photocatalytic system, comprising Nickel (Ni)-doped Titanium Dioxide (TiO₂) synergized with graphitic carbon nitride (gC₃N₄). This system demonstrated a notable 82.3% degradation efficiency of sodium salicylate, a precursor and active component of one of the most widely used medications (aspirin) in the world, within 4.5 hours. Utilizing the Central Composite Design and Response Surface Methodology (CCD/RSM), we optimized the Ni to TiO₂ ratio, the gC₃N₄ to Ni-TiO₂ proportion, and catalyst dosage. Detailed characterizations, including SEM, XRD, XPS, UV-VIS spectrophotometry, and electrochemical studies, revealed the catalyst's superior properties. Beyond sodium salicylate degradation, this system exhibits potential for broader organic pollutant remediation, presenting a promising avenue in wastewater treatment and environmental cleanup strategies.

5:00 PM EN11.03.05

Breaking Barriers in Chalcogenide Perovskite Synthesis Kiruba Catherine Vincent, Shubhanshu Agarwal, Jonathan Turnley and Rakesh Agrawal; Purdue University, United States

Chalcogenide perovskites are emerging semiconductor materials with attractive optoelectronic properties. These materials have been shown

computationally and experimentally to possess high absorption coefficient, tunable bandgap, and high dielectric constant. In contrast to their lead halide counterparts, they are known to be stable, and earth-abundant with nontoxic constituents, making them potential candidates for a variety of electronic applications.

However, the existing rudimentary synthesis techniques have limited the growth of these materials. Traditional solid-state and vacuum processing methods demand temperatures in excess of 800-1000 °C, which bring about difficulties in identifying suitable substrates and subsequent device fabrication. To address these issues, we have identified the key barriers in the synthesis of these materials and succeeded in reducing the synthesis conditions to moderate temperatures (<600 °C) and time periods of 1-2hrs. Our work also identifies a potential liquid flux that enables to overcome the diffusional limitations between precursors.

5:00 PM EN11.03.06

Structure and Phase Transition Study of Emerging Sb and Bi Chalcogenides by X-Ray Diffraction [Ivan Caño Prades](#)¹, Alejandro Navarro¹, Mykhailo Kolstov², Maria Del Barrio¹, Marcel Placidi¹, Josep Lluís Tamarit¹, Xavier Alcobé³, Nicolae Spalatu², Joaquim Puigdollers¹ and Edgardo Saucedo¹; ¹Universitat Politècnica de Catalunya, Spain; ²Tallinn University of Technology, Estonia; ³Universitat de Barcelona, Spain

Sb and Bi-based Van der Waals chalcogenides with formula MChX (M=Sb or Bi, Ch=S or Se and X=Br or I) are constituted by relatively earth-abundant and non-toxic elements, they have bandgaps in the 1.5-2.0 eV range, and they can be synthesized at low temperatures. In addition, their low-dimensional structure leads to enhanced transport properties, which make these largely overlooked materials very attractive for advanced energy applications, including photovoltaics. Furthermore, chalcogenides have been reported to possess ferroelectric properties, whereby a small displacement along their *c*-axis switches between centrosymmetric and non-centrosymmetric structures.¹ However, despite previous studies and theoretical calculations, there is a general lack of information on their structural properties regarding the impact of elemental substitution and temperature on the cell parameters, phase stability, and ferroelectricity.

In this work, the eight materials obtained from MChX permutations have been synthesized as thin films by physical vapor routes. Then, they have been characterized by X-ray diffraction (XRD), and Le Bail and Rietveld refinement techniques have been performed to acquire the cell parameters and volume, phase composition, texture characteristics, and other structural features. Various trends and correlations have been observed, revealing the impact that the metal, chalcogenide and halogen have on the structure of the material respectively. For example, it is shown that the halogens have a bigger impact on the cell volume and parameter *a* but the chalcogenide has the strongest effect on parameter *c* (covalently-bonded ribbons). On the other hand, changing the metal (M), the unit cell is compressed in direction *a*, but expands in the other crystallographic directions. Also, it has been observed that the volume and cell parameters are highly correlated with the ionic radii, and that compounds with larger electronegativities have lower cell volumes. Overall, it is demonstrated that halogens have the biggest impact on all the structural properties.

Secondly, thermal characterization and temperature-dependent X-ray diffraction experiments have been performed on selected samples, aiming at studying phase stability and transitions. For instance, SbSI powders have been analyzed by differential scanning calorimetry and XRD, identifying the phase transition between paraelectric and ferroelectric structures with Curie point at room temperature. Thin films have also been characterized using temperature-dependent XRD, giving bigger insight on the stability of chalcogenide phases and the effect of temperature on their structure.

1 *Energy Environ. Sci.* **8**, 838 (2015)

5:00 PM EN11.03.07

A Figure of Merit to Quantify The Efficiency Potential of your Favorite Emerging PV Material [Andrea Crovetto](#); Technical University of Denmark, Denmark

The pace of exploration of new photovoltaic (PV) materials has accelerated in recent years, but we are still lacking methods to (i) quantify their efficiency potential during early development stages, (ii) guide their optimization, and (iii) help researchers make rational decisions on which materials are worth investigating.

To help achieve these goals, I propose a human-derived figure of merit for PV materials based on 30,000 drift-diffusion simulations. The applicability of the figure of merit is demonstrated on a sample of 25 PV materials of current research interest, but the method can immediately be applied to experimentally synthesized or computationally examined materials at any development level, as long as seven of their bulk material properties have been determined by experiment or first-principles calculations.

This figure-of-merit approach helps understand whether imperfect PV performance is intrinsic to the material (inadequate bulk properties at the current stage of development), or if it “only” requires a different device structure, contact layers, or improved interface properties. For example, the reasons for the lack of and NaBiS₂ and BaZrS₃ solar cells with notable PV efficiencies are completely different for the two materials.

Using a local version of the proposed figure of merit, a material-specific optimization strategy can be laid out for any experimentally synthesized PV absorber, by specifying the bulk properties that should most urgently be improved to increase their PV efficiency.

Come by my poster and estimate the maximum efficiency of your favorite emerging PV material!

5:00 PM EN11.03.08

Photoluminescence of BaCd₂P₂ as a New Defect-Insensitive Solar Material [Gideon Kassa](#)¹, Smitakshi Goswami¹, Zhenkun Yuan¹, Muhammad R. Hasan², Andrew Pike¹, Shaham Quadri³, Yihuang Xiong¹, Victoria Kyveryga², Diana F. Dahliah⁴, Gian-Marco Rignanese⁴, Romain Claes⁴, Andriy Zakutayev³, David Fenning⁵, Obadiah Reid⁶, Sage Bauers³, Kirill Kovnir², Geoffroy Hautier¹ and Jifeng Liu¹; ¹Dartmouth College, United States; ²Iowa State University of Science and Technology, United States; ³National Renewable Energy Laboratory, United States; ⁴Université Catholique de Louvain, Belgium; ⁵University of California, San Diego, United States; ⁶University of Colorado Boulder, United States

Searching for earth-abundant, defect-insensitive solar materials can play a significant role in future photovoltaics. Here we experimentally verify BaCd₂P₂ as a promising candidate for low-cost, high-efficiency photovoltaic material, as predicted by high-throughput screening of nearly 40,000 semiconductors. Its optimal band gap of 1.45 eV and properties such as temperature stability and long carrier lifetime make BaCd₂P₂ a strong photovoltaic candidate. We were able to experimentally demonstrate the optical performance of BaCd₂P₂ by comparing its photoluminescence (PL) intensity with that of GaAs. The relatively low-purity (99.9%) BaCd₂P₂ powder had direct gap PL intensity in the same order as GaAs powder obtained from a prime single crystalline wafer, suggesting that it is insensitive to impurities and defects. We further present an in-depth investigation of the PL spectrum of this promising material

by studying the impact of temperature, excitation laser power, and composition variations. Nearly all our experimental data have agreed with our theoretically calculated properties of BaCd₂P₂. The calculated band structure suggested a direct gap of 1.45 eV and an indirect gap of 1.48 eV. The PL spectrum of BaCd₂P₂ at 298 K, had a peak at 847 nm (1.46 eV), aligning well with the predicted band structure, and another, broader, peak at 980 nm. At 78 K we observed a separate peak on the lower wavelength side of the 847 nm peak resulting from the indirect gap transition, further validating our computed band structure. This material also showed great temperature stability, increasing the temperature to 368 K had only a slight decrease in the PL emission by ~5%, which fully recovered when going back to 298 K. Our work on excitation power dependence of PL intensity has enabled us to confirm the nature of 847 nm peak and gain a better understanding of the 980 nm peak. We did this by modifying the well-known equation $I_{PL} = C * (P_{laser})^\alpha$ (meant to model the change in PL peak intensity with power) to account for competing nonradiative processes such as Auger recombination at higher excitation powers and consider the potential saturation of available states. We developed a more generalized equation that treats PL intensity as a function of thermal excitation, laser excitation, and nonradiative recombination. For the 847 nm peak, we repeatedly got a value of the α parameter that was strongly indicative of a band-to-band transition. We saw that the 980 nm peak does not blueshift with decreasing temperature and that it had a strikingly similar response to PL laser excitation power variations as the radiative defect of Si-doped GaAs, appearing at 950 nm, leading us to hypothesize that the 980 nm peak of BaCd₂P₂ is due to a shallow radiative defect. We conducted an evaluation of the change in the 950 nm defect PL peak when using off-stoichiometric BaCd₂P₂ samples. We observed that the peak intensifies and is slightly redshifted in Ba-poor samples. We further used the data from our studies of PL intensity change with temperature to calculate the activation energy of the prominent nonradiative defects.

5:00 PM EN11.03.09

Enhancing Photocatalytic Hydrogen Production with Nanocone-Structured Z-Scheme Photocatalysts [Jihun Kim](#), Ryun Na Kim, Sungwan Kwon, HyungYong Ji, Jeongyeol Kim and Whi Dong Kim; Korea Institute of Industrial Technology (KITECH, Korea (the Republic of

Z-scheme photocatalysts have emerged as a promising solution to address the efficiency challenges in solar-assisted water splitting, thanks to their capability to efficiently absorb visible light and maintain the essential charge potential required for overall water splitting. To ensure the successful operation of Z-scheme photocatalysts, it is crucial that the two constituent photocatalysts and the charge recombination layer are precisely arranged in a specific sequential order. However, previous research has predominantly utilized Z-scheme photocatalysts in a randomly mixed configuration, thereby preventing the full exploitation of the unique attributes inherent to Z-scheme photocatalysts.

This study demonstrates fabrication of a nanocone-structured BiVO₄/SrTiO₃ Z-scheme photocatalytic thin film, enabling effective Z-scheme charge transfer. The fabrication process involves the preparation of a nanocone BiVO₄ structure on a glass substrate, the formation of a BiVO₄/reduced graphene oxide (RGO) composite nanocone structure, and the deposition of SrTiO₃ nanoparticles to form BiVO₄-RGO-SrTiO₃ Z-scheme photocatalyst. The resulting structure comprises BiVO₄, RGO, and SrTiO₃ arranged sequentially. A comparative analysis between randomly mixed Z-scheme photocatalysts and the arranged Z-scheme photocatalyst demonstrates a significant enhancement in hydrogen production efficiency for the latter, underscoring the pivotal role of precise arrangement in Z-scheme photocatalysis.

Additionally, the study investigates how the superhydrophobic surface properties of the nanocone structure influence the capture of hydrogen and oxygen gas bubbles generated during the water splitting reaction in photocatalyst module. The nanocone-structured Z-scheme thin film efficiently captures gas bubbles due to its superhydrophobic surface characteristics, while the randomly mixed Z-scheme photocatalyst experiences reduced gas bubble detachment, resulting in decreased photocatalyst production efficiency.

This study underscores the importance of meticulous Z-scheme photocatalyst arrangement and highlights the advantages of the nanocone structure in improving gas bubble capture during the water splitting process, thus contributing to the advancement of photocatalytic hydrogen production.

5:00 PM EN11.03.10

Enhancing Photocatalyst Efficiency through Type-II Core/Crown Nanoplatelets for Improved Charge Separation Ryun Na Kim, Jihun Kim, Sungwan Kwon, HyungYong Ji and [Whi Dong Kim](#); Korea Institute of Industrial Technology, Korea (the Republic of

Semiconductor nanocrystal-based photocatalysts have garnered significant attention for their potential applications in diverse fields, including hydrogen production, CO₂ conversion, and pollutant removal. However, a major hurdle to improving their efficiency arises from the fact that the radiative recombination rate of semiconductor nanoparticles (~hundreds of nanoseconds) is much faster than the rates of photocatalytic reactions (~microseconds to ~milliseconds). This leads to the loss of the majority of charges before they can actively participate in the desired photocatalytic reactions, resulting in low efficiency. Therefore, it is crucial to develop structures that facilitate efficient charge separation to address this efficiency issue in photocatalysts. The most common approach to tackle this challenge involves utilizing core/shell structures to create a type-II band alignment structure. However, this approach has a drawback: while it enhances charge separation, it tends to trap electrons or holes within the core, limiting their participation in photocatalytic reactions.

In this research, we explore the influence of type-II core/crown nanoplatelets (NPLs) on photocatalytic reactions. These NPLs possess a type-II band alignment structure while exposing both the core and crown regions externally, enabling active participation of both electrons and holes in photocatalytic reactions. To maximize the efficiency of charge separation in this open structure, we prepared core/crown nanoplatelets with various compositions, including CdS, CdSe, and CdTe, while carefully controlling the surface area of both the core and crown regions.

We conducted femtosecond laser-based time-resolved photoluminescence measurements and transient absorption measurements to analyze the carrier dynamics of the prepared NPLs. Then, we performed water-splitting experiments under light irradiation to clarify the relationship between charge separation and photocatalytic activity. The results revealed that as the carrier lifetime of the photocatalyst increased, the hydrogen generation rate also significantly increased. This highlights the significance of the charge carrier lifetime as a pivotal parameter impacting photocatalytic activity.

Furthermore, to validate the significance of an open structure, such as the core/crown configuration, we prepared type-II core/shell quantum dots with the equivalent composition and similar lifetimes to the core/crown nanoplatelets. Surprisingly, despite the efficient charge separation structure of the type-II core/shell quantum dots, their photocatalytic efficiency decreased. These findings underscore the importance of an open structure that facilitates the active participation of both electrons and holes in photocatalytic reactions while concurrently prolonging the carrier lifetime, ultimately resulting in enhanced photocatalyst efficiency.

5:00 PM EN11.03.12

Aspects Relevant to Developing Solar Cells of Tin Sulfide-Selenide of Cubic Crystalline Structure produced by Vacuum Thermal Evaporation [Fabiola De Bray Sanchez](#), M.T. Santhamma Nair and P. K. Nair; Universidad Nacional Autonoma de Mexico, Mexico

In recent work (2023), thin films of tin sulfide selenide of cubic crystalline structure were prepared at a substrate temperature of 450 °C at a low deposition rate of 3 nm/s by vacuum thermal evaporation (TE) of SnS-SnSe/Se powder sources. This opens up methodologies for preparing novel photovoltaic

absorber materials of a cubic crystalline structure with optical bandgap (E_g) 1.45 – 1.65 eV, which permits to achieve a light generated current density of 25 – 35 mA cm⁻² and a relatively high open circuit voltage, unlike in the more commonly known orthorhombic polymorph of SnS or SnSe with E_g of 1.1 or 1 eV, respectively. The development of SnS or SnSe of cubic crystalline structure by TE eluded until recently because of a deposition rate of > 10 nm/s typical in vacuum deposition techniques resulting in films of orthorhombic structure. The relatively higher content of Se in a SnS-Se-CUB helps to modify the E_g of the films toward 1.5 eV. It also helps to increase its p-type conductivity from 10⁻⁶ to nearly 10⁻³ Ω⁻¹ cm⁻¹. With less than 1% of Se in the SnS-CUB film, the vacancies at the S-sites are compensated, while maintaining the E_g of 1.7 eV (inherent in a SnS-CUB film) along with an increased electrical conductivity of 10⁻³ Ω⁻¹ cm⁻¹, which is higher by three orders of magnitude than that of the SnS cubic film. These results offer many options for solar cell configurations. Basically, they help to improve the proof-of-concept solar cell of FTO/CdS/SnS-CUB (TE)/C with V_{oc} of 0.478 V, but with a low conversion efficiency of < 1% by providing a back surface field p-type layer of SnS-Se-CUB:Se. The use of an SnS_{0.45}Se_{0.55}-CUB layer of thickness 120 nm with E_g , 1.57 eV of σ_p , 0.02 Ω⁻¹ cm⁻¹ produced by vacuum thermal evaporation in the FTO/CdS/SnS-CUB (TE)/SnS-Se-CUB:Se (TE)/C cell illustrates such prospects.

5:00 PM EN11.03.13

First Principles Thermodynamic Model of BaZrS₃ Synthesis Prakriti Kayastha, Giulia Longo and Lucy Whalley; Northumbria University, United Kingdom

The BaZrS₃ chalcogenide perovskite shows strong light absorption, high chemical stability, is nontoxic, and is made from earth-abundant elements. These properties make it a promising candidate material for application in optoelectronic technologies, including next-generation photovoltaic absorber materials [1]. It has been proposed as a more chemically stable alternative to the widely studied lead-based metal halide perovskite family [2]. Although the chemical and physical properties of this perovskite are favorable, a scalable synthesis technique remains an open challenge. Standard solid-state synthesis requires temperatures that are not suitable for device integration (>900°C).

Several studies have now established that the perovskite forms at moderate temperatures (500-600°C) through liquid-flux assisted synthesis [3]. This method is based on the formation of BaS₃ in a sulfur-rich environment. Other methods based on molecular precursors or nanoparticles have also been proposed, but no good quality crystalline thin films have been formed to date [4,5]. Progress is hindered by our limited understanding of the underlying reaction thermodynamics.

In our work, we use density functional theory and lattice dynamics to calculate the thermodynamic and vibrational properties of BaZrS₃ and its competing ternary, binary, and elemental phases. We consider the experimentally reported BaS_x, ZrS_x (x = 1, 2, 3) and BaZrS₃ phases. Using our open-source code ThermoPot [6] we calculate the temperature and pressure-dependent Gibbs free energy of formation with reference to competing ternary, binary, and elemental phases.

We find that to promote the formation of BaZrS₃ through liquid-flux there is a “goldilocks” zone for temperature and sulfur partial pressure. This is driven by the high sensitivity of Gibbs formation energy to the sulfur gas allotrope. At intermediate temperatures (500°C) and higher pressures (>10³ Pa) the S₈ allotrope dominates [7] and suppresses the formation of BaS₃. At lower pressures (<10² Pa) the S₂ allotrope dominates and BaS₂ forms. At intermediate pressures, the S₂ allotrope dominates and forms BaS₃ (10²-10³ Pa). We find good agreement between our results and those reported in the experimental literature [5]. Our work provides insights into the reaction thermodynamics of this promising material and suggests the experimental regimes to target for future synthesis.

References:

- [1] Sopiha et al, Adv. Opt. Mater. 2022 10 2101704.
- [2] Comparotto et al, ACS Appl. Energy Mater. 2022 5 6335.
- [3] Yang et al, Chem. Mater. 2023 35 4743.
- [4] Pradhan et al, Angew. Chem. 2023 62 202301049.
- [5] Yang et al, J Am Chem. Soc. 2022 44 15928.
- [6] <https://github.com/NU-CEM/ThermoPot>
- [7] Jackson and Walsh, J Mater. Chem. A 2014 2 7829.

5:00 PM EN11.03.14

Investigating Light-Induced Metastabilities in Kesterite Solar Cells: Implications and Applications Axel Gon Medaille¹, Alex Jimenez Arguijo¹, Romain Scaffidi², Yuancai Gong¹, Kunal Tiwari¹, Sergio Giraldo¹, Marcel Placidi¹, Edgardo Saucedo¹ and Zacharie Jehl Li-Kao¹; ¹Polytechnic University of Catalonia, Spain; ²Interuniversity Microelectronics Centre, Belgium

Kesterite solar cells have recently achieved a significant efficiency milestone, now **at the edge of the 15% threshold**, thanks to the innovative solution-based approach developed by Gong et al [1]. While thin-film chalcogenides are renowned for their **stability** in comparison to organic or perovskite counterparts, the phenomenon of **light soaking has persisted as a recurring characteristic in solar cell devices**. Light soaking refers to the alteration of a solar cell's characteristics after being exposed to illumination for a specific duration. Importantly, this property, whether enhancing or diminishing efficiency, often exhibits reversibility, highlighting a **fundamental metastability** within the system. Typically, light soaking is conducted under AM1.5g illumination for several minutes, in order to reach a stable state before assessing the performance of the device.

In this study, we aim at offering a comprehensive exploration of these instabilities by manipulating the **illumination power density and varying the wavelength** during the light soaking process, done both in short circuit and open circuit conditions. We systematically monitor the resultant dark current-voltage (JV) curve and observe noteworthy, reversible changes. These changes can be attributed to **interface defects**, which are investigated using wavelengths that are minimally absorbed by the absorber. Our approach is supported through optical modelling, utilizing a self-developed code to validate the optical characteristics.

Leveraging numerical electrical modelling via SCAPS1D, we propose a physical interpretation based in the **bandgap position of interface defects and their charge states**. This comprehensive analysis combines theoretical insights with practical observations, to analyze the complex mechanisms at play during light soaking. Additionally, the results and hypotheses derived from our results are rigorously tested against materials characterizations, including Raman spectroscopy and Photothermal Deflection Spectroscopy.

Beyond the implications for solar cells, these instabilities offer promising possibilities for applications extending **beyond the energy sector**. One such application is the potential for creating **optically controlled memristors**, a novel development with significant ramifications in the field of neuromorphic computing and beyond. This research offers a new perspective on light-induced metastabilities in Kesterite solar cells, shedding light on their potential for controlled applications in emerging technologies.

5:00 PM EN11.03.16

Unlocking The Potential of Silicon Clathrate films for Photovoltaics and Beyond Anil K. Bharwal¹, Romain Vollondat¹, Daniel Stoeffler¹, Céline

Chevalier², Stéphane Roques¹, Aziz Dinia¹, Abdelilah Slaoui¹ and Thomas Fix¹; ¹University of Strasbourg and CNRS, France; ²University of Lyon and CNRS, France

Silicon materials in various forms, including mono-, poly-, and amorphous, have been actively studied since their use in solar technology seven decades ago. Exotic, low-density silicon forms, namely silicon clathrates, have recently received attention for their attractive semiconducting and optical capabilities, which are equivalent to normal silicon materials [1–3]. The type II clathrate ($\text{Na}_x\text{Si}_{136}$), an open cage polymorph of silicon with unusual structural properties capable of accepting or releasing Na atoms, was discovered in powder form in 1965 [4]. However, type II clathrate investigation in films is relatively new, which is of great significance to thin-film technologies. Specifically, commercial solar cells employing d-Si with an indirect bandgap may see a large increase in energy conversion efficiency when using Si clathrate with a direct bandgap. Interestingly, inserting or removing Na from these cages can significantly alter their electrical characteristics, making them suitable for a wide range of applications in optoelectronics and energy conversion devices [5]. The removal of Na from the cages allows the guest-free clathrates to be used for various applications such as electrodes in Li-ion battery [6,7] and has great potential in H_2 -storage [8]. Nevertheless, further work needs to be done to understand the precise mechanism of Na insertion or removal within the empty Si_{136} cages.

The present research focuses on investigating, in premiere the electronic properties resulting from the insertion and removal of Na atoms in type II clathrate films using Kelvin Probe-Ambient pressure photoemission spectroscopy (KP-APS) characterization and density functional theory (DFT) calculations. The films were prepared using three different types of silicon substrates: intrinsic, n-type, and p-doped wafers and are characterized thoroughly. By manipulating the Na composition parameter x from 0 to 23 within $\text{Na}_x\text{Si}_{136}$ films, a transition from the semiconducting to a metallic state is achieved [5]. We investigated the energy levels and precisely drew the band diagram for each of the studied clathrate systems using KP-APS and optical measurements. This communication also highlights the use of clathrate film preparation and doping strategies for achieving efficient photovoltaic devices with a unique and novel heterojunction configuration, as well as great potential in maximizing their employment in LEDs, H_2 -gas storage, and lithium-ion batteries.

Acknowledgement

The present project is financed by ANR Exosil- Exotic Silicon: silicon clathrate films (project-ANR-22-CE50-0025).

References

- [1] Fix et al., J. Phys. Chem. C. 124 (2020) 14972–14977.
- [2] Vollondat et al., J. Alloys Compd. 903 (2022) 163967.
- [3] Iwasaki et al., Adv. Mater. 34 (2022) 2106754.
- [4] Kasper et al., Science. 150 (1965) 1713–1714.
- [5] Vollondat et al., J. Chem. Phys. 158 (2023) 164709.
- [6] Dopilka et al., Adv. Energy Sustain. Res. 2 (2021) 2000114.
- [7] Liu et al., Inorg. Chem. 62 (2023) 6882–6892.
- [8] Neiner et al., Inorg. Chem. 49 (2010) 815–822.

5:00 PM EN11.03.17

Improved Photovoltaic Performance and Robustness of Inverted AgBiS_2 Nanocrystal Solar Cells by Sodium Doping Bosen Zou and Jonathan E. Halpert; Hong Kong University of Science and Technology, China

Silver bismuth sulfide (AgBiS_2) is a third-generation photovoltaic material used in solution-processed solar cells. The material's high absorption coefficient enables it to generate a theoretical current density of over 28 mA/cm^2 with an ultra-thin active layer of approximately 30 nm. However, the innate traps from AgBiS_2 nanocrystals cause a non-negligible loss in open-circuit voltage (V_{OC}) and operating lifetime. To address this issue, we employed a sodium doping strategy in AgBiS_2 nanocrystals (NCs). Our findings suggest that sodium doping is particularly effective in improving solar cell performance by trap filling and by obtaining larger-sized NCs. Partial substitution between Na and Ag provides a reduced-trap density surface that can bind with a higher density of oleate ligands after purification, resulting in higher power conversion efficiency (PCE) and operational stability. The champion device achieved a PCE over 4.6% and light-soaking stability over 200 hours, making it one of the best-performing AgBiS_2 solar cells based on an inverted, p-i-n structure. Our metal-doping strategy offers an alternative approach to enhance the performance of AgBiS_2 -based solar cells.

5:00 PM EN11.03.18

Using Inorganic Chemistry to Design New Functional Semiconductors with a Computer Joseph W. Bennett; University of Maryland Baltimore County, United States

The design and discovery of new inorganic semiconductors to be used as platforms for functional properties can be expedited by investigating already synthesized and characterized compounds whose merits may have been previously overlooked. Here we use data-enabled methods that combine searchable crystallographic databases, group theory, and first-principles density functional theory calculations to create new semiconductors to function over a wide range of chemical environments. We investigate a family of known A_2BX_3 compounds as solid-state materials for applications such as solar harvesting and energy storage, and then use inorganic chemistry and group theory to explain how distortions in the 1D chains present in the structure types can lead to the microscopic mechanisms of ferroelectricity and antiferroelectricity that we predict. We then use compositional tuning to determine the optimal chemical formulas and ground state properties of a new class of inorganic semiconductors to be used for solar energy harvesting and storage. Ultimately, we would like to create a family of materials whose compositions span a wide set of cations and anions, specifically oxide and chalcogenides, to complement well-established semiconductors like the ABX_3 perovskites, Dion-Jacobson, and Ruddlesden-Popper phases.

5:00 PM EN11.03.19

Direct Solar Energy Storage with Doped Metal Oxides Nanocrystals Luca Rebecchi^{1,2}, Andrea Rubino¹, Irene Martin^{1,3} and Ilka Kriegel¹; ¹Istituto Italiano di Tecnologia, Italy; ²Università degli Studi di Genova, Italy; ³Politecnico di Torino, Italy

The profound impacts of the ongoing energy and climate crises are escalating the need for sustainable energy solutions within our society. To counteract these challenges, scientific research has directed its focus towards the investigation of novel technologies for the direct storage of solar energy. Notably, the utilization of doped metal oxide nanocrystals (MO NCs) has emerged as a promising avenue. Recent research has shown that different materials, such as Zinc Iron Oxide (ZIO) and Indium Tin Oxide (ITO) NCs can undergo photodoping^{1,2}, a process in which multiple photo-generated electrons after illumination beyond the bandgap accumulate in the NCs and remain stored within the NCs for a prolonged time in inert atmosphere¹. These properties make these materials attractive as prospective solution for the photon energy conversion and storage. However, to date this process has been observed only in solution, while for application in energy storage, it is mandatory to develop solid-state electrodes based on these nanomaterials.

In this contribution, we present our results obtained on thin film photo-electrodes made from ITO NCs. We show that these electrodes display typical supercapacitor behaviour in the dark with capacitance values in the order of mF. When excited with UV light, beyond the bandgap of ITO, we see with respect to dark conditions an increase in the time required to discharge the electrodes, while charging time decreases. This behaviour is typical of the

generation of an external photo-current, induced by light absorption. Finally, in this contribution we will show the first attempts to broaden the spectral range that the system can harvest by sensitizing the electrode with a visible absorber. We then characterized the electrodes photo-electrochemically to investigate how interaction with different wavelength ranges influences their behaviour.

1. Kriegel, I. *et al.* Light-Driven Permanent Charge Separation across a Hybrid Zero-Dimensional/Two-Dimensional Interface. *J. Phys. Chem. C* **124**, 8000–8007 (2020).
2. Brozek, C. K. *et al.* Soluble Supercapacitors: Large and Reversible Charge Storage in Colloidal Iron-Doped ZnO Nanocrystals. *Nano Lett.* **18**, 3297–3302 (2018).

SESSION EN11.04: Multi-anion PV/PEC
Session Chairs: Galina Gurieva and Rasmus Nielsen
Thursday Morning, April 25, 2024
Room 335, Level 3, Summit

8:30 AM EN11.04.01

The Defect Chemistry of Emerging, Wide-Bandgap Absorber BiOI Adair Nicolson¹, Seán R. Kavanagh², Alex M. Ganose² and David O. Scanlon³;
¹University College London, United Kingdom; ²Imperial College London, United Kingdom; ³University of Birmingham, United Kingdom

Wide bandgap solar absorbers are seeing significant interest for a variety emerging photovoltaic technologies, from top-layers in tandem cells to single junction devices for indoor applications. V-VI-VII materials have been studied for photocatalysis, but have recently gained interest as “perovskite-inspired” materials (PIMs) for solar absorber applications.^[1] These are materials which stray from the perovskite structure, but share an elemental space, thus keeping the strong antibonding character at the band edges and large dielectric constant, which are associated with the defect tolerance observed in lead halide perovskites.

From the family of bismuth-based absorbers, BiOI has emerged as a leading candidate due to its improved air stability and lack of ultrafast charge-carrier localization, which can pose a challenge for many Bi containing PIMs originating from the reduction in dimensionality.^[1,2,3] However, large concentrations of electron traps have been measured in BiOI thin films, the potential source of poor device performance.^[4]

Therefore, in this project we perform the first, complete investigation into all intrinsic point defect in BiOI at the hybrid DFT level, using the shakenbreak method to thoroughly search the complex defect potential energy surface.^[5] This will allow the identification of harmful defects and guide the development of fabrication processes to reduce their impact.

[1] Y.-T. Huang, S. R. Kavanagh, D. O. Scanlon, A. Walsh, R. L. Z. Hoye, *Nanotechnology*, 2021, 32, 132004.

[2] D. S. Bhachu, S. J. A. Moniz, S. Sathasivam, D. O. Scanlon, A. Walsh, S. M. Bawaked, M. Mokhtar, A. Y. Obaid, I. P. Parkin, J. Tang and C. J. Carmalt, *Chem. Sci.*, 2016, 7, 4832

[3] A. M. Ganose, M. Cuff, K. T. Butler, A. Walsh, D. O. Scanlon, *Chem. Mater.*, 2016, 28, 1980

[4] S. Lal, M. Righetto, A. M. Ulatowski, S. G. Motti, Z. Sun, J. L. MacManus-Driscoll, R. L. Z. Hoye, L. M. Herz, *J. Phys. Chem. Lett.*, 2023, 14, 6620–6629

[5] I. Mosquera-Lois, S. R. Kavanagh, D. O. Scanlon, A. Walsh, *npj Comput. Mater.*, 2023, 9, 1 —11

8:45 AM EN11.04.02

Air-Stable Bismuth Sulfobromide (BiSBr) Visible-Light Absorbers: Optoelectronic Properties and Potential for Energy Harvesting Xiaoyu Guo¹, Yi-Teng Huang¹, Hugh Lohan^{1,2}, Junzhi Ye¹, Yuanbao Lin¹, Juhwan Lim³, Nicolas Gauriot³, Szymon Zelewski³, Daniel Darvill², Aron Walsh², Huimin Zhu^{4,1}, Akshay Rao³, Iain McCulloch¹ and Robert L. Hoye¹; ¹University of Oxford, United Kingdom; ²Imperial College London, United Kingdom; ³University of Cambridge, United Kingdom; ⁴University of Strathclyde, United Kingdom

ns² compounds have recently attracted considerable interest due to their potential to replicate the defect tolerance of lead-halide perovskites and overcome their toxicity and stability limitations. However, only a handful of compounds beyond the perovskite family have been explored thus far. Herein, we investigate bismuth sulfobromide (BiSBr), which is a quasi-one-dimensional semiconductor, but very little is known about its optoelectronic properties or how it can be processed as thin films. We develop a solution processing route to achieve phase-pure, stoichiometric BiSBr films (*ca.* 240 nm thick), which we show to be stable in ambient air for over two weeks without encapsulation. The bandgap (1.91 ± 0.06 eV) is ideal for harvesting visible light from common indoor light sources, and we calculate the optical limit in efficiency (i.e., spectroscopic limited maximum efficiency, SLME) to be 43.6% under 1000 lux white light emitting diode illumination. The photoluminescence lifetime is also found to exceed the 1 ns threshold for photovoltaic absorber materials worth further development. Through X-ray photoemission spectroscopy and Kelvin probe measurements, we find the BiSBr films grown to be n-type, with an electron affinity of 4.1 ± 0.1 eV and ionization potential of 6.0 ± 0.1 eV, which are compatible with a wide range of established charge transport layer materials. This work shows BiSBr to hold promise for indoor photovoltaics, as well as other visible-light harvesting applications, such as photoelectrochemical cells, or top-cells for tandem photovoltaics.

9:00 AM EN11.04.03

Photoanodes and Thin-Film Solar Cells Based on SbSBr, SbSeI and BiSeI Absorbers Edoardo Maggi^{1,2}, Ivan Caño Prades¹, Alejandro Navarro¹, Cibrán López Álvarez¹, Oriol Segura Blanch¹, Hao Zhe Chun², Joaquim Puigdollers¹, Jordi Llorca Pique¹, Lluís Soler Turu¹, Lydia H. Wong² and Edgardo Saucedo¹; ¹Universitat Politècnica de Catalunya, Spain; ²Nanyang Technological University, Singapore

Emerging quasi-1D (Q1-D) van der Waals materials, (Sb,Bi)(S,Se)(Br,I), hold the potential to be a breakthrough in photovoltaic (PV), photocatalytic (PC), and photoelectrocatalytic (PEC) applications, aiming to address some of the main issues affecting even the more mature PV, PC, and PEC technologies. Although this materials family has rarely been explored for these applications, mixed chalcogenides fulfill the urgent need for innovative and renewable energy sources based on earth-abundant, low-toxicity, thermally stable, and defect-tolerant compounds.

This materials class has the peculiarity of possessing a crystallographic structure in which the atoms are held together by strong covalent bonds along one of their crystallographic directions and weak van der Waals bonds along the other two directions. When properly oriented, it results in a highly anisotropic material composed of nano/micro-ribbons with unique conductive properties. The high tunability of these materials and the results obtained in the present

work place these semiconductors in the spotlight for a wide range of applications, including next-generation PV tandem and transparent applications, photocatalytic hydrogen production, and oxygen and hydrogen evolution reactions (OER, HER) among others.

The nano/micro-ribbon structure, coupled with the extremely uniform single-crystal phases, leads to an increased number of photons that reach the space charge region, and the light-trapping effect reduces reflection. This morphology enhances the optoelectronic properties of SbSBr and BiSeI-based solar cells, the OER of Q1-D van der Waals-based photoanodes, and the photocatalytic activity of such-based photocatalysts. The dense coverage of properly oriented nano/micro-ribbons increases the surface area, a key parameter for improving photons and reactant absorption, enabling the synthesis of efficient, photoactive, photostable, and nontoxic photoanodes and photocatalysts. Furthermore, the band gaps of the obtained materials range between 1.25 and 2 eV, making them active to visible light and allowing an optimal usage of the solar spectrum.

The above-mentioned reasons are indicative of what can be achieved with this relatively unexplored technology. To date, no mixed chalcogenide compounds have been synthesized using physical vapor deposition (PVD) techniques, primarily due to the complexity of the material and the varying vapor pressures involved. This work marks the very first successful attempt to synthesize and investigate Q1-D van der Waals-based semiconductors using an innovative methodology that involves the co-evaporation of chalcogenides followed by high-pressure annealing under a halogen atmosphere. Various characterization techniques (XRD, XRF, SEM, EDX, PDS, UV-Vis, Raman spectroscopy, and DFT calculations) have demonstrated the high tunability of the morphology of this compound family by modifying the annealing conditions, confirming the possibility of synthesizing high-quality single-phase material with PVD techniques for the first time.

The versatility of the system allows for the optimal distribution of nano/micro-ribbons in terms of height, thickness, density, and orientation, according to the final device's use. An array of operational Q1-D van der Waals-based solar cells and photoanodes, each derived from distinct stack combinations, will be showcased and thoroughly examined, together with some preliminary results about photocatalytic hydrogen production under visible light. Notably, solar cells have exhibited open-circuit voltages reaching up to 600 mV, and photoanodes, even when utilizing non-protected absorbers, have achieved a photoanode current of nearly 2 mA/cm². This study demonstrates how these novel compounds represent a promising development in advanced energy conversion applications.

9:15 AM EN11.04.04

Exploring The Impact of Physical Vapor Synthesis Regime on The Properties of Pnictogen Chalcogenides for Solar Cell Applications [Alejandro Navarro](#)¹, Mykhailo Kolstov², Ivan Caño Prades¹, Nicolae Spalatu², Ilona Oja Acik², Atanas Katerski² and Edgardo Saucedo¹; ¹Polytechnic University of Catalunya, Spain; ²Tallinn University of Technology, Estonia

Recent advances in the study of van der Waals (vdW) materials have led to an increase in the effort devoted to their development for energy applications. In particular, the photoconversion efficiencies of Sb₂(S_{1-x}Se_x)₂ compounds highlight the potential of vdW semiconductors as photovoltaic absorbers. Significantly, their unique structure based on covalently-linked chains in the z-direction (low-dimensional structure) gives rise to anisotropic optoelectronic properties, which can result in enhanced charge carrier transport when the material is correctly oriented in the (001) crystallographic direction. Sb-chalcogenides also have high absorption coefficients, optimal bandgap for solar energy conversion, and they are constituted by earth-abundant low-toxic elements. Similarly, pnictogen chalcogenides are recently gaining a lot of attention, showing great potential as PV candidates. In addition to the aforementioned properties originating from vdW structure, the antibonding character of their valence band together with the conduction band consisting of an extension of p-states, results in a highly dispersive character for both bands, which can lead to defect tolerant properties, similar to those of Pb-halide perovskites. However, the particular vdW structure also leads to a complicated morphology consisting of randomly oriented needle-shaped crystals, which is clearly inadequate for the design of conventional thin film solar cells. Therefore, it is necessary to explore new alternatives to obtain more compact and uniform morphologies.

In this work, the formation dynamics of SbSI and SbSeI compounds from the selective halogenation of precursors Sb₂S₃ and Sb₂Se₃ has been investigated. In particular, the effects of different reaction pathways are analyzed in detail. These reactions are divided into convection-controlled and diffusion-controlled processes. For the first case, a series of experiments are carried out in high pressure and large volume tubular furnaces, where the effects of pressure and temperature as well as duration have been studied. In this case, high pressures are necessary to prevent the decomposition of the resulting compound at high temperatures. In the second case, the same reactions are carried out in the reduced volume of a close-space sublimation (CSS) reactor. A thin film deposition system is innovatively used as a reaction medium. In this case, the control of the decomposition is facilitated by the saturation of the atmosphere with the halide source (i.e., SbI₃). In addition to the effect of convection or diffusion-controlled processing, other synthesis routes have been investigated, including the reaction of previously deposited chalcogen and halide layers (solid-solid or solid-liquid reaction), which offers interesting possibilities for very high-pressure systems where evaporation is disabled and a fully diffusive solid-state reaction is favored. The differences between the two reaction pathways are clear, confirming that the diffusion-controlled process has much slower kinetics. Indeed, it has been observed that for processes of the same duration, the reaction is not complete in the diffusion-controlled case, suggesting that longer processes are necessary. The study is supported by microscopy and energy-dispersive X-ray spectroscopy analyses, which demonstrate the formation of large and compact micro-columns. The evolution of the reaction has been studied by X-ray diffraction in order to evaluate the reaction kinetics. In addition, photovoltaic devices have been developed using both methodologies. Temperature-dependent current-voltage and external quantum efficiency measurements have been performed.

9:30 AM EN11.04.05

Theoretical and Experimental Characterization of Highly Anharmonic Chalcogenide Anti-Perovskites for Energy Applications [Pol Benítez Colominas](#)¹, Ivan Caño Prades¹, Cong Liu¹, Cibrán López Álvarez¹, Jonathan Turnley², Rakesh Agrawal², Edgardo Saucedo¹ and Claudio Cazorla¹; ¹Universitat Politècnica de Catalunya, Spain; ²Purdue University, United States

Silver chalcogenide antiperovskites (AH) are a family of materials with chemical formula Ag₃BC where B=S, Se and C=Cl, Br, I. These are interesting energy materials that present suitable thermal stability and optoelectronic properties for applications in photovoltaics, solid-state batteries and fuel cells [1, 2]. Few experimental works have already reported the structural and ionic transport properties of Ag₃sBr and Ag₃SI [3], and recently a facile synthesis method has been proposed for them [4]. Nevertheless, a detailed description and understanding of the phase competition and thermodynamic properties of AH is still lacking, both at the experimental and theoretical levels, hence their thermodynamic and structural properties remain relatively unknown to date. Here, we present a comprehensive computational and characterization study of this family of materials, based on first principle calculations (DFT), as well as structural and optoelectronic measurements, which endorse the validity of the employed simulation approaches. Ag₃SBr and Ag₃SI polycrystalline thin films have been synthesized by a low-temperature solution-based methodology using thiol-amine molecular precursor inks. Then, structural and optical properties have been investigated by X-ray diffraction, microscopy and photothermal deflection spectroscopy experiments, demonstrating cubic anti-perovskite structure for both Ag₃SBr and Ag₃SI (Pm-3m and Im-3m respectively), and measured bandgaps in the 0.9-1.0 eV range. Interestingly, Ag₃S(Br1-xIx) solid solutions have been successfully synthesized, showing a bandgap bowing effect (bandgap increases, saturates after a certain value of x, and then decreases again). Thin film prototype solar cells have been prepared using Ag₃SBr and Ag₃SI absorbers (FTO/TiO₂/AH/P3HT/Au superstrate device structure), showing photo-active response and Voc values up to 150 mV. For theoretical calculations, we performed a thorough exploration of the

zero-temperature polymorphism of AH by using advanced crystal structure prediction and DFT methods. Several previously overlooked stable phases were thus predicted and studied for the six analysed parent compounds; for example, a cubic phase with space group P2₁3 for Ag₃SBr and an orthorhombic phase with space group P2₁2₁1 for Ag₃SeBr. Ab initio molecular dynamics (AIMD) simulations were also performed at different temperatures to take into account the effects of anharmonicity (i.e., electron-phonon coupling) and ionic diffusivity on the optoelectronic properties of AH. Remarkably, it was found that temperature-renormalization effects on the band gap of AH are giant (i.e., decrease it around 40% decreasing for Ag₃SBr) and necessary to provide good agreement with the experiments. Thus, these materials could be exploited for applications in which materials with strongly temperature-dependent electronic properties are required.

[1] PALAZON, Francisco. Metal chalcogenides: next generation photovoltaic materials?. *Solar RRL*, 2022, 6.2: 2100829.

[2] LIU, Zhiyang, et al. Bandgap engineering and thermodynamic stability of oxyhalide and chalcogenide antiperovskites. *Ceramics International*, 2021, 47.23: 32634-32640.

[3] HOSHINO, S., et al. Phase transition of Ag₃SX (X= I, Br). *Solid State Ionics*, 1981, 3: 35-39.

[4] SEBASTIÁ-LUNA, Paz, et al. Chalcogenide Antiperovskite Thin Films with Visible Light Absorption and High Charge-Carrier Mobility Processed by Solvent-Free and Low-Temperature Methods. *Chemistry of Materials*, 2023, 35.16: 6482-6490.

9:45 AM EN11.04.06

Photovoltaic Cu₃PS₄ Films via a Combinatorial Synthesis Platform Dedicated to Multi-Anion Semiconductors [Lena A. Mittmann](#), Javier Sanz Rodrigo and Andrea Crovetto; Technical University of Denmark, Denmark

Inorganic phosphosulfides – materials containing phosphorus, sulfur, and at least one metal – are a vast and chemically-versatile family of materials. Since metal phosphides and metal sulfides are among the highest-performing optoelectronic semiconductors, it seems reasonable to consider the phosphosulfide family as a potential pool of materials for solar cells, photoelectrochemical cells, and light-emitting diodes. Nevertheless, phosphosulfide semiconductors have very rarely been characterized with these applications in mind.

Only 258 out of over 320,000 chemically plausible phosphosulfides (up to quaternaries) have been synthesized in some form, and just a handful of them have been optoelectronically characterized. Thus, there is significant opportunity for new discoveries, but conventional synthesis approaches would be inefficient and tedious.

In the first part of this contribution, we will present our unique suite of high-throughput thin-film deposition tools dedicated to phosphosulfides and other sulfur-containing multi-anion semiconductors. The main high-throughput synthesis method we use for this project is based on reactive sputtering to generate combinatorial material libraries with two perpendicular gradients. The first gradient goes from sulfur rich to phosphorus rich while the second gradient goes from metal A rich to metal B rich, resulting in a variety of different stoichiometries for, e.g., quaternary phosphosulfides. The deposition suite also includes a rapid thermal annealing furnace with access to reactive sources of sulfur and phosphorus, as well as a separate evaporator for incorporating volatile metals. The whole system is glove-box integrated.

In the second part of this contribution, we will show the first experimental results on Cu₃PS₄ films, the first directly deposited phosphosulfide film specifically intended as a PV or PEC absorber.[1–4] The experimental results are complemented by computational studies carried out within our group. The computational track has been of crucial importance for obtaining properties that are difficult to measure experimentally, and for interpreting experimental results. Importantly, we show that the photoluminescence decay time of unoptimized Cu₃PS₄ films is already above 100 ns, demonstrating that phosphosulfides deserve close attention by the PV and PEC research community.

[1] Shi T, Yin W-J, Al-Jassim M and Yan Y 2013 Structural, electronic, and optical properties of Cu₃-V-VI₄ compound semiconductors *Appl. Phys. Lett.* **103** 152105

[2] Itthibenchapong V, Kokenyesi R S, Ritenour A J, Zakharov L N, Boettcher S W, Wager J F and Keszler D A 2013 Earth-abundant Cu-based chalcogenide semiconductors as photovoltaic absorbers *J Mater Chem C* **1** 657–62

[3] Foster D H, Jieratum V, Kykyneshi R, Keszler D A and Schneider G 2011 Electronic and optical properties of potential solar absorber Cu₃PS₄ *Appl. Phys. Lett.* **99** 181903

[4] Yin X, McClary S A, Song Z, Zhao D, Graeser B, Wang C, Shrestha N, Wang X, Chen C, Li C, Subedi K K, Ellingson R J, Tang W, Agrawal R and Yan Y 2019 A Cu₃PS₄ nanoparticle hole selective layer for efficient inverted perovskite solar cells *J. Mater. Chem. A* **7** 4604–10

10:00 AM BREAK

SESSION EN11.05: Computational PEC/PV I
Session Chairs: Geoffroy Hautier and Rachel Woods-Robinson
Thursday Morning, April 25, 2024
Room 335, Level 3, Summit

10:30 AM *EN11.05.01

Computational Approaches for Clean Energy Materials: Defect Graph Neural Networks, Equilibria with Interacting Defects and Interface Structure Prediction [Stephan Lany](#); National Renewable Energy Laboratory, United States

Currently, 80% of the global final energy consumption occurs in form of fuels and only 20% as electricity. On the other hand, renewable energy additions come almost exclusively in the form of electricity (dominantly photovoltaics and wind). Thus, a successful energy transition will require enormous growth in renewables, sufficient to convert excess electricity into fuels, as well as the development of non-electricity based solar fuel technologies. As such as photovoltaic capacities have grown over the past 20 years, it is far from clear that current technologies and materials are up to the task to grow from here by yet another factor 100 until 2050. Therefore, sustained research efforts on emerging inorganic semiconductors for solar electricity and fuels are essential for facing the double challenge of climate change and energy security. Computational materials science can make important contributions, guiding and supporting research activities through both materials search and discovery and through detailed studies that help to develop a mechanistic understanding of materials performance and bottlenecks. This presentation will highlight three recent computational projects with relevance for photovoltaics and solar fuels (1) Defect graph neural networks (dGNN) for materials discovery in solar thermochemical hydrogen (STCH) [1]. The dGNN approach facilitates broad and fast materials screening for defect properties. (2) Modeling highly off-stoichiometric systems by evaluating the free energy of defect interaction [2]. This approach allows quantitative prediction of H₂ production in complex STCH oxides. (3) First-principles atomic structure prediction for interfaces [3]. This work showed how an atomically thin CdCl₂ interlayer phase enables in principle ideal electron transport across the incommensurate SnO₂/CdTe interface.

[1] M.D. Witman, A. Goyal, T. Ogitsu, A.H. McDaniel, S. Lany, Nat. Comput. Sci. (2023).

DOI: <https://doi.org/10.1038/s43588-023-00495-2>

[2] A. Goyal, M.D. Sanders, R.P. O'Hayre, S. Lany (submitted).

[3] A. Sharan, M. Nardone, D. Krasikov, N. Singh, S. Lany, *Appl. Phys. Rev.* 9, 041411 (2022).

DOI: <https://doi.org/10.1063/5.0104008>

11:00 AM EN11.05.02

Statistics of Crystal Defects from Dilute Limit to Alloys, Excluded Volume Exchange Interaction and Effective Energetics of Defect Ensembles Mike Scarpulla; University of Utah, United States

Point defects determine the properties of otherwise-perfect semiconductors and insulators, thus computing their concentrations accurately is of prime importance. Typically, the dilute limit is assumed leading to Boltzmann statistics, however it is obvious that multiple defects or defect complexes cannot occupy the same site at the same time. Herein, we present closed-form expressions for point defect statistics applicable for all concentrations; thus unifying defect and alloy theories. These expressions prevent unphysical prediction of more defects than available sites when either a) any defect of type j in charge state q has zero or negative formation energy ΔE_j^q (e.g. charged defects at certain Fermi energies) or more interestingly b) when multiple defects and/or charge states have small ΔE_j^q compared to the thermal energy $k_B T$. An important insight is that different statistics arise if 1) host atom or 2) site conservation is assumed: Case 1 corresponds to a finite crystal with N_0 sites and moving displaced host-crystal atoms to extra unit cells on the surface, while Case 2 corresponds to an infinite crystal with N_0 sites per volume and moving displaced host-crystal atoms into external reservoirs (e.g. the case corresponding to modern DFT supercell calculations).

Analogously to quantum Fermions but classical in origin, the mutual exclusion between defects of any type can be conceptualized as an exchange interaction energy. Additionally, we demonstrate that multiple charge states of a defect, multiple configurations of a charge state, or other arbitrary subgroups of defects and complexes can be gathered together into objects having effective formation energy. This allows, for example, plotting the finite-temperature formation enthalpy of a defect having multiple charge states as a continuous function of Fermi level or using an effective chemical potential to enforce constraints on subgroups of defects, amongst other applications.

These fundamental tools add flexibility and accuracy to quantitative defect calculations and join smoothly to thermodynamics of solutions and alloys while adding only minor computational costs.

11:15 AM EN11.05.03

Doped: A Python Package for Solid-State Defect and Dopant Calculations Seán R. Kavanagh¹, David O. Scanlon² and Aron Walsh³; ¹Harvard University, United States; ²University of Birmingham, United Kingdom; ³Imperial College London, United Kingdom

Defect-induced non-radiative recombination typically represents the dominant limiting factor in the efficiencies of emerging inorganic solar cells / photocatalysts.^{1,2} Computational methods are widely used to predict defect behavior in solar materials, before combining and comparing theoretical predictions with experimental measurements. However, there are many critical stages in the computational workflow for defects, which, when performed manually, not only leave room for human error but also consume significant researcher time and effort. Moreover, there are growing efforts to perform high-throughput defect investigations,³⁻⁵ necessitating robust, user-friendly and efficient software implementing this calculation workflow.

Here we report *doped*, our python package for the full generation, calculation setup, post-processing and analysis of defect supercell calculations.^{2,6-9} The generation and thermodynamic analysis (i.e. defect formation energy diagrams, chemical potentials, doping analysis etc.) are agnostic to the underlying first-principles software, while input file generation is supported for several of the most widely-used DFT codes, including VASP, FHI-aims, CP2k, Quantum Espresso and CASTEP. A defect charge state prediction algorithm is implemented, which is shown to significantly outperform previous oxidation-state approaches in terms of both efficiency and completeness. Moreover, *doped* is built to be compatible with other computational toolkits for advanced defect characterisation, including *ShakeNBreak*¹⁰ for defect structure-searching, *py-sc-fermi*¹¹ for in-depth concentration, doping and Fermi level analysis, and *CarrierCapture.jl*¹²/*nonrad*¹³ for non-radiative recombination calculations. Its object-oriented python framework make it readily-usable in high-throughput architectures such as *atomate*(2) or *AiiDA*, with examples included in the documentation.

We will discuss the key features of *doped* for computational defect workflows, exemplified with relevant solar cell materials (CdTe, Sb₂Se₃, *t*-Se). We anticipate that *doped* will serve as a highly useful tool for computational defect researchers, being an efficient platform for conducting reproducible calculations of solid-state defect properties.

1 Y.-T. Huang et al, *Nanotechnology*, 2021, **32**, 132004.

2 S. R. Kavanagh et al, *ACS Energy Lett.*, 2021, **6**, 1392–1398.

3 D. Dahliah et al, *Energy Environ. Sci.*, 2021, **14**, 5057–5073.

4 pymatgen-analysis-defects, <https://materialsproject.github.io/pymatgen-analysis-defects/intro.html>

5 D. Broberg et al, *npj Comput Mater*, 2023, **9**, 1–12.

6 Y.-T. Huang & S. R. Kavanagh et al *Nat Commun*, 2022, **13**, 4960.

7 S. R. Kavanagh et al *Faraday Discuss.*, 2022, **239**, 339–356.

8 A. Nicolson et al, *Journal of Materials Chemistry A* 2023.

9 S. R. Kavanagh, *doped* v.2.0.5 Zenodo 2023.

10 I. Mosquera-Lois & S. R. Kavanagh et al, *Journal of Open Source Software*, 2022, **7**, 4817.

11 A. G. Squires et al, *Journal of Open Source Software*, 2023, **8**, 4962.

12 S. Kim et al, *Journal of Open Source Software*, 2020, **5**, 2102.

13 M. E. Turiansky et al, *Computer Physics Communications*, 2021, **267**, 108056.

11:30 AM EN11.05.04

High-Throughput Virtual Screening of Novel Ternary Phosphosulfides for Photovoltaic Applications Javier Sanz Rodrigo, Andrea Crovetto, Lena A. Mittmann and Ivano Eligio Castelli; DTU, Denmark

In order to improve the efficiency of solar cells, stable materials with suitable optoelectronic properties must be found. For this purpose, phosphosulfides offer a large and varied range of semiconductors with very diverse compositions, structures, and therefore, optoelectronic properties. This is mainly due to the wide range of oxidation states that phosphorus can take in this class of materials (from -3 to +5). We are currently studying phosphosulfides for solar energy by a multi-faceted approach, including first-principles calculations, high-throughput experiments, and machine learning.

It is estimated that the number of chemically-plausible ternary phosphosulfides is close to 1800, yet just around 100 have been synthesized, and only a handful have been investigated for PV or PEC applications. A high-throughput screening is reported here for over 800 of these materials, obtained from metal substitution in 67 structural prototypes reported in the Materials Project, resulting in some completely unknown potential candidates as wide-gap solar cell absorbers in tandem solar cells. On top of these simple elemental substitutions, we have also explored some previously unreported phosphosulfide stoichiometries, based on analogy with other pnictogens (N, As, Sb) and chalcogens (Se, Te). Unlike the case of most of the already-known phosphosulfides, these structures have phosphorus-rich stoichiometries, which appears to be correlated with favorable optoelectronic properties.

The initial criteria for the screening process are thermodynamic stability, intermediate band gaps and low effective masses. As a result, around 100 new phosphosulfide materials potentially suitable for solar cell applications are obtained from this virtual screening. Most of these compounds are not present in computational materials databases and have never been synthesized. More detailed calculations on a selected subset of these new materials suggest that a few of them deserve experimental investigation as PV absorbers.

The large volume of materials screened gives us a unique opportunity to identify composition-structure-property trends in phosphosulfides with special emphasis on optoelectronic energy conversion applications. We will show how these trends can be used to design new optoelectronic phosphosulfides beyond ternary systems.

11:45 AM EN11.05.05

First-Principles Studies of The Role of Cation Disorder on The Electronic and Optical Properties of Photoactive ZnTiN₂ Sijia Ke^{1,2}, John Mangum³, Andriy Zakutayev³, Annie Greenaway³ and Jeffrey B. Neaton^{1,2,4}; ¹University of California, Berkeley, United States; ²Lawrence Berkeley National Laboratory, United States; ³National Renewable Energy Laboratory, United States; ⁴Kavli Energy NanoScience Institute, United States

The recently synthesized wurtzite-derived nitride semiconductor ZnTiN₂ exhibits promising properties for photoelectrochemical (PEC) applications, including an optically measured band gap appropriate for PEC reactions, high potential for integration with high-performing semiconductors, and the formation of self-passivating surface layers under operating conditions. Similar to other heterovalent ternary nitrides, experimentally synthesized ZnTiN₂ thin film features a large concentration of antisite defects, or cation disorder, which can have significant effects on its electronic and optoelectronic properties, and which has been used to rationalize the large difference between experimental absorption onset around 2 eV and theoretical fundamental band gap of cation-ordered ZnTiN₂ of 3.4 eV. Using state-of-the-art first-principles density functional theory calculations with non-empirical optimally-tuned hybrid functionals on nearly one hundred large supercells, we compute the energetics, electronic structure, and optoelectronic properties of cation-disordered ZnTiN₂. Energetically preferable and undesirable local atomic arrangements are identified. We also demonstrate that cation disorder-induced local charge imbalance broadens the valence and conduction bands near band edges, leading to a reduction in band gap relative to the cation-ordered phase, a mechanism that can be extended to the family of multivalent ternary nitrides. Accounting for cation disorder, our calculated optical absorptions agree well with experiments. Our work reveals the nature of cation disorder and its influence in ZnTiN₂ in light of possible solar energy applications.

This work is supported by the Liquid Sunlight Alliance, a DOE Energy Innovation Hub; computational resources provided by NERSC.

SESSION EN11.06: Computational PEC/PV II
Session Chairs: Annie Greenaway and Sebastian Siol
Thursday Afternoon, April 25, 2024
Room 335, Level 3, Summit

1:30 PM *EN11.06.01

Accelerating The Search of New Solar Absorbers for Thin-Film Photovoltaic Using High-Throughput Computational Screening [Geoffroy Hautier](#); Dartmouth College, United States

Thin film photovoltaic technology has advantages to single-crystal silicon in terms of flexibility, lower energy manufacturing needs or potential for tandem cells. However, the high efficiency technologies available (e.g., CIGS, CdTe or halide perovskites) have all issues in terms of cost, abundance or long-term stability. Finding new solar absorber is a cumbersome process involving complex synthesis and characterization. First principles computations on the other hand offers an attractive way to speed up this process. Here, we will report on a large scale high-throughput computational search for new solar absorbers among known inorganic materials. Importantly, the need for high carrier lifetime is taken into account by considering in the screening intrinsic defects and their role as potential Shockley-Read-Hall recombination centers. Screening 30,000 known inorganic compounds, we identify a handful very promising solar absorbers combining large optical absorption in the visible, good transport properties and high carrier lifetime. I will discuss the chemistries that we found and highlight a few interesting new materials. I will especially focus on BaCd₂P₂, a new phosphide where our experimental follow-up work confirms the promising properties including adequate band gap but also long carrier lifetime. We also show that this new material is extremely stable even in harsh conditions. I will finish my talk by discussing how large data sets of defect computations can also be used to test and develop design principles for solar absorbers with “defect-tolerance”.

2:00 PM EN11.06.02

First Principles Phase Diagram and Electronic Structure Properties of Potassium-Based Copper Chalcogenide Alloys for Photocathode Applications [Arini Kar](#), Balasubramaniam Kavaipatti and Dayadeep S. Monder; Indian Institute of Technology Bombay, India

A recent high throughput study of copper-based semiconductors has identified potassium-based copper chalcogenides as optimal light absorbers in PV/PEC devices. In this work, we investigate the applicability of KCuTe_{1-x}Se_x and KCuSe_{1-x}S_x as photocathode materials. We first calculate the temperature-composition phase diagram of KCuTe_{1-x}Se_x and KCuSe_{1-x}S_x via solid solution model and cluster expansion-based Monte Carlo simulations. Our calculations predict a miscibility gap up to a maximum critical temperature of 243 K beyond which the alloy forms a solid solution in the hexagonal structure over the entire composition range. Similarly, KCuSe_{1-x}S_x forms a solid solution in orthorhombic structure, although ordered ground states at x = 0.25, 0.333, 0.5, 0.667, 0.75 and 0.833 are present at low temperatures. Based on the stable structure of the alloys we calculate the electronic structure properties via DFT. Unlike the bandgap bowing typical of highly mismatched alloys, predicted by band-anticrossing (BAC) model the electronic band gap of potassium-based copper chalcogenide alloys obeys Vegard's law. The conduction band of these alloys is appropriately aligned with respect to the hydrogen reduction reaction and suggests the utility of these alloys as a photocathode.

2:15 PM EN11.06.03

Computational Screening of Pre- and Post-Transition Metal Oxides and Sulfides for Photocatalytic Hydrogen Generation [Simon Gelin](#)¹, Nicole E. Kirchner-Hall¹, Rowan R. Katzbaer¹, Monica J. Theibault², Yihuang Xiong¹, Cierra Chandler¹, Mohammed Khan¹, Steven Baksa¹, Matteo Cococcioni³, Iurii Timrov⁴, Hector Abruna², Raymond Schaak¹ and Ismaila Dabo¹; ¹The Pennsylvania State University, United States; ²Cornell University, United States; ³University of Pavia, Italy; ⁴École Polytechnique Fédérale de Lausanne, Switzerland

Discovering efficient and scalable photocatalysts for water splitting is a major challenge for the sustainable production of carbon-free hydrogen. In this presentation, we tackle that challenge and expand the list of known water-splitting photocatalysts using data-intensive screening based on accurate first-principles calculations of band gaps, band edges, and free energies of electrochemical decomposition. Building on previous studies [1,2] which show that

inserting pre-transition (*s*-block) metals in binary metal oxides can improve redox activity while preserving solar absorption, we specifically target the family of post-transition (*p*-block) metal oxides. We analyze the influence of adding *s*-block cations on the band gaps and band edges of these materials and on their photocatalytic efficiency. Based on this analysis, we screen 109 ternary metal oxides and identify nine candidates, among which two appear to not have been previously proposed as water-splitting photocatalysts [3]. We then extend these results to the family of ternary *s*- and *p*-block metal sulfides, leading to the discovery of additional photoactive compounds, which warrants further studies [4].

[1] Xiong et al., *Energy Environ. Sci.* (2021) 14, 2335–2348. DOI: 10.1039/D0EE02984J

[2] Katz et al., *Adv. Energy Mater.* (2022) 2201869. DOI: 10.1002/aenm.202201869

[3] Gelin et al., submitted to *PRX Energy* (2023). arxiv:2303.03332

[4] Katz et al., submitted to *ACS Energy Letters* (2023)

2:30 PM *EN11.06.04

Navigating The Vast Materials Landscape for Photovoltaics with NOMAD Jose Marquez Prieto; Humboldt University of Berlin, Germany

Accelerating the development of innovative solar materials demands a fundamental transformation in lab methods, particularly in enhancing efficiency in production, characterization, and device integration. Numerous research labs are beginning to adopt more efficient methods to achieve the necessary acceleration, including high throughput computation and experimentation, and the emergence of some autonomous labs. All these efforts generate a massive volume of data that needs to be organized, automated and made ready for AI analyses and programmatic access.

This talk offers insight into how NOMAD (<https://nomad-lab.eu>), an open-source platform developed by the NFDI (Germany's National Research Data Infrastructure) consortium FAIRmat (<https://fairmat-nfdi.eu>), can help individuals and labs in this task. NOMAD is designed to tackle these challenges by enhancing the accessibility and usefulness of materials science data following the FAIR principles - making data Findable, Accessible, Interoperable, and Reusable. I will overview the dynamic improvements within the NOMAD infrastructure beyond computational materials science, specifically tailored for experimental solar cell research, and highlight an application created for detailed visualization and investigation of a broad, AI-ready solar cell dataset. As an illustration, I will examine the historical advancement of charge transport layers for perovskite solar cells using network analysis, demonstrating how it is possible to navigate effectively this extensive materials space.

To provide a digitization platform for experimental developments, the NOMAD platform incorporates a flexible electronic lab notebook (ELN), configured for customization to meet the specific needs of individual research laboratories, thereby facilitating the efficient capture, transfer, and processing of AI-ready data and metadata within a well-organized FAIR database framework.

Ultimately, this presentation aims to illuminate the path forward in the realm of semiconductor materials for solar applications, guided by data-centric methodologies and collaborative infrastructures like NOMAD, which are indispensable in accelerating the journey toward efficient and sustainable solar energy solutions.

3:00 PM BREAK

SESSION EN11.07: Nitride PEC

Session Chairs: Jose Marquez Prieto and Vladan Stevanovic

Thursday Afternoon, April 25, 2024

Room 335, Level 3, Summit

3:30 PM *EN11.07.01

Accelerating The Development of Semiconductor Thin Films through Advanced Automated Characterization. Sebastian Siol; Empa-Swiss Federal Institute of Materials Science and Technology, Switzerland

The discovery of new functional materials remains a key challenge in the development of next-generation sustainable technologies. Fueled by advances in high-throughput computation, new exciting materials are being predicted at an ever-increasing rate. Combinatorial high-throughput materials science techniques hold the promise to match this rate by facilitating the rapid exploration of complex phase spaces. Today, combinatorial materials science workflows are employed in many laboratories around the world. While gradient deposition of combinatorial thin-film libraries can be implemented in most standard deposition equipment, a comprehensive tool box for rapid materials characterization which is just as crucial is often harder to realize. In this presentation, it will be shown how accelerated thin-film materials development is performed in the Coating Technologies group at Empa. We employ a workflow consisting of reactive combinatorial physical vapor deposition, automated characterization and semi-automated data analysis which covers most common thin-film characterization techniques as well as functional property mapping. In recent years, we extended this infrastructure to include high-throughput surface analysis, but also optical measurement setups for accelerated aging studies. This extension not only complements the existing workflows, but provides additional insights that were previously much harder to obtain. It will be shown how surface analysis mapping can facilitate the discovery of new semiconductor materials in complex phase spaces, such as the wide band gap nitride semiconductors $Zn_2VN_3[1,2]$ or $Zn_2TaN_3[3]$. In addition, it will be shown how accelerated optical aging studies combined with machine-learning assisted data analysis can generate insights into the operational stability and degradation kinetics of more volatile materials.[4] The results presented here showcase the potential of integrating advanced characterization techniques into high-throughput materials science workflows for the rapid development of new energy materials.

[1] S. Zhuk, A. Kistanov, S. Boehme, N. Ott, F. La Mattina, M. Stiefel, M. V. Kovalenko, S. Siol, *Chem. Mater.* 2021, 33, 23, 9306–9316

[2] S. Zhuk, S. Siol, *Appl. Surf. Sci.* 2022, 601, 154172.

[3] S. Zhuk, A. Wieczorek, A. Sharma, J. Patidar, K. Thorwarth, J. Michler, S. Siol, *Chem. Mater.* 2023, 35, 17, 7069–7078

[4] A. Wieczorek, A. Kuba, J. Sommerhäuser, L. N. Caceres, Q. Guesnay, C. Wolff, S. Siol, *unpublished results*

4:00 PM EN11.07.02

Co-Design of Zinc Titanium Nitride Semiconductor towards Durable Photoelectrochemical Applications John Mangum¹, Sijia Ke^{2,3}, Andriy Zakutayev¹, Jeffrey B. Neaton^{2,3,2} and Annie Greenaway¹; ¹National Renewable Energy Laboratory, United States; ²University of California, Berkeley, United States; ³Lawrence Berkeley National Laboratory, United States

Development of photoelectrochemical (PEC) systems requires, among other advances, photoelectrode materials that are both photocatalytically active and stable in harsh electrochemical environments. We have intentionally searched for a candidate photoabsorber based on co-design principles, wherein design for photoactivity is based on the ability to integrate the new material with established semiconductors and design for stability is based on the propensity for

the photoabsorber to self-passivate during operation. This has led to the first synthesis and substantial development of wurtzite ZnTiN₂ as a photoabsorber. Initially, high-throughput combinatorial synthesis was used to identify the radio-frequency co-sputtering parameter space for ZnTiN₂.¹ Cation disorder in these films reduced the bandgap to ~2.0 eV, appropriate for solar fuel generation, and the ZnTiN₂ surface was found to transform to stable oxides under CO₂R-relevant electrochemical conditions. Together, these characteristics indicate that ZnTiN₂ could be used as a photoelectrode, but the optoelectronic and crystalline properties of the material would require substantial improvement before operation in PEC applications. Next, experimental integration of ZnTiN₂ with established semiconductor systems allowed us to rapidly improve the crystalline and optoelectronic properties of the sputtered ZnTiN₂ films, paving the way for high photocatalytic activity for PEC to be demonstrated using this semiconductor. We will report on materials quality advances in ZnTiN₂ thin films as well as progress toward demonstration of this material as a photoelectrode. Future work will focus on developing PEC device structures based on the improved ZnTiN₂ photoelectrode films by optimizing semiconductor properties (e.g. doping) and interfaces with surrounding device layers.

(1) Greenaway, A. L.; Ke, S.; Culman, T.; Talley, K. R.; Mangum, J. S.; Heinselman, K. N.; Kingsbury, R. S.; Smaha, R. W.; Gish, M. K.; Miller, E. M.; Persson, K. A.; Gregoire, J. M.; Bauers, S. R.; Neaton, J. B.; Tamboli, A. C.; Zakutayev, A. Zinc Titanium Nitride Semiconductor toward Durable Photoelectrochemical Applications. *J. Am. Chem. Soc.* **2022**, *144* (30), 13673–13687. <https://doi.org/10.1021/jacs.2c04241>.

4:15 PM EN11.07.03

Defect Engineering of Ta₃N₅ Photoanodes: Enhancing Charge Transport and Photoconversion Efficiencies via Ti Doping [Laura I. Wagner](#)^{1,2}, Elise I. Sirotti^{1,2}, Oliver Brune^{1,2}, Gabriel Groetzner^{1,2}, Johanna Eichhorn^{1,2}, Saswati Santra^{1,2}, Frans Munnik³, Simone Pollastri⁴, Luca Olivi⁴, Dennis Friedrich⁵, Verena Streibel^{1,2} and Ian D. Sharp^{1,2}; ¹Walter Schottky Institute, Germany; ²TU Munich, Germany; ³HZDR, Germany; ⁴Elettra, Italy; ⁵HZB, Germany

Ta₃N₅ shows great potential as a semiconductor photoanode for solar fuel applications. However, its performance is hindered by poor charge carrier transport and trapping due to a high density of defects that introduce electronic states deep within its bandgap. Here, we demonstrate that controlled Ti-doping of Ta₃N₅ can dramatically reduce the concentration of deep-level defects and enhance its photoelectrochemical performance, yielding a seven-fold increase in photocurrent density and a 300 mV cathodic shift in onset potential compared to undoped material.[1] Comprehensive characterization, including structural, compositional, optical, electrical, and photoelectrochemical methods, reveals that Ti⁴⁺ ions substitute Ta⁵⁺ lattice sites, thereby introducing compensating acceptor states, reducing concentrations of nitrogen vacancies, and reduced Ta³⁺ states, and suppressing trapping and recombination. Importantly, Ti doping offers distinct advantages compared to Zr, an intensively investigated dopant in the same group. Specifically, Ti⁴⁺ and Ta⁵⁺ have more similar atomic radii, allowing for substitution without introducing lattice strain, and Ti exhibits a lower affinity for oxygen than Zr, enabling its incorporation without increasing the oxygen donor content. Consequently, we demonstrate that Ti doping decreases the conductivity immensely by lowering the charge carrier density but simultaneously increases the mobility of free charge carriers due to reduced recombination at nitrogen vacancies. Thus, these findings provide a powerful basis for precisely engineering the optoelectronic characteristics of Ta₃N₅ and to substantially improve its functional characteristics as an advanced photoelectrode for solar fuel applications.

[1] L.I. Wagner, *Adv. Funct. Mater.* **2023**, 2306539

4:30 PM EN11.07.04

Transition Metal Coated Single Crystalline BiVO₄ Photoanode for Photoelectrochemical Chlorine Generation [Zhaoyi Xi](#)^{1,2}, Chenyu Zhou¹, Kim Kisslinger¹, Xiao Tong¹ and Mingzhao Liu¹; ¹Brookhaven National Laboratory, United States; ²Stony Brook University, The State University of New York, United States

Bismuth vanadate (BiVO₄) is an outstanding photoanode material for photoelectrochemical water splitting. In this work, a series of single crystalline BiVO₄ photoanodes are synthesized by pulsed laser deposition (PLD). Once coated with a thin layer of cobalt oxides (CoO_x) co-catalyst, also by PLD, the photoanodes support efficient photoelectrochemical generation of chlorine (Cl₂) from brine under simulated solar light. Activity of the chlorine generation reaction (CIER) is optimized when the thickness of CoO_x is about 3 nm, with the faradic efficiency of CIER exceeding 60%. Detailed studies show that the CoO_x co-catalyst layer is amorphous, uniform in thickness, and chemically robust. As such, the co-catalyst also effectively protects the underlying BiVO₄ photoanodes against chlorine corrosion. The other metal oxides cocatalysts are also compared, detailed mechanism on how the cocatalyst layers influence the performance of BiVO₄ photoanode is revealed. This work provides insights on using artificial photosynthesis for by-products that carries significant economic value while avoiding the energetically expensive oxygen evolution reactions.

4:45 PM EN11.07.05

Heterostructured Hematite Photoanodes featuring C₃N₄ with In-Situ Grown Ni-CoP_x for Boosted Photoelectrochemical Water Oxidation [Mengya Yang](#), Anna Hankin and Salvador Eslava; Imperial College London, United Kingdom

The high demand for renewable and clean energy resources has led to the rapid development of cutting-edge materials for photoelectrochemical (PEC) water splitting. However, the question of how to enhance solar conversion efficiency remains a persistent challenge. In line with this, we present a novel constructive strategy for a ternary-material-system photoanode, aimed at simultaneously improving charge separation and transfer, as well as water oxidation efficiency. Specifically, we demonstrate the PEC efficiency of composite Ti-Fe₂O₃/CN/NCP photoanodes obtained by loading hierarchical C₃N₄ (CN) nanosheets anchored with in-situ grown Ni-doped CoP_x (NCP) onto porous Ti-doped hematite (Ti-Fe₂O₃) photoanodes. The resulting Ti-Fe₂O₃/CN/NCP photoanodes exhibit a remarkable enhancement of photocurrent density (2.01 mA cm⁻² at +1.23 V_{RHE}) compared to Ti-Fe₂O₃ photoanodes (0.28 mA cm⁻² at +1.23 V_{RHE}). It is noteworthy that CN and NCP serve to deplete photogenerated electrons and remove photogenerated holes directionally from the surface of Ti-Fe₂O₃. This leads to the facile transfer and separation of electron-hole pairs necessary for exceptional catalytic performance. Moreover, we undertake a systematic analysis of the role of CN and NCP to gain deeper insights into the underlying mechanisms for the superior PEC water oxidation process.

SESSION EN11.08: Poster Session II
Session Chairs: Andrea Crovetto and Xiaojing Hao
Thursday Afternoon, April 25, 2024
Flex Hall C, Level 2, Summit

5:00 PM EN11.08.02

Stress-Induced Charge Redistribution at Grain Boundaries in Various Alkali Treated Flexible Cu(In,Ga)Se₂ Solar Cells [Ha Kyung Park](#)¹,

Kanghoon Yim², Jiyeon Lee¹, Jihye Gwak², Kihwan Kim² and William Jo¹; ¹Ewha Womans University, Korea (the Republic of); ²Korea Institute of Energy Research, Korea (the Republic of)

In recent development, efficiency of flexible Cu(In,Ga)Se₂ (CIGS) solar cells has exceeded 22%, marking a significant step towards commercial viability. [1] In particular, the deliberate alkali treatment boosted their efficiency, yielding a comparable effect to diffused alkali from soda-lime glass substrate. Besides alkali treatment, understanding stress-induced properties is crucial to maximize their performance. In this study, effects of alkalis on charge distribution under stress was investigated. Four flexible CIGS solar cells using a polyimide substrate were prepared with various alkali post deposition treatment including heavy alkalis (Rb and Cs). Among the CIGS solar cells, Na only treated sample showed the highest performance with an efficiency of 16.9% due to the highest carrier density and fill factor. Segregation of alkalis towards grain boundaries (GBs) was observed through transmission electron microscopy. Especially, Rb and Cs added after Na treatment occupied the GBs repelling the existed Na. Furthermore, surface charge transport under stress were probed via conductive-atomic force microscopy with curved holder. [2] Alkali treated CIGS thin film showed enhanced surface current along the GBs compared to CIGS without alkalis. Notably, surface current was degraded under convex bending state and the degradation was lower in the alkali treated CIGS. To explain the current distribution, defect energy levels were calculated using density functional theory and alkali related defects induced additional acceptors contributing to an increase in surface current. Additionally, energy level of electrically active defects changed with existence of compressive or tensile stress. As part of the future work, degradation of surface current will be quantitatively analyzed focusing on the redistribution of charges under stress.

[1] <https://www.pv-magazine.com/2022/10/11/swiss-scientists-achieve-22-2-efficiency-for-flexible-cigs-solar-cell/> (access: October 16th, 2023)

[2] H. K. Park et al., *npi Flexible Electronics* 6 (2022) 91.

5:00 PM EN11.08.03

Influence of The Growth Method of Sb₂Se₃ Absorber Layer for Thin-Film Solar Cells Víctor Bonal¹, Yudania Sánchez², Sanja Djurdjic Mijin¹, Iván Martín-Infantes¹, Fernando Chacón³, Snezana Ladic¹, Rosalia Serna³ and Raquel Caballero³; ¹Universidad Autonoma de Madrid, Spain; ²IREC, Catalonia Institute for Energy Research, Spain; ³Instituto de Óptica, IO-CSIC, Spain

In recent years, photovoltaic devices have gained considerable attention due to their potential to address the environmental problems associated with traditional energy resources, offering a clean and sustainable solution to meet the growing global energy demand through the direct conversion of solar radiation into electricity. Thin film solar cells (TFSC) have emerged as a suitable alternative to the traditional silicon technology. The best results in TFSC have been produced using CIGS and CdTe, but they use materials that are either toxic or scarce in the earth crust, limiting the future implementation of this technology. Other promising materials such as perovskite present toxicity and stability problems and the complexity of the growth control of CZTSSe kesterite-type material limits the device performance.

This is why there is a need for simple and stable compounds, with a low toxicity and earth-abundant materials. Among the many available candidates, binary Sb chalcogenides have emerged as promising alternatives due to their optoelectronic properties and good stability. Among them, Sb₂Se₃ has attracted interest not only as an absorber for photovoltaics, where it has already reached efficiencies above 10% [1], but also in battery and photochemical applications. Sb₂Se₃ presents a high absorption coefficient, which allows to reduce the absorber film thickness to 100-500 nm, a band gap energy of 1.2 eV, p-type conductivity, a high stability, and a low melting point, requiring low processing temperatures. In addition, this material presents a quasi-1D crystal topology, which could be one of its main advantages for high performance PV. This chain-structure provokes anisotropy in electrical conductivity, edge absorption and carrier transport. For this, the control of the fabrication process is crucial to obtain high efficiency solar cells.

In this work, we propose two different methods to prepare Sb₂Se₃ films to be used as absorber in a photovoltaic solar cell. The first one consists in the evaporation of a Sb film on top of Mo/SLG and SLG substrates followed by a thermal treatment in the presence of elemental Se under Ar atmosphere. The second method is the direct evaporation of Sb₂Se₃ into the substrate using vapor transport deposition (VTD). Both methods have been studied to prepare Sb₂Se₃ thin films of different thicknesses in the range 400-1000 nm. The goal of this work is to investigate and compare the properties of Sb₂Se₃ thin films grown by the two deposition methods. For that, the effect of the different fabrication parameters, such as deposition time, maximum temperature, amount of Se added or the temperature difference between source and substrate, on the orientation, morphology, structural, vibrational and optoelectronic properties of Sb₂Se₃ are investigated. The properties of the absorber layer are studied by GIXRD, SEM, AFM, Raman spectroscopy and transmittance measurements. In the case of the VTD process, the variation of substrate temperature is critical for the formation of a compact layer, observing a nanoribbon-type structure when temperature increases up to 400°C. In addition, there is a significant difference on the structure of Sb₂Se₃ when Mo is selenized before the deposition of the absorber layer. However, the selenization of evaporated Sb film leads to a much more compact and uniform morphology. First SLG/Mo/Sb₂Se₃/CdS/iZnO/ITO substrate configuration photovoltaic devices are fabricated, achieving efficiencies of 3.8% for the thinnest active layer of 400 nm. Further studies are being performed to optimize the different growth processes that result in an enhanced solar cell efficiency.

[1] Z. Duan et al., *Adv. Mater.* 2022, 34, 2202969.

5:00 PM EN11.08.04

Synthesis of Complex Pnictide Semiconductors Kirill Kovnir; Iowa State University, United States

Synthesis of complex inorganic materials is often a bottleneck of the materials by design concept. For complex pnictides, thermodynamic and kinetic limitations of conventional synthetic approaches areas are complicated with phase segregation of volatile components, such as P and As, together with extreme reactivity of alkali and alkaline-earth metals towards container materials. Such limitations often resulted in inability to synthesize predicted materials in ternary and quaternary systems with drastically different reactivities of the constituent elements. Several strategies to advance synthesis and produce challenging phases will be discussed, such as averaging precursor reactivity by atomic mixing of refractory components; and prebuilding chemical bonds in the precursor. In-situ studies are crucial for the development of effective synthesis, especially when backed-up with ex-situ synthetic explorations and DSC results.

5:00 PM EN11.08.05

Unveiling The Impact of Subtle Defect Fluctuations on Kesterite Thin Film Solar Cells: An Analysis of CZTSe/CdS Interface with 400 Devices Pedro Vidal-Fuentes¹, Jacob Andrade-Arvizu¹, David Payno¹, Fabien Atlan¹, Alejandro Perez-Rodriguez^{1,2}, Maxim Guc¹ and Victor Izquierdo-Roca¹; ¹IREC, Spain; ²Universitat de Barcelona, Spain

Renewable energy generation is intimately linked with the advancement of innovative photovoltaic technologies. The realization of large-scale production hinges upon emerging thin-film materials and device architectures built upon stable, environmentally conscious resources. Cu₂ZnSnSe₄ has surfaced as a promising contender in this realm, owing to its attributes such as stability, affordability, adaptability to flexible substrates, and tunable bandgap. While efficiency of the devices based on this promising material might not match conventional PV technologies, their potential for swift industrialization remains noteworthy. This transition from laboratory-scale small cells to more expansive formats is essential. It paves the way towards diverse applications, not just

extensive solar farms, but also for distributed implementations like IoT, indoor PV, and various emerging paradigms.

This shift, however, uncovers challenges that warrant early attention. In mature technologies such as CIGS, the cell-to-module efficiency gap ($\Delta PCE_{cell-module} = 5\%$) underscores the importance of addressing limitations upfront. For CZTSe, achieving precise control over thin film composition is pivotal due to its profound impact on material properties and photovoltaic performance. Even subtle compositional deviations can detrimentally influence device efficiency by exacerbating defects and grain boundaries, which are known to impede charge transport and place a limit to the V_{oc} . The interactions between the commonly used CdS electron transport layer (ETL) and the absorber layer in kesterite-based solar cells are equally crucial. Upscaling magnifies lateral inhomogeneity due to the augmented area-to-thickness ratio, necessitating highly uniform deposition methods. Failure to achieve homogeneity in the absorber layer can lead to compositional irregularities, thereby altering optoelectronic properties.

This research investigates two samples ($5 \times 5 \text{ cm}^2$ each), representing the initial step towards large-scale $\text{Cu}_2\text{ZnSnSe}_4$ device fabrication. Each sample is subdivided into $3 \times 3 \text{ mm}^2$ devices, facilitating discrete surface information for statistical analysis. Raman spectroscopy (RS), photoluminescence (PL) spectroscopy and current voltage characteristics (J-V) constitute the array of employed characterization techniques. This combination elucidates the interplay of physicochemical attributes within the CZTSe/CdS heterojunction and its consequent impact on device output. By scrutinizing a comprehensive dataset of 2×196 devices, noteworthy correlations emerge. Fluctuations in the CdS buffer layer, encompassing slight thickness variations, bandgap shifts, and non-uniform defect distribution, closely correlate with the efficiency of individual cells. These CdS layer dynamics establish patterns in optoelectronic performance across the $5 \times 5 \text{ cm}^2$ surface. Subtle in-process changes, often masked in small discrete samples or those subjected to wide fabrication variations, wield substantial impact on device efficiency. This underscores the significance of comprehensive data analysis, which can guide quality control in CZTSe module fabrication.

This study underscores the intricate interplay of optoelectronic properties and defect characteristics in CZTSe/CdS photovoltaic technology. The investigation of large-area samples through a comprehensive suite of characterization techniques has unraveled significant insights. The unexpected lack of a direct correlation between open-circuit voltage (V_{oc}) and CZTSe quality control parameters highlights the complex nature of V_{oc} loss, predominantly governed by CdS layer defects. Notably, defects localized on the CdS surface exhibit a distinct correlation with V_{oc} , indicating their pivotal role in device performance. The correlation between CZTSe photoluminescence quantum yield and V_{oc} , although significant, does not fully elucidate V_{oc} loss.

5:00 PM EN11.08.06

Electronic and Defect Properties of BaCd₂P₂ as a Solar Cell Absorber [Zhenkun Yuan](#)¹, Diana F. Dahliah^{2,3}, Romain Claes², Andrew Pike¹, Gideon Kassa¹, Muhammad R. Hasan⁴, Shaham Quadir⁵, Gian-Marco Rignanese², Andriy Zakutayev⁵, David Fenning⁶, Obadiah Reid^{5,7}, Sage Bauers⁵, Jifeng Liu¹, Kirill Kovnir^{4,8} and Geoffroy Hautier¹; ¹Dartmouth College, United States; ²Université catholique de Louvain, Belgium; ³An-Najah National University, Palestine, State of; ⁴Iowa State University, United States; ⁵National Renewable Energy Laboratory, United States; ⁶University of California, San Diego, United States; ⁷University of Colorado Boulder, United States; ⁸Ames National Laboratory, United States

We present the electronic and defect properties of BaCd₂P₂, a new solar cell absorber identified from our high-throughput computational screening and experimental follow-up synthesis and characterizations. Using first-principles calculations, BaCd₂P₂ is shown to have attractive optoelectronic properties, including a direct band gap of 1.45 eV, high carrier mobilities, and large optical absorption coefficients. HSE hybrid-functional defect calculations show that BaCd₂P₂ is an intrinsically semi-insulating material but can be doped *p*-type. Crucially, BaCd₂P₂ presents only a few deep defects that have either high formation energies or small capture coefficients. The calculated nonradiative recombination rates in BaCd₂P₂ are slower than or comparable to those in high-efficiency solar absorbers such as the halide perovskites. The favorable defect properties of BaCd₂P₂ are confirmed by photoluminescence (PL) and time-resolved microwave conductivity (TRMC) measurements. We will discuss these experimental results. In addition, a comparison of bulk and defect properties between BaCd₂P₂ and existing phosphide solar absorbers (InP and Zn₃P₂) will be made.

5:00 PM EN11.08.07

First principles modeling of polaron formation and optical signature on titanium-based oxides for oxygen evolution reaction photocatalysis. [Shay McBride](#)¹, Michael Paolino², Tanja Cuk² and Geoffroy Hautier¹; ¹Dartmouth College, United States; ²University of Colorado Boulder, United States

The exact mechanism and surface coverage present on (photo)-catalysts used for the oxygen evolution reaction (OER) remain elusive. Ultra-fast spectroscopy on model single crystal surfaces has started to clarify these questions but would benefit from more first principles theoretical support to facilitate the interpretation of the spectroscopic signatures. Here, we focus on the first principles modeling of the optical signature of polarons on OER intermediates on titanium-based photocatalysts (e.g., SrTiO₃ and TiO₂). The trapping of photo-generated holes by polarons on adsorbs at the catalyst surface is a key step in the photo-driven OER. We report from first principles on how the polarons formation process and optical signature changes with adsorbates (OH₂, OH, O) on different surfaces and compare with experimental results when available. Our work is a first step towards a better connection between ultra-fast spectroscopy and first principles computations.

5:00 PM EN11.08.08

Enhancing Photoelectrochemical Water Splitting Performance via Controllable Deposition of BiVO₄ on YSZ(110) [Zhaoyi Xi](#)^{1,2}, Chenyu Zhou¹ and Mingzhao Liu¹; ¹Brookhaven National Laboratory, United States; ²Stony Brook University, The State University of New York, United States

Bismuth vanadate (BiVO₄, BVO) is an outstanding photoanode material for photoelectrochemical water splitting. In our recent work, single crystalline BVO photoanodes were synthesized by pulsed laser deposition (PLD) method on YSZ(110) substrates. Through tuning different characters of BVO films deposited, they were found to be effective and influential in photoelectrochemical water splitting. Generally, the various characters of BVO were realized by tuning the deposition conditions of PLD, the growth mechanism of BVO thin films between YSZ(110) and conventional substrate orientation YSZ(100) was also compared. Furthermore, all the differences will have a direct influence on photoelectrochemical water splitting. Detailed surface characterizations and mechanistic research were performed to understand the inherent correlation between BVO growth conditions and performance, which will have a heuristic effect towards future photoanode design for solar water splitting.

5:00 PM EN11.08.09

BaZrS₃ – Single Crystals, Growth and Properties [Yvonne Tomm](#)¹, Galina Gurieva¹, Joachim Breternitz² and Susan Schorr^{1,3}; ¹Helmholtz-Zentrum Berlin, Germany; ²FH Münster, Germany; ³Freie Universität Berlin, Germany

Perovskite chalcogenide materials have gained increasing interest as potentially stable materials with promising optoelectronic properties owing to their structure type. These materials have the general formula of AMX₃ with A being a group II cation (i.e., Ca²⁺, Sr²⁺, or Ba²⁺), M a group IV transition metal (i.e., Ti⁴⁺, Zr⁴⁺, or Hf⁴⁺), and X a chalcogen anion (S²⁻ or Se²⁻). These materials have been known for a long time and attempts to prepare them have been made in many ways. Single crystals of this group of materials were prepared by the flux method. However, most of the data regarding structure and optoelectronic properties were determined on polycrystalline thin films (e. g. [1, 2]).

BaZrS₃ as a representative of this class of materials crystallizes in the orthorhombic perovskite-type structure. For thin films of BaZrS₃ a band gap energy of 1.95eV [3] and 1.99eV [2], respectively, has been determined.

Here we report on the growth of single crystals of BaZrS₃ and their crystal structure and optoelectronic properties compared to thin films. The BaZrS₃

crystals were grown by chemical vapor transport (CVT) using iodine as a transport agent. The resulting material and grown crystals were characterized by powder X-ray diffraction (XRD) and LeBail analysis of the diffraction pattern, as well as by single-crystal X-ray diffraction. The chemical composition of the crystals was determined by X-ray fluorescence. The band gap energy was determined from the diffuse reflectance measured by UV-VIS spectroscopy.

Reference:

- [1] Ramanandan, S. P. et al., Journal of Physics: Energy 2023, 5, 014013
- [2] Marquez, J. A. et al., Journal of Physical Chemistry Letters 2021, 12, 2148
- [3] Nishigaki, Y. et al. Sol. RRL 2020, 4 (5), 1900555

5:00 PM EN11.08.10

Solution Based Synthesis of Low Dimensional Pnictogen Chalco-Halides based on (Sb,Bi)(S,Se)(Br,I) for Sustainable Energy Applications David Rovira Ferrer, Ivan Caño Prades, Joaquim Puigdollers and Edgardo Saucedo; Universitat Politècnica de Catalunya, Spain

Quasi one-dimensional (Q1-D) structures based on van der Waals materials are gaining increasing interest in the search for novel energy applications such as photocatalysis, energy storage or photovoltaics. This attention is driven by the high stability and low environmental impact of chalcogenides and chalcogen halides in contrast to third generation solar cells, especially Pb-based perovskites. The optoelectrical properties of these materials can be easily tuned through compositional engineering. A wide bandgap range (from 1 to 3.5 eV) can be achieved with available candidates for single-junction solar cells. The Sb/Bi chalcogen halide compounds, generally formulated as MChX (M = Sb, Bi; Ch = S, Se; X = I, Br), crystallise in an orthorhombic Pnma space group consisting of covalently bonded ribbons along one crystallographic direction, while they are stacked together by van der Waals interactions in the other directions. This feature gives rise to unique optoelectronic properties when the material is properly oriented, such as enhanced carrier transport and increased mobility. In addition, it has been suggested that these compounds might possess a defect-tolerant electronic structure due to the trivalent metal cation, which is encouraging their development.

Despite these encouraging properties, the correct synthesis of these materials containing a halogen and a chalcogen in the structure is still a big challenge. Binary materials such as (Sb,Bi)₂(S,Se)₃ can occur as secondary phases, as well as sub-optimal morphologies. Uneven and uncompact films with uncontrolled ribbon orientation can form. This presentation will introduce a new methodology to synthesize mixed chalcogen halides developed by the authors of this work. Thin films of the complete set of ternary van der Waals (Sb,Bi)(S,Se)(Br,I) chalcogen halide semiconductors have been synthesized by dissolving MX₃ and selenourea/thiourea in N,N-dimethylformamide (DMF), followed by multiple spin-coating and hot-plate annealings at low temperatures (< 400 °C). Additionally, antisolvent incorporation during spin-coating, followed by a drying step at a temperature below the solvent's boiling point, have been applied to ensure that all organic residues are removed. This one step methodology provides less complexity compared to previous sequential procedures relying on diffusion of one precursor in a previously deposited film, which can lead to a gradient in the composition. Different surface treatments over the molybdenum substrate are explored to selectively orient texture in the (001) direction by improving the solution adhesion and increasing the nucleation sites.

In the second part of the presentation, the fundamental properties of these compounds obtained by electrical and optical characterisation will be discussed. The measurement of the bandgaps, band structures, optical and transport properties will be shown.

The last part of the presentation will be dedicated to the challenges and possible technological solutions for the fabrication of solar cell devices using this innovative absorber synthesis route. The use of different electrons and holes transport layers, and architectures inspired in bulk-heterojunction devices using blended ribbons of BiSI and BiSBr/SbSI as donor and acceptor, respectively, will be discussed. These solar cell prototypes will be shown, with very encouraging open circuit voltages around 500 mV, and conversion efficiencies exceeding 1%. Finally, the perspective of these materials and the possible advantages with respect to current chalcogenide and halide technologies, will be presented and discussed.

5:00 PM EN11.08.11

An ALD-Grown Al-Doped Zinc Oxide/n-Si Isotype Heterojunction for Solar Water Splitting C. S. Wang¹, P. H. Tseng², Y. S. Lai³ and Klaus Y. Hsu¹; ¹National Tsing Hua University, Taiwan; ²National Yang Ming Chiao Tung University, Taiwan; ³Taiwan Semiconductor Research Institute, Taiwan

It is well known that zinc oxide (ZnO) films are good passivation layers to semiconductor solar cells. Doped ZnO also serves as an excellent transparent electrode material. The efficiency of many solar cells has been enhanced by adopting this oxide material in the device structures. Besides, ZnO can be prepared by several large-area growth methods such as sputtering, evaporation, CVD, sol-gel, spray, ALD, etc. This benefits the use of ZnO in solar applications. In addition to being a transparent passivation layer or conducting electrode, n-type doped ZnO thin film can directly form an anisotype heterojunction with p-type silicon (p-Si) or an isotype heterojunction with n-type silicon (n-Si). These heterojunctions function simply as solar cells. When converting light power to electrical power, compared with conventional semiconductor p-n junctions, the ZnO/Si heterojunctions show no power loss at the near-surface region in the devices if the incident light comes from the ZnO side, because the ZnO films are transparent to visible light. This advantage further extends the application of ZnO to the active region of devices. In particular, the current flow in the n-ZnO/n-Si heterojunction should be easier since it involves only majority carriers. While numerous studies on the n-ZnO/p-Si anisotype heterojunction were conducted, much fewer works on the n-ZnO/n-Si isotype heterojunction can be found in the literature. In this work, an aluminum-doped ZnO (AZO) thin film was grown on an n-Si substrate by atomic layer deposition (ALD) with in-situ doping technique to form an isotype heterojunction. And a self-powered solar water splitter formed by serially connecting several of such heterojunctions was demonstrated.

The device was fabricated by first using the ALD system to grow a 53 nm thick AZO film on a 0.685 mm thick n-Si (2-7 Ω-cm resistivity) substrate. The growth temperature was low and set at 280 °C for best (002) crystallinity of the AZO film. The AZO film thickness was designed for minimum visible light reflection. The aluminum doping was performed by using an in-situ doping technique which involves the introduction of the Al₂(CH₃)₆ (TMA) precursor during the deposition process, which helps precise film thickness control. The resultant AZO film was characterized by Hall measurement to have a low resistivity of 2.48 x 10⁻³ Ω-cm and a high electron concentration of 1.3 x 10²⁰ cm⁻³. Therefore, the fabricated AZO/n-Si junction behaves like a Schottky junction, and the AZO itself can be the anode contact. TiN was coated at the backside of the Si substrate as the cathode. When serially connecting several devices, copper tape was used as the interposer.

The rectifying dark I-V curve of the AZO/n-Si junction was measured, from which the Schottky barrier height was extracted as 0.632 eV. When illuminated by the light from a tungsten-halogen lamp with an irradiance of 100 mW/cm², the open-circuit photovoltage was measured to be 0.38 V and the short-circuit current density was about 1 mA/cm². To demonstrate the usefulness of the AZO/n-Si isotype heterojunction device, we tried to use it to split DI water under illumination. By using the linear sweep voltammetry (LSV), it was found that the threshold voltage of DI water splitting for the fabricated AZO and TiN electrodes is 1.6 V. This indicates that at least 5 fabricated AZO/n-Si junctions must be connected in series to initiate splitting DI water under illumination. Such experiment has been carried out and the production of hydrogen gas was successfully observed.

5:00 PM EN11.08.12

Electron Transport Layers for CO₂ Reduction: Conductivity, Selectivity and Stability Rajiv Ramanujam Prabhakar and Joel W. Ager; Lawrence Berkeley National Laboratory, United States

Electron transport layers (ETLs) used as components of photocathodes for light-driven CO₂ reduction (CO₂R) in aqueous media should have good electronic transport, be stable under CO₂R conditions, and, ideally, be catalytically inert for the competing hydrogen evolution reaction (HER). Here, using

planar p-Si (100) as the absorbing material, we show that TaO_x satisfies all three of the above criteria. TaO_x films were synthesized by both pulsed laser deposition (PLD) and radio-frequency (RF) sputtering. In both cases, careful control of the oxygen partial pressure during growth was required to produce ETLs with acceptable electron conductivity. p-Si/TaO_x photocathodes were interfaced with ca. 10 nm of a CO₂R catalyst: Cu or Au. Under front illumination with simulated AM 1.5G in CO₂-saturated bicarbonate buffer, we observed, for both metals, faradaic efficiencies for CO₂R products of ~50% and ~30% for PLD TaO_x and RF sputtered TaO_x, respectively, at photocurrent densities up to 8 mA cm⁻². p-Si/TiO₂/Cu photocathodes were also evaluated but produced mostly H₂ (>97%) due to reduction of the TiO₂ to Ti metal under CO₂R conditions. In contrast, a dual ETL photocathode (p-Si/TiO₂/TaO_x/Cu) was selective for CO₂R, which suggests a strategy for separately optimizing selective charge collection and the stability of the ETL/water interface. The maximum photovoltage obtained with p-Si/TaO_x/Cu devices was 300 mV which was increased to 430-460 mV by employing ion implantation to make pn⁺-SiTaO_x/Cu structures. Photocathodes with RF sputtered TaO_x ETLs are stable for CO₂R for at least 300 min. Techno-economic analysis shows that the reported system, if scaled, could allow for an economically viable production of feedstocks for chemical synthesis under the adoption of specific CO₂ credit schemes, thus becoming a significant component to carbon-neutral manufacturing. Further to understand the why PLD TaO_x electron transport layer exhibits higher product selectivity over RF sputtered TaO_x, we investigated using ambient pressure x-ray photoelectron spectroscopy (APXPS) how the Cu catalyst oxidation state changes with different CO₂ partial pressures. There was evidence on favorable change in the oxidation state of Cu towards Cu²⁺ when exposed to higher partial CO₂ pressures with different TaO_x supports.

5:00 PM EN11.08.13

Co-Solvent Engineering for Solution-Processed CZTSSe on a Transparent Substrate Alice Sheppard¹, Raphael E. Agbenyeye¹, Jacques Kenyon², Robert Harniman¹, Laurie King¹, Jude Laverock¹, Neil A. Fox¹ and David J. Fermin¹; ¹University of Bristol, United Kingdom; ²Loughborough University, United Kingdom

Recent breakthroughs in efficiencies of up to 14.9%¹ for Cu₂ZnSn(S,Se)₄ (CZTSSe) solar devices have reignited interest in CZTSSe as an inorganic thin-film solar absorber. Traditionally, Mo-coated soda lime glass (SLG) substrates have been the standard for chalcogenide thin-film photovoltaics (PVs). Such substrates, however, can hinder the applications of thin-film PV, namely, semi-transparent and bifacial irradiation for building integrated PV applications. In this study, we explore the deposition of CZTSSe directly onto fluorine-doped tin oxide (FTO) by solution-based methods. The precursor solutions containing copper(II) chloride dihydrate, tin(II) chloride, zinc chloride and thiourea are formulated by employing mixtures of dimethyl formamide (DMF) and isopropanol (IPA).^{2,3} We also investigate the effect of adopting a one- or two-step heat treatment process at each layer during spin coating, prior to the reactive annealing step in the presence of Se. The effect of solvent composition and adopting an additional heat treatment step have been studied here by exploring the thin-film crystallinity, composition, secondary phase formation, and device performance, featuring CdS as buffer layer. Our data shows that solutions with a DMF:IPA mixture of 1:3 result in the most homogeneous grain growth and suppression of secondary phases, with a champion front illumination power conversion efficiency of 5.2%. We rationalise device performance in terms of the topography and surface electronic properties, as probed by energy-filtered photoemission electron microscopy.^{4,5}

1. NREL, Best Research-Cell Efficiency Chart, 2024

2. D. Tiwari, T. Koehler, X. Lin, R. Harniman, I. Griffiths, L. Wang, D. Cherns, R. Klenk, David J. Fermin, *Chem. Mater.* 2016, **28**, 4991–4997

3. R. E. Agbenyeye, J. Kenyon, A. Sheppard, N. Benhaddou, N. Fleck, M. A. Alkhalifah, D. Tiwari, J. W. Bowers, D. J. Fermin, *in progress*, 2024

4. D. Tiwari, M. Cattelan, R. L. Harniman, A. Sarua, A. Abbas, J. W. Bowers, N. A. Fox, D. J. Fermin, *iScience*, 2018, **9**, 36-46

5. D. Tiwari, M. Cattelan, R. L. Harniman, A. Sarua, N. A. Fox, T. Koehler, R. Klenk, D. J. Fermin, *ACS Energy Lett.*, 2018, **3**, 2977-2982

5:00 PM EN11.08.14

Photolithography Technologies for Metallic Meshes and Local Contacts on CIGS Thin Film Solar Cells with NIR-Transparent TCO Layers SeongYeon Kim, Si-Nae Park, Dong-Hwan Jeon, Van-Quy Hoang, Jaebaek Lee, Ali Amanat, Shi-Joon Sung and Dae-Hwan Kim; Daegu Gyeongbuk Institute of Science and Technology, Korea (the Republic of)

A transparent conducting oxides(TCO) for CIGS thin film solar cells, Al-doped ZnO(AZO) is widely used because of their wide band gap energy(Eg = 3.37 eV), high optical transparency, conductivity and based on earth-abundant materials. However, for the application of TCO layer for modules fabrication, AZO has an issue about optical loss in the visible and near-infrared spectrum. This causes electrical, optical and fill factor(FF) losses in the integration of solar cells in a module, which is known as cell to module(CTM) losses. To solve those issues, we have fabricated CIGS solar cells with hybrid electrodes of metallic grids / TCO layers.

Photolithography is versatile technology to make the patterns as we desired and demanded for semiconductor devices. We have patterned metallic meshes on AZO layer of CIGS solar cells using by photo lithography technique with negative photoresists. We fabricated photoresist template by exposure and development processes and deposited aluminum or silver metallic layers on the template about 1 μm of thickness and lifted off the photoresists to complete metallic meshes with attempting to minimize the linewidth by 2~3 μm and also minimize transmittance loss controlling by grid distance about 100 to 200 μm.

As a result, Al meshes occupying from 2.20 to 2.84% in a cells whereas reference devices have 3.94 to 4.66% of grid area. In both case of Al and Ag meshes devices, Jsc has been improved to 27.98 mA/cm² than 27.73 mA/cm² of the reference devices. In the case Ag meshes devices, Voc has been improved to 0.65 V which is closer to 0.66 V of the reference cell. By these results, we will discuss how to fabricate the solar cells with composite transparent electrode better way.

On the other hand, we have fabricated Hydrogen-doped Indium Oxide(In₂O₃:H) by sputtering process with H₂ and O₂ reactive gases with various mass flow controlling to improve NIR transmittance and high mobility. We have fabricated CIGS solar cells with In₂O₃:H instead of AZO layer and compare the parameters to clarify how NIR transparency and mobility improves the power conversion efficiencies.

Also, we fabricated local contacts with MgF₂ passivation layer with dot-shaped local contacts with various diameters and spacings on Mo back contact before CIGS deposition. we will discuss how those diameter and distance affecting on solar cells power conversion efficiency improvements.

SESSION EN11.09: Chalcogenides PV/PEC I
Session Chairs: Sage Bauers and Andriy Zakutayev
Friday Morning, April 26, 2024
Room 335, Level 3, Summit

8:00 AM *EN11.09.01

CdSe Solar Cells with Voc > 1V Sachit Grover¹, Mohammad Taheri¹, Taylor Hill^{1,2}, Elline Hettiaratchy¹, Xiaoping Li¹, Dmitry Krasikov¹, Gang Xiong¹, Darius Kuciauskas³, Craig Perkins³ and Angus Rockett⁴; ¹First Solar, United States; ²Colorado State University, United States; ³National Renewable

Energy Laboratory, United States; ⁴Colorado School of Mines, United States

An efficient, low-cost, scalable, and stable top-cell photovoltaic absorber is needed to make thin-film based tandem solar cells. Using cadmium selenide (CdSe) as an example, we highlight our methodology for rapid assessment of novel photovoltaic absorber materials and identify challenges towards making high efficiency devices.

With a bandgap of 1.72eV, CdSe is well suited as a top-cell absorber in a two-junction tandem solar cell. We assess the potential of CdSe as an absorber through several measurements including external radiative efficiency (ERE), carrier density, polycrystalline grain-size and orientation. Well formulated thin films of CdSe are found to be n-type, hexagonal, and exhibit high ERE (>0.2%). Photoluminescence and sub-band external quantum efficiency confirm that this absorber is capable of implied open-circuit voltages above 1.1 V. A transparent conducting oxide coated on glass forms the electron-contact to the CdSe thin-film grown on top of it. The hole-contact is formed by organic hole-transport layers used in conjunction with a bilayer of transition metal oxide and thin-gold. Solar cells with measured $V_{OC} > 1$ V have been demonstrated with this device structure.

Despite good V_{OC} , the devices made so far exhibit a limited fill factor and short-circuit current that cannot be completely accounted for by resistive or optical losses. By connecting a multitude of metrology techniques to device modeling results we conclude that the minority carrier collection is limited as the mobility and lifetime product ($\mu^*\tau$) product is about 10^{-9} cm²/V. This is attributed primarily to low hole mobility. Another key challenge is the unusually large ionization potential of CdSe at -6.5eV. SCAPS simulations indicate that improving the $\mu^*\tau$ and reducing the band-offset at the hole contact should lead to improved carrier collection. Defect signatures identified through sub-band photoluminescence measurements suggest selenium vacancies could be problematic.

In conclusion, well researched p-type transparent contact layers with a deep valence-band alignment are needed as hole contacts for CdSe solar cells. Options for designing a CdSe device that can be used in a thin-film based tandem are limited by the n-type absorber and require improved minority-carrier diffusion length.

8:30 AM EN11.09.02

Cation Mutation in $\text{Cu}_2\text{Zn}(\text{Ge}_x\text{Si}_{1-x})\text{Se}_4$ Solid Solution as a Path Towards CRM-Free Top Absorber Layer for Tandem Solar Cells Galina Gurieva¹, Sara Niedenzu¹, Alicia Manjon-Sanz², David C. Matzdorff¹, Melanie Kirkham² and Susan Schorr^{1,3}; ¹Helmholtz-Zentrum Berlin, Germany; ²Oak Ridge National Laboratory, United States; ³FU, Germany

The search for sustainable, efficient, and cost-effective photovoltaic materials continues to be a challenge in the field of solar energy production. In particular, the development of critical raw material free top absorber layers for tandem solar cells is crucial in the effort to transition away from fossil fuels and towards a greener energy future. The emergence of compound semiconductors has provided an opening into low-cost fabrication of thin-film solar cells, made possible a reduction in absorber layer thickness, and therefore lead to a decrease in production costs.

In this work, we explore the potential of tetravalent cation mutation in Cu-based quaternary chalcogenide semiconductors ($\text{Cu}_2\text{ZnSi}_x\text{Ge}_{1-x}\text{Se}_4$ [1]) with the aim of finding a material with increased bandgap (ideally around 1.7eV) and reduced structural disorder, which is considered to be the main culprit of the low V_{OC} in the only CRM-free material used in PV technology at the moment ($\text{Cu}_2\text{ZnSn}(\text{S,Se})_4$). One of the ways, previously shown to completely block structural disorder, especially the Cu/Zn disorder, is a change of the atomic crystal structure, e.g. [2]. The substitution of the tetravalent cation in the compound semiconductor brings a drastic structural change from the tetragonal kesterite type structure in $\text{Cu}_2\text{ZnGeSe}_4$ to the monoclinic wurtz-kesterite type structure in $\text{Cu}_2\text{ZnSiSe}_4$, with a significant increase in the bandgap as well [3].

We studied crystal structure, cation distribution and intrinsic point defect scenario in $\text{Cu}_2\text{ZnSi}_x\text{Ge}_{1-x}\text{Se}_4$ mixed crystals (powder samples) by neutron diffraction. This method enables us to differentiate the isoelectronic cations Cu^+ , Zn^{2+} and Ge^{4+} in the crystal structure analysis. These investigations enabled us to deduce the structural transition scenario of the $\text{Cu}_2\text{Zn}(\text{Ge,Si})\text{Se}_4$, series which is going via a region where two phases with different crystal structures but with the same chemical composition coexist. Interestingly both quaternary phases show the same cation distribution within the element specific cation sites. In the $\text{Cu}_2\text{Zn}(\text{Ge,Si})\text{Se}_4$, series the distortion of the coordination tetrahedra is increasing with increasing Si content thus indicating that the structural transition from the kesterite type to the wurtz-kesterite type structure is distortion driven.

The results of this study highlight the importance of considering alternative materials beyond the known kesterites in the search for CRM-free top absorber layers and demonstrate that cation mutation in quaternary chalcogenides is a promising path towards the development of highly efficient tandem solar cells.

[1] Niedenzu, S. et al. In: IEEE, 2018. - ISBN 978-1-5386-8529-7, p. 3290-3293

[2] Gurieva, G. et al. Phys. Rev. Mat. 4 (2020), p. 054602/1-8

[3] Schorr, S. Sol. En. Mat. and Sol. Cells 249 (2022), p. 112044

This work has received funding from the European Union's Horizon 2020 research and innovation program under grant agreement no.952982. A portion of this research used resources at the Spallation Neutron Source, a DOE Office of Science User Facility operated by the ORNL.

8:45 AM EN11.09.03

Enhancement of Open-Circuit Voltage in $\text{Cu}_2\text{ZnSn}(\text{S,Se})_4$ Solar Cells with Defect Passivation via LiF Post-Deposition Treatment Geumha Lim¹, Ha Kyung Park¹, Wook Hyun Kim², Seung-Hyun Kim³, Kee-Jeong Yang², Jin-Kyu Kang², Dae-Hwan Kim² and William Jo¹; ¹Ewha Womans University, Korea (the Republic of); ²Daegu Gyeongbuk Institute of Science and Technology (DGIST), Korea (the Republic of); ³Research Institute, YK Sintering Co., Korea (the Republic of)

$\text{Cu}_2\text{ZnSn}(\text{S,Se})_4$ (CZTSSe) is a promising candidate for low-cost, non-toxic, and highly stable alternatives to traditional light-absorbing materials. The incorporation of light alkali metals in CZTSSe solar cells has considered as a possible way to address limited power conversion efficiency caused by a significant open-circuit voltage deficit. In this study, fine interface engineering with effective passivation of detrimental defects via LiF post-deposition treatment (LiF PDT) was reported.[1] Three samples, the sample without a LiF layer, the sample with an as-deposited 0.7 nm LiF layer, and the sample with an 0.7 nm LiF layer followed by additional annealing at 200 °C, were prepared. Secondary ion mass spectroscopy shows that the diffusion of Li occurred only with additional heat treatment. Meanwhile, as-deposited LiF was lost during the CdS deposition process. Energy dispersive spectroscopy shows the possibility of Zn(S,Se) secondary phase migration to the surface of the absorber through additional heat treatment. To investigate the interface properties directly, mechanical dimpling of solar-cell devices was utilized. Uniform grinding condition was confirmed through Raman spectroscopy. Kelvin probe force microscopy reveals that the work function difference between bulk and interface reduced as the sample was subjected to the LiF PDT process, resulting in a lower conduction band offset at the CdS/CZTSSe interface. Furthermore, an increase in surface photovoltage signal indicates reduced defect-assisted carrier recombination through Li incorporation. Li modified the dominant defect types from Cu_{Zn} and Zn_{Cu} to shallower Li_{Zn} and Li_{Cu} antisites, preventing recombination losses and promoting charge transport. As a result, the sample with LiF PDT process achieved 10.4 % efficiency with significant enhancement of V_{OC} .

[1] G. Lim et al., *Journal of Materials Chemistry A* (2023), In press

9:00 AM EN11.09.04

In-depth carrier recombination mechanism at grain boundaries in flexible kesterite thin film solar cells with 12.2% efficiency Ha Kyung Park¹,

Dae-Ho Son², Shi-Joon Sung², Dae-Kyu Hwang², Jaebaek Lee², Dong-Hwan Jeon², Yunae Cho^{1,1}, Dae-Hwan Kim², Jin-Kyu Kang², Kee-Jeong Yang² and William Jo^{1,1}; ¹Ewha Womans University, Korea (the Republic of); ²Daegu Gyeongbuk Institute of Science and Technology, Korea (the Republic of)

Kesterite $\text{Cu}_2\text{ZnSn}(\text{S,Se})_4$ (CZTSSe), an earth-abundant and non-toxic material, is widely regarded as a promising light absorber for photovoltaic devices. Extensive research has focused on understanding recombination mechanism at the surface grain boundaries (GBs) which detrimentally impacts device performance, while their behavior within the material's bulk remains relatively unexplored. In this study, in-depth carrier recombination mechanism was investigated using atomic force microscopy-based characterization. A flexible CZTSSe thin film solar cell with an efficiency of 12.2% was prepared using a sputtering method on a Mo foil substrate. In particular, the sample was subjected to mechanical etching using a focused-ion beam to expose a plane at the specific depth. After that, electrostatic potential at the revealed surface was obtained by Kelvin probe force microscopy. At the surface and subsurface, formation of both conduction (E_C) and valence (E_V) upward bending was observed due to the widen band gap and increased charged defects at the GBs than in intra grains. This type of band bending is efficient for carrier separation as it repels electrons from the GBs while collects holes. [1] Additionally, large upward band bending contributed to a formation of conduction path along the intra grains. In contrast, center of absorber presented E_C downward and E_V upward band bending besides the E_C and E_V upward band bending, that is unfavorable as it can be the recombination sites. Hence, in-depth carrier recombination mechanism exhibited non-uniform behavior between the materials' surface and the bulk. In conclusion, the uniform E_C and E_V upward band bending at the GBs across the entire absorber layer is desirable to minimize the recombination. [2] Additionally, our research suggested the in-depth characterization methods that can be applied other materials beyond the kesterite thin film solar cells.

[1] H. K. Park et al., npj Flexible Electronics, 6 (2022) 91.

[2] D.-H. Son, H. K. Park, and K.-J. Yang et al., Carbon Energy, (2023) Accepted.

9:15 AM EN11.09.05

Manganese-Containing Quaternary Chalcogenides: New Earth-Abundant Semiconductors for Solar Energy Conversion Susan Schorr^{1,2}, Galina Gurieva¹ and David C. Matzdorf^{1,2}; ¹Helmholtz-Zentrum Berlin, Germany; ²Freie Universitaet Berlin, Germany

The need of eco-friendly compound semiconductors in thin film photovoltaics has constantly pushed the research towards more environmental friendly materials, such as the Kesterite-type compounds $\text{Cu}_2\text{ZnSnS}_4$, $\text{Cu}_2\text{ZnSnSe}_4$ and $\text{Cu}_2\text{ZnSn}(\text{S,Se})_4$ (CZTSSe). They present the only critical raw material (CRM) free thin film PV technology with tunable band gap energy and excellent long-term stability. The current record efficiency for CZTSSe solar cells of 14.9 % [1] highlights the great potential of this abundant chalcogenides to support a sustainable energy transition.

Recently, other quaternary semiconductors have raised attention: $\text{Cu}_2\text{MnSnS}_4/\text{Se}_4$. Photovoltaic devices based on their solid solution reached an efficiency of 1.8% [2]. An efficiency of 20.3% was calculated for a $\text{Cu}_2\text{MnSnS}_4$ based solar cell [3]. Including $\text{Cu}_2\text{MnGe}(\text{S/Se})_4$, a band gap energy range of 1.2 to 2.1 eV can be covered by the respective anion as well cation mutations. Moreover Mn is more abundant than Zn (1100 ppm against 79 ppm) [4], leading to a potentially cheaper final device. Thus Mn-based quaternary compound semiconductors have a strong potential in solar energy conversion technologies. In this work, we study four cation and anion mutation series: $\text{Cu}_2\text{Mn}(\text{Ge,Sn})\text{S}_4$ and $\text{Cu}_2\text{Mn}(\text{Ge,Sn})\text{Se}_4$ as well as $\text{Cu}_2\text{MnSn}(\text{S,Se})_4$ and $\text{Cu}_2\text{MnGe}(\text{S,Se})_4$ aiming for insights into the crystal structure, structural disorder and their band gap energies. In contrast to the kesterite-type materials discussed above, these Mn-containing quaternaries crystallize in the tetragonal stannite-type (when Sn is the four-valent cation) or orthorhombic wurtz-stannite-type (in case Ge is the four-valent cation) structure. This change in the crystal structure, with respect to the kesterites, can block Cu/B^{II} disorder (Cu/Zn disorder in kesterites), as shown before [5].

We studied the crystal structure, cation distribution and intrinsic point defect scenario in the mixed crystals of these four series (powder samples) by neutron diffraction. This method enables us to differentiate the isoelectronic cations Cu^+ and Ge^{4+} as well as electronic similar Mn^{2+} in the crystal structure analysis giving the possibility to conclude on anti site defects including these cations. From our experimental findings it became evident, that the off-stoichiometry type model developed for kesterites [6] also applies in Mn-containing quaternaries despite their different crystal structure.

We observed Cu-Mn swapping (very small fractional amount of Cu_{Mn} and Mn_{Cu} anti sites) in all compounds and mixed crystals with the exception of $\text{Cu}_2\text{MnSnSe}_4$ [7]. This type of cation swapping was also observed in $\text{Cu}_2\text{MnSnS}_4$ thin films [8].

We found that in the $\text{Cu}_2\text{Mn}(\text{Ge,Sn})\text{S}_4/\text{Se}_4$ series Sn-rich mixed crystals adopt the stannite structure, whereas Ge-rich mixed crystals adopt the wurtz-stannite structure. Within the intermediate range, two chemically identical but structurally different quaternary phases coexist, adopting the tetragonal and the orthorhombic structure respectively. The structural transition is driven by an increasing structural distortion with increasing Ge-content. Both end members of the $\text{Cu}_2\text{MnSn}(\text{S,Se})_4$ and $\text{Cu}_2\text{MnGe}(\text{S,Se})_4$ series crystallize in the same structure type, avoiding a structural transition. But a change in the structural disorder can be noticed within these series, showing an increase around the center of the solid solutions.

Finally, the band gap energy variations within these four cation and anion mutation series will be presented, showing the correlation between crystal structure and this important optoelectronic material property.

[1] www.nrel.gov/pv/cell-efficiency.html

[2] Sun et al., Sol. En. Mater. Sol. Cell. 219 (2021) 110788

[3] Pansuriya et al., Opt. Mater. 126 (2022) 112150

[4] Le Donne et al., Front. Chem. 7 (2019) 297

[5] Gurieva et al., Phys. Rev. Mat. 4 (2020) 054602

[6] Schorr et al., J. Phys.: Energy 2 (2020) 012002

[7] Gurieva et al., Faraday Discuss. 239 (2022) 51

[8] Rudisch et al., Phys. Stat. Solidi B 256 (2019) 1800743

9:30 AM EN11.09.06

Depth-Profiling of High Efficiency Kesterite Solar Cells: The Role of Co-Alloying Alex Jimenez Arguijo¹, Yuancai Gong², Tariq Jawhari³, Lorenzo Calvo-Barrio³, Alejandro Perez-Rodriguez¹, Sergio Giraldo² and Edgardo Saucedo²; ¹Institut de Recerca Energètica de Catalunya, Spain; ²Universitat Politècnica de Catalunya, Spain; ³Universitat de Barcelona, Spain

The kesterite ($\text{Cu}_2\text{ZnSn}(\text{S,Se})_4$, CZTSSe) absorber family is composed of low-toxicity, earth-abundant elements, and offers an unmatched stability which aligns with low-cost applications such as building-integrated and indoor photovoltaics. Moreover, it has recently experienced a breakthrough thanks to the research centered on solution-based precursors, showcasing a remarkable efficiency of 13% in 2022, which has now been further improved to 14.9%. This new paradigm for the Kesterite community has been possible through the smart design of solution chemistry in organic polar solvents yielding amorphous kesterite films, together with optimized thermal annealings for direct phase conversion from precursor to absorber, and the implementation of beneficial low-temperature heterojunction heat treatments. In addition, the alloying with isovalent elements (Ag, Cd, and Ge) has been shown to be crucial to achieve record efficiencies, suppressing lattice defects by improving the synthesis pathway.

A thorough understanding of the actual role of isovalent element alloying could enable the synthesis of high quality kesterite absorber materials without the need to use expensive, toxic and scarce elements during the synthesis. In this work, the role of additional elements will be studied by comparing the device performance of absorbers without alloying, with Ag alloying and with Ag,Cd co-alloying. Thus, demonstrating the beneficial role of these alloying strategies on the optoelectronic properties of the devices. Furthermore, the effects on the grain growth mechanism of Ag and Ag,Cd co-alloying will be

thoroughly investigated by secondary electron microscopy (SEM), X-ray diffraction (XRD) and Raman spectroscopy combined in break-off experiment at different temperatures. Finally, to shed more light on the performance improvement, depth gradient ion-milled samples will be fully analyzed by combining micro-Raman (325, 532 and 785 nm excitation wavelengths), micro-photoluminescence (PL) and X-ray and ultraviolet photoelectron spectroscopy (XPS and UPS), thereby showing the actual role of Ag and Ag,Cd alloying in high efficiency kesterite absorbers. In particular, the distribution of secondary phases, grain quality, defect concentration, sulfur content and carbon residues will be assessed by micro-Raman spectroscopy. Also, the in-depth compositional homogeneity as well as Sn and Cu oxidation states will be characterized by XPS, revealing insights on the deep-defect density (Sn, lifetime related) and the shallow defect density (Cu, doping related). Moreover, the combination of XPS, UPS and PL will allow reconstructing the in-depth band diagram, revealing key insights on the charge carrier transport of high quality kesterite materials. Overall, the present study will reveal the most relevant factors induced by the Ag and Cd incorporation in the lattice of high efficiency kesterite absorbers, paving the way for further improvements without requiring the use of expensive, scarce and toxic elements.

9:45 AM EN11.09.07

Exploration, Prediction and Experimental Verification of Structure and Optoelectronic Properties in I₂-Eu-IV-X₄ (I = Li, Cu, Ag; IV = Si, Ge, Sn; X = S, Se) Chalcogenide Semiconductors [Max McWhorter](#), Tianlin Wang, Garret C. McKeown Wessler, Yi Yao, Ruyi Song, Volker Blum and David B. Mitzi; Duke University, United States

Recent extensive research into the defect-resistant I₂-II-IV-X₄ (I = Li, Cu, Ag; II = Ba, Sr, Eu, Pb; IV = Si, Ge, Sn; X = S, Se) family of quaternary chalcogenide semiconductors suggests excellent potential for applications in photovoltaics, thermoelectrics, and nonlinear optics. Among these compounds, Eu containing members are understudied, with only five previously synthesized members. Herein, we undertake a comprehensive study of the possible structures and electronic properties of all eighteen of the Eu-based combinations within I₂-Eu-IV-X₄ (I = Li, Cu, Ag; IV = Si, Ge, Sn; X = S, Se). To further understand the broader I₂-II-IV-X₄ family and test the geometric tolerance factor (reported in our previous work) as a tool for predicting potential stable structures, we first use hybrid density functional theory to systematically study these rare-earth-including I₂-Eu-IV-X₄ semiconductors. Lowest-energy quaternary structure candidates, energy band structures, and densities of states are computationally predicted for all eighteen compounds. Following this screening process, the previously unknown compound Cu₂EuSnSe₄ was selected and synthesized due to its predicted photovoltaics-relevant direct band gap. Optimal synthesis conditions were determined, and the experimentally derived structure, lattice parameters, and bandgap of Cu₂EuSnSe₄ were found to be consistent with the predictions from both geometric tolerance factors and hybrid DFT, validating our predictive approaches and confirming a 1.55 eV band gap. Along with strong optical absorption in the visible range, this band gap suggests potential for Cu₂EuSnSe₄ in photovoltaic and other optoelectronic applications.

10:00 AM BREAK

10:30 AM *EN11.09.08

AgBiS₂ Nanocrystals: An Emerging Chalcogenide Absorber for Solution Processed Ultra-Thin Film Solar Cells [Gerasimos Konstantatos](#); ICFO, Spain

In this talk I will discuss recent progress in our group on the development of a new class of thin film solar cells employing Silver Bismuth Sulfide as an emerging absorber for solution processed eco-friendly solar cells. I will first introduce our first report on AgBiS₂ colloidal nanocrystal solar cells reporting power conversion efficiency of ~6% [1]. Then I will discuss on the opportunities of tuning the optical properties of this ternary compound via controlling cation disorder homogenization. We demonstrated that by homogenizing cation disorder in this compound we can drastically increase the absorption coefficient of this material as one with the high absorption amongst the semiconductors considered for photovoltaics. This taken together with advances on the device architecture led us to reach power conversion efficiencies of ~9% albeit using an absorber of only 35 nm [2]. In the last part of my talk I will describe our initial efforts on developing AgBiS₂ nanocrystal inks and their use with environmentally friendly solvents that led us to achieve efficiencies in excess of 7% [3]. I will conclude my talk with our most recent findings towards an improved passivation strategy of AgBiS₂ nanocrystal inks along with the formation of a double heterojunction in the device stack that led to power conversion efficiencies in excess of 10% with Voc of 0.5V, FF of 0.75 and Jsc of 28 mA/cm².

References:

[1] Solution-processed solar cells based on environmentally friendly AgBiS₂ nanocrystals, M Bernechea, N Cates, G Xercavins, D So, A Stavrinadis, G Konstantatos, Nature Photonics 10 (8), 521-525, 2016

[2] Cation disorder engineering yields AgBiS₂ nanocrystals with enhanced optical absorption for efficient ultrathin solar cells, Y Wang, SR Kavanagh, I Burgués-Ceballos, A Walsh, DO Scanlon, G Konstantatos, Nature Photonics 16 (3), 235-241, 2022

[3] Environmentally Friendly AgBiS₂ Nanocrystal Inks for Efficient Solar Cells Employing Green Solvent Processing Y Wang, L Peng, Z Wang, G Konstantatos, Advanced Energy Materials 12 (21), 2200700, 2022

11:00 AM EN11.09.09

Generalizing Synthesis Approaches for BaMS₃ Chalcogenide Perovskites and Related Materials [Shubhanshu Agarwal](#), Kiruba Catherine Vincent, Jonathan Turnley and Rakesh Agrawal; Purdue University, United States

Over the past decade, lead halide perovskites have witnessed a remarkable surge in solar device efficiencies. They possess a defect-tolerant crystal structure, showcasing outstanding optoelectronic and charge transport properties with tunable bandgaps. However, their progress is hindered by limited air, moisture, and thermal stability. While research on these exceptional materials should continue, there is a need to identify stable alternatives that exhibit similar appealing properties. Chalcogenide Perovskites have emerged as promising substitutes for lead halide perovskites. These materials also display defect tolerance and boast one of the highest light absorption coefficients. They demonstrate considerable stability against air, moisture, and thermal conditions, and their bandgaps can be tailored for either single-junction or tandem solar cell applications.

Nevertheless, Chalcogenide Perovskites face a challenge in high-temperature synthesis. Historically, they have been synthesized at temperatures exceeding 900°C, either as powders or vacuum-deposited thin films. Such high-temperature syntheses restrict the choice of substrates for material deposition. Additionally, not all the intermediary layers in a solar cell can endure such high temperatures. Therefore, it is imperative to synthesize these materials of the highest quality at low to moderate temperatures (<600°C). In recent years, multiple research groups have successfully synthesized nanoparticles or inhomogeneous solution-processed films at low temperatures. However, a comprehensive understanding of the critical parameters enabling this achievement is still lacking.

In this work, we present a comprehensive framework for the synthesis of low-temperature BaMS₃ compounds (M=Zr, Hf, Ti) while discussing the interplay of precursor reactivity, availability of a transport agent, and an oxygen sink as the primary factors governing low-temperature synthesis with

limited contamination. Furthermore, to validate our framework, we introduce four novel methods to synthesize BaMS₃ compounds at low temperatures, adhering to the guidelines outlined in the framework. Our results highlight a unique opportunity to synthesize BaMS₃ compounds using cost-effective precursors at low temperatures, offering guidance for future research on these materials.

11:15 AM EN11.09.10

Solution-Processed Chalcogenide Perovskite Thin Films Utilizing Amine Thiol Chemistry [Kiruba Catherine Vincent](#), Jonathan Turnley, Shubhanshu Agarwal and Rakesh Agrawal; Purdue University, United States

Growing technological advancements necessitate the development of versatile semiconductor materials capable of addressing diverse challenges. These materials must demonstrate robust stability, natural abundance, environmental friendliness, and tunable properties to cater to diverse applications, such as transistors, photovoltaics, thermoelectrics, LEDs, and more. Additionally, they should enable efficient and high-throughput synthesis. In the domain of photovoltaics, we can recognize two material systems competing to meet these requirements – emerging chalcogenides and lead halide perovskites. Emerging chalcogenides, such as Cu₂ZnSn(S,Se)₄, offer low toxicity and earth-abundant elements but have struggled to achieve high efficiencies. On the other hand, lead halide perovskites are breaking efficiency records but are extremely sensitive to air, and moisture and suffer from toxicity issues. An emerging class of materials that offers a compelling blend of the exciting properties of chalcogenides and lead halide perovskites are chalcogenide perovskites. Chalcogenide perovskites have shown superior stability and abundance in nature. They exhibit intriguing optoelectronic properties such as a tunable bandgap, high absorption coefficients, defect tolerance, and a high dielectric constant. However, despite their potential, chalcogenide perovskites have been constrained by their basic synthesis procedures, often requiring temperatures as high as 1000°C for extended periods, limiting their practicality. Solution processing has generally been seen as a low-temperature, ambient-pressure route to synthesize chalcogenide materials with high throughputs. Recent reports by Pradhan et.al provide promising results for solution-processed chalcogenide perovskites. They utilized CS₂ insertion chemistry to enable the synthesis of BaMS₃ materials at moderate temperatures. However, their method produced rough and cracked films with significant residual carbon (DOI: 10.1002/anie.202301049).

This study presents a versatile, moderate-temperature solution-processing synthesis approach for BaZrS₃, a notable chalcogenide perovskite for tandem solar cell applications and for the related BaHfS₃ perovskite, suitable for LED and water-splitting applications. We utilized the well-known alkahest amine-thiol solvent system to blade coat our films. This method produced crack-free films with minimal carbon residue and hence provided a promising step forward for the chalcogenide perovskite research. Subsequently, we conducted comprehensive material, morphological, and optoelectronic characterizations on these films to gain valuable insights that can guide the fabrication of high-performance devices.

11:30 AM EN11.09.11

Preparation, Structural and Optical Properties of Copper Chalcogenide Nanostructures and Thin Films (including 2D) for Photovoltaics, Thermoelectric and Electrochemical Applications [Richard A. Taylor](#), Kimberly A. Weston, Sarika V. Chandoo, Sean Persaud and Stefan C. Ghany; University of The West Indies, Trinidad and Tobago

Copper chalcogenides have emerged as attractive materials because of their wide-ranging applications involving photovoltaics, thermoelectrics, electrochemical and light emitting/down-conversion. This is because as nano- and microstructures, their properties can be controlled by their composition including defects, phase structure, morphology, dimensionality, optical, electrical, and electrochemical properties. However, in several ternary phases such as copper indium sulphide (CIS), copper antimony sulphide (CAS) and the two-dimensional (2D) copper molybdenum sulphide (CMS), there remains a challenge in controllable scalable preparation. To address this, we have been exploring facile colloidal and template-assisted syntheses, and aerosol-assisted chemical vapor deposition (AACVD) to selectively prepare these materials and control their properties. For example, tetragonal I-phase multilayered 2D CMS nanosheets and nanorods prepared colloiddally and by AACVD displayed tunable bandgaps (1.6 – 2.6 eV). Additionally, we demonstrated selective preparation of non-stoichiometric famatinite CAS nanoparticles at notably low temperatures (60 – 70 °C) with tunable bandgaps (1.9 – 2.2 eV) and high-quality non-stoichiometric tetrahedrite phase CAS thin films with Zn²⁺ ions incorporated with tunable bandgaps (1.7 – 2.1 eV) influenced by Zn²⁺ ion by point defects. Data from HR-SEM/TEM, EDS, XPS, confocal Raman and time-resolved PL spectroscopy, and cyclic voltammetry, suggest electronic properties implicated by point defects, and structural, morphological, optical characteristics dependent on synthetic conditions. We have also prepared tunable highly emissive CIS nanoparticles doped with Zn²⁺/Mn²⁺ ions and alloyed/passivated with ZnS/MnS as candidates for nanocomposite emissive luminescent down-shifting films for windows in controlled environment agriculture systems. As a novel approach, we have demonstrated template-assisted growth of large domain sized (30 – 200 nm) 2D nanosheets of ZnS, CuS, CIS and CAS, which typically form 3D or 0D nanostructures. Overall, our synthetic methodologies demonstrate control over tuning structure, morphology, composition including defects and their attendant electronic properties of these copper-based nanostructures and microstructured thin films for luminescent downshifting, photovoltaic and photoelectrochemical applications.

11:45 AM EN11.09.12

Routes Towards Improved Open Circuit Voltage in Sb₂Se₃ Solar Cells [Thomas Shalvey](#) and Jonathan D. Major; University of Liverpool, United Kingdom

Sb₂Se₃ is a defect tolerant, earth-abundant, stable semiconductor which has shown promise for low cost thin film photovoltaic power generation. It has a large absorption coefficient, suitable band gap, simple binary composition and benign grain boundaries compared to typical 3D materials. These attributes have helped solar cell efficiencies to surpass 10% with relatively little research effort in comparison to other absorber technologies. Despite this encouraging progress, the rate of improvement appears to have slowed recently as record devices approach the detailed balance limit of short circuit current density. This means that further improvements are likely to originate primarily from increasing the open circuit voltage (Voc) and/or fill factor (FF).

Interfaces within a solar cell play a key role in both the Voc and FF, and therefore we have carried out a detailed study of the partner layers in the Sb₂Se₃ device structure either side of the absorber layer. We have replaced the standard CdS front contact with TiO₂, which has a wider band gap and is far more robust, making it more amenable to the subsequent high temperature processing steps required for large grain, crystalline Sb₂Se₃ thin films. The initial solution processed TiO₂ layer has been replaced with a sputter deposited film which improved device uniformity and increased FF, however was prone to run-to-run variations in TiO₂ film quality and the inconsistent appearance of 'S'-shape JV curves. This issue has now been resolved through careful control of the sputtering process, which has led to exceptionally high short circuit current densities and significantly improved FF, however the impact on Voc has been limited. The back interface was then studied to determine the role of the hole transport material (HTM) in Sb₂Se₃ devices, and assess whether this could be an area for improvement. Several commonly used organic HTM layers were compared against one another, and to a simple Au contact. The direct Sb₂Se₃-Au contact is limited by a secondary barrier causing 'rollover' in JV curves, despite seemingly favourable band positions. Each of the HTM layers demonstrated the ability to eliminate this secondary barrier, thereby lowering the series resistance and improving the fill factor. Whilst this increases the champion efficiency, the improvement is relatively minor, especially considering the gradual oxidation of the Sb₂Se₃ back surface produces a similar self-passivation effect. Instead, the HTM layers have a far more drastic effect on the average efficiency, which is attributed to a pinhole blocking effect by the solution processed organic films. Nonetheless, Voc remains below 500mV for all devices tested.

After thoroughly investigating the partner layers, we are now turning our attention to the Sb₂Se₃ layer itself. We are currently exploring several routes to

improve the quality of the absorber layer. This includes a comprehensive study of dopants and defects in Sb₂Se₃, whereby the growth of high purity single crystals with the controlled addition of selected extrinsic dopants will inform the most suitable compositions to target in thin films, both in terms of stoichiometry and p-type dopant incorporation. This is particularly important given the apparent chalcogen-poor stoichiometry reported by most groups, especially for PVD processed films, as well as the lack of rigorous control over doping type typically found in literature reports. The transfer of knowledge gained from this single crystal study towards full devices will be accelerated via the use of a novel dual source close space sublimation chamber. This will allow co-deposition of different source material with varying stoichiometry and dopant concentration, and therefore allow a wide range of material compositions to be rapidly deposited. These compositions will then be assessed in terms of their implied Voc in order to carry out a loss analysis to identify the different contributions to the remaining deficit.

SESSION EN11.10: Chalcogenides PV/PEC II
Session Chairs: Sachit Grover and Gerasimos Konstantatos
Friday Afternoon, April 26, 2024
Room 335, Level 3, Summit

1:30 PM *EN11.10.01

Raman Spectroscopy at The Nanoscale: From Materials to Devices for Energy Conversion [Mirjana Dimitrievska](#); Empa–Swiss Federal Laboratories for Materials Science and Technology, Switzerland

The pace at which major technological changes take place is often dictated by the rate at which new materials are discovered, and the timely arrival of new materials has always played a key role in bringing advances to our society. Machine learning and advanced simulation and modeling techniques have recently massively accelerated the fast screening and discovery of new materials. There is however today a bottleneck in the exploitation of these emerging materials. Indeed, after the materials' existence and/or properties are predicted in silico, their synthesis and integration in devices to demonstrate functionality remain major challenge. Fast and reliable characterization can significantly accelerate materials optimization and bring them to the forefront of applications.

This talk will give an overview on the key role that Raman spectroscopy plays in accelerated semiconductor materials development for optoelectronic and energy conversion applications. I will show how Raman spectroscopy could be effectively used for probing fundamental properties of materials, such as crystal quality, phase purity, and defects. This will follow with presenting Raman-based methodologies for nanoscale detection of defects and impurities in materials, leading to establishing accurate phase diagrams and predictive synthesis-structure-property relationships. I will focus on wide range of material systems, from thin films to 1D and 2D materials. Finally I will discuss Raman-based mapping of the defect structure/space of thin film solar cells to optimize device structure.

2:00 PM EN11.10.02

Exploring Selenium Viability for Semi-Transparent Photovoltaics [Arnau Torrens](#)¹, Ivan Caño Prades¹, Alejandro Navarro¹, Axel Gon Medaille², Dioulde Sylla², Jose M. Asensi López³, Sergio Giraldo¹, Kunal Tiwari¹, Edgardo Saucedo¹, Zacharie Jehl Li-Kao¹, Joaquim Puigdollers¹, Pablo Ortega¹ and Marcel Placidi^{1,2}; ¹UPC, Spain; ²IREC, Spain; ³UB, Spain

Selenium (Se) holds historical significance as the first material used in a solar cell [1], in 1883, marking the initial exploration of materials capable of harnessing solar energy. However, it took over a century before being seriously considered for photovoltaics, achieving at this time an efficiency of 5% [2] with the following Au/Se/TiO₂/FTO architecture. In 2017, Todorov improved the device architecture with more suitable selective contacts (Au/MoO₃/Se/ZnMgO/FTO) and achieved the current worldwide efficiency record of 6.5% [3]. This breakthrough reignited interest in selenium for photovoltaics, resulting in many recent research publications, with a particular focus on its potential use as a top cell in tandem configurations, due to low temperature processing (melting point around 200 °C) and a direct bandgap of approximately 1.95 eV. However, Se appears also well suited for semi-transparent and/or indoor applications. Although its energy bandgap may initially not seem ideal for semi-transparency, recent findings suggest that very thin (less than 50 nm) amorphous silicon devices can achieve high visible transparency and impressive efficiencies, with promising light utilization efficiencies (LUE) of 0.7% [4]. Notably, the current worldwide efficiency record involved a 100 nm layer, but there is variability in the literature regarding the optimal absorber thickness, ranging from 100 nm to several micrometers, which could compromise its suitability for semi-transparent applications.

To check the viability of Se for semi-transparent PV, several amorphous layers of different thicknesses were prepared using an evaporation system. These layers were optically characterized before and after hot plate crystallization at temperatures around 200 °C, a process widely reported in literature. This crystallization step, both on glass and FTO, resulted in the formation of separated Se crystallized islands. In an effort to enhance the Se adhesion during crystallization, we initially avoided the use of Te, known to improve it, but potentially detrimental for device performance. Additionally, we explored the option of performing the crystallization step on complete device architectures, incorporating various selective contact layers before Se deposition, both in substrate and superstrate configurations, yielding valuable insights. All the results of this work will be presented at the MRS Meeting and the viability of selenium for semi-transparent photovoltaics discussed.

[1] C. E. Fritts, On a new form of selenium cell, and some electrical discoveries made by its use, *Am. J. Sci.* 26, 465 (1883).

[2] A. Kunioka et al., Polycrystalline thin-film TiO₂/Se solar cells, *Jpn. J. Appl. Phys.* 24, L536–L538 (1985).

[3] T. K. Todorov et al., Ultrathin high band gap solar cells with improved efficiencies from the world's oldest photovoltaic material, *Nature Communications* 8, 682 (2017).

[4] A. Lopez-Garcia et al., Ultrathin a-Si:H/Oxide Transparent Solar Cells Exhibiting UV-Blue Selective-Like Absorption, *Solar RRL* 7, 2200928 (2023).

2:15 PM EN11.10.03

Monolithic Selenium/Silicon Tandem Solar Cells [Rasmus Nielsen](#), Andrea Crovetto, Alireza Assar, Ole Hansen, Ib Chorkendorff and Peter C. Vesborg; Technical University of Denmark, Denmark

Elemental selenium, the world's oldest photovoltaic material, is reemerging as a promising inorganic thin-film PV absorber. With a direct bandgap of 1.95 eV in its trigonal phase and a high absorption coefficient ($>10^5$ cm⁻¹) in the visible region, it is a promising candidate for the top cell in tandem devices. Furthermore, its long-term air stability, monoatomic composition, and low melting point of 220°C makes processing simple, low-cost, and compatible with most bottom cells.

We present the first monolithically integrated selenium/silicon tandem solar cell, demonstrating a highly encouraging open-circuit voltage of 1.68 V.

Guided by device simulations, we identify critical energy barriers restricting the flow of charge carriers and investigate the potential of using other carrier-selective contact materials, resulting in a tenfold increase in the overall power conversion efficiency. In parallel with the tandem devices, we fabricate and characterize bifacial single junction selenium solar cells to gain insights into the polarity-dependent PV performance. In view of these results, we set forth strategies for further improving the device performance to realize higher efficiency selenium/silicon tandem solar cells.

2:30 PM EN11.10.04

Advancing CO₂-to-Fuel Conversion: Synthesizing Tellurium-Based Semiconductors Shaham Quadir, Sage Bauers and Andriy Zakutayev; National Renewable Energy Laboratory, United States

Converting CO₂ into energy-dense liquid fuels through the use of renewable energy sources is considered as an important component of addressing ongoing and future energy crises. The most elegant method for this conversion is the photoelectrochemical (PEC) reduction of CO₂, but the key challenge in realizing this process effectively lies in the development of highly efficient photoelectrode materials. In particular, operationally stable p-type photocathodes that can provide electrons to facilitate the required CO₂ reduction processes are required.

In this study, we synthesized new semiconductor thin film absorber material, Zn_x(GaTe₂)_y, via combinatorial sputtering approaches. The material was prepared using a 2-step process wherein room-temperature growth was followed with flash lamp annealing from 300 °C – 550 °C. Our X-ray diffraction study shows that Zn_x(GaTe₂)_y goes through a phase transition from cubic (F-43m) to tetragonal (I-42m) upon increasing Ga content, indicating a nearly complete ordering of atoms and vacancies on the zincblende lattice. Upon changing the cation ratio, a new peak observed in the X-ray diffraction pattern at an angle of ~35° with cubic structured Zn_x(GaTe₂)_y alloy, suggesting an intermediate amount of order can be achieved. At an optimal ratio of Zn:Ga:Te, Raman scattering reveals longitudinal optical (LO) peaks up to the third order when excited with a wavelength of 532 nm and displays superior photo luminescent properties, suggesting its potential to enhance CO₂ reduction capabilities. In the room temperature photoluminescence (PL) spectra, a defect emission is observed at 1.6 eV for all ratio of Zn_x(GaTe₂)_y. Time-resolved photoluminescence (TRPL) data indicates a shift in lifetime during the transition from an ordered to a disordered state.

2:45 PM EN11.10.05

Photovoltaic Efficiency of Transition Metal Dichalcogenides Thin Films by *Ab Initio* Excited-State Methods Pedro Venezuela¹, Enesio Marinho Jr², Cesar Villegas³ and Alexandre Rocha²; ¹Universidade Federal Fluminense, Brazil; ²Unesp, Brazil; ³Universidad Privada del Norte, Peru

Transition metal dichalcogenides (TMDCs) have garnered significant interest in optoelectronics, owing to their scalability and thickness-dependent electrical and optical properties. In particular, thin films of TMDCs could be used in novel photovoltaic devices. In this work, we employ *ab initio* many-body perturbation theory within G₀W₀-BSE approach to accurately compute the optoelectronic properties of thin films of 2H-TMDCs composed of Mo, W, S, and Se. Subsequently, we evaluate their photovoltaic performance including exciton recombination effects, and show this is a key ingredient. We obtain efficiencies of up to 29 % for a 100-nm thick film of WSe₂, thus providing an upper limit. We also include other phenomenological recombination mechanisms that could be present in current samples. This slightly reduces efficiencies, indicating that even with current synthesis technologies, there is still potential for further enhancement of TMDCs' performance in photovoltaic applications.

3:00 PM BREAK

SESSION EN11.11: PEC, Other Materials
Session Chairs: Andrea Crovetto and Mirjana Dimitrievska
Friday Afternoon, April 26, 2024
Room 335, Level 3, Summit

3:30 PM EN11.11.01

Integrated Photoelectrochemical Systems for Scalable Water Splitting and CO₂ Reduction Virgil Andrei; University of Cambridge, United Kingdom

Photoelectrochemical (PEC) systems hold the potential to lower the costs of sustainable solar fuel production by integrating light harvesting and catalysis within one compact device.^[1] However, current deposition techniques limit their scalability, while fragile and heavy bulk materials can affect their transport and deployment. Here, we first demonstrate the fabrication of lightweight artificial leaves by employing thin, flexible substrates and carbonaceous protection layers.^[2] Lead halide perovskite photocathodes deposited onto indium tin oxide coated polyethylene terephthalate achieve an activity of 4266 μmol H₂ g⁻¹ h⁻¹ using a platinum catalyst, whereas photocathodes with a molecular Co catalyst for CO₂ reduction attain a high CO:H₂ selectivity of 7.2 under a lower 0.1 sun irradiation. The corresponding lightweight perovskite-BiVO₄ PEC devices display unassisted solar-to-fuel efficiencies of 0.58% (H₂) and 0.053% (CO), respectively. Their potential for scalability is demonstrated by 100 cm² standalone artificial leaves, which sustain a comparable performance and stability of ≈24 h to their 1.7 cm² counterparts. Bubbles formed under operation further enable the 30-100 mg cm⁻² devices to float, while lightweight reactors facilitate gas collection during outdoor testing on a river. The leaf-like PEC device bridges the gap in weight between traditional solar fuel approaches, showcasing activities per gram comparable to photocatalytic suspensions and plant leaves.^[2] The presented lightweight, floating systems are compatible with modern fabrication techniques,^[3] and may enable open water applications, while avoiding competition with land use. The carbonaceous protection layers and rational design principles are successfully applied to an underexplored BiOI light absorber, increasing the photocathode stability towards hydrogen evolution from minutes to months.^[4] Similar PEC systems approaching a m² size can take advantage of the modularity of artificial leaves,^[5] whereas thermoelectric generators can further bolster water splitting by utilizing waste heat to provide an additional Seebeck voltage.^[6,7]

[1] Andrei, V.; Roh, I.; Yang, P. *Sci. Adv.* 2023, 9, eade9044.

[2] Andrei, V.; Ucoski, G. M.; Pomrungraj, C.; Uswachoke, C.; Wang, Q.; Achilleos, D. S.; Kasap, H.; Sokol, K. P.; Jagt, R. A.; Lu, H.; Lawson, T.; Wagner, A.; Pike, S. D.; Wright, D. S.; Hoye, R. L. Z.; MacManus-Driscoll, J. L.; Joyce, H. J.; Friend, R. H.; Reiser, E., *Nature* 2022, 608, 518–522.

[3] Sokol, K. P.; Andrei, V. *Nat. Rev. Mater.* 2022, 7, 251–253.

[4] Andrei, V.; Jagt, R. A. et al. *Nat. Mater.* 2022, 21, 864–868.

[5] European Commission; Directorate-General for Research; Innovation. Artificial photosynthesis : fuel from the sun : EIC Horizon Prize; Publications Office of the European Union, 2022. DOI: 10.2777/682437.

[6] Andrei, V.; Bethke, K.; Rademann, K. *Energy Environ. Sci.* 2016, 9, 1528–1532.

[7] Pomrungraj, C.; Andrei, V.; Reiser, E. *J. Am. Chem. Soc.* 2023, 145, 13709–13714.

3:45 PM EN11.11.02

Photocorrosion of CuBi₂O₄ Monitored by Operando Surface-Sensitive X-Ray Scattering Davide Derelli¹, [Francesco Caddeo](#)¹, Kilian Frank², Kilian Krötzsch¹, Patrick Ewerhardt¹, Marco Krüger¹, Sophie Medicus¹, Lars Klemeyer¹, Marvin Skiba¹, Charlotte Ruhmlieb¹, Olof Gutowski³, Ann-Christin Dippel³, Wolfgang Parak¹, Bert Nickel² and Dorota Koziej¹; ¹University of Hamburg, Germany; ²Ludwig-Maximilians-Universität München, Germany; ³Deutsches Elektronen-Synchrotron DESY, Germany

The low stability of most semiconducting materials is one of the key factors that hinders the development of efficient and durable PEC water splitting cells. Monitoring the semiconductor-electrolyte interface during operation is crucial to understand all the underlying photocorrosion processes and in turn establish appropriate mitigation strategies.

In this work, we show a novel method to study operando the semiconductor-electrolyte interface during PEC operation. In particular, we developed a custom-built PEC cell that allows to assess operando the crystalline and morphological evolution of the semiconductor surface by grazing-incidence X-ray scattering, making use of two detectors to collect simultaneously the total scattering (TS) and the small-angle X-ray scattering (SAXS) signals. We applied the technique to monitor the evolution of CuBi₂O₄ films, a promising p-type semiconductor to be used as a light harvesting material in the cathodic compartment of a PEC cell.

Our operando approach, together with complementary X-ray absorption near edge spectroscopy (XANES) and inductively coupled plasma mass spectroscopy (ICP-MS) measurements, allows us to uncover the multiple degradation pathways affecting CuBi₂O₄ films performance during PEC operation. We find that CuBi₂O₄ reduces to metallic Bi and Cu, with the first one being the fastest process. We also find that Cu ions are released in the electrolyte during long-term stability tests, while at the same time BiPO₄ is formed at the surface of the CuBi₂O₄ film, due to the presence of PO₄³⁻ ions in the electrolyte. Our work provides a detailed picture of the degradation mechanisms occurring at the surface of CuBi₂O₄ electrodes under operation and poses the methodological basis to study the photocorrosion processes of a wide range of PEC materials.

4:00 PM EN11.11.03

Spectroscopical Study on Electron Storage in Nano-Sized Tungsten Oxide [Irene Martin](#)^{1,2}, Luca Rebecchi^{1,3}, Andrea Rubino¹ and Ilka Krieger¹; ¹Istituto Italiano di Tecnologia, Italy; ²Politecnico di Torino, Italy; ³Università degli Studi di Genova, Italy

Dark photocatalysis is a promising technology for fuel production, which combines light harvesting properties with energy storing materials. The system involved would both work as a photocatalyst and rechargeable solar battery under illumination, so that electrons released during the discharge could be exploited for 'dark' reactions, e.g. CO₂ reduction reaction (CO₂RR) and hydrogen evolution reaction (HER). Thus, it also implies the investigation of materials capable of storing electrons for hours [1]. Tungsten(III) oxide (WO₃) has drawn interest owing to its ability of trapping electrons through intercalation of positive ions, accommodating negative charges at W centres [2], and being utilised for prolonged anti-corrosion activity in the dark (*i.e.* photocathodic protection) [3].

In the work herein presented we investigated the potential use of WO₃ nanoparticles for dark photocatalytic CO₂RR by means of photo-doping process. We analyzed the charge storing properties of the WO₃ colloidal nanoparticles via UV-VIS-NIR spectroscopy, by monitoring absorption changes under illumination. The increase of the LSPR peak and the blue shift of the band gap due to the Moss-Burstein effect indicate that WO₃ undergoes electron accumulation, similar to what has already been reported for indium tin oxide (ITO) and other metal oxide nanocrystals (MO NCs) [4]. The results obtained in our study suggest that these materials can be valid candidates for next generation of photocatalytic systems.

[1] Rogolino and Savateev, *Adv. Funct. Mater.* **2023** 2305028

[2] Ng et al., *Phys. Chem. Chem. Phys.* **2011** 13 13421-13426

[3] Zhou et al., *Corros. Sci.* **2009** 51 1386-1391

[4] Ghini et al., *Nanoscale* **2021** 19 8773-8783

4:15 PM EN11.11.04

Layered Intergrowths with SrBi₃O₄Cl₃ and Bi₂GdO₄Cl as Building Blocks Towards Stable Visible Light Mediated Photocatalysis. [Nayana Christudas Beena](#) and Sara Skrabalak; Indiana University, United States

Photocatalysts capable of visible light absorption that are also durable against photocorrosion are crucial to achieving overall water splitting. A unique layered intergrowth comprised of SrBi₃O₄Cl₃ and Bi₂GdO₄Cl building blocks is achieved by a flux-based approach. The feasibility of tuning the intergrowth's optoelectronic properties was investigated by varying the stoichiometry of the intergrowths. Intergrowth formation resulted in the destabilization of the O-2p and Cl-3p orbitals, elevating the valence band maximum position. In addition, local symmetry changes around the Bi sites due to the presence of Sr²⁺ and Gd³⁺ cations play an important role in lowering the conduction band minimum position. Furthermore, the minimal recombination of photogenerated charge carriers can be attributed to the charge separation due to the presence of an internal static electric field between the layers. The systematic study of these materials conducted using X-ray diffraction and electron microscopy provides insights into how intergrowth stoichiometry serves as a lever to optoelectronic properties and photocatalytic performance of visible-light responsive multi-metal oxyhalide intergrowths.

SYMPOSIUM ES01

Next-Generation EV Battery Materials—Bridging Academic, Government and Industry Research
April 23 - May 9, 2024

Symposium Organizers

Jeffrey Cain, General Motors

Zachary Hood, Argonne National Laboratory

Matthew McDowell, Georgia Institute of Technology

Yue Qi, Brown University

Symposium Support

Bronze

Georgia Tech Advanced Battery Center
Vigor Technologies (USA) Inc

* Invited Paper

+ JMR Distinguished Invited Speaker

^ MRS Communications Early Career Distinguished Presenter

SESSION ES01.01: Research and Collaboration Across Academic, Government and Industry Sectors

Session Chairs: Jeffrey Cain and Zachary Hood

Tuesday Morning, April 23, 2024

Room 425, Level 4, Summit

11:00 AM *ES01.01.02

Advanced Battery Materials from Labs to Markets Yi Cui; Stanford University, United States

This presentation covers two examples of how battery materials innovations take place in an academic lab and how these innovations are translated into products in markets. The first example is on Si anodes to enable high energy density batteries. Demonstration of Si nanowire anodes sparked global efforts on a variety of Si anode designs, leading to the formation of many startup companies and R&D effort in major battery companies. The second example is on metal-hydrogen gas batteries for grid-scale energy storage to integrate renewable electricity into the grids. I will highlight the lessons and guiding principles learnt from labs to markets.

11:30 AM *ES01.01.03

Empowering Advanced Battery Chemistries for “All-Electric Future” Mei Cai; General Motors, United States

As GM continues marching towards an all-electric, zero emission future with 25+ yrs experience in vehicle electrification, this mission has never been more important and urgent to our society than now. To accelerate EV adoption, the advancement of battery technology, in particular, battery chemistry requires starting with a solid and deep understanding in customer pain points. In this talk, we will discuss: 1) how to apply the approach of “begin with the end in mind” to further unleashing the power of advanced battery chemistry for EV; 2) a case study comparing EV battery systems integrated with different advanced chemistries by using above approach. Finally, the key aspects in battery chemistry advancement toward mass EV-adoption will be highlighted.

SESSION ES01.02: Advanced Battery Materials and Chemistry

Session Chairs: Udochukwu Eze, Colton Ginter and Zachary Hood

Tuesday Afternoon, April 23, 2024

Room 425, Level 4, Summit

1:30 PM ES01.02.01

Deciphering The Interfacial Chemistry and Degradation Pathway of Layered Cathode Materials Linqin Mu; Arizona State University, United States

The ever-increasing demand for renewable energy and electric vehicles calls for high-energy-density rechargeable batteries. Cathode materials such as layered oxides play a crucial role in determining batteries' energy density and safety. $\text{LiNi}_x\text{Mn}_y\text{Co}_z\text{O}_2$ (NMC), as the dominating cathode, has been successfully commercialized for many years. In addition, there is a consensus that integrating NMC cathodes into all-solid-state batteries (ASSBs) is an effective way to achieve high energy densities. However, NMC cathodes are still facing many challenges, particularly, during the perusing of the high Ni concentration and high cut-off voltages. In the presentation, we will discuss the interface degradation of the NMC cathode at multiple length scales. By comprehensive imaging and spectroscopic techniques, we could bridge the degradation phenomenon from the electrode scale to the atomic scale. We will present the challenges of characterizing the surface properties of the cycled layered cathode and summarize our strategies that can enhance the surface stability of NMCs. Our fundamental understanding will inform the design principles at multiple length scales in batteries. Shifting our focus to solid-state batteries (SSBs), there is a growing body of research on SSBs incorporating NMC cathodes and argyrodite solid electrolytes (SEs). However, these advanced ASSBs face significant challenges in terms of low initial Coulombic efficiency and rapid capacity degradation. Therefore, we will also explore the interfacial degradation mechanisms in composite SE-NMC cathodes utilizing the NMC/ $\text{Li}_6\text{PS}_5\text{Cl}$ combination as a platform.

1:45 PM ES01.02.02

Unlocking The Full Capacity of Ni-Rich Layered Oxide Cathodes: The Impact of Lithium Site Defects on Diffusion and Stability Leonhard Karger^{1,2}, Svetlana Komeychuk¹, Wessel Van den Bergh^{1,2}, Aleksandr Kondrakov^{2,3}, Jürgen Janek^{4,2} and Torsten Brezesinski^{1,2}; ¹Karlsruhe Institute of Technology, Germany; ²BELLA, Germany; ³BASF Corporation, Germany; ⁴Justus-Liebig-Universität Giessen, Germany

The automotive industry's transition to renewable energy relies, among others, on layered oxides, like $\text{LiNi}_x\text{Co}_y\text{Mn}_z\text{O}_2$ (NCM) and $\text{LiNi}_x\text{Co}_y\text{Al}_z\text{O}_2$ (NCA), for high-performance applications. These materials promise enhanced capacities within a stable cycling range. While the theoretical specific capacity is above 270 mAh/g, in reality only around 240 mAh/g can be realized under conditions closely resembling real-world applications. Interestingly, specific capacities exceeding 260 mAh/g can be achieved upon very slow cycling, highlighting that capacity loss is caused by sluggish lithium diffusion. A structural characteristic strongly linked to charge transport is the presence of intercalation site defects, including Ni_{Li} substitutional point defects, which are inherently found in state-of-the-art Ni-rich layered oxide materials. To investigate the effect that these defects have on cycling performance, we have developed a synthesis method for perfectly layered LiNiO_2 (LNO) through sodium to lithium ion exchange. Our analyses, including X-ray techniques and NMR spectroscopy, confirm that this route produces a material entirely devoid of Ni_{Li} defects. Overall, this method serves as a foundation for re-evaluating the impact of factors that are well recognized for influencing the cyclability, such as nickel content, defect concentration and particle size.

We attribute an ambivalent role to Ni_{1-x}Li_x defects, recognizing their negative effect on lithium diffusion, particularly limiting the discharge capacity. However, we also identify a secondary contribution of Ni_{1-x}Li_x defects, which is not readily observable in state-of-the-art LNO materials due to the intrinsic presence of substitutional point defects. As the defect concentration approaches zero, the high-voltage regime (high SOC) becomes unstable, as evidenced by increased oxygen release and capacity loss of more than 10%. Owing to the ambivalent nature of Ni_{1-x}Li_x defects, we propose a hypothesis that achieving an optimal balance between diffusion and stabilization is crucial to fully harness the material's capacity.

2:00 PM ES01.02.03

LiNi_{0.5}Mn_{1.5}O₄ Cathode Deterioration in Lithium-Ion Batteries Tracked through Intermittent Post-Mortem Material Characterizations [Kelsey L. Duncan](#) and Byron D. Gates; Simon Fraser University, Canada

Identifying high performing and cobalt-free transition metal-based energy storage solutions are a key feature for a cost-effective transition away from the fossil fuel economy. To inform the design of new materials, and the engineering of existing battery materials, a strong understanding of fundamental processes within the device is required. Lithium-ion batteries (LIB) are periodically evaluated by post-mortem (PM) autopsy, wherein a battery is disassembled and each cell component is analyzed separately, providing insights towards which areas of study are most critical to prevent device failure. When investigating cathodes in this manner, typically only whole-cathodes are studied where active material particles are encased in polymeric binders and adhered to a current collector. This provides some access to PM characterization through surface imaging, but cannot demonstrate a full understanding of the consequences of electrochemical cycling on the inner and base layers of cathode particles. Additionally, completing structural and composition characterizations are challenging due to the organics present. Seeking to develop a more detailed understanding of how cathodes particles deteriorate within an LIB cell, a procedure has previously been developed in the Gates Research Group to non-destructively harvest single cathode particles from their binder matrix for comprehensive post-mortem study. Building on this methodology, a systematic investigation into single cathode particles is presented.

In this work, cobalt-free LiNi_{0.5}Mn_{1.5}O₄ cathode particles are harvested at different points in their cycle life and characterized as PM isolated single particles to identify and track trends of cathode deterioration over time. High-resolution scanning electron microscopy images of hundreds of individual particles are systematically assessed for physical features of deterioration from cycling. These assessments are supported by x-ray diffraction and standard electrochemical analyses. With use of statistical analyses applied to the detailed imaging data, a template is created to enhance failure mechanism diagnostics and contribute experimental evidence to models of cathode degradation, informing the design of future cost-effective materials.

2:15 PM ES01.02.04

A Multimodal Investigation of Controlled Oxygen-Vacancy Formation to Prevent the Degradation in Ni-Rich NMC811 Cathode [Sumaiyatul Ahsan](#) and Faisal Alamgir; Georgia Institute of Technology, United States

Ni-rich LiNi_xMn_yCo_zO₂ (conventionally known as NMC, where $x+y+z=1$ and $x>y$; $x>z$) is one of the most used cathode materials in electric vehicles due to its low cobalt concentration and high capacity¹. One of the significant degradation mechanisms of this material has been attributed to intragranular crack formation and propagation that can lead to mechanical failure of cathode particles²⁻⁴. Due to cracking, the electrolyte can attack the newly exposed surfaces, releasing oxygen species such as radicals, ions, and molecules^{5,6}.

To mitigate crack propagation to the surface, we can synthesize a heterogeneous particle with a dislocation-dense (oxygen-deficient) layer^{3,7-9}. This surface layer can improve the stability of the cathode particles by shielding the core from electrolyte and annihilating the cracks generated in its core. Furthermore, the controlled oxygen vacancy (OV) layer on the surface of different transition metal cathodes has improved high C-rate capacity retention and cyclability³. Hence, it is crucial to investigate the control parameters for creating a dense OV layer on the surface of Ni-rich NMC material and associated lattice and oxidation change.

Herein, we explore a simple method for creating OV on the surface of NMC811 (LiNi_{0.8}Mn_{0.1}Co_{0.1}O₂) under a controlled atmosphere at elevated temperatures. The effect of different annealing temperatures has been analyzed using the in-situ X-ray diffraction (XRD) measurement. The intensity ratio of planes (003)/(104) decreases for oxygen-reduced structure, indicating a disordered cation layer with increased Oxygen loss³. Oxygen occupancy reduces from 0.99 to 0.975, indicating the presence of ~1.52% oxygen vacancy in the structure. Ni occupancy in the Li layer rises from 0.17 to 0.217, indicating increased Ni²⁺/Li⁺ mixing. Increased concentration of Ni²⁺ induces more cation mixing⁴. Hence, the oxidation state of modified NMCs has been investigated with X-ray absorption near-edge spectroscopy (XANES). The coordination structure was further examined through extended XAS fine structure (EXAFS)^{10,11}. A first-principal calculation-based computational model¹² was employed to calculate oxygen vacancy formation energy and a Quantum Espresso-based Xspectra¹³⁻¹⁵ package was used to reproduce the experimental metal K-edge XANES data to analyze further the optimum vacancy concentration required for the higher oxidation state of Ni (3+,4+). Finally, an ex-situ transmission electron microscopy study of the modified structure reveals the crack propagation in surface layers and the effect of the dense dislocation layer in crack annihilation.

References:

- 1 Manthiram, A. et al. *Adv Energy Mater* 6, (2016)
- 2 Su, Y. et al. *Journal of Energy Chemistry* 65, 236–253 (2022)
- 3 Su, Y. et al. *ACS Appl Mater Interfaces* 12, 37208–37217 (2020)
- 4 Jiang, M. et al. *Advanced Energy Materials* 11, (2021)
- 5 Gan, Q. et al. *EnergyChem* (2023)
- 6 Bak, S. M. et al. *ACS Appl Mater Interfaces* 6, 22594–22601 (2014)
- 7 Gu, Y. J. et al. *Int J Electrochem Sci* 12, 9523–9532 (2017)
- 8 Chen, B. et al. *J Mater Sci Technol* 35, 994–1002 (2019)
- 9 Song, J. et al. *Chemistry of Materials* 24, 3101–3109 (2012)
- 10 Alamgir, F. M. et al. in 79–108 (2015)
- 11 Yu, Y. et al. *ACS Appl Mater Interfaces* 12, 55865–55875 (2020)
- 12 Cui, S. et al. *Adv Energy Mater* 6, (2016)
- 13 Bunau, O. et al. *Phys Rev B Condens Matter Mater Phys* 87, (2013)
- 14 Gougoussis, C. et al. *Phys Rev B Condens Matter Mater Phys* 80, (2009)
- 15 Taillefumier, M. et al. *Phys Rev B Condens Matter Mater Phys* 66, 1–8 (2002)

2:30 PM *ES01.02.05

Single Crystal Ni-Rich Cathodes for Advanced Li-Ion Batteries [Jie Xiao](#)^{1,2}; ¹Pacific Northwest National Laboratory, United States; ²University of Washington, United States

High energy Ni-rich cathode will play a key role in advanced Li-ion batteries, but it suffers from moisture sensitivity, side reactions and gas generation. Single crystalline Ni-rich cathode has a great potential to address the challenges present in its polycrystalline counterpart by reducing phase boundaries and materials surfaces. However, synthesis of high-performance single crystalline Ni-rich cathode is very challenging. This talk will discuss a cost-efficient

drop-in approach to synthesize and scale-up high-performance single crystal Ni-rich cathode materials enabled by nanoscale phase segregation during calcination process.

3:00 PM BREAK

3:30 PM *ES01.02.06

Ceramic Nanowires for Li-Ion Batteries with Improved Safety, Energy and Power Gleb Yushin^{1,2}; ¹Georgia Institute of Technology, United States; ²Sila Nanotechnologies, Inc., United States

The recently discovered low-cost and highly scalable synthesis of ceramic nanowires or nanofibers enable their applications in high-performance Li-ion batteries, solid-state batteries and supercapacitors. Highly flexible ceramic separators produced from aluminum or magnesium oxide or oxyhydroxide nanowires of tunable dimensions enhance the safety, rate capabilities and energy density of a broad range of electrochemical energy storage devices. Compared to polymer or ceramic-coated polymer separator members, ceramic nanowire separators are not flammable or combustible and offer outstanding thermal stability, thereby improving battery safety. The higher porosity, smaller thickness and excellent wetting of ceramic nanowire separators by electrolytes result in lower resistance, higher efficiency, higher power, faster charging and often improved cycle stability of Li-ion batteries. Their lower attainable thickness also contributes to higher specific and higher volumetric energy densities in Li-ion cells. This invited talk will provide an overview of our progress in synthesis and energy storage-related implementations of this promising technology.

4:00 PM ES01.02.07

Porous Boron Nitride as Scaffold for Silicon Composite Anode Material Michael Karl^{1,2}, Alena Kalyakina², Johanna Rannigner², Christoph Dräger², Stefan Haufe² and Simone Pokrant¹; ¹University of Salzburg, Austria; ²Wacker Chemie AG, Germany

Aiming for higher specific energies and energy densities, lithium-ion battery (LIB) research explores silicon (Si) as an alternative high-capacity negative electrode/anode material. One of the challenges associated with employing Si materials in LIBs is their strong volume expansion upon lithiation (more than 300%), leading to significant stress in the particles. In the case of micrometre-sized Si particles, they tend to crack or detach from the conductive network of the electrodes. An effective way to overcome these issues is to apply nano-structured Si. However, reducing structure dimensions to the nanoscale results in increased specific surface areas, which promote a larger amount of electrolyte decomposition and subsequent solid electrolyte interface (SEI) formation. This irreversible process consumes electrolyte and diminishes the energy density of a LIB cell by immobilizing lithium.^[1]

Composite materials address this challenge, one possible concept is combining carbon and nano-Si to micrometre-sized particles.^[2] A successful approach to synthesize such composites is infiltrating silicon in porous carbon particles (~65% porosity) by chemical vapour deposition (CVD) using silane. Due to the micrometre particle size, the resulting composite exhibits a moderate surface area (below 25 m² g⁻¹), significantly limiting SEI formation. The reduced volume expansion of the particles leads to promising electrochemical performance,^[2] but some drawbacks persist. Porous carbon is not temperature stable in ambient atmosphere and may ignite at temperatures above 250 °C.^[3] In addition, exposed carbon surfaces are conductive and promote electrolyte decomposition as well as subsequent Li consumption upon lithiation.^[4]

Because of these drawbacks there is a growing interest in non-conducting and more safe alternatives. Hexagonal boron nitride (h-BN) fulfils the necessary requirements to replace carbon scaffolds in Si composites. It features a comparable low bulk density, and can be fabricated with a similar porosity to the previously employed carbon particles.^[2,5] In addition, hexagonal boron nitride exhibits a high temperature stability of up to 800 °C in oxygen atmosphere^[5], improving safety during material handling and cells in operation. As h-BN is an insulator, residual BN surfaces in contact with the electrolyte are not able to provide electrons for decomposition reactions. Thus, using insulating scaffolds is another factor reducing the undesired SEI formation, in addition to the generally low particle surface area of the Si composite concept.

In this work we present novel silicon-boron nitride composite materials, their fabrication, and their electrochemical performance as a negative electrode/anode material in a LIB. The synthesis of the highly porous h-BN scaffold is carried out in a furnace under nitrogen flow, using boric acid and an amide as precursors. Ammonia atmosphere forms inside the furnace upon heating, allowing the formation of h-BN sheets. By adjusting the processing time and temperature, a highly defective h-BN structure forms, exhibiting porosities of over 65%. The porosity is similar to those achievable for the porous carbon particles.^[2,4] In the next step, pores are filled with silicon using the same CVD-process as reported in literature for carbon composite materials.^[2] Employed in a LIB electrode, the composites show competitive cycle lives of over 500 cycles with 80% capacity retention at a capacity exceeding industry standard graphite by more than a factor of two.

References:

^[1]Ozanam, F. and M. Rosso., *Mater. Sci. Eng. B*, 2016. **213**: p. 2-11.

^[2]Liu, Y., et al., *J. Mater. Chem.*, 2013. **1**(45): p. 14075-14079.

^[3]Buettner, L.C., C.A. LeDuc, and T.G. Glover, *Ind. Eng. Chem. Res.*, 2014. **53**(41): p. 15793-15797.

^[4]David Linden, T.R., *Handbook of batteries*, 4th ed. 2011, Portland: Ringgold, Inc: Portland. p.26.17-26.25

^[5]Saha, D., et al., *ACS Applied Materials & Interfaces*, 2017. **9**(16): p. 14506-14517.

4:15 PM ES01.02.08

Pre-Regulated Solid-Electrolyte Interphase for High-Energy Density Silicon -Containing Anode-Based Lithium-Ion Batteries Gebrekidan G. Eshetu¹, Viviane Viviane Maccio-Figgemeier¹, Hyunsang Joo², Michel Armand³ and Egbert Figgemeier^{1,2}; ¹RWTH Aachen University, Germany; ²Helmholtz-Institut Münster/Forschungszentrum Jülich GmbH, Germany; ³Centre for Cooperative Research on Alternative Energies (CIC energiGUNE), Spain

Next - Generation Lithium (Li) - based high-energy density rechargeable battery technologies utilizing silicon (Si) - containing anode materials coupled with high-capacity/high-voltage insertion-type layered ternary oxide cathodes (IC, e.g.: Nickel-rich Lithium Nickel Manganese Cobalt Oxide, LiNi_xMn_yCo_{1-x-y}O₂) have reaped significant courtesy from both the academic and industrial sectors.¹ This ensues from their unparalleled high theoretical specific capacity (e.g., Si: 4200 mAh g⁻¹ for Li_{4.4}Si phase at 415°C and 3590 mAh g⁻¹ for Li_{3.75}Si at 20 °C, which is 10 times higher than that of the state-of-the-art Graphite); natural abundance in the earth's crust and thus competitive price, environmentally friendliness and suitable operating potential window (0.2 – 0.4 V vs. Li/Li⁺), all cumulatively offering a new possibility towards the large-scale adoption of electric vehicles and effective integration of renewable energy sources.

However, despite the above-mentioned benefits, Silicon-containing anode materials are featured with inherent shortcomings that deter their large-scale commercialization, including their colossal anisotropic crystallographic volume change (≥ 300 %), much lower diffusivity (σe⁻ and DLi⁺), unstable and fragile solid electrolyte interphase (SEI), high reactivity with electrode and electrolyte constituents at high states of charge, electrode swelling, and

electrolyte drying.

Among taming strategies, in-vitro electrochemical prelithiation making use of lithium chloride (LiCl)-based electrolytic medium has been hailed as one of the most effective approaches. This is attributed to the high solubility of LiCl in gamma-Butyrolactone (GBL). However, such electrolytic medium has been proved to result in notable amounts of gaseous chlorine (Cl₂) product that dissolve in the electrolyte, leading to a self-discharge Cl₂/Cl⁻ shuttling mechanism between the electrodes, lowering pre-lithiation efficiency, and thus causing current collector corrosion and rapid capacity decay after few cycles, even in the presence of state-of-the-art electrolyte additives such as Fluoroethylene carbonate (FEC).² Moreover, there could be a possibility for chlorination of GBL, leading to ring opening, and thus formation of soluble species concomitantly to the prelithiation process.

In this study, an alternative salt that result in inert gases instead of reactive shuttling species has been employed and proved to significantly improve the initial Coulombic efficiency, usable (reversible) capacity, long-term cyclability, and rate capability of Silicon-oxide/Graphite | NMC622 full cells compared to cells fabricated using LiCl salt-based electrolytic solution mediated electrochemically prelithiated and non-prelithiated (reference) SiO_x-Gr anode materials without any additive. The improvement could be attributed to the pre-formation of a highly tuned SEI layer with regulated properties. In-depth electrochemical analysis and investigations using various arsenal instruments proved different working mechanisms among the state-of-the-art salt, LiCl, the newly investigated salt-anion based electrolytic medium and reference battery cell.

The newly designed approach in this paper will spur a new avenue towards developing a highly tuned and pre-regulated solid electrolyte interphase via in-vitro electrochemical prelithiation to realize high Silicon Oxide (SiO_x)-containing SiO_x/Gr anode-based high-energy density lithium-ion batteries.

References

(1) Eshetu, G. G.; Zhang, H.; Judez, X.; Adenusi, H.; Armand, M.; Passerini, S.; Figgemeier, E. *Nature Communications* **2021**, *12* (1), 5459.

<https://doi.org/10.1038/s41467-021-25334-8>.

(2) Haneke, L.; Pfeiffer, F.; Bärmann, P.; Wrogegmann, J.; Peschel, C.; Neumann, J.; Kux, F.; Nowak, S.; Winter, M.; Placke, T. *Small* **2023**, *19* (8), 2206092. <https://doi.org/10.1002/smll.202206092>.

4:30 PM *ES01.02.09

Low Melting Alkali-Based Inorganic Molten Salts as Battery Electrolytes [Chibueze Amanchukwu](#); University of Chicago, United States

Lithium metal batteries (LMBs) promise high energy densities for electrified transport. Liquid electrolytes are currently state-of-the-art, but they are highly volatile and flammable and exacerbate safety concerns. Solid state batteries promise to address the safety concerns plaguing liquids but suffer from highly resistive electrode/electrolyte interfaces. In our work, we explore the use of low melting inorganic molten salts as electrolytes for LMBs. These electrolytes do not contain organic moieties and are not susceptible to the reactions that plague organic moieties in conventional ionic liquids and small molecule electrolytes. Furthermore, they are non-volatile and nonflammable, retaining the promise of solid-state systems. We show these electrolytes have high ionic conductivities at ~80°C, enable smooth lithium deposits, support high Coulombic efficiencies, and can support battery cycling. These inorganic molten salts with accessible melting temperatures open a new class of electrolyte media for both conventional and next generation battery chemistries.

SESSION MT02.03/ES01.03: Joint Keynote Presentation

Session Chairs: Jeffrey Cain and Feng Wang

Wednesday Morning, April 24, 2024

Room 321, Level 3, Summit

8:00 AM *MT02.03/ES01.03.01

U.S. DOE Supports Data-Driven Strategies to Accelerating Battery Commercialization [Changwon Suh](#); U.S. Department of Energy, United States

The Department of Energy's Advanced Materials and Manufacturing Technology Office (AMMTO) focuses on developing and deploying advanced manufacturing and materials technologies to support the DOE's mission to ensure America's energy security and environmental well-being. AMMTO invests in energy storage research, development, demonstration, and deployment (RDD&D) to help stakeholders improve efficiency, cut costs, and make materials, devices, and systems with superior performance. It is recognized in the energy storage space that effective utilization of data-driven experimentation, analysis and modeling is critical to accelerating the development and optimization of new technologies, improving manufacturing processes and reducing cost, leading to reduced time to commercialization and deployment of transformative technologies.

In this talk, AMMTO's approach to data-driven technology development and manufacturing will be highlighted. In addition, there will be a robust discussion of a wide variety of DOE's efforts in the context of technical and manufacturing challenges regarding scale-up and performance that still prevent the battery manufacturing community from achieving cost targets and commercial viability.

SESSION MT02.04/ES01.04: Joint Session: Materials, Manufacturing and Emerging Opportunities in Data-Driven Analysis and Modeling

Session Chairs: Jeffrey Cain and Feng Wang

Wednesday Morning, April 24, 2024

Room 321, Level 3, Summit

8:30 AM *MT02.04/ES01.04.01

Resource-Aware Materials, System and Process Design for Battery Materials [Elsa Olivetti](#)¹, Kevin Joon-Ming Huang¹, Karan Bhuwalka¹, Mrigi Munjal¹, Richard Roth¹, Romain Guillaume Billy², Daniel Beat Müller², Thorben Prein³ and Jennifer L. Rupp³; ¹Massachusetts Institute of Technology, United States; ²Norwegian University of Science and Technology, Norway; ³TU Munich, Germany

This presentation will provide a systems perspective on scaling needs in battery materials for electric vehicles ranging from our use of language model methods to source micro-challenges in the academic literature around electrode/electrolyte interfaces to materials supply chain issues including the impact on local communities for extraction of these materials. By providing a systems analysis on the extraction, beneficiation and refining complexities

associated with these technologies linked to the more fundamental research activities at the bench, this talk aims to provide insight at multiple length scales of the challenge in realizing next-generation EV battery materials.

9:00 AM MT02.04/ES01.04.02

Paradoxical Role of Structural Degradation of High-Nickel Layered Oxides and Electrode Crosstalk in Capacity Retention upon Storage of Lithium-Ion Batteries Hyejeong Hyun¹, Hyojung Yoon², Subin Choi¹, Juri Kim², Tom Regier³, Zachary Arthur³, Seokkoo kim² and Jongwoo Lim¹; ¹Seoul National University, Korea (the Republic of); ²LG Energy Solution, Korea (the Republic of); ³Canadian Light Source, Canada

Batteries undergo both active cycling and prolonged idle storage throughout their lifespan. While degradation mechanisms induced by cycling and their mitigation techniques have been deeply studied, the specific effects of storage without cycling remain largely underexplored. Notably, battery performance also sees a unique decline over time, contingent on the state-of-charge (SoC) when the batteries are at rest. Capacity decline during SoC70 storage primarily arises from electrode slippage and Li inventory loss in a full cell. This is accompanied by a minor structural breakdown of Ni-rich layered oxide cathodes. Conversely, SoC100 storage leads to a more pronounced structural impairment of Ni-rich cathodes and pronounced side reactions. Intriguingly, these severe side reactions curb the Li inventory loss, electrode slippage, and the reduction of full-cell capacity during SoC100 storage. In addition to standard degradation processes, such as Li/Ni cation mixing, the formation of surface reconstruction layers, and the emergence of exhausted phases, cathodes stored at SoC100 displayed an unexpected contraction of interlayer spacing during post-storage cycling, highlighting the atypical effects of storage. Based on the mechanisms of capacity reduction highlighted in this study, we propose strategies to counteract the aging caused by storage. This research offers valuable perspectives for refining battery production and management to enhance their calendar lifespan.

9:15 AM MT02.04/ES01.04.03

Improving Rate Capability in High-Energy Thick Lithium-Ion Batteries through Graded and Structured Electrodes Chih-Hsuan Hung¹, Srikanth Allu² and Corie L. Cobb¹; ¹University of Washington, United States; ²Oak Ridge National Laboratory, United States

Next-generation electric vehicles (EVs) made with Lithium-ion batteries (LIBs) require both higher energy density and higher power density to reach \$80/kWh at a 300-mile range as laid out by the US Department of Energy.¹ LIBs made with Nickel-rich layered oxide cathodes and graphite anodes can maintain energy densities around 250 – 300 Wh/kg at low charge and discharge rates.^{2,3} However, due to slow ion transport encountered with increasingly thick electrodes, these LIBs exhibit poor rate capability, with more than 50% capacity loss experienced at 4C and higher charge/discharge rates.⁴ Graded electrodes (GEs) are one approach that have been proposed to improve the efficiency of lithiation in thick electrodes. GEs assemble two or more electrode layers with differing porosity values into a single thick electrode. In addition to GEs, structured electrodes (SEs) are another means to enhance transport in thick electrodes by re-distributing electrode materials on a micron-scale into line- and grid-pattern electrode architectures. The controlled electrode architecture introduced by SEs reduces the effective electrode tortuosity and enables better electrolyte infiltration in thick battery electrodes.^{5,6} Our research aims to uncover new SE and GE electrode designs for EV batteries. In this study we explored the individual and combined benefits of SEs and GEs for improving the rate capability of high-energy LIBs through computational modeling in VIBE,^{7,8} a suite of multi-scale and multi-physics battery modeling tools developed by Oak Ridge National Laboratory. A three-dimensional physics-based continuum-scale electrochemical model was used in VIBE to model a series of electrode designs for a comparative electrode design analysis, including conventional electrodes, GEs, SEs, and combined SE and GE geometries. A LiNi_{0.6}Mn_{0.2}Co_{0.2}O₂ cathode and graphite anode are used as model material systems due to their current relevance for EVs. To ensure a consistent analysis, the active material loading is held constant for all models to allow us to study the effect of mass distribution and electrode design on LIB rate capability. Our current results show that at high discharge rates of 2C, 4C, and 6C, SE LIBs demonstrate a 33 – 37 % improvement in energy density, and the combined SE and GE LIB electrode designs demonstrate a 46 – 67% improvement in energy density over conventional cells. This study demonstrates the advantage of implementing SEs and GEs for thick electrode LIBs with improved rate capability. These results affirm the need to pursue new manufacturing approaches that enable SE and GE electrode designs to enhance the performance of existing LIB materials.

References

1. Energy Storage Grand Challenge Roadmap, *Energy.gov* (2020) <https://www.energy.gov/energy-storage-grand-challenge/articles/energy-storage-grand-challenge-roadmap>.
2. C. Heubner et al., *Journal of Power Sources*, 419, 119–126 (2019).
3. T. Placke, R. Kloepsch, S. Dühnen, and M. Winter, *J Solid State Electrochem*, 21, 1939–1964 (2017).
4. L. Kraft, J. B. Hadedank, A. Frank, A. Rheinfeld, and A. Jossen, *J. Electrochem. Soc.*, 167, 013506 (2019).
5. K.-H. Chen et al., *Journal of Power Sources*, 471, 228475 (2020).
6. C. L. Cobb and S. E. Solberg, *J. Electrochem. Soc.*, 164, A1339–A1341 (2017).
7. S. Allu et al., *Journal of Power Sources*, 325, 42–50 (2016).
8. S. Allu et al., *Journal of Power Sources*, 246, 876–886 (2014).

Acknowledgement

This material is based upon work supported by the U.S. Department of Energy's Office of Energy Efficiency and Renewable Energy (EERE) under the Advanced Materials and Manufacturing Technologies Office, Award Number DE-EE0010226. The views expressed herein do not necessarily represent the views of the U.S. Department of Energy or the United States Government.

9:30 AM *MT02.04/ES01.04.04

Battery Informatics in Devices & Discovery Steven B. Torrisi; Toyota Research Institute, United States

The increasing accessibility of battery data, both on the device and materials level, is driving exciting new questions in battery science and engineering. These span the full materials life-span, from how fleet-level users can best leverage on-vehicle diagnostic data to how R&D scientists can identify promising new materials. In this talk, I will highlight recent work which explores both device prediction tasks related to vector databases for batteries and history-agnostic degradation prediction as well as data-driven discovery of new principles in cathode design. Attention will be paid to the ways in which industrial, governmental, and academic labs can complement each other's strengths in the collection and use of data.

10:00 AM BREAK

Wednesday Morning, April 24, 2024
Room 425, Level 4, Summit

10:30 AM *ES01.05.01

Where does Na-Ion Fit in The EV space? Active Materials Chemistry, Commercial Scale-Up and Applications [Daniel Friebe](#); Natron Energy, Inc., United States

The acceleration of electric vehicle adoption has elicited perceived and sometimes real shortages in raw materials supplies for Li-ion batteries that lead to price volatility [1] and motivate the search for alternative “post-Lithium” cell chemistries. This presentation will begin with an overview of existing Na-ion cell chemistries and showcase their strengths and limitations in a comparison of currently achievable cell-level energy densities between Na-ion cells and Li-ion cells. Then, Prussian Blue analog (PBA) materials will be discussed in depth as active materials for Na-ion cells. Natron Energy has commercialized the first Na-ion battery that is entirely based on PBA active materials in both positive and negative electrodes. In contrast to earlier concepts that rely on hexacyanoferrate redox couples, we invented a PBA negative electrode material based on hexacyanomanganate(II/I) redox chemistry. Upon charging, sodium manganese hexacyanomanganate accepts an unusually high occupancy with intercalated Na ions, while the C-coordinated Mn site attains a +I oxidation state with low-spin configuration that is typically only encountered in organometallic Mn compounds. The combination of these two unique properties leads to a low sodiation potential near 1.9 V vs. Na/Na⁺. When sodium manganese hexacyanomanganate negative electrodes are paired with positive electrodes based on hexacyanoferrate PBAs, full cell voltages up to 2V can be achieved. While the open structure of PBAs and low voltage limit cell energy density, these cells are capable of extremely fast full charge (up to 20C) and deep discharge (up to 60C) with high energy retention and no risk of thermal runaway. Owing to the minimal structural changes of the PBA host lattice (less than 3% volume change during cycling), this PBA-PBA cell architecture can achieve exceptionally long service life with tens of thousands of cycles [2]. Insight into Natron’s progress in scaling up active materials production and mass manufacturing of cells will be given, and the unique high-rate deep-discharge capabilities will be discussed in the context of commercial applications where Na-ion batteries can close important gaps that are not addressed with Li-ion batteries, especially behind-the-meter applications such as uninterruptible power supplies, demand charge management, and support for electric vehicle fast charging.

[1] “2H 2021 Battery Metals Outlook: The Long Road to Recovery,” BloombergNEF, December 16, 2021.

[2] “Assessment of the first commercial Prussian blue based sodium-ion battery,” He, Minglong, et al, J. Power Sources 548 (2022) 232036.

11:00 AM ES01.05.02

Chemical Pre-Processing of Transition Metal Chalcogenide Electrode Materials [Joseph Stiles](#), Brianna L. Hoff, Fang Yuan, Scott B. Lee, Craig Arnold and Leslie Schoop; Princeton University, United States

We have identified H_xCrS₂, which is produced through proton exchange of NaCrS₂, as a new sodium ion battery electrode with improved performance over its parent material. H_xCrS₂ sees a measured capacity of 728 mAhg⁻¹ and an improvement in diffusion constant of three orders of magnitude better than NaCrS₂. Notably, the structure of H_xCrS₂ consists of an alternating crystalline/amorphous motif as a result of Cr migration during desodiation which is seemingly responsible for the improvement in performance. The alternating structure enables access to reversible Cr redox in the material which supports the high capacities. A range of techniques is used to study the mechanism by which the presence of the amorphous phase allows for these improvements. We then apply similar synthetic conditions to a library of other materials in which removal of the alkali ion results in transition metal migration to identify candidates which may feature similar structural motifs and study their electrochemical behavior. Through the development of pre-processing techniques such as proton exchange, we can re-explore electrode chemistries which may have previously been rejected due to migration of the transition metal in the absence of capacity limiting side reactions.

11:15 AM ES01.05.03

Developing Manganese- and Iron-Rich Cathodes for Sodium-Ion Batteries [Iwnetim I. Abate](#); Massachusetts Institute of Technology, United States

Decarbonizing transportation, grid and industries require low-cost batteries made from abundant, environmentally friendly, sustainable elements in the critical minerals supply chain. To this regard, Mn- and Fe-rich sodium-ion battery cathodes are particularly interesting. However, the practical use of these materials is inhibited by their structural instability upon deep desodiation. In this talk, I will present how my group is combining insights from advanced computational (both ground and excited state) experimental (electrochemistry, x-ray scattering and electron microscopy) techniques 1) to prevent structural disorder during deep desodiation via thermodynamic and kinetic design principles and 2) to develop environmentally sustainable cathodes

11:30 AM *ES01.05.04

Pathways to Commercially Relevant Lithium Metal Batteries for EVs and Electric Aircraft [Brett A. Helms](#); Lawrence Berkeley National Lab, United States

Lithium metal batteries are widely regarded as essential to the greater effort to electrify transportation beyond EVs, while also providing opportunities for fast charge and extended driving range. Yet, while energy density considerations have primarily driven this perspective and R&D investments, there are ongoing challenges in managing ion fluxes across interfaces, which impacts aspects of both performance and cycle life. Here, I will discuss the design of ion-transporting materials, both solids and liquids, which enable lithium metal cell chemistries to meet demanding performance requirements in conventional and emerging uses cases, including eVTOL. I will discuss data-driven research paradigms that accelerate the identification of ion-transporting materials and those that create useful interphases capable of high areal ion fluxes relevant to high power batteries and those capable of fast charge. I will further discuss how these discoveries have been translated into larger cell formats and provide context into how to advance to packs and modules.

SESSION ES01.06: Materials and Manufacturing
Session Chairs: Zachary Hood and Justin Sadowski
Wednesday Afternoon, April 24, 2024
Room 425, Level 4, Summit

1:30 PM ES01.06.01

NiFe₂O₄/N-Doped rGO as Anode Material for Li-Ion Batteries [Yi-Pin Chan](#) and Che-Ning Yeh; National Tsing Hua University, Taiwan

Lithium-ion batteries (LIBs) have become an indispensable part of modern energy storage technologies, characterized by their high energy density, lightweight design, long lifespan, and low self-discharge rates. However, the relentless pursuit of innovation seeks to further elevate LIB capabilities. This study focuses on the development of a high-performance anode material for LIBs, introducing a composite combining nickel iron oxide (NiFe₂O₄) and nitrogen-doped reduced graphene oxide (N-doped rGO). NiFe₂O₄ is well-established for its high theoretical capacity, while N-doped rGO offers excellent conductivity and environmental sustainability. The NiFe₂O₄/N-doped rGO composite material exhibits several advantages. Firstly, it exhibits a high capacity, thanks to the synergistic combination of NiFe₂O₄ and N-doped rGO, resulting in increased energy storage capabilities. Secondly, the outstanding conductivity of N-doped rGO enhances charge transfer kinetics, enhancing the rate of lithium-ion transport and reducing energy losses during charging and discharging processes. Moreover, the NiFe₂O₄/N-doped rGO composite material demonstrates exceptional cycling stability, minimizing capacity degradation over extensive cycles. Its superior rate performance ensures efficiency even at high current rates, making it particularly suitable for high-power applications or scenarios requiring fast charging. Finally, the use of N-doped rGO and nickel iron oxide reduces reliance on finite natural resources and minimizes adverse environmental impacts, aligning with the vision for sustainable energy storage solutions. In conclusion, the NiFe₂O₄/N-doped rGO composite material developed in this work presents a promising solution to meet the present energy storage demands and provides a route for the development of environmentally friendly and sustainable energy technologies.

1:45 PM ES01.06.02

Solvent Design for Earth-Abundant, Mn-Rich Cathodes [Qian Liu](#)¹, [Qijia Zhu](#)^{1,2}, [Jingtian Yang](#)^{1,3} and [Zhengcheng Zhang](#)¹; ¹Argonne National Laboratory, United States; ²Northern Illinois University, United States; ³The University of Chicago, United States

As concerns regarding safety, cost, and material availability continue to rise, cathode chemistries based on earth-abundant, sustainable Mn become an appealing choice. The Li-rich, Mn-rich (LMR) layered-structure cathode materials are promising candidates as they have greater galvanometric energy density compared to conventional cathode materials like LFP and LCO. Existing LMR cathodes still encounter issues such as capacity degradation and surface impedance rise, which highly associated with Mn dissolution/deposition. In this presentation, we will discuss the design of electrolyte solvents that mitigate Mn dissolution. By eliminating highly solvating solvents like ethylene carbonate (EC) and introducing low-solvating solvents, it becomes possible to effectively inhibit Mn dissolution, resulting in significantly enhanced cyclability.

2:00 PM *ES01.06.03

Anti-Corrosive Electrolyte Designs for Lithium Metal Batteries [Jang Wook Choi](#); Seoul National University, Korea (the Republic of)

Electrolyte is a very critical component in lithium metal batteries (LMBs). It is recognized that the solvation structure near the Li ion plays a crucial role in determining the solid-electrolyte-interphase (SEI) properties and thus the reversibility of Li plating and stripping. The concepts of highly concentrated electrolyte (HCE) and locally highly concentrated electrolyte (LHCE) have received much attention these days because of their ability to induce inorganic-rich SEI that is beneficial in improving the cycle life. Nonetheless, most of fluorinated solvents used as diluents in LHCEs have low LUMO levels such that Li metal can easily corrode upon in contact with the electrolytes. I will introduce my group's recent approach of adding an inert solvent in the electrolyte to serve as a kinetic barrier for fluorinated diluents in the so-called swollen SEI layer. The given approach can be expanded to a variety of electrolyte combinations with which both the cycle life and calendar life of LMBs can be improved simultaneously.

2:30 PM BREAK

3:30 PM *ES01.06.04

Challenges and Solutions to Lithium Metal Battery Design for High Performance Applications [Ali Firouzi](#); Cuberg, United States

Cuberg designs and manufactures high energy density, liquid electrolyte-based, lithium metal battery systems for an array of electric aviation and high performance automotive applications. The challenges and phenomena associated with reversibly cycling a lithium metal anode are numerous: the consumption electrolyte in side-reactions, the formation of thick and resistive solid-electrolyte interphases, and the formation of mossy, high surface area lithium deposits. The emergence of these phenomena and their role in limiting cycle life performance are also well-established in literature, but mostly limited to simple constant current charge and discharge profiles. However, when evaluating the cycle life performance of lithium metal pouch cells during realistic aviation flight missions or high-performance automotive drive profiles, these degradation phenomena can be considerably more subtle and complex. In this talk, we will discuss some of the challenges we observe, considerations we have, and design approaches we take when constructing lithium metal batteries for these realistic and high-performance applications.

4:00 PM ES01.06.05

Charging Ahead/All Charged Up: New Technology Goes The Extra Mile for Extreme-Fast Charging of Electric Vehicles [Zhijia Du](#); Oak Ridge National Laboratory, United States

Realizing extreme fast charging (XFC) in lithium-ion batteries for electric vehicles is still challenging due to the insufficient lithium-ion transport kinetics, especially in the electrolyte. Herein, a novel high-performance electrolyte is proposed and tested in pilot-scale, 2-Ah pouch cells. The origin of improved electrochemical performance is comprehensively studied via various characterizations, suggesting that the proposed electrolyte exhibits high ionic conductivity and excellent electrochemical stability at high charging rate of 6-C. Therefore, the high performance electrolyte filled pouch cells deliver improved discharge specific capacity and excellent long-term cyclability up to 1500 cycles under XFC conditions, which is superior to the conventional state-of-the-art baseline electrolyte.

4:15 PM *ES01.06.07

Updates in Lithium-Metal Battery Development [Amal Mehrotra](#); QuantumScape Corporation, United States

Today's conventional lithium-ion batteries fall short of meeting the needs of many automotive, consumer electronics, and stationary storage applications. Many believe that the unique cell design of solid-state lithium-metal batteries will help bridge this gap – particularly when it comes to electric vehicles – because the technology is designed to enable longer range, faster charging and enhanced safety compared to conventional lithium-ion batteries. In this talk, QuantumScape Senior Director of Cell Development, Amal Mehrotra, will highlight recent developments in solid-state lithium-metal technology and review some of the challenges in transitioning from R&D to a commercial product.

SESSION ES01.07: Poster Session
Session Chairs: Jeffrey Cain, Zachary Hood and Yue Qi
Wednesday Afternoon, April 24, 2024
Flex Hall C, Level 2, Summit

5:00 PM ES01.07.01

A Glycerol Triacetate based Flame Retardant High-Temperature Electrolyte for The Lithium-Ion Battery Xinsheng Wu, Tong Liu, Young-Geun Lee and Jay Whitacre; Carnegie Mellon University, United States

Rechargeable batteries that can operate at elevated temperatures (>70 °C) with high energy density are long-awaited for industrial applications including mining, grid stabilization, naval, aerospace, and medical devices¹. However, the safety, cycle life, energy density and cost of the available high-temperature battery technologies remain an obstacle primarily owing to the limited electrolyte options available². Here, we demonstrated a flame-retardant electrolyte that can enable stable battery cycling at 100 °C by incorporating triacetin into the electrolyte system. Triacetin has excellent chemical stability with lithium metal and conventional cathode materials can effectively reduce parasitic reactions and promises a good battery performance at elevated temperatures. Our findings reveal that Li-metal half-cells can be made that have high energy density, high coulombic efficiency, and good cycle life with triacetin-based electrolytes and three different cathode chemistries. The high-temperature failure mechanism of different cathode chemistries was also investigated and compared. Moreover, the nail penetration test in a commercial-scale pouch battery using triacetin-based electrolyte system demonstrated suppressed heat generation when the cell was damaged and excellent safety when using the triacetin-based electrolyte. These results demonstrated a new low-cost high-temperature flame-retardant electrolyte candidate which holds significant importance in developing a more robust electrolyte system for high-temperature secondary battery applications.

[1] Chen, T.; Jin, Z.; Liu, Y.; Zhang, X.; Wu, H.; Li, M.; Feng, W. W.; Zhang, Q.; Wang, C. *Angewandte Chemie - International Edition* **2022**, *61* (35).
[2] Ren, D.; Feng, X.; Liu, L.; Hsu, H.; Lu, L.; Wang, L.; He, X.; Ouyang, M. *Energy Storage Mater* **2021**, *34*.

5:00 PM ES01.07.02

Bi-Doped Low-Cost P2 Layered Sodium Ion Battery Cathode with Improved Cycling Stability Xinsheng Wu and Jay Whitacre; Carnegie Mellon University, United States

Sodium-ion batteries, free from material scarcity concerns, offer potential for versatile applications across various industries. However, the development of an optimal cathode material for sodium ion batteries remains a challenge in part due to long term stability issues. Among the various cathode chemistries explored for sodium-ion battery applications, those based on layered transition metal oxides have displayed promise, primarily due to their high energy density and scalability. Our work demonstrated a novel modified P2 layered sodium ion cathode material created via the introduction of bismuth into a manganese and iron-based layered transition metal oxide material, specifically $\text{Na}_{0.8}\text{Mn}_{0.75}\text{Fe}_{0.2}\text{Al}_{0.05}$. Our research has demonstrated that even a small amount of bismuth doping can have a profound impact on the cycling stability of this cathode material, both in half cells and also in hard carbon anode full cells. Furthermore, ambient environment storage of the Bi-doped materials (even in humid environments) does not reduce performance and in some cases seems to improve it. This finding holds promise for enhanced feasibility and reliability in sodium-ion batteries and could be beneficial for advancing the application of sodium-ion batteries in large-scale applications.

5:00 PM ES01.07.03

Low-Cost Silicon from Natural Sand for Lithium-Ion Batteries and Its Electrochemical Response to Oxygen Content Zhigang Z. Fang, Zehua Lin, Pei Sun and Chengshang Zhou; University of Utah, United States

The cost-effectiveness is an essential factor to be considered for the commercial viability of Silicon (Si) anode for lithium-ion batteries, alongside factors such as electrochemical performance and safety considerations. Here, we utilized low-cost natural sand as raw material and employed the magnesiothermic reduction method to produce battery-grade silicon with an impressive ~98% yield rate. Additionally, Si with varying oxygen content was produced by adjusting the stoichiometry of magnesium and reduction temperature. We also explored the effect of oxygen content on the electrochemical performance as an anode. Our findings indicated a linear decrease in both the initial discharge capacity and initial coulombic efficiency with increasing oxygen content. In contrast, the capacity retention at the 20th cycle and the lithium-ion diffusion coefficient exhibited an opposing trend. By comparing the electrochemical impedance spectroscopy and lithium-ion diffusion coefficient of those samples, we observed that the sample with high-oxygen content samples displayed less change in charge transfer impedance after cycling, while their lithium-ion diffusion coefficient exhibited a more pronounced increase.

5:00 PM ES01.07.04

The Correlation between The Mechanical/Rheological Properties of Fibrin, a Novel Binder used in Silicon Anodes of Lithium-Ion Batteries, and Its Performance Woong-Ju Kim and Dong-Wan Kim; Korea University, Korea (the Republic of)

Silicon binders, in the context of lithium-ion batteries, refer to polymers that are used to hold the silicon particles together and adhere them to the current collector. These binders play a crucial role in maintaining the structural integrity of the electrode during the repeated lithiation and delithiation cycles. The unique properties of silicon binders can be described as functional groups for hydrogen bonding, flexibility and elasticity, adhesion and cohesion. In this work, to optimize mechanical/rheological properties, the fibrin was modified through mixing with alginate and cation cross-linking. Fibrin is class of bio-polymer which contains abundant amino acids, also structured as 3D-network. When fibrin is mixed with alginate and then cross-linked, they stand as interpenetrating network, therefore enhances the mechanical strength. Furthermore, bonding mechanism with silicon was classified by FT-IR measurement. To measure mechanical properties of fibrin-based binder, peel test and advanced rheometric expansion system (ARES) were performed. Due to structural difference, fibrin based binder exhibits higher adhesion forces (3D network for fibrin, linear structure for alginate). In ARES measurement, alginate behaves like a viscous fluid ($G'' > G'$). In contrast, for fibrin-based binders, G' dominates over G'' at all ω values, indicating that they are more like elastic solids. However, in close look, at $\omega = 1 \text{ rad s}^{-1}$, fibrin exhibits the highest stiffness ($G' = 29 \text{ kPa}$) and the lowest stress relaxation ($G'' = 5.4 \text{ kPa}$). When fibrin is mixed with alginate at a 4:1 mass ratio (F4A1), the stiffness ($G' = 26 \text{ kPa}$) decreases by only ~12%, but the relax stress ($G'' = 8.6 \text{ kPa}$) is enhanced near by 60%. Due to ionic cross-linking of the alginate chains of F4A1 (F4A1-10Ca), finally optimized mechanical and rheological properties. F4A1-10Ca exhibits G' (28 kPa), which is comparable to the fibrin while maintaining G'' (7.9 kPa) that is comparable to the F4A1. As a result, when using a binder as F4A1-10Ca, it is expected to tightly hold electrode components while effectively relaxing stress. Upon these data, the electrochemical performance was conducted. As consequence, cycle stability was series of alginate<fibrin<F4A1<F4A1-10Ca, which is coincide with ARES prediction.

ACKNOWLEDGEMENTS

This work was supported by a National Research Foundation of Korea (NRF) grant funded by the Ministry of Science and ICT (2022R1A2C3003319).

5:00 PM ES01.07.05

High-Performance CuO as an Anode Material via Facile Synthesis for Lithium-Ion Batteries Nischal Oli¹, Sunny Choudhary¹, Brad Weiner², Gerardo Morell¹ and Ram Katiyar¹; ¹University of Puerto Rico, Rio Piedras, United States; ²University of Puerto Rico at Río Piedras, United States

While carbon matrices have demonstrated effectiveness in enhancing the electrical conductivity and accommodating the volume expansion of CuO-based anode materials in lithium-ion batteries (LIBs), achieving an optimized utilization ratio of the active CuO component remains a challenging obstacle. In this investigation, we have devised a straightforward synthesis approach to fabricate ultrafine CuO nanoparticles integrated within a high surface area carbon matrix denoted as CuO@C. We discovered that with the use of sodium carboxymethyl cellulose binder and fluoroethylene carbonate additives, this anode exhibits enhanced performance compared to previous reports. This material, owing to its distinctive architecture, reveals a notable reversible capacity of 800 mA h g⁻¹ at 100 mA g⁻¹ following 100 cycles and exhibits prolonged cycling stability, recording a reversible capacity of 450 mA h g⁻¹ at 400 mA g⁻¹ over 500 cycles. The exceptional lithium-storage performance of CuO@C is attributed to its high surface area carbon matrix and the presence of ultrafine CuO nanoparticles, which afford a greater abundance of exposed active sites favorable to electrochemical reactions.

Keywords: CuO, high surface area, carbon matrix, lithium-ion batteries, electrochemical reactions

5:00 PM ES01.07.06

Investigation of 3-Dimensional Structured Anodes for Fast Charging in Lithium-Ion Batteries Michelle E. Katz¹, Vinh Q. Nguyen¹, Daniel Abraham² and Corie L. Cobb¹; ¹University of Washington, United States; ²Argonne National Laboratory, United States

Lithium-ion batteries (LIBs) with fast charging capabilities are a critical component in electric vehicles (EVs) to reduce charging times to 15 minutes or less.¹ Current research and development efforts are focused on optimizing fast charge behavior with graphitic and silicon-based anodes. However, these anode materials face challenges which include irreversible side reactions, lithium plating, and cracking caused by volumetric strain, all of which limit their fast charge behavior. As an alternative to graphite and silicon, the use of Li₄Ti₅O₁₂ (LTO) anodes in LIB cells has been discussed.^{2,3} LTO is considered a zero-strain material and, furthermore, does not develop a solid-electrolyte-interphase (SEI) during electrochemical cycling. These properties help improve cycling stability and safety at high discharge rates. Although the higher nominal voltage of LTO (~1.5 V vs. Li⁺/Li) leads to lower energy density, recent research into material modification and discharge strategies that improve LTO energy density make it more attractive for fast charging.⁴ Additionally, 3-dimensional (3D) electrodes have been investigated by researchers over the last few decades to improve power density of battery cells.^{5,6} In this work, we take this concept a step further and investigate the impact of 3D structural design on the fast charge performance of LTO anodes. Our objective is to determine if a re-design of electrode architecture can enable better fast charging behavior for rates up to 10C and make these LTO anodes competitive with graphite-based anodes.

Acknowledgement

This work was funded in part by a Defense Advanced Research Projects Agency (DARPA) Young Faculty Award and Director's Fellowship under grant number D19AP00038. The views, opinions, and findings expressed in this work are those of the authors and should not be interpreted as representing the official views or policies of the Department of Defense or the U.S. Government, and no official endorsement should be inferred. This is approved for public release and distribution is unlimited.

(1) Vehicle Technologies Office. *Batteries 2021 Annual Progress Report*; Department of Energy, 2021.

(2) Wu, Y.; Wang, W.; Ming, J.; Li, M.; Xie, L.; He, X.; Wang, J.; Liang, S.; Wu, Y. An Exploration of New Energy Storage System: High Energy Density, High Safety, and Fast Charging Lithium Ion Battery. *Advanced Functional Materials* **2019**, *29* (1), 1805978. <https://doi.org/10.1002/adfm.201805978>.

(3) Jin, X.; Han, Y.; Zhang, Z.; Chen, Y.; Li, J.; Yang, T.; Wang, X.; Li, W.; Han, X.; Wang, Z.; Liu, X.; Jiao, H.; Ke, X.; Sui, M.; Cao, R.; Zhang, G.; Tang, Y.; Yan, P.; Jiao, S. Mesoporous Single-Crystal Lithium Titanate Enabling Fast-Charging Li-Ion Batteries. *Advanced Materials* **2022**, *34* (18), 2109356. <https://doi.org/10.1002/adma.202109356>.

(4) Yuan, T.; Tan, Z.; Ma, C.; Yang, J.; Ma, Z.-F.; Zheng, S. Challenges of Spinel Li₄Ti₅O₁₂ for Lithium-Ion Battery Industrial Applications. *Advanced Energy Materials* **2017**, *7* (12), 1601625. <https://doi.org/10.1002/aenm.201601625>.

(5) Cobb, C. L.; Solberg, S. E. Communication—Analysis of Thick Co-Extruded Cathodes for Higher-Energy-and-Power Lithium-Ion Batteries. *J. Electrochem. Soc.* **2017**, *164* (7), A1339–A1341. <https://doi.org/10.1149/2.0101707jes>.

(6) Ashby, D. S.; Choi, C. S.; Edwards, M. A.; Talin, A. A.; White, H. S.; Dunn, B. S. High-Performance Solid-State Lithium-Ion Battery with Mixed 2D and 3D Electrodes. *ACS Appl. Energy Mater.* **2020**, *3* (9), 8402–8409. <https://doi.org/10.1021/acsam.0c01029>.

5:00 PM ES01.07.07

Novel Design and Scalable Synthesis of Silicon Anodes for High-Energy Lithium-Ion Batteries Muqiao Su and Min-Kyu Song; Washington State University, United States

As the world races toward achieving net-zero emissions by 2050, there will inevitably be a surge in demand for high-energy batteries. Silicon is one of the most promising anode materials for next-generation lithium-ion batteries because it possesses a theoretical specific capacity that is almost ten times higher than that of the current graphite anode. However, silicon-based anodes usually suffer from a short cycle life due to the particle pulverization caused by the substantial volume change of Si (~300%) during the lithiation and delithiation process. To improve the cyclability of silicon anodes, we developed a novel scalable process for synthesizing bulk-core, porous-shell silicon that can alleviate the detrimental effects caused by volume expansion. By precisely controlling the processing parameters, both the size of the bulk core and the thickness of the porous shell can be tailored. The silicon with novel structure exhibits excellent electrochemical performances, much greater than 3D porous and bulk silicon counterparts. To further enhance the cycling performance of silicon, carbon coating was implemented via polydopamine precursor. The resulting Si-C composites showed good cycling performance up to 500 cycles. Our research offers a novel, scalable, low-cost production route for silicon anodes for high-energy lithium-ion battery applications.

5:00 PM ES01.07.08

Single-Pot Hydrothermal Synthesis, Characterization and Electrochemical Properties of SnO₂ Nanostructures Mushtaq Ahmad Dar¹, Hany Sayed Abdo¹, Mohammad Rezaul Karim¹, Nabeel H. Alharthi¹ and Dong-Wan Kim²; ¹King Saud University, Saudi Arabia; ²Korea University, Korea (the Republic of)

Nanostructured materials have gained significant interest in the field of science owing to their exceptional characteristics and efficacy in numerous fields. Tin oxide (SnO₂) shows potential as a material for energy storage purposes, namely in lithium-ion batteries. The electrochemical properties of this material make it a promising candidate for anode materials, allowing for effective storage and release of lithium ions during charging and discharging processes. Tin

oxide's effective electrical conductivity enhances battery performance, making it a crucial constituent in the development of advanced and efficient energy storage technologies. This investigation into the electrochemical characteristics of tin oxide represents a significant advancement in the effort to enhance the efficacy and reliability of battery technology across several fields.

In this research, we successfully produced tin dioxide (SnO₂) nanostructures inspired by sea-urchins by using a hydrothermal process strategy. The hydrothermal approach, known for its low cost and effectiveness, enables the specific development and distribution of tin dioxide nanoparticles, replicating the unique structure of sea-urchins.

The growth of radially arranged rutile-SnO₂ nanostructures with a size range of 1.5-2 μm was confirmed by conducting an in-depth analysis using a variety of methods, such as x-ray diffraction (XRD), thermogravimetric analysis (TGA), fourier-transform infrared spectroscopy (FTIR), field-emission scanning electron microscopy (FESEM), and transmission electron microscopy (TEM). The combined results from these investigations have verified the formation of nanostructures with a high level of purity, that have a unique radial pattern. The nanostructures had a unique morphology consisting of separate nanorods, each measuring roughly 300 nm in length and with widths varying from 30 to 50 nm. The building of rutile-SnO₂ nanostructures exhibited a high degree of homogeneity and accuracy, as evidenced by the extensive characterization techniques. Interestingly, electrochemical experiments used to evaluate these nanostructures features revealed their remarkable reversible lithium storing ability. The nanostructures demonstrated a consistent and reversible lithium storage capacity of 590 mAh. g⁻¹, even after undergoing 30 cycles of charging and discharging. This demonstrates their potential as exceptional materials for lithium-ion battery applications.

The controlled synthesis of radially ordered rutile-SnO₂ nanostructures with excellent electrochemical characteristics is demonstrated in this work, which offers significant insights into the process.

This project was funded by the National Plan for Science, Technology, and Innovation (MAARIFAH), King Abdulaziz City for Science and Technology, Kingdom of Saudi Arabia, Award Number (2-17-02-001-0053)

5:00 PM ES01.07.09

Structure Relaxation Contributes to Spinel-Like Phase Transformation in High-Mn-Content Disordered Rock Salt Cathode Materials [Tianyu Li](#) and Raphaële Clement; University of California, Santa Barbara, United States

Li-excess Mn-based disordered rock salt structures (DRXs) are potential cathode materials due to the low cost of Mn and their high theoretical capacities. Recently it was discovered that high Mn content DRXs exhibit gradually enhanced capacity during cycling, potentially due to the formation of a new spinel-like phase (delta phase). We hypothesize that the formation of the spinel-like structure is driven by the thermodynamic stabilization of delithiated high Mn DRXs. To verify our hypothesis and isolate the influence of delithiation, chemically delithiated DRX is prepared. We systematically studied its structure behavior under heating to mimic the thermal relaxation process of the delithiated DRX in battery cycling. We confirmed that the thermal relaxation of delithiated DRXs leads to the formation of the spinel-like phase and the spinel-like phase contributes to the capacity enhancement. With synchrotron X-ray and neutron diffractions, we studied the structure of spinel-like phase in detail. Through comparing the thermal relaxation behavior of delithiated High-Mn and low Mn DRX, we revealed the potential origins of the phase transformation in high Mn DRX under battery cycling.

5:00 PM ES01.07.10

A New High-Valent Fe-Based Redox Couple in Intercalation Electrodes [Hari Ramachandran](#)¹, Edward W. Mu¹, Eder Lomeli¹, Augustin Braun¹, Masato Goto², Kuan Hsiang Hsu¹, Jue Liu³, Grace Busse¹, Yuichi Shimakawa², Edward Solomon¹, Wanli Yang⁴, Thomas Devereaux¹ and William C. Chueh¹; ¹Stanford University, United States; ²Kyoto University, Japan; ³Oak Ridge National Laboratory, United States; ⁴Lawrence Berkeley National Laboratory, United States

Layered transition metal (TM) oxides (LiTMO₂) are attractive positive electrode materials for use in portable energy storage applications such as electric vehicles, primarily due to their high energy densities and their robust charge-discharge behavior. However, the persistent use of TMs such as Co and even Ni, which are both limiting in their cost and abundance, will restrain current technology from keeping up with the rapidly growing demand for portable batteries. There is, therefore, a great incentive to incorporate inexpensive, earth-abundant elements in commercial batteries. Iron is the perfect candidate, given its availability and low mining/refining cost. However, high-voltage Fe-based redox systems based on the Fe^{3+/4+} couple always exhibit simultaneous anionic redox and O₂ release, and as a result, always display highly hysteretic charge-discharge behavior.

Surprisingly, the compound Li(Li_{1/3}Fe_{1/3}Sb_{1/3})O₂ (Li₄FeSbO₆, referred to as LFSO henceforth) does form a layered system and exhibits remarkably stable electrochemical charge/discharge characteristics with < 0.2 V of hysteresis. LFSO forms a layered structure, with Li⁺, Fe³⁺ and Sb⁵⁺ sites having honeycomb ordering in the TM layer. Upon electrochemical cycling, this material exhibits a voltage plateau at ~4.2 V, which is stable for multiple cycles and corresponds to an extraction of almost 2 Li⁺ per formula unit during the first discharge. Several details about the electrochemistry of this material are striking. Firstly, the discharge potential is 4 V vs. Li⁺/Li, which is greater than the reported average potential of conventional NMC-based systems (~3.8 V). The first cycle charge capacity is close to 175 mAh/g, which is similar to the theoretical capacity of LiFePO₄ (165 mAh/g, operating at 3.2 V). Many questions remain regarding the mechanism behind the electrochemical performance of LFSO. For instance, the nature of the electronic charge compensation that accompanies (de)lithiation is poorly understood. Additionally, the structural transformations that accompany the redox plateau have not been thoroughly characterized. Investigating the electronic and lattice structures of LFSO is of great importance, as Fe-based redox in layered systems has not been studied before.

In this work, we address this gap using a variety of synchrotron and lab-based characterization techniques. We use X-ray absorption spectroscopy (XAS)-based techniques to investigate the electronic charge compensation mechanism during (dis)charge. We use Fe-L edge Resonant Inelastic X-ray scattering (RIXS) in conjunction with O-K edge RIXS (both of which are known to be sensitive to TM-3d orbitals) to accurately characterize the changes in Fe and O valence orbital occupancies during (dis)charge. Coupled with ⁵⁷Fe Mössbauer spectroscopy and charge-transfer multiplet calculations, we present a complete picture of the electronic structure changes that accompany electrochemical (de)lithiation and identify the redox-active species in the reaction. We also perform X-ray diffraction (XRD) experiments to study the structural transformations during the (dis)charge.

Our results show that the 4.2 V plateau is accompanied by a classical two-phase transition, and the electronic charge compensation stems from a novel high-valent Fe-based redox couple. While the presence of Sb in the system limits its commercial interest, LFSO serves as the ideal model system in which to characterize high-valent Fe redox. Some preliminary work carried out into substitution/doping strategies opens the door to achieving low-hysteresis, high voltage Fe redox in layered oxides using earth-abundant elements, which could serve to reduce our dependence on Co/Ni-based positive electrodes.

5:00 PM ES01.07.11

Accessing p- and n-type Polyimide Covalent Organic Frameworks via Post-Synthetic Linker Exchange for High-Performance Cathodes in Sodium-Ion Batteries [Swati Jindal](#), Zhengnan Tian, Osama Shekhah, Husam N. Alshareef and Mohamed Eddaoudi; King Abdullah University of Science and Technology, Saudi Arabia

Rechargeable metal-ion batteries have become a viable portable technology to fulfill the growing global energy demand and diminishing fossil fuel supply. Due to their abundance of reserves and wide operating temperature range, sodium-ion batteries (SIBs) have been predicted to be a rapidly emerging field in the post-lithium era. However, the sluggish intercalation kinetics of Na⁺ ions with cathode materials have limited their usefulness.

Recently, researchers have been looking into alternate cathode materials to get around these limitations and enhance the energy density and cycle performance of SIBs. Therefore, we have done this study, which focuses on the synthesis of highly crystalline and porous bipolar redox-active polyimide-linked covalent organic framework (COF), and deployed it as a cathode material for SIBs. For this purpose, we have designed and synthesized a **TPDA-NDI-COF** by incorporating n-type carbonyl-based reversible redox centers into the p-type triphenylamine-based structure via a post-synthetic linker exchange technique. This approach was successful and led to the formation of a highly crystalline and purposeful polyimide, which was not achievable via direct synthesis. The **TPDA-NDI-COF** exhibits a wide potential window of 1.0 to 3.6 V vs. Na⁺/Na, making it a good candidate as a cathode for SIBs. An advantageous specific capacity of 120 mAh/g at 0.02 A/g can be achieved by doping 50% CNT into the COF. This allows the capacity to be maintained at 92 mAh/g at 1.0 A/g, and even after 5000 cycles, COFs demonstrate the cathode's extraordinarily extended longevity. Our synthetic TPDA-NDI-COF shows an average discharge voltage of 2.1 V, outperforming most recently published COF hosts. We believe this approach will pave the way for boosting the synthesis and design of COFs with more desired properties for energy storage and other various applications.

5:00 PM ES01.07.12

Achieving a 3.0 V Cl-CHBC||LFP Battery via Antisolvent Crystallization-Induced Contorted Polycyclic Aromatic Hydrocarbons Jee Ho Ha and Seok Ju Kang; Ulsan National Institute of Science & Technology, Korea (the Republic of)

Organic materials, both small and polymeric, play vital roles in rechargeable Li-ion batteries (LIBs) due to their cost-effectiveness, tunability, and lightweight nature. Polymeric materials, known for their binding and insulating properties, serve as essential components, acting as binders and separators in LIBs. Recent advancements have explored organic materials as active components in both cathodes and anodes, displaying promising electrochemical performance.

Organic anodes, in particular, offer reliable performance compared to traditional graphite-based anodes but face challenges like solubility in electrolytes and conductivity issues. To address these limitations, crystalline conjugated small molecules, especially polycyclic aromatic hydrocarbons (PAHs), have emerged as potential organic anode materials. PAHs enable efficient Li-ion intercalation and deintercalation, enhancing rate performance.

Among these materials, Cl-CHBC, featuring large Cl atoms, stands out as a versatile anode applicable to LIBs, NIBs, and KIBs. Its crystalline structure accommodates various cation sizes, facilitating diffusion-controlled intercalation. Cl-CHBC exhibits superior rate performance and a single lithiation process, comparable to expensive LTO anodes.

In comprehensive battery experiments with LFP as the cathode and Cl-CHBC as the anode, superior electrochemical performance was observed compared to conventional setups. Cl-CHBC, when combined with inorganic cathode, offers potential cost-effective alternatives to conventional anodes, addressing previous limitations and improving power densities.

5:00 PM ES01.07.13

Topotactic Transformation of Lithium-Excess Spinel to Layered LiMn_{0.5}Ni_{0.5}O₂: The Interaction of 3D and 2D Li-Ion Diffusion Boyu Shi¹, Jihyeon Gim¹, Anh Vu¹, Tianyi Li¹, Dewen Hou^{1,2}, Yuzi Liu¹, Jacob Jorne³, Jason Croy¹, Michael Thackeray¹ and Eungje Lee¹; ¹Argonne National Laboratory, United States; ²Boise State University, United States; ³University of Rochester, United States

The cathode material plays a crucial role in shaping batteries' energy density and cycling performance, driving intensive research efforts for improvement.¹ Cathode materials such as LiNixCoyMnzO2 (NCM) and LiNixCoyAlzO2 (NCA) (Co ≤ 33%) have merged as prospective options for electric vehicle (EV) cathodes.² Despite their advantages in higher specific capacity and cost reduction when compared to cobalt-based cathodes, the high-nickel cathodes encounter challenges such as capacity degradation and instability, aggravated by the rising nickel prices. Consequently, the pursuit of novel cathode materials from economically viable and earth-abundant elements gains increasing attention, holding potential for enhanced thermal stability and cycling performance.³

Our recent study unveiled a novel Co-free, LxS-LiMn_{0.5}Ni_{0.5}O₂ (LxS-LMNO) cathode based on a cubic lithium-excess spinel structure type. The LxS structure surpasses conventional spinels such as LiMn₂O₄ and LiMn_{1.5}Ni_{0.5}O₄ by doubling the Li concentration in its pristine state, while maintaining its cubic symmetry. The Li/LxS-LMNO cell shows remarkable energy density, delivering ~225 mAh/g capacity from 2.5 – 5.0 V, with ~96% retention after 50 cycles. Additionally, the 3D Li-ion diffusion channels provided by its spinel framework allow faster lithium diffusion compared to layered LiMn_{0.5}Ni_{0.5}O₂ polymorph, showing promise as a high-performance cathode.⁴

Our previous work demonstrated that LMNO stabilizes into the LxS structure at lower synthesis temperatures, while favoring the layered phase at higher temperatures. Such observation suggests a temperature-driven phase transition and structural integration occurring within the range typical for solid-state reactions. This dynamic interplay between these phases likely impacts the material's structure and electrochemical properties significantly. Gaining a comprehensive understanding of the temperature-dependent phase transitions holds promise for innovative cathode material design.

Thus, this study focuses on varying LMNO synthesis temperatures to probe the phase transition and its implications. Results indicate a parabolic relationship between the electrochemical performance of LMNO materials and synthesis temperature. This trend primarily stems from the dynamic transformation of Li-ion diffusion channels. This study not only enhance our understanding of LMNO materials but also lays the groundwork for the future development of cutting-edge cathode materials relying on the LxS structure.

(1) Mekonnen, Y.; Sundararajan, A.; Sarwat, A. I. A review of cathode and anode materials for lithium-ion batteries. In *SoutheastCon 2016*, 2016; IEEE: pp 1-6.

(2) Choi, J. U.; Voronina, N.; Sun, Y.-K.; Myung, S.-T. Recent Progress and Perspective of Advanced High-Energy Co-Less Ni-Rich Cathodes for Li-Ion Batteries: Yesterday, Today, and Tomorrow. *Advanced Energy Materials* **2020**, *10* (42), 2002027.

(3) Gutierrez, A.; Tewari, D.; Chen, J.; Srinivasan, V.; Balasubramanian, M.; Croy, J. R. Earth-Abundant, Mn-Rich Cathodes for Vehicle Applications and Beyond: Overview of Critical Barriers. *Journal of The Electrochemical Society* **2023**.

(4) Shi, B.; Gim, J.; Li, L.; Wang, C.; Vu, A.; Croy, J. R.; Thackeray, M. M.; Lee, E. LT-LiMn 0.5 Ni 0.5 O 2: a unique co-free cathode for high energy Li-ion cells. *Chemical Communications* **2021**, *57* (84), 11009-11012.

5:00 PM ES01.07.14

Unveiling The Correlation between Synthetic Parameter and Structural Stability of O-Redox Cathodes via Time-Resolved XRD Analysis on The Solid-State Synthesis Seungmin Lee¹, Sang Hyuk Gong¹, Kyungwo Choi², You Seung Rim³, Teakjib Choi³ and Hyungseok Kim¹; ¹Korea Institute of Science and Technology, Korea (the Republic of); ²Sungkyunkwan University, Korea (the Republic of); ³Sejong University, Korea (the Republic of)

The demand for high-energy-density sodium-based batteries has led to the investigation of the oxygen-redox (O-redox) reaction to increase the theoretical

capacities of conventional cathodes. This O-redox reaction is triggered by introducing substitutes or vacancies in the transition metal (TM) layer, which generate the non-bonding electrons of lattice oxygens, thus providing additional capacity [1]. In terms of O-redox stability, the atomic arrangement of substitutes or vacancies in TM layer, which affects the distance between redox-active oxygens and TM migration barrier, is considered crucial for determining O-redox stability [1-2]. However, the construction mechanism of O-redox cathodes during synthesis and its correlation with O-redox stability has not been fully understood.

Herein, we aim to investigate the construction mechanism of O-redox cathodes during solid-state synthesis and evaluate their O-redox stability. Specifically, we monitor the evolving structure of cathode precursors using time-resolved X-ray diffraction (TR-XRD) analysis by controlling the synthetic parameter. Subsequently, in-depth structural studies on the cathodes are conducted using advanced characterization tools such as high-resolution electron microscopy (HR-TEM) and X-ray absorption spectroscopy (XAS). Our structural analyses reveal how the synthetic parameter influence the final cathode structure, and we further correlate these findings with the O-redox stability using the electrochemical tests.

5:00 PM ES01.07.15

Thermo-Electrochemical Characterization of $\text{LiNi}_{0.8}\text{Co}_{0.15}\text{Al}_{0.05}\text{O}_2/\text{Graphite}+\text{Si}$ Full Cells Across Commercial and Academic Form Factors Patrick J. West^{1,2}, Nicolas Lepout³, Rachel Carter¹, Corey T. Love¹, Laurent Pilon^{3,3,3} and Gordon Waller¹; ¹US Naval Research Laboratory, United States; ²American Association for Engineering Education, United States; ³University of California, Los Angeles, United States

As electrochemical systems increase in size from academic coin cells to commercial 18650's and beyond, so too do concerns about how excess heat generation can compromise the cell's safety and performance. Heat generation in lithium ion battery systems can be attributed to a number of factors, including (1) reversible heat from desired electrochemical reactions (2) joule heating from polarization effects (3) heat of mixing from concentration effects and (4) unwanted side reactions, all of which are influenced by the system's state of charge (SoC) and operating c-rate. Coupling galvanostatic cycling with isothermal calorimetry enables the observation of heat flow during cell operation and the quantification of the system's thermodynamic parameters, like enthalpy and entropy. Enthalpy calculations (kJ/mol of Li^+), found experimentally by the monitoring of heat flow during cell operation, must carefully correlate observed heat signatures and electrochemical processes. This requires low c-rates where overpotentials are suppressed and the observed heat flow is dominated by reversible heat. On the other hand, systematically recording the relationship between temperature and equilibrium voltage at various SoCs provides entropic information and informs the thermodynamics of the system at rest. [1] Theoretically, these thermodynamic measurements should be material specific that rely on the electrochemical redox pair's SoC, but experimental measurements are also influenced by form factor. When thermo-electrochemical characterization is performed on commercial 18650's, slow c-rates (<C/10) can be used to ensure that the observed heat is dominated by reversible heat from electrochemical reactions, but thermodynamic conclusions are limited to the cell level because both the cathode's and anode's active material exhibit changing entropic behavior with respect to their lithiation state. Academic coin cells, on the other hand, allow for entropic behavior to be attributed to the working electrode's active material through Li metal half-cell experimentation, but are not as robust as commercial cells.

In this work, entropic and enthalpic experiments were performed on a commercial $\text{LiAl}_{0.8}\text{Co}_{0.15}\text{Al}_{0.05}\text{O}_2$ (NCA)/Graphite+Si Li-ion 18650 cell using isothermal calorimetry coupled electrochemical testing. Then, in order to observe contributions from the anode and the cathode separately, the commercial 18650 was disassembled and the recovered electrodes were used to create coin cell half cell with Li metal anodes and coin cell full cells. Coin cell level calorimetry found that the majority of heat generation during (dis)charge originated from the electrode undergoing delithiation. Additionally, full cell entropic potential measurements were reconstructed from coin cell half-cell data, elucidating which electrode-specific processes dictate the system's thermodynamics at different SoCs. Together, heat signature collected across commercial and academic form factors and cell configurations compile an index of thermodynamic and kinetic behaviors of the NCA/Graphite+Si system. These findings will be discussed through a lens meant to inform decisions around commercial cell operation conditions while also serving as an experimental template for thermo-electrochemical comparisons of Li-ion battery systems across commercial and academic form factors.

1. Baek, S.W., et al., Potentiometric entropy and operando calorimetric measurements reveal fast charging mechanisms in $\text{PNb}_9\text{O}_{25}$, Journal of Power Sources, 2022. 520: p. 230776.

5:00 PM ES01.07.16

Synthesis and Electrochemical Properties of Si_xO Composite Anode Materials for Li Secondary Batteries Seunghyeok Jang and Jae-Hun Kim; Kookmin University, Korea (the Republic of)

The rising popularity of electric vehicles and advanced portable electronic devices has intensified the demand for power sources with higher energy density. Among the available options, Li-ion batteries (LIBs) emerge as a pivotal power source, appreciated for their elevated energy density, cost-effectiveness, and prolonged cycle life. Presently, graphite-based materials dominate as anode materials in LIBs due to their superior cycle performance. However, their capacities are constrained, necessitating the exploration of alternative materials.

Li-alloy-based materials have garnered significant attention due to their high reversible capacities achieved through Li-alloying reactions during Li insertion and extraction cycling. Among these materials, silicon (Si) stands out as a promising anode material, boasting a theoretical capacity (3580 mAh g⁻¹, $\text{Li}_{3.75}\text{Si}$ phase) approximately 10 times higher than that of graphite. However, the substantial volume fluctuations experienced by Si during repetitive Li-alloying/dealloying cycles in charge and discharge processes can result in the mechanical breakdown of the electrode. Consequently, electrical contact loss occurs between Si active material particles and the current collector.

Silicon oxides (SiO_x , $0 < x < 2$) have also become subjects of active investigation as Li-alloy-type anode materials. Their cycling performance is generally superior to Si-based materials because oxygen can mitigate the volume changes in active Si. However, the widespread use of silicon oxide is hindered by its low initial Coulombic efficiency.

In this study, we introduce a new SiO_x composite material that combines the advantages of both Si and silicon oxide. The materials were synthesized through a straightforward milling process, demonstrating remarkable electrochemical performance when utilized as an anode for LIBs.

5:00 PM ES01.07.17

Enhancing Interfacial Reaction Rates in Extremely Fast Charging Li-Ion Batteries Using Linear Carbonate-Based, High-Concentration LiPF_6 Electrolytes Hyuntae Lee¹, Hyeongguk An¹, Hongjun Chang², Janghyuk Moon², Sujong Chae³ and Hongkyung Lee¹; ¹Daegu Gyeongbuk Institute of Science and Technology, Korea (the Republic of); ²Chung Ang University, Korea (the Republic of); ³Pukyong National University, Korea (the Republic of)

With the growing reliance on battery-operated vehicles, addressing the safety concerns associated with lithium plating, exacerbated by high cell polarization during extremely fast charging (XFC) of Li-ion batteries, becomes imperative. This research probes into the effects of Li^+ desolvation and the solid-electrolyte interphase (SEI) chemistry on cell polarizations through the use of linear carbonate (LC)-based, high-concentration LiPF_6 electrolytes (LPCEs). Within the LC group, dimethyl carbonate (DMC) is identified as the most thermodynamically favorable for enhancing desolvation kinetics, thus reducing the charge-transfer resistance at the graphite anode. To facilitate effective graphite passivation and accelerated Li^+ transport through the SEI, fluoroethylene carbonate (FEC) is employed to form a thin, fluorinated SEI layer. This enhances the XFC cycling stability in graphite|NMC622 full cells

(3.0 mAh cm⁻²; N/P ratio = 1.1), achieving a remarkable 94.3% capacity retention after 500 cycles under a 10-minute charging regime. Compared to traditional electrolytes, the excellent XFC performance is further substantiated in a practical 1.2-Ah pouch cell, showcasing a tripling in capacity retention over 200 cycles and effectively mitigating Li plating-induced cell swelling. Unraveling the intricate mechanisms of cell polarization, as dictated by the electrolyte chemistry, furnishes pivotal insights for developing future electrolyte designs for XFC capabilities of Li-ion batteries.

5:00 PM ES01.07.18

X-Ray Photoelectron Spectroscopy Study of Solid Electrolyte Interface Formed on 3D NW Si Anodes Using RTIL-Based Electrolytes [Abinaya Sankaran](#); University of Limerick, Ireland

Silicon, capable of delivering high specific capacity (3579 mAh/g) at low working voltage, is a promising alloying anode for next-generation LIB chemistry. Despite this benefit, the cycling stability of Si anodes is limited by large volume expansion, leading to pulverization and solid-electrolyte interphase (SEI) layer instability. The SEI layer formed on the Si due to electrolyte decomposition at low potentials acts as a protective film that allows for facile Li-ion transport, which is a crucial factor for achieving high reversible capacity. The electrolyte compositions directly impact the formation of the SEI, thus determining battery cycle life. This work studies the electrochemical stability of core-shell a-Si@Cu₁₅Si₄ nanowire anodes under different carbonate and ionic electrolytes. To synthesize the anode, we modify the commercially used copper foil using a facile solvent vapor growth (SVG) system to grow copper-rich silicide Cu₁₅Si₄ Nanowire architectures as a robust and electrochemically stable current collector. Using the PECVD technique, the structured copper-rich silicide foils were directly deposited with amorphous silicon (a-Si), forming a core-shell nanowire architecture. The electrochemical performance of these synthesized binder-free electrodes with active areal loading up to 0.75 mg/cm² was evaluated using conventional carbonate (1M LiPF₆ in EC/DMC+3%FEC and LiPF₆ in EC/DMC+3%FEC) and ionic liquid electrolytes (0.2LiFSI-0.8EMIFSI, 0.2LiTFSI-0.8EMITFSI, 0.2LiTFSI-0.8EMIFSI) in a half-cell LIB configuration. The anode delivers superior performance compared to bare Cu foil with a reversible discharge capacity of 1350 mAh/g and 2000 mAh/g at C/5 rate in 1M LiPF₆ in EC/DMC+3%FEC and 0.2LiFSI-0.8EMIFSI ionic electrolyte—the improved adhesion and increased porosity help in preventing anodes' structural deterioration. The chemical composition and morphology of the SEI layer formed on the anodes were studied using ex-situ XPS and FIB-cross-sectional analysis. The chemical components of the SEI (inner and outer) developed using carbonate and Ionic electrolytes are explained. These findings could shed light on the decomposition pathway of Ionic electrolytes.

5:00 PM ES01.07.19

Fabrication of High-Performance Organic Electrodes through Field-Induced Charge Transfer for Li-Ion Batteries Jihye Park¹, Jun Hyung Gu², Dong Hwa Lee², Hosun Shin¹, Jung-Yong Lee³ and Jae Yong Song²; ¹Korea Research Institute of Standards and Science, Korea (the Republic of); ²Pohang University of Science and Technology, Korea (the Republic of); ³Korea Advanced Institute of Science and Technology, Korea (the Republic of)

Despite promising theoretical predictions, the practical performance of organic-based electrodes often falls short of expectations due to a low density of active sites, limited ion diffusivity, and high solubility in the electrolyte. In this study, we present an organic nanocomposite cathode with exceptional electrochemical stability achieved through an electric field-induced charge-transfer reaction in the nanocomposite, comprising 5,10-dihydro-5,10-dimethylphenazine (DMPZ) and perylene-3,4,9,10-tetracarboxylic dianhydride (PTCDA). Cryogenic milling was adopted to form a porous nanocomposite structure. The charge-transfer reaction effectively suppresses elution, and the porous structure increases the density of active sites. As a result, the porous nanocomposite showed a remarkable improvement in organic cathode performance, including an unprecedented high capacity retention of 90% over 600 cycles, a high initial capacity of 209 mAh g⁻¹, and excellent reversibility at high current densities. The performance enhancement mechanism of the organic nanocomposite cathode is elucidated through experimental analyses, including ex-situ XPS, PiFM, FTIR, and DFT calculations on the energy levels of organic components.

SESSION ES01.08: Battery Analysis, Recycling and Sustainability
Session Chairs: Jeffrey Cain and Zachary Hood
Thursday Morning, April 25, 2024
Room 425, Level 4, Summit

8:15 AM ES01.08.01

In-Silico Investigation of Promising Anode Materials for Li-Ion Batteries [Priya Johari](#); Shiv Nadar University, India

Development of computational resources and methods have taken a lead in current times to reliably predict promising electrode materials for the rechargeable batteries in a cost and time effective manner. This may provide an efficient route to guide experimentalists in improving the battery performance and realizing the next-generation energy efficient batteries for grid storage and electrical vehicles in terms of capacity and energy density. In view of that, using various approaches like the first-principles density functional theory and evolutionary algorithms, we comprehensively study a variety of materials to develop an understanding at the atomistic level and predict efficient anode materials for the Li-ion batteries.

8:30 AM ES01.08.02

Multiscale Modeling of Phase Evolution and Li-Ion Transport Kinetics in Boron Nitride Membranes [Yilong Zhou](#), Marcos Calegari Andrade, Bo Wang, Tae Wook Heo, Tuan Anh Pham, Sergei O. Kucheyev and Liwen Wan; Lawrence Livermore National Laboratory, United States

Boron nitride (BN) has gained attention in the field of electrochemistry due to its controllable surface chemistry and adjustable bandgap, along with mechanical robustness, thermal stability, and chemical inertness. In this work, we examine Li-ion migration behavior in defected hexagonal BN (hBN) using first-principles methods, towards applications as a separator or protected membrane in Li batteries. By comparing the activation energies of Li-ion diffusion along in-plane (between the BN layers) and out-of-plane (across the BN layers) pathways, we find that pristine hBN permits in-plane Li-ion diffusion with a relatively low energy barrier of 0.34 eV, while prohibiting out-of-plane Li-ion diffusion due to a high energy barrier (6.68 eV). Introducing defects is found effective to unlock the out-of-plane diffusion pathway despite the fact that local vacancies can trap Li and influence its consequent in-plane diffusion near the vacancy sites. In addition to the investigation of Li-ion transport behavior in hBN, we evaluate its phase stability by directly extracting its phase evolution kinetics from large-scale molecular dynamics simulations enabled by a machine-learning interatomic potential. We further investigate the impact of microstructure on the BN phase evolution kinetics and link it to various experimentally relevant conditions, which can ultimately allow us to establish strategies to fabricate BN membranes with desired properties.

This work was performed under the auspices of the U.S. DOE by Lawrence Livermore National Laboratory under Contract DE-AC52-07NA27344.

8:45 AM ES01.08.03

Electro-Chemo-Mechanics and Multiscale Battery Architecture [Giovanna Buccì](#); Lawrence Livermore National Laboratory, United States

The properties of rechargeable lithium-ion batteries are determined by the electrochemical and kinetic properties of their constituent materials as well as by their underlying microstructure. The discovery of novel 2D and 3D mesoscale architectures tailored to diverse applications remains an open challenge and it cannot be fully addressed empirically. It requires comprehensive modeling, embedding multiple time and length scales, with dynamic coupling of thermo-electro-chemo-mechanical phenomena. In this talk we will showcase multiscale modeling integration, prototyping, and an optimization algorithm to design energy storage devices that are tailored to function under a wide set of environments and use cases. This integrated workflow is also used to guide fundamental mechanistic understanding of the phenomena that degrade device performance, namely ion transport, morphological evolution, and solid mechanics.

9:00 AM ES01.08.04

On-Demand Capacity Extraction of Cu Current Collector for Li Batteries [Jun Ho Lee](#), Wenbo Zhang, Sanzeeda B. Shuchi, Sarah Holmes, Sang Cheol Kim and Yi Cui; Stanford University, United States

Irreversible loss of lithium due to its high reactivity lead to decrease in the energy density of lithium batteries. The decomposition of electrolyte forms electrochemically inactive solid electrolyte interface (SEI) layer on the surface of anodes, and lithium used to form SEI cannot be retrieved. Especially, large portion of Li^+ from cathodes are consumed during the initial cycle of LIB, and the energy density of full cells are significantly decreased afterwards. In order to supplement this loss, various prelithiation strategies such as introducing additional lithium compounds on either anodes or cathodes have been reported. However, Cu current collector, has not been considered as a source of extra lithium and considered as dead weight, mainly due to its electrochemical inactivity with lithium.

Here, we introduce a novel concept that involves utilizing Cu current collector as a lithium reservoir and extracting lithium on-demand during cycling to enhance the capacity of lithium batteries. By annealing Li and Cu, we show that Li-Cu alloy, a two-phase alloy, is formed with controllable capacity of lithium at an extraction potential of 1.2 V vs Li/Li^+ . Electrochemical and structural analyses revealed the irreversible extraction of Li during the phase transformation of the alloy. Based on electrochemical analyses, we demonstrated that Li-Cu alloy can serve as a prelithiated current collector in LIB, resulting in substantial increase of initial coulombic efficiency of anodes of half cells. Furthermore, relatively high extraction potential of Li-Cu alloy enabled on-demand extraction of lithium during discharging in full cells. In addition, prelithiated current collectors can also be employed to anode-free Li metal batteries, and capacity retention and cycle life of were observed to be improved. We anticipate that using current collector for lithium storage could enhance energy density of batteries while reducing reactivity of Li.

9:15 AM *ES01.08.05

Exploring Electrolyte Corrosion and Compatibility Across Lithium-Ion and Lithium-Metal Batteries [Chengcheng Fang](#); Michigan State University, United States

Developing next-generation electric vehicle (EV) batteries remains challenging regarding improving energy density, cycle life, and safety. Efforts are required to understand the materials' failure mechanisms quantitatively and develop new battery chemistry that breaks the energy density bottleneck. In this presentation, I will first talk about a systematic re-evaluation of the low-concentration ether-based electrolyte (LCEE), which is a promising, low-cost electrolyte system for lithium metal batteries (LMBs) but has long been believed to have "inferior" anodic stability. We identify the true failure mechanism of this electrolyte to be various electrochemical corrosion reactions with different working electrodes, while the intrinsic anodic stability window of LCEE is above 4.5 V, a value feasible for practical LMB operation. We also provide and verify design rationales to mitigate electrode corrosion and thus improve the full-cell performance of LMBs under realistic conditions. I will then introduce our recent work in designing electrolytes that are compatible with both graphite and lithium metal, enabling controlled lithium metal plating on graphite to realize hybrid lithium-ion/lithium-metal batteries with improved energy density (> 300 Wh/kg) and cycle life (> 1000 cycles) at fast charging conditions (up to 4C).

9:45 AM BREAK

10:15 AM *ES01.08.06

Direct Recycling in The ReCell Center [Jessica Durham](#); Argonne National Laboratory, United States

The Department of Energy's ReCell Center for Advanced Battery Recycling has recently expanded its program scope to cover Direct Recycling of Materials, Advanced Resource Recovery, Design for Sustainability, and Modeling and Analysis. The Center continues to scale-up its existing technologies and develop new technologies, applying them to the processing of both manufacturing scrap and end-of-life batteries. The presentation will highlight the expansion and progress of the Center's Direct Recycling of Materials focus area.

10:45 AM ES01.08.07

Styrene-Butadiene Rubber Patterned Current Collector for Enhanced Li-Ion Kinetics for High Energy Density Li-Ion Batteries [Seungcheol Myeong](#)¹, Seungwoo Lee¹, Insung Hwang¹, Joonhyeok Park¹, Jaeik Kim¹, Ganggyu Lee¹, Chanjin Park¹, Han Seung Min^{1,2}, Taeseup Song^{1,1} and Ungyu Paik¹; ¹Hanyang University, Korea (the Republic of); ²Korea Institute of Ceramic Engineering and Technology, Korea (the Republic of)

During the drying process, the migration of the styrene-butadiene rubber (SBR) binder, driven by capillary forces, can lead to a concentration gradient in the anode. This gradient adversely affects the adhesion strength at the interface between the anode film and the Cu current collector, as well as the Li-ion kinetics. In this study, we propose a solution to this issue through the use of a Cu current collector patterned with SBR. The pre-patterned SBR demonstrates strong adhesion to the Cu current collector, effectively preventing migration during the drying process. A uniform distribution of SBR along the longitudinal direction of the anode enhances both adhesion strength and Li-ion kinetics. Improved adhesion strength also allows for a reduction in SBR content in the anode, further enhancing Li-ion kinetics. Anodes utilizing this patterned SBR on Cu exhibit enhanced constant current charging capacity retention and improved cycling stability compared to those with a pristine Cu current collector.

11:00 AM ES01.08.08

Stress Evolution Prediction for Silicon Anode Particle during Charging/Discharging and a Comparison with *In-Situ* Test Results [Jifa Mei](#), Wenqing Zhou, Yao Ren, Peiran Ding, Weiran Jiang and Hui Li; Farasis Energy USA, United States

To unleash the potential of high-capacity Si-based anode in lithium-ion battery application, stress evolution and volume expansion mitigation within Si particles is of utmost importance in overcoming early degradation and side reactions caused by pulverization. An extensive and critical overview of the volumetric expansion, elastic, elastic-plastic behaviors of lithiated silicon at different concentrations is carried out by reviewing experimental and simulation studies available thus far. We summarized for the first time a quantitative characterization of these properties that are generally reached by

researchers through looking into these research progress as a whole. A coupled diffusion-mechanical model is then proposed to simulate the silicon lithiation process by incorporating concentration-dependent volumetric change and elastic-plastic properties. The stress state within a Si anode particle is studied when a charging and discharging profile is applied. It is found that the stress evolution throughout the lithiation and de-lithiation process is in good agreement with in-situ experimental measurements reported. Furthermore, the current modeling methodology has the potential to be applied to Si-C related anode composites for microstructure evaluation and design optimization.

11:15 AM ES01.08.09

Manufacturing Structured Lithium-Ion Battery Electrodes Using Acoustophoresis Emilee Armstrong¹, Keith E. Johnson², Ozgenur Kahvecioglu³, Matthew R. Begley² and Corie L. Cobb¹; ¹University of Washington, United States; ²University of California, Santa Barbara, United States; ³Argonne National Laboratory, United States

Scalable manufacturing of high-energy and high-power Lithium-ion batteries (LIBs) with fast charge behavior is crucial for lowering the cost and enhancing the performance of LIBs for electric vehicles (EVs) to meet DOE's current target of \$80/kWh by 2030.¹ Commercial LIBs are composed of planar electrode cell stacks that can be optimized for energy or power, but not both simultaneously. Structured electrodes (SEs) mitigate these performance trade-offs by using three-dimensional architecture in the anode or cathode to engineer porosity and tortuosity to enable fast ion transport in thick battery electrodes.^{2,3} However, a scalable manufacturing process for creating SEs over the large areas at the time scales required for cost-effective LIB manufacturing is still needed. To address this, we have developed a manufacturing process based on principles of acoustophoresis. Using acoustic forces, acoustophoresis rapidly assembles particles in a fluid on a micron scale, generating SE patterns over large, cm-scale areas.^{4,5} To date, we have used acoustophoretic principles to pattern SE cathodes made from size specific Lithium Nickel Manganese Cobalt Oxide (NMC-622). NMC-622 was selected as our electrode patterning material due to its relevance for EV applications. We have investigated how processing conditions can be used to tune the thickness and features of NMC-622 SEs and have conducted initial electrochemical testing.

References

1. Department of Energy, [Energy Storage Grand Challenge Roadmap], U.S. (2020).
2. C. L. Cobb and S. E. Solberg, *J. Electrochem. Soc.*, **164** (7), A1339-A1241 (2017).
3. K. Chen et al., *J. Power Sources*, **471**, 228475 (2020).
4. D. S. Melchert et al., *Mater. Des.*, **202**, 109512 (2021).
5. K. E. Johnson et al., *Mater. Des.*, **232**, 112165 (2023).

Acknowledgement

This material is based upon work supported by the U.S. Department of Energy's Office of Energy Efficiency and Renewable Energy (EERE) under the Advanced Manufacturing Office (AMO) Award Number DE-EE0009112. The views expressed herein do not necessarily represent the views of the U.S. Department of Energy or the United States Government. This work was partially carried out at the Materials Engineering Research Facility (MERF) at Argonne National Laboratory, which is supported by the DOE, Office of Energy Efficiency and Renewable Energy, and the Vehicle Technologies Office, under the Contract No. DE-AC02-06CH11357. The MERF synthesized size-specific NMC-622 for the project.

11:30 AM *ES01.08.10

On Advancements toward Sustainable and Environmentally Friendly Battery Technologies Rana Mohtadi^{1,2}; ¹Toyota Research Institute of North America, United States; ²Tohoku University, Japan

Current Li-ion batteries are considered the key driver toward societal electrification, however, limitations in the performances of these batteries coupled with their reliance on critical elements call for the consideration of alternative energy storage systems. A variety of batteries are poised in theory to offer improved performances, such as those utilizing metallic anodes and cathode incorporating earth abundant elements. Herein, we will discuss these technologies and share important advancements made in our laboratories.

SESSION ES01.09: Solid-State Batteries
Session Chairs: Matthew McDowell and Thomas Yersak
Thursday Afternoon, April 25, 2024
Room 425, Level 4, Summit

1:30 PM ES01.09.01

Argyrodite Solid-State Electrolytes: Overcoming Barriers to Interfacial Stability for Advanced Manufacturing of Solid-State Batteries Udochukwu Eze^{1,2} and Zachary D. Hood¹; ¹Argonne National Laboratory, United States; ²Georgia Institute of Technology, United States

Lithium argyrodite solid-state electrolytes (SSEs) exhibit many desirable properties such as high ionic conductivity (>1 mS/cm) at room temperature^{1,2,3} and greater ductility than most oxide SSEs,² enabling roll-to-roll cell fabrication relevant for EV battery packs. However, their instability in ambient air and at the Li||SSE and cathode||SSE interfaces presents challenges for scaled production and limits their cell performance.^{3,4} In this presentation, we present two interfacial strategies – those that involve dopants as well as pseudocapacitive interlayers – to overcome interfacial stability issues associated with argyrodite-type SSEs (Li₆PS₅Cl) in solid-state batteries. By using zinc, oxygen, and chlorine as dopants, we show that members within the Li_{6-2x-y}Zn_xPS_{5-x}_yO_xCl_{1+y} (x ≤ 0.25, y ≤ 0.25) phase space exhibit reduced reactivity under dry and H₂O-saturated oxygen as well as improved room temperature symmetric cell cycling performance at relatively high capacity and current densities. We also demonstrate a scalable, liquid-phase processing method for spraying adhesive pseudocapacitive interlayers on copper current collectors. These interlayers, constructed of MXenes (Ti₃C₂T_x) decorated with metal nanoparticles, can regulate the morphology of lithium metal during plating and stripping. Both strategies take advantage of Li alloy formation at the Li||SSE interface to form beneficial decomposition products that improve cycling performance and enhance the stability of the SSE with Li metal anodes as shown in recent work.⁵ Development of high performance next-generation solid-state batteries, those envisioned for EVs, will require interfacial tailoring, such as those presented in this work, in order to reduce impedance, alleviate poor rate performance, and reduce side reactions that lead to capacity fade.

Acknowledgements:

This project was supported by Laboratory Directed Research and Development (LDRD) funding from Argonne National Laboratory, provided by the Director, Office of Science, of the U.S. Department of Energy under Contract No. DE-AC02-06CH11357. This research used resources of the Center for Nanoscale Materials, U.S. Department of Energy (DOE) Office of Science user facilities operated for the DOE Office of Science by Argonne National

Laboratory under Contract No. DE-AC02-06CH11357. U.D.E. was supported by the Department of Defense (DoD) through the National Defense Science & Engineering Graduate (NDSEG) Fellowship Program as well as the Quad Fellowship. The authors gratefully acknowledge Natalie Holzwarth and David Cory Lynch for their modeling work of the $\text{Li}_{6-2x-y}\text{Zn}_x\text{PS}_{5-x-y}\text{O}_x\text{Cl}_{1+y}$ system.

References:

- ¹L. Zhou, N. Minafra, W. G. Zeier, and L. F. Nazar. "Innovative Approaches to Li-Argyrodite Solid Electrolytes for All-Solid-State Lithium Batteries" *Acc. Chem. Res.* (2021)
- ²Z. Zhang, Y. Shao, B. Lotsch, Y. Hu, H. Li, J. Janek, L. F. Nazar, C. Nan, J. Maier, M. Armand, and L. Chen. "New horizons for inorganic solid state ion conductors" *Energy Environ. Sci.* (2018)
- ³T. Schmaltz, F. Hartmann, T. Wicke, L. Weymann, C. Neef, J. Janek. "A Roadmap for Solid-State Batteries" *Adv. Energy Mater.* (2023)
- ⁴K. T. Kim, J. Woo, Y. Kim, S. Sung, C. Park, C. Lee, Y. J. Park, H. Lee, K. Park, and Y. S. Jung "Ultrathin Superhydrophobic Coatings for Air-Stable Inorganic Solid Electrolytes: Toward Dry Room Application for All-Solid-State Batteries" *Adv. Energy Mater.* (2023)
- ⁵Z. D. Hood, A. U. Mane, A. Sundar, S. Tepavcevic, P. Zapol, U. D. Eze, S. P. Adhikari, E. Lee, G. E. Sterbinsky, J. W. Elam, and J. G. Connell. "Multifunctional Coatings on Sulfide-Based Solid Electrolyte Powders with Enhanced Processability, Stability, and Performance for Solid-State Batteries" *Adv. Mater.* (2023)

1:45 PM ES01.09.02

Low-Temperature, Scalable Synthesis of Electrolyte Films: Spray Deposition of Sulfides and Oxides Colton Ginter^{1,2} and Zachary D. Hood¹;

¹Argonne National Laboratory, United States; ²The University of Chicago, United States

Given the projected tenfold increase in global battery demand over the coming decade,¹ it is imperative to prioritize the advancement of cost-effective, secure, and high-energy-density energy storage solutions for electric vehicles. Solid-state synthesis methods, those that are traditionally used for inorganic solid-state electrolytes (SSEs), generally require higher process temperatures, are incompatible with roll-to-roll processing, and produce millimeter-thick pellets, barring integration in energy-dense solid-state batteries (SSBs).² New, scalable methods for low-temperature manufacturing of SSEs at thicknesses comparable to polymer separators (~20 μm) are required for widespread adoption of SSBs.^{2,3} Here, we describe a spray deposition process to form dense $\text{Li}_x\text{PS}_2\text{Cl}$ (LPSCl) and Li_3BO_3 (LBO) films with room-temperature ionic conductivities greater than or equal to 10^{-4} S/cm and 10^{-8} S/cm, respectively, as determined by electrochemical impedance spectroscopy (EIS). Through precise control of spray parameters (including total mass, concentration, deposition rate, and substrate temperature), we successfully crafted dense, crack-free amorphous films, reaching thicknesses of 14.2 ± 0.3 μm for LPSCl and 0.188 ± 0.054 μm for LBO, all at remarkably low temperatures, below 200 °C. We augmented our findings with concurrent in situ Raman spectroscopy and EIS during the film annealing process, which revealed the presence of polymorphism in the deposited films and a crystallization process occurring at temperatures lower than conventional solid-state methods. Our research also delves into the diverse applications of these materials in SSBs and other next-generation electrochemical devices.

Acknowledgements:

This work was supported in part by the U.S. Department of Energy, Office of Science, Office of Workforce Development for Teachers and Scientists (WDTS) under the Science Undergraduate Laboratory Internships (SULI) program. This project was supported by Laboratory Directed Research and Development (LDRD) funding from Argonne National Laboratory, provided by the Director, Office of Science, of the U.S. Department of Energy under Contract No. DE-AC02-06CH11357. This material is based upon work supported by the National Science Foundation Graduate Research Fellowship under Grant No. 2140001. This research used resources of the Advanced Photon Source, a U.S. Department of Energy (DOE) Office of Science user facility operated for the DOE Office of Science by Argonne National Laboratory under Contract No. DE-AC02-06CH11357. The authors also acknowledge seedling funding provided by the Applied Materials Division, contributions by Nick O'Reilly, as well as assistance by George Sterbinsky from the APS.

References:

1. Zhou, Yan, Gohlke, David, Rush, Luke, Kelly, Jarod, & Dai, Qiang. Lithium-Ion Battery Supply Chain for E-Drive Vehicles in the United States: 2010–2020. United States. <https://doi.org/10.2172/1778934>
2. Balaish, M., Gonzalez-Rosillo, J. C., Kim, K. J., Zhu, Y., Hood, Z. D., & Rupp, J. L. (2021). Processing thin but robust electrolytes for solid-state batteries. *Nature Energy*, 6(3), 227–239. <https://doi.org/10.1038/s41560-020-00759-5>
3. Hood, Z. D., Zhu, Y., Miara, L. J., Chang, W. S., Simons, P., & Rupp, J. L. (2022). A sinter-free future for solid-state battery designs. *Energy & Environmental Science*, 15(7), 2927–2936. <https://doi.org/10.1039/d2ee00279e>

2:00 PM *ES01.09.03

First-Principles Calculation Study on Degradation-Related Phenomena around Cathode/Solid Electrolyte Interfaces in Solid-State Battery

Yoshitaka Tateyama^{1,2,3}; ¹National Institute for Materials Science, Japan; ²Tokyo Institute of Technology, Japan; ³Waseda University, Japan

Control of battery degradation has been a critical issue for the EV application, and a variety of technologies have been developed so far. However, understanding of the microscopic behavior of ions and electrons is still very lacking, and thus the degradation control has room to be improved. In this respect, we have investigated the microscopic interfacial and mechanical phenomena around cathode / solid electrolyte interfaces via density-functional-theory (DFT) based first-principles calculations, and drawn general theories effective for larger-scale consideration. In this talk, I introduce our recent works related to degradation; (1) stress/strain effects on Li^+ diffusion in Li_xCoO_2 [1], (2) oxygen evolutions and cation migrations around the surfaces of Li_xCoO_2 [2], (3) Li^+ transfer around cathode/coating layer/solid electrolyte interfaces [3,4]. (1) We found that the barrier in the single vacancy mechanism decreases with biaxial expansion, contrasting with an increase in the double vacancy mechanism. This phenomenon is attributed to the c-axis position in the Li^+ diffusion pathway. Our DFT-MD simulations revealed that compressive biaxial strain enhances Li^+ diffusivity in Li-deficient Li_xCoO_2 (decreased to 0.22 and 0.21 eV), while tensile biaxial strain and hydrostatic pressure hinder it. Surprisingly, "Co layer distances" play a pivotal role in Li^+ diffusion, and our study uncovers intricate interactions between Li-Li Coulomb interactions, state-of-charge (SOC), and Li^+ diffusion in Li_xCoO_2 . Besides, we reported the activation volume of LiCoO_2 under hydrostatic pressure and show that compressive biaxial strain weakens Li-O bond interactions, reducing the Li intercalation potential. (2) We examined oxygen release and Co-ion migration both in the bulk and on the surfaces (001), (104), and (110) of Li_xCoO_2 , taking into account the process of spinel-like Co_3O_4 formation. The calculated oxygen vacancy formation energies are 2.38, 2.42, 1.46 and 1.10 eV for bulk, the (001), (104) and (110) surfaces, respectively. These trends are reasonably consistent with the experiments. We also clarified the significant reduction in activation energies of Co-ion migration in the presence of oxygen vacancies, indicating the correlation among the oxygen vacancy formation and the Co-ion migration. (3) Focusing on LiCoO_2 / LiNbO_3 / Li_3PS_4 interfaces in typical solid-state battery, we calculated ionic PES across the interfaces by first-principles calculations, and demonstrated how such energy profiles look like around the interfaces. The results correspond to the discharging situation, and indicate how to understand the charging situation by separating ion and electron movements. Our interface analyses also suggested a way of understanding interfacial ion and electron transfer by DFT-based standard electrochemical potentials of Li, Li^+ and e⁻. The picture well accounts for the mitigation of ionic interface resistance by insertion of oxide coating layer between cathode and sulfide electrolytes. This DFT-based framework gives a crucial insight

into ion as well as electron transfer across general interfaces.

These works were done in collaboration with Mr. Z. Zhou, Dr. H. D. Luong, Dr. R. Jalem in NIMS, Prof. B. Gao in Jilin Univ., and Prof. H.-K. Tian in National Cheng-Kung Univ. The works were partly supported by MEXT as “Program for Promoting Researches on the Supercomputer Fugaku / Fugaku Materials Physics & Chemistry Project” (JPMXP1020230325) and JSPS KAKENHI “Interface IONICS” (JP19H05815).

References: [1] Z. Zhou, Y. Tateyama *et al.*, under review. [2] H. D. Luong, Y. Tateyama *et al.*, in preparation, [3] B. Gao, R. Jalem, Y. Tateyama ACS Appl. Mater. Interfaces, 13, 11765 (2021). [4] H.-K. Tian, Y. Tateyama *et al.*, ACS Appl. Mater. Interfaces, 12, 54752 (2020).

2:30 PM BREAK

3:00 PM *ES01.09.04

Mechano-Electrochemical Phenomena in Solid-State Batteries Jeff Sakamoto, University of Michigan, United States

There is tremendous interest in making the next super battery, however Li ion technology continues to improve and has inertia in several commercial markets. Recent material breakthroughs in solid-electrolytes (SE) could enable a new class of non-combustible solid-state batteries delivering twice the energy density (>1,300 Wh/L) compared to Li-ion. However, technological and manufacturing challenges remain, creating the impetus for fundamental and applied research.

This discussion will consist of fundamental aspects such as the mechano-electrochemical phenomena at solid interfaces as well as manufacturing challenges related to the integration of Li metal electrodes. The underlying physics that control the stability and kinetics of Li/SE interfaces are fundamentally different from interfaces in Li ion technology. Moreover, the mechano-electrochemical phenomena that occur during discharge and charge at the Li/SE interface are considerably different. For example, during charging at higher rates Li metal filaments can initiate at defects and propagate through relatively hard ceramics. During discharge, if the Li stripping rate is sufficiently high and the temperature is sufficiently low, voids form at the interface causing delamination at of the interface.

In another example, novel mechano-electrochemical phenomena are emerging when analyzing the formation of Li anodes in using the Li⁰-free manufacturing approach. Using this approach for solid-state batteries, Li metal in interposed between a current collector and the SE. The mechanics at this interface will determine the feasibility of this approach by controlling the homogeneity of the *in situ* formed Li anode. While significant progress is advance the technological maturity of solid-state batteries, there remain fundamental questions regarding the physics at interfaces and whether or not they exhibit sufficient stability and kinetics that are relevant to EVs.

3:30 PM ES01.09.05

Recent Breakthroughs in All-Solid-State Sulfide Ceramic Batteries: Performances, Safety and Future Developments Benoit Fleutot, Emmanuelle Garitte, Fabien Nassoy, Benjamin Cruel, Steve Duchesne, Jean-François Filion, Isabelle Filteau, Amélie Forand, Marie-Claude Girard, Karine Tremblay and Chisu Kim; Hydro-Québec, Canada

Despite some progress performed, state-of-the-art lithium-ion batteries still require improvements in energy and power to extend the range of electric vehicles and reduce charging time. In this domain, all-solid-state batteries are viable alternatives to conventional batteries employing organic electrolytes because of their benefits, i.e., high power density, high energy density, long-life operation and safety. These advantages stem from the great features of inorganic solid electrolytes, which are single ion conductor, so a high lithium-ion transport number, and no-liquid nature. In particular, the sulfide-based solid electrolytes possess favorable mechanical properties, high ionic conductivity allowing improved all-solid-state batteries performances at room temperature but suffer of moisture exposure that could induce H₂S generation.

Sulfide-based solid-electrolytes can potentially be employed in conjunction with a lithium metal negative electrode and 5V-class high voltage positive electrode material. Indeed, lithium metal is believed to be the most promising negative electrode due to its specific large capacity (3862 mAh.g⁻¹) and the lowest electrochemical potential (-3.03V vs ENH). Ceramic solid electrolytes and especially sulfide composite solid electrolyte have been considered to be the ideal solution to prevent dendrite growth because of their high shear modulus and high lithium transference number. At the same time, the chemical nature and composition of ceramic solid electrolyte can affect the dendrite growth by the interfacial chemical and electrochemical stability with lithium metal. In parallel, the sulfide solid electrolyte reacts with all components constituting the positive electrode as active material, electronic conductor, binder, current collector... Hence, all interfaces can generate side reaction, increase of polarisation, and so rapid battery fading. As demonstrated in literature, an important average pressure increase during cycling and aging can't allow a future commercialisation of this technology. The safety is a crucial point and the generation of H₂S in the case of all-solid-state battery based on sulfide electrolyte during scale-up phase and operation must be take into account and evaluated specifically.

In this field and since a few years, Hydro-Quebec has decided to conduct specific research on all-solid ceramic batteries and especially in the field of sulfide-based ceramic electrolytes. Based on Hydro-Québec's knowledge with polymers, a solution of all-solid composite battery with ceramic tendency has been developed by generating several industrial properties at the different levels of the battery. The interaction previously observed in positive electrode mixture without binder have been resolved and integrated in slurry. In parallel, the impact between solid electrolyte ceramic film composition, density, reactivity with lithium metal and flexibility were studied to offer high conductivity and easily manipulation. Unlike the general perception that the sulfide electrolyte is not compatible with lithium metal, we successfully stabilized the lithium metal interface reaching the cycle life more than 500 cycles under industry-relevant pressure conditions at moderate temperature under pouch-cell configuration. The constraints of the use of li-ion equipment's, cost reduction and safety have been considered at each level with quantitative measurements. The different improvements in positive composite electrode, in solid electrolyte ceramic film and in lithium metal interfaces will be explained. The presentation will show how technical and economical issues of sulfide electrolyte can be addressed to bring the technology closer to the market.

3:45 PM ES01.09.06

Comprehensive Safety Assessment of All-Solid-State Batteries: Using Calorimetry, X-Ray Radiography and Blast Testing Techniques Juliette Charbonnel^{1,2}, Rémi Vincent^{1,3} and Pierre-Xavier Thivel²; ¹CEA, France; ²LEPMI, France; ³Laboratoire, France

In the context of the energy transition, researches on batteries are devoted to improving their energy density, i.e. their autonomy and their safety, particularly in relation to the risk of fire. Among the different types of battery, all-solid-state batteries are promising because of their high energy density. A ceramic or a glass electrolyte replaces some traditional components of lithium-ion batteries as the liquid electrolyte and the polymer separator. However, safety concerns related to ASSBs have remained relatively unexplored. This investigation is focused on understanding the behaviour of reassembled all-solid-state batteries subjected to overheating abuse. Specifically, two batteries compositions: Gr|LLZO|NMC811 and Li|LLZO|NMC81 are

studied. The first cell aids in comprehending the impact of the electrolyte (liquid or solid) safety and the second enables to assess the safety of a reconstructed lithium-metal all-solid-state cell.

An innovative approach to assess the safety of all-solid-state cell in-development has been devised. This approach incorporates three distinct techniques: calorimetry, X-ray radiography and blast testing. This methodology could significantly contribute to the development of future battery technologies.

Ensuring the integration of safety concerns right from the beginning is crucial, encompassing both cell performance and safety aspects.

Substituting liquid electrolyte with a solid electrolyte, the initiation and the maximal temperatures remain unchanged. It reduced by 10 % the heat released and reduced by 40 % the amount of gas released and the duration of thermal runaway. Using solid electrolyte no prevent from thermal runaway.

Substituting liquid electrolyte with a solid electrolyte and substituting the lithiated graphite with a lithium-metal foil, the initiation temperature remains unchanged. The maximum temperature is at least increased by 40 %; the amount of gas and the duration of thermal runaway are decreased by 90 % and 95 %. Furthermore, the Li_{0.5}LLZO|NMC811 cell is not an explosive but a 188 mbar aerial pressure has been measured. It corresponds to a mass equivalent TNT of 2.7 g.

Furthermore, the characteristic parameters of thermal runaway are different. Therefore, the means to mitigate its thermal runaway are different and should be taken into account when all-solid-state batteries are developed.

The impact of blast wave on the casing and battery pack integrity should be taken into when all-solid-state batteries are developed.

To conclude, all-solid-state batteries are neither safer nor less safe than lithium-ion batteries. However, their the characteristic parameters of thermal runaway are different. This work underlines the importance of evaluating the safety of all-solid-state batteries with respect to users and the environment.

4:00 PM ES01.09.07

Transforming EV Battery Materials into Reserve Batteries via Advanced Manufacturing Justin A. Sadowski^{1,2} and Zachary D. Hood², ¹Air University, United States; ²Argonne National Laboratory, United States

The expanding electric vehicle (EV) market fuels research into advanced battery materials, particularly solid-state electrolytes (SSEs), to enhance energy storage technology, offering the promise of higher energy density, improved safety, and cost-efficiency. These materials show potential for deployment in reserve or primary batteries, addressing issues found in current technologies such as self-discharge, inadequate energy density, limited operational temperature ranges, and safety concerns associated with flammable liquid electrolytes. Our investigation centers on argyrodite-type sulfide-based SSEs, boasting exceptional Li⁺ conductivity (>1 mS/cm) at room temperature, lithium metal anodes with substantial energy capacity (theoretical limit: 3860 mAh/g)¹, and cathode active materials (CAMs) meeting the criteria for reserve or primary battery applications.² This study investigates the pivotal role of advanced manufacturing techniques in addressing the challenges associated with reserve batteries, focusing on sulfide-based SSEs and lithium metal, with a positive outlook on potential solutions. We present a comprehensive review of state-of-the-art solid-state battery technology in current reserve or primary battery applications, discuss CAMs' performance in sulfide-based SSE composites in half cells, and provide detailed postmortem analyses. These insights serve as fundamental guidelines for future optimizations in advanced battery material manufacturing, transcending the scope of EV-specific applications.

Acknowledgements:

This project was supported by Laboratory Directed Research and Development (LDRD) funding from Argonne National Laboratory, provided by the Director, Office of Science, of the U.S. Department of Energy under Contract No. DE-AC02-06CH11357. This research used resources of the Center for Nanoscale Materials, U.S. Department of Energy (DOE) Office of Science user facilities operated for the DOE Office of Science by Argonne National Laboratory under Contract No. DE-AC02-06CH11357. The views expressed in this academic research paper are those of the author(s) and do not reflect the official policy or position of the US government or the Department of Defense.

References:

1. W. Xu, J. Wang, F. Ding, X. Chen, E. Nasybulin, Y. Zhang, and J. Zhang. Lithium metal anodes for rechargeable batteries. *Energy & Environmental Science*, **2014**, 7, 513.
2. R. Silbergliitt, J. Bartis, and K. Brady. Soldier-Portable Battery Supply. RAND Corporation, **2014**.

SESSION ES01/ES05/MT02: Joint Virtual Session
Session Chairs: Ertan Agar, Jeffrey Cain, Ruozhu Feng, Zachary Hood, Deyu Lu and Feng Wang
Thursday Morning, May 9, 2024
ES01-virtual

8:00 AM *ES01/ES05/MT02.01

Development of Oxide-Based Solid-State Batteries Kazunori Takada; National Institute for Materials Science, Japan

Solid-state batteries they provide high reliability to lithium-ion batteries are regarded as promising next-generation batteries. Solid-state batteries with sulfide electrolytes were reported to attain higher performance than lithium-ion batteries, and they are under development aiming at vehicle application. However, sulfide electrolytes are unstable and hygroscopic materials, and the batteries should be assembled under strictly-controlled atmosphere. Therefore, replacement of the sulfides with stable oxides is strongly required; however, performance of the oxide-based solid-state batteries is much lower than that of the sulfide systems.

Although the highest conductivities having reported for oxides are of the order of 10⁻³ S cm⁻¹, which is lower than that of sulfides by one order of magnitude, they are not the main reason for the poor battery performance: the conductivities are almost comparable to lithium-ion conductivities of organic-solvent liquid electrolytes used in the current lithium-ion batteries. High resistance of oxide-based solid-state batteries originates from the interfaces.

Oxide-based solid electrolytes often show high grain boundary resistance. The grain boundary resistance can be lowered by increasing sintering temperature, indeed; however, it does not lead to high performance in the solid-state batteries. The solid electrolytes are in contact with active materials in the batteries. Sintering at high temperatures induces mutual diffusion between the solid electrolytes and active materials, which forms resistive impurity layers at the interfaces. Sulfide-based solid-state batteries have achieved the high performance not only by the high ionic conductivities of sulfide-based solid electrolytes but also by their deformability. Since sulfide solid electrolytes are deformable, they can be closely contacted to active materials only by cold pressing, where mutual diffusion takes place. Therefore, it is necessary to lower sintering temperature of the oxide solid electrolytes for realizing oxide-based solid-state batteries. I have been leading some research projects on oxide-based solid-state batteries. Achievements in the projects will be presented at the meeting.

8:30 AM *ES01/ES05/MT02.02

This searchable program is up-to-date as of April 15th, 2024.

Sudden Capacity Loss in Lithium Metal Cells [Louis G. Hector](#)¹, Meinan He¹, Mei Cai¹, Charles Wampler¹, Surya Kolluri¹, Michael Dato², Khalil Amine¹ and Chi Cheung Su²; ¹General Motors Global Research and Development Center, United States; ²Argonne National Laboratory, United States

Rechargeable Li-metal batteries have higher energy density relative to batteries based upon intercalation electrodes. They are therefore attractive energy storage candidates for electric vehicles. However, a main barrier to their commercial deployment is a relatively short cycle life. Re-engineering the electrolyte offers advantages towards acceptable cycle life; however, the cells exhibit a sudden capacity loss. In this presentation, we detail a new method for analyzing voltage profiles during cycling to differentiate between the capacity loss originating from loss of cathode capacity loss versus growth in cell resistance. We show that sudden capacity loss is preceded by acceleration of the rate of growth of cell resistance. Cycling of multiple cells suggested that this behavior is sensitive to the initial quantity of electrolyte. Alternatively, the cathode capacity degraded at a constant rate independent of the electrolyte quantity. Loss of active lithium and/or the loss of active cathode material were not the primary causes of sudden capacity loss. Rather, consumption and decomposition of electrolyte led to the drastic capacity loss at end of life.

9:00 AM *ES01/ES05/MT02.03

Challenges for Organic Active Materials for Stationary Electrical Energy Storage [Michael J. Aziz](#); Harvard University, United States

We have developed high performance flow batteries based on the aqueous redox behavior of small organic and metalorganic monomers composed of earth-abundant elements. These redox active materials can be inexpensive and exhibit rapid redox kinetics and high solubilities, potentially enabling rapid scaling of flow batteries at reduced cost. Adequate molecular lifetime has been one of the most challenging requirements to satisfy. We have shown that the amount of lost capacity is determined by the molecular calendar life, which can depend on state of charge, but is independent of the number of charge-discharge cycles imposed. I will discuss problems in measuring extremely small capacity fade rates and how an understanding of molecular decomposition mechanisms has permitted us to design molecules with decadal projected lifetimes and even to reverse capacity fade by recomposing decomposed molecules within the functioning battery electrolyte.

9:30 AM *ES01/ES05/MT02.04

Semantic Technology for Accelerated Battery Materials Research and Innovation [Simon Clark](#) and Eibar Flores; SINTEF Industry, Norway

Materials research and innovation are pivotal to advancing battery technology and enabling the green transition. However, widely used trial-and-error approaches are too slow and under-utilize the valuable data that they generate. This presentation explores the pivotal role semantic technology - a fusion of artificial intelligence and web technologies - plays in accelerating research efforts towards next-generation battery materials. Semantic web technology like ontologies and knowledge graphs, helps researchers integrate heterogeneous data sources. This not only simplifies data retrieval by enabling precise, context-aware queries, but also augments the capabilities of machine learning. With semantically enriched data, researchers can craft models that are more adept at predicting material behaviours and identifying promising compositions.

This talk introduces the fundamentals of semantic technology and presents real case studies from battery materials research. This includes a specific focus on examples coming from both experiments and simulations. It is shown how semantic annotations can enable both human- and machine-readability of battery data to automate analysis and enable interoperability between different modelling frameworks. Harnessing the power of semantic technology in materials research not only expedites the development of next-generation battery materials but also fosters data-driven innovation and collaboration across diverse research domains.

SYMPOSIUM ES02

Operando Characterization of Energy Storage Materials
April 24 - April 25, 2024

Symposium Organizers

Raphaële Clement, University of California, Santa Barbara
Feng Lin, Virginia Tech
Yijin Liu, The University of Texas at Austin
Andrej Singer, Cornell University

* Invited Paper

+ JMR Distinguished Invited Speaker

^ MRS Communications Early Career Distinguished Presenter

SESSION ES02.01: Operando Electron and Optical Microscopy of Energy Storage Materials
Session Chairs: Feng Lin and Yijin Liu
Wednesday Morning, April 24, 2024
Room 424, Level 4, Summit

8:30 AM *ES02.01.01

Real-Time Probing of Solid-Liquid Interfaces for The Alkaline Oxygen Evolution Reaction of Oxides [Vaso Tileli](#); EPFL, Switzerland

The design of active and stable oxygen-evolving oxide catalysts can be aided by their real-time probing, which provides information on how the catalysts perform and evolve under operating conditions [1]. Among the operando characterization techniques applied to electrocatalysis, electrochemical liquid-phase transmission electron microscopy (ec-LPTM) is capable of visualizing the electrochemically induced processes in liquid environments at the single particle level. In this talk, I will discuss the progress made in the application of ec-LPTM for monitoring solid-liquid interface processes occurring on Co-based and iridium oxide OER catalysts [2,3]. By analyzing the contrast of the lateral liquid electrolyte surrounding the catalyst particle in TEM images, the surface wetting dynamics with respect to the applied potential is revealed. The overall decrease in the lateral liquid thickness indicates a switch from hydrophobic to hydrophilic character under anodic potential due to electrowetting induced by ion accumulation at the interface. Within the pre-OER potential, the change in the surface wetting behavior on Co-based oxides suggests a link to the underlying Co II/III redox reaction and surface transformation of the oxyhydroxide phase. I will also demonstrate the direct probing of electrocatalytic molecular oxygen using operando electron energy-loss spectroscopy (EELS). Progress toward facet selectivity probing of the evolving molecular oxygen will be discussed and evidence of highly-pressurized electrocatalytic gas formation in the microcells will be presented.

References

- [1] J. T. Mefford et al., *Nature* **593**, 67 (2021)
- [2] T.-H. Shen, L. Spillane, J. Peng, Y. Shao-Horn, and V. Tileli, *Nature Catalysis* **5**, 30 (2022)
- [3] T.-H. Shen, R. Girod, J. Vavra, and V. Tileli, *The Journal of The Electrochemical Society* **170**, 056502 (2023)

9:00 AM *ES02.01.02

Operando Studies of Dynamic Evolution of Cu Nanocatalysts during CO₂ Reduction Yao Yang; Cornell University, United States

In an era of shifting the energy paradigm from fossil fuels to renewable energy, CO₂ reduction reaction (CO₂RR) emerges as a promising approach to convert greenhouse gas into valuable chemical fuels and close the carbon cycle for a sustainable energy supply. Since Cu remains the sole element for CO₂RR to multicarbon products (C₂₊), significant efforts have been devoted to developing Cu electrocatalysts with higher selectivity and activity. However, the complex nature of active sites and the intrinsic structures under reaction conditions have remained largely elusive due to the lack of *operando in situ* methods. In this work, we present a comprehensive *operando* correlative study of size- and potential-dependent dynamic evolution of Cu nanoparticle electrocatalysts under CO₂RR conditions. *Operando* electrochemical liquid-cell scanning transmission electron microscopy (EC-STEM) and 4D-STEM, driven by machine learning, resolve microscopic dynamic morphological and structural evolution at the nm scale. Correlated *operando* synchrotron-based high-energy-resolution fluorescence-detected (HERFD) X-ray absorption spectroscopy (XAS) reveals dynamic macroscopic changes in valence states and coordination environment. The methodology described herein can serve as a general strategy to resolve the electrocatalytic interface of nanoparticle catalysts under real-time operating conditions across multiple time and length scales.

9:30 AM ES02.01.03

Recovery of Isolated Lithium through Discharged State Calendar Aging Wenbo Zhang¹, Philaphon Sayavong¹, Xin Xiao¹, Solomon Oyakhire^{1,2}, Sanzeeda B. Shuchi¹, Rafael A. Vila¹, David T. Boyle¹, Sang Cheol Kim¹, Munsek Kim¹, Sarah Holmes¹, Yusheng Ye¹, Donglin Li¹, Stacey F. Bent¹ and Yi Cui¹; ¹Stanford University, United States; ²University of California, Berkeley, United States

Rechargeable Li-metal batteries (LMBs) have the potential to more than double the specific energy of the state-of-the-art rechargeable Li-ion batteries (LIBs), making Li metal a promising anode material for future generation rechargeable batteries. However, Li metal anodes suffer from greater cycle degradation compared to their Li-ion counterparts due to excess formation of capacity depleting byproducts.¹ Two major byproducts generated are: 1) the solid electrolyte interphase (SEI), a product of Li, salt and organic species reactions at the Li metal and the electrolyte interface to form a 'passivation' layer and 2) 'dead' or isolated Li, which traps capacity as Li metal detached from the electrochemical circuit. Recent studies have revealed that charged state calendar aging promotes further corrosion reactions between active Li and the surrounding electrolyte, leading to additional byproduct generation and further capacity loss.^{2,3} Although these studies highlight the detrimental effects of calendar aging in the charged state, they have not reported on the effects of discharged state calendar aging on cell performance. In the discharged state, all electronically active Li has been stripped away leaving only isolated Li and SEI on the anode.⁴ In this environment absent of active Li corrosion, the effects of rest on isolated Li, SEI, and cycle performance have not been explicitly explored and remain unknown.

In this work, we report calendar aging in the discharged state improves capacity retention through isolated Li recovery, a surprising contrast to the well-known phenomenon of capacity degradation observed during aging in the charged state. Discharged state rested cells achieve a sustained greater than 1% average CE increase over both continuously cycled and charged state rested cells. Additionally, running cells on a hybrid continuous/discharged state rest cycling protocol in combination with titration gas chromatography (TGC) reveal isolated Li recovery as the main contributor to capacity gain. Furthermore, a novel operando optical setup in combination with electrochemical quartz crystal microbalance (EQCM) reveal that the process of SEI dissolution during discharged resting promotes excess isolated Li recovery. These insights into a new pathway for capacity recovery through discharged state calendar aging emphasize the significant effects cycling strategies have on LMB performance.

1. Han, B. et al. Conformal three-dimensional interphase of Li metal anode revealed by low-dose cryoelectron microscopy. *Matter* **4**, 3741- 3752 (2021).
2. Boyle, D.T. et al. Corrosion of lithium metal anodes during calendar ageing and its microscopic origins. *Nat. Energy* **6**, 487-494 (2021).
3. Merrill, L.C., Rosenberg, S.G., Jungjohann, K.L., Harrison, K.L. Uncovering the relationship between aging and cycling on lithium metal battery self-discharge. *ACS Appl. Energy Mater.* **4**, 7589-7598 (2021).
4. Xiao, J. et al. Understanding and applying coulombic efficiency in lithium metal batteries. *Nat. Energy* **5**, 561-568 (2020).

9:45 AM ES02.01.04

Quantitative Operando Mapping with Nanoscale Resolution of 3D Mechanical Properties of Surface Electrolyte Interphase in Li-Ion and Na-Ion Batteries Oleg V. Kolosov¹, Yue Chen², Mangayarkaras Nagarathinam¹, Svetlana Menkin Bachbut³ and Dominic Wright³; ¹Lancaster University, United Kingdom; ²Fujian Normal University, China; ³University of Cambridge, United Kingdom

A nanoscale thin but extremely important component of any rechargeable battery is the solid electrolyte interphase (SEI), a passivation layer that defines the fundamental battery properties - capacity, cycle stability and safety. Local mechanical properties of SEI hold a clue to its performance, but their *operando* characterisation is very difficult as one has to probe nanoscale surface features in electrochemical environment that are also dynamically changing. Here, we report novel 3D nano-rheology microscopy (3D-NRM) that uses a tiny (sub-nm to few nm) lateral dithering of the sharp SPM tip at kHz frequencies to probe the minute sample reaction forces. By mapping the increments of the real and imaginary components of these forces, while the tip

penetrates the soft interfacial layers, we obtain the true 3D nanoscale structure of sub- μm thick layers. 3D-NRM already allowed us to elucidate key role of solvents in SEI formation and predict the conditions for building SEI for robust, safe and efficient Li-ion batteries [1]. We combine 3D NRM with magnetic excitation to investigate molecular-level solvation force spectroscopy and use molecular dynamics simulations to understand two morphologically dissimilar but chemically identical surfaces of typical carbon electrode material (basal and edge graphene planes) and different solvent-electrolyte systems (strong and weakly solvating electrolytes, as well as ionic liquid electrolyte). These approaches allowed us to get direct insight into the atomistic pictures for the underlying influence of cation's intercalation and solvation structures on the initial SEI formation.

Furthermore, here we explore the extension of these studies on smooth HOPG and inhomogeneous and rough copper anodes as sodium ion battery electrodes. Essentially, the new approach allows nanoscale characterisation of SEI with a few nm precision on the electrodes with 1000 nm roughness, and, importantly, to quantitatively evaluate the real and imaginary parts of the elastic moduli over the whole thickness of SEI layer. The observation of the change in moduli and the tip-surface distance helps to evaluate the growth of SEI as a function of the electrolyte, additives, electrode material and charge-discharge rate. Our understanding of these key interfacial structural factors in SEI formation allows targeting an electrochemically and mechanically robust surface passivation layer and guiding the development of efficient and safe rechargeable batteries. We believe that such evaluation of key interfacial nanomechanical properties of SEI will allow us to develop the electrochemically and mechanically robust SEI surface passivation layer and the development of efficient and safe rechargeable batteries.

[1] Y Chen, W Wu, S Gonzalez-Munoz, L Forcieri, C Wells, SP Jarvis, F Wu, R Young, A Dey, M Isaacs, M Nagarathinam, RG Palgrave, N Tapia-Ruiz, OV Kolosov, Nature Comm 2023, 14, 1321.

10:00 AM BREAK

10:30 AM *ES02.01.05

Real Time Electron Microscopy Observations of Electrode Materials for Li-Ion Batteries Sooyeon Hwang; Brookhaven National Laboratory, United States

Transmission electron microscopy (TEM) has played a vital role in providing nano- and atomic-scale insights into the morphology, microstructure, and chemical properties of Li-ion batteries at both anode and cathode materials. Moreover, improvements of in-situ capabilities, as enabled by specialized biasing TEM sample holders, offers an exciting opportunity to monitor the changes taking place in the electrode materials under external stimuli at an unparalleled resolution, enabling a deeper understanding of how the materials behave under various operating conditions. In-situ capability is also applicable to investigate structural changes of electrode materials during lithium removal or insertion under biasing conditions. Such operando characterization of the electrode materials is critical for gaining a fundamental understanding of how lithium-ion batteries function and degrade. My presentation will focus on real-time TEM observations of the phase transformations that take place in electrode materials during lithium migration. A dry-cell setup was developed inside the TEM column based on the Nanofactory STM-TEM sample holder, and lithium movement was controlled by applying bias to the samples. A multi-step lithium insertion reactions within tin sulfide will be presented as a proof-of-concept, and the nanoscale structural evolutions in these solid-state-cells will be further discussed. My talk will illustrate that dynamic investigations of electrode materials not only enhance our understanding of the structural changes induced by lithium but also provide intriguing insights into the underlying origins of battery performances.

11:00 AM *ES02.04.07

Unravelling Battery Interface: Speciation and Structure Feifei Shi; The Pennsylvania State University, United States

Interface speciation and structure significantly influence a battery's energy density, cycle life, and safety. However, the reduced signal strength and inherent fragility pose significant challenges when conducting the ex-situ and destructive characterizations. In this talk, I will initially provide an overview of surface science methodologies tailored to address interface-related issues in batteries, showcasing their practical applications. Subsequently, I will delve into the considerable promise of angle-resolved spectroscopy for discerning intricate interfacial speciation. Finally, I will introduce an innovative technique, time-resolved electrocapillarity, capable of offering precise insights into potential and concentration distribution across the electrode/electrolyte interface.

Acknowledge: This work is supported by U.S. Department of Energy under contract DE-NE0009286 and the National Science Foundation under Grant No. 2239690.

11:30 AM ES02.01.07

In Situ Imaging of Ion Transport in Electrochemical Cells for Predictive Solar Fuel Generation Livia Belman-Wells¹, James Utterback², Anwesha Maitra¹, Alex King^{3,1}, David Larson³, Leo Hamerlynck¹, Adam Weber³ and Naomi S. Ginsberg¹; ¹University of California, Berkeley, United States; ²Sorbonne Université, France; ³Lawrence Berkeley National Laboratory, United States

Ion transport underpins the functionality of many modern electrochemical devices involved in energy generation and storage. Despite its importance, label-free spatiotemporal imaging of ion transport in the solution phase in-operando has not been widely explored. Here we have performed interferometric reflection microscopy (IRM) measurements of voltage-induced ion transport in aqueous solution, spatiotemporally mapping ion concentration gradients and extracting transport parameters. We developed an electrochemical cell composed of a narrow channel etched into a microscope coverslip with vertical electrodes running along its sides to drive a reaction in a ferricyanide-based aqueous redox electrolyte. Applying a voltage while imaging the cell, we measure the evolution of concentration profiles through their changes to the local refractive index. Analysis of the evolving ion concentration gradients allows us to extract a diffusion coefficient consistent with that of aqueous ferricyanide, demonstrating the ability to do label-free optical imaging of ion transport in an aqueous electrolyte. This work serves as a basis to proceed to study CO₂ reduction for solar fuel generation. We anticipate imaging in situ mass transport to characterize the involved reactions and to compare local and global efficiency and durability across photoelectrode systems for improved device performance.

SESSION ES02.02: Operando X-ray Microscopy of Energy Storage Materials
Session Chairs: Raphaële Clement and Feng Lin
Wednesday Afternoon, April 24, 2024
Room 424, Level 4, Summit

1:45 PM *ES02.02.01

Characterizing The Morphological and Crystallographic Behavior of Ni-Rich Li-Ion Cathodes [Donal Finegan](#); National Renewable Energy Laboratory, United States

High Ni content cathodes display large volumetric changes and can incur crystallographic phase changes during formation and initial activation. The heterogeneous geometric and crystallographic evolution of the electrodes greatly influence their cycle-life performance. This work will focus on the application of advanced electron and X-ray microscopy techniques to characterize the evolution of heterogeneous particle morphology and crystallographic phases during formation, activation, and throughout the cycle-life of the cathodes. Focused-ion beam electron back scatter diffraction (FIB-EBSD) is applied to characterize the grain size distribution and orientations through the particle architectures. X-ray nano-computed tomography (nano-CT) is applied before and after formation and cycling to quantify morphological change such as crack growth throughout the life of the cathode materials. Finally, synchrotron X-ray diffraction computed tomography (XRD-CT) captures the efficacy of high-voltage activation steps during formation to irreversible form a stable layered phase for high performance long-life cycling. The multi-modal approach provides a comprehensive description of the morphological and crystallographic phenomena that determine the performance of earth-abundant cathodes and sheds new light on performance limiting material properties.

2:15 PM ES02.02.02

Advanced Operando Analysis for Interface Observation using Synchrotron X-Ray Computed Tomography for Lead-Acid Batteries [Seongjun Kim](#)^{1,2}, [Mark Wolfman](#)^{1,2}, [Tiffany Kinnibrugh](#)^{1,2}, [Alan Kastengran](#)^{1,2}, [Tim Fister](#)¹ and [Paul Fenter](#)¹; ¹Argonne National Laboratory, United States; ²Advanced Photon Source, United States

In the realm of battery technology, a field that has profoundly influenced various industries, including the automotive sector with the widespread adoption of lithium-ion batteries (LIBs), trust in these energy storage solutions remains challenged by issues related to safety, cost, and environmental impact. This has ignited an ongoing competition between traditional and emerging battery technologies.

Lead acid batteries (LABs), a technology dating back to 1859, have endured as preferred secondary power sources in many applications, primarily due to their economic advantages. Nevertheless, LABs face significant hurdles in order to compete effectively with other battery types. Deep discharges can lead to rapid sulfation, while the irreversible crystallization of lead sulfate (PbSO₄) can compromise battery lifespan and performance. Therefore, understanding the structural transformations of two critical components, the positive active material (PAM) and negative active material (NAM), becomes imperative for enhancing battery capacity and cycle life. Variations in internal morphology can influence electrode porosity and surface area, both pivotal factors in determining battery performance. Traditional post-mortem analysis methods, such as scanning and transmission electron microscopy (SEM and TEM), fall short in capturing real-time changes during cycling.

Synchrotron X-ray computed tomography (XCT) emerges as a non-destructive methodology for characterizing material morphology and interfaces across a wide spectrum of scales, from sub-micron to centimeters. This technique facilitates both two-dimensional (2D) and three-dimensional (3D) visualization, proving invaluable for investigating interface transformations in solid-phase materials. In situ or operando measurements enable the identification of morphology changes due to phase transitions during cycling. XCT-generated images can be reconstructed into 2D slices and further assembled into 3D representations, aiding in the interpretation of porosity and particle evolution across different states of charge (SOC). Additionally, complementary synchrotron X-ray techniques, such as diffraction (XRD) and transmission X-ray microscopy (TXM), contribute to unveiling the intrinsic chemo-mechanical dynamics within lead-acid batteries.

This presentation promises to shed light on LABs, offering insights into their mechanism through various synchrotron X-ray techniques. The application of in situ and operando X-ray measurements enhances our understanding of LABs, contributing to broader comprehension of this enduring energy storage technology.

2:30 PM BREAK

3:30 PM *ES02.02.04

The Applications of Operando X-Ray Fluorescence Microscopy in Electrochemical Systems [Luxi Li](#)¹, [Feng Lin](#)² and [Barry Lai](#)¹; ¹Argonne National Laboratory, United States; ²Virginia Tech, United States

X-ray Fluorescence Microscopy (XFM) has been an invaluable tool for investigating the elemental composition of specimens in both 2D and 3D contexts. Its versatile application spans across various scientific domains, including biology, medicine, and environmental science. Recently, operando XFM has emerged as a powerful technique for monitoring the transition element dissolution and redeposition in electrochemical systems. This method enables us to measure both the projective 2D elemental distribution and the interfacial elemental distribution through in-situ and operando XFM approaches [1,2].

The Advanced Photon Source (APS) 2-ID-D/E beamlines are the state-of-the-art hard X-ray microprobe XFM beamlines. In this presentation, I will provide an overview of the current instrumentations at 2-ID beamlines, followed by a selection of compelling showcase applications. To conclude, I will explore future perspectives in post-APS-U in-situ/operando research with multiscale and multimodal approaches.

1. Hu, Anyang, Yuxin Zhang, Fan Yang, Sooyeon Hwang, Sami Sainio, Dennis Nordlund, N Evan Maxey, Luxi Li, et al. "Manipulating Interfacial Dissolution-Redeposition Dynamics to Resynthesize Electrode Surface Chemistry." ACS Energy Letters 7, 2588 (2022).
2. Yuxin Zhang, Anyang Hu, Evan Maxey, Luxi Li, Feng Lin, "Spatiotemporal visualization and chemical identification of the metal diffusion layer at the electrochemical interface" J. Electrochem. Soc. 169, 100512 (2023).

4:00 PM ES02.02.05

Operando Bragg Coherent Diffraction Imaging of Commercial NMC811 Electrodes [Alice V. Llewellyn](#)¹, [Jiecheng Diao](#)², [Hamish Reid](#)¹, [Charlie Kirchner-Burles](#)¹, [Ian Robinson](#)¹, [Paul Shearing](#)³ and [Rhodri Jervis](#)¹; ¹University College London, United Kingdom; ²ShanghaiTech University, China; ³University of Oxford, United Kingdom

Commercial candidates for electric vehicle batteries include Ni-rich Li(Ni_{0.8}Mn_{0.1}Co_{0.1})O₂ (NMC811) cathodes due to their high specific capacity (200 mAh/g) and reduced cobalt content, which has positive socio-economic repercussions. Despite all of the advantages, these materials suffer from a range of degradation modes, many of which are associated with the redox and crystallographic behavior at high states of charge and are thought to be the cause of rapid capacity fade. NMC811 suffers from anisotropic changes in the crystal structure during cycling, which induce strain and can then lead to issues such as particle crack formation. Gathering data at multiple length scales is imperative for understanding the discrete mechanisms at play. Bragg Coherent Diffraction Imaging (BCDI) is a key tool for obtaining data at the nano-scale by providing high spatial resolution images of individual particles. BCDI also affords the unique opportunity to resolve the strain of individual crystals at the picometer scale, producing data with the highest quantifiable imaging resolution of battery electrodes and allowing for the detection of evolving defect modes such as shearing and stacking faults in the crystals during cycling. NMC811 typically employs the archetypal cathode particle morphology, consisting of a secondary particle agglomerate (~ 10 μm) made up of nanometer-sized primary particles. It is widely accepted that crack formation occurs at grain boundaries between primary particles. One mitigation method is to switch

to a single crystal morphology, reducing the number of grain boundaries within particles and therefore improving overall performance. However, there is still a limited understanding of the subtle mechanistic differences between the two morphologies during cycling. In this work, Operando BCDI was employed to study both polycrystalline and single crystal NMC811 electrodes in both pristine and aged states. Non-uniform distributions of inter- and intracrystal strain were observed for both polycrystalline and single crystal morphologies, even in the pristine state. The nucleation of crystal splitting was observed for a pristine single crystal during cycling, which could subsequently result in intergranular cracking. This feature is only resolvable with extremely high-resolution techniques such as BCDI. This work ultimately adds to the understanding of the central role of crystal-scale dynamics during cycling and the potential ramifications for a cell's electrochemical performance, leading to informed material design.

4:15 PM ES02.02.06

GRAPES Analysis of Particles in ElectrodeS (GRAPES); Data Workflows and Analytics for Computed Tomography (CT) Data of Degradation in Battery Materials [Matthew P. Jones](#) and Rhodri Jervis; UCL, United Kingdom

GRAPES is a python module designed to help researchers analyze electrode particles in tomography data. GRAPES transforms 3D image data into tabular dataframes that facilitate the rapid and intuitive processing of particles and particle properties relevant to the study of battery materials. Each row in the dataframe represents a unique particle with 20+ columns of particle characteristics such as sphericity, surface area, and volume. Additionally, battery degradation specific properties are included such as damage factor, and radial layer damage factors. The data transformation from image volumes to GRAPES dataframe can be executed in one line and allows users to more rapidly understand the relationship between different particle characteristics in their datasets. Furthermore, this format of large tabular data can be easily integrated with open-source machine learning libraries in python (sklearn, pytorch, etc.) to train classical machine learning models such as multiple linear regression, random forests, and gradient boosting.

In this work we report on two use case examples with a specific focus on the underlying data workflow used. These case examples are the degradation of silicon anode particles and NMC cathode particles during cycling. We cover the image processing, image registration, and image segmentation (binary and instance segmentation) required to prepare a time-lapse CT dataset. Additionally, we will discuss the importance of removing edge cases from the GRAPES dataset. This allows us to use GRAPES and other analytics to track how particles are damaged at different cycles, the spatial distribution of damaged particles, the regions of highest damage within particles, and track the percentage of particles that observe particular behaviors during cycling. Through this work we have demonstrated a state-of-the-art data workflow for processing CT datasets of electrode particle degradation. This method allows for large statistically relevant volumes to be analyzed during cell cycling whilst still tracking the changes in individual particles throughout time-lapse datasets. We believe that moving forward this workflow can be replicated for a broad range of electrochemical materials that observe volume and density change during use.

4:30 PM ES02.02.07

Operando Detection of Cracking in High Ni Battery Cathode Materials by X-Ray CT [Huw Parks](#)^{1,2} and [Rhodri Jervis](#)^{1,2}; ¹University College London, United Kingdom; ²Faraday Institution, United Kingdom

In a drive for ever-increasing energy density and reduction in use of cobalt in lithium ion battery cathodes, high-nickel content layered cathodes (Ni>80%) of the form $\text{LiNi}_x\text{Mn}_y\text{Co}_z\text{O}_2$ (NMC) have received significant recent attention. These materials undergo considerable anisotropic lattice changes during cycling (lithiation and delithiation) which has been attributed to the creation of microcracks in polycrystalline agglomerate cathode particles. This cracking behaviour has long been suspected to cause increased surface reactions leading to impedance rise, reduction of electronic conductive pathways and eventually complete particle detachment from the conductive matrix and pulverisation; however, the pre-existence of particle cracks and defects from manufacturing and calendaring of the electrodes can make it difficult to assess the contribution of the electrochemical history alone in causing cracks[1]. In a bid to reduce this, so-called single-crystal materials have been proposed to be more resistant to degradation[2] due to their resilience to cracking[3] and lower surface exposure to electrolyte, which can cause parasitic reactions and drive oxygen loss[4].

Assessing the origins of cracking and its evolution with battery ageing is complex due to the small and internal nature of the cracks, often requiring either destructive imaging techniques (such as FIB SEM or TEM on lamella) or small sample sizes in non-realistic environments to facilitate non-destructive imaging by methods such as X-ray computed tomography (CT). In previous work, we have developed methods for producing electrodes with optimised tab geometries for in situ and operando X-ray CT and related characterisation methods[5, 6], which we use here to allow for a pseudo-in situ nano-CT study of electrochemically induced cracking in NMC811 particles with minimal pre-existing damage[7]. This allows for direct observation of first-cycle cracking within the particles using lab-based CT on identical particles in the discharged and charged state, showing that even on the first cycle, significant intergranular cracks can develop in the polycrystalline materials. Additional ex situ studies on non-identical particles have revealed cracking in polycrystalline materials occurs at relatively low potentials, in the early stages of charging, and is at least partially recovered on discharge[8].

In this presentation we will extend this methodology to assess the progression of first cycle cracking throughout the charge and discharge range on thousands of identical particles from the same electrode within a realistic pouch cell environment. The use of the tab electrode geometry within a working pouch cell and larger field of view afforded by synchrotron micro-CT studies, combined with automated image processing and analysis, allows us to follow the behaviour of around 5,000 NMC particles through multiple states of charge, revealing the diversity of cracking behaviour within working, commercially relevant, Li ion battery electrodes. Advanced grey-scale analysis of the data reveals sub-resolution limit information about the damage to the particles throughout their states of (de)lithiation and provides a statistically relevant quantification of the extent of crack closure behaviour.

[1] T. M. M. Heenan et al., *Advanced Energy Materials*, vol. 10, 2020

[2] H. Li et al., *Journal of The Electrochemical Society*, vol. 165, 2018/04/05 2018

[3] S. S. Pandurangi et al., *Journal of The Electrochemical Society*, vol. 170, 2023/05/23 2023

[4] T. Li et al., *Electrochemical Energy Reviews*, vol. 3, 2020/03/01 2020

[5] C. Tan et al., *Journal of The Electrochemical Society*, vol. 167, 2020/04/06 2020

[6] C. Tan et al., *Cell Reports Physical Science*, vol. 2, 2021/12/22/ 2021

[7] H. C. W. Parks et al., *Journal of Materials Chemistry A*, 10.1039/D3TA03057A vol. 11, 2023

[8] A. Wade et al., *Journal of The Electrochemical Society*, vol. 170, 2023/07/14 2023

4:45 PM ES02.02.08

Heterogeneous Lithium Transport within Individual Single-Crystalline NCM Battery Particles [Bonho Koo](#)¹, [Jinkyu Chung](#)¹, [Danwon Lee](#)¹, [Chihyun Nam](#)¹, [Martin Z. Bazant](#)² and [Jongwoo Lim](#)¹; ¹Seoul National University, Korea (the Republic of); ²Massachusetts Institute of Technology, United States

Probing the lithiation kinetics in solid-state electrodes is foundational for advancing high-efficacy battery technologies. Typically, a consistent and monotonic lithium gradient is anticipated across solid-solution single-crystalline battery constituents throughout the cycling process. Our exploration, centered on the heterogeneous lithium distribution within single-crystalline $\text{LiNi}_0.333\text{Mn}_0.333\text{Co}_0.333\text{O}_2$ nanostructures, utilized operando scanning

transmission X-ray microscopy for precision. Contrary to the prevailing Fickian diffusion paradigm, our insights highlight the emergence of regions both rich and deficient in lithium, which exhibit dynamic behavior across battery cycles. This intricate interplay of intra-particle strain fields, capable of either concentrating or dispersing lithium, was authenticated using Bragg coherent X-ray diffraction methodologies. Significantly, we elucidated that regions with sparse lithium proximal to the particle surface can modulate the overarching charge transfer resistance and offer avenues for in-situ optimization. This investigation provides a renewed perspective on the intricacies of nanoscale solid-state guest diffusion, heralding implications for battery rate performance and durability.

SESSION ES02.03: Poster Session
Session Chairs: Livia Belman-Wells and Wenbo Zhang
Wednesday Afternoon, April 24, 2024
Flex Hall C, Level 2, Summit

5:00 PM ES02.03.01

Substitution Effects on Nucleation and Crystal Growth of Lead Sulfate on Barite for Battery Applications Shannon J. Lee¹, Carinna Lapson^{1,2}, Colin T. Campbell¹, Ajay Karakoti¹, Dan Thien Nguyen¹, Celsey Price² and Vijayakumar Murugesan¹; ¹Pacific Northwest National Laboratory, United States; ²University of Oregon, United States

The common and widespread use of lead-acid batteries is due to the reliability and cost-efficiency of this energy storage option. These batteries contain a Pb anode, PbO₂ cathode, and a microporous separator, all saturated with H₂SO₄ electrolyte. The common failure mechanism of “hard sulfation” involves the irreversible large crystal growth of non-electroactive PbSO₄ on the surface of the anode. Expanders are chemical additives, such as BaSO₄, used to uniformly distribute PbSO₄ nucleation sites and to minimize hard sulfation in the battery. Our studies combine methods using both *in-situ*, *ex-situ*, and *in-operando* imaging using 3D optical microscopy during electrochemical cycling to observe and better understand the nucleation and growth mechanisms of PbSO₄ on crystals of expanders BaSO₄ and Ba_{1-x}Sr_xSO₄. Fine tuning the ability of expanders (by Sr-substitution) to limit large crystal growth of PbSO₄ may improve overall lead-acid battery cycling.

SESSION ES02.04: Operando Spectroscopy of Energy Storage Materials
Session Chairs: Raphaële Clement and Andrej Singer
Thursday Morning, April 25, 2024
Room 424, Level 4, Summit

8:30 AM *ES02.04.01

Improving The Sensitivity of Operando Nuclear Magnetic Resonance for Electrochemical Studies Khashayar Bagheri^{1,2}, Ludivine Afonso de Araujo^{1,2,3}, Raphaël Praud^{1,2,3}, Vincent Sarou-Kanian^{1,2}, David Sicsic³, Michael Deschamps^{1,2} and Elodie Salager^{1,2}; ¹CNRS-CEMHTI, France; ²Réseau sur le Stockage Electrochimique de l'Energie (RS2E), France; ³Renault SAS, France

Nuclear Magnetic Resonance (NMR), as a bulk technique, is nicely suited for studying, *operando*, multi-component electrochemical cells. The NMR signal of atoms can be detected in many phases, independently of their degree of order: liquid, crystalline or amorphous. In addition NMR measurements deposit little power into the material, so that there is no risk of battery or material degradation during measurement. This comes however at the cost of a relatively low intrinsic sensitivity, which results in a limited temporal resolution.

In this talk we will present our latest developments to improve the sensitivity of *operando* NMR studies of batteries. Our approach is two-pronged: we work on reducing parasitic signals and on increasing intrinsic sensitivity, while controlling electrochemical behavior.

A first part will report on how we improved the *operando* setup and analysis for the early detection of the onset of metallic Li plating in NMC622/graphite cells at low temperature and fast charge [1]. Direct detection of metallic Li in the cell for various conditions of temperature and charging rate is precious to identify the exact conditions favoring metallic lithium plating and its evolution. A better grasp of this degrading phenomenon could lead to optimized charging protocols.

The second part explores how the sensitivity of the measurement itself can be increased. Most *operando* NMR measurements follow the signal of ⁷Li or ²³Na atoms, as they are taking part in the redox reactions. The NMR signals from the paramagnetic solid electrodes however suffer from large broadenings, due to the interaction of the atomic spins with unpaired electrons. Here we approached the problem from another side and explored ways to exploit the NMR signal of the liquid electrolyte solvent inside the battery. Sensitivity is enhanced thanks to the narrower signal of liquid, and the intrinsic sensitivity of ¹H higher than that of ⁷Li and ²³Na. We demonstrate that the ¹H NMR spectrum of the carbonates in the liquid electrolyte is mainly sensitive to the redox state of the positive electrode. This parameter is difficult to obtain without a three-electrode measurement, but is essential for understanding the mechanisms of capacity loss and developing adequate models for battery management systems.

Finally, proper electrochemical behavior may require pressure applied to the cell during cycling. This brings an additional challenge to NMR sensitivity, as the metallic parts applying pressure tend to disturb and shield the radio-frequency waves used for the measurement. We will present our progress on a design for *operando* NMR that is compatible with applying greater pressure on large pouch cells.

[1] L. Afonso de Araujo, V. Sarou-Kanian, D. Sicsic, M. Deschamps, E. Salager, Journal of Magnetic Resonance. 354 (2023) 107527. <https://doi.org/10.1016/j.jmr.2023.107527>.

9:00 AM ES02.04.03

Lab-Scale Operando X-Ray Emission and Absorption Spectroscopy to Monitor Redox Processes of Transition Metals in Lithium-Ion Batteries

Abiram Krishnan¹, Dong-Chan Lee², Ian Slagle¹, Sumaiyatul Ahsan¹ and Faisal Alamgir¹; ¹Georgia Institute of Technology, United States; ²Hongik University, Korea (the Republic of)

Tracking changes in the electronic structure of transition metal during cycling of lithium-ion batteries (LIBs) is crucial to investigate the nature of redox reactions occurring at the electrodes. X-ray absorption spectroscopy (XAS) is often utilized to study the role of individual elements in the redox processes during the cycling of batteries through oxidation state information in real-time (operando). In this study, X-ray emission spectroscopy (XES), a complementary core-hole method to XAS is presented as an alternate method to study the characteristic emissions from battery to investigate chemical and spin state changes in electrode material during C/10 constant current cycling.

XAS measures the energy-dependent absorption coefficient of a material in the process of generating core electron holes. Chemical state sensitivity from the XAS near-edge structure (XANES) and local atomic structure sensitivity through extended x-ray absorption fine structure (EXAFS) allows us to keep track of changes in the constituent elements during cycling. XES, a complementary method is obtained by capturing characteristic photons resulting from quenching generated core holes. K β emission line (3p-to-1s transition) of XES obtain their chemical state sensitivity through interaction between the 3p and valence orbital (exchange interactions). Element-specific emissions of sufficient energy resolution are simple to process and inform us on the chemical state, spin state, and local structure of transition metal allowing us to study the redox processes in real-time (operando) during charge/discharge of batteries. The high flux requirement of such real-time (operando) experiments often limits these studies to synchrotron sources. Limited access to synchrotron radiation has hastened the development of lab-scale instruments that employ bremsstrahlung sources and monochromators with sufficient energy resolution. The lab-scale instrument used in this study can perform both XAS and high energy-resolution XES experiments using a scanning setup which employs the Rowland circle geometry.

Here, we present the spectral changes of transition metal K $\beta_{1,3}$ and K β' features of XES are utilized to track state of charge (SoC) and study redox processes during C/10 operando cycling for the following cathode materials: LiCoO₂ (LCO), Li[Ni_{1/3}Co_{1/3}Mn_{1/3}]O₂ (NMC111), Li[Ni_{0.8}Co_{0.1}Mn_{0.1}]O₂ (NMC811), and LiFePO₄ (LFP). The results obtained from operando K β XES are compared with K-edge XAS, which serves as a benchmark. Additionally, the sensitivity of XES towards the total spin of the transition metal valence is used to investigate the change in magnetic properties resulting from nucleation of a new phase in electrochemically delithiated LCO samples in the range of 2-10% lithium removal.

9:15 AM ES02.04.04

Investigation on Photocorrosion of TiO₂ during The Photoelectrochemical Process by *In-Situ* ICP-MS Characterization Yiqun Jiang; Max Planck Institute for Iron Research, Germany

With the growing environmental deterioration and ever-increasing energy demand, exploring a renewable and clean energy for human development has been regarded as a promising research subject. Hydrogen is one of the most desirable energy carriers because of its abundance, high energy density and only byproduct of water. A breakthrough was made by Fujishima and Honda in 1972, who founded that hydrogen could be generated from water splitting on a TiO₂ photoelectrode under UV light. However, the energy conversion efficiency of TiO₂ semiconductor for photo(electro)catalytic process is relatively low owing to their fast recombination of electron-hole pairs and its large bandgap (3-3.2 eV). Fortunately, various methods are designed to improve the performance of photo(electro)catalyst which is closely associated with its nanostructure.

TiO₂ is considered to be quite stable since its redox potential has been calculated to be more positive/negative relative to the water oxidation/reduction potential, which means that photogenerated charge carriers participate in driving the desired redox potential rather than oxidizing or reducing semiconductor photoelectrodes. Nevertheless, the real photocorrosion (decomposition or degradation) depends on specific kinetic parameters such as illumination intensity, electrolyte property, radiation adsorption, charge transport and mass transport. We use inductively coupled plasma mass spectrometry (ICP-MS) to reveal the dissolution products of TiO₂ photoelectrode during PEC water splitting. It is unveiled that TiO₂ photoanode experiences photocorrosion from its oxidation with photogenerated holes. We demonstrate how the atomic scale structure of TiO₂ correlates with its PEC performance and photocorrosion process to enable a better understanding of the complex structure-activity-stability relationship in photoelectrocatalysis. ICP-MS analysis under solar water splitting conditions reveals the chemical instabilities that are not predicted from thermodynamic considerations of stable solid oxide phases represented by the Pourbaix diagram. Our investigation of photochemical corrosion pathway of TiO₂ thin film proves the competition between water splitting and semiconductor oxidation experimentally.

9:30 AM ES02.04.05

Operando Raman Spectroscopy for Aqueous Organic Redox Flow Batteries Lara Lubian, Rubén Rubio-Presa, Virginia Ruiz, Álvaro Colina and Edgar Ventosa; University of Burgos, Spain

Generation of electricity from renewable sources is crucial for achieving the transition to a sustainable and decarbonization energy system. While solar and wind power are becoming increasingly popular, their intermittency requires the deployment of efficient and cost-effective energy storage systems (ESSs) to match energy production and demand. Among the various EESSs, redox flow batteries (RFBs) that are featured by their independent scalability of energy and power are promising ESSs candidates for stationary energy storage application. The all-vanadium redox flow battery (AVRFB) is currently the state-of-art of RFB, but the large-scale implementation of AVRFBs presents an intrinsic challenge; vanadium is considered a critical material. Aqueous organic redox flow batteries (AORFBs) gaining much interest as vanadium-based species are replaced by organic redox-active species. While many organic molecules have demonstrated suitable redox potentials, kinetics and solubilities, their cycle stability should be further improved for large-scale deployment. Therefore, advanced techniques are required to investigate the capacity fading mechanisms in operando conditions.

In this contribution, the implementation of Raman spectroscopy for AORFBs will be discussed. Raman spectroscopy is a very useful technique that provides chemical information on redox-active molecules. Surprisingly, this powerful analytical technique has not been exploited in RFBs despite its intrinsic advantages to investigate highly concentrated solutions of strongly colored active species over more commonly used UV-Vis spectroscopy. Overall, the aim of this contribution is to promote the use of Raman spectroscopy within the RFB community by disclosing technical details for its implementation and discussing a couple of case-studies. Specifically, this contribution will be structured in three sections. First, the specific design, fabrication and practical implementation of Raman spectroscopy in a redox flow system for RFB research will be disclosed. Second, Raman spectroscopy will be used to monitor the state-of-charge and potential degradation of the catholyte of ferrocyanide-based redox flow batteries (both in alkaline and neutral pH). Finally, results on degradation of viologen-based analytes in the unavoidable presence of oxygen traces will be presented. Importantly, the methodology presented here may be of interest to other communities since it is implementable for other electrochemical flowing systems such as semi-solid flow batteries, electrochemical oxidation of pollutants, electrosynthesis, etc.

Acknowledgments

This work has received funding from the European Union's Horizon Europe research and innovation program – European Innovation Council (EIC) under the grant agreement No 101046742.

9:45 AM BREAK

10:15 AM *ES02.04.06

Hollow-Core Optical Fibre Sensors for *Operando* Raman Spectroscopy on Li-Ion Battery Liquid Electrolytes Ermanno Miele^{1,2}, Wesley Dose^{3,2}, Michael Frosz⁴, Zach Ruff^{3,2}, Michael De Volder^{3,2}, Clare Grey^{3,2}, Jeremy J. Baumberg^{1,2} and Tijmen G. Euser^{1,2}; ¹Cavendish Laboratory, University of Cambridge, United Kingdom; ²The Faraday Institution, United Kingdom; ³University of Cambridge, United Kingdom; ⁴Max Planck Institute for the Science of Light, Germany

Liquid-filled hollow-core fibres (HCF) are excellent sample cells in which light propagates in well-defined modes at the centre of a microchannel. The internal sample volumes in HCF can be as small as a few nL per cm interaction length, while long optical paths enable sensitive absorption, fluorescence, and Raman spectroscopy [1,2]. This talk will introduce optofluidic hollow-core fibres and briefly review their applications as microreactors. It will then demonstrate a new *operando* Raman spectroscopy method that tracks the chemistry of liquid electrolytes during battery cycling. An optofluidic hollow-core fibre is integrated into a working Li-ion cell and used to analyse sub-microlitre electrolyte samples at different stages of the charge-discharge cycle by background-free Raman spectroscopy. The observed changes in electrolyte composition are related to the solid electrolyte interphase (SEI) formation [2]. In addition, Raman measurements over multiple cycles reveal early signs of battery electrolyte degradation and we demonstrate that lost capacity can be recovered by infiltration of fresh electrolyte into a degraded cell. The new methodology contributes to understanding better the limitations of Li-ion batteries and paves the way for studies of degradation mechanisms in different electrochemical energy storage systems.

References

- [1] A. M. Cubillas *et al.*, Chem. Soc. Rev. **42**, 8629 (2013). <https://doi.org/10.1039/C3CS60128E>
[2] Ermanno Miele *et al.*, Nature Commun. **13**, 1651 (2022). <https://doi.org/10.1038/s41467-022-29330-4>

10:45 AM *ES02.04.08

***Operando* electrochemical Raman and IR spectroscopic studies of covalent organic frameworks for energy storage and conversion systems** Hye Ryung Byon; Korea Advanced Institute of Science and Technology, Korea (the Republic of)

I present designs of covalent organic frameworks (COFs) and underpin their significant applications in organic Li-ion batteries and electrochemical CO₂ reduction. Our COF designs encompass various tunable characteristics such as pore sizes, functional groups, and film thickness, ranging from nanometers to micrometers. These COFs serve as versatile platforms for Li⁺ storage electrodes, electrolytes, and CO₂/CO gas adsorption, which have been explored using *operando* electrochemical Raman and IR spectroscopy.

As a representative example, we have successfully incorporated redox-active azo groups into COFs to facilitate two-electron transfer, examining their potential as organic electrodes. Ensuring reversibility and stability proved crucial, with results highly contingent on neighboring functional groups. We explored three distinct linkages: beta-ketoenamine, imine, and thiazole-fused rings, each exhibiting varying cycling stabilities under identical operational conditions. It underscores the significance of fully conjugated organic systems. Furthermore, the overlap of vertical pi orbitals stemming from the azo moiety enhanced rate capability. *Operando* electrochemical Raman spectroscopy for the surface of cross-sectional COF electrode demonstrated reversible azo reaction with Li⁺ during the charging and discharging process.

11:15 AM ES02.04.09

The Local Structure in Zn-Cl Electrolytes and The Potential for *Operando* Study of The Interfacial Electrolyte Structure in Zn Ion Batteries using Valence-To-Core X-Ray Emission Spectroscopy Gerald Seidler¹, Diwash Dhakal¹, Darren Driscoll², Tim Fister², Niranjan Govind³, Andrew Stack⁴, Nikhil Rampal⁴, Gregory Schenter³, Christopher Mundy³, John Fulton³ and Mahaling Balasubramanian²; ¹University of Washington, United States; ²Argonne National Laboratory, United States; ³Pacific Northwest National Laboratory, United States; ⁴Oak Ridge National Laboratory, United States

The determination and modeling of the local structure around ions in electrolytes is a classic problem in physical chemistry that also has contemporary impact spanning electrical energy storage, geochemistry, and ionic liquids (broadly defined). This problem is greatly enriched by the occurrence of cation-anion correlations, such as in contact ion pairing, giving at its extreme the 'water in salt electrolyte' (WiSE) regime that poses extreme theoretical challenges while also showing improved energy density in some batteries. Here, we report several studies of ion pairing in the aqueous Zn-Cl solutions as a function of concentration, anion activity, nanoconfinement, and temperature. To this end, we demonstrate that laboratory-based valence-to-core x-ray emission spectroscopy (VTC-XES) gives an improved method to determine the local symmetry and average composition of the Zn(II) first shell coordination. Starting with bulk solutions at ambient conditions, analysis of VTC-XES gives a robust characterization of the first coordination shell without the analytical complications of extended x-ray absorption fine structure (EXAFS), for which the changing second-shell population at high concentrations generally requires independent theoretical modeling by advanced molecular dynamics simulation. Next, we find that nanoconfinement by nanoporous carbon electrode material increases the mean ion pairing and also, in agreement with prior WiSE results, increases the electrochemical window for Zn-ion batteries. Finally, we return to the bulk system to study the temperature dependence of ion pairing, giving new insight into the geochemical problem of Zn transport in brines while also clearly demonstrating the limitations of models based on extrapolation of solubility and thermodynamic information from the dilute regime.

These results illustrate the power of VTC-XES to investigate electrolyte structure, even when measured in the laboratory rather than at synchrotron x-ray light sources. The future extension to non-aqueous electrolytes would have even more direct relevance for beyond-Li-ion batteries. In addition, the work here lays important groundwork for future *operando* studies of the near-electrode interfacial structure of Zn-ion and other metal-ion electrolytes via synchrotron-based measurements. Such studies would immediately interrogate the connection between electrolyte structure and the operating voltage window for Zn-ion and other metal-ion battery systems.

11:30 AM *ES02.04.10

Understanding Electrochemical Properties of LiNiO₂ as a Cathode for Lithium-Ion Batteries Minkyung Kim; Kwangwoon University, Korea (the Republic of)

Cathode materials have been developed toward having high energy density and low cost with decreasing cobalt and increasing nickel. However, as Ni content increases, structural and electrochemical stabilities become poor. Cathode materials exhibit a trade-off relation between capacity and stability. It is challenging to break the trade-off relationship because 'high capacity' generally accompanies high structural and volumetric change. However, both properties are important to utilize materials. Recently single crystal cathodes are paid attention to solve the issue. Here, we synthesized single crystal LiNiO₂ and investigated the electrochemical properties depending on surface planes, crystal sizes and anti-site defects. Its impact will be addressed in this presentation.

SESSION ES02.05: Operando Diffraction and Scattering of Energy Storage Materials
Session Chairs: Yijin Liu and Andrej Singer
Thursday Afternoon, April 25, 2024
Room 424, Level 4, Summit

1:30 PM *ES02.05.01

Characterization of Advanced Positive Electrode Materials for Li-Ion Batteries [Naoaki Yabuuchi](#); Yokohama National University, Japan

The demand for electric vehicles equipped with Li-ion batteries is growing to develop low carbon society. Ni-enriched layered materials are used as electrode materials of Li-ion batteries for electric vehicle applications. However, available reversible capacity of Ni-enriched layered materials is approaching its theoretical limit. Therefore, innovation and development of new positive electrode materials are necessary. Recently, many cation-disordered rocksalt oxides have been proposed as a new series of electrode materials. Nevertheless, insufficient electrode kinetics for the cation-disordered rocksalt system limits its use for practical applications. One simple strategy is synthesizing nanosized materials to overcome a problem of electrode kinetics (for electrons, holes and ions), and electrode kinetics are significantly improved through nanosizing.¹⁻⁴⁾ Structural disordering also triggers unique electrode properties associated with different local environments for cations/anions.⁴⁻⁷⁾ From these results, we discuss the advantage and uniqueness of nanostructured cation-disordered rocksalt materials for high-energy advanced Li-ion batteries.

References

- 1) Y. Kobayashi et al., and N. Yabuuchi, *Materials Today*, **37**, 43 (2020).
- 2) M. Sawamura et al., and N. Yabuuchi, *ACS Central Science*, **6**, 2326 (2020).
- 3) J. Yun et al., and N. Yabuuchi, *PNAS*, **118**, e202496911 (2021).
- 4) N. Yabuuchi, *Current Opinion in Electrochemistry*, **34**, 100978 (2022).
- 5) R. Fukuma et al., and N. Yabuuchi, *ACS Central Science*, **8**, 775 (2022).
- 6) I. Konuma et al., and N. Yabuuchi, *Nature Materials*, **22**, 225 (2023).
- 7) A. Kanno et al., and N. Yabuuchi, *ACS Energy Letters*, **8**, 2753–2761 (2023).

2:00 PM *ES02.05.02

Understanding The Dynamics of Electrodes (Crystalline and Amorphous) and Interphases in Lithium Batteries [Enyuan Hu](#), Muhammad Rahman, Sha Tan and Nan Wang; Brookhaven National Laboratory, United States

Lithium batteries are complicated systems of electrodes and electrolytes. The inherent thermodynamic instability between the electrode and the electrolyte frequently results in the formation of an interphase. Understanding the dynamics of the electrodes and this interphase during battery operation is pivotal to advancing battery technologies. However, several challenges render the characterization process particularly daunting: 1. the processes can be far from equilibrium, making them unpredictable through traditional methods like phase diagrams; 2. instead of a well-defined crystalline structure, the electrode may assume an amorphous form, complicating our understanding; 3. the interphase exists in extremely trace amount, making its observation and study very demanding. We will discuss how we address these challenges using synchrotron-based scattering tools.

2:30 PM ES02.05.03

Revealing the Sodium Storage in Hard Carbon Pores [Luis Kitsu Iglesias](#), Emma Antonio and Michael Toney; University of Colorado Boulder, United States

Sodium-ion batteries (NIBs) are an attractive candidate to support the increasing demand of energy, especially amid growing concerns about the sustainability of lithium resources for lithium-ion batteries. NIBs provide advantages due to the abundance of sodium, its low cost, and electrochemical performance. Hard carbon (HC) is the most promising anode for the commercialization of NIBs, however, due to its structural complexity, a general mechanism for sodium storage in HC remains unclear, obstructing the development of highly efficient anodes for NIBs. To elucidate the mechanism of sodium storage in HC pores, we combined *operando* synchrotron small-angle X-ray scattering, wide-angle X-ray scattering, X-ray absorption near edge structure, Raman spectroscopy, and galvanostatic measurements. Through this multimodal investigation, we provide mechanistic insights into the sodium pore filling process across various HC microstructures including the pore sizes that are preferentially filled, the extent to which different pore sizes are filled, and how the defect concentration influences pore filling. We observe that sodium in the larger pores exhibits an increased pseudo-metallic sodium character, indicative of larger sodium clusters. Furthermore, we show that the hard carbons prepared at higher pyrolysis temperature have a larger capacity from sodium stored in the pores, and that sodium intercalation between graphene layers occurs simultaneously to the pore filling in the plateau region. Our results suggest that the engineering of defect sites in pore walls, together with increasing the pore size distribution and/or volume fraction of closed pores are key to designing superior HC anodes. Moreover, our study also gives a systematic approach to study other porous functional materials and to understand how ions store in the pores.

2:45 PM ES02.05.04

Comparing the Insertion Properties of Mg²⁺ into V₃O₇·H₂O in Organic and Aqueous Electrolytes [Daniela Söllinger](#) and Simone Pokrant; University of Salzburg, Austria

Batteries are indispensable in our society due to their ability to store renewable energy efficiently and provide it on demand. [1] In this context, lithium-ion batteries offer one of the highest energy densities and are already used in numerous mobile applications. However, lithium reserves and their accessibility are limited, which motivates researcher to find alternatives with similar electrochemical properties, i.e. low redox potentials and high volumetric/gravimetric specific capacities as counter electrode in batteries compared to lithium.

In this context, magnesium is attractive because it is more abundant, has a low redox potential vs. SHE and a small ionic radius, comparable to lithium. [2] The double charge of magnesium results in advantages and disadvantages; on the one hand it offers the possibility to store a higher amount of charge, while on the other hand the stronger polarization of Mg²⁺ compared to Li⁺ leads to challenges concerning the intercalation process. Therefore, cathode materials, which allow the reversible intercalation of Mg²⁺, offer high theoretical capacities and are stable in various chemical environments *e.g.* in organic and aqueous electrolytes, are of great interest in current magnesium-ion battery research. One promising cathode material, which can fulfil these requirements, is hydrated vanadium oxide V₃O₇·H₂O. [3]

In this context, we show via *operando* XRD how the structural evolution of V₃O₇·H₂O during ion insertion is affected by adding small quantities of water to the organic electrolyte. In addition, we study Mg²⁺ insertion into V₃O₇·H₂O in a completely aqueous electrolyte for the first time. Then we compare the structural properties of hydrated vanadium oxide as cathode material with respect to Mg²⁺ insertion in organic and aqueous electrolytes.

In the next step we investigate to which extent the chemical environment influences the electrochemical properties. Hereby, $V_3O_7 \cdot H_2O$ shows promising initial specific capacities of $\sim 300 \text{ mAh g}^{-1}$ in a pure aqueous electrolyte at practical current densities of 100 mA g^{-1} , which demonstrates the versatility of $V_3O_7 \cdot H_2O$ as cathode material for Mg^{2+} insertion.

Literature:

- [1] P. Wang *et al.*, *Energy Storage Materials*, **2022**, *45*, 142–181
- [2] P. Cunyuan *et al.*, *Small*, **2021**, *17*, 2004108
- [3] D. Söllinger *et al.*, *Electrochimica Acta*, **2022**, *434*, 141294

3:00 PM BREAK

3:30 PM *ES02.05.05

Operando Synchrotron-Based X-Ray Characterization of Battery Degradation Johanna N. Weker; SLAC National Accelerator Lab, United States

Synchrotron-based X-rays are a powerful characterization tool that can probe across many relevant length scales (from atomistic to millimeter) with different techniques that are sensitive to distinct features such as microstructure, chemistry, and morphology. Because of the high flux available and penetrating power of synchrotron-based X-rays, batteries can be probed under realistic (*operando*) conditions, which enables us to understand and overcome failure mechanisms of the next generation of battery materials. At the Stanford Synchrotron Radiation Lightsource at SLAC National Accelerator Laboratory, we have a suite of advanced X-ray characterization tools and have enabled a robust means of multimodal, *operando* characterization using a standard pouch cell geometry. With transmission X-ray microscopy (TXM), we capture morphology changes on either the cathode or anode during battery operation. Combined with absorption spectroscopy, the TXM provides maps of the local state of charge of active material particles. With high speed X-ray diffraction and X-ray absorption spectroscopy, we track the changes in crystallographic phases, local coordination, and chemistry. Results from all of these techniques can be combined together to get a more complete picture of the key degradation pathways of active battery materials to develop mitigation strategies for longer lasting energy storage.

4:00 PM ES02.05.06

Operando X-Ray Diffraction from Tape Casted Electrodes to All-Solid-State Batteries Kriti Kriti, Jean-Noël Chotard and Vincent Seznec; LRCS, France

The ever-growing field of energy storage needs the development of fast cycling rate and high energy density batteries and substantial research efforts are required to characterize them for improved performances. Operando X-ray diffraction is the most effective and convenient laboratory technique to get a deep insight into structural and electrochemical changes during operating conditions of batteries. In this work, we presented our newly developed operando LeRiChe'S Cell v2 which has been used to study NMC electrode materials not only with liquid electrolyte but also in solid-state batteries. The high brilliance of our laboratory diffractometer combined with our newly developed operando LeRiChe'S Cell v2 allowed us to investigate electrode materials at high C rates in a very short span of time. Moreover, we can also use our cell at low and high temperature to study battery materials. The operando cell has been tested not only for X-ray diffraction but also for X-ray absorption spectroscopy, coherent diffraction and X-ray photoemission spectroscopy on different beamlines at large scale synchrotron facilities.

4:15 PM ES02.05.07

Using Operando XRD to Characterize High-Temperature Oxidation and Reduction of Fe-X Energy Storage Materials Samuel M. Pennell and David C. Dunand; Northwestern University, United States

High temperature reduction/oxidation cycling of Fe materials is an attractive energy storage paradigm for the solid-oxide metal-air rechargeable battery (SOMARB). Using laboratory XRD sources, *operando* characterization of different Fe-X alloys during cycling enables detailed examination of the effects of the alloying element on the redox cycling process. Using these techniques, the extreme degradation resistance of hierarchically porous Fe-Mo and Fe-W metallic foams during redox cycling is shown. The foams are able to maintain their multi-level porosity through sintering inhibition, chemical vapor transport during reduction, and phase evolution that encourages mixing rather than segregation. These factors result in faster reaction kinetics with increased cycling, particularly over the first five cycles. These results are contrasted with Fe-Ni, Fe-Co, and Fe-Cu foams which show enhanced reduction kinetics but ultimately degrade due to poor sintering inhibition and lack of microscale porosity. These results guide further development of the energy storage material for SOMARBs and can be translated across domains into carbon utilization and chemical looping combustion.

4:30 PM ES02.05.08

Insights into Vanadium Electrocatalysis with High-Resolution In-Situ X-Ray Spectroscopy: Bi Nanoparticles on Graphene for Enhanced V Redox Flow Batteries Yue Wen and Rhodri Jervis; University College London, United Kingdom

Aqueous redox flow battery systems present notable benefits such as affordability, safety, and superior ionic conductivity. However, a central obstacle across all applications lies in effectively functioning within the limited electrochemical stability range of aqueous electrolytes, preventing their decomposition. Our research here is centred on investigating the side reaction of hydrogen evolution (HER) in the context of an all-Vanadium redox flow battery (VRFB), using it as a representative case [1]. VRFB is a crucial technology for large-scale energy storage on the grid, although they presently suffer from performance challenges and suboptimal coulombic efficiency due to detrimental side reactions. The hurdle lies in finding suitable catalysts for VRFBs—ones that promote essential redox reactions without concurrently promoting hydrogen evolution.

Leveraging a novel synthesis approach employed in creating robust Pt/graphene catalysts for fuel cells [2], we have successfully engineered a novel Bi-based catalyst tailored for VRFB. A precise and gentle synthesis method ensures the uniform dispersion of bismuth metal nanoparticles on a highly conductive graphene support, resulting in a substantial boost to battery performance that demonstrates an impressive energy efficiency of 75% over 100 cycles at a relatively high current density of 200 mA cm^{-2} . To unravel the catalytic mechanism, we conducted in situ X-ray absorption near edge structure (XANES) experiments, employing high energy resolution fluorescence detection (HERFD) and extended X-ray absorption fine structure (EXAFS) at the Bi L_{III} and L_I edges within electrolytes containing H^+ or both H^+ and V^{3+} . The XANES experimental data, enriched by HERFD, were meticulously compared with ab initio calculations to elucidate the relationship between electronic structure and potential. Utilizing density functional theory-based theoretical simulations, we unveiled a concentration-dependent relationship between H-ions and V-ions on Bi crystal surfaces. Given their inherent high V-ion concentration in the electrolyte to boost energy density, Bi holds promise for significantly suppressing HER side reactions. This work also provided insights into the role of ionized water molecules (H^*) and their implications on electrochemical processes, which is of utmost importance for advancing the development of efficient electrocatalytic systems in aqueous environments.

References:

- [1] Y. Wen, T.P. Neville, A. Jorge Sobrido, P.R. Shearing, D.J.L. Brett, R. Jervis, Bismuth concentration influenced competition between electrochemical

reactions in the all-vanadium redox flow battery, *J Power Sources*. 566 (2023) 232861. <https://doi.org/10.1016/J.JPOWSOUR.2023.232861>.
[2] G.M.A. Angel, N. Mansor, R. Jervis, Z. Rana, C. Gibbs, A. Seel, A.F.R. Kilpatrick, P.R. Shearing, C.A. Howard, D.J.L. Brett, P.L. Cullen, Realising the electrochemical stability of graphene: Scalable synthesis of an ultra-durable platinum catalyst for the oxygen reduction reaction, *Nanoscale*. 12 (2020) 16113–16122. <https://doi.org/10.1039/d0nr03326j>.

4:45 PM ES02.05.09

***Operando* X-Ray Absorption Spectroscopy for Lithium-Sulfur Batteries** Xueli Zheng; Stanford University, United States

Operando sulfur K-edge X-ray Absorption Spectroscopy (XAS) has emerged as a powerful tool to unravel the complex sulfur redox chemistry in lithium-sulfur (Li-S) batteries. Li-S batteries are promising as a compelling alternative to conventional lithium-ion batteries due to their exceptional theoretical energy density. However, their practical implementation faces challenges related to capacity fading, limited cycle life, and complex sulfur redox chemistry. *Operando* XAS plays a crucial role in understanding and addressing the above-mentioned challenges.

In this abstract, we first explore the application of *operando* sulfur K-edge XAS to gain real-time insights into the sulfur redox chemistry occurring at the sulfur cathode during Li-S battery operation. Using *operando* sulfur K-edge XAS, we revealed the dynamics of intermediate polysulfide species and the sulfur electrochemical conversion. Furthermore, the result guides us to design the multi-metal interaction with polysulfides. Li-S battery performance significantly enhanced by incorporating multi-metal to accelerate the Li-S reaction kinetics.

Then, we designed the cross-sectional Li-S battery cell to quantify polysulfide diffusion rate using sulfur K-edge X-ray spectromicroscopy. We found that elemental sulfur discharged to higher-order polysulfide species (Li_2S_8 and Li_2S_6) on the cathode and quickly diffused to the entire separator. This polysulfide diffusion resulted in the majority capacity decay in Li-S batteries.

In summary, we highlight the crucial role of *operando* XAS and X-ray spectromicroscopy as a transformative tool to overcome the fundamental challenges in Li-S batteries. Our study offers the potential for high-energy-density and sustainable energy storage solutions.

SYMPOSIUM ES03

Solid-State Batteries
April 23 - May 7, 2024

Symposium Organizers

Pieremanuele Canepa, University of Houston
Robert Sacci, Oak Ridge National Lab
Howard Qingsong Tu, Rochester Institute of Technology
Yan Yao, University of Houston

Symposium Support

Gold

Neware Technology LLC

Bronze

Toyota Motor Engineering and Manufacturing North America

* Invited Paper

+ JMR Distinguished Invited Speaker

^ MRS Communications Early Career Distinguished Presenter

SESSION ES03.01: General Session I

Session Chairs: Pieremanuele Canepa and Howard Qingsong Tu

Tuesday Morning, April 23, 2024

Room 423, Level 4, Summit

10:30 AM *ES03.01.01

Lithium Penetration through Solid Electrolyte Porosity and The Effect of a Ag-C Buffer Layer Gerbrand Ceder; University of California, Berkeley/Lawrence Berkeley National Laboratory, United States

Growth of lithium through connected porosity is one of the ways that Lithium filaments can penetrate through the solid electrolyte. By performing experiments on electrolyte pellets with controlled porosity we show that the relation between time to short-circuit and porosity is highly non-linear. I will also discuss the mechanism by which buffer layers, and in particular a Ag-C buffer layer can lead to highly efficient and uniform Li plating. By combining continuum + ab-initio modeling we can understand how Ag nanoparticles regulate the Li nucleation and growth. The understanding from this work also enables a rational selection of which other metals may or may not work.

11:00 AM *ES03.01.02

Materials Design for Super-Ionic Conductors for Solid State Li, Na, and Li-S Batteries Z. Lu, Y. Yu, Y. Wang, B Singh and Linda F. Nazar:
University of Waterloo, Canada

All-solid state Li-ion and Li-S batteries (ASSBs) have emerged as very attractive alternatives to conventional liquid electrolyte cells for e-mobility, owing to their enhanced safety and higher energy densities. Similarly, low-cost solid state Na-ion batteries may prove an promising alternative for stationary applications.

ASSBs are founded on high performance fast-ion conducting electrolytes, and in the important search for new materials, alkali thiophosphates (sulfides) and (oxy)halides are particularly promising classes of materials owing to their excellent mechanical properties. Sulfide-based solid catholytes are especially promising materials for high-performance solid-state sulfur cells that operate on the reversible conversion of S \leftrightarrow Li₂S. However, their electrochemical decomposition above 2.5 V vs Li⁺/Li causes progressive degradation in the operating window of the cell, because the free S²⁻ ions are oxidized to sulfur at a similar potential as Li₂S. Oxyhalides show particular advantage owing to their good interface stability with high voltage NMC-type cathodes.

The talk will cover an overview of the state-of-the art in the field, followed by a focus on recent findings in our laboratory and the understanding of superionic conductivity in these materials using a combination of structural elucidation via single crystal X-ray/powder neutron diffraction, ion conductivity mechanisms, and *ab initio* molecular dynamics simulations. We correlate crystal structure with ionic conductivity in a range of our newly developed fast ion Li and Na conductors. These considerations lead to an overarching understanding of the relative importance of interstitial alkali ion migration, defect concentration, and the factors that govern thermodynamic (meta)stability. The talk will also highlight their application in solid state batteries and factors that govern the cathode-electrolyte interface.

11:30 AM *ES03.01.03

Crystal Chemistry of Argyrodites and A₃PS₄-Type Solid Electrolytes (A=Li, Na) for Batteries Christian Masquelier¹, Ulas Omer Kudu¹, Dhanush Y. Shanbhag¹, Duy Linh Pham¹, Theodosios Famprikis¹, Jean-Noël Chotard¹, Virginie Viallet¹, Elodie Salager², Pieremanuele Canepa³, Saiful Islam⁴, Marc-David Braida⁵, Thierry Le Mercier⁵ and Florencia Marchini⁶; ¹Université de Picardie Jules Verne, France; ²Université d'Orléans, France; ³National University of Singapore, Singapore; ⁴University of Bath, United Kingdom; ⁵Solvay R & I, France; ⁶Umicore, Belgium

Solid electrolytes are crucial for next-generation solid-state batteries and immense activity is going on worldwide on many structural families of interest, including the ionic conductors Na₃PS₄, Li₃PS₄, Li₄PS₄I and Argyrodite Li₆PS₅(Cl,Br,I). We will present our recent crystal chemistry findings on these materials.

Li₃PS₄ is an attractive solid-electrolyte material that possesses high RT ionic conductivity (10⁻⁴ S.cm⁻¹) but the effects of specific synthesis parameters on the material's local structure and transport properties still demand clarifications. In particular, mechano-chemistry induces the formation of a variety of P_xS_y^{a-} moieties that strongly influence the global transport properties of Li₃PS₄.

Na₃PS₄ is another very interesting material with complex crystal chemistry that we will present. The effects of mechanochemical synthesis that lead to increased ionic conductivity in an archetypical sodium ion conductor Na₃PS₄ were not fully understood and we undertook comprehensive analysis based on diffraction (Bragg and pair distribution function), spectroscopy (impedance, Raman, NMR and INS), and *ab initio* simulations.

References

- Ö. U. Kudu, T. Famprikis, S. Cretu, B. Porcheron, E. Salager, A. Demortiere, M. Courty, V. Viallet, T. Le Mercier, B. Fleutot, M.D. Braida & C. Masquelier, *Energy Storage Materials*, **44**, 168-179 (2022)
T. Famprikis, H. Bouyanfif, P. Canepa, M. Zbiri, J. Dawson, E. Suard, F. Fauth, H. Playford, D. Dambournet, O. Borkiewicz, M. Courty, O. Clemens, J.N. Chotard, M.S. Islam & C. Masquelier, *Chem. Mater.*, **33(14)**, 5652-5667 (2021)
T. Famprikis, U. Kudu, J. Dawson, P. Canepa, F. Fauth, E. Suard, M. Zbiri, D. Dambournet, O. Borkiewicz, H. Bouyanfif, S. Emge, C. Grey, S. Cretu, J.N. Chotard, W. Zeier, M. S. Islam & C. Masquelier, *J. Amer. Chem. Soc.*, **142(43)**, 18422-18436 (2020)

SESSION ES03.02: General Session II
Session Chairs: Robert Sacci and Yan Yao
Tuesday Afternoon, April 23, 2024
Room 423, Level 4, Summit

1:30 PM *ES03.02.01

Exploring The Mechanism and Mitigation of Lithium Dendrites in Solid-State Batteries Dominic L. Melvin¹, Ziyang Ning¹, Dominic Spencer-Jolly¹, Guanchen Li², T. James Marrow¹, Charles Monroe¹, Peter Bruce¹ and Dominic Melvin¹; ¹University of Oxford, United Kingdom; ²University of Glasgow, United Kingdom

Solid-state batteries based on a ceramic electrolyte and lithium metal anode promise to revolutionise battery safety and energy density, but charging these batteries at practical current densities while avoiding dendrites remains a barrier to progress. Dendrites (filaments of lithium) penetrate the ceramic, resulting in short-circuit and cell failure. Important efforts have been made to understand dendrites in ceramic electrolytes and to mitigate them.

In recent work, we used *operando* X-ray computed tomography (XCT) to image a lithium anode solid-state cell during the charging process to understand the formation and progression of lithium dendrites through the solid electrolyte. Dendrites are found to follow a two-stage process of initiation then propagation, with different mechanisms for each. Initiation occurs in sub-surface pores where pressure builds to exceed the local fracture strength at the grain boundaries, by the mechanism of slow lithium extrusion. Propagation involves dry cracks, with Li driving the crack forward from the rear by a wedge-opening mechanism, rather than lithium at the crack tip, as has often been assumed previously. Reducing pressure at the lithium/solid electrolyte interface from 7 MPa to atmospheric pressure can significantly extend cycle life before cell failure.

Informed by the description of dendrite cracks, we control the microstructure of an Argyrodite (Li₆PS₅Cl) solid electrolyte and examine the impact of different microstructures, including pore size and distribution, crack length and width, on the dendrites. These studies consider how microstructure influences critical current densities for dendrite growth.

2:00 PM *ES03.02.02

Electrodeposition and Dissolution of *In Situ* formed Lithium and Sodium Metal Electrodes Jeff Sakamoto: University of California, Santa Barbara,

United States

Solid-state batteries consisting of lithium or sodium metal electrodes made using the anode-free manufacturing process are garnering significant interest. Anode-free manufacturing eliminates the need to handle and prevent oxidation and produces pure metal electrodes. However, little is known about the properties and mechano electrochemical behavior of these metal electrodes. Collaborative research conducted within the Department of Energy, Energy Frontier Research Center (Mechano-chemical Understanding of Solid Ion Conductors (MUSIC)) is exploring methods to characterize the behavior and properties of electrodeposited and electro dissolved lithium and sodium. Two model solid electrolyte systems were selected for this research based on their high conductivity and stability against their respective metal electrodes; LLZO for lithium and NaSICON for sodium. The results of this work will deepen the fundamental understanding of *in situ* formed lithium and sodium and advance commercialization of viable solid-state battery technology.

2:30 PM *ES03.02.03

Fast and Cooperative Ion Transport in Polymer Based Materials Valentino R. Cooper and Catalin Gainaru; Oak Ridge National Laboratory, United States

A major bottleneck limiting the advancement of energy storage and conversion technologies is the development of multifunctional, selective, and highly conductive membranes and solid electrolytes. State-of-the-art batteries rely on liquid electrolytes that exhibit low ion selectivity, poor electrochemical and thermal stability, and are plagued by potential safety hazards associated with dendrite formation, high volatility, and flammability. Similarly, polymer membranes in flow batteries and fuel cells have not achieved the necessary conductivity and selectivity for fast ion transport and suffer from water management issues that restrict operating temperatures due to the need for water (i.e., hydrogen bonding networks) to transport protons. In this presentation, I will discuss progress in the Energy Frontier Research Center on Fast and Cooperative Ion Transport in Polymer-Based Materials (EFRC FaCT) to understand and control fast, correlated ion and proton transport at multiple length and time scales. In particular, I will highlight two recent outcomes: (i) examining the mechanisms controlling the energy barriers for ion hopping in polymer electrolytes and (ii) the design of nanorod-composite systems exhibiting fast ion conductivity. These showcase the synergistic research across the center and the potential for the discovery and design of novel, fast ion conducting polymer electrolytes for next generation storage devices.

This work was supported as part of the Fast and Cooperative Ion Transport in Polymer-Based Materials (FaCT), Energy Frontier Research Center funded by the U.S. Department of Energy, Office of Science, Office of Basic Energy Sciences at Oak Ridge National Laboratory.

3:00 PM BREAK

3:30 PM *ES03.02.04

Interface Potentials inside Solid-State Batteries: Origins and Implications Yue Qi¹, Michael Swift², Elliot J. Fuller³ and Alec Talin³; ¹Brown University, United States; ²U.S. Naval Research Laboratory, United States; ³Sandia National Laboratories, United States

Interface resistance has become a significant bottleneck for solid-state batteries (SSBs). Most studies of interface resistance have focused on extrinsic mechanisms such as interface reactions and imperfect contact between electrodes and solid electrolytes. Interface potentials are an important intrinsic mechanism that is often ignored. Here, we highlight Kelvin probe force microscopy (KPFM) as a tool to image the local potential at interfaces inside solid-state batteries, examining the existing literature and discussing challenges in interpretation. Drawing analogies with electron transport in metal/semiconductor interfaces, we showcase a formalism that predicts intrinsic ionic resistance based on the properties of the contacting phases, and we emphasize that future battery designs should start from material pairs with low intrinsic resistance. We conclude by outlining future directions in the study of interface potentials through both theory and experiment.

4:00 PM *ES03.02.05

Understanding Fundamental Mechanisms of Materials and Interfaces in Solid-State Batteries through Atomistic Simulations Yifei Mo; University of Maryland, United States

The improvements of solid-state batteries are limited by the performances of the materials and their interfaces. We will present our recent atomistic simulation studies on the fundamental mechanisms underlying these critical materials and interfaces, in particular, what are the fundamental kinetic limitations in ion-conducting materials and solid-solid interfaces at the atomistic level. Through our atomistic level understanding, we will propose strategies for designing better materials and interfaces with faster kinetics.

4:30 PM *ES03.02.06

Constriction Susceptibility of Anode Materials in Solid State Batteries Xin Li; Harvard University, United States

This talk introduces a new concept of constriction susceptibility of anode materials found in all-solid-state batteries. X-ray diffraction, transmission electron microscopy, scanning electron microscopy, and elemental analysis techniques were used to characterize the structural and chemical details of the anode. Density functional theory simulation and high-throughput computation were used to analyze the constriction susceptibility of materials at anode, which helps categorize and design new anode materials. A proper utilization of the phenomenon can lead to fast plating and stripping of Li metal in the anode at high areal capacity in experiment. A pouch cell made by slurry-casting technique was used to demonstrate the stable and fast cycling capability of such anode design.

SESSION ES03.03: Poster Session
Session Chairs: Howard Qingsong Tu and Yan Yao
Tuesday Afternoon, April 23, 2024
Flex Hall C, Level 2, Summit

5:00 PM ES03.03.01

Formation of Intimate Interfacial Contact between The NCM and Li_{0.5}PS_{0.5}Cl Solid Electrolyte for All-Solid-State Batteries Jaeik Kim, Seungwoo Lee, Hyungjun Lee, Joonhyeok Park, Jiwoon Kim, Gunwoo Cha, Hongjun Park, Bobae Lee, Ungyu Paik and Taeseup Song; Hanyang University, Korea (the Republic of)

All-solid-state batteries (ASSBs) with sulfide-based solid electrolytes (SEs) have been considered the most promising next-generation energy storage

system due to their high energy density. However, mechanical instability such as initial insufficient physical contact and physical contact loss during cycling at the cathode active materials/solid electrolyte interface impede the practical use of ASSBs. Here, we report high-performance ASSBs using a Ni-rich NCM as cathode active materials coated with argyrodite-type sulfide solid electrolyte through the mechano-fusion method. The uniformly coated solid electrolyte layer guarantees solid physical contact between cathode active materials and solid electrolytes, enabling sufficient ion transport pathways. Furthermore, the firmly attached solid electrolyte does not detach from NCM when the cathode active material shrinks during de-lithiation. Making intimate initial physical contact and maintaining physical contact repress the interface resistance effectively. As a result, a full cell with argyrodite-coated NCM shows significantly enhanced electrochemical performances.

5:00 PM ES03.03.02

Multifunctional Covalent Organic Framework Solid Electrolyte Facilitating Fast Li-Ion Diffusion in Solid-State Batteries Jun-Hyeong Lee, Jaewoo Lee, Yoonhee So, Hong-Won Kim, Yujin Choi and Jong-Ho Kim; Hanyang University, Korea (the Republic of)

Ensuring the safety, high energy density, and long-term cycling performance of all-solid-state Li metal batteries (LMBs) requires the development of compatible organic solid electrolytes. However, it remains a challenge to develop an approach that enables organic solid electrolytes to easily dissociate strong Li-ion pairs and facilitate rapid Li-ion transport. In this study, a diethylene glycol-modified pyridinium covalent organic framework (DEG-PMCOF) with a well-defined periodic structure is prepared as a multifunctional solid electrolyte with a cationic moiety of high polarity, an additional flexible ion-transporter, and an ordered ionic channel for all-solid-state LMBs. The DEG-containing pyridinium groups within DEG-PMCOF lower the dissociation energy of Li salts as well as the energy barrier for Li-ion transport, resulting in an enhanced ion conductivity and a high Li-ion transfer number at room temperature in the solid electrolyte. Furthermore, the DEG-PMCOF solid electrolyte offers a wide electrochemical stability and effectively prevents the formation of Li dendrites and dead Li in all-solid-state LMBs. Molecular dynamics and density functional theory simulations provide insights into the mechanisms underlying the improved Li-ion transport in DEG-PMCOF, involving integrated diffusion processes such as hopping motion, vehicle motion, and free diffusion. The all-solid-state LMB constructed with a DEG-PMCOF solid electrolyte exhibits a high specific capacity, excellent retention, and outstanding Coulombic efficiency at various C-rates during long-term cycling. This DEG-PMCOF approach represents an effective strategy for designing a variety of solid-state Li batteries.

5:00 PM ES03.03.03

Enhancing Lithium Transport in Garnet-Type Solid Electrolyte for High-Performance All-Solid-State Batteries Young-Geun Lee and Jay Whitacre; Carnegie Mellon University, United States

Garnet-type $\text{Li}_{6.4}\text{La}_5\text{Zr}_{1.4}\text{Ta}_{0.6}\text{O}_{12}$ (LLZTO) is a promising solid-state-electrolyte for all-solid-state batteries; it has a good chemical stability in contact with Li metal and high ionic conductivity. However, insufficient interfacial contact and associated voids caused by poor wetting between Li metal and LLZTO can lead to a huge interface resistance and thus poor electrochemical performance including a high overpotential and limited critical current density (CCD). In addition, Li dendrites can be formed and will propagate through the LLZTO microstructure within the pores and grain boundaries, which can cause cell short circuiting. In this work, LiAlO_2 (LAO) was used as a sintering additive to improve a LLZTO microstructure with a denser structure, lower porosity, and compacted grain boundary regions. LLZTO with LAO (LLZTO-LAO) showed a higher relative density (~95%) and reduced porosity (~4.2%) compared to pure LLZTO (88% of relative density and 9.5% porosity). To calculate the ionic conductivity and activation energy of the LLZTO, a blocking electrode sputtered by gold on both side LLZTO was fabricated. LLZTO-LAO displays an improved ionic-conductivity (0.59 S cm^{-1}) and Li-ion activation energy (0.38 eV). In order to investigate interface resistances between LLZTO-LAO and Li metal, Li-Li symmetric electrochemical test cells were used. An enhanced interfacial resistance ($72.5 \Omega \text{ cm}^2$) was demonstrated for the LLZTO-LAO cell.

Li plating/stripping tests with critical current density (CCD) and cycling performance of Li symmetric cells were investigated by galvanostatic cycling experiment. While LLZTO delivers a lower CCD of 0.1 mA cm^{-2} , a higher CCD of 0.3 mA cm^{-2} is demonstrated within the symmetric cell with LLZTO-LAO. In addition, LLZTO-LAO showed lower overpotentials than LLZTO at the various current densities. The improved CCD and overpotential of LLZTO-LAO can be attributed to LAO additives that cause an improved microstructure with a reduced porosity resulting in a good interfacial contact between electrolyte and Li metal.

5:00 PM ES03.03.04

The Effect of Slurry pH Values on The Electrochemical Properties of Manganese-Based-Oxide Electrode for Solid-State Batteries Tzu-Hao Kuo, I-Han Lee, Chia-Chien Ma and Tri-Rung Yew; National Tsing Hua University, Taiwan

With the rapid growth of electric vehicles, their conventional lithium-ion batteries (LIBs) are suffered from insufficient energy density and potential safety risks. High-capacity, earth-abundance, and low-flammability make manganese oxides a promising active material for anodes. Furthermore, the pH value of solid-state batteries (SSBs) influences lithiation and delithiation reactions, which in turn impacts the lithium wettability and interface resistance of SSBs. It is critical to study the effect of pH range so as to optimize the active materials and binders in manganese-based-oxide anodes.

In this work, the different pH values of electrode slurries will be investigated to improve the stability of binders and active materials. Furthermore, the pH value will be optimized to inhibit the unnecessary irreversible reactions during charge and discharge. It is expected that the optimized pH value of electrode slurries will enhance the retention, Coulombic efficiency, and rate-capability of the manganese-based-oxide anode in SSBs.

For the optimization of the pH value for manganese-based-oxide electrode slurries, water-based slurries will be produced by mixing manganese oxide powders, carbon black (super P), carboxymethyl cellulose (CMC), and styrene-butadiene rubber (SBR). The pH value of slurries will be adjusted with an oxalic acid. After that, the premixed slurries will be coated on copper foils by using a doctor blade, and then baked in a vacuum oven. After battery assembly, the electrochemical impedance spectroscopy (EIS) and galvanostatic charge-discharge (GCD) analyses will be applied to analyze the Coulombic efficiency, cycling life, and impedance variation resulted from different pH values. The composition and structure of active materials will be characterized by field-emission scanning electron microscopy (FE-SEM), energy-dispersive X-ray spectroscopy (EDX), and X-ray diffraction (XRD). This work will shed a light on controlling the pH value of manganese-based-oxide electrode slurries, for the improvement of SSB retention.

5:00 PM ES03.03.05

Zwitterionic Covalent Organic Framework Solid Electrolyte with Ordered Ionic Channels for All-Solid-State Lithium-Metal Batteries Jaewoo Lee, Jun-Hyeong Lee, Jae-Hoon Shin, Yoonhee So, Yejoon Yu, Yujin Choi, Hong-Won Kim and Jong-Ho Kim; Hanyang University, Korea (the Republic of)

Organic solid electrolytes are considered a promising way to enhance the energy density of Li rechargeable batteries. However, practical applications of organic solid electrolytes have suffered from extremely low ionic conductivity at room-temperature due to strong ion pairs of Li salts and lack of ordered ionic channels for Li^+ diffusion. Covalent organic frameworks (COFs) with well-defined chemical and pore structures can be considered excellent candidates for solid electrolytes due to their uniform channels for the migration of ionic species. Herein, the zwitterionic covalent organic framework

(Zwitt-COF) was developed as a solid electrolyte with not only the superior ability to dissociate strong Li-ion pairs but also well-organized ionic channels for fast Li⁺ diffusion. Theoretical simulations revealed that zwitterion can effectively dissociate the strong Li-ion pairs, and the linear hexagonal ion channels can be reopened in the Zwitt-COF solid electrolyte by reconstructing AA stacking structures due to the dissociative adsorption of Li⁺ on Zwitt-COF. The Zwitt-COF electrolyte exhibited high ionic conductivity at room-temperature and stable Li plating/stripping performance without formation of Li dendrite and dead Li. Furthermore, the Zwitt-COF electrolyte displayed a wide electrochemical stability window and outstanding thermal stability. All-solid-state Li metal full cells prepared with a Zwitt-COF electrolyte exhibited excellent cyclic performance for a long duration with high retention of discharge capacity. The strategy for incorporating zwitterions into a COF structure can provide an effective way to develop various all-solid-state batteries.

5:00 PM ES03.03.06

Development of Solid Polymer Electrolyte with Excellent Electrochemical Properties Using High-Energy Electron Beam Irradiation Wookil Chae and Taeshik Earmme; Hongik University, Korea (the Republic of)

Lithium-ion batteries (LIBs), an energy storage system used in various fields such as electronic devices, electric vehicles, and unmanned aerial vehicles, consist of a cathode, anode, separator, and electrolyte. Currently, commercialized LIBs employ a liquid electrolyte that utilizes carbonate-based organic solvents. When an exothermal reaction is triggered by overcharge or external shock, the thermally unstable organic solvent can generate flammable gases and lead to ignition, ultimately causing a thermal runaway in LIBs. Due to the safety concerns associated with organic solvent-based liquid electrolytes, research has been conducted on solid electrolytes (SEs) as an alternative to liquid electrolytes (LEs).

Among various SEs, polymer electrolytes (PEs) have garnered attention for their advantageous interfacial properties, form factor, and processability. In this study, the fabrication method for PEs involves *in-situ* polymerization. PEs created through *in-situ* polymerization are prepared by injecting a liquid precursor comprising monomers, lithium salt, initiators, and other components into the cell. Typically, thermal initiation is employed as the primary method for PE fabrication. However, thermal initiation comes with drawbacks, including challenges in controlling precursor reactions and the requirement for extended heat treatments.

To address these issues, solid polymer electrolytes (SPEs) are prepared using high-energy electron beam irradiation. SPEs are produced with just tens of seconds of electron beam exposure. Optimized SPEs exhibit an average ionic conductivity of 0.54 mS cm⁻¹, a lithium transfer number (t_{Li^+}) of 0.69, a wide electrochemical window exceeding 5 V, and excellent properties in suppressing the growth of lithium dendrites. Furthermore, in the NCM811|SPEs|Li cell configuration, a discharge capacity of 183 mAh g⁻¹ (0.1 C, 25 °C) was achieved, with 80% capacity retention after 200 charge/discharge cycles at 0.5 C and 25 °C.

5:00 PM ES03.03.07

Rational Design of Electrolyte and Interface for High-Performance and Safer Solid-State Li Batteries Donggun Kim, Baozhi Yu and Ying Chen; Deakin University, Australia

Solid-state Li metal batteries (SSLMB) gained increasing attention from researchers. Free of flammable organic liquid electrolytes by replacing solid-state electrolytes (SSE) greatly enhances battery safety, and employing Li metal anode possessing ultrahigh specific capacity and lowest redox potential delivers higher energy density than current state-of-art Li⁺ ion batteries. However, the safety crisis still exists, due to the extremely high reactivity of Li metal and the uneven plating-stripping behavior of Li anode. Unwanted side reactions pulverize SSE and electrode-electrolyte interface. Dendritic Li deposition accumulates dead Li, penetrates SSE, and eventually invokes internal short-circuit. Moreover, incomplete solid-solid contact between SSE and electrode induces severe polarization during battery operation. The poor interfacial compatibility of SSE to Li metal, both (electro-)chemically and physically, hinders the practical application of SSLMB so far.

Here, we suggest some effective approaches to resolve interface issues in the SSLMB. Firstly, we prepared an artificial solid electrolyte interphase (SEI) layer using poly(vinyl alcohol) and hydroxyl-functionalized boron nitride nanosheets. The artificial SEI alleviates the side reaction between Li metal and electrolyte, which mitigates electrolyte degradation. We found that this artificial SEI also assists uniform Li plating-stripping and suppresses dendritic Li deposition, by boosting Li⁺ ion transport at the electrode-electrolyte interface.

Secondly, we designed multi-layered SSE with inorganic-gel hybrid SSE and *in-situ* prepared SSE. The inorganic-gel hybrid layer supports excellent mechanical stability and fast Li⁺ ion conduction with a high Li⁺ ion transference number. The *in-situ* prepared SSE greatly improves interfacial compatibility between SSE and Li metal anode. It provides intimate contact at the interface and prevents inorganic electrolyte decomposition in the hybrid. Moreover, by comparing different layered SSEs, we found that the bulk electrolyte layer assists cycling stability, while the interfacial layer dictates the practical current density of layered SSE. When this multi-layered SSE is applied in the Li-S full cell, the layered SSE only allows polysulfide dissolution in the *in-situ* SSE layer and halts its further diffusion into the bulk electrolyte.

5:00 PM ES03.03.08

Covalent Organic Framework Based Solid State Electrolytes Chaoqun Niu; Westlake EDU, China

The development of high-performance solid-state electrolytes is a key milestone in advancing the safety, performance, and energy density of energy storage technologies, particularly in lithium-ion batteries. Covalent Organic Frameworks (COFs), with their unique structural tunability, high thermal and chemical stability, and inherent porosity, have emerged as a promising candidate for solid-state electrolytes. Our work explores cutting-edge research in the design, synthesis, and characterization of COF-based solid-state electrolytes and their transformative potential in the realm of energy storage. We will discuss the rational design of COFs tailored for solid-state electrolyte applications, focusing on factors such as framework stability, and ion conductivity. By judiciously modifying COF structures, we can enhance their ion transport properties, leading to improved ionic conductivity and electrochemical stability. These studies shed light on the mechanisms of ion transport, electrochemical stability, and long-term performance of COF-based electrolytes.

In conclusion, this research represents a significant advancement in COF-based solid-state electrolyte development, offering solutions to the pressing challenges in energy storage technology. We anticipate that the insights and breakthroughs presented here will pave the way for the practical implementation of COF-based solid-state electrolytes, fostering discussions and collaborations within the materials science community, and catalyzing the transformation of energy storage technologies toward a safer and more efficient future.

References:

1. **Chaoqun Niu**, Wenjia Luo, Chenmin Dai, Chengbing Yu, Yuxi Xu*. High voltage tolerant covalent organic framework electrolyte with holistically oriented channels for solid state lithium metal batteries with nickel rich cathodes. *Angew Chem Int Ed*, 2021, 60(47): 24915-24923.
2. **Chaoqun Niu**, Yuxi Xu*. Two-dimensional polymers: Preparation, assembly and high-efficiency electrochemical applications. *Acta Polymerica Sinica*, 2021, 52(6): 549-564.
3. Kaige Zhang, **Chaoqun Niu**, Chengbing Yu, Li Zhang, Yuxi Xu*. Highly crystalline vinylene-linked covalent organic frameworks enhanced solid polycarbonate electrolytes for dendrite-free solid lithium metal batteries. *Nano Research*, 2022, 15(9): 8083-8090.
4. Zhen Hou, Shuixin Xia, **Chaoqun Niu**, Yuepeng Pang, Hao Sun, Zhiqi Li, Yuxi Xu*, Shiyong Zheng*. Tailoring the interaction of covalent organic framework with the polyether matrix toward high performance solid state lithium metal batteries. *Carbon Energy*, 2022, 4(4): 506-516.

5:00 PM ES03.03.09

Development of an All-Solid State Li-Ion System [Djamel Mourzagh](#); CEA - LITEN - Grenoble Alpes, France

Li-ion batteries are considered as the most suitable electrochemical energy storage systems for a wide range of applications including automotive applications in order to contribute to the reduction of CO₂ emissions responsible for climate change.

In recent years, the majority of the works on batteries has consisted in developing solid electrolytes with the goal to improve their safety and the possibility of using a negative electrode based on metallic lithium which will ultimately make it possible to achieve high energy densities.

CEA-Liten and Saft have jointly developed a solid-state polymer electrolyte system. The polymer PTMC (Poly trimethylene carbonate) has been selected for its high transport number, over 0.7, and its stability with respect to lithium both at high potential and at low potential despite its modest conductivity.

The Solid Polymer Electrolytes (SPE) realized is a crosslinked membrane based on PTMC, with good mechanical properties that allow an easy handling and integration into a complete system (Fig 1).

The electrodes containing PTMC and NMC622, Graphite or SiO_x as active material were manufactured with a surface capacities around 1mAh/cm². Their mechanical properties are similar to conventional Li-ion electrodes.

Solid-state prototypes with a capacity around ten milliampere-hours have been assembled with these components. The performances of the all-solid prototypes containing PTMC are encouraging. Indeed, they operate correctly at a C/20 rate at 80°C but also at room temperature with the addition of plasticizers.

5:00 PM ES03.03.10

Development and Characterization of Flexible PVDF-TrFE-Ti3C2 MXene-Based Composite Co-Polymer Solid Electrolytes: Towards Application in Solid-State Li-Ion Batteries [Harshkumar Bhatt](#)¹, Derek Xiong¹, Armando Correa¹, Prakhyat Gautam¹, Parshwa Khane¹, David Ryman¹, Saquib Ahmed^{2,2} and Sankha Banerjee^{1,3}; ¹California State University, Fresno, United States; ²Buffalo State College, United States; ³University of California, Davis, United States

Efficient energy storage systems are essential for renewable energy sources. While lithium-ion batteries are prominent in this regard, there are ongoing challenges related to safety and cycling stability. These issues can be addressed by adopting solid polymer electrolytes (SPE) as an alternative to the conventional separator/electrolyte setup. One of the issues with developing solid-state batteries is the development of functional materials and materials systems that have a combination of thermal stability, tunable surface chemistry, and charge carrier mobility characteristics. MXene and its composites have presented a fascinating opportunity in the realm of functional materials. This is due to their unique layered structures that exhibit several advantageous characteristics, such as higher electrical and thermal conductivity, increased charge carrier mobility, a high negative zeta-potential, strong mechanical properties, a tunable bandgap, excellent hydrophilicity, metallic properties, and rich surface chemistry. However, when considering applications in electrochemical energy storage, an inherent issue is the tendency for agglomeration and restacking of MXene nanosheets and nanoflakes that significantly hamper the accessibility of active surface sites for electrolyte ions. The following work involves the fabrication and characterization of PVDF-TrFE-Ti3C2 MXene-based co-polymer composite solid-state electrolytes. The microstructure of these composites will be studied using scanning electron micrographs. The dielectric and impedance characteristics will be tested using electrical impedance spectroscopy. The ionic conductivity characteristics will be categorized using electrochemical impedance spectroscopy.

5:00 PM ES03.03.11

Recent Advancements and Prospects Of Lithium-Ion Batteries: Smart Features, High Performance Anode, Cathode and Electrolyte Materials Shahria Ahmed, [S M Anayet Ullah Shohag](#), Md Wasikur Rahman and Jasim Uddin; The University of Texas, United States

Nowadays, lithium-ion rechargeable batteries (LiBs) are the predominant source for energy storage and have promising prospects in the future. Monitoring the health status of the LiBs has become a pressing need to prolong the life and increase the security of LiB-powered applications. This need has opened new possibilities for smart LiBs research, enhancing battery life and safety. Herein, the scheme of sensors for Li-ion smart batteries has been discussed, which use a straightforward beam structure towards the measurement of different parameters, for instance, force, temperature, and displacement. Besides, we have discussed the most recent high-performance anode, cathode, and electrolyte materials used for and the modification of the materials by using different techniques to make them suitable for high-energy density Li-ion batteries. Finally, it has been concluded with promising future outlooks of the LiBs research by using these high-performance materials.

5:00 PM ES03.03.12

Enhancing Sodium Ionic Conduction of β'' -Alumina-YSZ Composite Electrolytes by Controlling The Surface Composition Anisa R. Nurohmah¹, Yebin Cho¹, Junyeong Jeon¹, Keeyoung Jung² and Younki Lee¹; ¹Gyeongsang National University, Korea (the Republic of); ²Research Institute of Industrial Science and Technology (RIST), Korea (the Republic of)

β'' -alumina, a sodium aluminate with the non-stoichiometric formula of Na₂O·(5-7) Al₂O₃, has received considerable interest as a solid electrolyte in sodium batteries due to its high sodium ionic conductivity and remarkable thermal stability using inexpensive elements. Recently, a vapor-phase conversion process based on the reaction between Na₂O vapor and α -alumina has been reported, which allows for thinning and strengthening of β'' -alumina solid electrolytes (BASEs). The new process requires a composite with approximately 30 vol.% of yttria-stabilized zirconia (YSZ) to achieve O²⁻ diffusion during the entire α -to- β'' phase conversion. Nonetheless, the incorporation of YSZ, an O²⁻ conductor, reduces the Na⁺ transport pathway, so that a decrease in ionic conductance across the electrolyte is inevitable.

This study focuses on the effect of the proportion of β'' -alumina near the surface region of the composite electrolyte on the conductance. The lamination of α -alumina – 30 vol.% YSZ green tapes was used for the fabrication of BASEs, and the α -alumina content of both two outermost tapes was varied in 90 to 40 vol.% to create “core-shell” structure. Although the outermost layers, known as the “shell”, comprises only about 10% of the total thickness, the electrolyte with the surface incorporating more than 90 vol.% of β'' -alumina demonstrates 13.4 mS cm⁻¹, measured by blocking electrode method at 190°C; This value exhibits more than 20% increase as compared to the conventional electrolyte without the shells. When used with the symmetrical molten sodium electrodes at the same temperature, the novel electrolyte demonstrates 2.55 Ω cm⁻² of area-specific resistance; Additionally, this value represents a 28% reduction from the value of the conventional composite electrolyte without the shells. This finding suggests that adjustments to the composition of the surface region alone could considerably enhance ionic transport through the vapor-phase converted β'' -alumina-YSZ composites by expanding the conducting channels.

5:00 PM ES03.03.13

Investigation of Mechanical Characteristics of Catholytes in Composite Cathode of All Solid-State Batteries [Joseph M. Vazquez](#) and Howard Qingsong Tu; Rochester Institute of Technology, United States

All-solid-state batteries (ASSBs) are leading the path to safer and more efficient energy storage. The solid electrolyte is a critical component in determining the performance and stability of ASSBs, responsible for both ion transfer and resisting dendrite growth. A robust solid electrolyte that excels in these

functions is essential for advancing ASSB technology. Existing solid electrolytes face challenges like poor interfacial contact, mechanical debonding, and mechanical failure. While the field predominantly focuses on ion transfer and micro-scale mechanical properties, there is a noticeable gap in understanding macro-scale mechanics. This study addresses this gap by examining prevalent solid electrolytes, including $\text{Li}_6\text{PS}_5\text{Cl}$, Li_3YCl_6 , $\text{Li}_3\text{YBr}_3\text{Cl}_3$, and $\text{Li}_7\text{La}_3\text{Zr}_2\text{O}_{12}$. Through traditional compression testing supported by video analysis, we reveal the correlations between pellet density and slenderness with elasticity, strength, and toughness across sulfide, halide, and oxide solid electrolyte materials. Our findings underscore the macro-scale mechanical advantages of LPSCl, exhibiting a relatively large elastic range (5–83 MPa), high compressive strength (~103 MPa), significant toughness (~16 MPa), and semi-ductile nature. The notable differences in elastic, non-linear, and failure mechanics among solid electrolytes emphasize the relevance of macro-scale mechanical properties in predicting cell failures such as capacity fading, dendrite growth, and contact loss.

5:00 PM ES03.03.14

Long-Durable Three-Dimensional Garnet-Type $\text{Li}_{6.4}\text{La}_{1.4}\text{Zr}_{1.4}\text{Ta}_{0.6}\text{O}_{12}$ Solid-State Li-Metal Batteries Sung Ryul Choi, Seojeong Yoo and Jun-Young Park; Sejong University, Korea (the Republic of)

Lithium-metal (Li-metal) holds promise as an anode material for next-generation high-energy density lithium-ion batteries (LIBs) due to its exceptional theoretical capacity of up to 3860 mAhg^{-1} [1]. However, technical challenges are remained, notably concerning safety due to dendrite formation during charge-discharge cycles [2]. Even in conventional aqueous-LIBs, preventing the penetration of Li dendrites remains unresolved despite extensive efforts [3]. To address this challenge, solid-state electrolytes (SSEs) have emerged as promising alternatives due to their high ionic conductivity, stability against Li-metal, and wide electrochemical windows [4]. SSEs encompass various categories such as polymer electrolytes, inorganic sulfide electrolytes, and inorganic oxide electrolytes [5]. Among these, the garnet-type $\text{Li}_{6.4}\text{La}_{1.4}\text{Zr}_{1.4}\text{Ta}_{0.6}\text{O}_{12}$ (LLZTO) stands out for its excellent ionic conductivity, ranging from 10^{-4} to 10^{-3} Scm^{-1} , and its thermodynamic stability against Li-metal [6, 7]. However, the formation of Li dendrites persists even at low current densities, primarily due to the inhomogeneity between Li-metal and the LLZTO electrolyte, particularly poor Li-metal wettability on the LLZTO electrolyte [8, 9]. Efforts to address the lithiophobic nature of LLZTO electrolytes have involved surface polishing, which enhances lithium wettability [10-12]. Another approach for improving Li-metal wettability is the introduction of nanometer-scale metal/metal oxide interlayers at the Li-metal–LLZTO interface [13, 14]. However, these strategies have not completely prevented dendrite formation, evident from low critical current density (CCD) results [15]. In our study, we present a three-dimensional (3D) tri-layer structure created *via* the tape-casting technique. This structure comprises porous-dense-porous regions. The porous layer plays a crucial role in enhancing the heterogeneity of the interface between the Li-metal anode and LLZTO electrolyte, facilitating Li-metal wetting and infiltration into the pores. Additionally, the dense morphology acts as a protective layer, impeding Li dendrite penetration, as dendrites tend to propagate along porous regions and grain boundaries of the LLZTO electrolyte. This architecture resulted in stable Li-metal cycling at high current density and improved critical current density performance.

Keywords: Lithium-ion batteries, $\text{Li}_{6.4}\text{La}_{1.4}\text{Zr}_{1.4}\text{Ta}_{0.6}\text{O}_{12}$, solid-state electrolyte, dendrite.

References

- [1] J. M. Tarascon, M. Armand, *Nat.*, **414**, (2001) 359-367.
- [2] J. Qian, W. A. Henderson, W. Xu, P. Bhattacharya, M. Engelhard, O. Borodin, J. G. Zhang, *Nat Commun.*, **6**, (2015) 6362.
- [3] Y. Guo, H. Li, T. Zhai, *Adv. Mater.*, **29**, (2017) 29.
- [4] J. Janek, W. G. Zeier, *Nat. Energy.*, **1**, (2016) 16141.
- [5] A. Manthiram, X. Yu, S. Wang, *Nat. Rev. Mater.*, **2**, (2017) 16103.
- [6] L. J. Miara, S. P. Ong, Y. Mo, W. D. Richards, Y. Park, J. M. Lee, H. S. Lee, G. Ceder, *Chem. Mater.*, **25**, (2013) 3048-3055.
- [7] Y. Zhu, X. He, Y. Mo, *ACS Appl. Mater. Interfaces*, **7**, (2015) 23685-23693.
- [8] K. Ishiguro, H. Nemori, S. Sunahiro, Y. Nakata, R. Sudo, M. Matsui, Y. Takeda, O. Yamamoto, N. Imanishi, *J. Electrochem.*, **161**, (2014) A668.
- [9] L. Yang, Z. Lu, Y. Qin, C. Wu, C. Fu, Y. Gao, J. Liu, L. Jiang, Z. Du, Z. Xie, Z. Li, F. Kong, G. Yin, *J. Mater. Chem. A*, **9**, (2021) 5952-5979.
- [10] H. Huo, Y. Chen, N. Zhao, X. Lin, J. Luo, X. Yang, Y. Liu, X. Guo, X. Sun, *Nano Energy*, **61**, (2019) 119-125.
- [11] S. Lee, K. S. Lee, S. Kim, K. Yoon, S. Han, M. H. Lee, Y. Ko, J. H. Noh, W. Kim, K. Kang, *Sci. Adv.*, **8**, (2022) 153.
- [12] G. V. Alexander, I. M. S. R. Murugan, *Ionics*, **27**, (2021) 4105-4126.
- [13] R. H. Basappa, T. Ito, H. Yamada, *Electrochem. Soc.*, **164**, (2017) A666-A671.
- [14] X. Han, Y. Gong, K. Fu, X. He, G. T. Hitz, J. Dai, A. Pearce, B. Liu, H. Wang, G. Rubloff, Y. Mo, V. Thangadurai, E. D. Wachsman, L. Hu, *Nat. Mater.*, **16**, (2016) 572-579.
- [15] G. V. Alexander, C. Shi, J. O. Neill, E. D. Wachsman, *Nat. Mater.*, **22**, (2023) 1136-1143.

5:00 PM ES03.03.15

Converting Primary Alkaline Batteries to Rechargeable Solid-State Batteries via Single-Anion Conducting Polymer Electrolytes Eric G. Ruzicka, Hunter O. Ford, Brian Chaloux, Jeffrey Long, Debra R. Rolison and Megan B. Sassin; Naval Research Laboratory, United States

Demand for energy storage devices to supply society with its ever-increasing energy needs necessitates the development of portable power systems with enhanced energy efficiency, long cycle life, and improved safety. Lithium-ion batteries currently dominate the rechargeable battery market, but their reliance on expensive and non-US sourced active materials and flammable electrolytes leave the door open for researchers to develop rechargeable batteries based on alternative chemistries.

Here, we report on the synthesis and characterization of a polymeric hydroxide-conducting solid-state electrolyte (SSE) and demonstrate that this SSE facilitates rechargeability in alkaline Ag–Zn cells that are conventionally used as primary batteries. Utilizing a library of inhouse-synthesized styrenic monomers to generate custom SSEs, we found that the architecture of the polymer not only influences the stability of the SSE, but also the capacity and cycle life. Infrared (IR) and x-ray photoelectron spectroscopies (XPS) were utilized in conjunction with scanning electron microscopy (SEM) to assess the SSE and electrode chemistries before and after electrochemical cycling to evaluate for stability and active material-crossover. Combining electrochemistry (impedance spectroscopy, cyclic voltammetry, and galvanostatic cycling) with these results, we determined that crosslinking, chemistry of the quaternizing agent, and the electrode quality/geometry influence Ag–Zn cell performance.

5:00 PM ES03.03.16

Solid State Polymer Electrolyte for Lithium Ion Batteries Djamel Mourzagh, Lionel Picard and Thibaut Gutel; CEA - LITEN - UGA, France

Li-ion batteries are considered as the most suitable electrochemical energy storage systems for a wide range of applications including automotive applications in order to contribute to the reduction of CO₂ emissions responsible for climate change.

In recent years, the majority of the works on batteries has consisted in developing solid electrolytes with the goal to improve their safety and the possibility of using a negative electrode based on metallic lithium which will ultimately make it possible to achieve high energy densities.

CEA-Liten and Saft have jointly developed a solid-state polymer electrolyte system. The polymer PTMC (Poly trimethylene carbonate) has been selected for its high transport number, over 0.7, and its stability with respect to lithium both at high potential and at low potential despite its modest conductivity.

The Solid Polymer Electrolytes (SPE) realized is a crosslinked membrane based on PTMC, with good mechanical properties that allow an easy handling and integration into a complete system (Fig 1).

The electrodes containing PTMC and NMC622, Graphite or SiO_x as active material were manufactured with a surface capacities around 1mAh/cm². Their mechanical properties are similar to conventional Li-ion electrodes.

Solid-state prototypes with a capacity around ten milliampere-hours have been assembled with these components. The performances of the all-solid prototypes containing PTMC are encouraging. Indeed, they operate correctly at a C/20 rate at 80°C but also at room temperature with the addition of plasticizers.

SESSION ES03.04: Fabrication and Scale Up I
Session Chairs: Robert Sacci and Fengyu Shen
Wednesday Morning, April 24, 2024
Room 423, Level 4, Summit

8:15 AM ES03.04.01

Scale Up of The Synthesis and Processing of Halide-Based Solid Electrolytes for Li Metal Batteries Robert L. Sacci¹, Yan Yao², Liquan Guo², Teerth Brahmabhatt¹ and Jagjit Nanda³; ¹Oak Ridge National Lab, United States; ²University of Houston, United States; ³SLAC National Accelerator Laboratory, United States

Rare-earth alkali halides (REAHs) have been shown to have high ionic conductivity and are promising electrolytes for all solid state lithium batteries. Li₃InCl₆ and Li₃YCl₆ have been shown to adopt a layered structure with reported ionic conductivities approaching 2 mS/cm². A significant advantage these materials have over other solid electrolytes, such as garnets, is their low synthesis and processing cost. As an example, we will describe how Li₃InCl₆ and Li₃YCl₆ can be synthesized from concentrated aqueous solution through controlled dehydration. We probed the reactions by combining *in situ* neutron diffraction, thermogravimetry, differential scanning calorimetry, and *in situ* impedance spectroscopy. This presentation provides a pathway for the direct synthesis and processing of REAHs from concentrated aqueous solutions and we will discuss making thin membranes through dehydration and other casting methods.

The US Department of Energy's Energy Efficiency and Renewable Energy Vehicles Technologies Office provided funding for this work.

8:30 AM ES03.04.02

Unveiling The Mechanical and Electrochemical Evolution of Nano Silicon Composite Anodes in Sulfide based All-Solid-State Batteries Hongli Zhu; Northeastern University, United States

The utilization of silicon (Si) anodes in all-solid-state lithium batteries (ASLBs) provides the potential for high energy density. However, the compatibility of sulfide solid-state electrolytes (SEs) with Si and carbon is often questioned due to potential decomposition. To investigate this, operando X-ray absorption near-edge structure (XANES) spectroscopy, ex-situ scanning electron microscopy (SEM) and ex-situ X-ray nano-tomography (XnT) were utilized to study the chemistry and structure evolution of nano Si composite anodes. Results from XANES demonstrated a partial decomposition of SEs during the first lithiation stage, which was further accelerated by the presence of carbon. But the performance of first three cycles in Si-SE-C was stable, which proved the generated media is ionically conductive. XnT and SEM results showed that the addition of SEs and carbon improved the structural stability of the anode with fewer pores and voids. A chemo-elasto-plastic model revealed that SEs and carbon buffered the volume expansion of Si, thus enhancing mechanical stability. The balance between the pros and cons of SEs and carbon in enhancing reaction kinetics and structural stability enabled the Si composite anode to demonstrate the highest Si utilization with higher specific capacities and better rate than pure Si and Si composite anodes with only SEs.

8:45 AM *ES03.04.03

On The Journey toward Competent All Solid State Electrolytes Rana Mohtadi^{1,2}; ¹Toyota Research Institute of North America, United States; ²Tohoku University, Japan

Energy storage systems poised to offer improved performances beyond that afforded by Li-ion batteries are intensely being studied. Of these, all solid state batteries ASSBs promise to dramatically improve the energy storage densities and efficiencies by way of utilizing non-flammable solid state electrolytes SSEs that possess high compatibility with reactive anode and cathode materials, such as metallic anodes and high voltage cathodes. Unfortunately, all known families of SSEs fall short from fulfilling this demand and thus new SSE materials are required. We will herein discuss the status of these technologies and report critical SSEs advancements conducted in our group.

9:15 AM ES03.04.04

Fast Room-Temperature Mg-Ion Conduction in Clay-Like Solid Electrolytes Xiaochen Yang^{1,2}, Sunny Gupta³, Yu Chen² and Gerbrand Ceder^{1,2}; ¹University of California, Berkeley, United States; ²Lawrence Berkeley National Laboratory, United States; ³Rice University, United States

The discovery of mechanically soft solid-state materials with fast Mg-ion conduction is crucial for the development of solid-state magnesium batteries. Herein, we report a novel solid magnesium electrolyte that achieve high ionic conductivity of 0.47 mS/cm at room temperature. These Mg-ion conductors exhibit clay-like mechanical properties, enabling intimate contact at the electrode–electrolyte interface during battery cycling. With a combination of experimental and computational analysis, we identify that the soft-clay formation is induced by partial anion exchange. This partial anion exchange creates undercoordinated magnesium ions, yielding fast Mg-ion conduction. Our work demonstrates the potential of clay-like halide electrolytes for all-solid-state magnesium batteries, with possible further extension to other multivalent battery systems.

9:30 AM ES03.04.05

Scale-Up of Halide-Based All-Solid-State Batteries Fengyu Shen¹, Michael McGahan², John D. Pietras², Marca M. Doeff¹, Vincent S. Battaglia¹ and Mike Tucker¹; ¹Lawrence Berkeley National Laboratory, United States; ²SGR North America, United States

All-solid-state batteries (ASSBs) offer improved safety and potential higher energy density for energy storage. Among the components of ASSBs, the solid electrolyte plays an important role as it is the key component to prevent dendrite growth and forms interfaces with the cathode and anode. Halide solid electrolytes gain significant attention due to the high ionic conductivity, low processing temperature, good formability, oxygen resistivity and high-voltage

stability. Our previous study demonstrated the feasibility of scaling up halide electrolyte and halide-containing cathode by tape casting, using toluene as a solvent and MSB1-13 as a binder.¹ A low-voltage cathode (LiFePO₄) was used and cell performance was tested in button cell size with a 0.5 cm² area. In this study, pouch cells are manufactured, involving 80% cathode active material (LiNi_{0.82}Mn_{0.07}Co_{0.11}O₂) loading and Li/In alloy anode. A pouch cell is cycled under a lower stack pressure and results of long-term cycling will be reported. The interfacial resistance of pouch cells is higher than that of button cells with the same composition as the stack pressure for button cells is much higher (100 MPa). Cells with Li metal anode are also explored with an anode interlayer, cycling in a voltage window of 3-4.3 V, and the cell performance will be compared with that of the cells with Li/In alloy anode.

Reference:

1. F. Shen, M. McGahan, J. D. Pietras, G. Y. Lau, M. M. Doeff, V. S. Battaglia and M. C. Tucker, *J Electrochem Soc*, 2023, **170**, 100505.

9:45 AM ES03.04.06

Robot-Assisted Sol-Gel Exploration of Cation-Disordered Rocksalt (DRX) Materials for Li-Ion Batteries Tim Kodalle¹, Yuxing Fei^{1,2}, Nathan Szymanski¹, Yan Zeng¹, Gerbrand Ceder^{1,2} and Carolin M. Sutter-Fella¹; ¹Lawrence Berkeley National Laboratory, United States; ²University of California, Berkeley, United States

Rechargeable Li-ion batteries are omnipresent in our daily lives and demand is increasing. To satisfy the tremendous growth, there is a great interest in developing novel high-performance electrode materials at reduced cost, and nickel and/or cobalt free.[1] In this regard, Li-excess cation-disordered rocksalt (DRX) metal oxides have been identified as promising cathode materials with energy densities that can exceed traditional layered cathodes such as LiTMO₂ with TM being a combination of transition metals.[1,2] Some drawbacks of these DRX materials include significant first-cycle capacity loss, limited cycle life, and voltage fade.[1] Several factors have been identified to mitigate these drawbacks, including greater disorder of the TMs as well as controlled particle size and shape.[3] Each of these characteristics can be manipulated by modifying the choice of precursors and synthesis techniques. Conventionally, solid-state synthesis is employed for the fabrication of electrochemically active materials including Li-ion batteries.[4] The typical sequence of synthesis steps includes mixing, grinding, pelletizing, and annealing. Such reactions are driven by solid-state diffusion, which is predominantly controlled by time and temperature.[4] In comparison, the sol-gel approach to synthesis mixes elements at the molecular level by dissolving precursors in a solvent (e.g. water) with the addition of chelating agents (e.g. citric acid) to form a viscous gel. This is followed by solvent evaporation, gel decomposition, and annealing to form powders or thin films.[4] In this study, we compare the nucleation and crystallization pathway of Li-Mn-Ti oxide (LMTiO) deposited both by solid-state as well as sol-gel synthesis. Using automated, robot-assisted synthesis approaches, we systematically investigate the parameter space of both syntheses and the influence of precursors and precursor ratios on phase purity, final composition, oxidation states, reaction temperatures, and sample uniformity.

In the cathodes fabricated by solid-state synthesis, we find strong competition between two intermediate spinel-like phases, LiTM₂O₄ and Li₂TMO₃, depending on the oxidation state of the TMs as well as the Li-TM ratio in the selected precursors. While the intermediates forming in cathodes deposited via the sol-gel method appear to be less sensitive to these parameters, we find a strong dependency on the solvents and chelating agents used for fabrication. Additionally, we observe a strong interdependency between the choice of solvents and the ratio of Li:TMs influencing the reaction temperature of target phases and intermediates. Based on these findings, we will propose reaction pathways as well as a nucleation model for LMTiOs prepared by sol-gel synthesis.

References:

[1] J. Zheng *et al.*, *Adv. Energy Mater.*, vol. 7, no. 6, p. 1601284, 2017.

[2] Z. Lun *et al.*, *Nature Materials*, vol. 20, pp. 214-221, 2021.

[3] J. Zheng *et al.*, *Nano Lett.*, vol. 14, no. 5, pp. 2628-2635, May 2014.

[4] T. N. L. Doan *et al.*, *Front. Energy Res.*, vol. 2, 2014.

10:00 AM BREAK

SESSION ES03.05: Conductivity and Transport I
Session Chairs: Pieremanuele Canepa and Richard Remsing
Wednesday Morning, April 24, 2024
Room 423, Level 4, Summit

10:30 AM *ES03.05.01

Chloride Solid Electrolytes: Structural Complexity, Ion Transport and Reactivity Raphaële Clement; University of California, Santa Barbara, United States

Chloride solid electrolytes have spurred significant research interest over the past few years due to their high ionic conductivities and good stability against high voltage cathodes. While their bulk conduction properties depend sensitively on synthesis conditions, these materials often constitute a challenge for characterization due to their ability to accommodate various polymorphic structures, cation disorder, as well as planar defects. In this talk, I will show how solid-state nuclear magnetic resonance (NMR), when combined with X-ray diffraction, computational simulations, and other complementary tools, provides detailed insights into the links between ion transport and the complex structural landscape of this relatively new class of ion conductors, as well as their reactivity against sulfide electrolytes for dual electrolyte solid-state batteries.

11:00 AM ES03.05.02

Electronic Paddle-Wheels Facilitate Transport in Solid-State Ionic Conductors Richard Remsing; Rutgers University, United States

Solid-state ionic conductors (SSICs) are promising alternatives to liquid electrolytes in energy storage technologies. The rational design of SSICs and ultimately their deployment in battery technologies requires a thorough understanding of their ion conduction mechanisms. In SSICs containing molecular ions, molecular rotations couple to translational diffusion to create a “paddle-wheel” effect that facilitates conduction. This paddle-wheel mechanism explains many important features of molecular SSICs. However, we lack a similarly detailed explanation for anharmonic lattice dynamics and ion conduction in SSICs composed of monatomic ions. I will discuss our recent theoretical work that provides such an explanation. We predict that ion conduction in many SSICs involves “electronic paddle-wheels,” in which localized lone pair electrons rotate, and these rotations couple to and facilitate ion diffusion. After discussing our evidence from simulation results, I will make analogies to molecular SSICs and argue that the electronic paddle-wheel mechanism creates a unifying principle for understanding ion conductivity in both monatomic and molecular materials. We anticipate that a predictive

understanding of electron paddle-wheels in ionic conduction can be leveraged to create design principles for engineering solid-state electrolytes from the electronic level on up.

11:15 AM ES03.05.03

How Correlated are Ion Hoppings in Inorganic Solid-State Electrolytes? Cibrán López Álvarez^{1,2,3}, Edgardo Saucedo^{1,2} and Claudio Cazorla^{1,2}; ¹Polytechnic University of Catalonia, Spain; ²Barcelona Research Center in Multiscale Science and Engineering, Spain; ³Institute of Materials Science of Barcelona, Spain

Despite playing a central role in the design of novel solid-state electrolytes (SSE), little is known about the processes governing ionic diffusion in these materials and the spatio-temporal correlations acting on migrating particles. However, molecular dynamics (MD) simulations can reproduce the trajectories of individual diffusing ions with extraordinary accuracy, thus providing incredibly valuable atomistic data that in practice cannot be resolved by experiments.

The identification of hopping events from these simulations typically relies on active supervision and definition of arbitrary material-dependent geometrical parameters, thus frustrating high throughput screenings of diffusing paths and mechanisms across simulation databases and the assessment of many-diffusing-ion correlations.

Here, we introduce a novel approach for analyzing ion hopping events in MD simulations in a facile and totally unsupervised manner, that allows to determine key atomistic ionic diffusion descriptors. In particular, our approach identifies with precision which and when particles diffuse in a simulation and the exact migrating paths that they follow as well.

We apply such a powerful analysis tool to a comprehensive database of density functional theory ab initio MD (DFT-AIMD) simulations [1,2], comprising several families of SSE and tens of millions of atomic configurations. By doing this, we are able to (1) quantify correlations between many diffusing ions, (2) identify predominant collective migrating mechanisms and (3) determine how specific and novel migration descriptors such as the length and duration of individual ionic hops correlate with ionic diffusion coefficients, all under realistic finite-temperature conditions.

We show that the probability for N-ions to concertedly diffuse decreases exponentially with N, and that such many-ion correlations practically do not depend on temperature. Interestingly, it is found that despite N = 2 correlations are largest, higher order many ion (N > 2) coordination is more frequent in concerted diffusion. The explained unsupervised analysis approach has been implemented in the IonDiff software [3], a python code that is publicly available.

[1] C. López, A. Emperador, E. Saucedo, et al., Universal ion-transport descriptors and classes of inorganic solid-state electrolytes, *Materials Horizons*, 2023, doi: 10.1039/D2MH01516A

[2] C. López, A. Emperador, E. Saucedo, et al., DFT-AIMD database, 2023, url: <https://superionic.upc.edu>

[3] C. López, R. Rurali, C. Cazorla, Repository with all the developed codes, 2023, url: <https://github.com/IonRepo/IonDiff>

11:30 AM ES03.05.04

Path Integral Approaches to Ion Diffusion Jarvist M. Frost and Lucius Liu; Imperial College London, United Kingdom

Classical ion diffusion theories rely on simplified hopping models lacking concerted motion. Molecular dynamics can capture correlations but requires extensive sampling. This fairly brute-force approach has become the standard way to calculate ion diffusion rates, recently accelerated with the use of machine learning force-fields trained against density functional theory calculations.

We revisit path integral techniques to bridge this gap. Integrating state-of-the-art graph neural network potentials [1] with the 1990s path-integral approach of Chakraborty et al. [2] offers an efficient route to model correlated transport, and understand the physical processes. Generally these more sophisticated mathematical models developed in the 70s to 90s, have mostly been neglected as attention has shifted to explicit simulation on fast computers.

We show how a semi-numerical path integral approach parameterised by lighter weight machine-learning force-field molecular dynamics, can describe and understand correlation effects in representative lithium, sodium, and halide ion conductors.

[1] Batzner, S., Musaelian, A., Sun, L., Geiger, M., Mailoa, J.P., Kombluth, M., Molinari, N., Smidt, T.E. and Kozinsky, B., 2022. E (3)-equivariant graph neural networks for data-efficient and accurate interatomic potentials. *Nature communications*, 13(1), p.2453.

[2] Chakraborty, A.K., Bratko, D., Chandler, D., 1994. Diffusion of ionic penetrants in charged disordered media. *J. Chem. Phys.* 100, 1528–1541. <https://doi.org/10.1063/1.466632>

11:45 AM ES03.05.05

Enhancing Li-Ion Conductivity in Argyrodite Li₆PS₅Cl through Disorder Engineering Investigated by Machine Learning Potential Jiho Lee, Suyeon Ju, Seungwoo Hwang, Jinmu You, Jisu Jung and Seungwu Han; Seoul National University, Korea (the Republic of)

Solid-state electrolytes (SSEs) have emerged as promising candidates for next-generation batteries, offering improved safety and higher energy density compared to conventional liquid electrolytes. Nevertheless, the practical utilization of SSEs has been hindered by the challenge of achieving high ionic conductivity at room temperature. Among SSEs, argyrodite systems have achieved a high conductivity of 10 mS/cm at room temperature through strategies involving disorder engineering and doping. To further optimize ionic conductivity and gain a comprehensive understanding of the underlying mechanisms, theoretical calculations based on density functional theory (DFT) have been applied. However, recent DFT studies have faced challenges in accurately quantifying transport properties in argyrodite systems compared to experiments, primarily due to computational limitations. For instance, small simulation cells introduce spurious correlations in Li-ion motions between periodic boundaries, while a scarcity of diffusion events makes direct simulation at room temperature difficult.

In this presentation, we present the use of Behler-Parrinello-type neural network potentials (NNPs) to overcome the aforementioned challenges and obtain Li-ion conductivities in argyrodite Li₆PS₅Cl with varying S/Cl disorders (0–100%). Utilizing cost-effective and accurate NNPs allows for direct simulations at room temperature, unraveling the effects of S/Cl disorders. We select the SCAN functional, which reproduces the lattice parameter within 0.2% of the experimental value. To train the NNPs, we utilize the SIMPLE-NN package and employ strained bulk crystals and ab initio MD data at 600 and 1200 K. Several validations are conducted to ensure the quality of our NNP in terms of both structural and dynamic properties. To obtain the ionic conductivity with a statistical convergence error range of 10%, we carry out systematic tests on the supercell and ensemble sizes. As a result, NNP MD

This searchable program is up-to-date as of April 15th, 2024.

simulations are performed using 5×5×5 supercells containing 6500 atoms for up to 25 ns. In calculating the diffusivity, we neglect the initial 5 ns, where most of the Li-ions remain within the cage at room temperature, resulting in non-linear mean squared displacements. Our predicted activation energies and ionic conductivities align well with experimental data. Interestingly, the conductivity peaks at 25% S/Cl disorder. By analyzing the diffusion mechanism, we find that the peak observed at 25% disorder arises from the synergetic effects of two contributing factors; the enhancement of rotational motion and the disorder effect which facilitates the Li diffusion between cages. Additional free energy analysis shows that these structures are thermodynamically accessible, suggesting the potential for optimizing Li-ion conductivity through disorder engineering in Li₆PS₅Cl. This work paves the way for estimating and studying the transport properties of SSEs using accurate and cost-effective NNPs.

SESSION ES03.06: Electrode Interface I
Session Chairs: David Stewart and Howard Qingsong Tu
Wednesday Afternoon, April 24, 2024
Room 423, Level 4, Summit

1:30 PM *ES03.06.01

Interfacial Engineering for Lithium Metal Batteries Employing Garnet-Type Electrolyte Ju-Sik Kim¹, Sewon Kim¹, Gabin Yoon¹, Michael Badding², Zhen Song² and Dongmin Im¹; ¹Samsung Advanced Institution of Technology, Korea (the Republic of); ²Corning Incorporated, United States

Garnet-type solid electrolytes, represented by the composition Li₇La₃Zr₂O₁₂ and its derivatives, have recently garnered significant attention due to their good compatibility with lithium metal anode. However, several issues remain unsolved, hindering the commercialization of lithium metal batteries employing garnet-type electrolytes: (1) Carbonates and hydroxides easily form on the surface of garnet electrolytes, leading to high interfacial resistance when incorporated into batteries. (2) While the chemical stability of garnet-type electrolytes against lithium metal is reasonably good, it is frequently observed that lithium dendrites penetrate through the electrolyte layer, causing short circuits between the cathode and anode. (3) During cell discharge or lithium metal stripping, voids often form at the interface. This results in fluctuations in local current density, accelerates short-circuiting, and worsens cycling stability. In this presentation, we will demonstrate that surface treatment of garnet with acid and the introduction of a carbon or carbon-metal composite interlayer are highly effective in addressing these issues. Stable cell cycling performance is achieved even at room temperature, with an areal capacity comparable to that of commercial lithium-ion batteries. We will also discuss the working mechanisms of these methods.

2:00 PM *ES03.06.02

Sodium Solid-State Electrolyte and Electrode Interfaces Jin An Sam Oh¹ and Y. Shirley Meng^{1,2}; ¹University of California, San Diego, United States; ²The University of Chicago, United States

An ideal solid-state electrolyte requires a high ionic conductivity, low electronic conductivity, and matched electrochemical window with the electrode. Often, it needs to possess mechanical properties with rigidity to acts as a separator while having the ability to form intimate interface with the electrode to realize the all-solid-state batteries. In this talk, I will share our recent efforts in material development and architecture design to enable all-solid-state sodium batteries as a complimentary and safe energy storage system.

2:30 PM BREAK

SESSION ES03.07: Electro-Chemo-Mechanics
Session Chairs: David Stewart and Howard Qingsong Tu
Wednesday Afternoon, April 24, 2024
Room 423, Level 4, Summit

3:30 PM *ES03.07.01

High-Rate Cycling in 3D Dual-Doped NASICON Architectures toward Room-Temperature Sodium-Metal-Anode Solid-State Batteries Prem Jaschin, Christopher Tang and Eric D. Wachsmann; University of Maryland, United States

Sodium metal-based solid-state batteries hold tremendous potential for next-generation batteries owing to low-cost earth-abundant sodium resources. However, fabricating thin free-standing solid electrolytes that could cycle sodium at high current densities has been a major challenge in developing room temperature solid-state sodium batteries. By developing high conducting Zn²⁺ and Mg²⁺ dual-doped Na₃Zr₂SiPO₁₂ (NASICON) solid electrolytes and fabricating a 3D porous-dense-porous architecture (with an ultrathin, 25 μm, dense separator) coated with a nanoscale ZnO layer, an extremely low anode interfacial resistance of 3.5 Ω cm² was realized. This enabled a record high critical current density of 30 mA/cm² at room temperature with no stack pressure and a cumulative sodium cycling capacity of 10.8 Ah/cm² was achieved. Furthermore, pouch cells were assembled as a proof-of-concept with Na₃V₂(PO₄)₃ cathodes on dense-porous bilayer electrolytes with sodium metal anodes and cycled up to 2C rates at room temperature with no applied stack pressure.

4:00 PM ES03.07.02

Dyanmic Coupling of Internal Strain-Stress Field and Lithium Pathway within Individual Cathode Particles goverend by Solid Electrolyte in All-Solid-State Batteries Jinkyu Chung, Junho Bae, Hanbi Choi and Jongwoo Lim; Seoul National University, Korea (the Republic of)

In all-solid-state batteries (ASSBs), (electro)chemo-mechanical aspects such as uneven interfaces, cathode-electrolyte interphase formation, delamination, fracture, defects, etc., are the major factors in capacity fade but remain largely unknown.

Nonhomogeneous transfer of lithium ions can cause significant variations in strain and stress within battery electrodes, leading to degradation in battery performance. In all-solid-state batteries (ASSBs), the lithium pathway and the associated strain/stress field become more intricate due to the (electro)chemo-mechanical reaction at the electrode-electrolyte interfaces. The dynamic volume change in active particles are heavily influencing by strength of the solid electrolyte and interfacial conformality. This can continually alter the lithium pathway and the internal stress field, leading to recurrent redefinitions of (electro)chemo-mechanical environment.

Here, we have developed an operando coherent X-ray imaging platform and associated analysis methodologies. Named PICASSO (Primary particle In-situ X-ray imaging with Chemical-composition Analysis and Strain-Stress Observation), this technology can track the nanoscale transport of lithium and the strain evolution of individual electrode particles in ASSBs. With this platform, we gained a comprehensive electrochemical and mechanical understanding of the cycling properties of single electrode particles in ASSBs.

4:15 PM ES03.07.03

Competition Between Lithiation-Induced Stress and Concentration Gradients in 3D Geometries David M. Stewart, Paul Albertus and Gary W. Rubloff; University of Maryland, United States

A comprehensive understanding of electro-chemo-mechanical (ECM) phenomena in solid-state batteries (SSBs) requires not only theoretical models, but validation of the models by direct measurement in well-defined geometries. We will highlight a few intriguing results using 3D models of SSBs and measurements on thin film electrodes, which motivate novel methods for measuring local stress and Li concentration in situ. These results emphasize that the inclusion of ECM effects is essential in understanding the fluxes in 3D geometries.

Using multi-physics modeling we have simulated the electrochemical behavior of a battery operating in the confined space of a nanopore. The 3D geometry produces large concentration gradients that affect the Li flux: rather than a conformal flux field, largely along the radial axis of the pore, the Li flows up and down the pore. However, the same geometry, when including electro-chemo-mechanical coupling, has entirely different behavior. Due to the stress gradients produced by the confined volume expansion of the cathode, the Li flux is further influenced, and achieves the fully conformal distribution that we expected from intuition.

Experimentally, we have measured ECM coupling in two model systems using Si electrodes, whose electrochemical and mechanical properties are well known. We employed micro-Raman mapping to measure the shift in the Si peak, and ultimately translated that to a strain/stress profile in the electrode during lithiation. In single-crystal Si wafers we measured bi-axial stress maxima around 0.6 GPa, localized to the lithiation front, and post-mortem SEM shows lateral cracks that form at this same depth, causing delamination and breakdown the electrode. Furthermore, XPS depth profiles and EBSD cross sections show that the lithiation front is not sharp, as seen elsewhere in the literature. Due to ECM effects, the diffusion lengths in this experiment are 100x larger than predicted by concentration gradients alone.

In subsequent experiments, using a square Si island approximately 10 μm on a side, dynamic stress profiles are measured. The Raman stress measurement is fast enough to be done in operando, allowing us to see transient stress states for comparison with models. Existing literature treated the cracking and delamination of these islands entirely from a mechanical perspective. Our ECM models, parameterized to the experimental observations, reveal that the origin of the failure is not simply mechanical, but due to a competition between Li concentration gradients and stress gradients.

While the theory of ECM coupling is rather well studied, its application in 3D geometries is not well explored. At the same time, validation of the theory is nascent in electrochemical systems, where material properties change dynamically with state of charge. Together, our models and experiments are providing the fundamental understanding of SSB performance required for next generation designs.

4:30 PM ES03.07.04

Towards Improved All-Solid-State Batteries: A Multi-Scale Simulation of Cation Inter-Diffusion and Mechanical Failures at NASICON-Oxide/LiCoO₂ Interfaces Ming-Yuan Hong and Hong-Kang Tian; National Cheng Kung University, Taiwan

All-solid-state batteries (ASSBs) hold great promise, yet their commercialization has faced challenges due to interfacial complications, which encompass issues such as solid electrolyte decomposition, mechanical degradation, and Li dendrite growth. Specifically, NASICON-type solid electrolytes, like $\text{Li}_{1+x}\text{Al}_x\text{Ti}_{2-x}(\text{PO}_4)_3$ (LATP) and $\text{Li}_{1+x}\text{Al}_x\text{Ge}_{2-x}(\text{PO}_4)_3$ (LAGP), have attracted attention because of their stability against LiCoO₂ (LCO) and remarkable ionic conductivity (ranging from 10^{-4} to 10^{-3} S/cm). However, a decline in discharge/charge capacity due to mechanical breakdown at their interfaces has been a concern. Leveraging an integrated multi-scale simulation approach that combines Density Functional Theory (DFT) with Finite Element Analysis (FEA), we delved into the issues of cation inter-diffusion and the resulting mechanical challenges at LATP/LCO and LAGP/LCO interfaces. Our DFT studies pinpointed energetically favorable sites for Co to replace Ti atoms, mirroring atomic structures emerging from Co and Li inter-diffusion events. Evaluations of the elastic attributes of Co-LATP and Co-LAGP configurations showed a decline in modulus values (both Young's and Shear), signaling an interfacial softening. However, the diffusion of Co and Li away from LCO transforms into Co₃O₄, characterized by a greater Young's modulus compared to LCO and both LATP/LAGP. By channeling these insights into a 2D continuum model through FEA, we could visualize the Li-ion concentration gradient adjacent to the LCO particle and the subsequent stress distribution across various discharge phases. Our results identified peak first-principal stresses at the interfaces, reaching approximately 800 MPa for LATP/LCO and around 1000 MPa for LAGP/LCO. In comparison, non-interface scenarios registered values between 400-500 MPa. These findings accentuate the importance of inhibiting Co diffusion to safeguard ASSB integrity. Furthermore, simulations suggest that enhancing the interfacial contact area to 75% of optimal contact can effectively counteract peak stress induced by interfaces, underscoring the significance of this parameter in counteracting interface-induced mechanical degradation. In conclusion, this study offers a thorough exploration into the alterations in material properties and the potential mechanical decline triggered by cation inter-diffusion at these interfaces, urging its prevention in subsequent ASSB innovations. The analytical methods adopted here also present a valuable methodological framework for probing other ASSB material pairings, potentially guiding the prediction and alleviation of mechanical setbacks during the discharging phases.

4:45 PM ES03.07.05

Microstructure-Aware Mesoscale Modeling of Chemomechanical Stress Evolution during Cycling in Solid Electrolyte-Cathode Composite Bo Wang, Longsheng Feng, Kwangnam Kim, Liwen Wan, Tae Wook Heo and Brandon Wood; Lawrence Livermore National Laboratory, United States

The volume change of cathode active materials during charge-discharge cycling is responsible for the capacity fading of all-solid-state Li batteries due to mechanical degradation in the cathode such as delamination and crack formation. Many strategies to alleviate the chemomechanical stress buildup have been proposed in experiments but rationale of the stress release mechanisms at the mesoscale remain elusive. In this presentation, we present a microstructure-aware mesoscale model to quantitatively predict the stress distribution during cycling in a secondary particle agglomerate of the cathode active material embedded within a solid electrolyte matrix, taking the LiCoO₂-Li₇La₃Zr₂O₁₂ (LCO-LLZO) as a model system. We find that the mechanical stress hotspots develop at different stages within the grain boundaries of the LCO agglomerate and the LCO-LLZO interfaces. We investigate the influences of microstructural morphology (columnar versus equiaxial), grain orientations (textured versus random), mechanical properties at the grain boundaries and heterogeneous interfaces, and anisotropy of chemical expansion on the stress hotspot evolution and provide optimal mitigation strategies. The theoretical results can help gain mechanistic understanding on cathode degradation and inform guidelines for experimental design of mechanically optimized cathode materials for long-life solid-state batteries.

This work was performed under the auspices of the U.S. Department of Energy by Lawrence Livermore National Laboratory under Contract DE-AC52-07NA27344.

SESSION ES03.08: Electrode Interface II
Session Chairs: Imtiaz Ahmed Shozib and Kelsey Uselton
Thursday Morning, April 25, 2024
Room 423, Level 4, Summit

8:30 AM ES03.08.01

Phase Study of Lithium-Niobium-Tantalum Oxides as Cathode Coating Materials [Hengning Chen](#)¹, Zeyu Deng¹ and Pieremanuele Canepa^{1,2};
¹National University of Singapore, Singapore; ²University of Houston, United States

Although all-solid-state batteries (ASSBs) exhibit great potential for providing high energy density and enhanced battery safety, the stability of electrode–electrolyte interfaces is still a serious challenge. Niobate and tantalate materials have been widely applied as coating materials to mitigate the interfacial reactivities in ASSBs, especially amorphous LiMO_3 ($\text{M}=\text{Nb}$ or Ta) with high ionic conductivities and appreciable electronic resistance.¹ Compared with pure LiMO_3 ($\text{M}=\text{Nb}$ or Ta), partially-crystallized Li-Nb-Ta oxides were found to show even higher ionic conductivity and higher permittivity, which can be more effective for fast charge-transfer reactions at the cathode/electrolyte interfaces in ASSBs.² However, the mechanism behind Nb/Ta mixing and the improved properties needs to be further understood.

Leveraging a combination of density functional theory, cluster expansion formalism, grand canonical Monte Carlo (gcMC) simulations, and machine-learned molecular dynamics, we reveal the phase transition nature of $\text{LiTa}_{1-x}\text{Nb}_x\text{O}_3$ and the improved Li-ion conduction properties brought by Nb/Ta mixing. As studied in our previous work, the crystalline Li-M-O coating contains mixtures of LiMO_3 and Li_3MO_4 , and we extend the mixing study into Li_3MO_4 as well.³ Our investigation of the phase behavior and the structure-property relationships in the Li-Nb-Ta oxides helps to develop more suitable synthesis protocols to maximize the functional properties of these coating materials.

References:

1. Glass, A. M., Nassau, K. & Negran, T. J. Ionic conductivity of quenched alkali niobate and tantalate glasses. *J. Appl. Phys.* **49**, 4808–4811 (1978).
2. Yada, C. *et al.* A High-Throughput Approach Developing Lithium-Niobium-Tantalum Oxides as Electrolyte/Cathode Interlayers for High-Voltage All-Solid-State Lithium Batteries. *J. Electrochem. Soc.* **162**, 722–726 (2015).
3. Chen, H., Deng, Z., Li, Y. & Canepa, P. On the Active Components in Crystalline Li-Nb-O and Li-Ta-O Coatings from First Principles. *Chem. Mater.* **35**, 5657–5670 (2023).

8:45 AM ES03.08.02

Interplay of Interfacial Adhesion and Mechanical Degradation in Anode-Free Solid-State Batteries [Imtiaz Ahmed Shozib](#) and Howard Qingsong Tu; Rochester Institute of Technology, United States

Degradations at the interface between the solid electrolyte (SE) and the anode have been identified as one of the primary reasons for solid-state battery (SSB) failure. Interfacial adhesions and mechanical conditions are important factors need to be investigated for SSB. This article investigates the impact of assembling pressure on the performance of an anode-free solid-state battery (AFSSB) with an $\text{AgC} \parallel \text{Li}_6\text{PS}_5\text{Cl}$ (LPSCl) \parallel NMC811 full cell configuration. Results demonstrate that an optimal assembling pressure of 530 MPa significantly improves specific capacity. Notably, an increase in capacity is observed when the assembling pressure is increased from 350 MPa to 530 MPa, while pressures beyond this threshold lead to a significant decrease in capacity due to soft short effect. The highest discharge capacity was achieved at an optimal assembling pressure of 530 MPa, corresponding to a high gravimetric energy density of 409.62 Wh/kg. This notable enhancement over alternative assembling pressures is likely a result of the intricate interplay between interfacial adhesion and mechanical stability. This assembling pressure incrementally improves the interfacial adhesion between the SE and the AgC interlayer. At 450 and 530 MPa, where interfacial adhesion is moderately higher, lithium deposition predominantly occurs at the AgC/CC (current collector) interface, enhancing electrochemical performance by improving lithium transport to this interface. However, above 530 MPa, cracks form in the SE, disrupting performance despite increased interfacial adhesion between SE and AgC layer. This higher-pressure range (560 to 650 MPa) exhibits poorest mechanical stability due to SE cracks. This research provides insights into optimizing assembling pressure for enhanced capacity and energy density in LPSCl-based AFSSBs, offering a straightforward approach to improving overall battery performance.

9:00 AM ES03.08.03

Visualizing The Chemical Incompatibility of Halide and Sulfide-Based Electrolytes in Solid-State Batteries [Carolin Rosenbach](#) and Wolfgang Zeier; University of Münster, Germany

Because of the ongoing demand on energy consumption, high energy density batteries are needed. Solid-state batteries can lead to higher energy densities compared to commonly used liquid lithium batteries and avoid the flammable organic solvents. The class of halide electrolyte (Li_3MX_6 , $\text{M} = \text{metal}$, $\text{X} = \text{Cl}$, Br , I) provide promising characteristics in solid-state batteries due to their reasonable conductivity values and their larger electrochemical stability window compared to sulfides. Due to the good conductivity value of 1 mScm^{-1} , the broad theoretical electrochemical stability window and the water-based synthesis possibility the electrolyte Li_3InCl_6 is a good candidate for the use with high potential cathode materials like $\text{LiNi}_{0.8}\text{Mn}_{0.1}\text{Co}_{0.1}\text{O}_2$. It was shown that the Li_3InCl_6 is not stable at the lithium metal anode, therefore a bilayer setup with a sulfide and a halide layer is commonly used to study halides at the cathode side. Omitting the halide layer and only using a sulfide layer, like $\text{Li}_6\text{PS}_5\text{Cl}$, lead to a capacity loss over the cycling and decomposition products.

Based on this literature we studied three different cell setups with the halide electrolyte Li_3InCl_6 and sulfide electrolyte $\text{Li}_6\text{PS}_5\text{Cl}$ in combination with the cathode material $\text{LiNi}_{0.8}\text{Mn}_{0.1}\text{Co}_{0.1}\text{O}_2$. Cycling of the cells over 100 cycles revealed the fast capacity fading of the cell setup with the $\text{LiNi}_{0.8}\text{Mn}_{0.1}\text{Co}_{0.1}\text{O}_2$: Li_3InCl_6 cathode composite in direct contact to the $\text{Li}_6\text{PS}_5\text{Cl}$, whereas the cells with avoiding this triple phase boundary cycle more stable. Within the cycling process, electrochemical impedance spectroscopy was performed and showed a significant increase of the interfacial resistance in the fast capacity fading cell, which was not the case for the pure sulfide and the bilayer cell setup.

For further analysis of the fast capacity fade, time-of-flight secondary ion mass spectrometry and focused ion beam scanning electron microscopy analysis were performed to understand the interfacial resistance increase. At the buried interface of the cathode composite to the sulfide separator an indium-sulfide species could be detected, which were also slightly less present at the separator-separator interface of the halide and sulfide electrolyte. This indicates the incompatibility of the Li_3InCl_6 and $\text{Li}_6\text{PS}_5\text{Cl}$ electrolytes, which is more pronounced in the presence of $\text{LiNi}_{0.8}\text{Mn}_{0.1}\text{Co}_{0.1}\text{O}_2$.

This work highlights that in the search for new battery components the chemical stability of the materials to each other should not be overseen. Adding more components in a battery cell, like bilayers, increases the number of interfaces and possible degradation areas. Therefore, studies of solid-state batteries should also consider more properties besides electrochemical stability windows of single components.

9:15 AM ES03.08.04

Quantifying The Structural Properties of The Lithium-Solid Electrolyte Interface [Kelsey Uselton](#)¹, Dylan C. Hamilton¹, Elizabeth Allan-Cole¹, Samuel Marks¹, Annalise Maughan² and Michael Toney¹; ¹University of Colorado Boulder, United States; ²Colorado School of Mines, United States

All-solid-state batteries (ASSBs) are poised to meet the rising demand for high energy density electrochemical energy storage and safety in lithium-ion battery technology, a crucial aspect for the widespread adoption of electric vehicles [1]. However, the solid-electrolyte interphase (SEI) layer arising from chemical incompatibility and a narrow solid electrolyte electrochemical window poses a significant hurdle due to high resistance to ion transfer resulting in poor performance and cyclability of promising solid-state electrolyte materials [1]. Therefore, probing interfacial properties between the lithium and solid-state electrolyte is paramount to assess the interfacial changes that adversely impact battery performance through multiple charge-discharge cycles [2]. According to a review from Paul et al. there have been several studies characterizing the chemical composition of the SEI in ASSBs, but there is limited evidence probing the Li-SSE interphase structure [3]. Structural properties impact interfacial transport and are difficult to assess due to the limited quantity of material available for examination and for the “buried” nature of the interphase [4]. We implemented a Li/Li symmetric cell system to isolate the interactions between lithium and an argyrodite (Li₆PS₅Cl) solid electrolyte. To understand and quantify the structure of reaction layers that form and evolve at Li-SSE interfaces during cycling, we have performed interface-sensitive *operando* transmission X-ray Diffraction (XRD) experiments with high energy, high flux synchrotron radiation. Electrochemical cycling and electrochemical impedance spectroscopy paired with XRD measurements quantified SEI formation, degradation, and specific resistance contributions. Our results show evidence for crystalline reaction layers that evolve with time and potential providing insight into the formation and evolution of dominant crystalline phases throughout the interphase region.

References

1. Yu, C., Ganapathy, S., Eck, E.R.H. et al. Accessing the bottleneck in all-solid state batteries, lithium-ion transport over the solid-electrolyte-electrode interface. *Nat. Commun.* 8, 1086 (2017). <https://doi.org/10.1038/s41467-017-01187-y>
2. Bhaway, S. M.; Qiang, Z.; Xia, Y.; Xia, X.; Lee, B.; Yager, K. G.; Zhang, L.; Kisslinger, K.; Chen, Y.-M.; Liu, K.; Zhu, Y.; Vogt, B. D. Operando Grazing Incidence Small-Angle X-ray Scattering/X-ray Diffraction of Model Ordered Mesoporous Lithium-Ion Battery Anodes. *ACS Nano* 2017, 11 (2), 1443–1454, DOI: 10.1021/acsnano.6b06708
3. P.P. Paul, B.-R. Chen, S.A. Langevin, E.J. Dufek, J. Nelson Weker, J.S. Ko. Interfaces in all solid state Li-metal batteries: A review on instabilities, stabilization strategies, and scalability. *Energy Stor. Mater.* 45 (2022), pp. 969-1001, 10.1016/j.ensm.2021.12.021
4. Tan, S., Kim, JM., Corrao, A. et al. Unravelling the convoluted and dynamic interphasial mechanisms on Li metal anodes. *Nat. Nanotechnol.* 18, 243–249 (2023). <https://doi.org/10.1038/s41565-022-01273-3>

9:30 AM ES03.08.05

Impact of Structure and Interfaces on Li Ion Transport in Composite Solid Electrolytes [Markus Wied](#)¹, Christian Prehal², Moritz H. Futscher³, Anne Bonnin⁴ and Vanessa Wood¹; ¹ETH Zurich, Switzerland; ²University of Salzburg, Austria; ³Empa-Swiss Federal Laboratories for Materials Science and Technology, Switzerland; ⁴Paul Scherrer Institute, Switzerland

Increasing the Li ion battery energy density is a major challenge, which needs to be addressed in order to reduce their size and weight. Switching to metallic Li anodes would provide such a significant increase in energy density. However, this comes alongside many challenges, among them stability towards the electrolyte or Li dendrite growth. Solid electrolytes (SEs) are a promising replacement for state-of-the-art liquid electrolytes as they are electrochemically more stable and better at preventing Li dendrite growth. For high performance all-solid-state-batteries (ASSBs) the electrode-electrolyte interfaces and electrolyte ionic conductivity are crucial to reach high C-rates.

There are three major classes of SEs, consisting of inorganic ceramics, polymers, or composites of both. Ceramics generally feature high electrochemical stability, high voltage operation, and good ionic conductivity but they are brittle, difficult to manufacture and expensive. Polymers are cheap, easy to manufacture and compatible with slurry-based processes, and form and maintain SE-electrode interfaces well. Yet, their ionic conductivity at room temperature is limited. By combining both polymers and ceramics in composite-solid-electrolytes (CSEs), it is possible to take advantage of both material classes while maintaining the scalability of the fabrication process. However, there is a lack of understanding of lithium ion transport in CSEs.

We investigate the impact of the polymer ceramic structure and the properties of the polymers, ceramic, and their interfaces on transport in CSEs using 3D simulations on realistic CSE structures. We obtain realistic 3D x-ray tomography data on different CSEs made from Al-doped LLZO (LLZO) particles dispersed in a PEO (LiTFSI) matrix. We validate finite element simulations of the ionic conductivity of these 3D structures with experimentally obtained ionic conductivity data. With the simulation tools and the realistic structures we can gain insight into the relative importance of structure and material properties and their impact on heterogeneity of ionic transport with respect to the properties of the CSE heterostructure. This understanding is crucial as it shows that there can be quite significant local differences in ionic current that will affect cycle life or lithium plating behavior. Our findings emphasize the importance of interface treatments to minimize interface resistances in CSE heterostructures. We also highlight that properties such as mechanical stability and integrity or ionic current heterogeneity need to be considered for performance assessment besides the ionic conductivity.

9:45 AM ES03.08.06

Pulsed Laser Deposition and Characterization of Ceramic Battery Thin Film Bi-Layers: Interfacing a Solid State Electrolyte, Lithium Lanthanum Zirconate, with a High Voltage Cathode, Lithium Manganese Oxide [Isaac D. Dyer](#)¹, Hana T. Gobena², Jennifer L. Rupp² and Sossina M. Haile¹; ¹Northwestern University, United States; ²Technical University of Munich, Germany

Solid-state batteries have the potential to introduce higher energy densities and add improved safety into our power storage network. However, the electrochemical stability at the interface of a solid state electrolyte and a high voltage cathode remains an inhibitor of this technology. A precisely defined interface of phase pure constituents is needed in order to investigate this interfacial stability. Here, using pulsed laser deposition, we created such an interface by the formation of a thin film bilayer, a solid state electrolyte interfaced with a high voltage cathode. Tantalum doped Lithium Lanthanum Zirconate & Lithium Manganese Oxide bilayers were deposited onto Magnesium Oxide substrates. The resulting thin film bilayer was analyzed using X-ray Diffraction, Raman Spectroscopy, and Cross-Sectional Scanning Electron Microscopy. Here we show the capability to grow densified phase pure thin film bilayers of a solid state electrolyte and a high voltage cathode by pulsed laser deposition. This capability opens avenues towards the interfacial investigation of a precisely defined solid state electrolyte and high voltage cathode.

10:00 AM BREAK

SESSION ES03.09: Inorganic Electrolyte I
Session Chairs: Madan Saud and Joseph Vazquez
Thursday Morning, April 25, 2024
Room 423, Level 4, Summit

10:30 AM ES03.09.01

Design of Trigonal Halide Superionic Conductor by Regulating Cation Order-Disorder Seungju Yu, Joo-hyeon Noh and Kisuk Kang; Seoul National University, Korea (the Republic of)

Lithium-metal-halides have been recently revisited as promising solid electrolyte (SE) candidates that can provide solutions to the interfacial instability issues found in sulfide- and oxide-based SEs. Although early studies on halide-based SEs indicated that poor ionic conductivities (typically $< \sim 10^{-6} \text{ S cm}^{-1}$) constituted a major bottleneck, recent breakthroughs revealed that the ionic conductivity can be boosted by identifying appropriate synthetic routes, introducing a wide range of halide-based Li_3MX_6 ($\text{M} = \text{Y, Er, or In, X} = \text{Cl, Br, or I}$)¹. Notably, moving from the classical ampule synthesis to mechanochemical synthesis significantly improved room-temperature ionic conductivity up to $\sim 10^3$ order of magnitude for the Li_3MCl_6 ($\text{M} = \text{Y, Er}$)^{2,3}. It was speculated that the higher degree of cation disordering from the mechanochemical synthesis could open up the bottleneck transition triangular area for lithium diffusion. Although the factors leading to the hidden superionic conductivity of halide SEs remain unclear, these previous findings strongly suggest a close interplay between superionic conduction and cation arrangements/occupancies attainable from various synthetic methods^{4,5}. Hence, understanding the fundamental relationship between the superionic conduction mechanism and structural factors in trigonal Li_3MCl_6 halides is critical for realizing significant advancements in their ionic conductivities.

Herein, we employ first-principles calculations and experiments to investigate the conduction mechanism, propose, and validate our design strategies for enhancing ionic conductivity, using Li_3YCl_6 (LYC) as a model system. Consistent with previous reports, we find that the lithium diffusion occurs three-dimensionally in LYC, which exhibits anisotropic behavior with faster ionic conduction along the *c*-axis channel than in the *ab*-plane⁶. However, it is revealed that the lithium diffusion in the *ab*-plane leverages the superionic conduction in LYC, and, more importantly, it is primarily determined by the partial occupancies of the yttrium (Y) ion in the structure. Our theoretical calculations demonstrate that the presence of Y in the *ab*-plane interrupts the lithium diffusion with the electrostatic repulsion associated with the tetrahedral site hopping mechanism of lithium ions, resembling that of conventional layered lithium transition-metal oxides. Furthermore, the partial occupancy of Y over a certain ratio entirely disconnects the percolation diffusion pathways of lithium ions in the *ab*-plane. On the other hand, it is conversely observed that the lack of Y in the *ab*-plane leads to the collapse of the interlayer space, indicating that Y cations serve as a pillar of the layered lithium diffusion framework. This contradicting effect of Y in the structure signifies the importance of the composition/ordering of M cations in the trigonal Li_3MCl_6 . Accordingly, we propose a target region for M partial occupancy that can lead to cation arrangements with percolating and non-collapsed lithium diffusion pathways. Our design rules for the target cation arrangement are experimentally confirmed by an M-deficient $\text{Li}_3\text{M}_{0.8}\text{Cl}_6$ (i.e., $\text{Li}_3\text{Y}_{0.2}\text{Zr}_{0.6}\text{Cl}_6$), a new halide superionic conductor that exhibits the highest reported room-temperature ionic conductivity ($1.19 \times 10^{-3} \text{ S cm}^{-1}$) among trigonal halide superionic conductors. This study illuminates the detailed superionic conduction mechanism in halides for the first time and suggests that searching for a new compositional space that balances the lithium percolation and stacking slab distance is an unexplored and efficient pathway for the design of superionic halide SEs.

Reference

1. *Energy Environ. Sci.* **13**, 1429-1461 (2020).
2. *Z. Anorg. Allg. Chem.* **613**, 26-30 (1992).
3. *Adv. Mater.* **30**, 1803075 (2018).
4. *Adv. Energy Mater.* **10**, 1903719 (2020).
5. *Chem. Mater.* **33**, 327-337 (2021).
6. *Angew. Chem., Int. Ed.* **58**, 8039-8043 (2019).

10:45 AM ES03.09.02

Free-Standing Sulfide Electrolyte Thin Film for Solid-State Lithium Battery Applications Seokyoan Yoon^{1,2}, Dong Ok Shin^{1,2}, Seok Hun Kang¹, Jaecheol Choi¹, Ju Young Kim¹, Young-Gi Lee¹ and Young-Sam Park^{1,2}; ¹Electronics and Telecommunications Research Institute, Korea (the Republic of); ²University of Science and Technology (UST), Korea (the Republic of)

The great attention to low carbon economy through the electric vehicles grows the market of lithium ion battery (LIB) rapidly because of its high power and energy density. However, a liquid carbonate electrolyte employed in the LIB is flammable, thus being able to cause severe safety issues. To reduce the safety issues, a solid electrolyte (SE) instead of the currently commercialized liquid electrolyte has been introduced to fabricate solid-state lithium batteries [1,2]. Even though the prevailing SEs (that is, sulfide, polymer, garnet and sodium superionic conductor) do not simultaneously satisfy all the stability requirements such as mechanical, chemical, electrochemical and thermal stabilities, sulfides have the highest ionic conductivities and the favorable mechanical properties among them, thereby being considered to work reasonably well in the conventional sandwich battery structure [2].

To prepare the sulfide SE, a slurry coating technology has been generally used. However, the traditional wet method charges additional cost coming from using an environmentally harmful organic liquid solvent and the resulting production of a solvent recovery system. In addition, strong reactivity between a polar liquid solvent and the sulfide leads to the decrease in the ionic conductivity of the sulfide SE [2]. Thus, the introduction of a liquid-free dry process is necessary to obtain the sulfide electrolyte. Furthermore, thin and free-standing SEs are preferred for high efficiency batteries with a high degree of freedom of electrode material selection.

In this work, separate sulfide electrolyte films with a thickness of several dozens of micrometers are demonstrated by a dry procedure which is composed of the following three steps [3]: first, an agyrodite-type sulfide and a binder powders are mixed. Next, the two nonsticky powders are ground homogeneously to fabricate a sticky sulfide-binder dough. Then, the dough is fed into rollers to obtain the independent SE layer with a thickness of below one hundred micrometers.

Microstructural and elemental analyses are carried out utilizing a field emission scanning electron microscope and energy dispersive X-ray microanalysis, respectively. Alternating voltages are applied by a frequency response analyzer (10^{-1} - 10^5 Hz, Solartron HF 1225, AMETEK Scientific Instruments) to get Nyquist plots and calculate ion conductivities of dry- and wet-processed sulfide SE samples. Charging-discharging cycling experiments are performed under galvanostatic cycling condition from 3.0 to 4.3 V (Toscat-3000, Toyo System). The test results are presented and discussed in the talk.

- [1] D. O. Shin et al, *ACS Appl. Mater. Interfaces* 2023, 15, 13131-13143
[2] R. Chen et al, *Chem. Rev.* 2020, 120, 6820-6877
[3] S. Yoon et al, Korea patent, application number 10-2023-0030160 (Application date March 7th, 2023)

Acknowledgement

This work was supported by internal fund/grant of Electronics and Telecommunications Research Institute (ETRI). [23YB2600, Development of Fundamental Technology for Non-Lithium Resources Based Next Generation Aqueous-Type Multivalence-Metal-Ion Battery]

11:00 AM ES03.09.04

Fabrication of Y-Doped and Ce-Doped NaSICON through Integrated Mechanical and Thermal Activation Method [Madeline Barickman](#), Abigail Barickman and Shan-Ju Chiang; North Central College, United States

NaSICON (Na Super Ionic CONductor) materials have emerged as promising candidates for a wide range of applications such as all-solid-state Na-ion batteries, sodium-air batteries, electrochemical sensors, as electrolytes for thermoelectric generators, and membranes due to their high availability, profound ionic conductivity, high thermal and chemical stability, and good electrochemical compatibility. To be used in energy storage devices, the high ionic conductivity with relatively low interfacial resistance has to be possessed. However, the Na-ion conductance at room temperature remains several orders of magnitude lower than organic electrolytes even NaSICONs have relatively high ionic conductivity at elevated temperature. Therefore, there is still a need in developing a consistent manufacturing process to further increase the ionic conductivity of NaSICON and reducing the production cost for synthesizing NaSICON membranes.

This study aims to improve the density and ionic conductivity of yttrium and cerium-doped NaSICON materials through mechanical activation and one-step sintering process while suppressing the manufacturing cost of NaSICONs. Here, we report the feasibility of integrated mechanical and thermal activation method in doping the zirconium site in NaSICON. Fully densified Y-doped NaSICON has 100% higher total conductivity at the room temperature than the same material prepared from general solid-state sintering method, while Ce-doped NaSICON demonstrates the good bulk conductivity of 4.7×10^{-4} S/cm. This study will provide an alternate solution for synthesizing high ionic conductivity NaSICON at low cost for many energy storage systems.

11:15 AM ES03.09.05

Assessing Correlations between Phonon Features and Migration Barriers in Multivalent Solid Electrolytes [Samuel M. Greene](#) and Donald Siegel; The University of Texas at Austin, United States

Solid ion conductors with high ionic conductivity can enable the development of solid-state batteries with improved safety and performance. Most materials exhibit insufficient conductivity for commercial applications, particularly for multivalent ions. High-throughput computational approaches, which involve screening large databases of compounds, can accelerate the discovery of new materials with sufficient conductivity. Directly calculating ionic conductivity from first principles is expensive and difficult to automate, which renders such calculations incompatible with screening approaches. Previously, others have proposed the phonon band center (mean phonon frequency) as a metric that is easier to calculate and measure, and they have demonstrated that it is correlated with the energetic barrier for ion migration in lithium and sodium conductors. I will discuss our efforts to extend this approach to investigate magnesium, calcium, and zinc conductors using first-principles calculations of phonon features. In addition to frequencies, we consider the directions of phonon modes as predictors for migration barriers. We compare our results with previous trends for monovalent conductors.

SESSION ES03.10: Fabrication and Scale Up II
Session Chairs: Deok-Hwang Kwon and David Mitlin
Thursday Afternoon, April 25, 2024
Room 423, Level 4, Summit

2:00 PM ES03.10.01

Stable Anode-Free All-Solid-State Lithium Battery through Tuned Metal Wetting on The Copper Current Collector [David Mitlin](#); The University of Texas at Austin, United States

Stable anode-free all-solid-state battery (AF-ASSB) with sulfide-based solid-electrolyte (SE) (argyrodite $\text{Li}_6\text{PS}_5\text{Cl}$, LPSCl) is achieved by tuning wetting of lithium metal on "empty" copper current-collector. Lithiophilic $1 \mu\text{m}$ Li_2Te is synthesized by exposing the collector to tellurium vapor, followed by in-situ Li activation during the first charge. The Li_2Te significantly reduces the electrodeposition/electrodissolution overpotentials and improves Coulombic efficiency (CE). During continuous plating experiments using half-cells (1 mA cm^{-2}), the accumulated thickness of electrodeposited Li on $\text{Li}_2\text{Te-Cu}$ is more than $70 \mu\text{m}$, which is the thickness of Li foil counter-electrode. Full AF-ASSB with NMC811 cathode delivers an initial CE of 83% at 0.1 C, with a cycling CE of 99.5%. Cryo-FIB sectioning demonstrates uniform electrodeposited metal microstructure, with no signs of voids or dendrites at the collector-SE interface. Electrodissolution is uniform and complete, with Li_2Te remaining structurally stable and adherent. By contrast, unmodified Cu current-collector promotes inhomogeneous Li electrodeposition/electrodissolution, electrochemically inactive "dead metal", dendrites that extend into SE, and thick non-uniform solid electrolyte interphase (SEI) interspersed with pores. Density functional theory and mesoscale calculations provide complementary insight regarding nucleation-growth behavior. Unlike for conventional liquid-electrolyte metal batteries, the role of current collector/support lithiophilicity has not been explored for emerging AF-ASSBs.

2:15 PM ES03.10.02

A Unique Platform for High-Throughput Combinatorial Coating of Thiophosphate Thin-Film Electrolytes onto Bulk Battery Electrodes [Andrea Crovetto](#); Technical University of Denmark, Denmark

I will showcase a recently acquired, highly customized materials synthesis platform dedicated to air-sensitive materials containing sulfur and phosphorus. To the best of my knowledge, this is the only synthesis platform in the world where it is possible to deposit thin-film thiophosphate superionic conductors of any elemental composition in a high-throughput, combinatorial fashion.

This platform is of significant interest for solid-state battery research for two main reasons:

1) It enables intimate coating of bulk electrode particles with a thin solid electrolyte, with potentially improved interface properties and an increased energy density to a lower weight.

2) Bulk synthesis of solid electrolytes is not amenable to parallelized, high-throughput experimentation by combinatorial methods. Conversely, our thin-film deposition setup is designed to easily obtain compositional gradients (e.g., a P/S ratio gradient in one direction and a Li/Ge ratio in the perpendicular direction). Together with the automated, mapping-type characterization instruments in our laboratories, these combinatorial methods enable fast screening of multicomponent phase diagrams (as well as process parameters at constant composition) in the search for optimal properties in emerging or completely new battery materials. Materials of interest can be either electrodes or solid electrolytes.

As a synthesis-oriented material scientist within the optoelectronics field, I hope that this contribution will promote discussion and potential future collaboration with battery experts.

2:30 PM ES03.10.03

TiO₂(B) Epitaxial Thin Film Electrode for All-Solid-State Nanobattery Deok-Hwang Kwon¹ and Shinbuhm Lee²; ¹Korea Institute of Science and Technology, Korea (the Republic of); ²Daegu Gyeongbuk Institute of Science and Technology, Korea (the Republic of)

Due to its pseudocapacitive, one-dimensional, rapid ion channels, TiO₂(B) holds promise as a Li-ion rechargeable battery anode electrode. Despite its potential for high capacity and superior rate capability, realizing its theoretical capacity and full rate capability remained challenging. Partly owing to its metastability, instead of pure or single crystalline TiO₂(B) materials, multiphase or polycrystalline samples are synthesized. In this study, assisted by an isostructural VO₂(B) template layer, we successfully synthesized single-phase TiO₂(B) films epitaxially, with well-aligned ion diffusion channels. Using a liquid electrolyte, TiO₂(B) epitaxial electrode demonstrates a capacity close to the theoretical value of 335 mA h g⁻¹ and exceptional charge-discharge cyclability for ≥200 cycles, surpassing the performance of other TiO₂(B) or alternative phase nanostructures. Moreover, by applying LiPON as a solid electrolyte, we demonstrated the feasibility of an all-solid-state configuration, showing excellent stability. These findings suggest significant potential for downsizing all-solid-state nanobatteries for application in self-powered integrated circuits.

2:45 PM ES03.10.05

Large Area, Rapid Spray Plasma Processed Amorphous Lithium Lanthanum Zirconium Oxide Thin-Film Electrolytes for Solid State Batteries Thomas W. Colburn, Gabriel Crane, Sarah Holmes, Junyoung Lee, Yi Cui and Reinhold H. Dauskardt; Stanford University, United States

Lithium lanthanum zirconium oxide (LLZO) and other solid-state electrolyte (SSE) materials are widely heralded for their high lithium ionic conductivity, low electrical conductivity, and stability against lithium metal. However, the difficulty in manufacturing solid electrolytes, especially in the thin film geometry, has hindered widespread deployment. Multiple critical challenges need to be solved to produce low-cost SSEs for solid-state batteries at-scale: reproducibility of the thin-film deposition to achieve dense mixed-metal oxides, the intrinsic reactivity of lithiated metal oxides to environmental species like water and carbon dioxide that result in the formation of secondary surface phases like Li₂CO₃, and the necessity of low-throughput and energy-intensive curing steps.

Here, we present a rapid spray plasma process to manufacture large-area thin-film LLZO SSEs for solid state batteries. The LLZO is first generated via blade coating to form an oxide network. The oxide is then cured and densified in one step at 3.6 cm/min linear processing speed by a nitrogen plasma discharged into a low-humidity, ambient pressure environment. Plasma allows for a reduction in processing time by orders of magnitude compared with many traditional vacuum-based thin film routes owing to the combination of radical ions, ultraviolet photons, and heat present in the curing process along with the lack of vacuum. The resulting amorphous phase LLZO thin films have low carbonate contamination, high ionic conductivity of 1x10⁻⁵ S/cm at room temperature, low surface and through-plane defect density, and surface roughness of <40 nm. This work is a step toward the high-throughput manufacturing of LLZO for solid state batteries.

3:00 PM BREAK

SESSION ES03.11: Conductivity and Transport II
Session Chairs: Daniel Hallinan and Sanja Tepavcevic
Thursday Afternoon, April 25, 2024
Room 423, Level 4, Summit

3:30 PM ES03.11.01

Insights into The Reactivity and Lithium Plating Mechanisms of Ultra-Thin Metal Oxide Coatings for Anode-Free Solid-State Lithium Metal Batteries Sanja Tepavcevic¹, Michael J. Coughlan¹, Taewoo Kim¹, Teodora Zagorac², Yingjie Yang², Meghan Burns², Jordi Cabana², Robert F. Klie², Luke Hanley², Justin Connell¹, Anil Mane¹ and Jeffrey Elam¹; ¹Argonne National Laboratory, United States; ²University of Illinois at Chicago, United States

Solid-state batteries (SSBs) using lithium metal anodes are the best candidates for high energy density battery applications. The energy density can be further increased by eliminating the lithium metal excess in an “anode-free” cell format. However, low Coulombic efficiency from heterogeneous lithium metal plating and stripping along with charge loss due to solid electrolyte interphase (SEI) formation severely limit the cycle life of anode-free SSBs. Here, we explore the use of ultra-thin (5-20 nm) Al₂O₃ and ZnO coatings deposited by atomic layer deposition (ALD) on copper electrodes for anode-free cells with a solid polymer electrolyte. Voltammetry shows that lithium inventory loss due to SEI formation is reduced by over 50% with Al₂O₃@Cu electrodes, but these electrodes experience orders of magnitude higher interface resistances than bare Cu and ZnO@Cu electrodes due to their inherently low ionic and electronic conductivities. The electrochemical differences between Al₂O₃ and ZnO coatings are reflected in X-ray photoelectron spectroscopy (XPS) experiments that show Al₂O₃ undergoing a self-limiting lithiation reaction with Li metal, while ZnO reacts completely with Li to form a LiZn alloy and Li₂O. These chemical differences at the interface result in higher and lower lithium plating nucleation overpotentials for Al₂O₃ (up to 220 mV) and ZnO (down to 15 mV) coatings, respectively, relative to uncoated Cu electrodes (35 mV). Time-of-flight secondary ion mass spectrometry (ToF-SIMS) reveals lithium plating underneath a reacted Li_yAlO_x coating and through emergent defects and pinholes with Al₂O₃@Cu electrodes, while it plates exclusively on top of the electronically conductive converted ZnO@Cu electrodes. Scanning electron microscopy (SEM) corroborates these mechanisms by showing sparse coverage of isolated Li clusters plated with Al₂O₃@Cu electrodes, while Cu and ZnO@Cu grow more dense and interconnected lithium deposits. Despite both coatings improving different aspects of anode-free battery design, unmodified Cu electrodes show higher Coulombic efficiencies (~77%) than

Al₂O₃@Cu (up to 70%) and ZnO@Cu (up to 75%) electrodes. Increasing Al₂O₃ coating thickness decreases the practical current density compared to unmodified Cu (30 μ A/cm²) but increasing ZnO coating thicknesses can double or triple this value. These (electro)chemical and morphological observations lead to the proposal of two mechanisms, where less-reactive metal oxides develop lithium-ion conductivity through the metal oxide structure to plate lithium underneath the coating, while more-reactive metal oxides undergo full reduction and conversion reactions that allow lithium to plate above the coating. The fundamental research here opens paths for future work to leverage these mechanisms and explore other materials for high-efficiency anode-free SSBs.

3:45 PM ES03.11.02

Electrochemical Transport and Reaction in Polymer and Hybrid Electrolytes for Lithium Metal Batteries [Daniel Hallinan](#)^{1,1}, Anna Mills^{1,1}, Guang Yang² and Jagjit Nanda³; ¹Florida A&M University-Florida State University College of Engineering, United States; ²Oak Ridge National Laboratory, United States; ³SLAC National Accelerator Laboratory, United States

Increasing the energy density of lithium-ion batteries requires, among other advances, electrolytes that are compatible with lithium metal and next-generation cathodes. Polymer electrolytes play an important role in this regard, but overcoming slow ion transport is a major challenge. Recent advancements in time-resolved infrared spectroscopy to characterize salt diffusion in polymer electrolytes will be reported as well as efforts to electrochemically measure transference number and electrochemical reaction kinetics in these electrolytes. In addition to our efforts in developing characterization techniques, we will report recent progress in solid electrolyte development. Hybrid electrolytes that combine fast ion transport of ceramic electrolytes and processability of polymer electrolytes are promising. This requires either 1) low binder contents that maximize ceramic transport pathways or 2) unity polymer transference number that takes advantage of transport in both phases. Our progress in both of these directions will be discussed, focusing on 1) free-standing sulfide solid electrolytes with small amounts of inert binder and 2) polymer blend electrolytes. Both exhibit single-ion conduction, which yields numerous transport and efficiency advantages. The effect of processing solvent on binder-containing sulfide electrolyte properties will be covered. State of the art in the polymer blend electrolytes will also be reviewed including recent advancements from our team using precision polyanions with polyether solvating polymer. This presentation will cover miscibility, conductivity, and transference numbers as a function of composition and temperature. Distinct differences between blends containing different anionic forms will be explained in the context of ion correlation. Important future directions for polymer blend and hybrid electrolytes will also be discussed.

4:00 PM ES03.11.03

Enhancing Li Ion Conduction in Argyrodite Solid Electrolytes through Anion Site-Exchange [Jing-Sen Yang](#) and Ping-Chun Tsai; National Taiwan University of Science and Technology, Taiwan

The superionic solid electrolyte Li₆PS₅Cl (LPSC), featuring ionic conductivity on par with those of liquids, has gained intense interest in the development of all-solid-state batteries. However, the mechanisms behind such extraordinarily high ionic conductivity remain unclear. In previous works, a phenomenon involving positional exchange between S and Cl anions was observed, which we referred to as "S/Cl site-exchange." We disclosed the correlation between Li ion conduction and the S/Cl site-exchange by integrating DFT, AIMD and NEB simulations, along with ⁷Li PFG NMR diffusivity measurements for the first time. A remarkable increase of $\sim 10^2$ times in Li ionic conductivity and a substantial reduction of ~ 160 meV in energy barriers are observed when the S/Cl site-exchange is introduced. We found out that transportation bottlenecks of Li ions are overcome through beneficial neighboring Li configuration induced by the S/Cl anion exchange. The comprehensive understanding of ion transport mechanisms in LPSC would help the design of solid-state fast ion conductors.

4:15 PM ES03.11.04

Partial Transport Optimization and Mechanochemical Characterization of The Cathode Active Material Li₂FeS₂ in all Solid-State Batteries [Tim Berges](#); Inorganic and Analytical Chemistry, University Muenster, Germany

Solid-state batteries spark tremendous interest given their potential to overcome the limitations of energy density that are present in conventional Li ion batteries. At the same time, with current state-of-the-art cathode active materials (CAM) employing critical elements such as Nickel and Cobalt, concerns regarding their scarcity and cost are raised even before the wide-spread implementation of the technology. To overcome these concerns, in this work, we evaluated the cation- and anion-redox (cathode) active material Li₂FeS₂ as an alternative candidate for solid-state batteries with a promising theoretical specific capacity of 400 mAh/g. By combining electrochemical characterization with studies of the partial conductivities, cathode composites are optimized in regard to their CAM and solid electrolyte composition, leading to an optimum between high initial capacities and capacity retentions. Half cells employing 50 to 60 wt.% CAM are shown as most promising candidates, without the necessity of carbon additives due to the intrinsically high electronic conductivity of Li₂FeS₂ >30 mS/cm. The kinetic limitations of the cells are further elaborated by current density dependent cycling (rate testing), showing that higher electronic conductivities, i.e., higher intermediate CAM loadings, benefit faster charging rates in comparison. This is a promising result given that higher loadings are thought after to reduce the amount of electrochemically inactive materials in solid-state batteries.

The study of kinetic limitations is complemented by mechanochemical characterization of the cells. Tracing the pressure changes during cycling, both with lithium-indium and LTO as reference electrodes, is used to gather insights into the origin of capacity fading. While usage of lithium-indium allows to capture the mechanochemical response of the system including effects of lithium intercalation and deintercalation in the reference anode, the use of LTO, i.e., a zero-strain material during cycling, allows characterizing the response of the cathode specifically. Thereby, the latter approach could be utilized to characterize not only the general mechanochemical response of Li₂FeS₂ cathodes, but also to capture how these change as a function of cathode composition, ultimately providing insights into the failure mechanism of Li₂FeS₂ containing cathodes.

In conclusion, this work represents an initial introduction of Li₂FeS₂ as a cathode active material candidate for all solid-state batteries. Furthermore, partial transport and mechanochemical characterization are utilized to optimize the cathode composition to achieve both, high average specific capacities, i.e., active material utilization, and high capacity retention. With that, this work is a foundation for further optimization of cells employing Li₂FeS₂ as CAM, and allows a general comparison to established solid state battery CAM, e.g., Li(Ni,Mn,Co)O₂ (NCM).

4:30 PM ES03.11.05

Investigation of Microstructural Impacts on Ionic Transport in Li₇La₃Zr₂O₁₂-LiCoO₂ Composite Structures [Longsheng Feng](#), Bo Wang, Kwangnam Kim, Liwen Wan, Brandon Wood and Tae Wook Heo; Lawrence Livermore National Lab, United States

The ionic transport property of a solid composite cathode is sensitive to its microstructure, which has a critical impact on variability of the overall solid-state battery performance. In this presentation, we will discuss our recent microstructure-aware modeling effort on unraveling the relationship between microstructural features and effective ionic transport properties. Specifically, using Li₇La₃Zr₂O₁₂-LiCoO₂ composite cathode as a model system, we combine atomistically informed mesoscale modeling approach and machine learning (ML) analysis to examine how the local transport properties of individual microstructural constituents and their topological features affect the effective diffusivity of Li in the two-phase composites. In addition, our ML analysis identifies key microstructural descriptors for the effective transport property. Our framework can be extended for elucidating the intricate microstructure-transport property relationship in generic multiphase materials, which offers insights highlighting the importance of microstructure

engineering in tuning the properties of composite materials in diverse energy applications.

This work was performed under the auspices of the U.S. Department of Energy by Lawrence Livermore National Laboratory under Contract DE-AC52-07NA27344.

SESSION ES03.12: Inorganic Electrolyte II

Session Chairs: Stefan Adams and Xi Chen

Friday Morning, April 26, 2024

Room 423, Level 4, Summit

8:15 AM ES03.12.01

Mechanical Milling – Induced Microstructure Changes in Argyrodite Li₆PS₅Cl Solid-State Electrolyte and Influence on Electrochemical Performance Yixian Wang and David Mitlin; The University of Texas at Austin, United States

In the early stages of sulfide solid-state electrolyte (SSE) research, sulfides like Li₆PS₅Cl (LPSCI) were primarily synthesized in laboratories using fine precursors such as Li₂S, LiCl, and P₂S₅, employing meticulous synthetic procedures involving milling and sintering. This approach resulted in grams of as-synthesized SSE materials with a uniform particle size distribution and well-controlled morphology. Consequently, large-scale synthesis methods for LPSCI SSE have been developed, leading to the availability of commercial LPSCI SSE. Nonetheless, compared to lab-scale synthesis, commercial production of LPSCI SSE often yields a wide range of particle sizes and particle distributions. In-depth understanding is needed regarding how microstructural features such as the average particle size and distribution, and pore size and distribution, affect the compressed SSE's electrochemical performance.

In this presentation, we investigate mechanical milling – induced microstructure changes of LPSCI SSE and their influence on electrochemical performance. Planetary mechanical milling in wet media (m-xylene) is employed to alter commercial LPSCI powder. Quantitative stereology demonstrates how extended milling progressively refines grain and pore size/distribution, increases compact density, and geometrically smoothens the SSE-Li interface. Mechanical indentation demonstrates that these changes lead to reduced site-to-site variation in the compact's hardness. Microstructure, in turn, profoundly influences electrochemical behavior. For example, symmetric cells with 8 and 24-hour milled electrolytes remain stable after 190 cycles at 1 mA cm⁻²/2 mAh cm⁻², while the unmilled baseline cells short-circuit during initial activation. The Li/Ni asymmetric half-cells with milled electrolytes allow for stable electrodeposition of approximately 20 mAh cm⁻² (100 μm Li thickness), while the baseline shorts at 1.2 mAh cm⁻². Combined cryogenic focused ion beam (cryo-FIB) and X-ray photoelectron spectroscopy (XPS) demonstrate that milled microstructures promote uniform early-stage electrodeposition on foil collectors and stabilize solid electrolyte interphase (SEI) reactivity. Mesoscale modeling reveals the relationship between Li-SSE interface morphology and the onset of electrochemical instability, based on underlying reaction current distribution.

8:30 AM ES03.12.02

Formation of Lithium Lanthanum Zirconium Oxide Nanofibers: Insight from *In-Situ* Synchrotron X-Ray Scattering Study Jungkuk Lee¹, Michael J. Counihan¹, Wooseok Go², Pallab Barai¹, Sanja Tepavcevic¹, Mike Tucker², Marca M. Doeff², Venkat Srinivasan¹ and Yuepeng Zhang¹; ¹Argonne National Laboratory, United States; ²Lawrence Berkeley National Laboratory, United States

Lithium lanthanum zirconium oxide (Li₇La₃Zr₂O₁₂) with a cubic crystal structure is a promising candidate for a solid-state electrolyte due to its good ionic conductivity, thermal stability, and relatively large electrochemical window against Li metal anodes. The formation of the cubic phase usually requests elevated temperatures and a relatively long annealing time. However, we have observed cubic phase LLZO at significantly lower temperatures in nanofibers than their bulk counterparts. To understand the phase transformation and stability of the LLZO nanofibers, we performed in-situ simultaneous Small-Angle and Wide-Angle X-ray Scattering (SAXS/WAXS) for the LLZO precursor nanofibers during their annealing between RT and 800 °C. In this study, we investigate the structural evolution and microstructure changes of the nanofibers as a function of temperature. The electrochemical properties of the LLZO nanofibers were also evaluated.

8:45 AM ES03.12.03

The Effect of Particle Size and Spatial Distribution on The Ion Transport Barrier in Polymer-Ceramic Composite Electrolytes Xi C. Chen¹, Jiyoung Ock¹, Abigail Lee², Amit Bhattacharya³, Tao Wang¹, Catalin Gainaru¹, Md Anisur Rahman¹, Sheng Dai¹, Raphaële Clement³ and Alexei Sokolov¹; ¹Oak Ridge National Laboratory, United States; ²The University of Tennessee, Knoxville, United States; ³University of California, Santa Barbara, United States

Significant efforts have been made to develop composite electrolytes combining polymer matrix with Li-ion conducting inorganic solids for feasible construction of solid-state batteries. Two main mechanisms have been proposed to enhance the ionic conductivity of the polymer matrix: 1) through a fast ion-transport interface layer along the ceramic particle-polymer interface, and 2) through percolated ceramic particles. However, without proper selection of ceramic and polymer chemistries and control of interfacial interactions, the resulting composite often even exhibits decreased conductivity^{1, 2}. Furthermore, even with favorable interfacial interactions, the size and spatial arrangement of the ceramic particles may significantly impact the electrochemical performance of the composite electrolyte.

In this work, we investigate the effect of particle size and spatial distribution in polymer-ceramic composite electrolytes. Two sizes of ceramic particles, Li_{0.34}La_{0.56}TiO₃ (LLTO) nanorods with average diameter of approximately 20 nm, and commercial LLTO particles with average diameter of 1 μm are dispersed in two polymer matrices, a single-ion-conducting polymer electrolyte and a dual-ion-conducting polymer electrolyte. The total ionic conductivity in composites made with the single-ion-conducting polymer electrolyte shows a two-fold increase with the addition of LLTO nanorods, compared with neat polymer electrolyte. In addition, Li ion diffusion is also getting faster in this composite. In comparison, composites made from commercial LLTO does not show improvement in conductivity. We explain these results by increased Li ion mobility in the polymer interfacial layer surrounding nanoparticles. The ion transport energy barrier in the composites is analyzed and quantified as a function of temperature through broadband dielectric spectroscopy (BDS) analysis.

The spatial distribution of LLTO particles within the polymer matrix also plays a role in ion transport of the composite. Two morphologies of composites are created for this comparison, a relatively uniform morphology where particles dispersed throughout the matrix, versus a layered morphology where the majority of the particles reside on one side of the matrix. Constriction factor significantly decreases the total ionic conductivity in the layered morphology. Through these investigations, we shed light on how to design composite electrolytes to maximize favorable ion transport paths and minimize barriers.

Acknowledgements: This work was supported as part of the Fast and Cooperative Ion Transport in Polymer-Based Materials (FaCT), an Energy Frontier Research Center funded by the U.S. Department of Energy, Office of Basic Energy Sciences at Oak Ridge National Laboratory.

- (1) Chen, X. C.; Sacci, R. L.; Osti, N. C.; Tyagi, M.; Wang, Y.; Palmer, M. J.; Dudney, N. J. Study of segmental dynamics and ion transport in polymer-ceramic composite electrolytes by quasi-elastic neutron scattering. *Molecular Systems Design & Engineering* **2019**, *4*, 379-385.
- (2) Chen, X. C.; Liu, X. M.; Pandian, A. S.; Lou, K.; Delnick, F. M.; Dudney, N. J. Determining and Minimizing Resistance for Ion Transport at the Polymer/Ceramic Electrolyte Interface. *Acs Energy Letters* **2019**, *4*, 1080-1085.

9:00 AM ES03.12.04

Preparation of Structured Garnet LLZO Composite Solid Electrolyte Using Graphene Oxide as a Template Daniel Chang, Wan-Yun Lee and Chen-Ning Yeh; National Tsing Hua University, Taiwan

All-solid-state lithium-ion batteries are viewed as a promising candidate for next-generation batteries due to their safety and high energy density. Despite the enhanced safety of these batteries owing to the use of solid-state electrolytes (SSEs), there is still ample room for improvement in terms of their ionic conductivity. Among various types of SSEs, composite solid electrolytes (CSEs) stand out as they combine the benefits of polymer matrix and ceramic fillers. The ionic conductivity and transport behavior of CSEs is strongly influenced by the tortuosity and continuity of the ceramic fillers. Thus, achieving low tortuosity structures with straight, interconnected ion pathways in CSEs is highly desirable but challenging. In this work, we choose the garnet-type $\text{Li}_7\text{La}_3\text{Zr}_2\text{O}_{12}$ (LLZO) as the ceramic filler, because of its high ionic conductivity (10^{-4} - 10^{-3} S/cm) at room temperature and its great chemical stability against lithium metal anodes. Additionally, we use poly(ethylene oxide) (PEO) as the polymer matrix to form the CSE. While most aligned ceramic scaffold are made by templating fixed structures, such as wood, cotton, or cellulose, we harness graphene oxide (GO) as a template to fabricate oriented LLZO structures. This method allows us to establish versatile processing techniques for designing distinct ceramic structures with interconnected pathways, including honeycomb and layered structure. Utilizing a uni-directional freeze-drying process, we successfully create interconnected ceramic structures with low tortuosity. Consequently, the corresponding CSE exhibits significantly improved ionic conductivity compared to CSEs with randomly mixed ceramic fillers. Our work provides a promising approach to the realization of CSEs with superior ionic conductivity and further advancing the prospects of safer, more efficient, and higher energy density batteries.

9:15 AM ES03.12.05

Understanding The Reactivity between $\text{Li}_{1-x}\text{Al}_x\text{Ti}_2\text{x}(\text{PO}_4)_3$ and Sintering Aids to Minimize Densification Temperatures in All-Solid-State Batteries Morgan Guilleux^{1,2}, Christel Gervais¹, Arnaud Perez^{1,2} and Christel Laberty Robert^{1,2}; ¹LCMCP, Sorbonne Université, France; ²Réseau sur le Stockage Electrochimique de l'Énergie (RS2E), France

NaSICON-type materials like $\text{Li}_{1-x}\text{Al}_x\text{Ti}_2\text{x}(\text{PO}_4)_3$ (LATP) are considered promising solid electrolytes for all-solid-state batteries due to their good total ionic conductivity of 10^{-4} S.cm⁻¹ at room temperature. However, a critical issue concerns the processability of the solid electrolyte in the composite positive electrode¹. Indeed, LATP must be densified by heat treatment (>900°C) to approach its maximum ionic conductivity and form an intimate contact with the active material. Nevertheless, chemical reactivity in the composite cathode has been observed as low as 700°C for some systems^{2,3}.

To prevent this reactivity, one strategy is to lower the densification temperature of this solid electrolyte. Multiple reports in the literature propose to use lithium salts as a sintering aid to achieve this goal. For example, LiBF_4 and LiF have been shown to densify the solid electrolyte LATP to relative densities above 90% of the theoretical density at temperatures ranging from 800°C to 900°C, respectively^{4,5}. However, these sintering temperatures remain too high and close observation of powder X-ray diffraction data reported in the literature, confirmed by our own experimental results, shows that resistive impurity phases such as LiTiOPO_4 and $\text{Li}_4\text{P}_2\text{O}_7$ already form.

In this work, we investigated the chemical reactivity mechanism during the densification and sintering processes. We first studied the reactivity of several lithium salts with LATP ($x = 0.3$), using *in situ* and *ex situ* X-ray diffraction, Raman spectroscopy and *ex situ* solid-state NMR spectroscopy (⁷Li, ²⁷Al, ³¹P). We identified new intermediate phases for the first time, bringing a new light on the reactivity and sintering mechanisms. We show that lithium salts react with LATP at low temperature, long before they melt. This result interrogates the liquid phase sintering mechanism proposed in the literature and explain that the sintering temperature is not correlated to the melting point of the salt.

Decreasing the sintering temperature of LATP is a key challenge to achieve a viable composite positive electrode for all-solid-state batteries. Our work shows that the chemical reactivity between lithium salts and LATP is a limiting factor in decreasing the sintering temperature of the material below 700°C. This new knowledge enables us to reexamine sintering of oxide ceramics and explore new paradigms to address this challenge.

- (1) Banerjee, A.; et al. Interfaces and Interphases in All-Solid-State Batteries with Inorganic Solid Electrolytes. *Chem. Rev.* **2020**, *120* (14), 6878–6933.
- (2) Miara, L.; et al. About the Compatibility between High Voltage Spinel Cathode Materials and Solid Oxide Electrolytes as a Function of Temperature. *ACS Appl. Mater. Interfaces* **2016**, *8* (40), 26842–26850.
- (3) Yu, C.-Y.; et al. High-Temperature Chemical Stability of $\text{Li}_{1.4}\text{Al}_{0.4}\text{Ti}_{1.6}(\text{PO}_4)_3$ Solid Electrolyte with Various Cathode Materials for Solid-State Batteries. *J. Phys. Chem. C* **2020**, *124* (28), 14963–14971.
- (4) Dai, L.; et al. Influence of LiBF_4 Sintering Aid on the Microstructure and Conductivity of LATP Solid Electrolyte. *Ceramics International* **2021**, *47* (8), 11662–11667.
- (5) Kwatek, K.; et al. Structural and Electrical Properties of Ceramic Li-Ion Conductors Based on $\text{Li}_{1.3}\text{Al}_{0.3}\text{Ti}_{1.7}(\text{PO}_4)_3$ -LiF. *Journal of the European Ceramic Society* **2020**, *40* (1), 85–93.

9:30 AM ES03.12.06

Low-Density Fast-Ion Conductors for High Energy Density Batteries Nahong Zhao, Aniruddh Ramesh, Rayavarapu Prasada Rao and Stefan N. Adams; National University of Singapore, Singapore

In order to realize the promise of superior energy density, the solid electrolytes in solid state batteries have to combine fast ionic conductivity with a low contribution to the overall cell mass. While the dead mass of the “separator” solid electrolyte layer can be minimized by reducing its thickness to the extent limited by operational safety and processability, in high energy density batteries 80-90% of the electrolyte in the cell will be the catholyte material within the inevitably thick composite cathodes. Thus, in the absence of fast-ion conducting high energy density cathode materials, low density catholytes are of key importance for the achievable energy density of all-solid state batteries. Additional constraints for low-density fast-ion conducting solids include of course electrochemical and electromechanical compatibility, as well as interface wettability with the active materials.

Here we discuss examples for two design strategies to realize such low density fast-ion conductors. The first strategy involves ultrathin ceramic-in-polymer Composite Solid State Electrolytes (CSSEs). We developed CSSEs combining Li-doped polyacrylonitrile with various ceramic electrolytes ($\text{Li}_{1.5}\text{Al}_{0.5}\text{Ge}_{1.5}(\text{PO}_4)_3$, LiTa_2PO_8 etc.) with and without plasticizers. Optimized composites reach conductivities of 0.1 – 1 mS cm⁻¹ at densities < 2 g cm⁻³ and retain wide electrochemical windows. Temperature-dependent analysis of Li⁺ paths shows that the ceramic filler induces a percolating network of fast ion-conductive interphases below the glass transition of the bulk polymer. Spin coating and *in situ* UV-curing the precursor slurry on Li anode or composite cathode drastically reduces interfacial resistance. The electrochemical and mechanical performance of CSSEs are investigated. Symmetric cells cycled with up to 2 mA cm⁻² over 500h retain a stable overpotential and no dendrite growth is observed. LFP/SSE/Li cells achieve a maximum specific discharge capacity of 148 mAh g⁻¹ and retain 89% of that after 200 cycles. Stable room temperature cycling is demonstrated for cells with a cathode mass loading of 6 mg cm⁻². The strong binding and 3-dimensional architecture of the *in situ*-formed interfaces is crucial for the favourable cycling stability.[1]

An alternative all-ceramic strategy is to systematically explore the correlation between fast ionic conductivity, density and glass forming ability in crystalline and glass-ceramic oxides and oxyhalides [2]. The higher number of monovalent light halides required to balance the charges of (typically heavier) high valent glass-former cations helps to reduce the overall density and turns the materials less brittle. Compared to often close-packed halides, oxyhalides typically have reduced coordination numbers, which helps to create free volume for ionic motion. In view of their favorable oxidation stability yet limited reduction stability, oxyhalides should in particular be suitable for use as catholytes. The recent report of fast room temperature ionic conductivity of 10 mS cm^{-3} in LiMOCl_4 ($M=\text{Nb,Ta}$) [3] exemplifies the strong potential of the so far hardly explored class of oxyhalides. While the phases have originally been reported as orthorhombic and isostructural to moderate ion conductor LiVOF_4 , our redetermination of LiNbOCl_4 (density 2.7 g cm^{-3}) finds a simpler, but Li-disordered, tetragonal crystal structure with smaller unit cell. The revised structure model yields more plausible bond valence sums and is consistent with DFT energy minimizations. Molecular dynamics simulations utilizing our bond-valence related embedded-atom method type forcefield softBV-EAM reveal the ion transport mechanism and its relation to the local rotational mobility of the $(\text{MOCl}_4)_n$ chains [4].

References:

- [1] L. He et al. *Energy Stor. Mater.* 60 (2023) 102838.
- [2] R. Dai et al. *Chem. Mater.* 34 (2022) 10572.
- [3] Y. Tanaka et al. *Angew. Chem. Int. Ed.* 62 (2023) e202217581.
- [4] A. Ramesh et al. *in preparation*.

9:45 AM ES03.12.07

Electrochemical Performance of Si/C-Argyrodite Solid-State Composites: Limitations of The Effective Ionic Transport Yannik Rudel¹ and Wolfgang Zeier^{1,2}; ¹University of Münster, Germany; ²Helmholtz-Institut Münster Forschungszentrum Jülich, Germany

Silicon-graphite composite electrodes have emerged as an alternative to lithium metal or silicon anodes in all solid-state batteries due to their resistance to electro-chemomechanical failure, while maintaining low lithiation potential.¹ While those materials are designed for lithium-ion batteries, their limited intrinsic ionic conductivity hinders application in all-solid-state batteries requiring efficient charge carrier transport in the all-solid electrodes. Therefore, a design of the effective conductivities is imperative to achieve the best electrochemical performance. This can only be achieved by understanding the relations of charge carrier transport in the used materials as well as their composites under careful consideration of their preparation.² In our study, we focus on understanding the impact of charge carrier transport within a composite of silicon on graphite and argyrodite solid electrolyte on the electrochemical performance. Through a systematic variation of the Si/C to solid electrolyte ratio we show an exponential increase of the effective ionic conductivity in the anode composite with increasing content of solid electrolyte. Simultaneously, the electronic transport remains high ($\sim \text{S/cm}$) and virtually independent of the volume fraction. This enhanced effective transport in the composites translates to a substantial improvement in the specific capacities achievable when charging and discharging across various C-rates.³ In addition, we investigate the influence of temperature to gain information about the activation energy of the ionic transport in the composites. Our results underscore the importance of tailoring charge carrier transport properties in solid-state composite anodes to achieve optimal electrochemical performance.³

References:

- (1) Müller, J.; Abdollahifar, M.; Vinograd, A.; Nöske, M.; Nowak, C.; Chang, S. J.; Placke, T.; Haselrieder, W.; Winter, M.; Kwade, A.; Wu, N. L. Si-on-Graphite Fabricated by Fluidized Bed Process for High-Capacity Anodes of Li-Ion Batteries. *Chem. Eng. J.* 2021, 407, 126603. <https://doi.org/10.1016/j.cej.2020.126603>.
- (2) Janek, J.; Zeier, W. G. Challenges in Speeding up Solid-State Battery Development. *Nat. Energy* 2023, 8 (March), 230–240. <https://doi.org/10.1038/s41560-023-01208-9>.
- (3) Rudel, Y.; Rana, M.; Ruhl, J.; Rosenbach, C.; Müller, J.; Michalowski, P.; Kwade, A.; Zeier, W. G. Investigating the Influence of the Effective Ionic Transport on the Electrochemical Performance of Si/C-Argyrodite Solid-State Composites. *Batter. Supercaps* 2023, 6 (8), 1–6. <https://doi.org/10.1002/batt.202300211>.

10:00 AM BREAK

SESSION ES03.13: Organic Electrolyte
Session Chairs: Hunter Ford and Md Anisur Rahman
Friday Morning, April 26, 2024
Room 423, Level 4, Summit

10:30 AM ES03.13.01

Design of a Polymer Electrolyte with High Ionic Conductivity through an *In-Situ* Polymerization Approach Md Anisur Rahman, Catalin Gainaru, Georgios Polyzos, Xi C. Chen, Valentino R. Cooper and Alexei Sokolov; Oak Ridge National Laboratory, United States

Solid-state lithium metal batteries have risen as highly promising contenders for the next generation of energy storage systems, primarily because of their inherent safety, stability, and higher energy density. Nevertheless, they have yet to reach practical viability, primarily due to challenges related to solid-state electrolytes. In this study, we introduce a groundbreaking method for generating a polymer electrolyte with superior room-temperature lithium-ion conductivity and excellent interfacial stability. This approach involves the in-situ copolymerization of standard ionic-conducting and single-ion-conducting monomers in the presence of a lithium salt. This polymer significantly enhances the cation transference number and facilitates uniform contact with electrodes, resulting in the suppression of dendrite growth. This is attributed to the even distribution of charge at the electrolyte-electrode interface. This research presents a successful strategy for establishing a stable electrolyte/Li interface, thereby laying the foundation for the accelerated development of long-lasting solid-state lithium metal batteries. This presentation provides an overview of our ongoing endeavors to design a polymer electrolyte with exceptional ionic conductivity, aimed at enhancing the safety and stability of solid Li-Metal batteries.

10:45 AM ES03.13.02

TFSI-Based Single-Ion Conducting Polymer Electrolytes for Solid State Batteries Ain Uddin¹, Michelle Lehmann¹, Catalin Gainaru¹, Alexei Sokolov^{1,2} and Tomonori Saito^{1,2}; ¹Oak Ridge National Laboratory, United States; ²The University of Tennessee, Knoxville, United States

The development of high performance ion conducting materials that are lightweight and flexible with improved safety are imperative for next generation energy storage technologies, including lithium (Li)-ion batteries, sodium (Na)-ion batteries, supercapacitors, fuel cells, flow batteries, and many others.

High-performance solid-state polymer electrolytes have the potential to address various challenges in electrical energy storage devices if they can meet the requirements of (i) high ionic conductivity; (ii) sufficient mechanical strength; (iii) high transport number; and (iv) wide electrochemical stability window. However, dry polymer electrolytes lack sufficient ionic conductivity to meet cell power requirements. While improving ion conductivity of polymer electrolytes is generally a challenge due to a trade-off between ion conductivity and polymer segmental dynamics, mechanically robust single-ion conducting solid polymer electrolytes provide promise due to maintaining high transport number and enabling high conductance. This presentation will discuss our progress on the design of trifluoromethanesulfonimide (TFSI)-based single-ion conducting polymer electrolytes for Li- and Na- ion batteries, as well as other energy storage applications. Specifically, we have successfully synthesized TFSI-functionalized polynorbornene (PNB) derivatives. Due to the polyolefinic structure of PNB backbone, TFSI-PNBs form a new family of single-ion conducting polymers with particularly high mechanical and electrochemical stability. In addition, the ionic conductivity of TFSI-PNB is significantly higher (8 orders of magnitude) compared to other TFSI-based polymer electrolytes such as TFSI-polystyrene or TFSI-polymethacrylate. The structure-property relationships of ion conductivity, plasticization, mechanical and electrochemical properties as well as their cell performance will be discussed.

11:00 AM ES03.13.03

Covalent Organic Framework based Solid State Electrolytes: A Breakthrough for Safer and High-Performance Energy Storage Devices [Chaoqun Niu](#); Westlake Education, China

The development of high-performance solid state electrolytes is a key milestone in advancing the safety, performance, and energy density of energy storage technologies, particularly in lithium ion batteries. Covalent Organic Frameworks (COFs), with their unique structural tunability, high thermal and chemical stability, and inherent porosity, have emerged as a promising candidate for solid state electrolytes. Our presentation explores cutting-edge research in the design, synthesis, and characterization of COF-based solid-state electrolytes and their transformative potential in the realm of energy storage. We will discuss the rational design of COFs tailored for solid state electrolyte applications, focusing on factors such as framework stability, and ion conductivity. By judiciously modifying COF structures, we can enhance their ion transport properties, leading to improved ionic conductivity and electrochemical stability. These studies shed light on the mechanisms of ion transport, electrochemical stability, and long-term performance of COF-based electrolytes.

In conclusion, this research represents a significant advancement in COF-based solid-state electrolyte development, offering solutions to the pressing challenges in energy storage technology. We anticipate that the insights and breakthroughs presented here will pave the way for the practical implementation of COF-based solid-state electrolytes, fostering discussions and collaborations within the materials science community, and catalyzing the transformation of energy storage technologies toward a safer and more efficient future.

References:

1. Chaoqun Niu, Wenjia Luo, Chenmin Dai, Chengbing Yu, Yuxi Xu*. High voltage tolerant covalent organic framework electrolyte with holistically oriented channels for solid state lithium metal batteries with nickel-rich cathodes. *Angew Chem Int Ed*, 2021, 60(47):24915-24923.
2. Chaoqun Niu, Yuxi Xu*. Two-dimensional polymers: Preparation, assembly and high-efficiency electrochemical applications. *Acta Polymerica Sinica*, 2021, 52(6): 549-564.
3. Kaige Zhang, Chaoqun Niu, Chengbing Yu, Li Zhang, Yuxi Xu*. Highly crystalline vinylene-linked covalent organic frameworks enhanced solid polycarbonate electrolytes for dendrite-free solid lithium metal batteries. *Nano Research*, 2022, 15(9): 8083-8090.
4. Zhen Hou, Shuixin Xia, Chaoqun Niu, Yuepeng Pang, Hao Sun, Zhiqi Li, Yuxi Xu*, Shiyu Zheng*. Tailoring the interaction of covalent organic framework with the polyether matrix toward high performance solid state lithium metal batteries. *Carbon Energy*, 2022, 4(4): 506-516.

11:15 AM ES03.13.04

A Super-Ionic Solid State Block Copolymer Electrolyte [Stephan Foerster](#)¹, Daniel Krause², Beate Förster¹, Jürgen Allgaier¹, Monika Schönhoff² and Hans-Dieter Wiemhöfer²; ¹Forschungszentrum Jülich, Germany; ²Universität Münster, Germany

Lithium ion batteries are a key energy storage technology for electric vehicles and mobile portable devices. The related electrolyte materials are intensely investigated with respect to improvements in ionic conductivity, stability and safety. Solid polymer electrolytes represent a promising alternative, because of their compatibility with large-scale manufacturing processes, mechanical stability and toughness and good electrode adhesion, and improved safety. However, their low lithium ion conductivity, particularly at room temperature, has so far limited their applications. Ion conduction in solid polymer electrolytes is coupled to the segmental motions of the polymer chains, which is particularly slow for crystalline polymers and polymers with low glass transition temperatures. For polyethers such as polyethylene oxide (PEO), Li ion conduction occurs via coordination with the oxygen atoms by intersegmental hopping from one coordination site to another. Since PEO is crystalline below its melting temperature of ca. 60 °C, its segmental mobility at room temperature is very low, limiting its applications.

We systematically investigated the Li ion conductivity of PEO block copolymers loaded with LiTFSI-salt at high salt loadings from [Li:EO] = 0.1 – 10. We observe that super-stoichiometric addition of LiTFSI leads to the formation of a crystalline PEO/LiTFSI-phase that shows super-ionic conductivity. Concomitantly, the addition of LiTFSI increases the PEO-volume fraction in the block copolymers, thereby inducing a phase transition from hexagonally ordered cylinders to the bicontinuous gyroid phase. The crystalline superionic PEO/LiTFSI phase within the bicontinuous gyroid phase leads to solid electrolyte block copolymer membranes showing exceptionally high Li ion conductivities. We find ion conductivities of > 10 mScm⁻¹ at 0°C, and values of > 100 mScm⁻¹ at 80°C, which are in the range of the best inorganic Li ion conductors such as LGPS. The very low activation energies, in the range of 0.2 – 0.3 eV, the sharp increase of the ion conductivity at superstoichiometric addition, and the narrow relaxation time distribution as measured by ⁷Li-NMR indicate a super-ionic conduction mechanism in the solid polymer electrolyte. Therefore, these materials open the way for solid polymer electrolytes with sufficiently high ion conductivities for commercial applications.

11:30 AM ES03.13.05

Submicron-Thick Single-Ion-Conducting Polymer Electrolytes via Initiated Chemical Vapor Deposition [Hunter Ford](#), Ramsay B. Nuwayhid, Brian Chaloux, Michael Swift, Christopher Klug, Youngchan Kim, Xiao Liu, Battogtokh Jugdersuren, Jeffrey W. Long, Debra R. Rolison, Rachel Carter and Megan B. Sassin; U.S. Naval Research Laboratory, United States

Three-dimensional (3D) electrodes and architectures are becoming more prevalent in next generation batteries leading to enhanced performance. For instance, in the case of Zn-based batteries, a 3D Zn electrode alleviates current hotspots mitigating shape change¹, while in the case of Li-S batteries a 3D porous carbon nanofoam helps to prevent dissolution and diffusion of active material.² Additional functionality and flexibility can be unlocked via modification of the extensive surface area of the 3D components, such as incorporating coatings to enhance electrolyte wettability, serve as an artificial solid-electrolyte interphase, or as a solid-state electrolyte. Conformally and homogeneously coating the interior and exterior surfaces of a complex, macroscopically thick 3D structure necessitates the use of non-line-of-sight deposition techniques. Initiated chemical vapor deposition (iCVD) is a non-line-of-sight method that has demonstrated utility to generate conformal polymer coatings with tunable thickness on both 2D and 3D substrates. Recently, we have reported on the post-deposition modification of iCVD-derived polymer films to produce a submicron-thick anion-conducting polymer electrolyte.^{3,4} To build off of these results, we move to generate cross-linked co-polymer systems via iCVD,

based off of divinylbenzene and 4-dimethylaminomethylstyrene (DVB-co-DMAMS), and use post-processing protocols to impart specific performance functionalities. The co-polymer can be rendered as a single-anion conducting solid-state electrolyte (SSE) and we show that the ionic conductivity of the SSE depends upon the DVB/DMAMS ratio, the mobile ion identity, and network plasticization, with anion conductivity nearing $1 \times 10^{-4} \text{ S cm}^{-1}$ under optimal conditions. Molecular dynamic simulations are further used to probe ion transport, which coupled with mechanical property analysis enables structure-chemistry-property relationships to be determined. The iCVD generated SSEs facilitate anionic redox chemistry (Zn/ZnO, Ag/ZnO) without the use of an additional separator or free salt, a major advancement for improving specific cell capacity. Coupling iCVD with mass-scalable post-processing protocols to impart specific performance functionality of submicron-thick SSEs opens the door to advanced 3D electrodes and components to enable next-generation energy storage systems with high performance metrics.

- (1) Parker, J. F.; Chervin, C. N.; Nelson, E. S.; Rolison, D. R.; Long, J. W. Wiring zinc in three dimensions re-writes battery performance—dendrite-free cycling. *Energy Environ. Sci.* 2014, 7 (3), 1117-1124.
- (2) Neale, Z. G.; Lefler, M. J.; Long, J. W.; Rolison, D. R.; Sassin, M. B.; Carter, R. Freestanding carbon nanofoam papers with tunable porosity as lithium-sulfur battery cathodes. *Nanoscale* 2023.
- (3) Ford, H. O.; Chaloux, B. L.; Swift, M. W.; Klug, C. A.; Miller, J. B.; Kim, Y.; Jugdersuren, B.; Zuo, X.; Long, J. W.; Liu, X.; et al. Non-Line-of-Sight Synthesis and Characterization of a Submicron Isomerically Pure Cationic Polymer. *RSC Appl. Interfaces* 2023, in review.
- (4) Ford, H. O.; Chaloux, B. L.; Kim, Y.; Long, J. W.; Rolison, D. R.; Sassin, M. B. Submicron-Thick Single-Anion Conducting Polymer Electrolytes *RSC Appl. Interfaces* 2023, in review.

11:45 AM ES03.13.06

Facile Synthesis of Li Argpyrodite Materials as a Solid Electrolyte [JaeSeong Yoo](#) and Jae-Hun Kim; Kookmin University, Korea (the Republic of)

Recently, research on next-generation secondary batteries has been actively pursued to develop high-energy-density and safe battery technologies. Currently, liquid electrolytes are utilized in Li-ion batteries (LIBs), which are flammable and volatile. Replacing the liquid electrolyte with solid materials could facilitate a high-capacity Li metal anode and enhance the safety of LIBs. Solid electrolyte materials in all-solid-state batteries (ASSBs) are categorized into oxides, sulfides, and polymers. Among these, sulfide-based materials offer several advantages, including high ionic conductivity and excellent processability.

The Li-argpyrodite materials ($\text{Li}_6\text{PS}_5\text{X}$, X= Cl, Br, and I) are exemplary sulfide-based materials renowned for their high ionic conductivity and electrochemical stability. However, a challenge exists in the current synthesis of argpyrodite due to the elevated cost of lithium sulfide (Li_2S), an essential precursor for producing argpyrodite-type materials. The high expense associated with Li_2S amplifies the production costs of solid electrolytes, presenting a significant barrier that impedes the widespread commercialization of ASSBs. Consequently, there is a growing demand for an economical method to synthesize Li_2S at a lower cost. Another approach involves synthesizing sulfide-based materials without the reliance on Li_2S .

In this study, we introduce a novel method for synthesizing argpyrodite materials, employing Li_3N as the primary starting material instead of Li_2S . $\text{Li}_6\text{PS}_5\text{Cl}$ can be efficiently prepared through a one-step ball milling process. The resulting material ($\text{Li}_6\text{PS}_5\text{Cl}$) demonstrated an ionic conductivity of 1.1 mS cm^{-1} , comparable to the room temperature conductivity of established $\text{Li}_6\text{PS}_5\text{Cl}$ solid electrolytes. This approach has the potential to lower the cost of solid electrolyte synthesis and enhance time efficiency.

SESSION ES03.14: Virtual Session
Session Chairs: Xinrong Lin and Howard Qingsong Tu
Tuesday Morning, May 7, 2024
ES03-virtual

8:00 AM ES03.14.01

Sequencing Polymers for Room-Temperature Solid-State Batteries [Xinrong Lin](#)¹, Shantao Han² and Mao Chen²; ¹Duke Kunshan University, China; ²Fudan University, China

For decades, liquid electrolytes have been adopted in lithium-ion batteries to bridge the interspace between electrodes and transport ions. In an era aspiring deep electrification and decarbonization in transportation and power sectors, polymers are expected to double energy density at the system level when combined with lithium anode, and enable all-solid-state battery (ASSB) that offers enhanced safety, processability and flexibility. Unfortunately, the long-standing crux to designing high-performance polymer electrolytes is their poor ion conductivity, which is limited by chain mobility and number of dissociated ions in polymer matrix. Previously, researchers have almost always focused on increasing segmental chain motion to improve ion transport, such as adding plasticizing additives or changing molecular compositions, which could lead to compromised mechanical integrity and polarization-related transport loss. In the meantime, though the importance of dissociated ions is empirically considered, the sequence strategy to modulate polymer transport and achieve delicate control of ion dissociation is almost universally overlooked.

Inspired by natural macromolecules that can achieve complex regulation by delicately controlling sequential arrangement of the backbone, we envision that manipulating polymer sequence could facilitate ion dissociation and strengthen control of transport in polymers. Herein, with a combination of experimental and computational methods, we prove the fundamental significance of polymer sequencing in ion transport and create homogeneous Li^+ distributions, non-aggregated Li^+ solvation structures and enhanced Li^+ -anion dissociation in a designed solid-state fluorinated single-ion polymer electrolyte with alternating sequence (alter-SIPE). Perhaps most remarkably, in dry polymers, the alternately sequenced polymer leads to a concerted PEO- Li^+ -anion migration pathway, allowing conductivity tuned up by 1-3 orders of magnitude at 30 degC, which is comparable to that of liquid-state polyethylene oxide (PEO). In addition, we demonstrate that the exceptional ionic conduction capacity of our alter-SIPE could enable dendrite-free operation and reversible cycling in $\text{Li}||\text{LiFePO}_4$ (LFP) ASSBs with a high coulombic efficiency.

8:15 AM ES03.14.02

A Metal-Free Quasi-Solid-State Battery for Better Safety and Sustainability [Ying Wang](#); Louisiana State University, United States

Solid-state rechargeable batteries promise high energy, low cost, and improved safety/stability. Hence, they are considered as the new-generation battery technology for electric vehicles and grid-scale electricity storage, and expected to meet other critical needs for more compact and higher-capacity energy storage devices. On another note, current commercial batteries are mainly metal based, with metal elements in charge carriers and/or electrode materials, which poses potential economic and environmental concerns due to the heavy use of nonrenewable metals. Thus, metal-free batteries provide a more sustainable and environmental-friendly alternative to these batteries, though the relevant research is still in its infancy. Recently, rechargeable batteries based on aqueous electrolytes have shown high potential attributed to their low cost and intrinsic safety. An appealing choice is an aqueous battery using

non-metal ions as charge carriers, such as ammonium ion with a lighter molecular weight (18 g/mol) and a small hydrated ionic size of 3.31 Å, leading to faster ion diffusion in the electrolyte. Furthermore, by combining with organic electrodes, nonmetal ammonium-ion charge carriers make it possible to realize metal-free batteries that offer affordable, eco-friendly, and sustainable alternatives to current metal-based batteries.

In this work, a novel quasi-solid-state metal-free battery is assembled using a hydrogel electrolyte sandwiched between polypyrrole cathode and polyaniline anode. A hydrogel is a hydrophilic polymeric network containing large amounts of water. Herein, the quasi-solid-state hydrogel electrolyte is simply synthesized using ammonium sulfate, water, and xanthan gum that is edible and biodegradable. Concentrated salts are used to decrease the amount of free water molecules in the hydrogel electrolyte, and thus reduce hydrolysis and side reactions from water. Both the salt concentration and the polymer content in the hydrogel can be easily tuned and optimized, to minimize side reactions and maximize ionic conductivity and mechanical strength of the electrolyte, as monitored by XRD, SEM, XPS, Raman spectroscopy, electrochemical characterizations, impedance measurements, tensile and adhesion tests, leading to superior performance of the battery. As such, this study presents the first quasi-solid-state non-metal battery with lower cost and better performance, which opens the door to future metal-free electronics that would generate long-term benefits to environment.

8:30 AM ES03.14.03

Electrolytes for Lithium and Sodium Ion Batteries: The Road from Ionic Liquids to Deep Eutectic Solvents and from Solid Ionogels to Eutectogels An Hardy^{1,2,3}, Jonas Mercken^{1,2,3}, An-Sofie Kelchtermans^{1,2,3}, Bjorn Joos^{1,2,3}, Dries De Sloovere^{1,2,3} and Marlies K. Van Bael^{1,2,3}, ¹Hasselt University, Belgium; ²IMEC, Belgium; ³Energyville, Belgium

In order to increase the energy density as well as the safety of alkali ion batteries, efforts over the past years have focused on solid electrolytes, mainly for Li⁺ conduction. Among these, the solid composite electrolyte (SCE) consists of a liquid immobilized in a solid skeleton, for example the ionogel which confines an ionic liquid within an inorganic or hybrid solid matrix.

Since deep eutectic solvents have advantages over ionic liquids, such as ease of preparation, cost etc. we proposed a eutectogel (ETG) for lithium ion batteries composed of a DES (LiTFSI/NMA) in a solid silica matrix with a high ionic conductivity of 1.46 mS/cm, high thermal (130°C) and electrochemical stability (up to 4.8V)[1]. However, these materials also are brittle, which in the final cell will influence the interfacial resistance as the contact with the electrode may be limited, besides cracking, limiting the cell performance. Therefore, two strategies were followed for improvement. First, the silica matrix was replaced by a polymer matrix, called the P-ETG, achieving 0.78 mS/cm, stability up to 4.5 V and improved fire safety in comparison to the conventional liquid electrolyte (1M LiPF₆ in EC/DEC)[2]. Depending on the polymer that is used to build the matrix, the stability could be further improved (1.5-5.0V), which allows stable cycling with high energy density NMC622 cathodes[3]. Furthermore, insights into the DES-polymer interaction allow to optimize the conductivity from 0.4 mS/cm to 1 mS/cm at 25°C[4].

Second, turning to sodium ion batteries, the silica matrix was organically modified with phenyl groups in ionogels, which reduces the Young's modulus from 29 to 6 MPa. This improves the charge transfer resistance in Na/Na₂Ti₃O₇ half cells, but also decreases the ionic conductivity somewhat to 3 mS/cm; the anodic stability was 3.9V vs. Na⁺/Na [5]. The reason that the latter material was an ionogel, was that to the best of our knowledge, at the time there wasn't any suitable sodium ion conducting DES available in literature. Therefore, its development became the subject of our research as well. A first DES consists of NaTFSI and NMA, demonstrating that high concentrations of salt are needed to improve the electrochemical (up to 4.65 V) and fire hazard stability, while compromising the conductivity, which for the most stable electrolyte is 0.3 mS/cm at 20°C[6]. A remaining issue for this DES is that even the highest concentrated one is not stable in contact with Na metal. This is tackled by a novel composition, with optimized sodium metal compatibility and anodic stability up to 4.0 V vs. Na⁺/Na, and half cells with cycle life and coulombic efficiency on par with cells built with conventional carbonate-based electrolytes[7]. The development of these novel Na⁺ conducting DES, paves the way to their incorporation into a solid matrix towards the formation of Na⁺ ion conducting eutectogels[8].

In summary, in this presentation an overview of the group's work of the past 5 years will be given, to show that quite a distance has been travelled on the road from ionic liquids to deep eutectic solvents as liquid electrolytes for sodium ion batteries, and from ionogels to eutectogels in both lithium ion batteries and sodium ion batteries. This has allowed to achieve improvements in cell performance regarding energy density, stability, safety and compatibility with metal anodes.

[1] B. Joos et al, Chem. Mater. 2018

[2] B. Joos et al. Chem. Mater. 2020 32 (9) 3783-3793

[3] A.-S. Kelchtermans et al. ACS Omega 2023 8, 40, 36753-36763

[4] A.-S. Kelchtermans et al. Applied Polymer Materials, final technical revisions ongoing 2023

[5] J. Mercken et al. Small 2023 19, 40, 2301862

[6] D. De Sloovere et al. Adv. Energy & Sustainability Res. 2022 3, 3, 2100159

[7] A.-S. Kelchtermans et al. Submitted 2023

[8] J. Mercken et al. In preparation 2023

8:45 AM ES03.14.04

Effect of Li_x(MgCoNiCuZn)_{1-x}O as High-Dielectric Permittivity Fillers for Composite Polymer Electrolytes Sebastian I. Calderon Cazorla¹, Joseph Libera², Juan Carlos Verduzco¹, Kaiqi Zhang¹, Alexander Wei¹ and Ernesto Marinero¹; ¹Purdue University, United States; ²Argonne National Laboratory, United States

Composite polymer electrolytes (CPEs) are leading hybrid solid-state materials to replace flammable liquid electrolytes in lithium-ion, lithium-metal, and lithium-sulfur batteries (LIBs). Their advantage lies in the possibility to combine the flexibility and chemical stability of polymers with the mechanical and electrochemical robustness of ceramics, enhancing the typically poor ionic conductivity (σ) and transference number of the organic component. A full understanding of the mechanisms of ion conduction in such systems is still not fully well understood resulting in a limitation to produce materials having optimum transport properties. In previous work, we have observed that the increase in ionic conductivity of CPEs is not proportional to the low weight load of fillers utilized, suggesting that their surface properties may be more influential than their bulk features. One of such properties is the filler nanoparticle dielectric permittivity, which describes the ability of a material to be polarized in an electric field. In this regard, the Anderson-Stuart model suggests that dielectric permittivity is inversely proportional to the strength of interaction between Li⁺ and ether-O-atom in a polymer like PEO. In consequence, our work focuses on evaluating CPEs containing fillers with different dielectric constants such as Li₆La₂ZrBiO₁₂ garnets ($\epsilon \sim 30$) and high entropy oxides (HEO) such as Li_x(MgCoNiCuZn)_{1-x}O which are reported to have "colossal" dielectric constants reaching values of 10⁵ at 420°C and 20Hz. We propose to

understand whether the relationship between dielectric constant and ionic conductivity is expressed as changes in the microstructure of the polymer/ceramic interface, improvement in the salt dissociation and/or immobilization of the anion on the surface of these fillers. Dielectric spectroscopy results show a good correlation of dielectric permittivity at low frequencies versus ionic conductivity, for example EIS analysis show a monotonic overall increase in ionic conductivity of membranes when decreasing EO:Li, each series showing a σ_{\max} at 4% wt. HEO. More importantly, when decreasing the particles size from 2 μm to 200nm, we saw an order of magnitude increase in σ to $5.3 \times 10^{-5} \text{ Scm}^{-1}$ when keeping EO:Li as 20:1. To provide a mechanistic understanding of our observations, in addition to transport measurements, we utilize XRD, SEM, DSC, polarizing light microscopy and Raman spectroscopy to elucidate changes in polymer morphology and microstructure as well on Li-salt dissociation that are responsible for the improvements in ion transport observed.

9:00 AM ES03.14.05

Stable Hydroborate Solid-State Lithium Battery with High-Voltage NMC811 Cathode Hugo Braun¹, Ryo Asakura¹, Arndt Remhof¹ and Corsin Battaglia^{1,2,3}, ¹Empa-Swiss Federal Laboratories for Materials Science and Technology, Switzerland; ²ETH Zürich, Switzerland; ³EPFL, Switzerland

Hydroborate solid electrolytes offer high ionic conductivity and are stable in contact with alkali metal anodes, but are challenging to integrate into batteries with high-voltage cathodes [1-3]. Here, we demonstrate stable dis-/charge cycling of solid-state lithium-ion batteries combining a $\text{Li}_3(\text{CB}_{11}\text{H}_{12})_2(\text{CB}_9\text{H}_{10})$ hydroborate electrolyte with a 4 V-class $\text{LiNi}_{0.8}\text{Mn}_{0.1}\text{Co}_{0.1}\text{O}_2$ (NMC811) cathode, exploiting the enhanced kinetic stability of the $\text{LiCB}_{11}\text{H}_{12}$ -rich and $\text{LiCB}_9\text{H}_{10}$ -poor electrolyte composition [4]. Cells with lithium metal and indium/lithium anodes achieve a discharge capacity at C/10 of $\sim 145 \text{ mAh g}^{-1}$ at room temperature and $\sim 175 \text{ mAh g}^{-1}$ at 60 °C. Indium/lithium cells retain 98% of their initial discharge capacity after 100 cycles at C/5 and 70% after 1000 cycles at C/2. Capacity retention of 97% after 100 cycles at C/5 and 75% after 350 cycles at C/2 is also achieved with a graphite anode without any excess lithium. The energy density per cathode composite weight of 460 Wh kg^{-1} is on par with the best solid-state batteries reported to date.

[1] L. Duchêne, A. Remhof, H. Hagemann, D. Battaglia, Energy Storage Materials, 2020, 225, 782

[2] L. Duchêne, R.-S. Kühnel, E. Stilp, E. Cuervo Reyes, A. Remhof, H. Hagemann, C. Battaglia, Energy & Environ. Science, 2017, 10, 2609

[3] R. Asakura, D. Reber, L. Duchêne, S. Payandeh, A. Remhof, H. Hagemann, C. Battaglia, Energy & Environ. Science, 2020, 13, 5048

[4] H. Braun, Ryo Asakura, A. Remhof, C. Battaglia, ACS Energy Lett. in press

9:15 AM ES03.14.06

Synergistic In-Silico Design and Electrochemical Characterization of Solid-State Electrolytes with Fully Earth Abundant Chemical Compositions for Na/K-Metal Batteries Ivano Eligio Castelli, Chiara Spezzati, Benjamin Sjölin and Mohamad Khoshkalam; Technical University of Denmark, Denmark

The concept of corner-sharing frameworks is fundamental to the design of oxide solid-state electrolytes with superionic conductivity for alkali-metal ions such as Li^+ and Na^+ . These structures are composed of a highly covalent skeleton of corner-sharing polyhedra, allowing alkali-metal ions to diffuse through interconnected and highly metastable interstitial positions within the framework. In this study, our focus is on a class of earth-abundant rock silicates as solid-state electrolytes (SSE) for Na/K-metal batteries. Through a synergistic approach involving in-silico design and electrochemical characterization, we investigated the relationship between structural features—such as migration energy barriers for Na^+ and K^+ , bottleneck pathways in the skeleton structure, polyhedron packing ratio, and continuous symmetry measure—with SSE performance indicators such as ionic conductivity and phase stability under ambient conditions. Our preliminary investigations indicate that a high Continuous Symmetry Measure value in Na/K-polyhedra, along with a low packing ratio of the skeleton structure, are key features in achieving fast kinetic transport for Na^+ and K^+ . Experimental results demonstrate that by applying this hypothesis, it is possible to achieve Na^+/K^+ ionic conductivity levels in the range of 10-0.1 mS/cm at 50 °C, using a fully earth-abundant chemical composition without relying on rare-earth or multi-valent transition metal ions. An SSE based on the Na-Mg-Al-Ca-Si-O oxide system was fabricated into thin, self-standing tape-cast layers under ambient conditions. These thin, self-standing layers, in a symmetrical cell configuration of Na/SSE/Na, cycled for more than 50 cycles up to 1 mA/cm² at 50 °C. The utilization of earth-abundant rock silicates as SSE, demonstrated through synergistic in-silico design and experimental characterization, offers a promising avenue for the development of high-performance and sustainable solid-state batteries, showcasing significant potential in achieving enhanced ionic conductivity and phase stability without relying on rare-earth or multi-valent transition metal ions.

SYMPOSIUM ES04

Metal Anodes in Rechargeable Batteries—Electrolyte, Interface and Mechanism
April 23 - April 26, 2024

Symposium Organizers

Betar Gallant, Massachusetts Institute of Technology

Tao Gao, University of Utah

Yuzhang Li, University of California, Los Angeles

Wu Xu, Pacific Northwest National Laboratory

* Invited Paper

+ JMR Distinguished Invited Speaker

^ MRS Communications Early Career Distinguished Presenter

SESSION ES04.01: Li Metal—Solid State
Session Chairs: Tao Gao and Yuzhang Li
Tuesday Morning, April 23, 2024
Room 422, Level 4, Summit

10:30 AM ES04.01.05

Polymerized Acrylonitrile Artificial SEI for Long-Life Li-Metal Battery and Enhanced Stability for Li/Li₁₀GeP₂S₁₂ Interface [Binh K. Hoang](#)¹, Roya Damircheli¹, Madison Brausch¹, Victoria Castagna Ferrari², Nhi Nguyen¹ and Chuan-Fu Lin¹; ¹The Catholic University of America, United States; ²University of Maryland, United States

Lithium metal anode batteries have attracted significant attention as a promising energy storage technology, offering a high theoretical specific capacity and low electrochemical potential. Utilizing lithium metal as the anode material can substantially increase energy density compared to conventional lithium-ion batteries. However, the practical application of lithium metal anodes has encountered notable challenges, primarily due to the formation of dendritic structures during cycling. These dendrites pose safety risks and degrade battery performance. Addressing these challenges necessitates the development of a reliable and effective protection layer for lithium metal. This study presents a cost-effective and convenient method to produce lithium metal protective layers by creating ex-situ polymer layers using acrylonitrile (AN). This method extends the lifetime of lithium metal anodes by a remarkable factor of six under high current (1 mA/cm²) cycling conditions. While the cycle life of bare lithium metal is approximately 150 hours under high current conditions, AN-treated lithium metal anodes exhibit an impressive longevity of over 900 hours. Furthermore, with the increasing attentions on solid-state electrolytes – which address the safety concerns and energy density limitations associated with conventional liquid electrolytes in lithium-ion batteries, the interface between Li metal and solid-state electrolytes has been the major challenges. For example, Li₁₀GeP₂S₁₂ (LGPS) stands out among these solid electrolyte materials, boasting high ionic conductivity (1 × 10⁻² S cm⁻¹). Nonetheless, the severe instability of the interface between lithium metal anodes and solid electrolytes, including dendrite formation and electrolyte degradation, hindering their practical implementation. This work also goes deeply to explore the stability and performance of Li | LGPS systems by utilizing a polymerized acrylonitrile interfacial. By elucidating the mechanisms governing the interfacial layers, this low-cost fabrication of AN-treated lithium metal holds significant potential for advancing the commercialization of future lithium-metal batteries, surpassing the capabilities of traditional lithium-ion batteries.

10:45 AM ES04.01.06

Computational Analysis of a Promising Earth Abundant, Stable, Lithium Solid Electrolyte [Benjamin A. Williamson](#), Daniel Rettenwander and Sverre Selbach; Norwegian University of Science and Technology, Norway

Solid state electrolytes offer the potential to drastically increase the overall stability of rechargeable lithium batteries as well as provide the means to realise the use of Li-metal anodes maximising the charge capacity of a device. At present, batteries use liquid electrolytes such as [LiPF₆] which although they possess high ionic conductivities of 1 × 10⁻² S cm⁻¹ limit the safe temperature ranges a battery can be operated at as well as forbidding the use of Li-metal anodes due to dendrite formation leading to short circuiting and “thermal runaway”. Solid electrolytes such as the Li-rich garnet materials, LLZO, or antiperovskites, Li₃OCl, have demonstrated low migration barriers (<0.3 eV), however issues arise regarding stability or a competing lower conductivity phase. In this work, we have identified a promising Earth-abundant, non-toxic, stable Li-solid electrolyte. Using a combination of density functional theory and experiment, we show that this material possesses thermodynamic, dynamic and electrochemical stability, ideal defect chemistry and low migration barriers leading to undoped conductivities of ~10⁻³ S cm⁻¹ which are expected to rise to at least 10⁻² S cm⁻¹ with minimal doping.

11:00 AM *ES04.01.07

Lithium Metal Solid-State Batteries: Anode-Free vs. Lithium Excess [Matthew McDowell](#); Georgia Institute of Technology, United States

Solid-state batteries offer the promise of improved energy density and safety compared to lithium-ion batteries. The electro-chemo-mechanical evolution of materials at solid-solid electrochemical interfaces is different than at solid/liquid interfaces, and contact evolution in particular plays a critical role in determining the behavior of solid-state batteries. Lithium metal anodes in solid-state batteries are intrinsically limited by void formation during stripping and dendrite growth during plating. Anode-free solid-state batteries, in which there is no initial lithium metal at the anode interface, offer extremely high energy density, but there is a lack of understanding of how their behavior differs from excess-lithium electrodes. Using X-ray tomography, cryo-FIB, and finite-element modeling, we show that anode-free solid-state batteries are intrinsically limited by current concentrations at the end of stripping due to localized lithium depletion. This causes accelerated short circuiting compared to lithium-excess cells. Based on these results, the beneficial influence of metal alloy interfacial layers on controlling lithium evolution and mitigating contact loss from localized lithium depletion, including at low stack pressures, will be discussed. X-ray tomography is further shown to be particularly useful in observing the dynamic evolution of lithium metal, including void formation and filament growth. Finally, lithium metal composites offer a “middle ground” between lithium-excess and anode-free electrodes, and we show that composite electrode structure can act to enhance the effective transport of Li to the interface and therefore enable improved lithium operation at practical stack pressures < 2 MPa.

11:30 AM *ES04.01.08

Critical Current Densities for Short-Circuiting of Solid-State Electrolytes Ryo Kurose¹, Yasutoshi Iriyama¹ and [Munekazu Motoyama](#)²; ¹Nagoya University, Japan; ²Kyushu University, Japan

The cubic phase Li₇La₃Zr₂O₁₂ (LLZ) exhibits Li⁺ conductivity on the order of 10⁻⁴ S cm⁻¹ at room temperature and has sufficient stability even in contact with molten Li¹). Additionally, its shear modulus is several times greater than those of sulfide solid electrolyte materials²), and it is thus expected to act as a promising solid-state electrolyte for preventing dendrite growth of Li metal. However, it has been reported that repeated charging/discharging of Li metal anodes causes short circuits, even with LLZ. Similar results were reported by subsequent researchers, and it was gradually realized that the short-circuit problem was more difficult to solve than originally thought. Various models of the short-circuit mechanism of LLZ have been discussed^{3,4}), but there is no experimental confirmation of what determines the critical current density (CCD) that induces shorts. This is partly because Li voids are easily formed at the Li/LLZ interface, making it difficult to compare the CCD values under fair conditions. In the present study, the CCD was measured by keeping the Li/LLZ interface constant. The temperature dependence of the CCD was also clarified, and the short-circuit mechanism was discussed based on the activation energy values of the CCD.

Acknowledgments

This work was supported by JSPS KAKENHI Grant Number JP22H04611 (Grant-in-Aid for Scientific Research on Innovative Areas “Interface IONICS”), JP 22H02178, and JST GteX Grant Number JPMJGX23S5.

References

- 1) R. Murugan, V. Thangadurai, and W. Weppner, *Angew. Chem. Int. Ed.*, **46**, 7778–7781 (2007).
- 2) A. Sakuda, A. Hayashi, Y. Takigawa, K. Higashi, and M. Tatsumisago, *J. Ceram. Soc., Jpn.*, **121**, 946–949 (2013).
- 3) T. Krauskopf, F. H. Richter, W. G. Zeier, and J. Janek, *Chem. Rev.*, **120**, 7745–7794 (2020).
- 4) M. Motoyama, Y. Tanaka, T. Yamamoto, N. Tsuchimine, S. Kobayashi, and Y. Iriyama, *ACS Appl. Energy Mater.*, **2**, 6720–6731 (2019).

SESSION ES04.02: Li Metal—Electrolyte and Interface

Session Chairs: Tao Gao and Yuzhang Li

Tuesday Afternoon, April 23, 2024

Room 422, Level 4, Summit

2:00 PM ES04.02.01

Indigo as Single Additive in Liquid Electrolyte for Lithium Metal Batteries Charlotte Mallet, Emmanuelle Garitte and Rochon Sylviane; Center of Excellence in Transportation Electrification and Energy Storage, Canada

Rechargeable lithium ion batteries (LIBs) have been successfully developed and widely used to power today's portable electronic devices. The long term success in electric vehicles and energy storage system relies on rising the energy density, low temperature efficiency, safety and increased cycle life. In parallel, lithium metal batteries (LMBs), described as a system with Li⁰ as anode and metal oxide as cathode (NMC, LFP, LMO) are arising as aim of research for a plethora of groups. Lithium metal anode is considered as ideal anode due to high theoretical capacity (3860 mAhg⁻¹), lower negative electrochemical potential and lower density (0.534 g.cm⁻³).¹ Researchers used complex liquid electrolyte (ionic liquid, etc.) systems in order to avoid lithium dendrite and degradation, conventional liquid electrolyte (LiPF₆, carbonate solvents) degraded faster than expected, and consequently, generated cells fading. Therefore conventional liquid electrolyte in such cell was not used.

Use of organic additives in electrolyte and/or electrodes is considered as one of the most economical and effective approaches for solving many problems as cited previously. The additive can interact with electrolyte or anode to prevent degradation or enhanced cell performances.

This presentation will outline commercial organic compounds: Indigo and his derivatives use as single additive in NMC/Li batteries with conventional liquid electrolyte, which considerably increased the cycle life of Li metal batteries. Dyes such Indigoïd contain electron density donor (-NH-) and acceptor (-C=O) groups linked by conjugated bonds, which participate to their versatile electrochemical properties.

When used as additive in cathode materials or electrolyte, indigo modified the electrode structure and changed the composition of the Li-ions battery electrolyte and solid electrolyte interface (SEI) on lithium metal.

¹Zhang, H., Eshetu, G.G., Judez, X., Li, C., Armand, M., *Angew. Chem. Int. Ed.* 2018, 57, 15002-15027

2:15 PM *ES04.02.03

SINS of The SEI Layer: On The Origins of Electrode Passivity of Li-Metal Anode Robert Kostecki, Jonathan M. Larson, Andrew Dopilka and Asia Sarycheva; Lawrence Berkeley National Laboratory, United States

Li-ion and Li-metal batteries performance limitations are associated with physico-chemical processes at electrode/electrolyte interfaces, which lead to high impedance, electrochemical instability, and inhomogeneous Li plating and stripping. In fact, battery performance is largely determined by thermodynamic, kinetic, and mechanical properties of such electrochemical interfaces and interphases. These electrochemical systems tend to operate far away from equilibrium. A thin passive film, the so-called solid electrolyte interphase (SEI) layer, that forms at the electrode/electrolyte interface during battery assembly/formation, which gradually reforms during its operation is critical for its basic function and lifetime.

However, our overall understanding of heterogeneous ionic interfaces and interphases is still very limited due to two main reasons. First, characterizing such interfaces and interphases in their native environment is extremely challenging, as they are buried between two dissimilar materials. Second, the interfaces and interphases have complex structure and chemistry, and can even evolve by chemical inter-diffusion, lattice strain, defects, and space charge effects which lead to a variety of chemical reactions across multiple spatial and temporal scales. Interface evolution is further propelled by the large amount of charge and mass transfer between electrodes in a battery over its lifetime (generally leading to degradation, performance loss, and eventual battery failure).

In this work, we overview and exploit the nanoscale spatial resolution, chemical selectivity, and surface sensitivity of near-field infrared nanospectroscopy to characterize electrode/liquid and solid electrolyte interfaces. Near-field infrared measurements in combination with standard surface characterization tools reveal that intrinsic molecular, structural, and chemical heterogeneities at the interface. This work provides a unique insight into the mechanisms of early-stage interphase formation at electrochemically active buried interfaces, and an experimental diagnostic means to aid in the development of methods to control local nanoscale variations in electrolyte chemistry, structure, and ionic conductivity at the surface of the electrode.

2:45 PM ES04.02.04

Stable and Ion-Conductive Polymeric Lithicone for Lithium Metal Anode Protection Ridwan Ahmed¹, Xin Wang², Ju-Myung Kim¹, Xiangbo Meng², Ji-Guang Zhang¹ and Wu Xu¹; ¹Pacific Northwest National Laboratory, United States; ²University of Arkansas, Fayetteville, United States

Lithium (Li) metal batteries are becoming increasingly appealing for electric mobility and other high-tech applications as they offer high energy density advantage coming from the utilization of Li metal anode with an ultrahigh theoretical specific capacity and an extremely low reduction potential. However, the practical application of Li metal anode is hampered by a variety of issues. These include dendrite formation which poses a risk for fire, formation of unstable solid electrolyte interphase (SEI) and “dead” Li resulting in a fast capacity fading, which are aggravated at high current densities. In this work, we report Li metal protection by a lithium-glycerol lithicone (LGL) layer formed by utilizing *tert*-butoxide and glycerol precursors in a molecular layer deposition process. The as-formed protection layer shows a good stability and a high ionic conductivity. The performance of the LGL-protected Li metal anode (LGL@Li) is demonstrated in both symmetric and full cell configurations at high current densities. The LGL@Li|LGL@Li cells demonstrate improved cycling stability compared with Li|Li cells during Li metal stripping/plating process at ~ 2.3 mAcm⁻² (2C) and areal capacity of 1.1 mAhcm⁻². Furthermore, LGL@Li|NMC622 cells show a capacity retention of ~ 87 % compared with ~ 35 % for Li|NMC622 cells after 200 cycles at a high current density of 2.1 mAcm⁻² (C/2). Our results show that LGL protection strategy is promising for practical Li metal batteries.

3:00 PM BREAK

3:30 PM *ES04.02.05

Lithium Metal Batteries with Improved Thermal Stabilities Xia Cao, Wu Xu and Ji-Guang Zhang; Pacific Northwest National Laboratory, United States

Lithium Metal Batteries with Improved Thermal Stabilities

Xia Cao, Wu Xu, Ji-Guang Zhang^{*}
Energy and Environment Directorate, Pacific Northwest National Laboratory
Richland, Washington 99354, United States

Development of lithium (Li) metal batteries (LMBs) has attracted worldwide attention in recent years due to their much higher theoretical energy densities than those of conventional Li ion batteries.^{1,2} Other metal batteries (MBs), such as Na metal batteries (NMBs) and potassium metal batteries (PMBs) also attracted more and more attention due to their abundance in earth crust and low cost.^{3,4} Although long cycle life of metal batteries have been demonstrated,^{2,5,6} their large-scale applications are still hindered by several barriers. One of the main barriers is the thermal stability of the electrolytes, especially when they are in contact with high voltage cathode. Therefore, development of electrolyte with improved thermal stability is critical for large scale application of metal batteries

In this work, factors affecting thermal stability of electrolytes for Li metal batteries will be discussed. First, electrolyte components should be selected to enable preferential decomposition of its salt rather than solvent so an inorganic rich interphase layer can be formed on electrodes, especially on metal anode to block its continuous reaction with electrolyte. These inorganic rich SEI layers can also enable the formation of large size of metal particles instead of nano powders, therefore minimize the surface area of anode. Formation of a stable SEI layer can not only minimize the formation of powdered metal particles, but also can prevent exposure of large amount of pure metal powder to ambient air in case of mechanical damage of batteries. Second, electrolyte solvents with high boiling point, low vapor pressure, and low reactivity with oxygen species are desired. These features will largely slow down the formation of flammable vapor when the cell is exposed to ambient air. Third, electrolyte should be stable at elevated temperature even at fully charged (high voltage) conditions. In any case, selection of solvent properties should not compromise electrochemical properties of the electrolytes. At last, examples of novel electrolytes based on these design principles will be reported in this work.

1 Whittingham, M. S. History, Evolution, and Future Status of Energy Storage. *Proceedings of the IEEE* **100**, 1518-1534, (2012).

2 Niu, C. *et al.* Balancing interfacial reactions to achieve long cycle life in high-energy lithium metal batteries. *Nature Energy*, (2021).

3 Jin, Y. *et al.* Low-solvation electrolytes for high-voltage sodium-ion batteries. *Nature Energy*, (2022).

4 Zhang, W., Liu, Y. & Guo, Z. Approaching high-performance potassium-ion batteries via advanced design strategies and engineering. *Science Advances* **5**, eaav7412, (2019).

5 Hu, Q. Li-Metal Batteries. https://s29.q4cdn.com/695431818/files/doc_presentation/2022/03/March-2022-Investor-Presentation.pdf, (2022).

6 Zheng, J. *et al.* Extremely Stable Sodium Metal Batteries Enabled by Localized High-Concentration Electrolytes. *ACS Energy Letters* **3**, 315-321, (2018).

4:00 PM *ES04.02.06

Prediction of Electrode-Electrolyte Degradation through Data-Driven Massive Reaction Networks Kristin A. Persson^{1,2}; ¹UC Berkeley, United States; ²Lawrence Berkeley National Laboratory, United States

Despite decades of work, there is still considerable uncertainty regarding the major components of the solid-electrolyte interface (SEI) and its dynamic formation mechanism as a function of electrolyte and anode composition. Here we present a new data-driven first-principles framework using a combination of high-throughput calculations, reaction networks, machine learning and microkinetic modeling. Our automated methodology is based on a systematic generation of relevant species using a general fragmentation/recombination procedure which provides the basis for a vast thermodynamic reaction landscape, calculated with density functional theory. We explore this landscape using stochastic methods and shortest pathfinding algorithms, which yield the most likely reaction pathways which are then refined with transition state calculations and kinetic information. The results of the framework show promise in being able to automatically recover previous insights on single reaction pathways, as well as successfully predicting the early dynamics and competitive nature of the SEI formation. As examples, we present i) formation mechanisms of LEMC as compared to LEDC, ii) decomposition mechanisms of the lithium hexafluorophosphate salt and iii) recover the Peled-like separation of the SEI into inorganic and organic domains resulting from rich reactive competition. By conducting accelerated simulations at elevated temperature, we track SEI evolution, confirming the postulated reduction of lithium ethylene monocarbonate to dilithium ethylene monocarbonate and hydrogen gas. These findings furnish fundamental insights into the dynamics of SEI formation and demonstrate a path forward toward a predictive understanding of electrochemical passivation.

SESSION ES04.03: Li Metal—Characterization and Mechanism

Session Chairs: Tao Gao and Yuzhang Li

Wednesday Morning, April 24, 2024

Room 422, Level 4, Summit

8:15 AM ES04.03.01

Ultrafast Deposition of Faceted Lithium Polyhedra by Outpacing SEI Formation Xintong Yuan, Bo Liu, Matthew Mecklenburg and Yuzhang Li; University of California, Los Angeles, United States

Electrodeposition of lithium (Li) metal is critical for high-energy batteries. However, the simultaneous formation of a surface corrosion film termed the solid electrolyte interphase (SEI) complicates the deposition process, which underpins our poor understanding of Li metal electrodeposition. Here we decouple these two intertwined processes by outpacing SEI formation at ultrafast deposition current densities while also avoiding mass transport limitations. By using cryogenic electron microscopy, we discover the intrinsic deposition morphology of metallic Li to be that of a rhombic dodecahedron, which is surprisingly independent of electrolyte chemistry or current collector substrate. In a coin cell architecture, these rhombic dodecahedra exhibit near point-contact connectivity with the current collector, which can accelerate inactive Li formation. We propose a pulse-current protocol that overcomes this failure mode by leveraging Li rhombic dodecahedra as nucleation seeds, enabling the subsequent growth of dense Li that improves battery performance compared with a baseline. While Li deposition and SEI formation have always been tightly linked in past studies, our experimental approach enables new opportunities to fundamentally understand these processes decoupled from each other and bring about new insights to engineer better batteries.

8:30 AM *ES04.03.03

Integrating Multi-Functionality that enables *In-Situ* TEM probing of Solid Electrolyte Interphase Characteristics Chongmin N. Wang; Pacific

Northwest National Laboratory, United States

For better battery performances, solid electrolyte interphase (SEI) layer is expected to possess three ideal characteristics: electrically insulative, ionically conductive, and constant thickness. These three characteristics are interactively correlated, typically, the thickness of SEI layer is controlled by the electrical properties of SEI layer. However, SEI layers do not seem to behave the ideal characteristics, rather the thickness of the SEI continuously increases during charge-discharge cycling and shelf storage, indicating that the SEI does not behave as an electrical insulator. We use in-situ bias transmission electron microscopy to directly measure the electrical properties of SEI. We discover that the current-voltage characteristics of SEIs resemble certain electrical conductance, rather than electrical insulation as conventionally assumed. We further demonstrate by tailoring the solvation sheath of the electrolyte, the electrical properties of the SEIs can be readily tuned, which inherently correlate to electrochemical properties. The work highlights the significance of electrical properties of the SEI layer and their tuning towards the enhanced performance of an electrochemical cell.

9:00 AM *ES04.03.04

Real- and Reciprocal Space Characterization of Advanced Solid State Batteries [Kelsey B. Hatzell](#); Princeton University, United States

New and re-imagined energy materials play a critical role in decarbonizing a range of industries related to transportation, chemical fuels, separations, power production and beyond. Transportation accounts for approximately 23% of energy related carbon dioxide emissions and electrification approaches are widespread for personal vehicles. Batteries currently play an outstanding role in a range of applications including electric vehicles and portable electronic applications and there is a growing interests in expanding the frontier for batteries. Applications such as electric aviation, batteries in space applications, and undersea propulsion all present unique engineering and scientific challenges for electrochemical energy storage systems. In this talk I will discuss emerging battery systems which move ions (e.g. charge carrier) in a solid rather than a liquid. I will also discuss the materials and chemo-mechanical principles which impact ion transport and electron transfer reactions in this class of material systems. Understanding how to engineer materials for coordinated and/or concerted transport is critical achieving reversible operation of these materials and devices. Using real- and reciprocal- space techniques I will show how we can measure and visualize material utilization and reaction heterogeneity in solid state batteries in space and time. The talk will conclude by exploring emerging applications for energy and climate materials through highlighting some of our team's emerging directions that focus on batteries for space applications and novel moisture-swing direct air capture processes.

9:30 AM BREAK

10:00 AM ES04.03.05

Quantifying and Understanding Electron-Beam Radiation Induced Degradation of Lithium Battery Materials [Shuang Bai](#); University of California, San Diego, United States

The investigation of the solid electrolyte interphase (SEI) in Li metal batteries is crucial for advancing battery technology, improving safety, extending battery lifespans, and unlocking the full potential of Li metal as an anode material. Spatially resolved techniques, such as transmission electron microscopy (TEM), are widely applied to understand the continuous composition and structure evolution of SEI during battery cycling. However, electron beam-induced damage poses challenges to accurate data interpretation. In this study, we quantify the beam dosage limit for commonly reported SEI components, including Li_2CO_3 , LiF, Li_2S , LiOH, LiH, and Li_2O , demonstrating their chemical and structural evolution under electron beam irradiation. Our results reveal that these components exhibit varying susceptibility to electron beam damage, with Li_2CO_3 being the most easily damaged and Li_2O the least. The observed effects of repeated electron beam irradiation include surface atomic displacement, mass loss, and chemical reactions. To preserve pristine chemical environments, minimizing electron beam damage becomes crucial, and cryogenic protection during imaging proves to be an effective approach. Moreover, our study highlights the potential misinterpretation of experimental results due to electron beam damage, providing examples of SEI formed in two different electrolytes. This calls for special attention to ensure accurate characterization of SEI in Li metal batteries.

10:15 AM ES04.03.06

Mechanical Properties and Deformation Behavior of Lithium Metal [Lara C. Pereira dos Santos](#)^{1,2} and Robert Spatschek^{1,3}; ¹Forschungszentrum Jülich, Germany; ²RWTH Aachen University, Germany; ³JARA-Energy, Germany

Lithium metal is the ideal candidate as anode material for reaching higher energy densities. However, comprehensive and reliable research on its complex mechanical deformation remains scarce, hindering an in-depth understanding of Li-based solid-state batteries. Lithium mechanical properties vary widely depending on length scale, orientation, strain rate and temperature. Besides, lithium is extremely reactive, creeps at room temperature and has a strong anisotropy, making experimental characterization a considerable challenge. This work aims to study the mechanical properties and deformation of lithium using a combination of experimental and modeling tools. On the theoretical side, techniques such as first-principles, molecular dynamics and effective medium theory are applied. Information not only from the elastic parameters, but also from the plastic regime is obtained. Simulations are carried out for different temperatures, specimen sizes and crystal orientations. On the experimental side, micro-indentation is performed and the hardness of lithium foils is evaluated. With this study, we expect to support investigations regarding the size and orientation dependency of Li mechanical properties. Additionally, we aim to contribute to bridging the gap between theory and experiments, as well as understanding plasticity on small scales, high strain rates and high homologous temperatures.

10:30 AM *ES04.03.07

Liquid Madelung Potential as The "Beyond Debye-Hückel" Concept Validated for Several Metal Electrodes [Atsuo Yamada](#), Norio Takenaka, Atsushi Kitada, Seongjae Ko and Hinata Koyamada; The University of Tokyo, Japan

Achievement of carbon neutrality requires the development of electrochemical technologies suitable for practical energy storage and conversion. In any electrochemical system, electrode potential E is the central variable that regulates the driving force of redox reactions. However, quantitative understanding of the electrolyte dependence of E has been limited to the classic Debye-Hückel theory that approximates the Coulombic interactions in the electrolyte under the dilute limit conditions. Therefore, accurate expression of E for practical electrochemical systems has been a holy grail of electrochemistry research for over a century. Here we show that the "liquid Madelung potential" (E_{LM}) based on the conventional explicit treatment of solid-state Coulombic interactions enables quantitatively accurate expression of the electrode potential, with the E_{LM} shift obtained from molecular dynamics reproducing a hitherto-unexplained huge experimental shift for the several metal electrode. Thus, a long-awaited method for description of the electrode potential in any electrochemical system is now available. Examples of battery system optimization based on this new concept will be demonstrated.

11:00 AM *ES04.03.08

First-Principles Modeling of Deposition Processes at Metal Anodes [Axel Gross](#)^{1,2}; ¹University of Ulm, Germany; ²Helmholtz Institute Ulm (HIU), Germany

Metal anodes in batteries of the rocking chair type promise to lead to high energy densities as they yield the lowest possible binding energy for the metal atoms and require no host material. On the other, they are often rather reactive causing the decomposition of many commonly used electrolyte components. This may lead to the formation of a passivation layer known as the solid electrolyte interphase (SEI). A better understanding of these reaction mechanisms can lead to an improved electrolyte and substrate design to achieve highly reversible metal anodes. In this contribution, recent purely computational [1] and joint theoretical-experimental [2,3] studies addressing the most likely decomposition products of electrolyte components at a number of alkaline metal anodes are presented. It will be demonstrated how the analysis of the first-principles electronic structure calculations based on density functional theory (DFT) allows to identify the crucial steps in the decomposition reactions.

In addition, metal anodes also play a crucial role in batteries using anionic charge carriers such as chloride. Based on periodic DFT calculations, the initial steps in the conversion of a Mg anode to a magnesium chloride salt will be analyzed [4] which represents the driving force in the operation of such Cl-ion batteries.

[1] D. Stottmeister and A. Groß, *Batterie Supercaps* 2023, 6, e202300156.

[2] K. Forster-Tonigold, F. Buchner, A. Groß, R.J. Behm, *Batteries Supercaps*, 2023, 6, e202300336.

[3] D. Stottmeister, L. Wildersinn, J. Maibach, A. Hofmann, F. Jeschull, A. Groß, *ChemSusChem* (2023) e202300995.

[4] K. Sarkar, D. Hübner, D. Stottmeister, Axel Groß, *Phys. Rev. Mater.*, submitted.

11:30 AM *ES04.03.09

Unveiling Lithium Metal Anode Behavior through The Advancements and Applications of Titration Gas Chromatography Y. Shirley Meng^{1,2} and Wurigumula Bao¹; ¹The University of Chicago, United States; ²Argonne National Laboratory, United States

In the realm of energy storage technologies, lithium metal batteries have gained significant attention due to the global shift toward renewable energy systems. Accurate diagnosis and understanding of the attenuation mechanism of batteries are therefore essential for the development direction. Titration Gas Chromatography (TGC) is an effective tool for quantitatively understanding the anode materials' cycling behavior. The dead Li in the cycled Lithium metal anode consists of trapped Li (Li⁰) and Solid electrolyte Interphase (SEI) Li⁺, in which only trapped Li can react with the protic solvent to generate the hydrogen (H₂), while SEI (Li⁺) does not. The ideal protic solvent, therefore, must meet specific criteria: 1) exclusively reacting with Li⁰ to generate H₂ gas; 2) displaying chemical inertness with SEI components or refraining from producing H₂ gas. Adhering to these conditions, quantifying H₂ allows for the differentiation and quantification of trapped Li⁰ and SEI (Li⁺). With the optimal solvent selection, our investigations encompassed: 1) assessing corrosion effects on electrochemically deposited Li metal anode; 2) quantifying Li inventory in practical Li metal batteries³. We demonstrate the importance of using TGC techniques in quantitatively examining the Li inventory changes of the anode under various operating conditions. Beyond that, the results offer unique insights into identifying critical bottlenecks that enhance battery performance development.

SESSION ES04.04: Li Metal—Structure and Substrate

Session Chairs: Wu Xu and Yirui Zhang

Wednesday Afternoon, April 24, 2024

Room 422, Level 4, Summit

1:30 PM ES04.04.01

Lithium Planar Deposition by Microstructural Design. Alexey Rulev¹ and Artur Braun²; ¹Empa, Switzerland; ²Empa–Swiss Federal Laboratories for Materials Science and Technology, Switzerland

Lithium metal is the most energy-dense electrode material for Li-ion batteries. However, its application is limited by the extensive whisker growth during the charging process. Despite a variety of proposed solutions to the problem, stable Li metal anode was not achieved yet. Partially it could be explained by the fact that the mechanism of such morphological instability is still relatively unclear.

Previously we have proposed the mechanism of lithium whisker growth [1] that explains root-based growth (i.e. by insertion of atoms to the base of growing whisker) of lithium whiskers, which was later observed experimentally. The mechanism focuses on the rapid mass-transfer within the electrode (i.e., self-diffusion of metal lithium) that leads rapid whisker growth. The key elements for this mechanism are presence of the passivating film on top of the electrode and relatively fast solid-state self-diffusion. Both are inherent properties of lithium: the first is the always existing SEI layer; the second is best illustrated by room temperature being about 2/3 of lithium melting point, a point at which solid-state atomic mobility becomes sufficient.

The proposed mechanism also suggests the possibility of relatively smooth deposition of lithium without significant whisker growth. In this work we have used advanced techniques to demonstrate how and where lithium can deposit without loss of morphological stability. We deposited lithium on the idealized model electrodes and then, using focused ion beam (FIB) cross-sectioning and electron back-scatter diffraction (EBSD) on metal lithium we have shown that lithium deposits into the inclined grain boundaries just below the surface of the electrode. This way, the inclined grain boundaries have a certain "capacity" of lithium they can accommodate. Further we show how and to what extent this capacity may be increased by the microstructure engineering. Lithium itself is a fusible metal, which means that it would very easily recrystallize, making traditional ways of controlling the metal microstructure like quenching very limited. We used eutectic alloying with Ga as a way to reduce the size of Li grains. This way we significantly increase the areal density of shallow inclined grain boundaries on the surface of the electrode, this way increasing its "capacity" to accommodate lithium. We demonstrate that it lead to relatively smooth deposition of lithium for an extended time, which was much longer than for pure metal lithium electrodes. It should be noted that, in contrast to other alloy electrodes, like tin of silicon, here lithium constitutes 80 mass % of the electrode, and the deposition proceeds in form of pure metal.

The author acknowledges financial support from the EU Green Deal project "OpMetBat".

[1] Rulev, A. A.; Kondratyeva, Y. O.; Yashina, L. V.; Itkis, D. M. Lithium Planar Deposition vs Whisker Growth: Crucial Role of Surface Diffusion. *J. Phys. Chem. Lett.* 2020, 11 (24), 10511–10518. <https://doi.org/10.1021/acs.jpcclett.0c02674>

1:45 PM ES04.04.02

Vertically Orientated TiO₂ 1D Lepidocrocite Nanoflakes as Scaffold for Enhanced Li-Metal Anodes Neal A. Cardoza, Mary Qin Hassig, Taber Yim, Michel Barsoum and Vibha Kalra; Drexel University, United States

Lithium metal anodes have long been the ideal anode for a variety of cell chemistries owing to their high gravimetric capacity. Dendrite growth, during cycling, however, restricts their practical deployment. Here, a new class of nanomaterials TiB₂ derived 1-dimensional lepidocrocite quasi two-dimensional

nanoflakes (IDL) are used as basis for creating a Li scaffold, that can be used as an anode-free setup. The 2D nanoflakes comprised of IDL nanofilaments are synthesized with a bottom-up reaction, directly from commercial 3D-bulk solids at near ambient temperatures and pressures^{1,2}. The morphology of the IDL is highly tunable based on processing parameters and can be intercalated with a variety of cations^{3,4}. Here IDLs are orientated vertically to guide Li-metal deposition and serve as a Li metal scaffold. This is achieved with a control freezing of an aqueous blade cast slurry. Freeze-drying results in an organized vertically oriented structure. These vertical-IDLs enable easier Li nucleation, with lower overpotentials compared with bare Cu or a normal cast slurry of IDLs. The vertical-IDL shows an overpotential of -0.06 mA vs -0.08 mA for Cu, a 25% reduction. Leading to a more spatially uniform deposition of Li. Further, IDL flakes can be intercalated with lithiophilic cations to further improve Li metal deposition and nucleation. Lastly, the -OH rich surface groups on the IDL NFs surfaces help improve the formation of a uniform solid-electrolyte interphase. These properties enable IDL nanoflakes that are orientated vertically to serve as a Li-scaffold in an anode-free setup.

2:00 PM *ES04.04.03

Materials, Electrolytes and Tools for Lithium Metal Anodes Yi Cui; Stanford University, United States

This presentation covers the recent advances in my lab on enabling Li metal anodes. Topics include: 1) A breakthrough tool of cryogenic electron microscopy, leading to atomic scale resolution of fragile battery materials and interfaces. 2) Electrochemical measurement techniques for deep understanding of solvation entropy and free energy, charge transfer and electrodeposition kinetics. 3) Materials design to enable Li metal anodes. 4) New electrolyte design for stabilizing cycling of Li metal anodes.

2:30 PM BREAK

3:30 PM *ES04.04.04

Microstructural Design Principles for Achieving Stable Metal Anode Interphases with Liquid and Solid-State Electrolytes David Mitlin; The University of Texas at Austin, United States

Lithium metal battery systems (LMBs) are being sought as an ultimate replacement to LIBs, potentially increasing the cell energy by over fifty percent due to the high capacity and low voltage of the metal anode. Analogous improvement in energy is possible with sodium metal batteries (NMBs) and with potassium metal batteries (KMBs), where existing ion insertion anodes can be replaced by plating/stripping metal. However, in all three cases safety and performance are compromised by an unstable solid electrolyte interphase (SEI) that consumes metal ions and electrolyte, and ultimately leads to dendrites. This presentation provides a series of case studies derived from the group's LMB, NMB and KMB liquid and solid-state research on the microstructural design principles that provide for long-term cycling and fast-charge stability of metal anodes. The approaches may be categorized as the following: a) design of plating/stripping supports and templates with tuned geometry and functionality; b) design of secondary interlayers placed between the metal anode and the separator; and c) design of multifunctional hybrid separators to replace the conventional polymer separators employed with LIBs. It is demonstrated that despite appearing distinct, the efficacy of each in enabling electrochemical stability originates from three fundamental features that are directly interrelated. The wetting behavior of the electrolyte on the anode must be optimized, the wetting/stripping behavior of the metal anode on the current collector must be controlled, and a geometrically and chemically modified SEI must be established. Simultaneously achieving all three leads to stable plating/stripping, while missing even one leads to rapid dendrite growth. Cryogenic FIB cross sections and cryo-TEM are combined to yield new insight regarding film wetting behavior and early dendrite formation in optimized versus baseline specimens, analyzing growth in several representative electrolytes.

4:00 PM *ES04.04.05

Interfacial Pressure Improves Calendar Aging of Lithium Metal Anodes Katharine Harrison¹, Kimberly Bassett², Kathryn Small², Daniel Long³, Laura C. Merrill² and Benjamin Warren²; ¹National Renewable Energy Laboratory, United States; ²Sandia National Laboratories, United States; ³Air Force Research Laboratory, United States

Lithium metal is a very attractive anode material because its theoretical specific capacity is approximately 10 times higher than conventional graphite anodes. Despite great promise, Li anodes suffer from capacity fade due to instabilities with the electrolyte as well as stranding of active Li. We have previously shown that applied interfacial pressure improves Li anode cycling because the pressure reduces the propensity for Li isolation and enables easier reconnection. Many researchers have also shown that calendar aging can lead to Li capacity loss and this has been attributed to either electrolyte decomposition with concurrent Li corrosion or to the formation of stranded Li. Our prior research focused on calendar aging during cycling suggests the mechanism for calendar aging is largely related to stranding of Li during rest and reconnection of the stranded Li upon further cycling, evidenced by similar average Coulombic efficiencies and Li loss in cells with and without rest. Because our calendar aging studies suggest Li stranding as a major cause of Coulombic efficiency drops and our Li cycling studies suggest this can be mitigated partially through applied interfacial pressure, we hypothesized that applied pressure would improve calendar aging by reducing stranded Li and enabling reconnection.

We systematically varied applied pressure (0-1000 kPa) on Li metal anodes during cycling tests with and without intermittent calendar aging periods. Though the Coulombic efficiency decreases during aging periods, the lost capacity is recovered during subsequent cycles, as shown though average Coulombic efficiency and cumulative Li capacity loss analysis. We find that application of pressure partially mitigates calendar aging, in accordance with our hypothesis that calendar aging is caused by Li standing and can be mitigated to some degree with interfacial pressure. This is further supported by our results showing that the average Coulombic efficiency and cumulative Li capacity losses are similar over 50 cycles for cells that were continuously cycled and cells with periodic calendar aging periods. This result indicates that the losses during aging are reversible, which is consistent with Li stranding and reconnection. We show that pressure is one mitigation technique that helps reduce Li calendar aging in this study, but our finding that calendar aging is primarily governed by the stranding and reconnection of dead Li has wider implications. This research suggests that other mitigations which have been shown to prevent dead Li formation or encourage reconnection during cycling would also likely be successful for the purpose of improving calendar aging.

The authors were supported by a Laboratory Directed Research and Development (LDRD) program. This work was performed, in part, at the Center for Integrated Nanotechnologies, an Office of Science User Facility operated for the U.S. Department of Energy (DOE) Office of Science. Sandia National Laboratories is a multi-mission laboratory managed and operated by National Technology & Engineering Solutions of Sandia, LLC (NTESS), a wholly owned subsidiary of Honeywell International Inc., for the U.S. Department of Energy's National Nuclear Security Administration (DOE/NNSA) under contract DE-NA0003525. This written work is authored by an employee of NTESS. The employee, not NTESS, owns the right, title and interest in and to the written work and is responsible for its contents. This work was authored in part by the National Renewable Energy Laboratory, operated by Alliance for Sustainable Energy, LLC, for the U.S. Department of Energy (DOE) under Contract No. DE-AC36-08GO28308. Any subjective views or opinions that might be expressed in the written work do not necessarily represent the views of the U.S. Government.

4:30 PM ES04.04.06

Stress-Driven Diffusion of Lithium into Copper Current Collectors during Plating and Stripping Kurt Hebert; Iowa State University, United States

Stresses in lithium metal anodes determine their stability during inevitable volume changes experienced upon cycling. Lithium deformation during cycling in liquid cells can initiate surface morphological instabilities which lead to capacity loss, e. g. whiskers and moss (1-3). Evidence suggests that whiskers grow by solid-state diffusion to the whisker base (3), and that whiskers relieve compressive stress in the metal generated by electrodeposition (4,5). While quantitative characterization of these processes is challenging, diffusion accompanying morphology instabilities can be detected when lithium is deposited directly on copper current collectors (6,7). Lv et al. reported operando neutron depth profiling (NDP) measurement measurements of Li diffusion into Cu during plating-stripping cycles in pouch cells (7).

A model is presented for lithium diffusion in copper current collectors during cycling in a liquid cell. Diffusion is driven by gradients of elastic stress in the current collector, induced by the combination of misfit strain due to diffusing Li atoms and bending of the copper film due to the Li concentration gradient (8). The Li diffusion flux at the copper surface (inward and outward during plating and stripping respectively) is assumed to be a small constant fraction of the plating or stripping rate, consistent with the NDP measurements. We show that the model quantitatively accounts for all aspects of the measured concentration distributions. In particular, the model captures the unique "wave-like" concentration profiles revealed by NDP, in which the maximum lithium concentration is always at the copper surface, even when lithium diffuses out of the metal during stripping.

The constant flux boundary condition is justified by a model for surface morphology evolution, in which the lithium surface is covered by spheroidal protrusions that grow and contract, respectively, during plating and stripping (3,9). We show that plating on the spheroids through an intact solid-electrolyte interphase (SEI) layer generates inward stress-driven diffusion and outward creep within the protrusion. At the base of the spheroid, the diffusion flux continues into the substrate. This flux represents a small fraction of the plating rate, and thus accounts for the diffusion inferred from analysis of NDP measurements. Therefore, surface morphology evolution appears to be driven by stresses due to plating/stripping through an intact SEI layer.

REFERENCES

1. P. Bai, J. Li, F. R. Brushett, M. Z. Bazant, *Energy Environ. Sci.*, 9, 3221 (2016).
2. L. Frenck, G. K. Sethi, J. A. Maslyn, N. P. Balsara, *Front. Energy Res.*, 7, 115 (2016)
3. A. Kushima, K. P. So, C. Su, P. Bai, N. Kuriyama, T. Maebashi, Y. Fujiwara, M. Z. Bazant, J. Li, *Nano Energy*, 32, 271 (2017).
4. X. Wang, W. Zheng, L. Hong, W. W. Wu, H. K. Yang, F. Wang, H. G. Duan, M. Tang, H. Q. Jiang, *Nat. Energy*, 3, 227 (2018).
5. W. J. Boettinger, C. E. Johnson, L. A. Bendersky, K. W. Moon, M. E. Williams, G. R. Stafford, *Acta Mater.*, 53, 5033 (2005).
6. D. Rehnlund, F. Lindgren, S. Böhme, T. Nordh, Y. Zou, J. Pettersson, U. Bexell, M. Boman, K. Edström, L. Nyholm, *Energy Environ. Sci.*, 10, 1350 (2017).
7. S. Lv, T. Verhallen, A. Vasileiadis, F. Ooms, Y. L. Xu, Z. L. Li, Z. C. Li, M. Wagemaker, *Nat. Commun.*, 9, 2152 (2018).
8. L. B. Freund, J. A. Floro, E. Chason, *Appl. Phys. Lett.*, 74, 187 (1999).
9. C. C. Fang et al., *Nature* 572, 511 (2019).

4:45 PM ES04.04.07

The Influence of Copper Current Collector Crystal Orientation on Long and Short Term Lithium Metal Plating Josefine McBrayer, Alexander Heusser, Cooper Bryan and Noah Schorr; Sandia National Laboratories, United States

Lithium metal is a practical anode of choice for beyond lithium ion battery technologies due to its high capacity and low potential. However, recharging (plating) lithium metal has proven difficult because of the formation of lithium dendrites and an unstable solid electrolyte interphase (SEI). Both are root causes of poor performance and safety issues such as internal short circuits, fire, and thermal runaway. To mitigate these undesirable qualities of lithium anodes for secondary battery applications, more uniform lithium plating is necessary. Here we investigate the performance and lithium morphology on single crystal (111, 100, and 110) and polycrystalline copper current collectors to control Li plating, especially in early cycles. The 111 orientation was determined by cryo scanning electron microscopy (with focused ion beam cross sections) and energy-dispersive X-ray spectroscopy to lead to a more compact lithium morphology and uniform SEI. Plating/stripping experiments supported that this improved morphology also manifested in a greater coulombic efficiency in early cycles in lithium-copper cells.

SESSION ES04.05: Non-Li Metal—Non-Aqueous

Session Chairs: Yuzhang Li and Xintong Yuan

Thursday Morning, April 25, 2024

Room 422, Level 4, Summit

8:45 AM ES04.05.02

Low-Cost Carbonaceous Metal-Free Wetting Layer as Sodiophilic Treatment for Solid and Molten Na Batteries J Mark Weller¹, Hyungkyu Han¹, Eugene Polikarpov¹, Kee Sung Han¹, Keeyoung Jung², David Reed¹, Vincent Sprenkle¹, Vaithiyalingam Shutthanandan¹, Yilin Wang¹ and Guosheng Li¹; ¹Pacific Northwest National Laboratory, United States; ²Research Institute of Industrial Science and Technology (RIST), Korea (the Republic of)

Sodium-metal batteries are a promising alternative to Li-metal batteries due to the natural abundance of Na, especially for grid scale energy storage where the cost premium of Li puts strain on the economic feasibility of scalable renewables-plus-storage. Low temperature Na-metal batteries, like their Li-based counterparts, suffer from Na-dendrite formation and dangerous cell failure upon extended cycling or plating at high current densities. Also like their Li-metal counterparts, Na-metal solid-state batteries (SSB) are unable to prevent dendrite intrusion without careful engineering of the Na-metal/solid-electrolyte interface. An alternative approach is to use elevated temperature batteries with a molten anode, which can enable categorically higher current densities with no dendrite issues. Where classically molten Na-batteries such as high temperature Na-S or 'ZEBRA' batteries operate well above 200 °C, it is desirable to reduce operating temperatures to unlock lower cost materials of construction and increase energy efficiency by reducing thermal losses. Unfortunately, it is well known that molten Na has poor wettability in contact with common solid electrolytes like sodium beta-alumina solid-electrolytes (Na-β"-Al₂O₃, "BASE") or NaSICON (Na-Superionic Conductor) ceramic electrolytes.

Various wetting agents and interface modification strategies have been employed to improve wettability of molten Na and reduce interface resistance in Na-SSBs. Some rely on sputter deposition of a suitable metal such as Sn or deposition of metal precursors from solution followed by a heat treatment to form pure metals such as Pb, Sn, or Bi. Some strategies utilizing exotic phases of carbon such as graphene or carbon nanotubes have also been employed. Still others rely on high temperature annealing to drive off surface contaminants under vacuum or inert atmosphere. All of these strategies lack one or more crucial components such as low-cost, non-toxicity, simplicity, or scalability. This has motivated the development of a 'metal-free wetting layer' (MFWL)

based purely on low-cost carbon sources, that can be applied via scalable processes such as spin-coating, spray-coating, or even drop-casting from solution. Our MFWL shows excellent uniformity when applied to a suitable solid-electrolyte such as BASE or NaSICON, and facilitates excellent wetting of molten Na as low as the melting point of Na. The meso/microstructure of MFWLs and mechanism of Na-wettability will be discussed in detail. Symmetric Na-Na cell data confirm that cells with low specific resistance and excellent cycling stability can be obtained at elevated temperature ($T > 100\text{ }^{\circ}\text{C}$), forming extremely intimate contact between Na and the underlying solid-electrolyte. Further, the utility of this MFWL can be extended to solid-state symmetric Na-Na cells, showing that even without applied pressure, initial experiments with BASE electrolytes treated with MFWL demonstrate a critical current density of $\sim 0.5\text{ mA cm}^{-2}$ at $30\text{ }^{\circ}\text{C}$. This simple, inexpensive, and scalable interfacial modification strategy shows great promise for enabling pure Na-anodes across solid-state and elevated temperature batteries.

9:00 AM ES04.05.03

Advanced Hybrid Polymer/Ceramic PEO-SnF₂ Protective Mechanism for Sodium Metal Anodes [Roya Damircheli](#), Binh Hoang and Chuan-Fu Lin; Catholic University of America, United States

In the face of mounting global energy requirements and pressing environmental issues, the scientific community turned to lithium-metal batteries, celebrated for their superior capacity and efficiency. However, challenges arising from the scarcity and increasing costs of lithium have redirected research efforts towards sodium batteries. Sodium metal anodes, with their remarkable theoretical specific capacity of $\sim 1166\text{ mAh/g}$, low anode potential of -2.714 V vs standard hydrogen electrode, and cost benefits, are increasingly recognized as the promising candidate for conventional energy storage systems. Notwithstanding their advantages, the unstable and fragile solid electrolyte interphase (SEI) due to the spontaneous reaction between metallic Na and a liquid electrolyte remains a significant limitation. As this SEI layer expands, it hinders ion transport, causing increased polarization and diminishing the battery's energy efficiency. Specifically, during the plating process, Na ions are deposited beneath the SEI layer, causing significant expansion. This expansion fractures the fragile SEI, allowing dendrites to grow through these defects. As these dendrites grow, they can pierce the separator, posing a risk of short-circuiting the battery. While numerous studies have proposed designs for protecting sodium metal interphase, to overcome these challenges, this study amalgamates mechano-electrochemical protective strategies to enhance sodium metal anode stability, offering groundbreaking solutions to these challenges.

Central to our exploration were tin fluoride (SnF₂) and silicon nitride (Si₃N₄), both established as effective in generating robust artificial SEI layers on the sodium metal surface. These layers, rich in NaF and Na₃N respectively, demonstrated a notable improvement in cycling performance, effectively suppressing dendrite growth and enhancing the battery's cycling stability by nearly 3.5 times compared to bare sodium anodes.

Building upon these foundational insights, a novel approach was conceptualized: a hybrid protective mechanism combining polyethylene oxide (PEO) with the presence of SnF₂ as an additive, is particularly efficacious. This combination was specifically chosen to provide chemical stability, morphological conformality, and mechanical flexibility to accommodate the mechano-electrochemical instability upon sodiation/desodiation processes. Through this novel strategy, we aimed to amalgamate the strengths of both components, ensuring optimal outcomes. This composite artificial SEI under a 0.25 mA/cm^2 current density, delivering a cycling performance 10 times superior to bare sodium metal, and survived up to 1800 hours of cycling. Impressively, at a high current density of 0.5 mA/cm^2 , the hybrid system still performed much better than its untreated counterpart and continued cycling for up to 800 hours of cycling. The synergy of PEO and SnF₂ remarkably minimized electrolyte decomposition, inhibited dendrite formation, and stabilized Na plating/stripping processes, all of which consolidating its promise for sodium metal battery technology.

Keywords: Sodium Metal, Anode Protection, Polymer-Hybrid, Mechano-Electrochemical Effect

9:15 AM ES04.05.04

Cryogenic Focused Ion Beam Milling of Intact Na Metal Battery Stacks Reveals Separator Infiltration and Delamination Failure Mechanism [Kevin Matthews](#) and Jamie Warner; The University of Texas at Austin, United States

Metal anodes are the next frontier of high-energy-density rechargeable batteries. Sodium (Na) metal batteries are particularly promising due to the widespread abundance and low cost of Na precursors. The structure, composition, and function of the solid-electrolyte-interphase (SEI) as well as the metal growth mechanisms must be understood to improve and commercialize Na metal batteries. We developed a cryogenic workflow utilizing a cryogenic sample transfer system to prepare intact electrode:separator:electrode stacks, allowing us to probe the intrinsic structure and composition of undisturbed battery interfaces. By milling with a gallium ion beam at cryogenic temperatures, we produced clean milled surfaces of the electrodes and separator with minimal beam-induced artifacts allowing for high resolution imaging, spectroscopic mapping, and 3D reconstructions generated from serial milling and imaging. Using these techniques, we studied how the Na electrode, SEI, and separator evolve during cycling in both symmetric and asymmetric cells with a tri-layer porous polymer separator and either a carbonate- or ether-based electrolyte.

Though often discarded before characterization, we find that the separator is a crucial piece of the puzzle when investigating battery performance and failure. We found overwhelmingly that cells begin with a conformal interface between the Na metal and the electrolyte-filled polymer separator instead of being separated by a layer of electrolyte. After extended cycling, Na metal infiltrates the separator pores, growing towards the opposing electrode. At the interfaces between the tri-layers, the Na can grow laterally, delaminating the separator layers. High resolution imaging and electron dispersive X-ray spectroscopy (EDS) mapping capture the Na metal in-between and within the polymer layers. 3D reconstructions of the electrodeposited Na and SEI suggest that the robustness of the SEI and the heterogeneity of its distribution (or lack thereof) relates to the ability of the Na to grow into the porous network of the separator. We combine these results to suggest a new failure model that relies on short-circuiting via the formation of a conductive pathway of Na templated by the porosity of the separator, rather than a penetration of the separator by discrete dendrites.

9:30 AM ES04.05.05

Weakly-Coordinating Cyclic Ether-Based Electrolytes Improve Potassium Metal Battery Cycling Stability and Capacity Retention [Austin Choi](#)¹, [Zheng Li](#)^{2,1} and [Vilas Pol](#)¹; ¹Purdue University, United States; ²University of Maryland, United States

As the scientific community holistically seeks alternative energy sources to traditional fuels such as coal and natural gas, attention has turned towards renewable energy generation such as wind and solar. In tandem, methods of storing energy are also being developed as a way to mitigate the intermittent nature of such methods of energy generation. Among these, electrochemical energy storage solutions are of particular promise given their flexibility and performance, allowing them to suit the needs of an increasingly growing number of industries such as chemical production and automotive manufacturing that are trending towards electrification. Lithium-ion batteries (LIBs) especially have become a mainstay in this space owing to their portability, high energy densities, and cycle lifetimes, and are the principle driving force for the growth of the global battery market to beyond US \$100 billion today.

The "holy grail" anode material for LIBs is lithium metal itself, offering an excellent theoretical capacity of 3860 mAh g^{-1} , yet the scarcity and uneven distribution of lithium in the Earth's crust precludes its more widespread utilization. Hence, "Beyond Li-ion" batteries featuring more readily available charge carriers are also being thoroughly investigated to address this concern. Potassium-ion batteries (KIBs) in particular are suitable alternatives as potassium is available globally and at roughly 1000 times the abundance of lithium. Similar to Li metal, K metal is seen as a promising anode material for KIBs, but its proliferation is hindered by the propensity for dendritic growth, difficulty in maintaining a robust solid electrolyte interphase (SEI), and loss

of material in the form of “dead potassium.” Further, the larger ionic radius of potassium ions as compared to lithium ions further strains the SEI and corresponding cathode electrolyte interphase (CEI) during repeated cycling. Strategies to mitigate these effects are thus of paramount importance in successful realization of K metal anodes for KIBs.

As the SEI is derived primarily by decomposition of the electrolyte, electrolyte-based methodologies are the most direct avenue for improving SEI stability and performance. Specifically, the formation of a mechanically robust inorganic SEI and CEI is key in protecting the electrolyte from further degradation throughout repeated plating/stripping on the metal anode and (de)intercalation of the cathode. Specifically, components such as KF that are produced via the decomposition of the fluorine-containing salt are instrumental in the composition of an SEI/CEI that are resistant to internal stresses. Thus, electrolyte solvents that enable preferential salt decomposition rather than organic solvent decomposition are preferred. Such behavior is governed by the solvation structure around the dissolved cations in the electrolyte, where maintaining the presence of salt anions in the solvation shell is critical for development of an inorganic SEI/CEI and is influenced by a variety of factors including the solvent dielectric constant ϵ and steric effects.

As compared to conventional carbonate-based electrolytes, ether-based electrolytes have been shown to promote such behavior to an increased degree in LIBs, but this effect remains comparatively unexplored in KIBs, especially paired with the K metal anode. This work demonstrates the efficacy of two cyclic ethers in enabling increased cycling stability and Coulombic efficiency against a K metal anode with regards to plating/stripping performance when compared against a typical carbonate-based electrolyte system. Further, these benefits extend to KIBs with a conventional Prussian blue cathode and K metal anode. These performance enhancements are correlated with the corresponding solvation structures, establishing a framework by which electrolyte solvents can be assessed with metal anodes and presents opportunities for further electrolyte design in other metal anode systems.

9:45 AM ES04.05.06

Probing The Redox-Mediation of Transition Metal Phthalocyanine in Metal-Air Battery Subhankar Mandal and Aninda J. Bhattacharyya; Indian Institute of Science, India

Metal air batteries have garnered significant attention as a potential alternative to Li-ion batteries due to their high theoretical energy. In lithium-air batteries, during the oxygen reduction reaction (ORR), O_2 is reduced to solid insulating LiO_2 , Li_2O_2 and in the reverse charge process, which is the oxygen evolution reaction (OER), discharge products convert back to O_2 and Li^+ . However, the practical implementation of Li- O_2 batteries has been hindered by several challenges, primarily due to the sluggish kinetics of ORR and OER. In recent times, a liquid-based redox mediator (@ electrocatalyst) has been demonstrated as an effective approach to increase battery efficiency and modify the reaction pathways to alleviate side reactions. In this presentation, we have systematically explored the solution-based redox mediation behaviour of first-row transition metal phthalocyanines for lithium-oxygen batteries. Our findings, based on experiment and theory, convincingly demonstrate that d^5 (Mn), d^7 (Co), and d^8 (Ni) configurations function better compared to d^6 (Fe) and d^9 (Cu) in redox mediation of the discharge and charge step. The d^{10} configuration (Zn) and non-d analogs (Mg) do not show any redox mediation because of the inability to binding to O_2 . During the discharge process, the Li_2O_2 coordinate with metal phthalocyanines and leads to a solution phase reaction pathway and reverse process controlled by the RM, thus confirming a bifunctional redox mediator. Apart from the reaction pathways predicted based on thermodynamic considerations, density functional theory calculations also reveal interesting effects of electrochemical perturbation on the redox mediation mechanisms and the role of the transition-metal centre. In addition, to account for the interaction between RM mediator and the discharge products ($KO_2(LiO_2)$, Li_2O_2) and parasitic products (Li_2CO_3 and $LiOH$), further spectroscopic and theoretical investigations were conducted. Our finding reveals that discharge/parasitic product coordinated to metal centre with the unfilled d orbital and oriented in between to M-N bond. In the case of filled d system, the discharge/parasitic products along the M-N bond and interacting with the imidazole moiety of the phthalocyanine ring leads to the poisoning the catalytic activity in battery performance.

10:00 AM BREAK

10:30 AM *ES04.05.07

Low-Coordinating Borate Electrolytes for Metal Batteries Tianbiao Liu; Utah State University, United States

Metal batteries (LMBs) are promising alternatives to state-of-the-art Lithium-ion batteries (LIBs) to achieve higher energy densities. I will present our effort in developing novel borate based electrolytes to enable stable, reversible metal deposition. I will first share our results in Mg borate electrolytes as one of the first examples of Cl-free electrolytes for Mg deposition. Borate anion designs can be extended to other metal ion electrolytes because of their structural tunability. I will discuss our recent results on developing Li and Ca based borate electrolytes for Li and Ca metal batteries. This presentation emphasizes the interplay of ion solvation and ion pairing in turning interfacial chemistry between a borate electrolyte and a metal anode.

References:

Luo, J. (co-1st author); Bi, Y. (co-1st author); Zhang, L.; Zhang, X.; Liu, T. L.* "A Stable, Non-corrosive Perfluorinated Pinacoloborate Mg Electrolyte for Rechargeable Mg Batteries", *Angew. Chem. Int. Ed.* 2019, 58, 6967-6971.
Nielson, K. V.; Luo, J.; Liu, T. L.* "Optimizing Calcium Electrolytes by Solvent Manipulation for Ca Batteries", *Batteries & Supercaps* 2020, 3, 768-772.

11:00 AM ES04.05.08

Computational Insights Elucidating The Effect of Additives on The Stability and Reversibility of Rechargeable Mg-Ion Batteries (RMBs) Rishabh D. Guha¹, Chang Li², Linda F. Nazar² and Kristin A. Persson^{1,3}; ¹Lawrence Berkeley National Laboratory, United States; ²University of Waterloo, Canada; ³University of California, Berkeley, United States

In the ever-evolving landscape of energy-storage, lithium-ion batteries (LIBs) have been the traditional workhorse since their launch in 1991; an event that ushered in the personal electronics revolution. However, as the demand for high-performance storage systems continues to surge, factors such as limited volumetric energy densities, finite global resources, and the environmental and human costs associated with lithium extraction underscore the urgent need for the development of alternative technologies for “next-generation” batteries. In theory, multivalent batteries employing Mg^{2+} or Ca^{2+} can achieve high-energy densities with metallic anodes, but the bottleneck with these systems is the discovery of compatible electrolytes which allows reversible intercalation and plating/stripping at the respective positive and negative electrodes. If we specifically look at Mg-ion batteries, the higher charge per-ionic center inhibits ionic mobility in the electrolyte and often leads to the formation of solvated species which are prone to decomposition at the electrode/electrolyte interface. The commercial deployment of RMBs relies on the development of novel and accessible electrolyte systems that minimize these parasitic reactions and exhibit stable, reversible cycling at normal operating conditions.

Utilizing computational insights from classical molecular dynamics (MD) and density functional theory (DFT), this presentation delves into the atomistic-scale phenomenon contributing to the overall poor performance in commercial non-aqueous magnesium electrolytes. It then outlines design strategies for developing novel electrolyte systems that address these shortcomings, emphasizing the impact of solvation structures on efficient Mg^{2+} desolvation and electrolyte decomposition at the anode. The simulations reveal that the introduction of electronegative additives emerges as the key to tailor the solvation structures for enhanced stability. We then discuss the experimental development of an organic electrolyte with an easily accessible magnesium salt which

corroborates these computational takeaways and demonstrates stable plating/stripping for a remarkable period of 8.3 months at a practical areal capacity of 2 mAh cm⁻². The presentation will be concluded with some brief highlights on a cost-effective electrolyte system where solvent engineering enables outstanding coulombic efficiency (99.96%) and fast electrodeposition of pure magnesium on copper substrates.

11:15 AM *ES04.05.09

First Principles Investigation into The Dynamics at Ca Anodes and Electrolyte Interfaces [Hashan C. Peiris](#) and Manuel Smeu; Binghamton University, The State University of New York, United States

Motivated by recent experimental progress, we have utilized an approach combining density functional theory (DFT) and ab initio molecular dynamics (AIMD) to gain atomistic perspectives into the dynamic processes governing anode-electrolyte interactions. First principles based molecular dynamics allow one to capture the bond-breaking/forming processes, and interfacial interactions between the anode and the electrolyte, while preserving theoretical accuracy independent of empirical parameterizations. The DFT approach allows one to study the charge transfer during reactions energetics, capture transition states, and evaluate the potential energy landscapes in detail.

The transition to sustainable energy systems is predominantly influenced by the effectiveness of energy storage technologies. While Li-ion batteries have been the industry standard, there is a growing interest in multivalent ion battery systems. These alternatives offer advantages such as higher storage capacities, abundant material resources, and reduced geopolitical risks. Specifically, Ca-ion batteries garner attention as a promising option for high-energy density, low-cost batteries. Still at a nascent stage of development, understanding the interactions between the electrolyte and the Ca anode at the interface is crucial for optimizing the performance of these emerging battery technologies.

To gain insights into the initial formation of the solid-electrolyte interphase (SEI) at the interface, we first looked into the decomposition of pure ethylene carbonate (EC) and an EC/Ca(ClO₄)₂ electrolyte on a Ca metal surface. We found that CaCO₃, CaO, and Ca(OH)₂ are the most common byproducts of the initial interfacial reactions. A fast two-electron reduction reaction producing CO₃²⁻ and C₂H₄ is found to be thermodynamically and kinetically favorable, while a reaction producing C₂H₄O₂²⁻ and CO takes precedence when multiple EC molecules are considered. Investigating the EC-based electrolyte decomposition at Li, Ca, and Al anode interfaces, we found that pure EC only decomposes to CO and C₂H₄O₂²⁻ species on each surface. However, upon the introduction of a salt molecule into the electrolyte, a second EC decomposition route resulting in the formation of CO₃²⁻ and C₂H₄ begins to occur. Li and Ca surfaces are more active in EC breakdown than Al due to the rate of charge transfer being much faster due to lower electronegativity and ionization energies.

Thereafter, we looked at the use of preformed solid electrolyte interphase (SEI) using Al₂O₃ to retard the interfacial reactions with the electrolyte (EC) in Ca anodes. The amorphous oxide layer was found to be thermodynamically stable while allowing for the diffusion of Ca through the layer. The oxide coating remained insulating up to the equilibrium stoichiometry. More significantly, the calcinated oxide layer slowed or prevented the decomposition of solvent molecules.

Lastly, we examined the ether and ester electrolyte stability on Ca anodes with different solvent and salt combinations. Tetrahydrofuran (THF) was observed to be the most stable relative to EC, even in a highly reductive environment. We attribute this to the charge distribution in THF on its backbone while the EC concentrates charge on its ester oxygens and carbonyl carbon, resulting in decomposition. We find Ca(BH₄)₂ and THF to be the most stable solution in our investigation, corroborating experimental evidence of its suitability as a CIB electrolyte.

More recently, inspired by the recent advances in machine learning-assisted techniques for computational materials research, we have been actively investigating the interactions of Ca metal anodes with S-based cathodes. We report on our current progress in modeling the Ca anode interactions with polysulfides.

SESSION ES04.06: Li-ion and Li metal
Session Chairs: Tao Gao and Yirui Zhang
Thursday Afternoon, April 25, 2024
Room 422, Level 4, Summit

1:30 PM ES04.06.01

Investigating Large Deformation and Amorphous Intermediates in Sb Electrodes [Ananya Renuka Balakrishna](#) and Tao Zhang; University of California, Santa Barbara, United States

The key objective is to provide insight into how amorphous intermediates that form in high-capacity anodes during electrochemical cycling accommodate large volume changes and prevent microcracking in Antimony (Sb) electrodes. The electrochemical cycling of alloy anodes introduces an abrupt crystalline to amorphous structural transformation (in Na-based electrodes). This transformation, in turn, is accompanied by anisotropic volume expansion (>100%), abrupt changes to elastic stiffness, and an alteration to the Na-diffusion kinetics and alloying-reaction pathways. We hypothesize that these sudden changes to intrinsic material properties alter local stress distributions and phase transformation pathways in high-capacity anodes, which contributes to their characteristic mechanical response. We are developing a theoretical framework to understand the energy dissipation and deformation mechanism in large-volume change electrodes and to use these mechanistic insights to guide materials design.

1:45 PM *ES04.06.02

Quantifying Li Plating on Graphite during Fast Charging of Li-Ion Batteries [Bryan D. McCloskey](#); University of California-Berkeley, United States

Li-ion battery fast charge is limited due to challenges posed by lithium plating on the graphite anode, whereby the large overvoltage necessary to drive high Li⁺ insertion rates instead results in favorable thermodynamic conditions for Li metal deposition on the graphite surface. Li plating is difficult to detect, particularly in small quantities, and results in safety risks and capacity fade due to lithium metal's high reactivity with conventional electrolytes. Here, we present our efforts to develop both chemical and electrochemical methods to precisely quantify Li plating and detect the state-of-charge (SOC) onset of lithium plating on graphite electrodes during constant current fast charging. We will discuss titration mass spectrometry (TiMS), a highly sensitive (~20 nmol resolution, or 0.5 mAh of plated Li) chemical analysis where gases evolved from harvested graphite electrodes immersed in acid are used to quantify various solid electrolyte interphase species, including electrically isolated (inactive) Li metal.¹ TiMS is then used to determine the precise onset of Li plating and to distinguish between the various capacity fade mechanisms that arise during fast charge.² We then will discuss the use of simple

electrochemical cycling techniques to quantify irreversible Li plating in Li/Graphite half-cells as a function of energy density (electrode thickness), charge rate, temperature, and SOC.³ Similar methods are developed to quantify in-situ Li plating for commercially relevant Graphite/LiNi_{0.5}Mn_{0.3}Co_{0.2}O₂ (NMC) cells. In combination, all of these techniques provide a highly accurate measure of the onset of Li plating and quantitative insight into capacity losses during fast charging.

1. McShane, E. J.; Colclasure, A. M.; Brown, D. E.; Konz, Z. M.; Smith, K.; McCloskey, B. D., Quantification of inactive lithium and solid–electrolyte interphase species on graphite electrodes after fast charging. *ACS Energy Lett.* **2020**, 5 (6), 2045-2051.
2. McShane, E. J.; Bergstrom, H. K.; Weddle, P. J.; Brown, D. E.; Colclasure, A. M.; McCloskey, B. D., Quantifying graphite solid-electrolyte interphase chemistry and its impact on fast charging. *ACS Energy Lett.* **2022**, 7 (8), 2734-2744.
3. Konz, Z. M.; Wirtz, B. M.; Verma, A.; Huang, T.-Y.; Bergstrom, H. K.; Crafton, M. J.; Brown, D. E.; McShane, E. J.; Colclasure, A. M.; McCloskey, B. D., High-throughput Li plating quantification for fast-charging battery design. *Nature Energy* **2023**, 8 (5), 450-461.

2:15 PM ES04.06.03

Reaction and Ionic Migration at The Electrode-Electrolyte Interface in Solid State Batteries from Machine Learning Molecular Dynamics
Jingxuan Ding, Albert Musaelian, Yu Xie, Menghang (David) Wang, Laura Zichi, Anders Johansson, Simon L. Bätzner and Boris Kozinsky; Harvard University, United States

Atomistic-level understanding of the chemical reactions forming the solid-electrolyte interphase (SEI) in solid-state lithium batteries has remained challenging, primarily due to the limited resolution in experimental techniques and the insufficient accuracy in large-scale simulations. In this work, we combine on-the-fly active learning based on Gaussian Process regression (FLARE) with local equivariant neural network interatomic potentials (Allegro) to construct a machine-learning force field (MLFF) to perform large-scale long-time explicit reactive simulation of a complete symmetric battery cell with ab initio accuracy. The MLFF is validated with experimental values of mechanical properties of bulk lithium and diffusion coefficient of solid electrolyte. For the symmetric battery, we observe prominent fast reactions at the interface and characterize the dominant reaction products along with their evolution time scales, using unsupervised learning techniques based on atomic geometry descriptors. Our simulation reveals the kinetics and the passivation involved in the chemical reaction responsible for the SEI formation. The methods in this study are promising for acceleration analysis of atomistic mechanisms in complicated heterogeneous systems and provide design insights for the development of solid-state batteries.

2:30 PM ES04.06.04

Understanding Lithium Plating from Solid and Liquid Electrolytes Using Dynamic Impedance Spectroscopy Robert L. Sacci¹, Zhiao Yu², Ritu Sahore¹, Andrew S. Westover¹ and Zhenan Bao²; ¹Oak Ridge National Lab, United States; ²Stanford University, United States

A potential strategy for increasing energy density of lithium batteries is to implement the so-called anode-free design. Here, the lithium metal anode is solely sourced from the cathode, traveling through the electrolyte. However, such Li batteries suffer from short cycle life due to lithium loss from passivation layer formation (solid-electrolyte interphase), which require multiple cycles to stabilize. Anode-free batteries are required to have high Li metal coulombic efficiencies over the whole cycling life, particularly during the initial activation cycles. A holistic approach to electrolyte design, mechanism understanding, and battery engineering is needed to fulfill these requirements.

We used dynamic electrochemical impedance spectroscopy (dEIS) to probe the formation and evolution of the SEI during Li plating and stripping on copper current collectors. dEIS superimposes a multisine waveform atop the applied charge and discharge current. We applied a sliding window fast Fourier transform protocol that converts the complex ratio of the measured potential and current signals into complex impedance. We will discuss two Li plating systems, Lipon (an amorphous ceramic) and a liquid electrolyte with stabilizing additives. We observed drastic changes in the cells' impedance during plating and stripping. We will show how the passivation layer's impedance continues to evolve during Li cycling and accounts for a significant amount of the overall cell resistance. This knowledge enables us to predict the relative length of cycle life without long term continual measurements.

The US Department of Energy's Energy Efficiency and Renewable Energy Vehicles Technologies Office provided funding for this work under the US-German Cooperation on Energy Storage: Lithium-Solid-Electrolyte Interfaces program.

2:45 PM BREAK

3:15 PM ES04.06.05

Designing Stable Li Metal as Anode Electrode in Lithium Metal Batteries Junjie Niu; University of Wisconsin--Milwaukee, United States

Rapid increasing demand on electrical vehicles and portable electronic devices place expectation of battery with energy density at 400-500 Wh/kg or higher. Developing stable Li metal anode for both liquid and solid-state electrolyte based battery systems is critical to achieve this goal. Metallic lithium has the highest theoretical specific capacity of 3860 mAh/g and lowest electrochemical potentials of -3.04V versus the standard hydrogen electrode. However, the uncontrollable solid electrolyte interphase (SEI) and growth of mossy/dendritic Li induced safety concerns as well as low coulombic efficiency. Several strategies on stabilizing the Li metal-electrolyte interface have been reported such as adding electrolyte additives, constructing Li host for uniform Li deposition and regulating Li ion flux, and developing artificial SEI for Li metal-electrolyte interfacial stabilization.

Here I will talk about our recent progress in designing stable Li metal anode electrode by using a series of surface modifications. A polymer functionalized monolayer MXene shows better lithium regulation during plating and stripping process. Meanwhile, a dual-layer interphase that consists of an *in-situ* formed lithium carboxylate organic layer and an ultra-thin BF₃-doped monolayer MXene on Li metal surface was designed. The honeycomb-structured organic layer increases the wetting of electrolyte due to the large surface area, leading to a thin SEI. As a comparison, the MXene stacks coated on thin Li via rolling process also displayed uniform Li deposition/dissolution and suppressed dendrite growth. The battery displayed a high capacity retention under lean electrolyte condition. These results indicate that a reliable Li metal anode with dendrite suppression can be achieved by coating well-functionalized 2D materials.

References:

Mingwei Shang, Osman Shovon, Francis Wong, Junjie Niu. A BF₃-Doped MXene Dual-Layer Interphase For Reliable Lithium Metal Anode. *Advanced Materials*, 35 (2023) 2210111.

X Chen, M Shang, Junjie Niu. Pre-Solid Electrolyte Interphase-Covered Li Metal Anode with Improved Electro-Chemo-Mechanical Reliability in High-Energy-Density Batteries. *ACS Applied Materials & Interfaces*, 13 (2021) 34064-34071.

Z Hood, X Chen, R Sacci, X Liu, G Veith, Y Mo, Junjie Niu, N Dudney, M Chi. Elucidating Interfacial Stability Between Lithium Metal Anode and LiPON via in-situ Electron Microscopy. *Nano Letters*, 21 (2021) 151-157.

X Li, Y Zheng, Y Duan, M Shang, Junjie Niu, C Li. Designing Comb-Chain Crosslinker-Based Solid Polymer Electrolytes for Additive-Free All-Solid-State Lithium Metal Batteries. *Nano Letters*, 20 (2020), 6914-6921.

X Chen, M Shang, Junjie Niu. Inter-layer-calated Thin Li Metal Electrode With Improved Battery Capacity Retention and Dendrite Suppression. *Nano*

Letters, 20 (2020), 2639-2646.

M Shang, X Chen, B Li, Junjie Niu. A Fast Charge/Discharge and Wide-Temperature Battery with Germanium Oxide Layer on TiCA₃ MXene Matrix as Anode. *ACS Nano*, 14 (2020), 3678-3686.

X Chen, Y Lv, M Shang, Junjie Niu. Iron Controllable Lithium into Lithiotropic Carbon Fiber Fabric: a Novel Li Metal Anode with Improved Cyclability and Dendrite Suppression. *ACS Applied Materials & Interfaces*, 11 (2019), 21584-21592.

3:30 PM ES04.06.06

Proximity Matters: Interfacial Solvation Dictates Solid Electrolyte Interphase Composition Solomon Oyakhire^{1,2}, Yi Cui¹ and Stacey F. Bent¹;

¹Stanford University, United States; ²University of California, Berkeley, United States

The composition of the solid electrolyte interphase (SEI) plays a crucial role in controlling lithium-electrolyte reactions, yet the underlying cause of SEI composition differences between electrolytes remains unclear. Many studies have correlated SEI composition with the bulk solvation of Li ions in electrolytes, but this correlation does not fully capture the interfacial phenomenon of SEI formation. In our work, we present a direct mechanistic relationship between SEI composition and Li-ion solvation by forming SEIs using polar substrates that modify interfacial solvation structures. We avoid the deposition of Li metal by forming the SEI above the Li⁺/Li redox potential. Using theory and spectroscopy, we demonstrate that an increase in the probability density of anions near a polar substrate enhances anion incorporation within the SEI, establishing a direct correlation between interfacial solvation and SEI composition. We demonstrate the generalizability of this SEI-solvation correlation using three distinct classes of electrolytes. Finally, we employ this concept to generate stable, anion-rich SEIs, leading to high-performance lithium metal batteries. In summary, our work clarifies the mechanistic relationship between electrolyte solvation and SEI composition, resulting in a discovery that can be applied to the design of improved lithium metal batteries.

3:45 PM ES04.06.07

Stabilizing Anode/Electrolyte Interface in Li-O₂ Batteries by Molecular Sieves Huiping Wu, Xinbin Wu, Shundong Guan and Liangliang Li; Tsinghua University, China

Lithium-oxygen (Li-O₂) batteries with an ultra-high theoretical specific energy (3500 Wh kg⁻¹) has recently attracted enormous attention. Due to the difficulty in decomposing discharge product Li₂O₂, the charging overpotential of Li-O₂ batteries is high, which provokes parasitic reactions and worsens the cycling stability of the batteries. Redox mediators (RMs) are widely used to decrease the charging overpotential by altering the electrochemical processes in Li-O₂ batteries. However, unwanted side reactions between RMs and Li metal anode may severely damage both the anode and the RMs; therefore, it is necessary to suppress the shuttle effect of RMs to extend the lifespan of Li-O₂ batteries. To improve the interfacial stability of the Li anode, 4A zeolite, a molecular sieve with a narrow aperture size of ~ 0.4 nm, was used to restrain the diffusion of RMs in this work. A polymer membrane containing 4A zeolite was synthesized to evaluate the performance of the molecular sieve. With the membrane, the Li-O₂ batteries with 2,2,6,6-tetramethylpiperidinyloxy (TEMPO) as the RM showed greatly improved performance. The charging overpotentials were kept at low levels and the cycle life of the batteries was extended eight times. The results from Raman spectroscopy indicated that the small pores of 4A zeolite physically blocked the movement of TEMPO, thus stabilizing the interface between the Li anode and the electrolyte. Furthermore, lithiated 4A zeolite was directly coated on the surface of the Li anode to study its effectiveness in suppressing the shuttle effect of RMs. The protective layer composed of lithiated 4A zeolite not only suppressed the shuttle effect of TEMPO, but also reduced the formation of Li dendrites. As a consequence, the cycle life of Li-O₂ batteries was prolonged more than ten times and the full-discharge capacity of the batteries at room temperature was greatly enhanced. In summary, with the assistance of 4A zeolite-typed molecular sieves, it is promising to fabricate interface-stable, high-energy-density, and long-cycle-life Li-O₂ batteries.

4:00 PM *ES04.06.08

Spatially Resolved Operando Synchrotron Studies of Li Metal Anode Stripping and Plating - Heterogeneity and Correlations with Cathode Performance Peter Khalifah^{1,2}; ¹Stony Brook University, United States; ²Brookhaven National Laboratory, United States

Operando high energy lateral mapping (HELM) synchrotron diffraction studies have been used to carry out spatially resolved studies of the stripping and plating of Li metal anodes during battery cycling. Although it is very challenging to directly quantify the signal from Li metal layers that are only a few microns thick, this can be accomplished when the data collection is carried out in a carefully designed experiment at a modern synchrotron source and the subsequent Rietveld refinements are performed with suitably constrained structural models. In this manner, we have been able to interrogate the heterogeneity that develops during the cycling of "anode-free" pouch cell batteries with different metals used as the current collector. Furthermore, our data has enabled us to identify correlations between the heterogeneity in the anode and the cathode as well as to better understand the effect of this heterogeneity on the local current densities at different regions of the anode. Our synchrotron measurements probe local variations in electrochemical performance that cannot be resolved through traditional electrochemical testing, thereby providing novel insights into processes contributing to the loss of capacity and the reduction in the lifetime of pouch cell batteries.

4:30 PM ES04.06.09

Materials Processing to Create Fibrous Structures and its Application to Battery Manufacturing Jae Chul Kim; Stevens Institute of Technology, United States

We have developed electrospinning-based manufacturing processing applicable for battery systems that involve metallic lithium. With manufacturing feasibility, electrospinning is a widely used to create nano- and micro-porous layers of functional fibers. The electrospinning-produced layers can afford a wide variety of functionalities applicable to biomedical templates, separation membranes, and energy storage by tailoring fiber compositions. However, its manufacturing capability is limited at producing randomly-oriented fibrous structures. Topology and tortuosity of the electrospun fibers are poorly controlled, making it difficult to systematically investigate structure-property relationships for any given applications, especially electrochemical systems.

In this presentation, we will demonstrate how to we have obtained precise geometrical control of fiber construction by advancing the electrospinning method. Unlike conventional electrospinning, our approach employs a mobile stage that allows alignment of fibers. Produced fibrous structures will be used to construct the anode current collectors of an anode-free battery, one of the most promising energy-dense batteries beyond the Li-ion. While incorporating Li metal has proven difficult due to uncontrolled dendrite growth upon repetitive Li plating and stripping, we found that the anode current collector reinforced by the three-dimensional fibrous structure enhances Li storage efficiency over the extended number of cycles, compared to the planar current collector. We will discuss the effect of fiber compositions and controlled geometrical configurations on stabilizing Li plating and stripping morphologies to suppress Li dendrite growth. We will also provide a cell design principle to fundamentally extend the cycle life of anode-free batteries. Significantly, we consider that battery manufacturing advanced by this work will offer a systematic strategy to develop next-generation energy storage systems for a sustainable energy future.

SESSION ES04.07: Poster Session II
Session Chairs: Tao Gao and Wu Xu
Thursday Afternoon, April 25, 2024
Flex Hall C, Level 2, Summit

5:00 PM ES04.07.01

Excellent Reaction Kinetics and Low-Temperature Adaptability of Zinc Batteries Enabled by Water-Acetamide Symbiotic Solvation Sheath Shuyun Wang¹, Shengmei Chen¹, Yiran Ying², Gang Li³, Haipeng Wang⁴, Ka Kiu Keith Cheung¹, Qingjun Meng⁵, Haitao Huang², Longtao Ma⁶ and Juan Antonio Zapien¹; ¹City University of Hong Kong, Hong Kong; ²The Hong Kong Polytechnic University, China; ³Northwestern Polytechnical University, China; ⁴Yantai University, China; ⁵Shaanxi University of Science and Technology, China; ⁶South China University of Technology, China

Although rechargeable aqueous zinc batteries are cost effectiveness, intrinsic safety, and high activity, they are also known for bringing rampant hydrogen evolution reaction and corrosion. While eutectic electrolytes can effectively eliminate these issues, its high viscosity severely reduces the mobility of Zn^{2+} ions and exhibits poor temperature adaptability. Here, we infuse acetamide molecules with Lewis base and hydrogen bond donors into a solvated shell of $Zn[(H_2O)_6]^{2+}$ to create $Zn(H_2O)_3(ace)(BF_4)_2$. The viscosity of 1ace-1H₂O is 0.032 Pa s, significantly lower than that of 1ace-0H₂O (995.6 Pa s), which improves ionic conductivity (9.56 mS cm⁻¹) and shows lower freezing point of -45 °C, as opposed to 1ace-0H₂O of 4.04 mS cm⁻¹ and 12 °C, respectively. The acidity of 1ace-1H₂O is ~2.8, higher than 0ace-1H₂O at ~0.76, making side reactions less likely. Furthermore, benefiting from the ZnCO₃/ZnF₂-rich organic/inorganic solid electrolyte interface, the Zn||Zn cells cycle more than 1300 hours at 1 mA cm⁻², and the Zn||Cu operate over 1800 cycles with an average Coulomb efficiency of ~99.8%. The Zn||PANI cell cycles over 8500 cycles, with a specific capacity of 99.8 mAh g⁻¹ at 5 A g⁻¹ at room temperature, and operated at -40 °C with a capacity of 66.8 mAh g⁻¹.

5:00 PM ES04.07.02

Carbide-Mediated Catalytic Hydrogenolysis: Defective Carbonaceous Lithium Host for Liquid-Electrolyte and All-Solid-State Lithium Metal Batteries Namhyeong Kim¹ and Hyungyeon Cha²; ¹Pukyong National University, Korea (the Republic of); ²Ulsan National Institute of Science and Technology, Korea (the Republic of)

Commercial lithium-ion batteries based on intercalation carbonaceous anodes are reaching their limit in energy density due to the limitation of theoretical capacity of electrode materials. In this regard, lithium metal is an ideal anode owing to its high specific capacity. However, the practical use of the Li metal is still challenging. The Li metal anode suffers from dendrite formation, volume change, and severe side reactions, which lead to fatal safety issues and cell degradation.

Here, we propose a defective graphene shell grown on a carbon matrix as a stable lithium metal host via carbide-mediated catalytic hydrogenolysis. Unlike conventional carbon hydrogenolysis, the carbide-mediated hydrogenolysis provides not only channelling reaction but also the graphene shell with defects. These defects and nano-channels effectively mitigate the Li nucleation overpotential and achieve a stable cycle life with a comparable volume change with that of commercial graphite. Due to these features, the host exhibits good cycle stability (87.2% after 500 cycles) and low dimension variation (9 μm) in carbonate electrolyte full-cell evaluations. In addition to its good performances in the carbonate electrolyte, our versatile Li host, acting as a Li-ion flux regulating interlayer, also achieves an improved cycling performance in the argyrodite Li₆PS₅Cl based high energy density all-solid-state battery full-cell configuration.

5:00 PM ES04.07.03

Regulation of Outer Solvation Shell toward Superior Low-Temperature Aqueous Zinc-Ion Batteries Qianyi Ma, Zhongwei Chen and Aiping Yu; University of Waterloo, Canada

Aqueous Zn-ion batteries are well regarded among the next-generation energy storage technologies due to their low cost and high safety. However, the unstable stripping/plating process leading to severe dendrite growth under high current density and low temperature impedes their practical application. Herein, we demonstrate that the addition of 2-propanol can regulate the outer solvation shell structure of Zn^{2+} by replacing water molecules to establish a "eutectic solvation shell," which provides strong affinity with the Zn (101) crystalline plane and fast desolvation kinetics during the plating process, rendering homogeneous Zn deposition without dendrite formation. As a result, the Zn anode exhibits promising cycle stability over 500 hours under an elevated current density of 15 mA cm⁻² and a high depth of discharge of 51.2%. Furthermore, remarkable electrochemical performance was achieved in a 150 mAh Zn|V₂O₅ pouch cell over 1000 cycles at a low temperature of -20 °C. This work offers a new strategy to achieve the excellent performance of aqueous Zn-ion batteries under harsh conditions. It reveals electrolyte structure designs that can be applied in related energy storage and conversion fields.

Keywords: energy storage, solvation structure, aqueous Zn ion batteries, DOD

5:00 PM ES04.07.04

RF Sputtered Tungsten Oxide Based Electrochromic Devices for Energy Efficient Smart Window Applications Sang Ji Kim¹, Usha Krishnan Sundaram¹, Jin Young Hwang², Hyeon Dong Kim¹ and Sangyeol S. Lee¹; ¹Gachon University, Korea (the Republic of); ²Korea University, Korea (the Republic of)

In light of the global energy crisis and increasing environmental problems, reducing building energy consumption has become more important than ever. About 30 to 40% of the world's primary energy is used for heating, cooling, ventilation, and appliances in buildings. A smart glass window an electrochromic device, which works on electrochromism is a promising way to convert and save renewable energy because they have a high chromatic contrast, are affordable and are environmentally benign. Tungsten oxide based thin films were fabricated on ITO precoated substrate via RF magnetron sputtering technique. The film exhibited a maximum transmittance of 83%. SEM analysis revealed the uniform, and crack-free surface, revealing the low roughness of the thin film. The film exhibited smooth morphology with fine grains distributed evenly over the surface. Based on the electrochromic analysis, WO₃ thin films, showed larger optical modulation (ΔT) of 76%. We hope that this research sets the stage for developing high-performance electrochromic smart windows.

5:00 PM ES04.07.05

N, S-Doped Graphene Quantum Dots for Affordable and High-Performance Aqueous Zinc-Ion Battery Anna Chen¹, Qianyi Ma², Tingzhou Yang² and Michael Fowler²; ¹Laurel Heights Secondary School, Canada; ²University of Waterloo, Canada

The exorbitant costs linked to cutting-edge energy storage technologies, exemplified by lithium-ion batteries, present formidable obstacles to the widespread adoption and maintenance of new energy vehicles. As a result, there is an urgent call to expedite the development of the next generation of energy storage technology—one marked by both low cost and high performance. Aqueous zinc-ion batteries (AZIBs) have emerged as promising

candidates, offering an enticing blend of affordability and superior performance, positioning them as pivotal contenders for next-generation energy storage solutions. Nevertheless, the practical application of AZIBs faces significant challenges due to spontaneous surface corrosion and uncontrolled dendrite growth.

In pursuing a pragmatic solution while upholding cost efficiency, we propose a design strategy that involves N, S-doped graphene quantum dots (GQDs) derived from lemons and kitchen soda sources. This innovative approach aims to fabricate high-performance AZIBs. The introduction of GQDs serves a dual purpose: 1. it promotes the uniform distribution of zinc flux across the anode surface. 2. it mitigates the side reaction between the Zn anode and electrolyte. This optimization technique has the potential to substantially enhance the appeal and cost-effectiveness of the new high-performance battery energy storage technology.

Keywords: energy storage, nanomaterials, GQDs, aqueous Zn ion batteries

5:00 PM ES04.07.06

Enhancing Lithium-Ion Battery Safety in Hybrid Energy Systems: The Role of Triphenyl Phosphate (TPP) in Electrode/Solvent Dynamics and Fire Mitigation [Fernando Soto](#); The Pennsylvania State University, United States

Lithium-ion batteries (LiBs) are key in sustainable energy solutions such as Power-to-X (P2X). Their high energy density, long cycle life, and declining costs have made them especially appealing for broader deployments (1). However, with these advantages come inherent risks, particularly those associated with thermal runaway and potential fire hazards (2-3). Recent advances and the push for higher energy densities have led to the introduction of new materials and chemistries within LiBs (4). But these modifications, while enhancing performance, can sometimes exacerbate the underlying risks, especially when exposed to real-world conditions like extreme temperatures or physical damage.

This research focuses on Triphenyl Phosphate (TPP) as a flame retardant to enhance LiBs safety in hybrid energy systems. TPP's potential in mitigating fire risks without significantly impacting battery performance is examined. The study utilizes density functional theory (DFT)-based molecular dynamics simulations to explore the interactions of TPP with lithium surfaces and the implications for the Solid Electrolyte Interphase (SEI) layer. We present three computational models to analyze TPP's influence on LiB safety at high temperatures, simulating scenarios with and without TPP. The results reveal TPP's potential in stabilizing thermal degradation products and reducing gas evolution during thermal stress. The study also investigates TPP's impact on the SEI layer's formation and structure, critical to LiBs performance and safety.

The findings suggest that TPP could serve as an effective additive in LiBs, particularly in complex, interconnected hybrid energy systems, offering a safer and more reliable energy storage solution. This research bridges knowledge gaps about TPP's role in LiBs and paves the way for designing safer batteries in the context of evolving energy storage demands.

References

- (1) D. Stampatori, P.P. Raimondi, M. Noussan, Li-Ion Batteries: A Review of a Key Technology for Transport Decarbonization, *Energies*, 13 (2020) 2638.
- (2) Q. Wang, P. Ping, X. Zhao, G. Chu, J. Sun, C. Chen, Thermal runaway caused fire and explosion of lithium ion battery, *Journal of power sources*, 208 (2012) 210-224.
- (3) C. Un, K. Aydin, Thermal runaway and fire suppression applications for different types of lithium ion batteries, *Vehicles*, 3 (2021) 480-497.
- (4) K. Chayambuka, G. Mulder, D.L. Danilov, P.H. Notten, From li-ion batteries toward Na-ion chemistries: challenges and opportunities, *Advanced energy materials*, 10 (2020) 2001310.

5:00 PM ES04.07.07

Free-Standing Conversion-Type Ceramic Nanowire Interlayers towards Stable Lithium Metal Batteries [Kaixi Chen](#)¹, Wenbin Fu^{1,2}, Fujia Wang¹ and Gleb Yushin^{1,2}; ¹Georgia Institute of Technology, United States; ²Sila Nanotechnologies Inc., United States

Today, the growing demand for electric vehicles and consumer electronics necessitates the development of batteries with higher energy efficiency and lower costs [1]. Utilizing lithium metal anodes allows lithium batteries to provide a substantially higher energy density (3860 mAh g⁻¹) compared to those built with conventional anodes. However, crucial issues associated with Li metal anodes remain unresolved. Particularly, a major challenge is the development of lithium dendrites, which have the potential to induce short circuits and present significant safety risks [2].

To mitigate this issue, we introduce a novel design featuring a self-supporting conversion nanowire membrane, serving as a transformative interlayer to modulate lithium deposition, facilitating the development of stable and secure lithium metal batteries. This conversion interlayer is capable of producing a LiF-rich interface *in-situ* to guide heterogeneous lithium nucleation, fuse deposited lithium and suppress lithium dendrite growth regardless of electrolyte. When this interlayer is incorporated, Li metal full cells coupling with both LiFePO₄ (LFP) and LiNi_{0.8}Co_{0.1}Mn_{0.1}O₂ (NMC 811) cathodes exhibit substantially reduced capacity deterioration compared to those with bare Cu. Our results demonstrate that using a conversion nanowire interlayer offers significant promise for creating safe and high-energy lithium metal batteries.

[1] K. Turcheniuk, D. Bondarev, G. G. Amatucci, G. Yushin, *Materials Today* 2021, 42, 57.

[2] J. Liu, Z. Bao, Y. Cui, E. J. Dufek, J. B. Goodenough, P. Khalifah, Q. Li, B. Y. Liaw, P. Liu, A. Manthiram, Y. S. Meng, V. R. Subramanian, M. F. Toney, V. V. Viswanathan, M. S. Whittingham, J. Xiao, W. Xu, J. Yang, X.-Q. Yang, J.-G. Zhang, *Nature Energy* 2019, 4, 180.

5:00 PM ES04.07.09

Laminated Tin-Aluminum Anodes to Build Practical Aqueous Aluminum Batteries [Beier Jia](#) and Qingyu Yan; Nanyang Technological University, Singapore

Aqueous aluminum metal batteries (AAMBs) have emerged as promising energy storage devices, leveraging the abundance of Al and their high energy density. However, AAMBs face challenges such as unsuccessful Al deposition during charging or poor anode reversibility, passivation layer formation, and the competing hydrogen evolution reaction (HER). A promising approach to alleviate these issues is introducing foreign metals to interact with Al. In this study, Sn is selected for its appropriate standard reduction potential (-0.13 V), work function (4.42 eV), and compatibility with Al, facilitating Al underpotential deposition and enhancing anode reversibility. We first determine the feasibility of Al deposition on Sn substrate after three-electrode testing, which, however, results in low capacity. To increase the contact interface between Sn and Al and thereby improve capacity, we employ a scalable folding and rolling method to prepare Sn-Al laminate electrodes (Sn@Al). The Sn@Al heterostructure can effectively suppress Al passivation, reducing internal resistance. The Sn@Al electrodes demonstrate stable cycling for over 900 h in symmetric cells and superior performance in full cells when coupled with Al₂MnO₂ or KNHCF cathodes. To further enhance Sn@Al anodes, a polymer coating is applied to suppress HER. After 700 cycles, the p-Sn@Al|KNHCF cell shows 82% capacity retention compared to the 10th cycle. This study presents a strategy for designing effective and low-cost anodes for AAMBs and may provide insights into developing metal anodes for other aqueous batteries.

5:00 PM ES04.07.10

Facile Solvothermal Synthesis of Binder Free 1T-VS₂/MXene Hybrid Electrode Materials for Li-Ion Batteries [Rahul S. Ingle](#)¹, Kwangjun Kim¹, Minwook Kim¹, Yongtae Kim¹, Snehal L. Kadam² and Jong G. Ok^{1,1}; ¹Seoul National University of Science and Technology, Korea (the Republic of); ²Seoul National University, Korea (the Republic of)

The development of high-capacity batteries has become crucial to meet the growing demands for modern electric applications like electric vehicles, smartphones, and various smart wearable devices. However, their widespread adoption of Li-ion batteries is hindered due to the limited capacity, low energy density, poor cycling stability, and high cost of traditional electrode materials. To resolve these challenges continuous design and development of novel electrode materials are required. Due to their unique properties, transition metal chalcogenides (TMCs) and MXene hybrid composite materials have emerged as promising electrode materials for high-capacity Li-ion batteries. In this study, we explore the facile solvothermal synthesis of binder-free 1T-VS₂/MXene hybrid electrode materials for high-capacity Li-ion battery applications. The facile solvothermal synthesis offers several advantages, including simplicity, binder-free, cost-effectiveness, and scalability. It involves the simultaneous growth of 1T-VS₂ and MXene nanosheets within a single reaction vessel, resulting in a homogeneous growth of 1T-VS₂ on the MXene sheets. This method eliminates the need for separate synthesis and post-deposition steps, restructuring the fabrication process and improving the efficiency of electrode materials. The 1T-VS₂ decorated MXene serves various roles in the hybrid composite, firstly they act as conductive pathways, facilitating electron transport and reducing internal resistances. This results in enhanced charge/discharge rates and improved power density of the electrode material. Additionally, MXene provides mechanical stability to the fragile VS₂ nanoparticles, preventing agglomeration and ensuring long-term stability. The electrochemical properties of the binder-free 1T-VS₂/MXene hybrid electrode materials were systematically investigated using several techniques such as voltammetry, galvanostatic charge-discharge, C-rate, stability, and electrochemical impedance spectroscopy. The results demonstrated significant improvements in electrochemical performance compared to pure VS₂ electrodes. The hybrid composite electrodes revealed high capacity, improved rate performance, and excellent cycling stability. The binder-free 1T-VS₂/MXene hybrid electrode materials' enhanced electrochemical performance can justify the VS₂ and MXene synergistic effects. The MXene provides high conductivity, efficient ion diffusion, and structural stability, while the VS₂ nanoparticles offer large redox sites and high energy density. The amalgamation of these properties results from a well-balanced electrode material with improved Li-ion battery performance.

Keywords: 1T-VS₂/MXene hybrids, facile solvothermal, high-capacity, Li-ion battery

Acknowledgments:

This work was supported by the National Research Foundation of Korea (NRF) grants (No. 2021M3H4A3A02099204, and 2022M3C1A3081178 (Ministry of Science and ICT) and No. 2022R111A2073224 (Ministry of Education)) funded by the Korean Government.

5:00 PM ES04.07.11

Ag-Loaded Hollow Carbon Framework for Stable Anode-Free Li Metal Batteries [Jong Hun Sung](#) and Jong-Sung Yu; Daegu Gyeongbuk Institute of Science and Technology, Korea (the Republic of)

Anode-free lithium (Li) metal batteries are recognized as one of the most efficient battery systems with full merits of high capacity (3860 mAh g⁻¹) and low operating potential (-3.04 V vs standard hydrogen electrode) of Li. Removing the Li anode from rechargeable batteries can increase energy density and lower production costs. However, without continuous Li supply in the anode side, the anode-free design encounters huge challenges against high cycle stability. Herein, an N-doped hollow carbon framework (HCF) derived from zeolitic imidazolate framework (ZIF) is loaded with silver (Ag) as a lithiophilic element, and the resulting Ag@HCF casted on a copper (Cu) current collector (Ag@HCF/Cu) is proposed for stable Li deposition to achieve the long-term cycle life in anode-free batteries. The HCF has several advantages of N-doping, low weight, high specific surface area, and high electrical conductivity, which can help provide uniform Li nucleation and plating reaction and minimize energy density loss. In addition, Ag@HCF can effectively suppress the Li dendrite growth through uniform distribution of electrons. In this study, the Ag@HCF/Cu, which is prepared using in-situ Li plating reaction delivers the low nucleation overpotential, reduced voltage hysteresis, and high average coulombic efficiency (ACE) at high current density up to 4 mA cm⁻² under 4 mAh cm⁻². Furthermore, in a full cell system which is assembled with LiNi_{0.5}Co_{0.2}Mn_{0.3}O₂ (NCM) cathode of 4 mAh cm⁻² scale, Ag@HCF/Cu||NCM cell reveals superior capacity retentions of 80.9% for 100 cycles and 66.0% for 300 cycles, which can become an effective cornerstone for stable anode-free Li metal batteries.

5:00 PM ES04.07.12

Enhancing Zn-Ion Battery Performance with Thioacetamide Electrolyte Additive [Minji Yeo](#)¹, Yujin Kim¹, Jihoon Kim¹, Sukeun Yoon¹ and Kuk Young Cho²; ¹Kongju National University, Korea (the Republic of); ²Hanyang University, Korea (the Republic of)

Zn-ion batteries (ZIBs) are emerging as a next-generation energy storage solution, characterized by enhanced safety, cost-effectiveness, and a more abundant resource base compared to their flammable, naturally occurring counterparts. Distinctively, ZIBs employ a Zn-metal anode and a Zn-ion (Zn²⁺) storage cathode, resulting in a substantial theoretical capacity (820 mAh g⁻¹ or 5850 mAh cm⁻³) and a low redox potential of -0.76 V versus the Standard Hydrogen Electrode (SHE). Nevertheless, ZIBs confront several challenges, including limited charge-discharge reversibility attributed to the formation of Zn dendrites via the hydrogen evolution reaction (HER), uneven Zn electrodeposition, and the presence of electrochemically inert by-products such as ZnO, Zn(OH)₂, and ZnSO₄[Zn(OH)₂]₃·xH₂O. To resolve these issues, a range of methodologies has been explored, encompassing innovations in Zn electrode design, separator development, and the exploration of electrolyte additives.

In this study, the electrochemical characteristics and transformations on the Zn-metal surface were investigated by employing Thioacetamide (TAA) as an electrolyte additive within the aqueous liquid electrolyte of Zn-ion batteries. The primary objective of this research is to reduce the formation of the aforementioned Zn dendrites and byproducts while aiming to achieve a uniform Zn-metal surface deposition. TAA, characterized by primary amine functional groups, is recognized for its electrochemical activity, primarily attributable to the sulfur (S) present in the thioamide species, which tends to actively participate in electrochemical reactions. Furthermore, TAA undergoes hydrolysis within the electrolyte, resulting in the generation of weak acid by-products such as hydrofluoric acid and acetic acid, thereby facilitating the removal of impurities and contributing to a smooth deposition process. Consequently, TAA emerges as a promising functional additive capable of controlling the Zn electrodeposition process.

5:00 PM ES04.07.13

Functional Carbon-Based Zn Host Assisted with Ultra-Thin Hydrophilic ZnO Layer for Practical Aqueous Zn-Metal Batteries [Jung Been Park](#) and Dong-Wan Kim; Korea University, Korea (the Republic of)

Eco-friendly aqueous Zn-metal batteries (AZMBs) is considered a promising candidate for grid-scale energy storage system owing to its high theoretical capacity (5,854 mAh cm⁻³), low standard reduction potential (-0.76 V vs. Standard Hydrogen Electrode), and high compatibility with aqueous electrolyte. However, the inevitable dendritic Zn growth and side-reactions (hydrogen evolution reaction (HER) and Zn corrosion) during continuous cell operation block the practical utilization of AZMBs. Hence, we effectively ameliorate the growth of Zn dendrite and the side reactions of Zn-metal anode by developing the zincophilic porous carbon host (top layer) and ultra-thin ZnO layer (bottom layer) originating from native-oxide of metallic Zn. The functional carbon host provides many zincophilic Zn nucleation/growth sites due to its large specific surface area and oxygen doping effect, which inhibits Zn dendrite growth and volume expansion, as well as inhibits side reactions due to its low HER properties stemming from hydrophobicity of carbon. Also,

the hydrophilic ultra-thin ZnO layer (~10 nm) facilitates hygroscopicity of the aqueous electrolyte to the host to prevent "top accumulation" of Zn deposits on the carbon host, compensating low wettability of hydrophobic carbon host. Thus, the resonance between these two layers layer stably maintains low overpotential (~50 mV) even at ultra-high current density and high capacity (10 mA cm⁻² and 5 mAh cm⁻², respectively) during repetitive Zn plating/stripping. Furthermore, when combined with a MnO₂ cathode, the full-cell exhibits superior cyclability over 1,000 cycles at a low negative-to-positive electrode capacity ratio (~7.3), approaching practical AZMBs.

ACKNOWLEDGEMENTS

This research was supported by Basic Science Research Program through the National Research Foundation of Korea (NRF) funded by the Ministry of Education (NRF-2022R1A2C3003319).

5:00 PM ES04.07.14

Colloidal Synthesis and Defect Engineering of Vanadium Selenide: A High-Performance Anode Material for Li-Ion Batteries Chaeheon Woo and Jae-Young Choi; Sungkyunkwan University, Korea (the Republic of)

Defect engineering is essential for enhancing the performance of lithium-ion batteries (LIBs), particularly in transition metal chalcogenides (TMCs). Vanadium selenide, known for its outstanding electrochemical performance, has been extensively studied. In this study, we successfully synthesized Mo-doped V₂Se₉ at the nano-scale using a liquid-phase process. The resulting Mo-doped V₂Se₉ anode enhances reactive sites, facilitates Li⁺ ion transport, and exhibits high electronic conductivity. With these advantages, a reversible capacity of 1309.45 mAh g⁻¹ at 100 mA g⁻¹ was confirmed even after the 100th cycle. Furthermore, Mo-doped V₂Se₉ exhibits non-anomalous behavior, demonstrating a 30.34% increase in capacity after 100 cycles compared to the initial cycle. Herein, we elucidate the variation in capacity with doping concentration and provide insights into the reasons for the capacity increase. This study presents an expandable strategy for synthesizing doped TMCs, contributing to the enhancement of the lithium-ion battery anode performance in other TMCs.

5:00 PM ES04.07.15

First-Principles Study on The Interfacial Reaction of Cathode Coating with Organic Additive for Aqueous Zinc-Ion Batteries Moonwon Lee^{1,2}, Jin Hong Lee¹, Kyu-nam Jung¹ and Kanghoon Yim¹; ¹Korea Institute of Energy Research, Korea (the Republic of); ²Chungnam National University, Korea (the Republic of)

Aqueous zinc-ion batteries (AZIBs) are gaining great attention as a potential post-lithium-ion battery technology due to the advantages in safety and cost. However, numerous challenges still need to be addressed to improve the energy density and cycle stability for the commercialization of AZIBs. As an example, Mn-based cathodes which are widely used for aqueous ZIBs face a significant issue of Mn²⁺ dissolution into the electrolyte. To address this concern, various strategies are under investigation such as extra addition of Mn²⁺ into the electrolyte and crystal structure modification. In this work, we have utilized MnO₂ as the cathode material and introduced an organic additive to the electrolyte. The organic additive formed a protective coating on the cathode surface, effectively inhibiting Mn²⁺ dissolution and resulting in an enhanced battery performance. To understand the effect of organic coating and the atomistic mechanisms governing the formation of the coating film on the cathode and its role in surface protection, we employed density functional theory (DFT) calculations to theoretically investigate the interfacial reactions on the cathode surface and identify the origin of inhibition of Mn²⁺ dissolution.

5:00 PM ES04.07.16

Electrochemical Study of The Ti-V-Ni-A(A=Fe,Mn,Al) Alloy used as Anode in Nickel-Metal Hydride Batteries Gulhan Cakmak¹, Hakan Yüce¹ and Eli Grigorova²; ¹Mugla University, Turkey; ²Bulgarian Academy of Science, Bulgaria

While the energy crisis is on its way to becoming a crisis for the whole world, this problem and the storage of energy also emerge as an important problem. Although there are many energy storage methods, rechargeable batteries are of great importance. Accordingly, the development of highly efficient energy storage and conversion devices is more important than at any time in this century. Ni-MH batteries come first among these rechargeable batteries. In this direction, various alloys have been developed and continue to be developed to be used as anode materials in these batteries. Among these alloys, studies have shown that Ti-V-based alloys are especially useful for NiMH batteries and show critical technology advantages such as superior safety, environmental friendliness and excellent high/low temperature performance, and show a great development potential, especially in the field of low-temperature batteries. The electrode properties of AB alloys Continuous efforts are being made to develop and use new, high-performance versions for anode materials. Body-centered cubic (BCC) Ti or V-based alloys have an effective hydrogen storage capacity of more than 2 wt% and the pressure-composition (P-C) for absorption and desorption) shows a suitable plateau pressure in the isotherm curve and has been observed to be suitable for use as an anode material in Ni-MH batteries. This alloy electrode will be prepared by melting in a vacuum arc melting furnace under argon atmosphere and with the help of SPEX Ball Mill the alloy will be reduced below 45 microns and then Ti-V-Ni-A The crystallographic properties of the (A=Fe,Mn,Al) alloy will be examined. The electrochemical results are aimed at performing charge/discharge tests on NiMH batteries using potentiostat/galvanostat and collecting electrochemical impedance spectrum (EIS) data on the cell.

This work was supported by TUBITAK (The Scientific and Technological Research Council of Turkey) with project Number 121N774, which the authors gratefully acknowledge.

5:00 PM ES04.07.18

Characterization of Mg_{0.5}Al_{0.25}Cr_{0.25}Ni_{0.25}A_{0.25} (A=Nb,Ta,Co) Alloys as Anode Materials for NiMH Batteries Gulhan Cakmak¹, Hakan Yüce¹, Fatih Piskin¹, Berke Piskin¹ and Eli Grigorova²; ¹Mugla University, Turkey; ²Bulgarian Academy of science, Bulgaria

Hydrogen energy is becoming an important part of a viable solution to worldwide climate change and atmospheric pollution. In this regard, hydrogen storage materials direct the research of rechargeable batteries. High entropy alloys containing Mg consist of an attractive system because Mg is light, cheap, and abundant, and has a high absorption capacity. Mg-containing alloys are an attractive candidate for solid-state hydrogen storage and can be further applied in electrochemical systems where the hydrogen atoms occupy the interstitial forming metal hydride (MH). A Ni/MH battery is composed of a Ni(OH)₂ positive electrode, a metal MH negative electrode and an alkaline electrolyte (KOH solution). The family of hydrogen storage alloys based on transition metals (TM) – Mg – Ni has attracted increasing attention in recent years. They can meet the general electrochemical performance requirements by exhibiting high discharge capacity, long durability, good rate capacity, admirable discharge capacity at low temperature and low self-discharge characteristics. In this direction, it is aimed to add these properties to Mg-based alloys by adding transition metals to Mg-based alloys. In this direction, it is aimed to produce Mg_{0.5}Al_{0.25}Cr_{0.25}Ni_{0.25}A_{0.25} (A=Nb,Ta,Co) alloys. This alloy electrode will be prepared by melting in a vacuum arc melting furnace under argon atmosphere and with the help of SPEX Ball Mill the alloy will be reduced below 45 microns and then The crystallographic properties of the Mg_{0.5}Al_{0.25}Cr_{0.25}Ni_{0.25}A_{0.25} (A=Nb,Ta,Co) alloy will be examined. The electrochemical results are aimed at performing charge/discharge tests on NiMH batteries using potentiostat/galvanostat and collecting electrochemical impedance spectrum (EIS) data on the cell.

This work was supported by TUBITAK (The Scientific and Technological Research Council of Turkey) with project Number 121N774, which the authors

gratefully acknowledge.

5:00 PM ES04.07.17

Do Protons released from DRX Cathode Surfaces Initiate Decomposition of Ethylene Carbonate Electrolyte in Lithium-Ion Batteries? Rohith Srinivas Mohanakrishnan^{1,2}, Sudarshan Vijay^{1,2}, Jordan Burns^{1,2} and Kristin A. Persson^{1,2}; ¹University of California Berkeley, United States; ²Lawrence Berkeley National Laboratory, United States

The cathode-electrolyte interphase (CEI) is a critical, but not fully understood component of Li-ion batteries (LIBs). Ethylene Carbonate (EC), a commonly used electrolyte in LIBs, starts to decompose at approx. 3.8 V vs Li/Li⁺ to form this CEI [1]. One of the initial products formed due to this decomposition is vinylene carbonate (VC) which has been experimentally observed by in-situ FT-IR (Fourier Transform Infrared Spectroscopy) measurements at potentials as low as 3.8 V vs Li/Li⁺[2]. In this talk, we explore the feasibility of this reaction occurring through a mechanism involving transition metal ions on the cathode surface through density functional theory calculations performed under realistic surface conditions. Previous ab initio studies on the EC decomposition on NMC surfaces have been performed[3,4,5]. As a prototype for next generation cathode, we study Disordered Rocksalt(DRX) surfaces as cathodes and explore the equilibrium between EC, VC and abstracted hydrogen as a function of the potential. We find that surface adsorbed hydrogen is released as protons at a potential of 3.7 V vs. Li/Li⁺, which drives the conversion of EC to VC. We study the thermodynamics of proton release from the DRX surface at different lithiation stages from ab initio calculations to understand the potential dependence of proton release and further understand the thermodynamics of EC to VC decomposition. This will allow us to better understand the reactions occurring at the cathode electrolyte interface as well as crosstalk between anode and cathode materials.

Reference list

- [1] Y. Wu, X. Liu, L. Wang, X. Feng, D. Ren, Y. Li, X. Rui, Y. Wang, X. Han, G.-L. Xu, H. Wang, L. Lu, X. He, K. Amine, M. Ouyang, *Energy Storage Materials*. **37**, 77–86 (2021).
- [2] Y. Zhang, Y. Katayama, R. Tatara, L. Giordano, Y. Yu, D. Fraggedakis, J. G. Sun, F. Maglia, R. Jung, M. Z. Bazant, Y. Shao-Horn, *Energy & Environmental Science*. **13**, 183–199 (2020).
- [3] S. Xu, G. Luo, R. Jacobs, S. Fang, M. K. Mahanthappa, R. J. Hamers, D. Morgan, *ACS Applied Materials & Interfaces*. **9**, 20545–20553 (2017).
- [4] J. L. Tebbe, T. F. Fuerst, C. B. Musgrave, *ACS Applied Materials & Interfaces*. **8**, 26664–26674 (2016).
- [5] T. M. Ostergaard, L. Giordano, I. E. Castelli, F. Maglia, B. K. Antonopoulos, Y. Shao Horn, J. Rossmeisl *Journal of Physical Chemistry C*. **122**, 10442–10449 (2018)

5:00 PM ES04.07.19

Computational Study on a Variety of Lithium Diffusion Pathways Yevgeniya Kondratyeva and Artem Sergeev; N.N.Semenov Federal Research Center for Chemical Physics, Russian Federation

Lithium metal batteries are promising storage systems with better electrochemical characteristics than ubiquitous Li-ion. Lithium anode is the key to creating high-power batteries and the main challenge at the same time. One of the main flaws of using lithium as anode material is the formation of heterogeneous deposits on lithium surface during charge process. The most common type of such deposits is whiskers. Understanding of whiskers' formation and growth mechanism is required for solving this problem. Last studies have shown that solid-state processes run the whole show in the whiskers' formation processes.

In this study we investigated and compared different pathways of lithium diffusion within metal electrode: diffusion of point defects in the metal bulk, self-diffusion through grain boundaries and the influence of Li-Li₂O interface on the point defects. Due to high reactivity of lithium, we weren't able to provide all these investigations in chemical lab, we had to estimate diffusion processes with computational methods: Molecular Dynamics (MD) and DFT.

We have chosen MD for modeling all-lithium-systems (LAMMPS package) because this method can handle a relatively large system size and time scale. For avoiding inaccuracies, we have compared several force fields firstly. One of them was Machine-learning Interatomic Potential (MLIP), which we had trained ourselves. The results obtained with MLIP have shown DFT-level of accuracy. For instance, we calculated melting parameters and point defect energies obtained with 5 different potentials and compared these data with the published experimental and DFT data. Thus, we revealed the superiority of MLIP over other potentials and the possibility of using it to simulate large systems such a grain boundary with DFT-accuracy.

Further we simulated lithium grain boundary and calculated lithium diffusion coefficient from mean squared displacement slopes. Simulation cell consist of two lithium slabs rotated at a certain angle, which was chosen based on coincidence site lattice. We showed that the boundary is 3-5 atomic layers thick and is amorphous at room temperature. The mobility of grain boundary atoms was found to be extremely high and only 5 times lower than it is in supercooled molten lithium.

For comparison of the diffusion coefficients in the grain boundary and bulk we had to estimate self-diffusion value in solid lithium bulk. We investigated the mobility of point defects (vacancy and self-interstitial atom) in the lithium bulk and discovered an anomalous phenomenon. Temperature dependence of vacancy diffusion coefficient corresponds to Arrhenius law, simultaneously this dependence of self-interstitial atom does not correlate with Arrhenius law and even demonstrates an inverse dependence, i.e. diffusion coefficient decreases with the temperature increasing. We have further demonstrated that this anomaly is due to the interplay between ballistic motion of interstitial defect along <111> direction and its rotation which obeys to Arrhenius law.

There is the third way for lithium diffusion. It would be surface diffusion for any less reactive metal, but for lithium this way is not available due to presence of SEI. It is considered that the closest to lithium layer of SEI consists of lithium oxide, so we simulated Li-Li₂O interface using DFT (VASP) and estimated the behavior of point defects at the heterogeneous interface. We have studied the influence of space-charge at the interface on the defect energetics and mobility along the interface.

Eventually, we have been able to consider all possible mass-transfer pathways within the electrode to build a complete picture of processes during lithium deposition. We have discovered that solid-state diffusion along grain boundaries and Li-SEI interfaces is sufficient to realize the proposed mechanism of whiskers' formation and growth.

5:00 PM ES04.07.20

Ionic Peltier Effect in Concentrated Carbonate and Ether-Based Li-Ion Electrolytes Yu-Ju Huang, David Cahill, Zhe Cheng and Peilin Lu; UIUC, United States

Understanding the Li⁺ transport and solvation behaviors in electrolytes is crucial for electrolyte selection to optimize cell performance. The ionic Peltier effect is the phenomenon of heat generation or absorption at the interface of electrodes during a reversible electrode reaction. It can provide us with information on the solvation thermodynamics of Li-ion electrolytes. By using the temperature difference metrology developed by our group, we expand our ionic Peltier coefficient measurements and study more ether-based and carbonate-based electrolytes. The magnitude of Peltier coefficients of ether-based electrolytes is -70-80 kJ/mol, almost 2 times larger than that of carbonated-based electrolytes, around -20-30 kJ/mol. This difference indicates a larger change in partial molar entropy between the Li electrode and electrolyte at the interface in ether-based electrolytes. In addition, we also observe a decrease in the magnitude of the Peltier coefficient in ether-based electrolytes with increasing concentration, the same as in carbonate electrolytes. For carbonate

electrolytes, the binary mixture (EC/DMC) electrolyte has a Peltier coefficient between the values of pure solvents, EC and DMC. Peltier coefficients of different Li salt concentrations, from 0.5M to 3M, are slightly temperature dependent by being more negative with increasing temperature. Combining with the present Li solvation thermodynamic properties and the structures of different electrolytes, we provide information on the interaction between Li ion-solvent, and its correlation with solvent physical properties.

SESSION ES04.08: Non-Li Metal—Aqueous

Session Chairs: Tao Gao and Wu Xu

Friday Morning, April 26, 2024

Room 422, Level 4, Summit

8:15 AM ES04.08.01

Increasing The Cycle Life of Zinc Metal Anodes and Nickel-Zinc Cells Using Flow-Through Alkaline Electrolytes [Shuhua Shan](#)¹, Mihir Parekh², Rong Kou¹, Donghai Wang¹ and Chris Rahn¹; ¹Pennsylvania State University, United States; ²Clemson University, United States

Alkaline electrolyte flow through porous Zn anodes and Ni(OH)₂ cathodes can overcome diffusion limits, reduce dendrite growth, and improve cycle life. Zinc deposition morphology improves with low flow rates for KOH/ZnO electrolytes at current densities near the diffusion-limited regime. Zinc dendrites present without flow are suppressed by micrometer-per-second flow at concentrations ranging from 0.2 to 0.6 M ZnO dissolved in 6 M and 10 M KOH solutions. Zn-Cu asymmetric cell tests reveal that flowing electrolyte increases the lifespan by more than 6 times in the diffusion-limited regime by suppressing gas evolution and dendrite formation. Ni-Zn cell tests show that a flow-assisted battery cycles 1500 times with over 95% Coulombic efficiency (CE) at 35 mA/cm² current density and 7 mAh/cm² charge capacity, increasing the battery lifespan by 17 times compared with a stagnant electrolyte Ni-Zn cell. Flow-through electrolyte also stabilizes the Zn electrode in the over-limiting regime, achieving approximately 4 times increased lifespan and 297 cycles with over 90% CE at 52 mA/cm².

8:30 AM ES04.08.02

Mimicking Ion and Water Management in Poultry Breeding for Highly Reversible Zinc Ion Batteries [Zhi Li](#); University of Alberta, Canada

Aqueous Zn-ion chemistry has emerged as a promising energy storage technology yet suffers from severe irreversibility due to poor management of water and Zn²⁺ flows, leading to dendrite formation, parasitic reactions, and structural collapse of many cathode materials. To address these challenges, we turned to eggshell membranes (ESM), which have evolved over millions of years to regulate water and Ca²⁺ flows, ensuring the formation of well-defined hard shells and protecting chicken embryos during incubation. We discovered ESM, especially after denaturation, can effectively retard water, regulate Zn²⁺ flow, and self-concentrate Zn²⁺ at the electrode interfaces, thus achieving dendrite-free Zn plating/stripping at a Coulombic efficiency of ~99.8% over 500 cycles, steady charge/discharge beyond a half year, and capacity retention of 90.1% over 10,000 cycles for Zn-V full cells. To demonstrate scalability, we fabricated prototyped ESM-based papers, showing dual-electrode protection capability and long-term stability. This work also inspires bionic structures in batteries and beyond.

8:45 AM *ES04.08.03

Two Architected Battery Electrodes are Better than One! [Debra R. Rolison](#)¹, Jeffrey W. Long¹, Ryan H. DeBlock¹, Christopher N. Chervin¹, Samuel Kimmel^{2,1} and Christopher Rhodes²; ¹U.S. Naval Research Laboratory, United States; ²Texas State University, United States

Having removed the roadblock to rechargeable aqueous alkaline batteries by architecting the zinc in a sponge form factor, thus thwarting formation of cell-shortening zinc dendrites, our team at the US Naval Research Laboratory has turned to improving the performance of the opposing electrode. To do so, we again bring an architectural perspective to the positive electrode. Keeping the zinc sponge anode as a constant factor, we demonstrate two classes of Zn-based alkaline cells that derive improved discharge areal capacity and capacity retention, namely Ni-Zn and Zn-air, when the respective cathodes adopt either an architected form factor or deploy architected catalysts. We nucleate and grow Al(III)-substituted α -Ni(OH)₂ onto carbon nanofiber paper and achieve 1.5 electrons per Ni rather than the 1 electron per Ni characteristic of Ni cathodes. Using the 3D electron-wired cathode, the cell retains that extra per Ni capacity without fade over 80 cycles. To catalyze oxygen reduction (ORR) and evolution (OER) in the air electrode, we use aerogels as the design architecture. By blending aerogel versions of an excellent ORR catalyst (the 2×2 tunneled polymorph of MnO₂, cryptomelane) with an excellent OER catalyst (nickel ferrite) in a powder-composite electrode structure, we attain high areal capacity (mAh per geometric area) while achieving state-of-the-art low voltage hysteresis (700 mV) and charging voltage <2 V.

9:15 AM ES04.08.04

Advancements in Zinc Sponge Anode Fabrication for Scale-up, Manufacture and Battery Performance [Jeffrey W. Long](#), Ryan H. DeBlock and Debra R. Rolison; Naval Research Laboratory, United States

Zinc (Zn) anodes were historically prone to shape change, short-inducing dendrite formation, and suboptimal redox utilization in aqueous battery systems, particularly when subjected to extensive charge-discharge cycling. The Naval Research Laboratory introduced a 3D-architected Zn "sponge" design that mitigates many of the historic limitations of Zn anodes [1]. Over several years of development, the fabrication routes to Zn sponges have continued to evolve from early proof-of-concept examples with specialized chemicals and multistage thermal processing toward a more recent focus on methods that are fast, low-cost, readily scalable, and energy efficient. The latest protocols use simple inorganic porogens such as sodium chloride and potassium carbonate in conjunction with chemical sintering and simplified heating steps to produce robust Zn sponges in varied monolithic forms (discs, plates, cylinders) and scales (up to 20 cm on a side). We will discuss the latest advances in the fabrication, materials characterization, and electrochemical evaluation of Zn sponges as directed toward their use as anodes in aqueous batteries (alkaline to mild-pH).

1. J. F. Parker, C. N. Chervin, E. S. Nelson, D. R. Rolison, and J.W. Long. *Energy Environ. Sci.* 7 (2014) 1117–1124.

9:30 AM ES04.08.05

Colossal Capacity Loss during Calendar Aging of Zn Battery Chemistries [Bo Liu](#), Xintong Yuan and Yuzhang Li; University of California, Los Angeles, United States

Whereas previous research efforts in Zn battery chemistries have primarily focused on extending their cycle life, calendar aging has largely been neglected and is poorly understood. Here, we discover that Zn metal anodes lose 12-37% of their capacity after only 24 hours of calendar aging, which is more than

an order of magnitude greater than any other battery chemistry previously studied. We find that this large capacity loss occurs regardless of electrolyte chemistry, substrate composition, and calendar aging time, suggesting that the losses cannot be accounted for by corrosion alone. By leveraging titration gas chromatography, we distinguish corrosion losses from losses due to electrically disconnected Zn ("dead" Zn) and quantify dead Zn as the main contributor to capacity loss during Zn battery aging. More broadly, this study shows that large instabilities in seemingly non-reactive metals (e.g., Zn) can occur, highlighting the importance of understanding their underlying degradation mechanisms.

9:45 AM ES04.08.06

Characterization of Iron Anodes for Rechargeable Aqueous Batteries [Xiao Zhao](#)^{1,2}, Evan Carlson¹ and William C. Chueh¹; ¹Stanford University, United States; ²Lawrence Berkeley National Laboratory, United States

Metallic iron is an attractive anode material for aqueous batteries, particularly if the full 3-electron redox between Fe and Fe (III) can be accessed reversibly. However, oxidation of Fe (II) to Fe (III) causes drastic morphology change and irreversible formation of highly resistive phases. Yet, it remains unclear how these phases form at the nanoscale and, crucially, how they might be avoided. To achieve fully reversible Fe anodes, it is critical to obtain a mechanistic understanding of nanoscale morphology and phase evolution during electrode cycling. Here we investigated the electrochemical transformation pathways between Fe (II) and Fe (III) oxides using both ex-situ and operando techniques, including SEM, Raman, AFM, Infrared Nanospectroscopy (nano-FTIR) and Scanning Transmission X-ray Microscopy (STXM). Correlating the morphology evolution during this transformation to local Fe oxidation state and phase would offer fundamental insight into Fe (II)/(III) conversion and inspire novel engineering of the Fe anode to achieve higher capacity and cyclability.

10:00 AM BREAK

10:30 AM ES04.08.08

Peptide Gel Electrolytes for Stabilized Zn Metal Anodes [Yizhou Wang](#) and Husam N. Alshareef; KAUST, Saudi Arabia

The rechargeable aqueous Zn ion battery (AZIB) is considered a promising candidate for future long-duration energy storage due to its intrinsic safety features and low cost. However, Zn dendrites and side reactions (e.g., corrosion, hydrogen evolution reaction, and inactive side product (Zn hydroxide sulfate) formation) at the Zn metal anode have been serious obstacles to realizing satisfactory AZIB performance. The application of gel electrolytes is a common strategy for suppressing these problems, but the normally used highly crosslinked polymer matrix (e.g., polyacrylamide (PAM)) brings additional difficulties for battery assembly and recycling. Herein, we have developed a gel electrolyte for Zn metal anode stabilization, where a peptide matrix, a highly biocompatible material, is used for gel construction. Various experiments and simulations elucidate the sulfate anion-assisted self-assembly gel formation and its effect in stabilizing Zn metal anodes. Unlike polymer gel electrolytes, the peptide gel electrolyte can reversibly transform between gel and liquid states, thus facilitating the gel-involved battery assembly and recycling. Furthermore, the peptide gel electrolyte provides fast Zn ion diffusion (comparable to conventional liquid electrolyte) while suppressing side reactions and dendrite growth, thus achieving highly stable Zn metal anodes as validated in various cell configurations. We believe that our concept of gel electrolyte design will inspire more future directions for Zn metal anode protection based on gel electrolyte design.

10:45 AM ES04.08.09

Understanding, Quantification and Mitigation of Hydrogen Evolution Reaction for Aqueous Zinc Metal Batteries [Kingshuk Roy](#); Purdue University, United States

The study delves into the hurdles faced by aqueous zinc metal batteries (AZMBs), including challenges like the unwanted hydrogen evolution reaction (HER), corrosion of the zinc substrate, and dendrite growth, all of which hinder the overall effectiveness of these batteries. To thoroughly understand HER, the study introduces the use of in-situ electrochemical mass spectrometry (ECMS) for precise real-time monitoring of HER during zinc electrodeposition. It is highlighted that even a minute fraction (0.3%) of the total charge attributed to HER has a detrimental impact on the long-term cycling performance of AZMBs. The study establishes a significant platform by introducing a method to accurately determine the faradaic efficiency in zinc electrodeposition. This advancement becomes a valuable tool in evaluating additives and modifications aimed at enhancing the stability of AZMBs and suppressing the HER. Moreover, the text introduces a thoughtful approach to improving AZMBs by employing tetraalkylsulfonamide (TAS) additives. This additive is designed to tackle challenges like dendrite formation, HER, and ZnO passivation on the anode, which have historically impeded the development of AZMBs. Through various techniques such as nuclear magnetic resonance spectroscopy, mass spectrometry, and density functional theory studies, we demonstrate that TAS molecules displace water from Zn²⁺ solvation. This alters the solvation matrix, disrupting the hydrogen bond network in free water. The study reports promising outcomes with TAS additives, including suppressed dendritic growth and HER, along with a remarkable ~25-fold cycle life improvement—from approximately 100 hours to over 2500 hours—at a current density of 1 mA/cm². Techniques such as X-ray diffraction and X-ray photoelectron spectroscopy reveal impressive suppression of insulating side products and the formation of ion-conductive solid electrolyte interphase components. Post-cycling analysis further illustrates uniform, planar zinc growth in the presence of TAS, in contrast to the inhomogeneous, void-containing clusters observed in its absence. In conclusion, the findings from this study suggest that TAS additives offer a comprehensive framework for realizing robust zinc metal batteries, presenting a promising alternative to lithium-ion batteries.

11:00 AM ES04.08.11

The Preparation of Moldable Zinc-Ion Batteries Using Graphene Oxide Doughs [Min-Yen Tsai](#), Han-Shiuan Lin and Che-Ning Yeh; National Tsing Hua University, Taiwan

The increasing demand for electric vehicles has ignited a pursuit to enhance their energy density while simultaneously reducing manufacturing costs. Compared with Li-ion batteries, aqueous Zn-ion batteries show tremendous potential due to their attractive characteristics of having a high theoretical capacity (820 mAh g⁻¹) and a low potential (-0.76 V vs SHE). Furthermore, coupled with its safety and environmental friendliness advantages, this renders it with significant potential for large-scale applications. In this work, we use graphene oxide (GO)/carbon nanotube (CNT)/cellulose nanofibrils (CNF) composite dough as the 3D scaffold for the electrode. The composite dough is a binder-free and self-sustaining structure with moldable features. The characteristics of arbitrary shapes, highly processable and tunable microstructures endow it with significant potential for diversified applications. The composite dough combines the advantages of three different carbon materials. GO possesses a large surface area and, after annealing, maintains structural integrity to prevent collapse. CNT prevents the aggregation of GO after reduction and enhances the ionic conductivity of the composite. CNF improves the mechanical strength of the composite and its abundant hydroxyl groups enable the dough to maintain the viscoelastic state at high water content up to 90 wt%. The composite dough is then transformed into an electrode scaffold characterized by high porosity, excellent conductivity, and a large surface area. The anode features Zn powders (ZPs) integrated into the composite dough-based electrodes, which enhances control over the N/P ratio. However, zinc anodes normally suffer from issues including hydrogen evolution and corrosion. Coating TiO₂ nanoparticles onto the surface of the dough not only protects the ZPs from side reactions but also suppress dendrite growth. In addition, TiO₂ can also enhance the electrode's hydrophilicity, zincphilicity, and facilitate Zn ion diffusion. On the cathode side, α -MnO₂ is used as the active material and is incorporated into the composite dough. Our results indicate that the

MnO₂@composite dough-based electrode has higher gravimetric capacity and cycle stability compared to the MnO₂@carbon paper. The improved contact between MnO₂ and composite scaffold leads to enhanced charge transfer. The ZPs/TiO₂@composite||MnO₂@composite dough-based cell exhibits more stable cycle performance and higher discharge capacity than those of ZPs@carbon paper||MnO₂@carbon paper cell. This work offers an alternative approach for fabricating 3D and moldable electrodes, broadening the horizons for 3D electrodes in high-performance energy storage devices.

11:15 AM ES04.08.12

Promoting Room Temperature Aluminum Deposition Through Rapid Ligand Exchange Complexes [Dan Thien Nguyen](#)^{1,2}, Venkateshkumar Prabhakaran^{1,2}, Ying Chen^{1,2}, Karl Mueller^{1,2} and Vijayakumar Murugesan^{1,2}; ¹Pacific Northwest National Laboratory, United States; ²Joint Center for Energy Storage Research (JCESR), United States

Unlocking room temperature aluminum (Al) electroplating stands as a promising avenue for advancing multivalent energy storage systems and pioneering surface coating methods, pivotal in driving a zero-emission economy. Despite its potential, challenges such as electrolyte-induced parasitic reactions during Al deposition, high flammability risks, suboptimal Coulombic efficiency, and the costliness of organic-based electrolytes have persisted. Addressing these challenges necessitates reducing activation energy and expediting kinetics for the electrochemical reduction of aluminum cations in organic electrolyte solutions. This is pivotal for achieving efficient, reversible room temperature electrodeposition of Al. In our study, we introduce a novel electrolyte material—a highly concentrated aluminum chloride (AlCl₃) solution within weakly coordinating dialkyl-ether and sulfone compounds.^[1] These solvents swiftly form ligand exchange complexes with AlCl₃, enabling rapid Al electrodeposition at a minimal 0.2 V overpotential. Additionally, they effectively suppress the solvent's parasitic reaction, particularly in the low voltage regime. Our research delves into the intricate interactions between solvents and solutes in weakly coordinating environments, shedding light on their influence on electrolyte solution electrochemistry. This foundational understanding is pivotal for future electrolyte design and optimization, benefiting both electroplating and rechargeable batteries.

Reference

[1] Nguyen, D.T., Murugesan, V., Prabhakaran, V. and Mueller, K.T., Battelle Memorial Institute Inc, 2023. Aluminum-ether-based composition for batteries and ambient temperature aluminum deposition. U.S. Patent Application 18/130,281.

SESSION ES04.09: Lithium Metal and Beyond

Session Chairs: Tao Gao and Wu Xu

Friday Afternoon, April 26, 2024

Room 422, Level 4, Summit

1:30 PM ES04.09.01

Antraquinone-Based Silicate Covalent Organic Frameworks as Solid Electrolyte Interphase for High-Performance Lithium-Metal Batteries [Chen Li](#); The Hong Kong University of Science and Technology, China

Lithium (Li)-metal batteries (LMBs) possess the highest theoretical energy density among current battery designs and thus have enormous potential for use in energy storage. However, the development of LMBs is severely hindered by safety concerns arising from dendrite growth and unstable interphases on the Li anode. Covalent organic frameworks (COFs) incorporating either redox-active or anionic moieties on their backbones have high Li-ion (Li⁺) conductivities and mechanical/chemical stabilities, so are promising for solid-electrolyte interphases (SEI) in LMBs. Here, we synthesized anthraquinone-based silicate COFs (AQ-Si-COFs) that contained both redox-active and anionic sites via condensation of tetrahydroxy-anthraquinone with silicon dioxide. The nine Li⁺ mediated charge/discharge processes enabled the AQ-Si-COF to demonstrate an ionic conductivity of 9.8 mS cm⁻¹ at room temperature and a single-ion-conductive transference number of 0.92. Computational studies also supported the nine Li⁺ mechanism. We used AQ-Si-COF as the solid electrolyte interphase on the Li anode. The LMB cells with LiCoO₂ cathode attained a maximum reversible capacity of 188 mAh g⁻¹ at 0.25 C during high-voltage operation. Moreover, this LMB cell demonstrated suppressed dendrite growth and stable cyclability, with its capacity decreasing by less than 3% up to 100 cycles. These findings demonstrate the effectiveness of our redox-active and anionic COFs and their practical utility as SEI in LMB.

1:45 PM ES04.09.02

Modifying Li⁺ Transport and Interface Chemistry via Citric Acid-Treated Silica Carrier in Nanoparticle Colloidal Electrolyte toward Stable Li-Metal Batteries [Minhong Lim](#) and Hongkyung Lee; DGIST, Korea (the Republic of)

Tailoring the lithium ion (Li⁺) microenvironment is essential for achieving rapid ionic transfer and a mechanically strong solid-electrolyte interphase (SEI). This is key to the stable cycling of lithium-metal batteries (LMBs). Beyond the conventional approach of adjusting salt and solvent compositions, this study introduces a novel method. It involves simultaneous modulation of Li⁺ transport and SEI chemistry through a citric acid (CA)-modified silica-based colloidal electrolyte (C-SCE). The CA-tethered silica (CA-SiO₂) provides more active sites for attracting complex anions. This leads to a greater dissociation of Li⁺ from these anions, resulting in a high Li⁺ transference number (approximately 0.75). The intermolecular hydrogen bonds formed between solvent molecules and CA-SiO₂, along with their migration, serve as nano-carriers. These nano-carriers are responsible for transporting additives and anions to the lithium surface, thereby strengthening the SEI through the co-implantation of SiO₂ and fluorinated components. Notably, C-SCE has shown promise in suppressing lithium dendrite formation and enhancing the cycling stability of LMBs. This is a significant improvement over the CA-free SiO₂ colloidal electrolyte. The study highlights that the surface properties of nanoparticles play a crucial role in the dendrite-inhibiting capabilities of nano colloidal electrolytes.

2:00 PM ES04.09.03

Revitalizing Native Lithium-Metal Electrode Surfaces through Hydrohalic Acid-Assisted Pre-Halogenation [Jiyeon Seo](#), Jaeho Lee and Hongkyung Lee; Daegu Gyeongbuk Institute of Science and Technology, Korea (the Republic of)

Lithium metal anodes (LMAs) represent the ultimate choice for advancing beyond traditional Li-ion batteries due to their remarkable attributes, including a high capacity of 3860 mAh g⁻¹ and a low working potential of -3.04 V vs. SHE. However, the inherent challenges associated with LMA usage, such as their exceedingly high surface reactivity, uncontrollable dendritic plating, and unbounded volume expansion, have long hindered the development of practical lithium-metal batteries (LMBs). The primary culprit behind these issues is the formation of a non-uniform solid-electrolyte interphase (SEI) layer, arising from byproducts within the electrolyte and the inherent surface characteristics of LMAs. In light of these challenges, achieving uniform passivation of LMAs and the formation of a homogeneous SEI layer during the initial stages are imperative. Such uniformity is crucial to enable consistent Li⁺ ion flux. Additionally, the integration of halogenated SEI components holds great promise, offering enhanced mechanical strength, insulation properties, and thermodynamic stability.

In this study, we introduce a straightforward LMA treatment technique utilizing hydrohalic acids (HXs, X = F, Cl, Br, and I) to rejuvenate the native passivation layer (NPL) found on as-manufactured LMAs. This treatment ensures an even distribution of halogenated compounds across the LMA surface. A key aspect of this process involves the dissolution of existing inorganic Li-compounds, such as Li₂O, LiOH, and Li₂CO₃, present in the NPL by water molecules from aqueous HXs. This results in chemical reactions between HXs and pure Li, ultimately enriching the NPL with LiX compounds. A comparative analysis was conducted to identify the most advantageous LiX compounds for stabilizing the LMA surface and enhancing the cycling stability of LMBs. Furthermore, we elucidated the critical role played by LiX compounds in interfacial reactions when employing localized high-concentration electrolyte (LHCE) as an advanced electrolyte in LMBs. Through this comparative study, it was demonstrated that the establishment of a LiCl-rich SEI layer during the initial stages effectively lowers the energy barrier for Li nucleation and reduces interfacial resistances. This leads to significant enhancements in cycling performance for LMBs, even under practical operating conditions.

2:15 PM ES04.09.04

Tracking Dendrites and Solid Electrolyte Interphase Formation in Composite Electrolyte using Solid State NMR Spectroscopy [Ayan Maity](#), Asya Svirinovsky-Arbeli, Yehuda Buganim, Chen Oppenheim, Brijith Thomas, Arava Zohar and Michal Leskes; Weizmann Institute of Science, Israel

Solid-state lithium batteries have garnered significant attention in recent years as they are a promising technology with immense potential for development with diverse applications. Utilization of solid electrolytes is particularly appealing as it enables the use of lithium metal anodes and thus offer superior energy density with enhanced safety compared to traditional liquid electrolytes. Among the different types of solid-state batteries, polymer-based electrolytes are attractive due to their flexibility and non-flammable nature [1]. However, the practical implementation of polymer electrolytes in rechargeable batteries for high-energy applications faces challenges. These include limited room temperature Li-ion conductivity and formation of lithium dendrites at high current densities. To address these issues, one potential approach is to incorporate solid-state ceramic particles into the polymer matrix. However, there is still a limited understanding as to how ceramics incorporation impacts dendrite formation and propagation, as well as the composition and properties of the solid electrolyte interphase (SEI). The SEI plays a crucial role in the battery chemistry and gaining insights into its atomic-level structure and composition has the potential to transform the development of composites, enhancing their ability to suppress dendrite formation [2]. Unfortunately, there is a shortage of analytical tools capable of precisely identifying the SEI's chemical constituents at the atomic scale, and even more so, of understanding how these constituents affect ionic transport across the SEI. Here we introduce an innovative approach which allows to (i) quantify dendrites formation, (ii) determine SEI composition and its properties which allows us to (iii) determine the dendrite's propagation path within the composite electrolyte.

Using Li NMR spectroscopy, we successfully quantified the formation of dendrites in the cycled composites. Remarkably, we find a consistent rise in dendrite formation by increasing ceramic content up to 40 wt. %, when using Li_{1.5}Al_{0.5}Ge_{1.5}(PO₄)₃ (LAGP) and Li_{6.4}Al_{0.2}La₃Zr₂O₁₂ (LLZO) as ceramic fillers in polyethylene oxide. To determine the effect of ceramic content on dendrites formation, we employed dynamic nuclear polarization (DNP) [3], a method in which the high electron spin polarization is used to increase NMR sensitivity, to selectively enhance the SEI signal [4]. We make use of the inherent conduction electrons of the dendrites for DNP, enabling us to identify the chemical components and structure of the SEI, as well as the SEI permeability to Li-ions. We determined the chemical components of the SEI formed on dendrites in a pure polymer electrolyte and with the addition of varying content of LAGP and LLZO. Surprisingly, we found that SEI structures significantly differ not just with varying ceramic types but also with different ceramic contents, suggesting the nature of possible interaction of the dendrites with ceramic and polymer matrix. Furthermore, analysis of the SEI composition allows us to trace the dendrite propagation within the composite. We showed that in composites with 40 wt. % LAGP, dendrites chemically react with LAGP, hindering their growth towards the opposite electrode and impacting battery lifespan. Conversely, with 40 wt. % LLZO, dendrites are physically blocked without any chemical reaction. In summary, our study offers valuable insights into the SEI's composition, structure, and its correlation with dendrites and ceramic components. The approach can be used to identify the optimal ceramic material to reduce dendrite formation and enhance SEI's Li-ion permeability for improved battery performance.

References

1. Yu et al. *Energy Storage Materials* **2021**, *34*, 282–300.
2. E. Peled and S. Menkin, *J. Electrochem. Soc.*, **2017**, *164*, 1703-1719.
3. Rossini et al *Acc. Chem. Res.* **2013**, *46*, 1942.
4. Hope et al. *Nat. Commun.*, **2020**, *11*, 2224.

2:30 PM *ES04.09.05

Nondestructively Visualizing and Understanding Li Dendrite 'Soft Short' and Bulky Li Creeping in All-Solid-State Batteries [Hongli Zhu](#); Northeastern University, United States

All-solid-state Li metal batteries (ASLMBs) represent a significant breakthrough in the quest to overcome limitations associated with traditional Li-ion batteries, particularly in energy density and safety aspects. However, widespread implementation is stymied by the complex challenges surrounding ASLMBs. An essential part of the solution lies in a profound understanding of the complex mechano-electro-chemical behavior of Li metal in the ASLMBs. In this study, we leverage advanced techniques, operando neutron imaging and X-ray computed tomography (XCT), to nondestructively visualize Li behavior within ASLMBs. This novel approach gives us a unique window into real-time Li evolution, both pre- and post- the occurrence of a "soft short". Our utilization of two-dimensional neutron radiography, complemented by three-dimensional neutron tomography, enables us to chart the terrain of Li metal deformation operando. Concurrently, XCT offers a rich, three-dimensional insight into the internal structure of the battery following a "soft short". Despite the manifestation of a "soft short", we observe the persistence of Faradaic processes. To study the elusive 'soft short' behavior in solid electrolytes, we have coupled phase-field modeling with electrochemistry and solid mechanics theory. This has enabled us to simulate Li dendrite growth under varying external pressures. Our research unravels how external pressure plays a significant role in curbing dendrite growth, potentially leading to dendrite fractures and thus uncovering the origins of both "soft" and "hard" shorts in Li metal batteries. Furthermore, by harnessing finite element modeling, we dive deeper into the mechanical deformation and the fluidity of Li metal.

3:00 PM BREAK

3:30 PM ES04.09.06

Enhancing Lithium Stripping Efficiency in Anode-Free Solid-State Batteries through Self-Regulated Internal Pressure [Hongli Zhu](#); Northeastern University, United States

Anode-free all-solid-state lithium metal batteries (ASLMBs) promise high energy density and safety but suffer from low initial coulombic efficiency and rapid capacity decay, especially at high cathode loadings. Using operando techniques, we concluded these issues to interfacial contact loss during lithium stripping. To address this, we introduce a conductive carbon felt elastic layer that self-adjusts pressure at the anode side, ensuring consistent lithium-solid electrolyte contact. This layer simultaneously provides electronic conduction and releases plating pressure. Consequently, the first coulombic efficiency dramatically increased from 58.4% to 83.7% along with over tenfold improvement in cycling stability. Overall, this study reveals an approach to enhance

anode-free ASLMB performance and longevity by mitigating lithium stripping inefficiency through self-adjusting interfacial pressure control enabled by a conductive elastic interlayer.

3:45 PM ES04.09.07

Exploring Wet SEI Layer Dynamics and Stability in Lithium-Ion Batteries Through Salt Concentration: An *Ab-Initio* Molecular Dynamics and Machine Learning Study [Fernando Soto](#); Penn State University-Greater Allegheny, United States

The Solid-Electrolyte Interphase (SEI) layer plays a key role in the performance and longevity of lithium-ion batteries (LiBs) (1), with its stability being crucial for efficient reversible operation of LiBs. This study focuses on the dynamics of the 'wet SEI' – an inorganic layer in contact with electrolyte solution (2), comprising components such as lithium fluoride (LiF), lithium oxide (Li₂O), and lithium carbonate (Li₂CO₃). A combination of *ab-initio* molecular dynamics (AIMD) simulations and machine learning models is employed to identify a 'goldilocks' salt concentration that optimizes the stability of the SEI layer, a critical factor in enhancing battery performance.

The study provides a comprehensive analysis of the interaction dynamics of LiF, Li₂O, and Li₂CO₃ in various electrolyte environments. The changes in cluster stability, surface area, and bond dynamics are explored, particularly focusing on the effects of varying salt concentrations on these parameters. The goal is to characterize an optimal salt concentration that yields an ideal inorganic SEI layer, enhancing the layer's protective qualities and improving overall battery safety and efficiency.

The findings of this study are significant for advancing the understanding of wet SEI layer formation and its optimization in LiBs. The implications of achieving an optimal SEI layer are profound, potentially leading to batteries with higher energy density, longer cycle life, and improved safety profiles.

References

(1) A. Wang, S. Kadam, H. Li, S. Shi, Y. Qi, Review on modeling of the anode solid electrolyte interphase (SEI) for lithium-ion batteries, *npj Computational Materials*, 4 (2018) 15.

(2) S. Perez Beltran, P.B. Balbuena, SEI formation mechanisms and Li⁺ dissolution in lithium metal anodes: Impact of the electrolyte composition and the electrolyte-to-anode ratio, *Journal of Power Sources*, 551 (2022) 232203.

4:00 PM ES04.09.08

Unraveling The Impact of Pectin on Transport and Mechanical Properties of EC-LiTFSI Electrolytes [Sipra Mohapatra](#) and Santosh Mogurampelly; Indian Institute of Technology Jodhpur, India

Biocompatible electrolytes are becoming attractive alternatives for the existing counterpart technology for battery electrolytes, as they are sustainable, renewable, and easily degradable. We used all-atom molecular dynamics simulations to study the transport and mechanical characteristics of a new class of battery electrolytes containing ethylene carbonate (EC), Li-TFSI, and pectin at different weight percentages. Pectin is a polysaccharide exhibiting high ion solvating capability, making it a potential candidate for battery electrolyte applications. Our simulation results demonstrate that pectin reduces the coordination numbers of lithium ions surrounding the counterions (and vice versa) as a result of the strong lithium-pectin interactions in comparison to lithium-TFSI interactions. We observed that smaller ionic clusters are favored over larger ones due to strong ion-polymer interactions, which is different from the trend observed in conventional electrolytes. Moreover, the ion association probability shows an increase in free ions, which indicates an enhancement in the overall ionic conductivity of pectin EC-LiTFSI electrolytes. Interestingly, TFSI ionic diffusivities show a strong correlation with the ion-pair relaxation timescales, with a relationship of $D_{TFSI} \sim \tau_c^{-0.95}$. On the other hand, the diffusivities of lithium ions follow a different pattern, with $D_{Li} \sim \tau_c^{-3.1}$, suggesting a unique transport mechanism for lithium ions. Consequently, the Nernst-Einstein conductivities scale with the ion-pair relaxation timescales as $\sigma_{NE} \sim \tau_c^{1.85}$. Furthermore, the increase in viscosity and ion-pair relaxation timescales show that pectin can also enhance the mechanical stability of the electrolytes.

References:

1. O. Borodin and G.D. Smith, *Macromolecules*, 2006, 39, 1620.
2. S. Mohapatra et al., *Nanoscale*, 2024, doi:10.1039/d3nr04029a
3. S. Mogurampelly, J. R. Keith and V. Ganesan, *J. Am. Chem. Soc.*, 2017, 139, 9511–9514.
4. Y. Zhang and E. J. Maginn, *J. Phys. Chem. Lett.*, 2015, 6, 700–705.

4:15 PM ES04.09.09

Organic Electrode Materials for Li-Ion Batteries [Dwight Seferos](#); University of Toronto, Canada

Organic materials hold promise as less-scarce materials for electrodes in a range of emerging battery technologies. Despite this, they have significant hurdles to overcome in terms of capacity, stability, and conductivity. Here, I will discuss our efforts in the rational design of organic materials as electrodes, both anodes and cathodes, for Li-ion batteries. First, I will discuss functional groups to maximize theoretical capacitance. Second, I will discuss the arrangement of these functional groups as macromolecules that render them insoluble, which is a requirement for any electrode in both the charged and discharged state. And in both, synthetic strategies for developing the functional group chemistry and macromolecules will be discussed. We consider both linear and 2D/3D type macromolecular designs for this purpose. Finally, I will share some insight into designs that have afforded very high capacity as anodes, where the lithium intercalation exceeds the expected 1 Li per 6 carbon units. Overall, this presentation will describe chemical structures and electrochemical properties and then aim to rationalize performance at the molecular level.

SYMPOSIUM ES05

Symposium Organizers

Ertan Agar, University of Massachusetts Lowell
Ruozhu Feng, Pacific Northwest National Laboratory
Edgar Ventosa, University of Burgos
Xiaoliang Wei, Indiana University-Purdue University

* Invited Paper
+ JMR Distinguished Invited Speaker
^ MRS Communications Early Career Distinguished Presenter

SESSION ES05.01: Flow Based Energy Storage I
Session Chairs: Ruozhu Feng and Wei Wang
Wednesday Morning, April 24, 2024
Room 431, Level 4, Summit

8:30 AM *ES05.01.01

Molecular Engineering toward Highly Stable Redox Flow Batteries with High Energy Density Dawei Feng; University of Wisconsin--Madison, United States

An increasing amount of renewable energy sources are being integrated into the electric grid in the US and around the world. However, as intermittent wind and solar begin to approach more than a quarter of grid energy production, significant energy storage technology must be employed as well to mitigate the unbalanced energy production and demand in the grid. To meet the emission targets in an economically viable manner, low-cost grid-scale energy storage technology must be developed. This talk will compare different battery technologies and describe our efforts in development of new generation of inexpensive redox active species for redox flow batteries (RFB) that can offer extraordinary energy density and cycling stability. This involves identification of critical needs for redox couple design in RFB and development of simplest yet effective synthetic routes towards redox active molecules with desired performance.

9:00 AM *ES05.01.02

Ion-Coupled Electron Transfer of Naphthalene Diimide for Organic Redox Flow Batteries Hye Ryung Byon; Korea Advanced Institute of Science and Technology, Korea (the Republic of)

Organic redox flow batteries (RFBs) have been investigated for future energy storage systems (ESSs). Tailoring organic redox-active molecules tunes solubility, redox potential, and chemical stability, which gives the promise to enhance energy density, cyclability, and calendar life in RFBs. Numerous studies focused on increasing molecular solubility to satisfy Econo-technical levels. In addition, introducing electron-donating and withdrawing groups to the redox-active core modulated redox potentials to negative and positive shifts, respectively. The most effective way to multiply raising energy density is to find a redox-active core undergoing multiple electron-transfer processes. Quinone is the representative one providing a single two electrons transfer in an aqueous electrolyte solution. Fast redox kinetics and chemical stability are achieved by H⁺ coupling; The reduced form, hydroquinone, promoted the following electron transfer in the acidic solution. A similar concept is applied for non-aqueous electrolyte solutions and using cations of supporting electrolytes. However, such an ion-coupled electron transfer was rarely studied to date. Here, we demonstrated naphthalene diimide (NDI) and Li⁺ coupled electron transfer in acetonitrile (MeCN). The NDI is an excellent model for the stepwise two-electron transfer process. Its low solubility by the strong p-stacking interaction was surmounted by introducing ammonium cationic substituents to the NDI via simple condensation and *N*-alkylation. As a result, two ammonium-tethered NDI and bistriflimide (TFSI) as the counter anion showed 0.9 M solubility in MeCN. Two cathodic events made an anionic radical and dianionic NDI core, respectively. The received electron is delocalized over the NDI core and also stabilized by pairing it with the cation. Cyclic voltammograms showed ~120 mV of potential difference from two cathodic waves with Li⁺ of LiTFSI electrolyte in MeCN, which was narrower than ~370 mV with K⁺ of KTFSI. It suggested that the Li⁺ possessing high charge density was closely coupled with the anionic radical NDI, expediting the second electron-transfer process. The process was also dependent on non-aqueous solvents. High donor-number (DN) solvents widened the potential difference with Li⁺ because a thick solvation shell of Li⁺ weakened the ion coupling. We applied this system for non-aqueous RFBs. Unlike two distinct galvanostatic plateaus appearing with K⁺, the ammonium-introduced NDI with Li⁺ showed almost a single overlaid plateau caused by the rapid reduction of the anionic radical. The ammonium-tethered NDI/Li⁺ in MeCN cells performed high cyclability and low crossover through an anion exchange membrane, showing a capacity fading rate of 0.0089% for 1000 cycles in RFBs.

9:30 AM ES05.01.03

Water Self-Regenerative and Non-Flammable High-Performance Hydrogel Electrolyte with Anti-Freeze Properties and Intrinsic Redox Activity for Energy Storage Applications Nageh K. Allam; American University in Cairo, Egypt

Hydrogel electrolytes are essential components of a plethora of functional devices due to their flexibility and high electronic and ionic conductivity. However, they suffer from poor water retention (dehydration) during operation. Consequently, the overall performance of the hydrogel-based devices is severely declined as a result of conductivity fading of the hydrogel with poor self-regeneration. To this end, the rational tailoring of hydrogel electrolytes with high conductivity, self-regeneration, non-flammability, anti-freezing ability, stability, and intrinsic redox activity is necessary to enable the fabrication of highly durable devices. Herein, we demonstrate the design and synthesis of highly ionic conductive LiBr@PVA-based electrolytes. Upon the use of the synthesized hydrogel electrolytes in supercapacitor devices, they revealed intrinsic redox activity with outstanding water retention capability and self-regeneration characteristics. The mechanism of regeneration and water retention is thoroughly investigated. Also, the devices showed an improved self-discharge potential (SDP) rate compared to those previously reported using polymeric electrolytes with redox additives. Moreover, the synthesized LiBr@PVA-based electrolytes exhibited high anti-freezing properties with stable electrochemical performance before and after regeneration. Our study provides a universal method to fabricate large-scale hydrogel electrolytes with unique properties and opens the door to fabricating high-performance solid state devices.

9:45 AM ES05.01.04

Systematic Design of Active Materials and Membrane Separators for All-Organic Non-Aqueous Redox-Flow Batteries [Gan Chen](#)¹, Wenhao Zhang^{2,1}, Yiping Li^{1,2}, Kaushik Dey¹, F. Dean Toste^{2,1} and Brett A. Helms¹; ¹Lawrence Berkeley National Laboratory, United States; ²University of California, Berkeley, United States

Redox-flow batteries employ dissolved active materials separated by a semi-permeable membrane to store energy. Cell life and capacity are maximized when active materials can be sequestered in their respective cell compartments at high concentration. Here, I will discuss how the design of the semi-permeable membrane must be considered alongside that for the active materials, whose infinite miscibility with non-aqueous electrolytes allow for high volumetric capacity. The oligomeric design of these active materials makes them sufficiently large to be excluded by a microporous membrane, while maintaining substantially faster electron transfer kinetics than competing polymeric and colloidal active materials. I will discuss how these design features influence charge transfer with the electrode and other attributes that impact the efficiency of the flow cells as they relate to emerging applications in grid-scale energy storage.

10:00 AM BREAK

10:30 AM *ES05.01.05

U.S. DOE Initiatives Advancing Flow Battery Manufacturing Innovation [Changwon Suh](#); U.S. Department of Energy, United States

The Department of Energy's Advanced Materials and Manufacturing Technology Office (AMMTO) continues to invest in energy storage research, development, demonstration, and deployment (RDD&D) to help stakeholders improve efficiency, cut costs, and make materials, devices, and systems with superior performance. Despite recent promising advances, manufacturing capabilities are still necessary to meet the expected demand for energy storage as we move toward a clean energy economy. Strengthening the domestic manufacturing supply chains is also another important task to pursue in parallel.

AMMTO funded projects through Battery Manufacturing funding opportunity announcement and national laboratory call to address technical and manufacturing challenges in U.S. flow battery production, specifically targeting the optimization of flow batteries across commercial, industrial, and utility applications. These projects aim to and improve the manufacturability of flow batteries and reduce the cost of manufacturing battery components and systems by implementing advanced designs and processes.

In this talk, the status and accomplishments of the projects will be highlighted. In addition, there will be a robust discussion of a wide variety of AMMTO's efforts in the context of technical and manufacturing challenges regarding scale-up and performance that still prevent the flow battery community from achieving cost targets and commercial viability.

11:00 AM *ES05.01.06

Innovative Metal Complex Catholytes for Aqueous Redox Flow Batteries [Yu Zhu](#); University of Akron, United States

Aqueous Redox Flow Batteries (RFBs) have been recognized as potential candidates for large-scale grid energy storage. Nonetheless, commercial RFBs face material limitations, primarily due to the toxicity and cost of current active materials. To address this, there's an urgent need for next-generation RFBs that harness earth-abundant active materials, characterized by high solubility, optimal redox potential, and electrochemical stability. While organic and hybrid materials have been explored as alternatives, they present their own set of challenges, particularly when functioning as catholyte materials. This research will present a strategic design of metal complex catholytes for aqueous RFBs. By altering the symmetry of these metal complexes, we've achieved notable advancements in tackling solubility and crossover issues. Furthermore, our recent scattering experiments revealed the discovery that these materials form self-assembled particles in solution, paving new avenues for the design of active materials with enhanced water solubility.

SESSION ES05.02: Flow Based Energy Storage II

Session Chairs: Ertan Agar and Ruozhu Feng

Wednesday Afternoon, April 24, 2024

Room 431, Level 4, Summit

1:30 PM ES05.02.01

Embedded, Micro-Interdigitated Flow Fields for Flow-Based Electrochemical Desalination and Beyond [Kyle C. Smith](#); University of Illinois-Urbana Champ, United States

The delivery of fluids to porous electrodes is essential to the efficient functioning of flow-based electrochemical devices. To date this has been accomplished in flow batteries and fuel cells by using flow fields that employ millimetric channels embedded in ~1 cm thick bipolar plates that abut porous electrodes. Here, we demonstrate novel flow fields that use interdigitated microchannels less than 100 μm wide, embedded within porous intercalation electrodes for the purpose of water desalination [1]. We subsequently use these electrodes containing Prussian blue analog nanoparticles to achieve seawater-level salt removal (~500 mM NaCl) for the first time in a flow-based symmetric Faradaic deionization (FDI) device, while previous work had relegated such devices to brackish water desalination having >5X lower salinity. Physics-based modeling shows that the patently low hydraulic permeability of these intercalation electrodes (<0.5 μm^2) induces perpendicular flow within the electrode material between adjacent microchannels to promote reaction uniformity, despite parallel flow within electrode material being realized for the hydraulic permeability of flow battery and fuel cell electrodes (~10 μm^2). We fabricate these microfluidic patterns using laser engraving. Here, electrode wetting prior to laser engraving is shown to produce enhanced microchannel resolution and smoothness while maintaining the chemical and microstructural integrity of electrodes by suppressing the propagation of heat affected zones via the low thermal diffusivity and high latent heat of water. The resultant patterned electrodes exhibit as much as 100-fold increased apparent permeability relative to unpatterned electrode material, resulting in decreased pumping pressure and energy requirements. Consequently, simulated brackish water (~100 mM NaCl) and simulated seawater (~500 mM NaCl) solutions were desalinated to near-potable water with thermodynamic energy efficiencies (TEEs) of 40% and 7%, respectively. While TEEs show room for significant improvement relative to the thermodynamic limit, brackish TEE is at parity with reverse osmosis neglecting energy recovery. Such efficiency also shows the promise of embedded, micro-interdigitated flow fields for flow-based electrochemistry using low-permeability porous electrodes, such as those that contain nanomaterial conductive additives, catalysts, or active materials.

[1] V. Do, E. Reale, I. Loud, P. Rozzi, H. Tan, D. Willis, K. Smith, Embedded, micro-interdigitated flow fields in high areal-loading intercalation

electrodes towards seawater desalination and beyond, *Energy Environ Sci.* 16 (2023) 3025–3039.

1:45 PM *ES05.02.02

Manufacturing Electrodes with Tailored Structures for Efficient Mass Transport in Flow Batteries: Challenges and Opportunities [Ana Jorge Sobrido](#), Michael W. Thielke, Carlos Julando Junior Mingoos and Luis M. Murillo Herrera; Queen Mary University of London, United Kingdom

Deep and rapid decarbonisation of the global energy systems require the wholesale replacement of fossil fuels with renewable resources (e.g., wind, solar). However, these resources are intermittent and unpredictable challenging the existing grid infrastructure which is based on the just-in-time dispatchable generation enabled by combustion of fossil fuels. As such, flexible energy management systems, including electrochemical energy storage technologies, are urgently required to enable reliable electricity delivery from the variable assets. Among them, redox flow batteries (RFBs) are excellent candidates for large-scale, long duration energy storage due to their flexible design, long service life, high reliability, and environmental friendliness. Nevertheless, this technology is still in its infancy in terms of optimisation of materials and battery design that can lead to improvement in performance and cost. Our research seeks to improve upon one of their performance-determining components: the electrodes. In my talk, I will present our work on the use of electrospinning to produce self-supporting materials highly conducting and consisting of fibres of 500nm - 1micron diameter. I will also introduce our approach to replace commonly employed petrol-derived materials with biomass-waste carbon electrodes via electrospinning. Electrospinning is a versatile technique that allows the production of freestanding fibrous materials with tailored properties, including fibre diameter, surface chemistry and alignment of fibres. Finally, I will summarise the main challenges and opportunities to the development of efficient electrodes with optimised mass transport and charge transfer for redox flow batteries.

2:15 PM ES05.02.03

Designer Novel Deep Eutectic Electrolytes for Vanadium Redox Flow Batteries [Luis M. Murillo Herrera](#), Carlos Mingoos, Michael W. Thielke and Ana Jorge Sobrido; Queen Mary University of London, United Kingdom

Deep eutectic solvents (DES) are binary or ternary mixtures of Lewis acids and bases that exhibit significantly lower melting points than those of the original components. The application of these neoteric solvents in energy storage have recently started to gather attention due to its promising properties as low toxicity, high biodegradability, cost-effectiveness, high solubility for metal salts, conductivity and designer capability, which means that the DES can be specifically formulated for a desired application from among 10^6 possible combinations approximately.

Within the classification of DES, the second family composed of metal halides and quaternary ammonium salts has been applied to Li, Fe, and Al batteries, whereas DES of the third family made of quaternary ammonium, phosphonium or sulphonium halides and hydrogen bond donors have been recently applied as supporting electrolytes for redox flow batteries (RFB). Despite their huge structural flexibility, the application of DES to RFBs have been narrowed to mixtures of choline chloride with ethylene glycol, glycerol and urea, the three main archetypes of the third family. The chemistries studied so far are All-V(acac) and Fe/V. Although promising, these electrolytes suffer from high viscosities and low conductivities, which in consequence produces high cell polarisation resistance, low efficiencies, high pressure drop and small operational currents.

The overarching objective of this work is to transcend the prevailing DES archetypes to design and evaluate novel DES formulations tailored specifically for vanadium RFB applications based on family III DES. In the organic salt department, particular relevance is placed on the influence of the cation and the hydrogen bond donor in properties like cathodic window, viscosity/conductivity and vanadium solubility. Different counter anions are analysed in terms of anodic window, hygroscopicity, vanadium solubility and the potential to develop redox-actives DES (RADES), e.g bromide-based DES. In the hydrogen bond donor department, the impact of adjacent DES properties as pH, polarity and ionic strength on vanadium redox mechanisms is being under scrutiny. The most common separator technology studied for DES-based RFBs are proton-exchange membranes, which are not ideal for non-aqueous systems. As part of this project, the compatibility of DES with other membrane technologies as anion-exchange are explored, including membrane-less designs based on differences in negolyte and posolyte polarity.

Finally, new vanadium (III) complexes with electron-donating ligands capable of displacing V(II)/V(III) redox potential towards more cathodic values, while synergistically interacting with the web of intermolecular interactions of the solvents are proposed to leverage the larger cathodic windows of DES compared to aqueous electrolytes, thus increasing the active species concentration and the cell potential.

2:30 PM *ES05.02.04

Automated Electrochemical Characterization for Redox Flow Batteries Using The Electrolab: Molecules, Polymers, Electrolytes and their Complex Interactions [Zirui Wang](#), Michael A. Pence and [Joaquin Rodriguez-Lopez](#); University of Illinois at Urbana Champaign, United States

Designing superior redox flow batteries (RFBs) requires advanced electrochemical characterization techniques that elucidate manifold transport, reactivity, stability, and interactive properties of molecules, electrolytes, and other materials present in these systems. The modularity of many RFB designs enables significant flexibility in the choice of experimental conditions, thus making it imperative to swiftly identify those that lead to improved properties. This not only requires the ability to carry out many experiments in a timely fashion, but also to use electroanalytical approaches in a comprehensive and clever way. To accomplish these objectives, our group has recently introduced The Electrolab, an automated electrochemical platform that combines hardware, software, a dispensing robot, and custom designed e-chips which altogether enable characterization campaigns with minimal supervision while maximizing diagnostic power. The Electrolab is sufficiently versatile to enable both relatively simple but tedious experiments such as determining diffusion coefficients, to systematic experiments incorporating titrations, to more sophisticated measurements of lifetime of redox species using microelectrode e-chips.

In this presentation, we will first describe new opportunities in the use of redox-active polymers for the construction of redox flow batteries. Unlike small molecules, polymeric redox active materials exhibit dynamics that are highly dependent on aspects such as electrolyte concentration and type. I will then explain how the Electrolab incorporates functions to systematically explore these dependencies, including automated robotic titrations which enable to rapidly identify limiting factors. Finally, I will describe how a different type of redox titration experiment based on scanning electrochemical microscopy can be developed and automated to understand charge transfer performance between redox mediators and charge storage media such as redox polymers. Putting together automated electrochemistry, advanced techniques based on microelectrodes, and new concepts for energy storage based on polymeric materials, promises new directions in the identification of RFB systems.

5:00 PM ES05.03.01

Using Covalent Modification to Create Phenyl-, Butyl- and Fluorine-Modified Active Material for Deployment in Redox Flow Batteries [Robert Serrano](#)^{1,2}, Jennifer Bolibok¹ and Patrick Cappillino¹; ¹University of Massachusetts, Dartmouth, United States; ²Arizona State University, United States

In the United States, 13.6% of the country's power now comes from the two leading contenders for new sustainable energy projects: wind and solar. Since these two methods of generation are intermittent, it has been the prevailing thought that grid-level energy storage would be needed to balance when electricity is generated and when it is demanded. For this purpose, integrated battery technology such as lithium-ion manganese oxide (LMO) and lithium iron phosphate (LFP) have been adapted from the advancement of electric vehicle development in recent years, but can be expensive, require active thermal management, face longevity issues from deep cycling, and are not suitable for extreme temperatures. Redox-flow batteries have been proposed to solve these issues, but low energy density has been a limiting factor for wide-scale adoption. Using covalent modification, we are seeking to increase the energy density of a metal-organic compound for use as a non-aqueous redox-flow battery active material. Alpha substituted bromoacetic acids were used to synthesize the ligand of a vanadium complex in order to fine tune chemical properties of the complex, with α -bromophenylacetic acid and 2-bromohexanoic acid exhibiting great promise. The resulting ligands were characterized via NMR — specifically HSQC — which will be presented.

5:00 PM ES05.03.02

Investigation of The Dynamics of Extreme Redox-Active Molecule and Electrolyte Concentrations Relevant for Nonaqueous Redox-Flow Batteries [Anton S. Perera](#)^{1,1}, Nathan Stumme², Sashen Ruhunage^{1,1}, Andrew Horwarth², Scott Shaw² and Chad Risko^{1,1}; ¹University of Kentucky, United States; ²The University of Iowa, United States

Organic redox-active molecules have been explored for many uses including, acting as the active material in energy-storage systems for redox flow batteries (RFBs) and providing overcharge protection in lithium-ion batteries (LIBs). The concentration of the redox active species and the supporting electrolyte in an RFB play a significant role in determining the energy density of a battery. Nevertheless, at very high concentrations, the physicochemical relationship between the redox active molecule, electrolyte salt, solvent, and the electrochemical performance of an RFB has not yet been well studied. Herein we present a molecular-level understanding of the effect of concentration on physical properties of the redox-active solution to complement experimental observations using molecular dynamic (MD) simulations. To examine this relationship, we explored the redox-active molecule 2,2,6,6-tetramethylpiperidine 1-oxyl (TEMPO) and tetrabutylammonium hexafluorophosphate (TBAPF₆) electrolyte salts varied across concentrations of 1 mM to over 1000 mM in acetonitrile. We observed relationships between the transport properties of these solutions that were primarily based on solvation and ion-pairing effects. Furthermore, we also provide suggestions on obtaining optimum performance in such systems based on our theoretical insight.

5:00 PM ES05.03.03

Surface Decorated 3D Printed Electrodes as Viable Options for High Performance Redox Flow Batteries [Carlos Mingoes](#), Michael W. Thielke, Luis M. Murillo Herrera and Ana Jorge Sobrido; Queen Mary University of London, United Kingdom

In an era marked by rapid urbanization and industrialization, accompanied by increased demands for energy availability and utilization, the need for more large-scale application of reliable and sustainable energy sources has never been more pressing. As we take on the challenges of climate change and resource depletion, the need for efficient and scalable energy storage systems has emerged as crucial for the transition to a cleaner and more resilient energy landscape. Due to the intermittent nature of sustainable energy sources (Solar, wind...), energy storage systems are needed to bridge the temporal and geographical gaps that they impose.

Among the various energy storage technologies, Redox Flow Batteries (RFBs) has emerged as a particularly promising solution. A system wherein power and energy are decoupled affording the ability to scale each independently, rendering the system very flexible; different flow battery systems can be designed for different purposes, with different energy and power combinations.

In the quest to optimize flow battery technology, to make it more cost efficient and cost competitive, lots of research has been focused into enhancing the power density and efficiency of the electrochemical cell. This translates to refined engineering and in-depth study of electrode materials and structures to ascertain what characteristics makes them ideal for flow cells. Carbon based electrodes with porous structures are the standards in this regard. Providing large electrochemically active surfaces for the electrochemical reactions and having porous structures that facilitate mass, charge, and heat transport. Some conventional porous electrodes are carbon felts, cloths and papers, all electrodes composed of carbonized fibres and are prepared by methods, such as electrospinning, and weaving.

Recently, there has been increased interest in the potential of 3D printed electrodes for RFB. It is a very scalable manufacturing method, with numerous printing techniques and various material precursor types to choose from. In the scope of electrode designs, this method presents the ability to readily fabricate intricately designed custom electrodes, with well tune electrolyte transport channels for efficient mass transport. Depending on precursor type, printing method and thermal treatment steps, the structural, electrochemical and mechanical properties of the electrodes can be tuned. However, as demonstrated in other studies, preparing electrodes with high electrochemical surface area via this method can be challenging and thus surface decoration with other high surface area materials, such as carbon nanotubes and nanoparticles is a desirable option to increase this necessary characteristic for RFB electrodes.

In our work we aim to demonstrate the potential of surface decorated 3D printed electrodes to be a viable option in high performance RFB. 3D printed electrodes are thermally treated to induce conductivity and are subsequently surface decorated with nanomaterials to produce surface decorated 3D printed electrodes.

5:00 PM ES05.03.04

Architecting Electrospun Carbon Fibres for Redox Flow Batteries and The Influence of Fibre Size and Alignment [Michael W. Thielke](#)¹, Luis M. Murillo Herrera¹, Carlos Mingoes¹, Alexander H. Quinn², John N. Vergados², Fikile Brushett² and Ana Jorge Sobrido¹; ¹Queen Mary University of London, United Kingdom; ²Massachusetts Institute of Technology, United States

As one of the promising uprising technologies in the field of stationary energy storage, redox flow batteries are in focus for the future storage of sustainable energy harvesting. The carbon fibre-based electrodes in these batteries are a crucial component in achieving high efficiency and performance, which is significantly influenced by the composition and morphology of the utilized carbon fibres. Our work is based on the fabrication of carbon fibres by using electrospinning, a potential alternative to replace commercial carbon felts with higher performance based on the outstandingly high surface-to-volume ratio. This also allows the effective fabrication of doped and decorated fibres by an in situ doping of the fabricated fibre with catalytically active metal nanoparticles or through heteroatom-based doping of the fibre material itself.

Electrospinning has been proven to be a highly versatile technique to fabricate submicron carbon fibres and can be performed with alternative polymeric materials to synthesize carbon fibres, including biopolymers from renewable sources, such as lignin, opening the possibility of a fully sustainable future of

energy storage, without any dependence on petrol-derived resources. In recent years, different approaches to implementing bioderived carbon into the electrode have been reported, most commonly by using an additive method to enhance the commercial carbon felt with biomass-derived carbon particles, or by using given fibrous biomaterials from fibrous structure.

The versatility of the electrospinning process allows the fabrication of different fibre architectures. By modifying the collector of the electrospinning process to a rotating drum, the fibres can be collected in alignment with the rotation which can then be installed parallel or perpendicular to the flow field of a redox flow battery. The orientation can lower the pressure within the system and significantly influence the current density during the operation of the battery. To optimize the balance between pressure and performance, the degree of orientation of the fibres was gradually controlled through the rotation speed of the drum.

Another important factor that influences the performance of a redox flow battery is the fibre diameter, which can be controlled by changing the parameters of the electrospinning process. While electrospun carbon fibres are generally used due to their electrochemical active surface area compared to commercial felts, the process itself has the potential to form fibres in different sizes, in this case in the magnitude starting from 220 nm and up to 850 nm.

Changing the size of the fibres is a trade-off between the available performance through the higher surface area of the smaller fibres and lowering the pressure of the flow and favouring the mass transport of the larger fibres.

5:00 PM ES05.03.05

Gas Diffusion in Catalyst Layer of Flow Cell for CO₂ Electroreduction Toward C₂₊ Products [Nageh K. Allam](#); American University in Cairo, Egypt

The use of gas diffusion electrode (GDE) based flow cell can realize industrial-scale CO₂ reduction reactions (CO₂RRs). Controlling local CO₂ and CO intermediate diffusion plays a key role in CO₂RR toward multi-carbon (C₂₊) products. In this work, local CO₂ and CO intermediate diffusion through the catalyst layer (CL) was investigated for improving CO₂RR toward C₂₊ products. The gas permeability tests and finite element simulation results indicated CL can balance the CO₂ gas diffusion and residence time of the CO intermediate, leading to a sufficient CO concentration with a suitable CO₂/H₂O supply for high C₂₊ products. As a result, an excellent selectivity of C₂₊ products ~ 79% at a high current density of 400 mA.cm⁻² could be obtained on the optimal 500 nm Cu CL (Cu500). This work provides a new insight into the optimization of CO₂/H₂O supply and local CO concentration by controlling CL for C₂₊ products in CO₂RR flow cell.

5:00 PM ES05.03.06

1D Borophosphates for Use as Electrolyte Membranes in Solid Acid Fuel Cells [Brian Chaloux](#), James Ridenour, Michelle Johannes and Albert Epshteyn; US Naval Research Laboratory, United States

Although they are relatively new players in the field of hydrogen energy conversion, solid acid fuel cells (SAFCs) demonstrate several advantages compared to their more well-developed counterparts: polymer electrolyte membrane fuel cells (PEMFCs) and solid oxide fuel cells (SOFCs). The elimination of water as the proton carrier in solid acid electrolytes allows operation at intermediate temperatures (e.g., 200–350 °C), simultaneously improving catalytic activity and removing the need to manage liquid water while avoiding the high-cost, refractory materials required for operation under SOFC conditions. However, higher operational temperatures necessitate the discovery, design, and manufacture of electrolyte materials with improved thermal stability compared to PEMs.

Cesium hydrogen sulfate (CsHSO₄) and cesium dihydrogen phosphate (CsH₂PO₄, CDP) are two well-studied examples of solid acids: protic materials which remain solid at operational temperature while exhibiting proton conduction. CDP demonstrates particular promise as a SAFC electrolyte, as a superprotonic transition from a low-temperature monoclinic phase to a high-temperature cubic phase dramatically improves its proton conductivity above 225 °C. However, active humidification of the CDP electrolyte is required to prevent thermal decomposition (i.e., dehydration) below the superprotonic transition temperature, limiting the practical operational window of CDP-based SAFCs to 225–260 °C.

We synthesize and explore an isostructural family of one-dimensional inorganic polyelectrolytes, the “BOB” borophosphates – empirical formula M_{5-x}H_x[BOB(PO₄)₃] where M is a monovalent cation – as alternative proton conducting solid acids to commercially available membrane materials including PEMs and CDP. Comparing the previously described Rb₃H₂[BOB(PO₄)₃], Na₅[BOB(PO₄)₃], and the novel (NH₄)₅H₂[BOB(PO₄)₃], we find that the rubidium borophosphate (RbBOB) strikes an attractive balance between temperature- and humidity-dependent ionic conductivity and thermal stability. Exhibiting stability under air, inert atmosphere, and hydrogen up to 400 °C and exhibiting ionic conductivity up to 10⁻⁴ S cm⁻¹ under active humidification at elevated temperature, RbBOB is an exciting new solid acid for SAFC electrolyte membranes.

SESSION ES05.04: Flow Based Energy Storage III

Session Chairs: Ertan Agar and Ruozhu Feng

Thursday Morning, April 25, 2024

Room 431, Level 4, Summit

8:30 AM *ES05.04.01

Molecular Design for Redox Flow Batteries featuring Oligomeric Active Materials and Selective Polymer Membranes [Brett A. Helms](#); Lawrence Berkeley National Lab, United States

Nearly a decade ago, we introduced the concept of pairing microporous polymer membranes and oligomeric active materials for cross-over free redox-flow batteries. Since then, the field has advanced designs of considerable efficacy and rigor. Yet, there is more to do as use-cases evolve from multi-hour to long-duration. Here, I will discuss outstanding challenges with respect to different components in the devices as well as their thoughtful integration toward meeting technical specifications for these emerging use-cases. Increasingly, synthetic advances are coming from detailed understanding of specific electro-physioproperities of membranes and active materials as well as emergent failure mechanisms, which present differently at different stages of the battery's useful life and must be taken into account for there to be a credible pathway to commercialization and deployment.

9:00 AM *ES05.04.02

Understanding Cycling Stability of Redox Active Electrolytes in Aqueous Redox Flow Batteries [Tianbiao Liu](#); Utah State University, United States

Aqueous Organic redox flow batteries (AORFBs) have been considered a promising battery technology for scalable, long-duration energy storage. The presentation first highlights our research progress in developing viologen based AORFBs in the last 10 years. Then mechanistic studies regarding the cycling stability and crossover issues of viologen, ferrocene, ferrocyanide, and TEMPO based electrolytes will be discussed in detail. This presentation

This searchable program is up-to-date as of April 15th, 2024.

emphasizes data acquisition protocols and systematic spectroscopic studies for the energy storage performance of redox-active electrolytes in both half and full-flow batteries.

9:30 AM BREAK

10:00 AM *ES05.04.03

Accelerate Material Discovery and Expand Chemistry Space for Aqueous Organic Redox Flow Batteries [Wei Wang](#); Pacific Northwest National Laboratory, United States

Aqueous organic redox active materials have recently shown great promise as alternatives to transition metal ions as energy bearing active materials in redox flow batteries for large-scale energy storage due to their structural tunability, cost effectiveness, availability, and safety features. However, development to date has been limited to a small palette of aqueous soluble organics. This presentation will provide an overview of a data-driven approach to accelerate the discovery and development of aqueous organic redox-active molecules for flow batteries, including database curation, structure-property correlation, and automated property characterization and performance testing. This presentation will also use fluorenone as an example to showcase how a natively redox-inactive molecule can be tuned to possess two-electron redox reversibility through hydrogenation and dehydrogenation.

10:30 AM ES05.04.04

Understanding The Principles of Charge Transfer to Realize High Capacity Utilization in Redox Targeting Flow Batteries [Sam Kopfinger](#), Hongyi Zhang, Thai Boonme, Garrett Grocke and Shrayesh Patel; The University of Chicago, United States

Redox targeting systems represent a promising path for flow batteries, circumventing the solubility constraints encountered by various organic redox compounds. Yet, the pivotal challenge remains the attainment of high capacity utilization of the target within flow cell systems and a deeper comprehension of the mediator-target interplay. In addressing this gap, we present the development of a high solids accessibility redox targeting flow battery, alongside the formulation of an advanced yet clear thermodynamic model to unravel the intricacies of the mediator-target relationship. Our approach involves a ferrocene bearing insoluble polymer that is synthesized for use as a redox target and matched with different mediator systems: one with a single molecule that has a nearly identical potential and the other with a dual molecule system that has mediators with a voltage offset to encourage charge transfer. These two systems were then tested in a catholyte limited flow cell to determine the capacity accessibility of the mediator-target system. The single molecule system was able to increase the cell's capacity by 90% of the redox target's capacity and the dual molecule system was able to increase the capacity by >95% of the redox target's capacity. To better understand the thermodynamics of each system they are modeled using a Nernst analysis. For the single molecule system, this analysis builds on prior work to suggest that not only is a small voltage offset extremely important, but that the mediator's accessible state of charge range will determine the redox target's thermodynamic accessibility limits. For the dual molecule system, the model suggests that a medium voltage offset is ideal as it allows for high amount of charge transfer in the preferred direction with enough potential overlap to assist charge transfer in the reverse direction. In summary, our work not only demonstrates the achievable high accessible capacity of redox targeting systems within flow cells but also provides a comprehensive thermodynamic model to elucidate their operational mechanisms and crucial design considerations.

10:45 AM *ES05.04.05

Redox-Mediated Electrified Chemistry for Carbon-Neutral Energy Applications [Qing Wang](#); National University of Singapore, Singapore

Redox reaction involving charge transfer at the electrode-electrolyte interface represents an essential process for various electrochemical energy conversion and storage applications, such as fuel cells, electrolyzers and batteries, etc. As a result, the operation (*i.e.*, cell voltage, current density, number of charges, etc.) of the above devices is inherently dictated and constrained by the redox reactions at the electrode-electrolyte interface. The redox-mediated process — a chemical reaction between an electrolyte-borne redox species electrochemically generated on electrode and a material (generally insoluble in electrolyte) away from the electrode, provides additional flexibility in circumventing the constraints intrinsically confronted by the conventional electrochemical devices. One example is the redox targeting of energy storage materials for flow batteries. The redox-mediated reactions of high-capacity solid material stored in the tank with redox electrolyte flowing through it considerably boost the energy density of redox-flow battery without compromising its salient features of operation flexibility and scalability. Another example is the redox-mediated water electrolysis for spatially decoupled hydrogen production. The electrochemical-chemical cycle enables continuous reaction between an electrolyte-borne redox mediator and an HER or OER catalyst loaded in a fixed-bed reactor spatially separated from the cell, which is believed to be advantageous to enhanced safety and on-demand hydrogen production. So, with the assistance of redox mediators shuttling between the electrode compartment and reactor tank, the border of the conventional electrochemical reaction is spatially extended beyond the electrode compartment, which endows the system with intriguing features for various innovative energy applications.

SYMPOSIUM ES06

Sulfur and Sulfide Chemistry in High Performance Electrochemical Energy Storage
April 23 - May 7, 2024

Symposium Organizers

Yoon Seok Jung, Yonsei University
Dongping Lu, Pacific Northwest National Laboratory
Hui Wang, University of Louisville
Yang Zhao, University of Western Ontario

Symposium Support

Bronze
BioLogic

* Invited Paper
+ JMR Distinguished Invited Speaker
^ MRS Communications Early Career Distinguished Presenter

SESSION ES06.01: Lithium-Sulfur Batteries I
Session Chairs: Yoon Seok Jung and Dongping Lu
Tuesday Morning, April 23, 2024
Room 432, Level 4, Summit

10:30 AM *ES06.01.01

Lithium-Metal Stabilization through Tellurium Chemistry in Lithium-Sulfur Batteries [Arumugam Manthiram](#); University of Texas at Austin, United States

Lithium-sulfur (Li-S) batteries are appealing owing to the high specific capacity (1672 mA h g^{-1}) and low cost of sulfur. Lithium-sulfur cells involve a solid-liquid-solid conversion of sulfur species, from S to intermediate lithium polysulfides to the end discharge product Li_2S , which results in a sluggish reaction kinetics due to the insulating nature of S and Li_2S . Furthermore, the dissolution of polysulfides and their migration from the cathode to the anode severely hamper the reversible plating and stripping of lithium-metal anode. These problems impede the practical application of Li-S batteries. Numerous efforts have been devoted to overcoming these challenges, but the intrinsically low stripping and plating efficiency of Li and the corrosion from polysulfides necessitate excess Li and electrolyte.

This presentation will focus on the exploitation of the chemistry of tellurium, which lies in the same group as sulfur in the periodic table. The addition of a small amount of tellurium into sulfur cathodes helps enhance the cycle life of Li-S cells. However, due to the poor utilization of Te, a significant amount of Te is required to improve cell cycling performance, resulting in an increase in cost. To overcome this challenge, we have adopted two approaches: (i) use of tellurium nanowires (TeNW) synthesized *via* a hydrothermal method and (ii) incorporation of LiTe_3 synthesized by a one-step process as an additive into the electrolyte.

Coating TeNW onto the separator greatly enhances Te utilization and a significant improvement in cell cycle life. The versatility of TeNW is further demonstrated by utilizing it with carbon nanotubes as the anode substrate. The exceptional performance of TeNW is due to its high-surface area nanostructure and excellent conductive network, facilitating efficient electron transfer during cell cycling.

On the other hand, LiTe_3 reacts rapidly with polysulfides and functions as a redox mediator to significantly improve the cathode kinetics and the utilization of active material in the cathode. The formation of a $\text{Li}_2\text{TeS}_3/\text{Li}_2\text{Te}$ -enriched interphase layer on the anode surface enhances ionic transport and stabilizes Li deposition. By regulating the chemistry on both the anode and cathode sides, the LiTe_3 additive enables a stable operation of anode-free lithium-sulfur cells with only 0.1 M concentration in conventional ether-based electrolytes. With a high utilization of Te, the additive enables significantly longer cycle life of anode-free pouch full-cells under lean electrolyte conditions.

11:00 AM *ES06.01.02

Lithium Sulfur Batteries - What is The Future of this Battery Chemistry? [Y. Shirley Meng](#)^{1,2}; ¹The University of Chicago, United States; ²Argonne National Laboratory, United States

The research and development of lithium sulfur batteries have been decades, yet we still do not see its commercialization success. In this talk, I will give an examination of the literature and discuss the remaining scientific hurdles and technical challenges. With the advancement in all solid state batteries, our group has developed a unique approach in enabling lithium sulfur electrochemistry with solid state electrolytes. The progress made was enabled by fundamental understanding of the interfacial sciences and new scientific tools such as cryogenic microscopy and advanced spectroscopy.

11:30 AM *ES06.01.03

Design Interface Reactions in All-Solid-State Batteries [Xin Li](#); Harvard University, United States

Solid state battery is a mechanically more coupled device than the commercial liquid electrolyte Li-ion batteries. Mechanical constriction effect strongly modulates the electrochemical stability at all interfaces in a solid-state battery. This effect introduces some unique dynamical evolution of interface reactions upon battery cycling, understanding of which is challenging but also giving us an opportunity to design the battery performance beyond commercial Li-ion batteries. The talk will discuss the design of such a dynamic process at the electrolyte-electrode interfaces for a stable cycling of solid state batteries. The importance of the self-limiting interface reactions due to dynamic voltage stability will be emphasized.

SESSION ES06.02: Lithium-Sulfur Batteries II
Session Chairs: Hui Wang and Yang Zhao
Tuesday Afternoon, April 23, 2024
Room 432, Level 4, Summit

1:30 PM *ES06.02.01

A Long Cycle Li-S Battery with Minimum Shuttle Effect - Catalytic Disproportionation of Dissolved Polysulfide to Elemental Sulfur [Deyang Qu](#), Dantong Qiu and Dong Zheng; University of Wisconsin Milwaukee, United States

A Long cycle-life Li-S battery pouch cell with high sulfur loading (5 mg per cm^2) is reported with the mitigation of the shuttle-effect. The performance was achieved with a bifunctional carbon material with three unique features. The carbon can catalyze the disproportionation of dissolved long-chain polysulfide

ions to elemental sulfur; the carbon can ensure homogenous precipitation of Li sulfide on the host carbon and the carbon has honeycomb porous structure which can store sulfur batter. All the features will be demonstrated experimentally and reported.

Through an ex-situ, postmortem analysis in which a Li-S cell was disassembled after many cycles, few dissolved polysulfides were found in the electrolyte of the Li-S cell made with the bifunctional carbon in comparison with a control Li-S cell. A HPLC was used to determine the distribution of dissolved elemental sulfur and polysulfide ions in the electrolyte of the Li-S batteries during cycling. Only dissolved elemental sulfur was detected in the cell with the bifunctional carbon, while a distribution of polysulfide ions of various -S-S- chain length was observed in the control Li-S cell. A catalytic polysulfide disproportionation reaction mechanism was proposed, in which polysulfide ions can be catalytically disproportionate to elemental sulfur and Li_2S_2 and/or Li_2S precipitates. Since the dissolved polysulfides are the engine driving the shuttle effect, the detrimental shuttling in a Li-S cell can be mitigated through the removal of dissolved polysulfide ions in the electrolyte during the discharge and recharge.

The unique porous structure of the bifunctional carbon which was made from a raw silk was revealed by a SEM and a N_2 -absorption isotherm. The pore structure was believed to store sulfur uniformly and ensured the homogeneous deposition of Li_2S_2 and/or Li_2S . The N-containing functionalities that were introduced to carbon from the amino acids of raw silk can catalyze the disproportionation of the dissolved S_n^{2-} to solid S_8 at the cathode side, thereby mitigating the shuttle effect. In addition, the hierarchical honeycomb porous structures generated by a carbonization process can physically trap high-order lithium polysulfides and sustain the volume change of sulfur. With the synergistic effects of the unique structures and characteristics of the carbon, the sulfur/carbon composite using delivers a high reversible capacity of over 1000 mAh g^{-1} and over 600 mAh g^{-1} with a sulfur content of 1.2 mg cm^{-2} 5 mg cm^{-2} in a pouch cell, respectively.

2:00 PM *ES06.02.02

SPAN and Beyond: Sulfur-Based Cathodes Free of Polysulfides [Ping Liu](#); University of California, San Deigo, United States

Li-S battery is a highly desirable technology featuring high energy density and low-cost materials. However, the challenges with the technology are also well documented. In ether-based electrolytes, the redox of sulfur goes through a soluble polysulfide mechanism, which facilitates the reaction kinetics but greatly impacts the cycle life and practical energy density due to the need for elevated amount of electrolytes. Sulfurized polyacrylonitrile, SPAN, in contrast, does not involve the polysulfide mechanism. Instead, the material goes through a solid-solid conversion process. Coupled with the presence of a robust cathode electrolyte interface (CEI), the material has demonstrated exceptionally long life, well over 1000 cycles.

SPAN's limitation lies in its limited sulfur content (~ 43 wt%) and specific capacity (< 700 mAh/g). These values put a practical limit for the energy density of Li-SPAN battery at around 300 Wh/kg. In order to increase the capacity, we have embarked on a study to understand the structure and the capacity-limiting mechanism. During the first cycle, lithiation leads to a loss of H_2S which in turn improves the degree of conjugation and electronic conductivity. Both sulfur and the nitrogen on the pyridine ring are involved in the charge storage during the subsequent cycles. Recently, we have focused on further raising sulfur contents in SPAN by introducing sulfur species that resist the formation of long-chain polysulfide in the solid state. Structural analysis reveals the critical roles played by the nitrogen in facilitating the redox reaction of the additional sulfur. More than 20% improvement in capacity is obtained without the introduction of soluble polysulfide process. We will discuss in detail the reaction mechanisms of these high-sulfur SPAN materials and the pathway towards their implement in high energy density batteries.

2:30 PM ES06.02.03

Multifunctional Heterostructures for High-Energy-Density Lithium-Sulfur Batteries [Viet Phuong Nguyen](#)^{1,2}, [Jae-Hyun Kim](#)^{1,2} and [Seung-Mo Lee](#)^{1,2}; ¹University of Science and Technology (UST), Korea (the Republic of); ²Korea Institute of Machinery & Materials (KIMM), Korea (the Republic of)

A dense electrode with high sulfur loading is a straightforward approach to increasing the energy density of lithium-sulfur batteries, but the development of dense electrodes suffers from both fabrication challenges and electron/ion transport limitations. In addition, the shuttle effect of soluble lithium polysulfides and sluggish reaction kinetics cause declined utilization efficiency of the active material and poor cycling stability. In this study, we demonstrated that a novel heterostructure in the form of TiS_2 nanoribbons decorated with TiO_2 could function as an effective sulfur host to tackle these issues. We observed that TiO_2 with high adsorption capability anchors the lithium polysulfides, and TiS_2 with high electrical/ionic conductivity and catalytic activity can accelerate the charge transportation and enhance the kinetics of sulfur evolution reactions. Benefiting from these synergistic effects, the lithium-sulfur batteries using TiO_2 @ TiS_2 heterostructures exhibited high gravimetric and volumetric energy densities of 331 Wh kg^{-1} and 730 Wh L^{-1} , respectively, as well as superior cyclability at a high sulfur mass loading of 7.5 mg cm^{-2} and lean electrolyte of 2.5 $\mu\text{L mg}^{-1}$. The electrochemical performance was comparable to or even superior to the lithium-ion and lithium-sulfur batteries reported in the literature. This work provides an effective strategy for designing stable and high-energy-density lithium-sulfur batteries for practical energy storage applications.

2:45 PM ES06.02.04

Carbon Nanofoam Papers as Electrode Architectures for Chalcogens in Lithium- and Sodium-Based Batteries [Jeffrey W. Long](#)¹, [Zachary G. Neale](#)², [Matthew J. Lefter](#)², [Debra R. Rolison](#)¹, [Megan B. Sassin](#)¹ and [Rachel E. Carter](#)¹; ¹Naval Research Laboratory, United States; ²U.S. Naval Research Laboratory, United States

Sulfur has emerged as a promising charge-storage material for advanced rechargeable batteries based on the high capacity of the sulfur/sulfide redox reaction and earth-abundance of this element. The main limitations of sulfur-containing electrodes are the poor conductivity of sulfur and the propensity for release of soluble polysulfides into the electrolyte during redox cycling. These challenges can be mitigated by incorporating sulfur into porous, conductive carbon substrates to form cathodes for nonaqueous lithium- and sodium-based batteries. We find that carbon nanofoam papers (CNFPs) are highly effective materials for such purposes, providing the advantages of tunable pore size distributions (nm to μm), scalability in area (many cm^2) and thickness (100s of μm), and plug-and-play form factors for efficient battery construction [1]. Vapor deposition is a convenient route to coat the interior and exterior surfaces of CNFPs with nanometers-thick sulfur at effective weight loadings of up to 60 %; selenium and sulfur-selenium blends are also deposited in a similar fashion. We investigate the interplay of CNFP structure and chalcogen loading and composition with electrochemical performance in coin cells and pouch cells. In situ characterization with such techniques as optical microscopy and X-ray absorption spectroscopy provides additional details on redox mechanisms and associated side reactions.

1. Z. G. Neale, M. J. Lefler, J. W. Long, D.R. Rolison, M. B. Sassin, and R. E. Carter, *Nanoscale* (2023) in the press (DOI: 10.1039/D3NR02699J).

3:00 PM BREAK

3:30 PM ^ES06.02.05

Unraveling Mechanisms and Enhancing Kinetics in All-Solid-State Lithium-Sulfur Batteries [Hongli Zhu](#); Northeastern University, United States

All-solid-state lithium-sulfur batteries (ASSLSBs) hold promise for high energy density and improved safety compared to conventional lithium-sulfur cells using liquid electrolytes. However, low utilization of active sulfur caused by sluggish reaction kinetics has greatly hindered ASSLSB development.

Achieving efficient sulfur electron/ion accessibility in the cathode structure is critical. Porous carbon hosts, widely used in liquid cells, have been proposed to address these challenges. However, conventional porous carbons with buried pores are ineffective for ASSLSBs, as the non-mobile solid electrolytes cannot penetrate the pores to access enclosed sulfur. An ideal porous carbon should maximize surface area for sulfur while restricting pores to only the exterior surface. Despite works applying porous carbons in ASSLSBs, the optimal structure has not been well elucidated. Here, we pioneer discussion on the ideal carbon structure and develop polyacrylonitrile-derived porous carbon fibers (PPCF) with a unique core-shell morphology. A microporous shell on a dense core provides high surface area with accessible pores for electrolytes and sulfur. Consequently, ASSLSBs with PPCF show outstanding performance.

Furthermore, we grow MoS₂ nanosheets on carbon fibers. The chemical and electrochemical compatibility of MoS₂ with sulfur and sulfide solid electrolytes greatly improves cathode stability and ion/electron transport. Metallic 1T MoS₂ enables electron transfer, while the layered structure facilitates Li intercalation. This significantly enhances kinetics and relieves electrolyte decomposition. Our optimized ASSLSB delivers an ultrahigh initial capacity of 1456 mAh/g with high coulombic efficiency and 78% retention after 220 cycles.

Finally, we reveal the Li-S redox reaction undergoes a two-step transformation, producing polysulfide intermediates. Kinetic limitations can cause incomplete conversions, leaving polysulfides like Li₂S₂. Our mechanistic insights guide design principles for ASSLSBs.

4:00 PM ES06.02.06

Unravelling The Synergistic Effect of Cross-Linked Aqueous Binder and a Transition Metal Sulfide-Based Catalyst in High-Performance Lithium-Sulfur Batteries S B Majumder¹, D. Chatterjee¹, S Sahoo² and Suprem R. Das^{2,2}; ¹Indian Institute of Technology, Kharagpur, India; ²Kansas State University, United States

Commercial lithium-ion batteries (LIBs) generate a significant carbon footprint during the procurement of relatively scarce raw materials such as Li, Co, Ni, etc., manufacturing of cells, and their recycling. Lithium-sulfur batteries are far more environmentally friendly as they use only scarce lithium, have significantly higher specific energy density than LIBs, and easier to recycle. A facile one-step scalable process has been developed to increase the loading and conductivity of sulfur; retard long-chain polysulfides shuttling, tackle volumetric fluctuation of active particles and inhibit the lithium anode corrosion together with its dendritic growth during discharge-charge cycles. In the quest for this single-step scalable process, we have formulated a binder EA-PAA which can effectively anchor the polysulfides but is unable to escalate the conversion of low-order polysulfides to end discharge product-Li₂S₂/Li₂S, at a satisfactory level. The EA-PAA-based cathode delivers a capacity of 845 mAh/g, which decays to 539 mAh/g after 100 cycles. In order to augment the sluggish conversion kinetics of low order polysulfides, the catalytic effect is found to be a powerful solution. As a result, numerous catalysts have been developed and proved to exhibit catalytic effects in recent years. Unfortunately, none of them have been found to be as effective as using a catalyst alongside a polysulfide anchoring binder. Moreover, the polysulfide anchoring behavior could be facilitated in an alternative way by regulating the shape of sulfur particles by introducing polar capping agents such as PVP, which could additionally buffer the volume changes upon the conversion of sulfur to Li₂S. This would facilitate both anchoring the polysulfides while enhancing the conversion of low order polysulfides, in a single research study. So herein we are proposing a chalcogenide-based catalyst (e.g., ZnS) alongside the EA-PAA binder to formulate a cathode with high sulfur (>75%) content, which can deliver high discharge capacity (>1100 mAh/g) at C/2, with superior cycling ability (>85 % capacity retention at C/2 after 500 cycles), with high Coulombic efficiency (>90%) & rate performance (perform at 1C).

4:15 PM ES06.02.07

Binder-Free Manganese Iron Nitrides/N-Doped CNT Cathode for Lithium-Sulfur Batteries Yi-Jie Wang, Bo-Dong You and Che-Ning Yeh; National Tsing Hua University, Taiwan

Lithium-sulfur batteries (LSBs) hold promise due to their high energy density for commercialization. However, in lab-scale research, sulfur loading has typically remained below 2 mg cm⁻², far below the practical application requirements. The pressing need to increase sulfur loading inevitably intensifies a host of challenges, including poor conductivity, volume expansion, and notably, the shuttle effect. In this work, we present an innovative approach to address these formidable challenges. Our strategy involves the utilization of a composite composed of manganese iron nitrides and reduced graphene oxide (rGO). Manganese and iron are selected as host elements for their cost-effectiveness and substantial potential for cathode modification. Fe-N co-doped carbons demonstrate high adsorption-catalysis effectiveness for long-chain polysulfide reactions (LPR), while Mn-(O, N) coordination exhibits a strong adsorption effect for short-chain polysulfide reactions (SPR) and reduces charge-transfer resistance for Li₂S. Manganese iron nitrides are prepared by deriving the manganese-iron bimetallic metal-organic framework (MOF), which possesses high surface area and abundant active sites to adsorb the polysulfide and catalyze the conversion reactions. These bimetallic nitrides are assembled on a low tortuosity reduced graphene oxide (rGO) aerogel. The rGO aerogel, created through directional freeze drying, offers flexibility to accommodate volume expansion, high porosity to house sulfur, and creates direct pathways for fast charging of ions. By employing this directional rGO aerogel as the sulfur scaffold, manganese iron nitrides significantly mitigate the shuttle effect associated with various states of the polysulfides. Through the implementation of the S/rGO aerogel without additives as the cathode for LSBs, we can achieve a higher areal capacity while simultaneously preserving cycle stability. This advancement holds the potential to expedite the realization of LSBs for real-world applications.

4:30 PM ES06.02.08

Synergistic Effect of Anatase/Rutile Nanoparticle and Nitrogen Doping on NH₂-MIL-125(Ti)-Derived Porous Carbon as High Performance Lithium-Sulfur Battery Cathodes Seoyeah Oh¹, Seokhee Lee² and Jiwon Kim¹; ¹Yonsei University, Korea (the Republic of); ²Korea Institute of Ceramic Engineering and Technology, Korea (the Republic of)

Lithium-sulfur (Li-S) batteries have garnered significant attention as a future energy storage systems owing to their high theoretical capacity, energy density, and abundance of sulfur in nature. However, their development has been hindered by the polysulfide shuttle effect, which adversely affects the cycling stability of Li-S batteries. Various approaches – such as designing the pore structure of porous carbon, or introducing heteroatoms and/or metal oxides into the porous carbon – have been applied to address these issues. For instance, Yang et al. controlled the polysulfide adsorption on the porous carbon cathodes which depends on the phase of titanium dioxide (TiO₂) particles (*i.e.*, anatase or rutile) introduced in the electrodes^[1]. Furthermore, Kim et al. improved the retention of Li-S battery via coupled effects of nitrogen (N) vacancies and the rutile phase of TiO_{2,x}^[2]. However, the synergistic effects from the correlation among these factors (*e.g.*, heteroatom doping and phase type of TiO₂ particles) have not yet been systematically studied. In this work, we present a micro-sized NH₂-MIL-125(Ti) metal organic framework (MOF)-derived porous carbon (*micro*-cNMT) as a host material of sulfur for Li-S battery cathodes. *micro*-cNMT possesses a hierarchical micro-/meso-porous structure, N heteroatoms, and mixed phases of TiO₂ nanoparticles (*i.e.*, both anatase and rutile). These parameters collectively enhanced the performance of Li-S batteries through their synergistic effect. Specifically, *micro*-cNMT enhanced the prevention of polysulfide shuttle effects by the cooperation of physical and chemical adsorptions, facilitated by its hierarchical porous structure and N/TiO₂ nanoparticle doping, respectively. Porous structure of *micro*-cNMT not only accommodated active sulfur and its volume transition, but also facilitated Li-ion diffusion, which is confirmed by both cyclic voltammetry (CV) at various scan rates and Randles-Sevcik equation. Anatase and rutile phases of TiO₂ nanoparticles preferentially adsorbed short-chain polysulfide and long-chain polysulfide, respectively, preventing the loss of active sulfur throughout the entire discharging process. The long-chain polysulfide adsorption was confirmed by direct visualization of Li₂S₆ migrating from electrolyte to the *micro*-cNMT. Furthermore, scanning electron microscope (SEM) images of cathodes after 100 cycles of

discharge-charge and operando X-ray diffraction (XRD) measurement during the first discharge demonstrated that the *micro*-cNMT enhances short-chain polysulfide adsorption, thereby facilitating sulfur reduction reactions from polysulfide to Li₂S. As a result, the *micro*-cNMT cathode improved cycling stability owing to a synergistic effect from N and mixed phases of TiO₂ (0.39% decay at 0.1 C for 100 cycles), compared to the control group without N or with a single phase of TiO₂ nanoparticles (either anatase or rutile only).

References

Ziyi Yang, Chengxin Peng, Ruijin Meng, Lianhai Zu, Yutong Feng, Bingjie Chen,† Yongli Mi, Chi Zhang, & Jinhu Yang., *ACS Cent. Sci.*, 5, 1876-1883, (2019)

Kim, H., Yang, J., Gim, H., Hwang, B., Byeon, A., Lee, K. H., & Lee, J. W., *Electrochim Acta.*, 408, 139924, (2022)

4:45 PM ES06.02.09

Synthesis, Electronic Structure and Redox Chemistry of Li₂MnP₂S₆, A Candidate High-Voltage Cathode Material Yi-Ting Cheng¹, Fujii Yuta², Yu Nomata², Madhulika Mazumder¹, Nataly C. Rosero-Navarro², Aichi Yamashita³, Yoshikazu Mizuguchi³, Chikako Moriyoshi⁴, Takao Mitsudome⁵, Kiyoharu Tadanaga⁶, Akira Miura² and Chris Bartel¹; ¹University of Minnesota, United States; ²Hokkaido University, Japan; ³Tokyo Metropolitan University, Japan; ⁴Hiroshima University, Japan; ⁵Osaka Metropolitan University, Japan; ⁶Osaka University, Japan

While significant efforts have been made to harness the large capacity of sulfide-based cathodes, there has been limited focus on increasing their voltage. Here, by a novel iodide-assisted synthesis route, we successfully synthesized lithium metal thiophosphates Li₂MP₂S₆ (M = Mn, Fe, and Co), of which Li₂Mn_{0.902}P₂S₆ is a new compound. Electrochemical cycling revealed Li₂FeP₂S₆ and Li₂MnP₂S₆ can both be cycled at an equilibrium voltage of ~3 V, significantly higher than other sulfide-based cathodes. Despite the similar voltages, these two materials were found to operate by very different redox mechanisms. Density functional theory calculations show that while Li₂FeP₂S₆ exhibits traditional cationic redox, Li₂MnP₂S₆ involves participation and rehybridization of coupled Mn-S and S-S states. This work reinforces the promise of high-voltage sulfide-based cathodes for Li-ion batteries with the potential for significant capacity by combining both cationic (transition metal) and anionic (sulfur) redox.

SESSION ES06.03: Poster Session: Sulfur and Sulfide Chemistry for Electrochemical Energy Storage
Session Chairs: Dongping Lu and Hui Wang
Tuesday Afternoon, April 23, 2024
Flex Hall C, Level 2, Summit

5:00 PM ES06.03.01

Enhancing Aqueous Zinc Sulfur Battery Performance with a Novel Hybrid Electrolyte Yuqi Guo¹, Rodney Y. Chua¹, Yingqian Chen², Yi Cai¹, Ernest Tang¹, Nicholas J. Lim¹, Thu Ha Tran¹, Vivek Verma¹, Ming Wah Wong² and Madhavi Srinivasan¹; ¹Nanyang Technological University, Singapore; ²National University of Singapore, Singapore

Rechargeable aqueous Zn/S batteries hold significant promise due to their high capacity and energy density. However, their long-term cycling stability is hindered by sulfur side reactions and the growth of Zn anode dendrites in the aqueous electrolyte. In response, this research explores a simultaneous solution to these challenges through the development of a unique hybrid aqueous electrolyte incorporating ethylene glycol as a co-solvent. This innovative electrolyte design strategy facilitates the fabrication of Zn/S batteries with exceptional performance metrics on capacity, energy density and cycling stability under a high current rate. In addition, the investigation of the cathode charge-discharge mechanism reveals a multi-step conversion reaction. During discharge, elemental sulfur undergoes sequential reduction by Zn, ultimately forming ZnS. On charging, ZnS and short-chain polysulfides are oxidized back to elemental sulfur. This study not only offers a novel electrolyte design approach but also sheds light on the unique multi-step electrochemistry of the Zn/S system, paving the way for improved Zn/S batteries in the future.

5:00 PM ES06.03.02

Ultra Lean-Electrolyte Li-S Batteries Realized by Highly Solvating Electrolyte Design Zixiong Shi and Husam N. Alshareef; King Abdullah University of Science and Technology, Saudi Arabia

Lowering electrolyte usage is a key to attaining high energy density lithium-sulfur (Li-S) batteries. However, this remains a tremendous challenge in the conventional ether-based electrolytes with moderate polysulfide solubility. Highly solvating electrolytes, which can facilitate polysulfide dissolution, are considered a promising strategy to overcome this issue. They can also elevate sulfur utilization via altering reaction pathways and expediting redox kinetics. Nonetheless, mechanistic probing and kinetic evaluation on the complicated Li-S chemistry are still lacking. Herein, we design a highly solvating electrolyte via synchronous solvent and additive engineering. Spectroscopic investigations uncover that high-donor-number component can enable S₃⁻ radical-directed reaction path and three-dimensional Li₂S precipitation. Additionally, it has been revealed that ammonium ions promote the dissociation and dissolution of Li₂S by means of the H-S²⁻ bond. Benefiting from high polysulfide solubility and favored redox reaction, Li-S batteries with a low electrolyte and sulfur (E/S) ratio of 5 μL mg⁻¹ achieve a high capacity of 1092 mAh g⁻¹. Even at a harsh E/S ratio of 3 μL mg⁻¹, they still deliver an admirable capacity of 923 mAh g⁻¹ and sustain a stable operation over 40 cycles. Our work elucidates the polysulfide speciation and reaction mechanism in highly solvating electrolytes, which opens a new avenue for achieving pragmatic lean-electrolyte Li-S batteries.

5:00 PM ES06.03.03

Structural Properties and Ion Diffusion Pathways in Molybdenum Sulfide Materials of Interest for Li-S Batteries Sahar Bayat¹, Keerthan R. Rao¹, Taohedul Islam², Saiful M. Islam² and Chad Risko¹; ¹University of Kentucky, United States; ²Jackson State University, United States

Rechargeable battery systems, such as lithium-sulfur batteries, have garnered significant attention due to their high specific energies, lightweight form factors, and cost. However, challenges such as polysulfide shuttling and limited recharge cycles remain as shortcomings. Molybdenum sulfide-based chalcogels demonstrate potential to address these limitations as they show enhanced kinetics of lithium diffusion and the ability to mitigate polysulfide shuttling in lithium-sulfur (Li-S) systems. Here we are interested in developing structure-function relationships of molybdenum sulfide structures identified in the chalcogels through density functional theory (DFT) calculations and first-principles molecular dynamics simulations. We explore diverse sampling trajectories to extract structural factors, pair distribution functions, and bond structures to identify models that closely align with experiment. We then aim to elucidate ion diffusion pathways within the different molybdenum sulfide structures. The results of these studies provide fundamental understanding of the relationships among the composition, structure, and ion diffusion pathways in molybdenum sulfide-based chalcogels with the goal of delivering insights for future materials development.

5:00 PM ES06.03.05

Optimizing Lithium-Sulfur Battery Performance by The Integration of MgO Additive Sunny Choudhary¹, Nischal Oli¹, Rajesh K. Katiyar¹, Balram Tripathi², Gerardo Morell¹ and Ram Katiyar¹; ¹University of Puerto Rico at Rio Piedras, United States; ²S S Jain Subodh P.G.(Auto.) College, India

This study focuses on mitigating polysulfide dissolution in lithium-sulfur batteries by employing magnesium oxide (MgO) nanoparticles. We successfully incorporated MgO nanoparticles with sulfur through a commercially viable approach using a planetary ball mill. When integrated into the sulfur electrode, MgO led to improved capacity retention in the lithium-sulfur cell, surpassing the performance of cells with unaltered sulfur electrodes. This enhancement in cycling stability can be attributed to the robust chemical bonding between MgO and lithium polysulfide entities. This interaction effectively curtailed the shuttle effect of lithium polysulfides, thereby augmenting the utilization of the active sulfur material. The uniform dispersion of MgO nanoparticles on the surface of the sulfur demonstrates their effectiveness as additives for trapping lithium polysulfides. This research showcases the potential of MgO nanoparticles as a viable solution for the challenges associated with polysulfide dissolution in lithium-sulfur batteries. Our primary data exhibits stable reversible capacity more than ~ 600 mA h g⁻¹ over 100 cycles at 0.1C, surpassing a coulombic efficiency of ~99%. During the conference, we will present our insights into structural examination and electrochemical analysis.

5:00 PM ES06.03.06

Improving Low-Pressure Performance of Silicon Anodes in All-Solid-State Batteries using Ag Eunsuh Lee, Seungwoo Jun and Yoon Seok Jung; Yonsei University, Korea (the Republic of)

All-solid-state batteries (ASSBs) have emerged as promising alternatives to conventional lithium-ion batteries (LIBs), offering enhanced safety and superior energy density. Similarly to LIBs, Si stands out as an attractive anode candidate for ASSBs, owing to its high theoretical capacity (3580 mA h g⁻¹) and low voltage (<0.4 V vs. Li/Li⁺). However, it has been well documented that Si faces a significant challenge in LIBs; its immense volume change (>300%) during charge-discharge cycles leads to substantial pulverization and consequent electrical isolation of Si particles. In LIBs, this issue is often mitigated by combining Si with nanostructured carbonaceous materials, such as carbon nanotubes and graphene. Yet, in ASSBs, these same additives can consume Li⁺ sources and generate byproducts that exhibit poor Li⁺ conductivity. Recent advancements have demonstrated notable performance improvements in Si-based ASSBs by excluding SEs and carbon additives, albeit with minimal binder content and operation at 50 MPa. Nevertheless, from practical application, it is critical to evaluate and ensure performance sustainability at substantially reduced operating pressures. Herein, we provide a comparative analysis of the performance of Si ASSBs at varying operating pressures, emphasizing the significance of assessments at low pressures. We also introduce our approach to enhancing low-pressure performance through interfacial modification using metallic Ag. Lastly, we offer a series of complementary analytical results that delve into the underlying mechanism contributing to performance enhancement.

[1] Lee, Y.G., et al. Nat. Energy 2020, 5, 299–308.

[2] Lim, H., et al. Energy Storage Mater. 2022, 50, 543.

5:00 PM ES06.03.07

Electrochemistry of Deep Eutectic Fluorinated Ether Electrolyte in Li-SeS₂ Batteries Julio Zamora; Washington State University, United States

Lithium-Selenium disulfide (Li-SeS₂) batteries are a promising electrochemical system with much higher energy density compared to current Li-ion batteries. However, Li-SeS₂ batteries with conventional ether-based electrolytes undergo rapid performance degradation due to the “shuttle phenomena” associated with the formation and dissolution of polysulfide/selenide intermediates during battery cycling. Deep Eutectic Solvent (DES) electrolyte promises wide thermal stability and cost effectiveness compared to conventional commercial electrolytes. However, at high lithium salt concentrations, the high viscosity of DES hinders interfacial lithium-ion transport, and it can passivate Li-metal anodes. Dilute fluorinated ether has been implemented to improve bulk lithium-ion transport in other battery systems. In this study, we have designed novel, DES-based fluorinated ether electrolyte and investigated their thermal stability and lithium-ion solvation structure. Implementing novel DES-based electrolytes in Li-SeS₂ battery, we were able to reduce the performance degradation, retaining (>92%) of initial discharge specific capacity after high-rate cycling, achieve high coulombic efficiency (>99%), and achieve good battery cycling performance. This work provides new strategies for developing highly stable liquid electrolytes for high-energy Li-SeS₂ batteries.

5:00 PM ES06.03.08

Inorganic Porous Nanostructures Prepared by The Breath Figure Mechanism and Their Application in Lithium-Sulfur Batteries. Shu-Hao Chang and Yi-Jing Tsai; Chung Yuan Christian University, Taiwan

Lithium-sulfur batteries, recognized for their high theoretical capacity and plentiful sulfur source, are potential candidates for future energy storage devices. One significant challenge to commercialization is the polysulfide shuttle effect, which reduces the cycling stability and battery lifespan. We solved this issue by incorporating porous nanostructured metal sulfide into the battery's separator. We prepared metal sulfide nanoparticles through a simple hydrothermal synthesis and subsequently developed a porous thin film using the breath figure approach. Variables like substrate choice, temperature, and humidity were adjusted to refine the nanostructures. These modifications helped curb the shuttle effect by trapping the mobile polysulfides, thereby enhancing battery efficiency. The electrochemical attributes of these upgraded devices are elaborated upon in this research.

5:00 PM ES06.03.09

Hafnium Trisulfide Nanoribbons as a Promising Anode for High-Performance Lithium-Ion Storage Wei Shuangying; University of Chemistry and Technology, Prague, Czechia

Exploring the electrochemical characteristics of low-dimensional van der Waals materials is crucial for advancing novel rechargeable energy-storage devices, such as lithium-ion batteries (LIBs). Given their diverse band gaps, anisotropic conductivity, and high specific capacity, materials within the extensive family of transition metal trichalcogenides (TMTCs), including hafnium trisulfide (HfS₃), have garnered increased attention in recent years. Despite numerous theoretical and experimental studies focusing on the synthesis and physicochemical attributes of hafnium trisulfide, there remains a scarcity of experiments delving into its lithium-ion storage properties. Hence, HfS₃ material with a quasi-1D structure was applied as anode material for lithium-ion batteries. HfS₃ micro-belts were prepared using a simple solid-state reaction. Upon performing the relevant electrochemical tests, after 100 cycles, the HfS₃ electrode exhibits a high reversible capacity of 221.7 mAh g⁻¹ at a current density of 100 mA g⁻¹ and a great rate capability of 157.5 mAh g⁻¹ at the 101st cycle at a high current density of 800 mA g⁻¹. The excellent lithium storage performance can be related to the lithiation amorphization process, surface-controlled pseudocapacitive behavior, and low charge transfer resistance. The promising electrochemical characteristics of HfS₃ may shed new light on the design of transition metal trichalcogenides as viable anode materials for lithium storage. Nevertheless, the lithium storage behavior of ZrS₃ flakes is thus largely unexplored due to its low electronic conductivity and the challenges associated with its exfoliation.

5:00 PM ES06.03.10

Nickel-Based Sulfide Decorated Hydroxides as Cathode Materials for Hybrid Supercapacitors Ziwei Gan, Xiaohe Ren, Mengxuan Sun, Zhijie Li and Chunyang Jia; University of Electronic Science and Technology of China, United States

Due to their outstanding electrochemical properties, transition metal sulfides and hydroxides are often used as high-performance electrode materials for supercapacitors. The Mn-doped $\text{Co}(\text{OH})_2/\text{Ni}_3\text{S}_4$ electrode material in this study, due to the synergistic reaction mechanism among $\text{Co}(\text{OH})_2$ and Ni_3S_4 and the increased active sites by the addition of Mn, the $\text{Mn-Co}(\text{OH})_2/\text{Ni}_3\text{S}_4$ exhibits excellent electrochemical property. The electrochemical performance of the $\text{Mn-Co}(\text{OH})_2/\text{Ni}_3\text{S}_4$ hybrid electrode was measured in an electrode cell made of 2 M KOH solution, showing a superior specific capacitance of 1107.0 C g^{-1} at 0.5 A g^{-1} , in addition to the excellent capacity retention rate at 10 A g^{-1} is 72.7 % of that at 1 A g^{-1} . The performance of the hybrid supercapacitor (HSC) assembled with $\text{Mn-Co}(\text{OH})_2/\text{Ni}_3\text{S}_4$ compound and activated carbon (AC) was measured under the same electrolyte conditions, an well-specific capacity (157.2 F g^{-1} at 0.5 A g^{-1}) was achieved, along with superior long-term stable charge/discharge capability (88.9 % of the original specific capacity after 35,000 cycles at 8 A g^{-1}). Meanwhile, the most practical application is when the power density of 410.4 W kg^{-1} , the assembled HSC device has an energy storage capacity of 58.8 Wh kg^{-1} , revealing that the developed $\text{Mn-Co}(\text{OH})_2/\text{Ni}_3\text{S}_4$ has great application potential for supercapacitors in the future.

5:00 PM ES06.03.11

Hybrid Nanoarchitectures of $\text{Zn}_{0.76}\text{Co}_{0.24}\text{S}$ Nanoparticles@ $\text{Co}(\text{OH})_2$ Nanosheets for High-Performance Supercapacitor with Excellent Energy Density Xiaohe Ren, Ziwei Gan, Mengxuan Sun, Chunyang Jia and Zhijie Li; University of Electronic Science and Technology of China, China

It is a great challenge to achieve both high specific capacity and high energy density of supercapacitors by designing and constructing hybrid electrode materials through a simple but effective process. In this paper, we proposed a hierarchically nanostructured hybrid material combining $\text{Zn}_{0.76}\text{Co}_{0.24}\text{S}$ (ZCS) nanoparticles and $\text{Co}(\text{OH})_2$ (CH) nanosheets using a two-step hydrothermal synthesis strategy. Synergistic effects between ZCS nanoparticles and CH nanosheets result in efficient ion transports during the charge-discharge process, thus achieving a good electrochemical performance of the supercapacitor. The synthesized ZCS@CH hybrid exhibits a high specific capacity of 1152.0 C g^{-1} at a current density of 0.5 A g^{-1} in 2 M KOH electrolyte. Its capacity retention rate is maintained at ~70.0% when the current density is changed from 1 A g^{-1} to 10 A g^{-1} . A hybrid supercapacitor (HSC) assembled from ZCS@CH as the cathode and active carbon (AC) as the anode displays a capacitance of 155.7 F g^{-1} at 0.5 A g^{-1} , with a remarkable cycling stability of 91.3% after 12,000 cycles. Meanwhile, this HSC shows a high energy density of 62.5 Wh kg^{-1} at a power density of 425.0 W kg^{-1} , proving that the developed ZCS@CH is a promising electrode material for energy storage applications.

SESSION ES06.04: Sulfide-Based Solid-State Batteries—Electrolyte and Anode
Session Chairs: Yoon Seok Jung and Yang Zhao
Wednesday Morning, April 24, 2024
Room 432, Level 4, Summit

8:30 AM *ES06.04.01

Progress Towards New Sodium Mixed Oxy-Sulfide-Nitride Glassy Solid Electrolytes Steve Martin, Madison Olson, Alec Wakefield, Nicholas Oldham and Noah Riley; Iowa State University of Science and Technology, United States

While Lithium batteries are currently the most popular battery for grid scale energy storage, the rapidly increasing demands for Lithium to electrify transportation will soon outpace available geological reserves. For this reason, sodium batteries, with their comparable volumetric energy storage density, yet orders of magnitude lower cost, have been of interest for more than 50 years. The lack of a high conductivity, low cost, and electrochemically stable solid electrolyte has been a central reason for the current lack of a commercially available Na battery. In this talk, I will describe our more recent progress in developing new chemistries of Na-based glassy solid electrolytes that can be formed as thin films and in characterizing the many thermal, chemical, electrochemical, and mechanical properties needed of them.

9:00 AM *ES06.04.02

Thermal Runaway Behavior of Sulfide-Based Solid Electrolytes for All-Solid-State Batteries Taehun Kim, Kanghyeon Kim and Kyu Tae Lee; Seoul National University, Korea (the Republic of)

Lithium-ion batteries, which contain flammable liquid electrolytes, are susceptible to explosions when subjected to mechanical and thermal stress. Consequently, all-solid-state batteries (ASSBs), featuring solid electrolytes in place of liquid counterparts, have gained increasing attention as a promising alternative to current Li-ion batteries due to their potentially superior safety profile. Among these, thiophosphate-based solid electrolytes are considered particularly promising due to their high Li^+ ion conductivity and suitable mechanical flexibility, resulting in improved electrochemical performance for ASSBs. However, regrettably, the safety of sulfide-based ASSBs remains uncertain, as their thermal stability has primarily been assessed under specific, mild conditions, such as low state-of-charge (SOC) levels. In this presentation, we demonstrate the safety concerns associated with various solid electrolytes used in all-solid-state batteries with Ni-rich layered oxide cathode materials, particularly in the context of thermal and mechanical stress. Additionally, we propose not only the mechanisms responsible for the thermal degradation of solid electrolytes in the presence of Ni-rich layered oxide cathode materials but also the key factors that determine the thermal runaway of solid electrolytes. This discovery provides a deeper insight into the failure modes of all-solid-state batteries, shedding light on the broader understanding of their potential challenges and safety considerations.

9:30 AM ES06.04.03

Sulfide Solid Electrolyte with Better Safety and Cost Reduction Benoit Fleuot, Fabien Nassoy, Emmanuelle Garitte, Alexis Perea, Sergey Krachkovskiy, Steve Duchesne, David Rozon, Karine Tremblay and Chisu Kim; Hydro-Québec, Canada

All-solid-state batteries are viable alternatives to conventional batteries employing organic electrolytes because of their benefits, i.e., high power density, high energy density, long-life operation and safety. These advantages stem from the great features of inorganic solid electrolytes, which are single ion conductor, so a high lithium-ion transport number, and no-liquid nature. Solid oxide or sulfide are largely studied to allow the emergence of all-solid state battery based on solid electrolyte ceramic. In particular, the sulfide-based solid electrolytes possess favorable mechanical properties, high ionic conductivity comparable to liquid electrolytes but suffer of moisture exposure that could induce H_2S generation and very expensive precursor. Sulfide-based solid-electrolytes can potentially be employed in conjunction with a lithium metal negative electrode and 5V-class high voltage positive electrode material. Different families of sulfide electrolyte as glass ceramic, thio-LISICON, LGPS, argyrodites are synthesized by similar precursor as $\text{Li}_2\text{S-P}_2\text{S}_5$ and other component in function of composition. The composition must be designed to create stable passivating interface with lithium metal. In

parallel, the sulfide solid electrolyte reacts with all components constituting the positive electrode as active material, electronic conductor, binder, current collector... Hence, the optimal composition is a key issue. To hope for an emergence of this type of materials within all-solid batteries, it is necessary to avoid the use of heavy and expensive elements but also to improve the resistance of these materials towards humidity. This is possible thanks to the studies carried out on surface modification of sulfide electrolyte or the use of oxy-sulfide in the literature. Nevertheless, all these materials are based on the same precursor: Li_2S : very expensive and unsafe material. The ideal sulfide material would be one that is stable at high potential and low potential with lithium metal, a strong resistance to humidity allowing the handling of the material as well as its safe use in batteries with a low cost synthesis method in a minimum of steps using the minimum of expensive precursors.

In this field and since a few years, Hydro-Quebec has decided to conduct specific research on all-solid ceramic batteries and especially in the field of sulfide-based ceramic electrolytes. A specific study has been carried out to (1) optimize the composition of sulfide solid electrolyte with cheaper precursors to maintain or increase the properties as ionic conductivity and electrochemical stability, (2) better understand the reactivity at various dew points. Safety being in Hydro-Québec's DNA, emphasis has been placed on safety with a minimum step process as well as precise monitoring of H_2S generation of the precursors and the final material depending on temperature and humidity level. The complementarity between synthesis process, compositions, NMR analyses, XRD analyses, ionic conductivity, electrochemical stability, and safety measurements will be presented for the first time on sulfides prepared at Hydro-Quebec.

9:45 AM ES06.04.04

A High-Throughput Platform for Combinatorial Synthesis and Characterization of Thiophosphate Solid Thin-Film Electrolytes [Andrea Crovetto](#); Technical University of Denmark, Denmark

Research in thin-film battery materials is scarce, and reports of sulfur-based solid electrolytes and battery electrodes in thin-film form are particularly few. Even if we disregard the possible practical applications of thin-film materials in bulk solid-state batteries, dedicated work on sulfide battery materials in thin-film form would be highly beneficial for a very simple reason. Bulk synthesis of sulfide solid electrolytes is not amenable to parallelized, high-throughput experimentation by combinatorial methods. Conversely, an appropriately designed thin-film deposition system is an ideal platform for rapid exploration of new battery materials.

In this contribution, I will present our recently acquired, highly customized thin-film synthesis platform dedicated to air-sensitive sulfides, thiophosphates and related materials containing sulfur and phosphorus. To the best of my knowledge, this is the only synthesis platform in the world where it is possible to deposit thin-film thiophosphate superionic conductors of any elemental composition in a high-throughput, combinatorial fashion. Our thin-film deposition setup is designed to easily obtain compositional gradients (e.g., a P/S ratio gradient in one direction and a Li/Ge ratio in the perpendicular direction). Together with the automated, mapping-type characterization instruments in our laboratories, these combinatorial methods enable fast screening of multicomponent phase diagrams of sulfides (as well as process parameters at constant composition) in the search for optimal properties in emerging or completely new battery materials. Materials of interest can be either electrodes or solid electrolytes.

As a material scientist within the optoelectronics field specializing in sulfides, I hope that this contribution will promote discussion and potential future collaboration with sulfide battery experts.

10:00 AM BREAK

10:30 AM *ES06.04.05

Comparative Study of Oxides and Sulfides in Terms of their Dendrite Resistance: The Impact of Internal Defects and Interlayers [Yue Qi](#); Brown University, United States

The key challenge for the Li-metal electrode is to maintain a smooth surface at the microscopic scale during cycling. During lithium plating, it was found that the bandgap, tunneling barriers, and electron localization on internal defects, such as pores and crack surfaces and grain boundaries play a more important role in Li-dendrite nucleation and growth. A combined DFT and phase-field method was developed to demonstrate these effects. Several oxides (cubic $\text{Li}_7\text{La}_3\text{Zr}_2\text{O}_{12}$ (c-LLZO), $\text{Li}_1.17\text{Al}_0.17\text{Ti}_1.83(\text{PO}_4)_3$ (LATP), and $\text{Li}_2\text{PO}_2\text{N}$) and sulfide ($\beta\text{-Li}_3\text{PS}_4$ and Argyrodite $\text{Li}_6\text{PS}_5\text{Cl}$) electrolytes and their interlayer materials (Li_2O vs. Li_2S) were compared.

For the bulk solid electrolytes, the oxides tend to show much smaller bandgaps on the surface and grain boundaries than the corresponding bulk materials. While LLZO showed the most significant excess electrons on the surface and grain boundaries, $\beta\text{-Li}_3\text{PS}_4$, and argyrodite showed no such behavior. This is consistent with the observed trend and morphology of Li dendrite growth in different solid electrolyte materials.

Further, the Li_2O and Li_2S interface layers showed different lithium metal wettability. A combined density functional theory (DFT) and kinetic Monte Carlo (KMC) interface evolution simulations showed that the lithiophilic interface ($\text{Li}/\text{Li}_2\text{O}$) repels vacancies into the bulk Li, so Li atoms can quickly fill the Li vacancies near the interface and maintain a smooth Li surface. In contrast, the more lithiophobic interface (e.g. $\text{Li}/\text{Li}_2\text{S}$) traps Li vacancies toward the interface, and the accumulated Li vacancies form voids causing interface delamination. The appropriate alloying and stack pressure were predicted to avoid interface delamination at $\text{Li}/\text{Li}_2\text{S}$ interface during the stripping process.

11:00 AM *ES06.04.06

Unveiling Lithium-Solid Electrolyte Interface Evolution in All-Solid-State Batteries through Operando Characterizations [Yan Yao](#); University of Houston, United States

All-solid-state lithium metal batteries are projected to offer one of the highest specific energy among rechargeable batteries, positioning them as a front-runner for electric vehicle applications. Lithium metal anodes outperform conventional graphite anodes in terms of cell-level energy density. However, ensuring a conformal metal-electrolyte contact is a great challenge. In this presentation, I will illustrate the use of operando tools to understand issues like void formation and contact loss at the Li-electrolyte interface in all-solid-state batteries. I will first showcase a study where the Li-Mg alloy anode suppresses void growth. Operando scanning electron microscopy reveals voids coalescing into a gap at the pure-Li-electrolyte interface, but large voids split into smaller voids and collapse to ensure contact between Li-Mg alloy anode and solid electrolyte. This behavior is further supported by density function theory calculations, emphasizing the role of strong Mg-S interaction at the electrolyte interface in repelling vacancies and mitigating void formation. In the second example, I will introduce an interlayer strategy optimizing contact between the solid electrolyte and lithium metal, which enhances stripping/plating uniformity and suppress lithium dendrite formation.

11:30 AM ES06.04.07

Interfacial Evolution of Surface Modified Li Metal Anodes in All-Solid-State Batteries [Yoon Seok Jung](#); Yonsei University, Korea (the Republic of)

For decades, the pursuit of solidifying electrolytes using inorganic solid electrolytes (SEs) that display high mechanical strength has been regarded as a "Holy Grail" in the quest to enable Li metal anodes. Sulfide SE materials such as Li argyrodite (e.g., $\text{Li}_6\text{PS}_5\text{Cl}$) are particularly attractive due to their

mechanical sinterability and high ionic conductivities, making them subjects of extensive research for practical ASSBs. However, these materials encounter a critical limitation: their electrochemical instability in contact with Li metal. This instability leads to the reductive decomposition of sulfide SEs, producing byproducts like Li_2S , which substantially escalate interfacial impedance. More critically, Li metal tends to grow through the SE layers, inducing catastrophic short circuits. To address these challenges, various surface modification techniques have been explored. Inorganic materials (e.g., LiF) and alloying elements (e.g., Ag) have received considerable attention. However, despite advances in enhancing the performance of Li metal ASSBs, there is a noticeable gap in our understanding on the interfacial evolution, particularly concerning factors associated with cell fabrication methods and/or operating conditions.

In this presentation, we report our strategies for stabilizing Li metal anodes in ASSBs that use $\text{Li}_6\text{PS}_5\text{Cl}$, specifically through the incorporation of electroless-plated In or MgF_2 interlayers. Our findings indicate that neither intermetallic nor simple inorganic interlayers maintain stability throughout cell fabrication or operation. In contrast, MgF_2 interlayers exhibit substantial enhancements in these aspects. Furthermore, comprehensive analytical techniques, including operando electrochemical pressimetry, to probe the interfacial evolution in Li metal ASSBs, are also presented.

11:45 AM ES06.04.08

Insights into the Chemo-Mechanics of Sulfur Conversion Electrodes via Operando Acoustic Transmission for Lithium Batteries Kerry Sun^{1,1}, Gunnar Thorsteinsson^{1,1}, Alexandra Stiber^{1,1,1}, Libby Katzman^{1,1}, Wesley Chang², Richard May^{1,1} and Daniel Steingart^{1,1,1}; ¹Columbia University, United States; ²Drexel University, United States

The chemo-mechanics of the lithium-sulfur battery are unique in Li-ion batteries due to the sulfur electrode undergoing two first-order phase changes during discharge and charge. However, dissolution of sulfurous species in liquid electrolytes is a primary degradation mode in Li-S systems. Here, we use acoustic transmission to track the mechanical phasing of the sulfur electrode. We show that acoustic time of flight (or sound speed) is directly correlated to sulfur's physio-chemical phase dynamics. This is because the acoustic sound speed is a composite property dependent on the density and elastic modulus of the medium. By accounting for cell dilation, we show that inter-cycle and intra-cycle sound speed changes in time of flight are due to the sulfur dynamics alone. This understanding is linked with ex-situ techniques like XRD and TGA to track the effect of polysulfide shuttling.

SESSION ES06.05: Sulfide-Based Solid-State Batteries—Li Anode and Interface

Session Chairs: Yoon Seok Jung and Hui Wang

Wednesday Afternoon, April 24, 2024

Room 432, Level 4, Summit

1:30 PM ES06.05.01

High Performance MOF Separator for Li-S Battery using Langmuir-Blodgett Technology Seoyoung Yoon, Geonho Kim and Jiwon Kim; Yonsei University, Korea (the Republic of)

Lithium-sulfur (Li-S) batteries have been widely emphasized as alternatives to commercial lithium-ion batteries not only for their higher theoretical capacity (1,675 mAh/g) but also for abundance of sulfur in nature and being safe. However, the shuttle effect of lithium polysulfide limits long cycle life of batteries, and separators have been modified to effectively control reaction intermediates. For example, polymer-based separators have been coated with oxide or carbon in order to enhance filtration via pore or electrical attraction/repulsion. In particular, metal-organic frameworks (MOFs) as coating materials have advantages of porosity and electrochemical property which can be easily adjusted by the composition of metal clusters and ligands. However, most traditional coating techniques such as chemical vapor deposition (CVD) and vacuum filtration coating methods require heating process and produce relatively thick layer (at least microscale), thereby limiting its applicability.

Herein, we synthesized two types of MOF (i.e. MOF-5 and IRMOF-3) nanosheets using Langmuir-Blodgett (LB) technique to functionalize Li-S battery separator. A modified separator was uniformly formed (3.27 Å for R_a ; roughness average) by depositing five molecular monolayer films (total thickness of ~47.5 Å) at room temperature, while zinc acetate dihydrate and (2-amino)-terephthalic acid were used as MOF precursors. To note, polysulfide permeation test in H-cell revealed that a LB-coated MOF separator had comparable degree of filtration to a slurry-coated MOF separator despite of its thin thickness (c.a. 4,000 times thinner than slurry-coated one). Moreover, Li-S battery with a IRMOF-3 coated separator exhibited 1.13 times higher cycle stability (retention of 54.26% after 100 cycles) compared to one with non-coated separator (retention of 48.83% after 100 cycles). This suggests that heteroatom (i.e. nitrogen in IRMOF-3) and pore structure of MOF coating layer contribute to enhanced filtration ability of separators. Consequently, we can improve the cycle stability of Li-S batteries by applying a nanoscale MOF modification layer to separators via LB, which can further pave a way for commercialization of Li-S batteries.

1:45 PM ES06.05.02

Towards a Sealed Rechargeable Li-SO₂ Battery: Overcoming Slow Diffusion Kinetics and Side Reactions Gayea Hyun, Myeong Hwan Lee, Haodong Liu, Shen Wang, Victoria Petrova and Ping Liu; University of California San Diego, United States

Rechargeable lithium-sulfur dioxide (Li-SO₂) batteries are potentially of low-cost and high-energy density. The high SO₂ solubility in organic solvents has enabled cell operation under non-pressurized conditions. For example, superior electrochemical stability has been observed in carbonate-based electrolytes. However, most of the reports so far employ an "open cell configuration", where continuous SO₂ supply is provided. The needed accessories, such as gas diffusion layers and Swagelok-type cell construction with heavy steel frames, and gas handling systems, greatly impede the development of practical high-energy-density batteries.

Herein, we report our progress on understanding the behavior of electrolytes containing SO₂ within a closed system and to maximize the utilization of the active material. In comparison to other redox-active gases, SO₂ molecules, with their relatively high molecular weight (twice as heavy as O₂) and polarity, not only suffer from slow diffusion (~0.7 times lower diffusion coefficient compared to that of O₂) within the electrolyte but also exhibit a peculiar reverse osmotic behavior. When SO₂ is consumed in the electrolyte volume between the two electrodes, dissolved SO₂ in electrolyte outside the current path does not diffuse in. Instead, organic solvents are driven into the current path, leading to an evolution of SO₂ gas outside a cell stack. Our investigation confirmed that this behavior is driven by the molecular interactions between SO₂ and the organic solvents.

Based on the above insights, we have designed electrochemical cells to strategically place all SO₂ containing electrolyte within the current path, leading to maximize utilization. Our optimized bobbin-type battery, in which the electrolyte containing SO₂ is entirely contained within the cell stack, has proven highly effective in maximizing discharge capacity. This configuration allowed us to achieve exceptional utilization (~73%) of SO₂ along with an acceptable E/C ratio (~13 g/Ah, with discharge capacities of 2639 mAh/g_{KB} and 7.9 mAh/cm²). To further enhance the performance, we have developed a nanoporous lithium protective layer made of a composite of Nafion and alumina nanopowder, capable of retaining SO₂ reactant within the cell stack while minimizing continuous reactant loss from undesirable reactions with Li metal anode. In addition, we have achieved remarkable cycling stability by identifying catalysts

to reduce side reactions and polarization on the cathode. This research sheds new light on the working mechanisms of the Li-SO₂ chemistry and points to its potential as a low-cost, sustainable battery.

2:00 PM *ES06.05.03

Alloy Anodes in Sulfide-Based Solid-State Batteries [Matthew McDowell](#); Georgia Institute of Technology, United States

Alloy anodes offer high theoretical capacity, but they typically exhibit fast capacity decay in lithium-ion batteries because of excessive solid-electrolyte interphase growth. Here, we investigate a variety of alloy anodes in sulfide solid-state batteries, and we show that they can exhibit significantly improved interfacial stability and enhanced cyclability when engineered effectively. *In situ* measurement of stack pressure evolution during cycling shows that the volume changes of alloy anodes can lead to large pressure swings within the solid-state battery cell, giving insight into electrode composite evolution. We further investigate the fundamental electrochemical behavior of 12 different foil-based alloy anode materials in solid-state batteries, and we find that lithium trapping by the delithiated phase can play a key role in limiting performance. Based on these insights, we present a new design for dense foil aluminum-based alloy anodes with multiphase microstructure that offers significantly improved performance due to retained transport pathways within the foil. This design offers a paradigm that does away with slurry coating, potentially reducing manufacturing costs. In addition, we investigate solid-state dealloying of foil anodes to understand the interplay between densification and interfacial contact evolution at different stack pressures. Taken together, these findings show the importance of controlling chemo-mechanics and interfaces in alloy anodes for sulfide-based solid-state batteries for improved energy storage capabilities.

2:30 PM *ES06.05.04

Tuned Reactivity at The Lithium Metal – Argyrodite Solid State Electrolyte Interphase [David Mitlin](#); The University of Texas at Austin, United States

Thin intermetallic Li₂Te–LiTe₃ bilayer (0.75 mm) derived from 2D tellurene stabilizes solid electrolyte interphase (SEI) of lithium metal and argyrodite (LPSCl, Li₆PS₅Cl) solid-state electrolyte (SSE). Tellurene is loaded onto standard battery separator and reacted with lithium through single-pass mechanical rolling, or transferred directly to SSE surface by pressing. State-of-the-art electrochemical performance is achieved, e.g. symmetric cell stable for 300 cycles (1800 hours) at 1 mA cm⁻² and 3 mAh cm⁻² (25% DOD, 60 mm foil). Cryo-FIB sectioning and Raman mapping demonstrate that Li₂Te–LiTe₃ bilayer impedes SSE decomposition. The unmodified Li–LPSCl interphase is electrochemically unstable with geometrically heterogeneous reduction decomposition reaction front that extends deep into the SSE. Decomposition drives voiding in Li metal due to its high flux to the reaction front, as well as voiding in the SSE due to the associated volume changes. Analysis of cycled SSEs found no evidence for pristine (unreacted) lithium metal filaments/dendrites, implying failure driven by decomposition phases with sufficient electrical conductivity that span electrolyte thickness. Density Functional Theory (DFT) calculations clarify thermodynamic stability, interfacial adhesion, and electronic transport properties of interphases, while mesoscale modeling examines interrelations between reaction front heterogeneity (SEI heterogeneity), current distribution and localized chemo-mechanical stresses.

SESSION ES06.06: Sulfide-Based Solid-State Batteries—Cathode and Devices

Session Chairs: Dongping Lu and Yang Zhao

Thursday Morning, April 25, 2024

Room 432, Level 4, Summit

8:30 AM *ES06.06.01

Hot-Pressed FeS₂ Cathodes with Oxysulfide Solid-State Electrolyte for All-Solid-State Batteries [Hernando J. Gonzalez Malabet](#)¹, [Hayden Cunningham](#)² and [Thomas A. Yersak](#)¹; ¹General Motors Global R&D, United States; ²Optimal Inc., United States

The performance of all-solid-state batteries (ASSBs) is limited by poor interfacial contact between active material (AM) and solid-state electrolyte (SSE) particles. At the cell level, poor interfacial contact manifests as difficult operating specifications (e.g. high stack pressure, elevated temperature, or slow charge rate), or poor cell durability. This seminar investigates how an advanced processing technique can better consolidate electrode composites. It will be shown that the electrochemical performance of FeS₂/InLi ASSBs was improved when the cells were hot-pressed at a temperature > 200 °C. When cycled at 25 °C, a cold-pressed (CP) FeS₂/InLi ASSB delivered negligible capacity whereas a hot-pressed (HP) FeS₂/InLi ASSB delivered a 1st cycle discharge capacity in excess of 600 mAh g⁻¹. The improved performance is attributed to better interfacial contact between AM and SSE. This result was achieved by selecting thermally stable FeS₂ active material and highly processable Li₇P₃S_{9.75}O_{1.25} (LPSE) SSE.

9:00 AM *ES06.06.02

Tailored Ni-Rich Cathodes for All-Solid-State Batteries [Torsten Brezesinski](#); Karlsruhe Institute of Technology, Germany

Bulk-type solid-state batteries hold promise as an enabling technology for high density electrochemical energy storage. Especially layered (Ni-rich, low-Co or Co-free) oxide cathode materials [e.g., LiNi_xCo_yMn_{1-x-y}O₂ (NCM or NMC) and LiNiO₂ (LNO)] and superionic lithium thiophosphate solid electrolytes are being considered for high energy density solid-state battery applications. However, electro-chemo-mechanical degradation occurring during cycling is a major obstacle towards development of stable and long-lived cells. In this presentation, I will highlight the importance of tailoring Ni-rich cathodes for increasing performance of pellet-type and slurry-cast electrodes. In addition, I will show recent findings on the effect that protective surface coatings have on interfacial side reactions and mechanical degradation in thiophosphate-based cells.

9:30 AM ES06.06.03

Functional Surface Modification of Ni-Rich Cathode for All-Solid-State Lithium-Ion Batteries Employing Sulfide Solid Electrolytes [Jun Pyo Son](#) and [Yoon Seok Jung](#); Yonsei University, Korea (the Republic of)

Intensive research and development efforts have been directed towards lithium-ion battery (LIB) for electric vehicle applications. However, conventional LIBs utilize flammable organic liquid electrolytes, which pose inherent safety risks, including a propensity for fire-related incidents. These safety concerns have spurred heightened interests in all-solid-state batteries (ASSBs), which utilize inorganic solid electrolytes (SEs) instead. For ASSBs to meet the practical demands of high energy density, the use of Ni-rich layered oxide cathode active materials (CAMs), denoted as LiMO₂ (M = Ni, Co, Mn, and/or Al), which are prevalent in LIBs, is essential. However, a significant change arises with sulfide SEs, known for their high ionic conductivity but poor electrochemical stability. This instability necessitates the application of an insulating buffer layer on Ni-rich CAMs. Furthermore, Ni-rich CAMs are prone

to structural instability, leading to internal cracking and significant degradation, notably an irreversible H2-H3 phase transition when in high states of charge. To address the structural stability issues inherent in Ni-rich CAMs, metal doping techniques have been commonly employed. In this presentation, we propose a comprehensive strategy that addresses not only the poor electrochemical stability of sulfide SEs but also the detrimental phase transition of Ni-rich CAMs. This approach involves the development of multi-component functional coatings. Along with significantly enhanced electrochemical performance, interfacial evolutions probed by complementary analyses are presented.

9:45 AM ES06.06.04

In-Operando FTIR Study on The Redox Behavior of Sulfurized Polymers as Cathode Material for Li-S Batteries [Vibha Kalra](#); Cornell University, United States

Sulfurized polymers are an attractive cathode active material, promising to overcome the intransigent polysulfide shuttle effect sulfur cathodes face via the anchoring of sulfur by a carbon-sulfur (C-S) bond. Both sulfur-diisopropenylbenzene copolymers (SDIB) and sulfurized polyacrylonitrile (SPAN) contain C-S bonds which should function in this way, however, their performance in ether electrolytes still exhibit capacity fade associated with the polysulfide shuttle. We investigate this anchoring effect using in-operando ATR-FTIR spectroscopy to develop a molecular level understanding of the polysulfide speciation reaction in sulfurized polymers and cathode level molecular changes. We find that in SDIB copolymers with sulfur wt % of 80 and 30 wt %, the C-S bond is not active in the voltage window of Li-S batteries (1.8-2.6V vs Li/Li+). In SPAN, however, we found that the C-S bond is active in the typical voltage window (1-3V vs Li/Li+) contributing to the evolution of polysulfide species in electrolyte with low concentrations of lithium nitrate (LiNO₃), however this effect is mitigated when higher concentrations of LiNO₃ are used. We attributed the mitigation of the polysulfide shuttle to the formation of a cathode electrolyte interface (CEI), composed of lithium fluoride, established via ex-situ XPS studies on cycled cathodes. Additionally, we observed the reversible behavior of the C-S bond in IR at ~680 cm⁻¹ in electrolytes with high concentration of LiNO₃, as opposed to the irreversible behavior of the bond in electrolyte with low concentrations of LiNO₃. Moreover, we observed the lithiation of the cyclized PAN backbone, identified by the elimination of the aromatic region of the IR spectrum after the first cycle.

10:00 AM BREAK

10:30 AM *ES06.06.05

Polymeric Materials for Scalable, Reliable Sulfide-Based All-Solid-State Batteries [Jang Wook Choi](#); Seoul National University, Korea (the Republic of)

Sulfide-based all-solid-state batteries (ASSBs) are considered to be a next-generation energy storage concept that offers enhanced safety and potentially high energy density. Despite considerable progress in the development of materials, sulfide-based ASSB technology still remains at research stage without solution-based scalable manufacturing schemes having been established because of the incompatible polarity of binder, solvent, and sulfide electrolyte during slurry preparation. In this talk, I will introduce a novel binder design based on protection-deprotection chemistry, which resolves the tricky issue of polarity compatibility among the three electrode components (solvent, binder, and SE) in the slurry solution. Protection by the tert-butyl group allows for homogeneous dispersion of the binder in the slurry based on a relatively less polar solvent, with subsequent heat-treatment during the drying process to cleave the tert-butyl group. Upon deprotection, the polar carboxylic acid group is exposed, which enables hydrogen bonding interaction with the high-nickel layered oxide active material. Deprotection strengthens the electrode adhesion drastically, even beyond the levels of commercial LIB electrodes, and the key electrochemical performance parameters are improved markedly in both half-cell and full-cell settings. This study highlights the potential of sulfide-based ASSBs for scalable manufacturing and also provides insights that protection-deprotection chemistry could generally be used for various battery cells that suffer from polarity incompatibility among multiple electrode components.

11:00 AM ES06.06.06

Self-Templated 3D Porous Sulfide Solid Electrolytes for Solid-State Sodium Metal Batteries [Xiaolin Guo](#), Yang Li and Hui Wang; University of Louisville, United States

Rechargeable solid-state sodium (Na) batteries have gained great attention for their high-safety, high energy density and low cost. However, due to the high reactive Na anode, poor electrolyte/electrode interfaces compatibility is the biggest obstacle for inorganic sulfide solid electrolytes (e.g., Na₃MS₄, M=P, Sb) to achieve high performance batteries. Thus, it is necessary to design the nanostructure of sulfide solid electrolyte (SE) and modify interface to address that challenge on the electrochemical instability. In this talk, we will introduce a facile and simple synthesis to prepare Na₃SbS₄ (NSS) sulfide solid electrolyte with 3D porous framework, which can be further infiltrated with a phase transition polymer to form a composite solid electrolyte. The Na₃SbS₄-based composite (NSSC) exhibits enhanced interface stability towards Na metal compared with pristine NSS. The fabricated cells with structure of Na|NSSC|TiS₂ shows excellent cycling stability for 200 cycles with decent capacity retention. This result demonstrates great promise of achieving high-energy sodium metal batteries with sulfide solid electrolytes.

11:15 AM ES06.06.07

Investigating The Electro-Mechano-Chemical Coupling Phenomena of an Electrolyte in All Solid-State Battery [Kethsovann Var](#)^{1,2}, Christel Laberty Robert¹, Sofiane Maiza², David Sicsic² and Damien Bregiroux¹; ¹Sorbonne Université - Laboratoire Chimie de la Matière Condensée de Paris, France; ²Renault Group, France

Lithium-ion technology's energy density is constrained by negative electrode intercalation. The integration of lithium metal into solid-state batteries shows promise for a substantial enhancement of energy density. It would increase energy density from 372 mAh/g to 3862 mAh/g. However, several challenges persist, including cycling pressure, dendrite growth, and volumetric electrode variations that can lead to detachment and cracks in the electrodes, ultimately causing premature battery degradation.

This study primarily focuses on understanding the intricate relationships between electrochemical and mechanical properties within solid-state batteries. The chosen material is the argyrodite (Li₆PS₅Cl), which exhibits high ionic conductivity (10⁻³ cm⁻¹), comparable to that of liquid electrolytes. This material can be easily compacted through cold pressing due to its favorable mechanical properties. According to literature results, the material has a relatively low Young's modulus [E] 25-40 GPa [1,2], classifying it as a soft material, in contrast to oxide families.

The material's intrinsic properties (such as Young's modulus, hardness, viscoelasticity, etc.) were investigated using nanoindentation. In order to overcome the reactivity issues related to air and humidity, we have designed a specific device, inspired by Hikima [2] to conduct nanoindentation test in ambient atmosphere. Young's modulus values for the pure material were around 16 GPa which is lower than literature. The inconsistency in these results is attributed to the shaping process which introduces factors like porosity and surface inhomogeneity, necessitating refinement.

On the other hand we shown that the material has small elastic range, corresponding to its reversible deformation. It becomes evident that expanding the material's elastic range is imperative to accommodate electrode volumetric variations. We studied mechanical properties of argyrodite by a) modifying the particle size to manipulate macrostructural defects, and b) modifying the material's stoichiometry Li_{6+x}PS_{5-x-y}O_z by introducing elements like (F, Cl, Br, I). This modification is intended to affect the strength of chemical bonds, consequently influencing the Young's modulus.

Simultaneously, on a macroscopic scale, a testing cell is developed to monitor pressure variations during cycling. The $\text{Li}_4\text{Ti}_5\text{O}_{12} / \text{Li}_6\text{PS}_5\text{Cl} | \text{Li}_6\text{PS}_5\text{Cl} | \text{Li}_6\text{PS}_5\text{Cl} / \text{NMC811}$ (single or polycrystalline) system is the primary focus. The nearly negligible volumetric variation of LTO allows for the examination of pressure changes specifically at the positive electrode. Using this system, we were able to monitor the impact of electrolyte particle size on the pressure variation. Moreover, a composite with polymer is studied to accommodate volume variation and reduce pressure variation at macroscale. The ultimate goal of this research is to enhance our understanding of the intricate mechanisms involved in the electro-mechano-chemical coupling and the degradation processes within solid-state batteries.

[1] Ai, Q. et al High-Spatial-Resolution Quantitative Chemomechanical Mapping of Organic Composite Cathodes for Sulfide-Based Solid-State Batteries. *ACS Energy Lett.* **2023**, 8 (2), 1107–1113.

[2] Papakyriakou, M. et al. Mechanical Behavior of Inorganic Lithium-Conducting Solid Electrolytes. *J. Power Sources* **2021**, 516, 230672.

[3] McGrogan et al. - 2017 - Compliant Yet Brittle Mechanical Behavior of Li s

11:30 AM ES06.06.08

Bioinspired Multifunctional Nanocomposites for Energy Storage Applications [Ahmet Emre](#), Emine Turali-Emre and Nicholas A. Kotov; University of Michigan, United States

Bioinspired ion transport membranes have been extensively researched for energy storage applications. Sulfur, due to its natural abundance, low toxicity, high theoretical specific energy density (2600 Wh/kg), and high specific capacity (1675 mA/g), is attracting significant attention as an alternative battery system to replace traditional lithium-ion batteries that have limitations in terms of safety, capacity, and energy density in various applications. However, polysulfide dissolution and shuttling pose challenges that prevent the mass commercialization of metal sulfur batteries. We have developed a practical and comprehensive approach for developing high-performance metal sulfur batteries inspired by biological ion transport mechanisms. We used aramid nanofiber (ANF)-based composite ion transport membranes that prevent dendrite formation and confine polysulfides on the cathode side[1]. ANF composite battery separators provide diverse and opposing properties, including high mechanical properties, high ionic conductivity, and high thermal/chemical stability. These biomimetic separators have highly selective ion-sieving properties that make the batteries safe and high-performing. It is crucial to fabricate such biocompatible, affordable, flexible, and high-energy-density batteries to power next-generation EVs.

[1] M. Wang *et al.*, “Multifactorial engineering of biomimetic membranes for batteries with multiple high-performance parameters”, doi: 10.1038/s41467-021-27861-w.

SESSION ES06.07: Virtual Session
Session Chairs: Dongping Lu and Hui Wang
Tuesday Morning, May 7, 2024
ES06-virtual

8:00 AM *ES06.07.01

Characteristic Analysis of Single Particle Cathode Materials for Sulfide-Based All Solid State Batteries Jiwon Jeong^{1,2}, Kyoung Eun Kim^{1,3}, Mingony Kim^{1,3}, Sang Ok Kim^{1,3}, Woo Young Yoon², Ji-Young Kim¹ and [Kyung Yoon Chung](#)^{1,3}; ¹Korea Institute of Science and Technology, Korea (the Republic of); ²Korea University, Korea (the Republic of); ³KIST School, Korea University of Science and Technology, Korea (the Republic of)

All Solid State Batteries (ASSBs) have great attraction as next generation energy storage technology due to their nonflammable solid electrolytes (SE) and high energy density compare to commercial Li-ion batteries. However, there are still some issues that need to be addressed to move beyond lithium-ion batteries (LIB).

One of the troublesome challenges is the unstable contact between active material and SE. A typical cause of unstable interface contact is unwanted side reactions between active material and SE. In particular, among solid electrolytes, sulfide-based solid electrolytes with high reactivity and a narrow operating voltage accumulate ions and electrons at the interface in contact with the cathode active material, causing many side reactions. In order to prevent such a side reaction, there have been an efforts to such as coating the surface of the cathode material with stable polymer, metal oxide, and lithium metal oxide.

Another cause of interfacial contact loss is volume change. Whether ASSB or LIB, volume changes occur due to intercalation and deintercalation of lithium in the active material. In particular, materials that achieve higher capacities have larger volume changes because more lithium is accommodated. For this reason, composite anodes containing high-nickel NCMs in ASSB exhibit rapid capacity decline because it is difficult to restore contact between the cathode and the electrolyte once separated. To suppress volume changes, various methods are used, such as controlling the shape of active materials, surface coating using hard materials, and improving the physical properties of solid electrolytes.

Here, we adopt a method of strengthening physical properties of a material and suppress volume changes by growing a cathode active material as a single particle. The single particle cathode material was synthesized by growing the primary particles of the polycrystalline cathode precursor into large sizes. For performance comparison based on physical properties, poly and single particle cathode material is applied to a sulfide based ASSBs. The details will be discussed at the meeting.

8:30 AM *ES06.07.02

Sulfide Solid Electrolyte for Lithium/Sulfide All-Solid-State Batteries [Xiayin Yao](#)^{1,2}; ¹Ningbo Institute of Materials Technology and Engineering, Chinese Academy of Sciences, China; ²Center of Materials Science and Optoelectronics Engineering, University of Chinese Academy of Sciences, China

All-solid-state lithium batteries are considered as the most promising next generation electrochemical energy storage devices because of their high safety and energy density^[1]. Among all solid electrolytes, sulfide solid electrolytes have attracted increasing attention due to their high ionic conductivities and favorable interface compatibility with sulfur-based cathodes.

In the past decade, different sulfide solid electrolytes with room temperature ionic conductivity of $10^{-3} \sim 10^{-2}$ S/cm have been successfully synthesized. The moisture stability can be improved with oxide or halogen doping^[2]. Besides, according to process of water molecule adsorption and dissociation reactions, LiF-coated core-shell solid electrolyte can reduce the adsorption site, thus resulting in superior moisture stability when exposing in moist air^[3]. Meanwhile, the interfacial compatibility between solid electrolyte and lithium anode can also be enhanced. In order to reduce the sulfide solid electrolyte particle size, a liquid/solid fusion technology is developed to synthesize high ionic conductivity sulfide solid electrolyte with reduced particle size^[4]. Based on the high ionic conductive sulfide solid electrolyte powder, thin film can be obtained by cold press solid electrolyte with surface modification^[5], dry film method^[6] and wet coating approach^[7]. The obtained $\text{Li}_{5.4}\text{PS}_{4.4}\text{Cl}_{1.6}$ sulfide solid electrolyte membrane possesses a high ionic conductivity of 8.4 mS cm^{-1} with a thin

thickness of 30 μm .^[6] And the thickness of sulfide solid electrolyte film can be further reduced with relative high ionic conductivity above 1 mS cm^{-1} ^[7].

Due to similar chemical potential, sulfide cathodes show excellent interface compatibility with sulfide solid electrolytes. A series of transition metal sulfides or sulfur-based materials are employed as electrodes for all-solid-state rechargeable batteries based on intercalation/deintercalation and conversion reaction mechanisms. Nevertheless, transition metal polysulfides, such as FeS_2 ^[8], VS_4 ^[9], and MoS_6 ^[10], exhibit typical anionic redox driven electrochemical processes. Combination of electronic conductive carbonaceous materials and sulfide solid electrolyte coating can realize three-dimensional electronic/ionic conduction networks at the triple solid-solid contact interface. The well-designed transition metal polysulfide MoS_6 nanocomposite delivers a high reversible energy density of 1640 Wh kg^{-1} based on the active material at 0.1 A g^{-1} ^[10].

Although bright prospect of all-solid-state lithium batteries, there are still many challenges for their practical application. More attentions should be concerned on the high ionic conductivity and high chemical stable sulfide solid electrolytes, reducing the solid electrolyte thickness, electronic/ionic conduction network construction in the electrode layer, high specific areal capacity as well as alleviating stress/strain and volume changes.

References:

- [1] J. Wu, S. Liu, F. Han, et al., *Advanced Materials* 2021, 33, 2000751.
- [2] G. Liu, D. Xie, X. Wang, et al., *Energy Storage Materials* 2019, 17, 266.
- [3] Y. Jin, Q. He, G. Liu, et al., *Advanced Materials* 2023, 35, 2211047.
- [4] H. Wan, J. P. Mwizerwa, F. Han, et al., *Nano Energy*, 2019, 66, 104109.
- [5] G. Liu, J. Shi, M. Zhu, et al., *Energy Storage Materials* 2021, 38, 249.
- [6] Z. Zhang, L. Wu, D. Zhou, et al., *Nano Letters* 2021, 21 (12), 5233.
- [7] X. Zhao, P. Xiang, J. Wu, et al., *Nano Letters*, 2023, 23 (1), 227.
- [8] H. Wan, G. Liu, Y. Li, et al., *ACS Nano* 2019, 13, 9551.
- [9] Q. Zhang, H. Wan, G. Liu, et al., *Nano Energy* 2019, 57, 771.
- [10] M. Yang, Y. Yao, M. Chang, et al., *Advanced Energy Materials*, 2023, 13 (28), 2300962.

9:00 AM ES06.07.03

Iron Sulfides as High Energy Density Lithium Battery Cathodes Liping Wang¹, Zhendong Li², Jian Zou¹ and Hong Li³; ¹University of Electronic Science and Technology of China, China; ²Tianmu Lake Institute of Advanced Energy Storage Technologies, China; ³Institute of Physics, Chinese Academy of Sciences, Beijing, China

Conversion-type cathodes for lithium metal batteries are considered long-term targets due to their low cost and high energy density. However, they suffer from poor cycling life. In this talk, we present various interface engineering strategies, such as designing topotactic reactions and constructing a 3D ionic-electronic network to overcome this challenge. We demonstrate that micro-sized FeS_x cathode achieves a long cycling life at a high areal capacity ($> 4 \text{ mAh/cm}^2$) at high current rates. Meanwhile, we also demonstrate Li- FeS_x pouch cell prototype with an energy density up to 390 Wh/kg at room temperature without adding external pressure. It reveals the potential of conversion cathodes, even in micro-size, for practical applications.

Related works:

Liping Wang, Zhenrui Wu, Jian Zou, Peng Gao, Xiaobin Niu, Hong Li*, Lique Chen, Li-free cathode materials for high energy density lithium batteries, *Joule*, 3(2019) 2086-2102.

Zhendong Li, Ge Zhou, Shuai Li, Hongyu Liu, Liping Wang*, Hong Li*. Unlocking cycling longevity in micro-sized conversion-type FeS_2 cathodes, *Joule*, just-accepted, 2023

Jian Zou, Keguo Yuan, Jun Zhao, Bojun Wang, Shiyin Chen, Jianyu Huang, Hong Li*, Xiaobin Niu*, Liping Wang*, Delithiation-Driven Topotactic Reaction Endows Superior Cycling Performances for High-Energy-Density FeS_x ($1 \leq x \leq 1.14$) Cathodes, *Energy Storage Materials*, 43 (2021) 579-584.

Jian Zou, Jun Zhao, Bojun Wang, Shulin Chen, Pengyu Chen, Qiwen Ran, Li Li, Xin Wang, Jingming Yao, Hong Li, Jianyu Huang*, Xiaobin Niu*, Liping Wang*, Unraveling the Reaction Mechanism of FeS_2 as a Li-ion Battery Cathode, *ACS Applied Materials & Interfaces*, 2020, 12, 40, 44850-44857.

9:15 AM ES06.07.04

Irreversibility and Structural Distortion in Organic and Inorganic Fullerenes Arising from Electrochemical Cycling of Alkali-Metal-Ions. Arijit Roy, Sonjoy Dey, Shakir Bin Mujib and Gurpreet Singh; Kansas State University, United States

While large interlayer spacing allows for Na^+ and K^+ ion storage in transition metal dichalcogenide (TMD) based electrodes, side reactions, and volume change leading to pulverization of crystalline structure are persistent challenges for employing these materials in next-generation devices. Here in this study, we first investigate if irreversibility due to structural distortion resulting in poor cycling stability is also apparent in the case of quantum confined organic and inorganic (TMDs; such as MoS_2) fullerenes. To address these problems, we propose upper and lower voltage cut-off experiments to limit specific reactions. Differential capacity curves and derived surface plots highlight the continuation of reactions when a high upper cut-off technique is applied, indirectly suggesting the restriction of structural dissolution. Furthermore, structural preservation in half-cell electrodes during Li^+ , Na^+ or K^+ storage delivered better capacity retention with stable performance and higher coulombic efficiency, laying the ground for future works.

SYMPOSIUM MF01

Advances in Polymer-based Soft Matter for Additive Manufacturing
April 22 - April 26, 2024

Symposium Organizers

Emily Davidson, Harvard University
Michinao Hashimoto, Singapore University of Technology and Design

Emily Pentzer, Texas A&M University
Daryl Yee, École Polytechnique Fédérale de Lausanne

Symposium Support

Silver

UpNano US Inc.

* Invited Paper

+ JMR Distinguished Invited Speaker

^ MRS Communications Early Career Distinguished Presenter

SESSION MF01.01: Advances in Light-Based Printing / Multimaterial Printing I

Session Chairs: Emily Davidson and Daryl Yee

Monday Afternoon, April 22, 2024

Room 325, Level 3, Summit

4:00 PM *MF01.01.01

Biomaterials and Bioprinting to Enable Personalized Tissue Mimics Sarah C. Heilshorn; Stanford University, United States

Each individual is unique, yet pharmaceutical companies design the same therapies for all of us using lab mice. In the future, the biofabrication of personalized tissue mimics offers the exciting possibility of individualized therapies. However, current biofabrication methods are greatly hampered by a lack of materials that are simultaneously biofunctional and reproducible. A cell's behavior is directly influenced by its surrounding microenvironment; thus, ideally each cell type would be cultured in its own customizable biomaterial. To fulfill this need, my lab designs bespoke biomaterials that can be tailored to fit a range of applications. In one demonstration, I present a family of biomaterials that support the growth of patient-derived organoids, i.e. three-dimensional cell aggregates that demonstrate emergent, tissue-like behavior. While organoid cultures have the potential to revolutionize our understanding of human biology, current protocols rely on the use of Matrigel, a complex, heterogeneous material with large batch-to-batch variations. In contrast, our double-network hydrogels are formulated with recombinant biopolymers that can be fine-tuned to display a reproducible properties including printability. In a second example, I present a new "pick-and-place" 3D bioprinting strategy for the spatial positioning of organoids within a hydrogel support matrix. Using this method, we can fabricate large tissue structures composed of multiple organoids that fuse together. We demonstrate potential applications in the fabrication of neural "assembloids" composed of dorsal- and ventral-patterned neural organoids together with patient-derived brain cancer spheroids. We envision that these two technologies will be used together in the future to create personalized tissue models of individual patients.

4:30 PM *MF01.01.02

Orthogonal, Synergistic and Cooperative Precision Photochemistry for Multi-Wavelength Additive Manufacturing Christopher Barner-Kowollik^{1,2}; ¹Queensland University of Technology, Australia; ²Karlsruhe Institute of Technology, Germany

Over the last decade, our laboratory has employed monochromatic tunable laser systems to reveal a fundamental mismatch between the absorptivity of a chromophore and its photochemical reactivity in the vast majority of covalent bond forming reaction as well as specific bond cleavage reactions. Our data overturns the long-held paradigm that effective photochemical reactions are obtained in situations where there is strong overlap between the absorption spectrum and the emission wavelength. The lecture will demonstrate how a detailed action-plot driven precision mapping of photochemical reactivity enables the design of advanced multi-colour network formation and 3D printing modes with never-before-seen precision, exploiting wavelength orthogonal, synergistic, cooperative, and antagonistic photochemical reaction systems.

Selected References

Gauci, S. C.; Vranic, A.; Blasco, E.; Bräse, S.; Wegener, M.; Barner-Kowollik, C. *Adv. Mater.* **2023**, 2306468.
Gauci, S. C.; Du Prez, F. E.; Holloway J. O.; Houck, H. A.; Barner-Kowollik, C. *Angew. Chem. Int. Ed.*, **2023**, e202310274.
Thai, D. L.; Guimarães, T. R.; Chambers, L. C.; Kammerer, J. A.; Golberg, D.; Mutlu, H.; Barner-Kowollik, C. *J. Am. Chem. Soc.* **2023**, *145*, 14748.
Walden, S. L.; Rodrigues, L. L.; Alves, J.; Blinco, J. P.; Truong, V. X.; Barner-Kowollik, C. *Nat. Comm.* **2022**, *13*, 2943.
Nardi, M.; Blasco, E.; Barner-Kowollik, C. *J. Am. Chem. Soc.* **2022**, *144*, 1094.
Kodura, D.; Rodrigues, L. L.; Walden, S. L.; Goldmann, A. S.; Frisch, F.; Barner-Kowollik, C. *J. Am. Chem. Soc.* **2022**, *144*, 6343.
Walden, S. L.; Rodrigues, L. L.; Alves, J.; Blinco, J. P.; Truong, V. X.; Barner-Kowollik, C. *Nat. Comm.* **2022**, *13*, 2943.
Irshadeen, I.M.; Walden, S.L.; Wegener, M.; Truong, V.X.; Frisch, H.; Blinco, J.P.; Barner-Kowollik, C. *J. Am. Chem. Soc.* **2021**, *143*, 21113.
Menzel, J.P.; Noble, B.B.; Blinco, J.P.; Barner-Kowollik, C. *Nat. Comm.* **2021**, *12*, 1691.
Rodrigues, L. L.; Micallef, A. S.; Pfrunder, M.; Truong, V.X.; McMurtrie, J. C.; Dargaville, T.R.; Goldmann, A. S.; Feist, F.; Barner-Kowollik, C. *J. Am. Chem. Soc.* **2021**, *143*, 7292.
Kodura, D.; Houck, H. A.; Bloesser, F. R.; Goldmann, A. S.; Du Prez, F. E.; Frisch, H.; Barner-Kowollik, C. *Chem. Sci.* **2021**, *12*, 1302.
Kalayci, K.; Frisch, H.; Truong, V. X.; Barner-Kowollik, C. *Nat. Comm.* **2020**, *11*, 4193.
Houck, H. A.; Blasco, E.; Du Prez, F. E.; Barner-Kowollik, C. *J. Am. Chem. Soc.* **2019**, *141*, 12329.
Bialas, S.; Michalek, L.; Marschner, D. E.; Krappitz, T.; Wegener, M.; Blinco, J. P.; Blasco, E.; Frisch, H.; Barner-Kowollik, C. *Adv. Mater.* **2019**, *31*, 1807288.

SESSION MF01.02: Advances in Light-Based Printing / Multimaterial Printing II

Session Chairs: Emily Davidson and Daryl Yee

Tuesday Morning, April 23, 2024

Room 325, Level 3, Summit

10:30 AM *MF01.02.01

Multimaterial Actinic Spatial Control (MASC) 3D Printing [Andrew Boydston](#); University of Wisconsin–Madison, United States

Creation of multimaterial parts with complete 3-dimensional geometric freedom is a considerable challenge with potentially game-changing potential for manufacturing capabilities. Various approaches within the additive manufacturing and 3D printing communities have relied on equipment modifications that enable segregation of build materials and then selective deposition of different materials (from separate reservoirs) during printing. We propose a chemical approach to multimaterial parts fabrication that allows for a breadth of compositional diversity through orthogonal reaction mechanisms that can be mediated by different wavelengths of light. In this way, we are able to create multimaterial parts from single resin reservoirs (or vats) and control compositional gradients, heterogeneity, feature sizes, and colour without requiring complex compatibilization of vastly disparate build materials. Our published results already confirmed the ability to create soft-stiff materials combinations from a mixture of acrylate- and epoxide-based monomers. Our unpublished preliminary results have now confirmed the ability to create metallic components in the final parts, using photoredox catalysed reduction of soluble metal salts. Additionally, we have introduced some exciting resin features such as the ability to permanently alter colour through modulation of local pH via application of light, and a class of acrylate resin that produces soluble thermoplastics after photocuring. Specific targets of our program thus include: 1) creation of composite structures and open cell foams entirely via liquid-to-solid photocuring (no solids required in the resin feed), 2) creation of organic-inorganic combinations in multimaterial parts (e.g., circuitry, flexible electronics, antennae metamaterials), and 3) access to multicolor materials including custom camouflage patterns throughout a 3D part from a single resin composition.

11:00 AM MF01.02.02

Multi-Material Volumetric Additive Manufacturing of Hydrogels Using Gelatin as a Sacrificial Network and 3D Suspension Bath [Morgan Riffe](#)¹, [Matthew Davidson](#)², [Gabriel Seymour](#)¹, [Abhishek Dhand](#)³, [Megan Cooke](#)², [Hannah Zlotnick](#)², [Robert McLeod](#)^{1,1} and [Jason Burdick](#)^{1,2,3}; ¹University of Colorado Boulder, United States; ²University of Colorado-Boulder, United States; ³University of Pennsylvania, United States

Volumetric additive manufacturing (VAM) is an emerging layerless method for the rapid processing of reactive resins into 3D structures, where printing is much faster (seconds) than other lithography and direct ink writing methods (minutes to hours). As a vial of resin rotates in the VAM process, patterned light exposure defines a 3D object and then resin that has not undergone gelation can be washed away. Despite the promise of VAM, there are challenges with the printing of soft hydrogel materials from non-viscous precursors, including into multi-material constructs. To address this, we used a sacrificial gelatin matrix to modulate resin viscosity to support the cytocompatible VAM printing of macromers based on poly(ethylene glycol), hyaluronic acid (HA), and polyacrylamide. After printing, gelatin and unreacted resin are removed by washing at an elevated temperature (37°C). These constructs are soft due to the low polymer concentration and would be difficult to print in other types of additive manufacturing. Cell viability of various cell types (bovine mesenchymal stromal cells (MSCs), chondrocytes, and meniscal fibrochondrocytes) was also confirmed over 7 days of culture with an average viability of 96.4%. To print multi-material constructs, the gelatin-containing resin is also used as a shear-yielding suspension bath (including high molecular weight HA to further modulate bath properties) where an ink (also containing gelatin and high molecular weight HA) with a different photoreactive monomer can be extruded into the bath to define a multi-material resin that can then be processed with VAM into a singular defined object. Multi-material constructs of methacrylated HA (MeHA) used as the bath and gelatin methacrylamide (GelMA) used as the ink are printed (as proof-of-concept) with encapsulated MSCs, where the local hydrogel properties define cell spreading behavior with culture. After 1 day of culture, the cells spread in the GelMA regions and stayed rounded in the MeHA regions, due to the adhesion ligands and degradability present in GelMA. In future studies, this process can be applied to tissue engineering to help recapitulate the heterogeneous nature of complex tissues such as the meniscus.

11:15 AM ^MF01.02.03

Upconversion-Enabled Volumetric 3D Printing [Dan Congreve](#)^{1,2}, [Tracy Schloemer](#)^{1,2}, [Sam Sanders](#)², [Qi Zhou](#)¹, [Arynn Gallegos](#)¹, [Hao-Chi Yen](#)¹, [Mahesh Gangishetty](#)², [Daniel Anderson](#)², [Michael Seitz](#)^{1,2} and [Chris Stokes](#)²; ¹Stanford University, United States; ²Rowland Institute at Harvard University, United States

Triplet fusion upconversion, the manipulation of excited states in molecules to convert two low energy photons into one higher energy photon, has shown tremendous potential for a wide range of applications. Here, I will discuss how we can use this process to enable volumetric 3D printing, including the chemical, material, and optical designs required to do so and recent progress in pushing towards exciting applications.

11:45 AM MF01.02.04

Continuous Volumetric 3D Printing: Xolography in Flow [Lucas Stüwe](#)¹, [Matthias Geiger](#)¹, [Franz Röllgen](#)¹, [Thorben Heinze](#)¹, [Marcus Reuter](#)², [Matthias Wessling](#)^{1,3}, [Stefan Hecht](#)^{4,2,3} and [John Linkhorst](#)^{5,1}; ¹RWTH Aachen University, Germany; ²XOLO GmbH, Germany; ³DWI–Leibniz Institute for Interactive Materials, Germany; ⁴Humboldt-Universität zu Berlin, Germany; ⁵Technische Universität Darmstadt, Germany

Various printing techniques have emerged since Charles Hull's introduction of commercial 3D printing in 1980, with vat polymerization and technologies like stereolithography (SLA) and digital light processing (DLP) standing out with high resolution and fine surface finish. Despite impressive resolutions of up to 600 nm for SLA and about 75 µm for DLP, a fundamental trade-off between resolution and printing speed persists, limiting the applicability of 3D printing in high-throughput scenarios like scaffolds in bottom-up tissue engineering. For growing specific tissues on centimeter scale, millions of biocompatible building blocks with controllable micron-sized porosity are required to enable cell interpenetration and nutrient supply. Traditional AM methods that rely on the layer-by-layer approach, are not yet able to close the gap between high production rates and high resolution.

The next step in rapid additive manufacturing is represented by volumetric 3D printing, such as xolography. Unlike traditional layer-by-layer approaches, volumetric printing directly polymerizes a defined resin volume, allowing for arbitrary geometries while maintaining high resolution at rapid printing speeds. Xolography is a linear volumetric 3D printing method that utilizes dual-color polymerization for precise volumetric curing. A photoswitchable photoinitiator switches from a dormant to a latent state by illumination with the first wavelength in the UV-light spectrum. Upon illumination with the second wavelength, polymerization is initiated. Based on this principle, the polymerized volume can be set by projecting an image of the second wavelength onto a UV-light sheet. By moving the resin through the UV-light sheet and synchronizing a sequence of images with this movement, complex 3D geometries can be produced in seconds to minutes.

Xolography emerges as a possible choice for medical applications like tissue engineering, owing to its ability to achieve high printing speeds while maintaining high resolution, even with marginal photoinitiator concentrations (0.01wt%) - which can be a safety concern in biomedical contexts - and the use of high-viscosity resins, making it compatible with biodegradable high-molecular photopolymers.

In this study, Xolography is transformed from a batch process into a continuous fabrication method by vertically flowing resin through the UV-light sheet. The sequence of the projected images is synchronized to the resin velocity at the area of both intersecting wavelengths. The flow profile is visualized by computational fluid dynamic simulations. By designing a symmetrical flow cell with four inlets, the flow profile can be adjusted by the ratio of the volume flow through each inlet and is subsequently flattened in the intersecting area of both wavelengths for an enhanced printing resolution.

A second prerequisite for continuously printing objects via xolography is the circumvention of unwanted polymerization by the UV-light only. At increased radiant fluxes, polymerization occurs without the second wavelength. This is particularly the case at the glass-resin boundary where the resin velocity is reduced, and the radiant flux received by the resin is maximized. By integrating oxygen-permeable side windows to the flow cell, oxygen can

diffuse into the resin, quench the photoinitiator in the boundary layers and thus prevent unwanted curing.

With these modifications, the continuous xolography process achieves recognizable feature sizes of up to 10 μm in x/y and 25 μm in z-direction. Objects can be printed in parallel at a minimum object distance of 80 μm to utilize the entire printing area with constant resolution and print speed, showcasing the flexibility and potential for upscaling continuous volumetric 3D printing via xolography. This innovative approach closes the gap between high volume generation rate at high resolutions and holds great promise for biomedical applications.

SESSION MF01.03: Bioapplications
Session Chairs: Emily Davidson and Emily Pentzer
Tuesday Afternoon, April 23, 2024
Room 325, Level 3, Summit

1:30 PM *MF01.03.01

A Molecular Approach to Additive Manufacturing Medical Devices for Use in The Clinic Matthew L. Becker; Duke University, United States

The emergence of additive manufacturing has afforded the ability to fabricate intricate, high resolution, and patient-specific polymeric implants. However, the availability of biocompatible resins with tunable resorption profiles remains a significant hurdle to clinical translation. In this presentation, I will outline our strategies for synthesizing highly functional oligomeric resins that can be photochemically printed into a variety of structures possessing unique mechanical, chemical and degradation properties. I will also describe their use in a number of pre-clinical applications.

2:00 PM MF01.03.02

Materials Development for Additive Manufacture of Magnetic Resonance Imaging (MRI) Phantoms Brian Derby; University of Manchester, United Kingdom

Magnetic resonance imaging (MRI) is an important non-invasive probe used extensively for medical diagnostics. Phantoms are manufactured devices of controlled specific composition, dimensions and shape that are used for: instrument calibration, to provide common reference samples to allow the calibration of multisite research collaborations, they can act as replacements for human volunteers or live animal models during operator training or technique development. Additive manufacture is an attractive method for the production of phantoms with better physiological shape reproduction, if appropriate printable materials can be developed that provide the appropriate imaging contrast to mimic healthy and diseased tissue. Phantoms are more difficult to develop for MRI applications than other medical imaging techniques, such as X-Ray or ultrasonic imaging, because the imaging contrast is provided by the relaxation times, T1 and T2) of the nuclear magnetic resonance excitation of protons in biological systems. These relaxation times (T1 and T2) in biological tissue are much longer than in conventional polymeric materials because of the presence of water and the soft matter gel nature of biological tissue. Hence, conventional MRI phantom materials are either aqueous solutions or weak gels of biologically extracted hydrogels such as agarose gels, carageens and alginates, possibly doped with paramagnetic ions to further tune the relaxation times. These phantoms have a very limited shelf-life and are normally formulated prior to use and disposed of afterwards. They are not particularly stable and the relaxation may be affected by the local environment, e.g. humidity, ambient temperature or oxygen pressure (altitude of the site). Here we demonstrate a family of printable materials that have been developed using formulations of silicone resins that can access the T1 and T2 parameter space that encompasses most medically important organs and tissues. This tunability can be achieved using conventional silicone formulations and commercially available resins using simple variation of polymer and oligomer molecular weight and cross-linking density. A second strategy is also presented that uses a multiphase or composite approach with blends of immiscible materials. These formulations are shown to have the rheological properties appropriate for extrusion additive manufacturing methods. Simple demonstrator structures have been produced that show good imaging quality and stability.

2:15 PM MF01.03.03

3D Printed Core-Shell Structured Scaffolds with NIR-Triggered Dual Release for Cancer Therapy and Uterine Tissue Regeneration Shangsì Chen, Zhaohé Xu and Min Wang; The University of Hong Kong, Hong Kong

Gynecologic cancers and uterine fibroids can cause dysfunction of the uterus and hence result in female infertility. Various treatment options, including surgical resection, radiation therapy, chemotherapy and hormone therapy, are available for treating gynecologic cancers and uterine fibroids, aiming to restore fertility for women of the child-bearing age. Surgical resection is one of the most used treatments for cancerous tissues and uterine fibroids. However, insufficient clinical intervention can result in tumor recurrence, and the residual defective tissue after surgery can cause intrauterine adhesion (IUA) and further affect women's reproductive ability. Therefore, new and novel treatments that can effectively kill residual tumor cells and at the same time, regenerate new and healthy uterine tissues should be developed. In the current study, a dual drug/biomolecule release system, with the release being triggered by a near-infrared (NIR) laser that would deliver anticancer drug and biomolecules (for promoting uterine tissue regeneration) in a chronological manner, was designed and fabricated for the affected uterus. Specifically, gelatin (Gel) hydrogel/poly(L-lactide-co-trimethylene carbonate) (PLLA-co-TMC, "PTMC" in short) core-shell structured scaffolds with NIR-triggered dual releases of anticancer drug doxorubicin hydrochloride (DOX) and hormone estradiol (E2) were constructed via 3D printing for providing cancer therapy and for promoting uterine regeneration for postoperative females. DOX is a commonly used antineoplastic agent for treating many cancers and has been clinically used for uterine cancers. E2 is an estrogen steroid hormone extensively used to facilitate uterine regeneration. In our fabrication, Gel and DOX were homogeneously mixed first and 3D printed to form Gel-DOX scaffolds. E2-containing polydopamine (PDA@E2) microspheres were synthesized and homogeneously dispersed in PTMC-dichloromethane (DCM) solution. Gel-DOX scaffolds were then soaked in the PTMC-PDA@E2 solution for fabricating Gel-DOX/PTMC-PDA@E2 core-shell structured scaffolds. It was observed that the PTMC-PDA@E2 coating layer significantly enhanced mechanical properties of the scaffolds, making them comparably strong with the native uterine tissue. Furthermore, the coating layer protected the Gel-DOX core from rapid biodegradation and thus inhibited the burst release of DOX. Moreover, Gel-DOX/PTMC-PDA@E2 scaffolds could release DOX and E2 in a chronological manner, firstly delivering DOX together with photothermal therapy (PTT) to effectively kill Hela cells used in the *in vitro* experiments and then sustainably releasing E2 over 28 days of the experiment duration to promote uterine tissue regeneration. The *in vitro* experiments showed that DOX could be quickly released in 3 days and that the core-shell scaffolds exhibited excellent anticancer ability through the synergy of DOX release and hyperthermia cancer cell ablation. E2 via controlled release over the 28 days promoted the proliferation of bone marrow-derived mesenchymal stem cells (BMSCs) and induced their differentiation. The novel Gel-DOX/PTMC-PDA@E2 core-shell scaffolds have shown their high potential for postoperative management for female patients.

2:30 PM *MF01.03.04

An Ultrashort Aliphatic Self-Assembling Peptide Platform Supports Automated 3D Bioprinting for Large-Scale Tissue Constructs and 3D Tissue

Differentiation [Charlotte A. Hauser](#); King Abdullah University of Science and Technology, Saudi Arabia

Bioprinting is increasingly relevant for various applications in regenerative medicine. However, automated printing of stable large-scale constructs under physiological conditions with high shape fidelity and long-term cell survival are challenges that most existing bioinks cannot solve. Additionally, the required chemical or UV-cross-linking processes of current printing approaches compromise the encapsulated cells, resulting in restricted structure complexity. Rationally designed ultrashort self-assembling peptides are a promising class of biomaterials with different biomedical applications. We have rationally designed three self-assembling tetrapeptides as bioinks and demonstrated their potential for automated 3D bioprinting of large-scale cell constructs and their differentiation. The peptide bioinks overcome severe limitations in current bioprinting procedures, avoiding cell-compromising abrasive conditions such as chemical treatments or UV-cross-linking during the printing process. Using these peptide bioinks as a suitable body-like but synthetic material, we demonstrate an instant solidifying cell embedding printing process via a sophisticated extrusion procedure under true physiological conditions. Our printed large-scale cell constructs and the chondrogenic differentiation of printed mesenchymal stem cells point to the strong potential of the peptide bioinks for automated complex tissue fabrication.

3:00 PM BREAK

SESSION MF01.04: Bioapplications / Soft Polymers
Session Chairs: Emily Davidson and Emily Pentzer
Tuesday Afternoon, April 23, 2024
Room 325, Level 3, Summit

3:30 PM *MF01.04.01

Solvent-Cast 3D Printing with Multi-Material Inks to Independently Control Biochemical and Physical Properties [Lesley W. Chow](#); Lehigh University, United States

The biochemical and physical properties of a polymer-based biomaterial are commonly tailored to drive desired cellular responses for specific applications. However, modifying one property can lead to unwanted changes to another that make it difficult to fine-tune cell-material interactions. For example, surface chemistry can be controlled by changing composition, but this also impacts mechanical properties. Scaffold stiffness can be tuned without changing polymer type by changing porosity, but pore size and shape also affects cellular infiltration and nutrient and oxygen exchange. To address these challenges, we developed a versatile solvent-cast 3D printing platform using inks containing different polymer MW ratios and/or end-functionalized polymer conjugates to independently control surface chemistry, stiffness, and architecture. Blending different MW ratios of the same polymer allow us to change scaffold stiffness while the end groups of the conjugate become displayed on the surface during fabrication. In addition, using multiple printer heads enable us to spatially deposit different inks to organize biochemical and physical cues within the same construct. This talk will describe our platform and how we are 3D printing heterogeneously organized scaffolds to regenerate complex tissues like the osteochondral interface.

4:00 PM MF01.04.02

3D-Nanomaterials Printing for Tailorable Sensing and Flexible Electronics [Rahim Esfandyarpour](#); University of California, Irvine, United States

Over the past decade, three-dimensional (3D) printing technology has fundamentally transformed traditional fabrication and manufacturing, particularly for micro-scale structures, models, and devices. Recent advancements in 3D printing, especially in the domain of nanomaterials, offer benefits such as ease of operation, cost-effectiveness, rapid prototyping, high resolution, and the capability to tailor designs and fabricate sensors customized to specific model requirements, individual needs, or disease diagnostics. Notably, with the rising emphasis on in-situ real-time health monitoring, the demand for wearable sensors is surging. However, to achieve widespread adoption of wearable biosensors for large-scale population monitoring, there's a need for swift, reliable, cost-effective, and high-throughput integration of these platforms.

In this study, we demonstrate our innovative approach to 3D printing of nanomaterials, successfully producing multiplexed, cost-effective, and mechanically flexible wearable bioelectronic sensing patches. These patches comprise 3D-printed nanomaterial-based flexible sensors and flexible wearable microfluidic sample-handling units, all integrated within just a few hours.

Further, we demonstrated the mechanical and electrical robustness of these patches under repeated bending cycles. We characterized the performance of the sensing units ex situ with various target ion samples across a spectrum of concentrations. Negative control experiments further showcased the patches' capability for selective ion detection. Additionally, we highlighted the potential of our 3D-printed nanomaterial patches for continuous health monitoring. This was evidenced by the simultaneous in situ monitoring of multiple ions (e.g., H⁺, Na⁺, K⁺, and Ca²⁺) present in sweat.

Our work represents a significant stride towards enabling personalized health monitoring practices, deploying 3D nanomaterial printing technology for the facile and affordable development of tailored, integrated wearable, and flexible biosensing platforms, optimized for the noninvasive and continuous monitoring of individual health parameters.

4:15 PM *MF01.04.03

Room-Temperature 3D Printing of Super-Soft and Solvent-Free Elastomers [Christopher Bates](#); University of California, Santa Barbara, United States

This talk will discuss versatile strategies for designing new 3D-printable resins to efficiently access materials with unique properties.

4:45 PM MF01.04.04

Directed Self-Assembly of Thermoplastic Elastomers via 3D Printing for Mechanically Tailored Soft Architectures [Alice Ferguson](#), Ben H. Gorse and Emily C. Davidson; Princeton University, United States

Many biological systems utilize self-assembled hierarchically ordered structures to achieve complex functional properties. However, current methods cannot scalably achieve this level of control over structure and function across multiple length scales in synthetic systems. Here, we make progress towards bridging this gap by demonstrating the use of material extrusion 3D printing to induce tunable alignment of a commercial cylinder-forming polystyrene-*b*-poly(ethylene-*co*-butylene)-*b*-polystyrene (SEBS) thermoplastic elastomer along a controlled print path. We demonstrate that the extent of nanostructure alignment and resulting anisotropy can be tuned via the shear and extensional forces applied to the material during 3D printing. In addition, we show that

post-printing thermal annealing plays a critical role in maximizing domain alignment via relaxation of trapped stresses. Ultimately, we have demonstrated the ability to induce up to 85x greater tensile modulus along the print direction compared to perpendicular to the print direction. By designing custom print paths for these soft and mechanically anisotropic materials, we enable fabrication of soft architectures with tailored macroscopic mechanical behavior such as controlled localization of strain upon deformation.

SESSION MF01.05: Poster Session I: Materials Development
Session Chairs: Alice Ferguson and Daryl Yee
Tuesday Afternoon, April 23, 2024
Flex Hall C, Level 2, Summit

5:00 PM MF01.05.01

Development of Binding System for Metal Fused Filament Fabrication of AISi10Mg Alloy Gustavo M. Delfino^{1,2}, Kaue R. dos Santos^{1,2}, Leandro J. de Camargo³, Haroldo C. Pinto² and Tamires d. Nossa¹; ¹Federal Institute of Education, Science and Technology - IFSP, Brazil; ²University of São Paulo, Brazil; ³Federal Institute of Education, Science and Technology of São Paulo - IFSP, Brazil

Additive manufacturing technology through 3D printing can efficiently produce parts with complex geometries using smaller, portable equipment. 3D printing plays a significant role in manufacturing polymer prototypes and products in various areas. One promising area of research involves incorporating metal powder into polymer filaments for 3D printing, aiming to expand the versatility of the technique and provide an alternative to conventional approaches such as Fused Filament Manufacturing (FFF). The binder polymer formulation plays a crucial role in the success of the manufacturing process. This study presents the development of a specific binding system for the 3D printing of AISi10Mg filaments. The binder includes low-density polyethylene (LDPE) and thermoplastic starch (TPS). LDPE contributes to structural integrity during binder dissolution, reduces viscosity, and increases strength and stiffness. Meanwhile, TPS, besides being biodegradable, provides flexibility to the filaments. The study included an analysis of the shape and size distribution of metallic powder particles before their incorporation into the polymeric matrix. The composite filaments were produced using reactive extrusion (REX), being mechanically characterized and evaluated for their homogeneity. The reactive extrusion method demonstrated effectiveness in the production of homogeneous composite filaments in relation to the metallic filler incorporated into the thermoplastic polymer blend. Although extruded filaments exhibit inferior mechanical properties compared to thermoplastics generally used in FFF additive manufacturing, the method has potential for application in the manufacture of new composite filament compositions using LDPE and TPS blend matrix as a binding for application in 3D printing.

5:00 PM MF01.05.02

Different Strategies for Developing an Electrically Conductive and Flexible Composite by DLP 3D Printing Luca Montaina¹, Rocco Carcione², Francesca Pescosolido^{1,3}, Silvia Orlanducci¹, Silvia Battistoni⁴ and Emanuela Tamburri^{1,3}; ¹University Tor Vergata, Italy; ²ENEA, Italy; ³University of Tor Vergata, Italy; ⁴National Research Council, Italy

Additive manufacturing (AM), or 3D printing, is one of the main elements in the development of Industry 4.0, which can increase plant productivity and improve product quality. Indeed, thanks to the layer-by-layer manufacturing approach, AM opens up the possibility of mass customization of products by achieving complex designs, with minimal material waste. However, despite the several advantages of AM, the widespread usage of this technology is still limited by several factors, such as surface finish, standardization, and lack of materials. In this context, the primary contribution of this work involves the design and synthesis of a flexible and electroconductive composite, being the flexibility and conductivity essential properties in various industries, spanning from electronics, to sensors, and wearable technology. In particular, we are focusing our research on different strategies for including a conductive polymer, i.e. polyaniline (PANI), into a poly(ethylene glycol) diacrylate (PEGDA) matrix by using a Digital Light Processing (DLP) [et1] 3D printer. Such printing technique typically makes use of a light to selectively cure a thin layer of a photosensitive ink. However, the 3D printing technology for CPs is still in its early stages and faces many challenges, mainly related to poor solubility and printability of CP systems. In this context, we report two different protocols for producing PEGDA-PANI items by means of a DLP 3D printer. In the first, an in-situ approach is exploited to synthesize PANI inside a printed PEGDA substrate, by combining 3D printing with a subsequent chemical oxidation process. Conversely, the second approach exploits the printer UV light to start the photopolymerization of aniline monomers directly during a PEGDA printing process. The PEGDA-PANI systems produced by both the methods show suitable morphological and structural features, as well as electrical and electrochemical performances, making them potentially useful for various soft electronics applications.

The two distinct production methods developed highlight the versatility and adaptability of 3D printing in producing electroconductive materials. Moreover, the possibility to produce flexible and customizable electronics provides broader implications for various industries, as an expanded list of available materials for AM opens doors to novel product designs and functionalities.

5:00 PM MF01.05.03

Material-Process-Property Relationships for Direct-Ink-Writing of Ceramic Matrix Composites Caitlin Grover¹, Irmak Sargin², Scott Beckman¹ and Arda Gozen¹; ¹Washington State University, United States; ²Middle East Technical University, Turkey

Ceramic matrix composites (CMCs) consist of a reinforcing secondary material phase within a ceramic matrix. These material systems can resist corrosive/oxidizing environments and have high hardness even at high temperatures. Among the two types of CMCs, ones featuring chopped fiber reinforcements offer simpler processing compared to the ones continuous fiber reinforcement systems. However, chopped fiber CMCs remain inferior to their continuous fiber counterparts in terms of mechanical and thermal properties [1]. This is primarily because the conventional processing methods generally lack control over the part microstructure and produce a randomly distributed reinforcement phase, limiting the achievable property enhancement. Emerging material extrusion-based additive manufacturing methods such as Direct-ink-writing (DIW) offer an exciting potential to address this issue. In DIW, highly viscous inks including ceramic matrix powders and reinforcing fibers are deposited layer-by-layer as they are extruded out of small capillaries. It has been shown that the high shear and extensional stresses experienced by the inks during this process can align the reinforcing particles along the printing direction [2,3], providing means to control final part microstructure.

This study aims to understand the material-process-property relationships for DIW of CMCs including aluminum oxide matrix and chopped silicon carbide fiber reinforcements. Here, we formulate inks by combining aluminum oxide powder and silicon carbide fibers with a liquid phase polymer which is a precursor to silicon carbide. Through a custom DIW print head with integrated capillary rheometry [4] capability, we characterize the shear rates experienced by the inks during the printing process. We then examine the density, microstructure and mechanical properties of the printed and sintered CMCs to understand the influence of the DIW process on these outcomes. We expand the analysis to cover various ink compositions and nozzle sizes to explore the key material and process parameters to achieve microstructural control.

References:

- [1] J. Binner, M. Porter, B. Baker, J. Zou, V. Venkatachalam, V.R. Diaz, A. D'Angio, P. Ramanujam, T. Zhang, T.S.R.C. Murthy, Selection, processing, properties and applications of ultra-high temperature ceramic matrix composites, UHTCMCs—a review, *International Materials Reviews*. 65 (2020) 389–444. <https://doi.org/10.1080/09506608.2019.1652006>.
- [2] J.W. Kemp, A.A. Diaz, E.C. Malek, B.P. Croom, Z.D. Apostolov, S.R. Kalidindi, B.G. Compton, L.M. Rueschhoff, Direct ink writing of ZrB₂-SiC chopped fiber ceramic composites, *Addit Manuf.* 44 (2021) 102049. <https://doi.org/10.1016/j.addma.2021.102049>.
- [3] J.P. Lewicki, J.N. Rodriguez, C. Zhu, M.A. Worsley, A.S. Wu, Y. Kanarska, J.D. Horn, E.B. Duoss, J.M. Ortega, W. Elmer, R. Hensleigh, R.A. Fellini, M.J. King, 3D-Printing of Meso-structurally Ordered Carbon Fiber/Polymer Composites with Unprecedented Orthotropic Physical Properties, *Sci Rep.* 7 (2017) 43401. <https://doi.org/10.1038/srep43401>.
- [4] K.T. Estelle, B.A. Gozen, Complex ink flow mechanisms in micro-direct-ink-writing and their implications on flow rate control, *Addit Manuf.* 59 (2022) 103183. <https://doi.org/10.1016/j.addma.2022.103183>.

5:00 PM MF01.05.04

Dehydration Methodology for Poly (ethylene glycol) Diacrylate Hydrogels Using Silica Gel Samaher Shaheen¹, Sam Lloyd-Harry¹, Ozgul Yasar-Inceoglu¹ and Ozlem Yasar²; ¹California State University, Chico, United States; ²The City University of New York, United States

Poly (ethylene glycol) diacrylate (PEGDA) hydrogels have been proven to be a promising material in bone tissue engineering applications due to their remarkable capacity for the precise control of mechanical properties. The 3-dimensional structures of hydrogels play an important role in their biological efficiency and mechanical properties. Analysis of these nanoscale structures often requires the imaging of dehydrated hydrogels. The dehydration process is traditionally performed using freeze-drying or thermal techniques, which can be costly or cause damage to the nanostructures. This study uses silica gel to analyze a cost-effective dehydration methodology for PEGDA hydrogels. The 80% concentration hydrogels were prepared with an 85:15 PEGDA to PDMS volume ratio via sonication and subsequent UV light exposure. After photolithography, the weight and dimensions of the cured specimen were recorded. Then, a comparative dehydration study was initiated: one common method involving oven dehydration (190 to 200 F) and a narrative technique surrounding the specimen with dry silica gel beads inside a sealed container. Both dehydration methods were performed on multiple samples over (24, 48, and 72 hours). Post-dehydration, the specimens were measured and weighed. Characterization methods such as FTIR, SEM, XRD, Raman spectroscopy, compression testing, and hardness testing were performed. The preliminary findings of this study show that the silica gel method was more successful at preserving the 3-D structure and pore sizes than the thermal method. Furthermore, this study establishes that the silica gel dehydration method is a promising cost-efficient technique for preparing PEGDA hydrogel specimens for different types of analyses and can potentially extend the accessibility of tissue engineering materials research.

5:00 PM MF01.05.05

A Temperature-Dependent Framework of The Curing of Silicone Elastomers for Additive Manufacturing Te Faye Yap, Jasmine Klinkao, Anoop Rajappan, Marquise D. Bell, Barclay Jumet and Daniel Preston; Rice University, United States

Silicone elastomers offer a wide range of desirable mechanical properties, from extreme softness to high strain, that are not typically exhibited by additively manufactured parts. Direct ink writing (DIW) and vat photopolymerization (VP), two of the most commonly used layer-by-layer additive manufacturing methods for polymers, remain limited to materials with specific properties that allow for processing; for example, in DIW, the extruded inks should hold their shape post-printing, and in VP, photocurable thermosets are required. The additive manufacturing of parts from new materials, such as thermally polymerizable silicone elastomers, has only begun to be explored with layer-by-layer fabrication techniques, and the formation of elastomeric parts has largely remained limited to casting [1].

Development of new methodologies to allow for thermally polymerized silicone elastomers to enter the additive manufacturing design space must rely on a fundamental understanding of how temperature affects the rate of curing of these elastomers. Furthermore, the adhesion between layers in layer-by-layer printing processes must be well-understood. Recent work has shown examples of VP and DIW fabrication of parts using silicone elastomers, and the authors note the importance of considering the role of adhesion between layers in the performance of the final printed part; however, the adhesion strength between layers was not characterized or studied comprehensively [2, 3].

To facilitate development of future additive manufacturing processes, we developed an analytical model based on an Arrhenius framework that describes the rate of crosslinking as a function of temperature for commercially available platinum-catalyzed silicone elastomers. Our model, validated with experiments, serves as a guideline to determine the duration required for curing these silicone elastomers at any given temperature. For example, we show that the curing speed doubles with each ~10 °C increase in temperature. Furthermore, we highlight that the curing behavior exhibits self-similarity—using a nondimensional reaction coordinate, we can predict the extent of curing even for arbitrary spatiotemporal heating conditions. The nondimensional reaction coordinate serves as a powerful tool that allows us to study the adhesion strength between layers as a function of the curing time and temperature. Using the reaction coordinate, we are able to characterize the regimes where layer-to-layer adhesion would result in adhesive (versus cohesive) failure, and we can predict the adhesive or cohesive strength at different extents of curing. This work provides a framework to describe the relationship between temperature, the extent of the curing reaction, and the adhesion strength between layers, which will broaden the design space for the additive manufacturing of silicone elastomers and extend their processing beyond conventional casting.

References

- [1] D. W. Yee, “A HAPPI solution: Photothermal additive manufacturing of unmodified thermoset resins,” *Matter*, vol. 6, no. 8, pp. 2488–2612, Aug. 2023, doi: 10.1016/j.matt.2023.07.002.
- [2] S. Walker *et al.*, “Predicting interfacial layer adhesion strength in 3D printable silicone,” *Additive Manufacturing*, vol. 47, p. 102320, Nov. 2021, doi: 10.1016/j.addma.2021.102320.
- [3] C.-U. Lee, K. C. H. Chin, and A. J. Boydston, “Additive Manufacturing by Heating at a Patterned Photothermal Interface,” *ACS Appl. Mater. Interfaces*, vol. 15, no. 12, pp. 16072–16078, Mar. 2023, doi: 10.1021/acsami.3c00365.

5:00 PM MF01.05.06

Temperature Dependent Hygromechanical Behavior of Additively Manufactured Nylon (polyamide 6) and ULTEM (polyetherimide) Continuous Carbon Fiber Composites Madeline A. Morales, Bradley D. Lawrence and Todd C. Henry; DEVCOM Army Research Laboratory, United States

Fused deposition modeling (FDM) is used extensively for rapid prototyping with 3D printed thermoplastic materials. Nylon (polyamide 6) is a popular filament material; however, the mechanical properties are known to degrade in the presence of moisture and/or elevated temperature. In contrast, ULTEM (polyetherimide) has higher strength/stiffness and resistance to moisture/temperature but is more expensive. This work compares the impact of

hydrothermal conditioning on the flexural strength and modulus of Markforged Onyx (Nylon + chopped carbon fiber) and ULTEM 9085 samples with and without the addition of continuous carbon fibers printed using a Markforged FX20 3D printer. Samples for bend testing were conditioned at 90% RH at 22°C for 26 days, and mass/dimension increase was recorded. 3-point bend testing according to ASTM D7264 was conducted while varying temperature from 22°C (room temperature) to 50°C using an Instron load frame with an environmental testing chamber. The rate of flexural strength/modulus decrease with increasing temperature was compared for the four different materials (Onyx, Onyx + continuous carbon fiber, ULTEM, ULTEM + continuous carbon fiber) in the as-printed and conditioned state. Ductile vs. brittle failure mechanisms are discussed considering the polymer moisture content and microstructure. Fiber-polymer interfacial bonding is also discussed. The results will help inform end users of the optimal material to use given the operating load, moisture, and temperature conditions for their specific application.

SESSION MF01.06: Poster Session II: Biomaterials/Bioapplications
Session Chairs: Alice Ferguson and Daryl Yee
Tuesday Afternoon, April 23, 2024
Flex Hall C, Level 2, Summit

5:00 PM MF01.06.01

Additive Manufacturing of 3D Microchambers for Cell Culture Aman Singhal¹, Tejas Y. Suryawanshi¹, Arun Jaiswal², Shobha Shukla¹ and Sumit Saxena¹; ¹Indian Institute of Technology Bombay, India; ²The University of Sydney, Australia

Two-photon polymerization (TPP) has been developed as a direct laser writing technique for the preparation of complex 3D structures with resolution beyond the diffraction limit. Its remarkable characteristics, such as precise 3D fabrication, sub-diffraction resolution, material flexibility, and mild processing conditions, have made it suitable for several applications in biosciences. One such application is the fabrication of microchamber scaffolds for cell culture, which are three-dimensional structures that provide mechanical support and a three-dimensional environment for cells growth and differentiation. Here, we report the fabrication of 3D square microchambers scaffold using TPP technique. Fabricated scaffolds are made up of microchannels and microchambers interconnected to create a porous structure that mimics the extracellular matrix (ECM) of natural tissues that can provide a suitable environment for cell growth and differentiation. These scaffolds can be used in tissue engineering and regenerative medicine applications.

5:00 PM MF01.06.02

Carboxymethylation of Silk Fibroin and Injectable Microgel Assembly Prepared from Thereof Yeonwoo Yu, Seonghyeon Jo, Yehee Lee and Ki Hoon Lee; Seoul National University, Korea (the Republic of)

Silk fibroin (SF) from silkworm cocoons is a fibrous protein and found its application in various fields such as tissue engineering, drug delivery, soft electronics, etc., owing to its biocompatibility. SF can be fabricated into various different forms, such as films, macro-to-nano fibers, scaffolds, and hydrogels. Among these forms, SF hydrogel can be made by physical and chemical crosslinking. Physical crosslinking of SF is based on the formation of β -sheet structure, which results in a brittle mechanical behavior of the hydrogel. On the other hand, chemical crosslinking of SF through enzymatic crosslink or photo-crosslink results in elastic SF hydrogel. In 3D printing, various kinds of natural polymers are used as ink, and, in many cases, 3D constructs are formed upon the gelation of the polymer right after its extrusion. SF was also considered as a candidate natural polymer in 3D printing, but the inherent low viscosity of SF aqueous solution and its slow gelation kinetic were the technical hurdles. Therefore, blending with other 3D printable polymers or introducing photo-crosslinkable functional groups were suggested as a solution for SF. Meanwhile, microgel assembly has been applied in the 3D printing field. Microgels can be assembled into a macro-sized hydrogel through various interactions between the microgel particles. If the microgel assembly was formed by a reversible dynamic bonding, such microgel assembly can flow upon shear stress and recover back into a viscoelastic solid state when the stress is removed.

The aim of this study is to prepare a suitable SF microgel assembly for 3D printing. Many previous studies have been reported on preparing SF microgels, but they had to dissolve the SF fiber. However, large amounts of chemicals are required during this dissolution, and time-consuming dialysis should be followed. We have skipped this step by conducting direct modification of SF in its fiber state. Carboxymethylation was performed directly on the SF fiber, which resulted in a rod-like microgel. The carboxymethylation has been done primarily on the tyrosine of SF. The negative charges of carboxymethyl groups allowed high water uptake and swelling by the repulsive forces, but the dissolution was prevented by the intact β -sheet structure working as a physical crosslinker. By controlling the concentration and the degree of carboxymethylation of SF microgel, optimum conditions for microgel assembly formation were established. Rheological studies confirmed the injectability of SF microgel assembly, in which gel-like behavior under a low shear rate but flowability under a high shear rate. Finally, we have successfully built a standalone 3D construct of SF microgel assembly by extrusion 3D printer. The prepared SF microgel would have high potential in tissue engineering, and enhancing the structural stability of the 3D construct of SF microgel is currently underway.

5:00 PM MF01.06.03

Optimizing Collagen Bioprinting for Mechanically Strong and Resilient Ligament/Tendon Engineering Grace Hu¹, Karla Cebrero², Nandita Venkataraman², Zeqing Jin², Zev J. Gartner^{1,3,4} and Grace Gu^{2,1}; ¹University of California, Berkeley & San Francisco, United States; ²University of California, Berkeley, United States; ³University of California, San Francisco, United States; ⁴Chan Zuckerberg Biohub, United States

Ligaments and tendons coordinate and stabilize our body's movement, but damage to these soft tissues has been an enduring problem accounting for 30% of musculoskeletal clinical cases every year.^[1] While athletes who play contact sports are most commonly prone to sprains or ruptures of the anterior cruciate ligament (ACL), people can experience ligament and tendon injuries through falls, twists, or overuse. Traditional surgical interventions involve graft replacement from elsewhere in the patient's body, which often requires months of recovery and fails to achieve entheses healing or true regenerative capabilities. Promisingly, the development of synthetic biomaterials that mimic the native hierarchical structure of ligaments/tendons can facilitate tissue repair.^[2]

The overarching goal of our work is to optimize how type I collagen, the main component of tendons and ligaments, can be 3D-printed to serve as artificial implants. Our novel approach combines both a computational and experimental framework to iterate upon the bioprinted collagen. Numerical simulations are first implemented to characterize the swelling behavior of collagen, which are then compared to experimental testing.^[3] With an eye towards translation and ease-of-use, we utilize the commercially-available Cellink BioX bioprinter to control infill density, concentration, nozzle diameter, and heating duration throughout printing, observing vastly different mechanical properties in the resultant hydrogels. Secondly, we aim to fabricate gradient materials with directionally varying stiffnesses so that the printed collagen can achieve enhanced integration as a connective tissue. Overall, this synergistic approach will enable customizable, on-demand printing of ligaments and tendons for regenerative medicine.

- [1] Lim WL, Liau LL, Ng MH, Chowdhury SR, Law JX. Current progress in tendon and ligament tissue engineering. *Tissue Eng Regen Med*. 2019;16(6):549-571. doi:10.1007/s13770-019-00196-w
- [2] Lei T, Zhang T, Ju W, et al. Biomimetic strategies for tendon/ligament-to-bone interface regeneration. *Bioactive Materials*. 2021;6(8):2491-2510. doi:10.1016/j.bioactmat.2021.01.022
- [3] Jin Z, Hu G, Zhang Z, Yu SY, Gu GX. Modeling and analysis of post-processing conditions on 4D-bioprinting of deformable hydrogel-based biomaterial inks. *Bioprinting*. 2023;33(e00286):1-9. doi:10.1016/j.bprint.2023.e00286

SESSION MF01.07: Poster Session III: Novel Methods and Designs in Additive Manufacturing
Session Chairs: Alice Ferguson and Daryl Yee
Tuesday Afternoon, April 23, 2024
Flex Hall C, Level 2, Summit

5:00 PM MF01.07.01

Stimuli-Responsive Microscale Mechanical Logic Abhinav Parakh, Caitlyn C. Krikorian (Cook), Elaine Lee and Widiyanto P. Moestopo; Lawrence Livermore National Laboratory, United States

To overcome the operational limitations of conventional electronics, equivalent logic circuits composed of precisely fabricated mechanical systems have shown promise as a viable alternative. Here, we develop microscale, battery-free mechanical sensors in which stimuli-responsive materials are paired with micro-scale mechanical circuits to enable high mechanical computing power within a sensor system. We utilize additive manufacturing with micron-scale precision to fabricate structures that respond to thermal and chemical changes, and we perform computation by applying these stimuli. By integrating multiple stimuli-responsive actuators to mechanical logic gates, we demonstrate proof-of-concept computation of environmental cues in the microscale without electrical power. Our exploration of signal propagation dynamics in microscale mechanical logic circuits actuated by materials with different stimuli responsiveness will accelerate the development of smart, active, and sentient materials that can interface with extreme environments and respond to external changes without needing batteries. This work was performed under the auspices of the U.S. Department of Energy by Lawrence Livermore National Laboratory under Contract DE-AC52-07NA27344 (LLNL-ABS-850674). Support from LDRD Exploratory Research 22-ERD-030 and LDRD Feasibility Study 24-FS-018 are gratefully acknowledged.

5:00 PM MF01.07.02

Investigation of Mechanical Performance of Composites Based on ‘Hat’ Aperiodic Monotile Structures Jiyoung Jung, Ailin Chen and Grace Gu; UC Berkeley, United States

Disordered structures, as oftentimes found in nature, have the potential to have unique behaviors and higher mechanical performance in terms of stiffness, strength, and toughness compared to ordered structures. However, such a disordered structure increases the complexity of design and fabrication process, which can be resolved if the infinite plane can be aperiodically covered with a single unit cell (i.e. aperiodic monotile). With the long efforts of the mathematics community, a hat-shaped aperiodic monotile structure was recently discovered. This study proposes new composite designs using an aperiodic monotile structure and investigates mechanical performance and mechanisms. For tensile loading, aperiodic monotile composites consisting of stiffer material for core areas and softer material for boundaries are considered varying volume fractions of each phase. On the other hand, for compressive loading, the composites composed of stiffer material forming boundaries and softer material as filling are examined with different size of unit cells. The specimens are fabricated using multimaterial polyjet additive manufacturing processes. To probe further into the mechanisms, phase field modeling based fracture simulations are conducted for tensile loading cases and explicit dynamic fracture simulations are conducted for compressive loading cases. Simulations show that aperiodic monotile structure enables high strength and toughness compared to a honeycomb structure under tensile loading. In addition, the aperiodicity of the aperiodic monotile structure allows superior performance under compression compared to the periodic structure. This study shows that the aperiodic monotile composite structure can be next generation of composite structure showing superiority to other conventional composite structures in terms of stiffness, strength, and toughness.

5:00 PM MF01.07.03

Xerographic 3D Printing with Periodic Patterns Hyung Ju Ryu, Hadi Moeinnia, Omar Nemir, Sami Khan and Woo Soo Kim; Simon Fraser University, Canada

3D Printing, a form of additive manufacturing (AM) has gained widespread popularity for the fabrication of intricate structures. It is recognized as an innovative solution to overcome the limitations associated with traditional subtractive manufacturing methods. It also offers cost efficiency, design flexibility, rapid prototyping, and environmentally friendly attributes. In this research, we explore the Xerographic 3D printing method. The objective is to fully harness the potential of AM, capitalizing on the high productivity of the well-established Xerographic 2D digital printing techniques. In addition to the core electrostatic interactions underpinning the Xerographic dry copying process, our work introduces hydrophobic interactions between fluoropolymer particles and interim and final substrates, thus contributing to the formation of 3D structures by a transfer method. To implement this approach, we use a surface micro-texturing technique to create periodic structures on metal substrates followed by surface functionalization, which subsequently impacts hydrophobic properties. Thus, our research reveals that the supplementary hydrophobic effects substantially improve the fidelity and precision of 3D structures produced through Xerographic 3D printing. Our study is poised to advance the utilization of Xerographic 3D printing by providing a more efficient avenue for 3D structure fabrication while also deepening our understanding of the interaction mechanisms within the Xerographic setup.

5:00 PM MF01.07.04

Materials Design guided by Defects in Liquid Crystals Jeremy R. Money¹, Fakhreddin Emami¹, Andrew Gross¹, Jose A. Martinez-Gonzalez² and Monirosadat Sadati¹; ¹University of South Carolina, United States; ²Universidad Autónoma de San Luis Potosí, Mexico

Architected cellular materials represent a growing body of materials research encompassing a broad classification of materials, from open celled foams to sheet-based lattices. Comprised of unit cells of varying geometries and tessellation patterns, these material systems give rise to unique properties attributed primarily to their unit cell geometry as opposed to their bulk material chemistry. Enabled by additive manufacturing technologies, architected cellular materials are increasingly making their way into commercial design and production, offering solutions to many challenges faced by industries such as biomedicine and personal protective equipment and energy. However, additional barriers to ubiquity such as the stiffness/toughness tradeoff of lattice based architected cellular materials present opportunities for the development of novel unit cell geometries with tunable topological features. Current areas

of design inspiration are drawn from the intricate patterns displayed by nature or solid atomistic crystals. However, the opportunity for novel approaches to unit cell design presents a frontier ripe for exploration.

One such approach exists in the study of the behavior of liquid crystals and their interpenetrating networks of defects or disclination lines. This fascinating state of matter possesses the long range orientational ordering of solid crystals while retaining the fluidlike properties and response to confining geometries possessed by liquids. These material systems exhibit self-assembly of their constituent molecules, or mesogens, into interesting mesostructures which pack together forming 3D periodic arrangements. This behavior has been extensively investigated for its optical response; however, little is understood about the mechanical properties of the resultant disclination architectures. Through utilization of Landau-de Gennes guided simulations, these architectures can be readily predicted at the nanoscale and then upscaled for design and fabrication as promising candidates for architected cellular materials. Of the unique geometries which arise from the disclination arrangements in liquid crystal systems, is the interpenetrating double diamond lattice that shows promise for structural applications. Study of the mechanical response of these geometries indicate potential toughening mechanisms induced by contact between the bicontinuous lattice networks. In addition to its variable strut diameter and reinforced nodal regions, the relative density of these structures can be adjusted rapidly using the liquid crystal's scalar order parameter. The exploration of these disclination lattices offers a promising avenue for the enhancement of architected cellular materials, with tunable design parameters unique to the behavior of liquid crystal systems.

SESSION MF01.08: Poster Session IV: Devices and Applications
Session Chairs: Alice Ferguson and Daryl Yee
Tuesday Afternoon, April 23, 2024
Flex Hall C, Level 2, Summit

5:00 PM MF01.08.01

Dual-Function Hydrogel-Based Smart Wearables: AI-Driven Temperature Responsiveness & UV Index-Indicative Color Monitoring Mohamed Elnemr and Haider Butt Butt; Khalifa University of Science and Technology, United Arab Emirates

The integration of smart wearable technology with daily life necessitates materials that are not only responsive but also robust and user-friendly. This work introduces an advancement in smart wearables crafted from hydrogel composites, employing Digital Light Processing (DLP) 3D printing to achieve a level of durability comparable to conventional plastics. The enhanced hydrogels uniquely incorporate thermochromic & photochromic capabilities, allowing for a dynamic color response to temperature & UV light variations.

These color transitions are not merely aesthetic; they are intricately linked to an artificial intelligence (AI) model specifically trained to decode these hues into precise temperature measurements, providing a non-invasive method for monitoring personal thermal environments. In contrast, the photochromic aspect of the wearables acts as a visual sentinel against UV exposure, autonomously signaling when protective measures are advisable, bypassing the need for AI intervention.

These transformative hydrogel wearables challenge existing perceptions of material capabilities. With direct colorimetric feedback for UV protection and AI-assisted temperature monitoring, they offer practical, immediate environmental responsiveness in a user-friendly format.

5:00 PM MF01.08.02

Manufacturing Electrostatic Chucks via Ceramic 3D Printing: Formulation of Photopolymer Resin and Simulation-driven Structural Optimization Munseong Kim, Jihoon Kim and Sukeun Yoon; Kongju National University, Korea (the Republic of)

The electrostatic chuck is utilized to hold objects such as silicon wafers and LCDs securely. As advancements in related industries continue, research interest in electrostatic chucks is on the rise. Traditional manufacturing processes for these chucks primarily rely on APS (atmospheric plasma spraying) coating, a method that poses limitations in shape flexibility and consumes high energy. To overcome these challenges, this study introduces a method employing photopolymerization 3D printing, which combines ceramics with photopolymer resins. This 3D printing technology stands out for its exceptional precision and rapid production speeds. By integrating ceramic composite resin, it not only allows for the emulation of the physical properties of various ceramic materials but also vastly enhances design flexibility. To produce a ceramic composite resin tailored for photopolymerization 3D printing, a photopolymerization resin was formulated using two monomers: 1,6 hexanediol diacrylate (HDDA) and Trimethylpropane triacrylate (TMPTA). The resin's printing attributes and performance were assessed by monitoring the curing properties in response to varying monomer ratios. Following this, BaTiO₃ (BTO) powder was added in concentrations ranging from 0 to 30 vol.% to the best-performing resin to create a high dielectric constant BTO photopolymerization resin. To determine the optimal wavelength by evaluating the printability of the manufactured resin according to the optical characteristics of BTO, the curing characteristic behavior was analyzed according to the changes in the three wavelength bands of 385nm, 405nm, and 415nm. The dielectric properties of the 3D-printed BTO composite layers were evaluated to optimize the BTO content for peak dielectric performance, emphasizing both a high dielectric constant and breakdown strength. Based on this material insight, bipolar-type electrostatic chuck models were designed. Their structural optimization and corresponding chucking performance were enhanced using finite element analysis through COMSOL. In this study, by applying ceramic composite resin to photopolymerized 3D printing technology, we were able to fabricate electrostatic chucks with exceptional chucking performance through 3D ceramic printing.

5:00 PM MF01.08.03

Development of Conductive Aerogels for DLP-3D Printed Sensors Diana Cafiso^{1,2}, Federico Bernabei^{1,3}, Matteo Lo Preti¹, Ignazio Roppolo², Candido Fabrizio Pirri² and Lucia Beccai¹; ¹Istituto Italiano di Tecnologia, Italy; ²Politecnico di Torino, Italy; ³Scuola Superiore Sant'Anna, Italy

The growing demand for versatile soft sensors has propelled the research on novel materials and the use of technologies that ensure broad design flexibility, e.g., 3D printing [1]. Digital Light Processing (DLP) 3D printing is a promising approach for fabricating sensors with elaborate and scalable architectures due to the excellent resolution of the printed structures [2]. Still, developing printable and deformable materials is mandatory to fully harness the advantages of this technology for soft sensing.

In this work, we combined DLP 3D printing and lyophilization to manufacture conductive and soft aerogels featuring intricate morphologies. Hydrogels made of an insulating Polyethylene Glycol Diacrylate (PEGDA), poly(3,4-ethylenedioxythiophene) polystyrene sulfonate (PEDOT: PSS) and a photoinitiator were 3D-printed via DLP. Subsequently, the hydrogels were lyophilized to obtain conductive aerogels. The dual-step process limited the collapse of the printed samples during the solvent removal, leading to the fabrication of aerogels possessing elaborate 3D geometries with a remarkable resolution of 200 μm .

The aerogels' electrical, morphological and mechanical properties could be finely controlled by adjusting the chemical composition of the precursor hydrogels. The content of PEDOT: PSS was changed from 50%wt to 10%wt, and samples with tunable electrical conductivity were successfully fabricated.

The solvent ethylene glycol was used to further decrease the electrical resistivity from 70 k Ω *cm to 35 k Ω *cm. Moreover, SEM analysis of the obtained aerogels revealed a closed-cell porous morphology. The porosity increased with the amount of PEDOT: PSS from 58% to 96%, and the size of the pores ranged from 5 μ m to 60 μ m. The adjustable porosity played a crucial role in enhancing the deformability of the material and in tailoring the elastic modulus from 0.26 kPa to 1 MPa. Moreover, the softer aerogels endured repeated loading and unloading cycles.

A reactive diluent was added to the formulation to optimize the material's properties for force-sensing applications. The decrease in the crosslinking density and the formation of larger pores improved the deformability of the so-modified aerogels. Consequently, the electrical resistance under the application of compressive force decreased, demonstrating the suitability of these aerogels for the development of 3D force sensors. Different porous aerogel architectures were fabricated and tested, revealing the influence of the geometrical features on force sensitivity and paving the way for soft sensors with programmable design and performance.

Finally, despite their hydrophilicity, the samples exhibited remarkable stability upon humidity (up to 70% of relative humidity), proving their suitability for various working environments.

These results highlight the potential of the proposed material for developing 3D-printed soft structures with tailorable architectures and electro-mechanical properties, thus offering significant opportunities and versatility for soft sensing.

[1] Cafiso, D., Lantean, S., Pirri, C.F. and Beccai, L., Soft Mechanosensing via 3D Printing: A review. *Adv. Intell. Syst.* 2023, 5, 2200373.

[2] Joe, S., Bliach, O., Magdassi, S., Beccai, L., Jointless Bioinspired Soft Robotics by Harnessing Micro and Macroporosity. *Adv. Sci.* 2023, 10, 2302080.

5:00 PM MF01.08.04

Adaptive 3D-Printed Pressure Sensor Hadi Moeinina, Danielle Agron and Woo Soo Kim; Simon Fraser University, Canada

Pressure sensors have garnered considerable attention across a range of domains, including robotics, healthcare, and sports applications. Various pressure sensor designs have been proposed to enhance sensitivity and broaden the pressure detection spectrum. Nonetheless, creating a highly sensitive sensor capable of accommodating a wide range of pressure loads often demands the use of specialized clean rooms and costly equipment. In this study, we introduce a fully 3D-printed architectural pressure sensor equipped with a shape programmability feature. Leveraging the customizable 3D design capabilities of 3D printing, we fabricate pressure sensors tailored to individual patients. The pressure transduction mechanism relies on capacitance. Both experimental and simulation results affirm the precise adjustability of the sensor's detection range, spanning from 70 to 2,500 kPa. Sensitivity levels range from 0.01 1/kPa to 0.0002 1/kPa, with a remarkable response time of 800 milliseconds. Importantly, the cost of fabricating the entire sensor is under 5 cents per unit. The 3D architecture pressure sensor can be deployed in an array configuration for pressure mapping purposes, making it valuable in biomedical and robotic applications.

5:00 PM MF01.08.05

Controlling Dielectric Constant and Breakdown Voltage for Optimizing Chucking Force in 3D-Printed Electrostatic Chucks: A Combined Simulation and Experimental Investigation Yujin Kim, Jihoon Kim and Sukeun Yoon; Kongju National University, Korea (the Republic of)

Electrostatic chuck (ESC) is used to adsorb objects such as semiconductor wafers and LCD panels using electrostatic force and is attracting great attention as a device that can compensate for the shortcomings caused by mechanical clamps or vacuum chuck. The ESC is composed of an insulating layer (body), a dielectric layer, and an electrode in which the electrode is formed in a bi-polar type and interdigitated pattern. The chucking force is known to be enhanced by maximizing the dielectric constant and breakdown voltage of the dielectric materials. However, it is difficult to find a single material that simultaneously exhibit both required characteristics. In this study, distinct materials were selected for the body and dielectric layer of the ESC. Two different ceramic composite resins were formulated by varying the contents of BaTiO₃ (BTO) and Al₂O₃ (Alumina) between 0 to 30 vol% within a photocurable resin. BTO, which has a relatively high dielectric constant ($\epsilon_r \sim 23$) but a lower breakdown voltage (7 kV/mm), was used for the dielectric layer. In contrast, alumina, with a lower dielectric constant ($\epsilon_r \sim 6$) but a higher breakdown voltage (43 kV/mm), was chosen for the body. Using the DLP (Digital Light Process) 3D printing technique, a body comprising alumina with an interdigitated electrode pattern was created. Subsequently, this body was coated with a dielectric layer composed of BTO. The structural dimensions of the ESC were optimized through finite element simulation (COMSOL) to achieve the maximum chucking force. The simulation result and the measured chucking force of the fabricated ESC were compared and analyzed. The ESC made of a combination of alumina (body) and BTO (dielectric layer) exhibited superior performance compared to ESCs made solely of alumina or BTO for both body and dielectric layer. Additionally, these findings were consistent with the simulation results. In this study, using FEA-optimized structures and selective material choices, we successfully fabricated an ESC through 3D printing methods.

5:00 PM MF01.08.06

Printing of Micro-Lens Encapsulation Using Siloxane/Silica Nanocomposites for Highly Efficient Micro Light-Emitting Diode Arrays Byung Jo Um, Hyungshin Kweon, Junho Jang and Byeong-Soo Bae; Korea Advanced Institute of Science and Technology, Korea (the Republic of)

Nowadays, micro-scale light-emitting diodes (μ LEDs) have attracted tremendous attention as next-generation displays. Encapsulating materials are essential to protect μ LEDs from external environments and to increase light extraction efficiency (LEE) [1]. Conventional encapsulating materials face challenges in terms of thermal stability, and refractive index, limiting the long-term reliability and efficiency of μ LEDs [2]. To overcome these challenges, highly stable siloxane hybrid materials containing phenyl groups have been studied, suggesting that the phenyl group can improve optical performance [3]. In addition, lens-shaped encapsulation has been identified as a way to increase the light extraction efficiency of Chip-On-Board LEDs, but the existing method is complicated such as manufacturing unique supports on the substrate, making it difficult to apply to μ LEDs [4].

Herein, we have developed the highly stable μ LED encapsulating material with high refractive index (RI) and thixotropic index (TI), which greatly improved LEE and reliability of μ LED. To obtain μ LED encapsulating material, we fabricated phenyl-based siloxane hybrid (PSH) of thermal-induced hydrosilylation reaction of sol-gel synthesized linear vinyl-phenyl siloxane (LVS) and linear hydrogen-phenyl siloxane (LHS) resins. By using two phenyl-based siloxane resins, we can induce the high phenyl group contents in matrix, which lead to high RI of matrix. Polydimethylsiloxane-terminated hydrophobic fumed silica nanoparticles (FSNs) were dispersed in PSH that act as giving thixotropic properties for the formation of lens-shape and inducing scattering effect for the increment of LEE. We studied trade-off relationship among optical transparency, thermal stability, and TI of PSH by varying amount of FSN in matrix. Through optimization of FSN contents in PSH, we achieved excellent optical and rheological properties (RI: ~ 1.59 @ 486 nm, and TI: 3.96 from 0.1 to 100 s⁻¹) of PSH with 1.5wt% of FSN. Furthermore, the fabricated PSH with 1.5wt% of FSN showed the high thermal stability at 130 °C for 700 hours. After encapsulating μ LED arrays with PSH@FSN, the optical performance improved by 29.86% compared to the bare μ LED arrays. Furthermore, we confirmed the reliability of PSH@FSN-encapsulated μ LEDs under 85 °C/85% relative humidity, which exhibited almost similar luminous flux (86.4% retained) after 60 days aging.

[1] S. Lan et al., *Micromachines*, 10, 860 (2019).

[2] J. Shen et al., *Silicon*, 5, 2163 (2023).

[3] J.Y. Bae et al., *RSC advances*, 3, 8871 (2013).

[4] Y. Gan et al., *J. Mater. Chem. C*, 2, 5533 (2014).

SESSION MF01.09: Soft Polymers
Session Chairs: Emily Pentzer and Daryl Yee
Wednesday Morning, April 24, 2024
Room 325, Level 3, Summit

8:30 AM MF01.09.01

3D Printed Stretchable Soft Electronics with Metamaterials-Inspired Electromagnetic Architecture [LeiBin Li](#), Dwipak Sahu, Jared Anklam, Samuel H. Hales, Samannoy Ghosh and Yong Lin Kong; University of Utah, United States

The integration of electronics with soft and stretchable materials can enable active functionalities on the otherwise passive constructs. Previous works have demonstrated exciting success in imparting stretchability with geometrical designs but often require challenging microfabrication processes. Here, we propose a 3D printing approach that can create freeform electronics by selectively annealing micro-extruded nanomaterials *in situ* using a metamaterials-inspired electromagnetic architecture. This enables the creation of microscale three-dimensional interconnects and electronics with a desktop-sized platform that can resist strain and flexing – allowing the integration of stretchable active components on a soft substrate. We are also studying the integration of printed electronics into a broad range of soft materials by leveraging soft matter physics phenomena. Overall, we envision that this approach can enable new fabrication methodologies that lead to strategies that not only improve device compatibility and durability but also enable new classes of 3D-printed soft electronics.

8:45 AM MF01.09.02

3D Printing of Polyvinyl Alcohol Hydrogels (PVA) Enabled by Aqueous Two-Phase System (ATPS) [Michinao Hashimoto](#); Singapore University of Technology and Design, Singapore

The synthesis of PVA hydrogels (PVA-Hy) requires a high-concentration alkali solution (*e.g.*, sodium hydroxide, NaOH, 4.2 M), and the rapid physical crosslinking of PVA makes it challenging to ensure layer-to-layer adhesion for 3D printing. This work demonstrated the three-dimensional (3D) printing of PVA hydrogels in benign conditions (NaOH, 0.3 M) using a two-phase system (ATPS). Salting out of PVA to form ATPS allowed temporal stabilization of 3D-printed PVA structures while it was physically crosslinked by moderate alkaline conditions. Crucially, the layer-by-layer printing of PVA was enabled by delayed reaction at low alkaline concentrations. To verify this principle, we studied the feasibility of direct ink write (DIW) 3D printing of PVA inks (5 – 25% w/w, $m = 0.1 - 20$ Pa s, and MW = 22000 and 74800) in aqueous embedding media offering three distinct chemical environments: (1) salts for salting out (*e.g.*, Na₂SO₄), (2) alkali hydroxides for physical crosslinking (*e.g.*, NaOH), and (3) mixture of salt and alkali hydroxide. The presence of the salt did not compromise the stretchability and durability of PVA-Hy. Overall, our method demonstrated a unique concept of embedded 3D printing enabled by ATPS for temporary stabilization of the printed structures to facilitate 3D fabrication.

9:00 AM MF01.09.03

A Digital Exploration of The Mechanical Property Space of Self-Stabilizing Dynamic Printable Foams [Brett A. Emery](#)¹, Daniel Revier², Kelsey Snap³, Jeff Lipton¹ and Keith Brown³; ¹Northeastern University, United States; ²University of Washington, United States; ³Boston University, United States

Foams are versatile by nature, and are used ubiquitously in applications ranging from padding and insulation to acoustic dampening. Previous work established that foams additively manufactured via Viscous Thread Printing (VTP) are capable of enabling a greater degree of control over many of the key mechanical properties of conventional foams such as Young's modulus, fracture characteristics, and toughness while eliminating the need for chemical foaming agents. However, the relationship between input parameters and output properties is currently only accomplished via iterative empirical testing which limits generalizability and predictive control of desired output properties. Our work addresses this by combining high-throughput automated experimentation with machine learning to identify a subspace able to predict material behavior down to the stress-strain curve level. We identify a self-stabilizing microstructure trend in the VTP process, amplifying confidence in achieving desired output properties. Evidence for this self-stabilization is demonstrated by introducing various print height perturbations during the print process and measuring layer thickness as a function of the number of layers before restitution. This predictive mapping was developed utilizing data collected from thermoplastic polyurethane (TPU) specimens before being generalized by applying assumptions inherent to filament-based additive manufacturing to VTP's core physical models. This generalization was then validated using polylactic acid (PLA) and Nylon suggesting inherent compatibility with any material suitable for filament-based 3D printing.

9:15 AM MF01.09.04

Temperature-Responsive Dynamic Granular Hydrogels for 4D Printing Applications [Keisuke Nakamura](#), Nikolas Di Caprio and Jason Burdick; CU Boulder, United States

4D printing is an emerging technology to fabricate dynamic objects that can change their shape and properties in response to external stimuli (*e.g.*, temperature). Such 4D printed materials have a wide range of potential applications, including soft robotics, active drug delivery systems, and pharmaceutical models. Granular hydrogels, comprised of jammed microgels, are promising as 3D printable materials due to their shear-thinning and self-healing properties, as well as unique micropore structure. By introducing stimuli responsiveness (*e.g.*, volume transitions) into individual microgels, we anticipated that printed granular hydrogels would exhibit dynamic macroscopic and micropore structures; such dynamic granular hydrogels remain largely unexplored. To investigate this, we developed temperature-responsive microgels and assembled them into granular hydrogels to explore their application for 4D printing. Specifically, temperature responsiveness was achieved by crosslinking norbornene-modified hyaluronic acid (NorHA) with dithiol-terminated poly(N-isopropyl acrylamide) (DTPN) via a thiol-ene reaction, which showed a low critical solution temperature (LCST) transition. To form microgels, an emulsion of NorHA, DTPN, and photoinitiator was formed in stirring mineral oil and crosslinked via UV irradiation, which produced microgels with an average diameter of ~155 μm at room temperature (rt) after washing from the oil. Microgel diameters decreased by ~20% when heated (41°C), which was reversible when cooled back to rt. Granular hydrogels were prepared by centrifuging microgels, with structures exhibiting porosity and pore sizes of ~18 % and ~5360 μm^2 , respectively, at rt. The porosity and the pore sizes significantly increased (~28 % and ~10300 μm^2 , respectively) when heated (41°C), presumably due to microgel shrinkage and disconnection. To enhance the stability of granular hydrogels toward 4D printing, inter-particle photocrosslinking was introduced using a tetra-arm PEG thiol in the presence of a photoinitiator and light. Post-crosslinked granular hydrogels were stable and exhibited a bulk volume decrease by ~23% when heated. Interestingly, unlike granular hydrogels without post-crosslinking, increased temperatures reduced pore sizes (5848 μm^2 to 4283 μm^2) within post-crosslinked granular hydrogels. This is likely because there is no disconnection between the covalently crosslinked microgels during heating, resulting in isotropic shrinkage of micropores. Finally, control granular hydrogels (*i.e.*, non-responsive to

temperature) were used as suspension baths (i.e., shear-yielding and self-healing materials) to receive temperature-responsive granular hydrogel inks to create multi-material objects that actuate in response to temperature based on patterned responsivity. We envisage that our findings will facilitate the rational design of dynamic hydrogels that respond to various stimuli based on an innovative 4D printing approach that exploits the benefits of granular hydrogels.

9:30 AM *MF01.09.05

3D Printing-Assisted Casting of Soft Electronic Materials Yue (Jessica) Wang; University of California, Merced, United States

It is challenging to balance architectural complexity, electrical conductance, and material generality for the 3D printing of soft electronic materials. In this talk, I will discuss our efforts on 3D printing-assisted casting to alleviate this trade-off. Light-based 3D printing is used to create hollow molds, providing structural complexity and design freedom, whereas the casting nature imparts material versatility. The casting molds are made of superabsorbent polymers and printed in a partially hydrated state. Their dehydration provides significantly enhanced feature resolution and excellent thermal and mechanical properties, making them versatile for casting. After casting and curing desired materials within the mold cavity, over-hydration of the molds facilitate their energy-efficient removal. Using a polymeric conductor, poly(3,4-ethylenedioxythiophene) (PEDOT), as a model system, complex architectures such as octet and truncated octahedron can be achieved. Compositing silver flakes with PEDOT through a thermal injection process leads to prints with conductivity over 6000 S/cm. This method can also be applied to other hard-to-print soft materials and composites, and potentially enable multi-material structures through sequential casting.

10:00 AM BREAK

SESSION MF01.10: High Performance Polymers
Session Chairs: Emily Pentzer and Daryl Yee
Wednesday Morning, April 24, 2024
Room 325, Level 3, Summit

10:30 AM *MF01.10.01

The Practical Application of Additive Manufacturing for Extreme Environments Melissa A. Smith and Bradley Duncan; MIT Lincoln Laboratory, United States

In the automotive, aerospace, and defense industries, there is need for additively manufactured components that cannot only withstand extreme environments but to also be capable of multiple functions or enhanced capabilities. Existing material sets for additively manufactured components are often unsuitable for extreme environments, which limit their practical use and implementation. For example, organic or polymeric components are not rugged or suitable for temperature extremes. More rugged materials (metals and ceramics) can be difficult and expensive to process and are constrained in their compatibility to make composites or blends, hindering the fabrication of multifunctional structures. At MIT Lincoln Laboratory, our mission being technology in support of national security, we develop new materials sets to address shortcomings of the existing, well-established material sets. Success in this mission will facilitate not only the adoption of additive manufacturing for demanding or extreme applications, but also to provide a more far-reaching technological advantage. Specifically, this talk will highlight three distinct cases where new materials are implemented for (1) thermal, mechanical, and chemical stability extreme environments by using inorganic glass-based structures, (2) shielding of high energy particles or radiation for the localized protection of electronic components in space systems by designing composite materials consisting of materials with high and low atomic numbers, and (3) for obscuring transmission line designs in radio frequency systems using graded dielectrics. In all cases, the materials and composites were processed using direct write additive manufacturing, which features low processing temperatures and active mixing. Further, we show the ways our methods and materials outperform existing well-established materials. Due to the simplicity of our approach the consequential implications of its use, we expect the wide adoption of these materials and methods and also the increased acceptance of additively manufacture components for real applications (beyond prototyping and structural modelling), especially those in extreme environments.

DISTRIBUTION STATEMENT A. Approved for public release. Distribution is unlimited.

This material is based upon work supported by the Under Secretary of Defense for Research and Engineering under Air Force Contract No. FA8702-15-D-0001. Any opinions, findings, conclusions or recommendations expressed in this material are those of the author(s) and do not necessarily reflect the views of the Under Secretary of Defense for Research and Engineering.

11:00 AM MF01.10.02

3D Printed Electromagnetic Wave Absorber based on Carbon Black-Based Load-Bearing Metastructure Jeongwoo Lee¹, Daniel D. Lim², Jaemin Lee¹, Dowon Noh¹, Sujin Park¹, Grace Gu² and Wonjoon Choi¹; ¹Korea University, Korea (the Republic of); ²University of California, Berkeley, United States

As electronic equipment becomes more diverse and miniaturized due to advances in science and technology, addressing the issues of interference shielding and electromagnetic (EM) radiation absorption becomes increasingly important. Carbon-based composites combined with porous metastructures are lightweight, flexible and their EM properties can be modified in a desired frequency band, making them suitable for a variety of applications. However, the low density of these structures intrinsically limits their mechanical properties.

In this study, we report a multifunctional broadband metamaterial absorber (MBMA) with EM wave absorption, energy absorption, and constant relative stiffness using a bending-dominated lattice structure based on Kelvin Foam comprising carbon-black composite polylactic acid (PLA). Using computational simulation, EM wave characteristics are optimized by adjusting structural parameters such as beam diameter and unit cell size, and intrinsic material properties like dielectric constant according to carbon black filler concentration. Then, the optimized structure is additively manufactured for experimental validation to demonstrate the feasibility of actual implementation. The developed MBMA achieves an outstanding broadband (C-Ku band) EM wave absorption rate (>90%, average 95.9%) even at densities as low as cork (200 kg/m³), with a maximum absorption of 99.1% at 15.8. GHz. Regardless of the layer stacking direction, the relative density-to-relative stiffness ratio is close to 2.0, maintaining the theoretical stiffness of Kelvin Foam. The experimentally measured performances using 3D-printed MBMA are almost identical to the theoretically confirmed simulation results, validating the design and fabrication of the developed structure. This rational design strategy using 3D lattice structures can inspire multifunctionality of mechanical metamaterials including EM wave absorption, enabled by developing various polymer-based materials and unit cell structures.

11:15 AM MF01.10.03

Responsive 3D Printed Composites for Protective Applications [Miaomiao Zou](#) and Sebastian Pattinson; University of Cambridge, United Kingdom

Responsive materials that change their properties depending on their environment could enable diverse new medical, wearable, and other devices with exceptional function and compact form factors. Shear-stiffening gels (SSG) can be flexible but harden in response to rapid impact. This could enable protective devices amongst other applications. However, SSG can be easily deformed under external force and cannot recover its original shape, which limits its potential applications. In this work, we develop a 3D-printed elastic shear-stiffening composite to achieve shear-stiffening behavior alongside shape recovery. We find that the composite displays good anti-impact properties better than pure SSG, as well as shape recoverability. We also describe initial results describing further applications for these structures enabled by complex 3D printed geometries.

11:30 AM MF01.10.04

Digital Light Processing of Stiff yet Tough Single Network Hydrogels [Abhishek Dhand](#)¹, Matthew Davidson², Hannah Zlotnick² and Jason Burdick^{1,2}; ¹University of Pennsylvania, United States; ²University of Colorado Boulder, United States

Wide applicability of hydrogels towards tissue repair, drug delivery, or biomedical devices is often restricted due to weak mechanical properties and an inability to process them into structures that mimic tissue architecture. Conventional strategies to enhance hydrogel stiffness through increased number of crosslinks often result in embrittlement. To resolve the stiffness-toughness conflict, hydrogels with high degree of polymer chain entanglements have been developed, particularly with the use of low initiator concentrations and slow radical polymerization¹¹. Unfortunately, this approach is not directly amenable to processing methods such as Digital Light Processing (DLP), which relies on the rapid light-based crosslinking of liquid precursors to form 3D shapes in a bottom-up, layer-by-layer manner^{12,31}. To overcome this mechanical performance-processability conflict, we introduce one-step, Continuous curing after Light Exposure Aided by Redox initiation (CLEAR) printing approach towards formation of highly entangled networks. CLEAR printing is a dual-initiating approach that uses light to crosslink and set the shape of the part, while a complementary reaction (via redox initiators) slowly allows complete conversion of any unreacted monomer within the printed part under ambient conditions.

To demonstrate the advantage of CLEAR, we use acrylamide as a model monomer to form 3D printed, water-swollen highly entangled hydrogels with modulus (~250 kPa) and toughness (~600 kJ m⁻³) values far higher than those (~100 kPa, ~150 kJ m⁻³) attained with DLP alone. Despite their 85% water content, CLEAR printed hydrogels are also superior in compression and under shear than those printed with DLP alone. Interestingly, we also show that the CLEAR technique outperforms traditional approaches of improving green strength (e.g., light flood cure or thermal post-curing). We next leverage CLEAR to process highly entangled hydrogels into complex shapes with open, interconnected pores (e.g., trabecular structure), hollow channels, and knotted topologies with high print fidelity and resolution. These 3D printed structures can sustain cyclic (tensile or compressive) loading and recover their original shape with minimal hysteresis. Further, we show that CLEAR can be applied to other monomer systems through changing the type of monomer (e.g., N-isopropylacrylamide, acrylic acid) or the type of crosslinker (e.g., polyethylene glycol PEG diacrylate, gelatin methacrylamide) to obtain 3D printed, swollen single network hydrogels with modulus and toughness values as high as 300 kPa and 1.8 MJ m⁻³. Additionally, we establish the applicability of CLEAR towards 3D printing of highly entangled elastomers with toughness of 30 MJ m⁻³, nearly 10-fold higher than those printed with DLP alone.

As a potential biomedical application, we demonstrate the use of 3D printed, cytocompatible highly entangled hydrogels towards achieving robust adhesion onto wet tissues (e.g., *ex vivo* porcine heart, lung, stomach, intestine, tendon) with high interfacial toughness values ranging between 300 to 1000 J m⁻². We then process these hydrogels into 3D porous patches that can not only conform to curved tissue topology (e.g., heart) but are also compliant with the dynamic movement of native tissues. Finally, we show proof-of-concept hydrogel adhesives with 3D patterns to (i) form microfluidic connections directly onto tissues for delivery of drugs and (ii) metamaterial structures that enable directional, spatially selective adhesive strength.

Ref:

- [1] Kim+ *Science* **2021**, 374, 212.
- [2] Grigoryan+ *Science* **2019**, 364, 458.
- [3] Dhand+ *Adv. Mater.* **2022**, 34, 2202261.

11:45 AM MF01.10.05

Fracture Resistant Architected Polymers Using Material and Structural Size Effects [Zainab S. Patel](#), Abdulaziz Alrashed and Lucas Meza; University of Washington, United States

Strength and toughness are both highly desirable properties of structural materials, but they are often thought of as mutually exclusive, i.e., it is difficult to increase one without decreasing the other. Much work has gone toward developing materials that are both strong and tough using different composite architectures and material processing techniques, but they generally ignore the role of length scale and structural size-effects on toughness. In this work, we develop nanoarchitected polymeric materials that utilize heterogeneity and size-affected ductility to enhance their toughness without sacrificing strength. We create specimens with layered architectures in a micro-single edge notch bend configuration using two-photon lithography and various post-processing techniques. Gradually reducing the layer thickness (D) resulted in an increased fracture energy and slower, stable crack propagation, a phenomenon that became pronounced as the layer thickness approached or was smaller than the material fracture process zone ($D \leq FPZ$). This energetic size effect is quantified using Bazant's Size Effect Law. The thinnest of these layered structures demonstrated an increase in toughness by 5x from 60 J/m² to 300 J/m² as interlayer spacing was increased from 0 to 4 μ m, a value that is augmented by the creation of heterogeneity along the crack path. Cracks are observed to rapidly propagate in specimens with no interlayer spacing, but then show increasing blunting and deflection in structures with moderately spaced interlayers (~3 μ m). For larger interlayer spacings (>3 μ m), cracks do not propagate through; rather, deflect along the interlayer even at very large displacements. Notably, these materials do not show an appreciable loss in strength and stiffness up to an intermediate layer spacing despite a ~40% reduction in density. The results of this study not only demonstrate the large degree of tunability in these architectures but also show how to fundamentally utilize size effects to create architected materials with unprecedented properties.

1:30 PM MF01.11.01

Molecular Control via Dynamic Bonding Enables Material Responsiveness in Additively Manufactured Metallo-Polyelectrolytes [Seola Lee](#), Pierre Walker, Seneca Velling, Amylynn Chen, Zhen-Gang Wang and Julia R. Greer; California Institute of Technology, United States

Metallo-polyelectrolyte Complexes (MPEC) are a class of soft materials that exhibit unique mechanical and physical properties through reversible electrostatic interactions between dynamic crosslinkers (multivalent metal ions) and charged polymer chains. These molecular-level processes give rise to a wide range of material dynamic responses, for example, stimuli-responsiveness, self-healing, and high toughness through enhanced energy dissipation. The current state-of-the-art fabrication method based on the multistep nature of solution-based metallo-polyelectrolyte synthesis produces materials that suffer from poor long-term stability and inhomogeneity or relies on covalent crosslinking as a backstop for indirect synthesis. The range of scales involved in determining the behavior of MPECs (local bond liability, polymer configurations, and macroscale behavior) further presents computational challenges, which limits the broader application of models to guide experimental methods.

In this work, we demonstrate a facile, single-step fabrication method for MPECs via stereolithography, which produces homogeneous, stable, and high-longevity materials using a straightforward synthesis route. Then, aided by the robust fabrication platform, we present a theory-guided, physically-informed multi-scale study of MPECs. We have developed a roadmap that outlines the effect of different chemical species on the additively manufactured MPEC properties which can be used to tailor its functionality and responsiveness at material level. Our fabrication method enables easy compositional tuning by a simple swap of metal salt precursors during the resin formulation, which allows the wide selection of metal ions and produces a variety of metal-coordinated polymers.

We demonstrate the tunability of mechanical response by adjusting metal ion valency and polymer charge sparsity. We find that mono-, di-, and trivalent metal ions afford control of the coordination environment and bond strength, which propagate to the macroscale properties where higher valency ions result in stiffer and tougher materials. Polyanion charge sparsity, regulated by the pH of the precursor photoresin, also impacts the phase behavior of the gels, leading to changes in the mechanical response. Molecular Dynamic (MD) simulations and diverse polymer characterization methods (morphology, thermal and mechanical) demonstrate that the combination of these parameters controls the extent of dynamic crosslinking present in the system and the emerging polymer configurational distribution governing material properties of MPEC gels. We believe the development of a simple synthesis pathway via additive manufacturing, informed and guided by experimental investigation and molecular modeling, provides a comprehensive understanding of the parameter space and enables the selective design of advanced compliant and functional metallo-polyelectrolytes.

1:45 PM *MF01.11.02

Functional Polymers for 4D Additive Manufacturing with High Precision [Eva Blasco](#); Universität Heidelberg, Germany

4D printing has gained much attention during the last years and become a promising tool for the fabrication of dynamic and adaptive structures with potential application in different fields ranging from biomedicine to optics to soft-robotics. The additional fourth dimension refers to the ability of a 3D printed object to change its properties over time. We can imagine it as the addition of “life-like” behavior. While great progress has been made at the macroscale, the continuous miniaturization of today's devices has tremendously increased the demand for manufacturing at the smaller scales. Emerging technologies such as two-photon 3D laser printing have enabled the precise printing of structures at the micro and nanometer scale.

Our group has recently succeeded in the development of new functional materials for laser micro- and nanoprinting. In particular, we have focus on the incorporation of new features such as conductivity, subtractive manufacturing (inks allowing printing and erasing), superresolution and more recently, stimuli response for complex actuation. In this lecture, special attention will be paid to the design of inks based on functional polymers for 3D/4D microprinting. The challenges as well as the potential and perspectives of the field will be highlighted, too.

2:15 PM MF01.11.03

Free-Form Printing and Deformation Control Strategies for Liquid Crystal Elastomers [Devin Roach](#)^{1,2}, [Timothy White](#)³, [Jeremy Herman](#)³ and [Bryan Kaehr](#)²; ¹Oregon State University, United States; ²Sandia National Laboratories, United States; ³University of Colorado Boulder, United States

Fabrication pathways for liquid crystal elastomer (LCE) have remained a topic of intensive research interest in recent years. Photopatterning and two-stage reaction techniques were pioneering methods which enabled molecular patterning and fabrication of LCE networks in few, relatively simple steps. Recently, additive manufacturing (AM), or 3D printing, has become another promising approach for facile production of LCE networks. The combination of 3D printing with responsive materials, such as LCE, has led to a new generation of smart structures that not only possess a static shape but also can change their shape over time. This process is termed 4D printing, with the fourth dimension being time. The focus of this talk will be on the development of new 4D printing techniques to generate a new class of complex, multi-planar LCE geometries. One of the most notable 4D printing methods, direct ink write (DIW), enables simple fabrication of complex LCE structures by coupling the printing process with the LCE alignment step. This occurs due to the shear forces generated during extrusion through the DIW nozzle. By combining this approach with multiple materials, novel shape transformations can be achieved. For example, by combining LCE with the unique properties of another smart material called shape memory polymers (SMP), the shape transformation can be locked in place. Furthermore, LCE/SMP composites offer superior mechanical properties in both the deformed and undeformed state for functional engineering applications. The structures produced using this method, however, can only perform 2D to 3D shape transformations. Many smart structures applications require more complex 3D shapes to be fabricated. For this reason, we will discuss a recently developed printing method called embedded 4D printing. Here, LCE is extruded into a gel matrix to create complex 3D architectures which can generate unique 3D to 3D shape transformations. This approach enables LCE molecular programming in any 3D cardinal direction. The ability to 4D print complex 3D LCE structures without the need for supports opens new avenues for the design and development of functional and responsive systems such as soft robotics, biomedical devices, and advanced materials engineering.

2:30 PM BREAK

3:30 PM *MF01.11.04

Architected Soft Matter and The 4th Dimension [Howon Lee](#); Seoul National University, Korea (the Republic of)

Stimuli-responsive soft matter promises great potential for autonomous and intelligent engineering systems when precisely manufactured in specific architectures with programmed responses. Emerging pathway to create such dynamic systems involves additive manufacturing of stimuli-responsive and programmable soft matter. This approach has been termed “4D printing”, with the 4th dimension being time. In this talk, additive manufacturing of various soft matter using projection micro-stereolithography (PμSL) is presented. PμSL is a micro 3D printing technique that turns light into a complex 3D structure by utilizing digital light processing (DLP) technology. Combining rapid, versatile, and scalable micro 3D printing technique with various

functional soft matter, design principles and mechanics inspired by exquisite motions and morphologies in nature are physically realized. Micro-architectures that can transform and move are demonstrated by programming of dynamic response of various responsive hydrogels. Reconfigurable, deployable, and mechanically tunable lightweight material is created by employing shape memory polymers in mechanical metamaterials. Also presented is printing of liquid crystal elastomers with encoded molecular orientations for programming reversible shape change and soft robotic locomotion.

4:00 PM MF01.11.05

3D Printing of Polyelectrolyte Complexes: From Rheological Optimization to Biomaterials Rigoberto C. Advincula; The University of Tennessee/Oak Ridge National Laboratory, United States

Polyelectrolytes have a unique property of complexation when oppositely charged paired polymers form films or coacervates. They have found applications in diverse fields, including drug delivery, wastewater treatment, and tissue engineering. With 3D printing, using polyelectrolytes presents an exciting opportunity for precisely fabricating functional materials and devices. However, the strong electrostatic interactions and the complex formation as coacervates are unstable as viscoelastic materials hinder the flow and processability of inks during the direct ink writing (DIW) process. They have been mostly demonstrated by 3D printing in support media. This talk will focus on the use of polyelectrolyte complexes (PECs) suitable for DIW, in air to form complex shapes and objects. To make PEC-based inks amenable to 3D printing in air, a wash-out deplasticizing procedure was developed. Studies on different formulations were developed that meet the printability of polyelectrolyte complexes and their rheological requirements based on the use of nanoparticles, water-soluble polymers, and ampholytes. Our investigation entailed systematically exploring solvent composition, pH conditions, and the incorporation of specific additives. Furthermore, we evaluate how these ink formulations impact the final printed structures' fidelity, mechanical properties, and complexation behavior. The findings have the potential to enlarge the way we design and manufacture PEC functional materials across diverse applications, from biomedicine to electronics by harnessing the properties of polyelectrolyte complexes

4:15 PM MF01.11.06

Multi-Axis Magnetic 3D Printing of Magnetically-Responsive Architecture Brian Elder, Taylor Greenwood, Samannoy Ghosh and Yong Lin Kong; University of Utah, United States

The ability to program magnetic remanence in situ during extrusion-based 3D printing can enable the creation of soft, magnetically responsive architecture. Indeed, in comparison with other methods, such as folding or assembly, this freeform fabrication approach can create highly complex responsive architecture and actuators. Here, towards this goal, we developed a multi-directional magnetic 3D printing process that allows *in situ* programming of the magnetic domains during 3D printing. The multi-axis magnetic field enables the variance of magnetic remanence within a continuous filament, achieving complex deformation even in a single printed filament. This capability increases the range of possible motions, including bending, twisting, and contraction. As a proof of concept, we demonstrated the fabrication of a tunable propeller, magnetic-responsive textiles, and a magnetically-actuated ingestible device. We also demonstrated eight fundamental remanence pairs that produce deformation units, which we envision could enable the future design of tunable soft actuators and robots.

4:30 PM *MF01.11.07

Intelligentsia of Additively Manufactured Hierarchical Materials Julia R. Greer, Seola Lee, Seneca Velling, Wenxin Zhang and Cyrus Fiori; California Institute of Technology, United States

Creation of reconfigurable and multi-functional materials can be achieved by incorporating architecture into material design. In our research, we design and fabricate three-dimensional (3D) nano-architected materials that can exhibit superior and often tunable thermal, photonic, electrochemical, biochemical, and mechanical properties at extremely low mass densities (lighter than aerogels), which renders them useful and enabling in technological applications. Dominant properties of such meta-materials are driven by their multi-scale hierarchy: from characteristic material microstructure (atoms) to individual constituents (nanometers) to structural components (microns) to overall architectures (millimeters and above). Our research is focused on fabrication and synthesis of nano- and micro-architected materials using 3D lithography, nanofabrication, and additive manufacturing (AM) techniques, as well as on investigating their mechanical, biochemical, electrochemical, electromechanical, and thermal properties as a function of architecture, constituent materials, and microstructural detail. Additive manufacturing (AM) represents a set of processes that fabricate complex 3D structures using a layer-by-layer approach, with some advanced methods attaining nanometer resolution and the creation of unique, multifunctional materials and shapes derived from a *photoinitiation-based chemical reaction* of custom synthesized resins and thermal post-processing. A type of AM, vat polymerization, has allowed for using hydrogels as precursors, and exploiting novel material properties, especially those that arise at the nano-scale and do not occur in conventional materials. The focus of this talk is on additive manufacturing via vat polymerization and function-containing chemical synthesis to create 3D nano- and micro-architected metals, ceramics, multifunctional metal oxides (nano-photonics, photocatalytic, piezoelectric, etc.), and metal-containing polymer complexes, etc., as well as demonstrate their potential in some real-use biomedical, protective, and sensing applications. I will describe how the choice of architecture, material, and external stimulus can elicit stimulus-responsive, reconfigurable, and multifunctional response.

SESSION MF01.12: Sustainable Polymers
Session Chairs: Michinao Hashimoto and Daryl Yee
Thursday Morning, April 25, 2024
Room 325, Level 3, Summit

8:15 AM *MF01.12.01

Bacterial Cellulose-Based Inks: Enabling Mechanical Property Control in Sustainable 3D Printing Kuotian Liao, Mallory Parker, Hareesh Iyer, Aban Mandal, Taylor A. Hilton, Rebekah I. Brain and Eleftheria Roumeli; University of Washington, United States

Advancements in sustainable materials are needed to combat pressing challenges posed by synthetic plastics, such as non-renewable sourcing, environmentally detrimental manufacturing processes, and end-of-life fates. Biopolymers are attractive alternatives to petroleum-derived polymers, offering a reduction in environmental impact across their entire lifecycle. In parallel, additive manufacturing has revolutionized the production of polymer-based materials for numerous applications, particularly those challenging to manufacture using conventional techniques, utilizing sustainability practices such as minimal material usage and limited waste generation. Currently, the materials used in 3D printing applications are rather limited and majority of them are synthetic polymers. There is a clear need to provide more sustainable materials for the ever-increasing 3D printing applications. In this study, we present an entirely biobased material platform designed for direct ink writing (DIW), with the aim of enabling precise control over the mechanical properties of 3D-printed structures, both at the hydrogel and solid foam states. Utilizing polymer network principles, we use lab-cultured bacterial cellulose

(BC) as our primary, load bearing network element. We investigate the effects of chemical treatment with deep eutectic solvents on the BC fiber charge and degree of defibrillation, which ultimately exert a profound influence on ink rheology and hydrogel properties. BC holds particular promise due to its combination of high aspect ratio, molecular weight, and degree of crystallinity, and its capacity for scalable and tunable biosynthesis. Additionally, we explore the impact of introducing other biopolymers (e.g. proteins) and organic small molecules (e.g. lipids) on the rheological properties and mechanical integrity of the printed structures. By incorporating spatially modulated compositions, we open avenues for further fine-tuning of material properties. This comprehensive investigation aims not only to deepen our understanding of the structure-property relationships within BC-based networks but also to pave the way for tailoring the properties of resulting gels and foams for a diverse range of applications. These insights are poised to significantly advance our fundamental understanding of polymer physics and offer innovative solutions for sustainable material development.

8:45 AM MF01.12.02

Additive Manufacturing of Vitrimers with Circularity Sungjin Kim^{1,2}, Md Anisur Rahman¹, Karen C. Guzman¹, Zoriana Demchuk¹, Jeff Foster¹ and Tomonori Saito^{1,3}; ¹Oak Ridge National Laboratory, United States; ²The University of New Mexico, United States; ³The University of Tennessee, Knoxville, United States

Over 400 million tons of solid plastics are globally produced annually and only ~9% of those are currently recycled in U.S.. Establishing closed-loop circularity of plastics with a facile manufacturing path is critical for global circular economy. When commodity plastics are upcycled into higher-performance materials with facile processability, a sustainable closed-loop manufacturing would become reality. Additive manufacturing (AM) of such upcycled plastics to custom-designed structures accomplishes energy and resource efficient low-carbon closed-loop manufacturing. We hereby open a circular upcycling of a commodity plastic into a higher-performance vitrimer with fused deposition modeling or direct ink writing, resulting in robust printout properties comparable to crosslinked thermosets. Vitrimer exhibits mechanical robustness and chemical resistance because of its covalent network formation, but it can also be malleable by reconfiguring reversible crosslinks through the associative bond exchange at elevated temperature, making it recyclable. Due to its crosslinked nature, the upcycled vitrimers provide stronger, tougher, solvent-resistant 3D objects and separable from unsorted plastic waste. Tailoring the vitrimer composition overcomes the major challenge of (re)printing crosslinked materials, allowing multi-cycle printing. This presentation updates our efforts on AM of upcycled commodity plastics, especially upcycled vitrimers.

9:00 AM *MF01.12.03

Sustainability, Biodegradability and Circularity in Photopolymer Resins for 3D Printing Andrew P. Dove; University of Birmingham, United Kingdom

One of the unresolved consequences of the massive global production of plastic is the lack of proper waste management. As a consequence of technological limitations as well as inefficient collection and sorting methods, current recycling schemes are underperforming. In part this is a result of the inherent linear design of our polymer systems, and lack of consideration of waste management and environmental impact of the waste that does escape into the environment, at the polymer design stage. We, among others, are focussing on creating tools that could be applied to design polymers 'with the end in mind' – i.e. to incorporate chemical bonding that can be easily processed to make polymers but readily reversed either 'on demand' for recycling, or upon exposure to environmental triggers. To this end, one strategy in our research has focussed on the challenge to design photoset materials that can be processed by advanced methods such as additive manufacturing that are sustainably sourced but can be readily circularised. This talk will detail our efforts in this field to improve the sustainability of photopolymer resins through the use of sustainably sourced monomers, plastic upcycling and the development of closed loop recycling of photoset materials.

9:30 AM *MF01.12.04

Mechano-Responsive Protein-Polymer Networks for Sustainable Additive Manufacturing Alshakim Nelson; University of Washington, United States

Bio-sourced and biodegradable polymers for additive manufacturing could enable the rapid fabrication of parts for a broad spectrum of applications ranging from healthcare to aerospace. However, a limited number of these materials are suitable for vat photopolymerization processes. Herein, we report a process to fabricate protein-based constructs using commercially available vat photopolymerization printers. Bovine serum albumin (BSA) is a single-chain nanoparticle that can be chemically derivatized with acrylate and methacrylate functionalities. Aqueous resins were formulated from these materials to produce complex 3D geometrical constructs with a resolution comparable to commercial resins. While BSA is often used in cell culture protocols and diagnostic assays, we demonstrate that BSA can serve as junctions within polymer networks to afford stiff hydrogels and bioplastics with unique physical properties. Protein-based shape-memory objects and engineered living materials were 3D printed and will be highlighted as opportunities for future applications.

10:00 AM BREAK

SESSION MF01.13: Sustainable Polymers / Functional Materials
Session Chairs: Michinao Hashimoto and Devin Roach
Thursday Morning, April 25, 2024
Room 325, Level 3, Summit

10:30 AM *MF01.13.01

Dynamic 3D Printing of Bottlebrush Block Copolymer Photonics Ying Diao; University of Illinois at Urbana-Champaign, United States

Biological systems have evolved to exhibit dynamic, hierarchical structures that confer complex functionality, such as the adaptable, structural color in chameleons that allows them to match their environment. Attaining such dynamic complex structures at the nanoscale have been challenging to achieve in synthetic macromolecular systems. In addition, synthetic colors we use today constitutes one of the biggest environmental pollutants that severely impact human and aquatic life. Developing printable dynamic structure color will not only introduce new functionality that current synthetic color is not capable of, but also help address this urgent environmental issue. Towards this aim, we and collaborators developed a programmable 3D printing process that can modulate nanoscale assembly and structure color of bottle brush block copolymers on the fly. By understanding and controlling the polymer assembly pathways during processing, we demonstrated 3D printing structure color as chameleon patterns without changing the ink material. We and collaborators further unveiled the underlying mechanism by probing polymer assembly pathways via a combination of X-ray scattering, optical spectroscopy, electron microscopy and coarse-grained simulations – the programmable structure color was attained through arresting polymer chain extension and entrapping metastable structures by controlling the assembly kinetics during printing.

11:00 AM MF01.13.02

A 3D Printable Thermally Conductive yet Electrically Insulating Polymer Nanocomposite based on Ag@SiO₂ Nanowires Jean-Pierre Simonato^{1,2}, Antoine Bodin^{1,2}, Thomas Pietri^{1,2} and Caroline Celle^{1,2}; ¹Université Grenoble Alpes, France; ²CEA LITEN, France

What do high density batteries and up-to-date electronic chips have in common?

The problem of heat dissipation.

With the emergence of fast charging technologies, high energy density batteries and new generation microprocessors, the heat generation in such systems while in operation becomes significantly more intense. If this heat is not efficiently dissipated, a) the risk of thermal runaway in batteries increases and thus threatens the users safety, b) the performance, lifetime and reliability of electronic systems weaken. Improvement of batteries and electronic devices performances is therefore closely linked to the effectiveness of the thermal dissipation of such systems. Besides high thermal conductivity, very good electrical insulation of these structural materials is also expected to avoid issues such as short circuits or higher power consumption.

The use of thermoplastic polymers seems relevant due their intrinsic electrical insulation behavior and simple processability. However, such materials generally present low thermal conductivity ($< 0.4 \text{ W}\cdot\text{m}^{-1}\cdot\text{K}^{-1}$). An appropriate strategy for improving thermal conductivity while simultaneously preserving electrical insulation of polymer-based materials is to incorporate thermally conductive yet electrically insulating fillers to the polymer matrix.

In this presentation, we will show that the development of one-dimensional silver-silica core-shell nanowires (AgNW@SiO₂) is a relevant route to very efficient heat dissipative nanocomposites. We will present how the fine tuning of the silica nanolayer on silver nanowires is of utmost importance to reach optimized performances.

By adjusting the rheology of the nanocomposite, i.e. limiting the content of the nanofillers to 3 vol%, a proof of concept was 3D printed by FDM (Fused Deposition Modelling). Thanks to the alignment of the 1D nanofillers during the FDM printing process, as observed under various printing patterns, the thermal conductivity of the PC nanocomposite reaches an unprecedented value of $3.48 \pm 0.06 \text{ W m}^{-1} \text{ K}^{-1}$ in the printing direction, i.e. a fifteen-fold increase over the thermal conductivity of neat PC.

11:15 AM MF01.13.03

Integration of Thermoplastic Elastomers and Low Melting Point Alloys for 3D Printing of Multifunctional Composites Weinan Xu; University of Akron, United States

Due to the significant differences in physical and chemical properties of polymers and metals, their additive manufacturing is conducted using very different and incompatible methods or conditions. Such incompatibility is a significant limitation for multi-material 3D printing and fabrication of 3D functional composites. We address this issue by creating functional composites composed of thermoplastic elastomers, Field's metal, and graphene; and their 3D printability by fused filament fabrication is achieved. The 3D printable composites have widely tunable internal structures, mechanical, thermal, electrical properties, and full recyclability. Multiphysics modeling was developed to predict and elucidate the structure and properties. The 3D structures can be transformed from insulating to conductive based on the melting and coalescence of Field's metal nanoparticles. The incorporation of graphene bridges the adjacent Field's metal particles and significantly enhances the conductivity. Such 3D-printable polymer-metal hybrid platform will enable new advancements in soft electronics and robotics, and energy storage.

Ref: Bu, J., Shen, N., Qin, Z., & Xu, W. (2023). Integration of low-melting-point alloys and thermoplastic elastomers for 3D printing of multifunctional composites. *Cell Reports Physical Science*.

11:30 AM MF01.13.04

Interface-Modified Liquid Metal Elastomer Composites for Printing Stretchable Conductors Ren-Mian Chin, Youngshang Han and Mohammad H. Malakooti; University of Washington Mechanical Engineering Department, United States

Liquid metal alloys of gallium, such as eutectic gallium-indium (EGaIn), have garnered attention for their distinctive metallic and fluidic properties. These materials have been utilized in a variety of forms and device architectures, ranging from fluidic microchannels to polymer nanocomposites. Additionally, liquid metal can be embedded in the elastomer matrix to synthesize liquid metal elastomer composites (LMEC) which can augment various functional properties. These composites, with tailored material compositions, can also show high electrical conductivity while having excellent elasticity. However, creating a percolating network of liquid metal (LM) in low modulus elastomers, such as Ecoflex 00-30, is quite challenging. This is because the ultrasoft polymer matrix cannot deliver sufficient mechanical forces to the gallium oxide on the surface of the LM droplets. Since the oxide shell causes separation between the micro-sized LM particles, an innovative strategy for breaking this solid barrier is required to achieve conductive LM pathways in the low elastic modulus LMECs.

In this presentation, we will demonstrate how embedded EGaIn microdroplets in Ecoflex can be "mechanically sintered", or called "activated", to become electrically conductive. Surface modification of LM particles is a key for weakening the particle-matrix interface in LMEC, which results in the formation of a percolation network by strain-activation. Furthermore, we will discuss how the formulated composite can be used for printing stretchable conductors. The printed traces can be stretched over 900% tensile strain, and electromechanical testing results indicate minimal changes in electrical resistance under substantial deformations and strain rates. Finally, we will demonstrate the practical application of the formulated printable EGaIn-Ecoflex 00-30 inks in stretchable electronics circuits. Overall, this work highlights the potential of liquid metal elastomer composites for use in functional electronics and provides a promising approach for achieving high electrical conductivity in ultrasoft polymer matrices.

11:45 AM MF01.13.05

Advancing Semiconducting Polymer Patterning: Photothermal Approach for Sub-Micron Feature Fabrication for Electronic NIR Photodetectors Meghna Jha, Joaquin Mogollon Santiana, Megan L. Hong, Harishankar Manikantan and Adam J. Moule; University of California, Davis, United States

The industrial development of Semiconducting Polymers (SPs) faces a significant hurdle in the absence of an inexpensive, rapid, and viable patterning technology capable of producing sub-micron features. In this study, we explore Photothermal Patterning as a promising technique that leverages the solubility characteristics of SPs to address this challenge. The Photothermal Patterning process involves exposing an SP film to a semi-poor solvent mixture, rendering the polymer insoluble at room temperature. Subsequently, the SP film is exposed to laser radiation at a wavelength that is strongly absorbed by the SP in its solid state. The absorption of photons leads to localized heating, causing the SP to dissolve once the temperature surpasses its dissolution threshold, resulting in the formation of negative patterns. To validate the feasibility of this approach, we conducted experiments using the Alvéole PRIMO, a commercially available cleanroom equipment. Additionally, we developed a quasi-steady state model to investigate the dissolution behavior of SPs in solvent mixtures induced by a Gaussian laser beam's heating effect. Through our analysis, we successfully determined the depth and width of the patterns obtained and identified the influence of solubility kinetics on heat transfer dynamics. By gaining a comprehensive understanding of the heat transfer effects, we have been able to identify the regime in which these effects dominate, thereby enabling us to modify the shape of the patterns obtained. Leveraging this knowledge, we aim to employ the Photothermal Patterning technique to fabricate P3HT patterns over silver electrodes, with the goal of obtaining a functional NIR photodetector. This research significantly contributes to the development of a cost-effective and rapid patterning

technology for SPs, opening up new possibilities for their industrial applications in the field of electronic devices.

SESSION MF01.14: Functional Materials
Session Chairs: Michinao Hashimoto and Devin Roach
Thursday Afternoon, April 25, 2024
Room 325, Level 3, Summit

1:30 PM MF01.14.01

Direct Laser Writing of Composite Materials towards Bio-Inspired Photonic Actuators [Aoife Donohoe](#), Colm B. Delaney, Jing Qian and Louise Bradley; Trinity College Dublin, The University of Dublin, Ireland

Colour and colour changes play hugely important roles in the natural world, enabling organisms to camouflage, signal, and mimic. These responsive colour changes are a result of a phenomenon known as structural colour. The reflection of colour in these materials is dependent on a high refractive index and ordered structures with feature sizes comparable with wavelengths in the visible range. [1] In nature, this is often achieved through exploitation of naturally occurring crystals of chitin and guanine that can be ordered from the nano to millimetre scales.[2]

Synthetic analogues of structural colour have often been achieved through the use of liquid crystals, colloidal nanoparticles, and sol gel chemistry, resulting in colloidal crystal assemblies and photonic films.[3] Extrinsic structural colour has also been approached through the use of additive and subtractive manufacturing techniques such as etching, e-beam lithography, and nanoimprint lithography, often from dielectric material. [4] The combination of nanocomposite materials and Direct Laser Writing (DLW) using two-photon polymerisation (2PP) has emerged as a route to obtain ordering of a material in both an extrinsic and intrinsic manner mimicking that seen in biology.[5,6]

In this work we present DLW as a method to produce materials with controlled structural properties on the nm and micron scale in a precise manner resulting in a wide gamut of responsive colours through the exploitation of stimuli-responsive nanocomposite materials, to create responsive photonic materials inspired by those in the natural world. This presentation will encompass a range of nanocomposite materials including colloidal particles, liquid crystalline cellulose, polypeptides, and guanine nanocrystals. Upon incorporation into stimuli responsive materials, we present arrays of printed microstructure pixels, exhibiting dynamic structural colour to stimuli such as light, temperature, humidity and concentration. These materials offer a range of applications in technology such as active display technologies, steganography, and polarisation encryption.

[1] Parker, A.R., (2000). '515 million years of structural colour', *Journal of Optics A: Pure and Applied Optics*, 2(6), R15.

[2] Gur, D., Leshem, B., Pierantoni, M., Farsley, V., Oron, D., Weiner, S. and Addadi, L., (2015), 'Structural basis for the brilliant colors of the sapphirinid copepods', *Journal of the American Chemical Society*, 137(26), 8408-8411.

[3] Fenzl, C., Hirsch, T., and Wolfbeis, O. (2014), "Photonic crystals for chemical sensing and biosensing." *Angewandte Chemie International Edition* 53(13), 3318-3335.

[4] Zhu, L., et al. (2015) "Flexible photonic metastructures for tunable coloration." *Optica* 2(3) 255-258.

[5] Delaney, C., Qian, J., Zhang, X., Potyrailo, R., Bradley, A.L, Florea, L., (2021). 'Direct laser writing of vapour-responsive photonic arrays', *Journal of Materials Chemistry C* 9, 11674.

[6] Qian, J., et al. (2023) "Responsive spiral photonic structures for visible vapor sensing, pattern transformation and encryption." *Advanced Functional Materials* 2211735.

1:45 PM MF01.14.02

Direct-Ink-Write Crosslinkable Bottlebrush Block Polymers for On-The-Fly Control of Structural color [Sanghyun Jeon](#), Yash Kamble, Haisu Kang, Jiachun Shi, Matthew Wade, Bijal Patel, Tianyuan Pan, Simon Rogers, Charles Sing, Damien Guirounet and Ying Diao; University of Illinois at Urbana-Champaign, United States

The biological world offers exquisite examples of how simultaneous control over molecular composition and long-range macroscopic order gives rise to material properties unique to living organisms. One such phenomenon is structural color, found in various animals, arising from the periodic ordering of domains with different refractive indices on the nanometer scale. Structural color presents an eco-friendly alternative to synthetic color, as it avoids the environmental pollution associated with synthetic dyes. Additionally, it offers high brilliance and dynamic properties that are challenging to achieve through synthetic methods. Among various materials, bottlebrush block copolymers (BBCPs) show significant promise in mimicking biological structural color due to their ability to access a wide range of nanoscale morphologies, including lamellar, cylindrical, and spherical structures, resulting in visible-range structural coloration. In this study, we demonstrate "on-the-fly" modulation of structural color during printing by combining a UV-assisted DIW 3D printer with photo-crosslinkable BBCP chemistry. A key innovation is to realize dynamic control of assembly kinetics through programming the rate of photo-crosslinking, which serves to kinetically arrest assembly and lock in desired structural color "on-the-fly", or as we print. We then validate two key aspects of this hypothesis by combined coarse-grained simulations, rheological characterizations, and experimental structural analysis. First, using the implicit side-chain model developed by our team, we elucidate an evaporation-driven assembly pathway whereby the structural color evolves from blue to red due to backbone extension. This inference is affirmed by scanning electron microscopy and ultra-violet visible spectroscopy. Second, by rheology and in situ imaging, we show that the crosslinking timescale matches with the evaporation-driven assembly timescale, supporting the idea that assembly is arrested by crosslinking during evaporation-driven structural evolution. Enabled by this mechanistic understanding, we program the temporal profile of UV irradiance to demonstrate modulation of structural color "on the fly" as to access much of the visible spectrum and to create color gradients using a single ink material.

2:00 PM MF01.14.03

Additive Manufacturing via Direct Ink Writing: Printing Functional Hydrogels and Ceramics for Medical Applications [Philipp Schadt](#), Leonard Siebert and Rainer Adelung; Kiel University, Germany

Additive manufacturing (AM) also known as 3D printing is a highly versatile set of techniques for processing polymers, metals as well as ceramics into complex shapes. Among all AM techniques Direct Ink Writing (DIW) is the most versatile in terms applicable materials by employing a simple extrusion-based approach. Soft hydrogels, e.g., have been processed for biomedical applications using DIW. These polymeric materials offer not only tunable printing properties but also often show great biocompatibility. In combination with functional particles like ZnO these materials will exhibit advanced functionalities like antibacterial properties. This work presents an ink system for active wound dressings consisting of sodium alginate hydrogel as carrier

and ZnO particles in the shape of micrometer sized crystals (t-ZnO) with a tetrapod geometry. While the sodium alginate adjusts the inks rheological properties, the individual ZnO tetrapod arms penetrate through the hydrogels surface and have direct contact with the wound. This is due to the unique geometry of the t-ZnO as well as the selection of suitable concentrations for the alginate hydrogel and the particles. The penetration of t-ZnO enables to utilize the tetrapod's antibacterial properties. Additionally, rheological investigations have been performed improving the printing results. The sodium alginate shows a high yield point as well as a shear thinning behavior, which is highly desirable for a 3D printing process. These properties enable to print openly porous wound dressings with an oxygen access directly at wounds surface while the at same time the damaged tissue stays protected from contaminations. In order to improve the wound healing even further the t-ZnO particles can be decorated with a variety of functional proteins. These characteristics have been proven using cell and ex-vivo skin tests.

In contrast to these soft materials, DIW allows also to process hard ceramic biomaterials like zirconia. In combination with water soluble polymers like polyethylene oxide, pastes with high shape retention and strong shear thinning properties can be produced. These pastes are utilized in this work for the 3D printing of dental implant materials. The rheological properties have been tailored by changing the inks pH value allowing to process yttrium stabilized zirconia and reaching a high mechanical strength. In summary, this works presents an AM approach, which allows to manufacture soft hydrogels and polymers in combination with hard ceramic particles enabling the versatility of DIW and showing their great potential for biomedical applications.

2:15 PM MF01.14.04

Tuning Aging, Mechanical and Electrical Properties of Liquid Metal Polymer Composites for Improved Stretchable, Deformable and Robust Electronics and Robotics [Amanda Koh](#)¹, Anh Hoang¹, Chanyeop Park² and Omar Faruqe²; ¹University of Alabama, United States; ²University of Wisconsin–Madison, United States

Soft, stretchable electronics are a promising platform for wearable devices for monitoring health, movement, infrastructure damage, robotic environments, among many varied applications. While the literature demonstrates a wide range of strategies for achieving soft electronics, the incorporation of electronically active elements into a soft polymer (typically an elastomer for full stretchability) is one of the most successful. To get the most utility out of the elastomer composite, the electronic element must also be able to withstand repeated strain and not degrade the elasticity of the host. Room temperature liquid metal polymer composites (LMPCs) are composites of the metal alloy gallium-indium-tin (galinstan) and an elastomer matrix (most commonly polydimethylsiloxane, PDMS). As galinstan is liquid at room temperature, it inherently has no strain fatigue, and the research in Koh Lab has shown that galinstan can be composited into the matrix at concentrations greater than 70vol% without a dramatic increase in polymer modulus. Simultaneously, the LMPC exhibits dielectric properties with tunable relative permittivity up to and exceeding 160 based on liquid metal loading and polymer molecular weight. To realize the potential of this polymer composite material, it is necessary to fully explore its rheological, electrical, and sensing properties in order to transition it to a functional manufacturing platform. Additionally, it is necessary to understand the dielectric aging and fatigue properties of the composite as made in order to validate the long term utility of the composite as a sensor, wearable, or robotic component. The work presented will show recent data demonstrating how dielectric aging is impacted by LMPC formulation, and how these properties can be simultaneously tuned with mechanical/rheological properties to optimize the system for additive manufacturing or molding. Furthermore, this presentation will include new results related to the spatial homogeneity of the LMPC, which is a property that is both critical to manufacturing (the density of galinstan is greater than six times that of the host polymer) and largely unexplored in the literature. The data presented will demonstrate the boundaries within which spatial homogeneity does or does not impact mechanical, electrical, aging, and sensing properties as well as methods of improving homogeneity if necessary. The work discussed and presented here directly enables ongoing work in the Koh Laboratory to create components for wearable devices, robotic locomotion, and infrastructure hardening that rival and exceed the capabilities of ceramic and thermoplastic polymer dielectrics, expanding the possibilities for such systems.

2:30 PM MF01.14.05

Aggregation-Induced Emission to Visualize and Monitor Progression of Photopolymerization [Xiaoxing Xia](#), Sijia Huang, Elena Belk, Martin De Beer, Abhinav Parakh, Magi Yassa and Johanna J. Schwartz; Lawrence Livermore National Laboratory, United States

Light-induced polymerization is widely used in high-resolution fabrication such as additive manufacturing and photolithography as well as low-cost industrial processes such as UV curable coating and adhesives. Polymer parts made from acrylate-based resins exhibit a large variation in materials properties due to differences and inhomogeneities in the degree of conversion within each part and thus suffer from quality control challenges for high-precision applications. As new photochemistries are being actively developed, it is increasingly important to examine the uniformity of polymerization with high spatial resolution and monitor its progression kinetics with detailed temporal information. In this work, we introduced a class of fluorophores based on aggregation-induced emission (AIE) as an additive in the photo-resin formulation; their fluorescence intensity increases as the local rigidity of the cross-linked polymer increases. We conducted systematic ex-situ photo-rheology and FTIR measurements to establish the calibrated relation between fluorescence intensity and polymerization conversion for representative resin formulations. We used fluorescence microscopy and confocal microscopy to demonstrate high resolution grayscale mapping of polymerization conversion in 3D printed parts made by various photopolymerization methods including Digital Light Processing (DLP), Two-Photon Polymerization (2PP), and tomographic Volumetric Additive Manufacturing (VAM). With this unique visualization method, we observed the periodic variation of higher and lower conversion across each printed layer in DLP-printed dog-bone samples, which led to large differences in tensile strength as a function of the printing orientation with respect to the loading direction. Finally, we implemented a fluorescence monitoring setup to a VAM system that actively tracks the conversion of the 3D printed parts as tomographic printing progresses, which offers vast opportunities for real-time in-process metrology and feedback control to improve printing quality.

2:45 PM BREAK

SESSION MF01.15: Composites
Session Chairs: Michinao Hashimoto and Devin Roach
Thursday Afternoon, April 25, 2024
Room 325, Level 3, Summit

3:15 PM *MF01.15.01

Bioinspired Hierarchical Composite Hydrogels via Shear-Assembled Direct Ink Writing Technology [Wei Zhai](#), Tian Li and Quyang Liu; National University of Singapore, Singapore

Soft materials, such as hydrogels, have garnered significant attention in fields like wearable electronics, soft robotics, biomedicine, and energy technology, thanks to their unique combination of high electrical conductivity, stretchability, biocompatibility, and self-healing capabilities. Nevertheless, the inherent

brittleness of hydrogels has presented a challenge to their practical application. Biological soft tissues, like tendons and cartilage, exhibit remarkable strength, flexibility, and message-transmission capabilities due to their composite composition and intricate hierarchical structures. Drawing inspiration from nature, we have developed a promising approach—shear-assembled direct ink writing—to strengthen and toughen hydrogels by incorporating secondary-phase fillers and creating bioinspired hierarchical structures. This process involves applying shear-force-induced self-assembly extrusion printing of nanoceramic platelets enhanced hydrogel inks, providing control over nano- to sub-micro scale structures. Additionally, the filaments can be 3D printed into free-form bioinspired architectures, ranging from micro- to macro-scale, such as unidirectionally aligned, Bouligand, and crossed lamellar configurations. By tailoring the composition, nanoceramic alignment, and printing patterns, the composite hydrogel exhibits multiple strengthening and toughening mechanisms across different scales. Through the application of this technology, we have successfully produced flexible and robust nanoceramic-hydrogel composites with high ceramic compositions for creating reconfigurable structures. Furthermore, we have developed flexible bioceramic-hydrogel composites with potential applications in bone tissue engineering, as well as strong and tough conductive composite hydrogels for use in flexible electronics.

3:45 PM MF01.15.02

New Natural Polymer-Based Composite Hydrogels and Their 3D Printing into Scaffolds for Liver Tissue Engineering Xinyang Zhang, Xirui Zeng and Min Wang; The University of Hong Kong, Hong Kong

The liver is an important organ which performs many and diverse tasks in the human body. Chronic or acute liver failure occurs as a result of nonalcoholic fatty liver disease, alcoholic liver disease, hepatocellular carcinoma (HCC), etc. HCC is the fourth leading cause of cancer-related mortality and is also showing an increasing trend globally, with an estimated 500,000 to 1 million new cases annually. The primary treatment for early HCC is surgical resection. But surgery may not provide 100% removal of HCC tissue and hence tumor recurs in the liver in up to 80% of patients. On the other hand, liver transplantation, another main treatment option for HCC, can achieve a high survival rate with a low risk of recurrence. But this strategy has been severely limited in clinics due to the lack of liver donors, immune rejection, surgical complications, etc. Liver tissue regeneration (LTR) using the tissue engineering approach appears to be an important alternative treatment for the patients, and 3D printing provides a powerful platform for fabricating advanced liver tissue engineering (LTE) scaffolds for LTR. For LTR, the scaffolds should facilitate enhanced cell function and survivability, and hence inks/bioinks for 3D printing should closely resemble liver's cell-extracellular matrix (ECM) in composition and possess suitable gelling characteristics for different 3D printing or bioprinting processes. But the progress in 3D printing-based LTE has been hindered by the lack of inks that have adjustable properties and mimic the native environment of liver. Hydrogels based on natural polymers are attractive as printing inks for LTR because they also have the advantages of good biocompatibility and biodegradability. In the current study, we formulated and evaluated natural polymer-based hydrogel inks for 3D printing into LTE scaffolds. Double-bond modified hyaluronic acid and aldehyde-based hyaluronic acid were prepared first. They were then mixed with carboxymethyl chitosan and collagen to form composite hydrogels (designated as CHC hydrogels) for 3D printing. The gel-forming behaviour and effects of carboxymethyl chitosan amount of composite hydrogels (4CHC, 6CHC and 8CHC) were investigated, and the printability of these three composite hydrogels was studied. The hydrogel formation time was less than 1 minute, showing rapid gel formation and convenience for use. Rheological analysis revealed that hydrogel inks had good shear thinning behaviour and thixotropic properties, which would ensure successful 3D printing. Composite hydrogels contained abundant micropores, which are conducive for cell adhesion and proliferation. Compression tests showed that Young's modulus of composite hydrogels was close to that of healthy liver tissue, indicating that the composite hydrogels are biomechanically suitable for LTR. The hydrogels also showed good swelling efficiency and biodegradation properties. In extrusion 3D printing, the 6CHC hydrogel formed smooth filaments and could be printed into 15-layer, grid-type scaffolds with higher shape fidelity than 4CHC and 8CHC hydrogels. After UV crosslinking, printed 6CHC grid-type scaffolds could maintain their shapes without collapsing. Hepatocytes seeded on 3D printed scaffolds proliferated very well, indicating good biocompatibility and scaffold suitability for LTR. The new composite hydrogels appear to be suitable materials for 3D printing into LTE scaffolds which provide appropriate biomechanical and biochemical microenvironments in liver tissue regeneration.

4:00 PM MF01.15.03

Accurate Rheological Characterization of Highly-Filled Direct-Ink Write Pastes Jessica Kopatz, James Griebler, Jonathan Leonard, Alexander S. Tappan and Anne M. Grillet; Sandia National Laboratories, United States

Direct-ink write is an additive manufacturing technique that enables the creation of reproducible and complex hardware by depositing a viscous, shear-thinning liquid onto a substrate in a custom-pattern via extrusion through a syringe. The rheology of these inks is tailored through the addition of various filler materials. To successfully print highly-filled inks, we need to understand the effect of filler morphology, size, loading, and packing fraction on the ink rheology and corresponding printability. More importantly, characterization methods that accurately capture the ink's rheological properties that correlate to resin printability is imperative. Various filler particles and volume loadings of particles were dispersed in Polydimethylsiloxane (PDMS, Sylgard® 182) to investigate the change in zero-shear viscosity, shear-thinning behavior, and plateau modulus. Comparisons between capillary rheometer measurements versus parallel plate rheometer measurements were made. The extrusion force was measured at several volume loadings determine the highest attainable volume loading for printable resins as a function of different filler morphologies. The goal of this work is to understand effects of filler morphology on ink printability while determining adequate characterization techniques that accurately capture the rheological behavior.

Sandia National Laboratories is a multi-mission laboratory managed and operated by National Technology and Engineering Solutions of Sandia, LLC., a wholly owned subsidiary of Honeywell International, Inc., for the U.S. Department of Energy's National Nuclear Security Administration under contract DE-NA0003525.

4:15 PM MF01.15.04

3D Printed Soft Composites with Tunable Mechanical Properties Kimberlee Hughes and Arda Gozen; Washington State University, United States

The use of soft engineering materials such as silicones has been gaining more traction due to the emergence of technologies such as soft robotics, pre-surgical organ models, and wearable electronics, where compatibility with soft biological systems and the ability to mimic their functionalities are essential. For the continued advancement and broad utilization of these technologies, there is a need for further development of soft engineering materials with properties required in relevant applications. Particularly, the ability to precisely control the mechanical properties, as well as their spatial distribution towards development of functionally graded biomimetic compliant structures is a significant research interest. Additive manufacturing with multi-polymer systems have proven to be an effective method to achieve this goal, however, the commonly used Polyjet approach is highly expensive and limited in material capabilities. Towards addressing this challenge, this work presents novel soft composites, consisting of a silicone matrix and thermoplastic elastomer reinforcements, fabricated through low-cost extrusion-based additive manufacturing. Mechanical properties of these composites are functions of the reinforcement geometry that can be precisely controlled. We use a customized 3D printer with direct ink write (DIW) and fused filament fabrication (FFF) capabilities to print composites with a sinusoidal reinforcement pattern. We demonstrate that changes in the amplitude and frequency of these sine waves led to significant differences in the hyperelastic behavior of the composites. Specifically, decreases in amplitude and frequency led to an overall stiffening of the composite, while increasing these parameters led to a softer stress-strain response that approached that of a non-reinforced silicone sample.

Additionally, changing these parameters independently led to differences in strain-hardening behavior. Finally, we demonstrate the ability of this approach to seamlessly control the spatial compliance distribution of composites, by printing parts with sinusoidal reinforcements of spatially varying amplitude and frequency.

4:30 PM MF01.15.05

Freeform Additive Manufacturing of Carbon Fiber Reinforced Composites Using Dielectric Barrier Discharge-Assisted Joule Heating Smita Shivraj Dasari¹, Aniela Wright¹, Anubhav Sarmah², Jacob Carroll¹, Thang Quyet Tran³ and Micah Green¹; ¹Texas A & M University, United States; ²University of Minnesota, United States; ³Singapore Institute of Manufacturing Technology (SIMTech), Agency for Science, Technology and Research (A*STAR), Singapore

In this work, a novel out-of-oven additive manufacturing (AM) technique to rapidly print and cure thermosetting carbon fiber reinforced composites (CFRCs) using dielectric barrier discharge (DBD)-assisted Joule heating was developed. Conventionally, CFRCs are produced by automated fiber placement machines (AFPs) that use large, cumbersome molds and time-consuming oven/autoclave treatments to cure CFRCs in the desired shapes. Recently, out-of-oven AM has garnered attention as a method to manufacture CFRCs without the use of molds. AM allows for on-the-fly printing and curing of thermosetting CFRCs; however, current out-of-oven AM techniques are limited to UV-curable, low viscosity, or rapid-curing resins. Here, the DBD was used for in-situ heating and curing during AM of continuous CFRCs; this method is resin-agnostic, applying to most commercially available thermosetting resins. As the partially cured composite (prepreg) is deposited, Joule heating induced via a DBD applicator allows the part to cure in the desired shape; this is possible because of the conductive carbon fiber susceptors inside the part. Composites manufactured by this method show properties similar to those manufactured in conventional ovens. With the help of this technique, one can print composites in free space or on stationary and mobile substrates. 2D structures, and 3D multilayered structures can be printed. Automation of this process is also demonstrated. This technology leverages the advantages of AM techniques to enable the printing of high-performance and lightweight materials in any desired shape.

SESSION MF01.16: Composites / Devices / Methods
Session Chairs: Michinao Hashimoto and Seola Lee
Friday Morning, April 26, 2024
Room 325, Level 3, Summit

8:00 AM MF01.16.01

Squeeze Flow Induced Fiber Alignment in Fused Filament Fabrication of Carbon Fiber and PDMS Mixture Hoang Minh Khoa Nguyen and Dong-Wook Oh; Chosun University, Korea (the Republic of)

Fused Filament Fabrication (FFF) represents a significant segment of additive manufacturing processes, mainly known for its ability to fabricate complex structures using various materials. Among these, polymer composites integrated with short carbon fibers have gained immense attention due to their potential to exhibit augmented mechanical and thermal properties, positioning them as ideal candidates for high-performance applications in the aerospace and automotive industries. The optimization of these enhanced properties is intrinsically connected to the alignment of carbon fibers within the extruded filament. As current research indicates, this alignment is not a mere consequence of the filament extrusion but is significantly influenced by many factors. Primary among these are the configuration of the printing nozzle and the interactions occurring at the deposition bed. Despite widespread recognition of the merits of these composites, a conspicuous knowledge gap persists regarding the dynamics of fiber rotation during deposition. This paper seeks to bridge this aspect by incorporating experimental and computational methodologies.

Through flow visualization experiments, we observed fiber orientation in multiple focal planes during the extrusion process. This facilitated an in-depth assessment of the alignment angle, indicative of fiber rotations during extrusion. Initially, we examined the fiber rotations as exiting the nozzle, capturing their trajectory and orientation. This was followed by mapping the alignment angles as the extruded filament after the solidification, offering insights into the end-state orientation of the fibers. To foster a comparative analysis, we further performed a numerical flow simulation inside the nozzle and on the deposition bed. The computational calculation was done in a 2-dimensional incompressible Newtonian flow model, which provided velocity information within the filament. The flow field calculation paired with the Advani-Tucker orientation tensors was compared to the fiber orientation obtained from the flow visualization experiment.

We also varied configurations of the nozzle and the deposition bed design configurations. Specifically, by adjusting the gap between the nozzle tip and deposition bed, we introduced different squeeze flows, allowing us to delineate their impact on fiber rotation. Additionally, we varied in-nozzle flow geometries. By comparing the "straight channel" against the "orifice-embedded" nozzles, we manipulated flow fields, and each impacted fiber alignment during the extrusion and deposition process. Nozzle geometry significantly influenced the alignment of carbon fibers in the printed filament. The utilization of a "straight channel" nozzle led to fibers aligning parallel to the heating bed, while the "orifice-embedded" nozzle resulted in fibers aligning perpendicular to it. Moreover, the computational calculation revealed that squeeze flow introduced an additional factor to fiber alignment during the deposition process. In conclusion, our findings regarding nozzle gap, in-nozzle geometry, and squeeze-flow phases play a significant role in the fiber alignment within the printed filament. This study provides insights into the mechanics of fiber alignment in FFF and highlights advancements in customizing polymer composite materials, signaling a significant shift in additive manufacturing material science.

8:15 AM MF01.16.02

Customizable Flexible Pressure Sensors with Enhanced Performance via Ink Optimization and Microdome Integration Sina Hassanpoor, Kaliyah Shearod and Taeil Kim; Baylor University, United States

This research presents an extensive exploration of the development of customizable flexible pressure sensors through the application of Direct-Ink-Writing 3D printing technology. It places a primary focus on the optimization of ink formulations, varying filler ratios of carbon nanotubes (CNT) and silicon dioxide (SiO₂) in polydimethylsiloxane (PDMS) matrix. The research systematically examines how these optimized ink formulations offer precise control over the electrical and hyperelastic properties of the printed sensors and explains their influence on key sensor characteristics such as conductivity and sensitivity. The optimization process of ink formulation is at the core of this research. By adjusting the proportions of CNT, SiO₂, and PDMS, the printability of inks and the electrical properties of sensors could be effectively manipulated. This fine-tuning is essential for ensuring that the sensor operates efficiently in a wide range of environments and applications. Concurrently, the hyperelastic properties of the sensors, which encompass flexibility and elasticity, can be tailored to meet specific requirements. A crucial aspect of this research is the effect of these controlled modifications on the sensors' performance characteristics. The paper delves into how these adjustments can significantly impact the linearity and sensitivity of pressure sensors. Examining these attributes provides a comprehensive understanding of how customizability can enhance the sensors' precision and suitability for various applications. The integration of microdomes with various sizes and differing ink ratios as printed structures atop a flat printed layer introduces a dynamic

dimension to the pressure sensor design. These microdomes are meticulously tailored to function as responsive elements, each uniquely tuned for specific applications. When subjected to varying levels of pressure, these microdomes exhibit an array of behaviors, allowing the sensor to capture detailed data. This multifaceted approach enhances the adaptability of the sensor, making it well-suited for a wide range of applications where precise pressure sensing is imperative, such as touch-sensitive screens, medical devices, or robotic grippers. This adaptability and sensitivity are particularly relevant in healthcare and biomedical applications. Pressure sensors with these attributes can have a meaningful impact on patient care, providing accurate data for diagnosis and treatment. Moreover, integrating microdomes onto the sensor surface, each designed for specific functions, enhances the sensing capability to meet real-world healthcare needs. This integration enables tailored performance for practical applications like continuous blood pressure monitoring, prosthetic limb control, and minimally invasive surgical instruments that rely on precise pressure feedback. The comprehensive discussion in this research spans the methodology used in ink optimization, detailed results from experimental work, and the broad implications of this innovative technology for the domain of flexible pressure sensing. With a focus on precise control over sensor properties, this research aims to contribute to the ongoing advancement of sensor technology and its applications across various fields.

8:30 AM MF01.16.03

Adaptive 3D Printing of Resonant-Enhanced Microsensors Jared Anklam¹, Samuel H. Hales¹, LeiBin Li¹, Sanghoek Kim², John S. Ho³ and Yong Lin Kong¹; ¹University of Utah, United States; ²Kyung Hee University, Korea (the Republic of); ³National University of Singapore, Singapore

The ability to integrate wireless microelectronics on the surfaces of existing biomedical devices can functionalize an otherwise passive construct with advanced sensing capability. The digital freeform fabrication approach directly integrates sensors on a clinically proven device without requiring significant structural modification, lowering the clinical barrier for electronic integration. However, achieving microelectronics integration on biomedical devices (e.g., joint replacement implants) with microextrusion-based 3D printing remains challenging. Biomedical devices are typically geometrically complex three-dimensional constructs requiring extensive surface topological scanning, electronic design and calibration. Here, we develop a microscale closed-loop printing system aided with a laser displacement sensor capable of printing 3D resonant-enhanced microsensors with trace widths as small as 30 μm on a broad range of 3D constructs. The system adapts to the 3D surfaces, achieving conformal printing without requiring extensive alignment of the target substrate with the generated print path. As a proof of concept, we will demonstrate the ability to integrate sensors on biomedical devices such as joint-replacement implants and biological constructs such as bone. Finally, the sensors can be robustly and wirelessly interrogated with high sensitivity using readout techniques that leverage the enhanced sensitivity of systems at special degeneracies, enabling a fundamentally new approach to integrating electronics on existing biomedical devices.

8:45 AM MF01.16.04

Rapid Additive Manufacturing of Thermosetting Resins enabled via Radio Frequency Curing Ethan Harkin¹, Anubhav Sarmah², Thang Quyet Tran¹, Matthew Cupich¹ and Micah Green¹; ¹Texas A&M University, United States; ²University of Minnesota, United States

Direct Ink Writing (DIW) is an extrusion-based additive manufacturing method where the print medium is a liquid-phase 'ink' dispensed out of small nozzles and deposited along digitally defined paths. Conventional DIW methods for thermosetting resins rely on the use of viscosity modifying agents, novel crosslinking chemistries, and/or long curing schedules in an oven. Here we demonstrate the use of a co-planar radio frequency applicator to generate an electric field, which can be used to rapidly heat and cure nano-filled composite resins as they are printed. This method avoids the need for an oven or post-curing step. This process consists of a sequential print-and-cure cycle which allows for printing of high-resolution, multi-layered structures. Every extruded layer is partially cured using RF before depositing the next layer; this allows the printed part to maintain structural integrity without buckling under its own weight. The process enables both increased throughput and decreased touch time relative to traditional part manufacturing. Commercial epoxy resin with various carbon-nanotube loadings was examined as the primary DIW candidates. Rheological characterization was used to assess curing kinetics, extrusion behavior, and printability. After printing, the thermo-mechanical properties, surface finish, and shape retention of RF-cured samples were evaluated and found to be comparable against samples conventionally cured in an oven. This method of manufacturing establishes RF heating as a suitable alternative to conventional methods, facilitating rapid, free-form processing of thermosetting resins without a mold.

9:00 AM MF01.16.05

3D-Printing Liquid Crystal Polymers to Replicate The Anisotropic Complexity of Wood Kunal Masania; TU Delft, Netherlands

Anisotropic materials formed by living organisms such as cellulose fibres in wood grain and fibre bundles in osteons of bone can readily be found in Nature. Their microstructures can be shaped into any direction, with spatially tuneable gradients and sharp orientation changes. In contrast, engineered materials such as composite materials cannot be shaped with similar levels of anisotropy and directionality freedom. While the latter can be achieved with 3D printing, compatible anisotropic materials are typically fiber-filled. Paradoxically, these fibers restrict directionality freedom due to their intrinsic stiffness. Problems such as fiber breakage have been reported and often result in setting curvature constraints in the design space. Here, we present a new approach to replicate complex microstructures such as wood using 3D printing of self-assembling thermotropic liquid crystal polymers (LCPs). The LCPs can be reliably extruded to produce lines whose widths vary from half to three times the nozzle diameter, with stiffness ranging from 5 GPa to 35 GPa. This method allows shaping of anisotropic microstructures with tuneable stiffness and failure modes within a single material. By using a distance-aware toolpath generation algorithm, we can generate print lines of varying widths and curvatures that cover the shape domain homogeneously. We successfully 3D-print infills with no curvature constraint. By increasing allowed curvature, our method offers new design possibilities for composites, such as preventing crack propagation, or spatially distributing stress. Furthermore, this method creates the opportunity to study mechanical responses of natural anisotropic materials of intricate microstructures such as wood or bone.

9:15 AM MF01.16.06

Bridging the Gap to Higher Performance Silicone Elastomers for Direct Ink Write Spencer Schmidt¹, Jake Grondz^{1,2}, Michael Ford¹ and Jeremy Lenhardt¹; ¹Lawrence Livermore National Laboratory, United States; ²Case Western Reserve University, United States

Additive manufacturing via direct ink write (DIW) offers several advantages over traditional manufacturing processes, such as the ability to fabricate polymeric components of complex geometry with spatially dependent properties and reduced waste production. Formulation science is critical to new DIW feedstock development as typical inks must exhibit low yield stress thixotropy while avoiding nozzle swell and post-extrusion flow. These ink properties result from the intertwined effects of reinforcing filler, thixotropic additives, polymer molecular weight, catalyst type, and target mechanical response. For DIW silicones, some standard systems that retain ultimate tensile strength (UTS) of ca. 5MPa and 150 - 350% elongation with varying hardness (ca. 20 - 60 ShoreA) set a baseline from which higher performance feedstocks can be developed.

One approach to enhance silicone mechanical response is to chemically graft functional groups to the fumed silica surface, such as vinyl groups that enable covalent silica bonding to the polymer crosslink network. Systematic variations of polymeric components and in-house surface functionalized silica enable both control over cured mechanical properties in a new set of silicones (achieving ca. 8MPa UTS, 400 - 1200% elongation, and 20 - 50 ShoreA hardness) and direct comparisons across treatment type systems. When aggregated, these comparisons begin a detailed, empirical detangling of the reinforcing filler's

roll in silicone performance from other formulation components that will aid more streamlined development of future generations of printable silicones.

This work was performed under the auspices of the U.S. Department of Energy by Lawrence Livermore National Laboratory under Contract DE-AC52-07NA27344.

SYMPOSIUM MF02

Laser-Induced Nanomaterials—Synthesis, Properties and Applications
April 23 - May 7, 2024

Symposium Organizers

Antje Baeumner, Universität Regensburg
Jonathan Claussen, Iowa State University
Varun Kashyap, Medtronic
Rahim Rahimi, Purdue University

* Invited Paper

+ JMR Distinguished Invited Speaker

^ MRS Communications Early Career Distinguished Presenter

SESSION MF01/MF02/MF03/MT03: Joint Virtual Session

Session Chairs: Jonathan Claussen, Jie Xu and Daryl Yee

Tuesday Afternoon, May 7, 2024

MF02-virtual

1:30 PM *MF01/MF02/MF03/MT03.01

Matrix assisted Pulsed Laser Evaporation for Layer-By-Layer processing of Thin Films containing Biological Materials Andrew Sachan¹ and Roger Narayan²; ¹University of North Carolina at Chapel Hill, United States; ²North Carolina State University, United States

Matrix assisted pulsed laser evaporation has several advantages over dip coating, spin coating, and Langmuir-Blodgett coating for processing thin films that contain pharmaceutical agents and other biological materials. For example, matrix assisted pulsed laser evaporation allows for tight control of thin film thickness. Matrix assisted pulsed laser evaporation also allows for good control of thin film roughness. In addition, matrix assisted pulsed laser evaporation is a “cold” process that does not heat biological material. Matrix assisted pulsed laser evaporation has been used to deposit coatings of many types of biological materials; for example, it has been used to deposit thin films of the antiproliferative drug rapamycin on glass surfaces. Alamar Blue and Pico Green assays were used to evaluate the viability and proliferation rates of L929 fibroblast-like cells on the rapamycin coatings, respectively. The cells on the rapamycin thin films exhibited 70.6% viability ($p=0.0097$) and 53.7% proliferation ($p=0.0120$) compared to cells on the control material (borosilicate glass), respectively [1]. This result indicates that the rapamycin thin films deposited by matrix assisted pulsed laser evaporation successfully reduced cell viability and proliferation. Matrix assisted pulsed laser evaporation offers many potential opportunities to impart biological functionality to the surfaces of medical devices and other medically-relevant structures.

[1] Cristescu R, Negut I, Visan AI, Nguyen AK, Sachan A, Goering PL, Chrisey DB, Narayan RJ. Matrix-Assisted Pulsed Laser Evaporation-deposited Rapamycin Thin Films Maintain Antiproliferative Activity. *International Journal of Bioprinting*. 2020;6(1). doi: 10.18063/ijb.v6i1.188

2:00 PM MF01/MF02/MF03/MT03.02

Comparing The Effect of Single and Dual Sintering Methods Using Silver and Copper Nanoparticle Patterns for Flexible Electronics Applications Rajib Chowdhury and Seonhee Jang; University of Louisiana at Lafayette, United States

The utilization of metallic nanoparticle (NP) ink has gained significant attention in the fabrication of cost-effective and mechanically flexible printed electronic devices, including wearables, displays, sensors, and solar cells. The choice of metallic NPs is a crucial determinant of the electrical, material, and mechanical properties of the printed patterns. Commonly used NPs for ink formulation include silver (Ag), gold (Au), and copper (Cu). Ag NP ink is highly favored for its exceptional oxidation stability and electrical conductivity. Although Au NPs also offer good electrical conductivity and oxidation resistance, their high cost makes them less desirable. Cu NPs have good electrical conductivity and cost-effectiveness, but they have lower oxidation stability. The metallic NP ink is not electrically conductive after the printing process due to steric repulsion forces acting between the particles. These repulsion forces are caused by the introduction of organic additives and stabilizing agents to the ink, preventing the NPs from agglomerating due to Van Der Waals interactions between them. To achieve electrical conductivity, a post-processing step, known as the sintering process, is necessary to decompose the additives and stabilizing agents.

In this study, Ag NP ink (PSI-211, NovaCentrix) and Cu NP ink (CP-008, NovaCentrix) were chosen for printing and characterizing the conductive patterns. Flexible Kapton polyimide (PI) sheets with a thickness of 0.102 mm served as the substrate. The study explored the single and dual sintering methods on the printed Ag and Cu NP patterns. In the single sintering methods, the printed NP patterns were exposed to either laser irradiation (LO) or thermal treatment (TO). For the LO sintering condition, the Ag and Cu NPs underwent Nd: YAG laser irradiation at 600 mJ for 15 s and 800 mJ for 30 s,

respectively. For the TO sintering condition, the Ag and Cu NPs were placed in a formic acid (FA) environment at 140 °C for 1.5 min and 260 °C for 15 min, respectively. In the case of the dual sintering methods, one approach is to subject the printed metal patterns to thermal treatment followed by laser irradiation (TL), while the other method involves exposing the patterns to laser irradiation followed by thermal treatment (LT). The sintering parameters for TL and LT followed the same sintering conditions as LO and TO.

After analyzing the microstructure using the scanning electron microscope, the Ag NP patterns sintered using LT showed enhanced agglomeration and increased networking of particles through necking compared to the Ag NP patterns sintered using the other conditions. This pattern also displayed the highest roughness of 48 nm from atomic force microscopy (AFM) analysis, indicative of superior grain growth. Due to this fact, the Ag NP pattern sintered using LT demonstrated the lowest electrical sheet resistance with a value of 0.0031 Ω/Sq and the lowest resistance ratio (R/R_0) of 1.75 after the folding test. The highest hardness was found for the Ag NP pattern sintered using LT with a value of 4.28 N/mm^2 , which contributed to a better result in the adhesion test. On the other hand, the Cu NP pattern sintered using TO showed the most uniform grain growth through agglomeration and coalescence. Additionally, due to increased connectivity between NPs, the patterns sintered under TO showed the highest mechanical hardness of 55.36 N/mm^2 and the lowest R/R_0 value of 10.58 after the folding test. The lowest electrical sheet resistance was observed for the Cu NP pattern sintered using LT with a value of 0.0117 Ω/Sq , which thermogravimetric analysis (TGA) showed to be due to the complete removal of organic residue from the pattern. Additionally, the Cu NP pattern sintered under LT showed the highest roughness value of 51.36 nm.

2:15 PM MF01/MF02/MF03/MT03.03

Improvement of Laser-Induced Graphene-Based Electrochemical Biosensors through Graphene-Conductive Polymer Ink Coating for Sensitive Detection of Alpha-Fetoprotein Ridma Tabassum, Ali Ashraf, Nazmul Islam, Pritu Parna Sarkar, Ahmed Jalal and Robert Freeman; University of Texas Rio Grande Valley, United States

Hepatocellular carcinoma (HCC) is the most common type of primary liver cancer and is the sixth most commonly occurring cancer worldwide with the second-highest mortality rate [1] [2]. Since the 1970s, alpha-fetoprotein (AFP) has been used as a prominent biomarker for the diagnosis of HCC. But AFP is electrochemically inactive, thus, detecting AFP is unreliable for early detection of HCC [3]. In this study, we demonstrated the highly sensitive detection of alpha-fetoprotein (AFP) by developing an electrochemical biosensor using Kapton film. The electrochemical sensor was fabricated by laser scribing technique which is a one-step method that does not require any oxidative acid synthesis route or chemical vapor deposition (CVD) to obtain graphene structure which reduced the cost tremendously [4]. The laser-induced graphene (LIG) electrodes were modified with developed graphene polyaniline (G-PANI) ink to effectively enhance the detection of electrical signals. The peak potential voltage difference was 600 μV for the bare electrode, while after modifying with the ink the difference was reduced to 260 μV which indicates a 56% change. Therefore, the electrocatalytic effect of the electrode surface and electrochemical sensor signal was improved after modifying the electrode with ink. To evaluate the performance of the sensor, differential pulse voltammetry (DPV), and electrochemical impedance spectroscopy (EIS) techniques were performed in phosphate buffer saline (PBS) buffer with ferro-ferricyanide as the redox probe. For the DPV method, a significant surge in peak current was observed, increasing from 9.2 microamperes at a concentration of 20 pg/mL to 13.6 microamperes at 400 pg/mL which satisfied the fact that increasing the concentration of AFP, led to a higher number of analytes available for electron transfer, thus resulting in the observed current enhancement. The nearly identical current outputs in the DPV measurements were obtained consecutive 15 times which represents the sensor's stability with an RSD of 3.69% and exhibits high reproducibility (RSD=12.15%, N=5). The obtained EIS result showed good linearity in charge transfer resistance change (coefficient of determination, $R^2=0.87$) with the AFP concentration increment in the range of 20 pg/mL - 400 pg/mL , and the limit of detection (LOD) was 146 pg/mL at a signal-to-noise ratio of 3, indicating the sensor's sensitivity. The range was selected due to demonstrate high sensitivity in the picogram range and has the potential to cover the entire physiological range for a healthy adult. The specific selectivity of the sensor was evidenced by obtaining a random current peak when both AFP and estrogen were introduced simultaneously on the surface of the sensor. For both electrochemical techniques, a similar coefficient of determination was found from the calibration curves, suggesting that the fabricated biosensor offers high selectivity to the determination of AFP biomarker.

References:

- [1] S. F. Altekruse, K. A. McGlynn, and M. E. Reichman, "Hepatocellular Carcinoma Incidence, Mortality, and Survival Trends in the United States From 1975 to 2005," *J. Clin. Oncol.*, vol. 27, no. 9, pp. 1485–1491, Mar. 2009, doi: 10.1200/JCO.2008.20.7753.
- [2] L. A. Torre, F. Bray, R. L. Siegel, J. Ferlay, J. Lortet-Tieulent, and A. Jemal, "Global cancer statistics, 2012," *CA. Cancer J. Clin.*, vol. 65, no. 2, pp. 87–108, Mar. 2015, doi: 10.3322/caac.21262.
- [3] W. M. Hai-yong Wang and Li-song Teng, "Correlation analysis of preoperative serum alpha-fetoprotein (AFP) level and prognosis of hepatocellular carcinoma (HCC) after hepatectomy," *2013*, vol. 11, pp. 1–7.
- [4] R. Ye, D. K. James, and J. M. Tour, "Laser-Induced Graphene," *Acc. Chem. Res.*, vol. 51, no. 7, pp. 1609–1620, Jul. 2018, doi: 10.1021/acs.accounts.8b00084.

2:20 PM MF01/MF02/MF03/MT03.04

Laser-Induced Graphene (LIG) from Different Polymer Precursors Predicted Using Machine Learning Pranav Gupta¹, Dazhong Wu² and Gerd Grau¹; ¹York University, Canada; ²University of Central Florida, United States

The conversion of polymers to laser-induced graphene (LIG) is a facile and low-cost process to create a patterned conductive nanomaterial for applications such as sensing and energy storage. However, the complexity of the laser conversion process means that it is difficult to predict the effect of different laser parameters, especially for different polymer precursors. This research leverages advanced machine learning models to optimize and predict the laser parameters necessary for polymer conversion into LIG. Data to train the models was collected experimentally and extracted from the academic literature, after which preprocessing techniques were applied. A major input parameter studied in this work is the type of polymer precursor. To this end, we transformed the molecular structures of different polymers from their Simplified Molecular-Input Line-Entry System (SMILES) representation into molecular fingerprints, descriptors, and tokenized representations using RDKit and a pre-trained BERT model. A variety of predictive models including fully connected neural networks, random forest, gradient boosting, and XGBoost were trained, evaluated, and optimized. The cornerstone of the analysis was a specialized testing of feature importance across three distinct SMILES representations, illuminating the complex interplay between molecular structures and polymer properties. The superior performance of the random forest model highlights the vital importance of feature selection and optimization. This creates a comprehensive understanding of influential features in predictions including both laser parameters and different molecular representations. By integrating traditional molecular descriptors and advanced machine learning techniques, this research offers a robust framework for predicting LIG properties, potentially reducing extensive experimental needs. The results have broad implications in material science and flexible electronics.

2:25 PM MF01/MF02/MF03/MT03.05

Flexible Carbon Dioxide Sensors Based on Polyethyleneimine – A Study on Their Aging and Potential Solutions Tianyi Liu, Daniel Padilla, Kening Lang, Nickolas Boeser, Rishi Patel, Qihua Wu, Marriana Nelson, Christopher Landorf and Jiadeng Zhu; Brewer Science, United States

CO₂ sensors, being widely utilized in indoor air quality monitoring, ventilation systems, automotive emission control, and healthcare, can be constructed using various materials and technologies. In recent years, polymers have been considered a popular sensing candidate due to their low cost, outstanding processability, and excellent compatibility with other materials. Polyethyleneimine (PEI) is a polymer that can interact with CO₂ molecules and generate measurable responses; thus, it's been extensively explored in the development of CO₂ sensors. Even though many researchers have studied the stability of pure PEI, there are few studies for their real applications (i.e., CO₂ sensors) since it determines the sensor lifetime. Therefore, in this work, a systematic analysis of the screen-printed, PEI-based chemiresistive CO₂ sensors was conducted with emphasis on the sensors' aging behavior along with the mechanism. More importantly, we have demonstrated solutions to address the sensor aging by selecting the proper molecular weight PEI and doing the chemical modification on PEI. The produced sensors exhibit much better cycling stability compared to the control sample.

2:40 PM MF01/MF02/MF03/MT03.06

Laser 3D-Printing of Organic Semiconductor-Carbon Nanotube Microstructures for Flexible Microelectronics and Circuitry Omid Dadras-Toussi and Mohammad Reza Abidian; University of Houston, United States

3D printing is taking the stage in the forefront of technological and industrial advancements, particularly in the emerging field of organic micro/nano electronics. Amongst various 3D printing techniques, Direct Laser Writing based on Two-Photon Polymerization (DLW-TPP) reigns supreme, owing to its unique capability to construct arbitrary-shaped 3D architectures in sub-micron resolution. Herein, we have directly incorporated 2 organic semiconductor fillers, i.e. poly(3,4-ethylenedioxythiophene)-poly(styrene sulfonate) (PEDOT:PSS) and multi-walled carbon nano tubes (MWCNTs), in a photosensitive ink which can be fabricated into highly conductive microstructures via DLW-TPP.

The photosensitive ink contained polymer crosslinker poly(ethylene glycol) diacrylate (PEGDA), two organic semiconductors (PEDOT:PSS and MWCNTs), photo-initiator (ethyl (2,4,6-trimethylbenzoyl) phenylphosphine), and two miscible agents (dimethyl sulfoxide and pentaerythritol tetrakis (3-mercaptopropionate)). Formulation-wise, maximum content of PEDOT:PSS and MWCNTs in the conductive, homogeneous, and stable ink was found out to be 0.4 wt% and 0.15 wt%, respectively. Microstructures were constructed on flexible poly(dimethylsiloxane) substrates through 3D movement of XYZ stages and irradiation of 130 femtosecond pulses from two-photon laser, which solidified the resin at its focal point.

Current-voltage measurements revealed that conductivity of microstructures fabricated by the conductive ink was 140050 ± 29414 S m⁻¹, almost ten orders of magnitude higher than their counterparts fabricated with inks without added conductive agent, i.e. 0.0002 ± 0.0003 S m⁻¹ (n=5). Optical transparency of the conductive ink showed ink transmittance of 82% at 550 nm. Moreover, microstructures fabricated with the conductive ink presented average surface roughness of 258 ± 2 nm (n=4).

Fabrication and electrical/electrochemical characterization of various conductive microstructures were successfully demonstrated. In the space of flexible microelectronics and circuitry, printed circuit boards were fabricated via DLW-TPP based on the conductive ink. Functionality of sub-components such as resistors and capacitors were measured and confirmed. In another notable development, multi-site microelectrodes were constructed via DLW-TPP. Electrochemical impedance spectroscopy and cyclic voltammetry revealed that recording sites exhibited low impedance (18.28 ± 5.58 k Ω at 1 kHz) and high charge storage capacity (48.13 ± 4.67 mC cm⁻²), which promises their application in potential neural recording/stimulation. Development of these 3D-printed microstructures via DLW-TPP forges the path forward for development of advanced printed circuitry and wearable / implanted microelectronics.

2:45 PM MF01/MF02/MF03/MT03.07

3D-Printed Gyroid Architecture for Pressure Sensor Applications Danielle Agron, Chao Bao and Woo Soo Kim; Simon Fraser University, Canada

The gyroid structure represents a design renowned for its high strength and exceptional energy-absorbing qualities, rendering it a suitable choice for deployment as an energy damping device. Within the family of related gyroid structures, we have opted for the Slab single gyroid (Slab SG) model. This model has been meticulously crafted using the 3D printing method, with the intention of utilizing it as the basis for a capacitance-based pressure sensor. In this work, we introduce a simulation model to homogenize the variations introduced by the FDM manufacturing process. Our results indicate that the profile of the fused layer model, with a Young's modulus of 48.7%, exhibits performance closest to the isotropic model. To delve into the energy buffering capabilities of the Slab SG structure, we have developed a suite of closely related gyroid structures. Based on the model that demonstrates the highest linearity, we have fabricated a gyroid-based sensor. This sensor features an electrode network crafted with conductive ink via robot-assisted 3D printing. These electrodes are thoughtfully integrated into the parallel curved surface of the Slab SG structure to maximize the capacitance formed and, subsequently, the sensitivity of the sensor. We have devised a reinforced gyroid-based liner to ensure a uniform force distribution, thereby facilitating the assembly of components for an application in smart helmets.

2:50 PM *MF01/MF02/MF03/MT03.08

Sustainable Production of High-Energy Density Flexible Supercapacitors through Direct Laser Writing on Environmentally Friendly Substrates João Coelho^{1,2,3}, Rodrigo Abreu³, Maykel d. Klem^{3,4}, Sara Silvestre³, Tomás Pinheiro³, Neri Alves⁴, Elvira Fortunato³ and Rodrigo Martins³; ¹Universidad de Sevilla, Spain; ²Instituto de Ciencia de Materiales de Sevilla (Universidad de Sevilla-CSIC), Spain; ³Universidade Nova de Lisboa and CEMOP/UNINOVA, Portugal; ⁴School of Technology and Sciences, São Paulo State University (UNESP), Brazil

Supercapacitors (SC) and graphene are two cutting-edge technologies at the forefront of energy storage and materials science. Supercapacitors, often referred to as ultracapacitors or electrochemical capacitors, are energy storage devices that bridge the gap between traditional capacitors and batteries. They are known for their exceptional energy storage and rapid charge-discharge capabilities, making them essential components in a wide range of applications, from consumer electronics to electric vehicles and renewable energy systems^[1]. Graphene, on the other hand, promises to revolutionize the field of supercapacitors, offering significant improvements in terms of energy storage, charge-discharge rates, and overall performance. This effect is mainly due to graphene's high surface area, high electrical conductivity, exceptional capacitance and flexibility, and lightweight. Among a plethora of graphene synthesis and deposition methods, laser-induced graphene (LIG) is one of the most studied^[2]. This innovative technique has attracted considerable attention for its potential to improve energy storage devices and scalability. However, in terms of energy storage, LIG has mostly been fabricated in polyimide, which compromises the sustainability of the fabricated devices. In addition, as an electrical double layer (EDL) material, LIG-based supercapacitors will always have a relatively low energy density^[3].

In this work, we have developed a simple yet elegant sustainable strategy to fabricate LIG SC on paper and cork with improved electrochemical performance. Based on a fire-retardant treatment, the fabricated EDLC exhibited areal-specific capacitances as high as 4.6 mF cm⁻² (0.015 mA cm⁻²) for paper and 1.43 mF cm⁻² (0.1 mA cm⁻²) for cork. In addition, the devices have excellent cycling stability (> 10,000 cycles at 0.5 mA cm⁻²) and good mechanical properties^[4,5]. In order to increase the energy density of the device, two different strategies were explored. In one approach, the substrate was impregnated with a precursor that is converted to manganese oxide, a pseudocapacitor material, upon laser irradiation. The other strategy involved electrodepositing the manganese oxide onto LIG electrodes. Both methods resulted in supercapacitors with relatively high energy densities. The advantages

and disadvantages of both techniques will be discussed in detail in this talk.

Despite these promising advantages, it's important to note that graphene-based supercapacitors are still undergoing extensive research and development to optimize their performance and cost-effectiveness. Challenges related to scalability and production costs need to be addressed for widespread commercial adoption. Nevertheless, laser-induced graphene supercapacitors hold great promise for improving energy storage solutions and contributing to a more sustainable and energy-efficient future.

References

- [1] J. Coelho, M. P. Kremer, S. Pinilla, V. Nicolosi, *Curr Opin Electrochem* **2020**, *21*, 69.
- [2] R. Ye, D. K. James, J. M. Tour, *Acc Chem Res* **2018**, *51*, 1609.
- [3] Z. Peng, J. Lin, R. Ye, E. L. G. Samuel, J. M. Tour, *ACS Appl Mater Interfaces* **2015**, *7*, 3414.
- [4] J. Coelho, R. F. Correia, S. Silvestre, T. Pinheiro, A. C. Marques, M. R. P. Correia, J. V. Pinto, E. Fortunato, R. Martins, *Microchimica Acta* **2023**, *190*, 1.
- [5] S. L. Silvestre, T. Pinheiro, A. C. Marques, J. Deuermeier, J. Coelho, R. Martins, L. Pereira, E. Fortunato, *Flexible and Printed Electronics* **2022**, *7*, 035021.

SESSION MF02.01: Laser Assisted Manufacturing Off Flexible Circuits and Electronics
Session Chairs: Antje Baeumner and Varun Kashyap
Tuesday Morning, April 23, 2024
Room 324, Level 3, Summit

10:30 AM *MF02.01.01

Selective Laser Based Postprocessing to Convert Flexible Printed Circuits into Stretchable Circuits and Their Use in Biomedical Applications
Simon N. Dunham, Bobak Mosadegh, Varun Kashyap, Abdellatif A. Lahcen, Zixu Huang, Alex Caprio and Chris Liu; Weill Cornell Medical College, United States

Flexible printer circuit boards (Flex-PCBs) have become ubiquitous in commercial electronics and are pervasive across multiple industries. These components can bend and flex, allowing them to be used in a wide variety of interconnects and durable circuits, but they cannot accommodate significant in-plane strain. More recently, a wide variety of applications have been demonstrated based on the use of fully stretchable sensors, that can undergo this type of deformation. In particular, because tissues are intrinsically soft and stretchable, and anatomies tend to be complex and unique, there are a wide variety of biomedical applications where the ability of sensor to stretch and deform themselves to make intimate contact with tissue presents unique benefits.

A wide variety of wearable and soft robotics systems have been developed demonstrating the importance of these novel classes of devices. These are based on a wide variety of fabrication methods ranging from sophisticated approaches to use advanced fabrication of traditional brittle electronic materials, rendering them stretchable, to the use of novel materials that are intrinsically stretchable. We have demonstrated a low cost method to employ these design strategies, coupled with a self-aligned laser based postprocessing method to convert traditional Flex-PCBs into stretchable sensing arrays. We have demonstrated these approaches for both single and multilayer Flex-PCBs.

Here, we will describe this methodology. Furthermore, we will describe thermal simulations to understand the underlying mechanisms for this process. We use these simulations to understand the basic design trade-offs associated with this method, such as limits to resolution, number of layers, and other process parameters.

Separately, we describe the utility of these approaches by describing several practical demonstrations of biomedical devices that utilize these types of stretchable electronics, based on laser-based postprocessed Flex-PCBs. Here we describe the ability of these arrays to be easily integrated with stretchable biomedical grade polyurethanes for applications in cardiac mapping and patient intubation.

11:00 AM MF02.01.02

Enhancing The Conductivity of Laser-Induced Graphene with Functionalized Liquid Metal Particles Halil Tetik and Mohammad H. Malakooti; University of Washington, United States

The rapid and straightforward fabrication process of laser-induced graphene (LIG) has unlocked new possibilities in creating flexible sensors for emerging applications, such as wearable electronics and intelligent systems. While LIG exhibits remarkable sensitivity as a strain sensor, its application as a printed conductor on flexible substrates faces limitations.

In this talk, I will present our recent work on a versatile technique to significantly enhance the electrical conductivity and resistive heating capabilities of LIG, making it an ideal choice for flexible conductors in printed electronics. We achieve highly conductive traces by directly writing LIG onto a polyimide film using a CO₂ laser. Subsequently, we introduce functionalized liquid metal (LM), specifically eutectic gallium indium (EGaIn) particles, onto the LIG, leading to a remarkable ~400-fold increase in the electrical conductivity of LIG traces. This improvement is achieved while preserving mechanical flexibility and manufacturing scalability, all without the need for soldering. Electromechanical characterization of the LIG-LM traces reveals minimal resistance changes even under substantial bending deformations. Simultaneously, the enhanced electrical conductivity plays a pivotal role in improving the resistive heating performance, significantly reducing the input voltage requirement (by ~15 times) to achieve similar surface temperatures compared to pure LIG traces. By combining EGaIn with laser-synthesized graphene, we successfully fabricate flexible hybrid electronics, demonstrating the practicality of this technique through the creation of highly customizable patterns for flexible conductors and heating devices.

11:15 AM *MF02.01.03

Inkless Printing Multimaterial Electronics – A Multi-Laser-Based Additive Nanomanufacturing Approach Masoud Mahjouri-Samani, Zabihollah Ahmadi, Aarsh Patel and Adib Taba; Auburn University, United States

Printed flexible hybrid electronics (FHEs) have emerged as a remarkable technology in recent years due to the simple, cost-effective fabrication, reduced e-waste, and development of multifunctional devices. The rising demand for consumer and industrial electronic products that are uniquely fabricated/designed and increasing usage is boosting the demand for this technology. Current techniques rely on ink-based printing technologies such as inkjet and aerosol jet printers, which suffer from contamination, expensive formulation procedures, and limited materials sources, making it challenging to print pure and multimaterial devices. In this contribution, I will demonstrate a multi-laser-based additive nanomanufacturing (ANM) technique that allows dry, pure, solvent-free printing of electronics and functional devices on various substrates. The key technology advantages include 1) on-demand and in-

situ laser generation of various pure nanoparticles without contaminations, 2) in-situ and real-time laser sintering of nanoparticles on various substrates with no further post-processing, 3) multimaterial printing of hybrid and tunable nanocomposite materials and structures. Several different mechanical and electrical performance tests like bending, cycling, and surface adhesion are performed on the printed devices, which demonstrate their exceptional performance and the considerable impact this technique has on the future of printed sensors and devices.

11:45 AM MF02.01.04

Establishing a Virtual Look into Laser-Driven Shockwave Synthesis of Nanocarbon Materials [Rebecca K. Lindsey](#)^{1,1}, Yanjun Lyu¹, Sorin Bastea² and Sebastien Hamel²; ¹University of Michigan–Ann Arbor, United States; ²Lawrence Livermore National Laboratory, United States

Carbon nanomaterials are of tremendous interest due to the manifold of properties they can exhibit. For example, nanodiamond is renowned its hardness and biological inertness and is found in applications spanning industrial lubricants to biological implants and drug delivery vehicles; graphitic nanoparticles including quantum dots, nanotubes, and graphitic nanoions exhibit tunable electronic and optoelectronic properties that are being explored for quantum computing, energy harvesting, and electronic devices. However, exploration in this materials space remains nascent due to challenges associated with (1) establishing efficient, scalable synthesis strategies, and (2) navigating the massive design space.

Nanocarbon design and discovery efforts have primarily focused on low pressure synthesis methods including chemical vapor deposition and flame pyrolysis, for which synthesis output is measured in mg/hr rates, and accessible states of carbon are limited. High pressure methods hold significant promise for overcoming these limitations. Decades of explosive materials (EM) research have established that detonation can be used to produce *kg to ton quantities of nanodiamond in under a single microsecond*, and that a variety of unique, technologically promising nanomaterials can be produced in this fashion simply by changing the explosive material composition. However, when appropriating detonation for *intentional* materials synthesis, a key limitation is the inherent coupling between the driver and the precursor – that is, the temperatures (T), pressures (P), and the kinetics with which those conditions are realized during detonation is characteristic to the specific EM itself, precluding independent control over precursor composition necessary to tune properties of the emergent nanocarbon materials.

Recently we demonstrated that this limitation can be overcome by through use of an external shockwave source (e.g., via projectile or laser rather than detonation) to drive arbitrary precursors to high T/P in a finely controllable manner through a combined experimental and computational study. This presentation will overview the computational portion of the work including CHIMES, the unique physics-informed machine learning capability that enabled this work. Recent advances toward elucidating mechanisms and kinetics for the governing reactive phase transformation and phase separation processes will be discussed.

SESSION MF02.02: Laser-Induced 3D Structures and Their Applications

Session Chairs: Antje Baeumner and Jonathan Claussen

Tuesday Afternoon, April 23, 2024

Room 324, Level 3, Summit

1:30 PM *MF02.02.01

Laser Material Interactions for Soft Electronics [Keon Jae Lee](#); Korea Advanced Institute of Science & Technology, Korea (the Republic of)

This seminar introduces recent progresses of laser material interactions that can extend the application of self-powered soft electronics in both materials and processes. Laser technology is extremely important for the future of flexible electronics, allowing high-temperature processing on plastics vital for high-performance electronics, due to its ultra-short pulse duration; for example, low temperature poly-silicone (LTPS) process enables over 1000 °C process on plastics, without damaging the flexible substrates. Specifically, this seminar presents current laser usages in soft electronics, which are classified into four main categories: i) ultrashort heat treatment for annealing or sintering inorganic materials on flexible substrates, ii) laser-induced reaction that leads to a new type of material different from its initial state, iii) exfoliation that separates thin films and devices from their parent substrate for high performance flexible inorganic electronics, and iv) laser-induced etching (LIE), which consists of laser material modification and subsequent wet etching for flexible micro LED. These technologies can produce complex three-dimensional and stretchable structures for human oriented soft electronics. Additionally, various applications of laser–material interaction for inorganic-based flexible devices, including self-powered acoustic sensors, blood pressure monitor, massive transfer of optoelectronics and nanomaterial synthesis will be demonstrated.

2:00 PM MF02.02.02

3D Nanofabrication and Integration of Various Metal Oxides [Hu Huace](#)¹, [Wei Xiong](#)^{1,2}, [Chunsan Deng](#)¹, [Tao Han](#)¹ and [Hui Gao](#)¹; ¹Huazhong University of Science and Technology, China; ²Optics Valley Laboratory, China

Microsystems can achieve higher performance, smaller sizes, and lower power consumption through integrating three-dimensional (3D) functional structures of various metal oxides. However, the nanomanufacturing and heterogeneous integration of 3D functional metal oxides still face long-standing challenges. Currently, the mainstream 3D manufacturing techniques of metal oxide structures can be classified into two methods including particle-loaded bonding and femtosecond laser direct writing (FLDW). Particle-loaded bonding technology utilizes material's jetting or extrusion to achieve the 3D printing and heterogeneous integration of various kinds of metal oxides. However, its manufacturing resolution (>10 μm) and quality (high roughness, low stiffness) are difficult to meet the application requirements of integrated microsystems. On the other hand, although the FLDW technology has nearly unrestricted 3D design freedom at the nanometer resolution, the 3D metal oxide structures manufactured by this technology commonly suffer from serious shape distortions, limited material applicability, and difficulties in heterogeneous integration.

To address the above issues, we propose a method for 3D nano-printing and heterogeneous integration of various kinds of metal oxides by FLDW the water-soluble resin of metal ion-coupled coordination. This method has the following three main advantages: 1) The mechanism of mutual promotion between acrylic acid and 1-vinylimidazole in coupled coordination with metal ions has been proposed, which breaks through the concentration limit of metal ions in the 3D structure manufactured by traditional methods, increasing the metal ion content to 30.5% in the 3D structure, thereby significantly reducing the degree of morphological distortion. 2) The resin for FLDW is designed to be water-soluble, which may potentially extend this method to the processing of oxide of all water-soluble metal elements. 3) Sequential 3D printing according to the priority of metal activity enables the 3D heterogeneous integration of various functional metal oxides. The successful design of this printing method enables us to manufacture 3D nanostructures and heterogeneous integrated structures of various types of metal oxides, including MnO₂, Cr₂O₃, ZnO, NiO, and Co₃O₄. Furthermore, we demonstrate a high-sensitivity 3D ZnO micro-integrated sensor with a sensitivity of up to 1.113 million in a 200 ppm NO₂ environment, which is much larger than the sensitivity of the 2D device. Therefore, this printing method expands our capability to achieve the 3D manufacturing and integration of metal oxides at the nanoscale and demonstrate its significant application potential in the field of integrated sensing devices, integrated medical endoscopes, nanogenerators, and other 3D microsystem applications.

2:15 PM MF02.02.03

Selective Laser Sintering of Functional Polymer Powders for Precise Fabrication of 3D Hierarchical Composites Weinan Xu; University of Akron, United States

Selective laser sintering (SLS) (also named powder bed fusion) has been regarded as the most promising polymer 3D printing technology for many industrial applications. Its unique advantages compared with extrusion- or photopolymerization-based technologies include the ability to fabricate complex geometries without support structures, highly isotropic properties of the printed parts, and batch production of multiple parts in one printing. However, the major limitation of SLS is the limited polymer powder selection (95% is based on polyamide) and difficulty in multi-material printing. Here, I will present our recent progress in the development of new types of polymer/composite microparticles for SLS, and more importantly, the simultaneous laser-induced graphitization of polyimide microparticles into 3D hierarchical graphene structures with precisely controlled geometry and internal structure. 3D graphene-metal oxide structures can also be fabricated by this strategy, which have superior electrochemical properties for energy storage and catalysis applications.

2:30 PM BREAK

3:00 PM *MF02.02.04

Direct Freeform Laser Fabrication of Multimaterials for 3D Electronics Jian Lin; University of Missouri-Columbia, United States

In the past decade, direct laser fabrication (DLF) has been witnessed an exponential growth in various applications. Among them, one prominent field is sensor and electronics. Despite much progress, the mainstream application of DLF is restricted to planar fabrication capability. In this talk, we will discuss our recent progress in bringing such a capability in the conventional 2D plane to 3D free space. The first technological advance is to develop a 5-axis laser processing platform. With the two additional two degrees of freedom, the laser beam can be focused on any arbitrary surfaces for freeform laser induction (FLI) of representative laser induced graphene (LIG), metals, and metal oxides as high-performance sensing or/and electrode materials in 3D conformable electronics. To make a new stride based on this success, recently, we developed a freeform multimaterial assembly platform (FMAP) by integrating 3D printing (fused deposition modeling (FDM), direct ink writing (DIW)) with the FLI technique. 3D printing performs the 3D structural material assembly, while the FLI can fabricate and pattern the functional materials in predesigned positions of the 3D structures by synergistical, programmed system actuation. By this platform, crossbar LED circuit, touchpad for human-machine interaction, multiple sensors, sensor-enveloped springs, electromagnets, force feedback manipulators, and microfluidic reactors with embedded heating elements were fabricated to demonstrate the versatility and effectiveness of the technique.

3:30 PM MF02.02.05

High Temperature Reactions in Laser-Assisted Ceramic Additive Manufacturing Leonard Siebert, Philipp Schadte and Rainer Adelung; Kiel University, Germany

Ceramics are the most temperature- and oxidation-stable materials known. Usually only strong acids or bases are capable of inducing ceramics to react. When dealing with extreme temperatures over 3000 °C, however, oxide ceramics can be induced to lose an oxygen and become reactive. This can be used in laser-assisted additive manufacturing (AM) of ceramics. Lasers are used here to sinter or melt the ceramics layer-by-layer. Additionally, each layer and even each spot can be irradiated with almost arbitrary high power and thus extreme heating, which lead to extraordinary reaction kinetics. As an example, irradiating SiO₂ with a CO₂-laser ($\lambda = 10.6 \mu\text{m}$), it can be evaporated with ease, while more stable ceramics like ZrO₂ can be reduced to ZrO, losing one oxygen in the process. This state can be stabilized in inert gas atmosphere and quenched to room temperature, while in oxygen-rich atmosphere the recapture of oxygen takes place upon cooling. When in its reduced state (, i.e., ZrO) can react with other substances to form intermediaries that are usually hard to produce. For instance, by varying the gas atmosphere to forming gas (5% hydrogen, 95% nitrogen), the dark colored ZrO can be converted to the golden ZrN. The reaction zone is clearly molten, so that it can be concluded that the temperature for the reaction is above the melting point of both ZrO₂ (2680 °C) and ZrN (2980 °C). Thus, the gas phase can be employed as a reaction medium. Additionally, the solid phase can trigger certain reactions as well. The addition of Ti powder and a forming gas lead to the formation of an interpenetrating phase composite made from TiN and ZrO. The commonly weak interface between these two very different ceramics is stabilized through mechanical interlocking of the two phases, observed by cross-section elemental mapping in TEM. These TiN films are only a few 100 nm thick, yet present the excellent electrical conductivity that is common for this material. Since ZrO₂ is itself the solid electrolyte in solid oxide electrolyte fuel cells, such a conversion can be used to produce stable contacts for current collection. In additive manufacturing, the conversion technique can be employed to produce and partially convert ceramics to equip them with special functionalities. For example, Zn can be directly oxidized to the semiconductor ZnO in situ and thus produce functional nanostructures in the manufacturing process. In this contribution, I will show how high-power CO₂-laser treatments and additive manufacturing can be employed together to create in situ high temperature reaction and ultimately convert and stabilize these products.

3:45 PM *MF02.02.06

Rapid, Continuous Projection Multi-Photon 3D Nanoprinting enabled by Spatiotemporal Focusing of Femtosecond Pulses Xianfan Xu; Purdue University, United States

Two-photon lithography has become the dominant fabrication process for 3D nanoprinting for most applications today due to its capability to produce submicron features and true 3D printing of arbitrary structures. Still, the printing rate is often considered slow. Multiple methods have been proposed for improving two-photon 3D nanoprinting rates. Here, a rapid, continuous, layer-by-layer projection two-photon lithography process is described. To achieve 3D printing with submicron feature sizes, a spatiotemporal focusing effect due to a digital micromirror device (DMD) projection system applied to the femtosecond printing laser pulses confines the polymerization region of the photoresist to a thin 2D plane. By continuously changing the projected DMD pattern without pauses in printing layers while varying the height of the print plane in the photoresin, smooth 3D prints are achieved rapidly. Millimeter scale printing is demonstrated by printing various complex 3D geometries. This presentation will also discuss recent progresses toward grayscale printing, real time imaging and feedback, multiple beam printing, and machine learning to improve the speed and accuracy of 3D nanoprinting.

4:15 PM MF02.02.07

Direct Laser Writing of Complex 3D Metal Nanoparticle Patterns within Polymer Microstructures for Photothermal Micro-Actuators Luisa Lavelle¹, Srikanth Kolagatla¹, Paola Parlanti², Mauro Gemmi², Colm B. Delaney¹ and Larisa Florea¹; ¹Trinity College Dublin, Ireland; ²Istituto Italiano di Tecnologia, Italy

This work describes the fabrication of complex 3D structures comprising of metallic Ag nanoparticles (NPs) which were manufactured inside prefabricated polymer structures by direct laser writing (DLW). In recent years, DLW has been established as a powerful tool for the fabrication of 3D micro-objects with features below 300 nm. This additive manufacturing technology is an adaptable, high-resolution process, where structure fabrication can be achieved

via multi-photon polymerisation or metal photo-reduction.^{1,2} More recently, this technique has been applied to the fabrication of stimuli-responsive hydrogel microstructures. Due to their size, these structures offer dramatically improved response times, where the inherently slow diffusion-controlled hydrogel expansion is countervailed. In this context, stimuli-controlled hydrogel micro-actuators show improved performance compared to their macro-scale counterparts and find applications across many fields including micro-robotics, microfluidics and biomedical devices.³ The micro-structures described herein were realised using a two-step approach. The first step comprised the fabrication of polymer structures via DLW by free-radical polymerisation. Following their fabrication, the polymer structures were immersed in a solution of Ag⁺ and a second DLW process was conducted to induce photoreduction of the Ag⁺ ions, thereby creating complex patterns of Ag particles inside the 3D polymer microstructures. TEM characterisation of microstructure cross-section was used to characterise the metal particle size and the distribution of particles. The size of the obtained particles was also compared to the voxel size obtained under the range of laser powers and scan speeds, in order to establish a protocol for the realisation of controlled metal particle size via DLW.

The same two-step approach was used to create microstructures showing photo-induced actuation. In this case, the microstructures were fabricated in the thermo-responsive polymer poly(*N*-isopropylacrylamide) (PNIPAAm). PNIPAAm is vastly employed for the realisation of thermo-actuators, owed to its thermo-responsive properties associated with a phase transition at the lower critical solution temperature (32 °C).⁴ Ag NP patterns were then written *in situ* inside the PNIPAAm structure, to act as photothermal converters. Laser irradiation of the Ag NPs patterns caused localised heating, inducing fast, controllable and reversible actuation of the microstructures. We further demonstrate how the actuation direction and speed can be tuned by controlling the Ag pattern and by the laser writing/scanning speed.

References

1. Nishiyama H., Umetsu K., Kimura K., Versatile Direct Laser Writing of Non-Photosensitive Materials using Multi-Photon Reduction-Based Assembly of Nanoparticles, *Sci. Rep.*, 2016, 9, 14310.
2. Blasco E., Müller J., Müller P., Trouillet V., Schön M., Scherer T., Barner-Kowollik C., Wegener M., Fabrication of Conductive 3D Gold-Containing Microstructures via Direct Laser Writing, *Adv. Mater.* 2016, 28, 3592.
3. Bogue R., Recent developments in MEMS sensors: a review of applications, markets and technologies, *Sensor Rev.* 2013, 33, 300.
4. Ashraf S., Park H., Park H., and Lee S., Snapshot of Phase Transition in Thermoresponsive Hydrogel PNIPAM: Role in Drug Delivery and Tissue Engineering, *Macromol. Res.*, 2016, 24, 4, 297

SESSION MF02.03: Laser-Induced Functional Surfaces for Energy Storage Devices
Session Chairs: Antje Baeumner and Jonathan Claussen
Wednesday Morning, April 24, 2024
Room 324, Level 3, Summit

9:15 AM *MF02.03.01

Skin-Interfaced Wearable Biosensors based on Laser-Engraved Graphene Wei Gao; California Institute of Technology, United States

Laser-engraved graphene (LEG) has been applied increasingly in wearable and flexible electronics over the past decade owing to its unique physical and chemical properties. It has shown great promise in energy controls, chemical and physical sensing, and telemedicine. In this talk, I will introduce our efforts in developing LEG-based wearable biosensors for non-invasive molecular analysis. Such wearables can autonomously access body fluids (e.g., human sweat) across the activities and continuously measure a broad spectrum of analytes including metabolites, nutrients, hormones, proteins, and drugs. Laser engraving enables the manufacturing of high-performance nanomaterials-based biosensors at large scale and low cost. The clinical value of our LEG-based wearable systems is evaluated through various human trials toward precision nutrition, stress/mental health assessment, and chronic disease management (e.g., systemic inflammation monitoring). These wearable technologies could open the door to a wide range of personalized monitoring, diagnostic, and therapeutic applications.

9:45 AM MF02.03.02

E-Textile Enabled by Femtosecond-Laser-Induced Graphene Formation on Kevlar Dongwook Yang¹, Han Ku Nam¹, Truong-Son Dinh Le¹, Seung-Woo Kim¹, Soongeun Kwon² and Young-Jin Kim¹; ¹Korea Advanced Institute of Science and Technology, Korea (the Republic of); ²Korea Institute of Machinery & Materials, Korea (the Republic of)

Personal wearable devices are anticipated to have a pivotal role in advanced healthcare, sports, firefighting, and military contexts in the near future. E-textiles are a promising solution, as they can combine electrical and informative functions, incorporating various sensors, actuators, and energy storage components while maintaining a high degree of flexibility and adaptability. However, existing methods for e-textile production involve weaving conductive fibers and installing functional elements onto conventional textiles, which can be time-consuming, cause gradual wear and tear of conductive yarns, and create challenges in integrating different functional units seamlessly. To meet the growing demand for flexible and timely manufacturing of personalized e-textiles, a simpler design and patterning strategy is essential.

Graphene, with its remarkable electrical conductivity and mechanical and chemical stability, is a promising material for e-textiles. Laser-induced graphene (LIG) synthesis, which uses laser scanning to transform carbon precursors into graphene, has gained attention. Textiles, particularly Kevlar, have emerged as valuable LIG precursor materials. Previous attempts using CO₂ lasers to convert Kevlar to LIG resulted in textile damage and limitations in resolution and conductivity. To achieve advanced e-textiles, it's essential to explore direct LIG patterning with improved resolution and minimal ablation, eliminating the need for fiber weaving and preserving high LIG conductivity without degradation concerns.

Textiles can be categorized into nonwoven, knit, and woven types, each with distinct physical properties due to their unique structures. Understanding these structures is crucial for creating high-performance e-textiles. Nonwoven textiles consist of randomly aligned yarns mechanically bonded or adhered together. They have high strength but low stretchability. Knit textiles, made from intersecting yarn loops, are inherently stretchable, resembling a mechanical spring. Woven textiles involve interlacing weft and warp yarns, creating special bending sensing networks when subjected to strain.

In this study, we introduce a straightforward method for creating multi-modal e-textiles. We achieve this by one-step, maskless patterning of LIG using near-infrared ultra-short femtosecond laser pulses on various Kevlar textiles, including nonwoven, knit, and woven varieties. Our approach directly transforms common textiles into e-textiles in a cost-effective and simple manner, without the need for fiber weaving, while preserving their flexibility, adaptability, and air-permeability with minimal ablation. This direct laser writing method is faster, more accessible, and allows for better carbon ratio control compared to conventional techniques like chemical vapor deposition (CVD) and thermal reduction. Nonwoven textiles, with their high mechanical strength and resistance to external strains, are suitable for applications unrelated to mechanical strain, such as energy storage devices and temperature sensors. The supercapacitor demonstrates a specific areal capacitance of 36.17 mF/cm², and the temperature sensor exhibits a thermal coefficient of

resistance (TCR) of -0.097% per degree Celsius within the temperature range of 5 to 100 degrees Celsius. The knit structure, known for its wide stretchability, is ideal for creating strain sensors to detect human motion, with a gauge factor (GF) reaching 117.9 within a 0-3% strain range. The woven structure, characterized by a lattice-like network, is suitable for fabricating a bending sensor for voice recognition, with a GF of 230 within a 0-0.5% strain range. These demonstrations underscore the capability of femtosecond pulse lasers for one-step, maskless patterning of high-performance LIG sensors and energy storage devices, paving the way for future wearable multi-modal e-textiles.

10:00 AM BREAK

10:30 AM *MF02.03.03

Graphene Synthesis, Laser Scribing and Applications in Supercapacitors [Richard B. Kaner](#); University of California, Los Angeles, United States

Graphene is the ultimate two-dimensional material consisting of a single layer of sp^2 hybridized carbon. A facile, inexpensive, solid-state method for generating, patterning and electronic tuning of laser converted graphene will be discussed. Briefly, graphite can be converted into graphene oxide (GO) sheets, which readily disperse in water, and can then be reduced by various methods. Due to its unique ability to be solution processed and patterned, GO can be laser reduced to graphene directly onto various substrates without masks, templates, post processing, or transfer techniques. This work paves the way for the fabrication of inexpensive electrochemical energy storage devices that combine the energy density of batteries and the power density of capacitors. This technique can create more than 100 micro-devices in a single run on virtually any substrate.

References:

1. D. Li, M.B. Muller, S. Gilje, R.B. Kaner and G.G. Wallace, "Processable aqueous dispersions of graphene nanosheets", *Nature Nanotechnology* **3**, 101-105 (2008).
2. M.F. El-Kady, V. Strong, S. Dubin and R.B. Kaner, "Laser printing of flexible graphene-based supercapacitors with ultrahigh power and energy densities", *Science* **335**, 1326-1330 (2012).
3. J. Wassei, R. Kaner, "Oh the places you'll go with graphene", *Acc. Chem. Res.*, **46**, 2244-2251 (2013).
4. M.F. El-Kady, M. Ihns, M. Li, J.Y. Hwang, M.F. Mousavi, L. Chaney, A.T. Lech and R.B. Kaner, "Engineering three-dimensional hybrid supercapacitors and microsupercapacitors for high-performance integrated energy storage", *Proc. Nat. Acad. Sci.*, **112**, 4233-4238 (2015).
5. M.F. El-Kady, Y. Shao, R.B. Kaner, "Graphene for batteries, supercapacitors and beyond", *Nature Review Materials*, **1**, 16033-16046 (2016).
6. Y. Shao, M.F. El-Kady, J. Sun, Y. Li, Q. Zhang, M. Zhu, H. Wang, B. Dunn and R.B. Kaner, "Design and mechanisms of asymmetric supercapacitors", *Chem. Rev.*, **118**, 9233-9280 (2018).

11:00 AM MF02.03.04

Pulsed Laser-Induced Dewetting for The Formation of Monometallic and Bimetallic Nanoparticle Arrays on Patterned Dimpled Tantalum Substrates and Their Electrochemical Properties [Yujun Shi](#), Stephanie N. Bonvicini, Annie Hoang and Vilola Birss; University of Calgary, Canada

Highly ordered metal nanoparticle (NP) arrays have attracted great research interest due to their unique electronic, optical and magnetic properties, leading to their diverse applications as model electrodes for electrocatalysis in fuel cells, sensors, in magnetic memory arrays and catalyst arrays for the growth of semiconductor nanowires. Here in this work, we report the use of pulsed laser-induced dewetting (PLiD) for the fabrication of metallic NP arrays, including monometallic (Au, Pt) and bimetallic Au-Pt, on a pre-patterned dimpled Ta substrate. In PLiD, the metal is quickly heated to above its melting point within a short duration of the incident laser irradiation and the molten film breaks up to form metal NPs to reduce the free energy of the film-substrate-ambient system. The highly ordered dimpled Ta substrate, formed by anodization of polycrystalline Ta in a $H_2SO_4 + HF$ solution, consists of a self-assembled array of inverted hemispherical caps, or nanodimples. It has been shown that highly ordered Au, Pt, and Au-Pt NP arrays can be produced on the dimpled Ta substrate with excellent monodispersity, long-range order and good dimple coverage. Compared with thermal dewetting, which is a solid-state dewetting method driven mainly by surface diffusion, PLiD is more efficient and better suited for metals of high melting point. The size of monometallic Au and Pt NPs can be controlled by the initial film thickness as the dewetting process is shown to follow the spinodal dewetting mechanism. For the bimetallic Au-Pt NPs, the total bilayer metallic film thickness plays a determining role. We have also shown that the metallic NPs formed by PLiD are more spherical in shape than those by thermal dewetting. The produced bimetallic Au-Pt NPs have a configuration of a Pt-rich core and Au-rich shell. Finally, characterization of the electrochemical properties of the Pt-rich core/Au-rich shell NPs reveals strong Pt-O bonding on the bimetallic NP surfaces. In addition, while Au is enriched on the bimetallic NP surfaces, a significant Pt content, ranging from 10% to close to 40%, is still present on the NP surfaces, which makes the produced Au-Pt NPs useful for bifunctional electrocatalytic reactions.

11:15 AM MF02.03.06

Laser-Induced Oxidation and Defect Formation of Thin-Film Materials for High-Throughput Materials Discovery [Drake R. Austin](#)^{1,2}, Brian Everhart², Michael Altvater^{1,2}, Mario Hofmann³, Rahul Rao² and Nicholas Glavin²; ¹UES Inc., United States; ²Air Force Research Laboratory, United States; ³National Taiwan University, Taiwan

The discovery of nanomaterials is an exceptionally slow process requiring many years of development in order to translate fundamental research to real capabilities. Consequently, a rapid materials discovery approach is needed to understand and tailor the properties of materials for specific applications. In this work, we present a high-throughput laser-processing methodology for producing and characterizing hundreds of modified regions on a single precursor sample. In particular, laser-induced oxidation and defect formation in transition metal dichalcogenides is presented, where the thermodynamics of the process is controlled by scanning a continuous-wave laser across the sample surface at varying scan speeds and intensities. Coupled with in-situ Raman and photoluminescence spectroscopy, this allows for the generation of laser-processing diagrams indicating the conditions necessary to produce varying stoichiometries, crystal structures, and defect densities. With additional ex-situ optical and electrical characterization, this method can be used to identify novel materials with properties of interest for a variety of applications including sensing, photocatalysis, and neuromorphic computing.

11:30 AM *MF02.03.07

Laser-Matter Coupling Mechanisms Governing Nanoscale Damage on Particulate-Contaminated Optical Surfaces [Manyalibo Matthews](#); Lawrence Livermore National Laboratory, United States

The recent fusion ignition breakthrough at Lawrence Livermore National Laboratory's National Ignition Facility has generated a renewed interest in improving high damage threshold optical materials. While decades of improvements in optical material processing for high power laser systems has led to unprecedented levels of laser damage tolerance, surface contamination on surfaces generated during laser operation, optic assembly or handling can still lead to damage initiation and local failure of the optic. Laser micromachining of optics for damage repair and laser-induced damage cross-contamination can also introduce nanoparticulate debris, compounding the issue further. In addition to local damage initiated at the site of the debris and leading to failure, *non-local* mechanisms associated with contamination have been recognized wherein nano- to microscale particles on the entrance surface of optics can lead to Fresnel diffraction of incident light and damage on the exit surface. The dynamics of the laser-particulate interaction involve high gradients of pressure,

This searchable program is up-to-date as of April 15th, 2024.

temperature and corresponding changes to thermodynamic material properties, plasma formation and aerodynamic effects that drive nanoscale morphological changes to the optical surface. In addition, the formed plasma can interact with the laser pulse while the melted material layer on the particle is ejected and thus be the source of secondary nanoscale contamination/surface pitting.

In this talk, I will present a study of the interaction of microscale, metallic and glass particles bound to optical surfaces with nanosecond and picosecond laser pulses at 1064- and 355-nm that results in nanoparticle ejection and nanoscale modification of the optical surfaces. Our in situ experimental platform allows direct measurements of the particle velocity, plasma formation, and the kinetics of the ejected nanoscale material. Large aperture damage tests were also performed to assess damage probabilities and probe the stochastic nature of particle-induced damage events. We use FDTD, Fourier beam propagation and ray tracing to understand the effect of particle shape and particle-induced nano-pitting on beam propagation. By varying the combination of particle and substrate materials, we are able to gain important insights to the governing mechanisms of laser-particle interactions which could lead to improvements in inertial confinement fusion laser system designs. This work was performed under contract DE-AC52-07NA27344.

SESSION MF02.04: Laser-Induced Graphene Processing Methods and Applications

Session Chairs: Antje Baeumner and Rahim Rahimi

Wednesday Afternoon, April 24, 2024

Room 324, Level 3, Summit

1:30 PM *MF02.04.01

The Discovery of Laser-Induced Graphene [James M. Tour](#); Rice University, United States

Described will be the initial discovery of laser-induced graphene in 2013 and early rapid developments over the next few years. This will be a historical outlook, noting the initial post docs, graduate, and undergraduate students, that laid the foundation for this remarkably simple method to patterned graphene surface and devices. The science of materials conversion to graphene will be discussed. The surfaces will be outlined, starting with polyimide, and then branching into nearly any carbon surface through simple adjustments to the laser. Early devices will be presented, including energy devices and sensors that set the groundwork for enormous advances in engineering designs around the world.

2:00 PM MF02.04.02

ReaxFF Simulations of Laser-Induced Graphene Formation [Aniruddh Vashisth](#); University of Washington, United States

Polymer films subjected to CO₂ infrared laser irradiation in ambient conditions undergo a transformation, resulting in the formation of porous graphene known as laser-induced graphene (LIG). In this presentation, we will discuss finding from reactive molecular dynamics simulations (ReaxFF) to investigate LIG formation from five different polymers structures. Our research revealed that the initial molecular structure of the parent polymer significantly influences the resulting graphitic structure. During the early stages of LIG formation, the polymer transforms into an amorphous structure, releasing CO, and subsequently evolves into an ordered graphitic structure, liberating H₂ steadily. The resulting LIG exhibits out-of-plane undulations and bends due to the presence of numerous 5- and 7-member carbon rings throughout the structure. Our simulated molecular structure aligns well with recent experimental observations in the literature. Moreover, we observed that LIG yield is higher in inert conditions compared to oxygen-rich environments. Specifically, LIG derived from polybenzimidazole demonstrated the highest surface area and yield among the five polymers studied. These findings enhance our understanding of LIG formation mechanisms, offering valuable insights for various bulk LIG applications such as sensors, electrocatalysts, microfluidics, and precise polymer welding through targeted heating.

2:15 PM MF02.04.03

Exploring The Potential of Laser-Induced Graphene (LIG) from Polyfurfuryl Alcohol (PFA) for High-Performance Electrodes in Batteries and Supercapacitors [Michael A. Pope](#); University of Waterloo, Canada

Infrared (IR) lasers, such as the carbon dioxide laser popularly used by hobbyists and various industries for precision cutting and marking/engraving, are increasingly employed in the conversion of carbonaceous precursors into a mesoporous graphene-like carbon material, known as laser-induced graphene (LIG). In this presentation, I will delve into my research group's recent explorations into the potentials and limitations of utilizing this technique to create electrodes for batteries and supercapacitors. Our focus centers on the carbon precursor polyfurfuryl alcohol (PFA), a common component for crafting glassy carbon electrodes, derived from waste biomass. By amalgamating PFA with IR transparent salts, we aim to extend the laser's penetration depth, thus producing electrodes with an enhanced surface area or greater areal mass loading. Our findings reveal that typical salts, such as sodium chloride or sodium sulfate, not only achieve these objectives but also serve a dual role as a templating and doping agent, markedly improving the areal capacitance of symmetric supercapacitors. Furthermore, by incorporating this system with metal salts or catalyst precursors, we engineer unique compositions and nanostructures exhibiting significant electrochemical activity towards the oxygen reduction reaction. Our studies show that the process of direct laser writing on air-cathodes is a superior method to develop high-performance zinc-air batteries.

2:30 PM BREAK

3:30 PM *MF02.04.04

High-Performing Electrochemical Sensors enabled by Electrosun Laser-Induced Carbon Nanofibers [Nongnoot Wongkaew](#); University of Regensburg, Germany

Since its emergence, laser-induced carbon nanomaterial technology has revolutionized the fabrication of flexible electrodes applicable in several areas, which includes the development of high-performing electrochemical sensors at low cost. A wide array of substrates and composites have been successfully converted into carbon nanomaterials as well as their associated functional hybrids. Electrospun nanofibers as a substrate have caught our attention owing to their 3D-fibrous structure featuring high porosity and huge surface area-to-volume ratio, foreseeing the enhanced detection sensitivity when they are employed as electrochemical transducers. Moreover, doping the polymer solution prior to spinning allows tuning of properties and convenient modifications of fiber precursor, enabling facile fabrication of electrochemical transducers with favorable functionalities. In addition, their manufacturing process can be effectively controlled via spinning parameters, and easily scaled up at relatively low cost. However, when electrospun nanofibers are subjected to laser-processing their fluffiness and delicate structure pose significant challenges, which required thorough investigations to enable laser-induced carbon nanofibers (LCNFs) with desired properties. This talk will first highlight the parameters of the electrospinning and lasing processes, which critically govern the morphological and electroanalytical properties of the LCNF electrode. Afterwards, the talk will focus on how to implement the strategy to realize high performing enzyme-less electrochemical sensors. Here, the incorporation of metal salt precursor into the electrospun nanofibers

allows for further *in situ* formation of electronanocatalysts embedded with the LCNFs. Through electrospinning, the metal precursor can be uniformly distributed within the nanofibers, subsequently promoting homogeneous dispersion of the nanocatalysts within the LCNFs. As shown in an exemplary case, the immense electroactive surface area of LCNFs with highly dispersed Ni nanoparticles permitted the detection of glucose in sub μM range, which considerably outstands other reports where sophisticated procedure and costly instruments were required. Furthermore, the strategy for integration of LCNFs into miniaturized devices will be illustrated. Herein, the devices contained 3D-porous electrochemical transducers with pore sizes of ca. 5-10 μm (an order of magnitude smaller than the pores in comparable graphene foam) and unsurprisingly offered an impressive limit of detection for dopamine sensing (down to pM range). Finally, the talk will demonstrate LCNFs as part of a lateral flow assay (LFA). Here, 25-fold enhancement in detection sensitivity of a common redox marker could be obtained when compared to the LFA integrated with a flat screen-printed electrode. Overall, the investigations have proven that LCNFs are highly promising for the development of point-of-care testing where high analytical performance can be achieved together with high affordability.

4:00 PM MF02.04.05

Selective and Biocompatible Neural Probes with a Fluorous Sensing Phase Farbod Amirghasemi, Abdulrahman Al-Shami and Maral Mousavi; University of Southern California, United States

Laser engraving is becoming a widely popular method for producing porous graphitic carbon structures, known as Laser-Induced Graphene (LIG), for sensing applications. LIGs are produced by ablating carbon-rich polymers (mostly polyimide) using a laser beam, which creates local photothermal reactions converting sp^2 carbon atom hybridization into 3D porous graphitic structure. This method is a maskless, scalable, reproducible, cost-effective, and fast approach to producing graphene layers with high electrical conductivity and electrocatalytic nature, which makes LIGs superior over graphene created using conventional methods such as chemical vapor deposition (CVD) and wet chemistry.

Here, we developed the first use of a fluorous-phase potentiometric sensor for the measurement of acetylcholine (ACh), a vital neurotransmitter in brain activity. Fluorous compounds (molecules with high content of fluorine atoms) are extremely non-polar and non-polarizable to the extent that they are not miscible with both aliphatic compounds such as hexanes, and with water and other hydrophilic compounds. Therefore, fluorinated compounds are both hydrophobic and lipophobic. Since, the living systems are made of water and lipophilic compounds, makes fluorocarbons bio-orthogonal and nontoxic, meaning that they do not interfere with biology. Biocompatibility of fluorocarbons has resulted in many biomedical applications such as artificial blood, bio-orthogonal imaging contrast agents, and delivery and imaging vehicles. Fluorocarbons are used as coatings in biomedical devices to lower sensor biofouling and cell adhesion to the device. Exceptional selectivities that far outperform a conventional lipophilic sensing membrane were also reported for ionophore-doped fluorous sensing membranes. Such gain in selectivity is attributed to non-coordinating and poorly solvating properties of the fluorous-phase. The high selectivity, biocompatibility, and potentially exceptional resilience to biofouling make fluorous-phase sensors ideal for neural applications. Neurotransmitters present in nanomolar concentrations are a complex matrix (requiring high selectivity). Moreover, studying the dynamics of change and the correlation of such changes to behavior and stimulation is desired (requiring long-term in-vivo studies through implantable sensors).

We showed that selectivity gain in the fluorous phase resulted in more than an order of magnitude improvement in the limit of detection (LOD). Moreover, to move towards in-vivo application of the fluorous-phase ACh sensor (where probe size and flexibility are critical), we have developed the first compact and flexible solid-contact fluorous-phase potentiometric sensor. We fabricated the electrodes using laser-induced carbonization of flexible polyimide films.

Utilizing the laser engraving to fabricate neuroprostheses could enable more efficient fabrication approach toward neural probe by eliminating the intricate and expensive microfabrication approach. We are utilizing polyimide due to providing a pinhole-free, high flexibility, high mechanical strength, and biocompatible platform to construct implantable ACh-detecting sensors consisting of a working electrode (containing an acetylcholine organic sensing membrane) and a reference electrode (containing a reference membrane). The electrical potential (emf or electromotive force) between the ACh sensor and reference electrode correlates to the activity of ACh in the biofluid, according to the Nernst Equation ($E = E^\circ + (RT/nF) \log(a_{\text{ACh}})$), where E° shows the standard potential, R the universal gas constant, T temperature, F the Faraday constant, n the charge of the ion, and a_{ACh} the activity of ACh. A theoretical slope of 59.2 mV/decade is expected at room temperature and is defined as the Nernstian slope. The fluorous-phase solid-contact LIG ion exchanger electrode showed a near Nernstian slope of 54.9 ± 0.8 and a 42 nM limit of detection.

4:15 PM *MF02.04.06

Laser-Induced Graphene for Electrochemical Sensing: From Process Development to Real-World Applications Cicero C. Pola, Raquel Soares, Zachary T. Johnson, Gustavo Milião, Nathan Jared, Robert Hjort, Jonathan Claussen and Carmen L. Gomes; Iowa State University, United States

Graphene-based electrodes offers a promising solution for developing effective electrochemical sensors due to their high surface area ($2630 \text{ m}^2 \text{ g}^{-1}$), mechanical strength (Young's Modulus $\sim 1100 \text{ GPa}$), electrical conductivity ($\sim 64 \text{ mS cm}^{-1}$), chemical stability, biocompatibility, and tunable properties. Among graphene-based electrodes, laser-induced graphene (LIG) has emerged as a cost-effective, scalable alternative by directly converting sp^2 carbon found in carbon-rich substrates, such as polyimide into conductive sp^2 -hybridized carbon found in graphene through a laser scribing technique. We have demonstrated that the surface area and wettability of the LIG can be tuned to greatly improve the sensitivity of electrochemical enzymatic biosensors (detection limits down to the picomolar range) and reduce the water layer buildup between the ion-selective membrane and the electrode, which improves the accuracy of the sensor readings and its longevity. We have systematically characterized LIG formation and how the quality of graphene can be improved by varying the laser power, focus, DPI (dots per inch), and the number of repeat runs. We demonstrated that initial defocused lasing followed by focused lasing improves the quality of graphene produced, the surface wettability, and the resulting electrochemical sensors. The LIG electrodes have been used in a wide variety of electrochemical sensing applications including in food safety, environmental (soil and water) monitoring, wearable health sensors, and even for urinary potassium and ammonium, and salivary lactate and potassium sensing. All these electrochemical sensors have been validated in real-world samples and demonstrated to have limits of detection and linear sensing ranges that are relevant to their sensing applications. Additionally, we have demonstrated the ability to fabricate LIG electrodes using biodegradable substrates (i.e.; paper and cork) as a more sustainable approach to electrochemical sensing. The responses of the LIG-based ion-selective electrodes from cork and paper exhibited similarities to those made from the standard material, polyimide. In these studies, we show how high-quality, sensitive LIG electrodes can be systematically fabricated and integrated into electrochemical analytical devices for point-of-service and in-field applications.

5:00 PM MF02.05.01

Laser Reactive Sintering of Complex Oxides Jeldrik Schulte, [Martin A. Schroer](#) and Markus Winterer; Universität Duisburg-Essen, Germany

UV laser sintering allows densification and microstructural transformation of granular systems. The high photon energy of an UV laser leads to resonant heating if the energy is higher than the band gap of the irradiated material. Due to this effect, the heat load is strongly localized, and for nanostructured materials temperatures up to 2000°C and extremely high heating rates are reached at low laser powers [1]. Therefore, UV laser sintering is a versatile tool for materials engineering, as it enables reactive sintering of binary metal oxides to generate complex oxides with short process times. It is also feasible for processing (printed) electronic components with structures in the micrometer range.

The complex oxide CuAlO₂ is a transparent conductive oxide (TCO) with p-type conductivity [2]. TCOs are widely used in photovoltaics and optoelectronic devices like flat panel displays or solid-state lighting. However, the performance of p-type TCOs is still significantly lower compared to n-type TCOs. This impedes the production of high-performance p-n junctions, needed as key components for active electronic devices. Complex oxides with delafossite structure, like CuAlO₂, have shown great potential to overcome this problem [3].

The production of the CuAlO₂ delafossite is a challenge, because of the complexity of the binary phase diagram. In this contribution, we will present the generation of CuAlO₂ by reactive UV laser sintering of copper and aluminum nanoparticles and their characterization, including μ XRD diffraction.

[1] Sandmann, A., Notthoff, C., & Winterer, M. (2013). "Continuous wave ultraviolet-laser sintering of ZnO and TiO₂ nanoparticle thin films at low laser powers", *J. Appl. Phys.*, 113(4)

[2] Kawazoe, Hiroshi, et al. "P-type electrical conduction in transparent thin films of CuAlO₂.", *Nature*, 389,6654 (1997): 939-942.

[3] Zhang, K. H., Xi, K., Blamire, M. G., & Egdell, R. G. (2016). "P-type transparent conducting oxides." *J. Condens. Matter Phys.*, 28(38), 383002.

Acknowledgements:

Funded by the Deutsche Forschungsgemeinschaft (DFG, German Research Foundation): SCHR 1753/1 & WI 981/19-1 (project nr: 531185908), INST 20876/395-1 FUGG

5:00 PM MF02.05.02

Pyrolytic Jetting of Free-Standing Laser-Induced Graphene Fiber for Cost-Effective Supercapacitor [Hyunkoo Lee](#)^{1,2}, Dongwoo Kim³, Kounghun Min^{1,2}, Ji Hwan Lim^{1,2}, Sukjoon Hong^{1,2} and Habeom Lee³; ¹Hanyang University, Korea (the Republic of); ²BK21 Four Erica-Ace Center, Korea (the Republic of); ³Pusan National University, Korea (the Republic of)

In recent times, the significance of energy storage has surged due to the expanding use of renewable energy for achieving carbon neutrality. Efficient energy storage is crucial for stabilizing power grids amid the intermittent energy production from sources like solar and wind, as well as for meeting the escalating demand for reliable energy storage. Simultaneously, the rapid and widespread adoption of electric vehicles has highlighted the significance of energy storage solutions. As conventional combustion engines give way to electric-powered vehicles, an escalating demand emerges for energy storage systems that embody safety, reliability, and cost-efficiency while delivering requisite power. These advancements underscore the growing significance of energy storage in shaping our energy landscape and ensuring future energy security. As our society steadily progresses towards a sustainable, low-carbon trajectory, the need for versatile energy storage solutions is accentuated.

Supercapacitors offer distinct advantages, including higher power density, extended cycle life, and simpler material composition compared to batteries, making them a prominent energy storage solution. Graphene, particularly in the form of Laser-Induced Graphene (LIG), has emerged as a standout material for supercapacitors due to its rapid charging/discharging capabilities and extensive specific surface area. LIG's unique porous morphology holds great promise for various applications and has the potential to enhance energy storage performance by maximizing surface-area-to-volume ratios. Considering an environmentally conscious perspective, it becomes imperative to minimize energy consumption and material utilization during the fabrication process, while simultaneously maximizing storage capacity. A recent study in laser technology, known as pyrolytic jetting, has come to light under precise laser conditions (125 J/m). This innovation yields an incredibly porous, freestanding fiber-shaped LIG, demonstrating potential advantages for energy storage applications. In contrast to electrodes affixed to specific substrates, these fiber-shaped electrodes present significant merits as energy devices for diverse applications, notably through their remarkable characteristic. Despite its vast potential, research on its practical application in energy devices has been relatively limited.

Our study on laser pyrolytic jetting presents an efficient method to produce highly porous, free-standing graphene fibers from polyimide film. This process involves precise scanning of a continuous-wave laser, resulting in significant advantages over conventional LIG techniques. In this follow-up investigation, we demonstrate the superior potential of the laser pyrolytic jetting process for energy device applications, offering remarkable energy and material savings. Notably, the pyrolytic jetting process significantly increases the volume of the pyrolyzed product compared to conventional LIG, leading to an expanded surface area capable of storing a greater amount of electric charges. Raman measurement verifies the comparable attributes of the exfoliated material obtained through pyrolytic jetting and traditional LIG, making it exceptionally suitable for supercapacitor applications. Consequently, supercapacitors produced via pyrolytic jetting demonstrate a notable increase in capacitance, indicating an improvement of over 4.7 times compared to conventional LIG. This underscores the potential of pyrolytic jetting as a cost-effective fabrication technique for carbon-based energy devices.

5:00 PM MF02.05.03

Direct-Laser Scribing of Electrodes Using Metal-Organic Frameworks for Electrochemical Detection [Beatrice De Chiara](#), Fulvia Del Duca, Mian Zahid Hussain and Bernhard Wolfrum; Technical University of Munich, Germany

Electrochemical sensors have gained widespread recognition and utilization across diverse domains, encompassing applications such as clinical diagnosis, biochemical detection, and environmental monitoring. In the pursuit of enhancing these sensors, metal-organic frameworks (MOFs) have emerged as highly promising material candidates. MOFs are known for their porous structures, which exhibit substantial surface areas, remarkable stability, and a unique capacity for functionalization.

Here, we aim to integrate MOF structures into laser-induced graphitic (LIG) electrodes to improve the performance of electrochemical sensing devices. LIG electrodes present certain advantages over classical noble metal electrodes, such as reduced cost and ease of fabrication. We investigate the disparities between LIG sensors and LIG-MOF sensors, both of which are fabricated using direct laser scribing, a fabrication technique with the remarkable capability to convert non-conductive materials into active electrode materials, all the while generating desired patterns directly onto polymer substrates. Central to this investigation is the conversion of MOFs into patterned derived carbon utilizing an ultraviolet (UV) laser system. The process entails several steps. Initially, a solution containing MOFs is drop-cast onto a polyimide (PI) foil substrate. Once the MOFs composite is deposited onto the substrate, the

electrode is directly patterned with the UV laser. Importantly, the MOFs composites are confined to the electrode area, while the feedline and contact pad exclusively consist of LIG. For the passivation of the structures, Parylene C (poly(p-xylylene)), a flexible dielectric polymer, is chosen due to its good insulation properties and conformability. A thin film of Parylene C, approximately 5 micrometers thick, is deposited via chemical vapor deposition. Subsequently, the electrode area and contact pad are precisely opened using the laser. The characterization of the resultant sensors was conducted using scanning electron microscopy, Raman spectroscopy, impedance spectroscopy, cyclic voltammetry, and differential pulse voltammetry. These characterizations revealed the emergence of a highly porous carbonaceous material, with low-impedance observed in the case of the LIG-MOF sensors. This approach not only expands our understanding of MOF integration into electrochemical sensing but also underscores the potential for applications where high charge injection capabilities and low impedance at an electrode/electrolyte interface are required.

5:00 PM MF02.05.04

Electrochemical CO₂ Reduction to HCOOH Catalyzed by Ag_n(NO₃)_{n+1} Clusters prepared by Laser Ablation at The Air-Liquid Interface Tepei Nishi, Shunsuke Sato and Takeshi Morikawa; Toyota Central R&D Labs., Inc., Japan

Nanomaterials generated via laser ablation in liquid have been developed because of the capability to generate nanoparticles without chemical reagents. However, it is difficult to obtain monodispersed and small (< 2 nm) nanoparticles. We have reported laser ablation at the air-liquid interface to obtain monodispersed and small (ca. 5 nm) nanoparticles [1]. Here, we report laser ablation at the air-liquid interface using colloidal nanoparticles as a target to obtain smaller clusters [2]. Colloidal target was prepared by laser ablation of Ag powder precipitated on the bottom of the flask. Pulsed laser was irradiated through the bottom of the flask. After laser irradiation for 60 min, Ag nanoparticles stably dispersed in pure water was obtained. This colloid exhibited a large absorption peak at 400 nm. This colloidal solution was agitated in a measuring flask during laser ablation at the air-liquid interface. After laser ablation at the air-liquid interface, we obtained colorless and transparent solution, indicating the drastic size reduction. UV-Vis absorption spectra exhibited peaks in UV region. It indicated small cluster formation. The size was assessed by electro-spray ionization-mass spectrometry. It revealed Ag_n(NO₃)_{n+1} cluster generation. To investigate the electrocatalytic activity, Ag_n(NO₃)_{n+1} clusters were deposited on carbon paper substrate. Electrocatalytic activity for CO₂ reduction was assessed in CO₂ saturated aqueous 0.1 M KHCO₃ solution at an applied potential of -1.2 V vs RHE with Ag/AgCl reference electrode and Pt wire counter electrode. As well-known, micro and nano-sized Ag catalyst as comparisons generated CO via electrochemical CO₂ reduction. In contrast, Ag_n(NO₃)_{n+1} clusters generated HCOOH with a Faraday efficiency of 33%. The results indicated a drastic change in the selectivity induced by laser ablation at the air-liquid interface. Because the unique selectivity, carbon source of HCOOH was determined by isotope tracer analyses using ¹³CO₂ and KH¹³CO₃ together with ion chromatography-mass spectrometry. Because only H¹³COO⁻ peak was confirmed, it can be concluded that HCOOH was generated from CO₂. Both the catalyst size and modification by NO₃ potentially explain the results.

[1] T. Nishi et al., *J. Nanopart. Res.*, 2013, 15, 1569.

[2] T. Nishi., *Jpn. J. Appl. Phys.*, 2015, 5, 095002.

[3] T. Nishi., *Chem. Lett.*, 2021, 50, 1941-1944.

5:00 PM MF02.05.05

Quick and Reversible Superwettability Switching of 3D Graphene Foams via Solvent-Exclusive Microwave Arcs Soomin Cheon, Won-Jang Cho, Gi-Ra Yi, Byoungwoo Kang and Seung Soo Oh; Pohang University of Science and Technology, Korea (the Republic of)

For highly active electron transfer and ion diffusion, electrically and thermally conductive 3D graphene foams (3D GFs) heavily rely on precise control of their surface wettability with respect to different polarities of fluids. For their practical applications, either hydrophilic or hydrophobic 3D GFs are prepared in advance; even though there have been many different ways of controlling their surface wettability, such as solvent treatment, heteroatom doping, ultraviolet or laser irradiation, and plasma treatment, they are time-consuming and even high-cost processes, limiting them to be only applicable for 2D graphene or powders. Here, we present ultra-simple and rapid superwettability switching of 3D GFs in a reversible and reproducible manner, as mediated by solvent-exclusive microwave arcs. As the 3D GFs are pre-coated with vaporized solvents exclusively, short microwave radiation (≤10 s) leads to plasma hotspot-mediated production of polar or nonpolar radicals. Upon immediate radical chemisorption, the 3D surfaces become either superhydrophobic (water contact angle = ~170°) or superhydrophilic (~0°), and interestingly, the dramatic wettability transition can be repeated many times due to the facile exchange between previously chemisorbed and newly introduced radicals. Our microwave-mediated, quick and reversible wettability switching would be applicable for many different applications (e.g., energy storage, sensing, microfluidic transportation, and water-oil separation). Importantly, our superwettability switching is applicable for all kinds of carbon-based nanomaterials, including 2D graphene and carbon nanotubes.

5:00 PM MF02.05.06

Ultra-Thin Ultra-Light Planar Diffractive Lens with Laser-Induced Graphene (LIG) Younggeun Lee¹, Dongwook Yang¹, Hyeokin Kang^{1,2}, Han Ku Nam¹, Hyogeun Han¹, Seunghwan Kim¹, Joohyung Lee², Seung-Woo Kim¹ and Young-Jin Kim¹; ¹Korea Advanced Institute of Science and Technology, Korea (the Republic of); ²Seoul National University of Science and Technology, Korea (the Republic of)

By subjecting carbon-containing materials to a straightforward laser irradiation process, we can selectively transform them into laser-induced graphene(LIG), a material renowned for its outstanding electrical properties. This laser-induced graphene can be easily generated from carbon polymers like polyimide or even natural substances such as wood and leaves.

Polyimide, a leading precursor compound for Laser-Induced Graphene (LIG), is widely used in electronic devices for its remarkable chemical resistance and durability, particularly in circuits and displays. However, its application as an optical material, capable of effectively transmitting light, has been constrained by its selective performance in the visible light spectrum. To overcome this limitation, researchers have developed colorless polyimide(CPI), providing a solid foundation for polyimide to function as an optical material with exceptional performance in the visible light range.

We had converted this colorless polyimide(CPI) into laser-induced graphene(LIG) through femtosecond laser irradiation and embarked on research to create diffractive optical devices using it. The porous structure formed by the release of carbon dioxide and various gases during the laser-induced graphene(LIG) generation process leads to diffuse light reflection, resulting in significantly reduced transmittance. This unique property has enabled us to develop binary diffraction elements capable of blocking light beams through laser-induced graphene(LIG) structures. These elements are remarkably thin and lightweight compared to conventional refractive components, making them suitable for various optical applications crucial in modern society. With these innovative devices, we aim to introduce applications spanning a wide range of fields, from aerospace, which demands ultra-light lenses, to the bio-industry, where ultra-compact lenses are essential.

5:00 PM MF02.05.07

Arbitrary Three-Dimensional Alignment of Liquid Crystal Molecules via Laser Direct Writing Zexu Zhang¹, Wei Xiong^{1,2}, Chunsan Deng¹, Xuhao Fan¹, Mingduo Zhang¹, Xinger Wang¹, Fayu Chen¹, Yining Zhou¹ and Hui Gao^{1,2}; ¹Huazhong University of Science and Technology, China; ²Optics

Valley Laboratory, China

The precise construction of hierarchical ordered structures using nanomaterials as fundamental building blocks leads to enhanced optical, electromagnetic, and mechanical properties in functional devices. As one of the most promising functional nanomaterials, the three-dimensional (3D) assembly of liquid crystal (LC) molecules is crucial for the development of next-generation optical field modulation and stimulus response devices due to its distinct anisotropy and tunability. Spatial alignment of LC materials can be achieved through either contact or non-contact alignment methods. The contact alignment method can achieve orientation alignment of LC molecules through surface induced effects, shear forces, etc., but it is usually constrained by a low spatial resolution, material contamination and the lack of design freedom for processing. The non-contact alignment method can offer superior resolution and eliminate the contamination issue by aligning the LC molecules using electromagnetic fields. Nevertheless, it generally requires complex field-assisted (e.g. electric field, magnetic field) equipment and lacks the capacity for achieving arbitrary 3D alignment. Despite significant progress in LC alignment in recent years, a persistent challenge remains: the absence of a high-precision, non-contact, and straightforward method for achieving arbitrary 3D alignment of LC molecules.

To address the above issue, we propose a novel approach that enables us to align the 3D director of LC via two photon polymerization-direct laser writing (TPP-DLW). TPP-DLW is a non-contact method that utilizes femtosecond laser pulses to precisely align LC without any field-assisted devices. TPP-DLW's true 3D manufacturing capability facilitates the realization of arbitrary 3D spatial alignment. Its subwavelength resolution allows for the precise 3D assembly of LC with an accuracy of up to 140 nm. This method combines the advantages of both contact and non-contact alignment methods, achieving straightforward, high-precision, and high degree of design freedom 3D alignment of LC molecules. Finally, we have demonstrated the potential of this method by fabricating Fresnel zone plate devices for object imaging with polarization selection and spectral separation functions. We expect that this TPP-DLW alignment strategy will significantly contribute to the advancement of LC based optical processing, communication, and holographic displays and micro-robots, enabling extensive freedom and multifunctional capabilities.

5:00 PM MF02.05.08

Direct Patterning of Tungsten Oxide Nanoparticles via Laser Ablation Process for a Digital Informative Display [Jinhyeong Kwon](#)¹ and Junyeob Yeo²; ¹Korea Institute of Industrial Technology, Korea (the Republic of); ²Kyungpook National University, Korea (the Republic of)

This study focuses on the fabrication and characterization of a tungsten trioxide (WO₃) electrochromic device (ECD) *via* laser ablation. The fabrication process involves the deposition of a WO₃ thin film on a fluorine-doped tin oxide (FTO) substrate using spin coating and selectively removing the WO₃ and FTO layers through laser ablation. The resulting patterned WO₃ is assembled on the substrate with a gel-type electrolyte and a cover FTO substrate to construct the ECD. The fabricated ECD exhibits considerable color change and effectively blocks infrared wavelengths. X-ray diffraction analysis confirms the complete removal of the WO₃ and FTO layers during laser ablation. UV/VIS spectrometry and X-ray photoelectron spectroscopy analysis demonstrate the difference in transmittance and the changes in the tungsten ion oxidation state for the WO₃ ECD. The fabricated WO₃ ECD can be utilized for informative display applications, generating binary barcodes. In summary, this study presents the fabrication of a tunable WO₃ ECD with potential applications in display devices.

5:00 PM MF02.05.09

Laser-Induced Graphitic Electrodes as Rapid Fabrication of Thin-Film Implantable Multielectrode Arrays [Fulvia Del Duca](#), Lukas Hiendlmeier, George Al Boustani, Beatrice De Chiara, Mian Zahid Hussain and Bernhard Wolfrum; Technical University of Munich, Germany

In the field of implantable electronics, thin-film electrodes – usually made of polymeric substrates – have attracted attention for their flexibility and versatility. Common insulating polymer layers include parylene-C and polyimide. While thin-film technology offers many attractive advantages – such as increased compliance and minimal footprint – it also brings new challenges. Firstly, their patterning or selective removal requires a series of additional lithographic steps. Secondly, a major hindering factor is the stability of the polymer-metal adhesion under mechanically-challenging conditions within electrolyte environments.

Direct laser scribing of organic substrates has recently emerged as a rapid and straightforward method for patterning conductive tracks directly from insulating layers. Laser-induced graphite (LIG) electrodes are fabricated in a one-step process. A laser beam irradiation of suitable organic precursors thermally converts the insulating material into a multilayered graphite 3D structure with various degrees of porosity. Typically, CO₂ infrared lasers are employed for LIG fabrication over organic substrates with thickness down to 25 μm, but more commonly in the range of hundreds of μm. While LIG structures offer advantages such as direct fabrication, large charge storage for supercapacitor applications, and high effective surface area for biosensing, their higher feedline resistance compared to metals hinders their usability and advancement. Vomero et al. [*Sci. Rep.* (2018) 8:14749] fabricated parylene-based LIG electrodes over a 25 μm-thick metal foil, showing the possibility of employing LIG sensors in combination with metal feedlines.

Typically, the conductive layers used in microelectrode arrays (MEAs) and flexible electronics are hundreds of μm thin. Here, we present a method to fabricate graphitic carbon electrodes by direct laser scribing of insulating polymers over such thin metal layers, effectively opening the electrode sites with graphitic carbon without damaging the underlying metal tracks. The MEAs are fabricated by depositing an insulating layer of 5 μm parylene-C over a detachable substrate, then sputtering and patterning a conductive layer of 100 nm gold, and insulating again with 5 μm parylene-C. Then, a UV (355 nm) nanosecond pulsed laser is used to carbonize the parylene-C locally over the gold to open the electrode sites and contact pads. The 10-μm-thin electrodes are then released from the substrate. Therefore, no dry etching and hard mask patterning are required to open the electrode insulation, and the conductive material is directly generated from the insulating layer.

First, we test the fabricated electrodes by measuring the sheet resistance of the generated graphitic carbon material over gold, where we select the optimal laser parameters for best performance. Then, we test the electrodes in phosphate-buffered saline to measure the electrochemical impedance and the charge storage capacity, as well as the charge injection capabilities for neural stimulation applications. The mechanical stability of the adhesion between graphitic carbon and gold is also tested both in dry and aqueous environments, relevant to the contact pads and electrode sites, respectively. We also investigated the miniaturization limits of the fabricated electrode sites by laser scribing in different writing modes and with different line writing densities. In summary, we propose a new and rapid method for electrode fabrication applicable to thin-film and polymer-based electronics.

5:00 PM MF02.05.10

In-Field Monitoring of Plant Stress with a Low-Cost Electrochemical Sensor [Sina Khazaei Nejad](#) and Maral Mousavi; University of Southern California, United States

Environmental challenges, like drought, severe temperatures, pests, and diseases, have adverse effects on the growth, development, and yield of plants. Salicylic Acid (SA) serves as a plant hormone responsible for signaling in response to stress, and it plays a crucial role in plants' defense mechanisms against certain types of pathogens. Elevated levels of salicylic acid in plants serve as an indicator of stress. It is essential to monitor and assess plant stress to ensure the well-being and productivity of crops, as well as a steady food supply. The on-site measurement of salicylic acid aids in the early detection and diagnosis of plant stress, enabling prompt actions to reduce harm and sustain crop productivity.

Point-of-care diagnostic technologies have emerged as an advancement in medical analysis and monitoring. These technologies offer a decentralized and

cost-effective approach, making accessibility to crucial diagnostic services easier. As a rapid first line of diagnosis, they serve as a frontline defense.

In this work, we introduce an affordable electrochemical tool designed for the purpose of tracking plant stress by detecting Salicylic Acid (SA). The device is equipped with wireless connectivity, allowing it to transmit data to a smartphone via the Bluetooth Low Energy (BLE) protocol.

Methods

Electrochemical techniques have been used to monitor SA levels. We've utilized laser-induced graphene (LiG) electrodes, a low-cost and scalable 3D porous carbon material created through laser-based polymer-to-graphene conversion, which shows promise for electrochemical sensors.

We've developed an affordable, portable potentiostat to continuously monitor salicylic acid (SA) levels in plants, with the collected data being transmitted to a nearby smartphone via Bluetooth Low Energy technology.

Results

The ability to efficiently scale the production of LiG electrodes offers a cost-effective method for creating these systems. Examination of these electrodes reveals the formation of a graphene layer on the PI film. Moreover, by optimizing laser machine parameters, we have achieved electrodes that not only consistently reproduce but also exhibit impressive electrochemical capabilities.

Square-wave voltammetry measurements were conducted using the LiG sensors, with varying concentrations of SA in buffer. The peak current value demonstrates a linear relationship with the SA concentration, with a sensitivity of 130.54 $\mu\text{A}/\text{mM}$, and linearity range between 5 μM and 150 μM . The limit of detection is 1.75 μM .

Conclusion

An affordable device based on laser-induced graphene (LiG) for monitoring plant stress is created, and it is seamlessly integrated with a portable potentiostat. This device enables the detection of salicylic acid, a phytohormone vital for plant stress signaling. The detection is achieved using a 3-electrode LiG design, and our system has successfully demonstrated this capability.

5:00 PM MF02.05.11

A Nafion-Modified Laser-Induced Graphene Sensor for Spontaneous Monitoring of Caffeine and Vanillin Haozheng Ma, Stephanie Bartholomew, Jay Yoo, Caden Pak, Abdulrahman Al-Shami, Mona A. Mohamed and Maral Mousavi; University of Southern California, United States

Introduction: Coffee is a globally consumed beverage, widely known for its main active ingredient, caffeine. Although a daily caffeine limit of 400 mg is considered safe, exceeding this limit can lead to adverse effects such as depression, anxiety, irritability, and other health issues. Another frequently used compound in the food and beverage industry is vanillin, which provides a characteristic sweet and creamy aroma. Like caffeine, excessive consumption of vanillin can also lead to adverse effects like headaches and gastrointestinal disturbances. Despite the widespread consumption of caffeine and vanillin, accurately determining their content in different foods and beverages is challenging. This complicates the monitoring of daily intake, making it difficult to manage potential health risks effectively. Laser-Induced Graphene (LiG) is a specialized form of 3D porous carbon nanomaterial with unique properties. It is created through a process called direct laser writing, which is performed on certain polymer materials in ambient conditions. The technique is both simple and quick, making LiG an attractive material for a variety of applications. Due to its excellent physical and chemical attributes, including a large surface area and superior electrochemical performance, LiG has become particularly valuable in the development of medical sensing devices.

Methods: We fabricated Laser-Induced Graphene (LiG) with 30 W 9.3 μm CO₂ laser engraver (VLS 2.30, Universal Laser System), and used it as working electrode by applying a Nafion monolayer to its surface. The electrode was then dried at room temperature for 30 minutes. A LiG reference electrode was prepared using screen printing to cover silver ink on LiG, leaving the counter electrode blank. The sensor's performance was tested using varying concentrations of caffeine and vanillin in PBS (pH=7.26). Testing methodologies included cycle voltammetry and square wave voltammetry with an electrochemical working station (CHI760E, CH Instruments, Inc.).

Results: To facilitate the monitoring of daily caffeine and vanillin intake, we have utilized Nafion-modified LiG sensor to develop an electrochemical point-of-care sensor. Based on the extensive surface area and superior electrochemical performance of LiG and the protective Nafion layer that imparts high stability for long-term storage and multi reproducibility, this novel sensor can detect caffeine, that shows a peak around 1.4 V, and vanillin which has a peak around 0.6 V, both within a linear range of 10 μM to 200 μM .

Conclusions: The developed Nafion-modified LiG sensor offers a promising approach for effectively monitoring caffeine and vanillin consumption. This technological advance aids in better dietary management, thereby contributing to overall health.

Acknowledgment: Haozheng Ma would like to acknowledge the Viterbi Graduate School Fellowship.

5:00 PM MF02.05.12

Laser-Induced Pyrolytic Jetting of Porosity Variable Silica Thin Film for Fog Harvesting Kounghun Min^{1,2}, Hyunkoo Lee^{1,2} and Ji Hwan Lim^{1,2}; ¹Hanyang University, Korea (the Republic of); ²BK21 Four Erica-Ace Center, Korea (the Republic of)

Laser direct writing (LDW) is a renowned maskless manufacturing technology that employs laser beams for the direct creation of micro and nanostructured devices. It overcomes the limitations of conventional multi-step manufacturing processes such as lithography and molding. LDW has a significant impact in a multitude of sectors, spanning from microelectronics and optics to medical devices and beyond, thanks to its merits, including rapid prototyping, customization flexibility, precise control, and adaptability to various materials.

For PDMS, its exceptional optical transparency across a broad spectrum of wavelengths fundamentally constrains the potential applications of laser patterning technology. However, recently, successive laser pyrolysis (SLP) has been proposed as an on-demand laser-based transparent polymer patterning process, relying on the controlled sequence of photothermal pyrolysis phenomena guided by a continuous-wave (CW) laser. After effectively removing the pyrolysis by-product, SLP offers the rapid digital patterning of high quality 2D and even 3D PDMS microstructures, which can be directly utilized without the need for supplementary post-processing steps.

Moreover, the by-products generated in the SLP process, including SiC and the silica layer on the surface, present versatile opportunity for utilization as microstructure in various applications including surface treatment such as wettability modification. In our study, to harness the extensive utility of the surface silica layer, we employed the SLP process on a PDMS-glass hybrid substrate, facilitating the creation of a tunable silica film with controlled porosity through the pyrolytic jetting phenomenon.

The PDMS-glass hybrid substrate is prepared through the deposition of a thin PDMS layer onto a soda-lime glass substrate via a spin-coating method. During the SLP process, the gas generated as a result of PDMS pyrolysis is effectively contained by the glass substrate, directing gas concentration towards the PDMS surface, thereby facilitating the requisite pressure for the ejection of the silica film. Furthermore, the glass substrate plays a dual role by not only acting as a gas barrier but also composing the PDMS layer, thereby optimizing the efficiency of the silica film pyrolytic jetting process by providing a stabilizing counterforce.

In a more detailed approach, we have developed a microporous silica film with dimensions of approximately 10 μm through the optimization of laser

power, laser scanning speed, and scanning interval, in the pyrolytic jetting process. Furthermore, by adjusting these variables, we achieved the capability to tune porosity under 50%. Through water contact angle measurements, it was determined that silica films with approximately 45% porosity exhibited hydrophilic characteristics, while those with around 10% porosity demonstrated hydrophobic properties.

The microporous silica film was employed in a fog harvesting application, wherein it was affixed to a 2 cm x 2 cm surface area of a PTFE rod. Real-time measurements of the harvesting rate resulted in an average yield of approximately 55 mg/min. This level of performance aligns with that of several mesh-style fog harvesting applications sharing analogous structures, underscoring the potential viability of this approach in the field.

5:00 PM MF02.05.13

Laser-Induced Graphene Potentiometric Platform for At-Home Quantification of Choline in Infant Formula and Milk Powders [Abdulrahman Al-Shami](#)¹, Farbod Amirghasemi¹, Ali Soleimani¹, Sina Khazaei Nejad¹, Victor Ong¹, Alar Ainla² and Maral Mousavi¹; ¹University of Southern California, United States; ²International Iberian Nanotechnology Laboratory, Portugal

Introduction:

Choline (Ch⁺) is a water-soluble vitamin-like micronutrient used by the human body to regulate brain and nervous system functions such as mood, memory, and muscle control. Ch⁺ also has a structural function since it is involved in synthesizing phospholipids within cell membranes. Deficiency of Ch⁺ in infants' diet has been correlated with long-term visual and neurocognitive deficits and impaired learning capabilities and memory function. The U.S. Food and Drug Administration (FDA) and similar agencies have set guidelines and requirements for choline levels in commercialized infant formula. Not all families have access to well-standardized infant formula, and some families practice formula stretching due to economic limitations or difficulties obtaining infant formula, similar to the COVID-19 pandemic. In the U.S., 31% of families relying on infant formula for infant feeding encountered difficulties accessing these products during the COVID-19 pandemic. Moreover, 33% of infant formula users adopted adverse formula-feeding practices, encompassing the dilution of formula, the preparation of smaller feeding bottles, and the retention of partially used formula mixtures for subsequent utilization. These practices affect infants' choline intake and, therefore, their health. Precise quantifying of choline in infant formula is essential to ensure that infants receive the required nutritional intake, and yet there are no accessible tools for this purpose. Here, we report an innovative integrated sensor for the periodic observation of choline designed for at-home quantification of choline in infants' formulas and milk powders. This system comprises a choline potentiometric sensor and ionic-liquid reference electrode developed on laser-induced graphitic structure (LIG). The platform also includes a micro-potentiometer that conducts the potentiometric measurements and transmits results wirelessly to the parent's mobile devices.

Materials:

We fabricated the electrochemical electrodes through CO₂ laser ablation of a polyimide film using a laser cutter machine emitting at a 1060 nm wavelength. The choline-selective electrode was created by depositing a 40 μ L choline-selective membrane composed of a mixture containing 330 mg of poly(vinyl chloride) (PVC), 660 mg of o-nitrophenyl-octyl-ether (NPOE), 13.8 mg of sodium tetrakis [3,5 bis(trifluoromethyl)phenyl] borate, and 13.22 mg of calix 4 arene (ionophore) dissolved in 3 mL of THF, onto the electrode surface. The reference membrane solution was formulated by blending 50 mg of MeOctIm TFSI with 316 mg of PVC and 634 mg of o-NPOE in 3.0 mL of THF.

Results and Discussion:

The LIG structure electrochemical electrodes were characterized using Raman, EDX, XPS, and SEM. Characterization results confirmed the successful carbonization of P.I. film and the formation of a 3D multilayered porous graphitic structure with a thickness of 20 μ m. The obtained LIG-based choline-detecting platform showed a sensitivity of 55.3 ± 0.17 mV/decade, close to the Nernstian theoretical value of 59.2 mV/decade. The achieved limit of detection by our platform is about 95.4 μ M. The choline platform also showed an outstanding selective performance toward choline compared to other milk components such as vitamins, minerals, proteins, and sugars. Moreover, the reference electrode demonstrated a highly stable and sample-independent response, which is desired to obtain accurate and precise analysis results. The developed device was used to quantify choline in different commercially available infant formulas and milk powders, showing an accuracy between 100.4 and 108.6 %.

Conclusion:

The LIG-based choline sensing platform showed outstanding sensitivity, selectivity, stability, and accuracy in choline analysis. Leveraging the unique properties of LIG, the platform is flexible, portable, cost-effective, and efficient, making it a promising tool for choline periodic quantification in at-home settings.

5:00 PM MF02.05.14

Laser Induced Formation of Functional Metal Oxides for Enhanced Electrochemical Sensing [Devendra Sarnaik](#), Sotoudeh Sedaghat and Rahim Rahimi; Purdue University, United States

The use of electrochemical sensors in different sectors has highlighted the need for sensors with high sensitivity, low cost and high stability over time. However, the high cost, and low long-term stability of biomolecule electrochemical sensors have yielded the need for other approaches. Alternatively, metal oxides have shown promise to be used for sensing applications without the need of receptors but have yet to be widely adopted due to the complicated and expensive multistep manufacturing process associated with producing them. To develop the functional metal oxide surfaces, laser processing has been seen as an alternative, owing to the low costs, high degree of control and rapid processing time which can be adapted to more scalable manufacturing processes. The use of laser induced oxidation has shown great promise by creating highly localized modifications of the surface morphology without affecting the bulk properties of the metal, while providing a more stable and robust electrical connection between the oxide and bulk metal layer. Laser induced oxidation was used to develop of low cost, rapid detection electrochemical sensors, taking advantage of the create three-dimensional micro/nano oxide structures which exhibit enhanced electrocatalytic properties compared to that of bulk metal. Copper and nickel were laser processed to obtain the rapid, low cost and scalable manufacturing of electrochemical sensors for the detection of nonenzymatic glucose. The obtained laser-induced oxidized copper (LIO-Cu) and laser-induced oxidized nickel (LIO-Ni) contained highly nano/micro porous oxide structures which greatly increased the electrocatalytic activity enabling the detection of glucose. A systematic study of the composition, crystallinity, microstructure and wettability was conducted through the use characterization techniques including scanning electron microscopy (SEM), X-ray diffraction (XRD), Raman spectroscopy, and water contact angle measurement. The electrochemical sensing performance of the devised sensors were tested against a range of glucose concentrations to test sensitivity and detection limit. The LIO-Ni sensor demonstrated a high linear sensitivity of $5222 \mu\text{A mM}^{-1}\text{cm}^{-2}$ over glucose concentration range of $5 \mu\text{M}$ to 1.1 mM, and the LIO-CU sensor demonstrated exceptional sensitivity of $6950 \mu\text{A mM}^{-1}\text{cm}^{-2}$ over a wide range of 0.01 to 5 mM glucose concentration. The obtained results demonstrate the capability for laser processing to be adapted for a scalable manufacturing environment to produce rapid, low-cost and highly sensitive electrochemical sensors, which have application in various field of study including medicine and agriculture.

5:00 PM MF02.05.15

Laser-Induced Carbon Composite Electrode from Photoresist for High Performance On-Chip Energy Storage Devices Soongeun Kwon, Yunji Eom, Hak-Jong Choi, Junhyoung Ahn, Hyungjun Lim, [Geehong Kim](#), Kee-Bong Choi and Jaeyong Lee; Korea Institute of Machinery and Materials, Korea (the Republic of)

We report a laser-induced carbon composite (LICC) electrode prepared from a photoresist for a miniaturized electrochemical energy storage device. A photoresist material comprising of a conventional photoresist matrix and carbon black nanoparticles was photo-thermally converted to LICC by high-power carbon dioxide (CO₂) laser carbonization. Due to the high absorption of carbon blacks in the composite materials, the laser-irradiated composite material was directly exfoliated and carbonized, providing a hierarchically macro-porous, graphitic carbon composite with fewer defects. Depending on the precursor materials mixed with photoresist matrix, the LICCs with functional metal or metal oxide nanoparticles were successfully fabricated by one-step laser carbonization.

The experimental conditions of CO₂ direct laser writing were optimized to fabricate high-quality LICCs for on-chip micro-supercapacitor (MSC) electrodes with low sheet resistance and good porosity. In addition, the results revealed that the high-resolution electrode pattern in the same footprint as that of the LICC-MSCs significantly affected the rate performance of the MSCs.

Consequently, the proposed laser-induced carbonization technique using a photoresist provides simple and facile fabrication of porous, graphitic and high-resolution carbon composite electrodes for high-performance on-chip energy storage devices without high-temperature thermal pyrolysis.

5:00 PM MF02.05.16

Fabrication Defect-Insensitive Minimal Surface-Based 3D Metamaterial at Nanoscale Dahye Shin^{1,2}, Kisun KIM², Sanghyun Nam², Seokwoo Jeon² and Dongchan Jang²; ¹Agency for Defense Development, Korea (the Republic of); ²Korea Advanced Institute of Science and Technology, Korea (the Republic of)

Material scientists have been striving to break the conventional relationships between mutually exclusive materials' properties such as density-strength and to fill the white area in the materials' property space. One effective way to explore the empty space is harnessing nanoarchitectures to develop lightweight and strong artificial materials not only by the architectural designs but also by embedding the benefits of nanoscale effects of materials into hierarchical nanostructures. Generally, in fabrication aspects of those nanoarchitectures, multi-step procedures are required including fabrication of architecture frames and material conversions. During these complicated procedures, fabrication defects are almost inevitable, especially when we considering mass production too. Therefore, at some point, the design of architecture itself is demanded to be defect insensitive with high tolerance of fabrication defects.

For that purpose, we make the best use of 3D minimal surface structure to the design of nanoarchitectures. Since the minimal surface is a local minima of surface area under given constraints by its definition, it is energetically beneficial and efficient in the use of limited resources. Moreover, 3D minimal surface, so called Triply Periodic Minimal Surface (TPMS), exhibits smooth continuous surface without any self-intersections or singularities in all three dimensions avoiding the stress concentrations. And one important characteristic of them is that Gaussian curvature is negative everywhere on the surface by definition. This negative Gaussian curvature plays a key role to superior load carrying capacity and defect insensitivity which will be discussed in this study. Because of these fascinating features of TPMS structures, many engineers have been trying to use them for architected materials in macro- and microscale to achieve the best mechanical performance. However, many of the experimental works barely reach to the level of their initially designed performance due to the fabrication defects. Especially, for brittle ceramic materials, not many experimental works have been investigated and the performance of them has been severely affected by the imperfections resulting to the steep slope on the density-strength Ashby plots.

Therefore, in this study, we are suggesting nanoscale diamond-like 3D minimal surface shell made of brittle amorphous alumina by intertwining the advantages of TPMS structure and the nanoscale effect of the base material to overcome these limitations. Nanopatterning using near-diffraction patterns of laser with multi-phase masks enables us to fabricate the nanoscale TPMS structures with rapid large area production. In addition, it has been reported that the elastic body at nanoscale withstands high stress fields without catastrophic fracture so that to bring additional opportunities for the inelastic deformation even in intrinsically brittle materials. This unexpected inelastic deformation of the ceramic body makes the TPMS structure defect-insensitive.

Experimental data from monotonic and cyclic micropillar compressive tests reveals that our nanoarchitecture exhibits damping behavior, high strength and low scaling exponent of 1.07 in density-strength chart even with severe geometric defects. This new minimal surface nanoarchitecture will contribute to creating superior engineering ceramics with capability of mass production through its high defect tolerance.

5:00 PM MF02.05.17

Simultaneous Electrochemical and Fluorescence Sensing of Myocardial Infarction Biomarkers Using a Femtosecond Laser-Fabricated Fiber-Optic Platform Homayoon Soleimani Dinani¹, Bohong Zhang¹, Rex Gerald¹, Zheng Yan² and Jie Huang¹; ¹Missouri University of Science and Technology, United States; ²University of Missouri-Columbia, United States

The need for rapid and precise detection of biomarkers indicative of myocardial infarction has been emphasized in medical diagnostics and patient care. Conventional sensing approaches primarily utilize electrochemical or optical detecting mechanisms, each characterized by unique advantages and limits. This study aimed to design an advanced fiber-optic platform that integrates simultaneous electrochemical and fluorescence sensing. The integration of these two techniques enhances the reliability and comprehensiveness of biomarker identification. Microsized Laser-Induced Graphene (LIG) electrodes were fabricated on the outer surface of polyimide-coated optical fibers using femtosecond laser technology. The proposed innovation is presented as a scalable, reproducible, and economically viable approach to sensor manufacturing. The electrochemical sensing module was tailored explicitly to target myoglobin, an imperative biomarker for myocardial infarction. Enhanced sensitivity and specificity were achieved through a suite of electrochemical analyses encompassing Cyclic Voltammetry (CV), Square Wave Voltammetry (SWV), Differential Pulse Voltammetry (DPV), and Electrochemical Impedance Spectroscopy (EIS). The electrochemical sensing process was controlled by redox reactions and principles of charge transfer, facilitating high-accuracy measurements. Concurrently, fluorescence sensing was integrated into the platform, adding an auxiliary layer of biomarker validation. The fluorescence sensor was engineered to quantify the fluorescence quantum yield and absorption coefficients of specific fluorophores extant in the blood. This auxiliary mechanism offers supportive evidence and exhibits the potential for identifying other associated biomarkers or substances. The amalgamation of these bifurcated sensing modalities into a unified fiber-optic platform enriched the data acquisition process and accelerated the diagnostic timeline. The provision of multi-faceted, real-time data by the platform paves the way for sophisticated, point-of-care health monitoring systems. The research represents significant progress in sensor technology, particularly integrating electrochemical and optical sensing methodologies. The robust and versatile nature of the platform earmarks it as an optimum choice for diverse applications in medical diagnostics and real-time health monitoring applications.

5:00 PM MF02.05.18

Diagnosis and Monitoring of Milk Fever with a Laser-Engraved Calcium Sensor Ali Soleimani, Farbod Amirghasemi, Abdulrahman Al-Shami, Sina Khazaei Nejad, Alicia Tsung, Delaram Parvin and Maral Mousavi; University of Southern California, United States

Milk fever is a metabolic disorder that occurs in dairy animals and its occurrence is more prevalent a few months before and after calving and can lead to a range of clinical symptoms, including loss of appetite, muscle spasms, lateral recumbency, and eventually coma or death if left untreated. The primary cause of these symptoms is a decrease in blood calcium levels, hypocalcemia. Previous studies have categorized cows into three groups based on their serum calcium levels: normocalcemia (≥ 2.0 mmol/L), subclinical hypocalcemia (< 2.0 mmol/L but without any observable clinical signs), and clinical hypocalcemia (with clinical signs). Based on previous studies, the prevalence of subclinical hypocalcemia in the pasture-based system was around %50. Moreover, the productive life of dairy cows with hypocalcemia decreases by 3.4 years, which can have economic impacts on animal husbandry businesses.

Since subclinical milk fever does not have symptoms and frequent testing of calcium levels is expensive, subclinical milk fever is rarely diagnosed. Thus, having a Point-of-Use inexpensive sensor for frequent and on-demand calcium measurement is beneficial. For this purpose, we fabricated an inexpensive Laser-induced Graphene based potentiometric electrode to detect calcium levels in the clinically relevant range.

Materials and Methods:

We prepared the calcium selective membrane by mixing poly(vinyl chloride) (PVC) (33%), 2-nitrophenyl octyl ether (66%), calcium Ionophore (IV) and potassium tetrakis(4-chlorophenyl)borate (KTPCIB) (1%), with tetrahydrofuran. We fabricated the LIG sensors by directly operating a CO₂ laser on a Kapton film. Then, we drop-casted the membranes on the electrodes. We performed all the measurements at room temperature using a 16-channel potentiometer relative to a commercial reference electrode.

Results and Discussion:

We used laser engraving to pattern graphene on a low-cost polyimide film. SEM results indicated a 3D porous structure of LIGs with a thickness of 20 μm. Furthermore, EDX and RAMAN spectroscopy were performed on the sensors to confirm the presence of graphene on the PI films. The results indicate that the sensitivity of our LIG-based sensors is 26.58±0.28 mV/dec, which is close to the theoretically expected value (29.6 mV/dec). Moreover, the limit of detection (LOD) of the sensor is 1.87 μM, which is ~3 orders of magnitude lower than the clinically relevant range of calcium in the body. Another important characteristic of the sensor that ensures its reliability is the selectivity toward the ion of interest. The Selectivity results of the sensor indicates superior selectivity of the sensor over physiologically relevant ions and biologicals. Finally the sensor's performance in the bovine sample was evaluated. To this purpose, first the sensor where calibrated in two different solutions of artificial serum and then the sensors were exposed to the bovine serum. The results were compared with a commercial Calcium sensor indicating %104.54 recovery of LIG sensors.

Conclusion:

We fabricated a LIG-based potentiometric sensor that shows outstanding sensitivity and selectivity toward the ion of interest. Moreover, the sensor shows %4.54 error compared with a commercial electrode that is suitable and acceptable for in field detection of subclinical milk fever. Moreover, using a laser as an inexpensive, fast, and mass-producible method for fabricating the sensors makes them a suitable choice for in-field frequent use.

SESSION MF02.06: Laser Surface Modification for Enhanced Biocompatibility and Antibacterial Properties

Session Chairs: Varun Kashyap and Rahim Rahimi

Thursday Morning, April 25, 2024

Room 324, Level 3, Summit

8:45 AM *MF02.06.01

Designing Ti-Alloys Using 3D Printing for Load-Bearing Applications: Enhanced Biocompatibility, Minimized Tribo-Corrosion and Inherent Infection Resistance [Amrit Bandyopadhyay](#); Washington State University, United States

Metal 3D Printing was utilized to design novel Ti-alloys for load-bearing implant applications focusing on improving biocompatibility, minimizing bio-tribo-corrosion and related metal ion release, and adding inherent infection resistance. Successful alloy design can minimize adverse local tissue response (ALTR) from total hip implants (THAs) taper corrosion and septic loosening due to polymicrobial infections, eventually reducing implant failure in vivo. In one case, we designed a Ti-Ta-Cu alloy where Cu offers intrinsic microbial resistance and Ta-enhanced biocompatibility to mitigate potential Cu toxicity. Instead of using Ti6Al4V alloy, vanadium and aluminum contents were reduced to design a Ti3Al2V alloy for metallic implant applications. The biological and mechanical properties of Ti3Al2V alloy were measured. A 10% Ta and 3% Cu were added to the Ti3Al2V alloy to enhance biocompatibility and impart inherent bacterial resistance. Additively manufactured implants were investigated for resistance against *pseudomonas aeruginosa* and *staphylococcus aureus* strains of bacteria up to 48 h. A 3% Cu addition to Ti3Al2V showed an improved antibacterial efficacy, between 76 and 81% higher than CpTi and Ti6Al4V. Mechanical properties for Ti3Al2V-10Ta-3Cu alloy were measured, demonstrating excellent fatigue resistance, good shear strengths, and better tribological characteristics than Ti6Al4V. *In vivo* studies using a rat distal femur model showed improved early-stage osseointegration for alloys with 10%Ta addition than CpTi and Ti6Al4V. Ti6Al4V-ZTA-HA metal matrix composites were designed and investigated for load-bearing femoral heads in another alloy design. The composites were fabricated via 3D Printing. A rabbit distal femur 16-week *in vivo* study for implantation and histological characterization was conducted. An induced *in vitro* 16-week applied potential polarization study of the Ti6Al4V and Ti6Al4V-zirconia toughened alumina (ZTA)-hydroxyapatite (HA)-based composites was conducted to investigate the coupled taper-corrosion behavior. The Ti6Al4V-ZTA-HA composites displayed increased hardness, decreased wear volume, increased surface passivation during tribological testing, and faster re-passivation post-tribological testing, validated by increased contact resistance and more cathodic open circuit potential. Finally, a first-of-a-kind table-top joint simulator was designed and manufactured to simulate volumetric tribo-corrosion of femoral heads. The simulator mimics the gait-like motion of the hip joint. Ti6Al4V+ZTA+HA metal matrix composite femoral heads were produced via 3D Printing. The ability to move into volumetric articulating-based testing has shown promising results for improving these innovative materials to address the shortcomings of currently used metallic biomaterials in load-bearing orthopedic devices where corrosion and wear are of concern. The presentation will discuss 3D Printing-based alloy design and related characterization of next-generation Ti-alloys for load-bearing implants.

9:15 AM MF02.06.02

Laser Assisted Selective Texturing and Alloying of Titanium Implant surfaces for Enhanced Bactericidal and Osteointegration Properties [Akshay Krishnakumar](#), [Sotoudeh Sedaghat](#), [Vidhya Selvamani](#), [Sina Nejadi](#) and [Rahim Rahimi](#); Purdue University, United States

Orthopedic device-related infections (ODRIs) in implants represent a critical and multifaceted healthcare challenge, necessitating a comprehensive understanding of their impact on patient well-being, management, and prevention. While titanium-based (Ti) implants are commonly used due to their favorable corrosion resistance, excellent biocompatibility, and mechanical properties similar to that of bone, the development of bacterial infections owing to ORDI remains a daunting concern. Functionalizing the implant surface with antimicrobial agents, without altering the bulk properties of the Ti alloy, presents an effective approach to improving the efficacy of orthopedic implants and elevating patient outcomes. In this context, we have developed a two-step process involving laser texturing and alloying of silver (Ag) nanocomposites into the widely used titanium alloy (Ti6Al4V) implant surfaces, thereby conferring antibacterial properties. The process involved spray coating silver nanoparticles onto the implant surface, followed by heat sintering and laser-induced alloying of Ag into the Ti alloy. The local heat generated by the laser process enables simultaneous intermetallic alloying and texturing of the implant surface, enhancing its surface roughness without affecting its bulk mechanical properties. A systematic study was conducted by varying the laser beam power to analyze the structural, morphological, and elemental composition of the surface, utilizing X-ray diffraction (XRD), scanning electron microscopy (SEM), and energy-dispersive X-ray spectroscopy (EDX) analysis. The results demonstrated that the developed laser-textured surface exhibited enhanced wettability, increased surface roughness, and effective alloying of silver on the implant surface without compromising bulk mechanical properties. The optimized laser-textured surface was subjected to a seven-day antibacterial test against a model population of gram-positive (*Staphylococcus aureus*) and gram-negative bacteria (*Escherichia coli*). Furthermore, the osteointegrative properties of the developed surface were

assessed through in-vitro bone mineralization assays using Mesenchymal Stem Cells (MSC), and the calcified extracellular matrix levels were measured. The results indicated a two-fold increase in bone cell mineralization and long term antibacterial properties for the optimized laser-textured surface compared to the control Ti alloy surfaces. By modifying the implant surface, the antibacterial properties can help prevent bacterial colonization, while the enhanced osteointegration properties can promote bone cell adhesion and colonization. Ultimately, this scalable laser-assisted alloying approach holds the potential to enhance the long-term success of orthopedic implants and improve patient outcomes.

9:30 AM *MF02.06.03

Laser-Induced Graphene Composites for Electrically-Mediated Antimicrobial and Environmental Applications Christopher J. Arnusch; Ben Gurion University of the Negev, Israel

Laser-induced graphene (LIG) is a three-dimensional, porous, electrically conductive graphene material generated predominantly by irradiation of polymer substrates with a 10.6 μm CO₂ laser. Since 2014, this material has been shown to be useful in myriads of applications. In this presentation, I will discuss the synthesis and exceptional properties of LIG composites in antibacterial or antiviral environmental applications including air and water treatment technology. Electrical effects and electro- and photo-thermal heating for bacterial killing will be shown and insights into the mechanism of action will be discussed. Notably, LIG surfaces can deactivate bacteria when low currents are passed through the surface, when the surfaces are used as electrodes, or as heaters. Also, LIG on dense and porous substrates exhibited an electrically mediated antifouling effect. Other metal-doped LIG composites showed antibacterial effects due to the release of metal ions into the solution as well as contact with metal-embedded nanoparticles. This method to generate electrically conductive graphene on water treatment technology such as porous polymer membranes and dense substrates will enable many new applications in water treatment and separations.

10:00 AM BREAK

10:30 AM MF02.06.04

Laser-Induced Graphene (LIG) Membranes with Different Subsurface Morphologies for Electrically Dependent Microbial Decontamination Mauricio N. Kleinberg^{1,2}, Chidambaram Thamaraiselvan^{3,1}, Camilah D. Powell^{2,1} and Christopher J. Arnusch¹; ¹Ben-Gurion University of the Negev Sde Boquer Campus, Israel; ²The University of Texas at San Antonio, United States; ³Indian Institute of Science, India

Laser-induced graphene (LIG) is a graphitic material that can be easily formed by CO₂-laser irradiation on various carbon-based substrates, including porous polymeric membranes. LIG-membrane formation involves lasing the top surface of a polymeric membrane, and converts essential polymer separation structures to porous LIG foam. However, in previous studies, separation properties could be partly recovered by forming LIG polymer composite layers^(1,2) or by coating the polymeric membrane substrate with trimethylaluminum (TMA)⁽³⁾ or graphene oxide (GO)⁽⁴⁾ to avoid melting or damaging the subsurface polymeric structures during the lasing process. Herein, by optimizing the laser settings and fabrication conditions, we made LIG directly on uncoated porous polyethersulfone (PES) membranes while preserving the subsurface polymer.⁽⁵⁾ The effects of lasing on membrane properties were studied by comparing porous polymeric PES membranes fabricated using the non-solvent induced phase separation (NIPS) method with membranes obtained using the vapor-induced phase separation (VIPS) method. Membrane fabrication conditions, such as the polymer concentration of the casting solution and the exposure time to the non-solvent, were varied, and the NIPS method resulted in membranes with a finger-like polymer substructure morphology, while the VIPS method resulted in membranes with an asymmetric cellular morphology. LIG-membranes prepared on NIPS membranes resulted in large permeability changes, while LIG on VIPS membranes gave only very minor changes. The antimicrobial activity of these LIG-membranes as porous electrodes was dependent on applied voltage and solution contact time, and 4-6 log removal of bacteria at 10 V was achieved. Understanding LIG formation on porous polymeric membranes will minimize processing steps and might lead to electrically conductive membranes with controlled separation properties.

References

1. Thakur, Amit K., et al. *ACS applied materials & interfaces* 11.11 (2019): 10914-10921.
2. Thakur, Amit K., et al. *Journal of Membrane Science* 591 (2019): 117322.
3. Bergsman, David S., et al. *Nature communications* 11.1 (2020): 1-8.
4. Straub, Anthony P., et al. *Nano Letters* 21.6 (2021): 2429-2435.
5. Kleinberg, Mauricio N., et al. *Journal of Membrane Science* 673 (2023): 121481.

10:45 AM *MF02.06.05

Laser-Scribed Soft Bioelectronics and Robotics Zheng Yan; University of Missouri-Columbia, United States

Laser-assisted fabrication offers a simple, mask-free, cost-effective approach to pattern conductive materials on various substrates under ambient conditions. This process allows for high-precision customization and miniaturization, essential for emerging soft bioelectronics and robotics applications. With the ability to finely tune the porosity, morphology, composition, and electrical conductivity of the resultant patterns, a broad spectrum of applications can be realized, including biophysical and biochemical sensing technologies, as well as innovations in soft actuators for robotics. In this presentation, I will discuss our latest explorations into laser-scribed graphene and molybdenum dioxide on flexible substrates. I will highlight their significant contributions to the realms of soft bioelectronics and robotics. A showcase of various soft devices we have developed based on these materials will be provided, including sensors for hydration, temperature, electrophysiology, sweat biochemistry, UV, and gas. These demonstrate the material's aptitude in sensory technology. Furthermore, we will display our work in crafting reconfigurable three-dimensional architectures and light-driven smart worms using laser-scribed materials. These instances underscore the immense potential of laser-scribed materials in orchestrating devices with intricate behaviors and responses, paving the way for novel applications in a connected world.

11:15 AM MF02.06.06

Crystallization in Er/Yb:BaTiO₃ Perovskite Induced by fs-Laser Pulses Cleber Mendonca, Jose Clabel, Kelly Tasso, Marcelo Pereira-da-Silva, Jose Vollet-Filho, Filipe Couto and Euclides Marega; University of Sao Paulo, Brazil

Perovskite films have been attracting tremendous attention as promising candidates for applications in photonics and optoelectronics, including light-emitting diodes, photo-detectors, energy-harvesting devices, etc. Such applications are sensitive to changes in crystallization, size, and distribution of grains in the perovskite films. Hence, studies have been carried out to improve the quality of thin films and investigate the effect of sintering on the crystalline phase of the sample. Even though several sintering methods have been developed, fs-laser sintering has appeared as a versatile and rapid option, offering precise and localized energy distribution to the sample. The fs-laser sintering can produce highly crystalline devices with complex structures, although it depends on the processing parameters.

This study demonstrates the crystallization of amorphous Er³⁺/Yb³⁺:BaTiO₃ (BTEY) thin film upon fs-laser processing at 1030 nm. The threshold fluence to achieve laser processing was determined as 1.1 J/cm² at 1 kHz, as well as the irradiation conditions for crystallization. Raman spectroscopy confirmed

crystallization when irradiation was carried out at a 1 kHz repetition rate. Also, an increase in the sample emission was observed in the crystallized regions and on the surface potential. Such results provide insights into using fs-laser pulses for the crystallization of BTEY, which is relevant for device applications.

11:30 AM MF02.06.07

Laser-Induced Carbonization of Polyimide Films for Physically Unclonable Anticounterfeiting Applications Srinivas Gandla, Changgyun Moon and Sunkook Kim; Sungkyunkwan University, Korea (the Republic of)

Laser-induced carbonization (LIC) on polymers with aromatic and imide repetitive units, particularly Kapton polyimide (PI), has revolutionized the production of carbon-based devices and sensors. This includes supercapacitors, triboelectric nanogenerators, actuators, heater devices, as well as gas, humidity, strain, and biological sensors. Furthermore, PI demonstrates remarkable mechanical and thermal stability, positioning it as a compelling choice for a myriad of flexible electronic devices.

In contrast to traditional pyrolysis, where polymer materials undergo thermal decomposition in an inert atmosphere, the LIC technique offers a notable advantage in swiftly achieving patterned carbon. This is crucial for electrode fabrication and the creation of individual, isolated devices. Pulsed lasers emit high-intensity pulses with short durations, affecting only a small portion of the sample with limited penetration depth, thereby avoiding damage to the surrounding material. Various lasers, such as carbon dioxide (CO₂, 10.6 μm), infrared (IR, 1064 nm), ultraviolet (UV, 248 nm), and blue (456 nm), are commonly employed for carbonizing PI materials in diverse applications. Significantly, the carbonization mechanism varies with different wavelengths and other parameters such as laser power, speed, frequency, hatch distance, and pyrolysis environment. This is attributed to distinct absorptions by both PI and carbon. Although the exact mechanisms are not universally agreed upon, both photochemical and photothermal processes have been proposed to elucidate this phenomenon.

On the other hand, as the global population grows rapidly, there is an increasing demand for a larger quantity of goods to meet the needs and comforts of individuals. However, this heightened demand has inadvertently given rise to counterfeit markets. To combat this issue, the implementation of anti-counterfeiting tags on products has emerged as a practical solution. Various traditional anti-counterfeiting tags like quick-response codes, radio-frequency identifications, graphical elements, holograms, and watermarks have been utilized for consumer goods. Unfortunately, these tags are susceptible to cloning attacks and are primarily employed as "identifiers" rather than security tags for authentication. In response to the cloning issue, physically unclonable (PU) tags have been introduced. These tags, generated through stochastic processes, possess unique patterns of randomly distributed physical features that are extremely challenging to duplicate. Additionally, it is crucial for the tags to be low-cost and manufactured using easy, reconfigurable, and ultrafast processes. One effective technique for creating a unique and visually appealing PU tag is the LIC method. Notably, the creation of carbon content without the need for external matter eliminates the material cost drawback associated with tag production.

In this study, we demonstrate the fabrication of a unique and visually appealing PU tag based on a facile, low-cost, rapid, and scalable LIC approach. The LIC dot shapes, sizes, and density can be adjusted based on the input design and laser processing parameters, allowing the tags to be reconfigured according to the manufacturer's requirements. A PI sample with LIC spots of varying sizes distributed randomly in an array format is considered a tag. The LIC spot patterns, formed under the same laser beam energy incidence, are attributed to the heterogeneity of aromatic compounds in the PI film. The spot images are classified into three-level bits based on their sizes and brightness, serving as representations of an identity. The digitalized information encoded by these bits can be stored and utilized for authentication purposes. With this innovative approach, unique spot patterns can be directly engraved onto a flexible printed circuit board, providing a highly secure and customizable solution.

11:45 AM MF02.06.08

Development of Robust Superhydrophobic Surfaces Through Laser-Induced Micro/Nanoscale Armor Textured Structures Muhammad Bilal Asif; Hong Kong University of Science and Technology, Hong Kong

Superhydrophobic surfaces have attracted the attention of researchers across the globe due to their utility in a range of applications such as biotechnology, anti-corrosion, anti-fouling, and heat transfer. Super hydrophobicity is typically achieved through low surface energy and high micro to nano-scale surface roughness, allowing reduced contact between the liquid and the surface of solid material. However, during mechanical loading, this increase in surface roughness leads to high localized pressures due to reduced contact area between the interacting surfaces. This increase in local pressures makes such surfaces fragile and susceptible to damage during mechanical abrasion wear. As a result, the material underneath gets exposed which may cause a change in the hydrophobic property of the surface under abrasion. Therefore, most superhydrophobic surfaces are fragile and prone to damage when exposed to harsh environments.

In this study, we have proposed a methodology to achieve robustness in superhydrophobic surfaces on metals making them resistant to mechanical abrasion wear and can withstand harsh operating conditions, such as acidic and alkaline environments, sea water exposure, ultraviolet radiation (UV) exposure, exposure to water jet, and elevated temperatures. This was achieved by splitting the problem statement into two sections. The mechanical robustness is achieved through a single-step laser-induced micro-to-nanoscale surface texturing, obtaining interconnected armor grids of various shapes and sizes, whereas the low surface energy was achieved using the silica-based nanoscale superhydrophobic coating.

The microstructure armor shapes investigated in this study include interconnected hexagonal, triangular, and square-shaped holes. Optimization was carried out by testing eight different sizes of each microstructure shape. The interconnectivity in microstructure shapes was inspired by nature as observed in honeycomb structures and fish-scale skin structures.

The grid microstructure offers pockets to hold nano-coating and acts as protective armor for the superhydrophobic coating against abrasion wear. The water-repellent coating housed inside microstructure pockets offered superhydrophobic behavior to the surface. The influence of various geometric factors such as microstructure wall thickness, hole depth, and microstructure size on the superhydrophobic behavior was also investigated. The initial water contact angle (WCA) was measured to be around 168 degrees and after 1000 sandpaper abrasion cycles under loading, the surface retained its superhydrophobic property with WCA measuring above 150 degrees for most sizes of all microstructure shapes. The prepared surface retained its superhydrophobic property when exposed to; 30 days of UV radiation, 600 minutes of water jet impact test, 30 days in sea water, acidic and alkaline environments, and 30 cycles of thermal cycling testing as per ASTM D6644-15. The proposed methodology is a scalable process for achieving durable robust superhydrophobic surfaces and can be utilized for a range of materials in a variety of applications.

SESSION MF02.07: Laser Assisted Manufacturing of Functional Materials for Sensors and Actuators
Session Chairs: Jonathan Claussen and Varun Kashyap
Thursday Afternoon, April 25, 2024
Room 324, Level 3, Summit

1:30 PM *MF02.07.01

Laser-Assisted Synthesis and Texturing of Graphene Electrodes for Biosensing Devices Amit Barui and [Lia Stanciu](#); Purdue University, United States

The pressing global demand for rapid, point-of-care detection of enveloped RNA viruses necessitates innovative sensor manufacturing approaches. We present a biosensor manufacturing method, focusing on flexible electronics employing graphene inks printed on flexible polymeric substrates. These are subsequently cured and laser-textured under conditions specific to our experiments, incorporating optimized electrode geometries. A crucial component of our advancement is the novel 2D layered structure and electrode coating geometry. In conjunction, the precise laser texturing and curing protocols allow for functionalization using single-stranded (ss) DNA primers. These primers, interacting with graphene layers, play a significant role in constructing DNA sensors adept at detecting enveloped RNA viruses directly, without the need for PCR amplification.

Laser texturing significantly influences the hydrophobicity of these graphene sensors, enhancing their hydrophilic nature. Notably, differences were observed in hydrophilicity between different generations of sensors. Further, the methodology for DNA primer application is considered. While dip coating results in false negatives due to inadequate DNA ligand loading, drop casting amplifies the electrode resistance, denoting a superior yield in functionalization. Our evaluations further emphasize the superiority of unidirectional printing for sensor construction, evidenced by consistent, minimal resistance measurements.

The DNA sensor construction strategies reported in our research offer compelling insights into the manufacturing and deployment of highly specific, portable devices for enveloped RNA virus detection at point-of-care facilities, all within minutes. These findings underscore the role of laser-assisted processes, optimal electrode design, and DNA functionalization methods in advancing the field of RNA pathogen detection.

2:00 PM MF02.07.02

Potential Application of Laser Reduced Graphene Oxide Electrode for Pressure Sensing [Yijing Stehle](#); Union College, United States

Reduced graphene oxide (rGO) has attracted attention as an active electrode material for flexible electrochemical devices due to the high electric conductivity and large surface area. Compared to the other reduction strategy, laser reduction is a single-step, precise, low-cost, and chemical-free processing that can be directly applied on the graphene oxide (GO) membrane under ambient conditions. In general, the quality of the rGO is limited to that of pristine graphene due to incomplete reduction, and oxygenated defects involved in the reduction process. The partially removed oxygenated functional groups not only influence the impedance of the electrode, but also make it sensitive to the humidity of the working environment. Most of the studies are focused on the laser irradiation parameter optimization to achieve the lowest O/C ratio. This study aims to explore the potential of applying the Laser reduced graphene oxide (LrGO) for pressure sensing. Beyond the laser irradiation parameters including intensity, frequency, and scan speed, the impact of partially reduced GO on the bottom and the interlayer distance increase during the reduction is studied to improve the sensing performance of LrGO. Our results demonstrate the potential of applying LrGO in the pressure sensing field through facile post treatment.

2:15 PM MF02.07.03

Laser-Induced Graphene (LIG) based Green Gas Sensor [Cheolmin Kim](#), Hanku Nam, Mingu Kang, Kichul Lee, Youngjin Kim and Inkyu Park; Korea Advanced Institute of Science and Technology (KAIST), Korea (the Republic of)

In recent years, the global electronics industry has experienced rapid growth, driven by advances in technology and increasing demand for electronic devices. However, this growth has come at a significant cost to the environment, as electronic products consume vast amounts of energy and resources during their production, use, and disposal. As a result, there is a growing need for more sustainable and environmentally friendly electronics, also known as "green electronics". Green electronics refers to the design, production, and use of electronic products and systems that minimize environmental impact, reduce energy consumption, and promote sustainability throughout their lifecycle. The global green technology and sustainability market was valued at \$13.28 billion in 2021 and is expected to expand at a compound annual growth rate (CAGR) of 22.4% from 2022 to 2030. In the field of gas sensors, the development of green gas sensors that are easy to dispose of after use by using sustainable materials such as cellulose and gelatin has been actively developed in line with the changing times.

Recently, femtosecond lasers and their use to create laser-induced graphene (LIG) have received a lot of attention. The femtosecond laser used in this study to fabricate the gas sensor is a pulsed laser that can have a very high peak power of terawatts by focusing the photon energy of the laser beam in a very short time of femtoseconds. Femtosecond lasers are useful in many applications because they have a very high frequency, resulting in high energy and minimal heat transfer to surrounding materials. These characteristics make a process using femtosecond lasers suitable for fabricating the laser-induced graphene (LIG)-based gas sensors in this study. When certain materials containing carbon are irradiated with a laser beam, they carbonize and produce a three-dimensional porous material, which is known as LIG. LIGs have excellent electrical and mechanical properties, and their three-dimensional porous structure makes them ideal for use in gas sensors. In addition, LIGs created in wood do not require any special chemical treatments during fabrication, making them eco-friendly, easy and quick to manufacture, and inexpensive to make in any desired design.

In this work, we present a novel approach for the fabrication of a LIG-based eco-friendly gas sensor coated with a sensing material and patterned on wood substrates using a one-step process. The combination of LIG and the sensing material coating allows for the creation of a highly sensitive and selective gas sensor. This sensor is not only eco-friendly but also has the potential to be cost-effective due to the use of a renewable and sustainable wood substrate and a one-step fabrication process. The one-step patterning process allowed for precise and efficient production of the sensor, while the use of wood substrates made it environmentally sustainable and biodegradable. The gas sensors are reactive to CO, NH₃, and CH₄ gases, and are fabricated in an array by doping different materials to effectively detect different types of gases. The gas sensor also demonstrated its potential as a forest fire monitoring system by using deep learning algorithms to detect different types of gases in a fast time.

2:30 PM BREAK

3:00 PM MF02.07.04

Scalable Laser-Assisted Manufacturing of Chipless RFID Sensors on Metallized Films [Muhammad Masud Rana](#), Sarath Gopalakrishnan, Akshay Krishnakumar, Sotoudeh Sedaghat, Sina Nejati, Ulisses Heredia and Rahim Rahimi; Purdue University, United States

The global food packaging industry, valued at 311.4 billion dollars in 2020 and projected to reach 456.6 billion dollars by 2027, is witnessing growing demands for improved food quality and safety. Monitoring the quality of packaged food plays a vital role in reducing spoilage and enhancing food safety. Key indicators like humidity levels, pH, and chemical changes in meat products necessitate sensors for effective monitoring. Current solutions, such as colorimetric sensors and active sensors, have limitations. While colorimetric sensors are cost-effective and suitable for transparent packaging, they cannot be used in non-see-through packages, requiring labor-intensive manual inspection. Active sensors, though automated, are expensive and may not always be biocompatible due to batteries and electronic chips.

Battery-less chipless wireless sensors, due to their low cost and wireless capabilities, are becoming increasingly popular in food packaging. However, challenges in the commercialization of chipless sensors are associated with their manufacturing processes. Scalable manufacturing techniques like printing

This searchable program is up-to-date as of April 15th, 2024.

have been employed for chipless sensors in applications like moisture sensing, soil analysis, and identification. These techniques reduce the complexity and resources needed for sensor production but introduce challenges related to ink formulation, custom screens, and drying and sintering times.

Our Scalable Laser-Assisted Manufacturing (SLAM) process offers a solution for large-scale, roll-to-roll production. It enables one-step patterning of a conductive aluminum layer on paper or PET sheets while concurrently creating high-surface-area Al₂O₃ nanoparticles within the laser-ablated regions, enhancing the sensitivity of the wireless sensor.

This work presents a systematic investigation of different laser processing conditions on metalized paper films to optimize structures. These structures provide high-performance antennas while minimizing structural damage to the underlying paper substrate. Results demonstrate that optimized processing conditions yield concurrent patterning of the metalized film into desired antenna structures and high-surface-area metal oxide nanoparticles within the ablated region. This results in exceptional sensitivity (linear sensitivity of -87 kHz/RH in a relative humidity range of 0% to 85%), surpassing standard RFID sensors produced using conventional photolithography methods.

The second part of this work demonstrates the post-functionalization of laser-patterned resonators and antennas to achieve responsive sensitivity to pH and hypoxanthine (HX), biomarkers relevant to food spoilage and fresh meat and fish produce. This technology opens new possibilities for scalable and cost-effective sensor production, paving the way for their implementation in smart packaging to address the challenges associated with food waste.

3:15 PM MF02.07.05

Bandgap Engineering of Laser-Patterned Diamond-Like Carbon Structures [Naveen Narasimhachar Joshi](#), Ben Sekely, Pranay Kalakonda, Sachin Kadian, John Muth, Roger Narayan and Jagdish Narayan; North Carolina State University, United States

We report the formation of Si-DLC thin films on Si (100) and sapphire (0001) substrates via plasma-enhanced chemical vapor deposition (PECVD) technique. Subsequently, these thin films were irradiated with nanosecond ArF excimer laser pulses ($\lambda = 193$ nm; pulse duration = 20 ns) of varied energy density (0.6 Jcm⁻², 0.7 Jcm⁻², and 0.8 Jcm⁻²). The pulsed laser annealing (PLA) technique melts the Si-DLC films in a super-undercooled state that can be quenched rapidly. As such, the sp² content in the films can be modified by controlling the energy density of the laser pulse. We show that the optical bandgap of Si-DLC structures can be controlled by suitably tuning the sp² content in Si-DLC thin films through the PLA technique. Raman spectroscopy and XPS studies were employed to determine the sp²/sp³ ratio in the as-deposited and PLA-treated Si-DLC thin films. Absorption spectra were obtained by UV-Vis spectroscopy and used to determine the optical bandgap (Tauc's method) and Urbach energy and correlated with the sp² content in the films. This study shows that PLA is a powerful technique for controlling the functional properties of DLC thin films for state-of-the-art optoelectronic applications.

SYMPOSIUM MF03

Sustainable Polymers—From Fundamentals to Advanced Manufacturing and Applications
April 23 - April 26, 2024

Symposium Organizers

Yuanyuan Li, KTH Royal Institute of Technology
Kunal Masania, TU Delft
Gustav Nystrom, EMPA
Eleftheria Roumeli, University of Washington

* Invited Paper
+ JMR Distinguished Invited Speaker
^ MRS Communications Early Career Distinguished Presenter

SESSION MF03.01: Nanocellulose Fundamentals I
Session Chairs: Gustav Nystrom and Eleftheria Roumeli
Tuesday Morning, April 23, 2024
Room 323, Level 3, Summit

10:30 AM *MF03.01.01

Processing Fun with Nanocellulose [Jeffrey P. Youngblood](#); Purdue University, United States

Cellulose Nanomaterials (CNMs) are an attractive material class for possible applications in nanocomposites reinforcement, nanomaterials and biomedicine as they have high strength and stiffness, yet are renewable, biodegradable, non-toxic, and cheap. They are also of particular interest for rheology control. However, as nanoobjects they can prove challenging to process due to water binding ability and lack of dispersion. Here we detail our journey towards processing various materials with CNM. Of particular note will be our recent efforts at additive manufacturing with CNM and CNM as an additive in cement.

11:00 AM *MF03.01.02

Highly Effective Nanocellulose-Based Flocculants for Use in Freshwater and Saltwater Conditions [Wim Thielemans](#); KU Leuven, Belgium

The rigidity of cellulose nanocrystals and the ability to modify them at different surface planes makes them interesting candidates as flocculants for larger particles or organisms because they can flocculate using a patch mechanism and coiling under high salt conditions is avoided. Therefore, we investigate cationically modified CNCs for the flocculation of microalgae. Cellulose nanocrystals (CNCs), extracted from cotton via a standard H₂SO₄ acid hydrolysis, were chemically modified with methyl-imidazolium (MIM) and pyridinium (PYR) grafts at various degrees of substitutions (DS). The extent of grafting was determined by elemental analysis and FTIR and EXPS spectroscopy, while retention of crystallinity and morphology were confirmed by WAXS and AFM respectively.

When testing *Chlorella Vulgaris* (freshwater microalgae) flocculation, it was found that the flocculation efficiency did not vary significantly with surface graft or with DS. However, the required dose varied virtually linearly with DS and remained independent of graft type (Fig 1(a)). Applying these flocculants to marine microalgae *Nannochloropsis oculata*, flocculation remained effective and flocs could readily be removed using a large pore filter (Fig 1 (b)).

Adhesion force histograms and rupture distance measurements by securing (1) a microalgal cell on the AFM tip and probing a film of modified CNCs or (2) modified CNCs on the AFM tip and probing microalgal cells in solution, both showed that the interaction is governed by electrostatic interactions. This explains the linear relation between DS and required dose for flocculation. The interaction force for PYR-CNCs with *Chlorella vulgaris* was only a third of that for MIM-CNCs but that did not seem to affect its flocculation efficacy. Therefore, the strength of interaction does not seem to be a very important parameter so that our results show that increasing DS is more important than optimizing the type of cationic charge. This work was then extended to prepare fully biobased materials, using glycine betaine as the surface grafts on CNCs, giving similar results to pyridinium and methylimidazolium modified CNCs. We also investigate CO₂-sensitive grafts allowing us to add the CNCs to the microalgal growing medium, after which CO₂ could be bubbled through the medium rendering the CNCs positively charged thereby flocculating the microalgae. Finally, we are currently investigating in more detail the interaction strength between cationically modified CNCs with microalgal cell walls to be able to devise models capable of predicting flocculation performance.

Our work thus shows that CNCs offer great potential as biobased flocculants, even in high-ionic strength conditions. Extending this work to the removal of particulate matter in waste water is currently in progress and shows similar excellent flocculation performance, showing the wide applicability of cationic CNCs as flocculants.

11:30 AM *MF03.01.03

The Importance of Crystallite Bundles in The Chiral Self-Assembly of Cellulose Nanocrystals: Origin, Morphology and Function [Thomas G. Parton](#)^{1,2}, Kevin Ballu², Bruno Frka-Petescic², Richard M. Parker² and Silvia Vignolini^{1,2}; ¹Max Planck Institute of Colloids and Interfaces, Germany; ²University of Cambridge, United Kingdom

Cellulose nanocrystals (CNCs) are elongated negatively-charged nanoparticles produced by acid hydrolysis of cellulosic biomass (e.g. cotton, wood pulp). CNC suspensions spontaneously form a left-handed cholesteric mesophase, which has a periodicity (pitch) determined by the characteristics of the individual CNCs (e.g. morphology, surface chemistry) and the suspension formulation (e.g. solvent, additives). This helicoidal arrangement of CNCs can be preserved as the suspension is dried, resulting in films with vibrant structural color. The chiral self-assembly of CNCs is thus a promising route to create materials with a tunable optical response from a sustainable biopolymer feedstock, but understanding how the properties of the large-scale structure emerge from the behavior of individual nanoparticles has been a persistent challenge.

First, by gradually tuning the size and shape of cotton CNCs using ultrasonication, and correlating the morphology of individual particles with their cholesteric mesophase behavior in suspension, we found that CNC "bundles" (i.e. clusters of laterally-bound elementary crystallites) are essential for the formation of a cholesteric phase. These bundles appear to act as chiral dopants, analogous to those used for molecular liquid crystals, whereby an increase in dopant concentration leads to a decrease in cholesteric pitch (and blueshifted film color). We then compared common ways to induce aggregation in CNC suspensions (e.g., post-hydrolysis centrifugation or excess ionic strength). This investigation revealed that the formation pathway significantly affects the morphology of the bundles and thus their effectiveness as chiral dopants. These findings demonstrate that the "making" and "breaking" of crystallite bundles offers a facile way to tailor the self-assembly behavior of CNC suspensions.

SESSION MF03.02: Nanocellulose Fundamentals II
Session Chairs: Gustav Nyström and Eleftheria Roumeli
Tuesday Afternoon, April 23, 2024
Room 323, Level 3, Summit

1:30 PM *MF03.02.01

Making Active and Responsive Materials Using Rod Shaped Fillers: Structuring Nanocomposites [Johan Foster](#); The University of British Columbia, Canada

Cellulose nanocrystals (CNCs) are high-aspect ratio, mechanically stiff fibers which can serve as both a bio-renewable reinforcing agent in nanocomposites, as well as a handle for adding stimuli responsiveness. CNCs can be extracted from a wide range of natural cellulosic materials, with characteristics such as crystal structure, crystallinity and aspect ratio fluctuate widely between sources.

Here, we report functionalized cellulose prepared for reinforcing materials in a variety of environments, ranging from cement to implantable materials in the human body. Moieties attached to the surface of cellulose show that both irreversible and reversible changes can be induced by application of an external stimuli. These specifically designed materials are mechanically tunable, matching use conditions, while creating surprising mechanical properties.

2:00 PM *MF03.02.02

Agarose Facilitating Functional Hydrogels [Olli Ikkala](#) and Hang Zhang; Aalto University, Finland

Agarose is polysaccharide that is extracted from seaweed and has amply been applied, e.g., in biological characterizations. It forms hydrogels by physical crosslinks, showing thermoreversible sol-gel transitions, wherein nanoscopic bundles of semiflexible fibrils are formed in the gel state in comparison to polymer coils in the sol state. In hydrogels it allows strain stiffening (1). Here we show that agarose facilitates new hydrogelation functionalizations. We combine agarose physical gel networks with poly(N-isopropylacrylamide), PNIPAM, chemical gel networks. PNIPAM classically shows Lower Critical Solution Temperature (LCST) thermoresponsive behavior. Upon removing the agarose network, emptied channels remain facilitating rapid water flow (2). Such channelled PNIPAM gels are transparent at room temperature, but show intense white colour upon heating. Chemically modified agarose can also be

used as a chemical macro-crosslinker therein to allow even promoted whiteness upon heating (3). Similarly, upon removing the agarose network to allow channelled PNIPAm hydrogels allows rapidly thermally switchable underwater adhesion taken that PNIPAm has been functionalized with catechol (4). Finally, thermally trainable mechanical and volumetric properties are shown using networks consisting of PNIPAm and agarose or acrylated agarose (5). The approaches suggest that agarose is a versatile polysaccharide to functionalize composite hydrogels, relevant in foreseen applications.

1. L. Martikainen, K. Bertula, M. Turunen, O. Ikkala, *Macromolecules*, 53, 9983, 2020
2. A. Eklund, H. Zhang, H. Zeng, A. Priimagi, O. Ikkala, *Adv. Funct. Mater.*, 30, 2000754, 2020.
3. A. Eklund, S. Hu, Y. Fang, H. Savolainen, H. Zeng, A. Priimagi, O. Ikkala, H. Zhang, submitted, 2023.
4. A. Eklund, O. Ikkala, H. Zhang, *Adv. Funct. Mater.*, 2214091, 2023
5. S. Hu, Y. Fang, C. Liang, M. Turunen, O. Ikkala, H. Zhang, *Nat. Commun.*, 14, 3717, 2023

2:30 PM MF03.02.03

Latex-Based Pressure Sensitive Adhesives with Unmodified vs. Polymer-Grafted Cellulose Nanocrystals Julia Antoniw¹, Michael Kiriakou², Vida Gabriel³, Michael F. Cunningham⁴, Marc A. Dubé³ and Emily D. Cranston¹; ¹University of British Columbia, Canada; ²Anomera Inc., Canada; ³University of Ottawa, Canada; ⁴Queen's University, Canada

Meeting the requirements for “green” materials, cellulose nanocrystals (CNCs) have been demonstrated as good additives and stabilizers in emulsions, however their exact role is not always clear. Our work on miniemulsion, microsuspension, and seeded semi-batch emulsion polymerization has demonstrated that polymer latex properties (e.g. size, surface charge, surface roughness, polymer degree of polymerization) can be highly tuned through the incorporation of CNCs. Most notably, the addition of CNCs always improves all performance metrics in latex-based pressure sensitive adhesives (PSAs). This is uncommon given that additives that increase adhesive properties normally decrease cohesive properties and vice versa. We have investigated nano-scale adhesive properties and their link to macroscopic tack, peel and shear strength to elucidate how CNCs act as “anchor points” for polymer entanglement, improve wettability and latex film coalescence, and form percolated networks throughout PSA films. Most recently, we have studied the effect of CNC surface chemistry (sulfated vs. carboxylated) as well as polymer-modified CNCs on PSA properties – the trends are not straightforward as changing the CNC surface affects aggregation/dispersibility, colloidal stability, the location of CNCs in the latex, and the tendency for coagulation to occur during polymerization. This talk will explain the main conclusions across a series of papers on CNCs in latex-based PSAs and recommendations for when/if to modify CNC surface chemistry. While the focus is on latex-based PSAs we believe the work is translatable to a range of latex products including paints, coatings, inks, toners and rubbers.

2:45 PM BREAK

SESSION MF03.03: Lignin Based Materials
Session Chairs: Eero Kontturi and Yuanyuan Li
Tuesday Afternoon, April 23, 2024
Room 323, Level 3, Summit

3:15 PM *MF03.03.01

From Synthesis of Functional Lignin Nanoparticles to Their Catalyst-Free Ozonolysis: Closing The Loop Alexandros E. Alexakis and Mika H. Sipponen; Stockholm University, Sweden

Recent years have seen a growing interest in lignin nanoparticles (LNPs) based on technical lignins extracted from plant biomass. A common method to produce LNPs involves diluting a lignin solution in an aqueous organic solvent by adding water or evaporating the organic phase. Our group has contributed to overcoming obstacles of LNPs such as their instability in aqueous and organic solvents. These approaches aim to preserve the spherical shape and allow for chemical modification before or after particle preparation. Hydroxymethylation of lignin with subsequent production of colloidal particles and their hydrothermal processing gave rise to particles that remain stable at acidic media as well as alkaline pH 13 and anhydrous polar organic solvents.[1] Another means to produce LNPs with tailored functionality involves first fractionating lignin into solvent-soluble and insoluble fractions, epoxidation of one of these fractions, and their combination in original mass ratio.[2] When epoxidized high-molecular weight lignin fraction was combined with the low Mw fraction the particles could be internally cross-linked via simple heating at 100 °C in colloidal state. Moreno et al. (2023) established a method to stabilize LNPs using only natural components.[3] By co-aggregating urushi, a black oriental lacquer, with softwood kraft lignin, hybrid particles were formed. Owing to its catechol-type structure with unsaturated hydrocarbon chains linked to the aromatic ring urushi served as a renewable stabilizer through hydration barrier effects and thermally triggered internal cross-linking. The weight ratios of the components allowed adjustable stabilization levels. Hybrid particles with Urushi content >25 wt% underwent interparticle cross-linking, creating multifunctional hydrophobic coatings that enhanced water resistance of wood. Covalently stabilized lignin structures present in the aforementioned LNPs also pose questions regarding their resistance to oxidative degradation that occurs in natural environment due to oxidoreductive enzymatic activities. Likewise, if these particles were found to be persistent to advanced water purification processes there would be a risk of environmental pollution in the form of nanoplastics. Ozone is a well-known decomposition agent targeting the aromatic rings present in lignin. Because of the chemical robustness of the LNPs, their degradation should be investigated in order to close the loop. For this reason, the acidic aqueous LNP dispersion (non-covalently crosslinked) was treated with ozone and their degradation was monitored by means of DLS, SEM, FTIR, UV-Vis and ³¹P-NMR within three hours and it was compared with that of the most stable LNPs, i.e., the crosslinked hydroxymethylated ones.[4] Upon ozonolysis, the phenols were linearly converted to muconic acid structures and at longer times the degradation of LNPs was accompanied with the formation of small acidic compounds as identified by LC-MS. Although the chemical composition of the materials was significantly affected even after 15 min of ozonolysis, the size and spherical morphology of the LNPs was retained for one hour followed by their aggregation or complete degradation. Interestingly, mechanically homogenized softwood kraft lignin displayed considerable slower degradation rates compared to LNPs or HLNPs under similar conditions. The results of this study demonstrate that even chemically stabilized LNPs can be degraded with industrially relevant approaches. Further work should be directed to study biodegradation of LNPs that possess a high surface area under environmentally relevant conditions.

References

- [1] Morsali et al., *Biomacromolecules* 2022, 23, 11, 4597–4606.
- [2] Ferruti et al., *Green Chem.* 2023, 25, 639-649.
- [3] Moreno et al., *Urushi as a Green Component for Thermally Curable Colloidal Lignin Particles and Hydrophobic Coatings*. *ACS Macro Letters* 12, 2023, 759-766.

[4] Alexakis et al., Manuscript.

3:45 PM MF03.03.02

Greener Protocol for Chloromethylation of Lignin and its Diverse Applications [Yevgen Karpichev](#) and Mahendra Kothottil Mohan; Tallinn University of Technology, Estonia

Lignin, a highly abundant biopolymer characterized by its elevated carbon content and substantial aromaticity, holds immense potential as a valuable resource for fuel production and the synthesis of platform chemicals. However, despite its promising attributes, lignin remains underutilized within the spectrum of lignocellulosic biopolymers. Lignin's innate versatility can be harnessed through various chemical modifications at both "upstream" and "downstream" stages following its extraction. The chemically modified lignin exhibits the potential to serve as a precursor for the development of nanomaterials tailored for drug delivery, contingent upon its source, chemical alterations, and physicochemical properties. Efforts to improve lignin's utility have predominantly involved "upstream" chemical modifications, which either target the hydroxyl groups for alteration or introduce new chemically active sites, thereby expanding its applications³. Yet, the quest for a versatile and environmentally friendly method for these modifications persists. In this context, the concept of a greener chloromethylation process, currently experiencing renewed interest and offering extensive prospects for "greener" applications, remains unexplored within the realm of lignin. In this study, we present a novel method for the chloromethylation of lignin, which has paved the way for the creation of a diverse range of lignin-based products utilizing chloromethylated lignin (CLM) as the starting material. The resulting lignin-based materials encompass catalytic agents, antibacterial formulations, and thermoplastic additives. Our lignin-based catalyst exhibits several advantages over other catalysts, including straightforward synthesis, heterogeneity, recoverability, and recyclability. Furthermore, we have substantiated the efficacy of the lignin-based catalyst in a range of carbon-carbon bond formation reactions, such as Suzuki-Miyaura, Sonogashira, Heck reactions, click reaction, and hydrogenation. The introduction of various quaternary amines with variable chain lengths to chloromethylated lignin has resulted in a series of innovative surface-active materials with enhanced antibacterial activity against Gram-negative and Gram-positive clinical isolate bacteria. The products of CML esterification are shown to alter thermoplastic properties of biopolymer (PLA). This research, along with the greener chloromethylation approach for lignin, holds the promise of shedding new light on lignin valorization, rendering it economically attractive and environmentally benign.

4:00 PM MF03.03.03

Semicrystalline Polymers from Lignin-Derivable Monomers [Ty Christoff-Tempesta](#), Garrett F. Bass and Thomas Epps; University of Delaware, United States

Semicrystalline chain-growth polymers from lignin-derivable compounds are desirable for their potential to combine material sourcing from renewable feedstocks with performance-advantaged material properties (e.g., higher tensile strengths and improved barrier properties in comparison to their amorphous polymer counterparts). Despite significant effort in the synthesis of vinyl monomers from lignin-derivable molecules, the resulting chain-growth polymers to date have been dominantly amorphous. Here, we describe the chemical transformation of lignin-derivable molecules into monomers that enable the generation of semicrystalline macromolecules. We harness living polymerization strategies to synthesize these polymers with stereoregularity under mild conditions, and we further probe the impacts of synthesis conditions on molecular weights, crystallinities, and thermal properties. This work introduces a strategy for utilizing lignin-derivable molecules to generate semicrystalline polymers with tunable properties, providing a pathway to valorize lignin for a new range of polymer applications.

4:15 PM MF03.03.04

Sonochemical Synthesis of Lignin Nanoparticles and Their Applications in Poly(vinyl) Alcohol Composites [Dylan D. Edmundson](#), Anthony Dichiaro and Rick Gustafson; University of Washington, United States

Lignin is a common and abundant byproduct of the pulp and paper industry and is generally burned to produce steam. Opportunities exist to acquire greater value from lignin by leveraging the properties of this highly conjugated biomacromolecule for applications in UV absorption and polymer reinforcement. These applications can be commercialized by producing value-added lignin nanoparticles (LNPs) using a scalable sonochemical process. In the present research, monodisperse LNPs have been synthesized by subjecting aqueous dispersions of alkali lignin to acoustic irradiation. The resulting particle size distribution and colloidal stability, as determined by dynamic light scattering, transmission electron microscopy and zeta potential analysis, of LNPs can be adjusted by varying the solution pH and ultrasonication energy. As-synthesized LNPs with a mean diameter of 204 nm were incorporated into poly(vinyl) alcohol (PVA) to prepare thin and flexible nanocomposite films using a simple solvent casting method. The addition of 2.5 wt.% LNP increased the material's Sun Protection Factor up to 26 compared to 0 for neat PVA, while maintaining light transmission above 75% in the visible spectra. In addition, the tensile strength and elastic modulus of the PVA nanocomposites improved by 47% and 36%, respectively. The presence of LNP also enhanced the thermal stability of the materials. Significantly, the proposed sonochemical process may be generally applicable to the synthesis of a range of naturally-derived LNPs for a variety of value-added applications.

SESSION MF03.04: Poster Session I
Session Chairs: Kunal Masania and Eleftheria Roumeli
Tuesday Afternoon, April 23, 2024
Flex Hall C, Level 2, Summit

5:00 PM MF03.04.01

Synthesis and Antibacterial Properties of Lignin-Based Quaternary Ammonium and Phosphonium Salts [Mahendra Kothottil Mohan](#)¹, Harleen Kaur², Angela Ivask², Jean-Manuel Raimundo³, Tiit Lukk¹ and Yevgen Karpichev¹; ¹Tallinn University of Technology, Estonia; ²Institute of Molecular and Cell Biology, University of Tartu, Estonia; ³SINaM - Aix-Marseille University, France

Lignin, a naturally occurring aromatic polymer, possesses diverse biological functions, particularly in the defense mechanisms of plants against pathogenic microbes. The prospect of utilizing isolated lignin as an eco-friendly antimicrobial agent presents a promising avenue for enhancing the value of lignin. Furthermore, as lignin derives from plant photosynthesis, its integration into the antimicrobial industry carries the potential to reduce carbon emissions. While numerous studies have explored lignin's utilization for the development of antimicrobial agents across various applications, the highly heterogeneous nature of lignin, encompassing variations in monomer composition, linkages, molecular weight, and functional groups, has obscured the relationship between lignin's structure and its antimicrobial properties.

To bridge these knowledge gaps, we conducted a comprehensive study in which we synthesized forty-two quaternary ammonium/phosphonium organosolv lignin samples from Aspen, Pine, and Barley straw, representing hardwood, softwood, and grass sources, respectively, employing a recently developed versatile intermediate known as chloromethylated lignin. These lignin samples were systematically evaluated for their antibacterial potential against *E. coli* and clinical isolates of Gram-positive (MRSA) and Gram-negative (*K. pneumoniae*) bacterial strains.

Our findings indicate that the antibacterial activity of these lignin samples exhibits a notable increase with the length of the hydrophobic chain, up to C14, beyond which it begins to decline. Ongoing research is also exploring the antimicrobial activity of ammonium and phosphonium surfactant materials, both individually and in combination. This research underscores the significant enhancement in lignin's antimicrobial efficacy through chemical modification and highlights the potential for further improvements by incorporating additional chemical structures, such as cationic functional groups through chemical modification. This study opens new avenues for maximizing the antimicrobial potential of lignin, contributing to sustainable and eco-friendly solutions for pathogen control.

5:00 PM MF03.04.02

Tough 3D Printable Hydrogels Based on Force Responsive Protein Unfolding Ana Paula Kitos Vasconcelos, Naraa Sadaba, Antonio Vazquez and Alshakim Nelson; University of Washington, United States

The field of mechanochemistry has primarily focused on small molecules as the mechanophores that undergo mechanically-induced chemical transformations. Nature, however, uses macromolecules, such as proteins, as mechanically responsive elements in biological signaling and response. 3D printed thermosets based on the globular protein bovine serum albumin (BSA) as a biologically-derived mechanophore crosslinker have demonstrated high strength, ductility and shape memory, attributed to mechanically-responsive protein unfolding and refolding; however, these properties were not observed for the associated hydrogel. Herein, we develop a photopolymerizable hydrogel with a highly defined network topology based on norbornene functionalized BSA and poly(ethylene glycol) dithiol and a loosely-crosslinked interpenetrating network to observe mechanically-induced BSA unfolding. Harnessing BSA as a force-responsive crosslinker imparts high strength, toughness, ductility and tear resistance in 3D printable hydrogels, due to the disruption of the protein native structure and subsequent release of stored length as an energy dissipation mechanism to resist material failure. The development of this network enables the incorporation of a vast array of proteins as stimuli-responsive crosslinkers in vat photopolymerizable hydrogels.

5:00 PM MF03.04.03

Extrusion-Based 3D Printing of Gelatin-Carboxymethyl Cellulose Scaffolds for Tissue Engineering Applications Sule Yetis and Duygu Ege; Bogazici University, Turkey

3D printing in tissue engineering with natural polymers has significantly grown in the past decade. Gelatin (Gel) is a biocompatible polymer with high cell affinity due to its RGD groups; however it is not possible to 3D print it solely due to its low viscosity. Carboxymethyl cellulose (CMC) is another natural polymer used in tissue engineering and by blending CMC with Gel, the viscosity of the prepared ink can be increased and scaffolds can be efficiently 3D printed. In this study, Gel-CMC-based tissue scaffolds were prepared by using extrusion-based 3D printing. Tissue scaffolds were prepared for 3D printing using varying concentrations of Gel-CMC. The Gel concentration was adjusted within the range of 7.5% to 15% (w/v), while the CMC concentration remained constant at 7.5% (w/v), resulting in four formulations named as Gel7.5CMC7.5, Gel10CMC7.5, Gel12.5CMC7.5, and Gel15CMC7.5. Then, the samples were crosslinked with NHS:EDC to enhance their stability. The prepared inks were characterized with rheological study and the printed scaffolds were analyzed in terms of their Fourier Transformed Infrared Spectroscopy (FTIR), mechanical study, swelling, degradation and contact angle measurements. The rheological results showed that the dominance of the storage modulus (G') over the loss modulus (G'') highlights a prevalent elastic behavior, a solid-like response exhibited by all groups. The increase in Gel concentration resulted in higher viscosity values, printing temperature and pressure, primarily due to the enhanced electrostatic interactions between Gel and CMC. According to the mechanical test results, the elastic modulus ranged from 921 ± 23.50 kPa to 543.12 ± 42.42 kPa indicating a suitable platform for soft tissue engineering applications. Furthermore, as the amount of Gel increased, the tissue scaffolds swelled less, and G15-C7.5 had the lowest swelling ratio. This is because G15-C7.5 had the most covalent crosslinking, which made it swell relatively less than other groups. The contact angle measurements for the 3D printed scaffolds ranged from 45.69° to 71.68° , indicating that these scaffolds possess hydrophilic characteristics. Overall, Gel-CMC inks with different concentrations were printable, which are promising ink candidates for 3D printing for tissue engineering applications, and 3D printed Gel-CMC-based tissue scaffolds presented proper hydrophilic and mechanical properties.

5:00 PM MF03.04.04

Scalable Advance Manufacturing of Complex Multilayer Structures Film with Simultaneous Slot Dies Deposition Method Minwoo Jung; Georgia Institute of Technology, United States

The application of slot die coating manufacturing techniques has been widely studied due to their scalability, continuous process, and relatively cost-effectiveness. Slot die coating is applied to manufacturing organic thin film transistors (OTFT), organic capacitors, organic solar cells (OSC), and membranes. However, OTFT, organic capacitor, OSC have multilayer complex structures for their functionality, and advanced membrane often requires multilayer and patterned structure. Fabricating such products that have multiple-layer complex structures requires multiple manufacturing steps since the most widely used slot dies are limited to a single layer. With additional layers, a separate single-layer slot die and drying oven are needed, which often results in energy consumption and requires space for extra manufacturing tools. Therefore, reducing manufacturing steps to a minimum can be beneficial in terms of cost and environment. To overcome limitations of single-layer slot die, current technology allows depositing two layers at single steps using a bilayer slot die but limited to two layers and patterning deposition using a co-deposition slot die but limited to a single layer. However, these techniques still require more than two steps to fabricate the abovementioned products. To further reduce the extra steps for a multilayer complex structure, the co-deposition slot die, and Bilayer slot die can be deposited simultaneously on top of each other. Simultaneous deposition of co-deposition slot die and Bilayer slot dies can reduce the drying step, which consumes a large portion of the energy in the slot die process. Furthermore, negating drying ovens can reduce the footprint of the manufacturing line as mentioned above.

Using advanced manufacturing methods by simultaneous deposition of co-deposition and bilayer slot die, unique structure of simple capacitor can be achieved. Poly(3,4-ethylenedioxythiophene) polystyrene sulfonate (PEDOT:PSS) was used as conductive polymer, Polyvinyl alcohol (PVA) as insulating polymer, and Sodium carboxymethyl cellulose (CMC) as viscosity modifier. The surface tension and viscosity of the PEDOT:PSS was modified to stabilize the co-deposition film while the bilayer was deposited on top. Co-deposition slot die deposit alternating strip pattern that consists of PEDOT:PSS for conducting layer and PVA for insulation between PEDOT:PSS stripes. The bilayer deposits two layered films on top of the Co-deposition, without any drying step, that consist of PVA as the bottom layer and PEDOT:PSS as the top layer. The resulting film structure is a conductive polymer layer on the bottom of the film, an insulating layer for the middle layer, and another conducting layer on top resembling the capacitor's structure. Even though the resulting capacitor performance is subpar due to low-grade PEDOT:PSS, the advanced manufacturing method using simultaneous co-deposition and bilayer slot die can be applicable to a variety of products that consist of complex structure in reduced steps.

5:00 PM MF03.04.05

Nanocellulose Networks: Utilizing Colloidal Processing Principles to Tune The Mechanical Properties of Solid Foams [Aban Mandal](#), Hareesh Iyer and Eleftheria Roumeli; University of Washington, United States

In recent years, nanocellulose has emerged as a sustainable and environmentally friendly alternative to traditional petroleum-derived structural polymers. However, the widespread implementation of nanocellulose is hindered by high energy-intensive extraction and processing methods, limited quality reliability, and cost-effectiveness [1]. In addition, the required fundamental understanding of process parameters that govern the morphology and structure-property relationships of nanocellulose systems, from colloidal suspensions to bulk materials, has not been developed and generalized for all forms of cellulose. This further hinders the more widespread adoption of this biopolymer in applications.

In this study, we explore the tunability of mechanical properties of cellulose bulk structures, by investigating the intricate connections between thermodynamic, electrokinetic, and hydrodynamic interactions in nanocellulose networks, within the context of stability, phase transformations, and their profound impact on enhancing the properties of bulk materials. To delve into thermodynamic interactions, we examine different concentrations of various nanocellulose-solvent pairs with varying Flory-Huggins interaction parameters. Electrokinetic interactions are explored by manipulating surface charge densities, while hydrodynamic interactions are studied through concentration-based transitions. The interplay between thermodynamic and electrokinetic stability is elucidated through time-series polarized light and cross-polarized light imaging of the nanocellulose colloids. We employ Dynamic Light Scattering (DLS) to assess the Fuchs Stability Ratio and correlate the Diffusion Limited Cluster Aggregation (DLCA) and Reaction Limited Cluster Aggregation (RLCA) regimes[2] with the rheological properties of the colloids. This sheds light on the underlying mechanisms and the specific interactions responsible for the concentration-based Onsager's Isotropic to Nematic phase transition, and in addition, enables a co-relation of the properties at the colloidal state [3] and the final solid structures. Small-angle X-ray scattering (SAXS) is employed to comprehensively understand the influence of various processing parameters on the ordering of the final bulk structure and, subsequently, the structure-property relationships. Our study enriches the understanding of nanocellulose processing from a polymer physics and colloidal chemistry perspective. These findings hold the potential for extending to multicomponent biomass-based systems in the future, contributing to sustainable and high-performance materials development.

1. Dileswar Pradhan, Amit K. Jaiswal, Swarna Jaiswal, "Emerging technologies for the production of nanocellulose from lignocellulosic biomass", Carbohydrate Polymers, Volume 285,2022,119258, ISSN 0144-8617, <https://doi.org/10.1016/j.carbpol.2022.119258>.

2. M. Mellema, J. H. J. van Opheusden, T. van Vliet; Relating colloidal particle interactions to gel structure using Brownian dynamics simulations and the Fuchs stability ratio. J. Chem. Phys. 1 October 1999; 111 (13): 6129–6135. <https://doi.org/10.1063/1.479956>

3. Kummer, T., Kummer, N., Nordenström, M., Fall, A. B., Nyström, G., & Wågberg, L., The Colloidal Properties of Nanocellulose, ChemSusChem, <https://doi.org/10.1002/cssc.202201955>

5:00 PM MF03.04.06

Effect of Wet-Stretching and Confinement on Fiber Alignment in Bacterial Cellulose Films [Kuotian Liao](#), Julia Blair, Kwon-Teen M. Chen, Esther Nicolaou and Eleftheria Roumeli; University of Washington, United States

Recent progress in sustainable materials has provided viable solutions to address the escalating challenges posed by non-renewable sourcing, environmentally harmful manufacturing processes, and the ultimate fate of synthetic plastics. Within this context, biopolymers have garnered increasing interest for their potential as eco-friendly substitutes to petroleum-derived counterparts, offering the distinct advantage of reduced environmental impact across their entire lifecycle. Bacterial cellulose (BC) stands out as a particularly compelling candidate, combining a high molecular weight, high degree of crystallinity, and a scalable, adaptable biosynthetic manufacturing process. Unlike plant-derived cellulose, BC circumvents the need for extensive extraction procedures, rendering it more accessible and environmentally benign. Following drying, the naturally grown BC hydrogels, called pellicles, can be transformed into self-supporting, lightweight yet mechanically robust films with prospective applications in structural panels or protective garments. This study delves into the effect of mechanical stretching/confinement as means of aligning the fibers in BC pellicles and their impact on the overall mechanics of the resulting dried films, aiming to offer fundamental insights into the structure-property interplay of this networked polymer. The results will not only enrich our fundamental understanding of polymer physics pertaining to BC-based networks, but also pave the way for future tailoring of the properties of the resulting films to cater to a diverse array of applications.

5:00 PM MF03.04.07

Effects of Chemical Treatments and Additives on Bacterial Cellulose Foams [Hareesh Iyer](#), Michael Holden and Aban Mandal; University of Washington, United States

Renewable and biodegradable materials, including algae and cellulose, have emerged as promising alternatives to non-biodegradable petrochemical plastics. Bacterial cellulose (BC), a form of pure cellulose that is synthesized by bacteria, is an interesting alternative to plant cellulose due to the reduced processing required to harvest it. Here, we explore the utilization of BC as a biodegradable and renewable substitute for petroleum-derived plastic foams, both in its pure form and as a composite. The study investigates the chemical modification of cellulose, specifically using deep eutectic solvents (DES), to change its mechanical and morphological properties. Compression testing, Fourier transform infrared spectroscopy (FTIR), and X-ray photoelectron spectroscopy (XPS) are used to analyze the mechanical, morphological, and chemical bonding changes made to the cellulose. Subsequently, natural additives such as xanthan gum, glucomannan, pectin, and agar are evaluated as potential additives for BC composite foams. These additives are added with the aim to replicate the recoverability of commercial polymer foams made of materials such as polystyrene and polyurethane. By modifying the types of biopolymers, as well as their amounts and processing, we show significant changes in the mechanical and micromorphological properties of the cellulosic foams. We show that, especially with the addition of pectin, we are able to significantly improve the compressive strength and recoverability of BC foams while maintaining stiffness. Lastly, aiming to address the viscoelastic responses of the produced composite foams, we subject them to cyclic compression and stress-relaxation tests.

5:00 PM MF03.04.08

Understanding 3D Networks Structure during Biosynthesis of Cellulose from Bacteria [Julia Didier Amorim](#)^{1,2}, [Kuotian Liao](#)², [Hareesh Iyer](#)² and [Eleftheria Roumeli](#)²; ¹Universidade Rural de Pernambuco, Brazil; ²University of Washington, United States

Materials sourced from renewable sources and synthesized under mild conditions offer coupled benefits in terms of sustainability, in contrast to petroleum-derived polymers, which are known contributors to pollution and adverse health consequences. Bacterial cellulose (BC) consists of high aspect ratio fibrils that bundle into fibers, forming 3D networks which can be influenced by growth conditions. BC pellicles, which are produced in static conditions and are often used in research and applications, exhibit a layered structure at the mesoscale. These layers form as successive entangled fiber networks are deposited extracellularly during BC growth. The layered structure is a distinctive feature of BC pellicles and contributes to their unique mechanical properties. The growth conditions during BC fiber synthesis significantly influence the alignment, crystallinity, and 3D morphology of the formed network. However, there is a lack of understanding of the fundamentals of cellulose fiber aggregation into network assemblies. Understanding how nanoscale fibrils bundle, entangle, and form larger structures at the mesoscale is crucial for tailoring BC's properties for various applications, from biotechnology to materials

science. We investigate the intricate structural evolution of BC, spanning from the nanoscale to the mesoscale, with a specific focus on understanding entanglement phenomena. Furthermore, our investigation explores the significance of fibril entanglement in BC networks, providing insights into the intricate process by which individual nanofibrils interweave to construct the broader mesoscale framework. This research aims to provide a comprehensive understanding of BC's structural development.

5:00 PM MF03.04.09

Bio-Based Pickering Foams, From Fundamentals to Applications [Roozbeh Abidinejad](#)¹, Bruno Mattos¹, Eero Kontturi¹ and Orlando Rojas^{2,1}; ¹Aalto University, Finland; ²The University of British Columbia, Canada

Colloids are suitable options to replace surfactants in the formation of multiphase systems, while simultaneously achieving performance benefits. We introduce a synergistic combination of colloids for the interfacial stabilization of complex fluids that can be converted into lightweight materials. The strong interactions between high aspect ratio and hydrophilic fibrillated cellulose (CNF) with low aspect ratio hydrophobic particles afford Pickering foams. Compared to foams stabilized by the hydrophobic particles alone, the introduction of CNF significantly increased the foamability (by up to 350%) and foam lifetime. These effects are ascribed to the fibrillar network formed by CNF. The CNF solid fraction regulated the interparticle interactions in the wet foam, delaying or preventing drainage, coarsening, and bubble coalescence. Upon drying, such a complex fluid was transformed into lightweight and strong architectures, which displayed properties that depended on the surface energy of the CNF precursor [1].

Such systems can be further utilized for various purposes, including fire retardancy and thermal insulation. Many applications, including buildings and chemical and thermal processes, call for thermal insulation. Environmental awareness, however, is driving the industry toward more ecologically friendly and sustainable technologies. In this light, switching to renewable raw materials from petroleum-based foams is of importance [2,3]

References:

- [1] Roozbeh Abidinejad, Marco Beaumont, Blaise L. Tardy, Bruno D. Mattos, and Orlando J. Rojas. ACS Nano 2021 15 (12), 19712-19721
- [2] Wang, P., Aliheidari, N., Zhang, X., Ameli, A., 2019. Strong ultralight foams based on nanocrystalline cellulose for high-performance insulation. Carbohydr. Polym. 218, 103–111.
- [3] Lohtander, T., Herrala, R., Laaksonen, P. et al. Lightweight lignocellulosic foams for thermal insulation. Cellulose 29, 1855–1871 (2022).

5:00 PM MF03.04.10

Hydrogel-Ceramic Composite for Efficient Oil Water Separation in Emulsified System [Harsh Rohit](#), Shobha Shukla and Sumit Saxena; Indian Institute of Technology Bombay, India

Water pollution due to oil remains a prominent environmental concern, primarily driven by escalating incidents of oil spills, intensive petroleum operations, rapid expansion of the food industry, and the growth of textile, metal, and leather sectors. Oily wastewater discharged from these industries aggravates the problem, posing a significant threat to soil quality, water bodies, aquatic ecosystems, and human health. Ships discharge oily water which is governed by MARPOL. Although numerous techniques and materials are available for oil-water separation, filtration material systems exhibit promise due to their expansive surface area, appropriate pore sizes, lightweight structure, and cost-effectiveness. Filtration systems being invested across the community are majorly made of polymers and ceramics. Polysulfone (PSF), Polyacrylonitrile (PAN), Cellulose Acetate (CA), Sodium Alginate (NaAlg), Polyvinylidene fluoride (PVDF) are some of the polymers which, post morphological and chemical modification using functional groups are used for oil water separation. Across ceramic membranes, Titania (TiO₂), Silicon Carbide (SiC), Alumina (Al₂O₃), Silicon Nitride (Si₃N₄) etc. have been explored. A novel composite of Hydrogel with ceramic membrane made of Alumina, Zirconia and SiC has been tailored for efficient oil-water separation. The composite shows very high separation efficiency (beyond 99%) with very good antifouling properties. Furthermore, it is non-toxic and has very high pH and salinity resistance. The composite has potential to be used for pressure driven operations in industries for a high flux and better separation efficiency for continuous oil-water separation where water is in continuous phase.

5:00 PM MF03.04.11

Mycelium Bridge Behavior for Sustainable, Architected Biocomposites [Branden Spitzer](#), Sabrina Shen and Markus Buehler; Massachusetts Institute of Technology, United States

There is growing interest in the design of sustainable materials based on mycelium, the root network of fungi, due to its robust, interconnected growth and its degradable end of life. Our work aims to understand the fundamental interactions between mycelium, substrate materials, and void spaces, which can inform the design of complex and functional mycelium composites. In particular, here we investigate the ability of mycelium to bridge gaps of empty space within a waste-derived bio-composite material and observe the effects of varying nutritional content. The bio-composite substrate is suitable for 3D printing, which enables the creation of an array of complex forms. Understanding the formation and strength of mycelial bridges supports the future design of mycelium composite materials for self-healing, bio-welding, directed growth, and sustainable structure applications.

5:00 PM MF03.04.12

Sequence Control of Bioinspired Calcium-Responsive Protein-Based Polymers [Marina P. Chang](#), Gatha M. Shambharkar, Winnie Huang, Kenny M. Hernandez and Danielle J. Mai; Stanford University, United States

Protein-based polymers offer improved sustainability over fossil-based synthetic polymers because of their biodegradability and their composition from abundant, renewable materials. Natural proteins exhibit a wide range of functions, providing bioinspiration for engineering responsive protein-based polymers. Responsiveness to biological signals, such as calcium ions, allows protein-based polymers to mimic biological functions like muscle contraction. The amino acid sequence of protein-based polymers is often modified to tune the function of the polymers without requiring additional steps of chemical synthesis and purification. Tunability is advantageous for applications such as scaffolds for tissue regeneration, where the mechanical properties of the scaffold can be matched to specific tissues.

To create tunable, calcium-responsive, protein-based polymers, we take inspiration from a class of “Repeats-in-Toxin” (RTX) protein domains found in bacterial proteins. These RTX domains undergo a reversible conformation change from random coils to β -roll structures upon binding to calcium. RTX domains are characterized by the repetitive sequence GGXGXDXUX, in which glycine (G) and aspartic acid (D) are highly conserved in the calcium-binding region. For positions that are less conserved, U represents an aliphatic amino acid and X represents any amino acid. We explored the impact of amino acid substitutions at a non-conserved X site in the calcium-binding region. These amino acid substitutions probe the impact of monomer size, electrostatic interactions, and hydrophobicity on the calcium-responsive behavior of RTX domains. Additionally, we explored the impact of sequence variability by creating consensus RTX domains, which comprise tandem repeats of the simplified consensus sequence GGAGXDTLY. Circular dichroism reveals that some variants exhibit more ordered structures in the absence of calcium compared to wild-type RTX, particularly variants with smaller amino acid substitutions. By varying the amino acid sequence, we can tune the calcium sensitivity of RTX between 1 – 100 mM CaCl₂. Finally, RTX domains are incorporated into fusion protein polymers to create calcium-responsive materials with tunable stiffness for biomedical applications such as tissue scaffolds.

5:00 PM MF03.04.13

Rapid Photo-Triggered Release Kinetics of PPA Microcapsules [Yongsu Shin](#)¹, Jared Schwartz¹, Anthony Engler¹, Brad H. Jones² and Paul Kohl¹; ¹Georgia Institute of Technology, United States; ²Sandia National Laboratories, United States

Stimuli-responsive microcapsules have been investigated as a means to release special-purpose payloads such as catalysts inside solid polymer materials. These catalyst payloads have garnered recent interest in the recycling and upcycling of plastics. A microcapsule can be loaded into common commodity plastics and triggered to release a catalyst for depolymerization. Specific chemical conditions or structural changes have commonly been used to trigger microcapsules for controlled release, but these mechanisms tend to not be amplified or take substantially long times to induce release. Long times for release impact the cost of processing, especially for recycling that would otherwise require an outside-in mechanism. Unlike other stimuli, light has advantages in that it is readily available and convenient to use with low cost. This study utilized poly(phthalaldehyde) (PPA) microcapsules formulated with various UV-sensitive photo-acid generators (PAGs). Upon exposure to UV irradiation followed by heat treatment, PAGs generate and release strong acids that attack the PPA, which initiates rapid depolymerization back to the monomer. In the case of a microcapsule made with a PPA shell, the rapid depolymerization results in the immediate release of the capsule payload to its surroundings. PPA capsules were made using an oil-aqueous emulsification process in the presence of surfactants and their morphologies are a fraction of blueberry shapes (high loading of core) and a fraction of concave shapes (low loading of core). As UV dose increased, more capsules were depolymerized and more dodecane core was obtained, indicating core release. The percentage of dodecane release and depolymerized PPA were analyzed using ¹H NMR. The photo-triggered response was further tuned by varying PAG concentration, PAG type, and post-exposure heating time. The efficiencies of the PAGs were compared for their release kinetics and the energy required to fully decompose the shell. PPA microcapsules with UV-sensitive PAGs successfully released their core within a short time and with low UV doses.

5:00 PM MF03.04.14

Investigating The Pozzolanic Reactivity of Natural Zeolite as a Supplementary Cementitious Material: Correlations to Mechanical Performance [Brandon T. Lou](#), Dwayne Arola and Eleftheria Roumeli; University of Washington, United States

Cement, the binding material in concrete, produces a significant amount of atmospheric CO₂ during its production. Therefore, methods to reduce the amount of cement used in concrete production, while maintaining adequate strength and durability, has substantial environmental implications. Natural zeolites are being considered to replace a portion of cement content as a supplementary cementitious material (SCM) due to its high pozzolanic activity, which is attributed to their porous aluminosilicate framework. However, the detailed reactions between the zeolite and cement, namely the effect of the hydration reactions, as well as zeolite's contribution from physical characteristics, are not fully understood. Previous studies have characterized pozzolanic activity, assessed particle size and preprocessing contributions, mechanical properties, and performed chemical component analyses separately. However, there are inconsistencies among reported results and the materials science of the structure/processing/performance was not elucidated. Here, the pozzolanic activity of natural zeolite is characterized with respect to the degree of hydration of mortar mixes and correlated to the mechanical performance of concrete composites. The natural zeolite is first analyzed to understand its microstructure, elemental, and mineralogical composition using scanning electron microscopy (SEM), energy dispersive x-ray spectroscopy (EDS), and x-ray diffraction (XRD). Bound water measurements are utilized to quantitatively assess the pozzolanic reactivity of the zeolite, and over a range of particle sizes (achieved via milling). We then varied the percentage of natural zeolite in mortar composites at different particle sizes and concentration with respect to cement content. The effects of particle size on the micromorphology, degree of hydration, and development of bonding environments of the composites is observed via SEM, thermogravimetric analysis (TGA), and Fourier transform infrared spectroscopy (FTIR). The experimental results confirm that zeolite replacement of cement content in mortar composites enhances the mechanical performance at a discrete particle size and concentration. There are optimum parametric conditions to maximize strength that appear based on the increased degree of hydration stemming from increased pozzolanic activity of zeolite. Overall, this experiment demonstrates that natural zeolites are a viable SCM to reduce cement content in concrete composites and that further work could support the development of a truly superior sustainable concrete.

5:00 PM MF03.04.15

Energy-Efficient Manufacturing and Lightweight Applications of Expanded Ethylene-Propylene-Butene-1 Copolymer Bead [Peng Guo](#); SINOPEC Beijing Research Institute of Chemical Industry, China

Ethylene-propylene-butene-1 ternary copolymer (TPP) and ethylene-propylene copolymer (EPC) were fabricated to produce expanded polypropylene (EPP) beads through batch-foaming followed by steam-chest molding. The microstructure and thermal behaviors of both TPP and EPC were investigated by nuclear magnetic resonance, gel permeation chromatography, wide-angle X-ray diffraction, analytical temperature rising elution fractionation, and differential scanning calorimetry. EPP beads made of TPP and EPC were prepared by an autoclave batch-foaming process using compressed CO₂ as the blowing agent. Polypropylene micropellets (average diameter is approximately 1 mm) were obtained using an underwater micro-pelletizer system, which shorten the CO₂ diffusion distance. The effects of CO₂ content on the melting temperature of two types of polypropylene were studied. Magnetic suspension balance was used to measure the solubility of CO₂ in semi-molten PP. The effects of introducing comonomers on the foaming processing and cell structure of EPP beads were preliminarily investigated. The addition of 1-butene played a significant role in enhancing the mechanical properties and decreasing the energy cost during both batch-foaming and steam-chest molding with reduced carbon dioxide emissions.

5:00 PM MF03.04.16

Engineered Wood Materials Utilizing Seaweed Biomass as an Adhesive [Mallory Parker](#)¹, Paul Grandgeorge¹, Ian R. Campbell¹, Hannah Nguyen¹, Rebekah I. Brain¹, Scott Edmundson², Deborah Rose², Chinmayee Subban² and Eleftheria Roumeli¹; ¹University of Washington, United States; ²Pacific Northwest National Laboratory, United States

The increasing concerns associated with petroleum-derived resources call for sustainable renewably sourced alternatives. Engineered wood materials are widely used in the form of panels and particleboards in structural applications, construction and packaging. Wood-products provide multiple advantages such as sustainable feedstocks and lightweight final products that can meet load-bearing requirements for a plethora of applications. However, engineered wood products, such as medium density fiberboards (MDF), most predominately rely on formaldehyde-based adhesives to achieve wood particle/fiber bonding. Such adhesives are not only petroleum-derived but also have detrimental health effects during use (formaldehyde emissions) and at their end-of-life. To further mitigate the environmental impact of construction materials, more sustainable bonding agents need to be investigated. In this work, we hypothesize that the biopolymers within seaweed biomass can form a strong hydrogen bonding network with wood particles, that can be sufficient to create a set of fully biobased engineered wood composites. The use of seaweed as an adhesive would offer the benefits of carbon sequestering and renewable sourcing, as well as non detrimental end-of-life effects. We test our hypothesis using *Ulva expansa* (*Ulva*) as a proof-of-concept seaweed species and report the manufacturing of engineered wood composites with varying concentration of waste wood particles and *Ulva*, as well as a detailed study of their structure, bonding and mechanical properties. We demonstrate that upon hot-pressing, powdered *Ulva* flows in between the wood particles and provides a strong binding effect. We show that the flexural strength of produced engineered wood composites increases with increasing *Ulva* concentrations. We further report that the presence of *Ulva* attractively improves other properties such as water resistance and flammability. To highlight the bonding mechanisms at the biopolymeric level, we perform Fourier-transform infrared spectroscopy (FTIR) studies. We also show that the resulting wood panels can be machined using traditional drilling or laser-cutting methods. Finally, we perform an analysis of the environmental impact of ulva-bonded engineered

wood composites.

5:00 PM MF03.04.17

Recyclable Cellulose-Polymer Composites Using Silica Nanoparticle incorporated Nano- and Micron-Sized Cellulose Fibers [Jung-woo Park](#) and Young-soo Seo; Sejong University, Korea (the Republic of)

Interest in sustainable and biodegradable plastic fillers has increased due to environmental concerns and legislative regulations. Therefore, cellulose fiber (CF) with excellent mechanical properties has attracted attention recently. However, there are issues when it is mixed with plastics, which are lack of dispersion and limited thermal stability of CF. CF that aggregates immediately when dried due to capillary forces does not disperse well in plastic and oxidizes easily to render a brownish color during the melt mixing process reducing circularity. Here, to address these issues, the CF surface was modified with silica nanoparticles via a sol-gel reaction to provide some distance between fibers in the powder form of CF resulting in dispersion enhancement by reducing van der Waals interactions. At the same time, its thermal stability is improved due to the silica cladding that protects the CF surface from heat. We applied the silica-covered nano- and micron-sized CF to plastics such as polyamide (PA6) and polylactic acid (PLA) using melt-mixing processes including extrusion. Mechanical properties such as tensile and flexural strength of the composites and rheological and thermal properties such as glass transition and melting temperatures and heat distortion temperature will be presented.

5:00 PM MF03.04.19

Developing Sandwich Structure with Novel Biobased Composite Using Additive Manufacturing [Mahyar Fazeli](#); Aalto University, Finland

Sandwich structures are considered as promising designs for structural applications showing high stiffness, low weight, and high energy absorption properties. In this study, the sandwich panel is designed and fabricated using different plywood as the face sheet and thermoset-based composite as the core. The additive manufacturing (AM) method is employed to print the composite structure onto the plywood surface, enabling precise control over the material distribution and enhancing the bonding between the face sheets and the core. The optimized design and manufacturing process allowed for the integration of a thermoset-based composite core, which contributed to the overall weight reduction of the panel while maintaining its structural integrity. The flexural testing showed significant improvement in the sandwich panel compared to the plywood with the same thickness. The flexural strength and modulus increased up to 3.4 and 3.6 times, respectively. The resulting sandwich panel demonstrated exceptional load-carrying capacity and resistance to bending, making it a viable candidate for various structural applications where weight reduction and high performance are critical.

5:00 PM MF03.04.20

The Transfer to Sustainable Fashion: How The Textile and Clothing Industry Promote Waste Joud AlKhawashki¹ and [Mohammad Hayal Alotaibi](#)^{2,1}; ¹Alfaisal University, Saudi Arabia; ²King Abdulaziz City for S&T, Saudi Arabia

the textile industry is the second largest industry in manufacturing. The textile industry pays a huge contribution to the fashion and clothing industry by acting as its base, however with the high and on-going demand in clothing and garments “Fast Fashion”, and overconsumption are increasing as well moreover leading to a substantial and sequential rise in environmental issues and concerns such as pollution. The textile and fashion industry are the highest polluting industries, playing a critical role in water consumption and pollution, solid waste pollution as well as resource depletion. Due to its greatly negative impacts on our environment in addition to our environment’s current deteriorating state, global organizations such as the European Union (EU) as well as individual designers and the fashion and textile industry as a whole’s implementing techniques for sustainable fashion in order to sustain a green environment and lifestyle as well as promote a circular economy. Clothing has a significant influence on Saudi Arabia’s tradition and culture. Saudi Arabia’s vision 2030 is following a green initiative and in order to succor a sustainable approach Saudi designers and entrepreneurs are following sustainable fashion and clothing as an eco-friendly alternative. The essence of green chemistry as well as up-cycling redesigning are used in the sustainable clothing industry, in addition to implementing regulations and laws.

5:00 PM MF03.04.22

Non-Isocyanate Polyurethanes from Mixed Cyclic Carbonates: Carbonated Soybean Oil and Cyclic Carbonate Terminated CO₂-Based Poly(ether carbonate) [Ga Ram Lee](#), Eun Jong Lee, You Jin Jeon and Sung Chul Hong; Sejong University, Korea (the Republic of)

Non-isocyanate polyurethane (NIPU) has received significant attention in sustainability research due to its potential to be synthesized without the inclusion of toxic isocyanate raw material and catalysts. In this study, CO₂ is further employed as an eco-friendly resource to afford poly(ether carbonate) polyols, which is then chemically transformed to introduce cyclic carbonate terminal groups (PECC). Separately, soybean oil with cyclic carbonate functional groups (CSBO) is prepared as an example of sustainable raw material from bio-renewable resources. NIPU is then prepared through the ring-opening reaction of multi-amines and the cyclic carbonate functional groups of PECC/CSBO mixtures. Characteristics of the resulting NIPUs including physical and thermal properties are investigated, demonstrating reasonable and tunable tensile properties. This study demonstrates the preparation of industrially important polyurethane materials from eco-friendly renewable resources, well exemplifying our current and increasing endeavors to realize sustainable polymers. This work was supported by Korea Institute of Energy Technology Evaluation and Planning (KETEP) grant funded by the Korea government (MOTIE) (20208401010080, Development of Demonstration for Synthesis of High Value Chemical using Captured CO₂).

5:00 PM MF03.04.23

Towards The Recycling of Plastic Mixed Wastes: Noncatalytic C-H Insertion of Azidoformate-End Functionalized Polystyrene to modify Polypropylene for Compatibilized Polypropylene/polystyrene Blend [Ga Ram Lee](#), Rama Moorthy Appa and Sung Chul Hong; Sejong University, Korea (the Republic of)

Recycling of heterogeneous mixed plastic waste poses a formidable challenge due to the strong incompatibility arising from the different chemical and molecular structures of the constituent polymers. This challenge inspires us to study industrially viable method to enhance compatibility of polymer blends, leading to more homogeneous morphologies and improved mechanical performances. In this study, an azo-type radical initiator with azidoformate (AF) at both ends is firstly prepared, which is then employed for the radical polymerization of styrene to afford AF end-functionalized polystyrene (AFPS). The noncatalytic C-H insertion capability of AF group of AFPS allows the grafting reaction of AFPS onto polypropylene (PP) through industrially acceptable conventional melt process, affording PP-graft-PS. The characterization on the resulting PP-graft-PS demonstrates enhanced Young’s modulus and more elastic rheological behaviors, along with homogeneous fractured surface morphology and slightly decreased crystallinity. Given the substantial contributions of PP and PS in plastic consumption, the PP-graft-PS prepared in this study is expected to work as an *in-situ* compatibilizer in PP/PS, which may alleviate separation issue of mixed plastic wastes.

5:00 PM MF03.04.25

Production of Biodegradable Plastic Composites Using Agricultural Residual Biomass [Alexandrea Maerz](#), Anthony Dichiaro, Renata Bura and Rick Gustafson; University of Washington, United States

Global plastic pollution is a major environmental problem, with millions of tons of plastic waste accumulating in the oceans and landfills every year [2]. It becomes crucial to develop biodegradable alternative materials that generate less greenhouse gas emissions, can be broken down by microorganisms in the environment, and improve soil health and fertility when composted. Many currently available bioplastics, such as polylactic acid (PLA), fail to biodegrade effectively unless treated under conditions found in commercial composting facilities – high temperatures and forced air [4]. Other more biodegradable polymers are typically challenged by either high manufacturing costs or poor strength and barrier properties [3]. An innovative approach to imparting biodegradability to a polymer while achieving excellent mechanical characteristics consists of introducing fibrous structures into polymer matrices. This method not only endows the composite with good mechanical properties but also provides a vehicle for water and biodegrading enzymes to slowly penetrate the composite structure leading to complete biodegradation [7]. Recent research revealed that the incorporation of nanocellulose into polymer matrices can improve the composite performance both in terms of strength and biodegradability [1, 5, 7]. The present work reports the production of lignocellulosic nanomaterials from inexpensive wheat straw feedstock and alkaline peroxide pulping followed by mild peracetic acid treatment at pilot scale [6, 7]. The resulting cellulose nanofibrils have been extensively characterized and applied to prepare thin, flexible, and translucent composite films with low poly(vinyl) alcohol contents (i.e. below 40 wt.%) using a simple solvent casting method. The mechanical, optical, and barrier properties of as-prepared composites have been thoroughly examined. This novel bioplastic has the potential to replace petroleum-derived plastics across a broad range of industries such as aquaculture, agriculture, food packaging, and more; promising applications include ground covers, drip lines, goosy duck tubes, aqua nets, and paperboard lining or film covering for food packaging [2, 3, 8]. Furthermore, this work provides an analysis of the techno-economic performance of the system accounting for optimization of operational efficiency, cost-effectiveness, and sustainability factors. The findings contribute valuable insights into resource allocation and investment strategies in sustainable bioproduct systems.

- [1] Abraham, E., et al., X-ray diffraction and biodegradation analysis of green composites of natural rubber/nanocellulose. *Polymer Degradation and Stability*, 2012. 97(11): p. 2378-2387.
- [2] Huang, Y., et al., Agricultural plastic mulching as a source of microplastics in the terrestrial environment. *Environmental Pollution*, 2020. 260: p. 114096.
- [3] Kjeldsen, A., et al., A Review of Standards for Biodegradable Plastics. *Industrial Biotechnology Innovation Centre*, 2018.
- [4] Muniyasamy, S., et al., Mineralization of Poly(lactic acid) (PLA), Poly(3-hydroxybutyrate-co-valerate) (PHBV) and PLA/PHBV Blend in Compost and Soil Environments. *Journal of renewable materials*, 2016. 4(2): p. 133-145.
- [5] "Nanofibrillated Cellulose (Cellulose Nanofibril)". accessed 17 November 2021.
- [6] Pascoli, D., et al., A Robust Process to Produce Lignocellulosic Nanofibers from Corn Stover, Reed Canary Grass, and Industrial Hemp. *Polymers*, 2023. 15(4): p. 937.
- [7] Pascoli, D., et al., Lignocellulosic nanomaterials production from wheat straw via peracetic acid pretreatment and their application in plastic composites. *Carbohydrate Polymers*, 2022. 295: p. 119857.
- [8] Pearce, C.M., et al., Juvenile geoduck (*Panopea generosa*) predator protection with tubes: Assessing effects of tube diameter, length, and mesh size on growth and survivorship. *Aquaculture Reports*, 2019. 14: p. 100190.

SESSION MF03.05: Computational
Session Chairs: Gustav Nystrom and Eleftheria Roumeli
Wednesday Morning, April 24, 2024
Room 323, Level 3, Summit

9:00 AM MF03.05.01

A Computational Study of Cellulose Regeneration: All-Atom and Coarse-Grained Molecular Dynamics Simulations Igor Zozoulenko¹, Jiu Pang¹, Patrick Heasman¹, Sarbani Ghosh² and Aleksandar Mehandzhiyski¹; ¹Linköping University, Sweden; ²Birla Institute of Technology & Science, India

Processing natural cellulose requires its dissolution and regeneration. It is known that the crystallinity of regenerated cellulose does not match that of native cellulose, and the physical and mechanical properties of regenerated cellulose can vary dependent on the technique applied. In this paper, we performed all-atom molecular dynamics (MD) simulations attempting to simulate the regeneration of order in cellulose.¹ Cellulose chains display an affinity to align with one another on the nanosecond scale; single chains quickly form clusters, and clusters then interact to form a larger unit, but the end results still lack that abundance of order. Where aggregation of cellulose chains occurs, there is some resemblance of the 1–10 surfaces found in Cellulose II, with certain indication of 110 surface formation. Concentration and simulation temperature show an increase of aggregation, yet it appears that time is the major factor in reclaiming the order of "crystalline" cellulose.

Available experimental data indicates that regeneration of cellulose is a sluggish process. While we tried to push all-atom MD simulations to their limits in terms of the system size and simulation time, our findings demonstrate that to capture the order of the regenerated crystalline cellulose, evolution of much larger systems should be traced for much longer times. For this purpose, coarse-grained (CG) MD simulations based on Martini 3 force-field were developed and applied to study cellulose regeneration at a scale comparable to the experiments.² The X-ray diffraction (XRD) curves were monitored to follow the structural changes of regenerated cellulose and trace formation of cellulose sheets and crystallites. The calculated coarse-grained morphologies of regenerated cellulose were backmapped to atomistic ones. After the backmapping we find that the regenerated coarse-grained cellulose structures calculated for both topology parameters of cellulose I_β and cellulose II/III, are transformed to cellulose II, where the calculated XRD curves exhibit the main peak at approximately 20–21 degrees, corresponding to the (110)/(020) planes of cellulose II. This result is in good quantitative agreement with the available experimental observations.

Our results demonstrate that coarse-grained molecular dynamics simulations represent a powerful tool to provide a microscopic insight into the process of cellulose regeneration, which is not available by conventional experimental means.

(1) Heasman, P.; Mehandzhiyski, A. Y.; Ghosh, S.; Zozoulenko, I. A Computational Study of Cellulose Regeneration: All-Atom Molecular Dynamics Simulations. *Carbohydr. Polym.* 2023, 311, 120768. <https://doi.org/10.1016/j.carbpol.2023.120768>.

(2) Pang, J.; Mehandzhiyski, A. Y.; Zozoulenko, I. A Computational Study of Cellulose Regeneration: Coarse-Grained Molecular Dynamics Simulations. *Carbohydr. Polym.* 2023, 313, 120853. <https://doi.org/10.1016/j.carbpol.2023.120853>.

9:15 AM MF03.05.02

This searchable program is up-to-date as of April 15th, 2024.

Machine Learning-Aided Design of Biodegradable Polymers [Jessica N. Lalonde](#)¹, Ghanshyam Pilania², Babetta L. Marrone³, Chiho Kim^{4,5}, Huan Tran^{4,5}, Rishi Gurmani⁴ and Rampi Ramprasad^{4,5}; ¹Duke University, United States; ²GE Global Research, United States; ³Los Alamos National Laboratory, United States; ⁴Matmerize, Inc, United States; ⁵Georgia Institute of Technology, United States

In the pursuit of sustainable materials, biodegradable polymers have emerged as promising alternatives to traditional plastics, finding applications across diverse industries. Particularly, the degradation products of traditional plastic are of specific concern, and fully biodegradable and non-toxic plastic alternatives offer promising solutions to this ongoing challenge. However, a rational design approach to engineer biopolymers for degradation after their intended use still remains elusive. This is largely due to our inability to understand and model performance metrics (such as weight loss over time) capturing degradation behavior of these materials as a function of chemical, geometric and environmental factors.

As an exciting development in this direction, we have established predictive machine learning models which utilize physics-informed deep neural networks (NN) on previously established, manually curated experimental data that characterizes the weight loss behavior of fully biodegradable polyester copolymer samples in both water and soil natural environments. The models were applied in a series of experiments to predict the mass loss of approximately 10,000 structural and compositional variations of the 230 homo- and copolymers originally included in the original training set. The predicted mass loss for these candidate biodegradable polymers over a period of 365 days allowed us to identify novel copolymers with the potential to replace existing chemistries while matching property values to the desired performance metric ranges. This talk will discuss our findings and future directions, including the integration of critical properties, such as, thermal and mechanical characteristics, into the screening and design workflow and thereby bringing us one step closer to realizing the grand vision of a sustainable circular plastic economy.

9:30 AM *MF03.05.03

Experimental-Computational Design of Protein-Based Materials [Diego López Barreiro](#); University College London, United Kingdom

Nature leverages the self-assembly propensity of structural proteins like elastin, resilin, collagen, or silk to generate sustainable functional materials with remarkable performance and that span a wide range of mechanical and structural properties: from soft to stiff, from porous to densely packed, from static to dynamic... This is inspiring scientists and engineers to use structural proteins as a sustainable replacement for fossil-based polymers in the manufacture of synthetic functional materials with applications in food, healthcare, adhesives, energy, textiles, or membrane technology, to name a few.

Structural proteins are normally harvested from animal sources (e.g., silkworm cocoons, animal tissue), but these suffer from batch-to-batch variability, presence of contaminants, and cultural or religious concerns that limit their commercial use. Fortunately, developments in engineering biology allow us to overcome these issues and biofabricate non-animal-derived recombinant structural proteins. Furthermore, by carefully engineering their amino acid sequence, we can design entirely new structural proteins with properties inspired by natural structural proteins, but that do not exist in Nature, and use them to develop materials with e.g., adjustable mechanical properties, programmed functionalities, or the ability to adapt or respond to the environment.

However, a complete framework that connects amino acid sequence to material properties is unavailable. Thus, *de novo* recombinant structural proteins are normally developed through low-throughput trial-and-error experimentation, which impedes rapid prototyping. In this talk, we will showcase our work on the combination of computational and experimental tools to accelerate the exploration of the design space of structural proteins. Specifically, we will present examples of how this approach has aided us in the design of new protein-based materials including flexible conductive films, biominingalizing films, or injectable stimuli-responsive hydrogels.

10:00 AM BREAK

SESSION MF03.06: Biomatter Processing, Properties
Session Chairs: Kunal Masania and Eleftheria Roumeli
Wednesday Morning, April 24, 2024
Room 323, Level 3, Summit

10:30 AM MF03.06.01

Pathways to Biorenewable Circularity in Plastics [Brett A. Helms](#); Lawrence Berkeley National Lab, United States

Here, I will discuss how synthetic biology provides an inexhaustible toolbox for the creation of monomers useful for the creation of next-generation circular plastics collectively known as polydiketoenamides. I will highlight how materials properties are dictated not only by the diverse functionalization afforded such strategies, but also the importance of chirality, which is inherent to biology, but lacking or otherwise challenging to scale using conventional chemical approaches. From a materials perspective, not only is it interesting to understand factors governing materials properties stemming from biofunctionalization, but these choices also deeply impact how the materials undergo deconstruction to monomers. I will discuss a variety of phenomena unique to polymers compared to small molecules that guide our understanding of polymer reactivity, particularly as they manifest at different length scales and time scales. I will showcase operando X-ray and NMR capabilities that permit mechanistic studies underpinning deconstruction, which feedback into the materials design and biomolecular target selection.

10:45 AM *MF03.06.02

Engineering Microbes to Produce High-Strength Protein-Based Materials [Fuzhong Zhang](#); Washington University in St. Louis, United States

Microbially-synthesized protein-based materials (PBMs) present an appealing alternative to petroleum-derived synthetic polymers. However, their widespread adoption has been hindered by challenges such as the repetitive sequences, high molecular weight of proteins, and skewed amino acid compositions, particularly for high-strength PBMs. In this presentation, I will introduce our recent advances in synthetic biology aimed at overcoming these hurdles. We have developed a range of synthetic biology tools that enable the stable expression of high molecular weight and highly repetitive proteins within engineered microbes. These tools have been instrumental in the microbial production of recombinant spider silk of similar mechanical properties. We further engineered amyloid-silk proteins which have a remarkable propensity to form nano β -crystals, resulting in fibers that possess exceptional mechanical properties. Additionally, we have devised a universal strategy to augment material strength and toughness by incorporating intrinsically disordered mussel foot protein fragments at the termini of these proteins. This approach promotes end-to-end protein-protein interactions, leading to the creation of protein fibers that surpass natural spider silk and petroleum-derived nylon fibers in both strength and toughness. Moreover, these fibers can be produced at a yield of 8 g/L.

11:15 AM MF03.06.03

Macromolecular Composites as Physical Analogues for Biomatter Plastics [Jan R. Campbell](#)¹, Ziyue Dong², Paul Grandgeorge¹ and Ella Lee¹; ¹The

University of Washington, United States; ²University of Colorado Boulder, United States

Innovative and sustainable technologies intended to prevent the harmful effects of sourcing, manufacturing, and disposing of synthetic plastics are rarely both biobased and biodegradable. Even many biodegradable plastics will not fully decompose in natural settings and despite the best recycling efforts, a significant portion of the plastic produced annually escapes into the biosphere. In an effort to create a fully biobased and backyard-compostable plastic alternative, we recently reported a bioplastic produced directly from spirulina biomass, without the need for chemical extraction or other preprocessing. The application of heated compression molding was found to transform the spirulina biomass into a rigid, compostable biomatter plastic with mechanical performance comparable to polylactic acid and polystyrene. In this work, we investigate the mechanism governing the self-bonding of spirulina during thermomechanical processing by creating a representative analogue for biomatter plastics. Varying ratios of pure carbohydrates, lipids, and proteins are physically combined and subjected to heated compression molding to form materials similar to algal bioplastics. The effect of the varying macromolecular composition, and the contribution of each class of macromolecule to the morphology of the produced bioplastics and their mechanical properties are evaluated through scanning electron microscopy (SEM) and flexural testing. Specifically, the varying ratio of protein to carbohydrates is utilized to compare the mechanical performance of biomatter analogues to several species of algae. The bonding mechanism of the biomatter analogues is first assessed qualitatively during sequential reprocessing to isolate contributions of dynamic bonding. Fourier transform infrared spectroscopy (FTIR) and x-ray photoelectron spectroscopy (XPS) are then utilized to quantitatively measure both secondary and primary bonding interactions between different macromolecular components of the analogue composites. Experimental measurements of bonding and cohesion are complemented by molecular dynamic (MD) simulations of multi-component macromolecular systems and a mechanism is proposed for self-bonding in biomatter plastics.

11:30 AM MF03.06.04

Protein-Based Shape Memory Polymer Metamaterials with Strain-Induced Remodeling [Lucas Meza](#)¹, Naraa Sadaba¹, Eva Sanchez-Rexach², Curt Waltmann³, Shayna Hilburg¹, Lilo D. Pozzo¹, Monica Olvera de la Cruz³, Haritz Sardon⁴ and Alshakim Nelson¹; ¹University of Washington, United States; ²General Atomics, United States; ³Northwestern University, United States; ⁴POLYMAT, Spain

Mechanical deformation of a polymer network is transferred from the macroscale to nanoscale to cause molecular-level motions and bond scission that ultimately lead to material failure. Understanding how to mitigate polymer disentanglement and bond scission is a significant challenge, especially in the development of active and shape-morphing materials. We report the additive manufacturing of hierarchically designed mechanical metamaterial lattices made with a protein-based polymer network that undergoes a unique strain learning behavior that combines mechanical remodeling with shape memory. At the molecular level, protein mechanophores unfold in the presence of a mechanical force to release its “stored length”, thereby stiffening in the direction of applied load after undergoing a healing cycle. Incomplete refolding of proteins during shape recovery affords a network with enhanced stiffness. At the macroscale, architected lattices distribute stress across a 3D printed structure to mitigate damage and enable complete shape recovery, and the efficiency of this process varies with the lattice architecture. The combined hierarchical responses cause a mechano-activated remodeling of folded proteins in the network to afford up to a 2 to 3-fold improvement in the mechanical properties. These bio-inspired materials offer a unique opportunity to develop novel materials that can autonomously remodel under an arbitrary applied load.

11:45 AM MF03.06.05

Cannabinoid-Based Polymers Materials Ecosystem [Michael Sotzing](#)¹, John M. Toribio², Gregory Sotzing² and Alex Chortos¹; ¹Purdue University, United States; ²University of Connecticut, United States

To mitigate the negative health and environmental impacts of synthetic petroleum-based plastics, new methods to use natural resources must be developed. Materials such as poly(lactic acid) have established that cost-competitive polymers with favorable properties can be leveraged to replace plastics in some applications, notably additive manufacturing. Bio-derived polymers with a greater range of properties may help to increase the market penetration of products based on natural resources. This work explores printed electronics created with a new class of biopolymers created from polymerized hemp oil. Some benefits of cultivating hemp include an increased capacity as a carbon sink, improved water consumption, and scrubbing of heavy metals from soil (phytoremediation). The resurgence of hemp with the passing of the Farm Bill in 2018 has led to larger supplies of hemp oils (cannabinoids) such as cannabidiol (CBD).

Poly(cannabinoid)s are prepared through step growth polymerization of bifunctional carboxylic acids with hemp-derived cannabinoids containing two hydroxyl groups. With over 120 naturally occurring cannabinoids and hundreds of dicarboxylic acids, a large range of properties can be achieved. This is demonstrated notably with 3 plastics that possess different desirable properties, such as high glass transition temperature >100 °C, hydrophobicity with water contact angles >120°, and a block-copolymer with high adhesion to a variety of surfaces including skin.

Practical applications of these materials are demonstrated through the fabrication of additively manufactured biomedical devices. Electrocardiogram electrodes illustrate the advantages of these materials when applied in aqueous environments, not possible for long periods with conventional silver/silver chloride electrodes. Conformal on-skin heating elements that show self-limiting at 35 °C reducing the potential for thermal runaway present with conventional heaters. Devices were fabricated with multi-material additive manufacturing whereby conductive metal/polymer composites and adhesives were printed.

PolyCBD materials have been demonstrated to be susceptible to base-catalyzed hydrolysis leading to depolymerization of polyCBD into component monomers and varying molecular weight oligomers. Different base solutions such as sodium hydroxide, ammonium hydroxide and phosphene buffered saline impact the duration of the depolymerization and the number of oligomers left in solution. Identifying the right media that does not denature CBD or result in incomplete depolymerization will enable repolymerization of monomers.

SESSION MF03.07: Nanocellulose Fundamentals III

Session Chairs: Yuanyuan Li and Eleftheria Roumeli

Wednesday Afternoon, April 24, 2024

Room 323, Level 3, Summit

1:30 PM *MF03.07.01

Structuring Nanocellulose into Heat-Insulating Mesoporous Structures with Light Permeability [Tsuguyuki Saito](#); The University of Tokyo, Japan

Decreasing the heat loss in buildings and vehicles is important for the realization of the low-carbon society. A transparent insulator applicable to windows is effective in reducing such a heat loss. Conventional candidates for transparent insulators are silica aerogels, with optical transparency and high thermal insulation. However, silica aerogels prepared through an unscalable supercritical-drying process are mechanically brittle. Herein, we report a structurally aerogel-like “cryogel” comprising sustainable wood-derived, mechanically strong cellulose nanofibers (CNFs) through a scalable freeze-drying process.

Cryogels refer to freeze-dried porous structures. The optical transparency of the cryogels was achieved by suppressing the agglomeration of CNF during freezing. The CNF cryogels exhibited good insulating properties and circularity. Such a heat-insulating yet light-permeable cryogel of wood resource with scalability and circularity is expected to reduce CO₂ emissions in buildings and vehicles when used as the interspace material in double-glazed windows compared to normal heat energy-losing windows..

2:00 PM *MF03.07.02

Green Products for The Red Planet: Sustainable Materials for Human Exploration [Lynn J. Rothschild](#); NASA, United States

Synthetic biology – creating new capabilities with life – promises to create a greener future for planet Earth, from fields as diverse as pharmaceuticals to manufacturing, agriculture and nanotechnology. Progress can be stymied by such considerations as economics, politics, legal and philosophical issues surrounding GMOs. Often solutions to these problems already exist, so it is difficult for a new, superior method to displace the old. As we move humans beyond Earth, to long duration stays in the International Space Station, and then onward to the Moon and Mars, the challenges of supporting human life will need radical new solutions. For example, while life on Earth uses an enzymatic machinery which evolved over 3.5 billion years ago, synthetic biology promises to be able to engineer the systems to adapt to current natural or industrial environments. A focus on solutions off planet require a focus on a circular economy. While there are new constraints, such as worrying about the mass of a solution, constraints offer opportunities for game-changing solutions that will then allow revolutions back on our home planet. Example projects include biomining and fungal-based habitats off planet.

2:30 PM BREAK

SESSION MF03.08: 3DP/ELMs
Session Chairs: Kunal Masania and Lucas Meza
Wednesday Afternoon, April 24, 2024
Room 323, Level 3, Summit

3:30 PM *MF03.08.01

3D Printing Cell-Laden Living Materials [Gilberto Siqueira](#), Rani Boons, Tanja Zimmermann, Gustav Nystrom and André Studart; Empa–Swiss Federal Laboratories for Materials Science and Technology, Switzerland

Microbes are extensively used in industry to convert carbon sources into valuable end-product chemicals and have found applications in the food industry, waste treatment, water quality assessment and bioremediation. Among them, species of two microalgal groups, diatoms and dinoflagellates, that exhibit appealing features for sensing devices were selected and encapsulated in hydrogels with different degrees of complexity to create 3D printed biohybrid materials with sensing behavior. We explore the encapsulation of such microorganisms within multifunctional hydrogels that supports the growth and proliferation of those non-mammalian cells by designing a set of ink and methods (direct ink writing-DIW or digital light processing-DLP) that allow to shape them in complex functional 3D structures. To accomplish our goals, we have first investigated the effect of the ink composition on the rheological behavior, printability, mechanical properties and cell growth in the hydrogels. The hydrogel inks were mainly composed of a suspension of microalgae (diatoms or dinoflagellates), polymers, water and nutrients. Next, we explored different printing methods to develop sensors to access water quality- and mechano-sensing hydrogels. The cell survival and activity upon encapsulation was confirmed and correlated to the mechanical properties of the hydrogels. We concluded that the proposed methods are promising for the design and fabrication of living materials with sensing properties such as water quality and force impact sensors.

4:00 PM *MF03.08.02

You Are What You Eat: How Conditions of Growth Influence The Properties of Myco-Materials [Alicia Vivas Hernando](#), [Wenjing Sun](#) and [Tiffany Abitbol](#); EPFL, Switzerland

Fungi are remarkably adaptive organisms, modifying their behaviors and characteristics in response to their environment, including nutrient availability. Over the past 15 years, fungi have emerged as a promising source of sustainable materials, finding applications in areas such as packaging and building materials. However, there are still knowledge gaps in the field, compromising our ability to consistently produce reliable materials. In this presentation, we delve into the potential of manipulating growth environment to tune material properties, drawing both from the wider literature and our own research. Our aim is to contextualize the current state of the art and to ask the question: How can materials science leverage biological adaptation to develop functional mycelium-based materials?

4:30 PM MF03.08.03

Advanced Manufacturing with Engineered Living Materials for Sustainable Polymer Composites [Weinan Xu](#); University of Akron, United States

Engineered living materials (ELMs) are an emerging class of materials that combine living biological entities especially bacteria with functional soft materials. The incorporation of living bacteria provides the materials with biosensing, self-regenerative, and molecular computing capabilities. Recently, ELMs have also been used for direct ink writing-based 3D printing, which enables the fabrication of dynamic and active 3D structures for various applications. In this talk, I will discuss our recent progress on 3D printing with functional bacteria embedded in a supporting matrix or 3D printed bioreactors for advanced biofabrication. The bacteria can be genetically engineered to have specific functions, such as generating bacterial cellulose or reacting to external stimuli. We have demonstrated that 3D cellulose structures can be generated by in situ biosynthesis in the 3D printed templates followed by controlled shape transformation, which provides an efficient and versatile approach for fabricating 3D customizable bio-scaffolds for tissue engineering. More importantly, programmable microbial biosynthesis with two or multiple types of bacteria can be integrated with 3D printing, so that programmable biosynthesis of organic-inorganic biocomposites can be achieved in 3D printed bioreactors. We have shown that 3D hierarchical biocomposites with bionanofiber matrix and inorganic mineral nanoparticles with well-defined shape and internal structure can be produced, which provides a new platform for bone mimetic materials and tissue engineering.

Ref: Liu, S.; Yang, M.; Barton, H.; Xu, W. Designed Microbial Biosynthesis of Hierarchical Bone-Mimetic Biocomposites in 3D Printed Soft Bioreactors. *Adv. Mater. Technol.* **2023**

4:45 PM MF03.08.04

Enhancing Food Security with 3D Printing Technology [Woo Soo Kim](#); Simon Fraser University, Canada

The global challenge of food security is intensifying due to various factors such as population growth, insufficient agricultural investment, and inefficient distribution systems. As a result, food insecurity is often a complex interplay of elements including diseases, processing methods, and distribution challenges. These issues are particularly acute in vulnerable regions where traditional food safety testing methods are often impractical for detecting foodborne diseases. In response to these challenges, 3D printing technologies and 3D printed sensors emerge as a transformative solution. They provide a means to develop portable, precise, and cost-effective sensors that bridge the existing gaps in food security. This presentation explores the pivotal role of 3D printed sensors, specially such as disposable 3D printed sensors in addressing food security concerns, encompassing detection, processing, and quality monitoring in the food supply chain, ultimately ensuring reliable access to nutritious and affordable food. Furthermore, we discuss the applications of 3D printing technology in the agriculture sector, with a focus on the promising future of plant wearables and plant health detection. This innovative approach not only advances food security but also holds the potential to revolutionize agricultural practices, contributing to a more sustainable and secure global food supply.

SESSION MF03.09: Biomass Processing, 3DP
Session Chairs: Yuanyuan Li and Eleftheria Roumeli
Thursday Morning, April 25, 2024
Room 323, Level 3, Summit

8:30 AM *MF03.09.01

Developing a Technology Platform based on The Spinning of Bio-Based Nanostructured Fiber-Based Materials Daniel Soderberg^{1,2}; ¹KTH Royal Institute of Technology, Sweden; ²Wallenberg Wood Science Center, Sweden

Transitioning from promising scientific findings to practical engineering technologies often presents significant challenges. One such advancement lies in spinning high-performance reinforcement fibers from nanocellulose. We have been working broadly, spanning several projects, around a spinning technology built on the concept of flow-focusing spinning, which has shown some potential.¹⁻³ These previously published scientific results represent a substantial leap beyond current state-of-the-art techniques, particularly in achieving continuous and controllable conditions for nano assembly. This includes several routes for functionalization beyond the stress-strain curve.

The challenge has been pursued by addressing some key challenges related to conventional filament (fiber) spinning, such as e.g., winding, online drying, and multi-filament spinning. In addition, the need for consistent processing and material properties has been addressed, a specific challenge when working with nanocomponents.

An overview of recent results will be presented, considering the performance of continuously spun fibers and attempts to fabricate composite materials based on fabrics constructed from these fibers. One example is that the results show how the parameter space for processing and, specifically, drying strongly impacts the final material's properties. Another indicates that fibers spun using hydrodynamic flow-focusing show a surprisingly high thermal conductivity.⁴ Following this, the piezoelectric properties have been studied, as well as functionalization using other nanoparticles and polymers. Finally, the possibility to fabricate significant amounts has also made it possible to evaluate the compatibility with various polymer resins and the performance as a composite, where the apparent result is that the composites become more or less transparent.

Apart from the investigated property space, the vision is to develop further a technology platform that can provide society with innovative material solutions that are biobased, lightweight, functional, sustainable, and resilient.

- (1) K. M. O. Håkansson, A. B. Fall, . . . L. D. Söderberg, Hydrodynamic alignment and assembly of nanofibrils resulting in strong cellulose filaments. *Nature Communications* **5**, (2014).
- (2) N. Mittal, F. Ansari, . . . L. D. Söderberg, Multiscale Control of Nanocellulose Assembly: Transferring Remarkable Nanoscale Fibril Mechanics to Macroscale Fibers. *ACS Nano* **12**, 6378-6388 (2018).
- (3) N. Mittal, R. Janson, . . . L. D. Söderberg, Ultrastrong and Bioactive Nanostructured Bio-Based Composites. *Acs Nano* **11**, 5148-5159 (2017).
- (4) G. Wang, M. Kudo, . . . J. Shiomi, Enhanced High Thermal Conductivity Cellulose Filaments via Hydrodynamic Focusing. *Nano Letters* **22**, 8406-8412 (2022).

9:00 AM MF03.09.02

Unravelling The Governing Factors for Polysaccharide and Biopolyester Processing Cecile Chazot¹, Simona G. Fine¹, Eleanor C. Grosvenor¹, Sara Branovsky¹ and Gabrielle Wood^{1,2}; ¹Northwestern University, United States; ²Howard University, United States

The production, consumption, and disposal of polymers for textile and packaging applications pose several problems for the environment, including carbon emissions and the persistence of microscale and nanoscale debris in the ocean. In recent years, biopolyesters (e.g. Polybutylene adipate terephthalate or polybutylene succinate) have emerged as environmentally friendly alternatives to petroleum-derived polymers, due to their biodegradability, easy thermal processing and tailorable mechanical and barrier properties. Other biopolymer alternatives, such as polysaccharides (e.g. chitosan and cellulose ethers), are naturally abundant and have the potential to self-assemble in cholesteric liquid crystals with a tailored photonic bandgap, opening new opportunities for the development of functional optical materials. However, the widespread adoption of all these biopolymeric alternatives remains limited due to challenges in their large-scale synthesis and manufacturing. In this talk, we will discuss scalable processing of these polymers through fast and open-air reaction schemes, and their integration in the development of packaging and textiles with advanced functionality. We will discuss how chemical factors such as molecular weight and repeat-unit chemistry affect chain mobility and solution-based and thermal processing of biopolyesters and polysaccharides. We will also discuss how interchain interaction can be leveraged to result in long-range order such as liquid crystal self-assembly, therefore enabling new advanced functionality such as colorimetric sensing and circular dichroism. These relationships are expected to assist in the large-scale deployment of biopolymer-based functional materials with tailored structure and properties.

9:15 AM *MF03.09.03

Fundamental Issues Governing The Properties and Functions of Nanocellulose Networks Eero Kontturi; Aalto University, Finland

Nanocellulose networks have been extensively surveyed as so-called nanopapers for packaging applications on one hand and membranes for purification purposes on the other. Despite the two distinct ways of end use, the fundamentals of the network structure and its function remain the same. This presentation aims to introduce a fundamental discussion from both sides by consolidating both aspects. For example, hemicellulose is seen as a binder molecule when assessing the tensile properties of dry nanopapers but its water-accumulating capability in wet state is rarely discussed in membrane technology or even with hydrogels. Similarly, porosity is among the central properties of membranes but it is not usually considered with nanopapers, notwithstanding its pivotal role in strength development of any cellular material. The aim here is to address similar parameters from different application

perspectives.

9:45 AM BREAK

10:15 AM *MF03.09.04

Materials and Methods for Sustainable Soft Devices [Martin Kaltenbrunner](#); Johannes Kepler University, Austria

Soft devices provide unique opportunities in our quest for a more sustainable future. Among the key issues to overcome are the search for high performance green materials, end-of-lifetime considerations in complex (soft) systems, and their energy efficiency. This talk aims at suggesting solutions for some of these grand challenges. We introduce bioderived materials and fabrication methods for soft systems that biodegrade, yet are of high resilience. Based on highly stretchable biogels and degradable elastomers, our forms of soft electronics and robots are designed for prolonged operation in ambient conditions without fatigue, but fully degrade after use through biological triggers. Electronic skins provide sensory feedback, while stretchable and biodegradable batteries enable autonomous operation. 3D printing of biodegradable hydrogels enables omnidirectional soft robots with multifaceted optical sensing abilities. Going beyond, we introduce a systematically-determined compatible materials systems for the creation of fully biodegradable, high-performance electrohydraulic soft actuators. These embodiments reliably operate up to high electric fields, show performance comparable to non-biodegradable counterparts, and survive over 100,000 actuation cycles. Pushing the boundaries of sustainable electronics, we demonstrate a concept for growth and processing of fungal mycelium skins as biodegradable substrate material. Mycelium-based batteries with capacities as high as $\sim 3.8 \text{ mAh cm}^{-2}$ allow to power autonomous sensing devices including a Bluetooth module and humidity and proximity sensors, all integrated onto mycelium flexible circuit boards.

10:45 AM *MF03.09.05

Ever Ancient Ever New - Cellulose as The Material Platform for Sustainable Flexible Devices [Tian Li](#); Purdue University, United States

Cellulose, the main component in cotton, features a naturally occurred hierarchical structure down to the ångström scale, providing a scaffold with multiscale interspace and abundant functional groups. In this talk, I will talk about our work using cellulose as the material platform for flexible ionic and electronic devices. We will focus on the design principles as well as the application scenarios in energy generation, conversion and sensing.

11:15 AM MF03.09.06

Quasi-Two-Dimensional Marangoni Convection and Specific Polymer Deposition in Meniscus Splitting Phenomenon [Leijie Wu](#) and Kosuke Okeyoshi; Japan Advanced Institute of Science and Technology, Japan

Spontaneous pattern formation in polymer dissipative systems such as Turing patterns is highly valued in material design. However, the process of fixing patterns to the substrate through evaporation strategy involves a complex pathway from equilibrium to disequilibrium and back to equilibrium as the dispersed particles undergo deposition from saturation to supersaturation. Understanding the non-equilibrium process is essential for the advancement of materials innovation and applications. However, because of high viscosity, polymer dispersions have often received limited attention, presenting processing challenges. Inspired by the viscous fingering phenomenon, we use aqueous polysaccharide dispersions to induce stable spatial patterns within Hele-Shaw cells through controlled water evaporation. These spatial patterns effectively formed deposition patterns in the fluids, dividing the space from one into multiple with anisotropic polysaccharides membrane, splitting the meniscus.^[1,2] In this study, we meticulously tracked the evolving behavior of internal fluids of aqueous polysaccharide dispersion during the evaporation process using the Particle Image Velocimetry method. As the concentration of the dispersion increased, we observed that periodic convection gradually emerged within the cell. At higher concentrations of the dispersions, Brownian motion gradually loses its dominance, and evaporation-induced Marangoni flow under the influence of viscous forces triggers spatial periodic Marangoni convection, taking over as the dominant behavior. This quasi-two-dimensional convection encourages particles to aggregate at specific areas in the dispersion, which supplements the fluctuating flocculation caused by interfacial evaporation. Differing from the Rayleigh-Bénard convection, by the effect of capillary force, this spatial quasi-two-dimensional convection can be immobilized into polymer membranes with self-assembled polysaccharide structure through evaporating. This aggregation effect of convection is not limited to this kind of biopolymer but also can be extended to various functional polymer particles, complementing what has been achieved in assembling particles from fluids using convection fields.

[1] Saito, I., Wu, L., Hara, M., Ikemoto, Y., Kaneko, T., & Okeyoshi, K. *ACS Appl. Polym. Mater.* 4 (2022).

[2] Wu, L., Saito, I., Hongo, K., & Okeyoshi, K. *Adv. Mater. Interfaces*, 2300510 (2023).

11:30 AM MF03.09.07

Cellulose and Nanocomposite 3D Printing in Optimized Dispersions for High-Performance Properties [Rigoberto C. Advincula](#); The University of Tennessee/Oak Ridge National Laboratory, United States

The interest in renewable, natural, and bio-based polymers has a high potential, especially for commodity plastic replacement. From miscanthus grass, abaca fibers, chitin, and coconut coir, the key is determining their ability to form synergistic blends and composites. This means investigating their miscibility and dispersion properties, including a fundamental understanding of their secondary and tertiary structures (alpha-crystallinity and beta-sheets). The nanostructuring involves utilizing their sometimes high-aspect ratio or non-covalent interactions to determine the need for compatibilizations. Then, they must determine their minimum percolation threshold for the desired property at a minimum cost. These "optimization" protocols often unlock their true techno-economic value rather than simply using them to "replace the plastic". In this talk, we will describe strategies and projects where we have focused on preparing nanocomposites for high value in applications with coatings and 3D printing. Utilizing nanocellulose or cellulose nanocrystals, it is possible to unlock those advantages by emphasizing nanostructuring and derivatization. This is evident in their use with various dispersions in photopolymerizable resins, hydrogel metal precursors, and polyelectrolyte complexes. AI/ML strategies are emphasized as a method of improving optimization for additive manufacturing.

11:45 AM MF03.09.08

Quantifying The Softness of Wool via Structure-Property Relationships [Serafina R. France Tribe](#) and Cecile Chazot; Northwestern University, United States

State-of-the-art evaluation of textile touch sensation (e.g., scratchiness) follows broadly-adopted qualitative and time-intensive procedures that rely on consumer-based studies. This is due to the lack of understanding of how material properties and fiber morphology affect the surface interaction of the fabric with human skin. Wool, in particular, is an animal-derived fiber that can range from extremely soft to uncomfortably scratchy, due to the broad range of fiber properties depending on the source. Here, the morphological, compositional, and mechanical properties of a variety of natural wool fibers of reported consumer-based haptic feel are investigated. Using scanning electron microscopy (SEM) and a custom image analysis framework, we assessed the evolution of fiber morphology (e.g., diameter and surface roughness) across a large variety of animal sources. We also analyzed how fiber composition

varies between sheep breeds through Fourier transform infrared (FTIR) spectroscopy, thermogravimetric analysis (TGA), and x-ray diffraction (XRD). Last, we characterized the mechanical properties of the fibers such as tensile strength and viscoelastic moduli through dynamic mechanical analysis (DMA) and uniaxial tensile testing. This comprehensive study of wool fibers is essential in establishing structure-property relationships and quantifying how composition, microstructure, and mechanical properties impact fiber interaction with human skin and haptic feel. This will in turn enable the development of standardized human-subject-free test methods for fiber scratchiness and will guide the design of new fibers and textiles for the apparel and medical industries.

SESSION MF03.10: Upcycling, Recycling, Depolymerization I
Session Chairs: Megan Robertson and Eleftheria Roumeli
Thursday Afternoon, April 25, 2024
Room 323, Level 3, Summit

1:30 PM *MF03.10.01

Leveraging Stereochemistry to Advance The Design and Degradation of Sustainable Polymeric Materials [Andrew P. Dove](#); University of Birmingham, United Kingdom

Nature has evolved the ability to create large and complex molecules in which the precise control over both the sequence and spatial arrangement of the atoms is critical to their performance. The 3-dimensional control over the arrangement of bonds is as important to the function and behaviour of molecules as any other factor and is critical to the structure-function relationships that occur within biological systems. Specifically, the advantageous mechanical properties of most commodity plastics are intimately connected to their low glass transition temperature and crystallinity, the latter of which can be modulated by stereochemistry of the polymer. For polypropylene (PP), stereochemical control of the pendant methyl group on the polymer backbone (isotactic, or alternating bond orientation) contributes to its useful properties. While this concept has similarly been leveraged to improve the thermomechanical properties (i.e. increase the melting temperature or tensile modulus) of bioplastic polyesters (e.g. polylactic acid (PLA)) these materials are incessantly plagued by brittleness, lacking the flexibility and toughness of petrol plastics. By controlling the stereochemistry of polymer backbones, much more significant changes to polymer mechanics can be achieved. The most well known example is stereochemical differences between natural rubber (poly(cis-isoprene)) and Gutta percha (poly(trans-isoprene)), which lead to a complete change in physical properties from an elastomeric to plastic material. Despite this being well known, the state of the art in synthesis has not made it possible to readily exploit this effect more widely. To this end, our work has focused on developing polymerization methods that can result in materials in which the stereochemistry can be used to leverage a wide range of materials properties from thermomechanical to degradation, in both linear polymers and networks, with a high level of tuneability.

2:00 PM *MF03.10.02

Degradable and Thermally Stable Spiro Polycycloacetals from Renewable Resources [Megan Robertson](#), Elvis Enebeli, Justin Smith and Minjie Shen; University of Houston, United States

A series of partially bio-based spiro polycycloacetals were synthesized using bio-renewable feedstocks, such as vanillin and its derivative syringaldehyde, along with pentaerythritol and commercially available co-monomers including 4,4'-difluorobenzophenone and bis(4-fluorophenyl) sulfone. These spiro polycycloacetals displayed high thermal stabilities (degradation temperatures in the range of 343 – 370 °C, as quantified by 5% mass loss) and glass transition temperatures (in the range of 179 – 243 °C). Importantly, these polymers were effectively degraded to small molecules under acid-catalyzed hydrolytic conditions in less than 7 h. The kinetics of hydrolytic degradation was quantified through *in situ* NMR analyses.

2:30 PM MF03.10.03

Catalyst Development for Polymerization and CO₂ Capture, Storage and Upcycling to High Value Materials [James Hedrick](#)^{1,2}, Nathan Park¹, Luis Campos² and Dino Wu²; ¹IBM Research, United States; ²Columbia University, United States

Current strategies to reduce CO₂ emissions are insufficient—both point-source and direct-air-capture (DAC) must be considered to mitigate excessive atmospheric CO₂ concentrations. Given the urgency of climate change issues and the immense challenges of developing viable methodologies for CO₂ conversion, we posit that understanding structure–property relationships of organic/inorganic molecular reactivity across multiple length scales will lead to the evolution of remarkably efficient transformations of CO₂ and revolutionize chemistries to control the fate of this greenhouse gas. Thus, we sought to investigate families of superbases (SBs) that serve as CO₂ mitigating agents. This talk will focus on describing the wide-scope reactivity of a family of modular SBs that can be exploited in a variety of chemical transformations of CO₂ from dilute and pure gaseous sources as well as polymerizations. We found that the SBs can form zwitterionic complexes to activate CO₂, which can be readily mineralized into metal carbonates. Importantly, the highly reactive nature of SBs renders them widely useful to upcycle CO₂ into high value products.

2:45 PM MF03.10.04

Sustainable Polymer Networks that can be derived from Biobased or Waste Materials and Offer Reprocessability with Full Crosslink Density and Property Recovery [John M. Torkelson](#); Northwestern University, United States

Covalent adaptable networks (CANs), sometimes called vitrimers, offer promise for overcoming long-standing recycling and polymer circularity issues associated with conventional, permanently crosslinked thermosets that cannot be recycled for high-value use. It is also vital to demonstrate that properties of reprocessable networks can be optimized to meet the demands for high-performance materials. For example, it is important that the dynamic covalent bonds in CANs are robust at use conditions, including elevated temperatures where creep needs to be minimal, while ensuring reprocessability at yet higher temperatures that are well below conditions where degradation occurs. We have designed several classes of CANs that show that such performance demands can be met while contributing to polymer circularity and sustainability. Additionally, in many cases, such CANs can be derived from biobased or waste starting materials. We will provide examples ranging from non-isocyanate polyurethane networks, including both polyhydroxyurethane networks and non-isocyanate polythiourethane networks, that exhibit non-catalyzed dynamic chemistry of a dual associative and dissociative nature and can be made from a variety of biobased sources. We will also provide examples in which some polyolefins, including thermoplastic polyethylene, can be upcycled into CANs via simple one-step reactive processing with a radical initiator and an appropriate covalent crosslinker with dynamic chemistry that is strictly dissociative in nature, e.g. a dialkylamino disulfide or other disulfide-based crosslinker. For example, waste thermoplastic polyethylene can be transformed into crosslinked polyethylene exhibiting robust properties and reprocessability. Additionally, because of the dissociative nature of the dynamic chemistry, these CANs offer the possibility of being processed by conventional, continuous melt-processing methods such as melt extrusion.

3:00 PM BREAK

3:30 PM MF03.10.05

Depolymerizable and Recyclable Luminescent Polymers [Wei Liu](#)^{1,2}, Yukun Wu^{1,3}, Jianguo Mei³, Sihong Wang^{2,1} and Jie Xu^{1,2}; ¹Argonne National Laboratory, United States; ²The University of Chicago, United States; ³Purdue University, United States

Solution processable luminescent polymers are of great interest in a number of photonic technologies, including electroluminescence, bioimaging, medical diagnosis, bio-stimulation, and security signage. Ensuring the integration of depolymerizability and recyclability factors into the initial stages of the material design is of pivotal for promoting sustainability and mitigating environmental impacts throughout the entire product lifecycle. In this work, we unprecedentedly propose a general design concept utilizing cleavable moiety, herein tert-butyl ester, to create programmable depolymerizable and potentially recyclable thermally activated delayed fluorescence (TADF) polymers, without compromising their highly efficient luminescent properties. The programmable depolymerizability and remarkable luminescent properties of these polymers exemplify an innovative benchmark for endowing end-life environmental friendliness and circular economy to current photonic technologies.

3:45 PM MF03.10.06

Valorising Waste Plastics into Functional Materials and Industrially-Relevant Chemicals [Jason Y. Lim](#) and Derrick Fam; Institute of Materials Research and Engineering (IMRE), Singapore

Petroleum-based plastics are amongst the most versatile synthetic materials available today. They are produced in excess of 300 million tons a year and are ubiquitous in modern society due to their favourable combination of light weight, low cost and usefulness for a diverse range of applications. However, their existing life cycles are extremely linear, with most post-use plastics disposed unsustainably in landfills, incinerated or irresponsibly discarded in the environment, representing a huge loss of inherent material value. In recent years, these existing petroleum-based plastics are receiving increased attention as promising feedstock materials for production of functional polymers and chemicals essential for society. Herein, several examples of how plastics can be post-synthetically transformed into functional polymers will be described. These include upcycling waste poly(ethylene terephthalate) (PET) bottles into polymer electrolytes for energy storage, and synthesis of water-soluble antifungal polymers from polyethylene (PE). In addition, our recent methods for valorisation of waste polystyrene into benzoic acid, a commodity chemical with annual demand exceeding 500,000 tonnes, will be discussed. These proof-of-concept applications highlight the vast untapped potential for using waste plastics as a future source of raw material for producing high-value products for societal needs, ultimately reducing our collective reliance on petroleum sources for a more sustainable materials future.

4:00 PM MF03.10.07

A General Strategy for Upcycling Plastic Commodity Waste to Self-Healable and Fully-Recyclable Materials [Haixu Du](#); University of Southern California, United States

The rapid expansion of the plastic industry has led to significant environmental and ecological harm due to plastic waste. Considering the drawbacks of traditional recycling methods, as most of the plastic wastes are down-cycled into low-value products such as garden furniture or pots, upcycling has garnered increased attention for transforming plastic waste into high-value products. This study presents a general strategy to upcycle commodity plastic waste to a class of fully recyclable and self-healable polymers. Coumarin and its derivatives are light-sensitive and can self-react when triggered by ultraviolet (UV) light at varying wavelengths. Upon exposure to 365 nm UV light, coumarin undergoes dimerization and forms a cyclobutene ring. Conversely, exposure to 254 nm UV light results in the cleavage of the ring and a reversion to its original state. We demonstrate that after embedding the coumarin groups into our polymer matrix, thanks to the photodimerization and photocleavage occurring on the coumarin group C=C bonds under 254 nm and 365 nm UV light, our materials exhibit four distinct properties: light-tunable mechanics, reprocessing ability, light-activated self-healing, and recyclability. We show our strategy is universal to various commodity plastic wastes, such as PS, PP, PET, and PE. This transition from plastic waste to multifunctional materials offers a new strategy for upcycling various plastic wastes into a category of high-value products.

4:15 PM MF03.10.08

Effects of Nickel on The Acceleration of Radiation-Induced Decomposition of Polytetrafluoroethylene (PTFE) [Hao Yu](#), Akira Idesaki, Kimio Yoshimura, Akihiro Hiroki and Yasunari Maekawa; National Institutes for Quantum Science and Technology (QST), Japan

Introduction

High-performance plastics, such as PTFE (Polytetrafluoroethylene) and PEEK (Polyether ether ketone), have extensive applications in various industries. However, recycling and reusing these plastics pose challenges due to their exceptional heat resistance. This study presents our findings on a new method to reduce the decomposition temperature of PTFE. The method involves utilizing the catalytic effects of Nickel (Ni) for the radiation-induced decomposition of PTFE.

Materials and Methods

PTFE ($M_w=5,000\sim 20,000$) and Ni/NiO/Al₂O₃/SiO₂ powders were purchased and used. The PTFE or the mixture of PTFE with Ni was irradiated with an electron beam under air or argon gas. The maximum dose of the electron beam was 15 MGy, and the dose rate was measured using a cellulose triacetate (CTA) film dosimeter. Mixtures containing different mixing ratios of PTFE and Ni catalyst were prepared to investigate the impact of proportion of catalyst. The mixing time was varied before and after irradiation to observe the sequential effects of irradiation and catalyst. To perform quantitative analysis, the weight change of samples resulting from radiation was measured, and the solid residue remaining after irradiation was collected. The thermal decomposition of the samples with and without irradiation was measured using thermogravimetric differential thermal analysis (TG-DTA) from room temperature to 1000°C under argon gas. The gaseous products via thermal treatment were collected and introduced into a gas chromatograph-mass spectrometer (GC-MS) for their identification. Furthermore, the chemical groups were measured using Fourier transform infrared spectroscopy (FT-IR), the crystal structure changes were measured using X-ray Powder Diffraction (XRD), and the binding energy changes were measured using X-ray Photoelectron Spectroscopy (XPS), as a function of irradiation and temperature.

Results and Discussions

Both the use of Ni catalyst and irradiation accelerated the reduction of the decomposition temperature of PTFE. Increasing the proportion of Ni catalyst and irradiation dose had a positive effect on decomposition. In addition, the synergistic effect of Ni catalyst and irradiation had the greatest impact on the decomposition. In the presence of oxygen, when mixing was followed by irradiation, the 5% weight loss temperature of the solid residue was 103°C, which is 419°C lower than the pyrolysis temperature of pure PTFE (522°C). Under 15 MGy irradiation, approximately 40% of the PTFE equivalent experienced weight loss below 200°C.

During the irradiation, several changes were observed in the PTFE. In PTFE alone, the presence of carbonyl groups (-CO-) was confirmed, and GC-MS analysis indicated the occurrence of oxidation (C_nF_{2n} to C_nF_yO_z). These oxidative substances are responsible for the decomposition of irradiated PTFE at lower temperatures. There were no changes in crystal structure or binding energy (C 1s, F 1s). In the presence of Ni, the presence of -CO- was also

confirmed, but the gaseous products detected in GC-MS decomposed into smaller fragments (C₂F₄O₂ to CO₂/COF₂). Additionally, new crystalline structures were confirmed in the irradiation process involving oxygen. The binding energy of C 1s, Ni 2p_{3/2} remained unchanged, but a new peak of F 1s (F⁻, 685 eV) was confirmed, indicating the production of F⁻ from the original PTFE (p(CF₂-CF₂), 689 eV) during irradiation. In summary, the presence of oxygen played a crucial role in the degradation of PTFE, and we propose that Ni acts as a catalyst to accelerate the decomposition of PTFE.

Acknowledgment: This work was supported by JST, CREST Grant Number JPMJCR21L1, Japan. The authors would also like to thank the operators of the Takasaki electron beam irradiation system for their cooperation.

4:30 PM MF03.10.09

Selective Deconstruction and Upcycling of Step-Growth Polymers Nick Galan¹, Jackie Zheng^{2,1}, Md Arifuzzaman¹, Md Anisur Rahman¹, Jeff Foster¹, Bobby G. Sumpter¹ and Tomonori Saito^{1,2}; ¹Oak Ridge National Laboratory, United States; ²The University of Tennessee, Knoxville, United States

Engineering plastics based on step-growth polymerization such as poly(ethylene terephthalate) (PET), polyamides (PA), polyurethanes (PU), and polycarbonate (PC) comprise ~30% of the global plastic production. The catalytic deconstruction is one of the major paths for chemical recycling of step-growth polymers. Although there has been progress on their chemical recycling especially PET, most step-growth polymers are not recycled because of the difficulty in depolymerization to pure building blocks especially from mixed state in an energy efficient manner. Here, we have developed a tailored organocatalyst to enable low energy depolymerization pathways for step-growth polymers. Our catalyst allows glycolysis of PET, PA, PU, PC and their multiple mixture at moderate temperature with high yield. A wide range of post-consumer plastics waste, such as bottles, packaging, foam, carpet, etc. is readily deconstructed into monomers with high efficiency. The Life Cycle Assessment indicates that the reproduction of various engineering plastics from the deconstructed monomers will result in a significant reduction in greenhouse gas emissions (82-95% reduction) and energy input (68-94% reduction). Furthermore, we have developed a path to deconstruct those step-growth polymers to selective length of oligomers. We have utilized those deconstructed building blocks to synthesize upcycled polymers, and the upcycled polymers can be further deconstructed to reusable building blocks. Such circular design contributes to establishing new closed-loop circularity of polymers by energy efficient selective deconstruction and upcycling of various engineering plastics.

4:45 PM MF03.10.10

Itaconic-Based Copolyesters as Potential Replacement of Epoxy-Based Coatings in Metallic Food Contact Materials Jose Hector Ramirez Suarez and Julie Goddard; Cornell University, United States

Replacement of Bisphenol A (BPA) based coatings in food contact materials has been of industrial interest for decades due to health concerns and consumer perception. Although polyester- and acrylic-based resins have been introduced into the market as potential replacements, matching the chemical, mechanical, and thermal properties of BPA-based resins remain a challenge. Specifically, their remarkable performance into delaying the onset of corrosion in metal packaging, which protects the safety and quality of foods and beverages during their shelf-life.

Unsaturated polyesters (UP) are versatile, low molecular-weight thermoplastics that can undergo cross-linking reactions to yield thermosets or be functionalized to tailor their properties for potential use as additives in coating formulations. In an effort to improve the sustainability of petroleum-based UP thermosets, the incorporation of biomass-derived molecules in UPs, such as itaconic acid derivatives or short-length chain diols, has been explored. However, the thermal and mechanical properties of the resulting UPs is often negatively affected, limiting their potential use as coatings.

In this research, we present the synthesis of novel itaconic-based unsaturated copolyesters with improved mechanical and thermal properties by copolymerization with monomers of high structural rigidity (i.e. cyclic, substituted, or aromatic). We found that the nature of the catalyst played a role in favoring side reactions during the polycondensation affecting the structure and size of synthesized UPs. Zinc acetate as the melt-polymerization catalyst, yielded UPs with molar mass in the range of 3,000 to 4,000 g/mol and controlled and narrower molar-mass distributions (PDI < 2) in comparison to dibutyltin oxide (PDI > 10). Additionally, the backbone-integrated unsaturated moieties and the hydroxy chain-end groups were better preserved for post-functionalization.

Cross-linking of UPs was performed with branched thiol-functionalized or biomass-derived cyclic vinyl monomers by UV-initiated radical polymerization. Thiol-functionalized monomers yielded thermosets with a glass transition temperature of up to 60 °C, due to the high degree of cross-linking promoted by the introduction of branching to the linear UPs and high efficiency of thiol-ene reactions. Further, only UPs containing branched or cyclic diols were able to form flexible, thin, free-standing films (15 – 20 μm) while formulations containing aliphatic diols yielded brittle films.

Ongoing work involves the characterization of tensile properties and protective performance against corrosion over time in saline and alcoholic standard solutions by electrochemical characterization to assess their potential use as coatings.

Upon completion of this work, an industrially attractive and scalable UP-based thermoset capable of enhanced corrosion protection is developed as alternative to epoxy based resins. This research addresses the need for high-performance and environmentally sustainable materials for the food packaging industry in their quest to maintain the quality and safety of foods and beverages.

SESSION MF03.11: Poster Session II
Session Chairs: Kunal Masania and Eleftheria Roumeli
Thursday Afternoon, April 25, 2024
Flex Hall C, Level 2, Summit

5:00 PM MF03.11.01

Advancements in Biopolymer-Based Materials for Sustainable Packaging Applications Sezen Buell; Estee Lauder Companies, United States

This presentation aims to explore the diverse landscape of biopolymer-based materials and their promising applications in sustainable packaging. Focusing on innovative solutions derived from mycelium, yeast, plant and algae cells, the talk will delve into the unique properties and environmental benefits of each biopolymer.

Mycelium, as a rapidly renewable and biodegradable resource, offers a compelling alternative for packaging applications. Yeast-derived materials showcase versatility and potential for customization, while plant based materials highlight the rich biodiversity that can be harnessed for sustainable packaging. Additionally, protein-based materials present exciting possibilities for creating biocompatible and high-performance packaging solutions. The presentation will address key aspects of material synthesis, characterization techniques, and the inherent advantages of these biopolymers, including their biodegradability, low environmental impact, and potential for circular economy integration. Moreover, the discussion will extend to the scalability and commercial viability of these materials, exploring their potential to revolutionize the packaging industry and contribute to a more sustainable future. This comprehensive overview of biopolymer-based materials aims to inspire collaborative efforts and stimulate discussions within the material research

community and industry to further propel the development and implementation of these environmentally friendly alternatives in packaging applications.

5:00 PM MF03.11.02

Scalable Interfacial Polymerization of Thermally Processable Biodegradable Polyesters [Sara Branovsky](#) and Cecile Chazot; Northwestern University, United States

Aliphatic-aromatic polyesters (AAPE) have gained traction as sustainable alternatives to polyethylene-based packaging due to their superior biodegradability and comparable mechanical properties. Unfortunately, the large-scale deployment of these polyesters remains limited due to manufacturing challenges such as time- and energy-consuming syntheses and difficulty with thermal processing due to depolymerization. In this work we describe the implementation of a stirred interfacial polymerization (IP) framework to enable the rapid, open-air, high-yield synthesis of AAPE with tailored chemical structures and properties. We explore the effect of reaction conditions – such as aromatic vs aliphatic character and additive concentrations – on polymer yield and thermal properties. We characterize the mechanical properties of AAPE films made via hot pressing and compare the results with state-of-the-art synthetic packaging. This IP synthesis has potential as a scalable manufacturing pathway for biodegradable polyester-based packaging with enhanced thermal processability and mechanical properties.

5:00 PM MF03.11.03

Water-Based Sustainable Ink Composed of Regenerated Silk Fibroin and Upconversion Nanoparticles for Printing/Painting on Arbitrary Surfaces [Heeun Choi](#)¹, Junyong Ahn¹, Taehoon Kim², Fiorenzoomenetto² and Junyong Park¹; ¹Kumoh National Institute of Technology, Korea (the Republic of); ²Tufts University, United States

Regenerated silk fibroin derived from silkworm cocoons is considered as one of the promising sustainable materials for various fields such as biomedicine, photonics, and electronics. To date, a variety of unconventional material platforms have been demonstrated by engineering regenerated silk fibroin in various ways. In this study, we fabricate a nanocomposite composed of regenerated silk fibroin and upconversion nanoparticles (UCNPs) and demonstrate its printing/painting capabilities as an eco-friendly and biocompatible functional ink. The research is largely divided into three parts:

- 1) securing robust RGB emission spectra under 980 nm NIR excitation through systematic dopant control of citrate-capped hydrophilic UCNPs, which can be easily dispersed in aqueous silk fibroin solution;
- 2) selecting an appropriate auxiliary solvent that prevents the aggregation of silk fibroin and UCNPs to improve the room temperature storage and printability of ink;
- 3) expanding the color palette through mixing RGB inks and demonstrating printing/painting capabilities of the inks on arbitrary surfaces, including 3D curved substrates.

In conclusion, we developed a functional ink that can be designed with a total of six emission colors (RGBCMY), and succeeded in creating colorful patterns and tags that can be selectively revealed under NIR excitation on biological surfaces such as silkworm cocoons, pig skin, fruits, and leaves through stencil printing and brush painting. The natural product-based upconversion ink developed in this study may provide new opportunities for biocompatible and transient tattoos for medical purposes, anti-counterfeiting platforms, and sustainable nanophotonic devices.

5:00 PM MF03.11.04

Rapid Manufacturing of Smart Nanofibers: Solution Blow Spinning Polycaprolactone with Anthocyanins from Agri-Food Waste Sources [Josemar G. Oliveira Filho](#)¹, Henriette M. Azeredo², Luiz Henrique C. Mattoso² and Alexander L. Yarin¹; ¹University of Illinois Chicago, United States Minor Outlying Islands; ²Brazilian Agricultural Research Corporation, Embrapa Instrumentation, Brazil

The continuous advancement in rapid manufacturing techniques has played a crucial role in the fabrication of nanofibers intended to produce smart food packaging. This study aimed to employ the solution blow spinning (SBS) technique for the rapid production of intelligent nanofiber mats based on polycaprolactone (PCL) and red cabbage extract (CE) obtained from retail waste for application in monitoring food quality. The addition of CE to the PCL matrix increased the nanofiber diameter from 156 nm to values between 261.05 and 278.14 nm for PCL/CE10 and PCL/CE15, respectively. The addition of CE also improved the mechanical and water-related properties of the nanofibers, although it reduced thermal stability. CE-incorporated nanofiber mats exhibited visible color changes ($\Delta E \geq 3$) in response to buffer solutions with a pH range between 3 and 10, as well as when exposed to ammonia vapor. The smart nanofibers demonstrated the ability to monitor fish fillets through visible color changes during storage. Initially, at 0 hours, the PCL/CE10 and PCL/CE15 mats exhibited a lilac hue, but after 24 hours, this color became less saturated. After 48 hours, bluish-gray tones were observed, and after 72 hours, the blue color indicated deterioration of the fish fillets with a pH of 8.01. Thus, smart nanofibers produced by the SBS technique reveal potential as intelligent food packaging materials. The authors are grateful to FAPESP (processes 2021/13260-7 and 2023/02038-7) for financial support.

5:00 PM MF03.11.05

Facile Preparation of Anti-Mold Wood Fibers for Integration into Biocomposites [Yuqi Feng](#) and [Dendvid Lau](#); City University of Hong Kong, Hong Kong

Public awareness of energy and climate change drives the development of energy-efficient buildings, leading to increased indoor airtightness and bio-based building materials. Wood-based materials, known for their low embodied energy and sustainable life cycle, are highly valued in green building practices. Despite the energy-saving benefits of wood fibers, their susceptibility to mold contamination due to high moisture absorption is often overlooked. This challenges indoor air quality and human health, particularly in warm and humid climates and poorly ventilated buildings. While various coating strategies have been developed to make wood surfaces hydrophobic and mold-resistant, coating durability issues remain. Therefore, this study aims to modify wood fibers for creating wood fiber composites with inherent anti-mold properties. Wood fibers with mold-resistant behavior are prepared by in-situ growth of Zn-containing layered double hydroxides combined with a hydrophobic modification process by stearic acid. The mechanisms of antifungal action of the treatments on fibers and mold cells are understood through molecular dynamics simulations. Mold growth on the composites of untreated and treated wood fibers is then investigated by laboratory tests. The effects of anti-mold coating on the water resistance, dimensional stability, and mechanical properties of the composites are also evaluated. The mold-resistant biocomposites developed here provide a viable candidate for indoor and outdoor construction materials, with great potential for application in green buildings that advocate the healthy and harmonious coexistence of humans and the environment.

5:00 PM MF03.11.06

Designing Cellulose Nanomaterials to Craft Environmentally Conscious Polyurethane Nanocomposites [Teahoon Park](#); Korea Institute of Materials Science, Korea (the Republic of)

This research endeavors to manipulate the mechanical and thermal characteristics by optimizing the polymerization conditions of urethane foam while integrating cellulose nanomaterials (CNMs), known for their eco-friendly properties, through chemical reaction induction. Within the domain of urethane materials, foam variants, notably rigid urethane foam as an insulator and flexible urethane foam employed in memory foam and interior applications, are of particular interest.

Rigid urethane foam, primarily employed in construction and cooling sectors as insulation, is now gaining prominence in advanced insulation techniques for the transport and storage of liquefied natural gas (LNG). Its lighter weight and superior mechanical strength potential offer economic advantages by potentially reducing the material quantities required. Enhancing mechanical robustness while simultaneously reducing thermal conductivity holds promise for space optimization in LNG storage or transport contexts where superior thermal insulation and mechanical properties are paramount.

The surge in demand for environmentally sustainable construction materials aligns with the integration of cellulose, a sustainable alternative, to modulate properties. In addition, we need lighter materials. Glass fiber-reinforced insulation, prevalent in LNG transport, possesses a density of 2.5 g/cm³, significantly higher than the urethane foam material under consideration.

Flexible urethane foam, notably used in automotive seat interiors, demands heightened durability and toughness to withstand long-term usage and repeated stress conditions.

This study's focal objectives involve the development of eco-friendly cellulose nanomaterials and the refinement of urethane compositions to generate nanocomposite foams. The most important goal is to manipulate the physical properties of these nanocomposites through an intricate understanding and advancement of urethane reaction mechanisms. The study's scope encompasses thorough investigations into nanomaterials, polymerization processes, and optimized mixing methodologies to achieve desired material enhancements.

5:00 PM MF03.11.07

Understanding the Influence of Morphology and Chemical Compositions of Algae on the Hydration Reactions of Portland Cement [Meng-Yen Lin](#), Brandon T. Lou, Paul Grandgeorge, Li-Yuan Lin and Eleftheria Roumeli; University of Washington, United States

Cement accounts for up to 10% of global carbon dioxide emissions and has become one of the targets of recent decarbonization efforts. Algae is an abundant and easy-to-cultivate biomass, which can sequester carbon during growth and can be used to replace cement. Recently, we showed that certain microalgae hinder the primary hydration reaction of ordinary Portland cement at high concentrations, significantly hampering mechanical performance. To optimize the structural performance of algae-cement composites, here we focus on the effects of morphology and chemical compositions of algal biomatters on cement hydration. Applying a bottom-up approach, we first study the effects of algae-related biopolymer building blocks, including proteins, carbohydrates, and lipids, on the resulting hydration products through thermal gravimetric analysis (TGA) and scanning electron microscopy (SEM), and their relationships with the composites' compressive strength. To further characterize the influence of particle size, bonding structure, and chemical compositions of the algae on the composites, we then pretreat the microalgae and macroalgae through grinding, hot-pressing, and biopolymer extraction. SEM is used to investigate the effects of particle morphology on the binding interfaces and distribution in the cement matrix. Fourier transform infrared spectroscopy (FTIR) and X-ray photoelectron spectroscopy (XPS) are used to characterize the bonding environment and chemical compositions of the biomass, which are correlated with the hydration products in the algae-cement composites and their contribution to mechanical properties. We show that using specific pretreatment for both algal biomatters, the strength of composites can be improved by up to twofold compared to the unprocessed algal biomatter. The proposed processing methods allow for higher algae replacement content, effectively reducing the environmental impact of the cementitious binder.

5:00 PM MF03.11.08

X-Ray Tomography for Visualizing the Internal Structure of Paper Products and its Correlations with Mechanical Properties [Anderson Thiago Vasconcelos Veiga](#), James Drummond, Mark Martinez and Emily D. Cranston; The University of British Columbia, Canada

Mechanical pulp has traditionally been utilized in newsprint and low-value paper products. With emerging opportunities in bio-based products, mechanical pulp is now standing out as a greener alternative to plastics and fossil-based materials. The development of new sustainable products based on mechanical pulp involves exploring and combining different size fractions, creating composites with chemical and semichemical pulps, and forming layered or dispersed fiber structures.

The challenge in advancing the production of high-quality and specialty paper products based on high-volume mechanical pulp lies in elucidating the internal distribution and interaction of fibers within composites made from different kinds of pulp fibers. X-ray micro-computed tomography has proven to be a powerful tool for visualizing the 3D internal structure of materials, and its potential for elucidating paper structures at the fiber level has already been demonstrated. However, visualizing reinforcing pulp fibers or different phases of pulp fiber composites remains a challenge due to the similar chemical composition of fibers and the surrounding matrix.

In this work, we present a labeling protocol employing iron oxide nanoparticles to enhance the X-ray attenuation of added fibers or pulp phases, resulting in higher contrast fibers in X-ray tomographs. Through *in-situ* synthesis and deposition, iron oxide nanoparticles were deposited on the external and lumen surfaces of long fraction pulp fibers to prepare iron-labeled fibers. These iron-labeled fibers were then incorporated into paper handsheets at various loadings and examined via X-ray tomography. An in-house algorithm for the segmentation of iron-labeled and unlabeled fibers was developed based on tomograph histograms. To optimize the segmentation process, we embedded the handsheets in oil to eliminate the signals associated with air (background signal). After image processing, we successfully visualized the spatially and randomly oriented fibers within the handsheet plane at diverse loadings of iron-labeled fibers. Furthermore, we investigated the impact on mechanical properties of randomly oriented iron-labeled fibers in handsheets in comparison to unlabeled fibers to delineate the limitations of labeling fibers with iron nanoparticles as contrast agent for X-ray tomography.

This study not only provides valuable insights into the role of the large fraction of pulp fibers in reinforcing papers but also sheds light on how different kinds of pulp fibers are distributed in paper products and how the formation of a network impacts mechanical properties. A better understanding of the 3D distribution and network formation of fibers can be leveraged to support the development of high-value products based on high-yield mechanical pulp, aligning with opportunities toward sustainable and bio-based materials for the papermaking industry.

5:00 PM MF03.11.09

Oil-Paper-Umbrella-Inspired Passive Radiative Cooling Using Recycled Packaging Foam [Yang Liu](#) and Yi Zheng; Northeastern University, United States

Passive daytime radiative cooling (PDRC) is a promising energy-saving cooling method to cool objects without energy consumption. Although numerous PDRC materials and structures have been proposed to achieve sub-ambient temperatures, the technique faces unprecedented challenges brought on by complicated and expensive fabrication. Herein, inspired by traditional Chinese oil-paper umbrellas, we develop a self-cleaning and self-cooling oil-foam composite (OFC) made of recycled polystyrene foam and tung oil to simultaneously achieve efficient passive radiative cooling and enhanced thermal dissipation of objects. The OFCs show high solar reflectance (0.90) and high mid-infrared thermal emittance (0.89) during the atmospheric transparent window, contributing to a sub-ambient temperature drop of ~5.4 °C and cooling power of 86 W m⁻² under direct solar irradiance. Additionally, the worldwide market of recycled packaging plastics can provide low-cost raw materials, further eliminating the release of plastics into the environment. The OFC offers an energy-efficient, cost-effective and environmentally friendly candidate for building cooling applications and provides a value-added path for plastic recycling.

5:00 PM MF03.11.10

A Concept of Haze Matching for Cloaking of Bulk Anticounterfeiting Patterns Made of Silk Fibroin-Based Upconversion Nanocomposites [Seohan](#)

Yun¹, Taehoon Kim², Fiorenzo Omenetto² and Junyong Park¹; ¹Kumoh National Institute of Technology, Korea (the Republic of); ²Tufts University, United States

Since 2010, anticounterfeiting technology utilizing NaYF₄-based upconversion nanoparticles (UCNPs), which can emit visible light under invisible near-infrared (NIR) excitation, has been extensively studied. Typically, upconversion patterns and codes are realized by printing viscous nanocomposites composed of a polymer matrix and UCNPs. There are two technical issues: the first is to select a sustainable and environmentally friendly polymer matrix, and the second is to increase the concentration of UCNPs doped in the polymer matrix, considering the extremely low quantum yield of UCNPs. However, when a large amount of UCNPs are concentrated in a unit volume, scattering by nanoparticles increases, creating an opaque pattern. Because bulk patterns are intuitively identifiable, codes can be generated based solely on differences in the colors emitted by NIR excitation. One could consider making the pattern transparent to a level similar to the background by extremely reducing the concentration of UCNPs, but this would exponentially increase the output of the 980 nm light required for decoding. As alternatives, invisible UCNP-doped microbarcodes or microparticles have been proposed, but their processing involves expensive lithography and still requires inconvenient microscopy systems for decoding. Therefore, the practicality of UCNP-based anticounterfeiting platforms in actual fields outside the laboratory is very limited.

In this study, we propose for the first time the concept of haze matching, a convenient way to conceal bulk anticounterfeiting patterns by making the background opaque to a similar level as the pattern. This approach has the advantage of being able to easily control the optical characteristics of the background regardless of the haze level of the pattern, allowing the use of high-concentration UCNP patterns with bright upconversion emission. Regenerated silk fibroin extracted from silkworm cocoons was used as a sustainable and eco-friendly medium to disperse UCNPs. Dopant-free NaYF₄ nanoparticles synthesized under the same hydrothermal conditions were prepared as a medium for haze matching. Based on optical analysis of the transmittance and haze at various nanoparticle concentrations, we established the optimal conditions for the background to completely conceal the bulk pattern with extremely high concentrations of UCNPs. A variety of bulk codes and tags that appear selectively only under NIR excitation have been successfully demonstrated through printing/painting techniques. In particular, opaque anticounterfeiting films containing haze-matched codes and tags were more difficult to identify on white surfaces such as paper or ceramics.

The strategy for upgrading the sustainable nanocomposite-based anticounterfeiting platform proposed in this study will provide new options for the practical use of UCNPs.

5:00 PM MF03.11.11

Vat Photopolymerization-Based Multi-Material 3D Printing of Overhangs with Highly Removable and Recyclable Thiol-ene Photopolymer Supports Tengteng Tang, Prem Nawab, Parimal Prabhudesai, Saleh Alfarhan, Ivan Pesqueira, Kailong Jin and Xiangjia Li; Arizona State University, United States

Vat photopolymerization (VPP) based 3D Printing technology boasts the capability to print 3D structure with remarkable precision and rapidity. In the fabrication of complex structures beyond traditional capabilities, extensive additional support structures are often essential for creating overhanging and free-hanging features. Yet, these internal supports pose challenges as they are not directly removable, necessitating time-consuming manual removal and potentially causing unintended damage and surface imperfections. While specific materials like NaOH-soluble substances and wax have been employed for creating removable supports, these solutions are limited to specific printable materials and often result in considerable waste during the removal process. The current predicament lies in the fact that traditional vat photopolymerization 3D printing of overhangs employs a photocurable liquid resin, which forms a permanently crosslinked polymer. This invariably leads to disposal of body and especially support structure after its usage due to the material's non-recyclable nature.

To counter these drawbacks, this study leverages the properties of crosslinked thiol-ene photopolymer, such as polybutadiene and polyisoprene, which are renowned for their robust structures and excellent thermomechanical characteristics. The innovation lies in utilizing liquid polydiene elastomer as a building block in VPP-based 3D printing, a technique yet to be thoroughly explored. The research focuses on creating a chemically recyclable crosslinked polydiene elastomeric liquid resin, capable of undergoing photoinitiated thiol-ene click reactions with commercially available materials, apt for VPP-based 3D printing. The approach involves using liquid polysulfides with photoreactive thiol end groups and dynamic disulfide bonds, which react with polydienes' carbon-carbon double bonds (ene groups) through photo-crosslinking. The internal disulfide bonds in the resulting crosslinked polydiene elastomers allow for base-catalyzed thiol-disulfide exchange reactions, leading to the decrosslinking or degradation into photoreactive thiol oligomers. Combining conventional permanently crosslinked resin with developed recyclable resin allows for the printing of complex multi-material structures. Subsequent processing to recycle thiol-ene photopolymers can yield intricate overhangs, such as microfluidic channels, spinning tops, and interlocked da Vinci drones. In addition, the impact of surface to volume ratio and crosslinking rate under grayscale projection on the recycling rate is extensively investigated. The optimized porous support structures exhibit properties that are highly removable and recyclable. By demonstrating this scalable method, the study opens up new avenues for fabricating overhangs with easily removable and highly recyclable elastomeric resins via VPP, maintaining material properties across multiple recycling. This development not only offers a superior alternative to current casting/molding manufacturing methods for elastomeric materials but also paves the way for more sustainable and environmentally friendly practices in 3D printing technologies.

5:00 PM MF03.11.12

Biobased Epoxy Resin via Algae Curing Agent Keshan Lighty; North Carolina A&T State University, United States

A growing number of manufacturers are looking for environmentally friendly substitutes for conventional methods in order to cut down on carbon emissions. This research presents a viable path toward environmentally friendly manufacturing methods by investigating the creative use of bio-curing chemicals produced from algae as a novel technique to curing epoxy resin.

Given its abundance and quick development, algae provides a sustainable and renewable supply for bio-curing agents. The purpose of the study is to determine whether chemicals produced from algae may successfully replace traditional curing agents in epoxy resin formulations. Algae-based curing agents have the potential to perform on par with or even better than synthetic counterparts when their mechanical attributes, thermal stability, and curing kinetics are examined.

The use of curing agents generated from algae in epoxy resin formulations not only adds biodegradability and reduces toxicity, but also lessens the environmental impact of traditional curing agents. This move to bio-curing agents is consistent with the global movement toward a circular economy and more environmentally friendly industrial practices.

This research has important economic ramifications in addition to environmental benefits. The cultivation and processing of algae has the potential to generate additional revenue streams for bio-based material enterprises, hence promoting job development and portfolio diversification. Furthermore, the manufacturing industry benefits from increased resource security and resilience because of the decreased reliance on curing agents sourced from fossil

fuels.

By highlighting the crucial role that algae play in changing material science and advancing a more robust and sustainable future, this research provides the foundation for a paradigm change in the manufacturing sector.

5:00 PM MF03.11.13

Automotive Plastics Recycling in a Circular Economy through Molecular Recycling Technologies: Technology Status, Material Advances and Challenges [Mahshid Mokhtarnejad](#)^{1,2}, Gary Hawkins³ and Hendrik Mainka²; ¹The University of Tennessee, United States; ²Volkswagen Group of America, United States; ³Eastman Chemical Company, United States

The urgent need to address the global plastic waste crisis and its impact on climate change has created a demand for a materials revolution. Volkswagen Group of America Inc. (VWGoA) in collaboration with Eastman Chemical Company, is taking the lead in driving circular economy solutions for plastics through groundbreaking molecular recycling technologies. This innovative approach enables the conversion of difficult-to-recycle plastics from the automotive industry into raw materials for producing new specialty plastics and fibers, all while maintaining their quality and performance. Our primary focus lies in dealing with a wide range of plastic waste streams, including mixed plastics, colored plastic materials, post-consumer car carpets, and textiles. The collaboration between VWGoA and Eastman Chemical Company not only brings innovation but also addresses recycling challenges associated with these difficult materials, while providing environmental and sustainability metrics for the recycling process. The knowledge gained from this project contributes to global waste management efforts and fosters a cleaner and more sustainable future. With the molecular recycling process enabling the synthesis of various polymer types, it presents a direct alternative to virgin fossil-based plastics. This is particularly relevant as the automotive industry strives to reduce carbon footprints and divert plastic scrap and automotive shredder residue (ASR) from landfills, benefiting original equipment manufacturers (OEMs) and their suppliers. This molecular recycling process, developed by Eastman Chemical Company and successfully implemented by Volkswagen (VW), has proven to reduce greenhouse gas emissions by 25-50 percent compared to the conventional use of virgin-fossil-based raw materials in the automotive sector. Leveraging their expertise in automotive manufacturing, VW has successfully implemented initiatives to reduce CO₂ emissions through the use of lightweight body panels. This collaboration builds upon their past achievements of the VW's innovation hub in North America. Proof of concept is demonstrated through the Atlas Cross Sport Spoiler Assembly, Passat R-Line Diffuser, and Atlas Cup Holder Substrate, showcasing the successful recycling of mixed plastics. These components serve as examples of the effectiveness and viability of the mixed plastic recycling process to manage plastics from end-of-life vehicles in a sustainable way. In this study, by employing innovative molecular recycling technologies, these proof of concepts highlight the ability to transform challenging waste plastics into high-quality materials suitable for automotive applications. The successful recycling of mixed plastics not only demonstrates technical feasibility but also emphasizes the commitment to sustainability and circular economy principles within the automotive industry.

5:00 PM MF03.11.14

Dye Emission Solvatochromism to Monitor Local Environment in Polyhydroxybutyrate Nanoparticles [Gareth Redmond](#); University College Dublin, Ireland

In this work, the use of Nile red as a solvatochromic probe of biopolymer nano-environments was investigated. Firstly, relationships between measured dye fluorescence spectral maxima and solvent dielectric constant ϵ and Reichardt solvent parameter $E_T(30)$ were developed. Then, aqueous dispersions of NR-doped nanoparticles (NPs) of poly-hydroxybutyrate (PHB) were prepared using a batch-type emulsion process facilitated by tip sonication and the effect of NP preparation conditions on NR nano-environment was spectroscopically probed.

Photoluminescence spectra of aqueous dispersions of PHB/NR NPs indicated that NR fluorescence spectral maxima were redshifted for samples prepared with 2 min of tip sonication, blueshifting to similar values for samples prepared with 5 or 8 min of sonication. The data suggested that for NPs prepared with 2 min sonication, NR dye molecules were situated at locations ranging from highly dipolar aprotic to polar protic (H-bonding donor/HBD) in character. The dyes were comparatively poorly encapsulated in the PHB NPs being located near or at the interface in regions close to the PVA surfactant stabiliser and the surrounding aqueous medium. The data also indicated that for NPs prepared with 5 and 8 min sonication, the dye molecules were situated at locations that were mildly dipolar and non-HBD in character, i.e., the dyes were on average better encapsulated within the NPs, located away from the polymer-water interface and less exposed to H-bonding effects. Statistical analysis of emission maxima obtained for particles prepared with different sonication conditions showed a clear trend of shifting NR nano-environment character, from high polarity/HBD-type to lower polarity/non-HBD-type, on changing the NP batch preparation sonication time from 2 min to 5 or 8 min. The mean extracted value for the local dielectric constant ϵ in the 5/8 min PHB/NR NPs is estimated as 8.5 ± 1.5 , slightly larger than reported bulk values, suggesting that the dielectric response of these nanoparticles reflects contributions due to interfacial effects.

Photoluminescence decay data for aqueous dispersions of PHB/NR NPs were also acquired and fitted by a double exponential function, suggesting that the NR dye molecules were located in heterogeneous environments. The short emission decay component has previously been attributed to interaction between dye molecules and water molecules via H-bonding, leading to rapid non-radiative deactivation of the NR excited state. From the data, the relative amplitudes of the short and long decay components varied from 2 min through 5 min to 8 min sonication indicating a progressively decreasing contribution of the short decay process to the overall emission decay, consistent with reduced NR-H₂O H-bonding interactions due to improved dye encapsulation. To gain further information about the possible locations of NR molecules within the 5/8 min PHB/NR NPs, emission anisotropy studies were undertaken. Steady-state emission anisotropy spectra gave mean anisotropy values consistent with dye molecules being typically located in restricted environments. Time-resolved emission anisotropy decays were acquired, fitted by a double exponential function, and analysed using a "wobbling-in-a-cone" model that suggested that the measured anisotropy decays arise from rotational relaxation of dye molecules in the NPs by a wobbling-in-cone motion and by lateral (2D) diffusion relative to the NP surface. Trends in the extracted rotational relaxation parameters were consistent with inclusion of NR molecules in progressively more restrictive environments due to improved dye encapsulation with increasing sonication time.

The ability to employ a solvatochromic probe of nano-environments in novel polymer nanoparticles offers promising opportunities for future studies aimed at understanding the guest- and host-dependent mechanisms of encapsulation and controlled release of active ingredients in biopolymer nanostructures.

5:00 PM MF03.11.15

Biodegradable and Renewable Polymer Obtained from the Reactive Extrusion of Corn Derivatives Paula D. Santiago¹, [Tamires d. Nossa](#)² and Vagner R. de Mendonça²; ¹Federal University of Sao Carlos, Brazil; ²Federal Institute of Education, Science and Technology - IFSP, Brazil

The waste generation caused by human consumption of plastic has been growing exponentially in the last century, causing several environmental impacts. One of the alternatives to mitigate this effect is the development and application of biodegradable polymers. Starch is one of the most promising materials for this purpose, given its low cost, availability, and ability to be modified chemically, biologically, and physically. One of the sources of starch is corn, and its use is extremely attractive due to the high production of this food. However, starch has limited properties regarding its low mechanical strength and high hydrophilicity. Studies have been carried out to improve the properties of this material, making its processing and application more satisfactory. We can highlight the inclusion of glycerol, a residue from the biodiesel industry, as a plasticizing agent and coconut oil to increase mechanical resistance and water absorption. In this work, the effects of modifying products derived from corn, pre-gelatinized starch, were investigated for the processing of

polymers using glycerol and coconut oil through the reactive extrusion process to obtain a biodegradable product from a renewable source with potential application in the packaging industry. Thermogravimetric, Differential Exploratory Calorimetry and Fourier transform infrared spectroscopy analyses were carried out, and the mechanical properties, biodegradation, and moisture absorption were analyzed. It was possible to verify an improvement in the mechanical properties of the formulation with the addition of 20% by mass of coconut oil, with an increase of approximately 37.5% in the tensile strength limit and 32.1% in the elongation at break and a reduction in moisture absorption.

5:00 PM MF03.11.16

Thermoplastic Starch Reinforced with Bamboo Fibers: A Biodegradable Composite Alternative Nicolas A. Maricato, Vagner R. de Mendonça and Tamires d. Nossa; Federal Institute of Education, Science and Technology of Sao Paulo - IFSP, Brazil

Due to the large consumption of plastics and their frequent use in disposable applications, it is essential to direct studies toward the development of alternative materials that are biodegradable or come from renewable sources in order to reduce the impact generated by the disposal of these materials on the environment. This study focused on the production of a sustainable biocomposite, produced from a renewable and biodegradable source, using corn starch as a thermoplastic matrix, in which glycerol, a residue from the biodiesel industry, was used as a plasticizing agent. Different production parameters were studied through reactive extrusion in order to produce homogeneous filaments with a thermoplastic starch matrix (TPS), in the proportion 70:30 (% starch: % glycerol), reinforced with bamboo fibers with different filler addition proportions between 5%, 10%, 15%, 20% and 30% by mass. To incorporate the fibers, an alkaline treatment was carried out with sodium hydroxide (5% NaOH) in order to make the composite interface compatible. It was possible to observe that the presence of bamboo filler increased the mechanical tensile strength and modulus of the TPS while the elongation decreased. The presence of fibers also modified the TPS biodegradation profile, acting to preserve the proliferation of fungi, preserve the material, and increase the biodegradation time.

5:00 PM MF03.11.17

Curdlan Hydrogels as Sustainable Scaffolds for Cell-Based Meat Production Reyhaneh Sarkarat and Reza Ovissipour; Texas AM, United States

Cellular agriculture has drawn significant attention as a potential solution to challenges associated with traditional farming, such as environmental pollution, animal welfare, and sustainability. To support the cells to grow into desired tissues, a physical structure as a scaffold is needed. Scaffold development is a well-studied field in the tissue engineering discipline, more specifically for biomedical purposes. However, the biomaterial used in fabricating scaffolds for food products should meet different criteria. In addition to being biodegradable and biocompatible, cultured meat scaffolding biomaterial should be edible and be able to mimic meat texture and structure. This work aims to investigate microbial, plant, and insect-based biomaterials that have not been exploited for cultured meat scaffolding and introduce a new combination as a potential scaffolding biomaterial for food purposes. In this study, novel protein-enriched hydrogels have been developed, characterized, and applied to develop bio-based films supporting bovine muscle satellite cell growth. Curdlan, a microbial polysaccharide, was used as the gelling agent, combined with three different types of proteins, including hemp, alfalfa, and black soldier fly. To characterize the scaffold and assess the mechanical and chemical properties of the scaffold, FTIR, differential scanning calorimetry (DSC), and rheology tests were selected to be performed before and after seeding cells on biofilms. Additionally, patterned biofilms were developed to investigate the possibility of enhancing cell adhesion and differentiation.

5:00 PM MF03.11.18

Bacterial Cellulose Nanoparticles for Sustainable Drug Delivery Gabrielle Balistreri, Ian R. Campbell, Xinqi Li, Julia Didier Amorim, Shuai Zhang, Elizabeth Nance and Eleftheria Roumeli; University of Washington, United States

Sustainable nanomedicine is an emerging concept to address the challenges of scalability, reproducibility, thermostability, and waste free processing for nanotherapeutic manufacturing. This significant problem has created access barriers for patients in need of disease treatments in low-resource settings and under-developed countries. Bacterial cellulose (BC) is a nanomaterial with the potential to overcome these challenges and be a versatile drug delivery platform for disease treatments. The development of BC nanoparticles (BCNPs) for drug delivery is motivated by the material's biodegradability and biocompatibility properties, important for nanomedicine applications. BCNPs are nanoscale in all dimensions and are grown in a kombucha media in agitated and aerated conditions for 24 h and size separated utilizing polysorbate 80 surfactant solution. BCNPs are approximately 200 nm in particle size, and have a near neutral zeta-potential, and amorphous structure. Here, we study the morphology and structure of BC fibers within BCNPs over the course of 5-days. We find an increase in BC crystallinity and demonstrate significant differences in the hierarchical fiber organization with time of growth. Furthermore, we characterize the BCNPs thermal stability which is important for biomedical applications. Lastly, we demonstrate drug loading and unloading performance of BCNPs using bovine serum albumin (BSA) as a model. These results highlight the potential of BCNPs to be used in biological settings and in particular, their application as a sustainable drug delivery nanotherapeutic platform to treat critical diseases.

5:00 PM MF03.11.19

Texture and Pitch Evolution in Cholesteric Chitosan Mesophases Eleanor C. Grosvenor and Cecile Chazot; Northwestern University, United States

Chitosan has demonstrated value as a biodegradable packaging material due to its antibacterial and hydrophobic properties, but it has untapped potential in optical applications. This abundant, waste product-derived polysaccharide is known to develop chiral nematic liquid crystalline order upon suspension in various solvents. However, the thermodynamics of its self-assembly are not well understood. Through the measurement of cholesteric pitch using polarized light microscopy, we can pinpoint the critical concentration at which cholesteric mesophases begin to form. In concert with a phase diagram model to inform thermodynamic mesophase behavior, we have developed a framework to optimize the optical activity of chitosan suspensions for a variety of applications. We propose a quantitative relationship between cholesteric pitch and concentration, as well as other formulation and processing parameters like molecular weight, solvent choice, degree of deacetylation, and aging time. This relationship helps to elucidate the complex interactions occurring between chitosan and solvent. With a better understanding of this system, we open the door to new applications of structurally colored films, such as colorimetric sensing for food packaging.

5:00 PM MF03.11.20

Versatile Method to Produce Wood Particle Foams for Building Insulation Elizabeth Dobrzanski^{1,1}, Elisa Ferreira^{2,1,1}, Praphulla Tiwary³, Prashant Agrawal³, Richard Chen³ and Emily D. Cranston^{1,1,1}; ¹The University of British Columbia, Canada; ²Brazilian Nanotechnology National Laboratory, Brazil; ³Plantee Bioplastics Inc., Canada

Lightweight foams are excellent thermal insulators due to their structure, which traps layers of air pockets and results in low thermal conductivity. Modern buildings overwhelmingly use insulative foams derived from petrochemical sources, which not only contribute greenhouse gases during manufacturing but also end up in a landfill at the end of their life. Alternatives to petrochemical-based foams, such as mineral wool, have been linked to health concerns. As a result of these environmental and health concerns, the appetite for bio-based and environmentally-friendly materials is growing and may be awarded through building sustainability certifications like LEED or BREEAM [1].

Materials that are truly sustainable must be considered holistically, from their feedstock source to their manufacturing process to their end-of-life stage. Some examples of bio-based insulative foams are cellulose- and pulp-based foams, which are moving towards being fully sustainable but still require relatively high amounts of processing energy to transform them from their raw feedstock form. One feedstock source that is often overlooked is forest residues, materials generated by the forestry industry that have little to no economic value and includes bark, dead trees, off-cuts, and small-diameter trees. Due to their poor mechanical qualities, they are often used for low-value products [2].

We previously showed that we can circumvent the poor macro-scale mechanical properties of forest residue wood by milling the feedstock to < 1 mm and recombining the wood particles as a lightweight, high bio-based content foam [3]. This previous work focused on pine beetle-killed wood, which refers to trees that have been killed by mountain pine beetles and may contribute to high-intensity fires if left in the forest [4]. To produce these foams, waste wood particles are foamed in water with surfactant and a water-soluble polymer binder and then oven dried [5], a relatively facile and low-energy method of solid foam production. The resulting foams have mechanical (density ca. 0.12 g cm⁻³) and thermal (thermal conductivity ca. 0.042 W m⁻¹ K⁻¹) properties that are competitive with conventional petrochemical-based foams. The promising performance of our foams is attributed to their low density and hierarchical pore structure consisting of polyhedral cells templated by air bubbles and natural honeycomb pores from the wood cell walls [3]. The end-of-life stage is also considered, as the foams are able to be re-wetted, re-foamed, and re-dried while maintaining their original properties.

Our current research pushes this method further by exploring different waste wood feedstocks, different particle sizes, and the replacement of our surfactant and polymer binder with bio-based materials alternatives. Verifying the potential of alternative waste wood feedstocks and particle sizes is important for scalability and adaptability, while alternative surfactants and binders are important to create a fully bio-based product with no negative environmental impact. In most cases the thermal and mechanical properties of these alternative foams are competitive and have the potential to replace petrochemical-based foams. The alternative foams that do not meet ASTM or building standards may still be able to pass if the milling procedure is tweaked to allow for higher aspect ratio particles, which may result in more comingling of the wood particles and binder and produce a more cohesive solid foam structure.

[1] Schiavoni et al. *Renew. Sust. Energ. Rev.*, 2016, 62, 988

[2] Kizha & Han. *Biomass Bioenergy*, 2016, 93, 97

[3] Ferreira et al. *Mater. Adv.*, 2023, 4(2), 641

[4] Kurz et al. *PNAS*, 2008, 105(5), 1551

[5] Tiwary & Chen. Canada Patent WO 2022/073126, 2022

5:00 PM MF03.11.21

Physico-Mechanical Evaluation of Electrospun Nanofibrous Mats of Poly(3-hydroxybutyrate) / Poly(butylene succinate) Blends with Enhanced Swelling-Dynamics and Hydrolytic Degradation-Kinetics Stability for Pliable Scaffold Substrates [Harshal Peshne](#) and Bhabani Satapathy; Indian Institute of Technology Delhi, India

Biodegradable blends of PHB/Bio-PBS were successfully electrospun with solvent system 2,2,2-trifluoroethanol as the solvent to obtain electrospun mats (EMs) of fiber diameters ranging from 534 ± 135 nm to 181 ± 84 nm. The addition of CaCl₂ led to defect/bead free morphology of PHB and PHB/Bio-PBS blends with the exception for Bio-PBS at ~ 20 wt. % concentration. Bio-PBS based electrospun mats with CaCl₂ led to the lowest fiber diameter (due to high conductivity and low viscosity of solution). Further, our study indicates that PHB/Bio-PBS blends displayed shear-thinning behavior with reduction in solution viscosity which in turn remained in tune with increasing Bio-PBS concentration. DSC studies indicated a more significant drop in crystallinity for PHB/Bio-PBS blends and as well corroborated by WAXD. Mechanical properties were affected by immiscibility, resulting in lower tensile strength from ~ 4.0 MPa to ~ 2.0 MPa and tensile modulus from ~186 MPa to ~ 64 MPa, while strain-at-break increased from ~ 1.5 % to ~ 46.5 % with Bio-PBS content in PHB matrix. Electrospun mats with up to 50 % Bio-PBS loading demonstrated optimal ductility and strength and also exhibited a tensile modulus comparable to that of cancellous bone. Additionally, the blend with ~ 50 wt. % of Bio-PBS showed increased hydrophobicity (116°) and decreased swelling characteristics (84 %) compared to neat PHB (95° and 124 %). Hydrolytic degradation studies showed improved structural robustness and consistent morphology in Bio-PBS based electrospun mats even after 30 days in phosphate buffer solution compared to PHB based mats. Thus, up to 50 % Bio-PBS incorporation into Polyhydroxyalkanoates matrices, i.e. in the blends with 50:50 compositional the mats obtained showed enhanced pliability in combination with the desired extent of physico-mechanical properties and stiffness for soft bone tissue engineering.

5:00 PM MF03.11.22

Structure-Property Relationships of Lignin-Based Structural Building Materials [Malavika Bagepalli](#)¹, Priscilla Pieters², Jian Zhang¹, Kevin Miller³, Hemant Choudhary^{1,4} and Sumanjeet Kaur¹; ¹Lawrence Berkeley National Laboratory, United States; ²University of California, Berkeley, United States; ³Murray State University, United States; ⁴Sandia National Laboratories, United States

Buildings enable long-term storage of carbon due to their long lifespans (> 50 years). Engineered wood, including wood biopolymer composites, is a potential replacement for concrete and steel in construction to limit CO₂ emissions. However, current formaldehyde-based binders used in engineered wood are toxic and have environmental concerns, so there is a need to explore bio-based, formaldehyde-free binders. Lignin is one of the most abundant biopolymers on earth and is a natural glue which holds up a plant's structural framework. Currently, lignin (Kraft) is treated as a low-value waste product by the paper and pulp industry, with a significant amount burned for fuel. The use of lignin from waste streams and agricultural waste in building materials emerges as a cost-effective solution. However, the chemical composition of lignin is sensitive to lignocellulose source and method of extraction, leading to inhomogeneity. Extracting lignin through ionic liquids (IL) or deep eutectic solvents (DES), are environmentally friendly and energy efficient. However, the effects of lignin variability on adhesive performance have not been well explored. Specifically, ideal characteristics for the development of structural wood composites have not been systematically studied. To address this gap, this study aims to develop structure-property relationships of lignin-based adhesives from different sources and extraction methods. The study includes a comprehensive baseline characterization of the different lignin and repeated mechanical strength measurements of lignin-based adhesives.

SESSION MF03.12: Sustainable Structural Materials
Session Chairs: Kunal Masania and Eleftheria Roumeli
Friday Morning, April 26, 2024
Room 323, Level 3, Summit

8:45 AM *MF03.12.01

Bio-Inspired Biomineralized Bacterial Cellulose Composite Material [Marie-Eve Aubin-Tam](#); TU Delft, Netherlands

There is an important need for sustainable structural materials that combine high mechanical strength, possibility of control over 3D shape, and ease in upscaling material production. I will present how we use microorganisms to fabricate inorganic-biopolymer composite materials that show a layered structure reminiscent of tough biominerals in nature (nacre, bone, dentin). The inorganic component consists of calcium carbonate (CaCO₃) crystals formed by *Sporosarcina pasteurii* bacteria, and the organic components include bacterial cellulose and polyglutamic acid, produced by the bacteria *Gluconacetobacter hansenii* and *Bacillus paralicheniformis*, respectively. This 'bacterial nacre' reaches and exceeds the toughness of natural nacre, while being fabricated in an ecological, economical, and simple manner using bacteria. The 3D shape can be controlled via molding or direct ink writing. The resulting composite materials show promising applications as light weight structural materials.

9:15 AM MF03.12.02

MICP Biomineralization and Biotic Additive Manufacturing Toward The Design of Strong Biocomposites [Sabrina Shen](#)^{1,1,2}, [Ethan Viles](#)^{2,2}, [Chelsea Heveran](#)^{2,2} and [Markus Buehler](#)^{1,1}; ¹Massachusetts Institute of Technology, United States; ²Montana State University, United States

Microbial-induced calcium carbonate precipitation (MICP) has been explored as a more sustainable alternative for producing concrete-like load-bearing materials. Concurrently, additive manufacturing of biotic composites enables the production of complex hierarchical materials with minimally refined organic feedstocks. Such materials can be designed to be functional and highly biodegradable, however organic materials without a mineral phase are limited in mechanical strength, and material longevity is necessary for some applications. Here we explore MICP biomineralization of additively manufactured biotic composites, and investigate the interaction between mineral formation and biocomposite structure at multiple scales. We characterize the resulting materials and consider how MICP biomineralization and additive manufacturing can be used to design for strong and durable biocomposite materials.

9:30 AM MF03.12.03

Innovative Circular Building Technologies: Recycled Brick Sand, Geopolymer Mortars, Robotic Arm, Computer Vision and Low Carbon Emission Solutions [Mohammad Rizwan Bhina](#) and [Liu Kuang-Yen](#); National Cheng Kung University, Taiwan

The construction industry is undergoing a transformative shift towards sustainability due to environmental concerns and resource scarcity. The cement industry, responsible for 8% of industrial CO₂ emissions, exacerbates this issue. Haphazard and overbuilding construction practices also lead to a 3% annual increase in concrete demand, further contributing to global warming. This research explored innovative technologies, focusing on recycled brick sand, geopolymer materials, robotics, computer vision, and low-carbon solutions. Recycled brick sand reduces resource demand and minimizes waste, while geopolymer materials, derived from industrial by-products, cut carbon emissions and promote circularity. Automation, robotics, and computer vision enhance efficiency and safety. Moreover, AI-driven algorithms and drones improve site management, defect detection, and progress tracking. Addressing carbon emissions through carbon-capture technologies and renewable energy integration aligns with circular principles. This integration represents a significant step toward sustainability in construction.

Thus, as a result, the use of blend of low calcium fly ash and S4000 GGBS as a binder, 10 M NaOH as an activator, and recycled brick sand as a fine aggregate from recycled bricks used as a source material for evaluating the flowability and mechanical strength of geopolymer bricks in this study has been explored. For further study of the compressive strength of recycled brick, 0.363 was selected as the optimum binder-to-recycled brick sand ratio. In this study, it was found that brick sand is the most significant factor contributing to reduced flowability of geopolymer mixtures. Binder-to-recycled brick sand ratio of 0.363 with 10 M NaOH activator provided the highest 1-day compressive strength of 24.2 MPa. An inhomogeneous microstructure was observed with a binder replacement ratio of less than 0.35 in FESEM-EDS analysis of the specimens. Geopolymer materials bricks were more durable and mechanically strong when NaOH concentrations and curing temperatures were higher.

In conclusion, the integration of these innovative circular building technologies into construction practices was paving the way for a more sustainable and environmentally responsible industry. By reimagining materials, embracing automation, harnessing AI, and prioritizing low-carbon solutions, the construction sector is moving towards a circular economy model that aims to minimize waste, reduce resource consumption, and mitigate the environmental impact of building projects. These advancements hold the potential to reshape the future of construction and create a more sustainable built environment.

9:45 AM MF03.12.04

Deconvoluting The Effects of Chemical Composition and Structural Confinement of Algal Biomatter on The Hydration Reactions of Portland Cement [Meng-Yen Lin](#), [Brandon T. Lou](#), [Paul Grandgeorge](#), [Li-Yuan Lin](#) and [Eleftheria Roumeli](#); University of Washington, United States

Decarbonization of cementitious materials, which contributes to 10% global carbon emissions, is one of the primary targets to achieve carbon net zero by 2050. Utilizing the abundance, easy cultivation and carbon-sequestering ability of algal biomatters to reduce cement usage has received rising attention. We recently reported that certain algal strains in the unprocessed form hinder the hydration reactions of ordinary Portland cement, preventing the application of replacement at high algae content. Here, to understand the interactions between the algal biomatters and cement further, we aim to deconvolute the effects of chemical composition and structural confinement of algal biomatters on the performance of algae-cement composites. We first study the influence of algae-related biopolymers, including carbohydrates, lipids, and proteins, on the resulting hydration products using thermal gravimetric analysis (TGA) and scanning electron microscopy (SEM), and their contribution to composites' compressive strength. We then apply pretreatments, involving grinding, self-bonding induced by heat and pressure, and biopolymer extraction, to the macro- and microalgae respectively to investigate the impact of particle size, bonding structure, and chemical composition on the algae-cement interactions. The effects of varying particle size and morphology of biomass on the binding interfaces and distribution in cement matrix are evaluated by SEM. The modified bonding environment and chemical composition of biomass are measured with Fourier transform infrared spectroscopy (FTIR) and x-ray photoelectron spectroscopy (XPS), and then correlated with the hydration products and mechanical properties of the algae-cement composites. Compared to the unprocessed algal biomatter, we significantly improve the strength of composites by twofold using specific pretreatment for both algal biomatters. The proposed processing method and mechanisms enable higher algae replacement in cement with low energy trade-off, showing great potential for reducing cement usage and carbon footprint.

10:00 AM BREAK

10:30 AM MF03.13.01

Selective Mechanical Deconstruction of Multilayer Film Interfaces [Naomi Deneke](#), Natalie Stingelin and Blair K. Brettmann; Georgia Institute of Technology, United States

Studies have investigated the use of mechanically heterogeneous interfaces having compliant and rigid components for control of adhesion strength. From Kirigami-inspired tapes to composite micropillars. In a similar fashion, mechanically heterogeneous interfaces can be used to trigger delamination events due to localization of stress at the rigid-soft interface. This is especially useful for improving the circularity of multilayer films, which are difficult to recycle due to their multi-material chemistry and use of tie layer adhesives that prevent facile separation of the layers. I will present a material design that utilizes mechanically heterogeneous interfaces that when coupled with a mechanical trigger, selectively deconstructs a multilayer film. Rigid silica microparticles are placed at the tie layer (polyethylene acrylic acid (PEAA)) and aluminum foil interface of a tri-layer film comprised of polycarbonate, PEAA, and aluminum foil. A high intensity ultrasound pulse is sent through the sample, taking care to select a wavelength and voltage that will generate a pressure wave capable of generating significant mechanical stresses at the interfaces. Delamination of the foil layer was observed when 5 μm size particles were positioned at the interface and subjected to an ultrasound pulse, while no delamination was observed if no particles were used, suggesting that interfacial patterning with mechanically heterogeneous particles assists in delamination of the layers. Additionally, particle size, density, and location of within the bulk of the material play a significant role in the delamination mechanism. In this work, we design our multilayer materials with end-of-life in mind in order to improve recovery and reuse of layers used in multilayer films.

10:45 AM MF03.13.02

Biowaste Enabled Porous Carbon towards Ultrahigh Capacitance for Energy Storage [Yingchao Yang](#); University of Missouri, United States

Lignin is the second most abundant biopolymer and the most abundant aromatic-containing polymer in nature. Typically, lignin accounts for 15–30% of plants and serves as an adhesive by forming a lignin-carbohydrate complex to bind cellulose and hemicellulose together. Lignin is a waste product in the production of paper or chemicals (e.g. ethanol) from biomass. If not removed, the lignin could cause the paper-derived wood pulp to weaken and discolor rapidly.

Valorization of useless lignin to high value-added materials for advanced applications would help address the environmentally detrimental biowaste and satisfy the societal need. To date, lignin has been used as a functional component in polymer synthesis. For example, polyhydroxyalkanoate (PHA)/lignin shows better microbial resistance than PHA alone due to the formation of strong hydrogen bonds. Lignin blended polylactic acid (PLA) exhibits a great non-flammable capability. Furthermore, monomers in lignin have been used to synthesize polymers, such as polyester and polyurethanes. However, owing to the chemically recalcitrant nature, it is very challenging and costly to convert lignin into value added biopolymers.

Recently, the focus on using lignin and its derivatives has been shifted to fabricating energy storage devices, including lithium-ion batteries and supercapacitors. Regarding batteries, lignin has been used by either combining it with additives and binders as electrodes for lead-acid batteries or by fabricating it into three-dimensional (3D) hierarchical porous carbon as electrodes for lithium-ion batteries. Without a doubt, the lignin-based electrode is cheaper and greener, which is a great alternative to existing electrodes for energy storage.

In this presentation, a thick freestanding electrode coupled by lignin carbon and sodium without any binder and additives was fabricated demonstrating a specific area capacitance of 19.7 F cm^{-2} at a current density of 1 mA cm^{-2} , which is the highest among to date reported freestanding lignin carbon electrodes with similar thickness. This excellent electrochemical performance originates from high electro-positivity and oxygen content promoted by the sodium. Our brings a new strategy towards lignin utilization and energy storage through coupling lignin carbon and alkali metals.

11:00 AM MF03.13.03

Accessibility of Ring-Closing Depolymerization for Polycarbonates with Multiple Theory Validation [Brandi Ransom](#), Dmitry Zubarev, Nathan Park, James Hedrick and Kristin Schmidt; IBM Research, United States

We present an accelerated protocol to qualitatively screen polycarbonate monomers for viability of depolymerization in solvents of varying polarities. The largest barrier in the exploration of reaction kinetics is the necessary conformational analysis to identify lowest energy paths in depolymerization, which can depend on the solvent. Tight-binding DFT allows for an accurate quantification of depolymerization barriers as compared to DFT, with an increase in speed by up to 3 orders of magnitude. By a detailed featurization of over 30 compounds we verified that depolymerization barriers are not linearly correlated to the dielectric constant of the solvent. Volume of the molecules is explicitly not correlated with the depolymerization barrier; the solvent-molecule interactions and chemistry of the molecules is extremely influential due to the over coordinated oxygens in the transition state. Though computation of the solvent-solute interaction parameter is necessary for future predictive work in kinetic barriers, even alongside the 1800 Mordred features, conformational analysis is still necessary to determine the lowest kinetic barrier across solvents. We present multiple examples of the of lowest-barrier polycarbonates in acetonitrile, tetrahydrofuran, and toluene to highlight the large opportunity in this field for development in this multi-dimensional optimization problem. For the current available simulation and predictive models, our high-throughput protocol can evaluate the ideal solvent for 6-member polycarbonate depolymerization. From this work, further investigation into solvent-molecule interactions for quick computing features will lead towards the goal of data-driven methods for polycarbonate discovery and optimization.

11:15 AM MF03.13.04

Using Piezoelectricity to Make Force-Responsive Polymeric Materials [Sarah M. Zeitler](#) and Matthew Golder; University of Washington, United States

Stimuli-induced polymerizations continue to gain interest as synthetic polymers become more desirable for materials, industrial, and medical applications. While traditional stimuli such as heat, light, and electrochemistry have been extensively studied, they still have shortcomings such as unwanted side reactions, lack of consistent penetrability, and irregular and irreproducible equipment setups. Additionally, high energy inputs and large amount of solvent are regularly used with such stimuli. Many of these shortcomings can be overcome by using force as a stimulus for polymerization. As has been shown in organic small molecule synthesis, the use of piezoelectric nanoparticles enables force to initiate redox reactions, thus making force an even more useful, accessible, and sustainable stimulus for polymerization chemistry.

Herein, we show iodonium salts can initiate free and controlled radical polymerizations of acrylates upon the introduction of various types of force in the presence of piezoelectric nanoparticles, consuming less energy and solvent than traditional polymerization methods. These salts have demonstrated to be reactive with piezoelectric nanoparticles and useful in synthesizing high molecular weight polymers with relatively low dispersities. Furthermore, these polymerizations have been effectively carried out in both solid and solution states with multiple force sources, including ultrasound, ball milling, and vortexing. Preliminary data also indicates that force might be a new useful tool for crosslinking materials and for force-curing in additive manufacturing taking advantage of the mentioned multiple force sources. This iodonium initiated mechanoredox chemistry unlocks the possibility to better utilize force in synthesizing polymers and creating useful adaptable materials.

Acknowledgements: This work was supported by a seed grant from UW MEM-C, an NSF MRSEC funded under DMR-1719797

(1) Kubota, K.; Pang, Y.; Miura, A.; Ito, H. *Science*. **2019**, *366*, 1500–1504.; (2) Mohapatra, H.; Kleiman, M.; Esser-Kahn, A. P. *Nat. Chem.* **2017**, *9*, 135–139.; (3) Wang, Z.; Ayarza, J.; Esser-Kahn, A. P. **2019**, *58*, 12023–12026.; (4) Wang, Z. Z.; Pan, X.; Yan, J.; Dadashi-Silab, S.; Xie, G.; Zhang, J.; Wang, Z. Z.; Xia, H.; Matyjaszewski, K. *ACS Macro Lett.* **2017**, *546*–549. (5) Zeitler, S.; Chakma, P.; Golder, M. *Chem. Sci.* **2022**, *13*, 4131–4138. (6) Chakma, P.; Zeitler, S. M.; Baum, F.; Yu, J.; Shindy, W.; Pozzo, L.; Golder, M. *Angew. Chem. Int. Ed.* **2022**. Accepted Article

11:30 AM MF03.13.05

Recycled Polymers for a Circular Economy Model: Case Study of 3D Printed Wind Energy Generator Vitaliano Dattilo, Kunal Bachim, Nikhil Alagandula, Louis Sponton, Sarvenaz Ghaffari, Andrew Makeev and [Michael Bozlar](#); The University of Texas at Arlington, United States

Polymers are essential components of society as they are versatile, lightweight, and low-cost materials. On the other hand, the growing amount of plastic waste creates a global environmental concern. It is therefore necessary to investigate innovative methods and technologies to achieve a circular economy based on the recycling of plastic waste followed by a reprocessing. In this work, we focus on retrieving the original mechanical properties of polymers after recycling. We produce polymer composite fibers using recycled polyethylene terephthalate water bottles or polypropylene bottle caps, reinforced with various fillers, including graphene. We conduct tensile testing and analytical studies on these composites, and eventually demonstrate their 3D printing potential for application in vertical axis wind turbine rotors. The design process for the wind turbine, site selection, and wind climate analysis are briefly provided.

11:45 AM MF03.13.06

Trash to Treasure: 3D Printing of Waste-Based Polycotton Composite for The Production of Water Filters and Commodity Products [Varvara Apostolopoulou](#) [Kalkavoura](#), Natalia Fijol, Salvatore Lombardo, Maria-Ximena Ruiz-Caldas and Aji Mathew; Stockholm Univ, Sweden

The textile industry has been proven to be one of the most polluting industries worldwide due to the extensive use of virgin resources, the vast amount of water and land used and the emergence of fast fashion which resulted to double production of garments the last 20 years. Most of these textiles end up in landfills or incineration facilities. However, the recycling of textiles is still in seminal stage due to lack of proper sorting but also due to the limitations of recycling blended fabrics and the lack of upscalable technology. Polyethylene terephthalate (PET) dominates more than 50% of the textiles market and even if there are routes to recycle it, its presence in blended fabrics mostly in combination with cotton burdens its recyclability. Most of the recycling studies investigate either the depolymerization of PET or the dissolution of cotton in order to efficiently separate them. However, in most of the cases those processes are very energy and materials intensive.

Here we present an upcycling route in one-pot valorization of blended cotton-PET fabrics without separating the two constituents. We performed a mild chemical treatment of cotton-PET (1:1) fragmented post-consumer fabrics during which PET was inert but the cotton was functionalized with carboxyl groups and partially fibrillated. The reaction resulted in high yields (>90%) and the treated textiles were further mechanically disintegrated using a facile and short process in order to enhance their fibrillation and reduce their size. The treated textile mixture was then used for film casting which were oven-dried and cut into 1x1 cm pellets suitable for extrusion taking into account the thermoplastic nature of PET. The obtained filament was used as a feedstock for the Fused Deposition Modelling (FDM) 3D printer and several composite materials for water purification and commodity applications were printed. The presence of carboxyl groups enhanced the adsorption capacity of the polycotton filters making it possible to manufacture advanced materials from discarded garments for water purification applications. Furthermore, several fashion products with various designs were also successfully printed extending the use of the same waste feedstock in the preparation of every day polymer-based accessories.

The facile fabrication of customised waste-based pellets followed by extrusion and the successful 3D printing of the developed filaments into water purification filters and commodity accessories highlight the potential for upscaling and widespread commercialization. Compared to traditional 3D printing feedstocks, the waste-based filaments offer a cost-effective on-demand solution which can be widely accessible.

SYMPOSIUM MT01

Integrating Machine Learning and Simulations for Materials Modeling

April 22 - April 26, 2024

Symposium Organizers

Raymundo Arroyave, Texas A&M Univ

Elif Ertekin, University of Illinois at Urbana-Champaign

Rodrigo Freitas, Massachusetts Institute of Technology

Aditi Krishnapriyan, UC Berkeley

* Invited Paper

+ JMR Distinguished Invited Speaker

^ MRS Communications Early Career Distinguished Presenter

SESSION MT01.01: Machine Learning and Simulations I

Session Chairs: Raymundo Arroyave and Danny Perez

Monday Morning, April 22, 2024
Room 320, Level 3, Summit

8:15 AM *MT01.01.01

Structure Complements: A New Materials Taxonomy for ML-Guided Materials Discovery [James M. Rondinelli](#); Northwestern University, United States

Functional inorganic electronic materials design has undergone a shift from chemical-intuition-based strategies to data-driven synthesis and simulation. Numerous machine learning models have been developed to successfully predict materials properties and generate new crystal structures. Many existing approaches, however, rely upon physical insights to construct handcrafted features (descriptors), which are not always readily available. For novel materials with sparse prior data and insufficient physical understanding, conventional machine learning models may display limited predictability and are often applied to known structure types. In this talk, I will address this challenge by introducing a new paradigm of materials taxonomy, dubbed “structure complements,” by generalizing anti-structures (or inverse structures). Materials properties depend strongly on crystal geometry but also on the distribution of charge. Thus, our algorithm for classifying materials by geometry and cation/anion decoration proves not only useful as a novel categorization scheme but also as a framework for targeted materials discovery. As a use case, I will showcase our workflow which combines structure complement analysis, a transparent machine learning model, and high throughput density functional theory (DFT) calculations to discover novel ferroelectric materials. We then examine the microscopic origins of ferroelectricity in these new quasi-2D materials and compare them to state-of-the-art compounds. Finally, I propose how this workflow is designed to be integrated into an autonomous, closed-loop materials discovery platform which integrates a unified materials database, machine learning, simulation, and high-throughput synthesis and characterization.

8:45 AM *MT01.01.02

Combining Dataset Curation and Many-Body Calculations for describing Structurally Complex 2D and Quantum Materials [Felipe H. da Jornada](#)^{1,2}; ¹Stanford University, United States; ²SLAC National Accelerator Laboratory, United States

There is considerable excitement about the family of van-der-Waals-bonded materials, such as transition metal dichalcogenides (TMDs). They not only display unique electronic and optical properties when thinned down to a monolayer, but also allow for a radical new approach to making materials by judiciously stacking individual layers. However, there is a large phase space of possible layered materials when one considers the various possible interfacial stacking angles and layer chemical compositions, making a brute-force exploration of the problem via density-functional theory (DFT) unfeasible. We will discuss how to address these challenges with machine-learning- (ML-) parametrized classical force fields that capture the atomistic reconstruction in chemically nontrivial materials. In particular, we show how careful dataset generation and augmentation techniques can reduce the computational effort to train accurate ML force fields and yield structural information for chemically and symmetrically dissimilar materials. In parallel, we will comment on how similar techniques can be utilized to study the structural and dynamical properties of photoexcited materials. By combining accurate excited-state calculations based on the first-principles GW plus Bethe-Salpeter equation with machine-learning force fields, we can describe the dynamics of atoms after a material is optically excited, paving the way for the description of processes ranging from exciton-polaron formation to photochemical processes in structurally complex heterogeneous systems.

9:15 AM MT01.01.03

Ultrafast Nonadiabatic Dynamics in 2D Perovskites assisted by Machine Learning David Graupner and [Dmitri Kilin](#); North Dakota State University, United States

An exploration of the on-the-fly non-adiabatic couplings (NAC) for nonradiative relaxation and recombination of excited states in 2D Dion Jackobson Lead-halide perovskites is accelerated by a machine learning approach to *ab initio* molecular dynamics. Molecular dynamics of nanostructures composed of heavy elements is performed with use of machine learned force-fields (MLFF), as implemented in Vienna *Ab initio* Simulation Package (VASP). The force field parameterization is established using on-the-fly learning, which continuously builds a force field using *ab initio* MD data. At each step of MD it is determined whether to perform an *ab initio* calculation or to use the force field and skip learning for that step using a Bayesian-learning algorithm. The total energy and forces are predicted based on the machine-learned force field at each time step of the MD simulation and if the Bayesian error estimate exceeds a threshold an *ab initio* calculation is performed. Model training and evaluation were performed for a range of for a 2D Dion-Jacobson lead halide perovskite models of different thickness and composition. The MLFF-MD trajectories were evaluated against AIMD trajectories to assess level of discrepancy and error accumulation. To examine the practical effectiveness of this approach we have used the MLFF-based MD trajectories to compute NAC and excited-state dynamics. At each stage, results based on machine learning are compared to traditional *ab initio*-based electronic dissipative dynamics. We find that MLFF-MD provides comparable results to *ab initio* MDs when the MLFF is trained in a NpT ensemble.

9:30 AM MT01.01.04

Structure, Mechanical and Thermal Properties of Monolayer Amorphous Carbon and Boron Nitride [Yuyang Zhang](#)¹, Xi Zhang¹, Yupeng Wang², Shixuan Du¹ and Sokrates Pantelides³; ¹Chinese Academy of Sciences, China; ²Central South University, China; ³Vanderbilt University, United States

Amorphous materials exhibit various characteristics that are not featured by crystals and can sometimes be tuned by their degree of disorder (DOD). Here, we report results on the structures, mechanical and thermal properties of monolayer amorphous carbon (MAC) and monolayer amorphous boron nitride (maBN). The pertinent structures are obtained by kinetic-Monte-Carlo (kMC) simulations separately using empirical potential [1,2] and machine learning potentials (MLP) [3]. We find that despite conducting extensive validation on the reliability of empirical potentials for kMC simulations, and obtaining results consistent with DFT, kMC simulations using empirical potentials and more accurate MLP still yield significantly different results. Z-CRN containing crystallite instead of compositionally disordered “pseudocrystallite” is the favored structure of both elemental MAC and binary maBN. An intuitive order parameter, namely the areal fraction F_x occupied by crystallites within the Z-CRN, is proposed to describe the DOD. The mechanical and thermal properties of MAC and maBN were calculated via molecular dynamics simulation. The mechanical properties of MAC and maBN were found to be solely determined by F_x and are insensitive to the sizes and arrangements of crystallite. On the other hand, about two orders of magnitudes reduction in thermal conductivity was found in monolayer carbon after amorphization. The present results demonstrate the superiority of MLP over empirical potentials in the study of amorphous materials and reveal the relation between structures and properties in monolayer amorphous materials.

References:

- [1] Y.-T. Zhang, et al., Nano Letters, 22, 8018 (2022).
- [2] Y.-T. Zhang, et al., Applied Physics Letters 120, 222201 (2022).
- [3] X. Zhang, et al., <https://arxiv.org/abs/2309.15352>

9:45 AM BREAK

10:15 AM *MT01.01.05

Sampling Complex Energy Landscapes in Material Science Using Data-Driven Force Fields [Mihai-Cosmin Marinica](#); Université Paris-Saclay, France

Statistical methods, such as Machine Learning (ML) trained on physical data, can be invaluable when traditional approaches are limited or when their direct application is hampered by challenges like high computational costs. In materials science the interaction and transformation of crystal defects networks give rise to an extraordinarily diverse range of defect morphologies [1]. Additionally, accounting for chemical disorder presents another layer of complexity that is often overlooked in the emerging field of machine learning approaches. By utilizing the recently open-sourced MiLaDy (Machine Learning Dynamics) package [2] combined with accelerated Molecular Dynamics based on the Bayesian adaptive biasing force method [2], we aim to sample the intricate energy landscapes of defects by: (i) using methods that can identify complex networks of minima and saddle points at zero K; (ii) offering reliable force fields that handle intricate defects such as interstitials and dislocation loops; (iii) probing the atomistic free energy landscape of metals with ab initio accuracy up to the melting temperature [3]; (iv) examining chemical disorder in high entropy alloys (HEA); and, finally, (v) proposing surrogate models that sidestep traditional approaches to access challenging properties, like vibrational entropies [4].

[1] A. M. Goryaeva *et al.* *Nature Commun.* **14**, 3003 (2023); A. M. Goryaeva *et al.* *Nature Commun.* **11**, 4691 (2020);

[2] M.-C. Marinica, A. M. Goryaeva, T. D. Swinburne *et al.*, MiLaDy - Machine Learning Dynamics, CEA Saclay, 2015-2023: <https://ai-atoms.github.io/milady/>;

[3] A. Zhong, C. Lapointe, A. M. Goryaeva, J. Baima, M. Athènes, and M.-C. Marinica, *Phys. Rev. Mater.* **7**, 023802 (2023); C. Lapointe *et al.* (to be submitted);

[4] C. Lapointe, *et al.*, *Phys. Rev. Materials* **4**, 063802 (2020); C. Lapointe, *et al.*, *Phys. Rev. Materials* **6**, 113803 (2022).

10:45 AM *MT01.01.06

Physics-Based Molecular Modeling and Machine Learning for Accelerated Discovery of Metal-Organic Frameworks [Diego A. Gomez Gualdron](#); Colorado School of Mines, United States

Metal-organic frameworks (MOFs) are a class of crystals, whose chemically and structurally tunable pores have made them exciting prospects for a myriad of applications across chemistry, engineering, and materials science. MOF tunability stems from a modular structure that can drastically (or subtly) vary by “mix and matching” potential constituent building blocks. This tunability, however, gives rise to an overwhelmingly large material design space that cannot be efficiently explored by experiments, or even by relying solely on traditional computational methods such as molecular simulation. In this presentation, I discuss some of the ways molecular simulation and machine learning have been combined to accelerate the navigation of databases of MOF computational “prototypes” for applications seeking to exploit selective sorption of molecules into MOF pores.

First, I discuss how the switch to a physics-based approach allowed us to address the issue of (sorption) data scarcity by allowing us to create “synthetic data” that led to the training of an effective multitasking machine learning model to predict sorption of a diversity of molecules in MOFs at a variety of thermodynamic conditions. The use of this model to find promising MOFs from a 50,000+ MOF database for removal of Xe and Kr in nuclear fuel reprocessing is demonstrated.

Second, I discuss the combination of physics-based MOF representations, traditional descriptor-based hierarchical screening, and iterative machine learning model training to efficiently explore a 10,000+ MOF database to find promising MOFs for product extraction in plasma reactors used for synthesis of NH₃. The efficacy of the above combination of domain-knowledge and “off the shelf” machine learning tools is compared against more data-science involved approaches such as diversity-driven Bayesian optimization.

11:15 AM MT01.01.07

Large-Scale and Machine-Learning-Aided Investigations of Metal-Organic Frameworks for Water Harvesting [Li-Chiang Lin](#)^{1,2}, Yi-Ming Wang¹, Zhi-Xun Xu¹, Shiu-Min Shih¹, I-Ting Sung¹ and Archit Datar^{2,3}; ¹National Taiwan University, Taiwan; ²The Ohio State University, United States; ³Celanese Corporation, United States

Water adsorption in metal-organic frameworks (MOFs) has recently drawn considerable attention for its tremendous potential in mitigating water scarcity. An important key to the development of such water harvesting technology to capture atmospheric water is the selection of optimal adsorbent materials. To date, tens of thousands of MOFs have been reported experimentally, while orders of magnitude more candidates have been theoretically predicted. Given the large materials space of available MOF adsorbents, computational studies, by employing state-of-the-art molecular simulations, play an important role in the selection of potential materials. In this study, a large-scale *in silico* screening, employing state-of-the-art Monte Carlo techniques, is conducted to explore more than 10,000 MOF candidates that are included in the CoRE (Computational-Ready Experimental) MOF database for their potential in water harvesting. While the widely used grand canonical Monte Carlo (GCMC) simulations to compute water adsorption can converge very slowly may therefore yield unreliable results, the large-scale computations performed herein employ a method, denoted as the flat-histogram-based C-map method reported by some of us [1,2], to determine the water adsorption capability and capacity of MOFs. Through extensively studying a diverse set of MOFs, our results identify promising candidates as well as shed light on the structure-property relationships. Moreover, to facilitate the future development of optimal water adsorbents, machine learning models are also developed. Specifically, tree-based methods such as random forest as well as convolution neural networks (CNNs) are employed. For the former, aside from including commonly used structural features such as largest cavity diameter and surface area, a newly developed metric – the so-called continuously adsorption channel (CAC) recently developed by some of us [3], is also used to help develop more accurate models. For the latter, computer vision techniques are exploited to “see” the structures directly for model training, followed by making quantitative predictions. These machine learning models are also investigated to better understand the structure-property relationship in a quantitative manner. Overall, this work represents a synergistic effort between large-scale molecular simulations and machine learning studies, and we anticipate the outcomes achieved herein can facilitate future computational and experimental efforts on the development of optimal water adsorbents.

References:

[1] Datar, A.; Witman, M. & Lin, L.-C.* Improving Computational Assessment of Porous Materials for Water Adsorption Applications via Flat Histogram Methods, *J. Phys. Chem. C*, **125**, 4253-4266, 2021.

[2] Datar, A.; Witman, M.; Lin, L.-C.* Monte Carlo Simulations for Water Adsorption in Porous Materials: Best Practices and New Insights, *AICHE J.*, **67**, e17447, 2021.

[3] Xu, Z.; Wang, Y.; Lin, L.-C.* Connectivity Analysis of Adsorption Sites in Metal-organic Frameworks for Facilitated Water Adsorption, *ACS Appl. Mater. Interfaces*, **15**, 47081-47093, 2023.

11:30 AM MT01.01.08

Accelerating The Selection of High Uptake Covalent Organic Frameworks with Supervised Machine Learning for Methane Storage [Niraj Bhatt](#), Sandip Thakur and Ashutosh Giri; University of Rhode Island, United States

This searchable program is up-to-date as of April 15th, 2024.

Covalent organic frameworks (COFs) have been identified as ideal candidates for natural gas storage and catalysis applications primarily because of their tunable microstructure as well as the vast design space for their chemical makeup. COFs with high gas uptake values at workable pressures are highly desired for applications such as gas storage, carbon capture and catalysis. Methane (CH₄) storage is highly sought after because of the low carbon-hydrogen ratio, high calorific value and natural abundance. However, the vast design space for COFs makes the screening of high CH₄ uptake COFs very difficult as it requires time-intensive grand-canonical Monte Carlo (GCMC) simulations to calculate the uptake values. To overcome this challenge, we employ machine learning to develop a model that captures the structure-property relationship in COFs using a large in-silico database of hypothetical COFs. A machine learned regression model based on powerful random forest algorithm is developed that maps the structural and chemical features of the 5000 COFs used in training to their uptake values. The validated model is then used to find the uptakes of COFs in the experimental database eliminating the need of resource intensive GCMC. Thousands of diverse COFs are selected from the database and featurized using MATMINER, a powerful inbuilt python library used in material's informatics. The features are used to uniquely represent each COF which is mapped to their respective CH₄ uptake values during training of the ML model. The feature space includes the chemical features like elemental property features and structural features like radial distribution functions and density-based structural features. Various dimensionality reduction techniques like feature selection using co-relation analysis and feature extraction using principal component analysis are employed to make an accurate and efficient ML model. We employed this model to predict the CH₄ uptake values for an experimental database of ~ 600 COFs and screened top performers with CH₄ uptake values as high as 1260 molecules/unitcell.

11:45 AM MT01.01.09

Investigating The Binding Interactions between Newly Synthesized Metal-Organic Frameworks (MOF) and Organic Pollutants Using Computational Chemistry Melissa Mapula, Shiru Lin and Manal Omary; Texas Woman's University, United States

Benzene and toluene are hazardous organic pollutants due to their potential health effects. Benzene is a known carcinogen and exposure to high levels of toluene can cause central nervous system depression. Applying porous materials for the removal of benzene and toluene can be an effective approach for mitigating the environmental and health impacts of these organic pollutants. Metal-organic frameworks (MOFs) are a type of porous material consisting of metal nodes connected by organic linkers. MOFs have unique properties such as high surface area, tunable pore size, and the ability to selectively adsorb small molecules, making MOFs promising candidates for various applications including removing pollutants. In our study, we apply computational chemistry methods to investigate interactions of organic pollutants and synthesized MOF structures, such as MOF-TW1, which was formed from the crystals of the reaction of Cu(I) and Ag(I) precursors with pyrazine (Pyz) and piperazine (Ppz) and boasting a significant surface area of (1278 m²/g) and porosity of 23.7% void volume. We investigate the adsorption ability of MOF structures toward organic pollutants, which can guide the design and modification of MOFs for more organic pollutant absorptions and removals. Furthermore, we apply machine learning algorithms to predict organic pollutant absorption performances on synthesized MOF structures.

SESSION MT01.02: Machine Learning and Simulations II
Session Chairs: Raymundo Arroyave and Felipe H. da Jornada
Monday Afternoon, April 22, 2024
Room 320, Level 3, Summit

1:30 PM *MT01.02.01

Invariant Graph Neural Network Models for Accelerated Prediction of Equilibrium Structure, Defect Energetics and Electronic Properties of Semiconductor Materials Brian L. DeCost, Kamal Choudhary and Francesca Tavazza; National Institute of Standards and Technology, United States

Accelerated material property predictions are an important component of large scale search and optimization of new semiconductor device materials. We present ongoing work developing and applying invariant graph neural network models for modeling the properties of multicomponent semiconductor materials. We use such models to predict defect energetics in semiconductor materials. Initial results on prediction of equilibrium interface structures and electronic properties in semiconductor heterointerface systems will be discussed as well. Robust and fast uncertainty quantification methods are of particular concern for predictive design of semiconductor heterointerface systems, for which currently-available reference data is limited. We will discuss how we use graph neural network uncertainty quantification for active learning of force fields, out-of-distribution detection for predictive models, and for targeted allocation of theory-based modeling.

2:00 PM *MT01.02.02

Uncertainty-Quantification-Driven Autonomous Workflows for Upscaling of Complex Materials Properties Danny Perez; Los Alamos National Laboratory, United States

Many engineering models for require parametric or functional inputs that can in principle be obtained from lower scale simulations. For example, transport coefficients for radiation-induced defects computed from molecular dynamics can be used to inform kinetic Monte Carlo models, that can themselves inform cluster-dynamics simulation of microstructural evolution. However, in many cases, the number of lower-scale calculations required to obtain these higher-scale properties can be very large, which can lead to extremely long times-to-solution, especially when human intervention is needed at any step of the process. We demonstrate how tailored uncertainty-quantification approaches can be used to autonomously drive the execution of upscaling workflows at large computational scales. I will show how information can be systematically upscaled into different representations in order to develop reliable reduced-order models from simulation data.

2:30 PM MT01.02.03

A Physics Informed Bayesian Optimization Approach for Material Design Raymundo Arroyave; Texas A&M University, United States

The design of materials and identification of optimal processing parameters constitute a complex and challenging task, necessitating efficient utilization of available data. Bayesian Optimization (BO) has gained popularity in materials design due to its ability to work with minimal data. However, many BO-based frameworks predominantly rely on statistical information, in the form of input-output data, and assume black-box objective functions. In practice, designers often possess knowledge of the underlying physical laws governing a material system, rendering the objective function not entirely black-box, as some information is partially observable. In this study, we propose a physics-informed BO approach that integrates physics-infused kernels to effectively leverage both statistical and physical information in the decision-making process. We demonstrate that this method significantly improves decision-making efficiency and enables more data-efficient BO. The applicability of this approach is showcased through the design of NiTi shape memory alloys, where the optimal processing parameters are identified to maximize the transformation temperature.

2:45 PM MT01.02.04

Materials Discovery for High-Temperature Clean-Energy Applications (and Beyond) via Defect Graph Neural Networks [Matthew Witman](#)¹, [Anuj Goyal](#)², [Tadashi Ogitsu](#)³, [Anthony McDaniel](#)¹ and [Stephan Lany](#)²; ¹Sandia National Laboratories, United States; ²National Renewable Energy Laboratory, United States; ³Lawrence Livermore National Laboratory, United States

We present a graph neural network (GNN) approach that fully automates the prediction of defect formation enthalpies for any crystallographic site from the ideal crystal structure, without the need to create defected atomic structure models as input [1]. Using density functional theory (DFT) reference data for vacancy defects in oxides, we trained a defect GNN (dGNN) model that replaces the DFT supercell relaxations otherwise required for each symmetrically unique crystal site. Interfaced with thermodynamic calculations of reduction entropies and associated free energies, the dGNN model is applied to the screening of oxides in the Materials Project database, connecting the zero-Kelvin defect enthalpies to high-temperature process conditions relevant for solar thermochemical hydrogen production and other energy applications. The dGNN approach is applicable to arbitrary structures with an accuracy limited principally by the amount and diversity of the training data, and it is generalizable to other defect types and advanced graph convolution architectures. It will aid tackling future materials discovery problems in clean energy and beyond.

[1] Witman, M. et al. *Nature Computational Science*, **3**, 675–686 (2023)

3:00 PM BREAK

3:30 PM *MT01.02.05

Machine Learning Based Electronic Structure Prediction: From Nanostructures to Complex Alloys [Amartya S. Banerjee](#)¹, [Shashank Pathrudkar](#)², [Shivang Agarwal](#)¹, [Susanta Ghosh](#)², [Stephanie Taylor](#)¹, [Hsuan Ming Yu](#)¹ and [Ponkrshnan Thiagarajan](#)²; ¹University of California, Los Angeles, United States; ²Michigan Technological University, United States

I will describe our work on using specialized first principles calculations with machine learning tools to enable prediction of the electronic structure of various nanomaterials and bulk systems. I will focus on two related but independent directions. First, I will show how helical and cyclic symmetry adapted density functional theory calculations may be used to train interpretable machine learning models of the electronic fields of quasi-one-dimensional materials. The descriptors in this framework are global geometry and strain parameters. Through examples involving distorted carbon nanotubes, I will show how the framework can be particularly accurate in its prediction, even with limited training data. I will discuss the use of this framework for automated materials discovery, and in multiscale modeling.

Second, I will discuss the use of high-throughput first principles calculations to train machine learning models of bulk systems, possibly featuring some degree of disorder in atomic arrangements. The descriptors in this framework are local in nature and the prediction of electronic fields occurs in a pointwise manner spatially. I will describe how a combination of strategies, including transfer learning, thermalization, and the use of Bayesian Neural Networks can allow the development of machine learning models that are systematic, reliable, and very efficient (both in terms of training and prediction). I will discuss the use of this framework for calculation of the electronic structure of bulk solids with defects, and compositionally complex alloys, from which, other material properties of engineering interest may be inferred. I will end with a discussion of future research directions.

4:00 PM MT01.02.06

Learning Polarization Using Equivariant Neural Networks [Stefano Falletta](#)¹, [Andrea Cepellotti](#)¹, [Albert Musaelian](#)¹, [Anders Johansson](#)¹, [Chuin Wei Tan](#)¹ and [Boris Kozinsky](#)^{1,2}; ¹Harvard University, United States; ²Robert Bosch Research and Technology Center, United States

Polarization is an essential physical quantity for understanding the properties of dielectrics and ferroelectrics [1]. The modern theory of polarization [1] and further developments on electric enthalpy functionals [2] have enabled the study of polarization in periodic electronic structure calculations. Interestingly, predicting the polarization over a molecular dynamics allows for the determination of experimentally-relevant quantities such as infrared and Raman spectra from first principles. However, this remains a challenging problem in electronic structure calculations, because of their high computational cost.

Here, we introduce an equivariant neural network approach to efficiently learn and predict polarization for each atomic configuration, building on and extending state-of-the-art machine learning force field architectures. This allows one to determine the autocorrelation function of polarization over long-lasting molecular dynamics, thereby giving access to infrared spectrum, frequency-dependent dielectric constant, and Raman cross section from first principles. We implemented our scheme in the E(3)-equivariant NequIP/Allegro framework [3,4], and interfaced it with the LAMMPS code for performing molecular dynamics calculations.

[1] R. Resta, Macroscopic polarization in crystalline dielectrics: the geometric phase approach, *Rev. Mod. Phys.* **66**, 899 (1994).

[2] P. Umari and A. Pasquarello, Ab initio molecular dynamics in a finite homogeneous electric field, *Phys. Rev. Lett.* **89**, 157602 (2002).

[3] S. Batzner, A. Musaelian, L. Sun, M. Geiger, J. P. Mailoa, M. Kornbluth, N. Molinari, T. E. Smidt, and B. Kozinsky, E(3)-equivariant graph neural networks for data-efficient and accurate interatomic potentials. *Nat. Commun.*, **13**, 2453 (2022)

[4] A. Musaelian, S. Batzner, A. Johansson, L. Sun, C. Owen, M. Kornbluth, and B. Kozinsky, Learning local equivariant representations for large-scale atomistic dynamics *Nat. Commun.*, **14**, 579 (2023)

4:15 PM MT01.02.07

Ab Initio Investigations of a Two Dimensional form of Silicon featuring Dispersionless Electronic States [Chenhaoyue Wang](#) and [Amartya Banerjee](#); UCLA, United States

Materials with dispersionless electronic states (or flat bands) have been intensely investigated in recent years, owing to their association with strongly correlated electrons. Due to the negligible kinetic energies of electrons in such states, the electron-electron interaction dominates, thus resulting in superconductivity, ferromagnetism, and other exotic phases of matter. While a number of bulk materials and heterostructures have been investigated for their connection with flat-band physics, the discovery of new, simple low-dimensional materials with such electronic features, continues to be an alluring possibility. Following this line of thought, and motivated by the consideration that silicon is a versatile material with many known low-dimensional allotropes that have already been experimentally synthesized, we investigate here a two-dimensional form of silicon in the decorated honeycomb (or star) lattice. The proposed material has a buckled structure similar to silicene, consists of dodecagonal rings, and features electronic flat bands near the Fermi-level. We describe extensive first principles investigations into the static and dynamic structural stability of the material and observe that in-plane strains stabilize it. Furthermore, the bandwidth of the flat band is found to be highly tunable with strains. Finally, we investigate the possibility of using substrates to apply such stabilizing strains, suggesting the fabricability of this novel two dimensional material under experimental conditions.

4:30 PM MT01.02.08

Atomistic Modeling of Advanced Transistor Gate Stack Using Graph Neural Networks [Pratik Brahma](#)¹, Krishnakumar Bhattaram¹, Jack Broad^{2,2}, Sinead M. Griffin^{2,2} and Sayeef Salahuddin^{1,2}; ¹University of California, Berkeley, United States; ²Lawrence Berkeley National Laboratory, United States

Modern microelectronic devices such as silicon transistors are composed of multiple material interfaces whose electronic interactions significantly affect electron transport and, ultimately, device performance. These complex interfacial interactions between various materials of crystalline, polycrystalline, and amorphous phases, as well as boundary effects such as quantum confinement, present a significant challenge to the atomistic modeling of electronic devices. Traditional modeling approaches often use ab-initio methods such as density functional theory for molecular dynamics and electronic structure calculations. However, these methods scale poorly with increasing system size as they rely on diagonalization of the quantum Hamiltonian, posing a challenge for fast and accurate simulations of electronic devices that contain thousands of atoms and various structural phases.

In this work, we demonstrate the viability of graph neural networks (GNNs) [1, 2] to overcome this scaling challenge. Our architecture is designed to accelerate ab-initio molecular dynamics and electronic structure calculations by characterizing the relationships between local chemical environments and global electronic transport properties such as carrier injection velocity and gate capacitance. For given macroscopic transistor dimensions, we use our neural network predicted atomic forces to generate the heterogeneous crystalline silicon channel–dielectric gate stack (amorphous SiO₂-amorphous HfO₂), with bond lengths within 3% of experimental values. Furthermore, we predict global electronic (density of states) and transport properties (injection velocity) of crystalline nanoslab silicon channels, showing good agreement—within 0.18% for density of states and 5.4% for injection velocity—with the baseline material simulation model for channel thicknesses outside the training domain, while also accelerating the simulation speed by four orders of magnitude. The obtained accuracies demonstrate that our neural network captures the structural confinement effects of thin silicon channels in advanced transistors. Overall, the scalability and accuracy of our predictions over a wide range of material and transport properties demonstrate the efficacy of GNNs to accelerate advanced electronic device simulations, paving the way for rapid design and modeling of next-generation transistors.

[1] Schütt, K. T., Saucedo, H. E., Kindermans, P. J., Tkatchenko, A., & Müller, K. R. (2018). SchNet - A deep learning architecture for molecules and materials. *Journal of Chemical Physics*, 148(24). <https://doi.org/10.1063/1.5019779>

[2] Unke, O. T., Chmiela, S., Gastegger, M., Schütt, K. T., Saucedo, H. E., & Müller, K. R. (2021). SpookyNet: Learning force fields with electronic degrees of freedom and nonlocal effects. *Nature Communications*, 12(1). <https://doi.org/10.1038/s41467-021-27504-0>

4:45 PM MT01.02.09

Electronic Stopping Power Predictions from Machine Learning [Andre Schleife](#)¹, Logan Ward², Cheng-Wei Lee³, Ben Blaiszik² and Ian T. Foster²; ¹University of Illinois at Urbana-Champaign, United States; ²Argonne National Laboratory, United States; ³Colorado School of Mines, United States

We aim to develop an affordable computational approach that provides the electronic stopping power for arbitrary trajectories of ions impacting a target material with an accuracy comparable to that of modern quantum mechanical first-principles simulations. Currently, real-time time-dependent density functional theory can accomplish this in reasonable agreement with experiment. However, the computational cost of this method is high which limits the number of trajectories and host material atomic geometries that can be studied. This prevents a routine integration of electronic-stopping power, e.g. in the molecular dynamics simulation of radiation damage cascades. We use cutting-edge descriptors of atomic geometries to train modern machine-learning models on data from real-time time-dependent density functional theory. We find very low error bars and very high accuracy at million-fold reduced computational cost of the trained model for proton irradiated aluminum. We also are able to predict velocity dependent electronic stopping and entire Bragg peak simulations with our models. In this presentation we discuss our framework in detail as well as its broad applicability in the particle-radiation community, including target materials with complex atomic geometry or low-dimensional materials.

SESSION MT01.03: Machine Learning and Simulations III

Session Chairs: Joshua Agar and Elif Ertekin

Tuesday Morning, April 23, 2024

Room 320, Level 3, Summit

10:30 AM *MT01.03.01

Ultra-Compact and Parsimonious Machine Learning Frameworks for High-Velocity Scientific Discovery in Materials Microscopy [Joshua Agar](#); Drexel University, United States

Machine learning (ML) offers unparalleled opportunities for accelerating advancements in materials microscopy. Yet, practical implementation often stumbles due to the lack of models that are both machine-interpretable and conforming to underlying physical laws, as well as the absence of specialized computational infrastructure for automated data analytics. We address these bottlenecks by focusing on the codesign of microscopy technique, ultra-compact physics-aware ML models, connection to physics-inspired models, and bespoke hardware solutions.

Our contribution is three-fold. First, we present a robust infrastructure for the automated aggregation and management of high-velocity synthesis data, including real-time in-situ diagnostics. We introduce a federated, searchable scientific data management system optimized for high-throughput analysis. This infrastructure allows robust linkages between experiment and theory. Second, we go beyond traditional ML approaches by introducing highly parsimonious, physics-conforming neural networks specifically tailored for real-time analysis of band-excitation piezoresponse force microscopy data. These models are meticulously codesigned to be executable on field-programmable gate arrays (FPGAs) for edge-real-time analytics.

Lastly, we unveil a neural network architecture aimed at automating 4D-scanning transmission electron microscopy strain mapping. Leveraging a cycle-consistent spatial transforming autoencoder, we incorporate an affine transformation layer to parsimoniously capture the governing equations of geometric transformations. This is further optimized through advanced compression, regularization, and optimization strategies to facilitate the otherwise computationally intensive training process. Remarkably, our method outperforms traditional template-matching techniques, achieving a sub-pixel precision of 0.3, as benchmarked against py4DSTEM.

In sum, this work offers a comprehensive blueprint for seamlessly incorporating ultra-compact and parsimonious AI systems into the analysis of large-scale, high-velocity, and noise-prone experimental datasets. This facilitates closer connections between experiments and theory thereby revolutionizing the practical utility of AI in scientific discovery.

11:00 AM MT01.03.02

Learning Latent-Variable Representations of Microstructure Accounting for Materials Stochasticity [Sajad Hashemi](#)¹, Michael Guerzhoy^{1,2} and Noah H. Paulson³; ¹University of Toronto, Canada; ²Li Ka Shing Knowledge Institute, St. Michael's Hospital, Canada; ³Argonne National Laboratory, United States

Over the past decade, generative machine learning has found application in the design of materials with tailored properties. Generative latent-variable models represent high-dimensional data in low-dimensional spaces. The original data is n-dimensional, for example, 2-D/3-D image-based representations of materials microstructure with k pixels/voxels. New plausible examples of image-based representations can be generated from points in the low-dimensional space. The variational autoencoder (VAE) is a popular latent-variable model. The VAE is learned by optimizing the L2 distance in data space (2-D/3-D) between real and generated examples (in addition to regularization). This is suboptimal, since materials microstructure is stochastic. Therefore, image-based representations should be considered similar if their statistical properties are similar rather than just if they are close in Euclidean data space. We develop a novel VAE architecture to prioritize statistical representations of materials microstructure and the generation of statistically similar microstructure examples from a single location in the latent space. A successful implementation of this architecture would greatly aid materials development and optimization through iterative materials simulations. This novel capability will be demonstrated on both synthetic and natural microstructure datasets.

11:15 AM MT01.03.03

Spatial Atomic Structure Reconstruction for Transmission Electron Microscopy Images Using a Deep Learning Algorithm [Congjie Wei](#)¹, Chenglin Wu¹ and Jiaxin Zhang²; ¹Texas A&M University, United States; ²Intuit, United States

With the significant improvements and developments in transmission electron microscopes (TEM) techniques, accurate observation and identification is now more commonly adopted in angstrom-level precision, which reveals as sequential images about the real-space information. However, it still has difficulties to analyze the spatial defect distribution, phase transformation and dynamic phenomena since the TEM images can only record the appearances of the surface atoms while the out-of-plane information is severely missing. In this work, a first principle based deep learning algorithm is proposed and adopted to reconstruct the 3D transition states of a MXene healing process experimentally observed. Starting from the TEM image, all related Ti and C atoms around or within the laser-made hole could be categorized into 3 groups based on the confidence of the information obtained from the TEM images. Around hole atoms are assumed to have crystalline structure and set as the input along with the in-plane information of atoms that can be observed directly within the hole. Out-of-plane information of the latter group of atoms are then treated as the output of the algorithm along with the spatial distribution of all underlying atoms. The input and output information are reformed into graphical representations and treated as a graph reference problem. The trunk of this algorithm is set as a deep convolutional neural network incorporated with attention-based and non-attention-based components. To conform to the distance prediction, smooth potentials are constructed for Ti-Ti, Ti-C and C-C interactions based on first principle calculation. Simplified potentials are constructed based on this calculation as well as possible bond length ranges from all type of structures. The minimum potential energy accumulation of all atoms within the hole is set as one of the convergence conditions of the algorithm along with the fitting of the training data sets. Our models are trained on defected MXene structures optimized with DFT, where different sizes and number of atoms are considered. The predictions of this algorithm fit well with the TEM images and help with the understanding of the healing processes observed in MXene materials.

11:30 AM MT01.03.04

A Flexible Formulation of Value for Experiment Interpretation and Design [Matthew Carbone](#); Brookhaven National Laboratory, United States

Optimal design of experiments is an outstanding challenge in the materials science community. Standard techniques such as Bayesian optimization can address this challenge as long as the goal of an experimental campaign is maximizing some observable. While useful in a wide variety of cases, it is insufficient to address more epistemic goals, such as thoroughly exploring a sample space when an explicit objective is lacking. In this work, we showcase a formulation of "scientific value," a scalar representation of local uniqueness. Our method scalarizes arbitrarily high-dimensional data, allowing for the traditional optimization toolbox to be applied to any problem. Intuitively, our method, which we call the Scientific Value Agent, explores regions of space in which observables change rapidly, whilst exploring other areas sufficiently, wasting minimal experimental budget. It is also robust to the cold start problem, and can be utilized with no prior knowledge and next-to-no data. We demonstrate this technique by exploring a variety of simulated and real-world examples, including phase boundaries, autonomously changing the temperature measurement of a ferroelectric material, and analyzing nanoparticle synthesis data. Our method can be seamlessly extended to studies with multiple outputs, or fidelities, and can seamlessly integrate into existing autonomous experimentation frameworks with minimal added effort to the user.

11:45 AM MT01.03.05

Simultaneous Analysis of Wide Angle X-Ray Scattering Data (WAXS) and Extended X-Ray Absorption Fine Structure Spectroscopy (EXAFS) of Very Small Nanoparticles [Markus Winterer](#) and [Jeremias Geiss](#); University of Duisburg-Essen, Germany

Although experiments investigating the atomistic structure of disordered materials are today facile through modern instruments for X-ray scattering and spectroscopy, it is still a challenge to extract the relevant information especially in case of very small nanoparticles with a diameter smaller than 10 nm. In our contribution we will present recent advances in data analysis of this inverse problem using Reverse Monte Carlo (RMC) analysis [1].

RMC simulations enable the analysis of WAXS data as well as EXAFS spectra via partial pair distribution functions (pPDF) obtained from a physical, structural model. In case of nanoparticles and scattering data this approach suffers from the termination of the pPDFs due to the finite size of the particles. This produces artifacts in the computed scattering intensity due to the long-range probing distance of scattering which are eliminated by using the Debye scattering equation (DSE) for computing the scattering intensity from a particle model. Computational efficiency is provided by binning the distance distribution of atom pairs in the DSE.

Data fusion, i. e. simultaneous refinement of WAXS data and EXAFS spectra of small nanoparticles, is thus enabled using a mutual structural model. Therefore, this method allows the self-consistent extraction of complementary information on the local structure contained in EXAFS and on the long-range order in WAXS data. We describe this novel method for the nanocrystalline complex oxide LaFeO_3 [1]. The results are highly relevant for example for heterogeneous catalysis [2].

The method described can be further developed to additionally include small angle scattering data and provides an interface either via the (atomistic) structural model or the pPDFs to other physics simulation and materials modeling methods such as molecular dynamic (MD) simulations or density functional theory (DFT) modeling.

[1] M. Winterer and J. Geiß, *Combining reverse Monte Carlo analysis of X-ray scattering and extended X-ray absorption fine structure spectra of very small nanoparticles*, J. Appl. Cryst. **56** (2023) 103-109; doi.org/10.1107/S1600576722010858

[2] J. Geiss, J. Bueker, J. Schulte, B. Peng, M. Muhler, M. Winterer, *$\text{LaCo}_{1-x}\text{Fe}_x\text{O}_3$ Nanoparticles in Cyclohexene Oxidation*, J. Phys. Chem. C **127** (2023) 5029–5038; doi.org/10.1021/acs.jpcc.2c08644

This searchable program is up-to-date as of April 15th, 2024.

SESSION MT01.04: Machine Learning and Simulations IV
Session Chairs: Amartya Banerjee and Elif Ertekin
Tuesday Afternoon, April 23, 2024
Room 320, Level 3, Summit

1:30 PM *MT01.04.01

Campaign Design for Autonomous Experimentation in Materials Research [Benji Maruyama](#); AFRL/RXA, United States

The current materials research process is slow and expensive; taking decades from invention to commercialization. The Air Force Research Laboratory pioneered ARES™, the first autonomous experimentation system for materials development. A rapidly growing number of researchers are now exploiting advances in artificial intelligence (AI), autonomy & robotics, along with modeling and simulation to create research robots capable of making research progress orders of magnitude faster than today. We will discuss concepts and advances in autonomous experimentation in general, and associated hardware, software and autonomous methods.

Campaign design for autonomous experimentation or self-driving labs is complex and dependent on research objectives, experimental apparatus, analysis capabilities and decision strategies. Examples of autonomous experimentation campaigns to explore important aspects of campaign design will be given.

2:00 PM *MT01.04.02

Beyond Fingerprinting: Process Exploration and Optimization via High-Throughput and Machine Learning [Brad L. Boyce](#)^{1,2}; ¹Sandia National Laboratories, United States; ²Center for Integrated Nanotechnologies, United States

Material properties are governed by composition and associated microstructure dictated by the thermodynamics and kinetics of manufacturing processes. Often, the connectivity between process conditions and the resulting structure and properties is complex, evading full predictivity via high-fidelity modeling. In this work, we are exploring three manufacturing processes where material properties are difficult to predict directly from process settings: electroplating, physical vapor deposition, and additive manufacturing (laser powder bed fusion). Each of the three processes offer unique challenges and opportunities. Across these three exemplars, we are augmenting traditional process-structure-property investigations with an accelerated workflow to detect material structure/composition, prognose associated properties, and adapt the associated process to achieve improved product outcomes. This accelerated detect-prognose-adapt cycle is aided by three key elements: (1) automated combinatorial synthesis to enable rapid parameter sweeps, (2) high-throughput evaluation of both conventional and surrogate indicators of material chemistry, structure, and properties, and (3) machine learning algorithms to unravel correlations in high-dimensional spaces beyond expert cognition. In each of these three domains, we take advantage of previously developed capabilities, or where such capabilities are insufficient, we develop novel techniques. For example, in the domain of electroplating synthesis, we have employed an existing robotic pipetting system for formulation of solution chemistries while developing a custom 12-cell parallel electroplating system that enables hundreds of unique conditions to be explored in about a day. While we consider purely data-driven ML algorithms for some correlation analysis, a more interpretable and robust solution includes physical models based on established governing equations. In this regard, we have developed a physics-informed multimodal autoencoder that fuses data from multiple modalities alongside physical models to provide a deeper fingerprint of material state, enabling unsupervised detection of high-dimensional clusters and cross-modal correlations. SNL is managed and operated by NTESS under DOE NNSA contract DE-NA0003525.

2:30 PM MT01.04.03

Leveraging Physics and Machine Learning to Predict Battery Aging [Michael J. Kenney](#)¹, Maxim Ziatdinov², Katerina Malollari¹ and Sergei Kalinin³; ¹Amazon Lab126, United States; ²Oak Ridge National Laboratory, United States; ³The University of Tennessee, Knoxville, United States

A primary concern with lithium-ion battery technology is the performance deterioration over time. Capacity retention, a vital performance measure, is frequently utilized to assess whether these batteries have approached their end-of-life. Machine learning offers a powerful tool for predicting capacity degradation, leveraging both past data and physical knowledge in the form of simulations or phenomenological models. In this study, we showcase the utility of probabilistic machine learning and transformer-based deep learning modeling in battery health prediction. For our probabilistic models, which operate without pre-training, we employ: i) a structured Gaussian process (GP) - an enhanced version of the standard GP that integrates a phenomenological model as a probabilistic prior mean function, and ii) a multi-fidelity GP, augmented by prior physics-based simulations to boost its predictive power. Concurrently, we deploy time-series transformers pre-trained on existing datasets for forecasting purposes. Our findings juxtapose these models, offering insights into their optimal application scenarios, and the associated codes are open for access.

2:45 PM BREAK

3:15 PM *MT01.04.04

Understanding Complex Crystal Structures and Phase Transitions through Self-Assembly Simulations [Julia Dshemuchadse](#); Cornell University, United States

How do atoms come together to form crystal structures? Powerful theoretical and experimental tools exist to elucidate the structure of crystalline materials on multiple length scales. Directly observing the formation of their ordered structures, however, remains supremely challenging. How can we understand the path that a material takes to its crystalline state? We take a general approach toward understanding crystallization across multiple materials families by simulating their self-assembly using simple coarse-grained models, in order to investigate the emergence of long-range order from short-range interactions. In this way, we gain systematic insights into the phenomena that lead to the crystallization into even complex types of order, such as materials with large unit cells or aperiodic crystals. Our goal is to use these insights to find ways to tailor crystallization pathways and to create new materials. In this talk, I will discuss the broad spectrum of structural phenomena captured with particles that interact via simple isotropic pair potentials, which we apply to study crystal growth and solid-solid phase transformations. Our work promises to establish new pathways to materials design through simulations, which explicitly incorporate and explore phase transformation kinetics.

3:45 PM *MT01.04.05

Deep Learning Probability Flows and Entropy Production Rates in Active Matter [Eric Vanden-Eijnden](#); New York University, United States

Active matter systems, from self-propelled colloids to motile bacteria, are characterized by the conversion of free energy into useful work at the microscopic scale. These systems generically involve physics beyond the reach of equilibrium statistical mechanics, and a persistent challenge has been to understand the nature of their nonequilibrium states. The entropy production rate and the magnitude of the steady-state probability current provide quantitative ways to do so by measuring the breakdown of time-reversal symmetry and the strength of nonequilibrium transport of measure. Yet, their

This searchable program is up-to-date as of April 15th, 2024.

efficient computation has remained elusive, as they depend on the system's unknown and high-dimensional probability density. In this talk, building upon recent advances in generative modeling, I will present a deep learning framework that allows for the estimation of the gradient of the logarithm of this density, a quantity known as the score in the machine learning literature. This score, together with the microscopic equations of motion, gives direct access to the entropy production rate, the probability current, and their decomposition into local contributions from individual particles, spatial regions, and degrees of freedom. I will demonstrate the broad utility and scalability of the method by applying it to several high-dimensional systems of interacting active particles undergoing motility-induced phase separation (MIPS).

4:15 PM MT01.04.06

Programming Soft Materials with JAX-MD [Chrisy Xiyu Du](#)^{1,2}, Ella King^{3,2}, Qian-Ze Zhu², Samuel S. Schoenholz⁴ and Michael Brenner²; ¹University of Hawai'i at Mānoa, United States; ²Harvard University, United States; ³Simons Foundation, United States; ⁴OpenAI, United States

Soft Materials are ubiquitous in everyday life and are crucial in many different forms of revolutionary technologies. One property of Soft Materials is their ability to self-assemble into intricate structures from a finite set of building blocks with continuously tunable parameters. This giant design space of building blocks is a double-edged sword: on one side it provides researchers infinite possibilities to design building blocks for targeted functions, while on the other side it might take forever to search the design space. Here, we propose a new inverse design method that captures both interaction and geometry of building blocks. By enabling rigid body functionalities in JAX-MD, an end-to-end differentiable molecular dynamics engine, we can create soft materials model with components that are simple enough to design yet powerful enough to capture complex materials properties. In this talk, I will discuss the implementation of the methods alongside examples to showcase its potential applications.

4:30 PM MT01.04.07

Representation-Space Diffusion Models for Generating Periodic Materials Anshuman Sinha, Shuyi Jia and [Victor Fung](#); Georgia Institute of Technology, United States

Generative models hold the promise of significantly expediting the materials design process when compared to traditional human-guided or rule-based methodologies. However, effectively generating high-quality periodic structures of materials on limited but diverse datasets remains an ongoing challenge. Here we propose a novel approach for periodic structure generation which fully respects the intrinsic symmetries, periodicity, and invariances of the structure space. Namely, we utilize differentiable, physics-based, structural descriptors which can describe periodic systems and satisfy the necessary invariances, in conjunction with a denoising diffusion model which generates new materials within this descriptor or representation space. Reconstruction is then performed on these representations using gradient-based optimization to recover the corresponding Cartesian positions of the crystal structure. This approach differs significantly from current methods by generating materials in the representation space, rather than in the Cartesian space, which is made possible using an efficient reconstruction algorithm. Consequently, known issues with respecting periodic boundaries and translational and rotational invariances during generation can be avoided, and the model training process can be greatly simplified. We show this approach can provide competitive performance on established benchmarks compared to current state-of-the-art methods.

SESSION MT01.05: Machine Learning and Simulations V
Session Chairs: Aditi Krishnapriyan and Wennie Wang
Wednesday Morning, April 24, 2024
Room 320, Level 3, Summit

8:30 AM *MT01.05.01

Combining Data, Physics and Machine Learning for Accelerating Materials Computations Boris Kozinsky and [Albert Musaelian](#); Harvard University, United States

Discovery and understanding of next-generation materials requires a challenging combination of the high accuracy of first-principles calculations with the ability to reach large size and time scales. We pursue a multi-tier method development strategy in which machine learning (ML) algorithms are combined with exact physical symmetries and constraints to significantly accelerate computations of electronic structure and atomistic dynamics. First, density functional theory (DFT) is the cornerstone of modern computational materials science, but its current approximations fall short of the required accuracy and efficiency for predictive calculations of defect properties, band gaps, stability and electrochemical potentials of materials for energy storage and conversion. To advance the capability of DFT we introduce non-local charge density descriptors that satisfy exact scaling constraints and learn exchange functionals called CIDER [1]. These models are orders of magnitude faster in self-consistent calculations for solids than hybrid functionals but similar in accuracy. On a different level, we accelerate molecular dynamics (MD) simulations by using machine learning to capture the potential energy surfaces obtained from quantum calculations. We developed NequIP [2] and Allegro [3], the first deep equivariant neural network interatomic potential models, whose Euclidean symmetry-preserving layer architecture achieves state-of-the-art data efficiency and accuracy for simulating dynamics of molecules and materials. In parallel, we implement autonomous active learning of interactions in reactive systems, with the FLARE algorithm that constructs accurate and uncertainty-aware Bayesian force fields on-the-fly from a molecular dynamics simulation, using Gaussian process regression [4]. These MD simulations are used to explore long-time dynamics of phase transformations and heterogeneous reactions.

[1] K. Bystrom, B. Kozinsky, arXiv:2303.00682 (2023)

[2] S. Batzner et al, Nature Comm. 13 (1), 2453 (2022)

[3] A. Musaelian, S. Batzner et al, Nature Comm. 14, 579 (2023)

[4] J. Vandermause et al, Nature Comm. 13 (1), 5183 (2022)

This work was supported by DOE Office of Basic Energy Sciences Award No. DE-SC0022199 and Department of Navy award N00014-20-1-2418 issued by the Office of Naval Research; the NSF through the Harvard University Materials Research Science and Engineering Center Grant No. DMR-2011754, NSF OAC # 2118201, the Camille and Henry Dreyfus Foundation, and Bosch Research.

9:00 AM *MT01.05.02

Not as Simple as We Thought: A Rigorous Examination of Data Aggregation in Materials Informatics [Taylor D. Sparks](#)^{1,2}, Federico Ottomano², Giovanni De Felice² and Vladimir Gusev²; ¹University of Utah, United States; ²University of Liverpool, United Kingdom

Recent Machine Learning (ML) developments have opened new possibilities for materials research. However, due to the underlying statistical nature, the performance of ML estimators is heavily affected by the quality of training datasets, which are severely limited and fragmented in the case of materials

informatics. Here, we investigate whether state-of-the-art ML models for property predictions can benefit from the aggregation of different datasets. We probe three different aggregation strategies in which we prioritize training size, element diversity, and composition diversity by using novelty scores from the DiSCoVeR algorithm. Surprisingly, our results consistently show that both simple and refined data aggregation strategies lead to a reduction in performance. This suggests caution when merging different experimental data sources. To guide the size increment, we compare the use of DiSCoVeR, which prioritizes chemical diversity, with a random selection. Our results show that targeting novel chemistries is not beneficial in building a training dataset.

9:30 AM MT01.05.03

Leveraging Fragment-Based Representations in Active Learning and Reinforcement Learning Frameworks for Materials Design Daniel Tabor; Texas A&M University, United States

This talk will focus on the development and application of two types of methods for accelerating materials design. First, we will focus on developing reinforcement learning methods that are used to accelerate the design of functional materials, including radical-based polymers and organic optoelectronic materials. In our first demonstration of the reinforcement learning scheme, we show that this framework can integrate with quantum chemistry calculations in real-time, and through a careful design of the learning curriculum, we are able to find a diverse set of molecules with desired singlet and triplet energy levels. Second, we will describe our work on developing representations for predicting the polymer physics of disordered polymers at a much lower computational cost than current coarse-grained methods. One advantage of the new representation is that it avoids specifying the longest length of the chain in advance. In addition, this representation works well with a set of highly charged sequences, uncovering new insights to the fundamental interactions and scaling behavior of these systems. We will then discuss the compatibility of this representation with reinforcement learning methods.

9:45 AM MT01.05.04

Physics Supervised Deep Learning-Based Optimization (PSDLO) with Accuracy and Efficiency Hanqing Jiang and Xiaowen Li; Westlake University, China

Identifying efficient and accurate optimization algorithms is a long-desired goal for the scientific community. At present, a combination of evolutionary and deep-learning methods is widely used for optimization. In this paper, we demonstrate three cases involving different physics and conclude that no matter how accurate a deep-learning model is for a single, specific problem, a simple combination of evolutionary and deep-learning methods cannot achieve the desired optimization because of the intrinsic nature of the evolutionary method. We begin by using a physics-supervised deep-learning optimization algorithm (PSDLO) to supervise the results from the deep-learning model. We then intervene in the evolutionary process to eventually achieve simultaneous accuracy and efficiency. PSDLO is successfully demonstrated using both sufficient and insufficient datasets. PSDLO offers a new perspective for solving optimization problems and can tackle complex science and engineering problems having many features. This new approach to optimization algorithms holds tremendous potential for application in real-world engineering domains.

10:00 AM BREAK

10:30 AM *MT01.05.05

End-To-End Differentiability and Tensor Processing Unit Computing (TPU) to Accelerate Materials' Inverse Design Mathieu Bauchy; University of California, Los Angeles, United States

Numerical simulations have revolutionized material design. However, although simulations excel at mapping an input material to its output property, their direct application to inverse design has traditionally been limited by their high computing cost and lack of differentiability. Here, taking the example of the inverse design of a porous matrix featuring a target sorption isotherm, we introduce a computational inverse design framework that addresses these challenges. First, we adopt end-to-end differentiability to build a differentiable forward numerical simulation. Thanks to its differentiability, the forward simulation is used to directly train a backward deep generative model, which outputs an optimal porous matrix based on an arbitrary input sorption isotherm curve. Second, this inverse design pipeline leverages the power of tensor processing units (TPU)—an emerging family of dedicated chips, which, although they are specialized in deep learning, are flexible enough for intensive scientific simulations. This approach holds promise to accelerate the inverse design of novel materials with tailored properties.

11:00 AM *MT01.05.06

Accelerated Development of Materials Using High-Throughput Strategies and AI/ML Surya R. Kalidindi; Georgia Institute of Technology, United States

The dramatic acceleration of the materials innovation cycles is contingent on the development and implementation of high throughput strategies in both experimentation and physics-based simulations, and their seamless integration using the emergent AI/ML (artificial intelligence/machine learning) toolsets. This talk presents recent advances made in the presenter's research group, including: (i) a novel information gain-driven Bayesian ML framework that identifies the next best step in materials innovation (i.e., the next experiment and/or physics-based simulation to be performed) that maximizes the expected information gain towards a specified target (e.g., optimized combination of material properties, refinement of a material constitutive response), (ii) computationally efficient versatile material structure analyses and statistical quantification tools, (iii) formulation of reduced-order process-structure-property models that enable comprehensive inverse solutions needed in materials design (e.g., identifying specific compositions and/or process histories that will produce a desired combination of material properties), and (iv) high throughput experimental protocols for multi-resolution (spatial resolutions in the range of 50 nm to 500 microns) mechanical characterization of heterogeneous materials in small volumes (e.g., individual constituents in composite material samples, thin coatings or layers in a multilayered sample). These recent advances will be illustrated with case studies.

11:30 AM MT01.05.07

MACE-MP: A Foundation Model for Atomistic Materials Chemistry Janosh Riebesell; Lawrence Berkeley National Laboratory, United States

Machine-learned force fields have transformed the atomistic modelling of materials by enabling simulations of ab initio quality on unprecedented time and length scales. However, they are currently limited by: (i) the significant computational and human effort that must go into development and validation of potentials for each particular system of interest; and (ii) a general lack of transferability from one chemical system to the next. Here, using the state-of-the-art MACE architecture we introduce a single general-purpose ML model, trained on a public database of 150k inorganic crystals, that is capable of running stable molecular dynamics on molecules and materials. We demonstrate the power of the MACE-MP-0 model - and its qualitative and at times quantitative accuracy - on a diverse set of problems in the physical sciences, including the properties of solids, liquids, gases, chemical reactions, interfaces and even the dynamics of a small protein. The model can be applied out of the box and as a starting or "foundation model" for any atomistic system of interest and is thus a step towards democratizing the revolution of ML force fields by lowering the barriers to entry.

11:45 AM MT01.05.08

Machine-Learning Solar Cell Efficiency from a Dataset of Continuum Simulations [Andrea Crovetto](#); Technical University of Denmark, Denmark

Power conversion efficiency limits of solar cells based on ideal semiconductors are well known as a function of the semiconductor's band gap energy (Shockley-Queisser limit and their derivatives). However, it is notoriously difficult to estimate the maximum photovoltaic (PV) efficiency potential of real-world materials featuring a number of unavoidable imperfections.

In this contribution, I will show that this problem can be addressed by integrating a dataset of 30,000 drift-diffusion (continuum) simulations with machine learning to estimate the PV efficiency of a generic, non-ideal PV material. With this data-driven approach, and unlike any previously reported method, a generalized effect of, e.g., finite carrier mobilities and doping densities on the maximum PV efficiency can be modeled.

Importantly, the simulation dataset is not static but instead new data can be collected in a closed-loop fashion, depending on how the machine learning model performs with the available data at a given time. Furthermore, the relevant solar cell physics is incorporated into the model at various stages of our workflow, resulting in a favorable trade-off between statistical generality and physical understanding.

The relevance of the machine-learned PV efficiency is demonstrated on a sample of 16 PV materials of current research interest. The method can immediately be applied to experimentally synthesized or computationally examined materials at any development level, as long as seven of their bulk material properties (the basic descriptors) have been determined by experiment or first-principles calculations.

SESSION MT01.06: Machine Learning and Simulations VI

Session Chairs: Aditi Krishnapriyan and Taylor Sparks

Wednesday Afternoon, April 24, 2024

Room 320, Level 3, Summit

1:30 PM *MT01.06.01

Harnessing Materials Imperfections: Case Studies of 'Defects' in Materials for Energy Sustainability [Wennie Wang](#); University of Texas at Austin, United States

We present work in the Wang Materials Group (<https://wangmaterialgroup.com>) in understanding and harnessing defects in materials for energy sustainability applications that leverage and/or are inspired by aspects of machine learning. Our goal is to elucidate and predict the materials properties at the microscopic level using first-principles calculations, drive the exploration of novel materials platforms, and create strategies that directly couple to/guide experiments. Here, we present on two such case studies on next-generation memory and storage applications and electrocatalysts.

Memristors are an emerging memory technology that can help meet the capacity and energy efficiency demands. Non-volatile resistive switching (NVRs) between high- and low-resistive states has been broadly observed in various two-dimensional materials. As atomically thin systems, two-dimensional materials are promising as the active switching layer for two-terminal vertically stacked memristor devices. We examine one particular mechanism of NVRs based on the formation and dissolution of point defect complexes to describe the switching energetics and switching processes. In this talk, we will present our efforts in leveraging automated calculations to screen for defects capable of inducing NVRs in two-dimensional materials and extract materials-based scaling relationships for the switching energy.

In the second case study, we turn to the investigation of structure and catalytic activity relationships in electrocatalysts. Low-temperature electrocatalysis of water is at the forefront of strategies that could help realize a clean hydrogen economy. The (oxy)hydroxides are scientifically significant as electrocatalysts that electrochemically form on many pre-catalyst surfaces in the amorphous state. Interestingly, amorphous electrocatalysts have been reported to consistently outperform crystalline ones. Our goal is to connect the structural disorder in amorphous electrocatalysts to mechanism(s) in enhancing the electrocatalytic activity. We will discuss the considerations to appropriately describe the electronic and atomic structure and strategies in using point defects and genetic algorithms to understand local structural disorder.

2:00 PM MT01.06.02

Anion Charge Distribution Effects of Lithium Diffusion in Polymer Electrolytes Using End to End Force Field Parameterization through Machine Learning [Pablo A. Leon](#) and Rafael Gomez-Bombarelli; Massachusetts Institute of Technology, United States

Solid polymer electrolytes (SPEs) are seen as promising alternatives to conventional liquid electrolytes in lithium battery systems due to their low density, mechanical compliance, and low flammability but are challenged by lower ionic conductivity. Molecular dynamics (MD) simulations can be used to guide the design of novel SPEs by allowing quantitative determination of separable anion and cation diffusions as well as local solvation environments. Classical potential MD simulations update molecular conformations by the net force on each atom due to covalent and nonbonded interactions. However, these classical potentials require materials- and local environment-specific parameters such as nonpolarizable point charges on each atom that have historically been meticulously hand-tuned across decades.

In this work, we explore the effects of using distinct anion charge distributions based on minimum energy Lithium ion coordination on ionic solvation and conductivity in polymer electrolyte simulations. An in-house, machine learning-based workflow, named AuTopology, was used to autonomously learn the interatomic potential parameters of unique atomic environments for two different classical models from DFT forces as training data. In particular, the effect of machine learning regularization and chemistry-informed training data selection on resulting polymer-ion system behavior is highlighted. The learned harmonic OPLS model and anharmonic PCFF+ model parameters were then used to equilibrate condensed-phase simulations at a variety of experimentally-relevant concentrations. These simulations were allowed to run for hundreds of nanoseconds to determine the individual anion and cation diffusivities and resulting conductivities. Using this framework and an in-house database of molecular conformations, we have been able to reproduce wB97XD3-level DFT forces from trained OPLS force fields to within 5.5 kcal/mol-Å. Lithium solvation environments and ion diffusivities were found to match legacy parameterizations to the same order of magnitude.

2:15 PM MT01.06.03

Breaking Boundaries: AI-Driven Design of High-Temperature Polymer Dielectrics [Madhubanti Mukherjee](#), Shivank S. Shukla, Rishi Gurnani, Joseph D. Kern, Hari Krishna Sahu and Rampi Ramprasad; Georgia Institute of Technology, United States

In the domain of electrical and electronic applications, the demand for flexible polymer dielectrics capable of withstanding extreme temperatures and

electric fields is pressing. The dielectric breakdown strength, signifying the maximum electric field a polymer can endure while retaining excellent insulating qualities (i.e., sufficiently high bandgap (E_g)) is a pivotal parameter. Together with the dielectric constant of the polymer, it dictates the upper limit of electrostatic energy storage in a capacitor. Another key parameter for high-temperature energy storage is the high glass transition temperature (T_g), which ensures thermal and electromechanical stability, thereby preserving capacitive performance. Simultaneously obtaining high T_g , a high dielectric constant, and a high E_g for achieving enhanced energy density proves to be a formidable challenge due to the observed negative correlation between T_g and E_g , further complicated by potentially increased dielectric loss at higher T_g . Identifying such suitable candidates in the vast chemical landscape of polymers, entangled with the complexities of dielectric breakdown mechanisms is daunting. Artificial intelligence-driven screening methods have emerged as proficient tools for sifting through expanding polymer libraries, streamlining the selection process for experimental exploration [1]. The application of screening criteria based on readily accessible proxy properties has expedited the search process in contrast to the laborious manual extraction of chemo-structural attributes. These criteria include a high bandgap to ensure an insulating phase, a high glass transition temperature to ensure thermal stability, and a substantial dielectric constant that enhances energy density [2, 3]. Employing these criteria in conjunction with machine learning models, we conducted an extensive screening initiative encompassing over 14,000 previously synthesized polymers and an additional 6 million hypothetical polymers crafted from diverse reaction templates. This systematic approach has unraveled a multitude of promising candidates, boasting attributes such as a glass transition temperature reaching 400°C, a bandgap of 4 eV, and a dielectric constant within the range of 3-5. These characteristics hold the promise of remarkably high energy density. Furthermore, our study leverages density functional theory and molecular dynamics simulations to further validate the bandgap and glass transition temperature for a significant portion of these polymers. This study also provides valuable insights into the structural elements essential for designing robust, high-temperature polymer dielectrics with exceptional energy storage capabilities.

[1] Chem. Mater. 35, 4, 1560–1567 (2023)

[2] ACS Appl. Mater. & Interfaces 12, 33, 37182-37187 (2020)

[3] Matter, 5(9), 2615-2623 (2022)

2:30 PM BREAK

3:30 PM *MT01.06.04

Uncertainty Quantification in Machine Learning Models of Materials Properties [Dane Morgan](#)¹, Ryan Jacobs¹, Lane Schultz¹, Vidit Agrawal¹, Shixin Zhang¹, Glenn Palmer², Ben Blaiszik³, Aristana Courtas³ and KJ Schmidt³; ¹University of Wisconsin–Madison, United States; ²Duke University, United States; ³The University of Chicago, United States

Machine learning models are being increasingly used to predict an enormous range of materials properties. Such models are typically trained on computed and/or experimental data that has strong biases in terms of the sampled systems, potentially leading to models with limited accuracy and very specific domains. It is therefore of increasing importance to establish effective practices for uncertainty quantification of machine learning models used for materials properties. In this talk we share an approach that divides uncertainty quantification into separate challenges of error and domain determination, which together provide a strong framework for practical uncertainty quantification. This approach leads to uncertainty quantification that can guide users whether prediction on any given test data point is likely to be appropriate, and if it is appropriate, what accuracy might be expected. For determining errors, we demonstrate that, when properly calibrated, ensembles of models fit to bootstrap sampling of training data can provide robust and easily accessible estimates of test data point residuals[1]. For determining domain, we demonstrate that a kernel density estimate of training data density in feature space can be used to identify regions of feature space with inadequate sampling and therefore likely to be out of domain. Assessing any domain determination strategy is difficult as there is no unique ground truth for a test data point being in or out of domain. To manage this problem we propose a set of criteria for ground truth based on matching chemical intuition and expected large residuals and residual estimation errors with being out of domain. We show that a kernel density approach can generally categorize new test data points as in/out of domain with good accuracy (e.g., max F1 scores of about 80% or better) when using any of these criteria. Finally, we discuss how these methods can be trivially integrated into model fits through the MAST-ML[2] package and how such uncertainty aware models can be easily hosted in the cloud through the Foundry[3] service.

(1) Palmer, G.; Du, S. Q.; Politowicz, A.; Emory, J. P.; Yang, X. Y.; Gautam, A.; Gupta, G.; Li, Z. L.; Jacobs, R.; Morgan, D. Calibration after bootstrap for accurate uncertainty quantification in regression models. *npj Comput. Mater.* 2022, 8 (1), 9, Article. DOI: 10.1038/s41524-022-00794-8.

(2) Jacobs, R.; Mayeshiba, T.; Afflerbach, B.; Miles, L.; Williams, M.; Turner, M.; Finkel, R.; Morgan, D. The Materials Simulation Toolkit for Machine learning (MAST-ML): An automated open source toolkit to accelerate data-driven materials research. *Comput. Mater. Sci.* 2020, 176, 13, Article. DOI: 10.1016/j.commatsci.2020.109544.

(3) Blaiszik, B.; Schmidt, K.; Courtas, A. Foundry-ML. 2023. <https://foundry-ml.org> (accessed 2023).

4:00 PM MT01.06.05

Elucidating Structural Heterogeneity of Amorphous Materials with X-Ray Absorption Spectroscopy and Machine Learning Hyuna Kwon, Yu-Ting Hsu, Wonseok Jeong, Wenyu Sun, Liwen Wan, Michael Nielsen and [Tuan Anh Pham](#); Lawrence Livermore National Laboratory, United States

The ability to precisely determine the atomic structure of functional materials would have a transformative and broad impact on a broad range of emerging technologies, from energy storage and conversion to ion-selective membranes. In this talk I will summary our recent activities in integrating atomistic simulations, data science, and spectroscopic measurements to elucidate structural and chemical heterogeneities in disordered systems. I will show how machine learning potential is used to efficiently explore the vast configuration space of amorphous carbon nitrides and to identify the local structural motifs of the systems. Density functional theory simulations were used to establish a correlation between the local structure motifs and X-ray absorption spectroscopic signatures, which then serves as the basis for interpreting and extracting chemical content from experimental data. Beyond predicting the chemical content, I will also discuss a strategy to predict the three-dimensional atomic structure of amorphous systems from X-ray absorption spectroscopy via a generative diffusion model. Using amorphous carbon as a case study, it is found that the generative model exhibits a remarkable scale-agnostic property, enabling the generation of large-scale atomic structures, while being able to accurately predict the atomic structure from targeted spectroscopy. The methods developed here are general and can be broadly applied for inverse design of functional materials.

4:15 PM MT01.06.06

Decoding Structure-Spectrum Relationships in X-Ray Absorption Spectra with Physically Organized Latent Spaces [Deyu Lu](#), Zhu Liang, Matthew Carbone, Wei Chen, Fanchen Meng, Eli Stavitski, Mark Hybertsen and Xiaohui Qu; Brookhaven National Laboratory, United States

X-ray absorption spectroscopy (XAS) is a premier materials characterization technique, which is element specific and sensitive to the local chemical environment. However, the physical information in XAS, in particular, x-ray absorption near-edge structure (XANES), is encoded in the spectral function in an abstract form. First principles calculations are widely used to unravel the complex structure-spectrum relationship. However, this approach requires a great deal of domain expertise and is computationally expensive. These drawbacks limit the scope of XAS modeling for complex systems and in real-time analysis. To address this challenge, data-driven XAS analysis methods emerge, which take advantage of the fast developing machine learning tools for

spectral interpretation. Successful examples show that machine learning models can be used to accelerate XAS simulations and identify the physical origin of spectral trends in a statistically salient way.

In this study, a semi-supervised machine learning method for the discovery of structure-spectrum relationships is developed and then demonstrated using the specific example of interpreting XANES spectra. This method constructs a one-to-one mapping between individual structure descriptors and spectral trends. Specifically, an adversarial autoencoder is augmented with a rank constraint (RankAAE). The RankAAE methodology produces a continuous and interpretable latent space, where each dimension can track an individual structure descriptor. As a part of this process, the model provides a robust and quantitative measure of the structure-spectrum relationship by decoupling intertwined spectral contributions from multiple structural characteristics. This makes it ideal for spectral interpretation and the discovery of descriptors. The capability of this procedure is showcased by considering five local structure descriptors and a database of more than 50000 simulated XANES spectra across eight first-row transition metal oxide families. The resulting structure-spectrum relationships not only reproduce known trends in the literature but also reveal unintuitive ones that are visually indiscernible in large datasets. The results suggest that the RankAAE methodology has great potential to assist researchers in interpreting complex scientific data, testing physical hypotheses, and revealing patterns that extend scientific insight.

4:30 PM MT01.06.07

Physics Informed Disentangled Latent Space of X-Ray Absorption Spectra Sophie D'Halleweyn^{1,2}, Anatoly Frenkel¹ and [Prahlaad Kumar Routh](#)¹; ¹Stony Brook University, United States; ²The Bronx High School of Science, United States

X-ray absorption spectra provide insights into the atomic scale local structures of a wide range of materials with nanoscale dimensions. This information is often inaccessible to experimentalists through traditional structural analysis techniques. To analyze XAS spectra, theory-driven structural models are needed, particularly for fitting the extended part of the spectra (EXAFS). While the quantitative analysis of the near-edge part of XAS (XANES) remains an active research area, neural networks have proven their efficacy as universal approximators. They efficiently learn the mapping between theory generated spectra and structural descriptors in various cases of mono and bimetallic metallic nanocatalysts. However, challenges arise in uncertainty quantification and out-of-distribution performance when these networks are applied to experimental data. Recent studies have highlighted that low-dimensional embeddings of XANES, obtained via autoencoder frameworks, encapsulate these structural descriptors. To enhance the interpretability and utilize the generative capability of the autoencoder framework, a structured and continuous latent space is essential.

In our work, we introduce a physics-informed robust analysis of XANES spectra, striking a balance between reconstruction and descriptor-specific information. Our method, the Multitasking Algorithm for Variational Auto Encoder (MAVEN), achieves a disentangled, interpretable latent space through multi-objective optimization, focusing on reconstruction, denoising, autocompletion, and descriptor mapping. MAVEN stands out for its ability to disentangle and interpret latent space variables, offering a unique generative capability within the autoencoder framework. We've also developed a methodology to quantify the level of disentanglement achieved, rooted in information theory principles. We show the utility of MAVEN by interpreting experimental XANES of palladium and palladium hydride nanoparticles. These are renowned for their lattice expansion, which MAVEN distinguishes from particle size effects via coordination number analysis. The comparison of trends from the MAVEN algorithm to those obtained from extended X-ray absorption fine structure (EXAFS) spectral analysis using Demeter software indicates MAVEN's potential for high-fidelity real-time analysis of local structures. Our discussions will explore the applications of this technique in bimetallic nanoparticles systems and assess its effectiveness on experimental XANES spectra. The promising results suggest that MAVEN could be a vital tool for real-time analysis of local structures, especially in conjunction with experimental spectroscopy of functional nanomaterials like catalysts, batteries, and fuel cells.

SESSION MT01.07: Machine Learning and Simulations VII
Session Chairs: Rodrigo Freitas and Ryan Sills
Thursday Morning, April 25, 2024
Room 320, Level 3, Summit

8:30 AM *MT01.07.01

Learning Grain Boundary Thermodynamic Spectra in Polycrystals Christopher A. Schuh^{1,2}, [Nuttu Tuchinda](#)², Thomas Matson² and Malik Wagih²; ¹Northwestern University, United States; ²Massachusetts Institute of Technology, United States

The thermodynamics of alloy components determine material structures, properties and hence the processability and performance matrices of engineering alloys. Incorporating grain boundaries in thermodynamic models is not a simple task: grain boundary defects in polycrystals occupy a wide 5-dimensional configuration space, imposing a computational barrier in evaluating thermodynamic data across the chemical space. This complexity calls for a combination of recent advances in data science approaches and computational materials science. This talk will first discuss an isotherm approach in modeling equilibrium solute behavior at grain boundaries and show that relevant spectral thermodynamic quantities can be extracted from atomistic simulations. Then, data-science and machine-learning enabled accelerated models are presented to extend the work to many alloy systems. Finally, a full-spectral case study of a binary alloy system with the inclusion of rapid estimations of dilute segregation energies, solute-solute interactions at grain boundaries and excess vibrational entropy of segregation is presented. These accelerated models open opportunities to construct an embedded alloy grain boundary atlas, which ultimately can assist in alloy design.

9:00 AM *MT01.07.02

Artificial Neural Network Interatomic Potentials Developed for Grain-Boundary Modeling in Al₂O₃ Ceramics [Katsuyuki Matsunaga](#)^{1,2}, Tatsuya Yokoi¹ and Yu Ogura¹; ¹Nagoya University, Japan; ²Japan Fine Ceramics Center, Japan

Excellent structural and functional properties of ceramic materials often originate from their grain boundaries and interfaces. Therefore, it is essential to obtain in-depth understanding of electronic and atomic structures of the grain boundaries for materials design. However, crystal structures of ceramic components such as oxides are generally low symmetry and thus contain many atoms, so that a great number of atoms should be inevitably handled in the grain boundary modeling. This often makes it difficult to systematically treat the ceramic grain boundaries at the first-principles level. In the present study, artificial neural network interatomic potentials trained by first-principles data were developed for Al₂O₃, which is a representative ceramic oxide, and applied for their grain boundaries. Grain boundary structures thus obtained were compared with experimental STEM images to verify accuracy of the potentials. On the basis of the calculated grain boundary structures, first-principles calculations were again applied to investigate specific electronic structures of the grain boundary cores that are closely related to the grain boundary properties. Some other examples such as extension to multicomponent systems for the segregated grain boundaries will also be discussed.

9:30 AM MT01.07.03

On Neural Networks for Grain Boundary Dynamics [Fadi Abdeljawad¹](#), Malek Alkayyali² and Milad Taghizadeh¹; ¹Lehigh University, United States; ²Clemson University, United States

Nearly all structural and functional materials are polycrystals; they are composed of differently oriented crystalline grains that are joined at grain boundaries (GBs). Such interfaces play a critical role in controlling many engineering and functional properties. Understanding GB physics is, therefore, a key aspect of materials discovery and design efforts. Owing to their local atomic environments, GBs provide preferential sites for alloying elements to occupy. Indeed, the direct manipulation of GB chemical states has been found to influence a host of materials properties and processes, such as cohesion and fracture resistance, transport, electrochemical response, electrical conductivity, and processability during advanced manufacturing techniques. Of particular interest is the impact of GB solute segregation on boundary dynamics, as it influences microstructure formation and evolution pathways during processing treatments or under operating environments. For example, GB segregation has been used to mitigate grain coarsening and thermally stabilize nanograined structures. While GB solute segregation has been the subject of active research, most existing studies focus on the thermodynamics of GB segregation and the kinetic role (i.e., dynamic solute drag) remains unexplored. GB solute drag results when segregated alloying elements exert a resistive force on migrating GBs hindering their motion. The challenge here is that solute drag depends on several properties, such as alloy thermodynamics (e.g., heat of mixing), and dynamic processes including solute diffusion and boundary migration; solute drag is a hypersurface. In this talk, we unravel GB dynamic solute drag through theoretical analysis, mesoscale modeling, and machine learning studies. We establish design maps relating drag effects to relevant bulk alloy and GB properties. We find that solute drag is dominant in immiscible alloys with far-from-dilute compositions in agreement with experimental observations of GB segregation in metallic alloys. Further, asymmetric GB segregation is found to greatly influence solute drag values. On the whole, our work provides future avenues to employ GB segregation engineering to control GB dynamical processes.

9:45 AM MT01.07.04

Learning Grain Boundary Segregation Vibrational Spectra from Ni-Based Polycrystals [Nuttu Tuchinda¹](#) and Christopher A. Schuh^{1,2}; ¹Massachusetts Institute of Technology, United States; ²Northwestern University, United States

Polycrystalline systems consist of a broad range of planar defect configurations that cannot be represented by simplified boundary models such as small symmetric tilt boundaries. The multiple-site nature of grain boundaries calls for a spectral approach as opposed to a single-site McLean model. However, evaluating solute segregation thermodynamic quantities at every site in large polycrystals is an exhaustive process, especially for the segregation vibrational entropy. Here we show an attempt to integrate a data science approach with computational materials modeling for computational tractability. A modified local harmonic method is applied in combination with a statistical approach to quantify grain boundary segregation vibrational spectra of embedded dilute Ni-based binary alloy pairs. The database allows more rigorous predictions of grain boundary enrichment at a function of concentration, grain size and temperature which are critical for solute segregation-stabilized nanocrystalline alloys.

10:00 AM BREAK

10:30 AM MT01.07.05

Stability and Equilibrium Structures of Unknown Ternary Metal Oxides explored by Machine-Learned Potentials [Seungwoo Hwang¹](#), Jisu Jung¹, Changho Hong¹, Wonseok Jeong¹, Sungwoo Kang¹ and Seungwu Han^{1,2}; ¹Seoul National University, Korea (the Republic of); ²Korea Institute for Advanced Study, Korea (the Republic of)

Ternary metal oxides are extensively utilized across various applications and have been comprehensively cataloged in experimental materials databases. Nonetheless, there remains a substantial portion of unexplored combinations of cations with oxide forms in terms of their stability and structures. Discovering new ternary metal oxides solely through experiments is both time-consuming and resource-intensive. Alternatively, theoretical databases offer hypothetical structures based on known prototypes. However, it is possible to miss “hidden” ground state structures that are not represented by prototype structures. This challenge can be addressed through the application of crystal structure prediction (CSP), which employs heuristic methods, such as evolutionary algorithm, to identify the lowest-energy structure for a given composition without prior knowledge. Nevertheless, the effectiveness of this approach is limited due to its reliance on computationally expensive density functional theory (DFT) calculations and an exhaustive search of the structure space, which is often impractical for finding complex equilibrium phases of ternary metal oxides. Recent years have seen a growing interest in machine-learned potentials (MLPs) an effective alternative to the DFT method. MLPs can rapidly compute energy and atomic forces, achieving results comparable to DFT. Based on the concept that MLPs trained with disordered phases have been successful as surrogate models for DFT in CSP [1], a systematic CSP program called SPINNER (Structure Prediction of Inorganic crystals using Neural Network potentials with Evolutionary and Random searches) was developed, harnessing MLPs within an evolutionary algorithm [2]. In benchmark tests using experimental structure data, SPINNER identified 80% of the structures of 60 different ternary compounds with diverse crystal symmetries and identified 10^2 to 10^3 times faster than DFT-based heuristic methods. In this study, we extensively employ SPINNER to explore experimentally uncharted chemical spaces [3]. We investigate 181 ternary metal oxide systems, encompassing most cations except those with partially filled 3d or f shells, and search up to 60,000 crystal structures in representative compositions derived from common oxidation states and a machine-learned recommender system to determine the lowest energy crystal structure. Our exploration yields 45 systems containing stable ternary oxides that do not decompose into binary or elemental phases. Interestingly, many of these are noble metal-containing systems that have not yet been well studied and have equilibrium structures that do not belong to the known prototype structure. Comparisons with other theoretical databases highlight the strengths and limitations of informatics-based material searches and point to the synergistic effect between direct and data-mining searches. With a relatively modest computational resource requirement, we contend that heuristic-based structure searches, as demonstrated here, offer a promising approach for future materials discovery endeavors.

[1] C. Hong, *et al*, *Phys. Rev. B* **102**, 224104 (2020).

[2] S. Kang, *et al*, *npj Comput. Mater.* **8**, 108 (2022).

[3] S. Hwang, *et al*, *J. Am. Chem. Soc.* **145**, 19378 (2023).

10:45 AM *MT01.07.06

Neural Network of Defect Kinetics for Multi-Principal Element Alloys [Penghui Cao](#); University of California, Irvine, United States

The emergent multi-principal element alloys (MPEAs), commonly known as high entropy alloys, provide a vast compositional space to search for radiation-resistant materials for advanced nuclear reactor applications. However, the vast composition space of MPEAs makes identifying the desired composition and defect mechanisms a complex task. This presentation will introduce a machine learning strategy, specifically neural networks, to overcome this challenge. The machine learning-driven models have proven effective and efficient in predicting defect migration energy barriers across the complete compositional spectrum of MPEAs. The successful implementation of neural network kinetics model holds significant promise for harnessing

defect kinetics in the huge compositional space. It could significantly accelerate the alloy selection process, paving the way for engineering new alloy compositions with enhanced radiation performance.

11:15 AM MT01.07.07

Machine Learning Derived Periodic Table for High Entropy Alloys [Scott Broderick](#), Md T. Islam and Qinrui Liu; University at Buffalo, United States

This work explores new high entropy alloys (HEAs) which address the challenges in trade-offs between strength, ductility and various environmental effects. To address the limitations in traditional regression approaches which can generate large amounts of data rapidly but do not account for the complex interplay in correlating properties, we instead apply an unsupervised learning approach. By mapping the high dimensional nature of the systematics of elemental data embedded in the periodic table, the influence of specific combinations of elements on engineering properties of HEAs are captured. This approach is designed to capture the interplay between chemistry, microstructure and phase stability, which allows us to identify chemical design rules for improving mechanical properties with minimal trade-offs. This work uses a graph representation approach to capture the thermodynamic and structural complexity of high entropy alloys (HEAs). This approach has been used for materials discovery based on first principles, but now we are using it to design engineering alloys. We identify the potential existence of new combinations of phases not previously identified by tracking the connections in the network, which are analogous to tie lines in a traditional phase diagram representation. In this way, mechanical properties are rationally designed through proposed chemical design rules across the entire HEA search space, resulting in a machine learning based representation of a periodic table based on HEA properties.

11:30 AM MT01.07.08

Electronic Moment Tensor Potentials (eMTP): Application to Refractories and Shape-Memory Alloys Prashanth Srinivasan¹, [Yongliang Ou](#)¹, David Demuriya², Alexander Shapeev² and Blazej Grabowski¹; ¹University of Stuttgart, Germany; ²Skolkovo Institute of Science and Technology, Russian Federation

We present the electronic moment tensor potentials (eMTPs), a class of machine-learning interatomic models and a generalization of the classical MTPs, reproducing both the electronic and vibrational degrees of freedom, up to the accuracy of *ab initio* calculations (Srinivasan et al., 2023). Following the original polynomial interpolation idea of the MTPs, the eMTPs are defined as polynomials of vibrational and electronic degrees of freedom, corrected to have a finite interatomic cutoff. Practically, an eMTP is constructed from the classical MTPs fitted to a training set, whose energies and forces are calculated with electronic temperatures corresponding to the Chebyshev nodes on a given temperature interval. The eMTP energy is hence a Chebyshev interpolation of the classical MTPs. With eMTPs, one can access the temperature-dependent electronic and vibrational free energies and the coupling between the two, separately.

The performance is demonstrated on two classes of systems: (1) refractory Nb and TaVCrW high-entropy alloy, and (2) equiatomic Nickel-Titanium (NiTi) shape-memory alloy (SMA). The refractories demonstrate a significant electronic, vibrational, and coupling contribution to the free energy, all of which get captured accurately by performing a thermodynamic integration (Jung et al., 2022) to the eMTPs. We are able to reach full density-functional theory accuracy in thermodynamic properties all the way to the melting point without any further *ab initio* calculations.

The NiTi SMA is considerably more challenging to model owing to several energetically competing phases (body-centered cubic B2, monoclinic B19', orthorhombic B19 and base-centered orthorhombic B33). We train an eMTP to obtain the thermodynamic phase stability including all relevant contributions. The experimentally observed low-temperature martensitic (B19') and high-temperature austenitic (B2) phases get entropically stabilized. Both the vibrational and electronic contributions also significantly affect the B2-B19' phase transformation, bringing the behavior much closer to experiments. The eMTP-thermodynamic integration approach enables us to analyze the accuracy of different exchange correlation functionals and *ab initio* parameters. Lastly, to investigate kinetic effects, we perform large-scale molecular dynamics simulations using the eMTP to model the stress-induced and temperature-induced phase transformation.

References

- [1] Srinivasan P., Demuriya D., Grabowski B., Shapeev A.V.: preprint at research square <https://doi.org/10.21203/rs.3.rs-2643432/v1>, 2023
- [2] Jung J.H., Srinivasan P., Forslund A., Grabowski, B.: *npj Computational Materials* **9**, 3 (2023)

11:45 AM MT01.07.09

Machine Learning and Kinetic Monte Carlo Models of Transport in Concentrated Alloys Anjana Talapatra¹, Matthew Wilson¹, Ying Wai Li¹, Anup Pandey¹, Ghanshyam Pilania¹, Danny Perez¹, Sohah Chattopadhyay², Dallas Trinkle² and [Blas P. Uberuaga](#)¹; ¹Los Alamos National Laboratory, United States; ²University of Illinois at Urbana-Champaign, United States

With the increasing interest in so-called high entropy, multi-principal component, or compositionally complex alloys, there is a greater need to understand how transport is affected by the complex chemistry of these materials. As compared to a simple elemental solid, in which every lattice site is identical and transport can be described by a handful of saddle points, these materials exhibit a very rugged potential energy surface in which every site has a unique chemical environment. This means that every site exhibits a different defect formation energy and corresponding migration barriers for motion to neighboring sites. As the number of elements in these systems increases, it becomes increasingly challenging, and soon impossible, to enumerate the energetics of every site in the system. Alternative approaches are necessary.

Machine learning has become a popular choice to describe the chemistry-dependent properties of defects in these alloys. By training on atomistic data, machine learning models can predict the energetics of defects in unseen environments and be subsequently used in kinetic Monte Carlo simulations of defect transport. However, for the transport simulations to be thermodynamically valid, the underlying machine learning model must obey detailed balance.

Here, we describe various ways that detailed balance can be enforced in a machine learning model of defect formation and migration energies. Specifically, we consider a brute force model, a “soft constraint” model in which penalty associated with detailed balance is added to the loss function, and two “hard constraint” models in which detailed balance is explicitly included in the architecture of the model. We find that these physically-constrained models exhibit superior performance in maintaining detailed balance. This is demonstrated by determining the error in the energy of the system as defects traverse closed loops. We conclude that detailed balance must be considered to obtain valid trajectories.

We then use the machine learning model to determine the kinetic properties of defects. Using a recently-developed approach in which the complex correlated+uncorrelated kinetic Monte Carlo problem is mapped rigorously onto an uncorrelated surrogate, we then use this to identify which atomic scale events are most critical in describing the trajectory of the defect. This provides a route to close the loop, so to speak: to build an autonomous workflow in which the events that the trajectory is most sensitive to are further refined to improve the description of the material. We demonstrate the elements of this workflow for a vacancy in the simple Cu-Ni alloy, highlighting how we can then quickly determine the diffusion tensor for defects in complex alloys when

given appropriate computational resources.

SESSION MT01.08: Machine Learning and Simulations VIII
Session Chairs: Penghui Cao and Rodrigo Freitas
Thursday Afternoon, April 25, 2024
Room 320, Level 3, Summit

1:45 PM *MT01.08.01

Finite-Element-Based Physics-Informed Convolutional Neural Networks [Ryan B. Sills](#) and Pranav Sunil; Rutgers University, United States

Physics informed neural networks have become very popular as a technique for solving physics-derived partial differential equations. However, many PINN techniques do not allow for variation in geometry and parameters after training. Relatedly, PINNs are usually constructed with fully-connected NNs, making them costly to train. In this talk, we present a PINN methodology which leverages the finite element method to enable variation in geometry and parameters within a convolutional NN architecture. The heart of the method is a new type of convolutional operation called stencil convolution which utilizes the finite element inverse isoparametric map. We demonstrate the method with applications to deformations of linear elastic solids.

2:15 PM MT01.08.02

Probing Defect-Controlled Small Scale Plasticity via Machine Learning Approach and Defect Dynamics Modeling [Ill Ryu](#); The University of Texas at Dallas, United States

Mechanical behaviors of metals at small scale have attracted much attention due to their widespread applications in modern MEMS/NEMS devices due to their enhanced properties. To understand the underlying microscopic deformation mechanisms that control the mechanical properties of nanostructured metals, an insight into the intricate interaction of dislocations and grain boundaries is vital. Computational simulations of materials have advanced significantly in recent years, shifting from analyzing experimental observation to providing capability to predict mechanical behaviors for use in advanced material development. Machine learning has been a topic of great interest in recent years within the engineering community. In this study, we employed a multiscale modeling approach to investigate defect interaction. For the prediction of dislocation interactions with grain boundaries, we will present an efficient physically informed machine learning framework that has potential to significantly improve predictive capability of computational modeling, which in turn would reduce the number of prototypical experimental validation. With the atomistically informed mesoscale defect dynamics model, we explore the effect of varying misorientation angle for pure twist and pure tilt grain boundaries on plastic deformation of nanostructures, which could provide a better understanding of dislocation driven plasticity for polycrystalline metals at small scale. For complex loading and environmental condition, the unified defect dynamics model which coupled dislocation dynamics (DD) and finite element model (FEM) has used, which could play an important role in obtaining a fundamental understanding of deformation mechanism at small scale. The developed multiscale framework will shed light on fundamental investigation of “defect-controlled” mechanical behaviors in metallic materials.

2:30 PM MT01.08.04

Atomistic Dislocation Dynamics Using Bayesian Force Fields [Cameron J. Owen](#)¹, [Amirhossein Naghdi](#)², [Anders Johansson](#)¹, [Dario Massa](#)², [Stefanos Papanikolaou](#)² and [Boris Kozinsky](#)^{1,3}; ¹Harvard University, United States; ²NOMATEN Centre of Excellence, Poland; ³Robert Bosch LLC, United States

Dislocation dynamics present a difficult simulation task for existing classical and *ab initio* methods due to the simultaneous accuracy and length-scale requirements for reliable simulation and comparison to experimental data. These limitations ultimately prohibit advanced understanding of plastic deformation (e.g. via edge and screw dislocations) of materials. Here, we develop a Bayesian machine-learned force field (MLFF) from first-principles training data that extends quantum-mechanical accuracy to large length-scale molecular dynamics simulations which permit direct observation of high-temperature and high-stress dislocation dynamics in Cu with atomistic resolution. In concert, a generalizable training protocol is defined for the construction of MLFFs for description of dislocations, which can be trivially employed for other metal and alloy systems of interest. The resulting FLARE MLFF provides excellent predictions of static bulk properties (e.g. bulk modulus and elastic tensor), stacking fault energies, and reliable, dynamic evolution of edge and screw dislocations, as well as cross-slip mechanisms that allow for non-planar movement of screw dislocations across a broad range of temperature and applied stress. Each of these observations from molecular dynamics simulations are then compared to experimental data, including the screw and edge stacking fault widths, edge dislocation mobility coefficient, and screw dislocation cross-slip activation energy, where FLARE provides the best agreement among the methods tested. Such simulations permit increased understanding of material responses to extreme conditions by direct atomistic insight at the mesoscale with near quantum mechanical accuracy.

2:45 PM MT01.08.05

Aniso-GNN: Physics-Informed Graph Neural Networks Generalizing to Anisotropic Properties of Polycrystals [Guangyu Hu](#) and Marat Latypov; University of Arizona, United States

We present Aniso-GNNs -- graph neural networks (GNNs) that generalize predictions of anisotropic properties of polycrystals to arbitrary loading directions without the need in excessive training data. To this end, we develop GNNs with a physics-inspired combination of node attributes and aggregation function. We further propose a new efficient training strategy leveraging fundamental symmetries of crystallographic orientations and textures as well as tensor properties of individual grains and polycrystals. We demonstrate the predictive power of Aniso-GNNs in modeling anisotropic elastic and inelastic properties of polycrystalline alloys in a wide range of loading directions without training data in those directions.

3:00 PM BREAK

3:30 PM *MT01.08.06

Efficient High-Throughput *Ab Initio* Prediction of Liquidus Curves [Wenhao Sun](#); University of Michigan, United States

The liquidus curve captures the high-temperature eutectics, peritectics, congruent melting and incongruent melting regions of a phase diagram. Being able to predict liquidus curves would enable *ab initio* guidance of materials synthesis temperatures, as well as the design of materials stable under high-temperature operation conditions. Liquidus curves are available in databases like ThermoCalc or SGTE, but the available chemical spaces in these databases lag far behind computational materials discovery efforts. Direct simulation of liquid free energies across broad chemical spaces is probably infeasible (even using machine-learned interatomic potentials) given the wide range of temperatures and compositions that must be sampled. Here, we

present a CALPHAD-inspired approach to reference liquidus curves from experimental ASM phase diagrams to DFT convex hulls from the Materials Project. Using this technique, we fit non-ideal liquid mixing free-energies on a 50x50 matrix of binary alloy phase diagrams. Using very simple machine-learning models, we can then predict liquid free energies in novel chemical spaces, including ternary or quaternary+ spaces, at a computational cost low enough to be integrated with high-throughput DFT databases like the Materials Project. Our technique predicts liquidus curves, intermetallic melting temperatures, and three-phase invariant points (eutectics and peritectics) with surprisingly good accuracy, despite the known magnitude of formation energy errors in DFT convex hulls.

4:00 PM *MT01.08.07

Identifying The Transition State in Structurally Unstable but Dynamically Stabilized Phases: A GPR-Assisted First Principles Methodology
Seyyedfaridoddin Fattahpour and Sara Kadkhodaei; University of Illinois at Chicago, United States

Numerous materials of technological importance feature high-temperature phases that exhibit phonon instabilities. Leading examples include shape-memory alloys, ferroelectric and refractory oxides, and some metal hydrides. I will introduce a new model for diffusion barrier calculation in these phases. Our model efficiently explores the system's diffusive transition path using the dimer scheme based on a Gaussian process regression (GPR) of the temperature-dependent energy surface. Our model simultaneously samples the temperature-dependent energy surface and converges the system towards the saddle point. Our method provides a useful alternative to methods such as molecular dynamics, which directly simulate diffusive hops. I present the application of this model for some example metals and oxides.

References

S. Kadkhodaei and A. Davariashiyani, Phys. Rev. Materials 4, 043802, 2020
Fattahpour, S and Davariashiyani, A and Kadkhodaei, S. Phys. Rev. Materials 6, 023803, 2022

4:30 PM MT01.08.08

Machine Learning and Monte Carlo Simulations of The Gibbs Free Energy of The Fe-C System in a Magnetic Field Ming Li¹, Luke Wirth², Ajinkya Hire¹, Stephen Xie³, Michele Campbell⁴, Dallas Trinkle² and Richard Hennig¹; ¹University of Florida, United States; ²University of Illinois at Urbana-Champaign, United States; ³KBR, Inc., Intelligent Systems Division, NASA Ames Research Center, United States; ⁴University of California-Merced, United States

To model the thermodynamics and kinetics of steels in response to high magnetic fields requires knowledge of the magnetic Gibbs free energy, which involves millions of energy evaluations for the potential energy landscapes as a function of the applied field in the configurational space. Although sufficiently accurate, density-functional theory (DFT) calculations would result in high computational cost, hindering its direct application. To address this challenge, we take advantage of the ultra-fast force field (UF³) method [1], a machine-learning potential that combines effective two- and three-body potentials in a cubic B-spline basis with regularized linear regression, to approximate the DFT energy landscape. We assembled a database by performing DFT calculations using the Vienna Ab initio Simulation Package (VASP). This DFT database focuses on the information of the energies and forces as a function of magnetic field for a series of bcc and fcc Fe(C) structures, throughout which both structural and magnetic configurations are varied. The UF³ potentials are trained on this database to quickly evaluate the energies of ensembles based on the structural and spin configurations, and the accuracy of the resulting UF³ models predicting energies and forces is validated.

Subsequent Monte Carlo simulations take place with these machine learning models implemented. Thermodynamic integration is utilized to combine the simulations at different temperatures to achieve the magnetic Gibbs free energy models for the two Fe(C) phases as a function of temperature, atomic fraction of carbon, and magnetic field. Our calculations aim to investigate the origin of the experimentally observed shift in the transition temperature of tens of kelvins under an applied field of 10 T [2].

[1] Xie, S.R., Rupp, M., and Hennig, R.G., npj Comput Mater 9, 162 (2023)

[2] G. M. Ludtka, DOE technical report ORNL/TM-2005/79 (2005)

4:45 PM MT01.08.09

Engineering Relative Stability in Four Dimensions with The Generalized Clausius-Clapeyron Relation Jiadong Chen and Wenhao Sun; University of Michigan, United States

Sequential learning algorithms based on Bayesian optimization are routinely being deployed for materials stability optimization in high-parameter spaces. We anticipate these optimization methods would perform better if they were built upon stronger priors, for example, as derived from the fundamental thermodynamics underlying the equilibrium behavior of materials. Here, we present a thermodynamics-based technique to optimize the relative stability of a materials in high-dimensional thermodynamic space, based on a new derivation of a generalized high-dimensional Clausius Clapeyron relation. Using this thermodynamic infrastructure, we design several pathways to enhance the relative acid stability of Mn-oxides versus its dissolved states for potential electrochemical catalyst application. We construct a 4-D Pourbaix diagram with pH, redox potential E , particle radius $1/R$ and a chemical potential μ_K as axis. By exploring the gradients of the high-dimensional phase boundaries, we derive first-principles insights that nano-sizing ($1/R$) and certain doping ions (μ_K) can stabilize some metastable Mn-oxides polymorphs, where $1/R$ decreases acid stability and μ_K increases it. Our high-dimensional thermodynamic framework is a general method to engineer relative stability in parameter spaces that leverage multiple forms of thermodynamic work.

SESSION MT01.09: Poster Session I: Machine Learning and Simulations
Session Chairs: Chris Bartel, Rodrigo Freitas, Sara Kadkhodaei and Wenhao Sun
Thursday Afternoon, April 25, 2024
Flex Hall C, Level 2, Summit

5:00 PM MT01.09.01

Rapid Discovery of Lightweight Cellular Crashworthy Solids for Battery Electric Vehicles using Artificial Intelligence and Finite Element Modeling Edward J. Michaud^{1,2} and Dayakar Penumadu²; ¹Volkswagen Group of America, United States; ²The University of Tennessee, Knoxville, United States

Battery electric vehicles (BEVs) offer significant environmental benefits over traditional internal combustion engine (ICE) vehicles, including zero tailpipe emissions and improved energy efficiency. Despite this, typical BEV batteries can weigh up to 500kg, substantially heavier than a conventional vehicle's engine and fuel tank. This makes BEVs great candidates for lightweighting, offering improvements in driving range, acceleration, handling, and overall

efficiency. At the same time, these batteries must be protected from side-impact even further than a conventional ICE vehicle. In this study, we aim to leverage computational modeling and artificial intelligence (AI) methods to lightweight the battery's protective structures beyond capabilities achievable by a typical human. Specifically, we focus on the methods necessary to fully train an artificial intelligence architecture such that models can be rapidly generated and validated hundreds to thousands of times. Ultimately, this research will contribute to the development of more efficient and sustainable BEVs, which can help to mitigate climate change and reduce the environmental impact of transportation while maintaining or improving safety standards.

5:00 PM MT01.09.02

Chemical Environment Modeling Theory: Revolutionizing Machine Learning Force Field with Flexible Reference Points [Xiangyun Lei](#), Weike Ye, Joseph Montoya, Tim Mueller, Linda Hung and Jens Hummelshoerj; Toyota Research Institute, United States

This study introduces the Chemical Environment Modeling Theory (CEMT), a novel and powerful framework that generalizes the theory of machine learning force field (MLFF), which is widely used in atomistic simulations of chemical systems. The flexible and adaptable framework permits reference points to be positioned anywhere within the modeled domain rather than only atom centers, transcending this implicit constraint of traditional MLFFs, and enabling a diverse range of new model architectures. Leveraging Gaussian Multipole (GMP) featurization functions, several models with different reference point sets, including finite difference grid-centered and bond-centered models, were tested to analyze the variance in capabilities intrinsic to models built on distinct reference points. The results underscore the potential of non-atom-centered reference points in force training, revealing variations in prediction accuracy, inference speed, and learning efficiency. It clearly shows that the choice of reference points is an additional dimension of complexity that can be optimized for model performance, on top of environment featurization and model architecture. Finally, a unique connection between CEMT and real-space orbital-free finite element Density Functional Theory (FE-DFT) is established, and the implications include the enhancement of data efficiency and robustness by allowing the leveraging of intermediate results of DFT calculations. This framework could also serve as a cornerstone towards integrating known quantum-mechanical laws into the architecture of ML models.

5:00 PM MT01.09.03

A Self-Improvable Generative AI Platform for the Discovery of Solid Polymer Electrolytes with High Conductivity [Weike Ye](#)¹, Xiangyun Lei¹, Zhenze Yang², Daniel Schweigert¹, Ha-Kyung Kwon¹ and Arash Khajeh¹; ¹Toyota Research Institute, United States; ²Massachusetts Institute of Technology, United States

This study presents a novel generative AI-based approach for the efficient discovery and design of high-performance solid polymer electrolytes, crucial for next-generation battery technologies. The platform integrates three core components: a conditioned generative model, a validation module, and a feedback mechanism, creating a self-improving system for material innovation. To optimize the conditional generative model, we have compared different architectures including both the GPT-based and diffusion-based models, and employed pertaining and fine-tuning training strategies to achieve faster convergence and superior data efficiency. The implementation of validation from full-atom MD simulation and the feedback mechanism allows the platform to refine the output iteratively. We demonstrate that this platform facilitates the generation of hundreds of thousands of novel, diverse, valid, and synthesizable polymers, and more importantly, the effectiveness of the platform is underscored by the identification of 19 polymer repeating units, each displaying a computed ionic conductivity surpassing that of Polyethylene Oxide (PEO).

5:00 PM MT01.09.04

Adaptive Loss Weighting for Machine Learning Interatomic Potentials [Daniel Ocampo](#)¹, Daniela Posso², Reza Namakian¹ and Wei Gao^{1,†}; ¹Texas A&M University, United States; ²The University of Texas at San Antonio, United States

For atomistic simulations, machine learning interatomic potentials (ML-IAPs) have proven to accurately represent potential energy surfaces, overcoming some limitations of empirical force-fields and their functional form. Training such potentials involves optimization of multipart loss functions typically composed of potential energies, forces and stress tensors. However, the contribution of each variable to the total loss is typically weighted using heuristic approaches that yield either iterative or sub-optimal results. Therefore, we implement an adaptive loss weighting algorithm based on a mathematically intuitive and computationally efficient scheme, in which the contribution of each term is dynamically recalculated based on its learning performance; optimizing the imbalance of the widely used, heuristic fixed loss weighting approaches. Additionally, by adding a stress term to the loss function and using high convergence criteria for density functional theory (DFT) calculations we show that a ML-IAP with accurate predictive stress capabilities must include stress information during training. This approach results in more automated neural networks that can learn effectively potential energies, forces and stresses from *ab initio* calculations, producing reliable ML-IAPs that are usable in simulations involving mechanical deformations, phase transformations, or other stress-dependent phenomena.

5:00 PM MT01.09.05

High-Accurate and -Efficient Potential for BCC Iron based on The Physically Informed Artificial Neural Networks [Meng Zhang](#), Koki Hibi and Junya Inoue; The University of Tokyo, Japan

Atomic forces and energies, calculated by interatomic potential, are fundamental components of molecular dynamics (MD) and Monte Carlo (MC) simulations. Compared with traditional potential, machine learning (ML) potentials trained on extensive DFT databases offer enhanced accuracy in predicting physical and chemical properties of materials, but their transferability often faces constraints. To address this limitation, physically informed neural network (PINN) potentials have emerged. These models synergistically combine the strengths of ML with physics-based bond-order interatomic potentials, aiming for both improved accuracy and broader applicability. However, a major hurdle remains: the low performance of PINN potentials, hindering large-scale simulations. This work introduces a novel approach that significantly improves the performance of PINN potentials. The developed PINN potential for body-centered cubic (BCC) iron demonstrates exceptional accuracy in property predictions while boasting remarkable computational efficiency. Its performance overcomes both 12-MPI CPU-only ML potentials and GPU-accelerated ML potentials by achieving speedups of 168x and 22x, respectively. The proposed approach has a potential to provide a powerful way to develop high-performance and high-accuracy potentials even in the other systems.

5:00 PM MT01.09.06

Molecular Dynamics Simulation of HF Etching of Amorphous Si₃N₄ Using Neural Network Potential [Changho Hong](#), Sangmin Oh and Seungwu Han; Seoul National University, Korea (the Republic of)

Dry etching plays a key role in the fabrication of semiconductor devices. Recently, the requirement of high aspect ratios (40–60) of deep-trench structures and the introduction of through-silicon vias for 3D circuit integration demand precise etching control. Traditional macroscale models, such as the level set and Monte Carlo-based methods, have been employed to predict the outcomes of process parameter optimization. However, phenomenological fitting of model parameters can result in inaccurate predictions of feature profiles due to the omission of detailed chemical processes. Molecular dynamics (MD)

simulations can offer a close look into atomic processes in ion etching, overcoming the trial-and-error approaches for parameter determination in macroscopic interaction models. Classical potentials are an option but have limitations in both availability and accuracy. Density functional theory (DFT), although highly accurate, is computationally prohibitive for large-scale simulations. Recent advances in machine-learning potentials (MLPs) have demonstrated their efficacy in simulations involving surface catalysis, physical sputtering, and surface oxidation processes. However, application of MLPs for etching reactions between ions and solid-state materials is currently lacking. This is attributed to the complexity of predicting chemical reaction pathways, which creates challenges in constructing training sets for MLPs.

In this study, we investigate the mechanisms underlying Si_3N_4 etching by HF ions using MD simulations driven by a neural network potential (NNP). The NNPs are trained using SIMPLE-NN package. The training set is constructed through manual curation of relevant atomic environments and an iterative training process. The basic constituents of atomic configurations are both crystalline and amorphous bulk structures, as well as their slab counterparts. Additionally, guided MD is employed to sample the chemical reactions between HF molecules and the Si_3N_4 substrate; here, hydrogen and fluorine are displaced toward nitrogen and silicon respectively based on the assumption of bond preference. Alongside guided MD, high-temperature MD of a slab is used to facilitate the sampling of diverse local atomic environments that may emerge during energetic ion collisions. Using manually curated training sets, NNPs are iteratively validated and refined. This refinement is achieved by incorporating structures from NNP trajectories that exhibit significant energy discrepancies when compared against DFT calculations. Utilizing this optimized NNP, we conduct etching simulations on 4 nm^2 amorphous Si_3N_4 substrates over a 5 ns timescale, and analyze characteristics such as etching yield and surface modification. Our results demonstrate a square-root dependence of the etching yield on the incident energy. Furthermore, we observe modifications at the topmost surface, where the ratio of Si to N is 1:1. This ratio is intriguingly similar to observations from experimental studies utilizing different reactive plasma species. The primary etch products at normal incidence are SiF_2 , SiF_4 , N_2 , and NH_3 . This behavior is attributed to chemical sputtering, in which the surface is significantly modified by incoming reactive species, becoming susceptible to chemical etching. In contrast, at high angles of incidence, the surface remains largely unmodified, with the primary etch products being lower-coordinated molecules of Si and N, along with N_2 molecules. This suggests that under these conditions, the etching is more affected by physical sputtering. Our methodology offers a cost-efficient approach to achieving DFT-level accuracy in MD simulations, thereby elucidating etching mechanisms and contributing to the optimization of the etching process.

5:00 PM MT01.09.07

Deep Potential Model for Analyzing Enhancement of Lithium Dynamics at Ionic Liquid and Perovskite (BaTiO_3) Interface [Anseong Park](#), Sangdeok Kim, Chanui Park, Woojin Kang, Seungtae Kim and Won Bo Lee; Seoul National University, Korea (the Republic of)

Recently, ab-initio molecular dynamics (AIMD) based DeePMD (DPMD) potential has not only improved computational accuracy and speed but has also overcome the limitations of traditional force-field-based methods. In this study, we will discuss the technical details and considerations for utilizing this deep learning-based force field, particularly in multi-component systems such as ionic liquids. We will compare the results of structural & dynamical properties calculated from traditional force fields, scaled charge force fields, polarizable force fields, and DPMD force fields.

Finally, we will apply the DPMD force field to an ionic liquid and perovskite interface system, which is virtually impossible to simulate from using traditional force fields. Experiments have shown that the hybrid solid electrolyte (HSE), consisting of nanoscale perovskite particles mixed with an ionic liquid (IL), exhibits excellent flame retardancy, thermal stability, and improved ionic conductivity compared to pure IL electrolyte. We will analyze the structural and dynamical differences induced by the perovskite interface in comparison to bulk ionic liquid using DPMD force field simulations.

5:00 PM MT01.09.08

Autonomous AI generator for Machine Learning Interatomic Potentials [Bowen Zheng](#) and Grace Gu; University of California, Berkeley, United States

Machine learning interatomic potentials (MLIPs), which predict the system potential energy given an atomic configuration, have profoundly improved the accuracy and efficiency of molecular simulations. Learning from high-fidelity quantum chemistry-based data while interfacing with classical simulation frameworks, MLIPs inherit the quantum-level accuracy and the efficiency of classical molecular dynamics, achieving the best of both worlds. In recent years, MLIPs have witnessed great research efforts and various types of MLIPs have been proposed, tested, and documented. However, the development of MLIPs has largely been a manual, *ad hoc* process. Additionally, effective MLIPs are either scattered in online repositories such as Git-Hub or provided as supplementary materials of publications, making them difficult to locate and retrieve when needed. Here, we aim to create an autonomous AI generator for MLIPs, which consists of a Searcher, a Trainer, and an Evaluator. Given a request, for example, "generate an MLIP for Indium phosphide system", the Searcher is first up to the task, looking for available MLIPs online via web scraping or APIs. If such MLIPs do not exist, the Trainer then performs the following tasks in sequence autonomously: select an MLIP template (such as a neural network or a SNAP MLIP, upon request or by certain criteria), generate DFT-MD training trajectories, and train the MLIP. For an MLIP returned either by the Searcher or the Trainer, the Evaluator calculates various accuracy metrics such as the mean absolute errors (MAEs) and R-squared values. It is also viable to request training multiple types of MLIPs and compare their performances. Lastly, we propose a large language model (LLM)-based agent named ChatMLIP which accepts textual user requests and delivers appropriate responses. By way of AI, the present work may accelerate the development of MLIPs and potentially benefit broader research fields like carbon capture, protein engineering, drug discovery, among others.

5:00 PM MT01.09.10

Benchmarking, Visualization and Hyperparameter Optimization of UF_3 to Enhance Molecular Dynamics Simulations [Pawan Prakash](#), Ajinkya Hire and Richard Hennig; University of Florida, United States

Ab initio methods offer great promise for materials design, but they come with a hefty computational cost. Recent advances with machine learning potentials (MLPs) have revolutionized molecular dynamic simulations by providing high accuracies approaching those of ab initio models but at much reduced computational cost. Our study evaluates the ultra-fast potential (UF_3), employing linear regression with cubic B-spline basis for learning effective two- and three-body potentials. On benchmarking, UF_3 displays comparable precision to established models like GAP, MTP, NNP (Behler Parrinello), and qSNAP MLPs, yet is significantly faster by two to three orders of magnitude. A distinct feature of UF_3 is its capability to render visual representations of learned two- and three-body potentials, shedding light on potential gaps in the learning model. In refining UF_3 's performance, a comprehensive sweep of the hyperparameter space was undertaken, emphasizing finer granularity in zones indicative of optimal performance. This endeavor aims to provide insights into the smoothness of the UF_3 hyperparameter space, and offer users a foundational default set of hyperparameters as a starting point for optimization. While our current optimizations are concentrated on energies and forces, we are primed to broaden UF_3 's evaluation spectrum, focusing on its applicability in Molecular Dynamics simulations. The outcome of these investigations will not only enhance the predictability and usability of UF_3 but also pave the way for its broader applications in advanced materials discovery and simulations.

5:00 PM MT01.09.11

Generating Statistically Equivalent Thermal Spray Coatings Using Bayesian Optimization [David Montes de Oca Zapiain](#), Anh Tran, Nathan W. Moore and Theron Rodgers; Sandia National Laboratories, United States

Thermal spray deposition is an inherently stochastic manufacturing process used for generating thick coatings of metals, ceramics and composites. The generated coatings exhibit complex internal structures that affect the overall properties of the coating. The deposition process can be adequately simulated using rules-based process simulations. Nevertheless, in order for the simulation to accurately model particle spreading upon deposition, a set of pre-defined rules and parameters need to be calibrated to the specific material and processing conditions of interest. The calibration process is not trivial given the fact that many parameters do not correspond directly to experimentally measurable quantities. This work presents a protocol that automatically calibrates the parameters and rules of a given simulation in order to generate the synthetic microstructures with the closest statistics to an experimentally generated coating. The protocol starts by quantifying the internal structure using 2-point statistics and then representing it in a low-dimensional space using Principal Component Analysis. Subsequently, our protocol leverages Bayesian optimization to determine the parameters that yield the minimum distance between synthetic microstructure and the experimental coating in the low-dimensional space.

Sandia National Laboratories is a multi-mission laboratory managed and operated by National Technology and Engineering Solutions of Sandia, LLC., a wholly owned subsidiary of Honeywell International, Inc., for the U.S. Department of Energy National Nuclear Security Administration under contract DE-NA0003525. The views expressed in the article do not necessarily represent the views of the U.S. Department of Energy or the United States Government. SAND No. SAND2023-10921A

5:00 PM MT01.09.12

Anisotropic Assembly of Nanoparticles Explored through Molecular Dynamics Simulations, Global Optimizations and Machine Learning

Methods [Yilong Zhou](#)^{1,2}, [Tsungyeh Tang](#)³, [Sigbjorn L. Bore](#)³, [Francesco Paesani](#)³ and [Gaurav Arya](#)²; ¹Lawrence Livermore National Laboratory, United States; ²Duke University, United States; ³University of California, San Diego, United States

Novel applications of polymer nanocomposites like plasmonics often require anisotropic organization of nanoparticles (NPs) in polymers. However, achieving unique anisotropic assemblies of NPs in polymers is challenging since NPs tend to self-assemble into three-dimensional close-packed aggregates. In this work, we tackle this challenge of achieving anisotropic NP assembly in polymers through a combination of molecular dynamics (MD) simulations, global optimization, and machine learning. First, we present a new strategy for assembling NPs into anisotropic architectures in polymer matrices, which leverages the interfacial tension between two mutually immiscible polymers forming a bilayer and differences in the relative miscibility of polymer grafts with the two polymer layers to confine NPs within 2d planes parallel to the interface.¹ Through coarse-grained (CG) MD simulations, we demonstrate this strategy, showcasing the assembly of NP clusters, such as trimers with tunable bending angle and anisotropic macroscopic phases, including serpentine and branched structures, ridged hexagonal monolayers, and square-ordered bilayers. The above MD simulations are however inefficient for determining the equilibrium structures of NP assemblies, particularly those involving many particles or complex unit cells. To address this issue, we adapt the efficient Basin-hopping Monte Carlo algorithm to locate the global minimum energy configurations of NPs at interface, allowing us to explore the full breadth of NP structures possible at interface and uncovering many unique NP structures.² While exploring the assembly of polymer-grafted NPs at polymer interfaces using explicit CG MD simulations, we observe that many-body effects play an important role in the formation of quasi-1d structures. However, explicit modeling of the polymer grafts and melt chains is highly computationally expensive, even using CG models. We thus introduce a machine learning approach to develop an analytical potential that can describe many-body interactions between polymer-grafted NPs in a polymer matrix. The developed potential reduces the computational cost by several orders of magnitude and thus allows us to explore NP assembly at large length and time scales. Overall, the anisotropic NP structures discovered in this study hold significant potential for applications in various fields, including plasmonics, electronics, optics, and catalysis, where precise and anisotropic NP arrangements within polymers are essential for achieving desired functionalities.

[1] Tang, T. Y., Zhou, Y., & Arya, G. (2019). Interfacial assembly of tunable anisotropic nanoparticle architectures. *ACS nano*, 13(4), 4111–4123.

[2] Zhou, Y., & Arya, G. (2022). Discovery of two-dimensional binary nanoparticle superlattices using global Monte Carlo optimization. *Nature Communications*, 13(1), 7976.

Portion of the work was performed under the auspices of the U.S. Department of Energy by Lawrence Livermore National Laboratory under Contract Number DE-AC52-07NA27344.

5:00 PM MT01.09.13

Differentiable Gaussian Process Force Constants [Keerati Keeratikam](#) and [Jarvist M. Frost](#); Imperial College London, United Kingdom

The finite temperature properties of matter requires understanding thermal motion. In crystals this can be described by representing the collective excitation of the centre of mass motion as a phonon. Phonon frequencies (Energies) in the harmonic approximation come from the second order force constants (FC) of the potential energy surface (PES). The standard approach is to use a finite displacement method (FDM). Anharmonic contributions (required for finite thermal conductivity) require higher order force constants. FDM-based calculations scale poorly both with the size of the system, and the order of the force constants[1]. As an alternative approach, we can use a more sophisticated surrogate potential energy surface model [2].

Gaussian processes (GPs) are a supervised machine learning method which can describe an arbitrary function. GPs are naturally Bayesian (probabilistic). Our reference data is the electronic structure from which conditions the model (training) [3, 4].

Due to the underlying Gaussian form of a GP, the model is infinitely differentiable [5, 6]. This allows the model to be trained directly on forces (the derivative of energy), reducing the number of calculations required for a given accuracy of PES evaluation [7-9]. This differentiation can be extended to compute the second and the third derivative of PESs (harmonics and cubic anharmonic FCs) by using automatic differentiation (AD). By performing linear operations between arbitrary derivative orders of the GP, the covariance functions among PESs, forces and those FCs can be calculated.

We implement this method in the Julia language, in our `GPFC.jl` package. We first use our technique of anharmonic property calculations of Si, NaCl and PbTe which their atomic environments are represented on atomic Cartesian coordinates. To impose their space group symmetry, phonon coordinate representations are then used to describe the environment of these three materials resulting in faster convergence of anharmonic properties. To further impose a three-dimensional rotation symmetry, we aim to use an SO(3) representation (such as spherical harmonics) with our GP method to achieve accurate FCs with less data [3, 10]. We compare our results to standard approach of FDM (in `Phono(3)py.py`) [2] and cluster expansion (`HiPhive.py`) [11].

References

[1] A. Togo, L. Chaput and I. Tanaka, Distributions of phonon lifetimes in brillouin zones, *Physical Review B* 91 (2015) .

- [2] A. Togo et al., Implementation strategies in phonopy and phono3py, *Journal of Physics: Condensed Matter* 35 (2023) 353001.
[3] A.P. Bartók et al., Gaussian approximation potentials: A brief tutorial introduction, *International Journal of Quantum Chemistry* 115 (2015) 1051.
[4] H. Sugisawa et al., Gaussian process model of 51-dimensional potential energy surface for protonated imidazole dimer, *The Journal of Chemical Physics* 153 (2020) 114101.
[5] E. Solak et al., Derivative observations in Gaussian Process Models of Dynamic Systems, *NIPS'02: Proceedings of the 15th International Conference on Neural Information Processing Systems* (2002) 8.
[6] A. McHutchon, *Differentiating Gaussian Processes*.
[7] E. Garijo del Rífo et al., Local Bayesian optimizer for atomic structures, *Physical Review B* 100 (2019) 104103.
[8] S. Kaappa et al., Global optimization of atomic structures with gradient-enhanced gaussian process regression, *Physical Review B* 103 (2021) .
[9] K. Asnaashari et al., Gradient domain machine learning with composite kernels: improving the accuracy of PES and force fields for large molecules, *Machine Learning: Science and Technology* 3 (2021) 015005.
[10] V.L. Deringer et al., Gaussian process regression for materials and molecules, *Chemical Reviews* 121 (2021) 10073.
[11] F. Eriksson et al., The hiphive package for the extraction of high-order force constants by machine learning, *Advanced Theory and Simulations* 2 (2019) .

5:00 PM MT01.09.14

Understanding The Interplay between Anion Dynamics and Proton Conduction in Solid-Acid Compounds Using Machine Learning Molecular Dynamics Menghang (David) Wang¹, Cameron J. Owen¹, Grace Xiong², Jingxuan Ding¹, Yu Xie¹, Simon L. Batzner¹, Albert Musaelian¹, Anders Johansson¹, Nicola Molinari¹, Ni Zhan³, Ryan P. Adams³, Sossina M. Haile² and Boris Kozinsky¹; ¹Harvard University, United States; ²Northwestern University, United States; ³Princeton University, United States

Solid acid materials play a pivotal role as electrolytes for intermediate temperature hydrogen fuel cells. However, our current understanding of the relevant atomic motions that govern proton conduction remains incomplete, necessitating further investigation in different solid acid compounds. It is imperative to explore the atomic-scale correlation between anion and proton dynamics to design novel solid acid compounds with high proton conductivity.

In the superprotonic phase, solid acid proton conductors exhibit intricate behaviors, characterized by local proton hops in the O-H...O bond and anion reorientation. These phenomena comprise a two-step process necessary for long-range proton motion. Existing computational studies treat anion and proton dynamics as independent processes, while we find strong correlations between anion and proton dynamics in both CsH₂PO₄ (CDP) and CsHSO₄ (CHS) from machine learning molecular dynamics over nanosecond timescales. Achieving a nanosecond timescale is crucial to comprehensively study the diffusive regime. We observe that not all anion reorientations contribute to long-range proton motion, underscoring its multifaceted role in superprotonic behavior. Additionally, the contribution of anion reorientations to long-range proton motion exhibits distinctive characteristics in CDP and CHS. Furthermore, we confirm a significant O-H reorientation preceding the long-range proton motion, substantiating a previously hypothesized but unverified process. Our approach leverages machine learning interatomic force fields (MLFFs) developed through uncertainty-aware active learning [1] and equivariant neural networks [2]. By combining ab-initio precision with simulations of thousands of atoms over nanosecond timescales, our MLFFs support our findings on the correlations of anion dynamics and the long-range proton transfer with sufficient statistics.

This work bridges crucial knowledge gaps in the superprotonic behavior of solid acid proton conductors and has the potential to inform the design of advanced solid acid compounds for renewable energy technologies.

- [1] Xie, Y., Vandermause, J., Ramakers, S. et al. Uncertainty-aware molecular dynamics from Bayesian active learning for phase transformations and thermal transport in SiC. *npj Comput Mater* 9, 36 (2023).
[2] A. Musaelian, S. Batzner, A. Johansson, L. Sun, C. Owen, M. Kornbluth, and B. Kozinsky, Learning local equivariant representations for large-scale atomistic dynamics *Nat. Commun.*, 14, 579 (2023)

5:00 PM MT01.09.15

CRowdsourced Materials Data Engine for Unpublished X-Ray Diffraction Data Abhishek Daundkar, Mengying Wang, Hanchao Ma, Yiyang Bian, Alp Sehirlioglu and Yinghui Wu; Case Western Reserve University, United States

Modern multidisciplinary materials science routinely processes scientific workflows integrating different data resources (e.g., X-ray data, scripts, analytical results). This data resources are underutilized and sometimes tagged as ineffectual for the source problem. We propose to tackle the fundamental challenges of data-driven material science such as accessing extensive experimental data and relationship to the processing techniques of the discovered materials. Majority of machine learning models require significant number of training data that is not necessarily generated in materials research. Inspired by past work on discovery of high temperature piezoelectrics where the distributed nature of training and testing data was highlighted, we are creating CRUX, a CRowdsourced Materials Data Engine for Unpublished X-Ray Diffraction (XRD) to innovate and boost the utilization of this high-quality, unpublished material science data in collaboration with our industry partners and developer community. The core of CRUX is a materials knowledge graph (a semantic network of materials entities and their semantic relationships), build upon the materials data and materials ontology specifically developed to capture the processing meta-data. This knowledge graph represents abstract factual knowledge from XRD datasets, answers queries, and self-evolves to recommend newly shared datasets and facilitating the feature of querying itself to help users explore the underlying materials datasets. When working with materials research data the objective is to collect the most amount of critical data without overburdening the user submitting the information. We aim to enable a materials knowledge graph (KG) model, automatic data integration, and an exploratory query engine that support "Why" and "What-if" analysis for XRD analysis. As we expand on the experimental/modeling dataset we unleash the full potential of the data engine regardless of the state of model implemented for analysis. CRUX will enable an open, collaborative, and sustainable platform that can facilitate exchanging of unpublished XRD data and unlock new research problems (e.g., prediction of materials compositions with multi-phase data), and inspire the novel design of ML pipelines for data-driven materials science.

5:00 PM MT01.09.16

Do Computed Grain Boundary Energies Depend on Interatomic Potentials? Universal Trends Employing EAM-X Yasir Mahmood¹, Murray Daw¹, Michael Chandross² and Fadi Abdeljawad³; ¹Clemson University, United States; ²Sandia National Laboratories, United States; ³Lehigh University, United States

It is well established that grain boundaries (GBs) greatly influence the observable properties of a wide range of engineering and functional materials. Classical atomistic simulations employing the Embedded Atom Method (EAM) have emerged as a powerful technique to simulate GB phenomena. However, folded into such simulations is the dependency of GB structure and properties on the particular choice of EAM parameters. To address this question, we follow a direction of investigation that has not been generally explored, namely we simplify the EAM function space to a small but efficient set of parameters, called EAM-X [1]. Then, we study a set of GBs with various geometries and calculate their energies in the complete EAM-X parameter

space. We find that variations in GB energy with EAM parameters can be larger than variations due to GB geometry; an effect that has not been quantified before. The atomistic data are used to determine a fit of the GB energy in EAM parameter space, which can be used to obtain boundary energies in real FCC elements by selecting corresponding points in this parameter space. We find generally at best a moderate correlation between GB energy and shear moduli, and we discuss the relationship to prior work along these lines. Our work highlights the need to consider sensitivity to details of empirical potentials when performing quantitative studies of GB physics. *SNL is managed and operated by NTESS under DOE NNSA contract DE-NA0003525 (SAND2022-1056 A).*

[1] M. S. Daw, and M. Chandross. "Simple parameterization of embedded atom method potentials for FCC metals." *Acta Materialia* 248 (2023): 118771.

5:00 PM MT01.09.17

Atomistic Modeling of Bulk and Grain Boundary Diffusion for Solid Electrolyte Li₆PS₅Cl Accelerated by Machine-Learning Interatomic Potentials Yongliang Ou¹, Yuji Ikeda¹, Sergiy Divinsky² and Blazej Grabowski¹; ¹University of Stuttgart, Germany; ²University of Münster, Germany

Li₆PS₅Cl is a promising candidate for the solid electrolyte in all-solid-state lithium-ion batteries. For applications, this material is in a polycrystalline state with many grain boundaries (GBs) rather than an idealized single-crystalline state. Atomistic simulations of Li₆PS₅Cl with GBs, however, remain rare due to high computational cost. In this study, machine-learning interatomic potentials, specifically moment tensor potentials (MTPs) [1], are employed to accelerate the simulations while preserving the *ab initio* accuracy. In the initial stage, energies and forces of a small number of configurations are generated under the *ab initio* framework. MTPs are then fitted to the *ab initio* data, and active learning techniques are used to further stabilize the MTPs. The usage of MTPs enables molecular dynamics (MD) simulations in larger system sizes (up to 20 000 atoms) and longer time scales (several ns). Two tilt GBs Σ3[110]/(1-12), Σ3[110]/(-111) and one twist GB Σ5[001]/(001) are focused on, all of which show relatively low GB energies and an enhanced ionic conductivity for Li compared to bulk. Diffusion mechanisms specific to each GB are analyzed. This research offers new insights into the design of solid electrolytes through GB engineering and emphasizes the importance of considering GBs for materials modeling.

[1] A.V. Shapeev, *Multiscale Modeling & Simulation* **14**, 1153 (2016).

5:00 PM MT01.09.18

Exploring Reaction Pathways for Wet-Alkaline Etching of GaN with Machine-Learned Potential Purun-hanul Kim¹, Youngho Kang² and Seungwu Han^{1,3}; ¹Seoul National University, Korea (the Republic of); ²Incheon National University, Korea (the Republic of); ³Korea Institute for Advanced Study, Korea (the Republic of)

Micro-sized light-emitting diodes (μLEDs) based on gallium nitride (GaN) are building blocks for the development of augmented reality and virtual reality displays in our hyperconnected society. However, owing to the high surface-to-volume ratio, μLEDs are susceptible to surface defects, resulting in significantly lower performance compared to bulk LEDs. The surface structure of μLEDs is profoundly influenced by wet-etching processes in alkaline environments which are essential for fabricating microscale GaN. Hence, understanding the etching mechanism is pivotal to establishing optimal etching processes for μLED production. However, it remains elusive because of difficulties in experimental characterization and analysis. While *ab initio* molecular dynamics (AIMD) based on density functional theory (DFT) have been widely employed to investigate chemical reactions at an atomic level, they have limitations in terms of the system size and simulation-time scale. As such, AIMD is inadequate to explore intricate and diverse chemical reactions occurring at an interface between the solution and GaN during wet etching. Recently, Behler-Parrinello-type neural-network potential (NNP) based MD has emerged as an effective approach to overcome the limitations of AIMD. In this work, we explore wet etching of GaN using the NNP-MD simulation that is thousands of times faster than AIMD. To construct an accurate and reliable NNP for simulating etching processes, we generate a training set by sampling AIMD trajectories of GaN surface, KOH aqueous solution, and their interface models at wide ranges of temperature and pressure encompassing supercritical phase. Then, the NNP is trained using the in-house SIMPLE-NN code to reproduce the DFT energies, forces, and stress tensors. The generated NNP is thoroughly validated by comparing the results with DFT calculations. Afterward, we perform NNP-MD simulations to investigate the etching of GaN polar and nonpolar surfaces immersed in KOH solution applying a high-temperature and high-pressure to accelerate chemical reactions. Our simulation directly shows that an alkaline wet etching process transforms the slanted surface into the *m*-surface, which is consistent with experiments. Furthermore, the relative etching rates of different surface facets obtained from our simulations agree well with experiments. From the analysis of the atomic trajectories, we reveal the wet-etching mechanism of GaN surfaces in which the attachment of OH⁻ (*aq*) to surface Ga and subsequent passivation of a neighboring N dangling bond by H⁺ (*aq*) are the key processes. By providing atomic-scale insights into etching processes and surface structures of GaN that cannot be obtained with conventional DFT methods, our work will help develop high-performance μLEDs.

5:00 PM MT01.09.19

Open Large Language Models in The Service of Material Science Vineeth Venugopal and Elsa O; Massachusetts Institute of Technology, United States

The application of Open Large Language Models (LLMs) in material science is revolutionizing the traditional methodologies employed in Named Entity Recognition (NER), classification, and information extraction tasks. This study aims to explore the expansive capabilities and performance limitations of LLMs in the realm of material science, underlining their role in the creation of automated databases via Retrieval-Augmented Generation (RAG) pipelines and probing their behavior through the examination of activation functions.

LLMs are increasingly being used to automate the extraction of valuable insights from the expansive corpus of material science literature. They demonstrate high efficiency in NER tasks, effectively identifying and categorizing terminologies, material properties, and synthesis parameters. These capabilities extend to classification tasks, where LLMs can sort documents or data points based on pre-defined categories, such as material type, structural characteristics, or application domains.

Despite these promising features, LLMs are not without their limitations. One critical issue pertains to their tendency to produce spurious or "hallucinated" outputs. To mitigate this, our study incorporates ensemble methods and evaluates the outputs through metrics like F1-score for classification tasks and ROGUE-L score for text generation tasks.

The RAG pipeline is a notable development, automating the database creation process by combining the strengths of both retrieval and generation modules. We particularly focus on the application of RAG in creating a high-throughput, structured database of material structure-property-processing parameters. The RAG pipeline leverages LLMs to encode text documents into a large vector database. Queries, specified in natural language, are transformed into vector embeddings, followed by a vector similarity search. The output is then aggregated and structured, serving as a robust database for further scientific research.

To deepen our understanding of LLM behavior, we also investigate the activation functions within these neural networks. By scrutinizing how different layers and nodes respond to specific input types, we gain valuable insights into the model's interpretability and reliability. This examination allows us to optimize the model's performance further and provides a diagnostic tool for understanding the complexities inherent in LLMs.

In conclusion, this study offers a comprehensive evaluation of the utility and limitations of Open Large Language Models in material science. It elaborates on their role in automating complex NER, classification, and information extraction tasks, their implementation in RAG pipelines for database creation,

and the insights gained from analyzing their activation functions. As material science stands to gain significantly from these advancements, understanding and optimizing LLMs can pave the way for more efficient and accurate research methodologies.

5:00 PM MT01.09.20

Developing and Optimizing an Ultra-Fast Force Field (UF3) for Modeling The Crystallization of Amorphous Silicon Nitride Jason B. Gibson¹, Tesia Janicki², Ajinkya Hire¹, Christopher Bishop², J. Matthew D. Lane² and Richard Hennig¹; ¹University of Florida, United States; ²Sandia National Laboratories, United States

Crystallization of amorphous silicon nitride, as observed experimentally, can alter material properties in microelectronics process conditions as a layer-stacked component. Understanding the crystallization mechanism mandates a multi-scale approach in which quantum simulations inform atomistic simulations, which further inform continuum scale simulations and subsequently, experimental work. This talk will detail the progress and challenges faced in developing an Ultra-Fast Force Field (UF3) specifically designed to bridge quantum and atomistic simulations for the Si-N material system. The UF3 integrates effective many-body potentials within a cubic B-spline framework with regularized linear regression, creating a fast and interpretable machine-learned potential (MLP). First, we will cover the nuanced requirements of the MLP's training data: it needs to be diverse enough to avoid overfitting to Si₃N₄ stoichiometry, while maintaining enough specificity to prevent unneeded generalizations across the entire Si-N compositional range. Following this, we leverage the interpretability of UF3's 2/3-body terms to understand the MLP's behavior and identify areas for improvement. The presentation will conclude by detailing the simulation results that were used to validate the MLP and an analysis of the simulated crystallization results of the final MLP.

Sandia National Laboratories is a multimission laboratory managed and operated by National Technology and Engineering Solutions of Sandia, LLC, a wholly owned subsidiary of Honeywell International, Inc., for the U.S. Department of Energy's National Nuclear Security Administration under contract DE-NA-0003525.

5:00 PM MT01.09.21

Navigating Transition Path Sampling with Machine Learning Potentials: Insights and Challenges Nikita Fedik, Wei Li, Nicholas Lubbers, Benjamin Nebgen, Sergei Tretiak and Ying Wai Li; Los Alamos National Laboratory, United States

In the realm of molecular dynamics, capturing elusive transitions and unveiling potential energy landscapes is a paramount pursuit. Reactive events that lead a system from state A to state B through a transition path are often masked by an ensemble of energetically similar pathways. Transition path sampling (TPS) emerges as a potent tool to uncover these paths, although their infrequency in simulations due to high energy requirements and limited statistical occurrence remains a hurdle.

Machine learning potentials offer a promising avenue to model and discern these intricate transition paths, opening the door to new possibilities. The question that arises is: how do we select the right model and data?

Diverse machine learning potentials, such as HIPNN and ANI, have been shown to yield varying transition paths during sampling. An illustration is found in our exploration of alanine dipeptide, a system replete with multiple dihedral degrees of freedom. Intriguingly, even when accuracy metrics like mean absolute error (MAE) and root mean square error (RMSE) align, these static metrics assessed on a portion of the dataset may not suffice to identify the superior model. They serve as preliminary benchmarks, rather than comprehensive tests of model performance.

One avenue toward superior performance emerges through active learning sampling in the transition region. Our demonstrated approach significantly bolsters accuracy, reducing energy errors to a remarkable 0.5 kcal/mol. However, the path to progress is paved with caution when selecting transition paths for machine learning model testing. We emphasize this point using the example of azobenzene, a seemingly uncomplicated system with limited degrees of freedom, yet it poses a significant challenge for electronic structure calculations. Machine learning results may appear in perfect alignment with easily calculable paths, but this can be misleading if the unique open-shell nature of the transition state is overlooked. Establishing reliable benchmarks for machine learning, particularly in the context of transition path sampling, remains an intricate and ongoing endeavor.

Armed with these lessons of caution, our aim is to cultivate a deeper understanding of how to assess the accuracy of machine learning models in dynamical processes.

5:00 PM MT01.09.22

ChemChat | Conversational Expert Assistant in Material Science and Data Visualization Tim Erdmann, Sarathkrishna Swaminathan, Stefan Zecevic, Brandi Ransom and Nathan Park; IBM Research, United States

In recent decades, remarkable advancements have been made in the field of computational chemistry and machine learning (ML), yielding a plethora of sophisticated tools and artificial intelligence (AI) models. Despite their potential, these resources have yet to be fully harnessed due to their steep learning curves and their tendency to operate in isolation. Furthermore, the need for capabilities in programming and ML constitute access barriers to the targeted community – often experimental scientists. Concurrently, the advent of large-language models (LLMs) like (Chat)GPT has been revolutionizing various domains. Nevertheless, their efficacy in addressing chemistry-related challenges has been limited. Especially, these models lack knowledge about scientific workflows and the employed operations (e.g. in drug discovery), access to information sources providing up-to-date data, and the ability to accurately reference – but tend to hallucinate in their responses – what questions credibility, trust, and applicability. However, this crucial gap between AI and science can be overcome by integrating task-specific agents into the LLM-powered conversational application and allowing the LLM to reason over their appropriate usage based on provided instructions. It can be anticipated that this will result in a significant increase in the utilization of the developed cheminformatic tools and AI models and contribute to the scientific discovery overall.

Here, we present ChemChat, a web application and conversational assistant with a chatbot-driven user interface that is powered by non-GPT/OpenAI LLMs. Through the integration of existing cheminformatics tools and expert-developed AI models such as PubChem, CIRCA, RDKit, GT4SD, RXN, MolFormer and other knowledge sources the application is capable of assisting material scientists in tasks like property calculations, tailored design of molecules, retrosynthesis, forward reaction planning, data visualization, and literature research. Central to the talk we will be demonstrating use case-specific capabilities in comparison to related applications and the architecture and workflow behind ChemChat.

5:00 PM MT01.09.23

N-Body Fourier-Sampled Kernel for Machine Learning Potential Alexandre J. Dézaphie^{1,2}, Anruo Zhong¹, Clovis Lapointe¹, Alexandra Goryaeva¹, Jerome Creuze² and Mihai-Cosmin Marinica¹; ¹CEA, France; ²ICMMO, France

Irradiation induces the formation of vacancy and interstitial defects in crystalline materials, which can aggregate into larger clusters. The structure and mobility of self-interstitial clusters remain a largely unresolved issue. For the past 60 years, the scientific community has regarded the formation of interstitial clusters in metallic materials as an accumulation of mono-interstitials that, through diffusion, can aggregate into 2D dislocation loops with a well-defined Burgers vector, progressively growing to observable nanoscale sizes. Recently, we have shown that interstitial clusters in face centered cubic (FCC) metals can aggregate into 3D objects with a well-defined underlying crystallographic structure that ultimately dissociates into dislocation loops [1]. This results complete the puzzle of compact phase accumulation under irradiation, previously emphasized in body centered cubic metals (BCC) [2] and

seems to be a general phenomenon.

Further understanding the aging of these newly discovered nano-phases requires precise, large-scale molecular dynamics simulations. Studying the recombination mechanism of atomic scale defects into dislocations, as well as dislocation maturation, necessitates the development of new interatomic potentials. Machine learning potentials offer a compelling solution for atomistic simulations due to their unique ability to balance precision with computational efficiency. Therefore, we have embarked on the development of an innovative machine learning potential within the framework of kernel regression. The strength of our method is derived from: (i) introducing a novel descriptor that captures the many-body aspects of the metallic interatomic force fields, up to 5-body terms. To maintain invariance within the description of this local atomic environment, we employ and reformulate the permutation-invariant polynomials [3]. And (ii) solving the kernel regression in the descriptor space through the kernel-sampled Fourier transform method, avoiding the need for large matrix inversion. This force field was implemented in the Machine Learning Dynamics framework [4]. The intriguing aspect here is that while each of these approaches has previously existed independently, their integration marks a potential watershed moment, ushering in a new horizon of opportunities for atomistic simulations.

To investigate the mechanism governing the formation of compact clusters within FCC and BCC crystals, we conducted a series of simulations based on the newly developed interatomic potential. The kinetics of these processes were delineated through extensive molecular dynamics simulations at finite temperatures in Fe, Ni, and Al. Furthermore, we assessed the relative stability of these clusters through free energy calculations [5]. Lastly, we are actively engaged in the pursuit of intermediate states within the recombination mechanism of these nanophases. To achieve this, we will systematically explore the complex energetic landscape of these clusters at 0 K.

[1] A. M. Goryaeva, C. Domain, A. Chartier, A. D  zaphie, T. D. Swinburne, K. Ma, M. Loyer-Prost, J. Creuze, M.-C. Marinica, Nat Commun 14, 3003 (2023).

[2] M.-C. Marinica, F. Willaime, and J.-P. Crocombette, Phys. Rev. Lett. 108, 025501 (2012)

[3] C. van der Oord, G. Dussan, G. Cs  nyi, and C. Ortner, Mach. Learn.: Sci. Technol. 1 015004 (2020)

[4] M.-C. Marinica, A. M. Goryaeva, T. D. Swinburne *et al*, MiLaDy - Machine Learning Dynamics, CEA Saclay, 2015-2023: <https://ai-atoms.github.io/milady/> ;

[5] A. Zhong, C. Lapointe, A. M. Goryaeva, J. Baima, M. Ath  nes, and M.-C. Marinica, Phys. Rev. Mater. 7, 023802 (2023)

5:00 PM MT01.09.24

Data-Driven Crystal Growth Using Flux-Method Process Informatics Tetsuya Yamada^{1,2} and Katsuya Teshima^{1,2}; ¹Shinshu University, Japan; ²Shinshu University, Japan

Crystallographic characteristics such as crystallinity, crystal outline, and size are one of important factors to determine material performance, since they relates to physicochemical phenomena occurring on the surface and inside of materials. The flux method, which grow crystals in molten salts (fluxes) is a powerful technique for development of high-performance crystalline materials. However, its growth guidelines are not well established due to multi-step growth process with various phenomena. Therefore, it is necessary to explore the optimal conditions in a huge experimental space based on various experimental factors, including flux species. Thus, it takes several years to develop crystals using flux method.

Recently, we have studies flux-method process informatics (FPI), which is a data-driven approach to effectively explore favorable experimental conditions based on crystal growth prediction in the flux method. There are many issues to be solved to achieve high-accuracy FPI system. For example, description manner of feature values, big-data collection, expansion of materials target, and also effectivity of this method itself. In this study, we constructed an adaptive design of experiments (ADOE) system that can be used for FPI and applied to an anisotropic perovskite-type oxides.

The ADOE system accords to a Bayesian optimization cycle consisting of (I) acquisition of experimental data, (II) modeling by Gaussian process regression, (III) conduction of virtual experiments over 10000 ways, and (IV) proposal of experimental conditions based on the acquisition function. In this time, a layered perovskite oxide Ba₃Nb₄O₁₅ (BNO) with an anisotropic crystal structure was selected as one of the model materials. As the explanatory variables, experimental conditions, including raw material amounts, flux species, and heating conditions were used. Two types of crystal sizes were used as the objective variables to describe anisotropic crystal shape of BNO. The number of training data was about 70.

Firstly, we evaluated the efficiency of FPI using already collected dataset. The all dataset was divided into 10 as a training data and others as a test data. A prediction model was created using the training data, and the test data with high-likelihood one was selected as the goal candidate. If the selected test data was different from the goal, the data was added to the training data and continued the exploration until finding the goal. The cycles of modeling were output per 1 trial and scored the efficiency of ADOE after 100 trials. Comparing 100 random experiments, the average number of cycles by ADOE was 6 times smaller, indicating the better efficiency of this system than human-driven approach. In this presentation, we will also discuss the experimental results after applying the ADOE system, and contributing mechanism of each factor on the crystal growth.

Acknowledgements

This research was partially supported by NEDO Feasibility Study Program, NEDO Green Innovation fund projects, JST Open Innovation Platform with Enterprises, Research Institutes, and Academia (JPMJOP1843), JSPS KAKENHI (Grant Number 21K04807, 22H04533, and 22H00568), Knowledge Hub Aichi, TAKEUCHI Scholarship Foundation, and Wakasato association in Shinshu university.

5:00 PM MT01.09.25

Semi-Automatic Image Analysis Tool for Cellulose Nanocrystal Particle Size Measurement from Atomic Force Microscopy Images Saba Karimi¹, Sezen Yucel², Robert J. Moon³, Linda J. Johnston⁴ and Surya R. Kalidindi¹; ¹Georgia Institute of Technology, United States; ²Intel Corporation, United States; ³The Forest Products Laboratory, United States; ⁴National Research Council Canada, Canada

Cellulose nanocrystals (CNCs) are rod-like nanoparticles with that exhibit a unique combination of attractive characteristics for many applications: abundance, renewability, biocompatibility, desirable mechanical and chemical properties, and cheap production potential. Given these desirable properties, a broad spectrum of applications has been demonstrated in the literature for CNCs, from biomedical to composites, and from adhesives to sensors. Among the obstacles to the commercial utilization of CNCs is producing consistent quality, optimizing process parameters and reliable characterization protocols. Particle size and particle size distribution are particularly important when optimizing performance in any given application, for example as a rheology modifier in fluids or as a polymer reinforcement phase. Moreover, to optimize manufacturing processes, standardizing particle analysis is a crucial step. Currently the state-of-the-art approaches for characterizing CNC particle morphology are to manually measure individual particle dimensions in transmission electron microscopy or atomic force microscopy (AFM) images. This approach is not only time-consuming but also inconsistent because of bias or fatigue by human analyst. To address these characterization issues, a semi-automated image analysis framework based on MATLAB, called SMART, has been developed that segments AFM microscopic images into background and CNC particles, and classifies the identified CNC objects into isolated and agglomerated. This talk briefly introduces SMART, how it is applied to AFM image analysis by measuring the length and height of each CNC and reporting their distribution. This talk shows how the results are validated with the results of an inter-laboratory comparison study by Bushell et al., that assessed CNC size distribution using a reference CNC material that was characterized in four different laboratories. This talk critically compares the differences between the results obtained from SMART and from the traditional manual approaches. The results indicated that, while SMART's measurements were in good agreement with the manual approach, its advantages are (a) significant reduction in analysis times of CNC characterization — from hours to minutes, and (b) employing a consistent approach as opposed to analyst subjectivity in manual measurements. This talk will discuss how

SMART will facilitate CNC morphology characterization and how it may improve quality control assessment process and particle size optimization for a given application.

5:00 PM MT01.09.26

High Throughput Virtual Screening of Polymer Electrolytes for Li-Ion Batteries with Molecular Dynamics Simulations [Jurgis Ruza](#), Pablo A. Leon and Rafael Gomez-Bombarelli; Massachusetts Institute of Technology, Latvia

Developing high-power, high-density energy storage like lithium metal batteries is vital for sustainable, cost-effective electricity management in electric vehicles and intermittent renewables, reducing reliance on fossil fuels. Furthermore, lithium metal batteries have been proposed for high energy density applications to decarbonize the light- to heavy-duty vehicle sector, as well as for other applications with stringent energy density requirements. Unfortunately, the conventional carbonate-based liquid electrolytes used in lithium-ion batteries degrade both chemically and electrochemically when in the presence of solid lithium electrodes. Thus, alternative electrolyte systems are being investigated to increase diffusion kinetics and chemical stability to ultimately develop long-lasting batteries for electric vehicles and intermittent short-term renewable energy storage. Polymer electrolytes have been an interest in the field because of their enhanced electrochemical stability, increased safety as alternatives to liquid electrolytes.

We propose to use high-throughput molecular dynamics (MD) simulations to screen a large amount potential polymer electrolyte candidates for Li batteries. Using MD simulations for the screening of new materials accelerates the design and commercialization process and helps predict device-level performance using new candidates. However, the parameters historically used in interatomic potentials are inaccurate for new chemical systems, which limits the throughput of these simulations. Therefore, we use a machine learning pipeline to optimize interatomic potential parameters reproducibly for these species by using quantum chemistry simulations as training data across many unique polymer electrolyte systems. We show the capabilities of classical MD simulations with improved class I force fields are able to be used as a tool for ranking polymers based on their experimental conductivities and are able to simulate a large array of new polymer candidates, such as ether, ester, carbonate derivative as well as more different chemistries containing thiol, nitrile, and chemical groups.

5:00 PM MT01.09.27

Active Learning Protocols to Accelerate Galvanic Corrosion Predictions [Aditya Venkatraman](#), Ryan Katona, Demetri Maestas, David Montes de Oca Zapiain and Philip Noell; Sandia National Laboratories, United States

The current of a galvanic couple is generally treated as a surrogate measure of its resilience to or extent of galvanic corrosion. Experiments to measure cathodic current or obtain cathodic polarization curves incur a very high cost due to the need to explore a wide range of temperatures, salt concentrations, and specimen geometries that are used in engineering applications. To reduce these costs, Finite Element (FE) simulations are used to assess the cathodic current output. However, these simulations use the cathodic polarization curves as boundary conditions, which can only be discerned by performing experiments. Therefore, a protocol to accelerate the assessment of the cathodic current output for different chemistries under in-service environmental conditions is desirable. In this work, we develop an active learning protocol to minimize the total costs associated with performing the experiments and the simulations. We first calibrate a low-cost gaussian process surrogate model for the cathodic current output as a function of the environmental and geometric parameters that characterize the galvanic cell. The surrogate model is calibrated on a dataset of FE simulations, and it is used to calculate an acquisition function that identifies specific additional inputs with the maximum potential to improve the current predictions. The identification of additional inputs for further exploration is accomplished with the help of a staggered two-step workflow – (i) the influence of the geometric parameters are marginalized to identify the best configuration of environmental conditions for discerning the polarization curves, following which (ii) the geometric inputs best capable of refining the current predictions are identified. We demonstrate the efficacy of this protocol by minimizing the number of simulations necessary to obtain accurate predictions of the current output of a AA7075-SS304 galvanic couple. The protocols developed and demonstrated in this work provide a powerful tool for screening various forms of corrosion under in-service conditions. This work was supported by the Laboratory Directed Research and Development program at Sandia National Laboratories. Sandia National Laboratories is a multi-mission laboratory managed and operated by National Technology and Engineering Solutions of Sandia, LLC., a wholly owned subsidiary of Honeywell International, Inc., for the U.S. Department of Energy National Nuclear Security Administration under contract DE-NA0003525. The views expressed in the article do not necessarily represent the views of the U.S. Department of Energy or the United States Government. SAND2023-11065A

5:00 PM MT01.09.28

Exploring Multi-Type Crosslinked Architectures in Polymer Materials Using Graph Neural Networks [Connor Leavitt](#) and Mehdi Zanjani; Miami University, United States

Crosslinked polymer networks provide a promising route for developing novel material composites with a variety of applications in areas such as aerospace and biomedicine. These systems are typically made up of different combinations of backbone polymer chains and crosslinking agents of different kind. Understanding the relationship between the polymer network architecture and its properties is an important topic for design and development of new generation of polymer composites with on-demand functionality. While the study of crosslinked polymer networks has so far been mainly limited to systems with one or two types of crosslinkers, the existing synthesis techniques can readily be extended to devise more complex polymer networks with a larger number of crosslinkers and backbone chain types. However, the high-dimensional parameter space associated with such complex systems makes it difficult to predict the resulting architectures and properties of the materials developed through experimental trial and error.

In this work, we explore new designs for crosslinked polymer materials with multiple types of backbone chains and crosslinkers using a computational framework established based on graph theory (GT) and graph neural networks (GNNs). We demonstrate that including three or four types of backbone polymer chains can improve the mechanical behavior of the polymer composite provided that suitable structural features are established. We develop a graph representation of various polymer networks where graph edge features are defined according to the nature of crosslinking in the system, i.e. covalent or noncovalent bonds. We use a GNN framework to investigate the relationship between experimentally-controlled structural parameters, such as crosslinker density and type, and GT-based structural descriptors, such as graph connectivity and Wiener index. Following this step, we develop another GNN framework to study structure-property relationships using GT-based descriptors and mechanical properties obtained from Molecular Dynamics (MD) simulations. The trained GNNs will be used to predict the behavior of new potential structural morphologies in order to identify 'best-performing' configurations. The results of this work are aimed to be utilized for future experimental development of new crosslinked polymer composites.

Friday Morning, April 26, 2024
Room 320, Level 3, Summit

9:00 AM *MT01.10.01

The LAMMPS Particle Simulation Package: Bringing Together Innovative Physics Models, Machine-Learning Interatomic Potentials and Extreme-Scale Computing Resources Aidan P. Thompson; Sandia National Labs, United States

The molecular dynamics method (MD), as implemented in the LAMMPS[1] particle simulation code, is a powerful tool for explicitly sampling the phase space distribution of hundreds or billions of physically and chemically interacting atoms. It provides a wealth of information on how particular microscopic interactions lead to a vast range of emergent behaviors on much larger length and time scales, complementing theory and experiment. The overall usefulness of the method is sensitive to how well the chosen interaction potential approximates the true physical and chemical conditions. Over many decades, this has driven the emergence of many prominent interaction potentials that provide a good tradeoff between accuracy and cost. At the one extreme of minimal complexity are well-established models for simple fluids (Lennard Jones particles), polymer melts (FENE chains), and metals (EAM). In the case of chemical reacting systems, both organic and inorganic, the ReaxFF reactive potential has proven quite effective. More recently, relatively expensive machine-learning (ML) potentials have been found to approach the accuracy of very expensive quantum methods. These are trained to reproduce the energy and forces of many small configurations of atoms obtained from quantum electronic structure calculations e.g. Density Functional Theory. Examples of ML potentials implemented in LAMMPS include Behler-Parinello, GAP, SNAP[2], the Atomic Cluster Expansion (ACE)[3], and ALEGRO. In this talk, I will give a general overview of LAMMPS capabilities, as well as those the LAMMPS-integrated FitSNAP software [4] for generating quantum-accurate machine-learning interatomic potentials. I will describe several recent scientific applications of LAMMPS that combine innovative physics models, machine-learning interatomic potentials, and extreme scale computing resources.

[1] Thompson et al., *Comp. Phys. Comm.*, 271:108171, 2022. DOI 10.1016/j.cpc.2021.108171 (URL <https://www.lammps.org>) [2] Thompson et al., *J. Comp. Phys.*, 285:316, 2015. DOI 10.1016/j.jcp.2014.12.018 [3] Lysogorskiy, *npj Comp. Mat.* 7:1, 2021. DOI 10.1038/s41524-021-00559-9 [4] A. Rohskopf et al., *Journal of Open Source Software* 8, 5118 (2023). DOI 10.21105/joss.05118 (URL <https://fitsnap.github.io>)

9:30 AM ^MT01.10.02

Demystifying High Temperature/Pressure Material Synthesis through Physics-Informed Machine Learning Rebecca K. Lindsey; University of Michigan, United States

Design, discovery, and synthesis of new materials is a notoriously challenging problem, due largely to the massive associated design space and complex underlying phenomena. Simulations can provide a powerful means of navigating this problem space by providing both a capability for pre-screening and extracting otherwise inaccessible atomistically-resolved information on the underlying phenomena, but efforts are often limited by a lack of models exhibiting the necessary balance of accuracy and computational efficiency. In this presentation, we discuss recent efforts to overcome these challenges through development and targeted application of ChIMES, a physics-informed machine-learned interatomic model (ML-IAM) and supporting computational framework. We will present recent efforts to address grand challenges in ML-IAM development and application, e.g., toward reproducibility, reliability, and training efficiency as well as applications to high temperature/pressure nanocarbon synthesis.

10:00 AM BREAK

10:30 AM MT01.10.03

Molten Salt Crystallization studied by Machine-Learned Potentials Zhao Fan¹, Michael Whittaker¹, Piotr P. Zarzycki¹ and Mark Asta^{1,2}; ¹Lawrence Berkeley National Laboratory, United States; ²University of California, Berkeley, United States

Molecular dynamics (MD) simulations based on accurate interatomic force-fields are employed to calculate solid-liquid phase diagrams and investigate mechanisms of crystallization at the atomic level. The work is motivated by the potential relevance of molten salts in the context of lithium extraction. We report on the development of efficient and robust machine learning (ML) potentials for three unary salts (LiF, NaF and KF), three binary mixtures (LiF-NaF, LiF-KF and NaF-KF) as well as the ternary mixture of LiF-NaF-KF in the framework of Atomic Cluster Expansion and with the training datasets generated using density functional theory (DFT) with the strongly constrained and appropriately normed (SCAN) functional. We demonstrate that simulations based on these potentials produce properties consistent with DFT and available experimental data, including lattice constant, liquid density, melting point and latent heat of melting. The phase diagrams for the three binary mixtures and the ternary mixture calculated based on our ML potentials will be presented. In addition, we discuss results of simulations for homogeneous crystal nucleation, with focus on the crystallization pathways and role of metastable polymorphs. These studies are enabled by the attention paid in the potential development to accurate description of competing crystal phases, such as those with wurtzite, zinc blende and CsCl-prototype structures. The atomic-level mechanism of homogeneous melting of the rocksalt structure of LiF, NaF and KF will also be illustrated.

10:45 AM MT01.10.04

Tracing Molecular Reactions and Decomposition Using Machine Learning Force Fields and Active Learning Julia Yang^{1,1}, Whai Shin Amanda Ooi², Zachary Goodwin¹, Yu Xie³, Ah-Hyung Alissa Park⁴ and Boris Kozinsky^{1,1}; ¹Harvard University, United States; ²Columbia University, United States; ³Microsoft Research, Germany; ⁴University of California, Los Angeles, United States

Molecular reactivity spans extended length and time scales, making them costly to simulate using ab initio approaches or limited in chemical transferability/scope using reactive force fields. In this work, we describe how simulations of liquid structure and dynamics of organic molecules undergoing thermal decomposition reactions can be achieved using hybrid density functional theory (DFT), active learning [1], and machine learning force fields (MLFF) [2]. Active learning is essential for several reasons: 1) The overall computational cost of hybrid DFT is reduced dramatically as the uncertainty-aware force field collects only sufficiently-uncorrelated DFT frames; 2) High-temperature configurations with radicals or free gases, which are potential decomposition products, can also be collected on-the-fly; 3) The approach is useful in situations where classical force fields are either unavailable or lacking in expressivity.

When the training data from active learning are fed into a data-efficient equivariant neural network, molecular decomposition and reaction pathways can be traced with first-principles, all-atom resolution by identifying reaction pathways to product formation. We apply the approach to study the thermal decomposition of a “green” solvent used in battery recycling and validate our results against experimental characterization.

[1] Vandermause, J., Xie, Y., Lim, J.S. et al. *Nat Commun* 13, 5183 (2022).

[2] Musaelian, A., Batzner, S., Johansson, A. et al. Learning local equivariant representations for large-scale atomistic dynamics. *Nat Commun* 14, 579

(2023).

11:00 AM *MT01.10.05

Rational Design of Machine-Learned Interatomic Potentials [Megan J. McCarthy](#); Sandia National Laboratories, United States

The predictive capability of a molecular dynamics simulation is determined by how accurately the chosen interatomic potential (IAP) captures a material's bonding characteristics. Integrating machine learning techniques into IAP development has led to powerful improvements in that accuracy, while also introducing new levels of complexity to the training process. The choice of model (hyper)parameters, training set structures, validation tests, and whether and how to use tools such as active learning is frequently a material-specific, highly empirical process. To accelerate development and usage of machine-learned IAPs, new approaches to promote reproducibility and rational design of IAP are needed, ideally ones that are consistent with FAIR (Findable, Accessible, Interoperable, Reusable) research practices. In this talk, I will discuss promising developments in this area, amongst them software tools and techniques our group has developed while training machine-learned IAPs for multicomponent, chemically-complex materials used in extreme environments.

11:30 AM MT01.10.06

In Search of a More Perfect Forcefield: Considerations and Strategies for Parameterizing Complex Interatomic Potentials for Molecular Dynamics [Aravind Krishnamoorthy](#); Texas A&M University, United States

Molecular Dynamics (MD) simulations are an increasingly vital tool to understand molecular processes in a variety of material systems across mechanical, materials, and biological engineering. MD simulations require parameterized interatomic forcefields that capture complex interatomic interactions in materials. However, forcefield parameterization is a non-trivial global optimization problem involving quantification of forcefield variables in large-dimensional search spaces.

This talk will discuss currently used strategies to parameterize reactive and non-reactive interatomic potentials and will identify opportunities for improving these strategies through newly developed algorithms and software for performing multi-objective and global optimization, as well as schemes inspired by AI and ML training. Using EZFF, a Python package for parameterization of several types of interatomic forcefields using single- and multi-objective optimization techniques, I will describe a meta-analysis of the performance of forcefields for complex multi-phase materials generated using different strategies such as force-matching, energy-fitting and direct parameterization against dynamical properties. Approaches for parameterization of new forcefields against sparse ground truth data from experiments or expensive simulations will also be analyzed.

SESSION MT01.11: Machine Learning and Simulations X
Session Chairs: Rodrigo Freitas and Rebecca Lindsey
Friday Afternoon, April 26, 2024
Room 320, Level 3, Summit

1:30 PM *MT01.11.01

Machine Learning-Enhanced Physics-Based Modeling of Materials: From Atomistics to Microstructure-Property Relationships [Alejandro Strachan](#); Purdue University, United States

The synergy between principles-based modeling and data science is increasingly important in materials science and engineering. In addition to accelerating the design of new materials, there is significant interest in using machine learning (ML) tools to extract physical laws and structure-property relationships that govern materials' behavior from data. I will discuss recent progress by my group on machine learning applied to multiscale modeling and in the development of interpretable models that balance accuracy with parsimony.

I will discuss recent work on reactive ML interatomic potentials for materials at extreme conditions using an iterative approach to address the challenge of generating training data and the stochastic nature of NN training. The next step of the multiscale ladder is coarse-graining atomistic simulations, and I will discuss two applications. First, the use of dimensionality reduction techniques to extract physically interpretable collective variables from reactive MD simulations which are used to derive reduced-order chemical kinetics models. Finally, I will discuss our recent work on convolutional neural networks to develop models capable of mapping the initial microstructure of a composite material to the 3D temperature field induced by a shockwave.

2:00 PM MT01.11.02

Extracting Catalytic Reaction Mechanisms from Large-Scale Simulations Accelerated by Machine Learning Interatomic Potentials [Anders Johansson](#), Cameron J. Owen and Boris Kozinsky; Harvard University, United States

Machine learning interatomic potentials (MLIPs) have become a prevalent approach to bridging the gap between slow-but-accurate ab initio calculations and fast-but-inaccurate empirical potentials for molecular dynamics. Among MLIPs, there is a pareto front of models with different tradeoffs between accuracy and speed. The FLARE interatomic potential aims to push the boundary of scalability and performance, while maintaining sufficient accuracy to study complex, reactive systems.

In our recent work [1], we demonstrated the ability of FLARE to simulate heterogeneous catalytic reactions in systems of up to 0.5 trillion atoms using 27336 GPUs, with an accurate Bayesian MLIP efficiently trained using active learning. With the exceptional speed of FLARE on modern HPC architectures, we can combine the atomistic resolution of molecular dynamics simulations with the large length and time scales required for realistic simulations and sufficient sampling of rare catalytic events, while providing the near-quantum level of accuracy provided by the MLIP. In this talk, we will showcase how this combination of scales and accuracy enables new insights into chemically complex processes such as heterogeneous catalysis through high-resolution measurements of reaction rates and residence times.

[1] arXiv:2204.12573

2:15 PM MT01.11.03

Understanding Complicated Chemistry of Organic Materials Using Machine Learning Interatomic Potential [Cong Huy Pham](#)¹, Nir Goldman¹, Laurence Fried¹ and Rebecca K. Lindsey²; ¹Lawrence Livermore National Laboratory, United States; ²University of Michigan–Ann Arbor, United States

Understanding the chemical reactivity of organic materials under extreme conditions is important in many fields, such as chemistry, materials science, pharmaceutical, astronomy. Molecular dynamics simulations have become a powerful method that can provide insights into the detailed chemistry at the atomistic level. However, its accuracy depends strongly on the interatomic potential. Here, we present our effort to develop a quantum accurate Chebyshev Interaction Model for Efficient Simulation (ChIMES) many-body reactive potential to study the complicated chemistry of 1,3,5-Triamino-2,4,6-trinitrobenzene (TATB) under a shockwave. We discuss the techniques to control model accuracy and transferability as well as minimal training data selection. Our ChIMES potential has capability of reproducing the structural properties and chemistry of TATB at high accurate quantum level for a wide range of thermodynamic conditions. The shock simulations of TATB using ChIMES show good agreements with available experimental data.

2:30 PM MT01.11.04

Bayesian Interatomic Potentials for Thermodynamics Stability Predictions of Icosahedral Boron Crystals [Hao Deng](#) and Bin Liu; Kansas State University, United States

Elemental boron and icosahedral boron compounds (IBCs) are of surging interest due to their superior and versatile properties. For instance, boron suboxide (B_6O) and boron subphosphide ($B_{12}P_2$) derived from the α -rhombohedral boron lattice have extreme hardness and unusual electrical properties. These compounds display an extraordinary self-healing ability to repair the lattice defects generated from exposure to high-energy irradiation. Synthesis and control of the stoichiometry of IBCs are critical technical challenges. Computational tools, including Density Functional Theory (DFT) and molecular dynamics (MD) simulation, provide pathways to decipher the phase stability of IBCs. However, the structural and chemical complexity of IBCs hinder accurate DFT calculations and large-scale MD simulations.

In this talk, we report a unified sparse Gaussian process (SGP), a machine learning interatomic potential, for the phase stability predictions of boron allotropes (i.e., α -B, β -B, and γ -B). To account for the variety of lattice structures, on-the-fly training was employed for precise training set generation. The trained SGP yielded good agreement with DFT on predictions of structural, thermodynamics, and vibrational properties. Insights were gained from the generated P-T diagram and free energy composition analyses. The verified SGP training strategy is also employed in the phase stability prediction of B_6O . Factors affecting the phase stability of B_6O , including defect concentration and elemental composition, were investigated using SGP interatomic potentials implemented in large-scale MD simulations. We anticipate this computational approach will aid the understanding of the phase transition of complex crystals in future studies.

2:45 PM MT01.11.05

Benchmarking Anharmonicity in Machine Learned Interatomic Potentials [Sasaank Bandi](#)¹, [Chao Jiang](#)² and [Chris A. Marianetti](#)¹; ¹Columbia University, United States; ²Idaho National Laboratory, United States

Machine learning (ML) approaches have recently emerged as powerful tools to probe structure-property relationships in crystals and molecules. Specifically, ML interatomic potentials have been shown to predict ground state properties with near density functional theory (DFT) accuracy at a cost similar to conventional interatomic potential approaches. While ML potentials have been extensively tested across various classes of materials and molecules, there is no clear understanding of how well the anharmonicity of any given system is encoded. Here, we benchmark popular ML interatomic potentials using third and fourth order phonon interactions in fluorite crystals. An anharmonic hamiltonian was constructed from DFT using our highly accurate and efficient irreducible derivative methods, which was then used to train three classes of ML potentials: Gaussian Approximation Potentials, Behler-Parrinello Neural Networks, and Graph Neural Networks. We evaluate their accuracy in not only reproducing anharmonic interaction terms but also in observables such as phonon linewidths and lineshifts. We then present the results of the models trained on a DFT dataset, showing good and reasonable agreement with the DFT computed third and fourth order interactions, respectively. Finally, we discuss strategies to leverage anharmonic terms in the training procedure to improve the accuracy of ML interatomic potentials.

3:00 PM BREAK

3:30 PM *MT01.11.06

Data-Driven Approaches to Facilitate Inorganic Materials Discovery and Synthesis [Chris Bartel](#); University of Minnesota, United States

Machine learning is playing an increasingly prominent role in computational materials discovery. Recent advances in (universal) machine learning interatomic potentials allow practitioners to optimize the structure and compute the energy of inorganic crystals for arbitrary material compositions. These computed energetics can then be used as inputs to the convex hull analysis to determine if a hypothetical material is thermodynamically stable against potential competing phases. While stability is an important property for a candidate material, it does not determine if or how that material can be made in the lab. Whereas stability (at some set of conditions) is an intrinsic property of a material, synthesizability is not a similarly straightforward binary – it depends on experimental choices such as precursors, temperature, synthesis approach, etc. This talk will discuss recent efforts to use machine learning in the context of synthesis “recipe” generation, assessment, and optimization.

4:00 PM *MT01.11.07

Robust Machine Learning allows Accurate Modeling of Thermodynamics of Catalysts and Bulk Materials [Daniel Schwalbe-Koda](#); UCLA, United States

Recent advances in machine learning (ML) interatomic potentials (IPs) allow density functional theory (DFT) calculations to be bypassed with models that balance high accuracy and relatively low computational cost. However, MLIPs can be unreliable in regions of the configuration space not represented in the training data, which often hinders their use as universal predictors when modeling high-complexity systems. In this talk, I will describe how understanding robust generalization in ML can improve the development of next-generation ML models for materials simulation. First, I will demonstrate how extrapolation in atomistic systems can be rigorously defined in a model-free approach, thus without surrogate metrics such as variance of predictions. Then, I will describe how deep learning theory can be used to improve the generalization of MLIPs. These results are used to model several problems in materials simulation, from the thermodynamic of phase transformations to coverage effects in catalysis. In combination with automated workflows for combinatorial data generation, robustness in ML models can help drive the field towards the development of universal MLIPs towards length and time scales not accessible by ground truth calculations.

4:30 PM MT01.11.08

General Protocol for Training Machine Learning Interatomic Potentials for Ionic Liquids and Battery Solvents [Zachary A. Goodwin](#), [Nicola Molinari](#), [Julia Yang](#), [Albert Musaelian](#), [Simon L. Batzner](#) and [Boris Kozinsky](#); Harvard University, United States

We develop machine learning force fields (MLFFs), based on the equivariant graph neural networks with NequIP/Allegro [1,2], for representative ionic liquids and conventional battery solvents. As capturing the complex intermolecular interactions are subtle, and the dynamics of these electrolytes/solvents are quite slow, training a potential for these systems is not always straightforward. We develop a general, automatable protocol for training MLFFs for

This searchable program is up-to-date as of April 15th, 2024.

complex, multicomponent liquids, which efficiently samples representative structures, to collect diverse, uncorrelated molecular configurations for training. This approach is shown to yield reliable simulations in the NVT ensemble, but not always in the NPT ensemble, where we find densities significantly lower than expected from our DFT calculations. We develop an approach to remedy this issue, and test it on a number of electrolytes/solvents to ensure it is a robust method. In addition, we study the question of model transferability, the effect of long-range interactions and uncertainty of the model.

[1] S. Batzner, A. Musaelian, L. Sun, M. Geiger, J. P. Mailoa, M. Kornbluth, N. Molinari, T. E. Smidt, and B. Kozinsky, E(3)-equivariant graph neural networks for data-efficient and accurate interatomic potentials. *Nat. Commun.*, 13, 2453 (2022)

[2] A. Musaelian, S. Batzner, A. Johansson, L. Sun, C. Owen, M. Kornbluth, and B. Kozinsky, Learning local equivariant representations for large-scale atomistic dynamics *Nat. Commun.*, 14, 579 (2023)

4:45 PM MT01.11.09

Deep Learning-Assisted Analysis of Molecular Dynamics Simulations of LiTFSI/PYR₁₄TFSI Ionic Liquid Electrolyte Chanui Park, Sangdeok Kim, Anseong Park, Seungtae Kim, Woojin Kang and Won Bo Lee; Seoul National University, Korea (the Republic of)

Over the past decades, significant research has been conducted to understand microscopic behavior of ionic liquid electrolytes (ILEs) through molecular dynamics (MD) simulations. The development of polarizable force fields is one of the most remarkable achievements as they predict structural and dynamical properties of ionic liquid-based systems very accurately. However, even with the help of polarizable force fields, one cannot analyze atomic dynamics of a system in detail because most of the properties are evaluated by "averaging" individual atomic or molecular properties. A deep learning technique called Graph Dynamical Networks (GDyNets) has been suggested to learn atomic scale dynamics from MD simulations. GDyNets trains local environments around a specific target atom and classify them into states in an unsupervised manner. The classification model is trained in the direction where the VAMP loss decreases. The classification results are combined with conventional analysis techniques to calculate state-wise properties which can describe the system according to each state. Using this method, we analyzed MD trajectories of LiTFSI/PYR₁₄TFSI ILE with a range of lithium mole fractions, where the trajectories were generated under the APPLE&P polarizable force field. Li⁺ ions were treated as target atoms and classified into 3 local configurational states. State-wise radial distribution function, coordination number, spatial distribution function were defined and calculated to identify each state. The identified states were a Li⁺ ion coordinated by 2 and 3 TFSI⁻ ions, and a cluster composed of multiple Li⁺ and TFSI⁻ ions. Also, a transition matrix based on the Markov state model was generated from the classification results. With this matrix, dynamical properties of the states and transitions between states were measured to reveal which state or transition dynamics is faster than others. Finally, a design rule for ILEs with faster Li⁺ ion conduction was suggested.

SYMPOSIUM MT02

Battery Manufacturing—Emerging Opportunities in Data-Driven Experimentation, Analysis and Modeling
April 23 - April 25, 2024

Symposium Organizers

Alejandro Franco, Universite de Picardie Jules Verne
Deyu Lu, Brookhaven National Laboratory
Dee Strand, Wildcat Discovery Technologies
Feng Wang, Argonne National Laboratory

Symposium Support

Silver
PRX Energy

* Invited Paper

+ JMR Distinguished Invited Speaker

^ MRS Communications Early Career Distinguished Presenter

SESSION MT02.01: Battery Manufacturing: Challenges and Emerging Opportunities I

Session Chairs: Changwon Suh and Feng Wang

Tuesday Morning, April 23, 2024

Room 321, Level 3, Summit

10:30 AM *MT02.01.01

Small Data Challenge for Materials Research in Battery Manufacturing Krishna Rajan; University at Buffalo, The State University of New York, United States

The harnessing of data driven methods for materials design in battery manufacturing, demands the linking of data associated with the fundamentals of materials chemistry through to battery performance. A critical limitation of applying current informatics methods is that available data captures only small parts of the materials information spectrum. In this presentation we explore approaches to address this issue to track linkages between multiscale data regimes that allows one to explore connections between crystal chemistry to device performance.

11:00 AM *MT02.01.02

A Strategic Approach to Building a Secure Domestic Battery Supply Chain [Venkat Srinivasan](#); Argonne National Laboratory, United States

As the world embarks on widespread decarbonization, the supply chain crunch for batteries has become front and center around the world. In the United States, the issues are widespread, from material availability to the lack of cell and pack manufacturing. Recycling, which could bridge the supply gap, is still in its early stages. With the expected growth in the storage market, tactical approaches to solve the challenges will not suffice. What is needed is a comprehensive strategy that brings a holistic approach to solve the battery supply chain issues. This includes the search for alternative materials to the presently-constrained materials (such as nickel, cobalt, and lithium), examining opportunities for clean extraction of battery minerals, and recycling. In addition, an important part of the strategy is to examine leapfrogging materials and manufacturing methods that can enable deep decarbonization of transportation and grid sectors. The talk will examine the status of battery technology, and the opportunities for enabling widespread electrification with a sustainable and secure supply chain.

11:30 AM *MT02.01.03

Guiding New Battery Material Scale Up Through Automated Information and Relation Extraction [Elsa Olivetti](#)¹, Kevin Joon-Ming Huang¹, Mrigi Munjal¹, Thorben Prein² and Jennifer L. Rupp²; ¹Massachusetts Institute of Technology, United States; ²TU Munich, Germany

Improving the performance of novel electrode materials will enable competition with mature technologies like lithium-ion batteries (LIBs) at scale. To some extent novel electrode active materials can leverage the well-established manufacturing knowledge of lithium-ion batteries. However, several materials synthesis and performance challenges for electrode materials must be addressed for them to mature from lab to industrial scale. We employ natural language processing (NLP) tools to extract challenges from battery literature in the performance and synthesis of active battery materials. The tools also systematically review corresponding mitigation strategies. These selected mitigation strategies are then evaluated among a broad set of pre-existing lab-proposed mitigation strategies. These derived insights enable engineers in research and industry to navigate a large number of proposed strategies.

SESSION MT02.02: Battery Manufacturing: Challenges and Emerging Opportunities II

Session Chairs: Alejandro Franco, Krishna Rajan and Venkat Srinivasan

Tuesday Afternoon, April 23, 2024

Room 321, Level 3, Summit

1:30 PM *MT02.02.01

How Argonne's MERF Can Help Advance Your New Materials [Krzysztof Pupek](#); Argonne National Laboratory, United States

Rechargeable batteries are among the critical technologies in the decarbonization effort of increasingly expanded transportation and power grids. The demand for safer, longer-lasting, durable energy storage continues to fuel the need for battery innovation. This need, in turn, requires designing new materials, understanding how they function, and developing scalable processes to manufacture them. Electric vehicles (EVs) powered by lithium-ion batteries (LIBs) represent the most advanced and readily available energy storage technology to help the decarbonization of the world. There is an increased interest in deploying sustainable EVs powered by the new generation of rechargeable batteries, making energy storage scientists explore new, safer, cheaper, and earth-abundant materials to lower costs and dependence on foreign sources. The challenges ahead of battery researchers are complex, and it may take decades to convert the discoveries into full commercial adoption. These materials or better-performing new materials can quickly become a new quest for scientists. The current proven technologies to produce these materials most often may not work when the chemical composition and particle morphology requirement changes.

The Materials Engineering Research Facility (MERF) is a part of the Applied Materials Division at Argonne National Laboratory. Established in 2009, remodeled, and expanded in 2020, the MERF is a 28,000-square-foot research facility equipped with state-of-the-art instrumentation. It employs 40 researchers, engineers, and support technicians, with all key staff having an extensive industrial background. The facility is a home for Process R&D and Scale-up Group. It is a vital component of Argonne's Materials Manufacturing Innovation Center (MMIC), a significant, multi-year investment of discretionary laboratory resources to extend the Laboratory leadership in accelerating scalable materials synthesis and process development.

The presentation will familiarize the audience with MERF capability, including traditional process R&D technologies as well as a suite of emerging manufacturing technologies like Tailor Vortex Reactors, Hydro/Solvothermal Synthesis, Flame/Ultrasonic Spray Pyrolysis, and Continuous Flow Reactors. We will use systematic, data-driven approaches to develop efficient manufacturing processes and scale up the new materials to make sufficient amounts to support further research, prototyping, and industrial validation.

The team of researchers and engineers behind MERF aims to streamline the conversion of your discovery into commercial products.

2:00 PM *MT02.02.02

Linking Failure Mode Analysis and Machine Learning to Accelerate Life Prediction [Eric Dufek](#); Idaho National Laboratory, United States

Batteries continue to see rapid advancement both in materials selection and in emerging use cases. In all cases as new options for battery use and design arise there is a need to validate performance and to understand failure modes. Traditionally validation processes would require years of testing and immense use of resources to reach acceptable certainty that a new battery would function in an intended use case. Recent emergence of the use of combining failure mode analysis with machine learning and other advanced data analytics provides the opportunity to dramatically reduce the time needed for validation and to more quickly bring new discoveries and uses cases from the bench top to the consumer.

In this discussion several different approaches to reducing the time needed for performance validation will be discussed. This includes both the importance of appropriate and targeted data collection as well as the data analytic methods that can support rapid validation. The key to both the advanced analytics and data collection is the need to ensure a link to physical processes which aids in battery failure mode identification. The link also allows extended data sets to be generated using different modeling or synthetic data approaches to be used for enhanced training purposes.

Using a combination of experimental and synthetic data it will be shown that enhanced predictions are possible and that the time and resources needed to make predictions can be dramatically reduced. As an example set different predictions for graphite/NMC batteries used in standard and fast charge conditions will be highlighted.

2:30 PM *MT02.02.03

Data-driven Research for Aqueous Organic Redox Flow Batteries Wei Wang; Pacific Northwest National Laboratory, United States

Aqueous organic redox active materials have recently shown great promise as alternatives to transition metal ions as energy-bearing active materials in redox flow batteries for large-scale energy storage due to their structural tunability, cost-effectiveness, availability, and safety features. However, development to date has been limited to a small palette of aqueous soluble organics. This presentation will provide an overview of a data-driven approach to accelerate the discovery and development of aqueous organic redox-active molecules for flow batteries, including database curation, structure-property correlation, and automated property characterization and performance testing developed in PNNL's ARES (Automated Robotics for Energy Storage) lab.

Reference:

P. Gao, etc. "SOMAS: a platform for data-driven material discovery in redox flow battery development", *Scientific Data*, **9**, 740, 2022

Y. Liang, etc "High-throughput solubility determination for data-driven materials design and discovery in redox flow battery research" *Cell Reports Physical Science* **4**, 101633, 2023

3:00 PM BREAK

3:30 PM *MT02.02.04

DigitalDNA: Synchronizing Molecules to Machines to Build Smart Gigafactories Shailesh Upreti; Charge CCCV LLC C4V, United States

Lithium-ion battery (LIB) market size will grow at the compounded annual growth rate of +16%, surpassing 165 billion USD in revenue by 2030. While most of this growth is enabled by innovations in battery chemistry and performance, safety hazards remain a primary concern and a major restraint to market expansion. Safety incidences often result from errors introduced during high-volume manufacturing that, through a chain of events, leads to a thermal runaway and fire. C4V has teamed with leading Machine Learning (ML) and Artificial Intelligence (AI) experts to address the issue by developing tools that can not only track and minimize or eliminate manufacturing defects in the battery cells, but can warn users of an incipient catastrophic event ahead of time, thus preventing any damage to property or loss of life. The first generation of the DigitalDNA (DDNA) software is able to automatically capture key electrochemical data from cell cyclers installed at iM3NY, a New York based gigafactory that produces 50Ah prismatic cells. 2 DDNA automatically curates and analyse data generated at the production floor, and create actionable outputs for operator to take corrective measures in near real-time. DDNA is designed to be platform agnostic and can capture data in multiple formats. The next-generation of DDNA, with an in-built advanced data analytics algorithms can easily access and use these large data sets to train the ML models and implement AI to provide predictive insights and enable continuous improvements in electrochemical performance of LIBs. In addition, with a recent release of the Supply Chain module, DDNA can perform a full inventory control and management of +30 components that are required for battery cell production. With this module, DDNA can also track the progress of C4V's extensive raw material qualification program currently underway for more than 50 vendors globally. By integrating best-practices in laboratory information and data management systems, DDNA enables a high level of information flow control during the 5 discrete stages of phasegate qualification process starting with a preliminary assessments in a coin cell to a full scale evaluation in the commercial cell. When integrated with the warehouse management system and highlevel business systems such as ERP, the predictive capability of the software can use the raw material utilization data intelligently to create sourcing and procurement scenarios to achieve full inventory and cost optimization. By leveraging the fully digitized future gigafactories and the IIoT ecosystems, the future-generations of DDNA will seamlessly integrate with manufacturing execution systems to collect data at each step of the manufacturing process. By tapping into the real-time visualization of process and equipment performance data, the ML and AI analytics will be able to detect anomalies ahead of time. This ability to predict failure and perform preventive maintenance will increase equipment availability and performance and reduce disruptions and costly repairs. More importantly, DDNA will interface with the numerous in- or at-line quality control instruments implemented in a roll-to-roll process. Together with feedback control loop, access to statistically significant anomaly data set and advanced descriptive analytics, DDNA will enable processes that will reduce waste and improve yields. By quickly detecting and eliminating any debilitating defects at every step, DDNA will afford a highly reliable and safe battery products. We envision that DDNA will mature into a comprehensive software platform that will enable Smart gigafactories and predictive manufacturing and will make intelligent decisions informed by data gathered over the entire value chain of LIB from molecules (mines) to machines (vehicles and Energy Storage Systems).

Reference: 1. <https://www.fnfresearch.com/lithium-ion-battery-market> 2. <https://im3ny.com/>

4:00 PM *MT02.02.05

Exploratory Perspectives on Artificial Intelligence Enabled Autonomous Manufacturing Yuepeng Zhang¹, Noah H. Paulson¹, Santanu Chaudhuri^{1,2} and Jie Xu¹; ¹Argonne National Laboratory, United States; ²University of Illinois Chicago, United States

Manufacturing spans complex materials properties and process variables. Currently, process development relies on empirical analysis, trial-and-error, and ex-situ characterization, limiting production efficiency and yield. Recently, artificial intelligence (AI) coupled with in-situ, in-line metrology has enabled autonomous characterization, data analysis, and rapid development of process-property correlations — necessary components in a future accelerated manufacturing paradigm. In this report, we share perspectives on applying AI and machine learning (ML) to roll-to-roll (R2R) coating of formulated inks — a scalable high-throughput manufacturing process used for many energy storage and conversion technologies including lithium-ion battery (LIB) electrodes and fuel cell and water electrolyzer membrane electrode assemblies (MEAs).

4:30 PM *MT02.02.06

High-Throughput Approach to High Energy Lithium-Ion Cell Roadmap Development Gang Cheng, Ye Zhu, Ram Deivanayagam and Hui Wang; Wildcat Discovery Technologies, United States

As EV adoption has grown, there has been an increased focus in the battery industry on the development and implementation of high-nickel cathodes from 80% Ni to now 95 and above with increasing Si% in the anodes. These materials can deliver improved energy density relative to today's materials but suffer from poor lifetime and durability. Variations in electrode composition can impact the performance of the material. This presentation highlights Wildcat high-throughput strategy that can accelerate implementation of high-nickel cathodes paired with high Si% of anodes in applications. The presentation focuses on approaches other than compositional changes to the high nickel NMC/Si-C cells to improve cycle life in high-loading electrodes.

10:30 AM MT02.05.02

3D Printed Flexible Lithium-Ion Batteries with Improved Cycling Performance Xin Hu^{1,2}, Yimin Chen^{1,2}, Baozhi Yu^{1,2} and Ying Chen^{1,2}; ¹Deakin University, Australia; ²ARC Research Hub for Safe and Reliable Energy, Australia

3D printing technology, one of the additive manufacturing techniques, has shown remarkable promise in creating flexible and tailor-made high-performance batteries, which are in high demand for the upcoming era of intelligent and widespread energy usage. Nonetheless, a notable performance disparity, particularly in terms of cycling stability, still persists between 3D-printed electrodes and traditional counterparts, severely constraining the practical utility of 3D-printed batteries. This presentation discusses the development of a range of 3D-printed electrodes based on thermoplastic polyurethane (TPU) using fused deposition modeling for high-performance, flexible, and customizable lithium-ion batteries. The TPU-based electrode filaments are produced in significant quantities through a straightforward extrusion method. Consequently, the electrodes are printed with precision, offering excellent dimensional accuracy, flexibility, and mechanical stability. Notably, 3D-printed TPU-LFP electrodes demonstrate an impressive capacity retention of 100% after 300 cycles at 1C, representing one of the most robust cycling performances among all reported 3D-printed electrodes. This exceptional performance can be attributed to the outstanding stress-absorbing characteristics of the TPU-based electrodes, which effectively accommodate the volume changes during cycling and thus substantially prevent the collapse of the 3D-printed electrode structures. These findings not only open up new possibilities for creating adaptable and flexible batteries but also pave the way for bridging the performance gap between 3D-printed and traditional lithium-ion batteries.

10:45 AM *MT02.05.03

Sustainable LiFePO₄ and LiMn_xFe_{1-x}PO₄ (x=0.1 to 1) Cathode Materials for Lithium-Ion Batteries: A Systematic Approach from Mine to Chassis Atiyeh Nekahi, Anil Kumar Madikere Raghunatha Reddy, Karim Zaghib, Xia Li and Sixu Deng; Concordia University, Canada

We conducted a comprehensive literature review for LiFePO₄ (LFP) and LiMn_xFe_{1-x}PO₄ (x=0.1 to 1) (LMFP)-based lithium-ion batteries (LIBs), focusing primarily on electric vehicles (EVs), which account for approximately 90% of LIB consumption. Although numerous individual research studies exist, a unified and coordinated review that covers the subject from mine to chassis is notably absent. Accordingly, our review encompasses the entire LIB development process, starting with *I*) initial resources, including lithium (Li), iron (Fe), manganese (Mn), and phosphorous (P), their global reserves, mining procedures, and their demand in LIB production. Then, we examined *II*) the main Fe- and Mn-containing precursors of Fe⁰, Fe_xO_y, FePO₄, FeSO₄, and MnSO₄, focusing on their preparation methods, employment in LIBs, and their effect on the electrochemical performance (EP) of the final active cathode materials (ACMs). These two steps are followed by *III*) utilizing these precursors in synthesizing ACMs. Specific attention is paid to the pioneering synthesis methods in olivine production lines, particularly hydrothermal liquid-state synthesis (LSS), molten-state synthesis (MSS), and solid-state synthesis (SSS). Afterward, we described *IV*) electrode engineering and design and optimization of electrolytes and *V*) the production of cells, modules, and packs. Finally, *(VI)* our review underscored the challenges associated with the widespread utilization of olivines in LIBs, emphasizing safety, cost, energy efficiency, and carbon emission. In conclusion, our review offers a comprehensive overview of the entire trajectory involved in the fabrication of LFP/LMFP-based LIBs, spanning from the initial elements in the mine to the assembly of final packs that power EVs.

11:15 AM *MT02.05.04

Circular Manufacturing of Next-Generation Lithium-ion Battery Cathode Materials with R2R Molten Salt Electrodeposition Heng Yang; Xerion Advanced Battery Corporation, United States

For the past few years, Xerion has been developing a roll-to-roll (R2R) molten salt electrodeposition technology (DirectPlate™) for circular manufacturing of lithium-ion battery cathodes. Cathode materials such as LiCoO₂, Li(Ni_xM_yCo_z)O₂, and Li_{1-x}Mn_xO₂ are demonstrated with good electrochemical properties. DirectPlate™ cathodes are distinctly different from conventional slurry-cast electrodes combining several notable properties: they are very dense with less than 10% porosity, free of additives (carbon and polymer binder), and their crystal orientation can be accurately controlled, enabling high-rate operation at or beyond state-of-the-art areal capacity loading (3-4 mAh/cm²). As Li⁺ diffusion primarily occurs through the single crystalline domains aligned vertically to the current collector, DirectPlate™ LiCoO₂ cathodes delivers good electrochemical properties in a solid-state cell without the need to infiltrate electrolyte into the cathode. We further demonstrate that end-of-life DirectPlate™ cathodes can be efficiently re-lithiated and repaired with a short molten salt treatment; or they can be upcycled into another cathode material with a completely different composition. Finally, we demonstrate that the DirectPlate™ cathode can be employed as a redox membrane for direct lithium extraction from various lithium-containing solutions. Integrating the collective mineral refinement, electrode fabrication and recycling capabilities into the R2R DirectPlate™ platform enables next-generation circular battery manufacturing with much lower energy and environmental cost.

SESSION MT02.06: Data-Driven Battery Optimization and Health Prognosis

Session Chairs: Eric Dufek and Alejandro Franco

Wednesday Afternoon, April 24, 2024

Room 321, Level 3, Summit

1:30 PM MT02.06.01

Behind the Coulombic Efficiency Zonghai Chen, Jiyu Cai and Yingying Xie; Argonne National Laboratory, United States

Lithium-ion batteries have been widely adopted as the most practical energy storage technology for powering portable electronics and electric vehicles. Portable electronics generally require a battery calendar life of 2 years or less, which can be easily fulfilled by most state-of-the-art lithium-ion technologies. However, this is not the case for the emerging application in EVs, which generally require a substantially longer calendar life for 10 years or more. The assurance of calendar life must rely on certain mathematical prediction, such as multivariate regression and machine learning. On the other hand, coulombic efficiency has been generally used as an empirical indicator of cell performance, but the quantitative use of coulombic efficiency for prediction of cell life is not achieved yet. This talk will focus on the chemical and physical processes behind the measurement of the coulombic efficiency of lithium-ion cells, as well as its implication on the cell life prediction.

1:45 PM *MT02.06.02

AI Performance and Health Prognosis for Degradation-Aware Battery Development Noah H. Paulson, Joseph Kubal, Logan Ward, Saurabh Saxena, Wenquan Lu and Susan Babinec; Argonne National Laboratory, United States

This searchable program is up-to-date as of April 15th, 2024.

Battery development requires extensive experimental trials ranging from benchtop materials discovery, to scale up trials, to full production optimization, incurring costs that may exceed hundreds of millions of dollars. One principal barrier to a more efficient and accelerated development process is the requirement to consider the degradation of batteries with use, the experimental evaluation of which requires 12 to 18 months of laboratory cycling experiments to reach failure. Physics-based simulations of battery degradation are rapidly advancing, but the diversity and complexity of coincident degradation mechanisms precludes the complete replacement of experimental trials. Data-driven methods, however, do not require exhaustive description of degradation mechanisms, and in recent years have shown strong performance in predicting battery degradation and remaining useful life (RUL). In this presentation, we share recent work in predicting battery RUL from limited cycling for a dataset of 300 Li-ion pouch cells representing 6 cathode chemistries and a variety of anode and electrolyte compositions. RUL prognosis was performed with a mean absolute error of ~100 cycles for a model trained on all available cathode chemistries, and useful predictions were made for unseen chemistries. Furthermore, we present timeseries prognosis of a multivariate battery state of performance and health including capacity, energy, efficiency, resistance, and open circuit voltage quantities.

2:15 PM MT02.06.03

Harnessing AI: Accurate Predictions of Battery Capacity Fade and Battery Cycle Life Jordan Crivelli-Decker¹, Marc Cormier², Shivang Agarwal¹, Ty Sours¹, Steffen Ridderbusch¹, Dan Zhao¹, Stephen Glazier², Brian Wee¹, Don Fiander² and Ang Xiao¹; ¹SandboxAQ, United States; ²Novonix, Canada

Predicting battery degradation is pivotal for advancing material research and unlocking opportunities in battery design, utilization, testing, and recovery. This enables better battery management and ensures the maintenance of desired performance characteristics over an extended period including both up and downstream manufacturing processes such as material selection, design qualification, technology/cell selection (battery management), and warranty, etc. However, traditional models and machine learning techniques often fall short in capturing these characteristics.

Lithium-ion cells typically show a gradual capacity degradation up to a certain point, known as the knee-point, beyond which the degradation accelerates rapidly, leading to the cell's End-of-Life. SandboxAQ's collaboration with NOVONIX has resulted in a robust method to predict long-term cell capacity fade from early-life cycling data. The approach begins with extracting early-life current, voltage, and capacity data collected on NOVONIX's world-class Ultra-High Precision Coulometry (UHPC) cycler systems. Electrochemically relevant metrics are then combined with advanced feature engineering and sophisticated data transformations are employed to construct features conducive for machine learning.

Proprietary machine learning and deep learning models were trained on several comprehensive, but limited datasets. Despite limited training data, these models demonstrate a remarkable ability to accurately classify the cells with and without catastrophic failure at a given point in time, predict the cycle number at which 80% of cell's initial capacity remains, and estimate the remaining useful life of the cell, which provides key indicators of cell health and longevity.

One of the standout features of these models is their flexibility. They are designed to seamlessly incorporate new data as it becomes available, ensuring that the predictions remain relevant and accurate over time. This approach not only provides a more cost and time-efficient alternative to long-term experiments traditionally used to estimate battery life but also opens avenues for more dynamic and responsive battery management strategies.

In summary, our solution leverages AI to rapidly make accurate, physics-based, end-of-life predictions using early-life electrochemical data. We leveraged comprehensive manufacturing cell data to deliver custom machine learning and deep learning models that were able to reliably predict cycle life only from high fidelity early-life data. The models are designed to easily integrate any future data, offering a cheap and efficient alternative to lengthy benchtop experiments.

2:30 PM BREAK

SESSION MT02.07: Data-Driven Materials and Process Design I

Session Chairs: Deyu Lu and Noah Paulson

Wednesday Afternoon, April 24, 2024

Room 321, Level 3, Summit

3:30 PM *MT02.07.01

Data-Driven Battery Analysis with Machine Learning: From Laboratory to Field Application Weihan Li; RWTH Aachen University, Germany

Machine learning has emerged as a pivotal force within the battery industry, spanning research endeavors from the material level to the system level, encompassing both production processes and practical applications. Recent advancements in machine learning and data-driven methodologies have enabled innovative solutions for complex problems, particularly those scenarios where conventional physics-based models have fallen short.

In my talk, I will delve into our latest endeavors in the realm of data-driven battery analysis, encompassing both laboratory experimentation and real-world application in electric vehicles and stationary energy storage systems. Our research is centered on the development of deep learning models designed to augment and denoise CT images for in-depth battery electrode analysis. Additionally, we are actively engaged in harnessing machine learning and statistical learning techniques to scrutinize data from various testing and field sources, thereby improving aging diagnostics in the cloud.

This talk aims to offer a comprehensive overview of the diverse array of machine learning approaches employed in battery-related analyses while also shedding light on the unique challenges faced and the abundant prospects awaiting exploration.

4:00 PM MT02.07.02

Incorporating Domain Knowledge in Statistical Machine Learning to Efficiently Navigate Parameter Space and Test Durability for Energy Storage Maher Alghalayini, Marcus M. Noack and Stephen J. Harris; Lawrence Berkeley National Lab, United States

Given the urgency of addressing global warming and the need for sustainable energy solutions, the importance of efficient energy storage devices cannot be overstated. Of particular interest are the long-duration storage systems that are paramount for the integration of these sustainable sources, like renewables, in the power grid. Long-duration storage systems are designed to capture surplus energy during periods of high production and low demand, subsequently releasing it during periods of low production and high demand.

Developing such systems requires efficiently exploring their parameter spaces and assessing durability. Traditionally, this exploration process has been haphazard and inefficient, resulting in time and resource wastage, and an inadequate assessment of durability and failure probabilities. Machine learning and artificial intelligence are revolutionizing most aspects of science and engineering, including parameter space exploration, but adopting those advancements has been slow in the energy-storage community. The reasons are the expense of battery testing and the associated sparsity of datasets, the need to extrapolate instead of interpolate, the inherent stochasticity of the problem, and the deep connection between failure mechanisms and physical and chemical processes. All of this causes a purely data-driven approach to be suboptimal. In this study, we present an innovative method that harnesses statistical and machine learning techniques, specifically Gaussian Process regression and the expected information gain from future experiments, to streamline the exploration of energy storage systems parameter space. By incorporating the expertise of domain specialists to tailor our prior mean, kernel function, and noise model, our approach minimizes the need for extensive experimentation while accurately quantifying the failure probability distribution. Our results show that this method can, in fact, efficiently explore the parameter space and approximate failure distributions early in the testing process. In short, this work holds promise for expediting the development and optimization of energy storage, facilitating renewable energy integration, and contributing to a more sustainable future.

4:15 PM MT02.07.03

Exploring Secondary Phase Formation at The Solid-Electrolyte/Cathode Interface using Machine-Learning Interatomic Potential [Wonseok Jeong](#), Brandon Wood and Liwen Wan; Lawrence Livermore National Laboratory, United States

All-solid-state Li-ion batteries are attractive next-generation energy-storage devices, offering improved safety, energy density, and durability compared to conventional Li-ion batteries. A critical challenge in these batteries is the occurrence of side reactions at the solid-electrolyte/cathode interface, particularly at elevated temperatures during co-sintering. These reactions have the potential to result in the undesired formation of secondary phases that impede the transport of lithium ions. The dynamic formation of these secondary phases at the atomic scale and the conditions governing their emergence remain unclear.

In this work, we explore the nucleation and evolution of secondary phases, such as La-Co-O, at the interface between the $\text{Li}_7\text{La}_3\text{Zr}_2\text{O}_{12}$ (LLZO) solid electrolyte and the LiCoO_2 (LCO) cathode. Our investigation comprises three main components that employ atomistic simulations driven by a machine-learning potential (MLP) for accelerated and comprehensive analysis. Firstly, we utilize a crystal structure prediction algorithm in conjunction with an MLP to accelerate the identification of potential secondary phases that may form at the interface. Secondly, we conduct MLP-driven metadynamics simulations to investigate the relationship between local structural features and the energy landscape associated with the nucleation of secondary phases. This exploration helps us understand the conditions leading to the formation of bulk-like secondary phases. Finally, we perform large-scale MLP molecular dynamics simulations to directly observe the formation of secondary phases in a model interface structure.

Through this multi-level investigation, we offer a holistic understanding of the formation of secondary phases at the LLZO/LCO interface. This insight is critical for understanding battery degradation resulting from interface reactions.

This work was sponsored by the Office of Energy Efficiency and Renewable Energy, Vehicle Technologies Office and was performed under the auspices of the U.S. Department of Energy by Lawrence Livermore National Laboratory under Contract DE-AC52-07NA27344. A portion of this research was performed using computational resources sponsored by the Department of Energy's Office of Energy Efficiency and Renewable Energy and located at the National Renewable Energy Laboratory.

4:30 PM MT02.07.04

Reveal The Active Components of Crystalline Li-Nb-O and Li-Ta-O Coatings [Hengning Chen](#)¹, [Zeyu Deng](#)¹, [Yuheng Li](#)¹ and [Pieremanuele Canepa](#)^{1,2}; ¹National University of Singapore, Singapore; ²University of Houston, United States

As widely applied coating materials for high-voltage positive electrode materials, niobate and tantalate materials can mitigate the interfacial reactivities in Li-ion and all-solid-state batteries. Although crystalline LiMO_3 ($M=\text{Nb, Ta}$) coatings show substantial enhancements in the battery electrochemical performances, there exists an apparent contradiction between the low Li-ion conductivity of crystalline LiMO_3 coating and the good rate capabilities achieved in these cells.^{1,2} This contradiction needs to be well understood to optimize the functional properties of crystalline niobates and tantalates. Leveraging a combination of density functional theory, empirical bond valence mapping, nudged-elastic band calculations, and machine learning molecular dynamics, we reveal the multiphase nature of Li-M-O coatings, containing mixtures of LiMO_3 and Li_3MO_4 . The concurrence of several phases in Li-M-O modulates the type of stable native defects in these coatings. Li-M-O coating materials can form favorably lithium vacancies and antisite defects combined into charge-neutral defect complexes. Even in defective crystalline LiMO_3 , we reveal poor Li-ion conduction properties. In contrast, Li_3MO_4 introduced by high-temperature calcinations can provide adequate Li-ion transport in these coatings. However, the occurrence of intrinsic defects in niobates (and tantalates) remains conditional to the coexistence of LiMO_3 and Li_3MO_4 at synthesis conditions, which regulates the availability of Li vacancies. Our in-depth investigation of the structure-property relationships in the important Li-M-O coating materials helps to develop more suitable calcination protocols to maximize the functional properties of these niobates and tantalates.³

References

1. Glass, A. M., Nassau, K. & Negran, T. J. Ionic conductivity of quenched alkali niobate and tantalate glasses. *J. Appl. Phys.* **49**, 4808–4811 (1978).
2. Xin, F. *et al.* What is the Role of Nb in Nickel-Rich Layered Oxide Cathodes for Lithium-Ion Batteries? *ACS Energy Lett.* **6**, 1377–1382 (2021).
3. Chen, H., Deng, Z., Li, Y. & Canepa, P. On the Active Components in Crystalline Li-Nb-O and Li-Ta-O Coatings from First Principles. *Chem. Mater.* **35**, 5657–5670 (2023).

4:45 PM MT02.07.05

Data-Driven Electrolyte Design for Lithium Metal Batteries [Solomon Oyakhire](#)^{1,2}, [Sang Cheol Kim](#)¹, [Yi Cui](#)¹ and [Stacey F. Bent](#)¹; ¹Stanford University, United States; ²University of California, Berkeley, United States

Enhancing Coulombic efficiency (CE) plays a pivotal role in facilitating the adoption of high-energy-density lithium metal batteries. While liquid electrolyte engineering has emerged as a promising strategy for improving CE, its inherent complexity makes performance prediction and electrolyte design challenging. In this two-part presentation, we introduce machine learning methods and workflows that enable us to predict electrolyte performance, guide the design of new high-performing electrolytes, and extract important scientific insights.

In the first part, we introduce a novel workflow that combines principles of feature engineering, feature selection, and machine learning model assessment. This workflow allows us to extract insights that guide the design of five new, high-performing electrolytes. Leveraging simple features, such as elemental composition that encodes pertinent physics within the electrolytes, we constructed interpretable models using linear regression, random forest, and bagging techniques. Through the results derived from these interpretable models, we identified crucial electrolyte features that are instrumental in achieving high battery efficiency. One such feature is the atomic fraction of oxygen in the solvent, highlighting the significance of reducing solvent oxygen for achieving

This searchable program is up-to-date as of April 15th, 2024.

high Coulombic efficiency (CE). Equipped with this insight and a few others, we formulated five new electrolyte compositions with fluorine-free solvents, one of which attains a high CE of 99.70%.

In the second part, we employ data segmentation in conjunction with machine learning methods to discern crucial performance descriptors within distinct electrolyte efficiency classes. Through this approach, we made a surprising discovery. Common electrolyte performance descriptors like lithium morphology, ionic conductivity, solid electrolyte interphase chemistry, and lithium-electrolyte reactivity, **do not** explain performance variations in electrolytes beyond a Coulombic Efficiency (CE) of 98%. By utilizing new machine learning model assessment techniques, interpretable machine learning models, correlation analysis, and rigorous spectroscopy and electrochemistry characterizations, we unveil the pivotal role of **galvanic corrosion** in accounting for performance disparities within high CE (>98%) electrolytes.

This work underscores the potential of data-driven approaches in expediting the discovery of high-performance electrolytes for lithium metal batteries.

SESSION MT02.08: Poster Session
Session Chairs: Deyu Lu and Feng Wang
Wednesday Afternoon, April 24, 2024
Flex Hall C, Level 2, Summit

5:00 PM MT02.08.01

Image Enhancement and Feature Extraction for Battery Electrodes with Deep Learning [Thorsten Tegetmeyer-Kleine](#), [Adrian Mikitisin](#), [Dirk Uwe Sauer](#) and [Wei Han Li](#); RWTH Aachen University, Germany

In the field of battery material science, the use of advanced imaging techniques is paramount for a comprehensive understanding of electrode materials. Computed Tomography (CT) has become an invaluable tool, offering insights into the internal structures of battery components. However, the challenges of low-contrast materials and small feature sizes inherent to battery electrodes necessitate innovative approaches for image enhancement and feature extraction. In this study, we explore the application of a machine learning approach, i.e., UNets, for enhancing CT images and employ a Variational Autoencoder (VAE) for feature extraction and clustering.

Our focus centers on a graphite-silicon composite electrode, chosen due to its relevance in battery materials and the complex imaging challenges it presents. Notably, the smallest features, such as carbon black and chipped graphite flakes, exist at nanometer scales, contributing to a heterogeneous structure. Moreover, the materials, including graphite and carbon black binder, share similarities in their core charge numbers, leading to low signal contrast, making their distinction challenging.

The study primarily addresses three key aspects:

Image Enhancement: We utilize UNets to enhance CT images of the graphite-silicon composite electrode. These neural networks excel in denoising and super-resolution, improving the visibility of small features and enhancing the overall image quality. The application of UNets leads to clearer, more informative images, aiding researchers in the analysis of battery materials in a faster way.

Feature Extraction: Through the implementation of a VAE, we perform feature extraction and clustering on the CT images. This technique enables the identification and isolation of important structural features within the electrode, offering insights into the material's composition and distribution. The extracted features can be instrumental in understanding the electrode's behavior during battery aging.

Applications: We discuss the practical applications of enhanced CT images and feature extraction in battery material science. The enriched images facilitate the accurate characterization of small-scale structures and the spatial distribution of materials within the electrode. This information can be used in the development of battery materials and manufacturing processes, contributing to enhanced performance, safety, and longevity.

Our study underscores the potential of utilizing cutting-edge image enhancement techniques and feature extraction methods in battery material science. By enhancing the quality of CT images and extracting relevant features, researchers can gain deeper insights into the intricate structures of battery electrodes. This research bridges the gap between imaging technology and materials science, offering valuable tools for advancing the development and manufacturing of high-performance batteries.

5:00 PM MT02.08.02

Coral-Like Metal Oxide/C Hybrid Microspheres comprising a Porous Yolk and a Hollow Thin-Shell for Anodes in Li Ion Batteries [Jung Sang Cho](#); Chungbuk National University, Korea (the Republic of)

Nowadays, innovative anodes are in demand owing to the requirement for improvement in the performance of Li ion batteries (LIBs). Although yolk-shell structured transitional metal oxides (TMOs) with various compositions have been studied as anodes for LIBs thus far, their long-term cycle properties are unsatisfactory in practical implementation. In order to solve this problem, hybrids of TMOs and C could be an effective strategy, but with the traditional synthetic process for the yolk-shell structure, it is difficult to prepare the yolk-shell structured TMO/C hybrid. In this study, we introduce a novel synthetic strategy for the yolk-shell structured TMO/C hybrids. The yolk shows a coral-like structure with interconnected mesopores. The synergistic effects of the coral-like yolk-shell structure with well-defined interconnected mesopores and a highly conductive C content result in advanced anodes with excellent Li⁺ ion storage properties. The detailed formation mechanism of the structure and its electrochemical properties as anodes for LIBs were investigated, in detail.

5:00 PM MT02.08.03

A Novel Machine Learning Approach for Surface Roughness Quantification and Optimization of Cast-On-Strap Lead-Antimony Alloy via Two-Point Correlation Function [Nageh K. Allam](#); American University in Cairo, Egypt

Surface roughness has a negative impact on the materials' lifetime. It accelerates pitting corrosion, increases effective heat transfer, and increases the rate of effective charge loss. However, controlled surface roughness is desirable in many applications. The automotive lead-acid battery is very sensitive to such effects. In our case study, the cast-on-strap machine has the largest effect on the surface roughness of the lead-antimony alloy. In this regard, statistical correlation functions are commonly used as statistical morphological descriptors for heterogeneous correlation functions. Two-point correlation functions are fruitful tools to quantify the microstructure of two-phase material structures. Herein, we demonstrate the use of the two-point correlation function to quantify surface roughness and optimize lead-antimony poles and straps used in the lead-acid battery as a solution to reduce their electrochemical corrosion when used in highly corrosive media. However, we infer that this method can be used in surface roughness mapping in a wide range of applications, such

as pipes submerged in seawater as well as laser cutting. The possibility of using information obtained from the two-point correlation function and applying the simulated annealing procedure to optimize the surface micro-irregularities is investigated. The results showed successful surface representation and optimization that agree with the initially proposed hypothesis.

5:00 PM MT02.08.04

First-Principles Investigations of FeP@Graphene as Anode Material for Sodium-Ion Batteries [Qi-Jing Hong](#); National Central University, Taiwan

In recent years, numerous strategies have been proposed to tackle the challenges of large volume changes and capacity decay in conversion-type electrodes. Most studies have focused on experimental investigations, and only a few have centered on simulation studies. This research aims to apply density functional theory to study FeP and its modifications, which are one of the most widely recognized conversion-type electrodes in experimental studies due to its low cost and high theoretical capacity. Experiments have shown that combining FeP with graphene (FeP@graphene) can be a promising way to alleviate the volume variation issue. Furthermore, Cu doping in FeP has been reported to enhance conductivity and capacity.

The FeP@graphene model was constructed based on experimental results of X-ray diffraction (XRD), thermogravimetric analysis (TGA), and scanning electron microscopy (SEM), followed by a geometry optimization calculation using density functional theory (DFT). We conducted calculations on the adsorption energy of single sodium atom under various conditions, including distance from the graphene sheet and the nearest Fe and P of the FeP cluster. The results indicate that the adsorption energy is unaffected by whether Na is near Fe or P, while adsorption away from the FeP cluster results in weaker interaction, i.e., lower adsorption energy. The effect of Cu doping in FeP on material conductivity was studied by performing electronic structure analysis. The calculation results of the partial density of states (PDOS) did not exhibit substantial differences between models with and without Cu doping in FeP, but the adsorption energy of a single Na atom was significantly lower in the Cu doping system.

Analyses of electron density difference maps (EDDM) and partial atomic charges are performed to further discern the distinctions between FeP@graphene with and without Cu doping. Climbing image-nudged elastic band (CI-NEB) calculations are conducted to investigate the diffusion behavior of Na in the FeP@graphene structure.

SESSION MT02.09: Data-Driven Materials and Process Design II

Session Chairs: Gang Chen and Feng Wang

Thursday Morning, April 25, 2024

Room 321, Level 3, Summit

8:00 AM *MT02.09.01

Data-Driven Analysis on The Dynamics and Heterogeneity of Particle Network in Composite Electrodes of Li-Ion Batteries [Kejie Zhao](#); Purdue University, United States

We use a data-driven approach to assess the heterogeneous electrochemistry and mechanics in composite cathodes. We visualize the morphological defects at multi-scales ranging from the macroscopic composite, particle ensembles, to individual single particles. Particle fracture and interfacial debonding are identified in a large set of tomographic data. The mechanical damage of active particles is highly heterogeneous. The difference originates from the polarization of the electrolyte potential, various local conducting environments, and thus the non-uniform distribution of the activation energy for the charge transfer reaction. We model the kinetics of intergranular fracture and interfacial degradation to assess the heterogeneous mechanical damage in composite electrodes using microstructure-informed mechanics modeling. We quantify the influence of the mechanical damage on the metrics of battery performance. More interestingly, the interfacial failure reconstructs the conductive network and redistribute the electrochemical activities that render a dynamic nature of electrochemistry and mechanics evolving over time in the composite electrodes.

8:30 AM MT02.09.02

Navigating Phase Diagram Complexity to Optimize The Robotic Synthesis of Battery Cathodes and Solid-State Electrolytes [Jiadong Chen](#) and Wenhao Sun; University of Michigan, United States

There are a plethora of computationally-predicted battery 'wonder' materials, but only a limited number of them can be successfully synthesized. Efficient synthesis recipes are essential to accelerate the realization and manufacturing of theoretically-predicted electrodes. Oftentimes the solid-state synthesis of multicomponent oxide electrodes is impeded by undesired byproduct phases, which can kinetically trap reactions in an incomplete non-equilibrium state. We present a thermodynamic strategy to navigate high-dimensional phase diagrams in search of precursors that circumvent low-energy competing byproducts, while maximizing the reaction energy to drive fast phase transformation kinetics. Using a robotic inorganic synthesis laboratory, we perform a large-scale experimental validation of our precursor selection principles. For a set of 35 target quaternary oxides with chemistries representative of intercalation battery cathodes and solid-state electrolytes, we perform 224 reactions spanning 27 elements with 28 unique precursors. Our predicted precursors frequently yield target materials with higher phase purity than when starting from traditional precursors. Robotic laboratories offer an exciting new platform for data-driven experimental synthesis science, from which we can develop new fundamental insights to guide both human and robotic chemists.

8:45 AM MT02.09.03

Cathode Upcycling for Direct Recycling Using a Rapid Coprecipitation Approach [Eva M. Allen](#)¹, [Jessica Macholz](#)¹, [Feng N. Wang](#)¹, [Mansi Porwal](#)², [Tim Fister](#)¹, [Denis Keane](#)³, [Michael Guise](#)³, [Viktor Nikitin](#)¹, [Jordi Cabana](#)² and [Albert Lipson](#)¹; ¹Argonne National Laboratory, United States; ²University of Illinois at Chicago, United States; ³Northwestern University, United States

In line with carbon neutrality goals by 2050, the Li-ion battery market has surged. To enhance battery sustainability and circularity, direct recycling methods aim to recover intact cathode materials. However, end-of-life cathode materials are typically 15-20 years old and often have lower energy density compared to current cathode materials. In response, we have developed a rapid coprecipitation process to boost energy density by converting low Ni-compositions, $\text{LiNi}_{0.33}\text{Co}_{0.33}\text{Mn}_{0.33}\text{O}_2$ (NMC111), into higher Ni-compositions (NMC622). This process forms a Ni-rich coating that diffuses into the core, increasing compositional homogeneity upon high-temperature relithiation. Our technology leverages existing infrastructure, offering low capital cost and minimal additional chemical input. Through ex-situ tomographic transmission X-ray microscopy (TXM) and XANES, we quantify Ni:Co:Mn elemental ratios and Ni valence state, confirming that elemental content evens at the secondary particle level, but elemental gradients remain at the primary particle level upon relithiation. Ex-situ high-resolution and in-situ wide-angle X-ray diffraction reveals concurrent structural changes during the relithiation process. These findings guide further improvements in synthesis for increased initial capacity and retention.

9:00 AM *MT02.09.04

In Situ Insights into Cathode Calcination: A multimodal Assessment of the Crystallization Process of LiNiO₂ Akhil Tayal¹, Pallab Barai², Hui Zhong¹, Xiaohui Qu¹, Jianming Bai¹ and Feng N. Wang²; ¹Brookhaven National Laboratory, United States; ²Argonne National Laboratory, United States

Calcination is a crucial step in the solid-state synthesis of metal oxides, finding applications not only in manufacturing of cathode materials for batteries but also across various industrial sectors. However, the inherent complexity associated with the process, involving elusive kinetic intermediates, hindering in-depth understanding and predictive control over the production of high-performance metal oxide materials. In this presentation, we report our in-situ analysis of the calcination process of LiNiO₂, a potential high-performance cathode for Li-ion battery, to assess the course of crystallization and phase progression vs temperature and time. The composition phase evolution diagrams derived from quantitation Rietveld analysis over in-situ XRD patterns, extracted with multivariate curve resolution (MCR) fitting of the in-situ XAS data, simulated with a phase-field based continuum model, and constructed by using a cosine similarity based automated data analysis as an in-line tool for process monitoring, are examined individually and compared with each other to draw new insights over the calcination process in order to establish optimized processing parameters.

9:30 AM *MT02.09.05

PyBOP: A Python Framework for Battery Model Optimisation and Parameterisation Brady Planden, Nicola Courtier and David Howey; University of Oxford, United Kingdom

To maximise the benefits of battery models, we need to parameterise them accurately from materials and electrochemical data. However, this remains a significant challenge [1] due to the need for expert knowledge in experimental data acquisition, processing, and system identification. In response, we introduce a systematic software framework, PyBOP [2], to establish and formalise novel parameterisation workflows for various continuum battery models. We present initial results from synthetic open-source battery datasets for benchmarking our model parameter identification efforts, comparing traditional deterministic methods with advanced Bayesian inference techniques. We will also highlight PyBOP's capabilities for optimising cell design by discussing an electrode optimisation study on a high-voltage LNMO cathode and silicon-graphite composite anode cell. Throughout this work, we demonstrate PyBOP's ability to accommodate different levels of proficiency in model parameterisation and optimisation, including illustrative workflows tailored towards researchers or industrial users.

[1] E. Miguel, G. L. Plett, M. S. Trimboli, L. Oca, U. Iraola, and E. Bekaert, "Review of computational parameter estimation methods for electrochemical models," *Journal of Energy Storage*, vol. 44, p. 103388, 2021. [Online]. Available: <https://www.sciencedirect.com/science/article/pii/S2352152X2101077X>
[2] B. Planden, N. Courtier, and D. Howey, "Python Battery Optimisation and Parameterisation (PyBOP)." [Online]. Available: <https://www.github.com/pybop-team/pybop>

10:00 AM BREAK

SESSION MT02.10: AI/ML for Materials and Process Modeling I

Session Chairs: Deyu Lu and Feng Wang

Thursday Morning, April 25, 2024

Room 321, Level 3, Summit

10:30 AM *MT02.10.01

Nanoscale structures in battery cathodes from theory, ML, and microscopy/spectroscopy experiments Maria K. Chan; Argonne National Laboratory, United States

The determination of nanoscale structural evolution in battery materials during synthesis and cycling is of importance in order to understand battery performance and degradation. The integrated use of first principles density functional theory (DFT) modeling, machine learning (ML), together with microscopy (e.g. STEM), diffraction/scattering, and spectroscopy (e.g. XANES and EELS) measurements, has enabled more in depth understanding of such structural evolution. In this talk, we will discuss how this combination of techniques has allowed us to determine oxygen instability and reactivity, map local cation and defect concentrations, and determine intermediate phases in lithium battery cathode materials.

11:00 AM MT02.10.02

Designing 2D Janus MXene Zr₂CXT (X, T =O, S, Se, and Te) for Lithium-Ion Batteries using Computational Approaches Yu-Ting Lin and Szu-Chia Chien; National Central University, Taiwan

Lately, 2D MXenes have drawn significant attention owing to their potential applications in energy storage, optoelectronics, sensors, etc. Among various types of 2D MXenes, transition metal carbides with a general chemical formula of Mn_{n+1}X_nT_x, where M represents a transition metal atom, such as Ti, V, and Zr, X represents a C or N atom, and T represents the surface termination atom including S, O, Se, and Te, have become promising materials for electrodes in Li-ion batteries (LIBs) due to its high electrical conductivity and low diffusion barrier^{1,2}. Through chalcogen functionalization, the MXenes with higher capacity and relatively low diffusion barrier energy can be obtained^{3,4}. On the other hand, by functionalizing different surface elements on the two opposite sides of a single layer MXenes, instinct materials properties can be linked together, facilitating the realization of versatile functions and the expansion of various applications.

Janus Zr-based MXenes, Zr₂CXT, was recently found to possess excellent structural, elastic, electronic, and optical properties^{5,6}, making them promising materials in LIBs applications. It is of great interest to search for potential Janus 2D Zr₂CXT for broader applications. However, precise control of the functionalization on the MXenes surface by experimental methods is indeed very challenging. Therefore, this work aims to apply density functional theory (DFT) calculations to explore the promising Janus Zr-based MXenes for electrode materials in Li-ion batteries. Various Zr₂CXT with surface atoms, including O, S, Se, and Te are studied. The essential properties of suitable anode materials, such as the dynamical stability, electronic properties, and diffusion barrier, are calculated. Furthermore, the adsorption energy of the Li on the Zr₂CXT surface is also calculated, as well as the capacity. It is anticipated that this work will provide insights into designing good 2D Janus MXenes for LIBs applications.

References

Zhan, X.; Si, C.; Zhou, J.; Sun, Z., *Nanoscale Horiz.* 2020, 5, 235-258.
Salim O.; Mahmoud, K. A.; Pant, K. K.; Joshi, R. K., *Mater. Today Chem.* 2019, 14, 100191.

Chen, Z.; Huang, S.; Yuan, X.; Gan, X.; Zhou, N., *Appl. Surf. Sci.* 2021, 544, 148861.
Tang, C.; Wang, X.; Zhang, S., *Mater. Chem. Front.* 2021, 5, 4672-4681.
Jin, W.; Wu, S.; Wang, Z., *Physica E Low Dimens. Syst. Nanostruct.* 2018, 103, 307-313.
Wang, Y.; Tao, Y.; Zhang, Q.; Huang, R.; Gao, B.; Li, Z.; Li, G.; Hu, N., *Solid State Comm.* 2022, 354, 114893.

11:15 AM MT02.10.03

AI-assisted X-ray absorption spectral analysis: Data reproducibility, database, and machine Learning Deyu Lu; Brookhaven National Laboratory, United States

X-ray absorption spectroscopy (XAS) is a premier element-specific experimental technique widely used for materials characterization in battery research. XAS encodes rich local structural and chemical information around X-ray absorbing species, however such information is convoluted in an abstract form, making it very difficult and time consuming to analyze. In this talk, we will discuss the emerging opportunities in AI-assisted XAS analysis, which leverages first-principles theory, high-throughput computing and data analytics. Specifically, we will highlight key areas in this approach, including pipelines to ensure data quality and reproducibility, spectral database development, and machine learning applications. The AI-assisted analysis pipeline can enable real-time feedback in high-throughput studies and autonomous experimentation.

11:30 AM MT02.10.04

Robust Machine Learning Inference from X-Ray Absorption Near Edge Spectra through Featurization Yiming Chen^{1,2}, Chi Chen², In-Hui Hwang¹, Michael J. Davis¹, Wanli Yang³, Chengjun Sun¹, Shyue Ping Ong² and Maria K. Chan¹; ¹Argonne National Laboratory, United States; ²University of California, San Diego, United States; ³Lawrence Berkeley National Laboratory, United States

Machine learning (ML), used in conjunction with materials modeling, is reshaping the way that researchers analyze and interpret materials characterization data by greatly accelerating the process and providing underlying physics [<https://link.springer.com/article/10.1557/s43577-022-00446-8>]. One notable application is the extraction of essential materials properties, such as oxidation states and structural information, from X-ray absorption spectroscopy (XAS) data. Traditional ML models typically utilize raw spectral intensities as the model input, with limited exploration on transforming the spectra intensities to potentially boost model performance. In this presentation, we will compare and assess the effectiveness of both reduced-dimensional features and overcomplete representations to discover the optimal representation of x-ray absorption near edge structure (XANES) data. Our system of interest is LiNi_xMn_yCo_zO₂ (NMC), a typical cathode material for Li-ion batteries. This material presents challenges in studying detailed changes during electrochemical cycling due to the complexity arising from transition metal mixing. We will evaluate various input transformations for XAS through regression and classification tasks to demonstrating how such feature engineering improves prediction accuracy and interpretability of ML models. Furthermore, we will discuss model validation using unseen experimental datasets, illustrating the transferability and robustness of the feature. A thorough explanation will also be provided to elucidate why certain features outperform others, aiding in the data analysis of experimental spectra [arXiv preprint arXiv:2310.07049].

Acknowledgement

This work is supported by the U.S. Department of Energy (DOE) Office of Science Scientific User Facilities project titled "Integrated Platform for Multimodal Data Capture, Exploration and Discovery Driven by AI Tools". M.K.Y.C. acknowledges the support from the BES SUFD Early Career award. Work performed at the Center for Nanoscale Materials and Advanced Photon Source, U.S. Department of Energy Office of Science User Facilities, was supported by the U.S. DOE, Office of Basic Energy Sciences, under Contract No. DE-AC02-06CH11357. We also acknowledge the support provided the Data Infrastructure Building Blocks (DIBBS) Local Spectroscopy Data Infrastructure (LSDI) project funded by National Science Foundation (NSF), under Award Number 1640899. MJD was supported by the U. S. Department of Energy, Office of Basic Energy Sciences, Division of Chemical Sciences, Geosciences, and Biosciences operating under Contract Number DE-AC02-06CH11357.

11:45 AM MT02.10.05

Atomistic Modeling of Chemomechanics at Electrified Interfaces Veerendra Naralasetti, Himanshu Shekhar and Aravind Krishnamoorthy; Texas A&M University, United States

As the world moves to a more electrified future, addressing several mechanical and tribological challenges in electric systems ranging from electrical energy storage to electric vehicle powertrains requires a more fundamental understanding of chemomechanics of electrified interfaces. More detailed insights into the reactivity of surfaces under mechanical contact are needed to design novel materials/lubricants that are needed to improve the efficiency of electro-mechanical systems. In this study, we performed ab initio density functional theory (DFT) calculations and reactive molecular dynamics (RMD) simulations to understand the surface reactivity and evolution of tribolayers in surfaces under electrified and non-electrified contact. Atomistic simulations of Polyalphaolefin (PAO) lubricants on naturally-oxidized steel surfaces reveal the formation of amorphous non-stoichiometric iron-carbide tribolayers that are non-protective and contribute to surface wear, consistent with experimental observations. Reactive MD simulations, performed using a specially parameterized ReaxFF forcefield, were used to predict surface passivity and tribological performance at extreme conditions of temperature, pressure and electrification encountered near asperities in surfaces under mechanical loading and thus derive new design rules for surface structures and lubricants for electrified applications.

SESSION MT02.11: AI/ML for Materials and Process Modeling II

Session Chairs: Deyu Lu and Feng Wang

Thursday Afternoon, April 25, 2024

Room 321, Level 3, Summit

1:30 PM *MT02.11.01

Tackling Ion Transport and Interfacial Evolutions in Solid-State Batteries through "Intelligent" Machine-Learning Zeyu Deng¹, Abhishek Panchal², Xie Weihang¹, Sai Gautam Gopalakrishnan³ and Pieremanuele Canepa^{2,1}; ¹National University of Singapore, Singapore; ²University of Houston, United States; ³Indian Institute of Science, India

Computational material science is crucial to establishing a firm link between complex phenomena occurring at the atomic scale and macroscopic observations of functional materials, such as energy materials for solar cells, fuel cells, and rechargeable batteries. Storing and distributing green energy is

central to the modernization of our society. Rechargeable batteries, including lithium (Li)-ion batteries, contribute substantially to shifting away from oil and other petrochemicals. The 2019 Nobel Prize in Chemistry awarded to John Goodenough, Stanley Whittingham, and Akira Yoshino resulted in the Li-ion battery as a mainstream technology powering millions of portable devices, electric vehicles, and stationary applications. Commercial Li-ion batteries suffer from stability issues. All-solid-state batteries utilizing solid-electrolyte “membranes” separating the distinct chemistries of the electrode materials appear to be a safer alternative. Nevertheless, stabilizing solid-solid “buried” interfaces in all-solid-state batteries remains a poorly understood aspect. In my talk, I will showcase the power of simulations to inform the complex reaction mechanisms, which take place at these complex interfaces. My talk will address two main aspects: 1) The advancement of first-principles kinetic Monte Carlo to study transport in fast-ion conductors. 2) I will showcase how machine-learned potentials can bring insight into the metal-anode/sulfide electrolyte interfaces, such as that of Li-metal/Li₆PS₅Cl.

2:00 PM MT02.11.02

Graph Neural Networks for Accurate Prediction of Ionic Transport Properties of Solid-State Electrolytes Cibrán López Álvarez^{1,2}, Edgardo Saucedo^{1,2} and Claudio Cazorla^{1,2}; ¹Polytechnic University of Catalonia, Spain; ²Barcelona Research Center in Multiscale Science and Engineering, Spain

In the pursuit of energy-efficient and environmentally friendly energy storage devices, solid-state electrolytes (SSE) have emerged as promising candidates due to their substantial stability and performance. The discovery of new materials with enhanced ionic diffusion is essential for the advancement of SSEs. To address this challenge, we introduce a novel approach based on Graph Convolutional Neural Networks (GCNNs) to predict the ionic diffusion coefficient of materials in large datasets such as the Materials Project database.

Our GCNN model is trained on a large and diverse database of density functional theory ab initio MD (DFT-AIMD) simulations [1,2], comprising several families of SSE and tens of millions of atomic configurations, what allows extracting valuable insights from the underlying crystallographic and structural relationships.

The predictive power of our GCNN-based approach is demonstrated through extensive validation on the dataset, showcasing its ability to accurately forecast the electrolyte behavior of both known and yet to discover materials. The integration of GCNNs into the materials discovery pipeline holds great promise for the development of next-generation SSEs technologies, introducing here a framework which allows predicting on any desired dataset.

The scripts resulting from this study have been made publicly available as a Python package, that is user-friendly and easily adaptable [3] to any desired target database.

[1] C. López, A. Emperador, E. Saucedo, et al., Universal ion-transport descriptors and classes of inorganic solid-state electrolytes, *Materials Horizons*, 2023, doi: 10.1039/D2MH01516A

[2] C. López, A. Emperador, E. Saucedo, et al., DFT-AIMD database, 2023, url: <https://superionic.upc.edu>

[3] C. López, R. Rurali, C. Cazorla, Repository with all the developed codes, 2023, url: <https://github.com/IonRepo/IonPred>

2:15 PM *MT02.11.03

Calcination of Lithium-Ion Battery Cathode Materials: Addressing Scale-Up Challenges using Multiscale Modeling Techniques Pallab Barai, Feng N. Wang, Tiffany Kinnibrugh, Ozgenur Kahvecioglu, Xiaoping Wang, Mark Wolfman, Tim Fister, Juan C. Garcia, Hakim Iddir, Krzysztof Puppek and Venkat Srinivasan; Argonne National Laboratory, United States

Rapid electrification of the automotive industry requires the synthesis of battery cathode materials at large scale, where the high temperature calcination is considered to be the most energy consuming and expensive process. Oxidation and lithiation of the transition metal cathode precursors occur at elevated temperatures (around 700°C – 1000°C) during the calcination process. The various physicochemical processes that occur during the calcination process can be summarized as dehydration, oxidation, lithiation, layering, and sintering induced grain growth. Transport of reactants, removal of reaction byproducts, and maintaining uniformity of temperature within the reaction zone, are of significant importance for successful scale-up of the calcination processes. A multiscale computational methodology is developed, where the kinetics of chemical reactions are extracted at the smaller length scale, and the mass and energy transport related issues are addressed at the larger length scale. Collaboration with in situ characterization using X-ray diffraction (XRD) techniques provide experimental data required for the model development activities. Atomistic simulations are conducted to extract further insights regarding the energetics of the evolution of different phases during the high temperature calcination process. Overall, the developed modeling capability is able to help with the optimization of calcination protocols during their scale up procedure.

2:45 PM BREAK

3:15 PM MT02.11.04

Beyond Predictions: An Interpretable Machine Learning Approach for Battery Performance Forecasting Injun Choi¹, Jieun Kim^{1,2} and Inchul Park^{1,2}; ¹Research Institute of Industrial Science & Technology, Korea (the Republic of); ²POSCO NEXT Hub, Korea (the Republic of)

This presentation will discuss our recent study on the application of machine learning to predict the electrochemical behavior of batteries, a key aspect in the field of battery management systems and fast charging technologies. In a distinct departure from existing utilization-based degradation models, this research offers a fresh perspective that emphasizes material-focused performance prediction.

The core of this study is the extensive analysis of data from tens of thousands of charge-discharge cycles of Li-rich layered oxide in a single cell setup. This approach allows for a more focused study of material properties, while avoiding the complexities often introduced by cell configurations. A key achievement of the research is the application of deconvolution techniques to extract intrinsic material properties from the extensive dataset, a critical step in achieving improved prediction accuracy and understanding of material properties.

An integral part of this research is the detailed monitoring of these intrinsic properties over time. This enables not only broad trend predictions, but also a detailed understanding of the dynamic electrochemical behavior of the material. In addition, insights into the material's elemental composition ratios contribute to both performance prediction and a deeper understanding of its intrinsic properties.

The study demonstrates a high accuracy of over 98% in predicting battery performance, confirming the efficiency of the machine learning models and the robustness of the dataset. In addition, the research extends its applicability beyond LLO materials, suggesting its potential across different battery materials. This broad relevance underscores the significant impact of the study on battery material design and performance optimization.

In summary, this research represents a significant advancement in the application of machine learning to battery performance prediction. By focusing on intrinsic material properties and leveraging an extensive, detailed dataset, the study not only achieves high prediction accuracy, but also establishes a scalable model for materials analysis in battery technology. The methods and results introduced can lead to more efficient, reliable, and adaptable energy storage solutions for future battery technology.

3:30 PM MT02.11.05

AI + Quantum Chemistry: A Paradigm Shift in Lithium Battery Development - An Assessment of Potential Contributions Jie Liu^{1,2}; ¹Hong Kong Quantum AI Lab, Hong Kong; ²The University of Hong Kong, Hong Kong

The global lithium-ion battery market, achieving a shipment volume of 958 GWh in 2022 with an estimated average commercialized energy density of ~170 Wh/kg, is on the brink of a significant transformation. This equates to an annual consumption of approximately 6.38 Mt of battery materials, underscoring the substantial resource usage and the sustainability challenges facing industry growth. The global effort towards more efficient, resource-saving, and eco-friendly energy storage systems has positioned AI and Quantum Chemistry as key drivers in battery manufacturing and R&D, with their full potential impact yet to be completely realized.

In this study, we provide a comprehensive assessment of the potential contributions of AI and Quantum Chemistry to the future development of lithium batteries, with a focus on material efficiency and cost savings. Anticipating a compound annual growth rate of 22.8% over the next eight years (as per EV-Tank's forecast), lithium-ion battery shipments are projected to reach 4,952 GWh by 2030. We analyzed two scenarios of energy density improvements: a conservative estimate of a 3% annual increase, in line with traditional development pathways, leading to an energy density of 215 Wh/kg by 2030, and an optimistic projection incorporating AI, Quantum Chemistry, and Automation in R&D. This advanced integration could potentially elevate annual improvement rates from 3% to 5.1%, achieving an estimated commercial battery energy density of 234 Wh/kg by 2030. Such advancements could result in a significant variations in the required material volume, estimated at 23 Mt/year and 21.21 Mt/year by 2030, respectively. This approach could potentially lead to cumulative material savings of 4.3 Mt from 2023 to 2030, translating into substantial cost savings of approximately 41 billion USD over this period.

A sensitivity analysis was conducted to provide a more accurate reflection of these projections, taking into account different annual improvement rates and market dynamics. The findings underscore the significant advantages, both economically and in terms of resource conservation, of accelerating lithium battery R&D. There is a compelling case for seizing the opportunity to integrate AI and Quantum Chemistry in lithium battery R&D. This integration not only promises enhanced energy densities but also marks a significant stride towards more sustainable and cost-effective battery production, potentially yielding returns far greater than the current investments in these cutting-edge technologies.

3:45 PM MT02.11.06

Machine Learning Workflow to Track Degradation Mechanisms in Industrial Lithium Ion Battery Cells Amina El Malki^{1,2}, Mohamed Ati², Mark Asch³ and Alejandro A. Franco^{1,4,5}; ¹Laboratoire de Réactivité et Chimie des solides (LRCS), UMR CNRS 7314, Université de Picardie Jules Verne, Hub de l'Energie, France; ²Renault SA, France; ³LAMFA, CNRS UMR 7352, Université de Picardie Jules Verne, France; ⁴Réseau sur le Stockage Electrochimique de l'Energie (RS2E), FR CNRS 3459, Hub de l'Energie, France; ⁵ALISTORE-European Research Institute, FR CNRS 3104, Hub de l'Energie, France

The degradation of lithium-ion battery (LiB) cells is a complex process resulting from the interaction of multiple phenomena. Understanding LiB cell aging requires tracking measurable effects of different degradation mechanisms, known as degradation modes. These include the loss of active material in the electrodes, loss of lithium inventory, and conductivity loss. The aging mechanisms are directly correlated with electrochemical cycling protocols and operation conditions of the LiB cell, such as parameters related to the type and rate of current in the charge and discharge, voltage cutoff conditions, temperature, break periods, state of charge, and cycle number.

Using machine learning techniques to uncover the interrelations between aging conditions/protocols and mechanisms can trigger tremendous progress in designing battery management systems capable of extending cell lifetime in Electric Vehicle (EV) applications [1]. In this work, we introduce a novel workflow that combines various machine learning techniques with electrochemical LiB cell state of health diagnostic analysis, facilitating the discovery of the impact of a broad set of cycling conditions/protocol parameters on aging modes [2]. This approach allows for deriving the possible aging mechanisms that might manifest in each distinct condition.

While numerous studies have employed machine learning techniques on LiB cell datasets, they often focus on a limited number of cycling stressors (e.g., C-rate for charge and discharge), and the datasets typically originate from tests conducted in academic laboratories. In this study, a comprehensive industrial dataset, encompassing a broad range of cycling conditions and protocols to simulate real-world usage of LiB cells in Electric Vehicles (EVs), is utilized. We explore how more than 10 stressors impact the aging modes of cells and identify the predominant degradation mechanisms based on cycling conditions. The analytical capabilities of our machine learning tool are demonstrated through various application examples, and strategies for mitigating aging in automotive applications are discussed. Finally, we consider how our machine learning workflow holds the potential to propel current battery management systems in EVs to the next level.

[1] Artificial Intelligence Applied to Battery Research: Hype or Reality, Battery Research: Hype or Reality, Teo Lombardo, Marc Duquesnoy, Hassna El-Bouysidy, Fabian Arén, Alfonso Gallo-Bueno, Peter Bjørn Jørgensen, Arghya Bhowmik, Arnaud Demortière, Elixabete Ayerbe, Francisco Alcaide, Marine Reynaud, Javier Carrasco, Alexis Grimaud, Chao Zhang, Tejs Vegge, Patrik Johansson, and Alejandro A. Franco*, Chem. Rev. 2022, 122, 12, 10899–10969, 2021.

[2] Amina El Malki, Mohamed Ati, Mark Asch, Alejandro A. Franco, to be submitted (2023).

SYMPOSIUM MT03

Machine Learning Methods, Data and Automation for Sustainable Electronics
April 23 - April 25, 2024

Symposium Organizers

This searchable program is up-to-date as of April 15th, 2024.

Keith Butler, University College London
Kedar Hippalgaonkar, Nanyang Technological University
Shijing Sun, University of Washington
Jie Xu, Argonne National Laboratory

Symposium Support
Bronze
APL Machine Learning

* Invited Paper
+ JMR Distinguished Invited Speaker
^ MRS Communications Early Career Distinguished Presenter

SESSION MT03.01: Machine Learning for Experiments I
Session Chairs: Chibueze Amanchukwu and Jie Xu
Tuesday Morning, April 23, 2024
Room 322, Level 3, Summit

10:30 AM *MT03.01.01

Autonomous Experimentation for Materials Research [Benji Maruyama](#); Air Force Research Laboratory, United States

The current materials research process is slow and expensive; taking decades from invention to commercialization. The Air Force Research Laboratory pioneered ARES™, the first autonomous experimentation system for materials development. A rapidly growing number of researchers are now exploiting advances in artificial intelligence (AI), autonomy & robotics, along with modeling and simulation to create research robots capable of making research progress orders of magnitude faster than today. We will discuss concepts and advances in autonomous experimentation in general, and associated hardware, software and autonomous methods.

We will distinguish between non-iterative AI/ML approaches that use large data sets (e.g., CNN, LLM) and small data, iterative approaches that strive to identify & confirm scientific hypotheses using AI reasoning.

We consider the impact of autonomous experimentation on human scientists and the scientific enterprise: Changing roles for humans and robots, expectations. In the future, we expect autonomous experimentation to revolutionize the research process, and propose a “Moore’s Law for the Speed of Research,” where the rate of advancement increases exponentially, and the cost of research drops exponentially. We also consider a renaissance in “Citizen Science” where access to online research robots makes science widely available.

11:00 AM *MT03.01.02

Polybot: Accelerating Electronic Polymer Discovery through AI/ML and Automation [Henry Chan](#)¹, Jie Xu¹, Aikaterini Vriza¹ and Yukun Wu^{2,1};
¹Argonne National Laboratory, United States; ²Purdue University, United States

The increasing demand for flexible, wearable, and smart electronics has propelled the exploration of electronic polymers. To unleash their full potential, understanding the complex relationships between processing, structure, and properties is crucial, along with the development of scalable methods for producing high-quality thin films and devices. This task is particularly challenging due to the intricate interactions between processing parameters, including solution formulation, rheological behavior, and post-treatment procedures. In this presentation, we introduce Polybot, an advanced Autonomous Materials Acceleration Platform (MAP) that seamlessly integrates AI/ML, robotics, and automated characterization techniques for expediting the discovery and optimization of electronic polymers. Polybot exemplifies its prowess through closed-loop studies, demonstrating simultaneous enhancements in polymer processability and performance within a high-dimensional experimental parameter space. Furthermore, we delve into the intriguing realm of small data, addressing the integration of literature-derived insights and physics-based simulations within MAPs. Our discussion will illuminate both the challenges and the promising prospects associated with this integration, showcasing how it enriches the efficacy and robustness of the materials discovery process.

11:30 AM MT03.01.03

High-Throughput Structural Investigation of Block Copolymer and Conjugated Polymer Co-Assemblies Karen Li, [Kiran Vaddi](#) and Lilo D. Pozzo; University of Washington, United States

Conjugated polymers (CPs) have garnered much interest as semi-conducting materials for organic electronics. The properties of conducting polymers can be affected from induced long-range order. Block copolymers (BCPs) are commonly used as templating materials due to their ability to self-assemble into many crystalline structures. Blending structure directing BCPs and relatively rigid CPs may lead to materials with enhanced properties due to the formation of highly ordered structures. Thus, it is essential to understand the phase behavior of these co-assembled blends. The shape and order of these structures are also affected by many parameters including temperature, concentration, molecular weight, side chains, shear, etc. High-throughput characterization and analysis will be required to effectively investigate these factors. To demonstrate this, hydrogel blends of BCP polyethylene oxide-polypropylene oxide-polyethylene oxide and conjugated polyelectrolyte poly[3-(potassium-4-butanate)thiophene-2,5-diyl] were prepared at varying concentrations with an open-source liquid handling robot. The polymer blends were structurally characterized through high-throughput small angle x-ray scattering (HT-SAXS), utilizing a custom cartridge system that can enable thousands of measurements per day at a synchrotron. In addition, various temperatures and shear conditions were applied to the polymer blends to produce monolithic oriented gels and measured via small angle neutron scattering (SANS). A statistical analysis tool, *autophasemap*, was developed in our group to automatically generate phase maps that provide a hierarchical summary of the HT-SAXS experiments. This is accomplished by measuring the similarity between sampled profiles and data-based template functions and clustering the profiles based on this similarity. Multiple ordered phases of the polymer blends were then identified through the presence and position of Bragg peaks in 1D profiles and Bragg spots in 2D profiles.

11:45 AM MT03.01.04

Development of a High-Throughput Electrochemical Device for Data-Driven Electrolyte Materials Discovery Yangang Liang; Pacific Northwest National Laboratory, United States

Data-driven research in the field of electrolyte discovery for energy storage applications is growing rapidly. However, current characterization techniques struggle to analyze large numbers of samples accurately and efficiently. To address these limitations, we propose an innovative electrochemical measurement system to integrate with robotic platforms. This high-throughput system provides highly reliable and repeatable conductivity measurements, facilitating fast screening of battery materials and establishing materials-electrochemical property relationships. Our research contributes to advancing electrolyte materials for energy storage and demonstrates the potential of high-throughput characterization technologies in accelerating materials discovery.

SESSION MT03.02: Machine Learning for Experiments II
Session Chairs: Henry Chan and Reinhard Maurer
Tuesday Afternoon, April 23, 2024
Room 322, Level 3, Summit

1:30 PM *MT03.02.01

Machine Learning Accelerated Electrolyte Discovery for Batteries Chibueze Amanchukwu; University of Chicago, United States

Battery chemistries with high energy densities are required for long duration energy storage. Moving away from intercalation to electrodeposition endows lithium metal batteries (LMBs) with energy densities that surpass conventional lithium-ion. However, there are no electrolytes to date that can enable efficient electrodeposition and dissolution of lithium metal without significant degradation and lithium dendritic growth. Therefore, electrolyte discovery holds great promise for lithium metal batteries. Unfortunately, current approaches to electrolyte discovery have focused primarily on trial-and-error. In our work, we pursue a data-driven approach. We curate the largest dataset of important properties for small molecule electrolytes – ionic conductivity, oxidative stability, and Coulombic efficiency. We build machine learning models capable of predicting these properties and show that the models are consistent with known chemical principles and intuition. Deploying these models on large unlabeled datasets allowed us to identify new and promising electrolytes that have never been explored for LMBs. Our data science driven approach for electrolyte discovery is a paradigm shift that addresses challenges facing electrolytes in a wide range of electrochemical devices.

2:00 PM *MT03.02.02

Machine Learning Defect Properties of Semiconductors Arun Kumar Mannodi-Kanakkithodi; Purdue University, United States

Defects and impurities in semiconductors heavily influence their performance in optoelectronic applications. Quick predictions of defect properties are desired in technologically important semiconductors, but complicated by difficulties in assigning measured levels to specific defects and by the expense of large-supercell first principles computations that involve charge corrections and advanced functionals [1]. We address this issue by combining high-throughput density functional theory (HT-DFT) with machine learning (ML) to develop predictive models for defect formation energies (DFE) and charge transition levels (CTL) of native defects and functional impurities in Group IV, III-V, and II-VI zinc blende (ZB) semiconductors. Using an innovative approach of sampling dozens of metastable polymorphs each from defect configurations in thousands of distinct DFT computations, we generate one of the largest known computational defect datasets, containing many types of vacancies, self-interstitials, anti-site substitutions, impurity interstitials and substitutions, and defect complexes [2,3].

Two distinct types of ML methods are applied: (a) random forest, Gaussian process, and neural network regression models based on manual descriptors encoding the defect atom's elemental properties, coordination environment, and "unit cell" defect data [2,3], and (b) crystal Graph-based Neural Networks (GNNs) trained using entire defective structures as input [4], specifically using three established GNN techniques, namely Crystal Graph Convolutional Neural Network (CGCNN) [5], Materials Graph Network (MEGNET) [6], and Atomistic Line Graph Neural Network (ALIGNN) [7]. Root-mean square errors (RMSE) in predicting DFE are as high as 1 eV with the former, while ALIGNN yields errors of ~ 0.3 eV or less which represents a prediction accuracy of 98% given the range of values within the dataset, improving significantly on the state-of-the-art. While the first set of models yield only optimized energies based on a smaller dataset of ~ 1500 points, the GNN models are trained on > 15,000 data points and can be applied to predict accurate unoptimized, partially optimized, or fully optimized DFE values corresponding to any defective structure. The best models are eventually applied to perform screening across hundreds of thousands of hypothetical single defects/dopants and defect complexes to find stable defects which may or may not create energy levels within the band gap and affect the semiconductor's performance in optoelectronic devices. We also demonstrate that GNN models can be used as an effective surrogate for DFT computations to obtain low energy defective structures for any semiconductor-defect combination, which is very promising for screening over large chemical spaces without the need for expensive DFT.

REFERENCES

- [1] Freysoldt, C. et al. First-principles calculations for point defects in solids. *Rev Mod Phys* 86, 253–305 (2014).
- [2] Mannodi-Kanakkithodi, A. et al. Machine-learned impurity level prediction for semiconductors: the example of Cd-based chalcogenides. *NPJ Comput Mater* 6, 39 (2020).
- [3] Mannodi-Kanakkithodi, A. et al. Universal machine learning framework for defect predictions in zinc blende semiconductors. *Patterns* 3, 100450 (2022).
- [4] Rahman, H. et al., Accelerating Defect Predictions using Graph-based Neural Networks. *Under review*. Preprint: <https://arxiv.org/abs/2309.06423> (2023).
- [5] Xie, T. et al. Crystal Graph Convolutional Neural Networks for an Accurate and Interpretable Prediction of Material Properties. *Phys Rev Lett* 120, 145301 (2018).
- [6] Chen, C. et al. Graph Networks as a Universal Machine Learning Framework for Molecules and Crystals. *Chemistry of Materials* 31, 3564–3572 (2019).
- [7] Choudhary, K. et al. Atomistic Line Graph Neural Network for improved materials property predictions. *NPJ Comput Mater* 7, 185 (2021).

2:30 PM MT03.02.03

Analyzing The Impact of Design Factors on Solar Module Thermomechanical Durability Using Interpretable Machine Learning Xin Chen^{1,2}, Todd Karin³ and Anubhav Jain¹; ¹Lawrence Berkeley National Lab, United States; ²University of California, Berkeley, United States; ³PVEL, United States

Solar modules in utility-scale PV systems are anticipated to maintain a prolonged lifetime to effectively rival conventional energy sources. However, the

durability of these modules is often compromised by cyclic thermomechanical loading, emphasizing the need for a proper module design to counteract the detrimental effects of thermal expansion incompatibility. Given the complex composition of solar modules, isolating the impact of individual components on overall durability remains a challenging task. In this work, we constructed a comprehensive data set, capturing bill-of-materials and post-thermal cycling power loss from over 250 distinct module designs. Utilizing the data set, we developed a machine learning model to correlate the design factors with the degradation and applied the Shapley additive explanation to provide interpretative insights into the model's decision-making, investigating the impacts of design factors like the busbar number, wafer thickness, and others. Our analysis reveals that the type of silicon solar cell, whether monocrystalline or polycrystalline, predominantly influences the degradation, and monocrystalline cells present better durability. This finding was further substantiated by statistical testing on our raw data set. We also demonstrate that the thickness of the encapsulant remains another important factor, with thicker encapsulants correlated with reduced power loss. The study here provides a blueprint for utilizing explainable machine learning in an intricate material system and can potentially steer future research on optimizing solar module design.

2:45 PM MT03.02.04

Machine Learning Enhanced Optical Characterization of Hexagonal Boron Nitride Thickness on 300-nm Oxide Substrate [Kirsten L. Lina](#)^{1,2} and Masahiro Ishigami^{1,2}; ¹University of Central Florida, United States; ²NanoScience Technology Center, United States

This study integrates optical techniques with machine learning to achieve precise characterization of hexagonal boron nitride (hBN) thickness on 300-nm silicon oxide substrate. Conventional methods for interpreting large volumes of microscopy data are labor intensive, time consuming, and faulted by human subjectivity. The aim of this work is to mitigate these challenges by employing a regional convolutional neural network (R-CNN) to perform image segmentation and object detection on optical microscopy images, enabling real-time processing capabilities for thickness identification. The Mask R-CNN architecture featuring the ResNet101 backbone network, region proposal network, classification and mask subnets with bounding box regression generates feature maps to identify graphical features including shapes, flake sizes, contrast, and color. Initially, a robust theoretical mapping of hBN flake colors in the standard red, green, blue (sRGB) color space was developed, accounting for the oxide thickness. Theoretical RGB values corresponding to specific hBN thickness align remarkably well with those extracted from optical images, validating the use of colors as a reliable standard for hBN thickness identification. Our trained R-CNN predicts thickness of hBN flakes based on their mapped expected color variations with remarkable accuracy. This material characterization approach accelerates initial characterization of hBN while also holding potential for enhancing production efficiency across various 2D materials in nanoscience research.

3:00 PM BREAK

3:30 PM *MT03.02.05

Engineering Soft-Matter with Agent-Driven High-Throughput Experiments [Lilo D. Pozzo](#), Maria Politi, Brenden Pelkie, Kiran Vaddi, Huat Thart Chiang, Karen Li and Kacper J. Lachowski; University of Washington, United States

Artificial intelligence (AI), when paired with laboratory automation, can greatly accelerate materials optimization and scientific discovery. For example, it can be used to efficiently map a phase-diagram with intelligent sampling along phase boundaries, or in 'retrosynthesis' problems where a material with a target structure is desired but a synthetic route is not known. These approaches are especially promising in soft matter and polymer physics, where design parameters (e.g. chemical composition, MW, topology, processing) are vast and where properties and function are intimately tied to molecular design features. However, for AI algorithms to operate efficiently in these spaces, they must also be 'encoded' with relevant domain expertise specific to the problems being tackled. This talk will cover recent advances in hardware and software tools for accelerated materials optimization for polymers and soft matter systems. Finally, it will outline remaining challenges in practical implementations and identify future opportunities for research.

4:00 PM MT03.02.06

Accelerated Development of Ga₂O₃ Thin-Film Epitaxial Growth by AI Approaches with FAIR Data in NOMAD [Andrea Albino](#)¹, Ta-Shun Chou², Hampus Näsström¹, Amir Golparvar¹, Theodore Chang¹, Alvin Noe Ladines¹, Lauri Himanen¹, Mohammad Nakhuae¹, Andreas Popp², Jose Marquez Prieto¹, Sebastian Brückner^{2,1}, Markus Scheidgen¹, Claudia Draxl¹ and Martin Albrecht²; ¹Humboldt-Universität zu Berlin, Germany; ²Leibniz-Institut für Kristallzüchtung, Germany

Data-driven material science has the potential to transform the way we design and develop materials. This emerging field represents a significant departure from traditional trial-and-error methods and empirical approaches that have characterized materials science for decades. Experiments in this area involve a multidimensional parameter space, making analysis challenging and time-consuming. Finding predictive empirical relations that allow for precise control over various aspects of the synthesis process has posed a challenge to human cognitive abilities alone. This becomes even more complex when combining datasets from different labs or from different scientists due to the lack of established standards for data models and methods to capture the large number of experimental details, including elaborate workflows and a large diversity of instruments for characterization. It requires a radical shift in how information is handled and research is performed. Experiment data must be complemented with its rich-metadata context, also covering ontologies and workflows according to the FAIR (findable, accessible, interoperable, reusable) principles [1].

Opening new perspectives towards finding structure, correlations, and novel information with data-analysis and AI tools, therefore, is intimately connected to the challenge of integrating this information into a FAIR infrastructure [2].

Here we present growth optimization of β -Ga₂O₃ thin films by metalorganic vapor phase epitaxy (MOVPE) on (1 0 0) β -Ga₂O₃ semi-insulating substrates which is a successful example of applying ML/AI approaches in materials synthesis. Improving the efficiency of this synthesis is highly relevant due to the wide range of electronic device applications based on Ga₂O₃. Applying AI modeling on the experimental data related to thin film growth, we effectively improved the growth rate and prediction of doping level in MOVPE-grown Si-doped β -Ga₂O₃ [3,4].

We will present the implementation of this use case in NOMAD (nomad-lab.eu) [5] and discuss the functionalities developed to digitize the entire data lifecycle in crystal growth and epitaxy, with the ultimate goal of FAIR data for materials growth. We developed and deployed Electronic Laboratory Notebooks (ELN) to document all relevant synthesis procedures. We will show how structured data opens up the potential to create tools that facilitate and automate data management, and the sustainable application of AI-based analytics, dedicated to process optimization in synthesis.

[1] Wilkinson, M., et al. The FAIR Guiding Principles for scientific data management and stewardship. *Sci Data*. 2016; 3, 160018.

[2] Scheffler, M., et al. FAIR data enabling new horizons for materials research. *Nature*. 2022; 604, 635-642.

[3] Chou, T.-S. et al. Toward Precise n-Type Doping Control in MOVPE-Grown β -Ga₂O₃ Thin Films by Deep-Learning Approach. *Crystals*. 2022; 12(1), 8.

[4] Chou, T.-S. et al. Machine learning supported analysis of MOVPE grown β -Ga₂O₃ thin films on sapphire. *Journal of Crystal Growth*. 2022; 126737.

[5] Scheidgen et al. NOMAD: A distributed web-based platform for managing materials science research data. *Journal of Open Source Software*. 2023; 8(90), 5388.

4:15 PM MT03.02.07

Explainable Materials Informatics for Coherent Phonon Transport in 2D Heterostructures by Self-Learning Entropic Population Annealing
Wenyang Ding¹, Jiang Guo¹, Koji Tsuda^{1,2,3} and Junichiro Shiomi^{1,1}; ¹The University of Tokyo, Japan; ²National Institute for Materials Science, Japan; ³RIKEN Center for Advanced Intelligence Project, Japan

The exploration of coherent phonons demands flawless interfaces to circumvent phonon phase disruptions and inter-phonon interactions, a formidable challenge to achieve in practice. Van der Waals (vdWs) heterostructures, created through the precise layering of diverse two-dimensional materials, offer an optimal foundation for exploring coherent phonon transport because of their seamlessly integrated interfaces. Over the past decade, the comprehension of coherent phonon transport within superlattices has significantly advanced, propelled by the sophisticated field of materials informatics (MI) driven by machine learning techniques. Bayesian optimization, known for its efficiency in recommending structures with desirable properties, is a commonly adopted MI method. However, it's a black-box method with the potential for converging to local minima and limited representation of the entire sample space. In contrast, entropic population annealing (SLEPA) extended from entropic sampling with a machine learning model by Li et al. [1], efficiently captures the density of states, enabling comprehensive thermal conductivity assessments for vdWs heterostructures while evaluating few candidates without missing optimal results.

In this study, we obtain thermal conductivity distribution of graphene/WS₂ heterostructure in a candidate space of tens of thousands by combining SLEPA and atomistic Green's functions. Through analysis, we identified two factors that have a significant negative impact on the thermal conductivities of heterostructures: the average distance of WS₂ from the center of the heterostructure and the presence of specific sequences, such as '1 0 0 1', where '0' represents graphene and '1' represent WS₂. Moreover, by using mode-resolved atomistic Green's function (AGF), the underlying mechanism under these two factors are investigated. The findings reveal that, as the average distance of WS₂ from the center of the heterostructure decreases, there is an increase in the transmission of high-frequency phonons at oblique angles. Additionally, an increase in the number of '1 0 0 1' leads to higher transmission of low-frequency phonons that are normally incident. The combination of these two factors can suppress phonon transmission across a broad spectrum of frequencies and angles of incidence, leading to the optimized heterostructure with remarkably low thermal conductivity.

[1] J. Li, J. Zhang, R. Tamura, K. Tsuda, *Self-learning entropic population annealing for interpretable materials design*, Digital Discovery 1, 295-302 (2022).

4:30 PM MT03.02.08

Machine-Learning Minimization of Amorphous Heat Conduction by High-Throughput Deposition Process in The Loop Kunihiko Shizume¹, Ryohei Nagahiro¹, Michiko Sasaki^{1,2}, Masahiro Goto² and Junichiro Shiomi¹; ¹The University of Tokyo, Japan; ²National Institute for Materials Science, Japan

In Material Informatics, material exploration *via* high-throughput experiments has gained traction. This study utilizes a specially equipped combinatorial sputtering system and thermoreflectance method to explore amorphous materials with TC ~0.1 W/mK. There is a significant demand for solid-like thermal insulation materials combining mechanical strength, which can be applied to heat-mediated sensing devices and heat shields. Amorphous materials are promising candidates for dense thermal insulator since the disordered structure strongly suppress propagation of the vibrational modes. Their metastable nature can result in varied structures depending on the fabrication process. For instance, our prior research demonstrated that TC of amorphous Si (a-Si) and Ge (a-Ge) films varies with the deposition temperature during sputtering. This implies that amorphous structures can be modulated using sputtering process parameters (PP). Due to challenges in identifying structures, optimizing properties of amorphous materials has not been studied much. In this study, while treating the structure and the composition as a black box, we use the sputtering PPs as the explanatory variables and TC as the target variable to be minimized through Bayesian optimization. This high-throughput experiment also works as a materials screening process to identify interesting materials for the characterization analysis. It allows efficient experimental data accumulation on the relationships between the thermal conductivity and the characteristics of amorphous. As a further objective of this study, we also plan to implement machine learning to interpret the gathered data and enhance our comprehension of heat transfer in amorphous materials, which is not yet fully understood.

Samples were prepared using Combinatorial Sputter Coating System (COSCOS), which can deposit the target material with four arbitrarily controlled PPs: mixed gas composition, total gas pressure, sputtering power, and sample-target distance. The multiple holders enable automated deposition of 14 samples under a unique set of PPs, in a single batch. We prepared 40 of a-SiO_x, 35 of a-SiN_x, and 12 of a-Si₀Ge₀Sn₀ films with a thickness between 30-200 nm and measured the TC. Here, a-SiO_x and a-SiN_x were measured by frequency-domain thermoreflectance (FDTR) and a-Si₀Ge₀Sn₀ was measured by time-domain thermoreflectance (TDTR). Moreover, for the a-SiN_x, deposition was performed under 26 new conditions, as suggested by Bayesian optimization. 32 out of the 40 a-SiO_x films exhibited similar TC ranging from 0.6 to 0.9 W/mK except for the remaining 8 films with TC between 1.4-2.2 W/mK, likely due to contaminations of iron clusters from the equipment during sputtering. In contrast, a-SiN_x exhibited TC ranges from 0.6 to 1.5 W/mK with a wide-tailed distribution. This indicates the broader TC modulation range for a-SiN_x, compared with a-SiO_x. Among 26 of a-SiN_x films prepared under PPs suggested by Bayesian optimization, the one with the lowest TC achieved 0.5 W/mK. This result ensures the efficacy of our strategy to reduce TC. For a-Si₀Ge₀Sn₀ films, the lowest TC was 0.2 W/mK, lower than the reported TC of similar materials like a-Ge₃₀Si₅Sn_{1.5}O₃₆ (0.4 W/mK). TDTR also confirmed decreases in speed of sound as Sn content increases which contributes to the TC reduction. As a result, a-Si₀Ge₀Sn₀ emerges as a promising candidate for further optimization. Various characteristics like density and structure, beyond merely composition, might be modulated through the depositions across diverse PPs.

To enhance the experimental throughput, we employed the masking mechanism of COSCOS for multi-point deposition on a single substrate and FDTR/TDTR mapping measurements. This experimental scheme should facilitate data accumulation on the order of 100 samples per single deposition batch. We are currently continuing our material exploration in the a-Si₀Ge₀Sn₀ system and will report on these results in our presentation.

4:45 PM MT03.02.09

Accelerating The Development of Thin Film Photovoltaic Technologies: An Artificial Intelligence Assisted Methodology Using Spectroscopic and Optoelectronic Techniques Victor Izquierdo-Roca¹, Robert Fonoll¹, Enric Grau-Luque¹, Ignacio Becerri-Romero¹, Jacob Andrade-Arvizu¹, Pedro Vidal-Fuentes¹, Alejandro Perez-Rodriguez² and Maxim Guc¹; ¹IREC, Spain; ²Departament d'Enginyeria Electrònica i Biomèdica, IN2UB., Spain

Thin film photovoltaic (TFPV) materials and devices present a high complexity with multi-scale (from nm to μ m), multi-layer and multi-element structures and with complex fabrication procedures. To deal with this complexity, the evaluation of the compositional, structural, morphological, optical, and electrical properties, among others, of TFPV devices is critical to generate a model that allows pushing forward their development and optimization, especially in terms of PV performance. However, the intrinsic complexity of TFPV materials and devices requires approaching their research in a holistic way. This involves the performance of a holistic characterization approach which presents three main challenges: 1) performing a systematic combinatorial characterization (using different characterization techniques) of materials and devices, 2) automating characterization (data acquisition) for generating a statistically relevant amount of information (big data), 3) generating automatized, fast, and multidimensional data processing strategies.

In this work, an approach to solve these three challenges is presented through the creation of a modular and highly customizable automatized characterization platform and methods that provide a fast, holistic, and non-destructive characterization of complex material and devices. The above-

mentioned challenges are faced up by the platform in the following way:

1) Systematic heterogeneous characterization – integrating dedicated sensors for the evaluation of composition, morphology, crystal structure, thickness, and optoelectronic parameters by different techniques (X-ray fluorescence, Raman, photoluminescence and UV-Vis-NIR reflectance spectroscopies, visual imaging, elastic light scattering, I-V, EQE, electroluminescence).

2) Automate data acquisition – developing dedicated software and protocols for systematic and automatized data acquisition and a data storage structure for efficient data analysis.

3) Automatized and fast multidimensional data processing – developing flexible methodologies and algorithms to automatize data conditioning and processing using statistical and AI-assisted data analysis using machine learning algorithms to accelerate the big data analysis and identify correlation patterns and processes to push forward the development of the TFPV technologies.

A real case for the accelerated research of $\text{Cu}_2\text{ZnSnSe}_4$ -based TPV (CZTSe) devices is then used as practical example for the proposed platform. More than 20 samples (with $5 \times 5 \text{ cm}^2$ size) are systematically studied as the initial step for large-scale production of CZTSe based PV devices. The devices have Glass/Mo/MoSe₂/CZTSe/CdS/i-ZnO/ITO structure and small controlled and non-controlled fabrication processes variations are included in the samples. Each sample is discretized in $3 \times 3 \text{ mm}^2$ individual solar cells (up to 196 cells per sample), which allows achieving a complete data library that aids obtaining a considerable amount of cell-by-cell information to implement statistically relevant analyses. A systematic characterization combining optical and optoelectronic techniques as described above is performed in each cell. The analysis of the data obtained allows correlating the physicochemical properties of the TFPV materials with variations in device performance. This knowledge provides key information to understand the role of different materials and layers properties, their interrelations and, finally, the current technology limitations. This information is strongly relevant for the future development of the CZTSe technology towards high efficiencies and its future industrialization. Moreover, the proposed platform opens a way for the development of a process monitoring tool for controlling the production of TFPV devices that is easily adaptable to other optoelectronic technologies.

SESSION MT03.03: Poster Session: Machine Learning, Data, Software

Session Chairs: Keith Butler, Shijing Sun and Jie Xu

Tuesday Afternoon, April 23, 2024

Flex Hall C, Level 2, Summit

5:00 PM MT03.03.01

Mara - An Autonomous Synthesis System for Energy Materials [Clara N. Tamura](#), Arthur Chong and Shijing Sun; University of Washington, United States

The discovery and development of energy materials are crucial tasks to tackle the ongoing progression of climate change. Current research has focused on the exploration and synthesis of such materials, but current methods are time-consuming and do not allow for a larger scale of exploration and depth investigations. With the recent advancements in machine learning and robotics, autonomous synthesis and analysis to accelerate material discovery has become possible, allowing for widespread exploration and rapid prototyping.² Still, the field of autonomous laboratories is young, and integrating machine learning with robotics is yet to be explored.¹ At the UW Sun Lab, we are developing a fully autonomous materials synthesis system with AI instructing robots to make new materials. We are developing "Mara," an autonomous synthesis system consisting of an Opentron-OT2 liquid-handling robot, a microplate reader (96-well), and a camera system for monitoring the robotic movement and automated image analysis to create solar materials such as halide perovskite synthesized by drop-casting. Ultimately, Mara will autonomously synthesize material with desired properties, such as optimal absorption, without the need for human intervention. We set up the whole system from scratch in two months, and the Mara system is driven by the Python API commands. This will demonstrate the effective use of robotics and machine learning to accelerate material discovery and development, allowing a faster response to climate change.

Citations:

Higgins, K., Ziatdinov, M., Kalinin, V., Ahmadi, M., High-Throughput Study of Antisolvents on the Stability of Multicomponent Metal Halide Perovskites through Robotics-Based Synthesis and Machine Learning Approaches, *Journal of the American Chemical Society* 2021 143 (47), 19945-19955

DOI: 10.1021/jacs.1c10045

Li, Y., Xia, L., Fan, Y., Wang, Q., & Hu, M. (2022). Recent advances in autonomous synthesis of materials. *ChemPhysMater*, 1(2), 77-85.

<https://doi.org/10.1016/j.chphma.2021.10.002>

5:00 PM MT03.03.04

PV-VISION: An Deep Learning based Package for Automated Solar Module Inspection [Xin Chen](#)^{1,2} and Anubhav Jain¹; ¹Lawrence Berkeley National Lab, United States; ²University of California, Berkeley, United States

Solar photovoltaic (PV) modules are susceptible to manufacturing defects, mishandling problems or extreme weather events that can limit energy production or cause early device failure. Trained professionals use electroluminescence (EL) images to identify defects in modules, however, field surveys or inline image acquisition can generate millions of EL images, which are infeasible to analyze by rote inspection. We developed an open-source computer vision package PV-VISION to automatically process the EL images using deep learning models, covering automatic image preprocessing, cell defect detection and crack feature extraction. We demonstrated the functions of PV-VISION on two tasks: investigating fire impacts on solar farms by inspecting 2.4 million cells and quantifying crack growth in solar modules under mechanical aging tests. We anticipate that PV-VISION can offer a supportive platform for researchers in the solar field, facilitating a more efficient and data-driven approach to EL image analysis.

5:00 PM MT03.03.05

AI-Predicted Synthesis of Vertically Aligned Nanocomposite Structures [Jianan Shen](#), Tinghan Yang, Jiayi Liu, Benson Tsai, Yizhi Zhang, Chang Liu, Shiyu Zhou, Nirali Bhatt, Zedong Hu, Lizabeth Quigley, Jialong Huang, Jennifer Neville and Haiyan Wang; Purdue University, United States

The fabrication of self-assembled two-phase nanocomposite thin films through a one-step pulsed laser deposition process has garnered significant research interest. These films exhibit a wide range of functionalities, including ferromagnetic, ferroelectric, magnetoresistive, and multiferroic properties, as well as unconventional optical behaviors like plasmonic and hyperbolic properties. Typically, these nanocomposites self-assemble into two distinct structures: particles-in-matrix (PIM) nanostructures or vertically aligned nanocomposite (VAN) nanostructures with embedded nanopillars within the matrix phase. In rare instances, a solid solution structure emerges. Among these structures, VAN stands out due to its unique features, including vertical strain control and

highly anisotropic structure, which enable the epitaxial growth of materials with significant lattice mismatch. However, the successful synthesis of VAN structures has been challenging, often relying on time-intensive trial-and-error approaches due to the intricate underlying mechanics. Therefore, it is imperative to develop a predictive method capable of determining the most likely synthesis recipe for VAN structures. In this context, harnessing the capabilities of state-of-the-art artificial intelligence (AI) technology, we have created an automated pipeline tool helping predict the synthesis route of VAN structures. Our pipeline incorporates an automated data extraction process that leverages an advanced large language model (LLM) to extract information from our paper repository and combines it with laboratory-collected data to construct a comprehensive database. Subsequently, this database is utilized by a custom machine learning model for binary classification, distinguishing between VAN and non-VAN structures. The model achieves an impressive accuracy rate of 95%, validated through rigorous evaluations employing metrics such as precision, recall, and F1 scores. Furthermore, the model incorporates elements of a graph neural network, enabling it to comprehend the crystalline characteristics of materials and exhibit strong generalizability across a variety of materials, including metals, oxides, and nitrides, etc. The effectiveness of this model has been verified across multiple material systems in our laboratory. Looking ahead, we envision that researchers in this field can utilize our model to assess the likelihood of success for their VAN growth recipes, significantly reducing time and cost expenditures in experimental setups. In summary, our utilization of AI technology has yielded a robust tool for predicting VAN structure synthesis, highlighting the potential of AI in material science research.

5:00 PM MT03.03.06

Optimization of Bistable Clamp for Aerospace Thermal Systems Russell Laudone, Matthew Nakamura and Joseph Brown; University of Hawaii at Manoa, United States

Large spacecraft, launch vehicles, and hypersonic craft use a thermal protection system (TPS) consisting of tiles to mitigate potential thermal hazards while traveling through the atmosphere at high velocities. Historically, these tiles have been attached via silicone adhesive that mates tiles to the craft permanently. The proposed mechanism is a macroscale interlocking bistable compliant clamp that securely houses and rapidly exchanges thermal tiles attached to the TPS. Compliant mechanism design presents a significant learning curve due to large deflections requiring nonlinear mechanics models, and unexplored design space for analysis of deflection of flexible links and mechanisms. Despite their design challenges, compliant mechanisms present many desired characteristics not found in traditional multi-joint rigid-body components, including lower part cost, scalability, precise motion, zero off-gassing, and reduction in weight and friction. Here we report methodology, designs, and results that demonstrate use of optimization techniques to autogenerate revised compliant structures by comparing them against a specified fitness metric. This proposed method is less time-consuming and more efficient than traditional computational or “trial-and-error” methodology and exports parameterized structures in manufacturable file format. This paper's proposed bistable compliant clamp was fabricated in polylactic acid (PLA), assessed with finite element analysis (FEA), and mechanically cycled on a tensile tester. Results identified preliminary performance metrics regarding stress concentrations, retention force, and input force. It was theorized that these metrics depend on seven geometric parameters and could be optimized to maximize retention force and minimize input force, while keeping acceptable material-based stress concentrations and bistable characteristics. The design methodology implemented topology optimization techniques to identify potential parameter solutions that improve one or more of the defined performance metrics. Redesigned models were fabricated and tested against the original prototype to validate the algorithm's ability to enhance mechanisms' performance. The proposed compliant mechanism serves as a solution for a re-attachable TPS tile system and a methodology to optimize compliant structures that do not require extensive expertise in compliant design theory. This result also demonstrates optimal design of unit cells that may be tessellated to form an adhesive metasurface.

5:00 PM MT03.03.07

Machine Learning for Experimental Design of Ultrafast Electron Diffraction Mohammad Shaaban; Texas A&M University, United States

In the field of nanomaterials research, this study presents a groundbreaking approach to overcome the challenges associated with Ultrafast Electron Diffraction (UED) data analysis. We introduce convolutional neural network (CNN) models that enable real-time analysis of UED data, unveiling dynamic material processes and identifying signs of damage. Moreover, Generative Variational Autoencoder (G-VAE) models are introduced to interactively optimize experimental parameters. These machine learning techniques showcase their potential for self-correcting UED experiments and can be readily extended to other characterization methods. By using CNNs to classify UED images and C-VAEs for dimensionality reduction, this study identifies defect formation, lattice distortions, and phase transformations in real-space, offering a transformative shift in materials research. Transfer learning techniques are also demonstrated for practical application on experimental UED patterns, promising advancements in materials science experimentation.

5:00 PM MT03.03.08

Development of a Photovoltaics Research and Development Ontology Michael Goette¹, Tobias Roeschmann¹, Jens Hauch², Ulrich Paetzold³, Eva Unger¹ and Thomas Unold¹; ¹Helmholtz-Zentrum Berlin, Germany; ²HI-ERN, Germany; ³Karlsruhe Institute of Technology, Germany

Current efforts in energy materials research produce large quantities of data, most of which, however, are not published or stored according to FAIR principles. This can be an impediment to progress and makes it difficult to cooperate, reproduce results and enable machine-learning on these data sets. Ontologies provide a common syntactic and semantic framework for research domains and have been widely applied in many fields, such as finance and biomedics. Coupling ontologies with databases containing FAIR data can unlock the power of machine-learning across a whole research field. So far only few ontologies have been developed and applied in energy materials research and development, and to our knowledge no publicly shared ontology for photovoltaic materials and devices exists at present. We will present an ontology a thin film photovoltaic materials and devices which is based on the basic formal (BFO) top level ontology (<https://matportal.org/ontologies/TFSCO>). As a first use-case the PV ontology is used to integrate high-throughput research in halide perovskite photovoltaics at several research groups/institutes of the Helmholtz-Gemeinschaft in Germany, but could be in the future expanded to encompass further research and development areas in photovoltaics.

SESSION MT03.04: Machine Learning for Computation: Forward & Inverse Design

Session Chairs: Keith Butler and Rachel Kurchin

Wednesday Morning, April 24, 2024

Room 322, Level 3, Summit

8:15 AM MT03.04.01

Bayesian Optimization for Customizable Hierarchical Kirigami Piezo-Transmittance Strain Sensor Designs Jimin Gu¹, Bowen Zheng¹, Jiheyon Ahn², Inkyu Park² and Grace Gu¹; ¹UC Berkeley, United States; ²Korea Advanced Institute of Science and Technology, Korea (the Republic of)

The significance of IoT systems incorporating green and sustainable energy sources has grown exponentially. Simultaneously, the demand for sensing

systems integrated with low-powered and self-powered capabilities has emerged. Piezo-transmittance strain sensors, which operate on the optical transmittance change induced by mechanical deformation of the functional film, have demonstrated remarkable potential for in self-powered soft sensing applications integrated with solar cells. These sensors are notable for their reliability, rapid response, and long-term stability. While soft sensing systems offer advantages because of their compliance and stretchability, their suitability for vertical sensing platforms varies depending on the mechanical properties of the target objects. Consequently, there is a growing need to develop customized sensor characteristic optimization procedures within this field. The utilization of a kirigami structure in piezo-transmittance sensors addresses two benefits. First the repeated unit-cell pattern across the film area ensures sensor uniformity. Additionally, it offers design flexibility, allowing for the accommodation of predicted mechanical deformations within the pre-designed structure. In this research, we optimized a hierarchical kirigami-based structure, focusing on sensor sensitivity within different working ranges, as the functional film for piezo-transmittance strain sensors. First, we utilize the results obtained from finite element simulations as a training dataset to build a neural network surrogate machine learning model. This model accepts geometric variables as input and furnishes data regarding the desired performance metrics, thereby substituting the requirement for more costly physical simulations, facilitating the optimization process. The Bayesian optimization and the cross-entropy method were used to optimize the sensor's geometric structure, and a comprehensive analysis of the geometric factors was conducted through sensitivity analysis. Through sensitivity analysis, we can identify the major geometric factors that affect the sensor's performance. Additionally, in contrast to auxetic behavior, the sensor's performance is better in a simpler model, specifically at hierarchical level 1. Furthermore, through experimental testing, we can validate the superior performance of the designed kirigami piezo-transmittance strain sensors.

8:30 AM MT03.04.02

Physics inspired Machine Learning of Eliashberg Spectral Function for High-Throughput Screening of Novel Superconductors [Ajinkya Hire](#), Jason B. Gibson, Benjamin Geisler, Philip Dee, Oscar Barrera, Peter Hirschfeld and Richard Hennig; University of Florida, United States

The Eliashberg spectral function (α^2F) is at the core of understanding the electron-phonon superconducting properties of a material. But calculating α^2F from ab initio methods for a large number of materials is expensive, impeding the high-throughput search of novel superconductors. With machine learning models gaining prominence over the past decade for material properties, our work harnesses this potential for α^2F prediction. In this presentation, I will present our expansive database of theoretically calculated high-quality α^2F and introduce our state-of-the-art equivariant neural network models trained using it. This talk also elucidates the nuances of training models for predicting continuous properties such as α^2F , focusing on innovative physics-inspired node embeddings to bolster model performance. For the α^2F -derived properties like the electron-phonon coupling λ , and two moments of the frequency ($\langle \omega_{\log} \rangle$, and $\langle \omega^2 \rangle$), our base model, relying solely on crystal structure, achieves a Pearson correlation coefficient of 0.3, 0.7, and 0.8. In comparison, integrating moderately expensive node embeddings increases the Pearson correlation coefficients of 0.5, 0.8, and 0.9 on the derived properties. An intriguing power-law relationship between model loss and training dataset size is observed, emphasizing the imperative for community-collaborated expansion of α^2F databases.

8:45 AM MT03.04.03

AI Accelerated Computational Design of The Freeform Solar Cell Structures [Ruiqi Guo](#)^{1,2}, Wenqing Wang^{1,2}, Masahito Takakuwa², Kenjiro Fukuda¹ and Takao Someya^{1,2}; ¹RIKEN, Japan; ²The University of Tokyo, Japan

Artificial intelligence generated configurations (AIGC) have emerged as a game-changing approach for inverse design, demonstrating remarkable potential in the realm of free-form device structures. This innovation is especially valuable in the context of thin-film solar cell (SC) devices, where patterned meta-surfaces offer the potential to enhance both their electrical and optical properties.

Traditional human-designed periodic meta-surfaces, while effective, are inherently constrained by topological limitations and a limited set of parameters. The advent of free-form design liberates us from these constraints, allowing for the creation of intricate and unconventional shapes, as well as the exploration of a vastly expanded design landscape. This newfound design freedom holds the promise of unlocking unprecedented functional capabilities, potentially surpassing human intuition. Nevertheless, the efficient exploration of this expansive design space presents a significant computational challenge.

One of the primary obstacles to realizing high-throughput free-form designs is the computational cost associated with conventional numerical simulations. In our study, we tackle this challenge head-on by introducing a fully automated system that harnesses the power of high-speed Deep Learning (DL) surrogate solver alongside intelligent configuration optimizer. Compared to standard numerical methods, our DL surrogate model accelerates the prediction of outcomes by 22,700 times, resulting in a 98.47% reduction in computation costs, all while maintaining an average accuracy of approximately 99%.

Our extensive evaluation, encompassing a dataset of 600,000 configurations generated by the intelligent configuration optimizer, has led to the discovery of an optimized SC device design boasting a power conversion efficiency of 17.58%. This performance greatly surpasses the 14.70% baseline efficiency of SC device lacking patterns on the substrate layer. These findings underscore the immense potential of AIGC techniques in efficiently enhancing the performance of photovoltaic devices, paving the way for a brighter future in renewable energy applications.

9:00 AM MT03.04.04

Machine Learning to Construct Process-Structure-Property Relations of hBN Thin-Films [Dokwan Kook](#) and Satish Kumar; Georgia Institute of Technology, United States

Hexagonal Boron Nitride (hBN) is a 2D material with high in-plane thermal conductivity and low out-of-plane thermal conductivity. Due to its anisotropic properties, hBN films have high potential for the thermal management of next-generation electronics. The thermal conductivity of hBN film depends on the processing conditions and its thickness. The construction of Process-Structure-Property (PSP) relations of hBN film can help in accelerating the synthesis of hBN films with desired thermal properties. Machine learning (ML) techniques can help in utilizing both measurements and simulations to develop reliable PSP relations to guide the synthesis process. In this presentation, we will discuss how Gaussian Process Regression (GPR) can be applied to experimental and simulation data to construct PSP relations. Pulsed laser deposition (PLD) is used for the extraction of experimental data, and molecular dynamics simulations is used for the extraction of simulation data. The PSP relations will be constructed using SEM images as structure data and out-of-plane thermal conductivity as property for various process conditions.

A significant challenge is dimensionality mismatch which occurs from the large size of the structural data compared to process conditions and properties, e.g., SEM images are 2D images of a 3D structure, while process conditions or properties are typically 1D. Dimensional mismatch makes the ML model difficult to learn. To resolve this problem, we will apply two-point correlations and principal component analysis. Two-point correlations preserve spatial statistical information of the SEM images. This will allow original structural data from the samples to be converted into similar shapes, allowing the ML model to be trained efficiently. Applying principal component analysis will allow the structure data to be expressed as a linear combination of orthogonal vectors. The data will be represented by the matrix of coefficients of orthogonal vectors, which will be much smaller than an SEM image itself. Experimental data have high fidelity but low quantity, while simulation data can be produced in larger volume. Simulation data will be included with the

experimental data during the training of ML model to accelerate PSP relations and the model will identify process conditions corresponding to high thermal conductivities accurately.

9:15 AM *MT03.04.05

MaterialEyes – Looking into Renewable Energy Materials with Theory- and AI-Guided Characterization [Maria K. Chan](#); Argonne National Laboratory, United States

The understanding and design of materials for sustainability -- such as photovoltaics, optoelectronics, and energy storage materials -- rely on measurements not just of the functional properties, but also of fundamental structural and electronic properties. Data driven approaches such as machine learning (ML) for interpreting these measurements via microscopy and spectroscopy rely on labeled, reliable, balanced training data. We will discuss the use of AI including computer vision and large language models (LLMs) to obtain such training data from literature, and also the use of theory-guided AI approaches to interpret new microscopy and spectroscopy data. We will also discuss the use of generative AI to understand interfaces and structural evolution in renewable energy materials.

9:45 AM BREAK

10:15 AM *MT03.04.06

Physics and Uncertainty-Aware Ensemble-Based ML-Models for Interatomic Potentials and Prediction of Reaction Networks and Cell-Level Performance [Tejs Vegge](#); Technical University of Denmark, Denmark

Understanding the dynamic processes at solid-liquid interfaces in electrochemical devices like batteries is key to developing more efficient and durable technologies for the green transition. Fundamental and performance-limiting interfacial processes like the formation of the Solid-Electrolyte Interphase (SEI) [1] and dendritic growth [2] span numerous time- and length scales. Despite decades of research, the fundamental understanding of structure-property relations remains elusive. Ab initio molecular dynamics (AIMD) generally provides sufficient accuracy to describe chemical reactions and the making and breaking of chemical bonds at these interfaces [3]. Still, the cost is prohibitively high to reach sufficiently long time- and length scales to ensure proper statistical sampling [4]. Machine learning (ML) potentials offer a potential solution to this challenge. Still, training ML-based potentials capable of handling activated processes in organic or aqueous electrolytes remains a fundamental challenge since the potential must capture both intra- and intermolecular interactions in the electrolyte and during chemical reactions at the interface [4]. Here, we present new approaches using phase field models [2], graph neural networks [5] and new transition state training sets [6] for chemical reaction networks, and machine/deep learning models to predict the spatio-temporal evolution of electrochemical interphases [3]. We also discuss the development of methods like symbolic regression to learn the laws of electrolyte transport [8], the predictions of energy and forces with calibrated uncertainty quantification for interatomic potentials using neural network ensemble models [8,9]. Finally, we discuss how such models trained on multi-sourced and multi-fidelity data from multiscale computer simulations, operando characterization, high-throughput synthesis, and testing, to provide uncertainty-aware and explainable ML for early prediction of, e.g., of degradation trajectories for battery cells [10].

1. Diddens, Bhowmik, et al., *Adv. Mater. Inter.*, **2022**, 2101734
2. Jeon, Ho, Vegge, Chang, *ACS Appl. Mater. Inter.*, **2022**, 14, 15275
3. Bhowmik, Castelli, Garcia-Lastra, Jørgensen, Winther, Vegge, *Energy Storage Mater.*, **2019**, 21, 446
4. Bhowmik, Vegge, et al., *Adv. Energy Mater.*, **2021**, 2102698
5. Schreiner, Bhowmik, Vegge, Winther, *Mach. Learn. Sci. Tech.*, **2022**, 3, 045022
6. Schreiner, Bhowmik, Vegge, Winther, *Sci. Data*, **2022**, 9, 779
7. Flores, Wölke, Yan, Winter, Vegge, Cekic-Laskovic, Bhowmik, *Digital Discovery*, **2022**, 1, 440
8. Busk, Jørgensen, Bhowmik, Schmidt, Winther, Vegge, *Mach. Learn.: Sci. Technol.*, **2022**, 3, 015012
9. Busk, Schmidt, Winther, Vegge, Jørgensen, *Phys. Chem. Chem. Phys.*, **2023**, 5, 25828
10. Rieger, Flores, Nielsen, Winther, Ayerbe, Vegge, Bhowmik, *Digital Discovery*, **2023**, 2, 112

10:45 AM *MT03.04.07

Machine Learning Prediction of Electronic Structure for High-Throughput Inverse Design of Functional Organic Materials [Reinhard Maurer](#); University of Warwick, United Kingdom

Materials for electronic devices such as organic light emitting diodes need to have tailored optoelectronic properties and be synthetically viable. As devices are composed of organic thin films with different functionality, the optoelectronic properties of materials need to be designed in concert and the role of the interfaces between thin films must be understood. Computational high-throughput screening of molecular excited states can greatly facilitate this complex multi-objective design problem. I will present our recent work on deep machine learning models that are able to predict structure, electronic structure, and excited states of organic molecules and materials in general. Our models predict optical excitations, the fundamental gap, electron affinity and ionisation potential for large organic molecules of diverse composition. [1] While the models are trained on first principles electronic structure data, the prediction process requires no recourse to computationally expensive ab initio calculations. The accuracy and transferability of the models can be assessed against photoemission spectroscopy data. I will further showcase how such models can be used in combination with generative machine learning to discover novel organic compounds that satisfy specific optoelectronic properties. [2] We explore different applications with our approach from the design of organic electronics to plasmonic sensors and tailored nanoparticles. [1] *Chem. Sci.* 12, 10755-10764 (2021), [2] *Nature Comp. Sci.* 3, 139–148 (2023);

11:15 AM MT03.04.08

Proposal of Bayesian Framework for Inverse Inference to Predict Material Properties from Microstructures [Satoshi Noguchi](#)¹ and Junya Inoue²; ¹JAMSTEC, Jamaica; ²The University of Tokyo, Japan

This presentation introduces a Bayesian framework designed for inverse inference to predict material properties or process parameters from microstructure images. The basic strategy of the proposed framework is the integration of Bayesian inference methodologies with machine learning techniques. This enables us to not only predict target properties but also quantify the uncertainty associated with these predictions. Specifically, our focus lies on the development of a Bayesian framework based on generative networks which recently have received much attention in the field of computational material science. The integration could contribute to the examination of the prediction uncertainty.

In this presentation, we will explain the fundamental concepts of our framework and the outcomes of its application of this to a specific case study. Our chosen case is the prediction of material properties from artificial dual-phase steel microstructures. Also, we will discuss the comparison between our proposed Bayesian framework and a conventional inference method based on convolutional neural networks. By the end of this presentation, you will gain insights into the novel Bayesian approach and its potential advantages over conventional methods, providing a powerful tool for more robust predictions in the field of computational material science.

11:30 AM MT03.04.10

Physics-Informed Pre-Training of Graph Neural Networks for Materials Property Predictions Shuyi Jia, Fan Shu, Akaash Parthasarathy, Chandreyi Chakraborty and Victor Fung; Georgia Institute of Technology, United States

Pre-training of machine learning models, particularly in the form of self-supervised learning, is now an ubiquitous approach for improving model performance and robustness which has featured prominently in the fields of natural language processing and computer vision. To apply these similar concepts to the materials sciences, new domain-aware pre-training strategies need to be developed. We introduce a series of physics-informed pre-training strategies which align well to materials data and can be applied towards the widely used graph neural network class of machine learning models. We demonstrate the effectiveness of this approach on a wide range of benchmarks across multiple materials systems and properties. We discuss the benefits of pre-training for situations where datasets are limited in size and robust out-of-distribution performance is needed, as well as potential implications of pre-training towards developing foundational models for the materials sciences.

11:45 AM MT03.04.11

Using Domain Specific Languages to Enable Artificial Intelligence for Polymer and Catalyst Design Nathan Park¹, Jannis Born², Matteo Manica², James Hedrick¹, Tim Erdmann¹ and Pedro Arrechea¹; ¹IBM Almaden Research Center, United States; ²IBM Research-Zurich, Switzerland

Traditional research workflows in polymer chemistry, which often rely heavily on trial-and-error, stand to be profoundly reshaped through continued advances in automated experimentation and artificial intelligence (AI). However, the seamless integration of these advances within daily research activities still faces significant hurdles. To overcome these obstacles, we have focused our efforts in key areas which would be impactful for experimentalists. First, we have developed new systems and software for facilitating automated synthesis using readily available lab equipment, both for polymerization in continuous-flow reactors as well as small molecules in flow to batch systems. Second, we show how the use of a domain-specific language (DSL) can solve a host of issues surrounding experimental data representation and management—facilitating more straightforward development of AI models. Finally, we demonstrate how experimental data represented in a DSL can be utilized to develop effective generative models for materials and catalyst design.

SESSION MT03.05: Machine Learning for Computation: High-Throughput Computing

Session Chairs: Keith Butler and Arun Kumar Mannodi-Kanakkithodi

Wednesday Afternoon, April 24, 2024

Room 322, Level 3, Summit

1:30 PM MT03.05.01

Computational Design of Dual-Atom Catalysts for Sustainable Energy Conversion Guoxiang (Emma) Hu; Georgia Institute of Technology, United States

Dual-atom catalysts (M_1M_2 -N-C) are emerging as promising candidates for electrochemical reactions (e.g., oxygen reduction reaction) which are critical for clean and sustainable energy devices. However, due to the large chemical design space, myriad possible structural configurations, and dynamic structure evolutions of the metal centers under reaction conditions, the design of dual-atom catalysts has been challenging and cost-prohibitive for both experiments and computations. Here, using high-throughput density functional theory (DFT) calculations combined with machine learning, we rapidly and efficiently evaluate over 20000 dual-atom catalysts for oxygen reduction reaction. We first generate a DFT database of a subset of the dual-atom catalysts, and validate our computational predictions of the structure, stability, and catalytic activity with experimental data where available. With this benchmarked database, machine learning models based on neural networks were trained and applied to identify promising dual-atom catalysts in the search space which possess higher durability and activity than the state-of-the-art Pt and Fe-N-C single-atom catalysts. Furthermore, additional DFT calculations were performed on selected catalysts to reveal the origin of their improved catalytic performance and establish structure-property-performance relationships. The computational framework developed in this work can be generally extend to other important electrochemical reactions including carbon dioxide reduction reaction and hydrogen evolution reaction for sustainable energy conversion.

1:45 PM MT03.05.02

Sub-Trillion-Scale Atomic Data Integrated Deep Learning Approach for Predicting Thermal Transport Properties of 60,000 Inorganic Perovskites Ming Hu; University of South Carolina, United States

Although first-principles based anharmonic lattice dynamics method coupled with the phonon Boltzmann transport equation has been developed to obtain the phonon properties including lattice thermal conductivity at highest accuracy ever, the costly and time-consuming nature of the required interatomic force constants calculations renders high-throughput infeasible when facing tens of thousands of new materials. Here, a high-dimensional multi-element deep neural network with sub-trillion-scale atomic data is trained, dubbed Elemental Spatial Density Neural Network Force Field (Elemental-SDNFF), achieving a competitive force root mean square error and a speed-up of 4 to 5 orders of magnitude in comparison to first principles. The effectiveness and precision of the Elemental-SDNFF approach is demonstrated on a set of 150,000 inorganic crystalline structures spanning 63 elements in the periodic table by prediction of complete phonon properties such as phonon dispersions and lattice thermal conductivity. We then use our trained neural network model to predict and screen full phonon properties of 60,000 single and double perovskite structures. Due to the inherent structural feature of dynamical disorder, the perovskite structures have shown diverse thermodynamic and phonon transport properties. Dynamic stability of all 60,000 perovskite structures is predicted by screening negative frequencies in the Brillouin zone. Four-phonon scatterings and two-channel thermal transport are also analyzed and screened. The underlying mechanism is analyzed in deep at the electronic level. This study demonstrated that our algorithm is very powerful for predicting phonon properties of large-scale inorganic crystals and is also promising for accelerating high-throughput search of novel phononic materials for emerging applications.

2:00 PM *MT03.05.03

Understanding and Mitigating Bias in Autonomous Materials Characterization and Discovery Jason R. Hattrick-Simpers; University of Toronto, Canada

Since the publication of the Mission Innovation Materials Acceleration Platform, AI is increasingly responsible for driving automated experimental and computational tools. There have been multiple case studies for which autonomy was demonstrated to successfully drive materials optimization or discovery

problem and the world of scientific robots has moved from science fiction to reality. However, within the broader AI community it is well known that AI's carry with them their creators' biases and this has serious implications on model development and deployment. Using several case studies, I will illustrate how biases can arise in materials science and specific steps that can be taken to remove them. Specifically, I will discuss some of our recent work in (1) reducing human bias in label generation by applying robust statistics to spectroscopic data analysis, (2) identifying and mitigating search space bias through model disagreement, and (3) circumventing the big data bias loop by illustrating how the presence of information redundancy in large computational datasets and (4) how to construct an optimally informative dataset for model training.

2:30 PM BREAK

3:30 PM *MT03.05.04

Predicting The Structure and Properties of Bulk and Surface Perovskite Oxides with Machine Learning and Simulations [Rafael Gomez-Bombarelli](#), James K. Damewood, Jessica Karaguesian, Jaclyn Lunger, Jiayu Peng and Xiaochen Du; Massachusetts Institute of Technology, United States

Ceramics based on multicomponent oxides are a promising platform for catalysis and electronics. By controlled doping of multiple elements, it may be possible to tune electronic and transport properties of oxide materials towards high performance applications. This opens an exciting and high-dimensional design space for choosing the most promising choices and stoichiometric ratios of elements that fine tune desired properties.

Here we will describe how machine learning models, powered by electronic structure simulations can address property prediction and design in multicomponent space. In particular, we will explore how perovskite oxides, which can support quaternary or even more complex compositions, can be engineered in silico.

We will describe the use of elemental and electronic descriptors to predict whether perovskite oxide materials will exhibit chemical ordering when synthesized, we will evaluate the use of per-site deep learning models to predict atomically-project properties such as magnetic moments of catalytic site activity, the use of machine learning interatomic potentials to relax perovskite structures and to create surface phase diagrams, and the ability of equivariant models to capture symmetry-breaking relaxation and properties from idealized, unrelaxed prototypes.

These tools put together, alongside machine learning models for synthesis planning, will support the development of bottom-up data-driven design pipelines for multicomponent oxide materials with tailored properties.

4:00 PM *MT03.05.05

Fantastical Training Data and How To Generate It [Martijn Zwijnenburg](#); University College London, United Kingdom

In an ideal world we would train machine learning models for organic materials on training data generated using coupled-cluster singles-doubles-triples-quadruples or something similar and fully take into account the environment of the molecules. In practice this is impossible considering the number of training points required for most models. As a result, we have to make choices. Even more so when we want our model not to predict ground state energies and/or geometries but excited state properties, such as optical excitation energies or electron affinities/ionisation potentials, as well as to be transferable. Models that could accurately predict excited state properties for a wide range of organic materials would be very useful in virtual high-throughput screening of materials for organic LEDs, photovoltaics and photocatalysts.

In my contribution I'll discuss our work and that of others on training data generation for excited-state properties of organic materials. I'll consider which properties to aim for, what the best possible training data might look like and how hybrid schemes based on tight-binding methods calibrated to higher-level methods can be exploited.

4:30 PM MT03.05.06

Experiment Versus Computation, Physics Versus Machine Learning in The Inverse Design of Photovoltaic Materials [Andrea Crovetto](#); Technical University of Denmark, Denmark

As a practical case study to advance methods for the inverse design of photovoltaic (PV) materials, my group has been given the following task for the next 5 years: Identify and synthesize the best PV absorber out of the space of all inorganic materials containing sulfur and phosphorus (phosphosulfides). Within this family of materials ~10 compounds have already been considered as potential PV materials, ~260 have previously been synthesized, ~420 are present in the Materials Project database, and 200,000 phosphosulfide compounds from ternary and quaternary systems are chemically plausible according to charge-neutrality arguments.

To try to solve this puzzle within a 5-year timeframe, we have set up a multi-faceted inverse design platform. This platform includes:

1. High-throughput/high versatility modular synthesis apparatus for combinatorial growth of any inorganic phosphosulfide thin films, so that there are no excuses for excluding certain elements from experimental work. This includes sulfur- and phosphorus partial pressure control (both at atmospheric and low total pressures), separate chambers for volatile metal incorporation, and creation of perpendicular combinatorial gradients in the metal-to-metal ratio as well as in the S/P ratio.
2. High-throughput characterization apparatus, focusing on the properties that are expected to be correlated with the final PV performance and are difficult to simulate with sufficient accuracy.
3. A tiered approach to material property simulation, with a focus on complementing (rather than reiterating) the information available from experiment. The simulation tools can be roughly divided into first-principles quantum mechanical methods, semiclassical methods, and classical "rule-of-thumb" methods.
4. A data management tool to accommodate both experimental and simulation data.
5. Various artificial intelligence tools to be used both for decision-making in the lab and for understanding complex composition-structure-process-property-performance relationships.
6. Public access to the data generated by the tools listed above.

To make the presentation more concrete, I will discuss two practical examples that highlight the importance of a diversified methodological toolkit in

This searchable program is up-to-date as of April 15th, 2024.

modern materials research. The first example is the integration of computational and experimental approaches in the process of discovering new materials with new compositions and unknown crystal structures. The second example is the balance between physical soundness and statistical performance in the machine-learning-aided development of a phenomenological figure of merit to evaluate the quality of a generic PV material.

SESSION MT03.06: Data, Autonomy and Algorithms I
Session Chairs: Shijing Sun and Steven Torrisi
Thursday Morning, April 25, 2024
Room 322, Level 3, Summit

8:00 AM *MT03.06.01

Supervised and Unsupervised Machine Learning Applied to Challenging and Rapid Diffraction and Structural Problems [Simon J. Billinge](#); Columbia University, United States

Development of next generation materials for applications in sustainable energy and beyond require us to study the structure of real materials in real devices even as they operate: for example, putting operating batteries in the beam, studying spatially resolved labs-on-chip, doing real-time autonomous experiments and using computed tomography to see diffraction from cross-sections of bulk samples. These developments, powered by wonderful synchrotron and neutron source and detector developments, present major challenges on the data analysis side. Now we are putting heterogeneous devices in the beam and getting signals from different parts of them. We have bad powder averages (spotty data) because we can't spin the battery, and single crystal spots coming from some component in the setup that happens to be in the way of the beam. We have unknown and unexpected phases coming and going, and want to extract tiny signals from large backgrounds. I will present some of the data analysis, algorithmic and computational developments that are helping us to overcome these challenging situations and not only recovering from 'bad data', but also turning bad data into good data. Spotty powder patterns have more information in them than smooth powder rings. I will describe some new approaches, algorithmic, statistical, machine learning and otherwise, that are helping us move the goalposts in this domain, which can open up new opportunities for studying complex heterogeneous samples with hard x-rays.

8:30 AM *MT03.06.02

Designing Vitriimer Polymers with Molecular Dynamics and Machine Learning [Aniruddh Vashith](#); University of Washington, United States

Vitrimers are a new class of self-healing polymers that can heal by rearranging their molecular structure via dynamic covalent bonds. These polymers offer promise for improving the circular life-cycle and sustainability of various polymeric systems that are used in our day-to-day life ranging from fiber composites to electronics. A recently developed framework called Accelerated ReaxFF, uses the "bond boost" approach to speed up the MD simulations by providing reactive sites in the reactants with boost energy equivalent or slightly larger than the energy reaction barrier to overcome the cross-linking process barrier and form desired products. This approach avoids unwanted high-temperature side reactions while allowing for rejection of high-barrier events. This method can be employed not just for virtual characterization of vitriimer polymers but also to understand the rearrangement reactions in epoxy-acid vitriimer polymer chemistries. Further, using coupled molecular dynamics and machine learning, we design new vitriimer chemistries with targeted applications. This includes collecting a dataset of glass transition temperature of various vitriimer chemistries calculated through molecular dynamics (MD). This data is then used to train a latent space and property predictor. Finally, a search is performed within the latent space to uncover vitriimer chemistries with desired properties.

9:00 AM *MT03.06.03

Taming The Complexity of Materials Degradation with Machine Learning [Brett M. Savoie](#); Purdue University, United States

Limited stability and unacceptable degradation products are common reasons for otherwise promising materials to fail technological translation. The enduring state-of-the-art for establishing these properties essentially remains make-and-break testing, which is costly and provides information only at the end of the materials development process. The complexity of the reaction networks that govern degradation and the difficulty of data analysis pose tremendous obstacles to predictive approaches, however recent advances in automated reaction prediction and machine learning are increasingly making it possible to tractably describe and even predict degradation phenomena. In this talk I will highlight our group's recent work developing methods for predicting reaction outcomes and how they have been applied to several different materials classes. The second half of the talk will discuss machine learning approaches to the closely related problem of identifying degradation products on the basis of typical spectral information sources.

9:30 AM *MT03.06.04

Materials Cartography: The Role of Materials Representation [Steven B. Torrisi](#); Toyota Research Institute, United States

Within materials science, practitioners are concerned with modeling time and length scales that span many orders of magnitude, presenting differing challenges across the atomistic, mesoscale, and device levels. Moreover, problems where data are scarce pose challenges for applying machine learning in many scientific fields. When designing, training, and applying a model, the representation of input features can be just as important as the target and architecture of the model itself. Finding the appropriate way to represent a material of interest is not always straightforward and remains an active area of research. In this talk, I will highlight recent work which explores the concept of materials representation in applications ranging from materials and device-level informatics to molecular dynamics, highlighting intriguing results as well as lessons learned that may be useful for practitioners in diverse subfields of materials science.

10:00 AM BREAK

10:30 AM *MT03.06.05

Learning from Data and Distributions to Accelerate Engineering of Energy Materials and Devices [Rachel C. Kurchin](#); Carnegie Mellon University, United States

Whether or not we take an explicitly probabilistic perspective, and whether or not we are using black-box models or traditional physics-based ones, learning from and with distributions (of data, probability, and/or parameters) is an important tool in the data-driven modeler's toolbox. In this talk, I'll present two stories from my group's work emphasizing why this is important. First, I'll discuss some past and present work in using Bayesian parameter estimation to characterize materials and interfaces in photovoltaic devices. In

this work, we use a drift-diffusion solver to simulate current-voltage curves with a variety of different materials properties for both the layers and the interfaces within the device. By comparing these simulated curves to measured data we can effectively “invert” the device model to get posterior distributions reflecting our knowledge about the input parameters to the model as a function of measurements corresponding to the output. Next, I’ll shift to focus on some ongoing work utilizing diffusion models (the same type of machine learning model behind generative image tools such as DALL-E and Midjourney) to generate realistic microstructures of solid-oxide cell electrodes for use in device degradation simulations. A key aspect of validating these models is running their outputs through software that computes various microstructural properties of interest, including phase fractions, interfacial areas, and triple phase boundary densities. In particular, we examine the distributions of these properties in the generated data as compared to the training data and investigate whether, as has been reported in other work, diffusion models are less prone to issues such as mode collapse compared to other types of generative models such as generative adversarial networks. In both of these stories, understanding how we can learn from and with both data and distributions is paramount. The insights that we have on how physical processes in our systems of interest should affect values and distributions in our datasets are critically important to incorporate in the way we analyze and learn from that data.

11:00 AM MT03.06.06

Algorithmic Design and Implementation of an Automated Synthesis Platform for Rare and Exceptional Materials Discovery Alexander E. Siemenn¹, Armi Tiihonen^{1,2}, Basita Das¹, Eunice Aissi¹, Fang Sheng¹, Sebastian De Jesus¹, Lleyton Elliott¹, Sharil Maredia¹, James Serdy¹, Hamide Kavak^{1,3} and Tonio Buonassisi¹, ¹Massachusetts Institute of Technology, United States; ²Aalto University, Finland; ³Cukurova University, Turkey

Discovery of exceptional materials that have high-performance properties, such as perovskite materials with ideal band gaps and high stability, stands as an imperative challenge for developing sustainable electronic devices to tackle decarbonization and address the larger climate crisis. However, these exceptional materials are rare – existing only in narrow hypervolumes of vast and high-dimensional material search spaces, similar to a needle-in-a-haystack. With the rise in self-driving labs, it has become tractable to search larger volumes of these high-dimensional search spaces. However, current high-throughput self-driving labs are limited by their algorithmic performance in discovering needle-in-a-haystack exceptional materials as these labs are often guided using standard Bayesian optimization methods that inherently smooth over these regions containing exceptional materials within the search space. In this contribution, we present the design of DiSCO ([Di]scovery, [S]ynthesis, [C]haracterization, and [O]ptimization), an autonomous and high-throughput platform designed specifically to target the discovery of exceptional materials for sustainable electronic device applications. We highlight the following key contributions of DiSCO: (1) design of a zooming-based Bayesian learning with hypervolume penalization to maximize the number of exceptional materials discovered per unit time and (2) vectorization of the predicted exceptional materials for ultra-high-throughput synthesis and automated characterization within high-dimensional materials search spaces.

The DiSCO platform uses a method of ultra-high-throughput inkjet gradient deposition that synthesizes up to 100 unique material compositions within 20 seconds. Each material gradient is suggested by a custom Bayesian learning algorithm, entitled ZoMBI-Hop ([Zo]oming [M]emory [B]ased [I]nitialization). ZoMBI-Hop drives the discovery of exceptional materials within DiSCO by iteratively zooming the search bounds into regions of high-reward, in turn, capturing the true rough, non-convex nature of the needle-in-a-haystack optimum, rather than smoothing it over. Furthermore, ZoMBI-Hop jumps between high-reward basins in the search space, such that once an optimal region has been discovered, then that hypervolume becomes penalized for future iterations, resulting in only new high-reward regions being searched. Using this approach, we demonstrate the targeted discovery of up to 10x more exceptional materials from 6D materials search spaces, relative to previous ZoMBI implementations, given the same number of experiments. Each optimum suggested by ZoMBI-Hop is transformed from a single point into a vector that spans the extents of the search bounds using the angle of highest predicted cumulative reward along the vector. This vectorization of a single point generates a gradient of compounds that can be tractably synthesized in an ultra-high-throughput manner using DiSCO, hence, further increasing the resolution of the search space around each predicted exceptional material. In this version of DiSCO, the implemented reward function is derived from the optimization of band gap, computed autonomously for each deposited material using computer-vision-guided hyperspectral imaging. Future implementations will contain additional reward metrics such as electrical conductivity and stability. This automated characterization of band gap takes approximately 3 minutes to compute the band gap for every 100 uniquely synthesized material compositions. Overall, with the design of this DiSCO platform, it becomes tractable to acquire voluminous experimental data of exceptional materials as well as the regions surrounding those exceptional materials, resulting in the ability to confidently down-select optimal candidates with high precision for full electronic device scaled-up and testing. Discovery of high-performance band gap perovskite materials results in progress.

11:15 AM MT03.06.07

Atomistic Structure Search of Nanoscale Systems Using Generative Modeling and Evolutionary Algorithm Venkata Surya Chaitanya Kolluru, Nina Andrejevic and Maria K. Chan; Argonne National Laboratory, United States

Knowledge of the exact atomistic structure is crucial for computational analysis of unknown phases observed in experiments and for discovering novel materials. We previously developed the FANTASTX (Fully Automated Nanoscale To Atomistic Structure from Theory and eXperiments) package, a multi-objective evolutionary algorithm to determine atomistic structure from experimental characterization data. This approach relies on sampling the potential energy landscape of thermodynamically stable structures to find the best match between the simulated phase and observed experimental data. In this work, we develop a method for efficient sampling of candidate structures based on generative modeling.

Using a variational autoencoder (VAE), we transform the original, structure-oriented search space to a low-dimensional, property-oriented one. Structures are represented using an invertible point-cloud representation, and an auxiliary network is used to steer the latent space distribution according to the desired property. In this talk, we will discuss key components of this approach, including network optimization and sampling of the resulting latent space. We report the results of preliminary tests performed on CdTe and IrOx datasets, which utilize molecular dynamics and density functional theory for structure relaxation, respectively. This VAE-augmented approach enables more efficient sampling by refining the search space to meet expected property criteria, such as energy or mismatch to experimental data.

11:30 AM MT03.06.08

Advancements in Multimodal Emotion Sensing for Enhanced Human-Machine Interaction Anand Babu¹, Isabelle Dufour², Dipankar Mandal¹ and Damien Thuau³, ¹Institute of Nano Science and Technology, India; ²Université de Bordeaux, France; ³Bordeaux INP, France

Achieving effective human-machine interaction hinges on the recognition and response of machines to human emotions. However, the integration of emotions into robotics is a formidable challenge, primarily due to the intricacy and subjectivity of human emotional experiences. To enable the development of cognitive robotics capable of simultaneously perceiving and responding to human emotions, it is essential to make significant strides in emotional sensors driven by artificial intelligence (AI) and machine learning algorithms capable of accurately interpreting and responding to emotional cues. In this study, we introduce a novel approach to multimodal emotion sensing by harnessing non-invasive data collection of physiological indicators, including heart rate pulse, breathing patterns, and voice signatures. We utilize wearable printed organic piezoelectric sensors that offer rapid response times and are highly sensitive response a wide spectrum of force waveforms, frequencies, and pulse-width modulation. The responses obtained from these

wearable sensors are fed into a long short-term memory neural network algorithm, achieving remarkable classification in distinguishing various emotional states.

To further demonstrate the feasibility of transferring emotions to robotics, we have implemented Q-learning, demonstrating the effective training of a robotic model. By harnessing these multifaceted signals, our AI-driven emotional sensors aim to redefine the landscape of human-machine interaction. We envision a future in which machines possess the capability to discern and dynamically adapt to the diverse spectrum of human emotional states, fostering more seamless and responsive interactions between humans and machines.

11:45 AM MT03.06.09

Customized Acquisition Function Design for Materials Discovery Using Bayesian Algorithm Execution [Sathya R. Chitturi](#)^{1,2}, Akash Ramdas^{1,2}, Yue Wu², Brian Rohr², Stefano Ermon¹, Jennifer A. Dionne¹, Felipe H. da Jornada^{1,2}, Mike Dunne^{2,1}, Willie Neiswanger¹, Christopher Tassone² and Daniel Ratner²; ¹Stanford University, United States; ²SLAC National Accelerator Laboratory, United States

The development of advanced materials requires precise and efficient search through a vast range of possible material candidates and conditions to find the select few which satisfy highly customized or specific experimental goals. We focus on the area of AI-based sequential decision making where, at each step, the next candidate material is suggested based on previous accumulated data. We develop and extend the recently proposed concept of Bayesian Algorithm Execution to allow users to automatically convert a complex, targeted experimental goal into an adaptive data collection strategy, resulting in substantially improved performance compared to state-of-the-art methods.

SESSION MT03.07: Data, Autonomy and Algorithms II
Session Chairs: Janine George and Shijing Sun
Thursday Afternoon, April 25, 2024
Room 322, Level 3, Summit

1:30 PM MT03.07.02

High-Throughput Methods for Lead-Free Halide Double Perovskites: Computation and Experiment [Marina Selana Günther](#)¹, Oleksandr Stroyuk², Bernd Meyer¹ and Christoph J. Brabec¹; ¹Friedrich-Alexander Universität Erlangen-Nürnberg, Germany; ²Forschungszentrum Jülich GmbH, Germany

Lead-free halide double perovskites (LFHDP) have been an emerging material class for various applications in the field of optoelectronics over the last couple of years. In contrast to their lead-based counterparts they possess not only tunable optoelectronic properties but environmental friendliness and exceptional stability.^[1-2] Nevertheless only a small number of those perovskites have been evaluated up until today. The material class can be enlarged even further by substituting the Pb²⁺ ion not only with one M¹⁺ and one M³⁺ ion but with two of each resulting in a total number of six ions in the material.^[3-5] This adaption increases the number of possible materials immensely and gives rise to the demand for a different approach in material investigation: high-throughput (HTP) screening.

HTP screening aims to analyze a vast material range in a reasonable time by applying automation techniques and the restriction to swift measurement methods. Overcoming this issue can be done by applying not only HTP experimental methods but also HTP computational methods. Density functional theory (DFT) is able to examine a perfectly controlled range of material compositions for complementary features.

The combination of these strategies is a promising approach towards a HTP screening in novel materials discovery and is shown to be applicable on the example of Cs₂Ag_xNa_(1-x)Bi_yIn_(1-y)Cl₆. DFT has access to features like e. g. the lattice parameter, elastic properties and electronic properties whereas experimental methods investigate e. g. optical and vibrational material properties. By combining these two screening approaches a wider picture of the full material properties can be achieved.

Additionally DFT is not restricted by synthesis conditions and can therefore give an indication of what to expect of materials on the composition map which are not easily synthesizable or just reducing the time consumption of a certain measurement if only a random sample of the material range is measured and those measurements are then used as a calibration for the density functional data received for the whole composition map.

Using the variety of ion combinations in this LFHDP structure with interchangeable ion ratios opens up a whole new field of materials which can be evaluated by the methods developed on the example of Cs₂Ag_xNa_(1-x)Bi_yIn_(1-y)Cl₆ and therefore to build up a database. Using machine learning algorithms on this database can lead to a deeper understanding of the coupling between the ion exchange and macroscopic material properties.

Sources:

[1] E. Meyer, D. Mutukwa, N. Zingwe, and R. Taziwa, "Lead-Free Halide Double Perovskites: A Review of the Structural, Optical, and Stability Properties as Well as Their Viability to Replace Lead Halide Perovskites," *Metals*, vol. 8, no. 9. MDPI AG, p. 667, Aug. 27, 2018. doi: 10.3390/met8090667.

[2] L. Chu et al., "Lead-Free Halide Double Perovskite Materials: A New Superstar Toward Green and Stable Optoelectronic Applications," *Nano-Micro Letters*, vol. 11, no. 1. Springer Science and Business Media LLC, Feb. 27, 2019. doi: 10.1007/s40820-019-0244-6.

[3] H. Tang et al., "Lead-Free Halide Double Perovskite Nanocrystals for Light-Emitting Applications: Strategies for Boosting Efficiency and Stability," *Advanced Science*, vol. 8, no. 7. Wiley, Mar. 03, 2021. doi: 10.1002/advs.202004118.

[4] S. Li, J. Luo, J. Liu, and J. Tang, "Self-Trapped Excitons in All-Inorganic Halide Perovskites: Fundamentals, Status, and Potential Applications," *The Journal of Physical Chemistry Letters*, vol. 10, no. 8. American Chemical Society (ACS), pp. 1999–2007, Apr. 04, 2019. doi: 10.1021/acs.jpcllett.8b03604.

[5] O. Stroyuk et al., "'Green' synthesis of highly luminescent lead-free Cs₂Ag_xNa_{1-x}Bi_yIn_{1-y}Cl₆ perovskites," *Journal of Materials Chemistry C*, vol. 10, no. 27. Royal Society of Chemistry (RSC), pp. 9938–9944, 2022. doi: 10.1039/d2ct02055f.

1:45 PM *MT03.07.03

Materials Informatics for Polymer Materials: Experiments in The Loop [Junichiro Shiomi](#)^{1,2}; ¹The University of Tokyo, Japan; ²RIKEN, Japan

Materials informatics (MI) is to develop or study materials with an aid of informatics or machine learning. A typical approach is to train a black box model that relates basic descriptors (structure, composition, etc) and FoM (target properties) and predict or design a material with the largest FoM. At Thermal Energy Engineering Lab at University of Tokyo, together with the collaborators, we have been working on MI for heat transfer since 2015. One of the initial works was to design binary multilayered nanostructure to minimize or maximize thermal conductance by coupling thermal transport calculation and Bayesian optimization, which showed excellent efficiency. Later, the search space has been greatly expanded by utilizing quantum annealing. We have applied the methodology to computationally design and experimentally realize aperiodic superlattice that optimally impedes coherent thermal transport and multilayer metamaterial with wavelength-selective thermal radiation [1-8].

More recently, we have extended the machine-learning approach to that for polymers, aiming to functionalize them in terms of the thermal and dielectric properties. When molding or compounding polymers, the final properties are quite sensitive to the process parameters, therefore, the above approach of

serially connecting optimal design and experimental realization of materials is not sufficient. To this end, we have been developing a semi-automated MI system, where experimental fabrication and measurement are included in the optimization loop. This allows us to efficiently enhance the polymer properties. The MI optimization with experiments in the loop gives rise to various conceptual and practical questions; for instance, how to design and develop a robotic system that is adoptable to the existing material-development instruments and protocols, how to couple the property simulations and database with automated experiments, or how to appropriately define the search space for process parameters, etc. These aspects will be discussed in the talk.

- [1] S. Ju, T. Shiga, L. Feng, Z. Hou, K. Tsuda, J. Shiomi, *Phys. Rev. X* 7, 021024 (2017).
- [2] M. Yamawaki, M. Ohnishi, S. Ju, J. Shiomi, *Sci. Adv.*, 4, eaar4192 (2018).
- [3] A. Sakurai, K. Yada, T. Simomura, S. Ju, M. Kashiwagi, H. Okada, T. Nagao, K. Tsuda, J. Shiomi, *ACS Cent. Sci.* 5, 319-326 (2019).
- [4] R. Hu, S. Iwamoto, L. Feng, S. Ju, S. Hu, M. Ohnishi, N. Nagai, K. Hirakawa, J. Shiomi, *Phys. Rev. X* 10, 021050 (2020).
- [5] K. Kitai, J. Guo, S. Ju, S. Tanaka, K. Tsuda, J. Shiomi, R. Tamura, *Phys. Rev. Res.*, 2, 013319 (2020).
- [6] S. Ju, R. Yoshida, C. Liu, S. Wu, K. Hongo, T. Tadano, J. Shiomi, *Phys Rev. Mater.* 5, 053801 (2021)
- [7] J. Guo, S. Ju, Y. Lee, A. Gunay, J. Shiomi, *Int. J. Heat and Mass Transf.*, 195, 123193 (2022).
- [8] C. Lortaraprasert, J. Shiomi, *npj Comput. Mater.* 8, 219 (2022).

2:15 PM *MT03.07.04

Toward Accelerated, Experimental-Theoretical Closed-Loop Discovery [Austin Mroz](#), Rebecca L. Greenaway and Kim E. Jelfs; Imperial College London, United Kingdom

Novel chemical systems are necessary to fully address the major global challenges facing humanity, including the climate emergency, resource scarcity, and energy consumption needs. Traditional chemical discovery initiatives are founded on intuition-guided, "trial-and-error" processes. Here, small, iterative changes to chemical structure and experimental conditions are made by the researcher.¹ This is significantly resource and time intensive; after each small modification, the molecule must be synthesized (often a trial-and-error process in itself) and properties measured. As a result, these workflows are associated with long timescales (~20 years) and high costs.^{2,3} Recently, computation has accelerated this process via atomistic simulations and data-driven approaches.^{4,5} Yet, present applications of computation are largely often to post-rationalization of experimental observations or high-throughput screening of manually-curated databases of hypothetical systems.¹

The full utility of computation in the chemical discovery pipeline is only realized with the close integration of experiment and theory.⁶ This could be achieved via closed-loop, experimental-theoretical workflows, which are poised to efficiently identify high-performing candidate compounds for target applications. Here, AI-driven theoretical predictions guide high-throughput, automated experiments and these experimental results are used to improve the accuracy of the predictive models in an iterative process, which is repeated until convergence criteria are met. Often this process is directed using data-driven optimization strategies.

Despite the initial success of AI in closed-loop chemical discovery workflows, there still exist major challenges in their scalable implementation – the major bottlenecks being i) the degree of human intervention needed and ii) lack of methods to manage the number and quality of initial data points. This is further complicated by the necessary integration and accommodation of i) varying metadata formats, ii) non-compatible, proprietary characterization software, and iii) hands-on robotic platform calibration and manipulation, among others. Each of which needs to be explicitly addressed to realize coherent, automated closed-loop chemical discovery. Thus, data-driven solutions and supporting software are imperative to seamlessly close-the-loop in experimental-theoretical discovery workflows.

We address these bottlenecks and present an integrated, experimental-theoretical workflow that leverages high-throughput, automated experiments, and abstract computational models with data-driven optimization strategies to drive towards viable supramolecular materials for gas storage and separation applications.

References

- [1] *J. Am. Chem. Soc.*, **2022**, 144, 18730; [2] *Acc. Chem. Res.*, **2020**, 53, 599; [3] *Energy Environ. Sci.*, **2022**, 15, 579; [4] *Chem. Rev.*, **2020**, 120, 8066; [5] *Chem. Rev.*, **2021**, 121, 9816; [6] *Adv. Mater.*, **2021**, 33, 2004831.

2:45 PM BREAK

3:15 PM *MT03.07.05

New Opportunities for Data-Driven Chemistry and Materials Science Through Automation [Janine George](#)^{1,2}; ¹Federal Institute for Materials Research and Testing (BAM), Germany; ²Friedrich-Schiller-Universität Jena, Germany

In recent years, many protocols in computational materials science have been automated and made available within software packages (primarily Python-based).^[1] This ranges from the automation of simple heuristics (oxidation states, coordination environments)^[2] to the automation of protocols, including multiple DFT and post-processing tools such as (an)harmonic phonon computations or bonding analysis^[3]. Such developments also shorten the time frames of projects after such developments have been made available and open new possibilities.

For example, we can now easily make data-driven tests of well-known rules and heuristics or develop quantum chemistry-based materials descriptors for machine learning approaches. These tests and descriptors can have applications related to magnetic ground state predictions of materials relevant for spintronic applications^[4] or for predicting thermal properties relevant for thermal management in electronics.^[5] Combining high-throughput *ab initio* computations with fitting, fine-tuning machine learning models and predictions of such models within complex workflows is also possible and promises further acceleration in the field.^[6]

In this talk, I will show our latest efforts to link automation with data-driven chemistry and materials science.

References

- [1] J. George, *Trends Chem.* **2021**, 3, 697–699.
- [2] D. Waroquiers, J. George, M. Horton, S. Schenk, K. A. Persson, G.-M. Rignanese, X. Gonze, G. Hautier, *Acta Cryst B* **2020**, 76, 683–695.
- [3] J. George, G. Petretto, A. Naik, M. Esters, A. J. Jackson, R. Nelson, R. Dronskowski, G.-M. Rignanese, G. Hautier, *ChemPlusChem* **2022**, 87, e202200123.
- [4] K. Ueltzen, A. Naik, C. Ertural, P. Benner, J. George, *Article in Preparation* **2023**.
- [5] A. A. Naik, C. Ertural, N. Dhamrait, P. Benner, J. George, *Sci Data* **2023**, 10, 610.
- [6] C. Ertural, V. L. Deringer, J. George, *Article in Preparation* **2023**.

3:45 PM MT03.07.06

This searchable program is up-to-date as of April 15th, 2024.

Accelerated (Re)Design of Sustainable Formulations with The Autonomous Formulation Lab [Tyler Martin](#), Duncan Sutherland and Peter Beaucage; National Institute of Standards and Technology, United States

Industrial liquid formulations from electronics to nanoparticle coatings to drug delivery vehicles are often strikingly complex, with large numbers of components (10-100), complex multistep processing, and a wide variety of design requirements for a functional, sustainable, regulatory compliant product. This complexity often precludes physics-informed mapping between component fractions, processing, structure, leaving most formulation design to empirical trial-and-error or design of experiments strategies. I will discuss recent efforts by the Autonomous Formulation Laboratory (AFL) team at NIST to use machine learning driven, highly automated characterization to rapidly and intelligently map formulation phase space using structural characterization tools such as small-angle x-ray and neutron scattering (SAXS/SANS) together with secondary measurements, e.g. optical imaging, UV-vis-NIR and capillary viscometry. Our initial studies have resulted in an order of magnitude reduction in the time needed to map a model phase diagram and rapid cross-learning between model petroleum-based and biobased formulations. Other systems of interest from our personal care, biopharmaceutical, and alternative energy industrial collaborators will also be highlighted, including recent results on multimodal cooperative active learning.

4:00 PM MT03.07.07

A Low-Cost, Closed-Loop Nanomaterials Synthesis Automation Platform [Maria Politi](#), Brenden Pelkie, Blair Subbaraman, Fabio Baum, Kiran Vaddi, Nadya Peek and Lilo D. Pozzo; University of Washington, United States

Conventional nanomaterials synthesis schemes can be labor- and time-intensive, which significantly impedes the pace of new materials discovery and their applications. Semi-automated and fully automated platforms, in combination with data-science principles and artificial intelligence, have become an emerging paradigm for accelerated materials discovery. The combination of high-throughput experimentation and minimal human interactions with the system have allowed faster material synthesis, characterization, and analysis. However, many of these initiatives are still too costly to be implemented. In this context, open hardware principles have made the use of laboratory automation more accessible and more easily implemented for a variety of applications. We have demonstrated the use of a versatile automatic tool-changing platform (Jubilee) configured for automated ultrasound application, a liquid-handling robot (Opentrons OT2) and a well-plate spectrometer for the synthesis of CdSe nanocrystals. A total of 625 unique sample conditions were prepared and analyzed in triplicate with an individual sample volume of as little as 0.5 mL, which drastically reduced chemical waste and experimental time. Furthermore, we coupled the high-throughput workflow to a data-driven approach for the interpretation of the results provided a holistic view of the design space investigated. While successful, the previous study relied on three different instruments to conduct the workflow. Further improvements have allowed for integrating all the synthesis, processing, and characterization tools onto the same Jubilee platform for a closed-loop experimental campaign. This new ecosystem uses a simple Python API and allows for new tools to be easily integrated and interfaced, for simpler experimental orchestration. Thanks to the high-throughput capabilities of this low-cost and open-hardware platform, the ease in scalability of the system, and the modularity of the protocol, the overall workflow was adapted to study a variety of nanocrystal design spaces.

4:15 PM MT03.07.08

Understanding Design Rules of Colloidal Self-Assembly Using Autonomous Phase Mapping [Kiran Vaddi](#), Huat Thart Chiang, Sage Scheiwiller, Karen Li and Lilo D. Pozzo; University of Washington, United States

Automation in many experimental pipelines at laboratory and central facilities has shifted the bottleneck to autonomously driven data analysis and decision-making. Exponential growth in tools available for data-driven modeling resulted in the advent of self-driven laboratories (SDL) that aim to automate and accelerate the entire workflow starting from synthesis to characterization and device integration for emerging technologies and energy needs. Platforms based on solution-processible materials (polymers, colloids, and nanoparticles) are amenable to automation both at the synthesis and characterization levels. Techniques such as scattering and spectroscopy provide faster high-throughput alternatives to capture a signal of the underlying structure allowing us to construct composition-structure phase maps. However, one of the common goals in 'phase mapping' a system is to accurately identify phase boundaries that can have materials with interesting structures and properties. In the realm of SDL, the problem of mapping phase boundaries is tackled using a combination of Bayesian active learning and data clustering. These techniques however cannot predict the phase map by 'filling' in the unexplored space that can provide information about the type of phase transition a boundary represents. We address this problem by reformulating the closed-loop phase mapping as a Bayesian active learning of a surrogate model that predicts measurement curves (spectroscopy, diffraction, or scattering). We apply the proposed approach to several classes of nano-scale colloidal and polymeric materials to learn phase maps that can be effectively used in understanding design rules to engineer colloidal self-assembly.

SYMPOSIUM NM01

Advances in 2D MXenes
April 23 - May 8, 2024

Symposium Organizers

Stefano Ippolito, Drexel University
Michael Naguib, Tulane University
Zhimei Sun, Beihang University
Xuehang Wang, Delft University of Technology

Symposium Support

Gold

Murata Manufacturing Co., Ltd.

Silver

INNOMXENE Co., Ltd.

Bronze

Energy Advances

Progress in Materials Science The Institution of Engineering and Technology (IET)

* Invited Paper

+ JMR Distinguished Invited Speaker

^ MRS Communications Early Career Distinguished Presenter

SESSION NM01.01: Synthesis and Characterization I

Session Chairs: Stefano Ippolito and Michael Naguib

Tuesday Morning, April 23, 2024

Room 330, Level 3, Summit

10:30 AM NM01.01.01

High-Yield and High-Throughput Delamination of Multilayer MXene via High-Pressure Homogenization Alex Inman¹, Kateryna Shevchuk¹, Joseph Capobianco² and Yury Gogotsi¹; ¹Drexel University, United States; ²USDA ARS, United States

Two-dimensional (2D) MXenes are a large family of materials with unique properties and numerous potential applications. They are typically produced by selective chemical etching of MAX phase precursors, which is a top-down approach allowing for scalable manufacturing. Multilayer MXenes are then further processed by chemical intercalation and delamination to produce a stable dispersion of 2D flakes in water. The current process of delamination requires multiple time-, energy-, and waste-intensive steps and still fails to delaminate some MXenes. Herein, we demonstrate a method of high-energy delamination called high-pressure homogenization (HPH) that combines high shear, cavitation forces, and impact forces to delaminate MXene without any post-process refinement steps or chemical intercalants. HPH-delaminated MXene can be made at scale with high throughput and yield with virtually no waste. We demonstrate the viability of this process by fabricating free-standing films with the material for use as electrodes for energy storage and as an effective antimicrobial coating where any residual lithium is undesirable. HPH-MXene electrodes demonstrated comparable capacitance to that of lithium-delaminated films with better rate capability. HPH-MXene coatings proved effective as antimicrobial coatings with over a two-log reduction in pathogenic microbes without the concern of chemical leaching by the coating. We anticipate that this method will decrease the cost of MXene manufacturing and be applicable to a variety of MXenes, including those that cannot be currently delaminated via intercalation.

10:45 AM NM01.01.02

A-Modified MXenes: Interlayer Incorporation of A-Elements into MXenes via Selective Etching of A' from $M_{n+1}A'_{1-x}A''_x C_n$ MAX Phases Alexander Sinitkii; University of Nebraska -Lincoln, United States

MXenes are a large family of two-dimensional materials with a general formula $M_{n+1}X_nT_z$, where M is a transition metal, X = C and/or N, and T_z represents surface functional groups. MXenes are synthesized by etching A elements from layered MAX phases with a composition of $M_{n+1}AX_n$. As over 20 different chemical elements were shown to form A layers in various MAX phases, we propose that they can provide an abundant source of new MXene-based materials [1]. The general strategy for A-modified MXenes relies on the synthesis of a $M_{n+1}A'_{1-x}A''_x C_n$ MAX phase, in which the higher reactivity of the A' element compared to A'' enables its selective etching, resulting in A''-modified $M_{n+1}X_nT_z$. In general, the A'' element could modify the interlayer spaces of MXene flakes in a form of metallic species or oxides, depending on its chemical identity and synthetic conditions. We demonstrate this strategy by synthesizing Sn-modified $Ti_3C_2T_z$ MXene from $Ti_3Al_{0.75}Sn_{0.25}C_2$ MAX phase, which was used as a model system. Although the incorporation of Sn in the A layer of Ti_3AlC_2 decreases the MAX phase reactivity, we developed an etching procedure to completely remove Al and produce Sn-modified $Ti_3C_2T_z$ MXene. The resulting MXene sheets were of high quality and exhibited improved environmental stability, which we attribute to the effect of uniform Sn modification. We demonstrate a peculiar electrostatic expansion of Sn-modified $Ti_3C_2T_z$ accordions, which may find applications in MXene-based nanoelectromechanical systems. Overall, these results demonstrate that in addition to different combinations of M and X elements in MAX phases, an A layer also provides exciting opportunities for the synthesis of new MXene-based materials. Synthetic approaches to MXenes modified with A-elements other than Sn, as well as applications of such materials, will also be discussed.

[1] S. Bagheri, A. Lipatov, N. S. Vorobeva, and A. Sinitkii. *ACS Nano* 2023, 17, 18747.

11:00 AM NM01.01.03

Synthesis and Electronic Transport of Ultrathin Single Crystal WC and W_2C Alexander J. Sredenscheck, David Sanchez, Jiayang Wang, Da Zhou, Le Yi, Morteza Kayyalha, Susan B. Sinnott and Mauricio Terrones; The Pennsylvania State University, United States

The transition metal carbide (TMC) family has historically been studied and applied for their high hardness, chemical stability, and electrocatalytic activity. Initially studied in bulk, non-layered morphologies, TMCs have received renewed interest with the development of novel top-down and bottom-up approaches to isolate layered TMCs (MXenes)¹ and ultrathin, non-layered TMCs (UTHTMCs)², respectively. The MXene family is large, but challenges persist in phase control and isolation of tungsten carbide owing to the lack of appropriate precursor material.³ Following recent works in bottom-up synthesis of UHTMCs^{4,5}, we show the isolation of two tungsten carbide phases using a liquid-metal-assisted chemical vapor deposition (LMCVD). Moreover, in the tungsten carbide system, little attention has been given to the influence of diffusion barrier and reactive gas ratios on the thickness, morphology, and phase of the crystalline products.

In this work, we report the synthesis of WC (P-6m2) with copper/tungsten foil stacks, and W_2C (Pbcn) from gallium/tungsten substrates. We identify the phase of these compounds using a combination of X-ray diffraction and planar/cross sectional selected area electron diffraction. The chemical compositions of WC and W_2C are investigated by planar energy dispersive X-ray spectroscopy (EDX) in the scanning transmission electron microscope. Moreover, we probe the dependence of crystal morphology with changes in growth temperature as well as methane/hydrogen (CH_4/H_2) ratios. Another

aspect of the synthesis that we have investigated are byproducts in the synthesis of WC/Cu/W and W₂C/Ga/W by combination of scanning electron microscopy, EDX, and Raman spectroscopy. We find that an increase in the CH₄/H₂ ratio promotes the formation of graphene in both systems, yielding irregular shaped W₂C nanoplates with large thickness, and polycrystalline WC nanoplates. In the W₂C/Ga/W system, we also find that crystalline Ga₂O₃ is formed during the synthesis and can be limited using higher H₂ concentrations.

To explain how these distinct phases are isolated, we carried out a density functional theory study to probe thermodynamic properties of the WC and W₂C systems. We find that the carbon concentration and atomic terminations at the surface of WC and W₂C are critical to the preferential isolation of W₂C on Ga/W substrates. Finally, we report the electronic transport measurements of UThTMCs single crystals of WC and W₂C. In particular, we find that semimetallic WC does not enter a superconducting state down to 10 mK, while W₂C enters a superconducting state below 2.85 K. We then compare in-plane and out-of-plane magnetic field measurements to assess the dimensionality of this superconducting state.

References

- 1: Naguib et al. *Advanced Materials* **23**, 4248-4253 (2011)
- 2: Xu et al. *Nature Materials* **14**, 1335-1141 (2015)
- 3: Y. Gogotsi and Q. Huang *ACS Nano* **15**, 5775-5780 (2021)
- 4: Wang et al. *Advanced Electronic Materials* **5**, 1-7 (2019)
- 5: Zeng et al. *Nano Energy* **33**, 356-362 (2017)

11:15 AM NM01.01.04

Exploration of Stacked MXenes as Precursors to Ultra-High Temperature Ceramics [Kat Nykiel](#), Brian Wyatt, Babak Anasori and Alejandro Strachan; Purdue University, United States

Ultra-high temperature ceramic (UHTC) vacancy-ordered zeta phases are critical for applications over 2000°C due to their high melting temperatures, oxidation resistance, and fracture toughness. However, the synthesis of zeta phase systems typically requires high temperature processing at >1400°C with high pressures, making alternative synthesis pathways to UHTC phases highly desirable. In this work, we investigate the potential of layered 2D MXenes as nanoceramic building blocks for nanolamellar carbide and nitride zeta-like phases. Stacked MXenes can expand the domain of zeta-like phases via their large space of interfacial combinations. We employed density functional theory (DFT) to investigate the thermodynamic stability of stacked MXenes as UHTC precursors, with sequential quasi-random structures to study non-stoichiometric nanolamellar carbides. We identify both stoichiometric and non-stoichiometric nanolamellar carbides below the established convex hull. Furthermore, we use a workflow that combines DFT simulations and machine learning to predict key UHTC features, such as melting temperature and elastic constants. Our findings show that by using stacked MXenes the UHTC domain can be expanded beyond vacancy-ordered zeta phases and traditional UHTC transition metals via a lower-temperature synthesis pathway.

11:30 AM *NM01.01.05

Two-Dimensional Materials from Large-Scale Computations and Selective Etching of Laminated Solids [Johanna Rosen](#); Linköping University, Sweden

In 2011, the synthesis of 2D materials through selective etching of specific layers in laminated 3D precursors was demonstrated, leading to the discovery of MXenes. Since then, the quest for 2D materials via etching has relied primarily on experimental methods, given the lack of accurate and efficient computational protocols. We here present the first steps towards a general theoretical approach for predicting 2D materials formed by selective etching under acidic conditions. Among ~60,000 3D materials, we identify ~100 potentially exfoliable candidates, including several material families. We corroborate the existence of well-established materials such as both TMD and MXene. Furthermore, and as a proof-of-principle, we selectively etch Y from a Ru-based compound, resulting in freestanding 2D sheets of Ru-based material. Our discoveries hold promising implications for experimental realizations and further advancements in theoretical investigations.

SESSION NM01.02: Synthesis and Characterization II

Session Chairs: Stefano Ippolito and Michael Naguib

Tuesday Afternoon, April 23, 2024

Room 330, Level 3, Summit

1:30 PM *NM01.02.01

Synthesis Science between MAX phases and MXenes [Christina S. Birkel](#)^{1,2} and Rose Snyder¹; ¹Arizona State University, United States; ²Technische Universität Darmstadt, Germany

The synthesis of MAX phases and their two-dimensional siblings MXenes, especially when pushing beyond Ti-based compounds, is far from trivial. Our group uses diverse preparation techniques to access new versions of these intriguing types of materials, recent examples include Cr₂GaC in the shape of carbonaceous microwires,¹ hollow and full microspheres² as well as hitherto unknown carbonitride phases, such as Cr₂GaC_{1-x}N_x and V₂GaC_{1-x}N_x.³ We specialize in non-conventional methods, such as sol-gel chemistry⁴⁻⁶ and microwave heating⁷ to synthesize the MAX phases.

In this talk, I will highlight two of our recent projects: (i) Our work on a unique "514" MAX phase (Mo_{0.75}V_{0.25})₅AlC₄, its structural investigation and transition to the respective MXene including its electrocatalytic properties. (ii) The transition from a MAX-like "221" compound Mo₂Ga₂C to the fully exfoliated MXene Mo₂CT_x as well as Mn-doped variants. All materials are structurally characterized by diffraction and microscopy techniques and a deeper understanding of their chemical composition, formation mechanism and stability is obtained through spectroscopy and thermogravimetric methods.

2:00 PM NM01.02.02

Synthesis of High-Quality Monolayers of Cr₂TiC₂T_x MXene, Their Mechanical Properties, *p*-type Electrical Transport and Positive Photoresponse [Saman Bagheri](#)¹, Michael J. Loes¹, Alexey Lipatov^{1,2}, Haidong Lu¹, Alexei L. Gruverman¹ and Alexander Sinitskii¹; ¹University of Nebraska-Lincoln, United States; ²South Dakota School of Mines and Technology, United States

In the rapidly growing family of MXenes, Cr₂TiC₂T_x is one of the most intriguing materials as an ordered double-transition-metal MXene with peculiar magnetic properties. In this work, we developed a synthetic procedure for high-quality Cr₂TiC₂T_x and produced monolayer sheets with lateral sizes exceeding 15 μm for single-flake measurements. The results of such measurements on Cr₂TiC₂T_x further establish it as a unique material among the MXenes experimentally tested so far. Field-effect electrical measurements on monolayer Cr₂TiC₂T_x flakes reveal an average conductivity of 66.18 S cm⁻¹ and *p*-type transport properties, while established MXene materials, such as Ti₃C₂T_x and Nb₄C₃T_x, demonstrated *n*-type behavior in similar studies. The

experimental data are corroborated by DFT studies, showing that Cr vacancies are the major contributing factor to the p-type behavior of $\text{Cr}_2\text{TiC}_2\text{T}_x$. When illuminated with visible or infrared light, the $\text{Cr}_2\text{TiC}_2\text{T}_x$ devices exhibit *positive* photoresponse in contrast to the *negative* photoresponse that was recently reported for $\text{Ti}_3\text{C}_2\text{T}_x$ monolayers. Nanoindentation measurements of monolayer $\text{Cr}_2\text{TiC}_2\text{T}_x$ membranes yield a respectable value of effective Young's modulus of 220 ± 22 GPa. This work provides access to large high-quality $\text{Cr}_2\text{TiC}_2\text{T}_x$ flakes that can find numerous applications due to their attractive mechanical characteristics and transport properties that are complementary to other established MXene materials.

2:15 PM NM01.02.03

Evidence of Metallic Conductivity in $\text{Ti}_3\text{C}_2\text{T}_x$ by Temperature-Dependent Resistivity Measurements. [Alexey Lipatov](#)¹, Saman Bagheri² and Alexander Sinitnik²; ¹South Dakota School of Mines & Technology, United States; ²University of Nebraska - Lincoln, United States

$\text{Ti}_3\text{C}_2\text{T}_x$, the most popular MXene to date, is widely regarded as a metallic material based on numerous theoretical predictions and the results of experimental studies. Yet, despite this general consensus on the metallic nature of $\text{Ti}_3\text{C}_2\text{T}_x$, there have not been reports on its temperature-dependent resistivity (ρ) measurements that would demonstrate the expected increase of resistivity with temperature with $d\rho/dT > 0$ in a wide temperature range. Instead, all $\rho(T)$ data reported so far, mainly collected on macroscopic films of percolating $\text{Ti}_3\text{C}_2\text{T}_x$ flakes, demonstrate dependences with minima, which were observed in the range of 90-250 K in different measurements. In this work, we fabricated electronic devices based on individual high-quality $\text{Ti}_3\text{C}_2\text{T}_x$ flakes and measured their temperature-dependent resistivity. The resistivity of flakes was found to increase with temperature in the entire 10-300 K range, and the resulting $\rho(T)$ dependences can be accurately fitted by the Bloch-Grüneisen formula for the temperature dependence of resistivity of metals, confirming the metallic nature of $\text{Ti}_3\text{C}_2\text{T}_x$. We also demonstrate that oxidation of a $\text{Ti}_3\text{C}_2\text{T}_x$ monolayer transforms a monotonically increasing $\rho(T)$ curve into a dependence with a minimum that looks similar to the previously reported results for percolating MXene films. We also demonstrate that multilayer $\text{Ti}_3\text{C}_2\text{T}_x$ flakes retain their purely metallic $d\rho/dT > 0$ behavior even after annealing in air, suggesting that the outer layers of multilayer flakes effectively protect the core layers from oxidation. This result suggests that certain applications may benefit from multilayer flakes' improved environmental stability.

2:30 PM BREAK

3:00 PM NM01.02.04

Bottom-Up Synthesis of Two-Dimensional Transition Metal Carbides and Nitrides (MXenes) [Mark Anayee](#), Rahul Rao, Nicholas Glavin, Benji Maruyama and Dhriti Nepal; Air Force Research Lab, United States

MXenes represent the largest and fastest growing family of 2D transition metal carbides and/or nitrides, which exhibit unique combinations of properties, including metallic conductivity, hydrophilic surface chemistry, redox-active surface, and plasmonic behavior that make them attractive as electrodes for pseudocapacitive energy storage to coatings for electromagnetic interference shielding, transparent conducting displays for optoelectronics, conductive yarns for functional textiles, implantable electrodes for medicine, and many other applications. MXenes are typically derived via topochemical etching of atomically thick layers from precursor layered MAX phases using corrosive aqueous etchants. However, the chemical etching process leads to various atomic defects, contaminants, and inhomogeneity in surface chemistry. Herein, we explore bottom-up growth of MXenes using thermal and laser assisted Chemical Vapor Deposition (CVD). We conduct experiments using gradient samples (composition, film thickness, etc.) to demonstrate a combinatorial approach towards optimization of MXene synthesis and exploration of new MXene compositions. This work demonstrates the need to utilize high-throughput automated synthesis to investigate material systems with a vast chemical space such as MXenes. It also enables fabrications of MXene films with ordered morphologies that would not be possible using solution based deposition techniques.

3:15 PM NM01.02.05

Synthesis of Three Families of Titanium Carbonitride MXenes [Teng Zhang](#), Christopher E. Shuck, Kateryna Shevchuk, Mark Anayee and Yury Gogotsi; Drexel University, United States

Layered MAX phases and 2D MXenes derived from them are among the most studied materials due to their attractive properties and numerous potential applications. The tunability of their structure and composition allows every property to be modulated over a wide range. Particularly, elemental replacement and forming a solid solution without changing the structure allows fine-tuning of material properties. While solid solutions on the M (metal) site have been studied, the partial replacement of carbon with nitrogen (carbonitrides) has received little attention. By applying this concept, herein we report the synthesis of three families of titanium carbonitride $\text{Ti}_{n+1}\text{Al}(\text{C}_{1-y}\text{N}_y)_n$ MAX phases and $\text{Ti}_{n+1}(\text{C}_{1-y}\text{N}_y)_n\text{T}_x$ MXenes with one, two and three C/N layers. This greatly expands the variety of known MAX phases and MXenes to encompass 16 titanium carbonitrides with tunable X-site chemistries and different 2D layer thicknesses, including MXenes in the $\text{Ti}_4(\text{C}_{1-y}\text{N}_y)_3\text{T}_x$ system, which have not been previously reported. We further investigated the relationship between the composition, structure, stability, and synthesis conditions of the MXenes and their respective Al-based MAX phases. This range of materials will enable fundamental studies of the N:C ratio effect on optoelectronic, electromagnetic and mechanical properties of MXenes, as well as tuning those properties for specific applications.

3:30 PM *NM01.02.06

Organic and Inorganic Surface Chemistry of MXenes [Dmitri V. Talapin](#)^{1,2}, Young-Hwan Kim¹, Chenkun Zhou¹ and Di Wang¹; ¹University of Chicago, United States; ²Argonne National Laboratory, United States

Two-dimensional (2D) transition-metal carbides and nitrides (MXenes) show impressive performance in supercapacitors, batteries, electromagnetic interference shielding, and electrocatalysts. These materials combine the electronic and mechanical properties of 2D inorganic crystals with chemically modifiable surfaces, and surface-engineered MXenes represent an ideal platform for fundamental and applied studies of interfaces in 2D functional materials.

The comprehensive understanding of MXene surfaces is required for prescriptive engineering of their physical and chemical properties. We discuss general strategies to install and remove surface groups by performing topotactic substitution and reductive elimination reactions. Successful synthesis of MXenes with halido-, oxo-, imido-, thio-, seleno-, or telluro- terminations, as well as bare MXenes (no surface termination) can be synthesized both by traditionally (from MAX phases) and directly synthesized MXenes. We also successfully synthesized a series of hybrid organic-inorganic MXenes by covalently attaching dense carpets of organic surface groups. Since organic and inorganic materials are, in many aspects, complimentary to each other, organic-inorganic MXenes open a pathway to merge the benefits of both worlds into a hybrid matter that combines engineerability of molecules with the electronic, thermal, and mechanical properties of inorganic 2D materials. The description of MXene surface structure and reactivity requires a mix of concepts from the fields of coordination chemistry, self-assembled monolayers and surface science. MXene surface groups control biaxial lattice strain, phonon frequencies, electrochemical performance, the strength of electron-phonon coupling, making MXene surfaces not spectators but active contributors to conductivity, superconductivity, and catalytic activity.

SESSION NM01.03: Synthesis and Characterization III
Session Chairs: Stefano Ippolito and Ruocun Wang
Wednesday Morning, April 24, 2024
Room 330, Level 3, Summit

8:15 AM *NM01.03.01

About the structure, chemistry and stability of MXenes [Per O. Persson](#); Linköping University, Sweden

The properties and tailoring ability of MXenes has inspired research efforts across the globe, and the number of researchers, publications and applications associated with these materials is steadily accelerating. Despite this enormous and collective effort, fundamental properties, related to the MXene structure and the surface terminations remain unexplored.

At Linköping University, we have explored the structure and chemistry of individual MXene sheets, since the very first MXene publication. The method of choice for this purpose is advanced scanning transmission electron microscopy and spectroscopy methods with sub-atomic resolution.

In this talk I will review the current understanding of the structure, atomic defects and surface terminations. I will discuss which methods are available to generate, modify and tailor these through interaction with and exposure to the ambient environment. I will also review the current understanding of the stability of the structure, the surface chemistry, and how MXene interacts with water. For this I will provide in situ and ex situ results obtained using a number of different microscopy methods, microscopes, and special environmental holders.

8:45 AM NM01.03.02

Tuning The Microenvironment of Water Confined in $Ti_3C_2T_x$ MXene by Cation Intercalation [Mailis Lounasvuori](#)¹, [Teng Zhang](#)², [Yury Gogotsi](#)² and [Tristan Petit](#)¹; ¹Helmholtz-Zentrum Berlin, Germany; ²Drexel University, United States

The local microenvironment, which is often tuned by adding alkali metal cations to the electrolyte, has recently been found to play a major role in the electrocatalytic activity of nanomaterials.(1) Modulating the microenvironment can be used to either suppress hydrogen or oxygen evolution, thereby extending the electrochemical window of energy storage systems, or to tune the selectivity of electrocatalysts. MXenes are a large family of two-dimensional transition metal carbides, nitrides and carbonitrides that have shown potential for use in electrochemical energy storage applications. Due to their negatively charged surfaces, MXenes can accommodate cations and water molecules in the interlayer space. Nevertheless, the nature of the aqueous microenvironment in the MXene interlayer remains poorly understood. Here, we apply Fourier transform infrared (FTIR) spectroscopy to probe the hydrogen bonding of intercalated water in $Ti_3C_2T_x$ as a function of different intercalated cation and relative humidity. Being highly sensitive to different H-bonding states of water confined within the MXene layers,(2,3) especially in the O-H stretching mode region, FTIR spectroscopy enables the direct characterization of the H-bonding network of water and gives information on the relative amounts of water present in the samples. Because anions do not intercalate into MXene,(4) we are able to probe the hydration shell around isolated cations in a 2D confined environment. Strong changes in the hydrogen-bonding of water molecules confined between the MXene layers is observed after cation exchange. Furthermore, the IR absorbance of the confined water correlates with resistivity estimated by 4-point probe measurements and interlayer distance calculated from XRD patterns. This work demonstrates that cation intercalation strongly modulates the confined microenvironment, which can possibly be used to tune the activity or selectivity of electrochemical reactions in the interlayer space of MXenes in the future.

References

1. Schreier, M.; Kenis, P.; Che, F.; Hall, A. S. *ACS Energy Lett.* **2023**, *8* (9), 3935–3940.
2. Lounasvuori, M.; Sun, Y.; Mathis, T. S.; Puskar, L.; Schade, U.; Jiang, D.-E.; Gogotsi, Y.; Petit, T. *Nature Commun.* **2023**, *14* (1), 1322.
3. Lounasvuori, M.; Mathis, T. S.; Gogotsi, Y.; Petit, T. *J. Phys. Chem. Lett.* **2023**, *14* (6), 1578–1584.
4. Shpigel, N.; Chakraborty, A.; Malchik, F.; Bergman, G.; Nimkar, A.; Gavriel, B.; Turgeman, M.; Hong, C. N.; Lukatskaya, M. R.; Levi, M. D.; Gogotsi, Y.; Major, D. T.; Aurbach, D. *J. Am. Chem. Soc.* **2021**, *143* (32), 12552–12559.

9:00 AM *NM01.03.03

MXene Reactivity and Its Role in Development of Applications [Vadym Mochalin](#); Missouri University of Science and Technology, United States

A large family of two-dimensional transition metal carbides and nitrides (MXenes) raises interest for many applications due to their high electrical conductivity, mechanical properties [1], potentially tunable electronic structure [2], nonlinear optical properties [3], and the ability to be manufactured in the thin film state [4]. However, their chemistry that is key to development of these applications, still remains poorly understood [5,6]. In this presentation we will discuss recent progress in understanding fundamental MXene chemistry and harnessing it for suppressing unwanted reactions and prolonging stability of these materials.

For example, suppressing oxidation and hydrolysis at high pH was demonstrated as an effective way to prolong shelf-life and stability of MXene aqueous colloids [7]. Use of polyphosphate also has been shown to improve chemical stability of MXene aqueous colloids [8].

Other selected examples illustrating connections between understanding MXene chemistry and development of their applications will also be considered.

References

- Y. Li, S. Huang, C. Wei, C. Wu, V. N. Mochalin, *Nature Communications*, *10*, 3014 (2019)
M. Naguib, V. N. Mochalin, M. W. Barsoum, Y. Gogotsi, *Advanced Materials*, *26*(7), 992-1005 (2014)
J. Yi, L. Du, J. Li, L. Yang, L. Hu, S. Huang, Y. Dong, L. Miao, S. Wen, V. N. Mochalin, et al., *2D Materials*, *6*, 045038 (2019)
Y. Dong, S. Chertopalov, K. Maleski, B. Anasori, L. Hu, S. Bhattacharya, A. M. Rao, Y. Gogotsi, V. N. Mochalin, R. Podila, *Advanced Materials*, *30*(10), 1705714 (2018)
S. Huang, V. N. Mochalin, *Inorganic Chemistry*, *58*(3), 1958 (2019)
S. Huang, V. N. Mochalin, *ACS Nano* *14*(8), 10251-10257 (2020)
S. Huang, V. N. Mochalin, *Inorganic Chemistry*, *61*(26), 9877 (2022)
S. Huang, V. Natu, J. Tao, Y. Xia, M. W. Barsoum, V. N. Mochalin, *Journal of Materials Chemistry A* *10* (41), 22016 (2022)

9:30 AM BREAK

10:00 AM NM01.03.05

Defect Engineering of MXenes at Elevated Temperatures Brian Wyatt¹, Matthew G. Boebinger², Paul Kent³, Zachary D. Hood⁴, Shiba Adhikari⁴, Kartik Nemani¹, Murali Gopal Muraleedharan³, Annabelle Bedford¹, Wyatt Highland¹, Raymond R. Unocic² and Babak Anasori¹; ¹Purdue University, United States; ²Center for Nanophase Materials Sciences, United States; ³Oak Ridge National Laboratory, United States; ⁴Argonne National Laboratory, United States

The chemically diverse family of 2D MXenes have been widely adopted in areas such as energy storage, conversion, and electronics. From the ceramic perspective, MXenes uniquely enable the atomic control of its structure at the ~1 nm scale. In this presentation, we demonstrate the defect engineering of $\text{Mo}_2\text{TiC}_2\text{T}_x$, $\text{Ti}_3\text{C}_2\text{T}_x$, $\text{Mo}_2\text{Ti}_2\text{C}_3\text{T}_x$, and Nb_2CT_x MXenes at elevated temperatures using alkali cations. We demonstrate the improved phase stability of MXenes and control of formed carbide phases using *in situ* x-ray diffraction and scanning transmission electron microscopy techniques. Further, we present evidence for the role of partial occupation of alkali cations in defective sites in MXenes using computational methods paired with *in* and *ex situ* methods. Overall, this cation-based engineering of defects in 2D MXenes demonstrates the potential for improving their stability and further develops the tools for researchers to apply MXenes as a diverse and tunable family of nanoceramics for high temperature applications.

10:15 AM *NM01.03.06

Achieving Environmental Stability of MXenes in Air, Water and Electrolytes Asaph S. Lee, Mark Anayee, Mikhail Shekhirev and Yury Gogotsi; Drexel University, United States

MXenes display extraordinary electrical, optical, chemical, and electrochemical properties. There is a perception though that MXenes are unstable and degrade quickly in ambient environment, limiting potential applications and requiring specific storage conditions to last for a long time. However, significant developments in MXenes' synthesis, processing, and understanding of its chemistry led to dramatic increases in their environmental stability. Herein, we analyze delaminated $\text{Ti}_3\text{C}_2\text{T}_x$ MXene flakes in solution and on a substrate, electrodes in acidic electrolyte as well as free-standing films aged up to a decade. Structural, chemical and morphological characterization along with electronic conductivity measurements reveal the effect, or lack thereof, of prolonged storage under ambient conditions. Up to 90% conductivity was retained after 5 years of storage by the films dried after synthesis. Further, we show that decrease in electronic conductivity over time is largely caused by uptake of water by the hydrophilic surfaces of MXenes, and its effect can be, at least partially, reversed by vacuum drying at elevated temperature. MXene supercapacitor electrodes performed well over 500,000 cycles at 20 mV/s. The effects of $\text{Ti}_3\text{C}_2\text{T}_x$ stoichiometry, surface chemistry, defects, intercalants, interlayer spacing and storage condition on oxidation and hydrolysis are discussed. While no systematic data is available for other MXenes, we demonstrate that the same principles are applicable to V_2C , Nb_4C_3 and other 2D carbides.

10:45 AM NM01.03.07

Raman Spectroscopy Characterization of 2D Carbide and Carbonitride MXenes Kateryna Shevchuk¹, Asia Sarycheva^{1,2}, Christopher E. Shuck^{1,3} and Yury Gogotsi¹; ¹Drexel University, United States; ²Lawrence Berkeley National Laboratory, United States; ³Rutgers, The State University of New Jersey, United States

The first step to wider adoption of two-dimensional (2D) materials is understanding their fundamental properties by employing characterization methods, among which Raman spectroscopy plays a unique role, being a fast and nondestructive tool. The number, frequencies, and intensities of the modes (or bands) in the Raman spectrum have been used to identify the 2D materials' crystal lattice, bonding, and even the number of layers. MXenes, 2D transition metal carbides, nitrides, and carbonitrides, span diverse chemistries and structures, but only a few Raman spectra have been reported. This work is the first systematic experimental Raman spectroscopy study of the MXene family. We explore the vibrational spectra and provide peak assignments for ten MXenes with varying structures (from 2 to 4 atomic layers of transition metal) and compositions - Ti_2CT_x , Nb_2CT_x , Mo_2CT_x , V_2CT_x , $\text{Ti}_3\text{C}_2\text{T}_x$, $\text{Mo}_2\text{TiC}_2\text{T}_x$, Ti_3CNT_x , $\text{Nb}_4\text{C}_3\text{T}_x$, $\text{V}_4\text{C}_3\text{T}_x$, and $\text{Mo}_2\text{Ti}_2\text{C}_3\text{T}_x$ (terminated with -F, -OH, and =O) based on the experimental results and previously reported computational studies. We discuss the effects of MXene layer thickness, surface terminations, and MXene's metallic properties on Raman scattering. Additionally, we employ polarized Raman spectroscopy to identify out-of-plane vibrations and explain the higher frequency region of the spectra, and computational predictions to assign the peaks to the Raman-active modes. By creating the Raman spectra library of the most frequently used MXenes, we open the door for the use of Raman spectroscopy for fingerprinting of various MXenes.

11:00 AM *NM01.03.08

Insights into the MXene interfaces from simulations De-en Jiang; Vanderbilt University, United States

First principles molecular dynamics simulations of the MXene/water interfaces and the organic groups on the MXene surfaces will be presented. First, we will show how the proton transport across the interface and in confined water layers for MXenes and MXene/graphene heterostructures. Second, we will discuss the reactivity of MXene with water, to address the stability issue, including how the defects in the MXene layer impacts its reactivity with water. Hydrogen bond network, water dipoles, and Ti-water interaction are found to play important roles in the processes examined. Last, we will look at some organic groups on the MXene surface to examine the unique inorganic-organic interface on MXenes.

SESSION NM01.04: Synthesis and Characterization IV

Session Chairs: Alex Inman and Stefano Ippolito

Wednesday Afternoon, April 24, 2024

Room 330, Level 3, Summit

1:30 PM NM01.04.01

Local Surface Chemistry of $\text{Ti}_3\text{C}_2\text{T}_x$ MXenes in Aqueous Electrolyte Monitored by *In Situ* Scanning Transmission X-Ray Microscopy Peer Bärmann, Namrata Sharma, Faidra Amargianou, Tianxiao Sun, Markus Weigand and Tristan Petit; Helmholtz Zentrum Berlin, Germany

The pseudocapacitive behavior of $\text{Ti}_3\text{C}_2\text{T}_x$ MXenes promises high power and energy densities thanks to redox reactions occurring during the (de-)protonation of the MXene surface in acidic electrolyte. Nevertheless, local electrochemical processes occurring at the MXene-electrolyte interface and the associated changes of the MXene surface chemistry are currently largely unexplored. To this aim, soft X-ray spectroscopies are particularly relevant as they enable the selective characterization of either the electrolyte or the material of interest thanks to their element specificity.¹ Furthermore, the high spatial resolution (<30 nm) offered by X-ray Microscopy can provide precious information about local inhomogeneities at the nanoscale,² enabling the characterization of single MXene flakes. In this talk, the chemical bonding of Ti atoms in single few-layered $\text{Ti}_3\text{C}_2\text{T}_x$ MXene flakes was monitored in different electrolytes using synchrotron-based *in situ* Scanning Transmission X-ray Microscopy (STXM) at the Ti L-edge. Significant changes of the Ti

chemical environment are observed between acidic and neutral Li⁺-containing aqueous electrolyte and sub-flake inhomogeneities in the MXene surface chemistry was evidenced. Finally, potential-induced changes of MXene local surface chemistry will be discussed. *In situ* STXM will open new perspectives on the characterization of electrochemical processes in MXenes that can be monitored down to the single flake level.

1. Petit, T., Lounasvuori, M., Chemin, A. & Bärman, P. Nanointerfaces: Concepts and Strategies for Optical and X-ray Spectroscopic Characterization. *ACS Phys. Chem. Au* (2023).

2. Al-Temimy, A., Anasori, B., Mazzi, K., Kronast, F., Seredych, M., Kurra, N., Mawass, M., Raoux, S., Gogotsi, Y., Petit, T. (2020) "Enhancement of Ti₃C₂ MXene Pseudocapacitance after Urea Intercalation Studied by Soft X-ray Absorption Spectroscopy", *Journal of Physical Chemistry C*, 124, 5079.

1:45 PM NM01.04.02

A Mechanistic Study of MXene Current Collectors for Lithium-Metal-Based Batteries Ruocun Wang^{1,2}, Raymond R. Unocic³, Jaehoon Choi⁴, Yan Burets^{1,2}, Mark Anayee^{1,2}, Geetha Valurouthu^{1,2}, Wan-Yu Tsai³ and Yury Gogotsi^{1,2}; ¹A.J. Drexel Nanomaterials Institute, United States; ²Drexel University, United States; ³Oak Ridge National Laboratory, United States; ⁴University of Picardie Jules Verne, France

Lithium metal is widely investigated as a high-energy-density anode replacement for graphite in lithium-ion batteries. It is important for next-generation lithium-metal-based battery technologies. However, lithium dendrites tend to grow during deposition and stripping, resulting in poor battery life or short circuits. Literature shows that using MXene instead of copper as the current collector can mitigate lithium dendrite growth. Two mainstream hypotheses for dendrite suppression include forming a hexagonal close-packed structured lithium layer and a homogeneous growth of solid-electrolyte interphase (SEI) on the surface of MXene. However, there is a lack of experimental evidence to support those hypotheses. Here we used a suite of characterization techniques, including cryo-transmission electron microscopy (cryo-TEM), X-ray photoelectron spectroscopy (XPS), *in situ* Raman spectroscopy, scanning electron microscopy (SEM), and *operando* optical microscopy to investigate the crystal structure, SEI, and morphology of lithium nucleated on Ti₃C₂T_x MXene at different rates and capacity.

2:00 PM *NM01.04.03

Photoactive MBenes: the next generation of MXene-like 2D structures Agnieszka M. Jastrzebska; Warsaw University of Technology, Poland

MBenes family is a novel member in the flatland and a recent derivative of ternary MAB phases. However, MBenes differ from MXenes in many ways. Compared to MXenes, MBenes' structure is more complex due to multiple lattice arrangements. At the same time, boron opens the door to the rich structural chemistry of MBene, excellent reactivity, and energy harvesting abilities, to mention a few. In this talk, I will present a new synthetic approach to Mo₂B₂ MBene from its parental MoAlB phase, supported by theoretical calculations. In addition, I will demonstrate the tremendous photocatalytic potential of MBene compared to MXene. While research interest is rapidly accelerating, practical applications require better control over MBene's surface terminations and oxidation. MBene's vast compositional space and versatility provide almost limitless potential for designing structural variants with tailored optical and electronic properties. However, further research is needed to fully understand these novel materials and unlock their exotic light-driven phenomena. In summary, I expect MBenes to boost the fundamental research toward exploring their catalytic features in the next decade and development of MBene-based technologies that can manipulate light like never before.

2:30 PM BREAK

3:30 PM *NM01.04.04

A Systematic Study of MXenes for Hydrogen Evolution Reaction Anupma Thakur and Babak Anasori; Purdue University, United States

Two-dimensional (2D) transition metal carbides and nitrides (MXenes) are a large family of earth-abundant materials with more than forty compositions synthesized since 2011, such as Ti₂CT_x, Nb₂CT_x, Ti₃C₂T_x, and Mo₂Ti₂C₃T_x. MXenes have emerged as promising candidates for catalytic energy storage and conversion due to their electrochemically active surfaces combined with hydrophilicity, high electrical conductivity, and affinity to bond to molecules and nanomaterials to form hybrid structures. The ease of production of MXenes and their earth-abundant elements can overcome one of the major obstacles to the large-scale implementation of durable and efficient catalysts. In this talk, we will discuss the control of MXene transition metals and their surfaces to tune their electrocatalytic behavior. Specifically, we present a systematic study of 20 different MXenes, including novel compositions such as W₂TiC₂T_x and Mo₂Nb₂C₃T_x and high-entropy MXenes, and discuss how we achieve low overpotential for hydron evolution reaction (as low as ~160 mV).

SESSION NM01.05: Applications I
Session Chairs: Stefano Ippolito and Xuehang Wang
Thursday Morning, April 25, 2024
Room 330, Level 3, Summit

9:00 AM NM01.05.01

Ti₃C₂T_x MXene-Based Electrochemical Sensors for Phosphate Detection Thiba Nagaraja, Shiseido Robinson, Rajavel Krishnamoorthy and Suprem R. Das; Kansas State University, United States

The recent surge of the Internet of Things (IoT) has left an indelible mark on the global sensor market, spurring further research in a similar direction. At the heart of any sensor lies the sensing material and its intrinsic characteristics that define the key sensor metrics such as selectivity, sensitivity, limit of detection and dynamic range. Electrochemical sensors, known best for their dominance in rapid detection, cost efficiency and accuracy, are no exception to this paradigm. To date, many nanomaterials, including two-dimensional (2D) graphene, have been discovered and used as electrochemical sensing platforms for various biomedical and environmental applications. 2D transition metal carbides/nitrides (also known as *MXenes*), with their unique structure and presence of transition metals, have demonstrated large surface to volume ratio, high electrical conductivity, ease of functionalization and solution processibility. However, their electrochemistry and electrochemical stability have received limited exploration. Recently, there has been a growing focus on delving deeper into these aspects. Phosphate ions are intriguing molecules with significant relevance in environmental and biomedical applications. Understanding its detection in a solution environment using *MXene* as a sensing electrode will unveil *MXene*'s outstanding properties for unique applications as a phosphate sensor. Herein, we studied the performance of Ti₃C₂T_x *MXene* on a standard glassy carbon electrode in detecting phosphate ions in an electrochemical setup in the presence of molybdenum in an acidic media. The quality of Ti₃C₂T_x *MXene* was extensively characterized prior to serving as the sensing material in the electrochemical system. The proposed method demonstrated high selectivity in the presence of common interfering ions. The Ti₃C₂T_x *MXene* sensor also exhibited low detection limit and high sensitivity towards phosphate ions along with a large linear detection range

with reliable performance. This research lays the groundwork for the advancement of $Ti_3C_2T_x$ MXene-based phosphate sensors, promising future applications in environmental monitoring and sensing.

9:15 AM NM01.05.02

A Wide Look at MXene-Based CO₂ Reduction Electrocatalysts: Pioneering Pathways for Green Formaldehyde Production Sixbert P. Muhoza¹, Shiba Adhikari¹, Anupma Thakur², Babak Anasori² and Zachary D. Hood¹; ¹Argonne National Laboratory, United States; ²Purdue University, United States

Transition metal carbides, oxy-carbides, nitrides, and carbonitrides (MXenes) constitute an ever-growing class of two-dimensional materials with unique properties, including high conductivity and surface area as well as versatile and tunable surface chemistry.¹⁻³ Such a wide-ranging array of properties primes MXenes for various applications and, hence, provides them with the potential to tackle some of the most pressing challenges faced by our planet. Climate change is one such challenge, and the electrochemical CO₂ reduction reaction (CO₂RR) provides a potent pathway to alleviate the effects of CO₂ emission on the environment.⁴ The maturation of electrochemical CO₂RR, however, will require the development of electrocatalysts that maximize the value gained from converting the CO₂ feedstock. For this reason, we have developed a novel class of MXene-based electrocatalysts that leverage the unique properties of MXenes to convert CO₂ to formaldehyde. Formaldehyde is a key ingredient in manufacturing many value-added products, including resins, coatings, and vehicle components.⁵ However, formaldehyde is not typically generated with traditional electrocatalysts, indicating that the herein introduced MXene catalysts drive CO₂RR through new reaction pathways. This work highlights the behavior of a wide array of MXenes: ranging from single-layered traditional MXenes ($Ti_3C_2T_x$, $Mo_2TiC_2T_x$, and $W_2TiC_2T_x$) to multi-layered MXene/metal heterostructures ($Ti_3C_2T_x/CuM$, M = Ag, Sn, Zn, Ru, Ni, Fe). The $Ti_3C_2T_x/CuM$ heterostructures were developed through a novel electroless deposition of the bimetal onto the surface of MXenes by oxidizing the Ti moieties of the $Ti_3C_2T_x$ MXene. The reduction potential of the adsorbed metals dictated this process, with the strongly oxidizing metals reaching their lowest oxidation states while the weakly oxidizing metals were only partially reduced. In all cases, formaldehyde was generated and the highest efficiencies were achieved at low, industrially relevant, cell potentials (between -1.4 V to -2.2 V). These results, as they pertain to pioneering green formaldehyde production and favorability for industry adoption, warrant further exploration of the MXene-based CO₂RR electrocatalysts.

Acknowledgements

This material is based upon work supported by Laboratory Directed Research and Development (LDRD) funding from Argonne National Laboratory, provided by the Director, Office of Science, of the U.S. Department of Energy under Contract No. DE-AC02-06CH11357. This research used resources of the Center for Nanoscale Materials, U.S. Department of Energy (DOE) Office of Science user facilities operated for the DOE Office of Science by Argonne National Laboratory under Contract No. DE-AC02-06CH11357.

References:

1. Gogotsi, Y. & Huang, Q. MXenes: Two-Dimensional Building Blocks for Future Materials and Devices. *ACS Nano* **15**, 5775–5780 (2021).
2. Michalowski, P. P. *et al.* Oxycarbide MXenes and MAX phases identification using monoatomic layer-by-layer analysis with ultralow-energy secondary-ion mass spectrometry. *Nat. Nanotechnol.* **17**, 1192–1197 (2022).
3. Zhou, C. *et al.* Hybrid organic–inorganic two-dimensional metal carbide MXenes with amido- and imido-terminated surfaces. *Nat. Chem.* 1–8 (2023) doi:10.1038/s41557-023-01288-w.
4. Kuhl, K. P. *et al.* Electrocatalytic Conversion of Carbon Dioxide to Methane and Methanol on Transition Metal Surfaces. *J. Am. Chem. Soc.* **136**, 14107–14113 (2014).
5. Reuss, G., Disteldorf, W., Gamer, A. O. & Hilt, A. Formaldehyde. in *Ullmann's Encyclopedia of Industrial Chemistry* (ed. Wiley-VCH Verlag GmbH & Co. KGaA) a11_619 (Wiley-VCH Verlag GmbH & Co. KGaA, 2000). doi:10.1002/14356007.a11_619.

9:30 AM *NM01.05.03

MXene-based membranes for water-treatments Tae Hee Han; Hanyang University, Korea (the Republic of)

Seawater desalination presents a tremendous opportunity to utilize abundant water resources as approximately 70% of the Earth's surface is covered by the ocean. A recent advancement in the field involves an innovative approach that integrates reverse osmosis (RO) with feed heating through membrane distillation (MD), creating a hybrid thermal–membrane process to vaporize hot saline water and transport it through the pores of the hydrophobic membrane. However, this hybrid process still faces practical limitations, primarily due to the necessity of introducing an external heater, resulting in increased energy loss and thermal inefficiency. In this talk, I introduce a novel strategy to overcome these limitations by incorporating surface heating MD systems with MXene-based membranes. Specifically, MXene, known for their excellent electroconductivity, makes it an efficient material for Joule-heating. Additionally, surface-modified MXene exhibited remarkable oxidation stability and corrosion resistance. Ultimately, our MXene-based membrane demonstrated superior desalinating performance, achieving a high permeate flux and an outstanding heat utilization efficiency, all while maintaining excellent material stability.

10:00 AM BREAK

10:30 AM *NM01.05.04

Advancing wearable MXene bioelectronics to human translation. Flavia Vitale; University of Pennsylvania, United States

Wearable bioelectronics are widely adopted in clinical, research, and consumer electronics for health and fitness tracking. MXenes, and $Ti_3C_2T_x$ in particular, have emerged as ideal materials for soft, conformal, and multimodal wearable interfaces for sensing and modulating different body functions. In this talk, I will discuss our most recent works on designing, fabricating, and translating wearable MXene bioelectronics for use in humans. First, I will review how *ad hoc* manufacturing schemes allow leveraging the remarkable electronic, electrochemical, and magnetic properties of $Ti_3C_2T_x$ MXene at the molecular scale, while enabling full customization of the device functionality, geometry, and area coverage. Then, I will present examples of application of MXene wearables for non-invasive brain monitoring in outpatient clinical settings and neuromuscular diagnosis and rehabilitation in Achilles tendinopathy patients.

11:00 AM NM01.05.05

Hydrogel-Encapsulated MXene-Graphene Transistor for SARS-CoV-2 and E. Coli Bacteria Biosensing: Gel Gating and Transport Control Jiaoli Li¹, Jiabin Liu², Xinyue Liu², Shaoting Lin² and Chenglin Wu¹; ¹Texas A&M University, United States; ²Michigan State University, United States

Field-effect transistor (FET) biosensors have attracted huge interest in the multi-discipline, due to their effortless, time-saving, and label-free properties. However, its development is greatly restricted by its bare sensing surface and the liquid electrolyte, which will increase the nonspecific biomarkers absorption in complex environments. In this work, hydrogel encapsulation was applied to the MXene-graphene-based FET to detect SARS-CoV-2 and E. coli. Specific detection was also conducted to evaluate the feasibility of specific detection on our sensors. It demonstrated that hydrogel encapsulation

could achieve both gel gating and biomarker transport control and signal enhancement besides sensor encapsulation, which shows great advantages over the normal bare sensors. The investigation on the hydrogel encapsulated sensors shows great potential in the application of in-vivo monitoring and detection.

11:15 AM *NM01.05.06

Multispectral Electromagnetic Shielding Capabilities of 2D MXenes Chong Min Koo; Sungkyunkwan University, Korea (the Republic of)

The increasing prevalence of advanced electronics, mobilities, telecommunication, and medical devices operating across a wide range of EM waves (from ultralow kHz-level to high THz-scale frequencies) necessitates the development of EMI shielding materials operating in multispectral EM bands. MXenes, a class of two-dimensional materials comprising transition metal carbides, nitrides, and carbonitrides, have emerged as cutting-edge functional EMI shielding materials since their initial report in 2016. This is attributed to their exceptional metallic conductivity, expansive surface area, numerous surface terminations, and excellent solution processability. Here, this presentation aims to demonstrate that MXenes can deliver outstanding multispectral EMI shielding capabilities against radio-frequency (RF) waves, GHz-range microwaves, and THz/infrared (IR)-frequency waves, all achieved with minimal thickness and in various structural forms. Pristine MXene films with nanometer-scale thickness effectively interact with EM waves across the RF, GHz, and THz frequency ranges, while simultaneously demonstrating remarkably low IR emissivity. This low IR emissivity is a critical characteristic for applications such as selective thermal management, IR camouflage, stealth, and anti-counterfeiting measures. Through this exploration, we aim to highlight the versatility and efficacy of MXenes in addressing the evolving demands of EMI shielding across a wide range of electromagnetic frequencies and applications.

11:45 AM NM01.05.07

Integration of Mxene (Ti₃C₂T_x)-PVA-PAA Composite into Hanji: A Multifunctional Smart Fabric for Energy Harvesting, Thermoregulation, and EMI Shielding Yong Choi, Jiheon Kim and Byungseok Seo; Korea University, Korea (the Republic of)

Multifunctional smart fabrics have attracted a lot of attention due to the rapid downsizing of numerous electronic components and the emergence of wearable devices. One of the most advanced functions in such fabrics is energy harvesting in operating environments, while other multiple performances in terms of thermoregulation and electromagnetic interference (EMI) shielding would be desirable. Currently, heat, pressure, and triboelectricity are major energy sources that can be used with typical smart multifunctional materials. Herein, we report a novel smart fabric integrating energy harvesting using human perspiration and ambient moisture, as well as zonal heating for body temperature regulation and EMI shielding performances. In the smart fabric design, a blend of Mxene(Ti₃C₂T_x)-PVA-PAA is integrated into the environmentally friendly, traditional Korean paper, 'Hanji'. This composite exhibits high flexibility, oxidation resistance, hydrophilicity, and electrical conductivity. A precipitate of the mixture is obtained through ultrasonic treatment at room temperature, and then the asymmetric coating is applied to both sides of 'Hanji' using a vacuum filtration process. When the working fluid contacts the opposite side of the coated fabric, it rapidly penetrates through the coated interface of 'Hanji' and generates electricity through negatively charged nanofluidic channels. The introduction of hydrophilic polymer modulates the spacing of Mxene layers and prevents oxidation due to fluid exposure. The synergy between conductive Mxene and resistive hydrophilic polymer leads to achieving outstanding EMI shielding performance. Remarkably, even at low voltages, this composite shows efficient electricity-to-heat conversion and serves as a zonal heating element. The hydrophilic functional groups in the coating also provide humidity-sensing capabilities. The developed multipurpose smart fabric in this work will contribute to rationally designing multifunctional yet efficient energy harvesters using multiple sources.

SESSION NM01.06: Applications II
Session Chairs: Stefano Ippolito and Xuehang Wang
Thursday Afternoon, April 25, 2024
Room 330, Level 3, Summit

1:30 PM *NM01.06.01

Tailoring MXene Synthesis and Assembly for Enhanced Performance in Diverse Applications Yeonjin Baek¹, Kiandokht Pakravan¹ and Majid Beidaghi²; ¹Auburn University, United States; ²The University of Arizona, United States

Two-dimensional (2D) MXenes have garnered significant attention in recent years due to their exceptional properties and wide-ranging potential applications. This presentation showcases our group's recent research dedicated to optimizing the synthesis process and assembly techniques to enhance MXenes' electrochemical, mechanical, and membrane performance. The synthesis of MXenes plays a pivotal role in shaping their properties, including electrical conductivity and mechanical strength. Our studies reveal that the details of the synthesis process have a profound impact on MXene morphology, defect concentrations, and surface chemistry, ultimately influencing their electrical, electrochemical, and mechanical properties. Given the substantial impact of synthesis on MXene properties, the development of standardized synthesis protocols is imperative, as is the establishment of consistent performance reporting protocols across various fields of application. Furthermore, the performance of MXene-based devices is greatly influenced by how 2D MXene flakes are assembled into 3D structures. This presentation illustrates our research findings pertaining to the formulation of strategies aimed at enhancing MXene-based device performance through innovations in MXene assembly.

2:00 PM NM01.06.02

Exploiting Properties of MXenes to Improve Performance of Dry Reforming Catalysts Placidus B. Amama, Joshua Ighalo, Ahmed Al Mayyahi and Haider Almkhelfe; Kansas State University, United States

The development of efficient catalysts for dry reforming of methane (DRM) is critical for the sustainable production of syngas, an essential precursor for many industrial processes. DRM is known to have a high energy penalty due to the intrinsic chemical stability of the CO₂ molecule. The mechanism suggests that CO₂ is activated at the metal-support interphase while methane is activated on the surface of the active metals. Therefore, the reaction can be significantly improved by designing new catalysts that maximize the metal-support interactions (MSI) and consequently facilitate CO₂ activation. In this work, MXene (Ti₃C₂T_x) is used as support for Ni catalysts to address their low deactivation resistance during DRM. Wet impregnation was used to synthesize MXene-supported Ni catalysts (Ni/Ti₃C₂T_x) and a reference catalyst (γ-Al₂O₃-supported Ni) with 10 wt% loadings. The morphology and composition of the catalysts and the tailored surface functional groups of the MXenes obtained from electron microscopic and spectroscopic techniques have been correlated with their catalytic activity during dry reforming at atmospheric pressure. Simulations using Aspen Plus have been used to compare the experimental conversion with the thermodynamic benchmark by the Gibbs free energy minimization method.

2:15 PM NM01.06.03

Novel MXene-Based Electrified Air Filters for Enhanced Antiviral Airfiltration Performance [Marina Sefen](#); New Jersey Institute of Technology, United States

The COVID-19 pandemic has heightened concerns in public health regarding the transmission of airborne viruses. Many existing air purification methods primarily rely on physical barriers and filtration to arrest the spread of pathogens, but they often fall short in completely neutralizing microbiological agents. This deficiency poses the risk of secondary pollution and continued human infection. In this research, we developed MXene-coated non-woven air filters and achieved efficient antiviral air filtration at a low voltage of < 2V over the 4 x 4 cm² area. Uniform MXene coatings on commercial air filter membranes were fabricated by the spray coating of Ti₃C₂T_x MXene colloidal solution with varied loading amounts from 0.13 to 1.5 mg/cm². Under a voltage of 5 V, the current passing through an area of 2x2 cm² area was measured as 70 mA at 0.12 mg-MXene/cm² and 1500 mA at 0.75 mg-MXene/cm², much higher than the 2 mA for 1.5 mg/cm² graphene loading. This much-improved conductivity for the MXene-coated air filters can be ascribed to their excellent electrical conductivity. The antiviral air filtration tests revealed that the virus (MS2) removal rate was increased from ~50% for commercial air filters to ~75% for 0.12 mg/cm² and to >99% for 0.75 mg/cm² MXene coatings. Negligible pressure drop was achieved for MXene coatings up to a loading amount of 0.75 mg/cm². Notably, our findings indicated that the MXene-coated air filter exhibited significantly improved virus removal efficiency, surpassing the performance of graphene-based coatings. The affordability of MXene surface coatings further underscores their potential as a cost-effective solution for addressing critical public health concerns.

2:30 PM BREAK

3:00 PM NM01.06.04

Ti₃C₂T_x Co-Catalyst on CuO: Size Effects on Enhanced Photocatalytic Activity [Lu Chen](#)^{1,2}, [Taotao Qiang](#)¹, [Matyas Daboczi](#)², [Yasmine Baghdadi](#)² and [Salvador Eslava](#)²; ¹Shaanxi University of Science and Technology, China; ²Imperial College London, United Kingdom

Co-catalysts play a crucial role in photocatalytic reactions, and titanium carbide (Ti₃C₂T_x) is a promising alternative to expensive noble metal co-catalysts. However, size effects and charge transfer mechanisms of Ti₃C₂T_x co-catalysts on semiconductors for photocatalytic water splitting remain under-researched. Herein, we coupled copper (II) oxide (CuO) semiconductor with either Ti₃C₂T_x nanosheets (T2D) or Ti₃C₂T_x quantum dots (T0D) to create composite photocatalysts: T2D/CuO and T0D/CuO. The effects of size, morphology, and energetics of Ti₃C₂T_x were investigated and hydrogen production rates were tested. The results show that T0D are better co-catalysts for photocatalytic hydrogen production in comparison to T2D. The optimal T0D/CuO sample achieved a hydrogen production rate of 2174 μmol g⁻¹ h⁻¹, which is 19 times that of the optimal T2D/CuO samples, and more than 100 times that of pure CuO. The size of T2D in the composites is 200 nm, whereas the size of T0D is only 7 nm. This difference serves to decrease light obstruction and parasitic light absorption. Simultaneously, the surface area increases from 29 cm²/g for T2D/CuO to 43 cm²/g for T0D/CuO, indicating a higher abundance of active sites. This study highlights the impact of the size effects of Ti₃C₂T_x co-catalysts on photocatalytic performance and lays the foundation for the research of other quantum dot sized co-catalysts.

3:15 PM NM01.06.05

MXene Iontronics for Neuromorphic Computers and Actuators [Max M. Hamed](#); KTH, Sweden

2D materials and in particular MXenes can not only form passive metallic or supercapacitive structures but can also become active structures in which their optoelectronic or structural properties change as a function of doping. We term these materials 2D mixed ionic electronic materials (MIEC) or iontronics. Here we highlight two specific MXene MIECs devices that we have developed:

1) A component for in memory computers called **MXene electrochemical random-access memories (ECRAMs)**. The MXene ECRAM components has a channel like a conventional transistor, where the channel comprises a multi-layered MXene film formed using a highly accurate layer-by-layer self-assembly method developed by us.^[1] In the ECRAM, however, an electrolyte between the channel and gate is used instead of the dielectric used in a solid-state field-effect transistors (FET). As a result, we can electrochemically switch the redox state of the MXene MIEC material using a gate electrode. Conducting polymer ECRAMs were until now the only shown ECRAMs but can not be integrated into silicon chips because organic materials burn at the high temperatures used in CMOS fabrication. The multilayers of titanium carbide MXene^[1] can form ECRAMs with promising metrics for in-memory computation (also termed neuromorphic computers)^[2] and can withstand high temperatures for integration. In recent studies we analyze these components and describe their characteristics using equation derived for organic electrochemical transistors.^[3] We think our work paves the way for ECRAM based computers and MXene electrochemical transistors.

2) We recently developed an MXene based actuators that we call **Electrochemical Osmotic (ECO) actuators**.^[4] These actuators are formed from bulk composite electroactive hydrogels, fabricated from cellulose nanofibrils from trees, and 2D MXenes.^[5] These nanoparticles self-assemble into an anisotropic composite networks with an open mesoporous structure that can hold lots of water and be highly permeable to substances in their surroundings, while being mechanically very strong. The anisotropy of the network allows high expansion in one direction while maintaining very high strength and high electric conductivity in the other. The electrochemical charge/discharge of the MXene in the hydrogels controls the internal salt concentration and consequently their osmotic swelling. This allows direct electrically controlled actuation where around 700 water molecules expand/contract the structure for each ion/electron pair inserted/de-inserted at only ±1 volt, resulting in 300% electroosmotic expansion, with very high pressures reaching 1 MPa. This mode of electronic actuation has not been shown before, and has emergent properties not present in any previously known soft material. ECOs allow for monolithic integration of sensors and other functions into one composite, rendering a new form of smart soft material not achievable with other materials systems.

References

- [1] W. Tian, A. Vahidmohammadi, Z. Wang, L. Ouyang, M. Beidaghi, M. M. Hamed, *Nat. Commun.* **2019**, 10:2558.
- [2] A. Melianas, M. Kang, A. Vahidmohammadi, W. Tian, Y. Gogotsi, A. Salleo, M. M. Hamed, *Adv. Funct. Mater.* **2022**, 32, 2109970.
- [3] M. Kang, J. Shakya, J. Li, A. Vahidmohammadi, W. Tian, E. Zeglio, M. M. Hamed, *ArXiv* **2023**, 2303.10768.
- [4] L. Li, W. Tian, A. Vahidmohammadi, J. Rostami, B. Chen, K. Matthews, F. Ram, T. Pettersson, L. Wågberg, T. Benselfelt, Y. Gogotsi, L. A. Berglund, M. M. Hamed, *Adv. Mater.* **2023**, 35, 1.
- [5] W. Tian, A. Vahidmohammadi, M. S. Reid, Z. Wang, L. Ouyang, J. Erlandsson, T. Pettersson, L. Wågberg, M. Beidaghi, M. M. Hamed, *Adv. Mater.* **2019**, 1902977

3:30 PM NM01.06.06

Increased Sensitivity of Zero-Bias-Operated MXene via Lignin Hybridization for Chemiresistive Sensor [I Ketut Gary Devara](#), [Dhananjay D. Kumbhar](#), [MiJi Kwon](#), [Su-yeon Cho](#), [Dong Jun Kwon](#) and [Jun Hong Park](#); Gyeongsang National University, Korea (the Republic of)

High-sensitive and accurate environmental monitoring devices are essential to match the appropriate gas sensors to particular applications and requirements as global urbanization drives population density. MXenes is one of the 2D materials used as the active layer in chemical sensors. Since the bare MXene is nearly conductor, the dynamics of electric response upon chemical stimulation are not comparable to other solid-state chemiresistive devices. This work aims to enhance the sensitivity of chemiresistive sensors with different CO_{2(g)} and NO_{2(g)} gas concentrations without bias by reconfiguring the functional groups of MXene via hybridization lignin. Therefore, compared to MXene, MXene/lignin hybridization significantly showed better sensitivity. Besides that, it displayed a higher response and good repeatability for the target gases with various concentrations at room temperature. Under zero bias operation, the MXene chemiresistive sensor's sensitivity to NO_{2(g)} and CO_{2(g)} significantly enhanced with lignin hybridization at 15 ppm. In addition, the hybridized MXene/lignin was also applied on a curved composite substrate to determine the possibility for application in curvature objects. The MXene/lignin sensor shows a similar response and sensitivity to the value without curved, as exposure to 15 ppm of NO_{2(g)} and CO_{2(g)} gas at room temperature under zero gate bias operation. In addition, these chemical responsibilities of hybrid composite sensors are maintained after 50 bending cycles, consistent with mechanical stability. Consequently, MXene/lignin could be an attractive candidate sensing material for room temperature and zero bias NO_{2(g)} and CO_{2(g)} gas detection. The MXene/lignin hybridization sensor can be a model system for application in the advanced solid states sensory platform for curvature structure.

3:45 PM NM01.06.07

When MXenes Meet Machine Learning: A Promising Initiative Towards Data-Intensive Scientific Revolution [Moses A. Bokinala](#); University of Barcelona, Spain

Addressing the global challenge of sustainability and improving the quality of life for a growing population requires the development of advanced technologies, such as water-splitting devices, fuel cells, and rechargeable batteries. These technologies rely on materials that are both environmentally friendly and cost-effective. However, the path to discovering innovative materials faces a bottleneck due to complex trade-offs among material properties and challenges in optimizing high-dimensional spaces. Artificial intelligence (AI), employing data mining and machine learning (ML) tools, revolutionizes material discovery by automating and streamlining processes, empowering researchers to reveal hidden trends, and accelerating screening through efficient exploration of chemical space in vast materials datasets. Particularly, exploration of recently developed transition metal carbides/nitrides (MXenes), distinguished by their distinctive physical and chemical characteristics, has gathered widespread attention of material scientists, engineers, and chemists. Given the practical constraints of synthesizing the vast array of possible MXenes, a holistic approach that combines experimental and computational methods with ML gains prominence. This presentation highlights the pivotal role of ML in extracting knowledge from existing MXenes by using implicit data patterns and intricate correlations, providing intelligent guidance for purposeful MXene's development. Emphasizing the importance of SMART (specific, measurable, attainable, relevant, and timely) targets, the presentation illustrates how these objectives strategically shape the selection and transformation of data, promoting a comprehensive understanding of the challenges at hand. Subsequently, our recent work is showcased, featuring a versatile multistep procedure employing various supervised ML algorithms to develop well-trained data-driven models capable of predicting the hydrogen evolution reaction (HER) activity across a dataset comprising 4,500 MXenes configurations. A notable achievement in this exploration of ML modelling is the outstanding performance of the Gradient Boosting Regressor (GBR), demonstrating accurate and rapid prediction of the Gibbs free energy associated with hydrogen adsorption (ΔG_H). A detailed analysis of feature importance sheds light on key descriptors influencing HER performance, including d-band center variance, electron affinity, and the number of valence electrons in terminating groups. Overall, the adeptly trained ML model not only matches the predictive accuracy of DFT calculations but also exposes the factors shaping HER activity, opening up a coherent avenue to explore diverse configurations of MXenes.

SESSION NM01.07: Poster Session: Synthesis, Characterization and Applications

Session Chairs: Stefano Ippolito and Michael Naguib

Thursday Afternoon, April 25, 2024

Flex Hall C, Level 2, Summit

5:00 PM NM01.07.01

Multifunctional Single Component Epoxy System and MXene/Epoxy Composite with Polymeric Imidazole Latent Curing Agent [Sungmin Jung](#) and Chong Min Koo; Sungkyunkwan University, Korea (the Republic of)

A single-component epoxy system is necessary for industrial applications because of the convenience, productivity, and cost. Thus, there is a need for a latent curing agent that secures storage stability, while simultaneously triggering an immediate curing reaction above a certain temperature. Herein, we synthesize copolymers consisted of imidazole and furan groups in different ratios using controlled radical polymerization. Then, a microbead-type latent curing agent for epoxy resin is fabricated in an oil-in-water emulsion followed by Diels-Alder (DA) reaction between furan groups of copolymer and maleimide groups of bismaleimide (BMI) molecule at 40 °C. Compared to bare imidazole, the fabricated microbeads are able to effectively suppress reactivity due to the simultaneous operation of chemical modification and physical protection effect by DA network for 3 months at 60 °C. In addition, compared to epoxies made with imidazole, flame retardancy is secured by blocking heat and oxygen due to the high char residue formed by polymerization of BMI. Also, the increase in stiffness of specimen due to the rigid segment in the DA network results in the improvement of tensile, shear and impact strength. Lastly, as a proof-of-concept application, we incorporate functionalized-Ti₃C₂T_x MXene into epoxy to fabricate composite since MXene has received much consideration as a filler in polymer systems due to its remarkable electrical, electromagnetic interference shielding and flame-retardant properties. This proof-of-concept study demonstrates that MXene successfully endows the developed composites with high electrical conductivity and electromagnetic interference shielding and flame-retardant properties.

5:00 PM NM01.07.02

Ag-Ti₃C₂ MXene: A Promising Sorbent for Iodine Gas Capture in Nuclear Waste [Karamullah Eisawi](#)¹, Michael Naguib¹ and Brian Riley²; ¹Tulane University, United States; ²Pacific Northwest National Laboratory, United States

The capture and disposal of radioactive iodine gas, a byproduct of used nuclear fuel, are increasingly critical in the nuclear industry to ensure the sustainability of nuclear energy. There is a need for novel materials to capture such radioactive waste efficiently. MXenes, a family of 2D transition metal carbides, nitrides, and carbonitrides, exhibit intriguing physical and chemical properties, including customizable surface terminations, tunable interlayer spacing, high surface area, and excellent electronic conductivity. Their remarkable performance extends across diverse applications, encompassing energy storage, catalysis, water purification, and coating materials. In this study, we present a novel application for MXene hybrids, utilizing silver-MXene (Ag-Ti₃C₂T_x), as an effective sorbent for iodine gas at operating temperature of 150 °C. The hybrid was synthesized using a straightforward reduction of AgNO₃ to produce Ag nanoparticles that grow on the surfaces of Ti₃C₂T_x MXene layers. Our research demonstrates a notable iodine capture capacity in Ag-

Ti₃C₂T_x, surpassing widely reported iodine sorbents like silver zeolite (AgZ)¹ and Ag-aerogel². Specifically, the iodine loading in Ag-Ti₃C₂T_x reached 0.62 g_{Iodine}/g_{Sorbent}, outperforming AgZ and Ag-aerogel, which recorded 0.22 g_{Iodine}/g_{Sorbent} and 0.56 g_{Iodine}/g_{Sorbent} respectively. These findings highlight the potential of this synthesized hybrid material as effective sorbent for capturing iodine gas.

- [1] Asmussen, R.M., Turner, J., Chong, S., Riley, B.J., 2022. Review of recent developments in iodine wasteform production. *Frontiers in Chemistry*
[2] Matyáš, J., Ilton, E.S., Kovarik, L., 2018. Silver-functionalized silica aerogel: towards an understanding of aging on iodine sorption performance. *RSC Advances* 8

5:00 PM NM01.07.04

Design of an amperometric glucose oxidase biosensor with added protective and adhesion layer [Rongwei Gao](#); KU Leuven, Belgium

Electrochemical enzyme sensors have attracted tremendous attention due to their incomparable properties, such as specific selectivity, fast response, low cost, and easy miniaturization. Over the last decades, various electrochemical enzyme sensors have been reported, from simple test strips to wearable devices and implantable systems. Yet, only a few electrochemical enzyme sensors have practical application due to the instability and easy inactivation of enzyme. It is well known that immobilized enzymes display higher activities and stabilities compared to free enzymes, thus numerous works have focused on enzyme immobilization. Specifically, a total of 8398 documents was retrieved from the Web of Science when searching the keyword "Enzyme immobilization" over the past five years. Although many enzyme sensors have been reported in the literature, only a few that have been applied in various industries, such as blood glucose meters and pregnancy tests. In addition to the effective immobilization of enzymes, other factors may restrict the practical application of enzyme sensors and, thus, require further investigation.

Generally, enzyme sensors require a period of storage between preparation and use, which can affect their stability. Enzyme contamination denaturation and loss of activity can also cause sensor failure. Since the test system is inseparable from the liquid for both intrusive and non-invasive sensors, poor enzyme immobilization can cause the enzyme to leach from the immobilized layer or the entire modified layer to peel off the electrode into the test solution, resulting in detection failure. On the other hand, the electrochemical sensing process generally includes enzymatic reactions and heterogeneous electron transfer reactions. The key aims of this process are to achieve effective contact and accelerate the reaction kinetics between enzymes and detection molecules. Thus, it is pertinent to maintain the enzyme activity during the storage period, so that the active layer does not separate from the electrode surface under liquid operating conditions. The rapid realization and effective collection of the response signal of the enzyme toward target molecular are also highly important.

Herein, we propose an effective synergistic strategy to improve the stability and sensitivity of the enzyme sensor by combining the surface protective layer, intermediate reaction layer, and basic adhesion layer. Sodium hyaluronate (SH) is employed as the permeable protective film to protect enzymes from pollution and water loss, which is also beneficial to the diffusion of glucose towards the sensor's interface. The reaction layer is constructed with MXene-Ti₃C₂/GOD, in which MXene-Ti₃C₂ can ensure the highly dispersed loading of GOD. The adhesion layer consists of CS/rGO, whereby the large specific area of rGO strengthens the bond between the modification layer and current collector, preventing the sensing surface from peeling off the collector during the test. CS not only helps to bind MXene-Ti₃C₂ with rGO organically but also ensures high biocompatibility of the sensor. During the reaction, glucose passes quickly through the protective film (SH) into the reaction layer (MXene-Ti₃C₂/GOD) and reacts on the surface of GOD. Then, electrons are quickly released and effectively collected by the rGO-modified current collector. Results demonstrate that the repeatability of our designed sensor increased by 73.3% after improving the adhesion between the reaction layer and the current collector and that its response ability was greatly enhanced. Moreover, the long-term stability of the electrode surface with SH protective film proved to be superior than that without protective film, which suggests that this design can effectively improve the overall performance of the enzyme biosensor. This work proposed a multi-tier synergistic approach for improving the reliability of enzyme sensors.

5:00 PM NM01.07.06

A novel Zn single atom anchored Ti₃C₂T_x@ZIF-67 nanocomposites for effective deterioration of recalcitrant [Mohammed Askkar Deen F](#) and [Selvaraju Narayanasamy](#); Indian Institute of Technology Guwahati, India

Single atom catalyst (SAC) have garnered much attention owing to their atomic utilization efficiency, superior catalytic selectivity as well as engineerable catalytic sites. Despite this promising potential of SAC, the major challenge arises in their synthesis. Since SAC require chemically stable and high thermal substrates to stabilize metal atoms without sintering. Metal-Organic Frameworks (MOFs) offer vast surface area and enormous pore structure to be an immaculate template for synthesizing nanomaterials. However, its tendency to form nanoclusters during the synthesis renders them low mass transfer rate and poor catalytic activity. Hence, a pertinent substrate is required to enhance the MOFs stability, thereby regulating its electronic structure for optimized catalytic performance. MXene, a 2D nanomaterial with phenomenal conductivity, tunable surface terminations and remarkable mechanical pliability, exemplifies exceptional catalytic activity that can serve as a substrate for MOFs to exert a synergistic effect. Herein we developed a stable Zn single atom anchored Ti₃C₂T_x@ZIF-67 (Zn-SA/MXene/MOF) nanocomposites. The synthesized nanocomposites resulted in enhanced oxidation stability than pristine Ti₃C₂T_x MXene. Additionally, the nanocomposites exhibited a superior catalytic activity towards recalcitrant deterioration.

5:00 PM NM01.07.07

MXene Enabled Wearable Energy Storage Solutions [Alex Inman](#), Magdalena Zywołko, Lingyi Bi, Tetiana Hryhorchuk, Kyle Matthews and Yuri Gogotsi; Drexel University, United States

E-textiles can create new user experiences and provide comfortable monitoring of patient vitals. To realize their potential, there is a need for textile-based energy storage. However, devices reported in the literature don't store enough energy to power the electronics necessary to realize this vision. MXenes are conductive 2D materials with an electrochemically active surface and high energy storage capacity that can be integrated into textiles, making them an ideal candidate for textile-based energy storage. We demonstrate the use of MXenes in two different textile-based devices to power fully programmable microcontrollers capable of motion tracking and environmental sensing for extended times.

5:00 PM NM01.07.08

Stability of Pseudocapacitive Energy Storage in $Ti_3C_2T_x$ MXene in a Wide Temperature Range [Ruocun Wang](#)^{1,2}, Mark Anayee^{1,2}, Muhammad Nihal Naseer³, Teng Zhang^{1,2}, Yuan Zhang^{1,2}, Mikhail Shekhirev^{1,2}, Kateryna Shevchuk^{1,2}, Yong-Jie Hu² and Yury Gogotsi^{1,2}; ¹A.J. Drexel Nanomaterials Institute, United States; ²Drexel University, United States; ³University of Picardie Jules Verne, France

Pseudocapacitors have the potential to achieve high energy and high power density simultaneously, a holy grail for electrochemical energy storage. However, one obstacle facing pseudocapacitors is their shorter lifetime than commercial supercapacitors using the double-layer charge storage mechanism. In MXene-based pseudocapacitors, this concern is pronounced particularly at high temperatures due to the limited stability of the active material in aqueous solutions. This work shows that $Ti_3C_2T_x$ MXene thin-film electrodes in 5 M H_2SO_4 possess excellent rate capabilities from -50 °C to 70 °C but also a sufficient lifetime at 70 °C using a float test holding at -0.9 V vs. Hg/Hg_2SO_4 . Post-mortem characterization using X-ray photoelectron spectroscopy and Raman spectroscopy showed negligible signs of oxidation in the bulk of the film. This work suggests sufficient stability of $Ti_3C_2T_x$ MXene as a negative electrode in protic aqueous electrolytes across a wide temperature range rooted in thermodynamics, making it promising for pseudocapacitor energy storage.

5:00 PM NM01.07.09

Colorful MXene inks for multifunctional textiles [Lingyi Bi](#), Danzhen Zhang, Kseniia Vorotilo, Richard Vallett, Genevieve Dion and Yury Gogotsi; Drexel University, United States

Textiles are the ultimate wearables, providing 24/7 next-to-skin coverage of large areas of our body. They present large surface areas to host sensing devices. Great effort has been made to impart electronic properties - movement tracking, biological signal monitoring and actuation functions for haptic interactions—by incorporating conductive materials into traditional textiles. However, these metal and carbon-based conductive materials not only limit the hues to silver, black and grey but also require a large amount to be deposited for sufficient electrical conductivity – an approach that makes these textiles dull and harsh, deviate from the vibrant and comfortable textiles we love and experience every day. MXenes could pose a solution. MXenes are a family of two-dimensional transition metal carbides and nitrides with the highest electrical conductivity among solution processible nanomaterials. MXenes exhibit distinct colors from green, blue to purple, gold of different shades depending on the transitional metal(s) present (e.g., Ti, V, Nb, Mo, and Cr) and on their structuring. Moreover, the functional groups on the surfaces of MXenes allow them to establish strong interactions with the substrates, making them ideal conductive additives for durability and scale. Here, screen printing—a widely adopted technique in the textile industry—was demonstrated as an economical method for not only faithfully replicating MXene colors and achieving high conductivities on fabrics but also for carefully placing and combining MXenes for many electronic functions.

5:00 PM NM01.07.10

Annealing $Ti_3C_2T_z$ MXenes to control surface chemistry and friction [Kailash Arole](#), Hong Liang, Miladin Radovic, Jodie Lutkenhaus and Micah Green; Texas A&M University, United States

Although surface terminations (such as =O, -Cl, -F, -OH) on MXene nanosheets strongly influence their functional properties, synthesis of MXenes with desired types and distribution of those terminations is still challenging. Here, it is demonstrated that thermal annealing help to remove much of the terminal groups of molten salt-etched multi-layered (ML) $Ti_3C_2T_z$. In this study, the chloride terminations of molten salt etched ML- $Ti_3C_2T_z$ were removed via thermal annealing at elevated temperatures under an inert (argon) atmosphere. This thermal annealing created some bare sites available for further functionalization of $Ti_3C_2T_z$. XRD, EDS, and XPS measurements confirm the removal of much of the terminal groups of ML- $Ti_3C_2T_z$. Here, the annealed ML- $Ti_3C_2T_z$ were re-functionalized by -OH groups and 3-aminopropyl triethoxysilane (APTES), which was confirmed by FTIR. The -OH and APTES surface-modified ML- $Ti_3C_2T_z$ are evaluated as a solid lubricant, exhibiting ~70.1% and 66.7% reduction in friction compared to steel substrate, respectively. This enhanced performance is attributed to the improved interaction or adhesion of functionalized ML- $Ti_3C_2T_z$ with the substrate material. This approach allows for effective surface modification of MXenes and control of their functional properties

5:00 PM NM01.07.11

Graphene Quantum Dots enhanced MXene/Rare-earth Metal Oxide Nanohybrids based Printed Electrochemical Biosensor for Detection of Biogenic Amine Neurotransmitters [Sudip Das](#), Arghya Chakravorty, Aarcha A.M. and Vimala Raghavan; Vellore Institute of Technology, Vellore, India, India

With the expansion of science and technology, the healthcare business is flourishing with cutting-edge trends and innovations. Moreover, progress in the development of portable, real-time smart healthcare devices based on nanotechnological routes is of great collaborative interest between research and industry. Neuroscience is one such complicated, fascinating, but concerning genre of research in this current decade. Abnormal neurotransmitter levels and distributions can induce incurable disorders involving descending or ascending modulatory circuits or defective organs, according to neuroscience. One of the most promising methods for diagnosing brain illnesses is the detection of aberrant biogenic amine neurotransmitter levels. Hence, in this research, we have developed a novel graphene quantum dot enhanced MXene ($Ti_3C_2T_x$) and rare earth metal oxide-based (Gd_2O_3) printed electrochemical biosensor for simultaneous detection of Dopamine and Epinephrine. The nanocomposite has been characterized by some sophisticated characterization techniques like scanning electron microscopy, UV-vis spectroscopy, Fourier-transform infrared spectroscopy, energy dispersive x-ray spectroscopy, and powder x-ray diffraction. Cyclic voltammetry is employed for studying the chemical kinetics and absorbance of the nanocomposite, while differential pulse voltammetry, Linear sweep voltammetry, and electrochemical impedance spectroscopy have been performed to find out the lower-range detection limit of the analyte and wide linear range of the neurotransmitters present in the different biological fluids.

5:00 PM NM01.07.12

Efficient Delamination and Dispersion of 2D MXenes in Organic Solvents for Fabrication of Polymer Nanocomposites [James FitzPatrick](#) and Yury Gogotsi; Drexel University, United States

MXenes, a family of two-dimensional (2D) transition metal carbides and nitrides, have attracted significant attention in recent years for their unique optical, electronic, and chemical properties, to name a few. These nanomaterials have a general formula of $M_{n+1}X_nT_x$ where M is a transition metal, X is carbon and/or nitrogen, and T_x represents a variety of surface terminations. MXenes can be tailored for an incredibly broad array of applications, but are still often hindered by manufacturing, stability, and mechanical challenges. Many of these challenges can be overcome by integrating the 2D material into polymer matrices, leading to composites with distinct properties that can serve specific or multiple functions. To date, only a small portion of MXene research has been focused on polymer composites. Several hurdles exist for crafting high performance composites, including uniform distribution of flakes and interfacial compatibility with certain polymers, specifically hydrophobic ones. Current methods for compositing nanoparticles with polymers typically involve blending the two materials in an organic solvent, but dispersing the MXene in this medium either involves complex processing or lengthy sonication that can greatly reduce the average flake size and deteriorate properties. Herein, a more efficient approach to delaminating multilayer $Ti_3C_2T_x$ MXene in an organic solvent is proposed, forming stable colloidal solutions that can be used to process composites with highly uniform flake distribution. This delamination method requires little more work than typical methods for obtaining single-layer MXene flakes and does not require any sonication or

surface functionalization to improve interfacial compatibility and dispersion in a hydrophobic polymer matrix. Certain organic solvents such as propylene carbonate are highly effective in forming stable MXene solutions as well as enhancing formation of electroactive crystalline phases in polymers like PVDF. The properties of MXene-PVDF composites made through this process are examined through several characterization techniques, and potential applications of similar composite structures are explored.

5:00 PM NM01.07.13

Photoelectrochemical application of MoSe₂ decorated Ti₃C₂ MXene derived 2-D TiO₂ photoelectrode for simultaneous wastewater treatment and hydrogen generation Pooja^{1,2} and Pooja Devi^{1,2}; ¹Academy of Scientific and Innovative Research (AcSIR), Ghaziabad- 201002, India, India; ²Materials Science and Sensor Application, Central Scientific Instruments Organisation, Chandigarh-160030, India

To address the rising global energy demand, the world is transitioning to renewable sources, with hydrogen emerging as a clean and sustainable fuel option. While water is abundant, but availability of fresh water is very limited, and alternatively untreated wastewater can also be a source of pollution. Thus, using polluted/low quality water for hydrogen production presents a dual solution: managing wastewater while generating clean fuel. Photoelectrochemical (PEC) water splitting using photoelectrodes offers a promising approach. In this work hydrogen production from dye-contaminated water (utilizing methylene blue as a model pollutant) using MoSe₂-decorated Ti₃C₂ MXene derived TiO₂ photoelectrode in a PEC water-splitting system is demonstrated. The 2-D TiO₂ was synthesized from hydrothermal treatment of Ti₃C₂ MXene. Characterization confirms improved optical and structural properties of MXene derived 2-DTiO₂ as compared to commercial TiO₂. The 2-D TiO₂ hybrid electrode achieves better photocurrent density of as compared to P25-TiO₂. The condition will be optimized to yield remarkable dye degradation efficiency, and will be compared to MoSe₂ and TiO₂ alone. The optimized electrodes will also be studied for real waste water degradation by analysing the TOC and COD removal along with H₂ generation via gas chromatography investigation.

5:00 PM NM01.07.14

MXene as Electrochemical Sensing Chip for On-site Heroin Detection – New Era in Forensic Illicit Drug Monitoring Vimala Raghavan, Arghya Chakravorty, Sudip Das and Aarcha A.M.; Vellore Institute of Technology, India

In developing nations as well as across the globe, the abuses of narcotics are increasing drastically. In 2019, 1.3 million Europeans were heroin-addicted, while heroin production worldwide was 509-739 tons in 2022. Thus, a need arises to develop sensors that will lead to the detection of drugs even at lower concentrations. In this research study, we have fabricated titanium carbide MXene/Pt/Au nanocomposite on carbon paste screen printed electrode for developing a user-friendly, cost-effective sensing chip to detect illicit drug heroin. Scanning electron microscopy (SEM), X-ray powder diffraction (XRD), BET surface area analysis, and energy dispersive X-ray spectroscopy (EDX) are used for the characterization of composition and morphology of MXene/Pt/Au nanocomposite, demonstrating its high specific surface area of the synthesized material. The synthesized MXene possesses wall thicknesses of about 17 nm, nanoparticles' size was less than 70 nm on average. The mentioned properties provided rapid electron transfer and large electrochemically active surface area and assisted in the discrimination of analytes that reduce or oxidize under the same potentials. The enhanced electrode demonstrated appropriate sensing ability to heroin after performing fixation of MXene/Pt/Au nanocomposite. Kinetic factors charge transfer coefficient, standard heterogeneous electron transfer rate constant, and other different electrochemical factors are predicted using voltammetry methods. At a glance, the developed electrochemical chip ensures a unique LOD for device making and a wide linear range during detecting heroin. In addition, the mentioned suggested a suitable potential for profiling of heroin with appropriate long-term stability, repeatability, and reproducibility. The excellent efficiency for the measurement of real samples demonstrated the most significant future perspectives of this sensor.

5:00 PM NM01.07.15

MXene-Derived Sodium Titanate Nanoribbon/Lanthanum Composite as High-Performance Electrochemical Point-of-Care Sensor – A Step towards Achieving One Health Arghya Chakravorty, Aarcha A.M., Sudip Das and Vimala Raghavan; Vellore Institute of Technology, India

One Health is an approach to designing and implementing programs, policies, legislation, and research in which multiple sectors communicate and work together to achieve better public health outcomes. The One Health approach is critical to addressing health threats in the animal-human-environment interface. Among global health problems, antimicrobial resistance (AMR) is the one that best illustrates the One Health approach. In this context, the antibiotic enrofloxacin plays an important role in terms of therapeutic drug monitoring in humans, and administration in poultry, animals, and aquaculture, which includes the threat to food as well as environmental safety. Thus, a need arises to develop sensors that will lead to the detection of enrofloxacin even at lower concentrations in versatile real matrixes. In this research study, we have fabricated titanium carbide MXene-Derived Sodium Titanate Nanoribbon/Lanthanum nanocomposite on carbon paste screen printed electrode for developing a user-friendly, cost-effective sensing chip to detect illicit drug heroin. Scanning electron microscopy (SEM), X-ray powder diffraction (XRD), BET surface area analysis, and energy dispersive X-ray spectroscopy (EDX) are used for the characterization of the composition and morphology of MXene-Derived Sodium Titanate Nanoribbon/Lanthanum nanocomposite, demonstrating its high specific surface area of the synthesized material. The synthesized nanoribbon possesses wall thicknesses of about 15 nm, nanoparticles' size was less than 50 nm on average. The mentioned properties provided rapid electron transfer and large electrochemically active surface area and assisted in the discrimination of analytes that reduce or oxidize under the same potentials. The enhanced electrode demonstrated appropriate sensing ability to heroin after performing fixation of the nanocomposite. Kinetic factors charge transfer coefficient, standard heterogeneous electron transfer rate constant, and other different electrochemical factors are predicted using voltammetry methods. At a glance, the developed electrochemical chip ensures a unique LOD for device making and a wide linear range during detecting enrofloxacin in different real matrixes, viz. milk and food samples; human blood serum, and urine; waste water, and pharmaceutical industry effluents. In addition, the mentioned suggested a suitable potential for profiling of enrofloxacin with appropriate long-term stability, repeatability, and reproducibility. The excellent efficiency for the measurement of real samples demonstrated the most significant future perspectives of this sensor.

5:00 PM NM01.07.16

First-principles investigation of surface functionalization and CO₂ adsorption in MXenes Michelle Becerra and Cormac Toher; The University of Texas at Dallas, United States

Ever-increasing amounts of carbon dioxide (CO₂) are being expelled into the atmosphere, and without some type of countermeasure the environmental consequences will be dire. Motivated by the fact that CO₂ generators are a fixed part of our technological society which may be reduced, but not fully removed; research efforts have been directed towards utilizing these high concentrations of atmospheric CO₂ as a sustainable resource. Carbon capture, specifically post-combustion, captures CO₂ from a single source, removing it from the air and allowing further operations to be performed later. 2D early transition metal carbides and nitrides known as MXenes are investigated as an effective sorbent material thanks to their diverse composition, chemically active surface stemming from surface functionalizations and overall versatile and tunable nature. The computational characterization of MXene surface functionalizations, both the native surface inherited from synthesis and non-native surface groups introduced afterwards, are being systematically explored through calculated adsorption energies from density functional theory (DFT) as well as material optimization via machine learning (ML) methods. Molecules and surfaces being modeled are: pristine surfaces (Ti₃C₂, Mo₃C₂), attaching molecules (CO₂, H₂O, O₂, N₂, SO₂), native surface functional groups

(F, O₂, O, OH, Cl and H), non-native surface functional group (NH₂) and the interactions between them. The characterizations so far have shown that when adsorbing to a pristine Ti₃C₂ surface, single ions of F, O, OH, Cl and attaching molecules CO₂, H₂O and O₂ all preferred binding to hollow sites, while ions of H and NH₂ favored the bridge site before relaxing into a hollow site. Single fluorine ions bound to the surface were more thermodynamically stable when H₂O adsorbed, when compared to CO₂ and O₂, but saturation of the surface with fluorine resulted in CO₂ and H₂O having similar adsorption energies. The unknowns revolving around MXenes and their surface functionalizations is a knowledge gap that is preventing MXenes from being fully utilized in the field of sustainable chemistry. The characterizations and MXene designs generated by this research will not only fill in the divide between MXenes and carbon capture, but also unite industries and our environment through more accessible carbon capture methods.

5:00 PM NM01.07.18

Enhanced SERS Sensing via 3D Microstructures Hybridized with 2D MXenes Shehua C. Thor¹, Zihao Lin¹, Sodam Choi², Chiwon Ahn² and Jeong-Hyun Cho¹; ¹University of Minnesota, United States; ²Korea Advanced Institute of Science & Technology (KAIST), Korea (the Republic of)

Surface-Enhanced Raman Spectroscopy (SERS) is an analytical technique that can be used to detect target particles on a plasmonically enhanced surface. This has applications in fields such as medicine and environmental pollution. The advantage of SERS detection is that it can be used to detect very small amounts of a sample and it is noninvasive. However, traditional SERS requires that the target particles be in contact with the plasmonic materials on the sensing surface. For the detection of very low concentration target particles in a liquid, traditional SERS techniques are limited by the diffusion limit. More specifically, it can take hours for nanoscale target particles in a liquid at very low concentrations to diffuse to the sensing surface for detection. In this study, we address the diffusion limitation by merging MXenes, a 2D material, with a 3D microstructure, establishing a micro-scaled surface optimized for detecting minute concentrations of target particles in a liquid. The 3D configuration composed of SU-8 is a self-assembled twin-tubular microstructure that creates a nanogap at the center curvature. When fluid is flown through this tubular structure, an enhanced Raman signal can instantly be obtained. As fluid is flown from one end of the twin tubular structure to the other end, some fluid will flow between the center curvature (a nanogap). At this center curvature, some of the analytes will be caught in between the nanogap of the center curvature. Furthermore, both sides of this nanogap have MXenes. Hence, the analytes will be in contact with the plasmonic surface and be ready for instant Raman measurement. Furthermore, this Raman signal demonstrates two levels of enhancement. The first level of enhancement is from the MXenes. MXenes can be used as a plasmonic material that can enhance the Raman signal. The second level of enhancement is from the proximity of the two MXenes surfaces at the center of the twin tubular 3D microstructure. This proximity is a function of the twin tubular structure. The twin tubular structure curves itself into a shape where there is a nanogap at the center between the two tubes. At this nanogap, there is also MXenes on both sides of the gap. This nanogap is the plasmonic surface where the enhanced Raman measurement will be taken. Capitalizing on the combined advantages of 3D structures and low-dimensional (0D, 1D, and 2D) materials, which counterbalances the limitations of 2D materials like MXenes, the approach of fusing 3D microstructures with these low-dimensional materials offers broad application possibilities.

5:00 PM NM01.07.19

The fabrication and characterization of a water treatment system incorporating activated carbon, graphene nanoplatelets, and Ti₃C₂-based composite nanofiltration matrix: towards the development of multifunctional nanofiltration systems for targeted removal of emerging contaminants Prakhyat Gautam¹, Parshwa Khane¹, Derek Xiong¹, Edbertho Leal-Quiros², Saquib Ahmed^{3,3} and Sankha Banerjee^{1,4}; ¹California State University, Fresno, United States; ²University of California, Merced, United States; ³Buffalo State College, United States; ⁴University of California, Davis, United States

Researchers are exploring various strategies to address water scarcity, and one such approach involves the application of nanotechnology in water treatment and purification. There is also a great need for the targeted removal of Polyfluoroalkyl Substances (PFAS) and the recovery of useful nutrients from different wastewater sources. The ongoing research focuses on creating and refining a water purification system that combines activated carbon with graphene, and Ti₃C₂-based composite nanofiltration matrix. This system was tested using five different concentrations of methylene blue and deionized water solutions, which underwent filtration in three separate cycles. For potential consumer-level use, a cost-effective, small-scale water filter was developed. It utilizes activated carbon and graphene nanoplatelets, with filter paper serving as the medium to retain a mixture of these materials within the filter. To assess the water quality, measurements were taken for conductivity, total dissolved solids (TDS), and pH in both the untreated feed water and the processed water. These measurements were carried out using an Oakton PC2700 Benchtop Meter. A UV-Vis spectrometer was employed to gauge solution absorption. Additionally, scanning electron microscopy was used to observe the microstructure of the composite filtration matrix and the distribution and adsorption of dye particles.

5:00 PM NM01.07.20

Delamination of uniformly terminated MXene produced using the molten salt etching Teng Zhang, Kateryna Shevchuk and Yury Gogotsi; Drexel University, United States

MXenes produced by molten salt of MAX phases have attracted attention of the community due to their controllable surface chemistry. However, their delamination is challenging due to the hydrophobicity of multilayer MXene and strong interactions between halogen-terminated MX sheets. The current delamination method involves dangerous chemicals such as N-Butyllithium or NaH, making scale-up difficult and limiting practical application. In this work, we present a low-cost, sustainable, and eco-friendly methodology for the delamination of molten salt synthesized MXenes while maintaining their surface chemistry. We demonstrate successful delamination. MXene films produced from the delaminated MXene had a conductivity of 8,000 S/cm and it didn't change after exposure to 95% humidity conditions for a week. This validation of successful delamination, preservation of inherent surface properties, and stability under high-humidity conditions broadens the range of potential applications of MXenes. This research marks a significant leap towards the sustainable and economical production of two-dimensional materials.

SESSION NM01.08: Applications III
Session Chairs: Stefano Ippolito and Michael Naguib
Friday Morning, April 26, 2024
Room 330, Level 3, Summit

8:30 AM NM01.08.01

Enhanced Gas Sensing Performance of M₂CT_x/MO (M = Ti, V, Nb, Mo) Nanocomposites M S Bhargava Reddy and Shampa Aich; Indian Institute of Technology Kharagpur, India

Gas sensors are in high demand across various fields, from disease diagnosis through breath analysis to ensuring environmental safety and enhancing food and agriculture processes. The continuous discovery of new materials drives advances in gas sensor technology. Notably, 2D materials have gained significant attention for gas sensing due to their remarkable electrical, optical, and mechanical properties. Among them, 2D MXenes have emerged as compelling candidates due to their high specific area and their rich surface functionalities with tunable electronic structure make them compelling for sensing applications. MXenes are generally represented by $M_{n+1}X_nT_x$, in which M represents an early transition metal, X denotes either carbon or nitrogen or carbonitrides or oxy-carbides, T_x signifies surface terminations ($T_x = -OH, -O, -F, -Cl$), and n can be 1-4. M_2CT_x MXenes, in particular, show promise for VOC/gas detection based on theoretical calculations. However, research has predominantly focused on $Ti_3C_2T_x$ MXenes due to their established status, leaving limited exploration of other MXene variants as gas sensors. By altering the transition metal in MXenes, selectivity for specific gases can be achieved. Our research involves synthesizing MXenes from parent precursors (MAX and non-MAX phases) and conducting thorough property characterizations. We employ optimized synthesis methods to obtain single-/few-layered MXenes via selective etching and delamination. However, when comes to practical applications, pristine MXene-based gas sensors have low sensitivity, significant baseline drift, susceptibility to cross-interference, and a narrow band gap, which limits gas reaction and responsiveness. The self-stacking of MXene layers also impedes the diffusion of gas molecules and hinders surface-active sites, restricting the gas sensor response and limiting the detection of low-concentration gases [1]. To enhance gas sensing capabilities (response and stability), we fabricate M_2CT_x/MO ($M = Ti, V, Mo, Nb$) nanocomposites, introducing multiple in-situ Schottky barriers through surface oxidation to enhance VOC sensing capabilities. The MXene/MO nanocomposites were prepared by using the concept of in-situ conversion using MXene surfaces as reactants. MXene layers expose metallic atomic layers on their outer basal planes, which are highly oxophilic and prone to surface reactions like oxidation (e.g., Ti to TiO_2 in Ti_3CT_x , or $Ti_3C_2T_x$). The MXene surface is transformed partially, to form MO material in these processes. This approach lays the foundation for understanding the surface-sensitive behavior of MXenes in gas sensing by investigating the impact of surface chemistry. It represents a critical step towards expanding the scope of MXene-based gas sensors beyond $Ti_3C_2T_x$ and advancing the field of gas sensing technology.

Keywords: $Ti_3C_2T_x$; M_2X MXenes; surface chemistry; gas sensing; in-situ Schottky barriers.

References:

[1]. M Sai Bhargava Reddy, Saraswathi Kailasa, Bharat CG Marupalli, Kishor Kumar Sadasivuni, Shampa Aich*. "A Family of 2D MXenes: Synthesis, Properties, and Gas Sensing Applications". ACS Sensors 2022, 7, 8, 2132–2163.

8:45 AM *NM01.08.03

Two-Dimensional Graphene and MXene Electrodes for Stretchable Displays [HuanYu Zhou](#), Hyun-Wook Kim, Shin Jung Han and Tae-Woo Lee; Seoul National University, Korea (the Republic of)

Two-dimensional (2D) materials, exemplified by graphene and MXenes, hold immense potential for various flexible display applications. Nevertheless, the practical use of these materials has been hampered by the high charge injection barrier at the interface between stretchable electrodes and organic layers. In this study, we innovatively introduced a 2D graphene layer onto silver nanowire percolation networks, creating a comprehensive two-dimensional contact stretchable electrode (TCSE). This graphene layer effectively tailored the work function, facilitated charge distribution, and acted as a barrier against the ingress of oxygen and moisture. Our breakthrough enabled the development of intrinsically stretchable organic light-emitting diodes (ISOLEDs) boasting a remarkable efficiency of 20.3 cd/A. To further enhance electrode solution processability, we designed an environmentally stable MXene conductive electrode characterized by outstanding conductivity and a work function (WF) of 5.84 eV. Implementing the MXene electrode in ISOLEDs resulted in a substantial boost in current efficiency over 25 cd/A. These pivotal advancements not only establish a robust foundation but also offer a comprehensive blueprint for the creation of highly-efficient stretchable displays.

Reference

Adv. Mater. 2022, 34, 2203040.

Adv. Mater. 2022, 34, 2206377.

9:15 AM NM01.08.04

MXenes as Hydrogen Storage Materials Yi Zhi Chu^{1,2} and [Kah Chun Lau](#)¹; ¹California State University Northridge, United States; ²Michigan Technological University, United States

The ever-increasing need for electricity will require foremost increased efficiency in the uses of electric energy, more secure and sustainable energy resources and storages. To be better tailored to these challenges, novel materials for electrochemical and chemical energy storages that can efficiently store and deliver electric energy is highly important. In this case, hydrogen fuel stands out as a promising energy solution, and able offering a clean alternative to conventional energy sources while exhibiting the highest specific energy among many alternatives. Due to their high aspect ratio and tunable surface, slit-shape ion/mass transport channels, MXenes is a promising candidate in hydrogen storage materials. To address this issue, I will share with you our recent efforts based on theoretical studies with experimental supports from our collaborators. Based on our findings, some key avenues for future research that may help overcome the challenges and enable MXenes materials attain its full potential in this problem will be discussed.

Acknowledgement: This work is supported by the U.S. Department of Energy, Office of Basic Energy Sciences, Division of Materials Sciences and Engineering.

9:30 AM BREAK

10:00 AM NM01.08.05

Engineering 2D Mo-Based MXenes and Application in Ammonia Synthesis [Amanda Sfeir](#)¹, Christopher E. Shuck², Maya Marina³, Jean-philippe Dacquin¹, Yury Gogotsi², Said Laassiri⁴ and Sébastien Royer¹; ¹Université de Lille, CNRS, ENSCL, Centrale Lille, University Artois, UCCS-Unité de Catalyse et de Chimie du Solide, France; ²Drexel University, United States; ³Université de Lille, CNRS, INRA, Centrale Lille, Université Artois, IMEC – Institut Michel-Eugène Chevreul, France; ⁴Chemical & Biochemical Sciences, Green Process Engineering (CBS), Mohammed VI Polytechnic University, Morocco

Ammonia, which is one of the most important chemicals for synthesis of dyes, pharmaceuticals, and fertilizers, is conventionally produced by the reaction of molecular hydrogen with nitrogen, over an iron-based catalyst at 400-500 °C under pressure of over 200 bar, the Haber-Bosch process. While the H-B process is credited for providing a simple and cost-effective route for nitrogen-based fertilizer production, it is highly energy-intensive, accounting for ~ 2 % of the world's energy production, and as it relies on fossil-based resources, resulting in a staggering emission of 2.5% of global CO₂ annually. Decreasing the temperature and pressure of this century old, highly energy intensive process, would greatly decrease the energy consumption in the world and reduce carbon emissions. Fundamentally, producing ammonia at lower pressures is not thermodynamically prohibited, providing that the reaction takes place at temperatures below 300 °C. However, due to the high energy barrier for the activation/dissociation of the strong triple covalent NN bond (945 kJ mol⁻¹), most developed catalysts, including the industrial H-B catalyst, operate at temperatures over 400 °C. Consequently, high-pressure operation is

required to increase ammonia yields to acceptable industrial production (15% conversion per cycle). In this work, for the first time in the literature, we engineered Co decorated Mo_2CT_x MXene multilayers as catalysts for ammonia synthesis under mild conditions. The MXene functionalized by Co showed catalytic activity for ammonia synthesis from H_2 and N_2 at temperatures as low as 250°C , without any pre-treatment. The developed catalyst was highly active for ammonia synthesis, demonstrating a high rate up to $9500 \mu\text{mol g}^{-1} \text{ active phase h}^{-1}$ at 400°C under ambient pressure in steady state conditions, and did not suffer from any deactivation after 15 days of reaction. The apparent activation energy (E_a) was found to be in the range of 68 to 74 kJ mol^{-1} which aligns with the value reported for highly active catalysts such as Li-MT, $\text{Mn}_4\text{N-BaH}_2$, $\text{Ru/C}_{12}\text{A}_7\text{:e}^-$, and $\text{BaTiO}_{2.5}\text{H}_{0.5}$. This improved catalyst may decrease the energy consumption in synthesis of ammonia and its derivatives, as well as facilitate the use of ammonia as a hydrogen carrier for renewable energy storage. Numerous characterization techniques were used to analyze the catalysts including, XRD, SEM, TEM, H₂-TPR, XPS, EPR and ICP to understand their unique properties. Post-reaction analysis revealed partial substitution of lattice carbon with nitrogen, as well as partial reduction of Co^{2+} during ammonia synthesis. The catalytic activity profiles, supported by post-reaction catalysts characterization, suggest that active sites generated upon reaction might be cobalt decorated carbonitrides $\text{Co-Mo}_2\text{C}_{1-\delta}\text{N}_\delta\text{T}_x$. Upon reaching the steady state, the activity becomes stable upon cycling between low- and high-temperature conditions with no induction time. The results reported in this work demonstrate the appropriate modification of Mo_2CT_x resulted in a high-performance ammonia synthesis catalyst capable of operating under mild reaction conditions in the intermittent regime.

10:15 AM NM01.08.06

MXene Nanosheet-Derived N, S-Codoped Quantum Dots for Ultrasensitive Detection of 3-Nitro-L-Tyrosine in Biological Fluids Nguyen Thi Ngoc Anh, Van Thanh Nguyen and [Ruey-An Doong](#); National Tsing Hua University, Taiwan

3-Nitro-L-tyrosine (3NT) is an oxidative stress metabolite of neurodegenerative diseases, and the rapid and effective detection of 3NT in human fluids for early diagnosis is important. Herein, for the first time, the nitrogen, sulfur co-doped graphene quantum dots derived from nitrogen-doped $\text{Ti}_3\text{C}_2\text{T}_x$ MXene nanosheet via the hydrothermal method in the presence of mercaptosuccinic acid was synthesized as an optical sensing probe to detect 3NT in human serum. Tetramethyl ammonium hydroxide, the nitrogen source and delamination agent, was used to prepare nitrogen-doped MXene nanosheets via one step at room temperature. The as-prepared NS-MXene QDs (NSMQDs) are uniform with an average size of $1.2 \pm 0.6 \text{ nm}$, and can be stable in aqueous solution for at least 90 d to serve as the fluorescence probe. The N atoms in N-MXene reduce the restacking and aggregation of MXene nanosheets, while the sulfur dopant in NSMQDs increases the quantum yield from 6.2 to 12.1% as well as enhances the selectivity of 3NT over the other 12 interferences via coordination interaction with nitro group in 3NT. A linear range of $0.02 - 150 \mu\text{M}$ in PBS and $0.05 - 200 \mu\text{M}$ in human serum with a recovery of 97 – 108% for 3NT detection is observed. Moreover, the limit of detection can be lowered to 4.2 and 7 nM in PBS and $1 \times$ diluted human serum, respectively. Results obtained clearly indicate the potential application of the N- $\text{Ti}_3\text{C}_2\text{T}_x$ derived NSMQD for effective detection of 3NT, which can open a window for the synthesis of doped MQDs via 2D MXene materials for ultrasensitive and selective detection of other biometabolites and biomarkers of neurodegenerative diseases in biological fluids.

10:30 AM NM01.08.07

Thermoplastic Polyurethane (TPU) Reinforced with $\text{Ti}_3\text{C}_2\text{T}_x$ MXene: Synthesis, Characterization, Properties and Computational Modelling Rodrigo M. Ronchi, Rafael K. Nishihora, Jeverson T. Arantes and [Sydney F. Santos](#); Universidade Federal do ABC, Brazil

Thermoplastic polyurethanes are block copolymer consisting of alternating sequences of hard and soft segments (or domains). These materials are widely employed in industry for a wide range of applications which demands for high mechanical properties and wear resistance, good chemical stability, high formability at low temperatures, and high damping properties. Despite of these interesting properties, further improvements are still necessary to expand the use of TPU. In this context, the development of polymer based nanocomposites of TPU reinforced with MXenes appears as an attractive strategy to produce high-performance advanced materials with enhanced mechanical and tribological properties. Nanocomposite films of $\text{Ti}_3\text{C}_2\text{T}_x$ / TPU with concentrations 0, 0.25, 0.5, 0.75 and 1.0 wt% of MXene were produced and characterized by XRD, FTIR, XPS, SEM, DSC and TGA. Mechanical and tribological properties were assessed by nanohardness and nanotribological tests. Better results for mechanical properties and tribological behavior were found for the nanocomposites containing 0.5 and 0.75 wt.% of MXenes, respectively. In order to deeper understand the interaction between the TPU and $\text{Ti}_3\text{C}_2\text{T}_x$, the matrix / reinforcement interface was investigated by first principles calculation through DFT. The obtained results showed that the TPU adsorption on the surface of $\text{Ti}_3\text{C}_2\text{T}_x$ MXene is strongly affected by the surface functional groups and adsorption sites. While fluorine and hydroxyl terminations favored the interaction with the polymer, oxygen terminated MXene was unstable in three of the four configurations simulated. These results indicate the relevance of MXenes surface chemistry to the properties of these composites.

10:45 AM NM01.08.08

A Search for The Long-Duration Storage Medium of Ti_2CT_x MXene [Chiranjit Roy](#); Technical University of Denmark, Denmark

Recently, a new family of 2D transition metal carbides and nitrides named MXenes has gained significant attention due to their excellent electrochemical and mechanical properties. But, poor chemical/ oxidation stability of MXene acts as a barrier in its widespread application. To date, oxidation stability of $\text{Ti}_3\text{C}_2\text{T}_x$ MXene has been mostly studied among all Ti-based MXene, due to its excellent capacitance and metallic conductivity. The lightest Ti_2CT_x MXene has secured less attention in the research field, although it has comparable physiochemical properties. It also degrades rapidly over time in ambient conditions, limiting its widespread implementation. In this regard, we have resolved the two challenging tasks to broaden the application of the most unstable Ti-based Ti_2CT_x MXene: the improvement of oxidation stability and the prolongation of their shelf life for further practical applications. To solve these problems, we have dispersed the Ti_2CT_x MXene in different solvents (organic and water) for an extended period of time (3 months) under ambient as well as freezing conditions and observed how it affects the oxidation stability. Finally, the results suggest that the suitable medium to store Ti_2CT_x MXene for 3 months is IPA or DMSO at -20°C or Water at -80°C . This work is suitable for a wide range of readers working on synthesis, stability and characterization of Ti_2CT_x MXene to explore its application in the field of Supercapacitors, Li-ion batteries (LIBs), EMI shielding and Hydrogen storage etc.

11:00 AM NM01.08.09

Voronoi Inspired Conductive and Healable Covalent Adaptable Thiourethane MXene Nanocomposites [Michael Carey](#)^{1,2}; ¹Air Force Research Laboratory, United States; ²Riverside Research Institute, United States

A novel thiourethane vitrimer (TUV) chemistry is presented, along with a method to directly produce micron sized vitrimer powders through a simple precipitation polymerization. These TUV powders can then be passed through a colloidal suspension of conductive 2D MXene, $\text{Ti}_3\text{C}_2\text{T}_x$. With pH adjustment, electrostatic attractions allow for conformal MXene coatings on these TUV powders. Neat and composite bulk samples are produced by hot-pressing non-coated or MXene coated TUV powders into panels or thin sheets with minimal processing intensity. The unique Voronoi inspired microstructure obtained by the fusing of these TUV particles is characterized by micro and nano computed tomography (CT), scanning electron microscopy (SEM), electron dispersive spectroscopy (EDS) and transmission electron microscopy (TEM), revealing the presence of MXene at the boundaries between thiourethane rich domains. This microstructure facilitates conductive composites with a very low percolation threshold, a 275% increase in Young's modulus, and a 50% increase in toughness compared to the control vitrimer. This re-healable, conductive, and mechanically robust

platform has great potential for a next-generation smart composite for various advanced applications.

11:15 AM NM01.08.10

Vacancy and Growth Modulation of Cobalt Hexacyanoferrate by Porous MXene for Zinc Ion Batteries [Aiping Yu](#) and Maiwen Zhang; University of Waterloo, Canada

Prussian blue analogues (PBAs) featuring with three-dimensional open framework are recognized as promising cathode candidates for Zinc-ion batteries, but unsatisfactory active site utilization, low conductivity and abundant structural vacancies have impeded fulfillment of their potential. In this work, a highly conductive in-plane porous MXene is for the first time adopted as a multifunctional host material to enhance cobalt hexacyanoferrate (CoHCF) growth and crystallinity. Particularly, the uniform MXene surface charges are identified to induce anisotropic and highly crystalline CoHCF, which are critical to alleviating the practical drawbacks commonly associated with the PBA family. Empowered by the targeted modification, the CoHCF nanotube on porous MXene composite realizes high surface area and low defectiveness, achieving a high capacity of 197 mAh g⁻¹ at 0.1 A g⁻¹ and robust capacity retention of 94.4% even over 3000 cycles of operation at 2.0 A g⁻¹. This composition strategy, utilizing MXene as a multifunctional template, enhances PBAs' surface area, conductivity, and crystallinity, optimizing cathode capacity and stability for ZIBs, and showcasing the potential for large-scale energy storage.

Keywords: Zinc-ion battery, Porous MXene, Prussian blue analogues, induce growth, low vacancy

11:30 AM NM01.08.11

Strategy for Highly Absorption-Dominated Electromagnetic Interference Shielding through Electrical Polarization and Triboelectrification Synergistic Effect in Surface-Patterned Ferroelectric Poly[(vinylidene fluoride-co-trifluoroethylene)-MXene] Composite [Sol Lee](#) and Junghyo Nah; Chungnam National University, Korea (the Republic of)

Extensive utilization of electronic devices and wireless equipment require human to take affirmative measures to weaken unwanted electromagnetic wave radiations. Herein, a ferroelectric poly[(vinylidene fluoride-co-trifluoroethylene) (P(VDF-TrFE)-MXene)-poly(3,4-ethylenedioxythiophene) (PEDOT) multilayered film is developed that can increase electromagnetic interference (EMI) shielding performance through electrical polarization. The MXene is encapsulated by a P(VDF-TrFE) matrix, which inhibits oxidation, and a highly conductive MXene is created conductive network resulting in enhancement EMI shielding effectiveness (EMI SE). Furthermore, the surface pattern inducing multiple scattering and PEDOT layer contributes to the increasing absorption due to the electrically conductive PEDOT. Thanks to the electrically polarized and negatively charged P(VDF-TrFE)-MXene, the composite film demonstrates superior EMI SE and absolute EMI SE (SSE_a) are exhibited remarkable ≈61 dB and 15230 dB cm²g⁻¹ with high absorptivity (0.87) at thickness of 120 μm in X-band. Additionally, P(VDF-TrFE)-MXene composite film is applicable to motion and thermo-resistive sensor due to the negatively charged P(VDF-TrFE) and thermo-resistive property of PEDOT, respectively, for multifunctionality. This work provides a feasible avenue for flexible absorption dominant EMI shielding materials via electrical polarization with remarkable EMI shielding performance.

SESSION NM01/NM03: Joint Virtual Session
Session Chairs: Stefano Ippolito and Piran Ravichandran Kidambi
Wednesday Morning, May 8, 2024
NM01-virtual

8:00 AM NM01/NM03.01

Mxene Doped Supramolecular Composite Hydrogels for Antioxidant and Photothermal Antibacterial Studies [Zakia Riaz](#); Shanghai Jiao Tong University, China

Bacterial infections and the harm caused by various reactive oxygen species (ROS) present a significant danger to human health. There is a strong need to discover an ideal biomaterial system with wide-ranging antibacterial and antioxidant abilities. This study introduces a novel supramolecular hydrogel composite with both antibacterial and antioxidant properties. The composite is created using a chiral L-phenylalanine-derivative matrix (LPFEG) and Mxene (Ti₃C₂T_x) as a filler material. Fourier transform infrared and circular dichroism spectroscopy confirm the existence of noncovalent interactions (such as hydrogen bonding and π-π interactions) between LPFEG and Mxene, along with a reversal in the chirality of LPFEG. Rheological analysis reveals that the composite hydrogels possess enhanced mechanical properties. This hydrogel system also exhibits a photothermal conversion efficiency of 40.79%, enabling effective broad-spectrum photothermal antibacterial activity against both Gram-positive (*Staphylococcus aureus*) and Gram-negative (*Escherichia coli*, *Pseudomonas aeruginosa*) bacteria. Additionally, Mxene contributes to the hydrogel's exceptional antioxidant capabilities by efficiently scavenging free radicals like DPPH, ABTS, and OH. These findings suggest that the Mxene-based chiral supramolecular composite hydrogel, with improved rheological, antibacterial, and antioxidant properties, holds significant promise for biomedical applications.

8:15 AM NM01/NM03.02

Synthesis of Chromium Carbide MXene nanosheets and its electrochemical analysis for energy storage application [Shavita Salora](#)^{1,2}, [Suman Singh](#)^{1,2} and [Amit Lochan Sharma](#)^{1,2}; ¹CSIR-Central Scientific Instruments Organization, Chandigarh, India, India; ²Academy of Scientific and Innovative Research (AcSIR), India

MXene, a well known 2D transition metal carbide or nitride based material has been proved to be promising material for energy storage application. This material has gained significant attention due to their mechanical, electrical properties. In our study, the potential of chromium carbide MXene as an electrode material for energy storage applications has been investigated. The Chromium Carbide MXene opens up new avenues for energy storage owing to its electrical conductivity, mechanical properties, and high surface area. Chromium MXene was synthesized by using FeCl₃, well known etchant to etch Al layer for Cr₂AlC and Ascorbic acid was used for the removal of by-products. Delamination of the layers was done by sonication the sample in DMSO. A comprehensive characterization of chromium carbide MXene, including structural, morphological and electrochemical has been performed to understand this material. Electrochemical performance is evaluated as an electrode material for Supercapacitor application in different electrolyte i.e. acidic, basic and neutral medium. Cyclic voltammetry and galvanostatic charge-discharge studies demonstrated energy storage capabilities of synthesized chromium carbide MXene with capacitance 188 F/g and energy density of 26.11 Wh/Kg, excellent rate performance, and stability. This study sheds light on the potential of chromium carbide MXene as an electrode material for energy storage applications. The demonstrated electrochemical performance and the insights gained from this research pave the way for the design of MXene-based electrode materials, contributing to the development of energy storage devices.

8:20 AM NM01/NM03.03

Demonstration of Spin Hall Angle in Monolayer Xenes: A Proposed Template Swastik Sahoo¹, Satadeep Bhattacharjee² and Bhaskaran Muralidharan¹; ¹IIT Bombay, India; ²Korea Institute of Science and Technology, India

The capability of high-speed computing for spintronics has led to its development in the last two decades. The paramount acumen of controlling spin transport properties in non-magnetic materials is the usage of spin-orbit coupling (SOC). We propose a model to calculate the spin hall angle (SHA) for the elemental monolayers of group 4 with a buckled honeycomb structure, namely, silicene, germanene, and stanene. This model is based on Landauer-Buttiker formalism for quantum transport [1], and the device is introduced to some manual defects, manual dislocations, and interface-induced spin-orbit coupling. The SHA of these devices also illustrates the mesoscopic fluctuations, which can be a comparative measure for graphene and other metal devices. Further, the deviation of SHA of these Xenes follows the universal relationship regarding the longitudinal conductivity, which establishes the usefulness of the Xenes in the context of graphene. To validate our outcomes, we compare our results with experimental data and numerically exact real-space simulation results based on the nearest-neighbor tight binding (NNTB) model. This work will be a template to calculate spin-hall conductivity for all the elemental monolayers [2], considering the intrinsic scattering mechanism. Also, we look forward to calculate the spin transport parameters by taking heterostructures of monolayer Xenes, as mentioned above, with suitable materials like MoS₂ [3]. This work can be further extended to explore the possible spintronics applications for extrinsic scattering, which includes side-jump and skew-jump [4] scattering processes.

References:

- [1] da Silva, Juliana M., et al. "Spin Hall angle in single-layer graphene." *Journal of Applied Physics* 132.18 (2022).
- [2] Farzaneh, S. M., & Rakheja, S. (2021). Spin splitting and spin Hall conductivity in buckled monolayers of group 14: First-principles calculations. *Physical Review B*, 104(11), 115205.
- [3] Safeer, C. K., et al. "Room-temperature spin Hall effect in graphene/MoS₂ van der Waals heterostructures." *Nano letters* 19.2 (2019): 1074-1082.
- [4] Takahashi, Saburo, and Sadamichi Maekawa. "Spin current, spin accumulation and spin Hall effect." *Science and Technology of Advanced Materials* 9, no. 1 (2008): 014105.

8:35 AM NM01/NM03.04

Synthesis of Graphene Quantum Dots from Waste Material for Sustainable Application Dharmveer Yadav, Jyotiraman De, Saumaya Kirti, Sumit Saxena and Shobha Shukla; Indian Institute of Technology Bombay, India

As a 2D wonder material, graphene has excellent physical, chemical, and mechanical properties, leading to vast applications in electronics, water filtration, medicine and healthcare. Graphene quantum dots (GQD) can significantly enhance graphene's optical and electronic properties due to their size, expanding the scope of application in sensing, imaging, energy storage, and catalysis. However, their large-scale production often involves resource-intensive methods. Therefore, this study explores an innovative and eco-friendly method for synthesizing GQDs using waste materials as a carbon source. In this research, waste materials, such as biomass-derived precursors, are converted into high-quality GQDs through controlled pyrolysis to tailor the size, morphology, and surface functionalization of the GQDs. The resulting GQDs were characterized using advanced analytical techniques, confirming their structural and chemical properties. The sustainable GQDs obtained from waste materials demonstrated excellent performance in diverse water applications, including filtration and sensing of contaminants. Developed GQDs have been incorporated into polymer membranes to enhance membrane performance in terms of permeability and separation efficiency. Moreover, using waste materials as feedstock reduced the environmental impact and contributed to waste valorization and resource efficiency. The utilization of waste materials for GQD synthesis aligns with the principles of green chemistry and supports the transition towards a circular and sustainable economy. As the demand for GQDs continues to grow, this research provides a novel and eco-conscious approach to meet this demand while minimizing the environmental footprint.

8:50 AM *NM01/NM03.05

High-Dimensional Approaches for Immune Profiling of 2D Materials Lucia G. Delogu; University of Padua, Italy

We recently depicted the "Nano-immunity-by-design" where the characterization of 2D materials is not solely based on their physical-chemical parameters but also on their immunoprofiling. [1] The immune-profiling can be revealed on its complexity by unique, informative ways: high dimensional approaches. [2,3] We exploited high-dimensional approaches, such as single-cell mass cytometry and imaging mass cytometry on graphene and other novel two dimensional materials, such as transition metal carbides/carbonitrides (MXenes). [4-6] We revealed that the amino-functionalization of graphene oxide increased its immunocompatibility. [4] Moreover, we combined graphene with AgInS₂ nanocrystals, enabling its detection by single-cell mass cytometry on a large variety of primary immune cells. [5] Recently, we reported the immune modulation of specific MXenes, and their label-free detection by single-cell mass cytometry and other high dimensional approaches. [6-7] Together with our published works, I will present unpublished results on a wider variety of novel 2D materials, MXenes, MoS₂, WS₂, and bismuthene. Our results conceptualize that chemical and immunological designs of 2D materials offer new strategies for their safe exploitation in biomedicine.

- [1] Gazzi A et al... and Delogu LG*. Graphene, other carbon nanomaterials and the immune system: toward nanoimmunity-bydesign. *J Phy Mat* (2020).
- [2] Fusco L et al... and Delogu LG*. Graphene and other 2D materials: a multidisciplinary analysis to uncover the hidden potential as cancer theranostics. *Theranostics* (2020).
- [3] Weiss C et al... and Delogu LG*. Toward Nanotechnology-Enabled Approaches against the COVID-19 Pandemic. *ACS Nano* (2020)
- [4] Orecchioni M et al... and Delogu LG*. Single-cell mass cytometry and transcriptome profiling reveal the impact of graphene on human immune cells. *Nature Communications* (2017).
- [5] Orecchioni M et al... and Delogu LG*. Toward High-Dimensional Single-Cell Analysis of Graphene Oxide Biological Impact: Tracking on Immune Cells by Single-Cell Mass Cytometry. *Small* (2020).
- [6] Unal MA et al. and Gogotsi Y*, Delogu LG*, Yilmazer A*. *Nanotoday* (2021).
- [7] Fusco L, Gazzi A et al. and et al. and Gogotsi Y*, Delogu LG*, *Advanced Materials* (2022).

9:20 AM NM01/NM03.06

Multiwalled Carbon Nanotubes and CuO Nanoparticles Composite based H₂S Sensors Sumit Kumar and Mahesh Kumar; Indian Institute of Technology Jodhpur, India

H₂S is an extremely hazardous air pollutant that harms the human respiratory system and world ecosystems. The main sources of H₂S emissions are sewage, petroleum industries, and natural gas. The demand for some sensing mechanism to monitor its emissions is paramount. Herein, we demonstrate CuO nanoparticles and multiwalled carbon nanotubes (MWCNTs)-based H₂S sensors. The conventional chemical vapor deposition technique (CVD) is used for growing MWCNTs. The optimal amount of MWCNTs and CuO nanoparticles in the composite enhanced the H₂S sensor response. The experimental data confirmed that the bare CuO sensor response ($\Delta R/R_0$) for 1 ppm H₂S was 31%; further MWCNTs/CuO heterojunction sensor responses reached 53%. The enhanced sensing characteristics are a result of the formation of nano-heterojunctions between MWCNTs and CuO nanoparticles, which enhance the chemical and electronic sensitization properties. In addition, the heterojunction sensor demonstrated excellent H₂S selectivity over other

oxidizing and reducing gases.

9:25 AM NM01/NM03.07

New Mechanics in Cell-Nanomaterial Interactions: Boron Nitride Nanosheets Inducing Water Channels Across Lipid Bilayers [Xuliang Qian](#)¹, Matteo Andrea Lucherelli², Wenpeng Zhu³, Paolo Samori⁴, Huajian Gao¹, Alberto Bianco² and Annette von dem Bussche³; ¹Nanyang Technological University, Singapore; ²CNRS, Immunology, Immunopathology and Therapeutic Chemistry, France; ³Sun Yat-sen University, China; ⁴University of Strasbourg, France; ⁵Brown University, United States

Understanding the interaction between two-dimensional (2D) materials and cell membranes is pivotal for nanomedicine and safe nanotechnology applications. In this study, we investigate how hexagonal boron nitride (hBN) interacts with the cell membrane by combining molecular dynamics (MD) simulations and in vitro experiments. Our MD simulations reveal that sharp hBN wedges can penetrate lipid bilayers, forming cross-membrane water channels along their exposed polar edges, a behavior not exhibited by round hBN sheets. We hypothesize that such water channels can facilitate cross-membrane transport, potentially leading to lysosomal membrane permeabilization. To test this hypothesis, we prepared two types of hBN nanosheets, the former with a cornered morphology and the latter with a round morphology, and exposed human lung epithelial cells to both hBN nanosheets. The cornered hBN with exposed polar edges resulted in a dose dependent cytotoxic effect, whereas round hBN did not cause significant toxicity, thus confirming our hypothesis. These results highlight the significance of 2D materials in facilitating nanoscale water and molecular transport across lipid membranes and have substantial implications for the design of hBN-based drug delivery systems and safe design of future advanced hBN containing composites and devices.

9:40 AM NM01/NM03.08

Low Temperature Electron Transport study on Inkjet Printed Ti3C2Tx and Filtrated Ti3C2Tx-Ti3AIC2 Nanosheet Thin Films [Mi-Jin Jin](#); Institute for Basic Science, Korea (the Republic of)

Ti3C2Tx, most common structure of MXenes tunably show semiconductor behavior in their percolated thin-film structure. Magnetoconductance studies of thin-film MXenes are important to understanding their electronic transport properties and charge carrier dynamics, and also to appraise their potential for spintronics and magnetoelectronics. Also, it is desirable to develop deposition strategies such as inkjet printing, filtration that would enable direct patterning with complex structures/networks. Here, we investigate the extrinsic negative magnetoconductance of inkjet printed Ti3C2Tx MXene thin films and simply filtrated Ti3C2Tx-Ti3AIC2 nanosheet thin film. Both of inkjet-printing and filtration process has advantage for simple patterning of a device. Importantly, we report a crossover from weak anti-localization (WAL) to weak localization (WL) near 2.5K for both thin-film system but shows strong scale dependence for different materials element system. The WAL is consistent with strong, extrinsic, spin orbit coupling. From the magnetoconductance analysis, we estimate that the printed MXene thin-film has a strong spin orbit coupling field. Our results and analyses offer detailed understanding into microscopic charge carrier transport in Ti3C2Tx, and Ti3C2Tx-Ti3AIC2 nanosheet thin films

SYMPOSIUM NM02

Advances in Nanodiamonds
April 23 - April 24, 2024

Symposium Organizers

Jean-Charles Arnault, CEA Saclay
Huan-Cheng Chang, Academia Sinica
Shery Chang, University of New South Wales
Peter Pauzauskie, University of Washington

* Invited Paper

+ JMR Distinguished Invited Speaker

^ MRS Communications Early Career Distinguished Presenter

SESSION NM02.01: Quantum Sensing with Nanodiamonds
Session Chairs: Silvia Orlanducci and Peter Pauzauskie
Tuesday Morning, April 23, 2024
Room 338, Level 3, Summit

10:30 AM *NM02.01.01

Optical Hyperpolarization of Nuclear Spins in Nanodiamonds [Fedor Jelezko](#); Ulm University, Germany

Dynamic nuclear spin polarization allows to enhance signals in NMR and MRI by orders in magnitude. We show that electron spin of NV centers in diamond can be used as efficient source of nuclear spin polarization allowing to orient nuclear spins associated with ¹³C in nanodiamonds. We show that coherent control tools allow to realize efficient polarization transfer in randomly oriented nanodiamonds including isotopically engineered diamond nanoparticles. Efficient hyperpolarization together with long spin lattice relaxation time of diamond nuclear spins has the potential for applications in magnetic resonance imaging. Furthermore, hyperpolarized nanodiamonds can be employed as spin batterie for polarization transfer to external nuclear

spins.

11:00 AM *NM02.01.02

Engineering Nanodiamonds for Quantum-Enhanced Bio-Sensing [Philip Hemmer](#); Texas A&M University, United States

Diamond color centers like the nitrogen-vacancy (NV) have shown much promise for nanoscale sensing of magnetic and electric fields and temperature. So far however the quantum properties of the NV have not been used to full advantage, for example quantum entanglement of NV qubits has rarely been used for sensing. In this talk I will review recent advances in the fabrication of NVs, and other magnetic color centers in diamond, and in the growth of high quality nanodiamonds. Combining these advances, I will discuss the future prospects of engineering quantum-enhanced sensors in nanodiamonds.

11:30 AM *NM02.01.03

Long Spin Coherence and Relaxation Times of Nitrogen-Vacancy Centres in Nanodiamonds [Gavin W. Morley](#); University of Warwick, United Kingdom

The negatively charged nitrogen-vacancy center (NVC) in diamond has been utilized in a wide variety of sensing applications. The long spin coherence and relaxation times (T_2^* , T_2 and T_1) of the center at room temperature are crucial to this, as they often limit sensitivity. Using NVCs in nanodiamonds allows for operations in environments inaccessible to bulk diamond, such as intracellular sensing. We report long spin coherence and relaxation times at room temperature for single NVCs in isotopically purified polycrystalline ball-milled nanodiamonds. Using a spin-locking pulse sequence, we observe spin coherence times, T_2 , up to $786 \pm 200 \mu\text{s}$. We also measure T_2^* times up to $2.06 \pm 0.24 \mu\text{s}$ and T_1 times up to $4.32 \pm 0.60 \text{ms}$.

We also magnetically levitate micron-sized diamonds in vacuum towards putting them into a superposition of being in two places at once. This provides a platform for testing fundamental physics which could include, in time, a test of the quantum nature of gravity.

SESSION NM02.02: Biological Applications of Nanodiamond Sensors

Session Chairs: Yuen Hui and Alexander Shames

Tuesday Afternoon, April 23, 2024

Room 338, Level 3, Summit

1:30 PM *NM02.02.01

Diamond Quantum Sensing Microscopy of Spin Crossover and Cytochrome C Molecules [Abdelghani Laraoui](#)¹, [Suvechhya Lamichhane](#)¹, [Rupak Timalina](#)¹, [Kayleigh McElveen](#)¹, [Cody Schultz](#)¹, [Adam Erickson](#)¹, [Ilja Fescenko](#)², [Kapildeb Ambal](#)³, [Shuo Sun](#)¹, [Yinsheng Guo](#)¹, [Sy-Hwang Liou](#)¹ and [Rebecca Lai](#)¹; ¹University of Nebraska-Lincoln, United States; ²University of Latvia, Lao People's Democratic Republic; ³Wichita State University, United States

Diamond Quantum sensing (DQS) microscopy based on nitrogen vacancy (NV) centers has become a unique tool to probe weak static and fluctuating magnetic fields with an excellent combination of spatial resolution and magnetic sensitivity, opening new routes to study solid-state [1] and biological materials [2]. In this work, we present two examples of using DQS in wide-field geometry to probe nanoscale magnetic phenomena in molecules. First, we discuss DQS wide-field microscopy measurements on individual Fe(Htrz)₂(trz)(BF₄) (Fe triazole spin-crossover (SCO) nano-rods of size varying from 20 to 1000 nm. Fe triazole SCO molecules show thermal switching between low spin (LS) and high spin (HS) states which are applicable in thermal sensors and molecular switches. While the bulk magnetic properties of these molecules are widely studied by bulk magnetometry techniques, their properties at the individual level are not yet explored. Scanning electron microscopy (SEM) and Raman spectroscopy are performed to determine the size of the nano-rods and to confirm the spin state (LS vs HS) of the Fe triazole molecule respectively [3]. The stray magnetic fields produced by individual nano-rods are imaged by DQS microscopy as a function of temperature (up to 150 °C) and applied magnetic field (up to 350 mT) and correlated with SEM and Raman. We found that in most of the nanorods the LS state is slightly paramagnetic, probably originating from the surface oxidation and/or the greater Fe⁺³ presence along the nanorods' edges. NV measurements on the Fe-triazole LS state nanoparticle clusters revealed both diamagnetic and paramagnetic behaviors [3].

Then, we show DQS wide-field microscopy measurements on cytochrome C (Cyt-C) nanoclustered molecules. Cyt-C is an iron-containing biomolecule that plays an important role in the electron transport chain of mitochondria [4]. Under ambient conditions, the heme group remains in the Fe⁺³ paramagnetic state [5]. Initially, we performed NV T_1 relaxometry measurements on a carboxylated diamond chip doped with 8-nm thick NV-layer without any Cyt-C, which revealed a relaxation time T_1 of ~ 1.2 ms. Subsequently, we varied the concentration of Cyt-C from 6 mM to 54 mM and show a reduction of the NV relaxation time T_1 from ~ 800 μs to 150 μs respectively, explained by the spin noise generated from the intracellular iron spins in the Cyt-C molecules [6]. Additionally, we performed magnetic relaxometry imaging of Cyt-C proteins on a nanostructured diamond substrate by which we estimate the density of adsorbed iron from 1.44×10^6 to 1.7×10^7 per μm^2 [6]. [1] A. Laraoui, K. Ambal, Appl. Phys. Lett. 121, 060502 (2022). [2] I. Fescenko, A. Laraoui, et al., Phy. Rev. App. 11(3), 034029 (2019). [3] S. Lamichhane, A. Laraoui, et al., ACS Nano 17 (9), 8694-8704 (2023). [4] I. Bertini, et al., Chem. Rev., 106 (1), 90–115 (2006). [5] J. Liu, et al., Chem. Rev. 114 (8), 4366–446 (2014). [6] S. Lamichhane, A. Laraoui, et al., under review, arXiv:2310.08605 (2023). Acknowledgment: This material is based upon work supported by the NSF/EPSCoR RII Track-1: Emergent Quantum Materials and Technologies (EQUATE) Award OIA-2044049, and NSF Award 2328822. I.F. acknowledges support from Latvian Council of Science project lzp- 2021/1-0379. K.A. would like to acknowledge the support of the National Science Foundation/EPSCoR RII Track-4 Award OIA-2033210 and NSF Award 2328822. The research was performed in part in the Nebraska Nanoscale Facility: National Nanotechnology Coordinated Infrastructure and the Nebraska Center for Materials and Nanoscience (and/or NERCF), which are supported by NSF under Award ECCS: 2025298, and the Nebraska Research Initiative.

2:00 PM *NM02.02.02

On The Optimal Chemical Interface of Diamond for Quantum Biosensing [Petr Cigler](#); Institute of Organic Chemistry and Biochemistry of The CAS, Czechia

Non-perturbing sensing techniques applicable to biological systems are currently of central interest in the biosciences. Nanodiamond (ND) is a highly biocompatible nanomaterial for construction of nanosensors, which can accommodate nitrogen-vacancy (NV) centers. The NV spin properties can be read optically, which enables design of various probes based on quantum mechanical interactions. NDs can be exposed to biological environment and report sensitively on the spin-related processes occurring in a close vicinity of the particle employing for example the NV spin relaxometry measurements. ND relaxometry however reaches its limitations in terms of poor colloidal stability in physiological environment and non-specificity to detect only the magnetic field originated from the spins of interest.

To ensure colloidal stability in biologically-relevant environment we stabilize ND probes using thin polymer coatings that can be further modified to allow sensing of specific physical quantities or targeted molecules. To that end, we design molecular transducers for transposing the presence of particular analytes to a selective and unambiguous readout. Different types and concepts of surface architectures including those for selective measurements of pH, temperature, redox potential, and ascorbate concentration under physiological conditions will be discussed. Additionally, our recent developments of ND probes for detection of biomolecules using relaxometry together with a proof-of-principle results will be presented.

2:30 PM BREAK

3:00 PM NM02.02.03

Detection of Alzheimer's Disease Through Fluorescent Nanodiamonds-Based Spin-Enhanced Lateral Flow Immunoassay [Stefanny Angela](#)¹, Wesley Wei-Wen Hsiao¹, Gianna Fadhilah¹, Trong-Nghia Le², Huan-Cheng Chang² and Wei-Hung Chiang¹; ¹National Taiwan University of Science and Technology, Taiwan; ²Academia Sinica, Taiwan

Fluorescent nanodiamond (FND) has recently been regarded as a superior alternative reporter for lateral flow immunoassays (LFIA). The negatively charged nitrogen-vacancy (NV⁻) center in FND is a point defect with unique magneto-optical properties, giving outstanding characteristics to detect biomarkers of diseases. Alzheimer's disease (AD) is the most common form of dementia, characterized by decreased memory, thinking, cognition, behavior, personality, and ability to conduct everyday duties, which might result in complete brain failure and, eventually, death. The two most commonly used detection techniques to detect changes in the brain caused by AD are brain imaging (CT, MRI, PET) and lumbar puncture. However, while brain imaging is costly and time-consuming, lumbar puncture is controversial since 30% of patients get severe headaches followed by nausea and vomiting lasting more than a week. To this end, we have developed a Spin-Enhanced Lateral Flow Immuno-Assay (SELFIA) for non-invasive AD diagnostics utilizing the spin properties of the NV⁻ centers in FND to achieve background-free ultrasensitive detection. In addition, to enhance sensitivity and specificity, we employed a sandwich assay of SELFIA to further noncovalently conjugate FND to anti-pTau antibodies toward detecting pTau protein (a critical AD biomarker involved in AD pathology), while the capture antibody immobilized on the membrane. Note that we have a comparable result with Enzyme-Linked Immunosorbent Assay (ELISA), as our FND-based SELFIA only requires approximately 30 minutes to reach a detection limit of 7 pg/mL for pTau (the sensitivity/specificity threshold is 15 pg/mL in plasma). Hopefully, this study will contribute to developing a safe, simple, and accurate AD detection platform that can identify this illness in its earliest stages and might also be applied to other diseases in precision health.

3:15 PM *NM02.02.04

Intracellular Thermometry with Fluorescent Polymer Sensors and Nanodiamonds [Yoshie Harada](#); Osaka University, Japan

Intracellular temperature fluctuations are thought to be closely related to higher order cellular phenomena. We have developed a method for imaging the temperature distribution in single living cells using a fluorescent polymer thermometer and fluorescence lifetime imaging microscopy to study the effects of intracellular temperature on cellular physiological activity. Previous experiments using the developed method have shown that during the G1 phase, the temperature of the nucleus is approximately 1°C higher than the temperature of the cytoplasm, as well as some mitochondria and centrosomes. The mechanisms that maintain this intracellular temperature heterogeneity and its physiological significance are not well understood. Recently, however, the mechanisms of physiological phenomena caused by fluctuations in intracellular temperature have begun to be elucidated. We hypothesized that intracellularly generated heat is not only a product of reactions, but also drives cellular responses. To test this hypothesis, we focused on cell differentiation, in which cells dramatically change their protein expression patterns. Using the neuronal model cell PC12, we investigated the relationship between neuronal differentiation and intracellular temperature. The results showed that intracellular temperature is involved in neuronal differentiation and associated neurite outgrowth. In addition to the aforementioned fluorescent polymer temperature sensor and fluorescence lifetime imaging microscopy, we also measured temperature using fluorescent nanodiamond particles containing negatively charged nitrogen vacancy centers as temperature sensors. We have previously shown that fluorescent nanodiamonds are able to measure temperature independent of external environmental influences such as pH, salt, and viscosity. To measure intracellular thermal conductivity, we also fabricated nanoparticles coated with polydopamine, which generates heat when exposed to light, around fluorescent nanodiamonds. Although the intracellular thermal conductivity has been assumed to be the same as the thermal conductivity of water, whether this is true or not was verified by actually measuring the intracellular thermal conductivity using the fabricated hybrid particles of polydopamine and fluorescent nanodiamonds. The results showed that, although the data were very uneven, on average the thermal conductivity inside the cell was several times smaller than the conductivity of water. In the present study, it is clear from microscopic observations that the hybrid particles are present inside the cell, but it is not known where in the cell they are localized. The variability of the data suggests variations in thermal conductivity depending on the location within the cell. Future work will use techniques to chemically modify the surface of the polydopamine-fluorescent nanodiamond hybrid particles, such as localizing the particles in mitochondria and nuclei, to measure thermal conductivity at different local positions in the cell to clarify what exactly produces such low thermal conductivity.

3:45 PM NM02.02.05

Diamond-Based Quantum Sensing of Free Radicals in Migrating Human Breast Cancer Cells [Claudia R. Reyes San Martin](#)¹, Arturo Elias-Llumbet^{1,2}, Marcia Manterola², Aldona Mzyk³ and Romana Schirhag¹; ¹University Medical Center Groningen, Netherlands; ²University of Chile, Chile; ³Technical University of Denmark, Denmark

Cell migration is a crucial parameter for disease progression in cancer. It is known that ROS levels are involved in the regulation of the migration process, however, the exact role of free radical generation and where it occurs is unknown. Here we use a diamond-based quantum sensing technique to detect free radical generation during cancer cell migration in real time with subcellular resolution. We investigated highly metastatic MDA-MB-231 human breast cancer cells and observed free radical formation after 16 hours of starvation and 24 h of migration under low-serum conditions. Intracellular diamond dynamics was monitored at different migration points (0, 12, and 24 h), and cell morphology was evaluated. Additionally, the number of focal adhesions was analyzed as an indicator of the migratory potential of the cells. All the parameters were addressed using a homemade script on the FIJI platform. We further measured free radical generation under NOX2 inhibition by apocynin. We found that free radical levels decreased after 24 h treatment with 36 µg/mL apocynin while the levels of ROS increased and also the migratory capacity of the cells. Our results evidence the complexity of the redox regulation in migrating cancer cells and offer a novel approach to specifically and locally interrogate pivotal players of the oxidative network behind metastatic success.

4:00 PM NM02.02.06

Synergistic Effects of Nanoparticle Geometric Shape and Post Curing on Nanodiamond-Reinforced Epoxy Nanocomposites: Characterization, Microstructure and Mechanical Properties [Dawei Zhang](#), Ying Huang and Xingyu Wang; North Dakota State University, United States

Nanodiamond, a significant member of carbon-based nanoparticles, is characterized by a spherical geometric shape and typically classified as a 0-D material due to the extremely small diameter of individual nanoparticles. The unique characteristics of nanodiamonds distinguish them from other carbon-based nanoparticles and have gained considerable interest in the fields of medicine, electronics, sensors, and particularly as nanofillers in polymeric

nanocomposites. One of the primary challenges associated with nanoparticle-reinforced nanocomposites is achieving a homogeneous and consistent dispersion of the nanoparticles within the polymer matrix. Compared to other commonly used carbon-based nanoparticles such as cylindrical carbon nanotubes and planar graphene, the enormous differences in shape and dimension may inevitably lead to notable variations in dispersion, which further greatly influences the overall properties of reinforced nanocomposites. This study explores the dispersion characteristics of nanodiamond in epoxy nanocomposites and examines the resulting effects on viscosity, microstructure, and mechanical properties of the epoxy nanocomposites. Systematic comparisons are made between nanodiamond along with carbon nanotube and graphene, while also considering the synergistic effects with post curing of epoxy. Experimental results indicate that the nanodiamond-reinforced epoxy nanocomposite exhibit a more homogenous nanoparticle dispersion, lower viscosity, reduced porosity, and stronger pull-off adhesion, while the graphene-reinforced epoxy nanocomposites achieve a higher lap shear strength. Although post curing is effective in reducing porosity and improving adhesion properties of the nanocomposites, its impact became less pronounced with the addition of nanoparticles.

SESSION NM02.03: Poster Session
Session Chairs: Arsène Chemin and Peter Pauzuskie
Tuesday Afternoon, April 23, 2024
Flex Hall C, Level 2, Summit

5:00 PM NM02.03.01

Photophysical Characterization of Non-Covalently Bound Porphyrin-Nanodiamond Assemblies in Water [William A. Maza](#), Daniel Ratchford, Adam D. Dunkelberger and Jeffrey C. Owrutsky; US Naval Research Laboratory, United States

Photoinduced charge transfer dynamics between nanodiamond, ND, particles and adsorbed dyes can potentially provide the necessary driving force to induce chemical reactions. We present steady-state and time-resolved fluorescence and UV-visible absorption data of self-assembled aggregates of the free-base porphyrin meso-(tetracarboxyphenyl)porphyrin, H₂TCPP, and surface modified ND. Surface modification of H-terminated nanodiamond was carried out by the laser ablation method in water which has been reported to result in a OH-rich surface of ND, OHND. Interactions between H₂TCPP and OHND in water result in a bathochromic shift of the porphyrin Soret band and a quenching of both the porphyrin singlet and triplet state. The results are discussed in the context of what is known regarding the energetics of ND in solution and a model of porphyrin quenching by OHND is proposed.

SESSION NM02.04: Synthesis and Characterization of Nanodiamonds
Session Chairs: Peter Pauzuskie and Olga Shenderova
Wednesday Morning, April 24, 2024
Room 338, Level 3, Summit

8:30 AM NM02.04.01

Improving The Creation of SiV Centers in Diamond via Sub- Pulsed Annealing Treatment [Yan-Kai Tzeng](#); SLAC National Accelerator Laboratory, United States

Silicon-vacancy (SiV) centers in diamond are emerging as promising quantum emitters in applications such as quantum communication and quantum information processing. Here, we demonstrate a sub- pulsed annealing treatment that dramatically increases the photoluminescence of SiV centers in diamond. Using a silane-functionalized adamantane precursor and a laser-heated diamond anvil cell, the temperature and energy conditions required to form SiV centers in diamond were mapped out via an optical thermometry system with an accuracy of ± 50 K and a 1 temporal resolution. Annealing scheme studies reveal that pulsed annealing can obviously minimize the migration of SiV centers out of the diamond lattice, and a 2.5-fold increase in the number of emitting centers was achieved using a series of 200-ns pulses at 50 kHz repetition rate via acousto-optic modulation. Our study provides a novel pulsed annealing treatment approach to improve the efficiency of the creation of SiV centers in diamond.

8:45 AM NM02.04.03

Carbon Dots: Visible Light Activated Antimicrobial Functions and Their Property-Function Correlations [Liju Yang](#)¹, Yongan Tang¹ and Ya-Ping Sun²; ¹North Carolina Central University, United States; ²Clemson University, United States

Carbon dots (CDots), generally defined as small carbon nanoparticles (CNPs) with various surface passivation schemes, represent the nanoscale carbon allotrope at zero-dimension. Attributed to the π -plasmon-associated electronic transitions, CDots have remarkable broad optical absorptions in the entire visible spectrum, extending into both near-UV and near-IR, making them excellent visible light-excitabile agents. In recent years, a large number of studies have provided strong evidence to support the establishment of CDots as a new class of effective and efficient visible/natural light-activated antimicrobial agents. Experimentally, our teams have demonstrated the highly effective photoactive antimicrobial activities of CDots against various bacteria and viruses, ranging from laboratory model bacteria (*E. coli*, *Bacillus subtilis*), pathogenic foodborne pathogens (*Listeria*, *Salmonella*), to multi-drug resistant (MDR) nosocomial pathogens (*Enterococcus*), and biofilms, as well as various viruses (model MS2 virus, vesicular stomatitis virus (VSV), marine norovirus (MNV), and norovirus virus-like-particles (VLPs). Mechanistically, upon photoexcitation on CDots, there are rapid charge transfers and separation to form electrons and holes redox pairs, followed by the radiative recombinations of the separated redox pairs resulting in emissive excited states, which are responsible for the bright fluorescence as well as the photodynamic production of classical reactive oxygen species (ROS). It is the combined action of the initially separated redox pairs and the generated classical ROS that are responsible for the observed uniquely effective photoactivated antimicrobial function of CDots. Associated oxidative damages in CDots-treated bacterial cells have been confirmed, including elevated levels of lipid peroxidation, increased membrane permeability, and cytoplasmic structural disruptions. Degradation in viral proteins and genomic RNAs have also been confirmed. The presentation will also include the insights on property-function correlations in CDots for their photoactivated antimicrobial activities. Extensive experimental results have revealed that the optical properties, the surface functional groups and charges, the passivation layers of CDots, as well as the synthesis processes, are highly correlated with their photoinduced antimicrobial functions. Such correlations make CDots to be excellent tunable and expandable material platforms for further improvement in their desirable functions. Along with their non-toxic nature, CDots open up new opportunities for the development of highly potent carbon-based non-traditional photodynamic antimicrobial agents.

Acknowledgment: The research was supported by NSF grants #2102021, #2102056, & #1855905, and USDA grants #2019-67018-29689 & #2023-

67018-40681.

9:00 AM NM02.04.04

Mechanical Properties of 2D Hexagonal Diamond Fabricated by Electrodeposition Daniel Choj and Mohammed Afif; Khalifa University of Science and Technology, United Arab Emirates

Hexagonal Diamond is also popularly known as Lonsdaleite in an honor of Kathleen Lonsdale. Hexagonal diamonds are naturally occurred when meteorites strike surface of earth at very high velocities, due to high temperature and pressure of impact some parts of graphite present in meteorites turns in to hexagonal diamond. These hexagonal diamonds are unique and possess exceptional physical and electronic properties. Fabrication of hexagonal diamond using anodized aluminum oxide (AAO) nanoporous template is performed by two steps electrodeposition process. Initially, cobalt nanowires are deposited in the nanocavities of AAO template by applying constant current (galvanostatic) across the electrodes. Subsequently, hexagonal diamonds are deposited over cobalt nanowires by applying constant voltage (potentiostatic). Acetonitrile and methanol of 1:1 ratio homogeneous solution was used as an electrolyte in second stage diamond deposition process. The yield of diamonds was increased by keeping the crystallography of cobalt nanowires similar to crystal structure of hexagonal diamond by altering the pH of cobalt sulphate aqueous solution. HRTEM and STEM-EDS experiments were initially performed on the samples deposited. HRTEM with probe corrector, at operating voltage of 300 kV was used to analyze all the samples, occasionally. An elemental analysis was performed on AAO crystals and hexagonal diamond particles, spectrum from AAO and hexagonal diamond particles. HRTEM bright field and diffraction studies were performed on Individual Hexagonal diamond particles and acquired diffraction patterns are indexed with Lonsdaleite diffraction data obtained from crystallographic database. The ZA [001] of diffraction data matched with the experimental data and d-spacing of high-order reflections of experimental diffraction pattern matched with standard data with minimum deviation. Investigation of mechanical and electrical properties by Atomic Force Microscopy (AFM) is in progress. As preliminary results, the elastic modulus and thin-film resistivity of hexagonal diamond are found to be 800-900GPa and 10-100 GWm, respectively.

9:15 AM NM02.04.05

Imaging and Sensing Extreme Ultraviolet Radiation with Nanodiamonds containing Nitrogen-Vacancy Centers Yuen Y. Hui¹, Teng-I Yang² and Huan-Cheng Chang¹; ¹Academia Sinica, Taiwan; ²National Applied Research Laboratories, Taiwan

Extreme ultraviolet (EUV) radiation with wavelengths ranging from 121 nm to 10 nm has been applied for photolithography to fabricate nanoelectronic devices. This study demonstrates that Fluorescent NanoDiamonds (FNDs) containing Nitrogen-Vacancy (NV) centers as scintillators to image and characterize EUV radiations. The FNDs employed are ~100 nm in size; they form a uniform and stable thin film (~1 µm in thickness) on an indium-tin-oxide-coated slide by electrospray deposition. The film is non-hygroscopic and photostable and can emit bright red fluorescence from the neutral NV centers when excited by EUV light. An FND-based imaging device has been developed for beam diagnostics of 50 nm and 13.5 nm synchrotron radiations respectively, achieving a spatial resolution of 30 µm. The noise equivalent power density is 29 µW/(cm² Hz^{1/2}) for the 13.5 nm radiation. Our method can be extended to the imaging of Vacuum Ultraviolet radiation and soft X-ray.

Reference: T.-I. Yang, Y.-Y. Hui, J.-I. Lo, Y.-W. Huang, Y.-Y. Lee, B.-M. Cheng and H.-C. Chang, "Imaging extreme ultraviolet radiation using nanodiamonds with nitrogen-vacancy centers," Nano Lett. 23(21), 9811–9816 (2023).

9:30 AM NM02.04.06

Shape Induced Enhanced Fluorescence in Fluorescent Nanodiamond revealed by Correlative Transmission Electron Microscopy and Photoluminescence Microscopy Shery Chang; University of New South Wales, Australia

Fluorescent nanodiamonds (FNDs) are diamond nanoparticles containing color centers that emit visible light at room temperature. Among the color centers in FNDs, the nitrogen-vacancy centers (NV) have drawn the most attention due to its exceptionally stable optical properties and great prospect in sensing and biomedical diagnostic applications.

The current understanding of the optical properties of the FNDs relies largely on the optical measurement methods from either ensemble of materials or from few single particles. As most of the FND fabrication is a top-down process where larger diamond crystals are milled to desired nanometer size, FNDs generally have broad size distribution and irregular shapes. Therefore understanding of FNDs structure-property relationship using ensemble measurements only is insufficient.

We have developed a new method based on correlative transmission electron microscopy and photoluminescence (TEMPL)[1]. TEMPL allows a direct correlation of the fluorescence brightness and three-dimensional size and shape of individual nanoparticles. PL provides optical information with exquisite energy resolution, and TEM provides structural information with exquisite spatial resolution. Unsupervised machine learning (ML) with the generalized 3D shape descriptors, is used to analyse correlations between the PL brightness and 3D shape of FND particles. The automation provided by machine learning allows TEMPL to be applied to large sample areas (2-3 orders of magnitude larger than a typical TEM field of view) containing a statistically significant number of particles.

Using this new method, we directly reveal that the volume-averaged PL brightness of thin, flake-like nanodiamond particles is up to several times greater than that of three-dimensional-shaped, thicker particles provided the particle diameter is less than the sub-wavelength limit. With the assumption that the number of NVs within a particle is proportional to its volume, this implies that individual NVs within thinner particles are brighter. This experimental observation is supported by the theoretical simulations on simplified particle geometries on a range of supporting substrate and surrounding medium. The simulations indicates that the comparative brightness of thinner particles, either on a thin supporting substrate or in a low-index medium, is attributable, at least in part, to the constructive interference of partial light waves in these particles. With increasing particle thickness, such an effect becomes damped. The sub-wavelength dimension of the substrate plays an important role, as it results in higher effective reflectivity comparable to diamond particles in a low-index medium (e.g., a low-index solution).

In addition to correlative PL with TEM, we have also carried out correlative SEM and AFM for the study of FNDs supported on bulk substrate. Our overall results help to guide new routes of enhancing fluorescence brightness of FNDs for broad sensing applications.

References:

1. Wen, H. et. al. Correlative Fluorescent and Transmission Electron Microscopy Assisted by 3D Machine Learning Reveals Thin Nanodiamonds Fluorescence Brighter. ACS Nano, 2023. 17, 16491.

9:45 AM NM02.04.07

Control of Synthesis and Structural Analysis of Poly(glycerol) Functionalized Nanodiamonds Masahiro Nishikawa^{1,2}, Ming Liu¹, Taro Yoshikawa¹, Hidekazu Takeuchi¹, Naoyoshi Matsuno¹ and Naoki Komatsu²; ¹Daicel Corporation, Japan; ²Kyoto University, Japan

Poly(glycerol) (PG) functionalization is one of the most common surface functionalization methods for a variety of nanoparticles (NPs). The hyperbranched hydrophilic polymer on NP surface gives advantageous features; dispersibility in aqueous media with high ionic concentration and

extensibility for further functionalization through abundant -OH group. In addition, PG layer suppresses the adsorption of serum proteins in physiological environment to evade immune response or other non-specific interactions.

For PG functionalized nanodiamonds (ND-PG), to enable material and process design more quantitatively, we conducted the analyses of PG functionalization reaction, in which ring opening polymerization of glycidol (GD) on ND surface is done in ethylene glycol (EG) as a solvent, and structure of ND-PGs. As a result, we found that the amount of PG can be precisely controlled by the reaction conditions, use amount of GD and EG, and properties of ND core, oxygen content and particle size. In the structural analysis, the abundance ratios of substructures of glycerol unit in PG chain and the thicknesses of PG layer in dispersion for ND-PGs of different PG amounts and ND cores were elucidated by NMR, TGA and DLS.

M. Nishikawa et al, *Carbon* **2023**, 205, 463–474.

10:00 AM BREAK

10:30 AM NM02.04.08

Paramagnetic Defects in e-Beam Irradiated and Annealed Polycrystalline Nanodiamonds Produced by External Shock-Wave Detonation Synthesis Alexander I. Shames¹, Frederick T. So^{2,3}, Takuya F. Segawa⁴, Shinobu Onoda³, Hideaki Takashima^{2,5}, Takeshi Ohshima^{3,6}, Shigeki Takeuchi², Masahiro Shirakawa^{2,3} and Norikazu Mizuochi^{2,2}; ¹Ben-Gurion University of the Negev, Israel; ²Kyoto University, Japan; ³National Institutes for Quantum Science and Technology, Japan; ⁴ETH Zurich, Switzerland; ⁵Chitose Institute of Science and Technology, Japan; ⁶Tohoku University, Japan

PolyCrystalline NanoDiamonds (PCNDs), manufactured by an external shock-wave detonation (the DuPont method), are among directly synthesized diamond nanoparticles which attract growing interest to their use in biomedical and quantum sensing application. In contrast to detonation nanodiamonds (DNDs), origin and evolution of paramagnetic defects in PCNDs induced by various treatments such as thorough purification, irradiation, annealing were beyond the scope of diamond community. We report on results of room temperature electron paramagnetic resonance (EPR) experiments done on a series of PCND samples undergone purification and e-beam irradiation at increasing fluences up to 1×10^{19} e/cm² followed by standard annealing at 800 °C. The paramagnetic defects' pool in all samples consists of high abundant primary defects (mostly of $S = 1/2$) and low abundant triplet ($S = 1$) defects [1]. The total content of primary defects in the pristine PCND sample reaches 1280 ppm whereas the content of triplet NV⁻ centers does not exceed 35 ppb. Boiling acid treatment of the non-irradiated and non-annealed sample PCND-BA causes significant reduction of primary defects (down to ~780 ppm) but does not really affect triplet centers. Annealing of that sample retains the content of all defects untouched, however causes prolongation of spin-lattice relaxation times of primary defects. Deconvolution of the intense singlet quasi-Lorentzian line of primary defects into broad and narrow components allowed attributing these components to dangling bonds (broad) and exchange coupled P1 centers (narrow) [2]. The content of dangling bonds in the annealed PCND-BA sample was estimated as ~620 ppm and that of P1 of ~160 ppm. E-beam irradiation (fluences 1×10^{18} , 3×10^{18} , 5×10^{18} and 1×10^{19} e/cm²) increases the total content of primary defects at that contribution of the broad component practically does not change, the increase occurs due to the narrow one (up to ~400 – 500 ppm). At the same time content of the triplet centers in e-beam irradiated PCND-BA samples remains at the same low level. The PCND-BA sample irradiated with 1×10^{19} e/cm² fluence was further undergone the annealing treatment. It was found that annealing reduces total amount of primary defects (to ~400 ppm) due to reduction of both broad (~310 ppm) and narrow (~90 ppm) components. Some insignificant growth of NV⁻ content (up to 50 ppb) was observed as well. The observed findings allow attributing the increase of the content of defects contributed to the narrow component in e-beam irradiated samples to appearance of radiation-induced paramagnetic V⁻ centers. Annealing of these samples causes diffusion and recombination of V⁻ centers accompanying by formation of a certain amount of radiation induced NV⁻ centers. Surprisingly, the effect of NV⁻ centers formation in PCND samples by e-beam irradiation and annealing was found to be at least on the order of magnitude weaker than that in both NDs obtained by nanonization of HPHT diamonds and DNDs. In strong contrast, DNDs show an NV⁻ concentration of ~100 ppb in pristine sample, which increases up to ~500 ppb under identical electron irradiation and annealing condition [3]. This specificity of PCND samples is discussed within the framework of models recently proposed in the Ref. [3].

[1] A. I. Shames et al., *Phys. Status Solidi A* 212 (2015) 2400

[2] A. I. Shames et al., *Physica E* 146 (2023) 115523

[3] F. T.-K. So et al, *J. Phys. Chem. C* 126 (2022) 5206–5217

10:45 AM NM02.04.09

Excitation and Charge Transfers in Functionalized Nanodiamonds in Water Arsène Chemin¹, Ronny Golnak¹, Jie Xiao¹, Andreas Weisser¹, Benjamin Kiendl², Anke Krueger² and Tristan Petit¹; ¹Helmholtz-Zentrum Berlin, Germany; ²Institut für Organische Chemie, Germany

Generating solvated electrons from sunlight using diamond material has been proposed as a promising strategy to achieve CO₂ or N₂ reduction in liquid phase [Zhu, D. et al, *Nat. Mater.* (2013), Zhang, L. et al. *Angew. Chem.* (2014)]. The high conduction band energy and negative electron affinity of diamond surfaces facilitate easy electron transfer to water. Despite the diamond's large band gap (5.47 eV), reports have demonstrated CO₂ photo(electro)chemical reduction using visible light [Knittel, P. et al. *ChemCatChem.* (2020)] as well as the emission of solvated electrons from nanodiamonds [Buchner, F. et al. *Nanoscale* (2020)]. Our recent investigation of the sub-bandgap excitation on diamond materials has demonstrated the implication of the surface states in the photon absorption and the charge transfers in air [Chemin, A et al. *Small Methods* (2023)] by combining surface sensitive X-ray absorption spectroscopy (XAS) to surface photovoltage. However, ex-situ measurements have shown limitation in explaining charge transfers in liquid.

In this work, we investigate *in-situ* the nanodiamond-water interface to unravel the charge transfers and excitation process of detonation nanodiamonds functionalized with Ru complex, which showed promising photoelectrocatalytic properties [Kiendl, et al. Preprint (2022)]. While XAS characterisation is easily performed into vacuum, measurement in water is much more challenging due to the short penetration depth of soft X-ray in liquid. A recently introduced detection mode for XAS in liquid [Schön, D. et al. *J. Phys. Chem. Lett.* (2017)], performed at BESSY II synchrotron in Berlin, is used to characterize the unoccupied states at the nanodiamond surface as well as the structure of the water molecules at the interface with nanodiamonds. By comparing this measurement to XAS in vacuum, we determined that the interaction with the liquid lead to strong modification of the surface states. By coupling this information with UV-Vis absorption spectroscopy and photocurrent spectroscopy, we discuss further the impact of the water interface in the possible excitation path and charge transfer of the functionalized nanodiamonds.

This project has received funding from the European Commission under the Horizon 2020 grant agreement 665085 (DIACAT) and Volkswagen Foundation under the Freigeist Fellowship No. 89592.

11:00 AM NM02.04.10

Phonon Green's Function Method for Multiscale Modeling of Color Centers in Nanodiamonds Vinod K. Tewary and Edward J. Garboczi; National Institute of Standards and Technology, United States

Nanodiamonds are materials of strong topical interest because of their unusual properties and diverse potential applications in biomedical, communications, and sensing devices. Their dimensions range from a few to several hundred nanometers. There is special interest in color centers in nanodiamonds, which give them unique photonic and spin characteristics. These characteristics are useful for their applications in optical and quantum devices.

Color centers are lattice defects such as vacancies. A lattice defect causes a break in the translation symmetry of the lattice. Consequently, it causes a distortion or strain in the lattice, which also distorts the electronic wave functions and perturbs the associated energy levels. This effect is likely to be a serious material issue, which can affect the reliability and the performance of the finished device based upon the use of nanodiamonds. It is, therefore, of paramount importance to develop modeling and measurement techniques of the lattice distortion/strain field due to a color center in nanodiamond, which is the objective of this work.

A unified theory for lattice defects in nanodiamonds is a challenging problem because the nanodiamonds can be too small or too big for a conventional theoretical treatment. A 5 nm nanodiamond is too small for a standard bulk material continuum model to be accurate. One must use a discrete lattice theory such as molecular dynamics (MD). On the other hand, modeling a 100 nm nanodiamond, containing up to a billion atoms, using ordinary MD will be a formidable task, even with modern computer.

Further, in addition to variations in the size, there is also a need for seamless linking of the length scales in the same nanodiamond. Lattice distortion is a discrete function expressed as the displacement of atoms from their positions of equilibrium and needs to be calculated by accounting for the atomistic structure of the lattice. On the other hand, strain is a continuum model parameter defined in terms of the derivatives of the continuous displacement field. The inherent assumption in a continuum model is that the discrete lattice distortion is smeared out into a continuum, which is valid only at distances much larger than the interatomic separations. For the final results to be physically realistic, the near field and far field formulation must be seamlessly linked. We describe a Green's function (GF) method for modeling a color center in a nanodiamond of arbitrary size. The model is computationally efficient and can simulate even several hundred million atoms on an ordinary computer. It links the different length scales smoothly and seamlessly so can be used to estimate the nanodiamond size effect. We calculate the lattice GF by using a simple Born-von Karman model, in which each atom interacts with up to its second neighbor atoms. We also assume the harmonic approximation and the adiabatic approximation.

In this model, the main parameters are the interatomic force constants. These are given by the derivatives of the total potential energy, evaluated at the positions of equilibrium for each atom. In practice, the force constants are treated as adjustable parameters, which are determined phenomenologically by fitting them to elastic constants and phonon dispersion. Hence, an explicit knowledge of the interatomic potential is not needed. Our selected set of the force constants correctly reproduces the measured elastic constants of bulk diamond and gives a reasonable agreement with the observed phonon spectrum over the first Brillouin zone.

Numerical results will be presented for the strain field due to a color center, specifically a single vacancy, in a nanodiamond. The size effect on the strain field and the limitations and applicability of our model to interpretation of measurements will be briefly discussed.

11:15 AM *NM02.04.11

Real Effect of Size on the Raman Spectrum of sub-5 nm Nanodiamonds [Stepan Stehlik](#)^{1,2}; ¹Institute of Physics, AS CR, Czechia; ²University of West Bohemia in Pilsen, Czechia

Nanodiamonds (NDs) hold promise for a vast range of various distinct applications including drug delivery, cellular labeling and imaging, quantum sensing (such as thermometry and magnetic field/spin sensing), selective biomolecule binding or energy harvesting, and (photo)catalysis - to name a few. Although researchers employ nanodiamonds in all these applications, due to the great variety of this nanomaterial, the actual nanoparticles used can differ substantially. Sometimes to the extent that they could be defined as a different material.

In this contribution, specifics of the two most common ND types, detonation NDs (DNDs) and high-pressure high-temperature (HPHT) NDs will be highlighted. We will review recent experimental advances in the preparation of sub-5 nm NDs of both detonation and HPHT origin, including the HPHT NDs synthesized from molecular precursors (E. Ekimov et al., *Nanomaterials* 2022, 12, 351). The presentation aims to critically compare these two ND types from the Raman spectroscopy point of view as this technique is broadly used to assess not only the ND phase composition (C-sp³ and C-sp² content) but also the ND size. We show that the Raman spectra of DND and HPHT NDs on the 3-5 nm scale are size-insensitive yet significantly different from each other which limits the application of the current phonon confinement models for the ND size distribution analysis (S. Stehlik et al., *J. Phys. Chem. C* 2021, 125, 5647–5669). The diamond structural quality, and temperature (in)stability caused by laser irradiation during the measurement are the key features reflected in the NDs' Raman spectrum. The first time observed low-frequency (20–200 cm⁻¹) Raman scattering signals may correspond to "breathing-like" modes of NDs as these signals exhibit clear size dependence. The low-frequency Raman scattering may thus provide another way for size distribution analysis of nanodiamonds (A. Vlk et al., *J. Phys. Chem. C* 2022, 126, 6318–6324).

11:45 AM NM02.04.13

Size Sorting of Highly Crystalline High-Pressure High-Temperature Nanodiamonds [Marie Finas](#), Hugues A. Girard and Jean-Charles Arnault; CEA Paris Saclay, France

Due to their excellent crystalline quality, recent studies exhibited that milled high-pressure high-temperature nanodiamonds (MND) behave electronic properties very close to those of bulk diamond, with similar dependence on surface chemistry [1]. Those characteristics make them excellent candidates for photocatalysis applications. However, it is well known that particle size have a great influence on nanomaterial's properties, and HPHT nanodiamonds are no exception. Depending on nanodiamond size, modifications are expected especially dealing with specific area, spectroscopic signatures and electronic properties. According to literature, proton affinity is strongly facet-dependent [2] and thermal stability and structural properties are proved to be size-dependent in the range from 1 to 8 nm [3]. Moreover, the smaller the nanodiamonds, the greater the surface-to-volume ratio, which would influence the photocatalytic properties. Therefore, as MND exhibit a large polydispersity, it is crucial to fractionate them into different size ranges to assess their specific size-dependant properties.

Our strategy consists in implementing a density gradient made of mixtures of ethylene glycol and water in a vertical container, where MND will sediment with different velocities depending on their size during centrifugation [4]. This method was previously explored to fractionate with success detonation nanodiamonds and remove clusters [5]. We applied it for the first time to MND. To determine optimal separation conditions, experimental parameters like the centrifugation time, the MND initial size range and the fractionation values were tuned. By this mean, we succeeded to isolate larger MND (15-40 nm) from the smaller ones (< 15 nm). We used UV-Vis spectrophotometry to measure MND concentration after centrifugation, and DLS and SEM to evaluate size-sorting efficiency. The sorted MNDs were then characterized by FTIR, Raman and XPS to investigate the size influence on their surface properties.

References

- [1] Miliaieva, D. et al. (2023). *Nanoscale Advances*, 5(17), 4402–4414.
- [2] Barnard, A. S., & Per, M. C. (2014). *Nanotechnology*, 25(44).
- [3] Ekimov, E. et al. (2022). *Nanomaterials*, 12(3).
- [4] Qiu, P., & Mao, C. (2011). *Advanced Materials*, 23(42), 4880–4885.
- [5] Qu, J. et al. (2021). *Applied Nanoscience (Switzerland)*, 11(1), 257–266.

SESSION NM02.05: Characterization and Processing of Nanodiamond Materials

Session Chairs: Petr Cigler and Yuen Hui

Wednesday Afternoon, April 24, 2024

Room 338, Level 3, Summit

1:30 PM *NM02.05.01

New Techniques of Depositing Detonation Nanodiamonds onto Substrates and Their Applications Taro Yoshikawa^{1,2}, Akira Kaga¹ and Tomoaki Mahiko¹; ¹Daicel Corporation, Japan; ²Kanazawa University, Japan

Detonation nanodiamonds (DNDs) are considered exciting candidates for various applications, such as lubricant additives, semiconductor quantum dots, magnetic mapping sensors, protein mimics, and initial seeds for chemical vapor deposition (CVD) of diamond thin films on heterogeneous substrates. Essentially, these potential applications can be categorized into two groups: solution-based applications that use DND colloidal suspensions, and solid-state applications based on systems of DNDs supported by substrates, tips/probes, etc. The former applications have shown tremendous progress toward practical realization over the past decades. This progress is the result of thorough investigations and technological development in material preparation, including disassembling tightly bound aggregates, isolated/separated dispersion through graphitization or oxidization of surfaces, annealing in a hydrogen atmosphere, insertion of appropriate surfactants, surface functionalization with organic molecules, and stirred-media milling with ceramic or zirconia microbeads. Meanwhile, development of the latter applications has been primarily hindered by the technical challenge of depositing/coating DNDs on the surfaces of solid-state materials with the desired layer thickness, particle density, and surface roughness.

Recently, we have established two new techniques for depositing DNDs onto substrates. One technique involves the nanometer-scale ordered arrangement of DNDs on substrates. The signs of surface charges, i.e., zeta potentials, of substrate surfaces are locally inverted through a combination of electron beam lithography and surface functionalization with 3-aminopropyltriethoxysilane. As a result, selective electrostatic deposition of DNDs onto the substrates is performed with line-and-space and dot array patterns at a length scale of ≥ 20 nm. Another technique involves the electrostatic layer-by-layer deposition of DNDs onto substrate surfaces using DND colloidal suspensions with different zeta potentials. By treating substrate surfaces in DND colloidal suspensions with positive and negative zeta potentials alternately, DNDs are deposited homogeneously on the substrate surfaces layer-by-layer.

During the presentation, these techniques are introduced in detail, along with specific applications we have recently demonstrated. The nanometer-scale ordered arrangement technique is tested for the patterned growth of nanocrystalline diamond films. This could contribute to the manufacture of smaller diamond-based micro/nano electromechanical system devices through a bottom-up process, rather than the conventional top-down method that requires costly polishing and etching of the diamond films. Meanwhile, the electrostatic layer-by-layer deposition technique is applied to fabricate diamond photocatalytic electrodes, enabling CO₂ reduction with visible light irradiation. The results indicate that the DND layer thickness of the electrode strongly affects the photosensitivity of the CO₂ reduction reaction.

2:00 PM *NM02.05.02

Fluorescent Diamond Particles for Bioimaging and Quantum Sensing Olga A. Shenderova¹, Marco Torelli¹, Nicholas Nunn^{2,1}, Alex I. Smirnov² and Ashok Ajoy³; ¹Adamas Nanotechnologies, United States; ²North Carolina State University, United States; ³University of California, Berkeley, United States

Diamond nanoparticles containing fluorescent color centers exhibit a favorable combination of optical properties including photostability that outlasts quantum dots and molecular probes, a broad emission color palette, and excellent biocompatibility. Fluorescent nanodiamonds containing nitrogen-vacancy (NV) color centers enable unique quantum sensing capabilities by reporting on nearby analytes, such as free radicals and other paramagnetic species, by decoding fluctuating magnetic fields induced by these external spins. This information can be conveniently imaged optically by adapting conventional microscopes or via hyperpolarized magnetic resonance methods. For the latter, quantum sensing is based on hyperpolarizing ¹³C nuclei in nanodiamond particles by optical pumping of NV centers and then imaging chemical information by ¹³C NMR scanners at high resolution. In this presentation, material developments for quantum sensing applications will be highlighted. The progress of several projects on quantum sensing with a biological scope under development by our team will be presented, with a more detailed focus on a near-term application such as using nanodiamond particles as sensors of paramagnetic species in biological media.

2:30 PM BREAK

3:30 PM NM02.05.03

High Pressure High Temperature Synthesized Diamond Particles with Controlled Nitrogen Content Nicholas Nunn^{1,2}, Sergey Milikisiyants¹, Marco Torelli², Alexander Healey³, Roy Styles³, Brett Johnson³, Philipp Reineck³, Christopher Long⁴, Timothy Dumm⁴, Adam Dalis⁴, Takeshi Ohshima⁵, Emmanuel Druga⁶, Ashok Ajoy⁶, Alexander I. Shames⁷, Alex I. Smirnov¹ and Olga Shenderova²; ¹North Carolina State University, United States; ²Adamas Nanotechnologies, Inc., United States; ³RMIT University, Australia; ⁴Hyperion Materials & Technologies, United States; ⁵National Institutes for Quantum and Radiological Science and Technology, Japan; ⁶University of California, Berkeley, United States; ⁷Ben-Gurion University of the Negev, Israel

Diamond particles hosting nitrogen vacancy centers is a platform material for potential use in emerging nano and microscale sensing technologies. These envisioned quantum sensors are based on optical manipulation and readout of NV centers in response to external environmental stimuli (e.g., temperature, electromagnetic fields, mechanical strain). The important prerequisites for such measurement protocols are NV centers with suitable spin properties such as long coherence and relaxation times. While such properties are observed in bulk diamond crystals of suitable quality, the properties of diamond particles are often severely degraded by the presence of paramagnetic defects such as electronic spins associated with surface defects and other paramagnetic centers (primarily nitrogen P1 centers). Here we demonstrate HPHT grown microparticulate diamond with good crystal quality and a controlled nitrogen content in the range of ca. 5-50 atomic ppm. A resultant improvement in NV electronic spin coherence times by approximately 3-fold is directly observed by pulsed electron paramagnetic resonance (EPR) across the range of nitrogen concentration studied. These results may provide a foundation for the production of the next generation of fluorescent diamond particles, which thus far have relied exclusively on particulate diamond with nitrogen contents of ca. 100 atomic ppm.

3:45 PM NM02.05.04

Catalytic, Photocatalytic and Electrochemical Properties of Surface-Treated Nanodiamond and of Multifunctional Gold Decorated Nanodiamond Systems Emanuela Tamburri, Riccardo Salvio, Laura Micheli, Rocco Cancelliere, Giorgia Magnante, Emanuele Rea and Silvia Orlanducci; University of Tor Vergata, Italy

The unique surface properties of detonation nanodiamonds, such as their stability, high surface area, and the ability to be easily functionalized, make them a versatile and promising material for various catalytic applications. The large surface area and diverse surface functional groups on detonation nanodiamonds can promote heterogeneous catalysis and they can be used in a variety of reactions, including hydrogenation, reduction, oxidation, and other industrial processes. Here are some ways, developed in our laboratory, to modulate catalytic activities of ND by surface functionalization or by decorating ND with gold nanoparticles (AuNP). Gold nanoparticles and nanodiamonds are indeed remarkable nanomaterials with unique properties and a wide range of potential applications. The teamwork between AuNP and ND is related to the ability to control the shape and size of gold nanoparticles on the surface of nanodiamonds, modulate the colloidal properties, and the interactions with their surroundings. The hybrid system can exhibit unique catalytic and sensor activities, as both components contribute to these properties. In this communication, we will explore the use of AuNP-ND system as a platform for immobilizing enzymes and antibodies on electrode surfaces and test them in electroanalytical applications. Finally modified ND will be investigated as a catalyst in the reductive degradation of pollutants (nitrophenols class) and as enzyme mimics in the transesterification reaction. In summary, the combination of gold nanoparticles and nanodiamonds offers a powerful platform for a wide range of applications in various fields. Their unique properties, surface chemistry, and biocompatibility make them highly versatile, and the synergy between these two components can lead to innovative solutions in the areas of imaging, drug delivery, biosensing, and beyond. Research continues to explore and develop these hybrid systems to unlock their full potential for practical applications.

4:00 PM NM02.05.05

Surface Modification of Fluorescent Nanodiamond for Quantum Sensing Marco Torelli¹, [Nicholas Nunn](#)^{1,2}, Gary McGuire¹ and Olga Shenderova¹;

¹Adamas Nanotechnologies Inc, United States; ²North Carolina State University, United States

Developments in quantum sensing which surpass the capabilities of classical measurements will improve the understanding of complex events in molecular disease biology and enable new modalities for drug and biomarker discovery. The negatively charged nitrogen-vacancy (NV) center in fluorescent nanodiamond can sense local electromagnetic fields, free radicals, temperature, and pH with nanoscale resolution. However, charge transfer and electromagnetic noise from the particle's surface destabilize negatively charged NV⁻ emitters and convert them to non-sensing, neutral NV0 centers. This effect is important because sensing has a strong dependence on distance, and thus the quality of shallow NVs relates to sensing characteristics. Additionally, at small particle sizes the fraction of destabilized NV centers near the surface becomes significant. Here we report results for conversion and stabilization of NV⁻ by plasma surface modification with fluorine and nitrogen groups to provide enrichment and stabilization of NV⁻. The treatment is shown to be suitable for particles of differing sizes and initial surface chemistries, allowing for scalable production of nanodiamond particles adapted for quantum sensing applications.

4:15 PM NM02.05.06

Group-IV Split Vacancy Nanodiamonds Synthesized via High-Pressure High-Temperature Techniques for Enhanced Quantum Sensing [Chaman Gupta](#), Elena P. Pandres, Brittany P. Bishop, Alexander Bard, Christopher E. Woodburn, Alexey Soldatenko, Vincent C. Holmberg and Peter Pauzuskie;

University of Washington, United States

Rapid strides in quantum sensing have necessitated the development of robust, scalable, and efficient nanodiamond materials with well-defined point-defect microstructure. This research presents a novel method to further this pursuit by synthesizing nanodiamonds doped with group-IV elements (Si, Pb, Sn, Ge), aiming to harness the unique properties of their split vacancies in nanodiamonds for a range of quantum sensing and quantum communication applications. A chemical bottom-up approach was employed, where 4.5 nM of tetraethylorthoxysilane (TEOS) and 4.5 nM of tetraphenylgermane (TPG) were added as the dopants for Si and Ge, respectively, while trace amounts of organometallic Sn and Pb were included in the processing of carbon aerogel target materials. The doped resorcinol-formaldehyde (RF) gels were pyrolyzed to obtain the group 4-doped carbon aerogels. Subsequent laser heating to $1260 \text{ K} \pm 10 \text{ K}$ in high-pressure environments of $22 \text{ GPa} \pm 0.2 \text{ GPa}$ using diamond anvil cells yielded nanodiamond samples doped with group-IV point defects. Photoluminescence characterization showcased distinct zero-phonon lines (ZPLs) stemming from NV⁻ (638 nm), SiV⁻ (720 nm), SnV (620 nm), and Pb-related centers at ambient conditions. The observed shift in SiV ZPL with increasing pressure (0.85 meV/GPa) was in excellent alignment with existing density functional theory (DFT) calculations (0.83 meV/GPa). Further, we conducted lifetime measurements of the SiV centers at ambient conditions post nanodiamond recovery, resulting in a lifetime of $\sim 1.25 \text{ ns} \pm 0.03 \text{ ns}$, which matches very closely with the literature. A significant advancement of this research lies in its potential to modulate the relative concentration of dopants, enabling the precise ratio control of various quantum sensors in the resultant nanodiamonds. This study contributes to the development of the synthesis of nanodiamonds with split vacancy without damage induced by ion implantation. With future development, these group-IV split vacancies hold promise for quantum sensing and quantum communication applications.

SYMPOSIUM NM03

Nanoscale Mass Transport Through 2D and 1D Nanomaterials
April 24 - April 25, 2024

Symposium Organizers

Michael Boutilier, Western University
Ngoc Bui, The University of Oklahoma
Piran Ravichandran Kidambi, Vanderbilt University
Sui Zhang, National University of Singapore

* Invited Paper
+ JMR Distinguished Invited Speaker
^ MRS Communications Early Career Distinguished Presenter

SESSION NM03.01: CNT and Other 1D Structures I
Session Chairs: Piran Ravichandran Kidambi and Sui Zhang
Wednesday Morning, April 24, 2024
Room 329, Level 3, Summit

8:30 AM NM03.01.01

Growth of Carbon Nanotubes (CNTs) using Catalyst Stabilizers for Extended Growth [Michael J. Bronikowski](#); University of Tampa, United States

Recent results will be reported from investigations into Carbon Nanotube (CNT) growth using metal catalyst particles composed of catalytic metals such as iron mixed with heavy refractory catalyst stabilizers. The heavy refractory metals, which include high-melting-point elements such as tungsten, ruthenium and hafnium, act to slow down the erosion and Ostwald ripening of the nano-particles of catalytic metals from which the CNTs nucleate and grow, thereby allowing the particles to remain active for longer times and thus to grow longer CNTs. A number of different combinations of catalyst metal and heavy refractory stabilizer are investigated. Ethylene (C₂H₄) is used as the carbon source gas for nanotube growth, and growth parameters including temperature, pressure, and gas flow composition and rate, are varied for best CNT growth. Discussion will include implications for growth of CNTs to lengths great enough (tens of cm or more) for application in materials applications such as ultra-high-strength wires and cables.

8:45 AM NM03.01.02

Nanoconfinement Facilitates The Precipitation of Iron Hydroxides in Porous Amorphous Aluminum Oxides [Xiaoxu Li](#), Jianbin Zhou, Sebastian T. Mergelsberg, Xin Zhang and Kevin Rosso; Pacific Northwest National Laboratory, United States

In nature, nanoscale spaces where molecules are confined are ubiquitous, including within nanoparticle aggregates, biofilms, and fractures in rocks, leading to unique size-dependent chemical and physical interactions. Nanoconfinement also offers unique opportunities to manipulate and control reaction pathways and the properties of materials and substances in energy storage and conversion, carbon capture, catalysis, water purification and nanoelectronics. The well known tendency of nanoconfinement to lower the dielectric constant of water and limit diffusive mass transport rates leads to a common assumption that reactions are slower compared with their counterparts in bulk solution. Here, we report that the nanoconfinement can instead promote mineral replacement reactions. We examined the proton-promoted dissolution rate of porous amorphous aluminum oxide matrices of varying pore diameter when contacted with ferric chloride solution at acidic pH. Consumption of protons within the pores coupled to Al³⁺ release leads to oversaturation with respect to ferric hydroxides. Consequently, 2-5 nm Al-doped ferrihydrite and akaganeite nanoparticles heterogeneously nucleated on the dissolving surfaces of aluminum oxides pores, based on various solid characterization including SEM-EDS, TEM-EDS, XRD, and Mossbauer spectroscopy. Furthermore, the surface area normalized dissolution rates of the pores coupled to precipitation of ferric hydroxides exhibit an exponential increase of two orders of magnitude as pore diameter linearly decreases from 200 nm to 30 nm. This increasing rate trend of dissolution-reprecipitation with decreasing pore size aligns quantitatively with the principle of heterogenous nucleation of ferric hydroxides on curved surfaces. These results underscore the notion that nanoconfined space can accelerate dissolution-reprecipitation reactions by reducing the energy barrier to heterogenous nucleation of secondary phase, primarily due to the smaller pore size. Our results shed light on the underestimated and significant role of confined spaces in mineral replacement reactions that occur across a wide range of natural and materials synthesis environments.

9:00 AM *NM03.01.03

Nanofluidics under Extreme Confinement in 1D and 2D Channels [Aleksandr Noy](#)^{1,2}; ¹Lawrence Livermore National Laboratory, United States; ²University of California Merced, United States

Extreme spatial confinement in narrow fluidic channels strongly influences their transport properties and enables unconventional selectivity mechanisms that can often mimic some of the selectivity and transport characteristics of biological membrane channels. Modern nanomaterials have enabled experimental platforms that can recreate such extreme confinement in a range of 1D and 2D channels with defined geometry and controllable electronic properties. I will discuss several of these nanomaterials-based channel systems and show how confinement phenomena, coupled with the different electronic effects and dynamic charge equilibria in these channels can shape their transport properties and ion selectivity characteristics. Overall, these observations can pave the way for developing a new generation of precision separation platforms for biomedical and industrial use.

9:30 AM NM03.01.04

Mechanistic Study of Electroosmotic Pumping through Atomically Smooth Carbon Nanotube Membranes with Application in Programmed Drug Delivery [Bruce Hinds](#); University of Washington, United States

Mechanistic study of electroosmotic pumping through atomically smooth carbon nanotube membranes with application in programmed drug delivery
An important challenge for the membrane community is to mimic natural protein channels that outperform, by orders of magnitude, man-made systems based on pore size and coarse chemical selectivity. To mimic protein channel pumping on a robust engineering membrane platforms, applied bias can be used to actuate charged gatekeepers and induce ionic pumping. Carbon nanotubes have three key attributes that make them of great interest for novel membrane applications 1) atomically flat graphite surface allows for ideal fluid slip boundary conditions and extremely fast flow rates [1,2] 2) the cutting process to open CNTs inherently places functional chemistry at CNT core entrance for chemical selectivity and 3) CNT are electrically conductive allowing for electrochemical reactions and application of electric fields gradients at CNT tips. The CNT membrane, with tips functionalized with charged molecules, is a nearly ideal platform to induce electro-osmotic flow with high charge density at pore entrance and a nearly frictionless surface for the propagation of plug flow [3,4]. Use of the electro-osmotic phenomenon for responsive/programmed transdermal drug delivery devices for nicotine addiction [5]. Our recent work [6] shows highly energy efficient electroosmotic pumping of nicotine with optimal power consumption/flux efficiency of 111(μW/cm²)/μmoles/cm²/h. This allows watch-battery lifetimes of 7-62 days for conventional treatment dosing regimens. On/off nicotine flux ratios of 68 were achieved allowing programmed delivery between therapeutically relevant nicotine patch and nicotine gum levels. By varying degree of chemical functionalization at CNT tips and pH control of ionic/neutral species ratio, the relative contribution of electroosmosis and electrophoresis within atomically smooth CNT conduits was quantified. More recent work with the direct measurement electroosmotic flow in a capillary flow cell shows the enhancement is due to atomic smoothness of CNTs, as seen the reversible stopping of flow by benzyl alcohol adsorption but no effect by H-bond chain disrupter NaSCN. Increased cation size had minimal improvement in EO pumping through DWCNT conduits.

- 1 "Nanoscale hydrodynamics: Enhanced flow in carbon nanotubes" Majumder, M.; Chopra, N.; Andrews, R; Hinds, B.J Nature 2005, 438, 44.
- 2 'Mass Transport through Carbon Nanotube Membranes in three different regimes: ionic diffusion, gas, and liquid flow' Mainak Majumder, Nitin Chopra, B.J. Hinds ACS Nano 2011 5(5) 3867-3877
- 3 'Highly Efficient Electro-osmotic Flow through Functionalized Carbon Nanotubes Membrane' Ji Wu, Karen Gerstandt, Mainak Majumder, B.J. Hinds, RCS Nanoscale 2011 3(8) 3321-28
- 4 "Programmable transdermal drug delivery of nicotine using carbon nanotube membranes" J. Wu, K.S. Paudel, C.L. Strasinger, D. Hamell, Audra L. Stinchcomb, B. J. Hinds Proc. Nat. Acad. Sci. 2010 107(26) 11698-11702.
- 5 "Electrophoretically Induced Aqueous Flow through sub-Nanometer Single Walled Carbon Nanotube Membranes" Ji Wu, Karen Gerstandt, Hongbo Zhang, Jie Liu, and B. J. Hinds Nature Nano 2012 7(2) 133-39
- 6 'Electrically controlled nicotine delivery through Carbon nanotube membranes via electrochemical oxidation and nanofluidically enhanced electroosmotic flow' Gulati G.K., Hinds B.J. Biomedical Microdevices 2021 DOI: 10.1007/s10544-021-00580-1

9:45 AM BREAK

10:15 AM NM03.01.05

Nanofluidic Ion and Molecule Transport in Boron Nitride Nanotube Porins [Zhongwu Li](#)¹ and Aleksandr Noy^{1,2}; ¹Lawrence Livermore National Laboratory, United States; ²University of California Merced, United States

Biological membrane channels, which exhibit excellent efficiency and selectivity in ion and molecule transport, have sparked considerable interest in the development of their synthetic analogues. Numerous artificial nanochannels that can be integrated into lipid membranes have been designed and synthesized over the past decade, e.g., the remarkable one-dimensional carbon nanotube porins that exhibit exceptional nanofluidic transport properties. However, there is still a need to diversify the nanotube porin family to include nanochannels made of different materials that provide access to different geometries, surface properties, and electronic structure.

Here, we present the fabrication and nanofluidic transport studies of boron nitride nanotube (BNNT) porins. With the combination of liposome transport measurement and Cryo-EM imaging, we show that BNNT porins can insert into lipid membranes to form functional channels. Ion transport studies, which used the droplet interface bilayer setup, reveal distinct ion conductivity profiles and scaling behaviors at high ion concentrations. The ion transport also exhibits an inverted U-curve dependency on pH with the highest conductance at the neutral pH value. Reversal potential measurements suggest that BNNT porins have a high cation/anion selectivity. We attribute these observations to the strong ion interactions and pronounced surface adsorptions in the highly charged and extremely confined nanotubes. Furthermore, we present evidence of the ability of these BNNT porins to transport DNA molecules. Our findings position BNNT porins as a promising biomimetic platform for the investigation of nanofluidic transport and the development of membranes and biosensors.

10:30 AM NM03.01.06

Decoupling Entrance and Inner Resistances in CNT Channels Melinda L. Jue, Steven F. Buchsbaum, Sei Jin Park, Kathleen E. Moyer-Vanderburgh and [Francesco Fornasiero](#); Lawrence Livermore National Laboratory, United States

Due to their high transport rates, a great deal of attention has been recently given to 2D materials and slippery 1-D nanochannels as promising building blocks for next generation membranes. While in 2-D materials high flux is expected because of the classical inverse scaling of the flow rate with the pore thickness, in smooth channels such as carbon nanotubes (CNT), orders of magnitude rate enhancements with respect to classical theories are attributed to a vanishing friction at the pore wall. Irrespective of the high flux origin, in both atomically thin and thicker but slippery nanopores, the flow rates are largely dictated by the entrance/exit hydrodynamic resistance.

For CNT channels, experimental quantification of the magnitude of end and inner resistances is still lacking despite its importance for both practical applications and fundamental understanding. This has led to inaccuracy and disagreement in the calculation of slip lengths and flow rate enhancements from experimentally measured permeation rates, since often entrance/exit resistances are neglected altogether, or an arbitrary magnitude is assumed. Here, we quantified these resistances for both gases and liquids in CNT channels by fabricating membranes with controlled CNT length and known number of open pores. We found that the end resistance dominates the total resistance. For liquid water, measured viscous energy dissipation at the nanotube ends is quantitatively described by Sampson equation. For 2.4 nm wide single-walled CNTs, measured slip lengths approach several microns. A prevailing contribution of the end resistance was also found in pressure-driven gas transport, and recorded flow rate enhancements with respect to Knudsen theory appear to be independent of the gas type. These findings further advance the community understanding of the peculiar and often unusual CNT fluidic properties and may help reconciling "conflicting" literature reports on the subject.

10:45 AM NM03.01.07

Engineering Tunable Macrocyclic Subnanometer Pores as Biomimetic Channels for Ångstrom-Precision Separation [Yuhao Li](#)¹ and Jiachen Feng^{1,2}; ¹Lawrence Livermore National Laboratory, United States; ²The University of Nebraska Medical Center, United States

Efficient and selective membranes are essential for advancing sustainable water treatment processes, with the potential to address the separation of problematic contaminants and reduce environmental waste. The present landscape of conventional membrane fabrication techniques falls short in achieving the required solute-solute selectivity at the molecular level. Traditional approaches, such as interfacial polymerization for thin-film composite (TFC) membranes, were developed to enhance water-solute selectivity but lack precise control over local pore structures and chemical properties. Herein we demonstrate by using triangular macrocyclic hosts as biomimetic channels, offering a remarkable degree of tunability. By merely substituting the bridging groups, we can directly influence local pore size and structure, resulting in enhanced selectivity and efficiency. This innovation offers the possibility of a bottom-up approach to membrane fabrication that can be customized for specific separation needs, providing an array of advantages. These include precise control over sub-nanometer pore structures, size, and chemical environments through subcomponent modifications, excellent processability, and simplified assembly of subcomponents, thus offering a promising solution for advanced membrane fabrication.

11:00 AM NM03.01.08

Dynamic Memory Effects in Aqueous Ion Transport through 2D Nanopore Arrays [Ye Chan Noh](#)^{1,2} and Alex Smolyanitsky¹; ¹National Institute of Standards and Technology, United States; ²University of California, Berkeley, United States

Nanofluidic ion-conducting devices with built-in memory are gaining attention as potential components for brain-mimetic computing systems. Here we present examples of the dynamic memory effects in the aqueous ion transport through 2D nanopore membranes under alternating bias voltages. In the first example, we explore the transport of KCl and NaCl salt mixtures through arrays of graphene-embedded crown-like pores, known to selectively trap aqueous K⁺ ions. In this system, trapped K⁺ ions act as pore cloggers, while Na⁺ ions are the main charge carriers. We demonstrate that the dynamically

changing state of the system defined as the ratio of pores *unblocked* by K^+ (and thus the number of conductive paths available to Na^+) is marked by a basic time delay. This delay is shown to result in distinct memristive ion transport under alternating voltage bias.

In the second example, we investigate capacitive transport of water-dissociated $RbCl$ in the presence of sub-nm pore arrays in hexagonal boron nitride (hBN). In contrast to the first example, the pores are impermeable to Rb^+ and such a system behaves as a capacitor with a built-in chemical barrier, causing current spiking. The external bias voltage is shown to induce ordered adsorption of Rb^+ on one side of the membrane, representing the charging phase. Alternating the voltage direction triggers rapid ion discharge, leading to current spikes with current polarity dependent on the prior input.

The physical processes described in this work are remarkably illustrative, potentially extending beyond the presented examples. By focusing on the mechanisms, we provide a clear insight into the design of nanofluidic systems capable of memristive and spike ion transport within realistic timescales.

11:15 AM NM03.01.09

Exploring Confinement-Dependent Alkaline Silicon Etching in Nanochannels and Nanotrenches: Origins and Solutions [Yiding Zhong](#), Dohyun Park and Chuanhua Duan; Boston University, United States

Alkaline etching of silicon (Si) is one of the most fundamental processes for the semiconductor industry. Although its etching kinetics on plain substrates has been thoroughly investigated, the kinetics of Si wet etching in nanoconfinements has yet to be fully explored despite the practical importance of three-dimensional (3-D) semiconductor manufacturing. Herein, we report the systematic study of potassium hydroxide (KOH) wet etching kinetics of amorphous-silicon (a-Si) filled two-dimensional (2-D) planar nanochannels with heights ranging from 11 nm to 120 nm and polysilicon (poly-Si) filled 2-D vertical nanotrenches with widths ranging from 20 nm to 285 nm. We found that, while there is a positive correlation between the etching rate and the KOH etchant concentration similar to bulk Si etching, the etching rate would increase with the increase in nanochannel height/nanotrench width before reaching a plateau, indicating a strong nonlinear confinement effect. To investigate the fundamental mechanisms of the confinement effect, we further conducted Si wet etching using etching solutions with different ionic strengths and/or different temperatures. Our results show that both electrostatic interactions and hydration layer inside the nanoconfinement contribute to the confinement-dependent etching kinetics. To address the challenge of non-uniform etching rates in nanoconfinements of varying dimensions, we implemented various active or passive methods to modify nanochannel surface-etchant interactions, including DC bias gating, diffusio-phoresis, and etchant additives. Notably, we discovered that adding certain polymers and organic solvents resulted in excellent etching rate uniformity in poly-Si nanotrenches with spanning widths from 27 nm to 205 nm. These results provide new insights into the kinetic study of reactions in nanoconfinements and will shed light on etching process optimization in the semiconductor industry.

11:30 AM NM03.01.10

Controlled Ionic Transport and Electrical Sensing of DNA using Van der Waals Heterojunction Nanopores [Sihan Chen](#)¹, Siyuan Huang¹, Jangyup Son¹, Edmund Han¹, Kenji Watanabe², Takashi Taniguchi², Pinshane Y. Huang¹, William P. King¹, Arend M. van der Zande¹ and Rashid Bashir¹; ¹University of Illinois at Urbana-Champaign, United States; ²National Institute for Materials Science, Japan

Sequencing the human genome has helped to improve our understanding of disease, inheritance and individuality. Solid-state nanopores could potentially meet the demand for even cheaper and faster genome sequencing, owing to their superior mechanical, chemical and thermal robustness and durability, and potential for integration into high-density electronic arrays.¹ Despite the promise, solid state nanopores have yet to demonstrate DNA sequencing. Two key challenges remain, i.e., achieving few-base spatial resolution and slowing the translocation of the DNA molecule. 2D materials such as graphene² and MoS_2 ³ have emerged as attractive possibilities, since the thickness of these films is in the range of a few nucleotides. However, atomic membranes alone are not robust in fluid under an electric field.⁴ 2D materials sandwiched within dielectrics could provide a stable platform,⁵ but the resulting stack thickness limits the spatial resolution. Resolving these challenges requires new sensing mechanisms beyond ionic currents and translocation control.

This work reports a novel solid state nanopore sensor that has the desired sub-nanometer spatial resolution, integrated electrical sensing, and can potentially control the translocation of the DNA molecule. In this architecture, the nanopore is drilled through a vertical 2D heterostructure consisting of n-type MoS_2 and p-type WSe_2 using focused electron beams. The heterostructure forms an atomically thin out-of-plane p-n diode. The diode is passivated by atomic layer deposition (ALD) of HfO_2 for electrical insulation. We demonstrated modulation of ionic current by the interlayer potential of the van der Waals heterostructure diode. Ionic current modulation is more effective with smaller pores and lower salt concentrations, and thus is not caused by leakage or edge electrochemistry. Modulation of ionic transport is also more effective under forward bias than under reverse bias, as a larger fraction of in-plane bias drops across the vertical p-n junction under forward bias.⁶ Finally, we obtained signatures of DNA translocation in ionic and diode channels simultaneously. DNA translocation in 10 mM KCl resulted in current increase in ionic channel, as well as current increase in diode channel. Overall, this heterojunction architecture represents a new paradigm for nanopore mass transport control with simultaneous electrical sensing, which could be applied to applications such as gated molecular sieving and slowing translocation for molecular identification with solid-state nanopores.

References:

- (1) Lindsay, S. The Promises and Challenges of Solid-State Sequencing. *Nat. Nanotechnol.* **2016**, *11* (2), 109–111.
- (2) Garaj, S.; Hubbard, W.; Reina, A.; Kong, J.; Branton, D.; Golovchenko, J. A. Graphene as a Subnanometre Trans-Electrode Membrane. *Nature* **2010**, *467* (7312), 190–193.
- (3) Feng, J.; Liu, K.; Bulushev, R. D.; Khlybov, S.; Dumcenco, D.; Kis, A.; Radenovic, A. Identification of Single Nucleotides in MoS_2 Nanopores. *Nat. Nanotechnol.* **2015**, *10* (12), 1070–1076.
- (4) Graf, M.; Lihter, M.; Thakur, M.; Georgiou, V.; Topolancik, J.; Ilic, B. R.; Liu, K.; Feng, J.; Astier, Y.; Radenovic, A. Fabrication and Practical Applications of Molybdenum Disulfide Nanopores. *Nat. Protoc.* **2019**, *14* (4), 1130–1168.
- (5) Venkatesan, B. M.; Estrada, D.; Banerjee, S.; Jin, X.; Dorgan, V. E.; Bae, M. H.; Aluru, N. R.; Pop, E.; Bashir, R. Stacked Graphene- Al_2O_3 Nanopore Sensors for Sensitive Detection of DNA and DNA-Protein Complexes. *ACS Nano* **2012**, *6* (1), 441–450.
- (6) Lee, C. H.; Lee, G. H.; Van Der Zande, A. M.; Chen, W.; Li, Y.; Han, M.; Cui, X.; Arefe, G.; Nuckolls, C.; Heinz, T. F.; et al. Atomically Thin P-N Junctions with van Der Waals Heterointerfaces. *Nat. Nanotechnol.* **2014**, *9* (9), 676–681.

11:45 AM NM03.01.11

High-Performance Hemofiltration via Molecular Sieving and Ultra-Low Friction in Carbon Nanotube Capillary Membranes [Piran Ravichandran Kidambi](#); Vanderbilt University, United States

Conventional dialyzer membranes typically comprise of unevenly distributed polydisperse, tortuous, rough pores, embedded in relatively thick ≈ 20 – 50 μm polymer layers wherein separation occurs via size exclusion as well as differences in diffusivity of the permeating species. However, transport in such polymeric pores is increasingly hindered as the molecule size approaches the pore dimension, resulting in significant retention of undesirable middle molecules (≥ 15 – 60 kDa) and uremic toxins. Enhanced removal of middle molecules is usually accompanied by high albumin loss (≈ 66 kDa) causing hypoalbuminemia. Here, the scalable bottom-up fabrication of wafer-scale carbon nanotube (CNT) membranes with highly aligned, low-friction, straight-channels/capillaries and narrow pore-diameter distributions (≈ 0.5 – 4.5 nm) is demonstrated, to overcome persistent challenges in hemofiltration/hemodialysis. Using fluorescein isothiocyanate (FITC)-Ficoll 70 and albumin in phosphate buffered saline (PBS) as well as in bovine blood plasma, it is shown that CNT membranes can allow for significantly higher hydraulic permeability (more than an order of magnitude when normalized to

pore area) than commercial high-flux hemofiltration/hemodialysis membranes (HF 400), as well as greatly enhance removal of middle molecules while maintaining comparable albumin retention. These findings are rationalized via an N-pore transport model that highlights the critical role of molecular flexing and deformation during size-selective transport within nanoscale confinements of the CNTs. The unique transport characteristics of CNTs coupled with size-exclusion and wafer-scale fabrication offer transformative advances for hemofiltration, and the obtained insight into molecular transport can aid advancements in several other bio-systems/applications beyond hemofiltration/hemodialysis.

Cheng P. et al. Adv. Func. Mat. 2024 DOI: 10.1002/adfm.202304672

SESSION NM03.02: CNT and Other 1D Structures II
Session Chairs: Ngoc Bui and Luda Wang
Wednesday Afternoon, April 24, 2024
Room 329, Level 3, Summit

1:30 PM NM03.02.01

Pushing The Limits of Size-Selectivity in Nanoscale Solute Separations [Feng Gao](#)¹, Wen Chen^{1,2}, Jamila Eatman^{1,2}, Paul Nealey^{1,2} and Seth Darling^{1,2};
¹Argonne National Laboratory, United States; ²The University of Chicago, United States

Transport of a spherical solute through a cylindrical pore has been modeled for decades using well-established hindered transport theory, predicting solutes with a size smaller than the pore to be rejected nonetheless because of convective and diffusive hindrance; this rejection mechanism prevents extremely sharp solute separations by a membrane. While the model has been historically verified, solute transport through near-perfect isoporous membranes may finally overcome this limitation. We achieve encouraging solute rejections using nanofabricated, defect-free, thin silicon nitride isoporous membranes. The membrane is challenged by a recirculated feed of dextran molecules to increase the opportunity for interactions between solutes and the pore array. Results show the membrane completely rejects solutes with greater size than the pore size while effectively allowing smaller solutes to permeate through. A steep size-selective rejection curve takes shape in distinct contrast to the conventional S-shape rejection curve predicted by hindered transport theory. With this traditional hurdle overcome, there is new promise for unprecedented membrane separations through judicious process design and extremely tight pore-size distributions.

1:45 PM NM03.02.02

Soft Artificial Tissues based on Droplet Interface Bilayers and Their Application as Membranes for Electrically Driven Separations [Aida E. Fica Conejeros](#)¹, Harekrushna Behera¹, McKayla Torbett², A. Derya Bakiler¹, Elisabeth Lloyd³, Robert Hickey³, Berkin Dortdivanlioglu¹, Stephen A. Sarles² and Manish Kumar¹; ¹University of Texas at Austin, United States; ²The University of Tennessee, Knoxville, United States; ³The Pennsylvania State University, United States

Soft tissue-like materials mimicking biological tissues' functionality, responsiveness, and reconfigurability hold immense potential for revolutionizing robotics, sensing, computing, biomanufacturing, and separations. Key features involve replicating cell structure by compartmentalizing aqueous environments with lipid membranes and incorporating membrane proteins for ion and solute transport. Droplet interface bilayers (DIBs) emerge as a promising platform, forming cell-like compartments enclosed by lipid membranes, serving as building blocks for 2D and 3D soft, responsive tissues. Conductive pathways are established by associating membrane proteins with lipid bilayers, providing tunable transport properties.

A rapid, scalable protocol combining emulsification and centrifugation has been devised for creating artificial tissues based on DIBs. This process successfully produces tissues from lipids, and polymers, and integrates ion channels like self-inserting peptides, integral membrane proteins, and artificial channels. Additionally, a platform has been designed to employ these tissues as membranes for electrically driven separations. The process hinges on three main components: an aqueous solution, hydrophobic media, and a bilayer-forming amphiphile as the emulsifier. Emulsification leads to aqueous droplet formation enclosed by a monolayer. Centrifugation creates a tightly packed system and displaces the excess oil. The contact of monolayer-enclosed droplets creates a bilayer, forming a network of communicating water compartments. This process enables the formation of tissues from microliter to liter scale, with resulting material exhibiting exceptional properties including high electrical resistance, viscoelasticity, and self-healing behavior.

Modifications to the process can significantly alter tissue's electrical properties. By incorporating ion channels during emulsification, the tissue can become electrically conductive. This enables the creation of biomimetic membranes that replicate and amplify channel properties, such as selectivity and pore size exclusion. The system allows for the incorporation of various natural or artificial channels, as they self-arrange in the monolayer/bilayer due to the hydrophobic effect. Channels like gramicidin (self-inserting peptide), Outer Membrane Protein (OmpF), Ammonium Transporter Protein (AmtB), and artificial channels like LAP5n10, a highly selective lithium channel, have been successfully incorporated through this method.

The use of DIB-based artificial tissues as membranes for water treatment has been proposed and demonstrated at the laboratory scale. To fabricate the membrane, the tissue is placed in a glass or plastic container, separated by two hydrogel layers on each side, which are in contact with an aqueous media. The assembly order is aqueous solution/hydrogel/tissue/hydrogel/aqueous solution. Applying voltage between the two aqueous solutions drives the transport of charged molecules or ions across the membrane through ion channels. The membrane's selectivity is controlled by the tissue's width and the selectivity of the channels used, as each layer of droplets acts like a membrane. For example, two layers of droplets containing a channel with 90% selectivity for a specific molecule will behave like two 90%-selectivity membranes in series, yielding an overall 99% selectivity provided all droplets contain the selective channel. This feature allows fine-tuning of membrane selectivity even when using low-selectivity channels. Overall, this innovative platform for fabricating soft membranes holds tremendous promise for advancing water treatment separations.

2:00 PM *NM03.02.03

Nanofluidic Interfaces with Electrified Materials [Narayana R. Aluru](#); The University of Texas at Austin, United States

The coupling between liquids and solids at atomic limit is currently of great interest. In particular, understanding properties of simple and complex liquids interfacing with electronically active materials is an active area of research. In this talk, we will discuss how properties of liquids are affected by mechanically tuning the electrical properties of solids. In the second part of the part, we will discuss the quantum coupling between the electronically active solid material and the interfacing liquid.

2:30 PM NM03.02.04

Computationally Guided Study of Cross-Linked Covalent Organic Frameworks for Membrane Applications Althea E. Davies, Michael J. Wenzel, Cailin L. Brugger, Jordan Johnson, Bruce A. Parkinson, John Hoberg and Laura de Sousa Oliveira; University of Wyoming, United States

Two-dimensional covalent organic frameworks (2D-COFs) exhibit characteristics that are favorable for membrane applications including, but not limited to, their high stability and well-ordered nanopores. A challenge with fabricating these materials into membranes, however, is that membrane wetting leads to flake dispersion and increased interstitial flow of particles. Cross-linking, or “chemically stitching” two layers of the COF together has been shown to significantly improve the membrane performance. This work seeks to investigate the stability of cross-linked 2D-COFs via computational modelling coupled with synthesis, characterization, and membrane permeance testing. A quinoxaline-based COF was computationally modeled and cross-linked with oxalyl chloride (OC) and hexafluoroglutaryl chloride (HFG). Cohesive energy calculations indicate that both cross-linking moieties increase the intramolecular bond strength of the COF, thereby increasing the stability of the material. Based on enthalpy of formation, it was concluded that HFG is a marginally more favorable cross-linking moiety. This was attributed to the length of HFG which allows it to cross-link with the COF in more configurations than OC. Cross-linking with HFG was synthesized and characterized with Fourier transform infrared (FTIR) spectroscopy, X-ray diffraction (XRD), and water contact angles. The presence of HFG cross-linking was confirmed and it was concluded via membrane permeance testing that varying the amount of cross-linking reagent during synthesis had not changed the amount of cross-linking occurring. This was also supported by thermogravimetric analysis with differential scanning calorimetry (TGA-DSC). Enthalpy of formation and cohesive energy calculations suggest that reduced cross-linking has a negligible effect on framework stability, and *ab-initio* molecular dynamics also agreed with the temperature range of stability from TGA-DSC.

2:45 PM BREAK

3:15 PM NM03.02.05

Measurement of Liquid Transport in a Single Diatom Frustule via *In-Situ* Optical Microscopy Omer R. Caylan¹, Carlos D. Diaz¹, Suchitra Ambudipudi², Sunghwan Hwang², Jihoon Park², Joseph Flanagan², Ken Sandhage² and Lenan Zhang¹; ¹Massachusetts Institute of Technology, United States; ²Purdue University, United States

Diatoms are a type of microscopic phytoplankton that exist in various aquatic environments (oceans, lakes, rivers). They are unicellular organisms enclosed in intricate, silica-rich microshells known as frustules. Notably, diatom frustules can possess multilevel hierarchical 3-D pore patterns with the smallest pore sizes down to a few tens of nanometers. Such unique 3-D multiscale features cannot be easily achieved with state-of-the-art cleanroom fabrication techniques. For this reason, diatom frustules have attracted attention in a wide range of applications, from nanotechnology to biotechnology (e.g., for drug delivery, wastewater treatment, biomolecule, and gas sensors). To support these crucial applications, it is essential to possess a comprehensive understanding of the fundamental principles governing liquid transport within diatom frustules. However, characterizing liquid transport through the hierarchical pores in a single microscopic diatom frustule is fundamentally challenging. To overcome these challenges, we developed a microfluidic test rig equipped with high-resolution optical microscopy. This characterization apparatus is capable of detecting liquid propagation from multiple angles with high spatial resolution and with a high frame capture rate. We have used this apparatus to identify microscopic features affecting liquid transport in *Coscinodiscus wailesii* diatom frustules and, for the first time, obtained key liquid transport characteristics of such frustules (including capillarity, wickability, and permeability). The optical metrology-based test rig developed in this work can be a useful platform for evaluating microfluidic behavior in various complex structures. This study is based on work supported by the Air Force Office of Scientific Research under Award Number FA9550-23-1-0055. Diatoms are a type of microscopic phytoplankton that exist in various aquatic environments (oceans, lakes, rivers). They are unicellular organisms enclosed in intricate, silica-rich microshells known as frustules. Notably, diatom frustules can possess multilevel hierarchical 3-D pore patterns with the smallest pore sizes down to a few tens of nanometers. Such unique 3-D multiscale features cannot be easily achieved with state-of-the-art cleanroom fabrication techniques. For this reason, diatom frustules have attracted attention in a wide range of applications, from nanotechnology to biotechnology (e.g., for drug delivery, wastewater treatment, biomolecule, and gas sensors). To support these crucial applications, it is essential to possess a comprehensive understanding of the fundamental principles governing liquid transport within diatom frustules. However, characterizing liquid transport through the hierarchical pores in a single microscopic diatom frustule is fundamentally challenging. To overcome these challenges, we developed a microfluidic test rig equipped with high-resolution optical microscopy. This characterization apparatus is capable of detecting liquid propagation from multiple angles with high spatial resolution and with a high frame capture rate. We have used this apparatus to identify microscopic features affecting liquid transport in *Coscinodiscus wailesii* diatom frustules and, for the first time, obtained key liquid transport characteristics of such frustules (including capillarity, wickability, and permeability). The optical metrology-based test rig developed in this work can be a useful platform for evaluating microfluidic behavior in various complex structures. This study is based on work supported by the Air Force Office of Scientific Research under Award Number FA9550-23-1-0055.

3:30 PM NM03.02.06

Multimodal Characterization of Separation Membranes in Three Dimensions using Scanning Transmission Electron Microscopy (STEM) Tomography and Electron Energy Loss Spectroscopy (EELS) Matthew J. Coupin^{1,2}; ¹The University of Texas at Austin, United States; ²Texas Materials Institute, United States

For decades, thin film composite membranes, in particular those employing an aromatic polyamide active layer, have become the dominant technology for the purification of water by nanofiltration and reverse-osmosis [1]. The extreme physical and chemical requirements demanded of these membranes (selectivity, permeability, fouling resistance, mechanical strength) combined with unique difficulties in studying their structure-property relationships on the nanoscale, have largely frustrated efforts to develop viable membranes based off new technologies. After more than 40 years, synthetic polymer membranes, many of which were discovered serendipitously, remain state-of-the-art. As the world confronts a changing climate, growing demand for water, and a transition away from fossil energy it is increasingly important that new effective, energy-efficient separation technologies be developed [2]. This will require advances in computational modeling and synthesis, informed by new and improved methods of material characterization.

TEM has long been a powerful tool for the nanoscale characterization of membranes; however, all TEM methods fundamentally produce some sort of two-dimensional projection of the sample. Although there can be great value in 2D top-down and cross-sectional imaging of membranes [3], the structure of a membrane must be studied in more than two dimensions to fully describe its function. Unlike conventional TEM-tomography methods, which have been successfully employed to study 3D morphological properties of separation membranes [4] high angle annular darkfield scanning transmission microscopy (HA-ADF STEM) scans a focused probe over the sample and is capable of producing images at the highest achievable resolutions whose contrast is proportional to sample density and thickness. Further, each scan line can be acquired with a different defocus, allowing large areas of the sample to be kept in-focus even at high tilt angles [5]. Taken together, these qualities allow for three-dimensional images that accurately reflect the sample's scattering density to be computed from the HA-ADF tilt series data.

In this presentation I will discuss how HA-ADF STEM tomograms can be collected, calculated, and combined with electron energy loss spectroscopy data to produce three-dimensional images of chemistry and sample density to inform water transport simulations [6] and membrane synthesis. Particular emphasis will be given to the experimental and geometrical limitations on quantitiveness, such as the limited range of angles from which a membrane can

be viewed in TEM, and how optimization and machine-learning techniques can be employed improve quantitiveness beyond the current state-of-the-art. Last, prospects for a 'closed-loop' unifying synthesis, characterization, and computational design will be discussed.

- [1] Lee, K.P., Arnot, T., Mattia, D. A review of reverse osmosis membrane materials for desalination – Development to date and future potential. *Journal of Membrane Science* 2011, 370, 1, 1-22.
- [2] Park, H., *et al.* Maximizing the right stuff: The trade-off between membrane permeability and selectivity. *Science* 2017, 356, 6343.
- [3] Pacheco, F., *et al.* Characterization of isolated polyamide thin films of RO and NF membranes using novel TEM techniques. *Journal of Membrane Science* 2010, 258, 51-59.
- [4] An, H., *et al.* Mechanism and performance relevance of nanomorphogenesis in polyamide films revealed by quantitative 3D imaging and machine learning. *Science Advances* 2022, 8, eabk1888.
- [5] Culp, T., *et al.* Electron tomography reveals details of the internal microstructure of desalination membranes. *Proceedings of the National Academy of Sciences* 2018, 115, 35, 8695.
- [6] Culp, T., *et al.* Nanoscale control of internal inhomogeneity enhances water transport in desalination membranes. *Science* 2021, 371, 72-75.

3:45 PM NM03.02.07

Advanced Chemical Characterization of Sub-Nanometer Pores in 2D Hexagonal Boron Nitride Dana O. Byrne^{1,2}, Aleksandr Noy^{3,4}, Alex Smolyanitsky⁵, Jim Ciston² and Frances I. Allen^{1,2}; ¹University of California, Berkeley, United States; ²Lawrence Berkeley National Laboratory, United States; ³Lawrence Livermore National Laboratory, United States; ⁴University of California, Merced, United States; ⁵National Institute of Standards and Technology, United States

Understanding and controlling the local chemistry and structure of vacancy defect clusters (i.e. nanopores) in 2D materials is essential for the development of advanced membranes that leverage the unique transport properties of these systems. In particular, nanopores in solid state 2D membranes can be designed to finely control ion selectivity and molecule permeability, and are thus of great interest for advanced applications in filtration and molecular sensing. Recent theoretical work and simulation has demonstrated strain-modulated ion transport behavior in graphene-embedded crown ethers, where oxygen termination of the pore edges forms C^{δ+}-O^{δ-} dipoles radially aligned toward the center of each pore [1]. To investigate this mechanosensitivity effect experimentally, we turn to the heteroatomic 2D material hexagonal boron nitride (hBN). This is because geometric (specifically, triangular) nanopores can be fabricated in 2D hBN with radially oriented dipoles by default, eliminating the need for additional chemical functionalization steps. To fabricate nanopores in 2D hBN with controlled shape and size, we use ion beam [2], electron beam [3], and combined ion and electron beam methods [4]. The ion irradiation is performed using an ion beam microscope, whereas the electron beam manipulation is carried out in a transmission electron microscope (TEM) with in-situ imaging at atomic resolution to track the pore growth process. Although we have control over nanopore size and shape using the TEM, dangling bonds present on the nanopore edges will be susceptible to chemical changes. Environmental effects are thus expected to alter the nanopore transport properties, since ion transport is heavily dependent on the electrostatic and steric interactions inside the pore. Therefore, it is essential that we elucidate the chemical structures of the nanopores in order to understand how they behave in a real system.

We survey the local chemistry of our nanopores using monochromated electron energy loss spectroscopy (EELS) in the TEM, probing local bonding and chemical composition based on variations in the fine structure of the boron K-edge signals. We find that oxygen dopant defects are present in varying amounts in a range of hBN nanopore samples and that the local chemistry of the nanopores is susceptible to change both inside the vacuum environment of the microscopes as well as upon exposure to air. Furthermore, we find that nanopore stability in air is greatly affected by the presence of hydrocarbon surface contaminants. These results highlight the importance of thoroughly characterizing the chemical structure of 2D nanopores when they are exposed to different environments in order to enable accurate simulation and interpretation of ion transport data.

- [1] Fang, A., K. Kroenlein, D. Riccardi, and A. Smolyanitsky. 2019. "Highly Mechanosensitive Ion Channels from Graphene-Embedded Crown Ethers." *Nature Materials* 18 (1): 76–81. <https://doi.org/10.1038/s41563-018-0220-4>.
- [2] Allen, Frances I. 2021. "A Review of Defect Engineering, Ion Implantation, and Nanofabrication Using the Helium Ion Microscope." *Beilstein Journal of Nanotechnology* 12: 633–64. <https://doi.org/10.3762/bjnano.12.52>.
- [3] Meyer, Jannik C., Andrey Chuvilin, Gerardo Algara-Siller, Johannes Biskupek, and Ute Kaiser. 2009. "Selective Sputtering and Atomic Resolution Imaging of Atomically Thin Boron Nitride Membranes." *Nano Letters* 9 (7): 2683–89. <https://doi.org/10.1021/nl9011497>.
- [4] Dana O Byrne, Archana Raja, Aleksandr Noy, Jim Ciston, Alex Smolyanitsky, Frances I Allen 2023. "Fabrication of Atomically Precise Nanopores in 2D Hexagonal Boron Nitride Using Electron and Ion Beam Microscopes." *Microscopy and Microanalysis*, Volume 29, Issue Supplement_1 (August): 1375–1376. <https://doi.org/10.1093/micmic/ozad067.707>

4:00 PM NM03.02.08

Defect-Healed Carbon Nanomembranes for Enhanced Salt Separation: Scalable Synthesis and Performance Zhen Yao¹, Pengfei Li^{1,2}, Kuo Chen^{1,2}, Yang Yang¹, André Beyer¹, Q. Jason Niu³ and Armin Goelzhauser¹; ¹Bielefeld University, Germany; ²China University of Petroleum (East China), China; ³Shenzhen University, China

Ultrathin carbon nanomembranes (CNMs), fabricated from crosslinking self-assemblies of molecular precursors, are 2D membranes that possess well-defined physical and chemical properties.¹ Featuring a high density of sub-nanometer channels, CNMs enable superior salt separation performance compared to conventional membranes.² However, defect occurrence during synthesis and transfer processes impedes their technical realization on a macroscopic scale.

Here, we introduce a practical and scalable interfacial polymerization method to effectively heal defects while preserving the sub-nanometer pores within CNMs. Defects in CNM composites were successfully repaired by interfacial polymerization of polyamide using m-phenylenediamine as the aqueous phase monomer and trimesoyl chloride as the oil phase monomer. The defect-healed CNMs exhibit exceptional performance in forward osmosis (FO), achieving a water flux of 105 L m⁻² h⁻¹ and a specific reverse salt flux as low as 0.1 g L⁻¹ when measured with 1M NaCl as draw solution. This water flux is ten times higher than commercially available FO membranes. Through successful implementation of the defect-healing method and support optimization, we demonstrate the scalable synthesis of fully functional, centimeter-scale CNM-based composite membranes, showing a water permeance comparable to commercial membranes and a salt rejection of ~99.8%. Our defect-healing method presents a promising pathway to overcome limitations in CNM synthesis, unlocking their potentials for practical salt separation applications.

- (1) Turchanin, A.; Götzhäuser, A. Carbon Nanomembranes. *Adv. Mater.* **2016**, *28* (29), 6075–6103. <https://doi.org/10.1002/adma.201506058>.
(2) Yang, Y.; Hillmann, R.; Qi, Y.; Korzetz, R.; Biere, N.; Emmrich, D.; Westphal, M.; Büker, B.; Hütten, A.; Beyer, A.; Anselmetti, D.; Götzhäuser, A. Ultrahigh Ionic Exclusion through Carbon Nanomembranes. *Adv. Mater.* **2020**, *32* (8), 1907850. <https://doi.org/10.1002/adma.201907850>.

4:15 PM NM03.02.09

Interlayer-Shifting and Functionalization of 2D COF Membranes for Controlled Transport Sui Zhang; National University of Singapore, Singapore

2D COF membrane is a versatile platform for the understanding and control of ion/molecular transport with its microporosity, interlayer spacing and rich space of chemistry.

In the first part of our work, we attempted to regulate the interlayer alignment of 2D COF membranes by the use of different catalyst. In contrast to traditional acid, the Lewis acid is able to accelerate the polymerization of imine-based COF and drives the interlayer shifting between adjacent layers, thereby resulting in pore redistribution and reduced pore size. The membrane exhibits high permeance and reasonable selectivity for H₂/CO₂ separation. In the 2nd part of our work, we functionalized the COF with sulfonate groups and observed interesting coordination-facilitated ion transport in the mixed ion environment. While single ion tests do not show much selectivity towards divalent and monovalent ions, the ion transport is much accelerated in the mixed ion solution, enabling high Mg²⁺/Li⁺ selectivity.

SESSION NM03.03: Poster Session

Session Chairs: Ngoc Bui and Piran Ravichandran Kidambi

Wednesday Afternoon, April 24, 2024

Flex Hall C, Level 2, Summit

5:00 PM NM03.03.01

Novel Copper-Nickel Pc-Por-Based Electrocatalysts for Highly Selective CO₂ Reduction and Multi-Carbon Compound Synthesis Abebe B. Workie; National Taiwan University of Science and Technology, Taiwan

Efforts are focused on developing an efficient strategy to combat global warming while also advancing the electrochemical conversion of carbon dioxide (CO₂) into multi-carbon compounds and improving C-C coupling processes. For accelerating the transformation of CO₂ into high-value chemicals, Metallomacrocyclic compounds have shown great potential among the many materials under investigation. However, they have thus far run across issues including low current density, limited catalytic activity, poor product selectivity, and stability worries. In this work, we present a novel achievement in the form of stable and conductive ultrathin dimeric Copper-Nickel Pc-Por-based electrocatalysts, synthesized through a solvent-assisted strategy. The manipulation of electron polarization between metal atoms is made feasible by adjusting the functionality and size of ligands, which enhances catalytic activity. This, in turn, leads to heightened atom utilization efficiency, customized catalytic behaviors, and exceptional selectivity, surpassing the benchmarks in C-C coupling and multi-carbon product formation. Our electrocatalyst exhibits remarkable selectivity for acetylene production, as demonstrated in an H-type cell. When operating in a 0.5 M KHCO₃ solution, it achieves outstanding Faradaic efficiencies (FEs) for CO₂ reduction at 0.61 V (vs. RHE), yielding over 94% acetylene with a current density exceeding 85 mA cm⁻². These results surpass the performance of the majority of previously reported CO₂ electrocatalysts. This study introduces a practical approach for designing future generations of cost-effective, efficient, and selectivity electrocatalytic reduction of carbon dioxide, offering potential solutions to mitigate global warming.

5:00 PM NM03.03.02

Separation of High-Purity C₂H₂ from Binary C₂H₂/CO₂ with Robust Al-Based MOFs Constructed with Nitrogen(N)-Containing Heterocyclic Dicarboxylate Se Min Jeong^{1,2}, Donghyun Kim^{1,3}, Ji woong Yoon¹, Su-Kyung Lee¹, Jong Suk Lee², Donghui Jo¹, Kyung-Ho Cho¹ and U-hwang Lee¹; ¹Korea Research Institute of Chemical Technology, Korea (the Republic of); ²Sogang University, Korea (the Republic of); ³Yonsei University, Korea (the Republic of)

The separation of acetylene (C₂H₂) from carbon dioxide (CO₂) holds considerable industrial importance, primarily in acetylene purification. Indeed, the conventional distillation process poses significant energy-consuming due to the similar physicochemical properties, such as kinetic diameters and boiling points of these two gases. In this research, we investigate the potential of three aluminum-based metal-organic frameworks (Al-MOFs), namely Al-L₁, Al-L₂, and Al-L₃, built by nitrogen (N)-containing organic linkers for separating C₂H₂ from C₂H₂/CO₂ mixtures. Among these Al-MOFs, Al-L₃ shows the highest C₂H₂/CO₂ selectivity (4.86) owing to its relatively greater adsorption capacity for C₂H₂ (7.90 mmol g⁻¹) and lower adsorption capacity for CO₂ (2.82 mmol g⁻¹) compared to the other two Al-MOFs. In dynamic breakthrough experiments with an equimolar binary C₂H₂/CO₂ gas mixture, Al-L₃ demonstrates superior separation performance by yielding high-purity C₂H₂ (>99.95%) of 3.73 mmol g⁻¹ through a simple desorption procedure with helium (He) purging at ambient condition. Also, computational simulations employing canonical Monte Carlo and dispersion-corrected density functional theory (DFT-D) methods are conducted to explore the distinctive pore structures of Al-L₁ and Al-L₃. The results emphasize the changes of affinity from variations in the positions of N atoms within pyridine and secondary amine (H-N) groups of three different Al-MOFs. Consequently, Al-L₃ is considered a promising adsorbent for separating high-purity C₂H₂ from binary C₂H₂/CO₂ gas mixtures, and we expect to effectively address challenges related to gas separation in both industrial and scientific fields.

5:00 PM NM03.03.03

Single-Step Ethylene Purification from Ternary C₂ Hydrocarbon Mixtures in a Scalable Metal-Organic Framework Donghyun Kim^{1,2}, Bao Nguyen Truong¹, Donghui Jo¹, Ji woong Yoon¹, Su-Kyung Lee¹, Youn-Sang Bae², Kyung-Ho Cho¹ and U-hwang Lee¹; ¹Korea Research Institute of Chemical Technology, Korea (the Republic of); ²Yonsei University, Korea (the Republic of)

Single-step purification of the ternary C₂ hydrocarbon mixture to produce ethylene (C₂H₄) directly using adsorption-based technologies is desirable for reducing large energy consumption. However, it is challenging to develop an appropriate adsorbent, having preferential adsorption characteristics toward ethane (C₂H₆) and acetylene (C₂H₂) rather than C₂H₄ coupled with high adsorption capacity owing to their similar physicochemical properties. Herein, we present a highly stable, cheap, and scalable CAU-23 adsorbent, which enables single-step production of high-purity C₂H₄ (>99.9%) from the ternary C₂ hydrocarbon mixture. CAU-23 exhibited higher uptake capacity of C₂H₆ (4.0 mmol g⁻¹) and C₂H₂ (4.7 mmol g⁻¹) compared to that of C₂H₄ (3.8 mmol g⁻¹). Further, it showed the reasonable selectivity for both C₂H₆/C₂H₄ (1.54) and C₂H₂/C₂H₄ (1.5) with an equimolar binary mixture, indicating that the separation performance of CAU-23 is comparable to the benchmark porous materials for separating C₂ ternary gas mixture. The breakthrough experiments

demonstrated its capability to produce high-purity C_2H_4 (>99.9%) with various $C_2H_6/C_2H_4/C_2H_2$ compositions at 298 K and 1 bar with high recyclability. The origin of the separation performance was further explored by using computational simulations of the grand canonical Monte Carlo (GCMC) and density functional theory (DFT).

5:00 PM NM03.03.04

Metal-Organic Framework (MOFs)-Derived Carbon Nanotubes (CNT) Intercalated into Ultrathin Polyamide Selective Layers to Improve Ethanol Purification Performance Lei Jiang, Pengrui Jin and Bart Van der bruggen; KU Leuven, Belgium

With the growing severity of the energy crisis, the development of renewable and clean energy sources that can replace fossil fuels has become a hot research topic. Biofuel ethanol, mainly derived from biomass through processes like saccharification and fermentation, with a volume concentration of over 99% anhydrous ethanol, has emerged as a promising alternative energy source due to its natural abundance and non-toxic properties. Utilizing membrane separation technology to purify ethanol offers a more efficient alternative to traditional distillation techniques, significantly reducing overall production costs. The selective layer for the membrane is prepared through interfacial polymerization using d-sorbitol (DST) and trimesoyl chloride (TMC). DST is chosen for its higher number of hydroxyl groups, which provide a denser separation layer with the thickness less than 100 nm. Its linear structure reacts well with TMC, enhancing crosslinking and improving separation performance. Metal-organic framework (MOFs)-derived carbon nanotubes (CNTs) are a novel carbon material with the diameter of 10 nm obtained by high-temperature calcination of ZIF-67. During the pyrolysis process, there is no aggregation, and embedding MOFs-derived CNTs in the thin-film nanocomposite (TFN) membrane selective layer can create mass transport channels to increase the TFN membrane's flux without compromising separation efficiency. Therefore, post-treatment using MOFs-derived CNT intercalated into ultrathin polyamide selective layers can further enhance the flux and keeping a stable separation efficiency of TFN membranes with a stable performance over a long period of time.

5:00 PM NM03.03.05

Effect of Voids on Nanoscale Charge Transport Through 2D Networks Consisting of 1D Nanoscale Wires Sara Alzahrani, Devendra Kumar Gorle, Andrew Qiu and Ant Ural; University of Florida, United States

Two-dimensional (2D) networks consisting of one-dimensional (1D) nanoscale wires, such as carbon nanotubes, metal nanowires, and graphene nanoribbons, are promising candidates for many applications including nanoscale mass transport membranes, transparent conductive electrodes, flexible electronics, wearable systems, electronic skin, biosensors, and neuromorphic computation.

The nanoscale charge transport in 2D nanowire networks is governed by percolation, which deals with the formation of long-range connectivity in random networks. As a result, Monte Carlo simulations need to be utilized in order to compute the charge transport properties of these networks. Understanding the impact of voids, which could be present due to lack of control in the deposition/fabrication process or introduced intentionally, on nanoscale charge transport phenomena in nanowire networks is critical for many applications.

In this work, we study the effect of voids on nanoscale charge transport through nanowire networks. We generate two-dimensional square nanowire networks with square voids located at the center of the nanowire network. We define the relative void size as the ratio of the length of the side of the void to the length of the side of the nanowire network. We first study the impact of voids on networks consisting of randomly oriented and straight nanowires. We compute the percolation probability in these networks as a function of nanowire density for different relative void sizes ranging from 0 (i.e., a network without a void) to 0.8. Assuming a Gaussian percolation probability density function (PDF), we find that both the mean and standard deviation of the PDF increase with increasing relative void size. We then compute the relative conductivity change as a function of nanowire density for different relative void sizes and find that it increases approximately linearly with relative void size.

The conductivity of a nanowire network is found to exhibit a power-law dependence on nanowire density as predicted by percolation theory. In order to study the effect of voids on this dependence, we extract the local power-law critical exponent as a function of nanowire density for different relative void sizes. We find that the critical exponent approaches 2 at high density for all relative void sizes, in agreement with previous observations for junction-resistance dominated networks without voids.

Furthermore, we generate curly nanowires using third order Bezier curves characterized by the curviness angle and aligned nanowires using an orientation characterized by the alignment angle. Using the same procedure as randomly oriented and straight nanowires, we then investigate the impact of voids on the nanoscale charge transport through networks consisting of curly and aligned nanowires. We compute critical phenomena such as the percolation probability, mean and standard deviation of the percolation probability density function, relative conductivity change, and nanowire density critical exponent.

Our results demonstrate the impact voids have on nanoscale charge transport through 2D networks consisting of 1D nanoscale wires, such as carbon nanotubes, metal nanowires, and graphene nanoribbons. These results also show that Monte Carlo simulations are an essential predictive tool for providing insights into nanoscale charge transport in nanowire networks, which are promising candidates for a wide range of applications such as nanoscale mass transport membranes, transparent conductive electrodes, flexible electronics, wearable systems, and neuromorphic computation.

SESSION NM03.04: Graphene Membranes I
Session Chairs: Piran Ravichandran Kidambi and Sui Zhang
Thursday Morning, April 25, 2024
Room 329, Level 3, Summit

8:30 AM NM03.04.01

Ion-Selective Membranes for Critical Materials Separation Van T. C. Le, Quy Nguyen, Hien Duy Mai, Bin Wang and Ngoc Bui; The University of Oklahoma, United States

This study aims at the design and fabrication of an emerging adsorptive membrane platform for transition metal ion capture. Specifically, the membrane composes of a selective layer built from stacks of zinc imidazole salicylaldoxime (ZIOS) crystalline nanosheets on a polyvinylidene fluoride (PVDF) supporting layer pretreated with polydopamine and polyethyleneimine. The dimensional and morphological textures of ZIOS layers were tuned by varying the concentrations of poly(vinyl alcohol) (PVA, $M_w = 146,000-186,000$ g/mol) in the reaction media. Additionally, textural properties (e.g., morphology, crystal size, particle orientation, and uniformity) and the adhesion of the ZIOS selective layer to the PVDF-PDA-PEI supporting substrate were controlled by tuning the synthetic conditions. Our results show that these ZIOS/PVDF-PDA-PEI membranes feature distinct ion transport and adsorption efficiency, which are critical for selective metal ion capture. The Cu^{2+}/Ni^{2+} separating factor was calculated to be 193. We use in-situ Raman spectroscopy to elucidate the underlying mechanisms governing the preferential metal ion uptake by the adsorptive membranes, of which the ZIOS layer functions as a selective layer in discriminating the guest metal cations. Coupled with first-principles calculations, results from this study synergistically provide insight

into mechanistic understanding of metal ion separating behaviors of an emerging membrane platform based on ZIOS, a crystalline adsorbent system that we designed specifically for copper/nickel separation.

Keywords: supramolecules; nanosheet; organic-inorganic membrane; metal ion separation; insitu crystal growth; interfacial growth, in-situ Rama

8:45 AM NM03.04.02

Self-Assembled 3D Graphene-Based Framework for Supercapacitor [Xiaojun Ren](#)¹, Tongxi Lin¹, Bing Sun², Sophia Gu², Tobias Foller¹ and Rakesh Joshi¹; ¹School of Materials Science and Engineering, UNSW Sydney, Australia; ²UNSW Sydney, Australia

Numerous interests have been attracted to establishing graphene-based materials for energy storage applications in the past decades [1, 2]. Constructing 3-dimensional graphene-based architectures provides a promising conductive skeleton and surface area for surface charge transfer and storage [3]. Herein, we report a simple self-assembled approach utilising surface electrostatic force between graphene oxide (GO) and trimolecular layered double hydroxide (LDH) nanoparticles to construct a hybrid 3D functionalised graphene framework via freeze-drying method for supercapacitor. Surprisingly, the synthesised GO-LDH hybrid material exhibits a typical electro-double layer capacitor (EDLC) rather than a battery electrochemical profile contributed by LDH material [4]. Our experimental study confirmed that the GO-LDH hybrid presents a relatively high specific capacitance of 278 F/g at 1 A/g and impressive rate capability (77.6%) at a high current density of 50 A/g in the aqueous working environment. We further investigated the surface structure to discuss the unexpected electrochemical profile of the material. This work provides a new insight into the fabrication and understanding of the GO-LDH hybrid 3D framework. A simple synthesis method, high reproducibility, and effective energy storage performance open a broad potential pathway for further applications.

Reference

- [1] Noori, A., El-Kady, M. F., Rahmanifar, M. S., Kaner, R. B., & Mousavi, M. F. (2019). Towards establishing standard performance metrics for batteries, supercapacitors and beyond. *Chemical Society Reviews*, 48(5), 1272-1341.
- [2] Mohamed, N. B., El Kady, M. F., & Kaner, R. B. (2022). Macroporous graphene frameworks for sensing and supercapacitor applications. *Advanced Functional Materials*, 32(42), 2203101.
- [3] Shao, Y., El Kady, M. F., Lin, C. W., Zhu, G., Marsh, K. L., Hwang, J. Y., ... & Kaner, R. B. (2016). 3D freeze casting of cellular graphene films for ultrahigh power density supercapacitors. *Advanced Materials*, 28(31), 6719-6726.
- [4] Chen, S., Luo, J., Li, N., Han, X., Wang, J., Deng, Q., ... & Deng, S. (2020). Multifunctional LDH/Co9S8 heterostructure nanocages as high-performance lithium sulfur battery cathodes with ultralong lifespan. *Energy Storage Materials*, 30, 187-195.

9:00 AM NM03.04.03

CO2 Capture using Functionalized Graphene Oxide Dogukan Yazici and [Michael Bozlar](#); The University of Texas at Arlington, United States

In this work, we aim to address the urgent global issue of increasing CO2 levels. We conduct a comprehensive study that integrates both experimental and theoretical chemistry. Using Density Functional Theory (DFT) first-principle calculations, we determine the positions of functional groups on the graphene lattice. Furthermore, we investigate the nature of interactions between functionalized-Graphene Oxide and CO2 molecules, from first principles. We synthesize various types of functionalized-graphene membranes for CO2 capture and perform physical and chemical analyses using X-ray Diffraction (XRD), Proton Nuclear Magnetic Resonance (H-NMR), and Fourier Transform Infrared Spectroscopy. Our results demonstrate effective CO2 capture using amino-functionalized graphene under stationary conditions, consistent with theoretical predictions.

9:15 AM *NM03.04.04

Graphene Oxide Membranes for Purification and Separation [Rakesh Joshi](#), Tobias Foller, Xinyue Wen, Dali Ji and Xiaojun Ren; UNSW Sydney, Australia

We report graphene oxide (GO) based membranes with proper control of structure, in-plane pores and morphology for water purification, selective gas separation and moisture adsorption. We have investigated the water transport in cation-intercalated graphene oxide membranes and observed that cations act as water-attracting impurities on the channel walls. Via controlled water transport experiments, we show that the slip length of the nanochannels decays exponentially with the hydrated diameter of the intercalated cations. In collaborative projects with industries, we have successfully employed our GO membrane to remove natural organic matter and chlorine from water while maintaining high water flux. In addition, we introduce a straightforward electrochemical method utilising the angstrom confinement of laminar reduced graphene oxide (rGO) nanochannels to obtain a centimetre-scale network of atomically thin (0.4 nm) 2D transition metal oxides.

9:45 AM BREAK

10:15 AM NM03.04.05

Electrophoretically Deposited Graphene Oxide on Acid-Washed Nickel Foam Substrate for High-Performance Capacitive Ion Desalination [Jyotiraman De](#), Arun Kumar Singh, Sumit Saxena and Shobha Shukla; Indian Institute of Technology Bombay, India

Graphene Oxide (GO) comprises unique features that make it a potential material for capacitive deionization (CDI) of brackish and saline water such as Graphene Oxide's increased surface area provides more ion adsorption sites, chemical stability of Graphene Oxide across a wide pH and ionic strength range contributing to the longer operational time of the CDI electrodes, possibility of modification of the Graphene Oxide with various surface functional groups in order to alter the selectivity of CDI electrode for ions and easy dispersibility of Graphene Oxide in various aqueous media and solvents. However, the method of loading the Graphene Oxide as an active material on the current collector to prepare an electrode and the preparation of a current collector before loading of the active material affects the desalination performance. Hence, exploring an efficient loading method of Graphene Oxide on a high charge transfer capable current collector is required that would inherit a higher electrochemical performance along with higher salt removal capacity. In order to mitigate the drawbacks of currently employed materials and methods, here we report a facile, scalable, and efficient method of preparing CDI electrodes by electrophoretic coating of GO on acid-washed Nickel foam. The nickel foam as a current collector was subjected to acid washing with various concentrations of acid, and simultaneous material and electrochemical characterization were conducted to optimize the acid concentration. Further, the Deionised (DI) water and acid-washed Nickel foam current collectors were dip-coated and electrophoretically coated with Graphene Oxide which on performing the physicochemical and electrochemical characterization displayed the specific capacitance and current density in the order electrophoretically coated GO on acid-washed Nickel foam > dip-coated GO on acid-washed Nickel foam > electrophoretically coated GO on DI-washed Nickel foam > dip-coated GO on DI-washed Nickel foam. In comparison to the dip-coated GO on DI-washed Nickel foam, electrophoretically coated GO on acid-washed Nickel foam demonstrates a multi-fold increase in the specific capacitance and current density. The use of three-dimensional electrophoretically coated GO on acid-washed Nickel foam electrodes in a CDI device contributed to the efficient charge transfer ability of the CDI and resulted in a substantial increase in salt adsorption capacity with excellent recyclability and efficient regeneration of the electrodes.

10:30 AM *NM03.04.06

Nanoscale Transport of Water and Molecules within 2D Materials and Its Impact on Nanofluidic Circuitry Slaven Garaj; National University of Singapore, Singapore

The study of molecular transport within nanometer-scale confinements is a fundamental challenge in materials science, underpinning the rational design of advanced materials for diverse applications and novel nanofluidics circuitry. Two-dimensional (2D) materials, renowned for their atomically clean interfaces, sub-nanometer control over geometry, and precise manipulation of surface properties, present an exceptional model system for unravelling the intricate phenomena of molecular transport at the nanoscale.

Here we present a comprehensive exploration of the transport of water and molecules within atomically smooth 2D nanochannels and self-assembled laminar nanodevices. This investigation unveils distinct flux patterns for individual components of binary organic and ionic aqueous solutions, enabling a systematic investigation of the interplay between geometric factors, material properties and molecular correlations. Furthermore, our inquiry delves into the mechanical interplay between confined liquids and the channel walls, resulting in the intriguing phenomenon of elastocapillary-driven channel collapse, colloquially referred to as "switching." Armed with a comprehensive theoretical framework and a deep understanding of switching dynamics, we have engineered novel active nanofluidic components, specifically nanoswitches and nanocapsules. Notably, nanocapsules have demonstrated the remarkable ability to reversibly seal zepto-liter volumes of liquids, mirroring the volumes found within viruses.

11:00 AM NM03.04.07

Permeation Behavior of Stretchable Graphene-Based Films for High Performance Gloves Zidan Yang¹, Robert Hurt¹, Aidan Stone¹, Jiaman Wang¹, Aicha Sama¹, Rebecca Martin-Welp¹, Indrek Kulaots¹ and Francesco Fornasiero²; ¹Brown University, United States; ²Lawrence Livermore National Laboratory, United States

Graphene-based ultra-thin films are gaining attention for their exceptional performance as molecular barriers. Understanding how water vapor and hazardous organic molecules permeate these films is key to applications in for personal or product protection. We propose the use of pre-wrinkled graphene-oxide-based nanosheet films as high-performance coatings on gloves due to their stretchability, breathability and strong barrier performance for many organic molecules. Graphene oxide films, however, lack water stability and sufficient mechanical strength for the glove application. To address this, we explore three alternative stabilization methods: high-loading GO-polymer composites, embedded "sandwich" structures, and textured stretchable GO-based coatings. We fabricated these three types of barrier architectures, studied their behaviors under bending, tensile stress, stretching and water immersion, and measured their permeability to water, hexane and toluene as model molecules of widely varying polarity. This work identified several film formulations that show promising barrier properties in combination with breathability and mechanical/immersion stability suitable for glove applications.

11:15 AM *NM03.04.08

Mass Transport Phenomena in Low-Dimensional Space Hyung Gyu Park; Pohang University of Science and Technology, Korea (the Republic of)

Membrane technology poses the potential to bring process intensification to various industrial processes, such as energy-efficient separation of chemicals and energy storage. Membrane-based separation can enhance its efficacy if the membrane materials' selectivity, permeation, and durability can be rendered optimal. In this regard, understanding molecular transport phenomena under extreme confinement provided by low-dimensional materials can help understand and engineer the selective transport in the membrane interior, with which to innovate the pore design. This talk introduces the transport phenomena of molecules across 0D-, 1D-, and 2D-confined space that atomically thin orifices, nanotubes, and laminated 2D materials provide. As the confinement dimension increases, mass permeation tends to decrease from ultimate permeation to fast transport to molecular conduction, whereas chemical selectivity can be endowed to this space by engineering the confining material properties. From the perspective that one may tailor actual chemical selectivity through proper pore design and architectural modification, thus obtained knowledge and pore architectures could lay the cornerstone of advancing membrane transport properties toward process intensification.

11:45 AM NM03.04.09

PH-Dependent Water Permeability Switching and Its Memory in MoS₂ Membranes Chengyi Hu^{1,2,3}, Amritroop Archari^{1,2}, Kun Huang^{1,2} and Rahul Raveendran Nair^{1,2}; ¹National Graphene Institute, United Kingdom; ²The University of Manchester, United Kingdom; ³Xiamen University, China

Intelligent transport of molecular species across different barriers is critical for various biological functions and is achieved through the unique properties of biological membranes. Two essential features of intelligent transport are the ability to (1) adapt to different external and internal conditions and (2) memorize the previous state. In biological systems, the most common form of such intelligence is expressed as hysteresis. Despite numerous advances made over previous decades on smart membranes, it remains a challenge to create a synthetic membrane with stable hysteretic behaviour for molecular transport. Here we demonstrate the memory effects and stimuli-regulated transport of molecules through an intelligent, phase-changing MoS₂ membrane in response to external pH. We show that water and ion permeation through 1T' MoS₂ membranes follows a pH-dependent hysteresis with a permeation rate that switches by a few orders of magnitude. We establish that this phenomenon is unique to the 1T' phase of MoS₂, due to the presence of surface charge and exchangeable ions on the surface. We further demonstrate the potential application of this phenomenon in autonomous wound infection monitoring and pH-dependent nanofiltration. Our work deepens understanding of the mechanism of water transport at the nanoscale and opens an avenue for the development of intelligent membranes.

SESSION NM03.05: Graphene Membranes II
Session Chairs: Piran Ravichandran Kidambi and Luda Wang
Thursday Afternoon, April 25, 2024
Room 329, Level 3, Summit

1:30 PM *NM03.05.01

Covalently Linked Fullerene Membranes for Gas and Water Transport De-en Jiang; Vanderbilt University, United States

It is extremely challenging to create long-range-ordered sub-nanometer pores in carbon materials. Recent breakthroughs in synthesis of covalently linked fullerene networks in gram scales provide a great opportunity to realize 2D and 3D ordered sub-nanometer pores at the interstices among linked C60 units. Here we show from both first principles and molecular dynamics simulations that the square-latticed monolayer fullerene membranes based on the experimental quasi-tetragonal phase of the fullerene 2D network possess the pore size, shape, and geometry promising for gas separations and water

transport. Our simulation results suggest that there is a great potential in using covalently-linked-fullerene membranes for separations.

2:00 PM *NM03.05.02

Mechanistic understanding of oxidation of graphitic lattice for gaining control over the incorporation of Å-scale pores in graphene [Kumar Varoon Agrawal](#); EPFL, Switzerland

Porous two-dimensional (2D) selective layer hosting zero-dimensional pores is attractive for molecular differentiation because one can tune molecular selectivity (by tuning pore size) and molecular flux (by tuning pore density). Porous graphene is an attractive candidate for this given that single-layer graphene can be conveniently synthesized in single-layer polycrystalline film morphology by chemical vapor deposition. Several promising results towards molecular separation have been demonstrated by incorporating pores in graphene by a variety of methods including physical etching (bombarding lattice with energetic beams) and oxidative etching.

In this presentation, I will highlight the important role of oxidative etching of graphene in highly scalable and easy-to-implement porosity incorporation in graphene with excellent control in the incorporation of Å-scale pores. I will discuss our recent efforts in understanding the mechanism of incorporation of these pores in the graphene lattice, starting with a single oxidation event, followed by cooperative assembly of the chemisorbed oxygen (epoxy) into clusters which then regulate the final pore size. I will discuss how clusters have ordered superlattice of O (against expectations of amorphous structure), which then leads to a series of sequences resulting in the incorporation of pores. I will discuss further examples of oxidation reactions that allow one to tune the size of pores in a highly controllable manner. Finally, I will discuss recent activities in scaling up graphene membranes, thanks to a highly scalable graphene oxidation chemistry.

2:30 PM *NM03.05.03

Cascaded Compression of Size Distribution of Nanopores in Monolayer Graphene [Chi \(David\) Cheng](#)¹, [Jiangtao Wang](#)² and [Jing Kong](#)²; ¹The University of New South Wales, Australia; ²Massachusetts Institute of Technology, United States

Monolayer graphene with nanometre-scale pores, atomically thin thickness and remarkable mechanical properties provides wide-ranging opportunities for applications in ion and molecular separations, energy storage and electronics. Because the performance of these applications relies heavily on the size of the nanopores, it is desirable to design and engineer with precision a suitable nanopore size with narrow size distributions. However, conventional top-down processes often yield log-normal distributions with long tails, particularly at the subnanometre scale. Moreover, the size distribution and density of the nanopores are often intrinsically intercorrelated, leading to a trade-off between the two that substantially limits their applications. In this talk, we report a cascaded compression approach to narrowing the size distribution of nanopores with left skewness and ultrasmall tail deviation, while keeping the density of nanopores increasing at each compression cycle. The formation of nanopores is split into many small steps, in each of which the size distribution of all the existing nanopores is compressed by a combination of shrinkage and expansion and, at the same time as expansion, a new batch of nanopores is created, leading to increased nanopore density by each cycle. As a result, high-density nanopores in monolayer graphene with a left-skewed, short-tail size distribution are obtained that show ultrafast and angstrom-size-tunable selective transport of ions and molecules, breaking the limitation of the conventional log-normal size distribution. This method allows for independent control of several metrics of the generated nanopores, including the density, mean diameter, standard deviation and skewness of the size distribution, which will lead to the next leap in nanotechnology.

3:00 PM BREAK

3:30 PM *NM03.05.04

Nanoporous Graphene Based Nanofluidics, From Mechanisms to Applications [Luda Wang](#); Peking University, China

Nanofluidics has not only drawn significant research interest due to its abnormal behavior compared to bulk fluids, but also has numerous applications such as separation, sensing, and energy conversion. Graphene provides an ideal two-dimensional platform to investigate the transport of nanofluids owing to its ordered structure, chemical stability, and easy modification.

Nanopores in graphene membranes provide 0D confined spaces to study transport mechanisms. Controlling the pore size in graphene membranes is a prerequisite, as even a small variation in pore size can result in a significant difference in transport properties. By decoupling defect site nucleation and defect growth with two successive plasma treatments, we achieved a narrow pore size distribution from gas-selective sub-nanometer pores to a few nanometers in size for small molecule separation. Moreover, we used a new strategy and achieved high solvent flux via organic solvent forward osmosis. After the precise introduction of the confined space, we then focus on designing functional groups, which provide a new degree of freedom. Through controlled nitrogen plasma, a highly proton-selective membrane was fabricated. By controlling the grain boundary density, proton permeance can be tuned within a range of 2 orders of magnitude with high selectivity and high proton conductivity. Through the synergistic regulation of the pore size and chemical properties of *in-situ* covalent modification, asymmetric ion transport behaviors and efficient sieving of monovalent metal ions (K^+/Li^+ selectivity ~ 48.6) can be achieved. Meanwhile, it also allows preferential transport for cations. The resulting membranes exhibit a K^+/Cl^- selectivity of 76 and an H^+/Cl^- selectivity of 59.3. The synergistic effects of steric hindrance and electrostatic interactions impose a higher energy barrier for Cl^- or Li^+ to cross nanopores, leading to ultra-selective H^+ or K^+ transport.

Besides the proof-of-concept experiments, we tried to bridge the gap between theory and reality to utilize graphene membranes in specific applications. For large-scale production, decimeter-scale ($\sim 15 \times 10 \text{ cm}^2$) large-area nanoporous single-layer graphene membranes and stability-enhanced double-layer graphene membranes were fabricated. An application paradigm of graphene in a membrane-based precision instrument with higher precision and better stability was achieved. One step further, regarding realizing the module of graphene membrane, the poor resistance to deformation under tension and bending of composite membrane is the limit. We designed a large-area nanoporous graphene separation membrane supported by a fiber-reinforced structure, which exhibits excellent tensile and bending capabilities. The fracture stress, fracture strength, and tensile stiffness have been increased by 1-2 orders of magnitude compared to existing research. It can maintain stability under different curvature conditions and remain intact after 10,000 repeated bends, laying a foundation for the long-term development of graphene films in practical separation applications.

4:00 PM *NM03.05.05

Anti-Arrhenius Passage of Gaseous Molecules through Nanoporous Two-Dimensional Membranes [Petr Dementyev](#) and [Armin Goelzhaeuser](#); Bielefeld University, Germany

The passage of molecules through membranes is known to follow an Arrhenius-like kinetics, i.e. the flux is accelerated upon heating and vice versa. There exist though stepwise processes whose rates can decrease with temperature if, for example, adsorbed intermediates are involved. In this study, we perform temperature-variable permeation experiments in the range from -50 to $+50$ °C and observe anti-Arrhenius behaviour of water and ammonia permeating in two-dimensional free-standing carbon nanomembranes (CNMs). The permeation rate of water vapour is found to drop manifold with warming, while the passage of ammonia molecules strongly increases when the membrane is cooled down to the dew point. Liquefaction of isobutylene shows no enhancement for its transmembrane flux which is consistent with the material's pore architecture.

4:30 PM NM03.05.06

The Parameter Space for Scalable Integration of Atomically Thin Graphene with Nafion for Proton Exchange Membrane (PEM) Applications
Piran Ravichandran Kidambi; Vanderbilt University, United States

Selective proton permeation through atomically thin graphene while maintaining impermeability to even small gas atoms *i.e.* He or hydrated ions, presents potential for advancing proton exchange membranes (PEMs) across a range of energy conversion and storage applications. The incorporation of graphene into state-of-the-art proton conducting polymers *e.g.* Nafion can enable improvements in PEM selectivity as well as mitigate reactant crossover. The development of facile integration approaches are hence imperative. Here, we systematically study the parameters influencing the integration of monolayer graphene synthesized *via* scalable chemical vapor deposition (CVD) on polycrystalline Cu foils with a model proton conducting polymer (Nafion) *via* a facile hot-press process. The hot-press time (t), temperature (T) and pressure (P) are found to not only influence the quality of graphene transfer but can also introduce additional defects in the CVD graphene. Graphene transfers to Nafion performed below the optimum temperature ($T_{\text{opt}} \sim 115$ °C) remain patchy with ruptures, while transfers above T_{opt} showed defect features, and transfers near T_{opt} show minimal ruptures and defect features. We demonstrate Nafion/graphene/Nafion sandwich membranes using the optimal transfer conditions that allow for $\sim 50\%$ reduction in hydrogen crossover (~ 0.17 mA cm⁻²) in comparison to Nafion control membranes (~ 0.33 mA cm⁻²) while maintaining comparable proton area specific resistance < 0.25 Ω cm² (areal conductance $\sim 4-5$ S cm⁻²), that are adequate to enable practical PEM applications such as fuel cells, redox flow batteries, and beyond.

Chaturvedi P. et al. Materials Advances (2023) DOI: 10.1039/d3ma00180f

4:45 PM NM03.05.07

Programmable Synthesis of Atomically Precise Nanoporous Graphene Materials Mamun Sarker¹, Christoph Dobner², Percy Zahl³, Axel Enders² and Alexander Sinitskii¹; ¹University of Nebraska-Lincoln, United States; ²University of Bayreuth, Germany; ³Brookhaven National Laboratory, United States

The bottom-up synthesis is a powerful approach for fabricating graphene-based nanomaterials (GNMs) with atomic precision. This approach relies on well-defined chemical reactions between specially designed molecular precursors that dictate the structure of the resulting GNMs. Therefore, preparing a new GNM generally requires the design and synthesis of a new molecular precursor, which is often very challenging and laborious. In this work, we demonstrate a family of molecular precursors based on 7,10-dibromo-triphenylenes that can selectively produce different varieties of atomically precise GNMs, porous nanographenes (pNGs), and porous graphene nanoribbons (pGNRs), using different synthetic environments. More specifically, we show that upon Yamamoto polymerization of these molecules in a solution environment, the free rotations of the triphenylene units around the C-C bonds result in forming cyclotrimers at high yields. In contrast, in the case of on-surface polymerization of the same molecules on Au(111), these rotations are impeded, and the coupling proceeds toward forming long polymer chains. These chains can then be converted into pGNRs by annealing. Correspondingly, the solution-synthesized cyclotrimers can also be deposited onto Au(111) and converted into pNGs via a thermal treatment. Thus, both processes start with the same molecular precursor and end with an atomically precise GNM on Au(111), but the product type, pNG or pGNR, depends on the specific coupling approach. We also produced extended nanoporous graphenes (NPGs) through the lateral inter-ribbon cyclodehydrogenation of highly aligned pGNRs at high coverage. All synthesized products were atomically precise, including the NPGs, which were shown to be deterministic in terms of the nanopore shape and size and contain only [18]annulene nanopores if occasional defects are not considered. We demonstrate the generality of this approach by synthesizing two varieties of 7,10-dibromo-triphenylenes that produced six GNM products with different dimensionalities. By constructing different GNMs from the same building blocks, it is possible to tune the band gap in a wide range. The basic 7,10-dibromo-triphenylene is amenable to structural modifications, potentially providing access to many new GNMs. The fact that the synthesized GNMs possess nanopores suggests using these materials for fundamental studies of the nanopore effect on the electrical and mechanical properties of graphene and their potential use for electronic, optoelectronic, and molecular sieving applications.

This work was supported by the Office of Naval Research (N00014-19-1-2596)"

SYMPOSIUM QT01

Ultrafast Light-Matter Interactions in Quantum Materials
April 23 - May 9, 2024

Symposium Organizers

Nicolò Maccaferri, Umeå University
Ajay Ram Srimath Kandada, Wake Forest University
Chiara Trovatello, Columbia University
Ursula Wurstbauer, Technical University of Munich

Symposium Support

Bronze
LIGHT CONVERSION

* Invited Paper

+ JMR Distinguished Invited Speaker

^ MRS Communications Early Career Distinguished Presenter

SESSION QT01.01: High Harmonic Generation and Nonlinear Spectroscopy
Session Chairs: Chiara Trovatiello and Ursula Wurstbauer
Tuesday Morning, April 23, 2024
Room 420, Level 4, Summit

10:30 AM *QT01.01.01

Nonlinearities and High-Harmonic Generation with Strongly Coupled Photon-Matter [Prineha Narang](#); University of California, Los Angeles, United States

The ability to generate and control light at increasingly short time scales impacts wide-ranging areas of science and technology ranging from the investigation of material properties to the development of optical frequency combs suitable for metrology. Ultrafast light sources are often limited in terms of achievable photon energies though various techniques aimed at generating high harmonics of input light from solid-state materials have been pursued to push the upper energy limit to the extreme ultraviolet or x-ray regime. In this context, I will discuss a cavity-mediated approach to break the inversion symmetry allowing for highly tunable even-order harmonic generation naturally forbidden in such systems. This relies on a quantized treatment of the coupled light-matter system, similar to the driven case, where the molecular matter is confined within an electromagnetic environment and the incident (pump) field is treated as a quantized field in a coherent state. When the light-molecule system is strongly coupled, it leads to two important features: (i) a controllable strong-coupling-induced symmetry breaking, and (ii) a tunable and highly efficient nonlinear conversion efficiency of the harmonic generation processes. Both of these have implications for molecular quantum architectures. At the same time, being able to control molecules at a quantum level gives us access to degrees of freedom such as the vibrational or rotational degrees to the internal state structure. Towards this, we explore the role an excited cavity mode plays in the generation of entanglement between molecules in a strongly coupled cavity setup and the potential for generating non-classical states of light due to the strong interaction between the molecules and cavity field. Finally, I will present an outlook on connecting ideas in cavity control of matter and nonlinearities in such systems with quantum information science.

11:00 AM QT01.01.02

Probing Solid-State Matter with High-Order Harmonic Generation Spectroscopy [Andrea Annunziata](#)^{1,2,3}, Cristian Soncini², Nicolas Tancogne-Dejean³, Monica Bollani², Giovanni Isella¹, Umberto De Giovannini³, Hannes Huebener³, Michele Devetta², Angel Rubio³, Salvatore Stagira^{1,2}, Alberto Crepaldi¹, Eugenio Cinguanta², Caterina Vozzi² and Davide Faccialà²; ¹Politecnico di Milano, Italy; ²Istituto di Fotonica e Nanotecnologie, Consiglio Nazionale delle Ricerche, Italy; ³Max Planck Institute for the Structure and Dynamics of Matter, Center for Free Electron Laser Science, Germany

When an intense mid-infrared (MIR) laser pulse interacts with matter, photons with energies that are integer multiples of the incident photon's energy are emitted. This process, known as High-order Harmonic Generation (HHG), was first discovered in noble gases^{1,2}, and then applied to molecules³, solids⁴, and liquids⁵. Focusing on solid-state HHG, this process was described as a sequence of three steps. In the first step, the interaction of the material with the driving field promotes an electron in the conduction band, leaving a hole in the valence band. In the second step, electrons and holes are accelerated in the respective bands by the external driving field. Due to the non-linearity of the band dispersion, intra-band harmonics are emitted. In the third and last step, electrons and holes can recombine, thus generating inter-band harmonics.

This highly non-linear phenomenon conveys information about the originating medium, making high-order harmonic generation spectroscopy (HHGS) a powerful technique for probing matter in solid state. Significant examples are provided by all-optical band structure reconstruction and Berry phase measurement^{6,7}. HHG can also be used as a probe of electronic and lattice dynamics initiated by a secondary pump pulse preceding the HHG driving field. This time-resolved HHGS (tr-HHGS) approach has the capability to probe phase transition and phonon dynamics with unprecedented spatial and temporal resolution⁸.

In our work, we applied HHGS and tr-HHGS for the characterization of two semiconductor materials, germanium, and tellurium.

We performed HHGS measurements in bulk germanium (001) driven by a linearly polarized MIR field centered at 3.2 μm . By focusing an intense linearly polarized MIR field, and collecting the harmonics generated in reflection, we observed harmonics up to the 15th order and we fully characterized the harmonic yield as a function of the crystal axis direction. All the harmonics reflect the cubic symmetry of the material but show very different behavior as a function of the driving field intensity and polarization direction. This is a signature of the non-linear dynamics taking place during the process. Moreover, we fully characterized the polarization state of the emitted harmonics up to the 7th order as a function of the crystal axis direction, showing that it can significantly diverge from the driving field polarization and demonstrating the emission of light at specific wavelengths having strong ellipticity. This could be attributed to the interference of different harmonic emission pathways, which can allow us to extract information about the complex sub-cycle ultrafast electron dynamics in germanium when it undergoes strong field interactions.

Furthermore, we used tr-HHGS for probing phase transitions in tellurium, an elemental semiconductor with *chiral* crystal structure. Preliminary results show how the extreme sensitivity of HHGS can be used for tracking the lattice and electron dynamics induced by the pump.

References:

¹P. B. Corkum, Phys. Rev. Lett. 71, 1994 (1993)

²M. Lewenstein et al., Phys. Rev. A 49, 2117 (1994)

³Velotta R., et al., High-Order Harmonic Generation in Aligned Molecules, Phys. Rev. Lett. 87, 183901

⁴Ghimire, S., DiChiara, A., Sistrunk, E. et al. Observation of high-order harmonic generation in a bulk crystal. Nature Phys 7, 138–141 (2011).

⁵Luu, T.T., Yin, Z., Jain, A. et al. Extreme-ultraviolet high-harmonic generation in liquids. Nat Commun 9, 3723 (2018).

⁶Vampa G., et al., All-Optical Reconstruction of Crystal Band Structure, Phys. Rev. Lett. 115, 193603

⁷T. T. Luu and H. J. Wörner, Nat. Commun. 9, 916 (2018).

⁸M. R. Bionta, Tracking ultrafast solid-state dynamics using high harmonic spectroscopy, Phys. Rev. Research 3, 023250

11:15 AM *QT01.01.03

New Routes for Label-Free Super-Resolution Microscopy and Attosecond Science via Transient High-Harmonic Generation [Peter Kraus](#)^{1,2};

¹Advanced Research Center for Nanolithography, Netherlands; ²Vrije Universiteit Amsterdam, Netherlands

While the upconversion of infrared driving lasers into soft-X-ray pulses by high-harmonic generation (HHG) *in gases* has become an established technique for attosecond science and nanoscale imaging [1-3], HHG *in solids* is less explored. Gas-phase HHG is highly sensitive and thus controllable with regards to the microscopic generation mechanism, and the macroscopic buildup of emission via phase matching [4,5]. Parallels between solid and gas-phase HHG suggest that solid-state HHG may be controlled in similar manners, which would enable a generally applicable all-optical light switch with wide application potential.

In this talk I will introduce femtosecond resolved solid-state HHG and highlight the applications of solid-state HHG for metrology, spectroscopy and imaging with recent examples from our group.

On the nanoscale, we controlled HHG via engineering the surface topography of solids, which in turn demonstrates how solid HHG can be used for metrology on surfaces and tailored as a light source [6].

On the femtosecond time scale, we used the sensitivity of HHG to electronic band structure to follow ultrafast phase transitions in strongly correlated materials [7], and photocarrier dynamics in perovskites [8].

While the first set of measurements mentioned above showed nanoscale sensitivity, the second set of experiments demonstrated that photoexcitation can be used to control light emission via solid-state HHG.

Combining both efforts, I will outline and show first results how ultrafast control of solid HHG enables harmonic deactivation microscopy (HADES) - a label-free super-resolution microscopy below the diffraction limit of light [9].

Thinking ahead, the development of these techniques may enable resolution on the nanometer and femto- to attosecond scale fitted into a regular microscopy setting, with application potential ranging from strongly correlated materials to semiconductor metrology, photosynthetic processes, and medical imaging.

References:

- [1] P.M. Kraus, H.J. Wörner, *Angewandte Chemie International Edition* 57, 5228 (2018).
- [2] P.M. Kraus, M. Zurich, S.K. Cushing, D.M. Neumark, S.R. Leone, *Nature Reviews Chemistry* 2, 144 (2018).
- [3] P.M. Kraus et al., *Science* 350, 790 (2015).
- [4] S. Roscam Abbing, F. Campi, F.S. Sajjadian, N. Lin, P. Smorenburg, P.M. Kraus, *Physical Review Applied* 13, 054029 (2020).
- [5] S. Roscam Abbing, F. Campi, A. Zeltsi, P. Smorenburg, P.M. Kraus, *Scientific Reports* 11, 24253 (2021).
- [6] S.D.C. Roscam Abbing, et. al., P.M. Kraus; *Physical Review Letters* 128, 223902 (2022).
- [7] Z. Nie et al., Peter M. Kraus, *Physical Review Letters*, in review (2023).
- [8] M. v.d. Geest, J.J. de Boer, K. Murzyn, P. Juergens, B. Ehrler, P.M. Kraus, *Journal of Phys. Chem. Lett.*, in review (2023).
- [9] K. Murzyn et al., P.M. Kraus, in preparation.

11:45 AM QT01.01.04

Advances in Hands-Off Femtosecond Parametric Amplifiers for Solid-State Materials Investigation Stefan Piontek, Valdas Maslinskas, Jonas Berzinš and Marco Arrigoni; Light Conversion, Lithuania

Time-resolved and static nonlinear optics (NLO) experiments at surface and bulk of advanced solid-state materials require agile femtosecond and picosecond tunable sources with high peak power and excellent stability. Repetition rate agility, ease of use and a compact footprint enhance experimental productivity and eliminate the need for an “expert” laser user. Typical experimental set-ups for study of interfaces and bulk material properties on meso- and nanoscale include two-dimensional infrared (2D-IR)¹, sum-frequency generation (SFG)^{2,3}, as well as transient absorption (TA)⁴ spectroscopy. Until recently, these experiments required titanium-sapphire amplifiers with repetition rates of 1-5 kHz, or mode-locked lasers at 80 MHz with limited energy and tuning ranges. <!--[endif]-->

<!--[endif]-->With technological advancements provided by flexible Yb-based regenerative amplifiers, experiments can now be realized at 100 kHz-1 MHz repetition rates with significant improvements in signal-to-noise ratio¹⁻⁵. While for most experiments on solid-state samples, laser pulse energies in the microjoule range are perfectly adequate, some other benefits from higher energies that are now achievable in the latest generation of Yb amplifiers. After briefly describing recent advances in amplifiers, we will describe state-of-the-art tunable parametric amplifiers ranging from 190 nm to 16000 nm, allowing seamless access to most of the chemically relevant frequencies of interest⁶⁻⁸. We will provide application examples that benefit from technological improvements including sealed, hands-off configurations, enhanced efficiency and short pulse generation.

References:

1. Farrell, K. M.; Ostrander, J. S.; Jones, A. C.; Yakami, B. R.; Dicke, S. S.; Middleton, C. T.; Hamm, P.; Zanni, M. T., *Opt. Express* **2020**, 28 (22).
 2. Golbek, T. W.; Weidner, T., *The Journal of Physical Chemistry Letters* **2023**, 14 (44).
 3. Lackner, M.; Hille, M.; Hasselbrink, E., *The Journal of Physical Chemistry Letters* **2020**, 11 (1).
 4. Blaszczyk, O.; Krishnan Jagadamma, L.; Ruseckas, A.; Sajjad, M. T.; Zhang, Y.; Samuel, I. D. W., *Materials Horizons* **2020**, 7 (3).
 5. Donaldson, P. M.; Greetham, G. M.; Middleton, C. T.; Luther, B. M.; Zanni, M. T.; Hamm, P.; Krummel, A. T., *Acc. Chem. Res.* **2023**, 56 (15).
 6. Backus, E. H. G.; Schaefer, J.; Bonn, M., *Angewandte Chemie-International Edition* **2020**, (59),.
 7. Chattopadhyay, A.; Boxer, S. G., **1995**, 117 (4).
 8. Wang, Z.; Morales-Acosta, M. D.; Li, S.; Liu, W.; Kanai, T.; Liu, Y.; Chen, Y.-N.; Walker, F. J.; Ahn, C. H.; Leblanc, R. M.; Yan, E. C. Y., *Chem. Commun.* **2016**, 52 (14).
- <!--[endif]-->

SESSION QT01.02: Ultrafast Dynamics in 2D Materials I

Session Chairs: Veronica Policht and Ursula Wurstbauer

Tuesday Afternoon, April 23, 2024

Room 420, Level 4, Summit

1:30 PM *QT01.02.01

Manipulation and Non-Linear Propagation of Excitonic Complexes in 2D Materials Alexey Chemikov; Technische Universität Dresden, Germany

Two-dimensional transition metal dichalcogenides offer an excellent platform to study non-linear dynamics of tightly-bound exciton quasiparticles. The properties of the excitons and their optical response change drastically in the presence of free charges, leading to emergence of many-body states described as trions or Fermi polarons. The physics of such Bose-Fermi quasiparticle mixtures have attracted a lot of interest in the scientific community and motivated the development of methods to control them on ultrafast time-scales. In addition, excitonic complexes are known to be mobile both in monolayers and heterostructures, with the transport of optical excitations playing a central role from both fundamental and technological perspectives.

The first part of the talk will be focused on the use of intense THz pulses to transiently modify light-emission of exciton-electron ensembles in a monolayer semiconductor. We demonstrate a near complete, THz-induced trion-to-exciton conversion by monitoring time resolved photoluminescence after optical

excitation. It offers new pathways to manipulate exciton-electron mixtures in monolayer semiconductors, triggering a non-linear optical response by low-energy photons on picosecond timescales. In the second part, I will discuss linear and non-linear propagation of interlayer excitons in atomically reconstructed heterobilayers for an extended density range up to the Mott transition. Key results include demonstration of rapid exciton diffusion in absence of disorder- and Moiré-induced localization, role of the exciton-exciton interactions, and effectively negative diffusivity in the regime of dissociated excitons and dense electron-hole plasma.

2:00 PM QT01.02.02

Disentangling Many-Body Effects in The Coherent Optical Response of a 2D Semiconductor Chiara Trovattello^{1,2}, Florian Katsch³, Qiuyang Li^{1,4}, Xiaoyang Zhu¹, Andreas Knorr³, Giulio Nicola Felice Cerullo² and Stefano Dal Conte²; ¹Columbia University, United States; ²Politecnico di Milano, Italy; ³Technische Universität Berlin, Germany; ⁴University of Michigan–Ann Arbor, United States

Monolayer transition metal dichalcogenides (1L-TMDs) have received increasing attention because of their enhanced light-matter interaction, strongly bound excitons, exciton Rydberg states and many-body effects[1]. Transient absorption spectroscopy has been extensively used to study exciton scattering processes on an ultrafast timescale. While it has been shown that on a ten- to hundred-ps timescale, the exciton decay dynamics is dominated by thermal effects[2], **the physical origin of exciton dynamics on a ps and sub-ps timescale is still under debate**. In this temporal window, many-body effects lead to a renormalization of the bands, inducing a transient energy shift of the excitonic resonance. Simultaneously, the increase of the electronic temperature after photo-excitation, due to multiple electronic scattering events, broadens the excitonic linewidth. Broadening and shift of the excitonic peak overlap in time with an abrupt absorption reduction due to phase-space filling effect[3]. All these processes are difficult to disentangle, and their dynamical interplay determines the complex shape of the transient absorption spectra of TMDs across the bandgap at early pump-probe delays. Transient exciton energy shifts have been roughly estimated from pump-probe measurements with contrasting results, e.g., blue vs red shift, and values from meV to tens of meV.

In this work, we measure the transient optical response of 1L-WS₂ on SiO₂ across the A and B excitonic resonances. The sample is photoexcited on- and out-of-resonance with the A exciton, and at variable pump fluences below the exciton-Mott transition. In order to capture the origin of the different transient signal shapes for both excitations, we disentangle absorption reduction, energy shift and broadening of the excitonic peak from the transient optical response, using Kramers-Kronig constrained variational analysis. From the measured transient reflectivity ($\Delta R/R$) of 1L-WS₂ we retrieve the absorbance spectrum as a function of pump-probe delay.

When the sample is photo-excited the pump induces a dramatic change of the A exciton, resulting from several concomitant effects: a quenching of the exciton oscillator strength, a blue energy shift and an asymmetric lineshape broadening. All the spectra are well reproduced by a fitting function made by the sum of two Lorentz oscillators on top of a polynomial background. The transient energy shift persists over a timescale much longer than the temporal overlap of pump and probe pulses, excluding the possibility that it originates from optical Stark effect.

Microscopic calculations based on excitonic Heisenberg equations of motion quantitatively reproduce the non-linear absorbance spectra of the material. All the lorentzian parameters show a linear dependence with rising excitation power for both the pump photon energies, and many-body effects are strongly enhanced for resonant excitation, resulting in a transient blue shift of the A exciton. The shift progressively decreases as the pump is detuned from the resonance and turns into a small red shift when the energy of the pump is close to the B excitonic resonance. The energy shift originates from Coulomb-induced bandgap renormalization while the asymmetric broadening is related to excitation induced dephasing mechanism[4].

In conclusion, we provide a complete picture of the transient optical response of 1L-WS₂ which can finally explain the strong differences observed in the pump-probe spectra following on- and off-resonant excitation [4]. Our combined experimental and theoretical studies give important insights into the complex interplay between many-body correlations and excitonic interactions determining the non-equilibrium response of 1L-TMDs.

[1] Chernikov, A. et al. *Phys. Rev. Lett.* **113**, 076802 (2014).

[2] Moody, G. et al., *J. Opt. Soc. Am. B* **33**, C39–C49 (2016).

[3] Katsch, F., et al., *Phys. Rev. Lett.* **124**, 257402 (2020).

[4] Trovattello, C. et al., *Nano Letters*, **22**, 5322-5329 (2022).

2:15 PM *QT01.02.03

Ultrafast Charge Transfer Dynamics in Van der Waals Heterostructures Ermin Malic; Philipps University Marburg, Germany

Van der Waals heterostructures built by vertically stacked transition metal dichalcogenides (TMDs) exhibit a rich exciton energy landscape including spatially separated interlayer states, momentum-dark intervalley states, and hybrid exciton states. Recent experiments have demonstrated an ultrafast charge transfer in TMD heterostructures. However, the nature of the charge transfer process has remained elusive. Based on a microscopic and material-realistic exciton theory combined with time-resolved ARPES measurements, we reveal that phonon-mediated scattering via strongly hybridized dark intervalley excitons governs the charge transfer process [1,2]. We track the time-, momentum-, and energy-resolved relaxation dynamics of optically excited excitons and determine the temperature- and stacking-dependent charge transfer times for different TMD bilayers.

Furthermore, we demonstrate how the Coulomb interaction between the correlated electron- and hole-components of intra- and interlayer excitons facilitates the study of the ultrafast hole transfer mechanism in a twisted WSe₂/MoS₂ heterostructure. Intriguingly, we find an increase of the photoelectron energy in the ARPES spectrum upon the hole transfer process across the interface. This is surprising at first, because the electron remains rigid in the conduction band during the hole transfer process, and also because any relaxation mechanism is typically expected to cause an overall decrease of the measured electronic energies. However, we do not observe a free photoelectron, but the blue-shift is a direct consequence of the correlated nature of the Coulomb-bound electron-hole-pair.

Compared to the electron transfer occurring on a timescale of sub-100fs, we find both in experiment and theory that the hole transfer is considerably slower and occurs rather on a timescale of a few picoseconds. This can be traced back to different relaxation pathways: In the case of the electron transfer, optically excited intralayer excitons are subject to a relaxation cascade via layer-hybridized KA excitons to the lowest interlayer exciton states. In contrast, the hole transfer occurs via layer-hybridized Γ K excitons. Since the A valleys are three-fold degenerate, while there is only one Γ valley, the density of states for the electron transfer pathway is more efficient. Furthermore, the exciton energy difference between the initial optically excited intralayer exciton and the final interlayer exciton is roughly 200 meV larger in the case of the hole transfer, further contributing to a slower transfer dynamics of holes.

The provided insights present an important step forward in microscopic understanding of the technologically important charge transfer process in van der Waals heterostructures.

References:

[1] D. Schmitt, J. Bange, W. Bennecke, A. AlMutairi, G. Meneghini, K. Watanabe, T. Taniguchi, D. Steil, D. Luke, R. Weitz, S. Steil, G. Jansen, S. Brem,

E. Malic, S. Hofmann, M. Reutzel and S. Mathias, Formation of moiré interlayer excitons in space and time, *Nature* 608, 499 (2022)

[2] Meneghini, S. Brem, E. Malic, Ultrafast phonon-driven charge transfer in van der Waals heterostructure, *Natural Sciences*, e20220014 (2022)

[3] J. Bange, D. Schmitt, W. Bennecke, G. Meneghini, A. AlMutairi, K. Watanabe, T. Taniguchi, D. Steil, S. Steil, R. Weitz G. Jansen, S. Hofmann, S. Brem, E. Malic, M. Reutzel, S. Mathias, Probing electron-hole Coulomb correlations in the exciton landscape of a moire heterostructure, arXiv 2303.17886 (2023)

2:45 PM BREAK

3:15 PM QT01.02.04

Ultrafast Coherent Control of Valley Polarization in a 2D Semiconductor Francesco Gucci¹, Mattia Russo¹, Franco V. A. Camargo², Rui E. F. Silva^{3,4}, Misha Ivanov^{4,5,6}, Álvaro Jiménez-Galán^{4,7}, Stefano Dal Conte¹ and Giulio Cerrullo^{1,2}; ¹Politecnico di Milano, Italy; ²IFN-CNR, Italy; ³Centro Superior de Investigaciones Científicas, Spain; ⁴Max Born Institute, Germany; ⁵Humboldt-Universität zu Berlin, Germany; ⁶Imperial College London, United Kingdom; ⁷National Research Council of Canada and University of Ottawa, Canada

Today's information processing technology relies on electronics, with transistor switches reaching speeds as high as 800 GHz yet appearing to approach their limits. The next disruptive step in increasing speed of information processing should come from driving electronic response in two-dimensional materials with ultrafast controlled lightwaves. This so-called lightwave electronics aims to use ultrashort pulses of light to switch electric currents and can potentially operate at nearly PHZ rates. Lightwave valleytronics targets a new degree of freedom for information processing offered by excitons in two-dimensional materials with broken inversion symmetry: the valley pseudospin. The valley pseudospin is associated with the occupation of energy degenerate, but distinct valleys K and K'.

The optical selection rule, which couples the valleys with circularly polarized light, provides important implications for the development of valleytronics-based devices[1]. However, to this day, the short valley lifetime (i.e. few picoseconds) has prevented any practical implementation of valleytronics. Recently, the realization of a translating-wedge based identical pulses encoding system (TWINS) enabled the generation of phase-locked collinear pulses with a delay controlled on a sub-fs scale[2]. Exploiting this technology, we experimentally prove a new all-optical coherent ultrafast protocol to manipulate the valley polarization in two-dimensional semiconductors[3]. In our experiment, a couple of delayed phase-locked ultrashort laser pulses with perpendicular polarization enables us to induce a positive or negative valley polarization in a WS₂ monolayer. Our findings show that by making sub-cycle adjustments to the delay, we can continuously switch from exciting one valley to exciting the other.

Then, exploiting four phase-locked pulses, we realize an ultrafast switch of the valley polarization at room temperature: by carefully controlling the delays between the excitation pulses we quench and amplify the valley polarization on a sub-100 fs temporal scale. Our measurements also allow us to extract the excitonic dephasing time. Our experimental findings are validated by theoretical simulations calculated from first principles.

Our results demonstrate the possibility to control the valley polarization in two-dimensional semiconductors on an ultrafast timescale, opening a new route for ultrafast information processing with low-power few-cycle light pulses available today. We also provide a novel approach to investigate the properties of these materials.

[1] Mak, K. F., He, K., Shan, J. & Heinz, T. F. Control of valley polarization in monolayer MoS₂ by optical helicity. *Nature Nanotechnology* 7, 494–498 (2012).

[2] Brida, D., Manzoni, C. & Cerrullo, G. Phase-locked pulses for two-dimensional spectroscopy by a birefringent delay line. *Optics Letters* 37, 3027 (2012).

[3] Silva, R. E. F., Ivanov, M. & Jiménez-Galán, Á. All-optical valley switch and clock of electronic dephasing. *Optics Express* 30, 30347 (2022).

[4] Gucci, F *et al.*, *in preparation*

3:30 PM QT01.02.05

Ultrafast Switching of Trion Emitters in Monolayer MoSe₂ Marzia Cuccu¹, Tommaso Venanzi², Xiaoxiao Sun³, Takashi Taniguchi⁴, Kenji Watanabe⁴, Manfred Helm^{3,1}, Stephan Winnerl³ and Alexey Chernikov¹; ¹Technische Universität Dresden, Germany; ²Istituto Italiano di Tecnologia, Italy; ³Helmholtz-Zentrum Dresden-Rossendorf, Germany; ⁴National Institute for Materials Science, Japan

Excitons in two-dimensional transition metal dichalcogenides emerged as a unique nanoscale platform offering strong light-matter coupling, spin-valley locking and exceptional tunability. Moreover, their properties and optical response change drastically in the presence of free charges, leading to the formation of new quasiparticles known as trions or Fermi polarons. The physics of such Bose-Fermi quasiparticle mixtures have attracted considerable interest in the scientific community. However, there are limitations to how fast the optical response of these states can be manipulated, restricting the majority of applications to a static regime.

Here, we show how to overcome this challenge by using low-energy photons in the THz frequency range. We demonstrate the conversion of trions into excitons in two-dimensional materials on ultrafast timescales of a few picoseconds by applying short THz pulses after the optical excitation. Monitoring the time-resolved photoluminescence dynamics, a strong quenching of the trion population induced by the THz radiation is observed, accompanied by a simultaneous increase of the exciton emission. The process is highly sensitive to the energy of the THz photons, that has to match the trion binding energy of the material. Furthermore, the observed switching is found to be highly reproducible when both the THz power and the time delay between optical and THz pulses are tuned. Our results provide a promising experimental tool for fundamental research of light-emitting excitation mixtures and offer pathways towards technological developments of nanophotonic devices based on atomically thin materials.

3:45 PM *QT01.02.06

Ultrafast Processes in Atomically Thin Semiconductors Stefano Dal Conte; Politecnico di Milano, Italy

Two dimensional (2D) transition metal dichalcogenides (TMDs) have received increasing attention because of their optical and electronic properties, including enhanced light-matter interaction, strongly bound excitons, exciton Rydberg states, multiparticle excitonic complexes, and valley-selective circular dichroism [1]. Some of these properties are exploited in the realization of prototypical optoelectronic devices with improved performances and decreased size. Multiple layers of TMDs can also be stacked to form vertical heterostructures (HS) with tailored electronic and optical properties. Most of TMD-based heterobilayers have type II band alignment leading to fast charge separation and formation of interlayer excitons (ILX) characterized by ultra-long population recombination and twist angle dependence [2].

In my talk, I will report on the non-equilibrium optical response of 2D TMDs and their related HS measured by pump-probe optical spectroscopy techniques. In the first part of the talk, I will describe exciton formation and relaxation processes occurring on a sub-ps regime in isolated TMDs [1] focusing on the interplay between many-body and Coulomb correlation effects and excitonic population effects [3,4]. In the second part of talk, I will focus on the ultrafast processes occurring in TMD HS. I will show that it is possible to simultaneously detect interlayer hole and electron transfer processes on a 100 fs timescale [5] while the formation dynamics of ILX bleaching signal shows a distinct picosecond delayed growth dynamics significantly longer than that of intralayer excitons. Theoretical calculations based on microscopic Heisenberg equations of motion find that the delayed formation is mainly related

to phonon-assisted interlayer scattering of photo-excited carriers that give rise to finite-momentum (i.e. optically dark) hot ILX which quickly exchange energy and momentum with phonon population and become bright [6].

- [1] G. Wang *et al.* Rev. Mod. Phys. **90**, 021001 (2018)
- [2] Y. Jiang *et al.* Light: Science & Applications **10**, 72 (2021)
- [3] C. Trovatiello *et al.* Nat. Commun. **11**, 5277 (2020)
- [4] C. Trovatiello *et al.* Nano Lett. **22**, **13**, 5322–5329 (2022)
- [5] V. Policht *et al.* Nano Lett. **21**, **11**, 4738–4743 (2021)
- [6] V. Policht *et al.* accepted on Nat. Commun.

4:15 PM *QT01.02.07

Quantum Dynamics of Fermi Polarons in Doped Semiconductor Monolayers [Xiaoqin E. Li](#); The University of Texas at Austin, United States

In doped semiconductors, optically excited electron-hole pairs (i.e. excitons) can be treated as an impurity coupling to a Fermi sea. Atomically thin semiconductors provide a rich playground to explore the Fermi polaron problems where the electrons and excitons further acquire a valley index. The attractive interaction between the exciton and Fermi sea leads to an energetically favorable state --- the attractive polaron --- as well as a higher energy repulsive polaron, a metastable state that eventually decays into attractive polarons. Here, we study the emergence and evolution of attractive polarons and repulsive polarons in MoSe₂ and WSe₂ monolayers as the electron doping density increases. Using two-dimensional coherent electronic spectroscopy (2DCES), we follow the changes in resonant energy, oscillator strength, and quantum decoherence of the AP and RP branches. Because of their different band structures, polarons in MoSe₂ and WSe₂ monolayers exhibit distinct quantum quantum dynamics and coupling mediated by valley index. Because of the large oscillator strength associated with quasi-particles, their intrinsic dephasing dynamics occur on sub-picosecond time scales. On the other hand, long-lived population and valley dynamics have been reported in previous experiments. We attribute such dynamics from a few hundred picoseconds to a few nanoseconds to dark-to-bright exciton conversion processes.

We gratefully acknowledge funding the Department of Energy, Office of Basic Energy Sciences under grant DE-SC0019398 and the Welch Foundation grant F-1662 for sample preparation. Collaborations are enabled by National Science Foundation via MRSEC grants DMR-1720595 and DMR-2308817.

SESSION QT01.03: Poster Session I: Light Matter Interactions in Quantum Materials
Session Chairs: Veronica Policht and Ursula Wurstbauer
Tuesday Afternoon, April 23, 2024
Flex Hall C, Level 2, Summit

5:00 PM QT01.03.01

Z-Scan Spectroscopy of BaFeGaO₄ [Mark Swift](#), [Orrin Clarke-Delgado](#), [Jordan Palmer](#), [Leroy Salary](#) and [Doyle Temple](#); Norfolk State University, United States

There have been reliable methods in the past for determining the nonlinear optical properties of materials (i.e. nonlinear absorption and nonlinear refraction) that can be used for multiple applications such as optical limiting, multi-photon polymerization, and optical switching. Of these methods, z-scan, which was developed by Eric Van Stryland [1] is found to be the optimal method for determining the third order optical susceptibility of a material.

The goal of my Masters project was to build a z-scan system for nonlinear optical measurements of materials fabricated in the NSF CREST Center for Research and Education in Quantum-leap Science (CREQS) at Norfolk State University (NSU). The optical system uses 100 fs pulses emitted at a repetition rate of 1 kHz from a Spectra Physics Solstice regenerative amplifier. These pulses at 800 nm are converted to visible wavelengths using a Spectra Physics TOPAS Prime optical parametric amplifier. The wavelength used in this study was 650nm. Pulses were detected using standard silicon photodiodes that were amplified and fed into an AD converter for input into the computer. Labview was used to monitor all detectors and control the position of the sample using a Newport Corp. precision translator.

The sample used for system development was a BaTiO₃ crystal grown at NSU. The data was analyzed using a Mathcad Prime computer model of the z-scan process that was written as part of this project. This semester this includes computer modeling the z-scan technique using the computer program Mathcad, to determine the experimental parameters for building the Z-Scan system.

Preliminary results are consistent with the z-scan model but further refinements in the optical and detection system are underway and will be reported at the conference.

- [1] M. Sheik-Bahae, A. A. Said, and E. W. Van Stryland, "High sensitivity single beam n₂ measurement," Opt. Lett., vol. 14, 955–957 (1989)

5:00 PM QT01.03.02

Laguerre-Gaussian Laser Beam Shaping for Control of Optical Angular Momentum in Ultrafast Laser Spectroscopy of Quantum Materials [Alecia Gullede](#) and [Doyle Temple](#); Norfolk State University, United States

The project's main goal is to develop an optical system for generating and controlling laser pulses with desired states of Optical Angular Momentum (OAM) needed for experiments that will study spin states in quantum materials. A beam of light has a linear momentum which depends on the spatial distribution of an Optical Field (E) where E represents a specific electric field distribution which in this case is a Gaussian distribution. The specific OAM that's being desired is modeled using a helical mode in which the wavefront of the momentum is shaped like a helix.

The first step was to use MathCAD Prime to model the 2D patterns or filter needed to transform the Gaussian beam into the desired OAM wavefront. The point of this is to control the energy distribution of the laser wavefront so when it interacts with a material so that we can model the interaction of electron spins in the material with the OAM wave using quantum mechanics.

Second, we implemented the 2D patterns calculated using Mathcad on a spatial light modulator (SLM). An ultrafast laser beam was expanded to a diameter of 3 cm and passed through the SLM resulting in an OAM that could be observed by interfering the OAM beam with a plane wave beam split off from the original laser beam. Finally, the patterns generated in the experiment were compared with the modeled patterns and the results shows promise for future use in experiments of spin states in materials.

Future work includes refining the model used to generate the patterns on the SLM and implementing the system in the study of quantum materials which is

the subject of my PhD thesis.

5:00 PM QT01.03.03

Nanocavity-Mediated Purcell Enhancement of Er in TiO₂ Thin Films Grown via Atomic Layer Deposition Cheng Ji^{1,2}, Michael Solomon^{1,2}, Gregory Grant^{1,2}, Koichi Tanaka^{1,2}, Muchuan Hua², Jianguo Wen², Alan Dibos² and Supratik Guha^{1,2}; ¹University of Chicago, United States; ²Argonne National Laboratory, United States

Trivalent erbium (Er³⁺), typically embedded as an atomic defect in the solid state, has widespread adoption as a dopant in telecommunications devices and shows promise as a spin-based quantum memory for quantum communication. In particular, its natural telecom C-band optical transition and spin-photon interface make it an ideal candidate for integration into existing optical fiber networks without the need for quantum frequency conversion. However, successful scaling requires a host material with few intrinsic nuclear spins, compatibility with semiconductor foundry processes, and straightforward integration with silicon photonics.

Here, we present Er-doped titanium dioxide (TiO₂) thin film growth on silicon substrates using a foundry-scalable atomic layer deposition (ALD) process with a wide range of doping control over the Er concentration (from sub-ppm to a few percent). Even though the as-grown films are amorphous, after oxygen annealing at 400C, the anatase TiO₂ lattice structures can form and the embedded Er ions exhibit the characteristic optical emission spectrum from anatase TiO₂. Critically, this growth with an annealing process introduces the poly-crystalline grains of a few hundred nanometers, while maintaining the low surface roughness required for nanophotonic integration. This ALD process also offers potential advantages over other methods, such as molecular beam deposition of doped films and implantation of erbium ions in undoped films, in terms of translation to industry because of lower cost and increased scalability.

Furthermore, our optical measurements revealed distinct optical transitions and a substantially narrower homogeneous linewidth upper bound for the characteristic emission peaks around 1532 nm for the annealed films. Additionally, the films with low Er concentration exhibited a natural optical lifetime greater than 1 ns, typical of Er in anatase TiO₂. Finally, we interface Er ensembles with high-quality factor Si nanophotonic cavities via evanescent coupling and demonstrate a large Purcell enhancement (~ 300) of their optical lifetime. This enhancement plays a crucial role in achieving more efficient and controlled light-matter interactions.

Overall, our findings demonstrate a low-temperature, non-destructive, and substrate-independent process for integrating Er-doped materials with silicon photonics. To emphasize, this ALD deposition with annealing at 400C process is CMOS compatible, which ensures industrial scalability and can potentially lead to many applications in the integrated silicon photonics industry. For example, at high doping densities, this platform can enable integrated photonic components such as on-chip amplifiers and lasers, while dilute concentrations can realize single ion quantum memories.

5:00 PM QT01.03.04

Phase Dependent Ultrafast Light-Matter Interaction in Two-Dimensional Silver Matthew Liu, Arpit Jain, Chengye Dong, Joshua Robinson and Kenneth Knappenberger; The Pennsylvania State University, United States

Atomic-level control of two-dimensional materials provides a novel platform for nanoscale photonics and optoelectronics. Two-dimensional silver (2D-Ag) is stabilized via silver intercalation in epitaxial graphene on SiC. Two phases of 2D-Ag, termed Ag₍₁₎ and the Ag₍₂₎, have been distinguished through 1) in-plane phonon shear modes: Ag₍₁₎ at 17 cm⁻¹, and Ag₍₂₎ exhibiting two modes at 66 and 92 cm⁻¹ and 2) linear extinction: Ag₍₁₎ with two absorption peaks centered around 460 and 650 nm, and Ag₍₂₎ with a single band centered around 570 nm. Control of graphene chemistry enables the formation of single phase 2D-Ag, allowing us to explore the inherent differences between Ag₍₁₎ and Ag₍₂₎. The symmetry breaking at the SiC/2D-Ag interface creates an out-of-plane axial dipole, resulting in strong nonlinear optical (NLO) responses. Second harmonic generation microscopy is implemented to investigate the symmetry and second order susceptibility $\chi^{(2)}$ of Ag₍₁₎ and Ag₍₂₎. Both phases exhibit point group symmetry $3m$, verifying the epitaxial growth of the Ag layer on the modified SiC surface. The $\chi^{(2)}$ of Ag₍₂₎ is orders of magnitude greater than that of Ag₍₁₎. The carrier dynamics of 2D-Ag is studied with near-degenerate transient absorption (TA) spectroscopy. Both phases are excited near the resonance frequencies of 2D-Ag, setting pump wavelengths at 575 and 650 nm. Rapid decays (~2 ps) following the initial bleach are observed in the time-resolved TA spectra for both phases. The difference in coherent oscillations between Ag₍₁₎ and Ag₍₂₎ is attributed to electron-phonon coupling corresponding to the in-plane shear mode of each phase as confirmed with correlated Raman spectroscopy. The results suggest that we are able to tailor the NLO properties and carrier dynamics of 2D-Ag through phase engineering at the atomic level.

SESSION QT01.04: Ultrafast Magnetism in Quantum Materials

Session Chairs: Alberto De la Torre and Ursula Wurstbauer

Wednesday Morning, April 24, 2024

Room 420, Level 4, Summit

8:45 AM QT01.04.01

Terahertz Field-Driven Nonlinear Magnonics in Antiferromagnets Zhuquan Zhang¹, Frank Gao², Edoardo Baldini² and Keith A. Nelson¹; ¹Massachusetts Institute of Technology, United States; ²The University of Texas at Austin, United States

Coherent excitations of magnetically ordered materials, referred to as spin waves and their quanta, magnons, have emerged as prominent candidates for interference-based signal processing technologies. Despite growing interest in manipulating magnonic states beyond thermodynamic equilibrium, elucidating and inducing coherent couplings between distinct magnon modes remains a formidable challenge. By developing and employing a novel two-dimensional (2D) terahertz (THz) polarimetry technique facilitated by single-shot detection, we successfully uncover correlated magnonic states at the sum and difference frequencies of the two modes, as well as a second-order magnon upconversion response. These findings not only expand the domain of nonlinear magnonics by incorporating antiferromagnets but also lay the groundwork for further advancements in the ultrafast control of magnetism.

9:00 AM QT01.04.02

Terahertz Parametric Amplification of a Coherent Magnon Mode Zhuquan Zhang and Keith A. Nelson; Massachusetts Institute of Technology, United States

Parametric amplification is a ubiquitous process in nonlinear systems where a specific parameter can be varied to amplify a coupled degree of freedom. In

condensed matter systems, parametric amplification of collective excitations allows one to study non-equilibrium order-parameter physics and potentially control material properties. In this study, we use a pair of intense terahertz (THz) pulses to sequentially excite two distinct coherent magnon modes in an antiferromagnet and find that the lower frequency magnon mode is amplified by driving the higher frequency mode. The nonlinear excitation pathway of this parametric downconversion process is confirmed by two-dimensional THz spectroscopy measurements. Our work provides crucial insights into nonlinear magnonics in antiferromagnets, extending the frontiers of spintronics and magnonics into the ultrafast nonlinear regime.

9:15 AM QT01.04.03

Light Driven Spontaneous Phonon Chirality and Magnetization in Paramagnets [Yafei Ren](#)¹, Mark Rudner² and Di Xiao²; ¹University of Delaware, United States; ²University of Washington, United States

Spin-phonon coupling enables the mutual manipulation of phonon and spin degrees of freedom in solids. In this study, we reveal the inherent nonlinearity within this coupling. Using a paramagnet as an illustration, we demonstrate the nonlinearity by unveiling spontaneous symmetry breaking under a periodic drive. The drive originates from linearly polarized light, respecting a mirror reflection symmetry of the system. However, this symmetry is spontaneously broken in the steady state, manifested in the emergence of coherent chiral phonons accompanied by a nonzero magnetization. We establish an analytical self-consistent equation to find the parameter regime where spontaneous symmetry breaking occurs. Furthermore, we estimate realistic parameters and discuss potential materials that could exhibit this behavior. Our findings shed light on the exploration of nonlinear phenomena in magnetic materials and present possibilities for on-demand control of magnetization.

9:30 AM QT01.04.04

Coherent Magnon-Exciton Coupling in Magnetic Semiconductors [Youn Jue Bae](#); Cornell University, United States

Two-dimensional (2D) magnetic semiconductors possess tightly bound excitons with large oscillator strength and long-lived coherent magnons due to the presence of bandgap and spatial confinement. While magnons and excitons are energetically mismatched by orders of magnitude, their coupling can lead to efficient optical access to spin information. The ability to overcome energy mismatch between magnon and exciton combined with optical excitation and detection renders 2D magnetic semiconductors attractive candidates for quantum transducers. In this presentation, I will discuss strong magneto-electronic and magnetoelastic coupling and implications of these couplings in the 2D van der Waals antiferromagnetic semiconductor, CrSBr. Because of both magnetic and semiconducting properties in CrSBr, excitons are highly sensitive to spin environments. Optical excitation of coherent spin waves can dynamically modulate the dielectric environment and excitons can sensitively detect these changes. I will also discuss strong magnetoelastic coupling in CrSBr that induces transient strain fields to selectively launch a narrow range of wavevector and frequency of both coherent magnons and acoustic phonons.

10:00 AM BREAK

10:30 AM QT01.04.05

Extreme Nonlinear Opto-Magnonic Effects in a Layered Magnetic Semiconductor [Geoff Diederich](#)¹, John W. Calker¹, Jordan Fonseca¹, Sinabu Pumelo¹, Youn Jue Bae², Daniel Chica³, Xiaoyang Zhu³, Xavier Roy³, Di Xiao^{1,4}, Yafei Ren⁴ and Xiaodong Xu^{1,4}; ¹University of Washington, United States; ²Cornell University, United States; ³Columbia University, United States; ⁴University of Delaware, United States

The nonlinear dynamics of collective excitations offer both intriguing fundamental phenomena and significant practical applications. A prime illustration is the field of nonlinear optics, where diverse frequency mixing processes are central to advancing photonic technology. Demonstration of these frequency mixing processes in magnons holds considerable potential for practical applications in magnonics, an emerging frontier of spintronics and an important platform for developing quantum transducers and wave-based computing beyond traditional paradigms. In this talk, I will demonstrate the optical generation and detection of abundant magnonic frequency mixing processes in the antiferromagnetic semiconductor CrSBr by employing above-gap pump pulses to launch coherent magnons and optically measuring them via strong magnon-exciton coupling. The data shows a series of magnon sidebands arising from high-harmonic generation and, when breaking the system symmetry, the mixing of discrete magnon modes to produce sum and difference frequency generation (SFG & DFG). Further, we demonstrate control over the DFG in CrSBr by rotating an external magnetic field to tune its frequency over a broad range. This tuning allows us to push the DFG mode into resonance with one of the fundamental magnon modes, where we can controllably induce parametric amplification. These findings herald the opening of a new domain in nonlinear opto-magnonic coupling, offering innovative functionalities for hybrid quantum magnonics.

10:45 AM QT01.04.06

Thermally Driven Ultrafast and Deterministic Reversal of Magnetization in Ferrimagnets upon Single Pulse Photo-Excitation [Unai Atxitia](#); Instituto de Ciencia de Materiales de Madrid, Spain

The discovery of an ultrafast and deterministic reversal of magnetization upon single pulse excitation¹ in GdFeCo, dubbed as all-optical switching (AOS), holds promise for faster and more energy-efficient data storage. Followed by this discovery, a growing body of research has unveiled other magnetic systems exhibiting AOS, and has triggered extensive theoretical and experimental research efforts.

Although several micro- and macroscopic models have reproduced AOS, complete understanding of the role of electrons, lattice and spin sublattices, and their mutual interactions has remained a challenge. The existing criteria for switching rely on the existence of two antiferromagnetically coupled magnetic sublattices showing a distinct dynamical response to femtosecond laser photoexcitation, which heats the electron system at elevated temperatures. This allows the two sublattices to decouple and to dissipate angular momentum on their own time scales. While in single-species ferromagnets such as 3d transition metals, relaxation of angular momentum occurs via dissipation into other degrees of freedom in two-sublattice magnets; additionally, relaxation can occur via angular momentum exchange between sublattices— exchange relaxation. By driving the spin system into a nonequilibrium state where exchange relaxation dominates, a nonequilibrium ultrafast reversal path opens. One of the most outstanding open questions is about the conditions or criteria for the onset of the exchange-dominated relaxation regime.

In this talk, I present a general theoretical framework for the description of single-pulse switching of ferrimagnets². I provide explicit expressions for the relativistic and exchange relaxation parameters as a function of microscopic material parameters. This allows to uncover the criteria for the onset of the exchange-dominated relaxation regime and switching. In particular, I demonstrate that the magnetization dynamics transits from a relativistic relaxation path to an exchange-dominated regime due to the strong enhancement of the exchange relaxation under highly non-equilibrium situations. We demonstrate that switching occurs when the sublattice magnetization reaches a threshold value. Notably, this threshold scales inversely proportional to the number of exchange-coupled nearest neighbours considered in the model, which in the simplest case is directly linked to the underlying lattice structure. This dependence is related to the enhancement of the non-equilibrium spin fluctuations, which opens the door for a more efficient reversal in magnetic 2D ferrimagnets³.

Notably, by using the general theoretical framework, we have been able to guide experiments of AOS in ferrimagnets. First, to approach terahertz frequency of write/erase cycles with a minimum pulse to pulse separation of 7 ps⁴. Second, to determine that the minimum size for AOS in GdFe alloys, induced by a nanoscale periodic excitation, is around 25 nm and that this fundamental limit is governed by ultrafast lateral heat diffusion of electrons and by the threshold for optical damage.

References:

- [1] T. A. Ostler et al. Nat. Comm. 3, 666 (2012)
- [2] F. Jakobs and U. Atxitia, Phys. Rev. Lett. 129, 037203 (2022)
- [3] J. A. Vélez, R. M. Otxoa, and U. Atxitia, Appl. Phys. Lett. 123, 112402 (2023)
- [4]. F. Steinbach et al. Appl. Phys. Lett. 120, 112406 (2022); F. Steinbach et al. in preparation

11:15 AM *QT01.04.07

Light Control of Magnetism in Quantum Materials [Andrea Caviglia](#); Université de Genève, Switzerland

We will discuss light control of magnetism in van der Waals antiferromagnets and oxide interfaces and surfaces, focusing on the role of orbital angular momentum. In the first example, we will consider the control of magnetic ordered states using light. We will show that light-driven phonons can be utilized to coherently manipulate macroscopic magnetic states. Intense mid-infrared electric field pulses, tuned to resonance with a phonon mode of the antiferromagnet DyFeO₃, induce ultrafast and long-living changes of the fundamental exchange interaction between rare-earth orbitals and transition metal spins. [1-3]. In the second example we will discuss the emission and detection of a nanometre-scale wavepacket of coherent propagating magnons in the antiferromagnetic oxide dysprosium orthoferrite using ultrashort pulses of light [4]. In the third example we consider experimentally the relative merits of electronic and vibrational excitations for the optical control of zero orbital angular momentum magnets, focusing on a limit case: the antiferromagnet manganese phosphorous trisulfide (MnPS₃), constituted by orbital singlet Mn²⁺ ions. We study the correlation of spins with two types of excitations within its band gap: a bound electron orbital excitation from the singlet orbital ground state of Mn²⁺ into an orbital triplet state, which causes coherent spin precession, and a vibrational excitation of the crystal field that causes thermal spin disorder [5].

- [1] J.R. Hortensius, et al npj Quantum Materials 5, 95 (2020).
- [2] D. Afanasiev, et al Nature Materials 20, 607 (2021).
- [3] D. Afanasiev, et al Science Advances (2021).
- [4] J.R. Hortensius, et al Nature Physics 17, 1001 (2021).
- [5] M. Matthiesen, et al Phys. Rev. Lett. 130, 076702 (2023)

11:45 AM QT01.04.08

Photoexcited Electron Spin Resonance Properties of CrSrBr Lovia Ofori¹, Eric Walter², Luis Martinez¹, Xavier Roy³ and [Srinivasa Rao Singamaneni](#)¹;
¹The University of Texas at El Paso, United States; ²Pacific Northwest National Laboratory, United States; ³Columbia University, United States

The recent discovery of two-dimensional (2D) magnets offers excellent opportunities for the exploration of low-dimensional magnetism and for the development of novel magnetoelectric, magneto-optic, and spintronic devices. CrSrBr is an air-stable antiferromagnetic semiconductor and gained a great deal of attention in the community for its novel magneto-optical properties. In this work, we present our recent findings on the electron spin resonance (ESR) properties of quasi-2D CrSrBr upon photoexcitation as a function of temperature and time across the magnetic phase transition. We noticed that ESR spectral properties (line shape, g-factor, line width, and signal intensity) are strongly modified upon photoexcitation which infers the tunability of magnetic interactions. Our work demonstrates the unique importance of employing photons in tuning the magnetic properties and interactions of 2D van der Waals magnets.

SESSION QT01.05: Light-Matter Coupling in Quantum Materials I
Session Chairs: Alberto De la Torre and Chiara Trovatello
Wednesday Afternoon, April 24, 2024
Room 420, Level 4, Summit

1:30 PM *QT01.05.01

Light-Matter Control of Quantum Materials [Michael Sentef](#)^{1,2}; ¹University of Bremen, Germany; ²MPSD Hamburg, Germany

Advances in time-resolved pump-probe spectroscopies have enabled us to follow the microscopic dynamics of quantum materials on femtosecond time scales. This gives us a glimpse into the inner workings of how complex, emergent functionalities of quantum many-body systems develop on ultrafast time scales or react to external forces. The ultimate dream of the community is to use light as a tuning parameter to create new states of matter on demand with designed properties and new functionalities, perhaps not achievable by other means. In this talk I will discuss recent progress in controlling and engineering properties of quantum materials through light-matter interaction [a,b]. I will highlight work on Floquet engineering — the creation of effective Hamiltonians by time-periodic drives — on sub-cycle time scales [1,2] combining theory and pump-probe experiments at the limits of energy and time resolution. I will then showcase recent theories on inducing superconductivity with light by employing enhanced light-matter interaction in the near-field involving polaritonic excitations [3,4].

- [a] A. de la Torre et al., Rev. Mod Phys. 93, 041002 (2021)
- [b] F. Schlawin, D. M. Kennes, M. A. Sentef, App. Phys. Rev. 9, 011312 (2022)
- [1] M. Schüler and M. A. Sentef, <https://doi.org/10.1016/j.elspec.2021.147121>
- [2] S. Ito et al., Nature 616, 696-701 (2023), <https://www.nature.com/articles/s41586-023-05850-x>
- [3] C. J. Eckhardt et al., arXiv:2303.02176
- [4] S. Chattopadhyay et al., arXiv:2303.15355

2:00 PM QT01.05.02

Mapping The Ultrafast Transient Response of Cavity-Embedded WS₂ Monolayers with High Angular Resolution Veronica Policht¹, Jose J. Fonseca Vega², Samuel W. LaGasse², Nicholas Proscia², Jeremy T. Robinson², Cory D. Cress² and Paul D. Cunningham²; ¹NRC Postdoc Associate residing at U.S. Naval Research Laboratory, United States; ²US Naval Research Laboratory, United States

The behavior of Exciton-Polaritons (EP), arising from strong coupling between the photon mode of a high-quality microcavity and excitonic states in an embedded semiconductor material, have been of intense recent interest¹. EPs of cavity-coupled excitons in Two-Dimensional Transition Metal Dichalcogenides (TMD) are of particular interest due to promising potential applications including low threshold lasing² as well as the opportunity to study many-body physics at ambient temperatures³. Compared to the excitons in bare TMDs, TMD EP states show enhanced oscillator strengths, longer of excitonic and valley coherence times⁴, and may also mediate mixing between otherwise distinct excitonic species⁵. Despite recent progress towards TMD EP-based technologies, there remains significant ambiguity in our understanding of EP dynamics at early times, due in part to the ultrafast timescales (~100s fs) of EP relaxation. Additionally, previous studies of ultrafast EP dynamics have had limited angular resolution due to the use of microscope objectives which average over a large angle range and therefore obscure the EP response.

We study the ultrafast response of a WS₂ monolayer embedded in a metallic cavity measured with a transient reflectance technique with high angular resolution achieved in part through the use of large-area WS₂ monolayer flakes. With this approach, we are able to incisively pump and probe different EP branches as a function of the in plane angular momentum, k , with $<1^\circ$ angular resolution. We generate pseudo-dispersion maps as a function of k and photon energy for a given pump-probe delay time. We use this new approach to provide insight on the source of various nonlinear EP dynamics reported for cavity-coupled TMDs in literature and in particular resolve clear differences in the WS₂-cavity response under different pump energy conditions.

1. Zhang, L. *et al.* Microcavity exciton polaritons. In *Semiconductors and Semimetals* (Vol. 105), Elsevier Inc (2020).
2. Paik, E. Y. *et al.* Interlayer exciton laser of extended spatial coherence in atomically thin heterostructures. *Nature* 576, 80–84 (2019).
3. Luo, Y. *et al.* Manipulating nonlinear exciton polaritons in an atomically-thin semiconductor with artificial potential landscapes. *Light: Science & Applications*, 12(1), 220 (2023).
4. Hu, F., & Fei, Z. Recent Progress on Exciton Polaritons in Layered Transition Metal Dichalcogenides. *Advanced Optical Materials*, 8(5), 1901003 (2020).
5. Latini, S. *et al.* Cavity Control of Excitons in Two-Dimensional Materials. *Nano Letters*, 19(6), 3473–3479 (2019).

2:15 PM QT01.05.03

First-Principles Machine-Learning Quantum Dynamics at 0K in SrTiO₃: Light-Induced Ultrafast Ferroelectric Transition Francesco Libbi¹, Lorenzo Monacelli², Anders Johansson¹ and Boris Kozinsky¹; ¹Harvard University, United States; ²EPFL, Switzerland

Low temperature nonequilibrium quantum dynamics in crystals is extremely challenging, and has not been possible to perform on materials of realistic complexity. In this work we develop a novel technique, the time-dependent self-consistent harmonic approximation (TDSCHA [1]), and use it to simulate the quantum dynamics in SrTiO₃ at 0K. We combine TDSCHA with state-of-the-art machine learning force fields to accelerate calculations by multiple orders of magnitude compared to first principles dynamics.

We study the light-induced ferroelectric transition in SrTiO₃, where nuclear quantum fluctuations play a major role in stabilizing the paraelectric phase at low temperatures.

Our approach allows for an unprecedented description of the light-induced ferroelectric transition due to the absence of ad-hoc parameters, paving the way to the development of next-generation ultrafast nonvolatile memories.

[1] Lorenzo Monacelli and Francesco Mauri, Time-dependent self-consistent harmonic approximation: Anharmonic nuclear quantum dynamics and time correlation functions, *Phys. Rev. B* tel:103104305 (2021)

2:30 PM BREAK

3:30 PM *QT01.05.04

Exploring Electronic Band Structure of 2D and Quantum Materials by Time- and Angle-Resolved Photoemission Spectroscopy and KISS Exfoliation Method Antonija Grubisic-Cabo; University of Groningen, Netherlands

The fundamental physics of solids, including two-dimensional (2D) materials, is inherently linked to their electronic band structure. The investigation of the electronic band structure is therefore of paramount significance for understanding, tailoring and discovering new states of matter. In the case of 2D materials, such as graphene and single layer transition metal dichalcogenides, control of the electronic structure can be achieved by altering their surroundings, as the electronic structure of 2D materials is highly sensitive to the surrounding environment. However, robust methods for the determination of the electronic structure are required to ascertain the effects of those alterations. In this talk, I will present time- and angle-resolved photoemission spectroscopy (TR-ARPES) as a technique for the electronic structure studies on the ultrafast, femtosecond scale [1], and as means to achieve control over 2D materials by light [2].

Furthermore, I will introduce an innovative preparation method for 2D materials, kinetic *in situ* single-layer (KISS) method [3]. Using KISS method, exfoliation of 2D materials can be performed directly in ultra-high vacuum, and large flakes of excellent crystallinity and purity can be obtained. Multiple semiconducting and metallic transition metal dichalcogenides were exfoliated onto Au, Ag and Ge substrates, showing the versatility of the technique, and characterised by ARPES. Importantly, the proposed method is straightforward, simple, and does not require any specialised equipment. This technique is ideally suited for the electronic structure research of air-sensitive 2D materials since the sample preparation process happens entirely in ultra-high vacuum.

References:

1. Majchrzak, P., Volckaert, K., Grubisic-Cabo, A., Biswas, D., Bianchi, M., Mahatha, S. K., Dendzik, M., Andreatta, F., Grönborg, S. G., Markovic, I., Riley, J. M., Johannsen, J. C., Lizzit, D., Bignardi, L., Lizzit, S., Cacho, C., Alexander, O., Matselyukh, D., Wyatt, A., Chapman, R. T., Springate, E., Grioni, M., Lauritsen, J. V., King, P. D. C., Sanders, C. E., Miwa, J. A., Hofmann, P. & Ulstrup, S., "Spectroscopic view of ultrafast charge carrier dynamics in single- and bilayer transition metal dichalcogenide semiconductors", *Journal of Electron Spectroscopy and Related Phenomena* 250, 147093 (2021)
2. Beyer, H., Rohde, G., Grubisic-Cabo, A., Stange, A., Jacobsen, T., Bignardi, L., Lizzit, D., Lacovig, P., Sanders, C.E., Lizzit, S., Rosnagel, K., Hofmann, P. & Bauer, M., "80% valley polarization of free carriers in singly oriented single-layer WS₂ on Au(111)", *Physical Review Letters* 123, 236802 (2019)
3. Grubisic-Cabo, A., Michiardi, M., Sanders, C.E., Bianchi, M., Curcio, D., Phuyal, D., Guo, Q. & Dendzik, M., "In situ exfoliation method of large-area 2D materials", *Advanced Science* 2301243 (2023)

4:00 PM QT01.05.05

Probing Exciton Dynamics and Dispersion in C₆₀ Using TR-ARPES [Rysa J. Greenwood](#)^{1,2}, Alexandra Tully^{1,2} and Sarah Burke^{1,2}; ¹Quantum Matter Institute, Canada; ²The University of British Columbia, Canada

In organic semiconductors, photoexcitation generates strongly bound excitons which recombine quickly (generally 10's – 100's of femtoseconds). To achieve efficient charge separation in these materials it is necessary to drive the dissociation of the exciton prior to recombination. This is one of the limiting factors for organic photovoltaic (OPV) devices today. The mechanisms that result in efficient charge separation in these materials are still not well understood. Therefore, to better advise device design it is necessary to gain a deeper understanding of both the dynamics and delocalization of excitonic states that occur post- photoexcitation with femtosecond resolution.

While the ultrafast response of organic semiconductors have been studied using all-optical techniques for a number of years [1], a lack of momentum resolution has limited understanding of their delocalization and symmetry. Time-resolved, angle-resolved photoemission spectroscopy (TR-ARPES) is a powerful technique that allows a user to visualize the energy-momentum landscape of a material and monitor how the material responds to photoexcitation with femtosecond resolution. Recent developments in TR-ARPES (or similar techniques) are enabling investigation of organic semiconductors because of its capability to directly map the momentum dependent dispersion of the excitonic states with high temporal resolution [2-4].

Here, I show the capability to probe the fate of excitonic states in C₆₀, a prototypical OPV material, using TR-ARPES pumped with 3.1eV light. We have been able to track the dynamics of the excitonic states which decay into each other with lifetimes ranging from hundreds of femtoseconds to tens of picoseconds. Constant energy contours show momentum-space structure of each state across the first Brillouin zone which disperses energy. With this improved angular resolution, we aim to access the extent of delocalization of the excitons in the C₆₀ lattice.

[1] Askat E. Jailaubekov, X-Y. Zhu, et al., Nat. Mater., **12**, 66-73 (2013)

[2] Sebastian Emmerich, Benamin Stadtmuller, Martin Aeschlimann et al., J. Phys. Chem., **124**, 23579-23587 (2020)

[3] Kiana Baumgartner, Markus Scholz, et al., Nat. Comms., **13**, 2741 (2022)

[4] Bennecke Wiebke, Mathias Stefan et al., arXiv:2303.13904v1 (2023)

4:15 PM QT01.05.06

Spatially Heterogenous Structural Dynamics of NdNiO₃ Thin Films [Jugal Mehta](#)¹, Scott Smith¹, Nanna Zhou Hagström¹, Nushrat Naushin¹, Spencer Jeppson¹, Yu-Hsing Cheng¹, Pooja Rao¹, Marc Zajac², Burak Guzelturk², Donald Walko², Tao Zhou², Haidan Wen², Martin V. Holt² and Roopali Kukreja²; ¹University of California, Davis, United States; ²Argonne National Laboratory, United States

Rare earth nickelates display insulator-metal transition which is accompanied by a magnetic transition, charge ordering, and a crystal structure change. Laser-excitation drives the transition at ultrafast timescales providing an avenue to understand the role of coupled transitions in causing the transition. We utilized time-resolved x-ray diffraction to study the structural dynamics of epitaxial NNO thin film by observing the photoinduced changes in the (002) Bragg peak. The out of plane lattice parameter contracts for low fluences and expands for high fluences after laser excitation. A thermal model explains experimental trends revealing the potential for controlling structural dynamics via heteroepitaxial strain. Similar recovery timescales of structural and magnetism dynamics indicate a strong magneto-structural coupling is prevalent in the ultrafast recovery process. The change in integrated intensity and FWHM of the (002) peak indicate photoinduced domain dynamics which corroborates an ultrafast conductivity study proposing recovery via nucleating and growth in NNO. We present direct evidence of phase separation using time-resolved nanodiffraction. Spatiotemporally resolved characterization clearly shows the spatial heterogeneity of the structural dynamics in nickelates.

4:30 PM *QT01.05.07

Dynamic Control of Macroscopic Phases via Thermal Quench in 1T-TaS₂ [Alberto De la Torre](#); Northeastern University, United States

In materials with competing order parameters, quenching across a phase transition can lead to the system being trapped in a long-lived metastable phase, even if it is not the global free-energy minimum. Examples of this phenomenology can be found over multiple energies and length scales - from the evolution of the known Universe to supercooled liquids [1]. 1T-TaS₂, a layered dichalcogenide, is a unique platform for studying dynamic phase transitions in quantum materials [2]. Upon quenching 1T-TaS₂ after excitation with an ultrafast laser pulse, a low-temperature metallic metastable phase (H-CDW) emerges [3], which is different from any of the charge density wave (CDW) phases characterizing its thermodynamic phase diagram. I will show that a new metastable insulating phase with similar scattering signatures to the H-CDW [4] can be stabilized by intermediate quenching rates [5]. I will discuss the implications of this new phase in the controversy surrounding the presence of Mott physics and the role of c-axis correlations [6] in the equilibrium ground state of 1T-TaS₂.

[1] Zhiyuan Sun and Andrew J. Millis Phys. Rev. X **10**, 021028 (2020)

[2] B. Sipoš et al., Nat. Mat. **7**, 960 (2008)

[3] L. Stojchesvka et al., Science **344**, 177 (2014)

[4] Stahl et al., Nat. Commun. **11**, 1247 (2020)

[5] AdIT et al., in preparation

[6] S-H Lee et al., PRL **122**, 106404 (2019)

SESSION QT01.06: Poster Session II: Applications of Quantum Materials

Session Chairs: Youn Jue Bae and Nicolò Maccaferri

Wednesday Afternoon, April 24, 2024

Flex Hall C, Level 2, Summit

5:00 PM QT01.06.01

A Molecular Dynamics of Photo-Excited Ligand Exchange Dynamics in Tungsten-Complexes Kamrun N. Keya¹, Yulun Han², Wenjie Xia¹, Bakhtiyor Rasulev², Svetlana V. Kilina², Wenfang Sun³ and [Dmitri Kilin](#)²; ¹Iowa State University, United States; ²North Dakota State University, United States; ³The University of Alabama, United States

Transition-metal complexes (TMCs) play a pivotal role in areas such as optoelectronics, solar energy conversion, and biomedical applications. In this

study, we delve deep into the dynamics of ligand exchange reactions in six distinct $W(CO)_4(bpy)$ complexes using time-dependent excited-state molecular dynamics (TDESMD) based on Rabi oscillations between ground and excited states under optical irradiation. Our objective is to explore the mechanism of how the photo-induced charge transfer dynamics facilitates the mechanistic pathway in which a mix of $W(CO)_6$ and bipyridine (bpy) transforms into a $W(CO)_4(bpy)$ complex. Preliminary findings suggest that the photoreactions are facilitated by excited states corresponding more closely to ligand-to-metal charge transfer (LMCT) character. It is this photoactivation, particularly of the LMCT type, that weakens the W-C bonds, thereby facilitating the subsequent dissociation of CO ligands. Consequently, this gives rise to the reactive $W(CO)_5$ radical, which then establishes a coordination bond with the nitrogen of the bpy ligand. At the next stage, second CO ligand desorbs allowing for formation of two stable coordination bonds between tungsten and bpy. Several approaches have been committed to explore the possibility of the subsequent formation of $W(CO)_2(bpy)_2$ and $W(bpy)_3$ complexes. Our study enables the exploration of the pathways of photoactivated reaction dynamics and assessment of the intermediates formed during the reaction and the transition states along this path. Such insights are instrumental in interpreting synthetic endeavors, aiming for an efficient exploration of near-infrared (NIR) emitters composed of earth-abundant metals and a variety of organic ligands.

BR, SK, WS acknowledge support of DOE DE-SC0022239 for study of near-infrared emissive metal-organic complexes. KNK, YH, DK thanks NSF-1944921 for the support of excited state methods development.

[1] J. Phys. Chem. Lett. **2022**, 13 (39), 9210-9220. DOI: 10.1021/acs.jpcclett.2c02115.

5:00 PM QT01.06.02

Wearable Health Monitoring with Ultrathin Self-Powered Heavy-Metal-Free Cu-In-Se Quantum Dot-Photodetectors Jae Hong Jang¹, Shi Li², Jiwoong Yang² and Moon Kee Choi¹; ¹Ulsan National Institute of Science and Technology, Korea (the Republic of); ²Daegu Gyeongbuk Institute of Science and Technology, Korea (the Republic of)

Photodetectors (PDs), that transform light signals into electronic signals, are essential components in wearable electronics, finding wide-ranging applications in biological imaging, optical communication, and health monitoring. In particular, wearable health monitoring devices utilizing photoplethysmography (PPG) technology, which employs a light source and PDs to measure blood circulation variations, offer significant potential for non-invasive, cost-effective, and continuous real-time monitoring of vital signs and cardiac function. To enable effective real-time vital sign monitoring, PDs must exhibit high specific detectivity (D^*), rapid response time, and high mechanical deformability. Consequently, the development of mechanically deformable PDs with superior device performance and response times has been a paramount objective. While prior research advanced flexible and stretchable PDs, challenges endure, including limited deformability with thick inorganic films and reduced performance in organic PDs. Furthermore, most photodetectors rely on external power sources to generate photocurrent, restricting the evolution of point-of-care type wearable systems capable of independent, wireless, and sustainable operation.

Colloidal quantum dots (QDs) are highlighted for PDs, boasting size-tunable electrical and optical properties, high photo-absorption coefficients, narrow emission and absorption bandwidth, and robust photo- and air-stability. Nevertheless, the practical application of QD-PDs in wearable electronics faces challenges. Existing QD-PDs exhibit limited mechanical deformability due to their relatively thick light absorption layers (typically several hundreds of nanometers). Furthermore, the conventional use of toxic heavy-metal-containing QDs, including lead, mercury, and cadmium chalcogenide QDs, raises concerns about impact on human health.

Recently, heavy-metal-free Cu-In-Se (CISE) QDs been highlighted as a promising material for eco-friendly optoelectronic devices. CISE QDs offer advantageous characteristics, including a direct-bandgap structure, high absorption coefficient, broad absorption range spanning from ultra-violet to near-infrared, stable phase structure, cost-effectiveness, and nontoxicity. However, a dearth of research exists regarding the selection of optimal charge transport materials, specifically for the electron transport layer (ETL) and hole transport layer (HTL) materials, tailored to CISE QD-PDs. The electron mobility of typical ETLs is generally three orders of magnitude higher than that of general HTLs, causing the charge imbalance and recombination of photogenerated electrons and holes, leading to poor device performance. Therefore, the development of high-quality HTLs is essential to achieve high-performance CISE QD-PDs.

In this study, we present ultrathin self-powered CISE QD-PDs for the wearable PPG-based health monitoring system. We constructed PDs with CISE QDs capped with iodide ions as ultrathin light absorption layers (~40 nm), *p*-type colloidal MoS₂ nanosheets blended with poly(3,4-ethylenedioxythiophene):poly(styrenesulfonate) as HTLs, and *n*-type ZnO nanoparticles as ETLs. Fabricated ultrathin PDs (~120 nm except electrodes) feature high D^* of 2.10×10^{12} Jones, linear dynamic range of 102 dB, and spectral sensitive region from 250 to 1,050 nm at 0 V bias. These PDs utilize built-in potential created through the photovoltaic effect, facilitating the efficient separation and transfer of photogenerated electron-hole pairs without requiring an external power source. Their performance rivals that of conventional QD-PDs employing thick Pb-chalcogenide QD layers and typical self-powered PDs from previous researches. Furthermore, PDs fabricated on flexible substrates exhibit outstanding mechanical flexibility and device performance, surpassing that of flexible PDs employing alternative semiconductor materials. This realize skin-attachable PPG sensors capable of real-time vital sign monitoring.

SESSION QT01.07: 2D Quantum Light Sources
Session Chairs: Nicolò Maccaferri and Ursula Würstbauer
Thursday Morning, April 25, 2024
Room 420, Level 4, Summit

9:00 AM *QT01.07.01

Ultrafast Dynamics of Quantum Emitters in hBN Steffen Michaelis de Vasconcellos; University of Münster, Germany

Key challenges in the development of quantum networks and communications include the availability of efficient and robust quantum light sources and their optical coherent control. Recently, single-photon sources in atomically thin transition metal dichalcogenides and other 2D van der Waals materials joined the family of solid-state quantum light emitters [1]. In the 2D insulator hexagonal boron nitride (hBN), optically active states in the band gap have been discovered, efficiently emitting single photons even at room temperature. The wide variability of the emission wavelength, narrow emission lines and tunability makes this emitter particularly compelling for quantum sensing and wavelength division multiplexed quantum communications.

The quantum emitters in hBN can be found in commercially available nanocrystals, making them ideal for creating large arrays of single-photon emitters using the capillary assembly technique with high positioning yields up to 95% [2]. This method opens the way for systematic optical characterization of easily addressable single-photon emitters and offers the possibility of deterministically fabricating photonic nanostructures around individual emitters. Notably, photonic microstructures and components can be created using 3D direct-laser writing. This technique allows the printing of polymer microlenses in various shapes to effectively collect and direct light from embedded emitters. However, the auto-fluorescence of commercially available photoresins limits the application in quantum optics. To address this issue, we have developed an ultra-low-fluorescence photoresin for 3D direct laser writing. We demonstrate the 3D-printing of microlenses that effectively collect quantum light emission from the emitters and collimate the single photons into a low-

divergent beam [3].

Furthermore, we demonstrate the coherent state manipulation of a single hBN quantum emitter with ultrafast laser pulses using a double-pulse experiment [4]. The coherence properties of the two-level system are detected by measuring the emitted photons as a function of the pulse delay. Our joint experiment-theory study reveals the effects of different sources of spectral jitter on the ultrafast coherence dynamics. We also demonstrate that coherent control can not only be exerted resonantly on the optical transition but also phonon-assisted, provides profound insight into the internal phonon quantum dynamics. We find that increased decoherence rates in optical phonons are due to dephasing processes of the phonon states, partly due to their anharmonic decay. Similarly, dephasing induced by acoustic phonon generation results in a rapid decrease in coherence when propagating phonon wave packets are emitted. Our experiments on phonon-assisted coherent control of individual hBN color centers are a significant step towards hybrid quantum technologies that combine electronic and phononic excitations.

References

- [1] S. Michaelis de Vasconcellos et al., *physica status solidi (b)* 259, 2100566 (2022)
- [2] J. A. Preuß et al., *2D Materials* 8 035005 (2021)
- [3] J. A. Preuß et al., *Nano Letters* 23, 407 (2023).
- [4] J. A. Preuß et al., *Optica* 9, 522 (2022)

9:30 AM BREAK

SESSION QT01.08: Ultrafast Dynamics in 2D Materials II
Session Chairs: Chiara Trovatiello and Ursula Wurstbauer
Thursday Morning, April 25, 2024
Room 420, Level 4, Summit

10:00 AM *QT01.08.01

Controlling The Ultrafast Optical Properties of Graphene with Ionic Liquid Gating [Eva A. A. Pogna](#); CNR-IFN, Italy

Single-layer graphene is endowed with broadband optical absorption, largely dependent on the Fermi energy. Ionic liquid gating allows to tune the Fermi energy to hundreds of eV and control its optical response in the near-infrared and THz ranges. Transient absorption measurements in the near-infrared reveal that also the out-of-equilibrium optical properties can be largely tuned using ionic gating. By varying the Fermi energy via electrostatic gating, the sign of the transient optical response of graphene is switched while the recovery dynamics significantly slows down due to the quenching of the relaxation of the hot electrons through the emission of optical phonons. The electrostatic control of the recovery dynamics and of the sign of differential transmission, opens intriguing perspectives for applications of graphene as a tunable saturable absorber for generation of tunable near-infrared pulses or alternatively as optical limiter or logic gate. Moreover, ionic gating is exploited to conceive compact optoelectronic devices acting in the THz range as amplitude modulators, saturable absorber mirrors and frequency tuners. The large control of the THz optical response is used to compensate the cavity dispersion of a multimode THz quantum cascade laser and induced stable operation as frequency comb for metrological applications.

10:30 AM QT01.08.02

Ultrafast Exciton Dynamics in 2D Van der Waals Nanostructures: Probing The Hot Exciton Relaxation of Size-Controlled & Well-Dispersed Graphene Nanoflakes [Elsa Cassette](#)¹, [Sébastien Quistebert](#)¹, [Daniel Medina-Lopez](#)², [Stéphane Campidelli](#)² and [Jean-Sébastien Lauret](#)¹; ¹LuMin - Université Paris-Saclay, ENS Paris-Saclay, CNRS, CentraleSupélec, France; ²NIMBE/LICSEN - Université Paris-Saclay, CEA, CNRS, France

Graphene nanostructures, such as graphene quantum dots (G-QDs), graphene nanoribbons (G-NRs) and carbon nanotubes (C-NTs), combine the unique mechanical and electrical transport properties of sp²- hybridized carbon materials and the optical properties of direct semiconductors provided by the optical gap resulting from the reduction of dimensionality. Among them, the recent developments within the well-known synthesis of G-QDs through bottom-up approach [1] have led to exceptionally well-controlled nanostructures in terms of size, shape and dispersion [2]. The resulting graphene nanoflakes provide tunable emission in the red range, with fluorescence quantum yield close to one. Furthermore, these nanostructures have revealed to be promising stable emitters of single photons, as shown in our laboratory [2-5].

Here we use transient absorption of 30 fs temporal resolution with polarization-controlled configuration to probe the hot exciton relaxation (internal conversion, S_n→S₁) in rectangular G-QDs of various lateral lengths. The nanoflakes are composed of exactly 96, 114 and 132 conjugated carbons (respectively 2.30, 2.71 and 3.11 nm). While the ultrafast electronic dynamics in graphene nanostructures are often being blurred by large broadband photo-induced absorption signals [6-8] (in particular involving triplet states, T₁→T_n), here the suppressed aggregation in the studied graphene nanoflakes allows a clear observation and identification of the discrete ground state bleaching (GSB) and photo-induced emission (PIE) signals.

We selectively excite the different samples at the second optically active electronic transition and, thought the appearance of a PIE signal at the energy corresponding to the bandedge and red-shifted vibrational replica (*i.e.* at the position of the steady-state photoluminescence peaks), the dynamics of relaxation were unveiled. The resulting relaxation times range from 100 fs to 175 fs. These results allowed to discuss the mechanism of relaxation, with the effect of the length of the graphene nanoflakes and of the fluence excitation [[Quistebert et al.](#), in preparation].

References:

- [1] A. Narita, X.-Y. Wang, X. Feng, K. Müllen. *Chem. Soc. Rev.* 44, 6616 (2015).
- [2] D. Medina-Lopez, T. Liu, S. Osella, H. Levy-Falk, N. Rolland, C. Elias, G. Huber, P. Ticku, L. Rondin, B. Jousselme, D. Beljonne, J.-S. Lauret, S. Campidelli. *Nat. Commun.* 14:4728 (2023).
- [3] T. Liu, B. Carles, C. Elias, C. Tonnelé, D. Medina-Lopez, A. Narita, Y. Chassagneux, C. Voisin, D. Beljonne, S. Campidelli, L. Rondin, J.-S. Lauret. *J. Chem. Phys.* 156, 104302 (2022)
- [4] T. Liu, C. Tonnelé, S. Zhao, L. Rondin, C. Elias, D. Medina-Lopez, H. Okuno, A. Narita, Y. Chassagneux, C. Voisin, S. Campidelli, D. Beljonne, J.-S. Lauret. *Nanoscale* 14, 3826 (2022).
- [5] S. Zhao, J. Lavie, L. Rondin, L. Orcin-Chaix, C. Diederichs, P. Roussignol, Y. Chassagneux, C. Voisin, K. Müllen, A. Narita, S. Campidelli, J.-S. Lauret. *Nat. Commun.* 9 :3470 (2018).
- [6] M.L. Mueller, X. Yan, B. Dragnea, L.s. Li. *Nano Lett.* 11, 56-60 (2011).
- [7] D. Sebastian, A. Pallikkara, H. Bhatt, H.N. Ghosh, K. Ramakrishnan. *J. Phys. Chem. C* 126, 11182-11192 (2022).
- [8] M. Reale, A. Sciortino, M. Cannas, E. Maços, A.H.G. David, C.M. Cruz, A.G. Campana, F. Messina. *Materials* 16, 835 (2023).

10:45 AM QT01.08.03

Hot Carrier Cooling and Trapping in Atomically Thin WS₂ Probed by Three-Pulse Femtosecond Spectroscopy [Tong Wang](#)¹, Tom Hopper^{1,2} and Artem Bakulin¹, ¹Imperial College London, United Kingdom; ²Stanford University, United States

Transition metal dichalcogenides (TMDs) have shown outstanding semiconducting properties which make them promising materials for next-generation optoelectronic and electronic devices. These properties are imparted by fundamental carrier-carrier and carrier-phonon interactions that are foundational to hot carrier cooling. Recent transient absorption studies have reported ultrafast timescales for carrier cooling in TMDs that can be slowed at high excitation densities via a hot-phonon bottleneck (HPB), and discussed these findings in the light of optoelectronic applications. However, quantitative descriptions of the HPB in TMDs, including details of the electron-lattice coupling, and how cooling is affected by the redistribution of energy between carriers, are still lacking. Here, we use femtosecond pump-push-probe spectroscopy as a single approach to systematically characterize the scattering of hot carriers with optical phonons, cold carriers, and defects in a benchmark TMD monolayer of polycrystalline WS₂. By controlling the interband pump and intraband push excitations, we observe, in real-time (i) an extremely rapid ‘intrinsic’ cooling rate of $\sim 18 \pm 2.7$ eV/ps, which can be slowed with increasing hot carrier density, (ii) the deprecation of this HPB at elevated cold carrier densities, exposing a previously undisclosed role of the carrier-carrier interactions in mediating cooling, and (iii) the interception of high energy hot carriers on the sub-picosecond timescale by lattice defects, which may account for the lower photoluminescence yield of TMDs under above band-gap excitation condition.

11:00 AM *QT01.08.04

Revealing Ultrafast Phonon-Mediated Inter-Valley Scattering by Simulating Transient Absorption and High Harmonic Spectroscopies [Aaron Kelly](#); Max Planck Institute, Germany

Processes involving ultrafast laser driven electron-phonon dynamics play a fundamental role in the response of quantum systems in a growing number of situations of interest, as evidenced by phenomena such as strongly driven phase transitions and light driven engineering of material properties. In this presentation we will discuss how these processes can be captured in real-time from a computational perspective, focusing on simulating the transient absorption spectra and high harmonic generation signals associated with processes such as valley selective excitation under strong driving, and phonon-mediated intra-band charge carrier relaxation. We will show that the multi-trajectory Ehrenfest dynamics approach, implemented in combination with real-time time-dependent density functional theory and tight-binding models, offers a simple and efficient method to study ultrafast electron-phonon coupled phenomena in solids under diverse pump-probe regimes which can be easily incorporated into the majority of real-time *ab-initio* software packages.

11:30 AM +QT01.08.05

Quantum Floquet Engineering with an Exactly Solvable Tight-Binding Chain in a Cavity [Dante Kennes](#); RWTH Aachen University, Germany

Recent experimental advances enable the manipulation of quantum matter by exploiting the quantum nature of light. However, paradigmatic exactly solvable models, such as the Dicke, Rabi or Jaynes-Cummings models for quantum-optical systems, are scarce in the corresponding solid-state, quantum materials context. Focusing on the long-wavelength limit for the light, here, we provide such an exactly solvable model given by a tight-binding chain coupled to a single cavity mode via a quantized version of the Peierls substitution. We show that perturbative expansions in the light-matter coupling have to be taken with care and can easily lead to a false superradiant phase.

Furthermore, we provide an analytical expression for the groundstate in the thermodynamic limit, in which the cavity photons are squeezed by the light-matter coupling. In addition, we derive analytical expressions for the electronic single-particle spectral function and optical conductivity. We unveil quantum Floquet engineering signatures in these dynamical response functions, such as analogs to dynamical localization and replica side bands, complementing paradigmatic classical Floquet engineering results. Strikingly, the Drude weight in the optical conductivity of the electrons is partially suppressed by the presence of a single cavity mode through an induced electron-electron interaction.

SESSION QT01.09: Ultrafast Dynamics in 2D Heterostructures

Session Chair: Nicolò Maccaferri

Friday Morning, April 26, 2024

Room 420, Level 4, Summit

8:30 AM QT01.09.01

Exciton Multiplication and Dynamics in Two-Dimensional Transition-Metal Dichalcogenides [Suman Kalyan Pal](#), Ashish Soni and Bhuvan Upadhyay; Indian Institute of Technology Mandi, India

Two-dimensional (2D) transition-metal dichalcogenides (TMDs) have attracted considerable attention due to their notable optical, electrical, and mechanical characteristics [1]. Their potential for investigating many-body interactions at room temperature is rooted in the robust Coulomb interaction and diminished screening effects [2]. In recent years, ultrafast optical techniques have been employed to directly examine the many-body processes in 2D TMDs [3]. Our research has showcased effective multiple exciton generation (MEG) in monolayer MoS₂, discerned through the tracking of carrier dynamics at varying excitation photon energies. Our findings not only disclosed a low threshold energy for MEG but also highlighted a high MEG efficiency (86%) [4]. Furthermore, I will delve into the impact of vanadium (V) doping on the electronic structure and carrier dynamics of monolayer MoS₂ [5]. Our observations indicate that carrier recombination decelerates in V-doped samples, leading to prolonged charge carrier survival. To conclude the discussion, I will emphasize a distinctive aspect of our research involving the efficient dissociation of excitons at the interface of a WS₂/2D perovskite heterostructure. The electron transfer from WS₂ results in the formation of a longer-lived interlayer exciton in this van der Waals heterostructure. The experimental insights gleaned from our research bear significant implications for advancing mechanically flexible and highly efficient next-generation solar cells and photodetectors.

References

[1] Ermolaev G A, Grudin D V, Stebunov Y V et al., Giant optical anisotropy in transition metal dichalcogenides for next-generation photonics “*Nature Communications*” **854** 12 (2021).

[2] Lin Y, Ling X, Yu L, et al., Dielectric Screening of Excitons and Trions in Single-Layer MoS₂ “*Nano Letters*” **14** 5569-76 (2014).

[3] Soni A, Kushavah D, Lu L-S et al., Ultrafast Exciton Trapping and Exciton-Exciton Annihilation in Large-Area CVD-Grown Monolayer WS₂ “*The Journal of Physical Chemistry C*” **125** 23880-8 (2021).

[4] Soni A, Kushavah D, Lu L-S, et al. Efficient Multiple Exciton Generation in Monolayer MoS₂ “*The Journal of Physical Chemistry Letters*” **14** 2965-72 (2023).

[5] Upadhyay B, Sharma R, Maity D et al. Ultrafast carrier dynamics in vanadium doped MoS₂ alloys “*Nanoscale*” **15** 16344 (2023).

8:45 AM QT01.09.02

Microscopic and Spectroscopic Study on the Superfluorescence of Quasi-2D Perovskite [Aaron Wildenborg](#)¹, Ryan Munter¹, Francisco Freire Fernandez², Teri W. Odom² and Jae Yong Suh¹; ¹Michigan Technological University, United States; ²Northwestern University, United States

Halide perovskites have seen a surge in interest in optoelectronic devices beyond their uses in solar cells and batteries. By using buffer molecules in fabrication, it is possible to inhibit the growth of perovskites along one dimension, creating a few layers thick film called quasi-2D perovskite. With a sufficiently high excitation power at room temperature, quasi-2D perovskite exhibits the phenomenon of superfluorescence in which emitters undergo cooperative spontaneous emission. Our quasi-2D perovskite thin-films have shown pulsed emission of enhanced decay rate, an indicator of superfluorescence. Moreover, we perform scanning transmission electron microscopy on the samples to corroborate the quadratic dependence of output intensity on the number of emitters. We find that the formation of a superlattice plays a significant role in generating the superfluorescence of quasi-2D perovskite.

9:00 AM *QT01.09.03

Bidirectional Phonon Emission in Two-Dimensional Heterostructures triggered by Ultrafast Charge Transfer [Archana Raja](#); Lawrence Berkeley National Laboratory, United States

Atomically thin van der Waals crystals like graphene and transition metal dichalcogenides allow for the creation of arbitrary, atomically precise heterostructures simply by stacking disparate monolayers without the constraints of covalent bonding or epitaxy. While these are commonly described as nanoscale LEGO blocks, many intriguing phenomena have been discovered in the recent past that go beyond this simple analogy. In this talk, I will describe how we use ultrafast electron diffraction to uncover the role of layer-hybridized electronic states as a powerful route to control ultrafast energy transport across atomic junctions [1]. We measure the simultaneous heating of both WSe₂ and WS₂ in a WSe₂/WS₂ heterobilayer on a picosecond timescale after selective excitation of the WSe₂ monolayer. This observation cannot be explained purely by phonon transport across the interface. Through first-principles calculations, we identify electronic states hybridized across the heterostructure that allow phonon-assisted interlayer transfer of photoexcited electrons, which leads to bidirectional phonon emission and simultaneous heating of both the layers.

[1] Sood, A., Haber, J.B. et al. Bidirectional phonon emission in two-dimensional heterostructures triggered by ultrafast charge transfer. *Nat. Nanotechnol.* **18**, 29–35 (2023)

9:30 AM BREAK

SESSION QT01.10: Polaritonics in Quantum Materials

Session Chair: Nicolò Maccaferri

Friday Morning, April 26, 2024

Room 420, Level 4, Summit

10:00 AM QT01.10.01

Unveiling The Efficient Charge Transfer Cascade in Band-Tailored Two-Dimensional WS₂/ Ni Doped CsPbI₃ Heterosystem [Himanshu Bhatt](#)¹, Tanmay Goswami¹ and Hirenra N. Ghosh²; ¹Institute of Nano Science and Technology (INST), Mohali, India; ²National Institute of Science Education and Research (NISER), India

Band structure modulation in heterostructure has emerged as a highly effective strategy for fabricating advanced optoelectronic devices. In this work, we have designed a CsPbI₃-WS₂ (CPI-WS₂) heterosystem and employed transient absorption (TA) spectroscopy to gather a comprehensive understanding of charge carrier dynamics. TA study demonstrated the charge delocalization at the interface of CPI and WS₂. Due to the quasi-type II integration of CPI and WS₂, the charge separation in this heterosystem is not very effective, which would restrict their utilization in photovoltaic applications. To further improve the charge separation, Ni atoms were introduced as dopants into CPI nanocrystals. Ultraviolet electron spectroscopy (UPS) suggested that the homovalent doping elevated the band positions of CPI and resulted in a type II band configuration with WS₂. TA analysis revealed the spontaneous carrier's separation in band-modulated heterosystem due to the isolation of electrons and holes in discrete semiconductors. These spectroscopy findings were correlated with the optoelectronic performance of heterostructure-based devices. Enhanced charge separation within a doped heterosystem leads to superior optoelectronic performance compared to undoped heterosystems. Our findings showed that the band level of engineering encourages the segregation of charge carriers at the hetero-interface, which would be extremely impactful for designing heterostructure-based optoelectronic systems.

10:15 AM *QT01.10.02

Light Control of Charge Transport and Phase Transitions [Sheng Meng](#); Chinese Academy of Sciences, China

Photoexcitation is a powerful means in distinguishing different interactions and manipulating the properties of matter, especially for charge transport and phase transitions in complex quantum systems.

Here we show that laser-controlled coherent phonon excitation enables orders of magnitude enhancement of carrier mobility via accelerating polaron transport in a prototypical material, lithium peroxide (Li₂O₂). The selective excitation of specific phonon modes, whose vibrational pattern directly overlap with the polaronic lattice deformation, can remarkably reduce the energy barrier for polaron hopping. The strong nonadiabatic couplings between the electronic and ionic subsystem play a key role in triggering charge transport. These results extend our understanding of charge transport dynamics to the nonequilibrium regime and allow for optoelectronic devices with ultrahigh on-off ratio and ultrafast responsibility competitive with those of state-of-the-art devices. We also investigate photoexcitation induced ultrafast phase-transition dynamics in two-dimensional materials, where we identify a laser-induced collective pathway from 2H phase to 1T phase in MoTe₂ that is significantly different from thermal phase transitions. Our results provide insights from a new perspective on the coherent electron and lattice quantum dynamics in materials upon photoexcitation.

References:

H.M. Wang, X.B. Liu, S.Q. Hu, D.Q. Chen, Q. Chen, C. Zhang, M.X. Guan, S. Meng. Giant acceleration of polaron transport by ultrafast laser-induced coherent phonons. *Science Advances* **9**, eadg3833 (2023).

R.J. Zhao, P.W. You, S. Meng, Ring polymer molecular dynamics with electronic transitions, *Phys. Rev. Lett.* **130**, 166401 (2023).

C.Y. Wang, X.B. Liu, Q. Chen, D.Q. Chen, Y.X. Wang, S. Meng. Coherent-Phonon-Driven Intervalley Scattering and Rabi Oscillation in Multivalley 2D Materials. *Phys. Rev. Lett.* 131, 066401 (2023).
M.X. Guan, X.B. Liu, D.Q. Chen, X.Y. Li, Y.P. Qi, Q. Yang, P.W. You, S. Meng. Optical control of multi-stage phase transition via phonon couplings in MoTe₂. *Phys. Rev. Lett.* 128, 015702 (2022).
J.Y. Xu, D.Q. Chen, S. Meng. Decoupled ultrafast electronic and structural phase transitions in photoexcited monoclinic VO₂. *Science Advances* 8, eadd2392 (2022).

10:45 AM QT01.10.03

Light-Matter Coupling with Bound States in The Continuum in Van der Waals Metasurfaces [Luca Sortino](#)¹, Stefan A. Maier^{2,3} and Andreas Tittl¹; ¹Ludwig-Maximilians-University Munich, Germany; ²Monash University, Australia; ³Imperial College London, United Kingdom

The extraordinary properties of layered van der Waals (vdW) materials, like hexagonal boron nitride (hBN) and Transition Metal Dichalcogenides (TMDCs), make them an appealing platform to investigate and engineer light-matter interactions at the nanoscale. When reduced to atomically thin monolayers, they display attractive characteristics, such as strongly bound excitons and optically addressable spin defects, while in their bulk form they exhibit significant optical anisotropy and possess high refractive index values greater than 4, surpassing common semiconductor materials. This makes vdW materials highly desirable for achieving low-loss optical resonances and for vertically stacking different materials for developing novel all-dielectric nanophotonic structures.

Here, we exploit the concept of quasi-bound states in the continuum (qBIC) to create high-quality optical resonances in dielectric metasurfaces made of hBN and TMDCs. Our method is entirely monolithic, using only van der Waals materials, and achieves optical resonances with Q factors exceeding 10² through a two-step fabrication process. We demonstrate spectral tuning across the entire visible spectrum in hBN qBIC metasurfaces [1], and enhance light-matter coupling with intrinsic spin defects in hBN [2]. We observe a remarkable 25-fold increase in photoluminescence intensity and spectral narrowing of defect emissions, with a linewidth below 4 nm full width at half-maximum. Furthermore, our platform offers exciting possibilities for strong light-matter coupling, as seen in the distinct anti-crossing behavior between qBIC resonances and intrinsic excitons in monolithic TMDC WS₂ metasurfaces, achieving Rabi splitting values up to 116 meV under ambient conditions [3]. Our results illustrate how combining qBIC photonic metasurfaces with van der Waals materials paves the way for novel hybrid nanophotonic platforms and room temperature polaritonic devices.

[1] L. Kühner, L. Sortino, *et al.* "High-Q Nanophotonics Over the Full Visible Spectrum Enabled by Hexagonal Boron Nitride Metasurfaces" *Advanced Materials* 35, 13 (2023)

[2] L. Sortino, *et al.* "Optically addressable spin defects coupled to bound states in the continuum metasurfaces" arXiv:2306.05735 (2023)

[3] T. Weber, L. Kühner, L. Sortino, *et al.* "Intrinsic strong light-matter coupling with self-hybridized bound states in the continuum in van der Waals metasurfaces" *Nature Materials* (2023)

11:00 AM QT01.10.04

Optical Imaging of Ultrafast Phonon-Polariton Propagation through an Excitonic Sensor [Shan-Wen Cheng](#)¹, Ding Xu¹, Haowen Su¹, James M. Baxter¹, Luke N. Holtzman², Kenji Watanabe³, Takashi Taniguchi³, James Hone², Katayun Barmak² and Milan Delor¹; ¹Department of Chemistry, Columbia University, United States; ²Columbia University, United States; ³National Institute for Materials Science, Japan

Hexagonal boron nitride (hBN) hosts phonon polaritons (PhP), hybrid light-matter states that facilitate electromagnetic field confinement and exhibit long-range ballistic transport. Extracting the spatiotemporal dynamics of PhPs usually requires four-de-force experimental methods such as ultrafast near-field infrared microscopy. Here, we leverage the remarkable environmental sensitivity of excitons in two-dimensional transition metal dichalcogenides to image PhP propagation in adjacent hBN slabs. Using ultrafast optical microscopy on monolayer WSe₂/hBN heterostructures, we image propagating PhPs from 3.5 K to room temperature with sub-picosecond and few-nanometer precision. Excitons in WSe₂ act as transducers between visible light pulses and infrared PhPs, enabling visible-light imaging of PhP transport with far-field microscopy. We also report evidence of excitons in WSe₂ co-propagating with hBN PhPs over several microns. Our results provide new avenues for imaging polar excitations over a large frequency range with extreme spatiotemporal precision, and new mechanisms to realize ballistic exciton transport at room temperature.

11:15 AM QT01.10.05

Polaron Dynamics of The Photo-Induced Hidden Metallic Phase in La_{2/3}Ca_{1/3}MnO₃ [Shiyu Fan](#)¹, Feng Jin^{2,3,4}, Umesh Kumar⁵, Brandon Yalin¹, Jiemin Li¹, Taehun Kim¹, Vivek Bhartiya¹, Yanhong Gu⁶, Valentina Bisogni¹, Sobhit Singh⁷, Wenbin Wu^{3,4,2} and Jonathan Pellicciari¹; ¹Brookhaven National Laboratory, United States; ²University of Science and Technology of China, China; ³Anhui Key Laboratory of Condensed Matter at Extreme Conditions, China; ⁴Hefei National Research Center for Physical Sciences at the Microscale, China; ⁵Rutgers, The State University of New Jersey, United States; ⁶The University of Tennessee, Knoxville, United States; ⁷University of Rochester, United States

Creating new "hidden" phases that have no analog in thermodynamic equilibrium is becoming increasingly important in condensed matter physics. The use of ultrafast laser with femtosecond pulse width to trigger such quantum phase transition is appealing as some of the hidden phases can be long-lived, with a lifetime of hours or weeks, and reversible with temperature sweeping or extra laser pulses. However, investigating and understanding the microscopic interactions in those hidden phases are still on the early stage due to the lack of high-end spectroscopic techniques that are sensitive to all degrees of freedom, precluding the development of designing high performance devices. Here, by combining the femtosecond ultrafast laser as a switching knob with the state-of-the-art ultrahigh-resolution resonant inelastic X-Ray Scattering as a probe, we reveal the phonon and polaron dynamics, as well as the evolution of crystal-field excitations across the insulating to photoinduced hidden metallic phase transition in a strained La_{2/3}Ca_{1/3}MnO₃ thin film. Upon the ultrafast excitation, the Jahn-Teller distortion is suppressed due to the strain relaxation induced by the increasing itinerancy of the Mn e_g electrons. This renormalizes the energies of the polaron and Mn dd excitations, ultimately leading to the formation of a metastable long-lived ferromagnetic metallic phase. Our results demonstrate that the electronic properties of the mesoscopic photoinduced hidden phase evolve with laser fluence, as an evidence of the systematic softening of the polaron binding energy and Mn dd excitations, consistent with the trend extracted from the bulk phase comparison. However, the spectral weight of the phonon and polaron is different compared to the metallic as-grown film, proving that the photo-induced phase is unique and distinct from the bulk metallic phase. Our findings indicate the strength of electron-phonon coupling plays the key role to determine the conductivity of manganites.

11:30 AM QT01.10.06

First-Principles Quantum Electrodynamics Theory of Light-Matter Interactions at All Coupling Strengths [Yu Zhang](#) and Xinyang Li; Los Alamos National Laboratory, United States

This presentation introduces VT-QEDHF, a novel first-principles quantum electrodynamics method developed to understand light-matter interactions at any coupling strength. The intersection of QED with materials science has catalyzed significant advancements in manipulating materials properties.

Traditional computational approaches, while effective, have been limited by their applicability to specific coupling regimes. Our work breaks away from the limitations of conventional approaches, offering a universal and efficient way to study light-matter interactions across various coupling regimes. Our findings open up new possibilities for researching and manipulating material properties via light-matter couplings.

11:45 AM QT01.10.07

A Composite Electrodynamical Mechanism to Reconcile Spatiotemporally Resolved Exciton Transport in Quantum Dot Superlattices Rongfeng Yuan^{1,2}, Trevor Roberts¹, Rafaela M. Brinn¹, Alexander Choi¹, Ha Park¹, Chang Yan^{1,3}, Justin Ondry^{1,4}, Ke Xu¹, Paul Alivisatos^{1,4} and Naomi S. Ginsberg¹; ¹University of California, Berkeley, United States; ²The Hong Kong University of Science and Technology (Guangzhou), China; ³Shanghai Jiao Tong University, China; ⁴The University of Chicago, United States

Quantum dot (QD) solids are promising optoelectronic materials; further advancing their device functionality depends on understanding their energy transport mechanisms. The commonly invoked near-field Förster resonance energy transfer (FRET) theory often underestimates the exciton hopping rate in QD solids, yet no consensus exists on the underlying cause [1–3].

We elucidate a mixed near-field FRET and far-field emission/reabsorption mechanism excitonic energy transport by combining time-dependent exciton energy and exciton diffusivity measurements in a heterogeneous QD superlattice (QDSL) [4]. We first quantitatively characterize the heterogeneous energetic landscape of CdSe:Te/CdS QDSL monolayers by extracting inhomogeneous and intrinsic spectral components of QDs by single-particle emission spectroscopy [5]. We next track the time-dependent decay of the mean exciton energy by time-resolved emission spectra (TRES) upon QDSL photoexcitation. The enhanced dynamic redshift occurring in the QDSLs relative to the solution phase QDs immediately following excitation indicates excitons, on average, sample progressively lower-energy QDs as they explore the spatioenergetic landscape. Finally, we measure exciton transport by monitoring the spatiotemporal expansion of an exciton population after a local photoexcitation in QDSL monolayers with time-resolved ultrafast stimulated emission depletion (TRUSTED) microscopy [6]. The result is that the data may be fitted to a simple model of the TRUSTED protocol [6] to determine migration parameters, such as diffusivity.

We use all three types of experimental results to constrain parameters in a kinetic Monte Carlo simulation, and we find that FRET theory is incompatible with the TRUSTED and TRES results simultaneously. This approach is unique because we connect the exciton energy and diffusion dynamics directly, which puts stringent test on the existing FRET theory. We show that only by introducing far-field emission/reabsorption terms that allows hops well beyond the nearest neighbors, can the model reproduce both all three experimental results. Our inclusion of far-field coupling was inspired by Andrews *et al.* [7], who originally wrote down how the energy transfer rate between donor and acceptor TDM can most generally be written as a dipole-dipole coupling expansion, $\Gamma_{ij} \propto \frac{1}{r^2}$, where Γ_{ij} represents the FRET rate and dominates in the near-field. The far-field term (scales with r^{-2}) dominates when r is much greater than $\lambda/2\pi$.

The explanation of our own multimodal study also addresses a longstanding paradox in exciton transport within QD solids, i.e., the typically-employed FRET near-field model has repeatedly fallen short of explaining experimental results despite being perpetuated as a standard. We furthermore showed how our model reconciles the original report of this paradox from Tisdale and co-workers [1]. Overall, this work yields a much-needed unified framework in which to characterize transport in QD solids and new principles for device design.

References

- [1] G. M. Akselrod, *et al.*, *Subdiffusive Exciton Transport in Quantum Dot Solids*, Nano Lett. **14**, 3556 (2014).
- [2] A. J. Mork, *et al.*, *Magnitude of the Förster Radius in Colloidal Quantum Dot Solids*, J. Phys. Chem. C **118**, 13920 (2014).
- [3] K. Zheng, *et al.*, *Directed Energy Transfer in Films of CdSe Quantum Dots: Beyond the Point Dipole Approximation*, J. Am. Chem. Soc. **136**, 6259 (2014).
- [4] R. Yuan *et al.*, *A Composite Electrodynamical Mechanism to Reconcile Spatiotemporally Resolved Exciton Transport in Quantum Dot Superlattices*, Sci. Adv. **9**, eadh2410 (2023).
- [5] Z. Zhang, *et al.*, *Ultra-high-Throughput Single-Molecule Spectroscopy and Spectrally Resolved Super-Resolution Microscopy*, Nature Methods **12**, 935 (2015).
- [6] S. B. Penwell, *et al.*, *Resolving Ultrafast Exciton Migration in Organic Solids at the Nanoscale*, Nat. Mater. **16**, 1136 (2017).
- [7] D. L. Andrews, *A Unified Theory of Radiative and Radiationless Molecular Energy Transfer*, Chem. Phys. **135**, 195 (1989).

SESSION QT01.11: THz Dynamics in Quantum Materials

Session Chairs: Youn Jue Bae and Nicolò Maccaferri

Friday Afternoon, April 26, 2024

Room 420, Level 4, Summit

2:00 PM QT01.11.01

Time-Resolved THz-TDS Nanoscopy for Probing Carrier Dynamics in 2D Materials with Femtosecond Temporal and Nanometer Spatial Distribution Tobias Gokus¹, Jonas Albert¹, Artem Danilov² and Andreas Huber¹; ¹Attocube Systems AG, Germany; ²Attocube Systems Inc, United States

THz imaging and spectroscopy is attracting attention as a tool for contact-free characterization of free charge carriers and their dynamics in nano-electronic devices [1]. However, the optical resolution of traditional THz microscopy is restricted by the diffraction limit of light. Scattering-type scanning near-field optical microscopy (s-SNOM) surmounts the diffraction limit by focusing light to a metallic scanning tip and collecting and analyzing the tip-scattered light [2]. Deep subwavelength spatial resolution down to sub-15 nm ($\lambda/8000$) was recently demonstrated for s-SNOM measurements in the THz frequency range [3].

In this work we demonstrate THz-TDS based s-SNOM imaging and spectroscopy in combination with time-resolved THz-TDS spectroscopy based on a fully integrated pump-probe THz-TDS near-field optical microscope system. To illustrate these capabilities, we perform NIR pump – THz probe near-field imaging and spectroscopy of a MoS₂ flake with a thickness of about 250 nm deposited on a gold coated Si substrate.

Delivering broadband THz pulses (0.1 – 5 THz) for tip illumination, micron sized terraces with varying thickness on the MoS₂ can be well distinguished based on their characteristic near-field contrast, highlighting the capability of the system to achieve deep subwavelength spatial resolution. Further, a pronounced contrast is observed in the THz image between the MoS₂ and the highly reflective Au substrate.

Optical pumping of the flake with femtosecond laser pulses (center wavelength, 780nm (1.59 eV), pulse duration < 150fs) at photon energies larger than the direct/indirect bandgap of MoS₂ results in a general increase of the THz amplitude signal across the flake. Interestingly, the magnitude of the near-field

THz signal on the flake is now almost the same as for the gold substrate, indicating that the increase in THz signal of the MoS₂ flake originates from modification of the refractive index. Obviously, upon photoexcitation with the 780 nm pump pulse, the terahertz conductivity increases due to absorption by the photoinduced charge carriers [4,5]. It is to note, that the magnitude of the THz-near-field signal of the gold substrate remains unaltered during NIR laser illumination.

THz transients are measured by varying the timing between the NIR optical pump and THz probe pulses. The transients were recorded on two different areas on the flake separated only by a few microns. The decay of the THz near-field amplitude signal is on the order of a couple of hundreds of picoseconds with notably slower decay for the location with larger thickness. The observed long carrier relaxation dynamics up to the >100 ps time scale might result from slow carrier relaxation processes in the crystal [6].

Scattering type near-field microscopy is a powerful tool for optical investigation of nanoscale structures with wavelength-independent resolution < 20 nm. Its applicability has been successfully extended to the THz frequency range. Furthermore, we have expanded these capabilities successfully to enable time-resolved VIS/NIR pump and THz probe spectroscopy for studying the dynamics of photoexcited carriers in semiconductors. We envision even further opportunities for the investigation of low energy optical excitations in novel materials and their dynamics by implementing time-resolved THz-TDS spectroscopy to cryogenic s-SNOM microscopes.

- [1]. P. Kuzel and H. Nemeč, *Adv. Opt. Mater.* **8**,190062 (2020)
- [2]. F. Keilmann and R. Hillenbrand, *Phil. Trans. R. Soc. Lond. A* **362**, 787-805 (2004)
- [3]. C. Maissen et al., *ACS Photonics* **6**, 1279 (2019)
- [4] V. Pushkarev et al., *Adv. Funct. Mater.* **32**, 2107403 (2022)
- [5] M. Plankl et al., *Nature Photonics* **15**, 584 (2021)
- [6] S. Kar et al., *ACS Nano* **9**, 12, 12004 (2015)

2:15 PM QT01.11.02

Terahertz Emission Spectroscopy to Probe Ultrafast Spin to Charge Conversion at Perovskite/Ferromagnet Interfaces Yifan Dong¹, Matthew Hautzinger¹, Andrew Comstock², Aeron McConnell², Dali Sun² and Matthew C. Beard¹; ¹National Renewable Energy Laboratory, United States; ²North Carolina State University, United States

Understanding spin-to-charge conversion (SCC) allows efficient control and manipulation of the spin degree of freedom, which can pave the way for next generation spintronic devices. Unlike conventional transport-based measurements, terahertz (THz) emission spectroscopy offers great advantages including the capability of measuring transient charge currents with sub-picosecond time resolution. Using THz emission spectroscopy, we observed the ultrafast spin current injection at the interface between a ferromagnetic (FM) material and a chiral two-dimensional (2D) perovskite via inverse Rashba-Edelstein effect. In summary, we observed strong magnetic field- and polarization-dependence in both phase and intensity of the emitted THz signal, implying the great tunability in these chiral 2D perovskites for spintronic application. These results present a promising way to control charge and spin interconversion at perovskite/ferromagnetic interfaces and future spintronics devices. The unique asymmetry in THz emission due to SCC at chiral 2D perovskite/FM (i.e. (R-MBA)₂PbI₄/NiFe and (S-MBA)₂PbI₄) interface distinguishes them from three-dimensional perovskite materials which only exhibit symmetric THz emission. In this talk, I will discuss the measured THz emission signals including both the forward and backward THz emission (reflected at the air/substrate interface). The forward emission signal exhibits a π -phase shift when the in-plane magnetic field flips its sign, whereas the backward signal exhibits no phase shift at all. In addition, I will also discuss the asymmetry in THz emission intensity. Specifically, the THz emission intensity of the forward emission signal decreases by almost two-fold when the in-plane magnetic field reverses, while the backward emission signal increases by two-fold when the field direction reverses. Such asymmetry in THz emission can be explained with an in-plane momentum shift of the Rashba bands induced by the ultrafast laser pump.

2:30 PM BREAK

SESSION QT01.12: Light-Matter Coupling in Quantum Materials II
Session Chairs: Veronica Policht and Chiara Trovatiello
Friday Afternoon, April 26, 2024
Room 420, Level 4, Summit

3:00 PM *QT01.12.02

Quantum Material Research through Femtosecond Electron Crystallography, Spectroscopy and Microscopy Chong-Yu Ruan; Michigan State University, United States

The major potential advantage in using electron scattering data, compared to X-ray, is that electrons can be focused using an electromagnetic lens; thus, both images and diffraction patterns can be utilized for structural analysis under the same platform. Importantly, the different modalities are controlled by the post-specimen optics and aperture placement with additional sets of lenses. The lens combination offers great flexibility in creating either image, diffraction, or even spectroscopic signals from a large field of view or data for the microanalysis of small regions. Injecting ultrafast time resolution into the typical TEM modalities will not only allow ultrafast imaging and diffraction patterns to be obtained for studying material processes, but also the delicate control of timing between the pump and probe pulses can create a new contrast mechanism at various stages of the material's responses. Especially, the recent successful implementation of high precision control of electron probe dynamics enables the technologies to perform in the 10s femtosecond regime, opening new possibility of studying control-feedback mechanism.

We will discuss the uses of dynamical contrast to enhance the imaging and crystallography capabilities for the understanding of the evolutionary processes set forth from different types of laser pulse initiations in quantum materials. The evolutionary processes are probed through combined approach of ultrafast spectroscopy, diffraction, and microscopy that are conducted in situ to piece together information. Using vanadium dioxide nanocrystals and transition-metal dichalcogenide (TMDC) thin layers as examples, we demonstrate how the multi-modality ultrafast electron platform may provide useful new information regarding quantum material state evolution at different spatial and temporal scales. Through joint structure and spectroscopy probes we identify the common presence of nanoscopic transition intermediate as the cornerstone for the system's successful descend into the eventual state and adopting its functionality.

In the studies of TMDC (TaS₂, TaSe₂) first focusing on the dynamics on the ps and sub-ps timescale with time-domain contrasts over the optical signals and selected Bragg peaks, we observe that under different pump conditions different types of phonon modes in the hosting lattice of the charge-density-wave materials may be activated. Upon entering the phase transition regime, these phonon modes are hybridized with the emerging density-wave state observed through the dynamical crystallographic patterns. The transition becomes stepwise with the formation of nanoscopic domains that lock the emergent order with the host lattice in various formation. Remarkably, upon varying the pump power, the timescale for the multi-stage evolutions can be tuned by more than one order of magnitude. In the case of VO₂, multi-critical behavior also emerges but here we show the thermal and non-thermal controls manifest in different types of behavior. For the nonthermal control, in which, the initial step of ultrafast spectroscopic insulator-to-metal transition is observed over sub-100 fs timescale where the emergence of a nanoscopic excitonic polaron domain is simultaneously captured by the diffraction signals. Such evolution is different from the insulator-metal transition obtained under the thermal regime of control where no such polaronic domain is identified. These results indicate that the functional controls in correlated electron crystals may be more nuanced due to their sensitivity to more than one type of control parameter and our multi-perspective results may shed insight to address some highly debated open questions regarding these materials.

The work was funded by the U.S. Department of Energy, Grant DE-FG0206ER46309. The experimental facility was supported by U.S. National Science Foundation, Grant DMR 1625181.

3:30 PM QT01.12.03

Spatiotemporal Imaging of Waveguide Nonlinear Optics [Ding Xu](#) and Milan Delor; Columbia University, United States

Non-linear optical conversion is an essential aspect of modern photonic applications, and major efforts target the realization of efficient nonlinear processes in compact waveguides for miniaturization. Van der Waals structures, renowned for their pronounced light-matter interactions and nonlinear susceptibilities, have emerged as promising platforms to realize such nonlinear waveguides, but optimization requires precise knowledge of their linear and nonlinear optical properties, which are notoriously difficult to extract in highly anisotropic microstructures. I will describe an approach we developed to extract the optical properties and phase-matching conditions of nonlinear materials by directly imaging light propagation and harmonic conversion within van der Waals waveguides with extreme spatiotemporal resolution. Although it is generally assumed that waveguided light remains out the reach of far-field microscopy, our approach, based on far-field ultrafast microscopy, leverages strong light-matter interactions to track light fields even beyond the total internal reflection barrier, an unprecedented feat. We focus on slab waveguides of 3R-MoS₂, which were recently found to exhibit highly efficient second harmonic generation. We show that spatiotemporal imaging of both fundamental and second harmonic waves provides several self-consistent methods to determine the phase-matching angle, mode profiles, harmonic generation efficiency and losses in nonlinear waveguides without any a priori knowledge of material properties. Our approach thus enables rapid identification of promising materials and optimization of waveguide structures for efficient harmonic generation and optical modulation in nanophotonic architectures.

3:45 PM QT01.12.04

Ultrafast Infrared-Light-Driven Symmetry Control in Crystalline Materials Zhiren He and [Guru Khalsa](#); University of North Texas, United States

The interplay between structure, symmetry, and function is a fundamental and long-standing paradigm in materials physics. It dictates how we access physical properties, reveals hidden order, and guides both the search for, and the engineering of, new physical phenomena. Recent technological advances have enabled sub-picosecond manipulation of structure through the far-from-equilibrium drive of phonons — the mechanical modes of crystalline materials — using mid- and far-infrared light. How can we leverage these structural changes to induce new symmetries and functionalities?

In this talk, I will discuss our theoretical exploration of light-driven control of symmetry in crystalline materials via direct excitation of phonons. Focusing on strategies for tailored optical control of elusive symmetries and orders, I will demonstrate that new symmetries and length scales can emerge, that chemical environments not observed near equilibrium can be prepared, and that known or hidden phase boundaries may be traversed.

SESSION QT01.13: Virtual Session
Session Chair: Ursula Wurstbauer
Thursday Morning, May 9, 2024
QT01-virtual

8:00 AM QT01.13.01

Quantum Defects in 2D Materials for Terahertz Technologies [Su Ying Quek](#); National University of Singapore, Singapore

The emergence of stable terahertz (THz) sources and other THz optical components has spurred the development of many applications. However, THz technologies have thus far not been well integrated into the quantum regime. In this work, we predict that transition metal substitutional defects in two-dimensional transition metal dichalcogenides (TMDs) can serve as quantum defects for terahertz technologies. Central to this prediction is the finding that the zero field splittings between the spin sublevels in these defects are in the sub-terahertz to terahertz range. These zero field splittings are orders of magnitude larger than those found in other common quantum defects, due to the large spin-orbit coupling in these TMD systems. Based on the symmetries of the quantum states as well as first principles calculations of the optical transition energies, we identify defects that can serve as spin qubits, either through resonant excitation or through intersystem crossing channels. Such spin qubits are expected to have a longer spin coherence time compared to spin qubits with smaller zero field splittings. We further propose defects that can potentially be tunable quantum sources of terahertz radiation. Our research broadens the scope for advancements in quantum computing and information science, and lays a foundation for their integration with THz technologies.

Funding Acknowledgement:

Supported by the Singapore Ministry of Education under grant number MOE2018-T3-1-005.

8:15 AM *QT01.13.02

THz Driven Ultrafast Processes in Quantum Materials [Shovon Pal](#); National Institute of Science Education and Research Bhu, India

Quantum materials – a category of condensed matter systems – display strong electronic correlations where the very notion of electrons as non-interacting entities fails. The properties of quantum materials with the so-called strongly correlated states are, instead, determined by the collective interaction of many electrons via their charges and spins [1,2]. The complexity that arises from such interactions gives rise to emergent phenomena in a multitude of quantum materials, like high-T_c superconductors [3], heavy-fermion materials [4,5], ferroelectrics [6], topological materials [7], and multiferroics [8]. Because of the

multi-particle nature, microscopic understanding of their ground states with such strong-correlation phenomena is a demanding task and requires going away from the ground state and studying the nonequilibrium dynamics of such systems. In general, equilibrium studies ignore the temporal evolution of a physical process, and most importantly, neglect local fluctuations in the systems. In contrast, the non-equilibrium descriptions explain the roles of such fluctuations both in time and space. As the dynamics of many-body processes get even more critical in various quantum materials, we need to understand how the temporal evolutions of specific processes affect the underlying correlations between charge, spin, lattice and orbital degrees of freedom. In this talk, I will provide an overview on how the THz light has been used to drive quantum materials out of equilibrium and gain information on the associated correlation processes and the dynamics of low-energy excitations [9].

References:

- [1] D. N. Basov, et al., *Rev. Mod. Phys.*, **83**, 471 (2011).
- [2] B. Keimer, et al., *Nat. Phys.* **13**, 1045 (2017).
- [3] M. Budden, et al., *Nat. Phys.* **17**, 611 (2021).
- [4] C. Wetli, et al., *Nat. Phys.* **14**, 1103 (2018).
- [5] C.-J. Yang, et al., *Nat. Phys.* (2023).
- [6] X. Li, et al., *Science* **364**, 1079 (2019).
- [7] J. Reimann, et al., *Nature* **562**, 396 (2018).
- [8] T. Kubacka, et al., *Science* **343**, 1333 (2014).
- [9] C.-J. Yang, et al., *Nat. Rev. Mat.* **8**, 518 (2023).

8:45 AM *QT01.13.03

Non-Linear Light-Matter Interactions in Quantum Materials Su Ying Quek; National University of Singapore, Singapore

Non-linear optical phenomena are at the heart of many important technologies and spectroscopic techniques. In order to fundamentally understand, and predict, non-linear optical properties in quantum materials, it is necessary to incorporate the physics of excitons, or bound electron-hole pairs. In this work, we develop and implement a theory for the second-order optical susceptibility that takes into account excitonic effects with a first principles GW-Bethe-Salpeter-Equation (GW-BSE) approach. Using this theory, we elucidate the impact of excitons on sum-frequency generation and spontaneous parametric down-conversion in niobium oxydihalides (NbOX₂, X = Cl, Br, I) [1], a material of significant current interest in non-linear optics [2]. We also predict difference-frequency generation effects in quantum materials. In addition to shift current effects (the zero-frequency response), we consider the generation of terahertz pulses due to difference frequency mixing from incoming laser pulses. Our work provides a framework to predict and understand the non-linear effects arising from continuous-wave and ultrafast laser light incident on quantum materials.

- [1] F. Xuan, M. Lai, Y. Wu, S. Y. Quek, arXiv:2305.08345

- [2] *Nature* **613**, 53 (2023), *Nature Photonics* **16**, 644 (2022), *Advanced Optical Materials* **2202833** (2023), *Advanced Materials* **33**, 2101505 (2021)

9:15 AM *QT01.13.04

Ultrafast Thermodynamic Phenomena Involving Photons, Electrons and Phonons in (Twisted) Quantum (Meta)Materials Klaas-Jan Tielrooij^{1,2}; ¹Eindhoven University of Technology, Netherlands; ²Catalan Institute of Nanoscience and Nanotechnology, Spain

Quantum materials exhibit several exciting ultrafast physical phenomena that are moreover potentially technologically useful. This is particularly true for quantum materials with massless Dirac electrons, such as graphene and topological insulators. When light is absorbed in these materials, electron heating occurs through electron-electron interactions on a 10-100 fs timescale, followed by electron cooling, typically involving the emission of phonons on a picosecond timescale. We have exploited these ultrafast thermodynamics, and the heat-induced decrease in terahertz (THz) absorption, to generate harmonics in the THz regime [1]. This THz harmonic generation is particularly efficient in quantum metamaterials that consist of a quantum material and a metallic grating [2]. Thanks to an efficient “Coulomb cooling” mechanism between surface and bulk electronic states in topological insulators [3], we have recently demonstrated that the ultrafast thermodynamics can give rise to third-order terahertz harmonic generation approaching the milliwatt regime [4]. These results establish quantum (meta)materials as an excellent material platform for nonlinear terahertz photonics, with possible applications in next-generation wireless communication systems, among others.

Whereas these ultrafast thermodynamics in graphene and topological insulators are relatively well understood, this is not the case for twisted bilayer graphene near the magic angle. Using time-resolved photocurrent measurements, we have studied these ultrafast dynamics and found that the electron cooling dynamics in twisted bilayer graphene near the magic angle is very distinct from the dynamics in monolayer or non-twisted bilayer graphene. Specifically, the cooling time in near-magic twisted bilayer graphene is a few picoseconds all the way from room temperature down to 10 K, where non-twisted bilayer graphene becomes increasingly slow for lower temperatures. We ascribe this ultrafast cooling in magic-angle twisted bilayer graphene to Umklapp-assisted electron-phonon cooling, facilitated by the moiré pattern in twisted bilayer graphene [5]. Whereas Umklapp scattering is a very common phenomenon for phonons, it is very rare to observe such scattering processes for electrons. These results establish twist angle as control knob for steering the cooling dynamics and flow of electronic heat, and have possible implications for the development of ultrafast detectors operating at cryogenic temperatures, among others.

References

- [1] H.A. Hafez et al, *Nature* **561**, 507 (2018).
- [2] J.C. Deinert et al, *ACS Nano* **15**, 1145 (2021).
- [3] A. Principi and K.J. Tielrooij, *Phys. Rev. B.* **106**, 115422 (2022)
- [4] K.J. Tielrooij et al. *Light Sci. Appl.* **11**, 315 (2022)
- [5] J.D. Mehew et al. arXiv 2301.13742 (2023)

SYMPOSIUM QT02

Low-Dimensional Magnetic Quantum Materials
April 23 - April 26, 2024

Symposium Organizers

Zhong Lin, Binghamton University
Yunqiu Kelly Luo, University of Southern California
Andrew F. May, Oak Ridge National Laboratory
Dmitry Ovchinnikov, University of Kansas

Symposium Support

Silver
Thorlabs **Bronze**
Vacuum Technology Inc.

* Invited Paper
+ JMR Distinguished Invited Speaker
^ MRS Communications Early Career Distinguished Presenter

SESSION QT02.01: Emerging 2D Magnetic Materials I
Session Chairs: Andrew F. May and Dmitry Ovchinnikov
Tuesday Morning, April 23, 2024
Room 421, Level 4, Summit

10:30 AM *QT02.01.01

Graphene Nanostructures 3.0: Nanoelectronics, Quantum Phenomena and Properties [Xinliang Feng](#)^{1,2}; ¹Max Planck Institute of Microstructure Physics, Germany; ²Technische Universität Dresden, Germany

With the advances in emergent quantum technologies, such as quantum computing, quantum communications, etc., graphene nanostructures provide a unique molecular toolbox for accessing their unprecedented quantum phenomena and properties. In this lecture, we will introduce our recent efforts towards the precision graphene nanostructures as the defined quantum entities for the spin-spin coupling. Both in-solution and on-surface synthesis approaches will be discussed that provide synthetic access to this class of unique graphene nanostructures with controlled spin-orbital coupling behavior. Individual open-shell graphene molecules (Kekulé, non-Kekulé and concealed non-Kekulé structure motifs) with controlled singlet, triplet, as well as high-spin states, will be developed. Next, we will discuss the collective carbon magnetisms in the dimers of open-shell graphene molecules. Spin-chains with fractional edge excitations will also be presented. In the final section, we will also present our recent efforts towards graphene nanoribbon-based nanoelectronics. Various robust graphene nanoribbons with controlled edge structures and topologies will be synthesized and demonstrated to show their unique electronic and optoelectronic properties. The integration of single graphene nanoribbons into the nanoelectronic devices will be particularly highlighted.

11:00 AM QT02.01.02

Chemical Exfoliation of 1-Dimensional Antiferromagnetic Nanoribbons from a Non-Van der Waals Material [Mulan Yang](#)¹, [Guangming Cheng](#)², [Nitish Mathur](#)¹, [Ratnadwip Singha](#)¹, [Fang Yuan](#)¹, [Nan Yao](#)² and [Leslie Schoop](#)¹; ¹Princeton University, United States; ²Princeton Materials Institute, United States

As the demand for increasingly varied types of 1-dimensional (1D) materials grows, there is a greater need for simple and scalable methods to synthesize these materials. Chemical exfoliation is commonly used to make 2-dimensional (2D) materials, often in a way that is both straightforward and suitable for making larger quantities, yet this method has thus far been underutilized for synthesizing 1D materials. In the few instances when chemical exfoliation has been used to make 1D materials, the starting compound has been a van der Waals material, thus excluding any structures without these weak bonds inherently present. We demonstrate here that ionically bonded crystals can also be chemically exfoliated to 1D structures by choosing KFeS_2 as an example. Using chemical exfoliation, antiferromagnetic 1D nanoribbons can be yielded in a single step. The nanoribbons are crystalline and closely resemble the parent compound both in structure and in intrinsic antiferromagnetism. The facile chemical exfoliation of an ionically bonded crystal shown in this work opens up opportunities for the synthesis of both magnetic and non-magnetic 1D nanomaterials from a greater variety of starting structures.

11:15 AM QT02.01.03

Using High-Pressure Conditions to Access Novel Structures and Engender Magnetic Control in Layered Lanthanide Materials [Alison Altman](#), [Ebube Oyeka](#) and [Ryan O'Shea](#); Texas A&M, United States

A rational approach to designing the next generation of quantum magnetic materials requires hypothesis-driven synthesis. Yet, the complex phase space of solid-state systems and the small energy scales that determine magnetic order are such that subtle changes in composition can drastically change the structure and properties of the resulting material. In comparison, pressure provides an incrementally tunable vector, serving to increase orbital overlap and leading to more significant covalent and metallic interactions. In this work, we describe our multimodal approach combining high-pressure synthesis with spectroscopy and calculations to bring new chemical insight into the discovery of layered materials containing lanthanides primed to exhibit exotic magnetic behaviors. To realize promising synthetic targets, we turned to both traditional solid-state techniques as well as high-pressure experiments in diamond anvil cells. We note an established tendency towards layered structures in lanthanide halides that depends on the formal valence state of the lanthanide metal. Crucially, dimensionality is known to be sensitive to applied pressures, and can be harnessed to tune the structure of lanthanide systems to promote low-dimensional motifs. We will discuss our burgeoning chemical intuition for structure formation and metastability in this space, as well as present our ongoing efforts towards correlating new structures with magnetic properties both at ambient pressures and under high-pressure synthesis conditions.

11:30 AM *QT02.01.04

Antagonistic Pairs: A Pathway to The Discovery of New Quasi-Low Dimensional Materials [Tyler Slade](#); Ames Laboratory, United States

A foundational goal of materials chemistry is to develop general design principles for synthesizing materials with targeted structural motifs and physical properties. We propose that pairs of strongly immiscible elements, referred to here as antagonistic pairs,¹ can be used to reliably produce ternary compounds with low or quasi-reduced dimensionality intrinsically built into their crystal structures. Many pairs of elements offer essentially no miscibility, of which examples are Co-Pb, Cr-La, and Fe-Ag. The heart of our work is to leverage third elements that are mutually compatible with any given immiscible pair to form stable ternary compounds containing that pair. When such ternary compounds can be made, we discuss how the strong immiscibility of the antagonistic pair is remarkably preserved in the ternary crystal structures, with the third element separating the immiscible atoms into spatially separated substructures. Quasi-low dimensional structural units, such as chains or sheets, are the natural consequence of the immiscible atoms seeking to avoid close contact in the solid-state. Finally, we present the growth and characterization of single crystals of several new, 3d transition metal containing, ternary compounds based on antagonistic pairs and which feature quasi-2D structural motifs, concluding with an overview of their magnetic and transport properties.

[1] P. C. Canfield, "New materials physics", *Reports on Progress in Physics* 83, 016501 (2019)

Work at Ames National Laboratory was supported by the U.S. Department of Energy, Office of Science, Basic Energy Sciences, Materials Sciences and Engineering Division. Ames National Laboratory is operated for the U.S. Department of Energy by Iowa State University under Contract No. DE-AC02-07CH11358.

SESSION QT02.02: Topology and Magnetism in Emerging Moiré Materials

Session Chairs: Roland Kawakami and Dmitry Ovchinnikov

Tuesday Afternoon, April 23, 2024

Room 421, Level 4, Summit

1:30 PM *QT02.02.01

Helical Light Emission from a Moiré Chern Magnet [Xiaodong Xu](#); University of Washington, United States

Twisted MoTe₂ bilayer is an emergent fractional Chern insulator with spontaneous time reversal breaking. As semiconducting transition metal dichalcogenides famously exhibit spin-valley locking and circularly polarized valley-optical selection rules, a natural question arises as to how the interaction induced ferromagnetism couples to the optical response. Here, we demonstrate that the degree of circular polarization (DOCP) in the trion photoluminescence at zero magnetic field reaches near unity in the anomalous Hall metal phase, with the helicity controlled by the magnetization direction. Spin-valley Hall response is shown to tune the emission helicity, establishing the electric current as an additional control of the PL helicity. We further show that the PL DOCP is a sensitive probe of the integer and fractional quantum anomalous Hall effects, the putative zero-field composite fermi liquid state, as well as their electric field-driven topological quantum phase transitions. The unprecedented optical properties of this system promise to have profound implications for spintronics, valleytronics, and topological-optoelectronic devices.

2:00 PM QT02.02.02

Optics as a Probe and Control of Spin/Valley Order in Topological Moiré Magnet MoTe₂ [Eric Anderson](#)¹, [Xiaodong Xu](#)¹, [Jiaqi Cai](#)¹, [Heonjoon Park](#)¹, [Di Xiao](#)¹, [Ting Cao](#)¹, [Liang Fu](#)², [Wang Yao](#)³, [Kenji Watanabe](#)⁴ and [Takashi Taniguchi](#)⁵; ¹University of Washington, United States; ²Massachusetts Institute of Technology, United States; ³The University of Hong Kong, Hong Kong; ⁴National Institute for Materials Science, Japan; ⁵Kyoto University, Japan

In the past year, near-AA stacked homobilayer moiré MoTe₂ has been established as a robust, gate-tunable ferromagnet upon hole doping of the first moiré valence band. The system's spontaneous time reversal symmetry breaking enables the realization of an effective Haldane model and flat, topologically nontrivial bands. These unique characteristics of the moiré MoTe₂ system led to observation of quantum anomalous Hall and, for the first time, fractional quantum anomalous Hall states. Here, I discuss our optical measurements of tunable magnetic and topological states in the moiré superlattice. Additionally, I present our more recent studies leveraging the magnetic order in the system to control helical optical emission at zero applied magnetic field. The strong correspondence between the spin, valley, and optical degrees of freedom these results establish suggests that optics is not only a powerful probe of moiré MoTe₂, but could also be promising control knob for the magnetic states. Beyond the implications for spintronics, valleytronics, and magneto-optical devices, the link between magnetic order and topological index of the FQAH states presents a new path forward in the study of anyon physics – and perhaps, one day, towards topological qubits.

2:15 PM *QT02.02.03

Electrical Switching of The Edge Current Chirality in Quantum Anomalous Hall Insulators [Cui-Zu Chang](#); The Pennsylvania State University, United States

A quantum anomalous Hall (QAH) insulator is a topological state of matter, in which the interior is insulating but electrical current flows along the edges of the sample, in either a clockwise (right-handed) or counter-clockwise (left-handed) direction dictated by the spontaneous magnetization orientation. Such chiral edge current (CEC) eliminates any backscattering, giving rise to quantized Hall resistance and zero longitudinal resistance. In this work, we fabricate mesoscopic QAH sandwich (i.e. magnetic topological insulator (TI)/TI/magnetic TI) Hall bar devices and succeed in switching the CEC chirality through spin-orbit torque (SOT) by applying a current pulse under a suitably controlled gate voltage. The well-quantized QAH states before and after SOT switching with opposite CEC chiralities are demonstrated through four- and three-terminal measurements. Our theoretical calculations show that the SOT that enables the magnetization switching can be generated by both bulk and surface carriers in QAH insulators, in good agreement with experimental observations. Finally, I will briefly talk about the SOT switching-induced topological phase transition between the QAH and axion insulator states.

This work is supported by ARO award (W911NF2210159), AFOSR grant (FA9550-21-1-0177), DOE grant (DE-SC0023113), and Gordon and Betty Moore Foundation's EPIQS Initiative (Grant GBMF9063 to C.-Z.C.).

2:45 PM QT02.02.04

Observation of Fractional Quantum Anomalous Hall Effect [Heonjoon Park](#)¹, [Jiaqi Cai](#)¹, [Eric Anderson](#)¹, [Yinong Zhang](#)¹, [Jiayi Zhu](#)¹, [Xiaoyu Liu](#)¹,

Chong Wang¹, William Holtzmann¹, Chaowei Hu¹, Zhaoyu Liu¹, Takashi Taniguchi², Kenji Watanabe², Jiun-Haw Chu¹, Ting Cao¹, Liang Fu³, Wang Yao⁴, Cui-Zu Chang⁵, David Cobden¹, Di Xiao¹ and Xiaodong Xu¹; ¹University of Washington, United States; ²National Institute for Materials Science, Japan; ³Massachusetts Institute of Technology, United States; ⁴The University of Hong Kong, Hong Kong; ⁵The Pennsylvania State University, United States

The interplay of topology, magnetism, and strong correlation leads to intriguing quantum states of matter. A prominent example is the quantum anomalous Hall effect (QAHE), which displays integer quantum Hall effect at zero magnetic field due to topologically nontrivial bands and intrinsic magnetism. Realizing a similar analogue of the fractional quantum Hall effect at zero field, known as the fractional quantum anomalous Hall effect (FQAHE), has long posed a challenge due to stringent constraints in electron-electron interaction and quantum geometry. Here, we present the experimental observation of FQAHE and electrically tunable topological phase transition in twisted MoTe₂ bilayer using electrical transport measurements. In addition, an anomalous Hall state emerges near the filling factor -1/2. Its behavior mirrors that of the composite Fermi liquid in the half-filled lowest Landau level of a two-dimensional electron gas under high magnetic fields. The direct observation of the FQAH and associated effects opens the door to exploring charge fractionalization and anyonic statistics at zero magnetic field.

3:00 PM BREAK

SESSION QT02.03: Emerging Kagome and Magnetic Materials
Session Chairs: Zhong Lin and Andrew F. May
Tuesday Afternoon, April 23, 2024
Room 421, Level 4, Summit

3:30 PM *QT02.03.01

Topology and Correlation in Kagome Lattice Metals [Linda Ye](#); California Institute of Technology, United States

The two-dimensional kagome lattice comprised of corner-shared triangles is theoretically expected to host multiple exotic band features such as Dirac points, van Hove singularity and flat bands in its tight-binding model. The intricate interplay of these band features with spin-orbit coupling and electron-electron interactions renders the kagome lattice an exceptionally promising platform for the realization of topological and correlated electronic states. Recently, a growing family of transition metal-based intermetallic materials, known as "kagome metals," has been found to faithfully realize the anticipated model kagome electronic structure. In this talk, we will focus on the ongoing advancements in the pursuit of topological and correlated phases in binary kagome metals; in particular, we will highlight the band topology in the ferromagnetic phase, the emergence of flat bands as well as non-Fermi liquid behavior in these kagome metals.

References:

- [1] L. Ye and M. Kang et al., Nature 555, 638-642 (2018).
- [2] M. Kang and L. Ye et al., Nature Materials 19, 163-169 (2019).
- [3] L. Ye et al., arXiv:2106.10824

4:00 PM QT02.03.02

Above Room-Temperature Ferromagnetism in Van der Waals Material Fe₃GaTe₂ [Chaowei Hu](#), Jiayi Zhu, Sanae Tominaga, Jordan Fonseca, Yuzhou Zhao, Xiaodong Xu and Jiun-Haw Chu; University of Washington, Seattle, United States

The emergence of two-dimensional van der Waals magnets has introduced new prospects for vdW heterostructure and spintronic applications in the past decade. Recently a new member Fe₃GaTe₂ was found and stood out for its persistent ferromagnetism above room temperature. In this presentation, we will discuss our successful synthesis of single-crystalline Fe₃GaTe₂, as well as the following bulk characterization, transport, and magneto-optical measurements performed on our single crystal and exfoliated thin flakes. The magnetization and transport studies on the bulk Fe₃GaTe₂ crystals reveal a high Curie temperature of 355K and the thermodynamic investigations suggest the presence of a strong electron-electron correlation. Layer-dependent magneto-optical studies on thin Fe₃GaTe₂ flakes further unveil its robust ferromagnetism for room-temperature applications in 2D limits. Our work illuminates the remarkable magnetic properties of Fe₃GaTe₂, establishing it as a suitable vdW platform for realizing controllable 2D magnetism and spintronic applications in everyday environments.

4:15 PM *QT02.03.03

Kagome and Van der Waals Magnetic Topological Materials [Roland K. Kawakami](#); The Ohio State University, United States

Materials and heterostructures combining magnetic order and band topology are important for science and technology ranging from quantum anomalous Hall effect (QAHE) to highly efficient spin-orbit torque switching. Kagome lattice metals and van der Waals (vdW) heterostructures are two classes of materials that are particularly promising in this regard. The 2D kagome lattice has topological flat bands and Dirac cones inherent in its band structure and these features persist in compounds with layered kagome lattices. Meanwhile, vdW materials encompass 2D magnets and topological insulators that manifest the QAHE, most notably Cr-doped (Bi,Sb)₂Te₃ and MnBi₂Te₄. Our research has focused on the atomic layer-by-layer synthesis of kagome and vdW materials by molecular beam epitaxy and their characterization through magneto-optics, angle-resolved photoemission spectroscopy (ARPES), and magnetotransport. For kagome metals, we investigated spin-orbit torque effects in Fe₃Sn₂ by magneto-optic methods [1,2] and flat bands in CoSn by ARPES [3]. Recently, we demonstrated the first thin film growth of rare-earth kagome magnets (RMn₆Sn₆, R = rare-earth Tb, Er), which are prospective QAHE materials. For vdW materials, we developed thin films of layered antiferromagnetic topological insulator MnBi₂Se₄ [4], which cannot be stabilized in bulk vdW crystal form, and Fe₃GeTe₂/Bi₂Te₃ heterostructures. The latter are heterostructures combining topological insulators and 2D magnets, where the Curie temperature has been raised to above room temperature by varying growth conditions [5].

- [1] Shuyu Cheng et al., APL Materials 10, 061112 (2022).
- [2] Igor Lyalin et al., Nano Letters 21, 6975 (2021).
- [3] Shuyu Cheng et al., Nano Letters 23, 7107 (2023).
- [4] Tiancong Zhu et al., Nano Letters 21, 5083 (2021).
- [5] Wenyi Zhou et al., arXiv:2308.13620 (accepted to Physical Review Materials)

4:45 PM QT02.03.04

Half-Magnetization Plateau in The Kagome-Stripe-Lattice $\text{Na}_2\text{Co}_3(\text{VO}_4)_2(\text{OH})_2$ Yiqing Hao¹, Megan Smart¹, Jie Xing¹, Rongying Jin², Joseph Kolis³, Duminda Sanjeeewa⁴ and Huibo Cao¹; ¹Oak Ridge National Laboratory, United States; ²University of South Carolina, United States; ³Clemson University, United States; ⁴University of Missouri–Columbia, United States

Magnetization plateaus often signify quantum magnetic states arising from geometric frustration and/or quantum fluctuations. Here, we report a half-magnetization plateau in the kagome-stripe lattice (KSL) material, $\text{Na}_2\text{Co}_3(\text{VO}_4)_2(\text{OH})_2$. Our susceptibility measurements reveal the half-magnetization plateau under the applied field perpendicular to the quasi-one-dimensional stripe direction. To unravel the origin of the magnetization plateau, we used single crystal neutron diffraction to investigate the evolution of magnetic structures with field. At zero field, the ground state magnetic structure is a non-collinear antiferromagnetic order with reduced ordered-magnetic moments on both Co sites. Increasing the magnetic field flips the spins on one of the Co sites to ferromagnetic order, while the spins on the other Co site remain small to zero ordered-magnetic moments despite the strong magnetic field. Such robustness in reducing ordered-magnetic moments indicates strong magnetic frustration and/or quantum fluctuations in this KSL material. Furthermore, aided by the local magnetic susceptibility method using polarized neutrons, we concluded that the resulting ground state and the half-magnetization plateau are likely caused by the Dzyaloshinskii-Moriya (DM) interactions between spins on two Co sites and the strong quantum fluctuations within the 1D Co-spin chain.

The research was supported by the U.S. Department of Energy (DOE), Early Career Research Program Award KC0402020 and used resources at the High Flux Isotope Reactor, a DOE Office of Science User Facility operated by ORNL.

SESSION QT02.04: Emerging 2D Magnetic Materials II
Session Chairs: Dmitry Ovchinnikov and Tyler Slade
Wednesday Morning, April 24, 2024
Room 421, Level 4, Summit

8:30 AM *QT02.04.01

Next Level Two-Dimensional Quantum Materials Xavier Roy; Columbia University, United States

Two-dimensional (2D) materials have received widespread attention in the past two decades due to their remarkable physical, mechanical and chemical properties, and our ability to integrate them into devices. In this seminar, I will present our recent work in the development of the next generation of 2D materials. I will first discuss how magnetic order strongly couples to optical transitions in a new magnetic semiconductor developed in my laboratories, CrSBr. I will then introduce the synthesis and characterization of the first *f*-electron-based heavy fermion metal, CeSiI, that is also a 2D van der Waals (vdW) material. Conceptually, our synthetic design takes a traditional 3D intermetallic heavy fermion compound and slices it into atomically-thin vdW sheets by incorporating iodine into the structure. The resulting material is cleavable and effectively 2D electronically, even in bulk crystals.

9:00 AM QT02.04.02

Intercalation-Induced Magnetic Properties of Quasi-2D $\text{Fe}_{3-x}\text{GeTe}_2$ Van der Waals Magnet Srinivasa Rao Singamaneni and Daniel Rascon; The University of Texas at El Paso, United States

Among several well-known transition metal-based compounds, cleavable van der Waals (vdW) $\text{Fe}_{3-x}\text{GeTe}_2$ (FGT) magnet is a strong candidate for use in two-dimensional (2D) magnetic devices due to its strong perpendicular magnetic anisotropy, sizeable Curie temperature ($T_C \sim 154$ K), and versatile magnetic character that is retained in the low-dimensional limit. While the T_C remains far too low for practical applications, there has been a successful push toward improving it via external driving forces such as pressure, irradiation, and doping. Here we present experimental evidence of a novel room-temperature (RT) ferromagnetic phase induced by the electrochemical intercalation of common tetrabutylammonium cations (TBA⁺) into quasi-2D FGT. We obtained Curie temperatures as high as 350 K with chemical and physical stability of the intercalated compound. The temperature-dependent Raman measurements in combination with vdW-corrected *ab initio* calculations suggest that charge transfer (electron doping) upon intercalation could lead to the observation of RT ferromagnetism. This work demonstrates that molecular intercalation is a viable route in realizing high-temperature vdW magnets in an inexpensive and reliable manner, and has the potential to be extended to bilayer and few-layer vdW magnets.

9:15 AM *QT02.04.03

Room Temperature Néel-Type Skyrmions in a Van der Waals Ferromagnet Revealed by Multi-Modal Lorentz Electron Microscopy Yu-Tsun Shao¹, Hongrui Zhang², Xiang Chen², Zhen Chen³, Robert Birgeneau², Ramamoorthy Ramesh⁴ and David A. Muller⁵; ¹University of Southern California, United States; ²University of California, Berkeley, United States; ³Institute of Physics, Chinese Academy of Sciences, China; ⁴Rice University, United States; ⁵Cornell University, United States

Two-dimensional van der Waals (2D vdW) magnets offer a promising platform for exploring magnetic and topological phases, owing to their unique layered structure and crystallographic symmetries sensitive to stacking order. Real-space topological spin textures, such as magnetic skyrmions consisting of swirling spin configurations, are often stabilized by an antisymmetric Dzyaloshinskii-Moriya interaction (DMI) present in materials with broken inversion symmetry. Among the vdW materials for studying 2D magnetism, the Fe_xGeTe_2 (FGT, $N=3-5$) system is exceptional due to its tunability of magnetic properties with chemical doping and the existence of ferromagnetism above room temperature.

Here, we explore the chemically driven structural and magnetic phase transitions in $(\text{Fe}_{1-x}\text{Co}_x)_5\text{GeTe}_2$ (FCGT) using a combination of atomic resolution imaging, energy dispersive x-ray spectroscopy (EDS) mapping, and Lorentz four-dimensional scanning transmission electron microscopy (4D-STEM) along with an electron microscopy pixel array detector (EMPAD). Upon Co-doping, we find that the FCGT undergoes both structural and magnetic phase transitions from an antiferromagnetic, centrosymmetric AA'-stacking ($x=0.46$) to a ferromagnetic, polar AA'-stacking ($x=0.50$). This structural phase transition is accompanied by a change in Fe and Co ordering as revealed by atomic resolution STEM-EDS. More interestingly, room temperature Néel-type skyrmions emerge in the AA' phase as revealed by Lorentz 4D-STEM. In summary, our work paves the way for studying structural and magnetic phase transition in vdW magnetic materials.

Work supported by the AFOSR Hybrid Materials MURI, award # FA9550-18-1-0480 and USC Viterbi start-up. Facilities supported by the National Science Foundation (DMR-1429155, DMR- 2039380, DMR-1719875)

9:45 AM QT02.04.04

Magnetism in The Square Lattice Compounds YbBi_2IO_4 and $\text{YbBi}_2\text{ClO}_4$ Andrew F. May, Pyeongjae Park, Gabriele Sala, Thomas Proffen, Matthew Stone and Andrew Christianson; Oak Ridge National Laboratory, United States

The square lattice affords a simple platform to study quantum effects in two-dimensions (2D). This is because a two-interaction square lattice system is frustrated when the interactions are antiferromagnetic, with the phase diagram including the quantum spin liquid state. YbBi_2IO_4 and $\text{YbBi}_2\text{ClO}_4$ possess well-isolated layers containing square lattices of Yb^{3+} and are thus good candidates for realizing quantum effects on a square lattice. Here, we examine the magnetism and crystal field levels in the title compounds through a combination of specific heat, magnetization and inelastic neutron scattering measurements on polycrystalline samples. The results reveal that these materials host well-isolated Kramer's doublet ground states, with quasi-2D magnetic behavior as well as evidence for magnetic frustration. YbBi_2IO_4 and $\text{YbBi}_2\text{ClO}_4$ are therefore interesting candidates for future studies of 2D quantum magnetism.

10:00 AM BREAK

10:30 AM *QT02.04.05

Expanding The Portfolio of Two-Dimensional Magnetic Materials and Their Applications from First Principles Marco Gibertini^{1,2}; ¹Università degli Studi di Modena e Reggio Emilia, Italy; ²CNR-NANO, Italy

We have performed an extensive high-throughput screening of known inorganic materials, to identify those that could be exfoliated into novel two-dimensional (2D) monolayers [1]. The screening protocol based on density-functional theory simulations has identified a portfolio of close to 2,000 inorganic materials that appear either easily or potentially exfoliable [2], which has recently almost doubled [3] with further data ingestion and now provides an extensive pool to investigate promising properties. Specific interest has been devoted to the determination of the magnetic ground state [4], potentially considering supercells to accommodate non-trivial magnetic structures and systematically probing the energy landscape by effectively controlling and exploring the orbital occupation matrices of magnetic atoms through the Robust Occupation Matrix Energy Optimiser (ROME) workflow [5]. Among the possible applications of these novel 2D magnets, we have considered the possibility of creating heterostructures where the topological character and the dissipationless transport of the edge modes can be controlled by the magnetization direction [6].

[1] N. Mounet, M. Gibertini, P. Schwaller, D. Campi, A. Merkys, A. Marrazzo, T. Sohier, I. E. Castelli, A. Cepellotti, G. Pizzi and N. Marzari, Nat. Nanotechnol. **13**, 246 (2018).

[2] Materials Cloud 2D Crystals Database (MC2D) <https://www.materialscloud.org/discover/mc2d>

[3] D. Campi, N. Mounet, M. Gibertini, G. Pizzi and N. Marzari, ACS Nano **17**, 11268 (2023).

[4] F. Haddadi et al, in preparation.

[5] L. Ponet, E. Di Lucente and N. Marzari, <https://doi.org/10.21203/rs.3.rs-3358581/v1>.

[6] C. Cozza and M. Gibertini, in preparation.

11:00 AM QT02.04.06

Structural and Magnetic Properties of Entropy-Engineered Vanadium Rich 2D Thiophosphates Patricia E. Meza, Abishek Iyer, Roberto dos Reis, Mercouri G. Kanatzidis and Vinayak P. Dravid; Northwestern University, United States

Metal thiophosphates (MPX_3) have gained recent prominence for their intrinsic magnetic properties. These materials feature a layered, van der Waals structure with $[\text{P}_2\text{X}_6]^{4-}$ bipyramid anion units surrounded by octahedrally coordinated metal cations. By incorporating different metal cations, a diverse range of magnetic phases can be induced, making MPX_3 compounds promising subjects for condensed matter research into magnetic phases. Remarkably, V-based thiophosphates are comparatively understudied despite exhibiting the most stable antiferromagnetic ground state for the homogenous family of compounds, characterized by its large exchange parameter. [1] This is largely due to the difficulty of synthesizing the monometallic phase due to the formation of a parasitic V_xS_y species. Utilizing a flux method, [2] we have stabilized V in the MPS_3 structure by alloying with Mn, Fe, Co, or Ni. These V-rich compounds are expected to maintain the large exchange parameter while possibly exhibiting magnetic frustration.

Herein, we present a thorough investigation of novel $\text{V}_{0.56}\text{FeP}_2\text{S}_6$, and $\text{V}_{0.56}(\text{MnFeCoNiZn})\text{P}_2\text{S}_6$ thiophosphates including a study of structure, vanadium oxidation state, and chemical homogeneity. Elemental studies have confirmed the single crystal stoichiometry of these mixed cation systems. This is corroborated by structural refinement showing lattice expansion with increased alloying. Other mixed bimetallic thiophosphate systems demonstrate an inhomogeneous distribution of cations, resulting in heterostructures in the case CuInP_2S_6 or large composition fluctuations between exfoliated flakes in FeCoP_2S_6 . [3], [4] Conversely, electron energy loss spectroscopy (EELS) of $\text{V}_{0.56}(\text{MnFeCoNiZn})\text{P}_2\text{S}_6$ reveals a remarkable homogenous solid solution which is preferred for future magnetic susceptibility measurements to determine magnetic moment alignment. Additionally, we were able to clarify the oxidation state of V in these materials using bulk and nanoscale spectroscopy techniques. We confirm a mixed V^{2+} and V^{3+} state and observe a trend towards increasing V^{2+} as the system is alloyed from bimetallic to high entropy. Finally, we present synthesis techniques to grow phase pure V-rich thiophosphate powders and centimeter scale crystals to target both catalysis and magnetic measurements. Our findings highlight entropy engineering as a useful method towards stabilizing vanadium rich thiophosphates and provide in-depth chemical characterization which is vital for applications of V-rich thiophosphates in next generation electronic devices.

[1] B. L. Chittari et al., Phys. Rev. B, **94**, 184428 (2016).

[2] D. G. Chica et al., Inorg. Chem., **60**, 3502–3513 (2021).

[3] M. Cheng et al., Chem. Mater., **35**, 1458–1465 (2023).

[4] R. Rao et al., Chem. Mater., **35**, 8020–8029 (2023).

11:15 AM QT02.04.07

Magnetic-Electronic Coupling in The Van der Waals Metal-Phosphorous-Trichalcogenides Efrat Lifshitz; Technion-Israel Institute of Technology, Israel

The recent discovery of magnetic van der Waals materials- opens a new paradigm in solid-state research, offering an exploration of magnetism at the nearly atomistic limit, with an impact on the development of newly emerging spintronics, memory and information devices. In particular, antiferromagnetic (AFM) materials are catching special attention at the current time, due to their low stray magnetic field, and fast spin response (in the THz). The talk will include a thorough investigation of the fundamental magnetic properties and their coupling to the electronic nature of two representative materials: MnPS_3 and FePS_3 . With a single AFM layer, the metals are positioned in a honeycomb arrangement. The AFM character is generated via a spin-exchange interaction among metal next neighbours (NNs), when the metal spins are mainly oriented normally to the layer plane arranged either in Néel or zigzag configurations. It is important to note that second and third NNs intralayer interactions are not negligible in the MPX_3 layers, governed by super-exchange

AFM coupling through the metal(d)-chalcogen(p) bonding. An interlayer interaction adds small tuning with weak super-super spin-exchange interaction, which despite being weak, may change the magnetic properties by having either AFM or FM stacking or by inducing a magnetic torque. A MnPS₃ layer with a Néel magnetic configuration and lack of spin-orbit coupling was a suitable platform for examining the contribution of the long spin-exchange interaction. The study implemented dilution of the Mn content (forming alloyed compounds with the general chemical formula Mn_xZn_{1-x}S₃), examining the sustain of AFM arrangement down to a composition of x=0.5, hence, supporting the weight of 2nd and 3rd spin-exchange coupling to the long-range magnetic ordering. A FePS₃, having a zigzag magnetic configuration, represents a case with a pronounced distortion of the honeycomb symmetry, due to local distortion around a metal site by a strong spin-orbit coupling. The two examples mentioned here showed a strong correlation between the magnetic ordering and the optical transitions, showing obvious changes in the photoluminescence at the Néel temperature (a point possessing a magnetic transition from AFM to paramagnetic phase), as well as an optical polarization character along the magnetic directionality. It was mainly distinct in the appearance of an exceptionally sharp emission line in the FePS₃ single layer with a strong linear polarization along the zigzag direction. The accompanied DFT calculations simulated the spin-exchange coupling process and its impact on the electronic band structure (will be shown at the presentation by a short movie). Furthermore, the theoretical calculations exposed a fundamental character in which the electronic transitions show a hybrid property between local metal transitions and band-edge transitions. The exploration of these fundamental points is an ongoing process at the current moment.

Acknowledgement: The authors express their gratitude to the collaborators in the project: Dr. Milosz Rybak and Prof. Magdalena Birowska (Warsaw University) and Dr. Thomas Brume and Prof. Thomas Heine (The University of Dresden).

11:30 AM *QT02.04.08

Growth of 2D Magnets and Dielectrics Zdenek Sofer; Institute of Chemical Tech, Czechia

The recent progress in methods of high quality and low defect 2D magnetic materials will be discussed. Beside the group of transition metal halides and chalcogens also the rapidly growth family of mixed halogen-chalcogenides will be introduced. The dominantly explored material, chromium sulfo-bromide adopt FeOCl structure and possess A type antiferromagnetic ordering at low temperature. By various methods of exfoliation or defect formation, this material can be converted to ferromagnetic state. The chemistry of CrSBr including doping and possible covalent and non-covalent functionalization and its effect on magnetic and optical properties will be presented together with possible applications in electronic devices.

Beside the two dimensional magnets, the 2D dielectric exhibit important group of materials with crucial rule in device fabrication. The broad spectra of novel high-k 2D dielectric materials growth and applications will be presented together with large scale crystal growth of hexagonal boron nitride at atmospheric pressure using various metal flux.

SESSION QT02.05: Disorder and Magnetism in 2D Materials

Session Chairs: Chaowei Hu and Andrew F. May

Wednesday Afternoon, April 24, 2024

Room 421, Level 4, Summit

1:30 PM *QT02.05.01

Magnetic Dilution in The Magnetic Topological Insulators Derived from MnBi₂Te₄ Ekaterina Kochetkova^{1,2}, Manaswini Sahoo¹, Laura T. Corredor¹ and Anna Isaeva^{2,1}; ¹Leibniz Institute for Solid State and Materials Research Dresden, Germany; ²University of Amsterdam, Netherlands

Magnetic topological insulators were recently shown to host the quantum anomalous Hall effect (QAHE), albeit in a low-temperature range which is not yet technologically relevant. Extrinsicly doped Bi₂Te₃ and (Cr,V)Bi₂(Se,Te)₃ heterostructures demonstrate the QAHE below 1 K [1], whereas the intrinsically magnetic van der Waals material MnBi₂Te₄ sustains it up to 6.5 K [2]. Bulk MnBi₂Te₄ is an A-type antiferromagnet with T_N = 25 K, and its isostructural analogue Mn_{1+x}Sb_{2-x}Te₄ exhibits a ferri- or ferromagnetic ground state with an increased T_C up to 58 K [3] depending on the amount x of Mn excess.

Our combined x-ray and neutron studies of the Mn and Sb(Bi) distribution in MnSb₂Te₄ and MnBi₆Te₁₀ [4] highlight the importance of the Mn(II) distribution pattern in the crystal structure for the resulting magnetic ground state. Even subtle details of the atomic intermixing appears to influence the magnetic properties greatly.

In this talk, I will discuss our latest studies of the Mn-Ge-Sb-Te and Mn-Ge-Se-Te systems with the focus on how the site disorder of Mn(II) in the periodic crystal structure impacts the long-range magnetic order.

[1] C.-Z. Chang et al. Science 340, 167 (2013). [2] Y. Deng et al. Science 367, 895 (2020). [3] M. Sahoo, ..., A. Isaeva. *Tuning strategy for Curie-temperature enhancement in the van der Waals magnet Mn_{1+x}Sb_{2-x}Te₄*. Accepted to Mater. Phys. Today (2023). [4] A. V. Tcakaev, ..., A. Isaeva, V. Hinkov. Adv. Sci. 10, 2203239 (2023).

2:00 PM QT02.05.02

Near Room-Temperature Intrinsic Exchange Bias in an Fe Intercalated ZrSe₂ Spin Glass Zhizhi Kong and Kwabena Bediako; University of California, Berkeley, United States

Exchange bias is a magnetic phenomenon commonly manifested as the hysteresis-loop shift when a system hosting certain magnetic heterointerfaces is cooled under an applied external magnetic field. Despite the extensive use of the exchange bias effect, particularly in magnetic multilayers, for the design of spin-based memory/electronics devices, a comprehensive mechanistic understanding of this effect remains a longstanding problem. Recent work has shown that disorder-induced spin frustration might play a key role in exchange bias, suggesting new materials design approaches for spin-based electronic devices that harness this effect. Here, we design a spin glass with strong spin frustration induced by magnetic disorder by exploiting the distinctive structure of Fe intercalated ZrSe₂, where Fe(II) centers are shown to occupy both octahedral and tetrahedral interstitial sites and to distribute between ZrSe₂ layers without long-range structural order. Notably, we observe behavior consistent with a magnetically frustrated and multidegenerate ground state in these Fe_{0.17}ZrSe₂ single crystals, which persists above room temperature. Moreover, this magnetic frustration leads to a robust and tunable exchange bias up to 250 K. These results not only offer important insights into the effects of magnetic disorder and frustration in magnetic materials generally, but also highlight as design strategy the idea that a large exchange bias can arise from an inhomogeneous microscopic environment without discernible long-range magnetic order. In addition, these results show that intercalated TMDs like Fe_{0.17}ZrSe₂ hold potential for spintronic technologies that can achieve room temperature applications.

2:15 PM QT02.05.03

2D Heisenberg Ferromagnetism in Fe₃GeTe₂ Ankita Tiwari¹, Hyobin ahn², Jyoti Saini¹, Pawan K. Srivastava³, Budhi Singh³, Changgu Lee^{2,3} and Subhasis Ghosh¹; ¹Jawaharlal Nehru University, India; ²SKKU Advanced Institute of Nanotechnology (SAINT), Sungkyunkwan University, Korea (the Republic of); ³School of Mechanical Engineering, Sungkyunkwan University, Korea (the Republic of)

The van der Waals ferromagnets, such as CrI₃, CrTe₂, Cr₂X₂Te₆ (X = Si and Ge) and Fe₃GeTe₂ provide an excellent platform to investigate ferromagnetism in two dimension (2D) which is otherwise forbidden for short ranged exchange interaction mediated ferromagnetism, according to Hohenberg-Mermin-Wagner (HMW) theorem[1,2]. 2D van der Waals ferromagnets are being touted seriously as the materials for future spintronic devices. In particular, Fe₃GeTe₂ and Fe₅GeTe₂ are being investigated vigorously due to the exceptional tunability of their magnetic properties and high Curie temperature, which is near or above room temperature [3]. Short-ranged exchange interaction, such as 2D Ising and 2D XY driven phase transition, has been observed in Cr₂X₂Te₆ and CrI₃, respectively. However, the 2D-Heisenberg ferromagnet has not yet been observed in accordance with the HMW theorem. The presence of long-range (LR) interaction changes the scenario completely [4]. LR interactions have been shown to be responsible for (i) interesting finite temperature transitions, (ii) new critical phenomena, and (iii) continuously varying critical exponents in spin 1/2 Heisenberg systems in 2D systems. Though it is realized that LR-driven ferromagnetism is essential for circumventing the HMW theorem in 2D, but experimental realization remains elusive in condensed matter systems. Here, we show that Fe₃GeTe₂ is a 2D Heisenberg ferromagnet by breaking the limit of the HMW theorem. This has been possible due to the presence of both itinerant and local-moment magnetism in Fe₃GeTe₂ [5]. Temperature dependence of magnetization with the signature of 2D magnons, Rhodes-Wohlfarth (RW) and generalized RW-based analysis [6] established that Fe₃GeTe₂ is a 2D ferromagnet with itinerant magnetism which can be tuned by the magnetic field. So far, critical phenomena and second-order phase transition have been dealt with renormalization group theory. However, the same in the presence of long-range interaction is nontrivial [4]. Here we present an improvised method to deal with phase transition and critical phenomena mediated by long Heisenberg interaction in 2D in the presence of long-range Ruderman-Kittel-Kasuya-Yusida (RKKY). We show that critical exponents, in this case, can vary with external parameters. The critical exponents cross from the mean-field universality class to the 2D Heisenberg universality class as the field increases. We argue that variable critical exponents is the key signature for 2D Heisenberg ferromagnetism, as emphasized by recent theoretical calculations [7]. Fe in Fe₃GeTe₂ has two inequivalent charge states, i.e. Fe²⁺ and Fe³⁺, which lead to multi-orbital paths for different spin-spin interactions. In the case of a hexagonal crystal field, as in Fe₃GeTe₂, the five 3d orbitals of the Fe atom split into three groups of orbitals with differing localization is responsible for underlying long-range ordering for both itinerant and local-moment ferromagnetism.

References

1. N. D. Mermin and H. Wagner, Phys. Rev. Lett. 17, 1133 (1966).
2. P. C. Hohenberg, Phys. Rev. 158, 383 (1967).
3. Y. Deng, Y. Yu, Y. Song, J. Zhang et al., Nature 563, 94 (2018).
4. N. Defenu, T. Donner, T. Macri, G. Pagano, S. Ruffo, and A. Trombettoni, [Rev. Mod. Phys. (to be published)] 10.48550/arXiv.2109.01063.
5. Z. Fei, B. Huang, P. Malinowski, W. Wang, T. Song, J. Sanchez, W. Yao, D. Xiao, X. Zhu, and A. F. May et al., Nat. Mater 17, 778 (2018).
6. Y. Takahashi, Spin fluctuation theory of itinerant electron magnetism, Vol. 9 (Springer, 2013).
7. J. Zhao, M. Song, Y. Qi, J. Rong, and Z. Y. Meng, 10.48550/arXiv.2306.01044.

2:30 PM BREAK

SESSION QT02.06: Electronic and Magnetic Phases in Emerging Materials
Session Chairs: Zhong Lin and Daniel Pajerowski
Wednesday Afternoon, April 24, 2024
Room 421, Level 4, Summit

3:30 PM *QT02.06.01

Single Crystal Growth and Magnetic Anisotropic Study of SmCrGe₃ with Cr Linear Chain Mingyu Xu and Weiwei Xie; Michigan State University, United States

Mingyu Xu¹, Xianglin Ke², Sergey L. Bud'ko³, Paul C. Canfield³, Weiwei Xie^{1*}

1. Department of Chemistry, Michigan State University, East Lansing, MI, 48824
2. Department of Physics and Astronomy, Michigan State University, East Lansing, MI, 48824
3. Division of Materials Science, Ames Laboratory, Ames, IA, 50010

SmCrGe₃ was reported in the polycrystalline, which has ferromagnetic order occurring at 155 K [1]. To study the magnetic behaviors of SmCrGe₃, herein, the single crystals of SmCrGe₃ were grown using high temperature flux method. According to the single crystal X-ray diffraction, SmCrGe₃ crystallizes in the hexagonal LaCrGe₃-type structure with Cr linear chain along the *c*-axis, which forms the face-sharing Cr-centered octahedra aligned along the *c*-axis. Compared with itinerant magnet LaCrGe₃, SmCrGe₃ offers the opportunity to understand the interaction between localized 4*f* electron and itinerant electron in this quasi-one-dimensional system and the role of interaction played in domain pinning changing [2], which may explain “one domain” behavior in LaCrGe₃ single crystal. Transport, magnetization, and specific heat measurements are taken. SmCrGe₃ behaves as a hard ferromagnetic material, which is different from other RECrGe₃ (RE = La - Nd). Coercivity as the function of temperature and field-dependent pinning change are given, and the results will be discussed in detail.

[1] Haiying Bie, et al. *Chem. Mater.* **2007**, *19*, 4613-4620.

[2] M Xu, et al. *Phys. Rev. B* **2023**, *107*, 134437.

4:00 PM QT02.06.02

Unravelling Quantum Phases in The Shastry-Sutherland Lattice Huibo Cao¹, Kyle Ma¹, Brianna Billingsley², Madalynn Marshall¹ and Tai Kong²; ¹Oak Ridge National Laboratory, United States; ²The University of Arizona, United States

The Shastry-Sutherland lattice consists of a two-dimensional orthogonal arrangement of spin dimers. By varying the ratio of intra-dimer and inter-dimer

interactions, the rich phase diagram can emerge, encompassing various exotic quantum states. Single-ion and exchange magnetic anisotropies can further diversify the phased diagram and give rise to quantum states beyond the traditional antiferromagnetic Heisenberg Shastry-Sutherland lattice model. Neutron scattering is an important technique for characterizing magnetic states. Here, I will introduce our recent studies using neutron scattering to unravel the quantum states of spin dimers in the rare-earth (RE) Shastry-Sutherland lattice compound $\text{BaRE}_2\text{ZnS}_5$ (RE=Nd, Ce, and Pr).

The research was supported by the U.S. Department of Energy (DOE), Early Career Research Program Award KC0402020 and used resources at the High Flux Isotope Reactor, a DOE Office of Science User Facility operated by ORNL.

4:15 PM *QT02.06.03

Structural and Electronic Phases of 2D Transition Metal Dichalcogenides Oleg Yazyev; Ecole Polytechnique Federale de Lausanne, Switzerland

Layered transition metal dichalcogenides (TMDs) of chemical composition MX_2 (M = transition metal; X = S, Se, or Te) represent a broad family of materials with diverse electronic properties, including metals, insulators, as well as more complex states such as the charge-density-wave (CDW) and superconducting phases. More recently, the possibility of realizing single- and few-layer TMDs has brought the two-dimensional (2D) forms of these materials into the spotlight of prospective application in electronics, optoelectronics and beyond [1]. In my talk, I will review the “periodic table” of TMDs attempting to reveal systematic trends and develop chemical intuition across this family of 2D materials. Using a Wannier function approach, I will address the relevance of the crystal and ligand fields in determining the relative stability of 1T and 1H polymorphs as a function of the filling of the d-shell in 2D TMDs [2]. Then, I will present a unified picture of lattice instabilities in metallic TMDs that describes both the CDW phases and the strong-coupling scenario resulting in the formation of metal-metal bonds (as e.g. in the dimerized 1T' phases) [3]. In the rest of my talk, I will focus on topological and magnetic phases of TMDs. The 1T'-phase of Mo and W TMDs that have recently been shown to host the topologically non-trivial quantum spin Hall (QSH) insulator phase. The robustness of the QSH phase as well as the topological edge states [4] and interface states at the well-ordered 1T'-1H lateral heterojunctions will be discussed in conjunction with recent experiments on 1T'- WSe_2 [5]. I will also cover our recent discovery of magnetic ordering and magnetoresistive switching in metallic few-layer and insulating single-layer PtSe_2 [6,7].

1. S. Manzeli, D. Ovchinnikov, D. Pasquier, O. V. Yazyev and A. Kis, *Nature Rev. Mater.* **2**, 17033 (2017).
2. D. Pasquier and O. V. Yazyev, *2D Materials* **6**, 025015 (2019).
3. D. Pasquier and O. V. Yazyev, *Phys. Rev. B* **100**, 201103(R) (2019).
4. A. Pulkin and O. V. Yazyev, *J. Phys. Chem. Lett.* **11**, 6964 (2020).
5. M. M. Ugeda *et al.*, *Nature Commun.* **9**, 3401 (2018).
6. A. Avsar *et al.*, *Nature Nanotechnol.* **14**, 674 (2019).
7. A. Avsar *et al.*, *Nature Commun.* **11**, 4806 (2020).

4:45 PM QT02.06.04

Probing The Local Properties of Co-Honeycomb Magnets as an Avenue to Understanding Their Complex Magnetic Behaviour Megan R. Rutherford¹, Dalmau Reg-i-Plessis², Daniel Shaw³, Austin Ferrenti⁴, Solveig S. Aamlid¹, Graham King⁵, Tyrel McQueen⁴, Kate Ross³, Kenji Kojima^{6,1} and Alannah Hallas¹; ¹The University of British Columbia, Canada; ²ETH Zürich, Switzerland; ³Colorado State University, United States; ⁴Johns Hopkins University, United States; ⁵Canadian Light Source, Canada; ⁶TRIUMF, Canada

In the field of frustrated magnetism, the relationship between the crystal structure of a material and its magnetic properties has been a fruitful area of research for decades. A problem that has tormented materials scientists for an equal length of time, is the effect of small structural perturbations on the overall magnetic behaviour of a sample. An example of the interconnectedness of disorder sensitivity with rich magnetic phase spaces can be seen in well-studied examples of honeycomb magnets like RuCl_3 , where large differences in its physical characteristics emerge from subtle variations in stacking. A less well-understood example of this type of phenomena can be seen in the material $\text{BaCo}_2(\text{PO}_4)_2$ where the Co^{2+} ions form a highly frustrated, undistorted honeycomb lattice of Co^{2+} that are well separated by Ba and PO_4 spacer layers, hence this material is highly 2-dimensional. Neutron diffraction of $\text{BaCo}_2(\text{PO}_4)_2$ reveals not one, but two distinct short range ordered magnetic states that develop over two successive transition temperatures. In contrast, $\text{BaCo}_2(\text{AsO}_4)_2$, which is isostructural to the phosphate, long range orders into a single well-defined magnetic ordered state at low temperatures. Muon spin relaxation (μSR) is a local probe that is uniquely suited to the investigation of multiple coexisting, competing magnetic phases. A comprehensive μSR study has been performed on both the phosphate, and the arsenate for comparison, to determine how these competing magnetic phases develop with changing temperature across the temperature range of interest. The local structure of the material has also been investigated using total x-ray scattering techniques in an attempt to elucidate the origin of the unique magnetic behaviour of $\text{BaCo}_2(\text{PO}_4)_2$. The combined evidence from these local probes leads us to conclude that this phase coexistence in $\text{BaCo}_2(\text{PO}_4)_2$ is likely a result of synthesis-sensitive polymorphism.

SESSION QT02.07: Poster Session
Session Chairs: Yunqiu Kelly Luo and Dmitry Ovchinnikov
Wednesday Afternoon, April 24, 2024
Flex Hall C, Level 2, Summit

5:00 PM QT02.07.01

The Effect of Pr Doping and Sintering Temperature on The Structural, Magnetic and Transport Properties of $\text{La}_{1-x}\text{Pr}_x\text{Ca}_y\text{MnO}_3$ ($y = 0.30, 0.35, 0.40$; $x = 0.40$) Nanocrystals Dharmendra S. Raghav¹, Hari K. Singh² and Ghanshyam D. Varma³; ¹Invertis University, India; ²CSIR-National Physical Laboratory, India; ³Indian Institute of Technology Roorkee, India

Among the doped rare earth manganites, $\text{La}_{1-x}\text{Pr}_x\text{Ca}_y\text{MnO}_3$ (LPCMO) has been recognised as the prototypical of the phase separated doped rare-earth manganites. LPCMO perovskite manganites still attract the interest of materials, chemistry and physics communities. The structural, microstructural, magnetic and electrical transport properties have been correlatively studied to decipher the complex consequences of variation of intrinsic parameter, the average La-site cationic radii and extrinsic particle size on the magneto-electrical phase coexistence in $\text{La}_{1-x}\text{Pr}_x\text{Ca}_y\text{MnO}_3$ ($y = 0.30, 0.35, 0.40$; $x = 0.40$). Magnetization measurements show sequential paramagnetic (PM)-antiferromagnetic (AFM)-ferromagnetic (FM) transitions on lowering the temperature. The AFM-FM transition exhibits (i) pronounced hysteresis between field-cooled cooling (FCC) and field-cooled warming (FCW), (ii) substantial divergence between zero-field cooling (ZFC) and FCW curves. The lower temperature magnetic state is much closer to a spin glass at smaller ionic radius and larger particle size. At smaller ionic radius and smaller particle size, it shows a better resemblance to a cluster glass state. The presence of a large thermal hysteresis in the insulator-metal transition (IMT) coupled with the one in FCC-FCW magnetization at particle sizes ~ 200 nm-160 nm, and ~ 460 -

400 nm demonstrates that this particle size regime is the most conducive to the phase separation. IMT disappears at smaller ionic radii and larger particle sizes due to the enhancement of AFM and charge-ordering. The observed phenomena are explained in terms of the interplay between the ionic radii and particle size induced changes in the average apical bond angles and the average bond length.

5:00 PM QT02.07.02

Chromium Sulfide Bromide Down to Ferromagnetic Nanoribbons: The Study of Electrochemical Exfoliation Method and Magnetic Transitions in Bulk and Exfoliated CrSBr [Ksenija Mosina](#), Vlastimil Mazanek and Jan Luxa; University of Chemistry and Technology, Prague, Czechia

Recent advancements in the field of 2D materials have opened up exciting possibilities for applications in emerging technologies; however, the research focuses on magnetic atomically thin crystals that offer intriguing prospects in the realm of magnetoelectricity and magneto-optics is still in its infancy. In this study, we delve into the magnetic properties of chromium sulfide bromide (CrSBr), a material with a complex magnetic behavior. Recent reports have labeled chromium sulfide bromide CrSBr as an ideal candidate for studies of magnetism due to its antiferromagnetic state in bulk with a Neel temperature around 132 K and ferromagnetism in the monolayer. For the first time, we introduce the electrochemical exfoliation of CrSBr down to ferromagnetic nanoribbons in a non-aqueous environment. The exfoliated material preserves its orthorhombic crystalline structure and exhibits strong optical anisotropy, with Raman signals displaying polarization dependencies. The unique cleavage behavior of CrSBr is facilitated by its structural anisotropy and weak interlayer hybridization, allowing for efficient exfoliation along the crystal's a-direction. Interestingly, electrochemically exfoliated CrSBr exhibits a broad but clear FM transition with a T Curie around 130 K, which opens up the possibility of utilizing CrSBr nanoribbons in innovative magneto-optical and spintronic devices. Moreover, we demonstrate the potential application of exfoliated material in high-performance electrochemical photodetectors and their use as anodes in lithium-ion batteries, where they exhibit promising self-improving capabilities.

5:00 PM QT02.07.03

Characterization of Alloyed Fe_{3-x}Co_xSn₂ Kagomé-Lattice Films Grown Using Molecular Beam Epitaxy [Anna Li](#)^{1,2}, Prajwal Laxmeesha², Tessa D. Tucker² and Steven May²; ¹University of California, Berkeley, United States; ²Drexel University, United States

Materials in which transition metals form a kagomé lattice have generated interest in recent years due to their unique magnetic and electronic properties. Ferromagnetic Fe₃Sn₂ is one such example where the Fe kagomé sublattice results in the presence of Weyl fermions and flat bands. Being able to tune Weyl nodes has been an area of immense study, and hole and electron-doping are potential avenues for changing the position of Weyl nodes in energy and momentum-space, and as a result, as well as moving the Fermi level with respect to the Weyl points with respect to the Fermi level. We performed an experimental investigation on the effect of electron-doping in epitaxially-grown thin films of Fe₃Sn₂ through substitution of Co for Fe. We have grown Fe_{3-x}Co_xSn₂ films using molecular beam epitaxy (MBE) at various concentrations of Co (x = 0, 0.1, 0.5, 0.75, 1.0) on Al₂O₃ (0001) substrates buffered with a thin Co (111) wetting buffer layer. The Fe_{3-x}Co_xSn₂ films are capped with CaF₂ to prevent oxidation. Structural characterization of the heterostructures by *in situ* reflection high-energy electron diffraction (RHEED) confirms the growth of ordered films, and further surface characterization via X-ray reflectivity and atomic force microscopy identifies smooth surfaces. X-ray diffraction was used to confirm that the films have uniform c-axis orientation and that no secondary phases are present, while magnetometry was used to study the magnetic properties of the films. Further, it was observed that both the c-axis parameter and saturation magnetization decreases with increasing Co concentration, in agreement with previous density functional theory calculations (M. Adams *et al* 2023 *J. Phys.: Condens. Matter* **35** 265801). [PM4] Magnetometry measurements revealed a decrease in saturation magnetization as the Co content was increased. Our results provide the groundwork for further investigation on the changing magnetic properties and electronic band structure in doped alloyed epitaxial Fe₃Sn₂ heterostructures.

A.W.L. was primarily supported by NSF through the University of Pennsylvania Materials Research Science and Engineering Center (MRSEC) (DMR-1720530).

5:00 PM QT02.07.04

High-Frequency Electron Paramagnetic Resonance Properties of Kagome Crystal YMn₆Sn₆ Lovia Ofori¹, Johan van Tol², Nirmal J. Ghimire³ and [Srinivasa Rao Singamaneni](#)¹; ¹The University of Texas at El Paso, United States; ²Florida State University, United States; ³University of Notre Dame, United States

Kagome magnetic crystals received a great deal of research attention in the recent past for their intriguing magnetic properties. Recently, YMn₆Sn₆ has been shown to exhibit a number of nontrivial magnetic phases, and the origin remains elusive. We measured EPR/FMR at high fields and frequencies to investigate the local field at the magnetic Mn ions in YMn₆Sn₆. In particular, we studied the signals at 120 and 240 GHz (4 and 8 cm⁻¹, resp.) We observe the phase transitions and the coexistence of different phases in the transition region, which are approximately in line with the B-T phase diagram for YMn₆Sn₆. This work underscores the importance of employing the high/multifrequency EPR technique in probing for the microscopic mechanisms to better understand the observed new magnetic phases/textures.

5:00 PM QT02.07.05

Pressure-Dependent Magnetic and Optical Properties of Fe_{2.7}GeTe₂ Rubyan Olmos¹, Gilberto Fabbris², Rahul Rao³, Michael A. Susner³ and [Srinivasa Rao Singamaneni](#)¹; ¹The University of Texas at El Paso, United States; ²Argonne National Laboratory, United States; ³Air Force Research Laboratory, United States

van der Waals magnets offer a great opportunity for tunable magnetic properties as they are susceptible to external perturbations. Among all, pressure is a versatile tuning knob. In this work, we present our recent experimental findings collected on Fe_{2.7}GeTe₂ by employing SQUID magnetometry, Raman spectroscopy, and synchrotron-based XMCD measurements as a function of applied pressure. We observe that the saturation magnetization and the Curie temperature decreased as the external pressure increased. The Raman data showed the pressure-induced structural phase transition. This work signifies the application of pressure in tuning the magnetic properties of layered van der Waals magnets.

5:00 PM QT02.07.06

Epitaxial Growth and Magnetic Properties of Kagomé Metal FeSn/Elemental Ferromagnet Heterostructures [Prajwal Laxmeesha](#)¹, Tessa D. Tucker¹, Rajeev Kumar Rai², Shuchen Li³, Myoung-Woo Yoo³, Eric A. Stach², Axel Hoffmann³ and Steven May¹; ¹Drexel University, United States; ²University of Pennsylvania, United States; ³University of Illinois at Urbana-Champaign, United States

Binary kagomé compounds T_mX_n ($T=Mn, Fe, Co$; $X=Sn, Ge$; $m:n = 3:1, 3:2, 1:1$) have garnered significant interest due to the coexistence of topological band crossings and flat bands stemming from the geometry of the metal-site kagomé lattice. In order to harness these distinctive electronic band features for potential applications in spintronics, it is imperative to grow high-quality heterostructures. In this work, we detail the synthesis of Fe/FeSn and Co/FeSn bilayers on c-axis-oriented Al₂O₃ substrates, achieved *via* molecular beam epitaxy. The use of elemental buffer layers (Fe and Co) facilitates the growth of smooth and continuous FeSn films, while also enabling the formation of heterointerfaces between elemental ferromagnetic metals and antiferromagnetic

kagomé metal FeSn. Structural characterization using high-resolution X-ray diffraction, reflection high-energy electron diffraction, scanning electron microscopy and transmission electron microscopy revealed the FeSn films were flat and epitaxial with well defined interfaces. Rutherford backscattering spectrometry was used to confirm the stoichiometric window where single phase FeSn films are stabilized, while transport and magnetometry measurements were conducted to verify metallicity and magnetic ordering in the bilayers. We observe exchange bias in both bilayer systems, affirming the existence of antiferromagnetic order in FeSn, thus opening possibilities for further investigations into interfacial magnetism in kagomé heterostructures and the potential integration of these materials into spintronics devices.

Work at Drexel University and the University of Illinois at Urbana-Champaign was supported by the National Science Foundation, grant number ECCS-2031870. Work at University of Pennsylvania was supported by University of Pennsylvania Materials Research Science and Engineering Center (MRSEC) (DMR-2309043).

5:00 PM QT02.07.07

Synthesis of Mn-Doped Bi₂Te₃ via Chemical Vapor Deposition [Matthew E. Metcalf](#)¹, Bamidele O. Onipede¹, Shaan Dias², Alexander Glasgo¹ and Hui Cai¹; ¹University of California, Merced, United States; ²Carleton College, United States

Doping a topological insulator with magnetic elements can produce magnetic ordering within the material, breaking the time-reversal symmetry of the surface electronic states. Without this symmetry, topological insulators can exhibit many exotic quantum phenomena that are of theoretical interest and not well studied, including the quantum anomalous Hall effect, chiral Majorana modes, and topological magnetoelectric effects. In this work, we synthesized Mn-doped Bi₂Te₃, a topological insulator doped with a magnetic element, using atmospheric pressure chemical vapor deposition (CVD) and characterized our samples with optical microscopy, Raman spectroscopy, and X-ray photoelectron spectroscopy. The optimal values and acceptable ranges of several CVD growth parameters were determined by systematically varying each parameter one at a time. By utilizing CVD to synthesize Mn-doped Bi₂Te₃, this work demonstrates a simple, scalable, and low-cost process that offers precise control over the stoichiometry of grown crystals and opens the door to the production of high-quality atomically thin crystals—features which make CVD a useful and promising technique for future studies of magnetic topological insulators.

5:00 PM QT02.07.08

Strong Above Room Temperature Intrinsic Magnetism of Freestanding Layered CrTe₂ Crystal [Lihua Zhang](#)¹, Kim Kisslinger¹, Suji Park¹, Seng Huat Lee², Yu Wang², Zhiqiang Mao², Neha Dhull^{3,4}, Weichang Lin^{3,4}, Zonghuan Lu^{3,4}, Toh-Ming Lu^{3,4} and Gwo-Ching Wang^{3,4}; ¹Center for Functional Nanomaterials, Brookhaven National Lab, United States; ²2D Crystal Consortium, Materials Research Institute, The Pennsylvania State University, United States; ³Physics, Applied Physics and Astronomy Department, Rensselaer Polytechnic Institute, United States; ⁴The Center for Materials, Devices, and Integrated Systems, Rensselaer Polytechnic Institute, United States

Abstract: Magnetism in van der Waals (vdW) layered materials has attracted worldwide attention in fundamental condensed matter material research. Magnetism in low dimension materials has many exciting emerging properties and great potential for applications in low power spintronics, quantum computing, data storage, etc. Most monolayer (ML) vdW materials have been demonstrated to have Curie temperatures (T_c) below 300 K [1] or near room temperature [2]. This is because thermal fluctuations destroy the long-range magnetic order in a ML material according to Mermin-Wagner theorem. Thus, demands for the growth of bulk vdW layered materials to increase its T_c to above room temperature remains challenging. Only recently, bulk 1T-CrTe₂ crystal of mm size was synthesized from K deintercalation of KCrTe₂ and its room temperature T_c (310 K) was reported [3]. In this work, we present synthesized CrTe₂ crystals made from a similar method. We present their structure, chemical stoichiometry, vibrational, and magnetic properties of free standing CrTe₂ crystal measured by transmission electron microscopy (TEM), X-ray diffraction (XRD), electron backscatter diffraction (EBSD), energy dispersive X-ray spectroscopy (EDS), Raman scattering, superconducting quantum interference device (SQUID), and surface magneto-optical Kerr effect (SMOKE) techniques. TEM and XRD show CrTe₂ has crystalline layered structure with (0001) out-of-plane orientation with bulk lattice constants. EBSD shows a six-fold hexagonal crystal symmetry. EDS and Raman spectra show correct stoichiometry of 1 to 2 for Cr to Te ratio. All data support the synthesized crystals are of high quality. The temperatures dependent magnetization shows a phase transition at a T_c (317 K) above room temperature. The critical exponents extracted from the critical region are consistent with the classic 3D Ising model's prediction. SMOKE measurement of crystal at room temperature shows hysteresis loops with low coercivity (~20 Oe). Since the 632 nm laser wavelength's penetration depth depends on the laser incident angle, the probing depth is within sub-tens to tens of nm below surface, therefore the magnetic hysteresis loop measured by SMOKE is effectively from ultrathin layers of the CrTe₂ crystal.

Acknowledgements: This work is supported by the Center for Functional Nanomaterials, Brookhaven National Laboratory under DE-SC0012704, Penn State 2D Crystal Consortium –Materials Innovation Platform under NSF DMR-2039351, and the NYSTAR Focus Center at RPI, C180117.

References:

1. Huang, B., et al., Layer-dependent ferromagnetism in a van der Waals crystal down to the monolayer limit. *Nature*, 2017. 546: p. 270.
2. Bonilla, M., et al., Strong room-temperature ferromagnetism in VSe₂ monolayers on van der Waals substrates. *Nature Nanotechnology*, 2018. 13(4): p. 289-293.
3. Freitas, D.C., et al., Ferromagnetism in layered metastable 1T-CrTe₂. *Journal of Physics: Condensed Matter*, 2015. 27(17): p. 176002.

5:00 PM QT02.07.09

Diffuse Scattering in The Chiral Magnet BaCoSiO₄ [James W. Beare](#)¹, Huibo Cao¹, Chenyang Jiang¹, Zachary Morgan¹, Feng Ye¹, Yongqiang Cheng¹, Erxi Feng¹, Xiaojian Bai², Xianghan Xu³ and Sang-Wook Cheong³; ¹Oak Ridge National Lab, United States; ²Louisiana State University, United States; ³Rutgers, The State University of New Jersey, United States

In certain chiral magnets, a chiral arrangement of magnetic spins breaks both time reversal and spatial inversion symmetry, forming a toroidal moment. This symmetry breaking allows for the magnetoelectric effect, making these materials promising candidates for device applications. In BaCoSiO₄, Co ions form hexagonal layers in which magnetic interactions between the nearest five Co neighbors, as well as the antisymmetric DM interaction, are all important, leading to a complicated competition between interactions on this frustrated lattice. The ground state structure can be explained by a trimerization of Co ions into toroidal moments which form three interpenetrating sublattices, one of which has a toroidal moment opposite to the other two. Along with the frustration due to antiferromagnetic interactions within triangular trimers, there is structural short-range order which may contribute to additional frustration. In this talk, I will present diffuse scattering results which give insight into the short range magnetic and structural order within the material. Modeling both types of short-range order within the paramagnetic phase will improve our understanding of this exotic magnet. The research was supported by the U.S. Department of Energy (DOE), Early Career Research Program Awards KC0402020 and KC0402010, and used resources at the HFIR and SNS, DOE Office of Science User Facilities operated by ORNL.

5:00 PM QT02.07.10

Pillars of Discovery: Two Novel Divalent Transition Metal Germanates as Potential Multiferroics [Megan Smart](#)¹, Jie Xing¹, Colin McMillen², Joseph Kolis², Fankang Li¹ and Huibo Cao¹; ¹Oak Ridge National Laboratory, United States; ²Clemson University, United States

The pursuit of novel magnetic materials has driven inorganic crystal chemistry towards many exciting discoveries, from rare earth magnets to hexaferrites to elusive quantum materials such as spin liquids. One material class of interest are multiferroics, which combine the desirable properties of ferromagnetism and ferroelectricity, the latter of which requires crystallization in a polar space group. High-quality single crystals of inorganic oxides can be grown *via* hydrothermal synthetic methods using magnetic ions such as Co^{2+} and Cu^{2+} , with non-magnetic Ge^{4+} as a building block. Two such compounds were hydrothermally synthesized, $\text{Ba}_7\text{Rb}_2\text{Co}_6\text{Ge}_{18}\text{O}_{50}$ (**1**) and $\text{Sr}_7\text{K}_2\text{Cu}_6\text{Ge}_{17.3}\text{O}_{47.2}(\text{OH})_{2.8}$ (**2**), which crystallize in the acentric, polar space group $P6_3cm$. The polar feature of the unit cell is the ‘pillar’ propagating along each vertex on the *c*-axis. These pillars contain alternating trimers of TM^{2+} ($\text{TM} = \text{Co}, \text{Cu}$) in tetrahedral and trigonal bipyramidal geometries, and are separated by a central germanate cluster. With the conditions for ferroelectricity met, initial magnetic studies were performed, and their results are presented here. The Co-germanate shows two magnetic transitions in the susceptibility measurements, both suggesting magnetic short-range orders. The compound does not have structural disorder, therefore the magnetic short-range order likely originates from magnetic frustration. Two successive transitions possibly represent dimensionality cross-over transitions. The neutron scattering studies are underway to uncover the nature of magnetic transitions and phases in $\text{Ba}_7\text{Rb}_2\text{Co}_6\text{Ge}_{18}\text{O}_{50}$.

*The research was supported by the U.S. Department of Energy (DOE), Early Career Research Program Award KC0402020 and used resources at the HFIR, DOE Office of Science User Facilities operated by ORNL.

5:00 PM QT02.07.11

Quantum Criticality in Spin Dimer System $\text{BaNd}_2\text{ZnS}_5$ [Kyle Ma](#)¹, Brianna Billingsley², Madalynn Marshall¹, Xiaojian Bai³, Barry Winn¹, Cristian Batista⁴, Tai Kong² and Huibo Cao¹; ¹Oak Ridge National Laboratory, United States; ²The University of Arizona, United States; ³Louisiana State University, United States; ⁴The University of Tennessee, Knoxville, United States

We investigated the partial-disordered state of the Shastry-Sutherland system $\text{BaNd}_2\text{ZnS}_5$ utilizing the time-of-flight inelastic neutron scattering spectrometer HYSPEC at the Spallation Neutron Source (SNS) of the Oak Ridge National Laboratory (ORNL). Through modeling the field evolution of low-energy spin excitations up to 4T, we uncovered that the disordered states result from a delicate balance between the external magnetic field and antiferromagnetic (AF) inter-dimer Ising interactions. The intra-dimer interaction is predominantly Ising along the ordered moment direction, with a slight mixing of J_{++} and J_{--} .

Parametric measurements ranging from 0 to 4T of the order parameters of the ferromagnetic (FM) and antiferromagnetic (AFM) phases at 40mK were conducted using the DEMAND diffractometer at the High Flux Isotope Reactor of ORNL. The order parameter displays characteristics indicative of a quantum critical point and can be effectively modeled using semi-classical treatment based on $\text{SU}(4)$ coherent states. Although the longitudinal mode can not be quantitatively characterized, its presence is essential to explain the observed data, suggesting that the puzzling metamagnetic transition originates from the ordered antiferromagnetic state transitioning to the disordered quantum paramagnetic state.

SESSION QT02.08: Ultrafast Imaging and Control of Magnetism

Session Chairs: Dmitry Ovchinnikov and Veronika Sunko

Thursday Morning, April 25, 2024

Room 421, Level 4, Summit

8:45 AM *QT02.08.01

Engineering Quantum Geometry at Oxide Interfaces [Andrea Caviglia](#); Université de Genève, Switzerland

In oxide heterostructures, different materials are integrated into a single artificial crystal, resulting in a breaking of inversion symmetry across the heterointerfaces. A notable example is the interface between polar and nonpolar materials, where valence discontinuities lead to otherwise inaccessible charge and spin states. This approach paved the way for the discovery of numerous unconventional properties absent in the bulk constituents. However, control of the geometric structure of the electronic wave functions in correlated oxides remains an open challenge. Here, we create heterostructures consisting of ultrathin SrRuO_3 , an itinerant ferromagnet hosting momentum-space sources of Berry curvature, and LaAlO_3 , a polar wide-band-gap insulator. Transmission electron microscopy reveals an atomically sharp $\text{LaO}/\text{RuO}_2/\text{SrO}$ interface configuration, leading to excess charge being pinned near the $\text{LaAlO}_3/\text{SrRuO}_3$ interface. We demonstrate through magneto-optical characterization, theoretical calculations and transport measurements that the real-space charge reconstruction drives a reorganization of the topological charges in the band structure, thereby modifying the momentum-space Berry curvature in SrRuO_3 [1]. We will also report the discovery of the first material system having both spin- and orbital-sourced Berry curvature: $\text{LaAlO}_3/\text{SrTiO}_3$ interfaces grown along the [111] direction. We independently detect these two sources and probe the Berry curvature associated to the spin quantum number through the measurements of an anomalous planar Hall effect. The observation of a nonlinear Hall effect with time-reversal symmetry signals large orbital-mediated Berry curvature dipoles. The coexistence of different forms of Berry curvature enables the combination of spintronic and optoelectronic functionalities in a single material [2,3].

References

- [1] T. van Thiel et al., *Physical Review Letters* **127**, 127202 (2021)
- [2] E. Lesne et al., *Nature Materials* **22** (2023) 576
- [3] M.T. Mercaldo et al., *npj Quantum Materials* **8** (2023) 12

9:15 AM QT02.08.02

Exciton Transport in Van der Waals Antiferromagnet CrSBr [Florian Dimberger](#)¹, Sophia Terres¹, Kseniia Mosina², Zdenek Sofer², Akashdeep Kamra³, Mikhail M. Glazov⁴ and Alexey Chernikov¹; ¹Institute of Applied Physics and Würzburg-Dresden Cluster of Excellence, Germany; ²Department of Inorganic Chemistry, Czechia; ³Departamento de Física Teórica de la Materia Condensada and Condensed Matter Physics Center (IFIMAC), Spain; ⁴Ioffe Institute, Russian Federation

The recent discovery of *magnetic excitons* – a rare type of optical excitation that emerges from spin-polarized electronic states in magnets – raises important questions about elemental interactions between excitons, magnons, and light. In this contribution, we present the results of a study of the spatial transport of this intriguing type of exciton with particular focus on the role of crystal anisotropy, magnons and the magnetic order. We demonstrate highly non-linear exciton transport with unusual temperature dependence that culminates in substantially enhanced exciton propagation at the antiferromagnet-to-paramagnet phase transition. Observations of anomalous and effectively negative transport further indicate the substantial coupling of excitonic, vibronic,

and magnetic degrees of freedom.

9:30 AM *QT02.08.03

Spin-Orbit Torque in Magnetic Heterostructures: Exchange Interactions and Ultrasensitive Sagnac Magneto-Optic Interferometry Thow Min Jerald Cham¹, Saba Karimeddiny¹, Orion Smedley¹, Reiley Dorrian¹, Xiyue S. Zhang¹, Avalon Dismukes², Daniel Chica², Andrew F. May³, David A. Muller¹, Xavier Roy², Daniel C. Ralph¹ and Yunqiu Kelly Luo^{4,1}; ¹Cornell University, United States; ²Columbia University, United States; ³Oak Ridge National Laboratory, United States; ⁴University of Southern California, United States

In this two-part talk, we will first present our recent progress in advancing spin-orbit-torque metrology by adapting an ultrasensitive Sagnac magneto-optic interferometry originally developed for measuring time-reversal-symmetry breaking in exotic superconductors, and applying it for the first time to measuring spin-orbit torques. We will introduce the concept of Sagnac interferometry with an ultrahigh Kerr sensitivity of $\sim 5\mu\text{Rad}/\sqrt{\text{Hz}}$ and describe how such high sensitivity allows quantitative measurements of spin-orbit torque by sensing current-induced small-angle magnetization tilting. This method is especially advantageous for insulating magnets for which conventional transport spin-orbit torque metrology can be disrupted by magneto-thermal artifacts, but it can also be applied widely to broad classes of magnets regardless of conductivity and small net magnetization.

Secondly, we will present our recent work in identifying the gigahertz antiferromagnetic resonances within the easy-axis van der Waals (vdW) magnet CrSBr and understanding how their frequencies and intermode coupling can be controlled by the combination of external magnetic fields and magnetic anisotropy [3]. We will show that exchange bias from CrSBr acting on the van der Waals ferromagnet Fe₃GeTe₂ induces a spatially non-uniform spin configuration through the thickness of the Fe₃GeTe₂ that is not readily achievable with conventional magnetic materials, and can provide the symmetry breaking needed to enable field-free spin-orbit-torque switching in Pt/Fe₃GeTe₂/CrSBr heterostructures [4].

[1] S. Karimeddiny*, T. M. Cham, D. C. Ralph, and Y. K. Luo*, Sagnac interferometry for high-sensitivity optical measurements of spin-orbit torque. arXiv: 2109.13759 (2021)

[2] S. Karimeddiny*, T. M. J. Cham*, O. Smedley, D. C. Ralph, and Y. K. Luo*, Sagnac interferometry for high-sensitivity optical measurements of spin-orbit torque. Science Advances, 9 eadi9039 (2023)

[3] T. M. J. Cham*, S. Karimeddiny, A. H. Dismukes, X. Roy, D. C. Ralph, and Y. K. Luo*, Anisotropic gigahertz frequency antiferromagnetic resonance in layered van der Waals semiconductor. Nano Letters, 22, 6716-6723 (2022)

[4] T. M. J. Cham*, R. Dorrian, X. S. Zhang, A. H. Dismukes, D. G. Chica, X. Roy, A. F. May, D. A. Muller, D. C. Ralph, and Y. K. Luo*, Exchange bias between van der Waals materials: tilted magnetic states and field-free spin-orbit-torque switching. Advanced Materials, 2305739 (2023)

10:00 AM BREAK

10:30 AM *QT02.08.04

Nonlinear Optics in Magnetic Quantum Materials and Axion Electrodynamics Prineha Narang and Emily Been; University of California, Los Angeles, United States

Parametric optical nonlinearities are critical to a wide spectrum of photonic technologies, from optical parametric oscillators to frequency combs to quantum information processing. Optical nonlinearities also serve as a powerful method for mapping material properties including the symmetries of electronic structure. Optical nonlinearities are generally very small in conventional materials as they depend on higher order effects. Parallel to these technical needs, the field of topological materials has seen the prediction and discovery of a large number of massless, three-dimensional linear dispersion systems known as Dirac and Weyl semimetals. It was soon realized that these materials may offer a rich new material phase space for extending the nonlinear effects of graphene including the role of topology and Berry connection. In this context, I will present our recent work on predicting the optoelectronic and nonlinear properties of Dirac and Weyl semimetals with an emphasis on figures of merit (FoMs) that we will evaluate for these new Weyl and Dirac semimetals that capture the confinement and nonlinearity to describe the second and third order susceptibilities and electro-optic coefficients of the materials. Next, I will discuss our recent results on the multiphoton spectroscopy of a dynamical axion insulator. Here, the axion receives contributions from the collective motion of electrons, leading to a nonlinear topological magnetoelectric effect. Identifying this collective axion response faces a number of major experimental difficulties, which necessitate a theory-predicted smoking gun signature. We demonstrate a two-step protocol for the unambiguous optical identification of the collective axion mode in such a system. First, we show how collective oscillations of the axion mode can be induced by two-photon absorption or stimulated Raman spectroscopy, with the magnetoelectric nature of the excitation manifesting in the polarization dependence of the excitation beams. Second, we show how the axion oscillations can be confirmed through their manifestations in the time-resolved Kerr rotation, which again carries signature polarization dependence due to the magnetoelectric nature of the coupling. Looking ahead, I will discuss how collective responses in topological quantum materials can be unambiguously identified in nonlinear electro-dynamical probes, as well as identify potential avenues for intersections with particle physics in axion electrodynamics.

11:00 AM QT02.08.05

Scalable One-Dimensional Excitons in a Van der Waals Magnet Yinming Shao¹, Florian Dirnberger², Siyuan Qiu¹, Swagata Acharya³, Sophia Terres², Evan Telford¹, Dimitar Pashov⁴, Frank Ruta¹, Daniel Chica¹, Yiping Wang¹, Youn Jue Bae¹, Andrew Millis¹, Mikhail Katsnelson⁵, Mark van Schilfgaarde³, Kseniia Mosina⁶, Zdenek Sofer⁶, Alexey Chernikov², Rupert Huber⁷, Xiaoyang Zhu¹, Xavier Roy¹ and D. Basov¹; ¹Columbia University, United States; ²Technische Universität Dresden, Germany; ³National Renewable Energy Laboratory, United States; ⁴King's College London, United Kingdom; ⁵Radboud University, Netherlands; ⁶University of Chemistry and Technology Prague, Czechia; ⁷University of Regensburg, Germany

The discovery of two-dimensional (2D) van der Waals magnets has greatly expanded our ability to create and control nanoscale phases. A unique capability appears when a 2D magnet is also a semiconductor, which features tightly bound excitons with large oscillator strengths and potential tunability with magnetic field. While crystalline and geometric anisotropy can lead to anisotropic 2D (black phosphorus) and even 1D excitons (carbon nanotube), the superior excitonic properties do not easily scale up with increasing layer number/system size. Here we report scalable 1D excitons in the 2D A-type antiferromagnetic semiconductor CrSBr from few-layer to the bulk limit. The 1D confinement originates from a combination of in-plane crystalline anisotropy and inter-plane magnetic anisotropy. Magnetic confinement of the 1D excitons is established through the layer dependence and temperature dependence of the exciton properties, and further corroborated with *ab initio* theory calculations. Our work establishes a novel avenue towards the large-scale application of emergent functionalities of low-dimensional materials.

11:15 AM *QT02.08.06

Fast Light-Driven Domain Walls in a Parent Cuprate Kyle Seyler; University of Arizona, United States

Quantum materials exhibit fascinating phenomena when perturbed on short time scales or viewed at small length scales. For example, ultrafast light pulses can induce nonequilibrium behaviors that are thermally inaccessible. In addition, rich mesoscopic heterogeneity often exists in equilibrium, including the

presence of domain walls that lie at the interface between different domains. Merging direct spatial imaging with ultrafast time resolution therefore has tremendous potential to reveal intriguing light-induced domain wall dynamics but is often experimentally challenging. In this talk, I will show how ultrafast optical pulses can be harnessed to both image and dynamically manipulate the antiferromagnetic domain walls in a variant of the parent cuprates. In particular, I will highlight our discovery that antiferromagnetic domain walls can be driven to fast speeds by intense circularly polarized laser pulses. These results provide an unprecedented view of domain wall dynamics in quantum materials.

11:45 AM QT02.08.07

Angle-Resolved Photoemission Spectroscopy Studies of Flat Bands in Rhombohedral Graphene [Anil Rajapitamahuni](#), Turgut Yilmaz, Asish Kundu, Suji Park, Abdullah Al-Mahboob, Jerzy Sadowski and Elio Vescovo; Brookhaven National Laboratory, United States

The emergence of interaction driven phases in the twisted two-dimensional van der Waals heterostructures is due to the presence of van Hove singularities or flat bands where Coulomb repulsion energies dominate the kinetic energy of electrons. However, the correlated phenomena in twisted systems are extremely sensitive to angle disorder and strain, making them hard to achieve for experimental reproducibility. In this regard, graphene multilayers with rhombohedral or ABC stacking offers a different route to achieve flat bands. In this work, we have systematically studied the flat band electronic structure of ABC stacked multilayer graphene via high resolution angle resolved photoemission spectroscopy (ARPES). Few-layer (4 - 120) graphene flakes are directly exfoliated on to highly conducting Si (100) substrates using blue tape. We then identified ABC stacked flakes via Raman spectroscopy measurements. The thickness of the flakes is determined via atomic force microscopy (AFM). Synchrotron-based micro-ARPES experiments revealed intense flat bands around the K point, close to Fermi level (E_F). The presence of the flat bands over a large, measured photon energy range (44 - 235 eV) confirms their surface origin. From the energy distribution curves (EDCs) stacks a curvature in the ΓK and KM direction exists, and this dispersion extends over 25 meV. The width of the dispersion shrinks to ~ 10 meV, when the layer number is reduced to 4-5 layers, suggesting an increase in the correlation strength with the decrease of layer number in ABC stacked graphene. We have also performed temperature (12 - 300 K) dependent and polarization ARPES studies of the flat bands, to determine the magnetic origin of the curvature. Since RG is thermally more stable than twisted bilayers and naturally available, avoiding the need for fabrication, our work provides critical insights in understanding the correlated phenomena in chemically simple systems devoid of disorder.

SESSION QT02.09: Imaging and Control of Magnetism

Session Chairs: Ahmet Avsar and Kyle Seyler

Thursday Afternoon, April 25, 2024

Room 421, Level 4, Summit

1:30 PM *QT02.09.01

Symmetry-Breaking Pathway towards The Unpinned Broken Helix [Veronika Sunko](#)^{1,2}, Elizabeth Donoway^{1,2}, Thais Trevisan^{1,2}, Alex Liebman - Pelaez^{1,2}, Ryan Day^{1,2}, Kohtarō Yamakawa^{1,2}, Yue Sun^{1,2}, Rafael M. Fernandes³, Jian Rui Soh⁴, Dharmalingam Prabhakaran⁵, Andrew Boothroyd⁵, James G. Analytis^{1,2}, Joel Moore^{1,2} and Joe Orenstein^{1,2}; ¹UC Berkeley, United States; ²Lawrence Berkeley National Laboratory, United States; ³University of Minnesota, United States; ⁴Institute of Physics, École Polytechnique Fédérale de Lausanne, Switzerland; ⁵University of Oxford, United Kingdom

The search for materials exhibiting novel emergent properties relies on identification of their characteristic symmetries. A prominent example are materials in which magnetic symmetries promote topological phases, and consequently quantized responses to external stimuli.

EuIn_2As_2 attracted attention when ab-initio calculations predicted that it hosts the elusive axion insulator state, based on the assumption of a simple collinear antiferromagnetic structure. Recently, scattering measurements revealed a much more intricate magnetic ground state, characterized by two coexisting magnetic wavevectors, reached by successive thermal phase transitions. The proposed magnetic phases were a spin helix and a state with interpenetrating helical and antiferromagnetic order, termed a 'broken helix.' The symmetries of both deduced phases protected the axion state.

In this talk I will show results of magneto-optical experiments which are not compatible with the magnetic structures deduced by scattering. I will further demonstrate how combining the experimental information from scattering and symmetry-sensitive optics with an analysis based on group theory allowed us to uniquely identify the magnetic structure associated with each of the two phases. We find that the higher temperature phase hosts a 'nodal amplitude-modulated' structure rather than a helix, characterized by a variation of magnetic moment amplitude from layer to layer, with the moment vanishing entirely in every third Eu layer. The lower temperature structure is similar to the 'broken helix,' with one important difference: the relative orientation of the magnetic structure and the lattice is not fixed, resulting in an 'unpinned broken helix.' As a result of the consequent breaking of rotational symmetry, the axion phase is not generically protected in EuIn_2As_2 but we show that it can be restored if the magnetic structure is tuned with externally applied uniaxial strain. Finally, I will present a spin Hamiltonian that identifies the interactions needed to account for the complex magnetic order in EuIn_2As_2 , and how they arise from coupling to itinerant degrees of freedom.

Taken together, our results emphasize the power of a multimodal approach combining scattering and symmetry-sensitive optical probes in identifying complex magnetic structures, as well identifying EuIn_2As_2 as a remarkably tunable platform for exploration of magnetic symmetries.

2:00 PM QT02.09.02

Ferromagnetism in a Monolayer 2D Metal-Organic Framework [Egzona Isufi Nezir](#)^{1,2}, Karl-heinz Ernst^{1,2,3} and Christian Wäckerlin^{4,5}; ¹Universität Zürich, Switzerland; ²Swiss Federal Laboratories for Materials Science and Technology, Switzerland; ³The Czech Academy of Sciences, Czechia; ⁴Swiss Federal Institute of Technology Lausanne, Switzerland; ⁵Paul-Scherrer-Institut, Switzerland

Motivated by applications in information and energy technology, the search for new materials with stable long-range magnetic ordering continues. In this respect, metal-organic magnets, being built by coordination of metal-atoms with suitable ligands, have attracted significant attention in the recent years. Nanoscale magnetic materials with reduced dimensionality promise very interesting applications in information technology, e.g. information storage, information processing (spintronics) or quantum computing. The Mermin-Wagner theorem establishes that in systems with dimensions $D \leq 2$, governed by the isotropic Heisenberg exchange with short-range interactions, continuous symmetries cannot break spontaneously at finite temperatures. Only in presence of a significant magnetic anisotropy that counteracts random spin reorientations (or non-Heisenberg exchange interactions), ferromagnetism at low dimensions can occur. In this work, we show the existence of ferromagnetic coupling in a 2D metal-organic framework (MOF) consisting of Ni atom centers and tetracyanoethylene (TCNE) ligands on a Au(111) surface. Scanning tunneling microscopy (STM) shows a well-ordered MOF after co-deposition of Ni and TCNE. Analyses based on x-ray magnetic circular dichroism (XMCD) measurements reveal a strong out-of-plane magnetic

anisotropy and a square like hysteresis loop with a coercive field of 1 T. Origin of such 2D ferromagnetism will be discussed

2:15 PM QT02.09.03

Structural and Electronic Properties of Ti- and Ca-Doped Hexagonal TbInO₃ Kuntal Talit¹, Nabaraj Pokhrel¹, Yang Zhang², Johanna Nordlander², Ismail El Baggari², Julia Mundy² and Elizabeth Nowadnick¹; ¹University of California, Merced, United States; ²Harvard University, United States

Magnetic frustration combined with strong quantum fluctuations can create a quantum spin liquid ground state in that material. Doped spin liquids, which may host novel properties such as fractionalized charges and unconventional superconductivity are of fundamental interest and may hold promise for quantum computing applications. However, understanding what happens to added charge carriers in doped spin liquids remains a challenging problem. Recent research has demonstrated that hexagonal ferroelectric TbInO₃, characterized by anisotropic exchange interactions, substantial spin-orbit coupling, and f-electron magnetism, is a candidate spin liquid material. Low-dimensional frustrated magnetism in TbInO₃ arises from its layered crystal structure, consisting of nonmagnetic layers of corner-sharing InO₃ trigonal bipyramids alternating with layers of magnetic Tb³⁺ ions arranged in a distorted triangular lattice featuring two distinct Tb sites. In this work, we employ density functional theory (DFT) calculations together with scanning transmission electron microscopy (STEM) imaging to investigate the effects of doping hexagonal TbInO₃ thin films via chemical substitution. We explicitly introduce Ti⁴⁺ for electron doping and Ca²⁺ for hole doping, systematically exploring various dopant concentrations and configurations. We investigate the evolution of the structural and ferroelectric properties of electron- and hole-doped TbInO₃, finding good agreement between changes to lattice parameters and atomic displacement amplitudes from our DFT calculations and STEM measurements. We also combine DFT calculations of the density of states with electron energy loss spectroscopy measurements to probe the evolution of the electronic structure of TbInO₃ upon Ti⁴⁺ and Ca²⁺ substitution. This research provides new insight into the structural and electronic properties of doped TbInO₃ and their implications for conductivity in low-dimensional frustrated magnetic states.

Funding acknowledgement: This material is based upon research supported by Air Force Office of Scientific Research (MURI Grant No. FA9550-21-1-0429).

2:30 PM QT02.09.04

Inelastic Neutron Scattering of The Spin-Liquid Candidate Ba₃ZnRu₂O₉ and Diluted Ba₃Zn(Ru_{0.1}Sb_{0.9})₂O₉ Daniel M. Pajerowski¹, Daniel P. Phelan², Yu Li², Matthew Stone¹, David Dahlbom¹, Alexander Kolesnikov¹ and Duminda Sanjeeva³; ¹Oak Ridge National Lab, United States; ²Argonne National Laboratory, United States; ³University of Missouri–Columbia, United States

Ba₃ZnRu₂O₉ (BZRO) is a 6-H perovskite compound with layers of S=3/2 Ru⁵⁺ dimers arranged in a triangular lattice. There is no evidence of long-range magnetic order at temperatures as low as 37 mK, which suggests a potential spin-liquid ground-state.[1] Inelastic neutron scattering results are presented from from BZRO (powder, crystal arrays) and the diamagnetically doped Ba₃Zn(Ru_{0.1}Sb_{0.9})₂O₉. The BZRO shows highly dispersive excitations with no magnetic Bragg peaks. So, contrary to prior suggestions that a similar compound, Ba₃CaRu₂O₉, consists of magnetic dimers with negligible inter-dimer interactions,[2] these data show that BZRO clearly deviates from a dimer model. Different analysis techniques of the correlations are illustrated, including coarse-graining the system so that dimers are local entangled units.

[1] I. Terasaki, et al., J. Phys. Soc. Jpn. 86, 033702 (2017) [4 Pages]

[2] J. Darriet, et al., J. Phys. Chem. Solids 44 (1983) pp. 269-212.

2:45 PM BREAK

SESSION QT02.10: Spintronic Devices Based on 2D Materials

Session Chairs: Marco Gibertini and Yunqiu Kelly Luo

Thursday Afternoon, April 25, 2024

Room 421, Level 4, Summit

3:15 PM *QT02.10.01

Superlative Spin Transport in Two-Dimensional Black Phosphorus Luke Cording¹, Jiawei Liu², Jun You Tan², Kenji Watanabe³, Takashi Taniguchi³, Barbaros Ozyilmaz² and Ahmet Avsar²; ¹Newcastle University, United Kingdom; ²National University of Singapore, Singapore; ³National Institute for Materials Science, Japan

Exploitation of the intrinsic spin of an electron, spintronics, facilitates the development of multifunctional and novel devices which could play an important role in the Beyond-CMOS era. Two-dimensional (2D) crystals and their van der Waals heterostructures are particularly promising for spintronics device applications due to their unique properties, including strong responses to field effect gating and proximity interactions, which may enable new functionalities that are not possible with conventional bulk materials [1].

Two-dimensional black phosphorus is a promising material for semiconducting spintronics research due to its high charge mobilities, low atomic mass, and puckered crystalline structure, which are expected to lead to anisotropic spin transport with nanosecond spin-lifetimes. In this presentation, I will introduce ultra-thin BP as a unique platform for studying rich spin-dependent physics. Firstly, I will show that BP supports all electrical spin injection, transport, precession and detection up to room temperature [2]. Then, I will present our recent findings on the impact of the unique crystal structure of BP on its spin dynamics, revealing strong anisotropic spin transport along three orthogonal axes [3]. Finally, a van der Waals bonded spintronics device utilizing BP as channel material and 2D magnets for spin injection/detection will be introduced. The exceptional spin transport and strong spin-lifetime anisotropy we observe in BP add to the growing body of evidence for the potential of 2D materials in functional spin-based device applications.

[1] A. Avsar et al., Rev. Mod. Phys. 92, 021003 (2020)

[2] A. Avsar et al., Nat. Phys. 13, 888-894 (2017)

[3] L. Cording et al., Nat. Mater. (In press)

3:45 PM QT02.10.02

Current-Driven Magnetic Resistance in Van der Waals Spin-Filter Antiferromagnetic Tunnel Junctions with MnBi₂Te₄ Lishu Zhang; Forschungszentrum Jülich GmbH, Germany

The field of 2D magnetic materials has paved the way for the development of spintronics and nanodevices with new functionalities. Utilizing antiferromagnetic materials, in addition to layered van der Waals (vdW) ferromagnetic materials, has garnered significant interest. In this work, we present a theoretical investigation of the behavior of MnBi₂Te₄ devices based on the non-equilibrium Green's function method. Our results show that the current-voltage (I-V) characteristics can be influenced significantly by controlling the length of the device and bias voltage and thus allow us to manipulate the tunneling magneto-resistance (TMR) with an external bias voltage. This can be further influenced by the presence of the boron nitride layer which shows significantly enhanced TMR by selectively suppressing specific spin channels for different magnetic configurations. By exploiting this mechanism, the observed TMR value reaches up to 3690%, which can be attributed to the spin-polarized transmission channel and the projected local density of states. Our findings on the influence of structural and magnetic configurations on the spin-polarized transport properties and TMR ratios give the potential implementation of antiferromagnetic vdW layered materials in ultrathin spintronics.

4:00 PM *QT02.10.03

Proximity Spin Interactions in 2D Materials and Correlated Phases [Jaroslav Fabian](#); University of Regensburg, Germany

Graphene has weak spin-orbit coupling and no magnetic order. But when placed in contact with a strong spin-orbit coupling material, such as a TMDC, or a ferromagnet, such as Cr₂Ge₂Te₆, Dirac electrons acquire strong spin-orbit or exchange coupling, respectively. Such proximity effects render graphene suitable for spintronic applications that require spin manipulation [1]. In addition, graphene with strong proximity spin interactions can host novel topological states [2]. Fascinating new phenomena appear when bilayer graphene gets encapsulated by a TMDC from one side, and a ferromagnet from another. The resulting, so called ex-so-tic structure [3], offers spin swap functionality: switching spin-orbit and exchange coupling on demand by the gate. In this talk, I will review the recent developments in the proximity phenomena in graphene, and present some recent theoretical results on the control of the proximity spin-orbit and exchange coupling by twisting the van der Waals layers. I will show that the signature proximity spin-orbit coupling in graphene--valley Zeeman coupling--can be efficiently tuned by the twist angle [4], and that proximity exchange coupling can be switched by the twist angle, and even morph from ferromagnetic to antiferromagnetic [5]. Finally, I will also discuss the emergence of new correlated phases in AB bilayer and ABC trilayer graphene [6] due to the presence of proximity spin-orbit and exchange couplings. Support from DFG SPP1244, SFB 1277, FLAGERA 2DSOTECH, and EU 2DSPINTECH is acknowledged.

[1] J. Sierra et al, Nature Nanotechnology, 16, 856 (2021)

[2] P. Högl et al, Phys. Rev. Lett. 124, 136403 (2020)

[3] K. Zollner et al, Phys. Rev. Lett. 125, 196402 (2020)

[4] T. Naimer et al, Phys. Rev. B 104, 195156 (2021)

[5] K. Zollner and J. Fabian, Phys. Rev. Lett. 128, 106401 (2022)

[6] Y. Zhumagulov et al, arXiv: arXiv:2305.14277, 2307.16025

4:30 PM QT02.10.04

The Fabrication and Characterization of Spintronic Terahertz Emitter Using Magnetic/Non-Magnetic Bilayer with Nanometer Thickness

[Mikihiko Nishitani](#), Kohei Ejiri, Shinya Isosaki, Ruochen Dai, Shojiro Nishitani and Makoto Nakajima; Osaka University, Japan

The response time of electrons below the Fermi energy in solids to electromagnetic waves is known to be on the order of femtoseconds. As a result, the energy transfer between electromagnetic waves and spins is ultrafast, at the terahertz frequency [1]. Similarly, spin currents generated by spin polarization are described according to the LLG equation, i.e., the time dynamics of magnetization, and spin currents are expected to have a response time equivalent to that of electrons in the solid to electromagnetic waves. Furthermore, the effect of those spin currents being converted into electric currents by spin-orbit interactions is known as the inverse spin Hall effect, and the response time of those phenomena is also on the order of sub-picoseconds.

In 2013, Kampfrath et al. reported the emission of terahertz waves by femtosecond laser (photon energy of 1.55eV) irradiation of magnetic/nonmagnetic bilayers composed of nanometer-thick films [2]. Subsequently, those devices were named STE (Spintronic Terahertz emitters (STEs)), which have been actively studied in basic research as well as in application fields. We have been studying STE using ultrathin (several nanometer-thick) bilayers (Pt/Fe, W/Fe, etc.) of nonmagnetic/magnetic materials on inexpensive, large-aperture (large area) substrates such as glass substrates, and the intensity of terahertz radiation by femtosecond laser irradiation is comparable to that of conventionally used nonlinear optical crystal ZnTe, and further advances are being made [3,4]. Specifically, we have been studying 1) how to efficiently generate spin currents by femtosecond laser irradiation and 2) how to maximize the inverse spin Hall effect at the interface between magnetic and nonmagnetic materials.

In this report, we quantitatively evaluate the spin Hall angle, which is the figure of merit of the effect shown in 2) above mentioned, and investigate its relation to the experimental terahertz wave radiation intensity. The spin Hall angle was obtained by analyzing the magnetic field dependence of the spin Hall magnetoresistance [5], which is used to evaluate spintronic devices, and the terahertz radiation intensity was obtained using our TDS system. The obtained results show a good linear correspondence between the magnitude of the change in spin Hall magnetoresistance and the intensity of terahertz radiation. We plan to reflect these results in the fabrication conditions and in the progress of the technique to further improve the performance of this system.

References

[1] K. Yamaguchi, M. Nakajima, and T. Suemoto, Phys. Rev. Lett. 105, 237201 (2010).

[2] T. Kampfrath, M. Battiato, P. Maldonado, et al., Nat. Nanotechnol., 8, 256 (2013).

[3] Y. Koike, S. Tetsukawa, M. Nishitani, H. Kitahara, V. K. P. Mag-usara, M. Asakawa, M. Yoshimura, M. Tani, M. Nakajima, 45th International Conference on Infrared, Millimeter, and Terahertz Waves (IRMMW-THz) (2020).

[4] T. Matsunaga, V. K. Mag-Usara, K. Ejiri, S. Tetsukawa, S. Liu, V. C. Agulto, S. Nishitani, M. Nishitani, M. Yoshimura, M. Nakajima, 47th International Conference on Infrared, Millimeter, and Terahertz Waves, (IRMMW-THz) (2022).

[5] M. Kawaguchi, D. Towa, Yong-Chang Lau, S. Takahashi, and M. Hayashi, Appl. Phys. Lett., 112, 202405 (2018).

SESSION QT02.11: Imaging of Magnetism in Magnetic Materials

Session Chairs: Eric Fullerton and Zhong Lin

Friday Morning, April 26, 2024

Room 421, Level 4, Summit

8:30 AM *QT02.11.01

Synthesis and Ferroelectric Field Effect Studies of Few-Layer CrCl₃ [Xia Hong](#); University of Nebraska-Lincoln, United States

The van der Waals magnets CrX_3 ($X = \text{I, Br, and Cl}$) exhibit highly tunable magnetic properties and are promising candidates for developing novel two-dimensional (2D) spintronic applications. The ability to synthesize atomically thin CrX_3 samples and achieve voltage control of their magnetic states is critical for their technological implementation. In this talk, I'll discuss our recent progress in the synthesis and ferroelectric field effect studies of large size few-layer CrCl_3 flakes. Using the physical vapor transport technique, we have deposited high-quality CrCl_3 flakes down to monolayer thickness on mica. Both isolated flakes with well-defined facets and long stripe samples exceeding 60 μm length have been obtained. High-resolution transmission electron microscopy and Raman studies confirm the high crystallinity of these samples. The tunneling magnetoresistance of graphite/ CrCl_3 /graphite tunnel junctions reveals in-plane magnetic anisotropy and Néel temperature of 17 K of CrCl_3 . We encapsulate the tunnel junctions with free-standing ferroelectric $\text{PbZr}_{0.2}\text{Ti}_{0.8}\text{O}_3$ membranes and define the polarization state of the top-gate via conductive atomic force microscopy. Ferroelectric polarization reversal leads to nonvolatile modulation of the tunneling current, with an on/off ratio of 10^6 obtained at room temperature. Compared with the negative tunneling magnetoresistance observed in hBN encapsulated devices, the PZT-gated CrCl_3 tunnel junctions exhibit positive tunneling magnetoresistance at low temperatures, suggesting a change of magnetic state. Our study provides an effective strategy to design low power, scalable, flexible 2D nanoelectronics and spintronics.

This work was primarily supported by NSF through Grant No. DMR-2118828 and ERSCoR EQUATE Award No. OIA-2044049, and Nebraska Center for Energy Sciences Research.

9:00 AM *QT02.11.02

STEM Developments: Atomic-Resolution SE Imaging, Fast 4D STEM, Ultra-High Energy Resolution [Tracy C. Lovejoy](#); Nion, United States

A new type of secondary electron (SE) detector designed by Nion for a modern STEM combines SE detection with an atom-sized probe in the operating range 20-200 kV, clean (metal-sealed and bakable) UHV vacuum conditions, and state-of-the-art electron energy loss spectroscopy (EELS) and 4D-STEM capabilities [1,2]. Running experience reveals that common S/TEM samples (e.g. MoS_2 or metal nanoparticles on a carbon film) that give atomic-resolution annual dark field (ADF) images initially show only surface contamination in the SE signal. We use multiple methods for UHV surface cleaning, including resistive heating of the whole sample in a side entry holder (e.g. Protochips) and direct laser illumination of a small spot (20 mm x 40 mm). Direct laser illumination is particularly interesting because the laser light modulates the SE signal in some samples by changing the local charge distribution on the surface [3].

After cleaning, atomic-resolution SE signals are readily visible. Expanding on previous work with atomic-resolution SE imaging [4], lower operation voltage in a modern STEM avoids knock-on damage and enables atomic-resolution SE studies of 2D materials. We will show two examples: (1) combining atomic resolution ADF, SE, and 4D-STEM to study MoS_2 with intentional Vanadium dopants at 60 keV primary energy, and (2) combining atomic resolution EELS and SE analysis to study the origins of the SE signal in a model system that can tolerate very high electron doses -- monolayer graphene with Nitrogen and Boron dopants.

4D-STEM and especially EELS experiments on 2D materials have traditionally been complicated by slow detectors and readout noise. The latest direct detectors avoid readout noise and achieve high DQE and dynamic range with speed approaching that of traditional single-channel detectors (>10,000 frames/second). Combining these detectors with powerful open-source software for smart acquisition/compression and live processing makes multi-frame (time series) 4D-STEM or EELS imaging possible, bringing significant advantages when changing the sample environment (e.g. heating, cooling, light-, or gas-injection) causes sample drift that makes longer exposures impractical.

Doing these experiments in an instrument capable of <5 meV energy resolution [5] makes possible synergistic experiments such as mapping the absolute temperature of the sample in and around the spot illuminated by a laser using electron energy gain spectroscopy [6] and measuring the presence and local bonding configuration of hydrogen in the sample by detecting the "infrared absorption" signal of the H bonds with vibrational EELS [7]. Phonon spectroscopy of surface dopants visible in the SE signal is also very promising.

References

- [1] M.T. Hotz et al., *Microsc. Microanal.* 29 Suppl. 1 (2023) 2064-265
- [2] J. Martis, B. Plotkin-Swing et al., *Proceedings 20th IMC (Busan, 2023)*
- [3] J. Martis, N. Dellby et al., *Proceedings 20th IMC (Busan, 2023)*
- [4] Y. Zhu et al., *Nature Materials* 8 (2009) 808-812.
- [5] N. Dellby et al., *Microsc. Microanal.* 29 Suppl. 1 (2023) 626-627
- [6] J.C. Idrobo et al., *Phys. Rev. Lett.* 120 (2018) 095901
- [7] P. Rez et al., *Nature Comm.* 7 (2016) 10945

9:30 AM *QT02.11.03

Scanning NV Microscopy [Mathieu Munsch](#) and [Peter Rickhaus](#); Qnami AG, Switzerland

We introduce Scanning NV Microscopy (SNVM) as a non-contact characterization technique to investigate magnetic materials and thin films. We show that SNVM can be used to evaluate MRAM performance at the individual bit level. Magnetic random-access memory (MRAM) is a leading emergent memory technology that is poised to replace current non-volatile memory technologies such as eFlash. However, controlling and improving distributions of device properties becomes a key enabler of new applications at this stage of technology development. Here, We demonstrate magnetic reversal characterization in individual, < 60 nm sized bits, to extract key magnetic properties, thermal stability, and switching statistics, and thereby gauge bit-to-bit uniformity. We showcase the performance of our method by benchmarking two distinct bit etching processes immediately after pattern formation. Finally, we will provide other examples of the applications of SNVM for the study of multiferroics, 2D materials, and magnonics.

10:00 AM BREAK

10:30 AM *QT02.12.01

Spin-Orbit Studies of Ferrimagnetic, Antiferromagnetic and Oxide Weyl Semimetals [Eric Fullerton](#); University of California-San Diego, United States

Topology has emerged in many areas of magnetism that included both chiral spin structures and emergent electronic structures such as Weyl semimetals [1]. The further lowering of the symmetry of the crystal via strain or magnetic order can provide additional functionality. I will discuss recent studies of thin films of candidate Weyl semimetals and their potential use as sources of spin currents in spin-orbit torque devices. Materials studies include ferrimagnetically ordered CrPt₃ [2], antiferromagnetically ordered FeRh [3] and transition metal oxides such IrO₂ [4], CaIrO₃, and NdNiO₃. For each we have grown epitaxial chemically ordered films and studied the spin structure, magneto-transport properties, and spin-to-charge conversion that is a source for spin-orbit torques. For CrPt₃ we obtain large anomalous Hall conductivity of 2000 S/cm and large negative magneto-resistance consistent with Weyl semimetal properties. However, this, somewhat surprisingly, does not manifest itself in enhanced charge-to-spin efficiencies. For the antiferromagnetic FeRh phase we observe extremely large, strongly temperature-dependent exotic spin torques with a geometry that is tied to the magnetic ordering direction. Many 5d transition metal oxides such as IrO₂ and CaIrO₃ have unique electronic structures, where the density of states near the Fermi level is dominated by only 5d electrons with strong spin orbit coupling. IrO₂ is one of the simplest of these oxides is a Dirac nodal line semi-metal that exhibits a charge-to-spin conversion that is roughly 8 times larger than that of Pt. I will highlight the potential uses for complex materials that generate large, tunable spin-orbit torques. They may be used in conventional computing to non-volatile memory schemes, or for neuromorphic computing approaches exploiting spin dynamics in more complex magnetic systems. This work is supported by US Department of Energy under Grant No. DE-SC0019273

[1] M. J. Gilbert, *Comm. Phys.* **4**, 1-12 (2021).

[2] A. Markou et al., *Comm. Phys.* **4**, 104 (2021).

[3] J. Gibbons et al., *Phys. Rev. Appl.* **18**, 024075 (2022).

[4] B. Sahoo, A. Frano and E. E. Fullerton, *Appl. Phys. Lett.* **123**, 032404 (2023).

11:00 AM *QT02.12.02

Enabling Energy Efficient Logic through Magneto-Electric Spin Orbit (MESO) Device [Punyashloka Debashis](#); Intel Corporation, United States

Energy efficient and high functionality logic devices are key to sustain the long-term progression of Moore's law. The Magneto-Electric Spin Orbit (MESO) device is one such beyond-CMOS device that has attracted research attention recently. The MESO device uses an input voltage across a multiferroic material to switch the state of a ferromagnet and uses spin-orbit effects to transduce the magnetization state to an output voltage. This talk will present some of the key experimental advances in reducing the switching voltage, increasing the switching speed as well as improving the output voltage from spin-orbit module. Finally, some important challenges and opportunities towards achieving the target device specification will be discussed.

11:30 AM *QT02.12.03

Magnetic Tunnel Junctions for Enabling Novel and Neuromorphic Computing [Matthew W. Daniels](#)¹, William A. Borders¹, Advait Madhavan^{2,1}, Liam Pocher², Sidra Gibeault², Temitayo Adeyeye², Brian Hoskins¹, Daniel Lathrop², Mark Stiles¹ and Jabez McClelland¹; ¹National Institute of Standards and Technology, United States; ²University of Maryland, United States

Magnetic tunnel junctions (MTJs) are versatile devices with multiple modes of operation. Commonly thought of as memory elements in MRAM applications, magnetic tunnel junctions can also be used as stochastic bitstream generators or nanoscale oscillators. Among modern nanodevices of interest, magnetic tunnel junctions are also technologically mature and are already available in the back-end-of-line setting. In this talk, I discuss our group's recent work on utilizing these devices for alternative computing concepts, using properties like randomness and signal timing to generate energy-efficient brain-inspired computational patterns. We briefly consider the challenges of scaling device research from single-device experiments to the large numbers of devices needed for realistic computing demonstrations; to that end, I discuss NIST's Nanotechnology Accelerator Program and our upcoming hardware AI testbed that researchers can use to quickly close the technology transfer gap in moving from single-devices measurements to computing demonstrations utilizing advanced materials.

SESSION QT02.13: Devices and Control of Magnetism

Session Chairs: Matthew Daniels and Yunqiu Kelly Luo

Friday Afternoon, April 26, 2024

Room 421, Level 4, Summit

2:00 PM QT02.13.02

Low-Frequency Electronic Noise Characteristics of Vertical Quasi-Two-Dimensional Antiferromagnetic Semiconductor Devices [Subhajit Ghosh](#)^{1,2}, Zahra E. Nataj^{1,2}, Fariborz Kargar^{1,2} and Alexander A. Balandin^{1,2}; ¹University of California Riverside, United States; ²University of California, Los Angeles, United States

A new frontier in the search for the next-generation electronic, photonic, and spintronic devices is quasi 2D films of transition-metal phospho-trichalcogenides (MPX₃) where "M" is a transition metal and "X" is a chalcogen [1]. Recent studies have reported that MPX₃ structures are one of rare few-layer van der Waals (vdW) materials with stable intrinsic antiferromagnetism (AFM) even at mono- and few-layer thicknesses. The diverse properties of layered MPX₃ materials, tunable by proper selection and combination of the "M" and "X" elements make them an interesting platform for investigating novel low-dimensional device functionalities. The existence of weak vdW bonds between the MPX₃ layers allows one to scale them conveniently to individual atomic planes. The "M" element determines the AFM spin ordering. While FePS₃ shows an Ising-type phase transition at the Néel temperature (T_N), NiPS₃ follows XY-phase transitions, respectively. MPX₃ structures are semiconductors in nature and variation in the metal element modifies their bandgap from ~1.3 eV to ~3.5 eV. The latter opens up unique opportunities to design novel electronic and magnonic nanodevices suitable for optoelectronic and spintronic applications. However, the data on the electron transport properties and their interaction with spin ordering in these structures is scarce and requires detailed investigations. MPX₃ materials are highly resistive making electron transport measurements a formidable challenge in conventional lateral device structures. To overcome this challenge, we fabricated vertical *h*-BN/MPX₃ heterostructure devices with different MPX₃ components hosting various AFM spin orderings. In this presentation, we report the results of our temperature-dependent cross-plane electrical transport and noise measurements. The low-frequency noise spectroscopy was used to detect the magnetic phase transitions [2]. In vertical *h*-BN/FePS₃ devices with the active layer characterized by the Ising-type spin order, we observed a combination of two Lorentzian bulges appearing in the overall $1/f$ noise envelope at or close to T_N . These two features were attributed to the generation-recombination (G-R) and magnetic phase transition. The noise measurements of the

vertical devices with both FePS₃ and NiPS₃ active layers, characterized by the Ising and XY AFM spin orders respectively, revealed multiple noise peaks near the magnetic phase transitions. The intensity of the noise peaks in NiPS₃ was significantly higher than that in the FePS₃ device. The comparison of noise characteristics for devices fabricated with two materials of different AFM spin ordering shows a strong dependence of noise on the particular magnetic spin direction and suggests a strong interplay of the magnetic and electrical properties in these AFM materials.

F.K. and A.B.B. acknowledge funding from the National Science Foundation (NSF), Division of Material Research (DMR) via the project No. 2205973 "Controlling Electron, Magnon, and Phonon States in Quasi 2D Antiferromagnetic Semiconductors for Enabling Novel Device Functionalities."

[1] F. Kargar, E. A. Coleman, S. Ghosh, J. Lee, M. J. Gomez, Y. Liu, A. S. Magana, Z. Barani, A. Mohammadzadeh, B. Debnath, R. B. Wilson, R. K. Lake, and A. A. Balandin, "Phonon and thermal properties of quasi-two-dimensional FePS₃ and MnPS₃ antiferromagnetic semiconductors," *ACS Nano*, 14, 2, 2424-2435 (2020).

[2] S. Ghosh, F. Kargar, A. Mohammadzadeh, S. Rumyantsev, and A. A. Balandin, "Low-frequency electronic noise spectroscopy of quasi 2D van der Waals antiferromagnetic semiconductors," *Adv. Electron. Mater.*, 2100408 (2021).

2:15 PM QT02.13.03

Probing and Manipulating Spin States in Low-Dimensional Fe_xNbSe₂ for Antiferromagnetic Spintronics [Matthew Erodici](#) and Kwabena Bediako; University of California, Berkeley, United States

Magnetically intercalated, two-dimensional (2D) transition metal dichalcogenides (TMDs) represent a promising class of low-dimensional, magnetic materials for ultralow-power device applications based on the manipulation of electron spin. The ability to tune the magnetic properties of these compounds based on the choice of host lattice, intercalant, and relative stoichiometry offers a versatile platform for designing 2D magnetic materials, which would otherwise be difficult to access via direct exfoliation of bulk (3D) analogues. Recent work has shown that iron-intercalated tantalum disulfide (Fe_xTaS₂) exhibits long-range ferromagnetic order down to the bilayer limit, due to strong out-of-plane, magnetocrystalline anisotropy, showcasing the tremendous potential of this methodology to engineer non-trivial, low-dimensional magnetic systems.¹ While this approach endows one with a highly modular system of possible configurations, the materials phase space remains largely unexplored—and corresponding experimental demonstration of low-dimensional magnetic order is lacking. Here, we leverage this soft chemical intercalation process to synthesize few-layer iron-intercalated niobium diselenide (Fe_xNbSe₂) and probe the resultant magnetotransport response, in the pursuit of electrically manipulable, antiferromagnetic ground states akin to this family of iron-intercalated niobium-based dichalcogenides.² We utilize a suite of confocal Raman spectroscopy methods and electron microscopy-based imaging techniques to detect intercalant superlattice formation and examine the local atomic structure, as the distribution of magnetic sites in these compounds underpins the robustness of long-range magnetic order. These findings will bolster the possibility for engineering more complex magnetic heterostructures within this auspicious family of designer materials.

[1] Husremovic, S. *et al.* *J. Am. Chem. Soc.* **2022**, *144*, 12167–12176

[2] Nair, N. L. *et al.* *Nat. Mater.* **2020**, *19*, 153–157

2:30 PM BREAK

SESSION QT02.14: Devices Based on Magnetic Materials II
Session Chairs: Geoff Diederich and Dmitry Ovchinnikov
Friday Afternoon, April 26, 2024
Room 421, Level 4, Summit

3:00 PM QT02.14.01

Spin Dynamics and Exchange Interactions from a Van der Waals Antiferromagnet [Yunqiu Kelly Luo](#); University of Southern California, United States

This talk will present our recent progress in identifying the gigahertz antiferromagnetic resonances within the easy-axis van der Waals (vdW) magnet CrSBr and understanding how their frequencies and intermode coupling can be controlled by the combination of external magnetic fields and magnetic anisotropy [1]. We have recently advanced beyond the published results [1] to achieve direct electrical detection of the resonance dynamics in few-layer CrSBr devices via their effect on tunnel magnetoresistance, and to explore the effects of externally-applied spin-orbit torque on the mode damping. We have also demonstrated that exchange bias from CrSBr acting on the van der Waals ferromagnet Fe₃GeTe₂ induces a spatially non-uniform spin configuration through the thickness of the Fe₃GeTe₂ that is not readily achievable with conventional magnetic materials, and can provide the symmetry breaking needed to enable field-free spin-orbit-torque switching in Pt/Fe₃GeTe₂/CrSBr heterostructures [2]. These results will be of broad interest to the magnetism and spintronics community, for researchers interested in the fundamental physics of spin order in van der Waals materials, and for those working toward making practical devices using van der Waals antiferromagnets and ferromagnets.

[1] T. M. J. Cham, S. Karimeddiny, A. H. Dismukes, X. Roy, D. C. Ralph, and Y. K. Luo, Anisotropic gigahertz frequency antiferromagnetic resonance in layered van der Waals semiconductor. *Nano Letters*, 22, 6716-6723 (2022)

[2] T. M. J. Cham, R. Dorrian, X. S. Zhang, A. H. Dismukes, D. G. Chica, X. Roy, A. F. May, D. A. Muller, D. C. Ralph, and Y. K. Luo, Exchange bias between van der Waals materials: tilted magnetic states and field-free spin-orbit-torque switching. *Advanced Materials*, 2305739 (2023)

3:15 PM *QT02.14.02

Enhanced Magnetoelectric Coupling in Van der Waals Heterostructures [Li Yang](#)¹, Yan Lu² and Xilong Xu¹; ¹Washington University in St Louis, United States; ²Nanchang University, China

Multiferroic materials exhibiting coupled ferroelectric (FE) and ferromagnetic (FM) properties are vital for multifunctional devices. However, achieving enhanced magnetoelectric coupling remains a notable challenge. The emergence of ultra-thin, two-dimensional (2D) van der Waals (vdW) FE and magnetic materials offers unique opportunities to create artificial multiferroics through heterostructures. In this presentation, I showcase enhanced magnetoelectric couplings in two vdW heterostructures: CrI₃/Sc₂Co₂ and CrCl₃/CuCrP₂S₆. Our first-principles simulations predict that reversing FE polarization can efficiently switch their interlayer FM and antiferromagnetic (AFM) orders. Further analysis reveals that these observed magnetoelectric couplings stem from rich proximity mechanisms. In the first heterostructure, the magnetoelectric coupling is achieved through substantial changes in band alignment and subsequent charge transfer (doping effect). In the second heterostructure, the system remains insulating throughout the process, and the

mechanism primarily arises from the unique spin local field effect on interlayer exchange interactions. These results underscore the promising prospects of coupling electric polarization with correlated magnetic orders through the unique proximity physics in vdW multiferroic heterostructures.

3:45 PM QT02.14.03

Writing and Detecting Topological Charges in Exfoliated Fe_{5-x}GeTe₂ Alex Moon^{1,2}, Yue Li³, Conor McKeever⁴, Brian Casas², Moises Bravo⁵, Wenkai Zheng^{1,2}, Juan Macy^{1,2}, Amanda Petford-Long^{3,6}, Julia Chan⁶, Charudatta Phatak^{3,6}, Elton J. Santos⁴, Gregory McCandless⁵ and Luis Balicas^{1,2}; ¹Florida State University, United States; ²National High Magnetic Field Laboratory, United States; ³Argonne National Laboratory, United States; ⁴University of Edinburgh, United Kingdom; ⁵Baylor University, United States; ⁶Northwestern University, United States

Fe_{5-x}GeTe₂ is a promising two-dimensional (2D) van der Waals (vdW) magnet for practical applications, given its remarkable magnetic properties. These include Curie temperatures above room temperature, and topological spin textures – TST (both merons and skyrmions), responsible for a pronounced anomalous Hall effect (AHE) and its topological counterpart (THE), which can be harvested for spintronics. Here, we show that both the AHE and THE can be amplified considerably by just adjusting the thickness of exfoliated Fe_{5-x}GeTe₂, with THE becoming observable even in zero magnetic field due to a field-induced unbalance in topological charges. Using a complementary suite of techniques, including electronic transport, Lorentz transmission electron microscopy, and micromagnetic simulations, we reveal the emergence of substantial coercive fields upon exfoliation, which are absent in the bulk, implying thickness-dependent magnetic interactions that affect the TST. We detected a ‘magic’ thickness $t \sim 30$ nm where the formation of TST is maximized, inducing large magnitudes for the topological charge density ($\sim 6.45 \times 10^{20} \text{ cm}^{-2}$), and the concomitant anomalous ($\rho_{xy}^A \approx 22.6 \mu\Omega \text{ cm}$) and topological ($\rho_{xy}^T \approx 15 \mu\Omega \text{ cm}$) Hall resistivities at $T \sim 120$ K. These values are higher than those found in magnetic topological insulators and, so far, the largest reported for 2D magnets. The hitherto unobserved THE under zero magnetic field could provide a platform for the writing and electrical detection of TST aiming at energy-efficient devices based on vdW ferromagnets. The hitherto unobserved THE under zero magnetic field could provide a platform for the writing and electrical detection of TST aiming at energy-efficient devices based on vdW ferromagnets.

SYMPOSIUM QT03

Physics of 2D Halide and Chalcogenides Semiconductors
April 23 - April 26, 2024

Symposium Organizers

Michal Baranowski, Wroclaw University of Science and Technology
Alexey Chernikov, Technische Universität Dresden
Paulina Plochocka, CNRS
Alexander Urban, LMU Munich

Symposium Support

Bronze

LIGHT CONVERSION

Wroclaw University of Science and Technology

* Invited Paper

+ JMR Distinguished Invited Speaker

^ MRS Communications Early Career Distinguished Presenter

SESSION QT03.01: 2D Halide and Chalcogenides Semiconductors I

Session Chairs: Paulina Plochocka and Alexander Urban

Tuesday Morning, April 23, 2024

Room 444, Level 4, Summit

10:45 AM *QT03.01.01

Ultra-High Q Nanobeam Cavities for 2D Heterostructures Jonathan J. Finley; Technical University of Munich, Germany

In this talk, I will describe our recent investigations of the heterogeneous integration of 2D materials onto novel Si₃N₄ nanobeam optical cavities [1-5]. These nanobeam optical resonators host ultra-high cavity modes and allow us to explore novel light-matter and multimodal *vibronic* – *phonon* – *photon* couplings mediated by electronic excitations. For hBN-encapsulated MoS₂ monolayers, we observe a nonmonotonic temperature dependence of the cavity-trion interaction strength, consistent with the nonlocal light-matter interactions in which the extent of the centre-of-mass wave function is comparable to the cavity mode volume in space [1]. For MoSe₂ homo-bilayers [2], we study the twist-dependent moiré coupling. For small angles, we find a pronounced redshift of the K–K and Γ –K excitons, an effect that we trace to the underlying moiré pattern. Studies of thick hBN layers coupled to the high-Q nanocavity modes reveal intriguing dynamics: For example, we identify the zero-phonon line transition of charged boron vacancies () [3,4] and observe a novel tripartite coupling between the cavity photonic modes, lattice phonon and nanobeam vibrational modes. The fingerprint for this tripartite coupling is a pronounced asymmetry in the emission spectrum for cavities with a Q-factor above a threshold of $\sim 10^4$. Similar asymmetries are not observed for cavities without centers, or lower Q-cavities. To explain our findings, we model the system with phonon-induced light-matter coupling and compare it to the

Jaynes-Cummings model for usual emitters. Our results reveal that the multipartite interplay arises during the light-matter coupling of centers, illustrating that it is phonon-induced, rather than caused by the thermal population of phonon modes. Our results indicate how different photon (emission, cavity photonic) and phonon (phonon, cavity mechanical) modes provide a novel system to interface spin defects, photons, and phonons in condensed matter systems.

- [1] C. Qian *et al.* Phys. Rev. Lett. **128**, 237403 (2022)
- [2] V. Villafane *et al.* Phys. Rev. Lett. **130**, 026901, (2022)
- [3] C. Qian *et al.* Phys. Rev. Lett. **130**, 126901 (2023)
- [4] C. Qian *et al.* Nano Lett, 22, 13, 5137–5142, (2022)
- [5] R. Rizzato *et al.* Nat. Comm. 14, 5089, (2023)

11:15 AM QT03.01.03

Nano and Sub-Micro Scale Optical Characterization of Transition Metal Dichalcogenide Nanoribbons by AFM-Optical Spectroscopy T. Kien Mac¹, T.T. Trinh Phan¹, Ashley P. Saunders², Fang Liu², Dmitri Voronine³ and Tuan M. Trinh¹; ¹Utah State University, United States; ²Stanford University, United States; ³University of South Florida, United States

Two-dimensional (2D) transition metal dichalcogenide (TMDC) nanoribbons have attracted significant interest recently due to their intriguing optical, magnetic, and electronic properties, all of which can be controlled by manipulating their edges and ribbon width via quantum confinement. The specific termination, structure, strain, or defects at the edges play crucial roles in shaping the characteristics of TMDC ribbons. For instance, MoS₂ exhibits distinct signals in second harmonic generation (SHG) for S-zigzag versus S-Mo Klapin edges. However, understanding the correlation between optical properties and intricate ribbon edges is challenging largely due to the diffraction limits of conventional optical techniques. The integration of optical spectroscopy with an atomic force microscope (AFM) allows for nanoscale optical imaging by enhancing the optical signal through plasmonic confinement between the metallic AFM tip and the sample. The techniques could reveal more detail on the impact of the edge on the ribbons. In this study, we focus on optical nano-imaging of TMDC nanoribbons using tip-enhanced photoluminescence and second harmonic generation. Our observations reveal variations in emission energy across different locations on the ribbons, indicating the influence of defects and edges on photoexcited exciton and trion energies in TMDC ribbons. To delve deeper into the effects of ribbon edges, we conducted polarization-resolved SHG experiments both with and without the application of an external magnetic field. The results not only shed light on the influence of edges but also offer opportunities to tune and manipulate the optical and magnetic properties of these nanoribbons.

11:30 AM *QT03.01.04

Measuring and Controlling The Dimensions of Liquid-Exfoliated Nanosheets Claudia Backes; Kassel University, Germany

Liquid phase exfoliation (LPE) has become an important production technique for colloidal dispersions and solution-processable inks of a range of materials due to its versatility and applicability to a broad range of material classes. While mass production is possible, samples are inherently polydisperse and aspect ratios of lateral size/thickness are limited due to scission and delamination occurring simultaneously.[1]

In this talk, I will first discuss our state-of-the-art in measuring nanosheet dimensions through atomic force microscopy, highlighting the challenges associated with this measurement. I will then present our recent in-depth analysis of nanosheet dimensions of WS₂ samples produced by tip sonication in both aqueous surfactant solution and the organic solvent N-methyl-2-pyrrolidone in conjunction with the effect of the liquid environment in centrifugation-based size selection. This data shows that the solvent not only has an impact on the outcome of the centrifugation, but also during sonication with aqueous surfactant based nanosheets having slightly higher length-thickness aspect ratios.

In the second part of the talk, I will demonstrate that it is possible to derive and validate an accurate equation of motion of nanosheets in the centrifugal field accounting for nanosheet dimensionality by implementing length/thickness and length/width aspect ratios that are widely constant for a given material produced in LPE. We show that this equation allows us to predict the nanosheet dimensions in sediment and supernatant after centrifugation.

References

- [1] ACS Nano 2019, 13, 6, 7050–7061

SESSION QT03.02: 2D Halide and Chalcogenides Semiconductors II – Dynamics

Session Chairs: Michal Baranowski and Sascha Feldmann

Tuesday Afternoon, April 23, 2024

Room 444, Level 4, Summit

1:30 PM *QT03.02.01

Hot Exciton Dynamics in Two-Dimensional Organic-Inorganic Hybrid Perovskites Cherie R. Kagan; University of Pennsylvania, United States

Two-dimensional, organic-inorganic hybrid perovskites (2DHPs) are stoichiometric compounds composed of alternating sheets of corner-sharing, metal-halide octahedra and organoammonium cationic layers. We study 2DHPs containing single lead iodide layers separated by intervening substituted, phenethylammonium (PEA) cations with the chemical structure (x-PEA)₂PbI₄, where x=F, Cl, Br, or CH₃. These 2DHPs form type-I heterojunctions in which excitons and carriers are strongly confined to the lead halide layers with exciton binding energies > 150 meV. We use x-ray diffraction and variable-temperature steady-state and time-resolved absorption and photoluminescence (PL) measurements to uncover the correlation between their structure and photophysical properties. (PEA)₂PbI₄ excitonic absorption and PL spectra at 15 K show splittings into regularly spaced resonances every 40–46 meV.¹ Anti-Stokes hot exciton PL is observed at the same energy as the optical absorption resonances. Replacing a single atom in the *para* position of the PEA-cation phenyl group increases its length and therefore the interlayer spacing, but leaves the cross-sectional area unchanged and results in structurally similar metal halide frameworks.² As the cation length increases, the absorption spectra broaden and blueshift, but the PL spectra remain invariant. Substitution in the *ortho* position with progressively larger cations increasingly distorts and strains the inorganic framework.³ Ortho substitutions change the number of and spacing between the discrete excitonic resonances and increase the hot exciton PL by >10X. By correlating the atomic substitutions on the cation with changes in the excitonic structure, we show that the origin of the discrete excitonic resonances is consistent with a vibronic progression caused by strong exciton-phonon coupling to a phonon on the organic cation. We also show evidence of the structure-dependent formation of exciton polarons.⁴ The properties of 2DHPs can be tailored by the selection of the cation without directly modifying the inorganic framework.^{5,6}

(1) Straus, D. B.; Hurtado Parra, S.; Iotov, N.; Gebhardt, J.; Rappe, A. M.; Subotnik, J. E.; Kikkawa, J. M.; Kagan, C. R. Direct Observation of Electron–

Phonon Coupling and Slow Vibrational Relaxation in Organic–Inorganic Hybrid Perovskites. *J. Am. Chem. Soc.* **2016**, *138* (42), 13798–13801. <https://doi.org/10.1021/jacs.6b08175>.

(2) Straus, D. B.; Iotov, N.; Gau, M. R.; Zhao, Q.; Carroll, P. J.; Kagan, C. R. Longer Cations Increase Energetic Disorder in Excitonic 2D Hybrid Perovskites. *J. Phys. Chem. Lett.* **2019**, *10* (6), 1198–1205. <https://doi.org/10.1021/acs.jpcclett.9b00247>.

(3) Straus, D. B.; Hurtado Parra, S.; Iotov, N.; Zhao, Q.; Gau, M. R.; Carroll, P. J.; Kikkawa, J. M.; Kagan, C. R. Tailoring Hot Exciton Dynamics in 2D Hybrid Perovskites through Cation Modification. *ACS Nano* **2020**, *14* (3), 3621–3629. <https://doi.org/10.1021/acsnano.0c00037>.

(4) Hurtado Parra, S.; Straus, D. B.; Fichera, B. T.; Iotov, N.; Kagan, C. R.; Kikkawa, J. M. Large Exciton Polaron Formation in 2D Hybrid Perovskites via Time-Resolved Photoluminescence. *ACS Nano* **2022**, *16* (12), 21259–21265. <https://doi.org/10.1021/acsnano.2c09256>.

(5) Straus, D. B.; Kagan, C. R. Electrons, Excitons, and Phonons in Two-Dimensional Hybrid Perovskites: Connecting Structural, Optical, and Electronic Properties. *J. Phys. Chem. Lett.* **2018**, *9* (6). <https://doi.org/10.1021/acs.jpcclett.8b00201>.

(6) Straus, D. B.; Kagan, C. R. Photophysics of Two-Dimensional Semiconducting Organic–Inorganic Metal-Halide Perovskites. *Annu. Rev. Phys. Chem.* **2022**, *73* (1), 403–428. <https://doi.org/10.1146/annurev-physchem-082820-015402>.

2:00 PM *QT03.02.02

Realizing and Imaging Ballistic Transport in Van der Waals Semiconductors [Milan Delor](#); Columbia University, United States

Achieving long-range ballistic (coherent) electron flow in materials at room temperature is a long-standing goal that could unlock lossless energy harvesting and wave-based information technologies. The key challenge is to overcome short-range scattering between electrons and lattice vibrations (phonons). I will describe several avenues to achieve ballistic transport by harnessing strong interactions between coherent and incoherent excitations in solid-state lattices. The first is to leverage polaritons, part-light part-matter quasiparticles resulting from hybridization between photons and semiconductor excitations. The second is to leverage strong electronic and electron-phonon interactions, yielding either highly delocalized excitons or acoustic polarons that are intrinsically shielded from phonon scattering. In all cases, we develop ultrafast optical imaging capabilities enabling us to track the propagation of these quasiparticles with femtosecond resolution and few-nanometer sensitivity over a frequency range spanning the visible to the mid-IR, providing a precise measurement of quasiparticle velocity, scattering pathways, and transition from coherent to incoherent transport.

2:30 PM QT03.02.03

Probing the Hot Carrier Cooling Process in Low-Dimensional Halide Perovskites through Ultrafast Spectroscopy [Ziyuan Ge](#)¹, Ben Carwithen¹, Tom Hopper^{1,2} and Artem Bakulin¹; ¹Imperial College London, United Kingdom; ²Stanford University, United States

Halide perovskite has shown promising applications in perovskite-based optoelectronic devices, e.g., solar cells, and light-emitting diodes, owing to its superior properties including defect tolerance, long carrier diffusion distance, and significant absorption coefficient. Perovskites in nanoscale dimension to lower dimensional networks have recently emerged as having high luminescence efficiency, color purity, and stability. Owing to the soft nature of the perovskite lattice, these electronic properties are primarily governed by the carrier/exciton-phonon coupling strength. Understanding the role of individual phonons in modulating photophysical properties of these class of materials is largely limited to three-dimensional perovskites, (like MAPbI₃). Here in our research, we employ femtosecond Pump – push – probe and transient absorption spectroscopy in low-dimensional perovskite systems to study the influence of electron-phonons interaction in hot-carrier cooling to the fate of band-edge excitons. Furthermore, our spectroscopic approach allows us to discern the role of carrier-carrier interactions from carrier-phonon, which is otherwise difficult in conventional measurements. Our finding reveals that suppression of hot phonon bottleneck effect for systems with increasing quantum confinement (i.e., larger exciton binding energy). We predicted that electron-hole coupling within an exciton (in those confined systems) plays a dominant role in hot-carrier cooling over phonons and carrier-phonon coupling. On the other hand, band-edge electronic dynamics in low-dimensional excitonic systems studied through impulsive excitation provide direct evidence of involvement/coupling of various low-frequency phonon modes.

2:45 PM QT03.02.04

Propagation of Excitons and Trions in Two-Dimensional Hybrid Perovskites [Sophia Terres](#)¹, Jonas Ziegler¹, Kai-Qiang Lin², Barbara Meisinger², Yeongsu Cho³, Xiangzhou Zhu⁴, Manuel Kober-Czerny^{5,6}, Pabitra K. Nayak^{5,6}, Cecilia Vona⁷, Matan Menahem⁸, Takashi Taniguchi⁹, Kenji Watanabe⁹, Henry J. Snaith⁵, John Lupton², Claudia Draxl⁷, Omer Yaffe⁸, Timothy C. Berkelbach³, David A. Egger⁴ and Alexey Chernikov¹; ¹Technische Universität Dresden, Germany; ²Universität Regensburg, Germany; ³Columbia University, United States; ⁴Technische Universität München, Germany; ⁵University of Oxford, United Kingdom; ⁶Tata Institute of Fundamental Research, India; ⁷Humboldt-Universität zu Berlin, Germany; ⁸Weizmann Institute of Science, Israel; ⁹National Institute for Materials Science, Japan

Two-dimensional hybrid perovskites are a highly intriguing class of materials. They are considered natural quantum well systems composed of alternating inorganic and organic molecular layers. Their reduced dimensionality combined with weak dielectric screening leads to the formation of tightly bound excitons that are shown to be both efficient light emitters as well as highly mobile. However, external control of their optical response has proven difficult due to challenges to introduce electrical doping into these systems. Moreover, a key feature of some of these materials is the occurrence of a structural phase transition that can alter the electronic band gap as well as their optical response. To what extent the phase transition can affect these fundamental properties has been barely explored so far.

Here, we study the temperature-dependent exciton binding energy and exciton diffusion across the phase transition using a combination of time-resolved microscopy and non-linear spectroscopy. We demonstrate that neither exciton binding energy nor exciton diffusion are affected by the phase transition in contrast to initial predictions. These findings are unexpected considering the substantial changes of the free carrier masses and contrast the semi-classical understanding of their transport, highlighting the unusual behavior of excitons in 2D hybrid perovskites. To better understand excitonic equilibration and relaxation, we investigate non-equilibrium dynamics at cryogenic temperatures at both off-resonant and near-resonant excitation conditions. Beyond that, we report realization of electrically doped, ultrathin 2D perovskite layers, studied in ambipolar field-effect transistor geometries. We demonstrate formation of three-particle exciton complexes, known as trions, by detecting photoluminescence spectra as a function of gate voltage and we reveal the influence of exciton-carrier interaction on the exciton mobility. The experimental realization of both tunable and mobile trions encourages potential applications involving electrically guided charged exciton currents.

3:00 PM BREAK

3:30 PM *QT03.02.05

Phonon Bottleneck Slowing Down Exciton Dynamics in 2D Perovskites and Transition Metal Dichalcogenides [Ermin Malic](#); Philipps University Marburg, Germany

Monolayer transition metal dichalcogenides (TMDs) and 2D perovskites exhibit a rich exciton physics. The combination of spin-orbit and exchange coupling leads to a complex excitonic landscape of bright and dark states in 2D perovskites, which dictates not only optical signatures but also exciton formation, relaxation and decay dynamics. Despite having a lowest energy dark state, a surprisingly large photoluminescence from the higher-energy bright states has been observed. Combining low temperature magneto-optical measurements with a sophisticated many-particle theory we reveal the microscopic origin of the unexpected enhanced emission of bright excitons in 2D perovskites. We attribute the emission to a pronounced phonon-bottleneck effect, which considerably slows down the relaxation of excitons towards to energetically lowest dark states at low temperatures. We show that this bottleneck can be controlled by changing the bright-dark splitting and the energy of optical phonons by considering different perovskite materials and dielectric surroundings.

We demonstrate that a similar phonon bottleneck can also occur for exciton polaritons created in MoSe₂ monolayers integrated into a Fabry-Perot cavity. Efficient scattering into the exciton polariton ground state is a key prerequisite for generating Bose-Einstein condensates and low-threshold polariton lasing. However, this can be challenging to achieve at low densities due to the appearance of the polariton bottleneck effect that impedes phonon-assisted scattering into the lowest polariton states. However, the rich exciton landscape of TMDs provides potential intervalley scattering pathways to rapidly populate these polariton states. By exploiting phonon-assisted transitions between momentum-dark excitons and the lower polariton branch, we demonstrate that it is possible to bypass the bottleneck region and efficiently populate the low-momentum states in the lower polariton branch at room temperature.

Our work provides new insights on exciton dynamics in atomically thin semiconductors offering strategies for tuning the exciton emission in layered perovskites and populating the polariton groundstate in TMD monolayers that is crucial for many technological applications based on these materials.

4:00 PM QT03.02.06

Effect of Energy Bands Overlap in the Interlayer Energy Transfer Processes in 2D Heterostructures [Arka Karmakar](#); University of Warsaw, Poland

Heterostructures (HSs) made by the monolayers (1Ls) of transition metal dichalcogenides (TMDs) have shown great promises in designing next-generation optoelectronic device applications. Interlayer charge (CT) and energy transfer (ET) processes are the main photocarrier relaxation pathways in the TMD HSs. In semiconductor HSs, usually the CT processes happen at a faster timescale (~100s fs) than the nonradiative ET processes (~few ps). CT processes mainly occur due to the energy level offset between the materials and can survive only up to a few nm. Several studies have already been done using different ultrafast spectroscopic techniques to understand the different aspects of the CT process. Whereas, the interlayer ET process mediated by the dipole-dipole coupling between the donor and acceptor materials, can survive up to several tens of nm. Also, due to the experimental challenges to observe the dipole-dipole coupling, many key factors related to the ET processes remain incomprehensible. In this talk, I would like to present our recent studies to understand the effect of energy bands overlap in the ET process in TMD HSs. First, we study the effect of resonant overlaps between the optical bandgaps of two materials [1]. In this work, we showed that in the type-II HSs formed using the 1Ls of molybdenum diselenide (MoSe₂) and rhenium disulfide (ReS₂), an ET process dominates over the fast CT process, resulting 360% photoluminescence (PL) enhancement in the HS area. After completely blocking the CT process, this enhancement increased further up to more than 1 order of magnitude higher. In the second part, we showed that HS formed between the 1Ls of molybdenum disulfide (MoS₂) and tungsten disulfide (WS₂), an unusual ET process occur from the lower bandgap WSe₂ to higher bandgap MoS₂ due to the resonant overlaps between the high-lying excitonic states [2]. These works will help us to realize the complex ET processes in TMD HSs for better development of the TMD-based novel optoelectronic device applications.

References:

- [1] A. Karmakar, A. Al-Mahboob, C. E. Petoukhoff, O. Kravchyna, N. S. Chan, T. Taniguchi, K. Watanabe, K. M. Dani, "Dominating Interlayer Resonant Energy Transfer in Type-II 2D Heterostructure", *ACS Nano* 2022, 16, 3, 3861–3869.
[2] A. Karmakar, T. Kazimierzczuk, I. Antoniazzi, M. Raczynski, S. Park, H. Jang, T. Taniguchi, K. Watanabe, A. Babinski, A. Al-Mahboob, M. R. Molas, "Excitation-Dependent High-Lying Excitonic Exchange via Interlayer Energy Transfer from Lower-to-Higher Bandgap 2D Material", *Nano Lett.* 2023, 23, 12, 5617–5624.

4:15 PM QT03.02.07

Electronic Transport in 2D Chalcogenide Semiconductors [Yuan Yue Liu](#); The University of Texas at Austin, United States

Many commonly-used 2D chalcogenide semiconductors suffer from low carrier mobility at room temperature. There is a critical need to understand the transport bottleneck and improve. Here I will present our recent progress in developing and apply first-principles methods to accurately calculate and understand the electronic transport in 2D chalcogenides, including both phonon and defect scatterings. I will also present new materials with improved transport properties.

Ref: [1] Z. Xiao, R. Guo, C. Zhang, Y. Liu, "Point defects limited charge mobility in 2D transition metal dichalcogenides", under review; [2] C. Zhang, R. Wang, H. Mishra, Y. Liu, "Discovering and Understanding 2D Semiconductors with High Intrinsic Charge Mobility at Room Temperature", *Phys. Rev. Lett.*, 2023, DOI: 10.1103/PhysRevLett.130.087001; [3] L. Cheng, C. Zhang, Y. Liu, "Why two-dimensional semiconductors generally have low electron mobility", *Phys. Rev. Lett.*, 2020, DOI: 10.1103/PhysRevLett.125.177701

4:30 PM QT03.02.08

Interlayer Charge Transfer in 2D Hybrid Perovskites Containing Electroactive Ligands towards Enhanced Charge Carrier Transport [Wouter Van Gompel](#)¹, [Yorrick Boeije](#)^{2,2}, [Youcheng Zhang](#)^{2,2}, [Pratyush Ghosh](#)², [Szymon Zelewski](#)^{2,2,3}, [Arthur Maufort](#)¹, [Bart Roose](#)², [Zher Ying Ooi](#)², [Rituparno Chowdhury](#)², [Ilan Devroey](#)¹, [Stijn Lenaers](#)¹, [Alasdair Tew](#)², [Krishanu Dey](#)², [Hayden Salway](#)², [Richard Friend](#)², [Henning Sirringhaus](#)², [Laurence Lutsen](#)^{1,4}, [Akshay Rao](#)², [Samuel D. Stranks](#)^{2,2} and [Dirk Vanderzande](#)^{1,4}; ¹Universiteit Hasselt, Belgium; ²University of Cambridge, United Kingdom; ³Wroclaw University of Science and Technology, Poland; ⁴IMEC, Belgium

The family of hybrid organic-inorganic lead-halide perovskites are the subject of intense interest for optoelectronic applications. Due to the electronically inert nature of most organic molecules, the inorganic sublattice generally dominates the electronic structure and therefore optoelectronic properties of perovskites. However, over the past years interest in the incorporation of electronically active organic cations has been increasing.[1] We use optically and electronically active carbazole-based Cz-C_i molecules [2-3], where C_i indicates an alkylammonium chain and i indicates the number of CH₂ units in the chain, varying from 3–5, as cations in the 2D perovskite structure (Cz-C_i)₂PbI₄. We demonstrate a tunable electronic coupling between the inorganic lead-halide and organic layers. The strongest interlayer electronic coupling was found for (Cz-C₃)₂PbI₄. We measure ultrafast hole transfer from the photoexcited lead-halide layer to the Cz-C_i molecules, the efficiency of which increases by varying the chain length from i=5 to i=3. The charge transfer results in long-lived carriers (10 – 100 ns) and quenched emission. Electrical charge transport measurements using single-carrier devices show markedly

increased out-of-plane carrier mobilities compared to (PEA)₂PbI₄, with carrier mobility increasing from $i=5$ to $i=3$.^[4]

[1] Van Gompel, W.T.M.; Lutsen, L.; Vanderzande, D., *Journal of Materials Chemistry C* 2023, Advance Article (10.1039/D3TC02553E)

[2] Herckens, R.; Van Gompel, W. T. M.; Song, W. Y.; Gelvez-Rueda, M. C.; Maufort, A.; Ruttens, B.; D'Haen, J.; Grozema, F. C.; Aernouts, T.; Lutsen, L.; Vanderzande, D., *Journal of Materials Chemistry A* 2018, 6 (45), 22899-22908 (10.1039/c8ta08019d)

[3] Van Landeghem, M.; Van Gompel, W. T. M.; Herckens, R.; Lutsen, L.; Vanderzande, D.; Van Doorslaer, S.; Goovaerts, E., *The Journal of Physical Chemistry C* 2021, 125 (33), 18317-18327 (10.1021/acs.jpcc.1c05005)

[4] Boeije, Y.; Van Gompel, W. T. M.; Zhang, Y.; Ghosh, P.; Zelewski, S.; Maufort, A.; Roose, B.; Ying Ooi, Z.; Chowdhury, R.; Devroey, I.; Lenaers, S.; Tew, A.; Dai, L.; Dey, K.; Salway, H.; Friend, R. H.; Siringhaus, H.; Lutsen, L.; Vanderzande, D.; Rao, A.; Stranks, S. D., *Journal of the American Chemical Society* 2023, Just Accepted (10.1021/jacs.3c05974)

4:45 PM QT03.02.09

Towards In-Plane Control of Neutral Exciton Flux in Semiconducting 2D Materials Hassan Lamsaadi¹, Dorian Beret², Ioannis Paradisanos³, Pierre Renucci², Delphine Lagarde², Marie Xavier², Bernhard Urbaszek⁴, Ziyang Gan⁵, Antony George⁶, Kenji Watanabe⁷, Andrey Turchanin⁵, Takashi Taniguchi⁷, Laurent Lombez², Nicolas Combe¹, Aurelien Cuche¹, Vincent Paillard¹ and Jean-marie Poumirol¹; ¹CEMES-CNRS, France; ²INSA-CNRS-UPS, LPCNO, France; ³Institute of Electronic Structure and Laser, Foundation for Research and Technology-Hellas, Greece; ⁴Institute of Condensed Matter Physics, Technische Universität Darmstadt, Germany; ⁵Friedrich Schiller University Jena, Institute of Physical Chemistry, Germany; ⁶Abbe Centre of Photonics, Germany; ⁷Research Center for Functional Materials, National Institute for Materials Science, 1-1 Namik, Japan

For a wide range of next-generation applications in excitonic circuits, quantum optics and optoelectronics, neutral excitons in semiconducting 2D materials need to be controlled. Until now, and in particular in transition metal dichalcogenides, such control has been achieved through the local strain gradient engineering. However, the charge-neutral nature of the dominant exciton types in such materials limits their interaction with external electric or magnetic fields, still making their manipulation a challenging task. Recently, we demonstrated efficient unidirectional transport of excitons from high-gap to low-gap material at room-temperature in high-quality lateral heteromonolayer [1]. Tip enhanced Raman and Photoluminescence spectroscopies (~30nm resolution) performed on high-quality heteromonolayers reveal that excitons generated inside the high-gap material are able to pass through the junction before recombining inside the low-gap material, while propagation in the opposite direction is forbidden. Going further, we have shown that the abrupt change in exciton energy and effective mass has resulted in a strong Kapitza resistance-like effect, allowing excitons to be accelerated locally at the junction as they move from high-gap to low-gap material while being blocked in the opposite direction [2]. This effect causes a strong discontinuity in the excitonic density profile at the junction. As a result, a quenching of high-gap material-related PL is observed while low-gap material-related PL is enhanced near the junction. Finally, by using μ -Photoluminescence(μ -PL) imaging combined with a simulation-based statistical approach of randomly moving excitons through specific geometries of a high-quality CVD-grown MoSe₂-WSe₂ lateral heteromonolayer, we demonstrated that the exciton Kapitza effect enhances the exciton diffusion length, and is able to focus and confine excitons down to sub-wavelength dimensions [3]. We believe that our work provides new tools for manipulating neutral excitons in flat semiconducting 2D materials and will enable the incorporation of lateral heteromonolayers in next-generation excitonic devices.

References

- [1] Dorian Beret, Ioannis Paradisanos, Hassan Lamsaadi, et al. Exciton spectroscopy and unidirectional transport in MoSe₂-WSe₂ lateral heterostructures encapsulated in hexagonal boron nitride. **npj 2D Materials and Applications**, 6(1):84, 2022.
- [2] Hassan Lamsaadi et al. Kapitza-resistance-like in flat MoSe₂-WSe₂ lateral heterojunction. **Nature communications**, 5881(1):84, 2023.
- [3] Hassan Lamsaadi et al. Towards in-plane control of neutral exciton flux in transition metal dichalcogenide monolayers. in preparation.

SESSION QT03.03: 2D Halide and Chalcogenides Semiconductors III – Synthesis
Session Chairs: Cherie Kagan and Alexander Urban
Wednesday Morning, April 24, 2024
Room 444, Level 4, Summit

8:45 AM *QT03.03.01

Structure-Property Engineering in The 2D Hybrid Perovskite Family David B. Mitzi; Duke University, United States

Two-dimensional hybrid organic-inorganic perovskite (2D HOIP) semiconductors based on metal halide frameworks offer unprecedented opportunity to tailor structural and materials properties using the full flexibility afforded by the realms of inorganic and organic chemistry,¹ and such tunability offers wide-ranging potential for applications including solar cells, light-emitting devices, detectors, transistors and advanced computing devices. This talk will focus on examining the role that the organic cation plays in tuning one or more of the following: 1) self-assembling quantum well structures with predictable energy band offsets and charge carrier response,^{2,3} 2) chirality transfer and symmetry breaking within the inorganic framework,⁴ and/or 3) melting and glass formation/crystallization kinetics.^{5,6} Recent examples of such structure-property flexibility highlight the unique versatility and promise of using the organic component to control charge, light and spin within the wide-ranging 2D HOIP family.

1. D. B. Mitzi, K. Chondroudis, C. R. Kagan, *IBM J. Res. & Dev.* 45, 29 (2001).
2. D. Seyitliyev, X. Qin, M. K. Jana, S. M. Janke, X. Zhong, W. You, D. B. Mitzi, V. Blum, K. Gundogdu, *Adv. Funct. Mater.* 33, 2213021 (2023).
3. R. Song, C. Liu, Y. Kanai, D. B. Mitzi, V. Blum, *Phys. Rev. Mater.* 7, 084601 (2023).
4. Y. Xie, J. Morgenstein, B. Bobay, R. Song, N. Caturello, P. Sercel, V. Blum, D. B. Mitzi, *J. Am. Chem. Soc.* 145, 17831 (2023).
5. E. J. Crace, A. Singh, S. Haley, B. Claes, D. B. Mitzi, *Inorg. Chem.* 62, 16161 (2023).
6. A. Singh, Y. Kim, R. Henry, H. Ade, D. B. Mitzi, *J. Am. Chem. Soc.* 145 18623 (2023).

9:15 AM QT03.03.03

Growth of Arbitrary 2D TMDs Nanopatterns via Thermal Scanning Probe Lithography Giorgio Zambito, Maria Caterina Giordano, Matteo Gardella and Francesco Buatier de Mongeot; University of Genoa, Italy

Two dimensional (2D) materials have emerged as promising platforms for creating new generation, atomically thin devices in various fields, from nanoelectronics and nanophotonic, to quantum technologies and energy conversion [1–3].

These materials are generally manufactured from mechanically exfoliated flakes, which suffer from stochastic positioning and micrometric sizes. The re-shaping of 2D materials is attractive, since it opens interesting possibilities for engineering optoelectronic and photonic responses, as well as it enables the fabrication of devices with optimized geometries. Nanopatterning of exfoliated flakes is generally obtained by subtractive chemical etching methods [4] which, although effective for creating single demonstrative configurations, are not suitable for fabricating scalable devices for real-life applications.

Here we propose a process that allows the direct fabrication of few-layer MoS₂ nano-circuits with arbitrary geometries. Our approach combines i) a custom-developed sputtering growth for creating few-layers MoS₂ extended films and ii) a high-resolution lithography technique which makes use of a nanoscopic (~10nm) hot silicon probe (thermal Scanning Probe Lithography – t-SPL, NanoFrazor). By the accurate manipulation of such hot nanoprobe, transiently heated by Joule effect, we write deterministic nanopaths onto a sacrificial polymer layer; these nanopatterns spread over a large-area substrate are homogeneously coated by few-layer MoS₂ by the Ion Beam Sputtering (IBS) of a MoS₂ target, leading to MoS₂ nano-circuits with complex geometries and in-series scalability. After a proper high-temperature recrystallization process in a controlled atmosphere, these arbitrary MoS₂ nano-interconnections are characterized by the means of micro-Raman spectroscopy and Kelvin Probe Force Microscopy (KPFM). The observed vibrational and electronic responses confirm the presence of the stable 2H semiconducting phase confined inside the nano-circuits.

After the fabrication of a proper nano-device configuration, the local electrical transport properties of these MoS₂ nano-paths are investigated via conductive - AFM (ResiScope c-AFM), demonstrating the possibility to employ these 2D semiconducting nanocircuits as building blocks of integrated electronics devices.

Finally, we show some preliminary results on alternative applications of t-SPL on 2D materials, such as multilevel patterning of polymer films by 3D grayscale lithography. Indeed, the creation of three-dimensional patterns with arbitrary submicrometric features can serve as a tool to induce and study on-demand strain engineering of 2D materials.

[1] Q. H. Wang, K. Kalantar-Zadeh, A. Kis, J. N. Coleman, M. S. Strano, *Nat. Nanotechnol.* 2012, 7, 699.

[2] C. Martella, C. Mennucci, A. Lamperti, E. Cappelluti, F. B. de Mongeot, A. Molle, *Adv. Mater.* 2018, 30, 1705615.

[3] M. Bhatnagar, M. C. Giordano, C. Mennucci, D. Chowdhury, A. Mazzanti, G. Della Valle, C. Martella, P. Tummala, A. Lamperti, A. Molle, F. Buatier de Mongeot, *Nanoscale* 2020, 12, 24385.

[4] M. G. Stanford, P. D. Rack, D. Jariwala, *Npj 2D Mater. Appl.* 2018, 2, DOI 10.1038/s41699-018-0065-3.

[5] Giordano, M. C., Zambito, G., Gardella, M., Buatier de Mongeot, F., *Deterministic Thermal Sculpting of Large-Scale 2D Semiconductor Nanocircuits.* *Adv. Mater. Interfaces* 2023, 10, 2201408.

9:30 AM BREAK

10:00 AM *QT03.03.04

Layered Halide Perovskites: Rich Structural Chemistry and Untapped Potential in Optoelectronics [Constantinos Stoumpos](#)^{1,2}; ¹University of Crete, Greece; ²Saint Petersburg State University, Russian Federation

Halide perovskites have shown an immense potential as semiconductors in the past decade, exemplified by their remarkable prowess in photovoltaics, but also in other fields of optoelectronics with successful proof-of-principle demonstrations as radiation sensors, light-emitting devices and lasers. Halide perovskites hold great promise in the sense that they can match in performance the classical semiconductors, but in addition, they can exhibit unconventional behavior such as their unusual defect tolerance that derives from the dynamic nature of the crystal lattice. A specific branch of halide perovskite class of materials that have been drawn enormous attention in recent years, is the dimensionally reduced layered perovskites. Layered perovskites are produced by the incorporation of “molecular scissors” that disrupt the continuity of the inorganic lattice and produce nanoscale-sized two-dimensional sheets, periodically oriented in the form of macroscopic crystals. Layered perovskites possess all the privileges of the parent compounds, but in addition, they are subject to spatial and dielectric confinement effects, thus generating quantum phenomena within their multiple-quantum-well structure. In this talk, I will discuss the early developments in the field of layered halide perovskites and how this early work has led to the current state-of-the-art. I will outline the synthetic methods that have been utilized to obtain the materials in pure form and I will discuss the evolution of important homologous series that constitute the arch types of many related compounds. I will discuss how the optical properties of the materials vary in these systems, focusing of their ability to form stable excitonic states and the peculiar changes that occur in the spectra upon the numerous phase transitions observed in variable temperature experiments. I will conclude my talk by describing potential applications of layered perovskites that can benefit from the presence of stable excitons.

Acknowledgements: CCS acknowledges the Special Account for Research Funding of the University of Crete (grants KA10330 and KA10652), the project “NANO-TANDEM” (MIS 5029191), co-financed by Greece and the European Regional Development Fund, and the Ministry of Science and Higher Education of the Russian Federation (Megagrant no. 075-15-2022-1112) for financial support.

10:30 AM QT03.03.05

Extrinsic Doping and Compensating Defects in The 2D Hybrid Perovskite PEA₂PbI₄ [Gabrielle Koknat](#)¹, [Haipeng Lu](#)^{2,3}, [Yi Yao](#)¹, [Ji Hao](#)², [Xixi Qin](#)¹, [Chuanxiao Xiao](#)², [Ruyi Song](#)¹, [Florian Merz](#)⁴, [Markus Rampp](#)⁵, [Sebastian Kokott](#)⁶, [Christian Carbogno](#)⁶, [Tianyang Li](#)¹, [Glenn Teeter](#)², [Matthias Scheffler](#)⁶, [Joseph Berry](#)², [David B. Mitzi](#)^{1,1}, [Jeffrey Blackburn](#)², [Volker Blum](#)^{1,1} and [Matthew C. Beard](#)²; ¹Duke University, United States; ²National Renewable Energy Laboratory, United States; ³The Hong Kong University of Science and Technology, Hong Kong; ⁴Lenovo HPC Innovation Center, Germany; ⁵Max Planck Computing and Data Facility, Germany; ⁶The NOMAD laboratory at the Fritz Haber Institute of the Max Planck Society, Germany

2D hybrid organic-inorganic perovskites (HOIPs) are exciting materials for optoelectronic device applications due to their high degree of chemical and structural tunability. The ability to electronically dope these materials via incorporation of extrinsic dopants is essential for control over carrier concentrations. Conversely, the presence of intrinsic defects can negatively impact electronic doping efficiencies. Here, we present a systematic study of intrinsic point defects and extrinsic dopants (eg. Bi, Sn [*PRX Energy*, **2**, 023010 (2023)]), both in isolation and as combined defects, in phenylethylammonium lead iodide (PEA₂PbI₄). Using spin-orbit coupled hybrid density functional theory (DFT) and supercell models up to 3,383 atoms in size, we pinpoint the expected positions of dopant-derived electronic levels in the bandgap. Complementary experimental findings reinforce hypotheses of compensation mechanisms and limiting factors derived from DFT.

10:45 AM QT03.03.06

Interdigitation and Hydrogen Bonding in Benzotriazole-Based 2D Layered Perovskites: a Study of Organic Non-Covalent Interactions [Arthur Maufort](#)¹, [Jesús Cerda Calatayud](#)², [Kristof Van Hecke](#)³, [Davy Deduytsche](#)³, [Arne Verding](#)¹, [Bart Ruttens](#)⁴, [Christophe Detavernier](#)³, [Laurence Lutsen](#)^{1,4}, [Claudio Quarti](#)², [Wouter Van Gompel](#)¹, [David Beljonne](#)² and [Dirk Vanderzande](#)^{1,4}; ¹Hasselt University, Belgium; ²University of Mons, Belgium; ³Ghent University, Belgium; ⁴IMEC, Belgium

Extensive research in the past decade has shown that hybrid perovskites might become a cornerstone in the future global energy economy. Although three-dimensional 3D perovskites have been receiving a lot of research attention, their 2D layered counterparts have also been proven valuable to the field. In state-of-the-art 2D layered perovskites, alkylammonium and phenethylammonium cations are still mostly employed. Although these organic cations succeed in stabilizing the perovskite, they don't offer valuable properties of their own to complement the attractive optoelectronic properties of the perovskite layers. Synergy could be achieved by choosing larger organic cations with more suitable optoelectronic properties, [1,2] or by inserting organic charge-transfer complexes [3] or dipole stacks in the organic layers. However, the non-covalent interactions acting within these more advanced organic layers need to be fully understood in order to formulate design rules and structure-property relationships for this novel class of materials.

In this work, [4,5] benzotriazole-based organic cations are synthesized and subsequently successfully applied to 2D layered hybrid perovskites. The structural and thermal properties of thin films and single crystals of these perovskites are investigated. Single-crystal analysis reveals that benzotriazole-based organic layers in lead(II) iodide lattices show interdigitation, reducing the organic layer thickness and leading to an unusually dense aromatic stacking. Moreover, 2D layered benzotriazole perovskites contain hydrogen bridges – both inter- and intramolecular – within the organic layers. Through theoretical modelling using density-functional theory (DFT), we elucidate this interdigitation and hydrogen bonding and quantify the lattice stabilization. We relate the phenomenon of interdigitation to the available lattice space and to stabilizing non-covalent interactions. Finally, we show that these structural properties lead to enhanced thermal stability with respect to the state of the art.

References

- [1] R. Herckens, W. T. M. Van Gompel et al., *J. Mater. Chem. A* (2018), 6, 22899.
- [2] P.-H. Denis, M. Mertens et al., *Adv. Opt. Mater.* (2022), 10, 2200788.
- [3] W. T. M. Van Gompel, R. Herckens et al., *Chem. Commun.* (2019), 55, 2481.
- [4] A. Caiazza, A. Maufort et al., *ACS Appl. Energy Mater.* (2023), 6, 3933.
- [5] A manuscript by the authors on organic non-covalent interactions in 2D layered perovskites is being prepared.

11:00 AM QT03.03.08

Self Trapped Exciton Emission under Ambient Conditions in Two-Dimensional Halide Double Perovskites Triggered by Heterovalent Metal Substitution [Chunyang Chi](#); National University of Singapore, Singapore

Layered double perovskites (LDPs) possess soft lattice and strong exciton-phonon interactions, which represent an emerging class of materials as promising self trapped exciton (STE) emitters. However, few LDPs have been discovered with observable photoluminescence (PL) under room conditions hindered by the intrinsic parity-forbidden band transition. Herein, manganese (Mn) is incorporated into $(\text{PA})_4\text{AgInBr}_8$ ($\text{PA}=\text{CH}_3(\text{CH}_2)_2\text{NH}_3^+$) to form $(\text{PA})_4\text{Ag}_{1-0.5x}\text{Mn}_x\text{In}_{1-0.5x}\text{Br}_8$ ($0 \leq x \leq 1$) heterovalent-metal alloyed layered double perovskites. Halogen substitution is applied to characterize tunable optoelectronic properties of LDPs. Highly oriented thin films are fabricated and investigated via X-ray diffraction $2\theta/\omega$ and ψ scan. With this alloy-induced extrinsic exciton self-trapping strategy, broadband emission is obtained under room conditions via tuning STE states from dark to bright. Temperature-dependent PL gives insights to the emissive behavior and charge-carrier dynamics. The associated Huang-Rhys factors and exciton binding energies show the complexity of excitonic localization in this quantum-well-like structure. This study provides inspiration for designing novel lead-free PL-active perovskites and highlights the significance of understanding the intricate details of exciton-lattice coupling dynamics in LDPs.

SESSION QT03.04: 2D Halide and Chalcogenides Semiconductors IV – Devices
Session Chairs: Alexey Chernikov and Goki Eda
Wednesday Afternoon, April 24, 2024
Room 444, Level 4, Summit

1:30 PM *QT03.04.01

Low Dimensional Metal Halides: Optical and Electronic Properties of an Emerging 2D Semiconductor Class [Maria Antonietta Loi](#); University of Groningen, Netherlands

Low dimensional metal halides are currently under the spotlight for optoelectronic applications due to their remarkable photophysical properties. 3D compounds of similar chemical composition have been used to demonstrate highly efficient solar cells, light emitting diodes, and x-ray detectors. Very recently, 2D and quasi-2D Ruddlesden–Popper metal halide compounds, have also been explored for optoelectronic devices. Low dimensional metal halide affords specific advantages over other inorganic 2D materials such as transition metal dichalcogenides. As they are easily grown by both solution methods and vapor transport methods at low temperature, and they display a tuneable direct bandgap. In my presentation I will discuss the excitonic properties, transport and stability of two 2D perovskites based on Pb and on Sn, respectively. Concluding on the prospective for these materials in new optoelectronic devices.

2:00 PM *QT03.04.02

Optoelectronics of Atomic Dopants in 2D Semiconductors [Goki Eda](#); National University of Singapore, Singapore

Substitutional doping is a versatile approach for tailoring desired functionalities in 2D semiconductors. Unlike conventional semiconductors, dopants in 2D systems often possess a high activation energy due to reduced screening, leading to apparently minor effects on the host's electronic properties, even at relatively high concentrations. In this presentation, we will delve into the distinctive impact of atomic dopants on the optical, electrical, and optoelectrical characteristics of 2D semiconductors in contrast to traditional semiconductors. As an illustrative example, we will demonstrate that a single atomic impurity significantly enhances the local out-of-plane conductivity of 2D semiconductors by up to two orders of magnitude through resonant-assisted tunnelling. This breakthrough enables the rapid quantification of selected impurities in the dilute limit ($<10^{10} \text{ cm}^{-2}$) under ambient conditions, leveraging conductive atomic force microscopy [1]. Additionally, we will elucidate how atomic impurities create a narrow impurity band that facilitates in-plane conduction beyond a critical concentration. We conclude by showcasing the photovoltaic effect generated by individual atomic impurity dipoles within homobilayers of doped transition metal dichalcogenides, as observed using photoconductive atomic force microscopy.

- [1] Vu et al. "Single atomic point defect conductivity for dilute impurities imaging in 2D semiconductors" *ACS Nano*, 17, 15648 (2023)

2:30 PM BREAK

3:30 PM QT03.04.03

Emerging Van der Waals Heterostructures for Ultrathin Solar Cells: Implication of Type-II Band Edge Alignment on Photo-Conversion Efficiency Ponnappa K. Prasanna and Sudip Chakraborty; Harish Chandra Research Institute (HRI), India

The emerging two-dimensional (2D) materials, ZrSe₂ and HfSe₂, have been envisaged to construct the possible van der Waals heterostructures (vdW), for enhancement of solar cell efficiency. We have performed systematic first principles electronic structure calculations to explore the electronic band structures and optical properties of the heterostructures in order to determine the photo-conversion efficiency (PCE). We have considered both H and T phases of ZrSe₂ and HfSe₂ while constructing four different possibilities of heterostructures. From the analysis of band edge alignment, it has been found that the heterostructures are having Type-II band alignment, which helps in boosting the effective separation of electron-hole pairs, paving the way towards its application in materials for ultra-thin excitonic heterojunction solar cells. The electrostatic potential shows a huge difference in the dip which signifies the inbuilt electric field that is generated between two different surfaces therefore enhancing the transfer of electrons and holes between different layers. The optical absorption spectra of the heterostructures cover the wider range of the incident solar energy therefore better utilization of the incident radiation. The results show that the heterostructure formed by the H phase of ZrSe₂/HfSe₂ has attained a maximum power conversion efficiency of over 21%.

3:45 PM QT03.04.04

Spin LEDs Based on a Chiral Halide Perovskite Spin Injector Matthew Hautzinger, Kirstin M. Alberi and Matthew C. Beard; National Renewable Energy Laboratory, United States

The chirality induced spin selectivity (CISS) effect is the selective transmission of electron spin dictated by the handedness of chiral molecules (or structures). Materials exhibiting the CISS effect have great potential in acting as spin injectors, yet there are limited demonstrations of incorporating CISS active materials into spintronic devices. Here, we successfully integrate semiconducting chiral halide perovskites with semiconducting LED emitters. Based on the optical selection rules and conservation of angular momentum, we observe circularly polarized light emission as a result of the spin polarized injection from the chiral perovskite into the semiconductor. The large degree of spin polarization is enabled by the semiconductor-semiconductor interface. To further understand what parameters dictate CISS based spin injection efficiency, we have incorporated chiral perovskites with a variety of emitter materials to probe the impact of band offsets, spin lifetimes, and composition. This demonstration opens numerous opportunities to incorporate CISS materials with semiconductors as opto-spintronic technologies and provide some ground rules for achieving high CISS based spin injection efficiency.

4:00 PM QT03.04.05

Ultrathin Chalcogenide Light Harvesters: Charge-Carrier Transport and Fast NIR Photodetectors Robert Hoye; University of Oxford, United Kingdom

Bismuth-based semiconductors have gained increasing attention as potential nontoxic alternatives to lead-halide perovskites.^[1] Whilst most attention has been on bismuth-halide-based compounds, there is growing interest in broader families of materials, including chalcogenides, such as ABZ₂ materials (A = monovalent cation; B = Bi³⁺ or Sb³⁺; Z = chalcogen).^[2] However, the semiconductors explored thus far have gradually-increasing absorption onsets, and their charge-carrier transport is not yet well understood. The first half of this talk discusses our recent work on cation-disordered NaBiS₂ nanocrystals,^[3] which have a steep absorption onset, with absorption coefficients reaching $>10^5$ cm⁻¹ just above its pseudo-direct bandgap of 1.4 eV. Surprisingly, we also observe an ultrafast (picosecond-timescale) photoconductivity decay and long-lived charge-carrier population persisting for over one microsecond in NaBiS₂ nanocrystals. These unusual features arise because of the non-bonding *S p* character of the upper valence band, which leads to a high density of electronic states at the band edges, ultrafast localisation of spatially-separated electrons and holes, as well as the slow decay of trapped holes.

The second half of this talk covers our recent work on AgBiS₂, which also has high absorption strength, such that films only 50 nm thick are required to achieve adequate light absorption. Given the small bandgap of 1.2 eV, we demonstrate the utility of this material in near-infrared photodetectors. We achieve high cut-off frequencies reaching 0.5 MHz at 940 nm wavelength, along with >1 MHz cut-off frequencies in the visible wavelength range. Through detailed characterisation, we reveal the electronic-ionic transport properties of this material, and how these properties can be controlled to achieve fast NIR photodetectors. Finally, we demonstrate the practical application of these devices for heart beat monitoring.^[4]

Overall, in this talk, the critical role of cation disorder in these ternary chalcogenide systems is revealed, especially how they influence optical absorption and charge-carrier kinetics.

[1] Ganose, Scanlon, Walsh, Hoye,* *Nat. Commun.*, 2022, 13, 4715.

[2] *Nat. Photon.*, 2022, 16, 235.

[3] Huang, Kavanagh, ... Hoye,* *Nat. Commun.*, 2022, 13, 4960.

[4] Huang, Nodari, ..., Gasparini,* Hoye,* arXiv: 2308.12250

4:15 PM QT03.04.06

Optoelectronic Interactions of WS₂-ZnO for Scalable LEDs Based on Two-Dimensional Materials Osamah Kharsah¹, Leon Daniel¹, Denys Vidish², Dedi Sutarma¹, Stephan Sleziona¹, Peter Kratzer¹, Kevin Musselman² and Marika Schleberger¹; ¹Universität Duisburg-Essen, Germany; ²University of Waterloo, Canada

Recent advances in scalable large-area light-emitting diodes (LEDs) utilizing two-dimensional materials have spurred the investigation of promising architectures. Among the forefront LED architectures under investigation is the n-i-p design, featuring distinct layers comprising an electron-transport material (n), an intrinsic active material (i), and a hole-transport material (p). This framework facilitates efficient electron-hole recombination and subsequent light emission. Tungsten disulfide (WS₂) has attracted significant attention as an active material in such LEDs, given its direct bandgap, high stability, and robust photoluminescence (PL). Meanwhile, zinc oxide (ZnO), an n-type semiconductor, is under examination as a candidate for the electron-transport layer. This study investigates the interactions between WS₂ and both single-crystalline ZnO and spatial atomic layer deposition (SALD)-grown ZnO, with a primary focus on evaluating the optoelectronic interaction of this heterostructure. A comprehensive set of characterization techniques, including PL and Raman spectroscopy to probe optoelectronic properties, atomic force microscopy for morphological insights, Kelvin probe force microscopy for surface potential variations, and X-ray photoelectron spectroscopy to delve into chemical composition and electronic states at the WS₂-ZnO interface, is employed. Ultimately, this research aims to determine whether SALD-grown ZnO is a suitable candidate for integration into the n-i-p LED architecture, paving the way for scalable and efficient optoelectronic devices based on 2D materials.

SESSION QT03.05: Poster Session: Physics of 2D Halide and Chalcogenides Semiconductors
Session Chairs: Alexey Chernikov and Yana Vaynzof
Wednesday Afternoon, April 24, 2024
Flex Hall C, Level 2, Summit

5:00 PM QT03.05.01

Controllable Photoluminescence Modification of Monolayer Molybdenum Disulfide via Superacid Treatment and Atomic Layer Deposition of High- κ Dielectric Materials [Brendan F. Healy](#), Sophie Pain, Nicholas Grant and John D. Murphy; University of Warwick, United Kingdom

Transition metal dichalcogenides (TMDCs) are an exciting class of two-dimensional (2D) materials that exhibit exceptional physical and chemical behaviour at the monolayer limit. ¹ Molybdenum disulfide (MoS₂) is a prototypical TMDC that has emerged as a leading candidate for inclusion in numerous optoelectronic technologies, owing to its novel optical properties. ² With a direct bandgap in the visible spectral range, monolayer MoS₂ emits a relatively strong photoluminescence (PL) signal. ³ The ability to control the PL character of MoS₂ is important for full realisation of its optoelectronic application. The PL spectrum of MoS₂ has been shown to be sensitive to a range of external treatments, including oxygen plasma exposure, ⁴ annealing, ⁵ laser irradiation, ⁶ superacid treatment, ⁷ and dielectric encapsulation. ⁸ Each treatment will induce a change in response, potentially enabling tuneable modification of the PL behaviour of MoS₂ via the choice of treatment.

In this work, we present controllable variation of the PL signal from chemical vapour deposition (CVD)-grown MoS₂ monolayer films. We demonstrate selective alteration of the MoS₂ PL intensity, bidirectional energy shift and spectral reshaping via superacid treatment or atomic layer deposition (ALD) of a high dielectric constant (high- κ) material. By submerging monolayer MoS₂ in a solution containing the superacidic bis-(trifluoromethanesulfonyl)amide (TFSA), we achieve improvement of the PL character, in agreement with previous reports. ^{7,9} We find that superacid treatment induces significant enhancement of the absolute MoS₂ PL intensity, as well as blueshift in the energy of the emission and narrowing of the dominant peak. Conversely, we reveal opposing changes to the MoS₂ PL signal result from deposition of a high- κ dielectric. Grown by ALD, an atop layer of hafnium oxide (HfO₂) or aluminium oxide (Al₂O₃) layer is shown to attenuate the strength of the PL emission from monolayer MoS₂, with an accompanying redshift and broadening of the PL spectrum also observed. Via PL mapping, we confirm the treatment-induced modifications of the PL intensity to be prevalent across the MoS₂ surface following both TFSA and ALD-dielectric treatments. We utilise Lorentzian deconvolution of the PL spectra, coupled with a correlative analysis of the characteristic Raman peaks, to attribute the varying PL changes to differing charge doping and strain effects. ¹⁰ This work demonstrates facile control of the PL behaviour of CVD-MoS₂ monolayer films via application of an external chemical or dielectric treatment.

References

1. X. Duan; C. Wang; A. Pan; R. Yu; X. Duan, *Chemical Society Reviews* **44**, 8859 (2015).
2. B. Radisavljevic; A. Radenovic; J. Brivio; V. Giacometti; A. Kis, *Nature Nanotechnology* **6**, 147 (2011).
3. A. Splendiani; L. Sun; Y. Zhang; T. Li; J. Kim; C.-Y. Chim; G. Galli; F. Wang, *Nano Letters* **10**, 1271 (2010).
4. N. Kang; H.P. Paudel; M.N. Leuenberger; L. Tetard; S.I. Khondaker, *The Journal of Physical Chemistry C* **118**, 21258 (2014).
5. H. Nan; Z. Wang; W. Wang; Z. Liang; Y. Lu; Q. Chen; D. He; P. Tan; F. Miao; X. Wang; J. Wang; Z. Ni, *ACS Nano* **8**, 5738 (2014).
6. H.-J. Kim; Y.J. Yun; S.N. Yi; S.K. Chang; D.H. Ha, *ACS Omega* **5**, 7903 (2020).
7. S.L. Pain; N.E. Grant; J.D. Murphy, *ACS Nano* **16**, 1260 (2022).
8. S.Y. Kim; H.I. Yang; W. Choi, *Applied Physics Letters* **113**, 133104 (2018).
9. M. Amani; D.-H. Lien; D. Kiriya; J. Xiao; A. Azcatl; J. Noh; S.R. Madhupathy; R. Addou; S. Kc; M. Dubey; K. Cho; R.M. Wallace; S.-C. Lee; J.-H. He; J.W. Ager; X. Zhang; E. Yablonovitch; A. Javey, *Science* **350**, 1065 (2015).
10. H. Kim; T. Lee; H. Ko; S. Kim; H. Rho, *Applied Physics Letters* **117**, 202104 (2020).

5:00 PM QT03.05.02

Developing Bismuth Sulfoiodide Pellets for Low-Energy X-Ray Detection [Maia Momburu](#)¹, Kavya Reddy Dudipala², Hugh Lohan², Robert L. Hoye², Matthew C. Veale³, Laura Fornaro⁴ and Ivana Aguiar¹; ¹Universidad de la Republica, Uruguay; ²University of Oxford, United Kingdom; ³Science and Technology Facilities Council, United Kingdom; ⁴Universidad de la Republica, Uruguay

Bismuth based semiconductor materials are increasing in popularity due to their potential in optoelectronic applications such as solar cells and radiation detection. The latter application has uses spanning many fields, from medicine to homeland safety. Given the nature of soft and hard X-rays and gamma radiation, being able to correctly detect their presence and measure them is imperative. In particular, BiSI has been studied for solar cells, especially in film deposition, and for X-ray detection in pellets from nanostructures. In this work, we present the study of soft X-ray detection in BiSI pellets. BiSI nanorods were synthesized by either a solution or solvothermal method, using mono ethylene glycol as a reaction medium, and Bi₂S₃ and I₂ as reagents. The solution method yielded pure crystalline BiSI nanorods of 200 nm in average width, while the solvothermal method produced a composite of BiSI nanorods and amorphous carbon particles. Pellets were constructed with the powders by cold pressing in a uniaxial press. The orientation of the BiSI nanorods is parallel to the surface of the pellet, evidenced both by SEM and XRD characterization. In the case of the nanocomposite, this orientation is partly disrupted by the spherical nature of the carbon particles. Prototype devices were built by depositing Au contacts through evaporation in a sandwich configuration. I-V curves were measured both in the dark and under X-ray irradiation. Dark current was measured up to 600 V and the resistivity was two orders of magnitude higher for the nanocomposite versus the pure compound, with values of 10⁹ to 10¹¹ Ω.cm, respectively. This is in accordance to the fact that the composite has amorphous structure that limits the conductivity. The response to X-rays of 9 keV in energy was measured up to 20 V, and a linear response was obtained in both cases. When the dose was up to 4.2 μGy_{air} s⁻¹ at a fixed voltage of 20 V the current increased linearly. When comparing the two materials, the nanocomposite had a considerable better performance than the pure compound. The amorphous carbon particles lower the dark current, but do not contribute negatively to the photoconduction of the charge carriers generated by the X-rays. A notable advantage of this study is that the bias applied is considerably low with regards to usual operating voltages of direct semiconductor detectors, allowing for the possibility of using these devices in wearable technology, for instance in direct dosimeters. This work presents an easy, scalable and cheap way to produce low energy X-ray detectors with a suitable performance.

5:00 PM QT03.05.03

Observations and Maps of Second Harmonic Generation on 2D Chalcogenide MoS₂ Monolayers and Single Crystalline Thin Films [Xiaojuan Fan](#)^{1,2}, Lawrence Mubwika² and Lian Li²; ¹Marshall University, United States; ²West Virginia University, United States

Non-linear optical responses in 2D transition metal dichalcogenides (TMD) have attracted increasing attention due to unique layered structures and the ability to generate a series of non-linear harmonic waves, such as second harmonic generation (SHG). As an exotic class of atomically thin semiconductors, TMDs have emerged as a new generation of electronic and optoelectronic devices. MoS₂ monolayers and single crystalline thin films were deposited on Si substrates by a high-temperature tube furnace-based physical transport CVD system. MoS₂ monolayers showed SHG signals conducted by a homebuilt

optical microscope system with filters to block the fundamental and higher frequency lasers. It was found that powerful SHG signals can be generated from single crystalline thin films compared to monolayers, indicating that the intensity of the non-linear optical responses is proportional to the number of layers. We have successfully mapped SHG profiles on monolayers and thin films through reflection mode by an optical detector, and the maps are analogous to their optical microscopic images. The mapping technique utilizes the intensity contrast of reflected lasers between the SHG area and the substrate region, which is different from the general method used by others. Powerful SHG signals are generated from thick single crystalline thin films, potentially enabling immediate applications in optoelectronic devices and SHG light generators.

5:00 PM QT03.05.06

Understanding The Role of Defects in WS₂ Layer in Contact with ZnO Substrate [Dedi Sutarna](#) and Peter Kratzer; University of Duisburg-Essen, Germany

The remarkable properties of two-dimensional (2D) materials have garnered significant attention in recent years, and understanding their fundamental behavior is critical for developing next-generation technologies. In this study, we investigate the microscopic behavior of a 2D material, WS₂, with ZnO (1 -1 0 0) taking the role as the substrate as well as charge injection layer in this van der Waals (vdW) heterostructures. Unique combination of tunable optical properties and high carrier mobility of WS₂, as well as ZnO wide band gap, large exciton binding energy and compatibility with existing fabrication technique, provides an attractive outlook for optoelectronic devices. Specifically, we aim to elucidate the role of native defects in WS₂/ZnO, such as sulphur and oxygen vacancies. Using Density Functional Theory (DFT) calculations, we examine the structural and optoelectronic properties of the WS₂/ZnO, including the impact of point defects.

Herein, band alignment of the heterojunction is found to be type I, with the larger band gap in ZnO, which is desirable for using ZnO as an electron injector for radiative recombination in monolayer WS₂ forming the active layer in a light-emitting device. Our results demonstrate that defects can significantly modulate the electronic properties of the interface, including band alignment and charge transfer. Furthermore, absorption and Raman spectra are calculated to understand the optical behavior of this system. These insights give crucial information for the design and optimization of devices based on 2D materials, and offer a pathway for enhancing their performance in a wide range of applications.

5:00 PM QT03.05.07

Bandgap Opening in Monolayer MoSe₂ Induced by Selenium Vacancies [Zhuohang Yu](#), Natalya Sheremetyeva, Shreya Mathela, David Sanchez, Alexander J. Sredenschek, John Asbury, Vincent Meunier and Mauricio Terrones; The Pennsylvania State University, United States

Transition metal dichalcogenide (TMD) monolayers hold great promise for advancing next-generation electronics and optoelectronics. The synthesis of large-area TMD monolayers with a high degree of crystallinity is crucial for enabling mass production and real-world applications. However, the influence of structural defects on the optical properties of these two-dimensional (2D) materials remains unclear. In this study, we demonstrate a method for synthesizing MoSe₂ monolayers with high concentrations of selenium vacancies. Using liquid-assisted chemical vapor deposition and by controlling the duration of the selenium feedstock during synthesis, we were able to introduce selenium vacancies into MoSe₂ monolayer flakes. As the flakes grew, we observed that double-selenium vacancies became more frequent at the edges of the flakes when compared to the central regions, whereas the concentration of single-selenium vacancies remained relatively constant throughout the entire flake of MoSe₂. These observations were confirmed by atomic-resolution high-angle annular dark field scanning transmission electron microscopy (HAADF-STEM). Furthermore, femtosecond transient absorption spectroscopy revealed a notably accelerated decay rate at the edges of the flakes, implying a higher likelihood of nonradiative transitions related to defects (e.g. double-selenium vacancies). Interestingly, photoluminescence (PL) spectroscopy showed an increase of approximately 40 meV in the energy of emission for both excitons A and B at the flake's edges when compared to the central region. Laser power-dependent PL measurements performed at the edge of the samples indicated a linear power relationship with the emission on the edge, suggesting the nature of a free exciton. Through first-principles density functional theory calculations, we confirmed that the selenium vacancy concentration is correlated with an increased bulk bandgap, which confirmed our observations in the PL measurements. These findings not only unveil the growth mechanism of liquid-assisted chemical vapor deposition on MoSe₂, but also contribute to a better understanding of the role of double-selenium vacancies in tailoring the optical properties of MoSe₂ monolayers.

5:00 PM QT03.05.08

White-Light Emission and Diffusion of Self-Trapped Excitons in Antimony- and Bismuth-Based Hybrid Perovskites [Philip Klement](#)¹, Lukas Gumbel¹, Meng Yang², Johanna Heine² and Sangam Chatterjee¹; ¹Justus Liebig University Giessen, Germany; ²Philipps-Universität Marburg, Germany

Lead halide perovskites have set the stage for the emergence of main-group metal halide materials as promising candidates for next-generation optoelectronics, spanning applications like solar cells, light-emitting diodes, lasers, sensors, and photo-catalysis. Within these materials, efficient light-emission arises from self-trapped excitons, where excitations create transient defects in the crystal lattice that effectively capture excitons.

However, the complex interplay of factors, including ground- and excited-state lattice distortions, lattice softness, and electron-phonon coupling strength, presents a challenge in establishing the structure-property relationship. This complexity hinders the targeted design of optical properties and necessitates a deeper exploration of the influence of elemental composition and anion dimensionality.

In this study, we investigate two families of antimony and bismuth halide compounds that systematically vary in composition, anion dimensionality, connectivity, and the organic cation. These compounds possess crystal structures that facilitate self-trapped exciton formation, resulting in broad photoluminescence spectra with pronounced Stokes shifts. Our analysis identifies the relevant factors influencing bright white-light emission and quantifies the electron-phonon coupling strength, expressed by the Huang-Rhys factor (ranging from 5 to 22 in these materials). Furthermore, we investigate the diffusion of self-trapped excitons through temporally- and spatially resolved photoluminescence spectroscopy.

The insights gained from this research deepen our understanding of the emission mechanisms in hybrid halide perovskites, promising to guide the development of advanced optoelectronic materials.

5:00 PM QT03.05.09

Tunable White-Light Emission from Self-Trapped Excitons in Ultrathin Sheets of a Low-Dimensional Hybrid Perovskite [Philip Klement](#)¹, Natalie Dehnhardt², Chuan-Ding Dong³, Florian Dobener¹, Julius Winkler², Samuel Bayliff³, Detlev Hofmann¹, Peter Klar¹, Stefan Schumacher³, Johanna Heine² and Sangam Chatterjee¹; ¹Justus Liebig University Giessen, Germany; ²Philipps-Universität Marburg, Germany; ³Paderborn University, Germany; ⁴The University of Oklahoma, United States

Low-dimensional organic-inorganic perovskites complement the advantages of two classes of materials for next-generation optoelectronics: They combine customized building blocks for atomically thin, layered materials with the enhanced light-harvesting and -emitting capabilities of perovskites. These materials promise a playground for exploring novel phenomena driven by the dynamic interplay of electronic, photonic, and vibrational excitations.

Traditionally, the prevailing belief has been that in-plane covalent interactions are an absolute prerequisite for forming atomically thin materials. This belief has, in turn, limited the range of candidates for 2D materials.

In this study, we challenge this prevailing paradigm and present single layers of the one-dimensional organic-inorganic perovskite $[C_7H_{10}N]_3[BiCl_5]Cl$.^[1] Its unique crystal structure facilitates the exfoliation of single layers and the formation of self-trapped excitons, resulting in tunable white-light emission. Remarkably, the thickness-dependent behavior of exciton self-trapping leads to an unprecedented photoluminescence shift of 0.4 eV between bulk crystals and ultrathin sheets.

Our research demonstrates that even 1D covalent interactions suffice to create atomically thin materials, granting access to unique photophysics. These findings enable a versatile construction principle for identifying and creating two-dimensional materials, eliminating the prior constraint of covalently bonded 2D sheets.

[1] Klement, P.; Dehnhardt, N.; Dong, C.-D.; Dobener, F.; Bayliff, S.; Winkler, J.; Hofmann, D. M.; Klar, P. J.; Chatterjee, S.; Heine, J. (2021): Atomically Thin Sheets of Lead-Free 1D Hybrid Perovskites Feature Tunable White-Light Emission from Self-Trapped Excitons. *Adv. Mater.* **33**, 2100518, DOI: 10.1002/adma.202100518

5:00 PM QT03.05.10

Elucidating The Impact of Niobium Substitution in WSe_2 Nanosheets through Monochromated EELS, 4D-STEM and Deep Neural Networks [Tinsae Alem](#)¹, Kevin Roccapiore², Eric R. Hoglund², Pulickel Ajayan³, Jordan A. Hachtel², Kory D. Burns¹, Anand B. Puthirath³ and Anchal Srivastava³; ¹University of Virginia, United States; ²Oak Ridge National Laboratory, United States; ³Rice University, United States

Adding an additional degree of freedom to two-dimensional layered materials through alloying emerges as a suitable technique to tailor its thermal and optoelectronic properties. [1] Unfortunately, the relative concentration of the film can change drastically at micron-length scales, [2] making it difficult to directly correlate the true stoichiometry of a material with its respective properties. In this contribution, we first use aberration-corrected scanning transmission electron microscopy (STEM) and 4D-STEM to map out atomic positions in $Nb_{1-x}W_xSe_2$ and the crystalline phase of the material. Next, we use monochromated electron energy loss spectroscopy (EELS) to measure lattice phonon modes over a range of the alloying content. Last, with the assistance of deep neural networks, we extract coordinates and type/class of the atoms to correlate localized atomic displacements of atoms in the WSe_2 nanosheet and statistical inference on the atomic distributions. This work aims to help understand the correlation between phase, stoichiometry, and lattice phonon modes in ternary alloys of layered materials.

References

1. J. Yao and G. Yang. "2D Layered Material Alloys: Synthesis and Application in Electronic and Optoelectronic Devices." *Adv. Sci.*, 9, 2103036, 2022.
2. Y. Zuo et al. "Robust growth of two-dimensional metal dichalcogenides and their alloys by active chalcogen monomer supply." *Nat. Comm.*, 13, 1007, 2022.

5:00 PM QT03.05.11

Star-Shaped WS_2 Monolayers with Twin Grain Boundaries Promoted by Molybdenum Atoms [Na Zhang](#)¹, David Sanchez¹, Nadire Nayir^{2,1}, Yanzhou Ji³, Yueze Tan¹, Natalya Sheremetyeva¹, Swarit Dwivedi¹, Mengyi Wang¹, Nannan Mao⁴, Tianyi Zhang⁴, Da Zhou¹, Zhuohang Yu¹, Andres Fest Carreno¹, Adri Van Duin¹, Vincent Meunier¹ and Mauricio Terrones¹; ¹The Pennsylvania State University, United States; ²Istanbul Technical University, Turkey; ³The Ohio State University, United States; ⁴Massachusetts Institute of Technology, United States

Monolayers of transition-metal dichalcogenides (TMDs) exhibit fascinating properties that make them attractive in optics, electronics^a, spintronics, and valleytronics^b, and it is of vital importance to understand and control their morphology and tune their physical properties^c. However, the origin of their morphology evolution is still highly elusive, which hinders the synthesis of desired morphologies for specific applications. Herein, we report the controlled synthesis and formation mechanism of star-shaped WS_2 monolayers by adding trace concentrations of molybdenum using a liquid-phase precursor-assisted approach. Fluorescence imaging and photoluminescence (PL) mapping of six-arm stars revealed bright lines between adjacent arms. To correlate the morphology and optical properties with the microstructure, second harmonic generation (SHG) microscopy and dark-field transmission electron microscopy (DF-TEM) were implemented to confirm the presence of polycrystal domains with a 60° lattice misorientation and a mirror twin grain boundary. Detailed analysis of the grain boundary and molybdenum atom distribution was assessed using high-resolution, high angle annular dark-field scanning transmission electron microscopy (HAADF-STEM). The relationship of the growth morphology of WS_2 stars and the molybdenum to tungsten ratio of the precursor was also carefully investigated. In corroboration with the experimental results, we further developed a multiscale model which combines density functional theory, ReaxFF based molecular dynamics simulations, a Wulff construction and a phase-field model, which demonstrated that the anisotropy of grain boundary (GB) energy due to molybdenum doping can lead to the star morphologies of WS_2 . Our study provides further insights into controlling the morphology of crystalline TMD monolayers, with implications for the development of field-programmable semiconductor memristor devices.

References

- (a) Wang, Q. H., Kalantar-Zadeh, K., Kis, A., Coleman, J. N., & Strano, M. S. (2012). *Nature nanotechnology*, 7(11), 699-712.
- (b) Tong, W. Y., Gong, S. J., Wan, X., & Duan, C. G. (2016). *Nature communications*, 7(1), 1-7.
- (c) Dong, J., Liu, Y., & Ding, F. (2022). *NPJ Computational Materials*, 8(1), 1-11.

5:00 PM QT03.05.12

Self-Powered Photodetectors Based on Ruddlesden-Popper 2D Hybrid Perovskites with Carbazole Derivatives [Anna N. Alphenaar](#), Xiaoyu Zhang and Qiuming Yu; Cornell University, United States

Recently, carbazole-based organic cations have attracted the interests of scientists in a variety of fields for their potential application in 2D layered hybrid perovskite solar cells. These materials have demonstrated enhanced stability compared to other 2D and 3D hybrid perovskites which could allow them to achieve the level of self-sufficiency and environmental durability required of commercial solar cells. However, the potential incorporation of these highly efficient materials in photodetection has been largely unexplored. In this study, we synthesized CzeAP, a 2D layered organic-inorganic hybrid perovskite (OIHP) containing PbI_2 and a large organic ammonium 1-(9H-carbazol-9-yl) ethanaminium iodide (CzEAI) in a 1:2 molar ratio. We developed a series of thin films and devices in the configuration ITO/PEDOT:PSS/(CzEA)₂PbI₄/PCBM/BCP/Al using this novel OIHP. We conducted atomic force microscopy, UV Vis, photoluminescence, and external quantum efficiency measurements on these films and devices to assess their surface and optical properties. We also determined the hole mobility of CzeAP-based hole only devices in the configuration ITO/PEDOT:PSS/(CzEA)₂PbI₄/MOO₃/Ag. Through optimization of the deposition procedure for this perovskite, we constructed novel photodetector

devices with a specific detectivity of 6.95×10^{10} Jones at 485 nm illumination and the ability to operate in a self-powered condition at 0V. The development of highly efficient self-sustaining photodetectors is essential to the progression of a wide range of fields including optical communications, security, video imaging, biomedical imaging, motion detection, and gas sensing.

5:00 PM QT03.05.13

Triexciton Emission and Multiexcitonic Optical Gain in 2D Perovskites [Vadim Trepalin](#), Yang Ding and Masaru Kuno; University of Notre Dame, United States

Over the last decade the interest in 2D and quasi-2D perovskites has been growing rapidly thanks to their superior stability and unique optoelectronic properties as compared to the more commonly studied 3D perovskites. Spatially separated layers of metal-halide octahedra in these materials naturally form quantum wells with strongly pronounced excitonic effects due to both quantum and dielectric confinements. Exciton binding energies of up to several hundred millielectronvolts facilitate formation of stable multiexcitonic complexes such as biexcitons and even triexcitons under relatively low excitation intensities at cryogenic temperatures. Multiexciton radiative recombination enables a highly efficient pathway for light amplification and thus, these materials show a great potential in cost-efficient laser applications as optical gain media. Moreover, existence of stable triexcitons makes 2D perovskites a unique platform to study the exotic world of many-body physics.

In the present work we investigate the formation and radiative recombination of single excitons and multiexcitonic complexes, including rarely observed triexcitons, in the single crystals of phase-pure quasi-2D Ruddlesden-Popper perovskites $(\text{PEA})_2\text{MAPb}_2\text{I}_7$ and $(n\text{-BuA})_2\text{MAPb}_2\text{I}_7$ (PEA = phenethylammonium, MA = methylammonium, n-BuA = n-butylammonium). By means of time-integrated and time-resolved photoluminescence spectroscopies we confirm the existence of stable triexcitons at cryogenic temperatures after high-energy femtosecond pulsed laser excitation. We also support our experimental findings with a developed kinetic model of a dynamic equilibrium between excitonic species that qualitatively explains different laser fluence-dependent behaviors of each excitonic transition. Additionally, we observe Amplified Spontaneous Emission on single crystals of $(\text{PEA})_2\text{MAPb}_2\text{I}_7$ with threshold fluences as low as $\sim 2 \mu\text{J cm}^{-2}$ and estimate optical gain coefficient of $\sim 1100 \text{ cm}^{-1}$ using the Variable Stripe Length method. These promising lasing characteristics and strong excitonic effects together with low-cost solution-based synthetic methods, compositional tunability and enhanced stability make 2D perovskites a unique class of materials for future light-emitting applications and studies of higher order exciton physics.

5:00 PM QT03.05.14

Strain-Engineered Thermophysical Properties ranging from Band-Insulating to Topological Insulating Phases in β -Antimonene [Sumit Kukreti](#); Indian Institute of Technology Jodhpur, India

Employing strain may lead to unusual modifications in the material's properties. Low-dimensional materials having large mechanical strength are well suited for strain engineering. In our work, we present the structural, electronic, thermal, and vibrational characteristics along with the phonon and carrier dynamics of β -Sb elemental monolayers for achieving the band-insulating phase at no strain and topological insulating phase at $\sim 15\%$ biaxial strain. The weakened π and σ bonds under strain, leading to anharmonicity in the system. It is further reflected by the drop in lattice thermal conductivity (κ_l) from 4.5 to $3.1 \text{ W m}^{-1} \text{ K}^{-1}$ at $\sim 15\%$ strain, i.e., in the topological phase. Helical edge states at 15% strain and meeting the Z_2 invariant criterion confirm the non-trivial topological state. Here we noticed the significant contribution of the out-of-plane A_{1g} vibrational mode in the topological phase compared with the band-insulating phase. Importantly, the dominance of the out-of-plane optical modes contributes significantly to the topological phase along the band edges, which is primarily due to the reduced buckling height under strain. This work emphasizes the microscopic origin of the onset of the topological phase in strained β -Sb monolayers and provides strain-engineered structure-property correlations for better insights.

5:00 PM QT03.05.15

Charge and Energy Transfer Across the Organic-Inorganic Interfaces of Two Dimensional Lead Halide Perovskites [Angana De](#) and Libai Huang; Purdue University, United States

Creating heterojunctions enables the amalgamation of optimal properties from diverse materials, effectively bypassing individual bottlenecks. The essential photophysical phenomena in these materials are propelled by charge and energy transfer across these heterojunctions, making a comprehensive understanding of these processes imperative for optimizing such systems for energy conversion and harvesting applications. In our work on pyrene-based quasi-2D lead iodide perovskites, we explore how band engineering can instigate the formation of distinctive excited states and diverse optical phenomena. We conduct an in-depth analysis of their underlying mechanisms, also examining their competition with other parasitic processes. For the $n=1$ perovskite, efficient triplet energy transfer (TET) occurs from the inorganic sublattice to the organic layer, within the Marcus inverted domain. This transfer is driven by quantum tunneling, resulting in rarely witnessed temperature-invariant TET rates. On the other hand, the $n=2$ perovskite exhibits no TET. Instead, we observe the emergence of long-lived and mobile 'interlayer' excitons, originating from ultrafast charge transfer across the organic-inorganic interface.

SESSION QT03.06: 2D Halide and Chalcogenides Semiconductors V – Theory

Session Chairs: Tomer Amit and Ermin Malic

Thursday Morning, April 25, 2024

Room 444, Level 4, Summit

8:30 AM *QT03.06.01

Phonon-Induced Ultrafast Exciton Decomposition in Transition Metal Dichalcogenides: An *Ab Initio* Approach [Tomer Amit](#) and Sivan Refaely-Abramson; Weizmann Institute of Science, Israel

Underlying relaxation processes following light excitation in semiconductors are key in materials-based quantum information science. These processes are broadly studied in transition metal dichalcogenides (TMDs), where constructed atomistic design allows for tunable excited-state properties, lifetime, and stability. In this talk, I will describe our new *ab initio* theoretical approach to compute exciton decomposition in these systems, paving a route to explore microscopic processes occurring between optical absorption and emission. Our approach, based on a Lindblad density matrix formalism, captures quantum many-body effects by combining predictive assessment of the exciton states and a band-resolved analysis of their scattering with phonons. In particular, we explore the effect of mixed exciton states on both momentum and spin transitions, and study how these vary as a function of layer composition. Our findings supply an understanding of the underlying exciton relaxation mechanisms, offering new insights into the concept of excitons as stable quantum states in functional materials.

9:00 AM *QT03.06.02

Layered and Low-Dimensional Halide Perovskites: Electronic Structure, Optical Properties and Charge Carrier Mobilities from First-Principles.
George Volonakis; Université de Rennes, France

Ab initio calculations are becoming more and more efficient and have emerged as an indispensable tool to characterize and understand these complex systems. In particular, for halide perovskites and perovskite-like compounds, over the last decade, such computational approaches have been extensively employed and successfully unveiled the underlying atomic-scale physical mechanisms of these exciting materials. In this talk, I will overview our most recent results on prototypical structure of layered halide perovskites, vacancy ordered double perovskites, and low dimensional halide perovskite-like materials. I will present the key details of their electronic structure for each type of system that define their experimentally observed optical properties and achieved performances [1,2,3]. In the last part of my talk, I will show our latest findings on the effects of structural dimensionality on the charge carrier transport properties when comparing three-dimensional ABX₃ and layered halide perovskites.

References

- [1] ACS Materials Letters 5 (1), 52-59 (2023)
- [2] Chemistry of Materials 34 (21), 9685-9698 (2022)
- [3] Solar RRL, 2200718 (2022)

9:30 AM BREAK

10:00 AM *QT03.06.03

Mechanism of Circular Dichroism in Chiral 2D Halide Perovskites Peter C. Sercel¹, Ruyi Song², Matthew P. Hautzinger³, Volker Blum² and Matthew C. Beard³; ¹Center for Hybrid Organic Inorganic Semiconductors for Energy, United States; ²Duke University, United States; ³National Renewable Energy Laboratory, United States

A key motivator for research in hybrid organic-inorganic metal halide perovskites (HOIPs) is the potential to combine distinct characteristics of the inorganic and organic constituents to elicit desirable functional properties. For example, incorporation of chiral organic cations lacking a center of inversion into layered 2D halide perovskites with large spin-orbit coupling has been shown to result in structural chirality transfer, leading to Rashba/Dresselhaus-type spin-splitting while at the same time leading to the emergence of chiroptical effects such as circular dichroism (CD) [1,2]. Here we address the question: What is the connection, if any, between the spin textures that emerge by virtue of the structural chirality transfer and the emergence of chiroptical properties associated with the band edge exciton transitions? In this talk we explore the mechanism of excitonic CD in chiral 2D layered perovskites utilizing an analytical k.p/effective mass theory model, parameterized by hybrid density functional theory calculations. We develop analytical expressions for the electric and magnetic dipole transition matrix elements and show the direct connection between particular spin textures and the emergence of CD in these materials [3].

Acknowledgements

This work was supported through the Center for Hybrid Organic Inorganic Semiconductors for Energy (CHOISE), an Energy Frontier Research Center funded by the Office of Basic Energy Sciences, Office of Science within the US Department of Energy.

References

1. M. K. Jana *et al.*, Organic-to-inorganic structural chirality transfer in a 2D hybrid perovskite and impact on Rashba-Dresselhaus spin-orbit coupling, *Nat. Commun.*, 11:4699, (2020).
2. M. K. Jana, *et al.*, Structural descriptor for enhanced spin-splitting in 2D hybrid perovskites, *Nat. Commun.*, 12:4982, (2021).
3. P. C. Sercel, R. Song, M. P. Hautzinger, V. Blum, and M. C. Beard, Mechanism of circular dichroism in chiral 2D perovskites, in preparation, (2024).

10:30 AM QT03.06.04

Atomistic Mechanisms of Temperature-Induced Phase Transitions of 2D Lead Halide Perovskite by Molecular Dynamics Simulation Reza Namakian, Maria Garzón Vargas, Qing Tu, Ali Erdemir and Wei Gao; Texas A&M University, United States

A series of phase transitions has been experimentally observed in 2D lead halide perovskites within the Ruddlesden-Popper category in response to temperature changes. With increasing temperature, their crystal symmetry transitions from a low-symmetry phase to a high-symmetry phase, evident from the transition from a triclinic to an orthorhombic crystal system. This phase transition has been primarily attributed to the melting of organic spacer molecules. Separate experimental observations have also suggested that the transition is prompted by the disruption of hydrogen bonds between the ammonium headgroup of the spacer molecules and the iodides of the octahedra in the inorganic layers. To the best of our knowledge, there is a notable absence of atomistic modeling in the literature to provide a clear understanding of the atomistic mechanisms underpinning this transition.

In this study, we utilize molecular dynamics (MD) simulations to gain an in-depth understanding of the phase transition mechanisms in BA₂MAPb₂I₇, a compound containing n-butylammonium (BA) as the organic spacer molecule. In agreement with prior experiments, our results indicate that both the melting of the BA ligands and the hydrogen bond breakage play pivotal roles in facilitating the phase transition. At the onset of phase transition as temperature rises, the BA ligands begin localized rattling motion and undergo partial melting at the tail C-C bond. As the temperature continues to increase, the melting extends through the entire ligand backbone, intensifying the rotational motion of the ligands and causing the top and bottom ligands to swipe against each other. In addition, our study offers solid evidence supporting earlier experimental hypothesis regarding the in-plane shear deformation between adjacent organic layers at the onset of phase transition during the contraction of BA ligands. Intriguingly, our analysis unveiled another synchronized in-plane shear deformation within the inorganic layer. Such dual shearing effect results in notable octahedral distortions, which are characterized by the bond length distortion and bond angle variation of the octahedron.

In summary, our study bridges the gap between experimental observations and atomistic modeling and offers some unique understanding of the complex mechanisms underlying phase transition of 2D lead halide perovskites. Our findings pave the way for future research aiming to optimize the thermal stability and performance of these materials in various applications.

10:45 AM QT03.06.05

Magnetic-Field-Induced Wigner Crystallization of Charged Interlayer Excitons in Transition Metal Dichalcogenide Bilayers Igor Bondarev¹ and Yurii E. Lozovik^{2,3,4}; ¹North Carolina Central University, United States; ²Institute of Spectroscopy, RAS, Russian Federation; ³Tikhonov Moscow Institute of Electronics & Mathematics, Russian Federation; ⁴Russian Quantum Center, Russian Federation

We develop the theory of the magnetic-field-induced Wigner crystallization effect for charged interlayer excitons (CIE) discovered recently in transition-metal dichalcogenide (TMD) heterobilayers [1]. The Wigner crystal phase has been one of the longest anticipated exotic correlated phases, a phase that is very closely related to excitonic insulator, and originally was thought of as a periodic array of electrons held in place when their Coulomb repulsion energy

exceeds the Fermi and thermal fluctuation energies. Here, we derive the ratio of the average potential interaction energy to the average kinetic energy for the many-particle CIE system subjected to the perpendicular magnetic field of an arbitrary strength, analyze the weak and strong field regimes, and discuss the 'cold' crystallization phase transition for the CIE system in the strong field regime [2]. We also generalize the effective g-factor concept previously formulated for interlayer excitons [3], to include the formation of CIEs in electrostatically doped TMD heterobilayers. We show that magnetic-field-induced Wigner crystallization and melting of CIEs, the two correlated phases that block or allow the CIE transport in the system, can be observed in strong-field magneto-photoluminescence experiments with TMD heterobilayers of systematically varied electron-hole doping concentrations. Our results advance the capabilities of the TMD bilayers as a new family of transdimensional quantum materials. – [1] L.A.Jauregui, et al., Science 366, 870 (2019); [2] I.V.Bondarev and Yu.E.Loikov, Communications Physics (Nature) 5, 315 (2022); [3] P.Nagler, et al., Nature Communications 8, 1551 (2017).

11:00 AM QT03.06.06

Rational Design of Point Defects with Small Electron-Phonon Coupling in 2D Materials Fatimah F. Habis^{1,2} and Yuanxi Wang¹; ¹University of North Texas, United States; ²Jazan University, Saudi Arabia

Point defects in semiconductors have emerged as an attractive candidate for applications in quantum information science. Due to their ability to create well-localized states within the band gap, point defects can serve as effectively isolated atoms that can be utilized as single photon emitters (SPEs) and qubits.

Small Electron-phonon coupling is a key factor in producing higher photon indistinguishability which determines the suitability of defect systems as SPEs. Huang-Rhys (HR) factors are commonly calculated to measure the degree of electron-phonon coupling in a system. However, not only is the computation of HR factors a complex task, but once determined, they are often used solely as a numerical value without any effort to establish a meaningful connection between HR factors and the physical defect system. Establishing such a correlation would enable the development of a rational design principle for defects, with the goal of minimizing HR factors.

We propose that small HR factors are linked to the preservation of bonding-character between the initial (occupied) and final (unoccupied) states involved in a specific transition. We demonstrate this principle for realistic SPEs candidates in hBN defect systems. HR factors are first calculated through first-principles employing the one-dimensional configuration coordinate diagram (1DCCD) approximation, then compared with full calculations involving phonon spectra, where we carefully extrapolate spectral functions towards the dilute defect limit. These extrapolations are carried out through an embedding method that depends on the limited range of interatomic force constants within covalent semiconductors. Calculated HR factors are then related to the degree of bonding-character similarity between the excited and ground states.

11:15 AM QT03.06.07

Electronic Structure and Conductivity of Ge₂Sb₂Te₅ Heterostructures with Different Layer Orderings from Density Functional Calculations Tommi Ketola and Janne Kalikka; Tampere University, Finland

Chalcogenide phase change materials (PCMs) have been studied extensively in the past decades due to promising applications comprising e.g. memory devices and optical systems. In these materials, an external electric voltage can be used to transition from an amorphous phase to a crystalline one, leading to a significant change in the electrical resistivity and optical reflectivity. One scientifically interesting and technologically relevant chalcogenide PCM is Ge₂Sb₂Te₅.

Previous experimental studies suggest that a large contrast in the electrical conductivity of Ge₂Sb₂Te₅ can be achieved also in heterostructures comprising specific sequences of single-atom layers without the amorphous-to-crystalline phase transition. In this work, we explore the effect of different layer orderings on the electrical conductivity and basic electronic properties of Ge₂Sb₂Te₅ heterostructures. We employ the VASP code package based on density functional theory (DFT) along with the DFT-D3 van der Waals correction and BolzTraP2 code to compute electrical conductivity for six previously investigated stacking configurations. Furthermore, the lattice parameters, electronic band gaps, and electronic band structures are calculated for our set of 18-atom unit cells by using the DFT method.

Our calculations show that the in-plane (along the atomic layers) electrical conductivity is clearly larger than the out-of-plane (perpendicular to the atomic layers) electrical conductivity. Some layer orderings result in larger out-of-plane electrical conductivities than the other structures. The PBE band gap calculations show that some structures are metallic whereas others are semiconducting with band gaps of 0.2-0.4 eV. The PBE band structure calculations confirm these results. According to the HSE06 calculations, all structures are semiconducting with band gaps between 0.2 and 0.7 eV. Our studies indicate that the layer ordering in Ge₂Sb₂Te₅ heterostructures affects the electrical conductivity remarkably although the differences between the selected six structures are not as large as those observed experimentally in Ge₂Sb₂Te₅ heterostructures.

SESSION QT03.07: 2D Halide and Chalcogenides Semiconductors VI – Physics
Session Chairs: Alexey Chernikov and Milan Delor
Thursday Afternoon, April 25, 2024
Room 444, Level 4, Summit

1:30 PM *QT03.07.01

Optical Sensing of Strongly Correlated Electronic Phases in 2D Materials Tomasz T. Smolenski; ETH Zurich, Switzerland

When the Coulomb repulsion between itinerant electrons dominates over their kinetic energy, the electrons in solid state materials start to develop strong correlations. A paradigm state of matter that is expected to emerge in this regime is an electronic Wigner crystal, in which the electrons spontaneously break continuous translation symmetry and arrange themselves into a periodic lattice mimicking that of the real crystals. In this talk, I will review our recent experimental explorations of strongly correlated electronic phases in transition metal dichalcogenides (TMD) and their van der Waals heterostructures. In particular, I will present our novel spectroscopic technique allowing us to detect the Wigner crystal in a TMD monolayer through the periodic potential it generates for the excitons [1]. This potential allows the excitons to undergo a Bragg diffraction, which gives rise to a new, Bragg-umklapp transition in the optical excitation spectrum that heralds the presence of a crystalline electronic order.

In the second part of the talk, I will describe magnetic properties of the electrons forming a charge-ordered Mott insulating state in a MoSe₂/WS₂ bilayer that hosts strong moire potential. In particular, I will show that when such a Mott state is electron-doped, the system exhibits unusual ferromagnetism [2] that is driven not by Coulomb exchange interactions, but arises due to minimization of kinetic energy of itinerant electrons. This observation provides

direct evidence for the Nagaoka ferromagnetism in an extended two-dimensional system.

[1] T. Smolenski, P. E. Dolgirev, C. Kuhlenkamp, A. Popert, Y. Shimazaki, P. Back, X. Lu, M. Kroner, K. Watanabe, T. Taniguchi, I. Esterlis, E. Demler, and A. Imamoglu, *Signatures of Wigner crystal of electrons in a monolayer semiconductor*. *Nature* **595**, 53-57 (2021).

[2] L. Ciorciaro, T. Smolenski, I. Morera, N. Kiper, S. Hiestand, M. Kroner, Y. Zhang, K. Watanabe, T. Taniguchi, E. Demler, A. Imamoglu, *Kinetic Magnetism in Triangular Moire Materials*. arXiv:2305.02150 (2023).

2:00 PM *QT03.07.02

From Spin Dynamics of Charge Carriers to Fundamental Insights into The Band Structure of Lead Halide Perovskites [Erik Kirstein](#)¹, Dmitry R. Yakovlev¹, Mikhail M. Glazov², Evgeny A. Zhukov¹, Dennis Kudlacik¹, Ina V. Kalitukha¹, Victor F. Sapega², Grigori S. Dimitriev², Marina A. Semina², Mikhail O. Nestoklon¹, Evgeny L. Ivchenko², Natasha E. Kopteva¹, Dmitry N. Dirin³, Olga Nazarenko³, Maksym V. Kovalenko^{3,4}, Andreas Baumann⁵, Julian Höcker⁵, Vladimir Dyakonov⁵ and Manfred Bayer¹; ¹TU Dortmund, Germany; ²Ioffe Institute, Russian Federation; ³ETH Zürich, Switzerland; ⁴Empa–Swiss Federal Laboratories for Materials Science and Technology, Switzerland; ⁵Julius-Maximilians-Universität Würzburg, Germany

The emerging field of lead halide perovskite semiconductors offers a plethora of promising material compositions for applications. Experimentally exploring all of these combinations is challenging, especially in light of the increasing number of tandem devices. Theoretical models help predict suitable candidates, but require a fundamental understanding of the perovskite band structure. This is where our experimental methods come into play. Experimental spin physics helps improve, validate, and substantiate these models and provides insight into the underlying physics. The experimental method uses the optically oriented spin property of resident and photoexcited charge carriers as a probe. A strong and distinct charge carrier spin signal, typically the electron and hole spin simultaneously, can be observed and its spin precession resolved in time. The spin dynamics of the charge carriers is in the ns range and allows intense studies in different directions. The spin reveals the pronounced interactions between the charge carriers and their environment and is sensitive to band mixing, allowing, for example, the determination of the importance of distant bands as well as the study of the effective mass of the charge carriers. The methodological tools include time-resolved pump-probe Kerr spectroscopy, spin-flip Raman scattering, and optical orientation, which we have successfully applied to macroscopic perovskite crystals, nanocrystals, and 2D films.

2:30 PM QT03.07.03

Two-Dimensional Lead Organic Chalcogenide Materials with Strong Electron-Phonon Coupling [Hanjun Yang](#), Sagarmoy Mandal, Yoonho Lee, Jee Yung Park, Libai Huang, Ming Chen and Letian Dou; Purdue University, United States

Two-dimensional (2D) metal organic chalcogenides (MOCs) such as silver phenylselenolate (AgSePh) have emerged as a new class of 2D materials due to their unique optical properties. However, these materials typically exhibit large band gaps, and their elemental and structural versatility remains significantly limited. In this work, we synthesize a new family of 2D lead organic chalcogenide (LOC) materials with excellent structural and dimensionality tunability by designing the bonding ability of the organic molecule and the stereochemical activity of the Pb lone pair. The introduction of electron-donating substituents on the benzenethiol ligands results in a series of LOCs that transition from 1D to 2D, featuring reduced band gaps (down to 1.7 eV), and broadband emission. Furthermore, strong electron-phonon coupling is characterized by the presence of coherent optical phonons with long dephasing time, suggesting the low phonon anharmonicity in the LOC materials

2:45 PM QT03.07.04

Direct Observation of Polaron Vibronic Progression in 2D Layered Perovskites [Mateusz Dyksik](#); Wroclaw University of Science and Technology, Poland

Hybrid perovskites have emerged as a new class of materials with unique electronic properties, which are inherited from both their organic and inorganic constituents. The inorganic framework provides a basis for the semiconducting band structure, whilst the organic molecules stabilize the lattice, indirectly controlling the optical properties. These soft and ionic crystals possess many new and unexpected properties bridging the worlds of classic and organic semiconductors.

A direct consequence of the soft ionic lattice is the significant coupling of charge carriers to the ions of the lattice (i.e. the electron-phonon interaction). The microscopic description of the electron-phonon coupling is nontrivial, essentially due to the fact that it is mediated by a large anharmonicity and dynamic disorder, which requires the introduction of polarons – a quasiparticle representing charge carriers coupled to the lattice vibrations. Polarons are often regarded as a charge carrier “dressed” in a phonon cloud and are characteristic excitations for organic and ionic semiconductors. Polarons are widely invoked to understand the low mobilities of charge carriers, the long carrier lifetimes and diffusion lengths in metal halide perovskites.

Despite tremendous progress in understanding of the fundamental properties of 2D layered halide perovskite, unresolved questions of paramount importance remain to be elucidated. The most important is the origin of the complex optical response of these materials, which cannot be understood by considering only the band structure of these materials. Starting with the pioneering work of Noboru Miura, already 30 years ago, the peculiar line shape of both emission and absorption, composed of equidistant signals separated by tens of meV, is still under debate. Although multiple explanations were suggested in the intervening years, to date the understanding of linear optical response of 2D layered perovskites remains vague requiring further clarification, not only for fundamental understanding of these materials, but also for successful deployment in future opto-electronic devices.

In this work we provide, for the first time, a conclusive proof that the complex structure observed in the optical response of 2D layered perovskites is due to the formation of polarons. Using resonant Raman scattering to investigate various 2D layered perovskites, we observe a spectacular difference of the Raman response with respect to current literature data. Under resonant excitation conditions, the Raman scattering spectrum is dominated by a feature in the high-frequency region $>200\text{ cm}^{-1}$ ($>25\text{ meV}$), in striking contrast to typical non-resonant Raman spectra, where the scattering is dominated by the expected low-frequency optical modes ($<50\text{ cm}^{-1}$). This newly observed Raman signal is exactly at the energy corresponding to the spacing observed in absorption/emission (i.e. 280 cm^{-1} (35 meV) for $(\text{PEA})_2\text{PbI}_4$) and possess all the characteristics of polarons, allowing for the first time to comprehensively understand the emission and absorption spectra of 2D perovskites. This is the first direct correlation between absorption spectra and Raman studies in these materials.

An analysis of the polaronic response allows us to determine important physical parameters, such as the Huang-Rhys factor, and polaron binding energy. For all investigated samples, we find a consistently large Huang-Rhys factor $S>6$, indicating a charge carrier – lattice coupling approaching the strong coupling regime. Importantly, the parameters determined in this work are first of their kind for 2D layered perovskites, and could serve as a benchmark for future band structure theory of 2D layered perovskites, including carrier-lattice coupling.

3:00 PM BREAK

3:30 PM *QT03.07.05

Anomalous Interlayer Exciton Diffusion in WS₂/WSe₂ Moiré Heterostructure [Archana Raja](#); Lawrence Berkeley National Laboratory, United States

Stacking van der Waals crystals allows for on-demand creation of a periodic potential landscape to tailor the transport of quasiparticle excitations. We investigate the diffusion of photoexcited electron-hole pairs or excitons at the interface of WS₂/WSe₂ Van der Waals heterostructure over a wide range of temperatures. We observe the appearance of distinct interlayer excitons for parallel and anti-parallel stacking, and track their diffusion through spatially and temporally resolved photoluminescence spectroscopy from 30 K to 250 K. While the measured exciton diffusivity decreases with temperature, it surprisingly plateaus below 90 K. Our observations cannot be explained by classical models like hopping in the moiré potential. Using a combination of ab-initio theory and molecular dynamics simulations, we demonstrate that low energy moiré phonons, also known as phasons, may play a key role in describing and understanding this anomalous behavior of exciton diffusion. In particular, we show that the moiré potential landscape is dynamic down to very low temperatures. Our observations show that the phason modes arising from the mismatched lattices of a moiré heterostructures can enable surprisingly efficient transport of energy in the form of excitons, even at low temperatures.

Rossi, Antonio, et al. *arXiv preprint arXiv:2301.07750* (2023)

4:00 PM QT03.07.06

Understanding and Engineering Excitonic Properties in 2d Metal Halide Perovskites [John S. Colton](#)¹, Kameron R. Hansen², Cindy Wong³, C. Emma McClure⁴, Blake Romrell¹, Michele Eggleston¹, Daniel J. King⁵, Carter M. Shirley¹, Andre Schleife³ and Luisa L. Whittaker-Brooks²; ¹Brigham Young University, United States; ²The University of Utah, United States; ³University of Illinois at Urbana-Champaign, United States; ⁴University of Chicago, United States; ⁵University of Wisconsin–Madison, United States

As the field of 2d metal halide perovskites (MHPs) matures, state-of-the-art techniques to measure fundamental properties such as the band gap (E_g) and exciton binding energy (E_b), continue to produce inconsistent values which defy a coherent interpretation. In this work we present the results of a recently published paper [Hansen et al., *Matter* 6, 3463-3482 (2023)] in which we have used electroabsorption spectroscopy to precisely and unambiguously measure E_g and E_b for 31 different MHP compositions which include variations in metal atoms, halide atoms, organic cation molecules, and “n-number”. Among other things the results show a clear and direct correlation between E_g and E_b , and also a clear dependence of E_b on organic cation length which indicates that models of isolated quantum wells cannot in general be used to explain excitonic behavior in 2d MHPs. Instead, we have applied a known superlattice theory of repeating wells and barriers, which includes both quantum and dielectric confinement effects. This theory requires separate knowledge of dielectric constants for wells and barriers, which we were able to deduce in a self-consistent manner for many materials. Using the results of that theory we can tell that the most important parameters that affect E_b are well dielectric constant (metal halide layers), barrier length (organic molecules), and exciton reduced mass which we also relate to the MHP octahedral distortion; and we generate a parameter space map of realistically achievable (E_g , E_b) values. Finally, the dielectric constants required by the theory are between the microwave and optical-frequency dielectric values, indicating that the excitonic interaction is partially screened by phonons.

4:15 PM QT03.07.07

Magneto-Optical Studies of The Exciton Fine Structure in Two-Dimensional Perovskites [Katarzyna Posmyk](#)^{1,2}, Natalia Zawadzka³, Lucja Kipczak³, Mateusz Dyksik¹, Alessandro Surrente¹, Duncan K. Maude², Tomasz Kazimierzczuk³, Adam Babinski³, Maciej R. Molas³, Watcharaphol Paritmongkol^{4,5}, William Tisdale⁴, Michal Baranowski¹ and Paulina Plochocka^{2,1}; ¹Wroclaw University of Science and Technology, Poland; ²Laboratoire National des Champs Magnétiques Intenses, France; ³University of Warsaw, Poland; ⁴Massachusetts Institute of Technology, United States; ⁵Vidyasirimedhi Institute of Science and Technology, Thailand

Two-dimensional (2D) lead halide perovskites are a very interesting group of novel semiconducting materials, considered an alternative for applications in photovoltaics and optoelectronics. Their structure can be seen as the “natural” quantum wells, where slabs of metal-halide octahedral units are surrounded from both sides by large organic cations, acting as potential barriers. As a consequence of the quantum and dielectric confinement, the exciton binding energy can reach several hundreds of millielectronvolts, which results in significant splitting of states of the exciton fine structure. This makes them attractive objects for the investigation of exciton physics, since all excitonic effects are greatly enhanced in this system. Significant state spacing and whether or not the lowest excitonic state interacts with photons are also crucial aspects affecting the performance of a device based on 2D perovskites. Gaining a deeper understanding of the exciton fine structure is therefore very important from the point of view of potential applications.

We combine the optical spectroscopy techniques with the use of magnetic field to investigate the exciton fine structure of perovskite compounds with the general formula (PEA)₂(MA)_{n-1}Pb_nI_{3n+1}, where n=1,2,3,4 denotes the number of octahedra layers within a slab. For the thinnest quantum wells (n=1) we reveal the full exciton fine structure, including the optically inactive dark state. We also observe the bright state oriented out-of-plane of the crystal, located above the in-plane states - contrary to the theoretical predictions. For the first time in 2D perovskites, we observe the lower lying, brightened dark exciton state in the Faraday configuration. Knowing the energies of all four states of the exciton fine structure, we were able to quantify the bright-dark state splitting and the dark exciton g-factor along the c-axis of the crystal, which allowed us to estimate the values of the electron and hole g-factors along this direction [1,2].

Further magneto-optical spectroscopy studies on the perovskite compounds with n=2, 3 and 4 provide valuable information about the evolution of the properties of 2D perovskites with the change of confinement strength, as well as a solid base for further studies of the band structure and excitons in lead halide perovskites.

[1] K. Posmyk et al., *Journal of Physical Chemistry Letters* 13, 4463-4469 (2022)

[2] K. Posmyk et al., *Advanced Optical Materials*, 2300877 (2023)

4:30 PM QT03.07.08

The Phase Transition in HfS₂ Induced by The Pressure Non-Hydrostaticity Igor Antoniazzi¹, Amit Pawbake², Natalia Zawadzka¹, Magdalena Grzeszczyk³, Tomasz Wozniak¹, Jordi Ibanez⁴, Zahir Muhammad⁵, Weisheng Zhao⁵, Clement Faugeras², Maciej R. Molas¹ and [Adam Babinski](#)¹; ¹University of Warsaw, Poland; ²LNCMI, France; ³National University of Singapore, Singapore; ⁴Geosciences Barcelona, Spain; ⁵Beihang University, China

Layered van der Waals crystals are an exciting class of materials of properties, which strongly depend on their thickness. Their structure makes them very sensitive to the interlayer spacing, which can be modulated by temperature or strain. This motivates the recent interest in the strain engineering as an effective way to modify their mechanical, optical, and electronic properties.

We have addressed the effect of pressure on hafnium disulphide (HfS₂), material of promising electrical properties. We study Raman scattering (RS) in bulk HfS₂ using $\lambda=632.8$ nm (1.96 eV) and $\lambda=561$ nm (2.21 eV) at room temperature under pressure up to 10 GPa. A methanol-ethanol mixture or crystallographic oil were used in our diamond anvil cell (DAC) as the pressure transmitting medium (PTM).

HfS₂ under ambient conditions adopts the 1T octahedral structure with the RS spectrum dominated by the out-of-plane A_{1g} mode.

A systematic pressure-induced blue-shift of the RS features in the spectrum was observed when hydrostatic conditions of pressure were supported by a

methanol-ethanol mixture as PTM, confirming that no phase transition occurred in HfS₂ up to 10 GPa.

On the contrary, seven new modes appeared in the RS spectrum around P=7 GPa when crystallographic oil was used as PTM. The non-hydrostatic component of pressure in that case, which emerged around P=4 GPa was deduced from the characteristic splitting of ruby-related photoluminescence lines. Both "low-pressure" and "high pressure"-related peaks coexisted in the RS spectrum up to P=10 GPa with the former features systematically decreasing their intensity. The "high-pressure" peaks were observed under decompression down to P=1.2 GPa pointing out to a metastability of the observed transition.

Polarization angle-resolved measurements were performed at 7.4 GPa to study properties of all the observed RS peaks. A strong anisotropy of the RS for both the mode, evolving from the A_{1g} symmetry vibrations and the "high pressure" modes was observed. Moreover, the effect of excitation energy on the anisotropy was clearly appreciated. In particular for the A_{1g}-related mode, the two-fold (four-fold) polar symmetry of the RS intensity for co- and cross-polarization conditions was observed for l=561 nm (l=632.8 nm) excitation.

We conclude that the observed evolution of the RS spectra under pressure corresponds to the partial phase transition in HfS₂. The transition was triggered around P=7 GPa by the non-hydrostatic component of pressure. Both phases coexist up to P=10 GPa and upon decompression down to P=1.2 GPa. The anisotropy of the RS polar dependence at P=7.4 GPa points out to the distortion of crystal lattice in both co-existing phases. The effect of excitation energy on the A_{1g}-related mode was explained in terms of the non-resonant (λ=632.8 nm) and resonant (λ=561 nm) excitation conditions. Our results confirm the critical effect of the PTM on the pressure-induced phase transition in HfS₂, as revealed by the RS spectroscopy.

4:45 PM QT03.07.09

Dynamical Coulomb Screening in Atomically Thin Semiconducting Transition Metal Dichalcogenides Amine Ben Mhenni^{1,1,2}, Dinh Van Tuan³, Leonard Geilen^{1,1,2}, Marko M. Petrić^{1,1,2}, Kenji Watanabe⁴, Takashi Taniguchi⁴, Sefaattin (. Tongay⁵, Kai Müller^{1,1,2}, Nathan P. Wilson^{1,1,2}, Jonathan J. Finley^{1,1,2}, Hanan Dery^{3,3} and Matteo Barbone^{1,1,2}; ¹Technical University of Munich, Germany; ²Munich Center for Quantum Science and Technology (MCQST), Germany; ³University of Rochester, United States; ⁴National Institute for Materials Science, Japan; ⁵Arizona State University, United States

Reduced screening contributes to the particularly strong Coulomb interaction characteristic of 2D materials¹, which is behind the emergence of exotic quantum many-body phases found therein. While the 2D nature of these material systems complicates the screening description, its understanding is, to date, considered well-established, mainly based on static approaches². Here, we use exciton resonances as probes to study screening in monolayer WSe₂, which we embed in dielectric environments with dielectric constants ranging from 5 to more than 1000. At odds with previous reports³, we find evidence for an optical bandgap *blueshift* for larger dielectric constants. We understand the experimental findings by developing a fully dynamical approach to the environment dielectric response. Starting from the 3χ model⁴, we take the frequency dependence into account via the dynamical dielectric function, both in the bandgap renormalization and in the exciton binding energy calculations. While binding energy remains mainly controlled by low-frequency dielectric screening, we find that high-frequency dielectric response is predominant in bandgap renormalization. Our results show that a fundamental understanding of Coulomb interaction in atomically thin materials cannot ignore dynamical effects. The achieved tunability of the optical bandgap by more than 30 meV, together with the qualitatively different theoretical framework developed, offer new opportunities for tuning the optoelectronic properties of 2D semiconductors and advance the study of many-body interactions in layered materials and their heterostructures.

References:

- ¹ Chemikov, A., Berkelbach, T. C., Hill, H. M., Rigosi, A., Li, Y., Aslan, B., Reichman, D. R., Hybertsen, M. S., & Heinz, T. F. (2014a). Exciton binding energy and nonhydrogenic Rydberg series in monolayer WS₂. *Physical Review Letters*, 113(7).
- ² Cho, Y., & Berkelbach, T. C. (2018). Environmentally sensitive theory of electronic and optical transitions in atomically thin semiconductors. *Physical Review B*, 97(4).
- ³ Raja, A., Chaves, A., Yu, J., Arefe, G., Hill, H. M., Rigosi, A. F., Berkelbach, T. C., Nagler, P., Schüller, C., Korn, T., Nuckolls, C., Hone, J., Brus, L. E., Heinz, T. F., Reichman, D. R., & Chernikov, A. (2017). Coulomb engineering of the bandgap and excitons in two-dimensional materials. *Nature Communications*, 8(1).
- ⁴ Van Tuan, D., Yang, M., & Dery, H. (2018). Coulomb interaction in monolayer transition-metal dichalcogenides. *Physical Review B*, 98(12).

SESSION QT03.08: 2D Halide and Chalcogenides Semiconductors VII – Chirality

Session Chairs: Erik Kirstein and David Mitzi

Friday Morning, April 26, 2024

Room 444, Level 4, Summit

8:30 AM *QT03.08.01

Phase Purity in Chiral 2D Perovskites Yana Vaynzof^{1,2}; ¹Technical University Dresden, Germany; ²Leibniz Institute for Solid State and Materials Research Dresden, Germany

The introduction of chiral organic spacers in low-dimensional metal-halide perovskites triggers chiroptical activity, making these materials of great interest for spintronic applications. To enable such applications, it is necessary to develop a deep understanding of the structure formation of chiral two-dimensional (2D) perovskites and its impact on their optical properties. In the first part of the talk, I will discuss how changing the processing conditions impacts on the phase purity, microstructure, and chiroptical properties of chiral 2D perovskites. In the second part, I will focus on the optical properties of these materials, focusing in particular on the origin of the common observation of asymmetric shape of their photoluminescence.

9:00 AM *QT03.08.02

Novel Chiroptical Probes to Track Spin & Light in Space and Time in Semiconductors Sascha Feldmann; Harvard University, United States

Solution-processable semiconductors like halide perovskites and certain molecules are promising for next-generation spin-optoelectronic applications [1]. Yet, we still don't fully understand what governs the excitation and spin dynamics in these materials, and how these are affected by chirality.

In this talk, I will give an overview of our recent efforts to understand the spin-optoelectronic performance of these materials by developing time-, space- and polarization-resolved absorption spectroscopy and microscopy. For halide perovskite films, we find here that locally varying degrees of symmetry-breaking drive spin domain formation within picoseconds [2].

I will then briefly explain the fundamentals and artifacts involved in measuring circularly polarized luminescence (CPL) reliably [3], and finally show our most recent development of full Stokes-vector polarimetry with unprecedented time- and polarization resolution to track the emergence of chiral light emission in these fascinating materials [to be submitted].

- [1] Crassous,...., Feldmann, Nature Reviews Materials 2023
[2] Ashoka,...., Feldmann & Rao, Nature Materials 2023
[3] Kitzmann,...., Feldmann, Advanced Materials 2023

9:30 AM BREAK

10:00 AM *QT03.08.03

The Impact of Anisotropy and Anharmonicity on The Magneto-Optical Properties of Bulk 3D and 2D Lead Halide Perovskites Efrat Lifshitz;
Technion-Israel Institute of Technology, Israel

The renaissance of interest in halide perovskites, triggered by their unprecedented performance in optoelectronic applications, elicited worldwide efforts to uncover various intriguing physical properties, with a particular interest in spin-orbit effects. The current work presents magneto-optical experimental evidence for anisotropic electron-hole interactions in the 3D orthorhombic MAPbBr₃ and the 2D (PEA)₂PbI₄ bulk single crystals. The evidence was seen in the magneto-photoluminescence spectra while monitoring several different crystallographic directions. The observations exposed a highly non-linear response to a magnetic field and asymmetry to the influence of the sign of the magnetic field. A theoretical model implementing anisotropy in the electron-hole interaction, Rashba effect, Landé *g*-factors, and a lesser contribution from an Overhauser effect corroborated the experimental results.

A continuation of the work involved the investigation of the anharmonic ground-state of the (PEA)₂PbI₄ compound, using complementary information from low-temperature x-ray diffraction (XRD) to the photoluminescence spectroscopy, which was also supported by density functional theory (DFT) calculations. The study extrapolated four crystallographic configurations from the low-temperature XRD. These configurations imply that the ground state has an intrinsic disorder stemming from two coexisting chiral sub-lattices, each with a bi-oriented organic spacer molecule (see scheme). We further show evidence that these chiral structures form unevenly populated ground states, portraying uneven anharmonicity, where surface effects may tune the state population. Our results uncover a disorder that may be associated with a dynamic Rashba effect. The current efforts include using a unique pump-probe experiment to follow a dynamic Rashba effect. Also, preliminary magneto-photoluminescence of (F-PEA)₂PbI₄ uncovered two opposing chiral structures alone through the entire temperature range under investigation. This result was already corroborated by XRD measurements, confirming the locking of the F-PEA degree of freedom. Further study is ongoing regarding the relation between anharmonicity, the Rashba effect, and the dependence on structure and composition.

Acknowledgement: The authors express their gratitude to the collaborators in the project: Liang Z. Tan (LBL, Berkeley, USA) and Prof. Leeor Kronik (Weizmann Institute, Rehovot, Israel)

10:30 AM QT03.08.04

Manipulating Chirality of 2D Lead Halide Perovskites via Mixed Chiral and Achiral Organic Ligands Xiaoyu Zhang, Adewale J. Babatunde and Qiuning Yu; Cornell University, United States

Hybrid organic-inorganic halide perovskites have emerged as an important family of materials for optoelectronics with broader applications in solar cells, photodetectors, light-emitting diodes (LEDs), and lasers. As ionic semiconductors, the flexible crystal structures and tunable compositions make it possible to rationally design hybrid halide perovskites with desired properties. Chiral halide perovskites demonstrate such possibility and the breakthrough with respect to the development of a new class of chiral semiconductors, which opens up new applications of hybrid perovskites to chiroptoelectronics, ferroelectrics, and spintronics. One type of chiral perovskites is based on two-dimensional (2D) hybrid organic-inorganic halide perovskites by incorporating chiral organic ligands between achiral inorganic single layers composed of corner-sharing metal-halide octahedra. As a new class of chiral semiconductors, the chirality of hybrid 2D perovskites is attributed to the symmetry-breaking in the inorganic framework induced by the enantiopure chiral organic cations via asymmetric hydrogen bonding interactions, which transfers the structural chirality across the organic-inorganic interface. In this work, we demonstrate that the chirality of 2D halide perovskites can be widely tuned via incorporation of mixed chiral and achiral organic ligands in the organic layer. A broad range of alkyl and aryl chiral and achiral cations are used in forming 2D chiral halide perovskites. Additionally, we also synthesized semiconducting organic cations and integrated into the 2D chiral halide perovskites. To reveal the origin of the chirality, we conducted density functional theory (DFT) calculations to gain the insights of hydrogen bonding and octahedral structure as well as their relationship to the electronic band structure and spin split. We also conducted time dependent DFT to calculate circular dichroism (CD) spectra and to understand the correlation of rotatory strength at the orbital symmetry level. We performed temperature dependent synchrotron powder X-ray diffraction (PXRD) and pair distribution function (PDF) measurements and analysis to reveal the structural properties. To understand the chiroptoelectronics embedded in these new chiral perovskites, we conducted temperature dependent circularly polarized photoluminescent (CPPL) and conventional and circularly polarized transient absorption spectroscopy (TAS) measurements. While many phenomena are unknown and needed further investigations, this work provides a new way to manipulate chirality of 2D perovskites, which could lead to broader applications.

10:45 AM QT03.08.05

Enhanced Circular Dichroism and Polarized Emission in an Achiral, Low Bandgap Bismuth Iodide Perovskite Derivative Philip Klement¹, Jakob Möbs², Gina Stuhmann³, Lukas Gumbel¹, Marius Müller¹, Johanna Heine² and Sangam Chatterjee¹; ¹Justus Liebig University Giessen, Germany; ²Philipps-Universität Marburg, Germany; ³Karlsruhe Institute of Technology (KIT), Germany

Lead halide perovskites and related main-group halogenido metalates exhibit unique semiconductor properties, positioning them as promising candidates for next-generation optoelectronics. Their applications span solar cells, light-emitting diodes, lasers, sensors, and photo-catalysis. The approach of assembling customized building blocks into materials with tailored properties opens doors to explore novel phenomena. Recent advances in incorporating chiral organic cations have given rise to chiral metal-halide semiconductors. These materials exhibit intriguing properties such as chiroptical activity and chirality-induced spin selectivity, enabling the generation and detection of circularly polarized light and spin-polarized electrons for applications in spintronics and quantum information.

However, understanding the structural origin of chiroptical activity presents a challenge due to macroscopic factors and experimental constraints.

In our study, we present an achiral perovskite derivative [Cu₂(pyz)₃(MeCN)₂][Bi₃I₁₁] (pyz = pyrazine; MeCN = acetonitrile), which displays remarkable circular dichroism (CD) arising from the material's noncentrosymmetric structure. CuBiI features a unique crystal structure as a poly-threaded iodido bismuthate, with [Bi₃I₁₁]²⁻ chains are intertwined within a cationic two-dimensional coordination polymer. The material exhibits a low, direct optical band gap of 1.70 eV. Notably, single crystals exhibit both linear and circular optical activity with a substantial anisotropy factor of up to 0.16. Intriguingly, despite the absence of chiral building blocks, CuBiI exhibits a substantial degree of circularly polarized photoluminescence, reaching 4.9%. This value is comparable to the results achieved by incorporating chiral organic molecules into perovskites, typically ranging from 3% to 10% at zero magnetic field.

Our findings shed light on the macroscopic origin of CD and provide valuable insights for the design of materials with high chiroptical activity.

[1] Möbs, J.; Klement, P.; Stuhmann, G.; Gümbel, L.; Müller, M. J.; Chatterjee, S.; Heine, J. (2023): Enhanced Circular Dichroism and Polarized Emission in an Achiral, Low Bandgap Bismuth Iodide Perovskite Derivative. *J. Am. Chem. Soc.* 2023, XXXX, XXX, XXX-XXX, DOI: 10.1021/jacs.3c06141

11:00 AM QT03.08.06

Photonic Ferromagnets: Leveraging Chemistry to Develop New Van der Waals Ferromagnets with Strongly Coupled Spin and Optical Functionalities [Kelly M. Walsh](#), Kimo Pressler, Thom Snoeren, Rachel Smith and Daniel R. Gamelin; University of Washington, United States

Materials with strongly coupled electronic, magnetic, and optical properties are highly desirable for application in next-generation spin-based devices. Magnetic van der Waals materials have been demonstrated to be attractive candidates for archetypal spin-based electronics, but such ferromagnets are often non-emissive or show only broad, nondescript luminescence. Moreover, their chemical parameter space is often largely unexplored. This presentation will describe the use of composition to develop new van der Waals materials that both are ferromagnetically ordered *and* show unique optical properties, with strong coupling between the two. In one example, we show that deliberate doping with optical impurities can transform the broad luminescence of the prototypical 2D ferromagnet, CrI₃, into sharp *ff* luminescence of the lanthanide impurity, sensitized by the CrI₃ host. We show that the impurity spin is pinned to the ferromagnetism of the CrI₃ lattice, reflecting strong dopant-host exchange coupling and providing sensitive magnetic control over lanthanide emission polarization at exceptionally low fields. In another example, we have developed solution routes to growth of ferromagnetic 2D perovskites with complex compositions. These materials show strongly temperature-dependent absorption whose intensity reflects coupling to thermally populated 2D magnons. We also show that the air stability of these compounds can be increased dramatically through composition tuning. These demonstrations illustrate the ability to leverage the chemical tunability of layered 2D materials to access new and unusual magneto-optical functionalities.

SYMPOSIUM QT04

Superconducting Materials

April 23 - May 7, 2024

Symposium Organizers

Liangzi Deng, University of Houston

Qiang Li, Stony Brook University/Brookhaven National Laboratory

Toshinori Ozaki, Kwansei Gakuin University

Ruidan Zhong, Shanghai Jiao Tong University

Symposium Support

Gold

Faraday Factory Japan LLC

* Invited Paper

+ JMR Distinguished Invited Speaker

^ MRS Communications Early Career Distinguished Presenter

SESSION QT04.01: Iron-based

Session Chairs: Takanobu Kiss and Qiang Li

Tuesday Morning, April 23, 2024

Room 445, Level 4, Summit

10:30 AM *QT04.01.01

Iron-Based Superconductors as a New Majorana Playground [Hong Ding](#); Shanghai Jiao Tong University, China

Majorana zero modes (MZMs) in solid materials and devices have attracted tremendous interest owing to their potential applications in robust quantum computation. Last ten years witness rapid progresses and serious setbacks in searching for MZMs. Recently iron-based superconductors (FeSCs) emerged as a new and promising Majorana platform due to relatively high temperature and high purity. In this talk I will report a series of our discoveries which help to establish this iron-Majorana platform. We have observed a superconducting topological surface state of Fe(Te, Se) by using ARPES, and a pristine MZM inside a vortex core of this material by using STM. We have also observed a half-integer level shift of vortex bound states and nearly quantized Majorana conductance in this material, which are hallmarks of MZMs. We have found that most of FeSCs have similar topological electronic structures. Finally, we found that uniaxial strain can be used as a good tuning method to control MZMs in FeSCs. The combination of intrinsic topological nature of vortex and large energy spacing among the discrete bound states, all of which can be tuned by pressure, offers compelling evidence for the Majorana nature of vortex zero-modes discovered in FeSCs, thus creating an exciting playground for realizing and manipulating Majorana modes.

11:00 AM *QT04.01.02

The Structural Origin of Superconductivity in K-Intercalated FeSe System Maw-Kuen Wu^{1,2}, [Guo-Tsung Huang](#)¹, Chih-Han Wang¹, Ming-Jye Wang¹, Phillip M. Wu³ and Kung-Yu Yeh¹; ¹Academia Sinica, Taiwan; ²National Tsing Hua University, Taiwan; ³National Chung-Hsin University,

Taiwan

The discovery of relatively high T_c in potassium (K) intercalated FeSe, where the sample composition labeled as $K_{0.8}Fe_2Se_2$, has attracted extensive attentions in order to better understand the exact origin of superconductivity in this intriguing system. It has been known right after the observation of superconductivity in this system that there exists two distinguished crystal phases, one with full Fe-occupation of I4/mmm symmetry, the other with ordered Fe-vacancy of I4/m symmetry. Most of the reports designated the I4/mmm phase to be the one superconducting. However, this assignment could not provide proper answers to several phenomena observed: (A) Small fraction of superconducting phase is observed in the well Fe-vacancy ordered $K_2Fe_4Se_5$ sample when it is quenched from high temperature annealing; (B) Bulk superconductivity emerges in $K_2Fe_{4.2}Se_5$, with extra Fe-content, and superconducting volume fraction varies with the quenching temperature; (C) Superconductivity in $K_2Fe_{4.2}Se_5$ sample disappears after being annealed at a temperature lower than 400°C; (D) Superconducting transition temperature reaches a maximum of ~48K under high pressure. In this report, based on the results of high resolution x-ray diffractions, we show unambiguously that the Fe-vacancy ordered I4/m phase is the parent phase, which became superconducting after additional Fe partially occupied the vacant sites. Furthermore, we also identify the presence of an intermediate phase embedded in a Fe-vacancy ordered phase and a fully-occupied phases within the I4/m symmetry to be the structural origin of superconductivity, which could satisfactorily explain those unanswered questions. Our results closely associate with the picture of the interface superconductivity, which can be at either a non-magnetic semiconducting-metallic interface or an antiferromagnetic insulating-metallic interface.

11:30 AM QT04.01.03

Superconducting and Possible Topological States in Fe (Te, Se) Thin Film on YSZ Substrate Using Pulsed Laser Deposition (PLD) Technique

Himanshu Chauhan, [Shivam K. Miglani](#) and Ghanshyam D. Varma; Indian Institute of Technology Roorkee, India

Since the initial discovery of superconductivity in iron-based superconductors (IBSs), thin films of Fe (Te, Se) superconductors are at the forefront of research in condensed matter physics and materials science. For the development of advanced superconducting devices, it is essential to fabricate the high-quality epitaxial thin films of IBSs. In recent years, several groups have been trying to understand the origin of topological states in thin films, but so far there is not much experimental agreement on these issues, and further studies are needed. In this approach, we have fabricated $FeTe_{0.55}Se_{0.45}$ thin film of different thicknesses on Yttria-stabilized zirconia (YSZ) single-crystalline substrates using pulsed laser deposition (PLD) technique. The effects of thickness on the structural, superconducting, and topological properties have been systematically investigated. The superconductivity in the grown thin film has been affirmed by the temperature-dependent resistivity measurements. It has been observed that superconducting transition temperature vary with the thickness of the films. Superconducting parameters such as upper critical field $H_{c2}(0)$ and corresponding coherence lengths (ξ) and activation energy (U_0) have been estimated using magnetotransport measurements. In addition, a non-saturating linear magnetoresistance (LMR) is also observed, suggesting the presence of a possible topological superconducting state in the grown thin films. Furthermore, current-voltage (I - V) measurements have been used to calculate transport critical current density, J_c of the grown thin films. In this paper a detail correlation between thickness and observed superconducting properties of the grown thin films will be presented and discussed. The study of the presence of possible topological phase in the grown film is relevant to the current focus of developing quantum devices.

11:45 AM QT04.01.04

Electronic Structure and Transport Properties of Partially Ni-Substituted Superconducting Iron Chalcogenide $FeSe_{0.45}Te_{0.55}$

[Juntao Yao](#)^{1,2}, Sarah Paone^{1,2}, Genda Gu² and Qiang Li^{1,2}; ¹Stony Brook University, United States; ²Brookhaven National Laboratory, United States

Iron chalcogenides bring together superconductivity, non-trivial electronic topology, and magnetism in a single material, making it a potential platform for hosting Majorana fermions which are the building blocks for topological quantum computing. We investigated the change of electronic structure and transport properties in a series of superconducting iron-nickel chalcogenides $(FeNi)Se_{0.45}Te_{0.55}$ by partial Ni substitution for Fe. Ni substitution increases the electron count. Ni 3d spin-orbit energy is ~ 50% higher than that of an Fe atom, leading to enhanced topological properties in this class of materials. From combined ARPES and transport measurements, we found that Ni substitution reduces superconducting transition temperature T_c and superconducting gap. Temperature dependent normal state resistivity changes from a weak metallic behavior to an insulating-like behavior with Ni-substitution level above 2% (nominal composition). A low level of Ni-substitution was found to enhance the critical current density in iron chalcogenide superconductors that peaks around 2% substitution level.

SESSION QT04.02: REBCO Films and Coated Conductors, HTS Applications

Session Chairs: Xavier Obradors Berenguer and Venkat Selvamanickam

Tuesday Afternoon, April 23, 2024

Room 445, Level 4, Summit

1:30 PM *QT04.02.01

Vortex Pinning in Complex Heterogeneous Microstructures in REBCO Thin Films Formed by High-Density Artificial Pinning Centers

[Kaname Matsumoto](#)^{1,2,3}, [Tomoya Horide](#)^{2,1,3}, [Yutaka Yoshida](#)^{2,3} and [Ataru Ichinose](#)^{4,3}; ¹Kyushu Institute of Technology, Japan; ²Nagoya University, Japan; ³JST-CREST, Japan; ⁴CRIEPI, Japan

Development of REBCO coated conductors is in progress, and it is desired to improve the superconducting current-carrying capability for equipment applications at operating temperatures near 20 K and 65 K. For this purpose, appropriate introduction of artificial pinning centers (APCs) into REBCO thin films is effective, and higher concentrations of APCs are needed. For example, the main pinning center in NbTi metallic wires is the α -Ti normal-conducting precipitate, with an upper limit of about 25-30% in volume fraction. However, the upper limit for the volume fraction of APCs in REBCO thin films is much lower. If it is possible to introduce APC in REBCO thin films up to the same level as the volume fraction of α -Ti, higher J_c performance is expected to be achieved. At present, it is known experimentally that the upper limit of APC concentration in REBCO thin films is about 5-10%. The reason for this is thought to be the increase in epitaxial distortion, formation of various lattice defects, and oxygen deficiency at the interface due to the introduction of APC, as well as the reduction of the superconducting current path due to the complex structure. Under such a complex and inhomogeneous structure, it is very difficult to find the optimal APC distribution for high magnetic field applications by a conventional screening method. We first investigate the microstructure of REBCO thin films near the upper limit of APC concentration and the degradation of superconducting performance caused by epitaxial distortion, in order to obtain clues for solving the upper limit problem of APC volume fraction. In this study, GdBCO thin films with BHO nanorods were fabricated on IBAD-CeO2 substrates by PLD method. The PLD targets were 4.0, 4.5, 5.0, and 5.5 wt% BHO-doped GdBCO, and the PLD conditions were as follows: deposition temperature 760-840°C, oxygen partial pressure 300 mTorr, distance between substrates 60 mm, laser frequency 10 and 100 Hz, and laser energy 300 mJ/pulse. The sample was subjected to structural analysis by XRD, evaluation of superconducting properties such as J_c

and T_c by PPMS, and microstructural observation by TEM and STEM. Degradation of J_c properties was observed along with a decrease in T_c at higher BHO concentration. Interestingly, in the films fabricated at 10 Hz, the BHO nanorods collapsed and a BHO layered structure appeared. Elemental mapping by STEM confirmed that these were BHO additives. The collapse of the nanorod structure clearly causes degradation of the c-axis J_c property. This structural transition from nanorods to layers is considered to depend on the competition between the release of strain energy stored in the thin film and the kinetic process of thin film nucleation and growth. To quantitatively evaluate the origin of the above structural transition, epitaxial strain energy was analyzed based on micromechanics theory. Furthermore, vortex pinning simulation using TDGL (time-dependent GL) was performed to evaluate the elemental pinning forces at the complex APC interface, and the optimized APC structures to be considered in the future were discussed.

2:00 PM *QT04.02.02

Materials Research on REBCO Superconductors to meet Application Requirements [Venkat Selvamankam](#); University of Houston, United States

REBCO superconductors are in great demand now for many applications, particularly compact fusion. While these superconductors are being implemented in prototype devices, several issues remain before they can be widely used in commercial applications. Cost, capacity, uniformity, mechanical properties, and quench damage are the main issues of concern. High and uniform critical current to reduce cost, high growth rates to increase capacity and reduce cost, alternate conductor architectures for improved strength, flexibility, and defect tolerance are ongoing areas of research. Progress in these areas at the University of Houston will be discussed in this presentation.

2:30 PM *QT04.02.03

Development of Novel Methodologies for Better Understanding and Manufacturing of REBCO Coated Conductors by Integrating High

Throughput Magnetic Microscopy and Machine Learning [Takanobu Kiss](#)^{1,1}, [Zeyu Wu](#)¹, [Kohei Higashikawa](#)^{1,1}, [Shinya Sera](#)¹, [Yuto Tanaka](#)¹, [Natthawirod Somjaijaroen](#)¹, [Roman Valikov](#)², [Miyuki Nakamura](#)², [Valery Petrykin](#)² and [Sergey Lee](#)²; ¹Kyushu University, Japan; ²Faraday Factory Japan LLC, Japan

Recent advances in manufacturing techniques have made it possible to obtain commercial RE₁Ba₂Cu₃O_{7-δ} (REBCO, RE: Rare Earth) coated conductor (CC) tapes having a length of several 100 m. Along with this trend, research on the development of CC applied equipment is also being vigorously promoted in various countries of the world. However, in developing REBCO CC based large-size superconducting equipment, unexpected quenching and lowering of critical current (I_c) and yield at coil-forming are noticed as problem. Technology development for obtaining more stable performance with good reproducibility becomes an urgent issue. The author considers that, as the cause, 1) the behavior of the long CC tape under the practical operation condition is not sufficiently understood, and 2) the problem of the complexity of the manufacturing process. In this study, the local nonuniformity of critical current density (J_c) in the tape-plane of the long CC is measured nondestructive and noncontact manner at high spatial resolution using a reel-type high-speed magnetic microscope. Integrating with image analysis by machine-learning (ML), we succeeded in the automated analysis of several thousands of magnetizing current images and clarified the presence of domains of the local nonuniformity in the long tape, which is difficult to be detected by the conventional inspection by local I_c criterion, and obtained detailed information on the J_c lowering domain such as the size, position, and statistical distribution. To improve the process conditions, we also developed a ML regression model which can quantitatively estimate I_c obtained by the manufacturing condition through a coupled analysis by high-speed I_c measuring and ML regression using a combinatorial sample in which the manufacturing condition was systematically changed in the longitudinal direction of the tape. Furthermore, using the Genetic Algorithm on the basis of this ML regression model, we have also succeeded in deriving the combination of control variables, i.e., the production conditions, to maximize the I_c as output as the solution of the inverse problem. These new methodologies enable us to elucidate the reason for local non-uniformity of long CC tapes, to develop CC tapes with better spatial uniformity, to derive process parameters quickly on PC to maximize the tape performance and are expected to greatly contribute to drastic shortening of lead times for CC tape development and realizing stable tape performance.

Acknowledgements: This work was supported by JSPS KAKENHI Grant Number JP19H05617.

3:00 PM BREAK

3:30 PM *QT04.02.04

Ultrafast transient liquid assisted growth of YBa₂Cu₃O₇ coated conductors: why is it a novel process? [Xavier Obradors Berenguer](#)¹, [Teresa Puig](#)¹, [Lavinia Saltarelli](#)¹, [Diana G. Franco](#)¹, [Kapil Gupta](#)¹, [Elzbieta Pach](#)¹, [Roxana Vlad](#)¹, [Aiswarya Kethamkuzhi](#)¹, [Carla Torres](#)¹, [Adrià Pacheco](#)¹, [Silvia Rasi](#)¹, [Albert Queraltó](#)¹, [Jordi Aguilar](#)¹, [Daniel Sánchez](#)², [Emma Ghiara](#)¹, [Ona Mola](#)¹, [Victor Fuentes](#)¹, [Laia Soler](#)¹, [Julia Jareño](#)¹, [Juri Banchevski](#)¹, [Natalia Chamorro](#)¹, [Cornelia Pop](#)¹, [Joffre Gutierrez](#)¹, [Susana Ricart](#)¹, [Jordi Farjas](#)², [Cristian Mocuta](#)³, [Ramon Yañez](#)⁴ and [Eduardo Solano](#)⁵; ¹Institute of Material Science of Barcelona (ICMAB-CSIC), Spain; ²Universitat de Girona, Spain; ³Soleil Synchrotron, France; ⁴Universitat Autònoma de Barcelona, Spain; ⁵Alba Synchrotron, Spain

Coated conductors (CC) of REBa₂Cu₃O₇ (REBCO, RE= Rare Earth) are an exceptional achievement in materials science which encompassed many scientific and engineering challenges. These superconducting materials have emerged as the most attractive opportunity to reach unique performances at high and low temperatures, particularly at high magnetic fields, while reducing the cost/performance ratio continues to be a key objective for a large scale marketability.

To address the challenge of reducing the cost/performance ratio it is unavoidable to develop ultrafast growth rate processes which will lead to high throughput manufacturing of CCs with high performance. Liquid assisted growth of epitaxial REBCO films appears as a very promising approach to reach growth rates beyond 100 nm/s. We have recently created a novel concept, the Transient Liquid Assisted Growth (TLAG) [1-3], which differs from previous growth paths because it is a non-equilibrium process, i.e. the Ba-Cu-O transient liquid with different stoichiometries leading to the formation of REBCO is not an equilibrium one and its properties can be manipulated through kinetic parameters [4]. We will show that different REBCO (RE= Y, Gd, Yb) films can be grown through TLAG using either the temperature or the PO₂ routes and also with different liquid compositions. The TLAG process is fully compatible with the use of preformed BaMO₃ (M=Zr, Hf) nanoparticles to prepare nanocomposite CCs when propionate metalorganic solutions are used in a Chemical Solution Deposition (CSD) route. Finally, we show that the TLAG process can also be extended to other precursors such as amorphous phases deposited by Pulsed Laser Deposition (PLD) at low temperatures [5]. The growth process has been analyzed by in-situ synchrotron X-ray diffraction analysis which have confirmed that ultrafast growth rates (> 1.000 nm/s) can be achieved. We will show that high critical current densities have been achieved up of 3-5 MA/cm² at 77K in thin films and CCs and the process has been transferred to thicker films and metallic substrates. An overall overview of the features of the TLAG process, as compared to other growth approaches, will be presented [6], together with an outlook of the future potential and the pending challenges of this novel technique.

References

- [1] L. Soler et al, Nature Communications 11, 344 (2020)
- [2] A. Queraltó et al, ACS Applied Materials and Interfaces 13, 9101 (2021)
- [3] L. Saltarelli et al, ACS Applied Materials and Interfaces 14, 48582 (2022)
- [4] S. Rasi et al, Advance Science, 9, 2203834 (2022)

[5] A. Queralto et al, Superconductor Science and Technology 36, 025003 (2023)

[6] T. Puig et al, Nature Review Physics (in press)

4:00 PM QT04.02.05

Ultra-fast Growth of REBCO Superconducting Thin Films by Transient Liquid Assisted Growth Elzbieta Pach¹, Diana G. Franco¹, Lavinia Saltarelli¹, Carla Torres¹, Daniel Sánchez², Jordi Farjas², Eduardo Solano³, Cristian Mocuta⁴, Xavier Obradors Berenguer¹ and Teresa Puig¹; ¹Institut de Ciència de Materials de Barcelona, Spain; ²GRMT, University of Girona, Spain; ³ALBA Synchrotron, Spain; ⁴SOLEIL Synchrotron, France

Cuprates, REBa₂Cu₃O_{7-δ} (REBCO, RE = Y or rare earth) are the most important class of High Temperature Superconducting (HTS) materials, due to their outstanding properties. They are the superconductors with the highest operational temperature and highest operational magnetic field, hence, nowadays the materials of choice for Coated Conductor (CC) technology in most of the high current applications. The synthesis of REBCO-type superconducting films is compatible with standard chemical solution deposition methods (CSD) and pulsed laser deposition growth (PLD). However, recently, the development of a novel synthesis approach promises the reduction of the cost/performance ratio in the CC field. The, so called “Transient Liquid Assisted Growth” (TLAG) method [1-3] is a high-throughput, ultra-fast, non-equilibrium, kinetic process of growth of REBCO type superconducting films and coated conductors compatible with industrial applications. The understanding of the TLAG process requires application of advanced tools and techniques for its characterization and optimization. Therefore, development of a specialized instrumentation for the characterization and optimization of TLAG process in real time and in real conditions by synchrotron radiation based in-situ X-Ray Diffraction, was achieved. This new instrumentation allows to follow the precursors reaction, the generation of intermediate phases and follow the dynamic growth of the superconducting phase while acquiring the resistance of the sample in real time and in-situ by XRD. Epitaxial REBCO TLAG growth at 1000 nm/s has been reached in superconducting films of 3 MA/cm² at 77 K. Furthermore, TLAG growth method was shown to be compatible with introduction of inorganic nanoparticles as vortex pinning centres to increase the performance of such films. In this presentation, I will mainly report on the present understanding of the TLAG process based on the results gathered from the in-situ instrumentation setup.

References:

[1] L. Soler et al., Nat Commun, 2020, 11, 344

[2] S. Rasi et al. Adv. Science 2022, 2203834

[3] L. Saltarelli ACS Applied Mater. Interf. 2022, 14, 43, 48582

4:15 PM QT04.02.06

Monte Carlo Simulation of Nanostructure Formation in BMO-Doped REBCO Films Yusuke Ichino^{1,2}, Noriyuki Taoka¹, Yoshiyuki Seike¹, Tatsuo Mori¹, Tomonori Arita^{3,2}, Tomoya Horide^{3,2} and Yutaka Yoshida^{3,2}; ¹Aichi Institute of Technology, Japan; ²Japan Science and Technology Agency, Japan; ³Nagoya University, Japan

When BMO-doped REBCO superconducting thin films (BMO+REBCO films) are prepared by vapor-phase-epitaxy (VPE) such as PLD and MOCVD, BMO self-organizes into nanorods and/or nanoparticles in the REBCO matrix. On the other hand, only incoherent BMO nanoparticles are observed in the solid phase growth method such as MOD. These experimental results suggest that the kinetics of the raw material particles at the surface of the thin film crystal growth contribute significantly to the self-organization of BMO. In fact, it is known that BMO exhibits various nanostructures depending on the growth temperature (T_G), the volume fraction of BMO added (V_{BMO}), and the deposition rate (DR) in the VPE. Therefore, we have developed a BMO+REBCO thin film growth simulation considering the kinetics using the Monte Carlo (MC) method to investigate the effect of deposition conditions on the nanostructure and the formation mechanism of nanorods.

As a result, the following trends were obtained.

(1) When T_G is high and DR is low, nanorods are formed perpendicular and linear to the substrate surface. In addition, the diameter of the nanorods becomes thicker.

(2) At a lower T_G and higher DR than (1), the nanorods are inclined and their diameters are narrower and their number density is higher.

(3) When DR is high enough, nanoparticles consisting of short nanorods are observed.

(4) Even if DR is high enough, linear nanorods can be obtained if T_G and V_{BMO} are sufficiently high.

The above trends are qualitatively in good agreement with experimental results and reported cases.

The time evolution of nanostructure formation can also be observed in the MC simulations. This indicates that nanorods are formed in the following steps. First, crystal nuclei of REBCO and BMO are generated on the substrate surface, from which crystal growth proceeds. Since the volume fraction of BMO is small, the BMO islands are eventually surrounded by the REBCO layer, and BMO can only grow in the direction perpendicular to the substrate surface.

This process is repeated, consequently, BMO nanorods are formed. On the other hand, at low T_G and high DR , more BMO crystal nuclei are generated, which slows down the growth rate of BMO islands in the vertical direction, resulting in tilted or shortened nanorods. In other words, the competition between REBCO and BMO growth rates results in the formation of various nanostructures.

The above are mainly MC simulations in the VPE. On the other hand, the VLS growth method, which is a thin film growth method via thin liquid layer on a films surface, has the advantage that high-quality crystals can be fabricated even at high DR . However, it is difficult to control the BMO nanostructure.

This is because the kinetics of the raw material particles is different from that of the VPE due to the presence of the thin liquid layer. Therefore, MC simulations concerning to the VLS growth method were developed and compared with the VPE for the formation of BMO nanostructures. MC simulations were also performed by intentionally adding screw dislocations to obtain a more detailed picture of the crystal growth environment.

In this presentation, we will discuss the growth conditions, nanostructure formation, and thin film crystal growth environment.

Acknowledgment

This work was partly supported by JST, CREST Grant Number JPMJCR2336, Japan.

4:30 PM QT04.02.07

A Novel Application of High Temperature Superconducting Cable for Seabed Coils in Ship Magnetic Deperming Megumi Hirota; Naval Ship M&UEP R.C., NPO, Japan

The zero electrical resistivity of superconducting materials makes them ideal for long-distance electric-current transmission. In particular, high-temperature superconducting (HTS) materials require only moderate cooling power, and a few trials have successfully demonstrated their capability for power transmission. Utilizing a long extended HTS cable to generate an external magnetic field is an emerging application with unique challenges. Our study introduces a conceptual design of a flat seabed coil, proportional to a ship's size, for the purpose of ship magnetic deperming. Magnetic deperming involves imposing a magnetic field on the ship's hull to saturate the magnetization of its steel components. The required field is estimated to be 2,400 A/m, achievable by the flat seabed coils in shallow water. The deperming process requires an alternating magnetic field with decreasing peak intensity. We have designed the coil for the largest destroyer and submarine ships of the Japanese Maritime Self-Defense Force. The parameters required for the coil design were obtained from publicly-available information. Our design features three racetrack-shaped coils, each carrying a maximum current of 200 kA,

spanning a total length of 1,200 m for a single coil, set flat at a depth of 12 m, and cooled by liquid hydrogen, using the currently available HTS materials and technologies.

4:45 PM QT04.02.08

Low-Temperature Fabrication of High- T_c NdBaCuO_y Films by Oxygen Partial Pressure Controlled KOH Flux Method Shuhei Funaki, Haruki Shigenobu, Eisuke Sasaki and Yasuji Yamada; Shimane University, Japan

To apply coated conductors operated at boiling temperature of liquid nitrogen (77.3 K) to various fields, an improvement of the superconducting properties is required. In the case of REBa₂Cu₃O_y (RE123; RE: rare earth elements) coated conductors, a biaxial orientation of RE123 crystals on substrate and the improvement of a critical current density (J_c) have been greatly conducted. However, this RE123 coated conductor needs a high growth temperature during film fabrication that causes degradation of superconducting properties due to impurity diffusion from metallic tape substrate. Moreover, for the achievement of high critical current (I_c), a particular technique for the fabrication of thick RE123 film is needed. A single crystalline REBa₂Cu₄O₈ (RE124) has been fabricated by a low-temperature liquid-phase growth process using molten alkali hydroxide (KOH) in an ambient atmosphere [1–3]. By this approach, we synthesized biaxial oriented RE124 epitaxial films on NdGaO₃ (001) single crystalline substrate at low-temperature of ~650°C [4]. Furthermore, by controlling the oxygen partial pressure (pO_2), we fabricated biaxial oriented Y123 epitaxial films [5]. The critical temperature (T_c) of Y123 film fabricated at 650°C was ~90 K, comparable to that of conventional Y123 films. Recently, we have focused on light RE123 (LRE123), which has potentially high T_c , and prepared the Nd123 on SrTiO₃ (100) single crystalline substrate with high T_c by a low-temperature crystal growth process using KOH [6]. We succeeded in obtaining biaxially oriented Nd123 films even at a low temperature of 425°C. However, the T_c was dramatically reduced due to the increase of Nd/Ba substitution as the deposition temperature was lowered. In contrast, by increasing the Ba/Cu composition ratio of the flux to Ba-rich, the T_c of the Nd123 film was slightly improved, but was much lower than the conventional T_c [7]. In addition to Ba enrichment of the flux composition, a low pO_2 is also reported to be effective in suppressing Nd/Ba substitution in Nd123 [8]. In this investigation, to establish the fabrication method of high performance LRE123 films by feasible simple process, we endeavored to fabricate the LRE123 films on single crystalline substrate at low temperatures by liquid phase epitaxial growth using KOH flux with controlled pO_2 . Obtained films of LRE123 (LRE=Gd, Sm, Nd, La) fabricated at 700°C in various pO_2 of 2×10^{-1} , 1×10^{-2} , 1×10^{-3} atm showed biaxial orientation of 123 single phase completely, and c -axis length was elongated to the stoichiometric value with decreasing pO_2 . Moreover, Nd123 films fabricated at 700°C in $pO_2 \leq 1 \times 10^{-2}$ atm showed high- T_c^{onset} of ~90 K. From these facts, we succeeded in the fabrication of high- T_c (> 90 K) Nd123 film using KOH flux method at low temperature by controlling of pO_2 .

References

- [1] D. Sandford, L. N. Marquez, and A.M. Stacy, Appl. Phys. Lett., vol. 67, no. 3, pp. 422–423, May 1995
- [2] Y. T. Song, J. B. Peng, X. Wang, G. L. Sun, and C. T. Lin, J. Cryst. Growth, vol. 300, no. 2, pp. 263–266, Mar. 2007
- [3] Y. Nagira, T. Hara, Y. Yamada, K. Kuroda, and S. Kubo, Trans. Mater. Res. Soc. Jpn., vol. 35, no. 1, pp. 11–13, Apr. 2010
- [4] S. Funaki, F. Nakayama, and Y. Yamada, Phys. Procedia, vol. 27, pp. 284–287, Apr. 2012
- [5] S. Funaki, Y. Yamada, Y. Miyachi, and R. Okunishi, Jpn. J. Appl. Phys., vol. 55, Mar. 2016, Art. no. 04EJ13
- [6] S. Funaki, Y. Yamada, Y. Miyachi, and R. Okunishi, Phys. Procedia, vol. 65, pp. 125–128, Jun. 2015
- [7] S. Funaki, Y. Yamada, R. Okunishi, and Y. Miyachi, IEEE Trans. Appl. Supercond, vol. 26, no. 3, pp. 7201404, Apr. 2016
- [8] M. Murakami, N. Sakai, T. Higuchi, and S. I. Yoo, Supercond. Sci. Technol., vol. 9, no. 12, pp. 1015–1032, Jun. 1996

SESSION QT04.03: Poster Session
Session Chairs: Liangzi Deng and Yusuke Ichino
Tuesday Afternoon, April 23, 2024
Flex Hall C, Level 2, Summit

5:00 PM QT04.03.01

Magnetic ac Susceptibility of Superconducting Ta Films for Quantum Computing Juntao Yao^{1,2}, Chenyu Zhou², Sarah Paone^{1,2}, Mingzhao Liu² and Qiang Li^{1,2}; ¹Stony Brook University, United States; ²Brookhaven National Laboratory, United States

Recently, breakthroughs were reported in the long coherence time (> 0.5 ms) transmon qubit using tantalum films (Ta). Identifying the loss mechanism in Ta films will help further improve the performance of Ta-based superconducting qubits. Here, we report a study of superconducting properties in two sets of Ta films grown on c-cut and a-cut sapphires respectively using contact transport and noncontact magnetic ac susceptibility measurements. Although the resistive transition appears to be similar in both films, we found strikingly different responses in their complex magnetic susceptibilities $\chi' + i\chi''$. χ' in the c-cut films exhibits a sharp peak at superconducting transition T_c and becomes featureless below T_c indicating a strongly coupled superconducting state. In contrast, χ'' in the a-cut films exhibits a broad peak near T_c and a second peak appears below T_c , indicating granular superconductivity behavior. This second peak in χ'' is associated with the hysteresis loss at weak-link-type grain boundaries, which is believed to be a leading source of decoherence in the a-cut Ta films. The derived magnetic loss tangent in the a-cut films is about one order of magnitude higher than in the c-cut films. This study demonstrates that ac susceptibility is an excellent probe for characterizing bulk superconducting properties of the constituent superconducting materials used in qubits.

5:00 PM QT04.03.02

Integrating Novel Nitride Barriers and Conventional Nitride Superconductors into Epitaxial Junctions: Early Steps toward New Materials Platforms for Quantum Computing Sage Bauers; National Renewable Energy Laboratory, United States

Although nitrogen is approximately four times more prevalent than oxygen in the Earth's atmosphere, the stability of dinitrogen leads to an order of magnitude fewer known nitrides than oxides. Despite this, many of the known nitrides are important technological materials. Transition metal nitrides (TMNs) in the rocksalt crystal structure are one such example: these chemically stable, high-symmetry superconductors are well suited for epitaxial thin film integration with common substrates. To extend the functionality of TMNs and create epitaxial superconductor–semiconductor heterojunctions, suitable rocksalt-structured semiconductors are required. Our team has discovered a series of new rocksalt-structured nitride semiconductors with band gaps ranging from $E_G=0.9$ – 2.4 eV, described as either MgTMN₂ (TM=group 4 transition metal) or Mg₂TMN₃ (TM=group 5 transition metal). The lattice parameters of these new materials are compatible with TMNs, suggesting the possibility for integration into epitaxial structures, such as Josephson junctions and other circuitry forming superconducting qubits. Here, we study the epitaxial integration of TMNs on Al₂O₃ substrates and of MgTMN₂ and Mg₂TMN₃ compounds onto TMNs. We optimize TMN growth to repeatedly achieve high T_c for epitaxial NbN (15K), TiN (5K), and Nb_{0.5}Ti_{0.5}N (13K). Using electron and X-ray probes we show that heteroepitaxy can be readily achieved between TMNs and the novel semiconductors. Epitaxial NbN-

Mg₂NbN₃-NbN trilayer heterojunctions grown on sapphire are demonstrated with barrier layers down to ~3 nm and crystal coherence across the entire heterojunction stack. However, we also find that the inherent polymorphism of NbN complicates its use, motivating the eventual use of other TMNs such as Nb_{0.5}Ti_{0.5}N alloys.

5:00 PM QT04.03.03

Electronic Transport Studies of InAs Quantum Well [Layla Smith](#)¹, Kent Smith², Leroy Salary¹, Doyle Temple¹ and Wei Pan²; ¹Norfolk State University, United States; ²Sandia National Laboratories, United States

Google researchers have recently demonstrated quantum advantage in a superconducting quantum computer by solving a specific problem that is beyond the most powerful classical computers. The next step is to construct a universal quantum computer to solve real world problems such as new-drug design and discovery. This formidable advance will require a much larger number of fully functional qubits. Unfortunately, a relatively low average qubit gate fidelity of ~99% in current transmon qubits has been detrimental in this pursuit.

A different approach, topological quantum computing, may overcome these difficulties, due to its enhanced tolerance to errors. In a topological quantum computer, a qubit would be constructed out of four Majorana quasiparticles (MQPs), with a gate performed by moving one MQP around another, or braiding MQPs. Because the braiding is topological and nonlocal, Majorana-based qubits would be intrinsically robust against local decoherence sources and thereby enable fault-tolerant quantum computing.

InAs has emerged as a promising material platform to realize topological superconducting states (TSSs) which can host MQPs: (1) It can form a highly transparent interface with aluminum (Al, a superconductor); (2) the strength of spin-orbit-coupling (SOC) is large and tunable, a key ingredient for realizing TSSs. Indeed, recent work by Microsoft Quantum shows exciting results in InAs-Al hybrid devices that are consistent with the observation of TSSs and MQPs.

In this work, we will present our recent low temperature electronic transport characterization in a high quality InAs quantum well (QW), grown by molecular-beam epitaxy. A specimen of a standard 5mm × 5mm geometry is cleaved from an as-grown wafer. Eight indium contacts are diffused symmetrically around the perimeter of the specimen to form ohmic contacts to the 2D electron gas (2DEG) realized in the InAs QW. The specimen is then cooled down to the liquid helium temperature, and the magneto-resistance R_{xx} and the Hall resistance R_{xy} are measured as a function of magnetic (B) fields. R_{xx} displays the typical Shubnikov-de Haas oscillations. For R_{xy}, it is linear with B in the low field range but displays quantized plateaus at high B fields.

Our low temperature measurements demonstrate high quality 2DEG in our InAs QW. In the future, we will examine the SOC strength in InAs by analyzing the weak-antilocalization effect. Results from this study will provide critical information for the realization of MQPs.

5:00 PM QT04.03.04

Investigating The Superconducting and Structural Properties of Trigonal PtBi₂ Single Crystals [Ting-Wei Kuo](#)^{1,2}, Liangzi Deng¹, Hung-Duen Yang² and Ching-Wu Chu¹; ¹Texas Center for Superconductivity at the University of Houston, United States; ²National Sun Yat-sen University, Taiwan

In our research, we report the intriguing structural and superconducting characteristics of trigonal PtBi₂ single crystals. Originating from the synthesis process using high-purity elemental powders of Pt and Bi, the mixture, sealed in a quartz tube, was heated to 850°C and cooled to 420°C. Excess flux from the resulting crystals was subsequently removed through centrifugation, ensuring the crystal's integrity and purity. Our primary focus revolves around understanding the intricate relationship between their unique structural attributes and their emergent physical properties. Significant potential in their superconducting capabilities, positioning trigonal PtBi₂ as a compelling subject in the realm of condensed matter physics.

5:00 PM QT04.03.05

Superconducting Materials Exploration for Quantum Devices [Aidar Kemelbay](#), Arian Gashi, Ed Barnard, Shaul Aloni and Adam Schwartzberg; Lawrence Berkeley National Lab, United States

The performance of quantum devices strongly depends on the quality of materials and interfaces between them, controlling which at every fabrication step is crucial. The parameter space for superconductor synthesis is typically very large and scales up rapidly with more complex material systems, for example when going from binary to ternary or quaternary alloy superconductors. As a result, understanding the fundamental underpinnings of growth and fabrication processes needed to fine tune the application-specific superconductor performance becomes increasingly important. To address this problem a cluster deposition and characterization system was designed and recently launched at the Berkeley Lab's Molecular Foundry user facility, that includes multiple nanofabrication tools (deposition, oxidation, ion milling), a characterization suite (XPS, ellipsometry, FTIR, OES) and automated robotic system — all combined in an integrated vacuum system. This new capability enables synthesis and characterization of materials at every fabrication step, as well as their integration into quantum devices in a single vacuum cycle, preserving pristine interfaces between various device layers. By using the synthesis - characterization - machine learning loop we can efficiently tune material properties and accelerate new materials discovery. For example, we have optimized multiple superconducting systems towards their integration into all-nitride Josephson junctions, or to improve phonon management in superconducting sensors. In this presentation I will discuss this new user accessible capability and the wide range of ongoing and future applications of it.

5:00 PM QT04.03.07

Acid-Assisted Soft Chemical Route for Preparing High-Quality Superconducting 2M-WS₂ [Brianna L. Hoff](#)¹, Xiaoyu Song¹, Ratnadwip Singha¹, Joseph Stiles¹, Grigori Skorupskii¹, Jason F. Khoury¹, Guangming Cheng², Franziska Kamm³, Ayelet Uzan¹, Stephanie Dulovic¹, Sanfeng Wu¹, Florian Pielnhofer³, Nan Yao² and Leslie Schoop¹; ¹Princeton University, United States; ²Princeton Materials Institute, United States; ³University of Regensburg, Germany

2M-WS₂ is a metastable, superconducting polymorph of the transition metal dichalcogenide (TMD) WS₂, comprised of layers of face-sharing distorted WS₆ octahedra. It is predicted to host non-Abelian quantum states, promising for topological computing. Due to its thermodynamic instability, 2M-WS₂ cannot be synthesized using solid-state synthesis. Rather, it requires a top-down approach in which K⁺ is deintercalated from K_xWS₂; so far, this process has been completed using a strong oxidizer, K₂Cr₂O₇ in dilute H₂SO₄. A disadvantage of such an indirect synthesis is that the harsh reaction condition may cause the crystal quality to suffer. To date, no studies have been performed to optimize the synthesis or understand the chemical nature of this reaction. In this study, we found that the K-deintercalation process from K_xWS₂ is spontaneous, and a non-oxidative acidic reaction environment is sufficient to facilitate the oxidation of K_xWS₂ to 2M-WS₂ while reducing H⁺ to H₂. By analyzing the superconducting transition in the heat capacity, we found that 2M-WS₂ made using less aggressive methods has higher superconducting volume fractions. We describe how to access the thermodynamically unfavorable superconducting 2M phase of WS₂ as high-quality crystals.

5:00 PM QT04.03.08

Anisotropic Superconductivity in Atomically Thin (Sn_{1-x}In_x)Bi₂Te₄ [Jack M. Barlow](#)¹, David Graf², Jared Madsen³, Salman Ahsanullah³, Chaowei Hu¹, Jiaqi Cai¹, Jordan Fonseca¹, Zhaoyu Liu¹, Jiun-Haw Chu¹, David Cobden¹, Jiaqiang Yan⁴, Michael McGuire⁴, Xiaodong Xu^{1,1} and Dmitry Ovchinnikov³; ¹University of Washington, Seattle, United States; ²University of Florida, United States; ³University of Kansas, United States; ⁴Oak Ridge National

Laboratory, United States

Combining superconductivity with non-trivial band topology has been an emerging research area in recent years. It is especially appealing to identify material candidates in the van der Waals family of compounds where atomically thin films may allow the control of carrier density and disentanglement of bulk and topological states. In this talk, I will describe our progress in measuring and understanding the thickness-dependent electronic response of topological superconductor candidate $(\text{Sn}_{1-x}\text{In}_x)\text{Bi}_2\text{Te}_4$. By decreasing the thickness from bulk to several layers we observe an increase in anisotropy of the superconducting state with high in-plane critical fields. Furthermore, I will discuss non-linear transport measurements above the critical temperature and their implications for the nature of superconductivity in this material.

5:00 PM QT04.03.09

Selective Area Epitaxial Growth of Magnesium Diboride on SiC using Epitaxial Graphene Patrick A. Rondonanski, Chengye Dong, Joshua Robinson, Qi Li and Joan M. Redwing; The Pennsylvania State University, United States

Magnesium diboride (MgB_2) has a bulk transition temperature (T_c) of 39 K, the highest temperature BCS s-wave superconductor at ambient pressure, and it has been shown to achieve an upper critical field (H_{c2}) larger than 60 T. Furthermore, MgB_2 possesses two superconducting energy gaps, a small gap of ~ 2.3 meV due to the π band and a larger gap of ~ 7.1 meV due to the σ band which contributes to the high T_c . Access to the desirable σ band carriers for proximity coupled superconductivity are largely confined to the *ab*-axes and is not readily available in standard *C*-plane films. Selective area growth of *C*-plane films would allow not only direct growth of superconducting devices, but it also affords the opportunity to fabricate high quality thin film-based lateral devices. To selectively deposit MgB_2 , a chemically inert masking material is preferred to isolate growth regions to the substrate. Graphene is a unique 2D material that is highly stable and is chemically inert due to its strong sp^2 bonding. Moreover, graphene possesses high mobility, Dirac bands, and has been observed to have a room temperature quantum Hall effect in relatively low magnetic fields. The Josephson effect across graphene has been a subject of intense research recently due to the predictions of exotic states due to its Dirac bands, gate tunability, and even in low Landau level quantum Hall states. However, current studies on this matter mostly utilize low T_c superconductors, such as Nb, and it is therefore desirable to employ higher T_c materials to increase the operational temperatures. The high T_c and H_{c2} of MgB_2 make it an ideal candidate to pair with the quantum Hall or fractional quantum Hall effect found in graphene to study the predicted chiral superconductivity.

In this work we present selective area epitaxial (SAE) growth of *C*-plane MgB_2 by hybrid physical-chemical vapor deposition (HPCVD) using patterned epitaxially grown graphene on semi-insulating 6H-SiC (EG). We find that EG patterned using positive resist photolithography and etched with a N_2 plasma restricts MgB_2 deposition predominantly to the exposed SiC and allows for fabrication of lateral MgB_2 /graphene heterostructures. Low surface energy combined with minimal available oxygen bonds prevents Mg from sticking to the graphene and allows high surface mobility of adatoms to the exposed SiC. Thus, this makes graphene a suitable candidate to mask MgB_2 growth. The SAE technique also allows for simple and direct synthesis of MgB_2 devices, such as thin film nanoribbons for applications as single photon detectors or as other quantum sensors, on a semi-insulating substrate without the contamination and degradation of the superconductor from standard lithography processing after deposition. We have fabricated 5 μm wide by 1 mm long *C*-plane MgB_2 nanoribbons of 30 nm thickness that retain the bulk T_c of 39 K. Scanning electron microscopy shows that parasitic deposition on graphene is largely limited to photoresist contaminated areas or point and edge defects of the masking material that allow for Mg bonds to form. Furthermore, XPS analysis suggests the graphene is decoupled from the substrate during the MgB_2 deposition process, which allows for greater carrier mobility in the graphene. Lastly, the van der Waals bonding of graphene allows for easy physical exfoliation of the mask without damaging the MgB_2 device. Thus, this allows for isolation of superconducting devices on the semi-insulating SiC substrate if desired for the device application. Discussions in this talk will include synthesis considerations of developing these structures, such as chemical modification of the graphene during MgB_2 deposition, and the electrical properties of as-grown nanoribbons and other devices fabricated.

5:00 PM QT04.03.10

High Entropy Analogues to The Superconducting Face Centered Cubic W-Pt Binary Denver P. Strong and Robert J. Cava; Princeton University, United States

We report single phase superconducting face centered cubic (FCC) high entropy alloys (HEAs) synthesized via splat cooling. The single phase materials fall at electron counts in the HEA superconductor alloy family where structural stability and optimal superconducting electron counts clash. The materials' superconducting properties follow the general trends published for metallic alloys. Insights are provided as to why an FCC structure may be stable.

5:00 PM QT04.03.11

Capping Effects in Parent and Superconducting $\text{Nd}_{1-x}\text{Sr}_x\text{NiO}_2$ Shiyu Fan¹, Harrison LaBollita², Qiang Gao³, Yanhong Gu⁴, Taehun Kim¹, Jiemin Li¹, Vivek Bhartiya¹, Yueying Li⁵, Jiangfeng Yang⁵, Shengjun Yan⁵, Xingjiang Zhou^{3,6}, Andres Cano⁷, Fabio Bernardini⁸, Yuefeng Nie⁵, Zhihai Zhu^{3,6}, Valentina Bisogni¹, Antia Botana² and Jonathan Pellicciari¹; ¹Brookhaven National Laboratory, United States; ²Arizona State University, United States; ³Chinese Academy of Sciences, China; ⁴University of Tennessee, United States; ⁵National Laboratory of Solid State Microstructures, Jiangsu Key Laboratory of Artificial Functional Materials, China; ⁶Songshan Lake Materials Laboratory, China; ⁷CNRS, Universite Grenoble Alpes, Institut Neel, France; ⁸Dipartimento di Fisica, Universita' di Cagliari, Italy

The discovery of superconductivity in infinite layer nickelates ($\text{Nd}_{1-x}\text{Sr}_x\text{NiO}_2$) has attracted a lot of attention. So far, superconductivity in $\text{Nd}_{1-x}\text{Sr}_x\text{NiO}_2$ is a prerogative of thin films making the role of substrates and interfaces crucial. On this end, capping has been shown to affect the interface structure highlighting its active role on the electronic and magnetic properties of nickelates. However, only few spectroscopic studies specifically address this topic. Here, we use Resonant Inelastic X-ray Scattering (RIXS) to investigate the influence of the SrTiO_3 capping layer on the excitations of $\text{Nd}_{1-x}\text{Sr}_x\text{NiO}_2$ ($x = 0$ and 0.2). Spin excitations are observed in $\text{Nd}_{1-x}\text{Sr}_x\text{NiO}_2$ regardless of capping. While doping softens the spin excitations, capping moderately hardens them in both parent and superconducting samples and increases their spectral weight. Additionally, the hybridization between Ni 3d and Nd 5d orbitals is reduced by capping, as evidenced by a weaker charge transfer peak at ~ 0.6 eV. These observations can be rationalized phenomenologically in the context of the polar discontinuity at the NdNiO_2 - SrTiO_3 interface leading to the atomic and electronic reconstruction, possibly extending to the whole film. Finally, our findings uncover the effects of SrTiO_3 capping on the spin and charge excitations in $\text{Nd}_{1-x}\text{Sr}_x\text{NiO}_2$ and pave the way for a general understanding of infinite layer nickelates thin films.

5:00 PM QT04.03.12

Memristively Programmable Josephson Junctions Julian Liedtke and Stefan Tappertzhofen; TU Dortmund University, Germany

Superconducting quantum interference devices (SQUIDS) can be used for realization of highly sensitive magnetic field sensors and qubits for quantum computers. SQUIDS rely on Josephson junctions and flux quantization. Achieving ultra-high sensitivity, low noise, and long coherence times demands precise tuning of the junction's critical current while simultaneously suppressing the sub-gap current. Nb/NbOx/Nb junctions are highly attractive due to the large gap-energy of Nb, which minimizes the sub-gap current. However, the inherent reactivity of Nb with its native oxide introduces considerable

variations of the critical current. Today, Al/AIOx/Al and Nb/Al/AIOx/Al/Nb junctions show the best and reliable performance. Nevertheless, even with the application of advanced fabrication techniques like laser annealing or high-voltage electron beam lithography, the critical current variation still extends up to 15% on the wafer level. Here, we introduce an innovative solution by utilizing a memristive Nb/NbOx/Nb heterostructure, serving as a programmable Josephson junction. By resistive switching at room temperature, a filamentary weak link (metallic quantum point contact) or tunneling junction between two electrodes formed, effectively operating as a Josephson junction at cryogenic temperatures. In this proof-of-concept, we analyzed in detail and modelled the electrical and physico-chemical properties of the Nb-based memristors. Particular attention is paid to the quantum charge transport at cryogenic temperatures and the statistical variations of the critical current. We demonstrate reproducible forming and erasing of the filamentary junction, which may transcend the limitations of conventional Nb-based junctions such as stress or degradation. The fundamental transport and switching studies are complemented by advanced spectroscopic and microscopy techniques. These memristively programmable Josephson junctions allow for precise tuning of the junction properties post-fabrication through simple programming steps. This may eliminate the need for sophisticated deposition or patterning techniques and unlock the full application potential of Nb-based superconducting electronics.

5:00 PM QT04.03.13

Tuning The Thermodynamic Stability of High Hydrogen-To-Metal Ratio Superconducting Hydrides [Vitalie Stavila](#); Sandia National Laboratories, United States

Superconducting superhydrides are typically formed under high pressures by densely packing hydrogen atoms in unique clathrate structures with strong electron-phonon coupling. The hydrogen-metal interactions in these clathrate networks lead to diverse stoichiometries and exceptionally rich, hypervalent compounds (e.g. CaH₆, YH₈, LaH₁₀). Typically, such compounds are thermodynamically stabilized in bulk at ultra-high pressures, of the order of tens and hundreds of GPa. Here we show that reducing the particle size has a remarkable effect on phase diagram of and thermodynamic stability of such clathrate structures. Spatial confinement of Ca, Yb, and La in the presence of ammonia borane leads to significant changes in the thermodynamic stability, and in selected cases allows stabilization of metastable superhydride phases at lower pressures compared to bulk. Examples of successful interplay between theory and experiment to identify new promising superhydride materials and provide fundamental insights into their stability will be also presented.

5:00 PM QT04.03.14

A Study on Oxygen Post-Annealing of GdBa₂Cu₃O_y Coated Conductors Irradiated with Low-Energy Ions [Toshinori Ozaki](#)¹, [Hiroyuki Okazaki](#)², [Hiroshi Koshikawa](#)², [Shunya Yamamoto](#)², [Tetsuya Yamaki](#)², [Morihiisa Saeki](#)², [Tetsuro Sueyoshi](#)³ and [Hitoshi Sakane](#)⁴; ¹Kwansei Gakuin University, Japan; ²National Institutes for Quantum Science and Technology, Japan; ³Kyushu Sangyo University, Japan; ⁴SHI-ATEX Co., Ltd., Japan

High-temperature superconducting coated conductors (CCs) based on REBa₂Cu₃O_y (REBCO, RE = rare earth) with high current carrying capacity are being developed for use in high magnetic field applications. For these applications, increasing critical current density J_c under magnetic fields is important considerations. The in-field J_c can be improved by the introduction of artificial pinning defects with nano-meter size, which can pin the vortices. The desired defect structures can be created by ion irradiation, which is a promising technique applicable to all superconducting materials. Depending on appropriate ion species and energy, ion irradiation enables the creation of a variety of defects, such as points, clusters and tracks in the materials. Recent studies show low-energy ion irradiation could be a viable option for creating uniform pinning defects in superconducting films¹⁻³. We have reported the effect of low-energy Au-ion irradiation on superconducting properties in GdBCO CCs. The superconducting transition temperatures T_c 's of the GdBCO films irradiated with 2 and 10 MeV Au-ions decrease gradually with increasing fluence up to around 8.0×10^{11} ions cm^{-2} and then significantly started to drop. The J_c in the GdBCO CCs irradiated with 10 MeV Au-ions shows over 70% enhancement at around 3 T and 30 K, indicative of effective pinning defects by the irradiation. In this talk, we will present a study on the oxygen post-annealing of GdBCO CCs irradiated with 2 and 10 MeV Au-ions. The oxygen post-annealing at 450 °C leads to a recovery of T_c , which is close to the pre-irradiation level up to 8×10^{11} ions cm^{-2} dose. We also observe an appreciable recovery of T_c above 8×10^{11} ions cm^{-2} dose, but these T_c values are much less than the one before the irradiation. These results indicate that the oxygen annealing is effective to restore the T_c of the GdBCO CCs irradiated 2 and 10 MeV Au-ions. We will present self-field and in-field J_c before and after the oxygen post-annealing in the irradiated GdBCO CCs. We will also report the effect of oxygen post-annealing temperature on superconducting properties of GdBCO CCs irradiated with 300 keV He-ions.

We would like to thank Sumitomo Electric Industries, Ltd. for providing the GdBCO CCs.

Ion beam irradiation was performed at the Takasaki Ion Accelerators for Advanced Radiation Application (TIARA) of Japan's National Institutes for Quantum Science and Technology (QST).

- 1) M. Leroux et al. Appl. Phys. Lett. 107, 192601 (2015)
- 2) T. Ozaki et al., Supercond. Sci. Technol. 33, 094008 (2020).
- 2) D. Huang et al., Supercond. Sci. Technol. 34, 045001 (2021).

5:00 PM QT04.03.15

Imaging Defects in Epitaxial β -Nb₂N /AlN/ β -Nb₂N Josephson Junctions via Multislice Electron Ptychography [Naomi Pieczulewski](#), John Wright, Debdeep Jena and David A. Muller; Cornell University, United States

Coupling of superconducting qubits to the external environment through dielectric traps, oxidized surfaces, defects, or inhomogeneous phases can introduce undesired energy levels in form of host two-level systems leading to quantum decoherence. Identifying and eliminating the defects responsible for the decoherence will lead to scalable quantum computers. Recent developments in epitaxial growth of single phase, atomically smooth β -Nb₂N has confirmed superconductivity with a critical temperature $0.35 < T_c < 0.6\text{K}$ [1]. This opens the opportunity for large single-crystal layers to be used in Josephson junctions and enables easier identification of defects in comparison to amorphous and polycrystalline materials.

Here, we investigate an epitaxial transition metal nitride (TMN) Josephson junction with β -Nb₂N /AlN/ β -Nb₂N trilayer structure grown by molecular beam epitaxy (MBE) on c-plane sapphire. We measure non-linear I-V characteristics showing superconducting current across the junction. Hexagonal (non-polar) β -Nb₂N and wurtzite (polar) AlN are symmetry-matched and have only a 1.8% lattice mismatch. Here, we use multislice electron ptychography on four-dimensional scanning transmission electron microscopy (4D-STEM) to obtain a three-dimensional reconstruction of the junction and its interfaces with atomic-scale imaging and depth sectioning to show the presence of polarity-inversion boundaries of AlN at β -Nb₂N step edges.

[1] Wright, J. et al., Phys. Rev. Mater. 7, 074803 (2023). DOI: 10.1103/PhysRevMaterials.7.074803

5:00 PM QT04.03.17

Probing Buried Interface Properties in Ta/Sapphire Superconducting Resonators [Aswin kumar Anbalagan](#)¹, [Rebecca Cummings](#)¹, [Chenyu Zhou](#)¹, [Junsik Mun](#)^{1,1}, [Jean-Jordan Sweet](#)², [Vesna Stanic](#)², [Kim Kisslinger](#)¹, [Conan Weiland](#)³, [Steve Hulbert](#)¹, [Nathalie P. de Leon](#)⁴, [Yimei Zhu](#)¹, [Mingzhao Liu](#)¹, [Peter V. Sushko](#)⁵, [Andrew L. Walter](#)¹ and [Andi M. Barbour](#)¹; ¹Brookhaven National Laboratory, United States; ²IBM T.J. Watson Research Center, United States; ³National Institute of Standards and Technology, United States; ⁴Princeton University, United States; ⁵Pacific Northwest National Laboratory, United States

Dielectric loss significantly impacts the coherence time of superconducting qubits, suggesting that surfaces and interfaces are the primary limiting factors. Despite constituting a smaller fraction of the qubit's electromagnetic mode, they have the potential to exert significant influence as sources of high-loss tangents. This study investigates the structure and composition of the interfacial layer in Ta/sapphire-based superconducting qubits. Ta (222) films, comprising a pure α -phase, were sputtered onto a C-plane sapphire substrate at a growth temperature of 750 °C. Characterization of the film, including thickness, roughness, and electron density, was performed using synchrotron-based X-ray reflectivity (XRR) and Hard X-ray photoemission spectroscopy techniques. Notably, our analysis revealed an unexplored layer at the metal-substrate interface that is not possible to detect with the lab-based XRR. To establish the composition and the spatial extent of this interface layer, high-angle annular dark field-scanning transmission electron microscopy (HAADF-STEM) coupled with core-level electron energy loss spectroscopy (EELS) was employed. HAADF-STEM technique provided evidence of an interfacial layer approximately 0.7 nm thick between the metal-substrate layer, aligning well with the measurements from synchrotron XRR fitting. Further examination of the elemental composition of these interface layers using HAADF-STEM with EELS revealed an intermixing layer containing Al, O, and Ta atoms. Ab initio calculations suggest the substrate-metal interface structure's dependence on the sapphire termination before Ta deposition, offering the potential to modulate the Ta film structure through pre-treatment of the sapphire surfaces. These findings offer valuable insights into controlling the structure and composition of the substrate-metal interface that may be able to increase qubit coherence times.

5:00 PM QT04.03.18

Additively-Manufactured YBCO Superconductor [Dingchang Zhang](#)¹, Cristian Boffo² and David C. Dunand¹; ¹Northwestern University, United States; ²Fermi National Accelerator Laboratory, United States

Due to its brittleness, the high-temperature superconducting cuprate $\text{YBa}_2\text{Cu}_3\text{O}_{7-x}$ is currently manufactured in simple shapes (e.g., thin films or pellets) as complex 3D architectures are very difficult to achieve. Here, we show that 3D ink-printing (an additive manufacturing method) can fabricate cuprate superconductors with complex 3D architectures and high performance. An ink is first created with Y_2O_3 , BaCO_3 , and CuO submicron powders of various shapes. The ink is extruded layer by layer to form green parts, which are then sintered to achieve $\text{YBa}_2\text{Cu}_3\text{O}_{7-x}$ with high density. The isothermal sintering and subsequent slow cooling prevent the formation of cracks induced by thermal shock, which are always found in laser-beam-based additive methods. 3D ink-printing is demonstrated for various $\text{YBa}_2\text{Cu}_3\text{O}_{7-x}$ items: horizontal and toroidal coils, magnetic shielding tubes, and Origami folded objects.

5:00 PM QT04.03.19

Strain-Switchable Field-Induced Superconductivity [Shua Sanchez](#)¹, Philip J. Ryan² and Jiun-Haw Chu³; ¹Massachusetts Institute of Technology, United States; ²Argonne National Laboratory, United States; ³University of Washington, United States

Field-induced superconductivity is a rare phenomenon where an applied magnetic field enhances or induces superconductivity. Here, we use applied stress as a control switch between a field-tunable superconducting state and a robust non-field-tunable state. This marks the first demonstration of a strain-tunable superconducting spin valve with infinite magnetoresistance. We combine tunable uniaxial stress and applied magnetic field on the ferromagnetic superconductor $\text{Eu}(\text{Fe}_{0.88}\text{Co}_{0.12})_2\text{As}_2$ to shift the field-induced zero-resistance temperature between 4 K and a record-high value of 10 K. We use x-ray diffraction and spectroscopy measurements under stress and field to reveal that strain tuning of the nematic order and field tuning of the ferromagnetism act as independent control parameters of the superconductivity. Combining comprehensive measurements with DFT calculations, we propose that field-induced superconductivity arises from a novel mechanism, namely, the uniquely dominant effect of the Eu dipolar field when the exchange field splitting is nearly zero. Finally, we introduce a device architecture which uses combined strain and field to make a metal/superconductor toggle switch.

SESSION QT04.04: High Tc Materials I
Session Chairs: Toshinori Ozaki and John Tranquada
Wednesday Morning, April 24, 2024
Room 445, Level 4, Summit

9:00 AM *QT04.04.01

Pairing Symmetry and Electronic Origin of High-Tc in High Temperature Superconductors [Xingjiang Zhou](#); Institute of Physics, Chinese Academy of Sciences, China

We will report our recent angle-resolved photoemission (ARPES) studies of the iron-based and cuprate superconductors:

1. Observation of high superconductivity pairing temperature up to 83K in single-layer Fe/SrTiO₃ films [1]. By preparing high-quality single-layer Fe/SrTiO₃ films, we observe strong superconductivity-induced Bogoliubov back-bending bands that extend to rather high binding energy ~100 meV by high-resolution ARPES measurements. They provide a new definitive benchmark of superconductivity pairing that is directly observed up to 83 K.
2. Nodal s₊- pairing symmetry in an iron-based superconductor with only hole pockets [2]. We carried out ultra-high resolution ultra-low temperature (<1 K) laser ARPES measurements on KFe_2As_2 which is a prototypical iron-based superconductor with hole pockets both around the zone center and around the zone corners. We have determined the superconducting gap distribution and identified the locations of the gap nodes on all the Fermi surface. The pairing symmetry in KFe_2As_2 is found to be of the s₊- type. These results unify the pairing symmetry in the hole-doped iron-based superconductors and point to the spin fluctuation as the pairing glue in generating superconductivity.
3. Ubiquitous coexisting electron-mode couplings in high-temperature cuprate superconductors [3]. We find that the electrons are coupled simultaneously with two sharp boson modes with energies of ~70meV and ~40meV in different superconductors with different doping levels, over the entire momentum space and at different temperatures above and below the superconducting transition temperature. These comprehensive results provide a unified picture of the two energy scales and key information to understand the role of the electron-mode couplings in cuprate superconductors.
4. Electronic origin of high-TC maximization and persistence in trilayer cuprate superconductors [4]. We observed for the first time the trilayer splitting in Bi2223 superconductor. The observed Fermi surface, band structures, superconducting gap and the selective Bogoliubov band hybridizations can be well described by a three-layer interaction model. The electronic origin of the maximum Tc in Bi2223 and the persistence of the high Tc in the overdoped region is revealed. They are consistent with the composite picture where high-Tc can be realized in an array of coupled planes with different doping levels. These results provide key insights in understanding high Tc superconductivity and pave a way to further enhance Tc in the cuprate superconductors.

References:

- [1]. Yu Xu, X. J. Zhou et al., Nature Communications 12, 2840 (2021).
- [2]. Dingsong Wu, Lin Zhao, X. J. Zhou et al., arXiv: 2212.03472 (2022), to appear in Nature Physics.
- [3] Hongtao Yan, X. J. Zhou et al., arXiv: 2201.08108 (2022), to appear in PNAS.
- [4] Xiangyu Luo, Hao Chen, Yinghao Li, X. J. Zhou et al., arXiv:2210.06348 (2022), Nature Physics (2023). <https://doi.org/10.1038/s41567-023-02206-0>.

9:30 AM *QT04.04.02

Impact of Intrinsic Disorder on Superconductivity in Cuprates John M. Tranquada; Brookhaven National Laboratory, United States

Theoretical analyses of superconductivity typically assume a compositionally-uniform lattice. In cuprates, the dopant ions, such as Sr²⁺ for La³⁺ in La_{2-x}Sr_xCuO₄ (LSCO), are randomly distributed in the lattice and are poorly screened, resulting in an inhomogeneous charge landscape that is commonly ignored by theory [1]. As a consequence of the inhomogeneity, features such as spin and charge stripe correlations evolve with doping through a percolation transition, rather than a quantum critical point [2]. In underdoped cuprates, the presence of charge disorder can help to explain why the *d*-wave superconducting gap does not appear to be coherent at the gap maximum [1,3]. In overdoped LSCO, the charge inhomogeneity leads to multiple superconducting transitions [4] and appears to underlie the strange-metal behavior in the normal-state resistivity [2]. I will discuss the evidence behind these claims.

Work at Brookhaven is supported by the Office of Basic Energy Sciences, Materials Sciences and Engineering Division, U.S. Department of Energy, through Contract No. DE-SC0012704.

1. J. M. Tranquada, Adv. Phys. **69**, 437 (2020).
2. P. M. Lozano *et al.*, arXiv:2307.13740 (2023).
3. Y. Li *et al.*, Phys. Rev. B **98**, 224508 (2018).
4. Y. Li *et al.*, Phys. Rev. B **106**, 224515 (2022).

10:00 AM BREAK

10:30 AM *QT04.04.03

2G-HTS Wire Research at Faraday Factory Japan Valery Petrykin, I. Matviian, J. Renel, M. Okube, A. Molodyk, Miyuki Nakamura, Roman Valikov, H. Nanjo, S. Samoilnikov and Sergey Lee; Faraday Factory Japan LLC, Japan

Over the past few years, the world has experienced a steadily increasing demand for high-temperature superconducting wires of the second generation (2G-HTS wires). A significant proportion of wires require the exceptional performance under moderate to strong magnetic fields at reduced temperatures of 4-65K. These wires are primarily used in applications such as fusion magnets, rotating machines, and accelerators. Among these, fusion applications are a key driver for the development and manufacturing of 2G-HTS wires, having specific property requirements at 20K and in 15-20T magnetic fields. In 2023, Faraday Factory Japan (FFJ) supplied over 2,000 kilometers of 4mm wide wires. The technology utilizes an electropolished Hastelloy substrate, alongside technologies involving the formation of an ion-beam assisted MgO (IBAD-MgO) textured buffer layer and pulsed laser deposition (PLD) of superconducting materials. Our research activities aim at improving the deposition process in all stages of the tape fabrication. This presentation will focus on our current research efforts to enhance the quality of the buffer substrate, improve the performance of superconducting materials in strong magnetic fields, and achieve higher uniformity in the Cu and solder layers. Our results have led to produce wires with an engineering critical current density (*J_e*) at 20K and 20T of approximately 900-950 A/mm², with an average piece length of 350 meters. We will also discuss further practical improvements in our 2G-HTS fabrication process, which includes development of the new equipment, improvement of quality management, and addressing the challenges related to the scaling up of daily production.

11:00 AM *QT04.04.04

Unconventional Characteristics of REBCO Containing CuO Double Chain and Similar Defect Structures Jun-ichi Shimoyama, Takanori Motoki, Tetsuya Matsushita and Haruto Niitsu; Aoyama Gakuin University, Japan

Crystal structure of RE247 (RE₂Ba₄Cu₇O_{15,δ}) can be regarded as alternate stacking of RE123 and RE124 along the *c*-axis direction. There are three copper sites in RE247, which are at CuO₂ plane, CuO_{1-δ} chain and CuO double chain. Among them, CuO_{1-δ} chain has large oxygen nonstoichiometry, $\delta = 0 \sim 1$, as in the case of RE123. Superconductivity with *T_c* above 90 K can be observed for Y247 with $\delta \sim 0$, while it does not disappear even in largely oxygen deficient composition, $\delta \sim 1$, because the mean valence of copper is always higher than 2. *T_c* of RE247 monotonically decreases with an increase in δ except for Pr247. Pr247 shows 20 K class bulk superconductivity at $\delta \sim 0.6$ where CuO₂ plane is insulating state due to hole trapping by Pr³⁺. Therefore, the superconductivity of Pr247 is considered to be originated in CuO double chain. In addition, reentrant superconductivity by changing oxygen composition from $\delta \sim 0$ to 0.7 was observed in partially Y doped Pr247, where superconductivity by CuO₂ plane is observed at $\delta \sim 0$ and that by CuO double chain appeared at $\delta > 0.4$. (Pr,Y)247 also shows bulk superconductivity at $\delta \sim 0.5$, however, its flux pinning properties are very poor reflecting very long interlayer distance between superconducting layer more than 2 nm. On the other hand, stacking faults similar to CuO double chain can be introduced in RE123 crystals by three new methods. For RE123 thin films, CuO double chain-like stacking faults was found to be introduced and their density and distribution were controlled by post annealing conditions, such as temperature, holding time and partial pressure of vapor. The defect introduced Y123 films show largely improved *J_c* in low field region. Similarly, CuO double chain-like stacking faults was introduced in silver coated RE123 films by oxygen annealing. Although the mechanism of defect generation due to diffusion of silver into the RE123 films is still unclear, some defect introduced films show improved *J_c*-*B* characteristics. High energy electron irradiation is one of the effective method to improve critical current properties of RE123 crystals. TEM observation revealed that CuO double chain-like short stacking faults generated in the crystal. Role of CuO double chain and similar defects on superconductivity and enhanced critical current properties of RE123 crystal will be discussed.

SESSION QT04.05: Novel Materials I
Session Chairs: Liangzi Deng and Shuhei Funaki
Wednesday Afternoon, April 24, 2024
Room 445, Level 4, Summit

1:30 PM *QT04.05.01

From LTS through HTS to RTS [Paul C. W. Chu](#); University of Houston, United States

Superconductivity has been an ever-self-reinvigorating discipline since its discovery in 1911. It continues to generate excitement in science, materials, and technologies. One of the obvious hurdles to its full fruition in technology is to bring its transition temperature T_c to room temperature. In this talk, I shall first briefly review the impressive advancements made in low-temperature superconductivity (LTS) and high-temperature superconductivity (HTS) before the arrival of room-temperature superconductivity (RTS). Accompanying the advancements made in superconductivity science and technology over the last century, a solid experimental framework concerning the search, development, and even authentication of new discoveries has been established. All these can serve as valuable references in the infancy of RTS research. In this spirit, we will comment on the current status of rare-earth hydride RTS and present our preliminary negative results on Lu-N-H and LK-99, the two most studied materials in the search for RTS in the last few months, although several reports of more negation than affirmation have appeared. However, I do believe that when old wishes are dashed, new hopes will arise.

Research is supported in part by the Enterprise Science Fund of Intellectual Ventures Management, LLC; the U.S. Air Force Office of Scientific Research Grants No. FA9550-15-1-0236 and No.FA9550-20-1-0068; the T. L. L. Temple Foundation; the John J. and Rebecca Moores Endowment; and the State of Texas through the Texas Center for Superconductivity at the University of Houston.

Collaborators: L. Z. Deng, Z. Wu, T. Habamahoro, T. Bontke, D. Schulze, T. W. Kuo, and M. Gooch

2:00 PM *QT04.05.02

Evidence for Near Ambient Superconductivity in The Lu-N-H system [Russell J. Hemley](#)¹, [Alexander C. Mark](#)¹, [Adam Denchfield](#)¹, [Nilesh Salke](#)¹, [Muhtar Ahart](#)¹ and [Hyowon C. Park](#)^{1,2}; ¹University of Illinois Chicago, United States; ²Argonne National Laboratory, United States

Superconductivity in the vicinity of room temperature has the potential to revolutionize both numerous technologies and our understanding of condensed matter. Zero electrical resistance and expulsion of magnetic field below critical temperature T_c are crucial tests of superconductivity. Previous work from our group has established near-room temperature superconductivity but only at megabar pressures (e.g., Ref. 1). Recently reported evidence for superconductivity at ambient P - T conditions in nitrogen-doped lutetium hydride (Lu-N-H) is promising but controversial² Our group has conducted independent measurements on the material synthesized by the methods described in Ref. 2. Four-probe electrical measurements on selected samples in diamond anvil cells show abrupt and reproducible loss of resistance at well-defined critical temperatures and pressures. Magnetic susceptibility measurements show reproducible signatures of field expulsion at similar critical temperatures. The T_c values from electrical resistance and magnetic susceptibility for these samples agree and are consistent with the previously reported data.² On the other hand, other samples prepared with similar procedures exhibit no measurable T_c , but instead show evidence for anomalous metal-insulator transitions that have been well-studied in lanthanide hydrides at ambient pressure (e.g., Ref. 4). Our measurements thus provide direct evidence for near ambient superconductivity in one or more Lu-N-H phases while some phases in the material are not superconducting. We also conducted first-principles DFT and DFT+U calculations to further understand the remarkable properties of these materials. Supercell calculations starting with N-doped $Fm\text{-}3m$ LuH₃ reveal configurations such as Lu₃H_{23-x}N that exhibit novel electronic properties such as flat bands, sharply peaked densities of states (van Hove singularities, vHs), and intersecting Dirac cones near the Fermi energy (E_F).⁵ These electronic properties are present when N substitutes H in the octahedral interstices of Fm3m LuH₃. These structures also exhibit an interconnected metallic hydrogen network, a common feature of high- T_c hydride superconductors. Electronic property systematics gives an estimate of T_c for one structure that is well above the critical temperatures predicted for structures considered previously. DFT+U has an especially strong effect on one of the structures considered, enhancing the vHs and flat bands near E_F . These results provide a basis for understanding the electronic properties observed for nitrogen-doped lutetium hydride. Additional work is needed to fully characterize the material, optimize its synthesis, stabilize it at ambient pressure, and accurately determine the range of critical temperatures possible.

1. M. Somayazulu et al., Phys. Rev. Lett. 122, 027001 (2019).
2. N. Dasenbrock-Gammon et al., Nature 615, 244-250 (2023).
3. N. P. Salke et al., arXiv:2306.06301.
4. J. Shinar et al., Phys. Rev. Lett. 64, 563-566 (1990).
5. A. Denchfield et al. arXiv:2305.18196.

2:30 PM BREAK

3:30 PM *QT04.05.03

Superconductivities in Twisted Interface of Atomically Thin Van der Waals Materials [Philip Kim](#); Harvard University, United States

Engineering moire superlattices by twisting and stacking two layers of van der Waals materials has proven to be an effective way to promote interaction effects and induce exotic phases of matter. After the discovery of superconductivity and correlated insulators in magic-angle twisted bilayer graphene, several different two-dimensional materials have been used to create twisted two-layer systems and various novel phases. In this talk, we will discuss the emergent electronic states observed in various twisted vdW materials. In the first part, we will discuss superconducting multilayer graphene, including twisted bilayer graphene, twisted trilayer graphene, and twisted quadrilayer graphene with alternative twist angles. In these twisted multilayer graphene systems, we also demonstrate a flat electron band tunable by perpendicular electric fields over a range of twist angles. Several correlated behaviors have been observed, including superconductivity and spontaneously broken symmetry states. In the second part of the talk, we will discuss twisted interfaces between stacked van der Waals cuprate crystals that enable tunable Josephson coupling. Using a novel cryogenic assembly technique, we fabricate high-temperature Josephson junctions with an atomically sharp twisted interface between Bi₂Sr₂CaCu₂O_{8+x} crystals. We find that near the 45° twist angle, we observe two-period Fraunhofer interference patterns and fractional Shapiro steps at half integer values, a signature of co-tunneling Cooper pairs necessary for high-temperature topological superconductivity.

4:00 PM *QT04.05.04

Spin-Orbit Coupling and Superconducting Stripes in an Oxide Heterostructure EuO/KTO(110) [Xianhui Chen](#); University of Science and Technology of China, China

Unconventional quantum states have been realized at the interfaces of oxide heterostructures, where they can be effectively tuned by the gate voltage. Recent studies reveal that the conductive interfaces in the SrTiO₃ (STO)-based and KTaO₃ (KTO)-based heterojunctions host a surprisingly enriched cascade of intriguing physical phenomena, most notably the emergence of two-dimensional (2D) superconductivity. Such 2D superconductivity is characterized by a Berezinskii-Kosterlitz-Thouless (BKT) transition; its unusual behavior in external magnetic fields and large tunability under varying electric fields render the superconducting oxide interfaces a promising platform for exploring the mechanism of unconventional superconductivity.

In this talk I will introduce our recent progress on the study of the interface between high-quality EuO (111) thin film and KTO (110) substrate. Both

oxides are insulating, yet the interface is metallic and shows superconductivity with onset transition temperature $T_{\text{onset}} = 0.6\text{--}1.4$ K depending on the carrier density. The 2D nature of superconductivity is verified by the large anisotropy of the upper critical field and the characteristics of a BKT transition. By applying gate voltages, T_{onset} can be largely tuned with an enhancement of ~70%; such an enhancement can be possibly associated with a boosted spin-orbit coupling (SOC) energy. Further analysis based on the upper critical field (H_{c2}) and magnetoconductance reveals complex nature of SOC at the EuO/KTO (110) interface with different dominant scattering mechanisms in the superconducting and normal states. Our results demonstrate that the SOC should be considered an important factor in determining the 2D superconductivity at oxide interfaces.

More interestingly, we discovered a peculiar band-filling-controlled dimension reduction at the superconducting interface between EuO and (110)-oriented KTO. In devices with low carrier densities, electrical transport measurements reveal different T_c and H_{c2} with current applied along the two orthogonal in-plane directions. Theoretical analysis suggests that strong coupling between Ta $5d$ and Eu $4f$ electrons occurs in the low-carrier-density samples, whereas in the high-carrier-density samples (wherein T_c becomes isotropic) such coupling is weakened. Complemented by experiments of local magnetic susceptibility imaging, our observations imply an unprecedented emergence of unidirectional stripe-like superconducting texture, presumably induced by the ferromagnetic proximity effect; we suggest that the superconducting phase coherence is first established within these “stripes”, leading to the peculiar directional dependence of T_c . The realization of such exotic superconducting states provides impetus for the study of novel physics in heterostructures possessing both magnetism and superconductivity.

4:30 PM QT04.05.05

Enhancement of Superconductivity by Isoelectronic Defects in The Fermi-Hubbard Ladder Fabio Pablo Mendez-Cordoba^{1,2}, Paula Giraldo-Gallo¹ and Juan J. Mendoza-Arenas³; ¹Universidad de los Andes, Colombia; ²Universität Hamburg, Germany; ³University of Pittsburgh, United States

In this work we show that superconductivity across a two-leg Fermi-Hubbard ladder can be enhanced by introducing changes of the hopping parameter at specific locations in each leg. Using density matrix renormalization group calculations, we obtain the ground state of the model with repulsive on-site interactions, open boundary conditions and below half filling. We find that modifying the hopping at the position of extremal values of the density Friedel oscillations can strongly increase the value of the superconducting correlations and Luttinger parameter, compared to the homogeneous case. We discuss the mechanism underlying this finding, and experimental platforms where it can be implemented. Our results provide a possible pathway to enhance the superconducting dome by disrupting the lattice structure without changing the number of charge carriers.

SESSION QT04.06: Novel Materials II—Nickelates
Session Chairs: Shiyu Fan and Danfeng Li
Thursday Morning, April 25, 2024
Room 445, Level 4, Summit

8:15 AM *QT04.06.01

Superconductivity in Thin-film Nickelates: Materials Synthesis Danfeng Li; City University of Hong Kong, Hong Kong

Developing new techniques to design and discover novel superconductors, especially those with unusual symmetries of superconducting order parameters and/or exotic pairing mechanisms, opens new doors to future applications in quantum devices. The recent discovery of superconductivity in infinite-layer nickelates has engendered reviving interest in the study of a cuprate-analog system [1]. Notably, superconducting nickelates display signatures of intriguing similarities and distinctions to the cuprates in their phase diagrams, proximity to strongly correlated electronic phases [2], antiferromagnetic interactions [3], superconducting anisotropy [4], etc. Partially owing to the non-trivial challenges in materials synthesis and their thin-film nature [5], experimental demonstration of the intrinsic properties of this materials family has still been limited. In this talk, I will introduce this new family of superconductors synthesized by a soft-chemistry approach and highlight the key aspects of their electronic and magnetic structure. I will also present our latest developments in synthetic approaches to the nickelate materials system and probing of their distinct features, in a broader context of the unusual role that rare-earth elements and chemical environment play.

[1] D. Li *et al.*, *Nature* **572**, 624 (2019).

[2] D. Li *et al.*, *Physical Review Letters* **125**, 27001 (2020).

[3] H. Lu *et al.*, *Science* **373**, 213 (2021).

[4] B. Y. Wang *et al.*, *Nature Physics* **17**, 473 (2021).

[5] K. Lee *et al.*, *APL Materials* **8**, 041107 (2020).

8:45 AM QT04.06.02

Disentangling Symmetry-Breaking Charge Order from Oxygen Order in Infinite-Layer Nickelates Lopa Bhatt¹, Christopher T. Parzyck¹, Kyle Shen^{1,1}, Berit Goodge², David A. Muller^{1,1} and Lena Kourkoutis^{1,1}; ¹Cornell University, United States; ²Max Planck Institute for Chemical Physics of Solids, Germany

As a $3d^9$ analogue to the cuprates, the recent discovery of superconductivity in infinite-layer nickelates has provided a promising direction to understand high-temperature superconductivity and its competing orders [1,2]. Despite their similarities in crystal structure and valence electron configuration, the cuprates and nickelates are distinguished by significant differences in T_c and competing ground states [3]. In cuprates, charge density waves break symmetry and compete with superconductivity at low temperature, while in nickelates charge order has been relatively elusive. There have been reports of charge order in the infinite layer nickelates [4,5], but it remains unclear whether these signatures arise from an intrinsic correlation-driven density wave or extrinsic modulation of the nickel valence from excess oxygen [6,7]. Due to the rich interplay between superconductivity and charge order found in cuprates and other superconducting systems, it is essential to build an understanding of the nature of charge order in the nickelates to shed light on universality in high temperature superconductivity.

In this work, partially-reduced capped NdNiO_{2+x} thin films with intentional excess oxygen are characterized using scanning transmission electron microscopy (STEM). Electron ptychography - a phase retrieval algorithm providing highest resolution and 3D information in STEM - directly probes the atomic structure of the thin films. Precise measurement of O, Ni and Nd sites reveals the presence of excess oxygen which order with $3a_0$ periodicity, a period similar to that of previously reported charge order. Associated oxygen octahedral rotations and accompanying periodic lattice distortions (PLDs) of Nd and Ni sites are present in regions with oxygen ordering. Superlattice peaks which arise from these structural distortions enable mesoscale visualization of the excess oxygen ordering using electron nano-diffraction. We find that the ordering is not uniform across the film but exists in dispersed domains. No

superlattice peaks are observed in areas outside of ordered excess oxygen domains, suggesting that the signatures of charge order in NdNiO₂ reflect the presence of excess oxygen rather than intrinsic correlation effects. This work exemplifies the unique capability of a highly localized and sensitive probe, such as electron ptychography, to directly differentiate and disentangle exotic phases arising in finely tuned systems such as nickelates.

- [1] Li D. et al. Nature 527, 624-627 (2019).
- [2] Osada M. et al. Advanced Materials 33, 45 (2021).
- [3] Li D. et al. Physical Review Letters 125, 027001 (2020).
- [4] Rossi M. et al. Nature Physics 18, 869-873 (2022).
- [5] Tam C. et al. Nature Materials 21, 116-1120 (2022).
- [6] Raji A. et al. ArXiv:2306.10507 (2023).
- [7] Parzyck C. et al. ArXiv:2307.06486 (2023).

*STEM characterization was performed at the Cornell Center for Materials Research Facilities supported by National Science Foundation (DMR-1719875). The microscopy work at Cornell was supported by the NSF PARADIM (DMR-2039380), with additional support from Cornell University, the Weill Institute and the Kavli Institute at Cornell. L.B and L.F.K. acknowledge support from Packard foundation.

9:00 AM QT04.06.03

Eu Self-Doping Induced Superconductivity in NENO Thin Films Using *In-Situ* Synthesis Wenzheng Wei¹, Dung Vu¹, Zhan Zhang², Fred Walker¹ and Charles H. Ahn¹; ¹Yale University, United States; ²Argonne National Laboratory, United States

First observed in 2019, the superconducting infinite-layer-nickelates represent a novel class of unconventional superconductors that are spurring intense research interest due to their electronic and structural similarities to cuprate superconductors. One well known challenge to studying these materials is the ability to synthesize these materials. The common approach is to synthesize alkaline-earth-doped high-valance perovskite nickelate and conduct a topotactical reduction, a testament to the remarkable achievements to date.

In this talk, we apply an all-*in-situ* synthesis thin film processing technique to induce superconductivity in a new nickelate composition. This technique relies on the unique properties of Eu and its 4f electrons as a dopant and uses metallic Al deposited on top of thin film Nd_{1-x}Eu_xNiO₂ to reduce the samples to the superconducting phase. The resulting Nd_{1-x}Eu_xNiO₂ has an onset superconducting temperature as high as 21K and an unusually large upper critical magnetic field.

Work at Yale University was supported by the US DOE, Office of Science, Office of Basic Energy Sciences under award no. DE-SC0019211.

9:15 AM QT04.06.04

Structural Basis for Topotactic Transformation toward Superconducting Infinite-Layer Nickelates Hua Zhou¹, Yan Li¹, Xi Yan¹, Zihua Zhu², Binod Paudel², Yingge Du², Chengjun Sun¹, Shelly Kelly¹, Hong Zheng¹ and Dillon D. Fong¹; ¹Argonne National Laboratory, United States; ²Pacific Northwest National Laboratory, United States

The meticulous experimental verification of the infinite-layer superconducting nickelates heralds a new chapter of superconductivity after a long time extensive pursuit in rare-earth nickelate compounds for achieving cuprate-like unconventional superconductors. Despite great attention to explore the new forefront, the thermodynamic fragility of the parent precursor phase and infinite-layer phase adopting an unfavorably low nickel valence has posed a formidable experimental challenge in the thin film synthesis and the subsequent chemical reduction to attain superconductivity in infinite-layer nickelate heterostructures. Therefore, significant effort to obtain the metastable nickelate precursor phase thin films (i.e. RE_{0.8}Sr_{0.2}NiO₃, RE = La, Nd, Pr...) with minimized extended defects has been undertaken to circumvent the main obstacles due to the chemical instability of high Ni valence and the concomitant Ruddeldsen-Popper or other competing phases, for instance optimizing the non-equilibrium deposition energetics and the selection of close-matched substrate for epitaxy. However, the succeeding chemical reduction process to attain the infinite-layer structure hosting superconductivity remains serendipitous in experimental practice, and the holistic prospect of individual key steps of the evolving non-equilibrium reduction process has not yet been clearly revealed. The decisive understanding of the intricate topotactic reduction remains elusive due to its non-equilibrium dynamics and the lacking of real-time structural insights during key transformation steps.

Here, in this talk, we will demonstrate our *in situ* synchrotron surface X-ray scattering study combined with element-specific spectroscopies to probe at individual key steps of the topotactic reduction of the prototypical epitaxial Nd_{0.8}Sr_{0.2}NiO₃ thin films into Nd_{0.8}Sr_{0.2}NiO₂. The reduction occurs through a low temperature reaction with CaH₂. The relationships between lattice structure, reaction temperature, and time within the strongly reducing environment are discussed. Our experimental observations provide much needed structural and chemical insights into formation of the square-planar structure key to the development of superconductivity in nickelate heterostructures, including clarifying the actual transformation pathway apart from other possible scenario. In particular, we uncovered that the infinite-layer phase initiates at the heterointerface and propagates toward the film surface. Notably, a dynamic surface boundary layer is present introducing hydrogen to the infinite-layer phase while removing and transferring apical oxygen ions to the reducing environment. Moreover, the measurements sensitive to the hydrogen distribution elucidate its intervening role in the intermediate reduction step, and further discount any significant contribution of hydrogen to stabilize superconductivity in the completely converted infinite-layer phase with fully suppressed oxygen octahedral rotations. These results timely address the pressing question whether superconductivity can still be realized in these nickelate compounds without hydrogen. Our study unveils the structural basis underlying the transformation pathway and provides precise experimental guidance to improve the effective reduction for obtaining intrinsic superconductivity behaviors.

9:30 AM BREAK

SESSION QT04.07: Tuning Superconductivity
Session Chairs: Michael Osofsky and Yoshihiko Takano
Thursday Morning, April 25, 2024
Room 445, Level 4, Summit

10:00 AM *QT04.07.01

Exploration of Superconductivity in Layered Perovskite Nickelate La₄Ni₃O₁₀ under High Pressure Yoshihiko Takano^{1,2}; ¹National Institute for Materials Science, Japan; ²University of Tsukuba, Japan

Recent discovery of superconductivity in layered perovskite nickelate $\text{La}_3\text{Ni}_2\text{O}_7$ ($T_c \sim 80\text{K}$) attract much attention due to its high superconducting transition temperature (T_c) and similarity of crystal structure to high- T_c cuprate [1]. And its mechanism of superconductivity is expected to be unconventional [2]. $\text{La}_3\text{Ni}_2\text{O}_7$ corresponds to the $n = 2$ case of the Ruddlesden-Popper phase represented by the general formula of $\text{La}_{n+1}\text{Ni}_n\text{O}_{3n+1}$, and it has two layers of NiO_2 plane. In general, Ruddlesden-Popper phase has two-dimensional crystal and electric structure which is suitable for appearance of superconductivity for instance $\text{KCa}_2\text{Nb}_3\text{O}_{10}$ [3]. Particularly, $\text{La}_4\text{Ni}_3\text{O}_{10}$, is corresponding to $n = 3$ case of the Ruddlesden-Popper phase having three layers of NiO_2 plane. Due to the similarity between these materials, we expect the possibility of superconductivity in $\text{La}_4\text{Ni}_3\text{O}_{10}$ under high pressure [4].

We synthesized polycrystalline samples, $\text{La}_3\text{Ni}_2\text{O}_7$ and $\text{La}_4\text{Ni}_3\text{O}_{10}$, via solid-phase reaction and Hot Isostatic Pressing process from La_2O_3 and NiO [4]. Samples are characterized by powder X-ray diffraction and thermogravimetry. High pressure was generated with Diamond Anvil Cell with boron-doped diamond electrodes designed for four-terminal resistance measurement [5]. Cubic boron nitride powder was used as a pressure-transmitting medium. $\text{La}_4\text{Ni}_3\text{O}_{10}$ displays metallic behavior across all measured pressures, with a slight upturn observed at temperatures below approximately 100 K. At 32.8 GPa, a drop in resistance suddenly appears below 5 K. With increasing the pressure beyond 46.2 GPa, the drop of resistance becomes significant. And the temperature where the resistance begins to drop elevated up to 23K at 79.2 GPa. Magnetic field dependence of resistance was measured at 69.4 GPa. As the magnetic field increases, the drop of resistance becomes smaller. Therefore, the drop in resistance is most likely to be the result of a superconducting transition of $\text{La}_4\text{Ni}_3\text{O}_{10}$ [4].

References:

- [1] H. Sun et al., Nature 621, 493 (2023).
- [2] M. Nakata et al., Phys. Rev. B 95, 214509 (2017).
- [3] Y. Takano et al., Solid State Commun., 103, 215 (1997).
- [4] H. Sakakibara et al., arXiv: 2309.09462.
- [5] R. Matsumoto et al., Rev. Sci. Instrum. 87, 076103 (2016).

10:30 AM QT04.07.02

Pressure-Induced Superconductivity and Phase Transitions in Thermoelectric Material (Bi, Sb)₂Te₃ Liangzi Deng¹, Clayton Halbert², Busheng Wang³, Melissa Gooch¹, Daniel J. Schulze¹, Xin Shi¹, Trevor Bontke¹, Ting-Wei Kuo^{1,4}, Shaowei Song¹, Nilesh Salke², Russell J. Hemley², Eva Zurek³, Hung-Duen Yang⁴, Zhifeng Ren¹, Xiao-Jia Chen¹ and Ching-Wu Chu¹; ¹University of Houston, United States; ²University of Illinois Chicago, United States; ³University at Buffalo, United States; ⁴National Sun Yet-Sen University, Taiwan

$\text{Bi}_x\text{Sb}_{2-x}\text{Te}_3$ is a thermoelectric material with a high room-temperature figure of merit, which can be further enhanced through the application of pressure. Recently, we discovered pressure-induced superconductivity up to $\sim 9\text{K}$ in this system, and the variation in its superconducting transition temperature with pressure indicates possible phase transitions. Systematic X-ray diffraction measurements conducted at room temperature and pressures up to $\sim 50\text{GPa}$ reveal two distinct structural phase transitions. Our experimental results also suggest possible topological electronic transitions induced by pressure. In addition, our theoretical calculations have helped us verify and shed light on the structural and electronic phase transitions driven by pressure, as well as the underlying mechanisms responsible for the emergence of superconductivity in this system.

10:45 AM QT04.07.03

Superconducting Properties of Transition-Metal Nitrides from First Principles: Prospects for Strain and Isotope Modification of Superconducting Critical Temperatures Betul Pamuk¹ and Guru Khalsa²; ¹Cornell University, United States; ²University of North Texas, United States

Epitaxial integration of metallic and superconducting transition metal nitrides into the Group IIIA-nitride semiconductor family opens new avenues for low-temperature electronics and quantum information systems. A challenge for superconducting devices in the nitride platform arises due to the incompatibility between the hexagonal GaN crystal structure and the cubic NbN phase, the main focus of existing experimental work. This incompatibility leads to twin domains that may hamper device design and functionality. Furthermore, due to epitaxial lattice mismatch, the superconducting material may be strained by several percent. Here we use first-principles theory to explore the structural polytypes of NbxN to gather insights into the microscopic physics at play in their metallic and superconducting properties. We focus this work on the prospect of using strain and isotopes to modify electron-phonon interactions and superconducting properties. We discuss the limitations of the theoretical approximations and present our results within the framework of current experimental capabilities. We weigh the desired properties against the constraints imposed by structural symmetry-dictated domains, aiming for the development of domain- and defect-free epitaxial devices.

11:00 AM QT04.07.04

Effect of Metamaterial Engineering on The Superconductive Properties of Ultrathin Layers of NbTiN Michael S. Ososky¹, Vera Smolyaninova¹, Grace Yong¹, Will Korzi¹, Anne-Marie Valente-Feliciano², David Beverstock^{2,3}, Joseph Prestigiacomo⁴ and Igor Smolyaninov^{5,6}; ¹Towson University, United States; ²Thomas Jefferson National Accelerator Facility, United States; ³College William & Mary, United States; ⁴US Naval Research Laboratory, United States; ⁵University of Maryland, United States; ⁶Saltenna LLC, United States

The electronic transport and optical properties of high quality multilayers of NbTiN/AlN with ultrathin NbTiN layers were characterized. The anisotropy of the dielectric function of the multilayers confirmed their hyperbolic metamaterial properties. The superconductive transition temperature, T_c , of these engineered superconductors was enhanced up to 32% compared to the T_c of a single ultrathin NbTiN layer while the resistivity per NbTiN layer remained unchanged. We have demonstrated that this T_c increase can be attributed to enhanced electron-electron interaction in superconducting hyperbolic metamaterials. The measured critical fields are high and have anomalous temperature dependence in the perpendicular to the magnetic field direction. These results demonstrate that the metamaterial engineering approach can be used to enhance H_{c2} .

SESSION QT04.08: Novel Materials III—Topological Materials
Session Chairs: Genda Gu and Juntao Yao
Thursday Afternoon, April 25, 2024
Room 445, Level 4, Summit

1:30 PM *QT04.08.01

Experimental Signatures of Higher Order Topology Richard Deblock; Laboratoire de Physique des Solides, France

In second-order topological insulators (SOTIs), the bulk and surfaces are insulating, while the edges or hinges conduct current in a quasi-ideal (ballistic)

manner, insensitive to disorder. As in the case of quantum spin Hall edges of 2D topological insulators, the current should be transported without dissipation by counter-propagating ballistic helical states with spin orientation locked to momentum. These edge or hinge states open up many possibilities, ranging from dissipation-free charge and spin transport to new avenues for quantum computing. Bismuth, although a semi-metal, has been shown to belong to this class of materials. In our group, we have studied Josephson junctions based on crystalline Bi nanowires and found that they exhibit robust sawtooth current phase relations in a high magnetic field, which is the signature of one-dimensional ballistic edge states. We also demonstrated the topological nature of Andreev states through the dissipative microwave response in a phase-biased configuration. More recently, in a SQUID constructed from a bismuth ring, we have identified the parity relaxation rate by exploring the statistics of the switching current. In order to find different topological insulators with reduced contribution from bulk non-topological states, we are now exploring the quantum transport properties of WTe₂, which has been shown to exhibit a quantum spin Hall effect in the few-layer limit, and Bi₄Br₄. The latter material is a SOTI with a high bulk band gap.

2:00 PM QT04.08.02

Observation of a Resonant Andreev Plateau from Topologically Protected Hinge Modes [Wenyao Liu](#); Boston College, United States

A key challenge in topological systems is finding unique signatures of their boundary modes. This is especially true in topological superconductors where the bulk is gapped, but the superfluid can short-circuit transport signatures seen in quantum Hall states. A particularly promising candidate is Fe(Te,Se), which is predicted to host a 1D high-order topological superconducting (1D-HOTSC) state. This can emerge either from the bulk sign-changing order parameter or from the combination of intrinsic magnetism and topological superconductivity. Here, we present systematic tunneling experiments to test the existence of 1D-HOTSC mode. Initially, we observe an anomalous conductance plateau signal centered around zero bias when electrons tunnel along the hinges of our Fe(Te,Se) device in the topologically nontrivial phase. Remarkably, this anomalous conductance plateau disappears when the current source and ground are no longer connected by the same hinge, suggesting the nonlocal resonant Andreev processes originating from a propagating TSC hinge mode. To confirm this originates from nontrivial topology, we have tested devices with different Te/Se composition that possess similar superconducting transition temperatures without the bulk topological band inversion. As expected, such resonant conductance signal disappears in these samples. Additionally, the conductance plateau is robust to applied magnetic field and temperature, so long as the long-range magnetic order detected by Kerr rotation is maintained. Thus, our results are consistent with chiral TSC modes rather than trivial superconducting states.

2:15 PM QT04.08.03

Searching for Ideal Topological Superconductors in Pb-Sn-In-Te System [Genda Gu](#), Ruidan Zhong, John A. Schneeloch, Yangmu Li, Qiang Li and John M. Tranquada; BNL, United States

The discovery of 3D topological insulator materials and topological superconductor open up a new research field in the condensed matter physics. In order to search for the topological superconductor, we have grown a large number of the single crystals of Pb-system (Pb-Sn-In-Te) topological superconductor. We have measured the physical properties on these single crystals by various techniques. We have studied the effect of crystal growth condition, impurity and composition on the bulk electrical conductivity of these single crystals. We try to find out which composition and crystal growth condition is the best for the ideal topological superconductor. We have got the bulk topological superconductor with $T_c = 5\text{K}$.

2:30 PM QT04.08.04

Absence of Nematic Instability in The Kagome Metal CsV₃Sb₅ [Zhaoyu Liu](#)¹, Yue Shi¹, Qianni Jiang¹, Elliott M. Rosenberg¹, Jonathan DeStefano¹, Jinjin Liu², Chaowei Hu¹, Yuzhou Zhao¹, Zhiwei Wang², Yugui Yao², David Graf³, Pengcheng Dai⁴, Jihui Yang¹, Xiaodong Xu¹ and Jiun-Haw Chu¹; ¹University of Washington, United States; ²Beijing Institute of Technology, China; ³National High Magnetic Field Laboratory, United States; ⁴Rice University, United States

Ever since the discovery of the charge density wave (CDW) transition in the kagome metal CsV₃Sb₅, the nature of its symmetry breaking is under intense debate. While evidence suggests that the rotational symmetry is already broken at the CDW transition temperature (T_{CDW}), an additional electronic nematic instability well below T_{CDW} was reported based on the diverging elastoresistivity coefficient in the anisotropic channel (m_{E2g}). Verifying the existence of a nematic transition below T_{CDW} is not only critical for establishing the correct description of the CDW order parameter, but also important for understanding the low-temperature superconductivity. Here, we report elastoresistivity measurements of CsV₃Sb₅ using three different techniques probing both isotropic and anisotropic symmetry channels. Contrary to previous reports, we find the anisotropic elastoresistivity coefficient m_{E2g} is temperature-independent except for a step jump at T_{CDW} . The absence of nematic fluctuations is further substantiated by measurements of the elastocaloric effect, which show no enhancement associated with nematic susceptibility. On the other hand, the symmetric elastoresistivity coefficient m_{A1g} increases below T_{CDW} , reaching a peak value of 90 at $T = 20\text{ K}$. Our results strongly indicate that the phase transition at $T = 20\text{ K}$ is not nematic in nature and the previously reported diverging elastoresistivity is due to the contamination from the A_{1g} channel.

2:45 PM BREAK

SESSION QT04.09: Device—Josephson Junctions, SQUID
Session Chairs: Nathalie de Leon and Jeffrey McCallum
Thursday Afternoon, April 25, 2024
Room 445, Level 4, Summit

3:15 PM *QT04.09.01

New Material Platforms for Quantum Computing [Nathalie P. de Leon](#); Princeton University, United States

Constructing fault-tolerant quantum processors based on transmon qubits will require significant improvements in qubit relaxation and coherence times, which are orders of magnitude shorter than limits imposed by bulk properties of the constituent materials. However, significant improvements in the lifetime of planar transmon qubits have remained elusive for several years. We have fabricated planar transmon qubits that have both lifetimes and coherence times exceeding 0.3 milliseconds by using tantalum as the capacitor material. Following this discovery, we have parametrized the remaining

sources of loss in state-of-the-art devices using systematic measurements of the dependence of loss on temperature, power, and geometry. This parametrization, complemented by direct materials characterization, allows for rational, directed improvement of superconducting qubits.

3:45 PM QT04.09.02

Josephson Junctions and NanoSQUIDs Grown by Focused Electron and Ion Beam Induced Deposition [Jose M. De Teresa](#), Fabian Sigloch, Amaia Sáenz and Soraya Sangiao; CSIC, Spain

Focused Electron and Ion Beam Induced Deposition (FEBID and FIBID, respectively) are direct-write resist-free nanolithography techniques enabling the growth of high-resolution nano- and micro-structures. They rely on a gas precursor that is injected into the area of interest and decomposed by a focused electron or ion beam. Using the $W(CO)_6$ precursor and Ga^+ or He^+ FIBID [1], we grow superconducting in-plane nanowires with high lateral resolution [2], as well as three-dimensional superconducting nanostructures [3]. In this contribution, we will present recent results on the fabrication of Josephson junctions and nanoSQUIDs based on FIBID- and FEBID-grown W-C deposits. First, results of W-C nanoSQUIDs patterned as two large pads connected by two short nanowires will be shown. In these devices, the critical current oscillates as a function of the externally-applied magnetic field, which results in a large output voltage to magnetic flux change (1.3 mV per magnetic flux quantum) [4]. Interestingly, these nanoSQUIDs can be implemented on a cantilever for application in scanning-SQUID technology [5]. Other experiments in which Josephson Junctions (JJs) are created with alternative geometries and also with FEBID will be shown here. In summary, FEBID and FIBID represent techniques that can be exploited for the direct-write fabrication of superconducting devices for application in quantum technologies [6].

- [1] P. Orús, F. Sigloch, S. Sangiao, J.M. De Teresa, *Nanomaterials* 12 (2022) 1367
- [2] P. Orús, R. Córdoba, G. Hlawacek, J.M. De Teresa, *Nanotechnology* 32 (2021) 085301
- [3] R. Córdoba et al., *Nano Letters* 19 (2019) 8597
- [4] F. Sigloch, P. Orús, S. Sangiao, J.M. De Teresa, *Nanoscale Advances* 4 (2022) 4628
- [5] M. Wyss et al., *Phys. Rev. Appl.* 17 (2022) 034002
- [6] J. M. De Teresa, *Materials in Quantum Technology* 3 (2023) 013001

4:00 PM QT04.09.03

Josephson Diode Effect in Chiral Carbon Nanotubes [Joseph J. Cuzzo](#)¹, Michael Sizemore², Francois Leonard¹ and Enrico Rossi²; ¹Sandia National Laboratories, United States; ²William & Mary, United States

Within superconducting electronics, the Josephson diode effect (JDE) has attracted interest in recent years. Josephson diodes are characterized by an asymmetry in positive and negative switching currents of a Josephson junction (JJ) and could potentially find utility in a growing number of applications at cryogenic temperatures in the Quantum Information Sciences. Despite extensive theoretical and experimental work investigating the JDE, little attention has been paid to nanotube devices where non-reciprocity can be introduced in chiral structures. In this talk, we will present analytic and numerical results on the JDE in chiral carbon nanotubes (CNT). We find that chiral nanotubes in JJs can exhibit diode efficiencies far exceeding those of superconducting chiral nanotubes when an external magnetic field is applied along the nanotube. Furthermore, our numerical simulations show the Josephson diode *polarity* can be tuned by electrostatically gating CNTs in a Josephson junction. We will discuss the microscopic details that give rise to large diode efficiencies and gate-tunability in chiral CNT JJs.

This work was supported by the U.S. Department of Energy (DOE), Office of Science, Basic Energy Sciences (BES), under Award DE-SC0022245. The work at Sandia is supported by a LDRD project. SNL is managed and operated by NTESS under DOE NNSA contract DE-NA0003525.

4:15 PM QT04.09.04

Fabrication of Superconducting Devices on Diamond [Manjith Bose](#)^{1,2} and Christopher I. Pakes²; ¹The University of Melbourne, Australia; ²La Trobe University, Australia

Recent advancements in Chemical Vapour Deposition (CVD) based synthetic diamond growth have opened new avenues for the development of electronic devices capitalising on diamond's exceptional properties, including its high critical field (H_C) and transition temperature (T_C). Achieving superconductivity in lab-grown diamond with high boron concentrations is well-documented in bulk diamond, but limited research focuses on superconducting devices in diamond. The focus of this study was on developing innovative methodologies to engineer micro and nano-scale superconducting diamond devices using thin films of boron-doped nanocrystalline diamond (BNCD) and single crystalline diamond (BSCD). We employ electron beam lithography (EBL) and reactive ion etching (RIE) to engineer highly overdamped and non-hysteretic sub-micron bridges with varying dimensions on superconducting diamond films and low temperature magnetotransport measurements were conducted. A novel fabrication methodology involving neon-ion milling was developed to further define Dayem bridge junctions that demonstrated Josephson effects. The first NCD diamond nano-SQUID was created using these nanobridges as weak links, with a 50 nm loop size.

The nano-SQUID showed a very low flux noise $\Phi_{noise} = 0.14 \mu\Phi_0/\sqrt{Hz}$ at 1 kHz, and concurrent spin sensitivity of 11 spins/ \sqrt{Hz} , comparable to that of the lowest noise nano-SQUIDs reported so far in established materials such as niobium. The successful fabrication methodologies on BNCD films were further translated to locally grown BSCD films and superconducting bridges were demonstrated for the first time. In this presentation, we will discuss our results on BNCD nano-SQUIDs and outline our current efforts in developing devices on BSCD films and their corresponding transport measurement results.

4:30 PM QT04.09.05

Towards Atomic Precision in Superconducting Qubits: Mechanisms of Ta Oxidation and Strategies for Oxidation Suppression [Peter V. Sushko](#)^{1,2}, Chenyu Zhou³, Junsik Mun³, Mohammad D. Hossain¹, Jeffrey Dhas¹, Ekta Bhatia², Satyavolu Papa Rao², Yingge Du¹, Yimei Zhu³ and Mingzhao Liu³; ¹Pacific Northwest National Laboratory, United States; ²NY Creates, United States; ³Brookhaven National Laboratory, United States

Coherence times of transmon devices can be affected by oxidation of the components made of superconducting metals, such as Nb and Ta. Spontaneous oxidation results in the formation of suboxide phases and surface amorphization that contribute to dielectric losses that are primarily attributed to two-level systems within such native oxide layers. Mitigating undesirable effects of surface oxidation requires understanding the mechanisms of interfacial interactions at the atomic scale.

We review recent experimental studies that provide new insights into the atomic structure and composition of the native oxide layer and focus on ab initio simulations of the mechanisms of Ta interaction with oxygen. In particular, we consider energetics and pathways of the early stages of the Ta(110) surface oxidation, including propagation of the oxidation front into the Ta subsurface and corresponding electronic structure changes. We also explore strategies for suppressing Ta oxidation with the help of reactive metal coating and discuss atomic-scale models of candidate two-level systems.

C. Zhou, J. Mun, J. Yao, A. K. Anbalagan, M. D. Hossain, R. A. McLellan, R. Li, K. Kisslinger, X. Tong, G. Li, A. R. Head, C. Weiland, A. L. Walter, Q.

Li, Y. Zhu, P. V. Sushko, M. Liu *Ultrathin Magnesium-based Coating as an Efficient Oxygen Barrier for Superconducting Circuit Materials*, arXiv preprint arXiv:2309.12603

4:45 PM QT04.09.06

Superconductivity in Nanowire Devices Formed by Al-Si Exchange Jeffrey C. McCallum¹, Brett Johnson², Manjith Bose¹, Michael Stuiber³, Daniel Creedon⁴, Sergey Rubanov⁵, Vincent Mourik⁶, Jared Cole² and Alex Hamilton⁷; ¹The University of Melbourne, Australia; ²RMIT University, Australia; ³Melbourne Centre for Nanofabrication, Australia; ⁴CSIRO Manufacturing, Australia; ⁵University of Melbourne, Australia; ⁶Julich Research Institute, Germany; ⁷University of New South Wales, Australia

Development of devices that contain both superconducting and semiconducting components on a single chip is an important area of investigation for emerging quantum technologies. We have investigated superconductivity in nanowire devices fabricated using the Al-Si exchange process in silicon-on-insulator wafers. Aluminum from deposited contact electrodes undergoes an Al-Si exchange process with prepatterned Si nanowire device structures along the entire length of the nanowire, over micrometer length scales and at temperatures well below the Al-Si eutectic. The phase-transformed material is conformal with the predefined device patterns. In magneto-transport measurements, nanoring structures formed by this fabrication process exhibit periodic features in the differential resistance and in the critical current that result from fluxoid quantization. The retrapping current also exhibits oscillations. The devices can be operated in temperature/magnetic-field regimes where some components of the device are in the superconducting state while others are in a resistive state. Under these conditions the magneto-transport data exhibit more complex features which may provide insight into how these mixed-state devices could be further developed for uses in magnetometry and other quantum technologies. The details of the Al-Si exchange process also suggest that it could allow a range of new nanoscale superconducting-semiconducting device structures to be formed. In this presentation, our exploration of these superconducting nanowire devices and their promise for quantum technologies development will be discussed.

SESSION QT04.10: On-Demand Presentation
Tuesday Morning, May 7, 2024
QT04-virtual

10:30 AM QT04.10.01

Uniformity of Orientation Degrees in Dy123 Superconductor through Linear Drive-Type Modulating Rotating Magnetic Field Walid B. Ali, Shintaro Adachi, Fumiko Kimura and Shigeru Horii; Kyoto University of Advanced Science, Japan

The rare earth-based cuprate superconductor REBa₂Cu₃O_y (RE123) has garnered significant attention due to its high critical temperature (T_c) of approximately 90 K, making it suitable for various applications like liquid nitrogen-operated superconducting bulk magnets and cables. This material features an anisotropic crystal structure, comprising alternating 2D superconducting CuO₂ layers and 1D Cu-O chains. This anisotropy results in varying critical current densities (J_c) in different directions, with J_c/c being lower than J_c/ab [1]. To enhance the practical use of RE123, it's crucial to achieve biaxial or triaxial orientation and densification of its grains. One non-epitaxial method for grain orientation enhancement is magnetic alignment. Magnetic alignment doesn't require a vacuum process and can be done at room temperature. It involves the generation of a modulated rotating magnetic field (MRF) with two or more axes. In this context, permanent magnets (PMs) have proven to be a cost-effective solution for creating a low-cost MRF and aligning RE123 grains.

A continuous production technique known as linear drive-type modulated rotating magnetic field (LDT-MRF) employs a PM array to achieve triaxial grain alignment [2]. This equipment can generate an MRF of ~ 0.8 T without physically moving the sample [3]. Using this approach, DyBa₂Cu₃O_y (Dy123) grains were successfully biaxially aligned, as evidenced by a four-fold symmetric (103) pole figure at $\Psi \sim 45^\circ$, similar to results achieved with a 10 T-MRF from a superconducting solenoidal magnet [4]. In prior work [3], we noticed location-dependent orientation degrees in the biaxially aligned sample. The center part displayed higher in-plane and c -axis orientation degrees of around 8.5° and 6.0° , respectively. The side portions also exhibited higher orientation degrees but with a shift of the four-fold symmetric spots toward the right and leftward of the (103) pole figures. To understand this shift in diffraction spots, 3D simulations using the Finite Element Method (FEM) software were conducted to analyze the behavior of flux lines in the air gap between the magnet arrays. The simulation revealed that the flux lines inclined toward the outside of the magnet array along the Y -axis (the width of the magnet array), causing a $\theta \sim 6^\circ$ shift in diffraction spots from the center. This indicated non-uniformity in the MRF at the side parts of the magnet array, resulting in flux line leakage outside the array.

To address this non-uniformity, we designed a new magnet array with an increased width along the Y -axis, expanding it from 20 mm to 48 mm. The 3D simulation of this new design showed that the inclination angle remained under $\sim 5^\circ$ up to $Y = 16.5$ mm from the center, ensuring high orientation degrees. Biaxial alignment experiments with Dy123 powders in the newly designed magnet array consistently displayed four-fold diffraction spots at $\Psi \sim 45^\circ$, extending from the center to $Y = 10.5$ mm, with a slight 3° shift at $Y = 14$ and 16.5 mm. Importantly, the experimental results quantitatively matched the simulation results, demonstrating a homogeneous MRF within the range of $0 \leq Y \leq 16.5$ mm in the newly designed magnet array, resulting in an in-plane orientation degree of $\sim 8.4^\circ$. This research suggests that LDT equipment, in combination with improved magnet array designs, has the potential to advance RE123 superconducting tape production. However, challenges in material production and equipment limitations still need to be addressed. The presentation will feature 3D simulation results for the previous and newly designed magnet arrays, along with an explanation of how increasing the magnet array's width helped overcome location-dependent orientation degree issues.

Reference:

[1] Iye et al., Jpn. J. Appl. Phys. 26, (1987). [2] Horii et al., J. Ceram. Soc. Jpn. 126, (2018). [3] W. B. Ali et al., J. Appl. Phys. 134, (2023) (to be published) [4] Horii et al., Supercond. Sci. Technol. 29, (2016).

SYMPOSIUM QT05

Advances in Detection Methods for Emergent Phases in Quantum Materials
April 23 - May 8, 2024

Symposium Organizers

Jessica Boland, University of Manchester
Shelly Michele Conroy, Imperial College London
Ismail El Baggari, Harvard University
Juan Carlos Idrobo, University of Washington

* Invited Paper
+ JMR Distinguished Invited Speaker
^ MRS Communications Early Career Distinguished Presenter

SESSION QT05.01 Advances in Detection Methods for Emergent Phases in Quantum Materials I
Session Chairs: Shelly Michele Conroy and Yang Zhang
Tuesday Afternoon, April 23, 2024
Room 446, Level 4, Summit

1:30 PM *QT05.01.01

'Seeing' Physical Properties of 2D Materials on Nanoscale [Olga Kazakova](#)^{1,2}; ¹National Physical Laboratory, United Kingdom; ²The University of Manchester, United Kingdom

We present a unique opportunity of 'seeing' physical (and chemical) properties of 2D materials and heterostructures on (sub)nanoscale. Using a combination of advanced functional scanning probe microscopy (SPM) techniques, we perform a detailed local study of electrical, electronic, optoelectronic, and thermal properties. These studies are complemented by development of scanning gate microscopy techniques, where the gate can be a local source of electric/magnetic field, heat or near-field. We thus combine functional imaging with an active control and manipulation of the device properties. We demonstrate that advanced functional SPM techniques are a very powerful tool to obtain detailed information on the unique sample properties (such as the effect of non-uniformity, defects, degree of molecular absorption, etc.), which are not assessable by more traditional methods. We also demonstrate the accuracy of the measurements, which allows us to eliminate the common artefacts, which are not usually taken into account in many other approaches. The present work facilitates development of realistic 2D materials devices and their faster and reliable implementation. We also aim to showcase the measurement capability associated with the quantum material nanoprobe facilities for the research and applications of materials for quantum technologies, at scales ranging from several micrometers down to individual atoms.

1. V. Panchal, et al., *Scientific Reports* **3**, 2597 (2013)
2. M. Munz, et al., *ACS Nano* **9**, 8401 (2015)
3. C. E. Giusca, et al. *ACS Nano* **10**, 7840 (2016)
4. Ch. Melios, et al., *2D Materials*, Topical Review **5**, 022001 (2018)
5. T. Vincent, et al., *2D Materials* **6**, 015022 (2019)
6. S. Ulstrup, et al., *Nature Communication* **10**, 3283 (2019)
7. Ch. Melios, et al. *Sci Reports* **10**, 3223 (2020)
8. D. Buckley, et al., *Advanced Functional Materials* **31**, 2008967 (2020)
9. T. Vincent, et al., *Applied Physics Reviews* **8**, 041320 (2021)
10. A. Weston, et al., *Nature Nanotechnology* **17**, 390 (2022)

2:00 PM *QT05.01.02

The Interplay of Topology and Symmetry in Non-Symmorphic Square-Net Tellurides Probed by Scanning Tunnelling Microscopy [Sarah Burke](#); University of British Columbia, Canada

The non-symmorphic square-net materials have been of interest due to their symmetry enforced band crossings giving rise to Dirac nodal loops and both topologically trivial and non-trivial surface states. Crystals of the P4/nmm space group feature a plane of atoms in a square net (e.g. the Si plane in the ZrSiX family or Sn plane in RESnX family) with a 2-atom unit cell due to the surrounding lattice. This doubling of the square net unit cell, along with glide plane symmetry enforces a degeneracy at the edge of the Brillouin zone driving a crossing of different orbital symmetry that prevent hybridization. These features give rise to wide-bandwidth linear crossings which revolve around the Brillouin zone enclosing regions of distinct topology.

I will describe our recent work on two of these materials: ZrSiTe which exhibits a topologically non-trivial surface state, and LaSbTe which has a doping-dependent structural distortion that gaps portions of the nodal loop. Using Scanning Tunnelling Microscopy and Spectroscopy (STM/STS), we have investigated the surface structure and electronic states through quasiparticle interference (QPI) measurements. In ZrSiTe, the large area between two nodal loops hosts a topologically non-trivial "drumhead" surface state, previously observed up to E_f by ARPES¹. However, the presence of spin-orbit coupling in this system gaps the nodal lines, raising the question of what happens to the drumhead state. Using QPI we observed strong signatures of the drumhead state below and above E_f confirming this topologically protected state persists, owing to the small energy scale of spin-orbit coupling relative to the large band width of the nodal lines². We find that the drumhead state disperses over an energy range of ~ 600 meV and is split, but not gapped by the presence of spin-orbit coupling.

Unlike the mild perturbation of spin-orbit coupling, changes in symmetry (perhaps obviously) break the symmetry-enforced protection of the nodal-lines giving the potential for much larger gap openings. While Si square net is held together by strong interaction with Zr, the square nets with rare-earths off plane are prone to distortion from the heavily nested Fermi surface. Indeed, stoichiometric LaSbTe forms in an orthorhombic phase featuring a buckled square-net with zig-zag chains, with a gap opening in the nodal-lines in Γ -S direction. Here we have investigated the surface structure and electronic states

of twinned *o*-LaSbTe. The zig-zag rows of the Sb lattice can be seen in STM images, and a soft-gap of ~300meV can be observed consistent with DFT calculations for the distorted structure. Twin-boundaries show the two perpendicular orientations with domain “walls” several unit cells wide that appear tetragonal. Highly directional QPI is seen around Sb-lattice defect sites and is consistent with scattering from the remaining pockets of the nodal loops appearing in the tetragonal phase. I will also discuss the potential for doping to traverse this phase diagram and topological implications of these structural changes.

1 L. Muechler, et al. PRX 10, 011026 (2020)

2 B. Stuart, et al. PRB 105, L121111 (2022)

2:30 PM BREAK

3:00 PM *QT05.01.03

Multiscale Characterization of Quantum Materials [Donald M. Evans](#); University of Warwick, United Kingdom

Quantum materials, defined by their unique electronic properties, are central to current scientific and technological research. Their distinct conductivity and complex phase behaviour present an intriguing puzzle with both opportunities and challenges. Central to this exploration is the interplay between microstructures, compositional changes, and the resulting electronic properties. Adopting a multiscale approach provides essential insights into the impacts of these atomic-scale changes on the material's functional properties. In this presentation, we utilize the topological superconductor Fe(Se,Te) to showcase the importance of applying advanced multiscale characterization techniques. Initial bulk characterization confirmed the quality of our material system, indicating high-quality homogeneous single crystals. However, local real-space mapping of the enhanced conductivity of the superconducting phase, via low temperature conductive atomic force microscopy (cAFM), revealed unexpected spatial inhomogeneities. Specifically, across five orders of real space imaging, we see that the majority of the crystal is relatively insulating, with only localized regions of heightened conductivity. To confirm and substantiate these observations, we use atom probe tomography (APT) and energy dispersive x-rays (EDX) to discern that the different regions have distinct chemical compositions. This highlights the vital role of multiscale characterization in quantum materials, illustrating their true complexities that may elude classical characterization techniques. Such approaches are essential for refining our methods and advancing quantum material research.

3:30 PM QT05.01.04

Revealing Emergent Magnetic Charge in an Antiferromagnet with Diamond Quantum Magnetometry Anthony Tan¹, [Hariom Jani](#)^{2,3}, Michael Hogen¹, Lucio Stefan¹, Claudio Castelnuovo¹, Daniel Braund¹, Alexandra Geim¹, Annika Mechnich¹, Matthew Feuer¹, Helena Knowles¹, Ariando Ariando³, Paolo Radaelli² and Mete Atature¹; ¹University of Cambridge, United Kingdom; ²University of Oxford, United Kingdom; ³National University of Singapore, Singapore

Whirling topological textures play a key role in exotic phases of magnetic materials and offer promise for logic and memory applications. In antiferromagnets, these textures exhibit enhanced stability and faster dynamics with respect to ferromagnetic counterparts, but they are also difficult to study due to their vanishing net magnetic moment [1]. One technique that meets the demand of highly sensitive vectorial magnetic field sensing with negligible backaction is diamond quantum magnetometry. Here, we show that the archetypal antiferromagnet, hematite, hosts a rich tapestry of monopolar, dipolar and quadrupolar emergent magnetic charge distributions [2]. The direct readout of the previously inaccessible vorticity of an antiferromagnetic spin texture [1] provides the crucial connection to its magnetic charge through a duality relation. Our work defines a novel paradigmatic class of magnetic systems to explore two-dimensional monopolar physics, and highlights the transformative role that diamond quantum magnetometry could play in exploring emergent phenomena in quantum materials.

References:

[1] [H Jani](#) et al., Nature 590, 74 (2021).

[2] AKC Tan*, [H Jani](#)* et al., arXiv:2303.12125 (2023) [In Press - Nature Materials].

3:45 PM *QT05.01.05

Exploiting The Coherence of Synchrotron X-Rays to Study The Dynamics of Quantum Matter [Sophie Morley](#); Lawrence Berkeley National Laboratory, United States

A challenging aspect of designing functional materials is to understand the impact of a wide range of characteristic spatial and temporal scales on stabilizing novel quantum phases. Commonly used mean field approaches often provide reasonable estimates for static properties at macroscopic length scales, however, it does not provide the requisite fundamental insight into the important processes governing deviations from these averages. Such fluctuations are critically important. Soft x-rays are a powerful element-specific probe to study such mesoscopic charge and spin textures. The coherence available at current and newly upgraded light sources will enhance our tools to give significantly more detailed information of otherwise difficult to probe quantum states. We select the coherent part of the x-ray beam to produce an interference pattern known as speckle. Here I will discuss how we use that speckle to look inside, and better understand, the transitions of orbital order, amorphous noncollinear magnets and metal-to-insulator materials.

4:15 PM QT05.01.06

Optimisation of CVD Diamond for Applications in Room-Temperature Masers [Daan M Arroo](#), Wern Ng, Yongqiang Wen, Philip Diggle and Neil McN. Alford; Imperial College London, United Kingdom

Masers are the microwave analogue of lasers and can be operated as oscillators and amplifiers with quantum-limited noise performance. Despite their exceptionally low noise, conventional masers have historically been limited to niche applications in radio astronomy and deep-space communications due to their requirement for ultrahigh vacuums and cryogenic temperatures.

Recently masers capable of operating continuously at room temperature have been demonstrated using ensembles of nitrogen-vacancy (NV) centres in diamond, opening a route to the widespread use of masers across a range of new applications in telecommunications, medical imaging and quantum sensing.

In order to realise these broad applications it will be necessary to build miniaturised, portable diamond masers that can be readily integrated into existing standards but to date this has been limited by the highly homogeneous magnetic fields required for diamond masers to maintain coherence. Here we discuss strategies for relaxing the field-homogeneity requirement by optimising the material parameters of CVD-grown NV-diamond and present results benchmarking the performance of diamond masers using diamond gain media in which the concentrations of ¹³C nuclei and nitrogen-vacancy spins are varied. We conclude by discussing recent progress in the development of miniaturised diamond masers.

4:30 PM *QT05.01.07

A Quantum Coherent Spin in a Two-Dimensional Material at Room Temperature [Hannah Stern](#)¹, Carmem M. Gilardoni², Qiushi Gu², Simone E. Barker², Oliver F. Powell^{2,3}, Xiaoxi Deng², Stephanie A. Fraser², Louis Follet², Chi Li^{4,4}, Andrew Ramsay³, Hark Hoe Tan⁵, Igor Aharonovich⁴ and Mete Atature²; ¹The University of Manchester, United Kingdom; ²University of Cambridge, United Kingdom; ³Hitachi Cambridge Laboratory, Hitachi Europe Ltd, United Kingdom; ⁴University of Technology Sydney, Australia; ⁵The Australian National University, Australia

Quantum networks and sensing require solid-state spin-photon interfaces that combine single photon generation and long-lived spin coherence with scalable device integration, ideally at ambient conditions. Despite rapid progress reported across several candidate systems, those possessing quantum coherent single spins at room temperature remain extremely rare. In this talk, I will show new results of quantum coherent control under ambient conditions of a single-photon emitting defect spin in a two-dimensional material, hexagonal boron nitride. I show that the carbon-related defect has a spin-triplet electronic ground-state manifold and that the spin coherence is governed predominantly by coupling to only a few proximal nuclei and is prolonged by decoupling protocols. These results allow for a room-temperature spin qubit coupled to a multi-qubit quantum register or quantum sensor with nanoscale sample proximity.

SESSION QT05.02 Advances in Detection Methods for Emergent Phases in Quantum Materials II

Session Chairs: Shelly Michele Conroy and Jessica Wade

Wednesday Morning, April 24, 2024

Room 446, Level 4, Summit

8:30 AM *QT05.02.01

Nanoscale Advanced Materials Engineering for Quantum Technologies Ravi Acharya^{1,2}, Maddison Coke¹, Mason Adshead¹, Kexue Li¹, Barat Achniuq³, Rongsheng Cai³, Baset Gholizadeh¹, Janet Jacobs¹, Jessica L. Boland¹, Sarah J. Haigh³, Katie Moore¹, David Jamieson² and [Richard J. Curry](#)¹; ¹Photon Science Institute, United Kingdom; ²The University of Melbourne, Australia; ³The University of Manchester, United Kingdom

The ability to engineer the electrical, optical and magnetic properties of advanced materials on the nanoscale is of increasing importance to the development of future quantum technologies. One approach to achieving this is through impurity doping, with increased control over the spatial resolution and isotopic purity enabled by the development of dedicated tools. To achieve this goal a new capability (the 'Platform for Nanoscale Advanced Materials Engineering, P-NAME', Facility) has been developed and applied specifically to the engineering of materials for quantum technology. We demonstrate how the combined utilisation of novel ion source and mass selection technology enables the direct-write creation of bespoke materials utilising ultra-high ion doses (>1E19 ions/cm²) down to single-ion doping. The validation of such capability requires the utilisation of advanced detection and characterisation techniques. We draw upon the combined use of electrical, photonic, mass spectroscopy and electron microscopy methods in order to enable this. Together this allows us to demonstrate the delivery of ultra-enriched ²⁸Si as a platform for quantum technology device fabrication, and also for the doping of single-ion impurity centres within solid-state systems. Of particular interest is the development of methods to reliably detect single-ion doping events. This is a key enabling step to overcome the inherent limitation that is otherwise imposed by Poissonian statistics. Progress within this area remains a key challenge if scaling to deliver qubit arrays of the order of 10⁶ is to be achieved in order to deliver full error corrected quantum computation.

9:00 AM *QT05.02.02

Magnetotransport for Dirac Semimetal Phase of Topological Insulator Sb₂Te₃ [Satoshi Sasaki](#) and Joshua T. Gretton; University of Leeds, United Kingdom

Antimony Telluride (Sb₂Te₃) makes up the second generation of Topological Insulator (TI) materials with other layered chalcogenides Bi₂Se₃ and Bi₂Te₃. The TI phase in these materials arises from a spin-orbit induced band crossing of opposite parity orbitals at the Γ point of the Brillouin Zone, resulting in a single topologically protected Dirac cone projected to all surfaces.¹ Another set of surface states have been identified in Sb₂Te₃: intrinsic Rashba spin-orbit split surface bands extending from 300 to 750 meV below the valence band edge exist within a partial valence band gap.²⁻⁵ Also, a strong linear character to the bulk valence band dispersion has been established in Angle Resolved Photo-Emission Spectroscopy (ARPES) experiments,⁴ where accidental band crossing points^{2,3,6,7} imply a Dirac energy spectrum and so Dirac semimetal phase.^{8,9} Sb₂Te₃ is usually heavily hole doped due to a combination of Te vacancies and Sb_{Te} anti-site defects,^{10,11} with $p \sim 10^{20} \text{ cm}^{-3}$ the typical carrier density for nominally stoichiometric samples.^{12,13} The intrinsic doping effects in this material class are typically difficult to overcome, however they should also place the chemical potential close to the Dirac-like spectrum of bulk bands,^{2,3,12} meaning these could contribute to the transport without significant tuning of the carrier density.

So far no studies of the electronic transport looking for indications of these states has been carried out. To better understand the material system and probe for these contributions, Sb₂Te₃ single crystals have been grown using a modified Bridgman method with excess Te in the melt, and the magnetotransport of (001) oriented single crystal Sb₂Te₃ with p-type carrier densities in the range $2.4 - 12 \times 10^{19} \text{ cm}^{-3}$ is studied up to 8 T. It is found that the semiclassical magnetotransport is described by a two-carrier band model, finding contributions from majority hole and minority electron bands, and clear Shubnikov de Haas Oscillations (SdHO) are resolved at 1.5 K across the carrier density range. The convolution of different frequency SdHO cause novel beating envelopes for samples with reduced carrier densities and non-trivial Berry phases are extracted for carrier densities in the range $4.1 - 7.9 \times 10^{19} \text{ cm}^{-3}$. Detailed consideration of the SdHO points away from either the Rashba or Dirac surface bands causing these, and instead the region of multiple pockets of linearly dispersive Dirac-like bulk band crossing points in the upper valence band is found responsible. This work therefore confirms a bulk Dirac semimetal phase in the well-known TI Sb₂Te₃.

References:

- 1 H. Zhang et al., Nat. Phys. **5**, 438 (2009).
- 2 L. Plucinski et al., J. Appl. Phys. **113**, 053706 (2013).
- 3 C. Pauly et al., Phys. Rev. B **86**, 235106 (2012).
- 4 C. Seibel et al., Phys. Rev. Lett. **114**, 066802 (2015).
- 5 C. Seibel et al., J. Electron. Spectros. Relat. Phenomena **201**, 110 (2015).
- 6 N. Shukla and G. A. Ahmed, Materials Today: Proceedings **45**, 4819 (2021).
- 7 S. K. Verma et al., IEEE Transactions on Electron Devices **69**, 4342 (2022).
- 8 N. Armitage, E. Mele, and A. Vishwanath, Rev. Mod. Phys. **90**, 015001 (2018).
- 9 S. Li et al., Front. Phys. **15**, 43201 (2020).
- 10 R. J. Cava et al., J. Mater. Chem. C **1**, 3176 (2013).

- 11 C. Drasar, P. Lostak, and C. Uher, *J. Electron. Mater.* **39**, 2162 (2010).
12 A. von Middendorff, K. Dietrich, and G. Landwehr, *Solid State Commun.* **13**, 443 (1973).
13 V. Kulbachinskii et al., *J. Phys.: Condens. Matter* **11**, 5273 (1999).

9:30 AM BREAK

10:00 AM *QT05.02.03

Intrinsic Magnetism in Infinite-Layer Nickelate Superconductors [Jennifer Fowlie](#); Stanford University, United States

Nickel and copper are nominally similar so the search for superconductivity in nickelates is a story as old as the quest to understand the high temperature superconductivity of the cuprates.

In this talk, I will introduce the recent discovery of superconductivity in infinite-layer nickelates [1] and the ever-growing family of nickelate superconductors. I will touch on some of the materials challenges involved before summarizing the key physics we have learned so far. In particular I will focus on results from low-energy muon spin rotation [2] that reveals local magnetism in these materials that 1) onsets at rather high temperature, 2) is independent of the rare earth 4f electrons, 3) appears to be robust to doping 4) is antiferromagnetic and possibly short-range-ordered in nature and 5) coexists with superconductivity at low temperatures.

Finally, I will come back to the comparison between nickelates and cuprates and discuss how the disparities in the magnetic properties may be understood.

[1] D. Li et al, *Nature* 572 (2019) 624

[2] J. Fowlie et al, *Nature Physics* 18 (2022) 1043

10:30 AM *QT05.02.04

Microstructural Effects of Topotactic Reduction in Nickelate Single Crystals [Y. Eren Suyolcu](#), Yu-Mi Wu, Pascal Puphal, Hangoo Lee, Masahiko Isobe, Bernhard Keimer, Matthias Hepting and Peter A. van Aken; Max Planck Institute for Solid State Research, Germany

Rare-earth nickel oxides, known for their intricate interplay between structure and properties, serve as a pivotal foundation for the exploration of novel quantum phases and advanced applications. Recent topotactic transformations of perovskite nickelates have enabled precise control over oxygen vacancies, thereby harnessing the consequential coupling effects in these materials. Gaining in-depth insights into the atomic-scale lattice and electrical structure during topotactic reduction is imperative for unraveling the potential of these phenomena. In this study, we employ atomic-resolution scanning transmission electron microscopy (STEM) imaging and electron energy-loss spectroscopy (EELS) to examine two distinct nickelate single crystal variants, namely $R_{1-x}Ca_xNiO_{3-\delta}$ (where R represents either La or Pr). These single crystals are synthesized through topotactic reduction of the perovskite phase, employing CaH_2 as a reducing agent. The presentation will provide a comprehensive analysis of the oxygen vacancies, hole doping into the material, and the influence of cation structure.

We primarily focus on $Pr_{1-x}Ca_xNiO_{3-\delta}$ single crystals, revealing an oxygen-deficient phase with $\delta \sim 0.25$ occurring during topotactic reduction. A novel arrangement of oxygen vacancies within the brownmillerite structure, diverging from previously observed reduced rare-earth nickelates. Precise quantification of polyhedral tilting and bond angles shows that a significant amount of internal strain drives wave-like variations in polyhedral tilting and rotations to accommodate the local lattice structure [1]. Subsequently, we studied $La_{1-x}Ca_xNiO_{3-\delta}$ single crystals subjected to topotactic reduction, resulting in the formation of an infinite-layer phase with a composition of $\delta \sim 1$ [2]. Additionally, we unraveled the microstructural effects of topotactic reduction on the undoped $LaNiO_2$ single crystals [3]. Our attention is devoted to a precise examination of the detailed lattice and chemical structures of these crystals, where our measurements of Ni–O bonding conditions and electronic structures affirm the existence of the infinite-layer structure following the reduction process. The removal of apical oxygen atoms forming NiO_2 planes within the infinite-layer phase results in metallic behavior reminiscent of weakly doped thin films. These discoveries establish a critical connection between the observable characteristics of nickelates and their underlying microscopic origins, paving the way for further exploration of nickelates with distinct crystal structures achievable only through topotactic reduction. [4]

References:

- [1] Yu-Mi Wu *et al.*, "Topotactically induced oxygen vacancy order in nickelate single crystals" *Physical Review Materials* **7**, 053609 (2023).
[2] Pascal Puphal *et al.*, "Topotactic transformation of single crystals: From perovskite to infinite-layer nickelates." *Science Advances* **7**, eabl8091 (2021).
[3] Yu-Mi Wu *et al.*, *unpublished*.
[4] This project has received funding from the European Union's Horizon 2020 research and innovation programme under grant agreement No. 823717 – ESTEEM3.

11:00 AM QT05.02.05

Visualizing Thermal Vibrations and Phonon Mode Softening in Real Space [Harikrishnan K. P.](#)¹, Yilin Li¹, Yu-Tsun Shao^{2,1}, Christo Gugushev³, Sang-Wook Cheong⁴, Darrell G. Schlom^{1,3} and David Muller¹; ¹Cornell University, United States; ²University of Southern California, United States; ³Leibniz-Institut für Kristallzüchtung, Germany; ⁴Rutgers, The State University of New Jersey, United States

Lattice vibrations lie at the very heart of exotic phases in quantum materials, either directly as in the case of phonon mode softening that drives the polarization in ferroelectrics or indirectly as in the phonon mediated interaction that creates Cooper pairs in superconductors. Typical methods for characterizing phonons like infrared or Raman spectroscopy and neutron scattering provide only spatially averaged measurements. Although vibrational electron energy loss spectroscopy offers high spatial resolution, the measurements often require detailed theoretical models for interpretation. Here, we demonstrate the capability of electron ptychography^{1,2} as a novel detection tool to directly visualize lattice vibrations in real space.

We illustrate the capability of the technique to directly visualize the thermal ellipsoid of metal atoms that are intercalated in the van-der Waals gap of layered materials. The in-plane vibrational modes of the intercalants have a larger amplitude in comparison to the quenched out-of-plane mode³ and is reflected in the anisotropic thermal blur of the intercalant columns. We also show how ptychography enables us to study lattice distortions associated with a spatially localized phonon mode that is on the verge of softening in barium hexaferrite, a candidate material for quantum paraelectricity and room temperature multiferroicity⁴. By analysing the potential landscape associated with this near-soft phonon mode in three dimensions, we detect the presence of nanometer-scale polar regions⁵ from short-range ordering in the material.

References

- ¹. Y. Jiang *et al.*, *Nature* 559, 343–349 (2018)
². Z. Chen *et al.*, *Science* 372, 826–831 (2021)
³. S. Fan *et al.*, *Nano Lett.* 21, 1, 99–106 (2021)
⁴. P. S. Wang and H. J. Xiang, *Phys. Rev. X* 4, 011035 (2014)
⁵. H. K. P. *et al.*, *Microscopy and Microanalysis*, 28(S1), 476–478 (2022)

11:15 AM QT05.02.06

Characterizing Coupled Order Parameters Across Successive Phase Transitions at Atomic Resolution in SmBaMn₂O₆ Noah Schnitzer¹, Yorick Birkholzer¹, Anna S. Park¹, Evan Krysko¹, Jacob Steele¹, Shigeki Yamada², Taka-hisa Arima³, Ismail El Baggari⁴, Berit Goodge⁵, Darrell G. Schlom^{1,6}, David Muller^{1,1} and Lena Kourkoutis^{1,1}; ¹Cornell University, United States; ²Yokohama City University, Japan; ³The University of Tokyo, Japan; ⁴Rowland Institute at Harvard, United States; ⁵Max-Planck Institute for Chemical Physics of Solids, Germany; ⁶Leibniz-Institut für Kristallzüchtung, Germany

Rich phase diagrams and highly tunable ground states arising from strong coupling between electronic, magnetic, and lattice degrees of freedom make complex oxides an ideal playground for exploring connections between material structure and exotic strongly correlated properties. The A-site ordered double-perovskite manganite SmBaMn₂O₆ is a paradigmatic example: a complex set of structural distortions host a charge and orbital ordered (COO) polar antiferromagnetic ground state [1,2]. With increasing temperature, the material undergoes a series of structural, magnetic, and COO transitions governed by competing order parameters [3]. Coupling of these order parameters to the lattice generates intricate structural distortions and offers a tuning knob to control and stabilize new phases such as an anticipated ferromagnetic metallic phase under biaxial compressive strain [4].

To characterize these distortions, we measure SmBaMn₂O₆ in bulk and epitaxial thin films at atomic resolution with *in situ* scanning transmission electron microscopy (STEM) and electron energy loss spectroscopy (EELS). Studying the ground states and successive phase transitions in both the strain-free single crystal and epitaxial thin films under a series of strain states allows the role of the lattice in stabilizing electronic and magnetic order to be systematically investigated. Cryogenic STEM reveals the polar COO distortion defining the ground state structure as well as the low temperature phase transitions which reshape the COO and extinguish the polar and antiferromagnetic order. Characterization at higher temperatures can in turn clarify the structural mechanisms at play as the system undergoes an insulator-metal transition into a charge disordered phase.

[1] Morikawa, et al. *J. Phys. Soc. Jpn.*, **81**, 093602 (2012).

[2] Sagayama, et al. *Phys. Rev. B*, **90**, 241113. (2014).

[3] Yamada, et al. *J. Phys. Soc. Jpn.*, **81**, 113711. (2012).

[4] Nowadnick, et al. *Phys. Rev. B*, **100**, 195129. (2019).

* This work made use of the electron microscopy and synthesis facilities of the Platform for the Accelerated Realization, Analysis, and Discovery of Interface Materials (PARADIM), which are supported by the National Science Foundation under Cooperative Agreement No. DMR-2039380. The authors acknowledge the use of facilities and instrumentation supported by NSF through the Cornell University Materials Research Science and Engineering Center DMR-1719875, a Helios FIB supported by NSF (DMR-1539918), and FEI Titan Themis 300 acquired through NSF-MRI-1429155, with additional support from Cornell University, the Weill Institute and the Kavli Institute at Cornell.

SESSION QT05.03: Advances in Detection Methods for Emergent Phases in Quantum Materials III

Session Chairs: Jessica Boland, Shelly Michele Conroy, Ismail El Baggari and Juan Carlos Idrobo

Wednesday Afternoon, April 24, 2024

Room 446, Level 4, Summit

1:30 PM *QT05.03.01

Brownian Electric Bubble Quasiparticles Jorge Iniguez^{1,2}; ¹Luxembourg Institute of Science and Technology, Luxembourg; ²University of Luxembourg, Luxembourg

In this talk I will describe our theoretical predictions on the possibility to stabilize a new kind of quasiparticle in ferroelectric nanostructures, by suitably controlling the elastic and electric boundary conditions. These novel particles are electric bubbles (e-bubbles) that present a non-trivial topology at low temperatures (skyrmion-like) and become spontaneously mobile upon moderate heating (Brownian diffusion). I will present the typical time scales for the e-bubble dynamics and discuss the basic inter-bubble interactions -- as predicted from our atomistic (second-principles) simulations. I will also show how the e-bubbles' diffusion speed and lifetime can be tuned by controlling the temperature and the defining features of the ferroelectric nanomaterials (thickness, epitaxial strain they are subject to). I will conclude by giving an outlook of the field; in particular, I will comment on the possible use of these objects in Unconventional Computing applications.

Work done in collaboration with Hugo Aramberri and Natalya Fedorova (Luxembourg Institute of Science and Technology). Work funded by the Luxembourg National Research Fund through Grant C21/MS/15799044/FERRODYNAMICS.

2:00 PM *QT05.03.02

Ultrafast Diffraction Microscopy for Revealing Emerging Phases and Their Dynamics Haidan Wen; Argonne National Laboratory, United States

Light-matter interaction has been an effective approach for producing emergent phases in quantum materials. However, these phases and associated dynamics often arise on nanometer scales and evolve on ultrafast time scales, making them challenging to capture. Combined with ultrafast laser excitation, x-ray and electron diffraction microscopes have become an essential tool for studying nanoscale structural evolution. In this talk, I will demonstrate the applications of laser-pumped x-ray and electron diffraction microscopy comparatively. In the first example, ultrafast x-ray diffraction imaging reveals ultrafast nanoscale phase transition in FeRh film and ferroelectric domain reconfiguration in BiFeO₃. In the second example, ultrafast electron microscopy reveals acoustic harmonic modes in FePS₃ mediated by defects. The strengths and limitations of x-ray and electron diffraction microscopy will be discussed. The exciting outlook of these techniques in the dawn of next-generation x-ray facilities will be presented.

These works are primarily supported by the US Department of Energy, Office of Science, Basic Energy Sciences, Materials Sciences and Engineering Division, under award no. DE-AC02-06CH11357 and DE-SC-0012509.

2:30 PM BREAK

3:30 PM *QT05.03.03

Characterizing Disorder in High Entropy Oxides at Every Length Scale Alannah Hallas; The University of British Columbia, Canada

The field of high entropy oxides (HEOs) flips traditional materials science paradigms on their head by seeking to understand what properties arise in the presence of profound configurational disorder. This disorder, which emerges as the result of multiple elements sharing a single crystalline lattice appears to imbue some HEOs with functional properties that far surpass their conventional analogs. However, there are significant questions surrounding the actual degree of configurational disorder, its role in stabilizing the HEO phase, and its effect on other physical properties. Grasping the true extent of the elemental disorder in HEOs requires advanced characterization across orders of magnitude in length scales - from the atomic scale to the average structure, preferably with elemental sensitivity.

In my talk, I will discuss my group's efforts towards addressing these questions using x-ray and neutron methods. Our measurements extend from the nanoscale (x-ray absorption and extended x-ray absorption fine structure, both of which are sensitive to the immediate environment at each metal site) to the microscopic (scanning electron microscopy and x-ray fluorescence microscopy) to the average (bulk diffraction). We find that the true configurational disorder is greatly influenced by synthesis method and that significant kinetic and thermodynamic control is needed to ensure the most random elemental distributions. The most profound differences between samples are, surprisingly, observed at intermediate length scales, in the mesoscopic regime. However, importantly, we find that these sample-to-sample variations do not strongly influence the functional magnetic properties. The most technologically important properties, including ordering temperature and saturated moment, are highly robust to preparation method, and therefore are highly suitable for real world applications.

4:00 PM *QT05.03.04

Probing Topological Phase Transitions in Real-Space Polar Textures Yu-Tsun Shao¹, Sergei Prokhorenko², Lucas M. Caretta³, Yousra Nahas², Sujit Das⁴, Zijian Hong⁵, Ruijuan Xu⁶, Fernando Gómez-Ortiz⁷, Pablo García-Fernández⁷, Long-Qing Chen⁸, Harold Y. Hwang⁹, Javier Junquera⁷, Lane W. Martin¹⁰, Darrell G. Schlom¹¹, Ramamoorthy Ramesh¹⁰ and David A. Muller¹¹; ¹University of Southern California, United States; ²University of Arkansas, Fayetteville, United States; ³Brown University, United States; ⁴Indian Institute of Science, India; ⁵Zhejiang University, China; ⁶North Carolina State University, United States; ⁷Universidad de Cantabria, Spain; ⁸The Pennsylvania State University, United States; ⁹Stanford University, United States; ¹⁰Rice University, United States; ¹¹Cornell University, United States

Real-space topological dipolar textures such as polar vortices, skyrmions and merons in ferroelectric heterostructures emerge resulting from the interplay of elastic, electrostatic and gradient energies. The emergence of these dipolar textures is often accompanied by functionalities such as emergent chirality and local negative capacitance for potential applications in next generation nanodevices. As these textures are intrinsically three-dimensional (3D), nm-sized objects, it poses a challenge for characterizing their detailed atomic structures as well as to understand and explore their potential topological phase transitions.

Here, we explore the topological phase transitions in epitaxial perovskite oxide heterostructures, for example in systems of (PbTiO₃)/(SrTiO₃) and (BiFeO₃)/(TbScO₃), using a combination of atomic resolution imaging, and four-dimensional scanning transmission electron microscopy (4D-STEM). Using 4D-STEM multislice ptychography, we found a new phase in multiferroic BiFeO₃, the 3D dipolar waves, which can be characterized by incommensurate periodicities and antiferrodistortive modes. Further, 4D-STEM-based approach enabled us to directly observe the transitions among polar skyrmions, merons and anti-merons, with some transitions accompanied by a change in their chirality.

Research supported by AFOSR Hybrid Materials MURI (FA9550-18-1-0480), ARO ETHOS MURI (W911NF-21-2-0162), and USC Viterbi start-up funds. Facilities support from the NSF (DMR-1429155, DMR-1719875, DMR-2039380). Researchers at the University of Arkansas also thank the Vannevar Bush Faculty Fellowship Grant No. N00014-20-1-2834 from the Department of Defense.

4:30 PM *QT05.03.05

Recent Developments and Applications of Magnetic-Field-Free Atomic-Resolution Electron Microscope Naoya Shibata; The University of Tokyo, Japan

In recent years, new magnetic objective lens system that realizes a magnetic field free environment at the sample position has been developed for (scanning) transmission electron microscopy. Combining this objective lens system with higher-order aberration corrector, atomic-resolution imaging under magnetic field free condition has been finally achieved [1]. This magnetic-field-free atomic-resolution electron microscope will be a powerful tool for characterizing many interesting topological structures in quantum materials. In this talk, recent developments and applications of this electron microscope with related new techniques will be presented.

[1] N. Shibata et al., *Nature Comm.* 10, 2380 (2019).

[2] This work is supported by JST ERATO grant number JPMJER2202 and the JSPS KAKENHI (grant number 20H05659).

SESSION QT05.04: Poster Session
Session Chairs: Jessica Boland, Shelly Michele Conroy and Ismail El Baggari
Wednesday Afternoon, April 24, 2024
Flex Hall C, Level 2, Summit

5:00 PM QT05.04.01

STEM-EELS/EDS Identification and Manipulation of Color Centers in Nanodiamond Bethany M. Hudak¹ and Rhonda Stroud²; ¹U.S. Naval Research Laboratory, United States; ²Arizona State University, United States

Single-photon-emitting color centers in nanodiamonds are studied extensively for their application in quantum systems. In addition to strong single-photon photoluminescence from the color centers, diamond has many advantages such as chemical inertness, mechanical hardness, and zero nuclear spin. Nitrogen-vacancy (NV) centers in nanodiamonds are a potential architecture for single-atom quantum systems. However, unambiguous identification of a single NV center in a nanodiamond is challenging. Computational work has predicted that the NV center produces a peak at 282.4 eV near the carbon K-edge in electron energy loss spectroscopy (EELS). Here, we perform simultaneous EELS and energy dispersive x-ray spectroscopy (EDS) spectrum imaging in an aberration-corrected scanning transmission electron microscope (STEM) to identify single NV centers by identifying pixels that contain both the EELS 282.4 eV peak and the EDS nitrogen signal at 0.39 keV.

Atomic-scale identification of NV centers is an important first step toward single-atom quantum device fabrication. We further demonstrate that the

focused probe of the STEM can be used to reposition N and NV centers in the diamonds. By scanning the electron beam over a single nanodiamond for an extended period of time, we demonstrate the ability to: 1. corral N atoms into one region of the nanodiamond; and 2. redistribute the N throughout the nanodiamond. This is a significant step toward single-defect manipulation in nanodiamond, and density functional theory (DFT) calculations will help elucidate the exact mechanism of this atomic-scale manipulation.

5:00 PM QT05.04.02

Fabrication of a Micro/Nano-Structure-Based Sensing Platform using Two-Photon Polymerization for Detecting Cadmium Ions [Akanksha Sharma](#), Rahul K. Das, Tejas Y. Suryawanshi, Sweta Rani, Arun Jaiswal, Sumit Saxena and Shobha Shukla; Indian Institute of Technology Bombay, India

The escalating global issue of heavy metal contamination, largely stemming from industrial activities, particularly those in mining, refineries, petrochemical plants, chemical synthesis, fertilizer, paint, and battery production, has significantly contributed to cadmium pollution in water and soil. The World Health Organization (WHO) has established a strict allowable threshold of 3 parts per billion (ppb) for cadmium in drinking water, underscoring the urgent necessity for a detection method that is both sensitive and specific. While conventional techniques like atomic absorption spectrometry and inductively coupled plasma mass spectrometry are highly precise, they are hindered by their high cost, bulkiness, and time-intensive nature. Modern methods, such as fluorescence, colorimetry, and chemical and electrochemical sensing, offer simpler and real-time solutions for monitoring cadmium levels. In this research, we present an innovative approach involving a polymerized 4D structure that incorporates nonmetal-doped carbon quantum dots (CQDs) to enable fluorescence-based detection of cadmium. Our investigation meticulously delves into the fabrication of this hybrid sensor using two-photon polymerization, demonstrating its potential for integration into the next generation of compact devices designed for cadmium detection.

5:00 PM QT05.04.03

Optoelectronic Properties of Cubic Phase of CsPbBr₃ Quantum Dots Prepared by Hot Injection for Perovskites-Based Photosensors [Yen Shuo Chen](#)¹, Pin Chia Tseng¹, Ching Chang Lin² and Fu-Hsiang Ko¹; ¹National Yang Ming Chiao Tung University, Taiwan; ²The University of Tokyo, Japan

In recent years, perovskite materials have been widely used in solar cells and photovoltaic devices, of which CsPbI₃ colloidal quantum dots (CQDs) have been reported to be able to reach 30% power conversion efficiency (PCE), due to their excellent optical properties and potential for large-scale applications. The photovoltaic properties of quantum dots are less frequently used in photoelectric sensors. In this study, we propose that the CsPbBr₃ QDs photosensor was structured with an ITO substrate as the bottom layer. A layer of silicon oxide (SiO₂) was deposited by chemical vapor deposition (CVD) as a dielectric layer. Finally, the CsPbBr₃ QDs were grown by hot injection method and spin coating process and deposited with Au electrodes of 100 nm. The objective of this study was to compare the photoelectric properties of cubic-phase CsPbBr₃ QDs under 395 nm UV light irradiation for photosensor applications.

For synthesis of the cubic phase CsPbBr₃ QDs we are using the hot-injection method, the first step is adding 0.752 mmol PbBr₂ (Lead (II) bromide) into 20 mL ODE (1-octadecene), add 2 mL OA (oleic acid) and 2 mL OAm (oleylamine) into the solution vial the three-neck bottle. The cubic phase of CsPbBr₃ quantum dots (QDs) was synthesized by a thermal injection method. The successful synthesis of CsPbBr₃ QDs was verified by ultraviolet-visible (UV-Vis), photoluminescence (PL), X-ray diffraction (XRD), Transmission electron microscope (TEM). To verify the accuracy of the encapsulated crystal structures, we performed a series of comprehensive analyses. The cubic phase CsPbBr₃ QDs emit a bright green color at room temperature. In the UV-Vis absorption spectra, the cubic phase exhibited an absorption edge at 517 nm. For PL response spectra, the photoluminescence of the cubic phase CsPbBr₃ quantum dots (QDs) are significantly high at an intensity of about 517 nm compared to that of CsPbBr₃ QDs, which suggests that cubic-phase CsPbBr₃ QDs have a high quantum yield. The average grain size of CsPbBr₃ QDs was calculated from TEM images to be 25.1 nm when the reaction temperature was 120°C. The CsPbBr₃ QDs show strong diffraction peaks consistent with the literature (Li Q. et al., 2017).

In this analysis, we employed a 395 nm wavelength light source. The primary function of the photodetector is to discern specific wavelengths of light. This validation is based on the observed significant difference between light and dark currents, exceeding the photocurrent properties by an order of magnitude, highlighting the efficiency and precision of the CsPbBr₃ QDs photosensors. In addition to considering light and dark currents, there are several other factors that play a critical role in evaluating the performance of a photodetector. One such factor is responsivity, which quantifies the input-output gain of a detector system. Compared with no 395 nm UV light, the responsiveness of the cubic phase inclusion layer after illumination was significantly improved by two orders of magnitude. Responsivity indicates how efficiently the detector responds to an optical signal, while detectivity (D*) reflects the detection capability of a photoelectric detector, for a photodetector is a figure of merit used to characterize performance. For detectors, the higher the detection rate, the better the detector performance. We found that the increase in detection efficiency under 395 nm UV irradiation may be due to the rapid recombination of electron-hole pairs after separation for faster detection. The results are consistent with the External Quantum Efficiency (EQE) results. CsPbBr₃ QDs-based sensor in a UV detector at a wavelength of 395nm provides good and fast detection. The most promising applications for photosensors.

SESSION QT05.05: Advances in Detection Methods for Emergent Phases in Quantum Materials IV

Session Chairs: Shelly Michele Conroy and Ismail El Baggari

Thursday Morning, April 25, 2024

Room 446, Level 4, Summit

8:30 AM *QT05.05.01

Capturing Excitons and Phonons in Quantum Materials [Sandhya Susarla](#); Arizona State University, United States

The interplay of spin, lattice, orbital and charge degrees of freedom controls most of the emergent properties in quantum materials. The detection of these parameters at the atomic scale can unravel novel structure-property relationship that could be used to create interesting device architectures. The recent developments of direct electron detectors in analytical scanning transmission electron microscopy (STEM) have made the detection of subtle electronic and structural features in quantum materials possible. In this talk, I will enlighten the contribution of our group towards measuring subtle features in quantum materials from 1) unravelling light-matter interactions in the twisted moiré materials, to 2) exploring vibrational properties across ferroelectric and multiferroic domain walls. I will end my talk with the current and future challenges that we need to address to unravel atomic scale structure-property relationship in quantum materials.

9:00 AM *QT05.05.02

Emergent Excitons in Two-Dimensional Organic-Inorganic Van der Waals Heterostructures [Jeffrey B. Neaton](#)^{1,2,3}; ¹University of California, Berkeley, United States; ²Lawrence Berkeley National Laboratory, United States; ³Kavli Energy NanoScience Institute, United States

The ability to synthesize new classes of chemically-diverse two-dimensional materials attractive for optoelectronic applications has driven the development

of new theory, computational methods, and intuition for predicting the nature of their excitons and how they may be tuned. Here, we describe the recent synthesis and measurements of an emerging class of van der Waals heterostructures, namely a bilayer consisting of atomically-thin monolayers of non-covalently bonded molecular monomers interfaced with a transition metal dichalcogenide (TMD) monolayer. Specifically, we consider different recently-synthesized monolayers of perylene-derivative monomers, whose relative orientation can be tuned via choice of functional group, on MoSe₂ and WS₂ monolayers. We use state-of-the-art first-principles calculations – based on density functional theory and the *ab initio* GW-Bethe-Salpeter equation approach – to reveal the nature of the 2D molecular monolayer-TMD interface, their excitons, and their polarization-dependent optical response. We will describe how their excitonic properties are influenced by lattice structure, dielectric screening, and carrier concentration, and compare the predicted spectral response to photoluminescence and device measurements. General implications for similar systems are also discussed. This work is supported in part by ASOFR-MURI and DOE-BES. Computational resources provided by NERSC.

9:30 AM *QT05.05.03

Quantum Monochromated EELS: Accessing Emergent Phenomena in The Electron Microscope with High Spatial and Spectral Resolution [Jordan A. Hachtel](#); Oak Ridge National Laboratory, United States

Monochromated electron energy loss spectroscopy (EELS) in a scanning transmission electron microscope (STEM) is a technique that has achieved the ability to combine ultrahigh energy and spatial resolution simultaneously. As a result, a new wave of experiments on ultralow energy excitations, such as phonons, phonon-polaritons, molecular vibrations, shallow electronic structure, and infrared optical excitations have achieved exciting results in the STEM.

Here, I will show recent work at ORNL on the monochromated EELS of quantum materials with an emphasis on the emergence electronic structure and quasiparticles generated from coupling between layers in quantum dot networks and oxide superlattices. I will also focus on recent efforts at ORNL to incorporate cryogenic cooling alongside monochromated EELS in the analysis of quantum materials and some of the challenges and progress that has been made on the spectroscopy of low-dimensional quantum materials at liquid nitrogen temperatures.

10:00 AM BREAK

10:30 AM *QT05.05.04

Design of Novel Low-Dimensional Heterostructures via *In Situ* Atomic-Scale Observation [Kate Reidy](#); Massachusetts Institute of Technology, United States

Control of material processes at the level of atoms and electrons is a ‘grand challenge’ of materials design. With the rise of quantum materials and increasing security, resource scarcity, and sustainability considerations, the need for alternative methods of manufacturing at the atomic scale is paramount. Direct visualization of atomic-scale mechanisms allows precise tailoring of nanostructures from the bottom up. *In situ* transmission electron microscopy (TEM) is powerful in achieving this goal due to its high spatial and temporal resolution, obtaining atomic-scale movies while the sample undergoes functional changes, for example during nucleation, phase transformation, or current-biasing. Such direct observation of atomic motion can uncover kinetic models of nucleation and growth, as well as allow direct comparison with *ab-initio* or molecular dynamics simulations.

Here, I will explore the atomic-scale structure and *in situ* growth of an emerging class of van der Waals bonded materials termed ‘mixed dimensional’ heterostructures, which consist of two-dimensional (2D) + nD (where n is 0, 1 or 3) materials adhered primarily through non-covalent interactions.¹ The weak quasi-van der Waals bonding in certain 2D/3D heterostructures (exemplified by Au/MoS₂) results in reproducible moiré patterns that modify the electronic structure at the interface.² In contrast, more strongly bound heterostructures, such as Ti/Gr, exhibit ordered arrays of dislocation networks that are strongly modulated by the 2D material layer number and compliance. We introduce a criterion for dislocation formation in such suspended systems and tailor the thin non-dislocated structures towards ultra-thin heterostructure stacks, of application in quantum sensors.³ We demonstrate the feasibility of forming epitaxial and single crystalline metal/2D/metal (3D/2D/3D) heterostructures using suspended 2D materials, with implications for next-generation Josephson junctions. Lastly, we explore the nucleation and growth of lower symmetry structures, such as 1D nanowires and nanoribbons, examining the influence of symmetry on nanostructure morphology. Such understanding of growth kinetics allows versatile design of heterostructures for next generation nanoscale devices and showcases the powerful role of *in situ* TEM in unraveling the intricacies of quantum materials at the atomic scale.

1. Jariwala, D., Marks, T. J. & Hersam, M. C. Mixed-dimensional van der Waals heterostructures. *Nat. Mater.* **16**, 170–181 (2017).

2. Reidy, K.*, Varnavides, G.*, Dahl Thomsen, J., Kumar, A., Pham, T., Blackburn, A. M., Anikeeva, P., Narang, P., Lebeau, J. M. & Ross, F. M. Direct imaging and electronic structure modulation of moiré superlattices at the 2D/3D interface. *Nat. Commun.* **12**, 1290 (2021).

3. Monticone, E., Castellino, M., Rocci, R. & Rajteri, M. Ti/Au Ultrathin Films for TES Application. *IEEE Trans. Appl. Supercond.* **8223**, 1–5 (2017).

11:00 AM *QT05.05.05

High-Energy-Resolution Dark-Field EELS for Quantum Materials: From Mapping Localised Vibrational Modes to Magnonics in The STEM [Quentin Ramasse](#)^{1,2}, [Demie Kepaptsoglou](#)^{1,3}, [Khalil el Hajraoui](#)^{1,3}, [Vlado Lazarov](#)³, [Paul Zeiger](#)⁴, [Keenan Lyon](#)⁴, [Jose Angel Castellanos-Reyes](#)⁴, [Jan Ruzs](#)⁴, [Anders Bergman](#)⁴, [Michele Lazzerrì](#)⁵ and [Guillaume Radtke](#)⁵; ¹SuperSTEM Laboratory, United Kingdom; ²University of Leeds, United Kingdom; ³University of York, United Kingdom; ⁴Uppsala University, Sweden; ⁵Sorbonne Université, France

State-of-the-art monochromated electron energy loss spectroscopy (EELS) in the scanning transmission electron microscope (STEM) now offers angstrom size electron beam and an energy resolution for EELS under 5meV [1]. These capabilities enable studies of the interplay between fundamental properties of matter such as charge, spin and local chemistry, at the atomic scale. A striking example is presented by epitaxial graphene grown on SiC(0001) by thermal methods, which is known to present a so-called ‘buffer’ layer, whereby the last layer of carbon in contact with the SiC substrate possesses a strikingly different electronic structure from the free-standing epitaxial graphene, impacting possible applications in quantum devices [2]. The use of a dark-field EELS (DF-EELS) geometry to probe the vibrational response of the system [3], atomic plane by atomic plane, reveals the true nature of the chemical bonds formed at this interface, a characterisation that would not be possible with any other technique. Further growing Bi₂Se₃, a topological insulator (TI) with topologically-protected helical two-dimensional surface states and one-dimensional bulk states associated with crystal defects, on top of the graphene layers, takes advantage of strong spin-orbit interaction and proximity effects and results in subtle and controllable electronic band structure changes. The same experimental geometry allows the observation of the Dirac plasmons in the TI layers, and the study of their dispersion in momentum space. DF-EELS was also proposed to be a leading candidate technique to attempt the detection of magnons, even down to at the atomic scale, thanks to a recently developed theoretical calculation framework and preliminary experimental investigations [4,5]. Magnonics is an emergent field within spintronics research whereby a spin-wave (or magnon) is propagated controllably in nano-dimensional magnetic structures allowing to build a new generation of devices for data processing and storage. In addition, it was recently demonstrated that magnons can be utilised to convert spin to charge currents and vice versa, a critical step for integration of spin and charge devices. Despite recent progress, many challenges hinder practical applications due a lack of fundamental understanding of these processes at the nanoscale in the vicinity of interfaces. DF-EELS experiments can be used to study the spin-to-charge conversion in a system consisting of Yttrium Iron Garnet (YIG)/platinum (Pt) bilayer, a widely and intensively used materials combination and a prototypical system to demonstrate the detection of magnons and magnon-phonon polarons in the STEM.

[1] O. L. Krivanek *et al.*, *Ultramicroscopy* **203**, 60 (2019)

- [2] G. Nicotra *et al.*, ACS Nano **7**, 3045 (2013)
[3] F.S. Hage *et al.*, Science **367**, 1124 (2020)
[4] K. Lyon *et al.*, Phys. Rev. B **104**, 214418 (2021).
[5] J.A. Castellanos-Reyes *et al.*, Phys. Rev. B, accepted (2023)

11:30 AM *QT05.05.06

EELS Compton Scattering and The Electronic Structure of Materials Alina Talmantaite¹, Yaoshu Xie², Assael Cohen³, Pranab Mohapatra³, Ariel Ismach³, Teruyasu Mizoguchi², Stewart Clark¹ and Buddhika Mendis¹; ¹Durham University, United Kingdom; ²University of Tokyo, Japan; ³Tel Aviv University, Israel

Electronic structure is fundamental to a large class of materials phenomena, including mechanical, optical, magnetic and electronic transport properties. Momentum based spectroscopies such as angle resolved photoemission spectroscopy (ARPES), electron-positron annihilation and Compton scattering are traditionally used to measure the electronic structure. Compton scattering in the transmission electron microscope (TEM) was first explored in the 1980s using electron energy loss spectroscopy (EELS) [1]. Despite early success it did not achieve widespread use, largely due to the limitations in EELS spectrometer detector efficiencies, and artefacts arising from Bragg scattering within a crystalline specimen. However, with modern advances in EELS spectrometers as well as computational techniques for modelling dynamical scattering artefacts [2] many of the challenges facing EELS Compton scattering are arguably now resolved. EELS Compton scattering in the TEM provides several benefits over standard X-ray and gamma-ray Compton measurements, such as a higher spatial resolution and the ability to extract useful information from even poly-crystalline materials.

In EELS Compton scattering the incident electron beam undergoes an inelastic collision with individual electrons in the solid. The Compton signal appears as a broad peak in an EELS spectrum acquired at large scattering angles (i.e. high momentum transfer). The width of the Compton profile, which can be as large as several hundred eV, is due to the intrinsic momentum spread of the solid-state electrons. The Compton profile shape is therefore directly related to $J(p_z)$, i.e. the density of solid-state electrons with momentum component p_z along the scattering vector direction. $J(p_z)$ provides a 1D projection of the electronic band structure in reciprocal space. We have applied EELS Compton scattering to examine the electronic structure of bi-layer WS₂ [3], with a twist angle of 18° between the two layers. EELS Compton scattering is particularly suitable to this problem, since the low dimensional nature of the WS₂ flakes make it difficult or impossible to analyse using conventional methods. The $J(p_z)$ acquired along the 100 reciprocal direction indicates that the electrons are more delocalised in the bi-layer compared to monolayer WS₂. Comparison with density functional theory (DFT) simulations reveal that the delocalization is due to a small amount of electronic charge (i.e. 0.1%) accumulating in the inter-layer region. The inter-layer charge accumulates between overlapping W atoms, thereby screening the 'wrong' bonds generated by the twist angle. The charge accumulation is also accompanied by a local dilation of the inter-layer spacing. Time permitting I will also present other examples of EELS Compton scattering that are of interest.

- [1] BG Williams, TG Sparrow, RF Egerton, *Proc. R. Soc. London A*, **393** (1984) 409.
[2] BG Mendis, A Talmantaite, *Microsc. Microanal.* **28** (2022) 1971.
[3] A Talmantaite, Y Xie, A Cohen, PK Mohapatra, A Ismach, T Mizoguchi, SJ Clark, BG Mendis, *Phys. Rev. B* **107** (2023) 235424.

SESSION QT05.06: Advances in Detection Methods for Emergent Phases in Quantum Materials V
Session Chairs: Jessica Boland, Shelly Michele Conroy, Juan Carlos Idrobo and Suk Hyun Sung
Thursday Afternoon, April 25, 2024
Room 446, Level 4, Summit

1:30 PM *QT05.06.01

Atomically Stable Cryogenic In Situ TEM Biasing Holder with Accurate Temperature Control Yevheniy Pivak; DENSsolutions, Netherlands

Cryo scanning transmission electron microscopy (STEM) becomes an indispensable tool to study phase transitions in various quantum materials [1-3] at the atomic scale. Detailed characterization of the structural and electronic properties of these samples across phase transitions necessitates the need of the double tilt capability of the sample holder, atomic image stability and a continuous temperature control of the specimen. The latter is achieved through using microelectromechanical systems (MEMS)-based heating and biasing chips [4] in combination with a cryo TEM sample holder.

To accurately control the temperature during in situ cooling and heating experiments, the chips need to be calibrated to correlate the resistance of the microheater with the temperature of the sample. Since not all heater materials possess a linear resistance-temperature response and the high temperature coefficient of temperature resistance might not be valid for negative temperatures, a dedicated calibration of chips on cooling is required. While the calibration above the room temperature is nowadays done routinely by different methods [5, 6], it's not so common in cryogenic conditions. In this talk we will present a novel method of subzero chip calibration based on Raman spectroscopy. The temperature calibration performed in a wide temperature range reveals the need for a correction factor for the R-T correlation at cryo conditions. The resulting calibration factor was used to continuously control the temperature of Au-Pd nanoparticles -175°C to +800°C while keeping the holder cooled. It was found that the atomically stable imaging at -175°C is maintained till the highest temperature of +800°C though the stabilization time increases as the difference between the holder and the sample temperature rises. Similar in situ cooling experiments with continuously varied temperature but in a smaller temperature range have been performed using ferroelectric FIB lamellas. With the help of electron diffraction and TEM imaging, we were able to follow all, known and unknown phase transitions, in these samples.

- [1] E. Bianco, *et al.*, Microscopy and Microanalysis **26**, 1090-1092 (2020).
[2] B. H. Goodge, *et al.*, Microscopy and Microanalysis **27**, 346-347 (2021).
[3] N. Schnitzer, *et al.*, Microscopy and Microanalysis **26**, 2034-2035 (2020).
[4] H. Perez Garza, *et al.*, *19th International Conference on Solid-State Sensors, Actuators and Microsystems (TRANSDUCERS)*, 2155-2158 (2017).
[5] J. Tijn van Ommen, *et al.*, Ultramicroscopy **192**, 14-20 (2018).
[6] I. K. van Ravenhorst, *et al.*, ChemCatChem **11**, 5505-5512 (2019).

2:00 PM *QT05.06.02

Spatially Structuring The Surface Energy of Monolayer Graphene through Selective Heterointerface Engineering Zakaria Al Balushi^{1,2}; ¹University of California, Berkeley, United States; ²Lawrence Berkeley National Laboratory, United States

Selective bottom-up chemical synthesis of low dimensional quantum materials with high spatial resolution has long been a goal of crystal growers. The challenge, however, lies in the spatial modification of the surface energy landscape of a substrate, a crucial factor that promotes the diffusion and

accumulation of adatoms and/or molecules along the surface energy gradient, consequently facilitating nucleation in regions of reduced surface energy. Herein, we demonstrate the achievement of a highly controllable surface energy landscape of monolayer graphene on diamond like carbon (DLC) substrate through a heterointerface containing trapped gallium in a uniquely designed spatial structure. The process involves three steps: (i) spatial-selectively Ga⁺ ion implantation into DLC substrate to create “hill” features with a step height of 4 nm; (ii) polymer-free transfer of monolayer graphene on top of Ga⁺-implanted DLC; (iii) *in-situ* high-vacuum annealing process above 300°C for gallium precipitation at the graphene-DLC heterointerface with low energy electron microscope (LEEM). During the annealing process, both gallium precipitation and gallium-catalyzed reconstruction of the DLC structure contribute to a shift in the local surface work function of graphene, resulting in a decrease in the surface energy of graphene compared to that of pristine graphene. At 300°C, the surface work function difference (between graphene residing on the “hill” features and unmodulated region) is -142 meV, corresponding to a surface energy difference (between the modulated graphene region and unmodulated region) of -0.23 mN/mm. However, at 500°C, it is 240 meV with a value of -14.5 mN/mm. Notably, this difference remains consistent even upon cooling down to 300°C due to the irreversibility of gallium precipitation. In summary, a surface energy landscape of graphene with a high level of complexity can be realized by carefully tuning annealing conditions and the spatial arrangement of “hill” features, facilitating the selective area growth of materials in various nanofabrication processes.

2:30 PM *QT05.06.03

Emerging Properties of Chiral Functional Materials for Next-Generation Technologies Jessica Wade and Kim E. Jelfs; Imperial College London, United Kingdom

The use of organic semiconductors as low-cost, lightweight, easy-to-process active layers in optoelectronic devices has attracted considerable research and technological interest for over thirty years. The functional properties of chiral organic semiconductors, including the absorption and emission of circularly polarised light or the transport of spin-polarised electrons, are highly anisotropic. As a result, the orientation of chiral molecules impacts the functionality and efficiency of chiral devices. We have developed a strategy to control the orientation of helicenes, prototypical chiral small molecules. Our approach forces the helicenes to adopt a face-on orientation and self-assemble into upright supramolecular columns oriented with their helical axis perpendicular to the substrate, or an edge-on orientation with parallel-lying supramolecular columns, which can independently switch on and switch off low- and high-energy chiroptical responses. Our templating methodologies provide a simple way to engineer orientational control and, by association, anisotropic functional properties of chiral molecular systems for a range of emerging technologies. In this talk I will speak about our efforts to control and characterise the orientation, order and supramolecular assembly of chiral small molecules and polymers, and the impact that has on the functional properties of chiral thin films and devices.

3:00 PM BREAK

3:30 PM QT05.06.04

Probing *In-Situ* Twisted Moiré Quantum Emitters with Near-Field Scanning Optical Microscopy Arnab Manna, Shiang-Bin Chiu, Laurel E. Anderson, Jiaqi Cai, Xiaodong Xu and Arthur Barnard; University of Washington, United States

Transition metal dichalcogenide (TMD) Moiré superlattices are formed when two layers of TMD materials are stacked with a slight twist angle. This creates a periodic potential that can trap electrons and holes to form an array of optically active single emitters and other exotic quantum states. Compared to other solid-state emitters, Moiré emitters exist in a planar crystal and do not rely on crystal defects, giving the advantage of scalability, electrical tunability, optimized photon extraction efficiency, and ease of integration with nano-photonics structures to realize single-photon nonlinear optical effects. The twist angle in TMD Moiré superlattices critically determines the properties of the superlattice potential and thereby the optical properties of the emitters. But twisted devices are generally fabricated with a fixed angle that cannot be modified once the device has been made. In addition, the Moiré unit cell is very small, making it difficult to address single emitters with free-space optics. In this work, we propose and develop a new platform for reliable creation and read-out of Moiré emitters. This platform combines two capabilities: 1) a “Twistronics” apparatus that can bring two vdW layers into direct contact and rotate them relative to each other which allows for precise *in-situ* control of the twist angle between the layers, and 2) a near-field scanning optical probe that can focus and collect light from a subwavelength scale spot, making it possible to address single photon emitters in Moiré superlattices. We discuss the merits and challenges of the design and report our progress in using it to study the optical properties of TMD heterobilayers. We believe that our proposed platform will be a powerful tool for exploring the correlated physics of Moiré superlattices and for developing new quantum technologies based on these materials.

3:45 PM QT05.06.05

Thermoelectric Probing of Flat Bands in Twisted Bilayer Tungsten Diselenide Chuting Cai, Yajie Huang, Devika Mehta and Li Shi; The University of Texas at Austin, United States

Due to the relatively strong electron coulombic interaction compared to the small kinetic energy of the flat bands, twisted bilayer graphene Moiré system exhibits strongly correlated behaviors including superconducting, insulating, and topological states at different band fillings. Compared to twisted bilayer graphene, transition metal dichalcogenides (TMDs) Moiré system with a large range of twisted angles can produce very flat bands and strong correlations based on tight-binding calculation. Transport measurements of twisted bilayer tungsten diselenide (WSe₂) reveal insulating and superconducting state at half-filling of the first Moiré valence band. With a twisted angle less than 3 degrees in this system, the topmost valence band appears at the Gamma-valley, with narrow bandwidths and strong correlation. Here, we employ thermoelectric measurement as a unique probe of the flat band structures and interactions in twisted bilayer WSe₂ of different twisting angles. As a measure of the average entropy per charge, the Seebeck coefficient is highly sensitive to the asymmetry of the electron density of states near the chemical potential and is expected to switch sign when the chemical potential is moved across a flat band. For a sample with a twisted angle near 3 degrees, the measured Seebeck coefficient shows pronounced modulation as the hole concentration is varied by a gate voltage. The observed dependences of the measured Seebeck coefficient on the band filling and temperature provide detailed insight into both the flat band features such as the bandwidth, as well as electron-electron and electron-phonon interactions that cause a deviation of the Seebeck coefficient from the semiclassical Mott relation.

4:00 PM QT05.06.06

Electronic Viscous Flow in Hexagonal Boron Nitride Encapsulated Graphene FETs Wenhao Huang^{1,2}, Tathagata Paul¹, Mickael Perrin^{1,3,3} and Michel Calame^{1,2,2}; ¹Empa (Swiss Federal Laboratories for Materials Science and Technology), Switzerland; ²University of Basel, Switzerland; ³ETH Zürich, Switzerland

In most conductors, electron transport primarily involves diffusive scattering from defects and interactions with lattice vibrations (phonons), resulting in Ohmic behavior. Alternatively, transport can become ballistic when the dimensions of the conducting channel become the smallest length scale in the system. However, an intriguing and relatively unexplored transport regime emerges when electron-electron interactions attain a level of strength where they induce correlated and momentum-conserving flow, akin to the Hagen-Poiseuille flow observed in classical fluids. Our research explores the fascinating realm of charge hydrodynamic transport effects, which unveil unique characteristics. These include width-dependent

channel conductivity and a significant reduction in resistivity at elevated electron temperatures. Furthermore, we observe the presence of charge vortices through non-local vicinity resistance measurements[1]. By combining various approaches, we validate the existence of viscous effects over a wide temperature range, extending even up to room temperature. This resilience of hydrodynamic transport in graphene, compared to other systems like two-dimensional electron gases (2DEGs) and WP_2 , is a notable finding. To underpin our experimental findings, we employ finite element calculations of the graphene channel. These calculations not only confirm our observations but also provide valuable insights into device geometries that can enhance viscous effects. The occurrence of viscous effects at room temperature opens up new possibilities for functional hydrodynamic devices, including geometric rectifiers like a Tesla valve and charge amplifiers based on the electronic Venturi effect. This research signifies a step forward in understanding and harnessing the potential of charge hydrodynamics in graphene-based systems.

Reference:

[1]. W. Huang, T. Paul, K. Watanabe, T. Taniguchi, M. L. Perrin, and M. Calame, Phys. Rev. Research 5, 023075

SESSION QT05/QT07: Joint Virtual Session
Session Chairs: Shelly Michele Conroy, Rafal Kurlito and Stephan Lany
Wednesday Afternoon, May 8, 2024
QT05-virtual

4:00 PM *QT05/QT07.01

Attosecond Quantum Technologies for Detecting Emergent Phases in Quantum Materials Margaret M. Mumane^{1,2}; ¹University of Colorado, Boulder, United States; ²KMLabs Inc., United States

The macroscopic properties of solids, such as the electrical conductivity, greatly depend on the electronic states and their low-energy excitations near the Fermi level. In strongly-correlated quantum materials, many-body interactions between charges, phonons and spins can lead to the formation of a lower-energy ground state characterized by a pseudogap, rather than a sharp energy gap. Pseudogaps and the absence of a clear Fermi edge are found in a broad class of materials including cuprates, colossal magnetoresistance manganites and quasi-one-dimensional (quasi-1D) materials, where its origin has been a long standing and important puzzle.

Many-body interactions occur on extremely short timescales: electron-electron interactions occur on femtoseconds (10^{-15} seconds) or faster, while phonons respond more slowly, within hundreds of femtoseconds. Traditionally, these interactions are probed by changing a material's temperature, pressure, or chemical composition and then measure its electrical properties to learn about the interactions. However, materials that host different interactions can exhibit very similar properties, making it challenging to pinpoint the exact nature of these interactions.

In recent work we showed that by gently exciting a quantum material with an ultrafast laser pulse and probing it with extreme ultraviolet high harmonic pulses, we can measure not only the response times, but also see precisely how the electronic band structure changes. In combination, this makes it possible to identify the many body interactions underlying the ground state of a quantum material and thereby the nature of the pseudogap.[1]

Specifically, we compared how the electrons in two different 1D materials responded after they were gently perturbed by light: $(\text{TaSe}_4)_2\text{I}$ and $\text{Rb}_{0.3}\text{MoO}_3$, also known as rubidium blue bronze. Historically, both materials were thought to have a small insulating gap due to the coupling between electrons and phonons, called polarons. However, recent theory suggested that the insulating gap in such materials could be produced by polarons interacting to produce bipolarons. By tracking the energy and location of the excited electrons using time- and angle-resolved photoemission, we could see the signatures of bipolarons melting into single polarons in $(\text{TaSe}_4)_2\text{I}$.

In contrast, electrons in $\text{Rb}_{0.3}\text{MoO}_3$ respond and relax ten times faster (in ~ 60 femtoseconds) to light, clearly showing that interactions between electrons (Luttinger-liquid behavior) must be responsible for the insulating gap in that 1D material.

More generally, ultrafast high harmonic probes provide an exquisite source of short wavelength light, with unprecedented control over the spectral, temporal, polarization and orbital angular momentum of the emitted waveforms, from the UV to the keV photon energy region. They enable powerful new tools for near-perfect x-ray imaging, for coherently manipulating quantum materials using light, and for extracting the functional transport, electronic, magnetic and mechanical properties of ultrathin films and nanosystems.[2-6]

Zhang et al., Nano Letters **23**, 8392 (2023).

Wang et al., Optica **10**, 1245 (2023).

McBennett et al., Nano Letters **23**, 2129 (2023).

Zhang et al., Structural Dynamics **9**, 014501 (2022).

Tanksalvala et al., Science Advances **7**, eabd9667 (2021).

Frazer et al., Physical Review Materials **4**, 073603 (2020).

4:30 PM *QT05/QT07.02

Non-Collinear Mn₃NiN Antiferromagnets Lesley F. Cohen; Imperial College, United Kingdom

Antiferromagnets (AFM) hold interest because of their potential for application in high density, high speed spintronic devices, as an active layer and also as a component in superconducting S/AFM/S Josephson Junctions. Frustrated non-collinear antiferromagnets offer additional attractive functional properties due to their magnetic space group symmetry. Stimulated by these predictions we embarked on a growth program of non collinear antiferromagnetic antiperovskite Mn_3NiN films on various perovskite substrates by pulsed laser deposition. We have used observation of the anomalous Hall effect [1] to piece together the experimental phase diagram of magnetic order with biaxial strain [2]. Theory predicts that compressively strained films should support a high temperature collinear ferrimagnetic phase [3]. We use polar MOKE spectroscopy which in combination with DFT calculations sheds light on the origin of the magneto-optical signal as the material evolves from antiferromagnetic to ferrimagnetic phase [4]. Employing a laser scanning technique to create an out-of-plane temperature gradient we can also use the anomalous Nernst effect to provide information about domain structure in our films [5]. Finally, I will review the evidence for piezomagnetism [6,7] predicted to exist in these materials and as time allows, our recent work on the role of piezomagnetism in films grown on highly mismatched substrates.

[1] Anomalous Hall effect in noncollinear antiferromagnetic Mn_3NiN thin films, D. Boldrin, David; I. Samathrakias, Ilias, J. Zemen et al., Phys. Rev. Materials **3** (9) 094409 (2019)

[2] The Biaxial Strain Dependence of Magnetic Order in Spin Frustrated Mn_3NiN Thin Films, D. Boldrin, F. Johnson, R. Thompson et al., Advanced Functional Materials **29** (40) 1902502 (2019)

[3] Frustrated magnetism and caloric effects in Mn-based antiperovskite nitrides: Ab initio theory, J. Zemen, E. Mendive-Tapia et al., Phys. Rev.B **95**,184438, (2017).

[4] Room temperature weak collinear ferrimagnet with symmetry driven, large intrinsic magneto-optic and magneto-transport signatures, F. Johnson et al., Phys. Rev. B **107** (1) (2023)

[5] Identifying the octupole antiferromagnetic domain orientation in Mn₃NiN by scanning anomalous Nernst effect microscopy, F. Johnson et al., Appl. Phys. Lett. **120**, 232402 (2022)

[6] Giant Piezomagnetism in Mn₃NiN, D. Boldrin, A.P. Mihai, Bin Zou, et al., ACS Applied Materials and Interfaces **10** (22) 18863 (2018)

[7] Strain dependence of Berry-phase-induced anomalous Hall effect in the non-collinear antiferromagnet Mn₃NiN, F. Johnson et al., Applied Physics Letters **119** (22) 222401 (2021)

5:00 PM *QT05/QT07.03

Imaging the Breakdown and Restoration of Topological Protection in Magnetic Topological Insulator MnBi₂Te₄, Mark T. Edmonds; Monash University, Australia

Quantum anomalous Hall (QAH) insulators transport charge without resistance along topologically protected chiral one-dimensional edge states. Yet, in magnetic topological insulators (MTI) to date, topological protection is far from robust, with the zero-magnetic field QAH effect only realised at temperatures an order of magnitude below the Néel temperature T_N , though small magnetic fields can stabilize QAH effect. Understanding why topological protection breaks down is therefore essential to realising QAH effect at higher temperatures. Here we use a scanning tunnelling microscope to directly map the size of the exchange gap ($E_{g,ex}$) and its spatial fluctuation in the QAH insulator 5-layer MnBi₂Te₄. We observe long-range fluctuations of $E_{g,ex}$ with values ranging between 0 (gapless) and 70 meV, uncorrelated to individual point defects. We directly image the breakdown of topological protection, showing that the chiral edge state, the hallmark signature of a QAH insulator, hybridizes with extended gapless metallic regions in the bulk. Finally, we unambiguously demonstrate that the gapless regions originate in magnetic disorder, by demonstrating that a small magnetic field restores $E_{g,ex}$ in these regions, explaining the recovery of topological protection in magnetic fields. Our results indicate that overcoming magnetic disorder is key to exploiting the unique properties of QAH insulators.

5:30 PM *QT05/QT07.04

Spiral Magnetism in a Weyl Semimetal Fazel Fallah Tafti¹, Xiaohan Yao¹, Jonathan Gaudet² and Predrag Nikolic³; ¹Boston College, United States; ²National Institute of Standards and Technology, United States; ³George Mason University, United States

We present evidence of spiral magnetic ordering in the Weyl semimetal SmAlSi from transport and neutron diffraction experiments. This material is a member of RAISi family where R is the rare-earth. We show that a large magnetocrystalline anisotropy in PrAlSi, CeAlSi, and NdAlSi prevents the spiral order although chiral interactions may be present. However, SmAlSi shows a nearly isotropic crystal electric field which leads to its spiral order. We map the phase diagram of this material and reveal an A-phase at finite field and temperature. Within this phase, we observe a sizable topological Hall effect. We also find that the magnetic k-vector observed in SmAlSi matches the nesting between its Weyl nodes on the Fermi surface. As such, SmAlSi seems to be the first topological semimetal where spiral order is established from the direct engagement of Weyl electrons in magnetic interactions.

SYMPOSIUM QT06

Quantum Phenomena in Oxide—Synthesis, Characterization and Automation
April 23 - May 7, 2024

Symposium Organizers

Lucas Caretta, Brown University
Yu-Tsun Shao, University of Southern California
Sandhya Susarla, Arizona State University
Y. Eren Suyolcu, Max Planck Institute

* Invited Paper

+ JMR Distinguished Invited Speaker

^ MRS Communications Early Career Distinguished Presenter

SESSION QT06.01: Oxide-Based Quantum Materials and Applications

Session Chairs: Yu-Tsun Shao and Y. Eren Suyolcu

Tuesday Morning, April 23, 2024

Room 447, Level 4, Summit

10:30 AM *QT06.01.01

Engineering Boundary Conditions to Stabilize Improper Ferroelectricity in Hexagonal LuFeO₃ Films Down to the Monolayer Limit Darrell G. Schlom^{1,2,3}; ¹Cornell University, United States; ²Kavli Institute at Cornell for Nanoscale Science, United States; ³Leibniz-Institut für Kristallzüchtung, Germany

Ultrathin ferroelectric films with out-of-plane polarization and high Curie temperatures are key to miniaturizing electronic devices, including low-power non-volatile memories. Most ferroelectrics employed in devices are proper ferroelectrics, where spontaneous polarization is the primary order parameter.

Unfortunately, the Curie temperature of proper ferroelectrics is drastically reduced as the ferroelectric becomes thin; nearly all proper ferroelectrics need to be thicker than several unit cells. The absence of an ultrathin limit has been predicted, but not verified for improper ferroelectrics. These are ferroelectrics where the polarization emerges secondary to the primary order parameter, such as a structural distortion. The prime issue in thin films of improper ferroelectrics has been that they clamp to substrates that lack a structural distortion; such clamping thwarts the needed structural distortion and thus ferroelectricity. In this talk I will describe the use of an insulating substrate covered by a conducting electrode and followed by a monolayer transition layer that are not improper ferroelectrics themselves, but that do possess a structural distortion akin to that of the improper ferroelectric deposited upon them by molecule-beam epitaxy. The result is ferroelectricity with an undiminished Curie temperature in a formula-unit-thick (0.5-unit-cell) improper ferroelectric hexagonal LuFeO₃ (*h*-LuFeO₃) film grown on a SrCo₂Ru₄O₁₁ bottom electrode with a carefully engineered monolayer transition layer. Our results* demonstrate the absence of a critical thickness for improper ferroelectricity and provide a methodology for creating ultrathin improper ferroelectrics by stabilizing its primary order parameter.

* This work was performed in collaboration with the following coauthors: Yilin Evan Li, Rachel A. Steinhardt, Megan E. Holtz, Kunhikrishnan Premakumari Harikrishnan, Rustem Ozgur, Zhuyun Xiao, Evan Krysko, Adriana LaVopa, Petrucio Barrozo da Silva, Charles M. Brooks, Mario Brützmann, Hai Li, Tanay A. Gosavi, Chia-ching Lin, Dmitri E. Nikonov, Ian A. Young, Dmitri A. Tenne, Rob N. Candler, Padraic Shafer, Elke Arenholz, Julia A. Mundy, Craig J. Fennie, Ramamoorthy Ramesh, David A. Muller, Robert J. Cava, and Christo Gugushev.

11:00 AM *QT06.01.02

Epitaxy enables emergent phenomena [Ramamoorthy Ramesh](#); Rice University, United States

The past decade has witnessed dramatic progress related to various aspects of emergent topological polar textures in oxide nanostructures displaying vortices, skyrmions, merons, hopfions, dipolar waves, or labyrinthine domains, among others. For a long time, these nontrivial structures (the electric counterparts of the exotic spin textures) were not expected due to the high energy cost associated with the dipolar anisotropy: the smooth and continuous evolution of the local polarization to produce topologically protected structures would result in a large elastic energy penalty. However, it was discovered that the delicate balance and intricate interplay between the electric, elastic, and gradient energies can be altered in low-dimensional forms of ferroelectric oxide nanostructures. These can be tuned to create and manipulate order parameters in ways once considered impossible, thanks to a fruitful, positive feedback between theory and experiment: advances in materials synthesis and preparation (with a control at the atomic scale) and characterization have come together with great progress in theoretical modeling of ferroelectrics at larger length and timescales. The new emergent states of matter join together with exotic functional properties (such as chirality, negative capacitance, and coexistence of phases) that, along with their small size and ultrafast dynamical response, make them potential candidates in multifunctional devices. Finally, some open questions and challenges for the future are presented, underlining the interesting future that is anticipated in this field.

11:30 AM *QT06.01.03

The Emergence of Highly Defective Oxides in Material Development [Nini Pryds](#); Technical University Denmark, Denmark

The array of intriguing characteristics found in complex oxides, including ferroelectricity, piezoelectricity, and pyroelectricity, consistently draws significant attention. Various approaches are utilized to disrupt lattice symmetry, thereby broadening the spectrum of functionalities. In this presentation, I will demonstrate that symmetry breaking provides exceptional opportunities. For instance, it can stabilize phases that are typically unstable by leveraging highly coherent interfaces. It can also amplify electromechanical effects at interfaces or generate piezoelectricity in systems that are usually centrosymmetric. This collection of opportunities opens the door to a diverse and rich realm of new functionalities in complex oxides and their interfaces, presenting unparalleled prospects.

SESSION QT06.02: Novel Synthesis for Complex Oxides

Session Chairs: Sandhya Susarla and Y. Eren Suyolcu

Tuesday Afternoon, April 23, 2024

Room 447, Level 4, Summit

1:30 PM *QT06.02.01

Unlocking The Promise and Simplicity of Atomically Precise Synthesis for 4d- and 5d Metal Oxides through Hybrid MBE [Bharat Jalan](#); University of Minnesota, United States

The ability to achieve atomically precise material synthesis has marked a profound advancement in the field of materials science. Yet, it is often the degree of ease and precision in the synthesis process that paves the way for groundbreaking application and discovery. Consider an element of periodic table that is hard to oxidize and also difficult to evaporate, how do we create an atomically precise thin films of such metals, metal oxides or their heterostructures? This has been a central question in the synthesis science for many decades. In this talk, I will present my group's effort to address this question. We have recently shown that both the low vapor pressure and difficulty in oxidizing a "stubborn" element can be addressed by using a solid metal-organic compound with significantly higher vapor pressure, and with the added benefits of being in a pre-oxidized oxidation state along with excellent thermal and air stability. Using this approach, we show, for the first time, the synthesis of Pt, RuO₂, SrRuO₃ and superconducting Sr₂RuO₄ films with the *same ease and control* as afforded by III-V MBE. Finally, I will present a detailed MBE growth study of SrRuO₃ films combined with structural and transport characterizations emphasizing the role of structural inhomogeneity on anomalous hump-like magnetotransport, which has long been interpreted as a signature of Skyrmions formation.

2:00 PM *QT06.02.02

Emergent Properties in SrIrO₃ Heterostructures Grown by Metalorganic MBE [Ryan B. Comes](#); Auburn University, United States

Transition metal complex oxides exhibit a host of intriguing properties for new technologies that can be tuned by the choice of ions from the 3d, 4d, and 5d blocks of the periodic table. This combination of properties, including superconductivity, ferromagnetism, and ferroelectricity, in a single class of materials offers rich opportunities for engineering of unusual combinations of behavior through the design of multi-layer thin films. Such heterostructures can exhibit topological phenomena due to interfacial coupling between distinct phases. Our work employs hybrid metal-organic MBE and *in situ* X-ray photoelectron spectroscopy (XPS) to explore oxide films that exhibit strong spin-orbit coupling and interfacial charge transfer. We have demonstrated the growth of hard-to-grow materials including SrNbO₃, SrIrO₃, and SrHfO₃ using metal-organic precursors and examined how interfacial phenomena can be tuned via charge transfer.

In this talk, I will discuss our work on SrIrO₃ heterostructures grown using an Ir(acac)₃ solid-source metal-organic precursor. We have synthesized epitaxial films under different thickness and strain conditions and examined the role that these play on the electronic transport and carrier dynamics. We show that the metallicity can be tuned via increasing compressive strain and employ time-domain THz spectroscopy to examine the origins of this behavior. Additionally, we have examined ways to tune the Fermi level in SrIrO₃ using SrNbO₃ as an n-type interfacial donor and SrCoO₃ as a ferromagnetic p-type interfacial acceptor. I will discuss how these interfaces change the transport behavior in SrIrO₃ through charge transfer using *in situ* XPS and *ex situ* X-ray absorption spectroscopy and scanning transmission electron microscopy. These new synthesis capabilities open routes to tuning of electronic structure in iridate films, which have been predicted to exhibit superconductivity in low-dimensional systems.

2:30 PM *QT06.02.03

Thermal Laser Epitaxy for Ultraclean Heterostructures [Hans Boschker](#)¹, Felix Hensling², Lena Majer², Brendan D. Faeth², Jochen Mannhart² and Wolfgang Braun^{1,2}; ¹Epiray GmbH, Germany; ²Max Planck Institute for Solid State Research, Germany

We have developed a new thin-film deposition technique that is especially suited to the growth of an extremely wide range of heterostructures with atomic precision. Thermal laser epitaxy (TLE) uses chemical elements as sources, which are evaporated with continuous-wave lasers [1]. The lasers' virtually arbitrary power density allows for the evaporation of practically all elements of the periodic table in the same setup [2]. Furthermore, a wide range of elements has been grown in oxygen environments up to pressures as high as 10⁻² mbar, yielding films of binary oxides [4,5]. In addition, extremely clean oxide surfaces can be prepared with the use of a CO₂ laser substrate heater that enables temperatures (*T*) up to 2000 °C [5]. Here, I will introduce the advantages of TLE for epitaxy and focus in detail on the epitaxy of ultraclean oxide heterostructures.

References

- [1] W. Braun, J. Mannhart, AIP Adv. 9 (2019) 085310
- [2] T.J. Smart, et al., J. Laser Appl. 33 (2021) 022008
- [3] D.-Y. Kim, J. Mannhart, W. Braun, Appl. Phys. Lett. Mater. 9 (2021) 081105
- [4] D.-Y. Kim, J. Mannhart, W. Braun, J. Vac. Sci. Tech. A 39 (2021) 053406
- [5] W. Braun, et al., Appl. Phys. Lett. Mater. 8 (2020) 071112

3:00 PM BREAK

SESSION QT06.03: Free-Standing Oxide Membranes and Advanced Applications
Session Chairs: Yu-Tsun Shao and Sandhya Susarla
Tuesday Afternoon, April 23, 2024
Room 447, Level 4, Summit

3:30 PM QT06.03.01

Novel Quantum Heterostructures enabled by Membrane Epitaxy [Varun Harbola](#), Yu-Jung Wu, Felix Hensling, Hongguang Wang, Peter A. van Aken and Jochen Mannhart; Max Planck Institute for Solid State Research, Germany

Engineering of sharp interfaces and heterostructures with thin films of quantum materials is a cornerstone of thin films epitaxy. However, there is an inherent constraint of lattice compatibility, concerning not only the lattice symmetry but also lattice size, limiting the realizability of epitaxially grown heterostructures. To solve this problem and overcome that constraint, we introduce "vector substrates", for which the template layer for epitaxy can be chosen independently of the bulk of the substrate. The fabrication of vector substrates leverages thin-film membrane technology. The process begins by growing a template layer on a parent substrate. The template layer is then transferred onto a carrier substrate, thereby generating the vector substrate. Furthermore, these vector substrates can be handled and utilized for growth in the same way a traditional substrate is used. We show that this approach allows the deposition of heterostructures of quantum materials with clean and novel interfaces, opening up an unprecedented variety of possibilities in quantum materials research.

References:

- V. Harbola et al., Vector Substrates: Idea, Design, and Realization, Adv. Func. Mater. (In press) Article DOI: 10.1002/adfm.202306289 (2023).

3:45 PM *QT06.03.02

Unfolding The Challenges to Prepare Epitaxial Complex Oxide Freestanding Membranes [Mariona Coll](#); ICMAB-CSIC, Spain

The possibility to prepare epitaxial complex oxide freestanding membranes has opened a whole new ground of research to investigate novel phenomena and device concepts envisaging new applications for complex oxides in next generation electronics. The use of the sacrificial layer approach emerged as one of the simplest and most versatile route to prepare complex oxide membranes. Yet, challenges remain on the synthesis level to accurately prepare and nanoengineer many complex oxide compositions, create new interfaces and exotic architectures.

Here it will be discussed the use of chemical methods to prepare high quality and ambient-stable Ca-doped Sr₃Al₂O₆ sacrificial layer [1] to deliver a series of freestanding complex oxide membranes including CoFe₂O₄, La_{0.7}Sr_{0.3}MnO₃ and BiFeO₃/La_{0.7}Sr_{0.3}MnO₃ bilayers.

We identified that calcium doping in Sr₃Al₂O₆ has a key role on the stability of the sacrificial and define the subsequent epitaxial growth, strain and interface quality of the functional complex oxide. [2,3] Then it will also be presented a thorough study of the influence of both sacrificial and complex oxide thickness on the strain and mechanical properties of the freestanding membrane.

Finally, we demonstrate that the magnetic, electrical transport and piezoelectric properties of the CoFe₂O₄, La_{0.7}Sr_{0.3}MnO₃ and BiFeO₃/La_{0.7}Sr_{0.3}MnO₃ membranes, respectively, are preserved when transferred on flat arbitrary substrates. [4]

Therefore, this study provides an innovative and versatile platform to synthesize transition metal oxide freestanding films and heterostructures that can be integrated in a wide variety of substrates and will empower the search for novel and enhanced properties with many technological benefits.

[1] P Salles, I Caño, R Guzman, C Dore, A Mihi, W Zhou, M Coll *Facile Chemical Route to Prepare Water Soluble Epitaxial Sr₃Al₂O₆ Sacrificial Layers for Freestanding Oxides* Advanced Materials Interfaces, 8, 2001643 (2021)

- [2] P Salles, R Guzmán, D Zanders, A Quintana, I Fina, F. Sanchez, W Zhou, M.Coll *Bendable polycrystalline and magnetic CoFe₂O₄ membranes by chemical methods*, ACS Appl. Mater. Interfaces, 14, 12845-12854 (2022)
- [3] P. Salles, R. Guzman, A. Barrera, M. Ramis, J. M.Caicedo, A. Palau, W. Zhou, M. Coll *On the Role of the Sr_{3-x}Ca_xAl₂O₆ Sacrificial Layer Composition in Epitaxial La_{0.7}Sr_{0.3}MnO₃ Membranes* Advanced Functional Materials 33, 2304059(2023)
- [4]P. Salles, M. Coll et al. *Multifunctional epitaxial BiFeO₃ membranes for flexible applications* Under evaluation (2023)

4:15 PM QT06.03.03

Self-Assembly of Nanocrystalline Structures from Freestanding Oxide Membranes Yu-Jung Wu¹, Varun Harbola¹, Hongguang Wang^{1,2}, Sander Smink¹, Sarah Parks¹, Peter A. van Aken^{1,2} and Jochen Mannhart¹; ¹Max Planck Institute for Solid State Research, Germany; ²Stuttgart Center for Electron Microscopy, Germany

We present a novel route to fabricating nanocrystalline oxide structures of exceptional quality utilizing freestanding oxide membranes. The thermally induced self-assembly of nanocrystalline structures is driven by dewetting oxide membranes once they are lifted off and transferred onto sapphire substrates. Upon annealing at temperatures below the melting point of the membranes, they self-assemble systematically into a variety of nanostructures such as nanovoids, nanowires, and nanocrystals. The orientation of the nanostructures is exactly provided by the crystal lattice of the transferred membrane. The microstructure of the nanocrystals exhibits exceptional quality, characterized by a pristine crystal structure and uniform stoichiometry, and their alignment exceeds the capabilities of lithography and ion-milling techniques. These findings illustrate the nanofabrication opportunities created by dewetting complex oxides. Furthermore, the physics underlying the self-assembly process in the membranes can potentially enhance our understanding of interface diffusion, which is important to epitaxial thin film growth.

4:30 PM QT06.03.04

Spatially Reconfigurable Antiferromagnetic states in Topologically-Rich Freestanding Nanomembranes Hariom Jani^{1,2}, Jack Harrison¹, Sonu Devi², Saurav Prakash², Proloy Nandi², Junxiong Hu², Zhiyang Zeng¹, Jheng-Cyuan Lin¹, Charles Godfrey¹, Ganesh Ji Omar², Tim A Butcher³, Jörg Raabe³, Simone Finizio³, Aaron Thean², Ariando Ariando² and Paolo Radaelli¹; ¹University of Oxford, United Kingdom; ²National University of Singapore, Singapore; ³Paul Scherrer Institute, Switzerland

Antiferromagnets hosting real-space topological textures are promising platforms to model fundamental ultrafast phenomena and explore spintronics. However, to date, they have only been fabricated epitaxially on specific symmetry-matched substrates, to preserve their intrinsic magneto-crystalline order [1,2]. This curtails their integration with dissimilar supports, markedly restricting the scope of fundamental and applied investigations. Here, we circumvent this limitation by designing detachable crystalline antiferromagnetic nanomembranes of α -Fe₂O₃, that can be transferred onto other desirable supports after growth [3]. First, we show that flat nanomembranes host a spin reorientation transition and rich topological phenomenology via transmission-based antiferromagnetic vector-mapping. Second, we exploit the extreme flexibility of oxide membranes to demonstrate reconfiguration of antiferromagnetic states across three-dimensional membrane ‘folds’ resulting from flexure-induced strains. Finally, we combine these developments using an in-situ strain manipulator to realise the first demonstration of non-thermal Kibble-Zurek-like generation of topological textures at room temperature. Integration of such freestanding antiferromagnetic layers with flat/curved nanostructures could enable spin texture designs via magnetoelastic-/geometric-effects in the quasi-static and dynamical regimes, opening new explorations into curvilinear antiferromagnetism and unconventional computing.

References:

- [1] H Jani et al., Nature 590, 74 (2021).
- [2] AKC Tan*, H Jani* et al., arXiv:2303.12125 (2023) [In Press - Nature Materials].
- [3] H Jani*, J Harrison* et al., arXiv:2303.03217 (2023) [In Review].

4:45 PM QT06.03.05

Quantum Sensing with Rydberg Excitons Arva D. Keni, Nithin Abraham, Akshay Agrawal, Kinjol Barua, Yong Chen and Hadiseh Alaeian; Purdue University, United States

Rydberg excitons are promising quasi-particles for quantum sensing applications due to their extended wavefunctions and strong dipolar interaction strengths at higher quantum states. Electromagnetic excitations surrounding the excitons can be accurately quantified and measured when pump-probe processes are performed on them. The transitions between high-lying Rydberg states are in the microwave to terahertz frequency range, thus the excitons can absorb resonant or nearly resonant electromagnetic fields and eventually get excited into a higher state. This will lead to characteristic photon emission when the excited state spontaneously decays to the ground state. Exciton-based sensors are stable and immune to manufacturing variations, aging, and calibration issues since atoms of the same isotopic species are the same everywhere.

To enable Rydberg sensing, a suitable material platform capable of hosting highly excited Rydberg excitons is crucial. Until now, cuprous oxide (Cu₂O) is the only known semiconductor in which Rydberg excitons having principal quantum numbers as high as $n = 25$ have been observed. This is because of its high binding energy and symmetric lattice structure, which allow it to support many Rydberg exciton states without succumbing to thermal ionization. However, reaching a defect-free condition in naturally occurring bulk cuprous oxide remains a challenge, necessitating a more controlled manufacturing technique to produce high-purity, customized synthetic cuprous oxide. Thin-film cuprous oxide samples with thicknesses less than the blockade radius are especially appealing because they make the Rydberg blockade utilizable for nonlinear behavior in semiconductors.

Here, we present photoluminescence and absorption measurements performed on Cu₂O grown on a Strontium Titanate (STO) substrate. The dielectric permittivity of STO shows a large temperature dependence and we probe this using Rydberg excitons in Cu₂O. The large temperature-dependent change in refractive index at terahertz frequencies sensitizes the transition between Rydberg states to the temperature, which can then be measured through the dynamics of the quasi-particle. The Cu₂O/STO also provides us with a platform to study the effects of dielectric screening and dipolar interactions on the exciton dynamics. In this manner, a CMOS-compatible, integrable, and scalable solid-state semiconductor sensing platform can be realized which can pave the way for microwave sensing technologies.

8:15 AM QT06.04.01

Independence of Antiferrodistortive and Ferroelectric Transition in Strained SrTiO₃ Revealed by STEM [Guomin Zhu](#), Alex Hallett, Nicholas Combs, Binghao Guo, Arda Genc, John Harter and Susanne Stemmer; University of California Santa Barbara, United States

Doped SrTiO₃ is a prominent example of an unconventional superconductor that cannot be described by the BCS-Eliashberg paradigm. One of the main open questions is how superconductivity is connected to two other order parameters in this material, namely an antiferrodistortive instability and a ferroelectric instability. Recently, we have revealed the presence of static polar distortions in the paraelectric phase of SrTiO₃, and have discussed their role in the superconducting transition.

Some studies have suggested that the antiferrodistortive distortion plays no role in the superconductivity, while others speculate that antiferrodistortive domain walls may enhance superconductivity. In this study, we use scanning transmission electron microscopy (STEM) to unveil the antiferrodistortive and ferroelectric distortion in the compressively strained, doped SrTiO₃ films. We identified the antiferrodistortive phase in real space by mapping out oxygen atoms using annular bright field (ABF) STEM. The dopant effects on the antiferrodistortive and ferroelectric phase are further elucidated by applying a free energy model with near density functional theory-level accuracy. The antiferrodistortive phase exhibits a single-domain structure, as expected due to the compressive in-plane strain. Using maps of the Ti column positions, we simultaneously measured the local polar domains. We find that unlike the local polar ferroelectric phase, which is suppressed by dopants, antiferrodistortive order persists in the presence of dopants. We show that the two transitions are largely independent of each other and the antiferrodistortive phase plays no role in the superconductivity.

8:30 AM *QT06.04.02

Cryogenic Electron Microscopy of Electronic Order in Oxides [Ismail El Baggari](#); Harvard University, United States

In correlated oxides, quantum-mechanical effects and strong electron-electron interactions give rise to superb electronic properties and a vast potential for future technologies. In these materials, electrons may self-organize into new spatial patterns that break the symmetry of the underlying crystal. These electron ordered states display a rich interplay between distinct degrees of freedom and may induce novel functionalities through the breaking of additional crystal symmetries. I will show vivid atomic-scale visualizations of electronic order enabled by the development of cryogenic capabilities (near 100 K) for scanning transmission electron microscopy. These measurements are combined with advanced analysis tools to reveal picoscale atomic displacements governing electronic transitions, the nature and symmetry of electronic order at the local scale, and nanoscale fluctuations that underlie macroscopic properties. Despite these advances, a persistent challenge in the field of cryogenic transmission electron microscopy is the lack of stable liquid-helium-cooled sample conditions. I will discuss recent developments that provide access to ultra-low temperatures, as low as 20 Kelvin, while maintaining atomic-resolution imaging performance, paving the way for broader explorations of ultra-low temperature phenomena in oxide and beyond.

9:00 AM *QT06.04.03

Applications of High Spatial and Energy Resolution EELS in Functional Oxides for Thermoelectric Applications [Demie Kepaptsoglou](#)^{1,2}, Shihao Wang¹, Feridoon Azough³, Robert Freer³ and Quentin Ramasse¹; ¹SuperSTEM, United Kingdom; ²University of York, United Kingdom; ³The University of Manchester, United Kingdom

Recent advances in instrumentation, such as the introduction of advanced, high-resolution monochromators have allowed for new exciting experiments in the electron microscope. Spectroscopic signatures of optical and acoustical phonons, excitons and defect gap states are now accessible with an atom size probe and in tandem with high precision imaging. Here, we present recent results on the phonon and electronic structure of thermoelectric (TE) materials systems for heat recovery applications, using advanced electron microscopy.

to be expanded...

9:30 AM *QT06.04.04

Probing the Magnetic Cations in Multiferroic Magnetoelectric Thin Films [Shelly Michele Conroy](#)¹, Geri Topore¹, Demie Kepaptsoglou², Quentin Ramasse² and Sinead M. Griffin³; ¹Imperial College London, United Kingdom; ²SuperSTEM, United Kingdom; ³Lawrence Berkeley National Laboratory, United States

Magnetoelectric multiferroic materials show considerable potential for use in low-power computer memory and storage devices due to their coupled ferromagnetism and ferroelectricity, meaning that one could use an electric field to induce ferromagnetic domain switching. The opposite is also true, whereby a magnetic field can also cause ferroelectric domain switching. One such multiferroic material system is Aurivillius-phase Bi₆Ti_xFe_yMn_zO₁₈ (B6TFMO) thin films, where this coupling has been shown to exist in a single phase at room temperature. A large contribution to the room-temperature ferromagnetic ordering is the preferential partitioning of the magnetic cations (Mn and Fe) towards the center of the perovskite layers. Furthermore, even more complex polar topologies such as vortices around antiphase boundaries have been observed using atomic-scale scanning transmission electron microscopy (STEM) and polarization mapping. Understanding the mechanisms behind the cation segregation in the crystal structure and around crystallographic defects is of great importance if one aims to exploit the magnetoelectric ordering in these thin films for the manufacture of low-power, multi-state memory devices.

While atomic-scale STEM alongside techniques like Electron Energy Loss Spectroscopy (EELS) and Energy Dispersive X-Ray (EDX) spectroscopy have been invaluable characterization tools in analysing this material system, they only provide a 2D-projected view for what really are 3D features, especially in the case of complex topologies such as polar vortices. Hence, Atom Probe Tomography (APT) will be used due to its unique 3D chemical and structural analysis capabilities and a correlated workflow will be presented. For the same sample, structural information and specimen shape measurements from STEM will be correlated with APT analysis, as well as aid in the correct choice of atom probe reconstruction parameters. This combined dataset will provide invaluable insight about the mechanisms behind the fascinating room-temperature multiferroicity in these thin film material systems.

With the aim of better understanding the cation segregation mechanisms, we will show a controlled experimental method whereby magnetic Mn cations are implanted on Bi₆Ti₃Fe₂O₁₈ and their segregation will be observed before and after annealing, and compared to B6TFMO in which Mn was incorporated during growth from chemical solution deposition.

10:00 AM BREAK

This searchable program is up-to-date as of April 15th, 2024.

Wednesday Morning, April 24, 2024
Room 447, Level 4, Summit

10:45 AM *QT06.05.01

Machine-Guided Understanding of Functional Oxides in Extremes [Steven R. Spurgeon](#)^{1,2}; ¹Pacific Northwest National Laboratory, United States; ²University of Washington, United States

Directing the evolution of functional oxides in extreme environments is a longstanding challenge that requires new approaches to precision synthesis, characterization, and analytics. Our current inability to acquire, interpret, and act on multi-modal signatures greatly limits our control of materials for emerging applications, including quantum computing and energy storage. There is presently a transformative opportunity to harness artificial intelligence (AI) and domain-specific machine reasoning to guide the evolution of functional oxides more richly than ever before. Here I will describe our new framework for AI-guided experimentation, analytics, and modeling to explore oxides in extremes. This framework is transforming the study of fast-evolving phenomena, allowing us to discover latent defect signatures and determine key design parameters to control materials performance.

11:15 AM QT06.05.03

Irreducible Phonon Interactions and Phonon-Strain Couplings in SrTiO₃ [Shenwei Wu](#)¹, Mark A. Mathis¹, Enda Xiao² and Chris A. Marianetti¹; ¹Columbia University, United States; ²National Institute for Materials Science, Japan

While strontium titanate (SrTiO₃) has undergone extensive first-principles analysis, there remains a need for a systematic study of the irreducible phonon interactions to gain a comprehensive understanding of the vibrational Hamiltonian within a given first-principles method. Here we accurately compute cubic, quartic, and selected sextic irreducible phonon interactions, employing both the lone and bundled irreducible derivative approaches. Furthermore, the leading order irreducible strain phonon couplings are computed, yielding a detailed Taylor series of the Born-Oppenheimer potential in terms of displacements and strains. Particular focus is placed on the *R*-point antiferrodistortive (AFD) soft mode and the Γ -point *T_{1u}* manifolds. We demonstrate that the three-fold AFD manifold has a potential that is nearly spherical, while the linear strain coupling mildly favors the experimentally observed tetragonal distortion. The full anharmonic Hamiltonian is solved within the Hartree-Fock approximation for phonons, and the resulting observables are compared to previous similar calculations and experimental data.

11:30 AM *QT06.05.04

Precise Calculations of Strong Electronic Interactions and Transport in Oxides [Marco Bernardi](#); California Institute of Technology, United States

Combining density functional theory with many-body techniques is enabling rapid advances in first-principles calculations of electron dynamics in materials. Yet, oxides remain challenging because of their intricate structure and electronic interactions.

In this talk, I will present new methods to model electronic interactions and transport from first principles, emphasizing their relevance to complex oxides. I will show calculations of electron interactions and transport in transition metal oxides with strong electron-lattice coupling, pronounced polaron effects, strong electron correlations, and their combinations. These results advance microscopic understanding of structure-property relationships in insulating and metallic oxides.

The talk will conclude with a discussion of PERTURBO, an open source code developed in my group providing quantitative tools to study electron interactions and dynamics in conventional and quantum materials. The recent addition of data-driven methods to compress electronic interactions and significantly speed-up their computation will be highlighted.

SESSION QT06.06: Advanced Metrology for Oxide Quantum Materials
Session Chairs: Lucas Caretta and Yu-Tsun Shao
Wednesday Afternoon, April 24, 2024
Room 447, Level 4, Summit

1:30 PM *QT06.06.01

Defect-Property Relations at Charged Interfaces in Ferroic Oxides [Dennis Meier](#); Norwegian University of Science and Technology, Norway

Oxide materials exhibit a broad range of tunable phenomena, including magnetism, multiferroicity, and superconductivity. Oxide interfaces are particularly intriguing, giving a new dimension to property engineering of functional materials. The low local symmetry at the interfaces, combined with their sensitivity to electrostatics and strain, leads to unusual physical effects, offering amazing opportunities for fundamental and applied research.

In my talk, I will discuss the unique electronic properties that arise at natural and artificially designed charged interfaces in ferroelectric and multiferroic oxides. To give an overview and demonstrate how structural, electric, and compositional degrees of freedom at such interfaces control the material's behavior, I will present three examples: (i) ferroelectric domain walls in BiFeO₃, (ii) grain boundaries in ferroelectric ErMnO₃ polycrystals, and (iii) epitaxial heterointerfaces in multiferroic (LuFeO₃)₉/(LuFe₂O₄)₁ superlattices. To characterize the different types of interfaces, we perform correlated microscopy measurements, combining scanning probe microscopy, electron microscopy, and atom probe tomography. The imaging experiments provide new insight into the atomic-scale structure and chemical composition at charged oxide interfaces, clarifying the key role polar discontinuities and point defects play for their emergent physical properties.

2:00 PM *QT06.06.02

Spin Structures and Spin Transport in Oxidic Heterostructures [Mathias Kläue](#); University of Mainz, Germany

Magnetic oxidic insulators are exciting as they exhibit low damping and can thus be potentially used for low power GreenIT devices. Recently topological spin structures have been observed in these systems [1] and spin-orbit torques and in particular orbital torques can be used to efficiently manipulate these [2].

The low damping also lends itself to magnonic spin transport for instance in antiferromagnetic oxides. For the spin transport, spin currents are generated by heating as resulting from the spin Seebeck effect and by spin pumping measurements and we find in vertical transport short (few nm) spin diffusion lengths

[3,4].

For hematite, however, we find in a non-local geometry that spin transport of tens of micrometers is possible [5,6]. We detect a first harmonic signal, related to the spin conductance, that exhibits a maximum at the spin-flop reorientation, while the second harmonic signal, related to the Spin Seebeck conductance, is linear in the amplitude of the applied magnetic field [5]. The first signal is dependent on the direction of the Néel vector and the second one depends on the induced magnetic moment due to the field. We identify the domain structure as the limiting factor for the spin transport [6]. We also achieved transport in the easy plane phase [7], which allows us to obtain long distance spin transport in hematite even at room temperature [7]. Beyond hematite, we recently identified representatives of the broad class of orthoferrites, such as YFeO₃ and others to exhibit long distance spin transport, which additionally is highly anisotropic [8].

References:

- [1] S. Ding et al., Phys. Rev. B **100**, 100406(R) (2019)
- [2] S. Ding et al., Phys. Rev. Lett. **125**, 177201 (2020); S. Ding et al., Phys. Rev. Lett. **128**, 067201 (2022)
- [3] L. Baldrati et al., Phys. Rev. B **98**, 024422 (2018); L. Baldrati et al. Phys. Rev. B **98**, 014409 (2018)
- [4] J. Cramer et al., Nature Commun. **9**, 1089 (2018)
- [5] R. Lebrun et al., Nature **561**, 222 (2018).
- [6] A. Ross et al., Nano Lett. **20**, 306 (2020).
- [7] R. Lebrun et al., Nature Commun. **11**, 6332 (2020).
- [8] S. Das et al., Nature Commun. **13**, 6140 (2022).

2:30 PM BREAK

SESSION QT06.07: Quantum Phenomena in Oxide Thin Films and Interfaces
Session Chairs: Lucas Caretta and Sandhya Susarla
Wednesday Afternoon, April 24, 2024
Room 447, Level 4, Summit

3:30 PM QT06.07.01

Boosting the Edelstein Effect of Two-Dimensional Electron Gases by Ferromagnetic Exchange Gabriel Lazrak¹, Annika Johansson², Borge Göbel^{2,3}, Ingrid Mertig^{2,3}, Agnès Barthelemy⁴ and Manuel Bibes¹; ¹Unité Mixte de Physique, CNRS / Thales, Université Paris Saclay, France; ²Max Planck Institute of Microstructure Physics, Germany; ³Martin Luther University Halle-Wittenberg, Germany

Strontium titanate (SrTiO₃) two-dimensional electron gases (2DEGs) have broken spatial inversion symmetry and possess a finite Rashba spin-orbit coupling [1], which endows the electronic bands with unique spin textures and couples the spin of mobile electrons to their momentum. This enables the interconversion of charge and spin currents through the direct and inverse Edelstein effects (EE/IEE), with record efficiencies at low temperature [2,3]. In this work, we show that making these 2DEGs ferromagnetic enhances the conversion efficiency by nearly one order of magnitude. Starting from the experimental band structure of non-magnetic SrTiO₃ 2DEGs [4], we mimic magnetic exchange coupling by introducing an out-of-plane Zeeman term in a tight-binding model. We then calculate the band structure and spin textures for increasing internal magnetic fields and compute the Edelstein effect using a semiclassical Boltzmann approach [5]. We find that the conversion efficiency first increases strongly with increasing magnetic field, then shows a maximum and finally decreases.

This field dependence is caused by the competition of the exchange coupling with the effective Rashba interaction. While enhancing the splitting of band pairs amplifies the Edelstein effect, weakening the in-plane Rashba-type spin texture reduces it. Experimentally, we are studying the 2DEG at the interface between SrTiO₃ and the ferromagnetic oxide EuO, to imprint ferromagnetism in the gas.

- [1] Y. Kim, R. M. Lutchyn, and C. Nayak, *Origin and Transport Signatures of Spin-Orbit Interactions in One- and Two-Dimensional SrTiO₃-Based Heterostructures*, Phys. Rev. B **87**, 245121 (2013).
- [2] A. G. Aronov and Yu. B. Lyanda-Geller, *Nuclear Electric Resonance and Orientation of Carrier Spins by an Electric Field*, Sov. J. Exp. Theor. Phys. Lett. **50**, 431 (1989).
- [3] V. M. Edelstein, *Spin Polarization of Conduction Electrons Induced by Electric Current in Two-Dimensional Asymmetric Electron Systems*, Solid State Commun. **73**, 233 (1990).
- [4] D. C. Vaz et al., *Mapping Spin-Charge Conversion to the Band Structure in a Topological Oxide Two-Dimensional Electron Gas*, Nat. Mater. **18**, 11 (2019).
- [5] A. Johansson, B. Göbel, J. Henk, M. Bibes, and I. Mertig, *Spin and Orbital Edelstein Effects in a Two-Dimensional Electron Gas: Theory and Application to SrTiO₃ Interfaces*, Phys. Rev. Res. **3**, 013275 (2021).

3:45 PM *QT06.07.02

Multipolar Ordering in CaIrO₃ Thin Films Regina Dittmann¹, Marjana Lezaic², Alexandros Sarantopoulos¹ and David Gustin²; ¹PGL-7, Germany; ²Forschungszentrum Jülich GmbH, Germany

5d-transition metal oxides, where correlations and spin-orbit coupling play at the same energy scale, create a great playground in search for high-T_C and unconventional superconductivity, spin liquids and novel magnetic ordering phenomena. The metastable perovskite phase of CaIrO₃ was previously grown in thin-film form and characterized as semimetallic by *ab-initio* calculations (Yang et al., J. Phys. Condens. Matter (2010)), although the optical conductivity spectra were inconclusive in this respect, leaving open the possibility of a small-gap insulating state. We performed first-principles calculations which yield a small insulating gap, despite a large spatial extent of Ir 5d wavefunctions. Ordering of higher-order magnetic multipoles is shown to go hand-in-hand with the gap formation. In order to verify our calculations we have grown CaIrO₃ thin films on SrTiO₃ by pulsed laser deposition. Due to the high volatility of IrO₃ significant off-stoichiometry is observed despite a high crystalline quality and the formation of a stable perovskite structure. In order to obtain stoichiometric CaIrO₃ thin films, we had to adjust the growth kinetics while reducing the oxygen partial pressure to prevent the formation of volatile IrO₃. We will discuss the electrical and magnetic properties of our films in the framework of the presence of multipolar ordering, gap formation and possible structural defects.

4:15 PM QT06.07.03

Epitaxial Synthesis of Oxide Dirac Semimetal CaNbO₃ Thin Films Yunkyung Park¹, Seoung-Hun Kang¹, Hua Zhou², Jong Mok Ok³, Hwangsun Kim¹,

Shan Lin¹, Andrew R. Lupini¹, Mina Yoon¹, Satoshi Okamoto¹ and Ho Nyung Lee¹; ¹Oak Ridge National Laboratory, United States; ²Argonne National Laboratory, United States; ³Pusan National University, Korea (the Republic of)

Dirac/Weyl semimetals exhibit massless behaviors, leading to high carrier mobility and exotic quantum transport phenomena. Until now, only a limited number of studies have been conducted to explore Dirac/Weyl semimetals in oxide system, because the observation of a topological band structure to enable quantum transport is rare in oxide materials. Here, we report epitaxial synthesis of high-quality CaNbO₃ thin films by pulsed laser deposition on various substrates and their structural and physical properties. While bulk CaNbO₃ is orthorhombic, thin films revealed a delicate change of the structure depending on the growth conditions, including the type of substrates, thickness, and strain. Both tetragonal and orthorhombic phases with different octahedral symmetries were observed through X-ray Bragg rod measurements. Epitaxial strain is found to effectively manipulate oxygen octahedral symmetry from $a^0a^0c^-$ to $a^+b^+c^-$ / $a^-b^-c^-$ along with structural phase transition from tetragonal phase to orthorhombic phase. Furthermore, high-mobility transport was achieved on CaNbO₃ films along with a large linear magnetoresistance (LMR), which is one of the representative signatures of a Dirac semimetal.

4:30 PM QT06.07.04

Directional Anomalous Skin Effect in ReO₃ Timothy Branch^{1,1}, Graham Baker², Mohamed Oudah^{1,1}, James Day^{1,1}, Alannah Hallas^{1,1} and Douglas A. Bonn^{1,1}; ¹The University of British Columbia, Canada; ²Max Planck Institute for the Chemical Physics of Solids, Germany

Rhenium oxide (ReO₃) is the most highly conducting oxide material due to its extraordinarily low residual resistivity[1]. Due to this property it has a remarkably long low-temperature electronic mean free path, similar to that seen in the ultrapure delafossites. Recent observations from broadband microwave spectroscopy have revealed a new directional anomalous skin effect (ASE) in the quasi-2D delafossite material palladium cobaltate (PdCoO₂)[2]. This effect has also been found in ReO₃. The anisotropic ASE response in these materials is influenced by the alignment of surface currents, the electromagnetic wavevector, and the facets on their Fermi surfaces. For PdCoO₂, recent nonlocal Boltzmann transport models for anisotropic metals accurately describe its behaviour, which falls between the ballistic and hydrodynamic electronic transport regimes[3,4].

However, the directional ASE in ReO₃ has more complexity due to its three-dimensional electronic structure and multiple Fermi surface sheets. In this study, we provide microwave spectroscopy results for high-purity single-crystal samples of ReO₃ at low temperatures. These results demonstrate the unique anisotropy that arises for surface currents flowing in different directions with respect to the Fermi surface facets. Our findings confirm the directional ASE in ReO₃, and we interpret these results using nonlocal skin effect transport models.

[1] J. Falke et al., Phys. Rev. B **103**, 115125 (2021).

[2] G. Baker, T. W. Branch et al., arXiv:2204.14239 (2023).

[3] D. Valentinis et al. Phys. Rev. Research **5**(1), 013212 (2023).

[4] G. Baker, University of British Columbia, Dissertation (2022).

4:45 PM QT06.07.05

Unusual Quantum Oscillations and Indications of Non-Trivial Electronic States in a Quasi Two-Dimensional Electron System at Intricate Oxide Interfaces Manish Dumen¹ and Km Rubi²; ¹INST Mohali, India; ²Los Alamos National Laboratory, United States

Two-dimensional electron systems (2DES) built from perovskite transition metal oxides are potential prospects for the next generation of spintronics and quantum computing due to the simultaneous occurrence of electric-field driven superconductivity and spin-orbit interaction. To enhance technological applications, it is necessary to fully comprehend the electronic bands and confirm the anticipated electronic states in these 2DES by experimentation. Here, using thorough studies of Shubnikov-de Haas oscillations in two distinct systems, EuO/KTaO₃ (EuO/KTO) and LaAlO₃/SrTiO₃ (LAO/STO), we give new insights into the electronic states of the 2DES at oxide interfaces. We performed transport tests in high magnetic fields up to 60 T and low temperatures down to 100 mK in order to precisely resolve these oscillations. We saw a progressive increase in oscillations for 2D confined electrons at both contacts. We saw a progressive increase in oscillation frequency and cyclotron mass with the magnetic field for 2D confined electrons at both interfaces. We analyze these fascinating results by taking into account the possibility of non-trivial electronic bands, for which both linear and parabolic dispersion relations are included in the E-k dispersion. The unconventional oscillations presented in this study not only establish a new paradigm for quantum oscillations in 2DES based on perovskite transition metal oxides, where the oscillations frequency exhibits quadratic dependence on the magnetic field, but also provide experimental evidence for topological-like electronic states in KTO-2DES and STO-2DES.

SESSION QT06.08: Poster Session: Oxide-Based Quantum Materials

Session Chairs: Sandhya Susarla and Y. Eren Suyolcu

Wednesday Afternoon, April 24, 2024

Flex Hall C, Level 2, Summit

5:00 PM QT06.08.01

Isotopic Purification of TiO₂ Obtained by Surface-Enhanced Interstitial Injection Heonjae Jeong, Ian I. Suni, Raylin Chen, Xiao Su and Edmund Seebauer; University of Illinois, United States

Use of isotopically pure semiconductors is important in the fabrication of devices for quantum computing, as spinning nuclei require isolation from environmental perturbation by isotopically pure layers having nuclear spins of zero. Raw materials of sufficiently high isotopic purity are expensive and difficult to obtain, so a post-synthesis method for removing isotopic impurities would be valuable. Through isotopic self-diffusion measurements of oxygen in rutile TiO₂ single crystals immersed in water near room temperature, we demonstrate fractionation of ¹⁸O by a factor of three below natural abundance in a near-surface region up to 10 nm wide.¹ Application of electrochemical biases increases the width of this region by a factor up to five. The submerged surface injects O interstitials that displace lattice ¹⁸O deeper into the solid due to the statistics of interstitialcy-mediated diffusion combined with steep chemical gradients of O interstitials. The steep gradients arise because lowered chemical coordination at clean metal oxide surfaces facilitates the creation of interstitial atoms from adsorbed atoms with energy barriers near or below roughly 1 eV.² The atomic configurations for interstitial injection resemble those for site hopping in the bulk, with barriers only slightly higher. The modest hopping barriers of many interstitial species in oxides, coupled with those for injection, make clean surfaces efficient pathways for populating the nearby bulk with O_i near room temperature. This physical picture is not restricted only to oxygen or TiO₂. Indeed we also show that, when metallic cations such as Mn are present in the aqueous phase, application of electrochemical bias enables the efficient injection of the corresponding metallic interstitials into TiO₂. Such an approach for the host cation (Ti in this case) should lead to

isotopic purification of the lattice cation.

References

1. Heonjae Jeong and Edmund G. Seebauer, "Strong Isotopic Fractionation of Oxygen in TiO₂ Obtained by Surface-Enhanced Solid-State Diffusion," *J. Phys. Chem. Lett.*, **13** (2022) 9841-9847.
2. Heonjae Jeong, Elif Ertekin and Edmund G. Seebauer, "Surface-Based Post-synthesis Manipulation of Point Defects in Metal Oxides Using Liquid Water," *ACS Appl. Mater. Interfaces*, **14** (2022) 34059-34068.

5:00 PM QT06.08.02

Crystal Growth of Mixed Crystal Perovskites for Efficient Down Conversion Matthew Turner and Doyle Temple; Norfolk State University, United States

Materials with large nonlinear optical susceptibilities, that are highly transparent, and possess appropriately fast response times are essential for future DOD needs in telecommunications, as optical power limiters for eye/sensor protection systems, and quantum computing entangled state photon sources. The objective of this research is the discovery of new ultrafast nonlinear optical materials with an effort that focusses on single crystal growth of new mixed perovskite oxides based on the BaTiO₃ system. This talk will summarize the crystal growth of two compositions: Ba_xCa_{1-x}TiO₃ and BaTi_xZr_{1-x}O₃. Single crystals were grown using the optical float zone method with x= 0.01 and 0.05. XRD analysis shows that the crystals grown were tetragonal symmetry perovskite structure. Optical measurements of the second order nonlinear susceptibility are currently underway.

5:00 PM QT06.08.03

Single Crystal Growth and Properties of BaFeGaO₄ using The Floating Zone Technique Orrin Clarke-Delgado¹, Kevin Allen¹, Leroy Salary¹, Sunil Karna² and Doyle Temple¹; ¹Norfolk State University, United States; ²Prairie View A&M University, United States

Materials with topological spin textures are in demand for applications like memory storage and quantum computing. The AB₂O₄ family of crystals has a spinel structure and has been extensively examined. However, there are cases where the typical spinel structure is replaced with a tetrahedral network. The cubic ferromagnetic CuOSeO₃ has been previously shown to contain skyrmions. BaFeGaO₄ (BFGO) is being grown to better characterize its magnetic and thermal properties.

We have successfully developed a polycrystalline sample of BFGO using the solid state method. Polycrystalline samples were prepared using stoichiometric quantities of BaCO₃, Fe₂O₃, and Ga₂O₃. Since BaCO₃ decomposes at 1000 C, samples were annealed for 6 hours to convert it to BaO. The powder mixture was annealed twice at 1100 C, with intermediate grindings after each step. Growth rods were prepared by pressing the powder with a hydraulic press into rods approximately 6 mm in diameter and 5 cm in length. BFGO crystallizes in the hexagonal crystal system with space group P6₃. Structural analysis revealed that the samples had the correct structure. Rietveld analysis of X-ray diffraction also indicated single phase samples. BFGO belongs to the hexagonal structure having space group P6₃. Lattice parameters at room temperature: a = 10.8137 (6) Å and c = 8.6734 (5) Å.

Magnetic measurements were conducted with a Quantum Design Dynacool PPMS. The BFGO sample shows an upturn in the magnetic susceptibility near 50 K, evidence of magnetic ordering. The M-H hysteresis curve was observed at a temperature of 2 K, indicating that the sample is ferromagnetic. To understand the underlying physics and intrinsic behavior of BFGO, a single crystal is needed. Therefore, single crystals of BaFeGaO₄ are being grown using the floating zone technique to control the spinel structural phase and characterize its morphology, thermal, magnetic, and electronic properties. Results of single crystal growth will be presented.

5:00 PM QT06.08.04

A Thin-Film Study of Iron/MgO Using Scattering Geometry of ⁵⁷Fe Mössbauer Spectroscopy Olivia Checkley¹, Natarajan Ravi¹, Yilin Li² and Darrell G. Schlom²; ¹Spelman College, United States; ²Cornell University, United States

An experimental technique known as Conversion Electron Mössbauer Spectroscopy (CEMS) is built in our laboratory to study the surface properties of thin films prepared by Molecular Beam Epitaxial method (MBE). Pure Fe (30% enriched with ⁵⁷Fe) deposited on MgO substrate of 100 nm thickness is used to calibrate the CEMS system. The Zeeman spectrum and its intensity ratios of the spectral lines are analyzed in relation to the single crystal orientation. X-ray data of the thin film is correlated with this single crystal orientation and the easy axis of magnetization is determined. Comparison to the conventional transmission geometry is made for a polycrystalline sample of natural Fe absorber. The theory behind the magnetic dipole transition and the origin of the intensity Mössbauer lines are explained. Lorentzian line functions are used to obtain the least-squares fit of the experimental data.

This work is supported by the NSF PREM – Emergent Interface Materials, Grant 2122147.

5:00 PM QT06.08.05

La-Doped Hafnia Thickfilms for Cryogenic Cooling Jalaja M A and Pavan Nukala; Indian Institute of Science, India

Cryogenic operation of devices is one of the essential requirement in the field of quantum technologies. Electrocaloric (EC) materials are promising as silent solid-state alternates to conventional refrigeration technologies. EC materials are generally Pb based materials, and work at their maximum efficiency only in a limited temperature range near the room temperature. The Pb-based ferroelectrics and polymers are reported to have large pyroelectric coefficients and output power while working in the vicinity of the phase transition temperature, however, struggle to generate voltage threshold (with thin films of nanometer scale) suitable for power electronics where thousands of volts are required. Thin film geometries offer a potential solution to this issue, as they can provide large, continuous power output and fast thermal cycling.

Here we explore the efficacy of unconventionally ferroelectric Hafnia systems which are promising candidates for nanoelectronics due to their CMOS compatibility, robust ferroelectricity at nano scale thicknesses, low dielectric constant, large bandgap, simple chemical structure and less toxicity. The ferroelectricity in hafnia is originating from orthorhombic crystal structure which is stabilised by means of various parameters like dopants, temperature, electrodes, oxygen vacancies etc. Achieving ferroelectricity in Hafnia below 5nm and above 30 nm is quite challenging as the depolarization field effect becomes prominent while scaling down and the non-polar monoclinic phase accompanies the orthorhombic phase while scaling up.

Our study presents the effect of dopant and electrode on achieving robust ferroelectricity in hafnia thick films prepared by solution deposition method. Defect based systems like hafnia generally requires thousands of wake-up cycles to produce the ferroelectricity which is a practical issue while integrating in to nanoelectronics. The solution processed- La doped hafnia thick films shows ferroelectricity with out the wake-up effect and the polarization values are stable till 10⁹ cycles. Surprisingly hafnia thick film shows a phase transition from ferroelectric to non-ferroelectric phase around 140K which is evident from the temperature dependent P-E loops and C-V loops. The pyroelectric properties and electrocaloric cooling effects in the system are well studied

correlating with the electrode induced phase transition in hafnia. The electrocaloric cooling effect in hafnia is significant with $\Delta T = -2.2$ (K) and offers new avenue to built cryogenic coolers at low cost.

SESSION QT06.09: Unconventional Superconductivity in Nickelates
Session Chairs: Yu-Tsun Shao and Y. Eren Suyolcu
Thursday Morning, April 25, 2024
Room 447, Level 4, Summit

8:15 AM QT06.09.01

Absence of Hydrogen in Highly Crystalline Superconducting Infinite Layer Nickelates [Martin Gonzalez](#)^{1,2}, [Kyuho Lee](#)³, [Yijun Yu](#)^{3,2}, [Woojin Kim](#)^{3,2}, [Jennifer Fowlie](#)^{3,2}, [Anton Leviev](#)⁴ and [Harold Y. Hwang](#)^{3,2}; ¹Stanford, United States; ²SLAC National Accelerator Laboratory, United States; ³Stanford University, United States; ⁴Oak Ridge National Laboratory, United States

Infinite-layer nickelates are promising candidates for studying unconventional superconductivity because of their electronic and structural comparison with the cuprates [1]. Superconductivity in the nickelates was first realized in strontium-doped neodymium nickelate (Nd,Sr)NiO₂, which has since sparked a plethora of studies investigating Ni-based compounds [2,3]. The synthesis of infinite-layer nickelate thin films (RNiO₂, R = lanthanide), is a two-step process: first involving the growth of the perovskite precursor phase followed by the deintercalation of apical site oxygen atoms via topotactic reduction [4,5]. The topotactic structural transition is commonly achieved using calcium hydride (CaH₂) as a reducing agent [6,7]. It remains debated, however, whether the use of calcium hydride results in the insertion of hydrogen into the infinite layer structure [8–10]. To determine whether hydrogen is present in the infinite layer nickelates, we performed secondary ion mass spectroscopy (SIMS) measurements on optimally doped (Nd,Sr)NiO₂ thin films to quantify the hydrogen content resulting from calcium hydride reduction. We find that hydrogen does not play a critical role for superconductivity in nickelates, and that the presence of hydrogen is a result of poor crystallinity in non-optimally synthesized thin films.

References

- [1] A. S. Botana and M. R. Norman, Phys. Rev. X 10, 011024 (2020).
- [2] D. Li *et al.*, Nature 572, 624 (2019).
- [3] X. Zhou *et al.*, Mater. Today S1369702122000591 (2022).
- [4] Z. Yang *et al.*, Small 2304146 (2023).
- [5] W. Wei *et al.*, Sci. Adv. 9, eadh3327 (2023).
- [6] K. Lee *et al.*, APL Mater. 12 (2020).
- [7] M. Osada *et al.*, Phys. Rev. Mater. 7, L051801 (2023).
- [8] X. Ding *et al.*, Nature 615, 50 (2023).
- [9] L. Si *et al.*, Phys. Rev. Lett. 124, 166402 (2020).
- [10] P. Puphal *et al.*, Front. Phys. 10, 842578 (2022).

8:30 AM ^QT06.09.02

Advances and Challenges in The Single-Crystal Synthesis of Infinite-Layer and Ruddlesden-Popper Phase Nickelates [Matthias Hepting](#); Max Planck Institute for Solid State Research, Germany

Unconventional superconductivity remains a key focus in condensed matter research, traditionally centered on material classes such as cuprates, iron pnictides, and heavy fermion compounds. Recently, rare-earth nickel oxides have emerged as a new class with potential for unconventional superconducting behavior. Within this nickelate family, two types of structures have drawn particular interest. The first type comprises nickelates with the infinite-layer crystal structure, such as Nd_{0.8}Sr_{0.2}NiO₂, showing superconducting transition temperatures (T_c) up to 20 K. The second type encompasses Ruddlesden-Popper phase nickelates, such as La₃Ni₂O₇, which under hydrostatic pressure manifest a remarkably high T_c of 80 K. Despite these promising observations, the possibly distinct mechanisms driving the superconductivity in these two types of nickelates are not yet fully understood.

To address this, further investigations employing advanced spectroscopic methods are warranted, which are capable of probing the complex interplay between electronic, magnetic, and lattice degrees of freedom typically found in unconventional superconductors. Accordingly, a tailored sample synthesis is desirable to meet the specific requirements of each spectroscopic technique, such as large sample masses for neutron scattering and cleavable single crystals for surface sensitive techniques.

Yet, both nickelate families present unique challenges in material synthesis that have previously hindered the application of certain spectroscopic methods. For infinite-layer nickelates, synthesis can only be realized via a topotactic reduction of the parent perovskite phase. This process is invasive for the sample surface and has previously been executed primarily on thin films and polycrystalline powders. In this talk, I will discuss our advances in the topotactic reduction of single-crystalline samples [1,2]. Furthermore, we have performed resonant inelastic x-ray scattering (RIXS) experiments on these crystals, providing unprecedented insights into spin excitations and charge ordering of the bulk phase [3]. The topotactic infinite-layer crystals are also suitable for future experiments using neutron or surfaces sensitive spectroscopies.

In the case of La₃Ni₂O₇, sizable single crystals can be readily grown using the optical floating zone method and do not necessitate topotactic treatment. However, we recently observed that these crystals exhibit multiple crystallographic phases and a pronounced sensitivity to oxygen stoichiometry, affecting their physical properties. I will delineate how a close feedback loop between advanced characterization methods and iterative adjustments of growth parameters facilitates control over the material's phases, thereby enabling the realization of single crystals optimized for subsequent spectroscopic studies.

[1] P. Puphal, Y.-M. Wu, K. Fürsich, H. Lee, M. Pakdaman, J. A. N. Bruin, J. Nuss, Y. E. Suyolcu, P. A. van Aken, B. Keimer, M. Isobe, and M. Hepting, Topotactic transformation of single crystals: From perovskite to infinite-layer nickelates, Sci. Adv. 7, eabl8091 (2021).

[2] P. Puphal, B. Wehinger, J. Nuss, K. Küster, U. Starke, G. Garbarino, B. Keimer, M. Isobe, and M. Hepting, Synthesis and physical properties of LaNiO₂ crystals, Phys. Rev. Materials 7, 014804 (2023).

[3] S. Hayashida, V. Sundaramurthy, P. Puphal, M. Garcia-Fernandez, Ke-Jin Zhou, M. Isobe, Y.-M. Wu, Y. E. Suyolcu, P. A. van Aken, M. Minola, B. Keimer, and M. Hepting, (unpublished)

9:00 AM *QT06.09.03

Probing The Electronic Dispersion of Superconducting Nickelates Gael Grissonnanche^{1,2}, Grace A. Pan³, Harrison LaBollita⁴, Dan Ferenc Segedin³, Qi Song³, Hanjong Paik², Charles M. Brooks³, Antia Botana⁴, Julia Mundy³ and Brad Ramshaw²; ¹École Polytechnique, France; ²Cornell University, United States; ³Harvard University, United States; ⁴Arizona State University, United States

The origin of unconventional superconductivity in the cuprates remains a mystery partly due to the complex interplay of several competing states and relatively strong disorder. Superconducting nickelates are a new family of materials [1,2] that also combine strongly correlated magnetism with unconventional superconductivity. While comparisons with the superconducting cuprates are natural, very little is known about the metallic state of the nickelates, making these comparisons difficult.

To investigate the electronic structure of the nickelates, we measured the Seebeck coefficient S of a superconducting 5-layer nickelate $\text{Nd}_4\text{Ni}_5\text{O}_{12}$ ($n = 5$ nickelate), whose resistivity is predominantly linear—indicative of strange metal physics—as well as a more-overdoped, non-superconducting, 3-layer nickelate $\text{Nd}_4\text{Ni}_3\text{O}_8$ ($n = 3$ nickelate) for comparison. We find that both the $n = 5$ and $n = 3$ nickelate share a similar temperature-independent, negative S/T , but dramatically differs from the positive Seebeck effect measured on cuprates at similar doping [3].

To interpret our measurements, we used Boltzmann transport theory to show that the electronic dispersion obtained from first-principles calculations accounts for both the magnitude and sign of the temperature-independent Seebeck coefficient in the nickelates. This demonstrates that the electronic structure obtained from first-principles calculations is a good starting point for calculating the transport properties of superconducting nickelates, and suggests that, despite indications of strong electronic correlations, there are well-defined quasiparticles in the strange metallic state of this family of materials.

Finally, we explain the differences in the Seebeck coefficient between nickelates and cuprates as originating in strong dissimilarities in impurity concentrations. Beyond establishing a baseline understanding of how the electronic structure relates to transport coefficients in the superconducting nickelates, this work [4] demonstrates the power of the semi-classical approach to quantitatively describe transport measurements in strongly correlated electron systems, even in the strange-metallic state.

[1] Li et al. *Nature* 572, 624 (2019)

[2] Pan et al. *Nature Materials* 21, 160 (2022)

[3] Gourgout et al. *Physical Review X* 12, 011037 (2022).

[4] Grissonnanche et al. arXiv : 2210.10987

9:30 AM QT06.09.04

Topotactic Reduction: From Brownmillerite to Infinite-Layer Strontium Ferrite Aarushi Khandelwal^{1,2}, Woojin Kim³ and Harold Y. Hwang^{1,2}; ¹Stanford University, United States; ²SLAC National Accelerator Laboratory, United States; ³Pusan National University, Korea (the Republic of)

Isostructural to high-temperature superconducting cuprates, other infinite-layer materials like nickelates, cobaltates, and ferrites have attracted significant interest in recent years. A popular route to synthesizing these infinite layers in thin films is growing perovskite or brownmillerite films and removing oxygen through topotactic reduction [1].

In strontium ferrite, there has been substantial work dedicated to understanding both the as-grown brownmillerite phase, which is notable for high ionic conductivity and interesting magnetic structure [2,3], as well as the reduced infinite layer phase, which is an antiferromagnetic Mott insulator studied for its correlated electronic, magnetic, thermal, and optical properties [4-8]. However, relatively little is known about the mechanism of the reduction process, which can depend on the orientation of oxygen vacancy channels in the brownmillerite films [4,9].

In this work, we grow epitaxially-strained brownmillerite $\text{SrFeO}_{2.5}$ thin films on various substrates using pulsed laser deposition and reduce them to the infinite layer phase, SrFeO_2 , through low-temperature topotactic reduction using CaH_2 reducing agent. During this reduction, we track the evolution of structure and topography, probing the spatial distribution of the brownmillerite and infinite-layer phases as a function of reduction time and strain. We also study the strain dependence of the final infinite layer phase. This work sheds light on the oxygen diffusion pathways relevant to the topotactic reduction process to enable further refinement and control of the transformation between the phases.

References

[1] Z. Meng et al., *Adv. Functional Mater.* (2023) 2305225

[2] A. Nemudry et al., *Chem. Mater.* **10** (1998) 2403-2411

[3] J. C. Waerenborgh et al., *J. Solid State Chem.* **205** (2013) 5-9

[4] C. Tassel et al., *Chem. Soc. Rev.* **41** (2012) 2025-2035

[5] T. Kawakami et al., *Nat. Chem.* **1** (2009) 371-376

[6] S. Ju and T. Y. Cai, *Appl. Phys. Lett.* **94** (2009)

[7] M. Raham, Y. Z. Nie, and G. H. Guo, *Inorg. Chem.* **52** (2013) 12529-12534

[8] C. Tassel et al., *J. Am. Chem. Soc.* **130** (2008) 3764-3765

[9] S. Inoue et al., *Nat. Chem.* **2** (2010) 213-217

9:45 AM BREAK

SESSION QT06.10: Advances in Complex Oxides
Session Chairs: Lucas Caretta and Sandhya Susarla
Thursday Morning, April 25, 2024
Room 447, Level 4, Summit

10:15 AM *QT06.10.01

Emerging Phase Transitions in Lead-Free Antiferroelectric Thin Films Ruijuan Xu; North Carolina State University, United States

As one of the prominent lead-free antiferroelectric alternatives, NaNbO_3 has received considerable research attention owing to its significant potential in energy storage applications. It is also renowned for being one of the most structurally complicated perovskite materials, exhibiting a rich set of structural phases characterized by distinct symmetries, ferroic orders, and oxygen octahedral tilting patterns. This intricate energy landscape in NaNbO_3 also opens up possibilities for inducing novel phase transitions through various external stimuli. In this presentation, I will introduce our recent studies on the intrinsic size dependence of antiferroelectricity in freestanding NaNbO_3 membranes. Through a wide range of experimental and theoretical approaches, we probe an

intriguing antiferroelectric-to-ferroelectric transition that occurs as the membrane thickness decreases. Additionally, I will present our recent findings regarding an intriguing strain-induced phase transition in NaNbO_3 films, where we observed the presence labyrinthine domain patterns that self-organize into topological polar domains. Our work demonstrates enormous potential of using NaNbO_3 as a fertile ground for exploring emerging phase transitions and phenomena.

10:45 AM QT06.10.02

Many Body Localisation in $\text{CeMnAsO}_{1-x}\text{F}_x$? [Abbie McLaughlin](#), Gaynor Lawrence, Struan Simpson and Eve J. Wildman; University of Aberdeen, United Kingdom

Transition metal oxypnictides are known to exhibit a range of exotic phenomena. For example, high temperature superconductivity in $\text{LnFeAsO}_{1-x}\text{F}_x$ and colossal magnetoresistance in $\text{LnMnAsO}_{1-x}\text{F}_x$ ($\text{Ln} = \text{Nd, Pr}$), where the resistivity reduces by 95% at 4 K in a 7 T field. We have been investigating $\text{CeMnAsO}_{1-x}\text{F}_x$ ($x = 0 - 0.075$) and here we show how the electronic properties change with F⁻ doping. CeMnAsO is a Mott insulator. Upon electron doping, via substitution of O^{2-} with F⁻, an unusual insulator – insulator transition is observed for $x \geq 0.035$. The resistivity increases by more than two orders of magnitude over a 2 K temperature range and a superinsulating state is achieved below the transition temperature T_{II} . The superinsulating transition temperature can be tuned by increasing x in $\text{CeMnAsO}_{1-x}\text{F}_x$. Variable temperature synchrotron and neutron diffraction studies confirm that there is no change in the crystal or magnetic structure at T_{II} . Results from AC transport and Hall measurements suggest this transition could be the first observation of many body localisation (MBL) in the solid state. The most significant characteristic of MBL systems is that below a transition temperature they become perfect insulators, exhibiting zero electronic conductivity. The MBL phase also acts as a quantum memory and can be used to protect quantum memory allowing the tantalising possibility of performing topological quantum computation at finite temperatures.

11:00 AM QT06.10.03

Spectro-Microscopic Investigation of 2DEGs in KTaO_3 Interfaces [Aravind Raji](#)^{1,2}, Srijani Mallik³, Hugo Witt³, Victor Porée², Alessandro Nicolaou², Manuel Bibes³, Jean-Pascal Rueff^{2,4} and Alexandre Gloter¹; ¹Laboratoire de Physique des Solides Orsay, France; ²Synchrotron Soleil, France; ³Unité Mixte de Physique CNRS, Thales, Université Paris-Saclay, France; ⁴LCPMR, Sorbonne Université, CNRS, France

Emerging thin-film technology, and its electronic applications rise in parallel with the advances in their atomic-scale synthesis and characterization. Oxide based heterostructures are one key player in it, and they possess remarkable functionalities. The two-dimensional electron gases (2DEGs) in the 5d perovskite KTaO_3 (KTO) based heterostructures exhibits intriguing properties such as superconductivity [1-3], spin-charge interconversion which can have direct applications in spin-orbitronics [4], etc. Depending on the orientation of the substrate KTO, the physical properties in these systems are varied. For instance, the EuO/KTO (111) systems exhibit superconductivity below 2.2 K [1] (0.9 K for an AlOx/KTO (111) [5]), while an EuO/KTO (110) exhibited superconductivity below 1.35 K [6]. The KTO (100) based systems were found to be superconducting only with ionic liquid gating, and at a very low transition temperature of 40 mK [2].

In this path, here we study the Aluminium deposited-pristine KTO substrates in (111), (110), and (100) orientations and EuO/KTO (111) heterostructures with a focus on the emergence of 2DEG and how it influences the physical properties of interest in these. A microstructural and spectroscopic understanding of these interfaces is much appreciated in this direction. With this motivation, we conduct a study involving Scanning Transmission Electron Microscopy (STEM), Electron Energy Loss Spectroscopy (EELS) (Done at STEM Lab in LPS Orsay) and Standing Wave - Hard X-ray Photoemission Spectroscopy (SW-HAXPES) and Resonant Inelastic X-ray Scattering (RIXS) (Done at GALAXIES and SEXTANTS Beamlines in Synchrotron SOLEIL). STEM-EELS provides insights into the changes in the local chemistry and electronic structure together with an atomic scale resolution. On the other hand, SW-HAXPES is a depth selective and non-destructive technique, with a strong sensitivity to chemical differences in each layer. This combination enables us to extract the photoemission spectra from the interface separately. RIXS measurements with a linear polarized light sheds light on the orbital polarization, and also acts as a probe for the in-gap states. The objective is the characterization and determination of the spatial extension of 2DEG encompassing the possible Ferroelectric (FE) type distortion near the interface in these systems.

STEM-EELS element map analysis on a superconducting AlOx/KTO (111) 2DEG system already shown less cation intermixing and a cleaner Al-KTO interface [5]. Our following studies on the structural aspect using STEM, 4D-STEM, geometrical phase analysis (GPA) and SW-HAXPES unraveled the plane termination, and lattice reconstruction along with a substantial FE-type distortion near the last unit cell. These distortions are not the same between the samples. However, on a larger scale, a tetragonal out-of-plane compression up to 1% is observed on the three differently oriented AlOx/KTO systems, and they extend upto 10 nm into the substrate from the interface. On the spectroscopic part, monochromated EELS measurements shown clear fine structure variations at the $\text{Ta-O}_{2,3}$ edge near the interface, which constitutes the real space imaging of the spectroscopic charge, harboring the 2DEG. RIXS measurements shown possible in gap states, and differential charge localization between the samples. Such a combined study with microscopy and spectroscopy unfolds the more interesting physics occurring at the interface, which is not accessible by many bulk probing techniques.

[1] Liu, Changjiang, et al. Science 371.6530: 716-721 (2021). [2] Ueno, K., et al. Nature nanotechnology 6.7: 408-412 (2011). [3] Chen, Zheng, et al. Physical Review Letters 126.2: 026802 (2021). [4] Vicente-Arche, Luis M., et al. Advanced Materials 33.43: 2102102 (2021). [5] Mallik, S., et al. Nature Communications 13.1 (2022): 4625. [6] Hua, Xiangyu, et al. NPJ Quantum Materials 7.1 (2022): 97.

11:15 AM QT06.10.04

Proton-Phonon Coupling, and Causality between Lattice Vibration and Proton Conductivity in Solid Electrolytes Artur Braun¹, [Alexey Ruliev](#)¹, Qianli Chen² and Stephen P. Cramer³; ¹Empa, Switzerland; ²Shanghai Jiao Tong University, China; ³SETI Institute, United States

Ion conducting materials are key components in solid-state electrochemical devices including high-temperature fuel cells (SOFC) and electrolyzers. One of the shortcomings of SOFC – a high operating temperature – may be avoided by using another class of ion conductive ceramics: ceramic proton conductors. Proton conductivity is usually observed at lower temperature than oxygen conductivity due to higher proton mobility.

Ionic transport in solid state is a very important process in many areas; however, compared to, for example, electronic transport, ionic mobility is much less understood and not very well developed. Protonic mobility in particular is a specific peculiar case due to small mass of protons and its high mobility. The temperature dependence of proton conductivity in perovskites suggests that there might be a polaron-like mechanism of proton movement [1]. It implies that there is a significant interaction between the lattice vibrations and moving ions, and it is therefore of great interest to explore lattice dynamics of the perovskite materials.

Such problems are usually studied with conventional methods of lattice dynamics study such as Raman or infrared spectroscopy. These vibration spectroscopy methods provide convoluted information about lattice dynamics without element specificity. However, nuclear resonant vibration spectroscopy (NRVS) can provide element specific projected phonon density of states, which makes the method very attractive for combined studies of molecular and vibrational structure. NRVS, however, only works on Mössbauer-active isotopes, which narrows down its applicability.

For this study we chose barium stannate (BaSnO_3), which is one of proton conductors of perovskite family and contains Mössbauer-active ¹¹⁹Sn isotope. We have performed NRVS on pure and yttrium-doped barium stannate in dry and water-loaded state; the data, backed up by precision neutron diffraction data of the dry and heavy water-loaded ceramic. Using these as of yet unpublished data and results of DFT calculations, we are able to pinpoint which ions play which role on lattice vibrations and then proton conductivity in perovskite-type solid electrolytes.

[1] Braun A, Chen Q: Experimental neutron scattering evidence for proton polaron in hydrated metal oxide proton conductors. Nat Commun 2017, 8:15830.doi: 10.1038/ncomms15830.

SESSION QT06.11: On-Demand Presentation
Tuesday Morning, May 7, 2024
QT06-virtual

10:30 AM QT06.11.01

New Insights into Magnetization Dynamics in Multiferroics: Role of Two-Dimensional Correlations in Three-Dimensional TbMnO₃ and DyMnO₃
Narmada Hegde¹ and Subray Bhat²; ¹S N Bose Physics Learning Center, India; ²Indian Institute of Science, India

In the multiferroic manganites such as TbMnO₃, DyMnO₃ and GdMnO₃, frustration, either geometric or that arising from competing microscopic interactions, is known to have a major effect in determining the phase diagram of the material [1,2]. Additionally, the complex incommensurate and cycloidal structures underlying the multiferroicity arise from freezing out of certain dynamical modes. The study of temperature dependence of Electron paramagnetic resonance (EPR) linewidth $\Delta H(T)$ provides valuable information about spin dynamics. For example, in TbMnO₃ [3] and DyMnO₃ [4] EPR studies showed the presence of frustrated magnetism and strong, short range antiferromagnetic fluctuations much above the antiferromagnetic transition temperature T_N . It turns out that the analysis of $\Delta H(T)$ requires fitting the data to an appropriate model. In the EPR studies on TbMnO₃ and DyMnO₃, following reference [5], the 'spin freezing model', where $\Delta H(T) = A \exp[-(T-T_s)/T_0] + mT + \Delta H_0$, where A is a proportionality constant, T_s is the critical transition temperature, e.g., T_N , and T_0 is an empirical constant, was used to fit the experimental data. mT and ΔH_0 account for linear T-dependence and T-independent value of the line width. However, the fits reported in the papers do not appear to be very good. In a recent detailed study of EPR $\Delta H(T)$ in certain doped rare earth perovskite manganites we showed [6] that a more appropriate model to use is the Berezinskii-Kosterlitz-Thouless (BKT) model which takes in to account the possibility that the correlations could be two-dimensional, either due to the nature of the exchange interactions in the material or/and due to the effect of the applied magnetic field. According to this model, $\Delta H(T) = \Delta H_\infty \exp[3b\sqrt{(T/T_{BKT} - 1)}] + mT + \Delta H_0$, where T_{BKT} is the BKT transition temperature, ΔH_∞ is a constant, b takes the value of $\pi/2$ for a square lattice but has been theoretically shown to take an arbitrary value. This result has been confirmed by a number of recent studies[7]. Following this work, we reanalyse the data on TbMnO₃ and DyMnO₃, the latter in both hexagonal and orthorhombic forms and find that indeed the BKT analysis leads to significantly better fits. We summarize the results below: for TbMnO₃, the spin-freezing model fits with the parameters $\Delta H_0 = 320.9$ (G), $A = 7863.5$ (G), $T_N = 50$ K, $T_0 = 49.5$ and the goodness of the fit factor $R^2 = 0.973$; whereas the BKT model fits better. According to this model $\Delta H_\infty = 7.92$ (G), $m = -0.134$, $T_{BKT} = 80.99$ K, $\Delta H_0 = 306.1$ (G) and a better fit with $R^2 = 0.996$. For hexagonal DyMnO₃ the spin freezing model values are $\Delta H_0 = 975.56$ (G), $A = 9866.28$ (G), $T_N = 79.37$ K, $T_0 = 24.02$ and the goodness of the fit factor $R^2 = 0.992$. The BKT model fits slightly better. The parameter values are $\Delta H_\infty = 30.32$ (G), $m = -0.058$, $T_{BKT} = 53.44$ K, $\Delta H_0 = 599.79$ (G) and a slightly better fit with $R^2 = 0.999$; however, we note that for orthorhombic DyMnO₃ the spin freezing model gives a better fit with parameters $\Delta H_0 = 1477.6$ (G), $A = 3069.9$ (G), $T_N = 70$ K, $T_0 = 189.69$ and the goodness of the fit factor $R^2 = 0.997$. The parameters for the BKT fit are $\Delta H_\infty = 185.26$ (G), $m = -4.88$, $T_{BKT} = 16$ K, $\Delta H_0 = 3263.4$ (G) and a slightly poorer fit with $R^2 = 0.994$. We discuss the implications of the subtle differences in the spin dynamics as reflected in these numbers.

[1] T. Kimura, T. Goto, H. Shintani, K. Ishizaka, T. Arima, Y. Tokura, Nature 426 (2003) 55.

[2] T. Lottermoser et al., Nature 430 (2004) 541.

[3] N O Moreno et al., J. Magn. Magn. Mater. 310 (2007) e364–e366

[4] S Hari Krishnan et al., J. Appl. Phys. 104 (2008) 023902

[5] E. Granado, et al., Phys. Rev. Lett. 86 (2001) 5385.

[6] A. Ashoka, K.S. Bhagyashree, S.V. Bhat., Phys. Rev. B 102, (2020) 024429 and

A. Ashoka, K.S. Bhagyashree, S.V. Bhat., MRS Advances, 5, (2020) 2251–2260

[7] S. Chaudhuri et al., Phys. Rev. B **106**, (2022) 094416 and references cited therein.

SYMPOSIUM QT07

3D Topological Semimetals—From Fundamentals to Applications

April 23 - April 25, 2024

Symposium Organizers

Rafal Kurlito, University of Colorado Boulder
Stephan Lany, National Renewable Energy Laboratory
Stephanie Law, The Pennsylvania State University
Hsin Lin, Academia Sinica

* Invited Paper

+ JMR Distinguished Invited Speaker

^ MRS Communications Early Career Distinguished Presenter

SESSION QT07.01: Fundamentals, Theory and Modeling I
Session Chairs: Stephan Lany and Stephanie Law
Tuesday Morning, April 23, 2024
Room 448, Level 4, Summit

10:30 AM *QT07.01.01

Fundamental Bound on Topological Gap [Liang Fu](#); MIT, United States

I will present a fundamental bound on the energy gap of Chern insulators, derived from the consideration of optical absorption of circularly polarized light. The topological gap bound provides a guiding principle for finding integer and fractional quantum anomalous Hall states at higher temperature. I will also describe its deep connections to quantum geometry and optical response of solids. Applications of the topological gap bound to semiconductor moire materials and magnetic topological insulators will be described.

11:00 AM QT07.01.02

Redox-Coupled Structural Distortions in the Quasi-1-Dimensional Au₂M_{1-x}P₂ System [Scott B. Lee](#)¹, Joseph Stiles¹, Fang Yuan¹, Fatmagül Katmer¹, Stephanie Dulovic¹, Tieyan Chang^{2,3}, Yu-sheng Chen^{2,3} and Leslie Schoop¹; ¹Princeton University, United States; ²Advanced Photon Source, United States; ³The University of Chicago, United States

Symmetry and Fermi-level filling are two variables that lie at the foundation in investigating topological materials. For example, in the GdSb_xTe_{2-x-δ} system, the Sb:Te ratio governs the electron-filling of the band structure, producing a tunable system of structural distortions in its square-net layer. At specific ratios, these distortions retain certain symmetry-protected bands, such as a Dirac node on the Fermi surface, and gap out topologically trivial bands at the Fermi surface. One interest now is to investigate tunable topological structural motifs beyond a square-net of atoms. A one-dimensional (1D) chain of atoms realizes analogous symmetry protected Dirac nodes as the square net. The first part of my presentation expands on previously reported Au₂MP₂ (M=Hg, Tl, Pb, and now Bi), which contains a 1D chain of M atoms. Surprisingly, this structure type stabilizes across a difference of four electrons per chain atom, while the Bi analogue also contains a monoclinic polymorph that retains the linear chain of Bi atoms. The second part of my presentation demonstrates the importance of chemical workup in solid state compounds. X-ray and electron diffraction characterizations indicate crystals of the Au₂MP₂ system undergoes a redox-mediated structural distortion whose resulting symmetry and size of supercell depends on the identity of M. Further characterization and computations suggest modulated coordination environments as a possible driving force for the distortions. Finally, electronic transport between the modulated and unmodulated compounds are compared. As a result of these insights, nearly isolated 1D chains can be further probed in differing chemical environments.

11:15 AM QT07.01.03

Theoretical Defect Model for Synthesis Control of The Fermi Level Position in Cd₃As₂ [Chase Brooks](#)¹, Mark van Schilfgaarde², Dimitar Pashov³, Jocienne Nelson², Kirstin M. Alberi², Daniel Dessau¹ and Stephan Lany²; ¹University of Colorado Boulder, United States; ²National Renewable Energy Laboratory, United States; ³King's College London, United Kingdom

Cd₃As₂ is a three-dimensional Dirac semimetal with sustained scientific interest. Intrinsic point defects, however, induce excess electron carriers that elevate the Fermi level E_F away from the Dirac point and limit accessibility to its topological features. By combining density functional theory (DFT) calculations of defect formation energies and quasiparticle self-consistent GW (QS GW) electronic structure calculations, we demonstrate an innate concentration dependence of defect formation energies, and we find that Cd interstitials are the primary source of this self-doping. We extrapolate formation energies to arbitrary electron concentrations, and we utilize a thermodynamic defect equilibria model to study how extrinsic electron accepting dopants (e.g. Si, Ge, Sn) and particular growth conditions can tune E_F closer to the Dirac point. Separately, Zn₃As₂ is a trivial semiconductor with a direct band gap of 1.0 eV that typically forms with intrinsic p -type doping, so the (Cd,Zn)₃As₂ alloy system is expected to undergo both a topological phase transition and a net doping crossover. Using Monte Carlo simulations, we determined representative alloy structures, which can serve as the basis for predicting electronic structure and defect properties of the alloy.

11:30 AM *QT07.01.04

Chiral Topological Semimetals: Next-Generation Quantum Materials at The Intersection of Topology, Correlations and Magnetism [Niels Schröter](#); Max Planck Institute of Microstructure Physics, Germany

The term chirality is derived from the Greek word for 'hand' χειρ (kheir) and generally describes objects that are distinct from their own mirror image. It is long known that chirality plays a crucial role in nature, providing powerful functionality to chiral molecules in living organisms. Our goal is now to extend this concept from the molecular to the solid state to discover new chirality-enabled functionalities in crystals that could form the basis for new technologies. One particular focus of our activities are chiral topological semimetals, a new class of quantum materials at the intersection of structural and electronic chirality. We discovered the first example of this material class a few years ago (1) and have since demonstrated that they host new fermionic quasiparticles without analogue in high-energy physics, which carry large and controllable topological charges (2).

In this talk, I will present new results that go beyond these initial works and demonstrate that these materials realize an isotropic parallel spin-momentum locking that can be considered the natural counterpart of Rashba spin-orbit coupling (3). Moreover, I will also present fingerprints of parallel locking of the linear momentum to the orbital angular momentum. Finally, I will discuss magnetic chiral topological semimetals and the effect of spin-dependent correlations on the quasiparticle lifetimes of bulk and chiral surface states.

1. N. B. M. Schröter, D. Pei, M. G. Vergniory, Y. Sun, K. Manna, F. de Juan, J. A. Krieger, V. Süß, M. Schmidt, P. Dudin, B. Bradlyn, T. K. Kim, T. Schmitt, C. Cacho, C. Felser, V. N. Strocov, Y. Chen, Chiral topological semimetal with multifold band crossings and long Fermi arcs. *Nat. Phys.* **15**, 759–765 (2019).
2. N. B. M. Schröter, S. Stolz, K. Manna, F. de Juan, M. G. Vergniory, J. A. Krieger, D. Pei, T. Schmitt, P. Dudin, T. K. Kim, C. Cacho, B. Bradlyn, H. Borrmann, M. Schmidt, R. Widmer, V. N. Strocov, C. Felser, Observation and control of maximal Chern numbers in a chiral topological semimetal. *Science* **369**, 179–183 (2020).
3. J. A. Krieger, S. Stolz, I. Robredo, K. Manna, E. C. McFarlane, M. Date, E. B. Guedes, J. H. Dil, C. Shekhar, H. Borrmann, Q. Yang, M. Lin, V. N. Strocov, M. Caputo, B. Pal, M. D. Watson, T. K. Kim, C. Cacho, F. Mazzola, J. Fujii, I. Vobornik, S. S. P. Parkin, B. Bradlyn, C. Felser, M. G. Vergniory, N. B. M. Schröter, Parallel spin-momentum locking in a chiral topological semimetal. arXiv arXiv:2210.08221

SESSION QT07.02: Synthesis and Characterization I
Session Chairs: Kirstin Alberi and Stephanie Law
Tuesday Afternoon, April 23, 2024
Room 448, Level 4, Summit

1:30 PM *QT07.02.01

Two-Dimensional Topological States in Thin Films of Cadmium Arsenide [Susanne Stemmer](#)¹, Binghao Guo¹, Alexander Lygo¹, Wangqian Miao¹ and Xi Dai²; ¹University of California, Santa Barbara, United States; ²The Hong Kong University of Science and Technology, China

In this talk, we will discuss two-dimensional topological states in high-quality thin films of cadmium arsenide (Cd₃As₂) grown by molecular beam epitaxy. Cd₃As₂ is known to belong to a class of topological materials known as three-dimensional Dirac semimetals, but, as we will discuss in this presentation, in thin films it can be tuned between a variety of topological phases. We will discuss the evolution of the electronic states of Cd₃As₂ films as their thickness is scaled. We also discuss a two-dimensional Weyl semimetal phase that is obtained under applied in-plane magnetic fields. We show that magnetotransport studies can distinguish between the different topological phases.

2:00 PM QT07.02.02

Extrinsic Doping Control in Cd₃As₂ Thin Films Grown via MBE [Anthony Rice](#)¹, Ian Leahy¹, Chase Brooks², Stephan Lany^{1,2} and Kirstin M. Alberi¹; ¹National Renewable Energy Lab, United States; ²University of Colorado, Boulder, United States

Cd₃As₂ is a prototypical Dirac semi-metal, a class of materials with gapless topologically protected electronic states. In this system, these topological electronic states are close to the intrinsic Fermi level and are well isolated from non-trivial bands. Additionally, this system is air stable and compatible with molecular beam epitaxy, including lattice matching to III-Sb and II-Te layers, and similar elements to conventional semiconductors. With applications including low-energy computing, optoelectronics, and thermoelectrics, these materials have the capability to impact a variety of areas. To achieve this, however, more capabilities for tuning their properties need to be developed. In particular, strategies for changing the intrinsic n-type carrier concentration beyond electrostatic gating must be explored.

Here, attempts to dope Cd₃As₂ further n-type, as well as p-type, are presented. First, Se and Te are introduced during growth, analogous to doping approaches in conventional semiconductors. This allows for films to be doped from 5e17 cm⁻³ up to slightly over 3e18 cm⁻³ for [112] oriented films before compensation occurs [1]. Prior to compensation, mobility vs n_{3d} follows an expected trend, and fundamental parameters pulled from oscillation fitting are consistent with shifting the Fermi level without major changes in the band structure. Recent results reveal more sensitive doping in [001] oriented films, with higher achievable n-type carrier concentrations. For lowering the Fermi level, (Zn,Cd)₃As₂ is pursued. Similar attempts in bulk crystals and films grown via pulsed laser deposition achieve p-type films at >20% Zn. Here, due to a lower starting n-type carrier concentration, multi carrier behavior is observed <10%, with reduced n-type concentrations also possible. Combined, these efforts allow for significant control in the Fermi level position of a Dirac semimetal.

[1] A.D. Rice et al. Appl. Phys. Lett. 122, 061901 (2023)

2:15 PM QT07.02.03

Probing The Low-Resistivity in Sub-5 nm Thin Nanocrystalline NbP and TaP Semimetals [Asir Intisar Khan](#)^{1,2}, Emily Lindgren¹, Akash Ramdas¹, Byoungjun Won³, Xiangjin Wu¹, Hyun-mi Kim⁴, H.S. Philip Wong¹, Felipe H. da Jornada¹, Il-Kwon Oh³, Yuri Suzuki¹ and Eric Pop¹; ¹Stanford University, United States; ²University of California, Berkeley, United States; ³Ajou University, Korea (the Republic of); ⁴Korea Electronics Technology Institute, Korea (the Republic of)

Ultrathin materials with low resistivity are important for energy-efficient nanoelectronics: from interconnects for dense logic and memory to spintronic devices and neuromorphic memristor arrays. However, the electrical resistivity of ultrathin metal films typically increases with decreasing film thickness due to electron-surface scattering, limiting the performance of metal-based interconnects and nanoelectronics [1]. To overcome this bottleneck, novel topological semimetals such as transition metal pnictides (NbP, NbAs, TaP, TaAs) have been suggested in the ultrathin film limit [2, 3]. These materials have been demonstrated to be topological Weyl semimetals in their single crystal forms [2], a class of materials wherein surface conduction is predicted to dominate thin-film transport even in the presence of disorder [3].

Here we uncover an unconventional (compared to metals) reduction of electrical resistivity with decreasing film thickness of thin nanocrystalline NbP and TaP semimetals. Our electrical measurements suggest surface-channel dominated transport with decreasing film thicknesses in these nanocrystalline semimetals.

NbP and TaP thin films are sputtered on both sapphire and MgO substrates at 400 °C, a process compatible with back-end-of-the-line semiconductor fabrication. High-angle annular dark-field (HAADF) scanning transmission electron microscope (STEM) imaging reveals nano-crystallinity of the ultrathin NbP films with short-range ordering at the NbP surface, irrespective of the film thickness. A thin seed layer of Nb (or Ta) is used to reduce lattice mismatch between the substrate and sputtered NbP (or TaP) thin films, which also helps promote the local short-range order within the NbP films. The compositional homogeneity of the NbP thin films is further confirmed by energy-dispersive X-ray analysis.

The electrical resistivity of NbP and TaP shows a decreasing trend with decreasing film thicknesses (from ~80 nm down to ~1-2 nm) measured across a temperature range from 5 K up to room temperature. The sub-5 nm thin TaP and NbP films show significantly lower resistivity (e.g., ~12 μΩ-cm for 1 nm thin TaP and ~34 μΩ-cm for ~1.5 nm NbP, at room temperature) compared to their bulk single-crystal counterparts, as well as topological insulators and most metals at similar thicknesses [1,2,5,6].

Temperature-dependent measurements of our thin NbP films show increased conductivity with decreasing temperature. In contrast, bulk thick NbP (~80 nm) shows an opposite trend indicating impurity- or disorder-limited transport [5]. Based on a two-channel (surface and bulk) model of the experimental transport data, we deduce that with decreasing film thicknesses, the surface-to-bulk conductance ratio increases. We simultaneously find that the surface conductance increases with decreasing temperature, consistent with metallic behavior [5, 6]. Hall measurements show a decreasing trend of carrier density with decreasing thickness, and thus the estimated mobility increases for thinner films (e.g., ~7.4 cm²/V/s for ~4.3 nm NbP vs. ~0.2 cm²/V/s for bulk NbP). This also allows us to estimate a high surface-area-normalized carrier density of ~10¹⁶ cm⁻², and a 2D surface mobility of ~12 cm²/V/s. As film thickness decreases, the surface mobility contribution becomes more pronounced, leading to an increased conductivity in ultrathin NbP.

In summary, we uncovered surface-state-dominated conduction in ultrathin nanocrystalline NbP and TaP films. This leads to an exceptional decrease in the

resistivity with decreasing film thickness in such semimetals, promising for next-generation nanoelectronics. This work was supported in part by the Stanford SystemX Alliance.

Refs: [1] D. Gall et al., *MRS Bulletin* (2021). [2] C. Shekhar et al., *Nat. Phys.* (2015). [3] N. Lanzillo et al., *Phys. Rev. Appl.* (2022). [4] Y-B. Yang et al., *Phys. Rev. Lett.* (2019). [5] P. Corbae et al., *Nat. Mat.* (2023). [6] C. Zhang et al., *Nat. Mat.* (2019).

2:30 PM *QT07.02.04

Light-Field-Driven Non-Ohmic Current and Keldysh Crossover in a Weyl Semimetal [Shin-ichi Kimura](#)^{1,2}; ¹Osaka University, Japan; ²Institute for Molecular Science, Japan

In recent years, coherent electrons driven by light fields have attracted significant interest in exploring novel material phases and functionalities. However, observing coherent light-field-driven electron dynamics in solids is challenging because the electrons are scattered within several ten femtoseconds in ordinary materials, and the coherence between light and electrons is disturbed. However, when we use Weyl semimetals, the electron scattering becomes relatively long (several hundred femtoseconds - several picoseconds), owing to the suppression of the back-scattering process. This study presents the light-field-driven dynamics by the THz pulse to Weyl semimetal $\text{Co}_3\text{Sn}_2\text{S}_2$, where the intense THz pulse of a monocycle electric field nonlinearly generates direct current (DC) via coherent acceleration without scattering and non-adiabatic excitation (Landau-Zener Transition). In other words, the non-Ohmic current appears in the Weyl semimetal with a combination of the long relaxation time and an intense THz pulse. This nonlinear DC generation also demonstrates a Keldysh crossover from a photon picture to a light-field picture by increasing the electric field strength [1].

[1] R. Ikeda, H. Watanabe, J. H. Moon, M. H. Jung, K. Takasan, S. Kimura, arXiv: 2306.08876.

3:00 PM BREAK

SESSION QT07.03: Interfaces and Surfaces
Session Chairs: Stephan Lany and Hsin Lin
Tuesday Afternoon, April 23, 2024
Room 448, Level 4, Summit

3:30 PM *QT07.03.01

Quantum transport and spintronics in topological semimetal heterostructures [Nitin Samarth](#); The Pennsylvania State University, United States

We provide an overview of the synthesis and study of epitaxially grown topological semimetal heterostructures, focusing on Dirac semimetals (Cd_3As_2 , ZrTe_2) and Weyl semimetals (TaAs, NbAs). Studies of the integer quantum Hall effect in high mobility films of Cd_3As_2 provide new insights into the effects of quantum confinement on the g-factor of Dirac states [1]. By interfacing Cd_3As_2 and TaAs with a ferromagnetic metal ($\text{Ni}_{0.8}\text{Fe}_{0.2}$), we probe efficient spin-charge conversion at room temperature, in agreement with first principles calculations of the spin hall conductivity [2,3]. We also observe surprising effects of an interfacial oxide on the magnitude and sign of the spin-charge conversion efficiency. Finally, we discuss the spin-charge conversion and spin orbit torque in $\text{ZrTe}_2/\text{CrTe}_2$ heterostructures wherein a Dirac semimetal is interfaced with a 2D ferromagnet [4].

This work is sponsored in part by SMART, a funded center of nCORE, a Semiconductor Research Corporation (SRC) program sponsored by NIST, the Institute for Quantum Matter under DOE EFRC grant DE-SC0019331, and the Penn State Two-Dimensional Crystal Consortium-Materials Innovation Platform (2DCC-MIP) under NSF Grant No. DMR- 2039351.

1. R. Xiao et al., "Integer quantum Hall effect and enhanced g factor in quantum-confined Cd_3As_2 films," *Physical Review B* **106**, L201101 (2022).
2. W. Yanez et al., "Spin and charge interconversion in Dirac semimetal thin films," *Physical Review Applied* **16**, 054031 (2021).
3. W. Yanez et al., "Giant dampinglike-torque efficiency in naturally oxidized polycrystalline TaAs thin films," *Physical Review Applied* **18**, 054004 (2022).
4. Y. Ou et al., " $\text{ZrTe}_2/\text{CrTe}_2$: an epitaxial van der Waals platform for spintronics," *Nature Communications* **13**, 2972 (2022).

4:00 PM QT07.03.02

Magnetic Field-Effect Transistors based on The Topological Semimetal NbP [Lorenzo Rocchino](#)¹, Federico Balduini¹, Heinz Schmid¹, Mathieu Luisier², Vicky Süß³, Claudia Felser³, Bernd Gotsmann¹ and Cezar Zota¹; ¹IBM Research-Zurich, Switzerland; ²ETH Zürich, Switzerland; ³Max Planck Institute for Solid State Research, Germany

In the ever-evolving landscape of electronics and semiconductor technology, the quest for faster and more efficient transistors has driven researchers to explore unconventional materials and device architectures. Topological semimetals, like Weyl semimetals (WSMs), are promising candidates for redefining transistor technology in this context¹. Their unique transport properties, such as linear electronic bands, chiral fermions, and topologically protected surface states, can enable innovative device architectures, potentially outperforming standard complementary metal-oxide-semiconductor (CMOS) technology. Linear energy dispersion, in particular, yields low carrier mass and ultra-high mobility, which translates to the extreme magnetoresistance, up to 10⁶ %, exhibited by these materials, such as Cd_3As_2 , NbP, WP_2 , and many others². In this work, we demonstrate a new type of transistor that operates through a magnetoresistive coupling between a WSM and a superconductor. The active material is a topological WSM, NbP, whose resistivity is modulated via a magnetic field generated by the nearby superconductor. By using magnetic fields as a control quantity, the performance of the realized device is not reliant on ultra-thin channels, such as is the case for semiconductor electric-field devices. More importantly, this type of device allows to modulate the resistivity of a semi-metallic channel material with extremely low resistivity, ρ , and high carrier density (up to 10²⁰ cm⁻³), which is also not possible in a traditional semiconductor field-effect transistor. A full characterization of the NbP crystallite, performed with an externally generated magnetic field (up to 9 T), reveals very high values of MR, consistent with the ones reported in the literature. The fit of quantum oscillation data according to the Lifshitz-Kosevich formula allows the extraction of the main transport-related quantities, such as electron mobility, carrier density, and effective mass. The superconductive gate is made of NbN, and it is implemented to eliminate the contribution of self-heating, caused by the power dissipated in the gate electrode, to the resistivity modulation. The SC transition of the NbN gate occurs in a temperature range of 13.1 to 13.4 K, above the operating point of the device (5 K). The device characterization was done superposing the locally generated field with an external field offset which is able to shift the operating point of the

device towards a region where the MR coupling, dp/dB , is maximized. Furthermore, we were able to accurately reproduce the resistivity variation of the external magnetic field with the local magnetic gate using point-wise measurements. Due to the exceptionally large electron mobility of this material, which reaches over 10^6 cm^2/Vs , and the strong magnetoresistive coupling, we show that the realized magnetic Weyl transistor operates with very high transconductance gain at nanowatt levels of power dissipation. Transconductance gain, together with overall low parasitic RC delay indicates the potential for improvements over standard cryogenic amplifier technologies.

We foresee qubit readout signal amplification as a highly attractive area of application for this device due to the increasing need for low-power cryogenic amplifiers, operating at power budgets that will continue to shrink as quantum computers advance. Moreover, our device presents a generalized scheme to control the transport properties of Weyl semimetals, many of which are sensitive to magnetic fields. Overall, the obtained results indicate a promising path forward for integrated Weyl semimetal electronics that can leverage the often extreme transport properties of such materials.

References:

1. Gilbert, M. J. Topological electronics. *Commun Phys* **4**, 1–12 (2021).
2. Shekhar, C. *et al.* Extremely large magnetoresistance and ultrahigh mobility in the topological Weyl semimetal candidate NbP. *Nature Phys* **11**, 645–649 (2015).

4:15 PM *QT07.03.03

Quantum Metric Nonlinear Hall Effect in a Topological Antiferromagnetic Heterostructure Anyuan Gao¹, Ted Liu¹, Barun Ghosh², Thais Trevisan³, Yugo Onishi⁴, Chaowei Hu⁵, Tiema Qian⁵, Shaowen Chen¹, Mengqi Huang⁶, Damien Berube¹, Hochen Li¹, Christian Tzschaschel¹, Thao Dinh^{1,1}, Zhe Sun⁷, Sheng-Chin Ho¹, Shang-Wei Lien⁸, Bahadur Singh⁹, Kenji Watanabe¹⁰, Takashi Taniguchi¹⁰, David Bell¹, Hsin Lin¹¹, Tay-Rong Chang⁸, Arun Bansil², Chunhui Du⁶, Liang Fu⁴, Ni Ni⁵, Peter Orth³, Qiong Ma⁷ and Suyang Xu¹; ¹Harvard University, United States; ²Northeastern University, United States; ³Iowa State University, United States; ⁴Massachusetts Institute of Technology, United States; ⁵University of California, Los Angeles, United States; ⁶University of California, San Diego, United States; ⁷Boston College, United States; ⁸National Cheng Kung University, Taiwan; ⁹Tata Institute of Fundamental Research, India; ¹⁰National Institute for Materials Science, Japan; ¹¹Academia Sinica, Taiwan

Quantum geometry - the geometry of electron Bloch wavefunctions - is central to modern condensed matter physics. Due to the quantum nature, quantum geometry has two parts, the real part quantum metric and the imaginary part Berry curvature. Berry curvature has led to countless breakthroughs, ranging from the quantum Hall effect in 2DEGs to the anomalous Hall effect (AHE) in ferromagnets. In contrast, the quantum metric has rarely been explored. In this talk, I will report a new nonlinear Hall effect induced by quantum metric dipole by interfacing even-layered MnBi₂Te₄ with black phosphorus. This nonlinear Hall effect switches direction upon reversing the AFM spins. It exhibits distinct scaling demonstrating the non-dissipative nature. Like the AHE brought Berry curvature under the spotlight, our results open the door to discovering quantum metric responses. Moreover, our data suggests that the AFM can harvest wireless electromagnetic energy, enabling applications that bridges nonlinear electronics with AFM spintronics.

A. Gao et al. Quantum metric nonlinear Hall effect in a topological antiferromagnetic heterostructure. *Science* **381**, 181 (2023)

SESSION QT07.04: Poster Session
Session Chairs: Kirstin Alberi and Stephan Lany
Tuesday Afternoon, April 23, 2024
Flex Hall C, Level 2, Summit

5:00 PM QT07.04.01

Theoretical Study of The Electronic Properties of a 3D Dirac Semimetal Ge₄Sn using First-principles Mahesh Balwade and Prabhakar Singh; Indian Institute of Technology Bombay, India

A recent theoretical study¹ has predicted the topological nature of two materials with tetragonal structures: Ge₅ and Sn₅. Building upon this research, we investigated the electronic properties of Ge₄Sn, which shares a similar crystal structure. Our study shows that Ge₄Sn is metallic and non-magnetic in nature. Notably, the lattice parameters of Ge₄Sn are somewhat larger than those of Ge₅, yet significantly smaller than Sn₅. This discrepancy can be attributed to the relatively smaller size of the Ge atom in comparison to Sn. The chemical bonds of Ge₄Sn have covalent characteristics confirmed by the charge density plot. Furthermore, we find a strong hybridization between Ge *4p* and Sn *5p* orbitals in the energy range -4 to 0 eV below the Fermi energy. The highly anisotropic Dirac cone appears near *the A* point in the band structure without spin-orbit interaction. However, the inclusion of spin-orbit interaction leads to a significant band-splitting around *A* point as well. Topological properties are studied by calculating topological invariant and surface states. These results collectively demonstrate that Ge₄Sn exhibits the characteristics of a 3D Dirac semimetal. Further study is needed to uncover novel properties of Ge₄Sn. [1] C. Zhong, *Front. Phys.* **16**(6), 63503 (2021).

SESSION QT07.05: Fundamentals, Theory and Modeling II
Session Chairs: Kirstin Alberi and Hsin Lin
Wednesday Morning, April 24, 2024
Room 448, Level 4, Summit

8:30 AM *QT07.05.01

Chirality and Topology Claudia Felser; Max Planck Institute, Germany

Chirality is a very active field of research in organic chemistry, closely linked to the concept of symmetry. Topology, a well-established concept in mathematics, has nowadays become essential to describe condensed matter [1,2]. At its core are chiral electron states on the bulk, surfaces and edges of the condensed matter systems, in which spin and momentum of the electrons are locked parallel or anti-parallel to each other. Magnetic and non-magnetic Weyl semimetals, for example, exhibit chiral bulk states that have enabled the realization of predictions from high energy and astrophysics involving the chiral quantum number, such as the chiral anomaly, the mixed axial-gravitational anomaly and axions [3-5]. Chiral topological crystals exhibit excellent chiral surface states [6,7] and different orbital angular momentum for the enantiomers, which can be advantageous in catalysis. The potential for connecting chirality as a quantum number to other chiral phenomena across different areas of science, including the asymmetry of matter and antimatter and the homochirality of life, brings topological materials to the fore [8].

References:

- [1] M. G. Vergniory, B. J. Wieder, L. Elcoro, S. S. P. Parkin, C. Felser, B. A. Bernevig, N. Regnault, *Science* 2022, 376, 6595.
- [2] P. Narang, C. A. C. Gracia and C. Felser, *Nat. Mater.* 2021, 20, 293.
- [3] J. Gooth et al., *Nature* 2017, 547, 324.
- [4] J. Gooth et al., *Nature* 2019, 575, 315.
- [5] D. M. Neno, et al., *Nat Rev Phys* 2022, 2, 682.
- [6] B. Bradlyn, J. Cano, Z. Wang, M. G. Vergniory, C. Felser, R. J. Cava and B. A. Bernevig, *Science* 2016, 353, aaf5037.
- [7] N. B. M Schroeter, et al., *Science* 2020, 369, 179.
- [8] C. Felser, J. Gooth, *Chiral Matter*. March 2023, 115

9:00 AM *QT07.05.02

Electron Hydrodynamics and Signatures of Unconventional Transport in Topological Semimetals Prineha Narang; University of California, Los Angeles, United States

The re-invigorated field of electron hydrodynamics in quantum matter has recently garnered considerable scientific interest, both due to its technological promise of designing near dissipation-less nanoelectronics, as well as its fundamental importance as an experimental probe of strong electron-electron interactions. Investigating the capacity to which observations of electron hydrodynamic flows can inform the nature of electron-electron interactions is particularly important and timely with the advent of spatially-resolved transport measurements which, having demonstrated the hallmark spatial signature of electron hydrodynamic channel flow, must now turn their attention to studying more spatially-complex geometries, enabling the observation of intricate fluid phenomena such as vortices. Recently we have explored the effects of crystal symmetry on electron fluid behaviors starting from the most general viscosity tensors in two and three dimensions, constrained only by crystal symmetry and thermodynamics. In our work we demonstrate the anomalous landscape for electron hydrodynamics in systems beyond graphene, highlighting that previously-thought exotic fluid phenomena can exist in both two-dimensional and anisotropic three-dimensional materials with or without breaking time-reversal symmetry. In this context, the first part of my talk will discuss our recent predictions of hydrodynamics beyond graphene, especially the role of phonons in hydrodynamics in Weyl semimetals. We identify phonon-mediated electron-electron interactions, computed with techniques developed in the group that I will discuss in this talk, as critical in a microscopic understanding of hydrodynamics. In the context of these results in electron hydrodynamics, I will introduce a theoretical and computational transport framework from our group, the SpaRTaNS (Spatially Resolved Transport of Nonequilibrium Species) framework. I will discuss applications of this method in nonequilibrium electron and phonon transport in quantum matter. Time permitting, I will present recent work on unconventional mesoscopic transport regimes in kagome magnets. The kagome magnets TbMn6Sn6 (a Chern ferrimagnet) and Mn3Ge (a Weyl semimetal antiferromagnet) have interesting electronic and thermal conductivities, with the two showing large and opposing deviations from the Wiedemann-Franz law and Mott relation. Leveraging the aforementioned approach, we study whether such conductivities can be decoupled into independent diffusive modes and explore the possible emergence of hydrodynamics in finite channel geometries.

9:30 AM *QT07.05.03

Quantum Geometric Detection and Control of Quantum Materials Qiong Ma; Boston College, United States

In the quantum world of electrons, there exists a geometric structure formed by their quantum wave functions. This quantum geometry, studied through quantum metric and Berry curvature and deeply connected with topology, significantly impacts the behavior of electrons in unique ways. In this talk, I will discuss a few examples of how the coupling between quantum geometry and electromagnetic fields or waves can be utilized to detect and control topological materials.

10:00 AM BREAK

SESSION QT07.06: Synthesis and Characterization II
Session Chairs: Kirstin Alberi and Hsin Lin
Wednesday Morning, April 24, 2024
Room 448, Level 4, Summit

10:45 AM *QT07.06.01

Insights into The Role of Disorder in Topological Semimetals Kirstin M. Alberi; National Renewable Energy Laboratory, United States

As a result of their bandstructures, three-dimensional topological semimetals (TSMs) exhibit phenomena that are of potential interest for device applications, including ultra-high electron mobility, broadband optical absorption, linear magnetoresistance and the chiral anomaly. These behaviors have largely been studied in bulk crystals, but thin films will be required for devices. Given that disorder, in the form of defects, impurities and interfaces, will inevitably be present in thin films, it is important to understand the role they play on the behavior of TSMs. In this talk, I will discuss our use of epitaxy to intentionally vary specific forms of disorder and thereby generate new insights into property-disorder relationships. Our studies, mostly performed in Cd₃As₂ grown by molecular beam epitaxy, suggest that point defects modestly affect electron mobility but can substantially influence magnetoresistance. Impurities also offer important control knobs for controlling the Fermi level, either as extrinsic dopants or through indirect influence on the balance of point defects. Finally, I will discuss challenges and outstanding questions that the TSM field must address to effectively implement these materials into device applications.

11:15 AM QT07.06.03

Properties of Topological Semimetal Cd₃As₂ Thin Films as a Function of Growth Optimization and Buffer Choice Thomas G. Farinha^{1,2}, Edwin Supple³, Gregory M. Stephen², Nicholas A. Blumenschein², Adam L. Friedman², Brian Gorman³ and Christopher J. Richardson^{1,2}; ¹The University of Maryland, United States; ²Laboratory for Physical Sciences, United States; ³Colorado School of Mines, United States

The Dirac semimetal Cd₃As₂ is a high mobility, 3D topological semimetal with potential for exploration of quantum phenomena and future information science devices. However, the dependence of its topological properties on growth and heterostructure design is not well explored. Such parameters include growth temperature, dislocation density, and biaxial strain owing to lattice mismatch. The growth of Cd₃As₂ on different abrupt metamorphic buffer layers

is therefore completed via molecular beam epitaxy. The aforementioned growth variables are considered for their effect on the final electronic and physical quality and characteristics of the thin film Cd_3As_2 . Cd_3As_2 is grown on relaxed AlInSb , GaInSb , and InAsSb layers with engineered lattice constants at temperatures ranging from 50 to 130 °C. X-ray diffraction and transmission electron microscopy are used to evaluate the buffer layer quality and threading dislocation density. Van der Pauw measurements are conducted to determine carrier mobility and density according to the experimental variables. With the objective of maximizing electron mobility, films are grown over a range of variables including layer thickness and annealing times.

11:30 AM *QT07.06.04

Unique Electromagnetic Responses of Unconventional Topological Semimetals [Junyeong Ahn](#)¹ and Barun Ghosh²; ¹Harvard University, United States; ²Northeastern University, United States

Elucidating the physical manifestations of nontrivial band topology in materials is of great interest in quantum materials science. Recent advances in the classification of topological band crossing have led to the discovery of various new kinds of low-energy excitations. Yet, the unique physical properties that qualitatively distinguish them from Weyl and Dirac fermions or conventional metals are rarely known. In this talk, we present our theoretical discovery of unique electromagnetic response properties in unconventional topological point-node semimetals [1,2]. First, we reveal the pattern of the divergent nonlinear responses as the chemical potential approaches the energy of an overtilted (i.e. the so-called type-II) nodal point, with the leading divergence determined by the dispersion and dimensionality [1]. Then, we show that chiral multifold nodal points feature the unique circular dichroism that is absent for Weyl or Dirac fermions [2]. Our finding demonstrates that new types of excitations indeed possess new responses, motivating further exploration of other unconventional fermions whose unique response properties are elusive.

This work was supported by the Center for Advancement of Topological Semimetals (CATS), an Energy Frontier Research Center funded by the U.S. Department of Energy Office of Science, Office of Basic Energy Sciences, through the Ames Laboratory under contract No. DE-AC02-07CH11358.

[1] Junyeong Ahn, Topological enhancement of nonlinear transport in unconventional point-node semimetals, Phys. Rev. B 107, L201112 (2023).

[2] Junyeong Ahn and Barun Ghosh, Topological Circular Dichroism in Chiral Multifold Semimetals, Phys. Rev. Lett. 131, 116603 (2023).

SESSION QT07.07: Transport
Session Chairs: Kirstin Alberi and Stephan Lany
Wednesday Afternoon, April 24, 2024
Room 448, Level 4, Summit

1:30 PM *QT07.07.01

Lattice-Geometry Driven Hybrid Nodal Fermions in Topological Semimetals Bahadur Singh¹ and Sougata Mardanya²; ¹Tata Institute of Fundamental Research Mumbai, India; ²Howard University, United States

Successful classification of topological electronic states based on the crystalline lattice symmetries led to the identification of many topological materials through high-throughput first-principles modeling. Such symmetry-to-topology characterizations, however, ignore the effects of various crystallographic or nanoscopic motifs and their associated wavefunction properties even though they are essential for describing the numbers, energy-momentum relations, and geometries of the nontrivial states. Here, we discuss how spatial arrangements of atoms dictate the nature of energy dispersions of topological states in materials [1]. Specifically, we focus on anisotropic lattice materials and demonstrate that the lattice geometry-driven effective mass anisotropies dictate the hybrid nodal-line states by considering transition metal tetraphosphides MP_4 (M = Transition metal) as exemplary materials. We also discuss a general theory of incorporating orientation-dependent carrier effective masses as experimental fingerprints for determining energy dispersion in topological materials.

[1] B. Patra, R. Verma, S.-M. Huang, B. Singh, arXiv:2304.13086 (2023).

2:00 PM QT07.07.02

Structural Goldilocks Effect in The Ultra-Pure Topological Semimetal PtSn_4 [Samikshya Sahu](#)^{1,1}, Dong Chen^{1,1}, Niclas Heinsdorf^{1,1,2}, Mohamed Oudah¹, Douglas A. Bonn^{1,1}, Sarah Burke^{1,3,1} and Alannah Hallas^{1,1}; ¹University of British Columbia, Canada; ²Max Planck Institute for Solid State Research, Germany; ³The University of British Columbia, Canada

The Residual Resistivity Ratio (RRR) serves as a pivotal metric to gauge sample quality for metals, where RRR is the ratio of the resistivity at room temperature (~ 300 K) to the resistivity at base temperature (~ 0 K). For common metals like Au or Cu, transport behavior at 0 K primarily reflects the inherent defects and disorders within the material. Whereas at room temperature, the electronic transport is substantially influenced by other factors, such as phonons. Therefore, a sample with a high RRR can be valued as possessing fewer intrinsic defects and less disorder. However, such pristine materials are tough to come by and often require a lot of effort to optimize the crystal growth technique to make defect-free samples.

PtSn_4 is a rare exception, and shows ultra-low resistivity around 2 K and remarkable RRR values exceeding 1000. One of the other dominating electronic properties of this material is its ultrahigh magnetoresistance (XMR), which onsets at 30 K. Magnetoresistance (MR) is the resistance that develops in a material as a response to the application of the magnetic field. PtSn_4 is also classified as a novel topological semimetal and hosts Dirac arcs in its momentum space such that the conduction and valence band touch in loops and not at a point or line. Previous studies have linked this high mobility and XMR in PtSn_4 to its distinctive Fermi surface and the band dispersion of nodal arc surface states. Yet, despite numerous reports suggesting a connection between these surface states and electronic transport properties, a clear physical relationship remains elusive. Therefore, it is crucial to understand the origin of the high mobility and XMR in PtSn_4 , which will also shed light on the underlying relation between the non-trivial band topology and experimentally observed electrical transport properties in PtSn_4 .

Through this work on PtSn_4 , we aim to resolve the question about the origin of the high carrier mobility by perturbing the system using defects and chemical substitution. This approach allows to disentangle whether the high mobility in PtSn_4 originates from forbidden backscattering, which results from topologically protected surface states, or whether it is related to an unusually low defect density. Using electrical transport measurements, scanning tunneling microscopy (STM) and density functional theory (DFT) calculation we confirm that PtSn_4 is remarkably robust against chemical substitution and resistant to defect introduction into its lattice. Comparing it with AuSn_4 and IrSn_4 , which form locally similar structures to PtSn_4 , we find significantly

lower RRR values in the latter two. This highlights the uniqueness of the PtSn₄ structure. The high electron mobilities in PtSn₄ can be attributed to the defect-intolerant Pt layers, which dominate electronic transport. Our STM mappings quantitatively assess the defect concentration in PtSn₄, revealing surprisingly low defects in the Pt layers compared to higher concentrations in the Sn layers. DFT calculations corroborate these findings, showing higher defect formation energies for Sn within the PtSn₄ lattice and the favorable energy associated with introducing defects into the AuSn₄ structure. Thus, we conclude that the crystal chemistry in PtSn₄ is a good example of a structural Goldilocks effect where the naturally defect-intolerant layers support the long electron-free paths.

2:15 PM QT07.07.03

Evidence for The Chiral Anomaly in The Cubic Type-II Dirac Metal Pd₃In₇ Aikaterini Flessa Savvidou^{1,2}, Andrzej Ptok³, Gargee Sharma³, Brian Casas², Judith Clark⁴, Victoria Li⁴, Michael Shatruk¹, Sumanta Tewari⁵ and Luis Balicas^{1,2}; ¹Florida State Univ, United States; ²National High Magnetic Field Lab, United States; ³Institute of Nuclear Physics, Poland; ⁴Department of Chemistry and Biochemistry, United States; ⁵Clemson University, United States

We report a transport study on Pd₃In₇ which displays multiple Dirac type-II nodes in its electronic dispersion. Pd₃In₇ is characterized by low residual resistivities and high mobilities, which are consistent with Dirac-like quasiparticles. For an applied magnetic field ($\mu_0 H$) having a non-zero component along the electrical current, we find a large, positive, and linear in $\mu_0 H$ longitudinal magnetoresistivity (LMR). The sign of the LMR and its linear dependence deviate from the behavior reported for the chiral-anomaly-driven LMR in Weyl semimetals. Interestingly, such anomalous LMR is consistent with predictions for the role of the anomaly in type-II Weyl semimetals. In contrast, the transverse or conventional magnetoresistivity (CMR for electric fields $E \perp \mu_0 H$) is large and positive, increasing by $10^3 - 10^4$ % as a function of $\mu_0 H$ while following an anomalous, angle-dependent power law $\rho_{xx} \propto (\mu_0 H)^n$ with $n(\theta) \leq 1$. The order of magnitude of the CMR, and its anomalous power-law, is explained in terms of uncompensated electron and hole-like Fermi surfaces characterized by anisotropic carrier scattering likely due to the lack of Lorentz invariance.

2:30 PM BREAK

SESSION QT07.08: Magnetic Semimetals
Session Chairs: Kirstin Alberi and Hsin Lin
Wednesday Afternoon, April 24, 2024
Room 448, Level 4, Summit

3:30 PM QT07.08.01

Experimental Observation of Nonreciprocal Reflection in a Magnetic Weyl Semimetal at Zero Applied Field Arun Nagpal¹, Ioannis Petrides², Chandra Shekhar³, Claudia Felser³, Prineha Narang² and Harry A. Atwater¹; ¹California Institute of Technology, United States; ²University of California, Los Angeles, United States; ³Max Planck Institute for Chemical Physics of Solids, Germany

The discovery of magnetic Weyl semimetals has inspired a flurry of investigation into the magneto-optical responses of such topological semimetals. In this work, we demonstrate modulation of the non-reciprocal p-polarized reflection coefficient by reversing the orientation remanent magnetization in a magnetic Weyl semimetal. Previously, measurements of nonreciprocity via the transverse magneto-optic Kerr effect, where the amplitude of the p-polarized reflection is modulated with respect to the polarity of a magnetization vector that is transverse to the optical plane, had remained elusive. We observe a net reflectance modulation of nearly 8% in the half-Heusler Co₃Sn₂S₂ at 80K without the concurrence of an external applied magnetic field, nearly an order of magnitude higher than previous measurements of the transverse magneto-optical Kerr effect in ferromagnets. Our results demonstrate the utility of magnetic Weyl semimetals for magneto-optical metasurfaces, applications in magnetic memory, and energy harvesting. Unlike traditional ferromagnets or magnetic semiconductors where the off-diagonal permittivity is a function of the cyclotronic resonance frequency, the nonreciprocal response of magnetic Weyl semimetals is believed to be governed by the nontrivial Berry curvature that exists between recombinant Weyl nodes. This unique topological effect paves the way for the realization of practical Berrytronic devices.

3:45 PM QT07.08.02

Pulsed Magnetic Field Studies of Topological Magnetic Kagome Compounds Joanna Blawat¹, Tyler Slade^{2,3}, John Singleton¹, Benjamin Ueland^{2,3}, Paul Canfield^{2,3}, Robert McQueeney^{2,3} and Ross McDonald¹; ¹Los Alamos National Laboratory, United States; ²Ames Laboratory, United States; ³Iowa State University of Science and Technology, United States

Magnetic Weyl semimetals provide an interesting opportunity to study the interplay between local spin texture, band topology and correlations. The rare earth 166 kagome materials are a prime example, which exhibit complex magnetic orders due to their geometrically frustrated 2D lattice, as well as an electronic structure that embodies both flat band and linear (Dirac) band crossings. Specifically, this includes ErMn₆Sn₆ which crystallizes in a hexagonal space group *P6/mmm* (No. 191). The recent neutron diffraction data shows that ErMn₆Sn₆ exhibits a first order transition from a planar-ferrimagnetic to distorted triple-spiral magnetic order at $T = 92$ K and the theoretical calculations using the mean-field theory predict a very rich magnetic phase diagram of ErMn₆Sn₆ [1]. We present the experimental measurements of magnetization in pulsed magnetic field with $H//a$, $H//b$ and $H//c$. The rich variety of magnetic phases gives us opportunity to study the behavior of Dirac fermions with control of the spin orientations tuned by the magnetic field. High field magnetoresistivity and Hall effect measurement helped us to identify novel magnetic and topological phases and probe Fermi surface topology via quantum oscillations. This combination of experiments reveals the possibility of tuning topological properties in ErMn₆Sn₆ via the application of strong magnetic fields.

[1] Riberolles, S. X. M, et al. arXiv preprint arXiv:2306.13206 (2023).

The work was performed at the National High Magnetic Field Laboratory (NHMFL), which is supported by National Science Foundation Cooperative Agreement No. DMR-2128556 and the Department of Energy (DOE). This research is supported by the Center for the Advancement of Topological Semimetals (CATS), an Energy Frontier Research Center funded by the USDOE Office of Science, Office of Basic Energy Sciences, through the Ames Laboratory. Ames Laboratory is operated for the USDOE by Iowa State University under Contract No. DE-AC02-07CH11358.

4:00 PM *QT07.08.03

Exotic Magnetotransport in Simple Magnetic Weyl Semimetal Films Masaki Uchida; Tokyo Institute of Technology, Japan

Magnetic Weyl semimetals host singularities called Weyl points in their band structures, and exotic magnetotransport phenomena involving the Weyl

points have been intensively studied. Magnetic Weyl semimetals discovered so far may be classified into two major groups. The first group includes Mn_3Sn , $\text{Co}_3\text{Sn}_2\text{S}_2$, and Co_2MnGa , which have $3d$ transition metal elements as magnetic elements and are characterized by high magnetic transition temperatures. On the other hand, these materials have high carrier density and complex band structures hosting Weyl points. The second group includes EuCd_2Sb_2 and GdPtBi , which have $4f$ rare earth elements as magnetic elements. Their magnetic transition temperatures are low, and it is necessary to apply a magnetic field for inducing the ferromagnetic Weyl phase. In these materials, their carrier density is low, and Weyl points occupy a large area compared to the Fermi surface. It is thus expected that exotic magnetotransport can be controlled and enhanced using thin-film techniques.

Based on our knowledge about film growth of II-V compounds such as Cd_3As_2 [1,2] and its combination to Eu magnetic elements [3-5], we have succeeded for the first time in fabricating single-crystalline EuCd_2Sb_2 thin films by molecular beam epitaxy [6]. While these films exhibit the same antiferromagnetic and field-induced ferromagnetic phases as EuCd_2Sb_2 bulks, they show a very large anomalous Hall effect compared to the bulks. We have systematically controlled the carrier density with electrostatic gating and have found that the anomalous Hall effect exhibits a sharp peak structure as function of carrier density. As also demonstrated by first-principles calculation, the intrinsic anomalous Hall conductivity is maximized reflecting the presence of Weyl points.

I will also present results about EuCd_2As_2 , another Weyl semimetal candidate, and extensively discuss exotic magnetotransport phenomena appearing in simple magnetic Weyl semimetal films.

References

- [1] Y. Nakazawa *et al.*, APL Mater. 7, 071109 (2019)
- [2] Y. Nakazawa *et al.*, Phys. Rev. B 103, 045109 (2021)
- [3] M. Ohno *et al.*, APL Mater. 9, 051107 (2021)
- [4] M. Uchida *et al.*, Sci. Adv. 7, eabl5381 (2021)
- [5] M. Ohno *et al.*, Phys. Rev. B 103, 165144 (2021)
- [6] M. Ohno *et al.*, Phys. Rev. B 105, L201101 (2022)

SESSION QT07.09: Heavy Fermions and Strong Correlation

Session Chairs: Stephan Lany and Stephanie Law

Thursday Morning, April 25, 2024

Room 448, Level 4, Summit

8:45 AM *QT07.09.01

Topological Semimetals in Heavy Fermion Compounds [Silke Buehler-Paschen](#); Vienna University of Technology (TU Wien), Austria

Gapless electronic topology driven by strong correlations is an emerging field of great interest, with heavy fermion compounds at its forefront. I will introduce the first such materials class, Weyl-Kondo semimetals [1-3], and report on the giant signatures of topology observed in $\text{Ce}_3\text{Bi}_4\text{Pd}_3$ [1,3] and the genuine topology control that can be achieved by magnetic field tuning [4,5]. I will also discuss design strategies for further correlation-driven topological phases, and discuss several realizations [6,7].

This work was supported by the Austrian Science Fund (FWF-I4047, I5868-FOR5249-QUAST, SFB F 86, Q-M&S), the European Union's Horizon 2020 Research and Innovation Programme (824109, EMP), and the European Research Council (ERC Advanced Grant 101055088, CorMeTop).

- [1] S. Dzsaber *et al.*, Phys. Rev. Lett. 118, 246601 (2017).
- [2] H.-H. Lai *et al.*, PNAS 115/1, 93 (2018).
- [3] S. Dzsaber *et al.*, PNAS 118, e2013386118 (2021).
- [4] S. Dzsaber *et al.*, Nat. Commun. 13, 5729 (2022).
- [5] S. E. Grefe *et al.*, arXiv:2012.15841.
- [6] L. Chen *et al.*, Nat. Phys. 18, 1341 (2022).
- [7] H. Hu *et al.*, arXiv:2110.06182.
- [8] D. M. Kirschbaum *et al.*, in preparation (2023).

9:15 AM QT07.09.02

Observation of Nodal-Line Semimetallic State in PrSbTe [Sabin Regmi](#)^{1,2}, [Iftakhar Bin Elius](#)¹, [Anup Pradhan Sakhya](#)¹, [Milo Sprague](#)¹, [Mazharul Islam Mondal](#)¹, [Nathan Valadez](#)¹, [Volodymyr Buturlim](#)², [Kali Booth](#)¹, [Tetiana Romanova](#)³, [Krzysztof Gofryk](#)², [Andrzej Ptok](#)³, [Dariusz Kaczorowski](#)³ and [Madhab Neupane](#)¹; ¹University of Central Florida, United States; ²Idaho National Laboratory, United States; ³Polish Academy of Sciences, Poland

Rare-earth(*R*) based *RSbTe* materials, which are isostructural to the nodal-line semimetal *ZrSiS*, are gathering research attention because of the possible elements of electronic correlation and magnetism that the *R-4f* electrons may bring. Here, we study the electronic structure in *PrSbTe* by utilizing angle-resolved photoemission spectroscopy (ARPES) in conjunction with first-principles calculations and thermodynamic measurements. Thermodynamic measurements show that no discernible phase transitions occur down to 2 K. ARPES results and their comparison with first-principles calculations reveal the presence of multiple nodal-line crossings in this system. This study contributes to the understanding of the role of spin-orbit coupling in the topological electronic structure within the *RSbTe* family of materials.

***This work is supported by National Science Foundation CAREER award DMR-1847962, Air Force Office of Scientific Research MURI Grant FA9550-20-1-0322, Idaho National Laboratory's Laboratory Directed Research and Development program under Idaho Operations Office Contract DE-AC07-05ID14517, and Division of Materials Science and Engineering, Office of Basic Energy Sciences, Office of Science of the U.S. Department of Energy (DOE).*

9:30 AM BREAK

SESSION QT07.10: van der Waals and 2D Materials

Session Chairs: Stephanie Law and Hsin Lin

Thursday Morning, April 25, 2024
Room 448, Level 4, Summit

10:00 AM *QT07.10.01

The Josephson Diode Effect in Junctions formed from 2D Van der Waals Metals [Stuart S. Parkin](#); Max Planck Institute of Microstructure Physics, Germany

Recently we have discovered a non-reciprocal Josephson diode effect in several Josephson junctions, both lateral and vertical, formed from conventional superconducting electrodes (Nb, NbSe₂) separated by several non-superconducting metals including the 2D van der Waals Dirac semi-metal, NiTe₂ [1]. We discuss a variety of other 2D metals that show a Josephson diode effect including WTe₂ [2], as well as those that do not show an effect such as MoTe₂. Each of these materials becoming superconducting by proximity to the conventional superconducting electrodes. The superconductivity can be sustained over long distances of, in some cases, up to ~1 micron. The critical supercurrent densities for current flowing in opposite directions within the junction are distinct and can vary by up to ~80%. The non-reciprocity is only observed in the presence of a small magnetic field oriented perpendicular to the supercurrent. For vertical Josephson junctions formed from WTe₂ we show that the non-reciprocity depends on the orientation of the magnetic field with respect to the crystal structure of the WTe₂, proving thereby the intrinsic origin of the Josephson diode effect. Such an effect could have important applications as a novel magnetic field detector at cryogenic temperatures, for example, to "read" magnetic domain walls in a cryogenic racetrack memory*. *Funded through an European Research Council Advanced Grant "SUPERMINT" (2022-2027).

[1] B. Pal *et al.*, "Josephson diode effect from Cooper pair momentum in a topological semimetal," *Nat. Phys.*, vol. 18, pp. 1228-1233, 2022.

[2] J.-K. Kim, K.-R. Jeon, P. K. Sivakumar, J. Jeon, C. Koerner, G. Woltersdorf, and S. S. P. Parkin, "Intrinsic supercurrent non-reciprocity coupled to the crystal structure of a van der Waals Josephson barrier," *arXiv:2303.13049*, 2023.

10:30 AM QT07.10.02

Engineering Van der Waals Heterostructures of Layered Dirac Materials for meV-Scale Quantum Sensing [Elizabeth Peterson](#) and Jian-Xin Zhu; Los Alamos National Laboratory, United States

Quantum sensing of meV-scale scattering and absorption of impinging particles with electrons in solid state detectors has important applications not only of interest for fundamental physics, such as the detection of astronomical phenomena and light dark matter, but also for quantum information, such as single photon detectors for quantum key distribution. Current sensing and detection schemes often use single-phase detectors, such as superconductors or narrow band gap semiconductors. These detector targets face challenges in differentiating between signals that come from impinging particles of interest and those from inherent quasiparticles, such as phonons and magnons, requiring operation at extreme cryogenic temperatures.

Heterostructures of layered massive Dirac materials offer a novel pathway to selective detection of impinging particles that can operate at more realistic temperature scales for scalable quantum sensing technology. In our scheme, by engineering interfacial orbital hybridization in van der Waals heterostructures of Dirac materials, interlayer charge transfer is promoted only for pre-selected types of impinging particles based on their dispersion relations (i.e. specific quantum mechanically allowed combinations of energy and momentum transfer). Here we present first-principles density functional theory calculations on exemplar heterostructures of the layered Dirac materials ZrTe₅ and HfTe₅ as a proof-of-principle of this novel quantum sensing scheme. As massive Dirac materials with narrow band gaps and strain-sensitive band structures, ZrTe₅ and HfTe₅ are ideal testbeds for detection of meV-scale absorption and scattering events. We demonstrate that the electronic structure of these heterostructures exhibits a promising distribution of regions of single-layer and hybridized interlayer orbital character necessary for selective interlayer charge transfer. We examine the effects of strain and layer number for tuning hybridization in the electronic structure and the type of impinging particle that may be detected. We suggest that by exploiting hybridization in heterostructures of Dirac materials, it is possible to construct "dispersion filters" for next-generation quantum sensors.

This work was supported by the U.S. DOE NNSA under Contract No. 89233218CNA000001. It was supported by the LANL LDRD Program, and in part by the Center for Integrated Nanotechnologies, a DOE BES user facility, in partnership with the LANL Institutional Computing Program for computational resources. Additional computations were performed at the National Energy Research Scientific Computing Center (NERSC), a U.S. Department of Energy Office of Science User Facility located at Lawrence Berkeley National Laboratory, operated under Contract No. DE-AC02-05CH11231 using NERSC award ERCAP0020494. LA-UR-23-31768

10:45 AM QT07.10.03

Exceptional Electronic Transport and Quantum Oscillations in Thin Bismuth Crystal Grown inside Van der Waals Materials [Amy Wu](#)¹, Laisi Chen¹, Naol Tulu¹, Joshua Wang¹, Adrian Juanson², Kenji Watanabe³, Takashi Taniguchi³, Michael T. Pettes⁴, Marshall Campbell^{1,4}, Chaitanya Gadre¹, Yinong Zhou¹, Hangman Chen¹, Penghui Cao¹, Luis Jauregui¹, Ruqian Wu¹, Xiaoqing Pan^{1,1,1} and Javier Sanchez-Yamagishi¹; ¹University of California, Irvine, United States; ²California State University Long Beach, United States; ³National Institute for Materials Science, Japan; ⁴Los Alamos National Laboratory, United States

Most materials are challenging to produce as uniform and thin crystals with large grain size. Varying the thickness of a material alters its electronic behaviors and enables new devices. We have developed a new synthesis technique to grow crystals in a nanoscale mold defined by atomically-flat van der Waals (vdW) materials. We heat and compress bismuth in a vdW-mold made of hexagonal boron nitride (hBN), resulting in controlled thickness such as ultraflat 10 nm to 100 nm thick bismuth. The vdW-molded bismuth at different thickness all shows exceptional electronic transport, enabling the observation of Shubnikov-de Haas quantum oscillations originating from the (111) surface state Landau levels, which have eluded previous studies. Our vdW-mold growth technique establishes a platform for electronic studies and control of bismuth's Rashba surface states and topological boundary modes. Other than molding bismuth, we have also successfully molded tin and gold. Beyond confining in thickness, we also molded bismuth into vdW-molds with predefined shapes. This vdW-molding approach provides a low-cost way to synthesize ultrathin crystals and directly integrate them into a vdW heterostructure.

11:00 AM *QT07.10.04

Symmetric State Topological Heavy Fermion Metal in Twisted Bilayer Graphene [Bogdan A. Bernevig](#); Princeton University, United States

We show that the noninteger filling low temperature state of twisted bilayer graphene is a symmetric metal which exhibits a kondo resonance. This fermi liquid state can then become susceptible to pairing, as it efficiently screens the coulomb interaction.

SESSION QT07.11: Devices
Session Chairs: Stephan Lany and Stephanie Law
Thursday Afternoon, April 25, 2024
Room 448, Level 4, Summit

1:30 PM *QT07.11.01

Nonlinear Hall Effect in Dirac/Weyl Semimetals and Terahertz Detection Yang Zhang; The University of Tennessee, Knoxville, United States

We propose a method for broadband long-wavelength photodetection using the nonlinear Hall effect in Dirac/Weyl semimetals with/without magnetic field. With intrinsically tilted spectrum or induced chirality imbalance, the net Berry curvature gives rise to a nonlinear current, with inherently quadratic relation between transverse current and input voltage. This effect is then used to rectify the incident terahertz or infrared electric field into a direct current, without invoking any diode. Our photodetector operates at zero external bias with fast response speed and has zero threshold voltage. Remarkably, the intrinsic current responsivity due to the Berry curvature mechanism is a material property independent of the incident frequency or the scattering rate, which can be evaluated from first-principles electronic structure calculations. We identify the Weyl semimetal NbP and ferroelectric semiconductor GeTe for terahertz/infrared photodetection with large current responsivity without external bias.

2:00 PM QT07.11.02

Zero-Field Josephson Diode Effect in Dirac Semimetal-Based Asymmetric SQUIDs Joseph J. Cuzzo¹, Wenlong Yu¹, Keshab Sapkota¹, Enrico Rossi², David Rademacher¹, Tina Nenoff¹ and Wei Pan¹; ¹Sandia National Laboratories, United States; ²William & Mary, United States

Conventional diodes are characterized by their non-reciprocal charge transport and are ubiquitous in electronic devices. Within superconducting electronics, the superconducting diode effect (SDE) has attracted interest in recent years. Superconducting diodes are characterized by an asymmetry in positive and negative switching currents and could potentially find utility in a growing number of applications at cryogenic temperatures in the Quantum Information Sciences. Currently, many superconducting diodes require an external magnetic field or ferromagnetic layers to break time-reversal symmetry and induce the SDE. In this talk, we will discuss the *zero-field* SDE in asymmetric superconducting quantum interference devices (SQUID) based on Dirac semimetals. In this case, the Josephson effects in the SQUID arms dictate the non-reciprocity (Josephson diode effect) and we theoretically explore the role of surface and bulk states in Dirac semimetals. We will discuss how coupling of surface and bulk states can give rise to a diode effect in the *absence* of external magnetic fields or ferromagnetic layers. We will then present experimental results showing a zero-field SDE in asymmetric SQUIDs based on Dirac semimetal Cd₃As₂.

J.J.C, E.R., and W.P. acknowledge support from DOE, Grant No DE-SC0022245. The work at Sandia was also supported by LDRD projects. Device fabrication was performed at the Center for Integrated Nanotechnologies, a U.S. DOE, Office of BES, user facility. Sandia National Laboratories is a multimission laboratory managed and operated by National Technology and Engineering Solutions of Sandia LLC, a wholly owned subsidiary of Honeywell International Inc. for the U.S. DOE's National Nuclear Security Administration under contract DE-NA0003525.

2:15 PM *QT07.11.03

Dark Matter Detection with Topological Materials Sinead M. Griffin; Lawrence Berkeley National Laboratory, United States

The last few decades have seen a huge surge of interest in matter that cannot be described by our standard theories. For instance, the nature of dark matter, which cannot be described by the Standard Model, remains one of the biggest mysteries in our current understanding of the matter in our universe. As ongoing experiments continue to rule out large regions of phase space for higher-mass dark matter (e.g. WIMPs), new ideas for the direct detection of low mass (sub-GeV) are needed. These lighter DM masses require us to rethink the fundamental requirements for dark matter detectors to be sensitive to these lower masses. In this talk I will discuss how low-energy excitations in condensed matter systems are apt for the detection of such low-mass DM. I will discuss some of our proposals for detecting such low-mass DM in topological materials. As examples, I discuss the coupling and detection of (i) particle-like DM in topological semimetals and (ii) wave-like axion dark matter in topological insulators and multiferroics. I will also discuss how topological materials provide a unique route for sensing these rare events. To finish, I will discuss current challenges and opportunities for the intersection of condensed matter approaches to dark matter detection.

2:45 PM *QT07.11.04

Applications of Topological Semimetals for Post-Cu Interconnects Ching-Tzu Chen¹, Hsin Lin², Christian Lavoie¹, Nicholas Lanzillo³, Guy M. Cohen¹, Oki Gunawan¹, John Bruley¹, Peter Kerns¹, Franco Stellari¹, Nathan Marchack¹, Vesna Stanic¹, Utkarsh Bajpai³, Ion Garate⁴, Gengchiao Liang⁵, Yi-Hsin Tu⁶, Shang-Wei Lien⁶, Ravishankar Sundararaman⁷, Sushant Kumar^{7,3}, Cheng-Yi Huang⁸, En-De Chu⁹, Jason Tran⁹, Peng Wei⁹ and Asir Intisar Khan¹⁰; ¹IBM T.J. Watson Research Ctr, United States; ²Academia Sinica, Taiwan; ³IBM Research, United States; ⁴Université de Sherbrooke, Canada; ⁵National Yang Ming Chiao Tung University, Taiwan; ⁶National Cheng Kung University, Taiwan; ⁷Rensselaer Polytechnic Institute, United States; ⁸Northeastern University, United States; ⁹University of California, Riverside, United States; ¹⁰Stanford University, United States

Conduction via the surface states in topological semimetals yields unconventional scaling behavior such that resistivity decreases with reduced device dimensions down to ~nm. This may provide a solution for the interconnect bottleneck in highly scaled integrated circuits. In the first half of the talk, we will present first-principles-based electrical transport calculations of a Si-CMOS compatible topological semimetal CoSi and a prototypical Weyl semimetal NbAs. We will summarize the simulation results of pristine films and films with point defects, line defects, or grain-boundaries. We will also report the contact resistance scaling between a topological semimetal and a conventional liner material.

In the second half of the talk, we will report detailed experimental studies of CoSi. We first present resistivity scaling data of both polycrystalline and highly textured thin films down to ~5nm. Our magneto-transport measurements reveal coexisting high-mobility surface carriers with low-mobility bulk carriers and their temperature dependence. Most notably, we observe that the room-temperature resistivity in nanoscale CoSi thin films can drop below the ideal bulk single-crystal limit. Last, we present the resistance scaling of wafer-scale CoSi nanowires, both polycrystalline and highly textured. Our proof-of-principle studies demonstrate the potential of topological semimetals as post-Cu interconnect conductors and lay out the key challenges to tackle next.

Acknowledgements

We thank Teodor Todorov, Jean Jordan-Sweet, Lerato Takana and Yuri Suzuki for the technical support in materials characterization. We thank Pavlo Sukhachov, Arun Bansil, Tay-Rong Chang, Judy Cha, and Chris Hinkle for the illuminating discussions.

SYMPOSIUM SB02

Charge Carrier Transport in Organic and Organic-Inorganic Hybrid Materials
April 23 - April 26, 2024

Symposium Organizers

Xiaodan Gu, University of Southern Mississippi
Chad Risko, University of Kentucky
Bob Schroeder, University College London
Natalie Stingelin, Georgia Institute of Technology

Symposium Support

Bronze
MDPI AG

* Invited Paper
+ JMR Distinguished Invited Speaker
^ MRS Communications Early Career Distinguished Presenter

SESSION SB02.01: Mixed Ionic and Electronic Transport in Organic Semiconductors
Session Chairs: Xiaodan Gu and Bob Schroeder
Tuesday Morning, April 23, 2024
Room 437, Level 4, Summit

10:30 AM *SB02.01.01

Ion Diffusion and Morphology of PEDOT:PSS. Insight from Molecular Dynamics Simulations [Igor Zozoulenko](#), Tahereh Sedghamiz, Mohsen Modarresi and Aleksandar Mehandzhiyski; Linköping University, Sweden

Poly(3,4-ethylenedioxythiophene) polystyrene sulfonate (PEDOT:PSS) is one of the most important mixed electron-ion conducting polymers, where the efficiency of the ion transport is crucial for many of its applications. Despite of the impressive experimental progress in determination of the ionic mobilities in PEDOT:PSS, the fundamentals of ion transport in this material remain poorly understood and the theoretical insight of the ion diffusion on the microscopical level is completely missing.

In the present paper, Martini 3 coarse grained molecular dynamics (MD) model for PEDOT:PSS is developed and applied to calculate the ion diffusion coefficients and ion distribution in the film.¹ A prerequisite to study the ion diffusion in PEDOT:PSS is to build its adequate morphological model properly describing its two-phase morphology as well as water intake and ion exchange. Using the coarse-grained calculations we developed this model by mimicking experimental process of film formation by drying the emulsion of PEDOT:PSS particles.² We demonstrate that PEDOT:PSS film is an essentially three component system, consisting of positively charged PEDOT chains, PSS chains with mostly deprotonated sulfonate groups, and protonated PSS chains.³ PEDOT-rich regions are predominantly composed of PEDOT and deprotonated PSS chains, whereas PSS-rich regions are composed of protonated PSS chains. Our calculations unravel how PEDOT-rich and PSS-rich regions are formed from the solution phase during drying process. We show that when the dry polymer film is immersed in water it swells by nearly 60%, and we demonstrate that the origin of swelling is related to deprotonation of the sulfonate groups in the PSS-rich regions. It is mostly PSS-rich regions that swell while the PEDOT-rich regions remain rather unchanged.

Using the obtained morphology we calculated the ion diffusion coefficients for Na⁺ ions and we found that they are practically the same in the PEDOT-rich and PSS-rich regions and do not show sensitivity to the oxidation level. We compare the calculated diffusion coefficients with available experimental results. Based on this comparison, and based on the MD morphology simulation of PEDOT:PSS revealing the formation of pores inside the film, we revised a commonly accepted granular morphological model of PEDOT:PSS. Namely, we argue that PEDOT:PSS films, in addition to PEDOT-rich and PSS-rich regions, must contain a network of pores, where the ion diffusion takes place.

We believe that our results demonstrate the power of the MD simulations for organic mixed electron-ion conductors providing the essential insight into polymer morphology and ion diffusion that is difficult to obtain by other means.

- (1) Sedghamiz, T.; Mehandzhiyski, A. Y.; Modarresi, M.; Linares, M.; Zozoulenko, I. What Can We Learn about PEDOT:PSS Morphology from Molecular Dynamics Simulations of Ionic Diffusion? *Chem. Mater.* **2023**, *35* (14), 5512–5523. <https://doi.org/10.1021/acs.chemmater.3c00873>.
- (2) Jain, K.; Mehandzhiyski, A. Y.; Zozoulenko, I.; Wågberg, L. PEDOT:PSS Nano-Particles in Aqueous Media: A Comparative Experimental and Molecular Dynamics Study of Particle Size, Morphology and z-Potential. *J. Colloid Interface Sci.* **2021**, *584*, 57–66. <https://doi.org/10.1016/j.jcis.2020.09.070>.
- (3) Modarresi, M.; Mehandzhiyski, A.; Fahlman, M.; Tybrandt, K.; Zozoulenko, I. Microscopic Understanding of the Granular Structure and the Swelling of PEDOT:PSS. *Macromolecules* **2020**, *53* (15), 6267–6278. <https://doi.org/10.1021/acs.macromol.0c00877>.

11:00 AM *SB02.01.02

Organic Electrochemical Transistor Materials for Bio-Interfacing Electronics [Ting Lei](#); Peking University, China

Organic electrochemical transistors (OECTs) are one of the most promising options for biointerfacing electronics, as they have high transconductance, low

operation voltage (<0.8 V), good biocompatibility, and intrinsic compatibility with ion-related biological events. Compared to the abundant high-performance p-type OECT materials, n-type and ambipolar OECT materials are rare, and more importantly, their performances lag far behind, which largely limits the development of OECT-based logic circuits and amplifiers for bio-interfacing electronics. To address this issue, we designed and synthesized a series of n-type and ambipolar materials and proposed a design strategy, namely "doped state engineering", which has greatly improved the performance and response speed of both n-type and ambipolar OECT materials. Based on these materials, we have realized high-performance logic circuits and amplifiers that exhibit high voltage gains, suitable for in vivo biosignal capture and amplification.

11:30 AM *SB02.01.03

Next-Generation Design Strategies for Organic Mixed Conductor Technologies [Alexandra F. Paterson](#); The University of Kentucky, United States

Organic mixed ionic-electronic conductors (OMIECs) and organic electrochemical transistors (OECTs) have enormous potential to impact everyday life and society – from low-cost biotechnologies in a widespread healthcare internet of things, to versatile neuromorphic computing technologies operating at the bio-hybrid interface. While significant research progress has been made, poor stability remains a critical bottleneck for OECTs. Additionally, identifying, enhancing, and measuring figures of merit that inform the 'material-device-circuit-application' research stack is essential for the success of emergent OMIEC electronics. Here, materials and device design strategies that increase important figures of merit will be discussed, as well as how the figure of merit, the μC^* product, can be overstated when extracted from OECTs.

SESSION SB02.02: Emerging Charge Transport Phenomena in Organic and Organic-Inorganic Hybrid Materials

Session Chairs: Christian Müller and Bob Schroeder

Tuesday Afternoon, April 23, 2024

Room 437, Level 4, Summit

1:30 PM *SB02.02.01

Narrow Bandgap Conjugated Polymers with Strong Correlations and Open-Shell Electronic Structures: Towards New Phenomena and Emergent Technologies [Jason D. Azoulay](#); Georgia Institute of Technology, United States

For over forty years, conjugated polymers (CPs) have been a source of enormous fundamental breakthroughs, enabling foundational insight into the nature of π -bonding and electron pairing, the creation of novel optoelectronic functionalities, and the development of commercially relevant technologies. Despite the achievement of significant technological milestones, the complex structural and energetic heterogeneities that define these materials preclude bandgap control at low energies, tailored interactions with infrared (IR) light, the study of fundamental physical phenomena, and the design and realization of new device functionalities. To address these modern challenges, we have developed precision synthetic methods that provide control of the frontier orbital energetics, coplanarity of the conjugated backbone, intermolecular interactions, and many chemical, electronic, and structural features that affect electronic coherence within these π -conjugated macromolecules, enabling unprecedented levels of bandgap control. The utility of these materials for understanding emergent light-matter interactions that enable the transduction of IR photons and the extension of CPs into high-performance IR optoelectronics will be discussed. We subsequently discovered that narrow bandgaps afforded through extended π -conjugation are intimately related to the coexistence of nearly degenerate electronic states. Through articulating novel mechanisms of spin alignment, topology control, and exchange, we have enabled the synthesis of neutral CPs with ground states that span the entire range from "conventional" closed-shell structures to biradicaloids with varying degrees of open-shell character, to diradicals in both singlet ($S = 0$) and triplet ($S = 1$) spin-states. These materials exhibit weaker intramolecular electron-electron pairing and stronger electronic correlations than their closed-shell counterparts, which imparts novel optical, transient, transport, thermal, spin, magnetic, quantum, and coherent phenomena not previously measured in soft-matter (polymer) systems. These novel attributes have enabled new optoelectronic and device functionalities that cannot be realized with current semiconductor technologies and provide a remarkable platform to study new phenomena at the interface of various fields such as chemistry, condensed matter physics, and quantum matter.

2:00 PM SB02.02.02

Effects of Processing-Induced Contamination on Organic Electronic Devices [Ian Jacobs](#)¹, [Dimitrios Simatos](#)¹, [Ilya Dobryden](#)², [Malgorzata Nguyen](#)¹, [Achilleas Savva](#)¹, [Deepak Venkateshvaran](#)¹, [Mark Nikolka](#)¹, [Jerome Charmet](#)³, [Leszek Spalek](#)¹, [Mindaugas Gicevičius](#)¹, [Youcheng Zhang](#)¹, [Guillaume Schweicher](#)⁴, [Duncan Howe](#)¹, [Sarah Ussel](#)¹, [John Armitage](#)¹, [Ivan Dimov](#)¹, [Ulrike Kraft](#)⁵, [Weimin Zhang](#)⁶, [Maryam Alsufyani](#)⁷, [Iain McCulloch](#)⁷, [Róisín Owens](#)¹, [Per Claesson](#)⁸, [Tuomas Knowles](#)¹ and [Henning Sirringhaus](#)¹; ¹University of Cambridge, United Kingdom; ²RISE Research Institutes of Sweden, Sweden; ³HES-SO University of Applied Sciences Western Switzerland, Switzerland; ⁴Université Libre de Bruxelles, Belgium; ⁵Max Planck Institute for Polymer Research, Germany; ⁶King Abdullah University of Science and Technology, Saudi Arabia; ⁷University of Oxford, United Kingdom; ⁸KTH Royal Institute of Technology, Sweden

Organic semiconductors are often touted as 'defect tolerant', however to date there have been relatively few systematic studies of the role of impurities on device performance. In particular, little attention has been paid to processing-induced contaminants, originating from e.g. the glovebox atmosphere or solvents, even though anecdotal reports have long indicated that such factors may be important.

Here,^[1] we present a systematic study of processing-induced contamination on the performance of indacenodithiophene-co-benzothiadiazole (IDTBT) organic field effect transistors (OFETs). We observe that glovebox vapor can result in film contamination, but that in gloveboxes with a typical carbon-based solvent trap, the dominant impurities are typically aliphatics such as vacuum pump oil, rather than aromatics typically used for spin coating. In clean gloveboxes, we observe that the solvent content in films is largely determined by the residual solvent vapor in the atmosphere, rather than annealing, due to the large surface to volume ratio of thin films.

In addition, we find that most common plastic laboratory consumables, such as pipette tips, syringes, and even metal needles, leach contaminants into organic semiconductor solutions. In some cases, such as poly(dimethylsiloxane) (PDMS) coatings on metal needles, contamination leads to improvements in film wetting and device performance. However, in other cases, such as leachates from micropipettes, we observe strongly degraded device performance. Using NMR, we identify two primary contaminants (oleamide and glycerol monostearate) leaching from micropipette tips. These chemicals are both amphiphilic, and therefore could plausibly lead to increased electrostatic disorder, or the formation of hydrophilic inverse micelles. Tellingly, quartz crystal microbalance measurements reveal that uncontaminated IDTBT films are entirely hydrophobic, while contaminated films swell by 20% upon exposure to water, suggesting that previous studies on the role of water uptake in IDTBT may have been dominated by impurities. Our results promisingly suggest that intrinsic OFET performance may actually be more stable than previously thought. However, they are also broadly relevant to a wide range of materials and devices fabricated from solution, and suggest important strategies to limit contamination and increase experimental reproducibility.

[1] D. Simatos,* I.E. Jacobs,* et al. *Small Methods*, 2023, 2300476

2:15 PM SB02.02.03

High-Performance Organic Thermoelectric Materials by Shifting up The Fermi Level [Jianyong Ouyang](#); National University of Singapore, Singapore

Organic thermoelectric materials are regarded as the next-generation thermoelectric materials because of their merits including low cost, high mechanical flexibility, and low intrinsic thermal conductivity. However, their Seebeck coefficient is usually quite low, which is lower than their inorganic counterpart by 1-2 orders in magnitude. Here, I will report a new strategy to greatly enhance the Seebeck coefficient of organic thermoelectric materials. This can shift up the Fermi level and thus increase the Seebeck coefficient, while it only slightly lowers the electrical conductivity. As a result, the organic thermoelectric materials can exhibit high Seebeck coefficient and high electrical conductivity.

2:30 PM *SB02.02.04

Dopant-Induced Morphology Changes and Their Impact on Thermoelectricity in Polymers [Oliver Fenwick](#); Queen Mary University of London, United Kingdom

Conducting polymers have attracted interest as thermoelectric materials because of their processability, light weight, flexibility, low toxicity and cost. In terms of performance, it is their intrinsically low lattice thermal conductivity (typically $0.2 - 0.5 \text{ W m}^{-1} \text{ K}^{-1}$) which is of particular interest to the thermoelectric community. However, can we assume that the thermal conductivity is always low in these systems? Doping these systems is required to obtain useful electrical conductivities, but causes significant morphological changes in order to incorporate the large molecular dopants and further structural adjustments occur to accommodate the polaronic charge carriers. How do these morphological changes impact the thermal conductivity of polymers? How does this impact zT ?

This presentation aims to shed some light on these questions, by investigating the cases of four polymers, poly(3-hexyl thiophene) [P3HT], poly(3,4-ethylenedioxythiophene) [PEDOT], poly[6,9-dihydro-6,9-dioxobenzimidazo[2,1-b:1',2'-j]benzo[1,2-b:1',2'-j]phenanthroline-2,12-diyl] [BBB] and poly[17-oxo-7,10-benz[de]imidazo[4',5':5,6]-benzimidazo[2,1-a]isoquinoline-3,4:10,11-tetrayl]-10-carbonyl] [BBL]. We measure in-plane thermal conductivity of different P3HT morphologies produced by spin-coating, drop casting and aligned by mechanical rubbing. We also compare doped and undoped analogues of these films. We do find an effect of morphology on thermal conductivity in aligned polymer films that we can link to structural changes. However, by far the biggest effect on lattice thermal conductivity comes from electrical doping, which induces a subtle change to the morphology but a significant increase in thermal conductivity. We find thermal conductivity states in the range of 0.2 to $> 1 \text{ W m}^{-1} \text{ K}^{-1}$. [1] In PEDOT, we de-dope the polymer to improve the Seebeck coefficient, but also aim to maintain or improve charge transport. We observe significant morphological changes in this process which we link to the macroscopic observables.

In the case of BBB and BBL we investigate the effect of ladderisation on polymers (BBL being a ladder-type polymer and BBB it's non-ladder type analogue). Ladder-type polymers should be more planar and more rigid than non-ladder types. Correspondingly, we find that the thermal conductivity in the ladder-type polymers can be >3 times that in the non-ladder-type analogue. When doped the lattice thermal conductivity increases to remarkably large values $>2 \text{ W m}^{-1} \text{ K}^{-1}$.

[1] Degoussé et al. *J. Mater. Chem. A*, 2021,9, 16065-16075

3:00 PM BREAK

SESSION SB02.03: Molecular Semiconductors
Session Chairs: Christian Müller and Alexandra Paterson
Tuesday Afternoon, April 23, 2024
Room 437, Level 4, Summit

3:30 PM *SB02.03.01

Structure-Property Relationships in Thienoacenes for Improved Transport Properties [Guillaume Schweicher](#); Université Libre de Bruxelles, Belgium

In spite of tremendous progress in molecular design, engineering and processing, only few small molecule organic semiconductors (OSCs) have reached charge carrier mobilities (μ) higher than $10 \text{ cm}^2/\text{Vs}$, typically with single-crystal devices. However, μ is a material property and not a molecular one. It is thus of paramount importance to take supramolecular order into consideration at all length scales. As recently evidenced, the best OSCs tend to self-organize into large plate-like single-crystals exhibiting a layer-by-layer herringbone packing motif.¹ Moreover, thermal lattice fluctuations cause temporal variations of transfer integrals (J) and impose a transient localization of charges leading to reduced macroscopic μ in these weakly bonded van der Waals solids.² We will present recent progress achieved in our group in terms of molecular design and understanding of the impact of thermal energetic disorder: design by theory, crystal engineering, quantum-chemical calculations and evaluation of transport properties in electronic devices.

References:

- Schweicher, *Adv. Mater.* **2020**, 32, 10, 1905909; Fratini, *Nature Materials* **2020**, 19, 491
- Fratini, *Adv. Funct. Mater.* **2016**, 26, 2292; Fratini, *Nature Materials* **2017**, 16, 998; Schweicher, *Adv. Mater.* **2019**, 31, 43, 1902407; Banks, *Adv. Funct. Mater.* **2023**, 33, 38, 2303701; Giannini, *Acc. Chem. Res.* **2022**, 55, 6, 819; Giannini, Di Virgilio, *Nature Materials* **2023**, 10.1038/s41563-023-01664-4

4:00 PM SB02.03.02

Polymorphic Organic Crystals of P(NDI2O-T2): Impact of Microstructure on The Charge Transport Properties [Chamikara D. Karunasena](#)¹, Hong Li¹, Casey Davis², Megan R. Brown³, Joel H. Bombile³, Veaceslav Coropceanu¹, Chad Risko³, Michael Toney² and Jean-Luc Bredas¹; ¹The University of Arizona, United States; ²University of Colorado Boulder, United States; ³University of Kentucky, United States

The electronic charge transport characteristics of organic semiconductors (OSCs) are intricately linked to their solid-state morphology. Deciphering the complex interplay of these OSC polymer properties with the supramolecular organizations in their (semi)crystalline structure is of importance in the pursuit of high-performance materials for next-generation optoelectronic technologies. However, currently available *in-situ* experimental characterization

techniques offer limited nano-scale insight, making it challenging to comprehensively describe the microstructure of fabricated films in terms of crystallinity and polymer conformations and orientations, and thus to rationalize the relationship of structure with associated electronic properties. In this study, we present an in-depth characterization of the supramolecular crystal organization and its impact on the electronic charge transport properties of polymorphic crystalline forms of the n-type hairy-rod polymer P(NDI2O-T2); this material can have low energetic disorder and high electron mobility, making it well-suited for a wide range of electronic device applications. Based on available experimental data from X-ray scattering techniques and infrared spectroscopy, we derive the crystal unit-cell structures of the three reported polymorphic forms at the atomistic scale, through a meticulously parameterized classical molecular dynamics force field in conjunction with periodic density functional theory (DFT) calculations. Furthermore, we extend our simulations to investigate the diverse morphological aspects of the semicrystalline structure following thermal treatment and account for the factors governing the polymorphic interconversion and selectivity. We sample the nano- to microstructure of the simulated thin films and quantify charge carrier transport through density functional theory calculations. These results serve as the foundation to establish critical and fundamental correlations between crystal transport properties and the nano- and microstructure of the polymer, as well as the associated disorder. This, in turn, allows the determination of the dominant transport microscopic parameters and provides insight into how these parameters can be tuned through precise processing techniques.

4:15 PM SB02.03.03

Synthesis and Functionalization of New Chromophores for Organic Electronics & Photonics [John Anthony](#), Tanner Smith, Karl Thorley and Dean Windemuller; University of Kentucky, United States

High-performance organic electronic and photonic devices require optimization of both the core chromophore and the chromophores' interactions in the solid state. Recently, we have been exploring the synthesis and implementation of larger chromophores - either linked trimeric systems or very long (> 8) fused-ring aromatic compounds to enhance both photonic properties and improve intermolecular contacts. Along with these new chromophores, we have developed new functionalization strategies to allow solution processing and to impart some control over the solid-state order of the cores. By this process, we have made a series of remarkably stable large aromatic systems with absorption well into the near-infrared. By tuning electronic coupling within chromophores, we have developed new singlet fission chromophores that yield quintet states exclusively. By tuning the functional groups on other systems, we have found approaches using C-H- π interactions to dramatically reduce disorder, and are studying the impact on charge transport. Due to their increased rigidity, we expect these larger polycyclic systems to demonstrate significant improvements in mobility. Thorough studies of decomposition mechanisms for these higher fused aromatic compounds have elucidated new reaction pathways, along with approaches to minimize reactions with oxygen or dimerization, yielding materials with unprecedented stability.

4:30 PM *SB02.03.04

Exploiting Charge Transfer States in Molecular and Organic Electronics [Oana D. Jurchescu](#); Wake Forest University, United States

The growing demand for smaller, faster, and more versatile electronics has led to a surge of interest in new device concepts. One promising approach is to exploit the charge-transfer (CT) state that forms at the interface between charge donor and acceptor molecules. However, establishing reliable relationships between donor/acceptor molecular structures, the resulting CT, and physical properties is challenging. In this talk, the implications of the hybrid electronic states will be discussed by examining two model systems: a monolayer of co-assembled molecules with strong electron donor and acceptor termini, and a polymorphic system based on a donor/acceptor charge transfer salt in the form of single crystals with varying donor-acceptor overlap. In the molecular rectifiers based on self-assembled molecules, the charge transfer state is responsible for the observed increase in the rectification ratio, despite the reduction caused in the film degree of order. These high-performance molecular diodes have been employed in circuits to effectively rectify an AC signal. In the single crystals, we correlate the solid-state packing with the degree of charge transfer and the resulting electrical properties. We also probe the sub-gap, trap states, through the measurement of field-effect transistors, an analysis which has so far seen little application in ambipolar devices. Our results provide evidence that small differences in donor/acceptor overlap can induce significant changes in electronic coupling and electrical properties of organic devices and highlight the potential of charge transfer states as a disruptive approach to engineering organic electronics.

SESSION SB02.04: Poster Session: Charge Carrier Transport in Organic and Organic-Inorganic Hybrid Materials

Session Chairs: Xiaodan Gu, Alexandra Paterson and Bob Schroeder

Tuesday Afternoon, April 23, 2024

Flex Hall C, Level 2, Summit

5:00 PM SB02.04.01

A Highly Conductive n-Type Conjugated Polymer Polymerized in Water [Qifan Li](#), Jun-Da Huang, Chi-Yuan Yang and Simone Fabiano; Linköping University, Sweden

Poly(3,4-ethylenedioxythiophene):poly(styrene sulfonate) (PEDOT:PSS) is a benchmark hole-transporting (p-type) polymer that finds applications in diverse electronics devices. Most of its success is due to its facile synthesis in water, exceptional water processability, and outstanding electrical performance. Applications in fields like bioelectronics and thermoelectric devices often necessitate the complementary use of both p-type and n-type (electron-transporting) materials. However, the availability of n-type materials amenable to water-based polymerization and processing remains limited. Here, we present a novel synthesis method enabling direct polymerization in water, yielding a highly conductive, water-processable n-type conjugated polymer. By adjusting the synthetic procedure and use of surfactants, we achieve an impressive conductivity of up to 66 S/cm (with an average of 48 ± 18 S/cm), ranking among the highest for n-type polymers processed using green solvents. The new n-type polymer also exhibits outstanding stability, maintaining 89% of its initial conductivity after 146 days of storage in air. Our synthesis approach, along with the novel polymer it yields, promises significant advancements in the field of printed electronics.

5:00 PM SB02.04.02

Spin Transport Modeling in The Small Tetraheme Cytochrome [William Livernois](#) and Anant Anantram; University of Washington, United States

Multi-heme cytochromes have attracted attention due to their conductive properties [1] and, more recently, their spin-selective properties [2]. The small tetraheme cytochrome (STC), a c-type cytochrome found in *S. oneidensis*, has been demonstrated experimentally to act as a spin filter [3], with the potential to be used in nano-scale spintronic devices. Building upon a spin-dependent transport model previously applied to related biomaterials and cytochromes [4], we investigated decoherent transport through the cytochrome and electron hopping between heme groups. This model incorporated spin-orbit coupling and a generalized spin model to explore non-collinear effects. Preliminary findings indicate that collinear effects, arising from electron exchange and spin state, predominantly influence the transport pathway while spin-orbit effects only cause minor shifts in orbital energies. Notably, the

peptide backbone functions primarily as a structural scaffold facilitating heme-to-heme electron transport, rather than directly contributing to electron conduction. We also examined the impact of solvation within our model and identified its role in modulating the coupling between heme sites and the overall conductivity of the cytochrome.

The research was supported by National Science Foundation NSF Grant Number 2317843, NSF Future of Manufacturing Grant No. 2229131, and the NDSEG fellowship.

References:

- [1] Dahl, Peter J., et al. "A 300-fold conductivity increase in microbial cytochrome nanowires due to temperature-induced restructuring of hydrogen bonding networks." *Science advances* 8.19 (2022).
- [2] Mishra, Suryakant, et al. "Spin-dependent electron transport through bacterial cell surface multiheme electron conduits." *Journal of the American Chemical Society* 141.49 (2019): 19198-19202.
- [3] Niman, Christina M., et al. "Bacterial extracellular electron transfer components are spin selective." *The Journal of Chemical Physics* 159.14 (2023).
- [4] Livernois, William, and M. P. Anantram. "A Spin-Dependent Model for Multi-Heme Bacterial Nanowires." *ACS nano* 17.10 (2023): 9059-9068.

5:00 PM SB02.04.03

Exploring DNA-Carbon Nanotube Interfacial Interactions and Transport Olaiyan M. Alolaiyan^{1,2} and M. P. Anantram¹; ¹University of Washington, United States; ²King Abdulaziz City for Science and Technology, Saudi Arabia

In the rapidly changing world of combined scientific studies, two standout materials are drawing attention: DNA and carbon nanotubes (CNTs). DNA, known for its central role in carrying genetic information, is a wonder of nature's design. On the other hand, CNTs, recognized for their strength and electrical properties, represent the best of modern material advancements.

Studying the interaction between DNA and carbon nanotubes (CNTs) presents a series of tangible challenges. One of the main obstacles is that the inherent differences in their chemical properties make direct interactions between them non-trivial. In addressing the challenges of understanding the intricate interactions between DNA and CNTs, our approach leverages the power of Molecular Dynamics (MD) simulations. MD simulations offer a dynamic and detailed perspective, allowing us to scrutinize the behavior of our DNA-CNT system. To initiate our study, we began by modeling the direct interaction between DNA and CNTs without forming any covalent bonds. This step was pivotal, setting the groundwork before introducing the linker and further constructing the comprehensive DNA-Linker-CNT system. The introduction of a linker in the system, studied under MD, can provide insights into creating stable bonds that bridge DNA and CNTs, ensuring their effective interaction without compromising their individual properties.

In our comprehensive study on the DNA-Linker-CNT system, we utilize a systematic methodology to elucidate the behavior and stability of the structure complex. Each component of the system was carefully constructed: the DNA, in its B-form comprises a 12-basepair double-stranded sequence denoted as (3G3C3G3C). The linker, a 10-atom amino linker, served as the bridge in our system. The CNT has a chirality of (6,6) and is 10 primitive cells long. Crucially, to ensure accurate simulations, we employed specific force fields: the Amber force field bsc1 for DNA, and GAFF (General Amber Force Field) for the linker and CNT. By having the individual components, our next step was to bring them together into a cohesive environment. This involved forming bonds between the DNA, linker, and CNT, followed by the application of force fields – with specific force fields parameters calculated for the linker and CNT. To simulate a realistic biological environment, we introduced a water solvent using the TIP3P model, encapsulating our system in an octahedral geometry with a 15-angstrom buffer. Then we ionized the structure to ensure it was ready for the Molecular Dynamics (MD) simulations.

The MD simulations were significant in revealing the dynamics of our system. Across multiple runs, a consistent observation was the pronounced attraction between the DNA and CNT, with the DNA segment nearing the CNT's surface, adopting a stable configuration involving the interaction between pi-orbitals on the DNA and CNT. This proximity between the pi-orbitals of the two subsystems, sustained over a significant portion of the simulation, is indicative of potential electron transport opportunities, a phenomenon further corroborated by RMSD analyses which underscored the stability of each component. Our observations so far paints a promising picture for the DNA-Linker-CNT system, hinting at potential channels for electron transport. Complementing our MD studies, we are performing transport calculations which will be presented to further enhance our understanding. These calculations shed light on the electron transfer between the DNA and nanotube subsystems under a variety of CNT-Linker-DNA-Linker-CNT configurations. Together, MD simulations and transport calculations provide a comprehensive and promising approach to unravel the complexities of the DNA-Linker-CNT interactions, paving the way for a deeper understanding of these systems. [We acknowledge NSF FMRG 2328217 and NSF SemiSynBio 2027165 grants.]

5:00 PM SB02.04.04

Carbon Nanotube-Poly(3-Hexylthiophene) Hybrid Thin-Film Phototransistors with Ultra-High Responsivity Zahra Bahrami¹, Kevin Schnitker² and Joseph Andrews^{2,1}; ¹University of Wisconsin-Madison, United States; ²University of Wisconsin-Madison, United States

Phototransistors (PTs) are photodetectors that combine light detection and signal amplification capabilities by modulating the charge-carrier density within the transistor's active channel upon exposure to light.¹⁻³ Solution-processable phototransistors (PTs) have gained prominence thanks to their outstanding attributes, notably their adaptability to various substrates, including flexible materials, facilitating large-area integration.⁴⁻⁷ Among PTs, hybrid material phototransistors stand out, leveraging the strengths of inorganic materials' high carrier mobility and organic materials' efficient light absorption and tunable bandgap.⁸ This synergy enhances light detection sensitivity and efficiency.^{8,9} Conjugated Poly(3-hexylthiophene) (P3HT) and carbon nanotubes (CNTs) are frequently employed in optoelectronics due to P3HT's flexibility, absorption coefficient, and cost-effectiveness, and CNTs' exceptional electrical and optical properties driven by their unique one-dimensional structure.¹⁰ In this study, we present a promising solution-processible technique to fabricate a phototransistor utilizing CNTs integrated with P3HT through heterogeneous crystallization as the channel of phototransistor, with the aim of investigating their capabilities in high-responsivity optical detection devices.

Our findings reveal that the devices demonstrate an exceptionally high photoresponsivity of 3.6×10^5 A/W at a wavelength of 470 nm. The exceptional photoresponsivity primarily stems from the high light-absorption characteristics of the conjugated polymer, complemented by the excellent mobility facilitated by the underlying CNT network. Additionally, we determined the device's detectivity by analyzing its noise profile at 10 Hz for various V_{GS} values. The device's maximum detectivity reaches approximately 0.9×10^{11} , a value that is approximately 5000 times higher than a control sample consisting solely of P3HT at the peak of responsivity. These results show the solution processed P3HT/semi-CNT hybrid platform is a promising approach for advanced photodetection applications.

References:

1. Nam, H. J., Cha, J., Lee, S. H., Yoo, W. J. & Jung, D. Y. A new mussel-inspired polydopamine phototransistor with high photosensitivity: signal amplification and light-controlled switching properties. *Chemical Communications* **50**, 1458–1461 (2014).
2. Huang, X., Ji, D., Fuchs, H., Hu, W. & Li, T. Recent Progress in Organic Phototransistors: Semiconductor Materials, Device Structures and Optoelectronic Applications. *ChemPhotoChem* **4**, 9–38 (2020).
3. Tavasli, A., Guranlu, B., Gunturkun, D., Isci, R. & Faraji, S. A Review on Solution-Processed Organic Phototransistors and Their Recent Developments. *Electronics* **2022**, Vol. 11, Page 316 **11**, 316 (2022).
4. Roslan, N. A., Abdullah, S. M., Haliza, W., Majid, A. & Supangat, A. Investigation of VTP:PC 71 BM organic composite as highly responsive organic

photodetector. *Sensors and Actuators A* **279**, 361–366 (2018).

5. Dou, L., Liu, Y., Hong, Z., Li, G. & Yang, Y. Low-Bandgap Near-IR Conjugated Polymers/Molecules for Organic Electronics. *Chem Rev* **115**, 12633–12665 (2015).

6. Park, J. B. *et al.* Visible-Light-Responsive High-Detectivity Organic Photodetectors with a 1 μm Thick Active Layer. *ACS Appl Mater Interfaces* **10**, 38294–38301 (2018).

7. Pace, G. *et al.* All-Organic and Fully-Printed Semitransparent Photodetectors Based on Narrow Bandgap Conjugated Molecules. *Advanced Materials* **26**, 6773–6777 (2014).

8. Zhu, H. *et al.* Perovskite and conjugated polymer wrapped semiconducting carbon nanotube hybrid films for high-performance transistors and phototransistors. *ACS Nano* **13**, 3971–3981 (2019).

9. Chang, P. H. *et al.* Ultrahigh Responsivity and Detectivity Graphene–Perovskite Hybrid Phototransistors by Sequential Vapor Deposition. *Scientific Reports* **2017 7:1** **7**, 1–10 (2017).

10. Kufer, D. & Konstantatos, G. Photo-FETs: Phototransistors Enabled by 2D and 0D Nanomaterials. *ACS Photonics* **3**, 2197–2210 (2016).

5:00 PM SB02.04.05

Ordered Inorganic–Organic Hybrids can Crystallize with Differing Organic Cation Species Megan Cassingham¹, Yang Goh¹, Sujeewa Lamahewage², Aaron Rossini², Mark E. Thompson¹ and Brent Melot¹; ¹University of Southern California, United States; ²Iowa State University of Science and Technology, United States

Hybrid organic–inorganic materials have been employed in a variety of applications including photovoltaics, optoelectronics, and nonlinear optics. Despite their unique and diverse properties, there is still potential to employ the organic molecules as more active contributors to the optoelectronic properties of these materials. In this work, we explore the possibility of applying more than one organic cation specie to these systems to investigate possible charge transfer properties. We look at three materials, 1-methylquinolinium lead iodide (1-MQPbI₃), 1-naphthylammonium lead iodide (1-NAPbI₃), and the mixed hybrid of these two ((1-MQ)(1-NA)PbI₃). These systems were chosen for their similarity in structure. While there is precedent for other hybrid systems such as 3D systems like methylammonium lead iodide to incorporate more than one organic cation in the structure, this is the first system we are aware of to show clear order without distinct regions of one cation or the other. We corroborated the single crystal X-ray data of the structure using solid state NMR techniques to discover the distances between the organic cations. We also investigated the photophysical properties of all three systems including temperature dependent emission and lifetime data. Dielectric data was also collected to gain a better understanding of the relationship between possible structural changes and the unique photophysical properties we observed. Although these two organic cations do not display strong charge transfer characteristics, this work opens the door to further studies into the mixed hybrid space and shows promise for new ordered systems which can better utilize charge transfer properties.

5:00 PM SB02.04.06

Chain Length Dependent, Reversible Switching of Spiropyran-PMMA Blend Dielectrics for Light-Gated Organic Transistors Sten Gebel, Parham Derakhshanfar, Shoupeng Cao, Lucas Caire da Silva, Paul W. Blom and Ulrike Kraft; Max Planck Institute for Polymer Research, Germany

The increasing demand for mobile and flexible electronics and the rising interest in the “Internet of Things” promotes research on lightweight organic electronic devices and concepts where the integration of silicon chips is too expensive. One promising approach to introduce additional functionalities for sensing and memory applications into conventional organic electronic devices is the introduction of molecular switches. These small organic molecules undergo reversible isomerization between (at least) two isomers when irradiated with light of different wavelength and this induces drastic changes in physicochemical properties such as frontier orbital energy levels, dipole moment and/or molecular geometry. These reversible changes in molecular properties can be exploited to deliberately modify charge transport in organic field-effect transistors (OFETs) and therefore enable optical control over device characteristics.

Spiropyran is a photoswitch that can be used to fabricate light-switchable organic electronic devices. The system is particularly interesting, because the UV light-induced isomerization of the neutral spiropyran (SP) to the zwitterionic merocyanine (MC) can be exploited to reversibly tune OFET characteristics [1–3]. One possible approach to incorporate spiropyran-based photoswitches into organic transistors is to blend them with dielectric polymers to obtain light-responsive gate dielectrics. However, there is no consistent explanation in the literature for how isomerization of the photoswitch alters charge transport and performance of OFETs, and several mechanisms have been proposed. We address this issue by blending spiropyran molecular switches with alkyl side chains of different lengths (i.e. C₁, C₄, C₁₀ and C₁₆) with poly(methyl methacrylate) (PMMA) and study the reversible switching of these functional blends using UV/Vis absorption spectroscopy, impedance spectroscopy and further electrical characterization in metal-insulator-metal capacitors and OFETs. The UV/Vis absorption data show that all four SP derivatives isomerize to their respective MC form upon UV irradiation. Thermal annealing induces the reverse reaction from MC to SP. In OFETs, the reversible switching between the SP and MC states translates into pronounced, reversible shifts of the threshold voltage.

Surprisingly, we find that the switching of both capacitor and transistor characteristics strongly depends on the length of the alkyl side chain of the photoswitch. This suggests that the change of the dipole moment (low versus high) and the charge (neutral versus zwitterionic) might not be the only cause for the altered device characteristics, but that the side chains must also be considered. This chain length dependent switching is further investigated by bias stress measurements using OFETs and a similar dependence on the chain length is found.

Such a chain length dependent reversal of the switching in light-gated devices has not been reported before. Hence, our results highlight the importance of the chemical design of photochromic molecules for well-controlled switchable devices.

1. Ishiguro, Y. *et al.*, *ACS Applied Materials & Interfaces*, 2014, **6**(13): p. 10415-10420.

2. Shen, Q. *et al.*, *Advanced Materials*, 2010, **22**(30): p. 3282-3287.

3. Shen, Q. *et al.*, *The Journal of Physical Chemistry C*, 2009, **113**(24): p. 10807-10812.

5:00 PM SB02.04.07

Herringbone-Patterned Asymmetric Electron-Blocking Material for Stable Blue Phosphorescent Organic Light-Emitting Diodes Eunhye Hwang¹, Wonyoung Choe¹, Jun Yeob Lee² and Tae-Hyuk Kwon¹; ¹Ulsan National Institute of Science and Technology, Korea (the Republic of); ²Sungkyunkwan University, Korea (the Republic of)

Blue phosphorescent organic light-emitting diodes (PhOLEDs) have been suffered from severe triplet leakage issues between interfacial layers, resulted in rapid degradation of the device performance as well as considerable efficiency roll-off. So far, electron-blocking materials (EBMs) with high triplet energy levels (E_T) have been introduced to achieve triplet confinement in emissive layers, but the large energy bandgaps required by typical EBMs often increase turn-on voltages (V_{on}) of PhOLEDs and then rather accelerate their degradation. However, there is a lack of studies on the development of EBMs suitable

for blue PhOLEDs considering their charge carrier mobilities to act as efficient hole-transporting as well as electron-blocking channels, which is closely related to the consequent V_{on} . Herein, we present a molecular design strategy of asymmetric EBMs for stable blue PhOLEDs with a focus on molecular packings and orientations to reduce their V_{on} . Adjusting photophysical properties and electrostatic interactions, four EBMs having high E_T are developed by fine-tuning of three-dimensionally twisted molecular structures. X-ray crystallographic analyses show that the compound containing a fully *ortho*-linked donor-donor- π -acceptor configuration achieves a herringbone-patterned crystal structure with a face-on-dominated orientation, advantageous for hole carrier transport. Resultingly, providing a decreased V_{on} and effective triplet confinement, power efficiency and operational lifetime of the corresponding blue PhOLEDs are successfully improved compared to a conventional symmetric EBM with a slow hole mobility. The structural modification of asymmetric EBMs considering their molecular arrangement will provide further insight into the design of interfacial layers, enhancing the device performance and stability in various optoelectronic applications.

5:00 PM SB02.04.08

Photoinduced Charge Transfer at Quantum Dot to Dye Interface [Svetlana V. Kilina](#); North Dakota State University, United States

Recent focus on assemblies of the QDs functionalized by various organic and metal-organic dyes is dictated by their promise to serve as a key element for both solar-to-electrical and solar-to-chemical energy conversion processes. Our simulations of QD/dye composites have led us to predictions of conditions that govern the direction and rates of the charge transfer from the QD to the dye and interpretation of transit-spectroscopy data.

5:00 PM SB02.04.09

Iteratively Synthesized, Atomically Precise Graphene Nanoribbons with Heteroatoms [Steven Kolaczowski](#), [Nicholas Angello](#), [Wesley Wang](#) and [Joseph Lyding](#); University of Illinois at Urbana-Champaign, United States

The semi-metallic electronic structure of graphene has been the major problem in the fabrication and integration of graphene electronic devices. While the thermal, optical, mechanical, and electronic transport properties of graphene vastly outperform silicon, the very low on-off current ratio prevents 2D planar graphene from being used as a controllable channel in field effect transistors (FETs). Graphene nanoribbons (GNRs), laterally confined, 1D structures of graphene exhibit a wide variety of bandgaps while maintaining similar physical properties. For example, GNRs are predicted to have electron mobilities and thermal conductivity over twenty-five times higher than that of Silicon. However, limitations in current GNR synthesis techniques prevent the use of heteroatoms from being incorporated into a length-controlled ribbon. Here, I discuss a solution-based iterative coupling technique capable of synthesizing GNR copolymers and GNRs with heteroatoms. This increase control over GNR synthesis arises from the use of tetramethyl *N*-methyliminodiacetic acid (TIDA) protected haloboronic acid difunctionalized GNR building blocks. By utilizing optimized catch-and-release purification methods and automated machinery, we've demonstrated the ability to create user-defined, atomically precise, length controlled GNR copolymers with no human intervention in as little as eight hours. Because TIDA-protected boronic acids can be deprotected under mild, basic conditions, these GNR building blocks can be synthesized with the inclusion of heteroatoms without degradation. GNR building blocks containing Oxygen, Sulfur, and Nitrogen have already been synthesized. The inclusion of these electron-rich species into the graphene lattice alters the electronic band structure and ribbon conductivity, effectively n-type doping the local environment. These synthesized GNRs and GNR copolymers are then exfoliated onto metallic and semi-conducting surfaces in situ in ultra-high vacuum (UHV) using dry-contact transfer. Finally, these on-surface GNRs probed using scanning tunneling microscopy (STM) to better understand their electronic structure, on-surface behavior, and stability. This procedure has the potential to open the floodgates to hundreds of novel GNRs and GNR heterostructures that can be used in post-silicon devices.

5:00 PM SB02.04.10

Active Learning Approaches to Predict Intermolecular Noncovalent Interactions in Organic Semiconductors [Moses Ogbaje](#)^{1,2}, [Vijaykumar Karthikeyan](#)³, [Kyle Eldridge](#)¹, [Vinayak Bhat](#)⁴, [Baskar Ganapathysubramanian](#)⁵ and [Chad Risko](#)^{1,2}; ¹University of Kentucky, United States; ²Center for Applied Energy Research, United States; ³Paul Laurence Dunbar High School, United States; ⁴Columbia College, United States; ⁵Iowa State University of Science and Technology, United States

The natures and strengths of intermolecular noncovalent interactions are critical to the formation of organic semiconductors (OSC) from their molecular or polymer-based building blocks. While there are several quantum-chemical approaches available to evaluate intermolecular noncovalent interactions, including symmetry-adapted perturbation theory (SAPT), these methods can be computationally expensive, especially for the types of large building blocks used in OSC. This computational cost limits the ability of machine-enabled searches of the OSC chemical and materials space. Machine learning (ML) models have emerged as powerful tools to provide fast predictions of a variety of molecular and material properties at a fraction of the computational cost when compared to quantum-chemical approaches, though they often require substantially large and labeled datasets, posing challenges when data is scarce or difficult to obtain. Here, we discuss an active learning approach that augments ML models trained to predict intermolecular noncovalent interactions by incorporating a prediction confidence. The active learning scheme is developed to enable the reduction of labeled data requirements by identifying regions in the chemical space where the model exhibits the most uncertainty. This combined approach demonstrates effective and fast determination of intermolecular noncovalent interactions in OSC.

5:00 PM SB02.04.11

Morphology Control Strategies for Efficient Charge Transport versus Injection in Solution-Processed Organic Electronic Devices [Minsoo Kim](#), [Woongsik Jang](#) and [Dong Hwan Wang](#); Chung-Ang University, Korea (the Republic of)

ABSTRACT BODY:

Organic electronic devices have attracted much attention owing to their advantages such as solution processable, low cost, superior absorption coefficient, flexibility, and so on. By developing of the non-fullerene acceptors (NFAs), organic photovoltaics (OPVs) achieved high power conversion efficiency (PCE) over 19% and organic photodetectors (OPDs) beyond the detectivity of 10^{14} Jones. These desirable results are thanks to the various morphology control strategies of organic semiconductor materials, and novel thin film formation process using their. In this study, we suggest the morphology control strategies in terms of materials engineering and thin film lamination process. Representative methods of controlling the morphology of photoactive materials include additive engineering (morphology regulator), and ternary strategies such as introducing the guest components, those enable efficient charge dynamics by controlling molecular orientation. The morphology of the photoactive material which composed of polymer donor PM6 and non-fused ring electron acceptors (NFREAs) TPDC-4F controlled by additive engineering which induce efficient vertical phase distributions of the donor and acceptor components through volatilization process of the high boiling point of additive. Accordingly, we successfully fabricated efficient OPDs (Detectivity of 1.27×10^{13} Jones) with suppressed dark current (3.55×10^{-9} A cm^{-2}) [1]. Moreover, the ternary strategy introducing the high LUMO level guest acceptor (EH-IDTBR) with PM6:BTP-4F-12 binary blend, can block the injected charge from external efficiently and robust transfer the photo-generated charge carrier, is promising method for morphology regulation. The devices with ternary strategy based on optimal ratio of EH-IDTBR showed advanced OPV (PCE of 16.20%), and OPD (Detectivity of 1.33×10^{13} Jones) performances [2]. In addition, morphology also can be adjusted by thin film

lamination process. To achieve a desirable thin film surface morphology with a well-distributed donor (PM6) and acceptor (BTP-4F-12) phase in the vertical structure, we developed a vacuum-free (VF) lamination process, in which the blend films with various thicknesses using the adhesion-optimized PUA mediators are transferred onto the target substrates without the vacuum process. Consequently, the VF-laminated devices achieved improved OPV (PCE of 15.97%) and OPD (D^* of 3.61×10^{13} Jones) performances. Additionally, the device prepared using the VF-lamination exhibited improved internal resistance, as well as photoresponse property, as observed by optical, electrical, and morphological analyses [3, 4].

- [1] M. S. Kim, W. Jang, B. G. Kim, D. H. Wang, *Adv. Optical. Mater.*, 2023, 11, 2202525
- [2] M. S. Kim, W. Jang, B. G. Kim, D. H. Wang, *J. Mater. Chem. C*, 2023, 11, 8776-8783.
- [3] M. S. Kim, W. Jang, T-Q. Nguyen, D. H. Wang, *Adv. Funct. Mater.*, 2021, 31, 2103705.
- [4] M. S. Kim, J. Lim, W. Jang, D. H. Wang, *Carbon Energy* (Accepted).

5:00 PM SB02.04.12

Impact of Dielectric Environment and Counterion Size on Polaron Characteristics in Electrochemically Doped π -Conjugated Polymers Megan R. Brown¹, Joel Bombile¹, Jean-Luc Bredas², Zhiting Chen², Chamikara Karunaseena², Hong Li², Erin L. Ratcliff² and Chad Risko¹; ¹University of Kentucky, United States; ²The University of Arizona, United States

Electrochemically doped π -conjugated polymers (CP) are central materials in several emerging applications such as semiconductors in optoelectronic devices, active materials in thermoelectric generators, and electrode or binder materials in batteries. In these systems, electronic transport is controlled by the formation of polarons, which act as charge carriers in the CP. As the CP interacts with counterions from an electrolyte source, the charge associated with the polaron is stabilized. While both the counterion and the solvent environment involved in this interaction can impact the optical and charge-carrier properties of CPs, a clear understanding of the governing mechanisms is still lacking. Here we focus on assessing how single-chain polaron properties are impacted by changes in the surrounding dielectric environment and counterion used. We use first-principles calculations based on density functional theory (DFT) and time-dependent density functional theory (TD-DFT) with a tuned range-corrected hybrid functional to determine various polaron characteristics in the model CP N2200 in assorted dielectric environments with and without counterions of varying sizes present. We find that the Coulomb interactions between the polaron and the counterion lead to smaller, more strongly bound polarons as reflected by changes in charge delocalization, bond distortion, and polaron features of the optical absorption spectra. These data provide valuable insight into how such variables impact the charge transport properties of electrochemically doped CP's.

5:00 PM SB02.04.13

Expanding The Compatibility of P3HT Hole Transport Layers for Stable NIP Perovskite Solar Cells David Hardy, Feng Wang and Feng Gao; Linköping University, Sweden

In order for perovskite solar cells to be commercially competitive, attaining robust environmental stability is of the utmost importance. In a standard nip device stack the material selection for the surface hole transport layer (HTL) is critical, as it will dictate the degree that air and moisture will penetrate into the sensitive perovskite layer. Present high performing devices rely upon the established small molecule: Spiro-OMeTAD due to its well aligned energy levels, high hole mobility and broad compatibility with differing perovskite chemistries and interfacial passivation layers.

Conductive organic polymers offer several advantages over small molecule materials like Spiro-OMeTAD, such as fast intramolecular transport, greater environmental stability, and reduced cost. Poly(3-hexylthiophene-2,5-diyl) (P3HT) is one such polymer, and has been successfully implemented as an HTL in numerous reported perovskite solar cells, attaining efficiencies up to 24.6% [1]. However, typically these high performances rely upon interfacial perovskite treatments to induce favourable P3HT orientation and packing, and thus introduce restrictions on choice of perovskite chemistry or passivation method, that are not present for Spiro-OMeTAD. While reports that rely on oxidative dopants such as F4TCNQ, to increase the conductivity of P3HT HTL, exhibit lower efficiencies [2]. Therefore, presently P3HT based devices lag behind their Spiro-OMeTAD counterparts, in terms of performance, and versatility.

Recently the novel "ion-modulated radical doping strategy" for Spiro-OMeTAD based HTLs has outlined a doping strategy that relies upon a stable radical (Spiro²⁺-TFSI) to increase conductivity, in conjunction with an ionic modulator (TMBP-TFSI) to improve hopping transport between molecules [3]. Drawing inspiration from the IM-Radical doping strategy, this work aims to develop an analogous co-doping approach, for P3HT (or other low-cost polymers). Oxidising dopants such as charge transfer materials, Lewis acids, photo-initiator salts, and electrophilic salts have been screened in order to maximise HTL conductivity, and thus short circuit current, while various ionic modulators have been employed to align material work-functions and maximise the open circuit voltage. Through this combined doping approach we aim to develop a low cost P3HT based HTL that can match the performance of established Spiro-OMeTAD based devices and offer improved environmental stability, without imposing material restrictions upon the underlying device stack.

References

- [1] M. J. Jeong, K. M. Yeom, S. J. Kim, E. H. Jung, and J. H. Noh, "Spontaneous interface engineering for dopant-free poly(3-hexylthiophene) perovskite solar cells with efficiency over 24%," *Energy Environ. Sci.*, vol. 14, no. 4, pp. 2419–2428, 2021, doi: 10.1039/d0ee03312j.
- [2] H. C. V. Tran, W. Jiang, M. Lyu, and H. Chae, "Tetrahydrofuran as Solvent for P3HT/F4-TCNQ Hole-Transporting Layer to Increase the Efficiency and Stability of FAPbI₃-Based Perovskite Solar Cell," *J. Phys. Chem. C*, vol. 124, no. 26, pp. 14099–14104, 2020, doi: 10.1021/acs.jpcc.0c03890.
- [3] T. Zhang *et al.*, "Ion-modulated radical doping of spiro-OMeTAD for more efficient and stable perovskite solar cells," *Science* (80), vol. 377, no. 6605, pp. 495–501, 2022, doi: 10.1126/science.abo2757.

5:00 PM SB02.04.14

Measuring Carrier Lifetimes in Organic Solar Cells Ally Hurd^{1,2}, Awwad N. Alotaibi², Obaid Alqahtani², James R. Doyle¹ and Brian A. Collins²; ¹Macalester College, United States; ²Washington State University, United States

Printable and flexible organic solar panels are promising sources of inexpensive, large-scale renewable energy, where panels can be manufactured by printing from polymer inks. There are some limitations to these types of solar cells, however. First, toxic halogenated solvents have historically been necessary to dissolve polymers to make the ink. In addition, organic solar cells typically have high rates of recombination, which limits their efficiency. Here, we use a transient photovoltage (TPV) technique to measure charge lifetimes in cells made from two different organic solvents. The first solvent is toxic, halogenated dichlorobenzene (DCB) which is typically used to make organic solar cells. The other is a less toxic, non-halogenated solvent, carbon disulfide (CS₂). By varying the processing methods in this way, we find that cells made from CS₂ have longer charge lifetimes and higher efficiencies than those made with DCB. Possible reasons for these differences are explored using semi-analytic and numerical modeling. This work demonstrates that we may be able to decrease the toxicity of organic solar cell manufacturing and simultaneously improve the efficiency of the devices, bringing this powerful method of capturing solar energy to the forefront of sustainable energy solutions.

5:00 PM SB02.04.15

Conductivity Control by Welding of Nanomembrane for Stretchable Electronics [Jeeyoung Kim](#)^{1,2}, Minjeong Kim^{1,2} and Dae-Hyeong Kim^{1,2}; ¹Seoul National University, Korea (the Republic of); ²Institute for Basic Science (IBS), Korea (the Republic of)

Welding is a technology that enhances conductivity by forming junctions of metal nanomaterials within a nanocomposite. Conventional nanocomposites have difficulty forming percolation because conductive nanomaterials are mixed with insulating polymers. Conductivity can be improved only through welding with harsh conditions, making it a challenge to control conductivity through welding. Herein, we introduce welding control technology to enable control over the conductivity of nanomembranes on a wide scale under mild conditions. Welding control is a technique that regulates the interparticle junction diameter of the nanomembrane by controlling the reactivity of the reduction solution, which removes ligands attached to the surface of nanoparticles. Reduction solutions can directly act on the nanoparticles exposed in the form of a monolayer in the nanomembrane. The reactivity of the reduction solution is directly proportional to the degree to which ligands are removed, thus increasing the junction diameter. By adjusting the diameter of these junctions, resistance can be tuned from a few ohms to several thousand ohms. This technology is applicable to various metal nanoparticles, such as Au and Ag, and can simplify circuit design when used for patterning. Hence, it can be used as a universal strategy in stretchable devices.

5:00 PM SB02.04.16

Disorder-Tolerant Efficient Doping Strategy of Conjugated Polymers for High-Performance Organic Thermoelectrics [Jimin Kim](#) and Kilwon Cho; Pohang University of Science and Technology, Korea (the Republic of)

Molecular doping has been a paramount technique to modulate the electronic properties of conjugated polymers (CPs) used in various organic device applications. However, conventional redox doping requires a sufficient energy level offset between the host and dopant; otherwise, doping occurs through the formation of a charge transfer complex, which strongly reduces doping efficiency. Moreover, especially in organic thermoelectrics (TEs), excessive dopants introduced to form highly doped CPs generally cause structural distortion and broadening of the density of states (DOS) in CPs (i.e., dopant-induced disorder), thereby deteriorating their charge transport properties. Herein, we present an efficient doping strategy to attain highly doped CPs with dramatically suppressed structural and energetic disorder using a promising Lewis acid dopant, tris(pentafluorophenyl)borane (BCF), which has recently shown potential for doping CPs regardless of their ionization energy and enabling efficient integer charge transfer by forming a BCF–water complex. Using a non-polar aliphatic solvent, hexane, which can effectively swell the CP films due to its good affinity with the side chains of CPs, we successfully infiltrate BCF into the lamellar spacing of poly[2,5-bis(3-tetradecylthiophen-2-yl)thieno[3,2-b]thiophene] (PBTTT) films via sequential doping, producing a remarkable electrical conductivity of 230 S cm⁻¹ and a TE power factor of 140 $\mu\text{W m}^{-1} \text{K}^{-2}$. Concomitantly, the resulting sequentially doped films show significantly high Hall carrier mobility and facilitated bipolaron formation within their high solid-state ordering compared to films doped by solution-mixing. In addition, the sequentially doped films exhibit highly delocalized transport characteristics through highly ordered domains with a narrow DOS, substantiated by charge transport modeling and quantitative investigation of crystalline ordering, charge carrier localization, and energetic disorder. This work would provide an approach for disorder-tolerant doping strategies with a comprehensive understanding of processing–structure–property relationships in highly doped CPs.

5:00 PM SB02.04.17

Ester Functionalized Di-Pyrrole Containing Chalcogenophene Based Semiconducting Small Molecules for Organic Field Effect Transistor Applications [Ashutosh Shrivastava](#), Michael C. Biewer and Mihaela C. Stefan; The University of Texas at Dallas, United States

Pyrrole is the most electron-rich molecule among five-membered heterocyclic molecules like furan, thiophene, and selenophene. These five-membered chalcogenophenes are isoelectronic to each other and have the potential to be utilized for organic electronics. In this study, we have designed and synthesized three different organic compounds containing Di-pyrrole molecules fused with different chalcogenophenes: diethyl 1,7-dihydrofuro[3,2-b:4,5-b']dipyrrole-2,6-dicarboxylate (FDP), diethyl 1,7-dihydrothieno[3,2-b:4,5-b']dipyrrole-2,6-dicarboxylate (TDP), and diethyl 1,7-dihydroselepheno[3,2-b:4,5-b']dipyrrole-2,6-dicarboxylate (SeDP). The molecular characterization of these compounds was done using ¹H, and ¹³C Nuclear Magnetic Resonance (NMR) spectroscopy. The crystal structure determination and phase purity analysis of these compounds were performed using Single Crystal X-Ray Diffraction and Powder X-Ray Diffraction respectively. The XRD analysis reveals that fused rings of these compounds have a planar structure in which two compounds (TDP and SeDP) form dimers and are interacted by N-H•••O hydrogen bonding. The optical and electrochemical properties were studied using UV-Vis Spectroscopy and Cyclic voltammetry respectively, that displays that these molecules are promising semiconducting candidates for electronic applications. The highest occupied molecular orbital (HOMO) and lowest unoccupied molecular orbital (LUMO) energy levels of these molecules were also calculated by density functional theory (DFT) calculations using Gaussian and are compared with experimental data. Thermogravimetric analysis and Differential Scanning Calorimetry studies show that these compounds are thermally stable (vary in the range of 150-200 °C) and do not have any phase transformation below decomposition temperature. These as-synthesized organic semiconducting molecules will be studied for organic field effect transistor applications.

5:00 PM SB02.04.18

Enhancing Stability and Thermoelectric Performances of Doped Oriented Regioregular Poly(3-Hexythiophene) Using Anion Exchange Doping [Shubhradip Guhait](#)¹, Aditya Dash², Antoine Lemaire¹, Laurent Herrmann¹, Martijn Kemerink² and Martin Brinkmann¹; ¹Institute Charles Sadron, CNRS – Université de Strasbourg, France; ²Institute for Molecular Systems Engineering and Advanced Materials, Heidelberg University, Germany

Doping polymer semiconductors is an elegant method to produce conducting polymer films for various electronic applications with effective structural control. In this contribution, we present an innovative method for preparing stable and efficient conducting polymer films by combining high-temperature rubbing with anion exchange doping using bis(trifluoromethylsulfonyl)imide (TFSI) as the dopant. We combine two doping methods i.e. anion exchange and incremental concentration doping to investigate the impact of progressive dopant introducing in the semi-crystalline structure of P3HT on the structural and thermoelectric properties of aligned thin films using a combination of Transmission electron microscopy, Polarized optical absorption spectroscopy and transport measurements. Our results demonstrate that anion exchange strongly depends on both the ratio of the dopants (F₄TCNQ and LiTFSI in n-butylacetate) but also on their concentration. Two regimes of doping are evidenced with different distributions of dopants in the semi-crystalline structure of P3HT: first crystalline domains are doped by exchange of F₄TCNQ⁻ with TFSI⁻ followed by a progressive doping of amorphous regions of P3HT. The best thermoelectric performances are comparable to the ones observed for P3HT doped with tris(4-bromophenyl)ammoniumyl hexachloroantimonate (magic blue) with power factors of 150-160 $\mu\text{W/mK}^2$. In addition, we demonstrate a long-term stability of the doped films under inert atmosphere over > 50 days. The enhanced stability of TFSI-doped P3HT films is directly related to the specific distribution of dopants inside the semi-crystalline polymer structure. The enhanced stability is analysed in the frame of a modulation-doping mechanism considering the dopant distribution in the polymer structure and its impact on the accumulation layer that is created at the crystal/amorphous interface.

5:00 PM SB02.04.19

Solubilizing Benzodifuranone-Based Conjugated Copolymers with Single Oxygen Containing Branched Side Chains [Diego Roperó Hinojosa](#)¹, Nathan James Pataki², Pietro Rossi², Andreas Erhardt³, Shubhradip Guhait⁴, Francesca Pallini⁵, Chris McNeill³, Christian Müller⁶, Mario Caironi² and Michael Sommer¹; ¹TU Chemnitz, Germany; ²IIT Milano, Italy; ³Monash University, Australia; ⁴CNRS Strasbourg, France; ⁵University of Milano-

Bicocca, Italy; ⁶Chalmers University, Sweden

Achieving simple methodologies to synthesize, scale up, and process organic polymeric materials from solution is paramount to simplify access to semiconductor devices. In this context, benzodifuranone-based copolymers have shown excellent performance in different electronic applications, such as organic field effect transistors or organic thermoelectric generators. Nevertheless, these materials commonly display limited solubility due to their highly coplanar structures, giving rise to significant aggregation. Large branched alkyl side chains are commonly used to circumvent this problem; however, these side chains suffer from long and cumbersome synthetic routes and high costs. In this work, single ether-containing branched side chains synthesized employing Williamson etherification were prepared to provide a straightforward strategy to attach long side chains to p-conjugated backbones. The starting materials used were cost-economic Guerbert alcohols and α,ω -dibromoalkyls. The robustness of the method allowed both spacers as well as side chain lengths to be varied. Molar masses of benzodifuranone-thiophene copolymers reached up to 50 kg/mol, and solubilities were as high as 90mg/mL. Furthermore, n-doping of the polymers with *N*-DMBI delivered conductivity values three times superior to similar copolymers reported in the literature. The synthetic approach is furthermore extended to different backbone structures.

5:00 PM SB02.04.20

Charge Carrier Transport in Individual Granules of Sepia Melanin [Shahid Khaleel](#), Zhaojing Gao, Anthony Camus and Clara Santato; Polytechnique Montreal, Canada

Sepia melanin, a naturally occurring pigment found in the ink sac of cuttlefish, has garnered significant interest for its intriguing electrical properties and potential as an organic semiconductor material. Sepia melanin exhibits unique characteristics, such as its moisture-dependent electrical response [1] and broadband optical absorption [2], making it a promising material for applications in organic electronics, energy harvesting, and bioelectronics. Sepia melanin exhibits properties of disordered organic semiconductors whose charge transport behavior is attributable to a combination of band-like and hopping transport mechanisms [3]. The electrical conduction in Sepia melanin is influenced by its complex hierarchical structure, which eventually leads to melanin nanoparticles ~150-200 nm-sized self-assembled into granules. These nanoparticles result from variety of arrangements of pi-pi stacked molecules [4].

In this study, we explored the charge transport properties of Sepia melanin at the nanoscale, with the aim to fully harness Sepia melanin's potential for sustainable optoelectronic technologies.

We focus our investigations on a nanoscale, inter-digitated planar geometry of patterns (inter-electrodes distance ~200-700 nm) as our goal is to detect signals generated by individual granules of Sepia melanin. Patterns are fabricated by Electron Beam Lithography.

Findings from our ongoing study reveal the influence of structural disorder on charge carrier transport in Sepia melanin, including charge carrier localization and trapping effects as it is confirmed from current-voltage measurement. Also, Temperature-dependent electrical characterizations are helping us shed light on aspects related to hopping transport and de-trapping of charge carriers, such as calculating the activation energy.

Such effects represent opportunities for tailoring charge transport characteristics in Sepia melanin-based devices. We observed that Sepia melanin granules reveal their remarkable high electrical conductivity.

Work is in progress to study the Electrochemical Impedance Spectroscopy (EIS) response in dry and wet atmosphere complemented by current-time measurement to confirm the nature of the charge carriers (electrons or ions or both).

1. Wunsche, J., et al., *Protonic and electronic transport in hydrated thin films of the pigment eumelanin*. Chemistry of Materials, 2015. **27**(2): p. 436-442.
2. Pullman, A. and B. Pullman, *The band structure of melanins*. Biochimica et biophysica acta, 1961. **54**: p. 384-385.
3. Haneef, H.F., A.M. Zeidell, and O.D. Jurchescu, *Charge carrier traps in organic semiconductors: a review on the underlying physics and impact on electronic devices*. Journal of Materials Chemistry C, 2020. **8**(3): p. 759-787.
4. Clancy, C.M. and J.D. Simon, *Ultrastructural organization of eumelanin from Sepia officinalis measured by atomic force microscopy*. Biochemistry, 2001. **40**(44): p. 13353-13360.

SESSION SB02.05/SB04.04: Joint Session: Advances in Organic Electronics

Session Chairs: Xiaodan Gu, Ulrike Kraft and Bob Schroeder

Wednesday Morning, April 24, 2024

Room 437, Level 4, Summit

8:00 AM *SB02.05/SB04.04.01

Bulk Doping of Conjugated Polymers and Interplay of Their Electrical and Mechanical Properties [Christian Müller](#); Chalmers University of Technology, Sweden

Chemical doping is widely used to modulate the electrical properties of conjugated polymers. Doping of thin films facilitates fundamental spectroscopic studies and, ultimately, is important for the operation of devices from transistors to solar cells. However, some applications such as thermoelectrics and wearable electronics require bulk materials, which complicates doping processes. This talk will explore some of the fundamentals of doping of both thin films and bulk materials. The impact of doping on the electrical as well as mechanical properties will be discussed, and it is shown how doping can be used to tune both the conductivity and stiffness of conjugated polymers. Finally, strategies are explored that permit to decouple the effect of doping on the electrical and mechanical properties.

8:30 AM *SB02.05/SB04.04.02

Doping Glycolated Polythiophenes with Lithium Salts [Christine Luscombe](#); Okinawa Institute of Science and Technology, Japan

Polymer-based mixed ionic/electronic conductors (MIECs) are receiving increased attention, in part due to their utility across a wide-range of applications. MIECs show valuable properties, including volumetric capacitance changes, transduction of ionic and electronic signals, and biocompatibility. These properties result in a number of useful features, enabling their use in applications such as batteries and ultracapacitors, (bio)sensors, actuators, and organic electrochemical transistors (OECTs). Homopolymer MIECs originally showed limited ionic mobility due to their highly hydrophobic backbones. There has been a significant improvement in their ionic conductivity by introducing polar groups into the solubilizing side chains; the most popular chemistry for the polar side chains is oligoethylene glycol (oEG). This strategy of introducing oEG has driven significant improvements in MIEC performance in a number of conjugated polymer backbones.

Side chains are known to have a profound influence on the morphology, crystallinity, charge carrier concentration, charge thermal stability and ion/water uptake properties of conjugated polymers. By studying a range of polythiophenes across LiTFSI doping concentrations, we are able to elucidate how variations in the side chain architecture influence the evolution of morphology with increasing levels of LiTFSI doping, highlighting the importance of the architecture of oEG side chains in determining the blended material's morphology and resultant ionic and electronic conductivity. The presentation will focus on how small changes in the side chain structure can affect where the LiTFSI is located and thus the conductivity of the materials.

9:00 AM *SB02.05/SB04.04.03

Soft PhotoElectroChemical Systems for Solar Fuels [Erin L. Ratcliff](#); University of Arizona, United States

Highly scalable, durable π -conjugated polymer materials provide control over local environments afforded through synthesis, long-lived charge carrier lifetimes, and flexible, low-cost, and scalable thin film formats which circumvent the shortcomings of inorganic materials (surface states, grain boundaries, challenges in processing, and mechanically unstable platforms). The Center for Soft PhotoElectroChemical Systems (SPECS) is an Energy Frontier Research Center focused on the basic science questions that underpin the development of low-cost, robust energy conversion and energy storage technologies based on new organic polymer (plastic) electronic materials. These materials are predicted to fill a critical position in the U.S. energy portfolio, providing for next-generation fuel-forming platforms (energy conversion) and batteries (energy storage) that cannot currently be achieved with conventional (hard) inorganic materials.

The realization of all-organic semiconductor systems that capture light energy and convert it into chemical energy requires a detailed understanding of structure-property relationships governing the interconnected dynamics of photo-generation, transport, and electron transfer across multiple interfaces. Dark electrochemical processes must be understood before increasing the complexity via light-matter interactions. This talk will focus on increasing complex, multiple interface platforms, towards the goal of photons-to-electrons-to-molecules energy conversion processes for all-polymer photocathodes. A number of emerging *in situ/operando* spectroelectrochemical and scanning electrochemical cell microscopy approaches will be discussed for this exciting new area of energy conversion.

9:30 AM *SB02.05/SB04.04.04

Organic Photodetectors for Shortwave Infrared Sensing Thuc-Quyen Nguyen and [Hoang Mai Luong](#); University of California, Santa Barbara, United States

Shortwave infrared (SWIR) has various applications, including night vision, remote sensing, and medical imaging. SWIR organic photodetectors (OPDs) offer advantages such as flexibility, cost-effectiveness, and tunable properties, however, lower sensitivity and limited spectral coverage compared to inorganic counterparts are major drawbacks. We develop a simple yet effective and widely applicable strategy to extend the wavelength detection range of OPD to a longer wavelength, using resonant optical microcavity. We demonstrate a proof-of-concept in PTB7-Th:COTIC-4F blend system, achieving external quantum efficiency (EQE) > 50 % over a broad spectrum (450 – 1100 nm) with a peak specific detectivity (D^*) of 1.1×10^{13} Jones at 1100 nm, while cut-off bandwidth, speed, and linearity are preserved. By employing a novel small-molecule acceptor IR6, a record high EQE = 35 % and $D^* = 4.1 \times 10^{12}$ Jones are obtained at $\lambda = 1150$ nm. This work emphasizes the importance of optical design in optoelectronic devices, presenting a considerably simpler method to expand the photodetection range compared to a traditional approach that involves developing absorbers with narrow optical gaps.

10:00 AM BREAK

SESSION SB02.06: Morphological Control in Organic Semiconductors

Session Chairs: Bob Schroeder and Guillaume Schweicher

Wednesday Morning, April 24, 2024

Room 437, Level 4, Summit

10:30 AM *SB02.06.01

Glassy Metallic Character in Amorphous Coordination Polymers of Tetrathiafulvalenetetrathiolate [John S. Anderson](#)¹, Jiaze Xie², Patrick Crossland¹ and Chen-Yu Lien¹; ¹University of Chicago, United States; ²Princeton, United States

New conducting coordination polymers featuring tetrathiafulvalenetetrathiolate (TTFt) linkers will be presented. These materials possess no long-range order, but are still highly conductive and display signatures of glassy metallic charge transport. Deeper characterization of these charge transport properties including Hall effect measurements will be discussed, as well as new efforts in processing these materials and altering their electronic structures via doping or metal ion exchange.

11:00 AM SB02.06.02

Understanding Polymorphism-Driven Thermoelectric Properties in Molecularly Doped Poly(Dodecyl-Quarterthiophene) through Microstructure Gradients [Shrayesh Patel](#); University of Chicago, United States

Our research delves into the intricate relationship between microstructure changes induced by thermal annealing and the resulting charge transport properties in poly(dodecyl-quarterthiophene) (PQT). Employing targeted characterization techniques, including GIWAXS and ellipsometry, the study unveils the polymorphism and chain orientation within PQT and emphasizes the crucial role of interdigitation of side chains. Through vapor doping with F4TCNQ, the study demonstrates that polymorphs strongly control doping efficiency, thereby significantly influencing charge transport properties. Specifically, the research reveals that the 100 °C annealed sample, characterized by tightly packed side chains, displays low doping efficiency and corresponding low electronic conductivity, whereas the 130 °C annealed sample exhibits markedly improved electronic conductivity from higher doping efficiency. Additionally, the study presents a novel method for fabricating continuously graded (CG) thin films of PQT using controlled thermal annealing, revealing diverse 1D in-plane microstructure gradient profiles modulating electronic conductivity and Seebeck coefficient across a 5 mm distance. Comparing these CG films to their equivalent uniform counterparts, the study showcases their enhanced cooling performance due to the effective redistribution of Joule heating and Peltier cooling effects. These findings underscore the significance of understanding the interplay between local order, polymorphism, and doping efficiency in molecularly doped conjugated polymers. In turn, this work provides valuable insights for the design of semiconducting polymers tailored for precise microstructure and doping levels for organic thermoelectric applications.

11:15 AM SB02.06.03

Operando X-Ray Fluorescence for Direct Ion Composition and Mobility Quantification in Organic Mixed Ionic/Electronic Conductors [Ruiheng Wu](#), Xudong Ji and Jonathan Rivnay; Northwestern University, United States

Organic mixed ionic-electronic conductors (OMIECs) represent a class of organic materials, mostly conjugated polymers, characterized by their ability to transport both electronic and ionic charges. Understanding the composition and mobility of ions within OMIECs is of paramount importance, as it directly influences the performance and fundamental mechanisms of OMIEC-based devices. Typically, such assessments have relied on indirect methods, often based on assumptions that may not always be accurate. Ex situ X-ray fluorescence (XRF) has been employed to quantify ion composition in OMIECs under different doping states, but potential errors could arise due to the need for sample washing to remove residual electrolyte. Instead, operando XRF emerges as a powerful and direct tool for investigating dynamic ion composition and transport in OMIECs during electrochemical operations. Herein, operando XRF was harnessed to probe ion transport in a model OMIEC material, poly(3,4-ethylenedioxythiophene) polystyrene sulfonate (PEDOT:PSS). The findings from this investigation are highly enlightening: the initial electrochemical cycle showed a slow electro-wetting and cation-proton exchange. Subsequent cycles demonstrated minimal cation fluctuation, around 5%, implying a rapid, stable response with small, consecutive steps of ion migration. The calculated effective ion mobility displayed thickness-dependent behavior, underscoring the significance of interfacial ion transport pathways with higher effective mobile ion density. This decoupling of bulk and interfacial effects on ion mobility enhances our comprehension of ion transport in both conventional and vertical organic electrochemical transistors (OECTs). Furthermore, the correlation between ion mobilities, domain boundaries, and mobile ion density suggests that ions within OMIECs migrate in a highly complex way. These findings promise to advance our understanding of ion transport in OMIECs and related devices, offering valuable insights that can guide molecular design, material processing, and charge/ion migration modeling. Ultimately, this research can contribute to enhanced device performance and faster response times. Importantly, this methodology is not limited to OMIECs; it can be effectively applied to investigate complex ion transport mechanisms in various mixed conductors, spanning diverse fields such as batteries and solar cells, holding the potential to revolutionize the design and optimization of a wide range of technologies.

SESSION SB02.07: Organic Semiconductor Design Through New Modeling Approaches

Session Chairs: Xiaodan Gu and Guillaume Schweicher

Wednesday Afternoon, April 24, 2024

Room 437, Level 4, Summit

1:30 PM *SB02.07.01

Theoretical Description of Phonons Controlling Charge and Heat Transport in Organic Semiconductors [Jerome N. Comil](#); University of Mons, Belgium

The charge mobility in molecular crystals is governed by the extent of delocalization of the charge carriers, in turn dictated by the extent of fluctuations of the transfer integrals by lattice phonons. The latter also act as heat carriers in organic semiconductors. In order to maximize electrical conductivity and minimize thermal conductivity (for thermoelectric applications), there is a need for a detailed description of the phonons impacting the most charge and heat transport and for the establishment of structure-property relationships. In this contribution, I will describe our recent efforts aiming at assessing the role of individual phonons in the thermal fluctuations of the transfer integrals as well as the impact of phonon dispersion. I will also present some recent simulations of heat transport showing that the extent of delocalization of the phonons controls the thermal conductivity.

2:00 PM *SB02.07.02

High-Throughput Models of Conjugated Polymers [Alessandro Troisi](#) and Hesam Makki; University of Liverpool, United Kingdom

Structural models of semiconducting polymers are challenging to generate, validate against experiments and interrogate for novel properties and research hypotheses. Despite their importance, producing a model of reasonable quality requires weeks/months of human and computer time. This situation is totally unsuitable for designing polymers, deriving structure-property relations from large data sets or simply engage with a very dynamic community of synthetic chemists and characterization experts. This lecture explores the recent advances toward high-throughput modelling for polymeric materials and the workflow derived to be deployed over hundreds of different polymers. Methods to extract relevant properties of charge transport will be discussed alongside recent advances in the study of highly doped polymers. As common in our research group, these large scale calculations are used to derive practical generalizations and design rules.

2:30 PM BREAK

3:30 PM SB02.07.03

Machine Learning Guided Prediction of Thermal Properties and Identification of Crystallizable Organic Semiconductors [Holly Johnson](#)¹, Filip Gusev², Jordan T. Dull¹, Yejoon Seo¹, Rodney D. Priestley¹, Olexandr Isayev² and Barry P. Rand^{1,1}; ¹Princeton University, United States; ²Carnegie Mellon University, United States

Crystalline organic semiconductors feature improved exciton diffusion length and charge carrier mobility compared to their amorphous counterparts. Certain organic molecular thin films can be crystallized at large-scale via annealing of initially prepared amorphous layers. These films ideally crystallize as platelets with long-range order on the scale of tens to hundreds of microns, but have also been seen to crystallize as spherulites or to resist crystallization entirely. Molecules that can transform into a platelet morphology feature high melting point and crystallization driving force (ΔG_c). Here, we employ machine learning to identify candidate organic materials that were predicted to crystallize into large-area platelets by estimating the aforementioned thermal properties. Six materials identified by the machine learning algorithm were evaluated for their bulk thermal properties using differential scanning calorimetry, and their crystallization behavior via thin film crystallization. Of these six materials, three crystallized as platelets, one crystallized as a spherulite, and two resisted crystallization, displaying a successful application of machine learning in the scope of organic thin film crystallization and reinforcing the principles of melting point and ΔG_c as metrics that govern the crystallization behavior of organic thin films.

3:45 PM *SB02.07.04

Strategies to Improve the Performance of n-Type Conjugated Polymers [Derya Baran](#); King Abdullah University of Science and Technology, Saudi Arabia

The development of organic semiconductors (OSCs) has gained significant attention in the realm of organic electronics (OEs). Organic thermoelectrics (OTEs) are of interest owing to their potential for harnessing power from residual waste heat and powering autonomous wearable devices. Although P-type OTEs showed robust thermoelectric performance from an early stage, the development of n-type OTEs has been slower in comparison, owed to limited doping efficiency and rapid degradation of electronic properties. [Here, we present DPP-based n-type conjugated polymers \(CPs\) for OTEs with three different strategies to enhance their charge transport and TE performance. Our strategies are based on the Hansen solubility parameter \(HSP\) framework and provide insight to improve charge transport in doped OSCs from morphology control to solvent-host-dopant interaction.](#) First, we utilize HSP to screen thousands of solvents to refine our selection and succeed in controlling the mesoscale morphology of DPP-based n-type CPs films transitioning from nanofibrils into nanofibers. We found that the nanofiber morphology can simultaneously maintain their electrical properties and enhance its mechanical robustness. Second, we address the limitations of the electrical conductivity (σ) of n-type CP by employing HSP to assess the suitable solvent that improves miscibility and charge transport. We found that solvent having higher solubility of dopant, and conjugated backbone of the CP can increase σ without sacrificing Seebeck coefficient (S). This work emphasizes the effectiveness of HSP-guided solvent selection in hindering σ -S trade-off and limitations from solution mixing doping. Last, we propose the idea of self-induced anisotropy in n-type OTEs which enhance the thermoelectric power factor (PF) by mitigating the trade-off between σ and the S. Utilizing HSP theory, we try to understand the solvent-host-dopant intermolecular interactions and elucidate the origin of self-induced anisotropy. We found that a preferential edge-on orientation would increase the in-plane delocalization length and thus improved the electrical conductivity without hindering the S.

SESSION SB02.08: Doping of Organic Semiconductors I
Session Chairs: Mariano Campoy-Quiles and Xiaodan Gu
Thursday Morning, April 25, 2024
Room 437, Level 4, Summit

8:15 AM *SB02.08.01

The Design, Synthesis and Application of Molecular Dopants for Electronics and Opto-Electronics [Seth R. Marder](#)^{1,2}; ¹University of Colorado Boulder, United States; ²National Renewable Energy Laboratory (NREL), United States

In this talk I shall describe issues related to the design and application of dopants for organic electronic and opto-electronics and highlight factors that influence how to select dopants to be paired with various materials. I will also discuss preliminary studies on doping materials with chiral dopants and doping chiral materials with an achiral dopant.

8:45 AM SB02.08.02

Ground-State Electron Transfer in All-Polymer Donor: Acceptor Blends enables The Aqueous Processing of Water-Insoluble Conjugated Polymers [Tiefeng Liu](#), Johanna Heimonen, Qilun Zhang, Mats Fahlman, Renee Kroon and Simone Fabiano; Linköping University, Sweden

Conjugated polymers offer a unique blend of solution processability, mechanical flexibility, and semiconducting properties, making them invaluable for diverse applications in industries ranging from displays and energy storage to healthcare. However, conventional processing methods often involve hazardous solvents, posing challenges for broad commercial and sustainable adoption. To address this, we introduce a novel approach based on mutual electrical doping in donor:acceptor polymer blends, which facilitates the dispersion of water-insoluble conjugated polymers in aqueous solutions. This approach leads to macromolecular charge-transfer salts with 10,000 \times higher electrical conductivities than the pristine polymers, low work function, and excellent thermal/solvent stability, providing a versatile platform for various electronic devices. The resulting conductive, water-processable inks demonstrate exceptional performance in non-fullerene organic solar cells, organic electrochemical transistors, inverters, and artificial neurons. This breakthrough offers a practical solution for achieving large-scale and sustainable implementation of organic electronics without the need for traditional chemical modifications.

9:00 AM SB02.08.03

Spontaneous Modulation Doping in Semi-Crystalline Conjugated Polymers Aditya Dash¹, Shubhradip Guhait², Dorothea Scheunemann¹, Vishnu Vijayakumar², Nicolas Leclerc³, Martin Brinkmann² and [Martijn Kemerink](#)¹; ¹University of Heidelberg, Germany; ²Institute Charles Sadron, France; ³Université de Strasbourg, France

The possibility to control the charge carrier density through doping is one of the defining properties of semiconductors. For organic semiconductors, the doping process is known to come with several problems associated with the dopant compromising the charge carrier mobility by deteriorating the host morphology and/or introducing Coulomb traps. While for inorganic semiconductors these factors can be mitigated through (top-down) modulation doping, this concept has not been employed in organics. Here, we show that properly chosen host/dopant combinations can give rise to spontaneous, bottom-up modulation doping, in which the dopants preferentially sit in an amorphous phase, while the actual charge transport occurs predominantly in a crystalline phase with an unaltered microstructure, spatially separating dopants and mobile charges. Combining experiments and numerical simulations, we show that this leads to exceptionally high conductivities at relatively low dopant concentrations.

9:15 AM SB02.08.04

Doping Effectiveness and Stability in Semiconducting Polymers [Meghna Jha](#), Joaquin Mogollon Santiana, Aliyah A. Jacob, Kathleen Light, Megan L. Hong, Michael R. Lau, Leah R. Filardi, Sadi M. Gurses, Coleman X. Kronawitter and Adam J. Moule; University of California, Davis, United States

Molecular doping of semiconducting polymers has emerged as a prominent research topic in the field of organic electronics with new dopant molecules introduced regularly. FeCl₃ has gained attention as a p-type dopant due to its low-cost, availability, ability to dope high ionization energy co-polymers, and its use as a dopant that can be used with anion exchange. Here, we use a combination of UV-Vis-NIR spectroscopy, four-probe sheet resistance measurements, and X-ray absorption near-edge structure (XANES) spectroscopy to perform lifetime measurements to assess the stability of the doped polymers over time, which is crucial for evaluating the long-term performance and reliability of the doped films. FeCl₃ can cause radical side reactions that damage the conjugated polymer backbone, leading to degradation of the electronic properties. The rate of this degradation is orders of magnitude higher when the film is exposed to air. Anion exchange doping can reduce the [FeCl₄]⁻ concentration, but does not necessarily improve the doping lifetime because anion exchange electrolytes can serve as co-reactants for the degradation reaction. By comparison, doping with (2,3,5,6-Tetrafluoro-2,5-cyclohexadiene-1,4-diylidene)dimalononitrile (F4TCNQ) as the reactive dopant results in lower initial conductivity, but the lifetime of the doped polymer is almost tripled as compared to FeCl₃ doped polymer films. These findings highlight that the use of FeCl₃ as a molecular dopant requires a cost/benefit analysis between higher initial doping levels and lower

film stability.

9:30 AM *SB02.08.05

N-Doped Conducting Polymer (n-PBDF): Polymerization and Doping Mechanisms [Jianguo Mei](#); Purdue University, United States

n-PBDF has been recently discovered. It distinctly departs from known n-type conducting polymers - being solution-processable, highly conductive, and environmentally stable. In this talk, I will introduce the synthesis of n-PBDF and the mechanistic understanding of its polymerization and doping mechanisms.

10:00 AM BREAK

SESSION SB02.09: Charge Transport in Organic Semiconductors I

Session Chairs: Derya Baran and Mariano Campoy-Quiles

Thursday Morning, April 25, 2024

Room 437, Level 4, Summit

10:30 AM *SB02.09.01

Charge Transport Physics of Organic and Metal Halide Perovskite Semiconductors [Henning Sirringhaus](#); Cambridge University, United Kingdom

Organic and metal halide perovskite semiconductors are soft functional materials that are emerging as a viable semiconductor technology in industries such as displays, electronics, renewable energy, sensing and healthcare. A key enabling factor has been significant scientific progress in improving the charge transport properties and carrier mobilities of these materials, which has been made possible by better understanding of the structure-property relationships and the underpinning charge transport physics. Here we aim to present a coherent review of how we understand the unique charge transport physics in these two classes of semiconductors and discuss similarities and differences. We are also interested in the use of these materials in thermoelectric devices and we will discuss approaches to their controlled doping and understanding of the relevant thermoelectric physics.

11:00 AM SB02.09.03

Effects of Nanoscale Morphology on Molecular Doping in Conjugated Polymers [Sung-Joo Kwon](#)¹, Rajiv Giridharagopal¹, Justin Neu², Wei You² and David S. Ginger¹; ¹University of Washington, United States; ²University of North Carolina at Chapel Hill, United States

Conjugated polymers are inherently nanostructured, with a mixture of crystalline and amorphous domains, investigating the underlying mechanism of doping benefits from nanoscale real-space imaging. Here, we studied the molecular doping on P(g₃2T-TT) in solution-dripping doping with varying film-casting condition and dopants. Firstly, we perform spectroelectrochemistry to calibrate the optical bleaching to known polaron levels, and calculate the doping efficiency of molecular doping. We further perform functional atomic force microscopy (scanning Kelvin probe and conductive atomic force microscopy) methods to visualize the dopant aggregation and heterogeneity of local extent of doping on CPs. We show that the doping efficiency and dopant aggregation are both correlated with the ability of the dopant/solvent solution to swell the conjugated polymer, with combinations that swell resulting in more efficient doping and smoother films with less aggregation. We use these methods to provide a link between optical measurements of doping and local work function variations for films that have been molecularly and electrochemically doped. These techniques provide spatial mapping of topology with work function and time-resolved doping behavior of high resolution (sub-micron scale). Additionally, we investigated further dopant aggregations upon modifying the solvent of the dopant solution, side-chain and crystallinity of CPs; it reveals that swelling of dopant solution, and crystallinity both govern the aggregation of dopant on CPs, thereby limiting the doping efficiency of the CPs. This work will provide significant insight to understand molecular or electrochemical doping of conducting polymers at the microscopic level.

11:15 AM *SB02.09.04

Impact of Chain Conformation and Interchain Contacts on Charge Transport in Conjugated Polymers [Jenny Nelson](#), Jack F. Coker, Jarvist M. Frost and Xingyuan Shi; Imperial College London, United Kingdom

Charge transport in organic semiconductors such as conjugated polymers proceeds through a combination of intrachain and interchain charge transfer events. Predicting transport properties for any new material requires an understanding of how the chemical structure and physical organisation of polymer chains influence these two processes. The polymer's conformational phase space influences intrachain charge dynamics through variations in the structure, and hence energy, of polaron states and also influences the type of interchain contacts that can be formed. We consider the case of the stiff, high-mobility indacenodithiophene-*co*-benzothiadiazole polymer (C16-IDTBT) and use a variety of electrical and structural measurements as well as molecular dynamics, electronic structure calculations and charge transport simulations to probe the nature of the intra and inter-chain charge transfer processes. We conclude that the polymer's unusually high connectivity, rather than high interchain coupling, is responsible for its hole mobility. We compare the behaviour with other conjugated polymers including polyfluorenes and polythiophenes, in terms of their chemical structure. We conclude by reviewing the factors that will ultimately limit charge transport in conjugated polymers.

SESSION SB02.10: Charge Transport in Organic Semiconductors II

Session Chairs: Ting Lei and Erin Ratcliff

Thursday Afternoon, April 25, 2024

Room 437, Level 4, Summit

1:45 PM *SB02.10.01

Charge Transport Properties of n-Type Conjugated Polymers and Photovoltaic Blends [Samson A. Jenekhe](#), Sarah West and Duyen Tran; University of Washington, United States

Understanding of the charge transport properties of conjugated polymers is central to their applications in organic electronic devices, including organic light-emitting diodes, thin film transistors, electrochemical transistors, organic photovoltaics, thermoelectric devices, etc. Nevertheless, the underlying

mechanisms of how molecular and supramolecular factors influence the charge transport properties of semiconducting polymers remain to be fully elucidated. In this talk, I will highlight some examples of our recent work in addressing this knowledge gap for n-type and p-type conjugated polymer films as well as for photovoltaic polymer blend films. Our studies in one area have investigated how polymer molecular weight influences the charge transport properties in two topologically distinct classes of n-type conjugated polymers – those with rigid-rod chain topology and those with semi-flexible chain topology – and found that the chain length dependence of carrier mobility and mechanism of electron transport depend on the polymer chain topology. A detailed characterization of the thin film microstructures of the materials provided insights on the structural disorder and energetic disorder as a function of polymer chain length. How side chain engineering and tuning of the donor-acceptor character on the ladder polymer backbone influence their thin film microstructures and charge transport properties are investigated in a series of p-type conjugated ladder polymers. In another example, we have investigated the charge transport properties of binary blends of interest in all-polymer solar cells, including the roles of the molecular weights of the polymer components in achieving bipolar-symmetric blend charge transport and optimal morphology, photophysics, and device efficiency.

2:15 PM SB02.10.02

Multi-Band Filling and Non-Equilibrium Charge Transport in Conjugated Polymers at Charge Densities on The Order of 10^{21} cm⁻³ Xinglong Ren¹, Dionisius Hardjo Lukito Tjhe¹, Ian Jacobs¹, Gabriele D'Avino², Tarig Mustafa¹, Thomas Marsh¹, Lu Zhang¹, Yao Fu¹, Ahmed E. Mansour³, Yuxuan Huang¹, Wenjin Zhu¹, Ahmet Hamdi Unal¹, Vincent Lemaure⁴, Claudio Quarti⁴, Jin-Kyun Lee⁵, Iain McCulloch⁶, Martin Heeney⁷, Norbert Koch³, Clare Grey¹, David Beljonne⁴, Simone Fratini² and Henning Sirringhaus¹; ¹University of Cambridge, United Kingdom; ²Institut Néel, France; ³Humboldt-Universität zu Berlin, Germany; ⁴University of Mons, Belgium; ⁵Inha University, Korea (the Republic of); ⁶University of Oxford, United Kingdom; ⁷Imperial College London, United Kingdom

Organic electrochemical transistors (OECTs) provide us a powerful tool for studying charge transport in conjugated polymers over a wide range of charge densities. It has been reported that in both n-type and p-type OECTs, charge densities on the order of one charge per monomer ($\sim 10^{21}$ cm⁻³) can be achieved. At such high charge densities, Coulomb interactions among electrons and between electrons and counter-ions are expected to play a role in charge transport. However, charge transport in this regime, as well as the many-body correlated physics, is still not as well understood as charge transport in devices with much lower charge densities (e.g., organic field-effect transistors).

In this work, we show that in OECTs based on a class of p-type donor-acceptor polymers, it is possible to completely empty the HOMO and eventually access the HOMO-1 orbitals without any degradation, which is supported by a combination of electrical, thermoelectric, and photoemission spectroscopic measurements. More interestingly, under such extreme band filling conditions, by adding a second field-effect back-gate to the OECT, we observe unusual field-effect response when the ionic motions are frozen. Both the shape of the back-gate transfer curve (graphene-like) and the magnitude of drain current modulation (up to 300%) are substantially different from what one would expect from a conventional field-effect device based on an ultra-heavily doped polymer. Temperature-dependent measurements suggest that the unusual back-gate field-effect response is a non-equilibrium phenomenon, which provides unique insight into the formation of a frozen, soft gap in the density of states driven by Coulomb interactions.

2:30 PM *SB02.10.03

Chiral Assemblies of Conjugated Polymers for Controlling Charge and Spin Transport Ying Diao; University of Illinois at Urbana-Champaign, United States

Intimately connected to the rule of life, chirality remains a long-time fascination in biology, chemistry, physics and materials science. Chiral structures, e.g., nucleic acid and cholesteric phase developed from chiral molecules are common in nature and synthetic soft materials. Chiral semiconductors have been long leveraged by Nature to efficiently transduce energy and transfer electrons. However, it has been rarely used in synthetic semiconductors due to synthetic challenges. We recently discovered chiral emergence from high performance achiral conjugated polymers, in which hierarchical helical structures spanning nano- to micron scales emerge from a multistep assembly pathway in an evaporating meniscus during coating and printing. We further show that such hierarchical helical structures can be largely modulated by non-equilibrium processing during solution printing as well as by subtle changes in the polymer structure. With the ability to widely tune helical structures, we set out to demonstrate the ability of chiral helical structures in enhancing chemical doping efficiency and conductivity in redox polymers, and in efficiently converting spin to charge promising for spintronic applications.

3:00 PM BREAK

SESSION SB02.11: Organic Thermoelectrics
Session Chairs: Jianguo Mei and Erin Ratcliff
Thursday Afternoon, April 25, 2024
Room 437, Level 4, Summit

3:30 PM *SB02.11.01

π -Conjugated Nickel Complexes as n-Type Organometallic Semiconductors for Thermoelectric Generators Michihisa Murata; Osaka Institute of Technology, Japan

Flexible thermoelectric generators, which convert waste heat into electricity, have received increasing attention as convenient and low-cost energy-harvesting devices. p-Type and n-type organic and organometallic semiconducting materials are particularly suitable for thermoelectric materials on account of their very low thermal conductivity, which affords significant advantages not only in realizing high efficiency, but also in generating a temperature gradient. However, the development of n-type organic materials has been hampered partially on account of their instability in air upon doping with an n-dopant.

One promising example of n-type organometallic semiconductors is π -conjugated nickel-ethenetetrathiolate (NiETT), which exhibits high air-stability and n-type thermoelectric behavior. We envisioned that the new design of π -conjugated ligands in nickel complexes should have a positive impact on the conductivity and the thermoelectric properties. In order to increase the accessible variety of this class of complexes, we have developed a versatile method for the synthesis of a variety of π -conjugated Ni complexes and examined their performance. Even though they are insoluble in virtually all common organic solvents, we found that the conductivity of the resulting films can be markedly improved by the choice of the π -conjugated core. For example, a nickel complex containing thieno[3,2-*b*]thiophene units was designed and synthesized. Composite films of the resulting nickel complex and polyvinylidene difluoride (PVDF), which can be fabricated via a simple solution process under atmospheric conditions, exhibit remarkably high n-type conductivity (>200 S/cm). Moreover, the thermoelectric power factor of the n-type composite film was proven to be air stable. A grazing-incidence wide-angle X-ray diffraction analysis (GIWAXD) indicated a significant impact of introducing the thieno[3,2-*b*]thiophene core into the backbone of the nickel complex on

the orientation within the composite films.

These results on the design and synthesis of air-stable n-type materials should contribute to the generation of advanced materials with potential applications in flexible thermoelectric generators.

4:00 PM SB02.11.02

Controlling Energetic and Structural Disorder of Doped Conjugated Polymers for High-Performance Organic Thermoelectrics [Kilwon Cho](#); Pohang University of Science and Technology, Korea (the Republic of)

Molecular doping is a fascinating technology that can easily increase the electrical conductivity of conjugated polymers. It is actively being explored as a fundamental approach for developing thermoelectric materials and flexible bio-integrated electronics. A variety of dopants, from inorganic salts to molecular dopants and Lewis acids, along with innovative doping strategies, have successfully pushed the electrical conductivity of conjugated polymers to approximately ~ 1000 S/cm. Despite these noteworthy outcomes, inherent limitations hinder further progress in this field. Conjugated polymers lack a three-dimensional crystal structure and contain structural imperfections, leading to a substantial energetic disorder with a broad distribution of the density of states in their energy landscape. Moreover, the incorporation of dopants introduces structural disorder in crystalline ordering, localizing charge carriers to just a few monomer units. This energetic and structural disorder acts as a significant hurdle to advancing doped conjugated polymers. In this talk, I will present a chemically doped conjugated polymer, indacenodithiophene-co-benzothiadiazole (IDTBT), which is able to maintain low energetic disorder due to the highly planar backbone chain structure. I will thoroughly introduce the relationship between the exceptional charge transport properties revealed by the Kang-Snyder model and narrow-band model, and the polymer chain structure inspected through Raman spectroscopy and DFT calculations. Also, I will discuss a doping strategy aimed at reducing dopant-induced disorder in highly doped conjugated polymers, with a particular focus on a promising Lewis acid dopant, tris(pentafluorophenyl)borane (BCF). The improvements in charge transport properties that result from this strategy will be substantiated through an analysis of structural disorder, energetic disorder, and charge carrier localization, including quantitative investigation using coherence length, paracrystallinity, and paramagnetic susceptibility. Lastly, I will provide a brief overview of the high thermoelectric performance achieved in our research and present the potential of thermoelectric materials based on doped conjugated polymers.

4:15 PM SB02.11.03

Unlocking The Potential of Solution-Processed PEDOT:PSS Thin Films for Efficient Thermoelectric Energy Conversion [Juhung Park](#) and Jeonghun Kwak; Seoul National University, Korea (the Republic of)

Thermoelectric (TE) generation using solution-processable conjugated polymers holds great promise for low-temperature energy harvesting due to their versatility in materials, processes and form-factors. Among these polymers, poly(3,4-ethylenedioxythiophene):poly(styrenesulfonate) (PEDOT:PSS) is considered a promising candidate owing to its high electrical conductivity, flexibility, and air stability. However, a lack of understanding on the relationship between microstructure and TE charge transport properties has been a significant obstacle, impeding further enhancements in performance of solution-processable PEDOT:PSS. Here, we present a solution-processed, high-performance TE device based on a PEDOT:PSS thin film and thoroughly investigate their microstructure–thermoelectric performance–charge transport property relationships. We first fabricated a highly conductive PEDOT:PSS films using a super acid, where the σ values increased up to ~ 3600 S cm^{-1} primarily due to the highly ordered microstructure with PSS removal. Through a successive reduction process, we achieved the highest power factor of $534.5 \mu\text{W m}^{-1} \text{K}^{-2}$ with delocalized charge transport properties. Additionally, high electronic tunability of the reducer allowed us to investigate the Seebeck–conductivity relation over a wide range of σ , suggesting that the maximum PF value may surpass the experimentally obtained values. To identify the origin of the discrepancy, we analyzed the macro- and micro-scale charge transport properties using the temperature-dependent σ , Hall effects, and magnetoconductance of the films, together with the morphology, and found out that the connectivity between crystalline domains and the resulting high degree of percolation for transport are important factors toward the theoretically ideal PF .

4:30 PM SB02.11.04

3D-Printed Bulk Organic Thermoelectrics with High Power Output for Stretchable Electronics [Francisco Molina-Lopez](#); KU Leuven, Belgium

Distributed electronics are gaining traction for application in wearables and the Internet of Things (IoT). The increasing complexity of these systems comes with an acute need for energy that batteries struggle to satisfy, either because they are too stiff to be seamlessly integrated into soft wearable electronics, or because their replacement is unfeasible for the numerous and highly distributed nodes of the IoT. In those scenarios, thermoelectric (TE) materials, which can convert directly waste heat into electrical power, hold great potential. Conveniently, it has been suggested that TEs are more efficient than other thermal engines for low-power applications[1] like wearables and the IoT. However, the widespread of TE generators (TEG) is hampered by their expensive fabrication process; the use of critical elements such as Bi and Sb; and their limited form factor (rigid, flat, and small).[2] The ubiquity of the IoT nodes and the particular form factor of wearable devices (stretchable and large-area) call for a new technology that strongly relies on clean and abundant materials like polymers, and on scalable and versatile fabrication techniques, like printing. While the development of conducting polymers for organic thermoelectrics (OTEs) has recently witnessed tremendous progress, the reality is that the integration of such materials in actual devices has been seldom attempted, and when attempted, the high performance of the materials did not translate into performing devices. The reason for such lackluster outcome resides in the fact that most OTE materials are developed as thin films using technologies borrowed from organic FETs and photovoltaics. In sharp contrast, performing TEGs (such as commercial Peltier elements) are inherently bulk devices, presenting low internal resistance and capable of sustaining large temperature gradients in the through-plane direction, none of which is possible for thin films.

In my research group, we are working towards the development of high-performing 3D-printed bulk OTEs, which can be directly printed over large areas on flexible/stretchable substrates. In particular, we are developing direct ink writing (DIW) of conjugated polymers, which requires the careful formulation of pastes with very particular rheology, namely shear thinning and high yield strength. Moreover, specific strategies for drying and post-processing are necessary to ensure high shape fidelity. In return, DIW is not only potentially cheap and suitable for soft substrates, but offers also enough processing versatility to tune material morphology while enabling original device architectures that allow on-skin integration (to power wearables using the heat emitted by the human body) and conformability to hot curved surfaces, like hot pipes or engines (to power IoT nodes).

Acknowledgments

This work was supported by the European Research Council (ERC) under the European Union's Horizon 2020 research and innovation programme: Grant Agreement No. 948922 – 3DALIGN.

[1] C. B. Vining, Nat. Mater. 2009, 8, 83.

[2] F. Molina-Lopez, In 2020 IEEE Sensors, IEEE, Rotterdam, 2020, pp. 1–4.

SESSION SB02.12: Doping of Organic Semiconductors II
Session Chairs: Jianguo Mei and Chad Risko
Friday Morning, April 26, 2024
Room 437, Level 4, Summit

8:30 AM *SB02.12.01

Dopant Complexes—A Highly Stable and Almost Universal Doping System for Organic Semiconductors [Mariano Campoy-Quiles](#); ICMAB-CSIC, Spain

Chemical doping of organic semiconductors (OSCs) is mandatory in order to improve charge transport to the level required for applications such as thermoelectrics. However, the typical dopants used, such as F₄TCNQ or FeCl₃, invariably present limitations in terms of processability, thermal stability and/or generality. In this contribution, we will present Lewis-paired complexes as an alternative class of high-performance dopants that, remarkably, address all of the aforementioned drawbacks. Focus is given to solution-processable complexes formed by the Lewis acid BCF and F₄TCNQ bearing Lewis-basic -CN groups. Due to its exceptionally high electron affinity of ~6 eV, BCF:F₄TCNQ is shown to dope a broad range of OSCs (over 20 of which were studied) including non-fullerene acceptors and polyfluorenes. State of the art mobilities (up to 900 S cm⁻¹) can be obtained with this dopant system, which, moreover, exhibits a 3-fold higher dedoping activation energy compared to the neat constituent dopants making this a promising dopant system for thermoelectrics. Then, we will discuss the mechanism of complexation subsequent doping by looking at several Lewis acids, molecular dopants, and microstructures, as well as looking at DFT calculations. Finally, the capability of this system to be used for local doping will be demonstrated.

9:00 AM SB02.12.02

Mapping Ions and Polarons in Organic Mixed Conductors at The Nanoscale [Connor G. Bischak](#); The University of Utah, United States

Organic mixed ionic-electronic conductors have emerged as promising materials for an array of devices that leverage mixed conductivity, including bioelectronics, biosensors, and neuromorphic computing. One challenge of understanding structure-function relationships in OMIECs is the heterogeneous nature of these materials at the nanoscale, which impacts both ionic and electronic transport processes. To uncover nanoscale structure-property relationships, our group has developed ways to image ion and polaron distributions with ~10 nm spatial resolution using photoinduced force microscopy (PiFM). We correlate these measurements with nanoscale stiffness mapping to directly relate local crystallinity to local ion and polaron concentrations. Our images show that ions and polarons preferentially reside in the crystalline regions of organic mixed conductors, consistent with previous bulk studies.

9:15 AM SB02.12.03

Pure Spin Current and Large Inverse Spin Hall Voltages in a Nonconjugated Radical Polymers [Hamas U. Tahir](#); Carsten Flores-Hansen, Kangying Liu, Brett M. Savoie and Bryan Boudouris; Purdue University, United States

Spintronics is emerging as a potentially efficient alternative to traditional electronic devices that use spin rather than electric currents. Despite this, state-of-the-art non-magnetic metals and highly doped conjugated polymers that are critical for spin manipulation suffer from fundamental performance and stability issues when transforming spin currents to transverse electrical currents via Inverse Spin Hall Effect (ISHE). Nonconjugated radical polymers with unpaired electrons offer a unique solution to these challenges owing to their paramagnetic nature and ability to transport pure spin currents by rapid radical-radical exchange interactions with in the material and at device interfaces. Thus, there is a critical need to investigate these class of materials for their spin transport properties in practical device applications. Here, we investigate the spin-transport characteristics of two non-conjugated radical polymers named poly(4-glycidioxy-2,2,6,6-tetramethylpiperidine-1-oxyl) (PTEO), and poly[3-(4-(1-(3-methoxy-2-methylpropyl)-1H-1,2,3-triazol-4-yl)phenyl)-1,5-dimethyl-1H-1,2,λ²,4,5-tetrazin-6(5H)-one], poly(verdazyl ethylene oxide) (PVEO). These polymers show excellent spin-filtering effect leading to giant magnetoresistance(GMR) effect of ~ 80 % in PTEO and ~ 35 % in PVEO at 4 K respectively. This relatively large GMR can be attributed to the radical-radical exchange interactions that promote spin-dependent charge transfer under the presence of external magnetic field. Large room temperature ISHE voltages of 0.10 mV in PTEO and 0.40 mV in PVEO demonstrate their exceptional capability in transporting pure spin currents. These values are comparable to many inorganic semiconductors and higher than many metal-free doped conjugated polymers. Our results demonstrate the first ever application of radical polymers in spintronic devices and thereby paves the way for further development of this field in spintronics community.

9:30 AM SB02.12.04

Electrically Programmed Doping Gradients Optimize the Thermoelectric Power Factor of a Conjugated Polymer [Jian Liu](#)¹, [Mariavittoria Craighero](#)¹, [Vandna K. Gupta](#)¹, [Dorothea Scheunemann](#)², [Sri H. Paleti](#)¹, [Emmy Järvvall](#)¹, [Youngseok Kim](#)¹, [Kai Xu](#)³, [Juan Sebastian Reparaz](#)², [Lambert Jan Anton Koster](#)⁴, [Mariano Campoy-Quiles](#)³, [Martijn Kemerink](#)², [Anna Martinelli](#)¹ and [Christian Müller](#)¹; ¹Chalmers University of Technology, Sweden; ²Heidelberg University, Germany; ³ICMAB-CSIC, Spain; ⁴University of Groningen, Netherlands

Functionally graded materials (FGMs) have been widely explored in the context of inorganic thermoelectrics, but not yet in organic thermoelectrics. Here, the impact of doping gradients on the thermoelectric properties of a chemically doped conjugated polymer is explored. The in-plane drift of counterions in moderate electric fields is used to create lateral doping gradients in films composed of a polythiophene with oligoether side chains, doped with 2,3,5,6-tetrafluoro-tetracyanoquinodimethane (F₄TCNQ). Raman microscopy reveals that a bias voltage of as little as 5 V across a 50 μm wide channel is sufficient to trigger counterion drift, resulting in doping gradients. The effective electrical conductivity of the graded channel decreases with bias voltage, while an overall increase in Seebeck coefficient is observed, yielding an up to 8-fold enhancement in power factor. Kinetic Monte Carlo simulations of graded films explain the increase in power factor in terms of a roll-off of the Seebeck coefficient at high electrical conductivities in combination with a mobility decay due to increased Coulomb scattering at high dopant concentrations. Therefore, the FGM concept is found to be a way to improve the thermoelectric performance of not yet optimally doped organic semiconductors, which may ease the screening of new materials as well as the fabrication of devices.

9:45 AM SB02.12.05

Polaron Characteristics in Doped Conjugated Polymers [Joel H. Bobile](#), Yusuf O. Augustine, Kyle N. Baustert, Kenneth R. Graham and Chad Risko; University of Kentucky, United States

Doping semiconducting polymers enables a variety of applications and is important for improving the performance of many devices. The process of doping involves injecting or transferring charges to a host material. The injected charges are stabilized by the reorganization of nuclei and electronic polarization to form polarons. Each polaron charge is balanced by a counterion, either an ionized dopant or a guest ion, to ensure electrical neutrality. The counterion interacts with the polaron, thereby influencing the polymer optical and electronic response and ultimately device performance. Elucidating how the counterion impacts the polaron characteristics in doped conjugated polymers (CP's) can provide an avenue for further optimizing performance. This work provides a detailed and comprehensive look at the characteristics of polarons in doped CP's and the different ways these characteristics can be impacted by the counterion. Focusing on a hole-transport (p-type) polymer, pDPP-4T, we use first-principles calculations based on density functional theory to

determine the ionization energy of single polymer chains for an excess charge sequentially stabilized by nuclei reorganization, electronic polarization and the counterion, relative to a non-stabilized charge. We also compute the associated polaron probability distributions. We observe that the resulting binding energies correlate with the polaron size and find that the counterion has the strongest stabilizing effect on the polaron. We also compute the optical response of the ionized chains and find that the position of the lowest energy polaron peak (P1) is increasingly blue shifted for more strongly bound polarons, with the polaron stabilized by the counterion exhibiting the highest energy P1 peak. The correlation between polaron binding and P1 peak position is explained using Koopman's theorem and the energy level of the polaron orbital within the electronic band gap. The different quantitative assessments of the counterion impact on the polaron point to an adverse effect on electronic transport. We examine the effects of counterion size and position relative to the polaron center of charge and conclude that the counterion impact on the polaron can be reduced with larger polaron-ion distances. The use of larger counterions, which sit at longer distances from the polymer backbone, is one way of achieving this.

SYMPOSIUM SB03

Materials, Devices and Systems for Neuromorphic Electronics—From Artificial Synapses to Bionic and Wearable Systems
April 23 - April 25, 2024

Symposium Organizers

Dimitra Georgiadou, University of Southampton
Paschalis Gkoupidenis, Max Planck Institute
Francesca Santoro, Forschungszentrum Jülich/RWTH Aachen University
Yoeri van de Burgt, Technische Universiteit Eindhoven

* Invited Paper
+ JMR Distinguished Invited Speaker
^ MRS Communications Early Career Distinguished Presenter

SESSION SB03.01: Mixed Conductors In Neuromorphic Applications
Session Chairs: Francesca Santoro and Benjamin Tee
Tuesday Morning, April 23, 2024
Room 436, Level 4, Summit

10:30 AM *SB03.01.01 **Stable Organic Electrochemical Neurons** [Simone Fabiano](#); Linköping University, Sweden

Recent progress in the design and synthesis of both p-type and n-type organic mixed ionic-electronic conductors (OMIECs) has led to the creation of power-efficient devices for diverse applications, including sensors, nervetronics, neural interfaces, and artificial synapses. A cutting-edge addition to the bioelectronic toolkit is the organic electrochemical neuron (OECN) with ion-modulated spiking, facilitating the development of event-based sensors capable of local sensing, signal processing, and stimulation/actuation. However, the current technology encounters stability challenges, primarily stemming from the degradation of the p-type organic electrochemical transistor (OECT) characteristics. Therefore, achieving stable p-type OMIECs is deemed essential for unlocking the full potential of high-performance OECNs. Here, we leverage the inherent stability of rigid ladder polymers, which can sustain a high degree of electrochemical doping. This intrinsic property results in exceptional operational stability, high charge carrier mobility, and large volumetric capacitance. By integrating both n-type and p-type ladder polymers with an engineered backbone to ensure efficient charge transport, we present integrate-and-fire OECNs exhibiting biologically relevant firing frequencies and unparalleled stability. Our findings represent a significant leap forward in OECN technology, addressing previous stability limitations and promising novel opportunities for the advancement of in-sensor computing and the broader field of bioelectronics.

11:00 AM *SB03.01.02 **Unlocking The Versatility of n-Type Mixed Conductors for Bioelectronic Applications** [Sahika Inal](#); King Abdullah University of Science and Technology, Saudi Arabia

Establishing close interactions between biological systems and synthetic materials is the key to forming biohybrid assemblies that find use in sensors, actuators, and robotics. In this talk, I will present n-type conjugated polymers as multifunctional bioelectronic interfaces. I will show how they can be tailored to form favorable interactions with catalytic enzymes.¹ When this biohybrid is used in an enhancement mode organic electrochemical transistor (OECT), the device detects glucose and lactate in blood serum or saliva with excellent sensitivity and selectivity over six orders of magnitude wide detection range. While showing the unique characteristics of these devices, I will discuss the possible pathways through which the polymer film generates charges as the enzyme reacts with its metabolites.² I will then show how these polymers respond to visible and NIR light by generating photocurrents in aqueous electrolytes.³ This system is then integrated into adaptable circuits with output controlled by various stimuli, mimicking the function of a neuron.

1 D. Ohayon et al *Nat. Mater.*, 2020, 19, 456.
2 V. Druet et al *Adv. Electron. Mater.* 2022, 2200065.
3 V. Druet et al *Nat. Commun* 2023, 14, 2023

11:30 AM SB03.01.03

A Novel Class of Soft Materials for Neuromorphic Electronics and Wearables: From Conducting Hydrogel to Semiconducting Hydrogel Shiming Zhang, Dingyao Liu and Yan Wang; The University of Hong Kong, Hong Kong

Thin-film semiconductor-based devices have revolutionized the field of microelectronics. In the realm of biomedical applications, conducting hydrogels have rapidly gained prominence due to their mechanical and biocompatible nature with biological systems. The realization of semiconducting hydrogel materials holds significant value within the field of bioelectronics [1]. Advancing towards flexible and stretchable semiconducting hydrogels can enable direct applications at the interface of soft biological systems [1].

However, the development of semiconducting hydrogels presents challenges, primarily due to the thin-film nature of semiconductors, which are generally less than 1 micrometer in thickness. In contrast, hydrogels tend to have thicker thicknesses and struggle to achieve good semiconductor properties.

The advent of organic electrochemical transistors (OECTs) has introduced a new paradigm that can be a powerful testbed to evaluate the performance of a semiconducting hydrogel. In this report, we present the development of the PEDOT:PSS semiconducting hydrogel and its application in the development of OECTs. Furthermore, we delve into the development of stretchable semiconducting hydrogels and explore how they can revolutionize applications in the field of biomedical research.

11:45 AM SB03.01.04

Neuromorphic Organic Electrochemical Transistors: High-Endurance Long-Term Potentiation induced by PEDOT:PSS Electrochemical Polymerization on the Gate Electrode Isacco Gualandi¹, Federica Mariani¹, Francesco Decataldo², Filippo Bonafè², Marta Tassarolo², Giada D'Altri¹, Tobias Cramer², Beatrice Fraboni² and Erika Scavetta¹; ¹Dipartimento di Chimica Industriale 'Toso Montanari', Università di Bologna, Italy; ²Dipartimento di Fisica e Astronomia, Università di Bologna, Italy

Organic electrochemical transistors (OECTs) are emerging devices in the field of artificial intelligence, as they are able to emulate several synapses functionalities. While short-term processes (short-term plasticity, spike-dependent plasticity, etc..) can be successfully simulated by exploiting peculiar features of OECTs ionic circuit, long-term potentiation (LTP) must be further investigated to increase the retention of the induced neuromorphic states [1]. A recent successful approach is based on electrodeposition occurring in the transistor channel [2].

This contribution describes the use of PEDOT:PSS electrodeposition on the gate electrode to obtain long-term potentiation [3]. The presynaptic signal (V_{pre}) is the potential applied to the gate electrode, which acts as a controller of the drain current, that represents the postsynaptic signal (I_{post}). The neuromorphic behavior does not stem from the channel employed as a memory element but from an enhancement of the gating efficiency and switching properties. The deposition of PEDOT:PSS film raises the gate capacitance and thus the ability of the gate electrode in modulating the current flowing in the channel. LTP depends on both the number of pulses used and the V_{pre} , which generates LTP when a threshold of +0.7 V is overcome. The synapse weight is evaluated by measuring the transconductance, which varies from 0.3 μ S for the native device to 30 μ S for the neuromorphic OECT with the highest LTP. In-operando atomic force microscopy shed light on operating principle by showing the modifications of the gate electrode induced by V_{pre} . The structural strengthening of the artificial synapse is stable for at least two months, and the behavior can be reset by inducing long term depression by applying V_{pre} pulses that leads to a PEDOT:PSS overoxidation and to the formation of a nonconductive layer on the gate electrode.

The artificial synapse also mimics short-term plasticity (STP), and in particular paired pulse depression, with two distinguishable exponential decay phases. The time constants associated with STP in our device, i.e., 0.4 and 2.0 ms, are considerably smaller than those characterizing the decay phases reported in some biological synapses. It is worth noting that PPD and LTP were induced using different shapes of V_{pre} waves with the same experimental setup. These results suggest that the proposed device could combine short-term plasticity and long-term plasticity in a hybrid process. The integration of these devices in neuromorphic circuits could open fascinating perspectives in the realization of advanced neuromorphic circuits based on OECTs.

REFERENCES

- [1] Y. Tuchman, T. N. Mangoma, P. Gkoupidenis, Y. van de Burgt, R. A. John, N. Mathews, S. E. Shaheen, R. Daly, G. G. Malliaras, A. Salleo, *MRS Bulletin* **2020**, *45*, 619.
- [2] J. Y. Gerasimov, R. Gabrielson, R. Forchheimer, E. Stavrinidou, D. T. Simon, M. Berggren, S. Fabiano, *Adv. Sci.* **2019**, *6*, 1801339.
- [3] F. Mariani, F. Decataldo, F. Bonafè, M. Tassarolo, T. Cramer, I. Gualandi, B. Fraboni, E. Scavetta, *ACS Appl. Mater. Interfaces*, **In press**, <https://doi.org/10.1021/acami.3c10576>.

SESSION SB03.02: Organic Electrochemical Transistors

Session Chairs: Dimitra Georgiadou and Sahika Inal

Tuesday Afternoon, April 23, 2024

Room 436, Level 4, Summit

1:30 PM *SB03.02.01

Organic-Based Synapses, Neurons and Dendrites Alberto Salleo; Stanford University, United States

Polymer-based artificial synapses have shown outstanding performance in terms of switching speed, switching energy and endurance. The working principle of these devices leverages the dynamics of ion diffusion in polymers. The same dynamics can be used to fabricate organic circuits that mimic spiking neurons that exhibit adaptive behavior. Furthermore, the same materials set is used to fabricate multi-gate devices that reproduce the features of dendrites, specifically spatial and temporal pulse sequences. Device and circuit design allows to tune the temporal response of organic synapses, neurons and dendrites. Semiconducting polymers are thus attractive to fabricate all components suitable for neuromorphic computing.

2:00 PM SB03.02.02

Unraveling The Bistability of Solid-State OECTs Lukas M. Bongartz^{1,2}, Garrett LeCroy², Tyler Quill², Adam Marks², Hans Kleemann¹, Alberto Salleo² and Karl Leo¹; ¹Technische Universität Dresden, Germany; ²Stanford University, United States

Organic electrochemical transistors (OECTs) are excellent building blocks for a new class of neuromorphic devices. Owing to a peculiar switching mechanism based on a redox reaction, the ions of an electrolyte couple with the electronic charge carriers of the active material and unique properties absent in other types of thin-film transistors emerge. Among these is often a pronounced switching hysteresis, an attractive feature widely applied as a non-

volatile memory. However, its physical origin has hardly been studied.

Using a specific electrolyte with the benchmark channel material PEDOT:PSS, we are able to report on OECTs of significantly enhanced hysteresis, as well as an off-state lowered to the regime of nA. Both of these properties, previously sought through complex material modifications, can be achieved here through the simple use of the commercially available ionic liquid [EMIM][EtSO₄], which does not require any further material processing. Based on a thermodynamic framework, we can describe this hysteretic behavior as a bistability and trace it back to the dominance of enthalpic effects over entropy. We substantiate this concept with experiments demonstrating the theoretically predicted scenario in which the subthreshold swing exhibits a non-monotonic dependence on temperature. This behavior is contrary to what is expected from classical transistor theory. Going further, we set out to investigate the microscopic origin of the bistability, that is, the interactions underlying the enthalpic effects. To this end, we have turned to spectroscopic methods, including *ex situ* XPS, GIWAXS, UV-Vis-NIR and Raman spectroscopy, which allow us to decipher the unique interplay between PEDOT:PSS and [EMIM][EtSO₄]. We find that the ionic liquid introduces significant changes to the channel material, as it removes excess dopant and induces an ion exchange, both of which contribute to the device's exceptional electrical performance. To further study this performance *in situ*, we employ spectroelectrochemistry, which reveals a unique de-/doping behavior compared to other electrolyte systems, and which we can quantify by fitting the spectral signals with a vibronic model. As such, we can draw a conclusive picture of the OECT performance, ranging from the broad ensemble-picture of thermodynamics to the narrow view on microscopic interactions underlying the bistability.

We are convinced that this work will not only expand the understanding of OECT physics, but also provide simple access to devices of remarkable performance based on the mechanisms revealed herein.

2:15 PM SB03.02.03

Top-Gate Organic Electrochemical Transistors: A New Paradigm for Fast and Energy Efficiency Operation Ali Solgi; Photonic Materials (IAPP) and Institute for Applied Physics, Technische Universität Dresden, Germany

Organic electrochemical transistors (OECTs) have garnered significant interest due to their ease of fabrication, flexibility, biocompatibility, and suitability for biosignal sensing, including applications in neuromorphic computing. However, power consumption is pivotal in neuromorphic computing and logic circuit applications. The central challenge in these applications lies in identifying the optimal balance between the operational speed of the device and the magnitude of current flowing through the channel, which is ultimately all defined by the transistor geometry. Consequently, much effort has been put into miniaturizing the OECTs, which unfortunately comes with the disadvantage of increasing integration complexity and cost.

Here, we propose a novel top-gate architecture for OECTs in pursuit of higher operational frequencies, power efficiency, and the ability to integrate using low-cost printing techniques seamlessly. We analyze the scaling of these printed, all-solid-state top-gate devices vs. side-gate structures, and we define a figure of merit describing how efficiently transconductance is utilized for device speed, which is most relevant for integrated circuits. Using this figure of merit, we should reduce the channel length and increase charge carrier mobility, or the mobility capacitance product does not make device operation more efficient. Instead, sub-millisecond device operation can be obtained even for devices with a channel length as long as 200µm, enabling, e.g., the design of fast and power-efficient spiking neurons using the top-gate architecture.

2:30 PM *SB03.02.04

Neuromorphic Sensing Data Transmissions and Soft Actuators Benjamin C. Tee; National University of Singapore, Singapore

Neuromorphic architectures can enable significant power efficiencies in machine learning tasks. The use of soft, organic materials can allow for integration of sensing, actuation and data transmission onto neuromorphic platforms. In this talk, I will share our work on developing asynchronous data transmission systems¹ for neuromorphic in combination with soft flexible electronic materials and devices². Using such systems, we can generate unique datasets containing high speed sensory data, for e.g., a MNIST like tactile dataset³ and apply them to use cases in robotics^{4,5}.

References

1. van de Burgt, Y., Melianas, A., Keene, S.T. *et al.* Organic electronics for neuromorphic computing. *Nat Electron* **1**, 386–397 (2018). <https://doi.org/10.1038/s41928-018-0103-3>
2. Lee, W. W., Tan, Y. J., Yao, H., Li, S., See, H. H., Hon, M., Ng, K. A., Xiong, B., Ho, J. S., & Tee, B. C. K. (2019). A neuro-inspired artificial peripheral nervous system for scalable electronic skins. *Science Robotics*, *4*(32), eaax2198. <https://doi.org/10.1126/scirobotics.aax2198>
3. Yao, H., Yang, W., Cheng, W., Tan, Y. J., See, H. H., Li, S., Ali, H. P. A., Lim, B. Z. H., Liu, Z., & Tee, B. C. K. (2020). Near-hysteresis-free soft tactile electronic skins for wearables and reliable machine learning. *Proceedings of the National Academy of Sciences*, 202010989. <https://doi.org/10.1073/pnas.2010989117>
4. ST-MNIST -- The Spiking Tactile MNIST Neuromorphic Dataset, 2020, <https://arxiv.org/abs/2005.04319>
5. Taunyazov, T., Sng, W., See, H. H., & Lim, B. (2020). Event-Driven Visual-Tactile Sensing and Learning for Robots. *Robotics: Science and Systems*.

3:00 PM BREAK

SESSION SB03.03: Neuromorphic Devices
Session Chairs: Paschalis Gkoupidenis and Alberto Salleo
Tuesday Afternoon, April 23, 2024
Room 436, Level 4, Summit

3:30 PM *SB03.03.01

Modeling Organic Electrochemical Neuromorphic Devices Ugo Bruno¹, Henrique Frulani de Paula Barbosa², Francesca Santoro³ and Bjorn Lussen²; ¹Istituto Italiano di Tecnologia, Italy; ²Universität Bremen, Germany; ³Forschungszentrum Jülich GmbH, Germany

Organic Electrochemical Transistors are seen as a key element for a fully flexible and wearable sensor technology. In addition, they can be functionalized to show short- or long-term depressive behavior, and long-term potentiation. These devices, often called electrochemical neuromorphic devices (ENODEs) have attracted intense research interest in the last couple of years, which led to a continuous increase in device performance. However, although the progress of the field has been impressive, their fundamental working mechanism is still under debate and an experimentally verified

model to discuss ENODE behavior has been elusive. Here, we discuss our progress towards such a model. A focus is put on a correct description of the steady-state and transient switching observed in OECTs, describing important dynamics of ions and holes. In addition, faradaic reactions are introduced in the model, enabling simulations of voltage-driven processes that are usually behind countless sensing applications. Lastly, an outlook is given towards the implementation of charge transfer and ion trapping in the device that form the basis for describing neuromorphic behavior.

4:00 PM SB03.03.02

Electrochemically Controlled Neurotransmitter Delivery for *In Vitro* Neuromodulation [Craig Milroy](#)^{1,2}, Eric Reed², Alena Veigl², Tyson Back³, Nicholas Glavin³, Rhonda Pitsch², Matthew Grogg², Tyler Nelson² and Steve Kim²; ¹NRC Postdoctoral Fellow, United States; ²711th Human Performance Wing, Air Force Research Laboratory (AFRL), Wright-Patterson AFB, United States; ³Materials and Manufacturing Directorate, Air Force Research Laboratory (AFRL), Wright-Patterson AFB, United States

The National Academies of Science and Engineering have issued a grand challenge to “reverse-engineer the brain”. Addressing this challenge requires a more complete understanding of how connections between individual neurons and groups of neurons are formed and maintained, as well as a more thorough elucidation of the signaling processes that drive neural network optimization. However, to achieve these goals, it is first necessary to develop the appropriate fundamental tools and protocols for adaptive biointerfacing, bottom-up neuroscience, and neuromodulation, which all involve a tightly coordinated synergy between sensors and specialized devices for neurotransmitter delivery. To date, extensive research efforts have been devoted to neurotransmitter sensing, but relatively little attention has been given to developing methods for electronically controlled *in vitro* neurotransmitter delivery.

To address this challenge, our research team has developed devices that can both sense and selectively dispense the biochemical cues that drive the formation, regulation, and modulation of *in vitro* cellular/neural networks. Here, we report electrochemically controlled dispensing of both excitatory and inhibitory neurotransmitters (*e.g.* glutamate, GABA, dopamine) from functionalized electrodes that operate at low voltage. The regulated uptake and release of neurotransmitters is mediated by electrochemically controlling the electrostatic affinity between the neurotransmitter and a polarized electrode that has been functionalized with an electroactive affinity molecule.

To optimize our devices, our team tested a variety of electrode functionalization approaches (*e.g.* alkane-thiol or silane chemistry, layer-by-layer or covalent modification) and a variety of electroactive affinity molecules (*e.g.* ferrocene, methylene blue, viologens). Our controlled dispensing devices function as a faradaic capacitor – when the functionalized electrode is anodically polarized, the redox affinity molecule becomes oxidized (*i.e.* positively charged), and the neurotransmitter loads on the functionalized electrode through electrostatic attraction to the oxidized redox affinity molecule. The neurotransmitter may be conveniently “stored” on the electrode by maintaining the applied electrode potential, and then released on demand by reversing the applied bias using controlled steps or pulses, which reduces the electroactive affinity molecule and releases the neurotransmitter. This controlled adjustment of applied electrode potential permits quantitative biochemical release. In addition, the electrochemical signature associated with the loading of different neurotransmitters permits sensing as well as delivery.

We confirm the operational principle through a variety of analytical and electroanalytical techniques, such as cyclic voltammetry, chronopotentiometry, open-circuit potentiometry, continuous enzymatic monitoring, electrochemical quartz crystal microbalance (EQCM), X-ray photoelectron spectroscopy, and triple quadrupole mass spectrometry. We then demonstrate that the functionalized electrodes may also be coupled with electrochemical transistors (ECT) for triggered neurotransmitter release in conjunction with changes in the concentration of important physiological ions (*i.e.* sodium, potassium, calcium) or biochemical messengers.

Finally, we will present the steps we have taken to implement these devices within organ-on-a-chip systems, and demonstrate the utility of our devices for studying the formation and longitudinal evolution of neural networks within *in vitro* neuronal colonies.

4:15 PM SB03.03.03

Organic Electrochemical Transistors based Decoding Hardware for Near-Sensor Brain Signal Processing [Yuyang Yin](#) and Paddy K. L. Chan; The University of Hong Kong, Hong Kong

As the thriving of brain-computer interface (BCI) technologies, signal decoding algorithm and hardware have been rapidly developing for information interpretation as a crucial part of the BCI system. Although state-of-the-art algorithms can be capable for successful brain wave decoding to realize tasks such as speaking intention prediction or robot arm manipulation, unconventional processing and computing hardware are indeed desired for low-cost and high-speed decoding. Neuromorphic hardware provides solutions in this regard, for which low-complexity protocol and true-hardware implementations have been pursued. Herein, reservoir computing (RC) hardware is constructed based on memristive organic electrochemical transistors (OECTs) for intention of decoding signals from brain. The OECT devices with PEDOT:TOS/PTHF channel layer can be electrically regulated to realize transition from short-term memory (STM) element to long-term memory (LTM) element, which benefits the one-batch fabrication of reconfigurable dual-modal memory device. Based on this merit, the reservoir unit of the RC system is constructed with STM elements and designed as an adjustable network to fit the feature of inputs, at the same time LTM elements are used as trainable weights of the neural network in the readout layer. It is beneficial that the reservoir maps temporal inputs into reduced-size vectors, allowing feasible hardware demonstration of the readout layer in a small network size and leading to desirable short-delay decoding. With this hardware system, simulated epileptic seizure signals can be detected online at decent accuracy, which further direct the generation of stimulus to form a close-loop BCI system for early depression of seizures. This function is transferable for varied types of brain signals at appropriate configuration, paving the way for further design of feasible decoding hardware for efficient online interpretation of brain disease or intentions.

4:30 PM SB03.03.04

Hemispherical Nanowire Array based Bionic Eye Devices with In-Sensor Neuromorphic Signal Processing [Zhenghao Long](#) and Zhiyong Fan; Hong Kong University of Science and Technology, Hong Kong

Vision plays a crucial role in artificial systems such as surveillance, manufacturing, and robotics. However, the capabilities of conventional cameras are constrained by their design. Planar image sensors often result in significant aberration issues. While complex multi-lens systems can mitigate aberrations, they also increase the size and weight of the camera and limit its field of view. Additionally, the separation of imaging, memory, and signal processing units can lead to excessive signal transmission, delays, and high energy consumption—all of which are detrimental to the rapid advancement of artificial intelligence applications.

Drawing inspiration from the natural vision of animals, we have developed bionic eye devices featuring a curved artificial retina equipped with onboard signal processing capabilities. These devices use high-density curved nanowire arrays that emulate a retinal neuron array, endowing the bionic eye with a compact design, superior imaging performance, and an ultra-wide field of view exceeding 120 degrees. We have embedded advanced neuromorphic signal processing functions at the pixel level, including capabilities for color distinction, contrast enhancement, noise reduction, and motion detection. Additionally, we have incorporated electrically switched working modes and adaptive optics to enhance the adaptability of our bionic eyes in a variety of application settings.

4:45 PM SB03.03.05

Dual-Function IGZO Phototransistor for Rate-Based Encoding and Photonic Synaptic Characteristics in Neural Networks [Ya-Chi Huang](#), Yu-Chieh Chen, Li-Chung Shih and Jen-Sue Chen; National Cheng Kung University, Taiwan

Machine vision has emerged as a pivotal technology with applications ranging from autonomous driving to intelligent vision systems. However, contemporary machine vision systems typically rely on separate imaging sensors and von Neumann computing architectures for real-time information perception and processing, respectively. This approach generates significant redundant data, leading to increased data latency, a substantial computing load, and reduced energy efficiency. In contrast, the human visual system efficiently processes visual information. Photoreceptors perceive images and ganglion cells convert this information into electrical spikes using neural encoding algorithms. These encoded signals are then transmitted to the visual cortex in the brain for further processing.

Taking inspiration from the human visual system, we introduce an indium gallium zinc oxide (IGZO) phototransistor capable of simultaneously perceiving and encoding information within a single device. To ensure effective perception and encoding capabilities, the IGZO phototransistor was exposed to 405 nm light of varying intensities while simultaneously being subjected to gate voltage pulses of stochastic intensity. These gate voltage pulses were randomly sampled from a Gaussian distribution with a mean (μ) of -0.4 V and a standard deviation (σ) of 0.2 V. Concurrently, the drain terminal generated spikes whenever it exceeded the threshold current (I_{TC}). As a result, as the light intensity increased, the spike rate also rose, demonstrating the IGZO phototransistor's ability to efficiently encode light intensities into spike rates.

Furthermore, to make the IGZO phototransistor suitable for integration into neural networks, we conducted tests to assess its photonic synaptic properties. Initially, we examined the temporal effects of light/voltage pulses by exposing the IGZO phototransistor to a 10 ms light pulse with a light density of 77 mW/cm² and a 10 ms voltage pulse of either 0.7 V or -0.1 V, while adjusting the time intervals between them. As the time interval between the light and positive voltage pulse (0.7 V) increased, the drain current of the device decreased. On the other hand, as the time interval between the light and negative voltage pulse (-0.1 V) increased, the current either decreased when the negative voltage pulse was supplied later or increased when the negative voltage pulse was supplied first. Subsequently, the IGZO phototransistor was exposed to 64 light pulses (for potentiation) and 64 negative voltage pulses (for depression), aimed at regulating the photonic synaptic weight of the device. As a result, the IGZO phototransistor exhibited the capacity to represent a total of 128 distinct conduction states. Finally, the IGZO was illuminated by 405 nm light for 10 ms at gate voltage of 0.1 V and 1 V, and the retention time after illumination was assessed. The result indicates that the retention time at $V_G = 1$ V is longer than at $V_G = 0.1$ V, suggesting that the photonic retention capability of the device can be adjusted by the gate voltage.

The results of the experiments discussed above reveal that the IGZO phototransistor exhibits both spike encoding and photonic synaptic functions, making it a promising candidate for neural networks applications. In our future work, we plan to utilize the IGZO phototransistor to encode the MNIST dataset into spike rates and subsequently train it using spiking neural networks (SNNs). With further development and exploration, our goal is to utilize a single device for perception and encoding, eliminating the need for separate light sensors and enhancing the efficiency of machine vision systems.

SESSION SB03.04: Wearable Neuromorphic Devices
Session Chairs: Dimitra Georgiadou and Ioulia Tzouvadaki
Wednesday Morning, April 24, 2024
Room 436, Level 4, Summit

9:00 AM *SB03.04.01

Materials for Neuromorphic Supercomputers [Jeffrey Shainline](#), Bryce Primavera, Jeffrey Chiles and Saeed Khan; NIST, United States

Many efforts in neuromorphic computing seek extreme energy efficiency for edge devices by leveraging principles of neural information processing. Fewer efforts aim to capture the full complexity and scale of biological brains, potentially implementing neural principles in technological hardware at a scale that surpasses that of the human mind. For this second thrust, which we term “neuromorphic supercomputing”, the materials challenges are quite unique.

Utilizing existing silicon microelectronics is a natural choice for neuromorphic supercomputing. Yet when implementing neuro-inspired circuits, architectures, and algorithms with existing silicon microelectronic hardware, communication bottlenecks emerge as a major limitation. Biological neurons make thousands of connections to near and distant synapses, whereas silicon neurons cannot achieve this level of fan-out due to wiring parasitics. Address-event representation of spikes is employed with a shared communication infrastructure. As the number of neurons grows, that infrastructure becomes overwhelmed, and the rate at which each neuron can spike drops below the rate of biological neurons, rendering the technological approach inferior to the biological one, even for relatively small systems. This is a severe obstacle for neuromorphic supercomputers.

To overcome this barrier, we use light for communication. A neuron spike is represented by a pulse of photons distributed to synaptic connections via nanophotonic waveguides, circumventing wiring parasitics that prevent direct electrical communication. Superconducting single-photon detectors allow communication to occur at the lowest possible light level for extreme energy efficiency. For computation, the photonic components must be paired with electronic devices and circuits. Using superconducting single-photon detectors requires low temperature operation, so other superconducting elements such as Josephson junctions can be used as well. To realize the full spectrum of synaptic, dendritic, and neural functions, a combination of cryo-CMOS and Josephson circuits are uniquely powerful.

The full hardware stack for this neuromorphic supercomputing platform includes conventional CMOS working in conjunction with superconducting electronics, semiconducting light sources, multiple planes of passive dielectric waveguides, and single-photon detectors integrated with those waveguides. To realize this full stack, multiple challenges in materials science remain. First and foremost, we must integrate light sources with CMOS electronics. Such a feat has been a goal of the industry, yet this context provides one crucial advantage: low-temperature operation. Silicon itself is a reasonable light emitter at low temperature, provided the crystalline lattice is modified to contain emissive centers. The optimization of silicon for this unique optoelectronic purpose represents an important objective of this research. A second objective relates to the single-photon detectors. For scalability, we seek to operate at 4.2K. Polycrystalline materials such as NbTiN make excellent single-photon detectors with superconducting transition temperatures above 4.2K, but the yield and detection plateau are sub-optimal. Other amorphous materials such as MoSi and WSi have much higher yield and detection plateau, but they typically must be operated between 1K and 2K. Finding a material with the best of both worlds remains an important goal for the project as well. Finally, to achieve large systems with the number of neurons and synapses as the human brain will require many planes of waveguides and active superconducting devices. Numerous materials integration challenges must be solved to realize this sophisticated microelectronics process at the 300mm scale. If these problems can be solved, the world will have access to a new domain of advanced computational technology for neural information processing, achieving several important fundamental physical limits of cognition.

9:30 AM SB03.04.02

Volatile Memristive Devices with Analog Resistance Switching Based on Self-Assembled Squaraine Microtubes as Synaptic Emulators [Gareth Redmond](#); University College Dublin, Ireland

In this work, the discovery of volatile memristive devices that exhibit analog resistive switching (RS) and synaptic emulation based on squaraine materials is presented. Specifically, organic microtubes (MTs) based on 2,4-bis[(4-(N,N-diisobutyl)-2-hydroxyphenyl)squaraine (SQ) are prepared by evaporation-induced self-assembly (EISA). The MTs are ca. 2 μm in diameter (aspect ratio: 10–130). While powder X-ray diffraction data for MTs identify monoclinic and orthorhombic polymorphs, optical data report the monoclinic phase with energetic disorder. By favorable energetic alignment of the Au work function with the SQ HOMO energy, unipolar (hole-only) symmetric metal–insulator–metal devices are formed by EISA of MT meshes on interdigitated electrodes. The DC I–V characteristics acquired exhibit pinched hysteretic I–V loops, indicative of memristive behavior. Analysis indicates Ohmic transport at low bias with carrier extraction by thermionic emission. At high bias, space-charge-limited conduction in the presence of traps distributed in energy, enhanced by a Poole-Frenkel effect and with carrier extraction by Fowler-Nordheim tunneling, is observed. These data indicate purely electronic conduction. I–V hysteresis attenuates at smaller voltage windows, suggesting that carrier trapping/detrapping underpins the hysteresis. By applying triangular voltage waveforms, device conductance gradually increases sweep-on-sweep, with wait-time-erase or voltage-erase options. Using square waveforms, repeated erase-write-read of multiple distinct conductance states is achieved. Such analog RS behavior is consistent with trap filling/emptying effects. By waveform design, volatile conductance states may also be written so that successive conductance states exhibit identical current levels, indicating forgetting of previously written states and mimicking the forgetting curve. Finally, advanced synaptic functions, i.e., excitatory postsynaptic current, paired-pulse facilitation, pulse-dependent plasticity, and a transition from short- to long-term memory driven by post-tetanic potentiation, are demonstrated. In conclusion, operating on the principle of purely electronic RS, these novel organic semiconductor MT mesh devices provide an attractive combination of large dynamic range, access to multiple conductance states, linear and symmetric conductance tuning, and biorealistic synaptic emulation.

9:45 AM SB03.04.03

Inkjet Printed Metal-Organic Framework Memristors for Non-Volatile Memory and Neuromorphic Applications [Yan Liu](#)¹, Franz Fischer², Hongrong Hu¹, Hartmut Gliemann¹, Carsten Natzeck¹, Christof Wöll¹, Ben Breitung¹ and Jasmin Aghassi-Hagmann¹; ¹KIT, Germany; ²RWTH Aachen University, Germany

Memristors, as fundamental electronic components, have the unique ability to retain a memory of its past electrical resistance state based on the charge that has flown through it. They have generated considerable interest in the field of electronics due to their potential to revolutionize memory and computing technology. Moreover, they offer a combination of non-volatile storage, high-speed operation, and the ability to perform analog computation, which can be advantageous in certain computing tasks and artificial intelligence applications.

Metal Organic Frameworks (MOFs) consist of metal ions connected by organic linkers, resulting in intricate structures with well-defined porosities, which leave spaces for ions, vacancies or guest molecules to immigration and provides an excellent environment for electrochemical metallization (ECM) memristors.

Integrating MOFs into additive manufacturing techniques like inkjet printing can revolutionize their applicability, opening doors to large-scale production of patterned MOF devices. In this talk, the first demonstration of inkjet printed HKUST-1 directly integrated into a printed electronic device, particularly a memristor, will be presented, marking a significant advancement in the field of printed electronics. Furthermore, the inkjet printed memristors can serve as both, non-volatile memories and artificial synapses, for neuromorphic computing. Additionally, the ability of inkjet-printed memristors to act as artificial synapses for neuromorphic applications under different forms of synaptic short-term plasticity was investigated. This study showcases the potential of inkjet printed MOF memristors and will pave the way for high performance memristors in the field of neuromorphic computing, thus, it will further advance the development of artificial intelligence.

10:00 AM BREAK

SESSION SB03.05: Photonic Computing
Session Chairs: Dimitra Georgiadou and Nripan Mathews
Wednesday Morning, April 24, 2024
Room 436, Level 4, Summit

10:30 AM SB03.05.02

Infrared Nanoimaging of Hydrogenated Perovskite Nickelate Memristive Devices [Sampath Gamage](#)¹, Sukriti Manna², Marc Zajac², Steven Hancock¹, Qi Wang³, Sarabpreet Singh¹, Mahdi Ghafariasl¹, Kun Yao¹, Tom Tiwald⁴, Tae Joon Park³, David Landau¹, Haidan Wen², Subramanian Sankaranarayanan², Pierre T. Darancet², Shriram Ramanathan⁵ and Yohannes Abate¹; ¹University of Georgia, United States; ²Argonne National Laboratory, United States; ³Purdue University, United States; ⁴J. A. Woollam Inc., United States; ⁵Rutgers, The State University of New Jersey, United States

Solid-state devices from correlated oxides such as perovskite nickelates are promising for neuromorphic computing by mimicking biological synaptic function. However, comprehending dopant action at the nanoscale poses a formidable challenge to understanding the elementary mechanisms involved. Here, we perform operando infrared nanoimaging of hydrogen-doped correlated perovskite, neodymium nickel oxide (H-NdNiO₃) devices and reveal how an applied field perturbs dopant distribution at the nanoscale. This perturbation leads to stripe phases of varying conductivity perpendicular to the applied field, which defines the macroscale electrical characteristics of the devices. Hyperspectral nano-FTIR imaging with density functional theory calculations unveils a real-space map of multiple vibrational states of H-NNO associated with OH stretching modes and their dependence on the dopant concentration. Moreover, the localization of excess charges induces an out-of-plane lattice expansion in NNO which was confirmed by in-situ - x-ray diffraction and creates a strain that acts as a barrier against further diffusion. Our results and the techniques presented here hold great potential in the rapidly growing field of memristors and neuromorphic devices wherein nanoscale ion motion is fundamentally responsible for function.

10:45 AM *SB03.05.03

Event Driven Optical Sensors based on Perovskites and Organic Semiconductors [John Labram](#); University College London, United Kingdom

While great progress has been made in visual object recognition in recent years, almost all strategies occur in software, relying on conventional video input. This represents a major bottleneck that could limit the speed at which objects can be identified. Recently, we have demonstrated simple capacitive event-

driven sensors inspired by the way that animals perceive visual stimuli. [1] These so-called *retinomorph sensors* provide a spiking voltage in response to changes in illumination, but no response under constant illumination. [2]

In this talk I will discuss our motivations for detecting light in this way, strategies to achieve this experimentally, and how we expect arrays of these sensors to interpret the visual field. We have demonstrated sensors which employ both metal halide perovskites and organic semiconductors as the absorber layer, with each system exhibiting vastly different behavior. Our latest devices can detect objects which spend less than 10 μ s in the visual field, and generate an output voltage with zero input voltage. [3] I will end my talk by describing a framework to quantify behavior in these devices, evaluate performance limits, and discuss strategies to improve functionality in the future. [4]

References:

- [1] E. D. Adrian and R. Matthews, *The Action of Light on the Eye*, J. Physiol. **64**, 279 (1927).
- [2] C. Trujillo Herrera and J. G. Labram, *A Perovskite Retinomorph Sensor*, Appl. Phys. Lett. **117**, 233501 (2020).
- [3] X. Zhang and J. G. Labram, *Role of Blend Ratio in Bulk Heterojunction Organic Retinomorph Sensors*, J. Mater. Chem. C **10**, 12998 (2022).
- [4] J. G. Labram, *Operating Principles of Zero-Bias Retinomorph Sensors*, J. Phys. Appl. Phys. **56**, 065105 (2023).

SESSION SB03.06: 2D Material Artificial Synapses
Session Chairs: Dimitra Georgiadou and John Labram
Wednesday Afternoon, April 24, 2024
Room 436, Level 4, Summit

2:00 PM SB03.06.02

Exploring the Potential of Combining Polyoxometalates (POMs) and 2D Materials with Nanogap Electrodes for Neuromorphic Computing.

Roshni S. Babu¹, [Emilie Gerouville](#)^{1,2}, Ioannis Zaimpekis^{1,2} and Dimitra G. Georgiadou^{1,2}; ¹University of South Hampton, United Kingdom; ²Optoelectronics Research Centre, United Kingdom

Neuromorphic computing, inspired by the human brain's remarkable computational capabilities, has emerged as a promising paradigm for advancing artificial intelligence and cognitive computing systems. In contrast to the Von Neumann computing architecture, the human brain relies on neurons and synapses for both storage and computation. Consequently, there has been a growing interest in exploring nanodevices that mimic synapses to achieve highly efficient computing. Among these nanodevices, memristors have gained a lot of attention due to their advantages, such as low power consumption, high integration density and the capability to replicate synaptic plasticity, which align with the requirements of neuromorphic computing. In this work, we explore two nanomaterial classes, namely polyoxometalates (POMs) and two-dimensional (2D) transition metal dichalcogenide (TMD) materials, to facilitate the development of efficient neuromorphic hardware. POMs, a class of nanoclusters composed of metal and oxygen atoms, exhibit tunable multi-redox properties. Their excellent electron-accepting ability, high stability, and photo-stimulable redox properties, render them suitable for mimicking synaptic plasticity and being employed in in-memory and neuromorphic computing devices. In this study, we have fabricated resistive switching memory devices based on Keggin-type POMs, bearing various counterions, and the role of these cations on memristive switching characteristics was investigated. The POMs are deposited by spin coating or drop casting on coplanar nanogap metal electrodes. The coplanar electrodes of Au and Al separated by a nanogap of 10 nm are prepared by adhesion lithography. This coplanar nanogap geometry is an ideal platform to accommodate such 1-nm sized molecular clusters. Preliminary results showed a resistive switching behaviour with a low operating bias voltage and high endurance and retention, while control over the reversible redox states can be used in neuromorphic and reservoir computing. Furthermore, our research involved an investigation into POMs, a class of nanoclusters composed of metal and oxygen atoms, exhibit tunable multi-redox properties. Their excellent electron-accepting ability, high stability, and photo-stimulable redox properties, render them suitable for mimicking synaptic plasticity and being employed in in-memory and neuromorphic computing devices. In this study, we have fabricated resistive switching memory devices based on Keggin-type POMs, bearing various counterions, and the role of these cations on memristive switching characteristics was investigated. The POMs are deposited by spin coating or drop casting on coplanar nanogap metal electrodes. The coplanar electrodes of Au and Al separated by a nanogap of 10 nm are prepared by adhesion lithography. This coplanar nanogap geometry is an ideal platform to accommodate such 1-nm sized molecular clusters. Preliminary results showed a resistive switching behaviour with a low operating bias voltage and high endurance and retention, while control over the reversible redox states can be used in neuromorphic and reservoir computing. Furthermore, our research involved an investigation into 2D memristors, employing coplanar nanogap electrodes with MoS₂ as the channel material. The MoS₂ is directly grown on to a Si/SiO₂ substrate using atomic layer deposition (ALD) process and transferred onto a coplanar nanogap electrode array. The utilization of MoS₂ in memristors fabricated with nanogap electrodes has demonstrated the potential to reduce switching voltages to a crucial minimum. In conclusion, as we delve into nanomaterials, such as POMs and 2D materials, and their incorporation into artificial neural networks, we can expect significant advancements in neuromorphic computing, bringing us closer to a future, where computational systems mimic the remarkable efficiency and adaptability of the human brain.

2:15 PM SB03.06.03

Integration of Sputtered Molybdenum Disulfide Layers into a Wafer Thin Film Technology for Memristive Devices [Anna Linkenheil](#)^{1,1}, Theresa Scheler^{1,1}, Jonas Schneegaß^{1,1}, Ole Gronenberg², Hendrik Groß², Benjamin Spetzler¹, Peter Schaaß^{1,1}, Lorenz Kienle² and Martin Ziegler^{1,1}; ¹TU Ilmenau, Germany; ²Kiel University, Germany

In the last decade, various classes of memristive materials have demonstrated promising properties for emerging information processing technologies such as neuromorphic computing. Among the innovative materials for memristive devices, the class of transition metal dichalcogenides (TMDCs) has attracted much attention, due to their excellent physical properties and scaling capability, which allows scaling to atomically thin layers with defined electronic structure. However, many of the physically relevant properties have so far only been demonstrated on single devices made from TMDC flakes produced by exfoliation which commonly suffer low reproducibility with the fabricated flakes/sheets being rather sensitive against ambient influences like humidity and light. Thus, to exploit their full potential in applications, reliable thin-film processes at wafer-level are requested to tailor the materials precisely for the desired application and integrate them into functional devices and systems. It is therefore beneficial to introduce homogeneous layers on a large scale, enabling to encapsulate targeted areas from the ambience and build vertical devices of controllable size fingerprints.

This contribution therefore presents a technology platform that allows TMDC materials to be integrated into a thin-film process. In detail, a wafer-level 4-inch thin-film technology for fully encapsulated molybdenum disulfide (MoS₂) memristive devices is presented, allowing for a systematic statistical analysis of electrical properties. The developed method, paired with material analyses, further enables us to compare the different material configurations and draw conclusions about the physical switching mechanism and suitability for integration into circuits. MoS₂ layers of 10 nm thickness were deposited in a tri-layer process, sandwiching the material between two 30 nm electrodes using magnetron sputtering. Devices were structured using an optical

lithography lift-off process, comprising more than 32,000 devices in six different sizes, areas ranging from 10x10 to 50x50 square micrometers. The sputtered MoS₂ was found to have an amorphous structure. Devices were encapsulated using high quality chemical vapor deposited silicon dioxide (CVD-SiO₂). To understand and tailor the switching mechanism of the memristive devices, the electrode material (active and non-active) was varied and the influence of the encapsulation of the MoS₂ were investigated in detail.

Experimenting with different electrode materials, Cu and Ag showed a strong interaction between electrode and MoS₂, deploying transmission electron microscopy (TEM). Even though these combinations tend to exhibit switching behavior, they have an undesirably high variability due to the material interactions.

Furthermore, comparing the current-voltage characteristics measured on both encapsulated and non-encapsulated devices revealed that in the encapsulated devices, no resistive switching could be observed. In contrast, I-V hysteresis could be found in non-encapsulated devices. To realize the objective of encapsulated, reliable, and reproducible devices, technology was then adapted from tri-layer to bilayer sputtering, introducing a defined oxidation step for the MoS₂ layer before the deposition of top electrode and encapsulation.

The therewith resulting devices were systematically evaluated, studying their current-voltage characteristics, number of resistive states, retention time, on/off ratio, and switching energy. Finally, a model of the switching is proposed, explaining the cause of memristive characteristics in sputtered MoS₂ and their link to external influences.

Funding by the Deutsche Forschungsgemeinschaft (DFG, German Research Foundation) – Project-ID 434434223 – SFB 1461 and the Carl-Zeiss Foundation via the Project MemWerk as well as support by the Center of Micro- and Nanotechnology (ZMN), a DFG-funded core facility at TU Ilmenau, is gratefully acknowledged.

2:30 PM BREAK

SESSION SB03.07: Phase Change Materials
Session Chairs: Simone Fabiano and Dimitra Georgiadou
Wednesday Afternoon, April 24, 2024
Room 436, Level 4, Summit

3:30 PM *SB03.07.01

Wearable Neuromorphic Device for Personalized Healthcare Wei Gao; California Institute of Technology, United States

The rising research interest in personalized medicine presents a tremendous opportunity for developing wearable devices toward predictive analytics and treatment. Emerging neuromorphic computing technologies that mimic the data processing properties of biological neural networks offer a promising solution for handling overflowing data related to personalized healthcare. In this talk, I will first introduce the implementation of a simplified, functionally flexible analog-type operator by physically defining short-term plasticity and long-term plasticity in a crossbar synapse array. The applicability of such neuromorphic processor consisting of short-term synapses and long-term synapses was evaluated by constructing a small-sized analog-type operator to conduct representative data-processing tasks for wearable applications. I will also introduce our latest works on the development of wearable, flexible, and multifunctional bioelectronic systems with multimodal physicochemical sensing and neuromorphic computing capabilities for personalized healthcare.

4:00 PM SB03.07.02

Reconfigurable Memristive Devices based on Phase Change Materials for Artificial Synapses and Neuromorphic Computing Sundar Kunwar, Nicholas Cucciniello, Di Zhang, Pinku Roy and Aiping Chen; Los Alamos National Laboratory, United States

Phase change materials such as vanadium oxide (VO₂) possess great potentials for artificial neuron application because of its inherent nonlinear characteristics such as metal-to-insulator (MIT) phase transition with an applied electric field and quick relaxation. Recent studies have demonstrated that the VO₂ based artificial neurons achieve superior biological neuronal activities at lower energy as compared to those based on the filamentary type devices. Our recent study on the VO₂ based memristive devices have suggested that a reconfigurable resistive switching (RS) i.e., both volatile (as neurons) and non-volatile (as synapse) can be achieved, enabling the creation of more energy and area efficient artificial neural networks for neuromorphic computing. In this talk, I will present the case of the VO₂/La_{0.7}Sr_{0.3}MnO₃ (LSMO) heterostructure devices and their dual RS properties. The movement of oxygen vacancies and the MIT phase change are deemed to be the main driving forces for such dual RS modes. A dual mode RS in a single device holds great promise for the application in memristive neural networks and neuromorphic computing.

4:15 PM SB03.07.03

Investigating The Interplay of Piezoelectricity and Synaptic Plasticity in Se-Based Photodiodes for Optically Controlled Memristors on Flexible Substrates Taizo Kobayashi¹, Kunal Tiwari², Sergio Giraldo², Marcel Placidi², Axel Gon Medaille², Arindam Basak^{3,2}, Edgardo Saucedo² and Zacharie Jehl Li-Kao²; ¹Ritsumeikan University, Japan; ²Polytechnic University of Catalonia, Spain; ³Kalinga Institute of Industrial Technology, India

Neuromorphic computing, situated at the forefront of the AI revolution, offers the promise of overcoming the Von Neumann bottlenecks in terms of energy consumption while excelling in tasks such as unsupervised learning, analysis of probabilistic and fast changing data. In the era of increasing significance for computer vision, visual learning, and soft robotics, **the fabrication of devices on flexible substrates becomes extremely relevant.**

This work proposes a pioneering investigation of **the synaptic plasticity in Selenium (Se)-based photodiodes** with a particular focus on the complex **interplay between piezoelectricity and memory.** These Se-based photodiodes are fabricated on flexible polyimide substrates, introducing a novel dimension to their functionality by exhibiting a substantial piezoelectric effect, leading to a remarkable variation of the open circuit voltage under different strains as previously reported.

Our research methodology involves using **both continuous and pulsed light to explore the relationship between piezoelectricity and memory within these Se-based devices.** Remarkably, we observe changes in the dark current-voltage (JV) characteristics both before and after a train of illumination pulses, indicative of the device's behavior being very similar to an **optically controlled memristor.** It should be noted that **this change in resistivity is fully reversible** and can be induced even at relatively low illumination power densities, as low as 5 mW.cm⁻².

To further investigate the interplay between piezoelectricity and memory, we follow a classic approach of sequential light write pulses and read voltage pulses. This monitoring process involves tracking the current at specific voltage pulses, thus providing indirectly the persistent photoconductivity. This dynamic data is collected as a function of time under various bending angles of the devices. Our findings bring important insights on the role played by the interface **band alignment between the Se absorber and the ZnMgO window layer** in driving the piezoelectric effect and affecting the memory effect. Our research makes use of different illumination wavelengths, ranging from 350nm to 1400nm, which shows that the system is also **wavelength selective.**

To assess the synaptic plasticity in these devices, we systematically characterize the device's short term and long-term plasticity in terms of the Recovery Time Constant. Additionally, we utilize paired pulse facilitation ratio and rate sensitivity as figures of merit to gauge the device's performance in neuromorphic computing applications.

This potentially seminal work is to our knowledge the first reported exploration of the **interplay between piezoelectricity and visual memory** within the context of Se-based photodiodes. Moreover, our research proposes a pioneering use of Selenium-based photodiodes in the frame of neuromorphic computing applications. These findings hold important promise for advancing flexible, optically controlled memristors and their diverse applications in the domains of visual AI, soft robotics, and beyond.

4:30 PM *SB03.07.04

Engineering Mixed Conductor Transport and Device Form Factor for Neuromorphic Applications [Jonathan Rivnay](#); Northwestern University, United States

Materials processing and synthetic design serve as ideal avenues to control the transport properties of organic mixed ionic/electronic conductors (OMIECs). Small changes in chemistry can affect the materials electronic mobility, swelling, ion uptake and stability. Devices based on these materials have thus opened up new opportunities in bioelectronics, energy, and neuromorphic computing. Furthermore, volumetric/bulk transport and charging in organic mixed conductors opens up opportunities for less common device form factors that can result in scaled down and co-localized function in circuits. In this talk I will present on the engineering of OMIECs for artificial synapses, as well as recent efforts to improve artificial neurons by engineering highly non-linear responses. I will first present a non-volatile organic electrochemical transistor (OECT) based on a poly(3,4-ethylenedioxythiophene):tosylate (PEDOT:Tos)/ Polytetrahydrofuran (PTHF) composite. This device can continuously and reversibly change its conductance state at a write bias less than 0.8 V and the state retention time can be longer than 200 min without decoupling the write and read operation. By incorporating a pressure sensor and a photoresistor into the gate terminal of volatile and non-volatile OECTs, a neuromorphic circuit is demonstrated with the ability to associate two physical inputs (light and pressure), which may have implications for biomimetic devices like electronics-skin and neuroprosthetics. I will then discuss recent developments in simple co-localized OECTs for on-site amplification, as well as for fine tuning of gaussian (or anti-ambipolar) responses in vertical OECTs for simplified spiking circuits, which present an exciting pathway for fully integrated artificial neurons that can directly interface with biological systems.

SESSION SB03.08: Poster Session

Session Chairs: Dimitra Georgiadou and Paschalis Gkoupidenis

Wednesday Afternoon, April 24, 2024

Flex Hall C, Level 2, Summit

5:00 PM SB03.08.01

Graphene/SiO₂ Nanoflakes as Reliable Bio-Photonic Synapse Integrating with Dual-Functionalities of Sensing and Memory Effects for Energy-Efficient Artificial Neural Networks [Kuan-Han Lin](#), Tsung-Yen Wu, Zhe-Hao Liu and Chia-Yun Chen; National Cheng Kung University, Taiwan

In recent years, the system of artificial intelligence is still suffocated by the traditional von Neumann computing architecture. This inherent limitation has led to the bottleneck of computing speed and the problem of high energy consumption that needs to be imperatively solved. To ameliorate von Neumann bottleneck in conventional computing, we began to adopt a neuromorphic computing model, which is inspired by the neural network in human brain and allows the system to actualize "Computing in Memory". Herin, the photonic synapse based on graphene/PMMA@silica nanoflakes is demonstrated to emulate fundamental synaptic behaviors endowed with sensing and memory functionalities. The bio-photonic synapse proposed in this work offers a series of fundamental synaptic functionalities, such as excitatory postsynaptic current (EPSC), paired-pulse facilitation (PPF), and short-term plasticity (STP) to long-term plasticity (LTP) conversion under weak light stimulation. It is found that the resulting PPF index of our graphene-based bio-photonic synapse stimulated by 365 nm light is 267.3% when the interval time is 0.1 s under the employment of -3 V in gate voltage. Additionally, after 24 pulses of light stimulation at a frequency of 0.40 Hz, the relaxation time constant still reaches up to 193.7 s, indicating the critical synaptic plasticity of our devices. The plasticity can be flexibly modulated by the gate voltage, which further contribute to a dynamic synapse with controllable weight. The learning ability of our bio-photonic synapse is confirmed by simulating the learning process with distinct moods via adjusting the gate voltages. Furthermore, due to the charge-trap rich center in silica nanosheets, the bio-photonic synapse can also act as non-volatile flash memory, well mimicking the long-term plasticity (LTP) and keeping long retention time. It should be pointed out that the implement of light-stimulated photonic synapses via the strategy of heterostructure engineering represent a potential avenue that allows the ultrafast processing speed, high bandwidth and low crosstalk than electrical-stimulated synapses. This bifunctional-photonic synapse is anticipated to bridge the gap between the neuromorphic computing and sensing data in our life and pave the way for "Computing in Memory", promoting the emerging artificial neural networks.

5:00 PM SB03.08.02

TaO_x-Based Memristor with Nanostructured Electrode towards Neuromorphic Computing [Patrick Chuang](#)¹, Fei Qin¹, Han Wook Song², Yuxuan Zhang¹, Lisa Bosman¹ and Sunghwan Lee¹; ¹Purdue University, United States; ²Korea Research Institute of Standards and Science, Korea (the Republic of)

In-memory computing technology has garnered significant attention in recent years due to its integration of memory and central processing within a single unit cell, along with its ability to efficiently process tasks in parallel like the human brain. This technology is anticipated to subvert conventional computer architectures. Memristors, a type of passive two-terminal electronic component that exhibits a unique resistance change in response to the time history of the applied voltage or current, play a crucial role in the development of in-memory computing technology due to their non-volatile characteristic, low power consumption, fast switching, and high-density integration. In this research, tantalum oxide (TaO_x) is applied as the switching layer of our memristors because of its controllable resistive switching characteristics. The challenge of the memristor we trying to overcome in this research is the random growth of filaments, which is the main cause of the large variations observed in different cycles or different devices. This performance variation is one of the major obstacles to hindering the advancement of memristor in practical applications. In this presentation, we report on two approaches to mitigate the variation issues. We first focus on the engineering of the oxygen vacancy defect density in the TaO_x switching layer by controlling the oxygen partial pressure in the reactive sputter gas. XPS was utilized to examine the oxygen vacancy concentration of TaO_x switching layers. Next, the electrode's structure was rationally modified to further reduce the performance variation. The TiN bottom electrode was well defined as nano pyramid pattern. We propose that these purposely introduced nanoscale features can induce periodic higher electric fields across the device, which in turn significantly reduce the randomness of filament growth. Finite element analysis was employed to theoretically validate the hypothesis about the nanostructure effect on the electric field and filament growth. Electrochemical impedance spectroscopy was also used to verify the filamentary switching mechanism of our TaO_x-based memristors. In addition, through pulse measurements, we demonstrate synapse behaviors, i. e. multi-conductance levels of our TaO_x-based memristors. Finally, a neural

network simulation was conducted utilizing the attributes of TaO_x-based memristors, demonstrating their capability of image recognition abilities when applied to the Fashion Modified National Institute of Standards and Technology database.

5:00 PM SB03.08.03

Scalable Microfabrication of Intrinsically Stretchable Organic Electrochemical Transistor Array for Neuromorphic Computing [Songsong Li](#)¹, Max Weires¹, Zixuan Zhao¹, Fangfang Xia² and Sihong Wang¹; ¹The University of Chicago, United States; ²Argonne National Laboratory, United States

Organic electrochemical transistors (OECTs) for on-body neuromorphic computing require mechanical stretchability and large-scale manufacturability. However, developing intrinsically stretchable OECTs using a standard cleanroom microfabrication process is challenging due to limitations in the integrated processing of multiple materials. In this work, we develop a standard cleanroom microfabrication process to fabricate intrinsically stretchable OECT arrays with patterned solid-state ion gel electrolytes. This fabrication process offers a higher resolution and density compared to existing printing techniques. Using this innovative technique, we fabricate a stretchable 10 x 10 neuromorphic array and further construct artificial synapse/neuron functions. Utilizing our neuromorphic array, various machine learning algorithms are implemented to detect acute disease and to control the movement of soft robotics. Overall, this work spotlights a promising strategy for fabricating intrinsically stretchable OECT arrays to realize on-body neuromorphic computing.

5:00 PM SB03.08.04

Modulation of Synaptic Functions via Charge Trap Layer in Oxide Semiconductor-Based Synaptic Transistor by Light Irradiation [Seokgyu Hong](#), Won Kyung Min, Jusung Chung, Dong Hyun Choi, Hyung Tae Kim, Moon Ho Lee and Hyun Jae Kim; Yonsei University, Korea (the Republic of)

Due to advancements in artificial intelligence (AI) technologies, such as machine learning, deep learning, and computer vision, computing systems are increasingly required to manage vast amounts of data storage and fast computational processing. However, current computing systems face limitations such as the bottleneck phenomenon associated with von Neumann architecture. To address these limitations, artificial synaptic transistors have emerged, emulating the intricate neural systems of humans, enabling them to store vast amounts of data while maintaining high-speed operation with low power consumption in computing systems. Nonetheless, as computing systems progressively demand enhanced learning capabilities in various environments of data, a necessity arises to distinguish the simple and complicated tasks by adjusting the modification of their synaptic properties as desired. Among the diverse research of synaptic transistors, oxide semiconductor-based synaptic transistors have attained prominence due to their relatively low off current, which contributes to low power consumption.

In this study, we propose a synaptic weight modulation layer (SML) in oxide semiconductor-based synaptic transistors by adjusting the quantity of charge trapping depending on the light irradiation. SML is comprised of ultra-violet (UV)-treated hafnium oxide (HfO_x), which generates varying amounts of oxygen vacancy (V_o) sites, acting as charge trap sites, simply by modifying the UV lamp (wavelength of 184.9 nm & 253.7 nm) exposure time. The devices are based on indium-gallium-zinc oxide (IGZO) thin film transistor (TFT) with two types of SMLs: low-synaptic weight modulation layer (L-SML) with 10 min UV-treated HfO_x and high-synaptic weight modulation layer (H-SML) with 1-hour UV-treated HfO_x located between the channel of a-IGZO and thermally grown silicon dioxide (SiO₂) from a heavily boron-doped p-type silicon substrate (p+-Si).

The hysteresis characteristics are measured to confirm the charge trapping phenomenon by threshold voltage shift (ΔV_{th}). IGZO TFT w/ L-SML and IGZO TFT w/ H-SML showed the ΔV_{th} of 5.15 V, and 10.10 V respectively. This result implies that the increment of ΔV_{th} is clearly influenced by UV treatment time, which occurs by the difference in charge trap density. To verify the UV effect on the HfO_x dielectric film, the current density versus electric field (J-E) curve is obtained in metal-insulator-metal (MIM) capacitors. The HfO_x dielectric film shows a dielectric strength of 10.13 MV/cm, L-SML shows 8.88 MV/cm and H-SML shows 7.35 MV/cm. The breakdown electric field decreases while UV exposure time increases. This phenomenon is expected by bond dissociation and X-ray photoelectron spectroscopy (XPS) analysis is performed to investigate the difference of chemical bonds in the HfO_x between L-SML and H-SML.

In general, the inhibitory post-synaptic current (IPSC) was measured to verify the synaptic characteristics of IGZO w/L-SML and IGZO w/H-SML-based synaptic transistors. These devices showed different synaptic characteristics through the ratio of post-synaptic current/pre-synaptic current in different pulse amplitudes. At 5 V, 6 V, and 7 V, the IGZO TFT w/H-SML ratios are 43.7%, 58.0%, and 75.0%, respectively, compared to the IGZO TFT w/L-SML ratios of 19.7%, 32.6%, and 49.8%. Additionally, potentiation and depression characteristics of IGZO TFT w/L-SML and IGZO TFT w/H-SML according to 128 consecutive pulses are measured to verify the difference in learning capability. The post-synaptic current (PSC) change in IGZO TFT with L-SML and H-SML exhibits a remarkable difference, with an increase from approximately 140 nA to 323 nA (2.3-fold) and 18 nA to 117 nA (6.5-fold), respectively. As a result, it was confirmed that the different characteristics of synaptic transistors via simple light irradiation method might be a candidate for enhancing the learning capability and computational efficiency of neural computing.

5:00 PM SB03.08.05

Solution-Processed Photosynapses Based on Graphene and Organic Dyes for Neuromorphic Computing [Jonathan D. Yuen](#), Jakub Kolacz, Paul A. Brown and Christopher M. Spillmann; Naval Research Laboratory, United States

Combining optical detection and neuromorphic computing to create a bionic optoelectronic nervous system offers great prospects towards mimicking one of the essential components of the human perception, the visual system. We demonstrate a novel and simple implementation of a photosynapse, the fundamental unit of the bionic optical nerve, using graphene and organic conjugated dyes as the materials basis. Through a facile and flexible fabrication process, large-scale devices were created that successfully mimic synaptic behaviors including short- and long-term memory, spiking rate-dependent plasticity, spiking number-dependent plasticity and paired-pulse facilitation. Our work presents a path toward large-scale fabrication of artificial photosynapses of varying length scales employing photoactive materials using a simple, low-cost process, easing the potential development of applications covering artificial visual perception and neuromorphic intelligent systems.

5:00 PM SB03.08.06

Exploring Electro-Thermal Localizations and Metal Insulator Transitions in Micron to Sub-Micron Thin Film Devices [Yeonju Yu](#)¹, Adelaide Bradicich^{1,2}, Timothy D. Brown², Fatme Jardali¹, Suhas Kumar², R. Stanley Williams¹ and Patrick Shamberger¹; ¹Texas A&M University, United States; ²Sandia National Laboratories, United States

Two separate mechanisms, namely electrically induced current density and temperature localization (electro-thermal localization) and temperature driven metal-insulator-transition (MIT), give rise to volatile electrical responses, such as negative differential resistance (NDR) and threshold switching. [1] Devices exhibiting such electrical responses have recently garnered significant interest due to their potential applications in hardware based neuromorphic computing. [2, 3] Within microscale devices, both phenomena are characterized by spatial inhomogeneity, leading to the formation of channels with high current density due to increased temperature or the emergence of a higher conductivity high temperature phase in the material.

In transition metal oxide materials like VO₂, the emergence of electro-thermal localizations and MIT has been observed to occur sequentially, [4, 5] with the current induced MIT believed to occur within the previously established steady state localized channel. Nevertheless, it remains unclear under what conditions localization behavior precedes MITs, and whether these spatial inhomogeneities disappear as device dimensions are reduced below a certain

critical size, along with the impact this may have on the device's electrical response. The objective of this study is to investigate the interactions between electro-thermal localizations and MIT with the goal of providing insight into how localization behaviors affect the onset and properties of the MIT and how these behaviors vary with variations in device dimensions.

Here, the interplay between spatially inhomogeneous electro-thermal localizations and phase transitions is studied in 3D finite element models of two terminal lateral thin film devices with varying lengths (0.7 to 6 μm) and widths (0.7 to 10 μm) using COMSOL Multiphysics. The Joule heating Multiphysics interface combining the electrical and heat transfer modules is used throughout the simulations. The device model contains four domains including a thin film domain, an underlying dielectric substrate domain, separated from the thin film domain by an interfacial thermal conductance, and two electrode domains that span the width of the device. Simulations were conducted by applying a constant electrical current to one electrode and then allowing the system to evolve over time to reach steady state thermal and electrical solutions.

We demonstrate that the dynamical localization of current density and temperature precedes the onset of the MIT, determining the location of the emerging high temperature phase (metallic phase) in micron scale devices. Furthermore, we observe that as device dimensions are reduced to sub micron scales, distinguishing the emergence of spatial phase and thermal inhomogeneities becomes challenging. These results highlight the significant role that electrothermal localizations play on the onset of MIT, offering insight into electrically induced behaviors and corresponding responses of thin films with variable dimensions. Understanding this behavior suggests a pathway for designing desired electrical responses in non linear oscillator type neuromorphic devices.

References

1. Chae, B.-G., et al., *Abrupt metal-insulator transition observed in VO₂ thin films induced by a switching voltage pulse*. Physica B: Condensed Matter, 2005. **369**(1): p. 76-80.
2. Goodwill, J.M., et al., *Spontaneous current constriction in threshold switching devices*. Nature communications, 2019. **10**(1): p. 1628.
3. Parija, A., et al., *Metal-Insulator transitions in β' -Cu₂V₂O₅ mediated by polaron oscillation and cation shuttling*. Matter, 2020. **2**(5): p. 1166-1186.
4. Brown, T.D., et al., *ElectroThermal Characterization of Dynamical VO₂ Memristors via Local Activity Modeling*. Advanced Materials, 2022: p. 2205451.
5. Das, S.K., et al., *Physical Origin of Negative Differential Resistance in V₃O₅ and Its Application as a Solid State Oscillator*. Advanced Materials, 2023. **35**(8): p. 2208477.

5:00 PM SB03.08.07

Lithium-Modulated 3-Terminal Artificial Synapse with Long-Term Memory Function Induced by Fluorinated Self-Assembled Monolayer Minho Jin, Haeyeon Lee, Jiyeon Kim and Youn Sang Kim; Seoul National Univeristy, Korea (the Republic of)

Neuromorphic computing has been introduced as a revolutionary computing architecture to overcome the limitations of von Neumann architecture. Neuromorphic computing is known for its low operational speed and high power consumption, especially when dealing with large volumes of data in areas such as artificial intelligence and big data. This new architecture conducts calculations and memory operations at the same time within a specific resistor, known as an 'artificial synapse'. These artificial synapses, which are structured in parallel circuits, can be distinguished by their adjustable analog electrical conductance. For use in neuromorphic accelerators, artificial synapses need to have the ability to adjust synaptic weights variably, linearly, and symmetrically with a high dynamic range, and they need to be able to maintain updated synaptic weights.

Electrolyte-gated transistors (EGTs) are seen as a potential option for their low switching voltage thanks to the high capacitance of the electrolyte, their simple production process, and the high flexibility in device configuration. The way EGTs work is by altering the channel conductance through physical or chemical interactions of cations or anions in the electrolyte with the channel, thereby representing changes in synaptic weight. However, due to the natural characteristic of electrolytes to balance charges, an EDL formed at the interface by an immediately applied electric field is likely to be transient. Therefore, considering charge interactions with ions at the interface becomes crucial for achieving adjustable conductance with high linearity and long-term retention. In this study, we present Heneicosafluorododecylphosphonic acid (F21-DDPA) as an interfacial monolayer in EGT, specifically highlighting its role in the physisorption of ions caused by large dipole moment at the channel/electrolyte interface. The device uses amorphous indium gallium zinc oxide (a-IGZO) as the channel material, which is notable for its low off-current and high field-effect mobility in n-type thin-film transistors, and water-in-bisalt lithium electrolyte as the polymer dielectric, which is remarkable for its high areal capacitance and large electrochemical window. With the introduction of F21-DDPA in EGT, a strong ion-dipole force is observed between the lithium ions and F21-DDPA, leading to the immobilization of lithium ions at the channel/electrolyte interface. As a result, the lithium EGT with F21-DDPA shows exceptional synaptic characteristics, such as switching conductance with near-linearity and high dynamic range (~ 10), and long-term retention (>30 min), even at a switching voltage below 3 V. Specifically, through chemical analysis and DFT calculations, we speculate that lithium ions become strongly trapped within the van der Waals gap of F21-DDPA. This finding suggests the potential of a specific capacity of lithium ions within F21-DDPA. We propose an EGT-based artificial synapse with multimodal behavior by suggesting a new method of integration for F21-DDPA, indicating its significant potential in neuromorphic accelerators performing both training and inference tasks.

5:00 PM SB03.08.08

Organic-Inorganic Hybrid Memristor for Neuromorphic Electronics. Abdulaziz Aldubayan, Antonio Facchetti and Natalie Stingelin; Georgia Institute of Technology, United States

In the era of big data, there is a growing demand for highly efficient technologies to facilitate the acquisition, storage, and analysis of vast volumes of information. The Resistive Switching Random Access Memory (ReRAM), having non-volatile memory attributes, synaptic-like behavior, and energy-efficient, high-density features, had emerged as a promising tool poised to transform and shape the development of neuromorphic computing and wearable electronics. In this work, an organic-inorganic hybrid poly (vinyl alcohol)/titanium oxide hydrate hybrid memristor device is developed. The device of the structure Au/PVA:TiOH/Au exhibits bipolar non-volatile resistive switching characteristics. We hypothesize that the operational mechanism of the PVA:TiOH layer is driven by the formation and rupture of local conductive Ti³⁺ filaments caused by Joule heating and electric field-assisted reduction of Ti⁴⁺, producing dioxygen, that induces a Schottky-like barrier behavior at one interface and a quasi-ohmic contact behavior at the other. This biocompatible memristor presents a compelling case for sustainable memory solutions in the increasing field of neuromorphic electronics.

5:00 PM SB03.08.09

Additively Manufactured 3D Membranes for Wearable Renal Assist Device Natalie Hwee¹, Kun Wang², Sijia Huang¹, Donglin Li², Wade Degraff², Longsheng Feng¹, Sangil Kim², Jianchao Ye¹ and Juergen Biener¹; ¹Lawrence Livermore National Laboratory, United States; ²University of Illinois at Chicago, United States

More than 400,000+ Americans require renal assist devices in the form of hemodialysis machines. This industry costs more than \$50 billion dollars a year. Two limitations of current hemodialysis membranes are that they are prone to biofouling and have low packing density of the membrane resulting in a large device. Developing a wearable device that has improved filtration and efficiency would change the lifestyle of thousands of Americans from relying on hemodialysis centers.

This searchable program is up-to-date as of April 15th, 2024.

We have developed a formulation for a material that has 3 times better antibiofouling properties than commercial materials while maintaining mechanical robustness. We have used a combination of additive manufacturing (AM) and polymerization induced phase separation (PIPS) to design a 3D membrane with controlled micropore size and two-phase flow. Our membrane has achieved over 10 times higher flow rate compared to commercially available membranes at similar pressure drop. This membrane design enhances filtration capabilities through the membrane wall by creating turbulent flow in the channels. Coupling material formulation and additive manufacturing is a way to develop high packing density membrane for a wearable renal device.

This work was performed under the auspices of the U.S. Department of Energy by Lawrence Livermore National Laboratory under Contract DE-AC52-07NA27344.

SESSION SB03.09: Theory and Modeling of Brain-Inspired Devices
Session Chairs: Paschalis Gkoupidenis and Bjorn Lussem
Thursday Morning, April 25, 2024
Room 436, Level 4, Summit

8:15 AM *SB03.09.01

Brain-Inspired Electronic Learning Metamaterials Douglas Durian, Sam Dillavou, Menachem Stern and Andrea Liu; University of Pennsylvania, United States

Neural networks in the brain and artificial neural networks (ANNs) in silico are both able to learn complex functionality. While each artificial neuron is updated based on global information, using a central processor (CPU) and memory, each real neuron in the brain updates itself without external CPU. In this talk I will describe the first laboratory realization of such self-learning without use of CPU or memory. Our systems consist of a network of identical variable-resistive elements that self-adjust using a local rule based on the voltage drops they experience under contrastive boundary conditions. As such, they have many brain-like advantages over ANNs and enable study of learning as a bottom-up emergent process.

8:45 AM SB03.09.02

2D Axisymmetric Continuum Model for RESET Kinetic Variations in Electrochemical Metallization Cells Milan Buttberg¹ and Stephan Menzel²; ¹RWTH Aachen IWE2, Germany; ²Forschungszentrum Jülich GmbH, Germany

Electrochemical metallization (ECM) cells operate on the principle of growing and dissolving a conducting filament (CF) in an insulator separating two metal electrodes. Typically, the thickness of the insulator is a few nanometres. The growth (SET) of the CF occurs by applying a positive voltage to the electrochemical active electrode (AE), which leads to oxidation of the electrode and migration by ion hopping within the oxide – also called switching layer (SL) – of the resulting metal ions. Reduction occurs preferentially on a critical nucleus at the inert electrode (IE), leading to growth of the CF. Reversal of the voltage leads to reversal of the above processes and dissolution (RESET) of the CF. A previously published 2D axisymmetric model^[1] contains Butler-Volmer equations to describe ionic currents, Simmons tunnel equation for electronic tunnel current between the conducting filament (CF) and the active electrode, Fuchs-Sondheimer model for resistivity of the CF, mechanical stress, to limit the lateral CF growth and a moving mesh approach for growth of the CF. This model was extended with tunnel junction heating, an additional energy dissipation when electronic tunnel currents occur, the dissolution of the anode and the previously current limiting resistor was exchanged by an ideal current limitation. The model was then modified to simulate not only SET but also RESET kinetics. In this work the dissolution of the AE and the combined influence of heating, mechanical stress variations, dissolution of the active electrode, the length of the SET voltage pulse (programming time) and the maximum SET current on the RESET time was investigated. It is shown, that mechanical stress – which crucially affects the lateral size of the CF – and the dissolution of the active electrode have the largest impact on the RESET time and that only tunnel junction heating allows significant heating of the CF even at low currents in the low microampere range. The integration of this findings into compact models should lead to better descriptions of measurement results and thus improving and boosting the design of memristive devices and neuromorphic circuits.

References:

[1] M. Buttberg, I. Valov, S. Menzel, *Neuromorphic Computing and Engineering* 2023, 3, 024010.

Acknowledgements

This work was supported in part by the Deutsche Forschungsgemeinschaft under project SFB 917 and in part by the Federal Ministry of Education and Research (BMBF Germany) in the project NEUROTEC II under Grant 16ME0398K and Grant 16ME0399.

9:00 AM SB03.09.03

Behavior Guided Design of Materials, Mechanics and Electromagnetics for Biosymbiotic Electronics Philipp Gutruf; University of Arizona, United States

Philipp Gutruf

Departments of Biomedical Engineering and Electrical and Computer Engineering, Bio5 Institute, Neuroscience GDP University of Arizona, Tucson, AZ 85721, USA.;

The concept of digital medicine, which relies on streams of continuous information from the body to gain insight into health status, manage disease and predict onset health problems, is currently relying on biosensors with limited chronic capabilities.^{[1][2]} Key technological hurdles that slow the proliferation of this approach are means by which clinical grade biosignals are continuously obtained without frequent user interaction.^[3] To overcome these hurdles, solutions in power supply and interface strategies that maintain high fidelity readouts and function chronically are critical. Current approaches for high fidelity recordings typically rely on adhesive interfaces that are subject to epidermal turnover, limiting sensor lifetime. Additionally, they rely on electrochemical power supplies which are subject to frequent recharge, add bulk and weight, require user interaction and introduce motion artefacts. Here we introduce a new class of devices that overcomes the limitations of current approaches by utilizing context aware mechanical and electromagnetic design facilitated through digital human behavior assessment to create unique personalized devices optimized to the wearer. Specifically, we introduce new methods to use behavioral analysis of a user group to shape design to enable indefinite device lifetimes.^[4] These elastomeric, 3D printed and laser structured constructs, called biosymbiotic devices, enable adhesive-free interfaces and the inclusion of high performance, far field energy harvesting to facilitate continuous wireless and battery-free operation of multimodal and multi device, high-fidelity biosensing in an at-home setting without user interaction. We present devices that can operate over weeks at the time, enable new sensing paradigms such as circumferential muscle strain, high fidelity

absolute position sensing, mK resolution thermography and 3D printed optofluidics to capture an encompassing and evolving record of health. The impact of this approach is also showcased in wearable devices that are low profile, soft and can transmit high fidelity biosignal data over tens of miles of distance without cell connection uninterrupted over weeks without user interaction.

References

- [1] T. R. Ray, J. Choi, A. J. Bandodkar, S. Krishnan, P. Gutruf, L. Tian, R. Ghaffari, J. A. Rogers, *Chem. Rev.* **2019**, *119*, 5461.
- [2] J. Heikenfeld, A. Jajack, J. Rogers, P. Gutruf, L. Tian, T. Pan, R. Li, M. Khine, J. Kim, J. Wang, *Lab Chip* **2018**, *18*, 217.
- [3] T. Stuart, L. Cai, A. Burton, P. Gutruf, *Biosens. Bioelectron.* **2021**, 113007.
- [4] S. Tucker, K. K. Albert, I. I. Christian, M. D. Thomas, P. Roberto, H. Jessica, J. Megan, F. Max, L. Thomas, U. Paul, G. Philipp, *Sci. Adv.* **2021**, *7*, eabj3269.

9:15 AM SB03.09.04

Neuromorphic Computing Using Long Short-Term Memory Models with Memtransistor-Enabled Short-Term Memory Manipulation Yu-Chieh Chen, Ya-Chi Huang and Jen-Sue Chen; National Cheng Kung University, Taiwan

The conventional von Neumann bottleneck, characterized by the separation of information processing and storage, presents architectural limitations in computational efficiency and energy consumption. As the growing demand for energy-efficient computing systems, neuromorphic systems, inspired by the parallel processing principles of the human brain, have gained significant attention. Within this domain, the memtransistor, integrating the functionalities of both a memristor and a transistor into a single device, exhibits distinctive memresistive switching characteristics controlled by an external gate terminal. To ensure compatibility with CMOS process technology, we fabricated a metal oxide-based memtransistor on SiO₂/p⁺ Si substrate. The memtransistor structure involves the stacking of hafnium oxide (HfO_x) as the gate insulator and indium gallium zinc oxide (IGZO) as the active layer. The redistribution of oxygen vacancies within HfO_x plays a crucial role in controlling the memristive conductance. Introducing an adequate number of oxygen vacancies near the HfO_x/IGZO interface can effectively modulate the Schottky barrier height between the IGZO channel layer and the aluminum (Al) metal source/drain (S/D) electrodes. Unlike traditional two-terminal memristors, the single-pulse measurements reveal the ability to manipulate short-term memory decay time by adjusting gate voltage levels, while the drain pulse waveform remains fixed, allowing us to simulate various degrees of short-term memory effects effectively.

The Long Short-Term Memory (LSTM) model provides distinct advantages for image recognition through controlled degrees of short-term memory states within the LSTM that adapt to varying image dynamics, ultimately enhancing accuracy and efficiency. In time-series data processing, we divide 4x4-sized black-and-white English letter images into four rows, each containing four pixels. The design of electrical pulse waveforms, based on stroke order, serves as inputs to the LSTM mode, enabling it to capture temporal relationships within image sequences. Our research advances memory and recognition technologies, promising enhanced accuracy and efficiency across diverse fields of application.

9:30 AM SB03.09.05

Brain Inspired Floating Redox Wiring for Neural Networks Roshani Madurawala, Maik-Ivo Terasa, Anna Lina Wyszkon, Soeren Kaps and Rainer Adelung; University of Kiel, Germany, Germany

The human brain is a remarkably complex and adaptable organ and its capability to change and adapt, is due to a phenomenon known as "neuroplasticity." Neuroplasticity in synapses refers to the brain's outstanding ability to change the strength and structure of the connections between neurons, which is crucial for information transfer. This has inspired the design and training of artificial neural networks (ANN), allowing them to learn and improve their performance over time. In the trend of implementing ANN in hardware, one specific challenge is the implementation of plasticity in the artificial synapses. Here we show a concept and a mechanism to incorporate plasticity into a system by means of electrochemical metallization in a liquid matrix, Dimethyl sulfoxide (DMSO). A liquid matrix inspired by the brain has been employed to facilitate the mobility of the ions in addition to its cooling purposes in this ionotronic system. These bio-inspired, dynamic and reconfigurable electronic connections are robust in DMSO while still being prone to manipulation upon applied external stimuli, because they float in DMSO. These connections are wires that grow as dendrites due to the redox reaction taking place at the electrodes. The thickness and the growth conditions of these wires influence their electrical properties, which could be altered by varying the initial experimental conditions such as the applied voltage. The manipulation of these wires could be done during the growth of the wire (filament) between two nodes or more, simultaneously. Furthermore, after the growth of one filament, the filament could be manipulated in a way to induce filament breakage which resembles synaptic properties. This process of plasticity in artificial synaptic connection equivalents, serves as a fundamental step in the refinement of network connectivity. Its replication within artificial systems marks a significant milestone in the quest to emulate the brain's adaptability. Intriguingly, this filament can grow in a span of over 200 μm. What is even more remarkable is their ability to overcome the limitations of traditional 2D growth, as they readily extend their presence into the 3D realm. Growth and manipulation of single 2D and 3D filaments and in extension, a filament network, using external stimuli will be shown along with electrical characterization of these filaments and possible applications. In essence, the groundwork laid in the field of dynamic filament growth within a liquid matrix holds the potential to reshape the landscape of technological advancement. With its capacity for synaptic mimicry, flexible growth, and 3D expansion, this innovation ushers in an era of transformative possibilities, making inroads into fields as diverse as neuromorphic computing, cognitive sciences, and advanced artificial intelligence. [1]

[1] M.-I. Terasa et al., *Materials Today* (2023), <https://doi.org/10.1016/j.mattod.2023.07.019>

The authors acknowledge financial support by the Deutsche Forschungsgemeinschaft (DFG, German Research Foundation) – Project-ID 434434223 – SFB 1461

9:45 AM SB03.09.06

Wireless Implantable Microwave Neural Device for Neural Inhibition Carolyn Marar, Ji-Xin Cheng and Chen Yang; Boston University, United States

Neuromodulation using electromagnetic wave allows manipulation of brain circuits in a minimally invasive manner. To date, researchers have explored a broad spectrum of electromagnetic wave and developed wireless neuromodulation methods. Microwave (MW), with frequencies between 300 MHz and 300 GHz, fills the gap between optical wave and magnetic wave, yet has rarely been explored for neuromodulation. Microwave has much longer wavelength than photons, which have been known to provide >50 mm penetration depth into the human brain noninvasively, while maintaining more than 50% of its energy. Yet, its wavelength is much shorter than that of magnetic wave, promising higher spatial resolution to specifically modulate subcortical regions. Here we will discuss a miniaturized millimeter size microwave antenna as a wireless implantable neural interface to inhibit neural activities in vitro, ex vivo and in vivo. The developed split-ring resonator (SRR) generates a localized and enhanced microwave field at the gap site of the ring with submillimeter spatial precision. The SRR breaks the microwave diffraction limit and greatly enhances the efficiency of microwave inhibition. With the SRR, microwaves at dosages below the safe exposure limit are shown to inhibit neurons within 1 mm from the gap site. Importantly, we measured the temperature at the neurons under microwave modulation using mCherry as a temperature reporter and found the temperature increase to be less than 1 degree, confirming a non-thermal effect for microwave inhibition. The inhibition effect was also confirmed in a crayfish nerve model using electrophysiology recording. Application of the microwave SRR to suppress seizures in an in vivo model of epilepsy is demonstrated. These results suggested that the millimeter microwave resonator is a novel platform for wireless, battery-free neuromodulation in the deep brain with high spatial precision. The device operates within safety limits and occupies a volume < 2 mm³. This approach opens up a broad potential of wireless deep neural

inhibition through miniaturized microwave implants treating neural disorders as well as managing pain.

10:00 AM BREAK

SESSION SB03.10: In-Memory Sensing
Session Chairs: Paschalis Gkoupidenis and Jonathan Rivnay
Thursday Morning, April 25, 2024
Room 436, Level 4, Summit

10:30 AM *SB03.10.01

Memristive Devices for Advanced and Ultrasensitive Bio/Chemical Sensing Systems. [Ioulia Tzouvadaki](#); Ghent University, Belgium

Memristive devices and systems, much akin to biological synapses, possess the intrinsic ability to simultaneously carry out computational tasks and store information at significantly reduced volumes and power consumption by modifying their memory state as a function of the integral of the input stimulus. These emerging technologies coupled with biological processes, opened new perspectives in the role of bio-inspired sensors introducing a versatile paradigm for label-free and ultra-sensitive bio/chemical sensing, holding great promise as intelligent bio-interfaces and sensory systems in the biomedical domain. The recent advancements in the transduction and processing of chemical biomarkers of the neural and immune system functions will be discussed while also providing a critical outlook on the prospective role of memristive devices as fundamental building blocks in advanced biosensing systems.

11:00 AM SB03.10.02

Artificial Thermomechanical Receptor for In-Sensor Multimodal Fusion [Junhyuk Bang](#)¹, Kyun Kyu Kim² and Seung Hwan Ko¹; ¹Seoul National University, Korea (the Republic of); ²Stanford University, United States

As wearable devices evolve in complexity, there's a surging demand for advanced multimodal sensing technologies. Especially the acquisition of thermodynamic information is essential, which allows human-like perception, sensor calibration, and hazard detection. While previous studies have succeeded in selectively capturing temperature and mechanical signals, these methods typically required individual measuring units of target stimuli, leading to increased structural complexity, and necessitating extra computational processes for signal matching. To address these limitations of traditional multimodal sensors, we introduce the neuromorphic sensor for in-sensor multimodal fusion. This innovative design is inspired by the sensory nerve system's efficient computing architecture, which represents multimodal information by interleaving signals across time. To replicate this neural-like computing architecture, we utilized a stretchable memristive nanowire network (the Ag@Cu₂O core-shell nanowires) as the sensing material. This random network, with numerous memristive junctions of a metal-metal oxide-metal configuration, experiences a binary phase transition related to material and network geometry during the memristive switching process. In the high-resistance state, the conductivity pathway primarily goes through a dense network of Cu₂O shells, while in the low-resistance state, it predominantly goes through a sparse network of conductive filaments. This unique feature empowers active alteration in sensing capability, allowing for the selective extraction of thermal and mechanical signals through a singular resistance measurement unit. Furthermore, by carefully manipulating the signal measurement voltage pulse scenario, thermomechanical information is integrated into a singular interleaving response profile. It enables the spatiotemporal synchronization of thermal and mechanical information itself without the necessity of an external computing unit. Owing to its design simplicity, our neuromorphic multimodal sensor is much more miniaturized than previous work, achieving a sensing channel size of under 0.1mm² and a device thickness of less than 40 μm. This advancement not only improves its conformability on curved surfaces but also ensures rapid response to external stimuli. To demonstrate the practical application of realizing human-like perception, we integrated our sensor with the deep neural network and recognized random objects. In-sensor multimodal fusion, which captures complex physical characteristics, shows superior recognition accuracy compared to datasets acquired by measuring single information (thermal information or mechanical information). These findings open new opportunities for wearable electronics with wearability, and functionality and pave the way for intelligent multimodal sensor systems.

11:15 AM SB03.10.03

High-Speed Edge Computing Implemented Using Reconfigurable Carbon Nanotube Transistor Memories [Jingfang Pei](#)¹, Lekai Song¹, Pengyu Liu¹, Teng Ma² and Guohua Hu¹; ¹The Chinese University of Hong Kong, China; ²Hong Kong Polytechnic University, China

The constant data transportation from the edges to the centralized cloud computing infrastructure causes considerable constraints over the computational power and latency as well as the energy cost. Decentralization of the computation with the computational tasks distributed to the edges is an emergent solution to address the problem. Processing onsite data in local memories holds great promise to implement the edge computing. Here, we demonstrate edge computing using reconfigurable nonvolatile carbon nanotube transistor memory arrays, and prove high-speed, real-time video processing.

We fabricate the transistors from solution-sorted semiconducting single-walled carbon nanotubes. The transistors exhibit fast switching with the switching times and delays down to tens of nanoseconds, a large switching ratio of over 10⁵, and, particularly, a significant memory window of ~12 V arising from charge trapping in the sorting polymer. The above characteristics endow the transistors with highly-stabilized reconfigurable nonvolatile memory states and a high data processing speed. Owing to solution processing, the fabrication is wafer-scalable, the transistors exhibit uniform characteristic memory metrics, e.g. with 1.8% variation in the memory window, suggesting an industrial-scale manufacturing capability of the fabrication. Using the transistor memories, we design and implement an edge computing device with a convolution unit connecting to a differentiator, and demonstrate the application of the edge computing device in edge detection and motion track tasks of video streams. Particularly, the edge computing device successfully performs local video processing at a speed of 10,000 fps, exceeding the conventional high-speed cameras. Given the efficacy of the edge computing device, and the scalability of the fabrication, we envisage a promising prospect of realizing large-scale edge computing devices in implementing practical edge computing in, for instance, autonomous driving, virtual and augmented reality, and robotics.

11:30 AM SB03.10.04

Interfacial Engineering of Metal Ion Injection in Threshold Switching Memristor for Neuronal Applications [Calvin Lee](#), Putu Andhita Dananjaya, Eng Kang Koh, Funan Tan, Lingli Liu and Wen Siang Lew; Nanyang Technological University, Singapore

Neural networks composed of artificial neurons and synapses mimicking the biological nervous systems have governed much attention because of their promising potential in high-density memory storage and large-scale neuromorphic computing. In this context, various resistive switching phenomena in memristors such as ionic charge transfer, oxygen vacancy ordering, and electrochemical metallization (ECM) have been utilized to replicate neuronal

dynamics. Among them, ECM threshold switching (TS) devices are favorable for realizing complex neural networks due to their simple structure, large on/off ratio, and low operation voltages. However, ECM TS device uniformity is relatively poor, which may affect the accuracy of artificial neural networks, limiting the practical applications of ECM TS memristors. In this work, we experimentally demonstrate a highly-uniform Ta₂O₅-based TS device with nanoporous Pt interfacial layer as the high-performance selector, which shows low leakage current (< 1 pA), high on/off ratio (> 10⁸), and high endurance (> 10⁸ cycles). Furthermore, the Ta₂O₅/Pt-nanoporous layer TS device exhibits self-oscillation behaviour at low voltage (<1 V), where the oscillation frequency increases with the applied voltage and decreases with the load resistance.

Based on the studies of the nanoporous Pt interfacial layer with Ta₂O₅-based TS devices, the overall variability of the operating voltages of TS devices with nanoporous Pt interfacial layer were reduced to levels below that achieved in TS devices without nanoporous Pt interfacial layer. Furthermore, the nanoporous Pt interfacial layer enables the TS devices to operate at higher current compliance levels (< 100 μ A). The insertion of the nanoporous Pt interfacial layer offers a simplistic technique of metal ions manipulation in ECM TS devices.

11:45 AM SB03.10.05

Revealing Oxygen Donor Level in Tungsten Oxide Films for Neuromorphic Applications with Parallel Dipole-Line Hall System [Hyunjeong Kwak](#)¹, Chaeyoun Kim², Byungha Shin², Oki Gunawan³ and Seyoung Kim¹; ¹Pohang University of Science and Technology, Korea (the Republic of); ²Korea Advanced Institute of Science and Technology, Korea (the Republic of); ³IBM T.J. Watson Research Center, United States

Electrochemical random-access memory (ECRAM) devices stand as key candidates for realizing analog cross-point array-based AI computation accelerators thanks to its excellent programmability driven by ion movement, high stability, low cycle-to-cycle and device-to-device variation(1). However, there have been limited efforts to investigate fundamental physical parameters of the key channel material, WO_{3-x}, that control ECRAM switching characteristics. Tungsten oxide serves as a channel layer since its conductivity can be modulated depending on the ion concentration, rendering it a fitting choice to realize the analog switching(2). In this work, we fabricate ECRAM devices in a multi-terminal Hall-bar structure and conduct Parallel Dipole Line (PDL) Hall measurements to investigate the essential electrical properties of tungsten oxide films, including resistivity, mobility, carrier density and activation energy. The AC Magnetic PDL Hall system, based on strong magnetic field generation and lock-in detection, offers high sensitivity, allowing for sensing even weak Hall signals from low mobility and high resistivity samples(3). Furthermore, we measure the mobility and carrier density of tungsten oxide as a function of temperature using variable temperature PDL Hall measurements. The observed Hall mobility in WO_{3-x} films reaches to 4.66 cm²/Vs at room temperature. At lower temperatures, a slight decrease in Hall mobility is observed due to impurity scattering from ionized centers. We extract the activation energy of the oxygen donor level in tungsten oxide thin films using Arrhenius plots. Our findings show the experimental access of the key variables that change during switching in ECRAM, which is not only crucial for enhancing ECRAM's performance but also essential for providing vital insights into neuromorphic applications.

1. P. Chen, F. Liu, P. Lin, P. Li, Y. Xiao, B. Zhang, G. Pan, Open-loop analog programmable electrochemical memory array. *Nature Communications* **14**, (2023).

2. K. Miyake, H. Kaneko, Y. Teramoto, Electrical and optical properties of reactively sputtered tungsten oxide films. *Journal of Applied Physics* **53**, 1511-1515 (1982).

3. O. Gunawan, S. R. Pae, D. M. Bishop, Y. Virgus, J. H. Noh, N. J. Jeon, Y. S. Lee, X. Shao, T. Todorov, D. B. Mitzi, B. Shin, Carrier-resolved photo-Hall effect. *Nature* **575**, 151-155 (2019).

SESSION SB03.11: Metal Oxide Memristors

Session Chair: Qiangfei Xia

Thursday Afternoon, April 25, 2024

Room 436, Level 4, Summit

1:30 PM *SB03.11.01

Halide Perovskite based Memristive Systems [Nripan Mathews](#); Nanyang Technological University, Singapore

Halide perovskites have been under the focus for photovoltaic applications where their power conversion efficiencies have soared to efficiencies exceeding 26%. They have also garnered tremendous research interest over recent years for the development of next-generation light-emitting diodes (PeLED) in optical displays and light sources. The spotlight on this class of semiconducting material stems from several of its enviable traits such as long carrier diffusion length, defect tolerance, high colour purity, and spectral bandgap tunability which spans across the visible and infrared spectrum.

This talk will focus on our efforts on utilising the ionic characteristics of halide perovskites to enable memristive devices that can be employed for neuromorphic applications. The influence of the ionic compositions, thicknesses and interfacial layers in the memristive properties would be described. Going beyond conventional 2 terminal memristors, other device configurations that exhibit memory and switching in light emission, photovoltages would also be described.

2:00 PM SB03.11.02

Niobium Oxide-Based Threshold Switching and Dynamic Memristors for Spiking Neural Network [Shuai Ming Chen](#), Kuan-Ting Chen and Jen-Sue Chen; National Cheng Kung University, Taiwan

Inspired by the human nervous system, neuromorphic computing based on spiking neural networks (SNNs) can offer numerous advantages including parallel processing, adaptive learning, energy efficiency, high fault tolerance, and high plasticity. However, implementing neuromorphic computing on traditional CMOS requires a substantially complex and extensive assemblage of components. The presence of the volatile threshold switching (TS) memristors simplifies the hardware structure of neuromorphic computing system, making hardware implementation more straightforward.

Niobium oxide (NbO_x) is a typical Mott insulator characterizing by its temperature-triggered insulator-metal transition. NbO_x-based memristors exhibit S-type negative differential resistance (NDR) during current-controlled I-V sweep measurement and show the volatile threshold switching (TS) characteristics when conducted voltage-controlled sweeping. Connected in parallel with a capacitor, TS devices can follow a Pearson-Anson-like relaxation oscillator circuit model, serving as a prototype for the Leaky Integrate-and-Fire (LIF) model. Due to the MIM (Metal-Insulator-Metal) structure of the TS device, the parasitic capacitance inherent in these components also simplifies the hardware implementation of the LIF model. When pulse strain is being applying to the NbO_x-based LIF circuit, it generates spiking signals of various frequencies when pulse voltage and input frequency exceed a certain value (spiking from 4kHz to 15kHz depending on the input conditions). However, when the voltage level or input frequency falls below a specific threshold, no

spike signals are generated, demonstrating an all-or-nothing characteristic.

With varying the thickness of the niobium oxide active layer, NbO_x-based devices can exhibit dynamic resistive switching (DS) as well. DS devices possess short-term memory characteristics that depend on operational history and duration, leading to dynamic resistance changes. After electrical stimulation with a 5V amplitude, 3ms pulse width square pulse, the DS device current value measured with 2V square pulse increased around 20 times larger than value measured before stimulation (from 10μA to 209μA). Applied the gradual increasing electrical wave from 0V to 3V, current level at 1.5V is 1.6μA and 3V is 590μA. This nonlinear growth in current value imparts DS devices with filtering capabilities.

DS devices also exhibit diode-like characteristics, enhancing their functionality within circuits. The combination of TS devices with DS devices allows for the realization of more complex LIF models, enriching the computational capabilities of SNNs, whether for controllable leakage behavior, gradual potential rise buffering, noise filtering or spatial summation characteristic. Both DS and TS devices utilize niobium oxide as active layer's material offering advantages in manufacturing, make the hardware implementation of neural networks more streamlined.

2:15 PM SB03.11.03

Inverse Design of Neuronal Action Potentials in Ge Implanted VO₂ Thin Films [Rebeca M. Gurrola](#)¹, John M. Cain², Timothy D. Brown², Fatme Jardali¹, Suhas Kumar², Tzu-Ming Lu² and Patrick Shamberger¹; ¹Texas A&M University, United States; ²Sandia National Laboratories, United States

Vanadium dioxide (VO₂) is a strongly correlated electronic material that exhibits a metal insulator transition (MIT) at 68°C. The MIT can result in up to four orders of magnitude change in the electrical conductivity, which is coupled with a structural phase transition (SPT) where VO₂ transforms from insulating monoclinic to metallic rutile. Its nonlinear transformation enables non-linear dynamics that make it a desirable material for neuromorphic computing applications. Yet, the use of VO₂ to emulate neuronal behavior requires control of the on/off ratio and aspects of the transition, such as the hysteresis and sharpness of transition. All these factors play a crucial role in extending the lifetime of a VO₂-based memristor. Previous research has focused on 1) chemical doping of VO₂, [1] 2) applying strain to the material via lattice mismatch [2] and/or 3) creation of defects in order to tune aspects of the transformation [3]. It is poorly understood how modification of intrinsic properties of the film or the MIT translate to desired neuromorphic behavior (e.g., the neuronal action potential of a computing primitive).

The goal of this research is to first establish the feasibility of chemically doping VO₂ thin films with Ge ion implantation at moderate ion energies and various doses. Second, to investigate the changes in the electronic transport behavior and the MIT caused by the addition of various types of defects introduced into the system. Previous work using He⁺ ions at low fluences showed the feasibility of modifying the resistivity of the insulating and metallic phases (ρ_{low} and ρ_{high} , respectively) without greatly altering the T_{MIT} or the on/off ratio [4]. Ideally, by controlling the ρ_{low} and ρ_{high} and by decreasing the sharpness of the transition we can maximize the interval at which negative differential resistance (NDR) occurs. This would result in a larger time frame in which device oscillations can occur within the NDR region. Finally, we aim to harness ion implantation as a technique to induce desired current oscillations or action potential-like behavior in simple neuromorphic computational primitives.

Polycrystalline VO₂ thin films were grown on SiO₂(100 nm)/Si substrate. These films were implanted with Ge⁺ ions at 110 keV, and at fluences ranging from 1x10¹⁴ to 1x10¹⁶ ions/cm². Photolithography was used to make a variety of 2-terminal and 4-terminal devices on the films to study device switching performance. Implanted devices were then subjected to rapid thermal annealing (RTA) at temperatures ranging from 300°C to 900°C to restore the VO₂ crystallinity. This allowed us to identify the RTA temperatures and fluence values that best modified the MIT without amorphizing the film. The present study describes changes to the electrical transport upon Ge⁺ implantation as well as explores different oscillating behaviors observed within the NDR regions for devices subjected to different implantation conditions. Further exploration on the limits of controlling different aspects of the electrical transport behavior will 1) enable a larger class of materials that can emulate the neuronal functions and diverse neuronal dynamics, and 2) introduce a strategy to engineer biomimetic functionality into computational primitives.

References:

1. P. Jin, & S.Tanemura, "V_{1-x}Mo_xO₂ thermochromic films deposited by reactive magnetron sputtering," *Thin Solid Films*, 281, 239-242, 1996.
2. E. M. Heckman et. al., "Electrical and optical switching properties of ion implanted VO₂ thin films," *Thin Solid Films*, 518(1), 265-268, 2009.
3. K. Nagashima et. al., "Stress relaxation effect on transport properties of strained vanadium dioxide epitaxial thin films," *Physical Review B*, vol. 74, no. 17, 2006-11-17 2006, doi: 10.1103/physrevb.74.172106.
4. R. M. Gurrola et. al., "Modulation of electronic transport in VO₂ induced by 10 keV helium ion irradiation". In progress

2:30 PM SB03.11.04

Coexistence of Both Digital and Analog Response in Ta₂O₅-Based RRAM Devices toward Neuromorphic Hardware [Eng Kang Koh](#)^{1,2}, Putu Andhita Dananjaya¹, Han Yin Poh^{1,2}, Lingli Liu¹, Calvin Lee^{1,2}, Young Seon You² and Wen Siang Lew¹; ¹Nanyang Technological University Singapore, Singapore; ²GlobalFoundries, Singapore

With the amount of digital data growth in recent years, although the von Neumann architecture-based processors can efficiently conduct logic computations on structured data, they do poorly in image recognition and natural language processing for unstructured data. This leads to a paradigm shift towards a Neuromorphic computing architecture. The Resistive Random Access Memory (RRAM), or in particular its integration with a transistor, 1T1R (1 Transistor - 1 RRAM) structure, is a popular solution to this problem. These devices emulate storing synaptic weights in terms of the conductance of the devices. However, an innate problem is that the RRAM's switching mechanism typically involves an abrupt switching current response. This means that its ability to be used as a neuromorphic computing memory device is hindered because the total number of states that can be stored within a single device is restricted. In this work, using different voltage schemes, the Ta₂N/Ta₂O₅/Pt RRAM device demonstrates both filamentary (digital) and interfacial (analog) resistive switching within a single device. A thorough evaluation of the underlying principles governing both switching modes revealed that the anomalous gradual switching is linked to the modulation of interfacial oxides that form between the active electrode and the oxide switching layer. The coexistence of the two switching mechanisms means it is possible to operate the filamentary switching RRAM as a storage device and the interfacial switching RRAM as a neuromorphic device element within a chip fabricated using the same fabrication process steps. The devices also demonstrate good scalability (<150 nm), low operational voltage (< 2.5 V), endurance (>10⁶ cycles), good retention (85°C at 10⁴s), and the possibility of reversibility of the mechanisms while having good multi-level cell properties. With the duality of these two switching modes, our device is poised for application in both memory storage and synaptic weight-storing applications.

2:45 PM SB03.11.05

Enhancing Synaptic Plasticity with Metal Oxide-Based IGTs for Neuromorphic Computing [Ramin Karimi Azari](#)¹, Luan Camargo^{1,2}, Patrick Dang¹ and Clara Santato¹; ¹Polytechnique Montreal, Canada; ²State University of Londrina (UEL), Brazil

Neuromorphic computing, which relies on analog neural networks, seeks to significantly reduce computational power by minimizing the necessity for data transfers between memory and logic components. Within neuromorphic computing, the artificial synapse serves a dual purpose as both a storage and computational unit, paving the way for resilient learning and power-efficient in-memory computing. Diverging from conventional computing paradigms,

neuromorphic systems replicate the structural and functional attributes of the human brain.

Metal Oxides (MOs)-based IGTs and the tailoring of their properties for synaptic behavior, achieved by leveraging their unique electronic structure, composition, crystallinity, morphology, intrinsic, and/or extrinsic defects, as well as doping, have gained significant attention.

In this study, we used tungsten trioxide (WO₃) as channel material. WO₃ is earth-abundant with non-toxicity, high stability under ambient conditions, and biocompatibility. WO₃ can exist in different crystal structures, including orthorhombic, monoclinic, and hexagonal phases. The current modulation in MO IGTs arises from both electrostatic and electrochemical processes. The crystal structure of the metal oxide is anticipated to have an impact on ion permeability, leading to variations in doping, channel conductivity, and redistribution time of the anions in the IGT channel.

In our WO₃ synaptic transistor, channel conductivity, analogous to excitatory postsynaptic current (EPSC), was modulated with amplitude, width, interval, and the number of applied input gate-source voltage (V_{gs}) pulses. The fluctuations in conductance correspond to the learning and forgetting processes of the artificial synaptic device, with an increase signifying learning and a decrease signifying forgetting.

Another fundamental aspect that we investigated in WO₃-based IGTs is their plasticity, denoting the strengthen of synaptic weight or connection. Synaptic plasticity is typically divided into two categories, namely short-term (STP) and long-term (LTP), determined by the duration of their persistence.

The spontaneous decay time of conductance, which is referred to as the response time, plays a critical role in artificial synapses and can be likened to the forgetting process in biological synapses. The presence of both fast and short response times is the key factor determining the occurrence of STP and LTP in artificial synapses. WO₃-based IGTs display a more prominent transition between STP and LTP, indicating superior synaptic performance.

The current modulation in IGTs is investigated also by changing the gating medium (including solvent-in-salt media).

The addition of Li to the ionic medium ([EMIM][TFSI]) of metal oxide IGTs can play a crucial role in modulating the conductivity and synaptic behavior of the transistor.

When Li ions are incorporated into the channel material or adsorbed at the interface between the transistor channel and the ionic medium, they can influence the diffusion dynamics and mobility of ions within the channel. This leads to an increase in the conductivity of WO₃ channels by almost 100 percent after applying V_{gs} to the gate.

This affects the ion redistribution and de-doping processes, leading to changes in the synaptic behavior of the transistor. In particular, when Li ions are readily diffusible back into the ionic medium after the removal of the low amplitude gate bias (under 1 volt), STP was observed. On the other hand, if the Li ions are intercalated into the channel material and do not diffuse back spontaneously, LTP effects were exhibited and response time increased.

In this sense, understanding metal oxide materials in IGTs and effectively tuning the presence and dynamics of Li ions through pulse parameters offers opportunities for tailoring the synaptic properties and performance of these transistors in developing new integrated circuits and neuromorphic devices.

3:00 PM BREAK

SESSION SB03.12: Memristive Circuits and Arrays
Session Chair: Douglas Durian
Thursday Afternoon, April 25, 2024
Room 436, Level 4, Summit

3:30 PM *SB03.12.01

Noise and Variation in Memristive Devices and Crossbar Arrays Qiangfei Xia; University of Massachusetts, United States

Memristors are resistance switches with reconfigurable multilevel resistance states modulated by an electric field. Crossbar arrays of such devices can perform analog computation at the site where data is stored (in-memory computing) by directly using physical laws, such as Ohm's law for multiplication and Kirchhoff's current law for summation. Analog in-memory computing reduces the time and energy needed to access system memory. The multiply-accumulate operations can be performed through a single current sensing operation, dramatically increasing the computing throughput. However, ionic-based devices have noises due to the random trapping/release of charge carriers at thin-film interfaces or defect sites (random telegraph noise) and the fluctuation of defect concentrations ($1/f$ noise). Together with thermal and shot noises, they impose a fundamental limit on the capability of analog computing. Furthermore, the device-to-device variation remains a challenge for large-scale crossbar arrays. In this talk, we will showcase how we mitigate these issues through precise conductance tuning of the devices to achieve an unprecedentedly large number of conductance states. We will then discuss the algorithm-hardware co-design approach for edge computing with the memristive crossbar arrays. Finally, we will explore utilizing the variation in the crossbar arrays for embedded hardware security applications.

4:00 PM SB03.12.02

Photo-Enhanced Output in Memdiodes based on Organic/Inorganic Hybrid Materials for Neuromorphic Synapses Jacob Lee¹, Dhriti Nepal², John Ferguson², Ajit K. Roy² and Xiaojuan Fan^{1,2}; ¹Marshall University, United States; ²Air Force Research Laboratory, United States

We report that memdiodes (MDs) have been created based on metal halide-embedded polymeric hybrids in ambient conditions, presenting unusual photo-enhanced electronic transport behaviors. The hybrid materials show nonconventional optoelectronic properties, providing alternatives to traditional semiconductors such as silicon. The blending of inorganic metal halides and organic polymers combined with an insulating polymer membrane facilitates resistive memory and diode behaviors. Two-terminal memristive devices are made of a hybrid photoactive layer of CuCl₂ blended with poly(ethylene glycol) (PEG) and a layer of poly(methyl methacrylate) (PMMA) deposited on substrates to form a *pn*-junction memdiode. Thin films were characterized using ATR-FTIR, SEM, UV-Vis-NIR microspectrophotometer, and *IV* curves. Cyclic voltage sweepings present polarity-related current curves, which manifest the MD characteristics as the current stays near zero in negative voltages, but significantly increases in positive voltages. Cyclic *IV* curves also present a moderate hysteresis, featuring a memory device. Surprisingly, the current magnitude increases by 4 times when the light radiation turns on, implicating that the electronic output is significantly enhanced by photoexcitation. The resistive transport mechanism is hypothetically attributed to electron-ion couplings, where both electronic mobility and ionic-hopping contribute to carrier transport as electrons migrate in an ionic "train", where dielectric dipoles induce *IV* hysteresis. All materials in the MD devices are bio-compatible, stable, and flexible, potentially applicable to bio-electronic circuits, artificial neuromorphic synapses, and brain-inspired quantum computing.

SYMPOSIUM SB04

Innovative Device and Characterization Concepts for Organic Electronics
April 23 - April 26, 2024

Symposium Organizers

Paddy K. L. Chan, University of Hong Kong
Katelyn Goetz, National Institute of Standards and Technology
Ulrike Kraft, Max Planck Institute for Polymer Research
Simon Rondeau-Gagne, University of Windsor

Symposium Support

Bronze

Journal of Materials Chemistry C
Proto Manufacturing

* Invited Paper
+ JMR Distinguished Invited Speaker
^ MRS Communications Early Career Distinguished Presenter

SESSION SB04.01: OFET I
Session Chairs: Katelyn Goetz and Ulrike Kraft
Tuesday Morning, April 23, 2024
Room 435, Level 4, Summit

10:30 AM *SB04.01.01

Probing The Microscopic Origins of Device Performance and Stability in Organic Semiconductors through Trap Density of States Spectroscopy
Oana D. Jurchescu; Wake Forest University, United States

Organic semiconductors (OSCs) are highly susceptible to defect formation, owing to their weak intermolecular interactions, leading to trap states in the band gap that can drastically alter their optoelectronic properties. Characterization techniques that can elucidate the mechanisms of defect formation and evolution are essential for guiding the processing and design of high-performance stable OSC devices. In this presentation I will discuss a highly efficient methodology to elucidate the microscopic processes occurring within the OSC when deliberately exposed to different external stimuli. The methodology relies on real-time access to the trap density of states (t-DOS) spectrum of the OSC using organic field-effect transistor (OFET) measurements. The t-DOS spectrum provides detailed information about the origin and energetic distribution of electronic traps in OSCs, as well as their time evolution. Several different trap states will be discussed as case studies, including those arising from impurities and isomer coexistence, microstrain at device interfaces, environmental and bias stress. Methods for minimizing the trap density to enhance performance and stability will be presented. Finally, the exploitation of trap formation for the development of radiation dosimeters for cancer treatment will be discussed.

11:00 AM *SB04.01.02

High-Frequency Flexible Organic Thin-Film Transistors Hagen Klauk; Max Planck Institute for Solid State Research, Germany

Organic thin-film transistors (TFTs) are potentially useful for flexible electronics applications, as they can typically be fabricated at temperatures no higher than approximately 100 °C and thus not only on glass, but also on polymeric substrates and even on paper. An important TFT performance parameter is the transit frequency, which is the highest frequency at which a transistor is able to switch or amplify electrical signals. The transit frequency of organic TFTs depends mostly on the contact resistance and on the lateral TFT dimensions (channel length, gate-to-contact overlaps). A better understanding of the factors that determine the contact resistance of organic TFTs has made it possible to fabricate organic TFTs that have a contact resistance within three orders of magnitude of the theoretical limit and an experimentally measured transit frequency of 21 MHz (at 3 V). Any significant further reduction of the contact resistance of organic TFTs to the levels commonly achieved in inorganic field-effect transistors now hinges mainly on the elimination of the Fermi-level pinning induced by metal-induced gap states at the metal-semiconductor interfaces. In terms of decreasing the lateral TFT dimensions, flexible organic TFTs with channel lengths and gate-to-contact overlaps below 1 μm were recently demonstrated that display reasonable static characteristics (turn-on voltage of 0 V, subthreshold swing below 100 mV/decade, on/off current ratio greater than 10⁹), but suffer from a relatively large contact resistance that limits the transit frequency to 36 MHz (at 3 V). One of the challenges in pushing the transit frequency of flexible organic TFTs to 100 MHz and beyond will be to minimize all three parameters (contact resistance, channel length, gate-to-contact overlaps) simultaneously.

11:30 AM SB04.01.03

Fully Edible Transistor: Towards Next Generation Edible Electronics Elena Feltri^{1,2}, Pierluigi Mondelli¹, Fabrizio Mario Ferrarese^{1,2}, Alessandro Luzio¹ and Mario Caironi¹; ¹Italian Institute of Technology, Italy; ²Politecnico di Milano, Italy

With the increased burden on healthcare workers in recent years, point-of-care medical devices for the gastro-intestinal tract that do not need external supervision (neither during ingestion nor for their retrieval) could be crucial for safe and early diagnosis, monitoring and treatment of many diseases. Edible electronics can enable such a vision through devices that are not only ingestible but are indeed digestible just like food, as they are made up of food-grade materials, thus zeroing the risks and health hazards posed by device retention and therefore the need for supervised administration. To turn this vision into reality, research efforts are steering towards functional edible electronic devices that can enable active signal monitoring and control of drug release inside the human body[1].

In this work, we present a printed fully edible transistor operating at low voltage (<1V). Inert metallic source-drain and gate staggered electrodes were inkjet-printed on top of an ethyl-cellulose edible substrate, while the chitosan solid electrolyte and the edible semiconductor Copper Phthalocyanine (CuPc) were drop-casted and thermally evaporated, respectively. The devices were characterized in terms of transport characteristics, air stability and reproducibility, showing performances comparable to conventional transistors based on the same semiconductor, an air stability of at least 12 months and a

high degree of reproducibility. To realize a proof-of-principle logic gate, the transistor was connected with a commercial resistor to create an inverter. We believe that the results of this work can pave the way to the development of edible circuitry for a broad range of future applications in the medical, food and entertainment industry.

[1] AS Sharova, F Melloni, G Lanzani, CJ Bettinger, M Caironi, "Edible electronics: The vision and the challenge" *Advanced Materials Technologies* 6 (2), 2000757

11:45 AM SB04.01.04

Development of Strain-Induced Organic Single-Crystalline Transistors Mizuki Abe¹, Taiki Sawada¹, Yu Yamashita^{1,2,3}, Naotaka Kasuya¹, Shun Watanabe¹ and Jun Takeya^{1,2,3}; ¹The University of Tokyo, Japan; ²National Institute for Materials Science, Japan; ³JST CREST, Japan

Organic semiconductors (OSCs) are known as flexible, solution processable, light-weight, and potentially low-cost materials which are applied in many electronic devices. There is considerable interest in developments in organic thin-film transistors (OTFTs) for applications such as flexible displays, sensors, and IC tags. Rapid developments in synthetic chemistry and device engineering allow us to explore high performance devices. However, there is limited study to improve static (DC) and dynamic (AC) performances of organic devices without employing synthesis and complicated device integration. A strain is used to control the electronic structure. Particularly in the case of single-crystalline OSCs, it has been demonstrated that a slight compressive lattice strain can modify the electronic structure via uniformly modified crystal structure, and enhances carrier mobility[1][2]. However, the method to apply strain into OSCs has been limited; bending substrate has been only the way to systematically control the strain in OSCs. Therefore, a novel method to introduce a persistently strain into OSCs particularly on a planar substrate will be highly desired.

Here, we establish a general method to persistently induce uniaxial strain into single-crystalline OTFTs to enhance the performance of OTFTs. OTFTs with single-crystalline films of 3,11-dicytyldinaphtho[2,3-d:2,3-d]benzo[1,2-b:4,5b]dithiophene (C₈-DNBDT-NW) as the active layer were fabricated on 15 μm thick polyimide (PI) substrate. To induce uniaxial compressive strain into OTFTs semi-permanently in a planar substrate, we developed following new method. First, OTFTs fabricated on PI substrate were adhered onto a convexly bent thick mother substrate (polyethylene terephthalate) by using cyanoacrylate adhesive. The OTFTs adhered on the extended surface of the bent mother substrate were compressed semi-permanently when the mother substrate is recovered in a flat state. In this method, the surface strain ϵ of the bent film was calculated by the following equation : $|\epsilon| = h / 2(R + h)$, where h is the thickness of mother substrate and R is the curvature radius of bent substrate.

By applying this method, the modulation of carrier mobility by the introduction of uniaxial compression is observed. By changing the curvature of mother substrate, the ratio of compressive strain into OTFT changes accordingly. In this measurement, the maximum compressive strain induced into OTFTs is evaluated to be 3.1% along c -axis. The intrinsic mobility increases monotonically by inducing compressive strain by a factor of 156% when compressive strain reaches 3.1%. This large enhancement of intrinsic mobility agrees quantitatively with our previous study[1], and originates from the suppression of molecular vibration, rather than from the effect of effective mass; a reduction of lattice constant of C₈-DNBDT-NW directly restricts the molecular vibration that contributes particular to electron-phonon interaction.

The enhancement of dynamic performances of OTFTs by the strain is also observed consistently in strain-induced OTFTs. Cutoff frequency (f_T), the parameter which determines operation speed of OTFTs, improves by a factor of 140% when 1.0% compressive strain is induced into OTFTs. Theoretically, cutoff frequency is proportional to the carrier mobility of OSCs. Therefore, this result indicates that enhancement of carrier mobility by the introduction of strain also improves dynamic properties of OTFTs. From these results, strain-induced OTFTs showed high carrier mobility and improved cutoff frequency. Inducing even larger strain is expected to further improve both static and dynamic performances of OTFTs. This simple, but versatile method will open opportunities for further developments in high frequency operation of OTFTs.

[1] T. Kubo, J. Takeya *et al.*, *Nat. Commun.* **7**, 11156 (2016).

[2] H. Choi, V. Podzorov *et al.*, *Adv. Sci.* **7**, 1901824 (2020).

[3] J. Soeda, J. Takeya *et al.*, *Appl. Phys. Express*, **6**, 076503 (2013).

SESSION SB04.02: Charge Transport
Session Chairs: Paddy K. L. Chan and Hagen Klauk
Tuesday Afternoon, April 23, 2024
Room 435, Level 4, Summit

1:30 PM *SB04.02.01

Charge Transport and Thermoelectric Properties of High Mobility Doped Conjugated Polymers Henning Sirringhaus; Cambridge University, United Kingdom

Doped conjugated polymers are critical to emerging device applications, including field-effect transistors, thermoelectrics, bioelectronics, and neuromorphic computing devices. We will present recent advances in controlling doping processes and understanding the resulting charge transport properties of doped polymers. This will include discussion of the role of Coulomb interactions between carriers and with the counterions at high doping densities, new experimental methods to study the electronic structure and transport properties of these doped polymers as well as recent advances in improving the electrical stability of FETs and thermoelectric performance.

2:00 PM *SB04.02.02

Charge Carrier Transport in Crystalline Organic and Hybrid Perovskite Semiconductors Investigated with a High-Resolution ac -Hall Technique Vitaly Podzorov; Rutgers University, United States

The importance of Hall effect measurements in evaluating the charge carrier mobility of novel materials is being increasingly recognized in materials science, semiconductor physics, and electronics. Hall measurements are advantageous over other mobility measurement techniques in that they: (a) allow a direct access to the mobile carrier concentration and mobility in a steady-state charge transport regime; (b) provide an alternative for mobility evaluation in systems where other techniques are hard to implement; (c) provide means of distinguishing between different transport mechanisms (e.g., hopping, band-like, or their combination); and (d) help disentangling the contributions of various carrier types or trap states. However, in many intrinsically low-mobility materials and devices, conventional (dc) Hall measurements are extremely hard to carry out due to typically weak Hall signals (and, thus, low signal-to-noise ratio).

High-resolution ac Hall and photo-Hall measurements recently developed in our group have resulted in a significant progress in our understanding of the charge transport and photophysical properties of organic semiconductors and lead-halide perovskites.[1,2] In this talk, I will discuss a few examples of the

transport physics studies using Hall-effect measurements. For instance, Hall measurements have led to elucidation of the role of grain boundaries in high-performance polycrystalline organic field-effect transistors (OFETs), where capacitively charged grain boundaries lead to an “underdeveloped” Hall effect.[3] In another example, the *intrinsic* mobility-strain relationship has been experimentally revealed in organic semiconductors for the first time, achieved by simultaneous measurements of FETs and Hall effect under a calibrated uniaxial strain in ultra-thin, flexible, single-crystal rubrene OFETs.[4] These measurements revealed an anisotropic and reversible modulation of charge mobility with strain. A photo-Hall effect has also been recently measured in organic semiconductors for the first time, with the developed model capable of correctly disentangling the mobilities and densities of the photogenerated mobile electrons and holes.[2] These photo-Hall effect measurements performed in high-mobility rubrene single crystals confirmed the older findings that photoconductivity in this material is due to the interaction of long-lived mobile triplet excitons with surface states [5,6]. Finally, high-resolution *ac*-Hall measurements have also proven very useful in the investigation of the intrinsic (trap-free) charge transport in epitaxial lead-halide perovskite FETs recently developed in our group.[7]

References:

1. Y. Chen, H. T. Yi and V. Podzorov, *Phys. Rev. Applied* **5**, 034008 (2016).
2. V. Bruevich, H. H. Choi and V. Podzorov, *Adv. Funct. Mater.*, DOI:10.1002/adfm.202006178 (2020).
3. H. H. Choi, A. F. Paterson, M. A. Fusella, J. Panidi, O. Solomeshch, N. Tessler, M. Heeney, K. Cho, T. D. Anthopoulos, B. P. Rand and V. Podzorov, *Adv. Funct. Mater.*, 1903617 (2019).
4. H. H. Choi, H. T. Yi, J. Tsurumi, J. J. Kim, A. L. Briseno, S. Watanabe, J. Takeya, K. Cho and V. Podzorov, *Adv. Science*, 1901824 (2019).
5. H. Najafov, B. Lee, Q. Zhou, L. C. Feldman and V. Podzorov, Observation of long-range exciton diffusion in highly ordered organic semiconductors, *Nature Mater.* **9**, 938 (2010).
6. P. Irkhin, H. Najafov and V. Podzorov, Steady-state photoconductivity and multi-particle interactions in high-mobility organic semiconductors, *Sci. Reports* **5**, 15323, DOI: 10.1038/srep15323 (2015).
7. V. Bruevich, L. Kasaei, S. Rangan, H. Hijazi, Z. Zhang, T. Emge, E. Y. Andrei, R. A. Bartynski, L. C. Feldman, V. Podzorov, Intrinsic (Trap-Free) Transistors Based on Epitaxial Single-Crystal Perovskites. *Adv. Mater.* **34**, 2205055 (2022). <https://doi.org/10.1002/adma.202205055>.

2:30 PM *SB04.02.03

Effect of Structural Dynamically Induced Disorder on Charge in Molecular Materials [Lisa A. Fredin](#); Lehigh University, United States

Describing charge carrier anisotropy in small molecule crystalline semiconductors with ab initio methods is challenging because of the weak intermolecular interactions which lead to both localized and delocalized charge interactions. Hopping models (localized) are generally used to describe materials with small charge carrier mobilities, while periodic band models (delocalized) are used to describe materials with high carrier mobilities. Noncovalent interactions between the molecular components mean that dynamic disorder in these materials can have a large impact on the electronic properties of these materials at room temperature. In particular, dynamically induced structural disorder can lead to non-linear changes of the electronic response. Here we build new real temperature computational methodologies based on either Marcus Theory (hopping) or the Boltzmann Transport Equation (band transport) that allow for direct prediction of electronic response of single crystal organics while capturing the weak electrostatic interactions between π -interacting organic molecules, the surrounding crystal environment through periodic symmetry, delocalization of charge in a single calculation, and zero-point energy corrections. In particular, very small atomic displacements can sometimes have a large effect on the localization of electronic density and thus charge transport.

3:00 PM BREAK

SESSION SB04.03: Materials I
Session Chairs: Ting Lei and Simon Rondeau-Gagne
Tuesday Afternoon, April 23, 2024
Room 435, Level 4, Summit

3:30 PM *SB04.03.01

Understanding The Device Stability Through The Lens of Semiconductive Polymer's Chain Dynamics [Xiaodan Gu](#); University of Southern Mississippi, United States

Organic semiconducting polymers were widely studied due to their unique optoelectronic and mechanical property. They are the key component in various functional electronic devices, such as organic photovoltaic devices, flexible displays, wearable sensors, neuromorphic computing, and more recently bioelectronics. Despite tremendous progress being made in improving the charge carrier mobility and optimizing energy bandgap, the conjugated polymer's physical property was not widely studied, particularly the glass transition phenomenon. However, it is important for device stability, preventing wide adoption of polymer-based organic devices.

In my talk, I will outline past works on studying the polymer dynamics for semiconductive polymers and provide an overview of our effort in this area using a wide range of unique characterization tools, from thin film to bulk. I will discuss the challenge associated with accurately measuring the glass transition temperature for rigid conjugated polymers. I will also discuss our approach to address this challenge using thin-film calorimetry and ellipsometry tools, as well as using molecular dynamic simulation and cheminformatics to accurately predict the glass transition temperature. Lastly, I will cover how dynamics could impact thin film morphology and device performance at different operation temperatures and should be carefully considered when designing new polymers and devices.

4:00 PM *SB04.03.02

Nanomechanics of Materials used in Flexible Electronics [Deepak Venkateshvaran](#) and Leszek Spalek; University of Cambridge, United Kingdom

Organic semiconductors are multifunctional soft electronic materials that play an impactful role in the flexible electronics industry. Their use spans printed electronic circuits, large area displays, flexible solar energy harvesters, and implantable bioelectronics. For their competitive optical, electronic, thermoelectric, and spin-based properties, these soft electronic materials attract significant academic engagement, seeding new technologies for the future. [1, 2, 3]

Although macroscopic flexibility on the centimetre to metre scale is a unique selling point for organic semiconductor technology, not much is known about their mechanical properties on the nanoscale. Quantification of these nanomechanical properties, together with an understanding of nanoscale stiffness tunability and homogenisation, holds significant potential for fundamental and applied science.^[4,5]

During the last decade, the development of high precision atomic force microscopes has made it possible to quantify the mechanical properties of organic polymers on the scale of a few polymer chains. Techniques such as higher eigen mode imaging make it possible to visualise molecular ordering on the nanoscale under ambient conditions with ease. These techniques allow one to correlate molecular ordering with the stiffness that such ordering manifests.

In this talk, the science and technology of precision nanoscale measurement of mechanics will be spotlight. The interrelation between molecular organisation and nanomechanical properties in high-performance polymers used for organic electronics will be shown.^[6,7] A quantification of differences in strain within organic nanocrystal polymorphs will also be demonstrated. The measurement techniques demonstrated in this talk are extendable to a wide variety of multifunctional materials with a broad range of elastic properties and have significant use in both academia and industry.

- [1] D. Venkateshvaran, M. Nikolka *et al.*, *Nature* **515**, 384–388 (2014)
- [2] S. J. Wang, D. Venkateshvaran *et al.*, *Nature Electronics* **2**, 98–107 (2019)
- [3] P. Skalski, O. Zadorna *et al.*, *Physical Review Materials* **6**, 024601 (2021)
- [4] L. Ouyang, C. Kuo *et al.*, *J. Mater. Chem. B* **3**, 5010 (2015)
- [5] C. D. Gerardo *et al.*, *Microsystems and Nanoengineering* **4**, 19 (2018)
- [6] V. Panchal, I. Dobryden ... D. Venkateshvaran, *Advanced Electronic Materials* **8**, 2101019 (2022)
- [7] I. Dobryden, V. V. Korolkov ... D. Venkateshvaran, *Nature Communications* **13**, 3076 (2022)

4:30 PM SB04.03.03

Discovering New Molecules for Organic Electronics from The Chemical Supply Chain [Alessandro Troisi](#) and Omer Omar; University of Liverpool, United Kingdom

We present our methodology to discover novel active molecular compounds for organic electronics combining high-throughput virtual screening and knowledge of the chemical supply chain. The talk will provide new recent examples of the discovery of (i) dual emitters, (ii) molecules with inverted single-triplet gap and (iii) low energy emitters. In all cases the discovery takes place in two steps, the exploration of a large chemical space of pre-computed properties followed by a refinement of the search through more computationally demanding screening steps. The approach is designed to allow facile experimental verification of the predictions and some verifications will be presented as part of the lecture. The web platform enabling similar workflows to be adapted to different properties is presented.

- [1] D. Padula, O.H. Omer, T. Nematiram, A. Troisi, *Energ. Environ. Sci.* **12**, 2412 (2019)
- [2] T. Nematiram, A. Troisi, *Chem. Mater.* **34**, 4050 (2022)
- [3] O.H. Omer, D. Padula, T. Nematiram, A. Troisi, *Scientific Data* **9**, 54 (2022)
- [4] O.H. Omer, X.-Y. Xie, A. Troisi, D. Padula, *J. Am. Chem. Soc.* **145**, 19790 (2023)

4:45 PM SB04.03.04

Manipulating Self-Healing Properties in Organic Semiconductors through Supramolecular Chemistry Megan M. Westwood, Peter Finn, Lewis M. Cowen and [Bob C. Schroeder](#); University College London, United Kingdom

Material degradation poses a significant concern for both material scientists and engineers, leading to costly repair efforts and more extensive consequences than mere failure. As a result, there is a growing interest in developing self-healing materials to eliminate the need for maintenance. In contrast to their inorganic semiconductor counterparts, organic semiconducting materials possess notably low Young's moduli, making them exceptionally well-suited for integration into wearable electronic devices that can be directly applied to the human skin [1]. However, wearable electronics are exposed to a myriad of environmental stressors, including mechanical wear, chemical exposure, temperature fluctuations, and radiation. The relentless impact of these stressors can lead to the deterioration of the chemical structure, ultimately resulting in the degradation and eventual loss of the material's physical properties. Within this context, we will delve into our strategic approach to mitigating the loss of physical properties through the development of intrinsically self-healing polymers. This significant achievement was made possible by harnessing the principles of supramolecular chemistry, with a particular emphasis on the utilization of intramolecular hydrogen bonds [2-4]. To gain a comprehensive understanding of how hydrogen bonding affects the viscoelastic and electrical characteristics of organic semiconductors, we devised two distinct material sets. The first consists of a conjugated polymer with integrated hydrogen bonding functionality, while the second involves a composite material comprising a conjugated polymer embedded within a self-healing polysiloxane matrix.

Our discussion will comprehensively cover the effects of these distinct approaches on charge transport and self-healing capabilities. Furthermore, we will outline how we can leverage the observed disparities to not only customize the electronic properties but also fine-tune the self-healing and mechanical attributes of the material to align with the specific demands of diverse applications.

- [1] J. Y. Oh & Z. Bao, *Adv. Sci.*, **6**, 1900186 (2019).
- [2] J. Y. Oh *et al.*, *Nature*, **539**, 411–415 (2016, 539).
- [3] A. Gasperini *et al.*, *Macromolecules*, **52**, 2476–2486 (2019).
- [4] J. Ma *et al.*, *Nature Comm.*, **12**, 5210 (2021).

SESSION SB04.05: Optoelectronics I
Session Chairs: Paul Blom and Katelyn Goetz
Wednesday Morning, April 24, 2024
Room 435, Level 4, Summit

10:30 AM *SB04.05.01

High-Performance Organic Devices based on Crystalline Stacks [Karl Leo](#); IAPP, Germany

The research on organic electronics is driven by new applications using properties like flexibility, easy manufacturing, biocompatibility, etc. While OLED

displays and organic solar cells are commercially successful, organic electronic circuits have not yet reached broad application, mainly since device performance is lacking. In this talk, I will discuss highly ordered organic multilayer structures which have the potential to increase device performance by orders of magnitude. For the highly ordered layers, rubrene crystals are created by heating of amorphous layers and can be electrically doped during the epitaxial growth process to achieve hole or electron conduction. Analysis of the space charge limited current in these films reveals record vertical mobilities of 10 cm²/Vs. Furthermore, these structures allow comparatively long minority carrier diffusion lengths, allowing to realize the first organic bipolar transistors. OLED from highly ordered layers show high current densities and excellent emission homogeneity. Furthermore, I will address highly ordered organic thin-film blends with a similar chemical structure and show the effect of band structure engineering by spectroscopic methods. In contrast to previous studies where the experimental results can be described by quadrupole effects, delocalization is a significant effect for the crystalline layers.

11:00 AM *SB04.05.02

Organic Semiconductor Thin Film Crystal Growth: Formation and Propagation Barry P. Rand; Princeton University, United States

Organic semiconductors are commercially validated regarding OLED displays, with considerable scope for future applications. Toward these future prospects, I will present recent work from our group that seeks to better understand how to form crystalline films of organic semiconductors, approaching single-crystal-devices, but in a thin film platform. Through proper control of processing, we are able to realize pinhole free organic semiconductor films with single crystal grains with millimeter dimensions. We have found that transport in these films is considerably improved compared to disordered films, and that organic solar cells incorporating these long-range-ordered films exhibit highly delocalized and band-like charge transfer (CT) states, contributing to noticeably lower energy losses. We will discuss these aspects and our understanding to-date of which molecules are amenable to the formation of such films, and how to propagate crystal growth both homoepitaxially and heteroepitaxially.

11:30 AM SB04.05.03

On The Importance of Chemical Precision in Organic Electronics – Fullerene Intercalation in Perfectly Alternating Conjugated Polymers and Implications on Device Performance Jochen Vanderspikken^{1,2}, Zhen Liu³, Xiaocui Wu⁴, Stefania Moro⁵, Tyler Quill⁶, Bart Goderis⁷, Vincent Lemaur⁸, David Beljonne⁸, Alberto Salleo⁶, Laurence Lutsen^{1,2}, Koen Vandewal^{1,2}, Bruno Van Mele³, Giovanni Costantini⁵, Niko Van den Brande³ and Wouter Maes^{1,2}; ¹Hasselt University, Belgium; ²IMEC, Belgium; ³Vrije Universiteit Brussel, Belgium; ⁴University of Warwick, United Kingdom; ⁵University of Birmingham, United Kingdom; ⁶Stanford University, United States; ⁷KU Leuven, Belgium; ⁸University of Mons, Belgium

The true structure of alternating conjugated polymers – the state-of-the-art materials for a number of organic electronics technologies – often deviates from the idealized picture. The presence of structural defects is inherently linked to the applied cross-coupling polymerizations (notably Stille) and varies according to the experimental conditions. Nevertheless, many polymers still perform excellently in the envisaged applications, which raises the question if one should even care about these defects. Here, this question is addressed by comparing a traditionally prepared alkoxy-PBTTT polymer to a newly synthesized homocoupling-free variant, as verified by scanning tunneling microscopy (STM). We (for the first time) quantify the amount of homocoupling by STM and shed new light on the actual distribution of these defects in the polymer material. Additionally, we demonstrate that matrix-assisted laser desorption-ionization - time of flight (MALDI-ToF) mass spectrometry only shows a fraction of the homocoupled species and hence gives an incomplete picture. Further, it is shown through a combination of experimental techniques (and supported by calculations) that these defects hinder fullerene intercalation, whereas this returns for the homocoupling-free polymer and then affords stronger intermolecular charge-transfer interactions. This demonstrates that molecular defects may (strongly) impact material and blend properties and calls for increased attention for defect-free materials.

11:45 AM SB04.05.04

Understanding of The Nanosprouts Structure Inhomogeneity of Organic Semiconductor and The Corresponding Optical Memory Property Lizhi Yan¹ and Paddy K. L. Chan^{1,2}; ¹The University of Hong Kong, Hong Kong; ²Advanced Biomedical Instrumentation Centre, Hong Kong Science Park, Hong Kong

The structure inhomogeneity of organic semiconductors had been widely observed in organic polycrystal or amorphous films. Detailed understanding of the crystal packing modes and orientations of these structure inhomogeneities has the potential to guide the design of advanced organic electrical, optical, mechanical, or magnetic devices for the corresponding properties difference of lattice planes. The identification of the crystal packing modes and orientations of organic inhomogeneity structures is a challenging part to research community for the limitations of commonly used characterization methods. For instance, X-ray diffraction can only identify the presence of these inhomogeneity structures but cannot be used to detect the specific packing mode and orientation of each structure; STEM, the commonly used method in inorganic materials show limited performance in organic materials for the severe damage of high-energy electrons to organic materials. Here in, we report a characterization approach which provides local structure information of organic thin films over a large area.

In this talk, a low damage, organic materials compatible characterization method-lateral force microscope test will be introduced. Detailed characterization results of the crystal packing mode and orientation of a commonly used evaporation-based 2,9-Diphenyl-dinaphtho[2,3-b:2',3'-f]thieno[3,2-b]thiophene (2,9-Dph-DNTT) organic film will be showed; the two inhomogeneity structures in the film-nanosprouts structure and terrace structure are corresponding to the molecular “face on” packing mode and “face up” packing mode, respectively. The electrical performance difference of the two nanostructures will be studied by conductive atomic force microscope test. The temperature dependent formation mechanism of the two structures will also be discussed in detailed.

Apart from the properties difference, the structure inhomogeneities in organic materials also have the potential to generate other interesting phenomenon, for instance, optical memory phenomenon for the charge trapping centers induced by the lattice mismatch in the interface of the inhomogeneity structures. Non-volatile optical memory transistor (OMT) based on the nanosprouts structure of 2,9-Dph-DNTT film is developed, combining with Al₂O₃ high-k dielectric, the OMT showed low operating voltage (less than 4V) and decent field effect mobility up to 3cm²V⁻¹s⁻¹ and promising data retention performance of binary states current ratio higher than 10⁴ for more than 12hours, the mechanism of the optical-electrical memory phenomenon will be discussed in detailed. At last, a demonstration of a 16×16 flexible low operating voltage active matrix OMT array of 45ppi with image processing capability will be showed.

SESSION SB04.06: Optoelectronics II
Session Chairs: Barry Rand and Simon Rondeau-Gagne
Wednesday Afternoon, April 24, 2024
Room 435, Level 4, Summit

1:30 PM *SB04.06.01

Charge Carrier Trapping in Organic Semiconductors Paul W. Blom, Oskar Sachnik, Xiao Tan, Yungui Li and Gert-Jan Wetzelaer; Max-Planck-Institute for Polymer Research, Germany

The efficiency and stability of single-layer polymer light-emitting diodes is compromised by unbalanced charge transport, absence of triplet-exciton harvesting and low photoluminescence quantum efficiencies. Especially charge traps have a triple negative effect: they give rise to non-radiative trap-assisted recombination, they dissociate singlet excitons leading to a reduced photoluminescence quantum yield and due to confinement of the emission zone at an electrode they lower the optical outcoupling efficiency. A strategy is developed that precludes trapping in large band gap organic semiconductors. We demonstrate that using thermally activated delayed fluorescence emitters in combination with trap-free transport high external quantum efficiencies for single-layer blue OLEDs can be obtained. Our results show that OLEDs with a simplified single-layer structure can rival the efficiencies of complex multilayer stacks.

2:00 PM SB04.06.02

Using Molecular Design to Engineer Solid-State Spin Qubits in Organic Semiconductors Robert M. Jacobberger; University of Wisconsin–Madison, United States

Molecular spin qubits promise to enable breakthroughs in quantum information science due to the ability of chemistry to (1) create atomically precise structures using synthetic methodologies; (2) tailor the magnetic, optical, and electronic properties of the molecular qubits; and (3) construct large-scale ordered arrays of qubits via crystal growth and self-assembly. Here, we present our work on engineering atomically precise hierarchical systems with tunable quantum states to serve as spin qubit arrays.

First, we engineer spin qubits based on high-spin multiexcitons photogenerated in organic semiconductors using singlet fission.¹ We engineer the packing of tetracene molecules within single crystals by using tailored linking groups to demonstrate multiexcitons that exhibit promising spin qubit properties, including a coherence time, T_m , of 3 μ s at 10 K, a population lifetime, T_{pop} , of 130 μ s at 5 K, and stability even at room temperature. The single-crystal platform also enables global alignment of the spins and, consequently, individual addressability of the spin-sublevel transitions. Decoherence mechanisms, including exciton diffusion, electronic dipolar coupling, and nuclear hyperfine interactions, are elucidated, providing design principles for increasing the spin coherence lifetime and operational temperature of the multiexciton spin qubits. By dynamically decoupling the qubits from the surrounding spin bath, T_m of 10 μ s is achieved. This material system provides an exciting path to realize dense arrays of optically addressable qubits that are generated on demand at specific locations.

Second, we harness a new class of organic framework materials, known as ion-paired frameworks, to develop atomically precise arrays of molecular spin qubits.² We learn how to control the density of the paramagnetic Cu(II) porphyrin spins by engineering the linker groups and crystal growth conditions. Pulse-electron paramagnetic resonance (EPR) spectroscopy is used to probe the spin coherence of these single crystals at temperatures up to 140 K. The crystals with the longest Cu–Cu distances exhibit a spin coherence time, T_m , of 207 ns and a spin–lattice relaxation time, T_1 , of 1.8 ms at 5 K, which are records for qubits in an atomically precise molecular system. The mechanisms of spin decoherence and spin-lattice relaxation will also be discussed. Incorporating molecular electronic spin qubits in ion-paired frameworks enables control of composition, spacing, and interqubit interactions, providing a rational means to extend spin relaxation times for next-generation quantum technologies.

[1] R. M. Jacobberger, et al. *J. Am. Chem. Soc.* **144**, 2276–2283 (2022).

[2] C. M. Moisanu*, R. M. Jacobberger*, L. P. Skala*, et al. *J. Am. Chem. Soc.* **145**, 18447–18454 (2023).

2:15 PM SB04.06.03

The Photo-Hall Effect in High-Mobility Organic Semiconductors Vladimir V. Bruevich and Vitaly Podzorov; Rutgers University Physics Department, United States

High-mobility single crystal organic semiconductors are important for applications in advanced organic electronics and photonics. Photogeneration and transport of mobile photocarriers in these materials, although very important, remain underexplored. For sustained progress in the field, understanding the intrinsic (i.e., not limited by static disorder) charge transport properties of crystalline organic semiconductors is important. The Hall effect represents one of the most efficient experimental tools for assessing intrinsic charge transport, as Hall effect in single crystal materials probes band-like (i.e., delocalized) mobile charges. The photoconductivity-based *photo-Hall effect* can be used to address the fundamental charge transport properties of these functional molecular materials. Photocarrier generation by light allows circumventing the challenging problem of carrier injection from contacts (especially when measurements of both electrons and holes are pursued), avoiding carrier trapping and scattering associated with the interfacial charge transport as in OFETs, and preventing added disorder associated with chemical doping. Therefore, photo-Hall effect opens new opportunities in probing the intrinsic charge transport in organic semiconductors.

The photo-Hall measurements in pristine, ungated organic semiconductors pose an even greater challenge than the Hall measurements in OFETs or chemically doped samples, because a much lower carrier density (and, thus, much higher sample's resistances) is typically generated by light. By taking advantage of a sensitive ac-Hall methodology previously developed in our group, we have performed reliable photo-Hall effect measurements in a benchmark organic semiconductor rubrene.

We present the first clear demonstration of a photo-Hall effect in organic semiconductors, using a benchmark molecular crystal rubrene as an experimental platform. The concept of a photo-Hall effect allows probing the intrinsic transport properties of pristine semiconducting materials in stand-alone crystals, free from the problems associated with charge injection from contacts, interfacial transport, or additional disorder typically encountered in the conventional approaches based on FETs or chemically doped materials. In photo-Hall measurements, the steady-state carrier density and mobility are measured independently, with no assumptions regarding the photocarrier generation efficiency or lifetime, thus providing a direct experimental access to these important parameters. We find that under a *cw* illumination in the visible range, only mobile holes are generated in pristine rubrene crystals, leading to a substantial p-type surface photoconductivity with the hole mobility $\mu_{photo-Hall} = 11 \pm 1 \text{ cm}^2\text{V}^{-1}\text{s}^{-1}$ and the density that follows a power law $n_{photo-Hall} \propto P^\alpha$, with the power exponent $\alpha = 1/4 - 1/3$. In addition, by intentionally inhibiting the surface transport via the gauge effect, we observed a small residual bulk photocarrier density governed by a bimolecular electron-hole recombination ($\alpha = 1/2$) with a higher true-bulk hole mobility of $\mu_{photo-Hall} = 16 \pm 1 \text{ cm}^2\text{V}^{-1}\text{s}^{-1}$. These experiments significantly advance our fundamental understanding of charge transport and photoconductivity in rubrene, based on triplet exciton diffusion and surface dissociation, in which the latter process is shown to be governed by electron trapping with a release of mobile hole. Overall, our work demonstrates that the photo-Hall effect is a powerful tool for addressing the intrinsic charge transport in organic semiconductors and potentially other emergent semiconducting materials.

Reference:

Bruevich, V., Choi, H. H., Podzorov, V., The Photo-Hall Effect in High-Mobility Organic Semiconductors. *Adv. Funct. Mater.* 2021, 31, 2006178. <https://doi.org/10.1002/adfm.202006178>

2:30 PM BREAK

SESSION SB04.07: OFET II
Session Chairs: Emily Bittle and Paddy K. L. Chan
Wednesday Afternoon, April 24, 2024
Room 435, Level 4, Summit

3:30 PM *SB04.07.01

Advanced Functionalities in Organic Permeable Base Transistors Hans Kleemann, Amric Bonil and Juan Wang; Technische Universität Dresden iAPP, Germany

Vertical transistor architectures offer sub-micrometer channel dimensions and hence, high-frequency operation, without the need for advanced patterning techniques. However, while the fabrication procedures for lateral thin-film transistors matured, fabrication techniques for vertical organic transistors are less developed and as a consequence, yield, uniformity, and reliability of such devices remain poor. Furthermore, reports with vertical organic transistors addressing circuits and advanced device functionalities are rare.

For more than one decade, we have been developing organic permeable base transistors (OPBTs) – a vertical transistor structure that resembles a solid-state triode where nano-scale pinholes allow the current to pass from the emitter to the collector electrode through a control base. Starting with investigations on the fundamental device physics, we advanced the performance of these devices towards the ultra-high-frequencies region, and recently, we demonstrated the integration of complementary inverters with adjustable tripping point. In this contribution, I will discuss recent significant progress concerning device integration using large-area electrochemical anodization. In particular, using this technique, the yield of fabrication is close to 100%, allowing us to integrate circuits. Furthermore, the anodization gives us control over leakage currents, and device capacitance, and increases the tolerances against thickness variation, resulting in an excellent current gain of $>10^7$. Moreover, the anodization technique is vital for the realization of devices with advanced functionalities such as vertical memory or reconfigurable devices, opening up the perspective for the design of ultra-high-frequency application-specific circuits based on organic semiconductors.

4:00 PM *SB04.07.02

High-Speed Organic Integrated Circuits and Applications Jun Takeya^{1,2}; ¹The University of Tokyo, Japan; ²Pi-Crystal Inc., Japan

Electronic devices in the future sustainable societies require maximum function with minimum amount of constituent materials and energy cost for production. Electronic functions are often originated from two-dimensional material properties so that device components of large area and small thickness saves material consumption. The fundamental electronic functions of both analogue and digital circuits mostly rely on only a nanometer-scale thin layer at the very surface of the semiconductor material due to the very short penetration length of electric field. The presentation focuses on material bases, methods of circuit fabrication, dynamic operation of the devices, and several applications for commercialization.

Recently developed ultrathin organic semiconductor single crystalline films is suitable for large-area production with low energy consumption; the films are easily formed to large area from solution at relatively low temperature at 80 degrees centigrade [1]. Extremely thin crystal films are controllably grown to a-few molecular layers with the thickness of only 10 nm, so that material cost can be highly limited. Due to a careful material design for restricting harmful molecular vibration, very high carrier mobility more than 10 cm²/Vs is achieved. Furthermore, development of technologies for printed integrated circuits provides a manufacturable process for low-cost platforms for RFID tags and sensing circuitries. Finally, a technology for large-area light-weight display sheets will be demonstrated.

A dynamic transistor model is developed using device parameters such as channel length and overlap length of gate and source electrodes, so that high-frequency transistors are physically designed appropriately including charge-injection resistance [2]. A high cut-off frequency above 45 MHz is actually achieved which are composing elements of organic integrated circuits. Typical integrated circuits of approximately 500 transistors are formed. Moreover, a wireless power-supply is demonstrated using newly developed high-frequency organic rectifiers to operate an RFID tag with the NFC frequency [3]. Such prospect bears increasing reality because of recent research innovations in the field of material chemistry, charge transport physics, and solution processes of printable organic semiconductors. With excellent chemical and thermal stability in recently developed new materials, we are developing simple integrated devices based on CMOS using organic p-type and inorganic n-type FETs. Particularly important are new processing technologies for continuous growth of the organic single-crystalline semiconductor “wafers” from solution and for lithographical patterning of semiconductors and metal electrodes. Successful rectification and identification are demonstrated at 13.56 MHz with printed organic CMOS circuits. Future ten-meter scale large-area display also needs to be more “two-dimensional” to save materials and save energies to carry and equip on billboards.

[1] S. Watanabe, J. Takeya et al., Communications Physics 1, 37 (2018); A. Yamamura, S. Watanabe, J. Takeya et al., Sci. Adv. 4, ea05758 (2018); T. Makita, S. Kumagai, A. Kumamoto, M. Mitani, J. Tsurumi, R. Hakamatani, M. Sasaki, T. Okamoto, Y. Ikuhara, S. Watanabe, and J. Takeya, PNAS (2019).

[2] T. Sawada, A. Yamamura, M. Sasaki, K. Takahira, T. Okamoto, S. Watanabe and J. Takeya, Nat. Commun. volume 11, Article number: 4839 (2020).

[3] A. Yamamura, J. Takeya et al., Adv. Electron. Mater. 3, 1600456 (2017).

4:30 PM SB04.07.03

Reversible Switching in Capacitors and Organic Transistors Employing Dihydroazulene/Vinylheptafulvene Photochromic Switches Sten Gebel¹, Oumaima Aiboudi², Franziska Lissel², Paul W. Blom¹ and Ulrike Kraft¹; ¹Max Planck Institute for Polymer Research, Germany; ²Leibniz Institute for Polymer Research, Germany

Organic field-effect transistors (OFETs) have been shown to rival or even outperform benchmark amorphous silicon-based devices. This has stimulated research efforts to further exploit organic transistors for more complex, multifunctional devices such as photodetectors or optical memories. One possibility to introduce additional functionality into OFETs is to employ molecular switches that undergo reversible isomerization under applied stimuli, such as irradiation with specific wavelengths in the UV-Vis regime. Both photoisomers exhibit different properties, such as frontier orbital energies, dipole moment or spatial extension resulting in a reversibly switchable electronic system once incorporated into an OFET device.

Here, we present that blends of semiconducting polymers and dihydroazulene (DHA)/vinylheptafulvene (VHF) photo/thermoswitches can be employed to fabricate OFETs with light/thermo-responsive device characteristics. Irradiation with UV light results in significant alteration of the transfer characteristics, especially of the subthreshold region of the gate voltage sweep. In contrast to previous work on spiropyrans or diarylethenes, the backreaction is induced thermally and not via visible light irradiation and reproducibly yields the characteristics of the pristine devices. Applying UV light of different doses shows that the magnitude of switching directly depends on the respective UV dose, hence enabling a multi-level electronic system.

This searchable program is up-to-date as of April 15th, 2024.

We further demonstrate that DHA/VHF molecular switches can also be used to introduce stimuli-responsiveness into organic transistors by incorporating them into the gate dielectric of the device. To systematically explore this approach, we firstly focus on the evaluation of the dielectric properties of DHA/VHF blends with the dielectric polymer poly(methyl methacrylate) (PMMA) in metal-insulator-metal capacitors using impedance spectroscopy. Afterwards, these switchable dielectric blends are used as gate dielectrics in OFETs, allowing optical control of device characteristics and figures of merit such as field-effect mobility and threshold voltage.

Additionally, our results show that DHA/VHF molecular switches (unlike the established spiropyran (SP)/merocyanine (MC) photoswitch) exhibit excellent resistance to cycling fatigue when incorporated into both the semiconductor and the PMMA gate dielectric.

Bias stress experiments on transistors with DHA/VHF-PMMA and SP/MC-PMMA blend dielectrics reveal that the mechanism by which transistor performance is affected is fundamentally different for these two families of molecular switches.

4:45 PM SB04.07.04

Advanced Organic Field-Effect Transistors with pn-Heterojunction beyond Von Neumann Device Architecture [Yutaka Wakayama](#), Debdatta Panigrahi, Junko Aimi and Ryoma Hayakawa; NIMS, Japan

In this presentation, we will introduce an antiambipolar transistor (AAT) as a key element for novel electronic device to overcome the limitation of conventional von Neumann architecture. The uniqueness of AATs is ascribed to their distinctive electrical properties; sharp increase and decrease in the drain current can be observed by monotonical increase in gate bias voltage. This characteristic Λ -shaped transfer curve is realized due to a pn-heterojunction formed around the center of a transistor channel. Particularly, negative differential transconductance (NDT), where the drain current decreases against increase in gate bias voltage, is the key property to yield various functionalities. By taking advantage of this character, we have been developing a variety of novel organic electronic applications.

These kinds of innovative electronic device are particularly required in the field of organic electronics. Despite their various advantages, such as mechanical flexibility, light weight, solution processability, and cost-effectiveness, organic electronics have been recognized to have weak points in terms of integration density and data processing capability because of their incompatibility with conventional lithographic processes. Meanwhile, organic AATs appear to offer means to overcome such weaknesses, and thereby open a new frontier in the field of organic electronics.

First, the fundamental mechanism of the carrier transport is discussed in terms of the characteristic device configuration. The essential part of the AATs is the pn-heterojunction at the transistor channels; thin films of a p-type and n-type organic semiconductors are partially overlapped. These films are contacted with respective metal electrodes (source and drain electrodes) to form a pn-heterojunction transistor. The carrier transport mechanism was analyzed by original measurement techniques: operando photoemission electron microscopy (operando-PEEM) and operando Kelvin probe force microscopy (operando-KPFM). These techniques allowed us to characterize carrier transport properties in the device operation status under bias voltage. Second, the AAT applications are introduced those are multi-valued (ternary and quaternary) logic circuits and reconfigurable logic circuits. Both are advantageous to increase integration density with less device elements. Other applications are logic-in-memory and artificial synaptic device. These were realized by combining AATs and non-volatile memory effects. These novel devices have a potential to overcome the weak point of the organic electronics and limitation of conventional von Neumann type devices. Therefore, we categorize these devices as beyond von Neumann type electronic devices.

SESSION SB04.08: OMIECS

Session Chairs: Katelyn Goetz, Ian Jacobs, Hans Kleemann, Ulrike Kraft and Simon Rondeau-Gagne
Thursday Morning, April 25, 2024
Room 435, Level 4, Summit

8:30 AM *SB04.08.01

A Persistent Challenge in Organic Electronics: How Does Structure Affect Electronic Transport? [Alberto Salleo](#); Stanford University, United States

Linking microstructure to transport remains the grand challenge preventing the rational design of new organic semiconductors. Indeed overcoming this hurdle might unleash the full power of organic synthesis to make materials with “designer” properties, be they electronic, excitonic or ionic transport. We have spent years developing complementary techniques that allow us to analyze the microstructure at different length-scales and from complementary points of view. In particular, the use of XRD, TEM and IR/UV-Vis spectroscopy allows to understand order from the molecular to the device level. We use these techniques coupled with transport measurements to understand the role of intra vs. interchain order as well as mesoscale order. These techniques can be extended to mixed conductors where the electrolyte controls order and provides one more knob to study the relationship between order and transport.

9:00 AM *SB04.08.02

Electrochemical Transistors: A Platform for Exploring Carrier Transport and Ion-Carrier Correlations at High Charge Densities in Organic Semiconductors [Daniel Frisbie](#); University of Minnesota, United States

Electrochemical transistors are a powerful platform for fundamental investigations of hole and electron transport in organic semiconductors as a function of continuously tunable charge up to very large densities of order 0.1-1 carrier per molecule. There is increasing evidence that ion-charge carrier interactions are profoundly important in these devices. This talk will describe ongoing experiments to examine transport in electrochemical transistors based on single crystals and thin films of organic semiconductors. In one study, electron transport on the surface of electrolyte-gated C60 single crystals is measured as a function of cation radius in the gate electrolyte. For small cations, surface conductivity versus electron density exhibits a peak near 0.5 electron/C60. Conductivity is completely shut down at 1 electron/C60. As cation size increases, this peaked conductance behavior becomes less prominent and average electron mobility increases, indicating that cation-electron interactions at the surface of the C60 crystal play an important role. For devices gated with the largest cations, temperature dependent transport shows the gate-induced electrons are significantly delocalized. In a second experiment, transport is examined in a series of polythiophenes as a function of side-chain length. Again, a strong peak in conductance versus carrier density is observed, with the peak occurring near 0.15 hole/monomer for all of the polymers. Further, there is a marked dependence of the conductance maximum on side-chain length, with longer side chains giving higher conductances. The results are interpreted in terms of ion-carrier Coulomb interactions and the implications will be discussed.

9:30 AM SB04.08.03

In-Operando Spectroscopic Characterization of Non-Equilibrium States in a Highly Doped Polymer [Ian Jacobs](#)¹, Dionisius Hardjo Lukito Tjhe¹,

Xinglong Ren¹, Gabriele D'Avino², Tarig Mustafa¹, Thomas Marsh¹, Lu Zhang¹, Yao Fu¹, Ahmed E. Mansour³, Yuxuan Huang¹, Wenjin Zhu¹, Ahmet Hamdi Unal¹, Vincent Lemaire⁴, Claudio Quarti⁴, Jin-Kyun Lee⁵, Iain McCulloch⁶, Martin Heeney⁷, Norbert Koch³, Clare Grey¹, David Beljonne⁴, Simone Fratini² and Henning Sirringhaus¹; ¹University of Cambridge, United Kingdom; ²Centre National de la Recherche Scientifique, France; ³Humboldt-Universität zu Berlin, Germany; ⁴University of Mons, Belgium; ⁵Inha University, Korea (the Republic of); ⁶University of Oxford, United Kingdom; ⁷Imperial College London, United Kingdom

Heavily doped organic semiconductors are critical to a variety of applications, including thermoelectrics, bioelectronics, and neuromorphic computing devices. Recent advances have enabled the routine doping of polymer films to extremely high carrier densities on the order of one charge per polymer repeat unit. In this regime charge transport is comparatively poorly understood due to the non-negligible effects of electron-electron and electron-ion interactions, in addition to the ever-present role of static and transient disorder.

Here, we report on dual-gated indacenodithiophene-co-benzothiadiazole (IDTBT) organic electrochemical transistors (OECTs) and corresponding ion-exchange doped films, in which a second field-effect gate enables us to modulate the carrier density independently from the ion density. These devices show unusual behavior; at low temperatures, field effect transfer curves are highly non-linear and in many cases even ambipolar, while at high temperatures a purely linear curve is obtained. Using solid-state NMR and infrared charge modulation spectroscopy, we demonstrate that this non-linearity at low temperatures is a signature of a non-equilibrium state resulting from freeze-out of ionic motion. Under these conditions, we see an enhancement in charge delocalization, electrical conductivity, and Seebeck coefficient, pointing to a new pathway to enhanced thermoelectric performance.

9:45 AM SB04.08.04

Electrochemical Doping Induced Crystallinity in Organic Mixed Ionic/Electronic Conductors [Lucas Flagg](#) and Lee Richter; National Institute of Standards and Technology, United States

Organic mixed ionic-electronic conductors (OMIECs) are an exciting class of new materials with a range of potential applications including biosensors, electrochromics, and neuromorphic computing. These applications all require ionic transport from an electrolyte into the organic active layer during operation. Characterization of this electrolyte and ion swollen state is essential to understanding device operation on a fundamental level. However, this swollen state is particularly difficult to study because it requires development of *in-situ* techniques. Here, we utilize *in-situ* Grazing Incidence Wide Angle X-ray Scattering (GIWAXS) to study the crystallinity of the swollen state of OMIECs as a function of applied potential. We study a variety of conjugated polymer active layers and find consistent doping induced crystallinity across a variety of different polymer backbones. Interestingly, we find a maximum in the crystallinity as a function of doping level for some polymers. At moderate doping levels the crystallinity is enhanced relative to the undoped state, but then at the highest doping levels achieved the crystallinity decreases. Finally, we use organic electrochemical transistors (OECTs) to correlate the electronic conductivity with these doping induced morphological changes. These results demonstrate the importance of *in-situ* characterization to develop a better understanding organic electronic devices.

10:00 AM BREAK

10:30 AM *SB04.08.05

Tuning Mixed Ionic-Electronic Transport in PEDOT:PSS [Laure V. Kayser](#); University of Delaware, United States

Organic mixed ionic-electronic conductors (OMIECs)—conjugated polymers that can transport and capacitively store both ionic and electronic charges—are fundamental to the development of bioelectronics, energy storage, and neuromorphic computing. In organic electrochemical transistors (OECTs) in particular, OMIECs are used in the channel of the transistor to generate large currents under small voltage bias, making them attractive amplifiers for biosensing applications. While new OMIECs are regularly reported, the most commonly used material is the polyelectrolyte complex PEDOT:PSS. This material is commercially available as a dispersion in water and provides excellent performance in OECT after a variety of post-treatments. In this talk, I will share how our laboratory uses controlled radical polymerizations to precisely synthesize PSS and its derivatives towards a better understanding of structure-property relationships in PEDOT:PSS. I will also present a novel strategy to ensure that the films remain stable in water under repeated cycling operations by using an adhesion monolayer between the substrate and the PEDOT:PSS films.

11:00 AM SB04.08.06

Morphological and Structural Engineering of Conjugated Polymers for Near-Infrared Electrochromic Devices [Robert M. Pankow](#)^{1,2}, Antonio Facchetti³ and Tobin Marks²; ¹The University of Texas at El Paso, United States; ²Northwestern University, United States; ³Georgia Institute of Technology, United States

The recent device engineering and material optimization of electrochromic devices (ECDs) has enabled new frontiers beyond the original focus of smart-window applications and display devices, including: NIR-IR optical filters, energy storage, active camouflage, and broadband communication. For conjugated polymer ECDs, the highly tunable polymer structures provide numerous handles for modifying the optoelectronic and physicochemical properties facilitating efficient optical switching across the visible wavelength range (400-700 nm) and into the NIR (>750 nm). Here, we first disclose the optimization of a porous nanostructured conjugated polymer morphology enabling vertically stacked redox-active p-type and n-type polymer multilayer ECDs. Specifically, efficient oxidative electrochromic switching at lower potentials (+0.4 V versus +1.2 V with a dense top layer) or dynamic oxidative-reductive electrochromic switching is found with a multilayered ECD architecture. Next, we disclose the synergistic optimization of the CP sidechain (either branched alkyl or EG_n) and the electrolyte cation identity for a series of diketopyrrolopyrrole (DPP) and 3,4-ethylenedioxythiophene (EDOT) or glycolated bithiophene (g2T) copolymers. It was found that by fine-tuning the extent of EG_n sidechain incorporation and the identity of the electrolyte cation a 2x increase in optical contrast (from 12 to 24%) and >60x reduction in switching time (from 20 to 0.3 s) could be realized in NIR-ECDs. To elucidate the influence of the polymer morphology/microstructure on these performance metrics, atomic force microscopy (AFM) and grazing incidence wide-angle X-ray scattering (GIWAXS) were performed. These findings provide material design guidelines for the development of next-generation CPs and mixed ionic-electronic conductors.

11:15 AM SB04.08.07

Stretchable, Enhancement-Mode PEDOT:PSS Organic Electrochemical Transistors [Yan Wang](#) and Shiming Zhang; The University of Hong Kong, Hong Kong

Stretchable organic electrochemical transistors (OECTs), based on the conducting polymer poly(3,4-ethylenedioxythiophene) doped with poly(styrene sulfonate) (PEDOT: PSS), have shown significant potential in bridging the gap between microelectronic devices and the soft biological environment [1,2]. However, there has been a lack of corresponding stretchable devices that can operate in enhancement mode, which has limited the development of low-power soft integrated circuits and systems.

In our research, we present the first stretchable PEDOT: PSS OECTs that operate in enhancement mode. This achievement is made possible by the

development of two key elements: A straightforward solution-based method that efficiently removes dopants from stretchable PEDOT: PSS thin films; A two-step soft annealing process that immobilizes the de-doping agents on the transistor's channel without affecting its functionality.

Experimental results have demonstrated that the combination of these two approaches allows for the creation of robust and stretchable enhancement-mode OECTs. These devices can be stretched between 0% and 50% strain and remain functional even after repeated stretching tests. These stretchable enhancement-mode PEDOT: PSS OECTs are expected to serve as new building blocks for the development of low-power organic biosensing and bioelectronics systems.

[1]. Zhang, Shiming, et al. "Patterning of stretchable organic electrochemical transistors." *Chemistry of Materials* 29.7 (2017): 3126-3132.

[2]. Bai, Jing, et al. "Tissue-like organic electrochemical transistors." *Journal of Materials Chemistry C* 10.37 (2022): 13303-13311.

11:30 AM SB04.08.08

N-Type Semiconducting Hydrogel [Peiyun Li](#), Wenxi Sun and Ting Lei; Peking University, China

Hydrogels are an attractive category of biointerfacing materials with adjustable mechanical properties, diverse biochemical functions, and good ionic conductivity. Despite these advantages, their application in electronics has been restricted due to their lack of semiconducting properties, as they have traditionally only served as insulators or conductors. We develop single and multiple network hydrogels based on a water-soluble n-type semiconducting polymer, thereby endowing conventional hydrogels with semiconducting capabilities. These hydrogels show good electron mobilities and high on/off ratios, enabling the fabrication of complementary logic circuits and signal amplifiers with low power consumption and high gains. We demonstrate that hydrogel electronics can sense and amplify electrophysiological signals with enhanced signal-to-noise ratios. Our work could enable more optoelectronic properties and greatly expand the applications of hydrogels in bioelectronics.

SESSION SB04.09: Materials II

Session Chairs: Paddy K. L. Chan, Katelyn Goetz, Ulrike Kraft and Simon Rondeau-Gagne

Thursday Afternoon, April 25, 2024

Room 435, Level 4, Summit

1:30 PM *SB04.09.01

Semiconducting Polymers for Organic Electrochemical Transistors [Iain McCulloch](#); University of Oxford, United Kingdom

Organic electrochemical transistors (OECTs) have been shown to be promising devices for amplification of electrical signals and selective sensing of ions and biologically important molecules in an aqueous environment, and thus have potential to be utilised in bioelectronic applications. The sensitivity, selectivity and intensity of the response of this device is determined by the organic semiconducting polymer employed as the active layer. This work presents the design of new organic semiconducting materials which demonstrate good OECT performance, through operation in accumulation mode, with high transconductance and low operating voltage.

We discuss here the design, synthesis and performance of novel intrinsic semiconducting polymers for efficient accumulation mode OECT devices. Key aspects such as ion and charge transport in the bulk semiconductor and operational voltage and stability of the devices are addressed in order to elucidate important structure-property relationships. A range of new semiconducting polymers, designed to exhibit facile electrochemical doping of either holes or electrons, facilitate ion penetration and migration, as well as have aqueous compatibility are reported. Optimisation of a series of polymer parameters including electrochemical doping, charge carrier mobility and capacitance are discussed.

2:00 PM *SB04.09.02

Chiral Organic Semiconductors [Yves H. Geerts](#)^{1,2}; ¹University Libre de Bruxelles, Belgium; ²International Solvay Institutes of Physics and Chemistry, Belgium

I will report on our latest results on the design, the synthesis, and the characterization of crystalline organic semiconductors with achiral and chiral pi-systems. Chiral induced spin selectivity (CISS) effect and electrical magnetochiral anisotropy e(MChA) have been investigated in organic field effect transistors (OFETs) with these materials. [Adv. Sci. 2023, 10, 2301914]

2:30 PM *SB04.09.03

Deciphering The Difference between Flexible Chain and Hairy-Rod Polymer Semiconductors [Natalie Stingelin](#); Georgia Institute of Technology, United States

Organic electronic materials possess unique opto-electronic and processing properties that provide broad opportunities for use in light-emitting diodes, solar-energy harvesting systems, to next-generation sensors and neuromorphic computing components. These technologies have been continually improving over the past decades, aided by advancements in materials chemistry and processing innovation. State-of-the-art polymer semiconductors typically have an electron donor-acceptor (D-A) backbone structure with a number of fused ring moieties, and complex aliphatic or, e.g., ethylene-oxide side chains that decorate the backbone to provide solubility. It is important to recognize that the physical properties of the side chains are substantially different from the backbone, constituting an amphiphilic-like characteristics transverse to the backbone reminiscent of phospholipid and surfactant molecular analogs, and simple classical descriptions of amorphous vs. semicrystalline structure no longer apply. Here, we discuss how the FSC technique can be used for the identification of thermodynamic transitions of next generation D-A polymers commonly used in the organic solar cell area to obtain important structural information of this new class of materials and, in turn, establish processing guidelines towards materials of specific optical or electrical characteristics, and improved materials design for organic optoelectronic devices.

3:00 PM BREAK

SESSION SB04.10: Optoelectronics III

Session Chairs: Paddy K. L. Chan and Deepak Venkateshvaran

Thursday Afternoon, April 25, 2024
Room 435, Level 4, Summit

3:30 PM *SB04.10.01

Novel Extended Chromophores as Organic Transistor Materials [John Anthony](#); University of Kentucky, United States

The field of organic electronics benefits from the synthetic diversity of conjugated chromophores, which can be further functionalized to tune everything from optical gap to crystal packing. The ability to vary structure allows an impressive variety of related compounds to be compared, enhancing our understanding of design rules for the development of new semiconductor materials. For example, we know that two-dimensional electronic coupling is critical to high-mobility devices, as is a layered / lamellar motif for the 2D interacting layers. Design guidelines beyond that are only now emerging - such as a desire for isotropic electronic coupling within the 2D interacting layers, and functionalization that minimizes core vibration in the solid state. With these emerging notions in mind, I will present an array of new and exotic aromatic backbones and functionalization schemes designed to further explore these newer potential design guidelines, to attempt to determine their impact on performance in organic transistors. In particular, the impact of chromophore twisting / curvature on charge transport studies will be discussed.

4:00 PM *SB04.10.02

Harnessing Exciton Transitions for Sensing Devices: OLED and Transistor-Based Magnetic Field Sensors [Emily G. Bittle](#); NIST, United States

The study of excitons has advanced optoelectronic device control and efficiency. Now, there is a growing interest in harnessing the unique exciton transitions of long-lived high-binding energy excitons (HBEE) for developing new device functionality. Our research has demonstrated the feasibility of using exciton dynamics in organic light-emitting diodes (OLEDs) as magnetic field sensors in fully electronic devices¹. Additionally, wide-field optical detection of OLED output in a graded magnetic field has been demonstrated that shows the promise of sub-micron sensing using excitons². By integrating exciton properties and functionality into LEDs and other electronic devices, we envision the potential for developing screens and lighting with built-in sensing capabilities. We are actively exploring the use of transistor-based sensors to refine exciton-based measurements within electronic devices^{3,4}. The flexibility of controlling parameters in transistors, such as traps, interfaces, field, structure, etc, offers a versatile approach to enhancing exciton properties for optimal field sensing. Our ongoing work investigates material and device properties to enhance signal sensitivity, extending beyond the conventional focus on optoelectronic efficiency studies.

1 S. Engmann, E. G. Bittle and D. J. Gundlach, *ACS Appl. Electron. Mater.*, 2023, **5**, 4595–4604.

2 R. Geng, A. Mena, W. J. Pappas and D. R. McCamey, *Nat. Commun.*, 2023, **14**, 1441.

3 E. G. Bittle, S. Engmann, K. Thorley and J. Anthony, *J. Mater. Chem. C*, 2021, **9**, 11809–11814.

4 H. J. Jang, E. G. Bittle, Q. Zhang, A. J. Biacchi, C. A. Richter and D. J. Gundlach, *ACS Nano*, 2019, **13**, 616–623.

4:30 PM SB04.10.03

Characterization of Relaxation and Transport Properties of OLEDs with The Cross-Correlation Noise Spectroscopy [Andrey Rogachev](#); University of Utah, United States

The state-of-the-art cross-correlation noise spectroscopy developed in our group significantly expands the sensitivity and bandwidth of the method. This in turn has allowed to characterize electrical noise of several systems beyond the 1/f term and access various contributions related to generation-relaxation and transport processes in both phosphorescent and fluorescent OLEDs. The unique feature of the method is that the relative noise contribution of the most resistive element of the system gets strongly enhanced. We found that it can be related to the bottle-neck step in the percolative propagation across a device or to a particular interface that impedes the transport. Application the method to solar cells and its expansion to the optical domain will be also discussed in the presentation.

4:45 PM SB04.10.04

Highly Efficient Intrinsically Stretchable OLEDs from Thermally Activated Delayed Fluorescence [Cheng Zhang](#), Wei Liu and Sihong Wang; Pritzker School of Molecular Engineering, United States

Light-emitting devices are crucial for human-machine interfaces, which would function as read out displaying platform, health sensors, therapy unit, or optical neurostimulator in optogenetics. Considering the operation scenario of these devices, mechanical stretchability and electroluminescence (EL) performance are two of the key aspects of device design. To achieve stretchability, we have reported a feasible method that is copolymerizing soft chain with conjugated functional unit. To achieve decent EL performance, among current light-emitting technologies, organic light-emitting diodes (OLEDs) stand out for their high efficiency, brightness, and low working voltage. To the best of our knowledge, most of the reported stretchable OLED are based on fluorescence emitters, 1st generation of OLED emitter. This kind of emitter has relatively simple requirements since it only harvest its singlet excitons, which leads to a theoretical internal quantum efficiency (IQE) as 25%. In contrast, thermally activated delayed fluorescence (TADF) emitters, the 3rd generation of OLED emitters, are more preferred due to its organic constituents as well as a near-unit IQE. However, its complicated device structure and requirement of energy alignment make the realizing of highly efficient fully stretchable TADF devices very challenging. Here, we want to bring up with a fully stretchable OLED devices based on TADF mechanism reaching an external quantum efficiency (EQE) around 20% and crack-onset strain exceeding 120%.

SESSION SB04.11: Poster Session

Session Chairs: Paddy K. L. Chan, Katelyn Goetz, Ulrike Kraft and Simon Rondeau-Gagne

Thursday Afternoon, April 25, 2024

Flex Hall C, Level 2, Summit

5:00 PM SB04.11.01

Low-Temperature Cross-Linkable Hole Transport Materials for High-Performance Solution-Processed Quantum Dot and Organic Light-Emitting Diodes [Youngjun Hwang](#), Athithan Maheshwaran, Hyejeong Bae, Jaehyoung Park and Youngu Lee; Daegu Gyeongbuk Institute of Science and Technology (DGIST), Korea (the Republic of)

Solution-Processed Quantum Dot Diodes (QLED) and Organic Light-Emitting Diodes (OLED) have seen significant progress in recent years, offering numerous advantages in the display technologies such as enhanced color purity, brightness, and suitability for large-scale manufacturing. However, it is difficult to fabricate efficient solution-processed QLEDs and OLEDs in conventional device architectures (anode/hole injection layer (HIL)/hole transport layer (HTL)/emitting layer (EML)/electron transport layer (ETL)/cathode). The main obstacle to the fabrication of solution-processed QLEDs and OLEDs is the interface mixing/interfacial erosion of solution-based emitting materials in a small molecular HTL, degrading the performance of QLEDs and OLEDs.

Recently, various studies were conducted to develop thermal/photo cross-linkable organic molecular hole transport materials (HTMs) for efficient and stable solution-processed QLEDs and OLEDs. In particular, thermal cross-linking of organic molecular HTMs is the most promising technique for achieving efficient solution-processed QLEDs and OLEDs because it does not require the use of the photoinitiator. However, previously developed thermal cross-linkable HTMs possessed poor hole transport properties, high cross-linking temperatures, and long curing times.

To achieve efficient cross-linkable HTMs with high mobility, low cross-linking temperature, and short curing time, we designed and synthesized a series of low-temperature cross-linkable HTMs comprising dibenzofuran (DBF) and 4-divinyltriphenylamine (TPA) segments for highly efficient solution-processed QLEDs and OLEDs. The introduction of divinyl-functionalized TPA in various positions of the DBF core remarkably affected their chemical, physical, and electrochemical properties. Interestingly, cross-linked 4-(dibenzo[*b,d*]furan-3-yl)-*N,N*-bis(4-vinylphenyl)aniline (3-CDTPA) showed a deep highest occupied molecular orbital energy level (5.50 eV), excellent thermal stability (T_d , 427 °C), high hole mobility ($2.44 \times 10^{-4} \text{ cm}^2 \text{ V}^{-1} \text{ s}^{-1}$), uniform surface morphology (RMS, 0.95 nm), low cross-linking temperature (150 °C), and short curing time (30 min). Furthermore, a green QLED with 3-CDTPA as the HTL exhibited an impressively high maximum external quantum efficiency (EQE_{max}) of 18.59% with a high maximum current efficiency (CE_{max}) of 78.48 cd A^{-1} . In addition, solution-processed green OLEDs with 3-CDTPA showed excellent device performance with an EQE_{max} of 15.61%, a CE_{max} of 52.51 cd A^{-1} . To the best of our knowledge, this is the first report on green solution-processed QLEDs and phosphorescent OLEDs showing high EQE, luminescence using DBF as the core and divinyl-functionalized TPA as the cross-linked HTL. These results reveal that TPA-functionalized divinyl moieties at suitable positions in the DBF core provide a new strategy to achieve high hole mobility, low cross-linking temperature, and short curing time in solution-processed QLEDs and phosphorescent OLEDs.

5:00 PM SB04.11.02

On-Site Amplification of Neural Signals by Organic Field-Effect Transistors Yifan Guo¹ and Paddy K. L. Chan^{1,2}; ¹The University of Hong Kong, Hong Kong; ²Advanced Biomedical Instrumentation Centre, Hong Kong

In the field of brain-computer interface, the transducing elements play a pivotal role in monitoring and recording neural signals. Compared to noise-sensitive microelectrodes, the high transconductance of organic electrochemical transistors enables on-site signal amplification, leading to an enhanced signal-to-noise ratio (SNR). However, the ion exchange process restricts its capability to record high-frequency (> 1 kHz) neural signals. Although lack of direct communication with the ions in the body, organic field-effect transistors (OFETs) exhibit not only high transconductance (up to 1 mS), low sensitivity to noise (down to 1 nA), and remarkable mechanical flexibility but also high operating speed (> 10 kHz). These combined merits may broaden the potential for full-frequency brain signals recording using active electrodes.

In this study, we developed an ultra-conformal OFETs (5 μm channel length) featuring a top-gate bottom-contact structure, achieving a transconductance of 100 μS and a cut-off frequency of 10 kHz. In comparison to microelectrodes (SNR = 10 dB), the electrocorticogram signals amplified by OFETs exhibit a superior SNR (over 50 % improvement) and an enhanced temporal resolution. The pre-ictal brain signals (500 μV) associated with epilepsy are effectively monitored by our OFETs array. With proper encapsulation, the devices demonstrate excellent stability and biocompatibility. We believe that the flexible organic active electrode paves a promising path for disease prediction and high-frequency neural signals recording.

5:00 PM SB04.11.03

Allrounder Strategy of Using a Photocrosslinker for Photopatterning Transparent Silver Nanowire/PEDOT:PSS Electrodes Wanho Cho¹, BongSoo Kim¹, JeongHo Cho², InCheol Kwak², Moon Sung Kang³ and TaeHyun Kwon³; ¹Ulsan National Institute of Science and Technology, Korea (the Republic of); ²Yonsei University, Korea (the Republic of); ³Sogang University, Korea (the Republic of)

This work aims to develop transparent conductive materials for various applications such as next-generation displays, sunlight harvesting, lighting, and smart windows. These materials need to have high optical transparency, electrical conductivity, and mechanical flexibility. Additionally, they must exhibit environmental stability and be suitable for practical manufacturing processes. Silver nanowires (AgNWs) are considered promising candidates that meet these demanding requirements. AgNWs form a percolated network that offers high optical transparency and electrical conductivity. This network structure is also tolerant to mechanical deformation. Furthermore, Ag NWs can be dispersed in various solvents and applied to flexible substrates using solution-based methods.

Despite these advantages, the widespread use of AgNWs in commercial applications has been limited. One key challenge is the need for scalable processing methods to create precise and high-throughput AgNW networks that meet industrial standards. One common approach is the surface-energy-controlled transfer printing of AgNW networks onto target substrates, but this method faces challenges related to uniformity and fidelity.

Photolithography, a prominent microfabrication technology, is also considered a reliable and scalable patterning technique for AgNWs. However, traditional photolithography methods, involving pre-patterned photoresist and subsequent etching or lift-off processes, are not fully compatible with AgNW networks due to their porous nature and poor adhesion to substrates.

To address these issues, we developed a direct photopatterning method for AgNW networks. This method requires only a small amount of photocrosslinking agent (<3 wt%). A crosslinker, (oxybis(ethane-2,1-diyl))bis(oxy))bis(ethane-2,1-diyl)bis(4-azido-2,3,5,6-tetrafluorobenzoate (2Bx-4EO), was designed and synthesized to induce crosslinking between AgNWs upon ultraviolet (UV) irradiation. This crosslinking approach allows for the precise patterning of AgNWs. To further enhance the electrode characteristics of the AgNW network, poly(3,4-ethylenedioxythiophene) polystyrene sulfonate (PEDOT:PSS) was selectively coated onto the AgNW patterns. The unique roughness-assisted wetting phenomenon facilitated the deposition of PEDOT:PSS, resulting in hybrid bilayer electrodes with low roughness, high oxidation resistance, and high mechanical stability. These AgNW/PEDOT:PSS hybrid transparent electrodes were used to create various electrochemical devices. Organic electrochemical transistors (OECTs) were employed as driver transistors, and they exhibited improved performance when using the hybrid electrodes compared to pristine AgNW network electrodes. This improvement was attributed to the low contact resistance and smooth surface of the hybrid electrodes.

Furthermore, the AgNW/PEDOT:PSS hybrid electrodes were integrated into electrochromic (EC) devices, demonstrating their stability and suitability for applications involving charge transfer reactions. The devices exhibited reversible color changes and maintained their performance over numerous voltage cycles.

Finally, a seven-segment active-matrix EC display was developed by integrating seven EC cells with their own driving OECTs. This display showcased the potential of the Ag NW/PEDOT:PSS hybrid electrodes for use in more complex optoelectronic devices.

5:00 PM SB04.11.04

Mitigation of Dark Current in Organic NIR Photodetector Achieved by Controlling Trap States in The Active Layer Using The Ternary Approach Alvin Joseph, Anitha B, Akhil Alexander, Muhammed Raees A and Manoj A. Namboothiry; Indian Institute of Science Education and Research, Thiruvananthapuram, India

Effective suppression of trap states or controlling the energetic disorder in the photoactive layer is of utmost importance to mitigate the dark current in near infrared organic photodetectors (NIR OPDs).^{1, 2} Energetic disorder in the density of states distribution of the devices is determined by the nanomorphology of the active layer. A ternary approach by introducing a third component to the bulk heterojunction of a binary device is a strategic technique to control the trap density in the active layer.³ In the present study, a recently developed non-fullerene acceptor (NFA), BTP-FTh is introduced as the guest component in the host system of donor polymer PCE-10 and a narrow bandgap NFA, COTIC-4F. The performance of the ternary organic photodiodes is systematically investigated by varying the weight ratio of the NFAs and studied its effect to control the trap density and energetic disorder in the active layer. The judicious selection of the guest component simultaneously regulated the nanomorphology, which further resulted in a significant reduction in the dark current density of the optimized devices to about 3.94 nAcm⁻² at -1V. The Mott-Schottky analysis and capacitance-frequency spectroscopy studies also revealed that the dark current density suppressed due to the reduction in the trap density of state and energetic disorder in the photoactive layer of the OPDs. Moreover, the introduction of the third component in the host system synergistically improved the charge collection efficiency of the host system. Furthermore, the optimised devices exhibit fast photoresponse and good storage stability even after one month.

References

1. J. Kublitski, A. Hofacker, B. K. Boroujeni, J. Benduhn, V. C. Nikolis, C. Kaiser, D. Spoltore, H. Kleemann, A. Fischer, F. Ellinger, K. Vandewal and K. Leo, Nature Communications, 2021, 12, 551.
2. H. F. Haneef, A. M. Zeidell and O. D. Jurchescu, Journal of Materials Chemistry C, 2020, 8, 759-787.
3. Y. Zhang, G. Cai, Y. Li, Z. Zhang, T. Li, X. Zuo, X. Lu and Y. Lin, Advanced Materials, 2021, 33, 2008134.

5:00 PM SB04.11.05

Engineering The Solid-State Aggregates in Brickwork Stacks of n-Type Semiconductors by Structural Alteration: A Way to Achieve High Electron Mobility Indrajit Giri and Ratheesh K. Vijayaraghavan; IISER Kolkata, India

Recent developments in the area of solution processed ambient stable organic semiconductors (OSCs) becoming promising towards lightweight, low cost and mechanically flexible aspects towards the next-generation electronic devices. It has got immense potential for industrial applications in organic field effect transistors (OFETs), solar cells, light-emitting diodes (LED), sensors etc. Specifically, the OFETs are diversely utilized in displays, logic circuits, amplifiers etc., and therefore OSCs with high carrier mobility and good ambient stability have been robustly demanded. Since the performance of electron-transporting n-type OSC materials are lagging behind p-type OSCs, and for the industrial advancement of OFETs, p-n heterojunction and integrated circuits assembled by both types of materials, the improvement of n-type OSCs including good environment stability and high electron mobility (μ_e) is in research hotspot.

In our work, the foremost importance was given to synthetic easiness to ensure the scalability and economic utility of active layer n-type materials. Need of strong intermolecular interactions to minimize the longitudinal slip between π -stacked molecules and to reduce the lattice vibrations, special care is devoted to the molecular design strategy. Additionally, the substitution should favor effective solid-state aggregation which is crucial in achieving high carrier mobility and device stability. Substitution of planar aromatics with electronegative atoms or groups to achieve n-type materials is a known concept. But, a deep insight on the required groups and the resultant molecular packing to enable efficient charge hopping is not well addressed. There are some random design concepts and examples known with the same strategy, but a lucid approach to investigate the structural features is limited. Such additional groups should not only endorse deep LUMO to ensure efficient electron injection at low operational bias, but also potentially lead to substantial electrostatic interactions in their aggregating solids states, particularly in the brickwork stack of molecular assemblies. Here, we were able to achieve an n-type OSC with excellent dopant-free field-effect electron mobility (μ_e) as high as 1.0 cm² V⁻¹ s⁻¹, and a very high on-off current ratio ($I_{on}/I_{off} \sim 10^9$) by solution process deposition (spin coating). μ_e retained up to ~60 % upon ambient exposure for 100 h under 75 % humidity storage, indicating good ambient stability.

5:00 PM SB04.11.06

Intrinsically Stretchable Full-Color Light-Emitting Films via Elastomer Blend for Polymer Light-Emitting Diodes MinWoo Jeong¹, Jin Hyun Ma¹, Jae Seung Shin¹, Jun Su Kim¹, Guorong Ma², Tae Uk Nam¹, Phuong N. Vo¹, Kyu Ho Jung¹, Xiaodan Gu², Seong Jun Kang¹ and Jin Young Oh¹; ¹Kyung Hee University, Korea (the Republic of); ²The University of Southern Mississippi, United States

For skin-like display, intrinsically stretchable light-emitting materials are key components. However, the previously reported materials have been still restricted super yellow series materials, which could be emitting just green-like yellow lights. Therefore, three primary light-emitting materials such as red, green and blue (RGB) are necessary to develop skin-like full-color displays. Herein, we report highly stretchable three primary light-emitting films enabled by polymer blend between conventional RGB light-emitting polymer semiconductors and a non-polar elastomer (SEBS). Through nano-phase separation, these films are composed of multi-dimensional nanodomains that are interconnected in an elastomer matrix for efficient charge transport and light-emitting performance under strain. The polymer light-emitting diode (PLED) exhibited over 1,000 cd/m² luminance with low turn-on voltage (< 5 V_{on}) and the stretched blend films on rigid substrate preserved their light-emitting performance up to 100% strain even after 10,000 multiple stretching cycles.

5:00 PM SB04.11.07

Silicone-Induced Microlithography of Small-Molecule Phosphorescent Emitters for High-Resolution Micro-OLEDs Soyeon Lee¹, Hyukmin Kweon¹, Borina Ha¹, Ryungyu Lee², Seonkwon Kim³, Seunghan Lee⁴, Hyobin Ham⁵, Hayoung Lim¹, Moon-Ki Jeong⁶, Gyurim Park³, Joon Hak Oh⁶, Moon Sung Kang⁴, Youngmin You³, Jeong Ho Cho³, BongSoo Kim⁵, Hojin Lee² and Do Hwan Kim¹; ¹Hanyang University, Korea (the Republic of); ²Soongsil University, Korea (the Republic of); ³Yonsei University, Korea (the Republic of); ⁴Sogang University, Korea (the Republic of); ⁵Ulsan National Institute of Science and Technology, Korea (the Republic of); ⁶Seoul National University, Korea (the Republic of)

Organic light-emitting diodes (OLEDs) have emerged as a leading display technology, known for their exceptional color purity, rapid response time, slim design, and expanded color gamut. In the group of OLED materials, small-molecule based phosphorescent OLEDs, referred to as host-dopant systems, are favored for their superior luminous efficiency. These materials efficiently capture both singlet and triplet excitons, resulting in enhanced quantum efficiency and prolonged operational lifespans. This heightened efficiency makes phosphorescent OLEDs a preferred choice for a wide range of applications, including microdisplays for augmented reality, virtual reality, and mainstream commercial displays.

Patterning small-molecule-based phosphorescent materials conventionally rely on fine metal masks (FMM) for deposition-based techniques. Recent demonstrations have achieved resolutions up to 3,000 pixels per inch (ppi) for small-molecule OLED microdisplays using FMM. However, FMM-based approaches have inherent limitations, including shadow effects caused by factors such as vapor path, deposition angles, and mask thickness. Alternative methods like template-directed growth and inkjet printing have been explored, but they often exhibit issues related to resolution, pattern fidelity, and fabrication yield which necessitates the exploration of novel approaches to achieve high-resolution patterning.

To address these challenges, there is growing interest in utilizing reactive ion etching (RIE)-based photolithography for high-resolution patterning. RIE-based photolithography shows promise in achieving precise patterning. Nevertheless, the intrinsic limitations of small-molecule phosphorescent materials, characterized by their poor physico-chemical durability, have hindered their compatibility with RIE-based photolithography. This incompatibility leads to pattern degradation and compromises luminous properties, impeding the realization of high-resolution OLED microdisplays.

Herein, we designed a novel paradigm by incorporating silicone into phosphorescent small-molecule networks. This silicone-integrated phosphorescent organic light-emitting network (SI-phOLEN), in which silicone molecules are homogeneously crosslinked with small-molecule light-emitting materials, can effortlessly achieve ultrahigh-resolution patterns via the photolithography process without degradation of their exceptional phosphorescent emission efficiency. On the basis of the unique features of SI-phOLEN, we firstly demonstrate ultra-fine patterns of the SI-phOLEN (down to 1 μm) and high-resolution full-color RGB OLEDs corresponding to 3,000 ppi (4 μm x 5 μm anisotropic pattern). Our SI-phOLEN represents a transformative step in the pursuit of high-resolution OLED microdisplays and promises both fine patterning and improved luminescence properties. It marks a significant advance in the field of display technology, offering the potential to maximize performance and resolution to unprecedented levels.

5:00 PM SB04.11.08

Coherent Arrangement of Interfacial Surface Assembly via a Functionalized Polymer for Organic Optoelectronics [Jihyun Lim](#), Woongsik Jang and Dong Hwan Wang; Chung-Ang University, Korea (the Republic of)

Organic semiconductors are promising next-generation materials for various electronic applications such as light-emitting diodes, thin-film transistors, thermoelectric devices, energy harvesting, and light sensing due to their light weight and versatility. Recently, non-fullerene acceptor materials, especially Y6, have attracted much attention in organic photovoltaics due to their excellent optoelectronic properties that lead to high reproducibility performance.[1] In the related research, we successfully achieved a favorable molecular orientation for charge transport by using a functionalized polymer process instead of the spin-coating process, which had been a barrier to the fabrication and modularization of large-area devices based on the PM6:Y6 active layer.[2,3] This was demonstrated through simulations based on the wetting coefficient of the surface, validating a high reproducibility range. Furthermore, by adjusting the alkyl groups of Y6, we developed an environmentally friendly organic photodetector (OPD) with excellent detectivity based on Y6-BO material, which enhances eco-compatible solvent solubility.[4] Additionally, through facile surface treatment of the electron transport layer (ETL), we confirmed the effective suppression of deep hole injection barriers and trap density, resulting in effective dark current suppression in the photodetector.[5] Also, we verified the enhancement of performance in optoelectronic devices through interfacial control of the ETL even in a conventional device structure. In particular, n-type perylene diimide (NPDI) has been widely utilized as an interlayer between the active layer and the cathode in optoelectronic devices due to its work-function tunability and excellent charge mobility. However, because it is a two-dimensional planar small molecule, NPDI exhibits strong self-assembly leading to undesirable molecular aggregation, thus raising the risk of an insufficient coverage of the entire surface of the active layer, resulting in a higher leakage current. To improve the performance and stability of organic electronics, this aggregation of NPDI can be solved through effective interfacial engineering. In this research, well uniformed dry-printing nanotechnology was developed for the first time to produce a coherent arrangement of NPDI layer. We successfully controlled the film formation rate by employing the alcohol-based solvent 2,2,2-trifluoroethanol. Our proposed printing process used a functionalized polymer delamination substrate for the facile fabrication of a coherent arrangement of NPDI layer.[6] The use of a coherent arrangement of NPDI in organic optoelectronic devices enabled the flat and uniform coverage of the active layer, thus suppressing the leakage current when the generated charge carriers migrated towards the cathode. The coherent arrangement of NPDI layer significantly increased the charge mobility and effectively suppressed the trap density at the interface, effectively suppressed the dark current of the modified NPDI-based OPD and significantly enhanced the detectivity. Therefore, the coherent arrangement of NPDI is a process that facilitates the formation of high-quality thin films at the interface, leading to the enhanced stability of the optoelectronic devices.

[1] R. Yu, G. Wu, & Z. A. Tan, *J. Energy Chem.*, 2021, 61, 29-46.

[2] M. S. Kim, W. Jang, T. Q. Nguyen, D. H. Wang, *Adv. Funct. Mater.*, 2021, 31(38), 2170278.

[3] J. Lim, M. S. Kim, W. Jang, D. H. Wang, *ACS Sustain. Chem. Eng.*, 2023, 11, 625–637

[4] Hong, L., Yao, H., Wu, Z., Cui, Y., Zhang, T., Xu, Y., ... & Hou, J., *Adv. Mater.*, 2019, 31, 1903441

[5] J. Lim, W. Jang, J. Lee, J. Y. Chun, D. H. Wang, *Inorg. Chem. Front.*, 2023, 10, 2995-3006

[6] M. S. Kim, J. Lim, W. Jang, D. H. Wang, *Carbon Energy* (Accepted)

5:00 PM SB04.11.09

Identity of T* Matters! Improved k_{rISC} by Modulating Locally Excited Triplet State in TADF Emitters [Madalasa Mondal](#) and Ratheesh K. Vijayaraghavan; IISER Kolkata, India

Abstract:

Effective triplet exciton utilization efficiency is an essential factor for constructing low-power operational OLED devices with high luminescence efficiency and durability. Thermally activated delayed fluorescence assists this 100% triplet harvesting by converting dark triplet excitons into radiative singlet excitons via a reverse intersystem crossing process. The enhancement of this rISC rate (k_{rISC}) is primarily realized by the low energy offset between lowest S & T states; to pursue an extremely large k_{rISC} , the involvement of high energy locally excited triplet states has become a hot topic in TADF-OLED research in present days. However, the regulation of the ^3LE states to match precisely with the ^1CT energy level by suitable molecular design is still under progress.

Here, we demonstrated an effective electronic coupling between ^1CT & ^3LE or hybridized triplet state in a series of newly designed and synthesized TADF emitters with strongly twisted D-A structure. The detailed theoretical and experimental investigation reveals that the addition of peripheral donor units to the core D-A backbone incorporates multiple triplet excited states of locally excited or hybridized nature between S_1 and T_1 states, and the close alignment of ^1CT & ^3LE states accelerates the spin-flip process and the sizeable radiative rate results in suppressed efficiency roll off with short (ns) delayed lifetime. On the contrary, the isoenergetic alignment of ^1CT and ^3CT states realized due to the near orthogonal structure promotes the rISC mechanism. Our work highlights the pivotal role of the electronic nature of the intermediate triplet states in controlling the k_{rISC} ; a thorough photophysical investigation was also performed by manipulating ^3LE states by introducing variable donor units to the D-A backbone.

5:00 PM SB04.11.10

Investigating The Mechanisms of Nucleation and Growth of [1]Benzothieno[3,2-*b*] Benzothiophene (BTBT) and its Derivatives Using Molecular Dynamics Simulations [Sashen Ruhunage](#), Chamikara D. Karunasena and Chad Risko; University of Kentucky, United States

[1]benzothieno[3,2-*b*] benzothiophene (BTBT) and its derivatives are of interest as the building blocks of organic semiconductors (OSC) for thin-film transistors. OSC charge-carrier mobility is influenced by the crystallinity and the molecular arrangements of molecules in their crystal lattice. To understand relationships between molecular structure and solvents used to process OSC, we investigate the nucleation and growth mechanisms of BTBT and its derivatives using constant chemical potential molecular dynamics (C μ MD) simulations. We explore how concentration, solvent choice, and temperature affect the nucleation and growth of crystals along different crystallographic (template) planes, then quantify and analyze atomistic-scale thermodynamic and kinetic properties of crystallization. Our goal is to provide atomic-scale insights that can be used as guides for OSC design and processing.

5:00 PM SB04.11.11

Enhancing Integrated Circuit Properties through Engineering Backbone Alignment of Conjugated Polymers [Jinseok Yoon](#), Nakhee Kang, Chae

Won Kim, Keon Joo Park, Sam Nyung Yi, Hyung Soo Ahn, Kyoung Hwa Kim and Young Tea Chun; Korea Maritime and Ocean University, Korea (the Republic of)

In recent years, there has been a growing fascination with polymer materials due to their lightweight and flexible properties. Furthermore, their highly cost-effective manufacturing processes, which employ simple solution methods, have significantly contributed to their surging popularity. Specifically, conjugated polymers of this nature have been widely utilized in various fields like transistors, logic circuits, and sensors, mainly owing to their scalability and affordability. However, it is widely recognized that polymer materials face numerous challenges in terms of their inferior performance compared to inorganic materials.[1] Consequently, extensive research is currently underway to bridge this gap and improve their overall properties. One of the key challenges in manufacturing a logic circuit with polymer is to achieve selectivity in coating a specific conjugated polymer on the target area. Different properties of various conjugated polymer semiconductor materials result in imbalanced operating characteristics of the integrated circuit, and this discrepancy is hard to eliminate. This is an issue that needs to be addressed in CMOS circuits based on conjugated polymers.[2] This study presents a simple method to align polymer chains in a desired direction, resulting in controlled orientation of polymers, confirmed by UV-Vis spectroscopy and polarized optical microscopy. In contrast, conventional spin-coating techniques show random carbon backbones tangled in various directions. Comparative analysis between transistors fabricated using the proposed method and those made using spin-coating shows higher mobility and on/off ratios in the former. Furthermore, the use of n-type and p-type conjugated polymer semiconductor materials in logic circuitry fabrication achieved superior region selectivity, high mobility, and on/off ratios, leading to enhanced gain values and noise margins. These findings highlight the potential of conjugated polymer backbone engineering in overcoming semiconductor performance imbalances without changing the geometric structure of components, thus enabling the design of simple symmetric logic circuits. This research provides a promising approach for applying organic semiconductors in various electronic devices.

Keywords: Conjugated polymers, Integrated circuits, Organic electronics, backbone engineering

Acknowledgement : This work was supported by the Basic Science Research Program through the National Research Foundation of Korea (NRF) funded by the Ministry of Science, ICT & Future Planning (NRF-2022R1C1C1006036). Also, this research was partially supported by Korea Institute for Advancement of Technology (KIAT) grant funded by the Korea Government (MOTIE) (P0012451, The Competency Development Program for Industry Specialist).

Reference

- [1] Yao, Y., Huang, W., Chen, J., Wang, G., Chen, H., Zhuang, X., Ying, Y., Ping, J., Marks, T. J., & Facchetti, A. (2021). Flexible complementary circuits operating at sub-0.5 V via hybrid organic-inorganic electrolyte-gated transistors. *Proceedings of the National Academy of Sciences of the United States of America*, 118(44).
- [2] Liao, C., Zhang, M., Yao, M. Y., Hua, T., Li, L., & Yan, F. (2015). Flexible Organic Electronics in Biology: Materials and Devices. In *Advanced Materials* (Vol. 27, Issue 46).

5:00 PM SB04.11.12

Skin-Conformable Electrophysiological Sensor Devices with Tailored Negative Poisson's Ratio Hyun Seok Kang¹, Yung Lee¹, Sumin Kim², Jang-ung Park² and Byeong-Soo Bae¹; ¹Korea Advanced Institute of Science and Technology, Korea (the Republic of); ²Yonsei University, Korea (the Republic of)

Electrophysiological sensing is a crucial functionality that provides valuable information in clinical diagnosis and treatment. Recent advances in wearable electronics enabled tracking electrophysiological information such as electrocardiogram (ECG) in a daily basis.[1] However, conventional elastomer substrate-based devices suffer from the lack of long-term adhesion and conformability to human skin due to Poisson's ratio mismatch. To address these limitations, the Poisson's ratio (PR) of the devices should match with human skin, especially in the vicinity of joint areas which have negative Poisson's ratio. One approach to achieve negative PR is to utilize auxetic mechanical metamaterials with negative PR as device substrates.

In this study, we demonstrate electrophysiology devices with enhanced skin conformability, consisting of seamless auxetic substrates and printed liquid metal electrodes. To achieve a highly conformal contact, we analyze the PR of the human wrist skin directly, using 3D digital image correlation (DIC) method. Through this information, the devices are tailored to match the PR of the human skin. The negative PR of the device is achieved by the auxetic structured glass-fabric reinforced substrate with optimized geometric parameters. Also, a soft elastomer with extreme modulus difference with the glass-fabric reinforced film fills the perforations of the auxetic structure to form a continuous surface. [2] Utilizing the advantage of the seamless surface, we employ high precision 3D printing technique to fabricate liquid metal-based electrocardiogram (ECG) sensors and electro-tactile stimulators with simple configurations.

The liquid metal electrodes maintain their conductivity during up to 30% of stretching and 100 times of repeated stretching. The resulting devices exhibit increased sensitivity and stability even under dynamic motion of the wrist thanks to their enhanced adhesion and conformability compared to pristine elastomer substrates. Precisely, the ECG sensors maintain signal to noise ratio of over 20 dB after 30 times of wrist bending, while pristine PDMS-based sensors showed degradation to 13 dB. Moreover, the electro-tactile stimulators showed high consistency of perceived sensation for 6 stimulated perception levels, even stable under bending.

[1] Ha M. et al., *J. Mater. Chem. B*, 2018, 6,24: 4043-4064.

[2] Kim M. S. et al., *Adv. Funct. Mater.* 2023, 33, 2208792

[3] Park Y.-G. et al., *Sci. Adv.* 5, eaaw2844 (2019)

5:00 PM SB04.11.13

The Host-Guest Interaction Effect in all Organic Room Temperature Phosphorescence Light-Emitting Electrochemical Cells Hee Jung Kim and Eunyoung Kim; Yonsei University, Korea (the Republic of)

A series of metal-free dyes, rooted in bromofluorene (BrFX) were synthesized to harness phosphorescence at room temperature within amorphous films and light-emitting devices (LECs). By incorporating aliphatic and aromatic side groups onto the bromofluorene structure, we achieved substantial control over the resulting color and fine-tuned the intensity of the room temperature phosphorescence (RTP). Our selection of host materials, including 3,3'-di(9H-carbazol-9-yl)-1,1'-biphenyl and poly(9-vinyl carbazole) was guided by their energy bandgap and their ability to facilitate energy transfer to BrFX, with the aim of achieving high electrophosphorescence in BrFX, with the aim of achieving high electrophosphorescence in BrFX based LECs. The intensity of the electrophosphorescence was strongly reliant on the chosen host. In-depth investigations employing theoretical computations based on density functional theory, infrared studies, and single crystal X-ray diffraction unveiled the crucial nature of the interaction between the host's ring structure and the guest material in influencing electrophosphorescence. This study sheds light on the impact of host-guest interactions and the role of energy transfer within the host material in enabling room temperature phosphorescence in a device.

5:00 PM SB04.11.14

Metal Nanoclusters as an Interfacial Modifier in Organic Solar Cells Yousuf Alishan^{1,2}, Alvin Joseph¹, Anitha B¹, Aparna R.K¹, Ranjini Sarkar², Sudip Chakraborty³, Sukhendu Mandal¹ and Manoj A. Namboothiri¹; ¹Indian Institute of Science Education and Research Thiruvananthapuram, India; ²Indian Institute of Technology-Madras (IIT Madras), India; ³Harish-Chandra Research Institute (HRI) Allahabad, India

Novel and diverse strategies are constantly under development to boost the efficiency and stability of organic solar cells (OSCs). Interface engineering involving various functional materials is currently a research focus because of its promising potential to enhance the device performance of OSCs¹⁻³. Atomically precise metal nanoclusters, with tunable properties and notable dipole moments resulting from surface ligand interactions that provide stability to the nanoclusters, can be a promising candidate as an interfacial modifier.^{4,5} Copper nanoclusters (Cu NCs), synthesized by a one-pot synthesis method, are shown to exhibit dipole moment and can cause work function modification on a surface. The novel approach of introducing Cu NCs as an interfacial modifier between the electron transporting layer and the active layer has yielded improved photovoltaic performance in both fullerene and non-fullerene based OSCs (PTB7-Th:PC₇₁BM and PM6:Y6 based OSCs). On insertion of Cu NCs, the best power conversion efficiency (PCE) obtained for the non-fullerene based system is 15.83% compared to that of 14.22% for the control device while the PCE enhanced from 7.79% to 8.62% for the fullerene based system. The interface modification has resulted in reduced recombination losses and charge accumulation at the interfaces. Impedance and transient measurements have also revealed efficient extraction of photogenerated charge carriers in Cu NC incorporated devices. The improved performance in Cu NC interfaced devices is attributed to work function modification, enabling reduced energy barrier and enhanced charge collection. Moreover, The Cu incorporated devices exhibit better operational stability under MPP tracking than the control device. This work demonstrates the potential of a new class of materials for interface modification and enhancing the performance of OSCs.

References

1. D. Luo, W. Jang, D. D. Babu, M. S. Kim, D. H. Wang and A. K. K. Kyaw, *Journal of Materials Chemistry A*, 2022, 10, 3255-3295.
2. L. Tian, Q. Xue, Z. Hu and F. Huang, *Organic Electronics*, 2021, 93, 106141.
3. H. Tang, Y. Bai, H. Zhao, X. Qin, Z. Hu, C. Zhou, F. Huang and Y. Cao, *Advanced Materials*, 2023, n/a, 2212236.
4. X. Liu and D. Astruc, *Coordination Chemistry Reviews*, 2018, 359, 112-126.
5. Y. Zeng, S. Havenridge, M. Gharib, A. Baksi, K. L. D. M. Weerawardene, A. R. Zieffuß, C. Strelow, C. Rehbock, A. Mews, S. Barcikowski, M. M. Kappes, W. J. Parak, C. M. Aikens and I. Chakraborty, *Journal of the American Chemical Society*, 2021, 143, 9405-9414.

5:00 PM SB04.11.15

Thienoacene-Based Host Material for Near-Infrared OLED with High Efficiency Yasuharu Ujiie, Yuki Maeda, Chiaki Takahashi, Mari Ichimura and Yoshio Goto; Sony Semiconductor Solutions Corporation, Japan

A wide variety of organic thin-film devices have been investigated, including light-emitting diodes, photodiodes, transistors, memories and so on. One of the advantages of organic thin-film devices is that elements with various functions can be freely and finely arranged on a single substrate by using vapor deposition and/or coating methods. This capacity in device design will contribute to the evolution of electronic devices, lower costs of products and reduce environmental loads in manufacturing. Our particular interest is in the devices with OLEDs and organic photodiode elements on the same substrate, which can be applied to biometric identification, vital sensing, touchless sensors and so on. While OLEDs and organic solar cells for visible light have been well investigated, there still remain potentials in improvement of the near-infrared OLEDs[1][2][3].

We focused on the intermolecular interactions between organic semiconductors to achieve high luminous efficiency at low voltage drive for near-infrared OLED. In this study, we developed a new naphthodithiophene derivative (NDT) which is expected to show moderate intermolecular interactions in the film. NDT was introduced in near-infrared OLEDs as the host material in its emission layer with the near-infrared dopant 1 vol% of Pt(TPBP)[4] that has an emission peak at 770 nm. Compared to the reference of the DMFL-CBP[5] that is reported to form fine amorphous thin films, the near-infrared OLED with NDT showed 1.5 times higher EQE and 1.1 V lower driving voltage at 10 mA/cm². As a result, the luminous power efficiency became 1.8 times higher, which is very important in terms of the power consumption of electronic devices. In this contribution, we present the synthesis and characterization of NDT, followed by the fabrication and evaluation results of near-infrared OLED elements.

[1] Andrea Zampetti, Alessandro Minotto, and Franco Cacialli, *Adv. Funct. Mater.* **2019**, 29, 1807623 [2] Yuxin Xiao, Hailan Wang, Zongliang Xie, Mingyao Shen, Rongjuan Huang, Yuchen Miao, Guanyu Liu, Tao Yu, and Wei Huang, *Chem. Sci.* **2022**, 13, 8906–8923 [3] Hae Un Kim, Taehyun Kim, Chanhyuk Kim, Minjun Kim, and Taiho Park, *Adv. Funct. Mater.* **2023**, 33, 2208082 [4] Yiru Sun, Carsten Borek, Kenneth Hanson, Peter I. Djurovich, Mark E. Thompson, Jason Brooks, Julie J. Brown, and Stephen R. Forrest, *Appl. Phys. Lett.* **2007**, 444, 213503 [5] Yasuyuki Gotou, Yuko Kobashi, Mitsuharu Noto and Masanao Era, *Mol. Cryst. Liq. Cryst.* **2006**, 444, 185–190

5:00 PM SB04.11.16

Doping and Interlayer Engineering for High-Performance Filterless Blue Organic Photodetectors Tianyi Zhang, Louis C. Winkler, Jakob Wolansky, Jonas Schröder, Karl Leo and Johannes Benduhn; Dresden Integrated Center for Applied Physics and Photonic Materials (IAPP) and Institute of Applied Physics, Technische Universität Dresden, Germany

Red, green, and blue (RGB) sensing units form the foundation of image applications. To obtain color discrimination, commercial RGB sensors usually incorporate expensive optical filters, which also compromise the incident light intensity. Here, we elegantly demonstrate a fully thermal-evaporated filterless blue organic photodetector (OPD) based on exploring the dual role of the hole-transporting layer (HTL). Adopting Rubrene and C₆₀ as the photoactive components, HTLs of our choice effectively quench short wavelength absorption to yield narrowband features. They also serve as charge-blocking layers to suppress dark current injection. By introducing a MoO₃-doped underlayer, the OPD achieves high external quantum efficiency (EQE) up to 50 % at 0 V while maintaining narrowband features in thin-film devices. This strategy boosts the EQE by 53% compared to the undoped sample. Such enhancement results from higher charge dissociation and extraction enabled by doping. However, the device with an intrinsic underlayer in planar junction configuration, sandwiched between efficient hole and electron blocking layers, achieves an ultralow dark current density (2.46×10⁻¹² A/cm² at -0.1 V). It has a calculated specific detectivity (D^*) reaching a record-high value of 6.35×10¹⁴ Jones at zero bias, outperforming commercial silicon photodetectors, and an ultrahigh linear dynamic range of 205 dB. Our work highlights the versatility of doping and interlayer in realizing high-sensitivity narrowband organic photodetectors in the visible spectral region.

5:00 PM SB04.11.17

Wearable Respirometer for Pulmonary Disease Prediction Anand Babu¹, Isabelle Dufour² and Damien Thuau³; ¹Institute of Nano Science and Technology, India; ²Université de Bordeaux, France; ³Bordeaux INP, France

Breathing is a multifaceted indicator of health and performance, with pivotal parameters including tidal volume, inspiratory capacity, and forced expiratory volume crucial for healthcare assessment and disease detection. However, real-time, accurate, and continuous monitoring of these parameters is hindered by the limitations of cumbersome instruments. In response, this research introduces an innovative approach to estimate these critical parameters and predict associated diseases. Our method leverages descriptors extracted from breathing signals captured non-invasively via a wearable organic piezoelectric electronic patch, eliminating the need for invasive procedures. The wearable respirometer boasts impressive features, such as high sensitivity, with an

exceptional signal-to-noise ratio, and a low limit of detection.

To achieve precise and robust disease predictions, we conducted an extensive examination of various machine learning algorithms. Among these, gradient boosting regression emerged as the most suitable choice for predicting Chronic Obstructive Pulmonary Disease (COPD). Notably, our method achieved an accuracy of over 94% in predicting different COPD diseases. This research opens new avenues for continuous, real-time monitoring and early disease detection, addressing a critical need in healthcare and paving the way for improved patient outcomes.

5:00 PM SB04.11.18

Effects of Coffee Grounds in Modified Natural Rubber Thin Film on Resistive Switching Memory Characteristics Muhammad Awais¹, Nadras Othman¹, Mohamad Danial Shafiq¹, Feng Zhao² and Kuan Yew Cheong¹; ¹University Sains Malaysia, Malaysia; ²Washington State University, United States

Modified natural rubber thin film as a sustainable and green material for next generation resistive-switching memory application has been investigated. The natural rubber latex (poly 1,4-cis-isoprene) was formulated, modified, and processed with the additional of coffee grounds to form into a thin film with the objective of enhancing the resistive switching memory characteristics. With an optimum weight percentage of coffee grounds incorporated in the natural rubber, ON/OFF ratio and stability/endurance of the memory test structure have been improvement. Reason of the improvement is correlated to the chemical functional groups established between the coffee grounds and natural rubber as well as the intrinsic chemical property of the coffee grounds. With this evidence, a possible resistive switching mechanism based on this material system has been proposed.

5:00 PM SB04.11.19

Metal-Dielectric Photonic Crystal Organic Light Emitting Diodes Matthew S. White¹, David Allemeier^{1,2}, Khadga Thakuri¹ and Thomas Cleary¹; ¹University of Vermont, United States; ²Boston University, United States

A periodic array of stacked microcavity organic light emitting diodes (OLEDs) creates a photonic crystal comprising alternating metal and dielectric layers, a metal-dielectric photonic crystal (MDPC). In these MDPC-OLEDs, the semitransparent metals layers serve dual function as both mirrors and either the anode or cathode in the OLED device enabling simultaneous electroluminescence from each unit cell. The angle-resolved electroluminescence spectra of the MDPC-OLED reflects the photonic dispersion of the crystal with rich, energy, momentum, and polarization dependent behavior depending on the physical geometry of the crystal and the optical properties of the constituent materials. The number of states in the band, the bandwidth, and mid-band Peierls distortion can be controlled by varying the physical dimensions of the crystal through additive manufacturing. Linewidths of the photonic states are reduced by improving the optical symmetry of the unit cell. Crystal defects can be included to introduce mid-gap photonic states. These properties are modeled using a computational transfer matrix simulation and experimentally verified. Lastly, we develop an analytical model based on coupled mode theory and quasi-normal mode theory to determine the relationship between optical constants (index of refraction and extinction coefficient) of the metal and organic layers to the resulting photonic band structure.

5:00 PM SB04.11.20

pH-Dependent Electrochemical Doping of an n-Type Conjugated Ladder Polymer Duyen Tran, Sarah West and Samson A. Jenekhe; University of Washington, United States

The rise of electrochemistry-enabled applications of conducting polymers, including organic electrochemical transistors, batteries/supercapacitors, and electrocatalysis, has prompted the needs for new n-type π -conjugated polymers with rugged stability, robust redox reversibility, and high charge storage capacity. However, insights regarding the structure-property relationships, the nature of charge carriers, and how they are formed in n-doped conducting polymers remain scarce. In this talk, I will discuss how we leverage pH-dependent electrochemical doping of a model n-type π -conjugated ladder polymer to systematically map out the formation of different types of polaronic species. We found that the model conjugated polymer could exhibit one to three acid-based coupled redox reactions depending on the pH. By means of *in-operando* optical, electrical, and structural characterization techniques, we show that singlet polarons are the dominant species in lightly to moderately doped polymer films, whereas other charge carriers are found in heavily doped polymer films. Our findings provide new fundamental insights on the nature of charge carriers and their formation dynamics in n-doped conducting polymers that could be broadly applicable to various electrochemistry-driven device applications.

5:00 PM SB04.11.21

UV-Activated Cyclisation of Luminescent Organic Molecules: Correlating and Tuning Structural and Optical Properties Arya Karappilly Rajan, Pravien Rajaram, Ryan D. Baxter and Sayantani Ghosh; University of California, Merced, United States

Luminescent organic molecules (LOMs) combine the photo-induced charge carrier generation and recombination of inorganic semiconductors with the lightweight and easy fabrication techniques common to organic materials. Hence, they offer the potential to be used in various applications, including the development of inexpensive, flexible, and tunable organic electronic and optoelectronic devices, such as organic light emitting diodes (LEDs), solar cells, chemical and biochemical sensors, field-effect transistors, and nonlinear optical media for lasing applications, as cost-effective alternatives to inorganic semiconductors.

This project focuses on correlating the structural and functional properties of a novel class of benzoyl pyrazinium molecules, which undergo ultraviolet (UV) light induced cyclization reaction. Spectroscopic and NMR characterization of these molecules indicate changes to both electronic and structural properties before and after cyclization. The optical properties of these molecules can be controlled by tuning the chemical structure, their concentration and their interaction with surrounding materials. As the molecules were exposed to UV light, the corresponding cyclized products were seen to exhibit strong emission in the visible, with higher emission intensity observed at lower concentrations. Strong emission in solid state was also observed in drop-casted thin films of the molecules dispersed in PVA. The high emissivity at lower concentrations implies that these molecules can have great potential for applications in solar concentrators where the molecules can serve as fluorophores and help in minimizing losses due to self-absorption.

Funding:

This work was supported with funding from: NSF-CREST: Center for Cellular and Biomolecular Machines at UC Merced (NSF-HRD-1547848)

5:00 PM SB04.11.22

Magneto-Electroluminescence Responses mediated by Magneto-Conductance in Polymer and Thermally Activated Delayed Fluorescence Emitter-Based Light Emitting Diodes Tzung-Fang Guo¹, Anas Mujahid¹, Yi-Ting Lee², Yulin Lin¹, Chih-Ting Li¹ and Wei-Cheng Liu¹; ¹National Cheng Kung University, Taiwan; ²Soochow University, Taiwan

We characterize the magneto-electroluminescence (MEL) responses of polymer and thermally activated delayed fluorescence emitter-based light-emitting diodes (PLEDs and TADF LEDs) under constant voltage and current regimes to elucidate that the current as regulated by magneto-conductance (MC) mediate MEL of devices. Through the analytical fitting of MC and MEL curves, we disclose that MC (as interpreted by the polar pairs model) partially

involves the changes in the curve features, magnitudes, shapes, etc. of MEL responses. We observe a sharp W-shape curve feature in the MEL response of the TADF LED under the electric bias at the low magnetic field regime in our study. This result should be attributed to the mediation of the MEL by the negative MC response due to the unbalanced carrier dynamics of the device. While the carrier dynamics were balanced, the specific feature of the sharp W-shape curve disappeared. Our work clearly depicts an accurate analysis of MEL with MC response based on the polaron pairs model for studying the insight dynamics of the light-emitting LEDs and that the assessment of MEL is reliable if conduct the measurement at the constant current regime.

5:00 PM SB04.11.24

Thermal Conductivity Switch due to Topochemical Polymerization of Organic Material Sara Makarem¹, Amalie Attasi², Shannon Yee², James Ponder², Brian M. Foley³ and Patrick E. Hopkins¹; ¹The University of Virginia, United States; ²Georgia Institute of Technology, United States; ³Laser Thermal, United States

A material that exhibits significant change in thermal conductivity due to external stimuli can be used as a thermal switch and can allow the active control of heat flow. These materials are of high importance in various thermal management applications such as refrigeration and waste heat recovery. Due to their sensitivity to external stimuli, organic materials are considered as a promising class of materials in this regard. This study shows a potential thermal switching mechanism due to topochemical polymerization of [2,2'-bi-1H-indene]-1,1'-dione-3,3'-diheptylcarboxylate (BIT-Hep₂). The forward polymerization reaction of BIT-Hep₂ monomer to polymer, P(BIT-Hep₂), occurs when exposed to light. Since polymerization alters the interchain interactions, breaking and reforming of bonds between repeat units can affect the thermal conductivity. This study examines how changes in bond order affects the microscopic thermal conductivity. The thermal conductivities of these samples are measured using time domain thermoreflectance (TDTR). TDTR is a transient, non-contact, optical thermometry technique that utilizes a pump-probe experimental configuration. In addition, steady-state thermoreflectance (SSTR) technique was used to compose a map of thermal conductivity as a function of spatial coordinate for individual monomer and polymer crystallites. The complementary characterizations of these samples confirms that the topochemical polymerization of BIT-Hep₂ to P(BIT-Hep₂) changes the bond order which affects the planarity of the repeat unit. Thus, the decrease in thermal conductivity due to this topochemical polymerization is likely due to a greater extent of disorder present in P(BIT-Hep₂). This study finds that the thermal conductivity within the crystallites differs significantly and reports the average values of 0.478±0.065 W/m/K and 0.110 ±0.060 W/m/K for the monomer and polymer, respectively.

5:00 PM SB04.11.25

Enabling Polymer Single Crystal to be High Performance Dielectric Min Chen¹, Wee-Liat Ong¹, Boyu Peng¹, Xuyun Guo², Jie Ren¹, Ye Zhu² and Hanying Li¹; ¹Zhejiang University, China; ²The Hong Kong Polytechnic University, Hong Kong

Polymer dielectrics hold great potential for electrical power applications and advanced microelectronics. Unfortunately, they exist commonly in semicrystalline form with disordered aggregating microstructures, such as amorphous regions, that limit their dielectric performances, including breakdown strength, dielectric loss, and temperature stability. Efforts to improve their performances are often hindered by the lack of understanding of the diverse dielectric properties in the complex structures of these semicrystalline polymer dielectrics (SPDs). Circumventing these gaps in knowledge by crystallizing homogeneously-ordered SPDs to remove these disorders has yielded little success to date. Here, taking a typical and widely used dielectric, polyethylene (PE) as a model, big homogeneously-ordered SPDs as lamellar single crystals are successfully crystallized and studied for their dielectric properties. We obtain high-quality PE single crystals by controlling the crystallization kinetics in a self-seeding method. Nanoscale MIM capacitors built on these crystals using a non-destructive strategy exhibit a high dielectric breakdown strength and low dielectric constant, with the measured values among the best-known for PE. By exemplifying a crystallization strategy for the ordered SPDs and elucidating the origins of their outstanding dielectric properties, this work illuminates a path for deepening the fundamental understanding and enhancing the electrical performance of SPDs.

5:00 PM SB04.11.26

Spatiotemporally Controllable Electrical Stimulator via Independent Photobending and Upconversion Photoluminescence Using Two Different Wavelengths of Near-Infrared/Visible Light as Dual Stimuli Jiyeon Lee, Dongjun Kim, Jaehyeok Ryu and Jiwon Kim; Yonsei University, Korea (the Republic of)

Multistimuli responsive materials are advantageous in that they can enhance the desired response or bypass unwanted reactions. Light is one of the most attractive stimuli since it allows remote spatiotemporal control and multiplexing of properties (e.g., wavelength, intensity, irradiation time, pulsed/continuous wave) for application on multiphotoreponsive materials. However, the operating wavelength for such photoreponsive systems often includes an ultraviolet (UV) range that limits its use in the biomedical field. Herein, we investigate near-infrared (NIR)/visible (Vis) light-responsive nanocomposite films composed of rare earth element (i.e., Yb, Er)-doped NaYF₄ nanoparticles (NPs) embedded in azobenzene-incorporated poly(dimethylsiloxane) (AzoPDMS), silk fibroin, and silver nanowire (AgNW) layers. Photobending (PB) of the nanocomposite film is induced by a Vis light of 400–700 nm, while upconversion photoluminescence (UCPL) of embedded NPs is activated by an NIR light of 980 nm. The excitation wavelength of photoluminescence (PL) is shifted to the NIR ($\lambda = 980$ nm) range via photon upconversion in rare earth element-doped NPs. Independent operation of PB and UCPL enables both on-demand electrical switching and real-time location monitoring for spatiotemporally controlled electrical pulse stimulation. As a result, the dual-photoreponsive nanocomposite film can be utilized as a remotely controllable electrical stimulator and location indicator via different wavelengths of light.

5:00 PM SB04.11.27

Defect-Engineering to Control The Photonic Band Structure of Organic Semiconductor based Metal Dielectric Photonic Crystals Khadga Thakuri¹, Thomas Cleary¹, David Allemeier^{2,1}, Naoya Aizawa³, Ken-Ichi Nakayama³ and Matthew S. White^{1,1}; ¹The University of Vermont, United States; ²Boston University, United States; ³Osaka University, Japan

Alternating layers of metal and organic semiconductor (dielectric) thin films have been shown to form one-dimensional photonic crystals with application in organic optoelectronic devices like OLEDs. In this work, we introduce crystal defect engineering as a method to tune the photonic band structure of such metal-dielectric photonic crystals (MDPCs). The physical properties of each unit cell are determined by the index of refraction, extinction coefficient, and physical thickness of the layers. Varying the thickness of a single organic layer within the crystal introduces a substitutional point defect resulting in a mid-gap photonic state with varying impact on the photonic band dependent on the location of the defect within the crystal. The number of defect layers in the crystal can be increased until the defects constitute half of the layers. If done so with periodic distribution, this results in a binary unit cell and a Peierls distortion splitting the photonic band. We explore this regime by controlling the thickness of even-numbered metal layers in the MDPC from 0% to 200% that of the odd-numbered mirrors, revealing photonic edge states within the Peierls bandgap.

5:00 PM SB04.11.28

Controlling Rigidity of The Conjugated Backbone Using Plasticizing Molecular Additives to Enhance Deformability in Organic Semiconductors Sein Chung and Kilwon Cho; Pohang University of Science and Technology, Korea (the Republic of)

Plastic electronics, featuring deformable polymer layers, have emerged as a promising technology in recent decades. Researchers have been focused on enhancing the deformability of conjugated polymers by fine-tuning both the intrinsic molecular structure, such as the conjugation length of the polymer backbone, and the characteristics of functional side chains, including their length, branching points, and hydrogen bonding capabilities. However, it has become evident that chemical tuning alone has its limitations in overcoming the inherent trade-off relationship between electrical performance retention and mechanical deformability. To address this trade-off phenomenon, recent studies have introduced extrinsic aids into conjugated polymers, which encompass elastomeric polymers, crosslinkers, dopants, and various molecular additives. This research explores the impact of the chemical structures of plasticizing molecular additives (PMAs) on the mechanical, thermal, morphological, and electrical properties of films containing PMAs under deformation. For the purpose of a comprehensive comparison, our study employs a solution-based rheology and small-angle neutron scattering (SANS) technique to elucidate the adjusted persistence length of conjugated polymer, Poly[2,5-(2-octyldecyl)-3,6-diketopyrrolopyrrole-alt-5,5'-(2,5-di(thien-2-yl)thieno [3,2-b]thiophene)] (PDPP2T-TT-OD) interacting with various species of PMAs. Our findings reveal a significant influence of the modified persistence length of PDPP2T-TT-OD on the thin films' mechanical deformability, as determined through pseudo-free standing tensile testing. Based on our systematic analyses, we propose that the uniform distribution of PMAs within a conjugated polymer substantially enhances the deformability of thin films. These results are anticipated to offer valuable insights into the establishment of design principles for plasticizing molecular additives in the realm of plastic electronics.

5:00 PM SB04.11.29

Improving The Performance of Organic Photodetectors with Removable Ultrathin Top Electrodes [Kosei Sasaki](#), Takao Someya and Tomoyuki Yokota; The University of Tokyo, Japan

Recently, Organic photodetectors (OPD) with removable top electrode have attracted much attention for systematic analysis of the degradation of the device. This new structure of OPD consist of a bottom and top electrode sheets. The bottom electrode sheet was fabricated by forming a transparent electrode, electron transport layer (ETL) and active layer on a glass or flexible substrate. The top electrode sheet contains an electrode and hole transport layer (HTL) on another substrate. The top electrode sheet can be attached to the bottom electrode sheet by intermolecular forces. The top electrode sheet can be easily removed from the bottom electrode sheet without damaging the organic semiconductor layer. Using this structure, our group has succeeded in directly and continuously evaluating the electrical properties of the OPD and the crystallinity and chemical analysis of the interface between active layer and HTL before and after operating the device by removing the top electrode sheet.^[1] In previous report, the thickness of the top electrode sheet is 1 μm. This thicker substrate shows the weak adhesion between the active layer and the HTL. So, the device cannot be operated as an OPD without applying pressure. However, continuous pressure distorts the active layer and accelerate the degradation and possibly change the crystallinity.^[2] Therefore, it is important to develop OPD with removable top electrode that can be operated without applying pressure.

In this study, we developed OPD with removable top electrode that can be operated without pressure by using an ultrathin rubber sheet as a substrate of top electrode. The ultrathin rubber sheet is an extremely tough, self-adhesive and gas-permeable polydimethylsiloxane (PDMS) nanofilm with a thickness of approximately 700 nm, fabricated by dip coating a thin polyurethane nanofiber sheet with PDMS.^[3] The fabricated OPD shows 67% EQE at 550 nm and -5 V (light intensity is 6.7×10^{-3} mW/cm²) without applying pressure. The specific detectability of OPD is as high as 2.9×10^{12} Jones. The photocurrent and dark current at -2 V were changed 42.9 % and 117%, respectively after 100 cycles of lamination and delamination the top electrode sheet.

Reference

- [1] Shimanoe, et al. "Development of Air Stable Photomultiplication Type Organic Photodetector and Analysis of Active Layer using Removable Top Electrode," *Advanced Electronic Materials*, 2200651, 2022.
- [2] Cheng, Pei, et al. "Stability of organic solar cells: challenges and strategies." *Chemical Society Reviews* 45.9 , 2544-2582, 2016.
- [3] Wang, Yan, et al. "Robust, self-adhesive, reinforced polymeric nanofilms enabling gas-permeable dry electrodes for long-term application." *Proceedings of the National Academy of Sciences* 118.38, e2111904118, 2021.

5:00 PM SB04.11.30

Efficient Electron Injection and Transport in Fully Stretchable OLEDs [Wei Liu](#) and Sihong Wang; The University of Chicago, United States

Fully stretchable electroluminescent devices have garnered significant attention due to their transformative potential in applications ranging from wearable displays to implantable light sources. Among the various approaches, OLEDs based on the thermally activated delayed fluorescence (TADF) mechanism hold much allure because of their unity internal quantum efficiency and environmental/bio- compatibility. However, the performance, based on the identical emitter, in stretchable OLEDs falls significantly short of that achieved in traditional rigid devices due to fewer n-type materials available for efficient electron injection and transport. Here we propose innovative solutions to bridge this efficiency gap. First, we develop a stretchable electron transport polymer that simultaneously achieves decent electron mobility, suitable HOMO/LUMO levels, high triplet state, good solution processability, and high stretchability. Secondly, we propose a stretchable cathode design with an extremely low work function that is on par with the conventional rigid cathode, which is unprecedented with previously stretchable cathode based on silver nanowires, carbon nanotubes, conducting polymers, and others. Based on those innovations, we remarkably narrow the efficiency gap and eliminate the turn-on voltage differential between the fully stretchable TADF-OLEDs and their rigid counterparts.

5:00 PM SB04.11.31

Accessing New Optoelectronic Devices and Architectures through The Solid-Phase Processing of Conjugated Polymers [Guillermo Esparza](#), Darren J. Lipomi and David Fenning; University of California, San Diego, United States

Optoelectronic materials and devices are ubiquitous in the modern world. Thin-film processing of these materials is essential in a tremendous range of applications such as consumer electronics, healthcare, defense, scientific instrumentation, and renewable power generation and storage, to name a few. Among optoelectronic materials, conjugated polymers are of significant technological interest and are typically processed from either the vapor, liquid, or solution phases. Unfortunately, all of these techniques come with various downsides and limitations. Processing restrictions (such as solvent orthogonality) or device architectures (such as textured surfaces) impose potential processing incompatibilities and therefore limits on the devices which may be realized. For this reason, exploring novel processing routes is pivotal to unlocking the full potential any material.

Processing and application of thin films directly from the solid phase (that is, the creation of standalone thin films which are subsequently transferred onto a substrate or undergo other processing) has not been well explored, but has the potential of addressing various pitfalls that arise in conventional processing methods. This talk will focus several techniques in this category, which have utilized pre-formed thin-films to form coatings on non-planar surfaces, coat sensitive substrates without exposure to heat or liquid solvents, as well as serve as a sacrificial vehicle in order to preemptively deposit materials which would otherwise damage the rest of a device stack. Special emphasis will be given to how these approaches can outperform conventional processing methods as well as how they can be leveraged to enable devices which may have been previously impossible to realize.

5:00 PM SB04.11.32

Continuous Production of Ultratough Semiconducting Polymer Fibers with High Electronic Performance [Zhi Zhang](#) and Ting Lei; Peking University, China

Conjugated polymers have demonstrated promising optoelectronic properties, but their brittleness and poor mechanical characteristics have hindered their fabrication into durable fibers and textiles. Here, we report a universal approach to continuously producing highly strong, ultratough conjugated polymer fibers utilizing a flow-enhanced crystallization (FLEX) method. These fibers exhibit one order of magnitude higher tensile strength (>200 MPa) and toughness (>80 MJ m⁻²) than traditional semiconducting polymer fibers and films, outperforming many synthetic fibers, ready for scalable production. These fibers also exhibit unique strain-enhanced electronic properties and exceptional performance when employed as stretchable conductors, thermoelectrics, transistors, and sensors. This work not only highlights the influence of fluid mechanical effects on the crystallization and mechanical properties of conjugated polymers but also opens up exciting possibilities for integrating these functional fibers into wearable electronics.

5:00 PM SB04.11.33

Highly Conductive and Stretchable Metal Film Cathode for Intrinsically Stretchable Organic Light-Emitting Diodes [Kun-Hoo Jeon](#) and Jin-Woo Park; Yonsei University, Korea (the Republic of)

Stretchable electronics have received significant attention due to the increasing demand for skin-like biomedical devices in wearable healthcare and soft robotics applications. Intrinsically stretchable organic light-emitting diodes (is-OLEDs), which are essential components of stretchable electronics, have been actively studied in recent years. However, their performance, including luminance and operational stability (both before and after stretching), lags behind that of rigid, conventional OLEDs by several orders of magnitude. Among several drawbacks, the absence of suitable stretchable electrodes has been known as a major bottleneck in achieving further performance improvements. Electrodes for is-OLEDs must possess high conductivity and a smooth surface, along with superior charge injection properties. However, materials used for stretchable electrodes thus far have failed to meet these requirements. Conducting polymers, such as PEDOT:PSS, exhibit intrinsically low carrier density and mobility. Metal nanowires have rough surfaces that result in severe short circuits within the devices. Low-dimensional carbon materials, such as graphene, inherently lack stretchability. Therefore, new electrode materials must be developed to overcome the current performance limitations. Metal films are the most conductive materials due to their large free carrier density, but they are rarely used for stretchable electrodes because their conducting paths can be easily disrupted even under small strains. Several studies aim to enhance the mechanical flexibility of metal films by utilizing ultrathin structures, grain or crack engineering, or promoting strong adhesion between the substrate and metal films. Nevertheless, metal films have never been applied as electrodes for is-OLEDs, except for the cases involving geometrically engineered structures. In this study, we first demonstrated the use of stretchable silver films as the cathodes for is-OLEDs. We fabricated highly conductive and highly stretchable silver films by controlling their microstructures. The growth of the silver film was controlled by deposition conditions (evaporation rate and thickness) and the addition of seed layers, resulting in different grain morphologies. We studied the relationship between thin-film structure and electrical and mechanical properties to develop the optimal stretchable cathode. Slow evaporation and an ultrathin film structure could enhance the strain resilience of metal films. Introducing cesium carbonate seed layers could further improve conductivity and stretchability by suppressing silver aggregates due to their strong adhesion to silver. Although micro-cracks developed throughout the films under deformation, our cathodes were able to maintain their conductivity under repeated cyclic stretching of 40% strain, demonstrating superior elastic behavior compared to other reported stretchable electrodes. At the same time, the electron injection properties of silver films could be improved by composite electron transport layer (ETL) structures. Our stretchable silver film was sandwiched between a cesium carbonate seed layer, which possesses a desirable energy level for electron injection, and cesium carbonate-doped PEIE (d-PEIE) layers, which reduce injection barriers of the cathode. Our thin silver cathode has partially continuous film structures, thus providing numerous channels throughout the films that allow the participation of the upper-coated d-PEIE only in the electron injection process, excluding its insulating properties and effects on silver film growth. In conclusion, is-OLEDs with stretchable metal film cathodes showed improved luminance and operational stability compared to conventional AgNW-based cathodes. They also demonstrated stable operation under static stretching of 60% strain and cyclic stretching of 40% strain. We expect that our stretchable metal cathodes could become a new alternative to current stretchable electrodes.

5:00 PM SB04.11.34

Ultraflexible Organic Active Matrix Sensor for Tactile and Biosignal Monitoring [Andreas Petritz](#)^{1,2}, [Esther Karner-Petritz](#)^{1,2}, [Takafumi Uemura](#)^{2,3}, [Naoko Namba](#)^{2,3}, [Christine Priet](#)¹, [Matthias Hammer](#)¹, [Elisabeth Schreck](#)¹, [Manfred Adler](#)¹, [Andreas Tschepp](#)¹, [Herbert Gold](#)¹, [Teppei Araki](#)^{2,3}, [Tsuyoshi Sekitani](#)^{2,3} and [Barbara Stadlober](#)¹; ¹Joanneum Research Forschungsgesellschaft mbH, Materials – Institute for Sensors, Photonics and Manufacturing Technologies, Austria; ²The Institute of Scientific and Industrial Research (SANKEN) – Osaka University, Japan; ³Advanced Photonics and Biosensing Open Innovation Laboratory AIST – Osaka University, Japan

Flexible sensors are currently the subject of intensive research, as they allow cost-effective and environmentally friendly production of large-area, flexible and, when fabricated on ultrathin substrates, highly conformable devices [1]. Among many intriguing applications, we focus here on tactile and biosignals monitoring, where light weight multi-parameter sensors with high wearing comfort are of particular interest.

The required spatiotemporal resolution of the signals is achieved by integrating the sensors in an active matrix configuration. We combine organic ferroelectric transducers of high uniformity, characterized by a sensitivity spread of only 1.5%, with similarly uniform ultralow noise level organic thin film transistors operating below 5 V, showing a threshold voltage variation of just 0.13 V in a 12x12 sensor array. The transistor's transition frequency of >10 kHz (linear range) allows for a high spatiotemporal resolution of ~ 3 mm at a frame rate of >1 kfps. The thickness of only 2.8 μm renders our organic active matrix sensor sheet sufficiently ultraflexible to make it virtually imperceptible on the human skin. We demonstrate real time monitoring of the pulse wave with simultaneous measurements of heart rate, augmentation index and blood pressure [2] and spatially resolved tactile modes [3].

All presented devices are manufactured by processes scalable to industrial throughputs, mainly screen-printing and shadowmask evaporation, with life cycle analysis already starting at the design and materials selection stage, maintaining the prospect of a smooth transition to production in the future.

References

- [1] (a) Stadlober et al., Chem. Soc. Rev., 48 (2019) 1787-1825 (b) T. Someya et al., PNAS 101 (2004) 9966 (c) Kaltenbrunner, M. et al., Nature 499, 458–463 (2013).
- [2] A. Petritz et al., Nat. Comm. (2021) 12, 2399;
- [3] E. Karner-Petritz et al. Adv. Electron. Mater. (2023) 9, 2201333;

5:00 PM SB04.11.35

Improved Thermally Activated Delayed Fluorescence based Electroluminescent Devices using Vacuum Processed Carbazole based Self-Assembled Monolayer [Nrita Gaur](#), Manas Misra, Kashimul Hossain and Dinesh Kabra; Indian Institute of Technology Bombay, India

Engineering of the interface between organic emissive layer thin films and charge transport layers has fuelled the development of Organic light emitting diodes (OLEDs) over the past decade. This paper shows a comparative study between conventional poly(3,4-ethylenedioxythiophene): poly(styrene sulfonate) (PEDOT: PSS) vs carbazole functional groups based self-assembled monolayer (SAM) as hole-injection layer (HIL). SAM enables an improved interface to achieve the charge carrier balance and reduced interfacial recombination to enhance the external quantum efficiency in the *p-i-n* OLEDs. An industry compatible vacuum processed SAM-HILs ((4-(3,6-Dimethyl-9H-carbazol-9-yl) butyl) phosphonic acid (Me-4PACz)) as a hole transport layer in

thermally activated delayed fluorescence (TADF) based OLEDs is reported for first time, which facilitate to overcome the issues of poor device stability. Deeper highest occupied molecular orbital (HOMO @ -5.3 eV) of Me-4PACz enables the efficient hole injection with reduction in leakage current by 1 to 2 orders of magnitude compared to PEDOT: PSS (HOMO @ -5.00 eV) HIL based OLEDs. Also, built in potential is 1.3 times reduced to 2.45 V for Me-4PACz based OLEDs. With the further optimized thickness of Me-4PACz (d= 6 nm), OLED maximum external quantum efficiency (EQE) gets enhanced from 18.30 % to 20.79 % with luminous efficiency 62.79 cd/A. Further, the Me-4PACz is also investigated on the basis of its deposition method. Vacuum processed SAM based OLEDs showed a reduced operating voltages and enhanced brightness levels, which correlated with an improved electronic coupling between SAM/ α -NPD interfaces. We note that, evaporated SAM-HTLs to complete OLED demonstrates comparable efficiency to their solution-processed counterparts. Furthermore, vacuum deposition SAM as HIL based OLEDs is found to provide a five- fold enhancement in the operational stability 60% (LT_{60}) of the initial luminance L_0 of the OLED in comparison to PEDOT: PSS as HIL based OLED. This study is further extended to a blue TADF OLED, with almost similar finding.

5:00 PM SB04.11.36

Development of Next-Generation OPLS Force Field for Accurate Modeling of Phosphorescent OLED Materials [Steven Dajnowicz](#), Owen Madin, Hadi Abroshan, Shaun Kwak, Mathew D. Halls and Edward Harder; Schrodinger, United States

To address the inherent challenges of modeling organometallic complexes, which are commonly used as phosphorescent emitters in OLEDs, the OPLS4 force field is extended in order to have a more suitable functional form. These new developments include a fluctuating charge model to describe charge transfer, a Morse potential to describe the metal-ligand bonding, and an angular overlap model to describe d-orbital effects. The initial force field coverage is centered around common chemistries found in Pt(II) and Ir(III)-based emitters. Our model accurately represents geometries when comparing against DFT and crystal structure references. In addition, the model was validated on a series of organometallic emitters doped into an organic host layer, generating configurations from molecular dynamics simulations that are used to predict photoelectronic properties. Future developments include the extension of chemical coverage in the effort to more broadly aid in material design.

5:00 PM SB04.11.37

All Printed Vertical Organic Electrochemical Transistor with Fast Speed and Good Flexibility for High Frequency Inverter [Yingjun Chen](#); Nanyang Technological University NTU, Singapore

Printing technologies have revolutionized the field of organic electronics through large-scale fabrication and low cost, but limitations in printing resolution and printable material selection have restricted the performance of printed devices. This work presents the first successful all screen printed vertical organic electrochemical transistors (V-OECTs) on a flexible substrate, exhibiting fast switching times of 0.8ms and 1.6ms from off to on and on to off, respectively. The vertical structure offers advantages over traditional planar structures such as higher transconductance, fast transient response, and symmetric switching performance. In this work, bending testing and various substrate printing confirm the flexibility and printability of the devices, while the application of the printed OECT in a unipolar inverter with high frequency (~100 Hz) demonstrates their potential in printed flexible circuit. The printed V-OECT can also be utilized as amplifier to detect the electrocardiogram (ECG) signal. These results suggest a potential method for producing high-performance printed OECTs, paving the way for the development of all-printed flexible electronics with fast response for various applications.

5:00 PM SB04.11.38

Interactions in GO/P3HT Layered Nanostructures: Spectroscopic Investigation for Organic Solar Cells [Fokotsa V. Molefe](#)¹, [Bakang M. Mothudi](#)², [Mokhotjwa S. Dhlamini](#)² and [Mmantsae M. Diala](#)¹; ¹University of Pretoria, South Africa; ²University of South Africa, South Africa

Herein, a simple and effective approach has been followed to deposit poly (3-hexylthiophene) (P3HT) and GO/P3HT layered nanostructures and fabricate their devices. Different structural, morphological, spectroscopic and electrical techniques were used to probe P3HT and GO/P3HT layered nanostructures properties. The X-ray diffraction (XRD) spectrum of GO/P3HT revealed a highly crystalline reflection of GO which is slightly shifted to higher diffraction angles as evidence of interaction with P3HT. As a proof of concept of interactions, the smooth surface morphology of P3HT translated to wrinkled structure for GO/P3HT presenting the existence of GO sheets in scanning electron microscopy (SEM). Fourier Transform Infrared spectroscopy (FTIR) confirmed the alteration of P3HT structure upon interaction with GO where the average conjugation length decreased from ~ 1.20 to ~ 1.12. The UV/VIS/NIR spectrum of GO/P3HT has an observable decrease in percentage reflectance leading to enhancement of the light absorption ability of P3HT with the inclusion of GO nanostructures. Furthermore, the bandgap energy decreased and resulted in a decrease in energetic driving force. The fluorescent decay curves revealed a decline in exciton lifetime depicting quicker charge transfer from P3HT to GO which resulted in a decrease in exciton diffusion length. Our findings suggest that the energetic driving force induced the mechanism involved during chemical interaction at the GO/P3HT interface. However, the calculated energetic driving force suggests that the interface between GO/P3HT be tuned, which agrees with J-V results where the GO/P3HT device revealed a low power conversion efficiency (PCE) of 3.07 %.

5:00 PM SB04.11.39

Pentacene Two-Dimensional Crystals with Layer-Dependent Morphologies and Mobilities Grown via Confined Molecular Flow Deposition [Zhichao Cheng](#) and [Xiaomin Xu](#); Tsinghua University, China

Pentacene has gained significant attention as a channel material in organic field-effect transistors (OFETs). In most cases, the mobility, a key performance metric of the device, is evaluated for the entire film. However, there is limited understanding of its layer-dependent electric transport properties in the two-dimensional (2D) limit, particularly when compared to inorganic 2D materials that have been more thoroughly investigated. Furthermore, in OFETs, the growth of molecules is especially crucial at the initial stage, as the electrical conduction predominantly occurs in the few molecular layers adjacent to the dielectric surface. Herein, we successfully grew pentacene 2D crystals with 1, 2, and 3 molecular layers on thermally oxidized wafer surfaces using the confined molecular flow deposition method, under conditions of both high deposition rates and elevated substrate temperatures. The electric transport properties of these crystals were measured, and the results aligned well with the theoretical calculations. In addition, the growth mode of these pentacene 2D crystals differs from the classical models: layer-by-layer, layer-plus-island, and island growth modes. This deviation arises because the nucleation of pentacene under these conditions does not follow the classical nucleation process. Instead, it develops through two distinct steps. Initially, pentacene molecules nucleate as liquid clusters with the molecules adopting a lying-down orientation. Subsequently, these liquid nuclei transition to a solid crystalline state, where the molecules flip upright. The final number of molecular layers in the pentacene 2D crystals corresponds to the layer number in their solid nucleus, with each layer within the crystal growing synchronously. Additionally, the crystals with different numbers of layers exhibit distinct shapes: ellipses, rounded hexagons, and hexagons for one, two, and three layers, respectively. This phenomenon can be explained by phase field modeling. We believe our work not only verifies the electric transport properties of 2D pentacene crystals with different molecular layers, but also may pave the way for exploring new physics using small molecules.

5:00 PM SB04.11.40

Record-High Surface Potential by Spontaneous Orientation Polarization in Organic Semiconductors [Albin Cakaj](#), [Alexander Hofmann](#) and

Wolfgang Brueetting; University of Augsburg, Germany

Molecular orientation in organic semiconductors has many different facets, such as optical anisotropy leading to birefringence, alignment of their optical transition dipole moments (TDMs) and/or their permanent electrical dipole moments (PDMs) [1]. While TDM alignment is well established and readily exploited to improve light outcoupling in organic light-emitting diodes (OLEDs) [2], PDM alignment and the resultant spontaneous orientation polarization (SOP) is by far less investigated, and it is not fully clear yet if it is beneficial or detrimental for device application [3].

SOP is observed in evaporated films of polar organic molecules and leads to a so-called giant surface potential (GSP), which can be measured by Kelvin probe, impedance spectroscopy or the displacement current method [4]. In general, the GSP slope is roughly proportional to the magnitude of the molecule's PDM. However, despite their very high PDM, many molecules exhibit only small SOP because they tend to aggregate in pairs with antiparallel alignment. Thus, the order parameter (i.e., the degree of net PDM alignment) is typically less than 10%.

Here we report a new class of materials with drastically enhanced PDM alignment, exceeding 30% for films grown at room temperature [5]. These phosphine oxides exhibit a highly polar phosphor-oxygen bond, which leads to large SOP despite the presence of different structural conformers. By evaporating them on a cooled substrate in combination with dilution of the polar species in a non-polar host, record-high GSP slope of almost 300 mV/nm (with an equivalent electric field of 3×10^8 V/m) can be achieved. This opens new perspectives for application of organic semiconductors in energy harvesting devices.

[1] A.J. Hofmann, M. Schmid, W. Brueetting; *Advanced Optical Materials* 9, 2101004 (2021)

[2] T.D. Schmidt, T. Lampe, D. Sylvinson, P.I. Djurovich, M.E. Thompson, W. Brueetting; *Phys. Rev. Applied* 8 (2017) 037001

[3] Y. Noguchi, Y. Tanaka, H. Ishii, W. Brueetting; *Synth. Metals* 288, 117101 (2022)

[4] Y. Noguchi, W. Brueetting, H. Ishii; *Jap. J. Appl. Phys.* 58, SF0801 (2019)

[5] A. Cakaj, M. Schmid, A. Hofmann, W. Brueetting; *ACS Appl. Mater. Interfaces* 15, 54721 (2023)

5:00 PM SB04.11.41

Color Tunable Stacked QD-OLED Hybrid Devices Sung-Cheon Kang, Eun-young Choi and Jang-Kun Song; Sungkyunkwan University, Korea (the Republic of)

Organic light-emitting diodes (OLEDs) and quantum dot light-emitting diodes (QLEDs) stand out as highly promising display technologies due to their notable advantages, including high efficiency, rapid response speed, and a high contrast ratio. Typically, flat panel displays incorporate distinct red, green, and blue subpixels placed side-by-side to replicate a full spectrum of colors. However, this design exhibits drawbacks such as a low geometric fill factor, reduced efficiency, and challenges in fabricating high-resolution displays. A potential solution to address these limitations lies in a multicolor-emitting pixel structure, enabling the selective emission of more than two colors from a single pixel. AC-driven color-tunable devices present a promising avenue to achieve this goal. In an AC tandem device, the emitted light's color is determined by the applied signal's polarity, resulting in different colors emitted under forward and reverse bias voltages. In this presentation, we introduce AC-driven multi-color OLED-QLED hybrid pixel structures. The foundational unit comprises two-pixel QDLEDs, fabricated using an inkjet process, with an OLED layer deposited atop these QDLEDs. Through the combination of these three pixels, a full-color display is achieved. Efficiency optimization is achieved by fine-tuning the materials and structures within the charge transport and charge generation layers. This device configuration features two horizontally arranged pixels and another vertically stacked pixel, enhancing the fill factor by 1.5 times. As a result, this approach holds promise for future display applications, offering high efficiency and resolution.

5:00 PM SB04.11.42

Micropatterned Elastomeric Composites for Encapsulation of Transient Electronics Choi So jeong; Korea University, Korea (the Republic of)

While transient electronic devices are biodegradable and intended to dissolve or decompose through environmental factors, the necessity of an effective waterproofing or encapsulation system remains critical for ensuring reliable and durable operation over a specified timeframe. Current protection methods rely on multiple layers of electrically inactive organic/inorganic elements combined with polymers. Nevertheless, their elevated mechanical stiffness poses challenges when applied to soft, time-dynamic biological tissues, skins, or organs. In this context, we present an innovative solution: a stretchable, bioresorbable nanoparticle-incorporated elastomeric composites, accompanied by surface morphology modifications. The introduction of nature-inspired micro-patterns reduces the diffusion area for water molecules, while embedded nanoparticles act to impede water permeation. This synergistic combination significantly enhances the water-barrier performance. The encapsulation mechanisms are empirically and theoretically validated under strains. A demonstration involving a soft, degradable shield with an optical component submerged in a biological solution underscores the potential applicability of the proposed encapsulation strategy.

5:00 PM SB04.11.43

Photoluminescence and Electroluminescence Confocal Imaging of an OLED Angela Flack, Paulina Carmona-Monroy and Matthew Berry; Edinburgh Instruments, United Kingdom

In recent years organic light-emitting diodes (OLEDs) have become one of the leading technologies for full-colour display panels in high-end smartphones and televisions. This rapid growth in use has occurred because OLEDs offer an all-around superior performance to liquid crystal displays (LCDs). For example, they are thinner, lighter, more flexible, less power consumptive, and brighter.

When new OLEDs are developed, the optoelectronic properties of individual components and the complete device can be characterised using photoluminescence (PL) and electroluminescence (EL) spectroscopy. In this poster presentation, we use a confocal Raman microscope to characterise and spatially resolve the optoelectronic properties of a fabricated OLED device with four imaging modalities: PL, EL, time-resolved PL (TRPL), and time-resolved EL (TREL). Using a confocal microscope to characterise an OLED's spectral and time-resolved properties provides much greater detail than bulk measurements.

SESSION SB04.12: Bioelectronics

Session Chairs: Lucas Flagg, Katelyn Goetz, Ulrike Kraft and Simon Rondeau-Gagne

Friday Morning, April 26, 2024

Room 435, Level 4, Summit

8:30 AM *SB04.12.01

In Situ Characterization of Electrochemical Transistors for High-Performance Biosensing Sahika Inal; King Abdullah University of Science and Technology, Saudi Arabia

Solid-liquid interfaces have garnered significant attention for applications in bioelectronics, electrochromics, energy storage/generation, neuromorphic computing, and thermoelectrics. These devices operate in electrolytes that render ions mobile in the film, making the coupling between electronic and ionic charges crucial. An example of such a device is the organic electrochemical transistor (OECT), a high-gain transducer commonly used to monitor bio-ionic signals. In this talk, I will demonstrate OECT-based protein sensors based on organic mixed conductors and discuss the importance of the semiconductor type used in the channel and device dimensions for high-performance biosensing, based on the results acquired through a combination of operando techniques. I will also introduce polymer design and processing approaches that endow organic bioelectronic devices with longer shelf life and operational stability.

9:00 AM *SB04.12.02

Stable and High Performing *n*-Type and Ambipolar Organic Electrochemical Transistor for Next-Generation Bioelectronics [Wei Lin Leong](#); Nanyang Technological University, Singapore

Organic mixed ionic-electronic conductors (OMIEC), which are capable of efficiently transporting and coupling ionic and electronic charge, have gained significant attention in recent years as emerging organic materials for bioelectronic, neuromorphic computing, circuits and energy storage systems. One emerging device that uses these OMIECs is the organic electrochemical transistors (OECTs), which offer the advantages of low operation voltage (< 1V), high sensitivity and excellent aqueous operating capability. To date, OMIECs for OECTs have predominantly been *p*-type materials, while their *n*-type counterparts lag far behind in performance and stability, hampering their adoption in complementary circuit designs, electrochemical energy storage, and sophisticated biosignal sensing that rely on electron transfer. In this talk, I will present our recent progress on developing new conjugated ladder-type polymers which exhibit good mixed ionic-electronic conduction properties, enabling stable and fast *n*-type organic electrochemical transistors. This is due to the polymer's predominant edge-on packing and enhanced backbone coplanarity which promote efficient charge transport, as well as its porous structure which facilitates efficient ion penetration and transport. These unique advantages make this polymer especially suitable for bioelectronics, such as being used as a pull-down channel in a complementary inverter for long-term stable detection of electrophysiological signals. Moreover, the developed device shows a reversible anti-ambipolar behavior, enabling reconfigurable electronics to be realized using a single material. In addition, my talk will present our studies on various conjugated polymer blends with ambipolar properties, providing a facile strategy to simplify the fabrication process and reduce the manufacturing cost while simultaneously obtain high performing logic circuits.

9:30 AM SB04.12.03

Electrolyte-Gated Organic Field Effect Transistor Integrated in Neurosignal Recording System for Monitoring Brain Activity [Deng Zou](#)^{1,2} and [Paddy K. L. Chan](#)^{1,2}; ¹University of Hong Kong, Hong Kong; ²Advanced Biomedical Centre Limited, Hong Kong

Electrolyte-gated organic field-effect transistors (EGOFETs) have emerged as promising candidates for neurosignal detection, due to their high operating speed, effective transduction of biological inputs into amplified transistor signals and ability to operate stably in aqueous environments. Key limitations in these current microelectrode neuroprobes stemming from high electrode impedance and voltage drift, have necessitated innovative neurosignal recording solutions. In this study, we present a neural recording system that utilizes EGOFETs for on-site signal amplification. We demonstrate the capability of EGOFETs, when integrated into our recording circuit, to record neurosignals with an exceptional signal-to-noise ratio (SNR) at 16 dB and high fidelity. These EGOFETs are based on top liquid gate and top contact configuration, which can operate under low source-drain voltage ($V_{DS} = -1.2$ V) and gate voltage ($V_G = 0$ V) conditions, achieving a remarkable maximum transconductance of up to 500 μ S. This achievement underscores the potential for broad applications of EGOFET technology in monitoring brain activity, encompassing both research and clinical domains.

9:45 AM SB04.12.04

On-Device Calibration of Organic Electrochemical Transistor Biosensors for Advancing Alzheimer's Diagnostics [Stefany J. Kissovsky](#), [Scott T. Keene](#), [Gabriele S. Kaminski Schierle](#) and [George G. Malliaras](#); University of Cambridge, United Kingdom

Alzheimer's disease is a progressive form of dementia, which affects more than 50 million people worldwide and is expected to impact three times more by 2050. Although its cause and progression mechanisms are still not fully understood, Alzheimer's disease has been associated with the misregulation of certain biomarkers.¹ The quantification of these biomarkers requires expensive elaborate equipment, substantial experience, and time-consuming analysis due to their sub-nanomolar concentrations in blood. A much faster, cost-effective, and more convenient *in-vitro* method with very high sensitivity and good specificity is needed to advance Alzheimer's research and diagnostics.

Organic electrochemical transistors (OECTs) have emerged as a promising point-of-care testing platform for enzymatic biosensing due to their exceptional signal amplification properties, stability in aqueous environments, and biocompatibility.² However, due to their high sensitivity, OECTs are susceptible to signal drifts caused by changes in the surrounding environment, such as variations in pH levels, temperature fluctuations, and the presence of interfering species in the sample of interest. In this work we present a new OECT configuration design to achieve real-time on-device calibration. This configuration is designed to effectively compensate for signal drifts and faulty analyte detection, thereby ensuring stability and reliable results.

Three-terminal OECTs have been designed and microfabricated with a poly(3,4-ethylenedioxythiophene) polystyrene sulfonate (PEDOT: PSS) channel. This ion permeable channel is extremely sensitive to biochemical reactions occurring in the electrolyte placed directly on top of the device for testing.² The design of the device incorporates two gates, and it has been optimised to create highly sensitive enzymatic sensors.³ An enzyme is immobilised via bioconjugation on the first gate electrode, while the second gate electrode acts as a reference. The system is tested in real-time by addition of varying concentrations of the target compound in the electrolyte, while the changes in current are recorded. This test allowed the on-device calibration of our OECTs, enabling the reliable measurement of the compound with high sensitivity and specificity. This is a new promising platform for achieving stability against signal drifts in the OECTs and robustness against interfering analytes in enzymatic sensors, outlining the pathway to very high sensitivity and low limit of detection of brain biomarkers.

1. Michel, Claire H., et al. Extracellular Monomeric Tau Protein is Sufficient to Initiate the Spread of Tau Protein Pathology. *Journal of Biological Chemistry*, 289.2, 956–967 (2014).

2. D. A. Bernards and G. G. Malliaras. Steady-State and Transient Behavior of Organic Electrochemical Transistors. *Advanced Functional Materials*, 17.17, 3538–3544 (2007).

3. Cicoira, Fabio, et al. Influence of Device Geometry on Sensor Characteristics of Planar Organic Electrochemical Transistors." *Advanced Materials*, 22.9, 1012–1016 (2010)

10:00 AM BREAK

10:30 AM *SB04.12.05

Retinomorph Motion Sensors and Integrated Energy Storage Systems Based on Donor-Acceptor Polymers Tse Nga Ng; University of California, San Diego, United States

Organic retinomorph sensors offer the advantage of in-sensor processing to filter out redundant static background and are well suited for motion detection. To improve this promising photodetector, here we studied the key role of interfacial energetics in promoting charge accumulation to raise the inherent photoresponse of the light-sensitive capacitor. Specifically, incorporating appropriate interfacial layers around the photoactive layer was crucial to extend the carrier lifetime, as confirmed by intensity-modulated photovoltage spectroscopy. Compared to its photodiode counterpart, the retinomorph sensor showed better detectivity and response speed due to the additional insulating layer, which reduced the dark current and the RC time constant. Lastly, three retinomorph sensors were integrated into a line array to demonstrate the detection of movement speed and direction, showing the potential of retinomorph designs for efficient motion tracking.

In addition to enabling motion detector, the class of donor-acceptor polymers showed highly delocalized redox states and operated as stable n-type anodes in energy storage devices. The redox polymer was used in supercapacitors and achieved a high areal power density of 227 mW/cm², allowing rapid charging and high power delivery. The capacitance retention was 84% after 11,000 full redox cycles, offering the critical benefit of long cycle life. This work demonstrated the application of a new class of stable redox-active materials suitable to meet the energy storage needs for short-range wireless electronics.

11:00 AM SB04.12.06

Organic Electronic Platform for Enhancing Plant Growth Eleni Stavrinidou; Linköping University, Sweden

To cover the food demands of the growing population in the changing climate we need to increase crop yield in a sustainable manner. Hydroponics cultivation minimizes water and fertilizers use while it can be integrated in the urban environment. However so far, the substrates used in hydroponics mainly offer support to the root system. Here we developed an active, organic electronic platform that stimulates the growth of plants in hydroponics culture. We demonstrate that Barley, one of the most important crops, grows well within the bioelectronic platform. When stimulated, the biomass of the Barley increases by 40%, and the effect is evident in both root and leaf development during the growth period after the stimulation treatment. Results also show that stimulated plants reduce and assimilate NO₃⁻ more efficiently than controls, a finding that can have implications on minimizing fertilizers use. Our work opens the pathway for enhancing plant growth in hydroponics settings using organic electronics that may result in more sustainable food production.

11:15 AM SB04.12.07

Spontaneous Recording of Cardiomyocytes' Action Potential by Electrolyte-Gated Field Effect Transistors: A Simple, Planar, Printed *In-Vitro* Platform for Cardiovascular Drugs Screening Giulia Z. Zemignani^{1,2}, Adrica Kyndiah¹, Luca Sala³, Aleksandr Khudiakov³, Carlotta Ronchi¹, Gabriele Tullii¹, Giuseppina Iachetta⁴, Rosalia Moreddu⁴, Stefano Chiodini¹, Francesco De Angelis⁴, Maria Rosa Antognazza¹ and Mario Caironi¹; ¹Center for Nano Science and Technology, Istituto Italiano di Tecnologia, Italy; ²Politecnico di Milano, Italy; ³Center for Cardiac Arrhythmias of Genetic Origin, Laboratory of Cardiovascular Genetics, IRCCS Istituto Auxologico Italiano, Italy; ⁴Istituto Italiano di Tecnologia, Italy

In the context of cell-based biosensors, extensive endeavours have been dedicated to find accurate, in-vitro bioelectronic platforms capable of directly recording the electrical activity of electrogenic cells, namely neurons and cardiac cells, in a non-invasive way. The amplitude, shape and duration of the Action Potentials (APs) contain significant information on the viability of cells. These attributes, in turn, facilitate the exploration of cardiac pathologies and the impact of novel pharmaceutical products.

To date, the available methodologies used to assess APs predominantly involve patch clamp techniques or complex 3D nanostructured electrodes, frequently combined with electro/opto-poration, thereby rendering them very invasive in nature.

To this end, the principal objective of this study is to propose a simple and cost-effective device able to record the electrical activity of *in-vitro* cell cultures in a non-detrimental manner.

Within this research, we have accomplished for the first time the spontaneous recording of intracellular action potentials of human induced pluripotent stem cells-derived cardiomyocytes (hiPSC-CMs) by direct plating or seeding of cells on top of the channel of our printed, planar Electrolyte-Gated Field Effect Transistor (EGFET).

The EGFETs were fabricated employing carbon-based semiconductors via a simple and cost-efficient printing technique, aiming to facilitate large-scale production.

The cardiac cells APs were obtained by simply recording the transistor current at a fixed gate voltage V_{GS} corresponding to the maximum transconductance. The natural APs of cardiomyocytes are able to change the effective gate voltage applied, which is transduced in a modulation of the source-to-drain current I_{SD} in our device. Remarkably, this modulation occurs without the need of any external stimuli.

Our planar architecture was able to record signals with shape and duration comparable with patch clamp performed on the same batch of cells, confirming the fact that we recorded a major fraction of the intracellular action potentials (estimation in the range of 40-60 mV).

The exceptional sensitivity of our device made it possible to detect the APs perturbations induced by the addition of different drugs targeting specific ion channels. The Action Potential Durations (APDs) recorded in our device exhibit close congruence with those attained with patch clamp techniques, thus positioning our platform as an ideal candidate for long-term monitoring of cardiac arrhythmias, chronic disease and the screening of cardiovascular drugs. The optimal EGFET-cell coupling enabled by our planar, printed, carbon-based semiconductors, reveals high stability and quality of the signal transduced, achieving excellent reproducibility over more than a hundred tested transistors.

Such a high-throughput device is opening the path to deeper comprehension of fundamental transduction mechanisms at the bio-electronic interface and possesses the potential to be further developed into a future cost-effective diagnostic tool.

11:30 AM SB04.12.08

Design of Injectable, Self-Adhesive and Highly-Stable Conductive Polymer Electrode for Sleep Recording Huilian Wang; The University of Texas at Austin, United States

High-quality and continuous EEG monitoring is desirable for sleep research, sleep monitoring and the evaluation and treatment of sleep disorders. Existing continuous EEG monitoring technologies suffer from fragile connections, long-term stability, and complex preparation for electrodes in real-life conditions. Here, we report an injectable and spontaneously-crosslinked, conductive polymer hydrogel electrode for long-term EEG applications. Specifically, our electrodes have a long-term low impedance on hairy scalp regions of 17.53 k Ω for > 8 hours of recording, high adhesiveness on the skin of 0.92 N cm⁻¹ with repeated attaching capability, and long-term wearability during daily activities and overnight sleep. In addition, our electrodes demonstrate a superior signal-to-noise-ratio of 23.97 dB in comparison to commercial wet electrodes of 17.98 dB and share a high agreement in sleep stage classification with commercial wet electrodes during multi-channel recording. These results exhibit the potential of our on-site formed electrodes for high-quality, prolonged EEG monitoring in various scenarios.

11:45 AM SB04.12.09

Selective Response of Organic Electrochemical Transistor by a Potentiodynamic Approach [Isacco Gualandi](#)¹, Federica Mariani¹, Luca Salvigni², Francesca Ceccardi¹, Danilo Arcangeli¹, Francesco Decataldo³, Marta Tessarolo³, Domenica Tonelli¹, Beatrice Fraboni³ and Erika Scavetta¹; ¹Dipartimento di Chimica Industriale 'Toso Montanari', Università di Bologna, Italy; ²Organic Bioelectronics Laboratory, Biological and Environmental Science and Engineering Division (BESE), King Abdullah University of Science and Technology (KAUST), Saudi Arabia; ³Dipartimento di Fisica e Astronomia, Università di Bologna, Italy

Organic electrochemical transistors (OECTs) are finding growing interest in the field of biological and chemical sensing. Although the OECT transduction is based on electrochemical reactions, the transistor architecture offers several advantages as compared to amperometric sensors such as signal amplification, use of easy and cheap readout electronics, low supply voltage (usually < 1 V), low power operation (< 100 μ W), bio-compatibility. Moreover, OECTs can be easily miniaturized and adapted to non-flat, flexible and even textile devices [1]. Since electrochemical transduction usually detects all redox-active compounds in a sample, selectivity remains an open issue that should be addressed to achieve a reliable measure. Our group has developed a potentiodynamic approach for the selective detection of dopamine (DA) in the presence of interfering compounds (ascorbic acid, AA, and uric acid, UA) [2]. The trans-conductance curves allow linear calibration plots for AA, UA and DA and to separate the redox waves associated with each compound with performances comparable or even better than those obtained by differential pulse voltammetry. This contribution describes the recent achievements of OECT sensors, based on the potentiodynamic approach, to the design of robust and selective devices able to perform real-time analyses that do not strictly rely on laboratory facilities. The detection of the fat-soluble Vitamin A has been carried out in organic environment [3]. The OECT behaviour was thoroughly characterized, its structure was optimised and both potentiostatic and potentiodynamic detections were investigated. The potentiostatic determination exhibited a gain of 100 with respect to the electrochemical signal represented by Vitamin A oxidation current and the limit of detection was as low as 115 nM, but it did not address selectivity issues. On the other hand, the potentiodynamic approach showed a higher detection limit, but the sensor displayed selectivity in the presence of α -Tocopherol. Excellent performances were found when analyzing commercial food fortifiers and a multivitamin premix powder, encouraging results to these bioelectronic devices beyond the watery part of life and biology, where they have already proved to provide uniquely performing electrochemical interfaces. Finally, ongoing research deals with potentiodynamic determination of uric acid in saliva with the aim to estimate oxidative stress.

REFERENCES

- [1] I. Gualandi, M. Tessarolo, F. Mariani, L. Possanzini, E. Scavetta, B. Fraboni, *Polymers* **2021**, *13*, 894.
- [2] I. Gualandi, D. Tonelli, F. Mariani, E. Scavetta, M. Marzocchi, B. Fraboni, *Sci. Rep.* **2016**, *6*, 35419.
- [3] L. Salvigni, F. Mariani, I. Gualandi, F. Decataldo, M. Tessarolo, D. Tonelli, B. Fraboni, E. Scavetta, *Sens. Actuators B* **2023**, *393*, 134313.

SYMPOSIUM SB05

Materials and Systems for Fully Implantable Organ Interfaces
April 22 - May 7, 2024

Symposium Organizers

Eric Glowacki, Central European Institute of Technology
Philipp Gutruf, University of Arizona
John Ho, National University of Singapore
Flavia Vitale, University of Pennsylvania

Symposium Support

Bronze
Diener Electronic GmbH + Co. KG

* Invited Paper
+ JMR Distinguished Invited Speaker
^ MRS Communications Early Career Distinguished Presenter

SESSION SB05.01: Neural Interface Technology
Session Chairs: Philipp Gutruf and John Ho
Monday Afternoon, April 22, 2024
Room 434, Level 4, Summit

3:00 PM *SB05.01.01

Fiber-Based Tools to Probe Brain-Body Physiology [Polina Anikeeva](#); Massachusetts Institute of Technology, United States

Complex interplay between the brain and the other body system governs our behavior, immunity, and disease progression. Yet, probing of the brain-body circuits is challenging, as peripheral nerves and organs are in continuous motion and are subject to stringent immunosurveillance. Our group applies fiber-

fabrication methods in combination with traditional solid-state electronics to create multifunctional wireless interfaces with peripheral organs such as the gastrointestinal tract to probe physiological functions with cell-type and regional specificity. Concomitantly, we create fibers to interface with multiple brain regions, and develop materials-based approaches to enable straightforward surgical placement of multi-regional neural interfaces spanning multiple organs.

3:30 PM SB05.01.02

Magnetic Guidewires Driven Deployable Electronics for Minimal Invasive Epidural Electroencephalographic Brain-Computer Interface [Tao Zou](#)^{1,2}, Na Xiao^{1,2} and Paddy K. L. Chan^{1,2}; ¹University of Hong Kong, Hong Kong; ²Advanced Biomedical Instrumentation Centre Limited, Hong Kong

Electroencephalographic Brain-Computer Interface (ECoG-BCI) has significantly contributed to both fundamental neuroscience research and clinical applications, including brain function recovery, speech neuroprostheses, epilepsy detection, and traumatic brain injury prognosis. Improving the recording coverage and density of ECoG-BCI are particularly valuable for analysing the activities correlations among the multiple brain regions and identifying the actual neural disease foci accurately. Traditionally, the deployment of large-area coverage devices commonly necessitates an equally substantial cranial opening, which expose significant brain tissue and could potentially cause brain tissue swelling, inflammation, heighten risk of cortical damage, and infection. As a result, diminishing the acceptance of these implants among BCI users.

Here we present a deployable ECoG-BCI platform operated via magnetically controlled guidewires in minimally invasive approach. The ECoG-BCI platform comprises a high-density array of flexible PEDOT:PSS/pHEMA electrodes (28.4 electrodes cm⁻²) covering a large surface area (9 cm²), sub-millimeter soft magnetic polymer guidewires, a robotic arm equipped with a permanent magnet for guiding the magnetic guidewire, and an automatic control system. The folded flexible electrode array can traverse the craniotomy and be unfurled by tracking the guidewires. The thin, 10 μm thick parylene based electrode array, featuring perfusion holes, ensures excellent conformability and close contact with the curved brain surface. We deploy the proposed ECoG-BCI platform within area V1 of the visual cortex in a macaca fascicularis, demonstrating chronic neural signal recording and cortical electrical stimulation capabilities. The monkey has responses to the phosphenes induced by the visual cortex stimulation. This deployable ECoG-BCI platform has the potential to restore effective vision for the blind with minimal invasive implantation injury.

3:45 PM *SB05.01.03

Miniature Battery-Free Implants for Distributed Bioelectronic Networks [Jacob T. Robinson](#); Rice University, United States

Direct neural and cardiac stimulation is a powerful method to treat disorders when drug therapies are ineffective, or their side effects are intolerable. Unfortunately, traditional implantable stimulation technologies are based on wires that connect the stimulator to the target, which can lead to challenges for writing the wires, lead fractions, migration, and infection. This is particularly true when attempting to interact with a network of devices.

Here, we describe how magnetolectric materials enable construction of distributed network interfaces with each node the size of a pea or smaller and capable of digitally programmable stimulation. With robust wireless data and power transfer it is possible to make miniature implants less than 1 cm across with the ability to deliver biphasic stimulation powerful enough to drive neural activity from above the dura. As an example, we show applications in brain and cardiac stimulation neuromodulation where minimally invasive devices can form a network of precisely timed stimulators. Our data from large animal and human studies show the kind of good misalignment tolerance and high-power bioelectronics capabilities that would enable networks of wireless, battery-free, neuromodulation technologies.

4:15 PM *SB05.01.04

Soft and Flexible Bioelectronics for Brain-Machine Interfaces [Jia Liu](#); Harvard University, United States

Large-scale brain mapping through brain-machine interfaces is important for deciphering neuron dynamics, addressing neurological disorders, and developing advanced neuroprosthetics. Ultimately, brain mapping aims to simultaneously record activities from millions, if not billions, of neurons with single-cell resolution, millisecond temporal resolution and cell-type specificity, across three-dimensional (3D) brain tissues over the course of brain development, learning, and aging. In this talk, I will first introduce flexible and soft bioelectronics with tissue-like properties that can track electrical activity from the same neurons in the brain of behaving animals over their entire adult life. Specifically, I will discuss the fundamental limitations of the electrochemical stability of soft electronic materials in bioelectronics and present our strategies to overcome these limitations, enabling a scalable platform for large-scale, long-term, stable brain mapping. Then, I will discuss the creation of "cyborg organisms", achieved by embedding stretchable mesh-like electrode arrays in 2D sheets of stem/progenitor cells and reconfiguring them through 2D-to-3D organogenesis, which enables continuous 3D electrophysiology during the development of human stem cell-derived brain organoids and animal embryonic brains. Next, I will highlight our current efforts that merge 3D single-cell spatial transcriptomics, machine learning, and electrical recording, enabling cell-type-specific brain activity mapping. In conclusion, I will envision the fusion of soft and flexible electronics, spatial transcriptomics, and AI for a comprehensive brain cell functional atlas to enhance future brain-machine interface applications.

4:45 PM *SB05.01.05

Soft Implantable Bioelectronics for Heart Disease [Dae-Hyeon Kim](#)^{1,2}; ¹Institute for Basic Science, Korea (the Republic of); ²Seoul National University, Korea (the Republic of)

Recent advances in soft electronics have attracted great attention due in large to its potential applications in personalized bio-integrated healthcare devices. The mechanical mismatch between conventional electronic devices and soft human tissues/organs oftentimes causes various challenges, such as the low signal-to-noise ratio of the biosensors, inflammations and/or excessive immune responses near the implanted devices, and unsatisfactory electrical/chemical stimulations in feedback therapies. Therefore, the ultra-flexible, stretchable, and bioresorbable electronic devices have been developed and applied, since their mechanical and material properties are compatible with the in-vivo environment and thus they have a high potential to solve the aforementioned issues. To develop such bioelectronic devices, nanomaterials, their composites, and biodegradable materials have been researched. In this talk, the unconventional electronic material and device strategies and their applications to the treatment of heart diseases are presented. The integration of wireless technologies with the unconventional bioelectronics could provide additional opportunities, and the related results of the wireless bioelectronics are also briefly introduced. These efforts in the development of various unconventional materials and bioelectronic devices are expected to contribute to addressing many unsolved issues in clinical medicine.

Tuesday Morning, April 23, 2024
Room 434, Level 4, Summit

10:30 AM SB05.02.01

Rubbery Bioelectronic Patch for The Heart Cunjiang Yu; The Pennsylvania State University, United States

Electronics that can seamlessly integrate with human body could have significant impact in medical diagnostic, therapeutics. However, seamless integration is a grand challenge because of the distinct nature between electronics and human body. Conventional electronics are rigid and planar, made out of rigid materials. Human body are soft, deformable and curvilinear, comprised of biological materials, organs and tissues. This talk will introduce our solution to address the challenge through the recent development of a new class of electronics, namely rubbery electronics. Rubbery electronics is constructed all based on elastic rubber electronic materials of semiconductors, conductors and dielectrics, which possesses tissue-like softness and mechanical stretchability to allow seamless integration with soft deformable tissues and organs. Rubbery electronic materials (semiconductors, conductors, dielectrics) and device innovations set the foundation. This presentation will describe the development the recent advances of rubbery electronics and rubbery bioelectronics. As a platform technology, rubbery electronics could address many challenges in biomedical research and clinical studies.

10:45 AM SB05.02.02

Effects of Leaflet Design on Structural Integrity and Pump Efficiency of Heart Valves Yu-En Yu¹, Lilian Lin¹, Ching-Chang Huang² and Hao-Ming Hsiao¹; ¹National Taiwan University, Taiwan; ²National Taiwan University Hospital, Taiwan

Heart valve disease results in inadequate blood supply from the heart to the body and could cause many complications, including heart attack, stroke, blood clots, heart arrhythmia, or even sudden death. Conventional heart valve treatments often involve risky and lengthy procedure that requires thoracotomy (open chest). In recent years, interventional transcatheter heart valve products have been launched on the market and becomes popular. The procedure includes deploying a transcatheter heart valve to the lesion site through a micro-catheter to restore normal blood flow.

This study proposed a novel design methodology for transcatheter heart valve leaflets. Unlike most transcatheter heart valves today, our heart valve designs deviated from conventional 3-D molding techniques and used 2-D quadrics sketches instead to save manufacturing cost. Polytetrafluoroethylene (e-PTFE) and e-PTFE with the addition of Polyethylene Terephthalate (e-PTFE + PET) were employed as the leaflet materials due to their high blood biocompatibility. The heart valve has to maintain appropriate valve orifice area during opening and ensure secured seal when closed. In addition, it is essential to withstand large dimensional changes and significant deformations during crimping (inside catheter) and deployment (to heart chamber). An interventional transcatheter heart valve was integrated by combining a nitinol scaffold with an expanded e-PTFE leaflet.

A series of tasks including design, computer simulation, laser cutting and its associated heat treatment, and bench testing were conducted. Ten leaflet designs were sketched using 2-D quadrics and cut from e-PTFE fabrics. Finite Element models were developed to facilitate the design iterations and evaluate the heart valve structural integrity from the crimping into a catheter to the deployment inside the heart chamber for both leaflet and nitinol scaffold. Computational Fluid Dynamics were also analyzed to evaluate the pump efficiency of the heart valve pre vs. post replacement. Laser cutting, heat treatment, electro-polishing, and bench testing were implemented to manufacture and test the prototypes for the proof of concept. Results showed that the leaflet design affected the pump efficiency of the heart valve and the 2-D quadrics leaflet designs were able to provide good performance with reduced cost.

11:00 AM SB05.02.03

Materials Considerations Enabling Chronic Validation of a Wirelessly-Powered, Implantable Drug Delivery System Joanna L. Ciatti^{1,1}, Abraham Vazquez-Guardado^{1,2} and John A. Rogers^{1,1,1}; ¹Northwestern University, United States; ²North Carolina State University, United States

Chronically implanted drug delivery devices face significant challenges that affect tolerance and effective dosage upon implantation in living organisms. Foreign body reaction, for instance, is a well-known adverse response to implants and various materials strategies have been proposed to circumvent it, including surface coatings, topography, and morphology, but often they are limited to non-functional implants. Herein, we present a wireless and battery-free, fully-implantable drug delivery system capable of on-demand drug release enabled by rational materials selection. The system relies on electrolytic pumps for drug delivery, which necessitate optimization of surface degradation mechanisms to allow for long-term stability *in-vivo*. Materials choice, design, and fabrication techniques will be discussed, as they pertain to facilitating the chronic implantation and tolerance of devices. Carefully engineered devices have demonstrated excellent biocompatibility in studies as long as 4 months post-implantation, and successful drug delivery to the bloodstream from the subcutaneous implant after many weeks implanted.

SESSION SB05.03: Organic Electronic Organ Interfaces

Session Chairs: Philipp Gutruf and John Ho

Tuesday Afternoon, April 23, 2024

Room 434, Level 4, Summit

2:00 PM SB05.03.01

Conducting Polymer-Based Bioelectrodes with Enhanced Wet Adhesion and Stretchability Jiwan Jeon and Jin-Woo Park; Yonsei University, Korea (the Republic of)

Bioelectronic devices are mounted on human skin and tissue to get physiological information, enable electrical stimulation, and treat diseases. To fulfill these challenging roles, bioelectronic devices must possess the same mechanical properties as tissues that are soft, stretchable, and conform to the tissue surface. Also, it requires high conductivity and tough adhesion for high-quality electrical communication with devices and organizations. However, traditional bioelectronic devices are typically constructed using rigid metals, carbon nanotubes (CNT), or graphene, which offer excellent electrical conductivity but suffer a significant mechanical mismatch when interfacing with biological tissues. This disadvantage leads to non-conforming electrode-tissue interfaces and can trigger pronounced inflammation. To address these issues, recently, soft bioelectronics have been developed that aim at improving compatibility between the devices and tissues and reducing inflammations by replacing rigid components with soft materials that closely mimic the characteristics of natural tissues. Therefore, bioelectronic devices composed of conducting polymers within a soft matrix have been thought as one of the ideal choices of materials. This combination offers excellent biocompatibility, mechanical properties resembling natural tissues, and desirable electrical

characteristics. Poly(3,4-ethylenedioxythiophene):poly(styrene sulfonate)(PEDOT:PSS) has been studied extensively in soft bioelectronics. However, pure PEDOT:PSS is brittle because PEDOT:PSS network cannot effectively dissipate strain energy. The methods for preparing stretchable electrodes using PEDOT:PSS can be broadly categorized into two main approaches: one involves the design of geometric structures, while the other entails blending with plasticizers, ionic liquids (IL), or polymers. Forming a second network within the existing PEDOT:PSS network to create an interpenetrating polymer network, can enhance the stretchability of the composite electrode. Polyurethane is a hydrophilic polymer that can be easily mixed with PEDOT:PSS. Blending with polyurethane can make low modulus and high stretchability, but it reduces electrical conductivity with increasing amounts of insulating polymer. A higher proportion of PEDOT:PSS is required to achieve higher electrical conductivity while blending with PEDOT:PSS. However, this may result in a more rigid and less stretchable blend due to the inherent properties of PEDOT:PSS. Here, we report a double-network conducting polymer electrode consisting of PEDOT:PSS and polyurethane with high electrical conductivity and large stretchability by using an additive method that effectively reduces the modulus of the matrix and increases conductivity. We use Triton-X as an additive material. Triton-X effectively infiltrates the space between PEDOT:PSS chains and the polymer matrix, thereby increasing the free volume within both PEDOT:PSS and the polymer. This augmentation in free volume contributes to enhanced stretchability. Additionally, serving as a secondary dopant, Triton-X plays a crucial role in elevating the conductivity of PEDOT:PSS. When compared to DMSO, it has shown a more substantial improvement in conductivity. However, excessive Triton-X content can weaken the property of reverting to its original length, making it essential to incorporate an appropriate amount to maintain elastic characteristics. Subsequently, for effective attachment to tissues, wet adhesive properties are essential for signal measurement and stimulation. Polyacrylic acid (PAA) and N-hydroxy succinimide (NHS) have been employed in this regard. PAA-NHS forms covalent bonds on the tissue surface, resulting in robust adhesion. Using this approach, we demonstrate the electrodes that exhibit a low modulus, excellent stretchability, and effective wet adhesion properties, which can be used for implantable bio electrodes for nerve stimulation and implantable sensor for ECG.

2:15 PM SB05.03.02

Materials Science of a Multifunctional/Low Cost / Optimun Bcomptible Ultrananocrystalline Diamond (UNCD™) Coating and Applications to New Generation Implantable Medical Devices/Prosthese and Biological Treatments [Orlando Auciello](#)^{1,2}; ¹The University of Texas at Dallas, United States; ²Original Biomedical Implants, United States

The presentation will focus on discussing materials science / technological applications of a unique material named ultrananocrystalline diamond (UNCD™) in film form integrated into new generations of medical devices/prostheses, as described below: UNCD™ coatings, developed/patented by Auciello and colleagues, are grown on many substrates by low-cost Microwave Plasma Chemical Vapor Deposition (MPCVD) and Hot Filament Chemical Vapor Deposition (HFCVD) techniques, using a patented Ar/CH₄ gas flow into high vacuum chambers, coupling microwave power, or current-induced heating (~ 2200 C) of tungsten filaments. Both processes produce C⁺, C⁰, CH_x⁺, CH_x⁰ (x= 1, 2, 3) species, which establish chemical bonds on substrates' surfaces, inducing nucleation/grow of polycrystalline diamond films with the smallest (2-5 nm) grains of polycrystalline diamond film available today, thus, the name UNCD™ (TM means trademark). UNCD™ coatings exhibit lowest friction coefficient (0.02-0.04) compared with metals (≥ 0.5) currently used in friction-prostheses like hips, knees. UNCD™ exhibits unique biocompatibility, because it is made of C atoms (element of life in human DNA, cells, and molecules). Original Biomedical Implants (OBI-USA and OBI-México) companies are developing new medical devices/prostheses based on the UNCD™ coating, namely: 1) UNCD™-coated silicon-microchip implantable inside the eye as key component of the future artificial retina (The Argus II device, implanted outside the eye, connected to the human retina from outside has been marketed in USA /EU, since 2011, returning partial vision to people blind by genetically-induced degeneration of photoreceptors); 2) New generation implantable prostheses (e.g., dental implants, hips, knees) coated with UNCD™ eliminates failure of current metal-implants due to mechanical wear / chemical corrosion by body fluids (Clinical trials, since 2018, implanting UNCD™-coated dental implants (DI) in 51 patients in clinic in Querétaro-México, demonstrated transformational UNCD™-coated DI performance); 3) UNCD™-coated masks may trap COVID-19 virus better, due to ≤ 20 nm pores vs micron size pores in current masks, and surface C atoms trapping COVID virus more efficiently; 4) Unique electrically conductive/water corrosion resistant Boron-doped UNCD-coated metal electrodes passing electrical current through water, generate ozone (O₃) on the surface of the UNCD coating, enabling O₃ killing all virus, bacteria, and pathogen in water; also, ozonated water jets enable disinfection in 5-10 minutes of surgical instruments without heating them to high temperature for extensive time as currently done.

2:30 PM *SB05.03.03

Stand-Alone Conformable Implantable Bioelectronics Based on Internal Ion-Gated Organic Electrochemical Transistors [Dion Khodagholy](#); Columbia University, United States

It is increasingly appreciated that individual variability can strongly affect response to clinical treatments, motivating approaches that enable long-term monitoring of physiologic signals and delivery of responsive therapeutics. Implanted bioelectronic devices are often critical components of such approaches. The incompatibility of traditional electronic components with physiologic media, risk of device-related tissue disruption, and limited means by which to interface and power implanted devices are key hurdles. Organic electronics can be biocompatible and conformable, enhancing the ability to interface with tissue. However, limitations of speed and integration have thus far necessitated reliance on silicon-based technologies for advanced processing, data transmission, and device powering. Here, we create a stand-alone, conformable, fully organic bioelectronic device capable of realizing these functions. This device is based on a novel transistor architecture that incorporates a vertical channel and miniaturized hydration access conduit to enable MHz signal range operation within densely packed integrated arrays in the absence of crosstalk (vertical internal ion-gated organic electrochemical transistor, vIGT). vIGTs demonstrated long-term stability in physiologic media, and were used to generate high performance multi-stage amplifiers, oscillators, multiplexers, and rectifiers. We leveraged the high speed and low voltage operation of vIGTs to link them with an ion-based powering and data transmission approach that provides power to the transistor in the form of MHz range alternating current and permits signal extraction via modulation of this applied current. The resultant stand-alone device was implanted in freely moving rodents to acquire, process, and transmit neurophysiologic brain signals. Such fully organic devices have the potential to expand the utility and accessibility of bioelectronics to a wide range of clinical and societal applications.

3:00 PM BREAK

SESSION SB05.04/SB08.04: Joint Session: Bioelectronic Technologies
Session Chairs: Philipp Gutruf and Huiliang Wang
Tuesday Afternoon, April 23, 2024
Room 434, Level 4, Summit

3:30 PM *SB05.04/SB08.04.01

Transient Bioelectronic Implants [John A. Rogers](#); Northwestern University, United States

Recently developed classes of electronic materials create an opportunity to engineer 'transient' electronic devices that dissolve, disintegrate, degrade or otherwise physically disappear at triggered times or with controlled rates. This talk describes the latest work in bioresorbable classes of transient devices, designed as temporary implants with therapeutic function. Presented examples range from ultraminiaturized, self-powered cardiac pacemakers, to electrical stimulators of the diaphragm, phrenic nerve and spinal cord - each with well-defined envisioned uses in clinical care.

4:00 PM *SB05.04/SB08.04.02

Technology for Bioelectronic Medicine [George G. Malliaras](#); University of Cambridge, United Kingdom

Neurological conditions affect nearly one in six people in the world, imposing significant health, economic and societal burden. Bioelectronic medicine aims to restore or replace neurological function with the help of implantable electronic devices. Unfortunately, significant technological limitations prohibit these devices from reaching patients at scale, as implants are bulky, require invasive implantation procedures, elicit a pronounced foreign body response, and show poor treatment specificity and off-target effects. Over the past decade, new devices made using methods from microelectronics industry have been shown to overcome these limitations. Recent literature provides powerful demonstrations of thin film implants that are miniaturised, ultra-conformal, stretchable, multiplexed, integrated with different sensors and actuators, bioresorbable, and minimally invasive. I will discuss the state-of-the-art of these new technologies and the barriers than need to be overcome to reach patients at scale.

4:30 PM SB05.04/SB08.04.03

Minimally Invasive Neuroelectronics [Anqi Zhang](#); Stanford University, United States

Neuroelectronic interfaces have enabled significant advances in both fundamental neuroscience research and the treatment of neurological disorders. However, current neuroelectronic devices have a clear trade-off between invasiveness and spatial resolution, and are unable to achieve seamless integration into the nervous system with cell-type specificity. In this talk, I will first introduce an ultra-small and flexible endovascular neural probe that can be implanted into sub-100-micron scale blood vessels in the brains of rodents without damaging the brain or vasculature. Second, I will describe a biochemically functionalized electronic probe that enables cell type- and neuron subtype-specific targeting and recording in the brain. Third, I will present a bottom-up approach for constructing neural interfaces from the cell surface, where neurons are genetically programmed to express membrane-localized enzymes that catalyze in situ assembly of functional materials. Finally, I will discuss future advances toward clinical translation of minimally invasive neuroelectronic interfaces capable of long-term monitoring and treatment of neurological disorders.

SESSION SB05.05: Central Nervous System Interfaces I
Session Chairs: Eric Glowacki and Flavia Vitale
Wednesday Morning, April 24, 2024
Room 434, Level 4, Summit

8:00 AM *SB05.05.01

Advancing Bi-Directional Electrophysiological Studies on The Intact Retina with Soft Multi-Electrode Arrays [Yael Hanein](#), Ieva Vebraite-Adereth and Chen Bar-Haim; Tel Aviv University, Israel

The intricate nature of neural tissues presents formidable challenges in the realm of electrophysiological investigations, particularly when examining intact neural circuits. This challenge is amplified when studying the intact retina, where achieving bi-directional electrophysiological interfacing remains a significant hurdle, and currently available methods fall short of addressing this issue. In this presentation, a novel approach is introduced, leveraging cutting-edge soft multi-electrode arrays to enable comprehensive bi-directional electrophysiological studies on the intact retina. This endeavor involved the development and testing of soft electrode arrays meticulously designed to establish stable electrical connections with the retina. These soft probes were crafted to seamlessly conform to the curvature of the retinal structure within the eye, providing an unprecedented opportunity to study the retina in its unaltered state. Notably, this presentation demonstrates, for the first time, the concurrent capabilities of electrical recording and stimulation directly from the intact retina. Of particular significance is our achievement in mapping retina responses to electrical stimulation. This revelation of the retina's responses under electrical stimuli unveils a striking stability, both in direct and indirect responses, in stark contrast to ex-vivo conditions. Our findings propose an intriguing scenario in which intact retinas exhibit superior stability and resilience compared to their ex-vivo counterparts, positioning them as a more suitable substrate for effectively mapping responses to electrical stimulation. These results not only enhance our comprehension of intact neural circuits but also inaugurate fresh avenues for pioneering research in the field.

8:30 AM *SB05.05.02

NeuroEdge: Graphene Nanoedge Electronics for Monolithic and Chronic Recording at Neuronal Density [Yuxin Liu](#), Yunxia Jin and John S. Ho; National University of Singapore, Singapore

Recording electrophysiological signals from every closely spaced individual neuron over long durations is crucial for understanding the brain micro-circuit and functionalities at the cellular level. However, existing probe technologies are limited by sparse sampling of neurons in the intralaminar plane due to large interelectrode spacing and the need for surface modification materials, which are susceptible to instability over time, in order to have small dimensions and low impedance. Here, we report a monolithic graphene-edge probe array (NeuroEdge) that achieves a density of >2000 electrodes/mm², approaching cortical neuronal density. NeuroEdge is composed of self-aligned reduced graphene oxide nanoflakes with well-exposed nanoedges and electrolyte-filling nanochannels at the end, achieving impedance < 0.2 MΩ at neuronal size. Owing to its monolithic material composition and exceptionally low impedance, NeuroEdge provides stable electrophysiological recording with a high signal-to-noise ratio > 20 dB over 6 months. We demonstrate the utility of NeuroEdge for interrogating closely packed neurons by revealing the heterogeneity of acoustic-triggered activity in mouse auditory cortex. NeuroEdge provides a tool for accurately discriminating spikes from neighboring neurons in microcircuits *in vivo*.

9:00 AM SB05.05.03

Scaling Effects on The Electrochemical Performance of Ti₃C₂T_x MXene Thin-Film Bioelectronics for Neural Recording and Stimulation [Spencer R. Averbeck](#)¹, Raghav Garg¹, Michael S. Beauchamp¹, Yury Gogotsi² and Flavia Vitale¹; ¹University of Pennsylvania, United States; ²Drexel University, United States

In the last few decades there has been a growing interest in the development of technologies for neural recordings and therapeutic electrical brain stimulation. In these applications, microelectrode arrays offer the advantage of high-selectivity and sensitivity approaching the spatiotemporal scales of individual neurons. Recently, 2D $\text{Ti}_3\text{C}_2\text{T}_x$ MXene has emerged as a promising candidate for microscale recording and stimulation, due to its high electrical conductivity and volumetric capacitance. Here, we investigate the scaling effects on the electrochemical performance of thin-film 2D $\text{Ti}_3\text{C}_2\text{T}_x$ MXene microelectrodes with diameters ranging from 500 μm to 25 μm and film thicknesses varying from 100 nm to 700 nm. Prior to all electrochemical characterization measurements, we measured contact diameters, surface roughness, and thicknesses with confocal microscopy, atomic force microscopy (AFM), and 2D profilometry, respectively, in order to accurately assess geometric surface areas and available volumes. We then tested the electrodes with electrochemical impedance spectroscopy (EIS), cyclic voltammetry (CV), voltage transients (VT), as well as 10,000 continuous cycles of biphasic stimulation pulses. Through these experiments, we calculated impedance modulus at 10 Hz and 1 kHz, charge storage capacity (CSC), and charge injection capacity (CIC) across the various electrode contact sizes and thicknesses. We also investigated the effects of pulse-width and waveform asymmetry on the calculated CIC values to determine the optimal stimulation parameters for the safe and effective delivery of electrical stimulation in thin-film $\text{Ti}_3\text{C}_2\text{T}_x$ MXene microelectrodes. We found there was an expected increase in the magnitude of impedances at 1 kHz as the contact diameters decreased from 500 μm to 25 μm with an average thickness of 100 nm, increasing from $9.1 \pm 1.9 \text{ k}\Omega$ in the 500 μm contacts to $506 \pm 220 \text{ k}\Omega$ in the 25 μm contacts. Similarly, CIC values also increased as the contact size decreased, increasing from $40 \pm 10 \mu\text{C cm}^{-2}$ to $400 \pm 50 \mu\text{C cm}^{-2}$ in the 500 μm and 25 μm contacts, respectively. Ultimately, our findings indicate that $\text{Ti}_3\text{C}_2\text{T}_x$ MXene microelectrodes are able to safely deliver electrical microstimulation, opening the door to further diagnostic and therapeutic research as well as improve our biological understanding of neural activity through electrophysiological recording and electrical stimulation.

9:15 AM SB05.05.04

Orbit Symmetry Breaking in MXene Implements Enhanced Soft Bioelectronic Systems [Wubin Bai](#); University of North Carolina, Chapel Hill, United States

Bioelectronic systems with soft mechanics, stable biocompatibility, and high-performance electronic recording and stimulation interfaces to internal organs offer paradigm-shifting potentials for advancing biomedical implants such as those for cardiovascular disease. Yet, challenges remain in the development of biocompatible materials with practical scalability for constructing bioelectronic systems that leverage performance and interfacial attributes to not only functionally approach those of conventional wafer-based technologies but also biologically compatible for long-term in-body operation. Here, we present the orbit symmetry breaking in MXene (a low-cost scalable, flexible, and conductive 2D layered material), implementing the improved electrode-tissue interface impedance, which stems from the out-of-plane charge transfer, and coupling with in-plane high conductivity comparable to precious metals. Besides, we compare MXene bioelectronics with commercial biotracers (gold, graphene oxide, and poly(3,4-ethylenedioxythiophene) polystyrene sulfonate), emphasizing its enhanced biocompatibility, durability, and imaging visibility in bioelectronic systems. Accordingly, we introduce an epicardial patch based on orbit-symmetry-broken MXene that integrates the matrix mapping of electrophysiological activity and therapeutic capabilities across large areas at high-fidelity spatiotemporal resolution. Last, a wireless and battery-free MXene module, combined with real-time recording and closed-loop stimulation, demonstrates high signal-to-noise ratio data transmission, and wireless power transfer within bioelectronic systems.

9:30 AM +SB05.05.05

Bioengineering Strategies towards Multielectrode Arrays for Chronic *In Vivo* Neural Recording and Chemical Sensing [Xinyan T. Cui](#); University of Pittsburgh, United States

Microelectrode array (MEA) devices, placed in the nervous system to record and modulate neuroactivity have demonstrated success in neuroscience research and neural prosthesis applications. Functionalizing the microelectrode sites on MEAs to enable electrochemical sensing adds additional dimensions of information, and such multimodal MEAs present tremendous potential for understanding neural circuits and treating neurological diseases. In this talk, I will introduce the methods by which we enable chemical sensing from MEAs. By incorporating nanocarbon into the conducting polymer electrode coating, we achieved direct detection of electroactive species such as dopamine, melatonin, and serotonin. By immobilizing enzymes or aptamers on nanostructured electrodes, we achieved multisite detection of glutamate, GABA, and cocaine. Multisite and multiple analyte detection along with neural recording have been demonstrated with these MEAs. Currently, the chronic recording and sensing performance of implantable MEAs is sub-optimum due to material limitations and undesired host tissue responses. Quantitative histology, explant analysis, and 2-photon imaging revealed biofouling, neuronal damage, inflammation, and oxidative stress at the site of implants. Meanwhile, material degradation also contributes to device failure. We use several bioengineering strategies to minimize these failure modes. First, materials and devices that mimic the mechanical properties of the neural tissue have been developed and shown to significantly improve device-tissue integration. Secondly, biomimetic coatings and drug delivery have been applied to reduce biofouling and inflammatory responses. These approaches may be combined to achieve long-term and high-fidelity neural recording and chemical sensing.

10:00 AM BREAK

SESSION SB05.06: Bioelectronic Medicine
Session Chairs: Philipp Gutruf and Flavia Vitale
Wednesday Morning, April 24, 2024
Room 434, Level 4, Summit

10:30 AM *SB05.06.01

A Thin-Film Optogenetic Visual Prosthesis [Jonathan Reeder](#); Science Corporation, United States

Retinitis pigmentosa and macular degeneration lead to photoreceptor death and loss of visual perception. Despite recent progress, restorative technologies for photoreceptor degeneration remain largely unavailable. Here, we describe a novel optogenetic visual prosthesis (FlexLED) based on a combination of a thin-film retinal display and optogenetic activation of retinal ganglion cells (RGCs). The FlexLED implant is a 30 μm thin, flexible, wireless μLED display with 8,192 pixels, each with an emission area of 66 μm^2 . The display is affixed to the retinal surface, and the electronics package is mounted under the conjunctiva in the form factor of a conventional glaucoma drainage implant. In a rabbit model of photoreceptor degeneration, optical stimulation of the retina using the FlexLED elicits activity in visual cortex. This technology is readily scalable to hundreds of thousands of pixels, providing a route towards an implantable optogenetic visual prosthesis capable of generating vision by stimulating RGCs at near-cellular resolution.

11:00 AM SB05.06.02

Implantable Bioelectronic Systems for Early Detection of Kidney Transplant Rejection [Surabhi Madhvapathy](#)¹, [Jiao-Jing Wang](#)¹, [Heling Wang](#)²,

Manish Patel³, Anthony Chang⁴, Xin Zheng¹, Yonggang Huang¹, Zheng Jenny Zhang¹, Lorenzo Gallon¹ and John A. Rogers¹; ¹Northwestern University, United States; ²Tsinghua University, China; ³University of Illinois at Chicago, United States; ⁴The University of Chicago, United States

Early-stage organ transplant rejection can be difficult to detect. Percutaneous biopsies occur infrequently and are risky, and measuring biomarker levels in blood can lead to false-negative and -positive outcomes. We developed an implantable bioelectronic system capable of continuous, real-time, long-term monitoring of the local temperature and thermal conductivity of a kidney for detecting inflammatory processes associated with graft rejection, as demonstrated in rat models. The system detects ultradian rhythms, disruption of the circadian cycle, and/or a rise in kidney temperature. These provide warning signs of acute kidney transplant rejection that precede changes in blood serum creatinine/urea nitrogen by 2 to 3 weeks and approximately 3 days for cases of discontinued and absent administration of immunosuppressive therapy, respectively.

11:15 AM ^SB05.06.03

Wireless, Battery-Free Bioelectronics for Fully Implantable, Living Medical Devices Siddharth Krishnan, Matthew Bochenek, Suman Bose, Claudia Liu, Amanda Facklam, Nima Khatib, Ben Walters, Derin Gumustop, Laura O'Keeffe, Robert Langer and Daniel Anderson; MIT, United States

Living cells are a novel class of therapeutics that offer possibilities in long-term protein replacement. Primary cells such as pancreatic islets can offer functional cures for Type I Diabetes via responsive insulin secretion, as can stem-cell derived products¹. Immortalized cell lines can be engineered or transfected to secrete nearly any protein of choice, to address a broad range of conditions from blood-borne disorders to degenerative neural disease and cancer^{2,3}. Two core challenges limit the clinical translation of these types of cell therapies: first, the potential for recognition and attack by the host immune system necessitates the use of chronic immunosuppressants to maintain graft viability, with mixed success. Second, the formation of fibrotic capsules around transplanted cells isolates them from native vasculature, resulting in hypoxia¹.

In this work, we demonstrate a wireless battery-free device system capable of housing and supporting therapeutic cells in vivo by providing both immune-isolation and oxygen supply⁴. Transplanted cells are separated from host tissue by nanoporous membranes that prevent infiltration and attack by immune cells, obviating the need for immune suppression. A multilayer materials system comprising a proton-exchange membrane electrolyzer and an elastomeric encapsulation allows for direct splitting of molecular water into oxygen and hydrogen. Oxygen is stored in an elastomeric chamber that diffuses directly into regions containing transplanted cells. The entire reaction is sustained by a wireless power harvesting circuit based on resonant inductive coupling, at a frequency (13.56 MHz) chosen for its low specific absorption rate in biological tissue and compatibility with existing commercial infrastructure for two-way data and power transfer.

Systematic numerical modeling, benchtop testing, and in vitro experimentation highlight key aspects of device and materials performance.

In vivo studies demonstrate high levels of performance. HEK293T cells engineered to secrete a model protein system (erythropoietin, EPO), demonstrate sustained, significantly elevated levels of protein production when transplanted in O₂-Macrodevices relative to cells encapsulated in non-oxygenated control devices over several weeks. Xenogeneic rat islets transplanted into immune competent, diabetic C57BL/6J mice resulted in complete diabetic reversal for several weeks, with explantation studies revealing viable, glucose response islets. Notably, all of these studies involved transplantation into minimally invasive subcutaneous sites, that are clinically attractive owing to their easy accessibility for implantation and explantation procedures.

Taken together, these results combine advances in materials, electrochemistry, wireless power transfer and bioengineering to support xenogeneic and allogeneic therapeutic cells in vivo without the need for immune suppression, in minimally invasive sites. These hybrid "living" medical devices, combining cellular and inorganic device materials, could provide pathways for functional cures for a broad range of organ-specific diseases.

References

- 1 Thanos, C. G., Gaglia, J. L. & Pagliuca, F. W. Considerations for successful encapsulated β -cell therapy. *Cell therapy: Current status and future directions*, 19-52 (2017).
- 2 Fomin, M. E., Togarrati, P. P. & Muench, M.O. *Journal of Thrombosis and Haemostasis* (2014).
- 3 Emerich, D. F., Orive, G., Thanos, C., Tornøe, J. & Wahlberg, L. U. Encapsulated cell therapy for neurodegenerative diseases: from promise to product. *Advanced drug delivery reviews* **67**, 131-141 (2014).
- 4 Krishnan, S. R. *et al.* A wireless, battery-free device enables oxygen generation and immune protection of therapeutic xenotransplants in vivo. *Proceedings of the National Academy of Sciences* **120**, e2311707120 (2023).

SESSION SB05.07: Engineered Materials for Biointerfaces

Session Chairs: Philipp Gutruf and Flavia Vitale

Wednesday Afternoon, April 24, 2024

Room 434, Level 4, Summit

1:45 PM SB05.07.01

Advanced Thermogel Biomaterials for Ophthalmic Applications and Drug Delivery Jason Y. Lim¹, Qianyu Lin¹, Xian Jun Loh¹ and Xinyi Su²; ¹Institute of Materials Research and Engineering (IMRE), Singapore; ²Institute of Molecular and Cell Biology, Singapore

Retinal detachment is amongst the leading causes of blindness globally. After vitrectomy surgery, vitreous endotamponades are implanted into the vitreous cavity to facilitate retinal reattachment and recovery. Existing endotamponade materials are suboptimal: silicone oil can lead to inflammation and require follow-up surgery for removal, while expansile gases such as sulfur hexafluoride results in raised intra-ocular pressure and require the patient to adopt prolonged face-down positioning due to their buoyancy. Recently, temperature-responsive hydrogels, also known as thermogels, have emerged as a new highly-promising class of vitreous endotamponades. Our self-assembled thermogels offer easy injectability, transparency, possess the same density and refractive indices as native vitreous humor, show low in-vivo cytotoxicity and have the ability to provide sufficient swelling counter-force to facilitate retina re-attachment. In this presentation, our team's efforts in developing new generations of biocompatible thermogel-based vitreous endo-tamponades will be discussed. We show that our thermogels can be naturally cleared from the vitreous cavity post-surgery, whilst allowing the regeneration of a vitreous-like body with high proteomic similarity as native vitreous – the first biomaterial known to do so. In addition, we show the profound influences of polymer branching on the in-vivo performance of thermogel endotamponades, and also demonstrate the importance of this often-overlooked parameter on applications such as sustained drug release. Our findings demonstrate the vast potential of self-assembled thermogels as a viable biomaterial that can

revolutionise ophthalmic treatment.

2:00 PM SB05.07.02

Enhancing The Properties of a Novel Mg-Ca-Mn-Sr Alloy using Phosphorus Ion Implantation for Potential Orthopedic Use [Saqlain A. Shah](#) and Mazhar Hussain Asdi; Forman Christian College, Pakistan

This research delves into the impact of phosphorus (P) ion implantation on the morphological, microstructural, mechanical, and electrochemical attributes of an innovative biodegradable Mg–2Ca–1Mn–1 Sr (XMJ211) alloy when exposed to simulated body fluid (SBF) for potential orthopedic implant applications. The distinctiveness of this study arises from the innovative alloy blend and the methodical enhancement of its features through P ion implantation at different levels. Through XRD assessments, we observed a rise in the proportions of secondary binary phases, notably Mg₃P₂, and a reduction in grain size, decreasing from about 71 μm to 39 μm as P implantation was escalated. The alloy's mechanical hardness saw an enhancement, moving from around 60 HV to 75 HV, owing to grain size reduction and an uptick in secondary binary particles. Electrochemical evaluations highlight the alloy's augmented bio-corrosion resistance, moving from 48 kΩ to 87 kΩ as we increased the P concentration, albeit with lesser impact at heightened levels. Our findings underscore the ability to strike a balance between the mechanical and electrochemical characteristics of the alloy using moderate phosphorus levels. This not only emphasizes its potential as a viable biodegradable material for orthopedic implantation but also underscores the elimination of a secondary surgical procedure post-recovery. The insights from this research fill an existing void in current scientific discourse, offering a fresh perspective on augmenting the efficacy of Mg-centric alloys in the realm of biomedicine.

2:15 PM SB05.07.03

Mechanical Properties of Hydroxyapatite Coatings via Plasma Spray Deposition [Craig Rosenblum](#)^{1,2}; ¹Hitemco Medical Applications LLC, United States; ²The Johns Hopkins University, United States

Hydroxyapatite (HA) coatings deposited via plasma spray deposition have gained significant attention in the field of biomaterials due to their excellent biocompatibility and bioactivity. Understanding the mechanical properties of HA coatings produced through this deposition technique is crucial for their successful application in various biomedical and dental fields. This review aims to provide a comprehensive overview of the mechanical properties of HA coatings produced via plasma spray deposition, including their adhesion strength, hardness, porosity, and fracture behavior.

Adhesion strength is a critical mechanical property of HA coatings, as it ensures their long-term stability and performance. The review highlights the factors influencing the adhesion strength, such as surface preparation, coating parameters, and substrate properties. Use of a resorbable blast media such as apatitic abrasive to roughen the substrate of medical implants prior to the application of HA coating will provide a residue-free, textured surface for effective coating adhesion. Various characterization techniques, including tensile testing, pull-off tests, and scratch tests, have been effectively used to evaluate the adhesion strength of HA coatings produced via plasma spray deposition.

The hardness of HA coatings is another crucial mechanical property, which determines their resistance against wear and deformation. The review discusses the influence of plasma spray parameters, such as feedstock particle size and distribution, spray distance, feed rate, and temperature, on the hardness of HA coatings. Hardness characterization techniques, including indentation testing, have been utilized to assess the mechanical hardness of these coatings.

Porosity is an inherent characteristic of plasma-sprayed HA coatings and significantly affects their mechanical properties. The review examines the impact of spray parameters, such as spray distance, gas flow rate, and powder feedstock, on the porosity of HA coatings. Various imaging and characterization techniques, including scanning electron microscopy (SEM), have been utilized to quantify the porosity of these coatings.

In conclusion, understanding the mechanical properties of hydroxyapatite coatings produced via plasma spray deposition is crucial for their successful application in biomedical and dental fields. By optimizing the deposition parameters and post-processing techniques, it is possible to tailor the mechanical properties of these coatings to meet specific application requirements of the subject implantable device. Further research is needed to explore advanced characterization techniques and develop innovative strategies to enhance the mechanical performance of plasma-sprayed HA coatings.

2:30 PM BREAK

3:30 PM *SB05.07.04

Towards Implantable Biohybrid and Regulated Cell Therapies [Jonathan Rivnay](#); Northwestern University, United States

The union of bioelectronics with engineered mammalian cells is a transformative opportunity in regulated, personalized therapeutics. This approach involves combining the strengths of synthetic biology – namely biological specificity that leverages the natural machinery of cells – with bioelectronic systems, which offer precision timing, dose control, and communication with established sensing technologies and clinical feedback. To this end, we show how implanted biohybrid devices rely on bioelectronics to initiate the production of native peptides, control therapeutic dose, and support the health and productivity of these “cell factories”. We demonstrate optogenetic induction of drug production, fluorescence feedback via photometry to probe cell factory viability, and on-site electrocatalytic oxygenation for maintenance of implanted cell health at high cell density. Current efforts focus on regulation of circadian rhythms; however, the biohybrid cell therapy concept can be broadly applied to chronic diseases including Type I diabetes, obesity, and cancer immunotherapies.

SESSION SB05.08: Central Nervous System Interfaces II

Session Chairs: Philipp Gutruf and Flavia Vitale

Wednesday Afternoon, April 24, 2024

Room 434, Level 4, Summit

4:00 PM SB05.08.01

Electrochemically Mutable Soft Metasurfaces for Light Manipulation [Siddharth Doshi](#)¹, Anqi Ji¹, Ali Mahdi¹, Scott Keene², Skyler P. Selvin¹, Philippe Lalanne³, Eric Appel¹, Nicholas Melosh¹ and Mark Brongersma¹; ¹Stanford University, United States; ²University of Cambridge, United Kingdom; ³CNRS, France

Active optical metasurfaces, capable of dynamically manipulating light in ultra-thin form factors, enable novel interfaces between humans and technology.

Miniaturized implantable devices for light delivery open new applications in biophotonics, including minimally invasive sensing, endoscopic imaging, and optogenetic stimulation. The next generation of human-photonics interfaces will require mechanically adaptive, minimally invasive devices that can dynamically manipulate the shape of optical wavefronts and their spectral properties. In such interfaces, soft materials bring many advantages based on their flexibility, compliance, and large stimuli-driven responses.

Here, we realise electrochemically-mutable, soft (EMuS) metasurfaces that capitalise on the swelling of soft conducting polymers to alter the shape and associated resonant response of metasurface elements. Previous approaches to dynamic metasurfaces that rely on index-tuning of materials are fundamentally constrained by Kramers-Kronig relations, which prescribe that significant tuning (i.e. index changes) naturally comes with notable absorptive losses. By leveraging the deformability of soft materials to modulate geometry we circumvent these limitations, allowing for effective, low-loss phase tuning. Using the commercial polymer, PEDOT:PSS, we demonstrate dynamic, high-resolution color-tuning and high-diffraction-efficiency (>19%) beamsteering devices that operate at CMOS compatible voltages (~1.5V). Our devices can be realised as ultra-thin, sub-micron coatings, and provide a building block for a new generation of active opto-electronic devices amenable for integration with the human body, potentially enabling new applications in implantable light guiding and bio-imaging.

4:15 PM SB05.08.02

Implantable Microfluidics for Membrane-Free Neurochemical Sampling in Freely Moving Animals Yi Zhang and Guangfu Wu; University of Connecticut, United States

Extensive studies in both animals and humans have demonstrated that high molecular weight neurochemicals, such as neuropeptides and other polypeptide neurochemicals, play critical roles in various neurological disorders. Despite many attempts, existing methods are constrained by detecting neuropeptide release in small animal models during behavior tasks, which leaves the molecular mechanisms underlying many neurological and psychological disorders unresolved. Here, we report a wireless, implantable microfluidic system for membrane-free neurochemical sampling with cellular spatial resolution in freely moving animals. In vitro studies demonstrate the sampling of various neurochemicals with high recovery (>80%). Open-field tests reveal that the device implantation does not affect the natural behavior of mice. The probe successfully captures the pharmacologically evoked release of neuropeptide Y in freely moving mice. This wireless push-pull microsystem creates opportunities for neuroscientists to understand where, when, and how the release of neuropeptides modulates diverse behavioral outputs of the brain.

4:30 PM *SB05.08.03

Multimodality Sense and Actuate Bioelectrical Interfaces Tzahi Cohen-Karni; Carnegie Mellon University, United States

My team's efforts are focused on the development and engineering of nanomaterials-based flexible platforms to interrogate and affect the properties of tissue and cells. A few of the major questions we strive to answer are: Can we make materials and platforms tailored to allow seamless and stable integration with cells and tissue as well as enable sensing and actuation? Can hybrid-nanomaterials allow new insights into biological processes such as tissue development and disease progression? Highly flexible bottom-up nanomaterials synthesis capabilities allow us to form unique hybrid-nanomaterials that can be used in various input/output bioelectrical interfaces, i.e., bioelectrical platforms for chemical and physical sensing and actuation. The outstanding electrochemical properties of the synthesized hybrid-nanomaterials allow us to develop highly efficient catalysts, and electrical sensors and actuators. We demonstrated sensors capable of exploring brain chemistry and sensors/actuators that are deployed in a large volumetric muscle loss animal model. Finally, using the unique optical properties of nanocarbons in the form of graphene-based hybrid-nanomaterials and 2D nanocarbons (MXene), we have formed remote, non-genetic bioelectrical interfaces with excitable cells and modulated cellular and network activity with low needed energy and high precision. In summary, the exceptional synthetic control and flexible assembly of nanomaterials provide powerful tools for fundamental studies and applications in life science and potentially seamlessly merge nanomaterials-based platforms with cells, fusing nonliving and living systems together.

SESSION SB05.09: Poster Session: Materials and Systems for Fully Implantable Organ Interfaces

Session Chairs: Philipp Gutruf and Flavia Vitale

Wednesday Afternoon, April 24, 2024

Flex Hall C, Level 2, Summit

5:00 PM SB05.09.01

High Molecular Weight Branched Polyurethane Thermogels as Vitreous Endotamponades Qianyu Lin¹, Zengping Liu^{2,3,4}, Jason Y. Lim^{1,3}, Xinyi Su^{2,3,4} and Xian Jun Loh^{1,3,5}; ¹Institute of Materials Research and Engineering, Singapore; ²Institute of Molecular and Cell Biology, Singapore; ³National University of Singapore, Singapore; ⁴Singapore Eye Research Institute, Singapore; ⁵Nanyang Technological University, Singapore

Vitreous endotamponades are essential medical materials employed to seal retina tears and promote retinal reapposition after vitrectomy. Current clinical endotamponades in use include silicone oil and expansile gases but they require patients to assume prolonged faced down position and offer poor immediate visual acuity due to their buoyancy and low refractive indices respectively. Additionally, they are frequently associated with complications such as cataracts, glaucoma, and retinopathy due to emulsification of the silicone oil. As such, there has been great interest to develop biocompatible hydrogel-based vitreous endotamponades that offer much enhanced optical clarity and comfort to patients with reduced risk of complications. Among hydrogel-based endotamponades, thermogels are particularly advantageous. Thermogels are supramolecular hydrogels capable of self-assembly gelation in response to applied temperature. It undergoes spontaneous sol-gel phase transition when warmed above its gelation temperature without additional chemical crosslinkers. This allows thermogels to be facily employed as vitreous endotamponades as clinicians can easily inject it as a sol and its gel phase will form spontaneously to fully fill the vitreous cavity and provide the required tamponading effect.

For hydrogel-based vitreous endotamponades, it is desirable to have low polymeric content to ensure low osmotic pressure; high osmotic pressure in the vitreous cavity is associated with mechanical damage to the retina. For a thermogelling copolymer, a high molecular weight would provide gelation at low polymeric concentrations (~ 5 wt%). However, our previous study had shown that a transparent thermogel of high molecular weight tend turned opaque after implantation in the vitreous cavity. We believe that the thermogel turned opaque in the eye due to protein adhesion and aggregation to the hydrogel matrix due to the high hydrophobicity of the high molecular weight linear copolymer used to formulate the thermogel. To address the current limitation, we propose to change the architecture of the thermogelling copolymer from linear to branched to allow the copolymer to possess brush-like capability to reduce protein adhesion and thus maintain optical transparency in the vitreous cavity. Herein, we demonstrate that a branched high molecular weight thermogelling copolymer is able to perform as a vitreous endotamponade and maintain optical transparency in the vitreous cavities of rabbit models.

We further demonstrated that there is an optimal amount of polymer branching to ensure biocompatibility of the thermogel in the eye. Molecular weight analyses showed that the copolymers become more globular with more branches. Subsequent critical micelle concentration (CMC) and thermodynamics analyses showed that the increasingly globular copolymers had reduced ability to form micelles. Further small angle X-ray scattering (SAXS) analysis of the sol-gel phase transition of the branched thermogels showed that higher degree of branching lowered the propensity of micelles to aggregate into a stable hydrogel matrix. This is later reflected as higher gelation temperatures, lower gel stiffness, and higher rate of thermogel erosion. Subsequent implantation into the vitreous cavities of rabbits showed that thermogels from highly branched polymers rapidly disintegrated into large floating gel blocks and debris, which significantly lowered the biocompatibility by causing retina atrophy. Overall, we identified a new family of branched thermogels that can function effectively as vitreous endotamponades and delineated the effects of polymer branching on the performance of thermogelling vitreous endotamponades.

5:00 PM SB05.09.02

Biodegradable Gel Electrolyte for Self-Electrified Implantable Biomedical Devices [Giheon Kim](#)^{1,2}; ¹Korea University, Korea (the Republic of); ²BK21 Four Institute of Precision Public Health, Korea (the Republic of)

Gel electrolyte have attracted increasing attention as one of compartment of battery system due to their mechanical strength and high capacitance-to-volume ratio. However, the non-biodegradable gel electrolyte is still challenging to apply to various applications because of the harmfulness to environment and the toxicity to human. Here, we developed the biodegradable gel electrolyte by blending the polyvinyl alcohol (PVA) with polyethylene glycol (PEG) to enhance their mechanical, electrical, and electrochemical stability for implantable bioelectronic devices. We synthesized the different ratio of blended hydrogel (PEG:PVA = 1, 2, 5, 10, 20 %) by freezing-thawing method. The biodegradable gel electrolyte is achieved by immersing the blended hydrogel into ion-rich solution (*i.e.*, Phosphate Buffered Saline (PBS) and ionic liquid etc.). The prepared gel electrolyte exhibits better **mechanical strengths** (tensile strength of ~30 kPa under 120 % of strain) and high **ionic conductivity** (~ 50 mS/cm) compared to pure PVA hydrogel and PEO hydrogel. Although the liquid electrolyte induces the corrosion of biodegradable electrode (Mg, W, Mo etc.) surface leading to poor electrochemical performance, the prepared gel electrolyte can increase the anodic reaction up to 3.7 V, which reduce the corrosion and hydrogen evolution reaction (HER) of biodegradable anode and cathode. In addition, the PEG:PVA blended hydrogel is degraded by 14 days at 37 °C, which can be applied to biodegradable bioelectric devices. We anticipated that the biodegradable gel electrolyte can be applied for the biodegradable self-powered electroceuticals and biodegradable supercapacitor for implantable biomedical applications.

5:00 PM SB05.09.03

Design, Simulation and Fabrication of Novel Flat-Wire Braided Flow Diverter for Cerebral Aneurysm [Yao-An Zhuang](#)¹, Lillian Lin¹, Chen-Hsin Lin¹, Ching-Chang Huang² and Hao-Ming Hsiao¹; ¹National Taiwan University, Taiwan; ²National Taiwan University Hospital, Taiwan

Cerebral aneurysm is a weakened cerebral artery which causes localized ballooning of the blood vessel. As an aneurysm grows, it puts pressure on adjacent tissues and may eventually rupture, leading to severe events or even sudden death. Today the flow diverter, a stent-like mesh device, has gained increasing popularity for the endovascular treatment of cerebral aneurysms. The mechanism is to stop the blood flow into an aneurysm via the fine-mesh structure of the flow diverter to reduce the risk of rupture. It also serves as a scaffold for endothelialization, effectively sealing off an aneurysm from the body circulation. The paradigm shift in the treatment preference from traditional craniotomy reflects the growing confidence in the effectiveness of the flow diverter for managing cerebral aneurysms.

Braided flow diverter is currently used to treat cerebral aneurysms, with the braiding technology adopted to build stent-like mesh devices. Braiding is considered to be more cost-effective when compared to other stent fabrication techniques such as laser-cutting. When braiding, round wires extending from bobbins can be secured to the end of a mandrel under tension to form a braided device around it. In this paper, instead of using round wires, a novel flat-wire design with the wire dimension of 25 µm in thickness and 127 µm in width was investigated. This unique wire geometry possesses a higher aspect ratio that results in thinner struts and greater metal coverage (less opening). It is believed that thinner struts reduce the low wall shear stress zones and thus the risk of in-stent stenosis, a significant complication of narrowed arteries. Therefore, using flat wires could reduce the occurrence of in-stent stenosis, while increasing the metal coverage to cut down the blood supply to the aneurysm simultaneously.

A flat-wire braided flow diverter was investigated in this paper. Finite element analysis (FEA, ABAQUS) and computational fluid dynamics (CFD, ANSYS) were conducted to evaluate the mechanical integrity and hemodynamic behavior under various conditions consistent with the current practice. CFD models were analyzed based on an ideal aneurysm assembly with a flat-wire braided flow diverter implanted to evaluate its therapeutic effects. Prototypes were fabricated in-house using a braiding machine with the capacity of up to 64 bobbins, followed by the validation of bench tests for proof of concept. FEA simulation results showed no material damage occurred during the manufacturing and deployment processes as the strains were within the safety range. CFD simulation results showed the flat-wire braided flow diverter stopped a significant portion of the blood flow into an aneurysm. The velocity streamlines helped visualize the effectiveness of the increased metal coverage. These conclusions suggest that the flat-wire braided flow diverter has a great potential to achieve the best possible clinical outcomes.

5:00 PM SB05.09.04

Porous, Antibacterial and Biocompatible GO/n-HAp/bacterial cellulose/ β -glucan Biocomposite Scaffold for Bone Tissue Engineering [Saqlain A. Shah](#)¹ and Mua Khan²; ¹Forman Christian College, Pakistan; ²University of Punjab, Pakistan

We developed a nanocomposite scaffold for bone tissue engineering (using bacterial cellulose (BC) and β -glucan (β -G)) *via* free radical polymerization and freeze-drying technique. Hydroxyapatite nanoparticles (n-HAp) and graphene oxide (GO) were added as reinforcement materials. The structural changes, surface morphology, porosity, and mechanical properties were investigated through spectroscopic and analytical techniques like Fourier transformation infrared (FT-IR), scanning electron microscope (SEM), Brunauer–Emmett–Teller (BET), and universal testing machine Instron. The scaffolds showed remarkable stability, aqueous degradation, spongy morphology, porosity, and mechanical properties. Antibacterial activities were performed against gram -ive and gram +ive bacterial strains. The BgC-1.4 scaffold was found more antibacterial compared to BgC-1.3, BgC-1.2, and BgC-1.1. The cell culture and cytotoxicity were evaluated using the MC3T3-E1 cell line. More cell growth was observed onto BgC-1.4 due to its uniform interrelated pores distribution, surface roughness, better mechanical properties, considerable biochemical affinity towards cell adhesion, proliferation, and biocompatibility. These nanocomposite scaffolds can be potential biomaterials for fractured bones in orthopedic tissue engineering.

5:00 PM SB05.09.05

Comparison of Tensile Properties of Amniotic Membranes Sterilized with Different Techniques [Abigail Poland](#), [Molly Post](#), [Olivia Logan](#), [Isabella Sledge](#), [Babak Safavieh](#) and [Mora Melican](#); Tides Medical, United States

The amniotic membrane has gained recognition as a promising biomaterial in the field of regenerative medicine. The market offers a diverse range of placental membrane products designed for various applications. When evaluating and characterizing the numerous amniotic products available, it becomes crucial to ensure that each product aligns with the specific user requirements, particularly concerning the mechanical characteristics for wound care

applications. One effective method for testing this characteristic involves tensile testing. In this study, the Instron 5544 was used to test tensile strength of two different amniotic products. A standardized and optimized procedure for conducting tensile tests on amniotic products has not been previously well-established. This study addresses this gap by introducing a standardized test method for the tensile testing of dehydrated amniotic membrane. Through this study, we compare the handling capabilities of Artacent Wound®, a dual layer amniotic scaffold, sterilized with electron beam (e-beam) sterilization, to Artacent Wound® sterilized using an alternative sterilization technique.

Multiple sterilization techniques, such as gamma irradiation, ethylene oxide (ETO) gas sterilization, e-beam, and several other approaches have been utilized to remove potential pathogens for products derived from human placentas. However, the sterilization method can lead to diverse impacts on the material's mechanical characteristics. To ensure that the mechanical properties are maintained with the alternative sterilization technique, the Artacent Wound® product is compared to the e-beam sterilized Artacent Wound® product.

Tensile tests were performed on two different Artacent Wound® products (one with e-beam sterilization and one with an alternative sterilization technique), and the products were tested for Failure Stress (MPa), Failure Strain (%), and Young's Modulus (MPa). The tests were used to characterize and better understand the product's mechanical properties and how the sterilization techniques impact these properties. By developing a method to test tensile strength for amniotic products, new products and new processing steps can be easily tested to determine the mechanical impacts to the product.

5:00 PM SB05.09.06

An Open-Source Platform for Clinical Autonomic Neuromodulation Therapies Mona A. Mohamed¹, Ali Soleimani¹, Farbod Amirghasemi¹, Ellis F. Meng¹, Victor Pikov², Raja Hitti³, Hangbo Zhao¹ and Maral Mousavi¹; ¹University of Southern California, United States; ²Medpace Inc., United States; ³Med-Ally LLC, United States

The field of bioelectronic medicine is rapidly progressing, with emerging therapeutic approaches necessitating precise closed-loop control of neural activity in peripheral nerves like the vagus nerve, sacral nerve, pudendal nerve, enteric nervous system, and others. However, transitioning neuromodulation therapies for human clinical application poses significant challenges due to the high costs and lengthy development timelines required for implantable devices suitable for human use. Presently, many clinical research teams rely on off-the-shelf commercial devices for testing on both large animals and humans. These commercial devices are often tailored to specific applications and may not align with the requirements of novel therapies. Collaborations with large corporations can be complicated by potential conflicts of interest that hinder successful partnerships. Furthermore, existing devices often lack the capacity to record biomarkers from multiple sites, limiting their therapeutic potential. As a result, access to customizable neuromodulation technology stands as a substantial obstacle to scientific breakthroughs and the advancement of new treatments.

The CARSS Center, a collaborative venture involving the University of Southern California, Medpace Inc., and Med-Ally LLC, aims to address this challenge. They are creating an open-source system for closed-loop autonomic neuromodulation specifically designed for human clinical investigations. The CARSS system consists of an implantable pulse generator (IPG) equipped with Bluetooth capabilities and native support for running machine learning algorithms. Additionally, it includes a variety of leads for both stimulation and sensing purposes. The initial set of leads comprises a vagus nerve cuff and a sacral nerve linear array with combined stimulation and neural sensing capabilities, as well as electrocardiography, electromyography, and motion sensing leads for physiological monitoring. Further leads in development encompass sensing leads for neurotransmitters such as acetylcholine and catecholamines, as well as physical sensing leads for strain and end-organ temperature. CARSS is actively seeking collaborators interested in utilizing the system to conduct comprehensive studies on large animals, with the goal of eventually advancing these therapies to initial use in human patients.

5:00 PM SB05.09.07

A Cellulose Aerogel-Based Drug Delivery System using Punica Granatum Extracts - Invention to Innovation Subharina Mahapatra¹, Jyotiraman De² and Manjula Hebbale¹; ¹Bharati Vidyapeeth Dental College and Hospital, India; ²Indian Institute of Technology Bombay, India

Oral lichen planus is a widespread chronic mucocutaneous, autoimmune inflammatory disorder affecting the oral cavity. Oral lichen planus is usually associated with pain, burning sensation and irritation of the oral mucosa. Multiple therapeutic approaches including both topical and systemic corticosteroids have been used in the management. As a consequence of the reported adverse effects of corticosteroids, different natural plant extracts have been suggested.

Pomegranates (*punica granatum*) have been identified for hundreds of years as natural treatment modality for their numerous benefits for health. Topical *punica granatum* extracts gel in management of oral lichen planus has been tried as a topical medication and according to research it has anti-inflammatory property, which help to subside the symptoms of oral lichen planus but the disadvantage is that *punica granatum* extracts gel dissolve quickly inside the oral cavity by saliva, thus providing less application time. Prolonged application time of the medication is required for faster recovery.

As a result, drug (*punica granatum* extracts gel) -loaded cellulose aerogel have been introduced as a promising drug delivery carrier to deliver medications to the affected area by controlled release. They prolong the time of application as the medication slowly dissolves in saliva and is released to the particular applied area of irritation caused by oral lichen planus. Cellulose is used in this process, as cellulose is the perfect raw material for cellulose aerogel due to its easy availability, biodegradability, biocompatibility, and nontoxicity. It also offers a high surface area, a highly porous, interconnected fibre network, and the availability of various functional groups required for drug encapsulation.

Hence, a cellulose aerogel-based drug delivery system is developed from the *punica granatum* extracts gel in the management of oral lichen planus as an alternative treatment plan to prolong the application time and control release of the medication.

After development of the product, it has been applied in the oral lichen planus patients. Total thirty patients were divided into two groups, group a patient with topical corticosteroids and group b patients with drug (*punica granatum* extracts gel) -loaded cellulose aerogel. The results were better in group b patient, who were using drug (*punica granatum* extracts gel) -loaded cellulose aerogel.

5:00 PM SB05.09.08

Comparative Analysis of Sterilization Methods for Placenta-Based Products using an Animal Model Molly Post, Olivia Logan, Denae Landry, Isabella Sledge and Mora Melican; Tides Medical, United States

Placenta-based products, known for their regenerative potential in various clinical applications, are either aseptically processed or require effective terminal sterilization methods to ensure safety and maintain their therapeutic properties. Providing an overview of a comparative analysis of healing rate in a full thickness animal model has been used to show the importance of evaluating the impact of sterilization on these materials in a biologically relevant context. The Sprague Dawley full thickness model is used to assess the in vivo response to sterilized placenta-based products, and to provide critical insights into immunogenicity, tissue integration, and the overall regenerative potential of these materials.

Several sterilization methods, including gamma irradiation, ethylene oxide (ETO) gas sterilization, electron beam (e-beam), and various other methods have been employed to eliminate potential pathogens from placenta-based products. However, the choice of sterilization method can have varying effects on the biological activity and safety. In this study, we discuss the utilization of an animal model to assess the effects of different sterilization techniques on

the safety and efficacy of placenta-based products. The placenta-based product tested is Artacent Wound®, a dehydrated dual layer amniotic graft, terminally sterilized with two different techniques. Furthermore, it addresses the importance of selecting appropriate animal models that closely mimic human physiology, ensuring that the findings are translatable to clinical applications. The animals are monitored for wound healing progress and adverse effects.

In conclusion, employing relevant animal models allows for a more comprehensive evaluation of the impact of sterilization on these materials, bridging the gap between in vitro assessments and clinical applications.

5:00 PM SB05.09.09

Soft, Bioresorbable, Transparent Microelectrode Array Platform for Heart Disease Diagnosis and Treatment [Zhiyuan Chen](#); The George Washington University, United States

Heart disease kills nearly 700,000 people in the United States each year, with an estimated annual cost of \$219 billion. A key factor contributing to these alarming statistics is the lack of tools that can unravel complex pathophysiology, facilitate intraoperative or postsurgical monitoring, and provide effective and timely clinical treatments.

Noble metal-based microelectrode arrays (MEAs) have been widely used to probe the patterns of cardiac excitation waves and identify the regions causing arrhythmias, while electrical pacemakers and defibrillators are the cornerstone of therapy in clinical medicine to correct abnormal heart rhythm. However, they are **problematic in detecting critical cardiac parameters** such as intracellular calcium dynamics, metabolic activity, or target-specific cell types.

Optical mapping using voltage/calcium-sensitive dyes or intrinsic fluorescence can complement these electrical approaches by uncovering the roles of above-mentioned cellular parameters in both health and disease conditions. However, conventional opaque MEAs are not compatible with this as they block the passage of excitation illumination and fluorescence signals, and obscure the bio-signals by artifacts due to the photovoltaic effect. Furthermore, given the mechanical dynamic nature of hearts, higher requirements are placed on the flexibility of the interface devices. Therefore, developing such technology that can **bridge electrophysiology and opto-physiology at cardiac interface is of significance but very challenging.**

Soft transparent MEAs show great promise in tackling this challenge, as they allow light to transmit in both directions for simultaneous artifact-free optical and electrical investigation of cell/tissue from the same field of view and visualize the spatiotemporal distribution of cardiac activities with multiple parameters. Additionally, optically transparent MEAs are highly desired during clinical procedures to allow direct observation of areas of interest under the microelectrodes for concurrent optical diagnostics/therapies (such as endoscopy) and guiding other procedures (such as catheters) on the hearts. However, **all existing transparent MEAs are designed for chronic biointerfacing** and require surgical removal when they malfunction or are no longer needed.

In comparison, bioresorbable electronics provide unique opportunities to investigate, monitor, and treat short-lived cardiac complications, including postoperative arrhythmias and heart failure on the order of a few days to weeks following ischemic events or surgery, which account for at least one-third of postoperative deaths. Those devices can subsequently dissolve into benign products via natural metabolic mechanisms to avoid the complications, infection risks, and additional costs associated with surgical retrieval. However, **soft transparent MEAs that exhibit bioresorbable functionality remain unexplored.**

Here, we report materials, device design, fabrication, characterization, and validation of **the first fully bioresorbable and transparent MEA platform.** The developed fabrication strategy achieves **nanoscale transient patterns for the first time.** The device enables multiparametric electrical and optical mapping of cardiac dynamics and on-demand site-specific stimulation to investigate and modulate cardiac physiology in rat and human heart models. In addition, the device can be used as a heart implant to perform the **continuous process of arrhythmia detection, monitoring, and bipolar-pacing treatment *in vivo*** over a clinically relevant period. The bioresorption dynamics and biocompatibility of the device are systematically investigated by histology and serology. The concept and design of this work lay the foundation for bioresorbable cardiac technologies that advance postoperative monitoring and treatment of temporary patient pathological conditions in certain clinical scenarios, such as myocardial infarction, ischemia, and transcatheter aortic valve replacement.

5:00 PM SB05.09.10

Structural and Biological Characteristics of a Novel Hydroxyapatite–Sodium Alginate-Based Biocomposite Material for Dental Implants [Hussein S. Alrobei](#); Prince Sattam bin Abdulaziz University, Saudi Arabia

Materials intended for bone and dental implants must possess biocompatibility and good mechanical strength. To enhance these qualities, a novel hydroxyapatite–sodium alginate-based biocomposite was created by using wet precipitation technique. The XRD of the original and modified specimen closely matched the hydroxyapatite (HAp), and the presence of distinct HAp peaks in FTIR spectra endorsed the successful synthesis of both HAp and modified hydroxyapatite–sodium alginate. The SEM images vividly exhibited porosity in the modified specimen, with a recorded density of 3.1 g/cm. The peak microhardness value, 26.4 GPa, was attained in the optimized composition. As the dopant concentration increased, the antibacterial activity of the hydroxyapatite–sodium alginate-based composite also increased. The absence of dopant ion leakage under physiological circumstances was confirmed by a 35-day examination of ion release in simulated body fluids. The results indicate that the developed composite holds substantial potential as a material suitable for teeth and bone implants, owing to its mechanical and biological characteristics.

5:00 PM SB05.09.11

Zwitterionic Conducting Hydrogel for Suppressing The Foreign Body Response against Implantable Biosensors [Shinya Wai](#), Nan Li, Seounghun Kang, Yahao Dai, Lavoie Tera, Wei Liu, Matthew V. Tirrell and Sihong Wang; The University of Chicago, United States

Implantable medical devices (IMDs) are playing an increasingly important role due to an aging population and the associated increasing prevalence of chronic diseases. However, an inflammatory and fibrotic process known as the foreign body response (FBR) has limited IMDs from realizing their full potential. The FBR leads to the production of degradative chemicals and enzymes that can damage the implant. Fibrotic encapsulation is particularly detrimental for biosensors and electrophysiological devices because it would impede the diffusion of analytes and ions. A class of materials with promising FBR suppressing properties are zwitterionic polymers which have been shown to nearly eliminate the FBR for at least a year in mice. As electronic materials for IMDs, poly(3,4-ethylenedioxythiophene):poly(styrene sulfonate) (PEDOT:PSS) is of interest because it is chemically stable, highly processable, non-cytotoxic, and has good mixed ion-electron conducting properties. Nonetheless, previous work addressing the FBR against PEDOT:PSS did not place their focus on long-term solutions or characterize FBR-related immune and tissue responses. We hypothesize that by combining PEDOT:PSS and a zwitterionic polymer into a double-network hydrogel and carefully tuning its phase separation morphology, the conductivity can be increased and the FBR can be suppressed indefinitely. In this work, we demonstrate a process for inducing PEDOT:PSS network formation in a pre-formed zwitterionic hydrogel matrix, which significantly improves its conductivity and reduces FBR-associated fibrosis. Our work demonstrates that controlling the phase separation morphology of composite materials can be an effective strategy for suppressing the FBR.

5:00 PM SB05.09.12

Advanced Multilayered Biodegradable Wireless Sensors: Combining Reference, Shielding and Extended Communication for Precise, Portable and High-Sensitivity Intracranial Pressure Monitoring Minki Hong, Seunghun Han, Kyung Su Kim, Sehwan Park, Sumin Kim, Daeun Sung and Jahyun Koo; Korea University, Korea (the Republic of)

Brain diseases have long posed significant health and economic challenges, with stroke being a prime example. In 2021, one in six cardiovascular deaths in the U.S. resulted from stroke, accounting for about 162,000 fatalities[1]. With a recurrent stroke rate of 25% and an economic burden of \$55.6 billion between 2018-2019, there is an urgent need for advanced diagnostic and treatment modalities[2]. One promising development is the wireless brain pressure sensor[3]. However, long-term implantation raises concerns, particularly regarding Healthcare-Associated Infections (HAIs), with surgical site infections posing a notable threat[4]. Addressing these challenges, recent innovations present biodegradable devices, specifically wireless biodegradable Intracranial Pressure (ICP) sensors, that decompose and assimilate post-operation, minimizing complications[5,6]. Key criteria for these sensors include accurate pressure readings by eliminating physiological noises like blood flow and micro-vibrations and ensuring small sensor size, high sensitivity (within the adult brain pressure range of 500-5000 Pa), and effective wireless portability for continuous monitoring. In our study, we validated the efficacy of these biodegradable ICP sensors, emphasizing material choice, device architecture, noise mitigation, wireless communication, and in-vivo testing on rabbits. The sensors, crafted using biodegradable polymers and metals, utilized shielding and reference electrodes for noise reduction. A layered design enhanced sensitivity without compromising size, and Bluetooth technology enabled continuous and long-distance monitoring. Post-insertion into a rabbit's parenchyma and subsequent pressure modulation tests, the sensors exhibited comparable or superior performance relative to conventional pressure sensors. This research signifies a progressive stride toward the realization and clinical deployment of biodegradable diagnostic tools.

5:00 PM SB05.09.13

Highly Conductive and Ultra-Thin Elastic Silver-Nanosheet Membrane for Neural Recording Sonwoo Jung^{1,2}, Minjeong Kim^{1,2}, Seungyeon Kim³, Tae-Wook Kim^{3,3} and Dae-Hyeong Kim^{1,2,2}; ¹Institute for Basic Science (IBS), Korea (the Republic of); ²Seoul National University, Korea (the Republic of); ³Jeonbuk National University, Korea (the Republic of)

Nanocomposites are gaining prominence as suitable materials for skin wearable and implantable electronics due to their tissue-like mechanical properties and adequate electrical properties. However, achieving both conformal adhesion and excellent electrical and mechanical properties is challenging, as thickness and conductivity are often in a trade-off relationship for most of the materials. To overcome the challenge, highly elastic and conductive nanomembranes have been developed by leveraging 1-dimensional nanowires to form a nanocomposite with enhanced percolation networks between conducting nanofillers. However, owing to the geometrical anisotropy of the nanowire, nanomembrane exhibited different properties depending on the directions. Here, we present a stretchable and laser-patternable nanomembrane using 2-dimensional(2D) silver nanosheets with isotropic and high electromechanical properties. The single layer of nanomembrane is ultrathin (~ 250 nm) and highly conductive (> 80,000 S/cm) yet remains stretchable since the elastomer layer separated from the nanosheets dissipates the stress induced to the membrane. Furthermore, 2-dimensional nanosheets endow the membrane with isotropic mechanical and electrical performances in every direction. Based on float assembly fabrication, silver nanosheets were tightly gathered and partially embedded into the elastomer on the larger surface area of the silver nanosheet and constructed partial face-to-face contact. This face-to-face junction decreases the contact resistance of the nanomaterials, contributing to the high conductivity of the membrane. In addition, the silver nanosheet membrane was able to be manufactured with different dimensions and thicknesses by controlling fabrication variables, displaying distinct characteristics in electrical conductivity, stretchability, impedance, and modulus in each variable-controlled membrane. Moreover, through the bilayer stacking process, the contacts between silver nanosheets created extra percolation networks, resulting in a significant enhancement of conductivity, reaching up to 125,000 S/cm. By patterning the encapsulated nanomembrane with laser, we fabricated a stretchable electrode array making a conformal adhesion to the skin and nerves, demonstrating the future potential of the membrane for broad application both in wearable and implantable approaches.

5:00 PM SB05.09.14

Etching of Failed Polymeric Heart Valve Leaflets Reveals Cross-Tie Craze Microstructure Nipa Khair¹, Katie Vinterella², Ethan Harrell¹, Julianne Kindsfater¹, Lakshmi P. Dasi² and Susan James^{1,1,1}; ¹Colorado State University, United States; ²Georgia Institute of Technology, United States

Rheumatic and calcified aortic heart valve disease presents a global health concern, impacting millions of individuals across various age groups. The gold standard medical treatments recommend replacing the sick heart valves with xenograft-based bioprosthetic valves that are chemically fixed using glutaraldehyde, commonly sourced from bovine or porcine. Clinical investigations over more than two decades have revealed fixed tissues are prone to premature calcification and tearing, thereby limiting their durability. Moreover, challenges related to supply chains, inconsistent mechanical characteristics, and high costs have been constant issues for tissue valves.

An innovative alternative approach involves enhancing polyethylene-based materials with hyaluronic acid (HA), a glycosaminoglycan naturally occurring in native heart valve leaflets. By incorporating small amounts of HA into a low-density linear polyethylene (LLDPE) thin film at the molecular level, a robust and hydrophilic biomaterial of *in vivo* anti-calcific and anti-thrombotic properties is achieved. The LLDPE thin film has high tear strength and excellent flexibility, making it an appealing choice for developing heart valves. Nonetheless, during durability testing according to ISO 5840-2005 standards, these valves exhibited premature failure. To uncover the fundamental mechanisms behind these failures, this study conducted a failure analysis of semicrystalline blown LLDPE thin film-based heart valves.

The valves consistently tear and wear around highly stressed (from finite element analysis) commissure posts. Six of these worn posts were retrieved from failed valves and chemically etched. Low-voltage scanning electron microscopy (SEM) imaging was taken before and after chemical etching. The semicrystalline LLDPE polymer, with a crystallinity of 36% as determined by DSC, underwent chemical etching using a standard 2% w/v permanganate etching solution, followed by multistep washing. The SEM analysis of pristine LLDPE unveiled distinctive spherulitic structures consisting of well-organized lamellae with diameters of approximately 3 μ m and lamellae thickness of 40-80 nm. The etching process effectively eliminated low-energy amorphous regions, revealing the spherulites. A similar study was carried out on the worn and torn LLDPE valves.

The SEM images of the worn surfaces displayed signs of surface wear and aligned fibrils oriented perpendicular to the principal stress direction, akin to a phenomenon known as crazing. Following etching, some fibrils remained partially intact, while others exposed the crystals beneath them. These crystals within the fibrils lost their spherulitic superstructure, exhibiting thickened and fractured lamellae. The presence of these fibrils after etching suggested a state of hyper-crystallinity, a characteristic often observed in polyethylene-drawn filaments. In contrast, the worn surfaces that had tears displayed multiple irregularities at the torn surface. These included bumps, holes, a visually rough texture, and a lack of exposed crystals. Crystal disruptions were notably concentrated within 200-300 μ m areas near the tear and wear, while the rest of the samples retained spherulitic morphology.

Remarkably, one of the worn samples unveiled the Kramer craze microstructure "cross-tie," composed of aligned and interlinked lamellae. The spacing between cross-tie lamella ranges between 100-200 nm, and the thickness remained 40-80 nm. To the best of the author's knowledge, the cross-tie structure has been only theorized with indirect evidence collected from lab-grown crazes. Direct evidence of cross-tie structure indicates crazing initiates the tears.

Stress disentangles polymer strands, causing lamella fibrillation, but some do not disentangle. Instead, they pile up to bridge between fibrils. This study holds the potential to shed light on preventing polymer disentanglement, thereby mitigating crazing and improving heart valve durability.

5:00 PM SB05.09.15

Effects of Temperature on the Mechanical Properties of PEGDA and PDMS Copolymer Scaffold for Tissue Engineering [Sam Lloyd-Harry](#)¹, Samaher Shaheen², Ozgul Yasar-Inceoglu¹ and Ozlem Yasar³; ¹California State University Chico, United States; ²California State University, Chico, United States; ³The City University of New York, United States

Tissue engineering is a growing field of materials research concerned with finding new materials and methods for the replacement or improvement of natural tissue structures. Previous studies have shown poly (ethylene glycol) diacrylate (PEGDA) to be a promising engineering tissue structure, or scaffold material. However, PEGDA scaffolds have been shown to lack sufficient mechanical properties that would be required for implantation in the human body. More research must be done to tune the mechanical properties of the scaffold. Many research institutions do not have access to all testing equipment needed to fully study the limitations of scaffold samples. Thus, the need for collaboration between institutions is often necessary. Numerous common testing methods require consistent environmental conditions to maintain the structure of scaffold to accurately collect data. The study of the limitations of environmental conditions is significant to avoid degradation of the structure and therefore keep the mechanical properties of scaffold samples. Experiments have shown PEGDA scaffolds to experience a decrease in strength and elasticity after refrigeration for 24 and 48 hours, but a restoration of mechanical properties was found after 72 hours. No studies have looked at mechanical properties beyond 72 hours of refrigeration. This study investigates the effects of temperature on the mechanical properties of UV cross-linked PEGDA and polydimethylsiloxane (PDMS) copolymer scaffolds. Utilizing Fourier Transmission Infrared Spectroscopy, Scanning Electron Microscopy, X-ray Diffraction, and Raman Spectroscopy, the characterization of the copolymer scaffolds was performed. Compression testing was then performed on a QT 50 Universal Testing Machine at a rate of .75 mm/min. These results were compared with that of refrigerated copolymer samples and plain PEGDA scaffold samples. Samples were refrigerated at 0 degrees Centigrade for 24, 48, 72, and 96 hours.

5:00 PM SB05.09.16

Alginate Microgels Synthesized using Click Chemistry: A Benign Approach for Delivering Beta Lactamase to Gut Microbiota. [Hema Choudhary](#) and Niren Murthy; University of California Berkeley, United States

Microgels are crosslinked networks of polymer swollen in water with a size of 1-100 μm. Microgels have been extensively studied in the biomedical field due to the ease of engineering structural and mechanical properties. These microgels are typically made from biocompatible polymers such as alginate, agarose, gelatin, etc. which can be easily crosslinked by non-covalent interactions of ionic/hydrogen bonding. However, due to physical crosslinking, these microgels are susceptible to dissolution and degradation. To overcome this issue, generally methacrylate groups are introduced for covalent crosslinking. It requires the generation of free radicals which is unsuitable for biological applications, especially if microgels are used for encapsulating proteins or cells. Herein, we developed a new system for making mechanically robust microgels using alginate. These microgels are covalently crosslinked using click chemistry, a benign approach. For this, first alkyne/azide functional moieties are introduced on alginate polymer. Then microgels are created with modified alginate using a T-junction microfluidic device. These microgels are robust and remain stable in the buffer for 7 days as opposed to non-covalently crosslinked alginate which dissolves away within hours.

We expect this technology to have many applications, one of which is protein delivery. In this regard, we successfully encapsulated beta-lactamase protein in these alginate microgels without compromising on activity. Beta-lactamase is an interesting protein that can neutralize antibiotics. Antibiotics affect gut microbiome health which increases the risk of secondary infections and antimicrobial resistance. If beta-lactamase is delivered successfully in the gut, it could neutralize the remaining antibiotics post-treatment. Data from the oral delivery of beta-lactamase and other proteins encapsulated in our alginate click microgels will be presented in this talk.

5:00 PM SB05.09.17

Degradation Effects on Mechanical Properties of Polyethylene Glycol Diacrylate (PEGDA) and Polydimethylsiloxane (PDMS) Copolymer Scaffolds for Tissue Engineering. Ozgul Yasar-Inceoglu¹, [Andre A. Fatchi](#)¹, Sam Lloyd-Harry¹, Samaher Shaheen¹ and Ozlem Yasar²; ¹California State University Chico, United States; ²The City University of New York, United States

The merging studies of innovative engineering and cell biology offers promising results for the repair and replacement of human tissues. The field of tissue engineering aims to address critical challenges in the medical field and to further advance research in the biomedical industry. Previous studies have shown engineered tissue scaffolds to degrade over time. Therefore, more research must be conducted on scaffold reliability and breakdown over time, to further understand the limitations of engineered materials inside of the human body. This study examines the degradation effects on the mechanical properties of polyethylene glycol diacrylate (PEGDA) and polydimethylsiloxane (PDMS) copolymer scaffolds submerged in a Phosphate-Buffered Saline (PBS) solution. PBS has been shown to mimic the environment of the human body in previously published studies. The characterization of the copolymer scaffolds was executed by performing Raman Spectroscopy, X-ray Diffraction (XRD), Scanning Electron Microscopy (SEM), and Fourier Transmission Infrared Spectroscopy (FTIR). Equilibrium Swelling testing was conducted by submerging samples in water over 15 minutes. Compression testing was conducted utilizing a QT 50 Universal Testing Machine at a rate of .75 mm/min. The tests performed on the degraded copolymer samples were also conducted on non-degraded copolymer, degraded PEGDA, and non-degraded PEGDA samples. The results of all samples were compared to understand the effects of degradation on the mechanical properties of copolymer scaffolds.

SESSION SB05.10: Engineered Materials for Organ Interfaces

Session Chairs: Philipp Gutruf and John Ho

Thursday Morning, April 25, 2024

Room 434, Level 4, Summit

10:00 AM *SB05.10.01

Engineering Conducting Polymer Hydrogels for Additive Manufacturing and Biointerfaces [Alexandra Rutz](#); Washington University in St. Louis, United States

Hydrogels are insoluble polymer networks swollen with water (>90% water by mass) and are used widely in biomedical applications for their similarities to native extracellular matrix. For bioelectronics, there are many efforts to build devices based on these materials to achieve tissue-matching stiffness and other tissue-inspired properties in order to improve the biointerface. For making electrodes and other device components based on semiconducting

This searchable program is up-to-date as of April 15th, 2024.

materials, conjugated polymers can be gelled into electronically conducting hydrogels. Such methods include simple mix-and-cast techniques, similar to other methods used widely in traditional (non-conducting) hydrogel processing. We have investigated conducting hydrogels based on the conjugated polymer poly(3,4-ethylenedioxythiophene) polystyrene sulfonate (PEDOT:PSS) fabricated by mixing in a gelling agent, ionic liquid. We have studied how the hydrogel precursor formulation and other fabrication variables of this method affect gel properties, such as swelling, conductivity, and elastic modulus. Further, we have evaluated the potential of these PEDOT:PSS hydrogels for biointerfacing applications and have found that these gels when processed appropriately are stable *in vitro* and support mammalian cell culture. Finally, we are developing these conducting polymer hydrogels for compatibility with additive manufacturing to grant structural control of these soft bioelectronic interfaces. Such techniques provide manipulation of dimensions and microporosity, important for assembling these hydrogels into functional devices and optimizing tissue integration.

SESSION SB05.11: Central Nervous System Interfaces III
Session Chairs: Philipp Gutruf and John Ho
Thursday Morning, April 25, 2024
Room 434, Level 4, Summit

10:30 AM *SB05.11.01

Seeing the Sound: An Ultrasound-Mediated Intravascular Light Source enabled by Colloidal Mechanoluminescent Materials [Guosong Hong](#); Stanford University, United States

Light is used in a wide range of methods in biology and medicine, such as fluorescence imaging, optogenetics, photoactivatable gene editing, photothermal and photodynamic therapies to treat cancers, and photochemotherapy to inactivate viruses *in vivo*. A critical challenge of applying light *in vivo*, such as deep-brain optogenetic neuromodulation and photochemotherapy in deep organs, arises from the poor penetration of photons in biological tissue due to scattering and absorption. Therefore, delivering light deep into the body requires invasive procedures, such as the insertion of optical fibers and endoscopes, as well as surgical removal of overlying tissues. The very invasiveness of these procedures also precludes easy repositioning and volume adjustment of the illuminated region in the same subject. To address these challenges, our lab has developed an ultrasound-mediated intravascular light source, leveraging the deep-tissue penetration of focused ultrasound. We capitalized on mechanoluminescent nanotransducers (MLNTs), which are colloidal nanoparticles of mechanoluminescent materials synthesized via a biomineral-inspired suppressed dissolution approach. These MLNTs can be delivered intravenously into blood circulation and emit light locally at the ultrasound focus. Owing to the deep penetration and fast temporal kinetics of ultrasound, we have demonstrated that this method can produce on-demand and dynamically programmable light emission patterns at elevated depths in different organs of live mice with millisecond precision. This ultrasound-mediated intravascular light source has allowed us to perform noninvasive “sono-optogenetic” neuromodulation in live mice, as well as brain-wide “scanning optogenetics” that activate different brain regions of the same mouse brain. Our development of the ultrasound-mediated intravascular light source has been published in *PNAS* (2019), *Science* (2020), *Science Advances* (2022), *JACS* (2022), *JACS* (2023), and *Nature Protocols* (2023).

11:00 AM *SB05.11.02

Neural Interfaces to Human Organoids Designed for *In Vitro* and *In Vivo* Studies [Duygu Kuzum](#) and Madison Wilson; University of California, San Diego, United States

Human cortical organoids, three-dimensional neuronal cultures, are emerging as powerful tools to study brain development and dysfunction. However, chronic monitoring of structural and functional maturation of organoids is challenging due to limitations of existing technologies. Here, we will present the state of the art in neural interfaces for human brain organoids. We will discuss electrical and optical methods of interrogating organoids *in vitro* and *in vivo* configurations. We will present multimodal data analysis for longitudinal monitoring of neuronal activity in the organoids and the surrounding neuronal circuits. We will highlight future applications of *in vivo* transplantation of human organoids for comprehensive evaluation of the development, maturation, and functional integration of neuronal networks.

11:30 AM *SB05.11.03

Flexible, Scalable, High Channel Count Stereo-Electrode for Recording in The Human Brain [Shadi A. Dayeh](#); Integrated Electronics and Biointerfaces Laboratory, United States

Over the past decade, stereotactically placed electrodes have become the gold standard for deep brain recording and stimulation for a wide variety of neurological and psychiatric diseases. Current deep brain electrodes commonly known as the stereoecephalography (SEEG) electrodes, are limited in their spatial resolution and ability to record from small populations of neurons, let alone individual neurons. Here, we will discuss a novel, customizable, thin-film (polyimide) human-grade flexible depth electrode with platinum nanorod contacts that is capable of recording and stimulation at a depth of 10 cm in brain tissue, an electrode referred to as the UCSD microSEEG electrode. This 15 μ m thin, stylet-guided depth electrode is capable of recording local field potentials and single unit neuronal activity (action potentials), validated across species including humans. This device represents an advance in manufacturing and design approaches which extends the capabilities of a mainstay technology in clinical neurology.

SESSION SB05.12: On-Demand Presentation
Tuesday Morning, May 7, 2024
SB05-virtual

10:30 AM SB05.12.01

Electromechanical Analysis of Silicon Nanomembrane Based Bendable MOS Capacitors with Ultrathin Nanolaminated Encapsulation [Chen Liu](#), Zhuofan Wang, Hongliang Lü, Yuming Zhang, Haonan Zhang, Shiyuan Cheng and Yi-Men Zhang; Xidian University, China

Flexible silicon nanomembrane (Si NM) based active implants as advanced biomedical electronics are essential for futuristic applications in sensing, healthcare, and human-machine interfaces. The development of thin-film encapsulation with excellent mechanical robustness and conformability is indispensable for ensuring the long-lived operation of Si NM based functional devices in a biological environment. Here, the electrical properties have been investigated on Si NM based metal-oxide-semiconductor capacitors (MOSCAPs) encapsulated with ultrathin Al₂O₃/alucone nanolaminates under

mechanical strain conditions. As illustrated in the capacitance-voltage curves under mechanical-bending stress, the variation of the accumulation capacitance (C_{acc}) is observed to be lower than 1 % at both inward and outward bending radii of 85 mm and 38.5 mm compared with the planar condition for the encapsulated MOSCAP with a gate area of 0.02 mm², respectively. However, the corresponding reductions of C_{acc} are approximately 2 % and 4 % for the bare device with the same gate area. Up to 4 % and 26 % reduction in the accumulation capacitance have been measured for the encapsulated MOSCAP with a gate area of 0.08 mm² at a bending radius of 85 mm under tensile stress and 38.5 mm under compressive stress, respectively. Furthermore, the relevant reductions of C_{acc} are promoted to 9 % and 36 % for the bare device with the same gate dimension. Suppression of the gate leakage current has also been observed clearly for the encapsulated Si NM based MOSCAPs with an active area of 0.08 mm² compared with bare devices during bending, while the phenomenon could not be found for the devices with smaller gate areas. These findings demonstrate the great potential of nanolaminated films of Al₂O₃/alucone as the excellent encapsulation. It is also noted that a comprehensive study of the impact of the device gate area on the electromechanical properties will be beneficial to optimizing the scalable layout for achieving high mechanical reliable and high-performance flexible Si NM based MOSFETs to create the next-generation bioelectronic implants.

SYMPOSIUM SB06

Biohybrid Materials and Devices for Sensing, Robotics, Energy and Biomedicine
April 23 - May 7, 2024

Symposium Organizers

Neel Joshi, Northeastern University
Eleni Stavrinidou, Linköping University
Bozhi Tian, University of Chicago
Claudia Tortiglione, Istituto di Scienze Applicate e Sistemi Intelligenti

Symposium Support

Bronze
Cell Press

* Invited Paper

+ JMR Distinguished Invited Speaker

^ MRS Communications Early Career Distinguished Presenter

SESSION SB06.01: Bioelectronics I
Session Chairs: Eleni Stavrinidou and Bozhi Tian
Tuesday Morning, April 23, 2024
Room 427, Level 4, Summit

10:30 AM *SB06.01.01

Functional neurological restoration of amputated peripheral nerve using biohybrid regenerative bioelectronics [Damiano Giuseppe Barone](#);
University of Cambridge, United Kingdom

The development of neural interfaces with superior biocompatibility and improved tissue integration is vital for treating and restoring neurological functions in the nervous system. A critical factor is to increase the resolution for mapping neuronal inputs onto implants. For this purpose, we have developed a new category of neural interface comprising induced pluripotent stem cell (iPSC)-derived myocytes as biological targets for peripheral nerve inputs that are grafted onto a flexible electrode arrays. We show long-term survival and functional integration of a biohybrid device carrying human iPSC-derived cells with the forearm nerve bundle of freely moving rats, following 4 weeks of implantation. By improving the tissue-electronics interface with an intermediate cell layer, we have demonstrated enhanced resolution and electrical recording in vivo as a first step toward restorative therapies using regenerative bioelectronics.

11:00 AM SB06.01.02

Skin-Preparation-Free, Stretchable Microneedle Adhesive Patches for High-Fidelity Electrophysiological Sensing and Exoskeleton Robot Control
Heesoo Kim¹, Juhyun Lee¹, Ung Heo¹, Dhileep K. Jayashankar², Karen-Christian C. Agno¹, Yeji Kim¹, Choong Yeon Kim¹, Youngjun Oh¹, Sang-Hyuk Byun¹, Bohyung Choi¹, Hwayeong Jeong¹, Woon-Hong Yeo³, Zhuo Li⁴, Seongjun Park¹, Jianliang Xiao², Jung Kim¹ and Jae-Woong Jeong¹; ¹Korea Advanced Institute of Science and Technology, Korea (the Republic of); ²University of Colorado Boulder, United States; ³Georgia Institute of Technology, United States; ⁴Fudan University, China

Ensuring highly reliable and comfortable recording of electrophysiological (EP) signals is vital in various applications, from medical care to human-machine interaction. Recent research has tried to address this issue by developing soft epidermal electrodes that offer time-dynamic accommodation to skin deformation. Although these sensors are suitable for long-term use and are conformable, the signals acquired using these approaches highly rely on skin conditions, thus requiring a cumbersome skin preparation setup. Microneedle electrodes can overcome the limitation by eliminating the need for skin pretreatment by providing direct access to the epidermis. Nevertheless, existing rigid or flexible microneedle electrodes face challenges related to mechanical elasticity and electrical reliability, particularly during dynamic body movement, hindering their suitability for accurate EP sensing over a

prolonged time.

To address these issues, we have developed a stretchable microneedle adhesive patch (SNAP) for skin-preparation-free, reliable EP monitoring. SNAP comprises gold-coated silicon microneedle arrays, stretchable serpentine gold interconnects, and electrically conductive adhesives. The microneedle array, with a height of less than 200 μm , ensures virtually pain-free penetration of stratum corneum and maintains consistently low and stable skin contact impedance regardless of skin conditions. The elastic, adhesive and conductive platform, featuring a serpentine mesh, enables dynamic adaptation to tissue deformations while also enhancing the electrical skin interface through the provision of an additional conductive pathway. Through this design, SNAP offers remarkable skin penetrability and establishes a robust electromechanical skin interface, ensuring prolonged and precise EP signal monitoring across diverse skin conditions. Analytical and experimental outcomes validate that SNAP enhances wearer comfort during intensive exercise and significantly decreases contact impedance under uncleaned skin, outperforming clinical gel electrodes and flexible microneedle electrodes. Demonstration using the wireless SNAP system in a human-machine interface (HMI) to control a back-support exoskeleton robot underlines its potential for high-fidelity HMIs, even in challenging scenarios involving time-varying skin conditions. We foresee that this SNAP system can be applied to various EP sensing, suggesting new strategies for enhancing comfort, reliability, and utility in applications ranging from healthcare and medical diagnostics to cutting-edge human-robot interactions.

11:15 AM *SB06.01.03

Hydrogel interfaces for merging humans and machines Xuanhe Zhao; Massachusetts Institute of Technology, United States

The last few decades have witnessed unprecedented convergence between humans and machines that closely operate around the human body. Despite these advances, traditional machines made of hard, dry and abiotic materials are substantially dissimilar to soft, wet and living biological tissues. This dissimilarity results in severe limitations for long-term, reliable and highly efficient interfacing between humans and machines. To bridge this gap, hydrogels have emerged as an ideal material candidate for interfacing between humans and machines owing to their mechanical and chemical similarities to biological tissues and the versatility and flexibility in designing their properties. In this talk, I will provide a comprehensive summary of functional modes, design principles, and current and future applications for hydrogel interfaces towards merging humans and machines.

11:45 AM SB06.01.04

An electroadhesive hydrogel interface for prolonged gastrointestinal theranostics Binbin Ying^{1,2,1}, Kewang Nan^{1,2,3}, Qing Zhu⁴, Tom Khuu², Hana Ro¹, Sophia Qin¹, Shubing Wang², Karen Jiang¹, Yonglin Chen², Guangyu Bao⁵, Joshua Jenkins^{1,1}, Andrew Pettinari^{1,1}, Johannes Kuosmanen¹, Keiko Ishida^{2,1}, Niora Fabian¹, Aaron Lopes^{1,2}, Jason Li^{1,2,1}, Alison Hayward¹, Robert Langer^{1,1} and Giovanni Traverso^{1,2,1}; ¹Massachusetts Institute of Technology, United States; ²Brigham and Women's Hospital, United States; ³Zhejiang University, China; ⁴Zhejiang Pharmaceutical University, China; ⁵McGill University, Canada

Establishing a robust and intimate mucosal interface that allows medical devices to remain for extended periods is valuable for theranostic purposes. However, achieving this goal has proven extremely challenging, particularly within the gastrointestinal (GI) tract. Here, we report the development of **e-GLUE**, an electroadhesive hydrogel interface for robust and prolonged mucosal retention following electrical activation. Notably, this novel mechanism can amplify the adhesion performance on the mucosa by up to 30-fold and extend in vivo GI retention of e-GLUE devices for up to 30 days. Strong mucosal adhesion occurs within one minute of electrical activation, despite the presence of luminal fluid, mucus exposure, and organ motility, thereby ensuring compatibility with complex in vivo environments. In swine studies, we demonstrate the utility of e-GLUE for instantaneous mucosal hemostasis, sustained local delivery of therapeutics, and intimate biosensing in the GI tract. This system can enable improved treatments for various GI conditions, including recurrent gastric bleeding, inflammatory bowel disease, and potentially early monitoring of GI cancers.

SESSION SB06.02: Bioelectronics II
Session Chairs: Eleni Stavrinidou and Bozhi Tian
Tuesday Afternoon, April 23, 2024
Room 427, Level 4, Summit

1:30 PM *SB06.02.01

Bioadhesive and immune-compatible polymer bioelectronics Sihong Wang; University of Chicago, United States

The use of bioelectronic devices for acquiring biological information and delivering therapeutic interventions relies on direct contact with soft bio-tissues. To ensure high-quality signal transductions, the interfaces between bioelectronic devices and bio-tissues must combine signal amplification with stable and conformable contact. Semiconductor-based transistors (e.g., organic electrochemical transistors) have been developed as one of the most advanced technologies for high-performance bio-sensing. However, the rigid mechanical properties and the lack of tissue/skin adhesion from transistors largely prevent the formation of such intimate and long-term stable bio-interfaces. Also, immune-mediated foreign-body response (FBR) stands as the most widely existing challenge, which can lead to the growth of fibrotic tissue at the tissue-device interface. In this talk, I will first introduce our material and device designs for introducing tissue-adhesive properties onto transistor-based biosensors. Then, to combat FBR, I will introduce a set of molecular design strategies for enhancing the immune compatibility of semiconducting polymers. I will also introduce the strategies and advantages of using these new biomimetic properties in bioelectrical and biochemical sensing.

2:00 PM SB06.02.02

Electroadhesion as a Surgical Tool: Successful Repair of an Intestinal Injury in Mice by Electroadhering a Gel-Patch Leah K. Borden^{1,2}, Michele Saruwatari^{3,4}, Morine Nader¹, David J. Boegner¹, Paula M. Atienza¹, Ian White¹, Anthony Sandler³ and Srinivasa R. Raghavan^{1,1}; ¹University of Maryland, United States; ²Massachusetts Institute of Technology, United States; ³Children's National Hospital, United States; ⁴MedStar Georgetown University Hospital, United States

We have demonstrated that cationic hydrogels can be permanently adhered to animal tissues by applying a low DC voltage (< 10 V) for a short time (< 60 s) [1]. This phenomenon is termed electroadhesion (EA). It works with tissues of many mammals (human, cow, pig, chicken, and mouse), and is especially strong in the case of the aorta, cornea, lung, and cartilage. Applying the DC field with reversed polarity reverses this adhesion and allows the materials to detach. Only cationic gels can be electroadhered to tissues, which suggests that the tissues have anionic character.

We then set out to study if EA could be used to repair an intestinal injury in mice without the use of sutures. A cut was made in the mouse intestine, and a cationic gel-patch was adhered over the cut by EA (9 V for 30 s). For comparison, the injury was repaired with sutures (positive control) or by weak

contact adhesion of the same gel-patch (negative control). After the surgeries, the mice were returned to their normal routine and were then assessed after six days. Mice in the EA group showed no complications due to the EA-based surgery and all of them were healthy at the time of assessment. When these mice had a laparotomy, their injuries were found to have healed, with the healing outcomes being equivalent to or better than the mice treated with sutures. These results suggest that EA can be a viable alternative to sutures, with advantages including the ability to achieve a fast and strong adhesion on-command, and moreover the ability to reverse the adhesion as needed.

References

[1] L. K. Borden, A. Gargava and S. R. Raghavan, "Reversible electroadhesion of hydrogels to animal tissues for suture-less repair of cuts or tears." *Nature Communications*, 2021, 12, 4419.

2:15 PM *SB06.02.03

Organic Bioelectronic Point-of-care Devices as Drivers of Precision Medicine [Anna-Maria Pappa](#); Khalifa University, United Arab Emirates

The development of micro-electronic devices that bridge the gap between traditional electronics with biological systems is highly desirable. The emergence of highly conjugated polymers has opened up exciting directions in biomedical research including point-of-care diagnostics. With the ultimate goal of fully integrated wearable sensors combined with IoT, and that of autonomous at-home diagnostic tests, organic bioelectronic technologies have been heavily explored the past decade resulting in novel device configurations. Multiplexing capability, ability to adopt to complex performance requirements in biological fluids, sensitivity, stability, literal flexibility and compatibility with large-area processes are only some of the merits of conjugated polymers for point of care diagnostics. This talk will summarize our recent efforts on developing biosensors for health monitoring, on rigid and flexible substrates showcasing the potential of conjugated polymers towards next generation point of care sensors.

2:45 PM SB06.02.04

Printable, Soft and Stretchable Conductor-Based Sensors for Human Body Interface [Tao Zhou](#); The Pennsylvania State University, United States

Soft and stretchable electronics have garnered significant attention owing to its wide range of applicability. The versatility of this technology has resulted in its utilization across multiple fields, such as soft robotics, skin-integrated electronics, biomedical devices, flexible displays, and human-machine interfaces. Here we present a hybrid material based on hydrogel and metal particles that simultaneously possesses high conductivity, stretchability, tissue-level modulus (<10 kPa), as well as 3D printability. This novel material was further applied to develop devices that can interact with the human body for motion sensor and EMG signal acquisition device, demonstrating huge potential for sensors and biomedical devices.

3:00 PM BREAK

3:30 PM *SB06.02.05

Organic semiconductors for regenerative medicine: optical modulation of the cell fate [Maria Rosa Antognazza](#); Istituto Italiano di Tecnologia, Italy

Use of light for selective and spatio-temporally resolved control of cell functions (photoceutics) is emerging as a valuable alternative to standard electrical and chemical methods. Here, we propose the use of smart materials, and in particular of organic semiconductors, as efficient and biocompatible optical transducers in the field of regenerative medicine.

Devices able to selectively and precisely modulate the fate of living cells, from adhesion to proliferation, from differentiation up to specific function, upon visible light will be presented. Examples of practical applications, recently reported by our group, include optical modulation of the activity of both excitable and non-excitable cells, the control of essential cellular switches like transient receptor potential channels and mechanosensitive channels, as well as effective modulation of intracellular calcium signaling for precise control of cell metabolic processes.

In more detail, we critically discuss the reliability and efficacy of our approach by focusing on a few, representative examples of possible applications:

- i. Non-toxic modulation of the cell redox balance, by functional interaction with intracellular proteins;
- ii. Optical modulation of cell differentiation, migration and wound healing processes, by hybrid interfaces with mesenchymal stem cells and epithelial cells;
- iii. Optical modulation of cardiovascular cells, namely endothelial cells and human induced pluripotent stem cells-derived cardiomyocytes (hPSC-CM). Novel materials to optically modulate angiogenesis and to optically induce an anti-arrhythmogenic effect will be presented. Interestingly, these results may represent a breakthrough, noninvasive approach to face the cardiovascular risk, in particular post-ischemic disease and arrhythmias.

The above-mentioned study-cases represent, to the best of our knowledge, first reports on use of organic semiconductors for optical modulation of the cell fate, with disruptive perspectives in cell-based therapies and regenerative medicine.

4:00 PM SB06.02.06

A Pixeless, Leadless Photoelectrochemical System for High Spatiotemporal Biosensing [Pengju Li](#) and Bozhi Tian; University of Chicago, United States

Microelectrodes and transistor-based biochemical sensors have paved the way for high-sensitivity electrical and electrochemical sensing of entities like reactive oxygen species (ROS), inflammatory cytokines, and metabolites. Yet, achieving leadless high spatiotemporal sensing remains a challenge due to the technical intricacies and spatial restrictions associated with micropatterned arrays. In this work, we introduce a leadless approach for photoelectrochemical sensing leveraging the plasmonic nanostructured Au-TiO₂ systems. These systems are characterized by their efficient light-to-current conversion capabilities, offering precise high spatiotemporal photocurrent mapping. Notably, our method facilitates the quantification of chemical concentrations in randomly defined regions-of-interest and provides a detailed profile of biochemical distributions via photoelectrochemical mapping. Additionally, we showcase the potential of bionic imaging on the pixelless device with micrometer resolution, reconstructing light-generated patterns with multimodal information including position, intensity, and color. The monolithic system can also be made on flexible substrates to enable tissue-level photoelectrochemical sensing in vivo.

4:15 PM SB06.02.07

Electrocatalytic on-site oxygenation for transplanted cell-based therapies [Inkyu Lee](#)¹, [Abhijith Surendran](#)², [Samantha Fleury](#)³, [Ian Gimino](#)¹, [Cody Fell](#)³, [Alexander Curtiss](#)², [Daniel J. Shiwarski](#)¹, [Omar Refy](#)¹, [Blaine Rothrock](#)², [Seonghan Jo](#)¹, [Tim Schwartzkopff](#)¹, [Abijeet S. Mehta](#)², [Yingqiao Wang](#)¹, [Adam Sipe](#)⁴, [Sharon John](#)¹, [Xudong Ji](#)², [Georgios Nikiforidis](#)², [Adam Feinberg](#)¹, [Josiah Hester](#)⁵, [Douglas J. Weber](#)¹, [Omid Veischi](#)³, [Jonathan Rivnay](#)² and [Tzahi Cohen-Karni](#)¹; ¹Carnegie Mellon University, United States; ²Northwestern University, United States; ³Rice University, United States; ⁴The Pennsylvania State University, United States; ⁵Georgia Institute of Technology, United States

Implantable cell therapies have been investigated as a promising approach for diseases requiring persistent treatment. However, oxygen insufficiency from a delay or lack of vascularization has been a key challenge. To address oxygen deficiency and support cells and tissues, exogenous oxygen delivery has

been studied. While targeted gas circulation and decomposition of peroxides were employed for pancreatic islets and engineered therapeutic cells, however, they require bulky implants and transcutaneous supply lines, and are limited in oxygen production and its regulation.

Here, we report an electrocatalytic on-site oxygenation (ecO₂) platform that enables controlled bioelectronic oxygen production in physiological environments to maintain cell viability and therapeutic functionality of high-density engineered cells under hypoxic stress. Nanostructured sputtered iridium oxide serves as an electrocatalyst for oxygen evolution reaction in neutral pH. It enables a low oxygen evolution onset and presents selective oxygen generation without deleterious by-products over a 300 mV window of operation. ecO₂ is capable of maintaining high cell loading (>60k cell/mm³) in hypoxia in vitro and in vivo. We demonstrate that the exogenous oxygen-generating device can be readily integrated into bioelectronics and accomplish high cell loadings in miniaturized form factor. Our ecO₂ platform can be deployed in broad bioengineering applications in cell therapies for chronic disease management.

4:30 PM *SB06.02.08

AI-driven cyborg tissue platform for functional maturation of human stem cell-derived organoids [Jia Liu](#); Harvard University, United States

The ability to control and monitor the functional specialization and maturation of human-induced pluripotent stem cell-derived tissues is critical for tissue engineering, regenerative medicine, pharmacology, and synthetic biology. This talk will introduce an AI-driven cyborg tissue platform that integrates tissue-like flexible electronic sensors and actuators with developing tissues to offer multimodal recording and control. First, I will discuss seamless implantation, integration, and distribution of stretchable mesh nanoelectronics with miniaturized multifunctional sensors and electrical stimulators across the entire 3D organoids through organogenesis for continuous, multiplexed sensing and actuation. Then, I will discuss the integration of single-cell spatial transcriptomics with bioelectronics as an in situ electro-sequencing platform, capable of combining spatially resolved single-cell gene expression with the functional readouts from the electronics for multimodal characterizations. Next, I will discuss the utilization of different machine learning algorithms to analyze, integrate, and interpret multimodal electrical activities, gene regulatory, and signaling networks to determine the functional maturation and specialization of the organoids. Finally, I will discuss the implementation of reinforcement learning algorithms for real-time feedback control, electrical stimulation optimization, and model refinement to improve the functional maturation of organoids. Collectively, the potential applications of this platform as a cyber-physical biological system for various human organoid systems in both in vitro and in vivo settings will be highlighted.

SESSION SB06.03: Poster Session I

Session Chairs: Eleni Stavrinidou and Claudia Tortiglione

Tuesday Afternoon, April 23, 2024

Flex Hall C, Level 2, Summit

5:00 PM SB06.03.01

Photosynthetic vs Photovoltaic Efficiency of *Limnospira Indica*, Perspective Cyanobacteria Strain for Space Mission Live Support Systems. Nikolay Ryzhkov¹, Nora Colson², Essraa Ahmed², Paulius Pobedinskas², Ken Haenen², Paul Janssen³ and Artur Braun¹; ¹Empa, Switzerland; ²Hasselt University, Belgium; ³SCK CEN, Belgium

Due to their excellent photosynthetic capability, which can be directly and efficiently applied in O₂ generation, CO₂ utilization, food and chemical production, as well as the photoelectrochemical production of fuels, cyanobacteria are being utilized by space agencies to establish life support systems in future space stations, planetary stations, and long-haul space missions [1].

In the harsh conditions of space, the use of live cyanobacteria is preferred over cellular components because cyanobacteria can adapt to and cope with stress, including ionizing radiation, enabling long-term autonomous operation.

Protein-pigment complexes located in intracellular structures (the thylakoid membranes) capture and transform photonic energies (in the wavelength range of 400-700 nm), leading to the liberation of electrons from water into an intricate electron flow that can be utilized for photosynthesis or driven into an external circuit of a photovoltaic or photoelectrochemical cell. Excess energy is also dissipated as heat. The productivity of photosynthesis can be estimated through a combination of electrochemical and spectroscopic methods. In an attempt to achieve the highest current output, electrical polarization of bio photovoltaic devices is required, either through external polarization bias or by implementing living cells into a self-biased device. Since photosynthesis, in a nutshell, is a process of electron transport involving a series of Redox reactions, it can be influenced by polarization, and electrical bias must be considered an environmental stress for cyanobacteria.

Pulse-Amplitude-Modulation (PAM) fluorometry, in conjunction with the saturation pulse method, has been successfully employed for studying the induction and quenching of chlorophyll fluorescence in plant physiological studies [2]. Here, we have employed PAM to investigate cyanobacterial photosynthetic performance under various polarization conditions and conducted in-situ spectroelectrochemistry to analyze the dependence of cyanobacterial pigment absorbance on electrical polarization.

We have found that negatively polarized bioelectrodes based on intact *Limnospira*, cyanobacteria reported to be resistant to Gamma irradiation and perspective for space applications [3, 4], demonstrate higher absorbance. Relative increase of absorbance in red region of visible light spectrum is higher compared to blue. As a result, biophotoelectrodes exhibit higher cathodic photocurrents under monochromatic red light than what can be expected from absorbance spectrum analysis. Furthermore, embedding cyanobacteria in either a conductive polymer matrix or a non-conductive matrix with a charge carrier facilitates higher photosynthetic efficiency, as measured by PAM, resulting in higher photocurrent output and improved efficiency in light-limited conditions.

This work was supported by the Research Foundation Flanders (FWO-Flanders) and the Swiss National Scientific Foundation under the Senior Lead Agency Project G0D4920N/189455.

[1] Poughon, L. et al, *Life Sci Space Res.* 25, 53-65 (2020).

[2] Miao, A. J. et al, *Environ.Toxicol.*, 24, 2603-2611 (2005).

[3] Yadav, A. et al, *Microorganisms*, 9, 1626 (2021)

[4] Poughon, L. et al, *Life Sci. Space Res.* 25, 53-65 (2020)

5:00 PM SB06.03.02

Stable hemoglobin-based biosensor based on coordination-assisted microfluidic technology for hydrogen peroxide determination [Rongwei Gao](#); KU Leuven, Belgium

Hemoglobin (Hb), a special redox protein, has received widespread attention because of its good selectivity to hydrogen peroxide, thus, has been employed in numerous sensing technologies. However, because Hb is easily inactivated after being separated from the biological environment, tremendous efforts have been devoted to enhance its stability and application potential. In recent years, a large number of bioconjugation strategies have been developed to

immobilize Hb, such as using (bio-) polymers, metal organic framework materials to encapsulate hemoglobin, sol-gel methods, porous materials to adsorb Hb, etc. Nevertheless, the factors affecting Hb activity are not only related to the strength of the interaction force between the immobilized carrier and hemoglobin, but are also affected by the immobilized microenvironment. Generally, the bio-friendly microenvironment for preparing an enzyme-based biosensor should: (i) maintain high intrinsic activity; (ii) limit exposure time to environmental stress; and (iii) not hinder the conformational dynamic mobility of the enzyme. While most traditional methods can improve the stability of Hb and enhance catalytic activity, only a few can maintain the conformational dynamic mobility of immobilized Hb.

In addition, hemoglobin is generally “inactive” and exhibits a closed form in aqueous media due to its active sites covered by hydrophobic amino acid chains. And the electroactive centers of Hb are deeply buried in its hydrophobic cavity, delaying electron transfer and subsequently limiting the practical application of hemoglobin sensors. HIL is composed entirely of anions and cations and takes on liquid form at or near room temperature, also showing good solubility, absorption, and stability. Interestingly, HIL can act as a “two-handed weapon.” On one hand, the imidazole cation of HIL coordinates with the ferrous ion of Hb, realizing the effective immobilization of Hb. The combination of HIL and hemoglobin driven by hydrophobic and electrostatic interaction, which helps the expansion of the temporal polypeptide of Hb and ensures the dynamic migration of its conformation. On the other hand, the hydrophobic surface of HIL helps to “open” Hb, thereby exposing its active center – a process called “interfacial activation” and enhancing its biocatalytic activity. However, because of the strong trapping power of HIL, Hb can easily aggregate in HIL, which greatly decreases its biocatalytic activity. The mussel foot protein is secreted by the shellfish, the concentrated protein solution and the metal were stored respectively. The two types of secretion capsules of ions are mixed in the microfluidic channel-like duct network and form protein-metal bonds in the newly formed bypass. Metal coordination provides strong adhesion and enhances the mechanical stability of silk protein. Herein, we used a microfluidic channel as a microreactor to immobilize Hb in HIL and construct an active layer of HIL@Hb, which can effectively prevent the aggregation of Hb. More wrinkles formed on the surface of the electrode surface synthesized using the microfluidic channel, subsequently enhancing the effective sensing area for more target molecules. Moreover, to obtain a sensitive biosensor, the effective collection and rapid transfer of electrons between Hb and the electrode is also highly important. Thus, ultra-thin MXene-Ti₃C₂ nanosheets were introduced to modify the electrode surface. The rough 2D structure of MXene-Ti₃C₂ is conducive to adhere HIL@Hb on the electrode surface; while the excellent conductivity of MXene-Ti₃C₂ can effectively reduce contact resistance and support fast electron transfer. Interestingly, the good selective sensing of MXene-Ti₃C₂ to H₂O₂ can improve the sensitivity of the sensor by synergistic catalysis. Overall, this work proposes an effective strategy to construct a stable and sensitive enzyme sensing platform, which is promising for enhancing the sensor's stability and sensitivity.

5:00 PM SB06.03.03

Real-time monitoring and Swarm-intelligence Nanorobots Enhancing Drug Delivery Precision Fan Wang^{1,2}; ¹Max Planck Institute for Intelligent Systems, Germany; ²ETH Zürich, Switzerland

In the evolving landscape of targeted drug delivery systems, the integration of advanced materials and nanotechnology is paving the way for next-generation medical treatments. This study explores the innovative conjunction of Zeolitic Imidazolate Framework-8 (ZIF-8) and iron-platinum (FePt) nanoparticles in the form of ZIF-8@FePt nanorobots, proposing a groundbreaking approach for precision drug delivery activated by radiofrequency (RF) stimulation.

ZIF-8, a renowned metal-organic framework (MOF), exhibits exceptional characteristics conducive to drug delivery, primarily due to its stable, porous structure capable of high drug loading and controlled release. Concurrently, FePt nanoparticles stand out with superior magnetic properties, including high magnetic anisotropy and responsiveness to external magnetic fields, marking their significance in biomedical applications.

This research underscores the synthesis of ZIF-8@FePt nanorobots, leveraging the symbiotic benefits of ZIF-8's drug encapsulation efficiency and FePt's magnetic navigability. The nanorobots are engineered for responsiveness to RF stimulation, a feature that sets them apart in controlled drug delivery scenarios. Upon RF exposure, the induced heat disrupts the MOF structure, triggering the release of the encapsulated therapeutic agents precisely at targeted sites. This mechanism not only promises enhanced drug delivery efficacy but also minimizes systemic side effects, presenting a favorable profile for cancer therapy, among other chronic conditions.

Furthermore, the study delves into the real-time monitoring aspect, facilitated by the inherent magnetic properties of FePt, allowing for tracking the nanorobots' journey within the biological system. The concept of swarm intelligence is also introduced, highlighting the potential for coordinated, intelligent behavior of nanorobots, significantly optimizing the therapeutic outcome.

However, the application of RF in such advanced drug delivery systems is not without challenges. The research emphasizes the need for meticulous optimization of RF parameters to prevent potential thermal damage and ensure patient safety. Additionally, extensive in-vivo studies are necessitated to ascertain the biocompatibility, efficacy, and safety of these ZIF-8@FePt nanorobots.

In conclusion, the ZIF-8@FePt nanorobots under RF stimulation herald a new era in drug delivery, merging materials science, nanotechnology, and medicine. While preliminary results are promising, comprehensive clinical trials are imperative for their transition from a theoretical model to a medical mainstay. This exploration marks a significant stride toward personalized, precision medicine, potentially revolutionizing healthcare paradigms.

5:00 PM SB06.03.04

Assessing Cellular Viability, Cytotoxicity, and Antimicrobial Susceptibility of Magnesium-Doped Hydroxyapatite Nanofibers in Primary Fibroblast Cultures: A Biological Characterization. Fabiola Hernández Rosas, José R. Alanís Gómez and Alana L. Villareal Campos; Anahuac Queretaro University, Mexico

Hydroxyapatite (HAp) is a bioceramic material of great interest in the field of tissue engineering and bone regeneration, given its high biocompatibility and bioactivity in the human body. HAp has been doped with different elements, including magnesium, strontium, silver, and others. Particularly, magnesium-doped HAp (Mg-HAp) appears to have high potential in biomedical applications. Therefore, it is relevant to characterize their biocompatibility. In this study, an in vitro model of fibroblasts obtained from chicken embryos was used to evaluate the effect of HAp-Mg on cell viability. HAp doped with 5% and 10% magnesium was synthesized by the Microwave hydrothermal-assisted method in a Monowave 300 [Anton Paar]. Subsequently, X-ray diffraction analysis was performed to characterize the HAp-Mg samples. The morphological and microstructural characterization of HAp-Mg was carried out using scanning electron microscopy (SEM). Additionally, chemical analysis was conducted using energy-dispersive X-ray spectroscopy (EDS) and FTIR-ATR spectroscopy. To evaluate the effect of HAp-Mg on cell viability, primary fibroblast cultures were obtained from 10-day-old chicken embryos. Cultures were maintained in DMEM medium supplemented with 10% FBS and incubated for 3 days in 5% CO₂ at 37°C. For the treatments, 5% and 10% HAp-Mg were diluted in DMSO at different concentrations (0.1-100 µg/ml) and added to the fibroblast cultures for 24 hours. Subsequently, cell viability was assessed using the MTT and AlamarBlue assays. Antimicrobial susceptibility tests were performed using the disk diffusion method to determine the antimicrobial activity against *Escherichia coli*, *Staphylococcus aureus*, *Enterococcus faecalis*, and *Candida albicans*. This helped determine its ability to inhibit microbial growth and prevent the formation of biofilms. In conclusion, this study explored the biocompatibility of HAp-Mg, an important material in biomedical applications. Using a fibroblast model, it characterized HAp-Mg samples and assessed their impact on cell viability. Additionally, the antimicrobial activity of HAp-Mg was evaluated against various pathogens. These findings have significant implications for tissue engineering and bone regeneration applications.

5:00 PM SB06.03.05

"Hydrogel Variability in Drug Delivery: Balancing Mechanical Strength and Stimuli-Responsiveness" [Ji Ha Lee](#); Hiroshima University, Japan

Hydrogels have garnered significant attention as eco-friendly, renewable soft materials in the context of achieving Sustainable Development Goals (SDGs). These hydrogels can be broadly categorized into two types based on the formation of the crosslinked gel network that holds water molecules: those held together by covalent bonds and those formed through non-covalent processes. Covalently bonded hydrogels exhibit robust mechanical properties, including tensile strength, viscosity, and elasticity, while non-covalent bond-based hydrogels offer the advantage of responsiveness to external stimuli. Specifically, hydrogels assembled through non-covalent molecular aggregates can be precisely tailored to achieve ordered structures and diverse functionalities, making them promising candidates for advanced intelligent drug delivery systems (DDS).

When hydrogels are employed in DDS applications, the preservation of their shape until they reach the target site, serving as carriers for model drugs, necessitates substantial mechanical strength.

Within our research group, we have successfully developed a range of hydrogels using both covalent and non-covalent bonds as binding mechanisms. These hydrogels have been fabricated from materials such as natural polysaccharides, proteins, and supramolecular compounds. We have rigorously assessed the mechanical properties of these gels and conducted investigations into the correlation between their mechanical attributes and drug encapsulation and release behaviors.

5:00 PM SB06.03.06

Development of NmeGA, a Dual Scavenger for NO and ROS in Inflammation Treatment [Yunyoung Nah](#) and Won Jong Kim; Pohang University of Science and Technology, Korea (the Republic of)

Inflammation, an immune response to external stimuli, can be developed into severe inflammatory diseases if left uncontrolled. This study introduces NmeGA, a novel dual scavenger designed to target both nitric oxide (NO) and reactive oxygen species (ROS), two pivotal factors exacerbating inflammation. NmeGA combines *N*-methyl-1,2,-phenylenediamine (Nme), a NO scavenger, and gallic acid (GA), a ROS scavenger, through an amide bond. The unique structure of NmeGA yields superior NO and ROS scavenging abilities compared to single scavengers; the amide bond and Nme's methyl group function as electron donating groups (EDG), enhancing NO reactivity. Meanwhile, GA's catechol group and the amide bond serve as EDG and electron withdrawing group (EWG), respectively, effectively scavenging ROS. NmeGA's reduced toxicity and enhanced bioapplication suitability due to increased lipophilicity, indicate its potential for inflammation management. *In vitro* studies on lipopolysaccharide (LPS)-stimulated RAW 264.7 cells demonstrate NmeGA's enhanced NO and ROS scavenging abilities and remarkable anti-inflammatory effects. Moreover, in an LPS-induced peritonitis model, NmeGA significantly reduced mortality rates, NO levels, and inflammatory cytokine levels. This research highlights NmeGA's promising potential for targeting various inflammatory diseases with minimal toxicity.

5:00 PM SB06.03.07

Development of Supramolecular Gels using Calix[4]arene and its Mechanical Property [Tomoyuki Tachibana](#) and Ji Ha Lee; Hiroshima University, Japan

The development of soft materials, particularly viscoelastic systems like organogels and hydrogels, has found diverse applications in controlled release, soft tissue reconstruction, energy capture, storage, and sensing. These systems create stable networks through physical or chemical interactions, with physical gels offering reversible networks and self-healing properties. Recent efforts have improved the mechanical properties of polymeric hydrogels through various methods, but conventional supramolecular hydrogel systems still lack high tensile strength. Supramolecular gels, such as cyclodextrin-based hydrogels, exhibit relatively weak mechanical properties due to the non-covalent interactions forming their network structures. Attempts to strengthen them with multivalent interactions have had some success but still fall short of achieving high mechanical strength. Additionally, low-molecular-weight gelators face solubility challenges in water, particularly macrocyclic gelators, which are often hydrophobic. While some reports show functionalized calixarene-based hydrogels can be effective, there is a scarcity of studies on the mechanical properties of organogels and hydrogels made from self-assembled low-molecular-weight gelators, mainly because these materials are inherently weak.

In this research, we developed the supramolecular gels using calix[4]arene and analyze its mechanical property.

5:00 PM SB06.03.08

Stimuli-Responsive Soft Microactuators For Dynamic Microfluidics [Chantal Barwig](#)¹, [Sadaf Pashapour](#)^{1,2}, [Tobias Spratte](#)¹, [Annabelle Sonn](#)¹ and [Christine Selhuber-Unkel](#)^{1,2}; ¹Institute for Molecular Systems Engineering and Advanced Materials (IMSEAM), Germany; ²Microfluidic Core Facility Institute for Molecular Systems Engineering (IMSE), Germany

Microfluidic tools spark interest as drug delivery systems, miniaturized cell cultures and lab-on-a-chip devices. The main advantages of microfluidic systems arises from the ability to reduce the sample size and decrease the reagents volume by miniaturizing large scale systems, facilitating the development of rapid diagnostic devices. Still, there is a limit in the flexibility of microfluidics and the devices that are commonly adapted to a single static application. By combining responsive hydrogels with microfluidic systems we provide a compelling option to improve functionality. Stimuli responsive hydrogels are gaining traction for applications in soft microactuators. One of the most prominent thermoresponsive hydrogels is poly(*N*-isopropylacrylamide) (pNIPAM). The actuation of pNIPAM is based on a globule-to-coil transition at the lower critical solution temperature (LCST). Additionally, pNIPAM offers a LCST of around $T \sim 32^\circ\text{C}$ close to physiological conditions. At this temperature pNIPAM undergoes a reversible volumetric change due to a transformation in its hydrophilicity. We observed a significantly higher volume change when using pNIPAM hydrogels engineered with 3D microchannels compared to the bulk pNIPAM hydrogel. Besides using such microengineering approaches, the modification of pNIPAM hydrogels with light-, pH-, or magneto-responsive molecules and particles led to multi-stimuli responsive soft actuators with new characteristics. Further, a variety of pNIPAM-based soft actuators have been developed. Recently, we fabricated a dynamic microfluidic system based on pNIPAM microactuators with a broad range of applications in analytical chemistry as lab-on-a-chip devices, biosciences, and diagnostic devices. Ultimately, the combination of microfluidic devices with stimuli-responsive hydrogels simplifies the fabrication of complex microfluidic systems, and additive manufacturing opens doors towards dynamic microfluidics.

5:00 PM SB06.03.09

Electrochemically Co-Deposited Au-Pt Bimetallic Nano-Clusters for Highly Catalytic Glucose Detection [Rashid M. Khan](#)^{1,1,2}, [Namyun Kim](#)¹ and [Yi J. Lee](#)^{1,1}; ¹Korea Institute of Science and Technology, Korea (the Republic of); ²University of Science and Technology, Korea (the Republic of)

Bimetallic nanoparticles (NPs) have been attention as attractive electrode materials owing to their unique and synergetic properties in many fields, especially in healthcare sensing platforms. Among them, Au-Pt bimetallic nano-clusters (NCs) are considered to be superior for their marked catalytic activity. We have confirmed this by comparing these bimetallic nanoclusters with dendritic Au (DenAu) NPs in glucose sensing applications. Since high standards like a broad range and a low limit of detection with utmost selectivity are primary concerns, the demand for materials with exceptional catalytic activity has been raised. Herein, we have fabricated the sensor by co-depositing the Au-Pt NCs onto the patterned seed Au layer at optimal

agitation rates and applied potential, it was characterized by its properties (interfacial impedance, cyclic voltammogram, and response to the various glucose concentrations) compared to DenAu. During electrochemical deposition, the optimal growth conditions for Au-Pt NCs and DenAu were -0.1 V for 1000 sec (stirring rate of 1000 rpm) and -0.07 V for 400 sec, respectively, which were relatively low potential as well as fast deposition time.

As a result, the sensor with Au-Pt NCs and DenAu showed remarkably high charge density yields of 309.21 $\mu\text{A}/\text{cm}^2$ and 73.74 $\mu\text{A}/\text{cm}^2$, respectively, while the sensor with plane Au electrode exhibited a charge density yield of 2.37 $\mu\text{A}/\text{cm}^2$. Moreover, they showed extremely enhanced interfacial impedance values of 1.3 k Ω (Au-Pt NCs), and 5.6 k Ω (DenAu) at 0.1 Hz compared to that of 92.5 k Ω (plane Au). Consequently, Au-Pt NCs are considered to be an optimal candidate for the highly catalytic glucose detection.

By virtue of the heightened catalytic activity of bimetallic NCs, our sensor with Au-Pt (NCs) could detect various concentrations of glucose at a wide range from 1 to 10000 μM without any use of a mediator. While considering the sensitivity and limit of detection (LOD), Au-Pt nano-clusters (NCs) exhibit exceptional sensitivity of 1715.46 $\mu\text{A m M}^{-1}\text{cm}^{-2}$ and a very low limit of detection of 1.5 μM , comparably, DenAu shows 678 $\mu\text{A m M}^{-1}\text{cm}^{-2}$ sensitivity and 6 μM limit of detection.

In the near future, the Au-Pt bimetallic nano-clusters (NCs) will be integrated into various sensing platforms (e.g., immuno-sensing, fuel-cell application, and electro-chromic system application, etc.), and their practical feasibility will be investigated.

5:00 PM SB06.03.10

Platinum Metallized Focus Rotary Jet Spun Anisotropic Fiber Flexible Electrodes Felita W. Zhang¹, Honor C. Pimentel², Paul D. Trackey¹, Garret A. Longstaff¹, Kennedy V. Munz¹, Rosemary L. Calabro^{1,3}, Enoch A. Nagelli¹, Stephen F. Bartolucci³, Joshua A. Maurer³, Kevin K. Parker² and John Burpo¹; ¹United States Military Academy, United States; ²Harvard University, United States; ³U.S. Army Combat Capabilities Development Command, United States

Flexible electrodes enable the development of wearable electronics, biosensors, and portable energy storage devices. Current flexible electrodes are often ink or silicon based with limited mechanical strength and flexibility.¹ To address challenges of mechanical strength and rigidity, we demonstrate a fiber and solution-based synthesis approach for flexible platinum electrodes. Platinum was chosen due to its resistance to oxidation, high catalytic ability, and biocompatibility. Focused rotary jet spinning (FRJS) was used to fabricate the fibers. FRJS is a method that uses focused air streams to direct flow of a fiber solution toward a rotating mandrel to produce aligned fiber scaffolds, which enable directional metallization.² Fiber scaffolds are composed of polycaprolactone and gelatin to possess both mechanical strength and charged amino acid side chains that facilitate binding to charged metal salt ions. Palladium salt solution was used to sensitize the fiber scaffolds for electroless deposition. Cu metal was deposited as continuous concentric shells around the fibers using an electroless deposition solution.^{3,4} Controlling electroless deposition time allows tunable shell thickness in the Cu phase. The Cu metal phase was galvanically displaced with Pt salt solution to achieve surface Pt metallization of the Cu shell. The metallized fibers were characterized using scanning electron microscopy, energy dispersive x-ray spectroscopy, x-ray diffractometry, x-ray photoelectron spectroscopy, thermogravimetric analysis, Fourier transform infrared spectroscopy, orientation order parameter analysis, and force extension modulus testing. Electrochemical performance of the platinum fiber flexible electrodes was determined with electrochemical impedance spectroscopy and cyclic voltammetry. The rapidly synthesized, aligned, metallized fiber sheets have tunable metal thickness, porous structures, high mechanical strength, and high specific surface area. The fiber metallization synthesis technique is envisioned as an approach for a wide range of noble metal porous flexible electrodes to address energy storage, sensing, and catalysis applications.

References

- (1) Leote, R. J. B.; Beregoi, M.; Enculescu, I.; Diculescu, V. C. Metallized Electrospun Polymeric Fibers for Electrochemical Sensors and Actuators. *Current Opinion in Electrochemistry* **2022**, *34*, 101024. <https://doi.org/10.1016/j.coelec.2022.101024>.
- (2) Chang, H.; Liu, Q.; Zimmerman, J. F.; Lee, K. Y.; Jin, Q.; Peters, M. M.; Rosnach, M.; Choi, S.; Kim, S. L.; Ardoña, H. A. M.; MacQueen, L. A.; Chantre, C. O.; Motta, S. E.; Cordoves, E. M.; Parker, K. K. Recreating the Heart's Helical Structure-Function Relationship with Focused Rotary Jet Spinning. *Science* **2022**, *377* (6602), 180–185. <https://doi.org/10.1126/science.abc6395>.
- (3) Burpo, F. J. Three-Dimensional Virus Scaffolds for Energy Storage and Microdevice Applications. *Thesis (Sc. D.)--Massachusetts Institute of Technology* **2012**, 1–156.
- (4) Ohmura, J. F.; Burpo, F. J.; Lescott, C. J.; Ransil, A.; Yoon, Y.; Records, W. C.; Belcher, A. M. Highly Adjustable 3D Nano-Architectures and Chemistries via Assembled 1D Biological Templates. *Nanoscale* **2019**, *11* (3), 1091–1102. <https://doi.org/10.1039/C8NR04864A>.

5:00 PM SB06.03.11

Synthetic Route of Au-Fe₃O₄ Janus Nanoparticles for Continuous Separation and Purification of Selected Biomaterials Yunji Eom, Jaeyong Lee, Soongeun Kwon, Hak-Jong Choi, Junhyoung Ahn, Hyungjun Lim, Kee-Bong Choi and Geehong Kim; Korea Institute of Machinery and Materials, Korea (the Republic of)

Magnetic nanoparticles (MNPs) have been received a great deal of attention in bio-applications such as hyperthermia, drug delivery, and biosensor. Recently, MNPs were one of the most promising candidates for separation and purification of biomaterials such as proteins, DNA, and exosome for disease diagnosis and treatment [1,2]. Magnetic separation is very useful technology to obtain specific biomaterial from whole blood or urine because it is simple process, high yield and non-toxic to biomaterials [3]. However, agglomeration by multiple binding sites on MNPs surface and biomaterials makes a little problem, such as insertion of undesired biomaterials and hindrance by precipitation, for separation and purification. The problems might be improved to apply MNPs based separation and purification to industrial level.

In this work, synthetic route of Au-Fe₃O₄ Janus nanoparticles (JNPs) has been developed for continuous separation and purification of specific biomaterials. First of all, Au nanocrystals have been synthesized by reduction of HAuCl₄. Then, Fe₃O₄ NPs have been attached on Au surface using thermal decomposition of Fe(CO)₅ as following literature to synthesize Au-Fe₃O₄ JNPs capped with oleic acid [4]. Each ligand on the surface of Fe₃O₄ and Au has been continuously exchanged with hydrophilic chain (PEG, COOH, etc.) functionalized phosphonic acid group and target binding head (antibody, biotin) functionalized thiol group, which makes stronger bind between ligand and surface. Target binding head on Au surface has been attached on the surface of specific biomaterials. Then, hydrophilic chain of opposite site of JNPs can provide high dispersibility in water and buffer solution and self-passivation to prevent undesired agglomeration between biomaterials and JNPs. In this study, biotin functionalized thiol, PEG functionalized phosphonic acid, and streptavidin functionalized polystyrene (PS) bead are employed as target bind head ligand, hydrophilic ligand, and artificial biomaterials to prove JNPs system works well, respectively.

To analyze the structural and morphological properties, as-synthesized and ligand-exchanged JNP were investigated using transmission electron microscopy (TEM). Then, magnetic properties of JNPs were observed using vibrating sample magnetometer (VSM). Finally, dispersibility of JNPs before and after binding with PS bead was measured using home-made dispersion analysis system and scanning electron microscopy (SEM). In this results, JNPs system is well operated with high dispersibility enables easy movement and continuous process for separation by magnetic force.

5:00 PM SB06.03.12

Self-Assembly Sugar Derivative-Linked Nucleic Acid Nanoparticle for Nucleic Acid Medicine Delivery Noriko Miyamoto and Yukio Kitade; Aichi Institute of Technology, Japan

DNA- or RNA-based nucleic acid structures (NASs) have garnered significant interest as potential carriers for nucleic acid medicine delivery due to their ability to create unique sequence-based structures. However, for the biological application of NASs, it is still challenging to create a nanostructure that is stable and avoidance of recognition as an immunogenicity under physiological conditions.

We have developed a novel type of NAS called RION (reversibly ionic oligonucleotide-based nanoparticles including microRNAs) through a self-assembly process involving RNA-RNA hybridization and electrostatic interactions facilitated by chemically modified oppositely charged ion oligo nucleic acids[Miyamoto N., et al., *Advanced therapeutics* 2023, 6, 2200265]. In this research, to demonstrate the versatility of the chemical modification of RION, we designed a sugar derivative linked to RIONs. The sugar derivative-linked RION nanoparticles exhibit a spherical shape with a diameter of less than 100 nm, as observed in transmission electron microscopy images. Moreover, we found that sugar derivative-linked RION, when loaded with tumor suppressor microRNA, effectively inhibits the growth of human colorectal cancer cells (DLD-1 cells) in a dose-dependent manner. On the other hand, the sugar derivative-linked RION demonstrated transfection efficiency in a floating cancer cell line, a well-known difficult transfection with commercialized Lipofection reagents. This report introduces RION technology as an innovative platform for delivering nucleic acid-based medicines, offering promising potential for applications in the field of cancer therapy and beyond.

5:00 PM SB06.03.13

Nanocrystalline Gadolinium-Doped Hydroxyapatite: Synthesis, Characterization and Cytotoxicity Assessment for Enhanced Drug Delivery Applications Fabiola Hernández Rosas¹, José R. Alanís Gómez¹, Rodrigo Velázquez Castillo² and Emilio Carnaya Bustamante¹; ¹Universidad Anahuac Querétaro, Mexico; ²Universidad Autónoma de Querétaro, Mexico

Hydroxyapatite (HAp) is a ceramic material predominantly composed of calcium phosphate, possessing a crystalline structure similar to natural human bone. It holds a wide range of applications in the medical field, such as dental implants, and serving as a bone filler in orthopedic surgery. Moreover, HAp can be enriched with rare earth elements to bestow its luminescent properties. This makes HAp-based nanocarriers ideal candidates for incorporation into polymeric nanoparticles, which can be designed as nanospheres or nanocapsules, functioning as channels for precise drug delivery within biological systems.

In this study, we synthesized gadolinium-doped HAp nanofibers (HAp-Gd) using the Microwave-Assisted Hydrothermal Method to evaluate their suitability as drug carriers. After this, the HAp-Gd samples were characterized through X-ray diffraction. HAp-Gd was identified by comparing the results with the ICDD PDF files provided by Bruker. Morphological analysis and the determination of the elemental chemical composition of HAp-Gd nanofibers were performed through scanning electron microscopy (SEM) and energy-dispersive X-ray spectroscopy. Subsequently, luminescence analyses were executed to examine the interaction between the drug intended for transportation and the HAp-Gd nanostructures. This assessment was performed by analyzing the samples using photoluminescence spectroscopy. Then, we conducted an AlamarBlue Assay to assess the biosecurity and cytotoxicity of HAp-Gd in a culture model of chicken embryo fibroblasts. Results obtained from X-ray diffraction, scanning electron microscopy, and energy-dispersive X-ray spectroscopy collectively demonstrated the exceptional characteristics of the synthesized HAp nanofibers. These characteristics include a high level of crystallinity, purity, a hexagonal morphology, and a preferential crystalline orientation.

Furthermore, the chemical composition was uniform, indicating excellent integration of gadolinium into the HAp structure. Additionally, the biomaterial exhibited notable photoluminescent properties, suggesting its potential as a facilitator for drug transport within biological systems. Also, the results of the AlamarBlue assay indicate that the HAp-Gd does not exert a cytotoxic effect on fibroblasts.

In conclusion, the microwave-assisted Hydrothermal Method proved highly effective in synthesizing gadolinium-doped hydroxyapatite nanofibers with unique morphological and structural characteristics. We also demonstrate that this material is safe at the cellular level. These findings reinforce its potential application as a secure drug carrier in biological systems.

5:00 PM SB06.03.15

Modifying Bio-Ingredients within an Integrated Food Printer using an In-Situ Corona Discharge Non-Thermal-Plasma Approach: A Step Toward Creating Innovative Methods for Characterizing Engineered Food Materials and Biomedicine Kaiyu Vang¹, Derek Xiong¹, David Ryman¹, Edbertho Leal-Quiros², Saquib Ahmed^{3,4} and Sankha Banerjee^{1,4}; ¹California State University, Fresno, United States; ²University of California, Merced, United States; ³Buffalo State College, United States; ⁴University of California, Davis, United States

The present research is focused on pioneering new in-situ non-thermal plasma treatment techniques for 3D printed bio-ingredients based on starch. Thanks to its natural abundance and cost-effectiveness, starch emerges as a highly pertinent raw material for substituting synthetic polymers in various applications. It enjoys a reputation for being non-toxic, biocompatible, and biodegradable, making it a secure choice for applications in the biomedical, food, and packaging sectors. Utilization of starch as a foundation for stabilizing, integrating, or releasing bioactive substances with applications as bioactive compounds incorporated within starch matrices in the pharmaceutical industry, with a particular emphasis on their use in orally disintegrating films. These methods aim to customize the attributes of the starch granule-surface proteins (SGSP). The study also involves assessing continuous and discontinuous gluten networks formed due to the interaction of SGSPs with quasi-static corona discharge plasma conditions. Additionally, the research investigates the bonding characteristics of starch-based bio-ingredients based on plasma current-voltage behavior. The surface of the cured starch-based samples will undergo profiling for characterization. The binding properties, gluten network formation, and porosity characteristics will be examined through electron microscopy for microstructural evaluation. Furthermore, advanced hybrid machine learning models will be developed in conjunction with analytical techniques and empirical datasets to create strategies for modifying both the surface and bulk properties of these materials.

5:00 PM SB06.03.16

An Open-Source Droplet Digital PCR (ddPCR) System for the Rapid and Accurate Detection of Bacteria from Environmental Water Samples Mason Brady, Ian M. Van Horn, Donald Ledvina, Albert Burkle, Paula Sanchez, Yiyang Li, Jerry Crawford, Micheal Grubb and Christie Chatterly; Fort Lewis College, United States

Droplet Digital PCR (ddPCR) is a method of rapid bacterial quantification in a liquid culture or solution. The development of an open source ddPCR system will allow this technology to become more affordable. The development of this open-source system utilized reused optical components, including a Photomultiplier Tube (PMT) from a flow cytometer, aligned using optical fittings. The signals received from the PMT were passed through a circuit containing passive bandpass filters and amplifier stages. FITC fluorescent microspheres were used to test the potential limits of the system's ability to quantify different concentrations of positive bacterial droplets in a sample. The system provided a large cluster of counts at 100% accuracy when particles were passed at a rate slower than 50 particles per minute. The functionality of the system was assessed by utilizing microfluidic droplets containing cultured *E. coli* samples. Different concentrations were used to test the system's accuracy through comparison. For each concentration the bacterial counts were within 10% of the expected values. To automate the quantification of signals from the system, a convolutional neural network is in development.

5:00 PM SB06.03.17

Potassium Hydroxide Etched Silicon Biomembrane Optimization and Characterization for Lung-on-a-Chip Applications Sahra G. Genc¹, Leif Gislason¹, Sally Thompson¹, Sarah M. Schreiner^{2,3}, Adrian Gestos⁴, Virginia Ferguson⁴ and Jeff Jessing¹; ¹Fort Lewis College, United States; ²STROBE

NSF, United States; ³JILA, University of Colorado Boulder, United States; ⁴University of Colorado Boulder, United States

Organ-on-a-chip technology is heavily studied as an alternative to animal and cell culture models. Most of these studies are primarily focusing on the biological aspects. There is a need to understand the mechanical and morphological properties and functionality of critical components of such devices. Our group is developing a Lung-on-a-Chip device based on a novel biomembrane formed from porous silicon (PSi) that mimics the interstitial space between the epithelial and endothelial cells in vivo, with a thickness of approximately 1 μm . The membranes are fabricated through a process of chemical thinning p-type silicon wafers and electrochemical anodization to create the porous structure. Previously published results from our group on membranes that did not undergo the chemical thinning characterized with nanoindentation and scanning electron microscopy show a correlation between the porosity of the PSi samples with their reduced modulus and thickness. This current work focuses on the development and refinement of the technique used to etch ultrathin (less than $\sim 5\mu\text{m}$) silicon membranes using a potassium hydroxide (KOH) etchant. Further, we show the results of a small parametric study by varying the formation conditions during the KOH etch. The specific formation conditions that affect the resultant membrane surface quality are etchant temperature, inclusion of a surfactant, and post-etch quench "rinse". The membranes mechanical and morphological traits are characterized using scanning electron microscopy, atomic force microscopy, and nanoindentation to discern the surface quality of the silicon biomembrane, considering parameters like roughness, defect density, and uniformity. These aspects are correlated to the different KOH process parameters to find the optimal approach, as well as its potential relationship with the membrane's morphological features. In general, the surface quality and membrane thickness uniformity improves with decreasing etch temperature, inclusion of propanol as a surfactant, and employing a multiple stage hot rinse following the KOH.

5:00 PM SB06.03.18

Bioprinting of photothermal responsive engineered biohybrid material for biomedical applications Prakriti Dhungana, Natalie Dando, Kyle Duke, Jonathan Caguiat and [Byung-Wook Park](#); Youngstown State University, United States

Bioprinting has been shown to be an effective method for biomanufacturing biohybrid materials with designed structures and dimensions. Engineered biohybrid materials from micro- to macroscales can be constructed using a bioprinter for various biomedical applications. Stimuli-responsive biohybrid materials that respond to environmental conditions have attracted the attention to create material system that mimic the functions of living systems. Herein, we present a new biohybrid material system and method capable of bioprinting hydrogel bioinks with genetically engineered probiotic *Escherichia coli* Nissle 1917 (EcN) as photothermal responsive component. The engineered bacteria heat shock response (HSR) is triggered by the localized heating nanocomposite. We first discuss the design and optimization of the biotic and abiotic components encapsulated in a hydrogel bioprinted as engineered biohybrid material. We then demonstrate an expression of green fluorescent protein (GFP) upon near-infrared photo stimulus. Finally, the bioprinted engineered biohybrid material can survive for a period of at least 3 days in the M9 minimal medium. We anticipate the developed engineered biohybrid material system is further enabled by bioprinting of the photothermal responsive bacteria for biosensing and biomedical applications.

5:00 PM SB06.03.19

Detection of Bacteria Using Near-Infrared Raman Spectroscopy and Deep Learning [Donald G. Ledvina](#), Sienna Mullin, Ian M. Van Horn, Mason Brady, Micheal Grubb, Jerry Crawford, Jeff Jessing and Yiyan Li; Fort Lewis College, United States

The process of identifying bacteria can often be challenging and time-consuming. Employing machine learning, Convolutional Neural Networks (CNNs), and Raman Spectroscopy, we strive to develop a rapid and effective solution to this problem. As a preliminary trial, we have designed a 4-layer CNN using TensorFlow, trained and evaluated on a recently published dataset comprising 30 different classes of bacteria isolates. Our CNN demonstrates enhanced accuracy in identification and reduced intricacy in comparison to other networks. Moving forward, we intend to utilize our in-house near-infrared Raman (785 nm) microscope spectrometer to gather our own bacterial spectra dataset. Bacteria samples will be cultured on agar plates and preserved until required. Subsequently, a small portion of the bacterial colonies will be spread onto a gold-coated slide for the spectrometer to analyze. This dataset will be employed for training the CNN, facilitating the development of a cost-effective, high-speed bacteria identification system.

5:00 PM SB06.03.20

Development of Artificial Joints Printed by 2-Photon-Laser-Printing and Actuated with pNIPAM [Annabelle Sonn](#), Barbara Schamberger, Gaurav Dave, Chantal Barwig and Christine Selhuber-Unkel; Heidelberg University, Germany

Soft actuators are flexible components that can adapt to dynamic environments based on responsive materials like polymers, fluids, or hydrogels, to name a few. Hydrogels made of e.g., thermoresponsive poly-*N*-isopropylacrylamid (pNIPAM) are excellent candidates for soft robotic applications due to their ability to change in volume depending on the surrounding temperature. Below the lower critical solution temperature (LCST), which is 32 $^{\circ}\text{C}$, pNIPAM is in its swollen, hydrated state, while it shrinks to the dehydrated state above the LCST. With 2-photon-laser-printing (2PP), which is making use of the absorption of two near-infrared (NIR) photons, it is possible to initiate highly precise polymerization of the hydrogel ink, in our case pNIPAM. This enables the generation of complex 3D structures on the microscale. Here, we show the design and printing of artificial joints with pNIPAM components in the micrometer range by two approaches: First, the structures are printed in two-steps consisting of a solid polymer base, surrounded by pNIPAM, which is mimicking muscle tissues. Second, a structure is printed entirely out of hydrogel resulting in a fully soft joint. After printing and mechanically analyzing the joints by nanoindentation measurements, the thermoresponsive actuation was evaluated by switching the ambient temperature between temperatures below and above the LCST of pNIPAM. In the future, the design of the soft joints may be improved to give more complex structures with sophisticated functionalities on the microscale.

5:00 PM SB06.03.21

3D Printing Conductive Hydrogels with Tunable Properties for Soft Robotics and Biosensing [Trevor Kalkus](#), Tamara Unterreiner, Laura Wächter, Christina Schmitt and Christine Selhuber-Unkel; Heidelberg University, Germany

Soft electronics can serve a central role in the development of biosensors, wearable devices, and soft electronics. For these applications, flexible circuits with complex and organic geometries will be necessary. The 3D printing of conductive hydrogels offers a simple manufacturing method for creating such structures and provides opportunities for rapid iteration and modification. Because different applications may call for various hydrogel properties, we demonstrate the ability to tune ink viscosity, hydrogel stiffness, and hydrogel conductivity. These functional hydrogels are based on acrylamide, due its stability and ubiquity, and PEDOT:PSS, a commonly used conductive organic polymer, is embedded to provide conductivity. With thorough characterization, we highlight the advantages of designing conductive hydrogels in this way. Ultimately, we demonstrate the ability to print the components suitable for soft electronics. While this work provides a preliminary demonstration, future steps will focus on applying this method to create biosensors and soft robotics.

5:00 PM SB06.03.22

Electrochemical sensing of cytokines utilizing carbon nanotube fiber-based electrodes [Megan N. Baker](#)^{1,2}, Allison Yorita², Anna Ivanovskaya², Razi haque² and Samantha Santacruz¹; ¹The University of Texas at Austin, United States; ²Lawrence Livermore National Laboratory, United States

Aptamer based biosensors are a promising tool for further understanding mechanisms underlying various systems in the body at a molecular level. Aptamers allow for indirect electrochemical sensing of chemicals and biomolecules. As a specific target molecule binds to the aptamer, there is a conformation change. Scientists have taken advantage of this conformation change and designed aptamers that bring the charged free end closer to the surface of an electrode, sensing an electrochemical change in response to the chemical concentration. However, the binding of aptamers to the surface of metal electrodes has shown to be very fragile, making the lifespan of such biosensors limited. For *in vivo* and even future clinical applications, the devices need to be stable both in and out of solution for long periods of time. We propose using carbon nanotube fibers (CNTf) to improve the adhesion of aptamers to the surface of electrodes. CNTfs have great chemical stability, electrical properties, and high effective surface area making them ideal candidates for the substrate of the devices. The chemical bond between carbon and the aptamers is more stable than that with gold, a conventional biocompatible electrode material, allowing for a more stable device. To test this device design, we use aptamers that selectively bind to IL-6. The IL-6 aptamers are immobilized and attached to the CNTf using electrochemical conjugations. After successful attachment has been validated, the sensitivity of the device and limit of detection are evaluated and optimized. After optimization, the response time, lifetime, and biofouling response are analyzed. This is initially done in phosphate buffered saline (PBS) solution, but further testing in animal models is planned. The functionalized device can be used to decode immune status in blood using pro- and anti-inflammatory cytokines at physiologically relevant concentrations. This opens the door to being able to both monitor and intervene in the immune system using bioelectronic interfaces, with the CNTf sensor recording real-time immune system status and a future electrical interface with the nervous system modulating the immune system based on data from the sensor, a systems-level approach which has not been done before.

5:00 PM SB06.03.23

Continuous Whole Blood Dialysis Based on Regenerated Dialysate Utilizing TiO₂ Nanowire Photo-Electrochemical Oxidation and Protective Forward Osmotic Membrane Guozheng Shao, [Mingyuan Zhang](#), Hao Tang and Bruce Hinds; University of Washington, United States

While a traditional 4-hour dialysis treatment uses up to 120L of fresh dialysate per session, a full-scale bench-top system was developed to remove clinically relevant amounts of uremic toxins in whole blood using only 0.5L of commercial dialysate solution over a 24-hour continuous dialysis process. Urea was removed by photoelectrochemical method through a UV/TiO₂ nanowires array device connected to a Forward Osmosis (FO) membrane in a protected close loop, while other non-urea toxins were removed by Activated Carbon (AC) in the dialysate loop. Here we demonstrate a daily urea removal rate of 14.2g using 0.4m² of hemodialyzer membrane and 2.3m² FO membrane with 0.18m² TiO₂ nanowires array in Photoelectrochemical Oxidative Urea Removal (POUR) unit. Other non-urea toxins represented by creatinine and phenylacetic acid with a daily removal rate of nearly 7g were achieved by 70g of AC absorbent in the dialysate loop. Urea, creatinine and phenylacetic acid were constantly infused to the saline solution with the speed of 15g/24h, 5.6g/24h and 1.4g/24h to simulate actual human toxins level. Urea is continuously removed in a 0.15M NaCl saline solution by the photo-oxidation reaction occurring on TiO₂ nanowire surface with the presence of UV source and applied bias to enhance the electron-hole pair separation within the single crystal TiO₂ nanowire. The POUR loop was also protected from the potential oxidative species generated from the photooxidation of urea by inline AC absorbent with real-time ORP and pH sensors, showing non-cytotoxicity to the blood loop. The FO membrane is also a key component to prevent small solute molecules from dialysate entering the POUR loop to lower its efficiency as well as forming harmful oxidative byproducts. Our results also showed a wide variety of treatment modes (ie. 4, 8, 12 hr daily times) by coupling different membrane components. More importantly, by eliminating the need for the external water source, our system offers possibilities of a variety of portable kidney dialysis treatment options for home, work and travel.

5:00 PM SB06.03.24

Characterization of Single and Dual-Consortium Microbial Systems in 3D-printed Multi-Material Hydrogels [LeAnn Le](#), Alshakim Nelson and Naroa Sadaba; University of Washington, United States

Engineered Living Materials (ELMs) capture the efficiency of cellular systems within polymeric matrices to provide bioreactor designs for production of commodities such as biofuels, vaccines, and the classic Seattle IPA. With extrusion-based 3D printing, we can print multi-material ELMs that afford controlled spatial organization of cell populations. With F127-bisurethane methacrylate (F127-BUM), an easily accessible triblock copolymer, we can synthesize bioinks with proper yield strain for extrusion-based printing while also gaining robust biocompatibility and free diffusion of metabolites across the material. We maintain a basic understanding of F127-BUM structure but have limited knowledge of how the network interacts with cells. While these hydrogel constructs display robust metabolic function, prior studies have shown cells escaping into the surrounding media despite complete encapsulation, suggesting random migration through the material. However, in studies that culture two microbial species in adjacent F127 gels, higher-order spatial organization is observed as cell populations consisting of one species do not migrate into gel areas occupied by another cell species. In our studies, we propose an alternative 3D-printed core-shell cube structure that consists of a cell-laden inner core surrounded by a cell-free outer shell. This construct affords a model to study cell behavior of single and dual-cell consortiums in F127-BUM hydrogels as we seek to improve cell containment and preserve metabolic function in 3D printed hydrogel designs for bioproduction.

Using the core-shell cube structure, we demonstrated robust multi-kingdom functionality with Green Fluorescence Protein (GFP)-secreting *E. coli* and betaxanthin-producing *S. cerevisiae*. After six days, the multi-material constructs showed continuous GFP and betaxanthin production and diffusion into the media. Optical fluorescence microscopy showed GFP *E. coli* distribution focused on the core-shell interface while *S. cerevisiae* distribution is uniform throughout the core. While visual spatial separation between the core and the shell elements was maintained, cell escape after 48 h was observed using SEM as a result of microscopic inconsistencies in the printing process and cross-contamination of the extrusion nozzles during printing. By altering flow speed and the print design g-code, we improved cell containment.

To investigate impact of form factor on microbial behavior, we proposed a rectangular prism design with improved surface area-to-volume ratio to investigate the impact of geometric parameters on bioproduction and diffusion. We saw improvement in the GFP-system but observed little difference in our betaxanthin system. Additionally, we tested the performance of both core-shell constructs in co-culture systems by placing gels containing one cell population into free media containing a different microbial species. With the gel system, viability was maintained in both cell species for 6 d.

Following the single consortia models, we expanded the core-shell design to contain a dual-microbial consortium. Inspired by symbiosis, this multi-kingdom hydrogel design contained a metabolically constitutive relationship consisting of engineered *E. coli* and *S. cerevisiae* strains. *S. cerevisiae* only produces betaxanthin in presence of L-DOPA.

During a six-day period, final betaxanthin production remained low as a result of the inner core consortia having limited access to oxygen as the outer shell consortia blocks nutrient access during overgrowth. As a result, we will adopt designs such as coaxial fibers or thinner dual-material biofilms to avoid limitations in oxygen and nutrient diffusion.

Overall, our investigation of multi-material F127-BUM hydrogels and their ability to afford a wide range of microbial systems and design possibilities establishes a necessary model to study the intricate relationship between hydrogel structure and cell behavior for bioproduction applications.

5:00 PM SB06.03.25

Spectrally-Resolved Ratiometric Multiphoton Fluorescence and Second Harmonic Imaging of Noninvasive Vascular Scaffolds Tolulope Ajuwon, Tochukwu Emeakaroha and [Steve Smith](#); South Dakota School of Mines and Technology, United States

We present spectrally-resolved multi-photon induced fluorescence (MPIF) and second harmonic generation (SHG) imaging of porcine arterial wall tissue sections, both native tissues and damaged tissues subject to a proprietary therapy based on photo-activated crosslinking of collagen and other structural proteins in the arterial wall, a proposed treatment for peripheral artery disease termed non-invasive vascular scaffolding (NVS). We employ a spectrally-resolved multi-photon imaging system, based on a closed loop piezoelectric stage, a transmission grating and an EMCCD. From the spectrally-resolved multiphoton emission, we form ratiometric images of select spectral bands associated primarily with collagen (SHG) and elastin (MPIF). The ratiometric images aid in identifying representative regions for comparing the native and treated tissue sections, as well as reducing sensitivity to variations in intensity caused by scattering or attenuation of the excitation beam. Our aim is to use these ratios as a metric of the tissue structure and composition, indicating the relative contribution of collagen and elastin to the observed nonlinear signals. We note the photo-chemical modification results in a recovery of SHG intensity similar to the native artery, with the hypothesis that cross-linking of the compressed collagen fibrils in the arterial wall during the light activation step results in the formation of the NVS. We analyze the polarization anisotropy of the SHG from these tissues and evaluate the spectral dependence of control samples designed to calibrate the relative contributions elastin (MPIF) and collagen (SHG) to the observed spectra.

5:00 PM SB06.03.26

Tough, Non-Drying, and Tissue-Adhesive Glycerogel Dressing with Ferrocene Nanoparticles for Improved Wound Healing Ji Won Kang¹, Jin Han Cho² and Byoung Soo Kim¹; ¹Korea Institute of Ceramic Engineering and Technology, Korea (the Republic of); ²Korea University, Korea (the Republic of)

The benefits of employing moist wound dressings were firmly established in the late 1900s, driving notable progress in the evolution of modern wound care products, such as hydrogels and hydrocolloids. Notably, hydrogel-based dressings have demonstrated the ability to provide a soothing, cooling effect on the skin, making them a promising option for treating burns and painful wounds. Furthermore, studies have indicated that hydrogel-based dressings effectively minimize eschar formation, preserving tissue integrity and expediting the migration of epithelial cells. However, current hydrogel dressings lack adequate moisture balance and oxygen exchange that potentially leads to skin maceration, infections, and tissue damage by the constant changing of the material. Many hydrogel dressings available in the commercial market exhibit brittleness, necessitating the incorporation of a supplementary support layer, such as adhesive silicone, to reduce the water-vapor transmission rate. In this study, we designed tough, non-drying, and self-adhesive hydrogel dressing, synergistically integrated with stimulus-responsive drug nanoparticles for enhanced wound healing. First, we synthesize a tough hydrogel by optimizing the balance between physical and chemical cross-links by entanglements and covalent bonds. The achievement of non-drying and self-adhesive features can be attained by incorporating glycerol into the tough hydrogel matrix, leading to solvent exchange and partial contraction of the hydrogel matrix. The resulting tough hydrogel containing hygroscopic glycerol maintained its hydration state for 6 months in air. Additionally, they exhibited a substantial adhesion strength (183.73 kPa), attributed to the increased local concentration of hydroxyl groups. For enhance wound healing efficacy, we integrate the hydrogel matrix with stimulus-responsive ferrocene nanoparticles. We will discuss about clinical impact upon wound healing and antioxidation effect in moist wound care environment based on the resulting tough hydrogel dressing, infused with ferrocene nanoparticles.

5:00 PM SB06.03.27

Micro-vibrator integrated wet adhesive glycerogel patch for enhanced transdermal drug delivery system [Seo Yoon Kim](#); Korea Institute of Ceramic Engineering and Technology, Korea (the Republic of)

Transdermal drug delivery system (TDDS) is a painless method of delivering drugs by applying patches directly onto skin. Among the evolving variations of TDDS, hydrogel patches gaining prominence for its capacity to facilitate skin hydration and efficiently deliver pharmaceutical agents across the skin barrier. However, in order to facilitate commercialization, hydrogel-based patches need to effectively tackle three key challenges: (1) minimizing moisture evaporation, (2) enhancing adhesion in wet environments, and (3) precisely controlling the release dosage of the contained medicine. Here, we introduce a novel glycerogel matrix that exhibits wet-adhesive properties, does not dry out, and possesses high toughness. This matrix is first designed to facilitate prolonged skin contact and enhance the absorption of drugs. Next, the glycerogel matrix was combined with a micro-vibrator film in order to enhance medication penetration through the stimulation of skin microcirculation. The glycerogel matrix exhibits rapid adherence to various surfaces in a wet condition, with a time frame of less than 10 seconds. The strength of adhesion is influenced by the size and composition of the silica nanoparticles used for surface coating. We also confirmed the vibrator-assisted drug release create a synergistic effect within the hydrogel, promoting efficient drug dispersion and enhancing skin penetration. This accelerates drug absorption and improves drug efficacy, resulting in faster drug release and shorter time to achieve therapeutic goals. We believe this synergistic integration of these components presents a novel paradigm in controlled drug release, allowing for precise modulation of therapeutic dosages.

Keywords? : Tough hydrogels, bioadhesives, transdermal drug delivery, micro-vibration film, active drug delivery

5:00 PM SB06.03.28

Biocompatible WSe₂ Nanosheet Antibiotics for The Therapy of Pathogenic Bacterial Infections [Yoonhee So](#), Jun-Hyeong Lee, Jaewoo Lee, Sin Lee, Yejoon Yu, Yujin Choi and Jong-Ho Kim; Hanyang University, Korea (the Republic of)

Abuse of broad-spectrum antibiotics not only causes intestinal microbial imbalance but also emerges bacteria resistant to drugs. Therefore, it is an urgent task to develop narrow-spectrum antibiotics and new bactericidal mechanisms to overcome the limitations of broad-spectrum antibiotics. Herein, we present ultrathin WSe₂ and MoSe₂ nanosheets exfoliated and functionalized with poly(acrylic acid) (PAA-WSe₂ and PAA-MoSe₂) in an aqueous solution as a narrow-spectrum antibiotic or a species-specific agent, respectively, for treatment of bacterial infection diseases. PAA-WSe₂ nanosheets exhibited bactericidal activity only against gram-positive bacteria including multidrug-resistant *S. aureus*, whereas PAA-MoSe₂ showed selective bactericidal activity against *S. aureus* only. Moreover, PAA-WSe₂ accelerated the oxidation-reduction reaction mediated by lipoteichoic acid, a component of the cell membrane of gram-positive bacteria, producing Se⁴⁺ for antibacterial activity. Subsequently, the PAA-WSe₂ nanosheets induced depolarization and disruption of the bacteria-cytoplasmic membrane for the complete eradication of gram-positive bacteria. PAA-TMD nanosheets, including PAA-WSe₂ and PAA-MoSe₂, also exhibited outstanding biocompatibility against normal cells and hemocompatibility with red blood cells. Finally, PAA-WSe₂ nanosheets effectively eradicated *S. aureus* infecting the wounds of mice, showing excellent therapeutic effects *in vivo*. These results suggest that PAA-WSe₂ has been developed as a narrow-spectrum antibiotic used for various bacterial infections.

SESSION SB06.04: Living Materials I
Session Chairs: Eleni Stavrinidou and Claudia Tortiglione
Wednesday Morning, April 24, 2024
Room 427, Level 4, Summit

8:00 AM SB06.04.01

Microbial encapsulation with polyethylene-glycol based hydrogel materials for protection against environmental stress factors Ryan Hansen, Niloufar Fattahi, Jeffrey Reed, E'van Heronemus, Priyasha Fernando and Prathap Parameswaran; Kansas State University, United States

Many emerging applications in microbial biotechnology require that microorganisms function under harsh or unfavorable environments. These environments may contain chemical toxins, reactive oxygen species, limited nutrients, extremes in pH and temperature, or exogenous microorganisms, among other stress factors. Microbial electrochemical cells (MxCs), which use electroactive biofilms of anode respiring bacteria (ARB) for current production, are often limited by loss of ARB electrochemical activity due to these stress factors. This inhibits the use of novel MxC systems in applications related to water treatment, sub-surface remediation, remote sensing, and self-powered bio-batteries. In this work, we report the use of polyethylene-glycol (PEG) based hydrogel materials for encapsulation, stabilization, and toxin protection of ARB biofilms in a MxC system.

Hydrogels were formed using PEG divinyl sulfone and PEG tetrathiol precursor molecules. These molecules couple together through base-catalyzed Michael addition reactions between thiol and vinyl sulfone end groups, generating highly crosslinked hydrogel networks with well-controlled, tunable mesh sizes. Precursor molecules were mixed together over anodic biofilms using an established dip coating procedure. The resulting hydrogels were resistant to acid or base hydrolysis over a range of pH values (pH = 3 to 10), appeared stable over ARB biofilms, and did not compromise biofilm viability over a 30-day trial period. The electrochemical activity of hydrogel-coated ARB biofilms was compared to uncoated ARB biofilms in a side-by-side manner, and it was found that the hydrogel coated anodes displayed higher current density under oligotrophic environments, higher current densities during exposure to high concentrations of ammonium toxin, and faster recovery after an ammonium shock. Hindered diffusion of ammonium ions through the hydrogel was identified as the cause for improved ARB performance during and after the ammonium shock.

These findings demonstrate the novel use of hydrogel materials to protect EAB from sharp chemical gradients that commonly occur during a chemical shock. Because hydrogel pore size can be modulated by controlling the molecular weights of the PEG precursor molecules, and catalytic functionality can be added to the hydrogel, these coatings can be further engineered to provide selective control of mass transport to functional microbes for their protection in a variety of applications. On-going work investigates enzymatic modification of these hydrogels to protect encapsulated bacterial cells from other chemical toxins for bioproduction and biomedicine applications.

8:15 AM *SB06.04.02

Living fabrications by the engineered bacteria Zhuojun Dai; Shenzhen Institute of Advanced Technology, Chinese Academy of Sciences, China

A key focus of synthetic biology is to utilize modular biological building blocks to assemble the cell-based circuits. Scientists have programmed the living organisms using these circuits to attain multiple delicate and well-defined functions. With the integration of tools or technologies from other disciplines, these rewired cells can achieve even more complex tasks. In this talk, we will present our recent work in versatile biomanufacturing of biologics and functional material fabrication by integrating the engineered cells and polymer physics and chemistry. By exploiting cell-material feedback, we are able to design a concise platform to achieve versatile production, analysis, and purification of diverse proteins and protein complexes, and also assembly of functional living materials. Our work demonstrates the use of the feedback between living cells and materials to engineer a modular and flexible platform with sophisticated yet well-defined programmed functions.

8:45 AM SB06.04.03

A deep insight into the mechanism of production of living conducting materials Marika Iencharelli¹, Giuseppina Tommasini², Vittorio De Felice¹, Natalia Dell'Aversano¹, Maria Antonietta Ferrara¹, Giuseppe Coppola¹, Francesca Di Maria³, Mattia Zangoli³, Maria Moros², Angela Tino¹ and Claudia Tortiglione¹; ¹Istituto di Scienze Applicate e Sistemi Intelligenti "E. Caianiello", Consiglio Nazionale delle Ricerche, Italy; ²Instituto de Nanociencia y Materiales de Aragón (INMA), Spain; ³Istituto per la Sintesi Organica e Fotoreattività, Consiglio Nazionale delle Ricerche, Italy

Living cells are able fabricate complex structure starting from simple building blocks, offering new paradigms to create new hybrid materials by combing synthetic and living features. We have previously shown the capability of the living tissue-like organism, the freshwater polyp *Hydra vulgaris*, to produce fluorescent and conductive interface embedded into the animal tissues, starting from thiophene-based compounds, demonstrating the feasibility to use these organisms as biofactories of novel biocompatible and conformable bioelectronic interfaces [1-2]. Here we show that the potential of biofiber production is broadly valid in other biological systems, and showed that it can be promoted by several human and murine cell lines and by other invertebrate *in vivo* models (such as the sea anemone *Nematostella vectensis*). The cell type and organism developmental stage influences the fiber shape, amount and optical properties. In order to understand the mechanism underlying the fiber biogenesis, on one side we performed a systematic chemical engineering approach to identify the structure/groups involved in the spontaneous fiber assembling. On the other, we performed several physical and chemical treatments to identify the cell machinery components involved in the biosynthetic process. Finally, by mean of advanced characterization methods and holographic imaging we shed light on the mechanism of biofiber production and the fine structure, paving the way to new bioengineering concepts to fabricate novel living conductive materials.

[1] G. Tommasini, G. Dufil, F. Fardella, X. Strakosas, E. Fergola, T. Abrahamsson, D. Bliman, R. Olsson, M. Berggren, A. Tino, E. Stavrinidou, C. Tortiglione, Seamless integration of bioelectronic interface in an animal model via *in vivo* polymerization of conjugated oligomers, *Bioactive Materials* 10 (2022) 107-116.

[2] M. Moros, F. Di Maria, P. Dardano, G. Tommasini, H. Castillo-Michel, A. Kovtun, M. Zangoli, M. Blasio, L. De Stefano, A. Tino, G. Barbarella, C. Tortiglione, *In Vivo* Bioengineering of Fluorescent Conductive Protein-Dye Microfibers, *iScience* 23(4) (2020) 101022.

9:00 AM SB06.04.04

Selective Hydrogel Membranes For Modular SynBio Processing Units Claire Benstead, Maria Politi, David S. Bergsman and Lilo D. Pozzo; University of Washington, United States

Industrial microbiology has great potential in modernizing chemical manufacturing, particularly in the synthesis of high value products (HVPs) and precursors. To further mitigate issues within manufacturing regarding high energy consumption, environmental pollution, and slow response times to demand fluctuations, we can look to decentralized production and modular processing units. Hydrogels are 3D networks of crosslinked hydrophilic polymers that can retain large amounts of water without dissolution. Their rheological properties, cytocompatibility, and structural capabilities allow them a wide range of applications, including cell encapsulation, drug delivery, and membrane technologies. By encapsulating engineered microbes in hydrogel

membranes, we can create engineered living materials (ELMs) capable of on-demand activation, continuous bioproduction using simple raw materials like glucose, and membrane-based separations of the biomanufactured HVPs. We first investigate the application of poly(ethylene glycol) diacrylate/glycerol (PEGDA-Gly) hydrogels as semi-permeable membranes, including morphological characterization with high-throughput screening of Small Angle X-RAY Scattering (SAXS) and automated permeability testing. We further investigate the performance of these PEGDA-Gly membranes as ELMs by encapsulating betaxanthin-producing *S. cerevisiae* and assessing cell viability and productivity.

9:15 AM *SB06.04.05

Cellular Proliferation Driven Function in Engineered Living Materials Taylor H. Ware; Texas A&M University, United States

Engineered living materials derive functionality from the characteristics of living and non-living components. We will describe two unique functions, growth and cell delivery, driven by the proliferation of embedded microorganisms within covalently crosslinked hydrogels. Living yeast-hydrogel and bacteria-hydrogel composites are capable of undergoing programmed shape change, where volume can increase by >5x. As the cells have higher modulus (~100x) than the gel, cell proliferation results in a macroscopic shape change of the composite. This growth can be used to create stimuli-responsive materials or to manufacture components with >95% biomass. When the proliferating cells reach a boundary of the material, these cells are released to the surrounding environment. We will describe systematic relationships that govern cell release. For example, the elastic modulus of the hydrogel can be used to tune the rate of cell release over a range of four orders of magnitude. The use of these composites to deliver probiotic bacteria in a controlled fashion will be described.

9:45 AM BREAK

10:15 AM SB06.04.06

Polymer-Coated Yeast Cells for Enhanced Biosynthesis of Medicine Rong Yang; Cornell University, United States

Metabolic engineering has made significant progress in producing complex and valuable medicinal products in microorganisms by reconstructing heterologous biosynthetic pathways. Such synthetic pathways often comprise a dozen or more sequential reactions. While the metabolic flux of the reaction intermediates could be optimized for improved productivity and/or efficiency, which holds enormous potential, there have been a limited number of reports on such efforts. That is partially due to a dearth of information on the trans-membrane transport mechanisms of the reaction intermediates. This talk will highlight the recent progress in the development of a new paradigm for the facile optimizing metabolic flux, thereby advancing the biosynthesis of medicines while reducing the optimizing cost. The paradigm is termed MetaLock, which involves creating a conformal ultrathin coating at the single-cell level to achieve perm-selectivity of nutrients and metabolites. We demonstrate that the coating does not inhibit the permeability of nutrients such as sugars and amino acids but creates a diffusion barrier for reaction intermediates to achieve high reaction rates and boost productivity. Through rational material design characterization and computational modeling, we systematically verify the effectiveness of this concept in regulating metabolic fluxes, first in a 6-step reconstructed reaction and then in an 11-step one, respectively. As such, MetaLock is a generalizable strategy that is applicable to improving the productivity of a variety of synthetic pathways. We seek to underscore the importance of understanding detailed microbe-material interactions and to provide an outlook on leveraging MetaLock to accelerate the development of engineered living materials.

10:30 AM SB06.04.07

Generation of Extracellular matrix protein-based Microcapsules by using Droplet-based Microfluidics Sadaf Pashapour^{1,2}, Christine Selhuber-Unkel^{1,3,2}, Joachim Spatz^{1,3,4}, Kerstin Göpfrich^{4,2,5} and Michael Platten^{6,2}; ¹Institute for Molecular Systems Engineering and Advanced Materials, Germany; ²Microfluidic Core Facility, Germany; ³Max Planck School Matter to Life, Germany; ⁴Max Planck Institute for Medical Research, Germany; ⁵Zentrum für molekulare Biologie Heidelberg, Germany; ⁶University Medical Centre Mannheim, Medical Faculty Mannheim, Germany

Interactions of cells with the extracellular matrix (ECM) are involved in many cellular responses *in vivo*, and consequently activate multiple signaling pathways that initiate, drive and regulate nearly all motions of a cell. Therefore, cell-ECM interactions also underscore their central physiological roles, as well as their involvement in a wide variety of infectious diseases. Consequently, engineering 3D ECM niche systems for controlled observation and manipulation of bacteria *in vitro* has become an important strategy, particularly in medical applications. In this research, we have established a novel droplet-based microfluidic approach for the controlled assembly of ECM-based protein microcapsules loaded with *Escherichia coli* (*E.coli*). Towards this end, water-in-oil emulsion droplets consisting of negatively charged block-copolymer surfactants are used as a template for the charge-mediated formation of a laminin- or laminin/collagen-based continuous layer on the inner droplet periphery. A double-inlet microfluidic flow-focusing device is implemented to encapsulate *E. coli*, proteins and divalent ions. The positively charged ions are attracted to the negatively charged block-copolymer surfactant layer at the inner periphery of the droplet wall. This in turn attracts the negatively charged proteins. After incubating the droplets at 37°C for at least 1h, the polymerized protein microcapsules are sequentially released into a physiological environment. Here, the droplets are covered with a layer of the release medium of choice and perfluoro-octanol is added dropwise from above. Perfluoro-octanol acts as a destabilizing surfactant, which allows the fusion of the inside aqueous phase to the outer release medium, placed above the droplets. Incubating this solution for approximately 20min at room temperature releases the established protein microcapsules into the layer of release medium. Collecting the medium layer containing the microcapsules and seeding them on a glass coverslip allows for the analysis of bacterial behavior inside the capsules over longer time periods. We discovered two distinct behaviors of the same bacterial strain, depending on the type of protein used for generating the microcapsules. In the case of laminin-111 based microcapsules, bacteria colonies grow inside the microcapsules and simultaneously expand the microcapsule walls. The microcapsules can only withstand this growth up to a certain point, after that, the capsules break and release a great number of bacteria at once. This system can be taken to hand to e.g., conduct infection studies *in vivo*. By injecting the protein microcapsules at a point of interest, the encapsulated bacteria grow in confinement until the microcapsules burst and hence generate a local source of infection. In contrast to the outburst, *E.coli* incubated inside laminin-111/collagenIV-mixed microcapsules undergo filamentation. Here, the *E.coli* turn into long filamentous bacteria and start shedding small bacteria from the end of the filaments. This behavior is widely distributed in uropathogenic infections. This model can be used to conduct antibiotic studies on filamentous bacteria. These are just two examples to show the purpose of this system. With our new method it is possible to generate different kind of protein microcapsules and further the content is also not limited. Exchanging the aqueous phase allows a wide variety of proteins, organisms and/or molecules being encapsulated inside water-in-oil droplets. Using microfluidics also allows us to tune the size of the microcapsules, which further increases the applicability of this system.

10:45 AM SB06.04.08

Active biointegrated living electronics for multi-dimensional inflammation management Jiuyun Shi and Bozhi Tian; The University of Chicago, United States

Life-like and seamless interfaces between electronic devices and biological tissues stand to revolutionize disease diagnosis and treatment. However, biological and biomechanical disparities between synthetic materials and living tissues present challenges at bioelectrical signal transduction interfaces. Here, we introduce the active biointegrated living electronics (ABLE) platform, encompassing capabilities across the biogenic, biomechanical, and

bioelectrical dimensions simultaneously. The living biointerface, comprising a bioelectronics layout and a *Staphylococcus epidermidis*-laden hydrogel composite, enables multi-modal signal transduction at the microbial-mammalian nexus. The extracellular components of the living hydrogels, prepared through thermal release of naturally occurring amylose polymer chains, are viscoelastic, capable of sustaining the bacteria with high viability, and facilitate freeze-storage of the ABLE device. Through electrophysiological recordings, and wireless probing of skin electrical impedance, body temperature, and humidity, ABLE monitors microbial-driven intervention in psoriasis (an intricate autoimmune skin disease) through the innate microbial activities. Comprehensive mechanistic studies show that *Staphylococcus epidermidis* from the living bioelectronics impedes activation of initiating dendritic cells and subsequent inflammatory phases of psoriasis pathogenesis. The ABLE platform offers a multifunctional and life-like biointerface solution for addressing intricate biomedical challenges, including autoimmune diseases and rehabilitation needs.

11:00 AM *SB06.04.09

3D Templating Biohybrids for Highly Efficient Growth of Decarbonizing Biocements Shu Yang; University of Pennsylvania, United States

Concrete is the second most consumed material in the world for the construction of various infrastructures. It also contributes 7-8% of total global carbon emissions due to the production of cement. Microbially induced carbonate precipitation (MICP) of calcium carbonate (CaCO₃), the main ingredient of concrete or biocement, catalyzed by urease offers a carbon neutral or carbon negative route to create environmentally friendly and CO₂ capturing biocement. To enhance the efficiency of biological processes in MICP, while reducing material cost and operational cost, and increasing carbon capturing for biocement production, we exploit the use of 3D printed minimal surfaces coated with biocompatible gels as templates to immobilize *non-pathogenic* ureolytic bacteria genus *S. pasteurii*. We show that the amount of CaCO₃ crystals deposited on the 3D templates are an order of magnitude more than those deposited on an agar gel in a petri dish.

11:30 AM SB06.04.10

Biological nanofibres from electroactive microorganisms towards e-Biologics Jean V. Manca¹, Koen Wouters¹, Robin Bonne^{1,2}, Roland Valcke¹ and Bart Cleuren¹; ¹University of Hasselt, Belgium; ²Aarhus University, Denmark

In nature, biological ‘nanofibers/nanowires’ in electroactive microorganisms such as *Geobacter sulfurreducens*, *Shewanella oneidensis* and the more recently discovered *Cable Bacteria* demonstrate remarkable electrical transport properties. These electroactive bacteria are receiving growing attention from diverse research fields, motivated by a fundamental interest in the underlying long-range transport mechanisms and in the potential future role in emerging domains such as bio-electronics, biodegradable electronics, and electronic biological materials (e-biologics). In the long-term these materials could open novel avenues for the growing problem of electronic waste in the upcoming era of ubiquitous electronics (cfr. the *Internet of Things*). Moreover, the emergence of biological electronic materials could play a role next to synthetic organic electronic materials in the diverse “*More than Moore*” technology platforms for future electronic applications, where new materials and heterogeneous integration technologies are indispensable for future breakthroughs and towards next generation sustainable electronics. The fundamental study of the electro-optical properties of biological nanofibers from *Cable Bacteria* and other electroactive microorganisms, and their behaviour in bio-hybrid electronic devices can therefore be situated in this broader technological context.

Cable Bacteria are filamentous microorganisms consisting of more than 10⁴ cells, forming unbranched filaments of up to several centimeters long, characterized by a distinct morphology with parallel ridges along the length of the filament. They have developed a unique energy metabolism which requires charge transport over centimeter distances. Electrical measurements at X-LAB on ‘dry’ cable bacteria filaments out of their wet natural aquatic habitat provided the first direct evidence of intrinsic electrical conductivity through the use of electrical probe measurements, with nanofiber conductivity values over 10 S/cm and an exceptionally long electron transport distance in the order of 1 cm. While nanometer-scale electron transport is known to occur in prokaryotes, chloroplasts and mitochondria, and micrometer-scale electrical currents are measured in the nanowire appendages of bacteria and archaea, the centimeter-scale electron transport by cable bacteria extends the known length scale of biological transport by several orders of magnitude.

To disclose the underlying electrical transport mechanisms occurring in *Cable Bacteria* several techniques are being introduced. Impedance spectroscopy provides an equivalent electrical circuit model, which indicate that dry *Cable Bacteria* filaments function as resistive biological wires. Recently, proof-of-principle biohybrid demonstrators have been prepared to investigate the electrical signal transmission possibilities in a broad frequency range. Temperature-dependent electrical characterization reveals that the conductivity can be described with an Arrhenius-type relation over a broad temperature range (-195°C to +50°C) indicative for hopping transport. Furthermore, when cable bacterium filaments are utilized as the channel in a field effect transistor, they show a type transport with electron mobility values of ~0.1 cm²/Vs at room temperature and display a similar Arrhenius temperature dependence as the earlier mentioned conductivity.

Overall, the obtained results so far demonstrate that the intrinsic electrical properties of the conductive fibres in *Cable Bacteria* are comparable to synthetic organic semiconductor materials, and so they offer promising perspectives for both fundamental studies of biological long-range electron transport as well as alternative organic electronic materials for the emerging field of bioelectronics, biohybrid electronics and for visionary technologies such as biodegradable electronics and other “*More than Moore*” technology platforms.

11:45 AM SB06.04.11

Spatially resolved charge transfer kinetics at the quantum dot-microbe interface using fluorescence lifetime imaging microscopy Mokshin Suri, Farshid Salimi Jazi, Jack C. Crowley, Younghan Park, Bing Fu, Peng Chen, Warren R. Zipfel, Buz Barstow and Tobias Hanrath; Cornell University, United States

Microbe-semiconductor biohybrids formed by integrating complex microbial enzymatic machinery with programmable optoelectronic properties of semiconducting quantum dots (QDs) have introduced compelling prospects for future photosynthetic solar-to-chemical transformations. Bringing these prospects to fruition requires a firm foundational understanding of charge transfer mechanisms at the nano- bio interface. One challenge is that the transfer of photoexcited carriers from a QD to drive redox reactions in a proximate microbe involves a complex interplay of photochemical and physicochemical sub-processes, and the governing thermodynamic and kinetic factors are just beginning to emerge. The inherent heterogeneities of both the microbe and QD ensemble presents additional challenges challenge to establishing robust mechanistic understanding and to ultimately translate basic insights to design principles for advanced biohybrids. In this study, we leveraged advanced spectroscopic imaging tools (fluorescence lifetime imaging microscopy, FLIM) to interrogate charge transfer kinetics at the interface of a CdSe quantum dot (QD) film and *Shewanella oneidensis* microbes with sub-cellular spatial resolution. We focused on electron transport under fumarate-rich conditions and observed that both the intensity and lifetime of the QD’s photoluminescence decrease at on-cell and inter-cell positions relative to the off-cell background. These trends provide a map of electron transfer rates (in the range of 10⁸ to 10⁹ s⁻¹) from QDs to the *S. oneidensis* cells for terminal reduction of fumarate. Our analysis of spatially resolved charge transfer rates reveals the role of cooperative effects in small groups of microbes, i.e., working together, small communities *S. oneidensis* exhibit faster charge transfer than isolated microbes. We attribute the cooperative effects to nanowire extrusions from *S. oneidensis* that facilitate charge uptake. Light driven electron transfer rates define the photo-chemical efficiency limits of photosynthetic semiconductor biohybrids, and this study provides important progress towards characterizing these electron transfer rates with enhanced spatial resolution.

SESSION SB06.05: Living Materials II
Session Chairs: Angela Tino and Claudia Tortiglione
Wednesday Afternoon, April 24, 2024
Room 427, Level 4, Summit

1:45 PM *SB06.05.01

Growth and Distribution of Microalgae in Photosynthetic Living Hydrogels Marie-Eve Aubin-Tam; Delft University of Technology, Netherlands

Engineered living materials are functional materials that encapsulate living components within a polymer matrix. Understanding the physical, chemical and biological factors affecting the spatial organization and growth of cellular populations within the matrix is key to predicting and improving the materials' functionality and responsive potential. We study the motility, growth, spatial distribution, and photosynthetic activity of eukaryotic microalga *Chlamydomonas reinhardtii* in a hydrogel matrix. 3D printing is used to control the shape of the biohybrid hydrogel material as a whole, while light exposure and access to carbon source controls the growth and location of the cells within the material. I will present a strategy to control cell growth for higher productivity of photosynthetic living materials that resembles the established adaptations found in multicellular plant leaves.

2:15 PM SB06.05.02

Green Algae-Based Microrobots for the Active *In Vivo* Delivery Zhengxing Li; University of California, San Diego, United States

Green algae-based microrobots display diverse advantageous features concerning consistent self-propulsion and their functionalization capabilities. The long-lasting swimming behavior of natural microalgae offers excellent motion behavior, which provides remarkable potential as the carrier for gastrointestinal (GI) tract delivery. When orally administered in vivo into mice, our green algae-based microrobots substantially improved GI distribution of the payload compared with traditional magnesium-based micromotors, which are limited by short propulsion lifetimes. Such appealing motion behavior and extended lifetime of green algae-based microrobots allow precise GI localization and enhanced cargo deliveries in GI tissue for practical biomedical applications. Taking one specific example, green algae-based microrobots can be equipped with macrophage membrane-coated nanoparticles to efficiently capture pro-inflammatory cytokines 'on-the-fly'. The dynamic green algae-based microrobots outperform static counterparts by enhancing cytokine removal through continuous movement, better distribution, and extended retention in the colon to ease inflammatory bowel disease free from side effects. The advantages are not restricted to GI applications, as green algae-based microrobots also excel upon treating the mouse model of acute pseudomonas aeruginosa pneumonia, where the algae microrobots effectively reduce bacterial burden and substantially lessen animal mortality, with negligible toxicity. Overall, these findings highlight the attractive functions of green algae-based microrobots for the active in vivo delivery.

2:30 PM BREAK

3:30 PM *SB06.05.04

Photosynthetic Bacteria-based Biohybrid Materials for Energy and Sensing Matteo Grattieri^{1,2}, Jefferson Franco¹, Pierluigi Lasala¹, Dario Lacalamita¹, Paolo Stufano², Rossella Labarile², Danilo Vona¹, M. Lucia Curri^{1,2}, Elisabetta Fanizza^{1,2}, Massimo Trotta² and Gianluca Maria Farinola¹; ¹Università degli Studi di Bari Aldo Moro, Italy; ²Consiglio Nazionale delle Ricerche, Italy

Photosynthetic bacteria can utilize sunlight, the most abundant energy resource on Earth, to sustain their metabolism by means of the photosynthetic process. Scientists and engineers have mimicked this fascinating process developing artificial systems that allow converting sunlight into electrical and/or chemical energy.¹ In recent years, the possibility to couple abundant and sustainable photosynthetic biological catalysts with electrodes has called particular interest to harvest solar energy without the need of platinum group metals or other critical raw materials.^{2,3} However, bacterial cells did not evolve to exchange electrons with an external electron acceptor/donor, making the transfer of photoinduced electron to (and from) an electrode the most critical challenge to be overcome.⁴

The talk will focus on the approaches that we are currently investigating to tailor the bacteria/electrode interface, specifically by (i) developing polydopamine-purple bacteria-based redox-adhesive matrices;⁵ (ii) modifying the cellular membrane of photosynthetic bacteria with inorganic nanoparticles; and (iii) developing bio-based electrode materials using polyhydroxybutyrate for enhanced bacteria colonization. Application of the biohybrid materials obtained with these approaches for the development of sustainable biosensors and the production of energy carriers will be discussed, together with the challenges and outlook of this fascinating technology.

References

1. B. Zhang and L. Sun, Chem. Soc. Rev. 2019, 48, 2216.
2. N. Kornienko, J.Z. Zhang, K.K. Sakimoto, P. Yang, E. Reisner, Nat. Nanotechnol. 2018, 13, 890-899.
3. M. Grattieri, K. Beaver, E.M. Gaffney, F. Dong, S.D. Minteer, Chem. Comm. 2020, 56, 8553-8568.
4. L. D. M. Torquato, M. Grattieri, Curr. Opin. Electrochem. 2022, 34, 101018.
5. G. Buscemi, D. Vona, P. Stufano, R. Labarile, P. Cosma, A. Agostiano, M. Trotta, G.M. Farinola, M. Grattieri, ACS Appl. Mater. Interfaces 2022, 14, 26631-26641.

Acknowledgments

Matteo Grattieri would like to acknowledge the funding from Fondazione CON IL SUD, Grant "*Brains to South 2018*", Project No. 2018-PDR-00914.

4:00 PM SB06.05.05

An n-Type Conjugated Oligoelectrolyte Mimics Transmembrane Electron Transport Proteins for Enhanced Microbial Electrosynthesis Glenn Quek¹, Guillermo C. Bazan¹, Ricardo J. Vázquez², Samantha R. Mccuskey¹ and Fernando L. Garcia¹; ¹National University of Singapore, Singapore; ²Indiana University Bloomington, United States

Interfacing bacteria as biocatalysts with an electrode provides the basis for emerging bioelectrochemical systems that enable sustainable energy interconversion between electrical and chemical energy. Electron transfer rates at the abiotic-biotic interface are, however, often limited by poor electrical contacts and the intrinsically insulating cell membranes. Herein, we report the first example of an n-type redox-active conjugated oligoelectrolyte, namely COE-NDI, which spontaneously intercalates into cell membranes and mimics the function of endogenous transmembrane electron transport proteins. The incorporation of COE-NDI into *Shewanella oneidensis* MR-1 cells amplifies current uptake from the electrode by 4-fold, resulting in the enhanced bio-

electroreduction of fumarate to succinate. Moreover, **COE-NDI** can serve as a “protein prosthetic” to rescue current uptake in non-electrogenic knockout mutants.

4:15 PM SB06.05.06

Bacteriophage-based self-propelled catalytic biohybrid nanomotor Xi Ding, Marina Achterman and Elaine D. Haber; University of California, Riverside, United States

Self-propelled biohybrid materials have potential applications in fields from drug delivery to environmental remediation. Microorganisms, such as bacteriophage, provide unparalleled targeting and assembly. Their structure and surface, including exact shape and site-specific functional groups, are genetically encoded and known with atomic scale precision. Synthetic inorganic nanoparticles facilitate superdiffusive motion. Their interactions with chemical fuels or physical fields convert energy into locomotion. Of specific interest, here, are viruses with asymmetric capsid proteins, like the M13 bacteriophage, that can serve as programmable low-symmetry templates for autonomous biohybrid materials. The M13 is a high aspect ratio, 880 nm long and 6.5 nm diameter filamentous virus. It contains approximately 2700 copies of p8 major coat protein along its length and 5 copies of p3 minor coat protein at the proximal end of the filament. Each of these proteins can be modified to promote motor form and function. In this work, the asymmetric structure and functionality of the M13 bacteriophage capsid was used to create nanoswimmers. A cysteine-rich peptide fusion was inserted into the minor coat protein (p3) at the virus tip and Pt nanoparticles were attached via metal-thiol bonding. The viral-based Janus particles were fluorescently tagged and exposed to low concentrations of H₂O₂ to fuel self-propulsion. Using confocal fluorescence microscopy, nanomotor trajectory and motion were evaluated.

4:30 PM *SB06.05.07

In situ control of cells and multicellular structures by two-photon lithography Christine Selhuber-Unkel; Heidelberg University, Germany

In vivo, the tissue environment often provides strong confinement to cells and multicellular assemblies, particularly in cancer. Therefore it is highly important to mimic such confined environments, in order to investigate the impact of confinement on cellular systems. Here, we employed two-photon lithography, which allows to print directly into and next to multicellular assemblies. For example, we printed dome-shaped confinements with micrometer-sized openings to confine cancer spheroids in order to investigate the migration behavior of the cancer cells and also to study the effects of confinement on the spheroid. We have shown that confinement of the spheroids leads to a decreased cell migration speed and affects actin alignment and dynamics. Furthermore, in situ two-photon lithography provides a novel way of analyzing the behavior of specific regions of multicellular structures, by enabling the separation of multicellular structures from a spheroid. This is possible, as the laser used for printing can reach into the almost transparent multicellular structure and the used material is biocompatible. Hence, two-photon lithography is suitable for controlling the growth, migration and morphological cues of live cells, which is highly relevant to study the impact of the physical microenvironment on biosystems.

SESSION SB06.06: Plants—Environment
Session Chairs: Pengju Li and Eleni Stavrinidou
Thursday Morning, April 25, 2024
Room 427, Level 4, Summit

8:45 AM SB06.06.02

The Multifunctional Use of an Aqueous Battery for a High-Capacity Jellyfish Robot Xu Liu, Shuo Jin, Yiqi Shao, Autumn Pratt, Duhan Zhang, Jacqueline Lo, Yong Joo, Lynden Archer and Robert Shepherd; Cornell University, United States

The batteries that power Untethered Underwater Vehicles (UUVs) serve a single purpose—to provide energy to electronics and motors; the more energy required, the bigger the robot must be to accommodate space for more batteries. This size dependency is further exacerbated by the high gravimetric density of batteries, requiring bigger hulls to displace water the equivalent weight of the batteries. With the increased size, comes increased moments of inertia, reducing maneuverability. By choosing batteries that are primarily liquid (i.e. Redox Flow Batteries, RFBs), the increased weight can be distributed for improved capacity with reduced inertial moment; and, when also being used as hydraulic fluid, reduce the overall weight of the AUV. In this paper, we formed an RFB into the shape of a jellyfish, using two redox chemistries and architectures: (i) a secondary ZnBr₂ battery with high power density, and (ii) a hybrid primary/secondary ZnI₂ battery with high capacity. Our choice of a Jellyfish shape demonstrates a low inertial moment architecture, a hemisphere, facilitated by the easy shaping of fluid batteries. In our robot, the RFB electrolyte also provides hydraulic force transmission to control the shape of the jellyfish's bell, causing it to sink or swim. Finally, our choice of catholyte to fill the bell allows us to quickly recharge the battery by emptying the fluid and replacing it with pre-charged electrolyte (analogous to a gas station).

9:00 AM SB06.06.03

Communication with Plants Using Wearable Electrophysiology Sensors Yifei Luo¹, Yi Jing Wong^{1,2}, Wenlong Li¹, Xian Jun Loh¹ and Xiaodong Chen²; ¹Agency for Science, Technology and Research, Singapore; ²Nanyang Technological University, Singapore

Different parts and organs of a plant communicate using various forms of signals to optimize resource allocation and coordinate systemic responses to environmental stimuli for survival and growth. Investigating these communication processes is important to understanding plants' perception of environments and well-being as well as engineering approaches to improve plant health or induce desired behaviors. We aim to achieve this through electrophysiology, the study of electrical signals in plants, due to the simplicity of sensor design and rich biological insights buried in the signals. In this talk, I will share my work on developing plant-interfacing materials for high-fidelity signal acquisition from plants having complex surface topography (e.g., hairy, rough, superhydrophobic), as well as achieving long-term stability during plant growth. The conformal adhesive attachment of the devices on plants makes them resistant to motion artifacts, and the noninvasive wearable form factor promises the potential for real-world deployment in farms and gardens.

I will discuss possible applications of this technology in plant health monitoring, environment optimization, crop breeding, and robotic control, by giving examples. Electrophysiology sensors, together with other modes of plant wearable sensors, will play a role in the sustainable development of human society.

9:15 AM *SB06.06.04

Engineering Nanotechnology for Precision Sensing and Targeted Delivery in Living Plants Tedrick Thomas Salim Lew; National University of Singapore, Singapore

Plant engineering plays a pivotal role in enhancing the productivity and resilience of future agricultural practices. Nevertheless, current efforts in plant engineering are hampered by the lack of universal and efficient techniques that can be applied across various plant species. In this talk, I will present the development of nanoparticle-mediated biomolecule delivery and analytical tools which can be interfaced with living plants of different species to enable diverse plant biotechnology and agricultural applications. First, I will describe the engineering of nanomaterials as optical nanosensors to monitor plant defense signaling pathways elicited by environmental stresses. By embedding nanosensors within plant tissues, the plant internal state can be accessed with portable electronics in a non-destructive and species-independent manner – a combination of features currently unattainable with existing analytical approaches. The optical sensing strategy is versatile and can be expanded for selective detection of abiotic and biotic stressors. Additionally, I will also present recent efforts in our group developing functionalized nanomaterials for targeted delivery to specific plant organs. These advances highlight the potential of nanomaterial-enabled platforms to engineer high-yielding and climate-resilient agriculture for our food security.

9:45 AM BREAK

10:15 AM SB06.06.05

Real-Time Monitoring of Iron Uptake and Transport in Plants with Optical Nanosensor Thinh D. Khong¹, Javier Jingheng Tan^{2,1}, Raju Cheerlavantha¹, Benedetto Marelli^{3,1}, Urano Daisuke^{2,1} and Michael Strano^{3,1}; ¹Singapore-MIT Alliance for Research and Technology, Singapore; ²Temasek Life Sciences Laboratory, Singapore; ³Massachusetts Institute of Technology, United States

Iron deficiency is a major global health concern, and dietary iron from plant consumption is a primary source for most people worldwide. However, the iron content in plants is heavily affected by various environmental and agronomic factors, including climate change such as rising temperature, water scarcity, and elevated atmospheric CO₂ level. Therefore, it is a pressing need to develop effective strategies to combat iron deficiency and ensure food security for the global population. Conventional analytical techniques to investigate the efficacy of foliar iron fertilization are not optimally suited to observe the nuances of foliar absorption, translocation, and iron speciation. This lack of information hampers the optimization of fertilization strategies and the development of more effective nutrient formulations.

In this work, we introduce a highly sensitive fluorescence iron nanosensor for elucidating the biochemistry of iron in plants, thereby enabling the formulation of precise fertilization strategies. This nanosensor can be easily incorporated into living plant species to monitor real-time iron uptake via both foliar and soil-based fertilizations. Our sensor, fabricated by conjugating a synthetic conjugated polymer onto single-walled carbon nanotubes, is designed to exhibit a unique orthogonal optical response that enables differentiation between Fe(II) and Fe(III).

Using hydroponically grown lettuce as a model for iron foliar application study, our sensor provides the means to monitor iron uptake, metabolism, and transport with high spatial and temporal resolution in the leaf tissues in real time. Our findings demonstrate that the plant's mechanistic responses to the source of iron species depend on the chelation state rather than the oxidation state. Under conditions of iron deficiency or simulated abiotic stress, such as drought or salt stress, the diffusion and transport rate of iron species are also affected. We also observe a shared mechanistic response to chelated iron species across various plant species, hinting at the existence of conserved foliar iron homeostatic mechanisms.

With its ability to offer detailed insights into the dynamics of iron uptake and transport in real-time, we believe this sensor technology has the potential to revolutionize the study of iron uptake and distribution in plants. This advancement can lead to improved plant growth and yield through the development of more precise and efficient micronutrient management strategies.

10:30 AM SB06.06.06

Microfluidic Microbial Fuel Cell Based Biosensors for Copper Ion and Formaldehyde in Water Monitoring Hao Ren; ShanghaiTech University, China

In this abstract, we present microfluidic microbial fuel cell (MFC) biosensors, which are based on biohybrid materials of microorganisms living on electrodes, for monitoring toxic chemical in water. We have built microfluidic MFCs with anode and cathode chambers of 100 μ L. Start-up process of the microfluidic MFC biosensors takes 3-5 days and we utilize the MFCs for copper ion and formaldehyde in water monitoring. It is found that for copper ion in water monitoring characterization, a linear relationship between the output current and the copper ion concentration is observed, while the MFC biosensor can recover after the initial current drop caused by the copper ion in water. However, when the MFC biosensor is exposed to formaldehyde in water, a sigmoid relationship is observed and the MFC biosensor cannot recover after formaldehyde causes the current to drop. The experimental results may further the development of microfluidic MFCs for toxic chemical in water monitoring.

Water pollution is a global health threat affecting 2 billion people, causing significant health issues. Traditional non-real-time methods such as atomic spectrometry are time-consuming and expensive. Therefore, many studies have been performed to monitor toxic substances in water with MFCs due to their real-time measurement and low cost. However, the state-of-the-art MFC biosensors are non-reusable and take at least 3 minutes. Therefore, a real-time MFC biosensor for toxic chemical in water monitoring is needed.

The microfluidic MEMS MFC biosensor is composed of anode, cathode and proton exchange membrane (PEM) with a chamber volume of 100 μ L. The anode/cathode are 100nm-thick Pt thin films deposited by magnetic sputtering. The start-up process of the MFC biosensor takes approximately 3-5 days and the polarization curve confirms its normal operation. Firstly, we measure the response of the MFC biosensors to copper ion in water. The MFC biosensors are exposed to 0.2-1.6mg/L copper ion respectively. The current is first inhibited and then recovers, demonstrating the reusability of the MFC biosensor for copper ion in water monitoring. The biosensor linearity characterization demonstrates a strong linear correlation between the current inhibition percentage and copper ion concentration with an R^2 of 0.997. The accuracy of the biosensor is calculated as 3.54% by testing a concentration of 1.3 mg/L, which is the EPA standard for the maximum allowable copper ion concentration in water. The average measurement time for the MFC biosensor is only 48 seconds. Afterwards, we measure the response the MFC biosensor to formaldehyde. When the MFC biosensor is exposed to a large formaldehyde concentration range from a low concentration of 1×10^{-3} mg/L to a high concentration of 3 mg/L in water, a sigmoid dose-response relationship of normalized current inhibition percentage versus formaldehyde concentration in water is observed, in agreement with traditional toxicology dose-response curve obtained by other measurement techniques. In addition, the current cannot recover after the inhibition due to the toxicity of the formaldehyde. We believe the different response of the MFC biosensors to copper ion and formaldehyde in water can help to improve the specificity of the MFC biosensors for toxic chemical in water monitoring.

10:45 AM *SB06.07.01

EcoRobotics: bioinspired and biohybrid soft robots for environmental monitoring and preservation [Barbara Mazzolai](#), Fabian Meder and Emanuela Del Dottore; Istituto Italiano di Tecnologia, Italy

Meeting the global challenges of climate change represents one of the most important frontiers for science and sustainable technologies. With this ambition, our research activity envisions environmentally responsible, bioinspired systems that can grow, adapt, and are built with recyclable, or biodegradable, or biohybrid materials. We refer to them as 'ecorobots'. These ecorobots are designed to imitate the adaptability of living organisms, allowing them to navigate and function effectively in complex and unpredictable environments. They are also designed to seamlessly integrate into natural ecosystems.

We primarily draw inspiration from soft invertebrates, such as cephalopods and earthworms, as well as plants, as they exhibit remarkable adaptive capabilities with smart, effective, and efficient strategies. Specifically, when studying plants, we can develop innovative ecorobots featuring structural-functional materials, distributed sensing and intelligence systems, and biohybrid energy-harvesting mechanisms. Much like their natural counterparts, these machines are envisioned to possess the ability to biodegrade at the end of their lifecycle, promoting sustainability.

In this presentation, I will outline our approach to designing and developing ecorobots inspired by the characteristics of plants. Our primary objectives are twofold: first, to identify and extract the fundamental principles that underlie the biological functions of plants and translate them into technological solutions; and second, to advance our scientific understanding of the biological systems we draw inspiration from.

Our examples will include the following ecorobots: the Plantoid robot, the pioneering plant-root-inspired robot, equipped with artificial growing roots, distributed sensors, actuation mechanisms, and intelligence systems, designed for soil exploration and monitoring; the GrowBots, machines inspired by climbing plants that move by growing, tailored for various exploration tasks; the I-Seed robots, soft, biodegradable miniaturized robots inspired by the morphology and dispersion abilities of plant seeds, serving purposes in environmental monitoring, plant monitoring and drug delivery systems featuring natural plant hooks; biohybrid energy harvesting systems; as well as solutions inspired by plant communication and emerging collective behaviors, paving the way for a new paradigm of robot networks and embodied AI.

Our ecorobots have been designed for a wide range of applications, including exploration and monitoring of natural environments and infrastructures, archaeological research, space missions, and search-and-rescue operations. Beyond introducing innovative technologies, we also aspire to engage in "reverse biology" by using bioinspired robots as experimental tools for investigating biological behaviors.

11:15 AM SB06.07.02

Time-controlled nanoscale delivery system [Jihyeon Park](#), Seoyeah Oh and Jiwon Kim; Yonsei University, Korea (the Republic of)

Molecular communication (MC), a bio-inspired technology, is emerging as an alternative way of communication by overcoming the limitations of conventional electromagnetic waves. As the demand for practical implementation of MC grows, physical components of MC (*e.g.*, transmitter and receiver) have been fabricated through the integration of nano-/micro-technology. However, challenges such as slow speed of information molecule (IM) transmission, dispersion of IMs into the surrounding medium, and interference between sequentially transmitted IMs persist in employing the transmitters. Furthermore, sequential delivery of multiple IMs with an adjustment of their time intervals to enhance the communication efficiency remains as a significant challenge. Herein, we report a time-controlled delivery system that utilizes nanomotors as transmitters achieving precise multi-cargo delivery with desired time intervals. Nanomotors consisted of multi-metal nanorod (*i.e.*, nickel head, gold bridge, silver flexible filament, and gold tail) are encapsulated with poly (N-isopropylacrylamide) (pNIPAm) based hydrogel, and nanomotors with various dimensions transport multi-cargo as IMs (*e.g.*, Indigo carmine and Carminic acid) at different speeds under the same magnetic field. Consequently, nanomotors release IMs on-demand at desired locations upon near-infrared (NIR) irradiation, leading to IM delivery with high spatiotemporal density. Continuous linear sweep voltammetry (LSV) confirmed the sequential delivery of multiple IMs with time intervals of several minutes, indicating that nanomotors can transport IMs at higher transmission rate compared to diffusion-based methods. Furthermore, IM delivery using nanomotors exhibited higher signal intensity and reduced intersymbol interference (ISI), which enables a continuous signal transmission with a lower error rate in communication. We believe our time-controlled multi-cargo delivery via nanomotors can serve as transmitters paving a way to realize practical MC systems, such as disease detection and monitoring. This will allow us to understand communications in biological/biomimetic systems or unexplored environments.

11:30 AM SB06.07.03

Computational Design of Solid-Binding Peptides for the Biohybrid Diagnostic Electronic Nose [Oliver Nakano-Baker](#), Richard V. Lee, Shalabh Shukla and John D. MacKenzie; University of Washington, United States

Trained dogs can detect COVID-19 or cancer from the odor of exhaled breath. Could your phone do the same? Diseases create a distinct shift in the volatile compounds (VOCs) in human breath - a compact breathalyzer capable of detecting this "VOC fingerprint" of disease could provide rapid diagnoses for a wide range of conditions. We recently demonstrated a biohybrid sensor platform for targeted gas detection, combining carbon nanotube transistors with surface-binding peptide molecules derived from olfactory proteins. Here, we present a pipeline strategy for combining multiple biomimetic sensors into engineered multiplexes, eNoses capable of performing diagnostic tasks. Molecular machine learning and dynamics are used to predict and optimize the binding affinity of peptides to targeted disease-relevant VOCs. Then, computer simulations are used to evolve sets of peptides, bootstrapping the multiplex design towards peptide makeup that can classify VOC fingerprints efficiently. Finally, rapid experimentation with simulated breath validates and feeds back binding profiles to the computational pipeline, improving the toolset. The peptide-sensitized multiplex sensors created by this process could be the key to unlocking mobile breathomics - phone-sized breathalyzers capable of detecting viral and bacterial infections, blood glucose levels, early-stage cancers, and more from the chemical signatures in exhaled breath.

11:45 AM SB06.07.04

PEDOT:PSS Fiber-Based Highly Sensitive Strain Gauge Force Sensor for Biohybrid Robots [Xinran Xie](#), Abhijith Surendran, Ruiheng Wu and Jonathan Rivnay; Northwestern University, United States

Integrating biological components of contractile living muscle tissues with careful microstructure design, biohybrid robots have realized various biomimetic behaviors and functions such as swimming, walking, and object manipulation. However, the inherent vulnerability to the stimulation and increased dexterity of biohybrid robots require perception of their function and surroundings for tissue protection and accurate control. Currently, most biohybrid robots are stimulated to output large forces without considering their health status, causing short lifetime and decreased performance. Therefore, biohybrid robots need to be equipped with sensors that can monitor muscle force and length similar to the Golgi tendon and muscle spindle in humans. The feedback signals would help with tuning stimulation parameters to better protect tissues from damage while generating stable and controllable force. This can be realized by incorporating a strain gauge force sensor within the muscle tissue to provide real-time strain and force information.

Poly(3,4-ethylenedioxythiophene):poly(styrene sulfonate) (PEDOT:PSS) is one of the most widely utilized conducting polymers with diverse applications

in bioelectronics, owing to its favorable electrical and mechanical properties, biocompatibility, stability, and commercial availability. By wet spinning of PEDOT:PSS into sulfuric acid bath, we successfully made fibers with diameters ranging 50-100 μm . These fibers remain elastic within 0-0.5% strain range, which is suitable for in vitro muscle strain monitoring. These fibers work like a resistive strain gauge and achieve a gauge factor of ~ 150 in the elastic range. The high gauge factor indicates a highly sensitive strain gauge from a single PEDOT:PSS fiber. We are able to incorporate the fiber-based strain gauge into a standard two-pillar muscle culture polydimethylsiloxane (PDMS) platform and calibrate it with a force transducer to generate the strain-force relationship. The PDMS platform can then be used to culture skeletal muscle tissues and measure the muscle strain and force production in real-time. This research sheds light on the perception and control of biohybrid robots.

SESSION SB06.08: Cells—Organoids Interface
Session Chairs: Maria Rosa Antognazza and Claudia Tortiglione
Thursday Afternoon, April 25, 2024
Room 427, Level 4, Summit

1:30 PM *SB06.08.01

Hybrid bioelectronic tissues: interfaces for monitoring and modulating function [Brian Timko](#); Tufts University, United States

Hybrid bioelectronic systems offer a unique route toward two-way electronic communication with living cells and tissues. Recent advances in bioelectronics and bioactive materials have enabled multiplexed, stable and seamless interfaces with surrounding cells and tissues, representing a distinct advantage over conventional systems such as patch clamp and optical dyes.

We recently developed a multi-electrode array (MEA) platform that could integrate with cardiac monolayers at up to 32 spatially-distinct locations in vitro. In the first part of this talk we will discuss our recent heart-on-a-chip platform which integrated both extra- and intracellular recording elements for monitoring cardiac electrophysiology during episodes of acute hypoxia. This system allowed us to monitor not only cell-cell communication (e.g., wavefront propagation) but also action potentials (APs) at several spatially-distinct regions simultaneously. Our platform provided a unique route toward understanding the role of hypoxia on ion channel dynamics. For example, we found that APs narrowed during hypoxia, consistent with proposed mechanisms by which oxygen deficits activate ATP-dependent K^+ channels that promote membrane repolarization.

In the second part of this talk we discuss an integrated optogenetic and bioelectronic platform for stable and long-term modulation and monitoring of cardiomyocyte function. Optogenetic inputs were achieved through expression of a photoactivatable adenylyl cyclase (bPAC), that when exposed to blue light caused a dose-dependent and time-limited increase in intracellular cyclic AMP concentration and, subsequently, autonomous cardiomyocyte beat rate. Bioelectronic outputs from the MEA provided real-time readouts of cardiomyocyte behavior in response to optical modulation. Irradiation at $24 \mu\text{W}/\text{mm}^2$ resulted in a ca. 17% increase in beat rate within 20-25 minutes of irradiation. Multiplexed readouts revealed that wavefront propagation rates throughout the monolayer remained constant between “on” and “off” states, demonstrating that optical modulation did not affect intercellular coupling. In addition, bPAC activation could be cycled through repeated “on” and “off” states via time-limited illumination or in a gradient fashion with $0.03\text{-}24 \mu\text{W}/\text{mm}^2$ illumination. Cardiomyocytes could be modulated reproducibly over at least four days, demonstrating that bPAC expression as well as the bioelectronic interface were stable throughout that period.

Taken together, our studies demonstrate the feasibility of bioelectronic and optical techniques for monitoring and modulating cardiac function. We will discuss recent efforts in our lab toward 3D bioelectronics-embedded tissues and closed-loop feedback systems. We will also discuss potential clinical applications for cardiac regulation including arrhythmia diagnosis and intervention.

2:00 PM SB06.08.02

Exploring 3D printed GelMA/hydroxyapatite scaffold from design to biological evaluation for bone tissue engineering Fabiola Hernández Rosas¹, Ana Paola Salgado Álvarez¹, José R. Alanís Gómez¹, Manuel Jaime Rodríguez² and [Ximena Mejía Delgado](#)¹; ¹Universidad Anahuac Querétaro, Mexico; ²Tecnológico de Monterrey, Mexico

Bone repair is a widely explored field in tissue engineering due to its significant impact on the human body's structural integrity. Biomaterials based on calcium phosphate, such as hydroxyapatite (HAp), have shown promise because of their ability to emulate the mineral composition and porous structure of bone. Additionally, the utilization of additive manufacturing has provided opportunities to create cellular scaffolds for bone grafts, allowing us to control properties like porosity, pore size, structural form, and mechanical characteristics. These designs are crafted using Computer-Aided Design (CAD) software. The primary objective of this project is to design, fabricate, characterize, and assess the bioactivity of 3D HAp scaffolds for tissue engineering applications. To achieve this, hydroxyapatite was initially synthesized using the microwave-assisted hydrothermal method. Consequently, HAp nanofibers acquired a hexagonal structure, enhancing their mechanical properties. Subsequently, the HAp nanofibers underwent characterization through X-ray diffraction (XRD) and Scanning Electron Microscopy (SEM) to determine dimensions, morphology, topology, orientation, and crystalline structure. In addition, various 3D bone scaffolds with interconnected pores, facilitating permeability similar to trabecular bone morphology, were designed using Rhinoceros 3D CAD software with the Grasshopper extension. These scaffolds were produced using a 3D bioprinter with methacryloyl (GelMA) and laminin as bioink. Gelatin methacryloyl (GelMA) hybrid hydrogel with hydroxyapatite has shown its ability to promote osteogenesis and enhance osseointegration, as supported by both in vitro and in vivo studies. In this research, 3D Voronoi bioprinted scaffolds with GelMA/HAp were designed and manufactured for in vitro biological evaluation using mesenchymal stem cells. Mesenchymal Stem Cells obtained through primary culture of pig bone marrow were cultured in DMEM medium with 10% inactivated fetal bovine serum at $37^\circ\text{C}/5\% \text{CO}_2$. The study included two groups: one with the GelMA/HAp scaffold and another with a control group containing only GelMA hydrogel without hydroxyapatite. The scaffolds were maintained for 21 days under these conditions. Then, Alizarin red staining was done to reveal the osteogenic differentiation of Mesenchymal Stem Cells. Subsequently, RNA was extracted from the cell suspension, and osteogenesis was evaluated through RT-qPCR with markers BMP-2, OCN, COL1A1, and OPN. The mean cycle threshold (Ct) value for each target gene was normalized against the Ct value of a housekeeping gene to determine relative expression. To calculate the fold change, the DDCT method was applied, comparing mRNA expressions between the treated groups (with GelMA/HAp) and the negative group (cells cultured in complete culture medium only). Based on robust scientific evidence, this biomaterial is expected to demonstrate its bioactive functions without harming the cells, as intended.

2:15 PM SB06.08.03

Incorporation of Gentamicin-Encapsulated Poly (lactic-co-glycolic acid) Nanoparticles into Polyurethane/Poly (ethylene oxide) Nanofiber Scaffolds for Biomedical Applications [Yu Sun](#)¹, Jesse Heacock¹, Yan Li^{1,1,1}, Jianguo Liu^{1,1}, Chuchu Chen² and Kaiyan Qiu²; ¹Colorado State University,

United States; ²Washington State University, United States

The development of novel wound-dressing materials has attracted significant research interests in recent years. With the advancement of nanofabrication, the application of nanoparticles (NPs) in drug delivery systems has become feasible. However, most existing work focuses on incorporation of metal, metal/semi-metal oxide, or organic particles into nanofiber scaffolds. There has been a lack of work on incorporation of drug-encapsulated polymeric particles into nanofiber scaffolds. In this study, gentamicin-encapsulated poly (lactic-co-glycolic acid) (PLGA) NPs were synthesized via a double emulsion solvent evaporation method. Electrospinning was used to incorporate gentamicin-encapsulated PLGA NPs into nanofiber scaffolds. Atomic force microscopy (AFM), dynamic light scattering, scanning electron microscopy (SEM), ultraviolet-visible spectroscopy (UV-vis), and an agar diffusion method were utilized to characterize the morphologies, release profiles, and antibacterial activities of various gentamicin-loaded PLGA NPs incorporated nanofiber scaffolds. The results indicated the PLGA NPs had a spherical morphology with an average diameter of 130nm. Purification of PLGA NPs was essential to eliminate the residual polyvinyl alcohol (PVA) and to prevent particle agglomeration. The purified PLGA NPs were uniformly and individually incorporated into the polyurethane (PU)/ poly ethenyl oxide (PEO) or PEO-only nanofiber scaffolds, but nearly none into the PU-only fiber scaffolds. PEO served as a continuous phase in the PU/PEO mixture, which significantly improved the compatibility of PLGA NPs and PU, resulting in a well-dispersed distribution of PLGA NPs in the monolithic nanofiber scaffolds. Excellent antibacterial properties against *E.coli* were found in both PU/PEO and PEO nanofiber scaffolds. This study of incorporating gentamicin-encapsulated PLGA NPs into fiber scaffolds provides insights for achieving successful incorporation of drugs-encapsulated polymeric NPs into fiber scaffolds. This offers a promising microfabrication technology for delivery of therapeutic molecules with controlled release for biomedical applications.

2:30 PM BREAK

3:00 PM *SB06.08.04

Kirigami electronics for chronic electrophysiological recording of human neural organoids [Bianxiao Cui](#); Stanford University, United States

Neurons transmit information via electrical signals. Recent advancement in neural organoids and assembloid technologies, derived from human stem cells, have offered a promising avenue for modeling aspects of nervous system development. To understand brain development and develop effective disease models, it is crucial to enable long-term, minimally invasive recordings from these three-dimensional systems. Current technologies, such as patch clamp, penetrating microelectrodes, planar electrode arrays, and substrate-attached flexible electrodes, do not, however, allow chronic recording of neural organoids in suspension, which is necessary to preserve their 3D architecture. Inspired by the art of kirigami, we develop flexible electronics that transition from a flat 2D pattern to a 3D basket-like configuration to accommodate the long-term culture of human neural organoids in suspension. This platform, named kirigami electronics (KiriE), integrates with and enables chronic recording of intact cortical organoids for 170 days while preserving their morphology, cytoarchitecture and cell composition. KiriE detects disease-related hyperactive phenotype. Furthermore, KiriE is compatible with simultaneous recordings from individual organoids in an assembloid and can capture activity in emerging cortico-striatal circuits. Moving forward, this flexible electronics system holds the potential to unveil disease phenotypes and reveal the activity patterns underlying the assembly of the nervous system.

3:30 PM SB06.08.05

Microstructures printed via 2-Photon Polymerization (2PP) to mechanically stimulate 3D multicellular systems [Federico Colombo](#), [Mohammadreza Taale](#), [Gent Dulatahu](#), [Teresa Debatin](#), [Philip Kollenz](#), [Maria Villiou](#), [Fereydoon Taheri](#), [Malin Schmidt](#) and [Christine Selhuber-Unkel](#); University of Heidelberg, Germany

In nature, cells live immersed in an extracellular matrix with other cells, forming tissues and organs. These three-dimensional environments are essential for a wide array of vital biological processes. As a result, many recent studies are now exploring the utilization of 3D multicellular systems such as spheroids, organoids, and organotypic cell cultures. These alternatives, when compared to conventional 2D cell culture methods, hold a significant advantage in closely resembling physiological conditions. Indeed, the mechanical forces acting upon cells can yield differing outcomes depending on whether the cells are in a 2D or 3D environment. Traditionally, most studies on mechanotransduction, especially in terms of the effects induced by mechanical stretching, have been conducted on two-dimensional cultures. This approach, however, has provided only a limited understanding of the effects within a 3D culture.

To address this limitation, we have developed a device for the mechanical stimulation of 3D multicellular systems using Two-Photon Polymerization (2PP). This device can be used to study the mechanical forces in the biological complexities of tissues at an exceptional micrometer-scale resolution. The design of the device allows the application of forces capable of stretching the encapsulated 3D multicellular systems with extreme precision, using a cantilever. Simultaneously, this system enables high-resolution imaging to assess the effects of stretching in vivo. Our findings have revealed that cyclic stretching over 30 minutes at a frequency of 0.5 Hz, and an average displacement of 0.22µm, leads to noteworthy alterations in the morphology and orientation of actin within the 3D multicellular system. Furthermore, this device can be easily customized to mechanically stimulate various types of multicellular systems, accommodating differences in shape and cell types.

3:45 PM SB06.08.06

Novel Virus-Templated Engineered Material for Photodynamic Treatments [Marika Ienharelli](#)^{1,2}, [Paolo Emidio Costantini](#)³, [Vittorio De Felice](#)¹, [Roberto Saporetto](#)⁴, [Angela Tino](#)¹, [Francesca Di Maria](#)², [Alberto Danielli](#)³, [Matteo Calvaresi](#)⁴ and [Claudia Tortiglione](#)¹; ¹CNR-ISASI Consiglio Nazionale delle Ricerche, Italy; ²CNR-ISOF Consiglio Nazionale delle Ricerche, Via Piero Gobetti, Italy; ³Alma Mater Studiorum—Università di Bologna, Italy; ⁴Alma Mater Studiorum, Università di Bologna, Italy

Thiophene-based materials **TMs**, due to their excellent electron transport properties, optical properties, soft material nature, stability, solution processability, and water dispersibility, have demonstrated significant potential in photodynamic (**PDT**) therapies. To increase the cell uptake and the permeation of physiological barriers recent studies reported the use of proteins (human serum albumin, HSA) [1] or phages (M13 bacteriophage) [2,3] as natural carriers of different photosensitizers (rose bengal, chlorin e6, oligothiophene ECB04), able to induce cell death by apoptosis in a variety of cell lines. Here we propose a novel engineered living material for photodynamic therapy, i.e. a virus-templated platform, based on the M13 bacteriophage, engineered to display targeting ligands on its surface. By covering the surface of the M13 phage with oligothiophene molecule, a 1-D thiophene nanoplatfom, M13EGFR(TNP) was synthesized and tested in vitro and in vivo. Cell culture experiments were carried out to validate the ability of the biohybrid material to maintain the EGFR-targeted tropism of the phage and to demonstrate photoactivity. The tissue-like animal model Hydra was employed to further confirm the possibility to use these engineered materials for photodynamic treatment and to screen for targeting properties. The transparency, softness and body simplicity together with the lack of ethical issue make *Hydra* a suitable model for this type of studies, enabling fast screening of cytotoxicity and identification of molecular pathways underlying necrosis or apoptosis pathways. Our work provides valuable insights into the potential of M13EGFR(TNP) for targeted photodynamic therapy, laying the groundwork for further exploration of this innovative living material in **nanotheranostic** applications.

[1] "Human Serum Albumin–Oligothiophene Bioconjugate: A Phototheranostic Platform for Localized Killing of Cancer Cells by Precise Light Activation", *JACS Au* 2021, 1, 7, 925-935

[2] "Orthogonal nanoarchitectonics of M13 phage for receptor targeted anticancer photodynamic therapy" *Nanoscale*. 2022; 14(3):632-641.

[3] "Advanced photodynamic therapy with an engineered M13 phage targeting EGFR: Mitochondrial localization and autophagy induction in ovarian cancer cell lines" *Free Radic Biol Med*. 2022;179:242-251

4:00 PM SB06.08.07

Using Metamaterials and Cardiac Tissue Engineering to Engineer Robust and Contractile Cardiac Tissue Patches Lewis S. Jones¹, Hector Rodriguez², Omer Dzemali² and Robert Katzschmann¹; ¹ETH Zurich, Switzerland; ²Universitätsspital Zürich, Switzerland

Ventricular Septal Rupture (VSR) is a challenge in cardiac medicine with a high mortality rate of 45-60%. Current treatment methods use bovine pericardial patches (BPPs), which are non-contractile, tend to calcify over time, and fail to integrate effectively with the myocardium. Therefore, patients do not tend to fully recover cardiac function. To address these limitations, we are engineering a cardiac tissue patch that uses human stem cell-derived cardiomyocytes in hydrogel, reinforced with a metamaterial lattice. This approach allows us to tune the patch mechanical properties and contractility, while enabling stable implantation within the intraventricular space. Here, we will showcase our current results on metamaterial design and manufacturing, mechanical characterization (tunable stiffness and anisotropic ratio), and biological characterization (biocompatibility, cell maturation, and tissue contractility). In summary, we will show how metamaterials can be combined with engineered cardiac tissues to fabricate centimeter scale, three dimensional, and implantable cardiac tissues.

4:15 PM SB06.08.08

Ion Detection in a DNA Nanopore FET Device Purun (Simon) Cao¹, William Livernois¹, Quanchen Ding¹, Soumyadeep Saha² and M. P. Anantram¹; ¹University of Washington, United States; ²University of Waterloo, Canada

Significant strides have been made to integrate biotechnology with semiconductor nanotechnology, but the ability to directly interface with living cells is still an emerging area of research. Such devices are being developed for interfacing directly with neurons, which can help monitor and treat chronic pain and Parkinson's disease. In this pursuit, an ion detection device that combines a DNA-origami nanopore and a field-effect transistor (FET) was designed and modeled to determine the sensitivity of the nanodevice to the local cellular environment.

Our design employed an "artificial gap junction" constructed using a DNA origami nanopore on a CMOS device as a direct interface between the cell and the electronic device. Inspiration for using a DNA Nanopore comes from naturally occurring transmembrane nanopores, such as the protein Gramicidin, which have been modeled as ion channels. In this work, we have modeled a synthetic nanopore pore that uses a six-helix bundle of DNA that has been previously synthesized as a cylindrical nanopore structure that spans a bilipid membrane. The DNA-origami structure is bio-compatible and can also be modified with ligands to anchor to the lipid bi-layer on a cell. This self-assembling structure would be compatible with the living system and convert signals generated by ionic currents directly into an electrical signal using a gated ion-selective field effect transistor. While typical nanopore sensors detect single molecules and ions by measuring the change in ion flow across a membrane, the proposed device would detect the ions as a buildup of charge across the gate of the FET. A blanket of ions (electrical double layer) would form on the nanopore inner wall and over the gate oxide in a manner dependent on the local environment, and the resulting source-drain current can be used to measure the presence of ions in the cell.

A continuum model was used to account for the ions in the electrolyte. Modeling of an electron distribution with the electric double layer theory was applied to verify the applicability of the model to a bio-sensing environment. The FinFET architecture was shown to increase sensitivity to ions even with a low drain-source bias. The device combined with the nanopore is shown to have high sensitivity to ion concentration and nanopore geometry, with the electrical double layer behavior governing the device characteristics. The logarithmic relationship found between ion concentration and FET current generates almost a microampere of current difference across varying concentrations with a small applied bias.

Our findings illuminate a promising pathway for refining cellular interfacing, potentially catalyzing advancements in in-vivo sensing technologies for biomedical applications.

We acknowledge the NSF SemiSynBio 2027165 grant.

4:30 PM *SB06.08.09

Measuring Transmembrane Ion Channel Activity Using Biomembrane Bioelectronic Circuits Susan Daniel; Cornell University, United States

Despite advancements in transmembrane protein (TMP) structural biology and a growing interest in their applications, this class of proteins remains challenging to study. Progress has been hindered by the complex nature of TMPs and innovative methods are required to circumvent significant technical hurdles. We offer two new approaches that facilitate the study of the activity of ion channel proteins based on a bioelectronic biomembrane platform we developed. First, we harvest materials from plasma cell membranes that contain the ion channel of interest and coat our electrodes with these "cellular biopsies." Second, we use cell-free protein synthesis using reconstituted components of the cellular transcription and translation machinery in vitro for integrating TMPs directly into a membrane coating the electrode. In this talk, I will highlight both approaches for functionalizing electrodes with biological materials and measuring their activity. The bioelectronic biomembrane platform used in these studies is made possible by using a biocompatible conducting polymer film that supports a lipid bilayer. Specifically, PEDOT:PSS films on electrodes, which are both transparent and electrically conductive, allow the assessment of protein activity by optical and electrical means. Here, fluorescence microscopy and electrochemical impedance spectroscopy (EIS) are used to characterize the ion channels in these devices. Examples of activity measurements from the human, plant, and bacteria world will be given with implications in health, agriculture, and sensing.

SESSION SB06.09: Poster Session II
Session Chairs: Eleni Stavrinidou and Claudia Tortiglione
Thursday Afternoon, April 25, 2024
Flex Hall C, Level 2, Summit

5:00 PM SB06.09.02

Force-Triggered Self-Destructive Hydrogels Tharindu R. Rajasooriya¹, Hiroaki Ogasawara¹, Yixiao Dong¹, Joseph Mancuso¹ and Khalid Salaita^{1,2}; ¹Emory University, United States; ²Georgia Institute of Technology, United States

Self-destructive polymers (SDPs) are defined as a class of smart polymers that autonomously degrade upon experiencing an external trigger, such as a chemical cue or optical excitation. Because SDPs release the materials trapped inside the network upon degradation, they have potential applications in drug delivery and analytical sensing. However, no known SDPs that respond to external mechanical forces have been reported, as it is fundamentally

challenging to create mechano-sensitivity in general and especially so for force levels below those required for classical force-induced bond scission. To address this challenge, the development of force-triggered SDPs composed of DNA crosslinked hydrogels doped with nucleases is described here. Externally applied piconewton forces selectively expose enzymatic cleavage sites within the DNA crosslinks, resulting in rapid polymer self-degradation. The synthesis and the chemical and mechanical characterization of DNA crosslinked hydrogels, as well as the kinetics of force-triggered hydrolysis, are described. As a proof-of-concept, force-triggered and time-dependent rheological changes in the polymer as well as encapsulated nanoparticle release are demonstrated. Finally, the kinetics of self-destruction are shown to be tuned as a function of nuclease concentration, incubation time, and thermodynamic stability of DNA crosslinkers.

5:00 PM SB06.09.03

Label-Free Laser-Induced Ni/AuNPs Micropore Reusable Electronic Sensor for Rapid Bacteria Detection and Quantification [Wing Yan Poon](#) and [Mitch Guijun Li](#); The Hong Kong University of Science and Technology, Hong Kong

The advancement of biosensors for microbes, especially pathogenic bacteria has been an important research area aiming to develop rapid and accurate detection, with its crucialness to various applications in healthcare, food safety and environmental monitoring. Laser-induced nanoparticles have emerged as a viable solution to stimulate and identify electrochemical properties of bacteria. In this study, we propose a label-free laser-induced Ni/AuNPs reusable electronic sensor that enables fast and precise detection of pathogenic bacteria.

The rapid bacteria sensor is achieved by two major innovative laser applications. The sensor is firstly fabricated by a laser-drilled micropore sized at approximately 1 μm on double sided laser-induced graphene (LiG) polyamide film. The size of the micropore is utilized to conduct selective resistive pulse analysis which allows identifications across different pathogenic bacterial species along with machine learning. It is then followed by controlled potential amperometric analysis of different pathogenic bacteria using Ni/AuNPs modified LiG as electrode, providing quantitative details of bacteria present in the sample solution. The Ni/AuNPs modified LiG is efficiently manufactured by laser ablation of Ni-consisting crystal and Au thin film to laser-induced graphene. This novel bacteria sensor requires no additional coating of antibodies and non-reversible conjugations between bacteria and ligands, enabling its robust reusability on bacteria detection and quantification.

This novel approach demonstrates simple yet highly functional applications for the detections and quantification of bacteria, microorganisms or even viruses. Through the techniques of laser-induced nanomaterials and micropores, the manufacturing of microbes related sensing instruments would be immensely enhanced in terms of time efficiency as well as financial cost. With indications of such capabilities, it is assured that the future of microbial diagnosis will be optimized with next generation rapid sensors developed from laser evolved technologies, paving ways for further applications in fields of food safety, epidemiology and Point-Of-Care testing.

5:00 PM SB06.09.04

Pushing the Limit of Self-Assembly Ultrashort Peptides Minimum Gelation Concentration for Advanced Biomedical Applications [Panagiotis Bilalis](#), [Dana Alhattab](#), [Cynthia Juarez](#), [Abdulelah Alrashedi](#), [Manola Moretti](#) and [Charlotte A. Hauser](#); King Abdullah University of Science and Technology, Saudi Arabia

Ultrashort amphiphilic peptides, characterized by a distinct sequence motif and comprising up to seven natural amino acids, display self-assembling dynamics under physiological conditions. Despite their small size, these peptides can adopt α -helical, β -sheet, and β -turn secondary structures in aqueous solutions. At higher concentrations, they spontaneously organize into nanofibers, resulting in hydrogels characterized by an exceptionally high water content (>99% w/w). Notably, these hydrogels exhibit biocompatibility, biodegradability, and low immunogenicity, making them versatile for various biomedical applications such as 3D cell culture, bioinks for 3D bioprinting, hemostatic agents, drug delivery systems, and materials for soft tissue repair. By strategically substituting certain amino acids in the sequence with non-natural counterparts, we achieved the lowest reported minimum gelation concentration for self-assembling peptides, thereby expanding their potential applications. In-depth analyses using 2D-NMR, Raman spectroscopy, and molecular dynamic (MD) simulations were conducted to further elucidate the self-assembly process. These peptides serve as scaffolds capable of supporting cellular viability and proliferation without compromising the mechanical properties of the hydrogel. The results demonstrate the potential of these scaffolds for advanced biomedical applications. Specifically, we demonstrated the capability of the developed peptide scaffolds to be combined with human platelet lysate up to 40% of its volume without compromising the self-assembly process. This forms a hydrogel scaffold that can self-sustain and promote cellular growth under xenofree 3D culture conditions. The hybrid peptide and platelet lysate hydrogel developed in this study holds immense promise for clinical applications in the field of regenerative medicine.

5:00 PM SB06.09.05

Engineering Cellular Alignment in Contractile Cardiac Tissues Using Coherent Light Biofabrication [Lewis S. Jones](#)¹, [Miriam Filippi](#)¹, [Mike Yan Michelis](#)¹, [Aiste Balcuniute](#)¹, [Oncay Yasa](#)¹, [Gal Aviel](#)², [Maria Narciso](#)¹, [Eldad Tzahor](#)² and [Robert Katschmann](#)¹; ¹ETH Zurich, Switzerland; ²Weizmann Institute of Science, Israel

Biofabricating three-dimensional cardiac tissues that mimic the native myocardial tissue is a pivotal challenge in tissue engineering. In this study, we fabricate three-dimensional cardiac tissues with controlled cellular alignment and directed contractility. We use coherent light biofabrication with optically tuned bioinks of high cell density (15-60 million cells/mL) to fabricate hydrogel microstructures for cardiac cell alignment. Cardiac tissues with microstructures expressed higher levels of protein alpha 1 (GJA1) (1.6x) and exhibited higher uniaxial contractility (3.8x) relative to unstructured tissues. Tissues that were bioprinted at high cell density (30-60 million cells/mL) contracted synchronously (27 μm uniaxially). However, cell-induced light scattering hinders microstructure formation and cellular alignment at increased light propagation depth (> 400 μm). Furthermore, cell-induced light attenuation caused anisotropic tissue remodeling and contractility. We mitigated these limitations by projecting light bidirectionally. This approach minimized the light propagation depth and allowed us to rapidly bioprint larger tissues with microstructures (ϕ 0.6 mm x 2 mm). Our approach provides a new strategy for engineering cellular alignment in cardiac tissues used for drug screening, regenerative medicine, and biohybrid robots.

5:00 PM SB06.09.06

Multi Electrophysiological Signal Collecting E-Textile System by Sponge Electrode [Chansoo Kim](#), [Junyi Zhao](#) and [Chuan Wang](#); Washington University in St. Louis, United States

Wearable electrophysiological signal sensors are essential for long-term health monitoring applications, and these electrodes lead us to pre-diagnose lots of diseases such as a cardiac disorder and muscle or nerve disorders before the diseases move to more dangerous step. However, most of the reported wearable sensors have collected signals individually or integrated into patch for multi-signal collection. As a result, the practical implementation is hampered by challenges such as process complexity, durability, and user experience.

Here, we introduce an interesting approach for long-term and multi-electrophysiological signal collecting electrode by E-textile system. This system is composed of simply screen printed textile electrodes with Poly(3,4-ethylenedioxythiophene)polystyrenesulfonate (PEDOT:PSS) and carbon black mixed

conductive PDMS sponge electrode. The porous structure of soft and conductive sponge electrode provides pressure sensitivity by changing the void (air gap) structure inside of the sponge. So, it shows sensitive resistance and capacitance change under small pressure changes (Under 300 Pa). For the electrophysiological signals, the sponge electrode can drastically increase the contact area between skin and electrode in water and gel condition. In addition, it also keeps the water or gel longer time compared to the planner electrode. So, to overcome the hydrophilicity of PDMS and carbon black, and maximize the absorption of water or gel into the sponge electrode, layer-by-layer (LbL) coating is utilized with poly-L-lysine. Eventually, we achieve $1.2 \times 10^4 \Omega \cdot \text{cm}^2$ skin contact impedance and 30 dB signal-to-noise ratio (SNR) for the electrocardiogram (ECG) and electromyography (EMG). Furthermore, the carbon black sponge electrode demonstrates better wet condition stability compared to other coated sponge electrodes. Finally, we utilized this E-textile system for the patient study to collect uterine contraction signals and predict childbirth (Washington University Institutional Review Board, IRB 201612140). We strongly believe that this E-textile system will lead to a new opportunity for stable long-term electrophysiologic signal collecting applications.

5:00 PM SB06.09.07

Colorimetric and Photothermal Dual-Mode Apta-Sensor for Selective Detection of Kanamycin Using Chitosan-Stabilized Platinum Nanozymes Han Been Lee, Sung Min Jeon, Dayeong Choi and Gi Hun Seong; Hanyang University, Korea (the Republic of)

Addressing bacterial infections, kanamycin (KAN) finds extensive use in aquaculture, livestock husbandry, and agriculture. Nevertheless, the overuse of KAN leads to an excess of biological residues in the environment and food, resulting in potential nephrotoxicity, ototoxicity, and other harmful side effects for humans. Consequently, it becomes imperative to develop a rapid, selective, cost-effective, and sensitive detection system for KAN to safeguard human health and ensure food safety.

Colorimetric assays employing antibodies have garnered significant attention due to their noticeable color change discernible by the naked eye, swift observation, cost-effectiveness, and ease of operation. Nonetheless, antibodies come with drawbacks such as high cost, sensitivity to storage conditions, and variability in quality from batch to batch, leading to decreased reproducibility. To address these challenges, we opted for aptamer molecules. These functional, single-stranded nucleic acids possess the ability to fold into specific 3-D structures, exhibiting high specificity for target molecules, whether they are small molecules, or even proteins.

Nanozymes, nanomaterials exhibiting natural enzyme-like activities, have been recognized as viable substitutes to emulate natural enzymes such as horseradish peroxidase (HRP). This is attributed to their advantages of low cost, straightforward preparation, easy modification, excellent stability, and remarkable catalytic activity. Platinum nanoparticles (PtNPs), in particular, have found extensive use in bioanalytical applications due to their superior peroxidase-like activity, biocompatibility, and high chemical inertness. The choice of suitable stabilizing reagents is crucial in the synthesis of efficient nanozymes, as stabilizers significantly impact the physicochemical and biological properties of nanoparticles. In our study, chitosan (CS) was employed. The positively charged nature of CS facilitates the electrostatic binding of the negatively charged KAN binding aptamer (KBA) to chitosan-stabilized platinum nanoparticles (CS/PtNPs).

Traditionally, immunoassays operate by detecting the target in a single mode. However, outcomes obtained through a single-mode signal readout can be susceptible to variations stemming from differences among operators, equipment disparities, and non-standard analytical protocols. In contrast, dual-mode sensing platforms not only possess the intrinsic characteristics of each response mode but also offer mutual validation of detection results obtained through diverse modes. Recent efforts have been directed towards establishing analytical methods that incorporate temperature changes as a signal, in addition to the colorimetric method, in immunoassays. Among various photothermal agents, oxidized TMB (TMB_{ox}) has emerged as a promising photothermal sensor due to its high photoconversion efficiency in near-infrared (NIR)-induced photothermal applications. TMB_{ox} exhibits distinct absorbance at UV-visible (652 nm) and NIR (808 nm) wavelengths, making it suitable for use as a probe in both colorimetric and photothermal detection.

In this work, CS/PtNPs and TMB_{ox} were used to construct a dual-mode colorimetric and photothermal aptasensor designed for the selective detection of KAN, relying on the KBA-derived enhancement of peroxidase activity in CS/PtNPs and its subsequent inhibition by KAN. The developed dual-mode colorimetric and photothermal aptasensor exhibited a linear detection range of 0.1–50 and 0.5–50 μM , with respective limits of detection (LOD) of 0.04 and 0.41 μM . Furthermore, the aptasensor effectively identified KAN concentrations in spiked milk samples, confirming its reproducibility and reliability in practical applications. Crucially, the proposed aptasensor eliminates the need for a washing step and demonstrates robust selectivity for KAN. These characteristics position the aptasensor as a versatile tool for the detection of small molecules with known aptamers.

5:00 PM SB06.09.08

Nanocarrier Incorporating Fucoidan/Chitosan for Co-Encapsulation of TMB, Glucose Oxidase and Prussian Blue: Applications in Chemotherapy, Photothermal Therapy and Glucose Starvation Treatment Dayeong Choi, Han Been Lee, Sung Min Jeon and Gi Hun Seong; Hanyang University, Korea (the Republic of)

Fucoidan, a naturally occurring sulfated polysaccharide derived from marine brown algae, has been explored as a promising therapeutic nanoparticle for cancer treatment. Effective strategies such as chemotherapy, photothermal therapy, and glucose starvation can create a conducive environment for successful cancer eradication. Harnessing the potential of functionalized fucoidan nanoparticles in combination with chitosan, acting as a nanocarrier, presents an opportunity for biological activation, particularly in abnormally acidic extracellular environments. In this study, we developed a fucoidan (Fu)-chitosan (CS) nanocarrier through a self-assembly technique and encapsulated it with 3,3',5,5'-tetramethylbenzidine (TMB), prussian blue (P), and glucose oxidase (GOx) (Fu/CS@TPGOx). The synthetic multi-stimuli-responsive Fu/CS@TPGOx nanoparticles were characterized using dynamic light scattering (DLS), zeta potential, UV absorption, scanning electron microscopy (SEM), and transmission electron microscopy (TEM) analyses. DLS analysis indicated an average particle size of 440 nm, consistent with the spherical morphological structures observed in TEM results. Moreover, the positive zeta potential of 22.9 mV affirmed the stability of the synthesized particles.

The catalytic efficacy of Fu/CS@TPGOx nanoparticles is confirmed through UV absorption studies, revealing specific absorbance spectra at 652 nm. Additionally, a prominent peak at 810 nm signifies substantial absorption in the near-infrared (NIR) range, rendering it particularly suitable for photothermal treatment. The photothermal performance of the newly developed Fu/CS@TPGOx nanoparticles was assessed by subjecting them to an 808 nm NIR laser at concentrations of 7.7, 3.85, and 0.77 $\mu\text{g}/\text{mL}$, with a power density of 0.75 W/cm^2 . Results indicated a proportional increase in temperature with nanoparticle concentration. Notably, at 7.7 $\mu\text{g}/\text{mL}$ Fu/CS@TPGOx nanoparticles, the temperature reached 55.2 $^{\circ}\text{C}$, providing an optimal condition for the targeted destruction of breast cancer cells (MDA-MB-231) following a continuous 10 minute exposure to an 808 nm laser with a power density of 0.75 W/cm^2 .

The WST-1 assay, a live-dead cell staining method, validates the anticancer properties of Fu/CS@TPGOx in MDA-MB-231 cancer cells. Fu/CS@TPGOx exhibited 40% cytotoxicity in MDA-MB-231 cells under chemodynamic treatment and glucose starvation conditions at a dose of 0.77 $\mu\text{g}/\text{mL}$. Furthermore, the cytotoxicity increased to 55% during photothermal effects with chemodynamic treatment and glucose starvation by exposing Fu/CS@TPGOx to an 808 nm laser at 0.75 W/cm^2 for 10 minutes. The live-dead cell staining experiment yielded similar results, highlighting Fu/CS@TPGOx's significant potential as a cancer therapeutic. Moreover, DCFH-DA analysis confirms that under photothermal conditions with chemodynamic therapy and glucose starvation, the generation of reactive oxygen species was higher in the 0.77 $\mu\text{g}/\text{mL}$ Fu/CS@TPGOx treatment. This suggests that Fu/CS@TPGOx played a crucial role in activating OH^{\cdot} in cancer cells.

The flow cytometry study provides evidence supporting the cytotoxic effects of 0.77 $\mu\text{g}/\text{mL}$ Fu/CS@TPGOx under laser conditions, yielding the highest rate of apoptosis (84.5%) compared to glucose starvation and chemodynamic treatment (60%). The utilization of three anti-cancer strategies—

chemotherapy, photothermal treatment, and glucose starvation—is evident in the findings, showcasing Fu/CS@TPGox's substantial anti-cancer impact at low concentrations. This research holds the potential to contribute to the development of more effective anticancer therapies for cancer treatment. A comprehensive investigation of these novel materials will be conducted to assess their in vivo efficacy and toxicity in comparison to other anti-cancer drugs in the future.

Keywords: Fucoidan, Chitosan, Photothermal therapy, Chemodynamic therapy, Glucose starvation

5:00 PM SB06.09.09

The Photothermal Efficacy of Silver and Rhenium Disulfide Nanoparticles for Cancer Eradication Seshu Subramanian Murugan^{1,2}, Venkatesan Jayachandran^{1,2} and Gi Hun Seong¹; ¹Hanyang University, Korea (the Republic of); ²Yenepoya Deemed to be University, India

Cancer is a deadly disease that usually manifests in its later stages or whenever medicinal treatments become ineffective. Tumor cell suppression in the malignant microenvironment is a significant impediment to anticancer therapy. Photothermal characteristics of nanomaterials are being investigated as a potential new cancer treatment. Rhenium disulfide (ReS₂) nanosheets were created in this work by liquid exfoliation with gum arabic (GA), and then coated with AgNPs to produce reactive oxygen species that destroy cancer cells. The developed AgNP-GA-ReS₂ NPs have been studied by photothermal, UV, DLS, SEM, and TEM assessments. UV analysis shows that produced AgNP-GA-ReS₂ NPs has significant responses to NIR irradiation at 808 nm which could potentially utilized for photothermal cancer treatments. The dynamic light scattering (DLS) results showed that the NPs had a zeta potential of +76 mV and were around 216 nm in size. The transmission electron microscopy (TEM) and scanning electron microscopy (SEM) analyses indicated that the AgNP-GA-ReS₂ produced single-layered nanosheets on which the AgNPs were scattered. Following 5 minutes of laser irradiation, the photothermal effects of 50 µg/mL AgNP-GA-ReS₂ NPs were investigated using 808 nm laser, operating at 1.2 W cm⁻² and temperature increased to 55.8 °C. This temperature represents the ideal death point for tumor cells. Within comparable testing settings, AgNP-GA-ReS₂ at 25 µg/mL had an average temperature of “40.71 °C”, indicating an evident link between the concentration and the substance's photothermal abilities.

The anticancer activity of the novel AgNP-GA-ReS₂ NPs was investigated in MBA-MB-231 cells for five minutes with and without laser irradiation to determine dose-dependent cytotoxicity, and the results confirmed that higher concentrations (50 µg/mL) of AgNPs-GA-ReS₂ are effective at killing cancerous cells. Calcein and EtBr staining confirmed the cytotoxic nature of AgNP-GA-ReS₂ NPs in laser conditions, with more dead cells in the laser boundary region stained with red EtBr. In addition, AgNP-GA-ReS₂ nanosheets exposed to NIR irradiation produce Reactive Oxidation Species (ROS) with strong anticancer activity, as confirmed by the DCFH-DA and flow cytometry investigations, along with photothermal effects.

Key Words: Cancer, Photothermal effects, Rhenium Disulfide and Silver nanoparticles

5:00 PM SB06.09.10

A Conformal Second Skin for Long-Term Electrophysiology Monitoring of Plants Yi Jing Wong^{1,2}, Xiaodong Chen¹ and Xian Jun Loh²; ¹Nanyang Technological University, Singapore; ²Agency for Science, Technology and Research, Singapore

Electrophysiological (EP) signals are important plant health indicators as they are pivotal in the growth development and plants' response to environmental stimuli or stresses. Long-term plant health monitoring through analysis of EP signals has become increasingly important with the growing risk of global agriculture instability. However, the long-term attachment of wearable electrodes has always been hindered due to hydrogel dehydration or poor conformability with plant surfaces.

In this presentation, I will share my work on the development of a long-term coupling layer to achieve stable monitoring of plant EP signals. The high conformality of the coupling layer allows the non-invasive recording of EP signals for a month with superior signal-to-noise ratio and minimal drift.

This work investigates the coupling mechanism and demonstrates potential applications, with the objective of laying the foundation for use of wearables in understanding plants' long-term responses to environmental changes.

5:00 PM SB06.09.11

A Fibrous Matrix Immobilized with Milk Exosomes for Improved Wound Healing Hoai-Thuong Duc Bui¹, Gayeon You², Hyuksang Yoo¹ and Hyejung Mok²; ¹Kangwon National University, Korea (the Republic of); ²Konkuk University, Korea (the Republic of)

This study aims to provide an advanced therapy for wound recovery by immobilizing pasteurized bovine milk-derived exosomes (mEXO) onto a polydopamine (PDA)-coated hyaluronic acid (HA)-based electrospun nanofibrous matrix (mEXO@PMAT) using a straightforward dip-coating technique. The goal of this study is to create a wound-healing biomaterial that is composed of mEXO-immobilized mesh. mEXOs that have been purified and measured at approximately 82 nanometers contain a number of microRNAs (miRNAs) that are associated with collagen synthesis, cell proliferation, and anti-inflammatory properties. These miRNAs include let-7b, miR-184, and miR-181a. These miRNAs are responsible for eliciting increased mRNA expression of keratin5, keratin14, and collagen1 in human keratinocytes (HaCaTs) and fibroblasts (HDF). During the course of fourteen days, the mEXOs that have been immobilized onto the PDA-coated meshes are progressively freed from the meshes without experiencing a burst-out effect. In the cells that have been treated with HaCaTs and HDF, the degree of in vitro cell migration is greatly increased in the cells that have been treated with mEXO@PMAT. This is in comparison to the cells that have been treated with unmodified or PDA-coated meshes. A further benefit of the mEXO@PMAT is that it facilitates substantially quicker wound closure in vivo without causing any noticeable toxicity. Therefore, the prolonged liberation of bioactive mEXO from the meshes has the potential to significantly promote cell proliferation in vitro and accelerate wound closure in vivo. This has the potential to be utilized by mEXO@PMAT as a promising biomaterial for wound healing.

5:00 PM SB06.09.12

Functionalization of Gold Electrodes with Aptamers for Impedimetric Biosensor for Detection of *Brucella Abortus* Merylin S. Jiménez^{1,2}, David Monge Castillo^{1,2,3}, Daniela Zuñiga Rivera^{1,2}, Leonardo Lesser Rojas^{4,5}, Giovanni Sáenz Arce^{6,7}, Caterina Guzmán Verrí⁸ and Claudia Villarreal^{1,2,9}; ¹Escuela de Ciencia e Ingeniería de Materiales, Instituto Tecnológico de Costa Rica, Costa Rica; ²Centro de Investigación y Extensión en Ingeniería de Materiales (CIEMTEC), Instituto Tecnológico de Costa Rica, Costa Rica; ³Maestría Ingeniería en Dispositivos Médicos, Instituto Tecnológico de Costa Rica, Costa Rica; ⁴Centro de Investigación en Ciencias Atómicas, Nucleares y Moleculares, Universidad de Costa Rica, Costa Rica; ⁵Escuela de Física, Universidad de Costa Rica, San Pedro de Montes de Oca, Costa Rica; ⁶Centro de Investigación en Óptica y Nanofísica, Departamento de Física, Universidad de Murcia, Spain; ⁷Departamento de Física, Facultad de Ciencias Exactas y Naturales, Universidad Nacional, Costa Rica; ⁸Programa de Investigación en Enfermedades Tropicales (PIET), Escuela de Medicina Veterinaria, Universidad Nacional, Costa Rica; ⁹Laboratorio Nacional de Nanotecnología (LANOTEC), Centro Nacional de Alta Tecnología (CENAT), Costa Rica

Brucella Abortus is a bacterium that causes brucellosis, considered one of the main causes of economic losses in the livestock sector, also causing a zoonotic risk. It's estimates that about half a million new cases of human brucellosis occur each year worldwide. Biosensors offer the necessary criteria to perform an early, accurate and efficient detection of *Brucella abortus*, to prevent the spread of the disease and minimize its effects on human and animal health, due to their ease of use and portability for complex samples. The objective of this work is to develop a selective platform for the detection of *Brucella abortus*, to be implemented in a microfluidic device based on an impedimetric aptasensor. The aptamers are covalently functionalized on the gold

electrodes via glutaraldehyde and cysteamine. The electrodes were characterized by Fourier transform infrared spectroscopy (FTIR) to confirm the presence of aptamers on the surface; scanning electron microscopy (SEM) Energy Dispersive Spectroscopy (EDS) and atomic force microscopy (AFM) were used to image the aptamer layer on the electrode surface and evaluate the morphology, quality, homogeneity, uniformity, and thickness. Electrochemical Impedance Spectroscopy (EIS) and Cyclic Voltammetry (CV) are applied to observe the biological interaction response and interfacial properties of the functionalized electrode.

5:00 PM SB06.09.13

TD-DFTB Investigation and Deposition of Au onto Ag Nanocubes for Enhanced Stability and Sensing Ayomide D. Oluwafemi, Tim Kowalczyk and Ying Bao; Western Washington University, United States

Silver nanocubes are appealing to scientists and significant in technology due to their optical, electric, and chemical properties. However, there are limitations to chemically modifying silver nanocubes and they are susceptible to oxidation leading to the loss of their shape, stability, and quality. A solution is to deposit a metal like gold on silver nanocubes that is resistant to oxidation and chemically modifiable. This prevents silver nanocube deterioration, ensuring their stability and modification potential. Unfortunately controlling the synthetic parameters that shape gold-coated silver nanocubes is difficult. The galvanic replacement reaction between gold and silver can erode, hollow, or disintegrate silver nanocubes. We conducted several tests to create a viable and reproducible gold-coated silver nanocube synthesis process. This research employed both thermodynamic and kinetic control to prevent galvanic replacement reaction by decreasing the gold precursor's reduction potential with potassium iodide and adjusting the pH to regulate the reduction power of the reducing agent. We also evaluated various experimental settings and parameters vital to the synthesis. The refractive index sensing potential of gold-coated silver nanocubes was assessed and chemically treated with MUTAB ((11-Mercaptoundecyl)-N, N, N-trimethylammonium bromide). The Time dependent density theory functional (TD-DFTB) computational methodology was used to better understand the synthetic process and the atomic system, focusing on gold and silver electronic interactions and the effects of Iodide (I⁻), Chlorine (Cl⁻), and Sulphite ions (SO₃²⁻) on the galvanic replacement reaction, nanostructure geometry and stability. Overall, this study expands on gold-coated silver nanocube research. It gives more insights on how gold-coated silver nanocubes are synthesized, maintains their shape, improves stability, and functionality.

5:00 PM SB06.09.14

In Situ Cell Purification by Biomolecule Induced Peptide Self-Assembly Cheuk Yin Li, Zhenghua Liang and Yi Kuang; Hong Kong University of Science and Technology, Hong Kong

Synthetic mRNA switches have emerged as valuable tools for the cell sorting in culture condition, particularly for purification of stem cell-derived cells. The efficiency of recovering target cells is however hindered by the undesired expression of toxic proteins, and the removal of non-target cells is also limited due to the absence of signal amplification. To address these challenges, we developed an innovative approach utilizing synthetic mRNA switches sensing intracellular marker molecule, that control the formation of an extracellular toxic assembly. Since this approach does not involve in expression of toxic proteins, it ensures a high effectiveness in recovering target cells. Furthermore, we implemented multi-level signal amplification to enhance the elimination effectiveness of non-target cells. This novel approach can be customized to suit diverse in situ cell purification requirements, offering a promising solution for achieving effective and efficient in situ cell purification in a broad biological and clinical applications.

5:00 PM SB06.09.15

Thermodynamically Stable Nanotubular mRNA Carriers made of Self-Adjusting Peptide Building Blocks Youjin Jung; Yonsei University, Korea (the Republic of)

While mRNA delivery technology holds significant promise, storage and safety-related problems still exist, which arise from the inherently low thermodynamic stability of conventional mRNA carriers. The existing mRNA carriers have generally spherical structures. Considering the filamentous nature of mRNAs and the exceptional thermodynamic stability associated with nanotubes among nano-assemblies, we could dramatically enhance the thermodynamic stability by developing mRNA carriers in the form of nanotubes. Through cooperative interactions, mRNA and peptides were fabricated into rigid nanotubes that resemble tobacco mosaic virus. The fluttering and irregular mRNA strand was coated by a single layer of peptide building blocks. The crucial factor in developing the mRNA nanotube lies in designing self-adjusting supramolecular building blocks (SABs). SABs contain α -helical coiled coils, that incorporate two contrasting properties, namely dynamic flexibility and stiffness, within a single molecule. mRNA nanotubes with bound ligands for targeting exhibited high uptake efficiencies and the tunable transfection efficiencies in mammalian cells. Consequently, mRNA nanotubes will provide underlying technology in advancing the development of more stable and safe mRNA vaccines and therapeutics.

SESSION SB06.10: Biosensing

Session Chairs: Matteo Grattieri and Tedrick Thomas Salim Lew

Friday Morning, April 26, 2024

Room 427, Level 4, Summit

8:15 AM SB06.10.01

Genetically Encoded Nanoparticles Synthesized Intracellularly Or Shemesh^{1,2}, Krishnashis Chatterjee², Puruv Ramakrishna² and Amanda Lin²; ¹The Hebrew University of Jerusalem, Israel; ²The University of Pittsburgh, United States

Despite major advances in detection and therapy, multiple cancers are still aggressive and incurable. Metal nanoparticles are being tested and used for tumor imaging, radiotherapy, and hyperthermia. However, using nanoparticles in living specimens is impeded as they often fail to reach the target cell or desired subcellular organelle, causing insufficient efficacy and safety concerns. Sophisticated chemical coatings and targeting aids such as vesicles and antibodies designed to address these pitfalls, provide only a partial solution, as they either increase off-target activity or hinder the clinical function of the nanoparticles. To solve this, we had the nanoparticles of interest made by the tumor cells, using their own genetic machinery. We expressed genes that encode nanoscale protein cages, able to stabilize metal ions inside tumor cells. The expressing tumor cells were presented with subtoxic concentrations of salts containing metal ions, which were stabilized to form metal nanoparticles. We are now testing the hypothesis that creating Genetically Encoded Nanoparticles Synthesized Intracellularly (GENSIs) can yield high-efficiency cancer therapy. We optimized the formation of GENSIs in glioma cell cultures and confirmed the formation of metal GENSIs by optical microscopy, transmission electron microscopy (TEM) and elemental analysis (EDX). We anticipate tumor cell photothermal killing, by expressing GENSIs in cancer cell lines and exposing them to near-infrared laser light. These studies will unlock the immense potential embedded in genetically encoded nanoparticles for cancer therapeutics and diagnostics applications.

8:30 AM SB06.10.03

Nanopillar Devices for Single Molecule Sensing in The Clinic Alain Wuethrich, Junrong Li, Selvakumar Edwardraja, Christopher Howard, Richard Lobb and Matt Trau; The University of Queensland, Australia

The precise and early detection of biomarkers serves as molecular evidence for managing emerging diseases, enabling timely interventions, and potentially saving lives. Nanomaterials and nanostructures, with their unique physico-chemical properties, can be harnessed to develop innovative sensing systems for multiplex biomarker detection, generating patient-specific molecular profiles from a simple blood sample. At the Centre for Personalised Nanomedicine at UQ, our focus is on developing translational nanotechnologies. We explore nanomaterials and nanostructures to design highly sensitive and multiplex sensing systems for profiling circulating biomarkers in the clinic. In this presentation, we will highlight our recent adventures into single molecule sensing and show how these sensing systems can provide a new window into complex diseases. We will introduce a nanopillar sensing device with single molecule sensitivity for monitoring the human immune system [1], cancer [2, 3] and post-acute sequelae of COVID-19 (unpublished). Furthermore, we exemplify the design of novel biohybrid nanopores for sensing of emerging infectious diseases [4].

References

- [1] J. Li, et al., *Nature Communications*. **2021**, *12*, 1087.
- [2] J. Li, et al., *Advanced Science*. **2023**, *10*, 2204207.
- [3] J. Wang, et al., *Science Advances*. **2020**, *6*, eaax3223.
- [4] J. Li, et al., *Nature Nanotechnology*. **2023**, in press (<https://doi.org/10.1038/s41565-023-01415-1>).

8:45 AM SB06.10.04

Rapid miRNA Detection Enhanced by Exponential Hybridization Chain Reaction in Graphene Field-Effect Transistors Zhaoli Gao and Ting Huang; Department of Biomedical Engineering and Shun Hing Institute of Advanced Engineering, The Chinese University of Hong Kong, Hong Kong

Point-of-care nucleic acid testing with speed, accuracy, and precision is crucial for early detection and timely treatment of diseases. Electronic biosensors that utilize target recycling and hybridization chain reaction (TRHCR) in combination with graphene field-effect transistors (GFETs) show great promise for highly sensitive diagnostics of nucleic acid, reaching the limit of detection down to 100 aM. However, a challenge arises from its linear kinetics, which results in prolonged sensing times for lower concentration oligonucleotides, e.g., approximately 15 hours for 100 aM oligonucleotides. Here, we report a 30-fold reduction in sensing time, from 15 hours to a mere 30 minutes, for detecting 100 aM miRNA, which is achieved by developing an exponential amplification reaction pathway, synergistically compatible with GFETs. This enables the target miRNA to exponentially trigger TRHCR, leading to long-nicked double-stranded polymers that can be detected by GFET through chemical gating. Consequently, our approach facilitates the detection of 22 mer miRNA at concentrations as low as 100 aM in human serum samples, achieving a time frame congruent with point-of-care testing and superior specificity against single-base mismatched interfering oligonucleotides. Our work paves the way towards highly precise, efficient, and label-free nucleic acid testing, thus facilitating early-stage detection of cancer and other diseases at the point of care.

9:00 AM *SB06.10.05

Superstrong Electronic Hydrogel Actuators (ECO) Max M. Hamedi; KTH, Sweden

Superstrong Electronic Hydrogel Actuators (ECO)

Intelligent systems combine sensing, actuation, and computation to achieve complex tasks and functions. Soft electrically controlled multifunctional materials, especially hydrogels, are the most promising materials for such systems as they are as adaptable as biological systems yet compatible with advanced systems through electronics.

We describe an electroactive hydrogel fabricated from cellulose nanofibrils from trees, and conductive nanomaterials, like CNTs or 2D MXenes.^{[1][2]} These nanoparticles self-assemble into an anisotropic composite networks with an open mesoporous structure that can hold lots of water and be highly permeable to substances in their surroundings. The anisotropy of the network allows high expansion in one direction while maintaining very high strength and high electric conductivity in the other.

The electrochemical charge/discharge of the conductors in the hydrogels controls the internal salt concentration and consequently their osmotic swelling.^[3] This allows direct electrically controlled actuation where around 700 water molecules expand/contract the structure for each ion/electron pair inserted/de-inserted at only ± 1 volt, resulting in up to 300% electroosmotic expansion, with very high pressures reaching 1 MPa.

This mode of electronic actuation has not been shown before. We call these electroosmotic (ECO) actuators. Our ECO hydrogel actuators have emergent properties not present in any previously known soft material.

ECO actuators represent a new form of smart soft material, opening possibilities not achievable with other materials systems: as they enable monolithic integration of sensors and many other functions into the same composite, for example using 3D printing techniques.

References

- [1] L. Li, W. Tian, A. VahidMohammadi, J. Rostami, B. Chen, K. Matthews, F. Ram, T. Pettersson, L. Wågberg, T. Bensselfelt, Y. Gogotsi, L. A. Berglund, M. M. Hamedi, *Adv. Mater.* **2023**, *35*, 1.
- [2] W. Tian, A. Vahidmohammadi, M. S. Reid, Z. Wang, L. Ouyang, J. Erlandsson, T. Pettersson, L. Wågberg, M. Beidaghi, M. M. Hamedi, *Adv. Mater.* **2019**, *1902977*.
- [3] T. Bensselfelt, J. Shakya, P. Rothemund, S. B. Lindström, A. Piper, T. E. Winkler, A. Hajian, L. Wågberg, C. Keplinger, M. M. Hamedi, *Adv. Mater.* **2023**, *35*, 1.

9:30 AM BREAK

10:00 AM SB06.10.06

A Breakthrough in Nanotechnology-Enhanced Glucose Sensors Yuan-Hao Hsiao, Rajan D. Chakravarthy, Yu-Hsiang Hsiao and Hsin-Chieh Lin; National Yang Ming Chiao Tung University, Taiwan

According to the International Diabetes Federation (IDF), 537 million adults worldwide suffered from diabetes in 2021, and it is expected that by 2045, one out of every eight adults will have diabetes. As a result, monitoring blood glucose concentrations is essential.

Recent breakthroughs in materials science have led to the creation of nanozymes, which mimic the catalytic functions of natural enzymes, typically comprising metals, metal oxide or metal-organic frameworks (MOFs), offering benefits of stability, precision, and rapid reaction rates for blood glucose measurement.

Nanozymes, though versatile, tend to lack the specificity of natural enzymes, limiting their practicality, and some may exhibit low biocompatibility.

Hence, we created enzyme nanoparticles, fusing nanomaterial attributes with enzyme benefits to preserve natural enzyme advantages and compensate for nanozyme limitations like reduced catalytic activity, specificity, and biocompatibility, tailored for utilization in glucose sensors.

The findings illustrate that by incorporating organic enzyme-based nanoparticles, the electrode can attain outstanding glucose detection capabilities through the utilization of nanotechnology, enabling reduced enzyme dosage, heightened reaction efficiency, and enhanced stability, thus presenting a promising prospect for the future development of a novel blood glucose sensor.

10:15 AM SB06.10.07

MXene-Based 3D-Nanomaterials Printed Wearable System: A Self-Powered Solution for Continuous Physiological Biosignal Monitoring [Rahim Esfandyarpour](#); University of California, Irvine, United States

The development of sustainable, self-powered wearable sensing systems capable of recording physiological biosignals is pivotal for personalized health monitoring, but such devices have remained elusive. In this study, we introduce a novel, self-powered, MXene-based 3D-nanomaterials printed flexible wearable system tailored for continuous, real-time physiological biosignals monitoring. This integrated system combines power-efficient triboelectric nanogenerators (TEG), highly sensitive pressure sensors, and multifunctional circuitry. MXene, a two-dimensional (2D) transition material known for its unique electronegative, conductive characteristics, and triboelectric properties, serves as the foundation of our device and is ideally suited for 3D-printing. We paired MXene with a skin-mimicking Styrene-ethylene-butylene-styrene (SEBS) substrate, which boasts a positive triboelectric characteristic and exceptional stretchability. Our wearable, MXene-based, self-powered physiological sensing system delivers an output power of $\sim 816.6 \text{ mW m}^{-2}$ for its TENGs, with a sensor sensitivity of $\sim 6.03 \text{ kPa}^{-1}$, a low detection limit of $\sim 9 \text{ Pa}$, and a rapid response time of $\sim 80 \text{ ms}$. This makes it possible to continuously monitor the radial artery pulse (RAP) waveform in real-time, without reliance on external power sources. Furthermore, the system's capabilities extend to on-demand RAP monitoring and wireless data and power transmission via near-field communication. This development represents one of the inaugural wearable systems for real-time physiological biosignal monitoring, fully powered by human motion, showcasing its tremendous promise in the field.

10:30 AM SB06.10.08

Artificial intelligence-powered electronic skin for stress monitoring [Changhao Xu](#) and Wei Gao; California Institute of Technology, United States

Stress and mental disorders have become a leading contributor to the global burden of disease, especially given that there is a sharp increase in anxiety and depression in the aftermath of the COVID-19 pandemic. While current stress assessment relies on subjective questionnaires and clinical surveys, there is an unmet need for continuous and precise quantification of stress response evaluations. While progress has been made in the development of wearable sensors and continuous health monitoring, these devices can only monitor a limited set of physical signals and suffer from poor operational stability in biofluids. To meet the demand for reliable long-term continuous monitoring and objective stress assessment, we developed a consolidated artificial intelligence-reinforced electronic skin (CARES) platform that deconvolutes the biological mechanism behind stress responses. Integrated with miniaturized iontophoresis module, microfluidic channels and system-level engineering, the platform is capable of monitoring three key vital signs as well as six molecular biomarkers in human sweat. To enable continuous long-term daily monitoring, we developed a general material strategy for biochemical sensors by introducing analogous composite materials into the sensor interface that achieves an unprecedented long-term sweat biomarker analysis of over 100 hours with high stability. The high performance of CARES platform was evaluated through continuous multimodal physicochemical monitoring over 24-hour real-life activities, and can differentiate physiological and psychological stressors, as well as quantification of psychological stress responses with a high accuracy and confidence level. Such fully-integrated CARES platform can be adapted to monitor a broad spectrum of disease diagnosis and pave the way for numerous practical wearable applications such as intelligent healthcare and personalized medicine.

10:45 AM SB06.10.09

Development and Characterization of Flexible PVDF-TrFE-BaTiO₃-Ti₃C₂ MXene-Based Composite Multi-Morphs: towards The Development of Electro-Active Biomedical-Wearable Devices [Derek Xiong](#)¹, Kaiyu Vang¹, Parshwa Khane¹, Prakhyaat Gautam¹, David Ryman¹, Edertho Leal-Quiros², Saquib Ahmed^{3,3} and Sankha Banerjee^{1,4}; ¹California State University, Fresno, United States; ²University of California, Merced, United States; ³Buffalo State College, United States; ⁴University of California, Davis, United States

Lead-based perovskite oxides have been used as sensors, actuators, and transducers, for sound generation and detection, and also in optical instruments and microscopes. Electro-polymers such as PVDF, and PVDF-TrFE based structures have also been used in several applications towards the development of flexible electroactive multi-morph systems for biomedical applications. but the systems have lower piezoelectric strain coefficients as compared to those of their lead-based piezoceramics. Though lead-free-based ceramic and electroactive polymer composites have been explored their property-performance characteristics are not comparable to that of the electro-active ceramics. The following work looks into the fabrication of non-toxic PVDF-TrFE-BaTiO₃-Ti₃C₂ MXene-based lead-free alternatives to perovskite oxides application in stacked biomedical wearable devices. Three-phase, PVDF-TrFE-BaTiO₃-Ti₃C₂ electroactive nanocomposite thin films were fabricated. The volume fraction of the MXene phase was held constant at 1%, while the volume fraction of the BaTiO₃ phase varied from 20–70%. The dielectric constant, capacitance, impedance, and piezoelectric properties of the samples were measured using an impedance analyzer, and a piezotester. The results were compared as a function of the volume fraction of BaTiO₃ to understand the electron transport performance of these thin films. The impedance and dielectric spectra of the nanocomposites were recorded over a frequency range of 20 Hz to 10 MHz. The microstructural properties and cross-section of the thin films were analyzed using a Scanning Electron Microscope. The high sensitivity and electron transport properties of the composite could be potentially utilized in biomedical devices at low- and high-frequency ranges.

SESSION SB06.11: Biomaterials
Session Chairs: Bozhi Tian and Claudia Tortiglione
Friday Morning, April 26, 2024
Room 427, Level 4, Summit

11:00 AM SB06.11.01

DNA-based Immunostimulatory Hydrogel Loaded with Nanoparticle-detained Toxins as a Toxoid Vaccine against Bacterial Infection [Zhongyuan Guo](#), Ronnie H. Fang and Liangfang Zhang; University of California San Diego, United States

Vaccines have been highly successful in protecting against many different types of infections. Unfortunately, there are still many high-priority pathogens for which there are no clinically approved formulations. Recently, nanoparticle-based strategies have been explored for more effective antigen delivery to the immune system. Nanotoxoids are an emerging platform that leverages cell membrane coating technology to safely deliver toxic bacterial antigens in their native form for antivirulence vaccination. In order to further boost their immunogenicity, we have formulated nanotoxoids against staphylococcal α -hemolysin by embedding them into a DNA-based hydrogel with immunostimulatory CpG motifs. The resulting nanoparticle–hydrogel composite is injectable and improves the *in vivo* delivery of the bacterial toxin while stimulating nearby immune cells. This resulting in elevated antibody production and stronger antigen-specific cellular immune responses. In mouse models of pneumonia and skin infection caused by methicillin-resistant *Staphylococcus aureus*, mice that are vaccinated with our new hybrid vaccine formulation are better protected. Our work highlights the benefits of combining nanovaccines with immunostimulatory hydrogels into a single platform. We believe that the approach can be readily generalized to a range of infectious diseases.

11:15 AM SB06.11.02

Advancing smart materials with cell-free synthetic biology [Marilyn Lee](#); US Army DEVCOM CBC, United States

Cells are a basic building block of biology, but what can transcription and translation processes do when we think outside the cell? Cell-free biological systems provide an open environment that illuminates new opportunities, particularly in field-based sensing, biosynthetic prototyping, and biomaterials science. This presentation will outline progress in scaling and processing of cell-free systems for the functionalization of smart materials, highlighting the advantages of enhanced stability and biosynthesis unbounded by a cellular format. We extend synthetic biology into solvent and heat cast polymer plastics, with potential applications in coatings, wipes, wearables, and personalized hazard detection, and other biologically driven devices.

11:30 AM SB06.11.03

Alginate-based Material System for Medical Applications: From Multipurpose Phantom to Chronic Disease Treatment [Haoyi Qiu](#), Fabian Schuett, Leonard Siebert and Rainer Adelung; Kiel University, Germany

Phantoms are specialized models designed to mimic the properties of human tissue or body structures for use in various medical and healthcare applications. These phantoms are usually made for single application. For example, calibration phantoms usually contain materials with known density, size, or other physical properties e.g., polyethylene, acrylic, and polycarbonate, which can be used in computed tomography (CT), magnetic resonance imaging (MRI), and ultrasound (US) to calibrate the imaging equipment, ensure accurate measurements, and detect potential issues or deviations. They are not applicable for utilization in surgery training. Phantoms for surgery training are usually made from soft materials like silicones, utilized for educational and skill development purposes. They replicate anatomical structures and allow medical students and professionals to learn basic surgical techniques, honing advanced skills, and improving the dexterity and coordination. However, these phantoms exhibit limited suitability for hands-on surgical training. Surgical practice inherently involves destructive procedures, thereby precluding the subsequent reutilization of the phantoms. Materials like silicones owing to their resistance to natural degradation processes, exhibit persistence in the environment over an extended period, thereby constraining its applicability in the context of surgical training. These commercial phantoms have relatively high cost, which limits their use, especially in developing countries.

Another type of phantom is the so-called multipurpose phantom, which integrates multiple imaging modalities and allows for surgery practice within a single construct. For example, these phantoms can be measured under CT and US, after which the students or surgeons can be trained to identify the tumor from the CT and US images and then practice removing the tumor. However, the cost of making such phantoms is usually extremely high due to the materials and complicated fabricating process. In this work, we have developed a facile material system based on alginate and vegetable fat for fabricating the multipurpose phantom. The mechanical, US and CT properties of the materials can be tuned independently to achieve the desired properties of the individual organ and tissue within one material system. The used materials are cheap and easy to obtain even in resource-constrained or developing countries. Moreover, they are 100% vegan, food safe and biodegradable, which is highly suitable for surgery practice that is destructive. These advantages also make it the perfect material system for fabricating patient-specific phantoms for difficult surgery planning and practicing.

In addition to the medical phantoms, the alginate-based hydrogel can be further functionalized with nanoparticles for cardiovascular and musculoskeletal disease treatment. By incorporation of nanoparticles, the injectability or printability of the hydrogels can be modified and the release of the bioactive substances can be achieved under controlled conditions.

SESSION SB06.12: On-Demand Presentation
Tuesday Morning, May 7, 2024
SB06-virtual

10:30 AM SB06.06.01

Ultrashort Self-Assembling Peptide Hydrogels Provide Mechanical and Adhesive Support for Tissue Engineering and Coral Restoration [Manola Moretti](#), Sherin Abdelrahman, Maria Hountondji, Rui Ge, Panagiotis Bilalis and Charlotte A. Hauser; KAUST, Saudi Arabia

Ultrashort peptides that self-assemble into hydrogel matrices can provide mechanical and adhesion cues by a slight change in their sequence. Here we report two examples of specific sequence designs for tissue engineering and coral restoration applications. Cells' interactions with their microenvironment influence their morphological features and regulate crucial cellular functions including proliferation, differentiation, metabolism, and gene expression. Most biological data available are based on *in vitro* two-dimensional (2D) cellular models, which fail to recapitulate the three-dimensional (3D) *in vivo* systems. This can be attributed to the lack of cell–matrix interaction and the limitless access to nutrients and oxygen, in contrast to *in vivo* systems. Despite the emergence of a plethora of 3D matrices to address this challenge, there are few reports offering a proper characterization of these matrices or studying how the cell–matrix interaction influences cellular metabolism in correlation with gene expression. In this study, two tetrameric ultrashort self-assembling peptide sequences, FFIK and FIIK, were used to create *in vitro* 3D models using well-described human dermal fibroblast cells. The peptide sequences are derived from naturally occurring amino acids that are capable of self-assembling into stable hydrogels without UV or chemical cross-linking. Our results showed that 2D cultured fibroblasts exhibited distinct metabolic and transcriptomic profiles compared to 3D cultured cells. The observed changes in the metabolomic and transcriptomic profiles were closely interconnected and influenced several important metabolic pathways including the TCA cycle, glycolysis, MAPK signaling cascades, and hemostasis. Data provided here may lead to clearer insights into the influence of the surrounding microenvironment on human dermal fibroblast metabolic patterns and molecular mechanisms, underscoring the importance of utilizing efficient 3D *in vitro* models to study such complex mechanisms.

This searchable program is up-to-date as of April 15th, 2024.

Coral reef survival is threatened globally. One way to restore this delicate ecosystem is to enhance coral growth by the controlled propagation of coral fragments. To be sustainable, this technique requires the use of biocompatible underwater adhesives. Hydrogels based on rationally designed ultrashort self-assembling peptides (USP) are of great interest for various biological and environmental applications, due to their biocompatibility and tunable mechanical properties. Implementing superior adhesion properties to the USP hydrogel compounds is crucial in both water and high ionic strength solutions and is relevant in medical and marine environmental applications such as coral regeneration. Some marine animals secrete large quantities of the aminoacids dopa and lysine to enhance their adhesion to wet surfaces. Therefore, the addition of catechol moieties to the USP sequence containing lysine (IIZK) should improve the adhesive properties of USP hydrogels. However, it is challenging to place the catechol moiety (Do) within the USP sequence at an optimal position without compromising the hydrogel self-assembly process and mechanical properties. Here, we demonstrate that, among three USP hydrogels, DoIIZK is the least adhesive and that the adhesiveness of the IIZDoK hydrogel is compromised by its poor mechanical properties. The best adhesion outcome was achieved using the IIZKDo hydrogel, the only one to show equally sound adhesive and mechanical properties. A mechanistic understanding of this outcome is presented here. This property was confirmed by the successful gluing of coral fragments by means of IIZKDo hydrogel that are still thriving after more than three years since the deployment. The validated biocompatibility of this underwater hydrogel glue suggests that it could be advantageously implemented for other applications, such as surgical interventions.

SESSION SB06.13: On-Demand Presentation
Tuesday Morning, May 7, 2024
SB06-virtual

10:30 AM SB06.05.03

Living Material Architecture as the Reciprocal Interactions Between Materials and Embedded Cells [Salman Karim](#) and Nakhiah Goulbourne;
University of Michigan, United States

The interface between biomaterials and synthetic biology leads to engineered living materials that have superior properties such as tunability, programmability, growth, self-healing, disturbance sensing, and adaptation to their surroundings, etc. This three-dimensional interaction between cells and hydrogels made from synthetic polymers or nature-derived biopolymers gives rise to a smart, complex, dynamic, and stimulus-responsive system which opens up a new frontier for tissue engineering, regenerative medicine, self-healing materials, and sustainable building materials. However, the engineering of living materials is still in its infancy as the control of the properties including mechanical properties such as elasticity, stiffness, plasticity; swelling behaviour, microscale architecture, biological signalling, response sensitivity, stability, and deformation etc, is not well understood. Additionally, advancements in the 3-D printing, manufacturing, and assembly of material architecture are required to engineer functional materials. Our focus is on the engineering of load-bearing structures by cell embedding during scaffold fabrication using 3-D bioprinting in a spatially organised manner. An attempt has been made to engineer living materials of distinctive chemical and physical living structures by developing algae-laden hydrogel motifs to gain mechanistic insights into their morphology, pattern formation, and stability. The encapsulation of microalgae *Chlamydomonas reinhardtii* in 3D hydrogel scaffolds with pre-designed geometries was carried out to examine different parameters such as material composition and its effect on bioprinting structures, mechanical properties of hydrogel such as swelling and stability in culture, pattern geometry, cell survival during the plotting, cell viability and growth by measuring oxygen release and chlorophyll, spatial distribution of cells within the matrix, and build structure stability. Further, the relationship between printing parameters and plotting material composition will be tested. Overall, the purpose of this study is to identify the mechanism of failure in 3-D living materials by identifying the role of algae-hydrogel interactions during the growth, stability, and deformation of *Chlamydomonas reinhardtii* in a hydrogel medium. The results from this study will facilitate the transition from microscale to macroscale living architecture.

SYMPOSIUM SB07

Lipid Materials—Theory, Fundamentals and Applications
April 23 - April 25, 2024

Symposium Organizers

Shelley Claridge, Purdue University
Aurelia Honerkamp-Smith, Lehigh University
Elizabeth Kelley, NIST
Cecilia Leal, University of Illinois, Urbana-Champaign

* Invited Paper
+ JMR Distinguished Invited Speaker
^ MRS Communications Early Career Distinguished Presenter

SESSION SB07.01: Fundamental Properties of Lipid Materials and Membranes
Session Chairs: Elizabeth Kelley and Cecilia Leal
Tuesday Morning, April 23, 2024
Room 439, Level 4, Summit

10:30 AM *SB07.01.01

Enabling Atomistic Modeling and Simulation of Complex Lipid Structures and Cellular Membranes with xMAS Builder Noah Trebesch and [Emad Tajkhorshid](#); University of Illinois, United States

As more powerful HPC resources are becoming available, there is a new opportunity to bring the unique capabilities of molecular dynamics (MD) simulations to cell-scale systems. Lipid bilayers forming cellular and organelle-level membranes are ubiquitous within cells and are responsible for a diverse set of essential biological functions, but building atomistic models of cell-scale membranes for MD simulations is immensely challenging because of their vast sizes, complex geometries, and complex compositions. To meet this challenge, we have developed xMAS Builder (Experimentally-Derived Membranes of Arbitrary Shape Builder), which is designed to take experimental lipidomics and structural (e.g., electron microscopy and tomography) data as input and use them to build MD-ready models of cellular membrane systems. To test xMAS Builder's capabilities, we have used it to build two large models (each ~12.0 million atoms) of a test system with a representative complex lipid composition and geometry. The two models, which differed only in their lipid packing densities, both maintained their membrane integrity during an extended MD simulation (on the order of 100s of nanoseconds), but their highly divergent relaxation dynamics indicate that the proper packing density of curved membranes is determined by leaflet volume rather than surface area. These results suggest that xMAS Builder's algorithms produce high quality models and that simulation of these models will provide profound biophysical insights into the behavior of cellular membranes.

11:00 AM SB07.01.02

Coarse-Grained Simulation of RNA-Containing Lipid Nanoparticle Self-Assembly via Dissipative Particle Dynamics [Douglas Grzetic](#)¹, Nick Hamilton^{1,2} and John Shelley¹; ¹Schrodinger Inc., United States; ²The University of Vermont, United States

Ionizable lipid-containing lipid nanoparticles (LNPs) have enabled the delivery of RNA for a range of therapeutic applications. In order to optimize safe, targeted and effective LNP-based RNA delivery platforms, an understanding of the role of composition and pH in their structural properties and self-assembly is crucial, yet there have been few computational studies of such phenomena. Here we present a coarse-grained dissipative particle dynamics model of ionizable lipid and mRNA-containing LNPs. Our model allows access to the large length- and time-scales necessary for LNP self-assembly, and is automatically mapped and parameterized with reference to all-atom structures and simulations of the corresponding components at compositions typical of LNPs used for mRNA delivery. Our simulations reveal insights into the dynamics of self-assembly of such mRNA-encapsulating LNPs, as well as the subsequent pH change-driven release of mRNA.

11:15 AM *SB07.01.03

Dynamics of Fluid Bilayer Membranes: Insights from GUV Flickering and Electrodeformation [Petia M. Vlahovska](#); Northwestern University, United States

A lipid bilayer is the main component of the membranes that envelope cells and cellular organelles. While the fluidity of the bilayer is known to control lateral mobility of embedded biomolecules, its importance in membrane shape transformations is less appreciated. In this talk, I will discuss the significant role played by membrane viscosity in the bending dynamics of highly-curved structures such as liposomes and sub-cellular organelles. We extend the model of Seifert and Langer [Europhys. Lett, 1993] for the dynamics of a planar viscous bilayer to a quasi-spherical vesicle. The theory predicts a slower relaxation rate, $\sim q^4$, for a spherical harmonic mode q , a drastic change from the classic result $\sim q^3$. Flickering spectroscopy, which is the analysis of experimentally recorded thermally-driven shape fluctuations of giant vesicles (GUVs), confirm the theoretical results in the case of phospholipid/cholesterol mixtures and, for the first time, demonstrate that membrane viscosity slows down bilayer undulation dynamics giving the appearance of an effectively stiffer membrane. For scattering techniques such as Neutron Spin Echo, the theory predicts an anomalous diffusion exponent of $1/2$ governing the Dynamic Structure Factor instead of the commonly used $2/3$ [Zilman and Granek, Phys. Rev. Lett. (1996)]. Furthermore, we extend the theory to viscoelastic membranes motivated by the flickering dynamics of block-copolymer vesicles and recent electrodeformation experiments that show a two-time scales response, consistent with Kelvin-Voigt viscoelastic material, in the transient ellipsoidal deformation induced by an applied uniform AC electric field of DMPC vesicles near the melting transition.

This research was supported by NIGMS award 1R01GM140461

11:45 AM SB07.01.04

Impact of Structurally Active Lipids on Lipid Nanoparticle Delivery Processes [Lining Zheng](#) and Cecilia Leal; University of Illinois, United States

RNA therapeutics have the potential to treat many diseases that are not targetable by small molecules. One of the biggest challenges in RNA therapy is RNA delivery. Lipid nanoparticles (LNPs) is one of the most successful RNA delivery systems to date, however the delivery efficiency of LNP systems is still hindered by inefficient endosomal escape. How LNPs impact the endosomal escape process is still poorly understood. In this work, we explore how structurally active lipids that can form bicontinuous cubic and inverse hexagonal phases impact the properties of active model endosomal membranes, to better understand the change of endosomes when lipids from LNPs diffuse into the endosomal membrane. We formed giant unilamellar vesicles (GUVs) with different molar percentages of structurally active lipids, and with fluctuation analysis showed that the bending modulus of the membrane reduces with the increase in structurally active lipid content. The presence of membrane protein can greatly impact endosomal membrane properties, so GUVs with V-ATPase, a membrane protein that is essential to the endosomal escape process, were also formed to model active endosomal membranes.

SESSION SB07.02: Phase Separation in Lipid Materials and Membranes

Session Chairs: Elizabeth Kelley and Cecilia Leal

Tuesday Afternoon, April 23, 2024

Room 439, Level 4, Summit

1:45 PM *SB07.02.01

Liquid-Liquid Phase Separation in Membranes is a Product of Universal Material Properties and Specific Biological Functions [Sarah Keller](#); University of Washington – Seattle, United States

Many lipid membranes reversibly phase separate to form large (micron-scale) liquid domains. These systems vary widely, from simple membranes

composed of only three lipid types to complex membranes of living yeast cells or giant plasma membrane vesicles. Independent of the source of the phase-separating membrane, the size, shape, and behavior of the resulting liquid domains is governed by the membrane's material properties and the physical conditions under which it is held. For example, small domains in flaccid vesicles grow larger as membrane tension increases and as temperature decreases. Similarly, the temperature at which a membrane undergoes liquid-liquid phase separation is influenced by its lipid composition and the surfaces it touches. In simple membranes, these experimental conditions are imposed by researchers. In contrast, yeast cells actively regulate their lipid composition to achieve a particular biological outcome, namely, to maintain an offset between their growth temperature and their membrane transition temperature.

2:15 PM *SB07.02.02

Monolayer Domain Shapes - Equilibrium or Kinetically Controlled? [Joseph A. Zasadzinski](#)¹, Cain Valtierrez-Gaytan¹, Zachary McAllister¹ and Benjamin Stottrup²; ¹University of Minnesota, United States; ²Augsburg University, United States

Lateral phase separation of lipid monolayers and bilayers into domains of different composition or local order is the basis of the "raft" hypothesis of cell membrane organization in which sub-micron domains, or rafts, of different local composition or order nucleate and grow from a continuous phase within the cell membrane. These physical and chemical inhomogeneities within the membrane provide sites for multiple different proteins to localize and carry out complex cell functions. Phase separation and domain formation is also important to the dynamic spreading and surface tension lowering ability of native and clinical lung surfactants (LS) used to treat neonatal respiratory distress syndrome (NRDS) in premature infants. The relative simplicity of two-dimensional lipid monolayer films makes them ideal systems to study the fundamental issues that govern lateral phase separation, the evolution of domain microstructure, and the effects of this microstructure on interfacial dynamics. Here we show that a myriad of domain morphologies that occur during monolayer compression are the result of the classic Mullins-Sekerka growth instability (1) that occurs during crystallization from a multicomponent melt. On compression of dipalmitoylphosphatidylcholine-hexadecanol (DPPC-HD) monolayers with 1-5 mol% cholesterol, originally circular domain develop finger-like growth patterns as the surface pressure is increased. The finger widths and number vary with compression rate and quench depth with semi-quantitative agreement with the predictions of the Mullins-Sekerka theory. The Mullins-Sekerka theory postulates a diffusion front instability that predicts that the finger widths are set by a balance between line tension, crystallization rate, and the local variation in chemical potential between crystal and melt. The fingers are purely kinetically driven but eventually evolve into equilibrium extended stripe domains whose width depend only on surface pressure and temperature. The stripe width is independent of the route by which the morphology is approached, suggesting thermodynamic equilibrium. These observations help explain the wide variety of domain shapes observed in lipid monolayers that depend on compression rate and monolayer history.

2:45 PM SB07.02.03

Tiny Forces from Flow Transport Membrane Proteins on Cell Surfaces [Aurelia Honerkamp-Smith](#); Lehigh University, United States

Many cells sense and respond to flow in their environment, and flow responses regulate important physiological processes such as blood pressure. A paradox in cardiovascular flow sensing is that shear forces applied by blood flow are extremely small, and it is currently unknown how cells detect them. We propose a mechanical solution to this problem: lipid-anchored membrane proteins can be rearranged even by tiny shear forces. We have previously shown that avidin linked to biotinylated lipids in supported membranes forms micron-scale concentration gradients in response to femtonewton-sized shear forces. We observe that in both living cells and glass-supported lipid bilayers, proteins move downstream when flow is on, forming a concentration gradient, and that the gradient disappears when the flow is turned off. This gradient is responsive to flow magnitude and direction and disappears when flow stops. We estimate protein diffusion constants and hydrodynamic areas by observing the gradient dynamics. Our recent work demonstrates the sensitivity of our method for measuring these forces, allowing us to correlate hydrodynamic force with the folded shape of lipid-anchored proteins, distinguish membrane drag on different lipid anchors, and demonstrate that similar protein transport can occur on the surface of living cells. Our results support the hypothesis that lateral transport of membrane proteins may contribute to flow sensing.

3:00 PM BREAK

3:30 PM *SB07.02.04

The Biophysical Tight Rope of Cell Membranes: Lessons Learned from Extreme Lipidome Adaptation in The Deep Ocean [Itay Budin](#); University of California, San Diego, United States

Lipid bilayers are the universal structure of all cell membranes and depend on the propensity of specific phospholipid classes to form fluid lamellar phases. However, no biological membranes are composed entirely of bilayer-forming lipids, instead balancing species with low and high intrinsic curvatures. I will describe how this dynamic plays out in organisms that have adapted to hydrostatic pressure, which increases by 1 atmosphere every 10m in the water column. Small angle x-ray scattering of lipid suspensions from deep sea comb jellies (ctenophores) collected at depths up to 4km revealed a remarkable ability to access non-lamellar lipid phases, which are inhibited by pressure. Lipidomic analysis across a wide range of species identified phospholipids with large, negative spontaneous curvature as a depth-specific adaptation across the phylum. High pressure molecular dynamics of lipidome-derived bilayers supports this adaptation. Using engineered bacterial strains, we found that lipid spontaneous curvature can modulate pressure tolerance. Based on these results, we propose a homeocurvature adaptation model for cell membranes, in which the effect of pressure on lipid shape can contribute to both fitness and specialization in the deep oceans.

4:00 PM SB07.02.05

Nanoscale Molecular Organization in Polymer-Lipid Hybrid Systems using Cryo-Electron Microscopy Analysis of Nanoparticles (NPs) [Nurila Kambar](#) and Cecilia Leal; University of Illinois at Urbana-Champaign, United States

Membranes play an essential role in diverse engineering fields such as biomedicine, energy generation and water treatment. Thus, development of new types of membranes with tailored properties has been an active area of research. Two-component hybrid materials where phospholipid (PL) membrane stacks are hybridized with synthetic block copolymers (BCP) are of great interest due to their ability to combine the unique properties of two different materials. Hybrid membranes can demonstrate a wide range of self-assembled structures and properties that can be tailored to specific applications. The nanoscale arrangement of hybrid membranes into distinct lateral domains with varying structures and compositions is considered crucial for membrane functionality. The precise understanding of this organization has been challenging, primarily due to the absence of direct methods for probing nanoscale membrane features. Utilizing machine learning for the domain analysis of hybrid multilamellar nano-sized vesicles in cryo-TEM images, we are able to precisely generate detailed high-resolution 2D thickness maps of the membranes. These maps provide insights into the distribution of polymer-rich, lipid-rich, and well-mixed domains within the vesicles. Despite the optical microscopy indicating homogeneous mixing in the hybrid membranes, we reveal the coexistence of two distinct membrane structures within homogeneously mixed lipid-polymer hybrid vesicles. In this study, we highlight the significance of our semi-automated technique for directly imaging nanodomains in both biomimetic and biological membranes.

SESSION SB07.03: New Structures in Lipid Materials and Membranes
Session Chairs: Shelley Claridge and Cecilia Leal
Wednesday Morning, April 24, 2024
Room 439, Level 4, Summit

9:00 AM *SB07.03.01

From 2D to 3D: Non-Trivial Membrane Transformation in a Flat World [Irep Gozen](#); Oslo University, Norway

Synthetic cell studies conventionally focus on freely suspended lipid compartments, e.g. micelles and vesicles. This approach is simple and largely satisfactory, but misses the full potential of the 2D fluidic lipid material. On many solid interfaces, non-trivial transformations of biomembrane assemblies occur autonomously. Lipid membrane patches develop into a variety of astonishing morphologies, ranging from unilamellar compartment networks interconnected with nanotubes to densely packed microbial colony-like structures.

In my talk, I will explain how we exploit the tiny energy gain arising from contact of molecular lipid films with solid interfaces to drive the transformation from 2D to 3D assemblies, their architecture, communication and transport properties. The presentation will highlight the implications of the new findings for synthetic cell design, and argue that materials properties-driven autonomous processes on solid interfaces might have had a greater role in the development of life than currently considered.

9:30 AM SB07.03.02

Lipid Cubic Phase Films: Fundamentals and Applications [Adam Squires](#); University of Bath, United Kingdom

We present work on films of lipid cubic phases: 3D periodic nanomaterials that spontaneously self-organise in the presence of water. We form these films at the solid-liquid and solid-vapour interface, and probe their structures using grazing-incidence small-angle X-ray and neutron scattering. We present fundamental work understanding the orientation of the films; and show how we use them in different applications, including templates for high area metal nanomaterials, matrices for biosensors, and as a method to probe curvature-driven localisation of membrane-incorporated molecules.

9:45 AM SB07.03.03

Molecular Structure and Dynamics of Lipid Nanoparticles via Small-Angle Scattering [Shayna Hilburg](#) and Lilo D. Pozzo; University of Washington, United States

Lipid nanoparticles have revolutionized human health outcomes, as evidenced by the mRNA vaccines used to combat COVID-19. Despite the success of these self-assembled nucleic acid therapeutics, the physicochemical fundamental properties of the non-viral delivery vectors must be better understood to be more easily tuned and optimized. In this work, we use small-angle X-ray (SAXS) and neutron scattering (SANS) to provide a nanoscale picture of the lipid nanoparticles. Specifically, we investigate how the environmental changes lipid nanoparticles experience during storage and delivery and the fundamental properties of macromolecular cargo impact particle structure and dynamics. The effects of lipid charge state and nucleic acid properties are studied through static SAXS and SANS measurements as well as time-resolved SANS, which provides insight into molecular exchange. Such information demonstrates what drives degradation in storage, what parameters can be changed to improve component dissociation allowing more efficient endosomal escape, and how nucleic acid properties can impact lipid formulation selection.

10:00 AM BREAK

10:30 AM SB07.03.04

How an Extra Terminal Group on Fatty Acids Leads to The Formation of Nanostructured Langmuir Films? [Honghu Zhang](#)¹, Benjamin M. Ocko¹, Alexei V. Tkachenko¹, Guangcui Yuan² and Sushil K. Satija²; ¹Brookhaven National Laboratory, United States; ²National Institute of Standards and Technology, United States

A characteristic of fatty acids (FAs) covalently associated with fur and hair is two terminal methyl groups rather than the single methyl group found in simple FAs. When these FAs form Langmuir monolayers, the geometric constraint of the extra methyl group leads to periodic lateral nanostructures, a feature that doesn't appear in simple FAs. To unravel the nature of these nanostructures on aqueous surfaces we use in-situ surface X-ray scattering techniques directly on Langmuir monolayers. In our experiments, we investigate surface films prepared using 19-methyleicosanoic acid (19MEA) at different surface pressures with X-ray reflectivity (XRR) and grazing-incidence small-angle and wide-angle X-ray scattering (GISAXS/GIWAXS) methods. Our in-situ results reveal that interfacial 19MEA molecules self-assemble into two-dimensional (2D) hexagonal lattices of objects that resemble squished half hemispheres with a lateral lattice constant of 40-50nm. Surprisingly, this length uncovered by the GISAXS measurements is nearly 100 times that of the molecular width. Complementary GIWAXS studies show that the lateral order between the individual hydrocarbon chains is similar to simple FAs. With increasing of surface pressure, the lattice constant shrinks and the surface roughness measured by XRR increases from that found for simple FAs to a value which is 3 times larger. We have also measured the phase diagram of mixtures of 19MEA with arachidic acid, a simple FA. With increasing of the arachidic acid composition, we have found a cross-over from a hexagonal to a 1D nanostructure. A real-space model and a theoretical framework have been developed to explain the self-assembly behavior of the FAs that have two terminal methyl groups. This combined experimental and theoretical work provides a basis for understanding the unusual nanostructures which form in these simple molecular systems.

10:45 AM SB07.03.05

Nanoscale Confinement of Dip-Pen Nanolithography Written Phospholipid Structures on CuZr Nanoglasses [Srivatsan K. Vasantham](#)¹, Evgeniy Boltynjuk¹, Harald Fuchs², Horst W. Hahn^{1,3} and Michael Hirtz¹; ¹Institute of Nanotechnology, Germany; ²Universität Münster, Germany; ³The University of Oklahoma, United States

In the realm of materials science, nanoglasses have intrigued researchers due to their unconventional properties. However, their interaction with biomaterials and their effects on living cells remain insufficiently understood. Previous studies hinted at proliferation effects, but distinguishing these from other material or topography effects has been challenging. In this research, we explored how nanoglass surfaces interact with phospholipids, crucial components of cell membranes. Our study uncovered a distinctive confinement effect exhibited by nanoglasses on lipid structures patterned with dip-pen nanolithography. Dip-pen Nanolithography with phospholipids (**L-DPN**) utilizes the fine tip of an atomic force microscope, covered with phospholipid mixtures, for writing nanostructures of lipid membranes onto various substrates. These structures are used as probes for the lipid/nanoglass interaction. Our study revealed distinct differences between homogeneous (regular) metal glasses and their nanoglass counterparts of same chemical composition in regard to lipid spreading and membrane organization. Our findings show that nanoglasses interact profoundly different with L-DPN written membranes, which suggests a potential influence on cell membrane structures. The results can shed light on a possible mechanism for their impact on cell behavior and can inform future studies on nanoglass/cell interactions.

SESSION SB07.04: Lipid Nanoparticles for Drug and Gene Delivery
Session Chairs: Elizabeth Kelley and Cecilia Leal
Wednesday Afternoon, April 24, 2024
Room 439, Level 4, Summit

1:30 PM *SB07.04.01

Acid Degradable Lipid Nanoparticles Efficiently Deliver mRNA to The Liver, Lung, Spleen and Multiple Other Organs [Niren Murthy](#)^{1,2};

¹University of California, Berkeley, United States; ²U.C. Berkeley, United States

The development of acid degradable linkers that rapidly hydrolyze at endosomal pHs is a central problem in the field of drug delivery. Acid degradable linkages are challenging to develop because of their instability. In this report we present a new acid degradable linker based on an azide-acetal, which rapidly hydrolyzes at endosomal pHs but has exceptional stability at pH 7.4. The azide-acetal linkage hydrolyzes via a two-step mechanism that requires reduction and acid hydrolysis and has a unique combination of stability and rapid triggerable hydrolysis. The azide-acetal has a hydrolysis half-life of days at pH 7.4 and can be conveniently synthesized and incorporated into delivery vectors, however after *in situ* reduction with DTT it hydrolyzes with a $t_{1/2} < 15$ minutes at pH 6.0. We used the azide-acetal linker to synthesize acid degradable analogs of the lipid components of lipid nanoparticles and demonstrate that these new lipids are significantly better at delivering mRNA to mice than traditional lipids. Lipid nanoparticles containing acid degradable lipids transfected multiple non-liver organs after an intravenous injection and efficiently transfected brain tissue after an intracranial injection. The azide-acetal linkage has the potential to solve the instability problems associated with acid degradable linkers and has numerous applications in drug delivery.

2:00 PM *SB07.04.02

Preformed Vesicle-Mediated Delivery of Messenger RNA for Retinal Gene Therapy [Gaurav Sahay](#); Oregon State University, United States

Quantitative nucleic acid encapsulation by lipid-based nanoparticles (LNPs) is often thought to be one of the main prerequisites for successful cargo delivery, as the lipid environment protects mRNA from degradation by external nucleases and assists in initiating delivery processes. However, here we report the delivery of mRNA via preformed vesicle approach (PFV-LNPs) that defies this precondition. PFV-LNPs possess superficial mRNA localization that proved exceptionally beneficial in delivering mRNA to the back of the eye. Successful delivery of GFP mRNA to retinal pigment epithelium and photoreceptors was observed in mice, non-human primates, and human retinal organoids. This approach was generally beneficial as indicated by improved EGFP transfection with PFV-LNPs containing benchmark lipids (We posit that the PFV architecture may be beneficial to transfect local targets like the back of the eye. We will also discuss the impact of surface modifications for LNP mediated gene editing.

2:30 PM BREAK

3:30 PM *SB07.04.03

Stimuli-Responsive Liposomes for Triggered Cargo Release and Activated Cell Delivery [Michael Best](#) and Jinchao Lou; University of Tennessee Knoxville, United States

Liposomal nanocarriers are effective for the encapsulation and delivery of a wide range of therapeutic cargo in a manner that improves drug pharmacokinetic properties. However, liposome therapeutic properties could be advanced by enhancing control over cell delivery as well as cargo release. This presentation will describe the development of stimuli-responsive liposomes designed to achieve both of these goals. One approach employs synthetic lipid switches engineered to modulate lipid membrane properties upon contact with disease-associated conditions, such as through programmed chemical reactions and/or conformational changes. In particular, we will focus on encapsulated cargo release triggered by the binding of chemical agents/molecules that are commonly upregulated in diseased cells. A second strategy involves chemically triggering of cell entry. In this design, liposomes are masked as neutral carriers until they encounter stimuli that generate cationic lipids, thereby activating cell entry. The presentation will include the design and synthesis of stimuli-responsive lipid switches, analysis of selectivity of cargo release in the presence of different stimuli, investigation of changes to liposome membrane properties, and evaluation of cellular delivery properties triggered by disease-associated stimuli.

4:00 PM SB07.04.04

Poly(N-Vinyl Amide)-Lipid Conjugates as Poly(Ethylene Glycol) Alternatives for The Modification of Lipid-Based Nanocarriers [Antoine Debuigne](#), Manon Berger, François Toussaint, Sanaa Ben Djemaa, Christine Jerome, Anna Lechanteur, Denis Mottet and Geraldine Piel; University of Liege, Belgium

Pegylation of drug nanocarriers, and of lipid-based vectors in particular, is a common strategy to grant them stealth properties and promote their prolonged circulation in the blood stream. However, PEG is also associated to the accelerated blood clearance (ABC) effect, leading to the fast elimination of the medicine from the body, and to the PEG *dilemma*, which consists in uptake issues due to the presence of the polymer layer around the carrier. For these reasons, the search for PEG alternatives in drug delivery systems is timely.

This work explores the potential of poly(N-vinyl amide)s, including poly(N-vinyl pyrrolidone) (PNVP), as PEG alternatives for the development of non-toxic, efficient and less immunogenic lipid-based carriers, in particular siRNA-loaded lipoplexes and lipid nanoparticles dedicated to gene therapy.^{1,2} For this purpose, novel poly(N-vinyl amide)-lipid conjugates were synthesized by reversible deactivation radical polymerization. This strategy allowed to control the molar mass of the hydrophilic polymer sequence and to functionalize its extremity with lipids, such as 1,2-distearoyl-sn-glycero-3-phosphoethanolamine (DSPE), to ensure their anchoring at the surface of the lipid carriers. The surface active properties of these poly(N-vinyl amide)-lipid conjugates and their interaction with phospholipid bilayers were studied by Langmuir film balance and quartz crystal microbalance with dissipation monitoring (QCM-D), respectively. The anchoring of the poly(N-vinyl amide)-lipid compounds at the surface of siRNA-loaded lipid nanocarriers and their ability to prevent protein adsorption were demonstrated by dynamic light scattering, zeta potential and nanoparticles tracking analyses. *In vitro* and *in vivo* studies demonstrated the non-toxicity, stealth properties and transfection efficiency of the accordingly modified siRNA-loaded lipid nanocarriers. Importantly, compared to their pegylated counterparts, lipid nanocarriers decorated by poly(N-vinyl amide)s showed lower immunogenicity in particular after the second injection which constitutes a key step to the development of safer lipid-based carriers.

1. Berger, M.; Toussaint, F.; Djemaa, S. Ben; Laloy, J.; Pendeville, H.; Evrard, B.; Jérôme, C.; Lechanteur, A.; Mottet, D.*; Debuigne, A.*; Piel, G.* Poly(Vinyl Pyrrolidone) Derivatives as PEG Alternatives for Stealth, Non-Toxic and Less Immunogenic siRNA-Containing Lipoplex Delivery. *J. Control.*

Release 2023, 361, 87–101. <https://doi.org/10.1016/j.jconrel.2023.07.031>.

2. Patent Application EP23171538.4 “Polymer Derivatives and their use as lipid nanoparticle modifiers”. Inventors : Antoine Debuigne,* Géraldine Piel,* Denis Mottet,* François Toussaint, Manon Berger, Sanaa Bendjema, Anna Lechanteur.

Funding: LIPEGALT-ARC project (Concerted Research Action program), National Fund for the Scientific Research FNRS.

4:15 PM SB07.04.05

Biodegradable Polymer-Lipid Nanoparticles for Effective *In Vivo* mRNA Delivery [Yiyang Yang](#)¹ and James Hedrick²; ¹Bioprocessing Technology Institute, Agency for Science, Technology and Research (A*STAR), Singapore; ²IBM Almaden Research Center, United States

Currently, only 2 mRNA Covid-19 vaccines from Moderna and Pfizer-BioNtech have been approved by the US FDA for human use. Both vaccines utilize SARS-CoV-2 mRNA as the antigen and lipids as the carrier. The lipids consist of 3 different types of lipids (PEG-lipid conjugate, ionizable lipid and helper lipid) and cholesterol. The ionizable lipid condenses mRNA into lipid nanoparticles (LNPs) through electrostatic interaction and self-assembly. The mRNA-loaded LNPs stimulate the immune cells for prophylactic response against the SARS-CoV-2 virus. The use of PEG-lipid (ALC-0159) makes the LNPs unstable *in vivo*, leading to delivery of mRNA primarily to the liver after *i.v.* injection of mRNA LNPs. In this study, we synthesize amphiphilic block copolymers of PEG and biodegradable polycarbonate with varying chain length and urea moiety to replace PEG-lipid conjugate. Urea functional groups are used to form hydrogen-bonding interactions within the LNPs to further increase the stability of LNPs. Luciferase-encoded mRNA is loaded into lipid nanoparticles by using a microfluidic device. Use of amphiphilic polycarbonate block copolymers enhances the stability of mRNA-loaded nanoparticles in serum-containing medium while yielding high transfection efficiency of mRNA in mice. The introduction of polycarbonates alters their biodistribution *in vivo*. The polymer-lipid nanoparticles with enhanced stability may be used to deliver mRNA to T cells for cancer therapy.

4:30 PM SB07.04.06

Membrane Fusion Mediated Drug Loading in Exosomes [Hojun Kim](#); Korea Institute of Science and Technology, Korea (the Republic of)

Exosome-based drug delivery gaining a significant interest from bioindustry. Compared with conventional delivery vehicles, exosomes offer minimized immunogenicity, increased circulation stability, and exceptional permeability across various biological barriers. Such distinct characteristics make exosomes as a promising next-generation delivery platform. Despite of the therapeutic potential, however, there are multiple challenges remained. Among many, drug loading in exosome is recognized as one of the major challenges. This is because current approaches not only show poor drug loading efficiency but lead to side effects such as hemolysis due to foreign components. In addition, the size of therapeutic molecules is also limited with conventional approaches. Therefore, developing a new way of loading technology in exosome is in urgent need.

Here we devised a novel drug loading approach utilizing a highly fusogenic lyotropic liquid crystal nanoparticles. We inspired from the fact that endosome and exosome share its biological origin. Because lipid-based lyotropic liquid crystal nanoparticles are known to easily fuse with endosome, we hypothesized that it can also easily fuse with exosome thereby delivering its cargo. Our synchrotron SAXS and FRET based study revealed that fusion-mediated drug loading shows a high loading efficiency with only innate materials. Our results indicate that the fusion-mediated loading method can be a fruitful approach for exosome therapeutics.

4:45 PM SB07.04.07

Block Polymers of Acryl Derivatives Using Raft Polymerization as PEG Alternatives for mRNA Delivery [Hema Choudhary](#), Rohit Sharma and Niren Murthy; University of California Berkeley, United States

Lipid nanoparticles (LNPs) have emerged as an important class of non-viral delivery methods for mRNA delivery for various applications including, gene editing, vaccine development, and protein replacement therapy. The performance of LNPs is influenced by several factors including stability to proteases, protein absorption, pharmacokinetics, and immunogenicity. Poly (ethylene glycol) (PEG) is the most used polymer in nanomedicine and is a gold standard for improving LNP performance. Nevertheless, this overwhelming use of PEG for biomedical applications is resulting in anti-PEG antibody formation in PEGylated drug-treated patients. This presents an immense challenge in mRNA-based vaccine development and protein replacement therapies which requires multi-dosage delivery over a period. Consequently, there is a great need to explore alternative polymers that mimic the physiochemical properties of PEG.

Here, we present a simple approach to synthesize PEG alternative polymers for mRNA delivery. Our approach involves a synthesis of block polymers with acryl derivatives monomers using a reversible addition–fragmentation chain transfer (raft) polymerization strategy. We have synthesized a library of hydrophilic polymers with various functional groups on the polymer backbone using commercially available monomers such as N-(2-Hydroxypropyl) methacrylamide (HMPA), acrylamide, (Hydroxyethyl)methacrylate as well as in lab synthesized sugar methacrylamides. To test the drug efficacy of these polymers, LNPs were formulated by complexing mRNA with standard lipids (Dlin-MC3, DOPE, cholesterol), and stabilized using our block hydrophilic polymers. These LNP/mRNA complexes were investigated *in-vitro* (HEK293 cells) and *in-vivo* in mice. Data from these studies will be presented in this talk.

We expect these functional groups on the polymer backbone to attribute interesting behavior to the LNPs. In this regard, our mannose-polymer stabilized LNPs showed spleen-targeted delivery of luciferase mRNA in comparison to PEG-stabilized LNPs.

SESSION SB07.05: Poster Session
Session Chairs: Shelley Claridge and Cecilia Leal
Wednesday Afternoon, April 24, 2024
Flex Hall C, Level 2, Summit

5:00 PM SB07.05.01

Angiopep2-Functionalized Lipid Cubosomes for Blood-Brain Barrier Crossing and Glioblastoma Treatment [Xudong Cai](#), Jiali Zhai, Nhiem Tran and Calum Drummond; RMIT University, Australia

Background: Glioblastoma multiforme is an exceptionally aggressive form of brain cancer known for its high malignancy and resistance to traditional treatments, leading to a bleak prognosis for patients. Various treatment methods, such as surgery, radiotherapy, and chemotherapy, have been developed to address brain diseases; however, they often come with significant side effects on healthy tissues. Additionally, delivering drugs from the bloodstream to the brain is hindered by the presence of the blood-brain barrier (BBB). Lipid nanoparticles have gained substantial interest because of their inherent benefits,

including biocompatibility, facile surface functionalization for targeted drug delivery, and improved solubility for poorly soluble drugs. These distinctive features make them promising carriers for bioactive agents to cross the BBB.

Aims: In this study, we have pioneered the development of Ang2-conjugated cubosomes, an approach aimed at enhancing BBB penetration and improving the uptake of glioblastoma cells. Our previous research successfully yielded a range of amphiphilic block copolymers, synthesized through RAFT polymerization, which included polyethylene glycol (PEG), poly(2-(dimethylamino)ethyl methacrylate) (PDMAEMA), and poly(4-(4,4,5,5-tetramethyl-1,3,2-dioxaborolan-2-yl)benzyl acrylate) (PTBA). These polymers served as effective stabilizers for monoolein cubosomes with pH nad H₂O₂ responsiveness. In this study, we selected PEG114-b-PDMAEMA17-b-PTBA9-RAFT polymer to craft Ang2-conjugated monoolein-based cubosomes, loaded with the anti-cancer drugs cisplatin (CDDP) and temozolomide (TMZ), which are known for their poor solubility.

Methods: A comprehensive analysis of these developed nanoparticles was conducted to assess their particle size, surface charge, and internal structures through dynamic light scattering and synchrotron Small-Angle X-ray Scattering. Furthermore, their potential to enhance BBB penetration was evaluated using three in vitro models: a Transwell BBB model based on the hCMEC/D3 human brain endothelial cell line, a 3D hCMEC/D3 spheroid model, and an innovative microfluidic BBB/GBM-on-a-chip model. This microfluidic model featured a unique setup with hCMEC/D3 cells in one channel (representing the blood channel) and U87 glioblastoma cells in an adjacent, interconnected channel (representing the brain channel). This design enabled the simultaneous investigation of the cubosomes' ability to cross the BBB and enter U87 cells. To further evaluate the anticancer effectiveness of CDDP/TMZ-loaded cubosomes, in vitro cytotoxicity studies on U87 glioblastoma cells was conducted.

Results: These developed lipid cubosomes exhibited a particle size of approximately 300 nm, possessed an internally ordered inverse primitive cubic phase, achieved a high conjugation efficiency of Ang2 on the particle surface, and displayed an encapsulation efficiency exceeding 70% for both CDDP and TMZ. We employed various in vitro BBB models, including hCMEC/D3 cell Transwell assays, 3D spheroid cultures, and microfluidic BBB/GBM-on-a-chip models, to evaluate the effectiveness of these cubosomes in crossing the BBB. The results demonstrated that Ang2-functionalized cubosomes exhibited superior BBB penetration. Furthermore, these modified cubosomes exhibited significantly increased uptake by U87 glioma cells, with a notable three-fold enhancement observed in the BBB/GBM-on-a-chip model compared to unmodified cubosomes. Moreover, CDDP-loaded Ang2-functionalized cubosomes exhibited a heightened toxic effect on U87 glioma spheroids.

Conclusion: These findings suggest that the Ang2-functionalized cubosomes hold great promise for improving BBB penetration and enhancing the delivery of therapeutics to glioblastoma.

5:00 PM SB07.05.02

Electrokinetic Enhancement of Membrane Techniques for Efficient Nanoparticle Separation and Enrichment Ji Hyo Park^{1,2}, Jae Sung Yoon^{1,3}, Do-Hyun Kang¹, Yeong-Eun Yoo^{1,3} and Kwanoh Kim¹; ¹Korea Institute of Machinery and Materials, Korea (the Republic of); ²Seoul National University, Korea (the Republic of); ³University of Science and Technology, Korea (the Republic of)

Separation and preconcentration of colloidal nanoparticles are pivotal in various biomedical applications, notably bioprocessing and biochemical detection. While membrane-based techniques are recognized for their efficiency and versatility, diminishing particle sizes pose challenges such as increased flow resistance, escalated back pressure, and issues with particle retrieval due to adsorption onto membranes. In this study, we introduced an electric field-assisted membrane system, integrating conductive metal-coated membranes. By leveraging the electrokinetic effects from voltage application to the membranes, our system adeptly separated and retrieved nanoparticles even finer than the membrane pores. Experiments with polystyrene nanoparticles demonstrated separation efficiencies surpassing 95% and enrichment factors approaching 1.8 folds within 10 minutes. The pressure drops measured across the membranes were significantly lower than that observed in conventional systems with narrower pore sizes, particularly at elevated flow rates. Moreover, the pressure drop exhibited consistent stability over time, suggesting reduced membrane fouling. This approach offers an energy-efficient, high-throughput method for nanoscale particle separation and enrichment, holding promise for point-of-care diagnostics and progressive biomanufacturing.

5:00 PM SB07.05.03

Diet-Induced Obesity Modulates Close-Packing of Triacylglycerols in Lipid Droplets of Adipose Tissue Kyungwon Ko¹, Sarith R. Bandara¹, Weinan Zhou¹, Leo Svenningsson², Marilyn Porras-Gomez¹, Nurila Kamar¹, Julia Dreher-Threlkeld¹, Daniel Topgaard², Diego Hernandez-Saavedra¹, Sayeepriyadarshini Anak¹ and Cecilia Leal¹; ¹University of Illinois at Urbana-Champaign, United States; ²Lund University, Sweden

Adipose-derived lipid droplets (LDs) are rich in triacylglycerol (TAGs), which regulate essential cellular processes such as energy storage. Although TAG abundance in adipocytes has been linked to metabolic disorders, including obesity and metabolic syndromes, how LDs dynamically package TAGs in response to excessive nutrients remains elusive. Here, we found that LD lipidomes display a remarkable increase in TAG acyl chain saturation under calorie-dense diets turning them conducive to close-packing. Using high-resolution X-ray diffraction, solid-state NMR, and imaging, we show that beyond size expansion, LDs from mice under varied obesogenic diets govern fat accumulation by packing TAGs in different crystalline polymorphs. Consistently, LD membrane tension and tissue elastic modulus in high-calorie-fed mice doubled compared to normal diet. Our data suggest that in addition to expanding, adipocyte LDs undergo structural remodeling in response to caloric overload, close-packing rigid and highly saturated TAGs. This work could enable the development of new therapeutics for LD-involved pathologies.

5:00 PM SB07.05.04

Outer Membrane Vesicles as a Multicomponent Lyme Disease Vaccine Stephanie Curley, David Krimer and Bennett Beaulieu; Union College, United States

Lyme disease, caused by the bacteria *Borrelia burgdorferi* (Bb), is the most common vector-borne disease in the United States. It is transmitted by ticks, causing symptoms ranging from mild (fevers, headaches, and the characteristic erythema migrans rash), to severe (arthritis, carditis, and neuroborreliosis) if left untreated. Although mainly prevalent in the northeastern U.S., due to the changing climate, Lyme is expected to become even more widespread in the coming decades. Current treatment is limited to antibiotics, which often do not fully treat the infection. While there previously was an FDA-approved vaccine for human use, it was withdrawn from the market because of low sales due to high consumer cost and unfounded public fear of side effects. Development of a cheap and effective alternative vaccine for Lyme is needed.

Outer membrane vesicles (OMVs), spherical lipid bilayers naturally produced by bacteria, may provide the simple, cost-effective platform necessary to develop an effective Lyme vaccine. OMVs hold a plethora of macromolecules in their membranes that can enhance the immune response to the antigen of interest when co-delivered. There have been two previous studies on an OMV-based vaccine against Lyme Disease using meningococcal OMVs carrying the *Bb* antigen outer surface protein A (OspA). However, research suggest that a multi-antigenic approach for Lyme disease vaccination may be crucial for proper immune recognition.

Here, we investigated whether Lyme antigens could be effectively expressed on the surface of OMVs derived from a strain of *Clearcoli* that have been genetically modified to hypervesiculate. Bacterial surface protein cytolysin A (ClyA) was used as a fusion partner to assist in surface presentation of the

antigen proteins. Three outer surface proteins from Bb (RevA, OspC, and OspA) were successfully expressed as fusion partners to ClyA, as shown by SDS PAGE and western blot. After efficient expression was confirmed, OMVs expressing ClyA-Lyme antigen fusion proteins were produced from Clearcoli. OMVs expressing fusion proteins were evaluated using dynamic light scattering, and showed an average size of ~140 nm, which is slightly larger than OMVs that did not contain the fusion proteins. Furthermore, surface presentation of the ClyA-Lyme antigen proteins was confirmed using the protease accessibility assay. Future work will focus on evaluating the adaptive immune response of these vaccine platforms an animal model.

5:00 PM SB07.05.05

Bioinspired Glycolipids - Applications for Mitigating Airborne Dust Pollution [Damask Grinnell](#), Taehee Lee, Raina Maier, David Hogan and Minkyu Kim; The University of Arizona, United States

Airborne dust particulates are a major constituent of total atmospheric pollution affecting global environmental and human health that must be urgently mitigated. Particulate matter (PM) with diameter < 10 µm is deeply inhaled into the lungs, causing significant human health risks particularly for cardiovascular and respiratory health. PM is also environmentally harmful, affecting global biogeochemical cycles, polluting water bodies and air masses, and impacting global climate. Control of fugitive dust emissions is a major operational challenge to various industries including construction, agriculture, transportation, energy, and mining. Previous dust suppressant materials have included amphiphilic synthetic polymers as water additives, which interact with dust particles after water evaporation due to their amphiphilic properties and encourage particle agglomeration, thus suppressing dust generation. However, these synthetic polymers and other conventional dust suppressant materials have short-term effectiveness, are corrosive to machinery, and increase toxicity concerns to both humans and the environment.

Herein, bioinspired glycolipids are being investigated as alternative dust suppressants to conventional amphiphilic polymers. Glycolipids are naturally-occurring molecules consisting of sugar and lipid moieties, thus making them amphiphilic molecules with both hydrophobic and hydrophilic properties. While glycolipids can be extracted from bacterial membranes, there are issues with batch size and ill-defined and inconsistent mixtures, causing further problems for quality control. By synthetically manufacturing glycolipids, quality control issues are mitigated, and the processing provides the ability to modify their molecular structures and physicochemical properties.

We have investigated the relationship between dust suppression performance and molecular structures of glycolipids by varying (1) sugar head type, (2) sugar head number, (3) lipid tail length and (4) lipid tail number. Static and dynamic characterization methods have revealed that specific sugar heads, lipid tail lengths, and number of sugar heads/lipid tails influence the self-assembled structures of glycolipids and their interactions with dust particles, resulting in enhancing or diminishing of dust suppression capabilities. Specifically, glycolipids with single rhamnose and xylose sugar head demonstrated up to 90% better dust suppression performance compared to the water control, and both types also produced further enhanced dust suppression properties as their lipid tail lengths increased. Furthermore, those glycolipids with double lipid tails demonstrated excellent dust suppression performance > 95% better than the water control, indicating that the addition of a second lipid tail may enhance the wetting interaction of the glycolipids with small particles. This was further investigated through ATR-FTIR, DLS and SEM, and specific details will be discussed. Additionally, thermal characterization via DSC shows that several glycolipid types undergo a phase change to liquid at approximately 50°C and maintain the liquid phase at normal temperature. Our previous work with liquid amphiphilic polymers has shown that they are highly effective dust suppressants because their liquid phase facilitates more efficient physical interactions between the polymer and small particles, and this glycolipid phase change mechanism appears to follow a similar mechanism to those previously observed.

This work presents that bioinspired glycolipids are promising dust suppressant materials, and the ability to tune their molecular structures allows us to further enhance their dust suppression performance. Our findings are expected to facilitate the development of highly-efficient glycolipid structures to effectively reduce airborne dust levels contributing to enhanced human health and environmental safety.

SESSION SB07.06: Lipid Materials and Membranes in Living Systems

Session Chairs: Aurelia Honerkamp-Smith and Cecilia Leal

Thursday Morning, April 25, 2024

Room 439, Level 4, Summit

9:00 AM *SB07.06.01

How to Build a Synthetic Virus without a Living Host for Vaccination [Susan Daniel](#)¹, Neha Kamat², Hector Aguilar-Carreno¹, Ekaterina Selivanovitch¹, Vivian Hu² and Shahrzad Ezzatpour¹; ¹Cornell University, United States; ²Northwestern University, United States

There are 1.6 million mammalian and waterfowl viruses (Bull.WHO, 2018; 96:292). Even though only a miniscule set of these are known to infect humans, the potential that additional zoonotic viruses exist is high. Moreover, the natural evolution of viruses is rapid and hard to predict. Our best defense against viral illness is to train our immune system to recognize a threat before we are exposed to it. While vaccines address this need, we are largely ill-prepared to design, manufacture, and distribute vaccines rapidly during a pandemic outbreak. To stay abreast of viral threats, we must transform our approach to vaccine science and engineering. mRNA vaccines are one approach, as are "virus-like particle (VLP) vaccines. Our team takes another approach; we use synthetic biology and engineering to build a proteo-lipid nanoparticle vaccine that is easy to synthesize, tunable in antigen(s) presentation, nonvirulent, and eliminates cell production currently required to generate both VLP vaccines or the expression of the antigen from mRNA lipoparticles. We have achieved the successful cell-free synthesis of Nipah virus viral coat proteins embedded into lipid vesicles using our synthetic biology approach and show that the nanoparticles we created elicit neutralizing antibodies in mice. We have also successfully synthesized into lipid vesicles the full transmembrane Spike protein from coronavirus and hemagglutinin from influenza into lipid nanoparticles using cell-free approaches. This synthetic approach enables molecular-level modification that can be guided by computational and data-driven design approaches, leading to a modular approach to vaccine optimization. New insights into fundamental mechanisms of immune response will be enabled by unprecedented homogeneity of the particle structure possible with this approach.

9:30 AM *SB07.06.02

Probing The Physical Properties of Therapeutic Carriers that Modulate Uptake by Clathrin-Mediated Endocytosis [Grant Ashby](#) and Jeanne C. Stachowiak; The University of Texas at Austin, United States

Cell surface receptors facilitate signaling and nutrient uptake. These processes are dynamic, requiring receptors to be actively recycled by endocytosis. Due to their differential expression in disease states, receptors are often the target of drug-carrier particles, which are adorned with ligands that bind specifically

to receptors. These targeted particles are taken into the cell by multiple routes of internalization, where the best-characterized pathway is clathrin-mediated endocytosis. Most studies of particle uptake have utilized bulk assays, rather than observing individual endocytic events. As a result, the detailed mechanisms of particle uptake remain obscure. To address this gap, we have employed a live-cell imaging approach to study the uptake of individual liposomes as they interact with clathrin-coated structures. By tracking individual internalization events, we find that the size of liposomes, rather than the density of the ligands on their surfaces, primarily determines their probability of uptake. Interestingly, targeting has the greatest impact on endocytosis of liposomes of intermediate diameters, with the smallest and largest liposomes being internalized or excluded, respectively, regardless of whether they are targeted. These findings, which highlight a previously unexplored limitation of targeted delivery, can be used to design more effective drug carriers. Our ongoing work is examining the coupling between multiple physical parameters – size, targeting, rigidity, surface charge – during individual particle uptake events, toward a better understanding of the design space for effective particle-based delivery of therapeutics to cells.

10:00 AM BREAK

10:30 AM *SB07.06.03

Smart Blood: Red Blood Cell based Drug Carriers Maikel Rheinstadter; McMaster University, Canada

The era of one-disease-one-pill is long gone. We are now tackling complex diseases such as Alzheimer's disease, cancer, and infectious diseases. With moderate progress, it has become clear in recent years that complex diseases require sophisticated solutions. A significant hurdle in this process is the effective delivery of drugs to specific targets within the patient's body to increase the drug's efficacy and reduce the side effects common with conventional drugs. To accomplish this goal, drugs are encapsulated in or conjugated to nanocarriers and selectively delivered to their targets. Potential applications include immunization, delivering anti-cancer drugs to tumors, antibiotics to infections, targeting resistant bacteria, and delivering therapeutic agents to the brain. Despite this great promise and potential, drug delivery systems have yet to be established, mainly due to their limitations in physical instability and rapid clearance by the host's immune response. Recent interest has focused on using red blood cells (RBC) as drug carriers due to their naturally long circulation time, flexible structure, and direct access to many target sites. This includes coating nanoparticles with the membrane of red blood cells and the fabrication and manipulation of liposomes made from the red blood cells' cytoplasmic membrane. The properties of these erythrocyte liposomes, such as charge and elastic properties, can be tuned through the incorporation of synthetic lipids to optimize physical properties, loading efficiency, and retention of different drugs. Specificity can be established through the anchorage of antigens and antibodies in the liposomal membrane to achieve targeted delivery. Although still at an early stage, this erythrocyte-based platform shows promising results in vitro and in animal studies. A large part of the challenge is related to material science, involving the manipulation of biological materials at the molecular level. I will review the current status and recent progress in the field.

11:00 AM SB07.06.04

Erythro-PmBs: A Selective Polymyxin B Delivery System using Antibody-Conjugated Hybrid Erythrocyte Liposomes Hannah Krivic, Sebastian Himbert and Maikel Rheinstadter; McMaster University, Canada

Due to the growing worldwide antibiotic resistance crisis, many currently available antibiotics have become ineffective as bacteria develop resistance mechanisms. Only a limited number of potent antibiotics can successfully suppress microbial growth; however, these are often considered a last resort due to their toxicity. We have developed a novel PmB delivery system by conjugating hybrid erythrocyte liposomes with antibacterial antibodies to combine high loading efficiency with targeted delivery [1,2]. The retention of PmB is enhanced through the incorporation of the negatively charged lipid, DMPS, into the red blood cell's cytoplasmic membrane through electrostatic interactions. Molecular dynamics (MD) simulations reveal an optimal fraction of DMPS in the hybrid erythrocyte membranes that allows for complete anchorage of PmB by inserting their acyl tail into the hydrophobic membrane core. Anti-Escherichia coli antibodies are attached to these hybrid erythrocyte liposomes using DSPE-PEG maleimide linkers. Our studies demonstrate that these erythro-PmBs have a loading efficiency of approximately 90% and effectively deliver PmB to E. coli, with minimum inhibitory concentration (MIC) values comparable to those of free PmB. However, the MIC values for Klebsiella aerogenes significantly exceeded the resistance breakpoint, indicating that the inclusion of anti-E. coli antibodies enables erythro-PmBs to selectively transport antibiotics to specific targets. MD simulations further suggest a fusion or lipid exchange mechanism between erythro-PmBs and the outer membrane of E. coli.

[1] Krivic, H., Himbert, S., Sun, R., Feigis, M. and Rheinstadter, M.C., 2022. Erythro-PmBs: A Selective Polymyxin B Delivery System Using Antibody-Conjugated Hybrid Erythrocyte Liposomes. ACS Infectious Diseases.

[2] Krivic, H., Himbert, S., and Rheinstadter, M.C., 2022. Perspective on the Application of Erythrocyte Liposome-Based Drug Delivery for Infectious Diseases. Membranes, 12(12), p.1226.

11:15 AM *SB07.06.05

How Anisotropic Surface Chemistry Changes The Nano-Biomembrane Interaction: From Janus Nanoparticles to Viruses Yan Yu; Indiana University-Bloomington, United States

The non-uniform surface chemistry is ubiquitous for both naturally occurring and engineered nanoparticles. Microbes, such as viruses, are known to have anisotropic presentation of proteins on their surfaces. Engineered nanoparticles are often designed to have heterogeneous surface chemistries to enable novel applications. How does the anisotropic chemistry of nanoparticles impact their interactions with biological membranes and cells? More importantly, can we take advantage of the anisotropic surface chemistry to reverse-engineer nano-bio interactions? In this talk, I will present my group's recent research progress toward addressing those questions. On the one hand, using engineered "two-faced" Janus nanoparticles with different surface chemistries on two hemispheres, we demonstrated that spatially separating charges and hydrophobicity on the nanoparticles renders them more potent in perforating lipid membranes and thereby in killing a broad range of bacteria. On the other hand, using non-enveloped viruses, we found that the partial hydrophobicity on the viral capsid enables the viruses to deform and penetrate the lipid membrane, leading to their infection of host cells. Our studies from both living and non-living worlds provide direct evidence that the spatial distribution of surface functionalities, rather than just its overall surface chemistry, on a nanoparticle, plays a crucial role in determining its interaction with biomembranes.

11:45 AM SB07.06.06

Multicellular Lipid Compartments for Scalable Micro-Compartmentalization with Environmentally Responsive Release. Richard Archer, Tsuyoshi Inaba and Shin-Ichiro M. Nomura; Tohoku University, Japan

Smart drug release systems have gained attention as a method of using existing medicines in a more effective manner. However, topically applied medicines still rely on uncontrolled diffusion for delivery. Here we propose the use of multicellular lipid compartments (MCLCs) to encapsulate, regulate and control the release of encapsulated drugs. MCLC systems are lipid-based, semi-solid, high internal phase emulsions (HIPEs) with an aqueous dispersed phase pressed into tightly bound micro-compartments with a multicellular-like morphology. The resulting micro-compartments are typically between 20-200 µm and delineated by a continuous lipid-hybrid membrane. The lipid membranes show high stability over months of observations and have semi-

This searchable program is up-to-date as of April 15th, 2024.

permeable properties, allowing water and other small molecules across while retaining larger target molecules. MCLC systems are easily formed on milliliter scales within seconds from desired aqueous solutions by simple application of “lipid-inks”. These lipid-inks are formed from a mixture of natural phospholipids, commercial surfactants, and oils. We show that phospholipids play a crucial role in driving the distinctive cellular morphologies while the surfactants help increase the stability of the system.

To create properties for real-world applications, we encapsulate MCLC systems within polysaccharide hydrogels to improve their stability and enable their use as practical, tangible devices. Using these MCLC-hydrogels we demonstrate the release of the encapsulated contents into external aqueous environments using membrane solubilization strategies. Release rates from the membrane are shown to be related to compartmentalization conditions due to sequential membrane breakdown. Additionally, we show membrane breakdown can be triggered and enhanced by introducing ionic species, leading to environmentally sensitive release conditions. The compartmentalization strategy also allowed for heterogeneous cellular mixing, creating single MCLC systems consisting of multiple different types of separated drugs, and multiple release conditions leading to multi-step or sustained delivery outputs. We believe this work could lead to medical patches for smart and customizable trans-dermal drug delivery. Their environmental sensitivity could lead to smart-release capabilities capable of modulating drug release depending on skin conditions, further increasing their effectiveness by introducing conditional delivery.

Beyond drug delivery, we also hope to develop MCLC systems into simple cell models, communicating permeable networks and bio-inspired soft-robots.

SYMPOSIUM SB08

Advanced Biomaterials and Bioelectronics for Neural Interfacing
April 22 - April 25, 2024

Symposium Organizers

Guosong Hong, Stanford University
Seongjun Park, Korea Advanced Institute of Science and Technology
Alina Rwei, TU Delft
Huiliang Wang, The University of Texas at Austin

Symposium Support

Bronze
Cell Press

* Invited Paper

+ JMR Distinguished Invited Speaker

^ MRS Communications Early Career Distinguished Presenter

SESSION SB08.01: Magnetic Stimulation I
Session Chairs: Seongjun Park and Huiliang Wang
Monday Afternoon, April 22, 2024
Room 434, Level 4, Summit

1:30 PM *SB08.01.01

Engineering Magnetic Nanomaterials for Modulation of Cellular Physiology Polina Anikeeva; Massachusetts Institute of Technology, United States

Negligible interactions with biological matter and versatility of magnetic fields, make them uniquely suited for signal delivery into the organ systems. In my talk, I will discuss how magnetic properties of materials can be engineered to transduce magnetic fields into a diversity of physical stimuli capable of altering neuronal signaling. By focusing on magnetic performance, the gamut of magnetic nanomaterials can be expanded allowing for finer control of cellular functions. By coupling nanomaterials with biological machinery, we can achieve targeting of specific cellular signals in genetically and anatomically defined populations.

2:00 PM *SB08.01.02

Designer Nanomachines for Biological Targets: The Case of Magneto-Genetics (MG) Jinwoo Cheon^{1,2}; ¹Yonsei University, Korea (the Republic of); ²Institute for Basic Science, Korea (the Republic of)

Nanochemistry has been essential to create “designer nanomachines” that come with mechanical functions in nanoscale precision for next-generation biomedical sciences for identifying and executing desired missions. In this talk, I will discuss “magneto-mechanical nanoparticles” as core platform materials and tools for a variety of functionalities such as targeting and signaling of cells and live animals in a selective and efficient way. These tools serve as a modulator for cell signaling of neurons via “magneto-mechanical-genetics (MMG)” for the behavior control of live animals. MMG serves as one of the most advanced technologies in controlling neurons for brain stimulations via remote and wireless fashion.

This searchable program is up-to-date as of April 15th, 2024.

SESSION SB08.02: Bioelectronic Interface I
Session Chairs: Alina Rwei and Huiliang Wang
Tuesday Morning, April 23, 2024
Room 433, Level 4, Summit

10:30 AM *SB08.02.01

Skin-Inspired Sensors, Integrated Circuits and Bioelectronics Zhenan Bao; Stanford University, United States

In this talk, I will present our recent progress in related areas.

11:00 AM *SB08.02.02

Pushing Limits of Neural Electrodes for Intracortical Recording and Stimulation Chong Xie; Rice University, United States

I will present our efforts in ultraflexible neural electrodes and recent progress in scaling-up their channel count and density. I will also discuss using these electrodes for recording and stimulation in animal models.

11:30 AM SB08.02.04

High-Density Flexible Neural Electrode and Application in Neurological Disease Monitoring Siting Yang; Mechanical Engineering, China

Neurological disorders have become the most common diseases affecting human health, such as epilepsy, Parkinson's disease and aphasia. Measuring the neuro-electrophysiology signals is the gold standard for characterizing brain activity. Long-term tracking of the electrophysiological signals and timely feedback for intervention is a promising therapeutic approach for some of these brain diseases. Currently, traditional rigid neural electrodes, dominated by silicon-based electrodes and microwire electrodes, will inevitably induce immune responses due to the significant mechanical mismatch between the rigid materials and the brain tissue. As a result, it is challenging to form a long-term stable neural interface between the electrode and the neurons. In contrast, flexible neural electrodes with small size and low Young's modulus can form a seamless interface with the brain, thus enable long-term signal detection. To date, however, it is still difficult to precisely implant flexible neural electrodes with large amount of electrodes into multiple deep brain regions. It is one of the factors that restricts the large-scale implantation of flexible neural electrodes.

Here, we demonstrated a multi-shank high-throughput 120-channel flexible neural electrode based on polyimide thin polymer substrate, which consists of 6 shanks. The thickness of the electrode is 4 micrometers, and the width of the electrode is only 100 micrometers. At the same time, we used tungsten wire with a diameter of 20 microns as an auxiliary implant shuttle to minimize brain damage. In addition, we designed a reliable and controllable plug-in shuttle device to perform implantation of electrode and retraction of shuttle which can not only completes high-density implantation of multi-shank electrodes, but also able to operate at different approaching and retraction speed. We demonstrated that the prepared high-density flexible electrodes can be implanted in multiple brain regions and deep brain regions and it demonstrated stable in vivo action potential signal detection for up to 6 months. At the same time, immunological tissue section also showed that the prepared high-density neural electrodes cause lower acute immune responses and long-term immune responses. With this technology, long-term brain-computer interfaces based on high-density neural electrodes can be realized in the near future, will benefit to patients with serious brain diseases.

SESSION SB08.03: Bioelectronic Interface II
Session Chairs: Guosong Hong and Alina Rwei
Tuesday Afternoon, April 23, 2024
Room 433, Level 4, Summit

2:00 PM *SB08.03.01

Nonfibrotic Bioelectronic Interfaces with Diverse Organs Xuanhe Zhao; Massachusetts Institute of Technology, United States

Implanted biomaterials and devices face compromised functionality and efficacy in the long term due to foreign body reactions and subsequent formation of fibrous capsules at the implant-tissue interfaces. Here, we demonstrate that an adhesive implant-tissue interface can mitigate fibrous capsule formation in diverse animal models, including mice, rats, humanized mice, and porcine models, by minimizing the establishment of the inflammatory microenvironment and subsequent infiltration of inflammatory cells at the implant-tissue interface. Histological analysis shows that the adhesive implant-tissue interface does not form observable fibrous capsules on diverse organs, including the abdominal wall, colon, stomach, lung, peripheral nerves, and heart, over 12 weeks in vivo. In vitro protein adsorption, multiplex Luminex assays, quantitative PCR, immunofluorescence analysis, and RNA sequencing are additionally performed to validate the hypothesis. We further demonstrate long-term bi-directional electrical communication enabled by implantable electrodes with an adhesive interface over 12 weeks in a rat model in vivo. This finding may offer a promising strategy for long-term anti-fibrotic implant-tissue interfaces.

2:30 PM SB08.03.02

Microelectrode Arrays for Electrophysiology of Astrocyte Lineage Cells Misaki Inaoka, Nataly Hastings, Elise Jenkins, Sagnik Midya, Filip Wronowski, Mark Kotter and George G. Malliaras; University of Cambridge, United Kingdom

Astrocytes, a type of glial cell present in the central nervous system, play a crucial role in brain information processing together with neurons. These cells prominently exhibit Ca²⁺ excitations and are also characterised by electrophysiological activities that derive from voltage-gated ion channels on their membranes. However, there are few tools specifically optimised to detect their low-amplitude and low-frequency membrane oscillations from the extracellular environment, despite the intrinsic benefits these recordings provide for long-term recording and network studies. In this report, we developed an in vitro 64-channel microelectrode arrays (MEAs). To reduce impedance, our MEAs incorporate a larger electrode size (100 µm in diameter) compared to those designed for neurons and features a coating of PEDOT:PSS on a gold electrode. PEDOT:PSS offers notable biocompatibility and electrical properties. We cultured rat cortical astrocytes on this device and subsequently conducted electrophysiological recordings. The results demonstrated that the device could detect low-amplitude activities in the low-frequency range, which were absent in control recordings both without cells and after cell fixation. Moreover, leveraging the transparency of PEDOT:PSS, we carried out simultaneous recordings of calcium dynamics and electrophysiology in astrocytes and human glioblastoma cells, which are cancer cells that originate from astrocytes. The comparison of results from these two different cell types suggests that the frequency of calcium events in astrocyte lineage cells correlates with the signal intensity of electrophysiological recordings.

2:45 PM SB08.03.03

A Multimodal Neural Probe for Seizure Signals Monitoring and Optical Stimulation Treatment to Epilepsy Na Xiao^{1,2,3}, Tao Zou^{1,2}, Ruihong Weng², Chung Tin³ and Paddy K. L. Chan^{1,2}; ¹The University of Hong Kong, China; ²Advanced Biomedical Instrumentation Centre, China; ³The City University of Hong Kong, China

Epilepsy is a central nervous system disorder which affects more than 65 million people worldwide. Seizures are often accompanied by abnormal discharges of a large number of neurons overall the brain, causing periods of unusual behavior, sensations, loss of awareness and even death. Electrical stimulation to deep brain regions has been demonstrated to be effective methods of seizure control for patients with drug-resistant seizures. However, the metal neural probes used in clinical applications for monitoring the neural signal or delivering electrical stimulation have significant disadvantages in the poor conformability, risk of tissue damage, long term stability issue and etc. Soft-material based electrode array has emerged as a promising alternative to metal probes for their small size, biocompatibility, and more importantly, their flexibility and conformability.

Here we demonstrated a soft multimodal device that contains 16-channel depth electrodes and 16-channel ECoG electrodes. The electrodes were fabricated with gold as conducting layer and parylene-C as the supporting layer, coated with PEDOT:PSS and pHEMA to reduce the impedance and enhance the biocompatibility. By using a 50 μm diameter thin optical fiber as shuttle, the depth electrodes were implanted to the focal region of seizure, meanwhile, the ECoG electrodes were placed on the surface of the brain cortex of a half-hemisphere. This design allows us to monitor the LFP signals from the seizure source region, such as hippocampus, and spreading ECoG signals from the brain surface, simultaneously. The optical fiber shuttle was also served for delivering light stimulation to the source region. Data analysis results show that when we input both of the ECoG and LFP signals recorded with our device into a seizure detection computer model, the detection accuracy is high then only use one of them. The correlation coefficient and phase locking value analysis between the LFP channels and ECoG channels further demonstrated the functional connections between the seizure focal region and different spreading regions. We also found that the optical stimulation delivered to the hippocampus region of AAV-ChR2-infused animals effectively suppressed the seizures signals at both LFP and ECoG levels.

3:00 PM BREAK

SESSION SB08.05: Poster Session
Session Chairs: Guosong Hong and Seongjun Park
Tuesday Afternoon, April 23, 2024
Flex Hall C, Level 2, Summit

5:00 PM SB08.05.01

Biocompatible Lactulose based Resistive Random Access Memory for Bio-Implantable Electronics Beom Soo Kim, Jong Bin An, Hyung Tae Kim, Dong Hyun Choi, Moon Ho Lee, Sun Min Song and Hyun Jae Kim; Yonsei University, Korea (the Republic of)

The growing interest in digital healthcare has spurred research into the development of bio-implantable devices capable of detecting various biosignals for convenient daily use. Non-volatile memory is an important component of these bio-implantable devices, especially the resistive random-access memory (RRAM) device, which is attracting attention due to its low power consumption, fast switching, and low fabrication cost. In general, RRAM for processing biosignals is often made of inorganic materials, which are not suitable for bio-implantable devices that require biocompatibility. Therefore, numerous studies on organic-based RRAM, which offers several advantages over inorganic-based RRAM, including biocompatibility, low power consumption, and high flexibility, are in progress.

To fabricate bio-implantable organic-based RRAM, we propose Lactulose as a suitable material for the switching layer of RRAM among biocompatible organic materials that are not harmful to the human body. Lactulose has proven its efficacy and safety, as it is registered on the World Health Organization (WHO) list of essential drugs and has the unique characteristic of not being digested or decomposed in the stomach or small intestine. Based on these properties, we determined that Lactulose could be used as a switching layer of bio-implantable RRAM that has a characteristic of biocompatibility.

In order to make a Lactulose-based RRAM device, a series of processes are required. The first step is to prepare a Lactulose solution, which is made by dissolving Lactulose powder (Sigma-Aldrich, USA) in deionized (DI) water as a solvent with a concentration of 3 wt%. Lactulose is completely dissolved by stirring the solution for 24 hours. Simultaneously, prepare a p⁺-Si wafer to deposit the solution. After cleaning process, the wafer undergoes hydrophilic treatment through O₂ plasma to help the Lactulose solution adhere well to the wafer's surface during the spin-coating process. The next step is to deposit the Lactulose solution on the prepared wafer through spin-coating at 3,000 rpm for 30 s. After deposition, the sample is annealed at 80 °C for an hour. Finally, the top electrode, Magnesium (Mg), is deposited on the device after annealing is complete. Since the switching layer is an organic material, an E-beam evaporator is used to minimize damage to the switching layer, and an Mg thin film of about 120 nm is deposited. This results in the fabrication of a two-terminal RRAM having a p⁺-Si /Lactulose/Mg structure.

Fabricated Lactulose-based RRAM had stable bipolar resistive switching properties with a set/reset behavior between the LRS and HRS. When a voltage sweep is applied to a fabricated Lactulose-based RRAM to check the current change, a set behavior was observed at approximately 3.1 V under positive bias, and a reset behavior was observed at approximately -2.8 V under negative bias. The conversion between the LRS and HRS was also verified through the log-scale I-V curve, which indicated that the switching mechanism of the device is likely due to the formation and rupture of conductive filaments in the switching layer. The device also exhibited a stable resistive switching window over 250 cycles without degradation when resistive switching operations in the LRS and HRS regions were performed. The device also shows a retention time of over 8,000 s. Through these endurance and retention results, it was confirmed that Lactulose-based RRAM exhibits high reliability as a memory device. Therefore, the results suggest that Lactulose can be a strong candidate for a bio-implantable RRAM with its performance. Building upon these characteristics and stability, Lactulose-based RRAM demonstrates its potential for use as bio-implantable devices.

5:00 PM SB08.05.02

Effect of Magnesium-Doped Hydroxyapatite Nanofibers on The Growth and Regeneration of Cortical Neurons in Fibroblasts Primary Cultures and its Biological Characterization Fabiola Hernández Rosas¹, Rafael Rangel Ibarra¹, José R. Alanís Gómez¹, Juan David Olivares Hernández² and Rodrigo Velázquez Castillo³; ¹Universidad Anáhuac Querétaro, Mexico; ²Universidad Nacional Autónoma de México, Mexico; ³Universidad Autónoma de Querétaro, Mexico

Hydroxyapatite (HAp) is frequently employed in various biomedical applications due to its chemical composition, making it one of the predominant calcium phosphate bioceramics in the tissue engineering field. Magnesium-doped synthetic hydroxyapatite (HAp-Mg) is a variant of hydroxyapatite bioceramic in which magnesium has been introduced in these crystalline structures. This allows it to obtain additional properties and characteristics that

may have specific benefits at the cellular level, such as stimulation of cell growth, differentiation, and regeneration. This study used an in vitro model of fibroblasts obtained from chicken embryos to investigate the effect of hydroxyapatite nanoparticles doped with magnesium on the growth and regeneration of cortical neurons. HAp doped with 2% magnesium was synthesized by the Microwave Hydrothermal Assisted Method. Subsequently, for its characterization, X-ray diffraction analysis was performed to characterize the HAp-Mg samples. The morphological and microstructural characterization and the chemical analysis of the HAp-Mg were carried out using Scanning Electron Microscopy and Energy Dispersive Spectroscopy. To evaluate the effect on cortical neurons, the primary culture of chicken embryo cortical neurons was carried out in Nb-B27 medium with 10% inactivated fetal bovine serum. These neurons were treated with different concentrations of HAp-Mg in the range of 0.1-100 ug/ml and incubated at 37°C and 5% CO₂ for 24 and 48 hrs. Subsequently, morphometric analysis was stained with β -III-tubulin and for dendritic length analysis, individual neurons were selected and drawn using the Simple Neuro Tracer plugin of FIJI-ImageJ software to evaluate neurite outgrowth and neuronal branching; also, RNA was obtained to perform real-time PCR experiments to assess the ability of HAp-Mg to stimulate the regeneration of cortical neurons to molecular level. This study suggests that HAp-Mg nanoparticles may positively affect the growth and regeneration of cortical neurons. These findings provide a promising basis for future research on the potential use of HAp-Mg in neuronal regeneration and central nervous system repair therapies.

5:00 PM SB08.05.03

FIB-SEM Investigation for Neurons-Electrode Interface Characterization and 3D Reconstruction [Claudia Latte Bovio](#)^{1,2}, [Csaba Forro](#)³ and [Francesca Santoro](#)^{4,1,5}; ¹Italian Institute of Technology, Italy; ²Università degli Studi di Napoli Federico II, Italy; ³Stanford University, United States; ⁴RWTH Aachen University, Germany; ⁵Forschungszentrum Jülich GmbH, Germany

The interaction between biological cells and non-biological surfaces plays a pivotal role in influencing cell attachment, shaping long-term tissue responses, and ultimately determining the success of medical implants and biosensors[1]. The cell-chip electromechanical coupling plays a key role in ensuring a long-term and stable interaction between the neurons and the active elect of the neuroelectronic devices[1, 2]. In this work we investigated the primary cortical neurons response to the biomimetic microelectrodes designed through two-photon lithography technique. The goal strategies involved the use of the Focus Ion Beam – Scanning Electron Microscopy (FIB-SEM) assisted milling and imaging. The technique used is called “salami slicing” technique, or Slice and view; it allows to mill and to save the whole neuron without loss resolution at a nanometer length scale (about 5nm) and stable alignment. Importantly, the procedure used, the ultra-thin plasticization (UTP)[3–5], required different steps allowing the preservation of the integrity of the neuron structure. Firstly, the chemically fixation, then the heavy metal embedding by osmium and uranyl based to stain the membrane and protein; and at the end the resin embedding and polymerization. By coupling these two techniques we bypassed the substrate removal since the cut can be applied to any type of material, preserve the subcellular structures due to the plastic layer embedding, moreover we obtained the 3D reconstruction of the neurons deform around microelectrodes allowing the quantify of the cleft between the neurons and the electrodes. This was instrumental in providing a comprehensive and precise representation of complex biological structures. It allowed to visualize intricate details that might be overlooked in conventional representations. By embracing this advanced imaging technique, we aim to deepen our understanding of cell-material interactions and their implications for medical implants and biosensors, ultimately advancing the field. Through our investigations into how cell membranes engage with topographical features, such as nanoscale protrusions and invaginations, a remarkable discovery has emerged. Neurons membranes exhibit a pronounced tendency to deform inward and conform to protruding structures, while displaying limited outward deformation when encountering invaginating features. This intriguing asymmetry in membrane response significantly influences the width of the cleft between the cell membrane and the nanostructure's surface.

1. Mariano A, Lubrano C, Bruno U, Ausilio C, Bhupesh Dinger N, Santoro F Advances in cell-conductive polymer biointerfaces and role of the plasma membrane.
2. Mariano A, Bovio CL, Criscuolo V, Santoro F (2022) Bioinspired micro- and nano-structured neural interfaces. *Nanotechnology*. <https://doi.org/10.1088/1361-6528/ac8881>
3. A. Belu, J. J. Schnitker, S. Bertazzo, E. Neumann, D. Mayer, A. Offenhausser, Santoro F (2015) Ultra-thin resin embedding method for scanning electron microscopy of individual cells on high and low aspect ratio 3D nanostructures. *Journal of Microscopy*
4. Dipalo M, McGuire AF, Lou H-Y, et al (2018) Cells Adhering to 3D Vertical Nanostructures: Cell Membrane Reshaping without Stable Internalization. *Nano Lett* 18:6100–6105
5. Santoro F, Zhao W, Joubert L-M, et al (2017) Revealing the Cell–Material Interface with Nanometer Resolution by Focused Ion Beam/Scanning Electron Microscopy. *ACS Nano* 11:8320–8328

5:00 PM SB08.05.04

Point-Of-Care Detection of Alzheimer's Disease Biomarkers using Reduced Graphene Oxide [Reza Mahmoodi](#); University of Denver, United States

In recent years, significant advancements in biosensing technologies have revolutionized the development of diagnostic tools, offering rapid and precise results that are vital for timely medical intervention. Gold, with its remarkable attributes encompassing high electrical conductivity, biocompatibility, and facile surface modification capabilities has emerged as a pivotal element in transducing complex biological interactions into quantifiable signals. The integration of gold electrodes has further enriched the immobilization of biomolecules, capitalizing on their substantial surface area-to-volume ratio to achieve heightened sensitivity in the detection of target molecules. Gold's innate inertness ensures minimal interference from non-specific binding events, rendering biosensing platforms precise and reliable even within intricate biological environments.

The integration of reduced graphene oxide (rGO) into gold-based biosensors represents a notable advancement, driven by rGO's outstanding electrochemical properties and expansive surface area. This synergistic combination not only accelerates electron transfer kinetics but also enhances biomolecular immobilization, leading to a substantial boost in sensitivity and specificity. Furthermore, rGO's intrinsic structural flexibility and robustness fortify the stability and durability of biosensing platforms, establishing their versatility across a broad spectrum of applications.

The methodology involves the immobilization of antibodies using 1-Ethyl-3-(3-dimethylaminopropyl) carbodiimide (EDC) and N-Hydroxysuccinimide (NHS) coupling with a primary focus on detecting Brain-Derived Neurotrophic Factor (BDNF) and Amyloid Beta (ab) from clinical human samples. The detection of change in ab and BDNF levels is crucial providing insight into the state of the nervous system. ab is a peptide that plays a major role in the development of Alzheimer's disease (AD) and BDNF is involved in learning, memory, and cognitive functions. Point-of-care detection of BDNF and A β biomarkers offers the potential for earlier and more effective diagnosis and management of neurodegenerative diseases like AD. It can improve patient outcomes, reduce healthcare costs, and advance research in the field.

Its levels have been linked to several psychiatric and neurological conditions, including depression, schizophrenia, and neurodegenerative diseases. Overall, detecting BDNF and Amyloid Beta levels can assist in the early identification of neurodegenerative disorders. Early detection is fundamental for effective treatment and management of these conditions, potentially leading to improved patient outcomes and quality of life.

The electrochemical sensor results were benchmarked against the Enzyme-Linked Immunosorbent Assay (ELISA) technique. This integrated approach holds significant promise for rapid and label-free electrochemical biosensing, ultimately contributing to the amelioration of diagnostic capabilities in biomedical and environmental fields. Furthermore, this research initiative strives to democratize lab-quality testing by increasing access to reliable point-of-care diagnostics, thus empowering individuals with more accessible and accurate healthcare options.

5:00 PM SB08.05.05

A Highly Stretchable and Conductive PEDOT:PSS/PEG-Coated Au Nanoparticle Nanomembrane for a Low-Impedance Biointerface [Yoona Lee](#)^{1,2} and [Dae-Hyeong Kim](#)^{1,2}; ¹Seoul National University, Korea (the Republic of); ²Center for Nanoparticle Research, Institute for Basic Science, Korea (the Republic of)

A biointerface, which denotes the interface between human biological systems and devices, plays an important role in the field of wearable and implantable electronics since mechanical mismatch leads to low signal-to-noise ratio, delamination of devices, and even tissue damage. However, achieving a conformal contact between the device and the tissue remains challenging due to its difficulty in simultaneously satisfying high stretchability, high conductivity, low impedance, and biocompatibility. Herein, we present a novel material of coating an Au nanoparticle nanomembrane (Au NP NM) with a mixture of polyethylenedioxythiophene:polystyrene sulfonate (PEDOT:PSS) and polyethylene glycol (PEG) to fabricate a biointerface with ultrathin thickness, low impedance, high elasticity, and metal-like conductivity. Au NP NM, made of the float assembly with gold nanoparticles partially embedded on a styrene-ethylene-butylene-styrene (SEBS) substrate, forms a conductive percolation pathway that remains intact even in 200% tensile stretching. Then, the interaction between PEDOT:PSS/PEG and Au NP NM creates optimal contact, which improves the conductivity and durability while stretching (400%). Therefore, the coating of PEDOT:PSS/PEG does not disturb the Au percolation pathway rather, it reinforces its connectivity, thus improving stretchability, resulting in a biointerface with high charge storage capacity and high conductivity. This material could be incorporated into brain interfaces to facilitate efficient stimulation and monitoring of electrophysiological signals.

5:00 PM SB08.05.06

Materials Strategies to Fabricate Metal-Like Stretchable Nanocomposites Using Locally-Bundled Nanowires for Wearable Devices [Hyunjin Lee](#)^{1,2} and [Dae-Hyeong Kim](#)^{1,2}; ¹Seoul National University, Korea (the Republic of); ²Institute for Basic Science (IBS), Korea (the Republic of)

Stretchable conductive nanocomposites are a key focus in the field of wearable bioelectronics. Achieving a balance between metal-like conductivity (over 100,000 S/cm) and significant stretchability (more than 100%) for advanced skin-compatible devices remains a formidable task. This paper introduces a method for creating such a nanocomposite, employing locally clustered silver nanowires, which are stabilized using a combination of 1-propanethiols and 1-decanethiols. The process involves solidifying the nanocomposite through solvent evaporation in a highly humid environment, which clusters and stabilizes the nanowires within the organic solution. This local bundling reduces contact resistance and preserves the percolation network, enhancing conductivity. The use of both 1-propanethiol and 1-decanethiol further enhances this effect. Consequently, a nanocomposite is produced with exceptional conductivity (approximately 122,120 S/cm) and stretchability (around 200%). These outstanding electrical and mechanical properties are vital for various skin-like electronic applications. The paper showcases the application of this material in a wearable thermo-stimulation device.

5:00 PM SB08.05.07

Investigating Biocompatibility of PEDOT-based Biopolymers for Enhanced Integration into Neuronal Networks [Nevena Stajkovic](#)^{1,2}, [Isabela Berndt Paro](#)^{2,1}, [Janic Töx](#)^{2,1}, [Valeria Criscuolo](#)^{2,1} and [Francesca Santoro](#)^{1,2}; ¹Institute of Biological Information Processing – Bioelectronics, IBI-3, Forschungszentrum Jülich GmbH, Germany; ²Faculty of Electrical Engineering and IT, RWTH, Aachen, Germany, Germany

In the neuroelectronics field, neuromorphic devices based on organic electrochemical transistors (OECTs) are important, as they emulate neuronal features such as short- and long-term synaptic plasticity and adaptivity¹ because of the characteristic mixed ionic-electronic conduction mechanism of conjugated polymers like poly(3,4 ethylene dioxythiophene) – PEDOT:PSS. Depending on the application, aside from PSS⁻, PEDOT can be doped with negatively charged counterions such as hexafluorophosphate (PF₆⁻) or perchlorate (ClO₄⁻).^{2,3} Moreover, functionalization of PEDOT:PSS with azobenzene group *via* click chemistry produces photo-responsive azo-PEDOT:PSS biopolymers.⁴ To achieve full integration of OECT-based neuromorphic devices into neuronal networks, the interface between biological cells and biopolymers is critical.⁵ The surface geometry, biomaterial roughness, and its chemical composition can affect the neuron-material interfaces, neuron morphology, and network development. Developing new biomaterials with improved features in terms of stability and conductivity are in demand to achieve seamless integration and broaden the biological applications of OECTs considering also the potential role of different counterions in triggering neuronal outgrowth at the cell-chip interface.

In this work, the interfaces of cells and semiconductive PEDOT-based biopolymers—PEDOT:PSS, PEDOT:PF₆, PEDOT:ClO₄, and modified PEDOT-crown:ClO₄ are investigated. The PEDOTcrown:ClO₄ is interesting owing to its ability to bind Na⁺, which can mimic sodium channels that are abundantly expressed in the nervous system. The interfaces of cells and N₃-PEDOT:PSS, N₃-PEDOT:PF₆, and N₃-PEDOT:ClO₄, which can be functionalized into photo-responsive azo-PEDOT, are also studied. The biocompatibility of the biopolymers is investigated by assessing the viability and morphology of HT22 neuronal cells on each material. To assess the HT22 survival rate and cytotoxicity, standard *in vitro* assays (Live/Dead, MTT, and cellular ROS) are used. Cell morphology is assessed by labeling the actin cytoskeleton. The focused ion beam/scanning electron microscopy (FIB/SEM)⁷ is used to gain a deeper insight into cell-biomaterial interfaces. Currently, biocompatibility assays and FIB/SEM are being carried out to investigate primary neuron-biomaterial interfaces. Also, neuron overgrowth on biopolymers is being studied by actin labeling in the growth cones and by immunostaining of axons and dendrites.

The results of this study are of importance since they will provide a characterization of new semiconductive biomaterials with potential applications in the neuro- and optoelectronics fields.

1. Bruno, U. et al., "Integration of Neuronal Networks" (Neuromorphic Comput. Eng. 2023).
2. Donahue, M. J. et al., "Tailoring PEDOT for Bioelectronics" (Mat. Sci. Eng. R Rep. 2020).
3. Skorupa, M. et al., "Dopant-Dependent PEDOT Functionality in Bioelectronics" (Polymers 2021).
4. Corrado, F. et al., "Azobenzene Transistors for Neurohybrid Building Blocks" (Nat. Commun. 2023).
5. Rinklin, P. & Wolfrum, B., "Recent Developments in Neuroelectronic Devices" (Neuroforum 2021).
6. Kousseff, C. J. et al., "Controlled PEDOT Film Morphology for Electrochromic Behavior" (J. Polymer Sci. 2022).
7. Santoro, F. et al., "Revealing the Cell-Material Interface with Nanometer Resolution by Focused Ion Beam/Scanning Electron Microscopy" (ACS Nano 2017).

SESSION SB08.06: Bioelectronic Interface III
Session Chairs: Seongjun Park and Alina Rwei
Wednesday Morning, April 24, 2024
Room 433, Level 4, Summit

8:45 AM *SB08.06.01

Miniaturised, Flexible Deep Brain Probes Noaf Alwahab and [Stephanie P. Lacour](#); Ecole Polytechnique Federale de Lausanne, Switzerland

Microfabricated brain electrodes offer a distinctive method for directly interfacing with individual neurons *in vivo*. However, their long-term reliability is compromised by the formation of scarring tissue around them. A primary factor contributing to this issue is the mechanical disparity between the electrode and the surrounding biological tissue, prompting the exploration of more adaptable neuroelectronic interfaces. Advances in soft coatings that mirror the brain's elasticity, along with the introduction of compact, flexible designs, are paving the way for enhanced compatibility and durability of these implants. In our research, we fine-tuned a micrometric zwitterionic hydrogel coating for neural implants, leveraging its softness and minimal fouling characteristics while minimizing the implant size. This specialized coating was incorporated into microfabricated polyimide neural probes. These were chronically implanted into deeper brain regions prone to micromotion. Consistent weekly recordings from freely moving rats demonstrated an enduring capability to record for a minimum of 8 weeks, showcasing a high signal-to-noise ratio.

9:15 AM SB08.06.02

Biomimetic Dendritic Electrodes Tune The Neural Network Behavior and Communication [Claudia Latte Bovio](#)^{1,2}, Anna Mariano³ and Francesca Santoro^{4,5,1}; ¹Italian Institute of Technology, Italy; ²University of Naples Federico II, Italy; ³Istituto Italiano di Tecnologia, Italy; ⁴RWTH Aachen University, Germany; ⁵Forschungszentrum Jülich GmbH, Germany

The interaction between electrogenic cells and external devices is indispensable for tasks like cell recording and stimulation. In particular, the physical cell-chip coupling has a crucial impact on the electrical conduction mechanism. A deepened comprehension of how cells interact with artificial materials is of utmost importance in the quest for effective interfaces. The process of cells adhering to and spreading on pseudo 3D micro-structures, is a well-coordinated mechanism that hinges on cell adhesion and the cell's capacity to adapt its cytoskeletal architecture to conform to vertically aligned structures[1, 2]. This scenario highlights a knowledge gap in our understanding of how to modulate neural network development and how cell membranes conform to protruding vertical electrodes, particularly for creating an effective 3D representation of the cleft to be integrated into the cell-electrode equivalent circuit for recording and stimulation modeling. On this purpose a biomimetic dendritic electrode[3] has been fabricated by using the two-photon polymerization lithography[4]. Firstly, three structures' geometry have been identified: thin that can initiate contacts with presynaptic terminals and are therefore essential in the initial stages of spinogenesis; the mushroom shape as a result of the plastic and dynamic reshaping of the neuronal circuits during synaptic development and the stubby. The experimental approach involved the primary cortical neurons. In our work, we've demonstrated the mechanical interactions occurring at focal adhesion sites. These interactions oversee the continuous remodeling and adjustment of cells on the material's surface and have the capacity to generate localized traction forces on the substrate. Neurons can utilize these forces to facilitate directed movement through contact guidance. Additionally, this mechanism promotes the engulfment event by facilitating membrane invagination, leading to the precise localization of transmembrane proteins, including integrins. This localization helps induce a specific cytoskeletal arrangement. Furthermore, our results indicate how microelectrodes can impact directionality and influence the remodeling of the neural network, particularly affecting the growth cone phase, shifting from pausing to a resting state. Importantly, we've demonstrated that the growth cone rate changes in response to different pitch configurations. Significantly, our research has revealed that biomimetic topographical cues can swiftly impact membrane adhesion proteins and enhance the efficiency, as demonstrated through the 3D reconstruction integrated into an electrical equivalent model. With an eye toward future applications in controlling signal dissipation, this work has the potential to enhance the recording of electrogenic cells.

1. Mariano A, Lubrano C, Bruno U, Ausilio C, Dinger NB, Santoro F (2021) Advances in Cell-Conductive Polymer Biointerfaces and Role of the Plasma Membrane. *Chem Rev* *acs.chemrev*.1c00363
2. Santoro F, Zhao W, Joubert L-M, et al (2017) Revealing the Cell-Material Interface with Nanometer Resolution by Focused Ion Beam/Scanning Electron Microscopy. *ACS Nano* *11*:8320–8328
3. Mariano A, Bovio CL, Criscuolo V, Santoro F (2022) Bioinspired micro- and nano-structured neural interfaces. *Nanotechnology* *33*:492501
4. Harinarayana V, Shin YC (2021) Two-photon lithography for three-dimensional fabrication in micro/nanoscale regime: A comprehensive review. *Optics & Laser Technology* *142*:107180
5. A. Belu, J. Schnitker, S. Bertazzo, E. Neumann, D. Mayer, A. Offenhausser, Santoro F (2015) Ultra-thin resin embedding method for scanning electron microscopy of individual cells on high and low aspect ratio 3D nanostructures. *Journal of Microscopy*

9:30 AM SB08.06.03

Ultra-Compliant and Biodegradable Stem Cell-Embedded Hydrogel Microelectrode Arrays Applied for Combined Neural Signal Diagnosis, Electrically Neuromodulation and Cell Therapy [Wei-Chen Huang](#); National Yang Ming Chiao Tung University, Taiwan

Biohybrid neural interfaces (BHNI) are a new class of neuromodulating devices that integrate neural microelectrode arrays (MEAs) and cell transplantation to improve treatment of nerve injuries and disorders. However, current BHNI devices are made from abiotic materials that are usually bio-passive, non-bioisintegratable, or rigid, which restricts encapsulated cell activity and host nerve reconstruction and frequently leads to local tissue inflammation. Herein, we propose the first MEA composed of all bioisintegratable hydrogel tissue scaffold materials with synergistic performances of tissue conformal adhesiveness, MEA technologies, tissue scaffolding and stem cell therapy on a time scale appropriate for nerve tissue repair. The device substrate is made of an enzyme-crosslinked gelatin/silk (GS) hydrogel with adhesiveness and controllable degradability that benefit nerve tissue integration and neural progenitor cell (NPC) transplantation. MEA circuits composed of graphene oxide (GO)/PEDOT/gelatin-based ECHs were designed with a double-crosslinked architecture to confirm robust ionic/electroconductive properties. With seamless lamination around peripheral nerve fibers, the device permits successive neural signal monitoring for wound condition evaluation, while demonstrating synergistic effects of spatiotemporally controlled electrical stimulation and cell transplantation to accelerate restoration of motor function.

9:45 AM BREAK

SESSION SB08.07: Optical and Non-Invasive Stimulation
Session Chairs: Guosong Hong and Huiliang Wang
Wednesday Morning, April 24, 2024
Room 433, Level 4, Summit

10:15 AM *SB08.07.01

Optoelectronic Biointerfaces: From Random-Access Photostimulation to Neuromodulation [Bozhi Tian](#); University of Chicago, United States

The development of new neural interfaces necessitates innovative materials and advanced device concepts. Our lab has introduced a monolithic system designed for optoelectronic interfaces that effectively interact with neural and cardiac systems. Utilizing semiconductor-enabled biomodulation interfaces, we have enhanced the capabilities of random-access photostimulation. The devices demonstrate significant translational potential for medical applications, ranging from cardiac system modulation to peripheral nerve stimulation. In this talk, I will also introduce a new electrochemical system for neuromodulation. Our lab's future focus will be on refining the performance and reliability of the random access systems. We aim to expand the range of medical applications, improve device efficiency, and ensure seamless integration into clinical practices.

10:45 AM *SB08.07.02

Implantable Photoacoustic and Microwave Neural Interface [Chen Yang](#); Boston University, United States

High precision neuromodulation is a powerful tool for fundamental studies in neuroscience and potential treatments for neurological disorders. Here we report new developments in implantable non-genetic photoacoustic and microwave neural interfaces for high precise neuromodulation in retina and brain. First, we will discuss our design of biocompatible soft photoacoustic retina prostheses. We confirmed successful blind retina stimulation through a PDMS-based photoacoustic film safely with a spatial resolution of 50 microns ex vivo and in vivo. These results show the potential of using photoacoustic signal to drive activity in photoreceptor-damaged retinas. Second, we will report an implantable miniaturized multifunctional fiber integrating with electrodes for simultaneous stimulation and recording in brain in vivo. Successful electrophysiology recording upon photoacoustic stimulation has been demonstrated in mouse brain acutely as well as up to 1 mon after implantation of the stimulator. Such devices open up potential for improved closed-loop stimulation in deep brain stimulation without the interference between the conventional electrical stimulation and recording. Lastly, we will discuss a miniaturized millimeter size microwave antenna as a wireless implantable neural interface to inhibit neural activities in vitro, ex vivo and in vivo. Suppression of seizure activities in brain in an epileptic rodent model has been achieved using low intensity microwave together with the implanted microwave antenna 6-10 time less than the FDA microwave threshold.

11:15 AM SB08.07.03

Flexible and Biocompatible Photoacoustic Film for Vision Restoration at Ultrahigh Spatial Resolution [Yueming Li](#)¹, Audrey Leong², H el ene Moulet³, Jean-Damien Louise³, Serge Picaud² and Chen Yang¹; ¹Boston University, United States; ²Sorbonne Universit e, France; ³Axorus, France

Retinal degenerative diseases represent a major factor leading to irreversible blindness. Despite extensive research efforts, a definitive curative treatment remains elusive. The development of retinal prostheses, encompassing bionic and photovoltaic devices, has aimed to address this unmet clinical need. However, these technologies face inherent issues such as crosstalk from current leakage impacting spatial resolution, limitations in electrode numbers limiting the visual angle, and difficulties related to internal strain during fabrication. To address these challenges, we introduce a novel solution utilizing a uniform and flexible photoacoustic film composed of candle soot and polydimethylsiloxane for high-precision retinal stimulation as a subretinal implant. This approach leverages on the advantages of light patterning flexibility to overcome the limitations of unit spacing, electrode numbers, and internal strain observed in other devices. Our experiments demonstrate that this photoacoustic film effectively stimulates the retinas of blind rats ex vivo, achieving a spatial resolution of 50 μm . Moreover, upon implantation in rats, this flexible photoacoustic film exhibits superior biocompatibility. Significantly, the photoacoustic stimulation induced visual responses that were recorded in the rat brain's visual cortex. These findings hold promise for the restoration of vision in individuals suffering from age-related macular degeneration and retinal dystrophy, offering a potential solution with improved spatial resolution and better biocompatibility.

11:30 AM SB08.07.04

Fabrication, Characterization and In Vivo Validation of Flexible Optical Cortical Probe [Am elie Albon](#)¹, Emma Butt², Keith Mathieson² and Charles Rezaei-Mazinani¹; ¹EMSE, France; ²University of Strathclyde, United Kingdom

Mechanically-flexible neurotechnologies based on soft and biocompatible organic materials have significant advances for neuroscience applications. However, integrating active electronic components into polymer-based neurotechnologies is still a challenge. This is particularly important for optogenetic applications where, despite important advances in light delivery technologies (such as optical fiber or inorganic μLED -based optoprobes) they mostly rely on rigid substrates. This is a key obstacle to their successful integration with neural tissue. In this work, we focus on the development of a novel optical cortical-probe (optoprobe), seamlessly integrating high performance inorganic μLED s for optogenetic stimulation, along with organic electrodes for electrical recording. This optoprobe offers a plastic and conformable interface with the cortex. Here, we present our fabrication method for the integration of 4 μLED s (100x100 μm , $\lambda = 450 \text{ nm}$) and 4 PEDOT:PSS based electrodes (50x50 μm) and fully characterize the optoprobe for optogenetic stimulation and electrical recording. This includes analysis of the electrical crosstalk between the drive currents for the μLED s and the electrical recording component (sensitive to 10s of microvolts). Driving the μLED s can also increase the optoprobe's temperature profile and influence the long-term stability of the optoprobe – both of these effects have been studied in accelerated testing. Furthermore, we show validation of the optoprobe performance in mouse auditory cortex *in vivo*. Integrating electrodes and μLED s on a common transparent substrate has the potential to improve stimulation control by facilitating real-time adjustments based on observed neuronal responses through a closed-loop system. Moreover, our results demonstrate the scalability of this fabrication process to a large μLED arrays. This technology marks a significant step forward in the development of flexible optogenetic devices.

11:45 AM SB08.07.05

Non-Invasive and Programmable Molecular Manipulation for Deep Brain Modulation Using Focused Ultrasound [Wenliang Wang](#)¹, Yanshu Shi², Wenrui Chai¹, Kai Wang K. Tang¹, Banglin Chen² and Huiliang Wang¹; ¹The University of Texas at Austin, United States; ²The University of Texas at San Antonio, United States

The precise control of mechanochemical activation within deep tissues via non-invasive ultrasound holds profound implications for advancing our understanding of fundamental biomedical sciences and revolutionizing disease treatments. However, a theory-guided mechanoresponsive materials system with well-defined ultrasound activation has yet to be explored. Here we present the concept of using porous hydrogen-bonded organic frameworks (HOFs) as toolkits for focused ultrasound programmably triggered drug activation to control specific cellular events in the deep brain, through on-demand scission of the supramolecular interactions. A theoretical model is developed to visualize the mechanochemical scission and ultrasound mechanics, providing valuable guidelines for the rational design of mechanoresponsive materials at the molecular level to achieve programmable and spatiotemporal activation control. To demonstrate the practicality of this approach, we encapsulate designer drug clozapine N-oxide (CNO) into the optimal HOF nanoparticles for FUS gated release to activate engineered G-protein-coupled receptors in the mice and rat ventral tegmental area (VTA), and hence achieved targeted neural circuits modulation even at depth 9 mm with a latency of seconds. This work demonstrates the capability of ultrasound to precisely control molecular interaction and develops ultrasound-programmable HOFs to minimally invasive and spatiotemporally control cellular events, thereby facilitating the establishment of precise molecular therapeutic possibilities. We anticipate that this research could serve as a source of inspiration for precise and non-invasive molecular manipulation techniques, potentially applicable in programming molecular robots to achieve sophisticated control over cellular events in deep tissues.

SESSION SB08.08: Magnetic Stimulation II
Session Chairs: Alina Rwei and Huiliang Wang
Wednesday Afternoon, April 24, 2024
Room 433, Level 4, Summit

1:30 PM *SB08.08.01

Magnetolectric Metamaterials for Remote Control of Neural Activity Jacob T. Robinson; Rice University, United States

Magnetolectric materials have applications in wireless data transmission, electronics, sensing, data storage, and biomedical applications. Recently there has been interest in using magnetolectric materials for direct neuromodulation, but existing magnetolectric materials struggle to provide millisecond-precision remote stimulation due to the high resonant frequencies of magnetolectric materials. Here we discuss how we can engineer composite materials that display magnetolectric properties not found in nature including magnetoluminescence and strong non-linear magnetolectric coupling. These meta-atoms have magnetic coupling that enables precise activation of nerves and remote control of cell activity.

Specifically, we introduce the concept of self-rectifying magnetolectric metamaterials (MNM) that rely on nonlinear charge transport across semiconductor layers in a trilayer laminate consisting of a piezoelectric layer and two magnetostrictive layers. This innovation enables us to generate arbitrary electrical pulse sequences with a time-averaged voltage exceeding 2 V. Consequently, we can remotely stimulate peripheral nerves with repeatable latencies of less than 5 ms, a significant improvement over previous neural stimulation approaches relying on magnetic materials. This achievement holds promise for applications requiring fast neural signal transduction, such as sensory or motor neuroprosthetics.

Our work showcases the potential of rational design to introduce nonlinearities into the magnetic-to-electric transduction pathway, opening doors to diverse MNM designs tailored for applications spanning electronics, biotechnology, and sensing. Ultimately, this breakthrough in remote neural stimulation can be used for medical therapies, facilitating less invasive treatments and advancing neuroscience research in freely behaving animals.

2:00 PM SB08.08.02

Probing The Origin of Alternating Field Induced Magnetic Heating with Lithographically Fabricated Colloidal Solutions of Compensated Ferrimagnets Noah Kent, Daniel Suzuki, Byunghun Lee, Geoffrey Beach and Polina Anikeeva; Massachusetts Institute of Technology, United States

Magnetic nanoparticles (MNPs), used as alternating magnetic field (AMF) transducers, are currently actively being researched as a non-invasive way of manipulating biological systems. The nanomagnetic transducers turn the AMF into a force or field that can interact with biology. Most ubiquitous is the use of AMF transducers to generate heat. This heat can be used to ablate cancer cells, trigger ion channels, or open the blood brain barrier. Optimizing the heating from MNPs allows one to reduce the amount of MNPs used for medical treatment or to selectively heat on a cellular scale due to better local heating.

Current theory says that the heating from a MNP in an AMF is proportional to the area of the hysteresis loop swept by the MNP. While this is an excellent approximation there have been some noticeable discrepancies observed in the current literature with this theory; it has been observed quite often that superparamagnetic nanoparticles have significant heating, but have no hysteresis loop area. Additionally, the Hamiltonian used when calculating energy loss in this theory lacks a term for ferromagnetic exchange.

We instead turn to theory that describes accurately the switching of a MNP dynamically and includes ferromagnetic exchange. This theory predicts the heating induced in a magnet in an AMF is proportional to the sum of the speed of all the spins squared ($(dM/dt)^2$). Intuitively one could think of this as a magnetic friction. This explains why superparamagnets have heating that is nearly the same as ferromagnetic nanoparticles but paramagnets do not. This also agrees with the previously put forward theory that larger anisotropy and larger hysteresis loops lead to larger heating.

To confirm this theoretical framework we consider a system which, under the old theory should not heat but, with the accurate nanomagnetic heating theory, should heat: compensated ferrimagnets. Compensated ferrimagnets are ferrimagnets where the magnetization of the two sublattices are nearly the same, and therefore, below spin flip fields, have near zero net magnetization, have no hysteresis loop area, but still have two dynamically switching magnetic sub lattices.

Turning films of magnetron sputtered amorphous near compensation GdCo (Gd = 25%) into colloidal solutions of lithographic microdisks we observe a net magnetization of 1.1emu/g (very small compared to 100emu/g for magnetite), and a near zero area hysteresis loop. However, we observe non-trivial AMF induced heating of 240 w/g (350w/g for magnetite in the same field conditions). These results demonstrate that magnetic heating is not purely proportional to hysteresis loop area but is a result of rapid, ferromagnetic exchange induced, magnetic motion.

2:15 PM SB08.08.03

Controlling Neuronal Cell Signaling within Three-Dimensional Magnetic Nanocomposites Dekel Rosenfeld; Tel Aviv University, Israel

Iron oxide magnetic nanoparticles (MNPs) with diameter of 20-25 nm dissipate heat when exposed to weak alternating magnetic fields (AMFs) with amplitudes <50 mT and frequencies of 100-600 kHz. This heat can be exploited to activate cells that have thermally sensitive ion channels on their membrane via magnetothermal modulation. AMF has a high penetration rate with no deleterious effects, and therefore suitable for the activation of cells within deep organs in the body. Iron oxide nanoparticles are biocompatible and being utilized in different biomedical applications, including drug delivery, cell signaling and imaging.

We exploit the magnetothermal approach to control calcium signaling in cells within deep organs and with a minimally invasive scheme. While the common approach of magnetothermal stimulation exploits MNPs in the form of ferrofluid, my lab recently pioneered a new design of a three-dimensional nanocomposite that can examine cell signaling under thermal effects in microenvironment that is suitable for cell organization and functionalities. We introduce a novel concept for the field of bioelectronic medicine with new materials design and in-depth nanocomposite characterization. One intriguing target of the magnetothermal approach is the heat sensitive ion channel, the transient receptor potential vanilloid 1 (TRPV1), the capsaicin receptor. TRPV1 is a non-selective cation channel that is calcium-permeable and can be activated by heat with temperature threshold above 42 Celsius. Previous studies have demonstrated the expression of TRPV1 in various peripheral organs as well as sensory neurons. We use this model to demonstrate our approach of cells activation in three-dimensional magnetic nanocomposites.

2:30 PM BREAK

SESSION SB08.09: Ultrasound/Mechanical Stimulation
Session Chairs: Guosong Hong and Seongjun Park
Wednesday Afternoon, April 24, 2024
Room 433, Level 4, Summit

3:30 PM *SB08.09.01

Piezoelectric Currents: Mechanical Deformation of Hydrogels Induces Ionic Currents that Stimulate Nerves [John D. Madden](#)¹ and Yuta Dobashi²;
¹University of British Columbia, Canada; ²University of Toronto, Canada

The nervous system operates at tens of millivolts and employs ionic currents. Similar voltages and ionic currents are generated when hydrogels are compressed. This opens the possibility of stimulating the nervous system directly using the electrical energy produced when ionically conductive materials are deformed. To demonstrate this effect, a finger was firmly tapped on a slab of polyacrylamide hydrogel containing 1.5 M of sodium chloride solution. The resulting current was fed into PEDOT-coated Pt-Ir electrodes wrapped around a rodent peripheral nerve. The mechanical input produced currents of 10 μ A at voltages of less than 100 mV. Hindlimb twitches were produced. This 'self-powered' sensing interfaces with nerves without any signal conditioning or amplification. We dub the underlying mechanism "piezoelectric", in loose analogy to piezoelectrics. A pressure gradient applied to the hydrogel produces a flow of electrolyte and ions within it. Some ions displace faster than others as they translate through the nanopores of the hydrogel, likely due to differences in size between anions and cations. Similar effects are seen in other ionically conducting polymers including conjugated polymers and ionically conductive membranes. Response times can be quite fast (~30 ms) when thin gels are used, which create large pressure gradients around the indentation area, and fast transport. The piezoelectric effect creates the possibility of a fully ionic artificial mechanoreceptor that can interface with the nervous system - though long distance, high density signal conduction may be best achieved using thin metal wires.

4:00 PM *SB08.09.02

Flexible Transducers for Ultrasound Neuromodulation Sang-Mok Lee, Taemin Lee, Seunghyeon Nam and [Hyunjoo J. Lee](#); KAIST, Korea (the Republic of)

Wearable ultrasound patches possess the potential to transform conventional medical ultrasound applications by enabling hands-free, prolonged, and uninterrupted diagnostic and therapeutic procedures. However, current flexible ultrasound transducers often lack the ability to govern their curvature and are limited in terms of production throughput and design flexibility. In this work, we present a method for fabricating flexible ultrasound transducers with controllable curvature, utilizing high-yield silicon microfabrication and employing flex-to-rigid structures. The transducer's curvature is modulated through Joule heating, utilizing a low-melting-point metal alloy. The transducer demonstrates remarkable electrical and acoustical performance at central frequencies of 1.5 MHz and 3.4 MHz when immersed. We deploy this flexible transducer to induce neuromodulation of immune responses within an internal organ, illustrating the potential for continuous therapeutic interventions via a wearable ultrasound patch.

4:30 PM *SB08.09.03

Deep Brain Stimulation by Blood-Brain-Barrier-Crossing Piezoelectric Nanoparticles Generating Current and Nitric Oxide under Focused Ultrasound [Won Jong Kim](#); POSTECH, Korea (the Republic of)

Neurodegenerative diseases entail the gradual breakdown of the central nervous system, leading to involuntary movements, cognitive decline, and memory issues. Deep brain stimulation (DBS), a successful treatment, uses implanted electrodes to modify neural signals and neurotransmitter release, though invasive electrode insertion poses side effects. Therefore, a wireless, non-invasive approach is essential. Piezoelectric materials generate electrical output when mechanically stimulated. Combining these materials with focused ultrasound might non-invasively stimulate localized neurons. However, the blood-brain barrier (BBB), a critical CNS barrier, limits nanoparticle delivery to the brain. A strategy to modulate BBB is crucial for effective treatment. Nitric oxide (NO), a vital gas molecule, shows potential in disrupting BBB, but the mechanism remains unclear. A NO release in response to specific stimuli could temporarily open BBB, facilitating nanoparticle accumulation in target areas. This study introduces a multifunctional system, combining ultrasound-responsive NO donors with piezoelectric nanoparticles for non-invasive neural stimulation. These nanoparticles release NO and direct current only under ultrasound, temporarily disrupting BBB for nanoparticle accumulation. The piezoelectric nanoparticles stimulate dopaminergic neurons. In an animal model, systemically administered nanoparticles under high-intensity focused ultrasound alleviated Parkinson's disease symptoms without toxicity. In conclusion, this innovative approach offers promise for non-invasive, wireless neural stimulation.

SESSION SB08.10: Non-Invasive Bio-Interfaces
Session Chairs: Seongjun Park and Huijiang Wang
Thursday Morning, April 25, 2024
Room 433, Level 4, Summit

8:30 AM *SB08.10.01

Sensing Applications of Conformable Organic Imagers [Tomoyuki Yokota](#) and Takao Someya; The University of Tokyo, Japan

Optical-based 3-axis pressure sensors, with delicate imaging systems, can offer detailed tactile pressure data vital for robotics and human interaction. However, their bulkiness complicates mounting and integration. We present a thin and flexible sensor construction approach to realize detection of 3-axis pressure distribution on a large area with wide sensing range and high accuracy. The sensor can detect the distribution of 3-axis pressure on an area of 3 cm \times 4 cm, with a high-accuracy normal and tangential pressure sensing up to 360 and 100 kPa, respectively. A porous rubber is used as a 3-axis pressure-sensitive optical modulator to omit the thick and rigid focusing system without sacrificing the sensitivity. In addition, by integrating thin and flexible backlight and imager, the sensor has a total thickness of 1.5 millimeter, making it function properly even when bent to a radius of 18 mm. The flexible imager uses a combination of organic photo diodes (OPDs) and low-temperature polycrystalline silicon (LTPS)-based thin-film transistors (TFTs) fabricated on a film substrate. The imager has a pixel size of 235 μ m, and a total of 126 \times 168 pixels are formed on a 3 cm \times 4 cm area. The organic photodiode designed for NIR light detection, optimized for maximum sensitivity at a wavelength of 850 nm, exhibits excellent air stability due to the implementation of an inverted structure.

9:00 AM SB08.10.02

Noninvasive E-Textile System for Long-Term Multimodal Electrophysiological Monitoring in Sports and Clinical Healthcare [Junyi Zhao](#) and

Chuan Wang; Washington University in St. Louis, United States

Textile-based electronic systems have emerged as a promising platform for creating noninvasive and comfortable human-machine interfaces across various domains, including sensing, display, and communication, which aligns with the contemporary drive for enhanced miniaturization and multifunctionality. This work presents a novel E-textile system comprising in-plane electrode layout and bioinspired conductive microfibers. This configuration allows for gel-free and motion-artifact-tolerant recording of multiple physiological signals, including electrocardiography and electromyography, capturing muscle activity triggered by motor neurons. More specifically, The base layout features a screen-printed array of poly(3,4-ethylenedioxythiophene) polystyrene sulfonate (PEDOT:PSS), with PEDOT:PSS-coated fluffy microfibers stacked on top. The vertically oriented hairy microfiber conductors ensure exceptional conformal and robust skin contact, while the dispersed microfiber electrodes substantially increase the effective contact area, significantly reducing the contact impedance between the electrode and skin. This feature enables comfortable all-day wear under dry conditions without the need for ionic gels. To ensure the durability and functionality of the textile in harsh conditions, a self-assembled monolayer (SAM) of trichloro(1H,1H,2H,2H-perfluorooctyl) silane is vaporized as a superhydrophobic coating. This treatment preserves the natural texture of the textile while maintaining the intrinsic conductivity of the electrodes. Additionally, portable miniaturized circuitry was meticulously designed and manufactured to enable multi-channel recording, signal processing, and wireless communications.

These advancements facilitate the seamless integration of the E-textile system into everyday life, broadening its potential applications. This study explores the application of E-textile systems in real-life scenarios, including strenuous exercise and clinical studies. We commence by demonstrating the robustness and stability of the E-textile system during professional cycling training sessions. Remarkably, the recorded signals remained clear and free from motion artifacts, even in the presence of intense sweating, maintaining a signal-to-noise ratio of approximately 30 dB. Real-time monitoring facilitated on-the-spot data analysis, including heart rate and muscle output. Next, we tested the waterproof capability of the system by integrating it into an E-textile-equipped swimsuit. Throughout the professional swimming training, the fully submerged E-swimsuit consistently delivered reliable electrocardiography recordings, demonstrating its resilience and suitability for aquatic environments. Even when encountering water flows, the E-swimsuit showcased robust performance, making it ideal for water sports. Finally, the textile-based E-patch with electrode arrays was employed in clinical studies to monitor maternal/fetal health. Multiple pregnant subjects were involved for capturing multichannel maternal-electrocardiography and uterine-electromyography signals. The recorded multichannel uterine-electromyography signals were further processed to generate noninvasive and high spatiotemporal resolution three-dimensional (3D) electromyometrial images with a fast frame rate. This groundbreaking achievement offers unique insights into neural activities within the uterus, aiding in the diagnosis of abnormal obstetrics symptoms and predicting the risk of potential preterm birth. These findings underscore the versatility and potential of wearable E-textile systems across a wide range of real-world applications, paving the way for professional sports tracking and personalized advancements in healthcare.

9:15 AM SB08.10.03

Development of Human-Scale Dry EEG based on 2D MXene and Benchmarking Against Clinical Gelled Electrodes [Sneha Shankar](#), Doris Xu, Francesca Cimino, Ashley Koluda, Eugenia Angelopoulos, Kathryn Davis and Flavia Vitale; University of Pennsylvania, United States

Electroencephalography (EEG) is a valuable tool for non-invasive monitoring of electrical activity from the scalp for clinical monitoring of neurological disorders. Clinical EEG typically involves gel-based electrodes, whose application is time-consuming and requires skin-irritating abrasives and pastes. Recently, we have introduced dry EEG electrodes based on Ti_3C_2 MXene materials. These electrodes offer enhanced comfort and ease of use, requiring minimal skin preparation. Furthermore, they are conformable to the scalp, providing a comfortable fit for users. Here, we advance this technology towards research and clinical use by fabricating two different configurations of EEG headsets. The first configuration is a reduced-montage headband consisting of 8 channels placed at equal spacing on FP1, FP2, F7, F8, T3, T4, T5. The second configuration is a standard 10-20 montage with 21 recording sites at the canonical scalp locations. In both devices, the dry electrodes are fabricated from porous pillars infiltrated with Ti_3C_2 MXene (diameter: 8 mm, height: 6 mm), enabling access to the scalp through hair without the need for gel or pastes. The electrodes are connected to the recording amplifiers via snap connectors attached to snap leads. Owing to the high electrical conductivity ($155 \pm 4 \Omega$, $n=5$ electrodes) and surface area, the average 10 Hz impedance with the scalp of these dry porous MXene-infused electrodes is $2.1 \pm 1.8 \text{ k}\Omega$ ($n=5$ subjects). To further validate the dry MXene EEG technology, we have benchmarked it against clinical gelled cup Natus electrodes. Briefly, we have recruited patients in the outpatient epilepsy clinic at the Hospital of the University of Pennsylvania. For each participant, we recorded EEG with the reduced-montage headband and MXene electrodes for 20 minutes prior to clinical EEG. We recorded EEG in the following conditions: resting state, eyes open/closed, and sleeping, which corresponded to the same tasks used during clinical EEG acquisition. A preliminary analysis of the recordings shows comparable quality of the EEG signals acquired with the dry MXene and clinical gelled electrodes, while the duration of the skin prep and electrode placement operation reduced by $\sim 2\times$. In conclusion, we have developed and validated a novel dry EEG technology that can improve user comfort, reduce electrode placement and skin preparation time, and reliably transmit signals of interest, providing a comfortable and efficient solution for EEG monitoring.

9:30 AM SB08.10.04

Detect The Undetectable in Wearables and Brain-Machine Interfaces: pM-Level Biomolecular Detection with Fast-Scanned Aptamer-OECT [Xinyu Tian](#) and Shiming Zhang; The University of Hong Kong, Hong Kong

Biomolecular detection is the next goal for wearable devices. The lower limit of detection (LoD) is a critical metric for wearable biosensors. In this study, we demonstrate that aptamer-based Organic Electrochemical Transistors (OECTs) can detect concentrations in the picomolar range (close to the dissociation constant, K_d) in a fully-integrated wearable context [1], which is not achievable with a standard electrochemical sensor. The high transconductance (g_m) of OECTs allows for a more significant variation in current, making the sensor highly resistant to ambient noise.

Specifically, we observed that a high scanning rate improves LoD to values close to the theoretical limit (K_d) of the aptamers. This improvement is achieved by operating OECTs at optimal high frequency range where the leaking reaction resistance most vibrates with the binding of the molecules [2]. Thus, microscale OECTs are essential for achieving a higher cutoff frequency for rapid scanning purposes.

9:45 AM BREAK

10:15 AM *SB08.11.01

3D Printed Flexible and Stretchable Tissue-Like Electronic Devices for Neural Recording [Tao Zhou](#); The Pennsylvania State University, United States

The utilization of neural recording technology has significantly transformed our comprehension of the brain, spinal cord, and other nervous systems. These technologies have provided essential insights into neural activity, hence facilitating the development of groundbreaking therapeutic approaches. Nevertheless, the development of neural recording devices that can match the properties of neural tissues remains a significant challenge. Furthermore, commonly used neural recording devices are usually time-consuming to fabricate and costly. This research presents a novel strategy to tackle the aforementioned obstacle, wherein we propose the utilization of 3D printable flexible and stretchable tissue-like electronic devices for the purpose of neural recording. The device exhibits a unique structure that offers remarkable characteristics like flexibility, stretchability, and conformability. These properties facilitate the seamless integration of the device with the brain and spinal cord. In addition, the 3D printing manufacturing process can allow rapid fabrication of designed neural electronic devices and is less costly than lithography-based manufacturing methods. This innovation exhibits remarkable ramifications, presenting significant prospects for the fields of brain-computer interfaces, neuromodulation, and neural prosthetics.

10:45 AM SB08.11.02

Aerosol Jet Printing Enabled High-Density and Customized Neural Probe Integration [Xiaokang Bai](#)¹, [Priyan Pathirana](#)², [Efrain Brizuela](#)¹, [Angel Nunez](#)¹ and [John Seymour](#)^{1,2}; ¹The University of Texas Health Science Center at Houston (UTHealth), United States; ²Rice University, United States

Advanced packaging and integration techniques play a pivotal role in the development of next-generation medical devices. These devices demand high-density and complex-shaped substrate integration, which poses challenges to traditional packaging methods. Aerosol jet printing (AJP) offers a novel solution to the packaging of thin film arrays and convenient customization through AutoCAD. To achieve consistent and precise structures with AJP, design of experiments (DOE) is often necessary to establish optimal printing parameters. In this report, we present an approach to packaging flexible, tubular circuits, including high-density neural probes for neurosurgery or smart catheters for medical diagnostics. We demonstrated the effective utilization of the DOE method on a 400 μm step structure while maintaining high-density connections (64- to 128- channels) and achieving fine features with linewidths of $\leq 60 \mu\text{m}$ and pitch sizes of ≤ 4 mils. Our method is versatile and can be easily adapted to various smart catheter and neural probe integration requirements. Furthermore, it has the potential to be extended to broader packaging and integration applications, such as ASIC integration, printed electronics, and various medical devices.

Acknowledgements:

This work was performed under the auspices of the National Institute of Neurological Disorders and Stroke of the National Institutes of Health (NIH) (Award IRF1NS133972).

11:00 AM SB08.11.03

3D Printable Bioresorbable Electronics [Jared Anklam](#), [Kyle Harshany](#), [Breanna Wong](#), [Sammi Yu](#), [Eric K. Tokita](#), [Samuel H. Hales](#), [Aarav Parikh](#) and [Yong Lin Kong](#); University of Utah, United States

The ability for bioelectronics to be resorbed to the body can obviate the need for surgical extraction, reducing potential complications and clinical burden in bioelectronics implantation. Advances in bioresorbable electronics have enabled a broad range of transient electronics, yet achieving three-dimensional integration with bioresorbable electronics remains a challenging goal. Microextrusion-based 3D printing can create freeform wireless electronics that can be directly integrated with a broad range of three-dimensional biomedical devices and biological constructs. Nevertheless, formulating a 3D printing ink that simultaneously possesses the rheological properties and electronics properties necessary for high-performance wireless electronics has not been demonstrated. Here, we developed a 3D printable ink that is bioresorbable and electrical conductive ink. Our ink demonstrates excellent electrical conductivity ($3 \times 10^4 \text{ S/m}$) and possesses rheological properties that allow the preservation of geometrical fidelity. We envision that our work can enable the direct integration of transient bioelectronics into a broad range of biomedical devices and biological constructs, improving the potential clinical outcome in 3D-printed bioelectronics.

11:15 AM SB08.11.04

3D Printing of Nanomaterial-Based Bioelectronics with a Metamaterial-Inspired Near-Field Electromagnetic Structure [Samuel H. Hales](#)¹, [Jared Anklam](#)¹, [Xin Yang](#)², [John S. Ho](#)² and [Yong Lin Kong](#)¹; ¹University of Utah, United States; ²National University of Singapore, Singapore

3D printing of nanomaterials can enable the creation of freeform architectures and multifunctional devices with unprecedented versatility. The full potential of this technology, however, has so far been limited by the inability to selectively anneal the printed nanomaterials, a critical step to enhance performance. Here, we demonstrate the ability to selectively and locally anneal 3D printed nanomaterials *in situ* on a broad range of temperature-sensitive substrates by focusing near-field electromagnetic waves using a metamaterial-inspired near-field electromagnetic structure (Meta-NFS). The near-field microwave 3D printing (NFP) enables exceptional control of printed nanomaterial annealing parameters, allowing the creation of spatially freeform microstructure where the electronic and mechanical properties can be locally programmed. NFP significantly broadens the possible class of materials compatible with an additive manufacturing process, enabling the creation of hybrid multi-functional constructs and printing of functional electronics even on temperature-sensitive substrates.

11:30 AM SB08.11.05

Multifunctional Fluorinated Coating for Improving Neural Implant Biocompatibility [May Yoon Pwint](#), [Paige Martin](#) and [Xinyan T. Cui](#); University of Pittsburgh, United States

Although implantable neural electrode devices have been used in animals and human for neuroscience research and clinical applications, they face the challenge of signal degradation due to a myriad of reasons including implantation trauma, glial scarring, biofouling, and loss of signal-generating neurons. During implantation, the neural probe inflicts injury to the brain tissue by breaking blood vessels and inducing mechanical stress to the surrounding tissue. The implantation then triggers a cascade of immune response involving non-specific protein adsorption, inflammatory cell adhesion followed by the encapsulation of the probe by glial sheath. The disrupted blood flow may cause hypoxia, which along with the trauma and inflammation may compromise neuronal survival and function.

Here, we used chemically and biologically inert perfluorocarbon (PFC) as a multi-functional coating for implantable neural interfaces providing 1) lubrication during insertion to reduce insertion trauma, 2) anti-fouling surface, and 3) oxygen supply to the injury site. Preliminary data shows that the PFC coating can reduce peak insertion force of a single-shank silicon probe by at least 50%, translating to less acute trauma. The PFC coating also effectively decrease non-specific protein adsorption and inflammatory cell attachment. In addition, the same coating is capable of carrying oxygen and passively

releasing it over at least six hours. We also studied the effect of the coating on the interfacial impedance of platinum electrodes and found no significant difference in impedance between the bare and PFC coated electrodes. Combined, these functionalities of the PFC coating showed great potential for reducing implantation trauma and improving neuronal survival near the neural electrode implants.

SESSION SB08.12: Organic Materials
Session Chairs: Alina Rwei and Huiliang Wang
Thursday Afternoon, April 25, 2024
Room 433, Level 4, Summit

1:30 PM *SB08.12.01

Development of Highly Biocompatible Ultra-Low Fouling Zwitterionic Materials, Coatings and Nanoparticles Shaoyi Jiang; Cornell University, United States

An important challenge in many applications is the prevention of unwanted nonspecific biomolecular and microorganism attachment on surfaces. We have shown that zwitterionic materials and surfaces are highly resistant to nonspecific protein adsorption and microorganism attachment from complex media. Typical zwitterionic materials include poly(carboxybetaine), poly(sulfobetaine), poly(trimethylamine N-oxide), and glutamic acid (E) and lysine (K)-containing poly(peptides). Unlike poly(ethylene glycol) (PEG), there exist diversified zwitterionic molecular structures to accommodate various properties and applications. Furthermore, zwitterionic materials are super-hydrophilic while their PEG counterparts are amphiphilic. In this talk, I will discuss the application of zwitterionic materials to implants, medical devices, stem cell cultures, and drug delivery carriers. With zwitterionic materials, coatings, hydrogels or nanoparticles, results show no capsule formation upon subcutaneous implantation in mice for one year, expansion of hematopoietic stem and progenitor cells (HSPCs) without differentiation, no anti-coagulants needed for artificial lungs in sheep, and no antibodies generated against zwitterionic polymers. I will also discuss a newly developed drug delivery system to deliver mRNAs or small molecules through the blood-brain barriers into the brain.

2:00 PM SB08.12.02

Tailoring Thermogels: A Versatile Strategy for Functionalized Injectable Hydrogels and Controlled Drug Release Joey H. Wong¹, Belynn Sim^{1,2}, Jason Y. Lim^{1,3}, Xian Jun Loh^{1,4,2} and Rubayn Goh¹; ¹Institute of Materials Research and Engineering, Singapore; ²Nanyang Technological University, Singapore; ³National University of Sciences & Technology, Singapore; ⁴National University of Singapore, Singapore

Biocompatible injectable hydrogels provide a minimally invasive strategy for biointerfacing. Depending on the encapsulated payload, these hydrogels can serve as a low-modulus interface for neural electrodes, provide localized and sustained delivery of drugs, or offer structural support to cells during proliferation and tissue regeneration. One strategy used to develop injectable hydrogels involves copolymerizing thermally-responsive blocks with a hydrophilic polymer (e.g. pluronics). These thermally responsive injectable hydrogels, known as thermogels, undergo a sol-gel transition above a critical gelation temperature, such as when being warmed to 37°C. This is triggered by the formation of micellar crosslinks of the thermo-responsive domain.

In this study, we have developed a versatile synthetic strategy for creating a library of functionalized thermogels and have investigated the three-way interactions between functional groups, gel scaffolds, and encapsulated drugs. Our work will illustrate the impact of these functional groups on the sol-gel transition, the physical properties of these gels, and the sustained release of drug analogs. As a proof of concept, we were able to achieve sustained release of anionic orange II and cationic crystal violet of 5 to 6 months, with release profiles varying depending on the functionalized moieties.

2:15 PM SB08.12.03

Advanced Microfabrication Strategies for Neuro-Inspired 3D Conductive Polymers Valeria Criscuolo^{1,2}, Claudia Latte Bovio³, Kevin Lengefeld^{1,2} and Francesca Santoro^{1,2,3}; ¹RWTH Aachen University, Germany; ²Forschungszentrum Jülich GmbH, Germany; ³Istituto Italiano di Tecnologia, Italy

Neuroelectronic platforms aim at recapitulating neuronal communication and functions to monitor and eventually restore lost functionalities. Indeed, engineering neuroelectronic devices that can be smoothly interfaced with brain and neurons can provide a step forward in a better understanding of hampered electrical communication in e.g., neurodegenerative diseases. In this scenario, conductive polymers, such as PEDOT:PSS, have gained a prominent position in the realization of seamlessly integrated bioelectronic devices and soft flexible probes.¹ However, existing polymer-based devices are not yet able to effectively mimic and reproduce the complex neuronal environment, being flat and bidimensional. Neurons indeed interact with and respond to a great variety of mechanical and topographical stimuli; thus it is imperative to take inspiration from the extremely complex architecture of the brain.² Moreover, the cell-device interface plays a crucial role for an effective electrical coupling between the cell and the device.³ Indeed, a cleft is typically formed between the cell and the electrode. For this reason, recent approaches demonstrated that non-planar substrates, featuring 3D and 2.5D structures,⁴ result in the reduction of the cleft and in an improvement of cell-device electrical coupling.⁵

In the light of the above, here we introduce innovative microfabrication strategies for the realization of neuroelectronic platforms based on PEDOT that can recapitulate distinctive morphological neuronal features such as dendrites and dendritic spines.

Dendrites were reproduced by the formation of PEDOT:PF₆ fibers by using AC electro polymerization⁶ on a multi electrode arrays (MEAs). By changing the parameters of the applied signal and the geometric relationship between the electrodes, the growth and morphology of the fibers was altered.

Additionally, the fibers geometry and branching was tuned by changing the shape of the applied AC-signal and the manipulation of the electrical field. The so obtained dendrite-like fibers were morphologically characterized by means of scanning electron microscopy (SEM) and atomic force microscopy (AFM) and the neurite elongation and branching was compared to real neurons. Additionally, electrochemical properties as well as long term stability in aqueous media was investigated via electrochemical impedance spectroscopy (EIS) and cyclic voltammetry (CV).

On the other hand, dendritic spines, biological structures essential in synaptic communication, were recreated by means of 2-photon polymerization (2PP) lithography, given its high resolution, versatility, and design freedom² both achieving non-conductive and conductive material patterning via electropolymerization. The resulting 3D microstructures were characterized by SEM and electrochemical measurements (CV and EIS).

Finally, biocompatibility assays were carried out for both dendrites- and dendritic spines-like structures with neuronal cells, and the local adhesion processes to the 3D structures was characterized by means of optical and electron microscopy.

Overall, the proposed strategies allow for the fabrication of 3D/2.5D electrodes with different levels of complexity that can effectively mimic neuronal features and enhance the cell-chip interface. Such systems will open the way to the possibility of sensing and/or stimulating cells and tissues in a more realistic environment.

2. A. Mariano, et al., *Nanotechnology*, **2022**, 33, 492501
3. G. Wrobel, et al., *J. R. Soc. Interface*, **2008**, 5, 213–222
4. M. E. Spira, et al., *Front. Neurosci.* **2018**, 12.
5. F. A. Pennacchio, et al., *J. Mater. Chem. B*, **2018**, 6, 7096.
6. M. Cucchi, et al., *Adv. Electron. Mater.*, **2021**, 7, 2100586.

2:30 PM SB08.12.04

A Simple Animal Model to Discover Neuroactive Function of Semiconducting Oligomers [Claudia Tortiglione](#)¹, Giuseppina Tommasini¹, Mariarosaria De Simone¹, Silvia Santillo¹, Marika Iencharelli¹, Gwennaë R. Dufil², Daniele Mantione³, Eleni Stavrinidou² and Angela Tino¹; ¹Istituto di Scienze Applicate e Sistemi Intelligenti, Italy; ²Linköping University, Sweden; ³University of the Basque Country, Spain

Modulating neural activity with electrical or chemical stimulus can be used for fundamental and applied research. Beside intracellular and extracellular electrodes delivering brief electrical pulses for neural stimulation, wireless methodologies based on functional materials may represent superior alternatives to modulate neuronal function. Here we show that the organic semiconducting oligomer ETE-S induces precise behaviors in the freshwater polyp *Hydra*, a small invertebrate with a nerve net controlling a limited repertoire of behaviors. Through pharmacological and electrophysiological approaches we found that the ETE-S induced behavioral response relies on the presence of head neurons and calcium, and is prevented by drugs triggering ionotropic channels and muscle contraction [1]. Moreover, ETE-S affects *Hydra*'s electrical activity enhancing the contraction burst frequency. The unexpected neuromodulatory function played by this conjugated oligomer on a simple nerve net opens intriguing research possibilities on fundamental chemical and physical phenomena behind organic bioelectronic interfaces for neuromodulation, and on alternative methods that could catalyze a wide expansion of this rising technology for clinical applications.

[1] G. Tommasini, M. De Simone, S. Santillo, G. Dufil, M. Iencharelli, D. Mantione, E. Stavrinidou, A. Tino, C. Tortiglione. In vivo neuromodulation of animal behavior with organic semiconducting oligomers. *Science Advances*, published on line 18 Oct. 2023

2:45 PM SB08.12.05

Polymer-Based Transparent Brains for 3D Evaluation of Brain Tumors without Tissue Sectioning [Maryam Golshahi](#), Hamed Arami and Layla Khalifehzadeh; Arizona State University, United States

Conventional tissue sectioning, staining, and optical microscopy are used as standard clinical methods for diagnosis of the brain tumors (i.e., glioblastoma multiforme or GBM), studying their anatomical phenotypes and evaluating their response to therapies. Sectioning of the tissues is destructive and stained and analyzed tissues cannot be re-used for evaluation of additional biomarker. Also, histological microscopy data obtained from each tissue section are limited to that area of the tumor and are not ideal representatives of the whole tumor mass, especially for highly heterogeneous tumors such as GBM. Here, we will discuss a method for transforming the whole brain tumor tissues to optically transparent hydrogel masses without losing any anatomical, extracellular or sub-cellular features within the tissues. Different types of orthotopic brain tumors (e.g., human-derived U87 GBM with GFP signal) were generated in mouse brains (n=3-5) and analyzed using magnetic resonance and bioluminescent imaging (MRI and BLI). Brains were excised and immersed in an acrylamide monomer solution, followed by the polymerization of these monomer molecules within the entire brain tissue at 37°C. Brains were clarified by removing the lipid molecules from the tissue microenvironment. Transparent brains were analyzed using confocal and light-sheet microscopy techniques after being immersed in Focus Clear solution to adjust their refractive index for optimized microscopy. Three-dimensional macroscopic and microscopic maps were generated from the whole brains for analyses of the tumor growth pattern and their response to therapies, without losing the intactness of the proteins and tissue structure. Using various monomer derivatives enabled the tuning of the cross-linking rate and optical transparency of the hydrogels for improved analysis of heterogeneous tumor masses. This method enabled series of reversible staining de-staining, and re-staining of the tissues for clinical analysis of different brain tumors and a variety of neuropathological biomarkers.

SYMPOSIUM SB09

Bioelectricity and Recapitulation of 3D Environment in Microbial and Tissue Engineering
April 23 - April 23, 2024

Symposium Organizers

Sina Jamali, UNSW Sydney
Nathalia Peixoto, George Mason University
Frankie Rawson, University of Nottingham
Paulo Rocha, University of Coimbra

* Invited Paper
+ JMR Distinguished Invited Speaker
^ MRS Communications Early Career Distinguished Presenter

SESSION SB09.01: Electrical Stimulation of Cells
Session Chairs: Leyla Esfandiari and Sina Jamali
Tuesday Morning, April 23, 2024
Room 438, Level 4, Summit

10:30 AM *SB09.01.01

What Happens When We Stimulate Cells with Electricity? [George G. Malliaras](#); University of Cambridge, United Kingdom

Electrical stimulation of cells can elicit a variety of biological outcomes, e.g. the firing of action potentials in neurons, or the promotion of apoptosis in dividing cells. Clinical uses of electrical stimulation include the treatment of cardiac arrhythmia, profound deafness, movement disorders and different forms of cancer. Still, a unified description of the phenomena elicited by electrical stimulation does not exist and different communities focus on particular aspects within the general field (electrophysiology, tissue engineering, electroporation, tumour treating fields). I will discuss a generalised framework for discussing these phenomena, starting with experimental ways to avoid the production of chemical species at the electrodes, following with a review of the physical phenomena that take place upon electrical stimulation and ending with the elicited biological outcomes.

11:00 AM SB09.01.02

Investigating Electrical Stimulation to Mitigate The Foreign Body Response in Neural Implants [Filip Wronowski](#) and [George G. Malliaras](#); University of Cambridge, United Kingdom

This research addresses a critical challenge in the field of neural interfaces: the foreign body response (FBR). Neural interfaces hold tremendous promise for treating neurological disorders and enhancing therapeutic outcomes, but the FBR often limits their long-term effectiveness.

The FBR is primarily driven by non-neuronal glial cells and results in chronic inflammation and fibrosis, ultimately compromising neural recording and stimulation capabilities. This study focuses on the potential of electrical stimulation to mitigate the FBR and enhance the performance and longevity of neural implants.

Preliminary findings indicate that electrical stimulation can influence astrocytes, fibroblasts, and other cell types involved in the FBR. The parameters of stimulation, including timing, intensity, and frequency are being investigated and can influence the glial response, ranging from driving cell alignment, affecting cell division and to exerting anti-inflammatory to pro-inflammatory effects.

To this end, we employ two novel in vitro platforms, followed by advanced microscopy techniques and cytokine assays. These insights will be further complemented by RNA sequencing. Our ultimate aim is to extend our findings to an in vivo context, enabling us to refine our understanding and improve strategies for addressing the foreign body response in neural implants.

This research sheds light on these complex interactions, offering potential strategies to enhance the effectiveness of neural interfaces and reduce the impediments caused by the FBR. Ultimately, this work has the potential to significantly impact the field of neural implant technology and improve patient outcomes in the treatment of neurological disorders.

11:15 AM SB09.01.03

Quantum Bioelectrochemistry for The Treatment of Hard-To-Treat Cancers [Akhil Jain](#)^{1,2}, [Jonathan Gosling](#)¹, [Padma-Sheela Jayaraman](#)¹, [Stuart Smith](#)¹, [David Amabilino](#)³, [Mark Fromhold](#)¹, [Yi-Tao Long](#)², [Lluïsa P. García](#)⁴, [Lyudmila Turyanska](#)¹, [Ruman Rahman](#)¹ and [Frankie J. Rawson](#)¹; ¹University of Nottingham, United Kingdom; ²State Key Laboratory of Analytical Chemistry for Life Science, School of Chemistry and Chemical Engineering, Nanjing University, China; ³Institut de Ciència de Materials de Barcelona (ICMAB-CSIC), Spain; ⁴Departament de Farmacologia, Toxicologia i Química Terapèutica, Facultat de Farmàcia i Ciències de l'Alimentació, Universitat de Barcelona, Spain

Quantum biological tunnelling for electron transfer (QBET) is involved in controlling essential functions for life such as cellular respiration and homeostasis. Understanding and controlling the quantum effects in biology has the potential to modulate biological functions. Here we merge wireless nano-electrochemical tools with cancer cells for control over electron transfer to trigger cancer cell death. Gold bipolar nanoelectrodes functionalized with redox-active cytochrome *c* and a redox mediator zinc porphyrin were developed as electric-field-stimulating bio-actuators, termed bio-nanoantennae. We show that a remote electrical input of alternating current (A.C.) at high frequency (3MHz) and low voltages (0.65V/cm) regulates electron transport between these redox molecules, which results in quantum biological tunnelling for electron transfer to trigger apoptosis in cancer cells from various hard-to-treat tumors. Transcriptomics data show that the electric-field-induced bio-nanoantenna targets the cancer cells in a unique manner, representing electrically induced control of molecular signaling. Arrhenius-kinetics confirmed the occurrence of moderate QBET in the system. *In vivo* studies in tumor bearing rats are underway to demonstrate first example of quantum medicine to treat cancers.

SESSION SB09.02: Morphic Bioelectronics
Session Chairs: Raquel Amaral and Paulo Rocha
Tuesday Afternoon, April 23, 2024
Room 438, Level 4, Summit

1:30 PM *SB09.02.01

Organic Neuromorphic Bioelectronics [Paschalis Gkoupidenis](#); Max Planck Institute for Polymer Research, Germany

Neurons are the fundamental elements of the nervous system, coping with a great diversity of electrobiochemical signals. Neuronal function is an archetype for biomimicry with neuromorphic electronics. However, artificial neurons based on electronics are insufficiently capable of operating in situ in biological environments, thus hampering the seamless sensing and biointerfacing as well as the bio-realistic neuronal emulation. A few examples of soft-matter artificial neurons are based on conventional circuit oscillators and therefore require many elements for their implementation. An organic artificial neuron consisting of a compact non-linear electrochemical element will be presented. The artificial neuron displays in situ operation in biologically relevant environments that displays spiking dynamics sensitive to common ions of the biological aqueous milieu, within physiopathological concentration ranges (~5-150mM), and with ion specificity. Small-amplitude (~1-150 mV) electrochemical oscillations and noise in the electrolytic medium shape the neuronal dynamics, while changes of ionic ($\geq 2\%$ over physiological baseline) and biomolecular concentrations (≥ 0.1 mM dopamine) modulate the neuronal excitability. The artificial neuron operates synergistically with bio-membranes, forming real-time biohybrid interfaces. This electrochemical artificial neuron opens new possibilities for the seamless communication and the realistic emulation of biology with electronics.

2:00 PM SB09.02.02

Ultrathin TiO₂ ALD Coatings Enhance Properties of Biomaterials used in Medicine Jana Bacova¹, Kaushik Baishya², Jan Capek¹, Raul Zazpe^{1,2}, Hanna Sopha^{1,2}, Lina M. Sepulveda¹, Tomas Rousar¹ and Jan M. Macak^{1,2}; ¹University of Pardubice, Czechia; ²Central European Institute of Technology, Brno University of Technology, Czechia

TiO₂ surfaces are in general recognized as excellent biocompatible materials owing to their resistance to body fluid effects, low ion release, high stability, antibacterial properties, and wetting ability. Various TiO₂ nanostructured surfaces show great properties enhancing cell interactions. Anodic TiO₂ nanotube (TNT) layers have emerged as extremely suitable and effective substrates for cell growth and proliferation. A pioneering study demonstrated that TNTs with a diameter of 15 nm are the most suitable surface for the growth of cells [1]. Several papers also showed that anodization is a great tool for surface modification of various materials used in biomedical applications, especially TiAlV.

Recently, we demonstrated that ultrathin coatings by metal oxides (e.g. TiO₂) using Atomic Layer Deposition (ALD) on TNT layers enhance cell adhesion, growth, and proliferation [2]. These properties make them excellent as the uppermost surfaces for bone and dental implants. The presentation deals with the comparison of the biological effect of ultrathin TiO₂ ALD coatings achieved by various numbers of TiO₂ ALD cycles on planar and nanotubular surfaces. For that Ti sheets and anodized TNT layers with a distinct inner diameter of 12 nm and 15 nm, were used as substrates, as they appear to be the most suitable for cell growth in general. We evaluated the cell adhesion, proliferation, and density of fibroblast, osteoblast, and neuroblast cells on these substrates [2,3].

Moreover, the single-cell adhesion of the cells to the TNT layers modified using ALD method was studied by the bio-Atomic Force Microscopy (bio-AFM) technique [3]. Finally, the biological effect of black form of TiO₂ nanotubes in comparison to their classical counterparts was investigated for the first time. The black TiO₂ nanotubes with TiO₂ ALD coating can be considered as a potential candidate in various applications due to the disappearance of mild toxic effects of white and black TiO₂ nanotubes due to the shading of carbon and fluorine species incorporated within the TiO₂ nanotube walls [4].

References:

1. Park, J., Bauer, S., Schlegel, K. A., Neukam, F. W., von der Mark, K., & Schmuki, P. (2009). TiO₂ nanotube surfaces: 15 nm—an optimal length scale of surface topography for cell adhesion and differentiation. *Small*, 5(6), 666-671.
2. Motola, M., Capek, J., Zazpe, R., Bacova, J., Hromadko, L., Bruckova, L., ... & Macak, J. M. (2020). Thin TiO₂ coatings by ALD enhance the cell growth on TiO₂ nanotubular and flat substrates. *ACS Applied Bio Materials*, 3(9), 6447-6456.
3. Baishya, K., Vrchovecká, K., Alijani, M., Rodriguez-Pereira, J., Thalluri, S. M., Goldbergová, M. P., ... & Macak, J. M. (2023). Bio-AFM exploits enhanced response of human gingival fibroblasts on TiO₂ nanotubular substrates with thin TiO₂ coatings. *Applied Surface Science Advances*, 18, 100459.
4. Sopha, H., Bacova, J., Baishya, K., Sepúlveda, M., Rodriguez-Pereira, J., Capek, J., ... & Macak, J. M. (2023). White and black anodic TiO₂ nanotubes: Comparison of biological effects in A549 and SH-SY5Y cells. *Surface and Coatings Technology*, 462, 129504.

2:15 PM SB09.02.03

Microalgal Growth Assessment using Fluorinated Ethylene Propylene Microcapillaries Raquel Amaral¹, David M. Silva¹, Nuno M. Reis² and Paulo R. Rocha¹; ¹University of Coimbra, Portugal; ²University of Bath, United Kingdom

Efficient microalgal bioanalytical microsystems are becoming crucial to address the industrial, agricultural and environmental increasing demands. Most microalgae farming continues to depend on a significant amount of manpower in monitoring and measuring growth of microalgae in open ponds and/or photo-bioreactors. This requires specialized operators, regular sampling from open ponds or photo-bioreactors, and the use of bulky laboratory equipment. In addition, many open ponds and water reservoirs are exposed to environmental factors such as temperature, nutrients or pH changes which may trigger algal blooms or cause difficulty in predicting microalgal growth, a critical challenge in the water industry.

In this work we demonstrate the use of a melt-extruded fluorinated ethylene propylene (FEP) Teflon microfluidic film coated with PVOH as a hydrophilic "dip-stick" microcapillary for *in-situ* power-free sampling and optical monitoring of microalgal growth. We ascertained the growth of *Chlorella* for 22 days in the 'dip stick' microfluidic strips matched well the growth in an aerated Erlenmeyer, yielding a logistic growth with a growth rate of 0.35 day⁻¹ and similar to large industrial bioreactors, without the need of nutrient renewal. The optical transparency of the 'dip stick' strip combined with good permeability enabled simultaneous tracking of cell cycle and growth rate using simple image analysis, which can easily be carried out with a smartphone camera.

Our new microanalytical solution enables micro-cultivation and individual cell monitoring over time, which may pave the way to innovative biocompatible materials for water management and also high throughput microalgal productivity assessment.

2:30 PM BREAK

SESSION SB09.03: Bioelectronic Interfaces and Devices
Session Chairs: Sonia Contera and Nathalia Peixoto
Tuesday Afternoon, April 23, 2024
Room 438, Level 4, Summit

3:00 PM *SB09.03.01

Mechano-Electrical Coupling in Neurons Sonia Contera; University of Oxford, United Kingdom

We have become used to studying the different aspects of biological function in isolation; biochemical, genetic, mechanical or electrical properties of

biomolecules, cells and organisms are studied by different fields. Yet, it is precisely the coupling of the different aspects inside “a living shape” that underlies the functional diversity and the information processing capacity of living systems. By coupling their properties, biological systems can induce behaviours acting against the direction imposed by thermodynamic forces, which are characteristic of *being alive*. For example, a protein is able to work with great efficiency because it couples electrostatics, mechanics and chemistry; an embryo grows its shape by coupling mechanical, chemical, genetic and electrical oscillations.

In neurons, evidence gathered over half a century shows that local mechanical changes in the membrane propagate along with the action potential in neurons. These observations effectively point towards the hypothesis that the action potential is not merely an electrical pulse, but a complex multiscale electro-mechanical “multiphysics” process that affects and is affected by all components of the membrane [1]. Due in part to the emergence of experimental techniques such as atomic force microscopy (AFM) that allow to measure and alter the mechanical properties of membranes and living cells in physiological environments, research interest in the role of mechanics of the neuronal membrane has grown, essentially driven by its potential in medical applications, e.g. in ultrasound neuromodulation (expected to find applications in the treatment of epilepsy and chronic pain, to promote neuroplastic repair mechanisms for post-stroke recovery).

Using new techniques that allow us to apply mechanical signals to living neurons from the Hz to the 100s of KHz range and to quantify correctly viscoelastic properties from these measurements [2], and coupling them to electrophysiological and fluorescence measurements, our work shows that alterations of electrophysiological activity (e.g., with anaesthetics or electrical potential) correlate linearly with a change in viscoelastic properties such as the loss tangent, the ratio of mechanical energy stored and dissipated in the cell [3]. And the other way around, ultrasound stimulation alters neuronal firing. I will discuss these results in the context of building a “multiphysics” nonequilibrium framework to study neurons that allows us to create models to predict/interpret the oscillatory systemic behaviours of physical/chemical properties of neuronal networks [1].

References:

- [1] Electrophysiological-mechanical coupling in the neuronal membrane and its role in ultrasound neuromodulation and general anaesthesia. Jerusalem A. ...Contera S (2019) *Acta Biomater.* 97, 116–140.
- [2] Nanoscale rheology: Dynamic Mechanical Analysis over a broad and continuous frequency range using Photothermal Actuation Atomic Force Microscopy, Piacenti AR, Adam C, ...Contera S (2023) S- arXiv preprint arXiv:2307.16844.
- [3] Action of the general anaesthetic isoflurane reveals coupling between viscoelasticity and electrophysiological activity in individual neurons, Adam C, Kayal C, Ercole A, Contera S, Ye H, Jerusalem A (2023), *Communications Physics*, 6(1).

3:30 PM *SB09.03.02

Bioactive Piezoelectric Nanofibers for Electromechanical Stimulation and Neuronal Regeneration [Leyla Esfandian](#)^{1,2}; ¹University of Cincinnati, United States; ²Cincinnati Children Hospital, United States

One of the important signaling networks in embryonic development, regeneration, and homeostasis of tissue is the endogenous bioelectricity. It has been observed that electric fields can promote axonal regrowth in nerve injury and bioelectric stimuli can be crucial to induce regeneration in peripheral and central nervous systems. Severe peripheral nerve injuries disrupt nerve pathways, connections, and the extracellular matrix (ECM) surrounding the nerve, which affects distal innervation targets. If the injury gap is large enough, functional recovery is extremely limited and adequate clinical therapies don't exist. A key reason for poor functional recovery is that neurons lack the proper guidance, alignment, and signaling from the damaged ECM to allow for targeted growth across injured tissue.

We have developed an ultrasound-mediated, bioactive scaffold that addresses these challenges by offering controllable electrical, physical, and chemical signaling capabilities. Piezoelectric poly(vinylidene fluoride-co-trifluoroethylene)(PVDF-TrFE) is integrated with decellularized ECM through electrospinning fabrication technique. The bioactive piezoelectric nanofibers are capable of producing controllable electrical stimulation in response to cellular mechanobiology and remote ultrasound activation without the need for electrodes due to its piezoelectric capacity. The tissue-specificity of the ECM combined with the piezoelectric scaffold improved the cell-biomaterial interactions and host immune response. Extensive characterization of material properties was conducted on resultant bioactive scaffolds. The bioactive scaffold's piezoelectric nature remained intact, and cell-material interactions showed enhanced cell viability, proliferation, and adhesion. This new and multi-parametric biomaterial is envisioned to be used as next-generation nerve guidance conduits (NGCs) and will be tested for its efficacy in the future.

4:00 PM SB09.03.03

Observation of Cell Behavior by Waveform Measurement using Lithium Niobate-Based Surface Acoustic Wave Device [Shun Koda](#)¹, Takahiro Yamada², Hiroaki Onoe³, James Friend² and Yuta Kurashina¹; ¹Tokyo University of Agriculture and Technology, Japan; ²University of California, San Diego, United States; ³Keio University, Japan

Introduction: Highly matured cells and tissues are essential to improve the quality of regenerative medicine and drug discovery research. Fluorescence observation by immunostaining with antibody labeling of maturation makers is one of the gold standards for evaluating such cells and tissues. To deliver antibodies to antigens in the cell membrane, fixation and permeabilization of cells are necessary for fluorescence observation. Recently, living cells can be observed by gene transfer (Kasahara et al., *Sci. Adv.*, 2023), but with the risk of altering the cellular morphology. That is, observation of living cells is difficult without damaging cells.

Here, we propose a non-invasive evaluation method of cultured cells using surface acoustic waves (SAW) for sensing cell behavior without administering any invasive chemicals to the cells or altering their genetic traits. For cell behavior observation, a cell evaluation system with surface acoustic waves transmitted from a SAW device to the cells was fabricated. The SAW device consists of lithium niobate (LN) substrates having a high mechanical quality factor. Thus, LN is suitable for the material of the SAW device because of its low elastic loss and low attenuation of surface acoustic waves.

Materials and methods: The waveform information from the transmitted and received waves was measured to observe cell behavior by this cell evaluation system. The cell evaluation system was composed of the SAW device and energizing probes. The SAW device was fabricated by a lift-off method using an LN substrate with chromium and aluminum deposited to form IDT fingers. To micropattern the cells to the measurement spot, the seeding area was limited by the dimethylpolysiloxane (PDMS) chamber sandwiched between acrylic covers to adhere the chamber to the SAW device. The slit surface was then cleaned using peracetic acid and plasma. The cells were incubated for 6 hours after modifying fibronectin on the surface of the SAW device. After incubation, the acrylic cover and cell-seeding chamber were removed from the cell evaluation system. After seeding cells, an alternating current of around 40 MHz band was applied to the IDT to measure the received wave with an oscilloscope.

Results and discussion: The resonance frequency of the SAW device on the transmitter side of the fabricated cell evaluation system was measured with an impedance analyzer at 37.8 MHz. The SAW devices freely control the frequency band of irradiating SAW by changing the design of the distance between the interdigital transducer (IDT) fingers. In this study, by setting the distance between the IDT fingers to 25 μm , the target resonance frequency of the SAW device was 40 MHz. From the measurement of the impedance analyzer, the SAW device with a resonance frequency close to the target resonance frequency was successfully fabricated. This reproduces a wavelength ($\approx 100 \mu\text{m}$) that provides sufficient resolution for observing cell behavior. The cell seeding area was a 1 mm \times 5 mm slit area considering that the attenuation length of the SAW surface displacement at the LN-water interface is 1.24 mm. The SAW was irradiated by applying an alternating current at around 40 MHz band to the IDT fingers of the SAW device on the transmitting side. Waveforms were measured at two different cell counts. The ratio of the amplitude of the received wave to the amplitude of the transmitted wave was 0.88

when the cell density was 627 cells/mm², and 0.97 when the cell density was 83 cells/mm², respectively. Comparing them, the surface acoustic waves were attenuated as the number of cells increased. These results suggest that this system is effective in measuring cell counts. Since ultrasound is capable of reaching deep into tissues, measuring waveforms using this system could be applied to the development of more effective biomaterials including 3D cellular tissues.

SESSION SB09.04: Bioelectronic Interfaces for Monitoring and Modulating Cells
Session Chairs: Frankie Rawson and Paulo Rocha
Tuesday Afternoon, April 23, 2024
Flex Hall C, Level 2, Summit

5:00 PM SB09.04.01

PEDOT:PSS Porous Electrodes for Probing Cohort Signaling in *Escherichia Coli* Felipe L. Bacellar¹, Francisco C. Cotta Jr¹, Raquel Amaral¹, Nuno M. Reis² and Paulo R. Rocha¹; ¹University of Coimbra, Portugal; ²University of Bath, United Kingdom

Bacteria are known to coordinate gene expression to control their phenotypic characteristics to the most favourable condition in harsh environments. This smart communication mechanism enables the bacteria cells to efficiently manage the behaviour of their surrounding community. One important mediator of communication processes in bacteria is the dynamics of their membrane potential, mainly studied through single-cell patch-clamp - which is difficult due to bacteria small size, and through the use of genetic modified bacteria that produce changes in fluorescence intensity as a function of membrane polarization. Despite being a direct response to the external electric stimuli and chemical agents (such as ion channel inhibitors, stimulants or antibiotics) these fluorescence methods usually require toxic fluorescent probes hindering stress-free long-term recordings and fail to probe important sub-thresholds regimes in the measuring cell or cellular cohort.

Non-invasively sensing the minuscule electrical activity of bacteria populations is therefore a major challenge in bioelectronics and microbiology. To overcome this challenge, we have devised a highly sensitive transducer based on Au/Polyurethane(PU)/poly(3,4-ethylenedioxythiophene) polystyrene sulfonate (PEDOT:PSS) electrodes, to visualize the electrogenic activity of cohorts of bacteria without the need of gene modification or the use of stimuli to address intercellular communication.

For the first time, the electrical activity of large *Escherichia coli* populations is directly measurable. By submerging the recording electrodes into LB broth with the model bacteria *E. coli* MG1655, we were able to sense the bacterial electrical behaviour without any physical disruption or interference into their physiology. *E. coli* demonstrated fluctuations of their basal voltage level, which is much higher in amplitude than the background acquisition noise of about 1 μ V. The extracellular analysis reveals asynchronous and synchronous electrical spikes, with amplitudes ranging from 10 μ V up to 100 μ V, spike widths from 50 ms to 2 s and sporadic events of quasi-periodic bursts with interspike intervals mostly between 0.5 to 10 s, which can be attenuated by using a protonophore carbonyl cyanide m-chlorophenylhydrazine (CCCP).

The electric noise analysis combined with compound screening indicated that the *E. coli* likely communicate through a diffusion-limited paracrine signalling mechanism where the diffusion of H⁺ plays an important role.

Our ultra-sensitive transducer is a unique screening tool to study the electrophysiological properties of large bacterial populations under different pharmacological compounds effects and metabolic states contributing to more effective drug developments.

5:00 PM SB09.04.02

Bioelectricity in Diatom *Phaeodactylum Tricornutum* Cohorts Raquel Amaral, Francisco C. Cotta Jr, Felipe L. Bacellar and Paulo R. Rocha; University of Coimbra, Portugal

Diatoms are a large and highly diverse group of photosynthetic microalgae, mostly oceanic, with a major environmental role on the planet due to a significant contribution to global fixation of carbon and to the biogeochemical cycling of silica. The peculiar evolutionary history of diatoms equipped them with a unique genetic and metabolic makeup which likely contribute to their ecological success in the contemporary oceans. The presence of intracellular signaling and intercellular communication mechanisms in diatoms upon stress plays a role in the acclimatory response to (a)biotic stressors. Diatoms thrive and may proliferate into pernicious harmful algal blooms through their resourceful communication mechanisms, not yet fully understood. We demonstrate that a population of diatoms under darkness show electrical oscillations. Cells of model diatom *Phaeodactylum tricornutum* were left to settle on planar gold printed electrodes. The setup was in a Faraday's cage connected to instrumentation tailored to record minute electric fluctuations stemming from extracellular signaling. Recordings of voltage as a function of time show fast signals, preceded by voltage elevation, which resemble neurons' "firing" action potential. The mean magnitude of these spikes was 0.0404 mV, with a mean duration of 0.444 s, they are possibly a result of collective participation of several cells as a response to voltage fluctuation. Since diatoms are not synaptically interconnected in a network as neurons are, signal transmission likely occurs by paracrine signaling, in which one cell diffuses a messenger molecule to nearby cells, causing a cascade effect by consecutive voltage-gated diffusion of ions through membrane channels. Slower signals were also recorded with a speed of 201.9 μ m/s across the 1.4 mm diameter electrode, similar to previously determined for another diatom species. These signals have an atypical shape resembling random telegraph noise. Messenger Ca²⁺ ions are involved in the mechanism, since their diffusion characteristics match those of the intracellular waves.

The translation of microalgal cooperative signaling paves the way for early detection and prevention of harmful blooms and an extensive range of stress-induced alterations in the aquatic ecosystem.

5:00 PM SB09.04.03

Cyanobacteria Growth Assessment using Fluorinated Ethylene Propylene Microcapillaries David M. Silva, Raquel Amaral and Paulo R. Rocha; University of Coimbra, Portugal

Due to global warming and other human-derived nutrient rich discharge, nutrient availability increases, causing anomalous proliferation of bloom-forming phytoplankton. This leads to eutrophication and the deoxygenation of bottom waters, with a dramatic toll on the affected food web and ecosystems. Cyanobacteria, also known as blue-green algae, are the main bloomers in freshwater ecosystems, including species of *Oscillatoria*, known to produce algal toxins with an unpleasant earthy/moldy taste and odor, contaminating water sources and drinking waters.

The study of filamentous cyanobacteria is hampered by technical problems stemming from the slow growth observed *in vitro*, even with nutrient-rich culture media. Their maintenance in laboratory conditions is demanding and requires frequent nutrient refreshing to prevent culture loss. Moreover, the conventional methodologies used to study growth over time, such as cell counting, are not applicable due to cells being packed into filamentous morphology. Also, dry weight estimations are inconsistent due to the presence of various filament sizes in culture.

To overcome the technical limitation of assessing the filamentary growth of cyanobacteria, we developed a transparent fluorinated ethylene propylene (FEP) microcapillary strips to sample, cultivate and monitor the loaded filaments of *Oscillatoria* over time.

Geosmin producer strain *Oscillatoria* sp. UHCC 0332 was cultivated in BG11 medium during 3 weeks, in a growth chamber. Filaments were dip-loaded into 3 cm long strips that were then cultivated in standard conditions for 2 weeks for image assessing and then up to 15 more weeks for confirming survival. The growth of two filaments was determined after 1 and 2 weeks. The estimation of growth was achieved by determining the area occupied by the filaments over time, with image analysis. This enabled the observation that filaments elongate over time with growth rates reaching up to 0.40 day⁻¹. Also, it was possible to estimate the number of cells which corresponded to elongation. Our microanalytical solution enables long-term micro-cultivation and individual *Oscillatoria* monitoring over time, which may pave the way to pioneering biocompatible materials for water management and productivity assessment.

5:00 PM SB09.04.04

A PEDOT:PSS Porous Electrode for Real-Time Monitoring of Microalgae Growth using Electrochemical Impedance Spectroscopy [Francisco C. Cotta Jr](#), Raquel Amaral, Felipe L. Bacellar and Paulo R. Rocha; University of Coimbra, Portugal

Microalgae are early Jurassic unicellular microorganisms globally used as sentinels to examine water ecosystems due to their ability to grow in most humid environments and quickly react to environmental stressors. Monitoring microalgal growth is currently an important area in water resource management and remains hindered by non-efficient measurements of, for instance, N and P nutrient fractions, temperature, and dissolved oxygen, or even biomass. Here, we show that electrical impedance spectroscopy (EIS) can be used as a non-invasive and real-time tool to probe microalgal growth, from the linear to stationary phases, on metal/polyurethane/poly (3,4- ethylenedioxythiophene) polystyrene sulfonate (PEDOT: PSS) electrodes.

A highly mucilaginous culture of *Chlamydomonas* was selected to promote cell adhesion to our Au/PU/PEDOT: PSS porous electrode. The cells were seeded on our transducer, within a homemade cultivation well and inside a standard algal growth chamber from ARALAB. The EIS recordings were continuously monitored inside the ARALAB, for 14 days, during which the cells grown from linear to stationary phases - as confirmed by our parallel and conventional cell counting methods. Contrary to the high frequency regime where minor changes occurred, at low frequencies, below the Maxwell-Wagner relaxation frequency at 0.1 mHz, a substantial change in impedance of over 3 kΩ was observed with culture time.

Interestingly, the EIS data and equivalent circuit modeling are consistent with standard microscopy analysis, cell-counting and extracellular matrix development. The growth followed a logistic function with exponential phase from day 2 until day 6 followed by a linear growth and then cell density started to decline at day 10. A growth rate of $k=0.85$ cells/day was extracted from standard growth curves. The EIS at 0.1 mHz followed a similar trend to the standard growth curve, with an Impedance increase at the beginning of the growth curve coinciding to the exponential and linear phase of growth, followed by an electrochemically stable stationary stage. By following the extracellular polymeric substances (EPS) formation in *Chlamydomonas* cells over time, we ascertained that the high production of EPS by each cell in the initial growth phase is quite significant and contributes to a higher Impedance, at the beginning of growth. In fact, by considering that the cells and EPS are both occupying the sensor surface area and causing the impedance to change, a growth curve obtained with the total area occupied by cells and EPS was by normalized with the corresponding EIS, which resulted in a near overlapping of the fitted logistic functions.

Here we show that Au/PU/PEDOT:PSS porous electrodes can be applied to sense, characterize and model microalgae growth with EIS, which may open new avenues for more effective and predictive water resource management.

SYMPOSIUM SB10

Bioinspired Organic Materials and Devices for Sensing and Computing
April 23 - April 26, 2024

Symposium Organizers

Simone Fabiano, Linköping University
Sahika Inal, King Abdullah University of Science and Technology
Naoji Matsuhisa, University of Tokyo
Sihong Wang, University of Chicago

Symposium Support

Bronze
IOP Publishing

* Invited Paper

+ JMR Distinguished Invited Speaker

^ MRS Communications Early Career Distinguished Presenter

SESSION SB10.01: Organic Electrochemical Transistors—Fundamentals and Materials I
Session Chairs: Hans Kleemann and Sihong Wang
Tuesday Morning, April 23, 2024
Room 429, Level 4, Summit

10:30 AM *SB10.01.01

Novel Approaches for High-Performance Organic Transistors Lukas M. Bongartz, Matteo Cucchi, Anton Weissbach, Ali Solgi, Hans Kleemann and Karl Leo; IAPP, Germany

The first organic transistors reported were organic electrochemical transistors (OECT, 1984) historically before the organic field effect transistor (OFET, 1986), the organic inversion transistor (2011), and the organic bipolar transistor (2022). After a longer phase of limited interest, OECT have recently been investigated intensively since they offer switching and sensing functionality in an electrolytic environment compatible with biological systems. The mixed electron-ion transport of the devices has consequence for many parameters of the devices including dynamics and hysteresis. In this talk, our recent work on a better understanding of OECT operation is discussed. Recently, we have shown that the so far used electrostatic “FET-like” description of OECT is needs to be extended to a model including entropic and enthalpic terms. The model elegantly describes a multitude of effects, including bistability and a peculiar temperature behavior of subthreshold slopes. Besides offering new insight into the basic operation, it also allows novel device applications.

11:00 AM *SB10.01.02

Novel Material for n-Type Organic Electrochemical Transistors [Thuc-Quyen Nguyen](#); University of California, Santa Barbara, United States

Organic electrochemical transistors (OECTs) are attractive for applications in chemical and biological sensors, neuromorphic computing, and reconfigurable electronics. An OECT consists of three electrodes (source, drain, and gate), an organic mixed ionic-electronic conductor (OMIEC) channel connecting the source and the drain, and an electrolyte between the gate and the channel. The development of OECTs has been strongly linked to advances in OMIECs. The OECT active material needs to accommodate ion transport, electronic transport, ion-electronic coupling, and air stability. For these reasons, early development of OMIECs has focused mostly on p-type polymer materials because of their superior air-stability and processability. As for n-type OECT polymer active materials, the bottle-neck is usually air-stability because n-type polymers with lowest unoccupied molecular orbital (LUMO) higher than -4.0 eV react with oxygen at ambient condition. In this work, we report an approach to make n-type OECTs from a solution-processable perylene diimide-based material. Our model material shows good n-type electronic transport, ionic transport, ion-electronic coupling, and air-stability. Via device engineering, we achieve n-type OECTs with high transconductance (49 mS) and good stability (stable after hundred-cycle weekly operation across five weeks stored in ambient air). We demonstrate the use of n-type perylene diimide-based OECTs in glucose sensors.

11:30 AM SB10.01.03

Electric Field Contributions to Ion Motion in Organic Electrochemical Devices [Loren G. Kaake](#); Simon Fraser University, Canada

Organic electrochemical devices include biosensors, transistors, electrochromic displays, and light emitting electrochemical cells. One key step in device operation is the movement of ions within the electronically conductive π -conjugated material. The mechanisms of ion motion and the structure-property relationships that govern those mechanisms continue to be a source of keen interest. One important vantage point to understanding this motion is through the fundamental equations of mass transport (the drift-diffusion equation). Because both electronic charge carriers and ions are in motion, the details of this coupling can, in principle, be quite complex. In order to develop a first order model that encapsulates typical behavior in the most common systems, we performed spectroelectrochemical measurements on thin films of PEDOT:PSS, a common mixed conducting material. Specifically we examined what role, if any, applied electric fields have on the transport of ions in PEDOT:PSS. This was accomplished by comparing a device with potential applied at the electrolyte interface to a device where a potential is applied across the PEDOT:PSS thin film, in an attempt to use fields to draw the ions more rapidly through the bulk of the material. No discernable difference in the electrochemical charging dynamics was observed, demonstrating that macroscopic fields are not an important influence in ion motion. To better rationalize this result, finite element simulations were performed. These simulations highlight the importance of local fields as established by both the electronic charge carriers and the intermolecular forces between the ions and the polymeric medium in which it is embedded.

11:45 AM SB10.01.04

Stable Organic Electrochemical Neurons Based on p-Type and n-Type Ladder Polymers [Han-Yan Wu](#), Jun-Da Huang, Chi-Yuan Yang and Simone Fabiano; Linköping University, Sweden

Organic electrochemical transistors (OECTs) are a rapidly advancing technology that plays a crucial role in the development of next-generation bioelectronic devices. Recent advances in p-type/n-type organic mixed ionic-electronic conductors (OMIECs) have enabled power-efficient complementary OECT technologies for various applications, such as chemical/biological sensing, large-scale logic gates, and neuromorphic computing. However, ensuring long-term operational stability remains a significant challenge that hinders their widespread adoption. While p-type OMIECs are generally more stable than n-type OMIECs, they still face limitations, especially during prolonged operations. Here, we demonstrate that simple methylation of the pyrrole-benzothiazine-based (PBBT) ladder polymer backbone results in stable and high-performance p-type OECTs. The methylated PBBT (PBBT-Me) exhibits a 25-fold increase in OECT mobility and an impressive 36-fold increase in μC^* (mobility \times volumetric capacitance) compared to the non-methylated PBBT-H polymer. Combining the newly developed PBBT-Me with the ladder n-type poly(benzimidazobenzophenanthroline) (BBL), we developed complementary inverters with a record-high DC gain of 194 V V^{-1} and excellent stability. These state-of-the-art complementary inverters were used to demonstrate leaky integrate-and-fire type organic electrochemical neurons (LIF-OECNs) capable of biologically relevant firing frequencies of about 2 Hz and of operating continuously for up to 6.5 h. This achievement represents a significant improvement over previous results and holds great potential for developing stable bioelectronic circuits capable of in-sensor computing.^[1]

[1] H. Y. Wu, J. D. Huang, S. Y. Jeong, T. Liu, Z. Wu, T. van der Pol, Q. Wang, M. A. Stoeckel, Q. Li, M. Fahlman, D. Tu, H. Y. Woo, C. Y. Yang and S. Fabiano, *Mater Horiz*, 2023, DOI: 10.1039/d3mh00858d.

SESSION SB10.02: Organic Electrochemical Transistors—Fundamentals and Materials II

Session Chairs: Christopher Proctor and Sihong Wang

Tuesday Afternoon, April 23, 2024

Room 429, Level 4, Summit

1:30 PM *SB10.02.01

Electrochemical Transistors Monolithically Integrated for Sensing Arrays [Antonio Facchetti](#)^{1,2}; ¹Georgia Institute of Technology, United States; ²Northwestern University/Flexterra Inc, United States

Organic electrochemical transistors (OECTs) have stimulated new research in biosensor, wearable/e-textile, and neuromorphic applications. However, limitations in micro/nanopatterning of organic semiconductors and topological irregularities often limit their implementation in monolithically integrated circuits as is common in silicon-based electronics. In this presentation we first report on a new vertical OECT architecture (vOECT) enabling excellent and

balanced behavior. Next, we demonstrate the successful realization of high-density (up to $\sim 7.2\text{M}$ OECT/cm²) and mechanically flexible vOECT arrays and circuits via facile and generalizable micropatterning of the semiconductor materials by electron-beam lithography. The resulting p- and n-type vOECT active-matrix arrays exhibit excellent electronic characteristics with transconductances of 0.08 – 1.7 S, fast transient times (<100 μm) and ultra-stable switching properties ($>100\text{k}$ cycles). Furthermore, we demonstrate vertically stacked complementary logic circuits, including NOT, NAND, and NOR gates, which are essential components for digital processing and logic operations.

2:00 PM *SB10.02.02

Organic Electrochemical Transistors Based on Polymer Blends [Shunsuke Yamamoto](#); Tohoku University, Japan

We examine the organic electrochemical transistors (OECTs) based on polymer blends of a mixed conductor (PEDOT:PSS) and an ion conductor (PSSNa) or other functional polymers, including thermoresponsive PNIPAM. The phase separation structures, especially surface segregation, were examined to discuss the distribution of PEDOT and other components in the channel layers. For example, we found that the blend films of PEDOT:PSS and PNIPAM have a surface skin layer of PNIPAM on top of the PEDOT layer. This talk will cover the tendency and driving force of the surface segregation phenomena in PEDOT:PSS-based blend films for a rational design of functional OECT devices.

2:30 PM BREAK

SESSION SB10.03: Neuromorphic Computing I
Session Chairs: Simone Fabiano and Wei Huang
Tuesday Afternoon, April 23, 2024
Room 429, Level 4, Summit

3:00 PM *SB10.03.01

Physical Reservoir Computing with Dendritic Polymer Structures – Understanding Internal Dynamics, Scale-up and Integration in All-Solid-Systems Anton Weissbach, Peter Steiner, Lukas M. Bongartz, Richard Kantelberg, Peter Birkholz, Karl Leo and [Hans Kleemann](#); Technische Universität Dresden iAPP, Germany

Physical Reservoir Computing is an emerging field of research as such recurrent neural networks offer power-efficient real-time classification on edge devices thereby utilizing the inherent temporal dynamics of the underlying physical, chemical or biological system. In particular, the use of organic mixed ionic-electronic conductors enables a close connection to biological systems due to the strong coupling between ionic and electronic conduction as well as the possibility to chemically modify the polymer to interact with bio-molecules. Previously, we have shown a first realization of a physical reservoir composed of polymer dendrites integrated onto a flexible substrate for on-chip heartbeat classification. However, these systems were limited due to an insufficient complexity and the use of an external delayed feedback line (single-node reservoir), requiring significant data pre-processing and increasing the power consumption.

In this contribution I will discuss the internal dynamics of such dendritic reservoirs and how we tuned them by external parameters such as the ion conductivity or ion mobility. Furthermore, I will demonstrate the integration of such reservoirs into a solid-state electrolyte, which allows us to scale-up the network to a large number of nodes covering the bandwidth relevant for bio-signal processing. The scale-up results in an improvement of the classification accuracy up to 95% without any silicon-based component. Moreover, the scale-up study shows us that the classification accuracy and power consumption can be decoupled in sparse network configurations, enabling us to achieve such a high accuracy with a power consumption of only 100nW. This integration strategy of sparse networks into a solid-state electrolyte opens up new perspectives to further increase the efficiency of intelligent edge devices based on organic semiconductors.

3:30 PM *SB10.03.02

Coordination Compound Materials for Neuromorphic Computing and Brain-Computer Interfaces [Alec Talin](#); Sandia National Laboratories, United States

As we near the limits of conventional digital Si based transistor technology, neuromorphic computing using analog devices based on functional materials that emulate neuronal and synaptic characteristics has emerged as a powerful approach to realize the energy efficiency and dynamic adaptability of animal brains. While most efforts have focused on inorganic materials due to their compatibility with Si CMOS processing and scalability, a wide range of neuromorphic functionality has also been demonstrated in devices based on organic polymers, coordination polymers and molecular coordination complexes. In my presentation I will give a snapshot of how these different materials are being explored for analog neuromorphic computing, and then focus on our recent work with the mixed valence coordination polymers like the Prussian blue analogues (PBAs), attractive because they have an open framework structure and ability to conduct both ionic and electronic charge. Using inkjet-printing, we demonstrate flexible artificial synapses that reversibly switch electronic conductance by more than four orders of magnitude based on electrochemically tunable oxidation state. Retention of programmed states is improved by nearly two orders of magnitude compared to the extensively studied organic polymers, thus enabling in-memory compute and avoiding energy costly off-chip access during training. We demonstrate dopamine detection using PBA synapses and biocompatibility with living neurons, evoking prospective application for brain-computer interfacing. By application of electron transfer theory to in-situ spectroscopic probing of intervalence charge transfer, we elucidate a switching mechanism whereby the degree of mixed valency between N-coordinated Ru sites controls the carrier concentration and mobility, as supported by DFT.

4:00 PM SB10.03.03

Large-Scale Stretchable Neuromorphic Computing Circuits for Acute Disease Detection and Soft Robotics [Songsong Li](#)¹, Max Weires¹, Zixuan Zhao¹, Fangfang Xia² and Sihong Wang¹; ¹The University of Chicago, United States; ²Argonne National Laboratory, United States

Developing wearable edge computing electronics with skin-like stretchability has a significant impact on precision medicine and soft robotics. To implement edge computing function, integrated neuromorphic systems with artificial synapses and neuron functionalities are necessary, which can emulate biological neural networks and enable the replication of complex cognitive abilities within an artificial system. Recent explorations have identified organic electrochemical transistors (OECTs) as a promising device platform for stretchable neuromorphic computing. However, challenges remain in the scalable fabrication of stretchable large-scale synaptic arrays and additional stretchable components, such as artificial neurons. In this work, we develop intrinsically stretchable integrated neuromorphic systems by fabricating stretchable 10 x 10 neuromorphic arrays via a standard cleanroom microfabrication process, subsequently constructing artificial neurons to realize neuromorphic activation functions. Various machine learning algorithms are deployed using our

neuromorphic integrated system to detect acute disease and regulate the movement of soft robotics. Overall, this work will shed light on the promising pathway toward realizing wearable on-body edge computing.

4:15 PM *SB10.03.04

Structural Plasticity with PEDOT-Based Dendritic Electropolymerization for Neuromorphic Engineering Kamila Janzakova¹, Corentin Scholaert¹, Ismael Balafrej², Ankush Kumar¹, Dominique Drouin³, Jean Rouat², Sébastien Pecqueur¹, Yannick Coffinier¹ and Fabien Alibert^{1,3}; ¹IEMN-CNRS, France; ²University of Sherbrooke, Canada; ³CNRS, Canada

Neuromorphic computing and engineering is capitalizing heavily on the new physical properties offered by nanotechnologies to engineer biological processes. At the frontiers in between bio-mimetism and bio-inspiration, various solutions have been proposed for synaptic plasticity or neuronal features based on discrete memory elements, bistable switches or transistors circuits. One missing element that has been missing in the neuromorphic toolbox is the ability to reproduce the complex 3D interconnections observed in biological neural networks. Here, we propose to take advantage of bipolar electropolymerization of PEDOT dendritic fibers to reproduce the ability of neural networks to generate complex topologies. The electropolymerization mechanism is used to realize structural plasticity based on Hebbian-like plasticity rules. We explore how such bottom-up process can find optimal topologies for specific computing tasks. We demonstrate that such optimal topologies results in a drastic reduction of interconnects for classification and reconstruction tasks, thus offering an interesting option for neural network design.

4:45 PM SB10.03.05

Ladder-Type Conjugated Polymers: Synthesis and Their Application in Organic Electrochemical Transistors/Artificial Neurons Chi-Yuan Yang^{1,2} and Simone Fabiano^{1,2}; ¹Linköping University, Sweden; ²n-Ink AB, Sweden

Organic electrochemical transistors (OECTs) are a rapidly advancing technology that plays a crucial role in the development of next-generation bioelectronic devices. Recent advances in p-type/n-type organic mixed ionic-electronic conductors (OMIECs) have enabled power-efficient complementary OECT technologies for various applications, such as chemical/biological sensing, large-scale logic gates, and neuromorphic computing. However, ensuring both high performance and long-term operational stability remains a significant challenge that hinders their widespread adoption. Ladder-type conjugated polymers, with their rigid backbone structure composed of double-strand chains linked by condensed π -conjugated units, can sustain high electrochemical doping levels without any conformational disorder, which leads to exceptional operational stability, high charge carrier mobility, and large volumetric capacitance. In this report, we demonstrate our recent development on ladder-type conjugated polymers, with p-type/n-type high mixed ionic-electronic conducting performance and high stability in long-term OECT operation. Reasonable molecular design and improvement of synthesis methods have enabled the synthesis of high-performance p-type/n-type ladder polymers with mobility increased by more than 10 times. Their unique ladder-type structure enables them to have long-term stability within >90% current remain after 6 hours continues operation, and enables them to accommodate more carrier injections with of up to two charges per repeat unit. Density of states filling and opening of a hard Coulomb gap around the Fermi energy at high electrochemical doping levels enable the ion-tunable antiambipolarity in these ladder polymers. The development of ladder-based polymer ink formulations has also enabled printed electronics. With these ladder-type polymers, we developed complementary inverters with a record-high DC gain of 194 V/V and excellent stability. We report the first organic electrochemical neurons (OECNs) with ion-modulated spiking, based on all-printed complementary organic electrochemical transistors. We demonstrate facile bio-integration of OECNs with Venus Flytrap (*Dionaea muscipula*) to induce lobe closure upon input stimuli. We report a biorealistic conductance-based organic electrochemical neuron (c-OECN) using a mixed ion–electron conducting ladder-type polymer with stable ion-tunable antiambipolarity. The latter is used to emulate the activation/inactivation of sodium channels and delayed activation of potassium channels of biological neurons. These c-OECNs can spike at bioplausible frequencies nearing 100 Hz, emulate most critical biological neural features, demonstrate stochastic spiking and enable neurotransmitter-/amino acid-/ion-based spiking modulation, which is then used to stimulate biological nerves in vivo.[1-5]

References:

1. Adv. Mater. 2018, 30, 1704916.
2. Adv. Funct. Mater. 2022, 32, 2112276.
3. Adv. Electron. Mater. 2022, 8, 2100907.
4. Adv. Mater. 2022, 34, 2106235.
5. Nat. Commun. 2022, 13, 901.
6. Nat. Mater. 2023, 22, 242–248.

SESSION SB10.04: Poster Session I
Session Chairs: Sahika Inal and Sihong Wang
Tuesday Afternoon, April 23, 2024
Flex Hall C, Level 2, Summit

5:00 PM SB10.04.01

Manipulating Physicochemical Properties of Biosensor Platform with Polysuccinimide-Silica Nanocomposite for Enhanced Protein Detection Rabi Saleh Ibrahim and Chaenyung Cha; Ulsan National Institute of Science and Technology, Korea (the Republic of)

As point-of-care testing (POCT) is becoming the new paradigm of medical diagnostics, there is a growing need to develop reliable POCT devices that can be conveniently operated in a minimally invasive manner. However, the clinical potential of POCT diagnostics is yet to be realized, mainly due to the limited and inconsistent amount of collected samples on these devices, undermining their accuracy. This study proposes a new biosensing platform modified with a functional polysuccinimide (PSI)-silica nanoparticle (SNP) composite system that can substantially increase the protein conjugation efficiency by modulating physicochemical interaction with proteins by several hundred percent from an unmodified device. The efficacy of this PSI-SNP system is further validated by applying it on the surface of a microneedle array (MN), which has emerged as a promising POCT device capable of accessing interstitial fluid through minimal penetration of the skin. This PSI-SNP MN is demonstrated to detect a wide array of proteins with high sensitivity on par with conventional whole serum analysis, validated by in vivo animal testing, effectively displaying broad applicability in biomedical engineering.

5:00 PM SB10.04.02

Polypyrrole/ Hydrogel Hybrid Films as Biomimetic Self-Sensing Macromolecular Motors Yahya Ahmed-Ismail, Shabeeba Aranhikundan and Lijin

Rajan; University of Calicut, India

Conducting polymers can be regarded as the simplest model materials that can be used to fabricate biomimetic sensing motors (intelligent devices) mimicking biological functions in which the driving and sensing signals can be read at any time, through the same two connecting wires. With a view to fabricate more flexible and mechanically robust conducting polymer-based sensing motors, polypyrrole/hydrogel hybrid films were fabricated through in-situ chemical polymerization. Like natural muscles, the reversible redox reactions of the hybrid films respond, adapt and sense, any variation in chemical, electrical and thermal working energetic conditions using electrical energy and/or electrical charge as the sensing parameters. The single faradaic electrochemical reaction of polypyrrole was responsible for the self-sensing property. Under galvanostatic conditions, the hybrid films modify the consumed electric energy to self-adapt the newly imposed energetic conditions and respond to the electrical, thermal and chemical energetic conditions. Under potentiodynamic conditions, the extension of the faradaic reaction defined by the coulombometric charges senses the working electrical, chemical and thermal ambient. The conformational and structural changes occurring through n consecutive steps of one electron extraction per step arises due to the cooperative actuation of the constitutive polypyrrole chains (the chemical machines) driven by the oxidation/reduction reactions make the coulombometric charge a self-sensor of the working energetic conditions. Accordingly, we have fabricated a self-sensing supercapacitor device using the hybrid film capable of sensing its working condition at any reaction moment, without physical separation through the same two connecting wires. The similarity of cooperative actuation of the polypyrrole/hydrogel hybrid film with natural muscles in simultaneously sensing the working energetic condition can serve as the foundation for the construction of biomimetic multifunctional devices.

5:00 PM SB10.04.03

Rapidly Deployable, Compact Airborne Detection Platform Using Bio-Inspired Molecular Probes to Counter Infectious Disease and Evolving Threats [Richard V. Lee](#), Oliver Nakano-Baker, Shalabh Shukla and John D. MacKenzie; University of Washington, United States

Rapid detection of VOC signatures from exhaled breath provides a simple and non-invasive way for determining states of health by assessing the breathomics signatures of conditions, diseases and chemical toxins that can endanger human performance and health. In response, we are advancing the fundamental science and engineering of biologically-inspired molecular probe-based sensing towards developing a compact, multiplexed sensor that can be rapidly deployed to detect and quickly diagnose existing and emerging infectious disease threats, toxicants, and biomarkers at low cost. The key to our approach is computationally-engineered chimeric peptides and modified protein biomolecules derived from computational derivation of target molecule binding sites and homology from natural odorant-binding olfactory receptor protein libraries. These bioinspired molecules are multifunctional and bind to specific airborne volatile and dissolved targets whose binding events are transduced directly into electrical signals in carbon-based field effect transistor (FET) sensors. These probes create a selective, compact, and customizable platform to directly sense disease or identify the human body's response following exposure to a toxin. For complex VOC profiles such as the trace components of human breath, multichannel FET sensor chips can be functionalized with sets of peptide or protein probes to sensitize the transistor array to a disease, condition or intoxicant's multicomponent signature thereby creating high selectivity. The FET sensor allows for detecting voltage threshold shifts versus target exposure and the gate voltage tuning of the sensor bias to achieve maximum sensitivity. The transistor-based biosensor identifies diseases and human body responses to antagonists using machine learning (ML) trained on typically multicomponent target profiles, recognizing their often complex volatile organic compound (VOC) signature profile in exhaled breath or ambient air using computationally designed and optimized sets of solid-binding peptides and protein probe molecules that can achieve high selectivity and exclude confounding factors. The platform technology could be deployed as handheld, wearable, or drone-mounted eNoses and as broadly capable chemical sensors. We have demonstrated the ability of our system to directly detect VOCs indicative of COVID-19 infection in simulated breath as well as sensing of human stress biomarkers in solution using sensor-adapted cortisol-binding proteins. Solution titration studies of protein-functionalized carbon nanotube FET sensors have enabled the determination of a target detection threshold of at least 10 parts per trillion (10 femtomolar) in a simple, direct chemical/electronic transduction signal. We are currently exploring the targeted detection of biotoxins, such as saxitoxin, with our molecular-probe functionalized FET sensor platform.

5:00 PM SB10.04.04

Zwitterion Dielectric Materials for Low Voltage Organic Field Effect Transistors [Jasleen Kaur](#) and Loren G. Kaake; Simon Fraser University, Canada

Achieving low voltage operation in organic thin film transistors (OTFTs) is crucial for their integration into sensing devices, smart packaging, and the internet of things. This is often accomplished through the use of liquid electrolytes which intercalate into the organic semiconductor film. However, this strategy can lead to undesirable structural changes and charge trapping phenomena. Inspired by polyelectrolyte dielectric materials, we explored solution processable zwitterion-based dielectric materials for OTFT applications. Zwitterion-based films are prepared using 4-(3-butyl-1-imidazolium)-1-butane sulfonate in poly (vinyl alcohol) (PVA) polymer matrix. Top gate bottom contact p-type OTFTs gated via zwitterion-based dielectric are fabricated using poly(3-hexylthiophene-2,5-diyl) (P3HT) as organic semiconductor and electrical characteristics are studied under dry and humid conditions. The operating voltage is found to be strongly humidity dependent with humidified devices operating below -1.2 V. Further, electrochemical impedance spectroscopy of zwitterion-based dielectric films confirmed that increased dielectric response with humidity aids in lower voltage operation in OTFTs. Impedance data is fitted with the Havriliak-Negami model and indicates that only one polarization mechanism is responsible for the electrostatic double-layer like capacitance. The simple formulation and tunable capacitance of zwitterion-based dielectric materials hints at a rich line of research where the interplay of intermolecular forces and applied field leads to materials with exceptional properties.

5:00 PM SB10.04.05

Machine-Learning Assisted Micropillar Assay for High-Throughput *In-Situ* Functional Analysis of Patterned Organoids [Shuai Wu](#); Auburn University, United States

An organoid is a 3D multicellular tissue structure cultivated in vitro, designed to closely mimic its corresponding in vivo organ. This enables the study of various aspects of that organ within the controlled environment of a tissue culture dish. Although 3D tissue culture techniques have been in use for decades. The detection and quantification of protein biomarkers in-situ is hampered by challenges in its sampling and analysis. Here we report the use of a micropillar-based patch for fast in vivo sampling and on-pillar quantification of target protein biomarkers in organoid. We used the micropillar patch functionalized with different size nanoparticles-antibody conjugates to detect the cytokines in a multiplex way with machine learning assisted image process. Micropillar patches for the minimally invasive collection and analysis of biomarkers in organoids might facilitate point-of-care diagnostics and longitudinal monitoring.

5:00 PM SB10.04.06

Intrinsically Stretchable Subthreshold Organic Transistors for Highly Sensitive and Extremely Low-Power e-Skin Temperature Sensors [Phuong N. Vo](#)¹, Jun Su Kim¹, MinWoo Jeong¹, Tae Uk Nam¹, Kyu Ho Jung¹, Tae Il Lee² and Jin Young Oh¹; ¹Kyung Hee University, Korea (the Republic of); ²Gachon University, Korea (the Republic of)

Body temperature is a vital physiological parameter used for health monitoring and early detection of infectious diseases or changes in one's physical

condition. The growing importance of continuous health monitoring has led to an increased demand for swift and accurate temperature measurement. To address this need, researchers are rapidly developing skin-mounted or wearable sensors that provide real-time insights into an individual's well-being. Nonetheless, challenges like the tradeoff between power consumption and responsiveness, as well as sensitivity to strain, continue to pose significant obstacles for electronic skin (e-skin) sensors. Recently, researchers have made substantial progress in the development of organic thin-film field-effect transistors (OTFTs) using inherently stretchable organic semiconductor materials. These advancements hold promise for OTFTs to serve as skin-like sensors, capable of offering low power consumption, exceptional responsiveness to physiological signals, skin-like flexibility, and maintaining stability in the face of strain, while also delivering strong electrical properties and sensing capabilities. This work introduces an intrinsically stretchable subthreshold OTFT designed for a highly sensitive and low-power active-matrix temperature sensor array, closely resembling human skin. The OTFT exhibited an impressively steep subthreshold slope at low voltage, leading to a high transconductance efficiency. Consequently, it achieved exceptional temperature sensitivity ($9.4\% \text{ } ^\circ\text{C}^{-1}$) with ultra-low power consumption (less than 1 nW, with a maximum of 670 pW), rapid response times (0.3 seconds), a minimal threshold voltage deviation (within $\pm 0.5 \text{ V}$), and high sensing accuracy ($0.5 \text{ } ^\circ\text{C}$) even when subjected to a 100% strain. Additionally, we successfully created a skin-like subthreshold organic transistor active-matrix array, which accurately detected surface temperature variations even under three-dimensional deformations.

5:00 PM SB10.04.07

Development of a Minimally Invasive Flexible Continuous Glucose Sensor [Anthony Fontana](#) and Ahyeon Koh; Binghamton University, United States

Every year, hundreds of millions of people worldwide are affected by diabetes mellitus. While the symptoms and treatment regimens vary from each individual, a lifelong commitment to monitoring and balancing blood glucose concentration can be expensive and psychologically exhausting. To provide patients with an increased ability to control this disease, continuous blood glucose biosensors are used to provide on demand measurements of relevant biomarkers. This allows users to readily regulate the concentration of glucose in their blood. Traditional sensor devices analyze small samples of blood, requiring invasive techniques of obtaining the sample. There is also a lack of continuous glucose measurements in these devices, as fluctuating analyte concentrations during day-to-day activities cannot be monitored. To address these limitations, a device that utilize soft and flexible materials that can integrate with the skin and offer a minimally invasive method to continuously detect glucose concentration is proposed. A temporary tattoo platform that incorporates a sensitive electrode system can provide the patient with the ability to comfortably monitor their condition. Flexible bioelectronics has emerged as a promising platform to develop biosensors because of their seamless integration into biological systems. The abundance of soft and flexible tissues within the body interacts well with other flexible systems, hence the need to develop devices that interact with the body in the same way.

This glucose sensor device extracts interstitial fluid from below the skin through reverse iontophoresis, a process by which low current is precisely applied to the epidermis. Following this extraction process, the fluid interfaces with a three-electrode system that utilizes a substrate-enzyme interaction to detect glucose through a hydrogen peroxide intermediate. The electrodes were fabricated utilizing a PCB printer to extrude conductive inks onto a flexible polyimide substrate. The system was created from a carbon-graphite Prussian blue mediator paste which contains redox active molecules necessary for detection of the hydrogen peroxide intermediate. Onto the surface of the working electrode, the glucose oxidase enzyme was immobilized along with a solution of single walled carbon nanotubes and chitosan. Upon binding of glucose within the interstitial fluid to the glucose oxidase enzyme, the hydrogen peroxide by-product can be measured in terms of current by the working electrode.

To determine electrochemical function of the sensors, a variety of experiments including cyclic voltammetry, linear sweep voltammetry, amperometry, and chronography were used. These techniques demonstrated the performance of the Prussian blue working electrode by recording oxidation and reduction peaks, which align precisely with commercially available alternatives. Additionally, characterization of the reference and counter electrodes indicate proper electrochemical function of the entire sensor system. Following this analysis, the ability for the electrode to detect the hydrogen peroxide intermediate was evaluated. In target concentrations ranging from 2mM/L to 12mM/L of hydrogen peroxide, the device clearly possesses the ability to systematically and consistently respond to various H_2O_2 concentrations. The current density response is then used to develop a linear response curve to correlate H_2O_2 with electrical output.

Within this flexible biosensor system, hydrogen peroxide concentration was related to electrical output quantitatively. Hydrogen peroxide's direct relationship with glucose upon binding with glucose oxidase suggests this platform can provide a promising alternative from conventional methods of detecting glucose within the blood.

5:00 PM SB10.04.08

Surface Electromyography Controlled Human-Machine Interface Using Upcycled Compact Disc Electrodes [Pauline Faith A. Macapinlac](#), Matthew Brown and Ahyeon Koh; Binghamton University, United States

In efforts of relieving the ever-amassing amounts of electronic waste produced a year, researchers are looking for ways to repurpose discarded devices into new technologies for biomedical purposes. Promising methods of repurposing compact discs (CDs) into stretchable and flexible biosensors called upcycled compact disc electrodes (UCDEs), have opened up new possibilities for providing accessible and affordable biotechnology for a variety of applications. One application is the implementation of UCDEs in human machine interfaces (HMI). Human controlled robotic interfaces have garnered growing interest in recent years due to its potential use in aiding disabled and elderly individuals or augmenting the performance of everyday tasks and occupations. This study focuses on creating an HMI to simulate hand movement based on surface electromyography (EMG) conducted with UCDE applications. The UCDEs are specifically designed and patterned to mimic the mechanical properties of the skin above the targeted muscles and are used to detect the electroactivity during contraction and relaxation. When integrated into an HMI, UCDEs have proven to be capable of consistent and reliable measurements of muscle detection capable of controlling the robotic interface.

To begin the UCDE fabrication process, Verbatim UltraLife Gold Archival Grade DVD-R CDs were soaked in acetone for 30 seconds to break down the polycarbonate substrate and release the metal layer. The metal was then mechanically harvested by adhering polyimide tape followed by a layer of water-soluble tape to the surface of the exposed metallic surface. At this stage, the metal is patterned using a Cricut Fabric Cutter and prepared to be integrated into the machine interface. Mechanical properties of the UCDEs were evaluated using tensile testing with a 25 N load at a 5.1 mm/min to failure and cyclic bending with a strain rate of 300 mm/min held at a bending radius of 3.5 mm. The Quad BioAmp PowerLab system was used to examine the material's capability of EMG measurements and find optimal UCDE placement for the machine interface. The HMI used in this study was built using the InMoov open-source 3D printed hand and forearm, powered by an Arduino Nano and wirelessly controlled with a nRF24 module. MyoWare 2.0 Muscle Sensors attached to the UCDE sensors were used for measuring and processing muscle activity that can then be used to control movement of the robotic hand and designed into a wireless wearable electronic device. The machine interface was connected and coded to utilize the signals from the muscle sensors using Arduino Software (IDE).

The polymeric-metal layers of the UCDE were patterned with ease using the mechanical cutter down to feature sizes of $25 \text{ } \mu\text{m}$ capable of up to 20% strain. Once patterned, the UCDEs demonstrated an elastic modulus of $5.59 \pm 0.16 \text{ MPa}$ and elongation of $62.35 \pm 1.81\%$ when tested to failure. Cyclic bending for 100 cycles with a radius of 3.5 mm demonstrated a 0.29% increase in UCDE resistance. The performance of the UCDEs have proved to be comparable to commercial electrodes when measuring EMG of various muscle groups. When integrating UCDEs with the HMI, the wearable electronic system and

UCDEs were attached in ideal placement on the forearm. UCDEs proved capable of controlling all five robotic fingers in three distinct motions by detecting EMG signals from three different muscle groups simultaneously within a small surface area. Performance of the machine interface was comparable between the use of UCDEs and commercially available electrodes.

UCDEs proved to be capable of controlling complex systems such as HMIs through the constant measurement of EMG signals. This discovery demonstrates the promising potential of this sustainable solution for upcycling electronic waste and the possibility of creating more accessible and affordable HMIs with the use of commonly available materials.

5:00 PM SB10.04.09

Artificial Intelligence-Enhanced Flexible Biocompatible Triboelectric Nanogenerator [Mohammad Abrar Uddin](#), Barrett Burgess and Taeli Kim; Baylor University, United States

Triboelectric nanogenerators (TEENG) have emerged as a promising technology for energy harvesting in wearable devices and self-powered sensors. However, the effective utilization of TEENGs in practical scenarios faces several challenges including limited power output, complexity of material combinations, wear and tear issues, complex integration into systems, sensitivity to frequency ranges, and miniaturization. A lot of work is being done addressing these challenges, however, the use of artificial intelligence in design optimization can pave new ways to reduce experimentation and can identify the optimal design parameters to obtain the best possible output from a range of variables. To unlock the full potential of TEENGs, we propose a novel approach that integrates artificial intelligence (AI) techniques with the design of experiment (DOE) method to optimize the design and performance of TEENGs. A microcavity-nanoparticle assembled microstructure with one triboelectric layer composed of porous polydimethylsiloxane (PDMS) sandwiched between a second triboelectric layer has been chosen as the initial prototype design. The use of porous PDMS in the structure with nanofillers allows the increase in surface area without the need for a spacer structure between the triboelectric films. This design structure can be well integrated with the human body motion in day-to-day life and provide improved energy conversion. A novel biogel material has been used as electrodes to ensure the biocompatibility of the TEENG with the human skin along with flexibility. This study includes variation of key parameters or factors such as material combinations, porosity in PDMS, surface area, thickness, frequency of applied force or pressure, and applied force to prepare different sample prototypes and identify the optimal combinations for TEENG performance. The frequency of the applied force mimics the human motion frequency range, which is from 0 to 20 Hz. The data generated from the prototype design with a range for each independent data point is analyzed by statistical tools and software to identify significant factors or parameters, and interactions between these factors are evaluated. After that, the optimization algorithms are applied to find the optimal levels of significant factors. Additional experiments are thereby conducted to validate the predicted performance and find the accuracy of the optimization. Finally, by refining the design parameters and conducting iterative experiments, a final optimized contact separation mode TEENG design has been generated that is flexible, biocompatible, and efficient to power wearable biosensors for health monitoring. By harnessing energy from human motion, this AI-enhanced TEENG offers a sustainable, reliable, and biocompatible power source for wearable healthcare applications.

5:00 PM SB10.04.10

The Importance of Electrode Material in Bioelectronic Electrophoretic Ion Pumps [Tiffany Nguyen](#), Narges Asefifeyzabadi, Houpu Li, Le Luo and Marco Rolandi; The University of California, Santa Cruz, United States

Bioelectronic ion pumps deliver ions and biomolecules from a source to a target biological system with high spatiotemporal control for bioengineering and regenerative medicine applications. A voltage between a working electrode and a reference/counter electrode delivers the charged ions and biomolecules from a source to the desired target. The source and the target are separated by an ion exchange membrane so that only the charged molecules of interest are delivered. Future wearable and implantable applications require high efficiency of delivery to minimize power consumption. The majority of recent efforts on improving ion pump efficiency have focused on optimizing the ion exchange membrane. However, the contribution of the working electrode material to the ion pump efficiency has been mostly overlooked. This work identifies how changing the working electrode material greatly affects the efficiency of delivery in ion pumps. With an electrical circuit model analysis, voltammetry studies on silver, platinum, and palladium hydride working electrodes, and implementation of the Butler–Volmer equation, results show that the material-dependent equilibrium potential at the working electrode surface has a large impact on ion pump efficiency. With this knowledge, a simple predictive model to optimize the working electrode material for delivering each specific ion or molecule of interest is designed.

5:00 PM SB10.04.11

Synthetic Smart Hydrogels Tailored for Sensing in Gaseous Environments Sitao Wang¹, Gerald Gerlach¹ and [Julia Koerner](#)²; ¹Technische Universität Dresden, Germany; ²Leibniz University Hannover, Germany

Stimulus-responsive, i.e. smart, hydrogels are polymers capable of exhibiting a reversible volume change in response to external physical and chemical influences, for example pH value, light, temperature or specific analyte molecules. This makes the material a very interesting candidate for novel sensing elements, especially since the properties can be tailored for specific applications from a wide variety of monomers and mixtures thereof, as well as additives [1,2].

The smart hydrogel's volume change is usually mediated by the uptake and release of liquid and consequently, most applications are centered on liquid environments. However, the hydrogel's capabilities for selective and sensitive analyte detection hold great potential beyond that and we have therefore started to explore how to harness the material's properties for sensing in gaseous media. The specific target application of our research is volatile organic compound (VOC) detection in exhaled breath to enable monitoring of disease biomarkers such as acetone.

For this purpose, synthetic acrylamide-based hydrogels were chosen as the model material. In a first step, different polymers comprising polyacrylic acid (PAA), polyacrylamide (PAM), poly(*N*-isopropylacrylamide) (PNiPAAm) and their co-polymer combinations were investigated with respect to their ability of maintaining a measurable volume change in air with relative humidity variation from 0% to 100%. These studies were performed without and with added acetone gas as test VOC (concentrations: 20 ppm - 100 ppm) and the hydrogel's swelling response was characterized by gravimetry and piezoresistive pressure sensing. PNiPAAm showed the best responsiveness in terms of humidity range, dependence of swelling response on the target analyte concentration and potential for selectivity [3].

However, these studies also revealed a significant challenge for using hydrogels in a gaseous atmosphere: A large surface area is crucial for a strong and fast response in VOC detection, hence the hydrogel should ideally feature a very porous structure (surface and bulk). While the porosity can be adjusted by the use of pore-forming additives or by ice-templating during polymerization, the pores are likely to collapse after polymerization and subsequent drying in air.

To address this challenge, the second step of our research focused on the development of a procedure enabling the creation of defined porosity which is maintained under the conditions of a gas atmosphere with varying humidity conditions. We found that templating with PEG during polymerization, followed by freeze drying (either at -196°C or -20°C, depending on the desired pore size) and subsequent conditioning in high relative humidity (90 – 100 %) is the key to achieve stable porosity.

The material properties were characterized and compared in scanning electron microscopy and FT-IR analyses, and the volume change performance again evaluated by gravimetry and piezoresistive pressure sensing [4].

These investigations have been conducted for PNiPAAm which was identified as the most promising material candidate for our target application.

However, the developed process for tailoring and stabilizing a porous polymer structure in gaseous environments is of general nature and can easily be applied to other types of hydrogel since there are no components or steps specific for PNiPAAm. To enhance the responsiveness (i.e. swelling strength, time constants, reversibility) of the smart hydrogel even further, the focus of our future work is on the integration of additives such as graphene- and MXene-based materials.

[1] M. Koetting et al., *Mater Sci Eng R Rep.* 93:1-49, 2015; doi:10.1016/j.mser.2015.04.001

[2] S. Yang et al., *Energy environ mater.* 2023; doi:10.1002/eem2.12646

[3] S. Wang et al., *Polymer* 278:126009, 2023; doi:10.1016/j.polymer.2023.126009

[4] S. Wang et al., *Biomacromolecules* 2023; doi:10.1021/acs.biomac.3c00738

5:00 PM SB10.04.12

Mechanically Heterogeneous Silk Fibroin Film for Wireless Hybrid Electronics Yanling Wang and Xiaodong Chen; Nanyang Technological University, Singapore

Hybrid electronics that integrate rigid silicon-based electronic modules and stretchable sensors have been demonstrated through the combination of rigid islands and stretchable interconnects, which offer enhanced functionality and conformability with human body. However, mass production of these devices utilizing conventional synthetic materials contributes to the burgeoning electronic waste predicament. The fabrication process, involving intricate procedures such as photolithography, not only amplifies complexity but also consumes substantial power, thereby impeding sustainability and ecological equilibrium. Furthermore, the limited electrical stretchability of these hybrid sensors compromises the system's robustness. Consequently, there is an imperative need to explore sustainable materials capable of substituting or complementing synthetic counterparts in stretchable hybrid electronics, aiming to mitigate their environmental footprint while upholding performance and functionality.

Here, we developed a mechanically heterogeneous silk fibroin film as the platform for a wireless hybrid electronic system which can be attached on skin to collect biological signals with simple manufacturing. By virtue of the solution-processibility and tunable mechanical property of silk fibroin, the CaCl₂ plasticized silk fibroin film is fabricated by solvent casting and the effective strain isolation is achieved by locally hardening with methanol treatment. The considerable contrast in Young's modulus between rigid and soft parts, reaching approximately ~100, arises from the conformational transition of silk induced by methanol, which can be verified by both experimental structural analyses and molecular dynamic simulations. Combined with printing technology, the trace printed on our plasticized silk film exhibit consistent conductivity even at 100% strain, maintaining a low resistance. Besides, the interconnected resistor on the treated area sustains functionality when subjected to a 50% strain, showcasing the suitability of our designed structure for integrating hybrid electronics. Lastly, a wireless hybrid electronic system has been developed to facilitate on-skin sensing. The system comprises stretchable interconnects with high printing resolution and rigid microelectronics dedicated to signal processing and data transmission on a mechanically heterogeneous silk fibroin film. The proposed methodology, involving the fabrication of the heterogeneous biomaterials merged with thin-film technology, presents a promising pathway toward establishing on-skin hybrid electronic systems tailored for real-time physiological detection.

5:00 PM SB10.04.13

Highly Stable Ladder-Type Conjugated Polymer Based Organic Electrochemical Transistors for Low Power and Signal Processing-Free Surface Electromyogram Triggered Robotic Hand Control Zhongliang Zhou and Wei Lin Leong; Nanyang Technological University, Singapore

Organic electrochemical transistors (OECTs) based complementary inverters have been considered as promising candidates in electrophysiological amplification, owing to their low power consumption, and high gain. To create complementary inverters, it is important to use highly stable p-type and n-type polymers with well-balanced current. In this work, we improved the electrochemical stability of p-type ladder-conjugated polymer based OECT through an annealing process where it maintained its doped-state drain current from 76 % to 105 % after 4,500 cycles in ambient environment. We next present an OECT-based complementary inverter made from p-type and n-type ladder-conjugated polymers (PBBTL and BBL) that possess ultra-low power consumption (~170 nW), high gain (67 V/V) and high noise margin (92%) with full rail-to-rail swing. Furthermore, we demonstrate its potential in amplifying the envelope of surface electromyography (EMG) for robotic hand control. The high variation in the output (0.35V) allows the amplified EMG signals to be directly captured by commercial analog-to-digital converter, which in turn controls the robot hand to grasp different objects with low delay and low noise. These results demonstrate the capability of OECT inverter based amplifier in future signal processing-free human machine interface, particularly useful for prosthetic control and gesture control applications.

SESSION SB10.05: Biosensing and Bioelectronics I

Session Chair: Sahika Inal

Wednesday Morning, April 24, 2024

Room 429, Level 4, Summit

8:15 AM SB10.05.01

Organic Mixed Ion-Electron Conductors for THz Metadevices Federico Grandi^{1,2}, Cristiano Bortolotti^{1,3}, Francesco Modena³, Lorenzo Gatto², Matteo Butti³, Iain McCulloch⁴, Caterina Vozzi², Mario Caironi³, Giorgio Ernesto Bonacchini³ and Eugenio Cinquanta²; ¹Politecnico di Milano, Italy; ²CNR-IFN, Italy; ³Istituto Italiano di Tecnologia, Italy; ⁴University of Oxford, United Kingdom

In the last decades, materials that can efficiently transport ionic and electronic charges become key in advancements in the fields of bioelectronic devices, energy storing or harvesting, and healthcare. Organic mixed ionic-electronic conductors (OMIECs) are organic materials that can transport both ionic and electronic charge¹. The large variety of organic molecules that can be synthesized and the number of ways in which they can be arranged provide a great number of degrees of freedom that influence the OMIECs' properties and device functionalities. Recent progress in the design and synthesis of organic mixed ion-electron conductors is actively contributing to developing exciting new technologies based on organic electrochemical transistors (OECTs). Among recent applications, OECT-based resonant devices have been proposed in the microwave spectral region showing excellent amplitude and frequency tuning performances in the sub-5GHz range². In these devices, the 3-dimensional charge modulation capabilities of OMIECs are key in achieving excellent tunability of both individual and arrays of microwave resonators, hence leading to a novel class of microwave photonic devices based on organic materials. The next step is to explore the applicability of this approach toward the THz frequencies, as well as the investigation of the OMIEC charge transport properties in this spectral range.

In this work, we study the far-infrared conductivity of a state-of-the-art OMIEC, namely p(g2T-TT), with field-assisted THz Time Domain Spectroscopy (THz-TDS). Through this technique, we non-destructively investigate the dielectric and electronic properties of the OMIEC during operation, thus gaining crucial insights for the physical modeling of charge transport at high frequencies. By varying the applied voltage bias from -800 to 600 mV, we modulate

the dielectric response of the polymer and obtain information about the charge injection and its effect on the polymer conductivity. We observe an increased conductivity by tuning the bias from 600 to -800 mV indicating an increase of the injected charge. More in detail, we report a positive real accompanied by a negative imaginary part of the conductivity, as already shown in the literature³. This behavior is well described by the Drude-Smith model that considers charge localization effects due to the finite polymer chain size and the energetic disorder. From the fit, we extract the charge density injected in the OMIEC as a function of the applied voltage bias and its carrier mobility.

To demonstrate the effectiveness of the charge carrier screening effects in p(g2T-TT) at THz frequencies, we investigate the amplitude modulation performances of a THz metadvice based on this OMIEC. The prototypical device is based on metallic Split Ring Resonators with a resonance at 0.7 THz, which are electrostatically tuned with the p(g2T-TT). We show that despite the relatively low mobilities of the charge carriers, their large density modulation leads to excellent modulation depth – exceeding 60% - with polarization voltages below 1 V.

Our results highlight the potential of organic THz devices based on OMIECs, for instance as optical modulators for telecom applications. Further research efforts in this direction could lead to a new generation of reconfigurable photonic technologies that take benefit of the many desirable properties of organic semiconductors, such as the ease of processability on large-area flexible substrates.

References:

1. B. D. Paulsen, K. Tybrandt, E. Stavrinidou, and J. Rivnay. Organic mixed ionic–electronic conductors. *Nat. Mater.* 19, 13–26 (2020).
2. G. E. Bonacchini, & F. G. Omenetto. Reconfigurable microwave metadevices based on organic electrochemical transistors. *Nat. Electron.* 2021 46 4, 424–428 (2021).
3. D. Tsokkou, P. Cavassin, G. Rebeteza & N. Banerji. Bipolarons rule the short-range terahertz conductivity in electrochemically doped P3HT. *Mater. Horiz.* 9, 482–491 (2022).

8:30 AM *SB10.05.02

Translational Neuroelectronics Dion Khodagholy; Columbia University, United States

Our understanding of the brain's pathophysiology relies on discoveries in neuroscience and neurology fueled by sophisticated bioelectronics enabling visualization and manipulation of neural circuits at multiple spatial and temporal resolutions. In parallel, to facilitate clinical translation of advanced materials, devices, and technologies, all components of bioelectronic devices have to be considered. Organic electronics offer a unique approach to device design, due to their mixed ionic/electronic conduction, mechanical flexibility, enhanced biocompatibility, and capability for drug delivery. We design, develop, and characterize conformable, stretchable organic electronic devices based on conducting polymer-based electrodes, particulate electronic composites, high-performance transistors, conformable integrated circuits, and ion-based data communication.

These devices established new experimental paradigms that allowed monitoring of the emergence of neural circuits during development in rodents and elucidated patterns of neural network maturation in the developing brain. Furthermore, the biocompatibility of the devices also allowed intra-operative recording from patients undergoing epilepsy and deep brain stimulation surgeries, highlighting the translational capacity of this class of neural interface devices.

In parallel, we are developing the fully-implantable, conformable implantable integrated circuits based on high-speed internal ionic gated organic electrochemical transistors that can perform the entire chain of signal acquisition, processing, and transmission without the need of hard Si-based devices. This multidisciplinary approach will enable the development of new devices based on organic electronics, with broad applicability to the understanding of physiologic and pathologic network activity, control of brain-machine interfaces, and therapeutic closed-loop devices.

9:00 AM *SB10.05.03

Organic Neuromorphic Electronics for Sensory Coding and Biohybrid Systems Yoeri van de Burgt; Eindhoven University of Technology, Netherlands

Neuromorphic engineering takes inspiration from the efficiency of the brain and focusses on how to utilise its functionality in hardware. Organic electronic materials have shown promising solutions for the manipulation and the processing of biological signals, with applications ranging from bioinformatics to brain-computer-interfaces and smart robotics.

This talk describes state-of-the-art organic neuromorphic devices and provides an overview of the current challenges in the field and attempts to address them. I demonstrate two device concepts based on novel organic mixed-ionic electronic materials and show how we can use these devices smart robotics and at the interface with biology. This can pave the way for novel architectures with bio-inspired features, offering promising solutions for the manipulation and the processing of biological signals and potential applications ranging from brain-computer-interfaces to bioinformatics and neurotransmitter-mediated adaptive sensing. I will highlight our recent efforts for such hybrid biological memory devices and artificial neurons.

9:30 AM SB10.05.04

Zwitterionic Hydrogel Design of PEDOT:PSS Suppresses The Foreign Body Response against Bioelectronic Conductors Shinya Wai, Nan Li, Seounghun Kang, Yahao Dai, Lavoie Tera, Wei Liu, Matthew V. Tirrell and Sihong Wang; The University of Chicago, United States

Implantable medical devices (IMDs) are playing an increasingly important role due to an aging population and the associated increasing prevalence of chronic diseases. However, the foreign body response (FBR) has limited IMDs from realizing their full potential. The FBR is characterized by inflammatory and fibrotic processes that surround the implanted material. Degradative chemicals and enzymes produced in the process can damage the implant. Fibrotic encapsulation is particularly detrimental for biosensors and electrophysiological devices because it would impede the diffusion of analytes and ions. A class of materials with promising FBR suppressing properties are zwitterionic polymers which have been shown to nearly eliminate the FBR for at least a year in mice. As electronic materials for IMDs, poly(3,4-ethylenedioxythiophene):poly(styrene sulfonate) (PEDOT:PSS) is of interest because it is chemically stable, highly processable, non-cytotoxic, and has good mixed ion-electron conducting properties. Nonetheless, previous work addressing the FBR against PEDOT:PSS did not place their focus on long-term solutions or did not carry out FBR-specific characterization methods. We hypothesize that by combining PEDOT:PSS and a zwitterionic polymer into a double-network hydrogel and carefully tuning its phase separation morphology, the conductivity can be increased and the FBR can be suppressed indefinitely. In this work, we demonstrate a process for inducing PEDOT:PSS network formation *in situ* in a zwitterionic hydrogel matrix, which significantly improves its conductivity and reduces FBR-associated fibrosis. Our work demonstrates that controlling the phase separation morphology of composite materials can be an effective strategy for suppressing the FBR.

9:45 AM SB10.05.05

Potentiometric Wearable Sensors with a Laser Engraved Graphene Layer as Transducer Farbod Amirghasemi, Abdulrahman Al-Shami, Victor Ong and Maral Mousavi; University of Southern California, United States

Laser-induced graphene has gained great attention recently for sensing devices. LIGs are generated through the process of irradiating carbon-rich polymers, primarily polyimide, using a laser beam. This procedure induces localized photothermal reactions, resulting in the conversion of SP³ carbon atom

hybridization into a three-dimensional graphitic-like structure. This maskless, scalable, simple, reproducible, cost-effective, and fast technique produces high-quality graphene layers with outstanding flexibility, electrical conductivity, and electrocatalytic properties instead of using the conventional time-consuming, expensive, and complicated methods such as wet chemistry, ink-jet printing, and chemical vapor deposition (CVD). In this work, we discuss surface modification and properties of graphene for achieving a stable interfacial potential in contact with a lipophilic sensing membrane, in a potentiometric readout mode. Specifically, surface topography and hydrophilicity of the material impacts the long-term and short-term properties of the wearable sensors. We will show how the engraving conditions impact water layer formation and drift of sensors, and how a highly stable readout can be achieved through surface modification. We use bio-inspired organic receptors to achieve ion specific binding at the electrode surface and generate biomarker specific signal.

10:00 AM BREAK

10:30 AM *SB10.05.06

Controlling The Optical Properties of Near-Infrared Nanotube Sensors through Bioengineering [Ardemis A. Boghossian](#); Ecole Polytechnique Federale de Lausanne (EPFL), Switzerland

Single-walled carbon nanotubes (SWCNTs) emit fluorescence that is ideal for a breadth of optical sensing applications. The near-infrared emissions are minimally absorbed by biological tissue, biofluids, and other visibly opaque materials. This property motivates their use for packaging and deep-tissue applications. The indefinite photostabilities and optical sensitivity to changes in their environment further justify the use of SWCNTs for continuous optical monitoring. However, SWCNTs require surface functionalizations to control the selectivity of their interactions and the specificity of the resulting sensors. Biomolecules like proteins and DNA show unparalleled molecular specificity towards various bioanalytes. Although they are commonly functionalized onto various surfaces to control the specificity of these surfaces towards analytes, their interactions with the surfaces themselves are often suboptimal. In the case of SWCNTs, these sub-optimal interactions limit sensor performance and response. This presentation highlights recent advancements that rely on bioengineering strategies, including directed evolution, mutagenesis, and xeno nucleic acids, for tuning the performances of bio-based optical SWCNT sensors.

11:00 AM *SB10.05.07

Ultra-Sensitive and Selective Ionic Sensors based on Vertical Organic Electrochemical Transistors for *In-Situ* Body Fluid Monitoring [Wei Huang](#); University of Electronic Science and Technology of China, China

Ions are ubiquitous biological and physiological regulators, while abnormal ion concentrations in human body fluids are often fingerprints of ongoing pathological states, diseases, and even organ malfunctions (such as heart or kidney failure, and dehydration). Therefore, accurate and timely detection/monitoring of various vital ion concentrations in body fluids is highly desired. Here, we demonstrate ultra-sensitive and selective ionic sensors based on vertical organic electrochemical transistors (vOECTs). By combining the advantage of high transconductance ($g_m > 0.2$ S) and small footprint ($< 30 \times 30$ μm) of the vOECTs with specific ionic selective membranes, ultra-high sensitivities up to 13.9 mA/dec (for Na^+), 2.2 mA/dec (for K^+), and 187 mA/dec (for Ca^{2+}) are achieved, along with decent selectivity, stability, and reproducibility. Such sensitivities are the highest values among reported ion-sensitive transistors (including ISFETs, EGOFETs, and OECTs). By integrating different vOECT-based ionic sensors in an array, in-situ monitoring of the ionic level in the externally circulated body fluid or the dialysate during an active continuous renal replacement therapy (CRRT) is demonstrated with high accuracy and reversibility. This work demonstrates the great potential of OECT-based sensors for complex sensing scenarios.

11:30 AM *SB10.05.08

Shape-Actuated Bioelectronics [Christopher M. Proctor](#); University of Oxford, United Kingdom

Significant advances have been made in the last two decades in interfacing electronic devices with the nervous system. To that end, research efforts are being pursued to develop minimally invasive, implantable bioelectronic devices integrating sensing, stimulating, and dynamic control of geometry. Here we report recent developments towards such multimodal devices for neural interfacing that take full advantage of the favorable properties offered by flexible electronics, conducting polymers and polymer substrates. It is shown that thin, flexible devices can incorporate microfluidic channels to enable new sensing and therapeutic functionalities. One such technology leverages the mixed conducting properties of conducting polymers and molecularly imprinted polymers for real time sensing of cortisol. Furthermore, we show fluidic components can open the door to novel implantation strategies that can reduce the surgical footprint required for implantation of widely used bioelectronic devices. We anticipate this work will accelerate the development of a new generation of bioelectronic devices for diagnostics and therapy.

SESSION SB10.06: Biosensing and Bioelectronics II

Session Chairs: Toshinori Fujie and Jin Young Oh

Wednesday Afternoon, April 24, 2024

Room 429, Level 4, Summit

1:30 PM *SB10.06.01

Biointegrated Living Electronics for Healthcare [Bozhi Tian](#); University of Chicago, United States

The emerging field of living bioelectronics aims to seamlessly integrate electronic devices with biological tissues, offering transformative solutions in healthcare diagnostics and therapeutics. In this talk, I will begin by discussing our earlier efforts centered around engineered tissue-integrated bioelectronics and the construction of tissue-mimetic materials. Progressing from these foundational works, I will transition into our latest explorations that harness the synergy between biology and electronics to address intricate biomedical challenges. Specifically, we present the active biointegrated living electronics platform. This unique interface, integrating a bioelectronics framework with a bacteria-laden hydrogel composite, facilitates dynamic signal transduction between microbial and mammalian systems. This platform has demonstrated its potential by monitoring microbial interventions in several skin conditions. As we forge ahead, our focus will be on optimizing device longevity, enhancing efficiency, and unveiling novel therapeutic solutions.

2:00 PM *SB10.06.02

Organic Optoelectronic Neurohybrid Devices [Francesca Santoro](#)^{1,2}; ¹Forschungszentrum Jülich GmbH, Germany; ²RWTH Aachen University, Germany

Exploiting the light-matter interplay to realize advanced light responsive multimodal platforms is an emerging strategy to engineer bioinspired systems

such as optoelectronic synaptic devices. However, existing neuro-inspired optoelectronic devices rely on complex processing of hybrid materials which often do not exhibit the required features for biological interfacing such as biocompatibility and low Young's modulus. Recently, organic photoelectrochemical transistors (OPECTs) have paved the way towards multimodal devices that can better couple to biological systems benefiting from the characteristics of conjugated polymers.

Neurohybrid OPECTs can be designed to optimally interface neuronal systems while resembling typical plasticity-driven processes to create more sophisticated integrated architectures between neuron and neuromorphic ends. Here, an innovative photo-switchable PEDOT:PSS was synthesized and successfully integrated into an OPECT. The OPECT device uses an azobenzene-based organic neuro-hybrid building block to mimic the retina's structure exhibiting the capability to emulate visual pathways. Moreover, dually operating the device with opto- and electrical functions, a light-dependent conditioning and extinction processes were achieved faithful mimicking synaptic neural functions such as short- and long-term plasticity.

2:30 PM BREAK

3:30 PM *SB10.06.03

Self-healing, Stretchable and Tissue-Adhesive Materials for Stable Bioelectronics Donghee Son; Sungkyunkwan University, Korea (the Republic of)

Conventional flexible/stretchable devices capable of monitoring bio-signals and delivering the feedback information have been considered as essential functional components in realizing the stable closed-loop bioelectronics. Despite such significant progress, their mechanical and electrical instability, originating from materials fatigue and the absence of tissue adhesion, still remains a challenge in pursuit of strain-durable tissue-interfacing capability. Here, we report optimal stretchable materials design strategies and device fabrication/integration technologies for the two different kinds of self-healing tissue-adhesive bioelectronics: i) A patch-type platform for either facile peripheral nerve repair (neurorrhaphy) in rodents and nonhuman primates or large-scale conformal cardiac interfacing; ii) A syringe-injection-type platform for instantaneous closed-loop rehabilitation. The patch-type self-healing bioelectronics consists of ionically conductive hydrogel adhesive and tough composite electrodes with solid and liquid micro-/nano-fillers, enabling both on-tissue strain-insensitive electrical performance and mechanical adaptation. In terms of the injectable type, tough hydrogel with irreversible yet freely rearrangeable biphenyl bonds and reversible coordinate bonds with conductive gold nanoparticles was applied to injured nerves/muscles for realizing immediate closed-loop robot-assisted rehabilitation and effective tissue regeneration.

4:00 PM *SB10.06.04

Thin-Film-Based Soft Electronic/Photonic Devices for Conformable Contact with Organs Kenjiro Fukuda¹ and Takao Someya^{2,1}; ¹RIKEN, Japan; ²The University of Tokyo, Japan

Electronic/photonic devices that are conformable to biological organs basically need to have extremely soft properties. Such devices usually have a multi-stack structure consisting of several functional layers, and can usually be realized using thin film devices. It is possible to reduce flexural rigidity and buckling load by simply reducing the film thickness of the device as well as reducing Young's modulus of each layer. This approach creates a system that does not inhibit the movement of organs, becomes possible.

One example of our recent achievements is the establishment of a method for mounting ultrathin-film organic solar cell films on insect abdomens [1]. The abdominal segments consist of multiple segments, abdominal deformation is achieved through the overlap of the segments. To not inhibit the movement of the abdomen, we developed an adhesive method in which part of the films have adhered to abdominal surfaces, and the unbonded area secures the room for deformation during the bend of the abdomen. In the case of polymer films with Young's modulus on the order of GPa, there is a tolerance threshold of around 5-10 μm in thickness to secure the basic motion ability of a specific insect, which was quantitatively clarified from the correlation with the bending load. Through such evaluations, we created a system of cyborg insects that can be recharged with ultra-thin organic solar cells adhered to abdominal surfaces.

Another example is the construction of stretchable electrode systems for stimulation and sensing on PDMS [2]. The use of extremely thin PDMS (approx. 1 μm), improves its adhesion to living organisms. We developed a stretchable conductor using micro-crack structured gold onto such thin PDMS films, which contributes to nerve stimulation with lower power than thicker film-based electrodes. In addition, by combining it with conductive polymers, stable adhesion on the skin is achieved, making it possible to construct systems that enable daily activities such as hand washing and swimming.

[1] Y. Kakei et al., *npj Flex. Electron.* 6, 78 (2022).

[2] Z. Jiang et al., *Nat. Electron.* 5, 784 (2022).

4:30 PM SB10.06.05

Plant Electrophysiology with Organic Electronics Eleni Stavrinidou; Linköping University, Sweden

Electrical signals in plants are mediators of long-distance signalling and correlate with plant movements and responses to stress. These signals are studied with single surface electrodes that cannot resolve signal propagation and integration, thus impeding their decoding and link to function. We developed a conformable multielectrode array based on organic electronics for large-scale and high-resolution plant electrophysiology. As a model system we studied the generation and propagation of the action potential (AP) in the carnivorous plant Venus flytrap. The AP in VFT is one of the fastest electrical signals in plants and it is generated when the mechanosensitive hairs in the trap are triggered. When two AP are generated within thirty seconds the trap closes. With organic bioelectronics we performed precise spatiotemporal mapping of the action potential in Venus flytrap and found that the AP actively propagates through the tissue with constant speed and without strong directionality. We also found that spontaneously generated APs can originate from unstimulated hairs and that they correlate with trap movement. Last, we demonstrate that the Venus flytrap circuitry can be activated by cells other than the sensory hairs. Our work reveals key properties of the AP and establishes the capacity of organic bioelectronics for resolving electrical signalling in plants contributing to the mechanistic understanding of long-distance responses in plants.

4:45 PM SB10.06.06

Chemical and Biosensing Using Enzyme Inspired Electropolymerized MIPs and Devices Rigoberto C. Advincula; The University of Tennessee/Oak Ridge National Laboratory, United States

Bioinspired macromolecules can be prepared by bio-conjugation or de-novo biopolymer substitutes. The lock-and-key templating process can mimic molecular complexes inspired by biological enzyme-substrate interactions. Using functional monomers that can be electrochemically polymerized enables the formation of cross-linked polymer films with cavities that enable high-binding assays of chemical and biological analytes. This talk will show the effective and bio-inspired artificial enzymes for detecting chemical and biological analytes. We will focus on demonstrating electropolymerized molecularly imprinted polymer (E-MIP) sensor elements and their ability to utilize transduction methods such as surface plasmon resonance (SPR) spectroscopy to enable high sensitivity and selectivity. The monomer and molecular design for optimized analyte interaction enables effective templating protocols in an electrically conducting polymer matrix with tunable redox states to enable a high volume of analyte-cavity sites. Optimized electropolymerization methods are important for film deposition and surface characterization based on SPM, XPS, and other microscopic and spectroscopic

methods to confirm surface specificity. Several analytes, including drugs, organic pollutants, nerve agents, and epitopes of larger proteins. This was recently demonstrated in the detection of dengue-expressed proteins for disease diagnostics.

SESSION SB10.07: Poster Session II
Session Chairs: Simone Fabiano and Naoji Matsuhisa
Wednesday Afternoon, April 24, 2024
Flex Hall C, Level 2, Summit

5:00 PM SB10.07.01

Electropolymerized Organic Mixed Ionic-Electronic Conductors Amel Besic and Connor G. Bischak; University of Utah, United States

Organic mixed ionic electronic conductors (OMIECs) are conjugated polymer systems that conduct both ions and electrons. These materials are promising for applications in healthcare and energy technologies, including biosensors and batteries. An obstacle for these novel materials is a lack of understanding behind the fundamental principles that underlie operation, particularly the coupled ion motion dynamics, electron transport, and morphological changes. This work presents the electropolymerization and characterization of several thiophene-based polymers and copolymers. An advantage of electropolymerization is the monomers do not require bulky side-chains to be made soluble in organic solvents, which allows these materials to pack more charge per unit volume. Using electropolymerization, we synthesize several polythiophenes with different side chain chemistries. We investigate ion injection kinetics in these materials using spectroelectrochemistry and find that injection kinetics depend on the identity of the electrolyte. We also characterize their morphology with atomic force microscopy (AFM), scanning electron microscopy (SEM), and Grazing-Incidence Wide-Angle X-ray Scattering (GIWAXS). Electropolymerized OMIECs may play an important role in the advancement of OMIEC-based technologies due to their unique morphologies which stem from this new synthesis method.

5:00 PM SB10.07.02

Amplifying Biosensor Sensitivity through Chitosan-Coated Nanoparticles Ariadna Schuck and Yong-Sang Kim; Sungkyunkwan University, Korea (the Republic of)

Chitosan, a biocompatible polymer derived from chitin, enhances biosensor sensitivity by facilitating precise recognition element immobilization and protecting against interference [1], [2]. When combined with chitosan-coated nanoparticles, it further amplifies sensitivity by increasing the surface area for binding and signal output, improving biosensor performance [3], [4]. To verify the effect of the chitosan-coated gold nanostructures on the surface of a screen-printed carbon electrode (SPCE) sensor, we modified gold nanoparticles and nanostars with chitosan and performed several morphological and electrical characterizations. Uniformity, diameter size, and dispersion of the nanostructures were investigated with atomic force microscopy (AFM), UV-Vis spectroscopy, and scanning electron microscopy (SEM) images. The electrical analysis was performed after electrodepositing the coated nanostructures on the working electrode of the SPCE sensor. First, the cyclic voltammetry (CV) technique was measured with a buffer solution where the peak currents were amplified after the functionalization step. The Nyquist plots were also recorded to verify the charge transfer resistance based on the equivalent circuit. To verify the nanostructures' performance for the detection of biochemicals, we decided to immobilize specific antibodies (100 ng/mL) over the nanostructures and detect apolipoprotein E4 (ApoE4), a specific allele of the ApoE gene associated with Alzheimer's disease. We performed differential pulse voltammetry measurements to quantify the biomarker (ranging from 0.41 to 40 ng/mL) in human serum samples (less than 20 μ L). The current peak variations showed high linearity, with a linear regression coefficient (R^2) of 0.9841, corresponding to the levels of ApoE4. Further studies will involve validation and interference tests, including the detection of other Alzheimer's disease (AD) biomarkers, such as Amyloid- β 42.

[1] S. Yu, X. Xu, J. Feng, M. Liu, and K. Hu, "Chitosan and chitosan coating nanoparticles for the treatment of brain disease," *Int. J. Pharm.*, vol. 560, no. February, pp. 282–293, Apr. 2019, doi: 10.1016/j.ijpharm.2019.02.012.

[2] C. O. Mohan, S. Gunasekaran, and C. N. Ravishanker, "Chitosan-capped gold nanoparticles for indicating temperature abuse in frozen stored products," *npj Sci. Food*, vol. 3, no. 1, p. 2, Jan. 2019, doi: 10.1038/s41538-019-0034-z.

[3] X.-X. Dong *et al.*, "Portable amperometric immunosensor for histamine detection using Prussian blue-chitosan-gold nanoparticle nanocomposite films," *Biosens. Bioelectron.*, vol. 98, pp. 305–309, Dec. 2017, doi: 10.1016/j.bios.2017.07.014.

[4] G.-C. Fan, X.-L. Ren, C. Zhu, J.-R. Zhang, and J.-J. Zhu, "A new signal amplification strategy of photoelectrochemical immunoassay for highly sensitive interleukin-6 detection based on TiO₂/CdS/CdSe dual co-sensitized structure," *Biosens. Bioelectron.*, vol. 59, pp. 45–53, Sep. 2014, doi: 10.1016/j.bios.2014.03.011.

5:00 PM SB10.07.03

Superelastic Hydrogels for Mechano-Electric Sensing Stephan Foerster, Tulika Sharma, Martin Dulle, Jürgen Allgaier and Guido Vehres; Forschungszentrum Jülich, Germany

Hydrogels are materials that can retain large amounts of water, making them broadly applicable to many areas, including wound care, tissue engineering, and soft electronics. Conventional hydrogels usually possess limited mechanical strength. The current concept of double network hydrogels provides largely increased mechanical stability, thus allowing also mechano-electrical sensing. However, the chemical and structural complexity of many double network hydrogels complicate understanding and tailoring their mechanical and electrical properties over a broad range.

We synthesized a new class of elastic and mechanically stable hydrogels based on alternating amphiphilic copolymers that in water spontaneously form physical networks that constitute the hydrogels, with no crosslinking chemistry required. The hydrophobic copolymer blocks consist of alkyl chains that form well-defined nanodomains acting as dynamic crosslinks. The mechanical and dynamic properties of the hydrogels can be directly controlled by the lengths of the alkyl chains and the hydrophilic repeat units. The highly elastic hydrogels allow elongations of more than 10000%, with tensile moduli in the kPa-range to MPa-range, adjustable to the range of moduli and deformation of skin at joints. We demonstrate *in situ* X-ray diffraction under tensile stretching and compression, together with conductivity measurements to relate the nanodomain structure directly to the mechano-electrical properties.

The intrinsic ion conductivity of the hydrogels allows mechano-electrical sensing of stretching and compression from very small to large deformations for thin films, over a broad range of frequencies, suitable to sense joint motion and speech.

5:00 PM SB10.07.04

Naturally Derived Chlorophyll Absorption Layers for RGB Color Recognition in IGZO Phototransistors Hyunji Son^{1,2}, Dong Hyun Choi¹, Kyungho

Park¹, Jusung Chung¹ and Hyun Jae Kim¹; ¹Yonsei University, Korea (the Republic of); ²LG Display Co., Korea (the Republic of)

With the continuous growth of various Internet of Things (IoT)-based industries – including mobile smart devices, autonomous vehicles, and medical equipment – there has been a sustained interest in the technologies that recognize and communicate information in real-time. Particularly, as a significant portion of information processing is visual, the study of optoelectronic devices, such as photosensors that detect visual information, has become increasingly important. Metal-oxide semiconductors have been a focal point as potential optoelectronic devices due to their advantages, such as high uniformity over large areas, high optical transparency, high mobility, and low off current. Past research has primarily aimed to expand the inherently limited light absorption range (ultraviolet and blue light) of these semiconductors, which results from their wide bandgap (>3.0 eV). This was usually achieved by introducing light-absorbing layers or by forming subgap states. However, most strategies focused merely on broadening the detection range into the visible or infrared spectrum without the ability to distinguish specific wavelengths of the absorbed light. It has been shown that even when absorbing different wavelengths of light, a consistent photo-response is generated based on its intensity, making it impossible to identify the specific wavelength of absorbed light. Therefore, conventional photosensor devices need additional color filters to identify different wavelengths, increasing costs and complicating high-density integration.

In this study, we propose an indium-gallium-zinc oxide (IGZO) phototransistor integrated with naturally derived chlorophyll as the light-absorbing layer to differentiate between different wavelengths without needing for color filters. Chlorophyll's characteristic green hue arises from its predominant absorption of blue and red light, while reflecting much of the green light. Utilizing the unique absorption properties of chlorophyll, we enhanced the light response range of the IGZO phototransistor. Specifically, absorption in the chlorophyll layer produces electron-hole pairs. These generated electrons then migrate to the IGZO channel layer, altering the transistor's electrical characteristics. For a chlorophyll concentration of 0.06 M, we measured the phototransistor's characteristics under red (635 nm), green (532 nm), and blue (405 nm) light irradiation. At an intensity of 1 mW/mm², results indicated photoresponsivity of 1607/641/3881 AW⁻¹, photosensitivity of $5.80 \times 10^7/3.51 \times 10^5/2.35 \times 10^8$, and detectivity of $3.86 \times 10^{12}/1.63 \times 10^{11}/3.58 \times 10^{13}$ Jones for red, green, and blue wavelengths, respectively. This is in contrast to conventional photodetectors, which typically show a light responsivity order of blue>green>red; our findings presented an order of blue>red>green. Exploiting this distinctive characteristic, combining a conventional phototransistor with our chlorophyll-induced version allows the design of an NMOS (N-type metal oxide semiconductor) inverter logic circuit capable of differentiating between 3 colors of blue, green, and red without color filters. Using SPICE (Simulation Program with Integrated Circuit Emphasis) simulations and the phototransistor's experimental results, we demonstrated that within a light intensity range of 0.1–5 mW/mm², the output voltage responded with low, high, and mid-values for red, green, and blue light inputs, respectively.

In conclusion, the IGZO phototransistor utilizing chlorophyll as an absorption layer has demonstrated the potential to differentiate between red, green, and blue light. This suggests the possibility of simplifying the actual fabrication process by eliminating color filters in the sensor. Moreover, it implies the potential for various applications, such as light-controlled logic circuits.

5:00 PM SB10.07.05

Ultrathin, Self-Adhesive, Sweat-Absorbing Janus Membrane Epidermal pH Sensor Wenqing Wang^{1,2}, Suksmadhira Harimurti¹, Kenjiro Fukuda², Sunghoon Lee², Tomoyuki Yokota¹ and Takao Someya¹; ¹The University of Tokyo, Japan; ²RIKEN, Japan

Wearable biomedical sensors have enabled non-invasive and continuous physiological monitoring for daily health management and early detection of chronic diseases [1,2]. Among the biomedical sensors, wearable pH sensors attracted significant interest as pH influences most biological reactions [3,4]. However, the conformable pH sensor which can be self-adhesive to human skin, has sweat-wicking ability and gas permeability remains largely unexplored. Here, we present a novel approach to this problem through the development of a Janus membrane-based pH sensor with self-adhesive on the skin. The sensor consists of a hydrophobic polyurethane-polydimethylsiloxane (PU-PDMS) porous nanometer-thick film and a hydrophilic polyvinyl alcohol-polyacrylic acid (PVA-PAA) nanofiber film. This Janus membrane exhibits a thickness of a few micrometers, providing a firm and comfortable adhesion to the skin. The sensor demonstrates fast-responsive, accurate, and long-term pH measurements, enabling reliable wearable applications. The simultaneous realization of solution absorption, gas-permeability, and self-adhesiveness, make it suitable for long-term, continuous monitoring without compromising wearer comfort. The pH sensor has been tested successfully for continuous monitoring over an hour, demonstrating its potential for stable analysis of skin health conditions. This innovative Janus membrane-based pH sensor holds significant promise for comprehensive skin health monitoring and wearable biomedical applications.

Reference

- [1] T. R. Ray, J. Choi, A. J. Bandodkar, S. Krishnan, P. Gutruf, L. Tian, R. Ghaffari, J. A. Rogers, Bio-integrated wearable systems: A comprehensive review. *Chem Rev.* 119 (2019), pp. 5461–5533.
- [2] Y. Luo et al., Technology Roadmap for Flexible Sensors. *ACS Nano.* 17 (2023), pp. 5211–5295.
- [3] S. Nakata, M. Shiomi, Y. Fujita, T. Arie, S. Akita, K. Takei, *Nat Electron.* 1, 596–603 (2018).
- [4] A. Koh, D. Kang, Y. Xue, S. Lee, R. M. Pielak, J. Kim, T. Hwang, S. Min, A. Banks, P. Bastien, M. C. Manco, L. Wang, K. R. Ammann, K.-I. Jang, P. Won, S. Han, R. Ghaffari, U. Paik, M. J. Slepian, G. Balooch, Y. Huang, J. A. Rogers, “A soft, wearable microfluidic device for the capture, storage, and colorimetric sensing of sweat” (2016).

5:00 PM SB10.07.06

Breathable, Structure-Gradient Pressure Sensing Textile for Rehabilitation Assistance Jinxing Jiang and Qiyao Huang; The Hong Kong Polytechnic University, Hong Kong

Triboelectric pressure sensing textile shows great potential in various wearable applications such as healthcare monitoring system due to their light weight, high permeability and flexibility. However, it's difficult to achieve high sensitivity and large pressure sensing range simultaneously. Here, we innovatively crafted a skin-inspired fiber mat (SIFM) with a gradient structure using a template-assisted layer-by-layer electrospinning technique. Drawing inspiration from the human skin, our SIFM mimics its natural micro-bump texture, gradually transitioning from soft to rigid as one moves from its outermost surface towards its core. The distinct structural design of SIFM has led to the development of a breathable, structure-gradient pressure sensing textile (PSPST) with simultaneously high sensitivity, wide detection range and high breathability. In comparison to conventional pressure sensing textiles constructed from homogeneous fiber mats, our PSPST exhibits a substantial enhancement in pressure sensing performance. Finally, We demonstrate its ability for rehabilitation assistance, including monitoring the quadricep, pulse and plantar pressure simultaneously.

5:00 PM SB10.07.07

Tissue-Like Skin-Device Interface for Wearable Bioelectronics by Using Ultrasoft, Mass-Permeable and Low-Impedance Hydrogels Yoonsoo Shin and Dae-Hyeong Kim; Seoul National University, Korea (the Republic of)

Hydrogels are composed of a cross-linked porous polymer structure with water molecules distributed within the gaps of the polymer chains. This unique composition renders hydrogels soft and hydrated, sharing mechanical and physical characteristics akin to human tissues. Consequently, hydrogels have the potential to emulate a tissue-like environment within the minuscule spaces between wearable devices and the human skin. In this study, we introduce

strategies at both material and device levels to establish a quasi-solid, tissue-mimicking interface between wearable bioelectronics and human skin. A crucial element of this approach involves an ultra-thin functionalized hydrogel exhibiting exceptional properties like high mass-permeability and low impedance. This specialized hydrogel acts as a liquid electrolyte on the skin, creating a highly conformal and low-impedance interface suitable for wearable electrochemical biosensors and electrical stimulators. Moreover, its porous structure and ultra-thin profile enable efficient transport of target molecules across the interface, thereby maximizing the performance of diverse wearable bioelectronics.

5:00 PM SB10.07.08

Highly Elastic and Ultrathin Nanomembrane Using Kinked Ag Nanowires for Epidermal Electrode [Minseong Kim](#)^{1,2} and Dae-Hyeong Kim^{1,2,1}; ¹Seoul National University, Korea (the Republic of); ²Institute for Basic Science, Korea (the Republic of)

Skin electronic devices require a flexible conductor with properties such as metal-like conductivity, high flexibility, extremely thin thickness, and the ability to create simple patterns. Achieving these characteristics simultaneously has proven to be quite challenging. Previous research introduced a nano-membrane fabrication method using a float assembly technique to successfully address a significant portion of these challenges in creating electrodes for skin electronic devices. However, conventional nano-membranes often struggle to precisely control conductivity and flexibility due to the dense packing nature of nanowires. In this study, an innovative approach is presented to create highly flexible nano-membranes using twisted nanowires. Incorporating twisted nanowires in the nano-membrane fabrication process facilitates the formation of percolation networks at low concentrations. Furthermore, the use of twisted nanowires not only enhances flexibility but also reduces the likelihood of nanowire breakage during vertical deformation. This innovation advances the development of skin electronic devices and holds significant potential for improved flexibility, conductivity, and durability in various applications.

5:00 PM SB10.07.09

Recognitive Tactile Sensor System Inspired by Human Skin Mechanoreceptors [Kyoung-Yong Chun](#), Seunghwan Seo and Chang-Soo Han; Korea University, Korea (the Republic of)

The human skin is an astonishing sensory organ that provides extensive information about our surrounding environment. It can detect various stimuli such as pressure, vibration, texture, temperature, and even chemical substances. Taking inspiration from ion channels and receptors, which are key components of cutaneous sensory organs from a biological perspective, a new approach is being pursued to address the limitations of conventional touch sensors and enable machines to interact with the world in a more human-like manner. Specifically, skin sensory organs perceive tactile sensations through the simultaneous and complex reactions of diverse and abundant receptors. Each receptor possesses a unique working mechanism that selectively responds to specific stimuli. Unfortunately, prior research has overlooked the significance of this aspect and instead focused on independent studies or functions of individual receptors, neglecting to mimic structure of the skin or incorporate it adequately.

The skin encompasses numerous transmission networks that detect stimuli and relay information to the brain. These networks consist of receptors that detect stimuli, ion channels that generate action potentials, and nerves that transport the electrical signals to the brain. Specifically, in the context of sensing physical stimuli, mechanoreceptors are generally classified into four types: Merkel discs (MD), Meissner corpuscles (MC), Ruffini endings (RE), and Pacinian corpuscles (PC). These mechanoreceptors play a crucial role in collecting information about the physical properties of objects we encounter in the environment, enabling us to perceive their shape, weight, texture, etc.

To truly mimic human skin functionality, it is essential to design and manufacture a diverse array of sensors capable of obtaining various information such as pressure, shear force, and tension from a limited size. This will allow for more accurate and diverse collection of mechanical stimuli from the surrounding environment. For instance, in our case, to emulate the vibrational touch sensing function observed in dermal papillae where MC is located, a bump-like structure and piezoelectric characteristics can be utilized for implementation. Additionally, to mimic the positional and functional features of piezo2, found in the MD, a cone-shaped ion gel and piezo gel can be employed. As for the RE, which has a dendritic branch form within the capsule and participates in stretch detection, this can be emulated using carbon nanotubes (CNTs) sheet with properties of tensile resistance within viscoelastic materials. Simulating the functions and features based on these receptor structures represents a future challenge that artificial skin should strive towards. This study aims to develop a tactile sensor system that recognizes objects by mimicking the mechanoreceptors present in human skin. The sensor system is designed by emulating the unique structures and functionalities of three types of receptors (MD, ME, RE) crucial for object recognition. These sensors are embedded in a material with similar elasticity to human skin. The integrated sensors are arranged in a way that separates receptors (stimulus detectors) and ion channels (signal generators), enhancing selectivity to specific stimuli. The manufactured sensors exhibit stretchability similar to human tactile organs and demonstrate trends comparable to biological touch experiments. Furthermore, to achieve effective object recognition, an AI-based signal processing algorithm is employed to analyze and learn from the data generated by the sensors. The material design for the object recognition sensor incorporates materials such as piezo gels and non-hydrogel ion gels, as well as substances like carbon nanotubes to control mechanical and electrical properties. The integrated sensor system successfully recognizes surface textures and various objects that are difficult to analyze using only one or two types of sensors.

5:00 PM SB10.07.11

Multiple Recycled Triboelectric Nanogenerators for Smart Waste Management [Nikhil R. Patra](#), Yuvraj S. Negi and Kaushik Parida; IIT Roorkee, India

The last decade has seen a mammoth rise in the progress of polymer electronic devices. This has in turn lead to the accumulation of non-degradable plastic material which has led to the degradation of the environment. Thus, for the sustainable progress of mankind, there is a need to recycle these polymer electronic devices. Although there has been reports on recycled nanogenerator, there is a need to develop nanogenerator which can be recycled multiple times. A multiple recycled triboelectric nanogenerator (MRTENG) derived from mixed plastic waste has been fabricated to achieve an environmentally sustainable energy harvesting device with an increase in lifetime in an order of magnitude¹. The triboelectric layer is prepared from plastic waste using a novel material design in the presence of a compatibilizing agent derived from e-waste for high stability and mechanical performance. This increases the lifetime of the energy harvester for ten rounds of recycling. The current collector is extracted by high-temperature pyrolysis of segregated mixed plastic waste, depolymerized polyester, and multiple recycled triboelectric layer that acts as a conducting layer in the single-electrode triboelectric nanogenerator^{2,3}. The fabricated device shows high performance even after multiple rounds of recycling, hence providing a sustainable solution in reducing environmental pollution. The device is installed in smart dustbins for digitalizing waste management using machine learning. As a waste disposal sensor the MRTENG monitors filling of bins and also identifies the type of waste disposed to alert and optimize the waste collection and segregation process, from the homes to the recycling industries.

5:00 PM SB10.07.12

Conductive Carbon Fiber-Hydrogel-Composites for Functional Tissue Engineering Sebastian Bihler and [Julia Koerner](#); Leibniz University Hannover, Germany

Materials for tissue engineering rely on the mimicry of extracellular matrix environments, easily achievable biocompatibility and favorable mechanical properties. Hydrogels are a type of polymer that incorporate these properties and are widely used as tissue scaffolds [1]. In general, hydrogels are a non-

conductive material and therefore tailoring their electrical properties to enhance conductivity opens the possibility of extending their applications to include sensing and actuation.

One technique to tailor and modify the conductivity and mechanical properties of hydrogels is to embed carbon fibers in the polymer matrix. To date, carbon fiber-hydrogel-composites (CHC) with random fiber distribution within the hydrogel have been used as flexible and biocompatible sensors [2]. In addition, composites of epoxy-based polymers and unidirectional fiber bundles have been investigated for their properties under high strain and have shown piezoresistive behavior [3,4].

Our work targets the application of unidirectional carbon fibers as a novel approach for tailoring the hydrogel's electrical conductivity. The aim of this research is to study the capabilities of CHCs for directed electric signal transmission along the fibers which could be a first step towards applications as bioelectrical elements, e.g. in nerve grafts. In this regard, two forms of current flow inside the CHC need to be considered: electron- and ion-based for the carbon fibers and hydrogel matrix, respectively. The initial investigation focused on studying the interplay between these two types of conductivity and how they influence the general electric signal transmission capabilities of CHCs.

Therefore, cylindrical polyacrylamide hydrogels containing a bundle of polyacrylonitrile carbon fibers (~1000 filaments) in the middle were fabricated by molding and UV photopolymerization, with the fiber ends protruding from the hydrogel for electrical connection. Two different types of samples were defined: Sample group (SG) 1 features a continuous fiber bundle throughout the hydrogel and SG2 a cut fiber bundle inside the matrix with a gap of a few millimeters. This enables the investigation of the transition between electron- and ion-based current flows. Furthermore, samples from both groups were stored in different concentrations of phosphate buffered saline (PBS) solution to study the influence of the hydrogel's ion concentration on signal transmission capabilities. Prior to the electrical measurements, the samples were immersed in PBS solutions ranging from 1x to 5x in increments of 1x for at least 24 hours. Please note that the CHC samples were always stored in PBS solution between experiments but the measurements itself were conducted in air.

Predefined signals with a frequency of 1 kHz were applied at one end of the CHC sample and the voltage at the other end captured with a digital oscilloscope. The received signal was evaluated for change in amplitude and phase with respect to the input.

SG1 showed no relation between ion concentration and amplitude or phase but good overall conductivity (~100 S/mm). SG2 samples showed a variation in signal phase shift as a function of increasing ion concentration.

These experimental results were accompanied by the electrical properties of the CHCs being modeled in a circuit model in order to gain insight into the causes of the different transmission behavior. This is a very first step towards characterizing and ultimately utilizing the properties of CHCs for active signal transmission. Further work will focus on different fiber bundle distributions and the influence of mechanical stress on the electrical properties.

[1] S. Naahidi et al., *Biotechnol Adv* 35:530, 2017; doi:10.1016/j.biotechadv.2017.05.006

[2] Y. Huang et al., *ACS Appl Polym Mater* 5:5707, 2023; doi:10.1021/acsapm.3c00983

[3] D. D. L. Chung, *Carbon* 50:3342, 2012; doi:10.1016/j.carbon.2012.01.031

[4] D. Wentzel et al., *Int J Eng Sci* 130:129, 2018; doi:10.1016/j.ijengsci.2018.05.012

5:00 PM SB10.07.13

Fluorescence Imaging of Self-Assembled Peptides on h-BN Using Thioflavin-T Hiroki Maeda and Yuhei Hayamizu; Tokyo Institute of Technology, Japan

Peptides possess the capability to self-assemble into well-ordered structures on two-dimensional (2D) materials, such as graphene, rendering them promising candidates for biosensor applications owing to their design flexibility and biocompatibility [1]. Recent research has highlighted the potential of graphene biosensors functionalized with peptides, emulating olfactory receptors for applications in odor sensing [2,3]. Investigating the surface structure of self-assembled peptides on 2D material-based biosensors is crucial for comprehending their performance. Atomic force microscopy (AFM) with high spatial resolution has conventionally been employed for the precise observation of these peptide structures [4].

Nevertheless, due to its limited field of view, AFM is unsuitable for the in-situ observation of macroscopic structures of self-assembled peptides with sizes ranging in the hundreds of micrometers. This study focuses on the in-situ observation of macroscopic structures of self-assembled peptides on hexagonal boron nitride (h-BN) surfaces using fluorescence imaging with Thioflavin-T (ThT) as a fluorescent marker. h-BN, transparent in the visible region, is well-suited for fluorescent microscopy as a transparent substrate. ThT is known to exhibit strong fluorescence when attached to β -sheet structures, commonly found in amyloid fibers associated with diseases like Alzheimer's. Given that the peptides in this study are expected to form β -sheet structures, we assessed the feasibility of using ThT for real-time observation of the macroscopic surface self-assembly process [5].

AFM measurements unveiled that peptides formed long-range ordered structures on h-BN. Subsequently, under fluorescent microscopy, we observed strong fluorescence in regions where the ordered peptide structures existed. The size of the domain of ordered peptides on the surface spanned over a few tens of micrometers in length. This size exceeds the field of view of AFM measurements, and the fluorescent measurement with ThT molecules enables us to visualize the macroscopic self-assembled structures of peptides. Furthermore, weak fluorescence was also detected on partial surfaces of h-BN containing amorphous peptides. These findings underscore the potential of ThT as a tool for assessing the macroscopic self-assembly of peptides over a wide area. The ability to monitor these processes in real-time under liquid conditions using fluorescence microscopy provides insights into the spatial uniformity of molecular thin films, a critical aspect for enhancing the activity of peptide-based bio-probes on graphene biosensors. This methodology opens avenues for the development of improved peptide biosensors with enhanced functionality and performance.

[1] Y. Hayamizu, et al. *Sci Rep* 6, 33778 (2016)

[2] C. Homma, et al. *Biosens. Bioelectron.*, 2023, 224, 115047

[3] T. Rungreunthanapol, et al. *ACS. Anal. Chem.* 2023, 95, 9, 4556-4563

[4] P. Li, et al. *ACS App. Mat. Inter.*, 2019, 11, 23, 20670-20677

[5] T. N. Tikhonova, et al. *Angew. Chem., Int. Ed.*, 2021, 60, 25339-25345

5:00 PM SB10.07.14

Synthesis of Shape-Programmable Elastomer for a Bioresorbable, Wireless Nerve Stimulator Chan-Hwi Eom; Korea University, Korea (the Republic of)

Materials that have the ability to manipulate shapes in response to stimuli such as heat, light, humidity and magnetism offer a means for versatile, sophisticated functions in soft robotics or biomedical implants, while such a reactive transformation has certain drawbacks including high operating temperatures, inherent rigidity and biological hazard. Herein, we introduce biodegradable, self-adhesive, shape-transformable poly(L-lactide-co- ϵ -caprolactone) (BSS-PLCL) can be triggered via thermal stimulation near physiological temperature (~38 °C). Chemical inspections confirm the fundamental properties of the synthetic materials in diverse aspects, and study on mechanical and biochemical characteristics validates exceptional stretchability up to 800 % and tunable dissolution behaviors under biological conditions. The integration of the functional polymer with a bioresorbable electronic system highlights potential for a wide range of biomedical applications.

Keywords: biodegradable polymers; shape-transformable elastomers; shape memory; self-adhesion; nerve stimulators

5:00 PM SB10.07.15

NIH Brain Behavior Quantification and Synchronization Program: Next Generation Sensor Technology and Related Materials Science Development Yvonne M. Bennett; NIH, United States

This session will highlight several Notice of Funding Opportunities (NOFOs) from the National Institutes of Health (NIH) Brain Research through Advancing Innovative Neurotechnologies® (BRAIN) Initiative that are intended to support the development of next generation sensor technologies and bioelectronic devices to further the goals of the Brain Behavior Quantification and Synchronization (BBQS) program. The BBQS funding opportunities broadly support 1) development of tools for simultaneous, multimodal measurement of behavior and synchronization of these data with simultaneously-recorded neural activity; and 2) development of novel conceptual and computational models that capture dynamic behavior-environment relationships. More information about the BRAIN Initiative including existing Notices of Funding Opportunities for the BBQS program can be found at www.braininitiative.nih.gov (search "BBQS") and there is a BBQS Sensors Request for Information at NOT-MH-24-125. The BBQS Program invites researchers in materials science to contribute to upcoming projects (large and small scale, and future sensor hubs) to develop next generation sensor technologies at the micro and nano scales, which must feature wireless, lightweight, compact designs with energy harvesting capabilities. Sensors must be noninvasive or minimally invasive in design. Sensor developer teams in a future Consortium will promote rigorous technology design, fabrication, testing, validation, and dissemination of information regarding sensors and bioelectronics toward improving our understanding of human and organismal behavior.

SESSION SB10.08: Flexible and Stretchable Electronics
Session Chairs: Sihong Wang and Cunjiang Yu
Thursday Morning, April 25, 2024
Room 429, Level 4, Summit

8:15 AM SB10.08.01

Wearable On-Skin Chemo-Sensors Le Yang^{1,2}; ¹Institute of Materials Research and Engineering A*STAR, Singapore; ²National University of Singapore, Singapore

In an increasingly health-aware population and a move towards remote diagnostics, remote healthcare monitoring and cloud-based med-tech, we tap on the ubiquitous and unlimited reservoir of on-skin biomarkers, including sweat metabolites, in developing a wearable, non-invasive, continuous and real-time sensor – a printed, multiplexed biosensor. Such a device can be colorimetric or electrochemical in its sensing mechanism. Our integrated devices are designed and developed with scalability and translation in mind – ensuring printability (for scalable manufacturing), ease of fabrication routes, and solid-state and miniaturised prototype.[1-8]

In particular, firstly, we introduce a newly-published fully-printed paper-based patch, printed from our development of a ceramic-based ink along with nanoparticle-functionalisation, for multi-metabolite and sweat rate monitoring.[1]

Next, we highlight the importance of enzymes in such enzymes-based biosensors (enzymatic reactions to detect target analytes), where their intrinsic instability poses a bottleneck in practical long-term use. Previous methods at enhancing enzyme stability had always been met with a trade-off in sensitivity, selectivity or performance/efficacy. Herein, we showcase a novel materials-based approach, a one-pot synthesis of co-encapsulating enzymes and carbon-dots in a metal-organic framework, overcoming the aforementioned compromise. We achieve an electrochemical highly-stable and highly-sensitive device, and demonstrate it as a touch-based sweat sensor. [2]

Lastly, we briefly highlight an even more holistic approach in developing a printable, non-invasive, real-time and continuous electrochemical sensor for sweat-based and 'dry-skin' based on-skin chemosensing. [3-7]

[1] XT Zheng, WP Goh, Y Yu, L Sutarlie, DY Chen, SCL Tan, C Jiang, M Zhao, T Ba, H Li, X Su, L Yang. Skin Attachable Ink Dispenser Printed Paper Fluidic Sensor Patch for Colorimetric Sweat Analysis. *Advanced Healthcare Materials*, 2302173 (2023). *Online 28 Oct 2023*.

[2] XT Zheng, MWN Leoi, Y Yu, SCL Tan, N Nadzri, WP Goh, C Jiang, XP Ni, P Wang, M Zhao, L Yang. Co-encapsulating Enzymes and Carbon Dots in Metal-Organic Frameworks for Highly Stable and Sensitive Touch Based Sweat Sensors. *Advanced Functional Materials*, 2310121 (2023). *Online 30 Nov 2023*.

[3] A graphite-based paste/ink for electrochemical sensors, WP Goh, CY Jiang, Y Yu, XT Zheng, YX Liu, LYang, PCT/SG2022/050407, Singapore (*PCT filed*), 2022.

[4] A kirigami paper fluidic channel for sweat sensors, CY Jiang, WP Goh, XT Zheng, Y Yu, YX Liu, L Yang, SG-10202113328Q, Singapore (*PCT filed*), 2023.

[5] Y Yu, L Yang et al, *Materials Today Advances*, 14, 100238 (2022).

[6] Stretchable biochemical interface for solid epidermal analytes, YX Liu, WP Goh, XT Zheng, Y Yu, SCL Tan, CY Jiang, RT Arwani, L Yang, SG-10202202318P, Singapore (*PCT filed*), 2023.

[7] RT Arwani, WP Goh, CY Jiang, XT Zheng, Y Yu, L Yang YX Liu et al, *Under Revision* 2023.

8:30 AM SB10.08.02

Breathable Electrode based on Hydrophobic-Hydrophilic Membranes with Water Stability for Stable Biosignal Monitoring on Wet/Sweaty Skin Suksmadhira Harimurti¹, Wenqing Wang^{1,2}, Sunghoon Lee², Tomoyuki Yokota¹ and Takao Someya^{1,2}; ¹The University of Tokyo, Japan; ²RIKEN, Japan

Realizing a breathable electrode, which can reliably monitor biosignal after being exposed to water or sweat is challenging. Depending on the stability of its polymer chain backbone towards water or sweat, some of the electrodes could be damaged when exposed to water or sweat. Besides, sweat could also introduce undesired noise artifacts, which lowers the quality of the acquired biosignal. Here, a water- and sweat-stable breathable electrode was demonstrated by utilizing a stack layer of ultrathin hydrophobic microporous Au/polyurethane-polydimethylsiloxane (Au/PU-PDMS) membrane and water-stable hydrophilic poly(vinyl alcohol)/poly(acrylic acid) (PVA/PAA) nanofibers membrane. The hydrophobic membrane was fabricated by dip-coating the PU nanofibers into PDMS-hexane solution. By controlling the dip-coating withdrawal speed, PU-PDMS membrane with pore density of 39% was achieved. Despite having pores on its surface, the PU-PDMS membrane exhibited hydrophobicity with a water contact angle (WCA) of ~108°. Meanwhile, the hydrophilic nanofibers membrane was fabricated using electrospinning followed by a partial crosslinking process to achieve the water stability yet maintain the hydrophilicity. The total thickness of the stack layer was below 15 µm. Along with its porous structure, the electrode exhibited an

excellent breathability equal to the open bottle with a water vapor transmission rate (WVTR) of 0.58 kg/m²day.

Moreover, the stack of these two membranes facilitated a spontaneous water/sweat pulling, of which the water/sweat could be pulled up vertically in antigravity direction. As a result, when the sweat was secreted to the skin surface, the sweat was spontaneously pulled away from the skin surface. Consequently, the skin-electrode interface could be kept dry, ensuring reliable biosignal monitoring. In addition, the hydrophilic membrane showcased an excellent stability in water that it did not break even after being continuously immersed in deionized (DI) water or phosphate-buffered saline (PBS) solution for up to 1 month. PBS solution was used in this study to simulate the ions contained in the sweat. More importantly, even after continuous immersion in both liquids, the hydrophilic membrane could maintain its hydrophilicity. From the WCA measurement at 37 s, the WCA of the membrane after the immersion in DI water remained stable at ~23.5° while after the immersion in PBS solution the WCA decreased to 14.4°, indicating that the membrane became more hydrophilic. Furthermore, electrocardiogram (ECG) signal was measured at rest (dry skin) and after doing a physical exercise (sweaty skin) to evaluate the biosignal acquisition stability against sweat. Exhibiting a sweat pulling property, the electrode was able to maintain a high signal-to-noise ratio (SNR) of 30 dB on the sweaty skin. This result could potentially provide more insight for the medical doctors, especially when evaluating cardiovascular health of a subject that may require the subject to do physical exercise or under a dynamic ambient (temperature/humidity) conditions.

8:45 AM SB10.08.03

Intrinsically Stretchable Subthreshold Polymer Transistors for Highly Sensitive Low Power Skin Like Temperature Sensors Jin Young Oh, MinWoo Jeong, Phuong N. Vo and Kyu Ho Jung; Kyung Hee University, Korea (the Republic of)

Stretchable wearable sensors ultimately require low power consumption and high response to physiological signals with skin conformability. However, power response tradeoff and strain dependent sensing instability remain key challenges for electronic skin (e skin) sensors. In this talk, I will address an intrinsically stretchable organic subthreshold transistor operating at low voltage (−1 V) is presented, leading to ultralow power consumption (<1 nW) for highly sensitive skin like temperature sensory devices. The highly temperature dependent hopping transport of the fully stretchable subthreshold transistor exhibits high temperature sensitivity (9.4% °C^{−1}) and excellent sensing stability up to 100% strain. A skin like subthreshold organic transistor active matrix array is successfully fabricated that sensed the surface temperature distribution under a 3D deformation.

9:00 AM *SB10.08.04

Biomimetic Rubbery Synaptic Electronics and Integrated Systems Cunjiang Yu; The Pennsylvania State University, United States

Synapses are unique and critical biological structures that allow for the transmission of electrical or chemical signals thus to enable neurons to communicate with each other. Embodied within human or animals, the synapse is usually soft and able to accommodate various forms of mechanical deformations. Artificial synapse electronics that can be stretched similar to those appearing in human or animals could be seamlessly integrated other soft functional systems towards enabled neurological functions. This presentation will show our recent efforts on developing stretchable synaptic electronics fully made out of rubbery electronic materials. Rubbery synaptic devices are enablers for various soft systems with implemented neurologic functions. Examples including soft neurobots, cognitive smart skins, neuromorphic imaging devices will be introduced.

9:30 AM *SB10.08.05

Nature and Human-Inspired Sensing Devices Benjamin C. Tee; National University of Singapore, Singapore

B10- Bioinspired Organic Materials and Devices for Sensing and Computing

Sensing systems provide timely¹ and requisite data for machines to operate in physical environments. Often, natural biological systems provide optimized concepts that could be applied to design and engineer artificial sensor systems. Novel organic-based materials can even provide self-healing capabilities to such sensor devices². In this talk, I will discuss our recent advances in nature- and human-inspired materials for designing high performance sensor devices^{3,4}. The exciting cross-disciplinary interplay of physical interfaces, materials chemistry and electronics become essential for optimizing sensitivity, linearity and speed for the sensor system.

References

1. Lee, W. W., Tan, Y. J., Yao, H., Li, S., See, H. H., Hon, M., Ng, K. A., Xiong, B., Ho, J. S., & Tee, B. C. K. (2019). A neuro-inspired artificial peripheral nervous system for scalable electronic skins. *Science Robotics*, 4(32), eaax2198. <https://doi.org/10.1126/scirobotics.aax2198>
2. Hashina Parveen Anwar Ali, Zichen Zhao, Yu Jun Tan, Wei Yao, Qianxiao Li, and Benjamin C. K. Tee, *ACS Applied Materials & Interfaces* **2022** 14 (46), 52486-52498, DOI: 10.1021/acsami.2c14543
3. Cheng, W., Wang, X., Xiong, Z. et al. Frictionless multiphase interface for near-ideal aero-elastic pressure sensing. *Nat. Mater.* (2023). <https://doi.org/10.1038/s41563-023-01628-8>
4. Yao, H., Yang, W., Cheng, W., Tan, Y. J., See, H. H., Li, S., Ali, H. P. A., Lim, B. Z. H., Liu, Z., & Tee, B. C. K. (2020). Near-hysteresis-free soft tactile electronic skins for wearables and reliable machine learning. *Proceedings of the National Academy of Sciences*, 202010989. <https://doi.org/10.1073/pnas.2010989117>

10:00 AM BREAK

10:30 AM *SB10.08.06

Self-Healing, Stretchable and Recyclable Electronics Fabio Ciccoira; Polytechnique Montréal, Canada

Materials able to regenerate after damage have attracted a great deal of attention since the ancient times. For instance, self-healing concretes, able to resist earthquakes, aging, weather, and seawater are known since the times of ancient Rome and are still the object of research. While several mechanically healable materials have been reported, self-healing conductors are still relatively rare, and are attracting enormous interest for applications in electronic skin, wearable and stretchable sensors, actuators, transistors, energy harvesting, and storage devices, such as batteries and supercapacitors.¹ Self-healable and recyclable conducting materials have the potential to reduce electronic waste by enabling the repair and reuse of electronic components, which can extend the lifespan of electronic devices. Furthermore, they can be used for wearable electronic and biomedical devices, which are often subject to mechanical stress causing damage to their components. Conducting polymers exhibit attractive properties that makes them ideal materials for bioelectronics and stretchable electronics, such as mixed ionic-electronic conductivity, leading to low interfacial impedance, tunability by chemical synthesis, ease of process via solution process and printing, and

biomechanical compatibility with living tissues. However, they show typically poor mechanical properties and are therefore not suitable as self-healing materials.

In our group, we produced several self-healing and stretchable conductors by mixing aqueous suspensions of the conducting polymer poly(3,4-ethylenedioxythiophene) polystyrene sulfonate (PEDOT:PSS) with other materials providing the mechanical characteristics leading to self-healing, like for instance polyvinyl alcohol (PVA), polyethylene glycol, polyurethanes and tannic acid.²⁻¹⁰ In this talk, various types of self-healing will be presented and correlated with the electrical and mechanical properties of the materials. The use of the self-healing gels and films as epidermal electrodes and other devices will be also discussed.

REFERENCES

- Y. Li, X. Zhou, B. Sarkar, F. Cicoira et al., *Adv. Mater.* 2108932, 2022.
Y. Li, X. Li, S. Zhang, F. Cicoira et al., *Adv. Funct. Mater.* 30, 2002853, 2020.
Y. Li, X. Li, R. N., S. Zhang, F. Cicoira, et al. *Flexible and Printed Electronics* 4, 044004, 2019.
N. Rossetti, F. Cicoira et al., *ACS Appl. Bio Mater.* 2, 5154-5163, 2019.
C. Bodart, N. Rossetti, F. Cicoira et al. *ACS Appl. Mater. Interfaces*, 11, 17226-17233, 2019.
S. Zhang, Y. Li, F. Cicoira et al. *Adv. Electron. Mater* 1900191, 2019.
S. Zhang, F. Cicoira, *Adv. Mater.* 29, 1703098, 2017.
X. Zhou, G. A. Lodygensky, F. Cicoira et al., *Acta Biomaterialia* 139, 296-306, 2022.
X. Zhou et al, *Advanced Sensor Research*, in press, 2023
P. Kateb et al., *Flexible and Printed Electronics*, in press.

11:00 AM *SB10.08.07

Integrated Biodevices for Smart Contact Lenses [Takeo Miyake](#); Waseda University, Japan

Smart contact lenses—contact lenses with built-in electronics—are a next-generation wearable product with capabilities beyond simple vision correction. Since the electrical lenses are in continuous contact with the eyeball surface, they have three main applications: (i) biomedical sensing of tears and intraocular pressure to monitor health conditions, (ii) wearable displays for augmented reality (AR), and (iii) actively regulating eye accommodation to ensure perfect vision. Thus, a smart contact lens has substantially greater functionality than an electrical eyeglass. We have developed several prototypes of an ultrasensitive diagnostic smart contact lens [1-5] with high sensitive biosensors and high efficient parity-time (PT) symmetric wireless transfer systems, a wireless electrochromic lens using conductive polymer-based film, and multi-electrode electroretinogram (ERG) lens system. I will present a detail in my invited talk.

- [1] T. Takamatsu et al, *Adv. Mater. Technol*, 8, 2201704, 2023.
[2] S. Azhari et al, *IEEE Sensors Journal*, 23, 7902-7909, 2023.
[3] L. Hu et al, *Sensors and Actuators A: Physical*, 344, 113766, 2022.
[4] T. Takamatsu et al., *Adv. Funct. Mater.*, 30, 29, 2020.
[5] T. Takamatsu et al., *Adv. Mater. Technol.*, 4, 5, 2019.

11:30 AM *SB10.08.08

Tissue-Interfaced Electronics for Directing Biological Functions [Toshinori Fujie](#); Tokyo Institute of Technology, Japan

Integration of flexible electronics into the living system is expected for advancing medical diagnostics and therapeutics. Such devices should be seamlessly conformed to the physical and mechanical environment of living body, in which acquired biosignals are expected to be transmitted wirelessly to external device. In this regard, we envisage the development of tissue-interfaced electronics for wearable and implantable applications based on polymer nanosheet technology. The polymer nanosheet shows tens- to hundreds-of-nanometer thickness close to the scale of biomembranes, in which various types of polymers (e.g., biodegradable polymers, conductive polymers, and elastomers) are formed into the ultra-thin structure. Free-standing polymer nanosheets showed flexible and adhesive properties derived from their ultra-small flexural rigidity ($< 10^{-2}$ nN m). In this talk, polymer nanosheet (or thin film)-based devices are introduced by combining polymer nanosheet and printing technologies with variety of unique inks. A microgravure coater was employed for the preparation of flexible substrates or electrodes, an inkjet printer allowed for the tailor-made design of multielectrode array, and a laser processing machine was used for making the microchannels for insulating the circuit. The ultra-conformable structure has been utilized as tissue-interfaced electronics to direct biological functions in the applications of healthcare and medicine, represented by the wirelessly-powered light emitting device for photodynamic cancer therapy, and the flexible, thin-film neural electrode for diagnosis and treatment of epileptic seizure.

SESSION SB10.09: Neuromorphic Computing II
Session Chairs: Simone Fabiano and Songsong Li
Thursday Afternoon, April 25, 2024
Room 429, Level 4, Summit

1:30 PM *SB10.09.01

Organic Neuromorphic Electronics for Emulating and Interfacing Biological Systems [Paschalis Gkoupidenis](#); Max Planck Institute for Polymer Research, Germany

Neurons are the fundamental elements of the nervous system, coping with a great diversity of electrobiochemical signals. Neuronal function is an archetype for biomimicry with neuromorphic electronics. However, artificial neurons based on electronics are insufficiently capable of operating in situ in biological environments, thus hampering the seamless sensing and biointerfacing as well as the biorealistic neuronal emulation. A few examples of soft-matter artificial neurons are based on conventional circuit oscillators and therefore require many elements for their implementation. An organic artificial neuron consisting of a compact non-linear electrochemical element will be presented. The artificial neuron displays in situ operation in biologically relevant environments that displays spiking dynamics sensitive to common ions of the biological aqueous milieu, within physiopathological concentration ranges (~5-150mM), and with ion specificity. Small-amplitude (~1-150 mV) electrochemical oscillations and noise in the electrolytic medium shape the neuronal dynamics, while changes of ionic ($\geq 2\%$ over physiological baseline) and biomolecular concentrations (≥ 0.1 mM dopamine) modulate the neuronal excitability. The artificial neuron operates synergistically with bio-membranes, forming real-time biohybrid interfaces. This electrochemical artificial neuron opens new possibilities for the seamless communication and the realistic emulation of biology with electronics.

2:00 PM *SB10.09.02

Thiophene-Based Trimers *In-Vivo* Polymerizes to Form Substrate-Free Organic Bioelectronics on Living Cell Systems Magnus Berggren; Linköping University, Sweden

An array of different thiophene trimers have been synthesized to form bioelectronics that is amalgamated with living cell systems. Depending on the trimer composition and attached side groups, we can control the ionization potential, aggregation characteristics and the affinity to different cell system components. To fuel the polymerization, we take use of metabolic components, naturally available of the biological system, and various shapes of conducting and electroactive structures are formed. From here, we aim at establishing fundamental electrode and device architectures to enable novel routes to record and trigger cell functions, especially targeting the nervous system. The chemical, physical and electrical characteristics of different polymerized structures formed on cells and within tissues will be reported along with microscopy images.

2:30 PM SB10.09.03

From a Single Dendrite to Dendritic Networks: Towards Multi-Terminal OECTs Corentin Scholaert¹, Kamila Janzakova¹, Yannick Coffinier¹, Sébastien Pecqueur¹ and Fabien Alibert^{1,2}; ¹CNRS IEMN, France; ²CNRS - Laboratoire Nanotechnologies & Nanosystèmes (LN2), Canada

In the quest to change the way we envision computing, the ability to create connections in between computing nodes on demand offers the very exciting possibility to explore bottom-up strategies when it comes to thinking the design of electronic devices and circuits. Recently, the growth of conductive polymer fibers via electropolymerization (most notably poly(3,4-ethylenedioxythiophene) doped with poly(styrenesulfonate), abbreviated as PEDOT:PSS) was employed in the realm of neuromorphic hardware, first as a way to tune the resistance of a connection,[1] and then to perform computing tasks, such as biosignal classification through reservoir computing,[2] thus establishing the advantages of the method.

In this work, we propose to demonstrate that electropolymerization is a useful tool for the creation of sensors that are able to realize computing tasks in an aqueous environment. By taking advantage of the morphology of the fibers, we show that PEDOT:PSS dendrites can discriminate between different types of voltage pulses emitted in their vicinity by a local gate electrode, thus performing *in materio* classification.[3] In addition, we discuss the growth of networks of polymer fibers on 2D substrates. The ability to create structures that cover several microelectrodes allows us to study the behavior of the whole system instead of a single dendrite, and it highlights the relationship that relates the morphology of the object and its electrical properties. In particular, we show that dendrites present an asymmetric non-linear behavior due to the volume of polymer that increases the capacitance of the device albeit not participating in conduction. Moreover, because of the ionoelectronic coupling that exists within an electrolyte, two active devices working concomitantly will influence one another. We demonstrate that it is a blessing for the realization of computing tasks, such as logic, and that it can also be used to program the dendrites into non-volatile conductance states. Therefore, dendritic networks could constitute a new building block for non-conventional information processing that fits into the larger framework of brain-inspired computing.

References

- [1] M. Akai-Kasaya *et al.*, “Evolving conductive polymer neural networks on wetware,” *Jpn. J. Appl. Phys.*, vol. 59, no. 6, p. 060601, Jun. 2020, doi: 10.35848/1347-4065/ab8e06.
- [2] M. Cucchi *et al.*, “Reservoir computing with biocompatible organic electrochemical networks for brain-inspired biosignal classification,” *Sci. Adv.*, vol. 7, no. 34, p. eabh0693, Aug. 2021, doi: 10.1126/sciadv.abh0693.
- [3] C. Scholaert, K. Janzakova, Y. Coffinier, F. Alibert, and S. Pecqueur, “Plasticity of conducting polymer dendrites to bursts of voltage spikes in phosphate buffered saline,” *Neuromorphic Comput. Eng.*, vol. 2, no. 4, p. 044010, Dec. 2022, doi: 10.1088/2634-4386/ac9b85.

2:45 PM SB10.09.04

Face-On Orientation Matches Vertical Organic Electrochemical Transistors for High Transconductance and Superior Non-Volatility Bingjun Wang¹, Yuxin Kong², Sen Zhang¹, Ziang Wu³, Shijie Wang¹, Jiaqi Ren², Han Young Woo³, Yuxiang Li² and Wei Ma¹; ¹Xi'an Jiaotong University, China; ²Xi'an University of Science and Technology, China; ³Korea University, Korea (the Republic of)

The recently developed vertical structure of organic electrochemical transistors (OECTs) can integrate volatile (sensing) and non-volatile (memory) functions into one reconfigurable device, making it highly promising. However, compared with the conventional planar OECT (c-OECT), the understanding of vertical OECT (v-OECT) working principles and device engineering strategies is still lacking, impeding rational optimization. Since a major difference between c- and v-OECTs is their charge transport directionality, which is highly influenced by crystallite orientations, the orientation-device structure match thus becomes an important yet outstanding topic for OECTs. Herein, using a newly synthesized n-type small molecule IDIC-MEG, we investigate how much impact such a match can have on OECT performance. The IDIC-MEG c-OECT fails to work due to the seriously hindered in-plane electron transport by face-on orientation. Surprisingly, simply changing the device structure from planar to vertical allows the resultant v-OECT to exhibit the highest reported transconductance (46.3 mS) among all small-molecule OECTs, thanks to the match between face-on orientation and the vertical structure. Such a match also leads to excellent non-volatility, including good conductance state retention, highly predictable programmability, and nice operational stability. This work, for the first time, explicitly demonstrates the significance of orientation-device structure match for OECT optimization. We envisage that this device engineering strategy may provide a new pathway to achieve high-performance, reconfigurable v-OECTs for homogenous in-memory sensing and computing systems, which entail volatile and non-volatile functions alike.

3:00 PM BREAK

3:30 PM *SB10.09.05

Artificial Organic Afferent Nerves with Tactile Enhancement for Closed-Loop Feedback of Intelligent Robot Wei Lin Leong; Nanyang Technological University, Singapore

In biological tactile somatosensory system, the cooperation of mechanoreceptors, neurons and synapses allows human to efficiently detect, transmit and process the tactile information. Emulation of the tactile sensory nerve to achieve advanced sensory functions in robotics with artificial intelligence is of great interest. Here, we report an artificial organic afferent nerve (AOAN) by integrating novel pressure-activated organic electrochemical synaptic transistor (OEST) and artificial mechanoreceptors. Owing to the effect of electrochemical ion doping and ion trapping in bulk conjugated semiconductor, external mechanical stimulation enables activation and modulation of OEST, endowing the system with the recognition/sensation of spatiotemporal tactile information and a low retention loss during signal transmission. Dendritic integration function for neurobotics is achieved to perceive directional movement of object. An intelligent robot with our system, coupling with a closed-loop feedback program is demonstrated for slip detection and prevent slippage of objects. This work provides a promising approach towards next-generation intelligent neurobotics and low power biomimetic electronics.

4:00 PM SB10.09.06

Environment-Adjustable Bilingual Synaptic Functions in Bio-Synaptic Transistors [Moon Jong Han](#)¹ and Vladimir V. Tsukruk²; ¹Gachon University, Korea (the Republic of); ²Georgia Institute of Technology, United States

The transmission of signals in the nervous system is controlled by neurotransmitters. Neurons can be either stimulated or suppressed depending on the specific neurotransmitter released by the sending neurons. It is crucial for the nervous system to maintain a balance between these excitatory and inhibitory responses in order to be versatile, flexible, and capable of parallel processing. One way to achieve the brain's adaptability and flexibility is by replicating this balance between excitatory and inhibitory responses. Despite extensive efforts to study how the nervous system achieves this balance, it has been challenging to simulate the intricate connections between excitatory and inhibitory synapses. Herein, we propose an optoelectronic synapse that achieves a balance between excitatory and inhibitory responses with color recognition. This is accomplished by utilizing the humidity-sensitive helical arrangement of chiral nematic phases within cellulose nanocrystals (CNCs). The level of absorbed water molecules fine-tunes the polarization of the CNC complex films, resulting in diverse hysteresis effects and subsequent excitatory and inhibitory nonvolatile behavior in bio-electrolyte-gated transistors. By applying voltage pulses and stimulating with chiral light, the artificial optoelectronic synapse not only adjusts synaptic functions but also enhances learning behaviors and the ability to recognize color signals. Through the interdisciplinary collaboration between CNC bio-nanotechnology and functional optoelectronics systems, the versatile synaptic transistors exhibit potential for applications in highly efficient parallel neuromorphic computing and advanced robot vision technology.

4:15 PM SB10.09.07

A Fully-Integrated Wearable In-Sensor Computing Platform based on Intrinsically Stretchable Organic Electrochemical Transistors [Dingyao Liu](#) and Shiming Zhang; The University of Hong Kong, Hong Kong

Organic electrochemical transistors (OECT) have emerged as a promising technology paradigm for in-sensor computing and wearable healthcare applications [1]. However, several major challenges limit their widespread adoption in real-world applications: 1) the lack of conformable and stretchable OECT units to reduce the mechanical mismatch between devices and the soft human body; 2) the lack of reliable fabrication methods to enable scalable manufacturing of intrinsically stretchable OECT arrays with smaller feature sizes and high density; and 3) the lack of miniaturized readout systems to enable wearable-sized assembly [2]. In this work, we present a wearable, integrated, and soft electronic (WISE) platform based on intrinsically stretchable OECT arrays, addressing all these challenges. The WISE-platform achieves: 1) intrinsically stretchability (>50%) by implementing a new material protocol for device assembly and improving strain-robustness at interfaces with a tough adhesive supermolecular buffer layer; 2) a scalable fabrication of stretchable OECTs arrays with feature size down to 100 μm using a high-resolution 6 channel inkjet printing system; and 3) a customized, coin-sized data readout system for easy acquisition of biosignals at their origin. As an example, we demonstrate the use of the coin-sized, smartwatch-compatible electronic module for wearable in-sensor computing at the edge, but other application scenarios can be easily imagined.

4:30 PM *SB10.09.08

Synaptic Plasticity on Demand for Neuromorphic Computing and Bio-Inspired Artificial Nerve Dae-Gyo Seo, Gyeong-Tak Go, Min-Jun Sung and [Tae-Woo Lee](#); Seoul National University, Korea (the Republic of)

Biological nervous systems possess versatile attributes, serving diverse functions; for instance, the central nervous system (CNS) governs learning and memory, while the peripheral nervous system (PNS) is responsible for sensory perception. Consequently, there is a need to engineer artificial synapses tailored to adapt to performance requirements in various applications. Brain-inspired neuromorphic computing aims to emulate the learning and memory capabilities of the CNS, being inspired from the long-term potentiation (LTP) observed in biological synapses. The application of artificial synapses in the fields of neurotronics and neuroprosthetics requires the emulation of the short-term plasticity (STP), enabling the rapid signal transmission and fast responses akin to those in the biological PNS. To demonstrate the broad applicability, spanning areas including neuromorphic computing and bio-inspired neurotronics, our study has explored the modulation of STP and LTP using ion-gel gated polymer synaptic transistors (IGPSTs). We have modulated the polymer semiconductor (PSC) film's crystallinity through post-deposition film annealing, self-assembly monolayer treatment, and the introduction of various sidechain length, leading to the conversion between STP and LTP properties in IGPSTs. Moreover, we have utilized a straightforward yet effective approach by blending two PSCs with the same backbone but different sidechains. This blend strategy has led to a substantial improvement in LTP characteristics, whereas IGPSTs employing each PSC individually show only STP properties. IGPSTs with enhanced LTP properties demonstrate their potential as neuromorphic computing devices, effectively simulating learning processes in artificial neural networks. Concurrently, IGPSTs featuring STP capabilities are used to demonstrate various artificial nervous systems, such as artificial reflex arcs, neuromuscular systems, and neuro-prosthetic nerves incorporating artificial proprioceptors. These pioneering studies on neuromorphic devices have expanded the scope of applications for artificial synapses and validate the feasibility of these innovative technologies.

SESSION SB10.10: Bioelectronic and Neuromorphic Systems

Session Chairs: Donghee Son and Shunsuke Yamamoto

Friday Morning, April 26, 2024

Room 429, Level 4, Summit

8:30 AM SB10.10.01

Colloidal Electronic Matter Jihpeng Sun and [Albert T. Liu](#); University of Michigan–Ann Arbor, United States

Arming nano-electronics with mobility extends artificial systems into traditionally inaccessible environments. Carbon nanotubes (1D), graphene (2D) and other low-dimensional materials with well-defined lattice structures can be incorporated into polymer microparticles, granting them unique electronic functions. The resulting colloidal electronic 'cells', comprised of microscopic circuits connecting artificial 'organelles' (e.g., generators, sensors, logic gates, etc.), combine the modularity of modern electronics with the characteristic mobility found in dispersive colloidal systems. In this talk, I will discuss our efforts to fabricate colloidal electronic systems that perform autonomous functions integrating energy harvesting, chemical detection and digital memory recording - all within a form-factor no larger than biological cells.

8:45 AM SB10.10.02

A Purely Electronic Analog Memristive Device Based on a Squaraine Nanowire Mesh [Gareth Redmond](#); University College Dublin, Ireland

Analog memristors offer the ability to gradually increment device conductance, akin to synaptic weight updating the human brain, and a path toward emulation of brain-like functionality on a chip. Specifically, purely electronic resistive switching device operation may provide good device stability, fast

device response, and microelectronics fabrication compatibility. In this context, nanowires (NWs) based on 2,4-bis[(4-diethylamino)-2-hydroxyphenyl]squinone were prepared by non-solvent-induced precipitation and characterized in detail. Symmetric, unipolar (hole-only) metal-insulator-metal-type devices were formed by simple deposition of NW meshes on interdigitated gold electrodes. The DC I-V characteristics acquired from devices displayed pinched hysteretic I-V loops indicative of memristive behavior. Analysis of I-V data indicated Ohmic transport at low bias with carrier extraction facilitated by thermionic emission. At high bias, devices exhibited trap-limited space-charge-limited conduction in the presence of traps distributed in energy, which was enhanced by a Poole-Frenkel effect, with carrier extraction facilitated by Fowler-Nordheim tunneling. Overall, the data were consistent with purely electronic conduction. This hypothesis was further supported by DC measurement data acquired from devices under illumination, by AC impedance data acquired in both dark and light conditions, and by variable temperature transport measurements. During voltage sweeps applied to NW mesh devices, I-V hysteresis was observed, consistent with modifications to current flow caused by carrier trapping/detrapping. Device conductance could be increased sweep by sweep, giving conductance tuning through distinct states, with wait time- or voltage-erase options, consistent with trap filling/emptying effects. On this basis, trap-enabled analog memristive device functionality was demonstrated in both rigid and flexible device formats by applying various voltage waveforms. Repeated erase-write-read of multiple distinct states over many voltage cycles during continuous use in air was demonstrated. Also, synaptic functions, e.g., pulse-dependent plasticity, and short- to long-term memory transition, were successfully emulated. Finally, the stable, repeated erase-write-read of multiple distinct conductance states over hundreds of voltage cycles during hours long periods of continuous use in an ambient atmosphere was demonstrated. Overall, squaraine NW mesh devices appear to exhibit many attractive characteristics that make them potential candidates for neuromorphic computing applications.

9:00 AM SB10.10.03

Paper-Based Electronic Tongue for Rapid and Reusable Quantitative Sensing of Water in Organic Solvents Using Principal Component Analysis Gregory Moore and Anthony Dichiara; University of Washington, United States

Rapid and quantitative recognition of trace amounts of water in organic solvents is of great importance in industrial operations. Currently the standard methods of determining water content in such cases include the Karl Fischer (KF) titration and fluorescence colorimetry, which are expensive, time consuming, and require skilled operators to perform. Electronic tongues are sensor systems with the ability to analyze and classify complex samples by their chemical composition [1]. Principal Component Analysis (PCA) is a multivariate statistical technique used to reduce the dimensionality of data while retaining as much of the initial variation as possible and is commonly used in electronic tongue applications [1], [2]. In this work, a multifunctional liquid sensing and classification system was developed based on paper comprising pulp fibers adsorbed with multi-walled carbon nanotubes. Papertronics is a field of increasing interest due to the biodegradable nature, flexibility, and light weight of lignocellulosic paper and its ability to be produced at large scale using well-established and cost-effective manufacturing processes [3]. The hygroscopic nature of cellulose fibers causes them to swell radially in response to water molecules, which alters the conductive pathway within the percolated carbon nanotube network present on their surface, leading to a significant change in the paper resistance when wet. Importantly, the swelling behavior strongly depends on the nature of the solvent, which makes it an exceptional material for liquid sensing applications [4]. The electrical response of the sensor was tested and replicated for several liquid solutions of different solvents, concentrations of water in solvents, and ionic strengths of water. Specific features were identified from the response profiles, generating over 800 data points which were implemented in the PCA and used to differentiate between the liquids. The sensing platform can quantify the amount of water in the organic solvent with a sensitivity below 100 ppm and high resolution which makes it competitive with the KF titration. The proposed paper-based electronic tongue demonstrates the ability to rapidly differentiate low concentrations of water in organic solvents, provides an economic alternative to current methods, and enables future discoveries in biosensing and bioelectronics.

[1] "Electronic Tongues—A Review | IEEE Journals & Magazine | IEEE Xplore." Accessed: Oct. 18, 2023. [Online]. Available: <https://ieeexplore.ieee.org/abstract/document/6516019>

[2] I. T. Jolliffe, *Principal Component Analysis*, Second. in Springer Series in Statistics. 2002.

[3] S. M. Goodman *et al.*, "Scalable manufacturing of fibrous nanocomposites for multifunctional liquid sensing," *Nano Today*, vol. 40, p. 101270, Oct. 2021, doi: 10.1016/j.nantod.2021.101270.

[4] A. B. Dichiara, A. Song, S. M. Goodman, D. He, and J. Bai, "Smart papers comprising carbon nanotubes and cellulose microfibers for multifunctional sensing applications," *J. Mater. Chem. A*, vol. 5, no. 38, pp. 20161–20169, 2017, doi: 10.1039/C7TA04329E.

9:15 AM SB10.10.04

Untethered Cardiac Stimulation and Pacing Enabled by Ultra-Thin Rubbery Bio-Optoelectronic Stimulators Zhouyu Rao, Faheem Ershad and Cunjiang Yu; The Pennsylvania State University, United States

Untethered electrical stimulation or pacing of the heart is of critical importance in addressing the pressing needs of cardiovascular diseases in both clinical therapies and fundamental studies. However, existing devices to provide untethered electrical stimuli are typically rigid, bulky, and complex in system architecture thus it is challenging to seamlessly integrate them with soft, deformable, and dynamic organs and tissues, which unavoidably causes device failure or tissue damage. Alternatively, light illumination induced electrical stimulation via the photoelectric effect without any genetic modifications to the beating cells/tissues or the whole heart has profound benefits. However, a critical bottleneck lies in the lack of a suitable material/device with tissue-like mechanical softness and deformability and sufficient optoelectronic performances towards effective cardiac stimulation and pacing. Specifically, concurrent deformation (i.e. ~20% strain) of a stimulating device with a beating heart during the stimulation while not constraining its beating is of paramount importance. However, materials and devices with these collective properties have never been developed. Here we introduce an ultra-thin (<500 nm), stretchy, and self-adhesive rubbery bio-optoelectronic stimulator (RBOES), in a bilayer construct of a rubbery semiconducting nanofilm and a transparent, stretchable gold nanomesh conductor. The RBOES can produce a potential response as high as 150 mV from the semiconductor-electrolyte interface under light illumination (2.8 mW/mm²) and could maintain its optoelectronic performance when it was stretched by 20%. The RBOES was validated to effectively synchronize the beating and pace the cultured human induced pluripotent stem cell-derived cardiomyocytes under optoelectronic stimulation with variable target beating rates (from 20-30 bpm before stimulation to 30, 48, and 72 bpm after stimulation). Furthermore, optoelectronic pacing of ex vivo perfused rat hearts with the self-adhered RBOES was achieved with repetitive pulsed light illumination. Systematic investigations on the materials strategy, device design, and biological validations illustrated the key aspects of the RBOES and its capabilities in cardiac stimulation and pacing. This work exploits an unprecedented cardiac stimulator in a rubber format developed through material engineering to form a unique rubbery semiconducting nanofilm based bio-optoelectronic interface for non-genetic biological stimulation. The RBOES is applicable to various electrically excitable tissues and organs, such as the brain, spinal cord, peripheral nerves, and skeletal muscles, which paves the way towards non-genetic, untethered stimulation for both fundamental biological studies and clinical therapy.

9:30 AM SB10.10.05

Flow-Cell Sensor for Bacteria Detection Using Gate-Modified Organic Electrochemical Transistor Jingchu Huang, Daewoo Han and Andrew J. Steckl; University of Cincinnati, United States

Organic electrochemical transistors (OECT) have been previously demonstrated in the sensing of cells and metabolic products. In this study, we report a

novel approach on the universal detection of bacterial contamination in home-liquid-goods through the utilization of a microfluidic flow-cell that has been integrated with OECT technology. The flow-cell device has been developed for the purpose of detecting minimal concentration ($\sim 10^3$ CFU/ml) of several bacterium types (*Escherichia coli*, *Pseudomonas fluorescens* and *Staphylococcus aureus*) in various commercial household liquid product blends (cf. Air Febreze, Tide, Old Spice bodywash). This process can be completed in a testing period of one hour or less and does not require amplification or a designated binding agent. The flow-cell configuration uses a microporous filter membrane (Au coated PETE, 0.2 μm pore diameter) designed to concentrate the bacteria within the chamber. The membrane also functions as a gate electrode for the operation of OECT. The presence of bacteria on the gate filter membrane leads to an increase in the total effective gate voltage (V_{eff}), which in turn causes a decrease in the OECT source-drain channel current (I_{DS}). Based on the shift of I_{DS} , the OECT provides good discrimination between bacteria and sterile solutions (0.4 mA difference). The OECT transconductance (g_m) exhibits a maximum value at different levels of V_{GS} for sterile and bacteria solutions. g_m shifts to positive value at lower gate operating voltage due to bacteria attachment on Au gate. The flow-cell filtration and OECT gate sensing approach has the capability to identify a diverse range of bacteria, encompassing both gram-positive and gram-negative strains, across multiple testing media. This approach exhibits potential for biosensing systems that will enable real-time monitoring at the production line.

9:45 AM SB10.10.06

3D-Printed Epidermal Microfluidic Systems: Opportunities to Expand Access to Personalized Health Monitoring Tyler Ray; University of Hawaii, United States

Persistent disparities exist in access to state-of-the-art healthcare and disproportionately affect underserved and vulnerable populations. Advances in wearable sensors enabled by additive manufacturing (AM) offer new opportunities to address such disparities and enhance equitable access to advanced diagnostic technologies. Additive manufacturing processes, particularly stereolithography (SLA)-based printing, offer powerful pathways for circumventing existing barriers to innovation for resource-limited settings by providing significant reductions in prototype development cost and cycle time while substantially expanding device capabilities with fully 3D device designs. Here, we present a simplified 3D-printing prototyping process to fabricate flexible, stretchable, epidermal microfluidic devices ("3D-epifluidics") suitable for direct on-body interfacing. These wearable sweat sensors integrate microfluidic channel networks with biochemical sensors and flexible electronics to enable the noninvasive, real-time monitoring of sweat-based biochemical signals associated with health and wellness. By reducing fabrication time to [O]min, this approach enables the integration of spatially-engineered features including 3D-structured passive capillary valves, monolithic channels, and reservoirs with spatially-graded geometries. With geometric features comparable to established epifluidic devices (channels $>50 \mu\text{m}$), benchtop and on-body testing validate the performance of 3D-epifluidic devices. We utilize these platforms to showcase how these devices hold the potential for addressing some of the formidable obstacles to delivering comprehensive medical care in under-resourced settings, especially in remote or geographically isolated areas.

10:00 AM BREAK

10:30 AM SB10.10.07

Transfer-Printed PEDOT:PSS on Stretchability-Enhancing, Biodegradable PVA Substrates towards Stretchable OECTs Carla Volkert¹, Renan Colucci¹, Mateusz Brzezinski¹, Pablo Gomez Argudo¹, Jasper Michels¹, Pol Besenius², Paul W. Blom¹ and Ulrike Kraft¹; ¹Max Planck Institute for Polymer Research, Germany; ²Johannes Gutenberg University, Germany

Extensive efforts have been invested in advancing flexible devices¹, including biosensors, optoelectronic devices, organic field effect transistors (OFETs), light emitting diodes (LEDs) and organic electrochemical transistors (OECTs)². Building on these achievements, stretchable electronic devices have evolved within the last decade^{3,4}. To further advance and fully exploit the next generation of stretchable electronics, the innovation of novel device fabrication processes and materials is needed. Poly(3,4-ethylenedioxythiophene): poly(styrenesulfonate) (PEDOT:PSS) stands out as a popular material in bioelectronic applications due to its high conductivity, optical transparency, mechanical resilience, commercial availability and biocompatibility. Consequently, significant efforts have been undertaken to transform PEDOT:PSS from a brittle into a flexible and stretchable material. Conventional approaches involve the addition of chemicals such as ionic liquids⁵, surfactants, plasticizers and other organic additives⁶. Here, we propose an alternative approach towards stretchable electronics: rather than inducing stretchability through such additives, we demonstrate that the mechanical properties of PEDOT:PSS can be adjusted by utilizing diffusion-active substrates. The substrates are infused with a plasticizer that diffuses into the PEDOT:PSS, modifies its glass transition temperature and consequently leads to an enhanced stretchability and an increased conductivity. Chain-alignment and -mobility during elongation are evidenced by a higher crack-on-set-strain ($>150\%$) and an increased conductivity upon strain. A comprehensive (concentration-dependent) analysis, including electrical measurements, atomic force microscopy, and Raman spectroscopy, was undertaken to study the substrate- and PEDOT:PSS-chain alignment upon strain and was correlated with the concentration-dependent diffusion of the plasticizer. This novel approach towards stretchable electronics is furthermore compatible with our recently developed transfer-printing method for (plasma-patterned) electronic devices and finally led to the successful fabrication of intrinsically stretchable organic electrochemical transistors on biodegradable substrates.

- 1) Y. Luo, X. Chen et al.: ACS Nano 2023, 10.1021/acsnano.2c12606
- 2) S. Zhang, F. Cicoira et al.: Chem. Mater. 2017, 10.1021/acs.chemmater.7b00181
- 3) S. Wang, Z. Bao et al.: Nature 2018, 10.1038/nature25494
- 4) N. Matsuhisa, T. Someya et al.: Chem. Soc. Rev. 2019, 10.1039/C8CS00814K
- 5) N. Kim, K. Tybrandt et al.: Nature Commun. 2020, 10.1038/s41467-020-15135-w
- 6) H. He, J. Ouyang et al.: Macromolecules 2021, 10.1021/acs.macromol.0c0230

10:45 AM SB10.10.08

Edible Logic Circuits Giulia Coco^{1,2}, Valerio F Annese², Valerio Galli^{1,2} and Mario Caironi²; ¹Politecnico di Milano, Italy; ²Istituto Italiano di Tecnologia, Italy

As single-use and disposable electronic devices are becoming widespread for food and gastrointestinal tract monitoring, safe and sustainable materials development is emerging as a fundamental objective for technological innovation. The EU-funded ROBOFOOD project explores food-derived materials - an unprecedented and unconventional approach - to fabricate robots that could be metabolized (or degraded) in the body (or environment) after performing their function. In this perspective, the challenge consists of realizing stable edible electronic circuits that can provide synchronization, perform simple computation, and serve as memory, starting from notoriously unstable materials.

Here we present the fabrication and characterization of edible logic circuits. For this aim, a printed edible electrolyte-gated transistor with a lateral gate configuration was fabricated using food-based inks. A comprehensive characterization was carried out revealing performance comparable with state of the art. Hence, edible logic gates operating at low voltage ($< 1 \text{ V}$) were demonstrated, integrating the transistor in unipolar configurations. Different edible materials and fabrication techniques compatible with the proposed transistor were also explored for implementing the required resistive load. Edible NOT and NAND gates were successfully fabricated and characterized using well-established metrics. More complex circuits, such as an edible ring oscillator working at a frequency around 1 Hz and a set/reset latch, were demonstrated. We believe that this work leads the way to edible logic circuits performing complex functions and to their integration into devices that can interact safely with humans and animals.

11:00 AM SB10.10.09

A Fingertip Force Microscope (FFM) for Micro-Scale Morphology Characterization [Jiaqi Tu](#) and Xiaodong Chen; Nanyang Technological University, MSE, Singapore

Texture sensing is an essential part of tactile sensing, which extracts morphology, roughness, and hardness information during object manipulation. However, biological texture sensing is only a qualitative description of object features and shows low spatial resolution. Current research on artificial tactile sensing systems mainly focuses on machine learning-based qualitative comparison of different surfaces with different roughness. Here, we present a wearable artificial fingertip consisting of two piezoelectric vibration tips for quantitative morphology characterization. Two sensing tips with fixed spacing will bend and recover while sliding the artificial fingertip over uneven surfaces. Piezoelectric films on the tips transform vibrations into voltage signals. The two-tip design enables the identification of instantaneous speed. By correlating voltage signals with the actual moving condition and the calculated instantaneous speed, the time-domain information indicates the groove width, bar width, and groove depth of the grating texture. Therefore, textures with height of 1 μ m~3mm and distances beyond 200 μ m can be detected without the need for controlled speed and pressing force. Further, the artificial fingertip can be worn on fingers and generates micro-scale morphology information. The artificial fingertip was further integrated into a robotic hand for obtaining morphology information from multiple slides. Three-dimensional (3D) reconstruction of fine micro-scale patterns can be generated through a quick sweep in real time.

11:15 AM SB10.10.10

QuantumDock: An Automated Computational Framework for Wearable Sensor Design [Daniel Mukasa](#), Minqiang Wang, Jihong Min, Yiran Yang, Samuel A. Solomon, Hong Han, Cui Ye and Wei Gao; California Institute of Technology, United States

Wearable sweat sensors have the potential to revolutionize precision medicine as they can non-invasively collect molecular information closely associated with an individual's health status. However, the majority of clinically relevant biomarkers cannot be continuously detected in situ using existing wearable approaches. Molecularly imprinted polymers (MIPs) are a promising candidate to address this challenge but haven't yet gained widespread use due to their complex design and optimization process yielding variable selectivity. Here, QuantumDock is introduced, an automated computational framework for universal MIP development toward wearable applications. QuantumDock utilizes density functional theory to probe molecular interactions between monomers and the target/interferent molecules to optimize selectivity, a fundamentally limiting factor for MIP development toward wearable sensing. A molecular docking approach is employed to explore a wide range of monomers, and to identify the optimal monomer/cross-linker choice for subsequent MIP fabrication. We further employ a molecular generation scheme that allows us to generate molecules with much higher sensitivities and selectivities than traditionally used monomers. Using an essential amino acid phenylalanine as the exemplar, experimental validation of QuantumDock is performed successfully using solution-synthesized MIP nanoparticles coupled with ultraviolet-visible spectroscopy. Moreover, a QuantumDock-optimized graphene-based wearable device is designed that can perform autonomous sweat induction, sampling, and sensing. For the first time, wearable non-invasive phenylalanine monitoring is demonstrated in human subjects toward personalized healthcare applications.

11:30 AM SB10.10.11

Development of Water-Resistant Au-PVA/WBPU Nanomesh Electrodes for Stable Monitoring of Skin Impedance [Maho Mimuro](#), Sunghoon Lee, Tomoyuki Yokota and Takao Someya; The University of Tokyo, Japan

Electrodermal activity, which is known to vary due to various factors such as psychological states like stress level [1], and environmental factors like temperature [2] and humidity [3] is one of the important biological signals for early detection of disease and preventive healthcare. Previously, ultrathin and lightweight Au-PVA nanomesh electrode which does not cause discomfort when they were attached on skin has been developed [4] and continuous measurement of skin resistance and skin impedance were achieved by using the nanomesh electrodes [5, 6]. However, these electrodes were vulnerable to water and prone to damage, requiring careful handling during attaching to the skin and being susceptible to breakage with slight movements or sweat. To address this issue, we developed nanomesh electrodes with excellent water resistance and stable measurement capabilities by mixing hydrophobic WBPU (waterborne polyurethane) with the conventional material PVA (polyvinyl alcohol). The Au-PVA/WBPU nanomesh electrodes were fabricated by following method. First, a mixture of a 15 wt% PVA aqueous solution and a 30 wt% WBPU solution in 2:1 ratio was made into a nanofiber sheet by electrospinning method. And then, a heat-press treatment was applied to the nanofiber sheet to improve the inner connect between fibers. After a heat-press treatment at 150°C for 1 minute, a 100 nm thick layer of gold was deposited by vacuum evaporation method. To check the water resistivity of the nanomesh electrode, we conducted a water immersing test. After a 1-minute stirring test in the pure water, the conventional Au-PVA nanomesh electrodes completely disappeared from the artificial skin, whereas Au-PVA/WBPU nanomesh electrodes remained more than 95% area on the artificial skin. In addition, we checked the stability of the nanomesh electrodes on the skin. After attaching the electrodes on the skin for 2 hours, the resistance of the Au-PVA/WBPU nanomesh electrodes were almost constant while that of conventional nanomesh electrodes showed a deterioration, increasing by 3 to 4 times.

[1] R. B. Malmo, Activation: a neurophysiological dimension., *Psychol. Rev.*, 66, 1959

[2] R. Gudivaka *et al.*, Effect of skin temperature on multifrequency bioelectrical impedance analysis., *Journal of Applied Physiology*, 81(2), 1996

[3] Y. Yamamoto, T. Yamamoto, Characteristics of skin admittance for dry electrodes and the measurement of skin moisturisation., *Med. Biol. Eng. Comput.*, 24, 1986

[4] A. Miyamoto *et al.*, Inflammation-free, gas-permeable, lightweight, stretchable on-skin electronics with nanomeshes., *Nat. Nanotech.*, 12, 2017

[5] A. Miyamoto *et al.*, Highly Precise, Continuous, Long-Term Monitoring of Skin Electrical Resistance by Nanomesh Electrodes., *Adv. Healthcare Mater.*, 11, 2022

[6] R. Matsukawa *et al.*, Skin Impedance Measurements with Nanomesh Electrodes for Monitoring Skin Hydration., *Adv. Healthcare Mater.*, 9, 2020

11:45 AM SB10.10.12

Elastic Metal Microtube for Flexible Ultralow-Hysteresis Tactile Sensor [Yanzen Li](#) and Xiaodong Chen; Nanyang Technological University, Singapore

Low-hysteresis and fast-response tactile sensors that mimic the human sense of touch can empower robotic systems to manipulate diverse objects rapidly and accurately. However, current tactile sensors, which mostly rely on viscoelastic polymers as functional materials, suffer from high hysteresis and slow response time, limiting their applicability in intelligent robotics. Here, we introduce an elastic metal microtube enhanced (EMME) tactile sensor with ultralow hysteresis and fast response. The microtube structure is achieved by utilizing the inner stress of thermally evaporated metal films after dissolving a sacrificial layer. The superior elasticity of the metal microtubes minimizes energy dissipation during deformation under external mechanical stimuli, contributing to ultralow hysteresis and fast response of EMME tactile sensor. Furthermore, the positive correlation between hysteresis and energy dissipation is theoretically established in capacitive tactile sensors based on parallel plate structure. Our flexible EMME tactile sensor possesses ultralow hysteresis (~0.8%), fast response time (<1 ms), high endurance (10000 cycles), and the ability to keep up with high-frequency vibration. Upon integration with the robotic hand, accurate and autonomous manipulation of shape-changing objects with a feedback loop is achieved, mimicking air pressure monitoring via balloon volume change in chemical experiments, exhibiting its potential in future intelligent and autonomous laboratory robotic systems.

SYMPOSIUM SB11

Bio-based and Biomimetic Polymers in Soft Robotics
April 23 - May 8, 2024

Symposium Organizers

Artur Braun, Empa
Minkyu Kim, The University of Arizona
Danielle Mai, Stanford University
Newayemedhin Tegegne, Addis Ababa University

* Invited Paper

+ JMR Distinguished Invited Speaker

^ MRS Communications Early Career Distinguished Presenter

SESSION SB11.01: Bio, Bionics, Robotics
Session Chairs: Michael Dickey and Danielle Mai
Tuesday Morning, April 23, 2024
Room 430, Level 4, Summit

10:30 AM *SB11.01.01

Leveraging Biological Motor Control for Soft Robotics Ritu Raman; Massachusetts Institute of Technology, United States

Human beings and other biological creatures navigate unpredictable and dynamic environments by combining compliant mechanical actuators (skeletal muscle) with neural control and sensory feedback. Abiotic actuators, by contrast, have yet to match their biological counterparts in their ability to autonomously sense and adapt their form and function to changing environments. We have shown that engineered skeletal muscle actuators, controlled by neuronal networks, can generate force and power functional behaviors such as walking and pumping in a range of untethered robots. These muscle-powered robots are dynamically responsive to mechanical stimuli and are capable of complex functional behaviors like exercise-mediated strengthening and healing in response to damage. Our lab uses engineered bioactuators as a platform to understand neuromuscular architecture and function in physiological and pathological states, restore mobility after disease and damage, and power soft robots. This talk will cover the advantages, challenges, and future directions of understanding and manipulating the mechanics of biological motor control.

11:00 AM ^SB11.01.02

Vapor-Deposited Polymeric Biointerface to Direct Living Behavior Rong Yang; Cornell University, United States

Polymer is often considered one of the most prevalent materials in the modern age. The interactions between polymers and a highly ubiquitous living system – bacteria – are of great interest in applications ranging from fouling control to living materials, but details of those interactions are poorly understood. The sub-micron size of most bacteria, whose sensory apparatus often operates on the nanoscale, requires precise placement of chemical functionalities and nanostructures at the synthetic-living interface. The need for nanoscale resolution challenges most traditional synthesis and processing approaches, which have been predominantly performed in solution. Recent advances in vacuum-based synthesis technologies, such as the initiated Chemical Vapor Deposition (iCVD), have enabled a new mode of control over polymeric material properties during polymerization. Distinct from prior research that has placed strong emphasis on the design of monomer molecular structure and controlled polymerization, the all-dry synthesis enables manipulation of the physical phenomena, such as nanoscale dewetting, Knudsen diffusion, and molecular complexing, to achieve programmable material properties. In this talk, we will discuss several strategies to achieve the nanoscale control over the vapor-deposited polymeric biointerface. Such control in turn led to improved understanding and manipulation of bacteria-material interactions, such as suppression of virulence. Taken together, the synthetic advances are poised to open up a new dimension in the design of polymeric materials for the programmable material-bacteria interactions, which extend beyond “kill or repel” towards signaling and control.

11:15 AM SB11.01.03

Programmable Tissue Folding in Magneto-Active Structured Hydrogels Zenghao Zhang, Avinava Roy, Claudia Loebel and Abdon Pena-Francesch; University of Michigan–Ann Arbor, United States

Biological tissues are structurally complex and heterogeneous, making the in vitro recapitulation challenging if using a traditional flat cell-culture substrate. Although recent development in engineering tissue patterns has been achieved through top-down approaches including micro-molding and 3D bioprinting, reversible and on-demand dynamic patterning is still underdeveloped. Among soft actuation systems, magnetic actuation shows little toxicity to cells, and can penetrate tissue and media to generate pulling forces and torques remotely, enabling fast and reverse untethered actuation. In this study, we developed hydrogel cell-culture systems based on bilayer folding hydrogels composed of a rigid hyaluronic acid (HA) hydrogel and a stretchable double-network (DN) with ferromagnetic particle dopants. Building upon recent advances in the design of magnetoactive soft materials, our approach further uses magnetoactive hydrogels to provide dynamic patterning upon applying magnetic fields. Using this method, we generated cell-laden hydrogel substrates that display on-demand folding/unfolding reversible shape transformations, providing a culture system for mimicking dynamic tissue folding in vitro and

recapitulating 3D complex structures to probe cellular mechanisms.

SESSION SB11.02: Ionics and Robotics
Session Chairs: Minkyu Kim and Rong Yang
Tuesday Afternoon, April 23, 2024
Room 430, Level 4, Summit

1:45 PM *SB11.02.01

The Synergy of Electronic Polymers and Self-Driving Laboratories for Innovations in Soft Robots Jie Xu; Argonne National Laboratory, United States

In the realm of soft robotics, electronic polymers have emerged as important materials owing to their unique combination of mechanical viscoelasticity and electronic properties. These materials, including conductive and semiconductive polymers, are instrumental in crafting flexible coverings that empower soft robots to sense intricate environments and relay information to human counterparts. However, the quest to identify electronic polymers capable of realizing desired functionalities remains a formidable challenge. Traditional, manual methods, relying solely on human expertise, could entail decades of arduous research and development. In this context, self-driving laboratories, leveraging robotic automation and artificial intelligence, are revolutionizing the exploration and development of electronic polymers and soft devices tailored for soft robotics. In this presentation, I will begin by introducing our autonomous laboratory, aptly named 'Polybot.' Subsequently, I will delve into recent research, exemplifying autonomous electrochromic polymer discovery for applications in optical communication and autonomous polymer electrochemical sensor discovery, with the potential to serve as bio-sensing platforms within soft robotic systems.

2:15 PM SB11.02.03

Liquid-Metal-Based All-Soft Pressure Sensor and Machine Learning Application for Multidirectional Detection Osman Gul^{1,2}, Jeongnam Kim^{2,3}, Yulim Min^{2,3}, Hye Jin Kim^{2,3} and Inkyu Park¹; ¹Korea Advanced Institute of Science and Technology, Korea (the Republic of); ²Electronics and Telecommunications Research Institute, Korea (the Republic of); ³University of Science and Technology, Korea (the Republic of)

Electronic skin needs to be able to sense different types of pressures, such as radial pressures, which require the development of a soft multidirectional pressure sensor. Although previous studies have developed multidirectional pressure sensors, the investigation into discerning the direction and magnitude of applied pressure remains an unexplored domain in multidirectional pressure sensor research. Multidirectional pressure sensors have been extensively developed in literature due to their vast application opportunities. Recently, the trend has shifted towards developing soft sensors with a focus on the design of the structure and sensing materials. The four-element sensing structure is the most commonly used structure for multidirectional sensors. In the case of the four-element sensing structure, the four sensing element is positioned at 90-degree intervals from one other, forming a cube-like structure. The four-element sensing structure facilitates the measurement of multidirectional forces. Wide-ranged 3D bump structures are used at the top of the four-element sensing materials to identify the applied multidirectional forces effectively. Lee et al. demonstrated trapezoid structure and CNT array as the sensing material. Jung et al. proposed a multidirectional force sensor with the sensing materials placed on the sidewalls of the 3D bump structure. Vogt et al. and Kim et al. presented liquid-metal-based multidirectional sensors with rigid pressure transmission structures on the top of the liquid metal channels. In these sensors, the multidirectional force is generated by applied shear pressure to the four-sensing structure of the sensor. Nevertheless, extracting directional information from a four-sensing element-based sensors' setup when exposed to applied radial pressure remains a formidable challenge, because the four-sensing element method is primarily designed for shear force-based applications.

In the present study, we present a new solution to address the limitations of existing multidirectional sensors. Our approach involves the development of a soft sensor using liquid metal with a dome-shaped design that enables discrimination of directional pressures. Additionally, we leverage machine learning algorithms to identify the direction and magnitude of applied pressure. The microchannels of the soft pressure sensor were created using fused deposition modeling (FDM). A 3D printed mold made of poly(vinyl alcohol) (PVA) was embedded into the elastomer and dissolved with water to create the microchannels. The empty microchannels were filled with liquid metal, and a vacuum process was applied to create the dome structure for multidirectional pressure sensing. The microchannels within the liquid-metal-based soft pressure sensor exhibit a transient response when pressure is applied. Specifically, each direction of the sensor indicates a distinct transient response when the pressure is applied, which helps to differentiate between different directions of pressure. The machine learning technique, we have implemented is based on dual-task 1D convolutional neural networks (CNN). This approach allows for real-time classification and regression of the magnitude of pressures applied on different directions of the sensor. We achieved direction identification in real-time using the transient response data from the soft pressure sensor. The developed liquid-metal-based soft pressure sensor can detect the direction (classification accuracy of 99.1%) and magnitude (regression error of 20%) of the multidirectional pressure in real-time pressure prediction through a 1D CNN algorithm. The effectiveness of the sensor and algorithm is demonstrated with a human-machine interface application where the sensor is used to control an RC model car. The machine learning predictions, including the direction and magnitude of the pressure, are used to control the vehicle's real-time movement.

2:30 PM +SB11.02.04

Ultra-Tough Ionogels for Stretchable Ionic Devices Michael Dickey and Meixiang Wang; North Carolina State University, United States

Ionogels are compelling materials for energy storage devices, ionotronics, and actuators due to their excellent ionic conductivity, thermal and electrochemical stability and nonvolatility. However, most existing ionogels suffer from low strength and toughness. Here, we report a simple one-step method to achieve ultra-tough and stretchable ionogels by randomly copolymerizing two common monomers in ionic liquid. Copolymerization leads to a single covalent network with controllable polymer- and solvent-rich phases that form in situ due to the phase behavior of the polymer in ionic liquid. The polymer-rich phase forms hydrogen bonds that dissipate energy and thereby toughen the ionogel during extension, while the solvent-rich phase remains elastic to enable large strain. The copolymer ionogels composed of acrylamide and acrylic acid exhibit extraordinary mechanical properties, including fracture strength (12.6 MPa), fracture energy (~24 kJ m⁻²), and Young's modulus (46.5 MPa), setting new records among reported ionogels. The tough ionogels are highly stretchable (~600% strain) and possess good self-recovery, as well as excellent self-healing and shape-memory properties. This concept extends to other monomers and ionic liquids, which offers a promising and general way to tune microstructure in situ during one-step polymerization that solves the longstanding mechanical challenges in ionogels.

3:00 PM BREAK

SESSION SB11.03: Stimuli-Responsive Soft Robots
Session Chairs: Danielle Mai and Abdon Pena-Francesch
Tuesday Afternoon, April 23, 2024
Room 430, Level 4, Summit

3:30 PM +SB11.03.01

The Design, Fabrication and Structural Modeling of Biomimetic Soft Materials for Robotic Applications [Qing Chen](#); EMPA, Switzerland

The prospects of endowing soft actuators with biomimetic functions are promoting the development of intelligent robotics. Harnessing the energy from the ambient environmental conditions, various stimuli-responsive soft robots have been fabricated and applied in artificial muscles, human-machine interfaces and smart wearable devices. For example, a humidity-responsive actuator based on a mono-layered [1], and a multi-stimuli-responsive actuator based on a double-layered conducting polymer thin film have been fabricated [2], which demonstrated an outstanding actuation force and sensitive responses to their respective stimuli. The actuation behavior of soft actuators largely relies on their energy conversion and the underlying structural reconfiguration ability of stimuli-responsive materials. More importantly, these two processes are also essential for the reorganization of their intrinsic structural network, which is the key to self-healing ability of the material. Despite the tremendous advances in stimuli-responsive soft actuators, it is still a challenge to incorporate multiple-stimuli sensitivity and self-healing ability into a single material system. To solve this problem, great efforts have been devoted to develop structural-reconfigurable materials based on dynamic non-covalent crosslinking. For sample, a cellulose-based packaging paper have been fabricated, of which the humidity-responsiveness and hydration-induced self-healing ability depends on reversible hydrogen crosslinking of cellulose [3]. In another case, two stimuli-responsive and structural-reconfigurable layers with complimentary thermal expansion and compatible mechanical properties are combined as a bi-layered actuator *via* hierarchical assembly. The actuator is self-healing through a sequential treatment of heating and humidifying as each of the bi-layer is healable with the aid of either of these two energy inputs. Moreover, by combining various analytical techniques, we introduced the models for structural reconfiguration of these stimuli-responsive materials at multiple length scales, which could be used as the design platform for more biomimetic materials. Based on these achievements, we anticipate that these actuators hold great promise in a plethora of fields wherever programmable structural reconfigurations are needed, such as applications in space explorations and intelligent robotics.

References

- [1] Q. Chen, X. Yan, H. Lu, N. Zhang, M. Ma, Programmable Polymer Actuators Perform Continuous Helical Motions Driven by Moisture. *ACS Appl. Mater. Interfaces* 2019, 11, 22, 20473-20481
- [2] X. Yan*, Q. Chen*, Z. Huo, N. Zhang, M. Ma. Programmable Multistimuli-Responsive and Multimodal Polymer Actuator Based on a Designed Energy Transduction Network. *ACS Appl. Mater. Interfaces* 2022, 14, 11, 13768-13777 (* equal contribution)
- [3] Q. Chen, B. Sochor, A. Chumakov, M. Betker, N. M. Ulrich, M. E. Toimil-Molares, K. Gordeyeva, L. D. Söderberg, S. V. Roth, Cellulose-Reinforced Programmable and Stretch-Healable Actuators for Smart Packaging. *Adv. Funct. Mater.* 2022, 32, 2208074

4:00 PM SB11.03.02

Soft Sensory Robots based on Stimuli-Responsive Hydrogels for Electronic Implants [Wubin Bai](#); University of North Carolina, Chapel Hill, United States

Living organisms with motor and sensor units integrated seamlessly exhibit effective adaptation to dynamically changing environments. Taking inspiration from coherent integration between skeletal muscles and sensory skins in human, we present a design strategy for soft robots, primarily consisting of an electronic skin (e-skin) and an artificial muscle, that naturally couples multifunctional sensing and on-demand actuation in a soft, biocompatible platform. here, we will describe an *in situ* solution-based method to create the e-skin layer with a series of sensing materials (e.g., silver nanowires, reduced graphene oxide, and poly(3,4-ethylenedioxythiophene) polystyrene sulfonate) incorporated within a polymer matrix (e.g., polyimide and polydimethylsiloxane), imitating human skin with complex receptors to perceive various stimuli. Biomimicry designs (e.g., starfish and chiral seedpods) of the soft robots enable various active motions (e.g., bending, expanding, and twisting) on demand and realize good fixation and stress-free contact with tissues. Furthermore, integration of a battery-free wireless module into these soft robots enables robotic operation and communication without tethering, thus enhancing safety and biocompatibility of the soft robots as minimally invasive implants. Demonstrated examples range from a robotic cuff enclosing around a blood vessel for precise detection of blood pressure, a robotic gripper holding onto a bladder for accurately tracking bladder volume, an ingestible robot residing inside stomach for pH sensing and on-site drug delivery, to a robotic patch wrapping onto a beating heart for quantifying cardiac contractility, temperature and applying cardiac pacing, highlighting the application versatilities and potentials of the bioinspired soft robots. Our designs of soft robots could establish a promising strategy to integrate a broad range of sensing and responsive materials, for forming highly integrated systems for medical technology and beyond.

4:15 PM SB11.03.03

Printable Liquid Metal Foams that Grow when Watered [Febby Krisnadi](#)¹, Seoyeon Kim², Sook Im¹, Dennis Chacko¹, Man Hou Vong¹, Konrad Rykaczewski³, Sungjune Park² and Michael Dickey¹; ¹North Carolina State University, United States; ²Jeonbuk National University, Korea (the Republic of); ³Arizona State University, United States

Pastes and “foams” containing liquid metal as the continuous phase (LMFs) exhibit metallic properties while displaying paste or putty-like rheological behavior. These properties enable LMFs to be patterned into soft and stretchable electrical and thermal conductors through processes conducted at room temperature, such as printing. The simplest LMFs, featured in this work, are made by stirring liquid metal in air, thereby entraining oxide-lined air “pockets” into the liquid metal. Here, we report that mixing small amounts of water (as low as 1wt%) into such LMFs gives rise to significant foaming by harnessing known reactions that evolve hydrogen and produce oxides. The resulting structures can be ~4-5x their original volume and possess a fascinating combination of attributes: porosity, electrical conductivity, and responsiveness to environmental conditions. This expansion can be utilized for a type of 4D printing in which patterned conductors “grow”, fill cavities, and change shape and density with respect to time. Excessive exposure to water in the long term ultimately consumes the metal in the LMF. However, when exposure to water is controlled, the metallic properties of porous LMFs can be preserved. We characterize the physical changes of water-containing LMFs and explore prospective applications including a “growing” conductor that fills a gap in a circuit and an untethered pressure-driven actuator. We also demonstrate the printability of LMFs and present a printed pattern that changes shape over time.

4:30 PM *SB11.03.04

Fast and Autonomous Soft Robots enabled by Snap-Through Instabilities [Shu Yang](#); University of Pennsylvania, United States

Soft robots offer a myriad of potentials due to their intrinsic compliance and adaptivity to unpredictable environments. However, most of them have limited actuation speeds and require complex control systems to maneuver various tasks. Inspired by the snap-through instabilities utilized by Venus flytrap to catch prey, the hummingbird’s beak to catch insects, and corkscrew-like stalk of Erodium seed, we combine materials intrinsic anisotropy and mechanical

metastructures to program the snapping behaviors, enabling several autonomous and unprecedented soft robotic functionalities. Specifically, I will discuss the design and performance of several examples of soft robots, including a centimeter-sized, sensor-less metacarp gripper that can grasp objects in 3.75 ms upon physical contact or pneumatic actuation, lobed loops made from liquid crystal elastomer fibers capable of gait-like synchronization and directed locomotion, and laminated wood enabled seed carrier with helical tails capable of soil drilling with high success rate upon exposure to water.

SESSION SB11.04: Self-Healing Soft Robots

Session Chair: Minkyu Kim

Wednesday Morning, April 24, 2024

Room 430, Level 4, Summit

8:30 AM SB11.04.01

Self-Healing Semiconducting Polymers for Uses in Soft Robotics via Coordination Chemistry Yun Liu and Bob C. Schroeder; University College London, United Kingdom

Robots are increasingly assisting humans in performing various tasks. The requirement for safe physical human-robot interactions has led to the emergence of the field of soft robotics. Typically, soft robots consist of flexible and deformable materials such as elastomeric polymers, which have an inherent compliance comparable to biological tissues (10^5 to 10^9 Pa), greatly enhancing human interaction safety.^{1,2} Their intrinsic softness and compliance further endow them with features such as resilience to impacts and collisions due to shock absorbance, making soft robots an ideal candidate for handling delicate tasks in uncertain and unstructured environments.³

Despite the many advantages of soft materials, their usage in robotics does present challenges in terms of damage resistance. Synthetic soft polymers are highly susceptible to fatigue, overload and cuts, tears and perforation by sharp objects arising from uncontrolled working environments, which would induce irreversible damage to the material, massively reducing the functional performance of robots.³ Inspired by a powerful feature of living organisms, an economic and ecological solution to this vulnerability is to construct future soft robotic systems out of self-healing semiconducting polymers, permitting the healing of microscopic and macroscopic damages as well as recovering material functionalities.

Various strategies have been applied to synthesise self-healable semiconducting polymers via non-covalent interactions such as hydrogen bonding, π - π stacking, host-guest interactions and ionic interactions.^{5,6} Multiple advantageous features are associated with metal-ligand complexes, in general, most coordination complexes can chelate spontaneously, resulting in easily processable materials.⁷ However, achieving high mechanical strength within self-healing semiconducting polymers remains a crucial challenge. Due to the broad variety of possible metal and ligand combinations, the coordination bonds are highly tuneable, with accessible bond energies ranging from strong covalent to weak supramolecular forces such as van der Waals.⁸ By tuning the coordination bond strengths, the presence of metal-ligand complexes in the polymer matrix could result in a synergistic effect on mechanical toughness and self-healing efficiency, offering new insights into the design of self-healing soft robotics.

Herein, we describe a new self-healing semiconducting polymer system based on metal-ligand coordination between transition metal ions (Cu^{2+} , Zn^{2+}) and bipyridine moieties incorporated in the cyclopentadithiophene-derived (CPDT) conjugated polymer backbone. Drastic changes to the polymer structure have been observed through spectroscopic measurements with varying ratios of bipyridine. Upon addition of the metal ions, a noticeable change in viscosity implied successful cross-links among polymer chains. Thermal analysis has revealed the stability temperature of the polymers to be as high as 400°C, giving the materials the potential to withstand extreme environments. In this presentation, we will discuss the self-healing and mechanical properties of the polymers from a coordination chemistry point of view, probing an understanding of the healing mechanism. Through the findings of our research, we hope that this creative combination of self-healing materials with robotics can present many opportunities for the future development of soft robotics.

Reference:

1. D. Rus and M. T. Tolley, *Nature*, 2015, **521**, 467-475.
2. E. Roels; *et al.*, *Adv. Mater.*, 2022, **34**, 2104798.
3. S. Terryn; *et al.*, *Mater. Today*, 2021, **47**, 187-205.
4. S. Y. Wang and M. W. Urban, *Nat. Rev. Mater.*, 2020, **5**, 562-583.
5. Y. L. Rao; *et al.*, *J. Am. Chem. Soc.*, 2016, **138**, 6020-6027.
6. H. Park; *et al.*, *Nat. Commun.*, 2023, **14**, 5026.
7. C. H. Li and J. L. Zuo, *Adv. Mater.*, 2020, **32**, 1903762.
8. H. C. Wu; *et al.*, *Adv. Funct. Mater.*, 2021, **31**, 2009201.

8:45 AM SB11.04.02

Untethered, Autonomously Self-Healable, and Self-Powered Actively-Perceiving and Energy-Harvesting Triboelectric Skins and Their Applications in Soft Robotics Ying-Chih Lai; National Chung Hsing University, Taiwan

Soft robots with organism-like adaptive bodies have shown great potential in vast robot-human and robot-environment applications. Developing skin-like sensory devices (that are e-skins) enables them to naturally sense and interact with environment. It would be better if the capabilities to feel can be active like real skin. However, conventional e-skins are developed using passive sensing technologies, including resistive, capacitive, and optical types. Such passive sensors suffer from limited materials, poor scalability, complicated architectures, scant stretchability, large driving-voltage, and huge power dissipation in large-area uses. Those drawbacks greatly hinder the development of untethered and deformable robotic skins.

In this talk, we will present diversified cutting-edge self-powered triboelectric skins (tribo-skins) [1-6] with various fascinating attributes, including autonomous ability of self-healing (30 min, 100% efficiency at 900% strain) [3], omnidirectional stretchability (>900%) [1-4, 6], transparency (88.6%) [3], environmental-inert (-30 to 60 °C) [4, 6], and electromagnetic and biomechanical energy-harvesting ability [5]. The tribo-skins can actively sense proximity, contact, and pressure to external stimuli via self-generating electricity. The driving-energy comes from natural triboelectrification effect involving a cooperation of contact electrification and electrostatic induction. We will demonstrate the first actively perceivable and responsive soft robots using the untethered and ultra-stretchable tribo-skins.[1,2] The perfect integration of the tribo-skins and soft actuators enables soft robots to perform various actively sensing and interactive tasks including actively perceiving their muscle motions, working states, textile's dampness, and even subtle human physiological signals. The diversified self-powered tribo-skins with various desired attributes will be introduced. Last, we will demonstrate a transparent, self-healing, and self-powered perceiving soft robotic hand. These works will inspire lots of great ideas and show tremendous potentials of wearable/stretchable/deformable electronics, artificial e-skins, smart interfaces, and soft robots.

[1] Ying-Chih Lai, et al, *Advanced Materials*, 2016, 28, 10024-10032.

- [2] Ying-Chih Lai, et al, *Advanced Materials*, 2018, 30,1801114. •This work is highlighted in Nature Perspective "The rise of intelligent matter", *Nature*, 2021, 594, 345. [Ref 47], presenting the first soft robots driven by self-generated electricity via the triboelectric effect, which can sense and embrace close objects. •This work is also highlighted in MIT Review Tech.
- [3] Ying-Chih Lai*, et al, *Advanced Functional Materials*, 2019, 190426.
- [4] Ying-Chih Lai*, et al, *Nano Energy*, 2021, 106525.
- [5] Ying-Chih Lai*, et al, *Advanced Energy Materials*, 2021, 202100411.
- [6] Ying-Chih Lai*, et al, *Advanced Science*, 2023, 202202815

9:00 AM *SB11.04.03

Autonomous Self-Aligned Multilayer Self-Healing Polymers and High Energy Density Artificial Muscle based on Periodic Non-Covalent Dynamic Polymer Networks Zhenan Bao; Stanford University, United States

Polymer networks formed through dynamic noncovalent or covalent bonds exhibit a range of interesting and tunable mechanical properties (e.g., tough, elastic, self-healable, stimuli-responsive, and reconfigurable). In nature, hierarchically ordered structures are formed through weak but cooperative interactions to perform precise functions. Learning from nature, we designed and investigated flexible polymer chains linked with periodically placed and directional dynamic bonds. Through understanding the structure property relationships, we discovered unique applications of designing such polymers for self-healing electronic materials, "morphing" electronics, artificial muscle and reconfigurable soft robots.

9:30 AM BREAK

SESSION SB11.05: Animate Matter in Soft Robots I
Session Chairs: Danielle Mai and Newayemedhin Tegegne
Wednesday Morning, April 24, 2024
Room 430, Level 4, Summit

10:00 AM *SB11.05.01

Bioinspired Protein Materials for Self-Healing Robotics Abdon Pena-Francesch; University of Michigan, United States

Recent progress in soft robotics has motivated the search for new robotic materials and actuators that can replicate biological functions and behaviors (such as sensing, healing, power, etc.) with various degrees of autonomy and complexity. Proteins are uniquely well-positioned to bring new solutions to these challenges, as they offer high versatility, specificity, and control in their self-assembly to regulate their emergent structures and properties. In this talk, we will introduce cephalopod-inspired proteins with a segmented block design that self-assemble into β -sheet nanocrystalline structures. These β -sheet nanocrystals act as physical and reversible crosslinking structures in supramolecular protein networks that regulate the physical properties. We demonstrate the dynamic properties of squid-inspired polypeptides in self-healing protein networks with healing strength and kinetics surpassing those typically found in other natural and synthetic soft polymers. This family of cephalopod proteins and their biosynthetic derivatives have opened new opportunities in bioinspired design for adaptive functional materials and soft devices with enhanced autonomy and durability, and we will demonstrate their implementation in self-healing and reconfigurable soft actuators and in self-powered microrobots for aquatic locomotion.

10:30 AM SB11.05.02

Harnessing Protein-Based Motors and Liquid Crystal Networks for Bioinspired Locomotion Control of Small-Scale Soft Robots Chuqi Huang¹, Natalie Pinchin², Chia-Heng Lin¹, Hamed Shahsavani² and Abdon Pena-Francesch^{1,1,1}; ¹University of Michigan–Ann Arbor, United States; ²University of Waterloo, Canada

The miniaturization of untethered robots poses new challenges in powering, actuation, and control since traditional electro-mechanical mechanisms are not applicable due to their inherent size and weight limitations. While different strategies based on different stimuli have been developed, there is a rising need for new biocompatible methodologies to power and control small-scale robots. Inspired by the surface locomotion of aquatic insects, we propose the use of structural proteins as a porous matrix for the development of surface tension-propelled micromotors. These protein motors can change their nanostructure and nano-porosity to regulate the diffusion of chemical fuel and thus regulate the propulsion. We integrated these protein motors into photomechanical liquid crystal networks to provide steering control via bending and surface deformation, mimicking the posture change of swimming insects. We demonstrated diverse locomotion control and active direction transition in milli swimmers across length scales. This new strategy offers orthogonal power and control solutions for autonomous swimming soft robots.

10:45 AM SB11.05.03

Engineering Biomolecular Actuators from Calcium-Responsive Repeat Proteins Marina P. Chang, Alana P. Gudinas, Kenny M. Hernandez and Danielle J. Mai; Stanford University, United States

Protein-based hydrogels provide a platform for functional, biocompatible materials in soft robotics. Stimuli-responsive protein hydrogels can function as soft actuators by transforming environmental signals into mechanical motions without the need for an external power source. For soft robotics systems to interface or integrate with biological systems, they must respond to physiological stimuli. Calcium ions act as critical signaling molecules for a wide variety of biological functions, including muscle cell contraction, cell replication, and neurotransmitter release. Calcium-responsive actuators would enable broad biomedical applications, such as artificial muscles and implantable, responsive materials.

The diverse functionality of naturally occurring proteins offers bioinspiration to develop engineered proteins that respond to specific stimuli. Calcium responsiveness emerges in a class of "Repeats-in-Toxin" (RTX) protein domains that undergo reversible conformation changes from random coils to β -roll structures upon binding to calcium. We characterize the changes in the overall size and tertiary structure of RTX domains in the presence and absence of calcium using small angle x-ray scattering (SAXS). The addition of calcium results in a 70% decrease in volume of an RTX domain, representing a large contractile range. To harness this mechanical response, we genetically fused RTX domains between hydrogel-forming associative domains. The mechanical properties of the resulting hydrogels were characterized using shear rheology, which revealed calcium-dependent increases in hydrogel stiffness. By incorporating RTX domains in hydrogel systems, we demonstrate a tunable platform for calcium-responsive biomolecular actuators. RTX-based biomolecular actuators are poised to enable the development artificial muscles to aid in the repair or replacement of injured muscle.

11:00 AM *SB11.05.04

Overcoming Challenges in Processing Biobased Materials for Soft Robotics [Blair K. Brettmann](#); Georgia Institute of Technology, United States

Electronic materials and robotic devices are pervasive throughout modern society and with increasing demand comes a growing interest in improving the sustainability of these products. One of the most promising methods to improve sustainability is to replace key components with biobased materials, which are derived from renewable biomass sources. However, these materials are often very challenging to process due to a large degree of heterogeneity, impurities from the feedstock, batch-to-batch variation, and abundance of functional groups with strong molecular interactions. This becomes even more important for applications such as soft robotics where small changes in microstructure can lead to large changes in performance. Applying systematic study of the formulation and the processing conditions in tandem, we can provide insights into how to overcome these unique challenges in biobased materials, working with materials from cellulose nanocrystals to sodium alginate to silk fibroin. Strong hydrogen bonding and the presence of charged functional groups leads to changes in rheology that require adjustments in processing parameters, while impurities from the biomass source lead to inconsistency in the materials and development of additional purification schemes to reduce variability in the output product and improve quality. Underlying the design of these soft materials from biobased sources is a strong link between the formulation and the process and only with this vision towards manufacturability can we realistically improve the sustainability of these complex products.

11:30 AM SB11.05.05

Biomimetic Nanostructures Incorporated with Synthetic Melanin for Advanced Soft Robot Materials [Suyoung Lee](#), Damask Grinnell, Mark Van Dyke, Roberto Guzman and Minkyu Kim; The University of Arizona, United States

Soft robotics opens up new opportunities in a variety of fields, including biotechnology, agriculture, manufacturing, and defense, by replacing traditional rigid robots in complex scenarios. Soft robots are designed to imitate the flexibility and adaptability found in natural systems. Moreover, the materials employed in soft robotics typically require durability, with the necessity of biocompatibility, contingent upon the desired performance. Keratin, a fibrous protein comprising a major biomatrix in hair, skin, nails, wool, and feathers, can be an ideal candidate for soft robotics. The natural keratin-based materials offer biocompatibility and attractive mechanical properties, such as high tensile strength, hardness, toughness, and flexibility. However, materials developed from extracted keratin from natural sources often exhibit inferior mechanical properties compared to their natural counterparts, limiting their application in soft robotics.

In natural keratin-based biomatrix, melanin is commonly observed, and its catechol groups are known for their contributions to self-healing, enhanced mechanical properties, and chemical stability, in addition to their primary role as pigments. Polydopamine (PDA) has garnered attention as an artificial melanin due to its similar chemical structure and properties to its natural counterpart. The customizable design parameters of melanin-like PDA particles (MLPPs) make them even more intriguing than natural melanin. In this study, we introduced MLPPs into the keratin biomatrix to investigate the relationship between MLPP design parameters and the mechanical properties of the biomatrix. Specifically, we synthesized MLPPs using PDA alone or by coating PDA onto various particles and then incorporated these MLPPs into the keratin matrix. We correlated the mechanical properties of the biomatrix with PDA coating thickness, particle sizes, and concentrations of embedded MLPPs. We anticipate that the improved mechanical properties of keratin-based materials achieved through the integration of MLPPs, along with the multifunctional capabilities offered by diverse MLPPs, will not only render them suitable for soft robotics but also broaden their potential applications, including light harvesting, 4D printing, color-switching, and metal scavenging.

11:45 AM SB11.05.06

Phase Transition in Polymeric Systems for Biomimetic Materials Working with Water [Kosuke Okeyoshi](#), Taisuke Hatta, Yuto Watanabe, Reina Hagiwara, Thi Kim Loc Nguyen and Leijie Wu; Japan Advanced Institute of Science and Technology, Japan

Inspired by history of natural environment and biomaterials, we are designing and fabricating functional soft materials through organizing polymeric materials [1-3]. To propose advanced energy converting systems, materials living with water are the target. From a viewpoint of biomimetics, the air-water interface is expected to play an important role in establishing a universal model of dissipative structures. Viscous fingering, as an example of nonlinear fluidic flow, is an unstable situation that is widely known as *tears of wine*. This has been explained through the Marangoni effect, coffee ring effect, Saffman-Taylor instability, etc. However, due to the transitional nature of these phenomena, there are few strategies for immobilizing such fluidically regulated interfaces. Recently, such phenomena have been applied successfully to an immobilized structure by controlling the evaporation of a mixture of biopolymer and water.

In this study, we present a brief discussion of nonequilibrium phenomenon, “meniscus splitting”. More precisely, an air-liquid interface is divided into multiple interfaces to partition a space. By using a mixture of polysaccharides and water, a macroscopic pattern following a specific rule could be confirmed. When the mixture is dried from a top open cell, the polymer forms deposits at specific positions to split the meniscus by bridging a millimeter-scale gap. Because water irreversibly evaporates from the liquid phase to the air phase through a gap, the air-liquid interface is in a nonequilibrium state between polymer deposition and water evaporation. The interfacial instability is comparable to the mechanical instability of gels at the phase transition or to the skin layer of gel surfaces during shrinking. Furthermore, by controlling the deposition, the polymeric self-assembly could act as vapor-sensitive materials or super moisturizing materials [1-2]. Here, the phenomenon and the material’s behaviour would be discussed from physicochemical viewpoints. References: [1] I. Saito, L. Wu, K. Okeyoshi, et al, *ACS Appl Polym Mater* 4, 7054 (2022). [2] K. Budpud, K. Okeyoshi, et al, *Small* 16, 2001993 (2020). [3] K. Okeyoshi, et al: *Angew Chem Int Ed* 58, 7304 (2019).

SESSION SB11.06: Animate Matter in Soft Robots II

Session Chairs: Artur Braun and Minkyu Kim

Wednesday Afternoon, April 24, 2024

Room 430, Level 4, Summit

3:30 PM *SB11.06.01

Charge and Energy Transfer Dynamics in Organic Solar Cells Using Extracts of Algae [Mmantsae M. Diale](#); University of Pretoria, South Africa

The relationship between photosynthesis and photovoltaics is often viewed from different positions by researchers, whilst in fact, these two are related. Photovoltaics is a direct copy of photosynthesis, where the green leaf is the oldest solar cell with almost 100% photo conversion efficiency. The mechanism of solar energy conversion in photosynthesis is sustainable and environmentally safe, has a great potential as an example of renewable energy device. The efforts to collect all photons in the visible light has been unsuccessful due to bandgap limitations of inorganic materials. Recent advances in the design of optimal organic solar cells include the creation of converters in which thylakoid membranes, photosystems and cyanobacteria immobilized on nanostructured electrodes are used. Application of carotenoids and thylakoids pigments has extended light absorption from ultraviolet to infra-red photons,

an effort to improve solar cell performance and photo conversion efficiency. This presentation aims review charge and energy transfer dynamics in organic solar cells to produce maximum efficiency using algae-related matter.

4:00 PM SB11.06.02

Microstructures of Anisotropic pH-Responsive Chitosan Hydrogels prepared by Meniscus Splitting Method [Thi Kim Loc Nguyen](#) and Kosuke Okeyoshi; School of Materials Science, Japan Advanced Institute of Science and Technology, Japan

Polysaccharides have been expected to be a useful material in wide fields of food packaging, drug delivery, cosmetics, etc., toward a sustainable society. In addition, numerous natural polymers, like chitosan and cellulose, have also demonstrated pH-responsive swelling behavior. However, the hierarchical structures have not been used for materials under physiological conditions. In this study, to reorganize the polymeric systems, aqueous mixtures of chitosan as viscous fluid are used through the meniscus splitting method, for preparation of a chitosan membrane. To understand the factors on the specific deposition in the meniscus splitting, the nucleus position is analyzed thoroughly verifying the effect of the cell width. Furthermore, the dried chitosan membrane shows anisotropic pH-responses as a hydrogel because of the oriented structures in submicron scale.

To clarify the characteristic anisotropy in ion- or pH-sensitive hydrogels, the pH-dependence of three-dimensional swelling ratios and the cyclic pH-changes were validated. Especially, the dried membrane was directly immersed into each buffered solution in a wide range of pH (pH2.2–pH8.0). Under the acidic conditions, the protonation allowed the water molecules to penetrate the interspace not only among the fibers but also among the chains in fibers. As a result, some of the crosslinking points by the hydrogen bond should be dissolved. Besides, toward the use of the membrane in the physiological pH condition, like pH7.4, the repeatability of swelling/deswelling as the hydrogel was validated. In the pH cyclic changes between pH8.0 and pH2.2, the gels showed no reversibility. Through a repeat test of stepwise pH-changes between pH8.0 and pH2.2, it was clarified that the sample continued swelling and redispersed into the aqueous solution, suggesting that the chitosan chain had irreversibly dissolved crosslinking points. In the pH2.2, the protonation of the chitosan chain would induce the dissolution of the hydrogen bonds between the hydroxyl groups and exchange of the citric acid. Interestingly, in the cyclic pH changes between pH8.0 and pH5.0, the chitosan gels had reversibility both in the *Y*- and the *Z*-directions. This result suggests that the water molecules can go in and out of the interval of the oriented structure without dissolution of the crosslinking points. The membrane would have a hierarchical architecture: nanofiber as a molecular bundle, and microfibrils as a nanofiber bundle. In the presentation, to clarify the nano-/micro anisotropic structure in DRY/WET states, the surface and cross-section positions of the chitosan membrane will be discussed.

4:15 PM SB11.06.03

Soft Robots Meet Bioelectronic Interfaces: A Promising Use-Case of Bio-Based and Biomimetic Polymers for Minimally Invasive Implantable Devices [Sukho Song](#)^{1,2}, Florian Fallegger¹, Alix Trouillet¹, Kyungjin Kim^{1,3} and Stephanie P. Lacour¹; ¹École Polytechnique Fédérale de Lausanne, Switzerland; ²Empa Swiss Federal Laboratories for Materials Science and Technology, Switzerland; ³University of Connecticut, United States

This presentation shares an emerging research field of minimally invasive implantable devices that utilize soft robotics, which offers promising applications for bio-based and biomimetic polymers. The talk first highlights a recent work published in *Science Robotics* (*J*) concerning the development of deployable electrocorticography (ECoG) electrode arrays enabled by soft robotic sensing and actuation. ECoG is a minimally invasive method commonly used to map epileptogenic regions of the brain. It aids in lesion resection surgery and is increasingly explored in brain-machine interface applications. However, current devices present limitations, leading to trade-offs in cortical surface coverage, spatial electrode resolution, aesthetics, and risk factors. These limitations often restrict the use of the mapping technology to the operating room.

The presented work introduces a scalable technique for fabricating large-area soft robotic electrode arrays. These arrays can be deployed on the cortex through a square-centimeter craniotomy using a pressure-driven actuation termed "eversion". The design of these eversion-based electrode arrays is akin to a rubber glove with finger-shaped air pockets. To prepare for deployment, this glove is inverted and folded within a cylindrical loader. During deployment, liquid is introduced into each "finger," enabling the array to revert and expand over the brain. Each section incorporates soft, microfabricated electrodes and strain sensors for real-time deployment monitoring. In a proof-of-concept acute surgery, the soft robotic electrode array was successfully deployed on a minipig's cortex to record sensory cortical activity without causing significant morphological damage.

The talk will also discuss insights into the future prospects of soft robotic implant technologies, which hold potential for multifunctional chronic health monitoring and treatment. Beyond the eversion actuation mentioned, there are opportunities to explore various soft robotic actuation to adapt to the geometries and movements of specific target organs, such as bending, unfolding, coiling, and undulating. Additionally, there are promising applications for these robotic implants to deploy a diverse range of sensing or stimulating components. Examples include strain sensors for cardiac activity monitoring, microfluidic systems for drug delivery, and optical elements for optogenetic stimulation. Bio-based and tissue-mimetic soft polymers are especially significant, ensuring the implants' long-term biocompatibility and reliability. While the deployable ECoG arrays mentioned above utilized a soft polydimethylsiloxane (PDMS) matrix—comparable in mechanical properties to the brain's dura mater—employing even softer and more flexible polymers like hydrogels can decrease mechanical irritation on tissues, thus minimizing immune responses. Furthermore, antifouling materials like zwitterionic polymers can inhibit protein adhesion on the implant surface, a key factor in mediating immune responses. The integration of soft robotic implants with bio-based and bio-mimetic materials can open high-impact avenues in active implantable device technologies, enabling minimally invasive, chronic health monitoring and therapeutic applications previously deemed impossible.

References

1. S. Song, F. Fallegger, A. Trouillet, K. Kim, S. P. Lacour, Deployment of an electrocorticography system with a soft robotic actuator. *Science Robotics* **8**, eadd1002 (2023).

4:30 PM *SB11.06.04

Bioderived and Biodegradable Materials for Sustainable Soft Robotics [Martin Kaltenbrunner](#); Johannes Kepler University, Austria

Soft robotics provides unique opportunities in our quest for a more sustainable future. Among the key issues to overcome are the search for high performance green materials, end-of-lifetime considerations in complex (soft) systems, and their energy efficiency. This talk aims at suggesting solutions for some of these grand challenges. We introduce bioderived materials and fabrication methods for soft robots that biodegrade, yet are of high resilience. Based on highly stretchable biogels and degradable elastomers, our soft robots are designed for prolonged operation in ambient conditions without fatigue, but fully degrade after use through biological triggers. Electronic skins provide sensory feedback, while stretchable and biodegradable batteries enable autonomous operation. 3D printing of biodegradable hydrogels enables omnidirectional soft robots with multifaceted optical sensing abilities. Going beyond, we introduce a systematically-determined compatible materials systems for the creation of fully biodegradable, high-performance electrohydraulic soft actuators. These embodiments reliably operate up to high electric fields, show performance comparable to non-biodegradable counterparts, and survive over 100,000 actuation cycles. We elucidate their fundamental operating principles and provide materials combinations that enable power-efficient electrohydraulic actuators void of detrimental interfacial charging. Finally, concepts for energy-autonomous soft aquatic robots and aerial drones are introduced.

SESSION SB11.07: Poster Session
Session Chairs: Minkyu Kim and Danielle Mai
Wednesday Afternoon, April 24, 2024
Flex Hall C, Level 2, Summit

5:00 PM SB11.07.01

Biomimetic Phenolic Hydrogels [Faisal Ali](#) and Kwang Su Seo; Chemence, United States

Hydrogels with versatile properties have undergone extensive research for applications in surgical adhesives, soft robotics, and wearable device development. These materials must be biocompatible, non-toxic, and have minimal foreign body reactions. However, several challenges such as poor adhesion, excessive swelling, undesirable degradation rate, and extensive preparation before application persist.

PEG (polyethylene glycol)-based hydrogels stand out as promising candidates for these applications. Nevertheless, many commercially available PEG-based adhesives or gels demand extensive on-site preparation and special storage conditions prior to use. The adhesion is often inadequate, and swelling rate cannot be controlled.

To that effect, here we report a non-toxic biomimetic hydrogel based on PEG polymer chains functionalized with phenolic functional groups (Gallol and Catechol) developed for robust adhesion and with customizable properties (for example, modulus, degradation and swelling rate). Our two-part device simplifies on-site preparation prior to administration, making it also suitable for use as a surgical adhesive. The hydrogel network consists of 4-arm PEG chains grafted with either catechol or gallol units, crosslinked using Ferric ions or sodium periodate as agents. Other polymer backbones like Polyethyleneimine (PEI) have also been investigated. The concentration of crosslinking agents with respect to that of phenolic groups dictate the dominant mode of interaction, either coordination or covalent crosslinking. Furthermore, the overall self-healing ability, adhesive strength, and cohesive strength are tunable by the crosslinker's concentration relative to the PEG chains. Likewise, various findings have suggested that incorporating nanocomposite clay into the network can enhance the gel's cohesive strength.

In a comparative adhesion study, our optimal formulations, when tested alongside commercial PEG based adhesives on leather, exhibited shear strength of up to 253kPa, which was almost 12 times higher than CosealTM's shear strength of 22kPa after two hours of application. No delamination from the substrates (e.g., pig skin, leather, or collagen) was observed.

5:00 PM SB11.07.02

Wirelessly Actuated Soft Miniature Robots with Integrated Microfluidic Modules for Targeted Drug Delivery [Emily Buckner](#)^{1,1,2}, Boyang Xiao^{1,1,1}, Yilan Xu^{1,1,1} and Xiaoguang Dong^{1,1,1}; ¹Vanderbilt University, United States; ²The University of Tennessee, Knoxville, United States

The inherent softness of soft robots offers unique advantages in medical applications where safe interaction with surrounding biological tissues is crucial. Soft robots made of smart soft materials allow for programmable functionalities by spatially patterning material properties. More recently, magnetic actuation has gained significant attention due to its ability to wirelessly control soft robots for medical operations. Despite recent advances, the development of wireless soft robots for minimally invasive medical procedures that can traverse complex terrains remains challenging. In this study, we propose an untethered soft robot actuated by magnetic fields and integrated with microfluidic channels to achieve on-demand and targeted drug delivery in complex, confined environments within the body, such as the gastrointestinal (GI) tract. The robot, constructed at the millimeter scale through laser lamination and layer-by-layer assembly, boasts optimized material properties and dimensions to facilitate multi-modal locomotion and targeted drug delivery functions. By employing a tailored magnetization profile design, the robot exhibits various modes of locomotion, including crawling and climbing. Furthermore, the integration of microfluidic channels into the robot body, along with an origami-inspired self-folding pump and flexible valve, enables precise control of drug delivery. To actuate the robot's movement, we have designed a customized electromagnet array that accurately directs and regulates the magnitude of the applied magnetic field. Finally, we experimentally validated the robot's locomotion and drug delivery capabilities in phantom structures. This novel soft robot design holds great potential to navigate complex terrains and serve therapeutic functions in biomedicine as well as on-demand and targeted drug delivery, minimizing the side effects of overdosing during medical treatments.

5:00 PM SB11.07.03

Silica Percolated Ionic Dielectric Elastomer with High Electromechanical Energy for Soft Robotic Application [Hanbin Choi](#)¹, Yongchan Kim², Seonho Kim³, So Young Kim¹, Joo Sung Kim⁴, Eseudeo Yun², Hyukmin Kweon¹, Minjeong Kim¹, Vipin Amoli⁵, U Hyeok Choi³, Hojin Lee² and Do Hwan Kim¹; ¹Hanyang University, Korea (the Republic of); ²Soongsil University, Korea (the Republic of); ³Inha University, Korea (the Republic of); ⁴RIKEN, Japan; ⁵Rajiv Gandhi Institute of Petroleum Technology, India

Efforts to introduce soft actuators based on ionic electroactive polymer (i-EAP) in futuristic soft robotic systems are steadily underway. The i-EAPs offer many advantages for improving the performance of soft actuators through lightweight, flexibility, a straightforward manufacturing process, and low power consumption. Despite these advantages of i-EAPs, there are some limitations to their use in various soft robotic applications. Among them, a critical limitation is that i-EAP based actuators have low actuation force due to the flexibility of the material. To overcome this limitation, many studies have been attempted to improve the mechanical modulus of i-EAPs. However, improved modulus of materials reduces the flexibility, which inevitably decreases actuation strain. Therefore, these endeavors have delayed their implementation into soft robots due to the conflicting relationships between force and strain of i-EAP actuators.

In this study, we introduced an innovative approach to overcome the trade-off relationship between force and displacement in soft actuators based on ionic electroactive polymers (i-EAP). We present a novel material referred to as an ions-silica percolated ionic dielectric elastomer (i-SPIDER), which exhibits ionic liquid-confined silica microstructures that effectively resolve the chronic issue of conventional i-EAP actuators. Furthermore, by incorporating resistive polymers (PEDOT:PSS) and using ionic liquids and DMSO as additives, we could control the interface between ionic polymers and electrodes. The i-SPIDER is combined with ionic liquid-confined silica microstructures, thus enhancing electromechanical conversion capabilities at low voltage, thanks to improved ion accumulation facilitated by interpreting electrode polarization at the electrolyte-electrode interface. Through these characteristics, we successfully demonstrated that i-SPIDER containing IL-confined silica microstructures shows simultaneous improvement in both force and strain of electrically driven soft actuators by overcoming the chronic conflicting inverse relationship between them. As a result, ion accumulation was improved on the i-SPIDER -electrode interface, achieving a unique combination of high strain (by approximately 1.52%) and force (by roughly 1.06 mN) even at low Young's modulus (merely 5.9 MPa) based on high electromechanical energy density at a low voltage (2 V) compared to conventional i-EAP soft actuators.

Additionally, by demonstrating arachnid-inspired soft robots endowed with user-desired tasks through control of various form factors, we have demonstrated the potential for i-SPIDER-based soft robots to concomitantly enhance strain and force, ushering in the next generation of miniaturized, low-powered, low-voltage soft robotics.

5:00 PM SB11.07.04

Flexible Bacterial Cellulose Substrates Coated with Chlorophyll Dye for Photoelectrochemical Water-Splitting [Nteseng D. Mosalakgotla](#) and Mmantsae M. Diale; University of Pretoria, South Africa

In this study, flexible silver nanowire bacterial cellulose membranes have been fabricated to serve as conducting substrates for a chlorophyll dye. The structural properties and crystallinity of the prepared thin films were examined using X-ray diffraction (XRD). The surface morphology of the prepared thin films was investigated using the Field Emission Scanning Electron Microscope (FE-SEM). Ultraviolet–visible spectroscopy (UV-Vis) was used to study the photoabsorbance of the films and the existence of chlorophyll was confirmed using Fourier Transform Infrared Spectroscopy (FTIR). Lastly the thin films were used as photoelectrodes in a three-electrode electrochemical system to study their PEC properties. The obtained photocurrent response of the films is attributed to the strong photoabsorbance of the chlorophyll, and low resistance of the transfer of charge carriers at the solid/liquid interface of the films. This study promotes the use of cellulose based membranes as low-cost, lightweight, and durable substrates for PEC applications. Furthermore, it demonstrates the promise of incorporating organic materials on PEC systems to enhance the production of hydrogen.

5:00 PM SB11.07.05

Stimuli-Responsive, Morphing Liquid Crystal Elastomer Structures for Intelligent Systems [Xueju \(Sophie\) Wang](#); University of Connecticut, United States

Intelligent systems with capabilities of sensing, actuation, and closed-loop control are promising for many applications such as augmented reality, rehabilitation, and soft robotics. In this talk, I will present our work on stimuli-responsive materials, structures, and electronics toward this effort. I will start with our study on liquid crystal elastomers (LCEs), a type of smart material that has capabilities of soft elasticity and large, reversible shape-changing behaviors due to liquid crystal-polymer network couplings. Through introducing a versatile mechanical programming technique, previously inaccessible reconfigurable three-dimensional structures made of LCEs and their magnetic composites are created and their potential applications in soft robotics are demonstrated. I will further present our facile strategy to locally tailor the stiffness and the morphing behavior of these reconfigurable LCE structures by harnessing molecular-material-structure interactions, i.e., locally controlled mesogen alignment and crosslinking densities. Selective photopolymerization of spatially aligned LCE structures yields well-controlled lightly and highly crosslinked domains of distinct stiffness and selective permanent mesogen programming, which enables various previously inaccessible stiffness-heterogeneous geometries, as demonstrated in diverse morphing LCE structures via integrated experimental and finite element analysis. Furthermore, reprogramming of the non-photopolymerized regions allows for reshaping, as shown in a sequentially shape morphing LCE rod and “face”. The heterogeneous morphing LCE structures have the potential for many applications including in artificial muscles, soft robotics, and many others. In addition, a simple strategy for creating 3D thermochromic LCE structures with synchronous shape-morphing and color-changing capabilities for biomimetic robotics will also be introduced. I will conclude my talk with soft sensing devices for in situ pressure measurements, beyond the actuation capabilities enabled by LCEs. The introduced actuation and sensing strategies and concepts are promising for many intelligent platforms.

5:00 PM SB11.07.06

Design Optimization of The Directly 3D-Printed Jamming Structure Using Machine Learning Models [Yuna Yoo](#), Zeqing Jin and Grace Gu; University of California, Berkeley, United States

Modifying the stiffness of soft robots presents a significant challenge, with the goal of enabling free deformations at low stiffness, while increasing the robustness of grasping at high stiffness values. Among the promising approaches, the utilization of jamming structure stands out for its ability to achieve high stiffness modification with minimal volume variation. However, most of the jamming structures require a complicated fabrication process, which limits the prototyping speed, repeatability, and reliability. To address this issue, attempts have been made to directly 3D-print jamming structures; however, these attempts were limited to 3D-printing the standardized jamming structures and the optimized designs relied on heuristic searches based on trial-and-error experiments. In this study, we introduce a directly 3D-printed jamming structure with optimized design through machine learning. The stiffness of the generated jamming structure design is estimated by finite-element-based simulations and the design is optimized using machine learning models. To validate the optimization results, benchmark designs and the optimized design are fabricated and the stiffness of the designs are compared. Finally, the feasibility of the optimized 3D-printed jamming structure is verified by grasping demonstrations, including its implementation into a pneumatically actuated soft gripper.

5:00 PM SB11.07.07

A Self-Healing Electrically Conductive Organogel Composite [Yongyi Zhao](#)^{1,2} and Carmel Majidi¹; ¹Carnegie Mellon University, United States; ²Massachusetts Institute of Technology, United States

Self-healing hydrogels use spontaneous intermolecular forces to recover from physical damage caused by extreme strain, pressure or tearing. Such materials are of potential use in soft robotics and tissue engineering, but they have relatively low electrical conductivity, which limits their application in stretchable and mechanically robust circuits. Here we report an organogel composite that is based on poly(vinyl alcohol)–sodium borate and has high electrical conductivity ($7 \times 10^4 \text{ S m}^{-1}$), low stiffness (Young's modulus of $\sim 20 \text{ kPa}$), high stretchability (strain limit of $>400\%$) and spontaneous mechanical and electrical self-healing. The organogel matrix is embedded with silver microflakes and gallium-based liquid metal microdroplets, which form a percolating network, leading to high electrical conductivity in the material. We also overcome the rapid drying problem of the hydrogel material system by replacing water with an organic solvent (ethylene glycol), which avoids dehydration and property changes for over 24 h in an ambient environment. We illustrate the capabilities of the self-healing organogel composite by using it in a soft robot, a soft circuit and a reconfigurable bioelectrode.

5:00 PM SB11.07.08

Fabrication of Reentrant Micromesh Suspended by Shape Memory Polymer for Liquid-Repellency [Ga-in Lee](#), Moon Kyu Kwak, Minsu Kim, Han Jun Park and Dokyung Kyeong; Kyungpook National University, Korea (the Republic of)

Omniphobic surfaces, which are referred as having both hydrophobic and oleophobic behaviors under environments involving interaction with liquids, have been vigorously studied due to its robust liquid-repellency. By its non-wetting properties, the liquid-repellent surfaces have potential to be utilized in various applications such as self-cleaning, oil/water separation, droplet manipulation, and antifouling. Accordingly, scientists are developing the liquid-repellent surface by forming microscale structures with a specific functional morphology. Among the representations of the morphology, reentrant topography inspired by springtail in nature have enormous influences on microstructure engineering fields for its exceptional wetting resistance even under

liquids with low surface tension than water. Reentrant structures show an overhanging profile, by which a surface can uphold liquids so as to have liquid-repellency. Surface engineers have been consistently trying to imitate the reentrant topography by 3D printing, capillary interaction, self-assembly, photolithography, and imprint lithography ever since the studies of omniphobic surfaces have manifested. Among the aforementioned methods, imprint lithography by the UV light is one of the most commonly employed techniques due to its ability to achieve micro/nanoscale resolution affordably and rapidly. However, imprinting has limited feasibility in complex topography due to the difficulties in demolding process, for which 3-D structures with a semi-freestanding feature that below the surface is excavated and penetrated can be hard to be achieved. This shortcoming limits the practical realization of functional structures present in nature such as springtails, gecko, and so forth. Shape memory polymer (SMP) is a switchable material that has double states which are defined as a permanent shape and a temporary shape. Through manipulation of the shape under external stimuli such as heat or light, the temporary shape can be newly formed and fixed. Then SMP switches back to the permanent shape if triggered again by a stimulus. Recently, scientists have been utilizing SMP's unique property in developing functional surfaces including wetting controllable structures, diffractive optical elements, and dry adhesive surfaces. Herein, we fabricated suspended micromesh structures along with three different periods of the meshes. The meshes were imprinted on temporary-shaped flattened SMP and recovered to its permanent pillar shape when heat was applied above the glass transition temperature. Accordingly, the meshes were suspended as SMP recovered to its initial pillar shape and reentrant topography was formed consequently. In comparison with simple meshes, suspended micromeshes can realize the Cassie-Baxter state even with a liquid that has the intrinsic contact angle under 90 degrees by the geometry of the reentrant structure. Also, the apparent contact angle of suspended micromeshes increased compared to the simple meshes because of the created air fraction of the surfaces. Considering the reentrant geometry, we calculated the breakthrough pressure of suspended micromeshes based on the Laplace pressure and compared its values to the measured breakthrough pressure. In addition, drag reducing effect of suspended micromeshes were also evaluated to prove its robustness in liquid-repellency. In this work, we proposed a new method to fabricate the reentrant topography with the meshes by a combination of imprint lithography and SMP's own property. Wettability and hydrostatic robustness of fabricated suspended micromeshes were investigated via measurements of the contact angle, and breakthrough pressure, by which it is demonstrated that the reentrant topography was successfully established based on the comparison between the calculated values and the measured values. In addition, slip lengths were measured to further present the liquid-repellency of the structures owing to its created air layers.

5:00 PM SB11.07.09

Multifunctional Droplet Manipulation of Heterogeneous Structures using Magnetic Responsive Shape Memory Ridge Arrays and Superhydrophobic Silicon Thin Film [Seungbeom Kim](#), Sangyeop Lee, Junhyung Kim, Uhyeon Kim and Seok Kim; Pohang University of Science and Technology, Korea (the Republic of)

The manipulation of droplets finds applications across diverse fields such as materials synthesis, healthcare, and chemistry. Traditional methods for droplet manipulation involve techniques such as electrowetting and fluidic-based platforms. In this study, we propose a novel approach to induce multifunctional droplet manipulation by utilizing nanostructured superhydrophobic silicon thin films integrated on magnetic particle-embedded SMP (Shape Memory Polymer) ridge arrays. Our approach capitalizes on the inherent Laplace pressure gradient resulting from the interaction between a created heterogeneous structure's ratchet surface and the droplet, overcoming challenges like biofouling associated with externally applied forces. The incorporation of SMP introduces elastic properties, while the silicon thin film contributes superhydrophobicity, optimizing both mechanical characteristics and hydrophobicity of overall platform.

Our choice of SMP is deliberate, as it allows for diverse functionalities through controlled magnetic torque. Unlike traditional magnetic responsive polymers, we employ SMP to perform various functions with partial heating and cooling of the platform. The heterogeneous structure comprising SMP exhibits shape fixing without the need for continuous external stimuli, enhancing energy efficiency.

We believe that this heterogeneous structure, exploiting Laplace pressure gradient, holds promise for applications beyond our study, extending to fields such as digital microfluidics, potentially impacting technologies like lab-on-a-chip devices. The unique combination of SMP and superhydrophobic silicon thin film offers a versatile and energy-efficient platform for advanced droplet manipulation.

5:00 PM SB11.07.10

Universal Anipulation of Macro-To-Microobjects by Controlling Adhesion of Nanotip Shape Memory Polymer Surface [Junhyung Kim](#), Sangyeop Lee, Seungbeom Kim, Uhyeon Kim and Seok Kim; Pohang University of Science and Technology, Korea (the Republic of)

Shape memory polymer (SMP) possesses the capability to undergo dynamic variations in stiffness when subjected to external stimuli such as heat or light. It exhibits the unique ability to be shape-fixed into desired shapes and can revert to its original form through the shape memory effect. Exploiting these attributes, SMP serves as smart adhesives in applications like soft grippers and transfer printing, providing a solution to challenges posed by the adhesion paradox, a feature distinct from traditional elastomer adhesives.

Here, we report a nanotip SMP surface with extreme reversible adhesion, demonstrating its adeptness in manipulating objects across a spectrum ranging from macro-scale ($\geq 10\text{cm}$) to micro-scale ($\geq 5\mu\text{m}$). This innovative approach leverages the distinctive features of SMP to effectively resolve challenges related to the adhesion paradox, while also capitalizing on the adhesion paradox through a return to the original rough surface, thereby achieving excellent reversible adhesion. The nanotip SMP surface, characterized by an RMS roughness (R_q) exceeding 100nm, mitigates surface adhesion to zero through its rough topography. In its rubbery state, this surface allows for conformal contact with the object by reducing roughness, while transitioning to a glassy state results in increased adhesion due to shape-locking effect. Then, to release the object, the SMP surface is reverted to its original nanotip surface through the shape memory effect, inducing a return to a rough state and enabling easy release.

This mechanism underscores the achievement of great adhesion reversibility across varying scales, marking the capability of programmable and precise large-scale transfer printing at the $5\mu\text{m}$ level chips. The applications of this approach, such as micro LED transfer and repair are showcased, suggesting its potential as a next-generation display solution with enhanced yield and precision.

5:00 PM SB11.07.11

Layer Jamming Enhanced by Micro-Structured Biomimetic Adhesive Sheets for Soft Robotics Applications [Shima Jalali](#), Hyun J. Chung and Dan Sameoto; University of Alberta, Canada

Layer jamming, in which the shape and the stiffness of a micro-structured sheets is modulated by regulating the friction force between layers, is a promising technology in the field of stiffness-tunable soft robotics. Biomimetic dry adhesive technologies utilizing the distinctive microstructures found on a gecko's foot, have been applied in applications ranging from climbing robots, pick and place assembly, skin-adhesives, and microfluidics. The biomimetic dry adhesive technology can be utilized to augment the friction force that induces layer jamming in reversible manner without the need of vacuum.

In this project, we create dry adhesive sheets employing Kraton G1645 - a styrene-ethylene-butylene-styrene (SEBS) thermoplastic elastomer. G1645 is used as the primary structural material and then modified by blending different weight percentages of polypropylene (PP) which is miscible and lower cost than SEBS. The blend is then used for micro-molding using a modified recipe of our previously reported compression molding processes.

The Setex gecko adhesive materials (DA910B) has proven to be a promising candidate for jamming applications, demonstrating favorable results as a layer jamming actuator in prior studies. While the material composition remains proprietary, it seems to be a relatively viscoelastic cured polyurethane. Our objective is to transition from the proprietary Setex adhesive to a more cost-effective and customizable alternative by employing a blend of SEBS (a recyclable, easy process and low-cost thermoplastic elastomer) and PP. Despite SEBS exhibiting commendable dry adhesive properties and strength on smooth surfaces which makes it an excellent reversible adhesive, challenges arise due to its low melt flow index, hindering the production of ultra-thin sheets through micro-molding techniques. Furthermore, its strength may not be sufficient to endure numerous cycles of attachment and detachment, as it is prone to mechanical tearing in low thickness and deformation of micro features under shear stress during detachment processes. Polypropylene (PP) as a cost-effective thermoplastic offers chemical compatibility for blending, and may increase the mechanical stability of individual fibers, allowing taller fibers to space out jammed layers which should in theory increase the effectiveness of the sheets at stiffness switching. Previous reports have also used PP microfibrers for self-cleaning and directional adhesion properties which inspires the idea of using it in a blend with SEBS to improve mechanical properties and preserve adhesion ability of SEBS simultaneously. The manufacturing process of gecko adhesive layers with a mushroom-shaped microstructure (the same structure as the Setex commercial type) involves the hot embossing technique using negative PDMS molds replicated from Setex masters. The SEBS/PP blends are produced using a single-screw extruder and then, using a hydraulic hot press, compressed into thin sheets with approximately 60 μ m thickness. The SEBS/PP blends are compared to pure SEBS using microscale tests based on JKR models to measure the adhesion properties of the samples. Additionally, mechanical tests are conducted to provide a complete comparison with commercial samples and to identify the optimum composition of SEBS/PP for maximum repeatability and longevity of the adhesive layers. The experimental results demonstrate good compatibility between SEBS and PP and the adhesive layers can be thermally bonded to thin PP films to complete a jamming actuator. These research results hold promising implications for the large-scale production of low-cost materials suitable for various applications, especially as stiffness tunable actuator in soft robotics.

SESSION SB11.08: Sensing, Actuation and Reconfiguration in Soft Robots
Session Chairs: Qing Chen, Stephan Roth, Newayemedhin Tegegne and Jie Xu
Thursday Morning, April 25, 2024
Room 430, Level 4, Summit

8:45 AM SB11.08.01

The Hole Dynamic in PEDOT:PSS/Bacterial Cellulose Actuators Sukesh Kumar^{1,2}, Aimin Yu² and Mudrika Khandelwal¹; ¹Indian Institute of Technology Hyderabad, India; ²Swinburne University of Technology, Australia

Actuators are one among numerous applications that have emerged from the utilization of conducting polymers. This class of material has attracted wide interest in the field of electronics, because they conduct both electronic and ionic charges through the bulk of their volume. This makes possible the application of electronic devices as electrochemical devices, which are termed as organic electrochemical transistor (OECT). Despite the extensive use as OECTs, there are still numerous discrepancies in the descriptions of the fundamental physics underlying the performance of these devices. Therefore, there is a growing emphasis on modeling the ion-electron interaction within conducting polymers. Recent publications have contributed fresh insights into the conduction mechanisms. However, the actuator community has yet to fully integrate these newfound understandings into their efforts to comprehend and model the mechanical response of conducting polymer actuators. Existing models for these actuators have primarily focused on ionic diffusion, which falls short of explaining all the existing experimental observations.

This study draws from three distinct bodies of literature, comprising the most pertinent existing model for conducting polymer actuators, advancements in the comprehension of ionic-electronic conduction in conducting polymers, and empirical observations that defy current models for conducting polymer actuators. Also, Electrochemical Impedance Spectroscopy (EIS) is used extensively to understand the actuation mechanism under dynamic conditions, considering the progress made in comprehending the physics of conducting polymers as previously mentioned.

The conducting polymer actuator is prepared using PEDOT:PSS and bacterial cellulose (BC) (as a substrate), which is operated in both depletion mode and enhancement mode, for different time scales. The doping (compensation) and dedoping (displacing) in PEDOT:PSS (using an electrolyte) results in displacement of the PEDOT:PSS/BC bi-layer. Notably, the actuator displacement is found to be asymmetric, contingent on the polarity, magnitude, and frequency/time period of the applied potential. The observed asymmetry in displacement as a function of these parameters remains unaccounted for by existing models for conducting polymer actuators.

Experimental Process

Electrochemical Impedance Spectroscopy (EIS) is performed on a PEDOT:PSS/Bacterial cellulose bi-layer actuator, while the actuator is subjected to various electrostatic potential. The displacements of the actuator under these potentials are also recorded for different time periods. The EIS data is used to model electrical circuit for actuators under given potentials. Mott-Schottky analysis is performed to understand the energy band structure of the actuator-electrolyte system. Density Functional Theory simulations are performed to aid the conclusions derived from experimental data.

Significance

The results and discussion which follows in this paper is significant in deriving an updated model for conducting polymer actuators, delving into quantum capacitance effects given the low charge density in conducting polymer, which is essential for reliable device performance and in defining the operating ranges for such actuators. This study becomes significantly important in the background of the development happening in the field of OECT, as it brings in the mechanical deformation corresponding to those findings.

9:00 AM SB11.08.02

Fabrication of Responsive 4D Micro-Structures for Dynamic Structural Color and Optical Sensing Teodora Faraone¹, Jing Qian², Louise Bradley², Larisa Florea^{1,3} and Colm B. Delaney^{1,3}; ¹Trinity College Dublin, Ireland; ²Trinity College Dublin, The University of Dublin, Ireland; ³Centre for Advanced Materials and BioEngineering Research, Ireland

Self-assembly of colloidal particles into crystalline colloidal arrays have attracted great interest from chemists, physicists and materials scientists alike due to their broad applications in the fields of optics and photonics¹. In particular, application of colloidal crystal arrays offers a means for controlling and manipulating light flow, and gives rise to some of the most brilliant structural colors. This phenomenon is also present in nature, where many species of birds, insects, butterflies, fish and even flowers, owe their vivid color to hierarchical assemblies of photonic structures.

Changing the structural color of photonic crystalline structures typically requires the synthesis of different size particles, in order to modulate inter-particle distance². This can add different degrees of difficulty as precise control of particle size and inter-particle distance in the self-assembly process can be time-consuming. In this work, we prove how using just one size polymer particle spheres, a wide gamut of reflected colours can be obtained in a range of different polymer matrices.

Using direct laser writing (DLW) in nanocomposite photoresists (at particle concentrations conducive to self-assembly), we can fabricate complex 3D microstructures with sub-micron feature sizes. Furthermore the DLW fabrication technique allows for fine control over a series of fabrication parameters, such as laser power, structure slicing and hatching, thereby providing minute control over the inter-particle distance in all 3 dimensions, to obtain hierarchically ordered nanocomposite microstructures showing a wide gamut of color.

We present the expansion of this work to encompass soft, stimuli-responsive polymers in which an external stimulus can be further used to vary periodicity of the ordered nanocomposite, thereby further changing the reflected colour in and out of the visible spectrum. We will show routes of exploitation for this approach which span sensing and encryption.

In conclusion, the strategy presented herein offers a novel and efficient route for creating responsive photonic microstructures that can be used qualitatively (for analyte determination) or qualitatively (for go/no go interventions).

1. Zhang, H., Bu, X., Yip, S., Liang, X., & Ho, J. C. (2020). Self Assembly of Colloidal Particles for Fabrication of Structural Color Materials toward Advanced Intelligent Systems. *Advanced Intelligent Systems*, 2(1), 1900085.

2. Li, R., Zhang, S., & Zhang, R. (2023). Recent progress in artificial structural colors and their applications in fibers and textiles. *Chemistry Methods*, e202200081.

9:15 AM *SB11.08.04

Functional Hybrid Materials on Bio-Basis for Sensors and Actuators [Stephan V. Roth](#)^{1,2}; ¹KTH Royal Institute of Technology, Sweden; ²Deutsches Elektronen-Synchrotron DESY, Germany

Cellulose nanofibrils (CNFs) are an abundant, bio-based, and renewable material with excellent mechanical properties. They show highest strength and allow for light-weight applications. In order to functionalize this sustainable material par excellence, the fabrication of hybrid materials is mandatory. These hybrid materials include functional polymers as well as advanced core-shell and metallic nanoparticles. Here, the knowledge of the nanostructure is crucial for its application. Starting from thin film technology, spray deposition is a scalable, facile, and industrially used method for fabricating tailored nanostructures with specific applications. To start with, sprayed CNF templates themselves act as nanoporous templates for optoelectronic applications. They comprise non-swelling polymer electrodes¹, sensor materials², flexible electrodes³, and tunable amorphous photonic crystals⁴. Being all water-based, the interaction with water is crucial⁵. Using water-based polymers and CNF in a hybrid material and facile solution casting, internal stresses and humidity sensitivity is exploited to fabricate self-healing actuators⁶.

In my talk I will present the fundamental aspects of using CNF and characterizing its response to water and humidity. The nanoporous structure of CNF thin films is the key-point for their functionalization. The nanostructure is extracted using advanced X-ray and neutron scattering methods, which allows to understand and exploit the interaction with water of the hybrid materials applied in soft robotics.

1. Brett, C. J. et al. Humidity-Induced Nanoscale Restructuring in PEDOT:PSS and Cellulose Nanofibrils Reinforced Biobased Organic Electronics. *Adv. Electron. Mater.* **7**, 2100137 (2021).

2. Chen, Q. et al. Biopolymer-Templated Deposition of Ordered and Polymorph Titanium Dioxide Thin Films for Improved Surface-Enhanced Raman Scattering Sensitivity. *Adv. Funct. Mater.* **32**, 2108556 (2022).

3. Betker, M. et al. Sprayed Hybrid Cellulose Nanofibril-Silver Nanowire Transparent Electrodes for Organic Electronic Applications. *ACS Appl. Nano Mater.* **6**, 13677-13688 (2023).

4. Harder, C. et al. Optical Properties of Slot-Die Coated Hybrid Colloid/Cellulose-Nanofibril Thin Films. *Adv. Opt. Mater.* **11**, 202203058 (2023).

5. Brett, C. J. et al. Water-Induced Structural Rearrangements on the Nanoscale in Ultrathin Nanocellulose Films. *Macromolecules* **52**, 4721-4728 (2019).

6. Chen, Q. et al. Cellulose-Reinforced Programmable and Stretch-Healable Actuators for Smart Packaging. *Adv. Funct. Mater.* **32**, 2208074 (2022).

9:45 AM BREAK

10:15 AM *SB11.08.05

Artificial Sharkskin: Fabrication of Staggered Overlapped Microdenticles [Jeong Jae Wie](#)^{1,2}; ¹Hanyang University, Korea (the Republic of); ²State University of New York College of Environmental Science and Forestry, United States

In liquid crystalline elastomers, anisotropy in molecular alignment governs direction of mechanical actuation upon exposure to external stimuli.¹ Similarly, the arrangement direction of magnetic particles determines magnetomechanical actuation of polymer composites. In micropillar arrays, chain-like arrangement of magnetic particles can induce bending or twisting actuation of micropillars under linear external magnetic field.² When magnetic particles are arranged along the principal axis of the micropillar, the perpendicular external magnetic field produces bending actuation. In the same magnetic field condition, twisting actuation is induced with magnetic particles arranged along the short-axis of micropillars.² The strain responsivity of magnetic actuation can be enhanced by employing anisotropic micropillar geometry for anisotropic stress distribution.³ Based on the magnetic bending actuation of anisotropic microdenticles, staggered-overlapped three-dimensional microarchitectures are constructed to mimic artificial sharkskin, a feat difficult to achieve by conventional microfabrication techniques.⁴ In this presentation, various anisotropic functionalities of this artificial sharkskin will be discussed.

Acknowledgment

This work was supported by Air Force Office of Scientific Research/Asian Office of Aerospace Research and Development (AFOSR/AOARD) (FA2386-22-1-4086), National Research Foundation of Korea (NRF-2022R1A2C2002911).

References

1. J.J. Wie, M.R. Shankar, and T.J. White, *Nat. Commun.* **7**:13260 (2016).

2. J. Jeon, J.E. Park, S.J. Park, S. Won, H. Zhao, S. Kim, B.S. Shim, A. Urbas, A.J. Hart, Z. Ku, and J.J. Wie, *ACS Appl. Mater. Interfaces*, **12**, 14, 17113-17120 (2020).

3. J.E. Park, J. Jeon, S.J. Park, S. Won, Z. Ku, and J.J. Wie, *Small*, **16**, 2003179 (2020).

4. J.E. Park, H. Je, C.R. Kim, S. Park, Y. Yu, W. Cho, S. Won, D.J. Kang, T.H. Han, R. Kwak, S.G. Lee, S. Kim, and J.J. Wie, *Adv. Mater.*, **35**, 2309518 (2023).

10:45 AM SB11.08.06

Micro-Robots with Fast and Reversible Actuation via Two-Photon Polymerization Yekaterina Tskhe¹, Srikant Kolagatla¹, Alex J. Thompson^{2,2}, Colm B. Delaney¹ and Larisa Florea¹; ¹Trinity College Dublin, Ireland; ²Imperial College London, United Kingdom

The additive manufacturing and its application in micro-robotics have demonstrated the high potential for the fabrication of tiny smart devices.¹ These microscale tools can be used in surgeries to manipulate objects with precision and control while reducing damage and making patient recovery faster. The key element for the movements and actuation of such microsystems is stimuli-responsive material.

In this work, we present functional microgrippers fabricated by direct laser writing via two-photon polymerization (2PP). This technique allows the creation of complex 3D structures on a microscale by scanning a polymer hydrogel with the femtosecond laser, building the structure layer by layer.² By tuning the fabrication parameters such as slicing and hatching as well as laser power and scanning speed it is possible to adjust the mechanical and chemical properties for the desired application.

The actuation of the microgripper is controlled by pH-responsive polymer materials which react to the pH changes of the environment. Their shape-morphing feature is inspired by the artificial muscles which can contract and expand in response to pH changes.³ The microgripper is powered by this type of responsive polymers that can move its arms to reversibly close and open. The actuation takes a few seconds due to the miniature scale of these devices. By mimicking the blood vessels, we can implement such microgrippers as valves and use them in the pH sorter microsystem. The characterization of such microstructures was complemented by optical microscopy, atomic force microscopy (AFM), and scanning electron microscopy (SEM). We showcased the effect of structure design, hydrogel composition and writing parameters on the performance of microgrippers.

These types of micro-robots open new opportunities for minimally invasive surgeries, sensing and photonics.^{4,5,6} We can incorporate multiple functionalities into a single microdevice by adapting the design and adjusting fabrication parameters. It offers a high degree of flexibility and presents a wide range of potential applications for 2PP-fabricated micro-robots.

References:

- (1) Ye, M.; Zhou, Y.; Zhao, H.; Wang, Z.; Nelson, B. J.; Wang, X. A Review of Soft Microrobots: Material, Fabrication, and Actuation. *Advanced Intelligent Systems* **2023**, *n/a* (n/a), 2300311. DOI: <https://doi.org/10.1002/aisy.202300311>.
- (2) O'Halloran, S.; Pandit, A.; Heise, A.; Kellett, A. Two-Photon Polymerization: Fundamentals, Materials, and Chemical Modification Strategies. *Advanced Science* **2023**, *10* (7), 2204072. DOI: <https://doi.org/10.1002/advs.202204072>.
- (3) Ma, Z.-C.; Zhang, Y.-L.; Han, B.; Hu, X.-Y.; Li, C.-H.; Chen, Q.-D.; Sun, H.-B. Femtosecond laser programmed artificial musculoskeletal systems. *Nature Communications* **2020**, *11* (1), 4536. DOI: [10.1038/s41467-020-18117-0](https://doi.org/10.1038/s41467-020-18117-0).
- (4) Kaufman, G.; Jimenez, J.; Bradshaw, A.; Radecka, A.; Gallegos, M.; Kaehr, B.; Golecki, H. A Stiff-Soft Composite Fabrication Strategy for Fiber Optic Tethered Microtools. *Advanced Materials Technologies* **2023**, *8* (12), 2202034. DOI: <https://doi.org/10.1002/admt.202202034>.
- (5) Zhang, Y.; Wang, J.; Yu, H.; Zheng, J.; Zhao, X.; Guo, H.; Qiu, Y.; Wang, X.; Liu, L.; Li, W. J. A chemotactic microrobot with integrated iridescent surface for optical-tracking. *Chemical Engineering Journal* **2023**, *472*, 144222. DOI: <https://doi.org/10.1016/j.cej.2023.144222>.
- (6) Liu, B.; Dong, B.; Xin, C.; Chen, C.; Zhang, L.; Wang, D.; Hu, Y.; Li, J.; Zhang, L.; Wu, D.; et al. 4D Direct Laser Writing of Submerged Structural Colors at the Microscale. *Small* **2023**, *19* (2), 2204630. DOI: <https://doi.org/10.1002/sml.202204630>.

11:00 AM *SB11.08.07

Flexible Electronic Skins for Sensing and Haptic Actuation John A. Rogers; Northwestern University, United States

Mechanoreceptors in the skin present compelling targets for selective and noninvasive neural interfaces. This presentation summarizes our recent work in systems for independently rendering sensations in these afferent channels using miniaturized mechanical actuators configured in programmable, dense arrays as untethered, wearable devices. The actuators combine with the skin as an elastic, energy storing module to support bistable, self-sensing modes for inducing controlled deformations at the surface of the skin. The result renders both dynamic and static stimuli, through either normal or shear forces. Studies in the context of rehabilitation with human subjects demonstrate this wireless, skin-conformable haptic array as an interface to a physical environment, reconstructed and tracked from an advanced suite of smartphone-based sensors. The diversity in modes of engagement, the density of power delivery, and the efficiency in operation of these small-scale mechanical transducers represent key, enabling advances over alternatives based on electrostatic, pneumatic, and electromagnetic approaches.

SESSION SB11.09: Virtual Session
Session Chairs: Artur Braun and Minkyu Kim
Wednesday Morning, May 8, 2024
SB11-virtual

10:30 AM *SB11.09.01

Bioinspiration from Photosynthetic Light-Harvesting Protein Complexes Tjaart Krüger; University of Pretoria, South Africa

Proteins execute their programmed functions in a finely regulated way with extraordinary efficiency, despite ample environmental disorder and densely crowded, heterogeneous environments. These capabilities serve as a useful source of inspiration for polymer design. The way in which photosynthetic light-harvesting proteins establish robustness to conformational disorder is particularly meaningful for conjugated polymers where such disorder gives rise to spatial localization of excitons and the formation of electronic traps, whereby exciton lifetimes and charge diffusion lengths are significantly reduced. In photosynthetic light-harvesting proteins, these limitations are largely overcome by the binding of chromophores in dense arrangements, allowing the formation of molecular excitons that are coherently shared across a number of neighboring chromophores. Having a significantly reduced susceptibility to structural disorder, these spatially delocalized excitations offer various functional benefits such as faster energy transport and less trapping and ensuing loss of excitation energy. These functions are often enhanced by mixing of the excitons with charge-transfer states. In the first part of the presentation, I will discuss molecular design strategies of conjugated polymers with enhanced robustness to static disorder. I will also show how subunit aggregation types can be quantified, using as an example the application of three computational methods to the experimental absorption and photoluminescence spectra of a benzodithiophene-isoidigo copolymer. In the second part of the presentation, I will discuss how the photosystem organization of cyanobacteria serves as inspiration for the design of conjugated terpolymers whereby the use of one donor and two acceptor units mimics the design of one main type of light-

harvesting complex channeling excitation energy to two different types of photosystems.

11:00 AM *SB11.09.02

Shape Change Mechanisms in Biological Materials [Peter Fratzl](#); Max Planck Institute, Germany

The shape change of plant and animal tissues fulfills a variety of functions from organ growth to locomotion or seed dissemination. Various physical mechanisms, from fiber contraction to osmotic pressure and atmospheric dehydration, are at the origin of such shape changes. Fiber orientation distributions control the geometry of shape change and constitute, therefore, the alphabet for such programmed transformations. The talk reviews recent work on seed locomotion and capsule opening, on collagen fiber contraction as well as fiber tension-controlled tissue growth.

11:30 AM *SB11.09.03

Shaping Soft Matter: From Live Cell Tattoos to Hydrogel Transformers [David H. Gracias](#); Johns Hopkins University, United States

Micro and nanopatterning of rigid materials such as semiconductors, metals, and dielectrics has revolutionized human life by enabling integrated circuits, microsensors, and smart phones. Imagine applying the same micro/nano patterning principles and multi-scale integration to hydrogels and living materials. We could then create adaptable implants, living robots, microphysiological systems, and homeostatic materials.

This talk will describe our efforts to apply micro and nanoscale patterning and heterogeneous integration to hydrogels and living cells/organoids. I will describe the first demonstration of the patterning of live cells with nanolithographic arrays of gold dots and wires using a biocompatible biotransfer process. Integrating lithographic patterns on live cells offers the potential to create living material interfaces and incorporate electronic/optical tattoos. I will also describe shape-changing temperature responsive and DNA polymerization gels that display diverse functions such as gripping, locomotion, and complex programmable shape change. I will give examples wherein such hydrogel transformers can be applied widely, including for adaptive implants, soft-robots, digitally programmable materials, and automata. These studies indicate the potential for the design of a range of intelligent materials, robots, and integrated devices that have the touch and feel of biological matter.

12:00 PM SB11.09.04

Ultra-Thin Graphene Oxide Composite DNA Polymerization Gels [Ruohong Shi](#), [Qi Huang](#), [Rebecca Schulman](#) and [David H. Gracias](#); Johns Hopkins University, United States

DNA polymerization gels exhibit high swelling, as high as a 100-fold volumetric increase, based on the sequential insertion of DNA hairpins. They offer programmability based on DNA hybridization with high specificity and the potential for the integration of biomolecular circuits, which is of broad relevance to tissue engineering and soft robotics. Here, we incorporated graphene oxide (GO) nanosheets into the polymerization gels to enhance functionality. The composites are stiffer and enable the gels to be structured in significantly thinner films, as thin as 8 μm . We observe that the GO-DNA polymerization gel composites retain their sensitivity to DNA-induced shape transformation, such as swelling and shrinking, akin to controls without GO, but with accelerated shrinking rates. We anticipate that the combination of thinner gels with more rapid shrinking, combined with the functionality of GO (such as optical absorbance), enhances their potential for use in flexible devices, soft robotics, and drug delivery. The study also highlights the potential to incorporate other nanoparticles (e.g., noble metal, semiconducting, ferromagnetic) into DNA polymerization gels to enhance optical, electronic, and magnetic functionality.

12:05 PM SB11.09.05

Harnessing Gradients for Self-Assembly of Peptide-Based Nanocapsules [Xuliang Qian](#)¹, [Haopeng Li](#)¹, [Harini Mohanram](#)¹, [Xiao Han](#)¹, [Huitang Qi](#)², [Guijin Zou](#)³, [Fenghou Yuan](#)², [Ali Miserez](#)¹, [Qing Yang](#)⁴, [Tian Liu](#)², [Huajian Gao](#)¹ and [Jing Yu](#)¹; ¹Nanyang Technological University, Singapore; ²Dalian University of Technology, China; ³A*STAR, Singapore; ⁴Chinese Academy of Agricultural Sciences, China

Biological systems ingeniously craft materials with complex structures for specialized functions, a feat often challenging to replicate in man-made materials. We report a serendipitous discovery where insect cuticle peptides (ICPs) spontaneously form nanocapsules through a single-step solvent exchange process. This phenomenon occurs as a concentration gradient, arising from the mixing of water and acetone, drives the localization and self-assembly of the peptides into hollow nanosized capsules. The intrinsic affinity of these peptides for specific solvent concentrations, coupled with the diffusion-driven gradient interface, triggers their localization and self-assembly. This gradient-mediated self-assembly process not only mimics biological systems in its simplicity and efficiency but also paves the way for next-generation drug delivery systems using ICP nanocapsules. Furthermore, it showcases the potential of protein/peptide-based materials in self-healable robotic skin, and stimuli-responsive sensors and detectors.

SYMPOSIUM SF01

High Entropy Oxides and Related Materials
April 23 - May 7, 2024

Symposium Organizers

Ben Breitung, Karlsruhe Institute of Technology
Alannah Hallas, The University of British Columbia
Scott McCormack, University of California, Davis
T. Zac Ward, Oak Ridge National Laboratory

* Invited Paper
+ JMR Distinguished Invited Speaker
^ MRS Communications Early Career Distinguished Presenter

SESSION SF01.01: Local Characterization of High Entropy Materials
Session Chairs: Christina Rost and T. Zac Ward
Tuesday Morning, April 23, 2024
Terrace Suite 1, Level 4, Summit

10:30 AM *SF01.01.01

Investigations of Local Structure in High Entropy Oxides [Christina Rost](#); Virginia Tech, United States

Many properties we observe in materials are a direct consequence of their composition and local structure. High entropy oxides are a unique class of systems that do not have a primary composition; rather they contain a near-equimolar distribution of several elements—where no single element serves as host. Such compositional disorder is accompanied by a unique distribution of localized structural distortions which may affect properties such as thermal conductivity, magnetic interaction, diffusion, and more. A key point of interest in these high entropy systems is the implied breadth of property tunability, which ranges in compositionally dependent functionalities from amorphous-like thermal conductivities to exotic magnetic states. In this talk, we review the beginnings of high entropy oxides then present ongoing work on the local characterization of several high entropy compositions exhibiting numerous crystal structures. X-ray absorption fine structure (XAFS), both near-edge and extended, is demonstrated to aid in understanding such chemical and structural disorder. The strengths and challenges of such characterization are discussed.

11:00 AM *SF01.01.02

Atomic Level Structural and Chemical Characterization of High-Entropy Oxides using Advanced (S)TEM Techniques Di Wang¹, Kai Wang^{1,2}, Abhishek Sarkar^{1,2}, Gleb Iankevich¹, Ziming Ding^{1,2}, Zhibo Zhao¹, Robert Kruk¹, Horst W. Hahn¹, Xiaoke Mu¹, Ben Breitung¹ and [Christian Kuebel](#)^{1,2}; ¹Karlsruhe Inst of Technology, Germany; ²TU Darmstadt, Germany

High entropy oxides (HEOs) exhibit unconventional properties, which have attracted intensive interest for a wide variety of applications such as electrochemical energy storage [1,2] and (electro) catalysis [3] as well as in fundamental studies on strongly correlated materials with competing magnetoelectric phases [4] giving rise to interesting properties such as colossal magnetoresistance (CMR) and metal-insulator transitions (MIT). The recent advances in (scanning) transmission electron microscopy (S)TEM have enabled a detailed structural analysis of HEOs providing atomic level chemical and oxidation state information together with local structural distortion and strain analysis as basis for a fundamental understanding of structure property correlations allowing to disentangle the complex high-entropy and 'cocktail' effects.

In this presentation, I will illustrate some of these advanced TEM capabilities for a detailed analysis of HEOs. I will discuss how this information enabled deciphering the synergistic effects of the cations in a $Mg_{0.2}Co_{0.2}Ni_{0.2}Cu_{0.2}Zn_{0.2}O$ electrode in lithium ion batteries [2] as well as the correlation between composition, oxidation state, structural distortions and magnetoelectric properties in strongly correlated high entropy manganates [4].

The TEM investigation of a $Mg_{0.2}Co_{0.2}Ni_{0.2}Cu_{0.2}Zn_{0.2}O$ electrode during various charging stages [3] revealed a nanoscale phase segregation during the initial discharging of the homogenous HEO into a metallic CoNiCu alloy phase, a Zn(Li) and a Mg oxide phase, which forms a highly defective, semi-coherent fcc composite structure. Although the material appears X-ray amorphous, 4D-STEM crystal orientation analysis shows that the composite structure extends throughout the originally single crystalline domains. Segregation of the metallic alloy at the grain boundaries gives rise to an interconnected conductive network throughout the composite particle. During recharging, Zn and partially Co are reoxidized (electrochemically active elements) forming a mixed fcc oxide with Mg (providing the structural stability) while the metallic NiCu(Co) phase (providing electrical conductivity) is maintained. This self-assembled nanostructure enables stable cycling of micron-sized particles and bypasses the need for nanoscale pre-modification required for conventional metal oxides. It demonstrates that the elemental diversity with a defined role of each element is key for optimizing these multi-cation electrode materials.

In a series of single-phase orthorhombic $(Gd_{0.25}La_{0.25}Nd_{0.25}Sm_{0.25})_{1-x}Sr_xMnO_3$ ($x=0-0.5$) HE-manganites, which combines the high entropy (HE) concept with property control by Sr^{2+} (hole) doping, we extend the HE approach to design strongly-correlated systems. [4] Using atomic resolution STEM imaging, an orthorhombic distortion has been identified for $x=0$, which is reduced with increasing Sr concentration to pseudo-cubic for $x=0.5$. Atomically resolved elemental maps reveal a homogenous distribution of the rare-earth cations and Sr on the A-site and Mn on the B-site sub-lattice. The oxidation state change of Mn has been evaluated by EELS using the O K and Mn L-edge features, unambiguously confirming that the Sr^{2+} doping results in increased Mn^{4+} . These electronic and structural changes correlate with a transition of the magnetoelectric properties from an insulating antiferromagnetic to a metallic ferromagnetic phase with good CMR values. This initial study signals the excellent potential to achieve complex magnetoelectric phase diagrams with unique temperature dependencies that stem from competing magneto-electronic interactions, which can be tuned by merging high entropy design with strongly correlated electron systems.

References

- [1] A. Sarkar *et al.*, *Nat. Commun.*, **2018**, 9, 3400.
- [2] K. Wang *et al.*, *Nat. Commun.*, **2023**, 14, 1487.
- [3] L. Lin *et al.*, *Small Structures*, **2023**, 2300012
- [4] A. Sarkar *et al.*, *Adv. Mater.*, **2023**, 35, 2207436.

11:30 AM *SF01.01.03

Short Range Ordering in Entropy Stabilized Oxides with the α -PbO₂ Structure [Solveig S. Aamlid](#)¹, Sam Mugiraneza^{1,1,2}, Mario Ulises Gonzalez Rivas^{1,1}, Joerg Rottler^{1,1} and Alannah Hallas^{1,1}; ¹The University of British Columbia, Canada; ²University of California, Santa Barbara, United States

The four-component medium entropy oxide (Ti, Zr, Hf, Sn)O₂ crystallizes in the α -PbO₂ structure. The formation of this structure type is interesting since it is distinct from the ground state structure of any of its precursor oxides. In itself, this is an indication that (Ti, Zr, Hf, Sn)O₂ might be an entropy stabilized compound. Conveniently, the two-component low entropy oxide (Ti, Zr)O₂ crystallizes in the same crystal structure, and is verified experimentally to be entropy stabilized.

Short range ordering (SRO) is an elusive phenomenon to characterize and quantize, but also potentially pivotal for the emergence of superior functional properties in high entropy materials. (Ti, Zr)O₂ possesses a well-characterized type of ordering where Ti and Zr cations order in alternating slabs. The degree of ordering can be controlled by the cooling rate and monitored through a simple measurement of the lattice parameters. In this work, we aim to

quantify and compare the degree of SRO in the two-component (Ti, Zr)O₂ and the four-component (Ti, Zr, Hf, Sn)O₂.

Pair distribution function measurements reveal large changes in the local structure of (Ti, Zr)O₂ depending on whether the sample has been quenched or slowly cooled, while (Ti, Zr, Hf, Sn)O₂ displays no discernible changes after heat treatments. In order to explain these observations and quantify the true configurational entropy of these materials, we use a computational approach based on density functional theory, cluster expansions, and Metropolis Monte Carlo simulated annealing. The calculations are able to reproduce the type of ordering and temperature range experimentally observed for (Ti, Zr)O₂. The same calculations are performed for (Ti, Zr, Hf, Sn)O₂, where the order-disorder phase transition temperature is lowered by hundreds of degrees relative to the two-component compound. Sluggish diffusion kinetics keep the cations frozen in place regardless of cooling rate, effectively hindering any degree of SRO or even a reversible phase transition, explaining the lack of changes in the pair distribution functions. The two-component compound on the other hand, shows signs of SRO even at synthesis temperature, indicating that the ideal configurational entropy state is never reached. As the energetics of cation-cation interactions are similar in these two materials, it is the increase in configurational entropy that causes the suppression of SRO. Finally, we introduce the possibility of heterovalent substitutions within this framework. In this case, short range order is expected to be strong due to the strong and long-ranged electrostatic forces involved.

SESSION SF01.02: Functional Properties of High Entropy Materials I—Batteries
Session Chairs: Ben Breitung and Torsten Brezesinski
Tuesday Afternoon, April 23, 2024
Terrace Suite 1, Level 4, Summit

1:30 PM *SF01.02.01

From High-Entropy Solid Electrolytes to Batteries [Torsten Brezesinski](#); Karlsruhe Institute of Technology, Germany

Solid-state batteries represent a promising next-generation energy storage technology, with the prospect of delivering higher energy densities and exhibiting better safety characteristics than conventional liquid-electrolyte-based batteries, but are currently limited by short cycle life, among others because of electro-chemo-mechanical degradation. Especially superionic lithium thiophosphate solid electrolytes are being considered for use in bulk-type solid-state batteries. Nonetheless, many of the solid electrolytes reported in the literature tend to lack in room-temperature ionic conductivity and stability; thus, the continuous search for materials with improved properties. High-entropy conductors may offer a potential solution by enabling tailorable properties through compositional design. However, the correlation between configurational entropy and ion mobility is largely unexplored. In this presentation, I will show recent findings on the effect that configurational entropy has on charge transport in chemically complex lithium thiophosphates for solid-state battery applications. In addition, I will demonstrate that performance improvements of high-entropy hexacyanoferrate cathodes are mainly due to suppression of phase transitions and gas evolution during cycling.

2:00 PM SF01.02.02

Entropy-Mediated Stable Structural Evolution of Prussian White Cathodes for Long-Life Na-Ion Batteries [Yueyue He](#)¹, [Sören L. Dreyer](#)¹, [Yin-Ying Ting](#)², [Yang Hu](#)³, [Thomas Diemant](#)³, [Maximilian Fichtner](#)³, [Horst W. Hahn](#)¹, [Jasmin Aghassi-Hagmann](#)¹, [Torsten Brezesinski](#)¹, [Yanjiao Ma](#)⁴ and [Ben Breitung](#)¹; ¹Karlsruhe Institute of Technology, Germany; ²RWTH Aachen University, Germany; ³Helmholtz Institute Ulm (HIU) for Electrochemical Energy Storage, Germany; ⁴Nanjing Normal University, China

The high-entropy approach is applied to monoclinic Prussian White (PW) cathode materials for sodium-ion batteries to address the issue of unfavorable multilevel phase transitions, leading to structural degradation and poor cycling stability. A series of Mn-based PWs was prepared, composed of up to six metal atoms sharing the N-coordinated positions (with Mn predominating), endowing the materials with unique structural properties. The high-entropy PW material of composition Na_{1.65}Mn_{0.4}Fe_{0.12}Ni_{0.12}Cu_{0.12}Co_{0.12}Cd_{0.12}[Fe(CN)₆]_{0.92}■_{0.08} was found to exhibit superior cyclability over medium-entropy, low-entropy and conventional single-metal PWs. In addition to the promising electrochemical performance, we report, to our knowledge for the first time, that the high-symmetry crystal structure (cubic form in this study) is favorable for high-entropy PWs during battery operation. Computational comparisons of the formation enthalpy of high-, medium- and low-entropy materials show that the compositionally less complex samples are prone to phase transitions that negatively affect the cyclability, especially in the deep de-/sodiated state. Based on data from complementary *operando* and *ex-situ* characterization techniques, an intrinsic mechanism for the stability improvement of the disordered PW structure during Na⁺ insertion/extraction is proposed, namely the dual effect of suppression of phase transitions and gas evolution.

2:15 PM *SF01.02.03

High-Entropy Disordered Rock-Salt Cathodes for Lithium-Ion Batteries [Bei Zhou](#)¹, [Elmar Kataev](#)², [Götz Schuck](#)², [Matteo Bianchini](#)^{1,3} and [Qingsong Wang](#)^{1,3}; ¹Bavarian Center for Battery Technology, Germany; ²Helmholtz-Zentrum Berlin für Materialien und Energie GmbH, Germany; ³University of Bayreuth, Germany

Traditional layered oxides consist of well-ordered alternating Li and transition metal (TM) with Li transport in two-dimensional (2D). In the disordered rock-salt (DRX) structure, Li and TM cations are randomly distributed at the 4a sites in the cationic sublattice.¹ The three-dimensional (3D) DRX cathodes are considerably more stable than the conventional layered oxides which often suffer from collapse of the interlayer spacing upon Li extraction at high voltages. The disordered arrangement of Li and TM opens the possibility of using a variety of TMs. The high-entropy DRX oxyfluorides, firstly reported by our group^{2,3}, of which the underlying reaction mechanism has been intensively investigated recently especially by synchrotron-based techniques, including *operando* soft/hard X-ray absorption spectroscopy (XAS) and *ex situ* resonant inelastic X-ray scattering (RIXS).

References:

Energy Environ. Sci. 13, 345–373 (2020)
Energy Environ. Sci. 12, 2433–2442 (2019)
Batter. Supercaps 3, 361–369 (2020)

2:45 PM SF01.02.04

Segregation Phenomena in Rock-Salt High Entropy Oxides for Lithium Battery Applications Studied by *In Situ* Annealing in a Scanning Transmission Electron Microscope [Albina Borisevich](#)¹, [Craig A. Bridges](#)¹ and [Sheng Dai](#)^{1,2}; ¹Oak Ridge National Laboratory, United States; ²The University of Tennessee, Knoxville, United States

Recently high-entropy oxides were proposed as promising materials for lithium battery anodes, with reports showing improvements in the storage capacity and cycling ability of the rock-salt type materials attributed to entropic stabilization due to random distribution of metal cations within the lattice (see e.g. [1]). However, multiple further studies suggested that these materials are not behaving as a homogenous mix of cations: *in situ* XAS investigation showed that lithiation-delithiation follows a multistep path, with some irreversible processes taking place [2], and recent localized spectroscopy results showed nanoscale segregation and differential movement of the constituent cations during charging and discharging [3]. It is therefore very important to evaluate the compositional stability of these materials at different elevated temperatures, given that charge/discharge processes can be highly exothermic.

In this study we are exploring the elemental distribution in the equimolar rock-salt high-entropy oxide of Li, Mg, Mn, Co, Ni, Cu and Zn using compositional mapping with Electron Energy Loss spectroscopy in a Scanning Transmission Electron Microscope using *in situ* Protochips Aduro platform to heat the powders to temperatures ranging from 500°C to 950°C. The initial powders are either the mixture of initial oxides or pre-annealed *ex situ*, ball-milled before the *in situ* heating experiment.

Our results suggest that, even with a highly homogenized precursors, the most uniform distribution of cations is only achieved at high annealing temperatures, such as 950°C, and thermal treatment much below that temperature results in swift segregation of primarily Cu into distinct agglomerates. It takes as little as 1.5 hours at 500°C for the powder pre-annealed at 950°C to show Cu segregation. We also find that the reducing vacuum atmosphere inside the microscope contributes to the driving force for the segregation; while the powders annealed at 950°C inside the microscope from the precursors are the most homogeneous, they still show some segregation compared to powders annealed *ex situ* at the same temperature which do not.

These results confirm earlier findings about differential behavior of cations in these materials as they undergo thermal treatment and chemical transformations and suggest that controlling heat distribution within these anodes during charging and discharging can be very important for cycling stability [4].

References

- [1] Sarkar, A., Velasco, L., Wang, D. *et al.* High entropy oxides for reversible energy storage. *Nat Commun* **9**, 3400 (2018). DOI:10.1038/s41467-018-05774-5
- [2] P. Ghigna, L. Airoldi, M. Fracchia *et al.* Lithiation Mechanism in High-Entropy Oxides as Anode Materials for Li-Ion Batteries: An Operando XAS Study, *ACS Applied Materials & Interfaces* **12**, 50344 (2020). DOI: 10.1021/acsami.0c13161
- [3] Wang, K., Hua, W., Huang, X. *et al.* Synergy of cations in high entropy oxide lithium ion battery anode. *Nat Commun* **14**, 1487 (2023). DOI:10.1038/s41467-023-37034-6
- [4] This work was supported by the DOE office of Science, Basic Energy Sciences, Materials Science and Engineering Division.

3:00 PM BREAK

SESSION SF01.03: Novel Magnetic and Electronic Properties of High Entropy Materials

Session Chairs: Alannah Hallas and Alessandro Mazza

Tuesday Afternoon, April 23, 2024

Terrace Suite 1, Level 4, Summit

3:30 PM *SF01.03.01

Accessing Novel Phase Space by The High Entropy Approach [Alessandro R. Mazza](#); Los Alamos National Laboratory, United States

Disorder and defects often dictate emergent phenomena in materials – such as electronic phase, magnetic ordering, and mechanical strength. Traditional thought pushes our understanding of phase order to rely on the idea of uniformity in materials, with disorder and defects resulting in lower ordering temperatures and prevention of long-range percolation. However, high entropy materials are challenging this understanding and disorder is emerging as a parameter which drives the local microstates into globally ordered behaviors. We demonstrate that this seemingly counterintuitive statement is not only true but that it simplifies the prediction of predominant functional phase in high entropy oxides. As a result, we design, grow, and characterize high entropy perovskite oxide films demonstrating the utility of this predictive materials approach.

We present these theoretical and experimental results on two classes of single crystal epitaxial films. Magnetism and charge disorder of the high entropy ABO₃ perovskite La(Cr_{0.2}Mn_{0.2}Fe_{0.2}Co_{0.2}Ni_{0.2})O₃ is a representative case, demonstrating how a seemingly chaotic landscape of spin and charge disorder can yield an ordered state. Second, to explore electronic phase, we demonstrate realization of extreme A-site cation disorder in (Y_{0.2}La_{0.2}Nd_{0.2}Sm_{0.2}Gd_{0.2})NiO₃, whose parent ternary oxides each have a large range of electronic (metal to insulator transition) and structural phase transition temperatures. These results suggest cation variance and disorder, such as that accessible only in high entropy oxides, can be a critical order parameter in the design of correlated oxides, and that this parameter can more broadly provide continuous tunability to emergent phenomena.

4:00 PM SF01.03.02

Engineering The Spin Transition and Carrier Type with High-Entropy Lattice Distortions in Rare Earth Cobaltates Alan Zhang¹, Timothy D. Brown¹, Sangheon Oh¹, Catalin Spataru¹, Eli Kinigstein², Jinghua Guo², Joshua D. Sugar¹, Arantzazu Mascaraque³, Enrique G. Michel⁴, Alison Shad¹, Jacklyn Zhu¹, Matthew Witman¹, Suhas Kumar¹, Alec Talin¹ and [Elliot J. Fuller](#)¹; ¹Sandia National Laboratories, United States; ²Lawrence Berkeley National Laboratory, United States; ³Universidad Complutense de Madrid, Spain; ⁴Universidad Autónoma de Madrid, Spain

There is growing interest in material candidates that provide knobs to tune their properties beyond traditional limits. Compositionally complex oxides, often called high entropy oxides, are excellent candidates, wherein a lattice site shares more than four cations, forming single-phase solid solutions with unique properties. Here, we demonstrate compositional complexity as a tunable parameter in a spin-transition oxide semiconductor La_(1-x)(Nd,Sm,Gd,Y)_xCoO₃, by varying the population *x* of rare earth cations. As the compositional complexity increases with *x*, localized and uniform lattice distortions occur that have profound effects on the material's semiconductor-to-metal spin transition and carrier type. Experimental measurements, together with first-principles calculations, demonstrate that atomic-range distortions from the varying rare earth radii induce a crossover from hole-majority to electron-majority conduction at *x* = 0.8 without the introduction of electron donors. Thus, we show that control of localized lattice distortions through compositional complexity is a facile knob to tune oxide semiconductors and spin transitions beyond traditional means.

4:15 PM *SF01.03.03

Magnetic-Electric Properties of High-Entropy Oxides [Horst W. Hahn](#)^{1,2}, Zhibo Zhao², Robert Kruk² and Abhishek Sarkar^{3,2}; ¹The University of Oklahoma, United States; ²Karlsruhe Institute of Technology, Germany; ³IIT Kharagpur, India

The quest for artificial, heterostructured magneto-electrics is driving the search for new magnetic materials that can exhibit enhanced sensitivity to external

stimulation. In principle, the system of choice for this purpose can be the new class of materials known as High Entropy Oxides (HEOs). HEOs are single phase solid solutions consisting of five or more elements in equiatomic or near-equiatomic proportions incorporated into the cationic sub-lattice(s). What sets HEOs apart is their remarkable chemical complexity, encapsulated within a single crystallographic structure, often resulting in unique functionalities. From a local structure standpoint, HEOs exhibit an exceptionally large number of distinct metal-oxygen-metal pairings. Consequently, the magnetic correlations in HEOs, influenced by the coordination geometry, valence, spin state, and type of hybridized metal cations, are naturally influenced by an extensive variety of neighboring ionic configurations. These conditions give rise to a complex magneto-electronic free-energy landscape within HEOs, potentially leading to the stabilization of unconventional spin-electronic states. This form of inherently imbalanced magnetism has the potential to be influenced by external stimuli, such as voltage, presenting opportunities for the development of artificial magneto-electrics. Examples of these systems, including perovskites and spinels, will be discussed in the context of their magneto-electronic properties, which are a consequence of the extreme local chemical disorder.

4:45 PM SF01.03.04

Correlated Electron Metals with High Entropy: Thin Film Growth and Properties Saeed S. Almishal¹, Pat Kezer², Jacob Sivak¹, Sai V. Ayyagari¹, Francisco Marques dos Santos Vieira¹, Christina Rost³, Vincent Crespi¹, Venkatraman Gopalan¹, Nasim Alem¹, Ismaila Dabo¹, Susan B. Sinnott^{1,3}, John T. Heron² and Jon-Paul Maria¹; ¹The Pennsylvania State University, United States; ²University of Michigan, United States; ³Virginia Tech, United States

Novel conducting complex oxides with high electron correlation are of keen interest for UV-transparent applications, and as hosts for fundamental studies of correlated electron systems and spin-hall effect. Sr based cubic perovskite oxides are appealing to explore due to their heavy cation solubility and tunable electrical conductivity and transparency. Utilizing a high configurational entropy formulation, the high symmetry perovskite phase can be stabilized with five cations on the perovskite B-site. Our results show that Sr_x(Ti,Nb,Cr,Mo,W)O₃ thin films grown by pulsed laser deposition are stabilized as single-phase perovskite. Derivative systems with four B-cations instead of five, exhibit chemical and/or phase segregation. Contributions from individual B-cations and their interactions result in unique overall transport properties. For instance, Cr markedly influences electrical transport. A-site vacancies and doping, too, influence electronic and optical properties, and structure stability. The experimental findings are supported by first principles calculations that highlight the cation coexistence effect on octahedral tilting, tolerance factor, band structure and orbital filling.

SESSION SF01.04: Poster Session: High Entropy Materials

Session Chairs: Ben Breitung, Alannah Hallas, Scott McCormack and T. Zac Ward

Tuesday Afternoon, April 23, 2024

Flex Hall C, Level 2, Summit

5:00 PM SF01.04.01

Potentiodynamic Polarization and Electrochemical Impedance Behavior in Co-Rich Co₄₀Cr₂₀Ni₁₅Fe₁₅Mo₁₀ High Entropy Alloy Moonkyu Lee¹, Zakiyuddin Ahmad² and Kwangmin Lee¹; ¹Chonnam National University, Korea (the Republic of); ²University of Indonesia, Indonesia

This study aims to investigate the corrosion characteristics of a high entropy alloy (HEA) composed of Co₄₀Cr₂₀Ni₁₅Fe₁₅Mo₁₀, which is designed as a metallic biomaterial. The Co-HEA was synthesized using vacuum arc remelting (VAR). To gain insights into the detailed mechanisms of corrosion reactions, we performed potentiodynamic polarization (PDP) and electrochemical impedance spectroscopy (EIS) experiments in Ringer's solution. The PDP analysis revealed an I_{corr} value of 1.358×10⁻⁸ A/cm² for Co₄₀Cr₂₀Ni₁₅Fe₁₅Mo₁₀, which was lower than that of 316L stainless steel and L605 Co-alloy. To further understand the corrosion behavior, we employed an electrical equivalent circuit (EEC) to extract fitting parameters from Nyquist plots at various time points after the EIS test. The Nyquist plot exhibited a gradual increase in the size of the semicircular radius with increasing immersion time, indicating the growth of the passive film. Notably, the Co-HEA consistently displayed higher R_{ct} values at all time points compared to 316L and L605, representing its superior corrosion resistance attributed to their excellent passivation ability. The passive films formed on Co₄₀Cr₂₀Ni₁₅Fe₁₅Mo₁₀ were primarily composed of oxides and hydroxides of Co, Cr, and Fe, with the highest Cr₂O₃/Cr(OH)₃ ratio observed. These findings suggest that the Co₄₀Cr₂₀Ni₁₅Fe₁₅Mo₁₀ HEA, with its robust and stable passive film, demonstrates better corrosion and electrochemical properties when compared to 316L stainless steel and L605 Co-alloy, suggesting that it is a promising candidate for future biomaterial applications.

5:00 PM SF01.04.02

The Investigation of Electrochemical Properties Using High-Entropy Spinel-Oxide as an Anode for Lithium-Ion Batteries Chia-Chien Ma, I-Han Lee and Tri-Rung Yew; National Tsing Hua University, Taiwan

The global demand for lithium-ion batteries (LIBs) is increasing, primarily because they can be used for various applications. To improve the energy density of LIBs, transition metal oxides are potential candidates for anodes owing to their high capacity and earth abundance. However, the issues such as low ionic conductivity, low Coulombic efficiency, and structural degradation during charge/discharge cycles limit the development of transition metal oxides in LIBs applications.

High-entropy oxides exhibit new chemistries and outstanding cycling stability for developing electrode materials. Nevertheless, they often contain expensive raw materials, and their effects on the application of LIBs are still unclear. In this work, a novel spinel-structure AMFCZ-based high-entropy oxide with five cost-effective and non-toxic oxides consisting of aluminum, manganese, iron, copper, and zinc ions is synthesized using a solid-state method with an ideal capacity of ~1000 mAh/g. Its cycling performance, electrochemical properties, and reaction mechanisms are investigated, showing good rate capability.

The slurries containing the AMFCZ-based active materials, carbon black (Super P), carboxymethyl cellulose (CMC), and styrene-butadiene rubber (SBR) are coated on a copper foil by using a doctor-blade process to form an electrode. After that, the electrode is dried in a vacuum oven, followed by assembling half-batteries in a glove box. The crystal structure of AMFCZ-based anode is characterized by X-ray diffraction (XRD) analysis. Scanning electron microscopy (SEM) and energy-dispersive X-ray spectrometry (EDX) are used to analyze the morphology and composition distribution of AMFCZ-based anodes. Galvanostatic charge/discharge (GCD), electrochemical impedance spectroscopy (EIS), and X-ray photoelectron spectroscopy (XPS) are used to analyze the cycling performance and electrochemical properties. This work reveals a novel high-entropy oxide as an anode and demonstrates its electrochemical properties as an anode for LIBs.

5:00 PM SF01.04.03

Inhibition Effect of Segregation and Chemical Order on Grain Boundary Migration in NbMoTaW Multi-Principal Element Alloy Xiao-Tong Li,

Xiaozhi Tang and Ya-Fang Guo; Beijing Jiaotong University, China

Wide-range applications of high entropy materials (HEA) requires their superior mechanical properties, which essentially relies on grain boundary (GB) stability for sustaining plastic deformation. While the fundamental mechanisms of GB migration in HEA differ from the ones in conventional materials due to lattice distortion and local chemical environments. Particularly the GB segregation in HEA always accompanies local chemical order (LCO) variations. To quantitatively and efficiently investigate the impacts of solute segregation and chemical order on GB migration, we applied atomistic simulations for the NbMoTaW multi-principal element alloy. Assisted by a contrived Nb-rich model, it is found that solute segregation and chemical order synergistically inhibit GB migration. Nb segregation increases the critical stress for GB migration, and the presence of chemical order further enhances the resistance of GB to plastic deformation. The destruction of local ordering structures is responsible for the difficult GB migration. Transition pathway analyses show that GB modified with both Nb segregation and chemical order requires high migration barrier, and the prior migration of GB sites tends to avoid regions with heavier chemical order. These results provide new insight into how chemical complexity affects elementary GB motion and contribute to manipulating the stability of MPEAs.

5:00 PM SF01.04.04

Theory-Guided Searching for Ductile Single-Phase Refractory Multi-Principle-Element Alloys [Hailong Huang](#), Rameshwari Naorem, Prashant Singh and Nicolas Argibay; Ames Laboratory, United States

The pursuit of materials exhibiting good high-temperature mechanical behavior has never faded. Multi-principal-element alloys (MPEAs, also called compositionally complex alloys) with nearly infinite design space which deviate from conventional design philosophy offer great potential. Refractory MPEAs (RMPEAs) are promising for aerospace and related industries usage due to their excellent mechanical performance and superior resistance to softening at elevated temperatures. Nevertheless, a great majority of such RMPEAs developed up to date suffer from poor room-temperature ductility, which makes them difficult to be processed and thus limits their practical applications. Here we proposed a density-functional theory (DFT) guided searching for single-phase RMPEAs with tensile ductility and high strength.

5:00 PM SF01.04.05

Tough NiTi-Based High-Entropy Intermetallic Compounds: Uniform Plastic Deformation and Small-Scale Defects [Ya-Jing Lee](#), Chun-Cheng Chen, Cheng-Yuan Tsai and Shou-Yi Chang; National Tsing Hua University, Taiwan

Owing to the advantages of superior elevated-temperature strength and good thermal stability compared to traditional engineering alloys, intermetallic compounds with an ordered structure are of great potential for applications in extreme high-temperature environments. However, the detrimental brittleness due to strong bonding-caused low plasticity is concerned. In this study, based on the synergy of the chemical ordering of intermetallic compounds and the active defects in high-entropy alloys, NiTi-based, ordered B2 medium- and high-entropy intermetallic compounds were thus developed. Substitutional elements to Ni or Ti lattice sites were selected in consideration of thermodynamic parameters and electronegativity. Their microstructures were characterized, macro-to-microscale mechanical behaviors were investigated, and defect activities were experimentally examined and molecular-dynamics simulated. Experimental results indicated that the medium- and high-entropy intermetallic compounds presented a much higher strength, plasticity and resistance to high-temperature softening as compared to the traditional binary NiTi low-entropy one (in the condition without martensitic transformation). The quaternary intermetallic compound with Zr showed a high yield strength of 2000 MPa at room temperature and 400 MPa at 800°C (only 60 MPa for NiTi), while the one with Hf showed a compressive strain of 18% before fracture at room temperature (5% for NiTi). The quinary intermetallic compound with both Hf and Zr showed a retained yield strength of 1600 MPa, improved plastic strain of 20% and enhanced softening resistance of 600 MPa at 800°C. With further addition of Fe, the senary intermetallic compound became harder and more brittle due to the precipitation strengthening of Fe₂Zr but much more softening-resistant with 900 MPa at 800°C. The micropillar compressive tests of the binary, quaternary (the harder one with Zr) and senary (prepared from the single-phase, solid-solution region without Fe₂Zr) samples revealed that the low- and medium-entropy micropillars catastrophically fractured in a rapid slip way, whereas the high-entropy ones plastically barrel-like deformed with high work hardenability. Additionally, both microscopic observations and molecular dynamics simulations suggested that, instead of the long-distance planar gliding of long dislocations, short-range randomly-oriented activities of abundant tangled small-scale dislocations dominated the uniform plastic deformation of the high-entropy intermetallic compound.

5:00 PM SF01.04.06

Investigating The Phase Stability and Thermal Properties of Compositionally Complex Titanate Pyrochlores [Joshua Safin](#), Xin Wang and Katharine Page; University of Tennessee at Knoxville, United States

In multicomponent ceramics there are varying factors that determine the phase selection and stability such as the configurational entropy of the system or the ionic radii of the constituent cations. The influence of each of the aforementioned factors can vary based on the complexity of the crystal structure of the material. Stability rules based on ionic radius ratios are well established for rare earth pyrochlores (RE₂³⁺B₂⁴⁺O₇). From these rules, members of the titanate pyrochlore family have been synthesized from the Lanthanide series (La to Lu, large to small) that take advantage of the wide range of ionic radii and stable +3 oxidation state across the majority of the series to create a series of samples with different combinations and distributions of cations as well as including cations that are not normally stable as pyrochlores in single component systems based on known stability rules. The trends in the crystal structure were studied through the use of X-Ray diffraction and Rietveld refinement. Thermal properties were investigated using the Transient Plane Source method and dilatometry. Altogether, the impact of the higher entropy configurations and the distribution of constituent cations on pyrochlore radius ratio rules, thermal properties, and other potential crystal-chemical effects will provide deeper understanding of possible design considerations for intrinsic property tuning in these and other multicomponent complex ceramics. In particular, tunable rare earth titanate pyrochlores would have a wide range of applications in various fields such as in magnetic materials because of the spin ice properties, in thermal barrier coatings due to low thermal conductivity and good coefficients of thermal expansion, and in ionic conductors.

5:00 PM SF01.04.07

A Phonon-Unfolding Based Method for Quantitative Assessment of Thermal Conductivity of High Entropy Ceramics [Yuxuan Wang](#), Guoqiang Lan and Jun Song; McGill University, Canada

Thermal barrier coating materials have been extensively used in fields of aerospace and power industry. It can protect the underlying substrate against hot gas streams while effectively isolating the heat flow. High entropy ceramics, with their unique disorder lattice structures, exhibit ultra-low thermal conductivity and good high temperature stability, which make them promising candidate materials for next generation thermal barrier coatings (TBCs). Unlike the conventional ceramic materials where the intrinsic thermal resistance largely comes from phonon-phonon interactions, the thermal resistance in high entropy ceramics predominantly arises from phonon-disorder scattering. In this study, we propose a new method based on the supercell phonon unfolding (SPU) technique to predictively assess the thermal conductivity of high entropy ceramics, focusing on the high entropy rocksalt oxide group as the representation. We demonstrated that our method could obtain an indicator in direct correspondence to the thermal conductivity, thus allowing quantitative comparison of the thermal conductivities of different high entropy ceramics. A good agreement has been found between our model predictions

and the experimental measurements, confirming the validity of our method. The method provides a valuable predictive tool for screening and design of high entropy ceramics for TBCs.

5:00 PM SF01.04.08

Development of High Entropy Perovskite Oxide Electrocatalysts for the Oxygen Evolution Reaction: A Combined Experimental, Density Functional Theory (DFT) and Machine Learning Approach to Predicting Oxygen Vacancy Formation Energies [Pan Sun J. Tukur¹](#), Jianjun Wei¹, Yirong Mo¹, Hanning Chen², Wei Yong³ and Yinning Zhang⁴; ¹UNC Greensboro, United States; ²The University of Texas at Austin, United States; ³High Point University, United States; ⁴University of West Georgia, United States

This research explores the design and development of high entropy perovskite oxide electrocatalysts for the oxygen evolution reaction (OER) through a comprehensive approach that integrates experimental investigations, density functional theory (DFT) calculations, and machine learning techniques. By harnessing the potential of high entropy materials, we aim to enhance the catalytic activity of perovskite oxides for the critical OER process. We investigate the formation energies of oxygen vacancies and molecular adsorption energies on these catalyst surfaces using state-of-the-art DFT simulations. Additionally, machine learning models are employed to predict these critical properties, providing insights into catalyst performance across a wide compositional space. The synergistic combination of these methods promises to accelerate the discovery of advanced OER electrocatalysts with improved efficiency and sustainability, contributing to the advancement of renewable energy technologies.

5:00 PM SF01.04.09

Predicting The Synthesizability of High-Entropy Rare Earth Disilicates by First-Principles Calculations with Machine-Learning [Debanjan Sarker](#) and Cormac Toher; The University of Texas at Dallas, United States

Silicon carbide based ceramics are promising alternatives to the conventional nickel-based superalloys to be used in hot temperature sections of the turbines for their low density, and outstanding resistance to creep and oxidation at high temperature. However active reaction with water vapor in high-velocity combustion environments degrade the stability of Si-based ceramics thereby reducing its strength. To increase the durability, environmental barrier coatings (EBC) can be used as a protective layer for silicon-based CMCs by limiting the chemical reactions between environment and the CMC. The current state-of-the-art EBC candidate materials are rare earth silicates, due to their good corrosion resistance and a coefficient of thermal expansion similar to that of SiC. However, rare earth disilicates display several different polymorphs, and undergo phase transitions with changing temperature. To increase the thermodynamic stability of these compounds, tune their CTE and elastic modulus and reduce the lattice thermal conductivity, high-entropy rare earth disilicates are being developed. To predict which compositions are most likely to form a high entropy single-phase, we are combining first-principles calculations using the AFLOW framework with experimental data and machine-learning to develop models and find descriptors to predict phase formation in these materials.

5:00 PM SF01.04.10

Ultra-Fast Synthesis of High Entropy Boride Layers and Their Characterization [Merve Uysal Komurlu](#) and Ali Erdemir; Texas A&M University, United States

In this study, we used an ultra-fast boriding process to quickly and uniformly produce thick boride layers on high entropy refractory alloys consisting of W, Re, Nb, Zr, Ta, and V. Boriding is performed at 1000°C and for 1 hour. Chemical, structural, and mechanical characterization of the boride layers was carried out using relevant test methods and confirmed that W and Re-containing alloys were among the very best in terms of boride layer thickness of 40 µm and hardness. While, Nb, Ta, and V containing alloys attained thickness values of around 3 µm. Nano hardness profiles across the boride layers revealed that W and Re-containing alloys possessed exceptional hardness, i.e., around 40 GPa. In the cases of other alloys, hardness values of boride layers fell between 18.5 GPa and 8 GPa. Such significant variations in thickness and hardness highlight the need for a more systematic and predictive modeling approach that can provide critical information on the selection of constituent refractory metals in high entropy alloy systems as well as desirable boride phases with superior mechanical, thermal, and oxidative properties.

5:00 PM SF01.04.11

Microwave Plasma Synthesis of MoNbTaVW High Entropy Alloy: A Novel Approach [Bria C. Storr](#) and Shane A. Catledge; University of Alabama at Birmingham, United States

We investigate a novel approach for synthesis of the high entropy alloy MoNbTaVW from metal oxide precursors via microwave-induced plasma. The process involves ball milling of the metal-oxides, followed by microwave plasma annealing at 1800°C for a duration of 1 hour. Hydrogen is used as the plasma feedgas for efficient reduction of metal-oxides. Analysis through X-ray diffraction, scanning electron microscopy/energy dispersive x-ray analysis, and Vickers hardness testing has revealed the characteristic structure/properties of high-entropy alloy. This includes a single-phase body-centered cubic structure with a uniform distribution of all five metals, and measured hardness of 6.8 ± 0.9 GPa. This hardness aligns closely with findings reported in literature for high entropy alloys sharing the same five-metal configuration. In addition to rapid volumetric heating enabled by interaction of microwaves with the dielectric precursors, the microstructure exhibits clear evidence of localized microwave sintering. The outcomes highlight the promising potential of microwave plasma as a rapid, cost-effective, and versatile processing tool for the production of high entropy alloys.

SESSION SF01.05: Functional Properties of High Entropy Materials II

Session Chairs: Ben Breitung and Katharine Page

Wednesday Morning, April 24, 2024

Terrace Suite 1, Level 4, Summit

8:30 AM *SF01.05.01

The Crystal Chemistry in Two Families of Compositionally Complex Oxide Electrocatalysts [Katharine Page^{1,2}](#); ¹The University of Tennessee, Knoxville, United States; ²Oak Ridge National Laboratory, United States

Integration of renewable feedstocks into the current energy infrastructure drives the development of electrocatalysts that can maintain high surface areas and selective electrocatalytic activities under a variety of challenging chemical and environmental conditions. Recently, several compositionally complex oxides (CCOs) have been reported with intriguing and tunable electrocatalytic properties. We present recent studies on compositionally complex Rare Earth cerate oxygen evolution reaction (OER) electrocatalysts and bifunctional OER and oxygen reduction reaction (ORR) spinel ferrite electrocatalysts. A

combination of local to long-range electron, x-ray and neutron scattering probes are employed to investigate their complex configurational diversity and associated structure-property trends. Relationships are explored between the cation site preferences, chemical-short-range order, and promising electrocatalytic properties achieved in the families through compositional tuning and variation in synthesis/processing conditions. Experimentally derived models are supported by Density Functional Theory calculations employing Special Quasirandom Structure models. This work highlights the importance of studying structure-property characteristics under reaction conditions and hints at the exquisite level of detail that may be required in computational and experimental approaches to guide structure-property tuning in emerging CCO OER and ORR electrocatalysts. Current challenges and future opportunities in this arena will be discussed.

9:00 AM SF01.05.02

Synthesis and Fundamental Studies of $Ce_{1-x}(YLaPrSm)_xO_{2-\delta}$ as Ionic Conductors Billy E. Yang¹, Saeed S. Almishal¹, Mary Kate Caucci¹, Sai V. Ayyagari¹, Nasim Alem¹, Christina Rost², Susan B. Sinnott^{1,1} and Jon-Paul Maria¹; ¹The Pennsylvania State University, United States; ²Virginia Tech, United States

High entropy oxide $Y_{1/5}La_{1/5}Ce_{1/5}Pr_{1/5}Sm_{1/5}O_{2-\delta}$ (F1) with both +3 and +4 preferred cations is considered a promising candidate for oxygen ion conduction since the anion sublattice will contain up to 25% unoccupied sites in a fluorite structure. However, depending on the thermal and kinetic history during its synthesis, F1 may exhibit local chemical ordering and form an unwanted bixbyite-like structure. Therefore, it is crucial to investigate the conditions that lead to the phase transformation and the stabilization of the desired fluorite symmetry in high entropy sesquioxides. In this work, we synthesized a series of bulk F1-derived systems with varying the Ce concentration ($Ce_{1-x}(YLaPrSm)_xO_{2-\delta}$) to investigate the structural dependence on composition. The XRD patterns indicate when the cation mixture is equimolar; the system favors bixbyite structure up to 1500 °C. As the Ce concentration increases beyond 20%, the material transitions into a single-phase fluorite structure without evidence of a bixbyite-like phase. The SEM images reveal that all synthesized $Ce_{1-x}(YLaPrSm)_xO_{2-\delta}$ bulk samples have consistent grain size with no significant chemical segregation, as evident from EDS. Moreover, the bandgap and oxidation states of $Ce_{1-x}(YLaPrSm)_xO_{2-\delta}$ were investigated by UV-Vis and XPS and supported by first-principles calculations.

9:15 AM *SF01.05.03

Electrocaloric Performance of High-Entropy Oxides from First Principles [Ismaila Dabo](#) and Tara Karimzadeh Sabet; The Pennsylvania State University, United States

The electrocaloric effect holds significant promise for advancing sustainable solid-state refrigeration technologies. High-entropy oxides [1] are potentially advantageous due to the thermal stability of their polar phases. In this work, we evaluate the phase stability and electrocaloric performance of the high-entropy perovskite (Na,Bi,Sr,Ba,Ca)TiO₃. A pivotal parameter in evaluating electrocaloric performance is the dependence of adiabatic electrocaloric temperature change as a function of temperature, which is intricately linked to the change of polarization with respect to temperature under a constant electric field [3]. To predict this parameter, we developed models for the temperature-dependent polarization $P(T)$ of high-entropy oxides taking into account chemical disorder and local distortions.

[1] Rost *et al.*, *Nature Communications* **6**, 8485 (2015)

[2] Kotsonis *et al.*, *Journal of the American Ceramic Society* **106**, 5587 (2023)

[3] Nair *et al.*, *Nature* **575**, 468–472 (2019)

Funding: The Center for Nanoscale Science at the Pennsylvania State University is a Materials Research Science and Engineering Center (MRSEC) supported by the National Science Foundation (DMR-2011839)

9:45 AM SF01.05.04

Ion Beam Modification of High-Entropy Oxides William J. Weber¹, Candice Kinsler-Fedon¹, Lauren Nuckols¹, Brianna L. Musico², Anamul H. Mir³, Ritesh Sachan⁴, David Mandrus¹, Yanwen Zhang^{5,1} and Veerle Keppens¹; ¹University of Tennessee, United States; ²Los Alamos National Laboratory, United States; ³University of Huddersfield, United Kingdom; ⁴Oklahoma State University, United States; ⁵Idaho National Laboratory, United States

High-entropy oxides (HEOs) have recently gained recognition for their low thermal conductivity and tunable mechanical capabilities, but little is known about their response to high energy heavy ion beams. In this work, the heavy-ion irradiation response of HEOs with the pyrochlore and perovskite structures has been investigated. The damage accumulation behavior at 300 K due to 4 MeV Au ion irradiation of a <100>-oriented HEO titanate pyrochlore single crystal has been investigated by Rutherford backscattering spectrometry in channeling geometry and transmission electron microscopy (TEM). In addition, in situ TEM irradiation using 600 keV Xe ions has been employed to reveal the dose and temperature dependence of amorphization in a HEO pyrochlore with the same composition. In another single-crystal HEO titanate pyrochlore composition, amorphization due to 23 MeV Ni ions has been characterized by Raman spectroscopy, which indicates a much higher dose for amorphization, suggesting significant athermal recovery during irradiation due to the high electronic energy loss of the Ni ions. Ion tracks formed in a HEO perovskite structure irradiated with 774 MeV Xe ions have been characterized by TEM, and the stability of these ion tracks under electron beam irradiation has been evaluated. The results obtained on these HEO structures are compared to those of their single-component counterparts.

10:00 AM BREAK

SESSION SF01.06: Formation and Stability of High Entropy Oxides

Session Chair: Alannah Hallas

Wednesday Morning, April 24, 2024

Terrace Suite 1, Level 4, Summit

11:00 AM SF01.06.02

Reaction Pathway in The Formation of Rocksalt Entropy-Stabilized Oxides [Avery-Ryan E. Ansbro](#)¹, Akira Miura², Wenhao Sun¹ and John T. Heron¹; ¹University of Michigan, United States; ²Hokkaido University, Japan

High entropy oxides (HEO) are characterized through the effects of configurational disorder. The wide combinatorial space offered by complex materials, however, challenges our ability to predict reaction dynamics leading to entropy stabilization. We investigate (MgCoNiCuZn)O and establish the importance of kinetics in single phase formation. Rapid movement and diffusion between 800 °C and 870 °C indicate a eutectic copper oxide transition

phase mediates the formation of the entropy-stabilized complex by solvating and localizing metal cations. Larger, constituent particles remain inactive until 1020 °C, where it then dissolves the liquid phase to form an entropy stabilized oxide. Modifying the composition and phase of the binary mixture, we find that the liquid copper phase is essential to the development of a single phase. We propose the possibility that engineered, selective melting may be utilized to realize and design other ESO and oxide phases.

11:15 AM SF01.06.03

High Temperature Decomposition of Entropy-Stabilized Oxide (MgCoNiCuZn)O Matthew J. Webb¹, Mike Gerhart², Avery-Ryan E. Ansbro¹, Peter Meisenheimer³, Tony Chiang¹, Christina Rost^{4,2} and John T. Heron¹; ¹University of Michigan, United States; ²James Madison University, United States; ³University of California, Berkeley, United States; ⁴Virginia Tech, United States

Entropy-stabilized oxides represent a unique class of single-phase, multicomponent oxides that achieve stability through a substantial configurational entropy, ΔS_{conf} , which counters a positive, unfavorable enthalpy. Although it is generally postulated that entropy-stabilized oxides will exhibit robust thermal stability due to the presence of the $-T\Delta S_{\text{conf}}$ term in Gibbs' free energy, their behavior at high temperatures remains largely unexplored. In this presentation, I will discuss the stability of the prototypical entropy-stabilized oxide, rocksalt (MgCoNiCuZn)O, in the 1300-1700 °C range in air. As temperatures exceed 1300 °C, a gradual reduction in the Cu and Zn content within the rocksalt phase is observed. We pose that the correlated partial loss of these elements is mediated by local distortions and defects that facilitate greater diffusion rates for these ions at elevated temperatures.

11:30 AM SF01.06.04

High-Entropy Layered Double Hydroxides as Precursors for High-Entropy Oxides Sujeong Lee¹, Juhwan Noh² and Ho Jin Ryu¹; ¹Korea Advanced Institute of Science and Technology, Korea (the Republic of); ²Korea Research Institute of Chemical Technology, Korea (the Republic of)

Layered double hydroxides (LDHs) consist of positively charged metal cation layers with anion interlayers and water molecules, as following by formula, $M_{1-x}^{2+}M_x^{3+}(\text{OH})_2[\text{A}^n]_{x/n}\cdot z\text{H}_2\text{O}$. This material has advantages such as tunable metal composition layers, exchangeable interlayer anions, and memory effect, actively applying to the research fields of catalysts, batteries, drug delivery, and adsorption.

Through the flexible design of tunable metal layers, LDHs can be expanded to a high entropy system. The reported high entropy system exhibits a lower adsorption activation in energy in comparison to conventional systems. This resulted from the various adsorption activation energy spectrums and the availability of multiple binding sites because of the mixing of multiple elements. Furthermore, high entropy LDHs can be easily transformed into high entropy layered double oxides (LDOs) through calcination. Nevertheless, there is a scarcity of research on high-entropy LDHs and high-entropy LDOs. To address this gap, 120 binary, and ternary LDHs were synthesized through co-precipitation, serving as a database for expanding to the quaternary and quinary systems with a machine-learning-based approach. Out of the 120 LDHs, 47 cases were successfully formed as LDH crystal structures, while 10 cases showed mixed phases with less than half consisting of the secondary phases, and the remainder failed to crystallize as LDHs. The thermal stability of synthesized 57 cases was conducted and the evaporation temperature of the parent interlayer anions varied depending on the combination of metal elements. Lastly, the order of iodate adsorption capacity within the ternary system was as follows: Mg-based, Mn-based, Co-based, Cu-based, and Ni-based. Furthermore, 70% of the ternary system showed an improvement in adsorption capacity compared to simple binary cases, underscoring the importance of expanding the high entropy LDH system. Moreover, the exploration of high entropy LDHs might be the role of precursors for expansion into the high entropy oxide research area.

11:45 AM SF01.06.05

Growth of High-Entropy Oxide Single Crystals by means of Floating Zone Technique Dongjoon Song and Alannah Hallas; The University of British Columbia, Canada

The high-entropy materials (HEMs) have been dealt with as a new play ground of the material engineering, since the functionality of the materials is expected to enhance by controlling the new degrees of freedom. Also, the field flips traditional condensed matter physics paradigms on their head by seeking to understand what properties arise in the presence of profound configurational disorder. However, the fundamental physics governing these materials, including the true degree of configurational entropy, its role in stabilizing the structure, and its effect on other physical properties such as magnetism and electrical transport all remain open questions. A key roadblock towards achieving a deeper understanding of HEMs has been the inability to study these materials in single crystal form. Although the imperative to study HEMs in single crystal form are clear, many crystal growth methods are excluded because the synthesis of HEMs requires high levels of both thermodynamic and kinetic control. We suggest that floating zone growth is the optimal method to unlock this new frontier. In this talk, we will report several high-entropy oxide single crystals grown by the floating zone technique and discuss the advantages of this method in achieving high quality crystals of HEMs.

SESSION SF01.07: Machine Learning and Data Driven Approaches

Session Chairs: Scott McCormack and Simon Schweidler

Wednesday Afternoon, April 24, 2024

Terrace Suite 1, Level 4, Summit

1:45 PM *SF01.07.01

Accelerating Material Discovery of New High-Entropy Materials through High-Throughput Synthesis, Characterization and Machine Learning Methods Simon Schweidler¹, Anurag D. Khandelwal¹, Jan Schütze¹, Leonardo V. Valesco², Pascal Friederich¹, Markus Reischl¹, Ben Breitung¹, Horst W. Hahn¹ and Jasmin Aghassi-Hagmann¹; ¹Karlsruhe Institute of Technology, Germany; ²Universidad Nacional de Colombia Sede La Paz, Colombia

New materials are synthesized and optimized with the explicit intention of enhancing current state-of-the-art materials in various fields of application, addressing the continually growing societal demands. In this context, high-entropy materials (HEMs) offer a huge research area for the development of novel material compositions and potential applications, e.g. as electrodes in batteries or fuel cell or in the field of electrochemical catalysis.[1] Unlike "classical" materials, HEMs intentionally maximize configurational entropy by increasing the number of elements to reduce free formation energy and stabilize a single-phase crystal structure. In addition, the "cocktail effects" describing the interactions between different elements often lead to partially unexpected properties, which may affect potential application areas. Therefore, the advantage of using HEMs lies in the possibility of influencing their elemental composition and electronic structure through the choice of design parameters. This flexibility offers the possibility to create materials with unique surface properties by changing the size of the e.g. catalytic centers and/or the electronic structure, as well as by selectively creating defects (e.g. oxygen vacancies). However, exploring the vast compositional space of high-entropy materials in a conventional approach, i.e., one experiment at a time is prohibitive in terms of cost and time. Consequently, the development of high-throughput experimental methods supported by machine learning and

theoretical predictions will facilitate the search for HEMs in their compositional diversity. This talk will therefore focus on the establishment of automated high-throughput methodologies in the field of synthesis and characterization for metallic and non-metallic (ceramic) HEMs, allowing the creation of material libraries of material properties.[2–4] This facilitates the analysis of material properties in terms of the overall composition, the effect of individual elements, morphological and/or structural differences. Machine learning-based data analysis and theoretical approaches also provide opportunities for virtual development of novel materials for functional and structural applications.

1. Ma, Y.; Ma, Y.; Wang, Q.; Schweidler, S.; Botros, M.; Fu, T.; Hahn, H.; Brezesinski, T.; Breitung, B. High-Entropy Energy Materials: Challenges and New Opportunities. *Energy Environ. Sci.* **2021**, 2883–2905, doi:10.1039/d1ee00505g.
2. Velasco, L.; Castillo, J.S.; Kante, M. V.; Olaya, J.J.; Friederich, P.; Hahn, H. Phase–Property Diagrams for Multicomponent Oxide Systems toward Materials Libraries. *Adv. Mater.* **2021**, 33, 2102301, doi:10.1002/adma.202102301.
3. Schweidler, S.; Schopmans, H.; Reiser, P.; Boltynjuk, E.; Olaya, J.J.; Singaraju, S.A.; Fischer, F.; Hahn, H.; Friederich, P.; Velasco, L. Synthesis and Characterization of High-Entropy CrMoNbTaVW Thin Films Using High-Throughput Methods. *Adv. Eng. Mater.* **2022**, 2200870, 1–7, doi:10.1002/adem.202200870.
4. Kumbhakar, M.; Khandelwal, A.; Jha, S.K.; Kante, M.V.; Keßler, P.; Lemmer, U.; Hahn, H.; Aghassi-Hagmann, J.; Colsmann, A.; Breitung, B.; et al. High-Throughput Screening of High-Entropy Fluorite-Type Oxides as Potential Candidates for Photovoltaic Applications. *Adv. Energy Mater.* **2023**, 2204337, 1–10, doi:10.1002/aenm.202204337.

2:15 PM SF01.07.03

Data-Driven Design of High-Entropy Ceramics for Extreme Environments Md T. Islam and Scott Broderick; University at Buffalo, United States

High-entropy ceramics present a promising material class but represent a design challenge due to the massive compositional design space. Through the use of machine learning approaches, design rules linking compositions, for example of CeO₂, Y₂O₃, and Eu₂O₃ components, with mechanical properties for accelerated selection of compositional refinement. These machine learning techniques identify optimal compositions and reveal underlying relationships by capturing the intricate multidimensional relationships between composition, processing conditions, microstructure, and mechanical performance. Our findings present a set of promising compositions that exhibit enhanced mechanical properties, ideal for extreme environment applications, such as hypersonic applications.

2:30 PM BREAK

SESSION SF01.08: Functional Properties of High Entropy Materials III—Electronics

Session Chairs: Jasmin Aghassi-Hagmann and T. Zac Ward

Wednesday Afternoon, April 24, 2024

Terrace Suite 1, Level 4, Summit

3:30 PM *SF01.08.01

High-Entropy Oxides for Electronic Applications: Present and Future Jasmin Aghassi-Hagmann, Ben Breitung, Yueyue He, Hongrong Hu and Anurag D. Khandelwal; Karlsruhe Institute of Technology, Germany

HEMs represent a class of materials characterized by the incorporation of a minimum of five distinct elements within a single-phase lattice structure. This incorporation serves to elevate configurational entropy, a measure of entropy arising from the mixing of dissimilar elements, thereby engendering the emergence of unique material properties. There exist various subtypes, with high-entropy alloys and high-entropy ceramics being the most prominent among them. While alloys are typically unified within a single lattice structure, ceramics exhibit a more complex arrangement, often comprising multiple sublattices, including cationic and anionic sublattices. Consequently, when evaluating configurational entropy, one must scrutinize these sublattices independently. The combination of dissimilar elements or ions, characterized by disparities in size, electronegativity, and other factors, induces lattice distortions and intricate inter-element interactions. This interplay initiates a cascade of electronic, physical, chemical, and structural effects within the material.

Given that the synthesis of many high-entropy materials typically results in powders, and the production of well-ordered crystalline layers is possible only in specific cases or with significant effort, a structuring technique capable of yielding the desired results with powders is imperative.

This presentation introduces printing techniques as a versatile technique for structuring high-entropy materials and delves into current applications in electronic devices and systems. More specifically the talk will discuss the properties of semiconducting high entropy oxides as revealed by Hall mobility measurements of flurite structures. While the mechanism is still unknown we show that mobility can be improved by the number of constituent elements. These materials can have a great potential for high performance absorbance layers. As a second example we will show HE Metal organic frameworks (HEMOFs) displaying interesting properties as active materials in memristive devices. Wet chemistry approaches at room temperature are used to fabricate Prussian blue HE MOFs with at least five different elements. The HE MOFs can easily be inkjet printed and keep their molecular structure after patterning which is important for device fabrication.

In conclusion we believe that while many mechanisms underpinning the enhancement of various properties remain to be discovered, there exist great prospects for employing high-entropy materials as active materials in components of electronic systems

4:00 PM SF01.08.02

Enhanced Electrical Conductivity caused by Phase Transformation and Interfacial Segregation in an Entropy Stabilized Oxide Hasti Vahidi, Alexander Dupuy, Benjamin Lam, Justin Cortez, Pulkit Garg, Timothy Rupert, Julie Schoenung, William J. Bowman and Huiming Guo; University of California, Irvine, United States

Research on entropy stabilized oxides (ESOs) has primarily focused on exploring new structures, chemistries, dislocations [1], or unique properties. However, few studies discuss the impact of secondary phases on functionality. Here, electrical transport mechanisms in the canonical ESO (Co,Cu,Mg,Ni,Zn)O were assessed as a function of secondary phase content [2]. When single-phase, the oxide is a small polaron electronic conductor. After heat treatments, Cu-rich tenorite particles form at grain boundaries, which enhances the grain interior rocksalt oxide electronic conductivity due to increased Cu cation vacancies and compensating small hole polarons. While Cu depletion tailors grain interior the conduction mechanism, Cu-rich tenorite grain boundary phases create a pathway for Cu²⁺/Cu³⁺ small hole polarons after longer heat treatment times. The ability to selectively grow secondary phases nucleated at grain boundaries enables tuning of electrical properties in entropy-stabilized and complex concentrated oxides using microstructure design, nanoscale engineering, and heat treatment, paving the way to develop many novel materials.

[1] Xin Wang, Justin Cortez, Alexander Dupuy, Julie Schoenung, W.J. Bowman (2023) "High entropy oxide (Co,Cu,Mg,Ni,Zn)O exhibits grain size dependent room temperature deformation" *Materials Research Letters*

[2] Hasti Vahidi, Alexander D. Dupuy, Benjamin X. Lam, Justin Cortez, Pulkit Garg, Timothy J. Rupert, Julie M. Schoenung, and William J. Bowman (In Revision)

4:15 PM *SF01.08.03

Functional High Entropy Oxides: From Electronic to Magnetic Properties [David Berardan](#), Adrien Moll, Claudia Decorse and Nita Dragoe; University Paris-Saclay, France

Since their first report by Rost et al. in 2015 [1], Entropy Stabilized Oxides and High Entropy Oxides (HEOx) have become a hot topic in the field of functional oxides, with many papers devoted to the synthesis of new compositions and structures and to the study of various functional properties. In the past few years, many compositions have been obtained with different crystal structures, with both entropy-stabilized and thermodynamically stable compounds. Some of them exhibit promising functional properties, among other: superionic Li conductivity or fast ionic conductivity, colossal dielectric constants, photocatalytic properties, unexpected magnetic ordering, (...). Although no clear link has been made to date between these properties and the possible role of entropy-stabilization (or even high-entropy nature), cocktail effects have been reported in some cases with functional properties of the multicomponent compounds significantly different from that of their single-cation counterparts. In this talk, I will give an overview of the electronic and magnetic properties of various systems studied in our group, and discuss the perspective they open for applications.

[1] C.M. Rost et al., Entropy-stabilized oxides, *Nature communications* 6, 8485 (2015)

4:45 PM SF01.08.04

Entropy-Stabilized Oxide Memristors [Sieuun Chae](#)¹, Sangmin Yoo², Emmanouil Kioupakis², Wei Lu² and John T. Heron²; ¹Oregon State University, United States; ²University of Michigan, United States

Memristor arrays have emerged as a promising hardware platform for efficient machine learning tasks. Traditional amorphous oxide-based memristor materials, however, suffer from device stochasticity and a lack of tunability which hinder applications requiring adaptive networks. Here I will present a study on tunable carrier transport and dynamics in single crystalline (MgCoNiCuZn)O entropy-stabilized oxide (ESO) thin films. We find that the ESO undergoes composition tunable hopping conduction in agreement with the composition dependent point defect formation and electronic structure from first principles calculations. Notably, the transport is bulk and non-filamentary. Pulsed measurements reveal a low resistance state with a short, composition-tunable retention time that can be harnessed for memristor function via temporal data processing. We interpret the carrier dynamics in terms of voltage modulated filling of deep level defects states that are controlled by composition as predicted by theory. The precise tunability of carrier transport in this ESO make it an excellent candidate for "task specific" neural network systems with record energy efficiency for temporal data processing.

SESSION SF01.09: High Entropy Perovskites
Session Chairs: Alan Farhan and T. Zac Ward
Thursday Morning, April 25, 2024
Terrace Suite 1, Level 4, Summit

8:30 AM *SF01.09.01

Element Sensitive Characterization of High-Entropy Oxide Perovskite Thin Films [Alan Farhan](#); Baylor University, United States

Employing the entropy-driven stabilization concept into the perovskite structure showed first promising results demonstrating the potential unlimited freedom in designing ferroic properties in high-entropy oxide perovskite (HEOP) thin films [1]. Here, I will show how element-sensitive characterization with x-ray absorption spectroscopy (XAS), employing x-ray magnetic circular- and linear dichroism (XMCD and XMLD) can shed light into how each transition metal element contributes to the overall ferroic order in HEOP thin films with a primary focus on rare-earth-based $R(\text{Ni}_{0.2}\text{Co}_{0.2}\text{Fe}_{0.2}\text{Mn}_{0.2}\text{Cr}_{0.2})\text{O}_2$ (R: Tb, Lu and Dy). The results highlight the important role of elevated Co^{2+} concentrations, likely induced via strain, in introducing long-range ferromagnetic order [2, 3] and the occurrence of spin-reorientations in Dy-based HEOPs [4].

References:

- [1] A. Mazza et al. *Advanced Science* **9**, 2200391 (2022).
- [2] A. Farhan et al. *Physical Review B* **106**, L060404 (2022).
- [3] A. farhan et al. *Physical Review Materials* **7**, 044402 (2023).
- [4] M. Cocconcelli et al. *in prep.*

9:00 AM SF01.09.02

Growth and Characterization of High Entropy Perovskite $(\text{La}_{0.2}\text{Nd}_{0.2}\text{Gd}_{0.2}\text{Sm}_{0.2}\text{Y}_{0.2})\text{MnO}_3$ Thin Films on Cubic and Orthorhombic Substrates [Maximilian Mijhm](#), Aladin Ullrich, David Stein, Christian Holzmann, Helmut Karl and Manfred Albrecht; Institute of Physics, University of Augsburg, Germany

With the discovery of high entropy oxides in 2015 many different oxides have been synthesized using the high entropy strategy [1]. Since 2018 many different high entropy perovskites have been synthesized, some of them contain five elements on the A- or the B-site [2]. Some high entropy perovskites were synthesized with ten different elements, five on the A-site and five on the B-site [2]. Most of them were produced as polycrystalline powders, only a few of them have been grown as thin film [2-5]. In the recent research, the focus has shifted to high entropy manganites-perovskites, because of their interesting magnetic properties, where the Mn-O-Mn exchange dominates the magnetic properties and the rare earth ion radii influences the strength of the exchange [3,4]. One high entropy manganite-perovskite is $(\text{La}_{0.2}\text{Nd}_{0.2}\text{Gd}_{0.2}\text{Sm}_{0.2}\text{Y}_{0.2})\text{MnO}_3$ which was previously produced as a powder [2]. We have grown thin films of $(\text{La}_{0.2}\text{Nd}_{0.2}\text{Gd}_{0.2}\text{Sm}_{0.2}\text{Y}_{0.2})\text{MnO}_3$ via pulsed laser deposition on three different substrates, one with a cubic structure SrTiO_3 (001) and two with an orthorhombic structure, NdGaO_3 (001), and YAlO_3 (001). All films were subsequently annealed. X-ray diffraction data confirmed epitaxial growth of $(\text{La}_{0.2}\text{Nd}_{0.2}\text{Gd}_{0.2}\text{Sm}_{0.2}\text{Y}_{0.2})\text{MnO}_3$ on all substrates. Wide-range reciprocal space mapping and electron-backscattered diffraction revealed,

that $(\text{La}_{0.2}\text{Nd}_{0.2}\text{Gd}_{0.2}\text{Sm}_{0.2}\text{Y}_{0.2})\text{MnO}_3$ has three different crystal orientations on SrTiO_3 and two on NdGaO_3 and YAlO_3 . On SrTiO_3 $(\text{La}_{0.2}\text{Nd}_{0.2}\text{Gd}_{0.2}\text{Sm}_{0.2}\text{Y}_{0.2})\text{MnO}_3$ grows in two different directions (001) and (110). The (001) orientated crystals are rotated by 45° with respect to the substrate, while the (110) crystals are aligned either to the substrate lattice or are also rotated by 45° . On NdGaO_3 we observed only (001) orientated crystals, but with two different in-plane orientations, either (001) or (110). On YAlO_3 two crystal orientations were observed (110) and (001), both are aligned to the substrate lattice. High-resolution transmission electron microscopy confirmed the perovskite structure and the epitaxial growth. All surfaces showed a grainy structure which was observed by atomic force microscopy. Zero-field-cooled and field-cooled measurements revealed a magnetic transition temperature around 38 K for $(\text{La}_{0.2}\text{Nd}_{0.2}\text{Gd}_{0.2}\text{Sm}_{0.2}\text{Y}_{0.2})\text{MnO}_3$ grown on SrTiO_3 , which is lower compared to most of the parent compounds. This is in good agreement with the magnetic measurements on corresponding powder. Below 25 K the rare earth elements couple antiferromagnetic to the manganese, which is indicated by a decrease of the magnetization in the field-cooled curve. All samples showed a small coercive field and a small remanent magnetization, which indicates a soft magnetic behaviour.

- [1] C. M. Rost, E. Sacht, T. Borman, A. Moballeghe, E. C. Dickey, D. Hou, J. L. Jones, S. Curtarolo, and J.-P. Maria, *Nature Communications* **6**, 8485 (2015).
- [2] A. Sarkar, R. Djenadic, D. Wang, C. Hein, R. Kautenburger, O. Clemens, and H. Hahn, *Journal of the European Ceramic Society* **38**, 2318 (2018).
- [3] R. Das, S. Pal, S. Bhattacharya, S. Chowdhury, S. K. K., M. Vasundhara, A. Gayen, and M. M. Seikh, *Physical Review Materials* **7**, 024411 (2023).
- [4] A. Sarkar, R. Djenadic, D. Wang, C. Hein, R. Kautenburger, O. Clemens, and H. Hahn, *Journal of the European Ceramic Society* **38**, 2318 (2018).
- [5] A. R. Mazza, E. Skoropata, J. Lapano, J. Zhang, Y. Sharma, B. L. Musico, V. Keppens, Z. Gai, M. J. Brahlek, A. Moreo, D. A. Gilbert, E. Dagotto, and T. Z. Ward, *Physical Review B* **104**, 094204 (2021).

9:15 AM SF01.09.03

Synthesis and Characterization of Multifunctional High-Entropy Perovskite Oxides [Rubayet Tanveer](#), William J. Weber and Veerle Keppens; University of Tennessee, United States

The scientific community has taken a keen interest in perovskite oxides (ABO_3) due to their unique electrical, magnetic, thermal, and optical characteristics with diverse potential applications. The addition of compositional diversity or “high entropy” in these oxide perovskites with five or more cations on a given lattice site offers the opportunity for property engineering by taking advantage of the high compositional disorder, large lattice distortion tunability, huge mass fluctuation, expansion in cation size variance and integration of diverse cation species [1-3]. High entropy perovskites have the potential to revolutionize applications in areas including energy storage, electronics, and photonics, however, designing such compositionally complex multifunctional perovskite oxides is challenging and needs to take into account several factors, including e.g. cation choice for property integration, tolerance factor of the desired structure, high mixing enthalpy, and changing oxidation states. Herein, we present the synthesis of a group of new entropy-stabilized perovskite oxides with a series of alkaline and rare earths on the A site and five transition metals on the B site in equimolar amounts. Such compositions are interesting due to their high cation size variance, and diversity in cation species. Energy dispersive X-ray spectroscopy (EDS) and room temperature X-ray diffraction (XRD) were used to confirm the elemental distribution and single-phase compositions. Electrical, magnetic, and optical properties will be presented for various cation combinations to explore possible multifunctionality.

1. Mazza, A.R., et al., *Variance induced decoupling of spin, lattice, and charge ordering in perovskite nickelates*. *Physical Review Research*, 2023. **5**(1): p. 013008.
2. Mazza, A.R., et al., *Designing magnetism in high entropy oxides*. *Advanced Science*, 2022. **9**(10): p. 2200391.
3. Zheng, Y., et al., *Electrical and thermal transport behaviours of high-entropy perovskite thermoelectric oxides*. *Journal of Advanced Ceramics*, 2021. **10**: p. 377-384.

9:30 AM SF01.09.04

Vacancy-Ordered Halide Perovskites for High Entropy Semiconductors [Seán R. Kavanagh](#)¹, Shanti Liga², Aron Walsh³, David O. Scanlon⁴ and Gerasimos Konstantatos²; ¹Harvard University, United States; ²ICFO–The Institute of Photonic Sciences, Spain; ³Imperial College London, United Kingdom; ⁴University of Birmingham, United Kingdom

Due to their quasi-0D / molecular-aggregate type crystal structure, vacancy-ordered double perovskites (VODPs) with the chemical formula A_2BX_6 , exhibit unusual material properties associated with both zero-dimensional and three-dimensional materials.¹⁻⁴ These include low thermal conductivity, high compressibility, and strong exciton binding despite relatively small semiconducting band gaps, making them potential candidates for a range of alternative applications, such as thermoelectrics, white-light emitters/phosphors, photocatalysts, non-linear optics and more.

In this study, we report a combined experimental and computational investigation on the mixing behavior of cations in this system. Remarkably, we find ultra-low enthalpic costs to cation mixing, resulting in entropy dominance and ideal mixing behavior. This facilitates the room-temperature and low-temperature synthesis of high-entropy materials (high-entropy semiconductors) from these compounds, as demonstrated experimentally by Folgueras et al in *Nature*, 2023.⁵ We elucidate the underlying structural and electronic origins of this facile cation miscibility in these systems, and analyze the resulting optical, thermodynamic and structural changes upon cation mixing.

Our work demonstrates that vacancy-ordered perovskites present an exciting new class of high-entropy semiconductors, synthesisable at much milder conditions than typical high-entropy materials. Moreover, we elucidate the origins of this behavior, allowing the extraction of general design rules for high-entropy semiconductors with tailored properties.

- 1 S. R. Kavanagh, C. N. Savory, S. M. Liga, G. Konstantatos, A. Walsh and D. O. Scanlon, *J. Phys. Chem. Lett.*, 2022, **13**, 10965–10975.
- 2 Y.-T. Huang, S. R. Kavanagh, D. O. Scanlon, A. Walsh and R. L. Z. Hoyer, *Nanotechnology*, 2021, **32**, 132004.
- 3 B. Cucco, C. Katan, J. Even, M. Kepenekian and G. Volonakis, *ACS Materials Lett.*, 2023, **5**, 52–59.
- 4 B. Saparov, J.-P. Sun, W. Meng, Z. Xiao, H.-S. Duan, O. Gunawan, D. Shin, I. G. Hill, Y. Yan and D. B. Mitzi, *Chem. Mater.*, 2016, **28**, 2315–2322.
- 5 M. C. Folgueras, Y. Jiang, J. Jin and P. Yang, *Nature*, 2023, 1–7.
- 6 S. M. Liga & S. R. Kavanagh, A. Walsh, D. O. Scanlon and G. Konstantatos, *J. Phys. Chem. C.*, 2023

9:45 AM SF01.09.05

An Insight into The Functional Properties of High-Entropy Perovskite Oxides [Anurag D. Khandelwal](#), Piyush Sharma, Simon Schweidler and Ben Breitung; Karlsruhe Institut für Technologie, Germany

In recent years, there has been a surge of research interest in high entropy materials, driven by the potential to engineer their functional properties. High entropy materials, with their diverse elemental compositions, exhibit distinctive characteristics compared to conventional materials due to the intricate interplay of inter-elemental interactions, some of which cannot be predicted.

Among these materials, oxide perovskites stand out as a versatile material class with applications ranging from catalysis and solid-state fuel cells to oxide solar cells, rendering them particularly captivating for high-entropy investigations. Noteworthy studies have already shown the exceptional performance of high-entropy perovskite oxides in critical applications such as electrochemical catalysis, high-energy-density capacitors, and thermoelectric systems. The extensive array of perovskite systems, coupled with the immense spectrum of high-entropy cation combinations within them, opens up a vast domain of possibilities for such diverse applications.

In this talk, a comprehensive study of lanthanum-based perovskite-type oxides containing various compositions of transition elements (Co, Cr, Cu, Fe, Mn, Ni and Zn) at the B site is given, with the aim of studying the effects of the different cations on the properties of these materials. Various analysis techniques are used to characterize the optical and electronic behavior of these materials and thus enable further optimization for specific applications.

10:00 AM BREAK

SESSION SF01.10: Novel Synthetic Approaches to High Entropy Oxides

Session Chairs: Alannah Hallas and Ayako Yamamoto

Thursday Morning, April 25, 2024

Terrace Suite 1, Level 4, Summit

10:30 AM *SF01.10.01

High-Pressure Synthesis of High-Entropy Spinel-Type Semiconducting Manganates and Perovskite-Type Ferroelectric Niobates Ayako Yamamoto¹, Haruka Yokoyama¹, Tomoki Nakayama¹, Riki Maeda¹, Kimitoshi Murase¹, Anna Laila¹, Yann-Andrev Kerneur² and Nita Dragoe²; ¹Shibaura Institute of Technology, Japan; ²Université Paris-Saclay, France

We have studied high-entropy (HE) chalcogenides[1] and oxides prepared at high pressure. The high-pressure method has several advantages in stabilizing HE compounds; for example, enclose the volatile elements and quick-quench from high temperature. Here, we report our recent study on HE spinel-type manganates as a thermistor and HE perovskite-type niobates, possibly as ferroelectric relaxors.

We focused on NiMn₂O₄ as a pristine that is a typical NTC (Negative Temperature Coefficient) thermistor compound. NiMn₂O₄ and partially (minor component) substituted ones show proper resistivity for monitoring temperatures between 300–500 K in various electric devices. The efficiency of a thermistor is evaluated with the B constant (corresponding to sensitivity) in general. Most commercial ones show B = 3,000–4,000 K. Our objective of this HE-spinel project is to expand the temperature range up to 700 K while keeping B = 3,000–4,000 K by controlling temperature dependence of resistivity with the HE techniques.

Two types of crystal systems appear in AMn₂O₄ (A=Mg, Co, Ni, Cu, and Zn) spinel: cubic in A=Ni and Co and orthorhombic in A=Mg, Cu, and Zn. It is interesting to see which structural system is stable in HE spinels and how to change a temperature dependence of resistivity depending on the composition and structure. We mixed up equal molar selected 2–5 elements among Mg, Co, Ni, Cu, Zn, plus Ti in assuming A site. TiMn₂O₄ could not be stabilized in spinel since tetravalent Ti in ilmenite-type MnTiO₃ and rutile-type TiO₂ are stable in the ambient condition. However, we expected Ti would be included in the spinel structure with the HE stabilized effect if we were starting from TiO with divalent in a closed golden cell of high-pressure synthesis assembly. We prepared a single phase of tetragonal spinel (Mg, Co, Ni, Zn, Ti)Mn₂O₄ with sintering at high pressure (4 GPa) and quenched from ca. 1250 K to 350 K in several seconds. In contrast, samples sintered in the air were a mixture of tetragonal and cubic phases or two sets of tetragonal phases, whether quench (liquid nitrogen) or slow cooling. The temperature dependence of resistivity showed semiconducting behavior with B = 5,000–5,500 K at 300–700 K. In addition, resistivity's absolute value is higher than conventional ones, an advantage in sensitivity at higher temperatures. Ti may be located in the B site, and part of Mn moved to the A site. The Cu version (Mg, Co, Ni, Zn, Cu)Mn₂O₄ showed lower B = 3,000 K at 300–700 K and lower resistivity. The properties look sensitive to cooling processes and oxygen deficiency. We are also preparing A and B double sites' HE spinel.

Another HE project is to obtain a ferroelectric relaxor in perovskite-type niobates. ANbO₃ (Li, Na, K, and Ag) are well-known ferro(antiferro)electric compounds. Structure types and or distortion types of these compounds differ depending on the A element; however, they allow partial substitution of each other. For example, in KNbO₃, Li and Ag could be substituted 5–10 % of K, and NaNbO₃ makes a complete solid solution with KNbO₃. In this study, we adapted KNbO₃ as a pristine and prepared HE niobates with equal molar selected 2–5 elements among Li, Na, K, Ag, and others in A site at ambient and high pressure. The high-pressure method effectively suppresses alkaline metals' vaporization (Li, Na, and K). We found LiNbO₃ is more stable in a LiNbO₃-type structure at high pressure. Therefore, equal molar HE compounds may be challenging in this system. Once it stabilized in a single phase, even if Li concentration is lower than other metals, it expected a ferroelectric relaxor in the temperature dependence of dielectric constant.

We also present our progress in XAS and XPS studies in HE pyrite (Fe, Co, Ni, Cu)X₂ (X = S and Se). It investigates a local configuration and interaction difference by comparing A element in a single metal AX₂ (A=Fe, Co, Ni, and Cu).

[1] AZ. Laila et al., J. Phys. Soc. Jpn. 91 084802.

11:00 AM SF01.10.02

Influence of Synthesis Method on The Properties of The Spinel High Entropy Oxide Mario Ulises Gonzalez Rivas¹, Solveig S. Aamlid¹, Megan R. Rutherford¹, Edgar E. Villalobos-Portillo², Hiram Castillo-Michel², Ronny Sutarto³, Ning Chen³, Robert J. Green⁴ and Alannah Hallas¹; ¹University of British Columbia, Canada; ²European Synchrotron Radiation Facility, France; ³Canadian Light Source, Canada; ⁴University of Saskatchewan, Canada

Understanding and controlling sample dependence is a critical step towards any material achieving widespread use in applications. High entropy oxides (HEOs) are a class of materials with immediate potential for an array of applications but whose sample dependence has the potential to be particularly profound due to their high degree of configurational disorder. In this work, we seek to clarify the extent of sample dependence in HEOs by directly comparing the structural, magnetic, and electronic properties of an HEO with the spinel structure synthesized by five distinct methods. These methods (solid state, high pressure, hydrothermal, molten salt, and combustion) each provide distinct levels of kinetic and thermodynamic control in the growth process. The spinel HEO's ferrimagnetic structure was determined from neutron diffraction, whilst the site distribution of the cations in each sample was calculated using x-ray absorption spectroscopy. This thorough structural and magnetic characterization allowed us to identify the likely origins of variation in the magnetic behavior of our samples. We find that while distinct differences in homogeneity, sharpness of the magnetic ordering transition, and cation

distribution are apparent, the most technologically important properties, including ordering temperature ($\gg 400$ K) and saturated moment ($\gg 1.8 \mu\text{B}/\text{F.U.}$), are highly robust to preparation method, with the most extreme cases remaining within 10 % of one another. On the other hand, we observe a 500% variation in the sharpness of the onset of magnetic order between the most and least spatially homogenous samples. Likewise, we observe a 250% variation in coercive field, highlighting the effect of spatial homogeneity in the properties of HEOs. We conclude that this overall robustness to synthesis method make HEOs excellent candidates for a variety of industrial processes.

11:15 AM SF01.10.03

Rapid Synthesis of Entropy Stabilized Oxides Using Radio Frequency Heating Aniruddh Vashisth; University of Washington, United States

Entropy-stabilized oxides (ESOs) represent an exciting new category of hybrid materials and single-phase metal oxides, composed of multiple ions, exhibiting material characteristics that lie between those of their constituent oxides or occasionally showcasing entirely novel properties. One drawback of ESOs is their energy expensive manufacturing process, which has hindered the pace of their development and scaling. In this study, we introduce an innovative, energy-efficient method for synthesizing ESOs. This approach leverages the rapid heating capability of carbonaceous materials when exposed to radio frequency (RF) fields within the 1–200 MHz range. By employing carbon fibers and graphene as RF susceptors, we successfully achieved the synthesis of $(\text{MgCoNiCuZn})_{0.2}\text{O}$ through RF-triggered combustion synthesis, achieving heating rates of $203^\circ\text{C}/\text{s}$ with a 20 W input power. This technique reduces the ESO formation time to less than a minute, significantly enhancing fabrication efficiency. The morphology and composition of the resultant ESO-carbon fiber and ESO-graphene composites were comprehensively examined using spectroscopy and characterization techniques. Moreover, single carbon fibers coated with ESO underwent testing for tensile strength and modulus, revealing minimal changes in mechanical properties compared to pristine fibers. In this study, for the first time, a new method for producing ESO-carbon composites has been demonstrated using out-of-oven electromagnetic heating using radio frequencies in the range of 1–200 MHz at low input power (less than 25 W).

11:30 AM SF01.10.04

High-Entropy Spinel Ferrite Nanoparticles via Low-Temperature Synthesis for The Oxygen Evolution Reaction Judith Zander, Julia P. Wölfel and Roland Marschall; University of Bayreuth, Germany

High-entropy oxides are a material class that is currently receiving rapidly increasing attention due to the large variety in composition and adjustable properties. Cooperative effects between different metal cations in the crystal structure in addition to entropic phase stabilisation have proven beneficial for electrocatalytic applications. Most synthesis methods, however, require high synthesis temperatures and long synthesis times, and often only yield selected samples in good phase-purity.

We herein present for the first time a microwave-assisted low temperature synthesis of earth-abundant high-entropy oxide nanoparticles. Phase-pure spinel ferrites (AFe_2O_4) of various compositions ranging from one to seven different A-cations were successfully obtained after only 30 min synthesis time at 225°C . A detailed characterisation of their properties in relation to their composition was performed, and they were also employed for the alkaline oxygen evolution reaction (OER).

A partial replacement of Fe by Co moreover shows the high versatility of the synthesis that also allows for the simultaneous variation of the B-ion.

J. Zander, J. P. Wölfel, M. Weiss, Y. Jiang, N. Cheng, S. Zhang, R. Marschall, submitted

11:45 AM SF01.10.05

Designing Nanostructure Exsolution-Self-Assembly in a Complex Concentrated Oxide Huiming Guo¹, Christopher Mead², Marquez Balingit¹, Soham Shah³, Xin Wang¹, Mingjie Xu⁴, Ich Tran⁴, Toshihiro Aoki⁴, Jack Samaniego¹, Kandis Abdul-Aziz³, Lincoln J. Lahun² and William J. Bowman^{1,4}; ¹University of California, Irvine, United States; ²Northwestern University, United States; ³University of California Riverside, United States; ⁴Irvine Materials Research Institute (IMRI), United States

Complex concentrated oxides (CCOs) are an emerging material class that includes high-entropy oxide (HEOs) and entropy-stabilized oxides (ESOs), whose unprecedented properties stem from disorder-induced distributions in electronic structure and chemistry caused by stabilizing many-cation (typically > 5) solid solutions¹⁻³. Integrating these materials into composites with nanoscale tunability will enable tailored (multi)functionality beyond what is possible in a single phase⁴⁻⁶. Here, we demonstrate a novel, highly extensible approach, *exsolution self-assembly* (ESA), to realize CCO-based nanocomposite thin films with intricate multi-element nanostructures. Using pulsed-laser deposition (PLD), we selectively reduce cations in a model perovskite CCO $\text{LaFe}_{0.7}\text{Ni}_{0.1}\text{Co}_{0.1}\text{Pd}_{0.05}\text{Ru}_{0.05}\text{O}_{3-\delta}$, inducing defect-interaction-driven exsolution and simultaneous self-assembly of metal nanorods and metal-oxide core-shell nanoparticles, depending on oxygen partial pressure (P_{O_2}). A correlated analysis using aberration-corrected scanning transmission electron microscopy (STEM) imaging, energy dispersive X-ray spectroscopy (EDS), electron energy-loss spectroscopy (EELS), geometric phase analysis (GPA) strain mapping, atom probe tomography (APT) with 3D mass spectrometry, and X-ray photoemission spectroscopy (XPS) was performed to characterize the ESA nanostructures and elucidate the nanostructure formation mechanisms underlying the highly tailorable synthesis approach.

With decreasing P_{O_2} from 3 mtorr, 0.15 mtorr, to 0.015 mtorr, concentration of oxygen vacancy increases, which tunes the extent of exsolution for different ESA nanostructures. At P_{O_2} of 3 mtorr, the LaFeO_3 -based CCO thin film matrix shows uniform cation distribution. When P_{O_2} drops to 0.15 mtorr, ESA Pd nanorods grow from bottom of the thin film to top surface, with growth restricted by compressive stress exerted by the matrix in the in-plane direction and Pd availability in surroundings. When P_{O_2} further reduce by 10 times to 0.015 mtorr, Pd- $\text{Ni}_x\text{Co}_{1-x}\text{O}$ metal-oxide core-shell nanoparticles embedded in the matrix form via seed growth effect triggered by growth of Pd followed by subsequent exsolution of Ni^{3+} and Co^{3+} in the CCO matrix. ESA is expected to synthesize complex and multi-dimensional nanostructures for electrochemical devices via integration of novel compositions and crystal structures of CCOs as well as PLD conditions.

References

- 1 Guo, H. *et al.* Designing nanostructure exsolution-self-assembly in a complex concentrated oxide. *In Revision* (2023). <https://doi.org/http://dx.doi.org/10.2139/ssrn.4542882>
- 2 Guo, H., Wang, X., Dupuy, A. D., Schoenung, J. M. & Bowman, W. J. Growth of nanoporous high-entropy oxide thin films by pulsed laser deposition. *Journal of Materials Research* **37**, 124-135 (2022). <https://doi.org/10.1557/s43578-021-00473-2>
- 3 Brahlek, M. *et al.* What is in a name: Defining “high entropy” oxides. *APL Materials* **10**, 110902 (2022). <https://doi.org/10.1063/5.0122727>
- 4 Misra, S. & Wang, H. Review on the growth, properties and applications of self-assembled oxide-metal vertically aligned nanocomposite thin films—current and future perspectives. *Materials Horizons* **8**, 869-884 (2021). <https://doi.org/10.1039/D0MH01111H>
- 5 Wang, J. *et al.* Exsolution Synthesis of Nanocomposite Perovskites with Tunable Electrical and Magnetic Properties. *Advanced Functional Materials* **32**, 2108005 (2022). <https://doi.org/https://doi.org/10.1002/adfm.202108005>
- 6 Kawasaki, S. *et al.* Photoelectrochemical water splitting enhanced by self-assembled metal nanopillars embedded in an oxide semiconductor photoelectrode. *Nature Communications* **7**, 11818 (2016). <https://doi.org/10.1038/ncomms11818>

SESSION SF01.11: High Entropy Materials—Catalysis and Beyond

Session Chairs: Ben Breitung and Sheng Dai

Thursday Afternoon, April 25, 2024

Terrace Suite 1, Level 4, Summit

1:30 PM *SF01.11.01

Entropy-Maximized Materials for Catalysis Applications [Sheng Dai](#)^{1,2}; ¹Oak Ridge National Laboratory, United States; ²The University of Tennessee, Knoxville, United States

Until recently the design and synthesis of heterogeneous catalysts have been dominated through enthalpic factors (e.g., charge-charge interactions, charge-transfer interactions). With emergence of high entropy materials (HEMs), another avenue to design and synthesize catalytic materials has opened up. The definition of HEMs is any material that consists of the solid solution of more than five components that allow great flexibility in tuning surface compositions and interfacial functionalities. Here we present the synthesis of high entropy electrocatalysts that potentially outperform the traditional catalysts in energy-related catalysis reactions. The synthesis strategies through entropy maximization will be discussed.

2:00 PM SF01.11.02

Sol-Gel-Derived Ordered Mesoporous High Entropy Spinel Ferrites and Assessment of Their Photoelectrochemical and Electrocatalytic Water Splitting Performance [Marcus Einert](#)¹, [Arslan Waheed](#)¹, [Stefan Lauterbach](#)¹, [Maximilian Mellin](#)¹, [Marcus Rohnke](#)², [Lysander Wagner](#)², [Julia Gallenberger](#)¹, [Chuanmu Tian](#)¹, [Bernd Smarsly](#)², [Wolfram Jaegermann](#)¹, [Franziska Hess](#)³ and [Helmut Schlaad](#)⁴; ¹Technical University of Darmstadt, Germany; ²Justus-Liebig-Universität Giessen, Germany; ³Technical University Berlin, Germany; ⁴University of Potsdam, Germany

With the introduction of high-entropy oxides (HEO) as a novel class of materials, unexpected and interesting properties have emerged and are currently under investigation. A HEO consists of five or more ions occupying a single crystallographic site and inducing a high degree of configurational disorder, which increases the entropic contribution to the Gibbs free energy of formation. This extra gain of energy stabilizes the formation of single-phase structures showing unique and, so far, unpredictable properties. Significant efforts have been devoted to the development of new HEO phases; however, the large majority of synthetic approaches are based on solid-state, rather than sol-gel chemistry allowing only the preparation of micrometer-sized, low-surface-area particles.

With respect to sol-gel synthesis, the precise control of hydrolysis and condensation reactions of the complex precursor is important in order to form uniform structures. The whole reaction system becomes even more complex when an additional component – such as a structure-directing agent – is added. This intricate interplay of reactants, such as control of reaction kinetics, is most likely the reason why the sol-gel preparation of highly ordered mesoporous HEO thin films by the well-established soft-templating and evaporation induced self-assembly (EISA) approach has not been reported yet.

For the first time the design of periodically ordered mesoporous high-entropy-assisted (CoNiCuZnMg)Fe₂O₄ spinels prepared by dip-coating and EISA process is reported. A synthetic route was developed, utilizing the unique diblock copolymer (poly(ethylene-co-butylene)-block-poly(ethylene oxide), known as KLE, in order to obtain periodically ordered and 15–18 nm sized mesopores within the high-entropy ferrite (HEF) network. The mesostructured HEF electrodes were found to be crack-free on the nano- and macroscale. Time-over-flight secondary ion mass spectrometry (ToF-SIMS) and electron microscopy analysis verified a homogenous distribution of all elements within the thin film structure. The mesoporous HEF electrodes were used to study the fundamental impact of a nanoscale framework on the electrocatalytic and photoelectrochemical properties. Hence, the HEF electrodes were investigated as oxygen evolution catalyst and n-type photoanode for solar water oxidation. For both applications the near-metallic electric conductivity, which was related to an electron hopping mechanism induced by the interaction of 3d-states of the inserted transition metals, was found to improve the performance. The photoresponse of HEF photoanodes is limited owing to severe surface recombination as evidenced by intensity-modulated photocurrent spectroscopy.

This novel high entropy oxide class can be considered as interesting candidate and nanostructure for energy applications where high surface-areas offering a large number of (catalytically) active reaction sites are advantageous. [1]

[1] Einert, Marcus, et al. "Sol-Gel-Derived Ordered Mesoporous High Entropy Spinel Ferrites and Assessment of Their Photoelectrochemical and Electrocatalytic Water Splitting Performance." *Small* 19.14 (2023): 2205412.

2:15 PM SF01.11.03

Size Controlled Monodisperse Alloy Nanocrystals via Colloidal Synthesis, from Medium to High Entropy and Their Excellent Catalytic Properties [Jasper Clarysse](#), Yunhua Xing and Vanessa Wood; ETH Zürich, Switzerland

High entropy alloy (HEA) nanocrystals (NCs) are solid solutions of 5 or more elements, while medium entropy alloy (MEA) NCs are solid solutions of 2 to 4 elements. Entropy alloy nanocrystals are an emerging class of materials which show intriguing properties such as enhanced resistance to oxidation and mixing of immiscible elements within nanocrystals. Furthermore, HEA NCs have recently been demonstrated as catalysts in various important reactions (e.g., water splitting and oxygen reduction reaction) with record or near-record activities, attributed to “synergistic” and “cocktail” effects originating from the combination of multiple metals within the NCs. Yet, the exact structure-activity relationships, leading to the excellent performance of high-entropy alloys in applications such as catalysis remain poorly understood. Furthermore, no synthesis method for highly monodisperse and size-controlled medium and high entropy alloy NCs exists yet. Here we show the colloidal synthesis of highly monodisperse entropy alloy NCs [1-2], employing oleylamine as a suitable reaction solvent and non-poisoning L-type ligand. Furthermore, we extend our synthetic method to achieve MEA NCs constituting of non-precious, environmentally benign metals (e.g., Ni-Zn) and we report the first size-tunable synthesis of HEA NCs (e.g., 1.8 nm, 2.5 nm, and 3.5 nm HEA NCs) [3]. The synthesis method is facile and easily scalable. We demonstrate that the resulting nanocrystals possess size-dependent catalytic properties and exhibit better catalytic performance compared to monometallic nanocrystals. We achieve MEA and HEA nanocrystals with excellent catalytic properties and study these for different reactions (e.g. semihydrogenation of alkynes and hydrogen-evolution reaction). We understand the crystallographic and electronic structure of the nanocrystals using a range of advanced characterization techniques (high resolution transmission electron microscopy and synchrotron-based X-ray diffraction, total X-ray scattering and X-ray absorption spectroscopy) and using density functional theory calculations and reveal the relationships between catalytic performance and structure of the MEA and HEA NCs.

[1] J. Clarysse, A. Moser, O. Yarema, V. Wood, M. Yarema; *Science advances*, 2021, 7 (31) eabg 1934.

[2] J. Clarysse, J. D. J. Silva, Y. Xing, S. Zhang, S. Docherty, N. Yazdani, C. Coperet, M. Yarema, C. Copéret, V. Wood; Submitted.

[3] J. Clarysse, Y. Xing, V. Wood et al.; In Preparation.

2:30 PM SF01.11.04

Entropy-Inspired Materials Design for Novel Electronic Materials: $A_6B_2O_{17}$ -Form ($A = \text{Zr, Hf}$; $B = \text{Nb, Ta}$) Oxides Robert J. Spurling and Jon-Paul Maria; The Pennsylvania State University, United States

In this work, we apply an entropy-inspired materials design approach to study the class of compositionally complex, disordered $A_6B_2O_{17}$ ($A = \text{Zr, Hf}$; $B = \text{Nb, Ta}$) family of phases. The availability of multiple local coordination sites on the cation sublattice coupled with substantial tolerance for extended chemical solubility makes this a unique system for studying the interplay between configurational entropy (controlled across multiple structural hierarchies) and properties. This work focuses on both the thermodynamic consequences of configurational entropy on phase stability as well as property characterization, with particular focus on dielectric and candidate ferroelectric behavior. This work spans studies in both the bulk and thin film regimes. First, we confirm the stability of ternary and quinary $A_6B_2O_{17}$ phases at high temperatures as well as substantial inherent cation sublattice disorder; moreover, we observe enhanced solid solubility in multi-constituent systems commonly associated with high-entropy material behavior. We develop a sintering procedure for producing dense ternary $A_6B_2O_{17}$ phases for use as both sputtering targets for thin film preparation and bulk dielectric measurements. Furthermore, we characterize the effect of sputter deposition conditions (i.e. O_2 partial pressure and total pressure) on film quality (crystallinity, roughness, and density); we also relate these parameters to observed dielectric performance. Collectively, this study leverages a range of advanced characterization techniques, including both *ex situ* and *in situ* X-ray diffraction, scanning electron microscopy, atomic force microscopy, and X-ray photoelectron spectroscopy. These results support continued interest in such unique structures with substantial configurational entropy and suggest new opportunities for research probing structure-property relationships in high-entropy systems.

2:45 PM SF01.11.05

Computational Design and Experimental Validation of Ductile Refractory Metal-Based High Entropy Materials Kate Elder¹, Brandon Bocklund¹, Adam M. Krajewski², Joel Berry¹, Benjamin Ellyson¹, Connor Rietema¹, Jibril Shittu¹, Hunter Henderson¹, Alexander A. Baker¹, Thomas Voisin¹, Scott McCall¹, Aurelien Perron¹ and Joseph McKeown¹; ¹Lawrence Livermore National Laboratory, United States; ²The Pennsylvania State University, United States

The vast design space of high entropy materials allows the tuning of designer materials with enhanced properties. The subset of high entropy materials consisting of refractory metals with a body centered cubic (BCC) structure are known to maintain a high yield strength at elevated temperatures. However, just tailoring refractory metal-based high entropy materials to be strong and BCC stable is insufficient and ductility, which is challenging to model, must be incorporated into any alloy design process. Ductility models are compared with experimental compression and elongation data to determine which model accurately predicts ductility in refractory metal-based high entropy materials. Through analytical calculations, we investigate high entropy alloys from the Hf-Mo-Nb-Ta-Ti-V-W-Zr element palette to identify ductile candidates and understand which compositional combinations, with varying entropy, lead to novel properties. The design strategy is then expanded to rapidly explore the space of high order non-equiatomically refractory metal-based high entropy materials by leveraging machine learning and high-performance computing capabilities. Selected compositions predicted to maintain high strength, BCC phase stability and acceptable ductility are manufactured and tested to validate the search for refractory metal-based high entropy materials with designer properties. Prepared by LLNL under Contract DE-AC52-07NA27344.

3:00 PM BREAK

SESSION SF01.12: Thermal and Mechanical Properties of High Entropy Materials

Session Chairs: Lavina Backman and Scott McCormack

Thursday Afternoon, April 25, 2024

Terrace Suite 1, Level 4, Summit

3:30 PM *SF01.12.01

Synthesis and Characterization of High Entropy Carbonitrides Lavina Backman, James Tsai, Heonjune Ryou, Eric Patterson, Sara Mills, James Wollmershauser, Edward Gorzkowski III and Jesse Maxwell; US Naval Research Laboratory, United States

The high temperature ($T > 1700^\circ\text{C}$), highly chemically reactive environments encountered during hypersonic flight present unique design challenges for materials scientists. Requirements for these materials include melting temperatures greater than 3000°C , high thermal and dimensional stability, good thermal shock resistance, low reactivity and low coefficients of thermal expansion. Before 2015, less than 15 elements or compounds were considered to have the thermochemical stability to be viable material system candidates for this application and development of materials with coincident mechanical stability (e.g. ductility, toughness) has lagged. The recent advent of the high entropy design paradigm has expanded the composition space for UHTCs significantly and provided unprecedented tunability of mechanical and chemical properties. This is of particular interest for hypersonic vehicle designs requiring both high temperature oxidation resistance as well as maintaining structural and dimensional integrity to maximize aerodynamic performance. This presentation will review design strategies for performance in high temperature environments and discuss material system candidates, with a special focus on carbonitride high entropy ceramics. Experimental work on the synthesis and characterization of high entropy carbonitrides will also be presented.

4:00 PM SF01.12.02

Rapid Down-Selection of Novel High-Entropy Materials and Insights into their Characteristic Energy Scales from Temperature-Dependent Elastic Properties Christopher Mizzi¹, Tannor Munroe¹, Osman El-Atwani², Saryu Fensin¹ and Boris Maiorov¹; ¹Los Alamos National Laboratory, United States; ²Pacific Northwest National Laboratory, United States

High-entropy materials have generated much interest owing to their exceptional performance and high tunability. However, there are significant challenges in optimizing high-entropy compositions for tailored applications, such as in nuclear reactors, stemming from the immense size of the high-entropy design space. There is a pressing need for rapid, quantitative property assessments to identify promising high-entropy candidates, down-select compositions for further study, and provide experimental inputs to facilitate model development. One enticing property to examine in this context is elasticity. Elastic constants describe the extent to which materials resist elastic deformation, providing important information on mechanical performance as well as microscopic details about the nature of bonding and characteristic energy scales in materials. These features mean elastic constants naturally connect experiment and theory, making them prime candidates to serve as a benchmark for materials design, model development, and model validation.

In this talk, I will share elastic constant measurements on a range of refractory high-entropy alloys at ambient conditions to exemplify how elastic constants and ultrasonic attenuation can be used to rapidly identify promising high-entropy compounds for further study. Then, I use elastic constant determination down to 2K to explore the effects of composition on characteristic phonon energy scales (*e.g.*, Debye temperature), anharmonicity, and mechanical performance. These results are compared with theoretical predictions. Resonant ultrasound spectroscopy (RUS) is used for these experiments because of its ability to non-destructively determine the entire elastic constant tensor from a single measurement with high accuracy and precision. This approach, which entails extracting elastic constants from mechanical resonant frequencies, is amenable to all high-entropy materials, from metals to ceramics, compatible with any amount of crystalline anisotropy or texture, and capable of providing rapid feedback on novel high-entropy materials. As such, elastic constant determination with RUS is ideal to rapidly identify promising high-entropy materials, examine their functional properties, and determine key energy scales to incorporate in predictive models.

4:15 PM SF01.12.03

Critical Assessment of Mass and Lattice Disorder in Thermal Conductivity Prediction for Medium and High Entropy Ceramics Yuxuan Wang, Guoqiang Lan and Jun Song; McGill University, Canada

Medium and high entropy ceramics, with their distinctive disordered structures, exhibit ultra-low thermal conductivity and high temperature stability. These properties make them strong contenders for next generation thermal barrier coating (TBC) materials. However, predicting their thermal conductivity has been challenging, primarily due to their unique phonon scattering mechanisms. Apart from the conventional phonon-phonon scattering mechanism, the phonon-disorder scattering, comprising both mass and force disorder, are also expected to make significant contribution in determining the thermal conductivity of medium and high entropy ceramics. However, it remains challenging to quantify the phonon-disorder contribution, particular in the aspect of force disorder. Here we demonstrated a relationship between the lattice disorder, a quantity more readily calculable, with force disorder, rendering it possible to substitute the force disorder by lattice disorder. Based on this relationship and drawing inspiration from Klement's equation of static imperfection, we have developed a model that quantitatively assess the connection between disorder and thermal conductivity. Applying our model to the medium/high entropy rocksalt and pyrochlore oxides as the representative, we found good alignment between the theoretical predictions and experimental measurements of thermal conductivities, confirming the validity of our model. The model developed offers a critical predictive tool for rapid screening of TBC materials based on medium and high entropy ceramics.

4:30 PM SF01.12.04

Local Chemical Fluctuation and Lattice Thermal Conductivity of High-Entropy Thermoelectric Materials Wu Wang, Shixuan Liu, Yan Wang and Jiaqing He; Southern University of Science and Technology, China

High-entropy materials, which consist of multiple elements occupying the same crystallographic site, have emerged as the promising materials for a variety of applications [1,2]. With the mutual interaction of different elements, local chemical fluctuation arises in high-entropy structures and largely enhances the properties of various materials included metallic alloys [3], Li-ion batteries [4], and catalysts [5]. Recently, this high-entropy strategy has also been applied to enhance the performance of thermoelectric materials with the combination of multiple elements [6,7]. The local chemical fluctuation could dampen the propagation of heat-carrying phonons and thus largely reduce lattice thermal conductivity of thermoelectric materials.

However, these studies of high-entropy materials have lacked the attention on the role of each constituent elements on local chemical fluctuation, which is crucial for tailoring the local chemical fluctuation by selecting specific element. Herein, we have identified the respective contributions of the element characteristics (atomic mass, radius, and electronegativity) on the local chemical fluctuation by determining atomic-scale distributions and concentrations of various elements in GeTe, SnTe and PbTe-based high-entropy thermoelectric materials. The electronegativity is found to have a comparable influence with the mass on the elemental fluctuations while the slight contribution is from the radius. The local chemical fluctuation is further tailored by selecting specific elements to induce large lattice distortion and strong strain fluctuation in the GeTe-based high-entropy materials for lowering lattice thermal conductivity independent of the increased entropy by adding more elements. With the comparison of GeTe-AgSbX (X=Sn, Mn and Pb) high-entropy materials, we have also identified the noticeable contribution of electronegativity difference to the lattice thermal conductivity in addition to the known effect of mass and size differences. Our findings of local chemical fluctuation and lattice thermal conductivity provide the basis for tuning the structure and property of high-entropy materials by selecting specific elements.

References

1. George E P, Raabe D, Ritchie R O. High-entropy alloys. *Nature Reviews Materials*, 2019, 4(8): 515-534.
2. Dragoë N, Bérardan D. Order emerging from disorder. *Science*, 2019, 366(6465): 573-574.
3. Ding Q, Zhang Y, Chen X, et al. Tuning element distribution, structure and properties by composition in high-entropy alloys. *Nature*, 2019, 574(7777): 223-227.
4. Sarkar A, Velasco L, Wang D, et al. High entropy oxides for reversible energy storage. *Nature Communications*, 2018, 9(1): 3400.
5. Yao Y, Huang Z, Xie P, et al. Carbothermal shock synthesis of high-entropy-alloy nanoparticles. *Science*, 2018, 359(6383): 1489-1494.
6. Jiang B, Yu Y, Cui J, et al. High-entropy-stabilized chalcogenides with high thermoelectric performance. *Science*, 2021, 371(6531): 830-834.
7. Jiang B, Wang W, Liu S, et al. High figure-of-merit and power generation in high-entropy GeTe-based thermoelectrics. *Science*, 2022, 377(6602): 208-213.

4:45 PM SF01.12.05

Investigating High Temperature Thermal Properties of Rare Earth Oxides for Thermal Barrier Coatings William T. Riffe, Hunter Schonfeld, Kristyn Ardrey, Prasanna Balachandran, Beth Opila, Patrick E. Hopkins and Saman Zare; University of Virginia, United States

Rare earth oxides (REOs) show promising thermal properties required of next generation thermal barrier coatings (TBCs) for ultrahigh temperature applications (1500 °C+). TBCs mitigate conductive heating between hot components by reducing thermal conductivity through increased phonon-phonon scattering. New research aims to explore the fundamental mechanisms for this reduction and explore other properties of interest such as melting temperature and emissivity.

In this work, we perform a series of thermal and optical studies via pump-probe thermoreflectance, laser radiometry, and spectroscopic ellipsometry to elucidate temperature-dependent thermal properties of REOs. With a novel laser-based metrology, thermal conductivities, melting temperatures and emissivities of ceramics over 2000 °C can be measured nondestructively. Understanding these trends is of utmost importance in choosing REOs that can endure cycling to operating temperatures. Additionally, through ellipsometry, the lifetimes of optical phonons can be understood. Anharmonic scattering dominates thermal transport at high temperatures so measuring lifetimes with changing temperature is important to understand fundamental energy transport in REOs. By investigating pertinent physical scattering mechanisms at relevant temperatures, we deconvolute key design considerations for next generation TBCs.

SESSION SF01.13: High Entropy Carbides, Borides, and Silicates

Session Chairs: Theresa Davey and Scott McCormack

Friday Morning, April 26, 2024

Terrace Suite 1, Level 4, Summit

8:30 AM *SF01.13.01

First-Principles Calculations of Structural Transitions within Multi-Principal Component Transition Metal Carbides [Theresa Davey](#)^{1,2} and Ying Chen²; ¹Bangor University, United Kingdom; ²Tohoku University, Japan

High-entropy or multi-principal component ultra-high temperature ceramics (UHTCs), such as rocksalt structured MC_{1-x} (where the cation M is an equiatomic or non-equiatomic mixture of metallic elements including Ti, Zr, Hf, Nb, and Ta, and the anion C is carbon), have recently generated significant interest due to their potential improved or tuneable properties such as melting point, hardness, ductility, and oxidation resistance. The single metallic element UHTC carbides, such as zirconium carbide, are known to have a wide range of stoichiometry facilitated by significant numbers of carbon vacancies (up to around 50% of the carbon atoms), where in different parts of the phase space, the vacancies exhibit long-range ordering, short-range ordering, or are randomly distributed. Until now, there have been no systematic investigations varying carbon stoichiometry in multi-principal cation carbides, either experimentally or theoretically.

Individually, all the MC_{1-x} carbides have a tendency to form long-range vacancy-ordered phases at low temperature, although these are extremely challenging to experimentally synthesise. In single cation transition metal carbides (e.g. ZrC_{1-x} , HfC_{1-x}), the short- and long-range carbon vacancy ordering is driven by differing local bonding surrounding different vacancy cluster configurations. However, similar but slightly different trends are observed in group IV and group V transition metal carbides, resulting in different symmetries, for example low temperature M_2C ($M = Ti, Zr, Hf$) has a cubic Fd-3m structure, whereas M_2C ($M=Ta$) has a trigonal P-3m1 structure.

This work uses first-principles calculations to explore multiatomic mixing (binary, ternary, quaternary, and quinary) on the metallic element lattice at different carbon stoichiometries. Within this, disordered vacancies, and various vacancy-ordered structures were considered. Special Quasirandom Structures (SQS) were generated for each composition, to provide a supercell approximation of random mixing. Density functional theory (DFT) calculations were used to obtain the ground state energy and structural and electronic properties. The atomic bonding is investigated, and trends are identified by considering the local atomic environments and cluster configurations.

The effects that the multi-principal cation lattice has on the carbon vacancy ordering on the anion lattice are explored, at absolute zero and considering finite temperature effects. The most stable crystal structures are identified for various multi-cation systems at different carbon stoichiometries. Miscible and immiscible mixtures are identified, where approximate temperatures of miscibility gaps are determined using the Bragg-Williams configurational entropy approximation for ideal mixtures. The tendency for phase separation is compared in equivalent composition multi-cation vacancy-disordered and vacancy-ordered carbides. Approximate order-disorder transition temperatures are obtained for mixed-cation substoichiometric carbides and compared with the miscibility gaps in the same system. On this basis, the possibility of synthesising certain vacancy-ordered multi-principal cation compounds is revealed, alongside the required range of synthesis temperatures.

9:00 AM SF01.13.02

Computational Investigation into Synthesis of Transition Metal Borides [Himanshu Shekhar](#) and Aravind Krishnamoorthy; Texas A&M University, United States

Borides of transition metals and high-entropy alloys offer novel opportunities to design materials that demonstrate phase stability, high strength, and thermal oxidation resistance at high temperatures and under extreme conditions. Identifying mechanically strong and chemically inert transition metal borides requires an understanding of the synthesizability of different transition metal borides, as well as their mechanism of growth during boriding of such metals. We performed *ab initio* Density Functional Theory simulations to quantify phase stability, formation energies of point and extended defects, and point defect migration barriers in crystalline borides of transition metals and their alloys. A point defect model based on the computed defect concentrations and ionic mobilities was used to explain the experimentally observed thicknesses of boride films formed by the boriding of different transition metals and alloys. Thermodynamic (formation energies and stability) and kinetic (energy barriers and mobilities) data from these *ab initio* simulations were also used to create a graph neural network model for the screening of compositional phase space of high-entropy borides to identify promising candidates with high phase stability and synthesizability.

9:15 AM *SF01.13.03

Predicting The Synthesizability and Properties of Disordered Materials from First-Principles [Cornac Toher](#); The University of Texas at Dallas, United States

The successful development and manufacturing of new materials, for applications ranging from wear resistant coatings for cutting tools and thermal protection barriers in aerospace engineering to new catalysts and photovoltaics, as well as materials for batteries and electronics, depends on computational thermodynamics to predict synthesizability and stability. Thermodynamic models for synthesizability must incorporate entropy, which is particularly important at high temperature for multi-element materials [1, 2]. Descriptors and thermodynamic models have been developed based on the thermodynamic density of states extracted from ensembles of ordered calculations in the AFLOW repository [3, 4] to predict the synthesizability of new disordered materials such as high entropy carbides [5, 6]. Similar methods are now being combined with machine-learning to investigate high-entropy rare-earth silicates for thermal and environmental barriers in gas turbines [7].

[1] Toher et al., *npj Comput. Mater.* 5, 69 (2019).

[2] Brahlek et al., *APL Mater.* 10, 110902 (2022).

[3] Oses et al., *Comput. Mater. Sci.* 217, 111889 (2023).

[4] Esters et al., *Comput. Mater. Sci.* 216, 111808 (2023).

[5] Sarker, Harrington et al., *Nature Commun.* 9, 4980 (2018).

[6] Oses, Toher, and Curtarolo, *Nature Rev. Mater.* 5, 295-309 (2020).

[7] Toher et al., *Materialia* 28, 101729 (2023).

9:45 AM SF01.13.04

In-Situ SEM Tensile Characterization of High Entropy MXenes [Yuxiang Gan](#), Congjie Wei, Jiaoli Li and Chenglin Wu; Texas A&M University, United States

The synthesis of high-entropy (HE) MXenes as a new emerging member of the MXene family was reported by implementing four transition metals. The resultant HE MXenes, TiVNbMoC₃T_x and TiVCrMoC₃T_x have great potential in the thermoelectricity, magnetic, and superconductivity fields due to their diverse compositions. The stability and reliability of these applications largely depend on the mechanical properties of HE MXenes. However, the tensile strength as a critical factor for its practical strength in engineering applications has not been investigated. In this paper, we employed an in-situ push-to-pull device under a scanning electron microscope (SEM) to measure the load-displacement data of suspended HE MXene films and observed an exciting tensile behavior during crack extension. When the number of HE MXene layers in a stack changes, the tensile strength variations can be recorded. Additionally, the crack tip behavior after fracture testing can be observed by transmission electron microscopy (TEM). Our combined experiment and modeling investigations have revealed that the tensile strength of HE MXene is much higher than that previously observed in MXene and other 2D Materials stacks. HE MXene can serve as an excellent structural reinforcement for multi-scale composite materials, as well as for other applications in which robust mechanical performance is required.

10:00 AM BREAK

SESSION SF01.14: High Entropy Intermetallics and Alloys

Session Chairs: Alannah Hallas and Cormac Toher

Friday Morning, April 26, 2024

Terrace Suite 1, Level 4, Summit

10:30 AM SF01.14.01

Boron Interstitial and Boride Strengthened Grain Boundary for Toughening Refractory High-Entropy Alloys [Ping-Hsu Ko](#), Ya-Jing Lee and Shou-Yi Chang; National Tsing Hua University, Taiwan

Refractory high-entropy alloys exhibit a high mechanical strength and an excellent structural stability at elevated temperatures, and are of great potential for applications to aerospace and nuclear power components. However, the drawback of poor grain boundary cohesion and consequent early brittle intergranular fracture renders their practical applications limited. According to the literature, boron interstitials (or borides) have been verified to improve the cohesion strength of grain boundaries and thus the ductility of some intermetallic compounds such as nickel aluminide(s). Introducing boron interstitials (or forming multicomponent borides) particularly at grain boundaries was hence considered in this study for enhancing grain boundary cohesion and toughening refractory high-entropy alloys. A very small amount (0.1 at.%) of boron was added in arc-melted Hf_{0.5}Mo_{0.5}NbTa_xTiV_{1.5-x}Zr_x refractory high-entropy alloys, and the microstructure, compositions and crystallographic orientations of the alloys were characterized. Macroscale compressive tests were conducted for measuring the stress-strain response of the alloys, and micropillar compressive tests and indentations were carried out for measuring the strength of grains and grain boundaries. Microstructure observations indicated that elemental boron was uniformly distributed in the refined single-phase, solid-solution grains, while some nanosized boride particles were dispersed at the grain boundaries. With the addition of boron, the hardness of weak grain boundaries (about 5.0 GPa) was markedly improved to the equivalent level of grain interiors (about 6.2 GPa). While the yield strength of the boron-added alloys did not change (about 1450 MPa), the ultimate compressive strength effectively increased from 1690 to 2240 MPa at a higher work hardening rate. The compressive strain increased from 20-25% to 35-40%, attributable to the inhibited boundary decohesion-caused brittleness as the distinct transition of intergranular-to-transgranular fracture. Micropillar compression tests suggested that the grain boundaries of the alloys without boron early decohered at a stress of below 700 MPa, whereas those with boron did not fracture even after the adjacent grains yielded. Owing to the high charge density-enhanced grain boundary cohesion, the boron-added alloys also showed a high structural stability at elevated temperatures, with a retained strength of 1190 and 990 MPa at 600 and 800°C, respectively.

10:45 AM SF01.14.02

Predictive Modelling of The Structure and Phase Stability of High-Entropy Materials: Case Study of Al_xCrFeCoNi [Christopher D. Woodgate](#)¹, [Laura H. Lewis](#)^{2,2} and [Julie Staunton](#)¹; ¹University of Warwick, United Kingdom; ²Northeastern University, United States

Advancing both fundamental understanding and technological application in the rapidly developing field of high-entropy materials, computational-forward modelling approaches are an important tool to help guide experiment. Starting from a given combination of constituent elements, we would like to be able to predict a material's crystal structure, its thermodynamic stability, as well as the nature of emergent atomic short- and long-range order, as this will enable us to go on to predict subsequent macroscopic materials properties. Here we present results from a first-principles-based, all-electron Landau theory which has previously been used with success to study the Cantor alloy and its derivatives [1,2], as well as the refractory high-entropy alloys [3]. We study the Al_xCrFeCoNi system for 0 ≤ x ≤ 2 and demonstrate successful reproduction of the experimentally observed crystal structure and phase behaviour of this material. We successfully predict the A1+B2 coexistence region of the phase diagram, explain the lack of observation of an atomically disordered A2 phase, and give insight into the preferred low-temperature atomic arrangements. As the methodology is first-principled, we are able to explain ordering tendencies in terms of materials' underlying electronic structure, and pull out qualitative rules to explain ordering tendencies in these complex systems.

Acknowledgements

We gratefully acknowledge the support of the UK EPSRC, Grant No. EP/W021331/1. C.D.W. is supported by a studentship within the UK EPSRC-supported Centre for Doctoral Training in Modelling of Heterogeneous Systems, Grant No. EP/S022848/1. This work was also supported in part by the U.S. Department of Energy, Office of Basic Energy Sciences under Award Number DE SC0022168 (for atomistic insight) and by the U.S. National Science Foundation under Award ID 2118164 (for advanced manufacturing aspects).

References

- [1] C. D. Woodgate and J. B. Staunton, Phys. Rev. B **105**, 115124 (2022).
- [2] C. D. Woodgate and J. B. Staunton, Phys. Rev. Mater. **7** 013801 (2023).
- [3] C. D. Woodgate D. Hedlund, L. H. Lewis, J. B. Staunton, Phys. Rev. Mater. **7** 053801 (2023).

11:00 AM SF01.14.03

Thin Film Combinatorial Sputtering of TaTiHfZr Compositionally Complex Alloys for Rapid Materials Discovery Reece Emery, Stephen B. Pupilampu, Dayakar Penumadu, Eric A. Lass, Shakti P. Padhy, Zachary Sims and Philip D. Rack; The University of Tennessee, Knoxville, United States

Combinatorially sputtered thin films can be leveraged as a rapid, materials discovery process in mechanical alloy design. Ta_wTi_xHf_yZr_z thin films were synthesized via combinatorial sputtering from pure Ta, Ti, Hf, and Zr targets. The substrate was not rotated to generate compositional gradients where 12.4 < w < 71.6, 6.40 < x < 55.6, 4.22 < y < 58.8, 7.25 < z < 48.9 over a 100 mm diameter substrate. The crystal structure, phase fraction, film morphology, mechanical (i.e. modulus and hardness), optical (i.e. n and k), thermal (i.e. phase stability, CTE, and thermal conductivities), and corrosion properties (i.e. corrosion current and rates) are all correlated to the Ta_wTi_xHf_yZr_z composition. Temperature dependent x-ray diffraction (TDXRD) reveals the thermal stability of the material system. TDXRD has shown the as-deposited material library is primarily stable in a single HCP phase below 60 at. % Ta at room temperature but will form increasing amounts of a BCC phase at elevated temperatures. Nanoindentation of as-deposited films shows good agreement between experimental, solid solution estimations of hardness via a simple rule of mixtures from bulk elements, and correlated to a few up-scaled bulk samples. Thin film modulus shows good agreement with bulk rule of mixture estimations after accounting for thin film substrate effects via King's correction. As-deposited and annealed film properties are compared. Compositions with an optimal combinations of the aforementioned properties were then upscaled to bulk materials for further investigation.

11:15 AM SF01.14.04

Accelerated Discovery of Structural Materials for Harsh Environments Rameshwari Naorem^{1,2}, Hailong Huang¹, Gaoyuan Ouyang¹, Prashant Singh¹, Duane D. Johnson^{1,2}, Jun Cui¹, Ryan T. Ott¹, Iver E. Anderson^{1,2}, Nicolas Argibay¹ and Brandon Krick³; ¹Ames Laboratory, United States; ²Iowa State University of Science and Technology, United States; ³Florida A&M University, United States

Multi-principal-element alloys (MPEA) have emerged as a promising group of advanced materials with unprecedented combinations of mechanical properties compared to conventional alloys. Materials that can tolerate harsh environments and retain high strength at elevated temperatures are needed to enable greater efficiency in applications including nuclear reactors, hydrogen combustion turbines, bearings, and hypersonic vehicles. We will present results from materials design efforts focused on refractory alloys that rely on high-throughput synthesis and characterization methods like additive manufacturing, tribology-based mechanical testing, and electronic-structure modeling. Discussion topics will include rapid screening of thermomechanical properties using surface (scratch)-based techniques to assess hardness, fracture toughness, and tensile ductility. We will also present preliminary results from composition tailoring of MPEA to understand and control the impacts of hydrogen exposure on selected refractory MPEAs and to develop alloy design criteria for mitigating hydrogen embrittlement.

11:30 AM SF01.14.05

Bridging the Gap between Modeling and Characterization to Unravel Short-Range Order and Properties of Si-Ge-Sn-Pb Alloys Shunda Chen, Xiaochen Jin and Tianshu Li; George Washington University, United States

Group IV concentrated alloys composed of Si-Ge-Sn-Pb are promising candidates for mid-infrared photonics owing to their tunable band gaps, low-cost, and CMOS-compatibility. Although group IV alloys have been long conceived as a random solid solution, our recent ab initio-based statistical sampling predicted substantial short-range order (SRO) behaviors in group IV alloys¹⁻⁴. The structural complexity was further shown theoretically to yield a substantial impact on the underlying electronic¹⁻³, topological⁴, and transport properties of group IV alloys. Although SRO may have a complicated implication on material quality, it also opens an emerging opportunity for engineering SRO to harvest new functionalities that are challenging to achieve through traditional heterojunctions. Emerging characterization evidence based on EXAFS⁵, Raman⁶, APT⁷ and 4D-STEM support our prediction of SRO, but important questions need to be addressed regarding the actual structures, spatial domain size and its distribution, and corresponding changes in the properties of SRO, before a practical strategy can be employed. The explicit answers to these questions require synergistic efforts from both characterization and modeling. Here I will discuss our ongoing theoretical effort to close the gap between theory and characterization to enable deciphering the fine structural details of complex alloys. We have developed a highly accurate, highly efficient machine-learning potential (MLP) based on neuroevolution potential framework for group IV system. The developed MLP is shown to reach a DFT-level accuracy by exhibiting a root mean squared error of energy < 1 meV/atom with respect to the DFT training data set and more importantly, enables a side-by-side comparison with APT and 4D-STEM on the same scale. Using this development, we discovered the spatial structural heterogeneity in group IV alloys. In particular, we show that structural details at a fine level, as reflected by the distributions of both atomic SRO parameter and spatial SRO domains, are vital for the underlying electronic structures of group IV concentrated alloys.

This work is supported by Department of Energy, Office of Basic Energy of Sciences under Award No. DE-SC0023412.

- (1) Cao, B.; Chen, S.; Jin, X.; Liu, J.; Li, T. Short-Range Order in GeSn Alloy. *ACS Appl. Mater. Interfaces* **2020**, *12*, 57245–57253.
- (2) Jin, X.; Chen, S.; Li, T. Coexistence of Two Types of Short-Range Order in Si–Ge–Sn Medium-Entropy Alloys. *Commun Mater* **2022**, *3* (1), 66.
- (3) Jin, X.; Chen, S.; Li, T. Short-Range Order in SiSn Alloy Enriched by Second-Nearest-Neighbor Repulsion. *Phys Rev Mater* **2021**, *5* (10), 104606.
- (4) Liang, Y.; Chen, S.; Jin, X.; West, D.; Yu, S.-Q.; Li, T.; Zhang, S. Group IV Topological Quantum Alloy and the Role of Short-Range Order: The Case of Ge-Rich GePb, Under Review 2023.
- (5) Lentz, J. Z.; Woicik, J. C.; Bergschneider, M.; Davis, R.; Mehta, A.; Cho, K.; McIntyre, P. C. Local Ordering in Ge/Ge–Sn Semiconductor Alloy Core/Shell Nanowires Revealed by Extended x-Ray Absorption Fine Structure (EXAFS). *Appl Phys Lett* **2023**, *122* (6), 062103.
- (6) Corley-Wiciak, A. A.; Chen, S.; Concepción, O.; Zoellner, M. H.; Grützmacher, D.; Buca, D.; Li, T.; Capellini, G.; Spirito, D. Local Alloy Order in a Ge1–xSnx/Ge Epitaxial Layer. *Phys. Rev. Appl.* **2023**, *20* (2), 024021.
- (7) Liu, S.; Covian, A. C.; Wang, X.; Cline, C. T.; Akey, A.; Dong, W.; Yu, S.; Liu, J. 3D Nanoscale Mapping of Short-Range Order in GeSn Alloys. *Small Methods* **2022**, 2200029.

11:45 AM SF01.14.06

Fabrication and Characterization of Two-Dimensional High-Entropy Sulfides and Tellurides Yingchao Yang; University of Missouri, United States

Since the discovery of graphene monolayers by mechanical exfoliation in 2004, many other two-dimensional (2D) materials have been synthesized, such as transition metal dichalcogenides (TMDs), hexagonal boron-nitride (*h*-BN), black phosphorous. Another category of materials, high entropy alloys (HEAs) are constructed by the combination of multiple principal elements at an equimolar or near-equimolar fraction. HEAs offer an extensive combinatorial space facilitating superior functionalities that are generally lacking in conventional alloys composed only of one or two principal elements.

The combination between 2D materials and HEAs results in a new 2D high-entropy materials (2D HEMs). Even though 2D HEMs has significant potential towards catalysis and energy storage, the rationale and criterion for designing 2D HEMs and demonstration of feasibility in synthesizing 2D HEMs are still missing.

In this presentation, we will demonstrate the successfully synthesized five-metal-element sulfide and tellurides. Sulfides have been synthesized through

chemical vapor deposition (CVD) method and tellurides have been obtained via the conventional solid-state reaction (SSR) approach. Advanced characterization techniques have been performed to confirm that uniform element distribution and single phase 2D HEM have been achieved. The designed and fabricated 2D HEMs adds an exceptional family member to the fast-growing field of 2D materials.

SESSION SF01.15: Virtual Session: High Entropy Materials
Session Chairs: Ben Breitung, Scott McCormack and T. Zac Ward
Tuesday Morning, May 7, 2024
SF01-virtual

10:30 AM *SF01.15.01

High-Throughput Experimentation for The Exploration of High Entropy Materials: From Alloys to Oxides and Nitrides [Alfred Ludwig](#)^{1,2,2}; ¹Ruhr-University Bochum, Germany; ²Ruhr-Universität Bochum, Germany

Discovery of new materials is a key challenge in materials science. New materials for sustainable production/storage/conversion of energy carriers are necessary to improve existing and to enable future energy systems. Compositionally complex materials, frequently called high entropy materials, offer a vast multidimensional search space, which provides opportunities for discovering new materials. Next to alloys compounds such as oxides and nitrides are of interest. However, efficient methods for the exploration and exploitation of this multidimensional search space are necessary, especially as oxides and nitrides need more sophisticated synthesis methods such as reactive sputter deposition. Here, the integration of high-throughput thin-film combinatorial materials science methods with simulation and materials informatics (1) is presented as an effective means to produce large datasets on new materials, which enables mastering of this immense search space. The approach combines theoretical predictions from high-throughput computations with production of large, consistent and complete experimental datasets, which are used for materials informatics. Thin-film materials libraries are fabricated by (reactive) combinatorial sputter deposition and optional post-deposition treatments, followed by high-throughput characterization, and finally the organization of the acquired multi-dimensional data in adequate databases as well their effective computational analysis and visualization, e.g., of polyelemental systems in the form of composition-processing-structure-function diagrams, interlinking compositional data with structural and functional properties. The talk will discuss examples of high-throughput exploration of compositionally complex metallic solid solutions as well as oxide and nitride thin-film libraries for electrocatalysis and solar water splitting (2-7). In the case of compositionally complex perovskites, we recently discovered a new platform for materials discovery (8). Furthermore, a new approach (9) to accelerate atomic-scale measurements for complex materials and their oxidation (10) is presented.

- (1) A. Ludwig (2019), *npj computational materials* 5, 70
- (2) T. Löffler et al. (2018), *Adv. Energy Mater.* 8, 1802269
- (3) T. A. A. Batchelor et al. (2021) *Angewandte Chemie* 60, 6932–6937
- (4) V. Strotkötter et al. (2022), *Chemistry of Materials*, 34, 10291–10303
- (5) E. Suhr et al. (2023), *Advanced Engineering Materials* 300550
- (6) S. Kumari et al. (2020), *Zeitschrift für Physikalische Chemie* 234, 867-885
- (7) M. Nowak, et al. (2020), *Zeitschrift für Physikalische Chemie* 234, 835-845
- (8) T. H. Piotrowiak et al., (2023), *Advanced Engineering Materials* 25, 2300437
- (9) Y. J. Li et al., (2018), *Materials Horizons* 5, 86 - 92
- (10) Y. Li et al., (2018), *J. Alloys and Compounds* 766, 1080 -1085

11:00 AM *SF01.15.02

Electrospun High-Entropy Spinel Oxides as Catalysts for as Electrocatalysts for Oxygen Evolution in Alkaline Environment [Saveria Santangelo](#); [Mediterranea University, DICEAM, Italy](#)

The generation of H₂ via the electrochemical splitting of water is a promising and sustainable technology. Nonetheless, the oxygen evolution reaction (OER) still represents the bottleneck of the process. Spinel-structured transition metal (TM) oxides have shown great potential as an alternative to platinum group metal-based electrocatalysts as they are Earth-abundant, inexpensive and stable. Among them, those based on the high-entropy concept, benefiting from the synergy among their multiple-metallic components, are in focus due to their interesting performance in various energy applications [1,2], including the OER in alkaline environment.

This contribution focuses on the case of electrospun spinel-type high-entropy oxide (HEO) nanofibers (NFs), which thanks to their granular architecture are suitable to the preparation of ink-jet printable OER electrocatalysts [3]. It presents the results of the evaluation of a large set of HEO NFs with oxygen-deficient surface as electrocatalysts in alkaline medium. HEO NFs based on different equimolar TM combinations, are prepared under different calcination conditions and characterized by a combination of benchtop analytical techniques to investigate the complex and interdependent changes in the morphology of the fibers, crystallinity and inversion degree of the spinel oxide, concentration of the oxygen-vacancies, cation distribution in the lattice produced by the variation of HEO composition and calcination temperature (400-900 °C) and to identify the relationships with the different electrochemical properties of the fibers. The electrocatalytic performance of HEO NFs are discussed in terms of the most common descriptors, namely outer 3d-electron number, e_g filling and occupation of 16d sites.

- [1] C. Triolo, W. Xu, B. Petrovičová, N. Pinna, S. Santangelo, *Adv. Funct. Mater.* **2022**, 32, 2202892.
- [2] C. Triolo, S. Santangelo, B. Petrovičová, M.G. Musolino, I. Rincón, A. Atxirika, S. Gil, Y. Belaustegui, *Appl. Sci.* **2023**, 13, 721
- [3] C. Triolo, S. Schweidler, L. Lin, G. Pagot, V. Di Noto, B. Breitung, S. Santangelo, *Energy Adv.* **2023**, 2, 667.

11:30 AM SF01.15.03

Autonomous Discovery of Triple-Conducting High-Entropy Oxides for Protonic Ceramic Fuel Cells [Ivano Eligio Castelli](#); [Technical University of Denmark, Denmark](#)

We develop and implement an autonomous multi-fidelity computational workflow to explore the chemical space of high-entropy perovskite oxide materials with general formula ABO₃, screening for stable, high-performance cathodes for low-temperature protonic ceramic fuel cells. The workflow, implemented in the framework of Density Functional Theory (DFT), is based on the calculation of thermodynamic, electric and kinetic properties, which include phase and electrochemical stability, electronic conductivity, and ionic diffusivity. To accelerate the calculation of the kinetic properties, we employ accelerated methods that leverage recent advances in machine learning for materials science to predict transition barriers for ionic diffusion. The

computational cost of the workflow is additionally decreased while retaining the quality of results through a thorough examination of the required level of theory for all descriptive properties. Moreover, the aim is a general and chemistry-neutral approach that can be applied to other crystal prototypes and materials screenings.

SYMPOSIUM SF02

Actinide Materials
April 23 - April 25, 2024

Symposium Organizers

Edgar Buck, Pacific Northwest National Laboratory
Sarah Hernandez, Los Alamos National Laboratory
David Shuh, Lawrence Berkeley National Laboratory
Evgenia Tereshina-Chitrova, Czech Academy of Sciences

* Invited Paper

+ JMR Distinguished Invited Speaker

^ MRS Communications Early Career Distinguished Presenter

SESSION SF02.01: Spectroscopy/Advanced Characterization

Session Chairs: Liane Moreau and David Shuh

Tuesday Morning, April 23, 2024

Terrace Suite 2, Level 4, Summit

10:30 AM *SF02.01.01

Micro-Focused X-Ray Absorption Spectroscopy Studies of Plutonium Materials Sarah Hickam¹, Arjen van Veelen¹, Daniel Olive¹, Kasey Hanson¹, Raymond Atta-Fynn¹, Nicholas Edwards² and Samuel Webb²; ¹Los Alamos National Laboratory, United States; ²SLAC National Accelerator Laboratory, United States

Synchrotron X-ray absorption spectroscopy (XAS) is an established technique for studying the local structure of plutonium materials, including oxides and metals. Modern imaging and high-resolution techniques provide detailed information that may elucidate questions regarding the fate of impurities with different Pu oxidation conditions and may also find utility in nuclear forensics investigations. Combining XAS with x-ray fluorescence (XRF) mapping provides the ability to quickly locate particles or areas of interest with up to 1 μm spatial resolution and then obtain local structure information from individual points. In this work, we apply micro-focused XRF+XAS techniques to the study of common impurities in plutonium oxides, such as gallium, iron, and nickel. We investigate the distribution and local structure of these impurities in plutonium oxides made from various synthetic routes, including corrosion and high temperature calcination of Pu metal. The results show that for some impurities, like Ga, local structure and distribution are highly dependent on processing conditions, such as temperature. We also discuss developments in micro-focused high energy resolution fluorescence detection (HERFD) XAS techniques and their applications to Pu particulate samples. Using a HERFD spectrometer significantly increases the resolution of the near-edge spectrum, providing greater confidence in oxidation state determination, and combining this technique with a micro-focused beam enables the generation of oxidation state distribution maps. Here, we present results for heterogeneous plutonium samples, demonstrating the utility of this technique for distinguishing between phases of interest (e.g. oxide and metal) and their distribution within a sample. Characterization using these advanced methods provides insight into impurity fate with plutonium processing and possible nuclear forensics signatures of plutonium materials.

11:00 AM *SF02.01.02

The Auger Parameter and Plutonium Paul Rousset; AWE, United Kingdom

The Auger parameter, α' , the sum of the binding energy of the most prominent core level transition and the kinetic energy of the Auger transition, as measured in a single X-ray Photoelectron Spectrum, can afford chemical state / chemical fingerprinting, non / local screening and initial / final state information. The use of the Auger parameter and the related chemical state plot offer advantages over chemical state / environment determination from the shift in binding energy of a single core hole transition as both charge referencing / binding energy scale calibration and work function corrections are not required, such that data from different laboratories can be easily compared. In the area plutonium XPS there are three separate reports on the Auger parameter and the associated chemical state plots [1-3]. The first two reports [1, 2] have both utilised the Pu P_{1VV} X-ray induced Auger transition combined with the Pu $4f_{7/2}$ peak and are very similar demonstrating reproducibility as the data were acquire at different laboratories using different samples. However, the most recent report uses the Pu N_{7O_5V} Auger peak with the Pu $4f_{7/2}$ core level, and the results are distinctly different [3]. The first two reports show that the Auger parameter for PuO_2 is approximately 2 eV higher than plutonium metal which is extremely unusual, indicative of enhanced screening / extra atomic relaxation behaviour in the oxide compared to the metal. In comparison, the most recent report [3] indicate that plutonium dioxide has a remarkably similar Auger parameter to plutonium metal, albeit this is based on an extremely limited data set. The object of this presentation is to investigate this discrepancy and if possible, to explain the differences by evaluating the key assumption used in the Auger parameter of equal binding energy shifts for all core levels involved in the definition of the Auger parameter. To enhance understanding the of the Auger parameter involving the Pu N_{7O_5V} transition the data set used has been expanded which has resulted in a greater understanding to the factors involved in measuring the Auger parameter on plutonium materials.

- [1] Detection of plutonium hydride using X-ray photoelectron spectroscopy, D. T. Larson, K. M. Motyl, J. Electron Spectrosc. Relat. Phenom., 50, 67 (1990).
[2] X-ray excited Auger transitions of Pu compounds, A. J. Nelson, W. K. Grant, J. A. Stanford, W. J. Siekhaus, P. G. Allen, W. McLean, J. Vac. Sci. Technol. A 33, 031401 (2015).
[3] XPS characterization of a PuGa-7 at. % alloy, P. Roussel, S. C. Hernandez, J. J. Joyce, K. S. Graham, T. Venhaus, J. Vac. Sci. Technol. A 41, 023204 (2023).

UK Ministry of Defence © Crown Owned Copyright 2024/AWE

11:30 AM SF02.01.03

Extraction of Branching Ratios from HERFD Data James G. Tobin¹, Sophie Nowak², Sw Yu³, R. Alonso-Mori², T Kroll², D. Nordlund², T.C. Weng² and Dimosthenis Sokaras²; ¹University of Wisconsin-Oshkosh, United States; ²SLAC National Accelerator Laboratory, United States; ³Lawrence Livermore National Laboratory, United States

Historically, Branching Ratio measurements with X-ray Absorption Spectroscopy (XAS) and related techniques have played a key role in the advancement of the understanding of 5f electronic structure. [1] Specifically, the transitions utilized were the N₄ and N₅ of the actinide elements, with electrons being moved from the occupied 4d states into unoccupied 5f states. For soft x-rays, the peak separations are small, allowing the doublet peaks to be collected together, in a single spectrum. The intensity calibration is intrinsic, within some small variations such as those due to storage ring beam current decay and fluctuations and other higher order effects. For tender and hard x-rays, the peak separations tend to be larger, often requiring two separate spectra and some sort of new normalization, especially for High Energy Resolution Fluorescence Detection (HERFD) XAS spectra. It will be shown that the step heights in the EXAFS regime can be used as a cross calibration between the M₄ and M₅ spectra, if two well characterized cases can be used as controls. (EXAFS is Extended X-ray Absorption Fine Structure, typically about 20 eV or more above the white-lines (sharp, intense peaks) at threshold, e.g. the 5f peaks.) Thus, a quantitative analysis method has been developed that allows the cross calibration of separate Uranium M₄ and M₅ X-ray absorption spectra (XAS), in particular those collected with the new High Energy Resolution Fluorescence Detection (HERFD) method. With this method, it is now possible to generate experimental Branching Ratio (BR) values from the U M_{4,5} XAS HERFD data.

1. J. G. Tobin, S. Nowak, S.-W. Yu, R. Alonso-Mori, T. Kroll, D. Nordlund, T.-C. Weng, D. Sokaras, "Extraction of Branching Ratios from HERFD Data," J. El. Sp. Rel. Ph. 262, 147285 (2023) <https://www.sciencedirect.com/science/article/abs/pii/S0368204823000026>

11:45 AM SF02.01.04

Site-Specific Morphological and Chemical Analysis of Nuclear Materials Brandon W. Chung¹, Alexander A. Baker¹, Scott Donald¹, Tian Li¹, Rachel Lim¹, Uday Mehta¹, Debra L. Rosas¹, Donya Servando-Williams¹, Vanna Som¹, Nicholas Cicchetti², Alexander Ditter³ and David K. Shuh³; ¹Lawrence Livermore National Laboratory, United States; ²University of Nevada, Las Vegas, United States; ³Lawrence Berkeley National Laboratory, United States

Nuclear forensics requires accurate identification of distinguishing material characteristics to delineate the material's origin-to-interdiction information. We developed the focused ion beam (FIB) methodology to reveal entrapped material clues such as internal morphological and chemical features within the surface/subsurface and bulk of nuclear materials. Our recent effort also established the capability of using the FIB-based micromanipulation technique to select, isolate, and extract a site-specific microscopic feature from bulk plutonium (Pu) and uranium (U) materials. Using a combination of scanning electron microscopy (SEM), transmission electron microscopy, three-dimensional (3D) spatial modeling, and synchrotron-based X-ray spectromicroscopy, we identified distinguishing morphological and chemical characteristics that are attributable to the material's provenances. Variations in the internal chemical composition and morphological structure were found to occur between materials from different origin, processing, and environmental exposures. The information is of potential use in identifying material characteristics related to the provenance, process, and pathways of interdicted nuclear materials.

SESSION SF02.02: Advanced Characterization
Session Chairs: Edgar Buck and Sarah Hickam
Tuesday Afternoon, April 23, 2024
Terrace Suite 2, Level 4, Summit

1:30 PM *SF02.02.01

Application of Ultra-High Temperature XAFS Measurement System for Actinide Materials Tsuyoshi Yaita; Japan Atomic Energy Agency, Japan

In order to clarify accident progression scenarios in the Fukushima NPP accident, it is essential to evaluate the behavior of fuel heated to high temperatures, and information on fuel behavior in the "ultra-high temperature region (around melting point)" is required. However, there is little information on the structural and electronic properties of actinides in this high temperature region. In this study, we developed a new measurement cell that enables high-temperature heating and constructed an in-situ observation system using synchrotron radiation XAFS and XRD to obtain information on the structure and electronic state of materials around the melting point. The validity of machine learning was also verified by comparison with the structural and electronic state information predicted by theoretical calculations using NN potentials. In this study, we mainly report the results obtained by synchrotron radiation analysis of yttrium-stabilized zirconia around the melting point as first step. The measurements were performed at the JAEA beamline BL22XU at SPring-8. The incident light intensity was measured with an ion chamber placed just in front of the sample, a CCD detector and imaging unit for X-ray diffraction, and a silicon drift detector for XAFS, each of which was placed horizontally displaced from the optical axis downstream or upstream of the sample, taking into account the position of the window in the measurement chamber. The heating system was a pulsed current heating furnace using W as the electrode, which is capable of performing structural analysis experiments up to ~3500K. In the radial structure function by XAFS, the distance of the first peak originating from Zr-O tends to shorten as the temperature increases, especially around 2000 K. This indicates a phase transition of zirconia, corresponding to the phase transition of zirconia from Tetragonal to Cubic. On the other hand, the second peak originating from Zr-Zr shows a trend of increasing distance as a whole, and the peak became so small that its order is almost unobservable near the melting temperature. The energy of the absorption edge also showed a tendency to shift to the lower energy side with the structural change due to the temperature increase.

2:00 PM ^SF02.02.02

Actinide Photosensitization in Macromolecular and Nanocrystal Hybrids Rebecca Abergel^{1,2}; ¹Lawrence Berkeley National Laboratory, United States;

²University of California, Berkeley, United States

The small absorption cross sections ($\epsilon < 10 \text{ M}^{-1} \text{ cm}^{-1}$) characteristic of Laporte-forbidden transitions in the f-elements have limited the practical implementation of lanthanide and actinide nanoparticles in devices for applications ranging from solar capture to sensing. While various strategies designed to circumvent the problems of low f-f oscillator strengths have been investigated, comparatively little work has explored the utility of organic ligands with high absorption coefficients ($\epsilon \approx 10^3\text{--}10^5 \text{ M}^{-1} \text{ cm}^{-1}$) in sensitizing excited states in f-element macromolecules and nanocrystals. Our approach investigates actinide hybrid architectures, in which sensitization is achieved with aromatic antenna functioning as terminal light absorbers to convert light into luminescence with unusually high external quantum yields. In addition, chiral constructs allow for luminescence circular polarization for sensing applications and forensics determination. Energy transfer mechanisms in these actinide compounds and particles will be discussed, with an emphasis placed on the generality of this material architecture for realizing ligand-pumped, photon conversion and polarization.

2:30 PM SF02.02.03

Elastic Properties of Pu Alloys using Resonant Ultrasound Spectroscopy [Boris Maiorov](#); Los Alamos National Laboratory, United States

Determining the elastic properties of Pu alloys and their changes as a function of temperature and time is a powerful tool to study thermodynamic and dynamic changes. Temperature dependence informs the nature of the free energy of the different phases, as elastic moduli are fundamental thermodynamic susceptibilities and connect directly to thermodynamics, electronic structure, and mechanic properties. Changes occurring as a result of self-irradiation change the elastic moduli and affect thermodynamic phase transitions. In turn, these changes are translated to changes in the hardness and brittleness of the compound. Similarly, sound attenuation provides information about dynamic processes such as dissipation associated with defect movement, annealing or re-crystallization. Thus, measurements of elastic moduli and sound attenuation help determine the origin of the phenomena found in ²³⁹Pu and its Ga alloys. By measuring the mechanical resonance frequencies of a sample, the Resonant Ultrasound Spectroscopy (RUS) technique can extract with extreme precision and accuracy the elastic moduli without corrections. Using RUS we perform time- and temperature-dependent measurements of the mechanical resonance frequencies of polycrystalline Pu with different Ga concentrations. From these measurements, elastic moduli and the sound attenuation can be extracted. I will show the changes in elastic moduli and sound attenuation with time for samples with different ages and Ga concentrations.

2:45 PM SF02.02.04

Soft and Tender X-Ray Synchrotron Radiation Spectromicroscopy for Nuclear Forensics [David K. Shuh](#)¹, Alexander Ditter¹, Nicholas Cicchetti^{1,2}, Joe Brackbill^{1,3}, Artem Gelis², Rachel Lim⁴, Shohini Sen-Britain⁴, Debra L. Rosas⁴, Alexander A. Baker⁴, Scott Donald⁴ and Brandon W. Chung⁴;
¹Lawrence Berkeley National Laboratory, United States; ²University of Nevada, Las Vegas, United States; ³University of California, Berkeley, United States; ⁴Lawrence Livermore National Laboratory, United States

The development of new methods and signatures is crucial to ensure that nuclear forensics activities remain effective. Synchrotron radiation analysis offers one way to extend the scope of nuclear forensics investigations in elemental, chemical, and structural analysis which all can be done in imaging modes that in some cases, reaches to the nanoscale. X-ray techniques are particularly useful because of their elemental specificity and non-destructive nature. The ability to use tunable, focused beams makes synchrotron radiation sources a potentially key tool for addition into the array of characterization techniques currently employed, particularly when it comes to the investigation of particles or areas of interest in very small specimens.

There have been recent efforts at the Advanced Light Source (ALS) conducting tender and soft spectromicroscopy using primarily x-ray fluorescence and chemical speciation coupled with selective X-ray absorption near-edge structure (XRF and XANES; Beamline 10.3.2); and with a scanning transmission x-ray microscope (STXM; Beamline 11.0.2). The tender XRF/XANES measurements provide elemental analysis at the low-single micron scale, whereas the STXM can probe electronic structure with ligand K-edge spectroscopy and chemical speciation via XANES with a spatial resolution of better than 25 nm. Several uranium, plutonium, and along with other relevant specimens, from both particle-based systems and monoliths fabricated by focused ion beam (FIB) methods, have been investigated utilizing these specific aforementioned techniques. The potential signatures obtained from this data, as well as the significance of the results, will be presented and discussed. The outlook for synchrotron radiation within nuclear forensics including the strengths and drawbacks of these techniques will also be discussed.

3:00 PM BREAK

SESSION SF02.03: Theory I
Session Chairs: James Tobin and Angela Wilson
Tuesday Afternoon, April 23, 2024
Terrace Suite 2, Level 4, Summit

3:30 PM *SF02.03.01

DMFT Theory of Elemental Actinides and Their Compounds [Gabriel Kotliar](#)^{1,2}; ¹Rutgers University, United States; ²Brookhaven National Laboratory, United States

Elemental actinides and their compounds have for many years posed a challenge to the electronic structure field, as their physical properties are not well described within density functional theory and its variants due to strong correlations. Dynamical mean field theory, on the other hand, has explained and predicted many surprising experimental features of these systems, as it captures non-perturbative correlation effects. We will describe some of these, such as spectral features and magnetic moments. We will then go into more depth about why these features arise because multiple energy scales (crystal field, spin-orbit coupling, Hund's rule coupling, Hubbard U and kinetic energy) are all important and have to be taken into consideration, as well as how it affects the physics of these compounds. Examples of the successes of DMFT + electronic structure will be drawn from a large number of materials. These include nuclear fuels such as UO₂, the phase diagram of elemental Pu and why its beta phase is the most correlated of all, superconductors, such as PuCoGa₅ and UTe₂, and ferromagnets such as UGe₂.

4:00 PM SF02.03.02

Strain Dependence of Phonons in α -Uranium [Mark Mathis](#) and Chris A. Marianetti; Columbia University, United States

The phonons in orthorhombic α -uranium have been well studied due to the charge density wave state, yet a systematic study of the phonons as a function of strain has yet to be accomplished. Here we compute the phonons and anharmonicity in α -uranium using the irreducible derivative method, guaranteeing the

highest computational efficiency for a finite displacement method. Various functionals within density functional theory are used to study the change in phonons with respect to the lattice parameters, with particular focus on changes in the soft-modes. Soft phonon modes other than the mode associated with the charge density wave are also found, which have not yet been identified in previous studies. Quartic phonon interactions associated with all soft modes are computed, allowing for the computation of thermal expansion within the Hartree-Fock approximation for phonons. Our findings are compared with existing experimental data.

4:15 PM SF02.03.03

Hydrogen and Oxygen Gas Dosing on α -Plutonium Using Time-of-Flight Secondary Ion Mass Spectroscopy and Density Functional Theory [Sarah C. Hernandez](#), Raymond Atta-Fynn and Connor Dozhier; Los Alamos National Laboratory, United States

Plutonium metal is highly reactive towards environmental gases by immediately forming an oxide layer when exposed to air and quickly forming a hydride when exposed to hydrogen. Previous work has shown that the monoclinic α -Pu phase readily oxidizes quicker than compared to the face-centered-cubic δ -phase. By using ToF-SIMS in conjunction with DFT calculations, we exposed α -Pu to hydrogen and oxygen gas to determine the reactivity. ToF-SIMS is a highly surface-specific analytic technique that probes $<1\text{nm}$ of the surface and can determine impurities at parts-per-million levels and chemical speciation, including hydrogen. After H_2 and O_2 gas exposures of an Ar^+ sputtered cleaned α -Pu metal, there was no apparent reaction to H_2 for up to 180 Langmuir (L), where at $\sim 20\text{-}30\text{L}$ of O_2 exposure oxide formation was evident. This is indicated by the relative intensities of the negative Pu-O ion fragments being $\text{PuO}_3^- > \text{PuO}_2^- > \text{PuO}^-$ as the surface is approaching a " PuO_2 " state. The experimental observations were supported by DFT studies, which indicated that H_2 physisorbs on the α -Pu surface at 0 K independent of coverage and partially dissociates at high surface coverage at 300 K, whereas O_2 strongly reacts to form oxide layers at 0 K at both low and high surface coverage.

4:30 PM *SF02.03.04

Electronic Structure of Uranyl Complexes probed by Valence and X-Ray Spectroscopy [Valerie Vallet](#)¹, Hanna Oher², Wilken Aldair Misael¹, Richard Wilson³ and Andre Severo Pereira Gomes¹; ¹Universite Lille, CNRS, France; ²Univ. Rennes, CNRS, ISCR, France; ³Argonne National Laboratory, United States

This presentation will showcase the capabilities of relativistic quantum chemistry approaches in exploring the electronic structure of actinide-containing compounds. The focus will be on luminescence properties and core-level spectroscopic observables of the uranyl moiety (UO_2^{2+}) within both linear and bent uranyl complexes. Given the challenges associated with nuclear waste management and the environmental impact of fission products, efficient extraction and characterization methods for actinide-containing compounds are of great societal importance.

The electronic structure of actinide compounds remains poorly understood compared to other elements in the periodic table. Valence- and core-level spectroscopic techniques offer valuable insights into this complex subject. The presentation will demonstrate how luminescence spectroscopy and X-ray spectroscopies serve as sensitive tools for probing the electronic structure and bonding nature between the uranyl moiety and its coordinated ligands.

Specifically, the talk will cover the application of relativistic Time-Dependent Density Functional Theory (TDDFT) with the CAM-B3LYP functional. This method has proven effective in providing accurate excitation/emission energies and vibronic progressions for linear uranyl complexes ($\text{UO}_2\text{Cl}_4^{2-}$, $\text{UO}_2\text{F}_3^{3-}$, $\text{UO}_2(\text{CO}_3)_3^{4-}$, $\text{UO}_2(\text{NO}_3)_2\text{L}_2$), enabling the assignment of experimental data [1]. Additionally, the impact of bending the uranyl moiety on spectroscopy and observed vibronic progressions will be discussed [2].

The presentation will also delve into TD-DFT simulations of the core spectra of the uranyl tetrachloride dianion ($\text{UO}_2\text{Cl}_4^{2-}$) in the $\text{Cs}_2\text{UO}_2\text{Cl}_4$ crystal. These simulations align with previously reported angle-resolved near-edge X-ray absorption spectroscopy (NEXAFS) at the oxygen K-edge and high-energy resolution fluorescence detected (HERFD-XANES) at the uranium M_4 - and L_3 -edges [3].

[1] H. Oher et al. *Inorg. Chem.* **2020**, *59* 5896; H. Oher et al. *Inorg. Chem.* **2020**, *59*, 15036; H. Oher et al. *Inorg. Chem.* **2022**, *61*, 890.

[2] H. Oher et al. *Inorg. Chem.* **2023**, *62*, 9273–9284.

[3] W. A. Misael, A. S. P. Gomes, *Inorg. Chem.* **2023**, *62*, 11589–11601.

SESSION SF02.04: Theory II

Session Chairs: Najeb Abdul-Jabbar and Sarah Hernandez

Wednesday Morning, April 24, 2024

Terrace Suite 2, Level 4, Summit

8:30 AM *SF02.04.01

Ab-Initio Spin-Fluctuation Hamiltonian for Delta-Pu at Finite Temperatures [Babak Sadigh](#), Kyoung Kweon, Per Söderlind, Michael Surh, Lorin Benedict and Fei Zhou; Lawrence Livermore National Lab, United States

Spin/orbital-polarized density functional theory has been used extensively in the past years to explore materials properties of the Pu metal, from its polymorphic phase diagram to energetics of formation and migration of lattice defects and impurities in the various Pu phases. Calculations to date have been conducted using one or other static low-energy spin configuration. The effect of allowing for non-collinear spin/orbital fluctuations is yet largely unexplored. We have thus developed a novel technique that allows for efficient calculations of adiabatic non-collinear spin/orbital excitations within spin-constraint density-functional theory. We use this technique to extensively explore the potential energy landscape of adiabatic spin fluctuations in delta-Pu. Several families of low-energy non-collinear spin configurations are found. We construct an effective Hamiltonian for thermal spin fluctuations in delta-Pu and study its statistical mechanics via Monte Carlo simulations. We report the impact of spin/orbital fluctuations on the structure and magnetic susceptibility of delta-Pu at finite temperatures.

This work was performed under the auspices of the U.S. Department of Energy by Lawrence Livermore National Laboratory under Contract DE-AC52-07NA27344.

9:00 AM SF02.04.02

Studying The Initial Corrosion of δ -Plutonium Through Density Functional Theory [Charles H. Fricke](#) and Sarah C. Hernandez; Los Alamos National Laboratory, United States

In this work, we will present results of density functional theory on the initial corrosion of δ -plutonium (Pu) due to hydrogen, oxygen, and water. We will explore the kinetics and energetics of water splitting on δ -Pu(100) and δ -Pu(111). Atomic oxygen and hydroxyl species are found to be strongly bound to the surface, with binding energies on the order of -2.2 eV for oxygen and -1.6 eV for the hydroxyl, when referenced to the chemical potential of water. In addition, we find that water and hydrogen have negative binding energies, but that the adsorption Gibbs free energies are highly sensitive to gas pressure and temperature variation. In the presence of water and oxygen gases, the metallic surface of the material is irreversibly coated in atomic oxygen, with energetic barriers for water splitting and oxygen dissociative adsorption low at room temperatures and pressures. A kinetic model was also developed, and when applied, oxygen is found to adsorb onto the surface close the experimentally defined Langmuir coverage for oxygen and plutonium surfaces. In addition, since hydrogen and oxygen are precursors to hydride corrosion and oxide formation, respectively, we will present results on surface to near-surface and bulk behavior of atomic hydrogen and oxygen. We find that the surface sites for oxygen and hydrogen are energetically preferred over the subsurface and bulk sites. Out of the two different interstitial sites in δ -Pu, the octahedral is significantly more stable than the tetrahedral interstitial site for oxygen and hydrogen. Gibbs free energies and the Sieverts constant for hydrogen will also be explored for these systems and compared to experimental values.

9:15 AM SF02.04.03

Ab Initio Studies of The Interaction of H with Pu₆Fe [Raymond Atta-Fynn](#) and Sarah Hernandez; Los Alamos National Laboratory, United States

The corrosion of plutonium (Pu) by hydrogen (H) is rapid, however the mechanisms which dictate the hydride formation process is not fully understood. Iron (Fe) is a common impurity in Pu and segregates to the grain boundaries and triple points to form the intermetallic compound Pu₆Fe. To understand the role played by Pu₆Fe in the hydride formation process, density functional theory was employed to compute the energetics and electronic structure of H in interstitial and vacancy sites in Pu₆Fe. H binding was exothermic, with binding energies around -0.4 to -0.2 eV/H atom. With the aid of ab initio molecular dynamics, the interstitial diffusion of H was modeled and the crystal structure for bulk Pu₆Fe hydride was predicted. The role played by the Pu 5f electron states in the hydride formation process will be elucidated.

9:30 AM *SF02.04.04

Ab Initio Heavy Element Composite Methodologies Bradley Welch¹, Sasha North², Nuno Almeida¹ and [Angela K. Wilson](#)¹; ¹Michigan State University, United States; ²Adrian College, United States

Providing the correct qualitative description much less achieving quantitative accuracy for the prediction of energetic properties can become challenging for the lanthanides and actinides due to increasing computational costs and, typically, increasing complexity of the methodologies required. Developments by our group and applications that have provided insight about both energetic predictions for species of the lower part of the periodic table and the theoretical strategies used for the predictions will be highlighted. Specifically, we will discuss the heavy element correlation consistent Composite Approach (*f*-ccCA) and the super correlation consistent Composite Approach (*s*-ccCA), which have been designed for elements of the lower periodic table. These methods are built upon the main group and transition metal correlation consistent composite approaches, which have been effectively utilized for many hundreds of species. Successes and challenges in describing heavy elements will be overviewed.

10:00 AM BREAK

SESSION SF02.05: Condensed Matter Physics I
Session Chairs: Ladislav Havela and Alice Smith
Wednesday Morning, April 24, 2024
Terrace Suite 2, Level 4, Summit

10:30 AM *SF02.05.01

Piezomagnetism in Uranium Dioxide: Actinide Science at High Magnetic Fields [Krzysztof Gofryk](#)¹, Marcelo Jaime², Daniel Antonio¹, Zahir Islam³, Myron Salamon⁴, Andres Saul⁵, Rico Schönemann⁴ and James Smith⁶; ¹Idaho National Laboratory, United States; ²Physikalisch-Technische Bundesanstalt, Germany; ³Advanced Photon Source, United States; ⁴National High Magnetic Field Laboratory, United States; ⁵Centre Interdisciplinaire de Nanoscience, France; ⁶Los Alamos National Laboratory, United States

The spin-lattice coupling in uranium dioxide remains an unsolved puzzle resulting from the lack of a thorough understanding of the strong coupling between 5f-electron magnetism and lattice vibrations. Besides being the main nuclear fuel material, UO₂ is a Mott-Hubbard insulator with well-localized 5f-electrons (U⁴⁺ electronic configuration) and its magnetic state is characterized by a non-collinear antiferromagnetic structure of 3k type and multidomain Jahn-Teller distortions. In the magnetic state, a UO₂ single crystal subjected to strong magnetic fields exhibits the abrupt appearance of positive linear magnetostriction leading to a trigonal distortion and piezomagnetism. This is the first example of piezomagnetism in the f-electron spin system. The unusually strong correlations between the magnetic moments in U-atoms and lattice distortions are a direct consequence of the non-collinear symmetry of the magnetic state that breaks time-reversal symmetry in a non-trivial way. The microscopic nature of these interactions, however, remains unclear. During the talk, we will demonstrate how detailed thermodynamic and structural measurements, performed in high and ultra-high magnetic fields, can be used to study these interactions and their couplings. We will discuss the implications of these results in the context of the origin of the piezomagnetic ground state in this material.

11:00 AM SF02.05.02

Strain-Driven Switching between Distinct Antiferromagnetic States in Frustrated Antiferromagnet UO₂ [Evgenia Tereshina-Chitrova](#)¹, Leonid Pourvorskii^{2,3}, Sergii Khmelevskiy⁴, Lukas Horak⁵, Thomas Gouder⁶ and Roberto Caciuffo⁷; ¹Institute of Physics, Czech Academy of Sciences, Czechia; ²École Polytechnique, Institut Polytechnique de Paris, France; ³Collège de France, Université PSL, France; ⁴Vienna Scientific Cluster Research Center, Vienna Technical University, Austria; ⁵Faculty of Mathematics and Physics, Charles University, Czechia; ⁶European Commission, Joint Research Centre (JRC), Germany; ⁷National Institute for Nuclear Physics, Italy

In materials containing magnetic atoms arranged in geometrically frustrated lattices, various magnetically ordered states can possess comparable energies with respect to the inter-site antiferromagnetic (AFM) exchange interactions. The concept of geometric frustration often intersects with broader phenomena in condensed matter physics, such as quantum spin liquids, topological states, and critical behaviour [1]. In recent decades, there has been a growing interest in intentionally manipulating magnetic states in collinear antiferromagnets, motivated by advancements in AFM spintronics [2]. In our study, we

demonstrate the fundamental potential to control spin orientations in frustrated antiferromagnets, paving the way for their utilization in realms of spintronics.

Our research focuses on the interplay of magnetic and exchange anisotropy effects in artificial heterostructures based on a canonical frustrated **3-k** antiferromagnet, UO_2 . We demonstrate that effective switching between the AFM states of different symmetries can be achieved by stretching the lattice of UO_2 . The phenomenon is probed experimentally using the exchange bias (EB) effect in stoichiometric $\text{UO}_2/\text{Fe}_3\text{O}_4$ bilayers. By employing many-body first-principles calculations based on the charge self-consistent Hubbard-I approximation [3,4] we identify magnetic configurations in the UO_2 layers. We show that a minor tetragonal distortion induces a transition between antiferromagnetic states of different symmetries, driven by appearance of a robust single-ion anisotropy. This impacts the arrangement of magnetic moments at the $\text{UO}_2/\text{Fe}_3\text{O}_4$ interface and thus influences the magnitude of exchange bias. Our findings showcase how epitaxial strain enables the manipulation of antiferromagnetic states in frustrated antiferromagnets by controlling single-site anisotropy.

We acknowledge the support of Czech Science Foundation under the grant no. 22-19416S. The samples were prepared in the framework of the EARL project of the European Commission Joint Research Centre, ITU Karlsruhe. Experiments were performed in MGML (mgml.eu), which is supported within the program of Czech Research Infrastructures (project no. LM2023065).

[1] F. Giustino et al., J. Phys. Mater. 3 (2020) 042006

[2] C. Marrows, Science 351 (2016) 558.

[3] M. Aichhorn et al, Comp. Phys. Commun. 204 (2016) 200; J. Hubbard, Proc. Roy. Soc. (London) A 276 (1963) 238.

[4] L. V. Pourovskii, Phys. Rev. B 94 (2016) 115117.

11:15 AM SF02.05.03

Thermal Expansion of α -U at Low Temperatures [Volodymyr Buturlim](#)¹, [Xiabin Ding](#)¹, [Sabin Regmi](#)¹, [Chris M. Marianetti](#)², [Michael Manley](#)³, [Jason Jeffries](#)⁴ and [Krzysztof Gofryk](#)¹; ¹Idaho National Laboratory, United States; ²Columbia University, United States; ³Oak Ridge National Laboratory, United States; ⁴Lawrence Livermore National Laboratory, United States

Uranium is one of the only elemental metals in which charge density waves have been observed (the phases are labeled α_1 , α_2 , and α_3). The first transition takes place at 43 K (α_1), the second at 38 K (α_2), and the last one stabilizes below 25 K (α_3). The structure below the transition is complex, consisting of small displacements of the atoms along all three of the orthorhombic axes. Despite the large experimental and theoretical effort, the nature of these transitions is still elusive, but it is believed to be associated with the unique coupling of 5f states, residing in the vicinity of the Fermi level, and the lattice vibrations. Here we present detailed experimental and theoretical studies of low-temperature thermal, thermodynamic, and electronic transport properties of the high-quality single crystals of α -U, across the CDW transitions.

**V.B. acknowledges the support from Idaho National Laboratory's Laboratory Directed Research and Development (LDRD) program under DOE Idaho Operations Office Contract DE-AC07-05ID14517. K.G. acknowledges support from the Division of Materials Science and Engineering, Office of Basic Energy Sciences, Office of Science of the U. S. Department of Energy (U.S. DOE).*

11:30 AM SF02.05.04

Phonon-Spin Scattering in U-Doped ThO_2 and its Suppression on Thermal Conductivity [Zilong Hua](#)¹, [Saqeeb Adnan](#)², [Amey Khanolkar](#)¹, [Cody A. Dennett](#)³, [James M. Mann](#)⁴, [Marat Khafizov](#)² and [David Hurlay](#)¹; ¹Idaho National Laboratory, United States; ²The Ohio State University, United States; ³Massachusetts Institute of Technology, United States; ⁴Air Force Research Laboratory, United States

We report on an investigation of thermal conductivity suppression in thorium dioxide with low-level uranium doping. Thermal conductivity of 6%, 9%, and 16% uranium-doped thorium dioxide is experimentally measured using a spatial domain thermoreflectance technique in the temperature range of 77K-300K, and the results are compared to the predictions of an analytical Klemens-Callaway model. With the impacts from different phonon scattering mechanisms isolated in the analytical model, we observed that phonon-spin scattering, i.e., the lattice distortion induced by the spin of paramagnetic electrons, has a stronger impact than the Rayleigh-type point defect scattering on reducing the phonon-mediated thermal conductivity in this temperature range. Moreover, the relative thermal conductivities among our samples with different uranium doping percentages and pure uranium dioxide suggest that the intensity of phonon-spin scattering is not linearly correlated to the doping percentage. This work shows the profound effect of introducing atoms with 5f electrons, populated in uranium but not in thorium, on the thermal transport behavior of fluorite oxides.

SESSION SF02.06: Condensed Matter Physics II
Session Chairs: [Krzysztof Gofryk](#) and [Evgenia Tereshina-Chitrova](#)
Wednesday Afternoon, April 24, 2024
Terrace Suite 2, Level 4, Summit

1:30 PM *SF02.06.01

Unusual High-Field Superconductivity in Uranium Ditelluride [Nicholas P. Butch](#)^{1,2}; ¹NIST, United States; ²University of Maryland, United States

Uranium ditelluride (UTe_2) hosts a rare form of low-temperature superconductivity that involves spin-triplet pairing and may be topologically nontrivial. Multiple superconducting phases can be stabilized through the application of large magnetic fields or modest pressure. A dramatic example of reentrant superconductivity, dubbed the "Lazarus" phase, is stabilized at fields greater than 40T, persisting to higher than 65T. In this talk, I will discuss recent experimental developments in the study of the high field superconductivity.

2:00 PM SF02.06.02

Lattice Dynamics and Thermodynamics for δ -Plutonium from *Ab Initio* Theory [Per Söderlind](#); Lawrence Livermore National Laboratory, United States

We present results from density functional theory (DFT) calculations of the lattice dynamics (phonons) and thermodynamics for δ -phase plutonium. The fully relativistic electronic structure is calculated assuming a three-dimensional noncollinear magnetic structure in conjunction with DFT and the general gradient approximation for the electron exchange and correlation interactions. The electronic-structure model is further enhanced by addressing strong orbital-orbital coupling via the conventional orbital-polarization (OP) scheme as has been successfully done for plutonium. The temperature dependence of the phonons is calculated within the self-consistent *ab initio* lattice dynamics approach. The obtained phonons compare very well with measurements

although a modest overestimation of the transverse L -point $[\xi\xi\xi]$ phonon is acknowledged. Calculated thermal vibration amplitudes and the associated Debye-Waller temperatures are close to experiments. Lattice, electronic, and magnetic contributions to the heat capacity are predicted and consistent to a few percent with that deduced from experimental data. Good agreement is only achieved when a magnetic contribution to the specific heat is recognized. The parameter-free DFT+OP electronic model is thus capable of predicting phonon properties and thermodynamic behavior of δ -phase plutonium rather accurately.

This work was performed under the auspices of the U.S. Department of Energy by Lawrence Livermore National Laboratory under Contract No. DE-AC52-07NA27344

2:15 PM SF02.06.03

5f and 4f States in Layered Zintl Phases: Half- and Semi-Metals Ladislav Havela¹, Martin Divis¹, Dominik Legut^{1,2}, Jindrich Kolorenc³ and Volodymyr Buturlim^{1,4}; ¹Charles University, Czechia; ²VSB, Czechia; ³Czech Academy of Science, Czechia; ⁴INL, United States

The term Zintl phases denotes compounds of one electropositive element donating electrons to a complex anion with covalent bonding. We focus on layered compounds with the trigonal structure type CaAl_2Si_2 , which are known both for actinides (U,Th) and divalent lanthanides (Eu, Yb). The lanthanide-based compounds are narrow-band antiferromagnetic semiconductors with transport properties very sensitive to magnetic fields. UCu_2P_2 is Ising-like ferromagnet. Its $T_C = 216$ K steeply increases with hydrostatic pressure. Calculations reveal that the spin splitting of the 5f band with only one spin direction at E_F brings to the Fermi level also practically full polarization of light electrons. Hence UCu_2P_2 is a combination of semi metal and half metal. High pressure experiments on EuZn_2P_2 indicate that the band gap is suppressed under hydrostatic pressure of 12 GPa. Interesting aspects is brought by the layered character of the crystal structure, with f -element basal-plane sheets distinctly separated by the anionic slabs. This gives much longer magnetic correlations length in the basal plane. There is a striking contrast between EuZn_2P_2 with practically no magnetic anisotropy due to the spin-only magnetism of the f^7 state and extremely strong ($E_d/k_B \approx 500$ K) in-plane 5f bonding induced anisotropy in UCu_2P_2 with the U moments locked into the c -axis. The results illustrate how the f -systems are affected by the polar bonding. The potential of the band-gap engineering can be used for designing thermoelectrics or materials for spintronics.

This work was supported by the Czech Science Foundation under the grant No. 21-09766S.

2:30 PM BREAK

SESSION SF02.07: Radiation Effects

Session Chair: Nicholas Butch

Wednesday Afternoon, April 24, 2024

Terrace Suite 2, Level 4, Summit

3:30 PM *SF02.07.01

The Role of Radiation-Induced Non-Equilibrium Plutonium Oxidation States in Solution Gregory P. Holmbeck¹, Travis S. Grimes¹, Amy Kynman¹ and Stephen Mezyk²; ¹Idaho National Laboratory, United States; ²California State University Long Beach, United States

Plutonium plays a key role in global actinide research and nuclear fuel cycle technologies, and yet, our fundamental understanding of its inherent radiation-induced chemical behavior is limited. These radiation-induced processes cannot simply be switched off, as they are as fundamentally inherent to plutonium as the impact of relativistic effects on its f -electrons. In less chemically complex actinide systems, such as aqueous solutions of neptunium and americium, both steady-state and transient radiolysis products play a significant role in the redox cycling of their oxidation states, which ultimately impacts their chemistry and transport. However, plutonium's multiple, coexisting, and chemically active oxidation states, which comprise of bare ions and dioxo cations, provide additional redox pathways that complicate the aforementioned radiation-induced competition kinetics. Mechanistically understanding the response of these multiple oxidation states, both equilibrium and non-equilibrium, to intense ionizing radiation fields is essential for predicting the behavior of plutonium under a host of conditions that support technological innovation in global nuclear energy and non-proliferation efforts. Here, advances in radiation-induced plutonium solution chemistry will be presented, including new results from time-resolved electron pulse and steady-state gamma and alpha irradiations.

4:00 PM SF02.07.02

Recovery in Stabilized Delta Pu and its Effects on Thermophysical Properties Najeb M. Abdul-Jabbar, Shane Mann and Jeremy Mitchell; Los Alamos National Laboratory, United States

Recent efforts at Los Alamos National Laboratory (LANL) have focused on thermodynamic measurements of aged and pre-conditioned delta alloys at temperatures in the vicinity of defect recovery and stored energy release. In both scenarios, quantifiable thermophysical property changes are observed across temperatures ranging from 125-225 °C. Analogous behavior in Pu has been observed via electrical resistivity measurements, which has been attributed to migration of point defects, dislocations, and vacancy clusters. Whether interactions between defects produced by pre-conditioning or natural aging can develop into alpha-like embryos, which can lead to decomposition of the delta phase, remains to be seen. Consequently, ongoing thermal analysis work is being conducted at LANL on a comprehensive series of pre-conditioned and naturally aged Pu-Ga alloys and the ensuing results in the context of delta phase stability will be discussed.

4:15 PM SF02.07.03

Effects of Repeated Alternating Temperatures Measurements on Lattice Behavior of δ -Phase ^{239}Pu -Ga Alloys Alice I. Smith, Franz J. Freibert, Sven C. Vogel, Jianzhong Zhang, Joan E. Siewenie, Scott Richmond and Michael Ramos; Los Alamos National Laboratory, United States

Elemental plutonium is an atypical element in the periodic table, highly unstable and presenting six allotropes from room temperature to its melting point: monoclinic α , body-centered monoclinic β , face-centered orthorhombic γ , face-centered δ , body-centered δ' , and body-centered cubic ϵ . These phases are unstable with temperature, pressure, and time, affecting the crystallographic structure, thermodynamic and mechanical properties in ways that are still inconclusive. The high temperature face-centered cubic (fcc) δ -phase is stable in elemental Pu between 320 and 450°C, and it can be stabilized to room temperature and below by alloying it with small amounts of trivalent elements (i.e., Ga, Al, Ce, Am, or Sc). The resulting alloys are in a metastable state, of great interest for several applications and more easily worked metallurgically than the other phases, exhibiting intriguing behaviors and unusual properties, such as negative thermal expansion, large low-temperature electronic specific heat, high electrical resistivity.

Self-irradiation, “the inside out” aging in plutonium and its compounds¹, results in radiation damage which will affect the microstructure of the materials, with significant changes of their structure and physical and mechanical properties. X-ray diffraction and dilatometry studies have shown that the room temperature self-irradiation of δ -phase Pu-Ga alloys results in swelling of the lattice that saturates after 0.1-0.2 dpa of accumulated lattice damage. At low temperatures, self-irradiation results in significant lattice damage, but the mechanisms associated with the evolution of defects at sub-ambient temperatures are still not fully understood.

For a more complete picture of the poorly understood “aging” processes of defect accumulation and damage evolution in δ -phase ²³⁹Pu-Ga alloys, we need to consider the radiation dose and rate, thermal history, and composition of the materials. This talk will present experimental results on the evolution of the average structure of δ -phase ²³⁹Pu-Ga alloys when exposed to repeatedly alternating-temperatures between ambient and cryogenic values, investigated by time-of-flight neutron diffraction.

4:30 PM SF02.07.04

Defect Chemistry and Radiation Stability of (Gd & Zr) Co-Doped UO₂ Solid Solutions [Ritesh Mohun](#); Bangor University, United Kingdom

The irradiation behaviour of pure UO₂ is well experimentally characterised, but little is known about the irradiation of UO₂ doped with fission products such as rare-earth elements that are formed during in-reactor operations where the fuels are exposed to extreme environments of intense radiation and high temperature. For this purpose, this study was carried out to investigate the effect of heavy Kr-ion irradiation of UO₂ (to simulate radiation damage within a reactor) when doped with both trivalent Gd (a common burnable poison) and tetravalent Zr (a high concentration fission product) at varied concentrations. The mechanisms by which the dopants incorporate the UO₂ lattice were explored experimentally. XRD measurements showed that Gd-addition creates an oxygen vacancy environment comparable to hypo-stoichiometric UO_{2-x}, and HERFD-XANES revealed the presence of U(V) species in proportion quantities to the trivalent dopant to compensate for the charge. Zr doping, on the other hand, induced a contraction of the unit cell and Raman characterisations showed the induction of a new defect species with O_h symmetry that includes the Zr cation in the 8-fold coordination of O²⁻ in the form of ZrO₈-complex clusters.

Kr-irradiation of the pristine samples showed that dopants modify the irradiation character of the UO₂ structure, with the undoped pellet accumulating the highest concentration of lattice disorder, indicating that the co-doped solid solutions are more radiation resistant. The cation Frenkel pair formation enthalpy was calculated using DFT+U, which revealed that uranium interstitials formed as part of displacement cascades in doped samples have a significant thermodynamic drive to displace Zr/Gd substitutional defects, increasing the defect recombination volume. This mechanism, however, is not observed in undoped UO₂. In this talk, the key mechanisms that occur near defect-boundary interfaces will be discussed to highlight the precise role of dopants in changing the lattice defects mechanisms in nuclear fuels.

SESSION SF02.08: Poster Session
Session Chairs: Edgar Buck and David Shuh
Wednesday Afternoon, April 24, 2024
Flex Hall C, Level 2, Summit

5:00 PM SF02.08.01

New Angles on Actinide Quantum Materials [Rosalie Greer](#)¹, Matthew Simmers¹, Lorianne R. Shultz-Johnson¹, Alex Bretaña¹, Binod K. Rai¹, Christopher Barrett¹ and Tina Salguero²; ¹Savannah River National Laboratory, United States; ²University of Georgia, United States

While actinide materials have seen an enormous swell of interest in recent years due to the surprising and fascinating quantum properties of materials such as UTe₂, this interest has largely been confined to a small set of compounds. The intrinsic obstacles to research the actinides present has greatly limited broader explorations into novel materials, novel analytical methods, and manipulation of actinide isotopics. Savannah River National Laboratory, in light of its unique position ameliorating many of the difficulties of actinide research, has pursued a research effort to begin those broader explorations.

Utilizing primarily chemical vapor transport and flux synthesis methods, SRNL has generated a number of actinide-based quantum materials, both those subject to contemporary mainstream interest and those which have been neglected for decades with insufficient characterization. High-quality crystals of materials such as UTe₃ have been prepared and characterized at much higher levels of fidelity than possible at the time of their discovery, clarifying disagreements in the existing literature and revealing new and compelling magnetic features. SRNL also plans to prepare a series of UTe₂ samples with tailored uranium isotopics, including the use of highly enriched uranium, enabling an unprecedented investigation of the impact of nuclear spin on the unusual quantum properties of that material.

Most importantly, this work results from the establishment of an actinide-based quantum material synthetic capability which will allow the synthesis of entirely new materials, including with actinides other than uranium. The richly complex correlation effects endemic to actinide species will no doubt lead to novel and intriguing quantum properties, offering a whole new realm of investigation.

SESSION SF02.09: Nanoscience
Session Chairs: Karen Kruska and Valerie Vallet
Thursday Morning, April 25, 2024
Terrace Suite 2, Level 4, Summit

8:00 AM *SF02.09.01

Nuclear Nanotechnology: Mechanisms behind The Formation of Uranium Oxide Nanoparticles [Liane M. Moreau](#); Washington State University, United States

Nanoparticles are interesting due to the unusual properties that they display based on quantum effects, which make their electronic structures intermediate between individual atoms and larger bulk materials. While nanochemistry has been well developed throughout the transition metals, little is known regarding how actinide materials behave when their sizes are reduced to the nanoscale. This is problematic due to the inherent relevance of nanoscale actinides to the nuclear fuel cycle. High burnup structure nuclear fuel results in nanometer-scale grain sizes, and it is well documented that nanoparticle

formation greatly affects actinide oxide corrosion and the ability of actinides to move through environmental systems. In order to elucidate size/property relationships in uranium oxides, we have developed procedures to control the size and morphology of uranium oxide nanoparticles through organic phase colloidal synthesis and seed-mediated anisotropic growth. Notably, we have learned the important role that water plays in UO_2 nanoparticle synthesis, which has important implications for nanoparticle synthesis throughout the periodic table. Methods will also be described towards scaling down organic phase colloidal synthesis to achieve actinide oxide nanoparticles that utilize less than 1 mg of precursor, making trans-uranium nanoparticles more feasible to study. Additionally, we demonstrate the formation of unusual uranium oxide nanoparticle 2D superlattices, and how this can be controlled by altering nanoparticle size and morphology.

8:30 AM *SF02.09.02

Nanoprecipitates and Nanostructures in Spent UO_2 Fuel Lingfeng He¹, Yunyuan Lu¹, Cameron Howard², Linu Malakkal², Chao Jiang², Sudipta Biswas², Dewen Yushu², Jatuporn Burns² and Wei-Ying Chen³; ¹North Carolina State University, United States; ²Idaho National Laboratory, United States; ³Argonne National Laboratory, United States

Spent nuclear fuel experiences substantial alterations in both its microstructure and chemical composition during its time in a reactor. While some fission products remain integrated within the UO_2 matrix, other inert gases like xenon (Xe) and krypton (Kr), as well as certain 4d group metals (molybdenum, technetium, ruthenium, rhodium, and palladium), form nanoprecipitates within the UO_2 matrix. In certain areas of the UO_2 fuel, these Kr/Xe precipitates and metallic precipitates can also come together to create paired structures at the rim regions. Furthermore, as the burn-up levels increase, grain subdivision within the UO_2 occurs, giving rise to a high burn-up structure (HBS) characterized by the presence of nanograins. This research aims to provide an in-depth examination of the in situ microstructural changes in nanoprecipitates and HBS in spent UO_2 fuel when subjected to Kr or Xe ion irradiation. To enhance our understanding of these changes, this study employs transmission electron microscopy techniques alongside density-functional theory and phase field modeling.

9:00 AM SF02.09.03

Solvent Directed Anisotropic Growth of Uranium Dioxide Nanoparticles Christian Wentzell; Washington State University, United States

Nanoparticles are of interest due to their unusual behavior as a result of having a high surface area to volume ratio. The nanoscale size regime results in increased surface energy due to steric strain and increased lattice vacancies. Still, certain surface facets are more stable than others, which are modulated as a function of particle size, leading nanospheres to be the preferred morphology. To stabilize higher energy surface facets and achieve anisotropic nanoparticle morphologies, either one of two approaches is typically employed: 1) a surface binding species is utilized that preferentially binds to certain surface facets over others or 2) trace elemental species are added to the species which cap high energy surface facets and slow their growth rate. While these two approaches have been widely observed for noble metal and to a certain extent transition metal nanoparticles, little research has considered anisotropic growth in underexplored materials such as uranium dioxide. Of particular interest, it is possible that solvent coordination may also play a role in anisotropic growth due to their differential charge distribution. To this end, our initial findings show that in fact solvents can play a role and control anisotropic growth in uranium dioxide. Specifically, we have investigated various high boiling point organic solvents, such as dibenzyl ether, dihexyl ether and dioctyl ether, which have all resulted in different nanoparticle morphologies. Additionally, we have explored the effects of mixed solvents and variable surfactant mixtures with different functional groups including ethers, amines, ketones, aliphatic and aromatic compounds, which therefore sample various surface binding possibilities. In order to probe anisotropic growth pathways, time course reactions using transmission electron microscopy along with small and wide-angle X-ray scattering have been conducted. Overall, this presentation will demonstrate initial and illuminating progress towards morphological control over actinide oxides.

9:15 AM *SF02.09.04

Spectroscopy for Plutonium Polynuclear Species in Solution and Application of Model Structures in Data Analysis Thomas Dumas¹, Matthieu Viro², Cyril Michaux², Manon Cot-Auriol², Julien Margate², Sandrine Dourdain², Serguei Nikitenko², Kristina Kvashnina^{3,4}, Lucia Amidani^{3,4}, Pier Lorenzo Solari⁵, Denis Menut⁵, Philippe Moisy¹, Geoffroy Chupin¹, Christelle Tamain¹ and Dominique Guillaumont¹; ¹Univ. Montpellier, France; ²ICSM, Univ Montpellier, CEA, CNRS, ENSCM, France; ³The Rossendorf Beamline at the ESRF, France; ⁴Institute of Resource Ecology, Germany; ⁵Synchrotron SOLEIL, MARS Beamline, France

Understanding the structure of polynuclear plutonium ions in aqueous solution is crucial to develop separations technologies, predict the long-term behavior of actinide materials in wet systems and model accurately solution to solid precipitation mechanisms. It is an euphemism to say that plutonium chemistry in aqueous solution is complex. Diverse and multifaceted species has been identified and, most often, several of which coexist with each other. In this context, the structural information provided by EXAFS measurements can be a lighthouse for the chemist and the rich visible/near infrared plutonium absorption properties is an excellent asset too. Nevertheless none of which are easy to interpret because few structural models are available for plutonium. This presentation aims to recall how multiple spectroscopic approaches can benefit from reference structures (crystallographic and/or theoretical) to identify plutonium compounds in solution focusing on plutonium hydrolysis compounds and polycondensation in aqueous solutions.

Single crystal X-ray diffraction and spectroscopies has been applied to describe small plutonium clusters in solution.[1-3] Apart from the structural description, this plutonium hexanuclear core resulted in a peculiar absorption spectrum in the visible range that is a valuable footprint to detect it in several systems. The other actinide cluster geometries known [4-7] are also useful to support spectroscopic analysis in complex plutonium solution including nanomaterials. EXAFS spectra derived from crystal structures and ab-initio calculations how the cluster geometry and nuclearity translates into EXAFS scattering paths and may help to identify the plutonium clusters in solution.[8] This approach is one among others that is used to study larger plutonium assemblies. Overall, several structural and electronic properties of the nanosized plutonium oxides and colloids may be compared and analyzed on the basis of molecular bonds from plutonium clusters.[9-10] And ultimately, in the plutonium ions route to from colloidal suspensions or PuO_2 nanoparticles, polynuclear plutonium clusters are found to be an intermediate species, that the appropriate spectroscopic tools may help to capture.

[1] C. Tamain, T. Dumas, D. Guillaumont, C. Hennig and P. Guilbaud, *European Journal of Inorganic Chemistry*, 2016, 2016, 3536-3540.

[2] C. Tamain, T. Dumas, C. Hennig and P. Guilbaud, *Chemistry-a European Journal*, 2017, 23, 6864-6875.

[3] T. Dumas, M. Viro, D. Menut, C. Tamain, C. Micheau, S. Dourdain and O. Diat, *Journal of Synchrotron Radiation*, 2022, 29, 30-36.

[4] K. E. Knope, S. Skanthakumar and L. Soderholm, *Inorganic Chemistry*, 2015, 54, 10192-10196.

[5] L. Soderholm, P. M. Almond, S. Skanthakumar, R. E. Wilson and P. C. Burns, *Angewandte Chemie-International Edition*, 2008, 47, 298-302.

[6] G. E. Sigmon and A. E. Hixon, *Chemistry-a European Journal*, 2019, 25, 2463-2466.

[7] R. E. Wilson, S. Skanthakumar and L. Soderholm, *Angewandte Chemie-International Edition*, 2011, 50, 11234-11237.

[8] G. Chupin, C. Tamain, T. Dumas, P. L. Solari, P. Moisy and D. Guillaumont, *Inorganic Chemistry*, 2022, 61, 4806-4817.

[9] C. Micheau, M. Viro, S. Dourdain, T. Dumas, D. Menut, P. L. Solari, L. Venault, O. Diat, P. Moisy and S. I. Nikitenko, *Environmental Science-Nano*, 2020, 7, 2252-2266.

[10] A. Romanchuk, A. Trigub, T. Plakhova, A. Kuzenkova, R. Svetogorov, K. Kvashnina and S. Kalmykov, *Journal of Synchrotron Radiation*, 2022, 29,

9:45 AM BREAK

SESSION SF02.10: Chemistry I
Session Chairs: Robert Surbella III and Jennifer Wacker
Thursday Morning, April 25, 2024
Terrace Suite 2, Level 4, Summit

10:15 AM *SF02.10.01

Visualizing Non-Classical Growth of *f*-Element Oxalates with Cryo-TEM [Karen Kruska](#), Gabriel Hall, Shalini Tripathi and Edgar C. Buck; Pacific Northwest National Laboratory, United States

Cryo-transmission electron microscopy (TEM) was utilized to observe the initial stages of *f*-element oxalate morphologies under varying solution conditions, tracking particle nucleation and growth. U and Pu nitrites were mixed with oxalic acid to produce their respective oxalates. The reaction was stopped by vitrification of the reactants on a TEM grid, enabling the examination of early, meta-stable particle stages. The size and shapes of precipitates were studied over different reaction durations. Chemical analysis of cryo-samples was conducted using EFTEM, while post-mortem STEM-EELS provided more detailed chemical insights into dried samples. Images taken after 10 seconds revealed larger particles formed by the aggregation of smaller particles through particle attachment. Cryo-TEM unveiled the intermediate phases of this non-classical growth process. These findings will be discussed as part of a comprehensive investigation into the complete growth cycle, utilizing a combination of optical and electron microscopy techniques.

10:45 AM SF02.10.03

Highly Stable and Hierarchical Porous Ce-Based MOF for Efficient Uranium Extraction from Seawater Muhammad Asim, Bhupendra K. Singh and [Wooyong Um](#); Pohang University of Science and Technology (POSTECH), Korea (the Republic of)

Owing to rapidly growing world population and swift industrialization, there is an escalating global demand for a sustainable and environmentally friendly energy resource, triggering the exploration of uranium source for nuclear energy. Seawater with a vast and untapped uranium reservoir (4.5 billion tons) is a promising source and holds an immense potential for uranium mining over an extended period. However, efficient, and selective uranium extraction from seawater (UES) is profoundly challenging due to ultralow concentration of dissolved uranium in seawater (about 3.3 ppb), complex chemical matrix, harsh and corrosive marine environments as well as economic viability.

To overcome these challenges, various approaches have been explored so far including ion exchange, precipitation, membranes, and electrochemical methods. However, these methods often suffer due to high cost, low selectivity, inefficient uranium extraction, susceptibility to degradation, and environmental concerns. Among the various methods utilized for UES, application of metal organic frameworks (MOFs) has grabs significant attention due to their high surface area and selective reactivity, tunable pore structure, tailored functionality, and optimal structural stability in ocean water.

This study aims to boost the uranium extraction efficiency as well as chemical and structural stability in marine environment by fabricating a hierarchically mesoporous Ce-based MOF (CeHMMOF). Leveraging efficient coordination between Ce and the ligand (2-amino terephthalic acid) incorporated with soft template (Pluronic, F127), a superstructure CeHMMOF (particle size; 1.5 - 2 μ m) was successfully synthesized via one pot solvothermal approach. The synthesized MOF was systematically characterized using X-ray diffraction (XRD), Fourier transform infrared spectroscopy (FTIR), and scanning electron microscopy (SEM) to ascertain its structural, chemical, and morphological attributes.

The stability test conducted in simulated seawater conditions ($\text{Na}^+ = 23,000 \text{ mg/L}$, $\text{Cl}^- = 35,500 \text{ mg/L}$, $C_0 = 100 \mu\text{g/L}$, $\text{pH} = 8.0$) revealed promising chemical stability and structural resilience of CeHMMOF during prolonged exposure to simulated seawater up to 21 days, signifying its potential for practical deployment of UES at a larger scale. In terms of affinity for uranium and extraction efficiency in simulated seawater conditions, CeHMMOF displayed robust uranium removal efficiency (>50% of 100 $\mu\text{g/L}$ initial U concentration in 12 minutes), surpassing reported materials concerning the extraction efficiency, and thus affirming the outstanding capability and considerable scope of synthesized Ce-based MOF sorbent for UES application. In this work, we have developed a highly stable hierarchically mesoporous Ce-based MOFs with an efficient uranium extraction performance in harsh seawater conditions and proposed as an emerging candidate material for a high-throughput and sustainable UES, aligning well with ongoing global efforts to develop a clean and renewable energy resource.

To ensure the practical utilization of CeHMMOF on commercial scale, our research is ongoing and in the subsequent phases of this study, firstly, we will comprehensively evaluate the irradiation stability of synthesized MOF to assure its material stability and structural integrity under induced irradiation for long term onshore UES applications. Thereafter, uranium removal mechanism will be investigated in conjunction with other parameters impacting UES performance, including regeneration rate and selectivity of fabricated MOF for uranium extraction in natural seawater.

11:00 AM SF02.10.04

Evidence for Particle Attachment of Plutonium Solids in TX-118 Hanford Tank Waste [Edgar C. Buck](#), Dallas D. Reilly, Sergey I. Sinkov and Eugene S. Iton; Pacific Northwest National Laboratory, United States

The accumulation of plutonium particles in waste tanks has been suggested as a process that could lead to a nuclear criticality event during the processing of wastes at the Hanford site, WA, USA. This concern was bolstered by the apparent discovery of a bismuth-plutonium phase in the wastes by Reynolds et al. Initial analyses of TX-118 solids with SEM-EDS matched the findings of Reynolds and co-workers with the observation of similarly large 5 to 10 micrometer particles of Pu-bearing particles that also appeared to contain bismuth and phosphorus. However, it was not clear from the SEM-EDS, how these elements were incorporated into the Pu-phase. We used Scanning Electron Microscopy, (SEM), Scanning Transmission Electron Microscopy (STEM) and found no evidence for a distinct plutonium (Pu) -bismuth (Bi) and phosphate (P) phase. The plutonium was present as PuO_2 with closely associated minor levels of Bi and P. Plutonium-bearing particles in Waste Tank TX-118 appeared to consist of agglomerates of nanoparticles of PuO_2 with other metal oxide nanoparticles that were both crystalline and amorphous. We propose a particle-particle attachment mechanism for the formation of the plutonium agglomerates in TX-118 wastes. Low solubility Pu-bearing solids formed in the highly alkaline tank waste conditions would have had extremely low particle growth rates through Ostwald ripening or similar mechanisms. We performed precipitation experiments and examined the resulting agglomerates with STEM showing a possible particle attachment mechanism of formation.

SESSION SF02.11: Chemistry II
Session Chairs: Marisa Monreal and Tsuyoshi Yaita

Thursday Afternoon, April 25, 2024
Terrace Suite 2, Level 4, Summit

1:30 PM *SF02.11.01

Exploring The Photochemistry and Bonding of Trivalent Americium within Metal–Organic Constructs Robert G. Surbella III¹, Ana Arteaga¹, Aaron Nicholas¹, Michael Sinnwell², Bruce K. McNamara¹ and Edgar C. Buck¹; ¹Pacific Northwest National Laboratory, United States; ²The University of Iowa, United States

Metal-organic frameworks (MOFs) are suitable platforms for studying the fundamental properties of the transuranium (TRU) elements. While the material properties that are common to MOFs, (e.g., structural variability, high surface area, and permanent porosity), are often exploited for their functionality, our motivations for studying TRU-MOFs are fundamental in nature. These robust, crystalline constructs are attractive hosts for immobilizing the scarce and often, highly radioactive isotopes of the TRU elements, providing both structural stability and a platform to explore structure–property relationships. The trivalent lanthanide (Ln(III)) containing MOF-76 family is of particular interest in this regard, given its high thermal stability and unique optical properties, which have been explored for use in color tuning and analyte sensing. The MOF-76 family is constructed from Ln(III) ions (where Ln = Eu, Sm, Tb, Nd...) and 1,3,5-tricarboxylic acid (BTC) ligands, forming a porous, three-dimensional architecture. Perhaps more importantly, the synthetic routes for preparing MOF-76(Ln(III)) are robust, being able to accommodate nearly all the 4f elements, and as such, is an ideal entry point for studying the trivalent actinides, like americium. An overview of this synthetic strategy and the crystal structure of MOF-76(Am) will be presented. Moreover, the utility of this platform for studying the optical properties of Am(III) will be highlighted. To this end, the focus will be in differentiating 4f vs. 5f element behavior with respect to ligand-to-metal resonance energy transfer and photoluminescence quenching.

2:00 PM *SF02.11.02

Protein Crystallization Provides Insight into Actinide Coordination Jennifer N. Wacker¹, Peter B. Rupert², Marc Allaire¹, Roland K. Strong² and Rebecca Abergel^{1,3,3}; ¹Lawrence Berkeley National Laboratory, United States; ²Fred Hutch Cancer Research Center, United States; ³University of California, Berkeley, United States

The diverse implications in understanding the biological chemistry of the actinides are profound, demonstrated in both the decontamination efforts of individuals after a nuclear accident and the remedial use of radionuclides for cancer treatments and diagnostics. Underpinning these efforts aimed to address critical societal challenges is a thorough understanding of *f*-element binding and coordination behavior in the presence of biologically-inspired systems. Despite advances in probing the fundamental properties of the actinides through methods such as X-ray Absorption Spectroscopy, opportunities to expand our current understanding at the interface between small molecule actinide complexes and natural systems can be further aided by the use of macromolecular hosts. By combining hard oxygen-donor chelators that bind actinides with high-specificity and utilizing a protein called siderocalin, which has been shown to selectively bind a diverse range of actinide complexes, these ‘actinide-chelator-macromolecule’ constructs can be crystallized to reveal the fundamental bonding of even the rarest of actinide elements. Protein crystallographic measurements collected at the Advanced Light Source (Beamline 5.0.2) enable actinide coordination to be revealed in the solid-state, and more broadly can help probe the interactions between biological scaffolds and actinide materials.

2:30 PM BREAK

SESSION SF02.12: Fuels, Environmental and Forensics
Session Chairs: Brandon Chung and Lingfeng He
Thursday Afternoon, April 25, 2024
Terrace Suite 2, Level 4, Summit

3:00 PM *SF02.12.01

Room Temperature Oxidation Kinetics of a U-Nb Alloy Scott Donald; Lawrence Livermore National Laboratory, United States

The reaction of atmospheric gases with metal surfaces plays a crucial role in driving many beneficial and detrimental processes such as heterogeneous catalysis, corrosion, protection from degradation, and environmental dispersal. The chemistry and kinetics of the oxide formed on uranium metal alloyed with 14 at.% Nb was investigated following exposure to dry and ambient air environments. Using a combination of x-ray photoelectron spectroscopy (XPS) and time-of-flight secondary ion mass spectrometry (TOF-SIMS), the evolution of the oxide as a function of time and oxygen partial pressure were determined. Segregation of the solute element was found to occur, resulting in the formation of a niobium rich oxide interfacial layer between the UO₂ surface and bulk metal. The potential role of this segregation on passivating the material against further oxidation will be discussed and comparisons will be made to the oxidation mechanism of unalloyed uranium under similar environments.

This work was prepared by LLNL under Contract DE-AC52-07NA27344. This support does not constitute an express or implied endorsement on the part of the government.

3:30 PM SF02.12.02

From Conversion to Fabrication and Fine Characterization of MOX Fuel Laure Ramond^{1,2}, Florent Lebreton^{1,2}, Julie Simeon^{1,2}, Paul estevenon^{1,2}, Anna Hautecouverture^{1,2} and Guillaume Bernard-Granger^{1,2}; ¹Commissariat à l'Énergie Atomique et Aux Énergies Alternatives, France; ²Université de Montpellier, France

MOX fuel is an intimate mixture of PuO₂ in a uranium oxide matrix, with plutonium content ranging from a few percent (light water reactor fuel) to several dozen percent (fast reactor fuel). In addition to conventional powder metallurgy processes, CEA Marcoule is studying other innovative ways of preparing MOX, such as advanced thermal denitration, SCS (solution combustion synthesis) and freeze granulation. The sintering of these different types of powder is being studied at the CEA, with the development of sintering maps and activation energy calculations. A wide range of tools are used to characterize sintered MOX pellets, from scanning electron microscopy (SEM) to Raman spectroscopy and transmission electron microscopy (TEM).

3:45 PM SF02.12.03

Multimodal Analysis of UO₂ Corrosion enabled by a Microfluidic Electrochemical Cell Jennifer Yao¹, Eugene S. Ilton¹, Bianca Schacherl², Bruce K. McNamara¹, Tonya Vitova² and Edgar C. Buck¹; ¹PNL, United States; ²Karlsruhe Institute of Technology, Germany

Understanding the corrosion kinetics and mechanisms of spent nuclear fuel (SNF) is crucial for accessing the long term risks associated with the geologic storage of SNF.¹ Traditional experimental approaches have posed serious challenges, given the need for substantial resources and access to shielded hot cell facilities to protect researchers from the intense radiation field. One response is to work with depleted UO₂, a close but ultimately unsatisfactory analogue to SNF. An alternative would be to downsize the amount of SNF required such that the need for shielded hot cell facilities would be diminished.

Indeed, an innovative solution has emerged—the Particle-attached Microfluidic Electrochemical Cell (PAMEC)—which has the proven potential to work with microgram quantities of material. Central to the PAMEC is the electrochemical method, which is widely employed for studying corrosion processes. With respect to UO₂ corrosion, the PAMEC electrode is a composite of microgram quantities of UO₂ powder, polyvinylidene fluoride (PVDF), and carbon black.^{2,3} The PAMEC has already proven effective in studying UO₂ redox behavior, providing consistent results with those from traditional bulk electrochemical studies.⁴

In more detail, the PAMEC is a vacuum-compatible microfluidic platform that provides precise control over experimental conditions (e.g., flow rates, dissolved volatile concentrations such as H₂), minimal resource utilization, and the ability to observe redox reactions in real-time and in situ. PAMEC's in situ and real time analytic and imaging capabilities, made possible by an ultra-thin 50 nm detection window, include scanning electron microscopy (SEM) combined with Energy-dispersive X-ray spectroscopy (EDS). The same set up allows for operando high-resolution X-ray absorption near-edge structure (HR-XANES) spectroscopy, which we used to track U oxidation states during multiple cyclic voltammetry scans of UO₂. The compact nature of the PAMEC simplified shipping the loaded device to the Karlsruhe Institute of Technology (KIT) synchrotron facility CAT-ACT beamline in Karlsruhe, Germany for operando HR-XANES analysis.

Our research has showcased the ability of the PAMEC using UO₂ corrosion as an example. We envision this approach can greatly reduce the risk associated with studying the corrosion of SNF under conditions that resemble repository environments, as well as allow for multimodal analyses for acquiring complementary characterization and more in-depth understanding of the corrosion process.

(1) Ewing, R. C. Long-term storage of spent nuclear fuel. *Nature Materials* **2015**, *14* (3), 252-257. DOI: 10.1038/nmat4226.

(2) Yao, J.; Lahiri, N.; Tripathi, S.; Riechers, S. L.; Ilton, E. S.; Chatterjee, S.; Buck, E. C. A microfluidic electrochemical cell for studying the corrosion of uranium dioxide (UO₂). *RSC Advances* **2022**, *12* (30), 19350-19358, 10.1039/D2RA02501A. DOI: 10.1039/D2RA02501A.

(3) Yao, J.; Tripathi, S.; McNamara, B. K.; Lahiri, N.; Riechers, S. L.; Chatterjee, S.; Reilly, D. D.; Ilton, E. S.; Buck, E. C. Advancing radioactive material research method: the development of a novel in situ particle-attached microfluidic electrochemical cell. *Frontiers in Nuclear Engineering* **2023**, *2*, Original Research. DOI: 10.3389/fnuen.2023.1206110.

(4) Sunder, S.; Strandlund, L. K.; Shoesmith, D. W. *Anodic dissolution of UO₂ in slightly alkaline sodium perchlorate solutions*; AECL--11440; Canada, 1996. http://inis.iaea.org/search/search.aspx?orig_q=RN:28006012.

4:00 PM *SF02.12.04

Improvement of The Fission Track Analysis Methods for Nuclear Forensics Simulation and Tools Itzhak Halevy¹, Rami Babayew², Yaacov Yehuda zada², Galit Katarivas Levy³, Jan Lorincik⁴, Itzhak Orion¹, Noam Elgad¹ and Aryeh Weiss⁵; ¹Ben-Gurion University of The Negev, Israel; ²NRCN, Israel; ³Ben-Gurion University of the Negev, Israel; ⁴Research Centre Rez, Czechia; ⁵Bar Ilan University, Israel

In order to address inquiries pertaining to nuclear forensics, our research endeavors involve the formulation of novel methodologies and strategies aimed at enhancing the dependability and precision of this analytical process.

At now, the analysis of microscope pictures is limited to individuals who have received formal training in research methodologies. Given that this analysis relies on the researcher's own aptitudes and competencies, it is evident that several researchers will yield slightly divergent outcomes.

At now, the analysis of microscope pictures is limited to individuals who have received formal training in research methodologies. Given that this analysis relies on the researcher's own aptitudes and competencies, it is evident that several researchers will yield slightly divergent outcomes.

The simulation of fission tracks was conducted using the Monte-Carlo software, GEANT4. This software incorporates various aspects of nuclear fission tracks, including thermal neutron flux, fission cross-section, radiation time, particle size, enrichment, and other relevant physics. The present investigation involves the utilization of Trainer2.0 software to compute the trajectories on our Lexan detector, as well as their corresponding projections. These calculations are based on many physical parameters, including neutron flux, particle size, isotope, and radiation duration. The outcome manifests as a "star" that is positioned at the center of the simulated particle. The entirety of our software is implemented using MatLab programming language.

The simulation of harsh conditions allows for the exploration of novel aspects inside the fission track technique. The simulation provides insights into determining the appropriate sample size for the FTA procedure.

The simulation has the capability to make predictions and may be compared to both the mini-bulk and micro-bulk analyses.

The novel concept of employing penetrating fluorescent colors provides the capability to perform three-dimensional (3D) scanning with our detector, as opposed to the conventional two-dimensional (2D) scanning. In this particular instance, the Dapi marker was employed as an initial approach. It is widely recognized in the field of biomedical research.

This new idea to investigate the FT Star more than just by his projection.

The determination of the source isotope in a given element can be achieved by analyzing the length and distribution of its tracks. This analysis involves examining the shape of the "fission products distribution" as well as the density of impurities present in the source.

4:30 PM *SF02.12.05

Examining Actinide-Molten Salts Across Length Scales: Local Structure, Thermal Properties Marisa Monreal, J. M. Jackson, Scott Parker, Alexander Long and Sven C. Vogel; Los Alamos National Laboratory, United States

Actinide-molten salts are complex systems central to pyroprocessing for actinide metal purification and recovery, to molten salt reactors (MSRs)—a next-generation nuclear reactor concept currently in rapid growth, and also to a growing number of new energy-related applications. There are gaps in the literature concerning the chemistry and thermal properties of these systems, especially in data collected with well-documented methodology and experimental detail, using salts with analytical data confirming purity, and reported with thorough error analysis and quantified uncertainty. With the overarching goal to contribute to a better understanding of these complex systems, enabling prediction of their behavior, a suite of advanced characterization techniques is being developed at Los Alamos National Laboratory for the accurate and precise measurement of actinide-molten salt thermochemical and thermophysical properties, and for the study of their local structure. The high-quality empirical data collected using these capabilities supports the optimization of pyroprocesses, the development of MSRs, and the validation and refinement of models. Efforts to examine actinide-molten

salts across length scales will be described, including recent results from studies both on local structure and on thermal properties of uranium- and plutonium-bearing chloride salts. A selection of techniques and results will be detailed, with a focus on pulsed neutron characterization at the Los Alamos Neutron Science Center (LANSCE), including progress using pair distribution function (PDF) analysis to gain insight into uranium-molten salt local structure, and recent results from measurements of the liquid density of uranium- and plutonium-molten chloride salts as a function of temperature and composition using neutron radiography.

SYMPOSIUM SF03

Ion Insertion—Fundamentals Processes and Applications to Switching
April 23 - April 25, 2024

Symposium Organizers

Iwnetim Abate, Stanford University
Judy Cha, Cornell University
Yiyang Li, University of Michigan
Jennifer Rupp, TU Munich

Symposium Support

Bronze

Journal of Materials Chemistry A

* Invited Paper

+ JMR Distinguished Invited Speaker

^ MRS Communications Early Career Distinguished Presenter

SESSION SF03.01: Synthesis of Ion Insertion

Session Chairs: Iwnetim Abate and Judy Cha

Tuesday Morning, April 23, 2024

Room 339, Level 3, Summit

10:30 AM *SF03.01.01

Hafnium, Titanium and Zirconium Intercalation [Kristie J. Koski](#), Kevin R. Rivera, Tiffany Teoh, Ethan Chen and Vicky Huynh; University of California, Davis, United States

We demonstrate an intercalation chemistry for titanium, hafnium, and zirconium in the highly oxidized state (Zr^{4+} , Hf^{4+} , Ti^{4+}) into 2D layered materials through formation of a soluble, molecular bis-tetrahydrofuran (THF) metal halide complex. This method overcomes challenges distinct to intercalation of highly oxyphilic group 4 metals through creation of a molecular species that is highly soluble in organic solvents and is kinetically competent in reactivity. Metal intercalation is demonstrated in several layered hosts including MoO_3 , Bi_2Se_3 , Si_2Te_3 , and GeS . This strategy intercalates, on average, 3 atomic % or less of Hf, Ti, and Zr, limited by the high oxidation state and charge transfer with the host. MoO_3 is chemochromically switched from transparent white to dark blue through Zr^{4+} , Hf^{4+} , Ti^{4+} intercalation. Contrast with methods for intercalation of zero-valent metals in 2D layered materials is demonstrated. We believe that this bis-THF chemistry offers a unique way to ionically switch properties of 2D layered materials and achieves a route to intercalate otherwise elusive guests.

11:00 AM SF03.01.02

Controlling Composition and Stoichiometry of Co-Intercalated Chevrel Phase Sulfides via Electrochemical and Solid-State Synthesis Pathways [Konstantina G. Mason](#); University of California, Davis, United States

Carbon dioxide levels (CO_2) in the atmosphere continue to rise exponentially as fossil fuels remain a primary energy source for many industrial processes. Consequently, alternative energy technologies, such as solar and wind, must be harnessed to convert CO_2 into liquid fuels through the development of electrocatalytic materials that exhibit high selectivity and efficiency for CO_2 reduction (CO_2R). One such class of materials that have shown promise for CO_2R are Chevrel phase sulfides (CPs), due to their ability to host a wide variety of metal cations that can alter the structural and electronic properties of the crystal framework and in turn CO_2 binding motifs. CPs with the general formula $M_nMo_6S_8$ (M = transition, alkali, alkaline, or post transition metals) are excellent materials to investigate ion (de)insertion mechanisms due to the channels and cavities formed by the extended array of Mo_6S_8 clusters. While electrochemical insertion of a single mono or multivalent metal cation into CPs has been thoroughly investigated, co-insertion of two or more metal cations remains underexplored, despite the potential to further stabilize binding intermediates for CO_2R . Alternate electrochemical synthesis pathways can be exploited to not only co-insert two or more metal cations into the CPs framework for CO_2R studies but to further understand the thermodynamics and kinetics of chemical and electrochemical processes occurring during co-insertion. Furthermore, insertion methods, such as open circuit potential (OCP) mechanisms, can be used to investigate the synergistic movement of metal cations throughout the channels formed in the extended Mo_6S_8 solid and their effect on the electronic properties of the crystal structure that could prove beneficial for understanding product selectivity in CO_2R and other catalytic reactions. Aside from electrochemical co-insertion in aqueous electrolytes, medium temperature solid-state synthesis can also be utilized as a synthesis pathway to CPs materials with multiple metal cations inserted. In this work, control of composition and stoichiometry of co-inserted transition metal CPs

was achieved through OCP and cyclic voltammetry (CV) electrochemical synthesis techniques, as well as medium temperature solid state synthesis methods. Materials were characterized with X-ray diffraction (XRD), scanning electron microscopy (SEM), energy dispersive spectroscopy (EDS), x-ray photoelectron spectroscopy (XPS), and x-ray absorption near edge structure spectroscopy (XANES).

11:15 AM SF03.01.03

Bulk Proton Acidity Modulates Structural Transformations in Hydrogen Titanates during Li⁺-Insertion Coupled Electron Transfer Saeed M. Saeed¹, Takeshi Kobayashi², Noah Holzzapfel¹, Eugene Mamontov³, Naresh Osti³ and Veronica Augustyn¹; ¹North Carolina State University, United States; ²Iowa State University, United States; ³Oak Ridge National Laboratory, United States

Nanostructured TiO₂-based materials are of interest for energy storage and conversion applications due to their high abundance, low toxicity, and chemical tunability. Lithium titanium oxides, such as spinel-type Li₄Ti₅O₁₂ and ramsdellite-type Li₂Ti₃O₇, have been extensively studied as electrode materials for Li-ion batteries. The synthesis of nanostructured metal oxide materials with high surface area has been a promising path for achieving high specific capacity for electrochemical energy storage. As such, it is important to expand the materials design strategies to synthesize titanium oxide materials for high Li-ion energy storage applications. Here we explore a series of layered hydrogen titanates (HTOs), H₂Ti_nO_{2n+1}•xH₂O (n = 3, 4, and 5), with varying degrees of structural protonation and interlayer water. These HTOs are metastable materials prepared via acid etching of alkali titanates. The complexity of the interlayer environment motivated us to understand the role of water content and structural protons on Li⁺-insertion coupled electron transfer from a non-aqueous electrolyte. We hypothesized that structural protons are necessary for high Li⁺ intercalation capacity, while the mobility of these protons determines the degree of structural change that occurs during Li⁺ insertion. To investigate these phenomena, we utilized electrochemistry as well as operando electrochemical XRD, ex situ solid-state NMR, and acid-base titrations. By employing these techniques, we correlated the relative acid strengths of the structural protons to the degree of structural change during Li⁺ intercalation. Our findings show that HTOs with more acidic protons undergo rapid, irreversible structural changes due to hydrogen evolution of bulk protons. Long term electrochemical cycling reveals irreversible structural transformations of the HTOs to lithiated titanates. This work provides a comprehensive understanding of the relationship between bulk proton acidity and structural transformations during electrochemical Li⁺ intercalation into titanates. In doing so, it informs the structural design of next generation ion-insertion coupled electron transfer materials for energy storage and conversion.

11:30 AM SF03.01.04

Medium Temperature Intercalation (MTI) through Microwave Irradiation to Access Catalytically Relevant Metastable Chevrel Phases, MM₆X₈ (M = Ag, Sn; X = S, Se) Rose Smiley and Jesus M. Velazquez; University of California, Davis, United States

The demand for large scale sustainable energy solutions for an energy landscape evolving post-haste calls for the development of transformative materials with the ability to mediate sustainable renewable energy conversion. Chevrel phases (CPs), M₆Mo₆X₈ (M = alkali, alkaline, transition, post-transition, and lanthanide metals; X = S, Se, Te) have shown promise as electrocatalysts for the hydrogen evolution reaction (HER), the reduction of carbon dioxide (CO₂R), and the oxygen reduction reaction (ORR). However, efficient, and selective electrochemical conversion is hindered by achieving controlled bonding affinity of key intermediates. CPs offer a unique platform to probe structure function relationships between active sites and key intermediates in part to their highly tunable framework. While classical high temperature synthesis methods can be used to access thermodynamically stable CPs, the same methods can yield impure material for metastable CPs. Medium temperature intercalation (MTI) can be used to diffuse cations of interest into existing Mo₆X₈ framework to access pure phase metastable CPs. This work reports a facile synthesis procedure developed using a commercial microwave to synthesize SnMo₆X₈ and AgMo₆X₈ (X = S, Se), full characterization of the materials, and highlight X-Ray Absorption Near Edge Structure (XANES) and Extended X-Ray Absorption Fine Structure (EXAFS) data to gain insight on local electronics and structure.

11:45 AM SF03.01.05

Ion Insertion into Confined Solid Ionic Channels for Separation of Rare Earth Elements Siqi Zou¹, Woo Cheol Jeon², Maoyu Wang³ and Chong Liu¹; ¹UChicago, PME, United States; ²Northwestern University, United States; ³Argonne National Laboratory, United States

Rare earth elements (REEs) play an indispensable role in the path towards a greener, renewable future. Despite its efficacy, the conventional industrial solvent extraction method suffers from substantial energy consumption and chemical intensiveness. Thus, there is an urgent need to develop sustainable methods for REEs separation. Ionic radius and Lewis acidity are the two key differences that have paved the way for many separation methods. Separation methods combining both size effect and binding affinity can promote selectivity among REEs, however, the effect of long-range confinement on separation is largely unexplored. Here we report a new method to achieve separation among REEs in aqueous systems without ligands via creating optimal long-range confinement to maximize the energy penalty among disfavored REEs. We observed two distinct group behaviors through ion insertion, based on which we achieved effective separation for cross-group elements. We further proposed a pinning strategy to boost the same-group separation by maintaining the confinement throughout the reaction process. As a result, we achieved a significant escalation in enrichment factors for La-Nd and La-Pr pairs from 1.6 ± 0.1 and 1.5 ± 0.1 without pinning, to 5.4 ± 0.1 and 4.2 ± 0.1 with pinning, respectively. This unique design delivers an impressive ~92.3% purity of Dy from a 1:1 Nd-Dy pair, and a ~97.0% purity of Nd from a 1:1 La-Nd pair, through a two-time separation process. Our work illuminates the potential of confinement design and its pivotal role in advancing sustainable REE separation methods.

SESSION SF03.02: Ion Insertion for Switching Devices

Session Chairs: Iwnetim Abate and Judy Cha

Tuesday Afternoon, April 23, 2024

Room 339, Level 3, Summit

1:30 PM *SF03.02.01

Harnessing Ion Tuning Mechanisms for Neuromorphic Computing: From Artificial Synapses to Dynamically Reconfigurable Architectures Alec Talin; Sandia National Laboratories, United States

Non-von Neumann computing using neuromorphic systems based on analog synaptic and neuronal elements has emerged as a powerful approach, but its full potential has not been realized due to the lack of materials and devices with the appropriate attributes. Recently, solid state electrochemical ion-insertion, also known as electrochemical random access memory (ECRAM) has emerged as a promising approach to realize the needed device characteristics. Unlike memristors which require large write currents to drive phase transformations or filament growth, every electron transferred through the external circuit in an ion tunable element corresponds to the migration of ~1 ion, which is used to store analogue information. Like static dopants in traditional semiconductors, electrochemically inserted ions increase or decrease the conductivity by locally perturbing a host's electronic structure but do so in a

dynamic and reversible manner. The resulting change in conductance can span orders of magnitude, from gradual increments needed for artificial synapses, to large, abrupt changes required for artificial neurons. In my presentation, I will briefly cover the history of ECRAM, the recent progress in devices spanning various types of materials, circuits, architectures, and discuss the rich portfolio of challenging, fundamental questions and how we can harness ECRAM to realize a new paradigm for low power neuromorphic computing.

2:00 PM *SF03.02.02

On-Chip Learning with Organic Neuromorphic Systems Yoeri van de Burgt; Eindhoven University of Technology, Netherlands

The process of neural network training can be slow and energy-expensive due to the transfer of weight data between digital memory and processor chips. Neuromorphic systems can accelerate neural networks by performing multiply-accumulate operations in parallel using non-volatile analogue memory. However, the backpropagation training algorithm in multi-layer (deep) neural networks requires information - and thus storage - on the partial derivatives of the weight values, preventing easy implementation in hardware.

In this talk I will highlight a novel hardware implementation of the well-established backpropagation algorithm that progressively updates each layer using *in situ* stochastic gradient descent, thus avoiding this storage requirement. We experimentally demonstrate the *in situ* error calculation and the proposed progressive backpropagation method using a multi-layer hardware implemented neural network based on organic EC-RAM, and confirm identical learning characteristics and classification performance compared to conventional backpropagation in software.

2:30 PM SF03.02.03

Tuning Resistive Switching in ZrTaO_x Devices Matthew Flynn-Hepford¹, Reece Emery¹, Jack Lasseter¹, Anton Levlev², Olga Ovchinnikova¹ and Philip D. Rack¹; ¹University of Tennessee- Knoxville, United States; ²Center for Nanophase Materials Sciences, United States

TaO_x chemistries have been widely studied as candidates for memristive switching memory and computation due to the non-linear conductance state transitions observed in these materials when exposed to applied electrical fields. Less effort has been put into studying the effects of doping and alloying TaO_x chemistries in order to optimize the mechanism of resistive switching. ZrTaO_x alloys offer promising properties for stable resistive switching devices due to tantalum's mixed oxide states and zirconium's flexible 5S outer valence bonding orbital. To explore this system, we have employed a combinatorial magnetron reactive sputtering of this Zr_xTa_{1-x}O_y system over a 100 mm diameter substrate and achieved a composition gradient such that 0.15 < x < 0.9. We confirm the composition via energy dispersive x-ray spectroscopy and generate a series of Pt/Zr_xTa_{1-x}O_y/Pt memristors along the gradient and correlate the resultant I-V to the composition as-deposited and as a function of annealing temperature. To gain insight into the switching mechanisms of the effective chemistries we leverage a workflow that couples conductive scanning probe microscopy (SPM) and spatially resolved time-of-flight secondary ion mass spectrometry (ToF-SIMS). Additional defects can then be introduced to these oxide systems, in the form of He, Ne and Si focused ion beams, in order to further understand how intentionally induced defects affect the oxygen motion that drives these devices.

2:45 PM SF03.02.04

Toward Tunable Conductance States in Layered Materials for Neuromorphic Computing using Metal Intercalation Michelle A. Smeaton, Katherine L. Jungjohann and Lance M. Wheeler; National Renewable Energy Laboratory, United States

As computing needs and accompanying energy costs continue to rise exponentially, neuromorphic (brain-inspired) computing has the potential to provide crucial improvements to computing speed and efficiency over traditional CMOS technology. Metal-intercalated, layered van der Waals materials present a promising strategy for tuning conductivity and insulator-metal transitions in devices for neuromorphic computing. Ion-insertion materials have been well studied for energy storage applications; however, the field focuses on high, reversible loading of ion materials. Here, we investigate the intercalation of metal heteroatoms into layered chalcogenide and oxide host materials, with the goal of understanding the associated modulation of the host electronic structure. We measure electrical transport of bulk materials and provide local insight into the structural and chemical effects of intercalation using scanning transmission electron microscopy (STEM) techniques. We further discuss how these effects differ based on host and intercalant species and intercalant concentration. These findings help provide insight into the dependencies of the host/guest interactions to understand the modulation of conductance and insulator-metal transitions for neuromorphic devices.

3:00 PM BREAK

3:30 PM *SF03.02.05

Dynamics of Electrochemical Ionic Synapses to Emulate Spike Timing Depending Plasticity and other Bio-Realistic Learning Rules Bilge Yildiz; Massachusetts Institute of Technology, United States

In our research, we aim to reduce the energy consumption in analog, brain-inspired computing, by focusing on designing materials and devices that use ions to perform data storage and computation in a single architecture. In this talk, I will share our work on the ionic electrochemical synapses, whose electronic conductivity we can control deterministically by electrochemical insertion/extraction of dopant ions across the active device layer. We are exploring protons and magnesium ions, which bring different advantages to the operation of the device. The protons present very low energy consumption, on par with biological synapses in the brain. Magnesium ions present with better stability without the need for encapsulation. The modeling results indicate the desirable material properties, such as ion conductivity and interface charge transfer kinetics, that we must achieve for fast (ns), low energy (< fJ) and low voltage (1V) performance of these devices. We are also exploring ion dynamics in these materials to emulate bio-realistic learning rules deduced from neuroscience studies. These include spike timing dependence achieved by electrochemical ionic synapses, as well as a local learning rule describing how song birds learn to sing. Our findings provide pathways towards brain-inspired hardware that has high yield and consistency and uses significantly lesser energy as compared to current computing architectures.

4:00 PM *SF03.02.06

Various Functional Devices Created by Ionic Nanoarchitectonics, such as Neuromorphic Properties. Kazuya Terabe, Takashi Tsuchiya and Tohru Tsuruoka; NIMS, Japan

Today's semiconductor devices continue to make remarkable progress, supported by technological developments in miniaturisation and integration, but there are fears that this progress will slow down in the near future. In order to evolve into the next generation information society, it is necessary to actively develop high-performance devices and new functional devices that operate on different principles from conventional semiconductor devices. Among these, solid-state ionic devices, which operate by utilising local ion transfer in solids, are expected to be very promising candidates. To date, we have developed ionic nanoarchitectonic methods that combine ionics and nanotechnology to create novel ionic devices with various unique functions and performances [1,2]. The ionic nanoarchitectonics controls the transport of ions, which are much larger in mass and size than electrons, and thus can control not only the electronic state of materials but also the crystal structures of surfaces and interfaces. As a result, it has been found that various functions and performances can be realised that could not be achieved by conventional electron transport control in semiconductor devices. This talk will focus on the development of

memristive, neuromorphic and artificial intelligence related devices such as artificial synapses, artificial vision and physical storage devices created by the ionic nanoarchitectonics.

Reference

- [1] K. Terabe et al. *Nanoscale* 148(29), 13873-13879, 2016
- [2] K. Terabe et al. *Adv. Electron. Mater.* 8(8), 2100645, 2022

4:30 PM SF03.02.07

Exploring Bioinspired Information Pathways: Bridging The Gap Between Science and Technology with The Intercalation of Alkaline-Ions in 3D-Aeromaterial of MoS₂ Pia Pooker, Soeren Kaps and Rainer Adelung; University of Kiel, Germany

The human brain works with an exceptionally low power consumption but high information output. Understanding the intricate information pathways found in nature, particularly in the human brain, has emerged as a pivotal source of inspiration for revolutionary technological advancements. This exploration into bioinspired information pathways has led to the development of artificial neurons, a key element in unraveling the mysteries of neural processes. This exploration extends its reach to various domains, including energy efficiency, information storage, and memristive systems, where the integration of bioinspired concepts promises transformative breakthroughs.

As the brain functions with a decentralized energy supply, there are some striking similarities to alkaline batteries as both function with a liquid electrolyte based electrochemical system and are able to store energy with different kinds of charge transport carriers. In order to mimic spatial arrangement of a neuron inside the brain, a 3D network with a spatial and highly scalable structure, inspired by the intricate architecture of the brain, is designed in this study.

Moreover, to mimic the function of the brain, researchers have turned to two-dimensional materials to display the working function of ion channels, an integral aspect of bioinspired information pathways. The application of (non)-equilibrium dynamics allows these materials to serve dual roles. They function not only as energy-efficient batteries but also as information storage devices, thus bridging the gap between energy and data storage.

Among the intriguing materials of bioinspired information pathways are Transition Metal Dichalcogenides (TMDs), such as molybdenum disulfide (MoS₂). As part of the broader bioinspired research, TMD materials enable not only efficient energy storage but also serve as a cornerstone for developing innovative information processing technologies. TMDs like MoS₂, with their atomically thin structure and tunable bandgap, play a pivotal role in the quest to mimic the remarkable capabilities of the human brain.

In this contribution an aero-material consisting of the exfoliated 2D-TMD MoS₂ and exfoliated graphene (EG) is used as the functional material. For the realization of the battery-like electrodes, the 3D-network is infiltrated with a dispersion of both, exfoliated MoS₂ and EG, before etching ZnO away, to have a light, mechanically stable and 3D shaped TMD.

In a quest to advance traditional lithium-ion batteries, we are exploring sodium (Na) as well as potassium (K) as a viable alternative as the intercalated species to expand the horizons of layered materials. This shift opens new possibilities for energy storage technologies and fosters sustainability in energy solutions.

For testing equilibrium dynamics with both, Li and Na, the battery-like aero material is incorporated as the anode material with metallic Li as the cathode. The electrolyte is varied with different conducting salts containing Na⁺/K⁺-ions. The different ion-radii lead to an expansion of the interlayer spacing and hence to higher capacities. For testing non-equilibrium conditions, a tuning of the intercalation pathway of the alkaline ions and hence a tuning of the resistivity of certain pathways can be reached, by contacting several points of the 3D structure and applying different signals. With this measurement, a training of the network can be achieved.

Funded by the Deutsche Forschungsgemeinschaft (DFG, German Research Foundation) –Project-ID 434434223 –SFB 1461

4:45 PM SF03.02.08

Phase-Field Modeling of 3-Terminal Protonic Transistor Switching Dynamics Michael L. Li and Martin Z. Bazant; Massachusetts Institute of Technology, United States

The need for increased computational efficiency for deep learning applications has led to interest in in-memory computing. One example, three-terminal synaptic transistors with ion or proton intercalation mechanisms [1,2], have been recently studied for their CMOS compatibility and relatively fast switching time. Given the young nature of this technology, there are fundamental unanswered questions about these devices, which creates a gap between the current available models and tools required to simulate and accelerate material and architecture design. Though ion-intercalation materials have been heavily studied in the context of batteries, the large applied voltages to trigger the resistance state switching and nanoscale structure of these films lead to uninvestigated effects on the material reaction and transport properties. Additionally, the impact of these devices' design and formation on performance is not fully understood. A fundamental investigation of the relationship between material properties and device performance metrics is needed.

Here we present a new phenomenological phase-field model to describe the resistance switching of WO₃ 3-terminal protonic transistors [1] by extending multiphase polarization theory outline by Tian and Bazant [3]. Through this process, we determine relationships between the effective surface reaction and material transport parameters and device performance parameters, such as switching time and energy. We address the importance of the underlying model for the surface ion-intercalation reaction, comparing different the phenomenological Butler-Volmer and the coupled ion-electron transfer reaction model [4]. Additionally, we investigate the impact of phase separation on these devices, which, due to the large electric fields needed to switch between resistance states, is shown to occur even when the bulk concentration exists in a single-phase region. Finally, preliminary extensions to 3d device topologies are investigated. This model will be indispensable in predicting the impact of material properties and architecture on device performance, accelerating design of similar synaptic transistor technologies.

References

1. Onen, Murat, et al. "CMOS-compatible protonic programmable resistor based on phosphosilicate glass electrolyte for analog deep learning." *Nano Letters* 21.14 (2021): 6111-6116.
2. Cui, Jinsong, et al. "CMOS-compatible electrochemical synaptic transistor arrays for deep learning accelerators." *Nature Electronics* 6.4 (2023): 292-300.
3. Tian, Huanhuan, Ju Li, and Martin Z. Bazant. "Multiphase Polarization in Ion-Intercalation Nanofilms: General Theory Including Various Surface Effects and Memory Applications." *Advanced Functional Materials* 33.23 (2023): 2213621.
4. Bazant, Martin Z. "Unified quantum theory of electrochemical kinetics by coupled ion-electron transfer." *Faraday Discussions* (2023).

Tuesday Afternoon, April 23, 2024
Flex Hall C, Level 2, Summit

5:00 PM SF03.03.01

A GFP-Chromophore-Based C3V-Symmetric Tripodal Receptor Material with Selective Hg(II), Fe(III) and Cr(III) Ion Insertion Kuangsen Sung;
National Cheng Kung University, Taiwan

A novel green-fluorescent-protein-chromophore-based tripodal receptor material is synthesized. Its single crystal X-ray diffraction structure looks like a straight, long tube with one end closed. The diameter of the inner cavity of the tripodal receptor material is 2.7 Å and its outer cavity is a little larger with the diameter of 3.5 Å. The three GFP chromophores in this material are packed like a propeller quite well and tightly through van der Waals forces. The tripodal receptor material selectively captures Hg²⁺, Fe³⁺ and Cr³⁺ in its inner cavity through four binding sites (one tertiary amine and three amide groups) to form a 1 : 1 complex with the binding constant K of 2.6 × 10⁴, 1.4 × 10⁵ and 4.3 × 10⁴, respectively. The fluorescence of the tripodal receptor material is quenched by Hg²⁺, Fe³⁺ or Cr³⁺ through a heavy-atom or a paramagnetic quenching mechanism.

5:00 PM SF03.03.02

In Situ Studies of SrCoO_x Heterostructures for Synaptic Memories Tadesse Billo Reta¹, Daniel B. Durham¹, Yan Li¹, Jill Wenderott², Hua Zhou¹, Supratik Guha¹ and Dillon D. Fong¹; ¹Argonne National Laboratory, United States; ²Drexel University, United States

Varying the oxygen concentration in many transition metal oxides can be used to tailor electronic properties, making oxide heterostructures of great interest in ionotronics and novel memory devices. We investigate epitaxial SrCoO_x heterostructures, depositing insulating SrCoO_{2.5} and conducting SrCoO₃ layers and bilayers on SrTiO₃ (001) substrates. The resistive switching properties of the heterostructures depend on structural and electronic phase transitions as governed by ion insertion and extraction. The volume fraction of the different phases significantly influences switch behavior, affording fine control and revealing distinct traits in low-voltage I-V sweeps, especially during DC forming. We employ coherent synchrotron techniques such as X-ray Photon Correlation Spectroscopy (XPCS) during ionic liquid gating to shed light on the dynamics of oxygen ion insertion and extraction. We will discuss these results and findings from electrical device characterization, emphasizing the reliability and performance of these structures.

5:00 PM SF03.03.03

Broad-Range Modulation of Guest-Species Interactions in MoS₂ Transistors for Electrochemical Phase Transitions Jaeeun Kwon and Hanbin Cho;
Ulsan National Institution of Science and Technology, Korea (the Republic of)

In the realm of two-dimensional (2D) transition metal dichalcogenides (TMDs), the utilization of ionic gating has emerged as a powerful means, advancing electrostatic and electrochemical manipulations in a wide range of electronic properties. In general, the conventional ionic gating approach is, however, performed within the conservative low-voltage regime, which cannot take advantage of its full range of gating power as well as electrochemical interactions. Herein, we present an all-inclusive ionic gating technique covering from electric-double-layer gating (low-voltage stage) to insulator-to-metal transition (high-voltage stage). In the latter, the structural/electronic phase transformation of MoS₂ is triggered by intercalation of guest ions, 1-Ethyl-3-methylimidazolium ([EMIM]⁺), which is one of the most conventional cation used in ionic gating devices and the greater details in its characteristics are studied as a versatile and fast-switching device. In such device operated under high-bias condition, it is critical to prevent undesirable chemical reactions, and so we introduce a very thin high-k dielectric passivation layer deposited through atomic layer deposition, strategically protecting the electrodes and also reducing leakage current (so, I_{on/off} > 10⁶) while operating in liquid-based electrolytes at room temperature. In addition, to effectively accumulate the charge in the channel and control the voltage range in which phase transition can occur, a dual gating method was introduced just adding simple process fabricating bottom gate using high-k dielectric and a way to effectively operate the device was explored. This work underscores the potential for phase-change-based devices and hybrid gating schemes as promising avenues for advancing the field of 2D materials and nanoelectronics, offering unprecedented control and functionality in future electronic systems.

SESSION SF03.04: Fundamentals of Ion Insertion Dynamics

Session Chairs: Iwnetim Abate and Judy Cha

Wednesday Morning, April 24, 2024

Room 339, Level 3, Summit

8:00 AM *SF03.04.01

Materials Approach to Control The Properties of Electrochemical Artificial Neurons and Synapses Iliia Valov^{1,2}; ¹Peter Grünberg Institute 7 and JARA-FIT, Germany; ²Bulgarian Academy of Sciences, Bulgaria

Memristive devices have significantly developed in the last decade, expanding their application horizon much beyond memory applications. Especially important is their functionalities as artificial neurons and synapses, making them promising building units for the next generation bio-inspired neuromorphic hardware. Despite a lot has been learned about materials design and the operation principles of memristors, recent research has shown that fundamentals can still be significantly amended, demonstrating new operation principles and functionalities.

In this contribution, the common electrochemical fundamentals of biological and memristive artificial neurons and synapses will be discussed as well as new aspects on materials design and its influence on the physicochemical processes and resulting functionalities of both ECM (CIBRAM) and VCM (OxRAM) devices. The effects of the materials and thicknesses of the capping layer appear of special importance and as well the thicknesses and combination of thicknesses of all involved layers. The selection of different materials is changing the electrochemical nanoionics processes and as well the performance of the memristors. For reliable performance the device stack should be considered as a whole, and materials used in the stack and their thicknesses should be coordinated and harmonised.

A special attention will be paid on controlling the energy barriers at the interface electrode / switching film, where Schottky barrier competes with the energy barrier of the redox reactions. A new switching mechanism will be presented, relying entirely on electrochemical processes of oxidation and reduction and depends on the valence state and thickness of filament. The ohmic memristive devices, demonstrate a number of advantages compared to Schottky-based devices, such as combination of digital and analogue switching in same devices, higher voltage window of stability, lower operating currents, higher OFF to ON ratio, high endurance and retention, high temperature stability. The importance of fundamental research will be highlighted, allowing for new functionalities and opportunities for applications.

8:30 AM *SF03.04.02

Origin of The Time Relaxation of Volatile Valence Change Memory [Regina Dittmann](#), Johannes Hellwig, Carsten Funck and Dimitris Spithouris; PGI-7, Germany

Memristive devices based on the valence change mechanism are highly interesting candidates for data storage and hardware representation of synapses in neuromorphic circuits. Although long-term retention is often required for data storage applications, a time decay of the resistance is advantageous for several applications where short-term plasticity is required. In this work, we investigate in detail the LRS relaxation of volatile SrTiO₃ devices. The decay is analysed in terms of the Schottky-Read-Hall model for the contribution of electron traps and in terms of the Gibbs free energy gradient for the contribution of oxygen ion migration. Based on this, we can exclude trapping effects as origin of the LRS decay. In contrast, we could nicely model the device behaviour by oxygen ion migration considering four reservoirs within the devices, connected by oxygen exchange. Our model serves as a tool for developing guidelines and design rules for future volatile memristive technology based on Schottky barrier mediated electron transport. As an example, we demonstrate the acceleration of the decay over 3 orders of magnitude by modifying the microstructure of the SrTiO₃ layer.

9:00 AM *SF03.04.03

Ionic Peltier Effect in Li-Ion Electrolytes [David Cahill](#), Zhe Cheng, Yu-Ju Huang, Benjamin Zahiri, Patrick Kwon and Paul V. Braun; University of Illinois, United States

The insertion of an ion from an electrode to an electrolyte involves changes in the thermodynamics properties and the transport of charge and heat. The coupled transport of charge and heat provides fundamental insights on the microscopic thermodynamics and kinetics of this process. We describe a sensitive ac differential resistance bridge that enables measurements of the temperature difference on two sides of electrochemical cell with a resolution of better than 10 μ K. We use this temperature difference metrology to determine the ionic Peltier coefficients of symmetric Li-ion electrochemical cells as a function of Li salt concentration, solvent composition, electrode material, and temperature. The Peltier coefficients Π are negative, i.e., heat is absorbed at the cathode and emitted at the anode, large in absolute magnitude, $\Pi > 30$ kJ/mol, become less negative with increasing concentration, and becomes slightly more negative with increasing temperature. The Peltier coefficient is approximately constant on time-scales that span the characteristic time for mass diffusion across the thickness of the electrolyte, suggesting that the heat of transport plays a minor role in comparison to the changes in entropy at the interface between the electrode and electrolyte. Our work demonstrates a new platform for studying the non-equilibrium thermodynamics of electrochemical cells and provides a window into the transport properties of electrochemical materials through measurements of temperature differences and heat currents that complement traditional measurements of voltages and charge currents.

9:30 AM BREAK

10:00 AM SF03.04.05

Cation Insertion Characteristics of Mesoporous Titania-Silica Composite Layers [Debargha Chakravorty](#)^{1,2,3}, Nina Plankensteiner^{1,2,3}, Maarten Mees^{2,3} and Philippe M. Vereecken^{2,1,3}; ¹KU Leuven, Belgium; ²Imec, Belgium; ³EnergyVille, Belgium

Innovative approaches in materials and concepts will be key to address the energy transition challenge. A key area involves ion insertion materials which are not only interesting for energy storage but also for energy conversion and low power electronics and optoelectronics¹. Titanium dioxide (TiO₂) is well known ion insertion electrode capable of accommodating lithium ions. The ion storage capacity and ion insertion/extraction rates can be enhanced significantly by nano structuring and doping^{2,3}. For nanostructured TiO₂, insertion of other cations such as K⁺, Ca²⁺, Mg²⁺ and Al³⁺ has been shown⁴. The versatility and stability of titania chemistry lends itself to tuning of its morphology by simple fabrication methods. In this paper, mesoporous titania-silica composite thin films were fabricated by a facile sol gel approach. The thin film was spin-coated and cured onto a metal coated silicon substrate, which served as current collector and loaded in a three-electrode cell for electrochemical characterisation. A facile and reversible ion insertion and extraction of the titania-silica composites was found upon, respectively, reduction of Ti(IV) to Ti(III) and oxidation of Ti(III) to Ti(IV) from aqueous and non-aqueous solutions. Interestingly, the results show that next to Li⁺, also facile reversible ion insertion/deinsertion can be carried with other monovalent cations and even bivalent cations. The morphology and composition of the thin films were determined before and after the ion insertion process using scanning electron microscopy and transmission electron microscopy, combined with EDS and EELS. These measurements provided insights into the charge-discharge characteristics of the composite material and the charge capacity was determined. Proton intercalation/extraction was found a competing reaction during the charge/discharge process in aqueous solutions and depend on the pH. The total charge capacity of the material is then the sum of proton and cation insertion charges. The electrochemical characteristics of the material thus can be tuned according to the application.

1. Sood, A., Poletayev, A.D., Cogswell, D.A. *et al.* Electrochemical ion insertion from the atomic to the device scale. *Nat Rev Mater* **6**, 847–867 (2021).

2. Moitzheim, S., De Gendt, S. & Vereecken, P. M. Investigation of the Li-Ion Insertion Mechanism for Amorphous and Anatase TiO₂ Thin-Films. *J. Electrochem. Soc.* **166**, A1–A9 (2019).

3. De Taeye, L. L., Mees, M. J. & Vereecken, P. M. Surpassing the 1 Li/Ti capacity limit in chlorine modified TiO₂₋₃Cl_{2-y}. *Energy Storage Mater.* **36**, 279–290 (2021).

4. Koketsu, T., Ma, J., Morgan, B. *et al.* Reversible magnesium and aluminium ions insertion in cation-deficient anatase TiO₂. *Nature Mater* **16**, 1142–1148 (2017).

10:15 AM *SF03.04.06

Collective Phenomena in Mixed Ionic & Electronic Conductors [William C. Chueh](#); Stanford University, United States

Mixed ionic and electronic conductors underpin many energy storage and conversion mechanisms. The coexistence of ionic and electronic charge carriers gives rise to critical functionalities and mechanisms that do not exist in pure ionic and pure electronic conductors, such as ion insertion (intercalation). Fundamentally, mixed transport of ions and electrons involves collective phenomena, similar to many-body effects in condensed matter physics. At the atomic scale, mobile ions and electrons interact as they migrate in the solid-state, affecting both the equilibrium configuration and the kinetic pathway. At the mesoscale scale, a large ensemble of “wired” particles interact in non-trivial ways.

Historically, the electrochemistry community has largely taken a mean-field approach towards these collective phenomena, which is reflected in widely used reaction-transport models. In the solid-state ionics community, mobile ions and electrons are often dissociated under typical experimental conditions (i.e., higher temperatures). As such, the standard approach is to consider bulk ion-electron interaction through local and equilibrium charge neutrality.

In this talk, I will overview two bodies work at Stanford on collective phenomena in mixed conductors that goes beyond the mean-field and local charge neutrality approach. First, at the atomistic level, I will deconstruct the coupling between mobile ions and localized electrons (polarons) and show how the local chemistry is determined by such couplings. I will use two model solids, Li₂-XMnO₃ and Na₂-XMnO₇ as examples. Second, at the mesoscale, I will

show that reaction-diffusion and phase separation occurring in an ensemble of wired particles give rise to vastly different behavior than their bulk, single crystal counterpart. I will use two additional model solids, LiXCoO₂ and LiFePO₄ to showcase these unusual collective phenomena occurring at the mesoscale. To conclude my talk, I will describe the ten-year vision to advance the understanding of ionic and electronic transport by embracing emergent experimental and theoretical tools that tackle transport at the intrinsic time and length scales.

10:45 AM *SF03.04.07

Switching the Properties of Layered Materials through Intercalation, Defects and External Fields from First Principles [Diana Qiu](#); Yale University, United States

Layered van der Waals materials, such as transition metal dichalcogenides (TMDs), are a promising platform for applications as diverse as optoelectronics, energy storage, and quantum information in large part due to the tunability of their electronic, optical and structural properties. Both ground- and excited-state properties can be sensitively modified both during and after synthesis through methods such as ion intercalation, stacking and twisting, the introduction of defects, and coupling to external fields. In this talk, I will explore three different pathways for switching the properties of layered TMDs. Firstly, I will present our recent first principles work on ion intercalation induced phase transitions in different TMD heterostructures, including an intercalation-induced charge density wave (CDW) phase transition in WTe₂. Secondly, we will explore structural defects present in TMDs, routes for passivating these defects, and magnetic order arising from defect complexes. Finally, we will explore how many-body effects modify the nonlinear optical response of 2D materials and the coupling to strong external fields beyond the perturbative regime.

11:15 AM SF03.04.08

Coupling Diffusion and Finite Deformation in Intercalation Materials [Ananya Renuka Balakrishna](#), Tao Zhang and Delin Zhang; University of California, Santa Barbara, United States

We present a multiscale theoretical framework to investigate the interplay between diffusion and finite lattice deformation in intercalation materials. In this framework, we couple the diffusion of a guest species (Cahn-Hilliard type) with the finite deformation of host lattices (nonlinear gradient elasticity). We adapt this theory to LiMn₂O₄ to investigate the delicate interplay between Li-diffusion and the cubic-to-tetragonal deformation of lattices. Our computations reveal fundamental insights into the microstructural evolution pathways under dynamic discharge conditions, provide quantitative insights into the nucleation and growth of twinned microstructures during intercalation, and identify regions of stress concentrations (e.g., at phase boundaries, particle surfaces) that arise from lattice misfit. These findings suggest a potential mechanism for structural decay in LiMn₂O₄. More generally, we establish a theoretical framework that can be used to investigate microstructural evolution pathways, across multiple length scales, in first-order phase transformation materials.

11:30 AM SF03.04.09

Tailoring The Optical and Electrical Properties of MoTe₂ via Electrochemical Intercalation of Lithium Ions [Alyssa Shiyu Xu](#); Cornell University, United States

Intercalation of lithium (Li) ions is one of the most effective methods to realize structural transformation and to tune the optical and electrical properties of two-dimensional transition metal dichalcogenides (2D TMDCs). Numerous studies have focused on the phase transition from semiconducting 2H phase to metallic 1T (or 1T') phase in MoS₂ and WS₂ induced by the intercalation of Li ions. However, few reports explore the effects of Li intercalation in other TMDCs, such as Mo- or W- ditellurides. In particular, novel electronic and energy devices can be achieved using the Li-intercalated MoTe₂ with its intriguing electrical, topological and catalytic properties.

Here, we report electrochemical Li intercalation into 1T'-MoTe₂ flakes. The 1T' phase is stable down to 0.9 V of the applied electrochemical voltage, and two new phases are observed at 0.7 V (phase I) and 0.4 V (phase II), respectively. The lightly Li-intercalated phase I is evidenced by the disappearance of the A_g peak at ~77.7 cm⁻¹ and the appearance of a peak at ~86.9 cm⁻¹ in Raman spectroscopy and a 10% increase of electrical resistance in two-terminal measurements. For the heavily Li-intercalated phase II, we observe a lattice expansion of ~7% in (001) direction in single-crystal X-ray diffraction, the emergence of new Raman peaks at 16.8 cm⁻¹, 109.0 cm⁻¹ and 132.8 cm⁻¹ in Raman spectroscopy and increase of electrical resistance for over 8 folds. *In situ* Hall effect measurements confirm the decrease in conductivity, which also decreases with decreasing temperature for the phase II, suggesting a semiconducting phase. The Hall carrier density falls from 10¹⁵ cm⁻² in pristine 1T'-MoTe₂ to 10¹⁴ cm⁻² in phase I and to 10¹² cm⁻² in phase II. Our results highlight the importance of electrochemical intercalation of Li ions as a powerful tool to manipulate phase stability and electron density of 2D TMDCs.

SESSION SF03.05: Characterization of Ion Insertion Dynamics
Session Chairs: Iwnetim Abate and Aditya Sood
Wednesday Afternoon, April 24, 2024
Room 339, Level 3, Summit

1:30 PM *SF03.05.01

Operando Dynamical Studies of Dynamics within Intercalated 2D Materials [Aaron Lindenberg](#); Stanford University, United States

I will describe two recent efforts probing the dynamics of ion transport and ion-induced metastable phases as probed by time-resolved optical, x-ray and electron scattering. In Li-intercalated WTe₂, we find a new metastable phase featuring an anomalously large in-plane chemical expansion coefficient (expansion per unit lithium inserted). It is common for 2D materials to expand in the out-of-plane direction upon intercalation, but large tunable uniaxial in-plane expansion is much more rare. The unusual actuation of Li_xWTe₂ is linked to the formation of a metastable crystallographic phase, potentially enabling novel means for strain modulation at high frequencies. In the second part of the talk I will describe recent efforts to visualize the dynamics of ion hopping in superionic materials.

2:00 PM SF03.05.02

Operando Optical Probes of Ion-Insertion-Driven Phase Change in Electrochemically Gated La_{1-x}Sr_xCoO_{3-δ} (LSCO) for Tunable Photonics [Rohan D. Chakraborty](#), Teslim A. Fasasi, Chris Leighton and Vivian Ferry; University of Minnesota-Twin Cities, United States

Electrolyte gating has enabled dramatic control of electronic, magnetic, and optical properties in materials *via* electrochemically driven ion insertion and extraction at the interface between electrolytes and active materials. In ion-gel-gated perovskite La_{1-x}Sr_xCoO_{3-δ} (LSCO) thin films with $x = 0.50$, strong interfacial electric fields can support sufficient oxygen vacancy formation/migration to drive a topotactic transformation from the as-grown metallic

perovskite phase to an insulating, oxygen-vacancy-ordered brownmillerite phase that extends from the surface through the depth of the film. Our recent *ex situ* refractive index studies uncovered large optical contrast before and after this electrochemically induced oxygen extraction, framing LSCO as an attractive phase change material for tunable photonics.

Here, we apply *operando* FTIR spectroscopy to ion-gel-gated LSCO films to carefully probe the reversibility and cyclability of the metal-insulator optical changes induced by oxygen insertion/extraction at the ion gel-LSCO interface. Specifically, we will show FTIR transmission measurements of $x = 0.50$ LSCO under ion-gel electrochemical gating that reveal a repeated opening and closing of an electronic bandgap by switching between the as-grown metallic perovskite phase and the voltage-induced insulating brownmillerite phase, over many cycles and at room temperature. The *operando* FTIR measurements of this electrochemically-mediated photonic switching are correlated with insights from XRD, spectroscopic ellipsometry, and electronic transport.

We find that the topotactic phase changes in ion-gel-gated LSCO films with $x = 0.50$ are nearly fully recoverable, with positive gate voltage driving oxygen extraction from the nominally metallic perovskite phase to form the insulating brownmillerite phase, and negative voltage driving oxygen reinsertion through the gel-LSCO interface to re-form the metallic perovskite phase. This opening and closing of an electronic bandgap is observed over many cycles in *operando* FTIR transmission measurements, with some hysteresis due to imperfect reconstruction of the original perovskite phase and asymmetric redox kinetics. These differences in electrochemical reduction vs. oxidation are further explored through *operando* measurements under different environments. A low-moisture environment further drives oxygen extraction in the brownmillerite phase of LSCO, while an ambient environment is preferred in the reverse direction to reinsert more oxygen through the LSCO-gel interface and recover the original perovskite phase. The enhanced ionic movement under these respective environments corresponds to lower optical loss in the insulating phase and higher loss in the metallic phase, widening the optical contrast in LSCO. Together, these findings answer important questions about the reversibility and endurance of the electrochemically driven optical changes in ion-gel-gated LSCO films, provide insight on how different environments affect ion insertion dynamics, and, combined with the nonvolatile and low-power nature of these optical changes, further highlight the powerful role that electrochemically driven ion insertion and extraction can play in developing tunable photonic devices for adaptive sensing, optical memories, and more.

2:15 PM SF03.05.03

Ion Exchange Pathways of Lithium and Sodium in Layered Oxides [Yu Han](#) and Chong Liu; University of Chicago, United States

Ion exchange in layered materials is one type of special ion transport process, which involves ion insertion and ion extraction simultaneously. This type of bi-directional ion transport requires the rearrangement of interlayer ions and will induce the phase evolution of layered host structures. More importantly, ion exchange is a powerful method to access metastable materials with advanced functionalities for energy storage applications. However, the ion exchange reaction pathways in layered materials remain elusive. Here, using layered oxides as model materials, we tracked the real-time phase evolution during Li-Na ion exchange in layered oxides. An interesting pseudo-charging behavior has been observed. Combining with the chemical composition information, the ion exchange pathway of phase separation between Li-rich and Na-poor phases was revealed. Depending on the chemical potential of exchange ions in the solution side, we identified two different exchange routes, the surface reaction-limited route and the diffusion-limited route. The phase separation behavior accompanied by the charge transfer is general in both ion exchange routes. Both DFT calculation and experiments point to that the co-existence of Li-rich and Na-poor phases is governed by thermodynamics. Besides, we demonstrate that structural vacancy level and lithium preference are critical in determining the feasibility of ion exchange. Guided by this understanding, Na_xCoO_2 was converted from the parent Li_xCoO_2 for the first time and $\text{Li}_{0.94}\text{CoO}_2$ was converted from Na_xCoO_2 at 1-1000 Li-Na (molar ratio) with electrochemical assisted ion exchange.

2:30 PM BREAK

3:30 PM SF03.05.04

Tuning The Insulator Metal Transition in Rare Earth Nickelates through Dynamic Electrochemical Ion Insertion Alan Zhang, Catalin Spataru, Joshua D. Sugar, Alec Talin and [Elliot J. Fuller](#); Sandia National Laboratories, United States

The rare earth nickelates have received renewed attention due to the discovery of superconductivity in infinite layered structures under substitutional doping[1] and the observation of widely tunable electronic behavior in perovskite structures for use in analog memory devices[2]. Recent work has demonstrated that interstitial dopants (H, alkali metals) can be introduced into nickelates to change the room temperature resistance by 10^6 - 10^8 . However, the evolution of the bond disproportionation transition as a function of interstitial dopants has not been reported and the doping fraction leading to rich correlated electronic behavior is often unknown. Therefore, the electronic phase diagram in nickelate compounds as a function of interstitial doping is of interest. Here, we carried out lithium doping of PrNiO_3 using a dynamic electrochemical process. We constructed electrochemical cells using epitaxial thin films as electrodes and then insert lithium using an electrolyte. For $\text{Li}_x\text{PrNiO}_3$, we find that increased lithium doping interrupts bond disproportionation causing a reduction in the ground state resistivity at small fractions $0 < x < 0.25$ with a successively smaller ON/OFF ratio. At larger fractions $x > 0.25$ we observe the disproportionation transition to be destroyed and fully insulating type behavior is observed over $T = 5$ -300K. Raman spectroscopy reveals that lithium introduces structural changes that affect A1g modes which are a sensitive probe of bond disproportionation. Density functional theory calculations confirm the disruption to bond disproportionation with an initial reduction in the bandgap at small fractions and an increase at larger fractions. The results point to interstitial doping as a powerful method to synthesize new phases in strongly correlated systems and for next generation memory devices.

[1] D. Li *et al.*, "Superconductivity in an infinite-layer nickelate," *Nature*, vol. 572, no. 7771, pp. 624-627, Aug 2019, doi: 10.1038/s41586-019-1496-5.

[2] H. T. Zhang *et al.*, "Reconfigurable perovskite nickelate electronics for artificial intelligence," *Science*, vol. 375, no. 6580, pp. 533-539, Feb 4 2022, doi: 10.1126/science.abj7943.

3:45 PM SF03.05.05

Redox-Free Ion Insertion: Discovery of Electride Materials for Electron-Anion Exchange [Rebecca Radomsky](#) and Scott C. Warren; University of North Carolina at Chapel Hill, United States

In order to maintain charge neutrality, ion insertion is accompanied by reduction or oxidation of the host lattice. However, a class of materials called electrides, where vacant crystallographic lattice sites are instead occupied by a bare anionic electron, exhibits a fundamentally different mechanism. The mechanism for anion insertion into electrides—which we have named Electron-Anion Exchange (EAX)—allows for the one-to-one swap of anions and electrons as the anion hops between “vacant” electride sites. Because the participating anionic electrons are not associated with any atomic nuclei, the surrounding atoms do not experience any reduction or oxidation throughout the insertion process. The consequences of redox-free EAX are substantial. Due to the similar size and charge of anionic electrons and simple anions, the host lattice experiences virtually no electrostatic change during ion insertion and the reorganization energy becomes negligible. In order to fully exploit the effects of EAX, including little to no lattice expansion upon intercalation and exceptionally low activation energies for ion diffusion, we have designed and synthesized a novel electride material, Y_6S_4 . Similar to previously known electrides such as Y_2C , Y_6S_4 has a layered structure with alternating layers of anionic electrons and host material. However, Y_6S_4 contains S pillars throughout the anionic electron layer that increase the interlayer spacing, causing the overlap with neighboring cations to be small. We predict the “pillared

layered" structure of Y_6S_4 to have not only a larger capacity, but also a significantly higher ionic conductivity than its layered electrified analogs. We therefore anticipate Y_6S_4 to be one of the most efficient anion intercalation materials to date—with natural applications as an electrode in anion shuttle batteries or electrochemical capacitors.

4:00 PM SF03.05.06

Optical Properties and Applications of Molecular-Intercalated MoS_2 Bo-An Chen, Sylwia Ptasińska and Prashant Kamat; University of Notre Dame, United States

Two-dimensional (2D) transition metal dichalcogenides have demonstrated intriguing tunability in optical and electrical properties through the intercalation of ions within the van der Waals gap of their layered structure. In this study, we present a spectroelectrochemical method for electrochemically intercalating quaternary ammonium molecules into a MoS_2 thin film while monitoring the optical properties through absorption spectra. Throughout the intercalation process, we observed attenuation in both A and B excitonic peaks, with complete quenching achieved at a sufficient applied potential ($E = -1.8$ V vs. Ag). Raman spectra indicated that the as-intercalated MoS_2 remains in a semiconducting phase (2H), with an additional out-of-plane (A_{1g}) vibrational mode appearing. Additionally, both X-ray and ultraviolet photoelectron spectroscopy (XPS and UPS) results showed the metallic-like properties of the as-intercalated MoS_2 , confirming successful intercalation of ammonium molecules and resulting in a high concentration of electron injection. In the second part, we demonstrate a potential application in solar energy storage using colloidal MoS_2 prepared through an electrochemical intercalation and exfoliation process. This study underscores the importance of further investigating ion intercalation in 2D materials and provides insights into the potential of Molecular-Intercalated MoS_2 for energy storage.

4:15 PM SF03.05.07

Implantation of Gallium into Layered Tungstene Disulfide Nanostructures is Facilitated by Hydrogenation Alex Laikhtman¹, Julio A. Alonso², Jose I. Martinez³ and Alla Zak¹; ¹Holon Institute of Technology (HIT), Israel; ²University of Valladolid, Spain; ³Institute of Materials Science of Madrid, Spain

In this work, experimental results and theoretical simulations for the implantation of Ga into WS_2 nanoparticles exposed to focused Ga^+ ion beams (FIB) with various doses are reported.

Multiwalled WS_2 and MoS_2 nanotubes and polyhedral fullerene-like nanoparticles were discovered in the earlier 1990s. An efficient synthesis method for the scaled-up production of high purity inorganic fullerene WS_2 nanoparticles was later developed, which allows to produce tens of kilograms per day. Additional efforts resulted in renewed synthesis of highly crystalline WS_2 and MoS_2 nanotubes in pure phase and scalable fashion. The availability of these nanomaterials led to investigation of their properties, and stimulated numerous applications in photoelectronics and nano-optics, tribology, and hydrogen storage.

Implantation of atoms into solid materials provides a way to modify their properties. Doping of layered MoS_2 and WS_2 nanoparticles with alkali metal atoms, Re, Nb, and possibly other elements is a promising technique to change the electronic (semiconductor to metal), magnetic (diamagnetic to paramagnetic), and optical properties, the surface characteristics, and the mechanical and chemical behavior of these materials. The modified materials could be used in nanotechnology applications, catalysts and sensors, as well as in tribology and lubrication. However, the implantation processes often have a damaging effect on the materials structure.

Bombarding WS_2 multilayered nanoparticles and nanotubes with FIB of Ga^+ ions at high doses, larger than 10^{16} cm^{-2} , indeed leads to drastic structural changes and melting of the material. At lower doses, when the damage was negligible or significantly smaller, the amount of implanted Ga was very small. A substantial increase in the amount of implanted Ga, and not appreciable structural damage, were observed in nanoparticles previously hydrogenated by a radio-frequency activated hydrogen plasma.

Density functional theory calculations reveal that the implantation of Ga in the spaces between adjacent layers of pristine WS_2 nanoparticles is difficult due to the presence of activation barriers. In contrast, in hydrogenated WS_2 the hydrogen molecules are able to intercalate in between adjacent layers of the WS_2 nanoparticles, giving rise to the expansion of the interlayer distances, that in practice leads to the vanishing of the activation barrier for Ga implantation. This facilitates the implantation of Ga atoms in the irradiation experiments.

SESSION SF03.06: Dynamical Switching of Electrons, Spins and Phonons
Session Chairs: Iwnetim Abate and Judy Cha
Thursday Morning, April 25, 2024
Room 339, Level 3, Summit

9:00 AM *SF03.06.01

Dynamic manipulation of thermal & structural properties using electrochemical & electrical stimuli Aditya Sood; Princeton University, United States

Beyond energy storage, ion insertion has emerged as a powerful method to dynamically tune the physical properties of materials[1]. While there have been numerous examples of electrochemical tuning of optical and electronic properties, the dynamic manipulation of thermal and structural properties is relatively less explored. I will first describe our efforts to create "thermal switches" – materials whose thermal conductivity can be tuned in real-time – using ion insertion. We show that the reversible intercalation of Li^+ into the van der Waals gaps in MoS_2 induces a ~8-10x modulation in the cross-plane thermal conductance[2], opening avenues for dynamic thermal management. Interestingly, we find that micron-scale heterogeneities in ion concentration can be imaged using spatially-resolved measurements of thermal conductance, suggesting that heat current measurements could enable operando microscopy in electrochemical systems. Next, I will briefly discuss how ion insertion can change the crystal structure and symmetry in layered crystals; in particular, we discover intriguing uniaxial in-plane lattice expansion caused by Li^+ intercalation in WTe_2 , a finding that has potential applications in electrochemical actuators[3]. Finally, I will describe our recent efforts to visualize nanosecond-timescale and picometer-lengthscale structural dynamics in materials driven electrically[4]. Such ultrafast operando techniques could provide fundamental insights into field-induced intermediate states, metastable phases, and transport pathways in ionic systems.

[1] Nature Reviews Materials 6, 847 (2021), [2] Nature Communications 9, 4510 (2018), [3] Advanced Materials, 33, 2101875 (2021), [4] Science 373, 352 (2021)

9:30 AM SF03.06.02

Unlocking Exotic Charge and Spin States in Layered Materials: A Dynamic Approach via Ion-Insertion Iwnetim I. Abate; Massachusetts Institute of

Technology, United States

Layered two-dimensional (2D) and quasi-2D materials, along with their heterostructures, offer a diverse range of electronic, optical, and magnetic properties. The tunability of charge, spin, orbital, and lattice degrees of freedom in these materials, both through static and dynamic methods, provides numerous avenues for addressing fundamental questions and exploring diverse applications. Electrochemical ion-insertion in these van-der-Waals materials serves as a delicate tool to dynamically adjust their properties, potentially leading to the emergence of exotic electronic and spin states that might not be attainable through traditional synthesis methods. In this presentation, I will share our group's research on layered oxide materials where we induce exotic charge and spin states using electrochemical ion-insertion. These unique states challenge existing theoretical models and experimental observations. I will delve into the novel theoretical framework we have developed, underpinned by rigorous computational formalisms, and the distinctive magnetic, optical, and phonon properties observed experimentally.

9:45 AM SF03.06.03

***Operando* studies of mixed-conduction polymers: Microstructural effects and carrier-induced ordering** [Alberto Salleo](#); Stanford University, United States

New families of conjugated polymers are being investigated as mixed conductors in applications as varied as biosensing, electrocatalysis and brain-like computing. Great advances are being made in developing materials properties and in device design and integration. A fundamental understanding of “how they work” is however still missing. In this talk I will show how we use a suite of state-of-the-art *operando* techniques, spectroscopic and diffraction-based implemented during electrochemical biasing to study organic mixed conductors and answer basic questions. In particular, we elucidate the effect of electrolyte and charge density on structure and properties, namely carrier mobility. Most of these materials are semicrystalline and microstructure has an effect on their operation. We find that charge density affects structure, which in turn affects the ability of the semiconductor to conduct charges